9th International Congress on the Chemistry of Cement New Delhi, India, 1992

Organised by

NATIONAL COUNCIL FOR CEMENT AND BUILDING MATERIALS

NEW DELHI

9th International Congress on the Chemistry of Cement New Delhi, India, 1992

CONGRESS REPORTS

Volume I



Organised by

NATIONAL COUNCIL FOR CEMENT AND BUILDING MATERIALS
NEW DELHI

Co-sponsored by:

Department of Scientific & Industrial Research
Ministry of Science & Technology
Government of India

Cement Manufacturers' Association, India

The India Cements Ltd

J K Cement Works

Madras Cements Ltd

Narmada Cement Co Ltd

Orissa Cement Ltd

This volume is a part of six-volume series of the Congress Papers.
Title of each volume is given below:

I	—	Congress Reports
II	—	Communication Papers - Theme I
III	—	Communication Papers - Theme II
IV	—	Communication Papers - Theme III
V	—	Communication Papers - Theme IV
VI	—	Reports on Special Panel Discussions and Poster Papers

Published by :
National Council for Cement and Building Materials (NCB)
M-10 South Extension Part II New Delhi-110 049 INDIA

No Part of this publication be reproduced without the written permission of the Publishers.

The views expressed in the technical papers printed in this publication are those of authors and not necessarily of the Publishers.

Printed in India by THE OFFSETTERS, New Delhi-110003

PREFACE

Commencing with a one-day meeting in London on 14 January 1918 arranged by the Faraday Society, to discuss "The setting of cements and plasters", which is taken as the first Symposium to deal solely with the chemistry of cement, the subsequent International Symposia and Congresses on the Chemistry of Cement have been held in Stockholm (1938), London (1952), Washington DC (1960), Tokyo (1968), Moscow (1974), Paris (1980) and Rio de Jenairo (1986). At the conclusion of the Rio Congress, it was decided that the next Congress will be held in India. Accordingly, the 9th International Congress on the Chemistry of Cement is being held in New Delhi, India, from 23 to 28 November 1992.

The preparatory and organisational work for this 9th Congress was commenced immediately after the 8th Congress. To start with, all the participants in the previous two Congresses and a large number of individuals and organisations interested in the subject of the Congress were contacted through an extensively worked out and widely distributed Questionnaire. The response was most encouraging. The responses were carefully analysed and the directions which would meet the views of the largest number of participants towards advancing the cement sciences were determined. Based on these findings the first Bulletin was issued in August 1988, providing the necessary preliminary information on the Congress and outlining its scope and essential organisational aspects.

The objectives of the Congress were set to advance the knowledge of chemistry of cements with emphasis on application of this knowledge in both the manufacturing aspects and utilization of cements in practice. Within this broad scope, the thrust was on tracking the scientific progress made in the field since the last Congress, assessing the status of exploitation of the results by the industry and the society, and mapping of the new frontiers of knowledge.

The overall organisation of the Congress was governed by a National Organising Committee which was responsible for all organisational aspects including financial arrangements. Taking into account the suggestions received from various quarters, the International Scientific Committee consisting of 67 experts from 39 countries all over the world was formed which was responsible to finalise : (a) the themes and sub-themes of the Congress, (b) procedures for inviting, receiving and reviewing of papers, (c) selection of authors for general and special reports, and (d) the system for conduct of the proceedings of the sessions and other related scientific and technical matters.

The International Scientific Committee held two meetings in New Delhi in November 1989 and in January 1991. In addition, informal meetings were held with representative groups in Seoul, Tokyo, Paris, Washington DC and Montreal. The International Scientific Committee finalised the Generic and Specific Themes of the Congress. It was decided that for each Generic Theme, there shall be one Principal Review Paper, which shall cover the progress achieved in the area of the Generic Theme between the two Congresses. For each Specific Theme, there shall be one Congress Paper highlighting trends of research and realisation of the results in the industry in the areas related to the Specific Theme. Under each Specific Theme, in addition to the invited Congress Papers, there shall also be Communication Papers. Both the principal review papers as well as the Congress papers were to be presented by the invited experts identified after deliberations of the International Scientific Committee.

Preliminary Abstracts of communication papers were solicited through the Second Bulletin in May 1991. 537 Abstracts were received which were scrutinised by a panel of Indian experts and 513 were short-listed. Authors were requested to send full manuscripts of the paper for detailed review and acceptance for publication and presentation. As many as 412 communication papers from 40 countries were received which were reviewed by a panel of international experts. As a result, 346 communication papers belonging to the four themes of the Congress were finally

accepted for presentation and publication. These were in addition to 21 State-of-the-Art Congress Reports received from invited authors; reports on two Specific themes could not be had because the authors selected expressed their inability at a late stage, making replacement difficult.

In addition to the papers on deliberative thematic sessions, a poster session is being organised on "Advances in Physico-Chemical Evaluation, Characterisation and Quality Control Techniques and Systems" for Clinkers, Particulate Cements, Hydrated Systems and Concrete Systems. The State-of-the-Art Report would be presented by an invited expert and 24 contributions made in the form of posters will be presented during the Congress. In addition, Special Panel Discussions are being organised to survey the newer frontiers of knowledge in the areas of computerisation in cement science and concrete systems; resource economy in cement and concrete making; and cement in hazardous waste management.

The proceedings in six Volumes contain all the above contributions received for the Congress. This **Volume I** contains the invited **State-of-the-Art Reports on the Generic and Specific Themes and the Poster Session.**

A novel feature of the 9th Congress will be that, in addition to the normal sessions as in the earlier Congresses, there will be three sessions to bring out the technological and techno-ecnomic impact of the scientific advances on the industry. These are intended to provide a better appreciation of the implications of the scientific advances specially on the process control machinery and related industries as well as on operational aspects related especially to energy conservation and environmental improvement. Texts of these Special Lectures will be published in Volume VII of the Proceedings to be brought out after the Congress, along with the texts of Addresses at the Inaugural and Concluding Sessions and List of nearly 550 delegates from 42 countries who are expected to attend the Congress.

I am grateful to the members of the International Scientific Committee for their whole-hearted co-operation, to those who reviewed the Abstracts, and to the International Panel of Reviewers of Manuscripts for providing very useful technical and editorial comments on the communication papers. The co-operation of the authors in accepting and implementing the reviewers' suggestions and revising their manuscripts accordingly is greatly appreciated. Thanks are also due to those authors whose communication papers could not be accepted essentially because the contributions did not fit in with the themes of the Congress and not because of any technical deficiency. We recommend that the authors have those papers published elsewhere.

The unstinted efforts put in by my colleagues in the National Council for Cement and Building Materials in all aspects of organising this Congress, is thankfully acknowledged.

A K Mullick
Chairman
International Scientific Committee
9th International Congress
on the Chemistry of Cement

New Delhi
14 September 1992

CONTENTS

Volume I

GENERIC AND SPECIFIC THEMES REPORTS

1. Chemistry, Structure, Properties and Quality of Clinker 3
M Moranville-Regourd and A I Boikova

2. Clinker Formation and New Processes 49
Vagn Johansen and T V Kouznetsova

3. Effect of Low Grade Fuels, Combustible Wastes and Non-traditional Raw Materials 83
S C Ahluwalia and C H Page

4. Mineralisers, Modifiers and Activators in the Clinkering Process 125
G K Moir and F P Glasser

5. Effect of Energy Conservation and Environmental Control Measures on Clinker Properties 155
S Sprung and M Delort

6. Special and New Cements 177
A K Chatterjee

7. Portland and Blended Cement 213
K C Narang

8. Advances in Portland and Blended Cements 261
R Sersale

9. Blended Cements 303
J B Udachkin

10. Development in Non-portland Cements 317
Su Muzhen, W Kurdowski and F Sorrentino

11. Advanced Cement Systems, Including CBC, DSP, MDF 357
Della M Roy

12. Chemistry of Hydration of Cements and Cementitious Systems 383
Franco Massazza and Masaki Daimon

13. Advances in Hydration at Low, Ambient and Elevated Temperatures 449
K L Scrivener and W Wieker

14. The Structure of Hardened Cement Paste 485
J J Beaudoin and P W Brown

15. Effect of Admixtures 529
Mario Collepardi and V S Ramachandran

16. Performance and Durability of Concrete Systems 571
P K Mehta, P Schiessl and M Raupach

17. Cement-aggregate Compatibility and Structure property Relationships Including Modelling 663
H M Jennings and Y Xi

18. Physico-chemical, Biological and Thermal Degradation Including Environmental Effects 695
A K Mullick and Satish Chandra

19. Fibre Reinforced Cement — Thin Sheets 737
A J Majumdar

20. Effect of Fibers-Matrix Interaction on Concrete Strength 775
Surendra P Shah and Chengsheng Ouyang

POSTER THEME: STATE OF THE ART REPORT

21. Advances in Physico-chemical Characterization and Quality Control Techniques for Cement and Concrete 794
Hiroshi Uchikawa

EXPLANATORY NOTES

The following symbols, which have been universally recognised by cement chemists for formulating more complex compounds, are used interchangeably with the respective oxide formulae throughout this volume:

A	:	Al_2O_3	K	:	K_2O
C	:	CaO	M	:	MgO
C	:	CO_2	N	:	Na_2O
$\overline{C}H$	:	$Ca(OH)_2$	P	:	P_2O_5
F	:	Fe_2O_3	S	:	SiO_2
H	:	H_2O	$\overline{S}$	:	SO_3

Commonly used abbreviations of more general nature are as follows:

DTA	—	Differential Thermal Analysis
EPMA	—	Electron Probe Micro Analysis
IR	—	Infrared
NMR	—	Nuclear Magnetic Resonance
RH	—	Relative Humidity
w/c	—	Water-cement Ratio
XRD	—	X-ray Diffraction.
SEM	—	Scanning Electron Microscope
EDAX	—	Energy Dispersive Analysis of X-rays

GENERIC THEME I

CHEMISTRY STRUCTURE PROPERTIES AND QUALITY OF CLINKER

Chemie, Gefüge, Stoffeigenschaft, Qualität, Zementklinker

CHEMISTRY, STRUCTURE, PROPERTIES AND QUALITY OF CLINKER

M Moranville-Regourd
Ecole Normale Superieure de Cachan, Paris, FRANCE

and

A I Boikova
Institute of Silicate Chemistry of the Russian Academy of Science, St Petersburg RUSSIA

SUMMARY

The width and specificity of each of the four problems of cement chemistry mentioned in the title put before the authors the task of choosing the optimum variant in describing the material. As we understand the impossibility of citation of the results of all papers published since the 8th ICCC, we gave preference to focussing on the main trends of investigations in the field of the cement chemistry. In particular, in recent years intense investigations have been dealt with the influence of both individual oxides Na_2O, K_2O, MgO, SO_3 and their combinations on the characteristics of separate phases, as well as clinkers and cements as a whole. Therefore it would be useful to make a comprehensive review of those works.

As for the chemistry of cement clinker, it was impossible not to touch upon the clinker formation process, the properties of the clinker liquid phase, nucleation and crystal growth of phases, mainly of alite.

The term "structure" was considered in two aspects: 1) atomic structure of phases, their change under the influence of various parameters, polymorphic forms, structure distortion, imperfection, fine texture of crystals; 2) mineralogy of clinkers, phase relations.

The properties and the quality of the material were described in the course of reporting and the quality of the material were described in the course of reporting the results of the respective research because these characteristics in each reviwed paper were closely related with the other data.

Широта и специфичность каждой из четырех проблем химии цемента, указанных в заглавии, поставили перед авторами задачу поиска оптимального варианта изложения материала. Поскольку невозможно представить результаты всех работ, опубликованных после 8-го Конгресса, авторы предпочли выделить основные направления исследованний в области химии цемента. В частности в последние годы проводились интенсивные исследования влияния Na2O, K2O, MgO, SO3 и их различных сочетаний на характеристики отдельных фаз и клинкеров и цементов в целом. Поэтому результаты этих работ представлены достаточно подробно.

При рассмотрении химии цементного клинкера невозможно было не коснуться процессов формирования клинкера, свойств клинкерной жидкой фазы, зарождения и роста кристаллов клинкерных фаз прежде всего алита

Термин "Структура" рассматривается в двух аспектах, а именно: I) атомная структура фаз, их изменение под влиянием различных параметров, полиморфные формы, искажение и дефектность кристаллов, их тонкая текстура, 2) минералогия клинкеров, фазовые соотношения.

Свойства и качество материала охарактеризованы в ходе рассмотрения соответствующей работы, так как эти характеристики как правило тесно связаны с другими данными цитируемого исследования. Тем не менее одна из работ общего характера представлена в отдельном параграфе "Качество материала".

1. GENERAL CONSIDERATIONS.

The existing necessity in the utilization of portland cement is inevitably related with the consideration of number of problems of cement chemistry which have been urgent for a long period of time. In particular, one of such problems is the development of new technique implying the decrease of energy consumption in cement processing.

The idea of the real possibility of improving the existing technology of portland clinker and development of new methods consists in the influence of impurities of initial raw materials on both the clinker formation and the crystallo-chemical state of phases and consequently on the properties of clinker and the quality of cement (1,2,3,4).

It is not fortuitous therefore that the chemistry of cement clinker begins with the chemical composition of raw materials as one of the main parameters having effect on all distinctive features of clinker formation (the temperature of the appearance of the liquid phase, melt viscosity, surface tension), on the nucleation environment and crystal growth of clinker phases, on their crystal chemical features, on the phase relations.

It should be noted that the chemical composition of impurities of raw materials is also one of their constantly varying parameters. This is connected with the working of new deposits of raw materials and the use of various industrial wastes.

Although the problem of industrial wastes is a special topic, it is worth mentioning, however, that the work on their utilization or more precisely on the study of the role of their chemical composition acquires increasing significance. This work implies also such important aims as: 1) the necessity of decreasing energy consumption for obtaining such expensive materials as clinker and cement due to the decrease of clinker formation temperature and activation of clinker phases; 2) the improvement of ecological situation in some regions owing to the utilization of wastes. Besides, the latter is related not only with the incorporation of impurities in the raw mixes but also with the possibility of partial substitution of exhausting raw materials.

This fact promotes the necessity of further research for receiving additional information on the influence of the chemical nature of impurities, their various combinations and quantity (with the necessary account of thermal schedule) on the above mentioned features of clinker processing, environment of its formation, mineralogy, crystallo-chemical states of phases (composition, structure, crystal form, imperfection, crystallinity), properties and quality of the proper material.

Recent studies on the chemistry of cement clinker (since the 8th International Congress) reviewed in this paper deal to some or other degree with the consideration of impurity effect on structure, properties and quality of clinker. Let us note that considerable attention of investigators was paid to the studies of the crystallo-chemical state of phases and phase relations concerned mainly with participation of oxides Na_2O, K_2O, SO_3, their different quantities and combinations. A special place among these investigations belongs to the research of environment of nucleation and crystal growth of the main clinker constituent – alite.

It seems useful to remind of the basic crystallo-chemical features of clinker phases taking into account the importance of this problem. Now this is also essential for the reason that from time to time there appear some papers in which the identification is made between C_3S and alite, C_2S and belite, C_4AF (or C_6A_2F) and the aluminoferrite phase, C_3A and the aluminate phase as the same phases.

"Pure" compounds are mere matrices with sufficiently convenient crystallo-chemical sites in the lattice for impurity atoms. It is well known that each of the real clinker phases contains a set of isomorphous impurities. From the physical- chemical standpoint such phases can be regarded as polycomponent solid solutions.

The occurrence of the individual set of impurities for each phase and the definite isomorphous capacity make it possible to predict the preferential distribution of some or other impurity among the phases on the base of the chemical composition of the initial raw mix.

The knowledge of the set impurities characteristic of each phase gives a possibility for varying the chemical composition of the phase and consequently its structure as well as the clinker properties.

Among the common features of the formation of real clinker phases - polycomponent solid solutions - attention should be drawn to heterovalence substitutions which are most characteristic of this group of minerals. These substitutions are also most advantageous for structure activation. Actually the requirement of charge compensation leads to structure distortion. In this case we observe not only the increase of structure imperfection but also the worsening of the quality of crystallinity.

The problem of supersaturation of silicate and aluminate phases with calcium oxide has been insufficiently studied hitherto. Nevertheless by EMPA determination of the chemical composition of phases directly in clinker an excess CaO has often been found in the silicate and especially in the aluminate phases. However the synthesis of analogous phases in laboratory conditions seems difficult.

The most important consequence of the occurrence of impurities in the lattices of matrix clinker compounds is a disagreement between the calculated and real amount of phases in clinker. At the same time up to now the calculated quantitative phase composition of clinker is most often determined based on "pure" C_3S, C_2S, C_3A, C_4AF.

It should be noted in addition that EMPA results concerning the composition of phases of various commercial clinkers showed (5) that in the ratio of oxides $CaO:Al_2O_3:Fe_2O_3$ the aluminoferrite phase is close to the 6:2:1 composition and not to 4:2:1 which is usually used in the calculation. The difference in Fe_2O_3 content between these two phases is rather significant, 22.8% and 32.8% respectively.

Very useful data related with the determination of quantitative phase composition of clinkers are reported by Taylor in his new book "Cement Chemistry" (6).

Let us also remind that impurities are one of the main factors of the stabilisation of various crystalline forms of C_3S (T_I, T_{II}, T_{III}, M_1, M_2, M_3, R), C_2S (γ, β, α' L, α' H,α), C_3A (cubic, orthorhombic, tetragonal and monoclinic forms (7) obtained by stabilization with Na_2O), according to (8) - cubic, orthorhombic and monoclinic forms.

Among the numerous directions of impurity effects on clinker formation the following fact is also worth mentioning. Complication of the chemical composition of phases (the general problem of materials science) due to the impurities in their lattices is the base of structure activation and improvement of the material properties. Impurities favour the formation of phases with defect structure, the distortion of lattices, the disorder in distribution structural elements of crystal lattices of phases. All these fine changes in structure of matrix compounds inevitably promote the change in properties of phases.

A considerable role in the chemistry and mineralogy of cement clinker belongs to quantitative changes in phase relations. First of all this concerns the silicate phases – alite and belite. Actually, at definite concentrations of such oxides as Na_2O, K_2O, Cr_2O_3, TiO_2, P_2O_5 in the batch solid solutions of alite become unstable and decompose yielding the other phases such as belite and CaO. The belite content in clinker increases in this case.

The fact related with the chemical composition of the starting raw mix and its impurity content is also worth noting. If the quantity of impurities in the initial raw mix exceeds somewhat the quantity to be distributed among the clinker phases, the appearance of secondary phases may take place in clinker, namely: K_2SO_4, intermediate compounds $2C_2S{\cdot}CaF_2$, $2C_2S{\cdot}CaF_2$, $3C_2S{\cdot}3CaSO_4{\cdot}CaF_2$; $2C_2S{\cdot}CaCO_3$, recently found $K_2O{\cdot}Al_2O_3$.

It should also be mentioned that some impurities of raw materials influence the size of nodules, dusting and formation of coating. Thus a compound $K_3Ca_2(SO_4)_3F$ was found in the cyclone heat exchanger. For practical purpose it is important to know the properties of secondary compounds. For instance, in presence of K^+, Na^+, P^{5+} and Mo^{3+} the decrease of surface tension of the clinker liquid phase is accompanied by a decrease in size of clinker granules.

The impurity chemical composition of the batch is responsible for nucleation and growth of crystals of the major silicate phase – alite, influences its fine texture dependent also on many other parameters. Thus with increasing MgO content in the raw mix large zoned crystals of alite transform into small faceted crystals practically representing the polymorphic form M_3. If more than 1% SO_3 is present in clinker, the formation of anomalous large alite crystals of irregular form, mainly of the M_1 modification, takes place. The SO_3 effect on the fine texture of alite can be delayed due to alkalis.

At present much attention is paid to the study of alite fine texture which can testify to the actual formation conditions of this clinker major phase. Quantitative calculations of clinker microstructure can be regarded as an attempt to predict the strength of cement after 28 days hydration (studies of India and Japanese scientists).

In the given General considerations we paid special attention to a number of problems which make up the chemistry of cement clinker. So far as the clinker phases and phase relations finally determine all the properties of clinker and the quality of cement, the problem of obtaining new data on their crystallo- chemical possibilities remains invariable.

2. CHEMISTRY AND PHYSICAL CHEMISTRY OF CLINKER.

2.1 Clinker Liquid Phase

Formation, structure and properties of the clinker liquid phase have been reviewed by Timashev at the 7th ICCC and in the investigations of his successors (3,9). The author regards the clinker liquid as a weakly associated high-base melt, analyses the acid-base equilibrium in the melt, concerns the problems of viscosity, electrical conductivity, surface tension whose value is typical of electrolytes.

The data on the influence of various impurity elements on the physical-chemical properties of clinker liquid phase are given in the papers mentioned above. In particular, viscosity of a melt decreases in the presence of s-elements in the series K ⇒Ba ⇒Na ⇒Sr ⇒Ca ⇒Mg in which their basic properties decrease. At the same time viscosity decreases under the effect of p-elements whose acid properties

decrease in the series $\{Al \Rightarrow P \Rightarrow B \Rightarrow S \Rightarrow Cl \Rightarrow F$. In presence of d- elements viscosity decreases with decreasing degree of oxidation of the elements and weakening acid properties, for example in the series Mo ⇒W ⇒Cr ⇒Ti ⇒Mn ⇒Fe ⇒Co ⇒Cu ⇒Ni ⇒Zn ⇒Zn ⇒Cd.

Not dwelling upon the peculiarities of the behavior of the liquid phase under the effect of both separate impurities and their combinations, let us pay special attention to the role of K, Na, Mg, and S. This will be necessary because we shall consider below the effect of various combinations of oxides of these elements on phase relations in clinker, on crystallo-chemical state of the phases and their hydration properties.

It was shown in (3) that an increase of viscosity under the effect of K and Na was compensated by magnesium. Thus the increase of viscosity due to the presence of 1,5% (K_2O + Na_2O) was fully compensated by 6,5% MgO. Further increase of MgO content brings about an increase of viscosity which can be due to supersaturation of the melt with magnesium. The SO_3 influence leading to a decrease of viscosity is weakened by the presence of sodium and potassium. But when K^+ and Na^+ are present together in amounts providing the formation of K_2SO_4 and Na_2SO_4, the melt viscosity decreases.

The authors of the present review do not have the aim of a detailed analysis concerning the dependence of physical-chemical properties of the clinker liquid phase on a number of various parameters. It should be noted, however, that one of the most important practical results from the study of properties of the clinker liquid phase, – the ways of a decrease of its appearance temperature – has not been widely discussed in the recent literature.

It is not accidental that this idea was not forward by Kakali et al (10) who studied the influence of compounds of transition elements MoO_3, Nb_2O_4, WO_3 and ZrO_2 on the properties of clinker and cement with a view of their improvement. The authors state that up to these days little attention has been paid to the effect of small amounts of impurities on the process of sintering and on the properties of the liquid phase.

They also mention that whereas the major part of alite is crystallized from the melt, the aluminate and aluminoferrite phases are crystallized after the liquid phase has been hardened; impurities cannot but influence the crystallization conditions and consequently the properties of clinker. It should be noted that the effect of the indicated compounds on the liquid phase properties has been estimated by the authors on the basis of mineralogical analysis of alite crystals. This fact attracts our attention because at present some works are being carried out with the aim of determination of nucleation and growth conditions of alite crystals from the study of their fine texture (11). This problem will be concerned with in our paper below.

The authors of the reviewed paper (10) showed that Mo and W as the most acid elements of the four elements under study decrease the liquid phase viscosity and thus increase the rate of diffusion of solid components through the melt. This results in the formation of large alite crystals. As to Zr and Nb, the increase of the C/R ratio (charge/radius) weakens the influence of these ions on the melt viscosity. The effect of the studied compounds on the crystallization of aluminate and aluminoferrite phases as well as on the texture of belite has been found by the authors.

It is worth mentioning that the influence of Mo, Nb, W and Zr on the temperature of appearance of the liquid phase is insignificant. In conclusion, the authors (10) remark that they are faced with the problem of clarifying the influence of transition elements on the properties of clinker, quality of

cement, energy consumption during sintering. They also established that adding these compounds to the raw mix is a promising way of controlling the clinker formation conditions and consequently clinker microstructure.

Ivashchenko studied (12) the influence of s-elements (K, Na, Ba, Sr, Mg), d-elements (Cd, Zn, Ni, Cu, Mn, Mo, V, W. Cr, Ti), p-elements (Sn, Pb, Cl, F, P, B) on viscosity, surface tension, density and electronegativity of the liquid phase. These studies formely guided by Timashev have been continued in the direction of practical use of the results of physical-chemical investigation. The initial clinker raw mix for obtaining the melt was of the following composition (mass %): CaO - 57.0 %; SiO_2 – 7.5 %; Al_2O_3 – 2.2 %; Fe_2O_3 – 12.9 %. The above indicated elements were introduced to the clinker raw mix in the form of appropriate oxides or other compounds as well as in the form of wastes of chemical and metallurgical industries, (magnesium- titanium processing, processing of pigmental titanium diopside and non-ferrous metallurgical slags). The wastes utilized, besides the oxides CaO, SiO_2, Al_2O_3, Fe_2O_3 usual for cement raw mixtures, contained compound of titanium, manganese, sulphur, chlorine, fluorine, zinc, copper, nickel, magnesium and others which exerted a positive influence on the methods of cement synthesis and hydration. The use of wastes was part of solving the ecological problem.

The authors of paper (12) attract our attention from the point of view that impurity components were added to the initial batch as optimally selected groups. Complex modifieres were selected in such a way that they would exert a considerable effect on the most energy consuming stages of firing - decarbonization of the lime component and sintering of raw mixes with participation of the melt. The composition of complex modifiers consisted of the elements accelerating the decomposition of calcium carbonate (Fe^{2+}, Mn^{2+} and others), increasing the SiO_2 activity (F^-, Cl^-, K^+, Fe^{2+}), accelerating the decomposition of crystal lattices of SiO_2, clay and other minerals (F^-, Cl^- a.o.) and intensifying the mineral formation process owing to the decrease of melt viscosity and to the lower temperature of the melt appearance (F, Cl, Zn, Mn, S a.o.) which led to accelerate the delayed stage of alite formation.

Addition of complex admixtures permitted to improve the granulometric composition of clinker, decrease dusting, improve the work of rotary kilns, increase the hydraulic activity of cement. Industrial tests showed that the doping of wastes as complex modifiers in amounts of 1.5 to 6 mass % led to a 2-9 % decrease of fuel consumption for clinker firing (by wet processing), to a 10-15% consumption decrease of electrical energy for grinding modified clinker and to a 2–7 MPa increase of compressive strength. The author (12) explains the increase of strength characteristics of cement stone by high activity of calcium aluminoferrite and alite formed in modified clinkers.

Tests of the studied cements in concretes showed that such concretes possessed a higher value of 28 days compressive strength (to 15.8% and more). The increase of compressive strength of test concretes is much intense. To conclude the review of the above paper (12), let us emphasize its practical importance. Distinctive features of the influence of complex modifiers on clinker synthesis revealed in this study permitted to develop energy-consuming technologies using industrial wastes. Cements and concretes obtained on their base such technologies show improved practical characteristics.

In the study of impurity influence on the properties of clinker melts the authors (13) indicate that impurity elements control both the temperature and the interval of existence of the clinker melt. The peculiarity of the experiments implies the addition of impurity by sharp firing at 1100°C into calcareous component which then interacts with belite clinker (LSF ≈ 0.67). It was shown that the melt in such two batch mixtures appeared at a lower (by ≈ 50°C,) temperature than in the usual batch of analogous chemical composition even in the absence of impurity, namely at 1283°C and 1335°C, respectively.

In a two-batch mixtures (calcareous component + belite clinker) the beginning of the clinker melt appearance and the temperature range of its existence are most influenced by two elements: Ba and Mn. In the presence of Ba the melt appears at a lower temperature (1290°C) and the crystallization is complete at 1217°C. In this case the greatest temperature interval of the existence of the clinker melt was observed.

The influence of manganese is opposite, namely: the temperature of the melt appearance increases by 50°C and the crystallization sharply accelerates and starts 60°C earlier, i.e. at higher temperature. In conclusion the authors (13) indicate that the appearance of the lower-temperature melt and the larger interval of its existence are characteristic of two- batch mixtures both containing or not containing additions of oxides of Zn, Ba, Bi, Sr in calcareous components.

The authors (14) studied the clinker formation using slags enriched with ferrous compounds including Fe^{2+} Slags were used as a ferrous component of the clinker raw mix. The authors found that the most energy-consuming stage of clinker formation - decarbonization - proceeds in the temperature interval 600- 800°C; the clinker formation temperature decreased by ~ 50°C. Microscopic analysis showed that the clinker obtained contained alite and belite crystals of small size. Industrial tests showed that the use of converter slags as a ferrous component of the raw mix is promising as it provides the decrease of energy consumption with simultaneous solution of some ecological problems.

Having considered one of the directions of cement chemistry, i.e. the processes of clinker formation, the authors of the present review did not pursue the aim of a detailed description of all the studies performed since the 8th ICCC. Our main task was to reveal the modern trends in the development of this problem. One of the trends concerns the crystallization of clinker phases. This is essential because the fine texture of crystals, their size, shape and surface peculiarities are indicative of the conditions of their nucleation and growth, environment of clinkering.

2.2 Clinker Phases.

2.2.1 Crystallization of Clinker Phases

2.2.1.1 Nucleation and Growth of Alite Crystals. – A significant contribution to the chemistry of clinker was made by Maki who studied the nucleation and crystal growth of alite, its fine structure, recrystallization and morphological instability, the influence of processing parameters (impurities, firing temperature, heating rate) on the character and texture of crystals. Maki emphasized that the fine texture of constituent clinker minerals and their chemical composition determine the quality of clinker and can serve the source of information as regards the actual clinker processing environment.

The main results of Maki's research have been reported at the 8th ICCC (11). In particular, nucleation and growth of alite crystals are regarded as processes taking place in the high-temperature solution. In clinker such a solution is an interstitial melt (liquid phase) that appears at 1300°C in an amount of ~ 20 %. As is known, the occurrence of the interstitial liquid phase in clinker decreases the C_3S formation temperature and promotes crystal growth.

The dissolution of CaO and C_2S in the melt leads to supersaturation providing nucleation and growth of alite crystals. The high-temperature melt, on the other side, is a source of various crystal defects. The chemical and physical properties of the interstitial melt exert a strong influence on the growth mode of alite. The rate of nucleation influences the average size of alite crystals. In general from the kinetic and thermodynamic points of view higher temperatures are more preferable for nucleation. For the analogous process to take place, but at a lower temperature, a stronger supersaturation is needed.

Maki makes an analysis of homogeneous and heterogeneous nucleation and concludes that the true homogeneous nucleation can never be attained in portland cement clinker.

Depending on the nucleation and growth conditions a number of morphologically unstable crystals are formed : celluar, skeletal and dendritic.

One of the reasons of growth instability is entrapment of the liquid phase by crystals which takes place at high rate of crystallization. At stable growth crystals grow without inclusions. This criterion of growth stability is especially useful in analysis of fine crystalline texture of alite in clinker.

Inclusions of liquid phase are usually concentrated in the core of the crystal which can also contain entrapments of belite and lime. Under unstable growth conditions bubbles of air or gas can be entrapped by the crystal.

Under conditions of unstable growth alite can crystallize mainly in the M_1 modification. At low growth rate the crystals develop without inclusions which is evidence of growth stability. In this case alite is mainly formed as M_3.

When the growth rate is decreased, the character of crystal growth of alite changes from the unstable to the stable state. The phase formed changes from M_1 to M_3, accordingly. The core of the crystal formed in the unstable state is more defective than its periphery formed at stable growth. The density of dislocations in the core of the crystal is much higher than in the periphery.

Recrystallization in the later stage of clinkering is rather characteristic of alite; it influences considerably its crystalline texure. This seems observable when clinker is kept at rather high temperature and the crystals formed earlier are small in size. During recrystallization the crystal form of alite changes significantly from tablets on (0001) to massive granules with the pyramidal faces $\{10\bar{1}1\}$ and $\{1\bar{1}\,02\}$ well-developed.

As a rule, the M_3-form of alite develops in clinker as the recrystallization product with a decrease of impurity in solid solution. If the clinker contains a small amount of impurity, in particular MgO, the recrystallization product appears as T_2, which shows low birefringence, oblique extinction and polysynthetic twinning.

Maki considers the interrelation between clinker formation conditions and fine crystalline texture of alite. In general the crystallization includes two processes - nucleation and growth. Different crystalline textures of alite depend on which of these two processes predominate .

Usually nucleation predominates when supersaturation is so high that crystallization occurs far from equilibrium conditions. The nucleation rate is increased with increasing firing temperature. At high nucleation rate a decrease of supersaturation takes place owing also to the limited growth environments in clinker which is accompanied by the formation of small faceted crystal individuals consisting mainly of M_3.

Under conditions when the growth of crystals predominates over nucleation, the unstable growth of crystal individuals continues. Such a situation can take place in actual clinker processing at relatively low temperatures. In this case the appearance of the new crystallization centres is depressed and the growth of individual crystals proceeds at sufficiently high rates. In the early stages of clinker processing

it is the M_1-form of alite that mainly develops; it may both contain or not contain inclusions of the melt which depends on growth rate.

A decrease of supersaturation, as a result of progress of clinkering reactions leads to the appearance of M_3 which grows from the nucleus of M_1 to produce zoned alite crystals. The new crystallization centres consisting of M_3 which continue to nucleate are rare.

As the processing conditions of M_1 and M_3 are similar, there exists a tendency toward the appearance of hybrid crystals as inclusions of one phase to another and more seldom as zoned crystals.

Maki analyzes the influence on the fine texture of alite of various processing parameters such as heating rate, maximum firing temperature, retention time, preparation of the raw mix, impurities.

Rapid heating of the raw mix to sufficiently high temperatures promotes the dissolution of CaO and C_2S in the melt thus stimulating supersaturation and predominance of nucleation. With decreasing heating rate or firing temperature, it is the growth process but not nucleation that comes to predominate. In this case the fine crystalline texture of alite changes systematically. At slow heating rate well-faceted crystals with M_1 and M_3 intergrown in patches tend to appear.

High growth rate of alite compared to the nucleation rate can be attained at relatively low firing temperatures; the growth is unstable and M_1 appears in preference to M_3 which is usually formed at lower growth rates. A great influence on the fine structure of alite is exerted by firing the raw mix below the temperature of the appearance of the liquid phase. Inhomogeneity of the raw mix leads inevitably to wide local variations of fine texture of alite.

The modula H.M., S.M., I.M., L.S.F characterizing the raw mix change significantly its burnability and as a result influence the fine texture. In particular, the A/F ratio (I.M.) influences the viscosity of the interstitial melt and consequently the growth mode of alite (11).

Maki gives a detailed consideration of the influence of impurities which mainly changes the physical properties of the liquid phase and consequently the dissolution rate of CaO and C_2S. Thus MgO decreasing the liquid phase viscosity accelerates the formation of C_3S. With increasing MgO content in the raw mix large zoned crystals of alite can be completely replaced by small faceted crystals consisting mainly of M_3.

In contrast to MgO, SO_3 influences the growth process of alite crystals and the increase of their size. Under normal clinker processing conditions the addition of a small amount of SO_3 favours to produce zoned crystals mainly as M_3. If the clinker contains more than 1 % SO_3, anomalously large alite crystals consisting practically of M_1 are developed. They are irregular in shape (skeletal, dendritic). The alite crystals entrap the interstitial melt. Fine grains of belite and lime can be entrapped by the alite crystals.

The influence of SO_3 on the dissolution of CaO and C_2S is not straightforward. Sulphate ions decrease the viscosity and make easier the dissolution of CaO. At the same time the decrease of surface tension which facilitates the dispersion of CaO grains and promotes their growth can reduce the first effect. In the presence of SO_3 and alkalis the formation of two liquids can take place. The influence of SO_3 on the fine texture of alite can be considerably decreased due to high alkali concentration. When analysing the mutual effect of MgO and SO_3 Maki mentions that high content of MgO in the raw mix improve the formation of M_3; SO_3 stabilizes M_1 (Fig.1).

By means of EPMA, the study of the distribution of impurities (Mg, Al, Fe) in zoned crystals of alite was made (15). It was shown that the Al + Fe content was much higher in the core of the crystal than in the periphery; the Mg content was practically the same in both parts of the crystal. The high concentration of (Al + Fe) in the core of the crystal may come from the high growth rate in the early stage of crystallization. It was also found that the Al concentration in the core of the crystal can be about twice as high as in its periphery. Fig.2 shows the concentration of Al, Fe, Mg in the core and on the periphery of zoned crystals of alite (11).

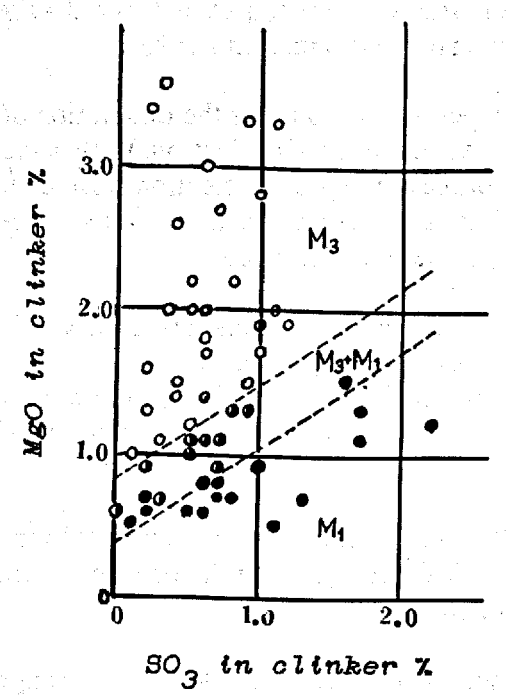

Fig.1. Phase constitution of alite against MgO and SO_3 contents in portland clinker. (Maki, 1986).

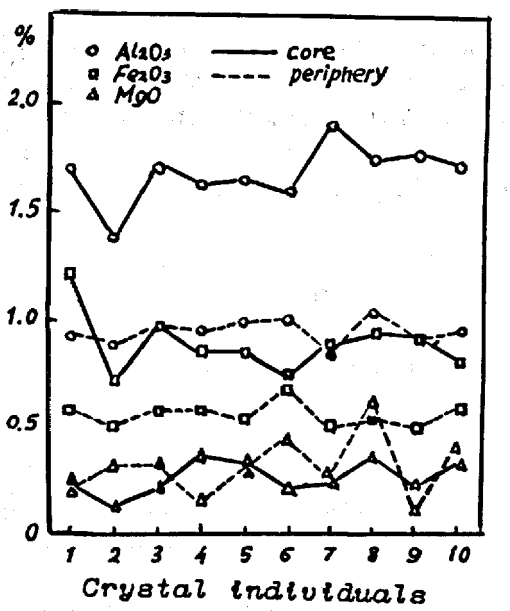

Fig.2. Distinction of chemical composition between the core and periphery of zoned alite crystals (Maki, 1986).

The study of the dependence of impurity concentrations on the crystallization temperature showed that the amount of all impurities in the crystal decreases with increasing crystallization temperature. This tendency shows up especially for Al and Fe. The amount of Mg in alite increases linearly with increasing amount of MgO in clinker. As to the correlation between the Al_2O_3 and Fe_2O_3 contents in the alite and clinker, there is some disagreement among the investigators (11). As shown in (12), the contents of Fe_2O_3 and Al_2O_3 in alite, belite and clinker are interrelated and can be represented as follows:

Fe_2O_3 (of alite) = (0,17 - 0,36)Fe_2O_3 (of clinker);
Fe_2O_3 (of belite) = (0,27 - 0,48)Fe_2O_3 (of clinker);
Al_2O_3 (of alite) = (0,09 - 0,23)Al_2O_3 (of clinker);
Al_2O_3 (of belite) = (0,21 - 0,38)Al_2O_3 (of clinker).

The existence of a correlation between Al_2O_3 and Fe_2O_3 at their incorporation in the alite lattice was indicated in (11).

Table 1 shows the growth mode and fine texture of alite according to the data of Maki (16).

TABLE 1

Growth mode of alite

Growth mode	Unstable	Stable
Growth rate	high	low
Liquid inclusions	abundant	scarce
Al, Fe concentration	high	low
Constituent phase	M_1 or M_3	M3 or M_1
Morphology	irregular	regular (faceted)
Direct concentration	high	low

Maki analyses the correlation between the environmental conditions and the growth mode of alite. According to (16), the conditions of alite crystallization in the early stage of clinkering can be classified into three categories with decreasing initial supersaturation of C_3S:

(1) high nucleation and low growth rate;
(2) low nucleation and high growth rate;
(3) low nucleation and low growth rate.

In this case the low initial supersaturation causes delayed nucleation and the crystal growth also proceeds at low rate. Maki reports that the size of alite grains depends on the ratio of the growth rate to the nucleation rate.

Maki considered the influence of various parameters on the environmental conditions such as the heating rate of the raw mix, the maximum firing temperature and retention time at this temperature, the particle size of the raw mix and the particle size distribution of impurities (16). He also studied the conditions of alite recrystallization which takes place in the later stage of clinker formation.

The recrystallization process of alite has been investigated by Mituzas (19). He has some reason to assume that just after the appearance of the liquid phase the R-form of alite is formed. Futher increase of firing temperature, as shown by X-ray diagrams, gives evidence in favour of the formation of monoclinic and then triclinic alite. The author also indicates that the rate of recrystallization depends mainly on the composition and viscosity of the liquid phase, other conditions being equal.

2.2.2 Phase Relation: Influence of Na_2O, K_2O, MgO, SO_3. Properties of Phases and Materials.

The formation medium of real clinker phases whose matrix bases are C_3S, C_2S, C_3A, C_4AF, C_6A_2F is polycomponent oxide system. Minor impurity components create favourable conditions to form clinker phases with a set of isomorphous impurities in the lattice at temperatures which are lower than the ones in "pure" systems.

The peculiarity of polycomponent clinker systems is the fact that one cannot neglect even small amounts of impurity components which are usually the participants of phase equilibria (together with CaO, SiO_2 a, o.). This can be well illustrated by the above metioned example of interaction between C_3S and such components as Na_2O, K_2O, Cr_2O_3, TiO_2, P_2O_5, SO_3.

2.2.2.1 Role of Na_2O, K_2O – At definite concentrations of each of the indicated compounds the solid solution decomposes yielding the formation of new phases, mainly C_2S and CaO. Thus, the limiting solid solution of C_3S with Na_2O contains less than 1 mass % of the alkali component (0.7 mass % Na_2O according to the data of Japanese scientists). In clinker alites the quantity of Na_2O in the solid solution is even less (~ 0.3 as reported in (20)). However, a small quantity of Na_2O in the solid solution (0.7 wt %) is quite sufficient for the C_3S triclinic lattice to transform into monoclinic one. At the same time the alkali cations Na(K) in the clinker batch always cause the change of phase relations between alite and belite towards the decrease of the amount of the first and increase of the latter.

Alkali elements make it difficult for alite to form, make its structure strongly distorted and unstable. The reasons of this phenomenon consist both in the peculiarities of C_3S atomic structure and isomorphous substitution of Ca^{2+} by $2Na^+$. One Na^+ atom occupies the Ca^{2+} site but there is no convenient site in the C_3S lattice (21) for the other Na^+ atom needed for charge compensation. Hence it is understandable why alite always contains a small amount of alkali elements and why the latter distort strongly the C_3S lattice. At definite concentration of alkali elements the solid solution of alite decomposes (as is usually spoken of) producing belite and CaO, but as reported by Japanese sientists, Na_2O,CaO, SiO_2 and CaO.

The increase of $Na_2O(K_2O)$ content in the clinker batch leads to a situation when no alite will be formed. This was shown in (22) when studying the influence of Na_2O, K_2O on phase relations in five-component clinkers (CaO, MgO, Al_2O_3, Fe_2O_3, SiO_2) with LSF of 0.87 and 0.92. With an increase of Na_2O in the batch from 0.3 to 5.0 and K_2O from 0.6 to 6% the quantity of alite decreased practically to zero and that of belite increased. The author (22) analysed the X-ray patterns of clinkers (LSF = 0.87) with 4.75% MgO in which the Na_2O amount changed. Clinker without Na_2O contained alite, β-modification of belite, the aluminate and aluminoferrite phases and periclase. When 0.3% Na_2O are added to the batch, the phase composition of clinker changes slightly namely: the intensity of the β-belite maximum increases somewhat. When 1.3% Na_2O are present in the sample, the changes of phase composition are rather strong: the amount of alite decreased markedly and that of belite increased; part of belite was formed as α'-modification.

With increasing Na_2O concentration a more intense decomposition of alite and an increase of belite content were observed. Besides, instead of the β-form, α'- and α- belites are formed. When the batch contains 5% Na_2O, no alite has been formed in the clinker, belite is present in α' and α-modifications; the sample contained periclase, free CaO. In this series of clinkers with increasing Na_2O concentration the quantity of the aluminate phase is increased and that of the aluminoferrite phase decreased. Besides the aluminoferrite phase becomes more ferrous.

A correlation between the content of free CaO and LSF and Na_2O is observed. At the same amount of Na_2O added to the clinker the quantity of free CaO is the greater, the higher the LSF value. This fact is obvious from analysis of phase relations in clinkers using the data of X-ray diagrams. When K_2O is added to the clinker batch, the decomposition of alite producing belite and CaO takes place at slightly higher K_2O concentration. With increasing K_2O content in the batch the quantities of α'- and α- modifications of belite also increase.

2.2.2.2 Role of MgO.– A special role in the formation of clinker phases and phase relations belongs to MgO. MgO acts in opposition to $Na_2O(K_2O)$ with respect to decomposition of solid solutions. Magnesium makes it difficult for solid solutions of C_3S with $Na_2O(K_2O)$ to decompose. Thus the X-ray determination of phase composition of clinkers with 2% Na_2O showed that the clinker with

4.5% MgO contains significantly higher quantity of alite (by 20% higher than the clinker with 1% MgO). This phenomenon was observed also in the case of solid solution of C_3S with Cr_2O_3 and C_3S with Cr_2O_3 and MgO (23).

A special role of MgO in its influence on the properties of the liquid phase and other processes was indicated by several scientists (1,3) whose studies dealt not only with Na and K but also with S. Thus, as shown in (24), the non-uniformity of volume change of cement containing more than 2% MgO was neutralized by such an amount of SO_3 that can be determined using the formula: $\%SO_3 = 0.67$ ($\%MgO = 2$). It is also reported that a method has been found to neutralize MgO in an amount of more than 3% by adding sulphates which permits to obtain a portland cement with higher MgO concentration and with the uniformity of volume change.

The study of the properties of the clinker liquid phase showed also the while the ions K^+ and Na^+ increase the melt viscosity, the ions Mg^{2+} decrease the latter, which was indicated above. Maki (11) also marked the influence of MgO opposite to that of SO_3 when he studied the nucleation and growth of alite crystals from the liquid phase. This was also mentioned by Gartner and Tang (25).

In the study of the MgO influence on phase relation in clinkers composed of CaO, Al_2O_3, Fe_2O_3 and SiO_2 it was shown (22) that the alite/belite ratio increases as much as 1.20-1.25 times, and the aluminoferrite phase / aluminate phase ratio as much as 1.5-1.7 times with increasing amount of MgO from 0 to 4%. On the contrary, with more than 4% increase of MgO the decrease of the indicated values was found to take place, i.e. the correlation between the decrease of alite content and increasing viscosity of the clinker liquid phase is observed when the MgO content exceeds 4.0%

According to the data reported in (3) the increase of viscosity of the clinker liquid phase proceeds at MgO content of more than 6%. The increase of viscosity makes difficult the crystallization of alite. Experiments showed that if the initial clinker mix contains more than 2.0% MgO, the formation of periclase takes place in clinker.

When discussing the role of MgO it is worth mentioning some papers dealt with clinkers and cements with elevated MgO content. This problem is actual as some countries are interested in the use of raw materials rich in MgO.

Luginina et al (26) investigated the possibility of utilizing clinkers with 6-7% MgO. As the magnesium-containing raw mix the authors used the marl with high content of dolomite. The clinkers studied contained also small quantities of Na_2O, K_2O, TiO_2, P_2O_5, SO_3. In some cases the quantity of K_2O reached 1.0-2.0% and that of SO_3 ~ 1.0%.

By means of EPMA, it was shown that in impurity composition in the lattices the clinker phases differ somewhat from the phases in clinkers with lower quantity of MgO. In particular, it was found that α'- belite contained increased quantity of MgO (3-4%) and also Al_2O_3 and Fe_2O_3. Belite also contained considerable amount of K_2O. It was also found that the quantity of impurities in α-belite was higher compared to β- belite. Alite contained a significant quantity of MgO, Al_2O_3, Fe_2O_3 (somewhat higher than 1% of each of these oxides).

The phase composition of clinker is represented by alite, β- and α'- belites, aluminoferrite and aluminate phase. It was observed that the quantity of aluminoferrite was much higher than that of

aluminate. All clinkers contained ~ 5% periclase. In clinker with increased SO_3 (1.16%) and K_2O (1.40%) contents the compound K_2SO_4 was found.

The authors indicate the expediency in obtaining cements based on such clinkers. Text cements met the demands of the uniformity of volume change, showed an intense increase of strength during the hardening in water and in air, possessed reduced values of shrinkage deformation, water separation and contraction; they exceeded low-magnesium cements in stability against aggressive media.

However, the qualitative indices of such cements depend significantly on the preparative conditions of the raw mix, firing and grinding of clinker. There is also a certain dependence of volume deformations of cement stone on the value of its moduli and LSF. The volume stability during testing in the autoclave is strongly influenced by the conditions of prehardening, by the duration and regime of curing in steam. The possibility of regulation of the magnesium-induced expansion of cements in the autoclave was established by means of a controlled process of their hardening. The authors also studied the possibility of using the reactive mineral admixture for preventing the non-uniformity of the volume change of cements in the autoclave.

2.2.2.3 Role of SO_3 in the Presense of MgO.– A significant role is played by sulphur in the formation process of clinker and clinker phases, in the change of phase relations and crystallo-chemical state of the phases.

Of practical and scientific importance is the study of separate and mutual influence of alkalis, MgO and SO_3 with regard for a number of factors, in particular, for the LSF (lime saturation factor) AR (alumina ratio) and SR (silica ratio), the firing temperature, the cooling rate. More often the investigators have no possibility to take all the process parameters into consideration, therefore the results of every work are useful and mutually complementary.

Fomicheva and Boikova studied the influence of SO_3 on the phase relations and crystallo-chemical state of the phases in five- component clinkers (CaO, MgO, Al_2O_3, SiO_2). Five series of clinkers were synthesized which contained different quantities of MgO (1.5; 3.0; 4.5; 5.5 and 6.5%). The quantity of SO_3 added to the batch of each series changed from 0 to 6.0%. The LSF changed from 0.80 to 0.85.

The main results of the study are as follows. Sulphur, like the alkali cations in certain concentrations, leads to a decrease of the amount of alite and to an increase of the amount of belite. Why does the amount of alite decrease? On the one hand, the solid solution of C_3S with SO_3 is extremely limited, namely it contains less than 1% SO_3. The crystal lattice of C_3S is inconvenient for the high amount of SO_3. to be distributed in it. The formation of such a solid solution is difficult due to the $[SiO_4]^{4-} \longrightarrow [SO_4]^{2-}$ substitution characterized by both the different charges and different sizes. This results in strong lattice distortion of the solid solution of C_3S with SO_3; when the SO_3 amount is slightly higher than the limiting concentration, the solid solution is destroyed yielding the formation of the new phases. On the other hand, when the SO_3 amount in the batch is increased to such a value that no alite is formed, it seems more correct to have in view the phase diagram. In the point of such a composition no alite should be formed according to the phase diagram.

The quantitative correlations between alite and belite depending on the SO_3 amount in the batch are shown in Fig.3.

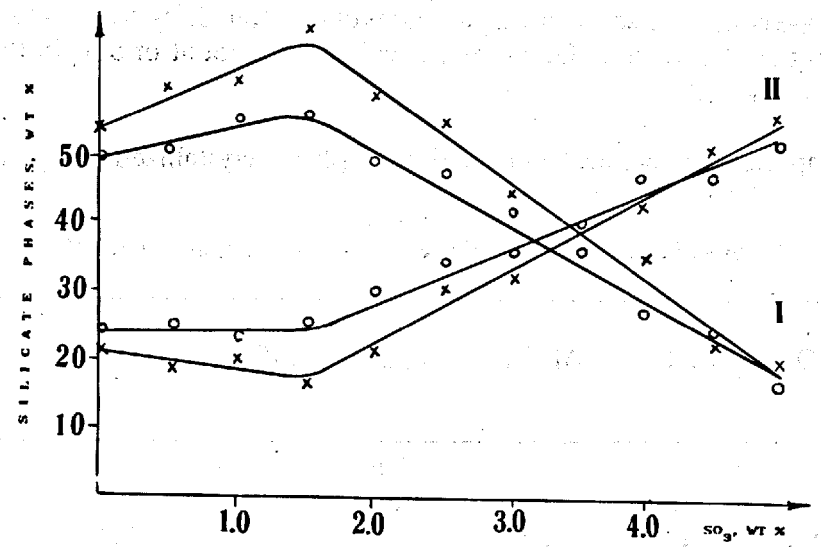

Fig.3. Dependence of the quantity of alite (I) and belite (II) on the SO_3 content in clinker. x-clinker with 4.5% MgO; o-clinker with 1.5% MgO

With increasing SO_3 content in the batch to 1.5% the amount of alite increases somewhat, and this increases is different for various clinkers. Alites from clinkers with 1.5% MgO and 4.5% MgO are shown in the Fig.3. The belite content in both series is decreased in this case. With increasing addition of SO_3 the amount of alite decreases and that of belite increases accordingly. As a matter of fact, the transition from alite to belite clinkers takes place.

A special role played by MgO is also shown in this case. MgO makes it somewhat difficult for alite with SO_3 to decompose. The increase of MgO content leads to a more significant growth of alite content in clinkers containing up to 1.5% SO_3. The MgO effect is opposite to that of SO_3.

Sulphur promotes the stabilization of α'- belite. It was shown by the X-ray method that the addition of SO_3 to the series of clinkers with 1.4% MgO leads to the appearance of the α'- form of belite. The α'-form quantity is increased with increasing SO_3 amount in the mix. At the same time clinker of this series free of SO_3 contains only the β-form of belite.

The increase of MgO content in the mix changes, however, the situation. In particular, MgO makes it difficult for α'-belite to form. Thus, in clinker with 3% (and more) MgO no α'– belite was found even at a considerable SO_3 content. The α– and α' – forms of belite were formed in sulphur-containing clinkers where the MgO content did not exceed 0.5 %.

One of the considerable effects of SO_3 is that sulphur distorts to a great degree the crystal lattices of belite and aluminoferrite phases. In the X-ray pattern this shows up in the diffused character of peaks and in the decrease of their intensity. It is worth noting that belite and aluminoferrite phases with strongly distorted crystal structure are characterized by greater impurity contents, in particular of SO_3, compared to more perfect crystals. In this case belite with high sulphur concentration contains a greater amount of Al_2O_3 in the solid solution.

The aluminoferrite phase in the clinkers studied also attracts attention. By means of X-ray and EPMA it was found that aluminoferrites with strongly distorted structure contain up to 10 % SO_3 in the solid solution, whereas crystals with more perfect structure contained less than 1 % SO_3. The aluminoferrite phase contains also significant amounts of MgO ans SiO_2 in the solid solution. However, attempts to synthesize the aluminoferrite phase with great amount of SO_3 in the solid solution in laboratory conditions failed.

Table 2 exemplifies the chemical compositions of phases crystallized in high sulphur clinkers.

Table 2
Chemical composition of phases in sulphur- magnesium clinkers.

Clinker Series	CaO	MgO	Al_2O_3	Fe_2O_3	SiO_2	SO3	Content in the initial mix, mass%	
							MgO	SO_3
				Alite				
I	70.2	1.4	1.0	1.0	26.2	0.2	1.4	0.5
I	69.7	1.6	1.3	1.0	25.8	0.7	1.4	4.0
IV	69.1	1.9	1.7	0.9	25.6	0.8	5.5	6.0
V	69.1	1.8	1.5	0.9	25.9	0.8	6.5	4.0
				Belite				
I	61.7	0.6	2.2	1.8	32.9	0.9	1.4	0.5
I	61.6	0.8	2.4	1.8	30.4	2.9	1.4	4.0
IV	59.3	0.5	3.2	1.8	31.0	4.3	5.5	6.0
V	59.3	0.7	3.4	2.0	31.2	3.4	6.5	4.0
				Aluminoferrite				
I	45.1	2.9	29.7	19.6	2.7	0.0	1.4	0.5
I	45.5	3.7	27.3	19.6	3.6	0.3	1.4	4.0
IV	47.6	3.0	18.9	17.1	3.0	10.3	5.5	6.0
V	44.9	2.1	22.2	18.2	2.3	10.3	6.5	4.0

It is well known that the character of the influence of one or another component of the clinker depends on many parameters and in some cases it seems difficult to take the majority of them into account.

In particular, when SO_3 occurs in belite-aluminoferrite clinkers, it exerts a different influence on both the phase relations and the crystallo-chemical state of phases. Thus, as shown in (28), in belite-aluminoferrite clinkers the influence of SO_3 depends to a greater degree on the Al_2O_3/Fe_2O_3 ratio. It was shown that in clinkers with Al_2O_3/Fe_2O_3 ratios of 1.75 and 1.0, three phases were formed: belite, aluminoferrite and calcium sulphoaluminate.

In more ferrous clinkers (A/F < 1) only two phases are formed: calcium aluminoferrite and belite. It was also found that sulphur promotes stabilization of high temperature forms of belite ($\alpha-$ and $\alpha'-$), whereas magnesium makes it difficult for this process to develop. For example, X-ray diffraction patterns showed that in clinkers with 6% MgO no $\alpha-$ and $\alpha'-$ modifications of belite were found even in the presence of 6 % SO_3.

EPMA studies permitted to establish that less ferrous aluminoferrite, namely C_4AF, contained high quantities of SO_3 (up to 6-7 %) in the solid solution. It also contained considerable amounts of MgO and SiO_2 which is characteristic of the aluminoferrite phase. More ferrous aluminoferrite solid solution (based on C_6AF_2) contained a small amount of SO_3 compared to C_4AF, namely in the limits of 0.1 to 0.6 % SO_3. It also contained much smaller amount of MgO (0.2-0.9 %). X-ray analysis showed that belite and aluminoferrite phase of these clinkers are products with extremely distorted lattices.

Fig.4 shows the X-ray patterns of belites with more or less distorted structures. The belite (II) has the following composition (mass %): CaO - 58.7; MgO - 0.5; SiO_2 - 31.8; Al_2O_3 - 3.4; Fe_2O_3 - 1.9; SO_3 - 3.6.

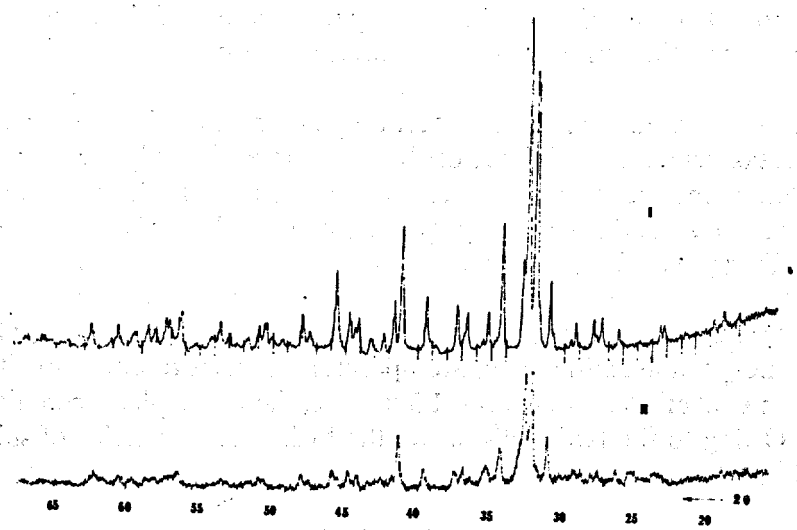

Fig.4. X-ray patterns of β-belites with weak (I) and strong (II) distorted structure.

The unit cell parameters of this β- belite are (A°): a=5.526; b=6.771; c=9.316; β =94.30°; for comparison the parameters of β-C_2S with B_2O_3 are as follows: a=5.48; b=6.76; c=9.28; β=94.83°. The composition of this belite was chosen from the EPMA results for belites crystallized in the clinkers investigated. β-belite (I) -C_2S+0.5% B_2O_3.

Measurements of compressive strength showed that its value is twice as high as for clinkers containing phases with imperfect structure (see the paper published in Proceedings of the present Congress).

Knöfel et al made a thorough study of the influence of alkalis and sulphur on cement properties (29, 30, 31, 32). The main results summarized in (33) are as follows. Both commercial clinkers and the ones synthesized in laboratory conditions were studied. The quantities of alkalis and sulphur as well as silica- alumina moduli and lime saturation factor varied. With increasing SO_3 content in clinker the alite content decreased and that of belite increased. At the same time the size of alite crystals increased. This fact is explained by the change of the liquid phase during the burning. Sulphur is bonded by the matrix phases and can form sulphates. Sulphur present in the structure of clinker phases accelerates cement setting, whereas sulphur bonded in the form of alkaline sulphates slows down the process.

Cement strength is decreased with increasing SO_3 content. Alkalis enter mainly the aluminate phase and belite. Sulphur preferably forms K_2SO_3 but not Na_2SO_4. The aluminate phase with alkalis is formed at low sulphur content and at high alkali content. With increasing alkali content the quantity of alite decreased significantly in presence of Na_2O and less in presence of K_2O. The belite content increased accordingly but no considerable change in contents of the aluminate and aluminoferrite phases is observed.

The degree of alkali sulphatisation in clinker influences the alite and belite contents as well as the behaviour of cement during the setting and its strength. The setting is always accelerated by Na_2O, in the case of K_2O this process is accelerated or hindered depending on the degree of sulphatization and on the chemical composition of cement. Alkalis promote the increase of strength at the early stages and the decrease at the later stages. The decrease of compressive strength can be fully or partly compensated by the optimal degree of sulphatization, by the increase of silica modulus and decrease of alumina modulus and/or by the increase of lime saturation factor.

Gies and Knöfel (34) studied the sulphur effect on phase relation in belite clinkers and on the technological properties of cements. In absence of alkali the increasing sulphur content stimulates the increase of belite content with simultaneous decrease of alite content. In this case the 2-days compressive strength decreased. The 28-and 90-days strengths are increased significantly by adding sulphates; this effect strengthens by rapid cooling of cement.

In belite-rich cement clinkers the greatest SO_3 amount enters belite and can also be present as sulphates, mainly as $CaSO_4$. Stabilization of high-temperature forms of α- and α'-belites is not reached if the quantity of SO_3 in clinker does not exceed 1.5 mass%; the belite phase contains 0.6- 0.8% SO_3 in the solid solution. Owing to the lattice distortion the hydraulic properties of sulphur-containing belite have improved.

In presence of alkalis and at 80-100 degree of sulphatization K_2SO_4 is more stable than Na_2SO_4 in both portland and belite clinkers. Na_2O enters both the belite and the aluminate phase; the latter being formed as the orthorombic modification. Addition of alkaline oxides in amounts of up to 1.0% at 80-100 degree of sulphatization exerts a positive effect on cement strength.

Gies and Knöfel (35) studied the alkali effect on phase relations in belite clinkers and on the technical properties of cement as well as the mutual effect of manganese and alkalis (36). With increasing alkali and manganese content in cement clinker the α- and α'- forms of belite are stabilized. The 28- and 90-days compressive strengths are increased.

When studying the role of Na_2O in belite clinkers Stark and Müller (37) showed that belite cement with high Na_2O content possess lower strength than K_2O-containing belite cements (at similar content of these oxides). α- and α'-belites stabilized by Na_2O possess similar hydraulic activity. The high cooling rate leads to high impurity content in belite owing to prevention of impurity segregation.

Jost et al (38) studied the formation of belite modification depending on the Na_2O content and on the cooling rate of belite clinkers (LSF = 70 and 80). They established that 3% Na_2O are sufficient to stabilize α-belite (along with the α') at a cooling rate of 300 K min^{-1}. At 1.3% Na_2O no stabilization of α-belite could be even at a cooling rate of 3000 K min^{-1}.

2.2.2.4 Mutual Role of Na, K, Mg, S.- Gartner and Tang (25) report that inspite of a great number of data published on sulphate clinkers there are still many uncertainties concerning the behaviour of SO_3 during clinker formation of high sulphate portland cement clinkers containing K, Na, Mg, $MgCO_3$,

Na_2SO_4, K_2SO_4, $CaSO_4$ were added to the initial clinker imx in such quantities that the content of alkalis, sulphur and magnesium could be varied. They studied the volatility of sulphur and alkalis during clinker formation and their mutual influence. For example, addition of $CaSO_4$ leads to a decrease of volatility of potassium and to an increase of that of sulphur.

Gartner and Tang also note that the results give evidence in favour of the hypothesis that K_2SO_4 and $CaSO_4$ form a mixed melt in the concentration limits of 1:0 to 1:2. The volatility of alkalis and sulphur observed in clinkers with average content of MgO is significantly lower than in clinkers with low MgO content. The authors also report some other important data concerning the mutual influence of alkalis and sulphur on their volatility.

The phase composition of clinkers was determined by means of microscopic and X-ray methods as well as by selective dissolution methods. The authors report that the phase composition of clinkers (phases relations) is greatly influenced by adding MgO and $CaSO_4$. X-ray and microscopic studies showed that with increasing MgO content in clinkers the quantity of the aluminate phase decreased and that of the aluminoferrite phase increased. If only $CaSO_4$ is added to the clinker mix, the quantity of alite decreased. However, the negative effect is weakened by adding MgO.

These results agree with those of Fomicheva and Boikova. Gartner and Tang note that the negative effect of $CaSO_4$ on the raw mix burnability can be compensated by adding from 0.5 to 1.5% MgO. The authors report the results of the EPMA study of the chemical composition of phases. In particular, they indicate that sulphur is present in the belite lattice. The alkali-containing aluminate phase and alkaline belites are also described in their work. Besides, at a definite chemical composition of the initial clinker mix some other products were found, namely: arcanite K_2SO_4, anhydrite $CaSO_4$, calcium langbeinite $K_2Ca_2(SO_4)_3$, aphthitalite or glaserite $Na_xK_{2-x}SO_4$. The authors also admit the possibility of of formation of an intermediate product – sulphate spurrite $[(Ca_5(SiO_4)_2(SO_4))]$.

The quantity of sulphur to be present in structure of the silicate phases depends on both the MgO content in clinker and the K/Na ratio. Clinkers with high sodium content and low potassium content show a strong tendency to form belite with both sodium and sulphur in the lattice regardless of the MgO content. According to EPMA data one of such belites contained 1% Na_2O and 2.7% SO_3. The sodium behaviour in this case differs from that of potassium whose presence in belite is not accompanied by the presence of sulphur. Summarizing the results on alkaline and sulphate phases the authors note (25) that although the equilibrium in the studied clinker systems was not reached and clinkers with the limited content of sodium, potassium and sulphur were studied, the summary table suggested by them can be useful.

Gartner and Tang studied the properties of cement pastes and presented the results of measuring 1-day, 7-days and 28-days compressive strengths. The pastes of high sulphate clinkers showed good workability in this case. The authors analyzed strength development of low and medium MgO clinker.

A correlation was made of compressive strength with water soluble alkalis in clinker and their total amount. Thus at the constant S:A ratio the correlation of 28-day strength with the total amount of alkalis is very good (for clinkers with low MgO content).

For medium MgO clinkers with low potassium content the 1-day strength decreases and is restored after 28 days. Low-alkali clinkers with high sulphate content show good 28-day strength. In the paper cited there are many other useful data of practical importance but only part of them can be discussed in this review. In conclusion Gartner and Tang summarized the main result of their study which consists

in the following. The authors showed potential advantages and disadvantages of interburnt sulphates as the replacement of interground gypsum in commercial cements. Cements prepared with SO_3 in the form of interburn calcium and potassium sulphates show better or similar strength development as compared to cements containing interground gypsum.

The harmful influence of Na_2SO_4 and $CaSO_4$ on clinker phases takes place if there is no sufficient amount of K_2SO_4 to form aphthitalite or langbeinite. The sodiums behavior differs from that potassium as regards the volatility and their presence in structures of clinker phases. Clinkers with high Na_2O content behave differently compared to clinkers with high K_2O. The explanation suggested agrees with the majority of data.

3. QUALITY OF MATERIALS

An important investigation dealt with the uniform criterion of cement quality was made by Bruggemann and Brentrup (39). The authors note that the cement strength will be an important quality criterion. The most important parameters were investigated to provide a basis for improved control strategies in cement production. For this purpose 27 industrial clinkers were studied by chemical and microscopical methods. The data obtained were correlated with the cement strengths. The authors showed that the content of soluble alkalis, of calculated C_3S, of alite determined by microscopy and the alite crystallite size proved to be important influencing variables.

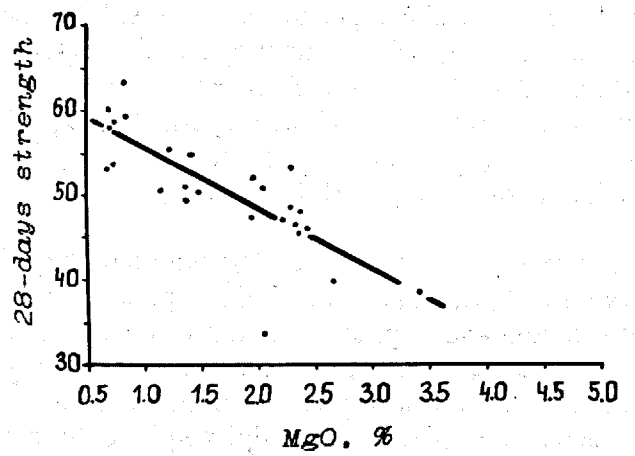

Fig.5. Relationship between MgO content and 28- day strength at 2800 cm^2/g Blaine, (by H. Bruggemann and L. Brentrup)

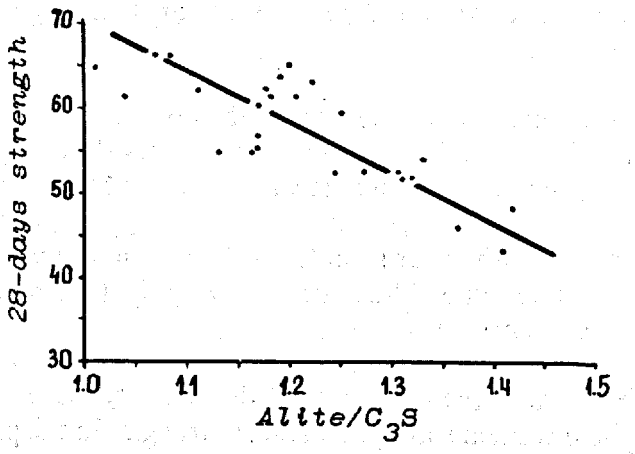

Fig.6. Relationship between the ratio of alite content determined by microscopy to the calculated Bogue C_3S content and the 28-day strength at 4800 cm_2/g Blaine. (by H Bruggemann and L Brentrup)

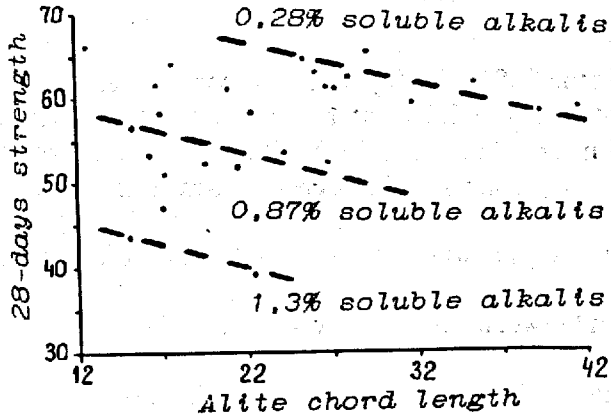

Fig.7. Relationship between the mean chord length of the alite determined by microscopy as a measure of its crystal size and the 28-day strength at 3800 cm^2/g Blaine. (by H. Bruggemann and L.brentrup)

These data could be used with the aid of an equation to calculate 28-day strength. The authors showed, that the error is smaller with finer cements than with coarser ones. The main results of the investigation are presented on figures 5, 6,7.

4. POLYMORPHISM AND STRUCTURE OF PORTLAND PHASES

At the 8th ICCC (1986), the solid solutions of clinker phases, polymorphism and crystal structure of C_3S were discussed by Boikova (4) and Maki (11) respectively, in two Principal Reports. In 1990, Taylor (6) published a book entitled Cement Chemistry. The chapter One details the polymorphism and crystal structure of Portland cement major phases. All structural data for the different polymorphs of the pure phases and their solid solutions have been determined from single crystal patterns. New calculated X-ray powder diffraction patterns using single crystal cell parameters are given for pure C_3S and clinker phases.

4.1 Tricalcium Silicate and Alites

4.1.1 Polymorphism of C_3S

As already reviewed in the previous international congress, seven forms of C_3S exist between the room temperature and 1100°C (11):

$$T1 \xrightarrow{620} T2 \xrightarrow{920} T3 \xrightarrow{980} M1 \xrightarrow{990} M2 \xrightarrow{1060} M3 \xrightarrow{1070°C} R$$

T = triclinic, M = monoclinic, R = rhombohedral

The M3 form, as discovered by Maki and Chromy (40) under microscopy, is stable within a narrow 10°C range. Birefringence, optic orientation and twinning structure clearly identified two kinds of triclinic phases between 620 and 920°C and two monoclinic forms between 980 and 1070°C. However, the T2 ——>T3 and M1 ——> M2 at respectively 980 and 990°C were not detected inspite of reversible DTA peaks. These transitions which have no influence on the "megascopic" optical properties may be attributed to the formation of a modulation structure (superstructure) or may be due to orientation disorder of the SiO_4 tetrahedra and changes in the Ca coordination (11).

4.1.2 C_3S Solid Solutions. Alites in Clinkers

Many foreign elements can be introduced in the C_3S lattice (4). The most common are magnesium, aluminium and iron. With increased contents, they stabilise at room temperature triclinic and monoclinic forms (11, 41, 42, 43,). The mutual interaction of Al, Fe, Mg, K and Na stabilises T1, T2, Ml and M3 molymorphs. It seems after electron diffraction and single crystal X-ray diffraction that the rhombohedral form is not stabilised, at room temperature, by Zn, La, Al + Mg + F (44). However Taylor (6) reports two cases of the R form, a single crystal with Sr^{2+} and a solid solution with fluorine.

In industrial clinkers there is an interaction between MgO and SO_3 (11):

* MgO favours the stabilisation of M3 by intensification of the nucleation process,

* SO_3 promotes the growth process (45, 46) and stabilises Ml crystals.

MgO and SO_3 counteract with each other. It can result in zoned crystals with M3 at the periphery and Ml in the core. EPMA of zoned crystals show that Mg is uniformly distributed but that Al and Fe are more concentrated in the core (15). Alite polymorphs will be different if alkalies are present as they produce alkali sulfates.

The crystallisation of alite is also influenced by the clinker processing (16, 41, 47, 48). In industrial clinkers the heating rate is low favours large faceted crystals. M1 is the first form to occur (16,41). M3 is the eventual product of recrystallisation (47). The clinker microstructure is also depending on the type of kiln (48). Edged alite crystals of 10-60 μm size with small inclusions of belite appear in the dry process. With a preheater kiln, alite is coarser (40-70 μm) and zoned.

The thermal stability of alites was studied by optical microscopy and DTA by Maki and Kato (43):

– with a high amount of MgO in the clinker (4%), M3 is a stable form which transforms reversibly into R,

– with a lower amount of MgO (1.1%), M3 reverts to T2 on heating beyond 700°C and then follows the polymorphism T2 ——> M1 ——> M3 ——> R. By rapid cooling M3 can be stabilised again at room temperature. By slow cooling Ml or T2 is the stable form.

– with a low amount of MgO (0.6%), Ml reverts to T2 above 600°C and gives the same sequence as the usual polymorphism. Ml occures after quenching and T2 by slow cooling.

Hudson and Groves (49) also observed the transformation of an M3 alite at 700°C on a heating stage of the 1 MV electron microscope. The new structure was characterised by superlattice reflections.

Industrial alites are, after Maki (11), usually M3 or M1 or M3 + M1. Hahn et al (50) also found M1, M1 + M3 and M3 forms in solid solutions with 0.9% Al_2O_3 + 0.5% Fe_2O_3 and with 0.5 to 2% MgO. By heating monoclinic industrial alites, Maki and Kato (43) stated that "there is no need to take into account the occurrence of M2 during heating. It seems that M1 can directly invert to M3 without passing through M2". However in their DTA diagrams of synthetic solid solutions with 1.5 and 2% MgO (M3 at room temperature which converted to Ml at 750°C), a peak at respectively 975 and 990°C was not indentified. This peak also remained approximatively at the same temperature and was reversible in the DTA diagrams of M3 solid solutions stabilised by ZnO (51). In pure C_3S this peak

corresponds to the transition M1——>M2. Accordingly it should disappear beyond the stability range of M1. As the M2 form is not distinguished from M1 by optical observation, this phase change, detectable by DTA only, is still open to discussion.

4.1.3 Crystal Structures of C_3S and Alites

Maki (11) reported the crystal structure of a rhombohedral form at 1200°C and a monoclinic M3 form. Both were C_3S solid solutions. The triclinic T1 structure was calculated by Golovastikov et al (21).

– Rhombohedral Structure (Fig.8)

Nishi and Takeuchi (52) refined the structure to R = 10% for 159 reflections. The unit cell has the following parameters:

a = 0.715 (6), c = 2.5586(15) nm, Space Group R3m, Z = 9

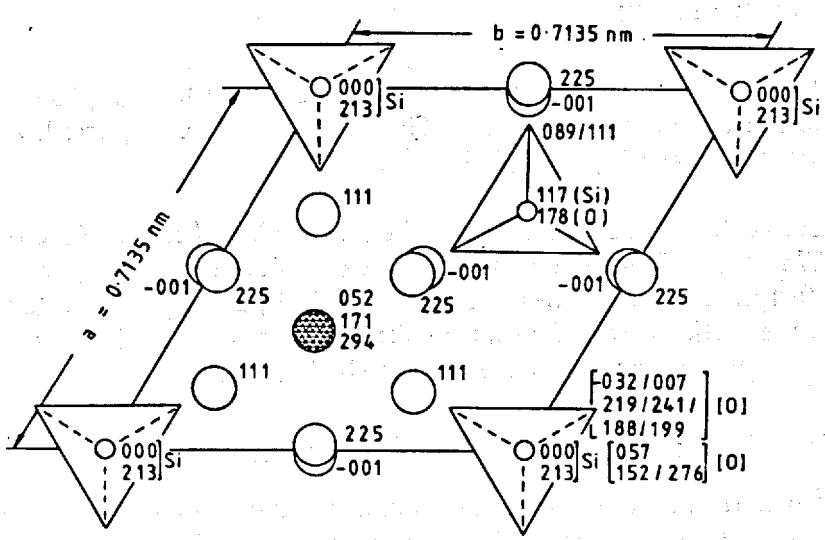

Fig.8 Crystal structure of the R modification based on the results of Nishi and Takeuchi (52) and after Taylor (6)

This structure differs from the structure determined by Jeffery (53) which was built from independent SiO_4 tetrahedra. Three tetrahedra Si(1), Si(2), Si(3) and three oxygen ions were on the trigonal axes. The calcium ions Ca(1), Ca(2), Ca(3) linked to the tetrahedra were octahedrally coordinated to three oxygen ions A,F,E which were not linked to Si. In the new structure:

1. the tetrahedron Si(1) has a different orientation: rotation of 60° around the trigonal axis,
2. the tetrahedron Si(2) points upward (U-orientation) at 30% and downward (D-orientation) at 70% at 1200°C,
3. the apical bonds of all the tetrahedra are tilted from the trigonal axis.

The coordination of Ca(1) and Ca(2) is sixfold as in the Jeffery's structure. The coordination of Ca(3) is however considered as fivefold. With a Ca-0 bond length of 0.215 nm the Ca coordination would be 5.66 on average.

- Monoclinic Structure: M3 form

Nishi, Takeuchi and Maki (54) refined the structure to R = 9.9% for the solid solution $Ca(2.89)Mg(0.11)SiO_5$. The unit cell is characterised by the following parameters:

a = 3.3083(8), b = 0.7027(2), c = 1.8499(4) nm, B = 94°12(2), SG = Cm, Z = 36. It is the same cell as that of Jeffery (53) derived from the alite C(54)S(16)AM. Three types of tetrahedra can be indentified on the trigonal axis:

1. fixed orientation: either U or D,
2. disordered in two orientations: U-D disorder,
3. disordered in three orientations: U-D-G disorder.

Half of the Ca ions are on the mirror plane and half on a plane close to y = 1/4. The coordination number is 6.15 on average.

— Triclinic Structure: T1 form

Single crystals of C_3S were studied either by X-ray rotation photographs by Golovastikov et al (21) or by electron diffraction by Groves (55). The same lattice was reported: A = 1.167, b = 1.424, c = 1.372 nm, $\alpha = 105.50°$, $\beta = 94.3°$ $\gamma = 90°$, SG = $P\bar{1}$, Z = 18.

Pure C_3S crystals exhibit reflection twins on the mirror plane $\{21\bar{1}0\}$ of the pseudolattice nearly trigonal with a = 0.7 and c = 2.5 nm. These twins may be considered as domains in an originally trigonal structure (55). In fact the same pseudo- lattice determined by Jeffery (53) occurs for all varieties of C_3S but superlattice reflections are different from C S and alites (55). So, lattices calculated earlier on the basis of X- ray powder photographs were found to be inapplicable.

4.1.4 Calculated X-ray powder diffraction patterns for C_3S and alites

X-ray powder patterns permit the determination of the dimensions of various lattices but give no information on the summary of the structures (51). One cannot distinguish for instance between a metrically rhombohedral and a true rhombohedral cell. Taylor (6) calculated the powder patterns from single crystal data for T1 and M3 forms. No data were available for the M1 form. For T1 and M3 the characteristic reflections used earlier are indexed with Golovastikov et al (21) and Nishi et al (54) crystal data (Table 3).

Table 3
X-ray characteristic reflections in T1 and M3 forms (6)

T1			M3		
dnm	I/Io	hkl	dnm	I/Io	hkl
0.2801	100	303	0.2778	100	$\bar{6}$ 06
0.2777	42	0$\bar{4}$4	0.2753	43	12.00
0.2755	45	042	0.2745	84	224
0.2741	44	$\bar{4}$02			
0.1780	34	0$\bar{8}$2	0.1768	58	14.24
0.1771	26	44$\bar{6}$	0.1763	52	040
0.1762	28	$\bar{4}$44			

4.2 Dicalcium Silicate and Belites

4.2.1 Polymorphism of C2S

Five forms of C_2S exist between ambient temperature and 1500°C but their stability ranges on heating and cooling are different:

– γ C_2S Stable form at room temperature:

* heating: $\gamma \xrightarrow{725-860} \alpha_L' \xleftarrow{1160} \alpha_H' \xleftarrow{1420°C} \alpha$

* cooling: $\alpha \xleftarrow{1420} \alpha_H' \xleftarrow{1160} \alpha_L' \xrightarrow{650} \beta \xrightarrow{500°C} \gamma$

– βC_2S stabilized at room temperature by rapid quenching of α_L'(<1160°C):

* heating: $\beta \xrightarrow{675} \alpha_L' \xleftarrow{1160} \alpha_H' \xleftarrow{1420°C} \alpha$

* cooling: $\alpha \xleftarrow{1420} \alpha_H' \xleftarrow{1160} \alpha_L' \xrightarrow{650} \beta \xrightarrow{500°C} \gamma$

The transformations $\beta \longrightarrow \gamma$ and $\gamma \longrightarrow \alpha'_L$ are irreversible. The $\beta \longrightarrow \gamma$ transition involves a considerable change of volume (dusting). According to Smith et al (56), the two transitions correspond to a rotation of SiO_4 tetrahedra and to major shifts of some of the Ca ions. Recent single crystal high temperature XRD patterns show that the phases are formed topotactically that is in a definite crystallographic orientation relative to the starting material. The dusting would be a fragmentation due to the large volume change (6). The $\beta \longrightarrow \gamma$ transformation is variable with temperature and can be incomplete. It is too a transition similar to the tetragonal- monoclinic transformation in zirconia (57) and to transformation toughening (58). A γ C_2S nucleation effect can be initiated by coarse crystals of β C_2S and by mechanical stresses (59,60).

The transformations $\alpha'_H \longleftrightarrow \alpha'_L$, $\alpha'_L \longleftrightarrow \beta$ and $\alpha \longleftrightarrow \alpha'_H$ are reversible and correspond to relatively small changes of the crystal structure.

4.2.2 C2S Solid Solutions and Belites

C_2S takes up a greater proportion of foreign elements such as Al, Fe, K, Na, P, Sr, Ti, V, Cr into solid solution than does C_3S. The nature and proportion of the foreign ions on one hand, the thermal treatment on the other, permits the synthesis of β,α'_L and α forms very similar to, those of pure C_2S.

C_2S solid solutions appear as products of imperfect crystallisation. A new β form called β^* has been identified by von Lampe and Seydel (61). Its XRD pattern is close to that of βC_2S and very similar β C_2S doped with B_2O_3 (62). This variety obtained from clinkers containing alkalis and rapidly cooled converts to α' around 400°C. The β^* belite contains more foreign oxydes (3.80%) than β (2.45%) but is closer to α' (4.75%). The formation of β^* C_2S has been related to the exsolution of foreign ions from the supersaturated solution in a very finely dispersed manner, not visible in the BSEE image of the EPMA. These sub-microscopic exsolutions cause irregularities of the belite crystal lattice reflected by the broadening of the 29 Si NMR signal.

The departure from stoichiometry of C_2S have been the subject of numerous publications reported at the Moscow Congress in 1974 (63). It was concluded that the β form was stabilized by an excess of CaO and that excess of SiO_2 favoured the $\beta \longrightarrow \gamma$ transformation. In an analytical electron microscopic study of doped dicalcium silicates, Chan, Kriven and Young (64) found that CaO/SiO_2 of β C_2S was always 2.0 ± 0.1. Thus the solid solution Ca(2.2)SiO(4.2) did not occur. K_2O and Al_2O_3 were used as dopants and it was shown that amorphous glassy phases and additional crystalline phases could account for the apparent departure (65,66). K_2O very low in C_2S was concentrated in an amorpuous grain boundary phase and more particularly in silica rich C_2S ($CaO/SiO_2 = 1.8$ in the starting composition). In the lime rich specimens ($CaO/SiO_2 = 2.2$) a twinned lamellar structure (type I) appeared as a "narrow banded microstructure". With K_2O the bands included the amorphous boundary phase. In Al_2O_3 doped specimens the bands were parallel cracks. Identified crystals were rankinite $Ca_3Si_2O_7$ in K_2O doped systems and gehlenite $Ca_2Al_2SiO_7$ for $CaO/SiO_2 = 1.8$ samples. Both appeared to be crystallising from the amorphous grain boundary phase. Large C_2S grains (10-50 μm cross) were in fact agglomerates of smaller grains (0.1-0.5 μm) identified by their twinning under TEM observation. For samples rich in lime ($CaO/SiO_2 = 2.2$) and above the Al_2O_3 saturation level (3% wt), C_3A and C_3S were detected. This study shows that EPMA data can account the contribution of the boundary phase that EDS/TEM does not. The low level of dopant substitution and K_2O more particularly might not be the major factor in βC_2S stabilisation. Physical parameters as critical particle size or matrix constraint might be more important than the chemical composition. The same type of amorphous phase between C_2S grains was also found in C_2S doped with phosphates (67).

$Ca_2Fe_2O_5$ as crystals appeared in an interstitial phase for Fe, Na or K stabilised C_2S (68). The Mossbauer spectrometry identified Fe^{3+} at octahedral and tetrahedral sites as follows:

* 30/70 in Na-Fe α substituted C_2S form,

* 63/37 in K-Fe α substituted C_2S form

In β C_2S, Fe^{3+} was mostly tetrahedral.

Sulfur is also a foreign element in C_2S. Lamellar β C_2S and non lamellar α C_2S were observed in high SO clinkers (45,46). In absence of alkalis and in belite-rich clinker, SO_3 is mainly incorporated in belite which is a lattice disturbed sulfate bearing phase (34).

The effect of minor elements on the stability of β C_2S is closely related to the polarization ability of the ions (69). Ions having smaller polarization ability than of Ca or higher than that of Si ion are able to affect the stability of β C_2S. On the contrary, ion groups like PO_4^{3-}, SO_4^{2-}, MnO_4^-, VO_4^{3-}, CrO_4^{3-} and AsO_4^{2-} substituting for SiO_4^{4-} stabilise βC_2S.

An idiomorphic belite was found in cements with a false setting tendency (70). These belites have a total amount in impurities of 6.6% with high SO_3 Fe_2O_3 and Al_2O_3 contents. The cement has undergone higher burning temperature than those contining round shaped belite. The cooling rate was moderate and there was an intense enveloping of belite and alite by the interstitial phase.

There are vacancies defects of Ca^{2+} in C_2S. These Ca^{2+} vacancies are equivalent to negative charges which capture the positrons due to the Coulomb attraction between positive and negative charges (71). So, the positron annihilation technique is useful for the defects in doped βC_2S. Na^+ replacing Ca^{2+} creates anion vacancies while P^{5+} replacing Si^{4+} creates cation vacancies. Sodium was concentrated on dislocations, at the grain boundaries and the surface of grains.

A reducing atmosphere has a minor effect upon the polymorphic transitions of the C_2S phase (72). Mn solid solutions are γC_2S (2.34% Mn) in reducing atmosphere and β C_2S (1.53% Mn) in air (73).

4.2.3 Crystal Structure of C_2S and Belites

The crystal structure of γ, β, α' and α C_2S forms determined from single crystals of solid solutions was reported at the Moscow Congress (63). Refinement of these structures was undertaken by Udagawa et al (74,75,76) and Jost et al (77). The relations between the structure of α, α_H', β and γ C_2S has been shown by Taylor (6).

γC_2S: single crystals of γ C_2S were synthesized by the flux method. The structure was refined to the final R value of 0.037 with 581 independent diffraction intensities collected by an automatic four circle single crystal diffractometer (74). The unit cell is characterized by the following parameters:

a = 0.5081(2), b = 1.1224(5), c = 0.6778(10) nm, SG = Pbnm, Z = 4.

The structure is similar to that of olivine $(Mg, Fe)_2$ SiO_4 and consists of a distorted hexagonal close-packed arrangement of oxygen atoms in which Ca atoms occupy one half of the octahedral sites and Si atoms occupy one-height of the tetrahedral sites.

The β ——>γ transformation proceeds not by a total reorganization of the structure as it was supposed earlier but by a topotactical reaction (6). The new form grows in a definite crystallographic orienteation relative to the starting crystal but the large volume expansion shatters the newly formed crystals into small fragments.

β, α', and α: $\alpha, \alpha_H', \alpha_L', \beta$ are very close polymorphs. Progressive decreases in symmetry result in different orientation of the SiO_4 tetrahedra and small movements of Ca^{2+} ions (Fig.9). The difference in orientation of the tetrahedra involves a difference in the coordination number of the calcium atoms.

Crystals of C_2S were grown from a $CaCl_2$ melt by Jost et al (77). The unit cell has the following parameters:

a = 0.5502, b = 0.6745, c = 0.9297 nm, β = 94.59°, SG = P21/n, Z = 4

Crystals of α_L', α_H' and β were stabilised with Sr, P_2O_5, anb Ba respectively. Their structure is characterised by:

– a = 2.0871, b = 0.9496, c = 0.5600 nm, SG = Pna21, Z = 12
– a = 0.949, b = 0.559, c = 0.685 nm, SG = Pcmn, Z = 4
– a = 0.5579, c = 0.7150 nm, γ = 120°, SG = P31c, Z = 2

The trigonal space group is that of the individual domains in the hexagonal structure

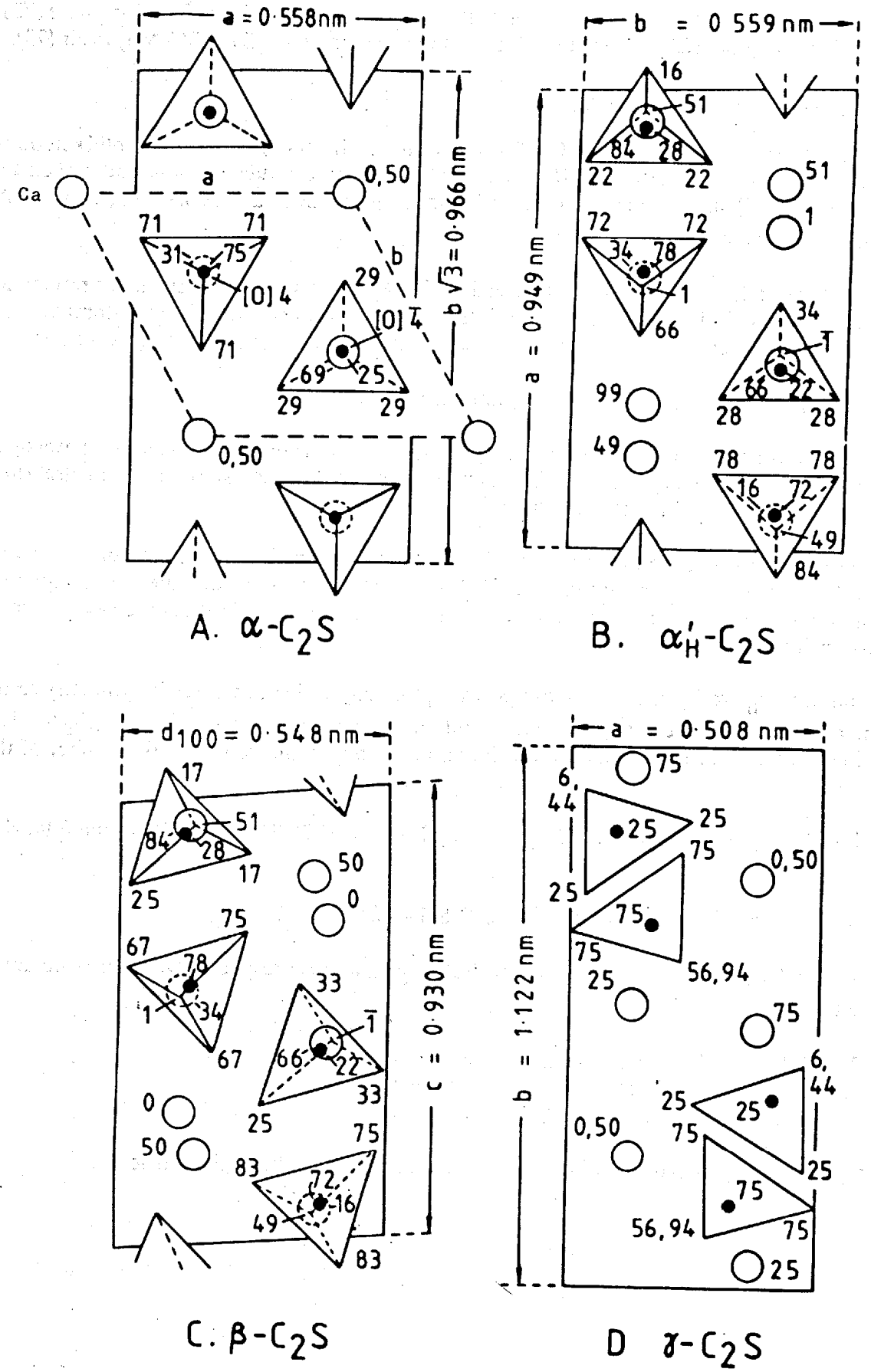

Fig.9 Crystal Structures of C_2S refined by Udagawa et al (74, 76) and after Taylor (6)

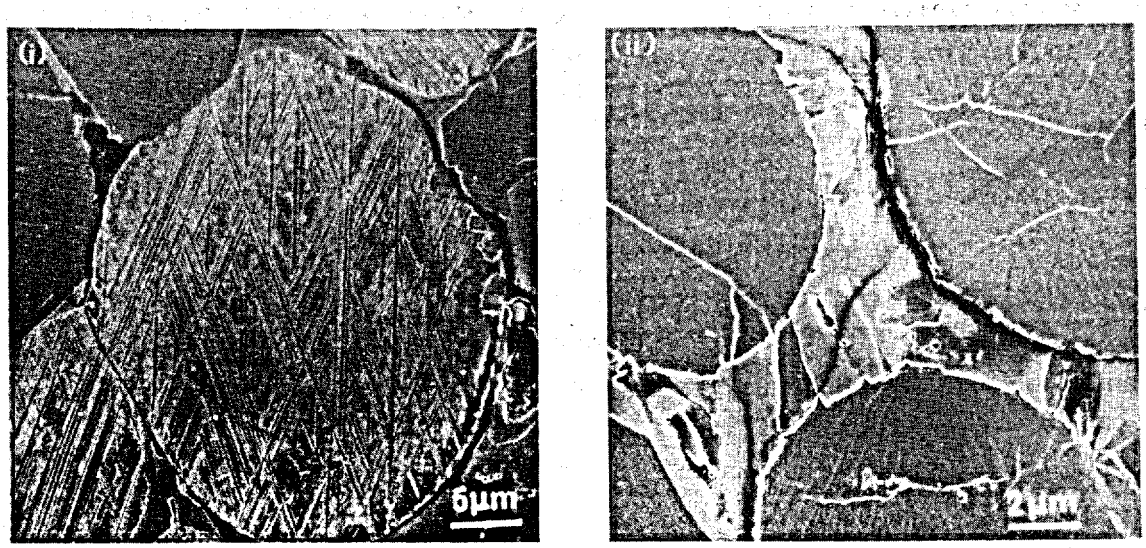

Fig. 10 SEM images of industrial belites
(i) Striated βC_2S, (ii) Smooth αC_2S

4.2.4 Lamellar structure of Belites

Belite usually occurs as rounded, striated grains with markedly laminated structure (Fig.10). The striations appear at the moment of the $\alpha \longrightarrow \alpha'$ and $\alpha' \longrightarrow \beta$ transformations. Two or more sets of striations are of Type I and twin lamellae singly orientated are of Type II (78).

Twins of C_2S have been examined by TEM (79), HEVM (80), HERM (81), optical microscopy and TEM (82):

Groves (79) prepared βC_2S by cooling $\alpha' C_2S$ or αC_2S. The transformation $\alpha' \longrightarrow \beta$ resulted in optically resolvable twins on a single set of planes $(100)\beta$. The $\alpha \longrightarrow \alpha' \longrightarrow \beta$ transformations gave TEM resolvable twins also on (100) planes with lamellae of 200 nm width grouped into domains having a common $< 010 >\beta$ direction, in the original grain. Local elastic strains and nucleated dislocations exist at domain interfaces. So, TEM observations lead to the hypothesis that twins result of alternating lattice transformation shear strains.

The HVTEM used by Barnes and Ghose (80) was able to directly detect narrow lamellae and fine substructure within each lamella (substriation or internally twinned structure). This fine substructure would indicate, a martensitic transformation, solid-state structural transformation involving small displacements of numerous atoms with a definite orientational relationship between the starting material and the newly formed phase. The effective driving force may be shear stress while the volume change is small.

Feng Xiuji et al (81) studied β C_2S doped with K_2O or Na_2O with a HERM. The (100) twins were confirmed and the (001) twins not observed by Groves (79) were identified. It was considered that the (001) twins occurred when α' C_2S transformed into β C_2S. A shear stress parallel to axis aα' turned the axis bα' into the axis cβ.

Fukuda and Maki (82) reexamined the orientation of βC_2S solid solution lamellae in the host α phase and confirmed earlier results about the orientation relationship between the β and α phases. Using optical microscopy and more particularly the measured birefringence, β and α phases could be clearly distinguished. The electron diffraction pattern showed the polysynthetic twinning on $(100)_\beta$, parallel to $\{ 11\bar{2}0 \}_\alpha$. The XRD precision photograph of a β crystal showed a cyclic twin around the b β axis and a polysynthetic twin on (100) β. The cyclic twin corresponded to the $\alpha \longrightarrow \beta$ transition during cooling (hexagonal ——> monoclinic) in such a way that $c\alpha\, b\beta$, $a\alpha\, a^*\beta$ and $a^*_\alpha\, c_\beta$. Three kinds of polished sections perpendicular to c_α, a_α, and a^*_α showed striations of different orientations. Striations parallel to the a^*_α intersected at an angle of 60° or 120° with another. Two sets of striation on the polished section containing a^*_α and c_α were parallel to a^*_α and intersected this axis at an angle of 23°. In the $a_\alpha\, c_\alpha$ plane, two sets of striation made angles of 15° and 27° with the a_α axis. The most probable face indices of the habit planes parallel to the a_α axes are $\{ 11\bar{2}5 \}_\alpha$. They difer from $\{ 10\bar{1}2 \}_\alpha$ determined by Yamaguchi and Ono (70).

The lamellar structure of industrial belites is able to indicate the clinkering temperature. The distribution of potassium in α + βC_2S belites is inhomogeneous, higher at the periphery (Fig. 11).

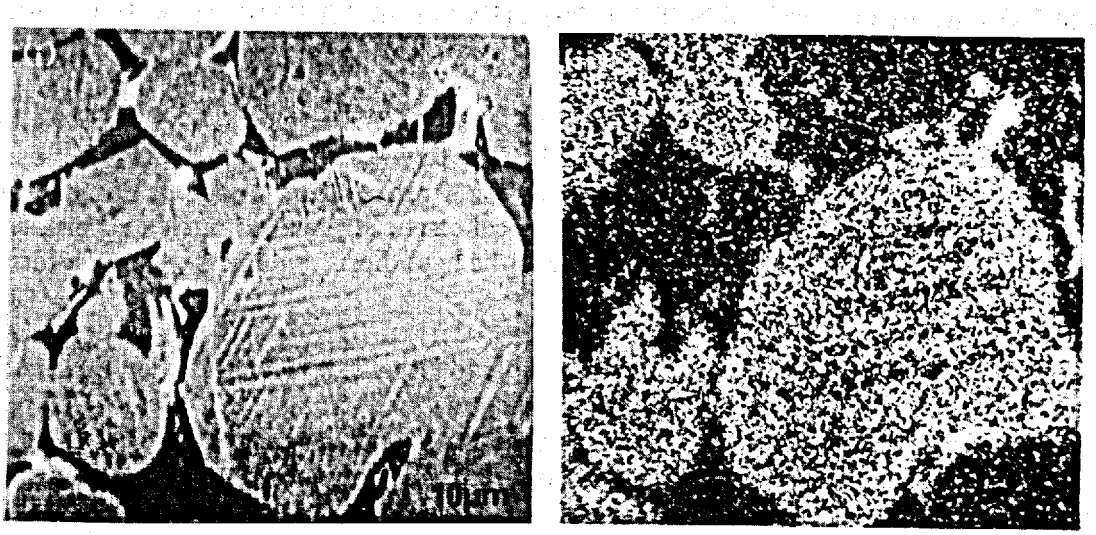

Fig.11 Distribution of potassium (EPMA) in a bistriated belite

4.3 Tricalcium Aluminate and Its Solid Solutions

C_3A is a definite compound showing no polymorphic transformations. However alkalis Na and K sustituting for Ca produce changes of symmetry in the pure C_3A crystal.

4.3.1 Crystal Stucture of $Ca_3 Al_2 O_3$ – The crystal structure of C_3A determined by Mondal and Jeffery (83) is cubic with:

a = 1.5263 nm, SG = Pa3, Z = 24

Eight $(Al_6O_{18})^{18-}$ rings of six AlO_4 tetrahedra are on the triad symmetry axes. They are interconnected by calcium ions located at the corners of the subcells. There are eight holes of 0.147 nm radius per formula unit (Fig.12). Two types of calcium can be distinguished:

1. the Ca(1), Ca(2) and Ca(3) atoms at the corners of the subcells are octahedrally coordinated to the oxygen atoms with short bond lengths, 0.2388 – 0.2354 nm,

2. the Ca(4), Ca(5) and Ca(6) atoms in centered positions are irregularly coordinated, the Ca-O bonds varying from 0.2444 to 0.2625 nm.

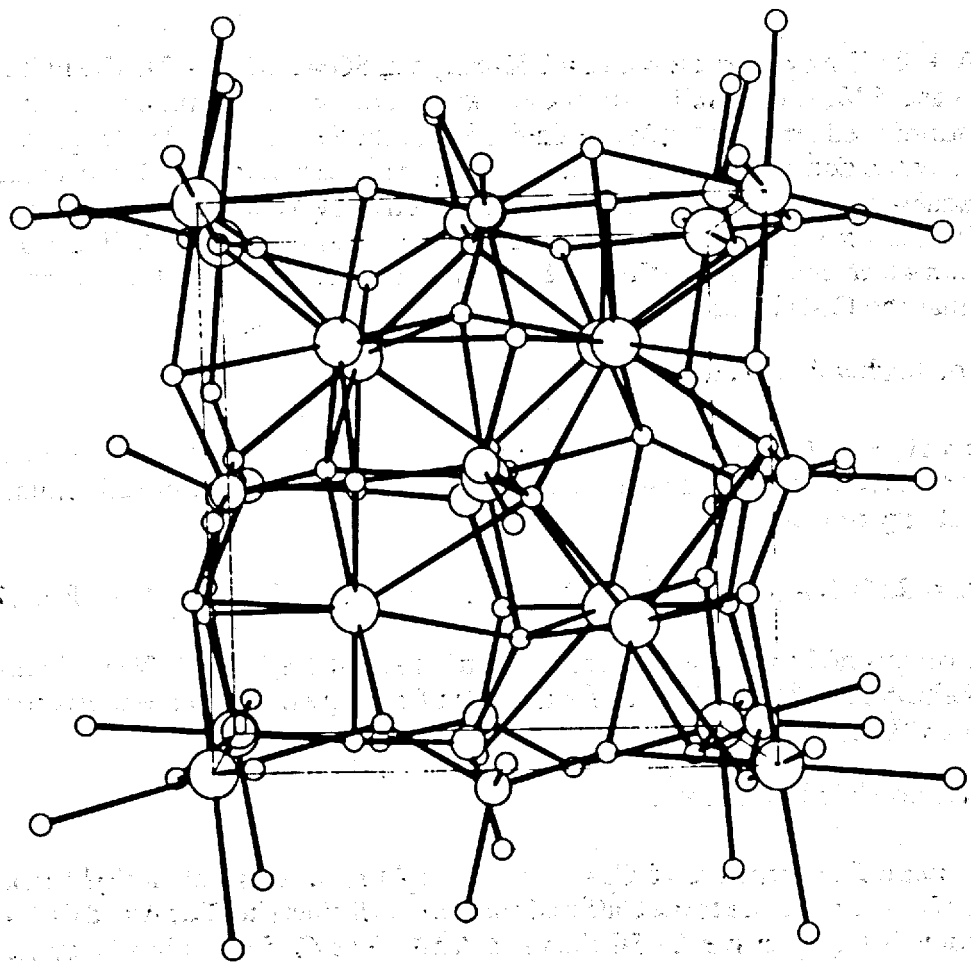

Fig. 12 Tricalcium aluminate structure; 1/8th of the cell viewed along the |010| axis. The hole in the Al_6O_{18} ring is at the bottom left (83).

4.3.2 Crystal Structure of C_3A – Na_2O solid solutions

Na substitutes for Ca in the crystal structure of $Ca_3Al_2O_6$. In order to preserve the neutrality, a second Na atom occupies the center of one of the Al_6O_{18} rings. Four domains of stability have been found:

1. 0 to 1.9% Na_2O by weight : CI
2. 1.9 to 3.7% Na_2O : coexistence of CII and O
3. 3.7 to 4.6% Na_2O : O
4. 4.6 to 5.9% Na_2O : M

Takeuchi et al (8,84), using X-ray precision photographs and a four circle diffractometer determined the structures of three single crystals containing respectively 2.4, 3.8 and 5.7% Na_2O which were respectively cubic II, orthorhombic O and monoclinic M. The structure of pure C3A has been called CI.

— The cubic CII structure

C_3A + 2.4% Na_2O is cubic with a = 1.5248(2) nm, SG = $P2_13$, Z = 24. The unit cell contains 69.5 Ca atoms and 5 Na atoms. Half of the sodium atoms are localised at the centres of Al_6O_{18} rings and half are substituted for Ca in Ca(3) and Ca(4) sites of the CI structure. The length of the Na-O bonds leads to a contraction of the rings and a decrease of the lattice parameter. Moreover the rings no longer remain aquivalent. The unit cell is non-centrosymmetric. Two kinds of calcium site appear: Ca A and Ca B. The Na occupancy in the B ring is larger than that in the ring A. The Ca 4B coordination polyhedron which contains 76% Ca and 24% Na is distorted due to the fact that the Na-O bonds are smaller than the Ca-O bonds.

— The orthorhombic O structure

The CII ——> O transformation corresponds to an important change in structure (85). If the lattice parameter c remains unchanged, the unit cell is now half the cubic cell volume with a different from b but very close to $\sqrt{2}$:

C_3A = 3.8% Na_2O: a = 1 0875(3), b = 1.0859(3), c = 1.5105(10) nm, SG = Pbca, Z = 12

The centers of the rings which were on the triad axes at 1/8, 3/8, 5/8, 7/8 positions are in c = 0 and c = 1/2 positions. Na atoms substitute for Ca in the Ca(5) site only and the rings are more contracted than in the CII structure.

— The monoclinic M structure

The monoclinic structure of C_3A + 5.7% Na_2O represents only a slight modification of the orthorhombic structure due to the Ca(5) splitting in two distinct sites Ca 5A and Ca 5B. The occupancy by Na atoms is higher in site Ca 5B than in CA 5A. The Ca 5B - O bonds are longer than in the orthorhombic structure but the Ca 5 - O bonds are shorter. The alternate stacking of these two sites leads to a slight distorsion only. The structure is characterized by:

a = 1.0877(6), b = 1.0854(13), c = 1.5135(13) nm, γ = 90.1°, SG = P21/a, Z = 12

The limit of solubility, 5.9% Na_2O, corresponds to the 75% occupancy rule at the ring centre. It is the limit corresponding to the permitted distorsion of the structure.

To conclude, the four structures of C_3A + Na_2O solid solutions can be classified into two groups, CI and CII on one hand, O and M on the other. In each group, the second variety is an ordered structure of the first one. The structure modifications are mainly due to the expansion of the Ca polyhedron when Na atoms substitute for Ca.

4.3.3 Other C_3A solid solutions

In the C_3A – Na_2O solid solutions, silicon atoms allow a complete occupancy of Ca 5B sites by Na atoms and 75% occupancy of the Al_6O_{18} rings (52, 53). The solid solution Ca(7.90)Na(1.73) Al(5.535)Si(0.465)Si(18) is monoclinic with a = 1.0844, b = 1.0855, c = 1.5122 nm, $\gamma = 90.38°$. In the presence of Si, the stability range of the orthorhombic form is enlarged. The excess of positive charge due to the introduction of Si^{4+} ions is compensated by a decreasing Na^+ occupancy in the ring while Ca 5B can be occupied by Na.

Potassium can also be introduced in the C_3A crystal lattice but the K substitution for Ca is not as easy as that of Na. The formation of K_2O solid solution is facilitated by the presence of Si and Fe. For example, the solid solution C_3A + (2.9% K_2O, 4.1% SiO_2, 10% Fe_2O3) is orthorhombic with a = b = 1.1.0867, c = 1.5120 nm (55). The crystal structure of solid solutions C_3A + Na, Fe, Si has been determined by Takeuchi et al (8,84). The single crystal |Ca(8.375)Na(0.875)| |Al(5.175)Fe(0.45) Si(0.375)| O(18) is orthorhombic with a = 1.0875, b = 1.0859, c = 1.5105 nm. Tetrahedral bonds Al-O, Fe-O, Si-O are not very different from Al-O bonds in the pure C_3A crystal structure: Al-O = 0.175, Fe-O = 0.188, Si-O = 0.162 nm. Silicon and iron atoms can stabilise, at room temperature, a pseudo-tetragonal orthorhombic O II form (87).

Mg substitutes for Ca but the solid solution C_3A + Mg remains cubic (88).

4.4 Aluminoferrite Phase

The aluminoferrite phase, a solid solution of composition C2 Ap F(1-p), is always orthorhombic.

4.4.1 Crystal Sructures of C2 Ap F(1-p) solid solutions

The orthorhombic structure of C2F is pseudo-tetragonal with a = 0.5599, b = 1.4771, c = 0.5429 nm, SG = Pcmn, Z = 4 (89). Along the b axis layers of FeO_6 octahedra alternate with layers of FeO_4 tetrahadra. Both types of layers are distorted.

In the C_2F structure, Al first replaces Fe in the tetrahedral sites up to p = 0.33 and then equally to both types of sites $|Fe^{3+}|$ and (Fe^{3+}). At p = 0.33 there is a change of space group from Pcmn to Ibm2. For p = 0.50, a = 0.55672; b = 1.4521, c = 0.5349 nm (90).

4.4.2 Other C2(Ap F1-p) solid solutions

Mg, Si, Ti, Mn and Cr can all enter into the lattice of C2(ApF1-p). There is only minor replacement of Ca^{2+} by Mg^{2+} (91). The total of Mg, Al, Si, Mn fills the tetrahedral and octaheral sites (92). The amount of Mg^{2+} ions is balanced by the total of Si^{4+} + Ti^{4+}, in agreement with previous EPMA data (94).

5. PORTLAND CEMENT MINERALS

The clinker phases crystallise from a partly melted composition. As described by Timashev (3), clinker is a non equilibrium multicomponent system of solid solutions. The minor elements are non uniformly distributed in the four main clinker minerals, their amounts being at least 4% in alite, 6% in belite, 10% in the aluminoferrite and 13% in tricalcium aluminate (93). As examples, Mg is preferentially dissolved in C2(AF) than in C_3S and C_3A, Na is concentrated in C_3A and K in C_2S, Al and Fe are twice as concentrated in C_2S than in C_3S.

Alites in industrial clinkers are mainly monoclinic. Belites are coexisting forms of β,α' and α C_2S identified by optical or electron microscopy. C_3A is cubic or orthorhombic, sometimes monoclinic. Two phases can coexist: cubic + orthorhombic and cubic + monoclinic. The ferrite phase is always orthorhombic with X-ray reflections broadened and often ill defined. Together, C_3A and C2(AF) constitute an interstitial phase of variable texture resulting from the thermal history as well as from the chemical composition (86).

There also exist some minor phases as free lime, periclase, sodium and potassium sulfates. Fillers introduced up to 5% in normalised Portland Cements can be calcite or calcite + dolomite and can contain minor phases like quartz and feldspars (95).

6. PROPERTIES OF CLINKER MINERALS

Portland cement is used as a powder. Its grindability and its reactivity related to its fineness are two characteristics to be taken into account. Some relations have been found between clinker microstructure and grindability. The fragmentation of clinker grains follows a process of liberation both fissural and mineral (96). The cracks progress respectively across the crystals and along the phase boundaries. Precracked and brittle C_3S crystals are easily fragmented (Fig.13). C_2S is more plastic than C_3S. Crystals or clusters of C_2S are detoured by the cracks up to an advanced stage of the fragmentation (Fig.14). These rounded grains give rise to a typical mineral liberation. Individual crystals are found intact in the coarser part (97,98). This phase segregation has been considered as detrimental (99). After grinding it is important to know the phase distribution at the surface of grains which will react (100). Vidick et al (101) have tried to measure the surface of silicate phases via the reaction of a chlorosilane with the silanol groups of alite and belite of cement powders used as polished sections, under an optical microscope equipped with an image analyser. This selective surface determination of silicates was found reliable. Scrivener and Pratt (102) used the back-scattered electron imaging technique in a SEM-EDAX producing X-ray maps. Scrivener (103) showed considerable differences between the surface composition of cements powders determined by X-ray diffraction and more particularly for the aluminate phases. ESCA and OAS (Opto-Acoustic Spectroscopy) used by Ball et al (104) showed that surfaces of commercial Portland cements have reduced cation and increased oxygen contents compared with the bulk material. Surface hydroxyl groups were also detected. Measurements of alite birefringence revealed that values from powders (Ono method) were twice those obtained by thin sections methods (105).

Sufficient quantity of small euhedral alite warrants high strength, high early strength being promoted by alkali sulfates (106) although K and S are in substitution in belite and K in C_3A, a mixture of cubic and orthorhombic forms. So alkali sulfate and fineness are two factors for a high strength cement (107). On the contrary, a poor strength cement has been characterised by large lamellar grains (40 μm average) euhedral to subhedral alite crystals (45 μm), profused growth of bladed Ca-K sulfate on alite and belite along the sets of lamellae (108).

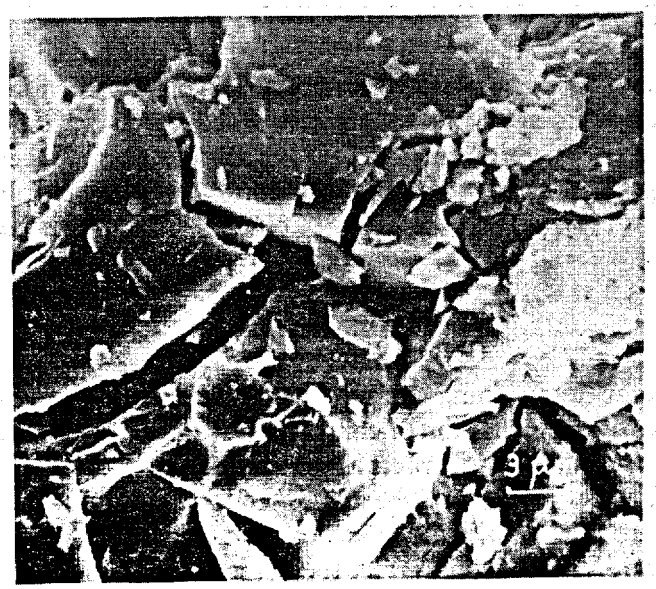

Fig. 13 Fissural liberation of C_3S fragments during grinding

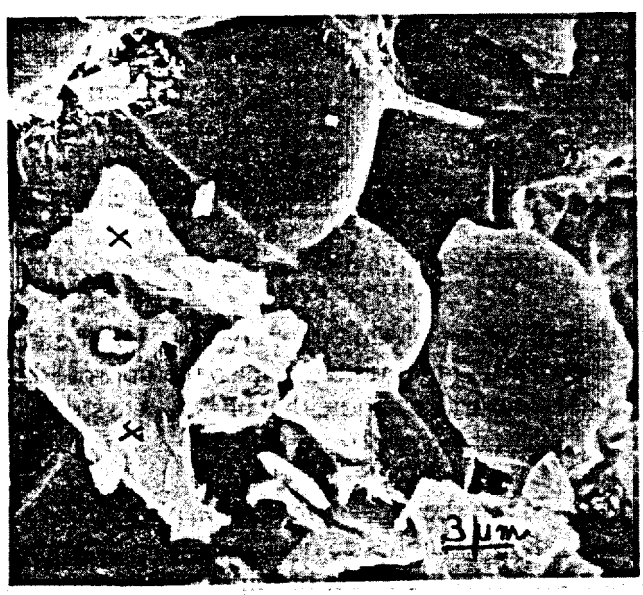

Fig. 14 Mineral liberation of C_2S rounded grains. Some sulfate flakes are visible on C_2S. Fragments of C_3S (x).

7. QUANTITATIVE PHASE ANALYSIS OF CLINKER

Quantitative phase anlysis can be done directly from X-ray diffraction (109) or optical microscopy data. Results of an international laboratory test published by Aldridge (110) leads to the conclusion that cement phase analysis by optical microscopy or X-ray diffraction needs an experienced operator and a careful sampling. Work is in progress in two committees, the RILEM 79 PAC and the ASTM Task Group Co1.23.01 (111), taking into account polymorphic phases like cubic and orthorhombic C_3A.

8. CONCLUSION

The main parameter determining the individuality of the chemistry of cement clinker, which involves the regularities of the formation of chinker phases and clinker, the mineralogical structure of clinker, the composition, the atomic structure, the fine texture of phases, their properties and the quality of the material as a whole, is the chemical composition of raw materials of the initial clinker mix. It is impossible here not to take into consideration the thermal conditions of the mixture firing (the maximum temperature, the heating rate, the retention time at the maximum temperature, the cooling rate). At the same time these conditions are known to be due to the chemical composition of the initial raw mix.

The set of impurity components in the raw mix as well as their concentration constantly change. Depending on this, changes also occur as regards the above mentioned processes, characteristics, properties, in particular the temperature of the appearance of the clinker liquid phase, its viscosity, surface tension, chemical composition and structure of the phases, their crystallo-chemical state, fine texture of crystal, phase relations.

It is worth mentioning once more that the formation medium of the clinker phases which finally determine the quality of the material is a polycomponent oxide system. One of the features of these systems is the impossibility of neglecting even small amount of impurity components in the analysis of phase relations. As mentioned above, when the raw clinker mix contains small amounts of such components as Na_2O, K_2O, Cr_2O_3, TiO_2, SO_3, the quantitative ratio between alite and belite changes significantly. When MgO is participating in the polycomponent clinker system, the behaviour of the phases and their ratio change. In this case the polymorphic forms of the phases can change as well as the distortion of crystal lattice and the quality of crystallinity.

The strongest lattice distortions are observed for crystals of the belite and aluminoferrite phases. These phases and materials containing them show up also the improved hydraulic properties, mainly the strength characteristics. It is important to note that phases with strongly distorted structure should be the subject of detailed investigation.

Mentioning the basic role of the chemical composition of raw mixes and taking into account the opinion of many scientists one should emphasize once more that a hopeful possibility of the development of new technological methods is the effect of impurity components. One cannot but mention, however, rather a weak intensity of the investigation of the action mechanism of impurity components, their chemical variety, various amounts and combinations in many processes responsible for the preparation of the high-quality material with lower energy consumption.

Meanwhile during the clinker production the processing parameters are so closely related with each other that consideration of the influence of only one of them (example, on the character of the clinker phases) can often lead to insignificant or inaccurate results if one neglects some other

simultaneously acting parameters. The results of each investigation need careful consideration so that one could really estimate the interrelation of the influence of several parameters with certain properties of the phase or the material. This also concerns the fine changes in atomic structure of the phases, the fine texture of crystals, the mineralogy of clinkers as a whole. The character of the crystals gives evidence for the environment of their formation.

The elucidation of the formation conditions of crystals with a reproducible fine texture makes it possible to reveal the correspondence with the hydration properties of separate phases and cements as a whole and with their quality. These data can also serve as the basis for the control of the features of clinker phases and consequently of the properties of the final material.

ACKNOWLEDGEMENTS

Dr A.I. Boikova is deeply grateful to Mrs I.G. Labetskaya for the assistance in translating her part of the paper into English and to Mrs O.I. Fomicheva who helped to prepare the manuscript for publication.

Prof M.Moranville-Regourd wishes to acknowledge Professor H.F.W. Taylor for his permission to reproduce some figures of the chapter One of his new book and to thank ATILH (Association Technique de l'Industrie des Liants Hydrauliques) for the access to its Service of Documentation.

REFERENCES

1. Bucchi, R. :"Influence of the nature and preparation of raw materials on the reactivity of raw mix". 7th ICCC, Paris, 1980, Vol I, I-1/3 - I-1/43.

2. Boikova, A.I. :"Isomorphous impurities in clinker phases - Main parameter ot their chemical activation". Tsement, 1986, N°9, 3-6.

3. Timashev, V.V. :"The kinetic of clinker formation. The structure and composition of clinker and its phases". 7th ICCC, Paris, 1980, Vol I, I-3/1 - I-3/17.

4. Boikova, A.I. :"Chemical composition of raw materials as the main factor responsible for the composition, structure and properties of clinker phases". 8th ICCC, Rio de Janeiro, 1986, Vol I, 19-33.

5. Boikova, A.I. :"Modern problems of impurity influence on mineralogy and crystal chemistry of clinker phases". Tsement, 1991, N°1-2, 20-24.

6. Taylor, H.F.W. :Cement Chemistry. Academic Press, London, 1990, 475 p.

7. Regourd, M, Chromy, S, Hjorth, L, Mortureux, B, Guinier, A. :"Polymorphisme des solutions solides du sodium dans l'aluminate tricalcique". J. Applied Crystallogr., 1973, N°6, 355-364.

8. Takeuchi, Y., Nishi, F. and Maki, I.:"Crystal-chemical characterization of the 3CaO Al2O3 - Na2O solid solution series". Zeit. Krist., 1980, 152, 259-307.

9. Al'bats, B.S., Osokin, A.P., and Burygin, V.V.:"Phase separation in the melts of commercial clinkers". (in Russian). 15th All-Union meeting of the chiefs of the laboratories of cement factories. Moscow, 1990, 86-88.

10. Kakali, G., Kasselouri, V.,Parissakis, G. :"Investigation of the effect of Mo, Nb, W an Zn oxides on the formation of Portland cement clinker". Cem. Concr. Res., 1990, 20, 131-138.

11. Maki, I.:"Relationship of processing parameters to clinker properties; influence of minor components". 8th ICCC, Rio de Janeiro, 1986, Vol i, 34-47.

12. Ivashchenko, S.I.:"Technology of modified cements with reduced energy consumption and improved properties". All-Union scientific-technical meeting on the chemistry and technology of cements, Moscow, 1991, Part I and II, 43-46.

13. Barbanjagre, V.D., Shamsburov, V.M., Timoshenko, T.I.:Effect of impurity elements on the properties of clinker melt". Ibid Ref 12, 12-14.

14. Zlatocrylov, M.R.:"A study of clinker formation on burning of Portland cement clinker mix based on converted slags". Ibid Ref 12, 12-14.

15. Maki, I., Takahashi, S., Hattori, M., Fukuda, K.:"Impurity distribution in zoned alite in Portland clinker as determined by CMA". Il Cemento, 1987, Vol 84, 351-358.

16. Maki, I.:"Processing conditions of Portland clinker and fine textures of alite". Il Cemento, 1985, Vol 85, 89-100.

17. Maki, I. and Hattori, M.:Influence of firing modes on the fine textures of alite in Portland clinker". Il Cemento, 1989, Vol 86, 131-140.

18. Maki, I., Tanioka, I., Imoto, Y; and Ohsato, H.:"Influence of firing modes on the fine textures of alite in Portland clinker". Il Cemento, 1990, Vol 87, 71-78.

19. Mitusas, A. :"Recrystallisation of alites in Portland cement clinkers". All-Union scientific-technical meeting on the chemistry and technology of cement, Thcherkessk, 1988, p13.

20. Fomicheva, O.I. and Boikova, A.I.:"Influence of sodium, potassium and magnesium oxides on formation of polycomponent solid solutions of di and tricalcium silicates (in Russian), All-Union meeting on the high temperature chemistry of silicates and oxides. Leningrad, 1988, 436-438.

21. Golovastikov, N.I., Matveeva, R.G. and Belov, N.V.:"Crystal structure of the tricalcium silicate 3CaO SiO2 = C3S". (in Russian), Crystallography, 1975, 20 (4), 721-729.

22. Fomicheva, O.I.:"Effect of alkali and magnesia oxides on the formation of clinker phases". (in Russian). Tsement, 1989, N°3, 17-18.

23. Boikova, A.I., Toropov, N.A., Pirytko, M.M. and Grum-Grzimailo, S.V.:"Effect of chromium oxide on structural transformations of tricalcium silicate". (in Russian), Izv. Academy of Science USSR, Neorgan Materialy, 1966, N°2, 1796-1802.

24. Schmitt-Henco, C.:"Magnesium oxide content of clinker, autoclave test and soundness". 6th ICCC, Moscow, 1976, VolI, 110-112.

25. Gartner, E.M. and Tang, F.J.:"Formation and properties of high sulfate Portland cement clinkers". Il Cemento, 1987, Vol84, 141-165.

26. Luginina, I.G., Konovalov, V.M. and Fadina, L.P.:"Peculiarities of cement production with high MgO content". All-Union meeting on the chemistry and technology of cement". (in Russian), Thcherkessk, 1988, C.120.

27. Luginina. I.G., Boikova, A.I., Fomicheva, O.I. and Konovalov, Y.M.:"Influence of high content of MgO on clinkers phase composition and properties of cements". 11 IBAUSIL, Weimar, 1991.

28. Boikova, A.I., Fomicheva, O.I. and Grishchenko, L.V.:"Effect of SO3 and MgO on the phase relation and crystal-chemical state of phases in the belite-aluminoferrite clinkers". All-Union scientific technical meeting on the chemistry and technology

of cement, Moscow, 1991, Part I and II, 20-24.

29-33. Strunge, J., Knofel, D. and Dreizler, I. :"Einflusse der Alkalien und des Schwefels auf die Zementeigenschaften.
Teil I. "Einflus des SO3 gehaltes auf die Zementeigenschaften". Zement, Kalk, Gips, 1985, N°3, 150-158.
Teil II. "Einflusse der Alkalien und des Sulfates unter Berucksichtigung des Silicatmoduls auf die Zementeigenschaften". Zement, Kalk, Gips, 1985, N°8, 441-450.
Teil III(a). "Einflusse der Alkalien und des Sulfates unter Berucksichtigung des Tonerdemoduls und des Kalkstandards auf die Zementeigenschaften". Zement, Kalk, Gips, 1986, N°7, 380-386.
Teil III (b). Einflusse der Alkalien und des Sulfates unter Berucksichtigung des Tonerdemoduls und des Kalkstandards auf die Zementeigenschaften". Zement, Kalk, Gips, 1986, N°8, 451-456.
Teil IV. "Zusammenfassende Betrachtungen". Zement, Kalk, Gips, 1990, N°4, 199-208.

34. Gies, A. and Knofel, D.:"Influence of sulphur on the composition of belite-rich cement clinker and the technological properties of the resulting cements". Cem. Concr. Res., 1987, 17 (2), 317-328.

35. Gies, A. and Knofel, D.:"Influence of alkalies on the composition of belite-rich cement clinkers and the technological properties of the resulting cements". Cem. Concr. Res.,1986, 16 (3), 411-422.

36. Knofel, D. and Gies, A.:"Einflusse erhohter Mangan and Alkaligehalte auf die Zusammensetzung belitreicher Zementklinker und die Zementeigenschaften". Silikattechnik, 1988, N°4, 119-120.

37. Stark, J, Muller, A. and Bimberg, R.:"Zur Rolle von Na2O in Belit-klinkern". Silikattechnik, 1989, N°5, 153-157.

38. Jost, K.H., Seydel, R;, Muller, A. and Stark, J.:"Zusammenhang zwischen Phasenzusammensetzung, Kuhlrate und Na2O-Gehalt in Belitklinkern". Zement, Kalk, Gips, 1988, N°4, 169-170.

39. Bruggemann, H. und Bentrup, L.:"Beziehungen zwischen der Zementfestigkeit und chemisch-moneralogischen Parametern des klinkers". Zement, Kalk, Gips, 1990, 30-33.

40. Maki, I and Chromy, S.:"Microscopic study on the polymorphis of Ca3SiO5". Cem. Concr. Res.,1978, 8 (4), 407-414.

41. Nagashima, M., Asakura, E., Uda, S. and Kawabata, H.:"Characteristics of alite in portland cement clinker and C3S solid solutions"., 8th ICCC, Rio de Janeiro, 1986, Vol II, 199-204.

42. Woermann, E., Eysel, W. and Hahn, Th.:"Chemical and structural investigations of solid solutions of tricalcium silicate. Part 5".,Zement, Kalk, Gips., 1969, 22, 414-422.

43. Maki, I. and Kato, K.:"Phase identification of alite in Portland cement clinker". Cem. Concr. Res., 1982, 12 (1), 93-100.

44. Sinclair, W. and Groves, G.W.:"Transmission electron microscopy and X-ray diffraction of doped tricalcium silicate'., J. Amer. Ceram. Soc., 1984, 67, 325-330.

45. Tagnit-Hamou, A. and Sarkar, S.L.:"The influence of varying sulfur content on the microstructure of commercial clinkers and the properties of cement"., World Cement, Sept 1990, 389-393.

46. Sarkar, S.L. and Tagnit-Hamou, A.:"Replacement of silica by sandstone in a raw meal. Its effect on the clinker microstructure"., 13th ICMM, Tampa, USA, 1991, 1-16.

47. Maki, I., Morikoshi, H. and Takashi, S.:"Processing of Portland clinker and microscopic textures of alites"., 14th Conf. Silicate Industry and Silicate Science, Budapest, 1985, Section C, 67-74.

48. Deshayes, S.M.:"Clinker microstructure. A comparison of dry process, preheater, and precalciner kilns"., 8th ICMM, Orlando, USA, 1986, 1-12.

49. Hudson, K.E. and Groves, G.W.:"The structure of alite in Portland cement clinker. TEM evidence3., Cem. Concr. Res., 1982, 12 (1), 61-68.

50. Hahn, Th., Eysel, W., Brenner, P. and Woermann, E.:"Modification M of Ca3SiO5". 5th ICCC, Tokyo, 1968, Vol I, 38-39.

51. Bigaré, M., Guinier, A., Mazières, C., Regourd, M., Yannaquis, N., Eysel, W., Hahn, Th. and Woermann, E.:"polymorphism of tricalcium silicate and its solid solutions"., J. Amer. Ceram. Soc., 1969, 50, 609-619.

52. Nishi, F. and Takéuchi, Y.:"The rhomboedral structure of tricalcium silicate at 1 200°C"., Zeit. Krist., 1984, 168, 197-212.

53. Jeffery, J.W.:"The crystal structure of tricalcium silicate"., Acta Crist., 1952, 5, 26-35.

54. Nishi, F., Takéuchi, Y and Maki, I.:"The tricalcium silicate Ca30 |SiO4|. The monoclinic superstructure"., Zeit. Krist., 1985, 172, 297.

55. Groves, G.W.:"TEM studies of some clinker compounds, their hydration and strong cement pastes"., Phil. Trans. R. Soc. Lond., 1983, A 310, 79-83.

56. Smith, D.K., Majumdar, A.J. and Ordway, F.:"The crystal structure of γ dicalcium silicate"., Acta Cryst., 1965, 18, 787-795.

57. Kriven, W.M.:"Displacive transformation mechanisms in zirconia ceramics and other non-metals"., Tailoring Multiphase and Composite Ceramics, Plenum Publ., 1986,223-237.

58. Moya, J.S., Pena, P. and de Aza, S.:"Transformation toughening in composites containing dicalcium silicate"., J. Amer. Ceram. Soc., 1985, 68 (9), C 259-262.

59. Yannaquis, N. and Guinier, A.:"Polymorphic β→γ transition of calcium orthosilicate"., Bull. Soc. Fr. Mineral. et Crist., 1959, 82, 126-136.

60. Gawlicki, M.:"The role of thermal treatment on dicalcium silicate polymorphic transitions"., 14th Conf. Silicate Industry and Silicate Science, Budapest, 1985, Section C, 67-74.

61. Von Lampe, F. and Seydel, R.:"On a new form of β belite"., Cem. Concr. Res., 1989, 19 (4), 509-518.

62. Regourd, M., Bigaré, M., Forest, J. and Guinier,A.:"Synthesis and crystallographic investigation of some belites"., 5th ICCC, Tokyo, 1968, Vol I, 44-48.

63. Regourd, M. and Guinier, A.:"The crystal chemistry of the constituents of Portland cement clinker"., 6th ICCC, Moscow, 1974, Vol I, 25-51.

64. Chan, C.J., Kriven, W.M. and Young, J.F.:"Analytical electron microscopic studies

of doped dicalcium silicates"., J. Amer. Ceram. Soc., 1988, 71, 713-719.

65. Chan, C.J., Ghose, A. ,Kriven, W.M. and Young, J.F.:"Microstructure of non stoichiometric dicalcium silicate doped with potassium oxide"., Int. Symp. Cement. Concrete, Beijing, 1985, Vol I, 11-28.

66. Chan, C.J., Kriven, W.M. and Young, J.F.:"Microstructure characterization of non stoichiometric dicalcium silicate doped with aluminium oxide"., 4th Annual Meeting of Electron Microscopy Society of America, Albuquerque, 1986, 452-453.

67. Matkovic, B. and Young, J.F.:"Dicalcium silicates doped with phosphates"., 8th ICCC, Rio de Janeiro, 1986, Vol II, 276-281.

68. Suzuki, K., Ito, S., Nishikawa, T. and Shinno, I.:"Effect of Na, K and Fe on the formation of α and βCa2SiO4"., Cem. Concr. Res.,1986, 16 (6), 885-892.

69. Feng Xiuji and Long Shizong.:"Investigation of the effect of minor ions on the stability of βC2S and the mechanism of stabilization"., Cem. Concr. Res., 1986, 16 (4), 587-601.

70. Oberste-Padtberg, R.:"Idiomorphic belites in Portland cements. A genetic model"., Cem. Concr. Res., 1986, 16 (5), 685-694.

71. Feng Xiuji, Long Shizong and Shen Dexun.:"Research ofpositron annihilation and hydration of doped βC2S"., Cem. Concr. Res., 1987, 17 (4), 532-538.

72. Rajczyk, K.:"Effect of reducing atmosphere on the properties of dicalcium orthosilicate"., Cem. Concr. Res., 1990, 20 (1), 36-44.

73. Puertas, F., Glasser, F.P., Blanco-Varela, Ma.T. and Vaquez, T.:"Influence of the kiln atmosphere on manganese solid solutions in Ca3SiO5 and Ca2SiO4"., Cem. Concr. Res., 1988, 18 (5), 783-788.

74. Udagawa, S., Urabe, K., Natsume, M. and Yano, T.:"Refinement of the crystal structure of γCa2SiO4"., Cem. Concr. Res., 1980, 10 (2), 139-144.

75. Udagawa, S;, Urabe, K., Yano, T., Takada, K. and Natsume, M.:"Studies on the dusting of Ca2SiO4. The crystal structure of α'Ca2SiO4"., CAJ 33th Meeting, 1979, 34-35.

76. Udagawa, S., Urabe, K. and Yano, T.:"Stabilization mechanism of polymorphism of C2S"., CAJ 34th Meeting, 1980, 35-37.

77. Jost, K.H., Ziemer, B. and Seydel, R.:"The crystal structure of C2S"., Acta Cryst, 1977, B 33, 1696.

78. Yamaguchi, G. and Ono, Y.:"Microscopic studies on the textures of belites in Portland cement clinker"., Semento Gijutsu Nenpo, 1962, XVI, 32-34.

79. Groves, G.W.:"Twinning in β-dicalcium silicate"., Cem. Concr. Res., 1982, 12 (5), 619-624.

80. Barnes, P. and Ghose, A.:"The microscopy of unhydrated Portland cement".,in Structure and Performance of Cements Ed by P.Barnes, Applied Science publishers, London, UK, 1983, Chapter 4, 139-203.

81. Feng Xiuji, Wang Lan, Long Shizong and Wang Yanguo.:"Investigations on C2S twins". Cem. Concr. Res., 1988, 18 (5), 753-757.

82. Fukuda, K. and Maki, I.:"Orientation of βCa2SiO4 solid solution lamellae formed in the host α-phase"., Cem. Concr. Res., 1989, 19 (6), 913-918.

83. Mondal,P. and Jeffery, J.W.:"The crystal structure of tricalcium aluminate"., Acta Crystallogr., 1975, B 31, 689-696.

84. Takéuchi, Y., Nishi, F. and Maki, I.:"Structural aspect of the C3A-Na2O solid solutions".,7th ICCC, Paris, 1980, Vol IV, 426-431.

85. Nishi, F. and Takéuchi, Y.:"The Al6018 rings of tetrahedra in the structure of Ca8.5 Na Al6 018". Acta Crystallogr., 1975, B 31, 1169-1173.

86. Regourd, M.:"Crystal chemistry of Portland cement phases" in Structure and Performance of Cements Ed by P.Barnes, Applied Science Publishers LTD, London, UK, Chapter 3, 109-138.

87. Lee, F.C., Banda, H.M. and Glasser, F.P.:"Substitution of Na, Fe and Si in tricalcium aluminate and the polymorphism of solid solutions"., Cem. Concr. Res., 1982, 12 (2), 237-246.

88. Puertas, F., Soria, J, Blanco-Varela, Ma.T. and Vasquez, T.:"Modification of the tricalcium aluminate phase in cements by manganese substitution"., Cem. Concr. Res., 1988, 18 (6), 837-842.

89. Colville, A.A.:"Crystal structure of Ca2Fe2O5 and its relations to the nuclear electric field gradient at the iron sites"., Acta Crystallogr., 1970, 26 (10), 1469-1473.

90. Colville, A.A. and Geller, S;:"The crystal structure of brownmillerite Ca2FeAlO6"., Acta Crystallogr., 1971, B 27, 2311.

91. Hahn, Th., Eysel, W. and Woermann, E.:"Polymorphism and solid solution of the ferrite phase"., 5th ICCC, Tokyo, 1968, Vol I, 54-60.

92. Harrisson, A.M., Taylor, H.F?W., and Winter, N.B.:"Electron optical analyses of the phases in a Portland cement clinker with some observations on the calculation of quantitative phase composition"., Cem. Concr. Res., 1985, 15 (5), 775-780.

93. Boikova, A.I.:"On the composition of clinker phases"., Il Cemento, 1978, 3, 137-146.

94. Zannei, Z. and Nanru, Y.:"A comparative study of the ferrite phase in high iron cements with the pure C2AxF1-x by MOssbauer spectroscopy"., Cem. Concr. Res., 1991, 21 (1), 31-37.

95. Regourd, M.:"Characteristics and activation of additive products"., 8th ICCC, Rio de Janeiro, 1986, Vol I, 199-229.

96. Hornain, H. and Regourd, M.:"Cracking and grindability of clinker"., 7th ICCC, Paris, 1980, Vol II, 276-281.

97. Sarkar, S.L. and Aitcin, P.C.:"Phase segregation in Portland cement during grinding" 10th ICCM, San Antonio, USA, 1988, 99-114.

98. Gutteridge, W.A.:"Quantitative X-ray powder diffraction in the study of some cementive materials"., in the Chemistry and Chemically Related Properties of Cement, 1984, Prc. Brit. Ceram. Soc., 35, Ed F.P. Glasser, 11-23.

99. Norris, D.:"Kiln feed homogeneity and clinker microscopy"., 10th ICCM, San Antonio, USA, 1988, 93-98.

100. Pratt, P.L.:"Physical methods for the identification of microstructures"., Materials and Structures, 1988, 21 (122), 106-117.

101. Vidick, B., Oberste-Padtberg, R., Laurent, J.P. and Rondelez, F.:"Selective surface determination of the silicates phases in portland cement powders using alkyl trichlorosilanes"., Cem. Concr. Res., 1987, 17 (4), 624_632.

102. Scrivener, K.L. and Pratt, P.L.:"The characterization and quantification of cement and concrete microstructures". , Proc 1rst RILEM Int. Congress, Versailles, France, 1987, Vol I, Chapman and Hall, London, 61-68.

103. Scrivener, K.L.:"The microstructure of anhydrous cement and its effect on hydration" Materials Research Society symposium Proceedings, 1987, Vol 85, 39-46.

104. Ball, M.C., Simmons, R.E. and Sutherland, I.:"Surface composition of anhydrous Portland cements"., Cem. Concr. Res., 1988, 18 (1), 29-34.

105. Pennel,J.:"Alite birefringence measurement. A problem and a solution"., 9th ICCM, Reno, USA, 1987, 1-15.

106. Sarkar, S.L.:"Parametric study of clinkering process and clinker microstructure of a high strength cement"., 3rd NCB Int. Seminar on Cement and Building Materials, New Delhi, 1991, IX, 1-13.

107. Sarkar, S.L.:"Develpoment of a high 24-hour strength clinker"., NSERC-Ciment Saint-Laurent-Université de Sherbrooke Co-operative Research Project, 1991, 60 pages.

108. Sarkar, S.L.:"Microstructural investigation of strength loss in a Type 10 cement" 11th ICMA, New Orleans, USA, 1989, 101-114.

109. Regourd, M.:"Application of X-ray diffraction to some problems of the cement industry"., Chemica Scripta, Vol 26 A, 1986, 37-45.

110. Aldridge, L.P.:"Accuracy and precision of phase analysis in Portland cement by Bogue, microscopy and X-ray diffraction methods"., Crm. Concr. Res., 1982, 12 (3), 381-398.

111. Struble, L. and Kanare, H.:"Cooperative calibration and anlysis of cement clinker phases"., NISTIR Report N°89-4164, USA, 1989, 44 pages.

Specific Theme I A

Clinker Formation Including New Processes

CLINKER FORMATION AND NEW PROCESSES

Vagn Johansen
G M Idorn Consult A/S, DENMARK

and

T V Kouznetsova
Moscow Institute of Chemical Technology, RUSSIA

Abstract

The relationship between the porperties of the raw mix and the clinker formation with respect to manufacture of Portland Cement is well understood.

The clinker melt formed has two important roles. It causes the load in the rotary kiln to form nodules, and it serves as the transport medium for the reactants in formation of the clinkerminerals. The presence of sulfats, chlorids and flourides have an effect on the rate of reaction and may cause the meltphase to separate into two liquids.

The most important process development has been in the grinding technology. There are activities in developing stationary kiln system, but no major step have been made.

NEW DELHI '92

Clinker Formation and New Processes

INTRODUCTION

Clinker formation is usually used in broad terms to describe the combined physical and chemical processes during the burning process of cement raw mixtures. These processes comprise several unit operations:

1. Drying and dehydrating the raw material components of the kiln feed.
2. Heating the kiln feed.
3. Decomposition of the $CaCO_3$ (calcining).
4. Agglomeration and formation of nodules of the calcined kilnfeed.
5. Synthesizing of the clinker minerals.
6. Cooling.

The increasing prices for energy and the regulation of the cement industry with respect to the environmental protection have been the driving force for the development towards more energy efficient cement plants.

The theoretical fuel consumption by the steps 1-6 is around 1800 kJ/kg clinker. This has to be compared to 3100-3300 Kj/kg clinker experienced for modern kiln systems. The difference is made up by the radiation loss and the heat in the exhaust gas. In addition to the fuel consumption comes the electrical power consumption which is around 100 KWh/t clinker. The major part of the electrical energy is used for processing the raw materials, grinding the raw mixture and grinding the clinker and gypsum to cement.

With respect to the total energy consumption the grinding process offers the largest potential for energy savings. Only a small fraction of the electrical power (1-2%) taken up by the conventional grinding installations is used for increasing the specific new surface of the material to be ground. Increasing this by 1 % would, therefore, increase the grinding efficiency considerably. The major developments in the cement industry through the 1980's have accordingly been in this field with the

introduction of high efficiency separators, high pressure roller mills and roller presses. The reduction in energy consumption is around 30 %. This development is, however, made by the suppliers to the industry, only very little research activity in the basics of the grinding process has been done.

The burning process does not present similar large potentials for energy savings. The calcining process is the step with the largest heat consumption: 1350 kJ/kg clinker. Concerning the production of ordinary Portland cement clinker from the usual raw materials not very much can be done to reduce this contribution to the over all fuel consumption. Production of clinker with other sources of CaO than limestone or with lower content of CaO i.e. belite clinker would, of course, decrease the theoretical heat consumption. The difference between a clinker with lime saturation 100 % and 80 % was shown by Meric[1] to be around 12 %.

Modern kiln systems are very compact and the heat loss due to radiation is at a minimum. Decreasing the burning zone temperature may have a marginal effect on this. The temperature has to be sufficiently high, however, for the clinker melt to form. The function of the clinker melt is two fold: it controls the agglomeration of the material in the burning zone, and the rate of clinker mineral formation by being the transport medium for the reactants. The effect of the clinker melt is demonstrated by comparing the production of ordinary Portland cement clinker with that of white cement clinker. They differ in their chemical composition in the content of Fe_2O_3: the white clinker contain less than 0.2-0.3% by weight. The clinker melt is formed at higher temperature for white cement clinker than for the grey clinker and the amount of clinker melt formed is usually smaller. The effect of this is that the production rate of white cement clinker on a given kiln is approximately 70 % of that of grey clinker. The specific heat losses will therefore be higher for the white cement clinker.

CLINKER FORMATION IN MODERN KILN SYSTEMS

Modern kiln systems using the dry process comprise a rotary kiln with suspension preheater and calcinator. There may be 4, 5 or more preheater stages. The more stages the better is the heat of the combustion gas utilized and the fuel economy therefore improved. More electrical power is, on the other hand, needed to overcome the pressure drop over the preheater. The optimum number of preheater stages is therefore determined by the relative prices of fuel and electrical power.

The first three steps of the clinker formation as listed above take place in a very short time compared to the total time for the clinker burning process. The kiln feed enters the kiln

within minutes after arriving at the preheater. The temperature of the material is then between 850 and 900°C and the degree of decomposition of the $CaCO_3$ of the kiln feeds lime component is 95 % in calciner kilns (45 % in kilns without calciner).

The retention time of the material in the kiln is 30 to 40 minutes of which the major part is in the burning zone. The temperature of the material increases rapidly from the 850°C to 1250-1300°C where the clinker melt is formed. In this part of the kiln there will be high concentrations of the volatile components of the raw materials and from the fuel. The volatile components are primarily the alkalies, sulfates and chlorides. These components volatilize and decompose in the burning zone and are carried with the combustion gas to the colder part of the kiln, where they condense on particles suspended in the gas stream as dust and on the material in the kiln. The repeated volatilization in the burning zone results in an internal circulation of these compounds and their concentration can be several times that of the kiln feed. These compounds have low melting points and may cause formation of liquid locally in the material prior to the formation of the proper clinker melt. In the charge of material at the entrance to the burning zone melt may also be formed locally at lower temperatures depending on the mineralogy of the raw materials used. For instance, quartz grains in the kiln feed will cause melt to be formed at or about 1200°C. The surrounding CaO, of which the mix is plentiful, will partly agglomerate, react and form crystals of belite. The belite crystals can be identified microscopically in the clinker as a pore surrounded by belite or coarse alite crystals. If secondary raw materials as slag or fly ash are used, particles high in silica will behave similarly. However, the large amount of clinker melt is formed within a narrow temperature interval and over a short distance in the rotary kiln.

The burning zone of the kiln is the part in which the material contains this liquid phase. In this part of the kiln the material has a temperature of up to 1450 - 1600°C. The liquid phase has two important functions. It causes the material to agglomerate into nodules, and it is the medium for the transport of the reactants in the mixture reacting to form the clinker minerals.

Formation of Clinker Nodules

After having reached the temperature for formation of the clinker melt, the material consists of particles and a liquid phase. During the rotation of the kiln, the tumbling material starts to agglomerate and form nodules. From the agglomeration physics it is known that good strong nodules are formed when 90-95 % of the void space of the densely packed particles is filled with the liquid. The particle size and the surface tension of the liquid are important parameters for the kinetics of nodulization and the size and the strength of the nodules.

(Optimum nodulization with water requires particles smaller than 200 μm, and the amount of water present is very critical with limits usually within 1 to 2 % by weight.) Too small amounts of liquid result in a few nodules in dust, too much in a paste-like mass.

For the material nodulizing in the kiln the amount of liquid necessary is between 15 and 25 % by weight. For some cement plants the amount of clinker melt is smaller because of the nature of the raw materials. The result of this is a very fine-grained, dusty clinker product. By adding, for instance, iron ore, the amount of liquid can be increased sufficiently to change the clinker granulometry towards coarser clinker nodules.

The two properties of the melt decisive for the rate of agglomeration and the strength of the resulting nodules are its viscosity and the surface tension[2,3]. The surface tension and the viscosities for a series of clinker melts with different admixtures have been extensively studied by Russian researchers[4]. The surface tension and the viscosity change relatively little when various compounds are added with values around $450*10^{-3}$-$500*10^{-3}$ N/m and 0.16 Pa*s respectively (values similar to the surface tension of Hg and the viscosity of olive oil). Only the simultaneously addition of K_2O and SO_3 is an exception. The surface tension is decreased to $150*10^{-3}$ N/m and since the strength of the agglomerates and nodules derives from that, this will result in weaker and smaller nodules and possibly clinker dust. This agrees with observations from industrial kilns. Increasing the SO_3 content of the kiln feed results in more dusty clinker. (From an industrial point of view is important to control the clinker granulometry because of its effect on the cooling process and the grindability of the clinker. In general, the specific power consumption for grinding clinker at a given grinding installation increases when the amount of the fine fraction, the dust, increases.)

The amount of melt is a discontinuous function of the temperature. There is a eutectic temperature, T_E, below which no liquid is formed. At T_E, most of the melt of a given composition is formed, and above T_E the increase in the amount of melt with temperature is very small. In the four component system, C-S-A-F, the eutectic temperature is 1338°C. In the system C-S-A it is 1460°C.

The amount of melt formed at T_E depends on the weight ratio Al_2O_3/Fe_2O_3. Al_2O_3/Fe_2O_3=1.4 gives the highest amount of melt at TE, and values larger or smaller than that give less melt at T_E [5,6,7]. Up to about 1550°C the amount of melt increases 3 % relative per 100°C increase in temperature. Above this temperature the slope of the curves are steeper and at approximately 1800°C, the typical Portland cement clinker will be completely melted.

The amount of the melt can be calculated according to the formula derived by Lea and Parker[8], or using Dahls formulae[9]. The formulae for calculating the amount of melt at given temperatures are derived assuming equilibrium and that solid solutions in the C_3S and C_2S phases present are negligible. The Lea and Parker formula for calculating the amount of melt at 1400°C in the C-S-A-F system is

$$\% \text{ liquid} = 2.95*(\%Al_2O_3) + 2.2*(\%Fe_2O_3)$$

Assuming that alite and belite have 1% Al_2O_3 and 1% Fe_2O_3 in solid solution[7], the formula overestimates the amount of melt with about 5 % absolute. This is according to observations made when the amount of melt is estimated by the amount of intermediate phase determined microscopically on quenched, synthesized clinker[10].

The effect of adding minor components to the C-S-A-F system is in general to lower the T_E and to increase the amount of liquid[7]. One of the important minor components is MgO. In the C-S-A-F system, the eutectic temperature is decreased to near 1300°C. In the system C-S-A, which is the model system for white cement clinker, the T_E correspondingly decreases from 1460 to 1400°C. Raw mixes for white cement are in general difficult to burn. 1-2 % MgO in such raw mixes, improves the burnability substantially compared to raw mixes without MgO.

Other important minor components are the alkalis; K_2O and Na_2O. Their presence in the melt decreases the T_E further by approximately 20°C. The simultaneous presence of sulfates and alkalis may complicate the situation since the sulfates form melts which are immiscible with the clinker melt[7,11,12,13].

The agglomeration and nodulization immediately after the formation of the clinker melt and the reduction of the porosity (sintering) of the clinker nodules during the burning process have been described by Petersen[10]. During the formation of the melt in which the particles are distributed the system is rearranged in a way to minimize the surface free energy. In the load of material small agglomerates are formed which grow together forming nodules. The process of nodulization is a combination of coalescence, by which small nodules of similar size collide and stick together, and by layering where small particles are rolled on the surface of the larger, in a way similar to the forming of snowballs[14].

After the rearrangement in the first part of the burning zone, the nodulization and the reduction of their porosity, q, take place under the influence of the rotation of the kiln and with the capillary pressure, ΔP, as the driving force. The packing properties of the individual clinker minerals have an effect on the development of the pore system[14]. Due to their crystal habit the alite crystals pack less densely than the belite or CaO crystals. For the isothermal sintering of clinker the following

relationship exists between the specific surface of the pore, S_K, the packing density of the clinker minerals and the porosity of the clinker:

$$S_K=(k/r)*(1-e)/e*q/(1-q)$$

S_K is defined as the surface area of the melt + crystals per condensed volume. The packing density is defined as 1-e where e is the void space between the clinker minerals, r is the average crystal diameter and k is a constant.

It has been shown that the grindability of cement clinker nodules are related to S_K[15,16,17]: the specific grinding energy increases with decreasing S_K. Clinker with high amount of clinker minerals with higher packing density should be more difficult to grind, all other parameters being equal. This is in qualitative agreement with experience from the industry, showing that the coarse fraction of the material (being the most difficult to grind) circulating in closed circuit cement grinding systems has a higher belite content compared to the average composition of the clinker.

The expression shows how the grindability of the clinker, by the correlation to S_k may be conceived as function of the mineralogy of the kiln feed and its chemical composition through the sintering structure:

1. The mineralogy and micro homogeneity of the raw mixture control the crystal size and thereby the capillary pressure through (k/r).

2. The chemical composition determines the amount of melt, the amount of clinker minerals and thereby the factor (1-e)/e.

3. The temperature and the retention time in the burning zone determines the porosity, q.

The reduction of the porosity during the burning process is a function of temperature and retention time, in the burning zone. At this stage the clinker behaves like a visco-elastic medium. For this system it can be shown in accordance with experiments that[10]

$$1/q-1/q_0=(t-t_0)\Delta P/(12\eta)$$

where η is the apparent viscosity of the system crystals plus melt, and t is the time of sintering.

The relations above are all valid for isothermal, stationary systems. They will, however, still be good approximations for the clinker formation in rotary kilns, because the texture of

the clinker is formed during the very fast rearrangement process in the very first part of the burning zone. The apparent viscosity is in the order of 10^6 times larger than the viscosity of the clinker melt, which means that the agglomerates and nodules formed are sufficiently strong to survive the transport through the kiln.

Formation of Clinker Minerals

Simultaneously with the agglomeration and nodulisation of the material in the burning zone, the formation of the clinker minerals by chemical reactions take place. In the nodules the reactants forming the clinker minerals are fixed relative to each other. The random nature of distribution of the raw material particles in the load results in variation in the chemical composition of the local elements on a microscopical level[18].

This can be illustrated by considering a simple model consisting of particles with diameters of 20 μm. Table I lists the probability for a local element 100 by 100 by 100 μm^3 to have a lime saturation factor larger than 125 %, for different overall average composition. A lime saturation factor larger than 100 % means that the local element after complete reaction will contain free, unreacted CaO. As shown in Table I, even for lime saturation factors in the interval 90 to 96%, which is a normal range for industrial clinker, the probability and thereby the concentration of these local elements, is high. Similarly, there must be local elements, in this system, with corresponding excesses of silica. In industrial kiln feeds, the particle size distribution is broad and there may be particles larger than 100 μm consisting of pure raw material components as for instance limestone and quartz. These coarse grains will enhance the differences in composition between the local elements. For coal fired kilns the absorption of ash will cause similar variations.

LSF %	90	91	92	93	94	95	96	97	98	99	100
100	6.6	7.6	8.1	8.9	9.5	10.4	11.7	12.7	13.6	14.7	15.9

Table I The probability, P, in %, that a local element, 100 x 100 x 100 u³, has a lime saturation factor larger than 125% as function of the average composition, constant silica ratio = 3 and varying LSF (Ref 65.)

The compositional variations between the local elements relative to the overall average composition of the kiln feed is reflected in the spatial distribution of the clinker minerals and the microstructure of the clinker nodules.

After a short time at the burning zone temperature, the material consists of CaO and C_2S in melt and the local microscopic elements may be assumed to be in local equilibrium. By this it is understood that the phase composition of the local element is in accordance with the phase diagram for the given local chemical composition and temperature and therefore each phase and phase boundary are in thermodynamic equilibrium.

Figure 1 is the isothermal section of the CaO-corner of the ternary system $CaO-Al_2O_3-SiO_2$ (CAS) system at 1500°C. It is divided into different fields D_1 to D_5. D_1, D_2 and D_3 are two phase fields with one solid phase in a melt of differing composition.

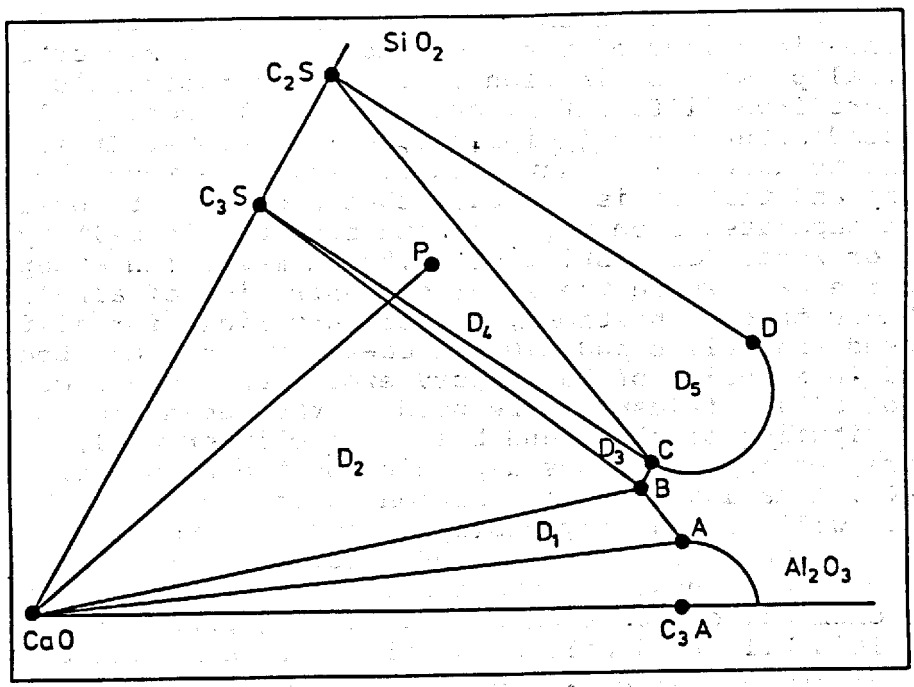

Fig. 1 Isothermal section of the CaO Corner of the $CaO-SiO_2-Al_2O_3$ system. 1500°C.

Compositions in D_1 are CaO in equilibrium with melt with compositions along AB. D_3 designates the compositions with C_3S in melt with compositions from B to C, and finally D_5 is the field of compositions with C_2S in melt CD.

The fields D_2 and D_4 are the three-phase fields, where two solid phases are in equlibrium with melt of one particular composition. D_2 is the field for CaO and C_3S in melt B, and D_4 the field for C_2S and C_3^c in melt with the composition C.

Contiguous local elements in the clinker nodules and agglomerates belonging to the same field constitute a region. In ternary systems only single-phase and two-phase regions can grow in size. Three-phase regions cannot form as a result of diffusion. They represent the boundary between two-phase regions[19,20]. If, for instance, a particle of CaO, belonging to D_1 is in contact with a region of composition P belonging to D_4 (Figure 1) the transport of CaO and SiO_2 in opposite directions result in a region belonging to D_3 :C_3S in melt. From microscopical examination of white Portland cement clinker, which can be represented in the C-A-S system, it is observed that regions with CaO/C_3S in melt always are divided from regions with either C_2S in melt or C_2S/C_3S in melt by regions with C_3S. Similar textures are observed in grey cement clinker.

Depending on the average chemical composition of the kiln feed and of the mineralogy of the raw materials, the microstructure and spatial phase distribution of the clinker minerals may vary in clinkers from different plants. They will however always be distributed after the principles described above. It is important to understand that the boundaries between the regions are sharp and that it is the rule that regions with belite in melt are separated from regions with free CaO in melt by regions or zones, consisting of alite in melt. (An exception to this is the case where the local concentration of alkalies is high. Under these conditions, the primary field for alite is suppressed and belite and CaO can co-exist. This has been observed in a series of laboratory experiments where coarse grains of alkali feldspar were used in the cement raw mixture). The distribution of alite and belite in clinker will, therefore, be inhomogeneous depending on the nature of the raw materials. A marl with a composition corresponding to P in Figure 1, will give a very easily burned mix and give clinker with a homogeneous distribution of alite and belite between each other. The opposite extreme will be a kiln feed with a similar chemical composition but containing pure limestone and quartz. This kiln feed will be difficult to burn and the clinker minerals will be inhomogeneously distributed. It is often seen in the literature that the quality of the clinker is measured by the degree of homogeneity by which alite and belite are distributed through out the clinker. This could lead to the erroneous conclusion that the phase distribution is controlled by the burning process. The spatial distribution of the clinker minerals is controlled by the properties of the raw materials used. An inhomogeneous distribution cannot be "burned away".

Rate of Reaction

Reactivity of the Ground Raw Mixture- The reactivity of cement raw mixtures, at equal conditions, is a function of the particle size distribution[21-35]. Laboratory experiments have shown[22] that the burning temperature may be decreased by 50°C for finely ground raw mixes.

This can be explained by the increased rate of diffusion caused by the increase in surface area and the correspondingly decreased diffusion distances. The shape of the particle size distribution plays a role, too. The more narrow it is the higher is the reaction rate[36].

The particle size distribution of the raw mixtures ground in vertical mills and roller presses is narrower compared to that of raw mixtures ground in conventional ball mills. It is therefore, at least in principle, to be expected that application of this kinds of mills for grinding raw mixtures also should have an effect on the kiln operation in terms of improved burnability.

Table II shows the development in the specific surface for three different type of grinding mills[21]. The longer time of grinding in the ball mill does not, however, increase the surface of the raw mixes. The reason is floculation of the fine particles. This may result in good homogeneity of the raw mixture but the grinding process becomes uneconomical.

Type of mill	Grinding Time							
	Minutes				Hours			
	2	5	10	20	1	2	3	4
Ball mill	-	-	-	-	26.5	24.7	22.3	20.7
Air-stream mill	-	22	23.2	22.4	-	-	-	-
Roller mill	21.1	24.8	24.3	24.4	-	-	-	-

Table II Influence of the grinding time on the surface of raw mixes ($m^2/kg \cdot 10^3$)

The development of new processes in the area of raw mixture production reflects the laboratory results shown in Table II. Vertical roller mills for grinding raw materials have been used for more than a decade. The high-pressure roller mill or roller press, which originally was introduced for grinding clinker to cement[37,38,39,40,41] is now also used for grinding the raw mixture[42,43,44,45].

Mechanical energy, which transfers to the structure of the solids, is the most effective method regarding the influence on the chemical and physico-chemical part of the material transformation.

The main act of the mechanical processing of the materials is the contact interaction between the particles of the raw materials and the working part of the mill. Kinetic energy is

liberated during the heating of raw materials, the destruction of the particles. During the grinding, the particle surface increases, and the morphology of the particles changes.

The internal energy increases as a result of the increase of the defect concentration and the stress concentration in the structure of the particles. These phenomena are the basis of the mechanical activation which intensifies the technological process.

Sulimenko[22] have shown that the impact shear grinding mill was the most effective. The microcrystalline structure blocks of the solid bodies ground by this mills were 4-6 times smaller than could be obtained by the impact grinding mill (Table III). The surface-active material used at the grinding of minerals reduces the microcrystals 5 times and the lattice distortion 3 times. As a result, the raw mixes' reactivity increases.

Method of failure	Minerals			
	Calcite		Quartz	
	D, Å	E, %	D, Å	E, %
Impact shearing	1640	0.14	1290	0.169
Crushing	6850	0.05	5040	0.089
Impact	7110	0.05	7910	0.034

Table III The influence of different kinds of grinding on the microcrystals size (D,Å) and lattice distortion of minerals (E, %)

Chodakov et al[24] have shown that, at the burning of calcite - quartz mix with the presence of surface-active material (SAM) - alite appeared at 900°C. The mechanism of alite formation they called mechano-sorptic. It includes the cracking of sorptic additives, and their chemical interaction with the centre of the surface layers of the solid bodies. The application of the SAM supplies the molecular density agglomeration of fine particles and their stoichiometric ratio. Temperature, time and energy activation are reduced compared with the classical grinding, due to the heat emission which is the result of the defect relaxation and the molecule mobility of the active surface layers of the particles.

The mechano-chemical activation of raw mixes is an especially effective method when using the equipment where the raw mixes are exposed to the high frequency of hydraulic impact and cavitation[24]. The researchers showed that this equipment (RPA)

The researchers showed that this equipment (RPA) makes it possible to obtain very fined grained material (Figure 2). The fine structure of the material is changed: the crystal parameters, crystal defects, phase transformation. Thus, by RPA-grinding, calcite transfers into aragonite. Grinding clay, the layer with the AlO_6 is fractured. As a result, material reactivity increases by up to 30% for clay and by 50-60% for limestone. In addition is the homogeneity of the mix improved. The results of the chemical analyses of the different fractions of raw mix are shown in Table IV.

The results reveal that grinding of raw mixes by RPA gives a more homogenic composition of the different fractions in comparison with the initial raw mix fraction.

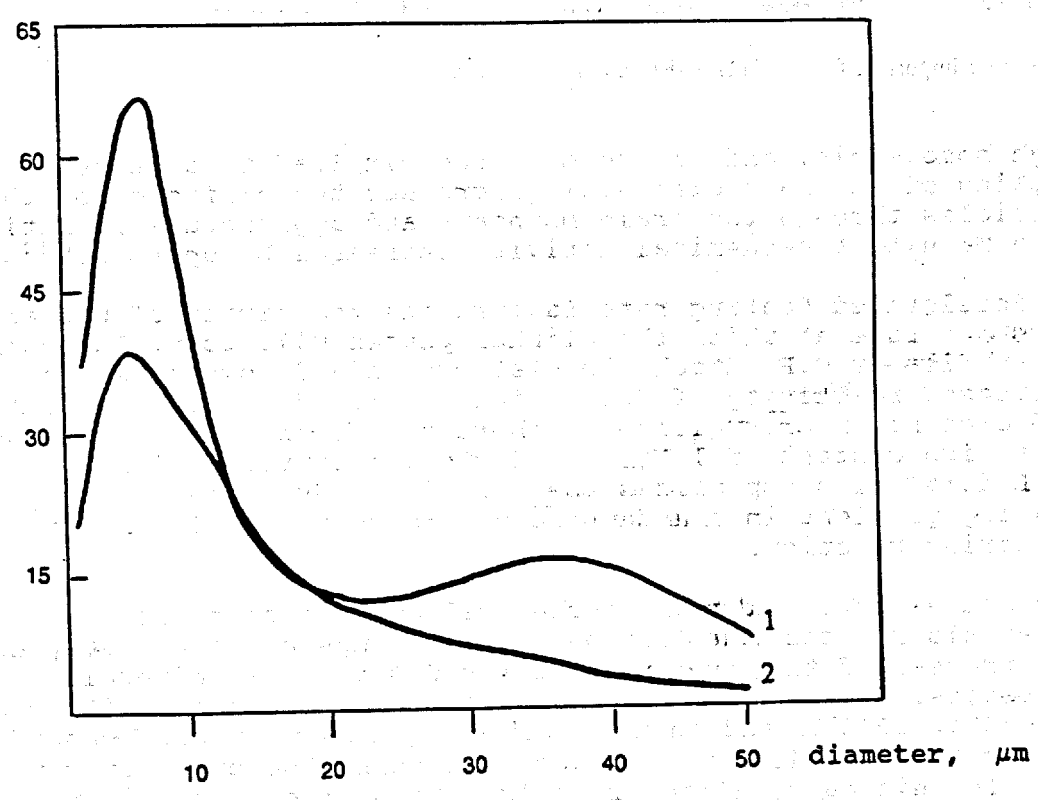

Fig. 2 Distribution of the particles of raw mixes:
1 - ordinary grinding 2 - [illegible] grinding

Kind of mix	Content %	Particle size, mm			
		60	40-60	15-40	less than 15
Initial	CaO	35.2	37.4	34.7	47.8
	SiO_2	23.7	21.8	15.2	7.6
	Al_2O_3	2.7	4.0	3.9	3.1
	Fe_2O_3	4.2	6.2	4.2	2.1
Activated	CaO	36.4	37.7	39.7	46.0
	SiO_2	19.3	17.4	16.8	13.6
	Al_2O_3	3.0	2.9	2.6	3.4
	Fe_2O_3	3.9	2.7	3.2	3.5

Table IV The chemical composition of the different fractions of raw mix.

One other important factor of (1) is the amount of melt, a.

High homogeneity and fineness of the mix lead to a dense packing of the particles. This increases the diffusion of the particles through the grain boundary and agglomerate formation. As a result, the chemical activity increases by up to 30%[25,26].

An accelerated heating rate favours the reactivity of CaO and thus the rate at which the clinker phases will form. According to studies by O.P. Mtschedlow-Petrossian and coworkers[31], the increased reactivity of CaO, which is formed at 800 to 900°C and does not recrystallize at short retention periods, is due to a high content of lattice defects and lattice voids. U. Ludwig[34] also emphasizes the technical advantage of a high heating gradient in the temperature range below 1000°C for the sintering reaction.

The above-mentioned mechano-chemical activation of raw materials reduces the decarbonization temperature of $CaCO_3$ and the process of the reaction between CaO and clay minerals increases. It was observed that a certain amount of alite was formed at 1200°C, and in the finished product it was 5-8 wt.% larger than in clinker obtained by burning the ordinary raw mix. In this case, alite crystals, which were formed in the solid phase, probably play the role of a seed in the formation of the main part of alite when the liquid phase appears. This changes the C_3S/C_2S ratio in the finished product. The most positive influence was observed when flyash was used as a raw component instead of clay.

The Rate of Alite Formation- The net reaction during burning of the cement raw mixture is the formation of alite:

$$CaO+C_2S \rightarrow C_3S$$

Quantitative information about the formation of C_3S in systems with melt[46,47,48,49] and without melt[50] have been obtained from a series of experiments using diffusion couples. The multi component diffusion of the reactants may be described as a pseudo binary diffusion problem making it possible to ascribe an effective binary difusion coefficient to CaO in the system[19,20]. Based on the assumption of transport controlled reactions, the growth of the reaction layer follow a parabolic rate[48,49]

$$X^2=kt$$
$$k=2a(D/\tau)(c_a-c_b)H\Delta c \qquad (1)$$
$$H=1/(c_1-c_a)+1/(c_b-c_2)$$

D is the effective binary diffusion coefficient for CaO in the melt. c_a and c_b are the weight fraction of CaO in the C_3S layer at the D_3-D_2 and the D_3-D_4 (Figure 1) interface respectively. c_1 and c_2 are the weight fraction of CaO in the endmembers (Figure 3). τ is the factor accounting for the tortuosity of the melt channels in the C_3S layer. c is the difference in CaO concentration between the melt in the C_3S-CaO endmember and the C_3S-C_2S endmember. a is the amount of melt. There is proportionallity between the rate constant and the amount of clinker melt. This is according to industrial experience. The higher amount of liquid phase at the burning temperature the easier the mix is to burn.

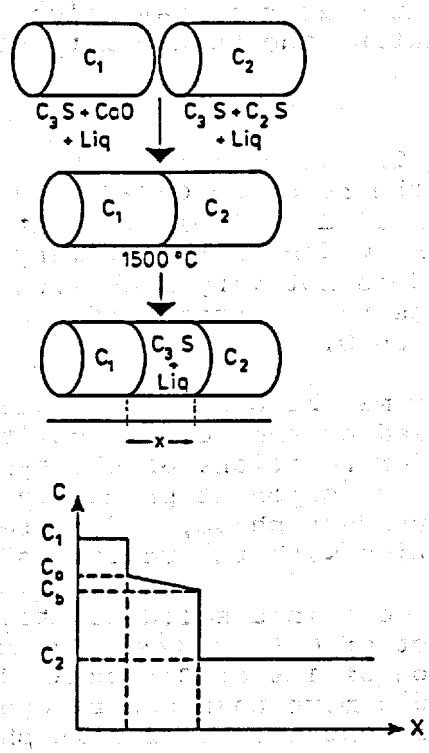

Fig. 3 **Principle of diffusion couple experiments and concentration profile. C is the concentration of CaO. (Ref. 48).**

Fineness and Homogeneity of the Raw Mixture- The factor H relates to homogeneity of the cement raw mixture and the microscopical distribution of the "local elements" described above. One extreme of raw materials is the marly raw materials with compositions close to the desired ("natural cement mix") which are homogeneous at a microscopical level. In this case H will have large values and the rate of C_3S formation will be high. These mixtures are "easy" to burn (part of the effect of RPA grinding summarized in table 3 may be explained in a similar way). The other extreme is the sandy type of raw materials in which the lime and silica components are separated into individual grains, the difference in concentration between the local elements is large, which gives small values of H and low rates of C_3S formation. These mixtures are "hard" to burn.

This has been dealt with in a direct way by Dreizler and Schäfer[51]. A number of raw mixtures were sieved in fractions: >125 μm, 90-125 μm, 63-90 μm, 32-63 μm and <32 μm. All fractions were analyzed, and the lime saturation factor (LSF), the silica module (SM) and alumina module (AM) were determined. Depending on the origin of the raw mixtures their fractions varied to different extend from the average compositions. The weighted deviation of the fractions LSF from the average correlated with the experience from the kiln operation. When the composition of the different fractions had large variations from the average composition the raw mixtures were more difficult to burn. The chemical compositions of the size fractions of the raw mixtures, have also been used by Chromy[51a] in a method correlating the burnability of the raw mixture with kiln operation.

The Driving Force- The Δc of (1) may be perceived as the driving force for the reaction $CaO+C_2S \rightarrow C_3S$. In the ternary system CAS it is small $\Delta c = 0.011$ (weight fraction) corresponding to the width of the primary field of C_3S of the phase diagram. It does not vary much with the temperature, so the influence on the rate constant of the temperature is mainly through the effect on D.

Modifications of Δc may be possible by adding minor components to the mixture. Based on thermodynamics it can be argued that the driving force for reactions of the type $CaO+C_2S \rightarrow C_3S$ will increase if the minor component primarily goes in solid solution with the product phase, and decrease if it primarily goes in solid solution with the reactants[52].

Fluorine primarily goes into solid solution with the alite phase and the effect of CaF_2 on the rate of alite formation is well known. Addition of 1 % of CaF_2 more than doubles the rate of the reaction, much more than can be explained by the possible increase of the amount of melt phase. The width of the primary field for C_3S in the C-A-S phase diagram increases with addition of CaF_2. This corresponds to a larger Δc[53] of (1) and

may be conceived as the thermodynamic effect.

Minor components as P_2O_5, Na_2O, K_2O and SO_3 primarily go into solid solution with belite[7]. The rate of CaO consumption in the alite formation is slowed down for mixtures with addition of these minor components. Müller and Stark demonstrated this for a raw mixture with LSF=80, MS=2.0, MA=2.1 and added K_2O (as carbonate) burned at 1350°C. The correlation between the free CaO and the K_2O was: $CaO_{free}(\%) = 0.43+2.31\ K_2O(\%)$[54,55].

The separate additions of alkali oxides or SO_3 have an inhibiting effect on the formation of the alite but combined addition as alkalisulfates does not decrease the rate to the same extent[56]. This is related to the fact that alkali sulfates form melts immiscible with the clinker melt, and therefore also reduce the amount going into solid solutions of belite.

Liquation- The amount of clinker melt has an effect on the rate of formation of the alite according to (1). The linear relationship between the amount a and the rate constant have been experimentally verified[49]. Addition of minor components may have an effect besides the thermodynamic effect mentioned above by causing separation of the melt, and thereby changing the effective transport area for the reactants in the alite formation as well as the agglomeration process. This is being dealt with in the following summary of the work by a number of russian researchers.

Similar to the liquid phase the clinker melt consists of Ca^{2+}, Mg^{2+}, O^{2-}-ions and the complexes SiO_4^{4-}, MeO_4^{5-}, MeO_6^{9-}, where Me = Al or Fe[27,29]. The melt may be conceived as micro-heterogeneous. The heterogeneity is a result of the irregular distribution of oxygen ions between stronger and weaker cations. This may cause liquation, i.e. the segregation, of the melt into two liquid phases which have viscosity and surface tension different from that the clinker melt[57,58].

For clinker melts with 1-5% fluorides, chlorides or sulfates the tendency to liquation increases when the minor components change as follows:

S → CL → F and Mg → Ca → Na →K.

Sulfated melts liquate only at the presence of alkaline cations. The addition of MgO, Mn_2O_3 and others to the liquid phase changes its properties and when the amount of Mg^{2+} in the melt is large, its liquation is suppressed completely.

The magnesium modulus may be used as a quantitative criterion of the melt liquation of industrial clinkers[59]:

$$m_{Mg} = MgO/(SO_3 + R_2O)$$

where MgO, SO_3, R_2O = the oxide quantity in raw mixture, wt%.

When the value of m_{Mg} is smaller than 1.5, the melt segregates without difficulty. If the value lies in the interval between 1.5 and 2.3, the probability of melt segregation in nearly 50%, and when m_{Mg} = 2.3 or more, microliquation does not occur.

For melts containing chloride or fluoride liquation phenomena take place at lower anion concentrations than in melts with sulfate anions.

Liquation salt melts in the system: R_2O-$CaSO_4$-MgO; CaF_2-$CaSO_4$; $CaCl_2$-$CaSO_4$; R_2O-CaF_2-$CaSO_4$ have a viscosity, which is 1-2 times lower, and a surface tension which is 2-4 times lower than that of the oxide melts which exist in the C-A-F-S-system.

The solubility of the salt melts in the oxide melts is around 2-3% at 1450°C. At lower temperatures their solubility decreases. However, if the salt melt (1%) dissolves at 1350°C, liquation takes place.

The solubilities for the oxides in the salt melts are as follows: CaO: up to 5.9%, SiO_2 up to 1.3%, Al_2O_3 and Fe_2O_3 up to 0.3%. In the melts of Na_2SO_4- K_2SO_4-$MgSO_4$, the oxide solubility increases as follows: CaO up to 13.5%; SiO_2 - 2.3%; Al_2O_3 and Fe_2O_3 - 1.1%, respectively.

In the melts which consist of chloride and fluoride, the oxide solubility is high even at 1100-1300°C. The $CaCl_2$-$CaSO_4$ melts have a maximum solubility and they decrease in the following succession: $Cl^- \rightarrow F^- \rightarrow SO_4^{2-}$. In such melts, CaO dissolves more intensively than C_2S. The experiments showed that chlorine and fluorine containing melts accelerate the mineral dissolution, but sulfo-alkaline melts reduce the rate of the reaction.

The kinetics of alite formation and microstructure of crystals depend on two factors: The composition of the oxide-salt melts and on the rate of CaO and C_2S dissolution[60].

At the presence of sulfo-alkaline melts, CaO dissolves slower than C_2S (Figure 4) and alite formation is limited by the rate of the interaction of CaO and the melt. In this case the large crystals of alite are formed. During growth they capture slowly dissolved particles of CaO which makes it impossible to obtain high alite clinker. The reduction of the liquation enables equal solubility of CaO and C_2S. The process of alite formation increases and its kinetics depends on the ion mobility in the melt. In this case the small crystal microstructure is formed.

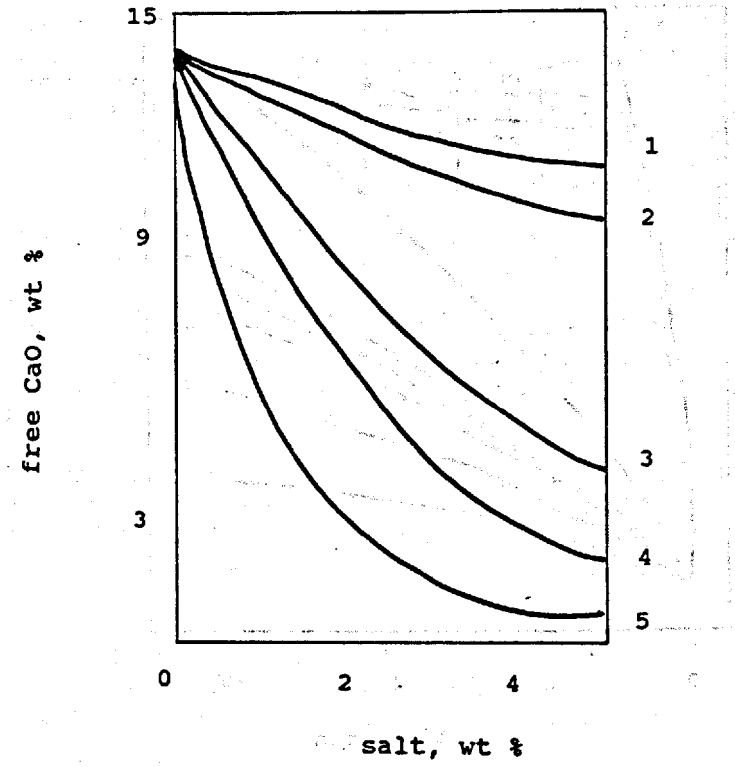

Fig. 4 Influence of salt content on free CaO content in sintering product at 1300 °C
1 - $CaCl_2$, 2 - CaF_2, 3 - $CaCl_2 + CaSO_4$
4 - $CaF_2 + CaSO_4$, 5 - $CaF_2 + CaCl_2$

The liquate melts which consist of chloride and flouride have the opposite regularity: If the quantity of the liquate fields in the melt increases, the process of alite formation increases and the alite crystal size reduces. The rate of the CaO dissolution exceeds that of C_2S.

The most intensive process of alite formation takes place at the presence of the composite melts (Figure 5). At 4-6% liquiate phase, alite formation is completed at 1350°C.

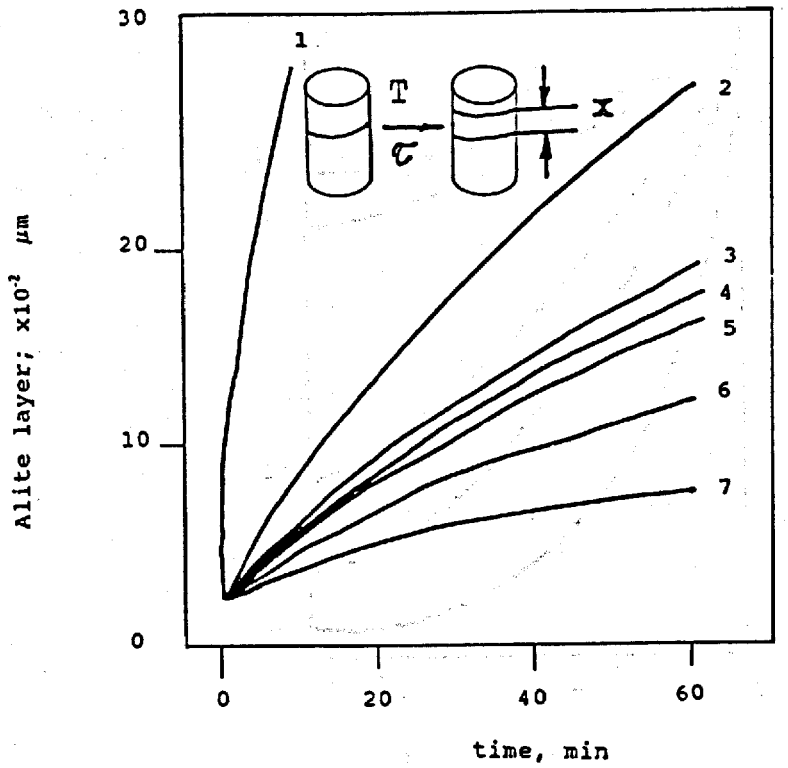

Fig. 5 Influence of sintering time (T=1450°C) on alite layer formed at the melt: 1 - CaF_2 + $CaSO_4$, 2 - F, 3 - R_2SO_4 + MgO 4 - R_2SO_4, 5 - MgO, 6 - ordinary melt without additives, 7 - R_2O

Clinker Phase Formation- Analyses of the composition of the clinker phases during heating give important information on the clinker phase formation and the probable scheme of the ion exchange between the silicate phases and the melt. Some experimental results which were obtained at the investigation of industrial raw mixes obtained from Russian cement plants are summarized below.

At heating rates of 5-7°C/min, alite formation in oxide melts which has a small content of sulphoalcaline liquate phase (2-8% relative), is the result of Ca^{2+} migration to the place where there is a concentration of ions $(SiO_4)^{4-}$.

The relatively fast growth of alite crystal at the first time up to 1350°C from the saturated melt causes the inclusions of the melt microvolumes and the unsoluble solid phases. First of all, growing alite crystals block the belite. The isormorhous capacity of alite reaches an average of 8 wt.% in crystal, and up to 10% at its surface layer.

At further heating the minimum amount of admixtures in alite is at 1375°C-1400°C. Their distribution remains the same in the surface and inside the layers. This indicates that alite crystal growth is not continuous. At definite conditions alite crystals disintegrate to small ones which can dissolve in the melt and are the basis for the further crystal formation.

Kouznetsova et al.[61] have shown that an insignificant change of the concentration of SiO_2 (23-24 wt% at the surface and 24-25 wt% at inner layers, at a temperature interval of 1350-1400°C) the concentration of CaO increases from 66 to 71 wt% in the surface layer and from 67.5 to 71.5 wt% at the inside layer. CaO/SiO_2 ratio reaches 3.2-3.3 at the surface and 3.1-3.2 at the inside of the crystals.

A maximum concentration of CaO and C/S ratio at 1375-1400°C corresponds to a minimum amount of Al_2O_3, Fe_2O_3 and other oxides. Simultaneously, the average concentration of CaO reduces from 52 wt% at 1350°C to 49.5 wt% at 1425°C in the melt. At 1425°C free CaO appears as a crystal phase.

The concentrations of Al_2O_3, Fe_2O_3 and MgO have a reverse relationship in the melt. The exchange of ions at the phase boundary is as follows:

$$Ca^{2+}_{melt} \rightarrow Al^{3+}/Fe^{3+}_{crystal} \quad \text{on} \quad Al^{3+}_{melt} \rightarrow Ca^{2+}_{crystal}$$

When Al and Fe-ions are replaced by Ca-ions some expansion of C_3S lattice is absorbed by the free space of the lattice, but in the opposite case the strong compressive strain of alite lattice destroys it. Free CaO and C_2S appear and dissolve in the melt.

At the cooling stage the Ca^{2+} and $(SiO_4)^{4-}$ are in the alumoferrite phase. The increase of the heating rate of the raw mix (20°C/min) leads to a fast dissolution of CaO and C_2S in the melt and rapid nucleation. This corresponds to the research of Maki[32].

The alite isomorphic capacity changes during the heating: from 6.4-7 wt% in the surface part to 4.6-6.6 wt% in the inside layer of the crystals. In the temperature interval 1350-1425°C the CaO concentration in the crystals increases and the SiO_2 concentration decreases (Figure 6). At first, the Al_2O_3 content decreases up to 1375°C and then increases. The concentration of Fe_2O_3, MgO, SO_3, Cr_2O_3, TiO_2, R_2O does not change. At fast burning, the composition of the alumoferrite phase changes and the amount of Al is larger than during ordinary burning.

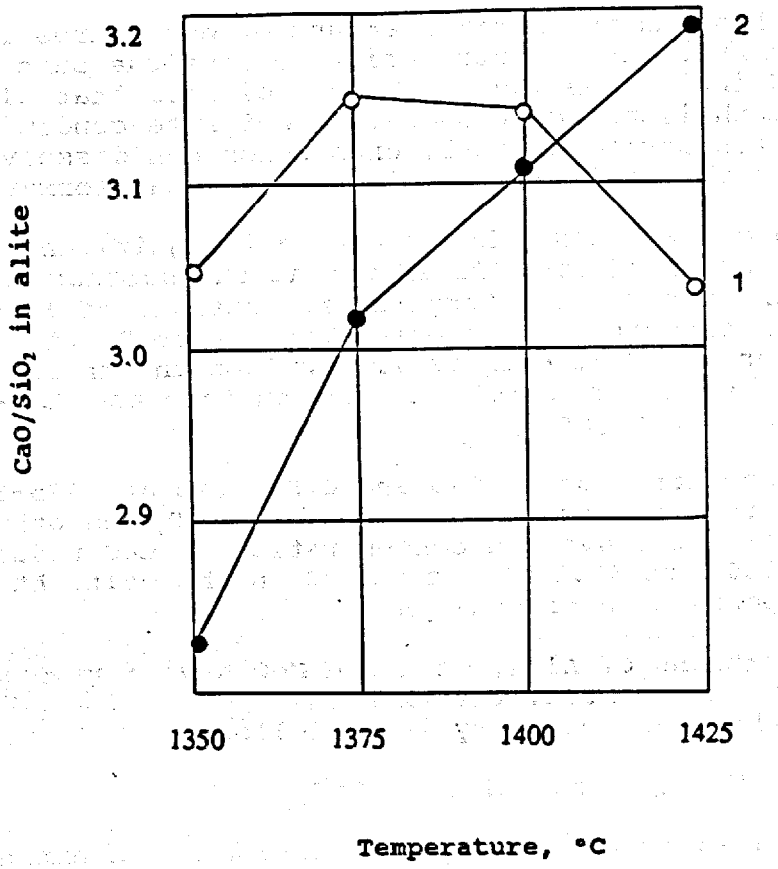

Fig. 6 CaO/SiO_2 ratio in alite crystals at the different temperature and rate of heating, °C/min 1-5 2-20

During slow heating the amount of SiO2 the A/F ratio increases in the alumoferrite phase. In this case alite crystals grow rapidly, and in the opposite case, during the fast heating, alite crystals grow slowly because the melt has a high viscosity. Minimum isomorphic capacity of silicate phases corresponds to their stoichiometric composition. It can be explained that the process of the clinker phase formation is accomplished by the replacement of heterovalency ions and their implantation into the lattice free space. But the dissolution of the stoichiometric amount of CaO in the silicate phase lattice, makes the lattice stronger and the binding of CaO increases up to 2.41-3.24 Å. Moreover, the admixture of oxides in the alumoferrite phase increases, especially that of sulphate ions. As shown by Samchenko[62] it enables the formation of the sulfoalumoferrite phase which is very important for the special cement manufacture.

NEW PROCESSES

A measure for the general development since the last congress may be the number of publications dealing with the different aspects of the cement manufacturing process. The basis for this has been the references in "Manufacture of Structural Cements" in Cement Research Progress[63] 1985 through 1990. The references have been grouped in papers with relation to [1]burnability and materials composition, [2]fuels, [3]special clinker and processes, [4]kiln operation, [5]grinding and finally [6]environment (Table V).

	Burnability & composition [1]	Fuel [2]	Special Clinker and processes [3]	Kiln operation [4]	Grinding	Environment
1985	30	7	6	17	24	11
1986	20	18	10	14	11	9
1987	15	12	6	24	12	23
1988	10	13	9	52	29	20
1989	20	19	15	62	38	19
1990	14	18	13	62	37	25

Table V Number of references dealing with cement manufacturer in Ref. 63

1) Mostly on the use of waste materials
2) Waste derived fuels (solid, liquid)
3) Belite clinker, white cement, oilwell cement
4) Optimization, Al-control

The number of papers on burnability and materials composition has decreased slightly through the years. These papers deal with application of waste materials as raw mix components and characterization of raw mixes with respect to their burnability.

The number of papers dealing with fuels are virtually constant, The fuels in question are primarily waste derived fuels, solids as well as liquid. New techniques for handling and controlling these types of fuels have been developed.

The papers on special clinker and processes show a small increase in number. These papers deal with the production of white cement and of low energy clinker, especially belite clinker. The possible lower content of calcium carbonate in the raw mixes for this type of clinker is important not only with respect to the reduced energy necessary for the decomposition of the carbonate but also with respect to reduced emission of CO_2. Table VI from Stark and Müller[64] gives an overview of low energy clinker.

	Main Clinker minerals	Properties application
Active Belite-Cement	α'-C_2S C_3S C_3A	Lower early age strength and higher later age strength compared to Portland Cement. Pilot scale experiments in former East Germany, India and SNG
Belite-Sulfoaluminate Cement	β-C_2S C_4A_3S CA, $C_{11}A_7$	High early strength, expansive, short setting time, good chemical durability. Special cements in USA, Japan and SNG
Belite-Sulfoferrite Cement	βC_2S C_4AF C_4A_3S CS	Short setting time, high early strength. Industrial production in Peoples Republic of China
Alinite-Cement	Alinit $2C_2S \cdot CaCl_2$ $C_{11}A_7 \cdot CaCl_2$ $C_4AF \cdot CaCl_2$	Chloride content up to 2,5%, high hydraulic activity, steel corrosion. Industrial production in SNG
Low temperature Cements	$3C_3S \cdot CaF_2$ $C_{11}A_7 \cdot CaF_2$	Still at the exprimental stage

Table VI Overview of low energi clinker. After Stark and Müller [64].

The number of contributions on kiln operation show a tremendous increase. This is partly an effect of change in the grouping of papers in reference 63. There is however a real increase through the years, reflecting the increasing automation and application of expert systems in process control of the rotary kiln and its auxilliary equipment; and the further development of preheaters and precalciners.

In the groups for grinding and environment there is an increase in numbers. This reflects the increased efforts by the industry to conserve energy and to control possible emmissions to the environments.

A strong development of systems for grinding raw mixes and cements have taken place since the last congress: high pressure grinding in roller mills and in roller presses. As mentioned in the introduction these processes are very energy efficient. The particle size distribution of the product from these mills tends to be more narrow than in the product from conventional ball mills and this has an effect on the reaction kinetics. The rate of hydration of cement[36] and rate of formation of clinker minerals during burning increases. An increased reactivity does not imply that the burning zone temperature can be decreased

very much. A possible minor decrease in temperature will only result in marginal energy savings in form of reduced radiation loss.

Work has been done for a long time on replacement for the rotary kiln by a stationary device. All the major suppliers of equipment to the cement industry have some activitites in this field. They all seem to involve the use of prenodulized kiln feed or kiln dust which is allowed to react and grow by coalescence at high temperatur in a fluid bed type reactor. One industrial stationary kiln for production of belite clinker have been refered to by Stark and Müller[64]. It is a 300 t/d fluid bed reactor, producing clinker nodules 3-5 mm in size which are quenched in a fluid bed from 1300°C to 900°C. From an operational point of view such a device has many advantages regarding the life time of the refractory lining and the mechanical maintenance. Considering the manufacture of portland cement it follows, however, that these types of reactors present challenging engineering and operational problems. Preheating and calcining of the kiln feed can take place in gas suspension without problems. The heat transfer from the hot gas to the raw meal is optimal in contrast to the conditions in a rotary kiln where it is limited to take place at the suface of the bulk material. When it comes to the formation of the clinker melt and the reaction between two or more raw material components the gas suspended state offers less optimal conditions than the rotary kiln. A certain degree of agglomeration is needed to make it possible for the reactants to meet and react; and a minimum retention time, of around 15-30 minutes depending on the fineness and mineralogy of the raw materials at the high temperature, is also needed for the completion of the reactions. These conditions are present in the burning zone part of a rotary kiln.

SUMMARY

In summary no really new processes have emerged. The most important developments have been in the grinding technology. The relationships between the properties of the raw mix and the clinker formation with respect to industrial cement manufacture seem to be well understood. There are interesting phenomenas still to be investigated regarding the behavior of the clinker melt containing sulfates, chlorides and fluorides and the growth of alite crystals . Manufacture of low energy clinker and especially belite clinker may play an important role by offering possibilities for reduction of the CO_2 emission.

REFERENCES

1 Meric, I.P.: "Low energy clinker formation". **Proceedings of the 8th International Congress on the Chemistry of Cement, Rio de Janeiro, Brazil,** 1986. **Vol. I,** p. 51-56.

2 Petersen, I.F.: "The ability of clinker module formation". **Proceedings of the 8th International Congress on the Chemistry of Cement, Rio de Janeiro, Brazil,** 1986. **Vol. II,** 21-24,

3 Johansen, V.: **"Coccion de clinker de cemento portland en hormos rotatorios".** Materiales de Construccion, 1977, **166-167,** 85-97

4 Albats, B.S., Filipova, L.S. & Krivoborodov, Y.R.: "Bases physico-chimique de la formation de granules des clinker". **Proceedings of the 7th International Congress on the Chemistry of Cement, Paris** 1980, **Vol II,** I145-I149.

4a Osokin A.P., Albaz B.S., & Potapowa E.N.: "Die Einwirkung der Liquation auf den Prozess der Klinkerbildung". TIZ-Fachberichte, Vol 11, No 8, 1987, pp.550-553.

5 Banda, R.M.H. & Glasser, F.P.: "Role of iron and aluminium oxides as fluxes during the burning of Portland Cement". Cem. Concr. Res., 1978, **8** pp. 319-324

6 Christensen, N.H.: "Modelling the Clinker Reaction". World Cement Technology, June 1981.

7 Taylor H.F.W: **"Cement Chemistry".** Academic Press, 1990.

8 Lea, F.M. & Parker, T.W.: Building Research Tech. paper No. 16, His Majestys Stationary Office, **"The Chemistry of Cement",** London 1935 in F.M.Lea, 3rd ed. Edwin Arnold 1970; p.128.

9 Bogue R.H.: **"The Chemistry of Portland Cement".** 2nd ed. Reinhold, New York 1955.

10 Petersen, I.F.: "Isothermal sinterning of Portland Cement Raw Mixes". World Cement June and July/August 1983.

11 Glasser, F.P. & Marr, J.: "Sulfates in cement clinkering, Immiscibility between sulfate and oxide melts at 1350°". Cem. Con. Res., 1980, **10**, 753-758.

12 Ossokin, A. & Potopov, E.: "Formation de mineraux dans les Bains fondus". **Proceeding of the 8th International Congress on the Chemistry of Cement, Rio de Janeiro, Brazil** 1986, **Vol II** 72-76,

13 Timashev, V.V.: "The Kinetics of Clinker Formation the structure and composition of clinker and its Phases". **Proceedings of the 7th International Congress on the chemistry of Cement, Paris** 1980, **Vol I** I-3/1.

14 Petersen, I.F.: "A model for the size Distribution of Rotary Kiln Cement Clinker. Part 1 and 2". World Cement Technology, Nov. & Dec., 1980.

15 Scheubel, B. & Balzer, H.J.: "Mikroskopische Untersuchungen an Zementklinkern mit Hilfe der Linearanalyse zur Bestimmung der Klinkermahlbarkeit". Zement-Kalk-Gips, 1983, **36**(11), 624-627.

16 Petersen, I.F.: "The Pore Structure and the Grindability of Clinkers". **Proceedings of the 7th International Congress on the Chemistry of Cement, Paris** 1980, **Vol II**, I73-I78.

17 Johansen, V.: **"Cement Production and Cement Quality"**. Materials Science of Concrete, ed by J.P.Skalny. The American Ceramic Society, 1989.

18 Petersen, I.F. & Johansen, V.: "Burnability and Clinker nodule Formation from a Statistical point of View". Cem. Con. Res. 1979, **9**, 631-639.

19 Christensen, N.H.: "Multiphase Ternary Diffusion Couples". J. Amer. Ceram. Soc. 1979, **60**(78), 293-296.

20 Christensen, N.H.: "Ternary Diffusion with Two Moving Boundaries". ibid 60, 1977, (1-2), 54-58.

20a Harrisson, A., **"Some Effects of coarse Raw Feed on Clinker Microstructure"**, World Cement December 1989, pp.440-441.

21 Sulimenko L. M. & Kouzntezova T. V. & Meipner S.: **"Mechanische Aktivierung carbonatischer und alumosilicatischer Materialien"**. - Tonindustrie - Zeitung, V. 109, n6, 1985.

22 Sulimenko L.M.: "Mechano-chemical and mechano-activative effects in the technology of raw materials". **The Conference on Cement Chemistry and Technology, Moscow**, 1991.

23 Locher F.W.: "Einfluss der Klinkerherstellung auf die Zementeigenschaften", Zement-Kalk-Gips, 1975, v.28, N7.

24 Ghodakov G.S. & Redkina H.I.: "Mechano-sorbtion activation of the reactions in solid phases". **The Conference on mechano-chemistry and mechano-emission of the solid bodies**, 1990, v.2.

25 Krivoborodov J.R., Plotnikov V.V. & Martens K.: "Mineral formation in the burning of the activative raw mixes". **10 International Baustoff und Silikattagung, Weimar** 1988, **v.1.**

25a Goswami, A., Panda, J.D. & Chatterjee, S., "A Study of Homogeneity of Cement Raw mixes Processed in Two Types of Mills". World Cement, November 1990, pp.489-492.

26 Johansen, V.: **"Cement production and Chemistry".** Symposium on Cement Manufacturing and Chemistry, Anaheim, California, USA, 1989.

26a Theisen, K., "The Influence of Raw Mix Burnability on Cement Clinker", World Cement, August 1992, pp17-23.

27 Bucchi, R.: "Influence of the nature and preparation of raw materials on the reactivity of raw mix". **7th International Congress on the Cement Chemistry, Paris** 1980, **v.1.**

28 Sprung, S.: "Effect of the burning process on the formation and properties of the clinker". **7th ICCC,** 1980, **v.1.**

29 Timashev, V.V.: "The kinetics of clinker formation. The structure and composition of clinker and the phases". **7th ICCC,** 1980, **v.1.**

30 Mchedlov-Petrossyan, O.P.: "Kinetics of clinkering". **8th International Congress on the Cement Chemistry, Brasil,** 1986, **v.1.**

31 Boikova, A.I.: "Chemical Composition of raw materials as the main factor Responsible for the Composition, Structure and Properties of Clinker Phases", **8th ICCC, Brasil**, 1986, **v.1.**

31a Puertas, F., Blanco-Valera, M.T., Paloma, A. & Vázquea, t., "Reactivity and Burnability of Raw Mixes made with Crystallized Blastfurnace Slags" Part I and Part II , Zement-kalk-Gips, 1988, **41**(8), 398-402, and 1988, **41**(12), 628-631.

32 Maki, I.: "Relationship of processing parameters to clinker properties; influence of minor components", **8th ICCC, Brasil**, 1986, **v.1.**

33 Glasser, F.P.: "Kinetics of cement - making reactions". **8th ICCC, Brasil**, 1986, **v.VI.**

34 Patent AS 2365152, 1973. Ludwig U.: "Verfahren und Vorichtung zum Brennen von zunentrohmeheen zu Zementklinkeren".

35 Kouznetsova, T.V.: **"Theoretical bases of clinker formation"**, J. "Cement", 1989, N2.

36 Osbaeck, B. & Johansen, V.: "Particle Size Distribution and Rate of Strength Development of Portland Cement", J.Am. Ceram. Soc. 1989 ,**72**(2) 197-201.

37 Kirsch, J.: "Use of high-pressure grinding rolls at cement plants of the Dyckerhoff AG", Zement-Kalk-Gips, 1990, **43**(7), 352-356.

38 Patzelt, N.: "Hybrid, combination and fine grinding with high-pressure grinding rolls" , 1990, ibid **43** (7), 347-351.

39 Odler, I. & Chen, Y.: "Influence of grinding in high-pressure grinding rolls on the properties of the Portland Cement", 1990, ibid **43**(4), 188-191.

40 Kupper, D. & Knobloch, O.: "Finish grinding of cement with polycom high-pressure grinding rolls" 1991, ibid **44**(1) 21-27.

41 Strasser, S.: "Partial finish grinding- Two-stage grinding of cement clinker", 1991, ibid **44**(1), 28-31.

42 Kellwessel, H.: "High-pressure material-bed comminution in practice", 1990, ibid **43**(2), 57-64.

43 Höidalen, Ö.: "Finish grinding of raw material with the Polycom high-pressure roll mill", 1989, ibid **42** (4), 184-187.

44 Thurat, B. & Wolter, A.: "High-pressure roll mills for cement raw meal, coal and lime grinding", 1989, ibid **42**(4), 179-183.

45 Chang, C.K.: "Operating experience with high-pressure grinding rolls in the Asia Cement Corporation (ACC), Taiwan", 1991, ibid **44**(1), 32-36.

46 Christensen, N.H. & Jepsen, O.L.: "Diffusion in a Three Component Clinker". J. Amer. Ceram. Soc.1971, **54**, 208.

47 Johansen, V., Jepsen, O.L., Christensen, N.H. & Ganborg Hansen, J.C.: "Termary Diffusion in Cement Clinker at 1500°C". Cem. Con. Res., 1978, **8**, 301-310.

48 Christensen, N.H., Jepsen, O.L. & Johansen, V.: "Rate of Alite-Formation in Clinker Sandwiches", 1978, ibid **8**, 693-702 .

49 Johansen, V. & Christensen, N.H.: "Rate of Formation of C_3S in the System $CaO-SiO_2-Al_2O_3-Fe_2O_3-MgO$ with Addition of CaF_2", 1979, ibid, **9**, 1-6.

50 Weissweiler, W. and Osen, E.J. "Kinetic Studies in the $CaO-SiO_2$-system. Part II. Reaction rate constants and activation energies of selected diffusion couples", Cem. Conr. Res., 1988, **18**, pp. 55-62.

51 Dreizler, I. & Schäfer, H.-U.: "Fraction analyses for evaluating the heterogeneity of raw meals",Zement-Kalk-Gips, 1990, **43**(9) pp. 445-451.

51a Chromy, S.: "Method for determining the reactivity and burnability of cement raw meals" (in German) TIZ-Facberichte, 1985, **109**(9), pp.654-656.

52 Christensen, N.H. & Johansen, V.: "Chemical Effect on Ceramic Reactions". J. Amer. Ceram. Soc., 1979, **62**(5-6), 313-315.

53 Sakar, A.K., Roy, D.M. & Smart, R.M.: "Mineralizers and Fluxers in the Clinkering Process". I Phase equilibria in the $CaO-Al_2O_3-Fe_2O_3-SiO_2$ system with Calcium Ferrosilicate". **Proceedings of the 7th International Congress on the Chemistry of Cement, Paris** 1980. **Vol II** I195-I200.

54 Müller, A. & Stark, J.: "Effect of alkalis on the strength development of active belite cement"(in German), Silikat Technik, 1987, **38**(9), pp. 301-305.

55 Strunge, J., Knöfel,D., & Dreizler,I.: "Influence of alkalis and sulphur on the properties of cement. Part IV: comprehensive survey", Zement-Kalk-Gips, 1990, **43**(4), pp 199-108.

56 Christensen, N.H. & Johansen, V.: "Mineralizers and fluxes in the clinkering process. II. Kinetics effects on alite formation". **Proceedings of the 7th International Congress on the Chemistry of Cement, Paris** 1980. **Vol II**, I1-I5.

57 Osokin, A.P., Potapova, E.N. & Burigin, V.V.: "Segregation of the oxide-salt melts." J. The melts, 1987, v.1, N2, (In Russian).

58 Harrison, A.: "Some effects of recirculating alkali loads on clinker microstructure and properties", World Cement, December 1991, p.24-26.

59 Kouznetsova, T.V., & Osokin A.P.: **"Clinker formation in the presence of Mg and SO_4^{2-} in the raw mix"**, J. Cement (in Russian), No 3, 1989.

60 Osokin, A.P. & Potapova, E.N.: "Clinker formation in the oxide-salt melts". **VNIECM, Moscow**, 1987. (In Russian).

61. Kouznetsova, T.V., Akimov V.G., & Panuschkin V.N.: "Hydraulic activities of the mineral, which are characterized by unstechiometric. **10 Intern. Baustoff und Silikattagung, Weimar**, 1988, **v.1.**

62 Samchenko, S.V.: "Mineral formation in alumoferrite systems at presence of calcium sulfate", J. Cement No3, 1989 (in Russian).

63 Chapter 1: "Manufacture of Structural Cements", Cement Research Progres, 1985, 1986, 1987, 1988, 1989 and 1990; ed Paul Brown, American Ceramic Society, Ohio, USA.

64 Stark, J., Müller, A.: "International development trends in low-energy cements" (in german), Zement-Kalk-Gips 41(4), pp. 163 (1988).

65 Johansen, V.**"Anwendung des gleichgewichtsdiagramms beim Klinkerbildungsvorgang industriell hergestellter Klinker"**, Zement-Kalk-Gips 32, pp. 176-181 (1979).

Specific Theme I B

Effect of Low Grade Fuels, Combustible Wastes and Non-traditional Raw Materials

Brennstoff, Ersatz, Verbrennung, Rohstoff (Zement), Recycling, Abfallverwertung

EFFECT OF LOW GRADE FUELS, COMBUSTIBLE WASTES AND NON-TRADITIONAL RAW MATERIALS

S C Ahluwalia
National Council for Cement and Building Materials, New Delhi, INDIA
and
C H Page
R C D, Associated Cement Companies, Thane, INDIA

SUMMARY

Depletion in the resources of good grade raw materials and the urgent need to conserve these, has made it imperative to find ways and means of utilizing low grade raw materials, industrial and agricultural wastes and waste fuels. Researches have established the feasibility of use for large number of low grade materials and industrial waste such as lime bearing carbonate sludges from paper, sugar and fertilizer industries, $Ca(OH)_2$ from acetylene plants, slags from iron, steel and other allied industries, flyash from coal based thermal power stations, red mud and γ -C_2S waste from aluminium industry etc. as alternate and substiute raw materials with specific technical advantages in some of the cases. Despite considerable efforts being made to find technical and technological solution to the problems of utilization, their actual use has remained limited primarily because of problems related to collection, handling, storage, transportation and the cost involved.

Recycling of hazardous and non-hazardous wastes fuels in cement manufacture has been a very promising development in past two decades. Considerable progress has been reported in design engineering and construction of waste derived fuel facilities for use of fuels such as rice husk and straw, bamboo dust, bagasse, sewage sludge, oil shale, rubber waste, scrap motor tyres, plastic waste, acid sludge, asphalt sludge etc. as part substitute to the conventional fuels in cement manufacture. Due to unique characteristics of cement kiln hazardous organic compounds are destroyed and trace elements present are bound in clinker and rendered harmless, in addition to providing a cost saving fuel and solving problems of disposal and environmental pollution without affecting the quality of clinker/cement.

Although the use of wastes as raw materials or alternate energy sources in manufacture of cement can result in significant saving and conservation of non-renewable materials, there is a need for comprehensive techinical and managment services in the area of utilization of wastes to make their use cost effective.

INTRODUCTION

The realisation that natural minerals and fossil fuels are going to get exhausted in foreseable future has made it imperative to look for ways and means for:

i/ Rational utilization of natural minerals and fuels and waste reduction.

ii/ Waste management particularly of industrial wastes and use them as substitute or alternate materials .

iii/ Use of unconventional and renewable sources of energy to supplement fossil fuels.

Cement manufacture offers unique opportunity both for utilization of industrial wastes such as lime bearing carbonate sludges from paper, sugar and fertilizer industries, $Ca(OH)_2$ from acetylene plants, slags from iron and steel works and other allied industries, flyash, from coal based thermal power plants, red mud and γ-C_2S waste from aluminium industry etc. as alternate and substitute raw materials. This is evident from the elemental composition of cement raw mix and some of the industrial wastes mentioned above.

Significant advancement has been reported in last decade on utilization of industrial wastes as raw materials and on use of low grade fuels and combustible wastes in cement manufacture. Waste fuels such as rice husk and straw, bamboo dust, bagasse, sewage sludge, oil shale, rubber wastes, scrap motor tyres, plastic wastes, acid sludge, asphalt sludge etc as part substitute to the conventional fuels have also been investigated and significant success reported.

This paper highlights the trends of research and results achieved in the area of utilization of non traditional raw materials and low grade fuels and combustible wastes on the chemistry of clinker formation, process of manufacture, quality of cement and impact on environment.

UTILIZATION OF NON-TRADITIONAL RAW MATERIALS

Since the discovery of Portland Cement in 1824 by Joseph Aspiden and perfecting the technology of manufacture by I C Johnson in 1840 the principal raw materials used are calcareous materials such as limestone and argillaceous materials like clay. Further improvement in clinker phase assemblage was evolved with the use of other corrective materials such as bauxite, iron ore etc to maintain the characteristic modulii values. Attempts have also been made to accelerate the rate of reactions at lower temperatures by use of mineralisers as an energy conservation measure and these have been successfully used on commercial scales (1-3).

The characteristics required for raw materials and significance of their constituents is well understood as also described in the article, "Cement Raw Materials and Raw Mixes" (4) . The complexity of various requirements of raw mix such as physical, chemical, mineralogical and thermal is depicted in Fig. 1 indicating the criticalities and their dependence in processing for cement manufacture.

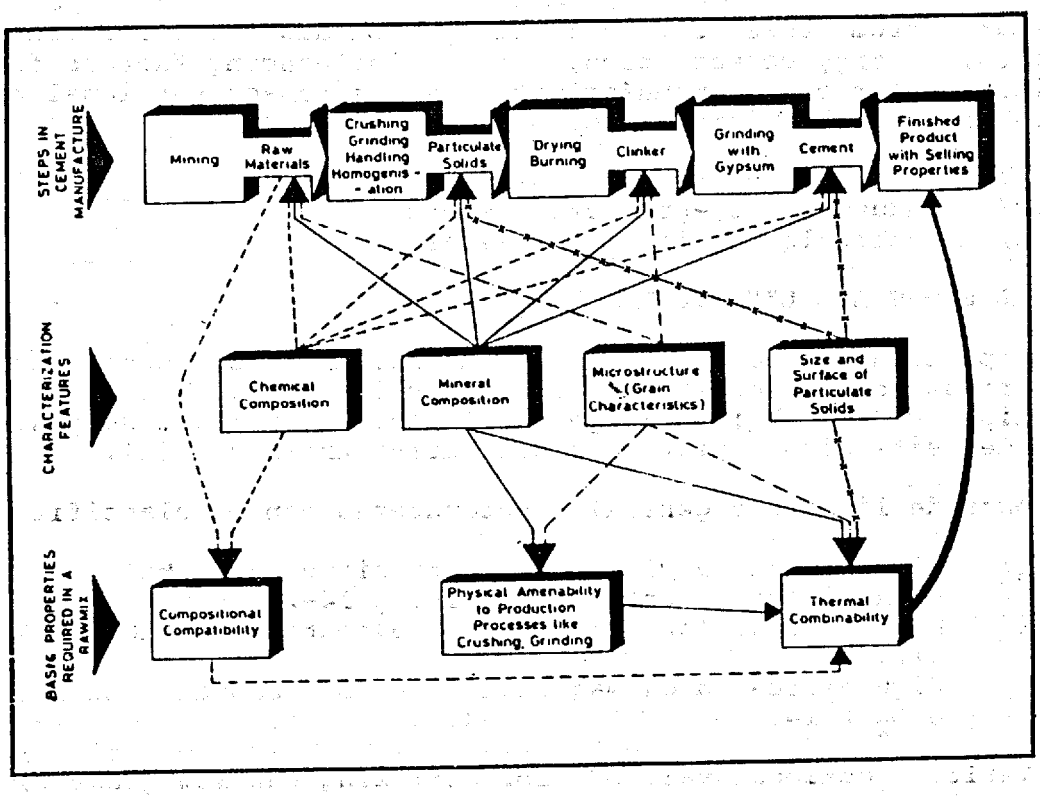

Fig.1 : Interrelation of Processing Steps along with Characterisation Features and Basic Properties of Cement Raw Mixes

Over the years, due to rapid industrialisation, lot of byproducts and waste materials are being generated creating environmental problems. The major constituent of these materials are the same as the cement raw mix (Table 1) which make these potential substitute/supplementry cement raw materials.

TABLE 1

ELEMENTAL COMPOSITION OF CEMENT RAW MIX AND SOME INDUSTRIAL WASTES

Material	Constituents (Percent)				
	O	Si	Fe	Al	Ca
1 Cement Raw Mix	23.0	6.0	2.5	2.0	31.0
2 Flyash	45.0	25.0	6.0	12.0	3.0
3 B F Slag	30.0	20.0	1.0	12.0	30.0
4 Fertilizer Sludge	47.0	1.6	0.7	0.8	34.0
5 Paper Sludge	48.0	3.7	0.7	0.5	34.0
6 Carbide Sludge	43.0	3.8	0.2	1.0	47.0
7 Red Mud	39.0	2.5	35.0	6.5	5.5
8 Carcasses	40.0	-	-	-	25.0
9 Rice Husk	30.0	25.0	-	-	-
10 Rice Husk ash	50.0	45.0	0.3	-	1.5
11 Rice Straw	35.0	22.0	-	-	-
12 Rice Straw ash	47.0	43.0	0.2	-	1.3

Apart from this, rational utilization and conservation of the deposits, energy conservation, etc are influencing factors for their utilisation for cement manufacture. These non-conventional materials can be broadly classified into;

i/ Natural sub-grade limestone
ii/ Industrial by-products / wastes
iii/ Materials bearing mineralisers

NATURAL SUB-GRADE LIMESTONE

Depletion of good grade limestone suitable for cement manufacture in various countries and particularly in India has put material scientist to relook into large available marginal and subgrade limestone deposits with a view to facilitating their use (5).

Lowgrade limestone generally encountered can be classified as;

i/ High magnesia limestone containiang 6-12% MgO
ii/ High silica limestone containing 14-21% SiO_2
iii/ High silica, low lime limestone containing CaO < 44%, SiO_2 > 14%.
iv/ High silica, high magnesia limestone containiang MgO > 3.5%, SiO_2 > 14%.

Various options available for utilizing the low grade limestone and problems and solutions have been discussed at length including beneficiation of high magnesia and marginal grade limestone and prospects and problems of utilisation of high magnesia and marginal grade limestone, are reviewed (6).

In order to cater to the desired requirements of raw mix the floatation technique for beneficiation of limestone is in use in a few wet process plants in India. Although more suitable for wet process techniques, this may have to be seriously reconsidered to cater to the future demands of limestone for cement manufacture. One of the wet process plant in India uses floatation technique for beneficiation of limestone in a semi-wet process using vacuum filtration technology and is used in a kiln with two stage preheater with calciner system to produce 1800 TPD of clinker (7-8). The chemical composition of kiln feed and clinker is given in Table 2.

TABLE 2

CHEMICAL ANALYSIS OF KILN FEED AND CLINKER USING BENEFICIATED LIMESTONE

Oxide	Kilnfeed	Clinker
SiO_2	13.5	23.5
Al_2O_3	2.3	4.9
Fe_2O_3	2.3	3.7
CaO	44.7	65.7
LOI	36.0	-
Na_2O	0.08	0.13
K_2O	0.20	0.35
SO_3	-	0.40
LSF	-	0.87
Ms	-	2.73
Ma	-	1.32
fCaO	-	1.0

The performance of the resultant cement is given in Table 3.

TABLE 3

PERFORMANCE OF OPC FROM SEMI WET PROCESS USING BENEFICIATED LIMESTONE

Properties	Value			
Sp Surface (m^2/kg)	300			
Setting Time (min)	Initial 135			Final 200
Compressive Strength (N/mm^2)	1 d	3 d	7 d	28 d
	14.5	30.0	44.0	54.0

The microstructural features of this clinker indicated well crystallised alite and belite. Alite is lathy, prismatic hexagonal with crystal size in the range of 13-79 microns with an average size of 37 microns. Belite is observed to be rounded to subrounded with crystal size of 8-50 microns with an average crystal size of 23 microns. The quantitative estimated phase composition of the clinker indicated C_3S 41%, C_2S 48%, C_4AF 5.0% and C_3A 6.0%. The microstructural features are shown in Plate 1.

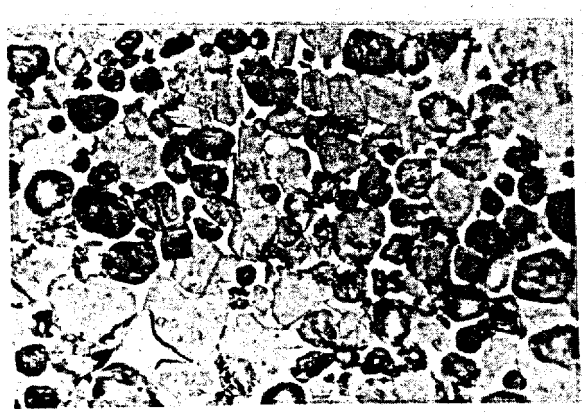

Plate 1: Optical Micrograph of Clinker Prepared with Beneficiated Limestone

The above observations are in agreement with the physical test data (Table 3). Floatation technique of beneficiation of limestone has proved to be useful in certain situations inspite of slightly higher energy consumption (~ 950 kcal/kg clinker).

The other beneficiation techniques of importance are :

i) Differential Grinding and Sieving (DGS)
ii) Electrostatic Separation (ESS)
iii) Photometric sorting
iv) Bacterial leaching

The investigations carried out using the above techniques have been reported (5). The Differential Grinding and Sieving, Electrostatic Separation and Photometric sorting are among the potential teqhniques of dry beneficiation of marginal grade limestone. These techniques are based on properties such as hardness, electrical conductivity and colour of minerals respectively. Further, the coarse grained limestone was found to respond well to both differential grinding and sieving and electostatic separation. However, differential grinding and sieving has been found to be more cost effective between the two. The photometric sorting technique is found to be promising in case of ores with different colours of acceptable and rejectable portions. The bacterial leaching technique which uses acid producing organisms in order to dissolve silica has also given encouraging results with some limitations in the application. However, these are only preliminary conclusions.

In view of various techniques of wet and dry beneficiation the utilisation of marginal/subgrade limestone appears to be promising. Alternative ways of using this limestone in production of special types of cement such as belite, alinite type etc has been reported (9,10).

INDUSTRIAL BYPRODUCTS/WASTES

The industrial wastes can be utilised as;

i/ Raw materials for clinker manufacture, and
ii/ Component of blended cements.

These wastes as a raw mix component can either replace calcareous component or the argillaceous component party or fully. Further these wastes which are used as a raw mix component can be classified into following groups.

i/ Lime bearing materials such as carbonate sludges from paper, sugar, fertiliser industries, $Ca(OH)_2$ from acetylene plants, dolomite fines, etc.

ii/ Industrial slags from iron, steel and other allied industries.

iii/ Flyash from thermal power stations.

iv/ Minerals and mineral wastes.

v/ Other industrial wastes such as red mud from aluminium industry, calcium silicate waste slurry from alumina production etc.

Lime Bearing Materials

Utilisation of lime sludge particularly the fertilizer sludge for the manufacture of cement is known for many years. The study using carbonate sludge from fertilizer industry has been reported in wet process plant of capacity 700 TPD(11). Calcium carbonate sludge was used to replace part of high grade and beneficiated limestone. The composition of raw materials is given in Table 4. The composition of the waste indicated that it contains sulphate, fluoride and phosphates and use of the sludge was primarily feasible upto 50% of the raw meal.

TABLE 4

COMPOSITION OF RAW MATERIALS AND CARBONATE SLUDGE

Constituents	High Gr Limestone	Beneficiated Limestone	Laterite	Carbonate Sludge
SiO_2	10.0	14.7	2.8	6.0
Al_2O_3	1.8	1.7	28.5	0.3
Fe_2O_3	1.0	1.1	45.5	0.3
CaO	48.0	45.0	1.5	46.5
MgO	0.8	1.0	0.8	0.5
LOI	38.0	36.2	20.0	37.5
SO_3	-	-	-	6.0
K_2O	-	-	-	0.13
Na_2O	-	-	-	0.04
P_2O_5	-	-	-	1.8
F	-	-	-	1.2

Incorporation of sludge adversely affected the setting time and compressive strength of resultant cement primarily due to high amount of P_2O_5 and F. However, the problem could be overcome by reducing the amount of sludge with an advantage of improved burnability and lower firing temperature (Table 5).

TABLE 5

BURNABILITY OF RAW MEAL WITH CARBONATE SLUDGE

Temperature ^oC	Free Lime (%)	Lime Combinability (%)
1250	5.5	91.6
1300	1.2	98.2
1350	0.6	99.0

$$\text{Lime Combinability} = \frac{CaO_{total} - CaO_{free}}{CaO_{total}} \times 100$$

Calcium carbonate sludge containing 48.18 percent CaO, 9.92 percent SO_3, 2.39 percent P_2O_5 and 2.01 percent F and used as a part substitute of limestone has been studied (12). The raw material used in the studies are limestone, marl, phosphochalk and sandstone. In view of operational problem, a maximum of 10% sludge could be used to substitute limestone in the raw mix. Also the use of phosphochalk beyond 10% as a raw mix component was not favoured because of the presence of high P_2O_5 and F^- contents. Microscopic analysis of clinker so prepared showed 48 and 31 percent well developed C_3S and C_2S respectively free lime indicating the quality of clinker to be good (Plate 2).

Investigations on the use of carbide sludge have shown that the sludge can be used as a source of calcareous component only as a part substitute to limestone due to the presence of high chloride content in the sludge. Taking into account the tolerable limit of chloride

content in the wet process and the rheological properties of raw meal containing sludge, not more than 30% of carbide sludge could be used (13). Large number of raw mixes were designed using carbide sludge and low grade limestone. The clinker so produced indicates well developed alite and belite phases (Plate 3) and had good performance characteristics.

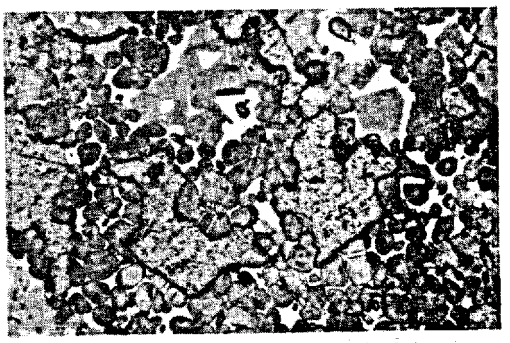

Plate 2 : Optical Micrograph of Clinker with PhosphoChalk

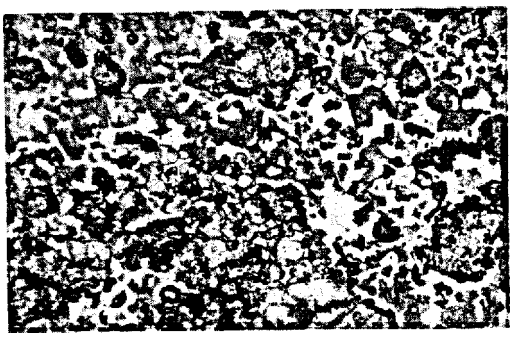

Plate 3 : Optical Micrograph of Clinker with Sludge

A case study using sludge in a wet process of 600 TPD capacity has been reported indicating the techno-economic feasibility of its use as a part substitute of limestone and highlights the design considerations for the process involving specific points such as settling characteristics of the slurries, storing and agitation devices, viscosity of the slurry at various moisture levels, filterability of the slurry etc (14). The burnability studies of the raw mix containing carbide sludge at various residue levels is given in Fig.2.

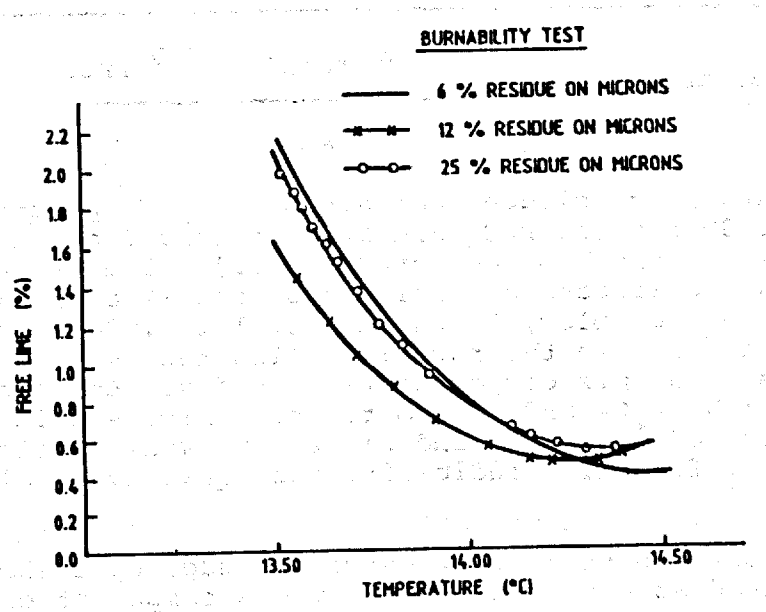

Fig. 2 : Burnability Studies of a Raw Mix Containing Carbide Sludge at Various Residue Levels

The data shows easy burning characteristics of the raw mix even with higher residue on 90 micron. This may be due to the better reactivity of the sludge.

NCB and others have carried out extensive investigations on the utilisation of carbonate sludge from paper industry, press mud from sugar industry, phosphochalk from fertilizer industry, calcium hydroxide sludge from acetylele industry, battery mud from sodium chromate industry and sludge from soda ash industry leading to the development of technologies for their use in cement manufacture (15-19). The paper from NCB highlights the problems inherent in the use of these materials and the prospects of their utilization. Handling and transportation of sludge which considerably influence the economics of their use have also been discussed. The lime bearing sludges from various sources for using as a raw material for mini vertical shaft kilns (MVSK) particularly with respect to material characteristics and process consideration has been highlighted (20).

Metallurgical Slags

Utilisation of metallurgical slags including blast furnace slag from iron and steel industry for cement manufacture both as a raw and blending material is well established (21-28). However the use of blast furnace slag as a raw mix component has not been fully explored on commercial scale. This might be because of preference to use slag as an admixture for manufacture of slag cements.

The burning behaviour of raw mixes using crystalline blast furnace slag with limestone and ferric oxide revealed that incorporation of slag in raw mix could alter the kinetics of clinker formation and conserve energy (29). The study was carried out on raw mix having LSF 98, MS 2.18 and MA 2.2 using 39% blast furnace slag and 2% pure Fe_2O_3. The raw mixes differed only in grain size of slag as follows:

Raw Mix	Grain size of slag (microns)
1	less than 32
2	between 45 and 32
3	between 63 and 45
4	between 90 and 63
5	between 125 and 90
6	greater than 125

The clinkers were studied for XRD and OM. The studies revealed that the grain size of slag has a significant effect on slag reactivity and liquid phase properties in the raw mixes studied. The microstructure of the clinkers obtained at 1450°C however, showed excellent development of silicate phases with adequate distribution. The slag grain size of above 90 u caused an increase in alite content at this temperature with hetrogeneous distribution of silicate phases caused by coarse slag.

Affect of use of blast furnace slag upto 20 percent as a component of cement raw mix on the reactivity and clinkerisation has been reported (30). Kinetics of combination of lime at various slag levels (Table 6) indicated good combinability at 1400°C and above.

TABLE 6

KINETICS FOR THE COMBINING OF FREE CAO

No	Quantity of Slag (%)	Free CaO (%) 1300°C	1350°C	1400°C	1450°C
1	0	16.42	7.22	2.42	0.70
2	5	10.67	3.43	0.85	0.35
3	10	8.91	3.09	0.68	0.28
4	15	7.80	3.00	0.42	-
5	20	7.63	2.85	0.20	-

Presence of BaO and Mn_2O_3 in cement raw mixes contributes to an increase in the alite content and improved performance of the cement (Table 7).

TABLE 7

PERFORMANCE OF CEMENT PREPARED IN LABORATORY

No	Slag (%)	Sp.Surface m^2/kg	Consistency%	Compressive Strength (N/mm^2) 1D	3D	7D	28D	1 Yr
1	0	410	28	14.0	32.0	40.4	55.8	68.8
2	5	415	28	14.4	32.5	41.0	56.6	67.5
3	10	425	28	14.2	33.0	41.5	60.2	69.0
4	15	395	28	15.0	31.0	43.5	61.6	68.5
5	20	405	28	15.1	32.5	42.8	60.9	69.7

The studies, however, have not dealt with the problem of volume stability likely to be caused by increased MgO content of cement. In an another study using 2 percent slag, raw mixes were prepared and investigated for lime combinability and performance (31). The data on clinker composition and performance are given in Table 8 and 9 respectively.

TABLE 8

CHEMICAL COMPOSITION OF CLINKERS PREPARED FROM RAW MIX WITH AND WITHOUT SLAGS

	Chemical Composition, % SiO_2	Al_2O_3	Fe_2O_3	CaO	MgO	F.CaO	LSF	MS	MA
Clinker-1 (Normal)	21.7	7.1	2.9	63.9	2.3	0.6	0.87	2.17	2.45
Clinker-2 (with air cooled slag)	22.4	7.3	2.9	63.7	2.0	0.5	0.84	2.19	2.51
Clinker-3 (with granulated slag)	22.9	7.1	2.8	63.8	1.8	0.5	0.83	2.31	2.53

TABLE 9

PERFORMANCE OF RESULTANT ORDINARY PORTLAND CEMENT

Sample	SO_3	Blaine's Surface m^2/kg	Setting Time (Minutes) IST	FST	Compressive Strength (N/mm^2) 3D	7D	28D
OPC-1 (Normal)	2.2	320	135	200	37.5	45.5	55.0
OPC-2 (Clk.2)	2.2	320	120	165	30.0	38.0	49.0
OPC-3 (clk.3)	2.2	320	85	140	35.0	43.0	52.0

Lime combinability was found to increase with the use of granulated and crystaline blast furnace slag compared with normal raw mix without slag (Fig.3).

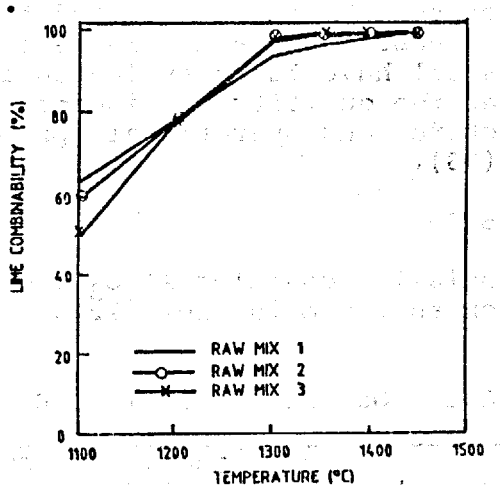

Fig 3 : Lime Combinability of Raw Mixes Prepared with Granulated and Crystalline Slag

The physical test data (Table 9) indicate that with even low LSF using slag comparable performacne could be obtained. Use of low carbon ferrochrome slags as a raw material component has been studied and a maximum of 50 percent slag was reported to have been used (32).

Flyash

Elemental composition of flyash (PFA) is similar to that of clay except that it generally contains more alumina. Typical chemical and mineralogical characteristics of flyash are given in Table 10.

TABLE 10
CHEMICAL AND MINERALOGICAL COMPOSITON OF A TYPICAL FLYASH

	Constituents Determined (%) LOI	SiO_2	Al_2O_3	Fe_2O_3	CaO	MgO	SO_3	Na_2O	K_2O
Flyash	4.30	55.59	26.64	9.50	2.30	0.60	0.44	0.23	0.40

	Major	Predominent	Small Amount	Glass Content %
Flyash	Quartz	Mullite	Haematite	26

Depending upon the efficiency of burning in the furnace, residual carbon varies from 4-12 percent. Use of flyash as a raw material substitute to clay will give some advantage of fuel saving. However, deficiency of iron has to be made up by using suitable corrective materials. Clinker designed with use of flyash as a raw meal component (Table 11) exhibited coarser grain size (average 60 μ) compared to that made without using flyash, which may be due to higher liquid content.

TABLE 11
MINERAL COMPOSITION AND RELATED COEFFICIENTS

Item	Mineral Composition (wt%)					Related Coefficients			
Clinker	C_3S	C_2S	C_3A	C_4AF	LSF	HM	SM	IM	AI
C-1,2	46.1	27.2	15.5	7.6	0.91	2.06	2.17	2.98	2.90
C-3,4	34.0	37.0	17.5	8.1	0.88	1.94	1.98	3.10	2.62

The analysis of heat balance indicated that about 15% of total heat input came from unburnt flyash. In general use of flyash as a raw meal component shall have to be evaluated from case to case basis taking into account the qualtity of limestone, quantity of flyash, process of manufacture and operational problems specific to the designed raw mixes (33).

OTHER INDUSTRIAL WASTES

Red mud essentially contains Al_2O_3 and Fe_2O_3 with a typical elemental composition as given in Table 12.

TABLE 12
CHEMICAL COMPOSITION OF TYPICAL RED MUD SAMPLE

Sample	Constituents Determined (%)									
	LOI	SiO_2	Al_2O_3	Fe_2O_3	CaO	MgO	Na_2O	K_2O	TiO_2	Mn_2O_3
Red mud	13.45	9.60	18.60	26.65	15.44	0.80	3.09	0.09	12.03	Traces

As evident from chemical composition, red mud contains alkalies and TiO_2 and therefore its use is likely to effect the liquid properties significantly (34). Extensive investigations have been carried out at NCB including plant trials. In a case study (35) using 8% red mud, good quality clinker could be produced with well developed alite and belite phases (Plate 4).

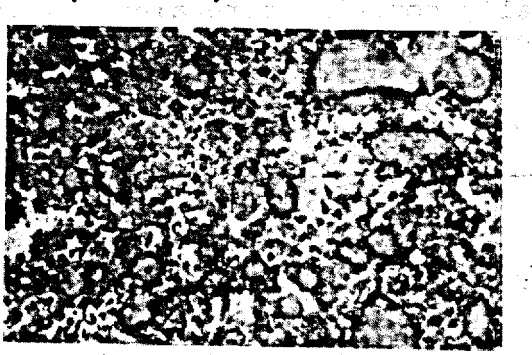

Plate 4 : Optical Micrograph of clinker prepared using Red Mud

In another plant trial use of 2.5% red mud in substitution of iron ore resulted in overcoming the problem of sulphur built up in the kiln system and also resulted in improved early strength of the clinker produced (Table 13 & 14)

TABLE 13
CHEMICAL COMPOSITION OF RAW MATERIAL AND PROPORTIONS

Raw Materials	Chemical Composition Percent							Raw Material Proportion	
	SiO_2	Al_2O_3	Fe_2O_3	CaO	LOI	Na_2O	SO_3	Normal	Modified
Quarry L/S	19.1	1.2	0.9	43.4	34.2	0.24	0.23	38.0	38.0
Floated L/S	8.9	1.1	1.0	49.3	49.3	0.21	-	56.5	56.0
Iron Ore	2.2	1.3	90.4	0.5	4.3	-	-	1.0	-
Red Mud	9.2	22.8	46.4	2.7	13.5	4.81	-	-	2.5

TABLE 14
PERFORMANCE OF ORDINARY PORTLAND CEMENT

Property	Normal	With Red Mud
Blaine's Surface (m^2/kg)	289	295
Setting Time (Mts)		
Initial	135	130
Final	200	190

Compressive Strength (N/mm^2)	1 d	3 d	7 d	28 d
Normal	14.5	30.0	44.0	54.0
With red mud	24.0	34.5	42.5	54.5

Use of red mud as a raw material for making ferrari cement with satisfactory hardening properties have been reported (36).

The post extraction slurry from alumina production in the sintering and disintigration method contains γ-C_2S and precipitated $CaCO_3$ (37). This post extraction slurry is a reactive raw material and results in improved burning of the raw mixes (Fig.4).

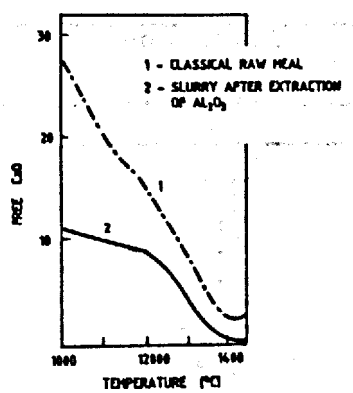

Fig 4 : Burnability of Raw Mix Prepared with Post Extraction Slurry

The cement produced with nearly 4.4% Al_2O_3 had highest compressive strength values which progressively decreased with increase in Al_2O_3 content in clinker (Table 15).

TABLE 15
COMPRESSIVE STRENGTH OF CEMENTS

Type	Al_2O_3 in Clinker %	Compressive Strength (N/mm^2) 3 d	7 d	28 d
A	3.0	25.2	33.5	47.5
B	4.4	25.0	38.2	60.4
C	6.8	16.3	20.4	35.8
D	7.8	6.9	9.3	18.8

The effect of Al_2O_3 could be offset by using waste containing barium (Fig. 5).

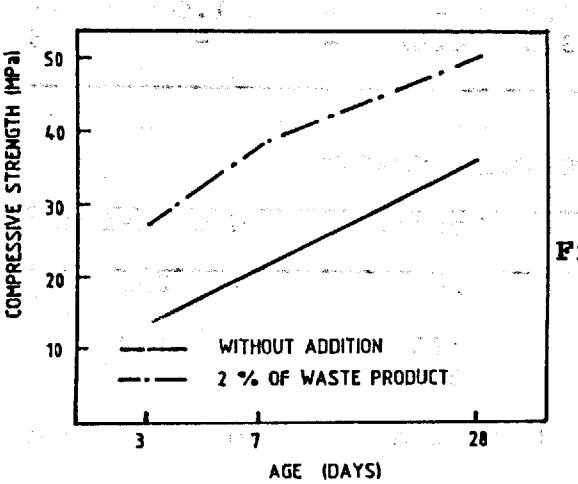

Fig 5 :Effect of Addition of Waste Containing BaO on Compressive Strength of Cement

MINERAL AND MINERAL WASTES

Mineral waste particularly copper-nickel tailings and raw taconite tailings have been used for making type 1 Portland cement (38). The work reported in these studies describes the use of non-conventional raw feed composed of beneficiated copper-nickel tailings as a replacement to argillaceous components in a conventional cement feed. The chemical analysis of kiln feed is given in Table 16.

TABLE 16
CHEMICAL ANALYSIS OF THE COMPONENTS OF KILN FEED

Constituents	Anorthite	Taconite Tailings	Limestone	Anhydrite
	..... Percent			
SiO_2	56.96	58.54	2.17	-
Al_2O_3	27.57	0.64	0.13	-
Fe_2O_3	0.62	27.40	0.37	-
CaO	8.80	4.40	53.96	41.20
MgO	0.16	3.10	0.33	-
SO_3	0.18	0.23	0.00	58.80
LOI	0.40	5.69	42.92	-
Na_2O	4.50	-	0.03	-
K_2O	0.81	-	0.06	-
TiO_2	-	-	0.03	-
P_2O_5	-	-	0.03	-

In order to take care of higher Na_2O content, 2% anhydrite was added to the kiln feed to reduce the formation of alkali aluminate phase. The resultant cement prepared showed that the cement adequately met the ASTM requirement of Type 1 cement. Concrete prepared using tailings based clinker, showed better strength development (Fig.6) which may be attributed to the presence of high C_3S content with C_3S/C_2S ratio of 3.29.

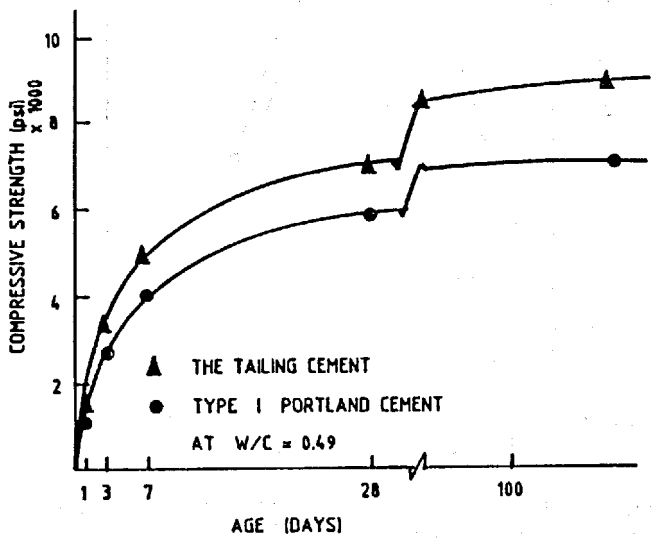

Fig 6 : Development of Compressive Strength of Concrete Specimen

Investigations on the use of basalt rock as a corrective material in portland cement manufacture has been described (39). Basalt is a family of rocks of volcanic origin abundantly available in nature and mainly used in building blocks and stone chips. The commonly occurring minerals in basalt are anorthite, albite, hypersthene, orthoclays, magnetite, iliminite and quartz. Most of the SiO_2 is in the form of silicates and almost all MgO is in the form of Magnesium ferrosilicates. In order to study the effect of Basalt on the reactivity of cement raw mix, raw mixes were prepared with and without Basalt (Table 17).

TABLE 17

RAW MATERIAL AND RAW MIX ANALYSIS WITH & WITHOUT BASALT

	Raw Material Proportions				Chemical Composition						
	Lime-stone	Bauxite	Iron-ore	Basalt	SiO_2	Al_2O_3	Fe_2O_3	CaO	LOI	LSF	MS	MA
	.....Percent.....											
Raw Mix-1	98.5	1.0	0.5	-	12.4	2.0	2.5	45.1	36.1	1.16	2.7	
Raw Mix-2	98.0	-	-	2.0	11.8	2.0	2.2	45.6	35.9	1.2	2.8	

Reactivity of these raw mixes was studied by firing the pelletised raw mix from 800 to 1450°C for a retention time of 20 min. The fired pellets were studied for physico-chemical and mineralogical characteristics. The volume changes in raw mixes with rise in temperature from 800-1450°C was determined by expansion shrinkage studies (Fig. 7) and residual free lime at each temperature determined (Fig. 8).

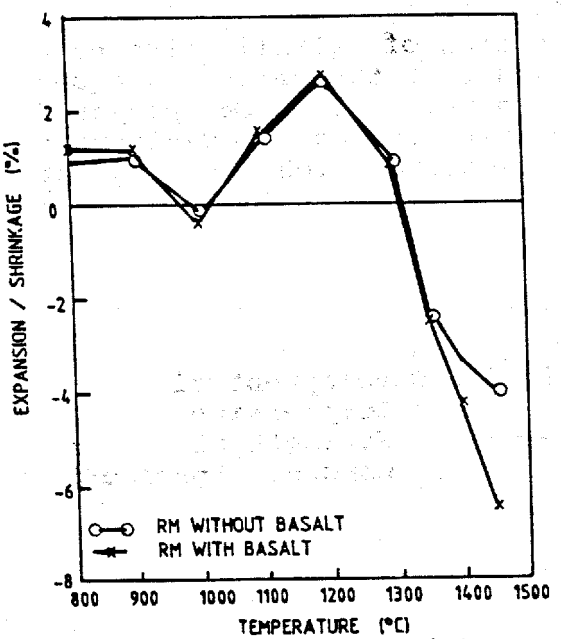

Fig 7 : Expansion/Shrinkage Studies of Raw Mixes

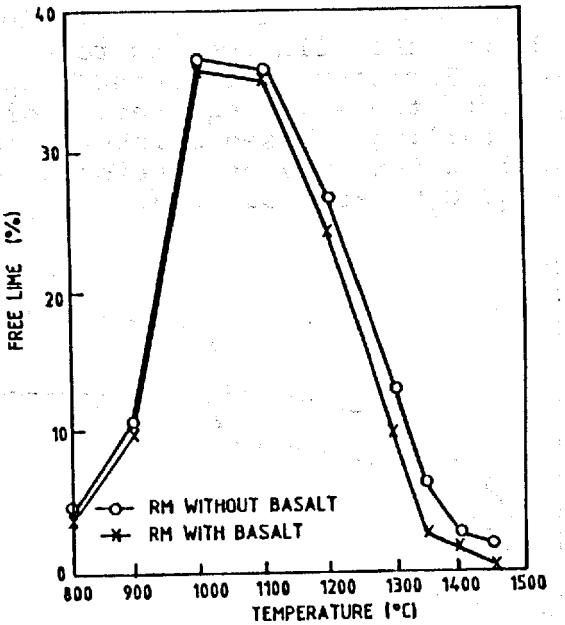

Fig 8 : Free Lime of Raw Mixes at Various Temperatures

The results of the studies indicate that the expansion upto 1100°C is more in raw mix 2 with Basalt than in raw mix 1 without Basalt, indicating higher rates of solid-solid reactions forming calcium silicates and aluminates. Higher shrinkage values in Basalt raw mix above 1300°C indicates higher quality of liquid formation and higher rates of C_3S formation exemplified by higher slope of the shrinkage curve. The lime combinability with Basalt is comparatively more compared with the raw mix without Basalt. The X-ray diffraction studies for sinters at various temperatures indicate appearace of C_3S formation at a lower temperature of around 1300°C in the raw mix with Basalt while the same is not observed in the raw mix without Basalt. Based on the results of the laboratory trials, a plant trial was carried out.

The data of the physical test results indicate that the cement produced from Basalt clinker shows higher compressive strength. The microstructure of clinkers with Basalt indicate well developed C_3S and C_2S crystals and finely crystalline matrix with presence of stabilised active polymorphs of belite which have higher hydraulic acivity inferred from higher compressive strengths (Plates 5, 6 & 7).



Plate 5 : Optical Micrograph of Clinker Without Basalt



Plate 6 : Optical Micrograph of Clinker With Basalt Showing Active Belite Polymorphs



Plate 7 : Optical Micrograph of Clinker using Basalt with Improved Microstructure

MINERALISERS BEARING WASTES

The merits and demerits of using mineralizers in clinker burning have been adequately reported in the literature on synthetic and industrial raw mixes (40-43). The potential use of mineraliser as possible means of energy conservation in cement is in principle well estalished and its use in economically profitable situations has been practised (44).

The utilisation of industrial wastes containing mineralising agents has been well established (45). The utilisation of phosphorous slags and phosphogypsum has been found to be interesting and prospective. The influence of fluorophosphorous slags as a compound mineraliser in clinker formation reaction both in solid and liquid phases has been reported.

Use of 1% phosphogypsum as a complex mineralising and modifying additive, leads to formation of fine grained and uniformly distributed alite and belite resulting in improved grindability as well as cement quality.

Use of barium bearing waste obtained in the manufacture of white mineral pigment has been reported (46). High strength cement could be obtained even with significantly higher belite content in the clinker, which has been attributed to higher solubility of barium in belite compared to alite, which was observed to be nearly 3 times. The clinkers containing 0.2-0.3% BaO were also reported to have improved grindability.

Zinc containing waste (47) in the raw mix was found to be excellent as a mineraliser for effectively improving burnability, (Fig 9a & b) activate alite and improve the early strength of cement.

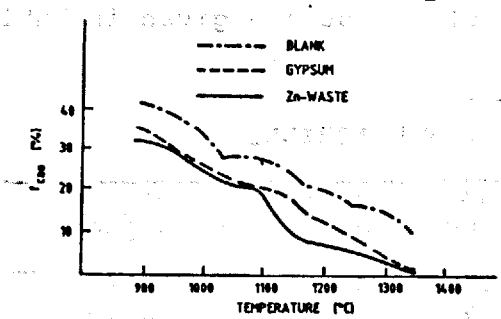

Fig 9a : Burnability Curves of Raw Mixes with Various Mineralizers

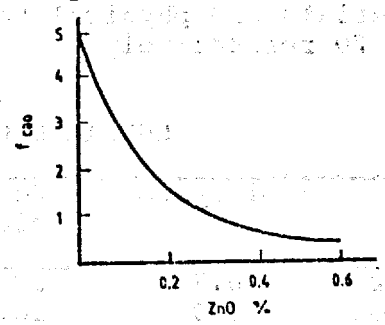

Fig 9b : Relation Between Free Lime and ZnO Contents

The zinc containing waste as a mineraliser has been found to give improvement in output and quality of clinker in a VSK. The improvement in compressive strength and other physical parameters are given in Table 18.

TABLE 18
PERFORMANCE OF CEMENT USING ZINC CONTAINING WASTE

No	KH	ZnO %	Setting Time (mts)		Compressive Strength N/mm^2			
			Initial	Final	ID	3D	7D	28D
1	0.96	0.00	150	190	12.2	29.3	58.3	89.0
2	0.96	0.20	122	163	14.0	29.8	62.6	95.3
3	0.96	0.60	102	142	15.4	45.0	74.7	107.4
4	0.80	0.00	73	324	-	8.8	22.5	70.4
5	0.80	0.20	130	343	-	8.5	22.3	70.1
6	0.80	0.60	291	379	-	9.1	24.3	85.3

The petrographic study of clinker containing ZnO shows that the size and axial ratio of alite crystals as well as crystalline tendency of interstial materials are all increased. Apart from these, ZnO improves burnability, decreases the viscosity of the melt and accelerates mass transfer process.

A dopant study reported (47) for alite formation in the rice husk ash and calcium carbonate system revealed that CuO is the most effective mineraliser. At 0.5%, CuO dosages more than 70% alite formation was obtained at 1400°C. Higher concentration of CuO had destabilising effect on alite. However, rapid cooling was necessary when CaF_2 and more than 0.5% CuO were used as mineralisers. The order of effectiveness of different mineralisers with 0.5% addition at 1350°C was CuO > ZnO > MnO_2 > SnO_2 > PbO while at 1400°C, it was CuO > MnO_2 > ZnO > SnO_2 > PbO.

In a case study reported for a dry process 2500 TPD plant with a precalciner and suspension preheater system where high free lime, poor kiln feed burnabiliy resulting into frequent unsoundness in cement was overcome by carrying out various raw mix studies by using suitable correctives and ore rejects (48). The correctives chosen were siliceous ore rejects with an average quartz grain size of 100 microns to replace the sand stone of average quartz grain size of 350 microns. The deficiencies in the raw mix were high LSF, low SM, and higher grain size of quartz in kiln feed. The chemical composition of raw materials and physical testing results of cement are given in Table 19 and 20 respectively.

TABLE 19
CHEMICAL COMPOSITION OF RAW MATERIALS

	Limestone	Calcareous clay	Sand stone	Silica Sand	Ore Rejects
SiO2	6.7	29.1	87.6	92.0	67.6
Al_2O_3	1.9	10.1	4.7	2.4	4.7
Fe_2O_3	1.5	7.3	0.7	0.4	5.7
CaO	48.4	24.2	2.1	2.2	10.7
LOI	39.6	25.0	3.8	2.3	3.1

TABLE 20

PERFORMANCE OF THE CEMENTS

	SO3	Compressive .Strength(N/mm2) 3D	7D	28D	Soundness
Normal Clinker	2.0	44.0	46.0	54.0	Failed
Clinker with ore rejects	2.0	40.0	46.0	68.5	Passed

The improved reactivity after utilising proper corrective and ore rejects is depicted in Fig 10.

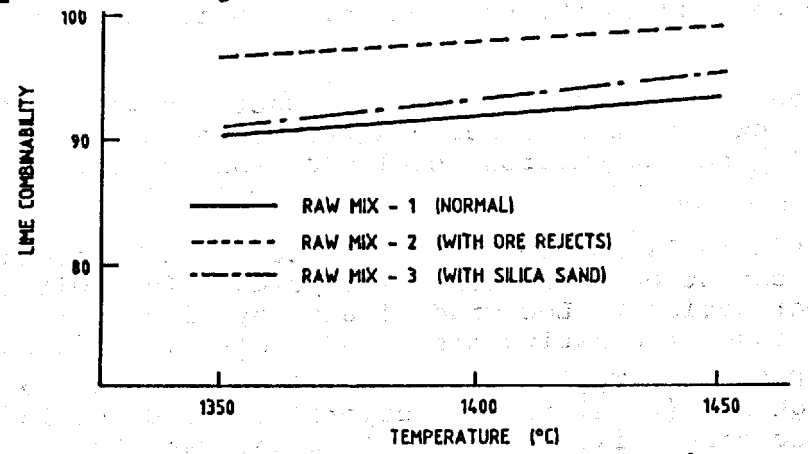

Fig 10 : Lime Combinability of Raw Mixes

The high reactivity of the raw mix (with ore rejects) is attributed to mineralising effect of one of the constituents of the ore rejects. Photomicrograph of improved clinker is given in plate 8.



Plate 8 : Optical Micrograph of Clinker Prepared With Ore Rejects

LOW GRADE FUELS AND COMBUSTIBLE WASTES

Coal and oil/gas are the most widely used fuels in the manufacture of cement (49, 50). Use of lignite as a fuel in cement manufacture is of more recent origin and technological developments have made it possible to use it as alternate fuel to coal (51-53). However its use

as a part substitue to coal has been widely practiced and its economic viability established. The problems relating to the use of these conventional fuels have been fully invesigated and it can be generally concluded that the factors effecting the techno-economics of their use broadly relate to the following aspects.

1 Volatiles in the raw materials and fuels
2 Flame characteristics
3 Ash content and composition of solid fuels
4 Raw meal-ash-clinker correlation

Use of oil and gas have an advantage over the use of coal in that even low grade limestone particularly with respects to lime content generally considered non-utilizable with coal, can be used to give good quality clinker. However because of higher content of sulphur, their use can add to the problems of volatile cycles during pryro-processing.

Low grade fuels and combustible wastes have gained importance from the view point of finding alternative to the fast depleting fossil fuels and the environmental problems posed by their disposal (54,55).

Low grade fuels for cement manufacture can be broadly termed as fuels which cannot be used alone as a primary fuel without beneficiation or upgradation . Low grade fuels may also be fuels which have high percentage of constituents such as alkalies, sulphur, chloride, titanium, P_2O_5 etc. Typical examples of such fuels are high moisture (>20%), high ash (>40%) and low calorific (<3500 kcals/kg) coals and low calorific gases like producer gas water gas etc.

Low grade fuels may be natural materials such as, high ash high sulphur coals, oil shales; agricultural by products such as, rice husk, bamboo dust, bagasse etc or synthetic materials such as paper and plastic wastes, industrial by product/wastes such as from petro-chemical industry, fertilizer plants aluminium industry etc. There is a long list of identified low grade fuels and combustible wastes which can be used in cement manufacture. These are classified and presented in Table 21.

TABLE 21
LOW GRADE FUELS AND COMBUSTIBLE WASTES USED IN CEMENT MANUFACTURE

A. NATURAL MATERIALS

(a) Agricultural

i/ Rice Husk
ii/ Straw
iii/ Coconut Husk
iv/ Peanut Husk
v/ Wood Waste
vi/ Bamboo Dust
vii/ Bagasse

(b) Others

viii/ Animal Waste
ix/ Sewage Sludge
x/ Oil Shales

C. INDUSTRIAL WASTES

1 Petro Chemical Wastes

i/ Petroleum Coke
ii/ Coke
iii/ Asphalt Sludge
iv/ Acid Sludge
v/ Chemical Waste

2 Carbon waste from fertilizer plant

3 Spent Pot Lining from Aluminium Industry

4 Waste oil and Hazardous Waste

B. SYNTHETIC MATERIALS

i/ Scrap Motor Tyres
ii/ Rubber Waste
iii/ Plastic Waste
iv/ Card Board
v/ Graphite Dust
vi/ Old Battery Boxes

D. OTHERS

i/ House-hold Waste
ii/ Municipal Refuse
iii/ Land Fill Gas

Cement rotary kiln is considered to be very a versatile incinerator and the kiln system can use almost any type of low grade fuel or combustible wastes under specific conditions (56) Compatibility with the cement raw materials particularly in cases where solid low grade/ waste fuels are used, is considered important as ash absorption may upset the delicate balance of raw meal composition required to produce quality cement without causing any operational problems.

PROBLEMS RELATING TO USE OF LOW GRADE/WASTE FUELS:

Use of low grade and wastes fuels throws up problems specific to each of these fuels and investigations and studies are still on to find solutions to enable their use. The problems relating to the use of these fuels can be broadly grouped into the following heads.

i/ Fuel preparation
ii/ Operational problems in the manufacturing process
iii/ Impact on quality
iv/ Environmental pollution

i/ Fuel Preparation

Depending upon the physical characteristics of the waste fuels, these may have to be processed for use in the cement rotary kiln. Some of the wastes such as rice husk, bamboo dust, coke and waste gases do not need much of fuel preparation and have to be fed through suitable firing mechanism at various points during the pyproprocessing. High moisture wastes will require predrying and pelletisation/pulverization while others will require cutting, shredding, pulverization etc (57). The problems related to fuel preparation for each category of wastes is dealt under the individual cases.

ii/ Operational Problems in the Manufacturing Process

Some of the operational problems relating to the use of waste fuels are : resistance to flow of materials in the preheater due to volatiles, fluctuation in temperature, coating formation, refractory lining life, grinding problems due to moisture and problems of storage and handling etc.

Though the solution to these problems vary from case to case and no single solution can be applied, considerable success has been reported in solving these problems.

iii/ Impact on quality

Quality is the single most important parameter governing the use of wastes in the manufacture of cement. The problem areas identified can be broadly considered to arise from;

(i) High residue content of the wastes,

(ii) Elemental composition of residue and its compatibility with other raw materials,

(iii) Impact of volatiles on composition and mineralogy of the clinker and

(iv) Problems relating to heavy metals and toxicity.

However, in general no serious problem relating to impact of use of waste fuels on quality of clinker and cement has been reported (58,59).

iv) Environmental Pollution

Cement rotary kiln is considered to be an ideal incinerator for waste fuels as the cement manufacturing process uses all modern pollution control devices relating to dust and gaseous pollutants. Several case studies have been reported to indicate that the level of pollutants emitted in the cement manufacturing process are well below the permissible limits laid down by the various regulating agencies the world over (60).

USE OF LOW GRADE/WASTE FUELS IN CEMENT MANUFACTURE

Use of low grade/waste fuel in cement manufacture and problems relating to their utilisation, quality of the resultant clinker and impact on environment have been presented here categorywise.

Agricultural Wastes as Fuel

Though the area under agriculture has been almost stagnant since 1975, crop production has registered a significant increase resulting in increase in the crop residues. The availability of agricultural residues depends not only on production levels but also on a variety of social and economic factors. In India 300 million tonnes of agricultural residues are generated every year. Add to this about 40 million tonnes of agro-industrial wastes mostly from the food processing industry which include pealings, pulps, stalks etc of fruits and vegetables. All agricultural residues essentially contain different proportion of cellulose, hemicellulose, lignin, ash, resin, wax, water soluble subastance and moisture. Carbon, oxygen and hydrogen are the major chemical constituents of agricultural residues. Small amounts of nitrogen, sulphur, chlorine and traces of other elements are also present. Volatile matter content is 60-75%. High ash content lowers the calorific value of residues, while the presences of oils, resins and wax raises the calorific value. The heat potentials of some of the selected agricultural wastes are given in Table 22 (61).

Amongst agro-industrial wastes, rice husk, bagasse, molasses, coconut residues, groundnut shells etc are more promising as fuels. However, rice husk obtained from rice milling industry has potentials for use in cement rotary kiln in view of its continuous supply and economics for use (62-64).

TABLE 22
HEAT POTENTIAL OF AGRICULTURAL WASTES

Agricultural Wastes	Moisture % wt basis	Ash %	Calorific Value Kcal/kg
Rice Straw/Husk	10.6	20.1	3000
Wheat Straw	9.2	18.0	3800
Cotton Sticks	12.0	13.5	3300
Maize Stalks	11.5	14.2	4700
Maize Cobs	8.6	13.8	3500
Bajra Stalks	11.2	17.5	3850
Pearl Millet Husk	-	-	3626
Groundnut Straw	12.1	1.3	4200
Castor Stalks	-	-	4767
Castor Shell	-	-	3665
Mustard Straw	-	-	4034
Mustard Stalk	-	-	3948
Gram Straw	9.2	13.2	3950
Moth Straw	-	-	3800
Masoor Straw	10.1	12.8	3810
Moong Straw	10.3	12.6	3820
Spent Coffee Grounds	-	-	5000

The chemical and proximate analyses of rice husk are given in Table 23 and 24 respectively.

TABLE 23
TYPICAL CHEMICAL ANALYSIS OF RICE HUSK AND BAMBOO DUST ASH (DRY BASIS)

Sl No	Constituents Determined	Rice Husk ..... Percent	Bamboo dust .....
1	SiO_2	85.0 97.0	69.89
2	K_2O	0.5 - 3.0	
3	Na_2O	< 2.0	4.05
4	CaO	< 2.0	9.18
5	MgO	< 2.0	3.56
6	Fe_2O_3	Traces - 0.7	6.05
7	Al_2O_3	-	6.69
8	P_2O_5	0.2 - 3.0	-
9	SO_3	0.1 - 1.5	-
10	Cl	Traces - 0.5	-

TABLE 24
PROXIMATE ANALYSIS OF TYPICAL SAMPLES OF RICE HUSK AND BAMBOO DUST (MOISTURE FREE BASIS)

Sl No	Property	Rice husk ..... Percent	Bamboo Dust .....
1	Volatile Matter	62	75
2	Fixed Carbon	15	18
3	Ash Content	22	10
4	Calorific value Kcal/Kg	3142	3796

Bamboo dust from paper industry has also shown potentials for its utilization in cement manufacture (65). The chemical and proximate analyses of bamboo dust are presented in Tables 23 & 24.

Both rice husk and bamboo dust are ready to use fuels and no preparation is required.

PROBLEMS RELATED TO UTILIZATION

Both rice husk and bamboo dust can be used in precalcinator and kiln. Various operational problem encountered are fluctuation in temperature of precalcinator, coating formation at riser duct and kiln inlet. When interground with coal the high initial moisture content adversely affect the grinding efficiency of the coal mill.

EFFECT ON QUALITY OF CLINKER

Use of rice husk as fuel is limited by the fact that it generally contains more than 90% silica with very little R_2O_3 (< 3%). It is compatible with raw mixes containing silica less than 12% when coal is used as a primary fuel. In the investigations carried out at NCB, the impact of substitution of coal by rice husk on the clinker composition was investigated and the results presented in Table 25 indicate that substitution can be tolerated upto 1 percent of coal ash without upsetting the various modulii values and the quality of resultant clinker.

TABLE 25
EFFECT OF RICE HUSK ASH ON CLINKER COMPOSITION

S No	Constituents	Clinker composition 6% coal ash	0.2% R H Ash 5% Coal Ash	0.5% R H Ash 5.5% Coal Ash	1% R H Ash 5% Coal Ash
1	CaO	64.46	64.45	64.43	64.42
2	SiO_2	22.79	22.79	23.00	23.18
3	Al_2O_3	5.39	5.34	5.27	5.17
4	Fe_2O_3	4.58	4.49	4.47	4.46
5	MgO	1.47	1.46	1.45	1.44
	LSF	0.88	0.88	0.87	0.87
	SM	2.29	2.33	2.36	2.41
	AM	1.18	1.19	1.18	1.16
	C_3S	46.51	46.00	45.65	44.93
	C_2S	30.28	30.95	31.50	32.56
	C_3A	6.52	6.55	6.40	6.15
	C_4AF	13.88	13.66	13.60	13.57

The alkalies and P_2O_5 present in the rice husk ash have not been found to adversely affect the setting and compressive strength upto 1 percent of rice husk ash absorption.

Bamboo dust on the other hand has chemical composition more favourable to clinker quality so far as silica & R_2O_3 are concerned. In addition, it has a lime content of 10 percent which can make up for deficiency in lime in case of use of marginal grade limestone.

Use of Sewage Sludge as Fuel

Sewage sludge, as obtained, contains high percentage of moisture which has to be reduced to less than 2 percent before it can be fired in the cement rotary kiln. The dried product is granuler/powdery, relatively stable and easy to store (66). The chemical composition, proximate and ultimate analyses of dried sludge are given in Tables 26 and 27 respectively.

TABLE 26
ELEMENTAL ANALYSIS OF SEWAGE SLUDGE ASH

Sl No	Constituents Determined	Percent
1	LOI	1.6
2	SiO2	30.5
3	Al_2O_3	13.6
4	Fe_2O_3	22.6
5	CaO	8.6
6	MgO	1.5
7	SO_3	1.3
8	K_2O	1.1
9	Na_2O	0.41
10	TiO_2	1.4
11	P_2O_5	17.9
12	Cl	0.01

TABLE 27

PROXIMATE AND ULTIMATE ANALYSIS OF TYPICAL SEWAGE SLUDGE SAMPLE (On Dry basis)

	Constituent	Percent	Constituent	Percent
a)	Proximate analysis		B) Ultimate analysis	
	Moisture	6.6	C	26.6
	Ash content	46.2	H	3.75
	Volatile matter	45.3	S	0.46
	Fixed carbon	1.9	Cl	0.05
			N	3.73
			O	16.00
c)	Calorific value	9850 kcal/kg		

The sludge contains high percentage of P_2O_5 and therefore the use of sludges has to be limited to not more than 10% to keep the P_2O_5 content within manageable limits. In addition sewage sludge also contains arsenic, cadmium, cobalt, chromium, copper, mercury, manganese, lead, nickel, zinc, etc in traces which are fixed in the clinker minerals. The properties of clinker or cement produced in a

kiln using sewage sludge as fuel are not significantly affected and cannot be distinguished from normal cement (66, 67).

Dried sludge can be fed pneumatically either into the main firing system or in the secondary firing system. The main firing system offers the advantage that the organic pollutants are destroyed by high gas temperature. From the combustion point of view the secondary firing system is not ideal. Kiln operation with sludge was reported to be smooth and without any change in kiln output. However, the CO content of flue gases measured after the preheater rose from 0.17 to 0.30 percent due to different burning conditions. The emission values obtained on burning sludge are presented in Table 28 and compared with the prescribed limits.

TABLE 28

EMISSION VALUES MEASURED WHEN BURNING SLUDGE

	Dried Sludge test (average value) compound/direct operation (mg/Nm^3)	Limits as per Clean Air Regulations compound/ direct operation (mg/Nm^3)
Dust	45.0/27.9	50
Hg + CD + Tl (class 1)	0.083/0.261	0.2
As + Cr + Co + Ni + Se + Te (class 2)	0.011/0.0057	1
Sb + Pb + Cu + Mn + V + Zn (class 3)	0.033/0.020	5
Be (cancerogenous)	0.0008/0.00014	0.1
Cl	0.067/0.045	30
F	0.023/0.017	5
SO_2	14/24	500
NO_2	4557724	1300/1800
Organic substances (hydrocarbons)	Organic gases as total organic C (TOC) 19/15	class 1= 20 class 2= 50 class 3= 150

The overall expenditure in burning dried sludge is high mainly on account of the drying cost. It has been reported that mercury in the sludge has to be limited or controlled and care must be taken to keep the quantity as low as possible.

Oil Shales as Fuel:

Oil shales have a composition (Table 29) of clay and can substitute argillaceous component of cement raw mix (68-69). Additionaly oil shales have oil as impurity and have a calorific value of 400-1500 Kcal/kg which can be utilized as a raw meal component in

the last stage of preheater after burning seperately in a flash furnace and then mixing it with limestone before entering the kiln.

TABLE 29

CHEMICAL ANALYSIS OF OIL SHALE

Sample	LOI	SiO_2	Al_2O_3	Fe_2O_3	CaO	MgO	SO_3	Na_2O	K_2O	Cl
	.....				Percent		.....			
Oil Shale	15.6	57.1	15.9	6.0	1.1	0.8	0.9	0.1	2.5	.003

A case study has been reported by using limestone, iron ore, sand and shale as components in the ratio 77.1:20.3:2.3:0.3 and the clinker produced has a chemical and mineralogical composition as given in Table 30 (70).

TABLE 30

CHEMICAL AND MINERALOGICAL COMPOSITION OF CLINKER USING OIL SHALES

Chemical Analysis (Percent)	SiO_2	Al_2O_3	Fe_2O_3	CaO	MgO
	22.9	5.3	3.4	66.4	1.7
Modulii Values	Silica Modulus			2.6	
	Iron Modulus			1.6	
	Lime saturation			0.91	
Mineral Analysis (Percent)	C_3S			55.76	
	C_2S			23.63	
	C_3A			8.29	
	C_4AF			10.35	

The problems related to choice of process and related issues have been reported. It has been concluded that oil shales do not affect the quality of clinker produced upto the quantity used in the raw mix design.

Rubber/Plastic Waste as Fuel

Wastes such as discarded automobile tyres, battery boxes, rubber chips etc are generally non perishable, occupy large space, and hazardous to burn without proper incinerating facilities. These wastes have high calorific value (5000-9000 Kcal/kg) and established suitability for use in pyroprocessing of cement raw mixes and therefore have found use in cement manufacture. Rubber tyres have been reported to be used in cement manufacture and considerable work has been reported (71-73). These have to be shredded and reduced to manageable size depending upon where these have to be fed in the pyroprocessing. System design detailing the use of these wastes have also been reported. Generally no operational problems have been observed when tyres are used. However, their use poses high demand on dust collection system with which most modern cement plants are

equipped. Though the CO and SO_x content in exit gases tend to increase, the peak values observed are generally within the acceptable emission levels. In case of tyres no HCN could be detected.

Use of tyres however affects the chemistry of clinker significantly. The slight change in colour has been observed due to reinforced steel in the tyres combining with cement raw meal forming small amount of FeO in clinker. This results in a yellow tint in clinker. Since the content of iron is variable, it affects both the silica and alumina ratios and this has to be taken into account while designing the raw mix and adjustments made to obtain uniform quality of clinker.

Chlorine rich rubber and plastic wastes, however may produce material flow problems in preheater due to volatalisation of alkalies which condense in preheaters.

By-product Coke as Fuel

i/ Sicco Fines

Sicco fines are produced in the low temperature carbonisation of coal. These fines can be differentiated into three categories based on size of coke. Analysis of these fractions are as follows:

On air dried basis	Size (mm) 15	15-12.5	-2.5
Moisture %	3-5	3-6	3-6
Ash %	32-36	34-38	34-40
VM %	4-8	6-10	6-10
FC %	52-58	50-56	50-56
Sulphur %	0.4-0.5	0.4-0.5	0.4-0.5
CV (K Cal/Kg)	4500-5500	4000-4500	4000-4500

ii/ Leco Fines

Leco fines are produced by the low temperature carbonization of lignite and non coking coals. The leco fines can be similarly categorised based on different size fractions.

1 -3 mm size carbonised sludge
2 -10mm size fine coke special and
3 -20mm size super fine coke

The proximate analysis of Leco fines is given in Table 31.

TABLE 31
PROXIMATE ANALYSIS OF VARIOUS FUELS

Properties	Leco Fines	Sample Petroleum coke	Carbon sludge	SPL
		..... Percent		
Moisture	5-8	0.67	1-3	0.25
VM	3-12	8.67	7-10	5.98
Ash	10-30	0.12	0.5-3	36.09
FC	-	90.54	85-90	57.68
CV (Kcal/kg)	>5000	8900	7000	47.47

iii/ Petroleum Coke

It is a carbonaceous material obtained as a refining residue by destructive heating of high molcular weight petroleum. The major products from coking are fuel gas, gasoline, gas oil and petroleum coke. It is a high calorific fuel having low ash content (< 0.5%) and high sulphur content (2-6%). Proximate analysis is given in Table 31.

Carbon Waste Sludge

Carbon sludge is a waste product of fertilizer industry using heavy petroleum fraction. Incomplete combustion of oil produces 2-3% carbon which is removed by simple scrubbing by water to remove carbon in the form of slurry. It has composition similar to coke on dry basis (Table 31).

Coke from various sources mentioned above contains high percentage of carbon and can be used in chemical industry, which is using most of these by-products produced in India. However, coke becuse of low volatile matter is considered an ideal fuel for manufacture of ordinary portland cement clinker by vertical shaft kiln process (74). Leco and Sicco fines though contain high ash content have also been found to be highly suitable as fuel in the VSK technology. The wet coke slurry can be directly used without drying in the Gotlieb process of cement manufacture by VSK technology (75).

These carbonaceous wastes can also be used as auxillary fuel along with primary fuel (oil, gas, or coal) in the pyroprocessing by the rotary kiln technology. Their use generally leads to minor operational problems such as control of heat input, and higher level of particulate emission. Laboratory studies have indicated that clinker quality is generally not affected by the use of these fuels except in cases where the presence of high sulphur may have to be offset by proper blend or use of alkali bearing additives in the raw mix.

Coking Coals

Coal beneficiation by washing is widely practiced the world over to upgrade the coal quality (76-82). Depending upon the petrography of the coal, its size, ash content and the washing characteristics, about 25-40% rejects having more than 50% ash are generated during beneficiation. Typical analysis of coal washery rejects are as under :

Sample	Coal I		Coal II	
	Ash (Percent)	Yield	Ash (Percent)	Yield
Raw coal	20-34	-	20-22	-
Middlings	36-37	34-54	32-34	17-27
Tailings	55-57	3-13	54-58	2-3

The rejects as well as the middlings obtained during beneficiation have high moisture, (50-70%). The middlings and rejects after drying can be used to a limited extent in precalcinator depending upon the ash absorbing capacity of the raw meal or as a supplementary fuel in the oil/gas fired kiln.

Non-coking Coals

Both wet and dry beneficiation of non-coking coals have been reported. The use of middlings and rejects after wet beneficiation of non-coking coals will have the problems of high moisture and high ash content as for the wet beneficiated coking coal.

In dry beneficiation of non-coking coal, however, the reduction in ash content is 5-7% wherein the beneficiated coal can be used in the kiln and rejects can be used in the precalcinator. The use of these do not seem to pose any serious problem both in the operation as well as quality of clinker.

Spent Pot Lining

Spent pot lining (SPL) from aluminium industry has almost the same calorific value as that of coke breeze (Table 31). It contains elements such as S, Cl, and Na which can reduce the burning temperature. However care should be taken to control these contents at suitable levels to avoid build up of volatiles.

Acid Sludge

Acid sludge is generated during the treatment of lube oil fractions with sulphuric acid at oil refineries. Small amount of acid sludge is also generated during purification of certain grade of wax. This sludge is acidic in character and dark brown in appearance with a pH of 2.5. The sludge has a mineral content of 1-3.5 percent. The chemical composition of ash is given in Table 32. The proximate analysis of the sludge is given in Table 33. The sludge has a calorific value varying from 8050 to 8697 Kcal/kg and thus has good potential for use as a fuel.

TABLE 32

ELEMENTAL ANALYSIS OF ACID SLUDGE ASH SAMPLE

Sl.No.	Constituents Determined	Percent
1	LOI	0.66
2	SiO_2	69.71
3	Fe_2O_3	9.87
4	Al_2O_3	10.22
5	CaO	1.07
6	MgO	2.19
7	SO_3	6.0

TABLE 33

PROXIMATE ANALYSIS OF ACID SLUDGE

Sl No.	Property	Percent
1	Volatile matter	82.26
2	Ash content	3.26
3	Moisture content	0.91

Due to viscous nature of the acid sludge, removal of the sludge from the dumps and its handling for further processing poses one of the major obstacles in its effective utilization. The various steps involved in its utilization are : excavation, pressing, solidification, crushing and grinding. The scheme for utilizing acid sludge as fuel is given in Fig. 11.

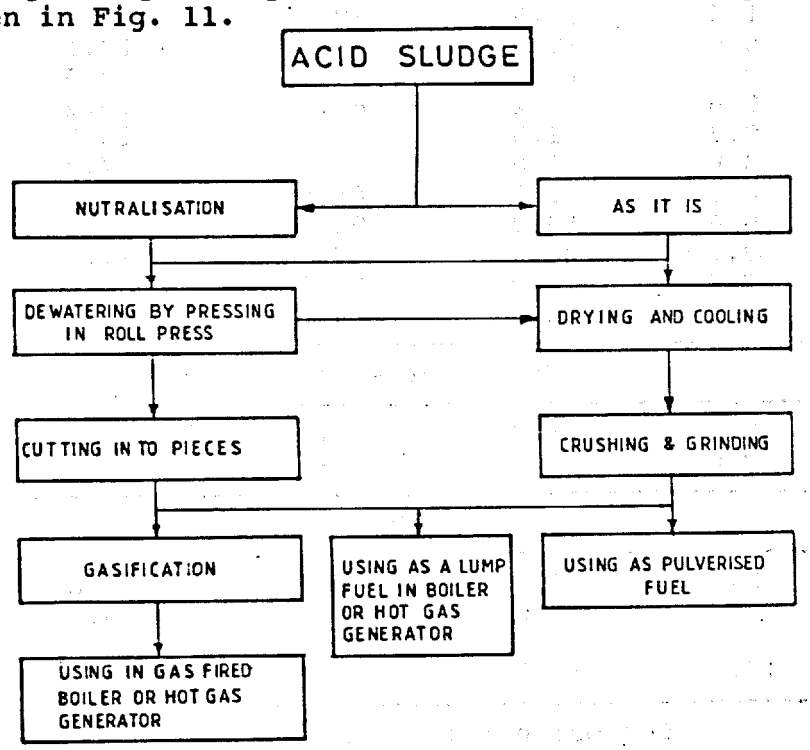

Fig 11 : Scheme for Utilizing Acid Sludge as Fuel

Due to high moisture and sulphur, sludge has been used only upto 1 percent replacement in cement plants.

Municipal Refuse

Municipal refuse is one of the combustible waste materials that can be used as fuel in cement manufacture (83-88). The refuse consist of several components depending upon the life style of the populace and societal rejects. The composition of the refuse along with the calorific values are presented in Table 34.

TABLE 34

COMPOSITION AND ANALYSIS OF A MUNICIPAL REFUSE SAMPLE ALONGWITH CALORIFIC VALUE

Component	% of all refuse by weight*	Moisture % by weight	Analysis Percent dry weight Volatile matter	Non-combus-tible	Calorific Value (BTU/lb)
		Rubbish 64%			
Paper	42.0	10.2	84.6	6.0	7572
Wood	2.4	20.0	84.9	1.0	8613
Grass	4.0	65.0	-	6.8	7693
Brush	1.5	40.0	-	8.3	7900
Greens	1.5	62.0	70.3	13.0	7077
Leaves	5.0	50.0	-	10.1	7096
Leather	0.3	10.0	76.2	10.0	8850
Rubber	0.6	1.2	85.0	10.2	11330
Plastics	0.7	2.0	-	16.3	14368
Oils, Paints	0.8	0.0	-	27.4	13400
Linolcum	0.1	2.1	65.8	2.5	8310
Rags	0.6	10.0	93.6	25.0	7652
Street	3.0	20.0	67.4	72.3	6000
Dirt	1.0	3.2	21.2		3790
Unclassified	0.5	4.0	-	62.5	3000
		Food wastes, 12%			
Garbage	10.0	71.0	53.3	16.0	8484
Fats	2.0	0.0	-	0.0	16700
		Non-combustibles, 24%			
Metals	8.0	3.0	0.5	99.0	124
Glass & Ceramics	6.0	2.0	0.4	99.3	65
Ashes	10.0	10.0	3.0	70.2	4172
		Composite refuse as received			
All refuse	100.0	20.7	-	24.9	6203

* Varies widely from place to place and country to country depending upon the life style of the populace and the total societal rejects.

Typical characteristics of the refuse derived fuel (RDF) as fired, before and after the installation of screens are given in Table 35.

TABLE 35

TYPICAL RDF FEED TO CEMENT KILN

	Unscreened	Screened
As fired :		
Net calorific value, kJ/kg	7,865	9,235
Water, wt %	31.9	34.6
Ash Analysis, wt %		
SiO_2	57.1	51.6
CaO	19.9	14.9
Al_2O_3	8.0	11.5
Fe_2O_3	3.3	4.7
Na_2O	7.2	5.7
K_2O	1.6	1.9

The data indicate that the effect of screening is to increase the gross calorific value of the refuse by 16-18%. Some of the energy potential available in the crude refuse is also discarded with the screen rejects. The ash analysis of refuse is presented in Table 34. However, its plastic content (PVC) give rise to chloride concentration which is likely to cause operational problems. Use of refuse as waste has not been found to affect the quality of clinker.

ACKNOWLEDGEMENT

One of the authors **Dr. S. C. Ahluwalia** thanks **Dr. K. M. Sharma, Mr. R. Bhargava** and **Dr. D. Yadav** for help in prepration of this paper.

REFERENCES

1 Chatterjee, A.K., C.H. Page "Industrial applications of mineralisers for improved clinker burning - illustrative cas studies" **Seminar on cement and allied building materials, Cem.Res.Inst.** India, Vol III, 1984, pp 192-209

2 Butt, Yu'M, "The mechanism of clinker formation process and the modification of its structure", **sixth international congress on chemistry of cement**, Moscow 1974.

3 Bucchl, R. "Influence of the nature and properties of raw materials on the reactivity of raw mix". **Proc. of Seventh ICCC**, 1980.

4 Chatterjee, A.K., "Cement raw material and raw mixes". **Pit & Quarry**, Sept, 1979, 103-111.

5 Gotecha, S.K., Giridhar K, S. and Narayana, N., "Beneficiation of limestone for cement manufacture", **NCB Quest**, February 1990, 1-13.

6 Ahluwalia, S.C., Laxmi, S. and Chopra, S.K. "High magnesia and marginal grade limestone prospects, problems and technology of utilization". **All India seminal on cement manufacture**, Vol I, 1981, 47-79.

7 Purohit, M.A., Rasal, S.M., Shaha, R.D. "Kiln feed filtration for semi dry conversion". **First NCB International Seminar on Cement and Building Materials**, New Delhi India 1987 Vol.2 III 59-74.

8 Shrinkhande, B.K., Tiwari, T.N., Chatterjee, A.K. "The conversion of ACC's Madukkarai Works to a semi-wet process" **World Cement**, Vol 22 No.10 Oct 1991. 18-21.

9 Karkhanis, S.V., Page, C.H., Rishi, B.K.G., Parameswaran, P.S., Chatterjee, A.K. "Technology of cement manufacture from low grade limestone and New approaches for Quality Control". **2nd Beijing International Conference** 1989, 377-384.

10 Vaidyanathan, Pradip D. and Kapur, P.C. "Production and properties of alinite cements from steel plant wastes". **Cement & Concrete Research**, Vol. 20 1990, 15-24.

11 Ghosh, D., Page, C.H., Chatterjee, A.K. "Potentials of cost reduction in raw meal preparation systems in running plants". **8th AFCM Tech. Symposium.**

12 **NCB** : Technical suitability of using calcium carbonate sludge as a part substitute to limestone for the manufacture of ordinary portland cement - Sponsored Project Report, October 1990.

13 **NCB** : Suitability of carbide sludge for the manufacture of cement - Sponsored Project Report, March 1987.

14 Vachani Pritam "Utilization of waste lime sludge for manufacture of cement". **World Cement Technology**, January/February, 1981, 29-36.

15 Ahluwalia S.C., Sharma K.M., Ali M.M. and Bapat J.D. : "Developments in the utilization of Indian Lime Sludgees in the manufacture of Building Materials". **National Seminar on role of Building Materials Industries in conservation of wastes into wealth**, March 1985, II-87-94.

16 Jain, H C, Nair, P.K. and Tondon, V.K. "Exploiting the use of calcium bearing industrial wastes as raw material for cement manufacture". **All India Seminar on Cement and Allied Building Materials**, Vol. 1, 1-97, New Delhi, 3-6 January 1984.

17 Banerjee, H.N. "Gainful utilization of waste lime sludge from paper mills". **All India Seminar on Cement and Allied Building Materials**, Vol. 1, I-123, New Delhi, 3-6 January 1984.

18 Narang, K.C. and Chopra, S.K. "Phosphochalk in cement manufacture". **State of art report, Cement Research Institute of India**, 1980.

19 **NCB** : "Utilisation of press mud for cement manufacture". Cement Research Institute of India, New Delhi, November 1987.

20 Ghosh, D. Chatterjee A.K. : "Lime sludge wastes of various sources as raw materials for mini cement material characteristics and process consideration". **All India Seminar on Cement and Allied Building Materials**, V.1, 103-122.

21 Royak, S.M. "Blast furnace slag-hydraulic activity and structure". **Tsement**, 1978, p4.

22 Taneja, C.A., Tehri, S.:. and Singh, M. "High manganese high alumina slags for cement manufacture". **7th International Cong. on chemistry of cement**, Paris, 1980, 111-48.

23 Ono, Y. et. al. "Strength of slag cement and contribution of basicity of vitrification degree". **Cement Association of Japan, 37th General Meeting**, Tokyo, 1983, p58.

24 Chopra, S.K. and Narang, K.C. "Blended Cements - raw materials including industrial waste". **All India Seminar on cement manufacture**, Vol.III, Jan 19-21, 1981, 493-532.

25 Nikifurov, Y.V. and Zozula, R.A. "Magnesia blast-furnace slags as raw material component and hydraulic additive in cement production". **All India Seminar on cement manufacture**, Vol.III, Jan 19-21, 1981, 533-36.

26 Panda, J.D., Goswami, G. "Utilisation of slags from different metallurgical industries". **National Seminar on role of building materials industries in conversion of waste into wealth.** March 1985, II-33-37.

27 Aoyogi, Yukio., Ishihara, Tohru Okuda Yoshimi. "Manufacturing and properties of a new type compound cement using coal ash as a substitute for clay".

28 Laxmi, S. and Mandal, P.K. "Metallurgical slags - potentials for conservation of energy and materials resources for building materials". **National Seminar on role of building materials industries in conversion of waste into wealth.** March 1985, II-51-66.

29 Puertas, F.M., Varela, Blanco T., Palomo, A., Vazquez, T. "Reactivity and burnability of raw mixes made with crystalised blast furnace slags". **ZKG**, Part I, 8-1988, 398-402.

30 Valkova, I.S., Dogandzhieva, R.G. "Producing portland cement clinker using blast furnace barric-manganese slag". **ICCC**, 19 pp I-79-I-83.

31 Chatterjee, A.K., Page, C.H., Ghosh, D. "Industrial experiences of using mineralisers". **International seminar on energy conservation, Beijing**, 1985, pp 174-190.

32 Utilisation of low carbon ferro-chrome slag for cement/ cementitious material manufacture - A feasibility study, **NCBM**, New Delhi, India, May 1978.

33 Ahluwalia, S.C., Sharma, K.M., Bhargava, R., Arora, V.K. and Narang, K.C. "Utilization of flyash for manufacture of building materials - Developments, prospects and problems". **National Seminar on role of building materials industries in conversion of wastes into wealth**, March 1985, II 67-86.

34 Laxmi, S., Parashar, A.K. "Potentials of utilisation of wastes from fertilizer and aluminium industries for building materials - An overview". **National Seminar on role of building materials industries in conversion of waste into wealth.** March 1985, II-101-111.

35 **NCB** : "Evaluation of red mud for its utilisation in the manufacture of OPC". Sponsored Project Report, March 1989.

36 Filippo, P. Amat di San. "Utilisation of red mud from Bayer process for producing ferrari cements". **ZKG**, No 11, 1989 pp. 584-86.

37 Werynski, B. Rajezyk, K., Kanas, A. "A study on the utilisation of the $-C_2S$ waste slurry from alumina production to the energy conserving manufacture of cement". **Beijing Conf.** 1989, Vol.2 pp. 370-76.

38 Bhatty, J.I. "Portland cement production using mineral wastes. **Cement and concrete research**, 1985, Vol. 15, pp 501-10.

39 Khadilkar, S.A., Ghosh, D., Page, C.H. "Investigation on the use of basalt as a corrective in portland cement manufacture - A case study". **2nd NCB International Seminar**, 1989, Vol. II, pp V1-12.

40 Budnikov, P.D. and Krochuk, L.A. "Intensification of clinker formation processes by mineralisers". **Zh. Vs. S. Khim. Obstchestrva im. D.I. Mendleeva**, 1965, 10(5) 545-50.

41 Sarkar, A.K., Roy, D.M. and Smart, R.M. "The Pennsylvania State University, USA. Phase Equilibria in the $CaO-Al_2O_3-Fe_2O_3-SiO_2$ system with calcium fluosilicate". N.H. Christensen and V. Johansen, F.L. Smidth & Co., A/S. Kinetic effects on alite formation. W.A. Klemm and I. Jawed, Martin Marietta Laboratories, USA. Burnability of synthetic and industrial raw mixes.

42 Palomo, A., Vazquez, T. Blanco, M.T., Varela, Puertas, F., Marid, E. "The Mineraliser effect on fluorspar in relation to the form of addition to an industrial raw mix". **T.Z. Fachberichete**, Vol. 109, 1985, No. 10, pp. 752-55.

43 Li Hao-Xuan Yang Jia. Zhi. "Influence of sintering temperature of clinker containing F and SO_3 on solid solubility of alite." **National Seminar on role of building materials industries in conversion of waste into wealth**, 1985, Vol.3, pp. 38-42.

44 Page, C.H., Ghosh, D. and Chatterjee, A.K. "Influence of mineralisers on constitution and properties of industrial clinkers". **8th International Congress on the chemistry of cement, Brazil**, 1986, Vol.II, pp. 152-57.

45 Goldshstein, L.Y.A. "Cement production from indusrial byproduct (wastes) utilisation". **Leningard, Stroiizolate** 1985.

46 Jinyu, Zhong., Yueming, Fan., Hui, Lu. andJiazhi, Vang. "Study on using Zn containing waste as mineraliser". **Beijing**, 1989, Vol.2 pp. 346-52, .

47 Misra, K.C. and Borthakur, P.C. "Alite formation in rice husk ash - $CaCO_3$ system, Influence of mineralisers on formation". **Regional Research Laboratory (Jorhat) Transactions of the Indian Ceramic Society**, September-October 1985 Vol. 44(5), pp. 101-106.

48 Khadilkar, S.A., Gore, V.K., Lele, P.G., Page, C.H. "Raw Mix optimisation for improved kiln performance - case studies". III **NCB International Seminar on cement & building materials**, 1991, Vol.I, pp. 59-68.

49 Saxena, J.P. and Sethi. Y.P. "Use of natural gas in Indian cement industry - problems & prospects". **Seminar on infrastructure support to cement industry - coal and railways**, 20 Sept 1991.

50 Arora, V.K. and Murthy, V.N. "Potential for utilizing natural gas with high ash coals". **Second NCB International Seminar on cement and building materials**, New Delhi. 30 Jan - 3 Feb 1989, Vol 2, pp III 102-113.

51 Verma, N.P. and Batra, V.K. "Use of lignite as primary fuel in rotary cement kiln firing". **Second NCB International Seminar on cement and building materials**, New Delhi. 30 Jan - 3 Feb 1989, Vol.2 pp III-86-93.

52 Balasubramanian, K., Arora, V.K. and Sethi, Y.P. "Uatilisation of lignite in cement industry - problems and prospects". **3rd NCB International Seminar on cement and building materials**, New Delhi. 21-25 Jan 1991, Vol 3. V-1-13.

53 Ahuja, I.C., Vasudevan, R., Ravi, K.K. "Lignite as fuel in Indian cement industry". **3rd NCB International Seminar on cement and building materials**, New Delhi. 21-25 Jan 1991, Vol.3 V-38-50.

54 Huhta, R.S. "Waste fuels in hot topic". **Rock Products**, July 1989, 55-57.

55 Goldmann & Wolt "Use of low grade coal in cement clinker klins" **Cement (Zagreb)**, 1979, 21 (3 - 4) pp 123 - 8.

56 Haley, C.A.C. "The use of refuse derived fuel in cement manufacture". **Cement betons plasters chaux** No. 754 - 3/85, pp 155-58.

57 William, H., Siemering, Parsons J.L. and Lochborunner, P. Jr. "Experiences with burning wastes". **Rock Products**, April 1989, 36-45.

58 Capon, B.M., Layne, P.B. and Watson, D. "The use of unconventional fuels in cement manufacture". **Cement, concrete and aggregates CCA GDP**, summer 1983, Vol.5, No.1, pp 30-34.

59 Sharipow, T.Y., et al. "Use of fuel byproducts from the Angren State electric power plant as a raw material component of cement production". **Uzls Khim. Zh.** 1980, (5), 38-40.

60 Waste burning an inside look : **Rock Products**, July 1988, pp 63-65.

61 Tyagi, P.D. "Fuel from wastes and weeds", 1989, pp 35.

62 Segal, R. Kiln Fulle. "Rice hulls, wood chips". **Proceedings, 19th International Seminar, Chicago, Illinois**, Dec 1983.

63 Freire, Paulo Mario "Rice husk in the production of portland cement". **Ceramica (Sao Paulo)**, 1981, 27(135), 105-113.

64 Borah, U.L., et al. "Carbonized rice husk, a fuel for black meal process of cement manufacture". **Trans Indian Ceramic Soc.**, 1989, 48(2), 36-8.

65 **NCB** : "Utilization of Bamboo dust in cement manufacture". Unpublished Report.

66 Obrist, A. "Burning sewage slugde in cement kilns". **World Cement**, March 1987, pp 57-64.

67 Nwesch, P.C., Kuenstkr H. and Kuepat, A.G. "Energy savings in rotary kilns in the production of cement through the addition of domestic waste and sewage sludge". **Recycling (Int. Recycling Cong.)**, 1979, 1, 318-23.

68 Milovanovic, Tomislav, Trifunovic Radomir. "Use of oil shales in the manufacture of cement". **Cement (Zagreb)**, 25(1), 29-32.

69 Kiyama, A. and Sakal. "Use of oil sludge for cement manufacture". **Jpn Kakoi Tokkyo Koho**, Jp 57, 188, 436, [82, 188, 436] (cl : c 04b7 / 44) 19 Nov 1982.Appl. 81/71, 334, 14 May 1981, 3 pp.

70 Nakamura, N. and Tominaga, S. "Malaysian cement plant utilizes oil shales". **World Cement**, June 1983, pp 175-186.

71 Watson, D. Matthee, H. and Robinson, D.W. "Refuse fuels in the portland cement industry". **The solid waste handbook edited by William D.R.**, pp 737-748.

72 Ono Takashi, Tsiya, Toshio, Nanbu, Atsushi Shiznoo, Veda Shunre, Kabaya, Masamichi Fr Demarde 2439168 (Cl. Co4B7/44) 16 May 1980, Japan Appl 78/127, 949, 18 Oct 1978, 13pp.

73 Naredi, R and Malmo : "Using solid fuels in supplementary firing of rotary cement kilns". **ZKG**, No 4, 1983, pp 185-189.

74 Rao, A.V.S, Imran, M & Raina, K : Plant trials with alternate fuels in CRI-MVSK cement plant. **Third NCB International Seminar on Cement and Building Materials**, New Delhi 1989, Vol. I, pp 90-103.

75 Gottlieb, S. and Swamy, R.K. "A new vertical kiln cement plant in India". **National Seminar on mini cement plant**, Vol. II, 26-27 May 1982, pp 1-4.

76 Fridman, I.A., Bikbau, M.Ya, Kaushanskii, V.E., & Barbaskev, G.K. : "Use of coal beneficiation and petro-chemical wastes in cement manufacture". **Tsement**, 1989 (12), pp 2-4.

77 Vusipov, N.Kh. : "Characteristics of raw mixes containing coal beneficiation wastes". **Tsement**, 1989 (12), pp 8-10.

78 Kraplya, A.F., Upolovnikov, A.B., Tsvang, A.S., Mokin, P.I. Sheiko, A.N. : "Use of coal beneficiation wastes and improvement of quality of clinker". **Tsement**, 1989 (12), pp 12-13.

79 Semchenko, I.A., Kougiya, M.V., Solovuskhov, N.E. Plotnikov, A.A. : "Computer use of coal beneficiation wastes and nickel slag". **Tsement**, 1989 (12), pp 13-15.

80 Kuznetsova, T.V., Tandilova, K.B., Kavsadza, Ts.E, Bibilashvili, B.V., Plevako, B.I. : "Coal beneficiation wastes in cement manufacture". **Tsement**, 1989 (12), pp 15-16.

81 Nikiforov, Y.V. : "Use of fuel containing wastes in the cement industry". **Tsement**, 1989, (12), 9-10.

82 Hradsky, T., et al : "Substitution of hydrocarbon fuel for low calorific solid fuels in cement industry". **Epitonayag**, 1989, 39(12), pp 353-7.

83 Duckett and Wiess, D. : "RDF as a kiln fuel". **Proceedings ASME, 9th National Waste Processing Conference, Washington, D.C.**, May 1980.

84 Weinberger, C.S. : "Evaluation of secondary shridding to enhance RDF production as fuel for cement kilns". **A Research Test, Proceedings ASME, 9th National Waste Processing Conference, Washington, D.C.**, May 1980.

85 Dorn, J.D. "Use of waste recyclable material in the cement industry". presented at **IEEE Cement Industry Technical Conference, Tucson, Arizona**, May 1976.

86 Watson, D. : "Combustible wastes and low grade fuels. Their use in cement manufacture". **Rock Products, 14th International Cement Seminar, Rock Products, Chicago**, December 1978.

87 Portland Cement Making and Municipal Refuse Conversion, **U.S Patent 4022630**, 10 May 1977.

88 Coomaraswamy, M, Haley, C.A.C, Giles, P.E. "Proceedings of Conference on Reuse of Solid Waste". **Institution of Civil Engineers, London**, 1982, pp 33-38.

Specific Theme I C

Effect of the Use of Mineralisers, Modifiers and Activators

Zementklinker, Klinkerphase, Reactivität, Stoffeigenschaft, Zusatzmittel, Eisenoxid, Siliciumdioxidstaub, Bauxit, Hochofenschlacke, Flugasche
f.sw.

MINERALISERS, MODIFIERS AND ACTIVATORS IN THE CLINKERING PROCESS

G K Moir
Blue Circle Industries PLC, Technical Centre, Kent, UK

and

F P Glasser
Department of Chemistry, University of Aberdeen, Scotland, UK

SUMMARY

The minor components normally constitute less than 4% of the chemical composition of Portland cement clinker, but can have a marked influence on clinkering reactions and cement properties. The sources of minor components in raw materials and fuels are discussed and recent published work is reviewed with reference to the position of the elements in the periodic table. Some typical clinker microstructures are illustrated, which have been strongly influenced by the presence of minor components. Lastly, the environmental impact of the components are considered and the future outlook assessed.

RESUME

Les composants mineurs constituent normalement moins de 4 % de la composition chimique du clinker de ciment Portland, mais peuvent exercer une influence sensible sur les réactions de clinkérisation et sur les propriétés du ciment. Les sources des composants mineurs dans les matières premières et les combustibles sont discutées et une revue faite de la littérature publiée relativement à la position des éléments dans le tableau périodique. Plusieurs microstructures typiques du clinker sont illustrées, qui sont fortement influencées par la présence des composants mineurs. Finalement, on considère l'impact sur l'environnement des composants et on évalue les perspectives futures.

1. INTRODUCTION

The major oxide components of Portland cement clinker (CaO, SiO_2, Al_2O_3 and Fe_2O_3) normally account for 96-97% of the chemical analysis. The relative levels of these four oxides control the proportions of the four principal clinker minerals, C_3S, C_2S, C_3A and C_4AF, and these proportions have a fundamental influence on cement properties. However, the minor components which account for the remaining 3-4% can have a very significant influence on the clinker-making process and the properties of the cement.

The cement maker currently faces increasing pressures from a number of different directions:-

- Customers have increasing expectations concerning cement performance. This particularly applies in markets where large sophisticated users source cement from a number of cement plants, and not unreasonably, expect equivalent levels of performance from different cements.
- Environmental legislation will require producers to meet certain limits for emissions of pollutants, such as SO_2, NO_x and particulates.
- Concern over the role of CO_2 as a so-called "greenhouse gas" is likely to result in pressures to reduce specific emissions of CO_2 per tonne of cementitious binder.
- Commercial and environmental pressures to utilise waste and by-product materials as fuels or as raw materials.

The minor components are very relevant to this situation as:-

- They are to a considerable extent responsible for the differences in cement characteristics from different sources.
- Certain components offer the potential to reduce the energy consumed in cement-making and emissions of NO_x and CO_2 by reducing the processing temperature required and/or increasing hydraulic activity.
- Wastes and by-products can be significant sources of minor components

This review seeks to identify the specific influences of the minor components relevant to cement making, and also the potential benefits which might be gained by the deliberate introduction of certain components.

2. SOURCES OF MINOR COMPONENTS

Table 1 indicates the levels of minor component oxides and elements found in 13 Portland cement clinkers, manufactured by Blue Circle Industries PLC in the UK. The analyses were determined on clinker samples accumulated at 2 hourly intervals over a 7 day period. Similar analyses for clinkers from continental Europe have been reported by Bucci(1).

The levels of minor components in the primary raw materials can have a strong influence on the decision where to locate a cement plant and the type of manufacturing process selected. The acceptable limits depend on local market circumstances (ambient temperatures, risk of alkali aggregate reaction, prevailing National Standards, etc.) and upon any interactions (reinforcing or compensating) between the individual minor components. An important distinction must be made between the commonly encountered components which are essentially non-volatile in the clinker-making process (eg MgO, TiO_2, P_2O_5, Mn_2O_3, BaO, SrO, NiO, Co_2O_3, CuO, Cr_2O_3) those which have a low volatility (V_2O_5, As_2O_3 and F) and those which are appreciably volatile (SO_3, K_2O, Na_2O, ZnO, Cl, PbO, CdO, and Tl_2O).

The volatility is relevant to

- process operation, particularly the tendency for deposits to form in the cooler parts of the kiln system
- the potential to lower the level in the clinker by operating a bleed of the kiln gases
- potential harmful emissions to the environment.
- volatile cycles leading to higher levels in the kiln than in the raw materials.

TABLE 1. Mean and range values for minor components in 13 Portland cement clinkers manufactured in the UK by Blue Circle Industries PLC.

	Mean	Range	
		min.	max.
weight %			
MgO	1.48	0.73	2.60
SO_3	0.80	0.51	1.58
K_2O	0.73	0.55	1.09
TiO_2	0.27	0.21	0.32
Na_2O	0.16	0.07	0.25
P_2O_5	0.10	0.05	0.20
SrO	0.09	0.03	0.20
F	0.07	0.03	0.17
Mn_2O_3	0.06	0.02	0.15
ppm			
ZnO	120	35	246
Cr_2O_3	103	75	140
V_2O_5	100	27	199
Cl	90	20	200
As_2O_3	57	13	211
CuO	55	20	240
PbO	16	0.5	95
CdO	0.5	<0.1	1.1
Tl_2O	0.3	0.04	0.5

Whilst the cement maker may be constrained in his choice of primary cement-making material, he is normally able to exercise choice in the selection of minor raw materials and fuels. These can be significant sources of minor components.

The following auxiliary raw materials are in fairly widespread use for clinker manufacture:-

	Typical Addition level in Raw Mix, wt %
- iron oxide	1-4
- silica sand	1-10
- bauxite	1-4
- blastfurnace slag	5-30
- fly ash from coal fired power stations	1-15

Care is necessary in the selection of iron oxide as elements such as chromium, arsenic, cadmium and thallium may be present at levels that may have some environmental consequences.

Bauxites normally have relatively high levels of TiO_2 (2-8%), and may also contain significant levels of Cr_2O_3 (0.04 to 0.4%).

Blastfurnace slags, by virtue of their high CaO content, can be used in much higher proportions than iron oxide, bauxite or sand. Table 2 indicates the levels of minor component oxides and elements found in 35 slag samples from 24 different worldwide sources. The level of MgO can be the main factor limiting the level of blastfurnace slag usage as a raw material, particularly if the level of MgO contributed by the indigenous materials is already high.

The range of potential raw materials from the metal refining industry is considerable (2). Within the limitations of present knowledge concerning the influence of minor component on cement properties, these materials are frequently rejected on account of the levels of such elements as Zn, Cr, P, F, Na, K. Other reasons include the relatively small tonnages available from a particular source, variable chemical composition and difficult handling characteristics, particularly if the material is only available in the form of a sludge.

The main fuel utilised by the cement industry worldwide is bituminous coal.

TABLE 2. Mean and range values for minor components in 35 slag samples from 24 worldwide sources

weight %	Mean	Range	
		min	max
MgO	7.2	3.3	11.7
S*	1.2	0.5	2.8
TiO_2	0.66	0.22	1.7
Mn_2O_3	0.64	0.25	1.2
K_2O	0.57	0.29	0.96
Na_2O	0.44	0.17	0.90
Cl	0.07	0.001	0.22
SrO	0.06	0.04	0.08
P_2O_5	0.03	0.01	0.25

*Total sulfur expressed as such.

The level of non-combustible inorganic material (ash) in coals used by the industry typically lies in the range 5-20%. Thus, for a modern dry process plant using a coal with an ash level at the lower end of the above range, the level of ash incorporation in clinker will be less than 1%, whilst for a wet process plant using a lower grade, high ash coal, it will be in excess of 5%. Fortunately, the ash in bituminous coals is essentially shale, and the levels of minor constituents contributed to the clinker are not normally of concern. Conversely, the levels of sulfur and chloride may vary considerably depending upon the country of origin or coal field. Some illustrative figures are given in Table 3.

TABLE 3. Illustrative sulfur and chloride levels in coals used by the European cement industry

Country of Origin	Sulfur %	Chloride %
UK	1.5	0.007
UK	0.8	0.30
UK	1.6	0.39
UK	1.0	0.04
UK	1.5	0.15
USA	1.1	0.25
Venezuela	0.8	0.007
Canada	1.3	0.15
Poland	0.8	0.23
Russia	0.5	0.012
S Africa	1.0	0.008

These analyses are not necessarily representative of the respective countries, but they serve to illustrate the range of sulfur and chlorine inputs from coals. Increasingly, a wide range of waste, or secondary fuels are being used by the cement industry to partly replace the primary fuel. Some of these are listed below:-

Petroleum coke
Used tyres
Impregnated sawdust
Waste oils (lubricants)
Sewage sludge
Metal cutting fluids
Waste solvents.

The cement kiln is an ideal reactor for the disposal of combustible wastes by virtue of:-

- the guaranteed high temperature >1400°C
- the relatively long residence times of combustible material in the kiln
- the highly alkaline nature of the solids in the kiln which prevent acidic emissions such as HCl.

- the ability of clinker to accommodate controlled levels of ash without detriment to cement properties.

These fuels are used to partially replace the main kiln fuel. The content of minor components (S, Cl, heavy metals) is one of the main factors restricting their use at most locations.

Petroleum coke has a low ash content (typically 1%) but most sources available also have high sulfur levels of ~ 5%. Thus this fuel can make a significant contribution to clinker SO_3 levels. The ash normally contains a very high level of V_2O_5 (up to 60%), but the low overall ash level means that the contribution to clinker V_2O_5 levels is relatively small (0.04% and 0.08% respectively for modern dry process and wet process plants using 50% replacement of coal by petroleum coke).

Used tyres have a very significant zinc content of 1.2 to 2.6% (3). However, even with 10% replacement of primary fuel the contribution to clinker ZnO content will be less than 0.1%.

The other types of waste fuels need to be assessed on their merits as the minor components present are specific to their source (4).

Additional sources of minor components are

- refractories
- wear on grinding media and mill internals.

In most countries the use of chromium containing refractories is being phased out on account of the environmental problems associated with the disposal of used bricks.

3. GENERAL INFLUENCES OF MINOR COMPONENTS ON CLINKERING AND CEMENT PROPERTIES

The main influences of the minor components can be summarised under the following headings:-

Fluxing action	- temperature of first liquid formation reduced - liquid viscosity modified - liquid surface tension modified - crystal morphology modified
Phase relations	- the relative thermodynamic stabilities of the clinker minerals can be changed by solid solution effects
Hydraulic activity	- the reactivities of the clinker minerals are modified by solid solution and/or crystal symmetry effects.

In general, the presence of minor components in addition to CaO, SiO_2, Al_2O_3 and Fe_2O_3 in the raw mix can be expected to reduce the temperature of first liquid formation [1338°C in the C-A-F-S quaternary system (5)]. The influence of the minor components on clinker viscosity and surface tension is much more complex, as was shown by the studies of Timashev and co-workers (6).

Ions of strongly electropositive elements, such as K^+ and Na^+, increase the viscosity whilst those of strongly electronegative elements, such as Cl^- and F^- decrease it. Surface tension is also subject to systematic influences, tending to increase with increasing electronegativity of the s-block elements, but to decrease with increasing electronegativity of the p-block elements. These trends can be overriden by any liquid immiscibility such as occurs when alkalis and SO_3 are present.

Viscosity is clearly important as it strongly influences the dissolution rate of CaO and C_2S in the clinker liquid and the rate of diffusion of Ca^{2+}, O^{2-} and SiO_4^{4-}, necessary to form C_3S. The surface tension is important in affecting the wetting of the surfaces of the reacting solids, and in particular, the penetration by liquid of the porous CaO particles created by the decarbonation of $CaCO_3$ particles.

Liquid viscosity and surface tension also affect nodulisation, clinker density/porosity and the penetration of refractories by clinker liquid.

In the pure four component system C_3S does not form below 1250°C. The presence of minor components can lower this temperature, thus facilitating C_3S

formation, or conversely, by stabilising C_2S, impede the formation of C_3S. In this review the term mineraliser will be confined to components which encourage the formation of C_3S by lowering this lower limit of stability of C_3S.

The hydraulic reactivity of the clinker minerals can be altered to a significant extent by the presence of minor components. Boikova (7) reviewed substitution mechanisms for minor components. It should be remembered, that whilst it is normally desirable to increase the reactivity of C_3S and C_2S, it is disadvantageous to increase the reactivity of the aluminate phase on account of the resultant increase in cement water demand, and the accelerated loss of concrete plasticity.

There are three main processes by which minor components can influence hydraulic activities

- introduction of defects caused by solid solution effects
- stabilisation at ambient temperature of a more reactive high temperature polymorph
- effects arising during the hydration process (eg coating of cement particles by insoluble basic salt.)

Akimov et al (8) correlated the concentration of defects in C_3S introduced by transition and alkali earth elements.

It is difficult to isolate the influence of polymorphism from the other two effects, but Aldous (9) confirmed in laboratory studies, the statistical observations of Gourdin et al (10) that rhombohedral alite identified by XRD is more hydraulic than the monoclinic forms. In contrast, Puertos and Trivino (11) found lower strengths with the rhombohedral polymorph which had been preserved by water quenching, a technique which may have modified reactivity by, for example, extraction of soluble alkali sulfates.

Boikova (7) showed that in C_3S solid solutions containing ZnO, as crystal symmetry changed from triclinic to monclinic to rhomobohedral with increasing ZnO level, the number of lattice defects and the hydraulic reactivity reached a maximum at the points of transition from one stabilised polymorph to another.

In general, those elements which have a marked retarding effect on cement hydration when added as soluble salts, (eg P, Zn, Cu, F), can be expected to display a similar influence when incorporated in clinker (12), but only when present at a much higher concentration..

4. SPECIFIC MINOR COMPONENTS

Alkalis

The role of alkali incorporated in the main clinker phases has been reviewed in previous symposia. Gies and Knöfel (13) conclude that in the absence of SO_3, Na_2O is preferentially incorporated in the tricalcium aluminate phase. Both Na and K are substituted into belite. The reactivity of the aluminate phase is somewhat reduced by sodium substitution, but overall clinker reactivity is enhanced by alkali. The authors used these principles to proportion an active belite clinker, containing a mixture of α and β dicalcium silicate polymorphs. High Na contents in the belite were associated with good strength development: at the same time, burning temperatures were typically reduced by ~100°C.

The role of impurity, especially alkali, in controlling the polymorphism of the C_2S (belite) phase has been re-examined by von Lampe and Seydel (14), who developed active belite clinkers. They found that quenching of belitic clinkers yielded α' belite at high alkali contents, about 1.49% Na_2O equivalent at the fastest cooling rate, ca 20 x 10^4 K min^{-1} or more. But at lower alkali contents, it was possible to develop a new Ca_2SiO_4 polymorph, designated β* belite. This could be distinguished from ordinary β by:-

(i) its monoclinic β angle, only 93.44° compared to that of β itself, 94.59°

(ii) the position of the fourth strongest powder reflection, at $\underline{d}$ = 2.612Å (Miller index 103) for β, but shifted to 2.63-2.64Å in β* and

(iii) its transformation, upon slow reheating of quenched material, to α at 260-380°C; ordinary β does not undergo any phase changes in this range.

In general, belitic clinkers with α gave the best strengths, followed by β*; ordinary β gave the lowest strengths. They conclude that the content of stabiliser, as well as cooling rate, are important to the successful development of belitic clinkers.

Strunge, et al (15) have reviewed the role of alkali and sulfate in clinkering and found that optimum clinker formulation ratios existed, especially in relation to lime saturation factors. K_2O was found to increase C_3A reactivity. On the other hand, alumina contents were less critical. Richartz (16) found that the role of alkali sulfate became important at higher alkali contents and suggested an approximate threshold at 1% K_2O content. The presence of SO_3 was found to reduce the extent of alkali solid solution in the aluminate, and hence reduce reactivity and improve cement properties.

Transition metal oxides

No major systematic studies concerning the influence of transition metals on the nature of the liquid phase, and the ease of combination, have been reported since the reports by Timashev (6) and Odler and Abdul-Maula (17) and (18). Several workers have investigated the influence of individual transition elements arising from the use of industrial wastes as raw materials (2), (19-21).

In detailed investigations of the influence of minor components on the properties of the clinker liquid phase, Russian studies (6) showed that the influence of transition metal ions on the viscosity of the liquid phase was related to the electro negativity of these ions. Figure 1 shows that viscosity increased with decreasing oxidation state (W^{6+} to Cd^{2+}) which also corresponds to weakening of their acidic properties and the strength of the Me-O bond. Surface tension also tended to increase (over the range 0.49 to 0.58 N/m) with decrease in acidic properties and weakening of Me-O bond, although the experimental data showed greater scatter.

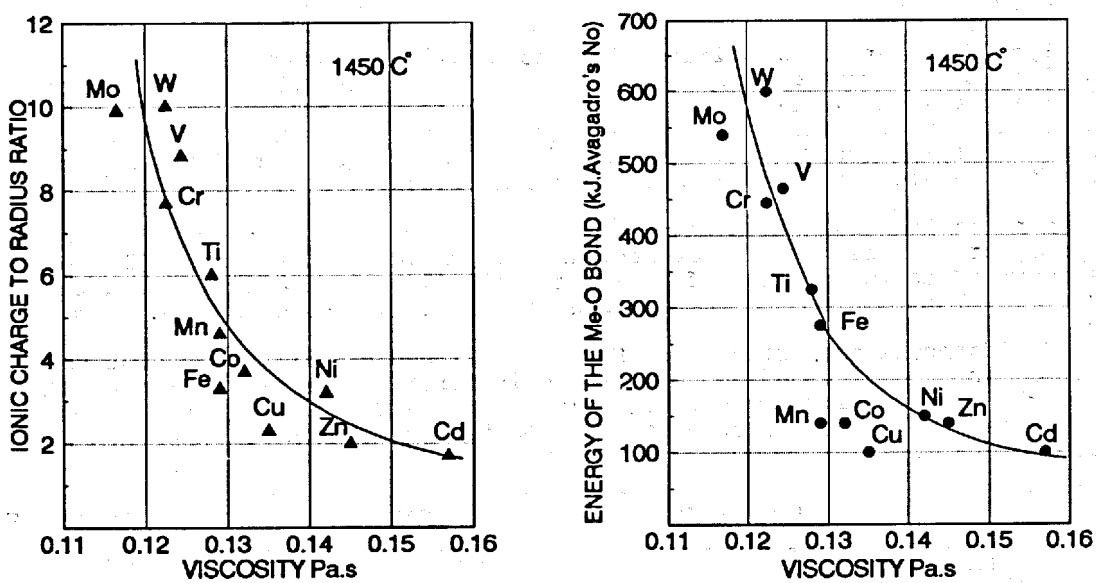

Fig 1. Influence of ionic charge to radius ratio and energy of Me-O bond on clinker melt viscosity (6).

Odler and Adbul-Maula (17 and 18) found that at 1200°C the effectiveness of the transitional metal oxides in aiding combination when added at the 1% level to a raw mix with parameters LSF 85%, SR 2.6, AR 1.8 was as follows:-

$$CuO > Co_2O_3 = V_2O_5 > Cr_2O_3 = ZnO > TiO_2$$

The CuO halved free lime, (from 19% to 8%), whilst the TiO_2, ZnO and Cr_2O_3 had a marginal effect.

The minimum free lime of 8% indicated that none of the oxides exerts a mineralising effect (ie the lower limit of stability of C_3S was not lowered significantly).

At 1300°C the relative effectiveness was

$$CuO = Co_2O_3 = ZnO > TiO_2 > CdO > MnO > V_2O_5 > Cr_2O_3$$

The CuO, Co_2O_3 and ZnO were particularly effective in promoting combination at this temperature, but V_2O_5 and Cr_2O_3 had a negative effect. These differences can not be readily explained by the viscosity and surface tension data of Timashev (6). This is not surprising as other influences such as solid solution effects will change the relative stability of C_3S and C_2S, and thus affect C_3S formation.

Hornain (22) found by microprobe analysis that, of the first series d-block elements, Cr and V had the highest relative concentration in C_2S, and thus the greatest potential stabilising effects.

It should not be overlooked that the effectiveness of a transition element as an aid to combination may be appreciably greater if the Al_2O_3 : Fe_2O_3 ratio of the clinker has not been optimised (23) at close to 1.38. In Odler and Adbul-Maula's studies the Al_2O_3 : Fe_2O_3 ratio was 1.8.

By entering into solid solution in the clinker minerals the transition metals have the potential to create defects or otherwise stress the crystal lattice and increase hydraulic activity. Potential benefits have been claimed for the inclusion of specific ions, or combinations of ions. The cause of the enhanced properties is often not known. It is not practicable to alter the chemical dopant levels independently of polymorphism or to change dopant levels without affecting phase equilibria. Many studies have concentrated on the influence of foreign ions on the polymorphism and reactivity of C_2S (24-30) as an active C_2S would enable significant savings in kiln fuel to be achieved.

Subba Rao and Narang (29) found that the hydraulic activity of low limed cements reached a maximum at a Cr_2O_3 level of 4-5%. However, the high toxicity and dermatological problems associated with chromium in cement make cements of this type impractical.

Feng Xiuji and Long Shizang (30) found that the effect of minor ions on the stability of βC_2S was closely related to the polarizing ability of the ions. The polarizing ability is defined as C^2/R where C is the ionic valence and R the Pauling ion radius. Of the transition metals, the strongly polarizing Mn^{7+}, Cr^{6+}, and V^{5+} are classed as stabilisers, whilst Mn^{4+}, Fe^{3+}, Ti^{4+}, Ni^{2+}, Zn^{2+}, Fe^{2+} and Mn^{2+} do not prevent inversion to γ C_2S at normal cooling rates.

None of the transition metals, apart from chromium, appears to have the property of increasing C_2S activity, although Ludwig and Pohlmann (27) found that the combined solid solution of Mn and the alkalis Na and K stabilised the α and α' forms of C_2S and that compressive strengths at 28 and 90 days were increased.

The comprehensive studies of Hornain (22) had earlier shown that chromium, and to a lesser extent, vanadium, were the only first series transition metals which enhanced the hydraulic activity of clinker with a C_3S level of 76%. Figure 2 illustrates the levels of transition elements found in the clinker minerals by microprobe analyses.

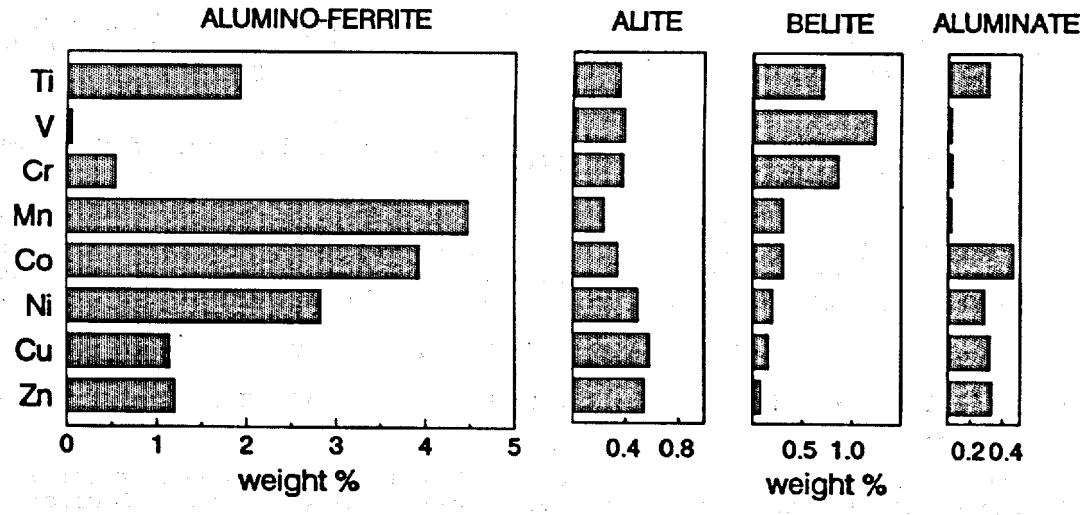

Fig 2. Distribution of transition elements in clinker minerals (22).

With the exception of chromium and vanadium, the highest concentration of the metal ions was found in the ferrite phase. Thus, these ferrite-soluble elements can be expected to have their greatest influence on the properties of the liquid phase formed during clinkering.

From the microprobe analyses and ionic size considerations, it was concluded that in the silicates Ti replaced Si, and Ni, Cu and Zn replaced Ca. For V, Cr, Mn and Cu, a more complex mechanism was proposed involving Ca, Si and interstitial sites, but with V and Cr substituting most readily for Si.

When present at levels above ~ 0.5% chromium appears to stabilise C_2S to the detriment of C_3S formation. (31).

Teoreanu et al (32) found that isovalent substitution of Si by Ti continues up to 3% TiO_2. Above 3%, substitution appears to be both by TiIV and by Ti in lower oxidation states. An increase in the mechanical strength properties of cement containing TiO_2 was noted at 7, 28 and 90 days. Earlier studies (33) had shown that initial reactivity and early strengths were progressively reduced by TiO_2 incorporation in clinker.

Marinho and Glasser (34) confirmed that Ti is preferentially soluble in the ferrite phase. The solid solution is accompanied by a series of complex changes with respect to both symmetry and order/disorder. With increasing levels of Ti the ferrite phase progressively adopts a perovskite type structure with diminished reactivity. The pattern of substitution of the ferrite phase in clinker is, however, much affected by the presence of other constituents such as magnesium.

In some parts of the world, it has proven difficult to obtain low MgO limestone resources. Palomo and Glasser (35) showed that titanium enhanced Mg solubility in the ferrite phase. Firing at 1300°C produced homogeneous, single phase ferrite solid solutions up to $2CaO(0.35Fe_2O_3.0.35Al_2O_3.0.3MgO.0.3TiO_2)$. This confirms numerous microprobe analyses showing that ferrite concentrates both Mg and Ti. It was envisaged that the substitution $Ti^{4+}+Mg^{2+} = 2(Al^{3+},Fe^{3+})$ occurred: infra-red evidence show that, as expected, Mg occurs preferentially in tetrahedral sites and Ti in octahedral sites.

Most of the transition elements have the potential to exist as oxides in several oxidation states, and this can clearly be expected to affect substitution mechanisms and possibly cement properties. Puertas et al (36) showed that for material fired in air and a reducing atmosphere respectively, the substitution limits for Mn in C_2S were 0.72% and 2.54%. For C_2S, the corresponding limits were 1.53% and 2.34%. In air Mn^{4+} is believed to substitute mainly for Si whilst under reducing conditions, isomorphous substitution of Mn^{2+} for Ca^{2+} occurs.

In a separate study, Puertas et al (37) found that for material fired in air the limit of solubility of Mn in C_3A (present mainly as Mn^{3+} and Mn^{4+}) was 0.78 ± 0.12%.

Feng Xiuji and Yan Peiyu (38) found that under oxiding conditions, Cr is present in C_2S as Cr^{4+} and Cr^{5+} co-ordinated in Si distorted tetrahedra. During hydration, Cr^{4+} and Cr^{5+} disproportionate to mixtures of Cr^{3+} and Cr^{6+}.

When manganese was incorporated into laboratory clinkers, Knöfel et al (39) found preferred incorporation in the ferrite phase. Alite content was increased up to 0.7% Mn, but reduced in favour of belite at higher levels. Cement early strengths were reduced progressively with increasing manganese addition, but unaffected at 90 days.

Odler and Schmidt (40) found that zinc can be accommodated in clinker up to ~ 0.5% Zn with little detriment to cement properties. At higher levels hydration is markedly retarded. As mentioned in section 3, Boikova (7) found that ZnO enhanced C_3S activity in synthetic preparations at ZnO levels which were transitional between those which stabilised triclinic, monoclinic or rhombohedral polymorphs.

The second and third series transition metals are less likely to be encountered than the first series, and consequently less is known about their effects on cement properties. A recent investigation by Kakali et al (41) found that incorporation of MoO_3, Nb_2O_3 and WO_3 into clinkers at levels up to 1.5% had no adverse effects on cement properties. However, ZrO_2 caused marked retardation of setting and strength development. The retardation is attributed to the precipitation of an insoluble calcium zirconate on the surface of the clinker minerals.

The recent published work has confirmed that chromium (and possibly vanadium) is the only transition metal which is a proven activator under normal clinkering

conditions. Explanations for this property have been offered, based on the substitution mechanism of Cr in C_3S, which results in calcium lattice vacancies (42) which produce semi-conductor type properties, and also the increased presence of structural defects, which could be detected by electron microscopy. Chromium is not unique in producing defects in C_3S. Akimov (8) found a correlation between the extent of early hydration and the concentration of defects introduced in C_3S by elements such as Co, Ni, and Ti. However, an important consideration is the behaviour of the metal oxides once they are released as initial hydration proceeds. It can not be unrelated that when added to cement in the form of the oxides or salts, V, Cu and Zn retard hydration (43-45) whilst those of Ni, Fe and Cr have little effect (46). Retardation is believed to be caused by the precipitation of either the insoluble hydroxide or a calcium salt, such as $CaZn_2(OH)_6.2H_2O$, on the surface of the clinker minerals. This explanation is, however, at best only partly correct as iron will also precipitate as an insoluble hydroxide.

Halogens

Chloride, bromide, iodide - The halogens Cl, Br and I have high volatilities in the cement-making process. They volatilise in the burning zone (normally as alkali halides) and condense in the cooler parts where they are associated with the formation of deposits which impair plant performance.

A volatile cycle is developed in which the level of halide in the partly clinkered materials and dusts may be many times that introduced by the raw materials and fuels. As a general guide, for efficient plant operation, it has been found that the chloride input (as a % expressed on clinker) to suspension preheater and precalciner kilns should be kept below 0.03% and 0.04% respectively. Higher levels can be tolerated if a proportion of kiln gases is bled from the system, but this increases fuel consumption. $CaCl_2$ has been added under these circumstances to aid alkali volatilisation and the production of a lower alkali clinker.

Grate preheater and wet process plants can tolerate higher Cl inputs, the limits depending upon the levels of dust return to the process and dust collecting efficiency.

Average levels of Cl retained in clinker are invariably less than 0.03%, irrespective of process type, and the influence of Cl on cement properties is therefore insignificant.

The levels of Br and I encountered in the raw materials and fuels used by the cement industry are very much lower than those of Cl. (47, 48). Similar process concentrations and retentions in clinker can be expected for these halides, should they occur in significant quantities.

The deliberate addition of Cl as flux has been investigated both as a chloride salt (17) or in combination with other salts (49). Odler and Abdul-Maula (17) found that when added at the level of 0.5-1.5%, $CaCl_2$ had a negative influence on combination.

The low temperature manufacture of chloride containing alinite cement generated a lot of interest at the 7th ICCC. (50). More recent studies (51), (52) have confirmed that alinite clinker can be formed at less than 1200°C, and cements produced with acceptable strength development characteristics.

The early strengths of the alinite cements were less than half of those of a conventional Portland cement, and thus Cl does not appear to qualify as an activator when present in the form of alinite or chloraluminate.

It is noteworthy that another calcium magnesium chlorosilicate, belinite $Ca_8Mg[(SiO_4)_4Cl_2]$ can be synthesized (53). The latter is structurally distinct from alinite, having cubic Fd3 symmetry, with $\underline{a}$ = 15.08Å. It is apparently not reactive towards water.

Even if the considerable process difficulties associated with high levels of chloride at temperatures of 1100-1200°C can be overcome, and acceptable levels of thermal efficiency achieved, the use of alinite type cements would have to be restricted to applications without steel reinforcement on account of the loss of protection to steel associated with the presence of chloride ions (54).

Kurdowski (55) has recently shown that the bromide analogue of chloride alinite can be synthesised.

Chloride and Sulfate - Tong Damao and Yao Daxi (56) reported a mineralising action for the combination of $CaCl_2$ + $CaSO_4$ with C_3S being formed at 1200°C. Cements

mineralised with $CaSO_4$ and $CaCl_2$ may develop several phases, and new characterisation data are recorded for both. One is calcium chlorosulfatosilicate, $Ca_{10}(SiO_4)_3(SO_4)_3\ Cl_2$. Chen and Fang (57) report its preparation and optical properties; it is uniaxial, negative with N_o = 1.665 and N_e = 1.659. From powder diffraction refinement, a = 9.688, c = 6.849Å. These would appear to confirm previous reports that it has an apatite type structure, specifically that of chloro-ellestadite. DTA and TG show that it decomposes with loss of Cl and SO_2 upon heating in air at or above 1200°C. The second phase is the analogue of spodiosite, $Ca_4(SiO_4)(SO_4)Cl_2$. Spodiosite itself is a phosphate; in its analogue PO_4^{3-} is replaced by equal numbers of (SO_4) and (SiO_4), ie.

$$2PO_4^{3-} = SiO_4^{4-} + SO_4^{2-}$$

thus maintaining charge balance. The sulfosilicate analogue has been synthesised (58) by direct heating of the reactants using $CaCO_3$, SiO_2 aerosil, anhydrite and $CaCl_2$ in excess. Calcination at 800°C (20 hr) following by slow cooling (20°C/hr) yielded 20 µm platy crystals together with $Ca_2SiO_4.CaCl_2$.

Fluoride - Fluoride has a unique combination of properties when present in a Portland cement raw mix. In addition to acting as a flux, lowering the temperature of first liquid formation and reducing the viscosity and surface tension of the clinker liquid (6), it has the unique mineralising action of enhancing the thermodynamic stability of C_3S relative to C_2S enabling it to be formed at temperatures below 1250°C. (59, 60).

Aldous (9) showed that beyond threshold values of F and Al the C_3S has a different symmetry which was identified as rhombohedral. This symmetry was also associated with enhanced hydraulic properties. Shame and Glasser (61) also found that above critical Al and F levels the C_3S in low temperature preparations retained rhombohedral symmetry at ambient.

When fluoride is used as a mineraliser in the preparation of pure C_3S it has an adverse influence on hydraulic properties. However, Moir (62) showed that if the levels of fluoride, alkalis, alumina and sulfate in the clinker were optimised and advantage taken of the strong mineralising action of F^- and SO_4^{2-} to maximise clinker C_3S, then cements with significantly enhanced strength properties could be produced. The C_3S in the cement was identified by XRD as rhombohedral. Figure 3 illustrates the relationship found between clinker F^- level, strength development and initial setting time at 20°C. The optimum fluoride level for maximum early strength was found to be ~ 0.2%. In the range 0.05 to 0.4% clinker fluoride, an increase in fluoride of 0.1% extended the initial (20°C) setting time by 40 minutes.

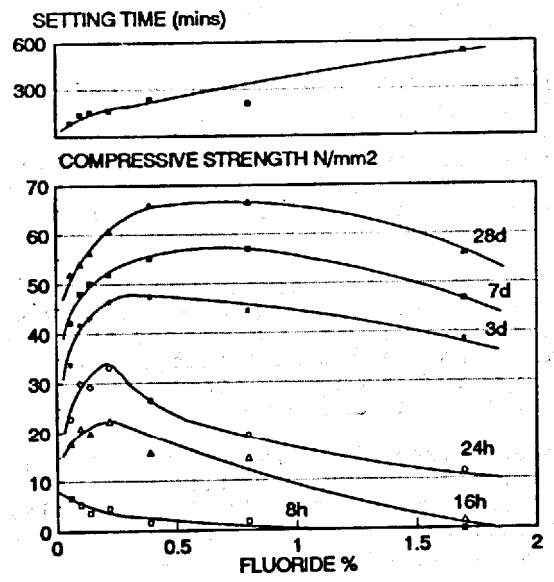

Fig 3. Influence of clinker fluoride level strength development and setting time of high alite cements (62).

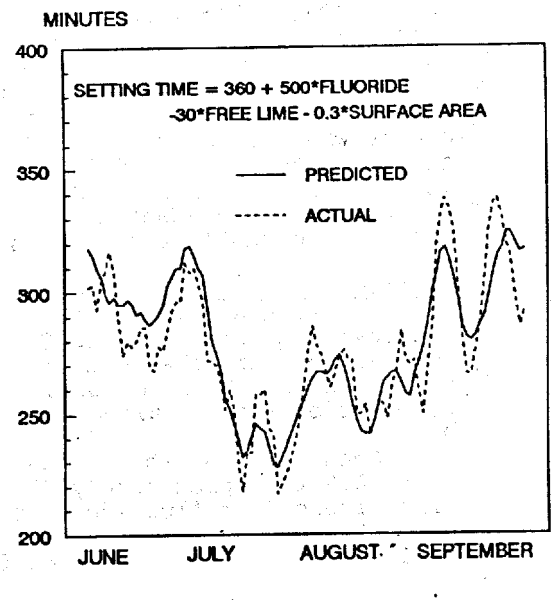

Fig 4. Influence of fluoride on 5°C setting time of production cement.

Production experience where fluoride occurs naturally in the raw materials confirms the importance of controlling the fluoride level. Figure 4 illustrates the influence of clinker fluorine on setting behaviour at 5°C. The relationship

involving surface area, free lime and fluoride has been derived by multiple linear regression analysis. As with the metals Pb, Cu and Zn the retarding action can be attributed to the formation of a barrier layer (in the case of F, insoluble CaF_2), on the surface of the clinker minerals.

Sinclair and Groves (63) found by electron diffraction that the 'rhombohedral' C_3S prepared by Aldous contained a variety of polymorphs, none of them possessing a true rhombohedral lattice. Maki (64) has questioned the existence of rhombohedral C_3S at room temperature. It is apparent that powder X-ray diffraction can disclose the approximate symmetry only, and that the true symmetry may be very complex: indeed, it may vary from crystal to crystal in the same preparation.

The role of fluoride in promoting C_3S formation was re-examined by Perez Mendez et al. Fluoride-substituted, C_3S-like phases were obtained (65). The mechanism of fluoride solid solution was determined by X-ray crystallography; F substitutes for oxygen with concomitant creation of cation vacancies. However, the introduction of F in this manner yields a product of poor reactivity and is thus not as effective in stabilising C_3S or improving its reactivity as is the simultaneous substitution of Si by Al and of O by F, as discussed subsequently.

Palomo, et al (66) studied a mix containing 33.9 wt % of a commercial raw meal to which was added additional limestone, clay, slate and 'pyrites ash' (86% Fe_2O_3) and commercial grade fluorspar (97% CaF_2). The sequence of mineral formation was monitored by infra red, X-ray diffraction and thermal methods. The evolution of phases upon heating differed from normal clinkers; fluoride promoted low-temperature formation of aluminates; fluorinated $C_{12}A_7$, C_3A, and gehlenite although burning at 1250°C and 1340°C gave a relatively normal clinker mineralogy. IR studies disclosed that the belite phase was preserved to ambient as the α'_L phase. The level of fluoride used, 0.2 wt %, did not significantly affect the final aluminate mineralogy; ferrite and C_3A were present at and above 1250°C.

The effect of fluoride at 0.5, 0.75, 1.0 and 1.5 wt % CaF_2 was studied on pellets of clinker raw materials (67). Samples were subject to static heating at one of four temperatures, 1000°, 1200°, 1280° and 1345°, and to dynamic heating, in a DTA. Supplementary examinations by X-ray diffraction and IR were used to confirm the phase development sequence. Clinkering reactions were virtually completed in 0.5 hr static heating at 1345°C; much C_3S developed, together with βC_2S, ferrite and C_3A. The X-ray pattern of the latter resembled proto-C_3A described by Han et al. (68).

Shame and Glasser (61) have suggested that a coupled substitution of F and Al is beneficial to combination and cement properties in agreement with the findings of Aldous (9). With finely divided raw materials it was possible to synthesise the C_3S - Al-F solid solution (named Alfluoral) by solid state sintering at ~1075°C.

As demonstrated in the studies of Imlach (69) the phase $C_{11}A_7.CaF_2$ is not encountered in conventional mineralised clinkers fired at 1350-1450°C and only occurs where clinker fluorine levels are above ~ 0.5% and the clinker has been fired at temperatures below 1320°C or cooled slowly through the temperature range 1340-1260°C. The presence of $C_{11}A_7.CaF_2$ results in rapid setting behaviour (Reg set type cement) in marked contrast to the influence of the same level of fluorine in clinker fired at 'normal' temperatures.

Fluoride and sulfate - Most of the recent research into the use of fluoride as a mineraliser has involved the combination of CaF_2 + $CaSO_4$ (49, 70, 76, 77 a-e). Much interest has been shown in China where the use of CaF_2 + $CaSO_4$ has the potential to improve both the operation of shaft kilns and the cement quality. The research has confirmed that F^- in combination with SO_4^{2-} is a much more effective aid to combination than F^- alone and that strength gains can be achieved at all ages.

Shen Wei (70) showed that in clinkers fired at 1360°C and containing F levels up to 0.91%, approximately 80% of the F is located in the silicates. The effectiveness of fluoride in overcoming C_2S stabilisation by SO_4^{2-} was also demonstrated and it was suggested that the presence of an appropriate level of SO_4^{2-} reduced the adverse effect of fluoride on early hydraulic reactivity.

Giminez-Molina et al (73) examined the combined impact of sulfate and fluoride on cement clinker phases. A reconnaissance of the system $CaO-Ca_2SiO_4-CaF_2-CaSO_4$ was made at temperatures up to ~1300°C, using quenching techniques, supplemented by DTA, XRD, etc. The subsystem $Ca_2SiO_4-CaSO_4-CaF_2$ was found to be ternary, and received the most detailed study. Fig 5 shows its liquidus surface and subsolidus compatibility.

The system contains a ternary phase, fluor-ellestadite, $3C_2S.3CaSO_4.CaF_2$, which is stable up to its incongruent melting point at ca 1240°C. This phase has the

apatite structure and is thus structurally distinct from other phases in this system. The liquidus surface has a large primary phase field of Ca_2SiO_4, the extent of which is of interest to cement making. Ca_2SiO_4 forms a ternary eutectic with CaF_2 and fluor-ellestadite at 1050°C which marks the commencement of melting in a wide range of mineralised C_2S-containing compositions. A critical limit for development of liquid at low temperatures is that the mole ratio of $CaSO_4.CaF_2$ in the charge should not exceed 3.0.

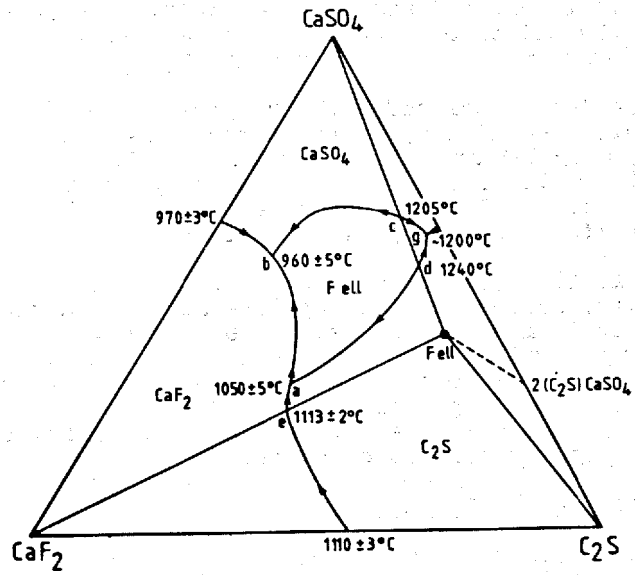

Fig 5. Phase diagram of part of the CaF_2-CaO-SO_3-SiO_2 system (73).

$CaSO_4$ and CaF_2 form joint solid solutions in C_2S. The crystallochemical nature and extent of these solid solutions were not determined, but the consequences are to extend the stability fields of α and α' polymorphs to lower temperatures, perhaps by up to 200°C, with the result that it is readily possible to obtain α and α' C_2S polymorphs at ambient without rapid quenching.

A reconnaissance of the system CaO-C_2S-CaF_2-$CaSO_4$ showed that C_3S was obtained above ~1250°C, but that the presence of F and SO_4 did not provide any special crystallochemical stabilisation for the C_3S phase. This contrasts with the behaviour of systems containing both F and Al, which together have a definite and relatively specific stabilising action for C_3S, permitting C_3S solid solutions to be obtained to as low as 1050°C. These data help confirm constitution of clinkers described by Blanco and colleagues (74, 75) in which partial substitution of CaF_2 and $CaSO_4$ for aluminate and ferrite phase decreased clinker formation temperatures to about 1350°C yet produced a clinker with above 70% alite content. The interstitial clinker phases included the usual aluminates and ferrites, together with fluor-ellestadite.

Several favourable production experiences with the combined mineraliser CaF_2 + $CaSO_4$ (62, 78, 79) and with CaF_2 (80) have also been reported.

Gimenez et al (78) found that during the trial production of 1500t of white Portland cement clinker using a 180 tpd wet process kiln, the addition of 5% gypsum and 2% fluorspar to the raw mix:-

- increased kiln output by ~10%
- reduced fuel consumption by ~15%.

Although the mean level of F and SO_3 in the clinker were 0.69% and 4.4%, which are both higher than considered optimum by Moir (62), cement properties were very satisfactory.

Humpola (79) also reported increased kiln outputs and improved cement strengths when 5% fluorogypsum was included in the raw mix.

The rather small strength improvement obtained by Page (80) when CaF_2 was used as a mineraliser may be attributable to the low potential C_3S contents of the clinkers (41% to 46%) and possibly the low levels of SO_3 in the clinkers (no data given).

In general the greatest 'activation' by F will be achieved when the levels of F, SO_3 and alkalis are controlled and the raw mix LSF, SR and AR are adjusted to maximise clinker C_3S content.

Fluoride and alkali - The phase $KF.2[Ca_6(SO_4)(SiO_4)_2]$ has been reported to occur in cement kilns; its structure, described in (81), is strikingly similar in many respects to that of C_3S and mistaken identification probably helps explain why K, F and S are occasionally reported to occur in large amounts in alite solid solutions. $KF.2[Ca_6(SO_4)(SiO_4)_2]$ is itself not stable to clinkering temperatures but the poor thermal stability of the silicate is enhanced, to at least 1200°C, by replacing (SiO_4) by GeO_4. Sulfate may also be replaced by CrO_4.

One potential problem associated with the presence of fluoride in the raw mix, apart from reduced early reactivity, is the formation of kiln deposits containing spurrite, $2\ C_2S.CaCO_3$ (82, 83) or fluor-ellestadite (84). An advantage however, in this respect, is that the lower burning temperature permitted by fluoride should enable the volatile cycle of alkalis and sulfates to be reduced and thus the tendency for alkali/sulfate based deposits to be reduced.

Fluoride and Boron - Little systematic work has been done on boron in conjunction with fluoride. However, synthesis of an apatite structured phase, $Ca_5(BO_3)_3F$ has been reported (85). It is monoclinic, Cm, a = 8.125, b = 16.051, c = 3.538Å, β = 100.90°. Its stability in melts at 1100°C suggests that it could be an important sink for these two ions in clinker: also, that the range of apatite solid solutions described previously (86) could perhaps be extended to include boron, with the result that apatite solid solutions are viewed as a potential sink for these (and other) ions in a range of mineralised clinkers.

P-Block Elements, including C, S and P

The most commonly encountered p-block elements in Portland cement clinker are sulfur and phosphorous in the forms of SO_4^{2-} and PO_4^{3-}. However carbon is used in fuel and is present, as carbonate, in the raw materials. Carbonate interactions occur in the early stages of clinkering. The interaction between SO_4^{2-} and the alkalis K and Na has a profound influence on the role of S in clinkering and on cement properties and these elements are considered jointly in a subsequent section.

Carbonate - Previous studies of carbonate mineralogy have shown that spurrite, $Ca_5(SiO_4)_2CO_3$ can form at appropriate points in the clinkering cycle. In synthetic studies, spurrite is observed to form slowly and with difficulty from the appropriate reactants. Bolio-Arceo and Glasser (87) reviewed the literature on spurrite formation, noting that various fluxes and combinations of flux, are indeed effective in promoting spurrite formation. Clinker rings in kilns are frequently observed to contain spurrite as well as various combinations of mineralisers - alkali sulfates, fluoride and chloride leading to the supposition that mineralisers are essential. However, spurrite is also observed to form in situations where only negligible concentrations of mineralisers are present, as evidenced by analysis of spurrite itself as well as the ring contents. The authors suggested that spurrite formed by reaction of Ca_3SiO_5 with CO_2: they showed that Ca_3SiO_5 was very reactive with CO_2 atmospheres: $2Ca_3SiO_5 + CO_2(gas) \rightarrow Ca_5(SiO_4)_2.CO_3 + CaCO_3$. Studies of the reaction kinetics showed that 50% of C_3S reacted with CO_2 at 1 bar, 900°C in 60h in the absence of mineralisers. Since C_3S is not stable below ~1250°C, it was suggested that the source of C_3S was kiln dust blown from hot zones, where C_3S was stable, into cooler zones where it collected and reacted with CO_2.

While not essential, mineralisers were effective, as little as 0.2 wt % of either CaF_2 or $CaCl_2$; markedly promoted reaction.

Carbonate-Sulfate - Carbonate also interacts strongly with other components, notably alkali sulfates. The fluxing action of mixed carbonate-sulfate systems was studied by Bolio-Arceo and Glasser (88). Initially the thermodynamics of the reciprocal salt system $CaSO_4$-K_2SO_4-$CaCO_3$-K_2CO_3 system were analysed. Thermochemical calculations showed that the join K_2SO_4-$CaCO_3$ is more stable than the alternative pair, $CaSO_4$-K_2CO_3. The stable join was studied in flowing CO_2 at 1 bar pressure with results in Fig 6. The eutectic, at 43 mol % $CaCO_3$ and 880°C could be attained with only slight decomposition. A noteworthy feature of the system is the extent of solid solution of $CaCO_3$ in K_2SO_4, reaching 20 mol % $CaCO_3$ at 880°C. The solid solution slows the α-β K_2SO_4 inversion. Normally, the transformation is non-quenchable, but the solid solutions are readily obtained at ambient.

The system K_2SO_4-$CaSO_4$ was re-examined and a hitherto unreported phase transformation in $K_2Ca_2(SO_4)_3$ encountered at 200°C. The inversion is associated with a 2.5% volume change which leads to 'dusting' of Ca-langbeinite.

The significance of stability relations was assessed. In the presence of alkali sulfates, $CaCO_3$ can dissolve in melts forming a CO_2-rich liquid phase at temperatures in the range 880°-900°C; at >900°C, the melt loses CO_2 rapidly.

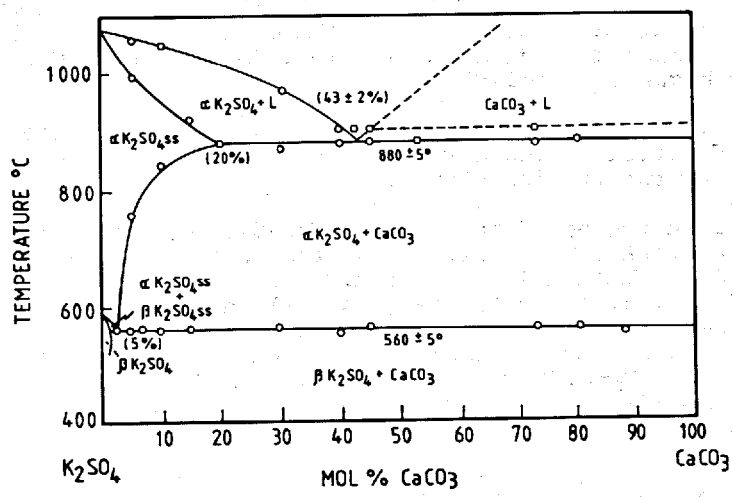

Fig 6. System K_2SO_4-$CaCO_3$ at 1 bar CO_2 pressure. (88).

Sulfur - Gies and Knöfel (89) investigated the influence of sulfur on the relative proportions of alite and belite using commercially available, grades of material. They were very successful in producing hydraulically active, high belite clinkers. They attributed this activity to the presence of 0.6 - 0.8 wt % SO_3 in the belite. Solid solution appeared to be favoured by high SO_3 contents. The rate of clinker cooling was not found to have significant effect on strength development.

Circulation of the alkali sulfates is known to be associated with this relatively high vapour pressure and tendency to evaporate congruently. Data are available for "simple" sulfates, Na_2SO_4 and K_2SO_4, although the literature shows large divergence in numerical values. Choi and Glasser (90) used the Knudsen effusion technique to obtain self-consistent values for Na_2SO_4, K_2SO_4 and a variety of more complex sulfates relevant to clinkering. Data are shown in Fig 7.

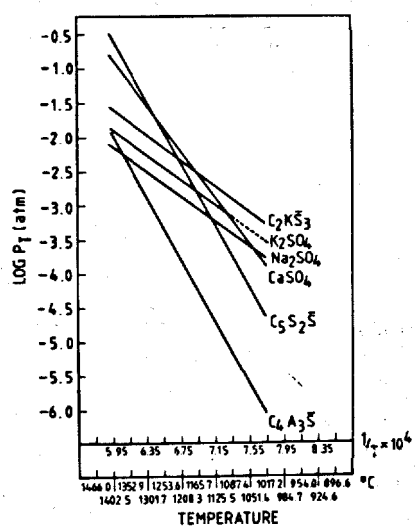

Fig 7. Log plot of the total pressure in atmospheres of the decomposition products of various sulfates occurring in the cement kiln. (90).

The more complex sulfates partially melt and decompose incongruently, eg to vapour and solid. The vapour pressure curves are in good agreement with experiment inasmuch as they predict an upper thermodynamic stability limit for $C_5S_2\bar{S}$, which decomposes above 1250 ±20°C to $CaSO_4$ and Ca_2SiO_4. The magnitude of the species responsible for the pressure function - SO_2, O_2 - is variable in the kiln, but lies roughly in the range 10^{-2} atm. The relative volatility of species is of course very sensitive to temperature, but at 1400°C the order is Na_2SO_4 < $C_4A_3\bar{S}$ ~K_2SO_4 < $C_2K\bar{S}_3$ < $CaSO_4$ < $C_5S_2\bar{S}$; thus the sulfosilicate, which has the lowest vapour pressure at 1000°C has the highest at 1400°C.

Phosphorous - P_2O_5 occurs in both limestone and shale in certain parts of the world and also in industrial by-products which may be used as raw materials, such as slags from the metal extractive industries.

The high lime region of the system, $CaO-SiO_2-P_2O_5$, was studied extensively by Gutt (91) and co-workers. At clinkering temperatures C_2S forms an extensive solid solution with C_3P ($3CaO.P_2O_5$). With increasing levels of P_2O_5 the C_2S adopts ß, then α symmetry. The dicalcium silicate is stabilised to the detriment of C_3S formation and with incremental additions of P_2O_5 a progressive reduction in C_3S content is observed (92). At P_2O_5 levels above ~1%, CaO is compatible at sub-solidus temperatures with a C_2S:C_3P solid solution and a C_3S solid solution containing 1.1% P_2O_5. The complex phase relations can be interpreted using the published phase diagrams (91).

The influence of P_2O_5 on combinability has been investigated by adding hydroxy apatite, $Ca_5(PO_4)_3.OH$, (17). At 1300°C, free lime levels increased in proportion to P_2O_5 content. This can be attributed to the stabilisation of C_2S ss and is predicted to occur from the revised phase relations (91).

Halicz (92) investigated the difficulties associated with using an oil shale containing up to 5% P_2O_5 as a secondary component. Although C_3S contents decreased markedly when P_2O_5 levels increased, satisfactory C_3S contents were achieved by including P_2O_5 in revised LSF and SR calculations and maintaining these at 1.0 and 2.75 respectively.

Figure 8 illustrates the influence of clinker P_2O_5 on the strength development of cements containing a range of clinker alkali levels (93). Calcium sulfate was incorporated in the raw mixes to ensure the clinker SO_3 level was slightly in excess of the molar eq Na_2O level. Thus, the alkalis were predominantly present in water soluble form (94). At 3 days, strengths were reduced progressively by P_2O_5, particularly at levels above 1.0%. This reduction was less, however, in the cements with high alkali contents. At 28 days, the expected reduction in strength with increasing alkali level was clearly evident in the cements with 0.05% P_2O_5. However, the highest 28 day strengths were given by high alkali cements containing P_2O_5 levels of 2.0%. Thus, appropriate levels of P_2O_5 have the potential to reduce the negative influence of clinker alkalis on 28 day strengths. In the clinkers with more 'normal', eg Na_2O levels of 0.8% the maximum 28 day strengths was obtained at a P_2O_5 level of 1.0%.

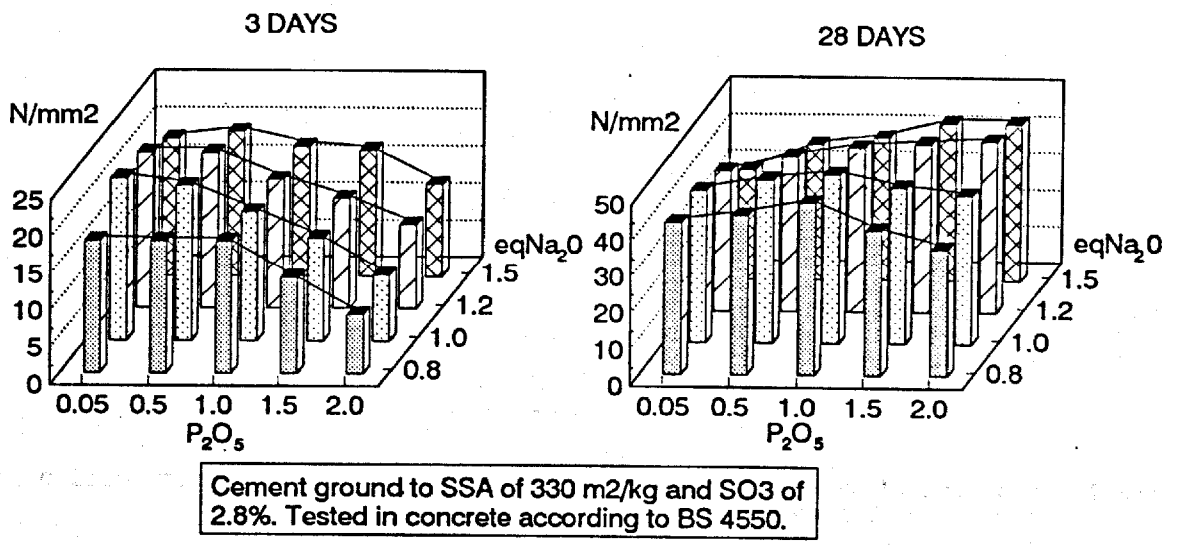

Fig 8. Influences of clinker P_2O_5 and alkali level on strength development. (93)

Matkovic (95) found that α' C_2S stabilised by P_2O_5 had a higher hydraulic activity than ßC_2S.

Fluorine appears to counteract the stabilising effect of P_2O_5 on C_2S (91). The quantity of F required to produce a clinker of normal microstructure is a function of the P_2O_5 level (96). Presumably the thermodynamics of the system favour the fluorine/aluminium C_3S solid solution rather than the phosphorous C_2S solid solution.

Boron - Boric oxide, B_2O_3, is a well-known flux in the ceramic industry and may be present in cement making raw materials. Its application to cement clinkering has, however, been less successful. Timashev (6) has noted that a correlation exists between electronegativity of the element and viscosity of melts; boron was found to be similar to phosphate and sulfate; its presence inhibits C_3S formation. Nevertheless other factors, notably the extent of solid solution of borate in the calcium silicates, affects stability relationships amongst the major clinker phases. It will be recalled that the free energy of formation of Ca_3SiO_5, relative to Ca_2SiO_4 and CaO, is only slightly negative ie, only slightly favourable for Ca_3SiO_5 formation at temperatures above ca 1250°C (97). The impact of boric oxide upon this balance of free energies is a paramount consideration in evaluating its success as a flux.

The $CaO-B_2O_3-SiO_2$ system has been studied previously (98, 99) but these studies disagree in several important respects. Flint and Wells (98) found a ternary phase, to which they assigned the composition C_5BS; Suzuki and Hira (99) found what is presumed to be the same phase, but reported its composition as $C_{11}S_4B$. They identified two polymorphs and inferred cell dimensions for the high temperature, or α, phase as a = 55.43, b = 10.65 and c = 6.89Å; α = β = = 90°C. Unpublished studies at the University of Aberdeen (100) confirm the occurrence of two polymorphs, but electron diffraction, while confirming the orthogonality of the α polymorph gave its cell dimensions as a = 17.828 12,, b = 15.950 (12), c = 6.877 (4)Å. The β, or low temperature polymorph, is monoclinic; a = 28.61, (2), b = 15.974 (9), c = 6.874 (8)Å; α = β = 90°C; = 104.1(1)Å: this non-standard setting is chosen to show similarity of the b and c dimensions between the two. Infra-red patterns were interpreted as indicating the presence of BO_3 groups in both α and β phases.

Borate-containing C_2S solid solutions were also examined by FTIR and XRD (100) and found to contain BO_3 groups; solid solutions extended along the join towards $3CaO.B_2O_3$. The general formula for the solid solution is:-

$$Ca_{2-0.5x}[SiO_4]_{1-x}[BO_3]_x$$

Substitution of borate for silicate is postulated to be accompanied by the introduction of Ca vacancies. After complete reaction, and with subsequent fast cooling to ambient temperature in 10 to 30 seconds, the relationship between the value of x and the belite polymorph obtained was as follows:-

C_2S	=	x =0
βC_2S:	=	x ~0.02
α'C_2S:	=	x ~0.16
α-like C_2S	=	x ~0.33

The nature of the product obtained at the higher limits of x was not conclusively determined.

Despite the extensive solid solution of boric oxide encountered with C_2S, little if any solid solution was found to occur in C_3S. Indeed, borate appeared to de-stabilise C_3S with respect to its decomposition:-

$$C_3S \rightarrow C_2S + CaO$$

Fig 9 shows the effect of borate. Phase pure C_3S, made by repeated firing of chemically-pure reagents in Pt crucibles, was used. This C_3S, verified by powder X-ray diffraction and chemical free lime determinations showing ≤1% free CaO was mixed with 2.8 wt % B_2O_3 and re-fired. The rapidly-cooled material was re-analysed for free lime.

Decomposition at 1200°C is not unexpected, in view of the lower limit of thermal stability of C_3S at about 1250°C, but at 1270°C and 1400° - especially at the latter temperature - Ca_3SiO_5 should be stable. Instead, decomposition occurred in the presence of borate at all temperatures up to 1700°C and the rate of decomposition became progressively more rapid upon increasing the isothermal firing temperature.

The levels of minor components, particularly heavy metals need to be monitored closely in raw materials and fuels, not only because of their influence on cement properties but also their potential environmental impact.

It was not possible to extend the results quantitatively to >1400°C, but qualitative observations showed that small amounts (1-2 wt %) of boric acid resulted in decomposition, with partial melting, of preformed phase-pure C_3S at temperatures up to ~1700°C. Fig 10 shows schematically a liquidus diagram of part of the CaO-SiO_2-B_2O_3 phase diagram. It illustrates the decomposition of C_3S above 1700°C at liquidus temperature: its decomposition allows C_2S, CaO and melt to co-exist at lower temperatures, including those relevant to clinkering. A fuller review, with new data is being prepared (101). Thus boric oxide is not a useful additive in

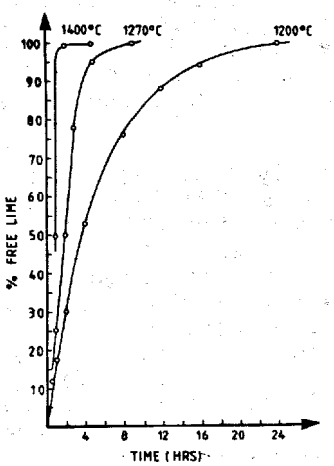

Fig 9. Time transformation curves for the decomposition of 2.8 wt % B_2O_3 doped C_3S.

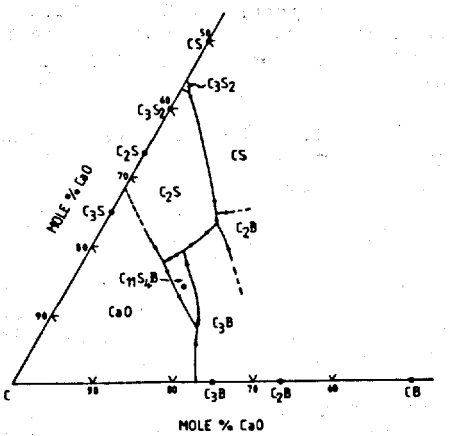

Fig 10. High lime portion of the CaO-B_2O_3-SiO_2 system.

those modern cements which depend on C_3S for early strength development but might be of interest as a mineraliser for belitic clinkers.

As with P_2O_5 the presence of fluorine overcomes the stabilisation of C_2S and a normal clinker microstructure results.

Other p-block elements - The elements As, Se, Tl, Pb are of interest on account of their toxicity and their volatility, and the consequent potential for emission to the environment. Most cement companies maintain close control over the inputs of these elements and no more than trace levels will be encountered in clinker and the influence on cement properties is thus negligible.

Miscellaneous - mixed fluxes systems

The use of mixed flux systems has been reported (71). These were applied in plants facing problems of low production, poor quality clinker and high fuel costs. Combinations which proved most effective were (CaF_2 + $MgCO_3$), ($CaHPO_4$ + $BaHPO_4$) and (CaF_2 + $MgCO_3$ + $CaSO_4$). The latter combination, giving a clinker batch with 0.5 wt % as F, 1% Mg as $MgCO_3$ and 1% S as SO_3, was found to give the best results. Another, only slightly less promising combination, was a mixture of ZnO + $CaHPO_4$. In general, mixed fluxes were always found to be superior to the same components used singly. Only general explanations were offered to explain the empirical test data.

5. MICROSTRUCTURE

The influences of clinker thermal history and the presence of minor components such as MgO and SO_3 on clinker microstructure have been reviewed by Maki (64, 102). The chemical and physical properties of the interstitial melt have a considerable influence on the nucleation and growth of alite crystals. The nucleation rate is strongly dependent on the degree of supersaturation and the viscosity of the liquid phase. In general, nucleation is favoured both theoretically and thermodynamically by high clinkering temperatures.

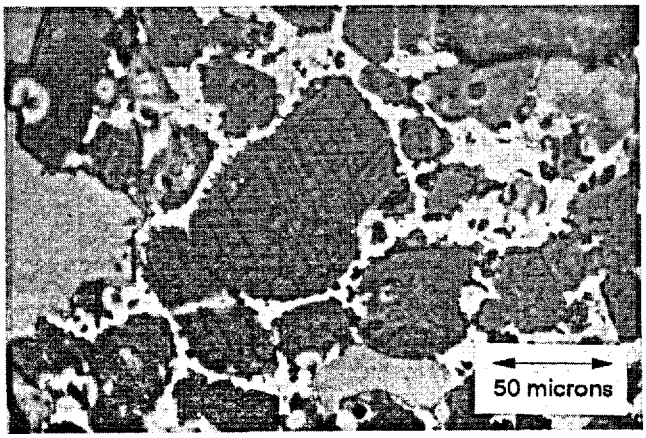

Figure 11. 1.1% Mn_2O_3. Partial reduction and re-oxidation.

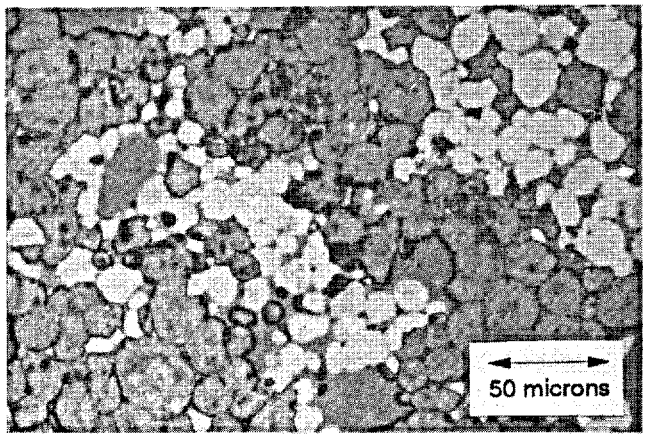

Figure 12. 3% B_2O_3 in white Portland cement clinker. Fired at 1500°C.

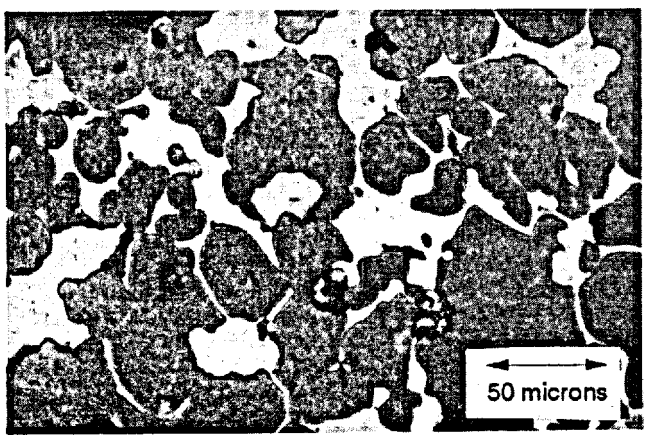

Figure 13. High SR clinker C_2S stabilised by SO_3. Fired at 1375°C.

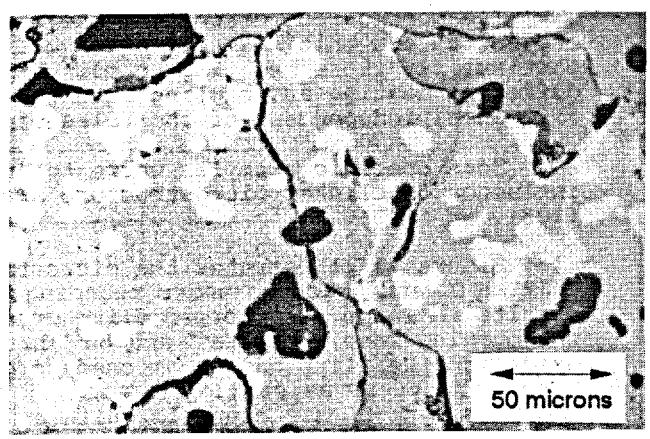

Figure 14. Same raw mix as Figure 13 but fired at 1525°C.

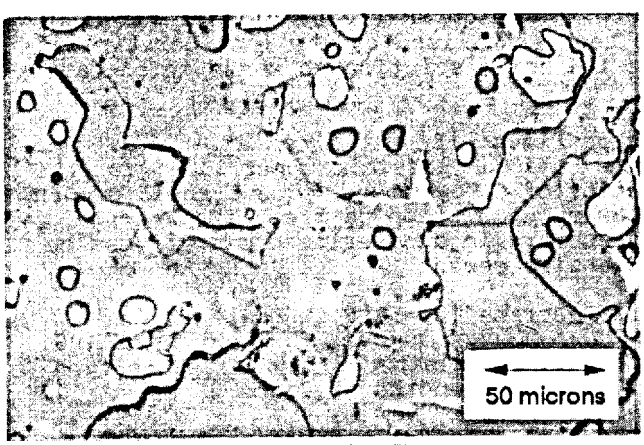

Figure 15. Mineralised clinker containing SO_3 and fluoride.

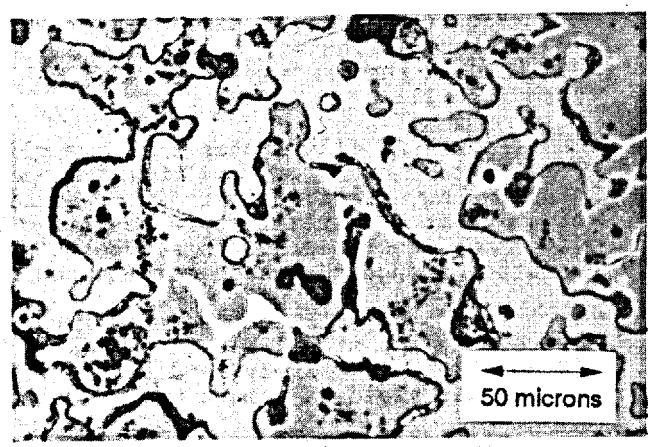

Figure 16. Mineralised clinker containing SO_3, fluoride and K_2O (in form of calcium langbeinite).

At high growth rates, in the early stages of crystallisation when the melt supersaturation is high, the alite can entrap inclusions of liquid, belite or free lime. At low growth rates, such as occur normally during the later stages of clinkering, no appreciable inclusions occur. Thus, defects and dislocations tend to be concentrated at the cores of the crystals.

Re-crystallisaton of alite can also occur in the later stages of clinkering, thus altering morphology to a considerable extent.

Rapid heating rates tend to favour nucleation and the production of a large number of relatively small alite crystals. Slower heating rates tend to produce a smaller number of large alite crystals.

The clinker microstructure is influenced to a considerable degree by the main chemical parameters of LSF, SR and AR, but also by the presence of minor components.

As discussed in previous sections, the minor components affect the

- temperature of first liquid formation
- liquid viscosity and surface tension
- relative thermodynamic stability of the clinker minerals
- polymorphism of clinker minerals.

The conclusions drawn from the microscopic examination of clinker can be rather subjective and this makes it difficult to compare observations in the literature, particularly those relating to clinker 'texture' and alite morphology. The different heating and cooling rates used by different workers also have a marked influence, independent of the roles of the minor components.

Some specific examples where the presence of minor components has had a clear influence on clinker microstructure are given in the remainder of this section, (103).

Figure 11 illustrates the microstructure of a production clinker containing 1.1% Mn_2O_3 and produced under reducing conditions. The low viscosity melt phase results in large well formed alite crystals. As a result of reducing conditions in the burning zone, both Fe^{2+} and Mn^{2+} have entered into solid solution. On re-oxidation the alite has decomposed to give ex solution lamellae of a Mn substituted C_2F which appear as striae in a matrix of C_2S. Mn^{3+} reduces more readily than Fe^{3+} and this type of structure is quite common in clinker from this source.

Figure 12 illustrates the stabilisation of C_2S in a white Portland cement clinker containing 3% B_2O_3. Although fired to a temperature of 1500°C (and water quenched from 1300°C) no alite has been formed and belite coexists in contact with free lime.

Figure 13 shows a similar microstructure in a high SR (10.0) clinker fired at 1375°C for 30 minutes, in which the C_2S has been stabilised by the incorporation of 8% $CaSO_4$ in the raw mix. As with B_2O_3, the C_2S solid solution coexists in contact with free lime.

Figure 14 illustrates the same clinker as Figure 13, but fired at 1525°C. The volatisation of SO_3 at the higher temperature (and the possible upper limit for the stabilising effect) results in de-stabilisation of C_2S with subsequent rapid growth of alite at high temperature resulting in the encapsulation of free lime. Long (104) has described how this type of microstructure in an overlimed clinker can be used to produce shrinkage compensated or expansive cement.

Fig 15 illustrates the effectiveness of fluorine (0.15% F in clinker) in overcoming the stabilisation of C_2S by SO_3. The clinker had LSF, SR and AR of 100, 10 and 2.0 respectively, and after firing at 1400°C contained 3.5% SO_3. This type of clinker yields a cement with exceptionally high strengths at 7 and 28 days.

Figure 16 illustrates a clinker with the same chemical parameters but with a K_2O content of 1.4% and a Na_2O content of 0.1%. The SO_3 is predominantly present in the form of calcium langbeinite ($K_2SO_4.2CaSO_4$). This type of clinker yields cements with exceptional early and late strengths as described by Moir (62). Note the high clinker porosity associated with the low volume and low surface tension of the melt.

6. ENVIRONMENTAL IMPACTS

The environmental impacts of the deliberate introduction of minor components (to achieve a mineralising, fluxing or activating effect) can be considered with reference to the following aspects:-

- toxic emissions and leachates
- NO_x and SO_2 emission
- fuel consumption
- CO_2 emission.

Toxic Emission and Leachates

The German Clean Air Regulations (1986) contain the following limits for emissions of trace elements. (105).

Cadmium, mercury and thallium are placed in category I on account of their volatility and toxicity.

Of the elements covered by the German Regulations, and therefore likely to have an adverse effect on the environment, only fluoride and possibly chromium are likely to be added deliberately to mineralise and/or activate clinker.

As discussed earlier, the deliberate introduction of chromium containing materials to the cement-making process should be discouraged on account of its association with dermatitis (106). Nevertheless, Weisweiler and Kromar (107 have confirmed that chromium has a very low volatility and remains fully combined in the clinker.

Class	Element	Mass flow in g/h	Limit in mg/m^3
I	Cd, Hg, Tl	>1	0.2
II	As, Co, Ni, Se, Tc	>5	1.0
III	Sb, Pb, Cr, F, Ca, Mn, Pt, Pd Rh, V, Sn	>25	5.0

Comprehensive sampling from operating cement plants (108) has confirmed that fluoride is not emitted in gaseous form on account of the large excess of CaO which ensures combination as CaF_2.

The fluoride enrichment in dusts arising from kiln systems is low (normally less than a factor of two compared to that in the kiln feed) and any fluoride which escapes the dust collecting equipment is in the form of CaF_2 which is insoluble and relatively harmless to the environment.

The concern has also been expressed that toxic minor components present in clinker could leach from concrete or mortar and cause contamination. Fortunately, the low solubility of the heavy metals in the high pH pore solution and the low permeability of cement paste (109) ensure a very low potential for leaching.

The levels of heavy metals in dusts arising from the less thermally efficient processes also need to be considered. Disposal to landfill could result in contamination of ground water.

NO_x Emissions

Nitric oxide, NO, is formed in the kiln system as a result of thermal oxidation of nitrogen in the combustion air and also from the decomposition of nitrogen compounds contained in the fuel. A proportion of the NO may be oxidised to NO_2 and N_2O_4 and the term NO_x is used to describe an uncertain or variable mixture of the three oxides.

The quantity of thermal NO_x formed is closely related to burning zone temperature (BZT). Lowes and Evans (110) showed that a reduction in BZT from 1500°C to 1300°C could reduce NO_x levels by 200/400 ppm.

The combined use of F^- and SO_4^{2-} in appropriate proportions, can enable BZT temperatures to be reduced by 100-180°C (62, 111). Thus, the use of mineralisers such as F^- and SO_4^{2-} could provide a viable means of lowering NO_x emissions.

SO_2 Emissions

It is expected that an SO_2 emission limit of between 400 and 800 mg/m^3 (dry)

will be introduced in most European countries in the near future. Emissions of SO_2 are dependent upon process type (wet, long dry, grate preheater, cyclone preheater, precalciner, etc.) and upon the forms in which sulfur is present in the raw materials (112).

The impending legislation is likely to inhibit the deliberate introduction of additional SO_4^{2-} to wet, long dry or grate preheater kilns on account of the losses of SO_2 which occur to the atmosphere. These can however, be minimised by ensuring an adequate excess of combustion air. In cyclone preheater and precalciner kilns there is minimal loss of S introduced either as sulfates in the raw material or sulfur in the fuel. Thus, in modern kiln systems, environmental considerations should not restrict the use of the mineraliser pair F^- and SO_4^-.

Fuel Consumption

Although some rather optimistic claims have appeared in the literature for potential energy savings realisable by the use of mineralisers and fluxes, when efficient heat recuperation from the clinker cooler is considered a BZT reduction of 200°C can be expected to yield an energy saving of less than 5%. (113).

CO_2 Emissions

Carbon dioxide is increasingly perceived as a pollutant because of its alleged contribution to 'global warming'.

Total CO_2 emissions per tonne of pure Portland cement produced are 0.90-1.25 tonnes. The lower figure is for an efficient cyclone preheater/precalciner plant and the higher for a wet process plant; the figures include electricity generation using fossil fuels (0.1-0.15 tonnes CO_2 per tonne of cement).

For an efficient plant, more than half of the CO_2 is derived from decarbonation. Thus, there would appear to be potential to lower emission by producing lower limed cements. However, a reduction in clinker C_3S from 60% to 35% only reduces CO_2 emissions by ~ 3%, even assuming a 100°C reduction in BZT.

One area where major reductions can be made is in increasing clinker hydraulic activity to enable increased replacement of clinker by materials such as quenched blastfurnace slag, fly ash and limestone, whilst maintaining satisfactory cement properties. Figure 17, taken from Long (104), illustrates that cement containing 40% fly ash can have similar strength development characteristics to pure Portland cement if the base clinker is mineralised using F^- and SO_4^-, has a high C_3S content and contains an appropriate level of alkali (114).

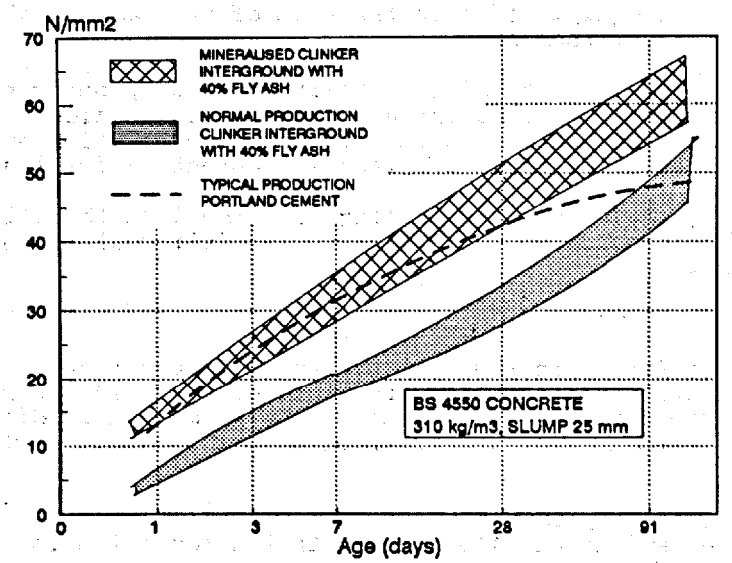

Fig 17. Figure illustrating increased clinker replacement by fly ash made possible by high alite mineralised clinker.

Thus, the application of mineralisation technology to maximise clinker strength properties, offers the potential to both reduce CO_2 emissions and also increase the utilisation of industrial wastes.

7. SUMMARY AND OUTLOOK

Minor chemical components are inevitably present in cement clinker, originating from raw materials and fuels. Their presence affects both the clinkering process and cement properties. During the period under review, substantial progress has been made in understanding the impact of selected minor components on clinker properties. The interactions between the major components and complex mixtures of minor components are, however, less well understood.

There nevertheless exist a number of technological pressures to quantify the impact of minor components on clinker properties. One such pressure is the need to produce cements with equivalent properties; the minor components are largely responsible for the differences in the characteristics of cements from different sources. Secondly, the industry is under pressure to curb emissions and, if possible, reduce specific fuel consumption. Minor components may be used to enhance the clinkering process, but a firm physiochemical basis for their action is only just being established; estimates of the potential energy savings vary, from marginally useful to substantial. The greatest energy savings are likely to be realised at thermally inefficient cement plants. Combustion of substitute fuels, including undesirable waste products, such as spent lubricating oils, industrial solvents, etc, offer the potential to reduce coal consumption and provide positive environmental benefits. Care is necessary in the selection of these materials as they may introduce undesirable levels of minor components.

The environmental implications of cement manufacture and use continue to receive study. The levels of minor components, particularly heavy metals, need to be monitored closely in raw materials and fuels; not only because of their influence on cement properties but also their potential environmental impact. Reduction of gaseous emissions, especially SO_2 and NO_x, will benefit from advances in combustion technology, but control over CO_2 emissions will be more difficult to achieve. One approach which shows promise is the utilisation of the mineraliser pair CaF_2 and $CaSO_4$ to produce reactive, high C_3S clinkers, which permit higher levels of replacement by materials such as fly ash and blastfurnace slag and thus a significant reduction in the quantity of CO_2 released per tonne of cementitous binder. The review of the literature has revealed that fluoride, either alone or in combination with sulfate, is the only minor component which has been successfully introduced at a number of locations on the industrual scale with benefit to the production process and cement properties.

Concrete emerges as an inexpensive, flexible, durable and relatively environmentally friendly material. Therefore, its future potential remains bright. However, improved manufacturing technology is essential if the basic raw material, Portland cement, is to realise its potential.

REFERENCES

1. Bucchi, R.: "Feature on the role of minor compounds in cement clinker - Part 1." World Cement Technology, 1981, June, 210-231.

2. Subba Rao, V. V. et al: "Utilisation of inferior grade raw materals and industrial wastes in cement manufacture." All India Seminar on Cement and Allied Building Materials, New Delhi, 1984, p.I, 136-152.

3. S. Sprung: "Technological problems in pyroprocessing cement clinker: cause and solution". 1985, VDZ Publication, Beton-Verlag, 129p.

4. Maury, H.D. and Pavenstedt, R.G. "Comparison of emissions of elements affecting the environment", Zem-Kalk-Gyps, 1989, No 2, 90-93.

5. Lea, F. M. and Parker, T. W.: "Investigation of a portion of the quaternary system $CaO - Al_2O_3 - SiO_2 - Fe_2O_3$: the quaternary system $CaO - C_2S - C_5A_3 - C_4AF$." Phil. Trans. R. Soc. 1934, 234, No 731, 1.

6. Timashev, V.V.: "The kinetics of clinker formation: the structure and composition of clinker and its phases." 7th ICCC, 1980, Vol 1, p.I-3/1.

7. Boikova, A.I.: "Chemical composition of raw materials as the main factor responsible for the composition, structure and properties of clinker phases". 8th ICCC, 1986, Vol 1, 17-33.

8. Akimov et al; "Defectuosites de structure et activite d'hydration des mineraux entrant dans le clinker du ciment portland." 8th ICCC, 1986, Vol III, 260-265.

9. Aldous, R.T.H. "The hydraulic behaviour of rhombohedral alite", Cement and Concrete Res., 1983, 13, 89-96.

10. Gourdin et al. "Polymorphisms de l'alite et du C_3A. Statistiques". 7th ICCC, 1980, Vol II, 223-228.

11. Puertos, F. and Trivino, F. "Modifications, clinker phase and mechanical strength in relation to type of quenching". 8th ICCC, 1986, Vol II, 228-233.

12. Baragano, J.R. and Campos, G., "Extension of setting time by means of mineralised clinkers", 8th ICCC, 1986, Vol III, 211-216.

13. Gies, A., and Knöfel, D. "Influence of alkalis or the composition of belite-rich cement and the technological properties of the resulting cements". Cement and Concrete Res., 1986, 16, [3], 411-422, 1986, 16 [3], 411-422.

14. von Lampe, F. and Seydel, R. "On a new form of β Belite". Cement and Concrete Res., 1989, 19, 509-518.

15. Strunge, J., Knöfel, D. and Driezler, I. "Influence of alkalis and sulfur on the properties of cement". Zem-Kalk-Gyps, 1986, 39, 380-386.

16. Richartz, W. "Effect of the K_2O content and degree of sulfatization on the setting and hardening of cement". Zem-Kalk-Gyps, 1986, 12, 678-687.

17. Odler, I. and Abdul-Maula, S. "Effect of mineralisers on the burning process of Portland cement clinker, Part 1: Kinetics of the process." Zem-Kalk-Gyps, 1980, No 3, 132-136.

18. Odler, I and Abdul-Maula, S. "Effect of mineralisers on the burning process of Portland cement clinker, Part 2: Mode of action of the mineralisers," Zem-Kalk-Gyps, 1980, No 6, 278-282.

19. Sersale, et al. "A study on the utilisation of an Italian steel slag". 8th ICCC, 1986, Vol II, 194-198.

20. Kuznecova, T. V., et al. "Application of cement modified by titanium-manganese production waste". C.T. URSS. 1985, No 12, 8.

21. Dmitrieva, G.G. et al. "The intensification of clinker formation with the aid of barium-manganese wastes", C.R., URSS, 1986, 3, 18.

22. Hornain, H. "Sur la repartition des elements de transition et leur influence sur quelques propriétés du clinker et du ciment". Revue des Materiaux de Construction, 1971, No 671-672, 203-218.

23. Herath Banda, R.M. and Glasser F.P., "Role of iron and aluminium oxides as fluxes during the burning of Portland cement". Cement and Concrete Res., 1978, 8, 319-324.

24. Knöfel, D. and Gies A. "Effect of high manganese and alkali contents on the composition of high belite clinker and on cement properties", Silikattechnik, 1988, 39, No 4, 119-120.

25. Fierens, P. and Tirlocq, J. "Nature and concentration effect of stabilising elements of βC_2S on its hydration rate". Cement and Concrete Res., 1983, 13, 267-276.

26. Bie, R. and Ludwig, U. "Hydraulic reactivity of belite rich Portland cement", Zem-Kalk-Gyps, 1990, 10, 506-510.

27. Ludwig, U. and Pohlmann, R. "Investigations on the production of low lime Portland cements. 8th ICCC, 1986, Vol II, 363-371.

28. Knöfel, D. and Gies A. "Effect of high manganese and alkali contents on the composition of high belite content clinker and on cement properties" Silikattechnik, 1988, 39, No 4, 119-120.

29. Subba Rao, V.V. and Narang, K.C." Potentials of making active belite cements with chromium oxide as modifier". Zem-Kalk-Gyps, 1987, 8, 434-437.

30. Feng Xiuji and Long Shizang. "Investigation of the effect of minor ions on the stability of βC_2S and the mechanism of stabilisation". Cement and Concrete Res., 1986, 16, 587-601.

31. Teorneau, I. et al. "The influence of Cr_2O_3 micro additions on the chemical and mineralogical composition of Portland cement clinkers". 7th ICCC, 1980, II, I-90-94.

32. Teoreanu et al. "Addition of titanium dioxide to Portland cement clinkers". Il Cimento, 1987, No 4, 397-404.

33. Knöfel, D. "Relationships between chemistry, phase content and strength in Portland cements". Zem-Kalk-Gyps, 1979, 32, 448-454.

34. Marinho, M. B. and Glasser, F. P. "Polymorphism and phase changes in the ferrite phase of cements induced by titanium substitution", Cement and Concrete Res., 1984, 14, 360-368.

35. Palomo, A. and Glasser, F. P. "Solubility of magnesium oxide in selected clinker phases". 1989, Advances Cement Res. 2, no 6, 55-59.

36. Puertas, F. et al. "Influence of the kiln atmosphere on manganese solid solution in C_3S and C_2S". Cement and Concrete Res., 1988, 18, 783-788.

37. Puertas, F. et al. "Modification of the C_3A phase in cements by manganese substitution". Cement and Concrete Res., 1988, 18, 837-842.

38. Feng Xiuji and Yan Peiyu. "Effect of the states of chromium ion on the colour characteristics of doped βC_2S", Advances in Cement Research, 1990, 3, No 10, 85-88.

39. Knöfel, D. et al. "Effect of manganese on the properties of Portland cement clinker and Portland cement". Zem-Kalk-Gyps, 1983, 7, 402-408.

40. Odler, I. and Schmidt, O. "Structure and properties of Portland cement clinker doped with zinc oxide". J. Am. Ceram. Soc., 1980, 13-16.

41. Kakali, G. et al." Hydration and strength development of cements produced from raw mixes containing MoO_3, Nb_2O_3, WO_3 and Zr_2O_3". Cement and Concrete Res., 1989, Vol 19, 968-972.

42. Sakurai et al. "The effect of minor components on the early hydraulic activity of the major phases of Portland cement clinker". 5th ICCC, 1968, I, 300-321.

43. Avliguie, G. and Grondet, J. "Influence of the composition of a cement on its hydration in the presence of zinc". Cement and Concrete Res., 1990, 20, 517-524.

44. Negro, A. et al. "Vanadium pentoxide: effect on hydration of C_3S and C_3A in the presence of gypsum and lime". Il Cimento, 1985, 1, 41-48.

45. Double, D.D. "New developments in understanding the chemistry of cement hydration". Phil. Trans. R. Soc. Lond., 1983, A. 310, 53-66.

46. Tashiro, C. "The effects of several heavy metal oxides on the hydration and microstructure of hardened mortar of C_3S," 7th ICCC, 1980, II-37-42.

47. Coerdt, W. and Mainka, E. "Versuche zur jodbestimmuns in boden-und staabfilterproben". 1985, Fresenius Z. Anal. Chem. 320, 656.

48. Berry, E.E. and McDonald, L.P. "Experimental burning of used automotive crankcase oil in a dry process cement kiln." 1975/76. J Hazardous Materials, 1, 137.

49. Osokin, A.P. and Potapora, E.N. "Alite formation in oxide salt melts". Silikatttechnik, 1989, 7, 229-234.

50. Nudelman, B. J. "Structure and properties of alinite and alinite cements". 7th ICCC, 1980, Vol III, V, 169-74.

51. Ftikos, C. et al "Preparation and hydration study of alinite cement." Cement and Concrete Res., 1991, 21, 1129-1136.

52. Agarwal, R.K. "Chloride salts as reactive medium for low temperature clinkerisation - a probe into alinite technology". 8th ICCC, 1986, II, 327-333.

53. von Lampe, F., Jost, K.H. and Wallis, B. "Synthesis, crystal structure and properties of a new calcium-magnesium monosilicate chloride $Ca_8Mg[SiO_4)_4Cl_2$". Cement and Concrete Res., 1986, 16, (5), 624-632.

54. Locher, F.W. "Low energy clinker". 8th ICCC, 1980, Vol 1, 57-67.

55. Kurdowski, W. "Bromide alinite", Cement and Concrete Research, 1987, 17. 361-364.

56. Tong Damao and Yao Daxi. "Using composite mineraliser of $CaCl_2$ and $CaSO_4$ in clinker formation of Portland cement." 1985, Beijing International Symposium on Cement and Concrete, Vol 1, p. 212.

57. Chen, M. and Fang, Y. "The chemical composition and crystal parameters of calcium chlorosulfatosilicate" Cement and Concrete Res. 91 184-188 (1989).

58. von Lampe, F., Grimmer, A.R. and Wallis, B. "Preparation and characterisation of the calcium silicate sulfate chloride $Ca_4(SiO_4(SO_4)Cl_2$" Cement and Concrete Res., 1989, 19, 595-602.

59. Gutt, W. "Manufacture of Portland cement from phosphate raw materials". 5th ICCC, 1968, I, 93-105.

60. Welch, J.H. and Gutt, W. "The effect of minor components on the hydraulicity of the calcium silicates." 4th ICCC, 1960, I, 59-68.

61. Shame, E.G. and Glasser, F.P. "Stable C_3S solutions containing fluorine and aluminium made between 1050°C and 1250°C". Br. Ceram. Trans. J. 1987, 86, 13-17.

62. Moir, G.K. "Improvements in the early strength properties of Portland cement". Phil. Trans. Roy, Soc., 1983, A 310, 127-138.

63. Sinclair, W. and Groves, G.W. "Transmission electron microscopy and X-ray diffraction of doped tricalcium silicate". J. Am. Ceram. Soc., 1984, 325-330.

64. Maki, I. "Relationship of processing parameters to clinker properties; influence of minor components". 1986, 8th ICCC, I, 34-47.

65. Pérez-Méndez, M., Faxos, J., Howie, R.A., Gard, J.A. and Glasser, F.P. "Calcium fluorosilicates: the $Ca_{6-0.5x}SiO_2O_{10-x}F_x$ phase". Cement and Concrete Res., 1985, 15, 600-604.

66. Palomo, A., Vásquez, T., Blanco-Varela, M.T. and Puertas, F. "The mineraliser effect of fluorspar in relation to the form of addition to an industrial raw mix". T1Z Fachberichte, 1985, 109, (10), 752-755.

67. Pérez Méndez, M., Trviño, Vásquez, F., Vásquez Moreno T. and Madrid, E. "Effect of fluorine on extracted phases from Portland cement clinker", T1Z Fachberichte, 1986, 110, (4), 286-291.

68. Hans, K.S., Gard, J. and Glasser, F.P. "Composition of stable and metastable C_3A solid solutions crystallised from simulated clinker melts". Cement and Concrete Res., 1981, 11, 79-84.

69. Imlach, J.A. "The influence of heating conditions on the production of fluorine containing Portland cement clinker". Cement Technology, 1974, 5, 403-406.

70. Shen Wei and Feng Minsfen. "A study on the effects of CaF_2 on clinker doped with compound mineraliser". 8th ICCC, 1986, Vol II, 111-116.

71. Surani, M.S. and Joshi, S.N. "Use of mineralisers and fluxes for improved clinkerisation and conversation of energy." Zem-Kalk-Gyps, 1990, 43, 43-47.

72. Damao Tong and Zongshau Lin. "The role of CaF_2 and $CaSO_4$ in cement clinkering". 8th ICCC, 1986, Vol II, 117-121.

73. Giminez-Molina, S., Teresa Blanco, M., Marr, J. and Glasser, F.P. "Phase relations in the system Ca_2SiO_4-CaO-$CaSO_4$-CaF_2 relevant to cement clinkering." Advances in Cement Research, 1991/2, 4 no 4, 81-86.

74. Blanco-Varela, M.T. and Vasquez, M.T., Ahorro de energia en la clinkerizacion empleando CaF_2 y $CaSO_4$ como mineralizadores. Estudio de la fluorellestadite. Mater. de Construccion, 1981, 181, 55-64.

75. Blanco-Varala, M.T. "A study of a new liquid phase to obtain low-energy cements". Cement and Concrete Research, 1986, 16, 97-104.

76. Blanco Varela, M.T., A study of a new liquid phase to obtain low-energy cements, Cement and Concrete Res., 1986, 116, 97-104.

77a. Xu Xianyu et al. "The formation of $C_{11}A_7.CaF_2$ and $C_4A_3\bar{S}$ in clinker".

77b Feng Peizhi et al. "The promoting effect of CaF_2 and $CaSO_4$ on the formation of C_3S".

77c Xue Jungan etal. "The formation rule of alumina bearing phases in clinker using F and SO_3 combined additives".

77d Feng Mingfen et al. "A study of the effects of sulfate on the clinker with addition of combined mineraliser".

77e Wang Tlandi and Chen Weiqiang. "Effect of burning temperature on the phase compositions, microstructure and quality of Portland cement clinker doped with CaF_2 and/or $CaSO_4$".

Refs 77 (a-e), 1985, Beijing International Cement and Concrete Conference, Vol 1.

78. Gimenez, S, et al. "Production of cement requiring low energy expenditure". Zem-Kalk-Gyps, 1991, 44, 12-15.

79. Humpola, H. "Practical control of the reactivity of cement raw meal". Zem-Kalk-Gyps, 1989, 42, 360-364.

80. Page, C.H. "Influence of mineralisers on the constitution and properties of industrial clinker". 8th ICCC, 1986, Vol II, 152-157.

81. Navarro, J.A. and Glasser, F.P. "Crystal chemistry of calcium silicates: germanate and chromate analogues of $KF.2[Ca_6(SO_4)SiO_4)_2O]$". Cement and Concrete Res., 1985, 15, (6), 1051-1054.

82. Goswami, G. et al. "Effect of fluorosilicate on cement raw mix burnability and kiln build-up". Zem-Kalk-Gyps, 1991, 44, 634-637.

83. Bolio-Arceo, H. and Glasser, F.P. "Formation of spurrite, $Ca_5(SiO_4)_2\ CO_3$". Cement and Concrete Res. 1990, 20, 301-307.

84. Gilioli, C. et al. Studies on clinker calcium silicates bearing CaF_2 and $CaSO_4$". Cement and Concrete Res., 1979, 9, 295-302.

85. Fletcher, J., Glasser, F.P. and Howie, R.A. "Pentacalcium triborate fluoride and its relationship to fluorapatite", Acta Cryst. 1991, C47, 12-14.

86. Pliego-Cuervo, Y. and Glasser, F.P. "Phase relations and crystal chemistry of apatite and silicocarnotite solid solutions". Cement and Concrete Res., 1978, 8 519-524.

87. Bolio-Arceo, H. and Glasser, F.P. "Formation of spurrite, $Ca_5SiO_4CO_3$". Cement and Concrete Res., 1990, 20, 301-307.

88. Bolio-Arceo, H. and Glasser, F.P. "Fluxing reactions of sulfate and carbonates in cement clinkering". I. Systems $CaSO_4$-K_2SO_4 and K_2SO_4-$CaCO_3$." Cement and Concrete Res., 1990, 20, 862-868.

89. Gies., A. and Knöfel, D. "Influence of sulfur on the composition of belite-rich cement clinkers and the technological properties of the resulting cements". Cement and Concrete Res., 1987, 17, 317-328.

90. Choi, Gang-Soon and Glasser, F.P. "The sulfur cycle in cement kilns: vapour pressures and solid-phase stability of the sulfate phases". Cement and Concrete Res., 1988, 18, 357-374.

91. Gutt, W. "Manufacture of Portland cement from phosphate raw materials", 1968. 5th ICCC, Vol I, 93-105.

92. Halicz, L. and Nathan, Y. "The influence of P_2O_5 on clinker reactions". 1983, Cement and Concrete Res., 1983, 14, 11-18.

93. Coleman, T. Unpublished report, Blue Circle Industries PLC.

94. Pollitt, H.W.W. and Brown, A.W.B. "The distribution of alkalis in Portland cement clinker", 5th ICCC, 1968, Vol I, 322-333.

95. Matkovic, B. and Young, J.F. "Dicalcium silicates doped with phosphates". 1986, 8th ICCC, Vol II, 276-281.

96. Gurevich, B.I. and Dobrynina, N.G. "Effect of calcium fluoride on the reaction capacity of alumino silicate components in the burning of phoshorous-anhydride containing raw batches", Proizvod. Stroit. Mater, 1977, 44-59.

97. Jøns, E.S. "Thermodynamic driving force for formation of tricalcium silicate". Cement and Concrete Res., 1980, 10, 103-106.

98. Flint, E.P. and Wells, L.S. "The system lime-boric acid-silica". Jour. Res. Nat. Bur. Stand. 1936, 17, 727-752.

99. Suzuki, K. and Hira, I. "Study of the system $2CaO.SiO_2$-$3CaO.B_2O_3$". Yogyo Kyokai Shi. (Jour. Ceram. Soc. Japan), 1970, 78, 189-195.

100. Fletcher, J.G. "Borate fluxes in ordinary Portland cement production : a feasibility study". PhD. Thesis, Univ. of Aberdeen, 1991.

101. Fletcher, J.G. and Glasser, F.P. In preparation.

102. Maki, I. and Hattori, M. "Influence of minor components on the fine textures of alite in Portland clinker". Il Cimento, 1989, 86(2), 131-140.

103. Long, G.R. Unpublished photomicrographs, Blue Circle Industries PLC.

104. Long, G.R. "The use of mineralisers to produce high strength cement", 1983, 5th ICCem. Microsc., 86-100.

105. Schutte, R. and Kupper, D. "The importance of recirculation considerations in relation to product quality and environmental compatability in cement production", Zem-Kalk-Gyps, 1990, 12, 565-570.

106. Fregert, S. "Chromium valencies and cement dermatitis", Brit. Journal Dermatology, 1981, 105, Supplement 21; 7-9.

107. Weisweiler, W. and Kromar, W. "Heavy metal balances of a cement kiln plant with grate preheater", Zem-Kalk-Gyps, 1990, 3, 149-152.

108. Sprung, S. and Seebach, H. M. V. "Fluorine balance and fluorine emission from cement kilns", ZKG, 1968, 1, 1-8.

109. Sprung, S. "Concentration build-up and measures for reduction", Zem-Kalk-Gyps, 1988, 6, 251-257.

110. Lowes, T. M. and Evans, L. P. "Optimisation of the design and operation of coal flames in cement kilns", J. Inst. Energy, 1989, 220-229.

111. Kumar, S. S. and Kataria, S. S. "Optimisation of burning characteristics of raw meal for fuel economy by special mineraliser", World Cement Technology, 1981, 279-285.

112. Nielsen, P. B. "SO_2 and NO_x emissions from modern cement kilns with a view to future regulations", Zem-Kalk-Gyps, 1991, 9, 449-456.

113. Gardiek, H. O. "Effect of the clinkering temperature on the specific energy consumption in cement clinker burning", Zem-Kalk-Gyps, 1981, 4, 169-174.

114. UK Patent No 1498057, 15 April 1976, "Improvements in hydraulic cements".

Specific Theme I D

Effect of Energy Conservation and Environmental Control Measures

EFFECT OF ENERGY CONSERVATION AND ENVIRONMENTAL CONTROL MEASURES ON CLINKER PROPERTIES

S Sprung
Forschungs institut der Zementindustrie, GERMANY

and

M Delort
Association Technique de l' Industrie des Liants Hydrauliques, FRANCE

Summary

Measures for energy conservation and environmental control can effect the clinker properties in a very different way. An important part play changes in the burning process and the composition of the kiln feed and furthermore also the use of secondary raw materials and fuels. By the conversion already completed in many cases from wet process either to the semi-dry or dry process equipped with preheaters and precalciners, the potential of energy savings in the clinker burning process recognizable from a process effectiveness of above 60 to 70 % has almost been exhausted and is liable to be further improved only in individual parts of the kiln system. The requirements on the quality, performance and environmental compatibility of clinker and cement and an economical production process as well are increasingly of importance when measures for energy conservation and environmental precaution are taken.

Zusammenfassung

Maßnahmen zur Energieeinsparung und zur Umweltvorsorge können sich in sehr unterschiedlicher Weise auf die Klinkereigenschaften auswirken. Eine wesentliche Rolle spielen hierbei Veränderungen am Brennprozeß und der Brenngutzusammensetzung, darüber hinaus auch die Verwendung von sekundären Roh- und Brennstoffen. Der bereits in vielen Fällen abgeschlossene Umstellungsprozeß vom Naß- auf das mit Vorwärmern und Calcinatoren ausgerüstete Halbtrocken- und Trockenverfahren hat bei Prozeßwirkungsgraden von 60 bis 70 % bereits zu einer weitgehenden Ausschöpfung des Energiesparpotentials geführt, die allerdings noch in einzelnen Bereichen des Ofensystems optimiert werden kann. Bei allen Maßnahmen zur Energieeinsparung und zur Umweltvorsorge gewinnen die Anforderungen an die Qualität, die Leistungsfähigkeit und die Umweltverträglichkeit von Klinker und Zement sowie an die Wirtschaftlichkeit des Herstellungsverfahrens zunehmend an Gewicht.

1. INTRODUCTION

The manufacture of cement requires a relatively high consumption of thermal and electric energy. In the example shown in figure 1, the total energy consumption is divided among the electric energy consumption with a proportion of approximately 27 % and the thermal energy consumption with a proportion of approximately 73 % [1]. Whilst the thermal energy is, above all, consumed in the burning process, drying of raw material, coal and blast-furnace slag included, the highest portion of electric energy is required for the production of the raw meal and the grinding of cement clinker. However, the distribution of the total energy consumption may vary considerably by nation and region and therefore be considered only as an indication value.

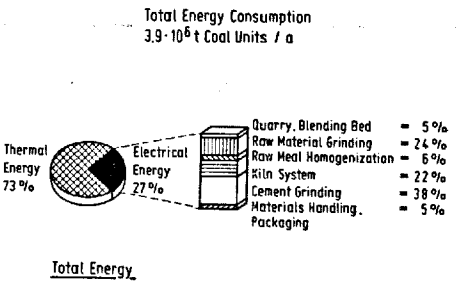

Figure 1: Thermal and electric energy percentage of total energy consumption

This, in particular, refers to the cost of energy. Its portion of the total production cost is high and, depending on the national and regional conditions, estimated to reach approx. 30 up to 50 % with roughly two equal halves distributed among fuel energy and electric energy. The portioning of the energy cost depends on the prices of fuel and electricity. Thus the cost of the electric energy, for instance, may exceed that of fuels in countries with particularly high prices for electric power, and vice versa. Apart from the nature of available fuel, the use of low-priced secondary fuels plays an important part.

Due to the high specific energy consumption, the cement industry has been making for more than 40 years considerable efforts to reduce the production cost by energy conservation. At the same time, the reduction of the specific energy consumption also leads to diminishing the emission of those exhaust gas compounds which, like CO_2, are considered to contribute to the impact on the global climate by the greenhouse effect. Therefore in many cement producing countries, steady improvement of energy and waste gas utilization has led to a reduction of about 50 % in the specific fuel energy consumption of rotary kilns. Figure 2 shows an example of the state of technology sofar attained in Germany [2, 3]. Thus at present only an average of roughly 3 000 kJ/kg of cement (716 kcal/kg of cement) with a clinker content of about 83 wt.-% are necessary compared with about 7 000 kJ/kg of cement (1 672 kcal/kg of cement) in 1950.

Approximately 2 000 kJ/kg of cement (478 kcal/kg of cement) of the total are needed to cover the theoretical heat demand and the drying of the different primary materials with an average moisture content of 5 to 8 wt.-%. On this basis, the energy demand for drying raw materials in approximation is represented as constant from 1950 to 1990. Although the particular figure may change from country to country, this portion of energy consumption as well as the theoretical heat demand can be regarded as unavoidable in the case of the modern dry process. Consequently, the mean energy losses, essentially caused by the kiln's shell, exhaust kiln gas, waste cooling air and clinker residual heat, amount to only about 1 000 kJ/kg of cement (239 kcal/kg of cement). This corresponds to a thermal efficiency of the process of about 67 % compared with almost 30 % in 1950. Moreover, this high effectiveness leads to a very low fuel-

based CO_2 emission of about 0,4 kg of CO_2/kg of clinker. On the other hand, the improvement of wet process plants makes it possible to decrease the consumption of thermal energy to a range of 4 600 to 5 000 kJ/kg of clinker (approx. 1 100 to 1 200 kcal/kg of clinker). The progress made so far remains remarkable in all those cases in which the kind of raw material or other circumstances still require the employment of the wet process. In this context differences in the consumption of electrical energy of the various processes cannot be discussed in detail.

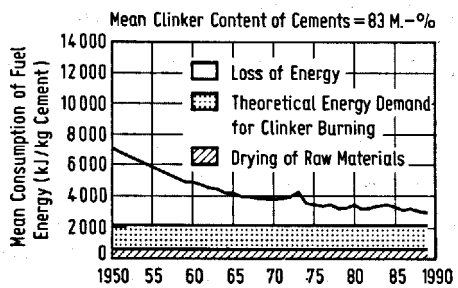

Figure 2: Development of mean thermal energy consumption of rotary kilns in Germany since 1950 (according to [2, 3])

The high degree of energy utilization as shown in figure 2 was mainly achieved by the substitution of the wet process and those dry process methods without preheater or with only a one-stage cyclone through modern energy saving processes and the close down of uneconomic kilns of low capacity. Additional savings in fuel energy are therefore to be expected only to a small extent and at individual parts of the kiln system, e.g. by further optimizing the burning process through improvement of the precalcining techniques, the preheating of combustion air and kiln feed as well as by reducing the heat losses of the kiln's shell [3].

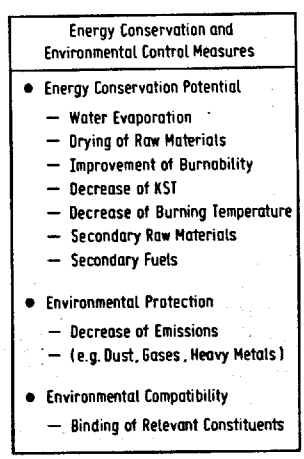

Figure 3: Energy conservation potential in clinker production process, environmental protection and environmental compatibility

When considering all measures for diminishing the fuel energy consumption, the cost of fuel energy or environmental precautions, the properties of clinker and of cements made of it must not be left out of consideration. Developments in recent years have shown that cement is no longer seen as an end product but as a preliminary product for the production of economical and durable concrete, when used expertly. For this reason, the market demands a great number of requirements on the properties, the quality level and the performance of cement. Apart from strengths development and

workability, the substantial quality and performance characteristics are above all derived from those properties which essentially influence the durability of concrete.

The cement plant must take these requirements into account considering the cost of production, particularly that of energy input, the rules of environmental protection and the compatibility of the product. The report presents the interrelationships shown in figure 3 as far as the clinker production is concerned. The effects of the measures to save energy in the cement grinding process and their influence on the properties of the product are not dealt with. This also relates to the use of interground and blended additions and their influence on the performance of cement in the concrete.

2. INFLUENCE OF MEASURES FOR ENERGY CONSERVATION

2.1 Burning Process

From figure 2 it can be seen that the expenditure of thermal energy for the clinker burning mainly depends on the energy demand for drying the raw meal constituents and the fuel, on the theoretical heat demand and the energy losses due to radiation, waste gas and remaining clinker heat. The conversion from wet process to modern dry processes with preheaters and calciners leads to an energy conservation of roughly 50 % or exceeding up to 3 000 kJ/kg of clinker (716 kcal/kg of clinker) [4, 5]. Accordingly the mean energy input for drying quarry-moist raw materials in Western Europe thus only amounts to about 200 to 300 kJ/kg of clinker (48 to 72 kcal/kg of clinker) and can nowadays be completely covered by utilization of the kiln exhaust gases. In the case of higher moisture contents of raw materials or if the installation of highly efficient multi-stage preheaters leads to a too low exhaust gas temperature, it sometimes may become adviceable to operate an additional hot gas generator. To reduce the investment and operation cost, the modification of the process is generally combined with an increase of capacity and the close down of small unprofitable kiln units. Consequently, this is above all a technological problem. Moreover, the conversion can also lead to improve the grindability of the clinker and the strengths development of the cements produced [6, 7]. This may result from higher heating rates of the kiln charge in a temperature range of above 900 °C, an often shorter residence time at sintering temperature and rapid cooling of the clinker. This leads, with a given raw meal composition, to the reduction of the mean crystal size of the alites as investigations of clinkers produced in an industrial plant [7, 8] and at laboratory scale [9, 10] have shown.

The lowest consumption of thermal energy is achieved in kiln systems with at least four suspension preheater stages for raw meal and integrated precalciners of different types of construction and operation [4]. The ratio length/diameter (L/D) is 14 to 18. A further improving development can consist in shortening the kiln to a L/D ratio of 10. At a nearly complete precalcination outside the kiln in a calciner with tertiary air ducting, the technically attainable gradient of heating up the kiln charge is about 25 to 30 K/min hence double as high compared with that of kiln systems without precalcination [11 - 13]. From the experiences hitherto gained, the accelerated clinker formation at a throughput time of 20 minutes turned out to be particularly favourable to decrease the grinding resistance and improve the properties of the cement. However, the substantial prerequisite for running this type of short kiln is a low degree of heterogeneity present in the raw meal [14]. If the raw meal is composed of several components special efforts have to be made as to the raw meal preparation and homogenization; in particular, quartz sand and limestone should be ground more finely and the residence time at sintering temperature and the sintering temperature should be increased [13]. As a result, the energy consumption may increase, too.

From present-day experiences, energy losses at existing kiln units equipped with preheater and, if applicable, additional calciner can only be lowered if the measures comprise the whole kiln system consisting of preheater, kiln and clinker cooler. These are, in the first place, process-technological measures. However, in order to satisfy

also the requirements on clinker quality, the process-technological procedure should appropriately be adjusted to the quality requirements. The operational optimization of the rotary kiln burner and the clinker cooler are typical examples which, however, cannot be further discussed in this context. The energy losses through the exhaust gas volume are the more decreased the lower the air excess factor is in dependence on the fuel energy consumption and the combustion behaviour of the fuel [15]. An incomplete combustion combined with partly reducing conditions is to be avoided for quality reasons. Similar interrelationships are valid for process technics to reduce NO_x emission.

Improvement of heat recuperation of the clinker cooler thus decreasing the fuel energy consumption of the whole unit can also be achieved by adjusting the clinker cooler operation to the particle size distribution of clinker, by equalizing the particle size distribution and by reducing the dust circulation between cooler and kiln. This can be achieved by appropriately changing the composition of raw meal and fuel [6], and suppression of clinker comminution, e.g. in counter-flow coolers [16, 17]. To attain favourable clinker properties, it is also of importance that the clinker is cooled down from sintering temperature to values below 1 000 °C by increasing the cooling rates as far as possible. When at the same time the heating rate of raw meal of normal composition and burnability is high and the residence time at sintering temperature limited, the so produced clinker, due to better grindability, requires less electric grinding energy than clinker containing coarse-grained alite [7]. Moreover it has been shown that high cooling rates in the high-temperature range are favourable especially for clinkers rich in C_3S und C_3A. By optimum calcium sulphate adjustment as to nature and quantity it is possible to produce portland cements with low water demand as well as favourable workability and strengths development [18].

2.2 Composition of the kiln feed

The governing factors for the burning behaviour, the fuel energy consumption and the properties of the clinker are a uniform composition and a sufficiently high fineness and homogeneity of the kiln feed, a current monitoring and control of uniform properties by the well known modern sampling, analyzing and evaluation methods [19 - 22] as well as adjusting the composition of the kiln charge to that of the fuels and the fuel energy consumption. The influence of the fuels, in particular coal and lignite, is the higher the higher their ash content, the more the ash composition differs from the composition of the clinker and the higher the requirements upon quality and quality level of the clinker are [18]. The quite considerable expense necessary for optimum adjustment leads not only to an equalizing of the clinker quality but also to a kiln operation which shows a noticeably lower frequency of disturbance. Systematical production planning and targeted energy management can contribute to further reducing the total energy consumption of about 3 to 5 %, increasing the kiln capacity and thus lowering the specific energy cost [23 - 25]. Above all a more uniform kiln operation contributes to reduce the emission of NO_x [26] and other exhaust gas compounds, such as for instance SO_2, CO, and fuel-derived CO_2.

In modern cyclone preheater kilns, cement clinker of high quality can therefore be produced at a process efficiency about 70 % with a thermal energy input of less than 3 100 kJ/kg (750 kcal/kg). The theoretical energy demand, i.e. the unavoidable enthalphy amount for clinker formation, summarizes to almost 60 % of the total energy demand. This refers to a clinker with a standard lime factor of above 95 which is burnt at a sintering temperature of 1 400 to 1 450 °C. The alite content generally exceeds 50 up to 80 wt.-%. In consequence, the belite content is low, varying from about 25 to less than 10 wt.-%. According to its fineness, the clinker allows the production of portland cements with high early strengths of above 10 to 30 N/mm^2 and 28-d standard strengths of above 55 N/mm^2, as required by the market. On this basis, cements can furthermore be manufactured with latent hydraulic, pozzolanic or inert main constituents having a performance which is equal to that of portland cements e.g. of the classes 35 F as per DIN 1164, CPA 45 as per NF P15-301 or 32,5 according to

ENV 197. Additionally, even cements of strength classes 45 (DIN), 55 (AFNOR) or 42,5 (ENV 197) can be produced with interground or blended constituents.

By reducing the $CaCO_3$ content in the raw meal, the theoretical energy demand necessary for clinker formation and the sintering temperature can be diminished. As shown in figure 4, the decrease is of about 110 kJ/kg of clinker (26 kcal/kg of clinker) or about 3.5 % related to the total consumption of thermal energy of 3 100 kJ/kg of clinker if the standard lime factor is decreased from 100 to 90. Lowering the standard lime factor however leads to a lower alite and an increasing belite content. The decreased hardening velocity, in particular the diminution of the early strength, can be compensated to a limited extent only by a higher fineness of grinding. However, this in general entails a higher consumption of electric energy which may amount to about 6 kWh/t of cement in modern closed-circuit mills when the fineness of grinding has to be increased e.g. by 400 cm^2/g. In most cases this compensates the savings in thermal energy or these are even offset by a higher consumption of expensive electric energy. In special cases, also the workability of the cement may be impaired due to the higher fineness of grinding.

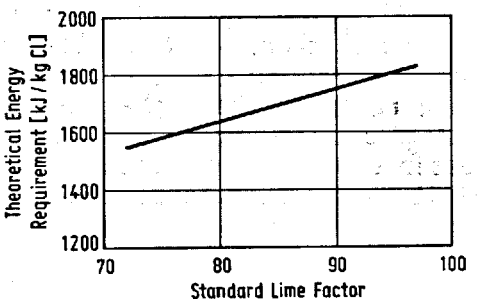

Figure 4: Change of theoretical energy requirement in dependence on the standard lime factor of raw meal from natural constituents

Furthermore, with decreasing standard lime factor of the clinker, above all the production of cements containing pozzolanas or fillers with a performance which is equal to that of the portland cement, is restricted. For cement plants which, on account of the market demand, are able to manufacture a large number of cements of various compositions and strength classes on the basis of a single high-quality clinker, the lowering of the standard lime factor and the altogether often uneconomical production of a second type of clinker are out of the question. Consequently, the lowering of the standard lime factor would theoretically permit small savings in thermal energy but the technical realisation is as a rule restricted by the requirements of the market on the cement properties and the quality level as well as by additional operational expenditure.

This relates in particular to the manufacture of special clinkers with a standard lime factor of less than 90 to 75, the properties and production techniques of which have often been investigated [27 - 39] and conclusively been evaluated in literature [33, 34]. From the view of process technology, the main conclusion is that the energy savings which result from decreasing the standard lime factor below 90 by reducing the theoretical energy consumption and the sintering temperature, are more or less compensated by increasing energy losses of the clinker cooler due to the necessary extremely rapid cooling rates of the clinker [15]. It is technically still not clear whether the energy losses can be avoided by using cooler types of special construction [25]. Moreover it has been shown that the grindability is impaired by increasing belite contents and consequently the specific consumption of electric energy increases [28]. Besides this the employment of those clinkers is practically impossible for the manufacture of cements with interground and blended constituents.

The influence of secondary raw materials on the theoretical energy demand and their effects on the clinker quality are dealt with in chapter 2.3.

By adding quantities up to 3 wt.-% of fluxing agents and mineralizers to the raw mix, the sintering temperature can be reduced to about 1 300 °C. Mineralizers promote the formation of clinker phases, in particular C_3S, whereas fluxing agents reduce the temperature at which the first melt formation occurs. They also influence the viscosity. The measures for reducing the sintering temperature and improving the burnability through fluxing agents and mineralizers are described and differently assessed in a large number of publications [6]. From a conclusive assessment of the state of knowledge at the 8th International Congress on the Chemistry of Cement 1986 [33, 34], it is still presumed that in general these additions positively influence the burnability in the laboratory test and contribute to lower the sintering temperature by about 200 K. However, the energy savings of about 100 kJ/kg of clinker respectively about 5 %, related to a thermal energy consumption of 3 140 kJ/kg of clinker which can be achieved with modern kiln systems equipped with cyclone preheater and precalciner, is often too small [36, 37] as to justify the additional cost of purchasing, conveying, the environmentally suitable storage and dosing of those additions in the cement plants. Furthermore, the savings in thermal energy may be compensated by a higher consumption of electric energy if the grindability of clinkers containing fluxing agents and/or mineralizers decreases [38]. Occasionally an impairment of early strengths development has also been observed in the uncontrolled use of secondary materials containing CaF_2 as mineralizers.

The questions that arise in connection with the manufacture of special clinkers and the energy consumption required cannot be further discussed here [29 - 31, 39].

2.3 Secondary materials

Raw materials and fuels of natural origin such as limestone, marl, clay, quartz sand, and coal, heavy fuel oil or natural gas respectively are regularly used at the industrial clinker burning process. Apart from these natural constituents, there are residual or waste materials from other industrial processes or from waste recovery which, under certain conditions, can be utilized as secondary constituents. Their employment, as a rule, does not directly but only indirectly lead to a reduction in the specific energy consumption of the clinker burning process. In general the specific energy consumption increases when e.g. the exhaust gas enthalpy losses increase [7, 40]. Their utilization however contributes to save natural raw materials and fuels, preserve natural resources and diminish the cost of fuel energy. Furthermore the utilization of secondary fuels also offers the possibility to reduce, though to a limited extent, the emission of CO_2 and other exhaust gas compounds by saving equivalent quantities of natural fuel and diminishing the impact of exhaust gas compounds on the greenhouse effect [67]. For technical reasons and for reasons of clinker quality, environmental precautions and the compatibility of the product, the overall economic potential is rather limited for the time being [41, 48]. Transport, storage and employment of secondary materials are in general regulated by national legislation on environmental protection and waste disposal [62] which is supplemented by international agreements within the OECD [42] and the EC [43].

The possibilities for waste or residual material recovery are presented schematically in figure 5 [41]. After collection, transport, preparation and storage, the stream of wastes divides in an employable portion and a non-utilizable portion. The non-utilizable portion has to be disposed, the employable portion is likable to be used as fuel for energy generation or as raw material component by utilizing its inorganic matter.

The energy content can be utilized in energy transformation processes, e.g. in thermal power stations, or in material conversion processes such as the clinker burning process. The residual materials such as slags and ashes which are obtained from power

stations or incinerators being sensibly reduced in volume can be further utilized or must be disposed. Both paths, either disposal or recovery, are marked by dashed lines. But if the energy content can be utilized in a material conversion process it is advantageous that the non-combustible portion participates, entirely and residual-free, in the clinker formation as a secondary raw material component.

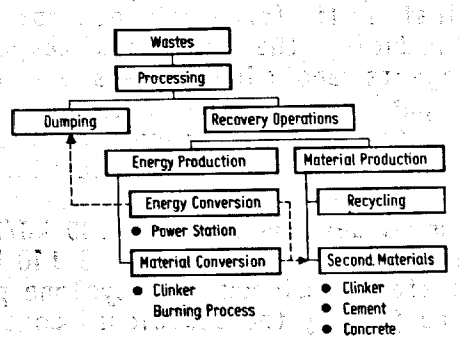

Figure 5: Possibilities of waste material utilization

When non fuel containing materials are recovered it may be distinguished by definition between recycling and utilization as secondary raw material. A recycling process exists when a distinct residual, such as glass, is used again to produce new glass products. Contrary to that, secondary materials are used to manufacture products of another kind. In the case of cement manufacturing, these secondary materials can be employed as raw material components for clinker burning or as additions for cement grinding. A further possibility consists e.g. in the utilization as addition to manufacture concrete or cement bound materials [44 - 46].

As a precondition and on the basis of the present experiences, secondary materials must satisfy a number of requirements for their utilization in the cement industry (figure 6). They shall not:
- deteriorate the structural properties of cement,
- infringe the environmental compatibility of cement and concrete,
- increase the environmental burdening by the production process,
- impair the uniformity and stability of the production process.

Furthermore, economical incentives should stimulate their use [41, 47, 48].

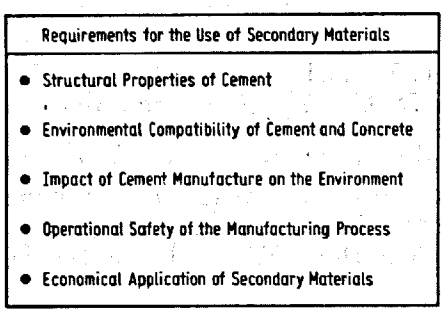

Figure 6: Requirements for the employment of secondary materials

2.3.1 Secondary fuels - A large number of experiences have been collected in the literature on the utilization of secondary fuels, e.g. [6, 7, 40, 48 - 59]. These are solid, fluid or gaseous substances which are obtained as synthetic products (e.g. used tyres, waste oil, solvents, plastics, paper, residual wastes) or remainders from the processing of natural materials (wooden waste, rice husks). Indications about the quantities used are rather poor. In Germany were used, e.g. in 1989/90, about 460 000 t

of secondary fuels which substituted a quantity of primary energy of about 420 000 t standard coal units per year. This corresponds to a proportion of merely 12 % of the total consumption of thermal energy [48]. Experiences from France show figures of a similar magnitude. In 1990, among others, about 200 000 t of secondary fuels, e.g. solvents, paint residues or waste lubricants, were employed representing roughly 120 000 t of petrol equivalent or 170 000 t of standard coal units.

It has been proved that only those secondary fuels can be used in continuous operation, provided that
- the required quantity is steadily available,
- their composition is as uniform as possible, and
- they are available in a high degree of uniformity.

In individual cases it has to be examined additionally whether and in what concentrations minor and trace constituents are contained in the secondary material. For instance, sulphur and chlorine cycles are liable to upset kiln operation by coating and ring formation, heavy metals may increase emissions or be concentrated in the clinker [6, 51, 60, 61]. The nature and concentrations of minor and trace constituents may therefore be a criterion for rejecting the recovery of secondary materials. It should also be further considered to what extent their utilization affects the economy of the production process. Additional costs may result for reasons of quality and environmental precautions, the liability of handling waste-derived residuals or from an increase of investment, operation and surveillance cost to ensure the indispensable control of the deliveries [41].

Due to the particularity of the clinker burning process with its high temperatures of gas and kiln feed which are needed to achieve clinkerization, the oxydizing gas atmosphere required for quality reasons and the alkalinity of the kiln charge, it is in general presumed that the secondary fuels which satisfy the criteria for their selection are entirely combusted and do not lead to an increase of environmental burdening if the prognosticable quantity limits are observed [62].

When high-ash coals with ash contents of above 15 wt.-% are used, impairments of the physical properties of the clinker and its hydraulic reactivity (figure 7) can only arise if the ash input and the thus lowered standard lime factor is not compensated by

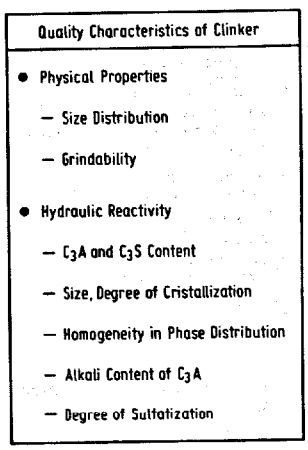

Figure 7: Influence of changing properties of raw material and fuel on the quality characteristics of clinker [64]

a respective increase of the $CaCO_3$ content in the raw meal. The use of fuels with a high ash content therefore requires a deposit of limestone with a high percentage of $CaCO_3$. The influence of the ash quantity and composition on the content of the clinker

phases C_3S and C_3A, their crystal size and their homogeneous deviation should be assessed the higher, the higher the requirements on the quality level of the clinker are defined.

When natural raw materials with a high content of alkalies and Al_2O_3 are used, the sulphur input from the fuel exceeding a degree of sulfatization of 80 % in the clinker may also entail disadvantages. This mainly affects the particle size distribution, the grindability and the reactivity of the clinker. It additionally happens when the properties of raw materials and fuels vary in an uncontrolled manner and no procedure of quality control and quality assurance exists. The introduction of such a system is of primary importance when secondary fuels are employed [6, 63, 64]. High deviations in the particle size distribution of the clinker, mainly a very fine-grained clinker, may impair the operation of the kiln and the cooler and therefore contribute to increase the thermal energy consumption of the kiln system [65].

Those heavy metals introduced into the kiln system by the materials used which are nearly entirely bound in the clinker, as a rule, do not measurably affect the cement properties when their concentration does not exceed 300 to 400 g/t (ppm). For reasons of environmental compatibility of the product and the market acceptance, the tendency is increasing as to impose that the quantities of heavy metals bound in the clinker should not exceed the contents obtained when exclusively natural constituents are used [41]. With increasing content of strongly colouring elements, such as e.g. Fe and Mn, it is presumed that not only white clinker is visibly coloured [66] but also the colour of normal clinker becomes darker. Moreover the reduction of the alumina ratio through a relatively small increase of the Fe_2O_3 content by 0.3 to 0.5 wt.-% may noticeably affect the 2-d and increase the 28-d standard strengths.

2.3.2 Secondary raw materials - For the selection and possibilities of using secondary raw matewrials, in principle the same requirements and selection criteria are valid as for the use of secondary fuels. Secondary raw materials can be subdivided in different groups according to the main element contained in them. Their use allows to substitute a limited portion of natural raw materials, correct the composition of a predetermined raw mix or prepare raw meals for the production of clinker with special properties. In figure 8, 6 groups of secondary raw materials are compiled with examples of those constituents which, according to present experience, are suitable for utilization in the industrial process to a limited extent and with certain restrictions [41].

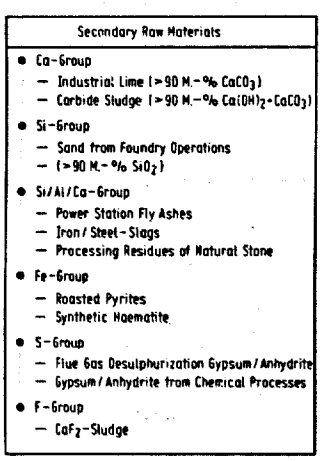

Figure 8: Subdivision in groups of industrially utilizable secondary materials [41]

In principle, all materials which have been properly prepared in a drying process, have lost their crystal water, are dissociated, contain glassy particles or are particularly fine-grained, present potentials of saving thermal or electric energy in the clinker production process. Savings in thermal energy can result from diminishing the theroretical heat consumption with materials which contain e.g. calcium hydroxides instead of $CaCO_3$, reactive mixtures of the oxides SiO_2, Al_2O_3, FeO_2 and CaO instead of clay minerals and other rock forming minerals or which contain these oxides nearly completely as glass like in fly ashes and slags [68 - 70].

For the time being, it is hardly possible to estimate the effective reduction of the theoretical energy consumption to be realized in the industrial clinker burning process since the transferability of investigations carried out in the laboratory in general has not been verified by balance measurements at industrial scale [69]. In other cases, secondary raw materials containing e.g. high chloride and/or heavy metal contents were used which have to be regarded as technically non-utilizable for reasons of operation safety of the kiln, clinker quality, environmental precautions and compatibility of the product [70, 71]. When glassy blast-furnace slag is used as a raw meal component, the lower theoretical heat consumption achieved by the gain of devitrification enthalpy may partly or wholly be compensated by an increasing consumption of electric energy to achieve a higher fineness of the raw meal during the grinding process which is indispensable for reasons of homogeneity and burnability [33]. In contrast, the use of silicious fly ashes instead of clay components appears more promising [72]. A precondition however is a given high fineness, a high glass content or content of reactive oxides in the fly ash as well as a limestone deposit with high $CaCO_3$ content.

When using fly ashes with a high lime content as a raw meal component the effects on the theoretical heat consumption were investigated with the aid of a model calculation and verified in a kiln system with suspension preheater of 1 200 t/d of capacity. From these investigations resulted a diminution of the theoretical heat requirement of about 135 kJ/kg of clinker (roughly 32 kcal/kg of clinker) and 105 kJ/kg of clinker (roughly 25 kcal/kg of clinker) respectively which were more or less attributed to the savings of decarbonation enthalpy. The raw meal however contained also 2.5 wt.-% of CaF_2 reacting as fluxing agent and mineralizer [73].

The high sulphur content, often present in fly ashes with a high lime content, may render their industrial use difficult for reasons of operation, quality and environment [73, 74]. This applies if the tendency of coating and ring formation [75] or the proportion of fine particles in the clinker increase and thus the clinker dust circulation by secondary air grows [6, 18], or if the grindability [7], the workability and the strengths development [76 - 80] are impaired and the SO_2 emission increases [6, 81].

A new development in this field is the manufacture of a binder consisting of portland cement clinker and up to 80 wt.-% of marl burnt in a fluidized bed kiln at about 800 °C. The binder is produced by intergrinding or blending [82]. The burnt marl already contains besides $CaCO_3$ calcium silicates, calcium aluminates and free lime. The hardening is mainly achieved by a pozzolanic reaction which is further incited by the hydration of the clinker component. With an almost equal performance compared with that of portland cement and assessed on account of its standard strength, the binder can be manufactured with a sensible reduction of thermal energy consumption since a corresponding clinker quantity can be saved.

A similar development is the manufacture of portland/oil shale cement. The difference however consists in the fact that, by intergrinding of burnt oil shale containing hydraulically hardening and pozzolanic components, not only the clinker content can be reduced at equal performance level but also the energy consumption compared with standardized cement is diminished. The reason is that during the combustion of the organic matter in the oil shale in a fluidized bed process to produce

burnt oil shale, thermal energy is gained which is used to generate electric energy, e.g. for the cement grinding process [83, 84].

3. MEASURES OF ENVIRONMENTAL PRECAUTION

Measures to be taken today for the sake of the environment comprise both the clinker burning process and the grinding of cement. In this context, the possibilities of reducing the specific CO_2 emission per ton of cement through the use of additions cannot be further discussed [85]. The amount of interground or blended additions in the cement and the reduction of the clinker content are in general determined by the requirements on the performance of the cement in the concrete. Besides the workability and strengths development, additionally the durability and corrosion protection have to be observed. In order to enable the employment of additions in amounts as high as possible, high-quality clinker is required, i.e. clinker with a standard lime factor of above 95.

3.1 Cycles

Measures to be taken to save energy and reduce emissions as well can partly, and even in a very different way, affect the clinker properties. Thus the conversion of the burning process, e.g. from wet to dry process and the simultaneous installation of an efficient precipitator to reduce dust emission, led to the buildup of internal and external cycles within the kiln system. This applies to such elements and compounds which volatilize from the kiln feed and are introduced into the kiln gas phase as vaporous or gaseous compounds. These are compounds of alkalies, sulphur, chlorine and fluorine as minor constituents as well as compounds of heavy metals contained as trace compounds in the raw materials and fuels. If volatile elements and compounds react with the kiln feed either in the kiln or in the preheater or if they condensate in the colder parts of the kiln system and subsequently reach again the hot kiln zones, internal cycles are established. External cycles are formed by waste gas utilization or if the precipitated dust is recirculated into the process together with the compounds contained in them [6, 86].

3.2 Minor constituents

As a rule, the clinker properties are affected if, due to an increased supply by natural constituents and particularly by secondary materials and cycles, the alkali and sulphur content of the clinker increases and the kind of alkali binding in the clinker phases changes [76 - 80]. Through a purposeful sulphur supply up to about 60 to 80 % of sulfatization of alkalies, the clinker properties can be improved without increasing the emission of SO_2. However, an increase of the SO_2 emission must be expected at sulfatization degrees of above 100 %, in particular, when in the operation of a secondary firing partly or locally reducing conditions in the kiln gas atmosphere occur [87]. The increase of SO_2 emission due to the oxidation of the pyrite content in raw materials in the preheater and the then required measures for reduction can be seen as a special case [88 - 91] which in general does not affect the clinker properties directly.

Minor constituents containing fluorine and chlorine do generally not require special measures of environmental precaution. Fluoride is bound in the clinker to above 95 %. At the contrary, chlorides mainly enrich in the internal cycle of rotary kilns. Fluorides as minor constituents may influence the properties of the clinker. The low degree of binding of the chloride in the clinker leads above all to coating and ring formation, additionally it may also promote the emission of heavy metals [6, 60, 61].

Organic constituents contained in certain secondary raw materials as part of the raw meal may increase the emission of environmentally relevant organic compounds when passing the grinding/drying unit or the preheater.

The content of alkalies as well as compounds of sulphur, chlorine, fluorine and carbon in secondary materials and fuels therefore is one of the main criteria for their selection and utilization which has to be observed not only for reasons of emission limitation but also for reasons of clinker quality and kiln operation safety. However, at present it seems not possible to recommend a uniform limitation as the requirements on the clinker quality, the kiln operation and the reduction of emissions can worldwide differ considerably, e.g. compared with the technical standard reached so far in Europe [2, 90] or other industrial countries.

3.3 Interruption of cycles

The buildup of disturbing cycles can be prevented in operation by partly or completely interrupting them. External cycles can be reduced through extraction of precipitated dusts, internal cycles can be prevented through a bypass. The frequency and duration of interfering in the kiln operation or the volume of a continuously operated bypass depend on the amount of the hourly input of minor and trace constituents into the kiln system and can be generally determinated by balance measurements and deduced model calculations [6, 61, 93 - 96]. The interruption of such cycles in principle allows, especially when secondary raw materials and fuels are used, to control emission and observe their limit values, avoid coating and ring formation and control, to a limited extent, the clinker properties as to their alkali and sulphur content. Effects of heavy metal cycles and accumulations on the clinker properties and the technological properties of the cement in concrete are not to be expected as long as their content does not markedly deviate from that contained in natural constituents when these are used exclusively. Comprehensive basic investigation in laboratory scale however showed that, e.g. some of the heavy metals may on principle influence the growth of alite crystals and can change the physical properties of the clinker melt as well, e.g. viscosity and surface tension [97].

The disadvantage of dust extraction from the external cycle, in particular the interruption of the internal cycle through a bypass, consists, apart from additional investment cost, in a noticeable loss of thermal energy, an increased electric energy consumption and the problem of utilization or disposal of the dust collected and discharged from the system [61]. Contrary to the suggestions of an exclusively technical resolution of the problem, there seems to be an increasing tendency, when the possibilities of utilizing secondary materials are examined, to make their utilization dependent also on the question whether or not a bypass operation is necessary. Such an exclusion criterion could, to a considerable extent, restrict their technical utilization, especially on account of the difficulties and cost of dust disposal on hazardous waste dumps or for reasons of product properties. The utilization of secondary materials would be further impeded also by the requirement on stricter emission limit values [98], especially in the case that this target could only be attained by an excessively high expenditure caused by special methods of exhaust gas cleaning [67].

4. CONCLUDING REMARKS

By the conversion already completed in many cases from wet process either to the semi-dry or to the dry process equipped with preheaters and precalciners, the potential of energy savings in the clinker burning process recognizable from a process effectiveness of above 60 to 70 % based on the thermal energy input, has almost been exhausted. Under these conditions, a further reduction of energy consumption seems at present possible only to a small extent by the optimization of individual process steps.

The developments of environmental precautions run concurrently. It is true that the individual measures taken and forced by the legislation considerably differ worldwide [2]. Altogether however, it is to be presumed that the emissions of dust, gaseous and vaporous components and of dust bound constituents will more and more be restricted.

On the other hand, the development over the last years has shown that in an open market the cement user makes increasingly requirements on the quality, the quality level and the performance of cement in concrete. It is therefore necessary to satisfy these requirements with every single step in the direction of further reducing the thermal energy consumption in the clinker burning process and also in the electric energy consumption for grinding. Additionally, these measures should equally comply with the increasing requirements on environmental precaution.

For the time being, the possibilites of lowering the thermal energy consumption concentrate on further improving the burning process, the composition of the kiln feed and the use of secondary materials. Since the introduction of modern burning processes with preheating and precalcining the raw meal and an improvement of the recuperation rate of clinker coolers, the energy consumption could above all been reduced through diminishing the heat losses and utilizing the waste heat as far as possible. Higher velocities in heating up the feed after precalcination and high cooling rates can positively affect the clinker properties such as e.g. the grindability and the strengths development if at the same time the clinker is of high homogeneity, optimal fineness and is burnt in an oxidizing atmosphere.

Lately, many attempts have been made to reduce the energy consumption by changing the composition of the kiln feed. This aimed, in the main, to lower the standard lime factor to values of below 90 and to use fluxing agents and mineralizers. However, both measures only ensure a relatively limited potential of energy savings which may more or less be compensated by losses of quality, process-technological problems and possibly even a higher consumption of electric energy in the cement grinding. In contrast, the manufacture of a high-quality clinker with a standard lime factor of above 95 is often more advantageous when cements with interground or blended additions and of equal performance like portland cement shall be produced and the effect of energy conservation can be obtained by a lower clinker consumption.

Experience has shown that there are principally a number of possibilities for the use of secondary raw materials and fuels in the clinker burning process. As a rule, the specific energy consumption is not or is only indirectly reduced. Nevertheless, natural resources can be preserved, the cost of fuel reduced and the emissions of the greenhouse gas CO_2 diminished. However, the potential of energy conservation is rather limited since, for technical reasons, for reasons of clinker quality, the environmental precaution and nowadays also the compatibility of the product, the requirements on the use of secondary materials are high and will probably even be increasing in future.

REFERENCES

[1] Bundesverband der Deutschen Zementindustrie: Zement-Jahresbericht 90-91.

[2] Kroboth, K., Kuhlmann, K., und Xeller, H.: Stand der Technik der Emissionsminderung in Europa. Zement-Kalk-Gips 43 (1990) Nr. 3, S. 121/131.

[3] Scheuer, A., und Ellerbrock, H.-G.: Möglichkeiten der Energieeinsparung bei der Zementherstellung. Will be published in Zement-Kalk-Gips 45 (1992) No. 5.

[4] Bonn, W., und Lang, Th.: Brennverfahren. VDZ-Kongreß Verfahrenstechnik der Zementherstellung 1985, Generalbericht, Fachbereich 5, S. 368/384.

[5] Kreft, W.: Modernisierung von Zementwerken - Umbau auf energiesparende Brennverfahren. Zement-Kalk-Gips 33 (1980) Nr. 7, S. 334/344.

[6] Sprung, S.: Technological Problems in Pyroprocessing Cement Clinker. Cause and Solution. (Translation of issue 43 (1982) of Cement Industry Publications, published by Verein Deutscher Zementwerke e.V., Düsseldorf). Beton-Verlag GmbH, Düsseldorf 1985.

[7] Kreft, W., Scheubel, B., und Schütte, R.: Klinkerqualität, Energiewirtschaft und Umweltbelatung - Einflußnahme und Anpassung des Brennprozesses. Teil 1: Basisbetrachtung. Zement-Kalk-Gips 40 (1987) Nr. 3, S. 127/133. Teil 2: Erfahrungen aus der Praxis. Zement-Kalk-Gips 40 (1987) Nr. 5, S. 243/258.

[8] Scheubel, B.: Investigations on the influence of the kiln system on clinker quality. Ciments, Betons, Plâtres, Chaux (1987) Nr. 766 = Nr. 3/1987, S. 185/188.

[9] Maki, I., Tanioka, T., Imoto, Y., und Ohsato, H.: Influence of firing modes on the fine textures of Alite in Portland clinker. il cemento 87 (1990) Nr. 2, S. 71/78.

[10] Chromy, S., und Maki, I.: Influence of heating rates on the kinetics of Portland clinker formation. il cemento 88 (1991) Nr. 1, S. 19/28.

[11] Billhardt, H.-W.: Erfahrungen mit einem Rohrkühler an einer 2500-t/d-Kurzdrehofen-Anlage mit Vorcalcination. Zement-Kalk-Gips 39 (1986) Nr. 3, S. 122/124.

[12] Wolter, A.: Development of the Short Rotary Kiln and the Use of Low Grade Coal in Cement Plants. TIZ-Fachberichte 111 (1987) Nr. 12, S. 905/909.

[13] Wolter, A.: Pyrorapid-Kurzdrehofen - Vorteile für alle Rohmaterialien. Zement-Kalk-Gips 43 (1990) Nr. 9, S. 429/432.

[14] Grigel, W., Oberhäuser, G., und Wolter, A.: Untersuchungen zur Heterogenität von Rohmaterialien und Rohmehlen und ihre Aussage hinsichtlich des Brennverhaltens. Zement-Kalk-Gips 38 (1985) Nr. 10, S. 589/590.

[15] Rosemann, H., Locher, F. W., und Jeschar, R.: Brennstoffenergieverbrauch und Betriebsverhalten von Zementdreh-Ofenanlagen mit Vorcalcinierung. Zement-Kalk-Gips 40 (1987) Nr. 10, S. 489/498.

[16] Scheuer, A.: Beurteilung der Betriebsweise von Klinkerkühlern und ihr Einfluß auf die Klinkereigenschaften. Zement-Kalk-Gips 41 (1988) Nr. 3, S. 113/118.

[17] Schürmann, W., und Scheuer, A.: Berechnung des Wärmeübergangs in einem Rohrkühler unter besonderer Berücksichtigung der Staubkreisläufe und der Zerkleinerung des Klinkers. Zement-Kalk-Gips 42 (1989) Nr. 10, S. 515/519.

[18] Sprung, S.: Einflüsse der Verfahrenstechnik auf die Zementeigenschaften. Generalbericht VDZ-Kongreß Verfahrenstechnik '85. Zement-Kalk-Gips 38 (1985) H. 10, S. 577/585.

[19] Martinez Ynzenga, J. I., Bergenfelt, C., und Pedersen, S. T.: Laboratory automation by robotics. Zement-Kalk-Gips 43 (1990) Nr. 6, S. 277/281.

[20] Mellies, F., und Vajk, I.: Adaptive Mischungsregelung, ein Baustein für das Laborautomationssystem POLAB®. Zement-Kalk-Gips 43 (1990) Nr. 6, S. 293/296.

[21] v. Eenbergen, A., und Gecks, W.: Neue Möglichkeiten der Röntgenfluoreszenzanalyse in einem modernen Zementwerk. Zement-Kalk-Gips 43 (1990) Nr. 6, S. 288/292.

[22] Mann, K.: POLAB® - Qualitätssicherung mit moderner Robotertechnik. Zement-Kalk-Gips 43 (1990) Nr. 6, S. 297/299.

[23] Nahamura, G., Aizawa, T., und Nakase, K.: Optimization of Cement Manufacturing Process. J. Res. Onada Cem. Co. JPN 40 (1988) Nr. 118, S. 29/40.

[24] MacDonald, L.P., Janik, A., und Blanck, M.: Reducing power costs with computerized production planning and energy management. Zement-Kalk-Gips 41 (1988) Nr. 6. S. 279/285.

[25] Blanck, M.: "Holderbank's" neue Wege im Energiemanagement für die Zement- und Aufbereitungsindustrie. Aufbereitungs-Technik 31 (1990) Nr. 1, S. 7/16.

[26] Scheuer, A.: Minderung der NO_x-Emission beim Brennen von Zementklinker. Zement-Kalk-Gips 41 (1988) Nr. 1, S. 37/42.

[27] Müller, A., Stark, J. und Rümpler, K.: Zum Stand der Entwicklung eines aktiven Belit-Zementes. Zement-Kalk-Gips 38 (1985) Nr.6, S. 303/304.

[28] Stark, J., Müller, A., Rümpler, K., Seydel, R., und Jost, K.: Manufacture of active Belite-cement with regard to the reduction of energy consumption. il cemento 84 (1987) Nr. 3, S. 239/250.

[29] Pöhlmann, R.: Zur Brennbarkeit von Portlandzementrohmehlen in Abhängigkeit vom Kalkstandard sowie Zusätzen und der hydraulischen Reaktivität beim Übergang von kalkreichen zu kalkarmen Portlandzementen. Dissertation RWTH Aachen 1986.

[30] Ludwig, U., und Pöhlmann, R.: Investigations on the production of low lime portland cements. Ciments, Bêtons, Plâtres, Chaux (1988) Nr. 773 = Nr. 4/1988, S. 257/262.

[31] Bei, R.: Herstellung und Eigenschaften von Portlandzementen mit niedrigerem Kalkstandard. Dissertation RWTH Aachen 1990.

[32] Philippon, Th., und Marinos, J.: On the strength behaviour and phase composition of low lime saturation clinkers. Cement and Concrete Research 18 (1988) No. 5, S. 804/811.

[33] Meric, J.P.: Low Energy Clinker Formation. 8th Intern. Congress on the Chemistry of Cement 1986, Theme 1.3 Vol. I, S. 51/56.

[34] Locher, F.W.: Low Energy Clinker. 8th Intern. Congress on the Chemistry of Cement 1986, Principal Rep. Theme 1.3, Vol. I, S. 57/67.

[35] Österreichische Patentschrift Nr. 383 341 B, 25.6.1987. Verfahren zur Herstellung eines aktiven Belitzements sowie Anordnung zur Durchführung des Verfahrens.

[36] Christensen, N.H., und Johansen, V.: Role of liquid phase and mineralizers. J. Skalny (Editor). Cement production and use. Engineering Foundation US Army Res. Off., 1979, S. 55/69.

[37] Gardeik, H.O.: Einfluß der Sintertemperatur auf den spezifischen Energieverbrauch beim Brennen von Zementklinker. Zement-Kalk-Gips 34 (1981) No. 4, S. 169/174.

[38] Staupendahl, G., Tauchmann, H., und Engelmann, Ch.: Einsatz CaF_2-haltiger Mineralisatoren im VEB Zementwerk Karsdorf. baustoffindustrie 1978, Ausgabe A, Nr. 5, S. 10/12.

[39] Vu Van Than und Seidel, G.: Brenntemperaturen unter 1200 °C - Möglichkeiten zur Zementherstellung. baustoffindustrie 1988, Nr. 3, S. 78/79.

[40] Rosemann, H.: Einfluß der Brennstoffart und des Einsatzorts auf Energieverbrauch, Betriebsverhalten und Emission von Drehofenanlagen. Zement-Kalk-Gips 41 (1988) Nr. 5, S. 231/236.

[41] Sprung, S.: Umweltentlastung durch Verwertung von Sekundärrohstoffen. Will be published in Zement-Kalk-Gips 45 (1992) No. 5

[42] OECD-Draft Decision of the Council on the Control of Transfrontier Movements of Wastes Destined for Recovery Operations. ENV/EPOC (92) 8 - 5.2.1992.

[43] Committee for the Adaption to scientific and technical Progress of Council Directive 91/156 CEE (Framework Directive on Waste) - List of wastes and hazardous wastes, Draft 19.12.1991.

[44] Sprung, S., und Rechenberg, W.: Einbindung von Schwermetallen in Sekundärstoffen durch Verfestigen mit Zement. beton 38 (1988) H. 5, S. 193/198.

[45] Sprung, S., und Rechenberg, W.: Bindung umweltrelevanter Sekundärstoffe durch Verfestigen mit Zement. Zement und Beton 34 (1989) Nr. 2, S. 54/61.

[46] Schmidt, M.: Verwertung von Müllverbrennungsrückständen zur Herstellung zementgebundener Baustoffe. beton 38 (1988) H. 6, S. 238/245.

[47] Wischers, G.: Möglichkeiten und Grenzen des Recycling in der Zementindustrie. Arbeitsgemeinschaft Industrieller Forschungsvereinigungen (AIF), Herbsttagung des Wissenschaftlichen Rates 1988, S. 7/14.

[48] Kirsch, J.: Umweltentlastung durch Verwertung von Sekundärbrennstoffen. Zement-Kalk-Gips 44 (1991) Nr. 12, S. 605/610.

[49] Capon, B.M., Layne, P.B., und Watson, D.: The Use of Unconventional Fuels in Cement Manufacture. Cement, Concrete and Aggregates 5 (1983) No. 1, S. 30/34.

[50] Maury, H.-D.: Brennstoff aus Müll - Ein Brennstoff für die Zementindustrie. Zement-Kalk-Gips 42 (1988) Nr. 10, S. 497/501.

[51] Maury, H.-D., und Pavenstedt, R.G.: Chlor-Bypass zur Erhöhung des Brennstoffeinsatzes aus Müll beim Klinkerbrennen. Zement-Kalk-Gips 41 (1988) Nr. 11, S. 540/543.

[52] Willing, E.: Stoffliche Abfallverwertung - Stand der Technik und Prognosen. Recycling - GIT Supplement Umwelt 1988, Nr. 2, S. 29/35.

[53] Krogbeumker, G.: Sicherheitseinrichtungen bei zusätzlicher Verbrennung PCB-haltiger Altöle im Zementdrehofen. Zement-Kalk-Gips 41 (1988) No. 4, S. 188/192.

[54] N.N.: Waste Burning: An Inside Outlook. Rock Products 1988, Nr. 7, S. 63/65, 84.

[55] Kreft, W.: Entsorgung im Zementwerk. Entsorgungspraxis 1988, Nr. 9, S. 360/368.

[56] Kreft, W.: Einsatz von Abfallstoffen als Energie- und Rohstoffersatz bei der Zementherstellung. TIZ International 112 (1988) Nr. 2, S. 123/127.

[57] Kreft, W.: Betriebskosteneinsparung durch rationelle Energieanwendung und Einsatz von Sekundärbrennstoffen beim Brennen von Zementklinker. TIZ International, Powder Magazine 113 (1989) Nr. 11, S. 915/922.

[58] Mantus, E.K., Kelly, K.E., und Pascoe, G.A.: All Fired Up - Burning Hazardous Waste in Cement Kilns, Environmental Toxicology International., 1992.

[59] Gerger, W., und Liebl, P.: Thermische Verwertung von Sekundärbrennstoffen bei den Gmundner Zementwerken. Zement-Kalk-Gips 44 (1991) Nr. 9, S. 457/462.

[60] Sprung, S., Kirchner, G., und Rechenberg, W.: Reaktionen schwer verdampfbarer Spurenelemente beim Brennen von Zementklinker. Zement-Kalk-Gips 37 (1984) Nr. 10, S. 513/518.

[61] Sprung, S.: Spurenelemente - Anreicherung und Minderungsmaßnahmen. Zement-Kalk-Gips 41 (1988) Nr. 5, S. 251/256.

[62] Kuhlmann, K., und Sprung, S.: The use of secondary raw materials and/or fuels in the clinker burning process - Impact on energy consumption, emissions and clinker quality. 9th Intern. Congr. Chem Cem., New Delhi 1992, Communication Paper.

[63] Opitz, D.: Korngrößenverteilung des Zementklinkers. Zement-Kalk-Gips 39 (1986) Nr. 12, S. 673/675.

[64] Sprung, S.: Maßnahmen und Möglichkeiten zur Qualitätssteuerung im Zementwerk. Zement-Kalk-Gips 43 (1990) Nr. 7, S. 340/346.

[65] Schürmann, W., und Scheuer, A.: Berechnung des Wärmeübergangs in einem Rohrkühler unter besonderer Berücksichtigung der Staubkreisläufe und der Zerkleinerung des Klinkers. Zement-Kalk-Gips 42 (1989) Nr. 10, S. 515/519.

[66] Kupper, D., und Schmid-Meil, W.: Verfahrenstechnisch- und rohstoffbedingte Einflußfaktoren auf die Helligkeit und Farbtönung von "weißem" Klinker und Zement. Zement-Kalk-Gips 40 (1987) Nr. 12, S. 589/597.

[67] Rose, D., und Kupper, D.: Ökologische und ökonomische Aspekte der Zementherstellung beim Einsatz von Abfallbrennstoffen. Zement-Kalk-Gips 44 (1991) Nr. 11, S. 554/559.

[68] Blanco-Varela, M.T.: Reactivity of Fly-Ashes when they are used as Constituent of Portland Cement Raw Mixes. TIZ-Fachber. 108 (1984) Nr. 5, S. 304/307.

[69] Puertas, F., Blanco-Varela, M.T., Palomo, A., und Vázquez, T.: Reactivity and burnability of raw mixes made with crystallized blastfurnace slags. Part I: Zement-Kalk-Gips 41 (1988) Nr. 8, S. 398/402. Part II: Zement-Kalk-Gips 41 (1988) Nr. 12, S. 628/631.

[70] Kusnezowa, T.W., Iwastschenko, S.I., und Kulikowa, G.F.: Die Verwertung von Abfällen als ein Weg zur Schaffung einer energiesparenden Technologie des Zements. TIZ-Fachber. 107 (1983) Nr. 89, S. 645.

[71] Patel, M.: Cement from chloride containing wastes. Silicates Industries 1989, Nr. 3/4, S. 55/60.

[72] Borgholm, H.E.: Umweltentlastung durch Verwertung von Flugasche als Rohmehlkomponente. Vortragsreferat: Zement-Kalk-Gips 44 (1991) Nr. 11, S. 584.

[73] Wächtler, H.-J., Urbanek, U., Just, Chr., Schwarzkopf, I., und Gewis, G.: Zur Frage der Klinkerbildung in Drehrohröfen. Teil 4: Theoretischer Wärmebedarf und spezifischer Brennstoffenergieverbrauch beim Klinkerbrennen. Silikattechnik 39 (1988) Nr. 5, S. 157/161.

[74] Saada, Y., und Seidel, G.: Wirkung sulfatischer Phasen in Abhängigkeit vom Alkaligehalt und Sulfatisierungsgrad in Portlandzementklinker und daraus hergestellten Zementen. Teil I: Einfluß des Alkaliträgers unter Berücksichtigung des Sulfatisierungsgrades. Silikattechnik 41 (1990) Nr. 4, S. 119/121.

[75] Sylla, H.-M.: Untersuchungen zur Bildung von Ansatzringen in Zementdrehöfen. Zement-Kalk-Gips 27 (1974) Nr. 10, S. 499/508.

[76] Locher, F.W., Richartz, W., Sprung, S., und Sylla, H.-M.: Erstarren von Zement. Teil III: Einfluß der Klinkerherstellung. Zement-Kalk-Gips 35 (1982) Nr. 12, S. 669/676.

[77] Locher, F.W., Richartz, W., Sprung, S., und Rechenberg, W.: Erstarren von Zement. Teil IV: Einfluß der Lösungszusammensetzung. Zement-Kalk-Gips 36 (1983) Nr. 4, S. 224/231.

[78] Strunge, J., Knöfel, D., und Dreizler, I.: Einfluß der Alkalien und des Schwefels auf die Zementeigenschaften. Teil 1: Einfluß des SO_3-Gehalts auf die Zementeigenschaften. Zement-Kalk-Gips 38 (1985) Nr. 3, S. 150/158.
Teil 2: Einfluß der Alkalien und des Sulfats unter Berücksichtigung des Silicatmoduls auf die Zementeigenschaften. Zement-Kalk-Gips 38 (1985) Nr. 8, S. 441/450.

[79] Knöfel, D., Gies, A., und Strunge, J.: Einflüsse erhöhter Alkaligehalte auf die Zusammensetzung der Portlandzementklinker und die Portlandzementeigenschaften. Silikattechnik 36 (1985) Nr. 5, S. 140/142.

[80] Verein Deutscher Zementwerke - Forschungsinstitut der Zementindustrie. Tätigkeitsbericht 1984/87, S. 36/39.

[81] Sprung, S.: Emissionsprognosen beim Einsatz von Abfallbrennstoffen. Zement-Kalk-Gips 37 (1984) Nr. 10, S. 519/522.

[82] Bailly, M., Makris, M., und Meynardi, G.: The K-Tech Process - High energy savings through the use of a new high-performance hydraulic component. Ciments, Bêtons, Plâtres, Chaux (1990) Nr. 785 = Nr. 4/1990, S. 228/232.

[83] Riedhammer, M.: The Rohrbach Process - The Economical Alternative Method of Utilizing Oil Shale. TIZ-Fachber. 109 (1985) Nr. 12, S. 941/944.

[84] Rohrbach, R.: Herstellung von Ölschieferzement und Gewinnung elektrischer Energie aus Ölschiefer nach dem Rohrbach-Lurgi-Verfahren. Zement-Kalk-Gips 22 (1969) Nr. 7, S. 293/296.

[85] Riedhammer, M.: Abbau und Verarbeitung von Ölschiefer zur gezielten Herstellung hochwertiger Ölschieferzemente. Zement-Kalk-Gips 40 (1987) Nr. 8, S. 393/398.

[86] Bucchi, R.: Features on the role of minor components in cement clinker. World Cement Technology 12 (1981) Part 1: Nr. 6, S. 210/231; Part 2: Nr. 7/8, S. 258/273.

[87] Schmidt, K.D., Gardeik, H.O., und Ruhland, W.: Verfahrenstechnische Einflüsse auf die SO_2-Emission aus Drehofenanlagen. Zement-Kalk-Gips 39 (1986) Nr. 2, S. 93/101.

[88] Rodenhäuser, F., und Herchenbach, H.: Verringerung der gasförmigen Schadstoff-Emission aus Zementanlagen. Zement-Kalk-Gips 39 (1986) Nr. 10, S. 575/577.

[89] Johansen, V., Egeløv, A.H., und Eiriksson, A.O.: Emission of NO_x und SO_2 from cement clinker burning. Zement-Kalk-Gips 39 (1986) Nr. 10, S. 558/560.

[90] Schütte, R.: Möglichkeiten zur Entstehung und Minderung von SO_2-Emissionen in Zementwerken. Zement-Kalk-Gis 42 (1989) Nr. 3, S. 128/133.

[91] Bonn, W., und Hasler, R.: Verfahren und Erfahrung einer rohstoffbedingten SO_2-Emission im Werk Untervaz der Bündner Cementwerke. Zement-Kalk-Gips 43 (1990) Nr. 3, S. 139/143.

[92] Locher, F.W.: Entwicklung des Umweltschutzes in der Zementindustrie. Zement-Kalk-Gips 42 (1989) Nr. 3, S. 120/127.

[93] Kreft, W.: Konzepte zum Umweltschutz in der Zementindustrie. Zement-Kalk-Gips 41 (1988) Nr. 4, S. 193/201.

[94] Kirchner, G.: Thalliumkreisläufe und Thalliumemissionen beim Brennen von Zementklinker. Zement-Kalk-Gips 40 (1987) Nr. 3, S. 134/144.

[95] Kreft, W.: Die Unterbrechung von Stoffkreisläufen mit Berücksichtigung der integrierten Weiterverwendung im Zementwerk. Zement-Kalk-Gips 40 (1987) Nr. 9, S. 447/450.

[96] Schütte, R., und Kupper, D.: Die Bedeutung von Kreislaufbetrachtungen für Produktqualität und Umweltverträglichkeit der Zementherstellung. Zement-Kalk-Gips 43 (1990) Nr. 12, S. 565/570.

[97] Maki, I., und Hattori, M.: Influence of Minor Components on the Fine Textures of Alite in Portland Cement Clinker. il cemento 86 (1989) Nr. 2, S. 131/140.

[98] EG Draft Council Directive on the Incineration of Hazardous Waste. Januar 1992.

GENERIC THEME II

ADVANCES IN PORTLAND BLENDED SPECIAL AND NEW CEMENTS

SPECIAL AND NEW CEMENTS

A K Chatterjee

Research & Consultancy Directorate
The Associated Cement Cos Ltd, Thane, INDIA

SUMMARY

Keeping in view the changing concepts of new and special cements with time, the historical trend of development prior to the 8th ICCC and the status of such novel products at the last Congress have been outlined. The why^{s} and how^{s} of eventual developments in the field of new and special cements have been traced. The relevant and significant growth of understanding and application of densified system of ultrafine particles, polymer-modified cements including macro defect-free binders, blended high-alumina cements, phosphatic materials, calcium aluminosilicate glass cements and calcium silicate cements of sol gel origin have been reviewed in reasonable details. An attempt has also been made to look into the prospects of new cements of yester decade like reactive belite, calcium sulphoaluminate and alinite cements.

PREAMBLE

One of the fundamental problems of dealing with special and new cements is the difficulty of delineating and defining the systems that could be categorised under this nomenclature. The difficulty ensues from the fact that the scope of special and new cements is a time dependant phenomenon. What was new or special cement two decades back does not belong to that category today any more. This is more evident when we try to trace the history of cements from the prehistoric days (Fig.1).

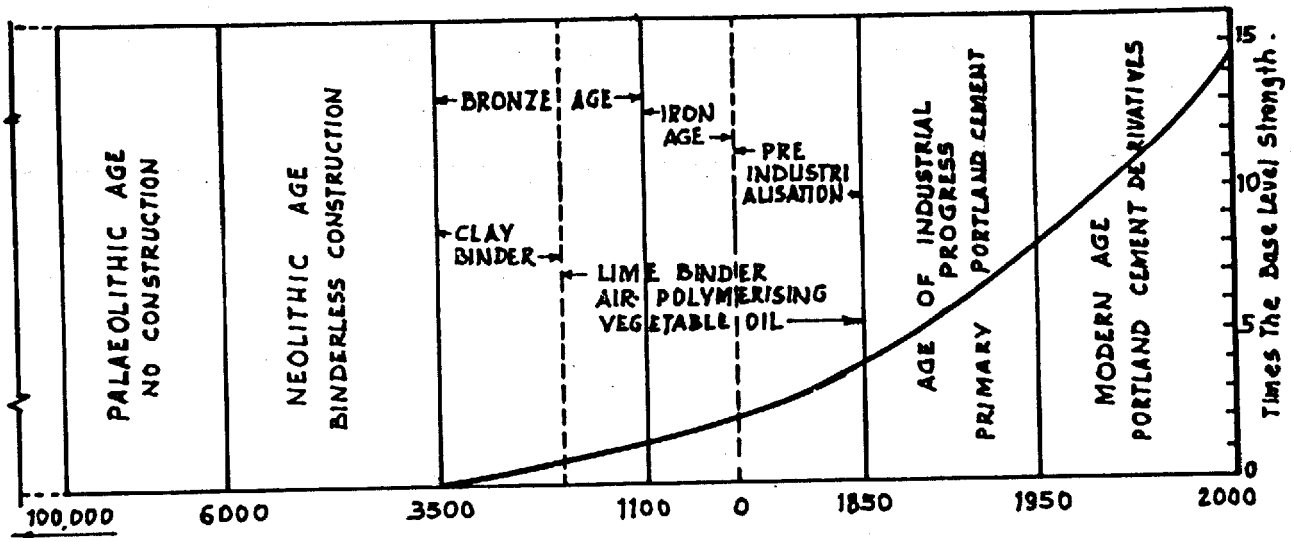

FIG.1 : CHANGE OF CEMENT CHARACTERISTICS WITH TIME

TRACING OF DEVELOPMENTAL TRENDS

From the above figure, it is observed that there was no human activity of construction in the palaeolithic age and the first concept of construction without any binders was introduced by man in the neolithic age when he started enclosing space with juxtaposition of stone blocks, animal skin, natural wood, etc. It is believed that in the Bronze Age, there was a chance discovery that the baking of wet clay would make it hard and could give rise to moulded shapes of some use like bricks. This also made clays as a binder in construction. Thereafter, with progress of time, the binding properties of lime, air polymerising vegetable oil and lime-pozzolana mixes were made use of in the construction during the period that preceded the known history of Portland cement and concrete. Since the advent of Portland cement over the last one and a half centuries, the developmental trends in cement applications branched off in the direction of obtaining high ultimate strength, higher early strength, greater durability and more effective conservation of materials usage in constructional concrete. Nagataki (1) has summarised the techniques (Fig.2) that are adopted today for attaining high strength in the constructional concrete. In the above figure, one of the requirements has been indicated as the high strength Portland cement. The steps taken to achieve this kind of product have essentially been to

- increase in C_3S content and ultimate optimisation.
- finer and finer grinding and ultimate control in particle size distribution.
- improvement in particle morphology.
- doping of mineral phases for higher reactivity.

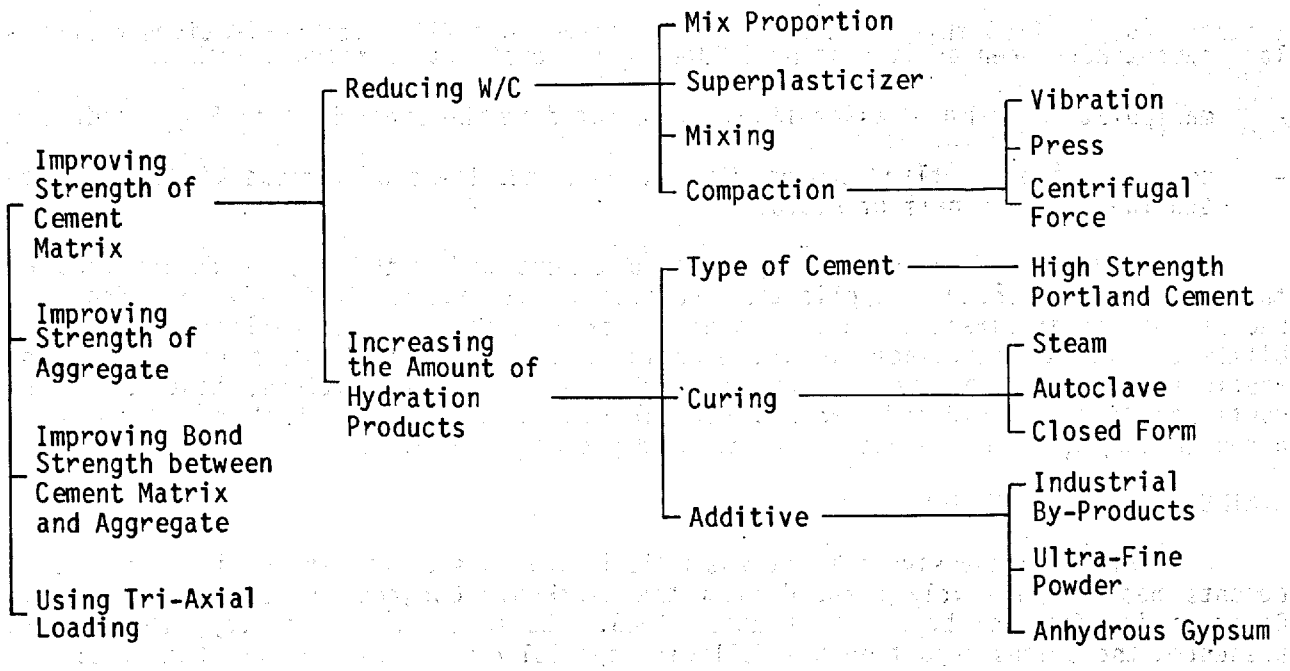

Fig.2 : Practical techniques for attaining high strength

With all these steps, the application properties of Portland cement could be improved with respect to its compressive strength but the intrinsic disadvantages of Portland cement with respect to its stiffness, tensile strength, fracture toughness and creep properties could not be overcome in any substantial manner. Hence, the researchers continued their efforts in developing various derivatives of Portland cement for special constructions. As a result, a host of derived formulations are produced and marketed all over the world today and these varieties are summarised in Fig.3.

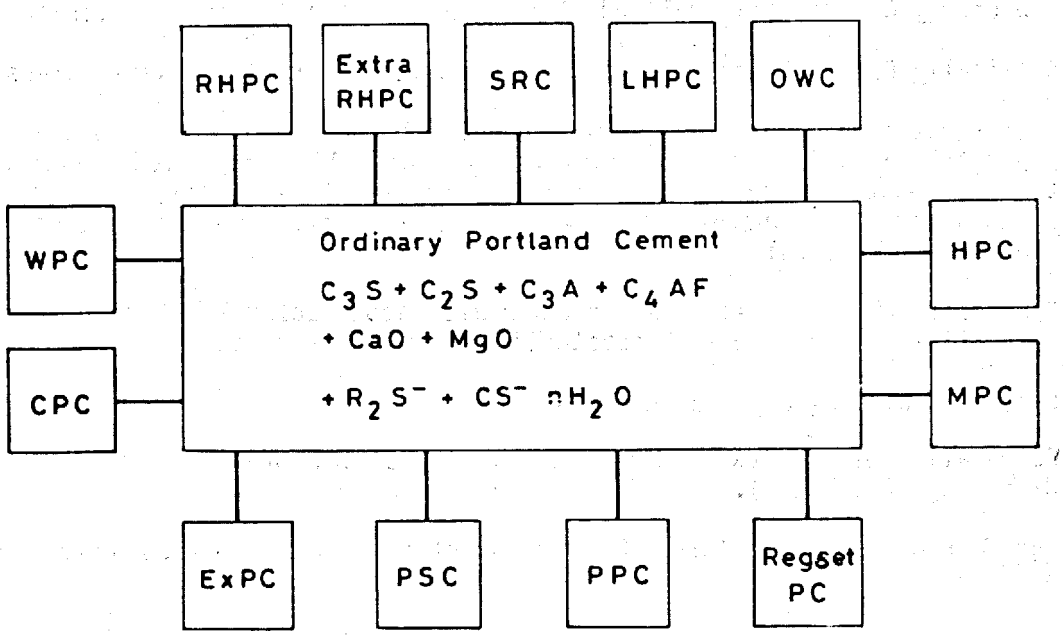

Fig.3 : Portland Cement Derivatives in Commercial Production

Interestingly, from this figure, one may observe that all these derivatives of Portland cement have been arrived at by following two distinct approaches such as

- manipulation of phase assemblages as depicted in the upper half of Fig.3 and
- compositing of Portland cement with external additives of various kinds as depicted in the lower half of Fig.3.

Both with the improved basic Portland cement and with diverse derivatives of this generic binder, the application horizon of cement substantially expanded, but because of the intrinsic shortcomings of the product as mentioned earlier the applicability of cement to replace metals, plastics and high-fired ceramics for engineering applications could not be resorted to. Most of these derivatives, however, were continued to be considered new and special cements during the last few decades, although they have turned out to be standard products today.

STATUS AT THE RIO CONGRESS

A fairly comprehensive attempt was made in (2) to show how the horizon of special cements has progressively changed from the Stockholm Congress in 1932 to the Paris Congress in 1980 and beyond till about 1985. Based on such a survey, the authors presented the status report on the following special cements at the last Congress:

* Alumina Cements (high alumina and calcium aluminate binders)
* Expansive Cements (K, S, M and AEC types)
* Fast Setting and Hardening Cements (hybrid formulations using binary OPC/HAC, ternary OPC/HAC/Gypsum, fluroaluminate and sulphoaluminate mixes)
* Very High Strength Cements (high strength concrete, high strength cement paste, DSP, MDF)
* Low Energy Cements (mineralised clinker cement, belite cement, alinite cement)
* Chemically Bonded Cements (phosphates, magnesia, dental and water glass cements).

Of the above varieties of special cements, the low energy cements were also dealt with separately in (3), where emphasis was laid on belite, modified belite and alinite cement. The above special cements were also dealt with in a large number of communication papers at this Congress, from which special mention may be made of the following interesting findings:

a) Synthesis of jasmundite, a compound with isostructural substitution of Cl^- by S in alinite structure with substantially lower hydraulicity (4).

b) Synthesis of MnF_3 doped alinite (5).

c) Formulation of complex binders with alkali activation of industrial wastes including slags (6, 7 & 8).

d) The lab-scale manufacture of hydrogarnet-gehlenite hydrates cement from C-A-S glass (9).

From this status of special and new cements at the conclusion of the Rio Congress, during the subsequent period, some significant changes have been noticed in the development of new cementitious materials.

PRESENT APPROACHES FOR DEVELOPMENT OF NEW CEMENTS

It has already been mentioned that despite significant developments in the field of cement chemistry and technology, the known binders continue to suffer from three important engineering properties - stiffness (resistance to bending), tensile strength (resistance to pulling) and fracture toughness (resistance to impact). This has been amply summarised in Table 1 (10). At the same time, it is interesting to note that there are naturally produced inorganic materials that do not suffer from such shortcomings.

TABLE 1

A SURVEY OF MECHANICAL PROPERTIES OF VARIOUS MATERIALS

	S*, MPa	E**, GPa	R#, J/m^2	K_{1c}##, MPa$\sqrt{m}$
Cement Paste	6.5	18	15	0.2
Concrete	8	25	80	1.2
DSP materials	?[1]	80	1[2]	?
MDF materials	150	50	200[3]	3
Polycarbonate	65	2.5	4000	3
'Typical' Ceramic	280	300	100	5
Mild Steel	280	210	140000	170
High-Strength Steel (4340)	1400	210	140000	170

* Tensile strength ** Young's Modulus # Fracture Energy ##Critical Stress Intensity Factor

1 Compressive Strength ca. 250 MPa . 2. 9,000 J/m^2 with addition of fibers
3 Said to approach 100,000 J/m^2 with addition of fibers

We know that living marine organisms have shells made of calcium carbonate, calcium phosphate and silica and their tensile strength is more than 100 MPa and toughness more than 1000 J/m^2 of new surface generated by fracturing, which makes it comparable in that respect to polystyrene and plexiglass. Being encouraged by such natural phenomena to create primarily inorganic materials of today's property requirements, scientists have tried to look at the formulation of hydraulic binders with fresh eyes so that products capable of replacing metals and plastics could be developed. The scientific community started from the fundamental aspects of hydration reactions and tried to establish the structure-property relationship in hardened cement pastes through intensive efforts in understanding porosity-strength behaviour and compliance of Griffith's theory of crack propagation. If we were to summarise some of these observations, we could refer to Fig.4. that shows the empirical laws relating the strength of cement to its volume porosity. The figure reveals that porosities occupying a volume fraction less than 0.2 are not attainable in ordinary cement mixing and that ordinary cements are intrinsically weak with a maximum compressive strength of about 130 MPa and a flexural strength of around 30 MPa at zero porosity (11-16).

From this kind of base level how to improve the properties further has been the concern of most researchers. The developmental trends can be summarised as in Fig.5 and the specific thrusts can be indicated as follows:

a) Development of non-Portland cements in systems other than the conventional silicate ones.

b) Compositing of Portland and non-Portland cements with ultra fine materials and dispersants.

c) Compositing of Portland and non-Portland cements with organic polymeric substances..

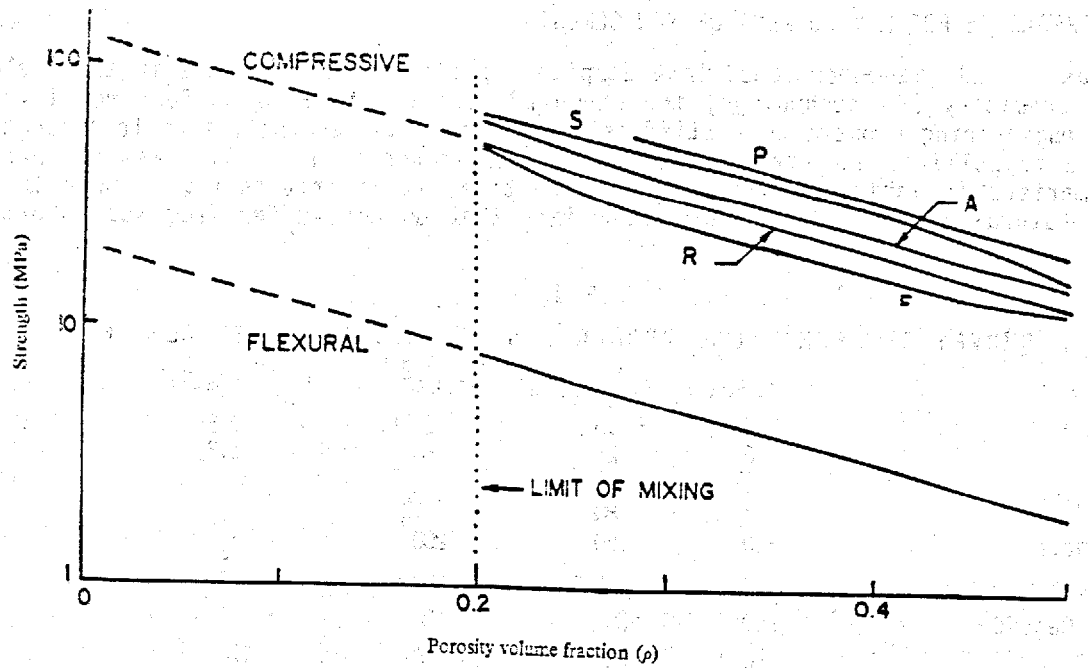

Fig.4 : Empirical laws relating strength of cements to their volume porosity (the compressive strength curves have been displaced vertically for clarity; the alphabets S, P, A, R and F refer to the initials of the authors in Refs.12-16 respectively), (after Kendall et al.)

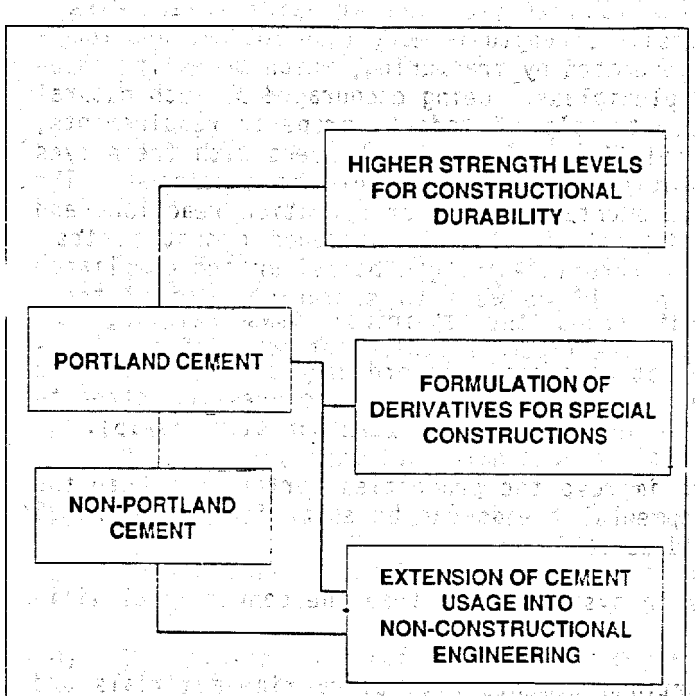

Fig.5
TRENDS OF DEVELOPMENTS IN CEMENT APPLICATIONS

These approaches have led to the generation of a new clause of materials called 'Chemically Bonded Ceramics (CBC)' which are defined as "Inorganic Systems that have been bonded into a cohesive unit through the use of chemical activation energies via a liquid-solid reaction" (17). Such reactions typically operate at much lower temperatures and such products make use of special processing techniques and special materials.

Taking note of the historical and eventual trends of developments in the binder technologies and keeping the basic Portland cement and its derivatives outside the purview, the scope of new and special cements that demands attention of the scientific world could be summarised as follows.

a) Composite cements with ultra fine materials and dispersants with or without fibres.

b) Composite cements with polymeric substances with or without fibres.

c) Multiblend cements with alkali activation.

d) Blended high alumina cements.

e) New cement systems

- Phosphatic materials
- Calcium alumino-silicate glass cements
- Sol-gel cements

In the present review, the above systems have been dealt with in some detail. Attempts have also been made to reflect on the status of reactive belite, sulpho-aluminate and alinite cements, which perhaps were new cements in the previous decade.

COMPOSITE SYSTEMS WITH ULTRA FINE MATERIALS AND DISPERSANTS WITH OR WITHOUT FIBRES

Developmental Background

It has already been indicated that the conventional concrete has a moderate compressive strength, a low tensile strength and poor ductility. When concrete is properly reinforced with steel bars or other reinforcing fibres, the material forms more reliable structures. In reinforced concrete, the reinforcing bars or fibres resist tensile stressess while the concrete resists compressive stressess and transmits forces to the reinforcement. A severe drawback of reinforced concrete is that the concrete cracks under tension at strengths that are only 2-5% of the yield strength of the reinforcement (18). This means that the reinforcement can only be effectively used at the cost of an internal coherence of the concrete in the form of cracks passing the reinforcement.

From the above, it is evident that internal coherence of concrete through denser packing of particles is of utmost importance in developing strong binder materials. The effort to pack cement densely could not yield positive results in the past as there were no effective dispersants suitable for ultra-fine cements and cements with special particle size distribution. With the appearance of effective dispersants for cement systems in the early 1970s, it became possible to establish denser packing of cement in aqueous suspensions. This development was primarily used to enhance the quality of conventional concrete with conventional cement, resulting in an increase in strength by 30 to 50%, corresponding to compressive strengths upto 120 MPa.

These possibilities have now been exploited to a fuller extent in the so called DSP materials, which is an acronym for "Densified Systems containing homogenously arranged ultra-fine Particles" and which were developed in seventies by Aalborg Portland in Denmark. These materials are based on very dense and strong binders with 70 to 80% cement and 20 to 30% ultra-fine materials having an average size of only 0.1 to 0.2 micrometers (19). The use of effective dispersants ensures dense packing of the cement with the ultra-fine materials placed homogenously in the spaces between the particles of cement, as illustrated in Fig.6 The ultra-fine materials used being less reactive than cement, it became possible to create dense and

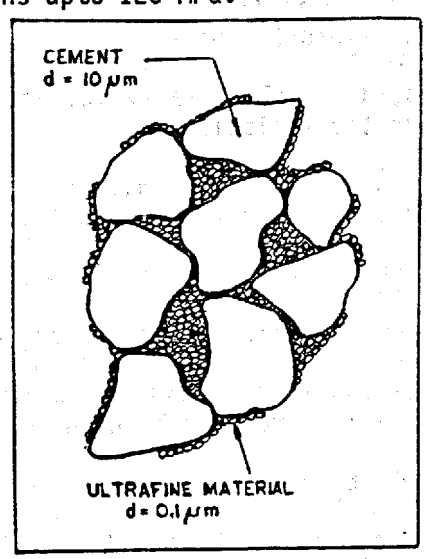

Fig.6: Structure of strong binder materials made from cement and ultra-fine material.

homogenous structures. The amount of water needed to achieve a plastic to fluid consistency in such materials is as low as 14% compared to 60% for conventional high strength concrete.

The compressive strength of DSP concretes is typically between 120 and 250 MPa. It is reported that DSP materials have been commercially used since the beginning of the 1980s for a variety of purposes including machine components, cutting tools, rods, etc. The characteristic limitation of most of these strong materials is their high brittleness. The brittleness of the very strong new materials is illustrated in Fig.7, which shows the problems of using very strong cementitious materials.

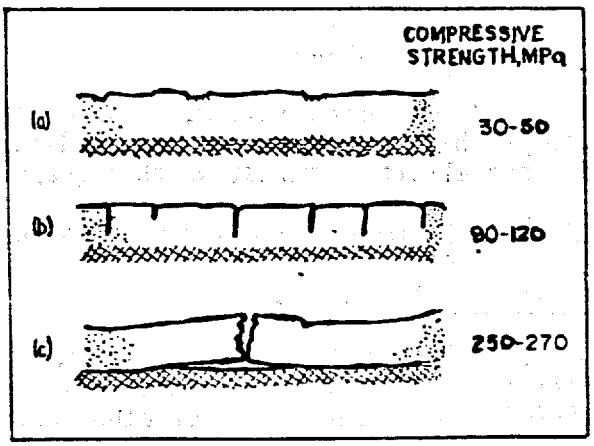

Fig.7 : Evidence of brittleness with strength : (a) normal quality, (b) material with higher strength showing shrinkage cracks and (c) much stronger material showing peeling of surface layer from base.

The morphology of hardening mechanism of DSP containing various types of cement and the mechanical properties of such DSPs have recently been studied and reported in (20). In this paper, an interesting observation has been made about the formulation of DSPs from calcium aluminate cements with low temperature calcination that improves the bending strength appreciably.

Fibre and Particle Reinforcement

The incorporation of fibres makes it possible to increase the tensile load capacity and provide ductility. However, in strong materials, it is necessary to ensure a higher concentration of fibres and as a result, it is not easy to produce such structures. The brittleness can be reduced by incorporating strong and stiff particles. The effective particle reinforcement would require much stronger and stiffer particles than the binder. For conventional concrete, this requirement is met with natural aggregates. However, in DSP systems, the requirements are not satisfied with normal aggregates. Hence, special types of strong aggregates are required for effective exploitation of such systems. With such special aggregates DSP systems with compressive strengths of 200 to 250 MPa are reported to be in the market with the use of cement, microsilica, alumina-rich aggregates and reinforcement (21).

Thus, for effective exploitation of the DSP composites, one may have to strive to achieve the following:

1. A very dense binder material based on hydraulic cement and ultra-fine materials with a low water/powder ratio.

2. A high concentration of fine and strong fibres.

3. A high concentration of strong and stiff particles.

4. Combining such modified materials together with densely arranged main reinforcement with a relatively high volume concentration.

Textural Features

This composite is built up of a strong paste matrix containing cement grains and ultra-fine particles, which is typically brittle in itself, but since it is heavily reinforced with fine fibres, it forms a stronger and more ductile body. This heavily

fibre-reinforced material, in turn, acts as a matrix in a composite that is further reinforced with a high concentration of main reinforcement which could even be steel bars. Thus, this new class of material has strong resemblance to conventional concrete but has a much higher load capacity not only in compression but also in tension (Fig.8).

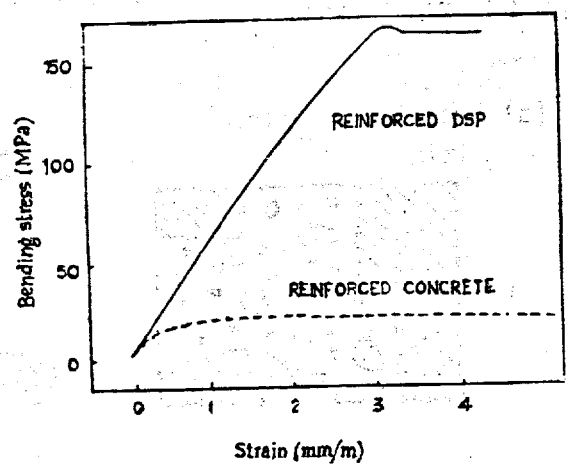

Fig. 8: Comparative behaviour of small beams of reinforced DSP and reinforced concrete (beam size 50 mm x 50 mm x 500 mm)

Application Potentials

It is reported that patent applications on DSP materials are quite extensive in different countries and the DSP materials and products are being primarily marketed by Densit A/S in Denmark and Elborg Technology Co. in U.S.A.(22). The first applications were overlays in concrete exposed to aggressive environments. Subsequently, more sophisticated applications of DSP have been attempted. Essentially, the new composite has served well as a substitute for cast basalt, rubber and steel as lining materials. Even engineering items like screw feeders, scoop feeders for cement mills, press tools for pressure-shaping steel plates in the car body industry, etc. have also been successfully made with DSP materials and gainfully used in industries (23). This composite material with compressive strengths of nearly half of structural steel, tensile strength of about one tenth of this compressive strength and very high strength to density ratio as compared to steel, has the potential of ushering in the possibility of building far bigger structures of bridges and towers than has hitherto been possible.

COMPOSITE CEMENT WITH POLYMERIC SUBSTANCES WITH OR WITHOUT FIBRES

Cement-Polymer Systems

Today the cement polymer systems are fairly widely known to the construction industry. At the Moscow Congress in 1974, a principal paper was devoted to the cement polymer system with special reference to the developmental work being carried out then on making concrete pipes from such composite materials (24). Surprisingly, in the subsequent Congresses, the cement-polymer systems were not emphasised to that extent, although, in the meantime, this system established itself as a preferred constructional material particularly for emergency repairs. A practical review of cement-polymer materials have been attempted in (25).

It is known that there are three modes of making polymer composites: polymer-modified cement mortars and concrete, polymer-impregnated concrete, and polymer concrete. Of these, the last variety would not strictly fall in the category of cement composites as it is generally made with coarse and fine aggregates embedded in polymers alone. According to the review mentioned above, the polymer-modified mortars and concretes have enjoyed popularity with the construction industry because of their process technology being similar to ordinary Portland cement mortars and concrete. The polymer dispersants widely used in such products are styrene-butadiene rubber(SBR), latex, ethylene-vinyl-acetate (EVA) and poly-acrylic ester (PAE) emulsions in Japan and Europe; and SBR latex, PAE and epoxy resin in USA. Generally in this mode of use, the polymer addition is in the range of 5 to 20%, cement to fine aggregate ratio being 1:2 to 1:3, water-cement ratio 30 to 60% and air content less than 6%. In the polymer impregnation mode, the methyl methacrylate monomer is normally used in the range of 5 to 15% with 20 to 30 mm impregnation depth. It is reported that this mode of use of polymer composite is not very cost effective and hence, not favoured in

the industry.

The principle of latex or emulsion modification in polymer modified mortar and concrete can be represented as a multi-step model of structure formation in which the hydrated cement phase and polymer phase interpenetrate into each other as represented in Fig.9 (26).

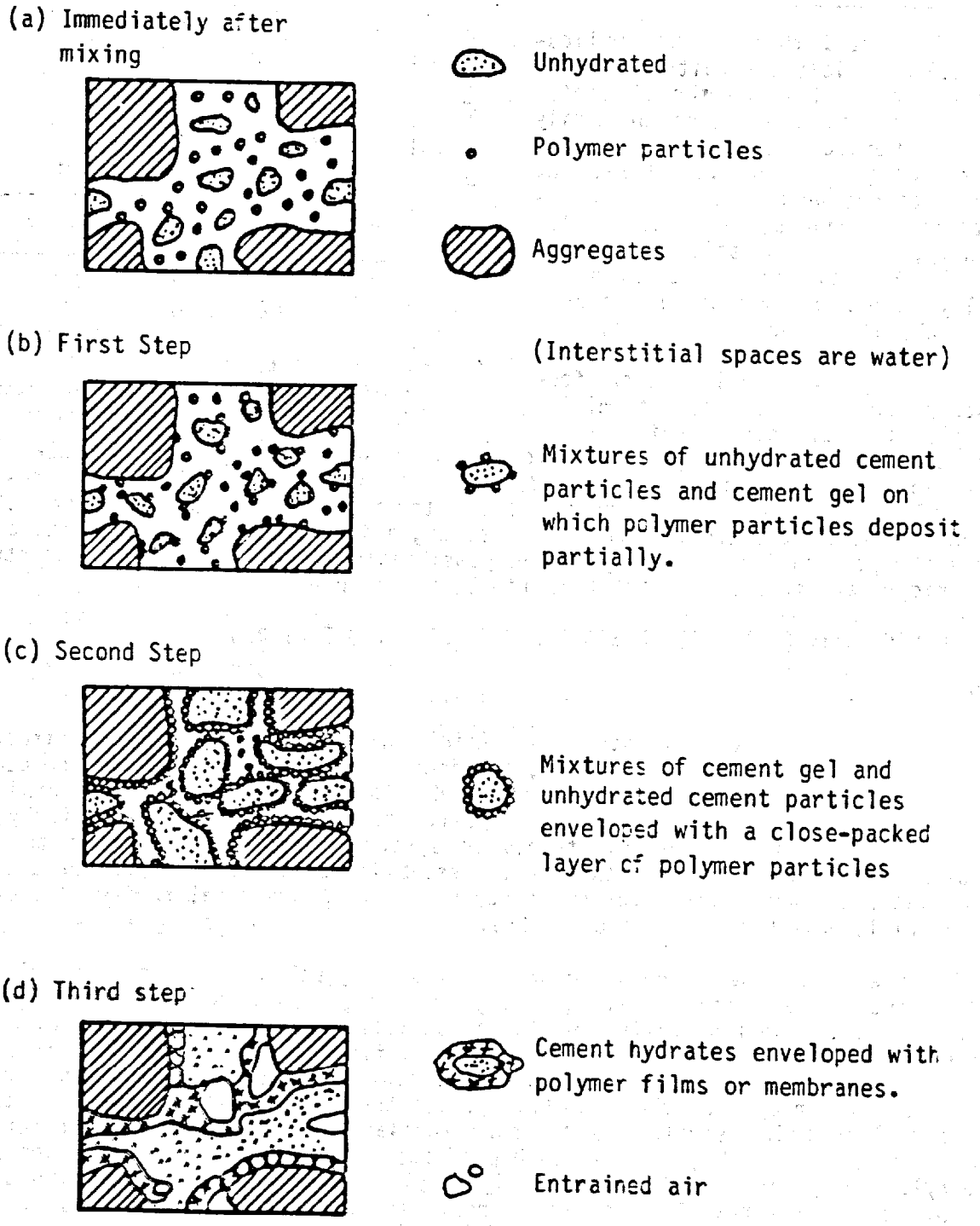

Fig.9 : Simplified Model of Structure Formation Process in Polymer-Modified Mortar and Concrete.

MDF Cements

Taking cue from the structure-property relationship of cement-polymer systems, MDF (Macro Defect Free) cement pastes were developed by Birchall and co-workers at ICI Mont Division more than a decade back. Before arriving at this formulation, the authors apparently carried out certain fundamental studies to understand the mechanism of optimum packing of particles in aqueous state. These studies revealed, in general terms, that as a suspension becomes concentrated, particles come into contact and bridge, and the interparticle friction is such that an adjustment to optimum packing by sliding cannot readily occur even under pressure. Therefore, both "dispersion" and "lubrication" of particles are necessary for optimum packing. While the chemicals used in the formulation of DSP materials help in "dispersion", the required effect of "lubrication" is not realised. On the other hand, both these effects can be achieved by the use of water soluble organic polymers in a cement-water mixture(27). Further, as mentioned earlier, the biogenic inorganic materials like "mother-of-pearl" show that the organic matrix in such materials controls the nucleation, growth and morphology of the inorganic crystallites. Based on these concepts, a new class of cement-polymer composites has appeared in the field (27-29).

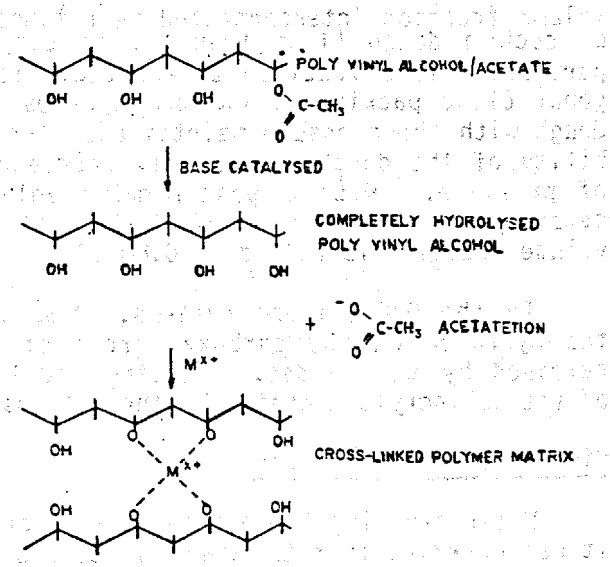

Fig.10 (a) Reaction of PVA with high alumina cement

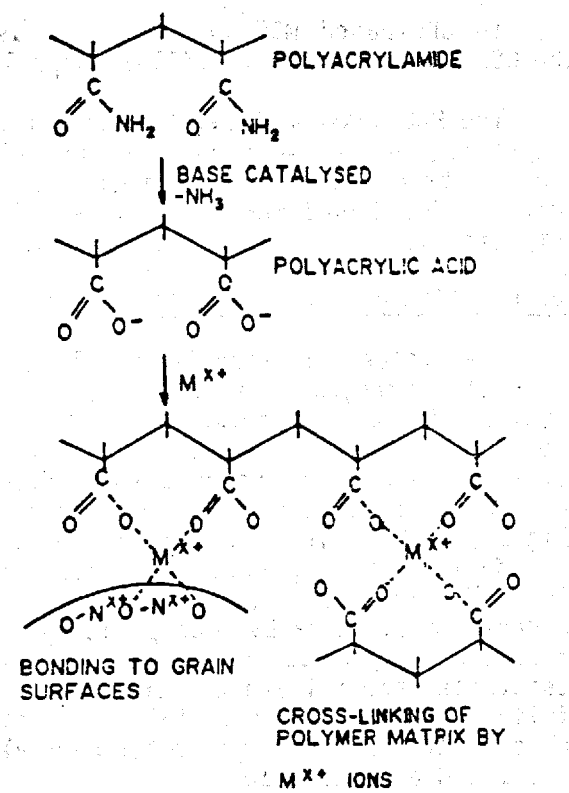

Fig.10 (b) Reaction between polyacrylamide and OPC

As already mentioned, in MDF cements, a water-soluble polymer is used to attain very high flexural strength (> 100 MPa). As the polymer gives a stiff gel with water, a high shear mixing is necessary. Two material systems have been worked upon in great details: high alumina cement with partially hydrolysed polyvinyl acetate and Ordinary Portland Cement with polyacrylamide (30-33). The cement-polymer-water reaction schemes as suggested by Rodger et al (33) are presented in Figs.10a and 10 b. In the high alumina cement system, when water is added to the cement mixed with polymer (PVA) the rising pH causes the hydrolysis of the acetate groups, leaving PVA in solution with acetate ions which subsequently react with calcium ions to form calcium acetate. The metal ions in solution will then crosslink the PVA chains; this causes the polymer matrix to become rubbery and thus allows the physical processing to continue as the cement-polymer mix attains a plasticine-like consistency. The polymer will also coordinate with metal ions on the surface of the cement grains, producing a cohesive matrix which links the anhydrous particles. As a result of such mechanisms the dough of such systems, formed by higher shear mixing, consists of packed particles of about 0.6

volume fraction interconnected by entangled hydrated polymer chains. A gentle pressure on such a dough (less than 5 MPa) compresses occluded air bubbles and raises the particle volume fraction to about 0.7 (as compared to 0.74 volume fraction for hexagonal close packing of uniform spheres). If a modest temperature is applied to the dough with the pressure maintained, the cement hydration is accelerated, the deformability of the dough is markedly decreased and no air pockets are reformed on release of pressure. With a post-forming volume contraction of about 10%, caused in this cement-polymer system by dehydration of polymer and hydration of cement, the particle volume fraction is raised to 0.80 (30).

In the OPC-polymer systems, when metal oxides are mixed with polyacrylic acid, the hydrogen on the carboxyl group of the acid becomes replaced by the metal ions released by the oxides. Setting and hardening then results from the cross-linking of the polyacrylate chains by the cations.

Microstructural Features

While studying the microstructure of high strength cement paste systems in general it was observed that the densification of microstructure is mainly due to lower porosity and formation of purely crystalline hydrates. In mortar specimens the bond between the cement paste and aggregate is moreover less porous and more finely crystallised than in normal mortars and concretes(32).

In OPC-based MDF cements, the usual hydration products are present; however, the CSH gel lacks the fibriller morphology often seen in conventional cements (34).

The HAC-based MDF cements do not contain the normal crystalline calcium aluminate hydrates, but a small quantity of gel containing the organic polymer forms a continuous network structure bonding clinker grains. The microstructure of the polymer phase in HAC-based MDF cements reveal the presence of Ca and Al ions, while Ca rich interstatial gel material was found in OPC-based MDF pastes (34).

Manipulation of Properties in MDF Cements

The value of Young's modulus, flexural strength and fracture energy obtained for a well formulated MDF paste are 50 GPa, 150 MPa and 1 KJ/m^2 respectively. With reinforcement with fibres the fracture toughness approaches 10^5J/m^2 (Fig.11) (30). The MDF pastes can also be filled with particulate materials like silicon carbide, alumina, metal powders, etc. thereby manipulating the properties such as hardness, abrasion resistance, thermal and electrical conductivity, etc. The materials can pick up pigments or the products can also be painted or metallized.

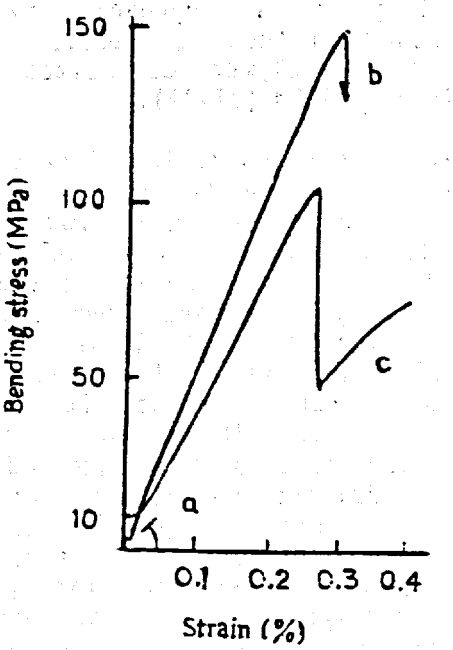

Fig.11: Comparative stress-strain relationship of (a) normal cement paste, (b) an MDF Calcium Aluminate cement and (c) the latter reinforced with 9% by volume Kevlar fibres.

Application Potentials

Those materials distinguish themselves as engineering materials because of their properties such as high flexural strength and fracture toughness, non-flammability, fairly good electrical, cryogenic and acoustic properties (Table 2) (35). Some of the potential applications in the field of acoustics are for making

TABLE 2

PROPERTIES OF MDF CEMENTS

Flexural Strength	150-200 MPa
Young's Modulus	50 GPa
Compressive Strength	300 MPa
Unnotched Charpy	3 KJm^{-2}
Unnotched Charpy (+ 15% Vol nylon fibre)	120 KJm^{-2}
Critical Stress Intensity factor	3 $MPam^{1/2}$
Poisson's ratio	0.2
Density	2500 kgm^{-3}
Porosity	1%
Permeability (Oxygen)	10^{-16} ms-1
Thermal Expansion	9.7 um/mk
Volume resistivity	10^{9}-10^{11} Ohm cm
Discharge Inception voltage	10 kV
Electric Strength	9 KV mm^{-1}
Shielding 30-1000 MHz, 30% vol iron	50 dB
Mean Dielectric Strength (1-10 KHz)	9
Acoustic tan delta	1

loudspeaker cabinets, turn-tables and Hi-Fi components, and in cryogenics, as cryogenic liquid containers. In an electrical field, because of good discharge inception voltage and electric strength, arc resistance and modest surface resistivity, possible applications can be found in arc chutes and fuse tubes. In the field of armour, some of the potential applications which are under extensive evaluation are for personnel and vehicle armour, building partitions and fragmentation protection in high threat areas.

Other potential applications are for load-bearing floors, ceilings, partition/cladding, decorative tiles and pipes for transporting gases and liquids. It may be relevant to mention here that Ube Industries in Japan has introduced into the market a commercial product under the name "mirrorgrace" based on MDF cement. The product is a decorative cladding for interior spaces in buildings as a competition to polished rock or marble panels (36).

Because of properties like high strength, stiffness, low permeability, solvent resistance and resistance to acid/alkalies, these composites can find applications in the field of nuclear waste containment and are being evaluated for this. Metal powder filled components are being evaluated for protection from electro-magnetic interference for equipment such as computers, motors, power cables, etc. Another application where extensive trials have been conducted is in the replacement of metals used in tool and die making. Today, these kinds of composites are commercially exploited in tooling for plastic fabrication, autoclave moulds (handling temperature upto 175°C) and compressive moulds (handling temperature upto 150°C). The advantages are ease of forming at low temperatures and no requirement of machining in contrast to metals (37). Other applications which may be commercially exploited in the near future are in brake-lining matrix as a replacement for phenolic resins which are presently being used.

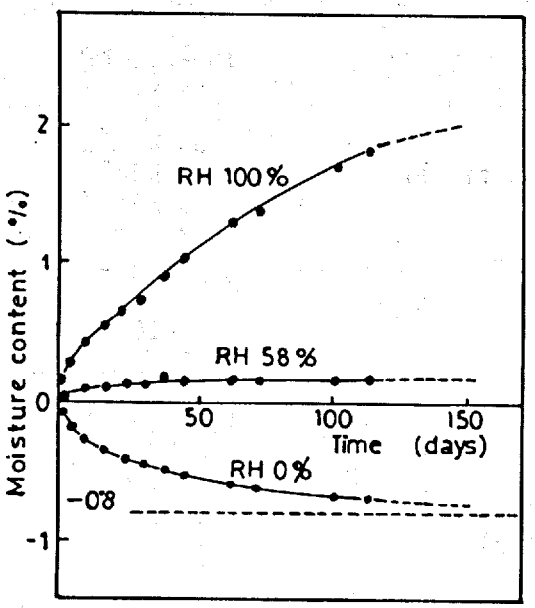

Fig. 12: Relationships between moisture content and time for PVA 5% sample.

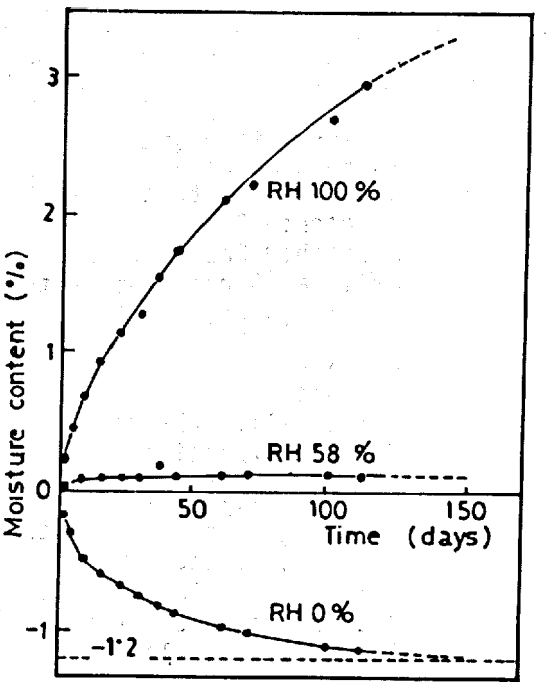

Fig.13: Relationships between moisture content and time for PVA 10% sample.

However, in expanding the horizon of application of MDF cements, one of the critical areas of research is the durability and effect of exposure to moisture. In (38) it has been observed that the MDF composite, prepared from high alumina cement and PVA, when exposed to RH 0%, desorbed moisture and when it was exposed to RH 58 and 100%, it adsorbed moisture (Figs. 12-14). The amount of adsorption depended on the content of PVA, the relationship between the moisture content, bending strength and elastic modulus are shown in Figs. 15-16. Apparently, the reduction in strength and elastic modulus by absorption of water is explained by the softening of PVA which is attributed to its solubility in aqueous medium. The diffusion co-efficient of water in MDF cement paste was of the order of 10^{-11} cm^2/S.

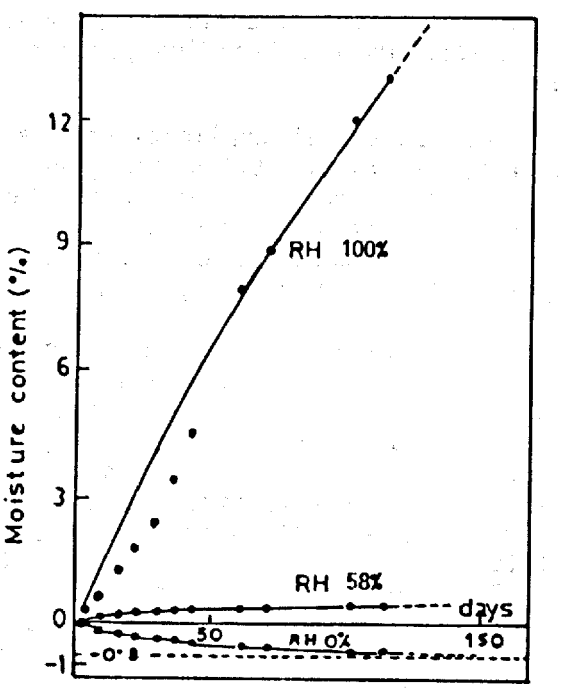

Fig.14: Relationships between moisture content and time for PVA 15% sample.

Polymer Modified Regulated Set Cement

It is known that regulated-set Portland cement was invented and patented by the researchers at the Portland Cement Association in USA in early 1970s (39). However, the main commercial application of this cement took place in Japan as Jet Cement. Today it is being commercially

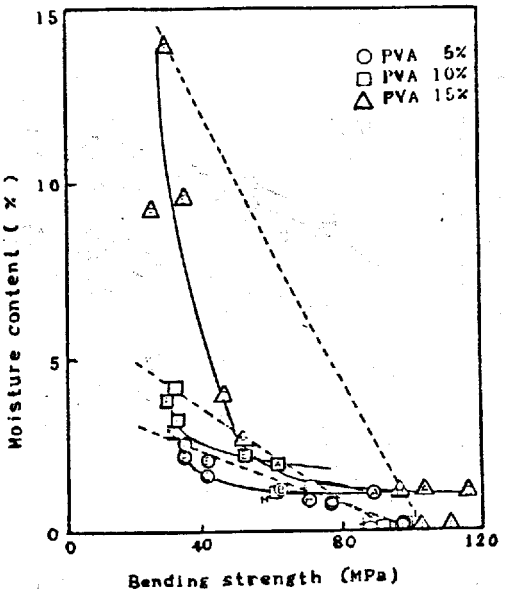

Fig.15: Relationships between moisture content and binding strength

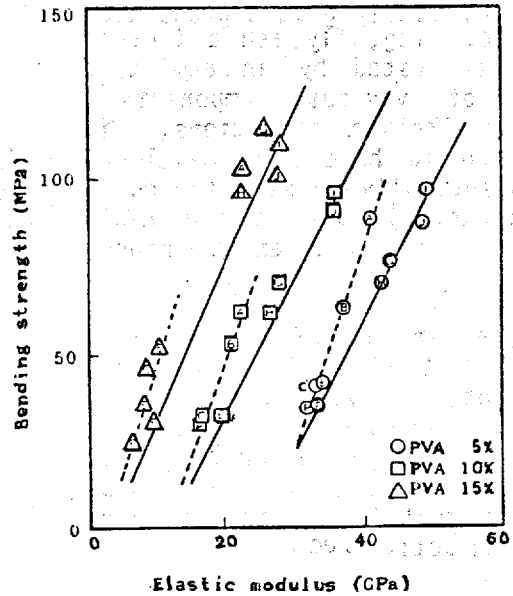

Fig.16: Relationships between bending strength and elastic modulus.

manufactured in various countries (40). It is also well known that this cement is derived from flouride modified Portland cement clinker in which $C_{11}A_7.CaF_2$ is present instead of C_3A.

In recent times, this variety of cement has also been taken up for production of composite cements with additions of polymers and fibres. It has been observed that the polymer modified regulated set cement (in which SBR has been used) showed improvement in proportion to the amount of polymer added. The tensile strength could be raised by two items, the bond strength by 2 to 3 times and water tightness by 5 times as compared to standard unmodified regulated set cement concretes (41). The improvement in terms of drying shrinkage has also been observed. Some of the findings are shown in Figs. 17 & 18. Similarly, attempts have also been made to use fibre reinforced regulated set cement, both with glass fibres as well as steel fibres (42). These kinds of modified regulated set Portland cements have been reported in the above references to have been successfully applied in fields.

MULTIBLEND CEMENTS WITH ALKALI ACTIVATION

The concept of making alkali activated slag cement is not new and perhaps owes its origin to some of the pioneering works of the Russian scientists like Glukhovskii. Later the Trief Cement was also developed on similar principles (43). Some of these developments have been reviewed in (44). In late 1970s, the interest in alkali activated slag cements faded out perhaps, to a large extent, due to the apprehension of general durability of such cements as well as of their vulnerability to alkali aggregate reactions.

However, from mid-80s, there has been a revival in the alkali activation approach not only for slag cements but also for multi-component alumino-silicate blended cements (45-47). The introduction of a new binder known as 'Pyrament' into the US market also indicates the revival of interest in alkali activation. This brand of cement is reported to be an alkali activated blended Portland pozzolana cement containing organic retarders and water reducers (48). A similar kind of product called 'F' Cement based

on the use of finely ground granulated blast furnace slag, fly ash and other pozzolana, activated by an admixture consisting of various components exhibiting alkaline reactions, is also reported to have been developed in Finland specially to meet the construction industry's need for a rapid hardening high strength binder (49).

The formulation of these kinds of activated binders have recently gained momentum in view of the large potential for saving energy and capital as well as for the opportunities that it presents for use of various industrial wastes that have latent properties of being activated.

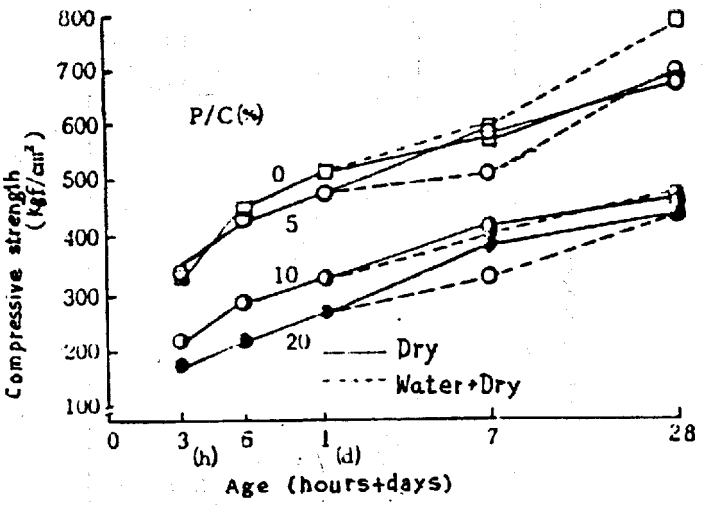

Fig.17. Compressive strength of polymer modified ultra rapid hardening cement concrete

For example, following this approach of alkali activation, it appears possible to make multiblend cements in which kiln dust, fly ash and slags can be used (Table 3) (47). It is interesting to note that such quarternary blends show higher strength at one year than cement alone although the one day strength was significantly lower. Similarly, from the study reported in (45), it seems that it is possible to use a combination of alkali activators like sodium hydroxide, sodium sulphate and hydraulic lime to activate blends of 60% slag and 40% fly ash which at a fineness of about 6000 cm^2/g shows a reasonable trend of strength development with different dosages of activators (Fig.19). Perhaps the most interesting possibility could be the formation of fly ash concrete with such alkali activators like limestone baghouse dust to yield a cement with low permeability, moderate strength and reasonable setting time, which would have the potential of being used as a filling agent (50).

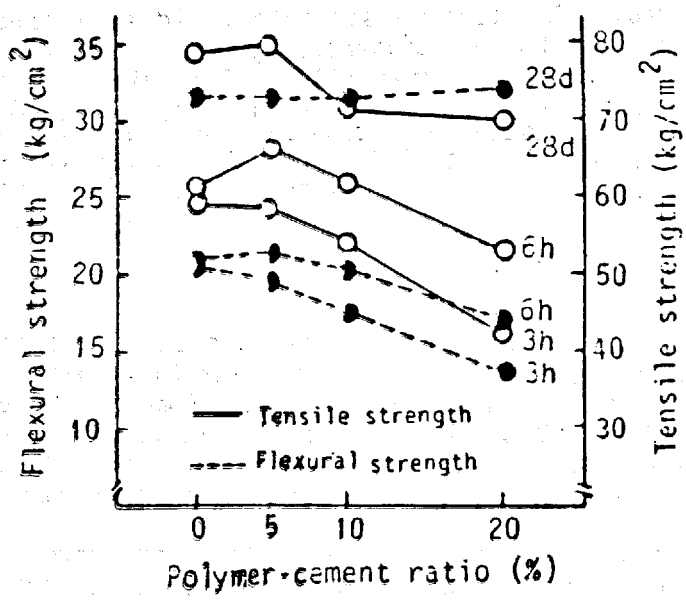

Fig.18. Tensile strength and flexural strength of polymer-modified ultra rapid hardening cement concretes

This approach of alkali activation of various industrial wastes may have the potential of being subjected to further processing under hydrothermal conditions to yield new generation of products. This can be predicted with reasonable certainties based on some of the work of Davidovits where a reference has been made to "Siliface Process" in which Kaolinite reacts with sodium hydroxide to form hydrosodalite at 150 to 180°C (51). This type of reaction is typical hydrothermal synthesis of zeolites. Davidovits has patented a number of similar systems and has introduced the terminology "geopolymers" to describe such binders.

The future of multiblend alkali activated cement is not very clearly visible. The hydration mechanism of

TABLE-3
PROPERTIES OF BLENDED CEMENTS MADE WITH CEMENT, KILNDUST, ASTM CLASS F FLY ASH AND SLAG

Blend	Blend Composition Wt. %				Autoc. Expan.	Drying Shrinkage %				Compressive Strength psi				
	C	KD	FF	SL	%	4d	11d	18d	25d	1d	7d	28d	90d	1Y
1	100	0	0	0	0.087	0.056	0.096	0.112	0.115	1320(100)	4920(100)	6030(100)	6150(100)	6830(100)
		Dust												
		S												
65	80	0	10	10	0.062	0.064	0.099	0.114	0.119	1050(80)	4320(88)	6200(103)	7230(118)	8130(119)
66	70	0	10	20	0.061	0.067	0.097	0.107	0.114	930(70)	4090(83)	7110(118)	8160(133)	9330(137)
67	70	0	20	10	0.052	0.052	0.085	0.095	0.105	1040(79)	3920(80)	5890(98)	6760(110)	7630(112)
68	60	0	20	20	0.068	0.058	0.081	0.086	0.097	775(59)	3480(71)	6270(104)	8210(133)	9300(136)
69	70	10	10	10	0.103	0.054	0.095	0.114	0.122	1150(87)	4230(86)	5980(98)	7000(114)	7730(113)
70	60	10	10	20	0.097	0.058	0.104	0.119	0.131	740(56)	4210(86)	6470(107)	7780(127)	9350(137)
71	60	10	20	10	0.100	0.055	0.092	0.102	0.113	760(58)	3750(76)	5640(94)	7060(115)	8490(124)
72	50	10	20	20	0.061	0.041	0.073	0.088	0.097	850(64)	3880(79)	5580(93)	6880(112)	8080(118)

C = Cement
KD = Kiln Dust
FF = Fly Ash
SL = Slag

such multiblend systems needs careful study. Little is known as yet about the long term creep, volume stability and chemical durability of concrete made from such multiblend cements. However, for the purposes of road building, land reclamation and environmental rehabilitation alkali activated binders of moderate strength and low permeability seems to hold high promise.

BLENDED HIGH ALUMINA CEMENTS

The high alumina cements are known since 1908 when the first patent was taken and this cement is in commercial production since 1913. Later on the manufacture and use of high alumina cements extended to many countries all over the world. Mineralogically, the high alumina cements consist primarily of CA, which is the main cementitious compound, along with many other phases. It is also known that compared to OPC, HAC is rather slow setting, but considerably rapid hardening. The heat of hydration in HAC is more than that of even rapid hardening Portland cement. Although HAC is not quick setting, but once it is set, it gains strength so rapidly that within 24 hours, the compressive strength of concrete can be as high as

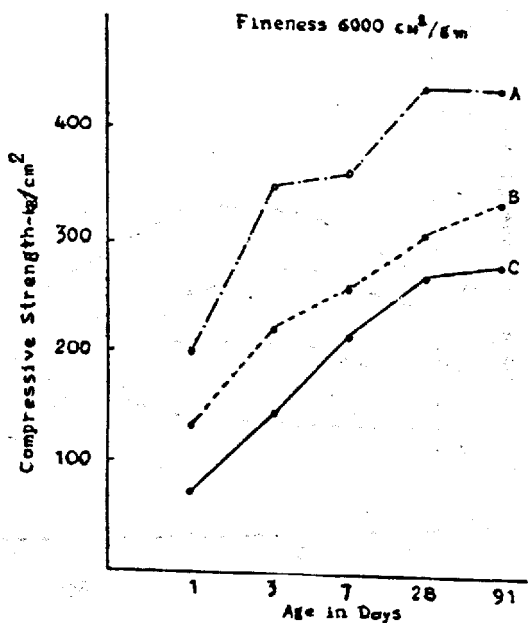

Activator % A-5, B-3, C-2.

Fig. 19: Effect of Activated dosage on slag (I) - Pozzolana (II PPA) Blends

90% of the ultimate strength. As a rule, beyond the age of 2 days the increase in strength is not more than 25% so that unlike OPC concrete the HAC concrete does not lead to increased safety with time. One of the characteristic features of HAC is the conversion of a hydrate phase. The hydration of CA leads to the formation of CaH_{10} with a small quantity of C_2AH_8 and alumina gel. The hydrate CAH_{10} belonging to the pseudo hexagonal crystal system is however chemically unstable both at low and high temperatures and becomes transformed into C_3AH_6 belonging to the cubic crystal system. This change is known as conversion which leads to a loss of strength in HAC concrete. Because of the conversion and strength loss phenomena in HAC concrete as well as the higher alkali attack known for this product, it is not favoured for use in structures.

In order to overcome the above shortcomings of HAC, systematic studies have been carried out at the Building Research Establishment in UK and it has been established that the deleterious effects of conversion in HAC concretes can be sufficiently counteracted, if not eliminated, by mixing a large proportion of ground granulated blast furnace slag with the cement. The hydration chemistry of cement and slag admixtures has been investigated and it has been observed that in wet environments hydration of calcium aluminates in HAC produces stratlingite (C_2ASH_8) in the presence of granulated slag and that at temperatures higher than the ambient this phase becomes a major constituent of the hydrated cement in a matter of months. The compressive strength of 100 mm concrete cube made from HAC and the HAC + slag admixture kept under water at 38 to 40°C for upto one year as given in Fig. 20 (52). It is evident that while the strength

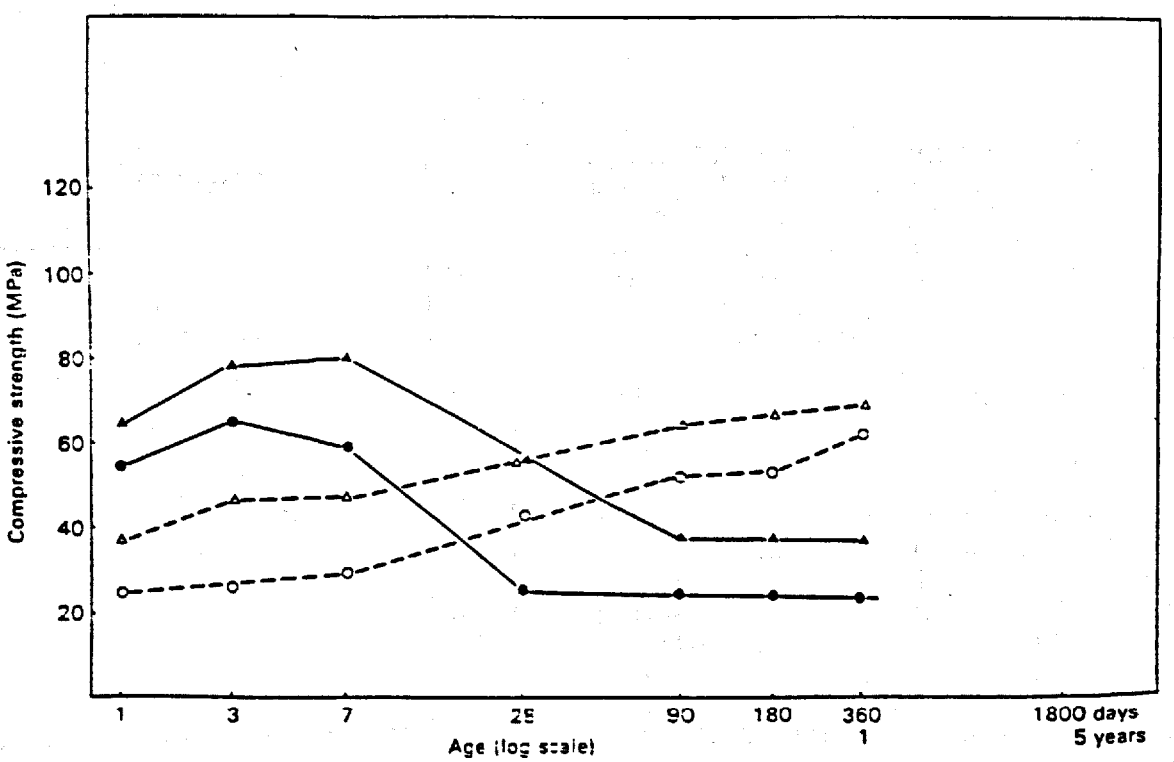

Fig.20: Compressive strength of 100 mm concrete cubes made from HAC with w/s ratios of 0.45 (▲—▲) and 0.56 (●—●) and from 1:1 HAC/ggbs mixture with w/s ratios 0.45 (Δ---Δ) and 0.56 (O---O). The cubes were stored under water at 38°–40°C.

TABLE - 4

COMPRESSIVE STRENGTH OF 1:3 MORTAR CUBES (w/s = 0.6)

Material	Storage condition	Compressive strength (MPa) 7 days	28 days	90 days	180 days
Ciment Fondu	De-ionized water	108	109	77	69
	Na_2SO_4 solution	75	41	29	27
	$MgSO_4$ solution	78	106	102	89
1:1 Mixture of HAC + ggbs	De-ionized water	44	49	61	62
	Na_2SO_4 solution	40	42	52	35
	$MgSO_4$ solution	48	58	61	66

of the concrete made from HAC alone has shown a reduction after the first 7 days, the strength of the cement plus slag mixture has increased progressively at both water and cement ratios. The authors claim that similar trends in strength results have been obtained for mixes of $C_{12}A_7$ plus slag and with different brands of HAC. The authors have also established that the sulphate resistance of HAC plus slag mixtures is as good and possibly better than that of HAC alone (See Table 4).

It seems, therefore, that the blended high alumina cements have the potential of overcoming the durability problems of the normal high alumina cements and may eventually open up the opportunities of structural use.

NEW CEMENT SYSTEMS

Phosphatic Binders

A cementitious material obtained from the reactions between an acid and a base is known for several decades. The reaction product, usually a salt or a hydrogel, forms the cement matrix in which the fillers are embedded. The acids can be mineral (viz. phospheric acid), Lewis (viz. magnesium chloride or sulphate) or even an organic chelating agent (viz. polyacrylic acid). The bases used for these cements are generally metal oxide such as magnesium oxide, gel forming silicate minerals such as wollastonite or an acid decomposible aluminosilicate type glass. Phosphatic binders belonging to this family of products, are generally based on the reactions between a metal oxide and acid salt or derivatives of phosphoric acid. It seems that a wide range of materials have been studied by various investigators to develop phosphate bonded materials for concrete repair applications. Most of these formulations have been developed by trial and error and are either recorded in patents or kept as secrets and hence their applications are reported to have many unsolved problems.

A fairly extensive review on magnesia phosphate cement (MPC) has been attempted by Sharp & Winbow (53). As summarised in this review, the acid sources for magnesia phosphate cements and the hydrates of relevance to MPC are given in Tables 5 and 6 respectively.

Microstructurally, MPCs appear as essentially composite materials in which a core of unreacted magnesia particles is surrounded by a matrix of hydration products of much greater surface area. Magnesium hydroxide is believed to be one of the reactants because the reaction rate can be controlled by the degree of dead burning of magnesia. The setting time can be controlled by retarders to the extent required. The incorpora-

TABLE - 5 Acid sources for magnesia-phosphate cements.

Name	Formula	Cement Notation	Abbreviation
Phosphoric acid	H_3PO_4	PH_3	---
Ammonium dihydrogen phosphate (or mono-ammonium phosphate	$NH_4H_2PO_4$	$(Am)PH_2$	ADP (or MPA)
Diammonium hydrogen phosphate	$(NH_4)_2HPO_4$	$(Am)_2PH$	DAP
Ammonium polyphosphate			APP
Aluminium orthophosphate	$Al(H_2PO_4)_3$	AP_3H_6	AOP

tion of retarders is known to increase the overall compressive strength of the composition.

It has been observed that use of APP solution, in place of DAP, significantly enhances the initial strength in the MPC system. Also strength enhancement as well as strength retardation will occur if part of the mono-ammonium phosphate is replaced by sodium tripoliphosphate or tetrasodium pyrophosphate. Such changes are generally related to the pH of the solution. It appears that for good bonding struvite is the most preferred phase to be formed in the paste and the other phosphate phases are the result of unwanted side reactions. This may still be controversial because real phosphate bonding is believed to be due to the formation of non-ordered or glassy or gel structure (54).

The mechanism of the formation of reaction products is probably based on a through-solution process. The acid dissolves instantaneously to give a relatively high concentration of phosphate ions in solution (and also of NH_4^+ and Al_3^{3+} ions). By comparison the magnesia is slow to dissolve. Under these circumstances, colloidal particle forms and coagulate through gel like interactions around excess NgO and filler particles.

TABLE - 6 Hydrates of relevance to magnesia-phosphate cements.

Mineral Name	Formula	Cement Notation
	$Mg(H_2PO4)_2.4H_2O$	MPH_6
	$Mg(H_2PO_4)_2.2H_2O$	MPH_4
	$Mg(H_2PO_4)_2$	MPH_2
Phosphorroesslerite	$Mg(HPO_4).7H_2O$	M_2PH_{15}
Newberyite	$Mg(HPO_4).3H_2O$	M_2PH_7
	$MgHPO_4$	M_2PH
	$Mg_3(PO_4)_2.22H_2O$	M_3PH_{22}
Bobierrite	$Mg_3(PO_4)_2.8H_2O$	M_3PH_8
	$Mg_3(PO_4)_2.4H_2O$	M_3PH_4
Struvite	$NH_4MgPO_4.6H_2O$	$(Am)M_2PH_{12}$
Dittmarite	$NH_4MgPO_4.H_2O$	$(Am)M_2PH_2$
Hannayite	$(NH_4)_2Mg_3(HPO_4)_4.8H_2O$	$(Am)M_3P_2H_{10}$
Schertelite	$(NH_4)_2Mg(HPO_4)_2.4H_2O$	$(Am)MPH_5$
Stercorite	$NaNH_4HPO_4.4H_2O$	$N(Am)PH_9$

The supply of magnesium ions in solution can be controlled with retarders such as STPP. At low temperatures nucleation of the product phases is slow and large crystals are formed while at higher temperatures large number of nucleii are formed which grow into crystals of smaller sizes (53).

Presently, magnesia phosphate cements are being used on a small scale like rapid hardening work with the apprehension that their strength still retrograde if they come into contact with a large amount of water for a reasonable length of time. Other practical problems may relate to the evaluation of heat and gases including H_2S and NH_3. Inspite of these points, the future of MPC materials seems to be good as successful repairs with good durability have already been carried out and with proper control of water very high compressive strength can be achieved within a few hours.

Calcium Phosphate Cements

Hydraulic calcium orthophosphates have turned out to be a subject of interest as a new cementing material. A review on this class of cements has been attempted by Brown and Chow (55). At present mainly α -$Ca_3(PO_4)_2$ (α -TCP), $Ca_4(PO_4)_2O$ (TeCP) $CaHPO_4$, $2H_2O$ (DCPD), $CaHPO_4$ (DCPA) and $CaCO_3$ are used for composing calcium phosphate cements. Only α -TCP can hydrate and harden by itself, while the hydraulic potential of TeCP and others appear by mixing at least one other calcium salt. The resultant hardened products are composed of hydroxyapatite (HAP) and octacalcium phosphate (OCP) [$Ca_8H_2(PO_4)_6\ 5H_2O$]. Most of these materials also harden with organic acids. All known hydraulic and acid-hardening calcium phosphates are listed in Table 7 (56).

TABLE 7 : Hydraulic or Acid-hardening Calcium Phosphates.

Cementing powder	Ca/P*	Mixing liquid
α-TCP	1.50	H_2O, Organic acids ,Polycarboxylic acids
TeCP	2.00	Organic acids, Polycarboxylic acids
TeCP + DCPD + (HAp)	1.67	H_2O, H_3PO_4
TeCP + DCPA + (HAp)	1.67	H_2O, H_3PO_4
TeCP + α-TCP	1.67	H_2O, Organic acids, Polycarboxylic acids
α-TCP + DCPD	1.33	H_2O
DCPD + CaCO	1.67	H_2O

The setting and hardening are considered to proceed with the networking of newly formed hydroxyapatite and/or octacalcium phosphate microcrystals. The hydraulic property can be modified widely by changing cement component, additive, mixing liquid, pH, temperature, etc. The hardened bodies have porosities of 50-80%, compressive strength upto 30 MPa and tensile strengths upto 3.5 MPa.

The product is being used for biorestoration of hard tissues and potential of its use as porous ceramics is being actively explored.

Al_2O_3-P_2O_5-H_2O $\pm SiO_2$ System

Systematic phase equilibria studies carried out in the above system have been summarised in (57). The stability diagram for high water regions in the Al_2O_3-P_2O_3-H_2O system at 60°C is reproduced in Fig. 21 and the phase equillibria at 200°C are shown in Fig.22. Anhydrous phases are formed in the vicinity of 200°C from $AlPO_4$ compositions

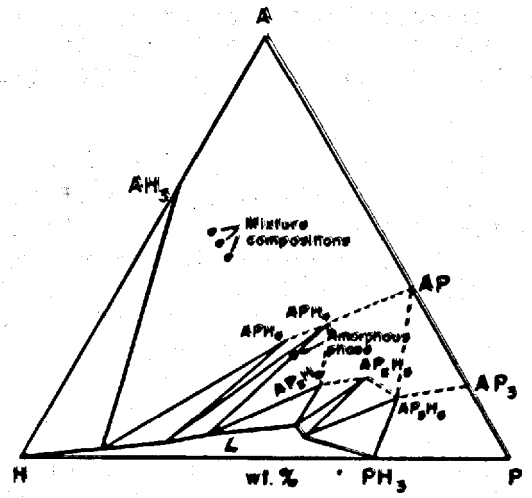

Fig.21: Proposed stability diagram for high water regions in the Al_2O_3-P_2O_5-H_2O system at 60°C. (Adapted from [27-29].)

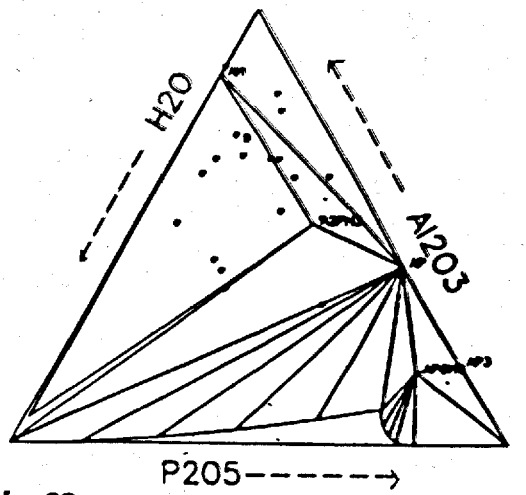

Fig.22: Phase equlibria in the system Al_2O_3-P_2O_5-H_2O at 200°C. Note stable anhydrous AP in equilibria with liquid. (Adapted from [26].)

while at lower temperatures, amorphous phases and crystalline hydrates dominate. These studies also revealed that phosphate bonded materials as a class gain strength faster than silicate materials and possess low K and low dielectric loss properties to qualify possibly as substrate material (Table 8). It was also possible to synthesize aluminophosphate ($AlPO_4$) and silicoaluminophosphate (SAPO) molecular sieves hydrothermally for hydrous gel precursor structures prepared with organic species. Thus, this system also holds promise for for new materials and cementitious compositions.

TABLE 8
PROPERTIES OF CHEMICALLY BONDED CERAMICS

Property	Silicates		Phosphates
	Super plasticized	Polymer Modified	Phosphate Bonded
Tensile Strength (MPa) Maximum	31	18	27
Density (kg/dm^3) Maximum	2.73	2.53	2.53
Porosity (percent) Minimum	1	12	
Dielectric constant (100 KH at 25°C) Minimum	-	5.8	2.0
Loss Factor (tan D x 100 for 100 KHz at 25°C) Minimum	-	0.42	0.05

Other Phosphate Systems

A compositional region surrounding the composition of the phase silicocarnotite $Ca_5(PO_4)_2SiO_4$ on the join C_3P-C_2S has been investigated (58). Tensile strengths of as high as 41 MPa but usually upto 35 MPa have been developed in pressed compacts cured for one day to one week at 35-90°C. The formation of hydroxyapatite appeared to play a major role in strength development.

In another study (59), phosphate hardened bodies have been formed by hydrothermal treatment of CA, CA_2 and CA_6 in H_3PO_4 solution at 100°C or 200°C under the pressure

of MPa for 3 days. At 100°C, the major phase was metavariscite ($AlPO_4.2H_2O$) which at 200°C it was berlinite. The compressive strength of hardened bodies increased with the increase of their A/C ratio going upto 150-290 MPa for CA_6 system at 200°C.

C-A-S Glass Cements

In the context of the conversion related risks involved in the structural use of HAC discussed elsewhere in this report, a developmental attempt has been made on the formation of cementitious material with hydraulic characteristics around C-A-S glasses along the C_2A-S compositional tie line (60,61). While earlier (62) it was reported that C-A-S glasses need activators to produce practical rates of hydration near the gehlenite stoichiometry, the study of MacDowell from Corning Glass Works (60,61) established that stable gehlenite hydrate cements were formed directly from glass cements without activators.

The cements were made from the compositional field shown in Fig.23 in one kilogram

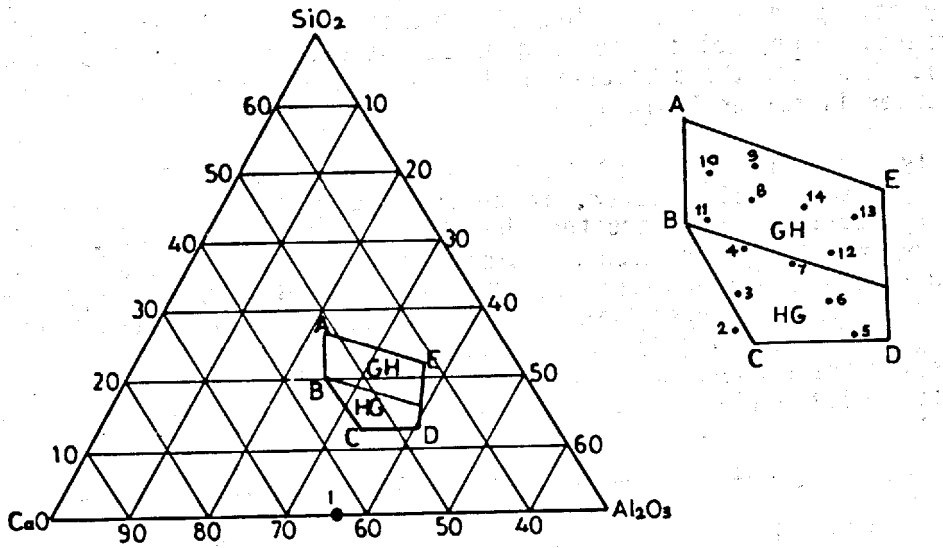

Fig 23: COMPOSITION AREA STUDIED

batches by melting at 1500-1650°C for 2 hours and quenching between water-cooled steel rollers or pouring into cold tap water. Cements were prepared by grinding to fineness of 350-500 m^2/kg. Glasses higher in SiO_2 than the enclosed polygon displayed poor hydraulicity while all cements within the enclosed area had at least 200 kg/cm^2 compressive strength. Glass cement paste compositions in the area marked HG in Fig.23 produced hydrogarnet solid solution as the major crystalline phase while in area GH, gehlenite hydrate was the dominant phase.

As reported so far, these glasses have only been tested in pastes and no mortar or concrete tests have been reported. Three component glasses with silica contents of 12-18% gave pastes that could be mixed and placed, set in a few minutes and were capable of giving compressive strengths as high as 80 MPa in some cases. The hardened pastes had fairly high porosities (20-32%) but appeared to be stable against thermal decomposition. Three component glasses with silica contents of 18-25% hydrated more slowly but the porosities were lower. In some cases strengths as high as 100 MPa were obtained. It was found that the incorporation of a few percent of titanium,

zirconium or cerium oxides in these glasses could accelerate the hydration and give a denser structure of radical spherulites made up of thin stratlingite platelets. Porosities as low as 2% (at 7 days) were reported for some of these four component compositions and their setting times were in the range of 2-8 hours (63). Proper explanations for many such phenomenological observations of the hydration mechanisms of these cements are yet to be established.

It seems that these cements have the potential of being used as thermally and chemically stable quick-setting binders. However, the upscaled manufacturing technology will have to be established first. The energy intensiveness of the process will have to be estimated and the cost effectiveness of this binder will have to be understood. The behaviour of this cement in concrete will have to be understood in terms of durability and other properties.

Calcium Silicate Cements by Sol Gel Technology

It is well known that the synthesis of fine powders by sol gel processing is being increasingly attempted in the fields of advanced electronic and structural ceramics for low temperature crystallisation and denser structure of ceramics than conventional methods (64). However, the application of this novel processing route to the synthesis of cement powder is rather limited.

Apparently, the first attempt to produce very reactive Ca_2SiO_4 powder was made by Roy and Oyefesabi (65). Later, in another study (66) powders in $CaO-SiO_2$ system with very high surface areas greater than 50 M^2/g even after 700°C calcination were synthesised by metallorganic decomposition. Phases like α-C_2S and β-C_2S were crystallised when C/S was greater than 2.0 but only β-C_2S when C/S ratio was equal to or less than 2. No crystalline calcium silicate was observed below 550°C. The powders obtained showed high hydraulic reactivity and dense CBC's were formed by unaxially pressing the powders and hydrating them at 60°C. The XRD results and hydration characteristics of the light calcined powders/pellets are reproduced in Figs. 24 & 25.

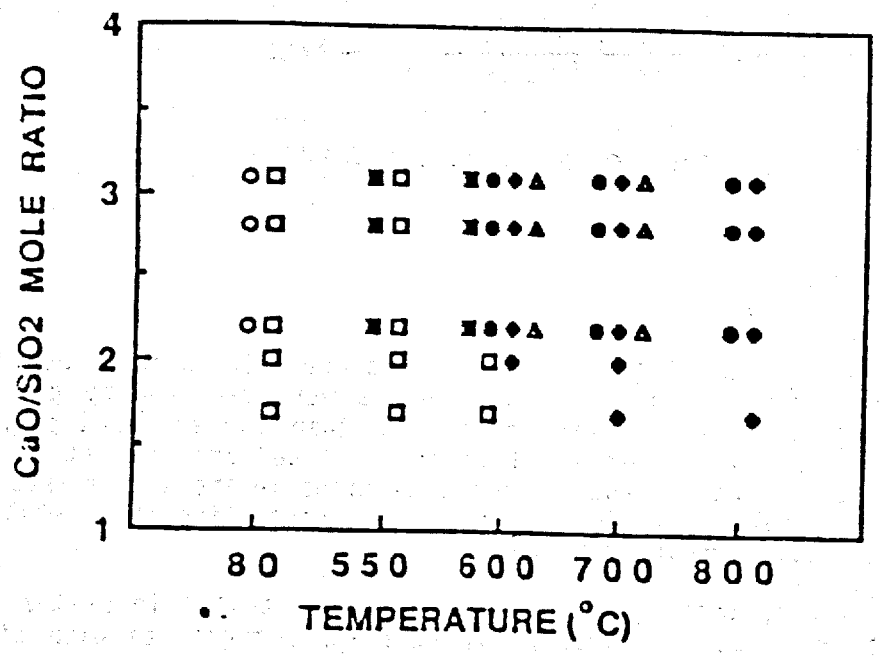

Fig. 24: XRD results of MOD powders calcined at various temperatures.
□ ; amorphous, ■ ; $CaCO_3$, o ; $Ca(OH)_2$, ● ; CaO, ♦ ; β-C_2S, ▲ ; α'-C_2S.

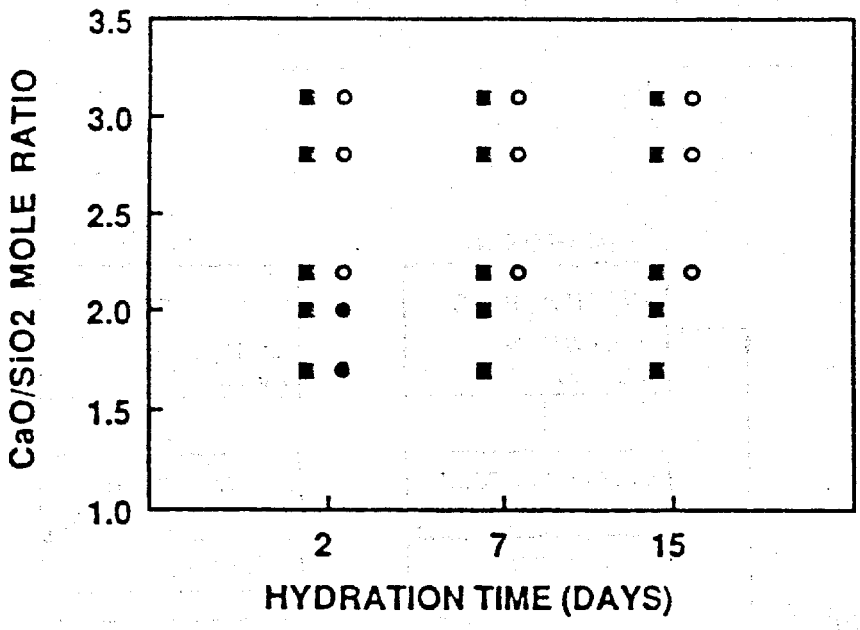

Fig. 25: Hydration of pellets formed with MOD powders calcined at 600°C.
■ CSH o Ca(OH)2 • β-C2S

A more elaborate study to develop the sol gel technology for the manufacture of cementitious materials has been reported in (67). This study covers the synthesis of binary calcium silicates by both aqueous and non-aqueous sol gel routes (Fig.26), effect of various additives such as alumina, fluoride, magnesia, sulphates and boron on the hydraulic characteristics of the final phases as well as scale-up and process optimisation feasibility. The opportunity of producing super white cement and coloured clinker through sol gel process has been emphasised in this study. The gel formation parameters and lime combinability characteristics of powders are reproduced from this paper in Tables 9 and 10. Excellent compressive strength characteristics were observed with the $CaO-SiO_2-Al_2O_3-F$ system with 28 day compressive strength of more than 70 MPa. The effects of dopants like boron, sulphate, magnesia and fluoride are seen in crystal size and reactivity and not in polymorphic transitions of calcium silicates. Dopants like alumina, fluoride and a combination of alumina and fluoride seem to help formation of C_3S, possibly of different crystallographic forms, and retains C_2S in beta form. The microstructural features of dried gels and sintered clinkers have been described in detail in this study. On the whole, the adaptability of sol gel technology for calcium silicate system has been well brought out as a future possibility of new cements.

PROSPECTS OF REACTIVE BELITE, CALCIUM SULPHOALUMINATE-BELITE AND ALINITE CEMENTS

Reactive belite, calcium sulphoaluminate (CSA)-belite, and alinite cements received a lot of attention of the scientific community in the past and particularly during the Paris and Rio Congresses. In the late eighties and early nineties studies leading to process upscaling, commercial applications, durability, etc. are often encountered in the literature, more specifically for belite and CSA-belite cements, while not much is reported on the status of alinite cement which was essentially a development in the former Soviet Union. Since these cements are widely known, no specific endeavour has been made in this report to review the status in general.

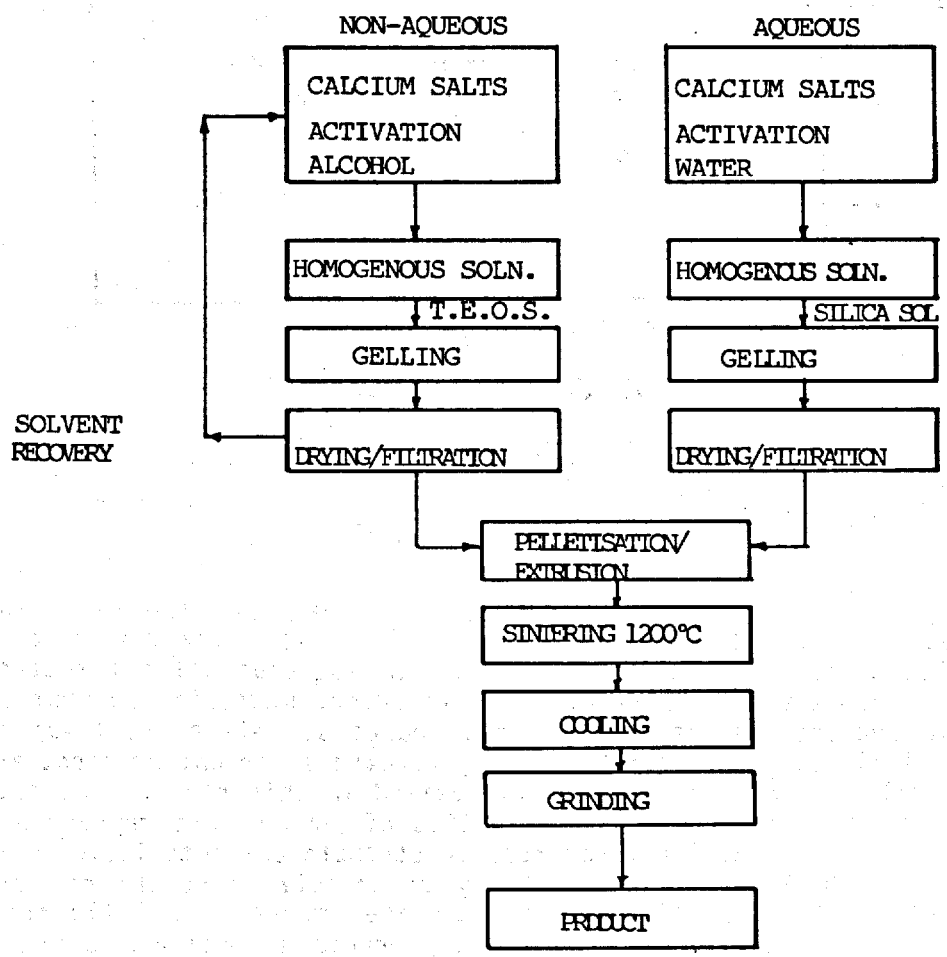

Fig.26: Sol-gel process scheme for manufacture of cementitious materials.

TABLE 9 : TYPICAL GEL FORMATION PARAMETERS

Solid content	70–100 g/L
Water in non-aqueous gel	4 mol/1 mol of TEOS
Acid catalyst	0.003 g mol/L
Viscosity of gel	2000 c.p.
Gel modifier	0.012 gmol/L
Time for gel preparation at isothermal condition	3 h
pH of gel	10–12

TABLE 10 : LIME COMBINABILITY AT VARIOUS TEMPERATURES

No.	System	Free CaO at °C			Lime combinability (%)	Phases formed at 1200°C
		1000°	1100°	1200°		
1	$CaO:SiO_2$	9.0	5.2	3.2	95.3	β C_2S
2	$CaO:SiO_2$:F	6.0	3.2	1.8	97.3	C_3S, β C_2S
3	$CaO:SiO_2:Al_2O_3$	5.0	4.0	2.5	96.2	C_3S, β C_2S
4	$CaO:SiO_2$ Al_2O_3:F	5.0	3.0	1.5	97.7	C_3S, β C_2S
5	$CaO:SiO_2$:MgO	11.6	8.3	4.4	93.4	β C_2S
6	$CaO:SiO_2:SO_3$	8.2	5.3	2.1	96.9	β C_2S, CS
7	$CaO:SiO_2:B_2O_3$	7.9	5.6	2.4	96.4	β C_2S
8	$CaO:SiO_2:Fe_2O_3$	10.5	8.3	3.4	94.9	β C_2S
9	$CaO:SiO_2$: $Al_2O_3:SO_3$:F: P_2O_5	4.0	1.9	1.3	98.0	C_3S, β C_2S $C_2S \cdot Ca_3(PO_4)_2$

Reactive Belite Cement

However, so far as reactive belite cement is concerned, reference may be made to some recent studies made to produce cements with high proportion of reactive belite (68, 69). In (68) specifically the use of plant raw materials has been tried. It showed that both alkalies and sulphates can be used to activate the belite phase in properly designed low LSF (0.8) raw mixes. The potential phase composition and compressive strengths development of these cements are shown in Table 11.

TABLE 11

POTENTIAL MINERAL COMPOSITION AND COMPRESSIVE STRENGTH DEVELOPMENT OF REACTIVE BELITE CEMENT

Cement	C_2S	C_3S	C_4AF	C_3A	kg/cm^2		
					3 D	7 D	28 D
SG-6	50	21	10	14	232	366	460
SG-7	59	13	12	13	61	124	387
SG-8	66	6	12	13	88	90	145
CBC-VII	53	22	11	8	280	375	485

Fineness 3000 cm^2/gm and W/C 0.4

The durability of reactive belite cements in comparison with commercial alitic cements or cement with high non-activated belite content has been attempted in (69). The clinker phase compositions of the cements studied are given in Table 12. Clinkers

TABLE 12

QUANTITATIVE CLINKER PHASE CONTENT MICROSCOPICALLY DETERMINED BY THE POINT COUNTING METHOD

Specimen	LS	Quantitative clinker phase content(ma %)			
		alite	belite	aluminate	ferrite
BL	80	21	60	12	8
BAL	80	23	52	20	5
BSL	80	13	67	14	6
PZL	88	54	29	0	16
PZ	93	60	24	9	7

designated as BL, BAL and BSL are high-belite laboratory-made ones with no sulphate/alkali activation, with only alkali incorporation and with both alkali and sulphate incorporation respectively, while PZL and PZ are commercially available Portland clinkers. The compressive strength data, the depth of carbonation and porosities of these five clinkers were studied in cement mortar samples, after converting all the clinkers to cements of same fineness (3000 and 4000 cm^2/g) and sulphate content (3.2%). The results of investigations are given in Figs. 27-28 and Table 13. From the results, it is evident that the reactive belite cements (BAL/BSL) have shown better strength development, lower depth of carbonation and higher impermeability with respect to non-activated belite cement and also the commercial alitic cements.

With such positive indications of better durability properties of reactive belite cements, it is quite likely that its commercialisation may catch up in near future. This might be particularly interesting for countries like India where clinker is produced with high ash coal resulting in relatively higher proportions of belite.

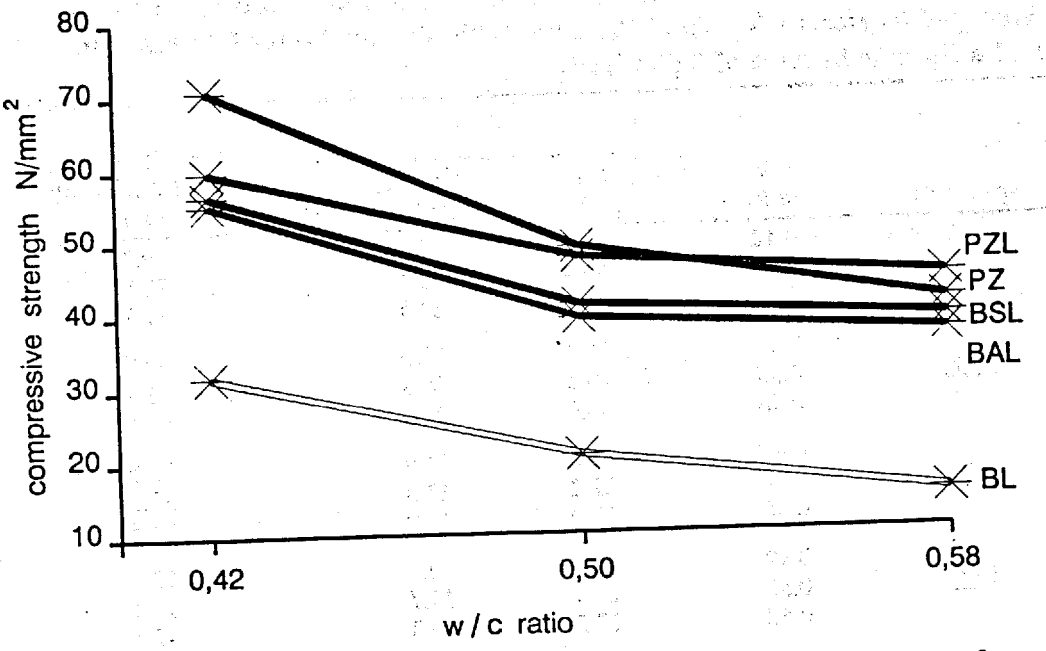

Fig. 27: Compressive strength of the cement mortars after 28 days as a function of the water/cement ratio (4000 Blaine, 27 days water storage).

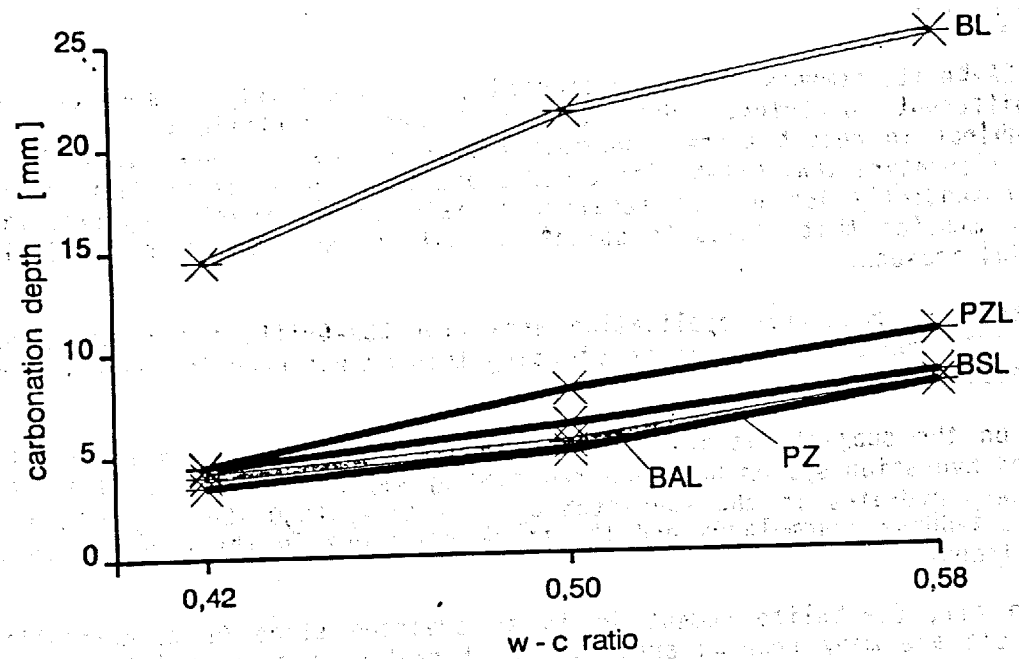

Fig. 28: Depth of carbonation of the cement mortar prisms after 90 days' exposure in 1 vol% CO_2.

TABLE 13: Porosities of Various Hardened Cement Pastes after 90 Days, Arranged by Decreasing Total Porosity, With Varying Water-Cement Ratios and a Specific Surface of 3 000 cm^2/g

specimen	w/c ratio	porosity		capillarity related to total porosity [%]
		total [vol%]	capillary [vol%]	
BL	0.42	26.7	18.5	69.3
	0.50	30.8	22.4	72.8
	0.58	34.4	24.5	71.2
PZL	0.42	25.1	15.0	59.8
	0.50	29.1	18.3	62.9
	0.58	34.0	22.0	64.6
PZ	0.42	20.0	11.9	59.5
	0.50	22.2	13.3	59.9
	0.58	25.9	16.0	61.8
BAL	0.42	19.6	10.3	52.3
	0.50	20.4	11.7	57.4
	0.58	23.2	13.3	57.3
BSL	0.42	16.4	7.4	45.4
	0.50	18.3	8.9	48.6
	0.58	23.0	13.3	57.8

An effective activation mechanism of the belite phase in such situations may help in significant upgradation of products.

CSA-Belite Cement

The CSA-belite cements have been studied quite extensively in seventies and eighties in different countries. Not much significant scientific work is encountered on this subject in recent times, whereas enough indications are available from the commercial literature that CSA-belite cements are in large scale production in various countries essentially for use as repair materials or in grouting applications (70). Needless to mention that access to scientific data on such products is difficult due to commercial reasons.

Nevertheless, potential application areas for CSA-belite cement have been highlighted in (71) where the experience of using this cement even in load-bearing structures has been mentioned.

While on the subject, it may be worthwhile to mention that an interesting study on a related hydration system has been reported by Kaprolik and Hamic (72). Formation of quarternary hydrates in the subsystem C_4A_3S - $CaSO_4.2H_2O$ -$Ca(OH)_2$-H_2O, the stability in the 4-phase assemblages and the phase relations in the given subsystem have been established.

All in all, CSA-belite cement is in an advanced stage of commercialisation, although there are many unknown areas in the hydration and durability of CSA-belite concretes.

Alinite Cement

It is quite widely accepted that alinite is a new chlorosilicate equivalent of C_3S with higher hydraulic reactivity and that alinite cement can be produced at

substantially lower temperatures (73, 74). Experimental production of alinite cement in a wet process kiln of 2.75 x 75 m size and the evaluation of the clinker has also been reported earlier (75).

It has also been known that the technical specifications of alinite cement had been adopted as a temporary standard in the former Soviet Union by the Ministry of Building Materials Industry (76). It is reported that 2-storied dwelling units were constructed with alinite cement in the outskirts of the city of Tashkent (77). However, the proliferation of this technology has been affected by the controversy of long-term durability of this cement in RCC construction due to the apprehension of chloride corrosion of steel reimbursements (3). Although it is believed that this technology is still being pursued in Uzbekistan by the group led by its inventor Noudelman, no widescale dissemination of information is presently encountered. As a result the present status or the future prospects could not be reliably ascertained.

CONCLUSIVE THOUGHTS

From the developmental trends of new and special cements over the last decade, it is evident that there are no threats to Portland cements as binders of future construction. This is accompanied with continuing demand of Portland cement derivatives.

However, the main thrust towards the radically new binders has come from the perceived needs of substituting metals, plastics and high-fired ceramics in engineering applications like manufacture of components, tools, dies, etc. This has opened up newer opportunities of using essentially inorganic binder-based novel composites in the family of CBCs, which has resulted in the crosslinking of ceramic manufacturing technologies with hydraulic binder systems. Consequently, one observes the gradual adoption of high shear mixing, use of ultrafine materials, chemical admixtures, polymers, etc. along with newer processing routes like solgel and hydrothermal synthesis of materials in non silicate systems.

In search of low-energy low-cost binders, the revival of alkali activation process is seen to gain ground, which may perhaps be of significance to the demands of environmental management, which is becoming more crucial in the world day by day.

The intrinsic short-coming of high-alumina cements as a structural material has attracted the attention of the scientific community, leading to the new finds of blended high-alumina cements and C-A-S glass cements.

The newer binders of yester decade like reactive belite, CSA-belite and alinite cements continue to hold promise of commercialisation in some form or other, permitting the exploitation of their low-energy characteristics.

It is evident, therefore, that the 21st century is expected to realise some breakthroughs of radically new cost-effective binder systems and technologies with predominance of inorganic materials for engineering applications, energy conservation and environmental protection.

REFERENCES

1. Nagataki S, Use of High Strength Concrete at Present Stage, Proceedings of the MRS International Meeting on Advanced Materials, Vol. 13, Advanced Cements and Chemically bonded Ceramics, ed by M.Doyana, S Somiya and R P H Chang, Tokyo, Japan, 1989, p.3-14.

2. Kurdowski W, George CM and Sorrentino FP, "Special Cements", Principal Report, 8th ICCI, Rio de Janeiro, Brazil, 1986, Vol. I, p.292-318.

3. Locher, F.W., "Low Energy clinker formation",ibid, p.57-67.

4. Bikbau M Y, "Formation, crystal chemistry and properties of alinite and jasmundite", ibid, vol. II, p.352-357.

5. Burger D and Ludwig U, "Synthesis of Calcium Silicates at low temperatures and influences on their reactivity", ibid, Vol. II, p.372-378.

6. Bhatty M S Y, "Properties of blended cements with Portland cement, cement kiln dust , fly ash and slag", ibid, Vol.IV, p.118-127.

7. Parameswaran P S and Chatterjee A K, "Alkali activation of Indian blast furnace slag", ibid, Vol.IV, p.86-91

8. Malolepszy J, "Activation of synthetic meliolite slags by alkalies", ibid, Vol.IV, P.104-107.

9. MacDowell J F, "Hydrogarnet-gehlenite hydrate cements from $CaO-Al_2O_3-SiO_2$ glasses", ibid, Vol.IV, P.423-428.

10. Diamond S, Very High Strength Cement-Based Materials - A PROSPECTIVE, very High Strength Cement-Based Materials, ed by J Francis Young, MRS, 1985, p.233-244.

11. Kendak K, Howard A J and Birchall J D, The Relation Between Porosity, Microstructure and Strength and the Approach to Advanced Cement-Based Materials, Technology in the 1990s : Developments in Hydraulic Cements, ed by Sir P Hirsch, J D Birchall, D D Double, A Relly, G K Moir and C D Pomeroy, The Royal Society, London 1983, p.139-53.

12. Schiller K K, Mechanical Properties of Non-Brittle Solids, ed by H Walton, Butterworth, London, 1958, p.35-49

13. Powers T C, "Physical properties of cement pastes", Proc.. 4th Intl. Symp. on the Chemistry of Cement, NBS Monograph, No.43, National Bureau of Standards, Washington D C, Vol.II, p.577-613.

14. Abrams D, Bull. Univ.Chicago, Struct. Mater. Ress. Lab., Lewis Instt., Chicago, No.1, 1918.

15. Ryshkewitch E, "Conpressive strength of porous sintered alumina and zirconia", J. Amer. Ceram. Soc., 36, 1953, p.65-68.

16. Feret R, Bull-Sol. Encour. Ind. Natn, Paris, II, 1987, p.1604.

17. Roy Rustom, "Workshop on chemically bonded ceramics", The pennsylvania State University, Materials Research Laboratory, July 1984.

18. Bache H H, "The new strong cements, their use in structures", Phys. Technol., 19, 1988, p.43-50.

19. Bache H H, "Densified cement/ultrafine powder etc. based materials", CBL Report No.40, Aalborg Portland, Denmark, 1981.

20. Mino I and Sakai E, "Engineering Concrete" Proceedings of the MRS International Meeting on Advanced Materials, Vol.13, Advanced Ceramics and Chemically Bonded Ceramics, Vol.13, ed by M Doyana, S Somiya and R P H Chang, Tokyo, Japan, 1989, p.247-256.

21. Mindess S, Relationships Between Strength and Microstructure for Cement-Based Materials : an Overview, Very High Strength Cement-Based Materials, Vol.42, ed by J Francis Young, Materials Research Society, Pittsburgh, USA, 1985, p.53-68.

22. Hjorth L, Development and Application of High-Density Cement-based Materials, Technolgy in 199C : Developments in Hydraulic Cements, ibid, p.167-173.

23. Wise S, Satkowski, Scheetz B, Rizer J M, Mackenzie M L, and Double D D, The Development of a High Strength Cementitious Tooling/Molding Material, Very High Strength Cement-Based Materials, ibid, p.253-264.

24. Idorn G and Fordos Z, "Cement-Polymer Materials", Principal Paper, Proceedings of the Sixth International Congress on the Chemistry of Cement, Stroiizdat, Moscow, 1976, Vol. III, P.287-304.

25. Ohama Y, Current State and Trend of Concrete-Polymer Composites, Proceedings of the MRS International Meeting on Advanced Materials, ibid, p.79-98.

26. Ohama Y, Concrete Admixtures Handbook, ed by V S Ramchandra, Noyes Publications, NJ, 1984, p.341.

27. Birchall J D, Howard A J, and Kewall K, Europen Patent No.0021682, 1981.

28. The Pennsylvania State University, "CBC in cement technology", USA, 1989, p.2 and 8.

29. Birchall J D, Howard A J and Kendall K, European Patent No.0055035, 1982.

30. Birchall J D, Cement in the Context of New Materials for an Energy-Expensive Future, Technology in the 1990s : Development in Hydraulic Cements, ibid, p.31-42.

31. Rodger S A, Sinclair W, Groves G W, Brooks S A and Double D D, Reactions in Setting of High Strength Cement Pastes, Very High Strength Cement-Based Materials, ibid, p.45-51.

32. Regourd M, Microstructure of High Strength Cement Paste Systems, Very High-Strength Cement-Based Materials, ibid, p.3-17.

33. Rodger S A, Brooks S A, Sinclair W, Groves G W and Double D D, "High Strength Cement Pastes", J.Mat. Sci., 20, 1985, p.2853-60.

34. Sinclair W and Groves G W, The Microstructure of High Strength Cement Pastes, Very High Strength Cement-Based Materials, ibid, p.31.33.

35. Alfred N McN and Birchall J D, The Properties and Potential Applications of Macro-Defect-Free Cement, Very High Strength Cement-Based Materials, ibid, p.265-276.

36. "R&D in advanced cement-based materials in Japan", ACBM Newsletter, Illinois, USA, No.1, 1991.

37. Seamwide K J, Miller L, Herzfeld C, Rodgers T and Melbourne T, "CBC - Versatile Materials for Composites Manufacturing Tooling Conference for Composites-90", Anaheim, California, USA, June 1990, p.90-183.

38. Goto S, Koyata H, Daimon M, Yasuda E, and Kimura S, Diffusion of Moisture in MDF Cement, Proceedings of the MRS International Meeting on Advanced Materials, Vol.13, Advanced Cements and Chemically Bonded Ceramics, ibid, p.207-212.

39. Greening N R, et al, "Modified Portland Cement and Process", US Pat. No.3628973, Dec. 21, 1971.

40. Parameswaran P S, Heble A S and Krishnan S, "Rediset - an ultra superhigh early strength cement", NCB International Seminar on Cement and Building Materials, 2nd, New Delhi, India, 1989, p.V-54-62.

41. Sekino K, Oshio A and Kawano T, Properties and Applications of Polymer-Modified Ultra Rapid Hardening Cement Concrete, Proceedings of the MRS International Meeting on Advanced Materials, Vo.13.Advanced Cements and Chemically Bonded Ceramics, ibid, p.105-114.

42. Minematsu T and Uchida Y, Application for Repair Work of Fiber Reinforced Shotcrete Using Jet Cement, Proceedings of the MRS International Meeting on Advanced Materials, Vol.13, Advanced Cements and Chemically Bonded Ceramics, ibid, p.15-168.

43. Trief L, "The new Trief cement process", Proceedings of the IV Fly Ash Symposium, St. Louis, USA, 1979.

44. Malone G, et al, "Potential applications of alkali-activated alumino-silicate binders in military operations", US Army Corps of Engineers Report GL-85-15, Washington D.C., 1985.

45. ACC Central Research Station, "Alkali-activated slag-fly ash Cement", Progress Report, Thane, India, 1984.

46. Malolepszy J, "Activation of granulated slags", 8 International Baustoff Und Silikattagung 'Ibausil', Weimer, 1982, Vol.I, p.158-164.

47. Bhatty M S Y, "Kiln dust cement blends evaluated", Rock Products, 88, 1985, p.47-52.

48. Heitzmann et al, "Cement Composition curable at low temperatures", US Pat. No.4842649, June 27, 1989.

49. Forss B, "F-Cement, a new low-porosity slag cement", Silicates Industriels, 3, 1983, p.79-82.

50. The Pennsylvania State University, "Large volume use of fly ash for environmental reclamation", Biannual CCBC Meet, 1991.

51. Daviovits J, "Geopolymers of the first generation : Siliface Process, Proceedings of the First European Conference on Soft Mineralogy (Geopolymer '88), France, 1988, Vol.I, p.49-67.

52. Majundar A J, Singh B and Edmonds R N, Blended High-Alumina Cements, Vol.16, Advances in Cementitious Materials, ed by Sidney Mindess, The American Ceramic Society Inc., Ohio, USA, 1991, p.661-678.

53. Sharp J H and Winbow H D, Magnesia-Phosphate Cements, Cement Research Progress, ed by P W Brown, American Ceramic Society, Ohio, USA, 1989, p.233-264.

54. Sarkar A, "Phosphate cement-based fast-setting binders", Ceramic Bulletin, 69(2), 1990, p.234-238.

55. Brown W E and Chow L C, A New Calcium Phosphate, Water-Setting Cement, Cement Research Progress, Rd by P W Brown, American Ceramic Society, Ohio, USA, 1986.

56. Monma H, On Hydraulic Calcium Phosphates, Proceedings of the MRS International Meeting on Advanced Materials, Vol.13, Advanced Cement and Chemically Bonded Ceramics, ibid, p.15-26.

57. Roy D M, Recent Advances in Phosphate Chemically Bonded Ceramics, ibid, p.213-228.

58. Steinke R A, Agrawal D K, Roy R and Roy D M, Reactions and Bonding of Sol-Gel Derived Chemically Bonded Ceramics in the System $CaO-P_2O_5-SiO_2$. ibid, p.229-238.

59. Yamazaki K, Yoshimura M and Somiya S, Formation of Phosphate-Bonded Bodies in the $CaO-nAl_2O_3-H_3PO_4(H_2O)$ System, ibid, p.239-246.

60. MacDowell J F, "$CaO-Al_2O_3-SiO_2$ glass hydraulic cements", US Pat. No.4 650443, Aug.12, 1986.

61. MacDowell J F, "Stratlingite and hydrogarnet from calcium aluminosilicate glass cements", Materials Research Society Annual Meeting, Boston, MA, USA, 1989.

62. Locher F W, "Hydraulic properties and hydration of glasses in the system $CaO-Al_2O_3-SiO_2$", Fourth International Symposium on the Chemistry of Cements, Washington D.C., 1960.

63. Gartner E M and Myers D F, New Cements and Novel Cement Matrices, Advances in Cementitious Materials, ed by S Mindess, The American Ceramic Society, Ohio, USA, 1991, p.621-642.

64. Ulrich D R, "Sol gel processing", Chemtech, April, 1988, p.242-249.

65. Roy D M and Oyefesabi, "Presentation of very reactive Ca_2SiO_4 powder", J.Am. Ceram. Soc., 60 (3), 1977, p.178-180.

66. Nagira T, Warner S A, Mecholsky J J and Adair J H, Alkoxide Derived Calcium Silicate Chemically Bonded Ceramics, Proceedings of the MRS International Meeting on Advanced Mataerials, Vol.13, Advanced Cements and Chemically Bonded Ceramics, ibid, p.255-262.

67. Page C H, Thombare C H, Kamat R B and Chatterjee A K, Development of solgel Technology for Cement Manufacture, Advances in Cementitious Materials, ed by S Mindess, American Ceramic Society, Ohio, USA, 1991, p.643-660.

68. Visvesvarya H C, Raina S J and Ghosh S N, Synthesis, Mineralogy and Performance Characteristics of Low Energy Cements, Proceedings of the MRS International Meeting on Advanced Materials, Vol.13, Advanced Ceramics, ibid, p.45-50.

69. Knofel D and Fuhr C, Durability of Activated Belite-Rich Cement Mortars, Advances in Cementitious Materials, ibid, p.715-727.

70. Associated Cement Cos. Ltd., Product Brochure on CASAL, Bombay, India, 1990.

71. Pai B V B, Bapat A D, Dhuri S S, Mudbhatkal G A and Chatterjee A K, "Role of a non-alitic cement in practical applications", Seminar on Cement Industry organised by the ASEAN Federation of Cement Manufacturers, Singapore, 1986.

72. Kapralok I and Hanic F, "Phase relations in the subsystem calcium aluminate sulphate ($C_4A_3\bar{S}$) - gypsum-calcium-hydroxide-water of the system calcia-alumina-calcium sulphate-water referred to hydration of sulphoaluminate cement", Cem. Concr. Res., 19(1), 1989, p.89-102.

73. Ilyukhin V V, Navsky N N, Bikbaou M Y and Howie R A, "Crystal structure of alinite", Nature, 269 (5627), 1977, p.397-398.

74. Noudelman B I and Gadaev A I, "Aspects physico-chimiques de la cristallisation des chlorsilicates lors de la clinkerisation on basse temperature dans le bain fondu de sel", 8th International Congress on the Chemistry of Cement, Rio de Janeiro, Brazil, 1986, Vol.II, p.347-351.

75. Agarwal R K, Paralkar S V and Chatterjee A K, "Chloride salts as reaction medium for low temperature clinkerisation - a probe into alinite technology", 8th International Congress on the Chemistry of Cement, ibid, Vol.II, p.327-333.

76. Ministry of Building Materials Industry, "Technical specifications of alinitic portland cement, No.TU 21-20-53-83, Moscow, 1983.

77. Noudelman B I, Personal Communication, Tashkent, 1989.

PORTLAND AND BLENDED CEMENT

K C Narang

Dalmia Cement (Bharat) Limited, New Delhi, INDIA

SUMMARY

State of art on portland cement, its derivatives and blended cements continued to be upgraded with special attention on improving the performance, particularly to obtain high early and ultimate strengths, greater durability and more effective conservation of energy and raw materials used in cement concrete and utility for specific applications. Control on mineral composition, microstructure, particle size distribution and their optimization are understood as the key contributors to control the performance of end product. Development of Mathematical models to correlate physio-chemical and mineralogical characteristics with performance has been a significant area of research in the last decade for formulation and hydration of Cement.

The use of advanced analy tical techniques and computer application softwares have started playing their role in understanding the role of phase composition of cement and its modifications due to incorporation of minor constituents. Reactivity of low calcium silicates is still in the process of being understood and exploited commercially. Developmental studies on new resource minerals like microsilica fumes and rice husk ash have progressed and have helped in understanding the mechanism of blended cements. It is expected that more precision techniques of manufacture and control and newer techniques of communition would play very important role in the years to come in the developmental work for improving performance of portland and blended cements. Besides energy saving processes, use of waste fuels and alternative non-conventional sources of energies are foreseen as the trend for future research.

INTRODUCTION

In the gradual evolution of development of Portland and Blended Cements, a number of modified portland cements and blends of portland cement have emerged and have been accepted based on their specific characteristics and applications (1, 2). While the basic chemistry of the cements has remained the same, it is through the modification of physio-chemical and mineralogical characteristics of basic portland cement model that the derivatives have been able to attain their specific characteristics. In this process of development a number of natural and artificial minerals other than conventional raw materials have been investigated for their suitability in the manufacture and application of cement. While with the use of natural pozzolana, Italy has a long tradition of producing portland pozzolana cements, the use of Fly ash is more recent(3). Blast Furnace Slag was used for making Slag Cement in Europe, particularly in France and Germany, for decades (4). The initial aim was of course to save money, but a further objective was to achieve special properties, in particular, resistance to aggressive substances such as water containing sulphates and lower heat of hydration. New objectives have been added to this approach as it has effectively helped to save energy, conventional raw materials and helped to solve pollution problem. Lately, the production of cement containing calcareous fillers has also been advocated and practised (5). Use of Micro silica is the latest to enter as the resource mineral for producing composite cement with advantage (6,7).

Besides the chemistry, the manufacturing process and its control have improved over the years both at clinkerisation and comminution stages (8, 9). Effective environment control and auto control in burning techniques, together with use of non-conventional fuels including waste fuels, and special comminution techniques, like Roll Press and High efficiency separators, have offered new areas of developmental work. Advancements in the experimental and analytical techniques, such as Scanning electron microscopy, X-ray microanalysis, Light electron Microscopy, Thermo-analytical methods and host of application of Computer Softwares have improved the understanding of Chemistry of Cement in manufacture and application.

DEVELOPMENT

There have been two distinct approaches in making variety of portland and portland based cements.

- Modification of chemical and mineralogical assemblage in portland cement at the pyro-processing stage;
- Manipulation of physical characteristics of raw materials and cement at grinding stage;

Incorporation of intrinsically hydraulic minerals and / or inert ingredients to obtain blended / composite cements.

The Ternary diagram (FIG.1) depicts integration of various resource minerals, cement minerals and types of cements, which form the basis of formulation of Portland Cement, its derivatives and Blended cements (5, 10, 11).

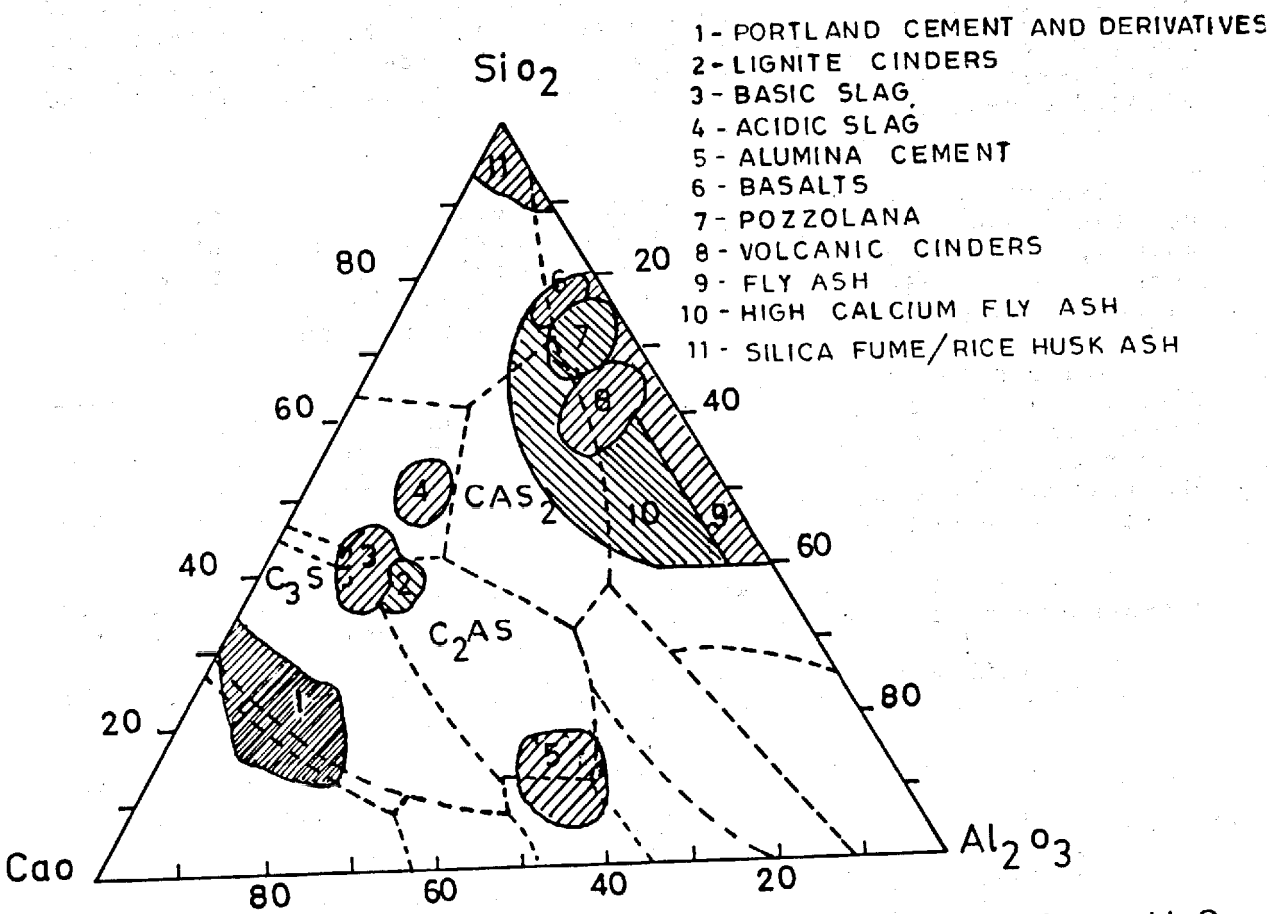

FIG. 1 – TERNARY DIAGRAM OF $CaO - SiO_2 - Al_2O_3$ DEPICTING POSITION OF VARIOUS RESOURCE MINERALS, CEMENT MINERALS AND TYPE OF CEMENT

State of art on portland cement, its derivatives and blended cements continued to be upgraded with special attention on improving the performance, particularly to obtain high early and ultimate strengths, greater durability and more effective conservation of energy and raw materials used in cement concrete and utility for specific applications (2,5,8,12,13). Control on mineral composition, microstructure, particle size distribution and their optimization are understood as the key contributors to control the performance of end product. Development of Mathematical models to correlate physio-chemical and mineralogical characteristics with performance has been a significant area of research in the last decade for formulation and hydration of Cement (14, 15, 16, 17).

Certain new concepts such as Sol-gel process for formulation of cement and alinite cement through modification of alite phases have been further investigated (18, 19). Addition of mineral additives, in quantum lower than the permitted levels (as in specifications) of pozzolana and slags, have widened the scope of investigations to understand the mechanism of filler concept and blended cement systems (20, 21). Tailor-made formulations are being seen as the state of art in portland, its derivatives and blended cements.

Excellent reviews on various aspects of developments on Portland and Blended Cements have been presented at Tokyo, Moscow, Paris and Rio Congresses on Chemistry of Cement and in recent publications. The number is so large that it is practically impossible to list all the contribution at one place.

Glasser and Regourd independently in their views on Future direction of Research in cement production identified certain areas of research relating to Pyroprocessing, grinding, use of alternate fuels and blended cement in 1979 (22, 23). It is interesting to note that these have been the areas mainly researched during the last decade.

Some of the issues which have attracted the attention of researchers since the Rio Congress can be summerised as under :

* Influence of minor constituents/mineralizers on the structure and performance of portland cements,

* Portland cement, its derivatives and low energy cements (Relationship between composition, microstructure, size distribution and performance),

* Properties of cement made through new size reduction techniques and classifier systems such as Roller Mills, Roll Press and High Efficiency separators, etc.,

* Blended cements with silica fumes and other inorganic additives,

* Non-portland blended cements based on slag, fly ash and other mineral additives, including activators.

INFLUENCE OF MINOR CONSTITUENTS/MINERALIZERS

Components of Portland Cement, i.e. C_3S,C_2S,C_3A and C_4AF undergo changes in their crystal structure, reactivity and performance with the incorporation of foreign ions/minor oxides which are inherent in the basic raw materials. Polymorphism and Crystal structure of these phases, therefore, continued to be investigated with combined application of advanced high temperature analytical techniques, such as DTA, XRD and Microscopy. Correlations have been found between percentages of individual oxides and their distribution in Clinker phases by Hahn,

Woermann, Boikova, Maki, Kristmann, Yamaguchi and Terrier both in individual phases and in commercial clinkers (24,25,26,27,28,29,30). Substitution by MgO, Al_2O_3 and Fe_2O_3 in C_3S, in commercial clinkers have been investigated alone and in presence of each other. The influence of alkalies on these incorporations is seen as further complexity in cement clinker. The temperature of formation and cooling rates further determine the incorpora-tion and type of polymorph present finally. Bucchi at the Paris Congress and Boikova and Maki at the Rio Congress presented a comprehensive review of effect of minor components in raw materials and other factors responsible for changes in the clinker structure and properties of clinker/cement (8,26,27).

What makes the issue very important is :

* Potential for decreasing energy consumption,
* Improve quality and Specific application potential,
* The shift from Oil/Gas firing to coal firing and use of certain low grade/waste raw materials and fuels in pre-calciner kilns.

$CaO-Al_2O_3-Fe_2O_3-SiO_2$ System

The Tetrahedral model of quaternary system of four major oxides defines the composition of Portland Cement. The system is divided into ternary sub systems for clarity of understanding the phase volume and other features of different phases (1,31). Subsequent studies have been carried out to determine the exact composition of these phases at equilibrium condition. Newkirk and Thwaite, Sorrentino and Glasser, Swayze and Gutt have extended knowledge of the system to wider range of compositions (32,33,34,35). Isomorphous substitution of atoms or formation of solid solution are seen as the basis of incorporation of various minor oxides, and their influence on properties. Practically all impurities can be distributed among the clinker minerals under certain conditions and based on limiting solubility, Aluminate being the largest adopter. MgO, Alkalies, SO_3 are the components studied extensively due to their direct influence on properties and extent of occurrence in the cement raw materials.

MgO

MgO has significant effect on equilibrium phase assemblage. Structure of alite and its thermal stability is dependent on the amount of MgO in the clinker. The liquid phase, presence of alkalies and sulphates and rate of heating and cooling the clinkers affect the modification of alite due to MgO as shown by Maki et.al.(Fig.2) (36,37).

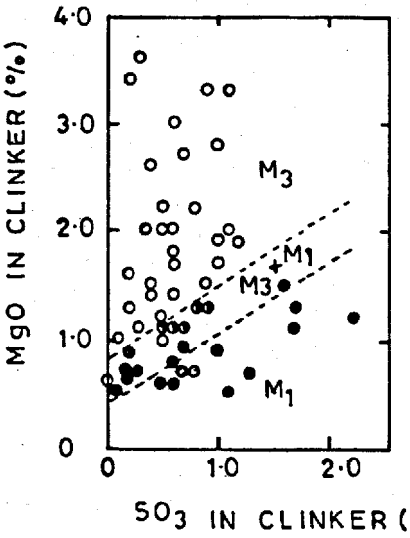

FIG.2-DEPENDENCE OF THE POLYMORPHIC MODIFICATION OF ALITE IN PRODUCTION CLINKER ON THE MgO AND SO_3 CONTENTS OF THE CLINKER

Correlation has been reported between MgO content in alite, belite individually and in clinker and the total impurity content of the belite and MgO of the clinker. Boikova proposed the equation I_a = 0.7 Me + 2.1 for MgO incorporation with total impurity (26).

Burnability of raw mixes can be improved significantly with small amount of MgO particularly at low temperatures. MgO is taken up in all phases but its influence on structure of alite and liquid phases is significant. Total MgO content in most cement specifications are limited to 5-6%. However, cements made with higher MgO content over 3.5% can show unsound behaviour under autoclave depending on the C_3S and C_3A contents, burning temperature and cooling history of the clinker used (38). Clinkers burnt at high temperature and cooled rapidly can incorporate large quantities of MgO and much of it can remain in aluminate and ferrite phases, leaving small quantity of periclase. Moir and Goswami et.al. studied the formation of phases in presence of MgO and Fluoride (39,40). The phase assemblage is reported to be different from the normal clinker containing only MgO. Spurrite and $C_{12}A_7$ occur as the intermediate phases. At higher levels of F, formation of $C_{11}A_7.CaF_2$ takes place. In the final clinker $C_{12}A_7$ and $C_{11}A_7CaF_2$ are replaced by C_3A. Periclase content decreases above 1200°C and enhances the growth of alite. The actual alite content is higher and C_2S and C_3A are lower in such clinkers. Cements made show high strength but erratic setting time characteristics. Efforts to make high MgO clinkers continue to be made (41). The expansive behaviour of higher MgO cements is controlled by increasing fineness of cement and making blended cements with Pozzolana/Slags effectively.

Alkalies and Sulphates

Alkalies in the raw meal affect both the clinker phase

formation and properties of cement and try to combine preferentially with each other to form alkali or potassium calcium sulphate. Boikowa and Regourd reported incorporation of alkali ions in the individual phases and found that Sodium ion was incorporated in the C_3A structure by substitution of calcium ion while a further sodium ion is included in the structure for balancing (42). According to Skalny sodium oxide can be incorporated in the C_3A structure upto a maximum of 7.6% by mass with the formation NC_8A_3 (43). Odler et.al. observed that K_2O is incorporated in the C_3A which accelerate hydration of pure C_3A phase (44). Woermann determined that upto 1.4% (by mass) of Na_2O and K_2O each can be incorporated in C_3S (24). In case of higher K_2O contents, free lime and alkali belite are formed apart from C_3S. In contrast to this Yamaguchi reported not more than 0.71% and 0.5% by mass of Na_2O and K_2O being incorporated in C_3S respectively (45). The effect of alkalies, in presence of SO_3 show a distinct influence on the formation and content of clinker phases, specially alite of larger crystal size are formed. The much higher growth rate of alite is due to lowering of viscosity of melt.

Maki reported that with more than 1% of SO_3 in the clinker very large alite crystals are developed, which are irregular in shape (27). The alite crystal growth is accompanied by entrapping small grains of belite and free lime. However, Butt et.al reported that excess addition leads to reduced alite formation (46). The effect of SO_3 on crystallisation mode of alite can be reduced considerably by increasing alkali concen-tration. Gutt and Smith observed that SO_3 could restrict formation of C_3S in absence of MgO (47). Trace amounts of alkali carbonate are also reported in some clinkers. Role of SO_3 making sulphoaluminate and belite type cement is very important.

Locher reported that increasing alkali content in conjunction with correspondingly reduced $Ca(OH)_2$ content of the liquid phase in the cement paste promotes recrystalisation of ettringite which accelerates setting (48). K_2O increases the viscosity of the melt reducing the rate of alite formation. Na_2O and SO_3 lower the viscosity of the liquid phase thus reducing the formation of alite and increasing belite and free lime content particularly with high Na_2O content. The effect of alkalies on water demand is not much pronounced. Na_2O clearly accelerates the setting but the effect of K_2O is ambiguous. Both acceleration and retardation of setting time occur in presence of K_2O which is due to formation of syngenite. In contrast the effect of alkalies on compressive strength is more obvious. The 2 days compressive strength is increased by K_2O percentage upto 1.5% by mass. Na_2O reduces 28 days and 90 days compressive strengths more distinctly than K_2O. Skalny further studied the effect of alkali sulphates and found that 28 days compressive strength is reduced by about 30% with 2% K_2SO_4 and setting time was shortened, however, the soundness was not affected (43).

The studies carried out by Driezler and co-workers on the influence of SO_3 content showed that sulphur was incorporated in all four clinker phases (49). The highest sulphur content was found to occur in the belite. Individual $CaSO_4$ were detected in alkali free clinkers with more than 5.3% SO_3 by mass. With

increasing SO_3 content, alite content decreases and belite content increases. The higher content of SO_3 was found to lower the strength. However, setting was more rapid.

Fluorides and Mineralisers

The influence of addition of fluorides and mineralisers on the clinkering process have been extensively investigated by various researchers. CaF_2 and fluorosilicates act both as flux and mineralisers. Mineralizers lower the temperature of liquid formation and in turn clinkerisation temperature by 50-150°C. The systematic study of phase equilibrium, relationship in C-A-S-F system with fluoride fluxes and presence of P_2O_5 impurities has been done earlier (50,51). There is an optimum level, say about 1% for CaF_2 at which the surface tension and viscosity are reduced significantly. The other effects are reduction in average crystal sizes and additional alite formation. With reduction of C_3A which is replaced by $C_{11}A_7.CaF_2$, resulting in extra lime for alite formation in the early stage. The properties of resultant clinker are affected appreciably.

Klemn indicates that with 1% CaF_2, a C-S-A-F raw mix can be converted into alite at 1300°C at the same rate as at 1450°C without CaF_2 (52). Further, he reported the production of alite at moderate rate from CaF_2 doped samples even at 1200°C.

Christensen and Johansen have carried out similar studies and reported that with 1% CaF_2 at 1350°C the rate of reaction is same as at 1450°C with no CaF_2, the former is more prone to form alite well below 1250°C (53). 1250°C is the inversion temperature at which CaO, C_2S and C_3S are in equilibrium with each other. Fluorides, therefore, lower inversion temperature. This lowering reflects a change in thermodynamic equilibrium properties and driving force for alite formation over a considerable temperature range. In the ternary system of C-A-S the width of primary field for C_3S represent a measure of this driving force for alite formation. The width of C_3S field dramatically swelled in case of CAF_2 (54). There is some uncertainty as to the extent to which F enters the C_3S and influence on the hydraulic characteristics of cement produced with CaF_2. Change of Triclinic form of C_3S to monoclinic was reported earlier. The strengths made with such cements were reported to be poor by Tanaka (55). However Moir reported high early strength with 0.16 F in the clinker (39). Klemn examined the influence of MgO and SO_3 together with CaF_2 and observed that MgO appears to increase the rate of alite formation and SO_3 decreases the rate of reaction (56). This is reported due to early formation of $C_{11}A_7,CaF_2$ in the liquid phases to be later distributed between silicate phases. Investigations on influence of Fluoride to modify C_3S and C_3A structure and control in the clinker was reported by Glasser and recently by Goswami et.al. (57,40). The presence of high MgO, high alkali and fluoride in the industrial clinker, as reported by Goswami altered the alite content and reduced C_3A content. Setting behaviour of such cements was also investigated. Retardation in setting time and lower early age strength have been observed.

Correlation between Composition and other parameters with Strength

Properties of cements are largely dependent on Chemical, Mineralogical and Physical parameters. As the outstanding importance of cement strength, especially of concrete strength, is not doubted, establishing exact relations between chemical characteristics, phases and strength is of great importance not only for predicting cement quality but also predesigning cement quality.

The correlation can be worked out in two stages :

* Raw Meal and Fuel parameters processing parameters and Clinker quality
* Fineness, gypsum content size distribution at grinding stage and hydration products

Ono reported that gradient of heat up, peak temperature, retention time, and rate of cooling, largely determine the activity of alite and belite which, in turn, govern the 28 days compressive strength more than that of free lime or fineness provided all other parameters are kept constant (58). Optical Microscopy is suggested as the control tool to determine and control the alite and belite size. Fundal reported that alite crystal size is determined by burnability of cement raw mix (59) and agreed that inter-relationship between the mineralogical structure and the cement quality does exist.

Hargave, et.al., considered the overall mineral content and sizes of alite and belite along with shape factor, twin and cluster formation as the parameters (60). Strunge, Knofel and Dreizler reported that Na_2O is having the strongest negative effect on 28 days strength (61). Gebaurer confirms that 28 days compressive strength is inversely related to content of soluble alkalies (62). Osbaeck reported the effect of C_3S, aluminate contents, soluble alkalies (63). Richartz reported optimum influence of K_2O on 28 days strength between 0.4 - 0.5% (64).

Bruggemann and Brentrup found the following parameters in order of their influence on cement strength in terms of correlation coefficient obtained from a statistical evaluation of data on number of cement samples (65).

* Soluble Alkalies (According to Pollit and Brown)
* $C_3S + C_2S$ (According to Bogue)
* $3C_3S+2C_2S$+Aluminate-Ferrite (Acc.to Knofel)
* Silica Ratio
* C_3S (According to Bogue)
* Alite + Belite
* MgO
* Belite

The best correlation with the smallest coeffient of error and the smallest standard deviation (1.2 N/mm^2 of desired strength) is achieved when combining soluble alkalies with the quotient of C_3S/Alite size (Fig.3) and Table 1.

FIG. 3 - RELATIONSHIP BETWEEN COMPRESSIVE STRENGTH AND SOLUBLE ALKALIES, C3S, ALITE CHORD LENGTH

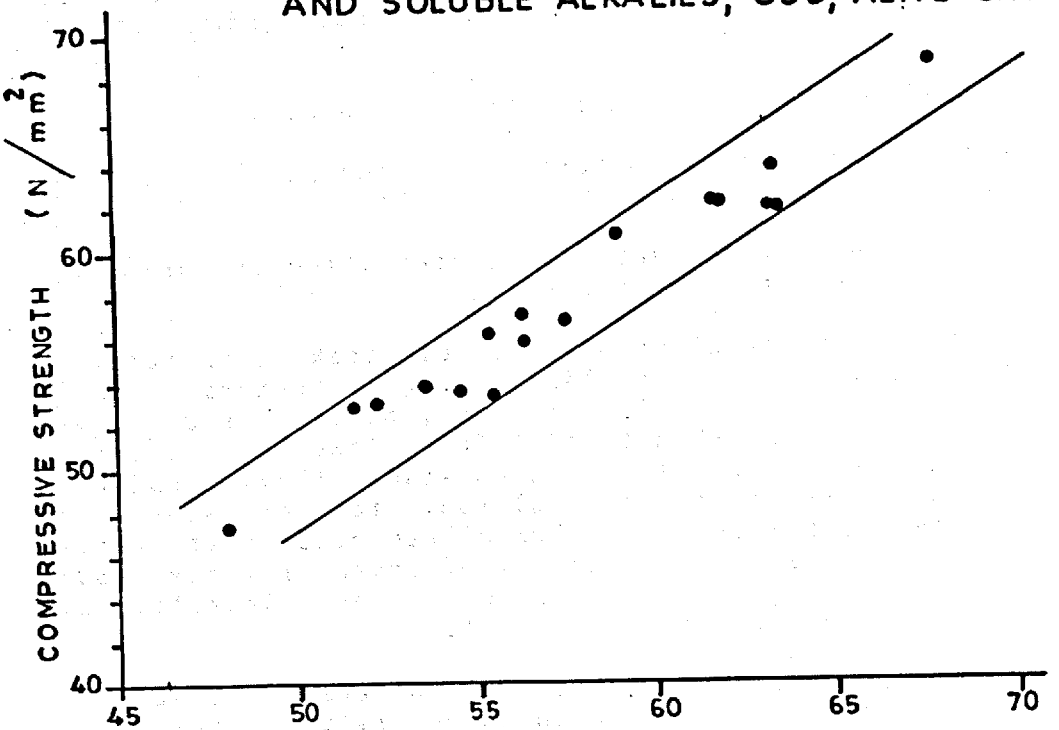

TABLE 1 : RESULTS OF MULTIPLE REGRESSION ANALYSES WITH COMPLEX PARAMETERS

1. Parameter	Coeffi cient	Coeffi. Error	:: 2. Parameter	Coeffi- cient	Coeffi. Error	:: 3. Para- meter	Coeffi- cient	Coeffi. Error	R	S N/mm^2
Soluble Alkalies	-15,75	1,55	::			::			0,93	2,0
-do- -do-	-15,66	1,5	:: Alite	0,14	0,10	::			0,94	1,9
-do- -do-	-12,80	2,36	:: $C_3S + C_2S$	0,34	0,21	::			0,94	1,9
-do- -do-	-14,92	1,96	:: Alite + Belite	0,11	0,16	::			0,94	2,0
-do- -do-	-14,03	1,59	:: C_3S	0,21	0,10	::			0,95	1,7
-do- -do-	-12,44	1,59	:: Knofel-Factor	0,15	0,05	::			0,96	1,5
-do- -do-	-17,12	1,34	:: Alite-size	-0,19	0,06	::			0,96	1,6
-do- -do-	-16,74	1,08	:: Alite/Size	1,27	0,30	::			0,95	1,3
-do- -do-	-16,39	1,08	:: Alite + Belite/ :: A-Size	1,21	0,29	:: ::			0,97	1,3
-do- -do-	-16,23	0,93	:: C_3S/ A-size	1,67	0,31	::			0,98	1,2
-do- -do-	-16,30	1,05	:: $C_3S + C_2S$ / :: A-size	1,30	0,30	:: ::			0,97	1,3
-do- -do-	-16,32	1,00	:: Knofel-F./A-size	0,46	0,10	::			0,98	1,3
-do- -do-	-14,46	2,28	:: $C_3S + C_2S$	-0,22	0,33	:: SM	2,6	1,3	0,96	1,7
-do- -do-	-16,00	1,36	:: C_3S / A-size	1,61	0,44	:: SM	0,13	0,71	0,98	1,2
-do- -do-	-15,8	0,78	:: C_3S / A-size	1,31	0,29	:: MgO	-0,74	0,28	0,99	0,97

Knofel recently examined laboratory and commercial clinkers to establish correlation and considered various raw meal moduli phases for correlation with strength to be more realistic (Fig.4).

Based on laboratory results, he proposed the following formula (66).

F28 = 3.Alite + 2.Belite + Aluiminate - Ferrite
(F28 = 28 days strength)

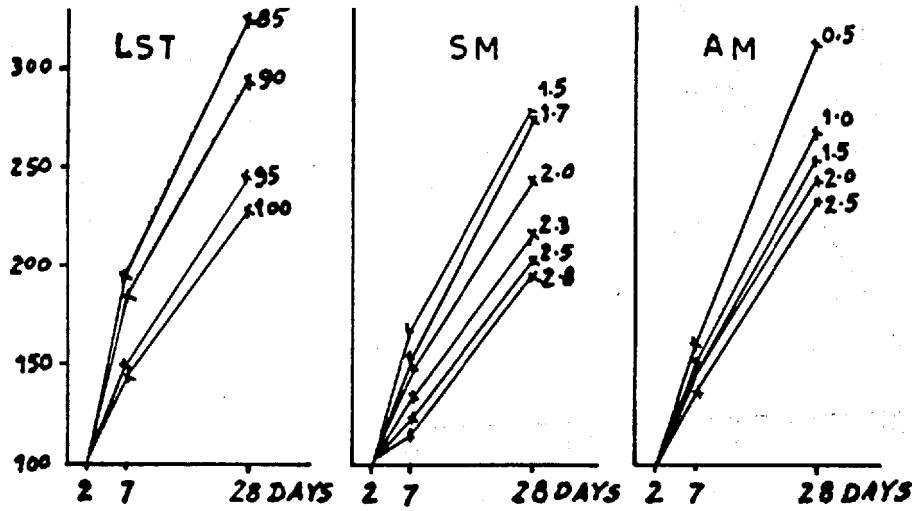

FIG.4 - RELATIVE COMPRESSIVE STRENGTH AS A FUNCTION OF LST SM AND AM AND OF AGE AT TESTING.

Fig.5 shows the relationship between strength characteristics (F28) and 28 day compressive strength in laboratory cements.

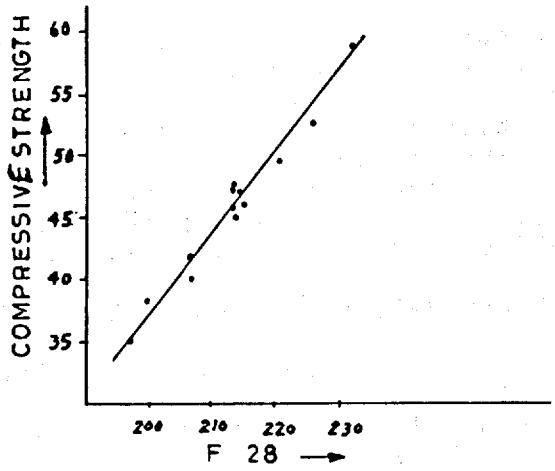

FIG.5-RELATIONSHIP BETWEEN STRENGTH CHARACTERISTIC F 28=(3 X ALITE+ (2 X BELITE)+ALUMINOFERRITE AND 28-DAY COMPRESSIVE STRENGTH IN LABORATORY CEMENTS

According to Knofel (66) the lab scale correlation did not work for industrial scale and he concluded that there do not exist any co-relation between the clinker phases and strength of randomly chosen cement samples. However, compressive strength after 28 days can be forecast with satisfactory accuracy from the clinker phases for a specific cement plant under similar production conditions. (Fig.6).

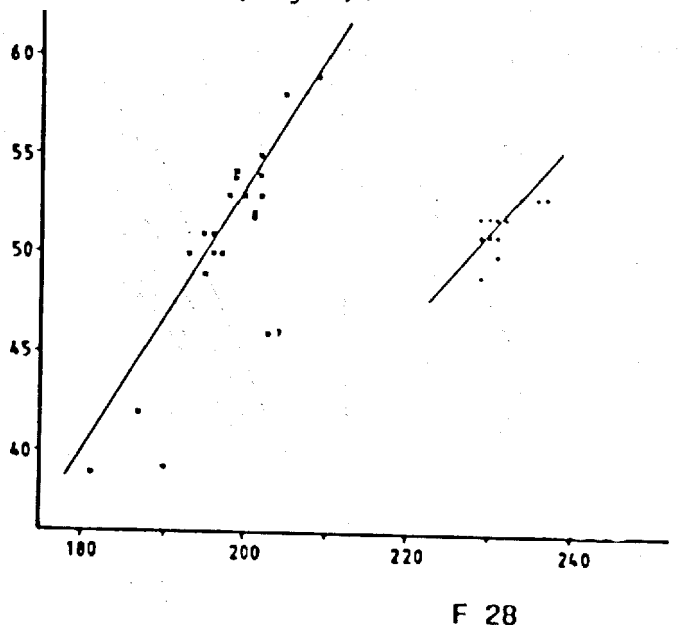

Fig. 6: Relationship between strength characteristic F 28 and 28-day compressive strength of industrial cements from individual cement works

Viswanathan and Narang studied relationship of size distribution, free lime, fineness and phase composition with strength at 3, 7 and 28 days and determined a specific factor using a mathematical model which can be used for quality control at the plant level (16). The influence of raw mix fineness, various moduli and size distribution were also determined and correlated with clinker quality. The relationship thus attempted, although have produced guidelines, are not universal.

PORTLAND CEMENT, ITS DERIVATIVES AND LOW ENERGY CEMENTS

Specification world over cover wide variety of Portland Cements (67). While the basic composition of cement is retained, it is the manipulation of chemical constituents, their ratios and resulting phases which help exploitation of one or more potential characteristics. The recent attempts hitherto have been more on quality of phases, i.e. microstructure and size distribution, etc, than on percentages.

The basic improvements, which have been sought in the performance of portland cement and its derivatives are in terms of :

* Control on setting characteristics, (Oil Well Cements, Rapid hardening cements, Early setting cements.)

* Performance under aggressive environment (Resistance to alkali aggregate reactivity, corrosion, sulphate resistance leading to formulation of low alkali, low heat, and low C_3A cements, etc.)

* Performance under high mechanical and environmental stresses (low/medium heat cement, expansive cements, oil well cements, and early and ultimate high strength cements.)

* Low Energy Cements and Newer processes of making Cements, (Belite Cement and Alinite Cement, etc).

Oil Well Cements

Oil Well cements, in principle, require the same raw materials as for Portland Cement, but due to restriction on C_3A, C_3S and total ferrite phases and its sensitivity to minor constituents, particularly for additive response, selected materials low in Al_2O_3, F, P_2O_5, TiO_2, MnO_2 and alkalies are used. Oil Well Cements are generally used together with components such as silica flour/bentonite/hematite to control setting, flow, density and strength characteristics. The most important requirement for Oil Well Cement are Sulphate resistance and Thickening time regulation and adequate strength development at high temperature and pressure (static/circulating) at the bottom of the well. American Petroleum Institute (API) has laid down specification for different classes of Oil Well Cement and its testing procedure (68). While investigations on different classes of cement have been carried out extensively, Class 'G' of American Petroleum Institute specifications forms the base cement for designing slurry with the help of additives to achieve the designed performance characteristics (69,70,71). The rheological characteristics of Oil well cement are governed by free lime content and size distribution, besides microstructure. Correlations of various parameters including microstructure with thickening time and strength of Oil Well Cement with and without the additives have been attempted (72). Each application agency finds out the compatibility of Oil Well Cement, additives under defined conditions and no universal model has emerged so far. In fact, each slurry has to be tailor-made for specific conditions prevailing in the well.

Bensted has outlined the main features for low hydraulic activity of oil well cement as low C_3S content, low C_3A content and low free CaO, SO_3 content, however, fineness should not be too high (73,74,75). Control on reducing conditions in Pyroprocessing and grinding temperature during grinding needs to be exercised. Cementing chemistry of oil well cements is generally the same as that of Portland Cement except lower rate of hydration. Thickening time and subsequent strength

development are principally due to hydration of silicate phases to form non-stoichiometric calcium silicate hydrate and $Ca(OH)_2$. In hot wells amorphous Calcium silicate hydrate in place of crystalline C-S-H and $Ca(OH)_2$ is formed. Benstad also reported the early hydration characteristics of Class G Oil Well Cement in presence of retarders and observed that retardation produced more ettringite and less C-S-H, increased dispersion and hindered crystal growth in addition to reduced chemical reactivity. Fig.7 shows the heat liberation curves on hydrating Class G Oil Well Cement (72).

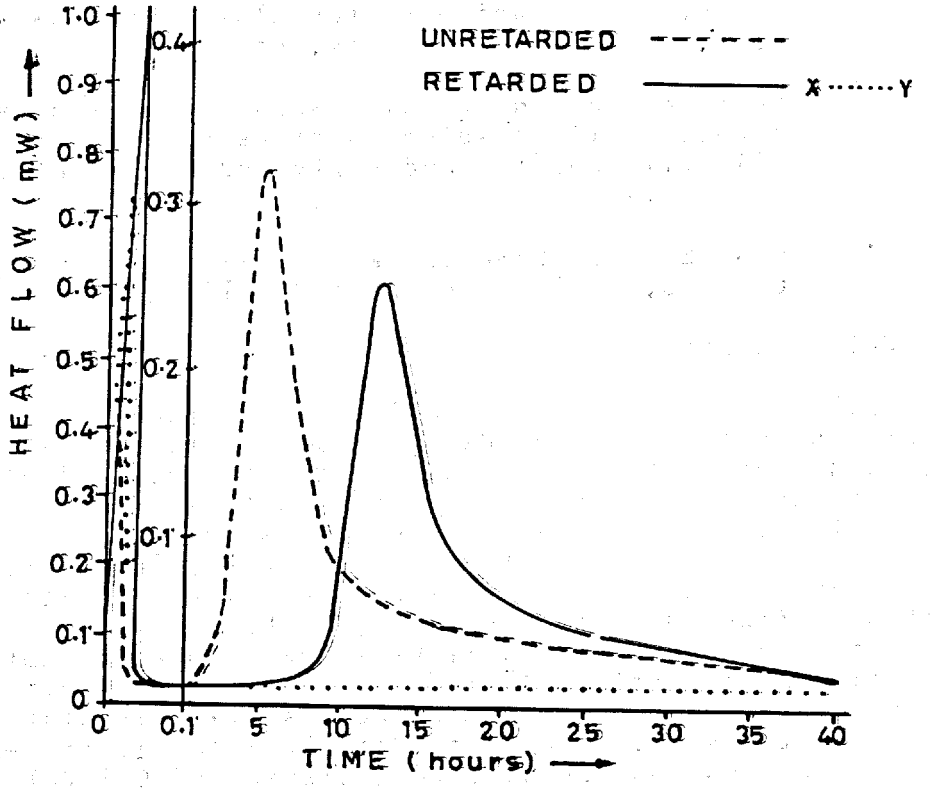

FIG.7-CONDUCTION CALORIMETRIC CURVES FOR THE CLASS G OILWELL CEMENT

Particle size distribution and SO_3 contents play significant roles. Prehydration state of gypsum mineral, i.e. synergite content is an important aspect in controlling performance. Oil Well Cements made with Coal as fuel show distinctly different crystal size of alite and hydraulic activity compared to those made with oil firing (76).

Lignosulphonates, modified lignosulphonates, various cellulose derivatives, latex admixture and saturated NaCl are among some of the additives used as retarders, accelerators and dispersants. At higher temperatures, in deep wells, pozzolanic admixture / silica flour are commonly used to arrest strength regogression (76).

A Special Cement (Class-J of American Petroleum Institute) consisting of dicalcium silicate and silica, interground in proportions of 60:40 by weight, (sometimes with small additions of calcium hydroxide have also been investigated for high temperature wells). In Class J cement, protection against

strength regogression is already incorporated. Narang et.al. carried out studies on Class J cement formulated from slag and different types of silica sources and also evaluated the effect of additives on the same (77). The permeability of such formulations is observed to be generally poor.

Grabowski reported Blended Oil Well cements in which silica flour was replaced by silica fume (78). These cements showed significant increase in compressive strength but decrease in water permeability (Fig.8).

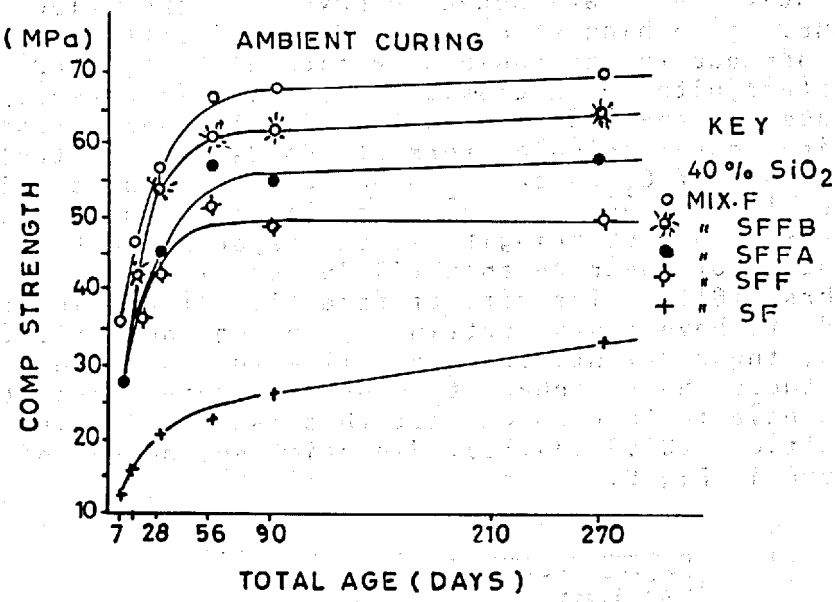

FIG. 8-COMPRESSIVE STRENGTH VS. PERIOD OF CURING IN FOG ROOM CONDITION

Very Rapid Hardening and High Early Strength Portland Cement

Portland cement in the absence of sufficient quantity of set regulator, i.e. calcium sulphate, will flash set and thus can be termed as the fastest setting cement, but this is characterised by very poor ultimate strength due to uncontrolled hydration of C_3A similar to MacDowell's glass (79). In order to overcome the poor early and ultimate strength of Portland cements, various modifications in the basic portland cement have been investigated. The concept of Rapid Setting cement was first introduced at Portland Cement Association and later in the form of jet cement in Japan (80). The basic approaches to achieve the objective are :

* Portland Cement with admixtures, (mixtures of Portland Cement with Calcium Aluminate Cement);
* Modify Portland Cement clinker to contain fluorides based mineral ($C_{11}A_7$, CaF_2 and C_4A_3S);
* Use of Polymer modifiers.

While formulations based on 1 and 3 are tailor-made, preferably at site and vary significantly, commercialisation of fluoride based cement is on more universal basis. Fluoride bearing raw mixes are clinkerised at low temperatures, thus incorporating fluorides in aluminate phases, instead of in silicate phases. $C_{11}A_7.CaF_2$ replace C_3A and formation of C_4AF is also hindered. The major phases in such cements are C_3S, C_2S, $C_{11}A_7.CaF_2$ ferrite and $CaSO_4$. The set control agents are anhydrite, which has low solubility. Certain other physico chemical controls (such as higher specific surface) and additives like citric acid, etc. are added to have setting time in a designed range. The high strengths and early setting in all these cements are due to the rapid hydration of $C_{11}A_7.CaF2$ which do not interfere with the hydration of silicate phases. The concept is based on the observation that C_3A is more reactive, thereby require more soluble form of $CaSO_4$ to control its hydration. In case of $C_{12}A_7$ or $C_{11}A_7CaF_2$ phases, stable single-phase hydrate layer can not be established. Uchikawa and Coworkers observed that Etteringite is the major product at early ages of hydration of these cements (40-45% of $C_{11}A_7.CaF_2$ having reacted at 3 hrs) (81). The rate of formation of ettringite can be controlled to have faster setting by using anhydrite. In other aspects, these cements compare well with Portland Cement except that these have inherent poor sulphate resistance. Investigations have further shown that this can be improved with Pozzolana addition (82,83,84,85). Hydration mechanism of such cements is shown in Fig 9.

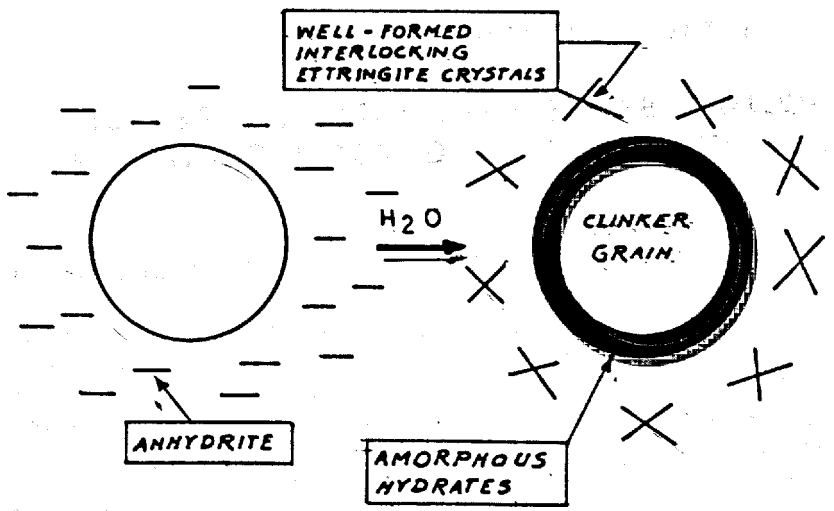

FIG. 9 FLUOROALUMINATE HYDRATION IN RSPC

Formulations, using Portland Cement, Calcium Aluminate Cement and $CaCl_2$ in specified quantities has been patented in India for specific application, such as bolting in coal mines. The study shows that the mixtures are very sensitive to composition, specially to quantum of $CaCl_2$ and fineness (86).

C_4A_3S based rapid hardening cements have been reported by Sudoh et al, with phase composition as C_4A_3S, C_2S(3%), C_4AF(5%) and free lime (9%) (87). The cements were made at such moderate fineness of 400 m^2/Kg^{-1} and had anhydrite as the set regulator. Ettringite is the main hydration product. Shelf life or stability under storage and preuse condition is of great importance. Long and coworkers suggested a specific application procedure in which C_4A_3S clinker containing slurry was mixed with another slurry containing anhydrite, $Ca(OH)_2$, bentonite and alkali salts at the site . Since C_4A_3S clinker hydrates slowly in the absence of $Ca(OH)_2$, it can be accelerated by the second slurry containing CH and alkali activator. Several blended cement system for high early strength and rapid hardening have also been developed from Portland Cement.

Low Energy Cements

Efforts to reduce energy consumption in clinkerisation and in comminutions have led to development of efficient techniques of pyroprocessing, formulation of modified Portland Cement and advanced techniques of comminution. The physio-chemical characteristics of the cements get influenced by each of these approaches. Heat consumption has been reduced to 700 K.Cal/Kg of Portland Cement clinker by efficient heat exchangers in the commercial production. Any further reduction in heat calls for changes in the Chemistry of mix to get appropriate mineral phases.

Locher and Meric reviewed the various ways of reducing energy consumption in the last Congress (89,90). The various methods include use of fluxes, producing cement containing reactive belite, and other reactive minerals, replacing alite by chloride containing phases i.e. alinite and making composite cements. Burning temperature can be decreased by about 150°C by fluxes and about 300°C by chlorides addition. There are different opinions on the extent of energy savings and the mechanism of clinker formation at low temperature, however, it is generally opined that it is achieved by reducing alite content and increasing belite. The basic approach being to obtain active belite or activated belite by activating phases like C_4A_3S. Reactive form of belite has been obtained in the laboratory by low temperature synthesis, but with doubts about its industrial application. Studies of Stark and Muller showed that clinker containing around 48% of C_2S gives higher early strength (91). Active belite cements, containing ~ 70% C_2S and near absence of C_3S was reported based on chromium oxides activator (88). The approach however, has problems on account of strict environmental controls. The main conclusion in the development of active belite cements is that it can be formulated with C_3S content as low as possible in the clinker. Stark and Mueller reported various approaches to low energy cements under development as

highlighted in Table 2.

TABLE 2 : DEVELEOPMENT TREND IN LOW ENERGY CEMENT

	MAIN CLINKER MINERALS	SPECIAL PROPERTIES / APPLICATION	RESEARCHERS
ACTIVE BELITE CEMENT	α' α C_2S	in comparision with portland	Stark and
	C_3S	cement; lower early and higher	Muller A.
		late strengths	
	C_3A	setting times, workability,	Gies,
		etc. as for ordinary portland	Knofel,
		cement	Sudakas,
			Ghosh
	C_4AF	pilot-plant tests in GDR,	Ludwig and
		India, USSR	Pohlmann
BELITE-SULPHO-ALUMINATE CEMENT	β-C_2S CA,	high early strength,	Ikeda
	C_4A_3S	short setting time,	Sudoh
	$C_{11}A_7$	high chemical resistance	Volke and
		special cement in USA, Japan,	MULLER
		USSR	
BELITE-SULPHO-FERRITE CEMENT	β β C_2S	short setting times,	Mehta
	C_4AF	high early strengths	Yanmou
	C_4A_3S	mass-produced cements in	Than
	$C\bar{S}$	China, Industrial production	
LTS / ALINIT CEMENT	Alinite	chloride content upto 2.5 %,	Nudel'man
	$2C_2S$. $CaCl_2$	high hydraulic activity,	
	$C_{11}A_7$. $CaCl_2$	steel corosion	
	C_4AF . $CaCl_2$	industrial production in USSR	
LOW-TEMP. CEMENT	C_3S . CaF_2	in the exploratory stage	Burger and
	$C_{11}A_7$. CaF_2		Ludwig

Belite-Sulphoaluminate /Ferrite Cements

This cement was referred to as Special Cement and was reported by Kurdowski and Sorrentino (92). C_2S-C_4A_3S cements are high early strength and are for expansion or shrinkage compensation. Sulphoaluminate-belite cement with extremely high strengths (15 MPa after 2 hours) and intended for use as an additive to portland cement was developed under the name of Besalit (93). Alumina belite cement consisting of 62-64% belite, CA, $C_{12}A_7$, C_4A_3S and C_5S_2S and having good strength and sulphate resistance was reported earlier. Typical properties of belite (good late strength development) and of $3CaO.3Al_2O_3.CaSO_4$ (high early strength) are appropriately combined. The standard strengths are reported to be similar to those of ordinary portland cement. These cements are also reported to have high sulphate resistance.

High iron rich hydraulic cements reported by Mehta can be termed as Energy Saving Cements (94). (Composition of cements is based on C_2S (30%), Ferrite (30%), C_4A_3S(20%) and CS(20%). Iron rich belite cements are produced in a number of small cement plants more particularly in the People's Republic of China. According to Yanmou and Jun'an, these cements are used in housing construction, in hydraulic engineering structures, etc (95). Their properties are adapted to suit the requirements of the job by variation of the proportions of clinker minerals (high-early strength cement, expanding cement, self prestressing cement). The hydrate phases found to be present were AFt,AFm, AH_3, C-S-H and a little $Ca(OH)_2$. The compressive strengths were in the range of 50-90 MPa. The good frost and corrosion resistance of these cements is highlighted. Subsequent modifications by introducing $C_{11}A_7.CaF_2$ together with C_4A_3S was reported by Xiuji to obtain higher early strength (96).

Low Temperature Alite Cement

Studies on Alinite Cement developed in USSR and also produced at industrial scale were reported in the last Congress at Rio. Evaluations of such cements was reported by Aggarwal et.al (97). It was observed that microstructure of alinite resembled that of Portland Clinkers and also confirmed the presence of $C_{11}A_7.CaCl_2$ and Calcium Chloride ortho-silicates. Hydration of alinite is likely to be similar to that of Portland Cement. As fixation of chloride was not complete in these cements and hence posed problems with use in reinforced concrete. Lampe observed that MgO is a indispensable ingredient of alinite (98). The formula worked out by him is

$$Ca_{9.9}, Mg_{0.8}, O_{0.3} (Si_{3.4} Al_{0.6}O_{16}) O_{1.9}, Cl_{1.0}.$$

Reports on work done on alinite cement at VDZ indicate complete corrosion on the surface on 5-year storage and was considered for use in unreinforced construction only.

Burger and Ludwig studied a fluoride bearing alinite which could be made at 1050°C using CaF_2 (99). Flourine alinite takes care of the steel corrosion problem, but results in lower hydraulic activity. Use of chemical activators (transition element), catalysts may be the futuristic approach to make low alite cements at low temperatures.

Expansive Cement

Excellent reports on development of expansive cements of various types and their applications have been presented at Moscow, Paris and at Brazil Congresses. Since the exciting reports of Klein and Co-workers, wherein C_4A_3S is an essential gradient of expansive cement, the composition of expansive cement have been varied incorporating changes in raw material composition but in all cases the objective is to achieve expansion due to ettringite formation from hydration of C_4A_3S only (100). The content of C_4A_3S decides the design characteristics of K type expansive cement. Durability of K type cement

has been the subject of further studies. Studies on Free CaO and MgO based have also been carried out during the last decade. The MgO based expansive cements have shown commercial potential.

Cohen reviewed theories of the expansion mechanism (94). While one school of researchers attribute expansion due to forces exerted by the growth of the ettringite crystals, Mehta attributed it to imbibition of water by the gelatinous layer of colloidal ettringite (101,102). On this hypothesis, expansion does not occur with the larger crystals formed at low CaO concentrations because these do not form aggregates that imbibe water. Ogawa and Roy's observations suggest that the above hypothesis is not the sole or even the major cause (103). Cohen proposed a model to explain the mechanism and kinetics of expansion in K type cement. With the help of this model .he explained the difference between expansion of S and K type cements. Cohen also reported the influence of parameters like fineness of C_4A_3S indicating that excessive fineness reduces the extent of expansion and the expansion in inversely proportional to the fineness. Besides the overall fineness,the effect of size distribution, specially the fineness fraction is considered important. The presence of coarse particles can resultin delayed expansion. That will damage the paste irreversibly.

Investigations on pore structure development of expansive cement paste as a function of expansion strain and curing time have been recently reported by Cohen (104). The expansion strain, bulk density, dynamic modulus, and evaporable water content of paste specimens were monitored periodically during and after termination of expansion . (Fig.10). Correlation with the pore size distribution data obtained by mercury intrusion porosimetry for both unrestrained and restrained expansion systems with various properties were also obtained.

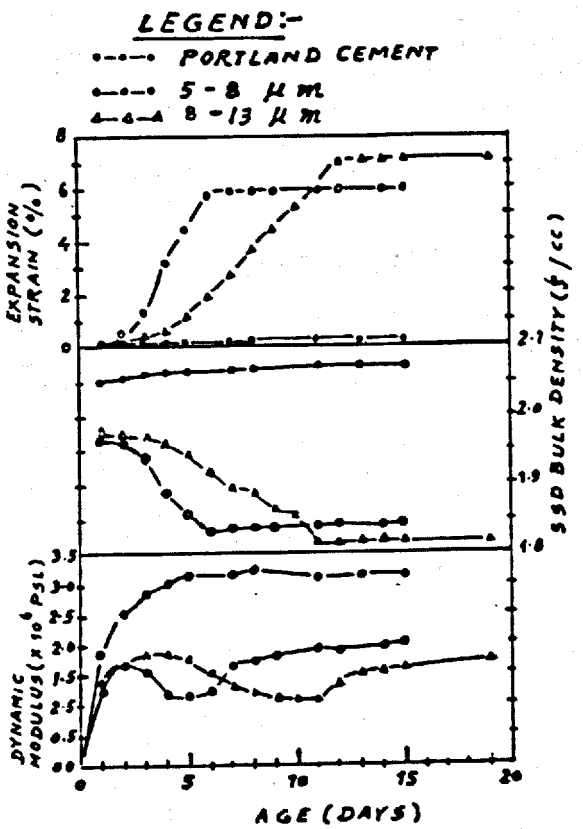

FIG.10- EXPANSION, BULK DENSITY AND DYNAMIC MODULUS CURVES OF FREE EXPANSION PASTES

It is shown that expansion results in the formation of large pores (and/or microcracks) in the paste. The mass of evaporable water appears to be a better way of characterizing changes in porosity during expansion, however, it does not reveal any information about pore size distribution.

The effect of restraint by steel reinforcement on pore structure development of expansive cement paste was also studied. It was found that restraining expansive cement paste results in reduction of the size of large pores. However, even with a large degree of restraint, expansive cement paste is still more porous and contains larger pores than portland cement paste of the same age. Under sulfate environment, if adequately sulfated, performs at equal or even more than that of portland cement. The new uses of expansive cement are under exploration, however, its use in prestressing concrete, water and oil wells, asbestos cement boards, airport pavements, etc. are already subjected for research and the results are encouraging.

Studies on Free CaO based expansion cements and Soft burnt MgO (periclase) based cements have been reported earlier. Author has studied various parameters (Calcination temperature, time, size distribution) and the influence of type of raw material used for making free lime and free MgO based expansive cements. The results indicate that free CaO based cement irrespective of their origin and formation expand too fast and the expansion is over in less than 24 hrs. Similar studies on MgO obtained from magnesite have also been carried out and it was found that activity of MgO as an expansive component can be controlled.

PROPERTIES OF CEMENT OBTAINED FROM NEW/MODIFIED GRINDING TECHNIQUES

Advances in comminution technology have offered number of energy efficient systems for crushing, grinding and classification. The new generation separators, roller mills and recently developed roll press, all influence the physio-chemical and microstructural characteristics significantly. These techniques enable the specific surface to be reduced and help in obtaining narrow particle size distribution and higher homogeneity. Kinetics of reaction at clinkering stage can be influenced due to narrow particle size distribution. It leads to formation of optimum size of crystals in the clinker. The problem related to overburning and underburning is also solved to an extent. For cement grinding, the system helps in saving energy by reducing specific surface without reducing strength. The increase in water demand of narrow grain size distribution and behaviour of cement in fresh concrete, particularly early stiffening have at times raised doubts on the quality of cement from such systems.

The lab scale study carried out by Gebauer shows that the reactivity of the clinker is influenced by factors such as aluminate phase C_3S and alkali content, kiln atmosphere, degree of burning and temperature of ground material (105). Reactivity increases with increasing alkali and alite content and under reducing kiln atmosphere with lower degree of burning. The higher temperature of ground material converts gypsum to

hemihydrate or anhydrite. In the wake of narrow particle size distribution of cement, the amount of sulphates adjusted such that all C_3A is bonded in the form of ettringite. If there is an excess of sulfate in the solution then this makes cement pastes to stiff rapidly. Apart from the above, the fineness of cement especially its grain size distribution also influence the workability of cement paste. Thus cements obtained from ball mill or mills with High Efficiency Separator exhibit poor workability more so when the soluble sulfate is not matched properly. With reactive clinker, the amount of soluble sulfate required increases if the cements have a narrow particle size distribution. Study also indicate that the effect of grain size distribution affect the water requirement on concrete less than in cement paste. Table-3 compare different properties of cement obtained from separate grinding and intergrinding.

TABLE 3 : EFFECT OF PARTICLE SIZE DISTRIBUTION ON CEMENT PROPERTIES.

Cement No.	1	2	3	4	5	6	7	8
Clinker Mill	A OPEN	A H.E.S.	B OPEN	B H.E.S.	B OPEN	B H.E.S.	C CLOSED	C ROLL
PSD of Cement								
d' (um)	28.7	27.2	15.0	13.0	25.0	27.0	19.0	19.0
n	0.86	0.95	0.93	1.11	0.86	1.13	0.86	0.97
Blaine (cm^3/g)	2930	2650	4405	4075	2940	2600	3990	3275
Paste								
Water demand (%)	23.0	26.0	30.3	33.8	26.0	28.0	26.3	29.0
Concrete (Slump 7.5 cm)								
W/C ratio	0.56	0.55	0.60	0.61	0.55	0.55	0.54	0.55
Strength (N/mm^2)								
2 days	19.9	22.3	28.4	30.4	24.0	23.1	32.4	28.9
28 days	33.1	37.7	39.1	43.2	37.1	37.2	46.5	44.4

Wustner and Coworkers investigated the characteristics of cement produced with Roll Press (106). The grain shape has been investigated with electron microscope, for size distribution between 32 to 63 microns and found to be sharp edged and platy. They further indicate that there was an increased water demand and a shortened setting time in cements which has been ground in high pressure rolls instead of in a tube mill due to narrow particle size distribution. Further tests showed that the cement properties can be improved by addition of precipitated dust and by selective reduction of content of the sulphate carrier. By doing so, the process of setting was normalised. However, the high water requirement still persisted, although this decreases with increasing percentage of dust and SO_3 content. Increased reactivity of C_3A in the clinker was also assumed to be another

cause of higher water demand. Tube mill cements showed a higher compressive strength, after two days, but lower values after 28 days, in contrast, with the cement produced in a closed circuit grinding system, with roller press. This is attributed to the fact that cement discharged from closed circuit grinding system lacks fines. The grinding system have now been optimised and strengths comparable to those obtained in ball mill are being produced. Effective use of roll press is also being made in making blended cement by separate grinding.

J.M. Brugan systematically studied the various properties of cement product obtained from High efficiency Separators (107). Results show that

* The fine particle content of cement (-10 microns, -3 microns) is basically the same as before the high efficiency separator, even though the Blaines is lower in most cases.

* The early strength development does not suffer much. This is attributed to the fact that fine particle content is more or less similar and the Particle Size Distribution slope is changed only in the coarse particle size region. 3-32 micron fraction is not appreciably affected in both the cases.

* The reduction in coarse particle content has resulted in only 0 to 2% increase in mortar water content. Coarse particles represent the strength controlling agent and their population reduction increases the strength of cement. Similar results have been obtained with high early strength cements, which confirms that fine particle content remains essentially the same. Fig.11 shows the comparison for cement obtained from High Efficiency Strength and Conventional Separators.

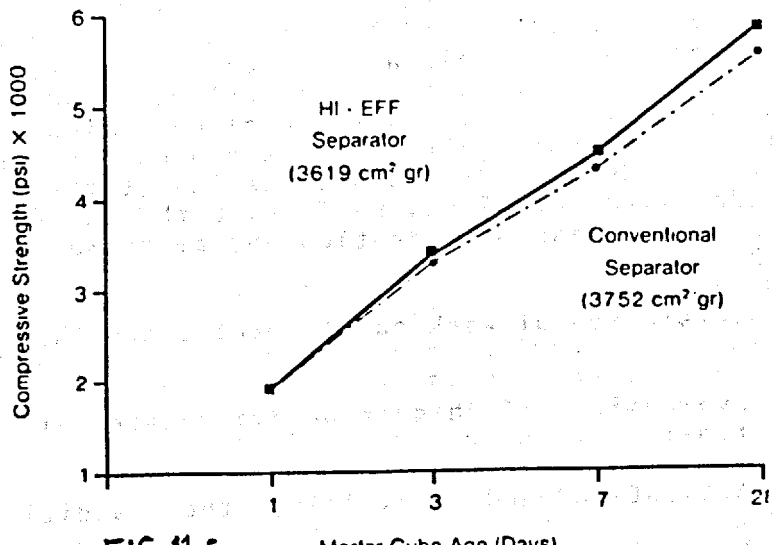

FIG 11 :

The various benefits with respect to quality of cement obtained from high efficiency separators are outlined as under :

* Ability to have better control of cement strength, and to enhance characteristics, such as coarse particle residue. Variations of these characteristics are minimized, resulting in higher confidence in cement quality.

* Lower cement temperature, minimizing the tendency of false or pack set in cement.

* Ability to make Special Cements such as coarse oil well and fine (binary / Ternary blends, including) masonry blends.

BLENDED CEMENTS

Formulations of blended cements based on natural or synthetic inorganic minerals are associated with conservation of energy, capital, environment and time. The mineral balance in the nature is disturbed with depletion of natural minerals on one hand and the rapid growth of by-products from increased industrial and agricultural activities creating handling, disposal and environmental problems on the other. While one has to spend energy to make the same hydraulic minerals in Portland Cement by clinkerisation and grinding, industrial wastes containing useful minerals having intrinsic hydraulic potential offer ready to use solution. Further with increasing demand on specific performance characteristics in concrete such as improved strength, low heat, sulphate resistance, improved impermeability and certain other applications, these minerals have imparted superior qualities to Portland Cement. The potential for formulation of blended cements can be seen from $CaO-SiO_2-Al_2O_3$ phase diagram (Fig. 1)where Zone of hydraulic minerals of Portland Cement can be extended to latent hydraulic minerals through activation by alkalies, sulphate and lime to obtain blended cements (5,10,11,108). Among the mineral additives, which are foremost in their acceptance, are granulated slag and fly ash. Quantum of Natural pozzolana and calcined clay pozzolana used widely is on the decline. Rice husk ash and microsilica or condensed silica fumes and calcareous fillers like limestone/kiln dust are the additives investigated most during last decade with promising results, both on formulation and application; Mechanism of hydration and performance is now better understood.

The developmental work carried out since the last Congress include :

* Evaluation of higher activity materials like Silica fume;

* Activation and maximising the additive content;

* Mechanism of contribution by additives;

* Durability of blended cements under certain critical conditions.

Report by Uchikawa at Rio Congress and composite cements by Taylor present a comprehensive review on the subject (11, 1). The properties of these mineralogical assemblage may vary with source and conditions of processing and need to be examined for

* Origin, Composition and Variation including minor constituents,

* Compatibility of components in terms of chemical / physical / mineralogical parameters, optimisation of their ratio, glass content and granulometry

* Choice of manufacturing techniques

* Product performance and economics

Slag and Slag Cement

Excellent reviews the physio-chemical and mineralogical characteristics of slag and slag cement have been reported (5,11,109). The influence of chemical composition, mineralogy, glass content and other activity parameters on the hydraulic properties of the slag have been recognised. The structure of glass, presence of crystallite for nucleation have been used to explain certain influences with regard to hydraulicity more clearly. Various hydraulic indices and basicity are reported as the measure of hydraulic activity. Studies on a large number of slags and the statistical inferences derived, however, indicate that the basicity ratio or any other parameter alone is not the criterion to predict the hydraulicity (110). Influence of Al_2O_3 (upto 13%) and MgO (upto 11%) were reported to increase the strength. Influence of MnO is negative while that of alkalies and P_2O_5 is rather complex. In several studies it is reported that presence of small proportion of crystalline material finely dispersed in glass improve grindability and/or reactivity. Demoulin found that the 5% crystalline phase could increase the strength at 2 and 28 days due to nucleation phenomenon in hydration (111). Regourd reviewed structural and other aspects of slags and concluded that neither periclase nor lime is found (5). MgO was present either in the glass or in the inert crystalline phase and thus MgO is not to be the cause of autoclave expansion.

The process of granulation is important and has been the subject of detailed investigation. In addition to Blast Furnace slags, a number of slags from other metallurgical processes have been investigated. Amongst those found useful are the Arc furnace slags, phosphatic slags, LCFC slags, copper and nickel slags. While arc furnace slags and phosphatic slags are lime rich and can be obtained in granulated form under controlled conditions for use in slag cement manufacture, LCFC slag is obtained in γ-C_2S form and can not be granulated as such. The efforts to granulate it also did not succeed due to high C/S ratio ($\simeq$ 1.7). Modification of composition of LCFC slag in molten slags enabled effective granulation. Through this process

granulated slag with latent hydraulic character is obtained and used for making slag cement in the usual way (112). Recent investigations have shown that vitrified non-ferrous slags, such as copper and nickel slags, have potential pozzolanic character and their blends with OPC can be used as binders of low cementing value. The pozzolanic action of these slags is slow and is suitable for making blends for high way construction, etc. The prospects of using these slags in the regular blended cement production therefore do not appear to be attractive excepting in masonry cements.

Regourd and Uchikawa have (5,11) reported that principal hydration products in Blast furnace slag cement are essentially similar to that of Portland Cement. But the quantity of CH is lower. The microstucture of such cements are also similar to that of Portland Cement apart from lower CH (5,11,113,114). The quantities of CH would vary with percentage of slag with a maximum of about 60%. Layers of the insitu reaction product form at the boundaries of the slag grain and gradually extend inwards. The size of these grains were 0.5 mm after 90 days as detected by light microscopy. Backscattered electron images show that these grains were barely detectable at 28 days but upto 10 micrometer wide at 6 months and 15 micrometer upto 14 months (115). Glasser et al have carried out study on the amount of reacted and unreacted slag but the results are varying (106, 116). The slag cements produced have higher sulfate resistance, improved durability, high ultimate strength and have controlled heat evolution. They find application in aggressive environments, in mass concrete structures and the areas of high strength requirements.

Newer techniques like Roll Press crushing and Separate blending are replacing the conventional Ball mill grinding system. These offer certain positive advantages in terms of control on size distribution and effective exploitation of hydraulic potential of slag and clinker, besides saving energy.

Natural and Calcined Clay Pozzolana

Natural sources of pozzolana (from volcanic origin) are well known in Italy, Greece, West Germany and USA. The physio-chemical composition of the pozzolanas from natural sources varies widely and is reported to have presented serious problems coupled with physically bound water organic substance and minor constituents (such as alkalies). The minerals which could be present in natural pozzolana are Silicate Glasses, calcite, quartz, feldspar and zeolites. The interest in natural pozzolana for cement manufacture is limited to specific locations and not much work is reported since the last Congress.

Clay minerals exhibit pozzolanic activity when calcined at temperatures between 600 - 900°C and ground to cement fineness. Under specified conditions, the pozzolana thus obtained consists of quartz, crystobalite, gehlenite, orthoclase, calcite, C_2S and muscovite besides glass and amorphous silica. All clays are not suited for manufacture of pozzolana. Some of the shales have also been found useful for making pozzolana. There appears to be no quantitative relationship between the various physico-chemical

and mineralogical parameters and the pozzolanic activity of the natural pozzolana or calcined clay, although it is clearly understood that addition of thermally or chemically activated clay significantly increases early hydration of Portland Cement due to absorption and ion exchange processes on the surface. Detailed investigations on effect of pozzolana addition on sulphate resistance, alkali aggregate reactivity and influence of environmental condition have been examined.

The activity of the pozzolana varies significantly with the type and source of clay, the heating schedule and the fineness to which these are ground. Very little control is exercised on the quantity of pozzolana as the main concern is to obtain the required strength in PPC. As a result, there are problems of large variations in the quality of PPC and its early strength development. Recently Galal et.al. reported kinetics of hydration of calcined clay pozzolana cement systems and tried to establish correlation between compressive strength and physico-chemical parameters (117).

Fly Ash

Fly Ash, a by-product from thermal power stations using pulverized coal, is pozzolanic in character and is accepted in the manufacture of blended cements. The chemical composition of fly ashes varies from source to source due to change in coal/lignite source and combustion condition at the Power Plants and broadly consists of SiO_2 (45-60%), Al_2O_3 (10-20%), Fe_2O_3 (4-6%), besides unburnt carbon and small amounts of CaO, alkalies and sulphates, except in lignite or brown coal flyashes which contain CaO in significant amount. The mineral contents of flyashes are characterised as quartz, mullite, hematite, magnetite, glassy phase and unburnt carbon. Excellent review by Kokubu, Regourd and others have explained the potential of fly ash and characteristics of cement made from fly ash (3,5,11).

Importance of spherical particles including hollow spheres called cenopheres which differ in size and shape due to differences in degree of pulverisation of coal, boiler type, power load and efficiency of collection systems is well recognised. The overall fineness (Blaine) (3000-6000 Cm^2/g) is, however, generally of the same order as that of Portland Cement used. The overall grading of particles is considered appropriate for mixing with Portland Cement to obtain fly ash cements.

The important parameters which dictate the use of fly ashes for cement manufacture, are the glass content, strains and fissures in glassy phase and the particle size distribution and unburnt carbon. The proportion of glass and other amorphous alumino-silicates may be determined by difference from QXDA on the superimposed peaks of crystalline phases for correlation (118). Hubbard established a relationship between K_2O/Al_2O_3 and amorphous alumino-silicate (119). It was postulated that the ratio obtained multiplied by ten may be used as pozzolanic

potential index (PPI). Mechanism of pozzolanic reaction is still not fully resolved. Physico-chemical and mineralogical parameter have been used to develop the relationship with performance. Tenoutasse recently proposed that the pozzolanic reaction model based on microscopic studies, involving three steps (123):

* Migration of ions from acquous phase to reaction sites at the surface of the particles,
* Precipitation of $Ca(OH)_2$
* Reaction between $Ca(OH)_2$ and vitreous phase of fly ash particle leading to the formation of C-S-H and C_2ASH_8

This model is shown through Fig.12. Role of filler mechanism is seen as an additional step by some Researchers.

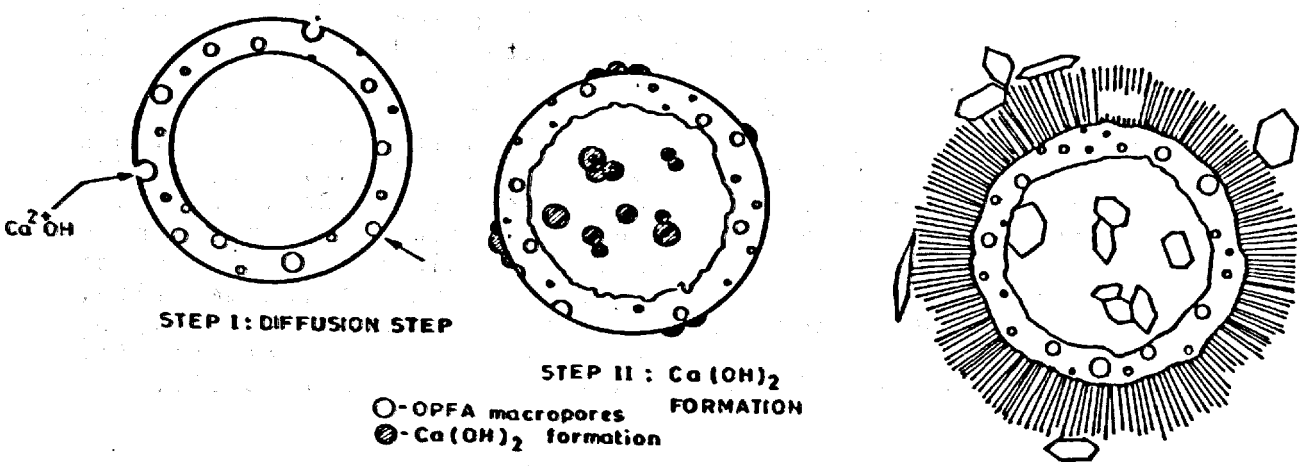

FIG.12-POZZOLANIC REACTION MODEL

The apprehensions with regard to the use of use of fly ash have arisen due to high variation in the quality of flyash even from single source and the handling and transportation problems. Increase in water demand is considered as the cause for reduction in strength and this is more pronounced if unburnt carbon is higher. Kokubu established that good quality fly ash in Portland

Cement should improve workability and thus produce a concrete with same slump and strength at 28 days as Portland Cement in suitably designed concrete (3).

It is recognised that there is no inter-relationship between individual characteristics of fly ash among themselves, i.e. between size of particles or sphere, fineness, and unburnt carbon or chemical composition, etc. and with strength performance of PPC. Various methods of predicting pozzolanicity have shown limited capability. Certain formulae involving various parameters, such as LOI, residue on 45 micron sieve etc are observed to have reasonable correlation with product performance. These are, however, only indicative and for any meaningful utilization, compatibility of flyash with clinker has to be established at the plant.

Ordinary flyash is not hydrated by itself but is hydrated with the addition of alkalies and $Ca(OH)_2$. The hydrates such as C-S-H $C_3A.CaCO_3.H_{12}(C_4AH_{13})$ and C_2ASH_8 are produced and hydro-garnet is formed at later age. There is decrease in Ca/Si ratio of C-S-H and CH contents. Uchikawa has reviewed the hydration mechanism of fly ash cement in the last Congress and reported that with the addition of $Ca(OH)_2$ and $CaSO_4.2H_2O$ the reaction degree is increased (11). Fly ash in general retards the hydration of C_3S in initial ages but increases at later ages. SEM study showed that C-S-H and CH are deposited on the surfaces of fly ash grains before they start to react (121). Further, the glassy phase was etched heavily for 7 days and that many particles upto 1 to 2 micrometer were consumed within 28 days. However, the crystalline phase appeared to be inert. QXDA study confirms that ratio of mullite to quartz does not change on hydration which supports the view that crystalline phase is inert (116). There are two Schools of thought on the hydration mechanism of interestial phase in fly ash cement. According to one, fly ash retards the hydration while other say the reverse. But from the point of view of availability of sulfate for the formation of ettringite, Uchikawa opined that ettringite formation is lowered in the presence of SO_4^{2-} in fly ash at C/A ratio of 3 or more with increasing $Ca(OH)_2$ saturation ratio (118). Further, mono sulfate hydrates are more produced in hardened flyash cement paste than in hardened ordinary portland cement paste. The rates of pozzolanic reaction are more sensitive to temperature than any other parameter.

Fly ash cements can result in concrete with low heat evolution, higher sulphate resistance generally. Tikalsky et.al observed that certain fly ashes in fact contribute to sulphate attack (122). Calcium content and the crystaline phase of alumina seem to play dominant role. Fig.13 shows the influence of these parameters.

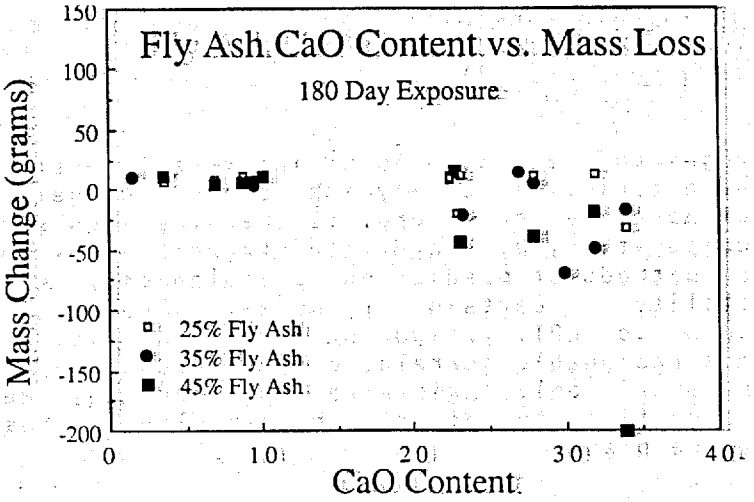

Mass loss of concrete specimens versus the calcium oxide content of the fly ash

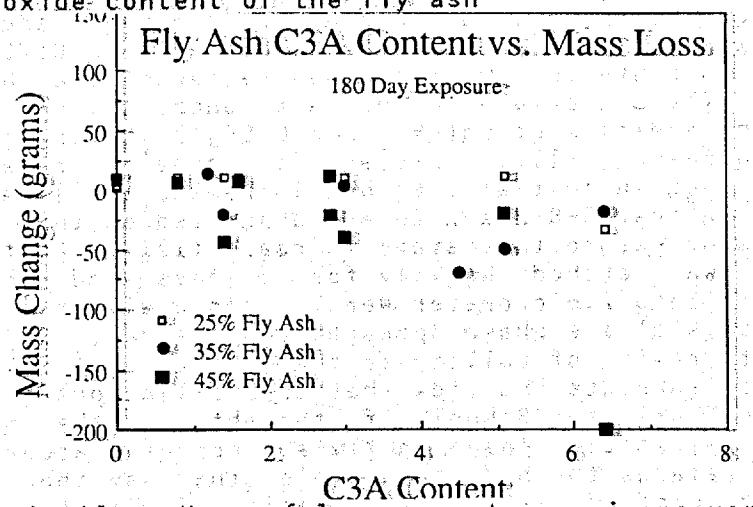

Fig 1.3 Mass of loss cncrete specimens versus the C_3A content of the fly ash

Microsilica

Microsilica (Silica fume/silica flour or dust) is a by-product obtained from the process of producing metallic silica and ferro-silicon by reducing quartz in an electric furnace. Some SiO vapours, oxidized by the air, get deposited as SiO_2 giving a very finely particulate solid. The characteristics may change in term of its purity and depends on the raw material, electrodes and reducing carbon quality. The material as such may require some beneficiation. The material formed in making elementary silicon typically contains 94-98% SiO_2, but for that formed in making the alloys 86-90% SiO_2 is more usual. The minor components are Fe_2O_3, P_2O_5, CaO, TiO_2 and Alkalies besides carbon and sulphur coming from reducing agent. Typically, the average particle size is about 100 nm and the specific surface area is in

the range of 15-25 m2 g-1. The true density is above 2000 kgm-3 but the bulk density of the freshly filtered powder is only 200 kgm^{-3}. The amorphous phase in silica fumes is similar to quartz glass (123). In most of the samples the diffused XRD peak from the glass accounted for 98-99.5% of the total diffracted intensity and that it peaked at the value of 0.405 nm characteristic of vitreous silica. The commonest crystalline impurities detected were KCl, quartz, metallic iron and iron silicide, and pozzolanic reactivity was found to depend more on the chemical composition and nature of impurities than on the fineness or SiO_2 content. A surface layer of carbon, if present, greatly decreased reactivity (124).

Viewed as a mineral addition in concrete, microsilica is characterized by its small particle size and high pozzolanic activity. In the absence of a water-reducing admixture, the percentage replacement of cement is probably effectively limited by the high water demand to about 5%, but this can be increased by adding superplasticizers. By lowering the w/s ratio in such mixes to 0.2-0.3, concretes with high compressive strengths can be obtained (125). Bleeding is also reduced. With special mixes and processing conditions, compressive strengths of up to 270 MPa have been obtained. Traetteberg showed that microsilica used as an addition with cement has considerable pozzolanic activity, mainly in the period 7-14 days after mixing, and that the reaction product formed with CH probably had a Ca/Si ratio of about 1.1 (126). Subsequent studies have shown that the pozzolanic reaction is detectable within hours and also that the early reaction of the alite is accelerated (127). Huang and Feldman (128,129) studied the hydration reactions in some detail. In pastes with 10% or 30% replacement and w/s ratios of 0.25 or 0.45, the CH content passed through maxima usually within the first day before beginning to decrease; in those with 30% replacement, it had reached zero by 14 days.

Uchikawa reported the hydration of cement composition with silica fume and rice husk ash and observed that specific surface area and particle size distribution are important besides strains in the structure of SiO_2. C-S-H produced has lower C/S ratio than that of slag and fly ash system. The hydration of C_3S is accelerated due to absorption of Ca^{2+} by SiO_2 followed by early diffusion of Ca^{2+} in the low C/Si C-S-H. X-ray microanalyses show that the Ca/Si ratio of C-S-H decreases markedly as the content of microsilica increases.

Rice Husk Ash as Pozzolana

Chemistry and Technology of making cement with Rice Husk Ash was first advocated by Mehta (130,132). Rice Husk Ash obtained by incinerating of Rice Husk under controlled conditions (350-600°C) and controlled supply of air is a super pozzolana in terms of its lime reactivity. SiO_2 content is >90% and impurities rather low. Rice Husk Ash pozzolana has high specific surface and contains amorphous silica retaining the cellular microstructure of the original material and can be ground with ease to a high fineness. In view of this, the rice husk ash portland pozzolana cement can replace in higher quantum of Portland Cement compared to burnt clay or flyash and also ensure

good early strength development. While early strengths are likely to be better, the late strengths are at par with Portland Cement. Due to low bulk density and handling problem, it has not become a regular input to Blended Cement (131).

Blended cements with rice husk ash are reported to have superior acid resistance, creep resistance and improved impermeability. Studies on working out the reaction mechanism, correlate physico chemical and morphological parameters with performance using XRD/electron microscopy and thermal analysers have been reported recently (132,133,134,135).

The decomposition of rice husk takes place through two major steps as observed under electron microscopy. The morphology of ash samples explains the higher surface area, porosity and reactivity of the low temperature ash samples in comparison to high temperature ash samples. It was also reported that the rate of formation of C-S-H is dependent on the ash/lime ratio, reactivity and fineness of the ash. The mechanism of rice husk ash cement hydration has been schematically shown in Fig.14.

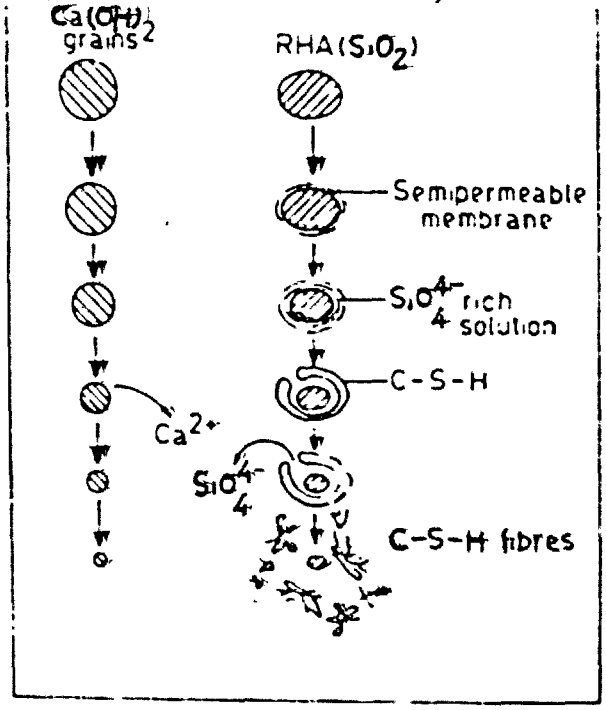

Fig.14: Mechanism of RHA cement hydration (Schematic)

Calcareous Additives

Blended Cements can also be made with inert calcareous materials like Limestone, Raw meal and Kiln dust from cement plant. In France, limestone upto 27% is used in various varieties of blended cements. Some of the world specifications permit use of inorganic mineral within 5% in normal Portland Cement. While it is recognised that water demand of such cement may change. The absence of clay and organic matter helps in maintaining expected quality. Regourd defined the role of fillers and derived mathematical correlations for the role of inert additives (5). Reports on use of kiln dust have appeared and have shown that these are effective additives to Portland

Cement for making blended cements. Authors have studied the effect of addition of limestone, kiln dust, ground slag and other materials in range <5% and 10-25%. It is concluded that effect of such filler is partly physical as it acts as a filler between the grains of clinker and accelerates the hydration of alite and aluminate phases forming C_4ACH_{11}. The filler effect of minerals could be graded with microsilica having the maximum effect and granulated slag as the minimum. With the increase in proportion of filler, the physical effect gets diluted and influences the hydration mechanism as the interface between clinker grain gets reduced affecting workability and strength. Clinker composition, i.e. alite and aluminate content and reactivity also influences the role and content of filler. Plasticity of such mixes is generally better.

Non Portland Blended Cement

Alkaline activation of slag is known for long when slag-lime binders were marketed and used in thirties. The use of such cements was, however, discontinued mainly due to apprehensions on their resistance to weathering conditions and relatively poor strength as compared to Portland Cement. Some studies on activation of granulated blast furnace slags with alkalies and their salts have since then been reported but commercialisation of pure activated slag cements has not been realised. Studies on systematic evaluation of slag activated binders gained momentum after the reported formulation LTP (Leant Trief Pur) of Trief (136). Studies published earlier indicated the potential of formulating activated non-portland cements using synthetic and commercial slags and in a manner that these can be marketed at par with normal cements (137,138,139,140).

Narang et.al. studied the microstructural behaviour and performance of non portland systems and established that activated slag and its blends with fly ash and other pozzolanic materials can be successfully formulated to have strength characteristics at par with Portland Cement. The optimum dose of sodium hydroxide is between 3-5 and optimum fineness of slags and slag fly ash blends is 4000-5000 cm^2/gm. Activation with combination of lime and other salts is more effective for slag with high alumina and low calcium contents. Activation mechanism of alkalies alone or in combination is nearly same in view of strength development and hydration product characteristics. Ternary blends consisting of Slag + Fly Ash, Activator and other inert materials can be formulated for masonry and other special cements through this mechanism.

It is well known that granulated slags can be activated in their hydration by variety of activators like lime, gypsum, alkalies and alkali salts. The degree of hydraulicity attained by the slag however depends on the quantity and composition of glass and activator. While slags rich in akermanite glass show strength development on hydration without activators, slags with gehlenite type glass composition need activator. It is observed that slags rich in lime possess higher intrinsic hydraulic value but the same is limited to an optimum CaO/SiO_2 ratio. Kondo reported that slag glasses with 50% CaO and below 20% SiO_2 only had hydraulic properties (141). Alumina content in slags plays an important role. Certain minor constituents like Mn_2O_3, P_2O_5

etc are known to influence both the granulation process and glass structure thereby influencing the hydraulicity of slags in the presence of activators. In his recent reports Kondo reported that the mechanism of slag activation and hydration with different activators was different (141). While lime and gypsum are considered as reactants, NaOH is considered as catalyst. It is also reported that with lime activation in quantities beyond 5%, slag activation becomes near independent of lime. While with increasing quantities of NaOH and gypsum the activation is both accelerated and is continued for longer durations, the two observations appear in contradiction. With NaOH the reactions are generally completed earlier. While mechanism of activatyion and hydrationwith lime resembles with that of slag portland cement,except that it results in hydration productions of lower C/S ratio and C_2ASG_8 is also not observed in this case, with gypsum the reactions are similar to those in supersulphated cement, with etteringite being themajor hydration product (112). Role of NaOH on the other hand is assumed that of sample catalyst (139). The products identified in soda activated slags are C_4AH_{13}, C_2ASH_8 and C-S-H. Sopdium silicate and sodium carbonate and their combination in the lime behaving nearly the same wayas NaOH.

The activation and significant strength development inslag-flyash blends can be explained on the basis that lime-rich slags activated in the presence of sodium hydroxide yielding calcium-silicate hydrates and lime in the initial stages. The lime thus liberated opens up more of silicate structures in slag and also reacts with silica/glass of fly ash to promote the pozzolanic react9ons. The removal of lime bypozzolana further changes the composition of solution resulting in liberation of more lime from slag and that is how a dynamic equilibrium is maintained. The nature and the quality of reaction products therefore is likely to be different from what is obtained from activation of slag alone. In case of activation by combination of Na_2CO_3 + $Ca(OH)_2$ and Sod meta silicate and lime; the first reaction is that of producingh NaOH together with accelerating the activation bysodium carbonate and silicates by providing lime from extra source in particular in low lime or C/S slags. In case of calcium sulphate, the reaction obviously is due to ettringite formation. While formulationof such cements has been investigated, the application and durability aspects are yet to be fully looked into.

Pyrament Cement

Development of Pyrament, recently introduced by Lonestar Cement in U.S. is based on alkali activated blended portland pozzolana cement containing organic additives (79,142). It is characterised as high early strength cement. A low w/c ratio (.2 - .26) is essential in order to obtain higher strengths in this type of system. The reportedly good setting time of this cement is due to high alkali hydrate concentration in the pore solution. However, the Pyrament cement produced in U.S. under U.S., Patent 4842 649 have very high early strength (2500 psi in 4 hrs) high ultimate strength (10,000 psi comp.strength in 28

days) and wide range of set time (30 mts to 220 mts). However, long term creep, vol.stability and chemical durability of this cement is yet to be established. In addition to slags and flyash, use of inert materials like limestone, kiln dust, etc can enhance the composition range of these cements.

REFERENCES

1. Taylor H.F.W : Cement Chemistry,. Academic Press Ltd. 1990. P. 1-4, 45-48, 277-344.

2. American Ceramic Society : "Advances in Cementitious materials; Ceramic Transactions, Ed. by Sidney Mindess S, Vol.16, 1991, P 289-318, 489-500, 621-642

3. Kokubu M : "Fly Ash and Fly Ash Cement". International Symposium on Chemistry of Cement, 5th, Tokyo, Japan. 1968, Vol. IV, P. 75-113

4. Schroder F : "Blast Furnace Slag and Slag Cements". International Symposium on Chemistry of Cement, 5th, Tokyo, Japan. 1968, Vol.IV, P 149-203

5. Regourd M : "Characteritiques et Activation des Produits D'addition". International Congress on Chemistry of Cement, 8th, Rio, Brazil, 1986, Vol.I, P 199-232

6. Hjorth L : "Microsilica in Concrete". Nordic Concrete Research, No.1, Paper 9, Aalborg, Portland, Denmark, 1982, P. 18

7. Popovic K, Djurekovic A, Ukraincik V : "Blended and Special Cements incorporating condensed silica fume". International Congress on Chemistry of Cement, 8th, Rio, Brazil, 1986, Vol.IV, P. 137-144

8. Bucchi R : "Influence of the nature and preparation of Raw materials on the Reactivity of Raw Mix". International Congress on Chemistry of Cement, 7th, Paris, 1980, Vol.VI, P. 4-43

9. Haspel D.W & Taylor R.A : "High Level Kiln Control", Zement Kalk Gips, No.4, Vol.38, April, 1986, P. 183-185

10. Calleja J : "Future trends in the research of the structure, properties & behaviour of blended cements". International Congress on Chemistry of Cement, 8th, Rio, Brazil, 1986, Vol.1, P. 233-248

11. Uchikawa H : "Effect of blending components on hydration and structure formation". International Congress on Chemistry of Cement, 8th, Rio, Brazil, 1986, Vol.1, P. 249-280

12. Hwang C.L. & Shen D.H.: "The effect of Blast furnace slag and fly ash on the hydration of Portland Cement", Cement & Concrete Research, Vol.21, July 1991, P 410-425

13. Miller F.M. & Venable R.L.: "Aspects of Cement Performance in Concrete as revealed by clinker microscopy". International Conference on Cement Microscopy, 10th, Texas, USA, 1988, P. 306-323

14. Bruggemann H & Brentrup L : "Correlations between mineralogical clinker parameters & cement strength", International Conference on Cement Microscopy, 11th, Louisiana, USA, April 1989, P.226-245

15. Knofel D : "Inter-relation between proportion of clinker phases and compressive strength of Portland Cement". International Conference on Cement Microscopy, 11th, Louisiana, USA, April 1989, P.246-262

16. Narang K.C. : "Mathematical Model for Correlation of Power, Particle Size Distribution and Performance oc Cement" under communication to Zement-Kalk-Gips.

17. Sychev M.M. : "Cement Hydration Control". International Conference on Chemistry of Cement, 8th, Rio, Brazil, Vol.III, 1986, P 277-280

18. Page C.H., Thombare C.H, & Kamat R.D, Chatterjee A.K. : Development of Sol-gel Technology for Cement manufacture, Advances in cementitious materials, Ed. by Mindess S. American Ceramic Society, Vol.16, 1990, P 643-660

19. Noudleman B, Bikbaou M, Iliukhine V & Sventsitski A : "Structure and Properties of Alinite & Alinite Cement". International Congress on Chemistry of Cement, 7th, Paris, France, 1980, Vol.III, P 169-174

20. Bhatty M.S.Y. : "Properties of Blended Cements made with Portland Cement, Cement Kiln dust, Fly ash and Slag", International Congress on Chemistry of Cement, 8th, Rio, Brazil, 1986, Vol.IV, P 118-127

21. Sharma R.B. and Narang K.C. : "Investigations of Cementitious Binders containing artificial Pozzolanic materials", Ph.D. Thesis , April 1986

22. Glasser F.P. : Fundamentals of Cement Chemistry - The Clinkering Process. Cement Production and Use, Edi.by Skalny J, New Hampshire, June 1979, P. 31-40

23. Regourd M. : Fundamental of Cement production : The Crystal Chemistry of Portland Cement Minerals, New Data", Cement production & Use, Ed.by Skalny J, New Hampshire, 1979, P. 41-50

24. Hahn T., Eysel W & Woermann E : International Symposium on Chemistry of Cement, 5th, Tokyo, Japan, 1968, Vol.I, P.61

25. Woermann E, Hahn T & Eysel W : Cement & Concrete Research, 9, 1979, P.701

26. Boikava A.I. : "Chemical composition of raw material as the main factor responsible for the composition, structure and properties of clinker phase". International Congress on Chemistry of Cement, Rio, Brazil, 1986, Vol.I, P.19-34

27. Maki I : "Relationship of processing parameters to clinker properties, influence of minor components", International Congress on Chemistry of Cement, Rio, Brazil, 1986, Vol.I, P.34-47

28. Kristmann M : Cement and Concrete Research, August, 1978, P.93

29. Yamaguchi C & Takagi S : International Symposium on Chemistry of Cement, 5th, Tokyo, Japan, Vol.I, 1968, P.181

30. Terrier P, Hornain H & Socroun G : Rev. Mater. Constr. 1968, P.109

31. Lea F.M., Parker T.W. : "The quaternary system $CaO-Al_2O_3-SiO_2-Fe_2O_3$ in relation to Cement Technology", Building Research Tech Paper 16, HMSO, London, 1935, P.52

32. Newkirk T.F & Thwaite R.D.: J.Res Natl Bur, Stand, 61, 1958, P.233

33. Sorrentino F, Glasser F.P. : Trans J. Br. Ceramic Soc. 75, 1976, P. 95

34. Swayze M.A. : American J. Sci, 244, 1946, P.1.

35. Gutt W & Welch J.H : J. Am. Ceram. Soc. 42, 1959, P. 11

36. Maki I & Kato K : Cement & Conc. Res., Dec. 1982, P. 93

37. Maki & Goto K : Cement & Conc. Res. Dec.1982, P. 301

38. CRI : "Unsoundness of clinker with MgO content well below permissible I.S. Limit", RB-22-82, CRI, Mar.1982

39. Moir G.K : Phil.Trans. R. Soc, London, A310, 1983, P.127

40. Goswami G, Mahapatra B & Chatterjee S : "Phase formation during sintering of a magnesium fluoride containing raw mix in a cement rotary kiln", Zement Kalk Gips, May 1990, P.253-258.

41. Long G.K :Phil. Trans. R. Soc. London, A 310, 1983, P.43

42. Boikova A.I., Domansky A.I., Paramonova V.A., Stavitskajii G.P. & Nikushchenko V.M. : "Influence of Na_2O on the structure and properties of $3CaO.Al_2O_3$". Cement & Conc. Res.1977, Vol.7, P. 483-493

43. Skalny J.K, Klemn W.A : "Alkalies in clinker - Origin, Chemistry, Effects". Conference on alkali aggregate reaction in concrete, Capetown, South Africa, 1981

44. Odler I, Wonnermann R : "Effect of alkalies on Portland Cement hydration - Alkali oxides incorporated into crystalline lattice of clinker minerals - Part I", Cement & Conc. Res. 1983, Vol.13, P. 477-482

45. Yamaguchi G & Uchikawa U. : "Unter Suchungen Uber Die Mischkristalle Im System C_3S-Na_2O", Zement Kalk Gips, 14, 1961, P. 497-509

46. Butt Y.M. & Timashev V.V : "The mechanism of clinker formation - Process & Ways of modification of clinker structure". International Symposium on Chemistry of Cement, 6th, Moscow, 19.

47. Gutt W, Smith M.A. : Trans. J. Br. Ceram.Soc, 66, 1967, P. 557

48. Locher F.W, Richartz W. & Sprung S : Zement Kalk Gips, 36, 1983, P.224-231

49. Strunge J, Knofel D & Dreizler I : Zement Kalk Gips, 38, 1985, P. 150-158

50. Locher F.W : "Influence of bruning conditions on clinker characteristics". Cement Prod. & Use, Ed. by Skalny J., New Hampshire, 1979, P. 81-96

51. Roy D.M. & Sarkar A.K. "Effect of fluoride fluxes & mineralizer upon phase equilibria". Cement Prod. & Use, ed. by Skalny J., New Hampshire, 1979, P.51-54

52. Klemn W.A., Holub K.J. & Skalny J : "The effect of fluxes & mineralizers in lowering cement kiln temperature". Progress Report 3, Martin Marietta Corp, Maryland,1978

53. Christensen N.H. & Johansen V. : Cement & Conc. Res., Sept., 1979, P. 1-6

54. Gutt W & Osborne G.J. : Trans. J. Br. Ceram. Soc. 69, 1970, P. 125-129

55. Tanaka M. Sudah G & Akaiwa S : International Symposium on Chemistry of Cement, 5th, 1968, Vol.,1, P.122

56. Klemn W.A : "Influence of clinker liquid on burnability". Cement Prod. & Use. Ed. by Skalny J., New Hampshire, 1979, P. 74-75

57. Glasser F.P. : "Kinetic of clinker formation". International Congress on Chemistry of Cement, 8th, Rio, Brazil, 1986, Vol.VI, P.

58. Ono Y. : "Microscopical observation of clinker for the estimation of burning condition, grindability & hydraulic activity". International Conference on Cement Microscopy, 3rd, Houston, Texas, USA, 1981, P. 198-210

59. Fundal E. : "Optical measurements of cement clinkers". World Cement, 13, 1982, P. 276-283, 318-324

60. Hargave R.V., Venkateswaran D., & Chatterjee A.K. : "Application of Optical Microscope as quality control tool in some Indian Cement Plants". International Conference on Cement Microscopy, 9th, Nevada, USA, 1987, P. 147-164

61. Strunge J., Knofel D., Dreizler J. : "Influence of alkalies & sulfur on the properties of cement" - Part I, II, III". Zement Kalk Gips - 3, 1985, P. 150-158, 441-450 Zement Kalk Gips - 7, 1986, P. 380-386

62. Gebauer J, Kristmann M : "The influence of the combination of industrial clinker on cement & concrete properties". World Cement, 3, 1979, P. 46-51

63. Osbaeck : "The influence of alkalies on the strength properties of portland cement". Zement Kalk Gips, 2, 1979, P. 72-77.

64. Richartz W. : "Effect of the K_2O content and degree of sulfatization on the setting & hardening of cement,". Zement Kalk Gips, 12, 1986, P. 678-687

65. Bruggemann H. & Brentrup L. : "Correlations between mineralogical clinker parameters & cement strength". International Conference on Cement Microscopy, 11th, Louisiana, Texas, USA, April 1989, P. 226-245

66. Knofel D : "Inter-relation between properties of clinker phases and compressive strength of portland cements". International Conference on Cement Microscopy, 11th, Louisiana, Texas, USA, April 1989, P. 246-262

67. NCB: "Cement Standards of the World - A comparative summary", NCB-SP-1-88, National Council for Cement & Building Materials, New Delhi, India, 1988

68. API : "Specification for materials & testing for well cements". API Specs (10), Fifth Edition, Ame. Petr. Inst. Publication, July, 1990.

69. Royak S.M. "Oil Well Cement", International Congress on Chemistry of Cement, 6th, Moscow, 1976, Principal Paper.

70. Montgomery C. & Smith D.K. : "Oil Well Cementing practices and materials", The Petroleum Engineer, June, 1961, P. 28-33

71. Bendsted J : "Class G & H Basic Oil Well Cements". World Cement, Vol.23, No.4, Apr. 1992, P. 44-51

72. Bensted J. & Shaunak R. : "Early hydration of Class G Oil Well Cement". International Conference on Cement Microscopy, 11th, Louisiana, Texas, U.S.A., 1989, P. 198-224

73. Bensted J. :"Effect of aeration on the property of Glass G Oil Well Cement". British Ceramic Proc. No. 35. The Chemistry & Chemically related Prop. of cement, Ed.by Glasser F.P., Br. Cer. Soc. 1984, P. 317-337

74. Bendsted J : "Retarded Oil Well Cements of API Classes D, E & F". World Cement, Vol.22, No.1, Jan.1991, P. 31-35

75. Bendsted J. : API Class C Rapid hardening Oil Well Cement", World Cement, Vol.22, No.5, May 1991, P. 38-41

76. Taylor H.F.W. : "Cement Chemistry - Admixtures & Special use of Cement". Academic Press Publication, 1990, P. 372-373

77. NCB : "Development of Oil Well Cement". CRI-RB--29-84, National Council for Cement & Building Materials, New Delhi, India, 1984

78. Grabowski E. & Gillott J.E. : "Effect of replacement of silica flour with silica fume on engg.properties of Oil Well Cement at normal and elelvated temp. & pressures". Cement and Conc. Res., Vol.19, May 1989, P. 333-344

79. Gartner E.M. & Myers D.F. : "New Cements and Novel Cement Matrices", Advances in cementitious materials. Ed.by Mindess S., Ceramic Transactions, Vol.16, Am. Cer. Soc. Publication, 1991, P. 621-642

80. Uchikawa H. & Tsukiyana K. : "The hydration of jet cement at 20°C." Cement and Concrete Res. Mar.1973, P. 263

81. Uchikawa H, Uchida S : "The hydration of "$CaO.7Al_2O_3$ CaF_2 at 20°C". Cement & Concrete Res. June 1972, P. 681

82. Majumdar A.J. : "New Rapid hardening Cement developed". Building Research Establishment, BRE News of Construction Research, April 1989

83. Della R. & Kumar A. : "Pore structure studies of high early strength OPC containing silica fume". Transation of Indian CeramicsSoc, 1988, P. 11-15

84. Nakugawa K., Watanabe Y, Daimon M. : "Hydration mechanism & quick hardening mechanism of amorphous calcium - aluminate with anhydrous gypsum". Gypsum & Lime, Jan.1989, P. 12-17

85. Chatterjee A : "Phase compositions, micro-structure, quality & burning of Portland Cement Clinker - Part I," World Cement Technology, 5, 1979, P. 124

86. Ali M.M., Handoo S.K. & Ahluwalia S.C. : "Improved formulations with high early strength and regulated set", NCB International Seminar on Cement & Building Materials, IIIrd, New Delhi, India, 1991, P. 21-27.

87. Sudoh G., Ohta T. & Haradar H. : "High Strength Cement in the $CaO-Al_2O_3-SiO_2-SO_3$ system and its application." International Congress on Chemnistry of Cement, 7th, Paris, 1980, Vol.III, V, P. 152-157.

88. Subba Rao V.V. and Narang K.C. : "Potentials of making active belite cementswith chromium oxide as modifier". Zement Kalk Gips, Vol.40, No.8, Aug.1987, P. 434-437

89. Locher F.W : "Low Energy Clinker formulation". International Congress on Chemistry of Cement, 8th, Rio, Brazil, 1986, Vol.1, P. 57-67

90. Meric J.P. : "Low Energy Clinker formulation". International Congress on Chemistry of Cement, 8th, Rio, Brazil, 1986, Vol.1, P. 51-56

91. Stark J.,Muller A. : "International Development trends in Low Energy Cements". Zement Kalk Gips, No.4, April 1988, P. 162-165

92. Kurdowski W, George C.M., Sorrentino F.P. : "Special Cements, Calcium alminate & other no silicate cements". International Congress on Chemistry of Cement, 8th, Rio,Brazil 1996, Vol.1, P. 292-318.

93. Kusnetsova T.V : "State of the art & prospects of special cements". International Congress on Chemistry of Cement, 8th, Rio, Brazil, 1986, Vol.1, P. 283-291

94. Mehta P.K : "Investigations on energy saving cements". World Cement Technology, Nov.1980, P. 166-177

95. Yanmou W., Junan D, Muzhan S : " An Investigation into Cement $CaO-SiO_2-Al_2O_3-Fe_2O_3$ system". International Congress on Chemistry of Cement, 8th, Rio, Brazil, 1986, Vol.2, P. 300-305

96. Xiuji F & Yufeng Z : "Research on an early strength cement containing high content of Iron". International Conference on Chemistry of Cement, 8th, Rio, Brazil, 1986, Vol.2, P. 285-292

97. Agarwal R.K., Parelkar S.V. & Chatterjee A.K. : "Chlorite salts as reaction medium for low temperature clinkerization - A Proble into Alinite Cement". International Congress on Chemistry of Cement, 8th, Rio, Brazil, 1986, Vol.II, P. 327-333

98. Lampe V., Oliew G, Pomansky A.L.: "Uber die hydrauliche Aktiritat Verelieden Substotwier ter Alinite". Silkatechn (in Vorb)

99. Burger D., Ludwig U.: "Synthesis of Calcium Silicate at low temp & influences on their reactivity". International Conference on Chemistry of Cement, 8th, Rio, Brazil, 1986, Vol.2, P. 372-378

100. Klein A, Troxell G.E. : Proceedings of American Soc. for Testing of Materials, 58, 1958, P. 986

101. Cohen M.D : Cement & Concrete Res. 13,1983, P. 809

102. Mehta P.K. : Cement and Conc. Res. 3, 1973, P. 1

103. Ogawa K., Roy D.M. : Cement & Conc. Res. 12, 1982, P. 101, 247

104. Cohen M.D., Lobo C. : "Pore structure development in type K expansive cement pastes". Cement & Concrete Res. Vol.21, No. 2/3, March 1991, P. 229-241

105. Gebauer J. : "Influence of Cement grinding on the properties of fresh concrete". Holderbank News, 5, 1988, P. 14-17

106. Wustner H., Dreizler I. & Oberheuser G : "Using roller press in grinding plants for coal, cement raw materials & cement". Zement Kalk Gips, Vol.40, No.7, July 1987, P. 345-353

107. Brugan J.M. : "High efficiency Separators - Problems & solutions", Zement Kalk Gips, Vol.41, No.7, July 1988, P. 350-355

108. Glasser F.P., Luke K : "Internal Chemical evolution of the constitution of blended cement." Cement & Concrete Res. Vol.18, No.4, July 1988, P. 495-502

109. Taylor H.F.W : "Cement Chemistry : Composite Cements". Academic Press Publication, 1990, P. 276-314

110. Smolczyk H.G. : International Congress on Chemistry of Cement, 7th, Paris, 1980, Vol.1, P. 111-1/3

111. Demoulian E., Gourdin P., Hawthorn F. & Vernet C. : International Congress on Chemistry of Cement, 7th, Paris, 1980, Vol.2, P.III-89

112. CRI : "Utilization of LCFC slag for cement/cementitious materials manufactured - A Feasibility Report", CRI-RB-8-78, Cement Research Institute, New Delhi, 1978

113. Uchikawa H., Uchida S. & Ogawa K. : International Congress on Chemistry of Cements, 8th, Rio, Brazil, 1986, Vol.4, P. 251

114. Harrisson A.M., Winter N.B. & Taylor H.F.W. : Mater. Res. Soc. Symp. Proc. 85, 1987, P. 213

115. Kondo R. & Ohsawa S : International Symposium on Chemistry of Cement, 5th, Tokyo, Japan, 1968, Vol.4, P. 255

116. Luke K. & Glasser F.P. : Cement and Concrete Res., 17, 1987, P. 273

117. Galal A.F. : "Hydraulic reactivity and microstructure of artificial pozzolana fine pastes". International Conference on Cement Microscopy, 12th, Vancour, Canada, 1990, P. 135-153

118. Dalziel J.A & Güttridge W.A : "The influence of pulverized fuel ash upon the hydrationcharacteristics and certain physical properties of a portland cement paste". Tech. Report 560, Cement & Concrete Asssociation, Slough, U.K, 1986, P. 28

119. Hubbord F.H, Dhir R.K & Ellis M.S. : Cement & Concrete Res, 15, 1985, P. 185

120. Tenoutasse N, Marion A.M : "Microscopial investigation on the pozzolanic behaviour of fly ashes". Proceedings of International Congress on Cement Microscopy, 10th,Texas, USA, 1988, P. 58-70

121. Diamond S., Ravina D. & Lovell J. : Cement and Concrete Res., 10, 1980, P. 297

122. Tikalsky P.J : "The effect of fly ash on the sulfate resistance of concrete". Proceedings of International Congress on Cement Microscopy, 10th,Texas, USA, 1988, P.250-264

123. Hjorth L : "Microsilica in concrete (Nordic Concrete Res. No.1, Paper 9), Aalborg, Portland, Denmark, 1982, P. 18

124. Aitcin P.C, Carles-Gibergues A, Oudjit M.N, Vaquier A. : International Conference on Chemistry of Cement, 8th, Rio, Brazil, Vol.4, 1986, P. 22

125. Aitcin P.C, Sarkar S.L, Diatta Y : Material Res. Soc, Symposium Proceedings, 1985, P. 261

126. Traetteberg A : Cement, 1978, P.259

127. Halse Y., Goult D.J. & Pratt P.L : British Ceramic Proceedings, 35, 1984, P. 403

128. Huang C.Y, Feldman R.F. : Cement & Concrete Res. 15, 1985, P. 285

129. Huang C.Y Feldman R.F : Cement & ConcreteRes. 15, 1985, P.585

130. Mehta P.K., Groney P.R : J. Am.Conc. Inst. (Proc) 74, 1977, P. 440

131. James J & Subba Rao M : Cement & Conc. Res, 16, 1986, P. 276

132. Mehta P.K : Proceedings of Ist NCB Int. Sem. New Delhi, India, IV-1

133. James J & Subba Rao M : Thermochim Acta, 97, 1986, P. 329

134. James J & Subba Rao M : Am.Ceram. Soc. Bull, 65(8), 1986, P. 1177

135. Mehta P.K : Proc. UNIDO/ESCAP/RCTT Workshop on rice husk ash cement, Pakistan, 1979, P. 113

136. Trief L : "The new Trief CementProcess", Proc. of 4th Ontermatopma, Fly ash Symposium St.Louis, 1979

137. Narang K.C : "Investigations on microstructural behaviour & performance of non portland binders". Int. Conference on Cement Microscopy, 10th, Texas, USA, 1988, P. 71-81

138. Smith M.A. & Osborne G. : "Slag/Fly ash cements", World Cement Technology, 8, 1977, P. 223-233

139. Voinovitch & Dron R. : "Effect of various activators on hydration of granulated slag", Silica Ind, 41, 1976, P. 209-212

140. Narang K.C., Das S. & Chopra S.K. : Indian Patent, a, Oct.1980

141. Kondo R. & Ueda S. : "Kinetics & mechanisms of the hydration of cement". International Symposium on Chemistry of Cement, 5th, Tokyo, Japan, 1968, Vol.II, P. 203-255

142. Malone P.G : "Potential applications of alkali activated alumina silicate binders in military operations", U.S. Army Corps of Engg Report GL-85-15, Washington, DC 1985

Specific Theme II A

Advances in Portland and Blended Cements

ADVANCES IN PORTLAND AND BLENDED CEMENTS

R Sersale

Department of Materials and Production Engineering
University of Naples, ITALY

SUMMARY. The Paper summarizes the advances having main interest in practical applications of blended cements. Traditional and up-to-date mineral additions are described, without omitting the role of the quality of Portland clinker on the behaviour of the resultant cement. Some aspects of Portland clinker manufacture, related to: composition, alkalis content, kind of fuel used, air pollution, are briefly outlined, too. Emphasis is laid on methods for estimating the reactivity of mineral additions, on "pozzolanic" reaction, on evaluation of the degree of hydration, without disregarding, though in a brief treatment, some aspects of the hydration chemistry and kind of hydration products. The influence of the porosity on mechanical behaviour, the most common causes of deterioration and the precautionary measures, the main factors affecting durability of hardened cement mortars and concretes, are discussed,with a brief mention on the actual situation concerning the Specifications for quality assurance of supplementary cementitious materials.

RÉSUMÉ. Ce Rapport tente de faire le point sur le progrès au sujet de la pratique des utilisations des ciments aux ajouts. On traite les ajouts réactifs ordinaires et nouveaux, sans omettre le rôle des caractéristiques de qualité du clinker de ciment Portland sur le comportement du mélange. Quelque aspect de la production du clinker, en ce qui concerne: composition, teneur d'alcali, type de combustible employé, pollution atmosphérique, a été aussi deliné. On porte plus particulièrement sur les méthodes d'évaluation de la réactivité des ajouts, sur la réaction "pouzzolanique", sur l'appréciation du degré d'hydratation, sans oublier, avec un aperçu sur la question, quelque aspect de la chimie d'hydratation et de la nature des produits qui se forment. L'influence de la porosité sur la résistance mécanique, les causes les plus récurrentes de détérioration et les rèmedes à conseiller, les facteurs qui assurent durabilité aux mortiers et betons durcis, ont été soulignés, avec une brève mention sur la situation actuelle au sujet des Normes pour la qualification des produits d'addition.

INTRODUCTION.

This Report makes an attempt at summarizing, with an approach outlining mainly the technical standpoint, some of the advances in the concerned theme, made in the period following the "8th International Congress on the chemistry of cement" and the valuable and exhaustive Papers of Bucchi R. (1), Regourd M. (2), Calleja J. (3) and Uchikawa H. (4).

As is well known, blended cements contain - in addition to Portland clinker and calcium sulphate - a latent hydraulic component (granulated blast-furnace slag) or a pozzolanic component (natural pozzolan, low-lime fly ashes, condensed silica fume, burnt clay or a "filler" component, such as limestone. It is also well known that blended cements allow an economy of 40% fuel and an increase of cement production computable in 1.5-2 times, without altering the quality and the performances of the resultant cement (5). During the past thirty years, a significant increase in the use of materials by-products in the manufacture of blended cements, or as addition to concrete, has been recorded, owing to unquestionable technical advantages (6), which above all include: improved resistance to sulphate and dilute acid attack; reduction in amount and rate of heat evolution (7), beneficial, in particular, in the casting of thick section of concretes; reduction in the alkali level of the blend, in order to minimize the risk of alkali - silica reaction; improvement in the characteristics of fresh concrete. Possible disadvantages, such as: slower rates of strength gain at early ages, particularly at lower temperatures, and higher sensitivity of concretes to poor curing (8) , are therefore largely overcome.

As concerns the burning question whether it is more advisable to use the mineral admixtures in the manufacture of blended cements rather than in the preparation or concrete mixer blend (9), from a theoretical view-point the answer is relatively simple. It is important, in fact, that both the concretes, that manufactured with a blended cement and the other, prepared through direct addition of the same mineral by-product at the concrete mixer, prove to be equivalent in terms of concrete strength grade and behaviour in the foreseen environment. This can be ensured only through a severe observance of the appropriate guidelines for the characterization of all the cementitious components, the settlement of the percentages, the proper manufacture, casting and curing of the mixture.

1. CONSTITUENTS OF THE BLEND.

The most important constituents of the blend are: Portland clinker and other finely ground, suitable reactive materials, in different but well defined percentages. The principal reason for blending ordinary Portland cement with these additions is economic, although in many cases blended cements perform better than ordinary Portland cement. For specification purposes, Portland and blended cements are designed by type, depending on their chemical composition and chemical, physical and mechanical requirements (10). All those reported in the Draft (September 1991) by the European Committee for Standardization belong to the category of Standard Cements (Tab. I).

Significant advances in the knowledge on these reactive materials have been made in the CANMET/ACI International Conferences on Fly Ash, Silica Fume, Slag and Natural Pozzolans in Concrete, held in Madrid (1986) and in Trondheim (1989).References are reported in this paper as: ACI SP-91 and ACI SP-114, V.M. Malhotra Ed., respectively.

To obtain a blended cement of excellent quality it is imperative to fully characterize (11) the raw materials in order to prepare the best clinker, to fully characterize the selected reactive material, to evaluate and possibly improve its activity, to comply within the appropriate guidelines. In fact when adequately characterized materials are used, the resulting blended cement pastes will frequently impart superior properties to the matrices of the concrete which they form.

1. 2. Clinker

The quality of a cement clinker is substantially determined by the nature and composition of the raw meal (12) and its thermo-physical treatment to achieve the clinker structure required for optimum

Table I: Cement types and composition (Draft March 1991. Massazza F. Private communication).
Proportion by mass[1].

Cement type	Clinker K	Blastf.slag S	Pozzolana natural Zn	Pozzolana industrial Zi	Fly-ashes siliceous Cs	Fly-ashes calcareous Cc	Burnt shale B	Limestone L	Silica fume D	Minor[2] additional constituents D
I	95-100	-	-		-		-	-	-	0-5
II/A[5]	80-94	S+Z+C+B+L+D[3]+F[4] = 6-20						-	-	-
II/B[5]	65-79	S+Z+C+B+L+D[3]+F[4] = 21-35						-	-	-
III/A	35-64	36-65	-		-		-	-	-	0-5
III/B	20-34	66-80	-		-		-	-	-	0-5
III/C	5-19	81-95	-		-					0-5
IV	60-90	-	0-40			-	-	-	0-10	0-5
V/A	40-64	18-30	18-30			-	-	-	-	0-5
V/B	20-39	30-50	30-50			-	-	-		0-5

1) The values in the table refer to cement nucleus, excluding calcium sulphate and addtives.

2) Minor additional constituents may be filler or may be one or more of the main constituents unless included as main constituents in the cement.

3) The proportion of silica dust is limited to 10%.

4) The proportion of a filler is limited to 5%.

5) If a Portland-composite cement consists beside clinker only of one other main constituent it shall be designated accordingly, e.g. II/A-S Portland-slag cement, II/B-C Portland-fly-ash cement etc.

cement quality (13). It is in fact undeniable that there is a relationship between mineralogical structure of the clinker and cement quality and that the hydraulic activity of alite and belite is in some way dependent upon crystal size,which also depends upon minor constituents, especially sulphur and alkalis (14). The total chemistry, especially the content of alkalis, sulphur and magnesium (15) in fact is reasonably of even greater importance than the crystal sizes. Minor constituents affect also alite-belite content, and structural modifications of C_3S induced by the trace-elements allow clinker reactivity to be improved (16). Percentage of hydrated MgO is reduced as the pozzolanic activity is increased (17). Experimental long terms results, in ordinary environmental conditions, have suggested (18) the possibility of increasing MgO content, generally restrained within 2.5-6%, beyond the maximum value reported by the Specifications, in Portland and blended cements.

The quality of limestone influences the sintering process and the characteristics of the clinker itself (19).

The best clinker is therefore achievable through a proper adjustment of the composition of raw meals and of the mineralisers (20), the grinding (21), burning (22) and cooling conditions (23), taking also into account the admixtures effect on sintering process (24). The activity of the clinker can be increased by the optimization of the composition of the raw meals and of the mineralisers, the control of amount and properties of the liquid phase and the adjustment of the burning and cooling conditions (25). As concerns clinker petrography, texture and distribution of phases give useful information on properties. Good clinkers have a regular distribution of alite and belite crystals in the interstitial matter, the alite crystals being in the range 20-30μm and a pseudo-hexagonal outline in single crystals. Belite is of type I, of dimension between 15-30μm and without belite clusters, in rounded forms (26). Recently new techniques have been set up for the study of clinker structure (27) and there has been considerable interest in the alkali content of Portland cement and Portland cement products.

The use of alkali- and sulphur - bearing raw materials and fuels for the production of Portland cement clinker, implies difficulties and frequently involves deteriorated cement qualities. The alkalis occur as water - soluble alkali sulphates depending on the sulphate content, or are incorporated in the clinker phases and the effects of alkalis on the phase composition of Portland cement clinker and on the technological properties of Portland cement have been throughly investigated. Alkalis have an influence on the rate of setting and hardening of Portland cement and on the ultimate compressive strength of mortar and concrete. Usually high alkalis accelerate setting and hardening, raising early strength and reducing the final one. Recently, great progress has been made in the acquisition of knowledge of the influence of alkalis and sulphur on the properties of industrial clinkers and industrial cement (14). By means of a systematic investigation it has been pointed out that increasing SO_3 content of the clinker, alite decreases with an increase in the crystals size (28) and belite increases. Sulphur combined in the clinker phases accelerates setting, whereas sulphate combined as alkali sulphate shows a retarding effect. Cement strengths falls with increasing SO_3 content. Alkalis are incorporated preferentially in the aluminate and belite (29). Alkalis sulphatization results in a stronger effect on potassium as K_2SO_4 than on sodium as Na_2SO_4. Alkali aluminate is found only at low degrees of sulphatization and high alkali-content. Alite content is reduced more by Na_2O than by K_2O, with increase in belite content and no substantial change in aluminate and ferrite content. The degree of alkalis sulphatization in the clinker significantly influences the content of alite and belite clinker phases, as well setting and strengths of cement. Setting proves to be accelerated by Na_2O and accelerated or retarded by K_2O, depending on the sulphatization degree and chemical composition of cement. It has been confirmed that setting and strength development of cements strongly depend upon optimum SO_3 content.

Alkalis, sulphur, chlorine and heavy metals create cycles in the kiln. It has been pointed out (31) that alkali and sulphur cycles are considerably affected by the amount of chlorine introduced in the burning system with the raw meal and fuel, owing to the effect of chlorine intakes on volatilities. Although the relationships between distribution of the cycle components entering the system and the volatilities require further confirmation, it has been emphasized that alkalis not combined by chlorine

react with sulphur to form Na_2SO_4 and K_2SO_4 with lower alkali and sulphur volatility. The left over sulphur forms $CaSO_4$ with high sulphur volatility, thus increasing alkali and sulphur cycles.

The SO_3 present in cement comes principally from the gypsum added during grinding, but significant amounts may also come from the clinker, if high-sulphur fuel is used in the clinker burning process. SO_3, from the combustion of sulphur compounds in the fuel, often forms sulphites and sulphates, which appear to be less effective than the interground gypsum in the controlling the setting. With the recent conversion to coal of cement plants, with regard to the change-over from natural gas or oil to pulverized lignite, a decreasing of alite content has been noticed (32) with increasing size of alite crystals, disintegration of alite and occurrence of secondary belites and an overall lower hydraulic activity, associated with lower early strengths. It is therefore appropriate to make an assessment of suitability of the available coal and of the variations in clinker quality likely to be associated with them.

1.2.1. Short account on ecological aspects - The production of blended cements, through a partial replacement of the clinker fraction in cement, significantly contributes to climate protection. Environmental protection in cement industry has for some time attracted attention. The possibility of reducing dust emission, combatting its nuisance, noise and vibrations abatement, have been carefully studied (33). As concerns gas emission, it has been pointed out that sulphur dioxide increases little if fuel rich in sulphur is used, owing to the excess of alkalis usually present in the kiln and that sulphur dioxide resulting from sulphides decomposition can be bound by calcium carbonate dispersed in the gas stream. As a general rule, no gaseous fluorine compounds make up the emissions, since the nearly total amount of fluorine entering the kiln as clay minerals is discharged with the clinker and that emitted with the clean gas is bound as calcium fluoride. Nitrogen oxides emission (about 90% nitrogen monoxide and 10% dioxide), arising from nitrogen chemically bound in the fuel, depends on clinker burning temperature and is to be fought with appropriate operating conditions (34). In general SO_2 or NOx emissions depend to great extent on the temperature and the conditions of combustion in the main and the secondary firing systems. Sufficiently high process temperatures favour clinker quality but show an adverse effect on the NOx emission of the kiln plant. Part of nitrogen monoxide is broken down via catalytic reactions, but favourable operating conditions for a non-catalytic reduction of nitrogen monoxide with ammonia water have been also set up (35). As regards carbon dioxide, which is to a great extent responsible for the increasing the greenhouse effect on the earth (36), considering that the total emission during clinker production amounts to 0.872 $kgCO_2/kg$ clinker (62% from limestone decarbonation and 38% from fuel combustion), there is evidence that using carbonate raw materials, the level of the CO_2 discharge is only influenced by the type of fuel (C-content) and heat energy consumption.

Investigations into the behaviour in the kiln of the heavy metals present as trace elements in the raw materials and fuels, have shown that lead and zinc are to a great extent incorporated in the clinker. Rather similar is the behaviour of vanadium, beryllium, nickel, cadmium, arsenic and chromium, the last forming poorly volatile arseniates and chromates, in alkaline and oxidizing atmosphere. Thallium in raw meal burning conditions, is volatile and the possibilities of reducing the proportion of trace elements have been throughly investigated (37). Studies on mercury cycle are in progress.

1.2.2. Clinker selection. - As concerns the selection of clinker composition when "pozzolanic" matters are employed in the manufacture of the resultant cements, results of regression analysis (38) indicated that in the case of fly ash, its strength contribution appears to be positively affected by K_2O and negatively by $CaSO_4$ and C_2S in the cement. Since K_2O does not promote strength development in Portland cement, such a disadvantage can be reduced by fly ashes addition. In the case of blast-furnace slag (39), alkalis content affects in a different way the clinker and the slag fractions. Soluble alkalis content in fact noticeably decreases compressive strength of Portland cement, but its effect on slag fraction is highly positive. Strength development will therefore be strongly influenced by the alkalis content of the blend, according to the clinker/slag ratio involved.

In general, in order to manufacture a blended cement with good performances, it is recommended to choose a clinker of high quality, with high C_3S, C_3A and soluble alkalis content higher than that of a clinker for plain Portland, so abating the disadvantage of low strengths at early ages (40).

2. GYPSUM ADDITION.

Gypsum continues to be an essential component in today's Portland cement. Added to Portland cement clinker during the final grinding process, gypsum controls both the setting time and strength development of the mortars. The reaction of gypsum with tricalcium aluminate and tetracalcium aluminoferrite during the early stages of Portland cement hydration process involves the formation of calciumsulphoaluminates, accountable for controlling setting characteristics of cement and optimizing strength development and drying shrinkage. However, the amount of gypsum added is established by the cement producers to optimize strength, to minimize drying shrinkage and to control time of setting and slump loss. The optimum gypum amount to be added can be evaluated according to strength development (41), or to heat evolution curves during hydration, as well by the ettringite formed at the beginning of hydration process, when SO_3 saturation reaches the maximum value, considering the role of the chemical and physical form of the sulphate. The initial high rate of aluminate phase consumption appears to be influenced significantly by the rate of solubility of the sulphate used and especially the rate at which it releases $CaSO_4$ into solution (42). It has been also assumed that soluble sulphate in Portland cement strongly retards initial aluminate phase hydration and that a reduced initial rate of aluminate phase consumption allows an improvement both of workability of fresh cement paste and of the ultimate strength of the hardened product (42). Interground gypsum appears to be more effective than interblended gypsum, of the same apparent fineness, in controlling aluminate hydration (42). Experimental investigations (43) gave evidence that, as with additions to ordinary Portland cement, gypsum remarkably affects strength development of blast-furnace slag cements, so that it is possible to double, too, strength values at early ages by means of an optimum gypsum addition. Specific surface affects strength characteristics of blast-furnace slag cement more than of Portland cement. The optimum gypsum amount needed to reach maximum strength increases with specific surface area for both cements and decreases with age, but the difference in the SO_3 amount is limited for Portland cement and higher for slag cement. That is why one must state beforehand whether maximum strengths are expected at early or at later ages. From the point of view of cement quality an accurate control of the proportioning of the amounts of slag and gypsum is fundamental (43).

A wide laboratory and industrial investigation (44) performed in order to systematically follow the compressive strength development of Portland cement and of high slag blast-furnace cement mortars, as a function of gypsum content and curing temperature, pointed out the opportuneness of a precise correlation between gypsum dosage and curing temperature. A direct technical result of such an investigation concerns the proper choice of the type of cement to be used according to climate conditions. Evidence has been obtained of employing Portland cement at lower temperature, taking into account the dependence of gypsum dosage on temperature, whereas at higher temperature the use of blast-furnace slag cement appears to be preferable, considering that gypsum dosage proves to be virtually independent of temperature. A noticeable influence of gypsum addition on properties and internal structure of pastes and mortars has been also pointed out. SO_3 content in fact significantly influences pore size distribution of Portland and blended cements. Fig.1 points out that both for pozzolanic and slag cement mortars at early and long ages, a continuous shifting towards smaller pores with gypsum content is to be seen (45), whereas for Portland mortars, beyond 2.5% SO_3 the shifting stops. A variation in the total porosity has been also observed, so that total porosity appears as the microstructural parameter governing the influence of SO_3 content on compressive strength, since the sole variation of pore size distribution negligibly influences strength.

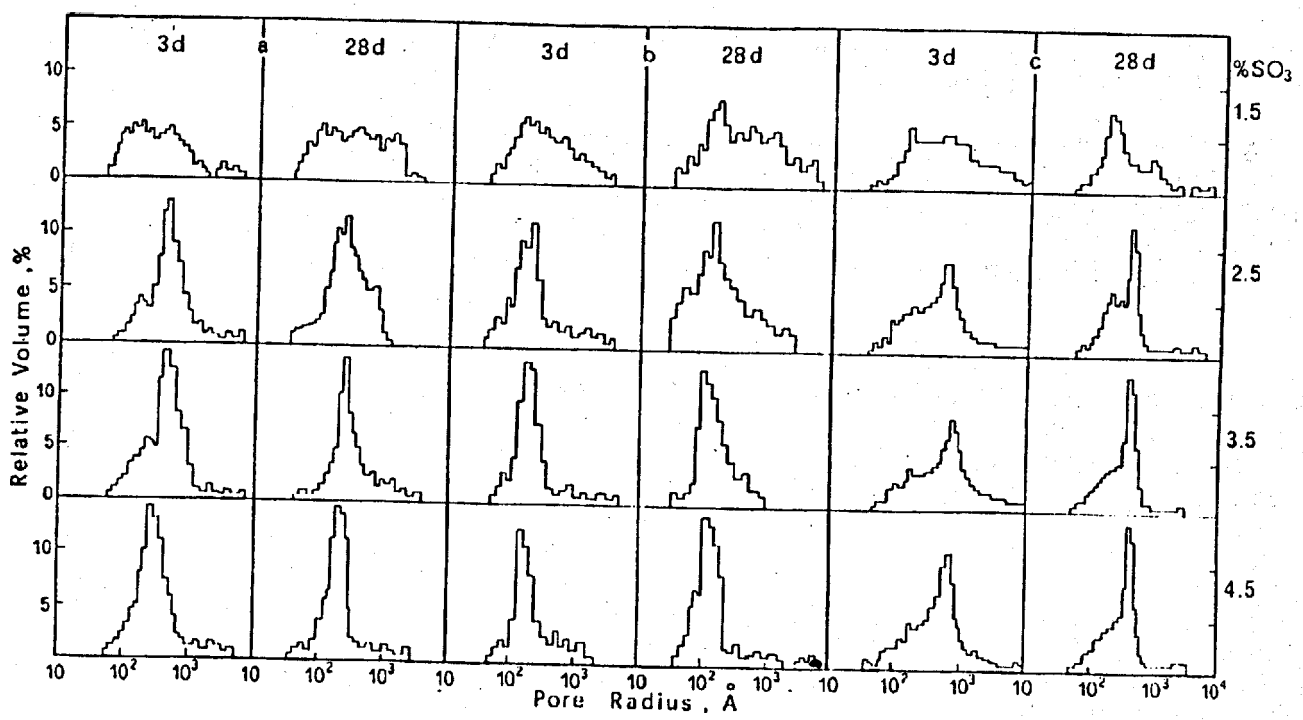

Fig. 1. Pore size distribution of mortars: a) 35% pozzolan in the blend; b) 70% blast-furnace slag in the blend; c) Portland cement (C_3A=8,4%).

2.1. Gypsum substitutes

It has been suggested substituting the amount of gypsum for fly ashes rich in SO_3 (46), or for a suitable mixture of ashes rich in SO_3 and ferrous silicon powder.

As concerns the use of chemical by-product gypsum, phosphogypsum (the by-product of phosphoric acid industry, consisting of $CaSO_4.2H_2O$ and impurities such as P_2O_5 and organic substances), has been used in the manufacture of some Portland cement, in lieu of the natural gypsum (47). Considering that the effect may vary with the variation in the content of some of its minor constituents, it has been pointed out that phosphogypsum increases later expansion with a somewhat increased drying-shrinkage at early ages, slightly improving later strength. However, phosphogypsum should be incorporated in the cement in smaller quantities than natural gypsum, it being a much more effective retarder. It has been also emphasized that untreated phosphogypsum can be used as a retarder directly in trass cement, whereas the reduction of strength induced in Portland cement suggests a refinement process by washing the product with milk of lime (48). Borogypsum is also used successfully as setting time regulator (49). Mention of the partial substitution of gypsum for limestone (50) and of the influence of limestone additions to Portland cement on the optimum SO_3 content (51) will be referred to later.

3. MINERAL ADDITIONS.

The term is used for inorganic materials, both natural minerals and industrial by-products, that are used in quantities of 5% or more by mass of the cement (52). Mineral additions may be blended or interground with Portland cement or added directly to concrete before or during mixing.

The class of the more well-known mineral additions- some of them called also "supplementary cementitious materials for use in concrete" includes: Fly ashes; Basic granulated blast-furnace slag; Condensed silica fume; Natural pozzolans; Zeolitized counterparts of the natural pozzolans (lithoidal

volcanic tuffs). More recent investigations suggest also the use of: finely divided substances: Ground limestone; Steelwork slag; Non- ferrous slag; Industrial wastes.

Fly ashes, blast- furnace slags and natural pozzolans are the most commonly used mineral additions today. Since the 1970's microsilica also has been increasingly used, but mostly for special purposes due to the limited availability. The predominant constituents in these additions is the amorphous silicate glass. Regourd (2) and Uchikawa (4) reviewed in full details the major characteristics and the effects of these mineral additions, so that only subsidiary data are reported here.

RILEM Commision 73 SBC presided by P.K. Mehta suggests classifying some of these products according to their performance in concrete, rather than by source of origin. A summary of the data on typical chemical and mineralogical compositions and particle characteristics is shown in Tab. II (53). Each of these products is available with a very wide range of composition and there is not always a full correlation between physical- chemical characteristics and performance.

It is generally accepted now that pozzolanic and cementitious properties of siliceous by products used as cement additions depend mostly on their particle characteristics and mineralogical composition, rather than their chemical composition and source of origin (53). So, from the standpoint of the effects of a mineral addition on the properties of the resultant cement, it appears less important whether the addition is a fly ash or a slag, but more important how fine is the particles size distribution and whether the non crystalline and the crystalline phases present are more or less active to hydration (53). All these materials are beneficial to concrete, too. The choice of slag or "pozzolan", is generally influenced by the availability of the materials, unless particular properties are desidered (54). Condensed silica fume is to be considered a premium product for producing high strength, low permeability or high electrical resistivity. Blast- furnace slag, fly ashes and pozzolans have the potential both for reducing the cost of concrete and for imparting improved sulphate resistance and inhibition to alkali- aggregate reaction.

3.1. Pulverized fuel ashes .

Fly ashes have a special characteristics different from the other supplementary cementitious materials (55). Ground granulated blast- furnace slag and natural pozzolan are products from quasi-homogeneous masses; as such, each particle, although it may be different in size and shape from its neighbour, has about the same chemical composition and the same internal structure. Silica fume is collected in particular form, but the indications are that individual particles are morphologically and compositionnally nearly identical to each other. In contrast, fly ashes constitute the fine particular residue of the responses of individual fragments of ground coal suspended in an air stream, moving rapidly through a brief exposure to high temperature,so that particles of similar size may be very different from each other in glass content, composition and content and type of crystalline matter included (55). Clusters of small spherical particles attributed to relicts of ground coal fragments containing high concentrations of fine mineral matter have been detected by SEM observations. The internal structure of certain particles has been revealed by selective dissolution of glass in hydrofluoric acid solution, emphasizing that susceptibility to HF attack between individual particles of the same fly ash accounts for variation in glass content. In contrast with blast- furnace slag, fly ashes, condensed silica fume, natural pozzolan, volcanic tuffs, rice husk, require calcium hydroxide as a necessary reactant during hydration.

Reactivity of fly ashes as a "pozzolan" primarily, depends upon calcium content (56), structure, specific surface area (57), quantity of glass phase, particles size distribution and total porosity. Important properties for use in blended cements are also the content of unburnt carbon, relatively unreactive and the ability to decrease water demand of mortars and concretes. Under normal operating conditions modern thermal power plants are capable of producing fly ashes that are generally low in carbon (<5%), high in glass (>75%) and have a fine particles size distribution (>40% under 10μm and <20% above 45μm). These fly ashes are well suited for use as a cement supplement in the cement and concrete industries (58).

Tab. II - Classification, composition, and particle characteristics of siliceous by-products used as cement additions, or as mineral admixtures in concrete (53).

Classification	Chemical and Mineralogical Composition	Particle Characteristics
I. Cementitious		
Rapidly-cooled blast furnace slag	Mostly silicate glass containing calcium, magnesium and aluminium. Crystalline compounds of melilite group and merwinite may be present in small quantities.	Unprocessed material is granular or pelletized and contains 5 to 15% moisture. Before use it is dried and ground to particles mostly less than 45 μm (400 to 500 m^2/kg Blaine). Particles have rough texture.
II Cementitious and Pozzolanic		
High-calcium fly ash (> 10% CaO)	Mostly silicate glass+ containing calcium, magnesium, and aluminium. The small quantity of crystalline matter present generally consists of quartz and C_3A; free lime and periclase may be present; $C\bar{S}$ and $C_4A_3\bar{S}$ may be present in the case of high-sulfur coals. Unburnt carbon is usually less than 2%.	Powder corresponding to 10-15% particles larger than 45 μm (usually 300-400 m^2/kg Blaine). Most particles are solid and spheroidal with less than 20 μm diameter. Particle surface is generally smooth, but not as clean as in low-calcium fly ash.
III Highly Pozzolanic		
a.Condensed silica fume	Consist essentially of silica in non-crystalline form.	Extremely fine powder consisting of solid and spheroidal particles mostly less than 0.1 μm (about 20000 m^2/kg surface area by nitrogen adsorption).
b.Rice husk ash produced by controlled incineration.	Consist essentially of silica in non-crystalline form.	Particles are generally less than 45 μm but they are highly cellular (about 60000 m^2/kg surface area by nitrogen absorption).
IV Normal Pozzolanic		
Low-calcium fly ash (< 10% CaO).	Mostly silicate glass containing aluminium and iron. The small quantity of crystalline matter present consists generally of quartz, mullite, hematite and magnetite. Unburnt carbon is usually less than 5%, but at times may be up to 10%.	Powder corresponding to 15-30% particles larger than 45 μm (usually 250-350 m^2/kg Blaine). Most particles are solid and spheroidal with average 20 μm diameter. Cenospheres and plerospheres may be present.
V.Others		
a.Slowly-cooled blast furnace slag.	Consist essentially of crystalline silicate minerals, and relatively small amount of non-crystalline matter.	The materials must be pulverized to very fine particle size in order to develop satisfactory cementitious or pozzolanic activity. Ground particles are rough in texture.
b.Bottom ash, boiler slag, field-burnt rice husk ash.		

+ In fly ashes containing more than 20% CaO, the composition and reactivity of the glass are much different than the glass in low-calcium fly ash; the glass in high-calcium fly ash is more reactive.

Test methods for determining chemical composition, particle density, glass content, fineness of fly ashes, have been the object of the work of RILEM TCFAB- 67 (59). Related International Standards have been also indicated. It has been stressed that activity of fly ashes depends not only on their own properties, but on the physical and chemical properties of the cement employed, even within the same cement type. Fly ashes should therefore be tested with the cement intended to be used in practice in mortar and concrete, unless otherwise specified. An ordinary Portland cement should be used to test basic activity. Pozzolan activity index according to ASTM designation C311 does not appear to be a decisive parameter for grading the relative reactivity of fly ashes. More useful information has been obtained from normally-cured test mortars containing 20% fly ashes by weight of cement and 0.485 ratio between water to cement plus fly ashes (58).

In antracitic or bituminous ashes-corresponding to type I or class F, according to American designation (ASTM C 618- 80), low in CaO and available to a greater extent - the glassy phase, the determining factor for pozzolanic activity, generally exceeds 70%. Crystalline minerals generally comprise quartz, mullite, magnetite or ferric spinel. Glass evaluation can be performed quantifying the crystalline particles via X-ray diffraction with the method of intensities ratio, using CaF_2 as diluent (60). Measurements can be improved with the choice of internal standard and the reduction of the particles (61).

In fly ashes containing more than 20% CaO (corresponding to type II or class C, ASTM C618-80 subbituminous) with pozzolanic and hydraulic properties, the composition and reactivity of the glass prove to be much different from the glass in low-calcium fly ashes, the glass in high calcium fly ashes being more reactive. Crystalline phases in subbituminous ashes include C_3A, $C_4A_3\bar{S}$, calcium sulphate and alkali sulphate (53), both of them being reactive. Ground high-calcium fly ashes proved to be characterized by strong chemical affinity to water (62) and exhibit large variability in chemical and phase composition for various grain size. Cements containing 70% high-calcium fly ashes exhibited compressive strengths between 33-48 MPa, depending on fineness. 28-day hydrated pastes examined by X-ray diffractometer were found to contain $3CaO.Al_2O_3.3CaSO_4.32H_2O$ and C-S-H and no $Ca(OH)_2$ from clinker phases. Ashes with high content of SO_3 do not require gypsum addition in the resultant cement. Good strength performance has been attributed to stabilization of ettringite in the structure of hardened paste.

A fly ash containing 40% wt free lime (CaO total being 72% wt) and 13% anhydrite, not corresponding to any of ASTM types because of a too high CaO content, has been suggested as component of a masonary cement (63): a mixture of 70% wt hydrated fly ashes and 30% Portland cement, and for a non structural -low strength pozzolanic cement concrete , a mixture of 70% wt hydrated fly ashes and 30% wt silica fume. Strength development in both the cements has been attributed to C-S-H and ettringite formation.

Advances in the characterization of the glassy aluminosilicate phases in coal fly ashes have been made in the Symposium held in Boston and organized by the Materials Research Society (64). Glass science has been applied to formation and structure of the glassy phases and summarized the structural insights obtained by a wide range of characterization methods. Notable advances have been made using electron microscopy (55), XRD (65), vibrational spectroscopy, thermal analysis and chemical methods. Structural differences have been pointed out between fly ashes glass types, and diagrammatically represented. Various chemical treatments provided further details on the crystalline and glassy phases (66). Evidence is given that heterogeneity in fly ash exists at all scales of investigation down to the structure of non-crystalline or glassy constituents. Many particles that appear to be non-crystalline also contain crystals of different type. The constituent glasses differ substantially in composition and these differences are expected to be responsible for a quite different behaviour with alkaline product of cement hydration.

The quality of fly ashes shows to be substantially improved by fine grinding (67). The coarse fractions have low particle bulk densities and as a consequence are easy to grind. Carbon, quartz, mullite and free lime concentrate in the coarser particle fraction; anhydrite and glass phase in the finer. Strength progress is strongly influenced by particle size distribution, even if the sole evaluation

of the fraction passing through a 45μm sieve does not in itself appear fully appropriate to foresee fly ashes technical behaviour. Laser diffraction technique, characterized by precision speed and reproducibility, is suggested as an alternative to sedimentation and sieving technique for granulometric analysis in dry and wet feeding systems (68).

In order to produce a product of high quality, it might be interesting to process fly ashes (69). Air classification and grinding are presented as a way for improving efficiency of fly ashes, positively influencing strength development at early ages, pozzolanic reactivity and sometimes workability, too.It has been emphasized that an increase in the fineness of fly ashes improves the solid structure of hardening mortars, leading to an increase in early strength. Moreover the pozzolanic reactivity increases by optimization in the fine particle range, both for the enlargement of the potential reaction surface and for the enrichment of chemically reactive constituents. Particles shape appears to be a further factor governing water - reducing effect: the more closely the particle shape approximates to an optimum spherical conformation, the more favourable appears the effect on workability. An unfavourable particle shape decreases the improvement of rheological properties due to increased fineness. Removal of coarse costituents through air classification generally improves effectiveness of fly ashes (70).

As regards the possible quantification of fly ashes, high resolution gamma spectrometry has been proposed (71) as a suitable method for calculating their percentage in a cement, provided that their source is known.

To sum up, the performance of a pulverized fly ash blended cement depends on the chemistry and mineralogy of the fly ashes and, besides the fineness, on the loss on ignition of the ashes, as well as on the free lime content of the clinker and the SO_3 content of the blend (57).

3.2. Blast-furnace slag

It is the non metallic product, consisting essentially of silicates and alumino-silicates of calcium and other bases, that is developed in a molten condition simultaneously with iron in a blast- furnace. The glassy, granular material is formed when the molten by-product is rapidly chilled, as by immersion in water. Such a by-product provides the greatest energy saving, in that it may be used with little (or no) Portland cement. Blast- furnace slags are made up from both glassy and crystalline phases, the first one in higher proportion as the slags are more acid. Typically, granulated slag contains 85- 90% glass. Crystalline compounds identified in the devetrified slags are mainly the melitite solid solution series with end members gehlenite and akermanite and lesser amount of monticellite, diopside, merwinite. Glassy phase content and basicity are still considered the most important factors governing hydraulicity, although some results contradicting a direct relationship: glass content- slag reactivity are not missing (72). A moderate amount (about 3-5%) of crystalline fraction could be considered in the same way as the unreacted slag micro- particles: a barrier against microcracks propagation.

As already emphasized, the glassy phase is much more homogeneous than is found in the pulverized fuel ashes. Its reactivity depends to a greater extent on composition. In general, the more basic the slag is, the greater its hydraulic activity in the presence of alkaline activators, including clinker, and the higher the glassy phase, the lime and alumina contents, the higher is the hydraulic property. In many Specifications basicity is defined as:

$$\frac{CaO+Al_2O_3+MgO}{SiO_2}$$

representing a quality factor. Cementitious properties are therefore positively influenced by an increase in lime and alumina and negatively by an increase in silica.

Cements manufactured by additions of vitreous - like acidic blast-furnace slag are reported (73) as blends characterized by a low water-demand and a small specific required quantity in concrete, a

high strength in mortars and concrete with normal hardening conditions, and in particular after steam - curing, a reduced heat release, a satisfactory sulphate and frost-resistance and a moderate shrinkage. Cements with main granulated blast-furnace slag also possess these properties but those manufactured with acidic slag exhibited higher frost resistance (73).

Factors affecting hydraulicity are in short: glass content, chemical composition, fineness of grinding, activation of slag glasses by chemical or thermal means. Although slag reactivity is reduced when devetrification increases, the relationship between glass content of slag and strength development in a blended Portland cement containing slag is not linear.

3.2.1. Slag activation.- Blast-furnace slag, when properly granulated or pelletized, is a cementitious material which reacts directly with water in the presence of activators. In absence of special activators, $Ca(OH)_2$ produced in the hydration of Portland cement serves as the activator. It is well known that slag hydration takes place after mixing with water and a protective layer is formed on the surface which inhibits the water penetration and further dissolution of ions from the slag. Numerous species serve as activators and accelerators: Portland cement, alkalis, gypsum, lime. NaOH has a higher activation effect than $Ca(OH)_2$. Gypsum accelerates hydration, but is less effective as activator without the presence of $Ca(OH)_2$.

Hydration of slag requires the breaking of bonds and dissolution of the three- dimentional network structure of glass. High pH values easily break the bonds in the network structure of glassy slag and promote hydration (74). The alkalis generally used such as NaOH, Na_2CO_3 and water glass, are expensive, often hygroscopic and potentially harmful. Neutral salts such as sodium sulphate and potassium aluminum sulphate have been suggested as alternative, having similar effects and being less expensive and harmful. The breaking of Si-O and Al-O bonds through the action of activators such as $Ca(OH)_2$, NaOH, KOH, allows the dissolution of Si and Al ions followed by precipitation of low-solubility calcium silicate, calcium aluminate and magnesium aluminate hydrates, due to increased ionic concentrations in the liquid phase. In the presence of gypsum (75), the concentration of Ca and Al ions are reduced, owing to ettringite formation. When pH of the liquid phase reaches approximately 12, ettringite is formed stably (76) and hydration of slag is most accelerated. In order to mantain active hydration of slag, it is therefore necessary to supply sufficient hydroxyl, to create a high pH to break glass network and stabilize the neo- formed ettringite, together with SO_3 and alumina for further ettringite formation. That is the assignment of activators, justifying the opportunity of using in some cases compound activators (77), rather than individual ones, deciding the relative amounts by detailed experiments. The role of activating agents has been also investigated in term of dissolution mechanism of slag constituents (78). Activation by anhydrite has been also investigated with the objective of preparing supersulphate slag cement, normally obtained from 80-85% high lime slag, 10-15% activators and 5% ordinary Portland cement. Experiments made on indian slag, relatively poor in lime (26-38%) and rich in alumina (20-30%) pointed out (79) that optimum quantity of anhydrite is in the range of 15-20%. Ettringite and calcium- silicate- hydrates have been indicated as the major hydration products and maximum quantity of the first one was formed in the early ages of hydration. Strength enhancement at later ages has been attributed to calcium- silicate hydrate formation. Activation of slag in supersulphated cements can be performed by various form of calcium sulphate: chemical gypsum or hard burnt gypsum. The ashes obtained from the filter cake in the refining of raw cane sugar and successively burned have been used in various amount (80). The maximum activation effect has been reached during the first day of hydration for pastes containing 5-10% ash. In the ash- free samples, hydrated calcium silicates and hexagonal tetracalcium aluminate have been found as the main hydration products; in the presence of ashes, calcium sulphoaluminate hydrates have also been detected. Supersulphated cements have however short utilization, because of the short protection that guarantee reinforcement.

As regards mechanical properties, it has been found (81) that addition of small amount of NaBr, NaCl, NaF or Na_2SO_4 increases strength at early ages; NaBr or NaCl increases strength even at 91 days. The microstructure of pastes with NaBr or NaCl addition showed a structure containing CSH gel, AFm, ettringite and other phases having a compact structure. Experimental results pointed out

(82) that the particle size distribution of the clinker affects more particulary the early strength, whereas that of the granulated slag primarily affects the 28-day and 91-day strength of cement, without a systematic influence upon water demand and setting behaviour of the blast- furnace cement. When slag amount exceeds 25%, separate grinding appears sometimes to be profitable from the power efficiency angle and the quality of the end product (83). The characteristics of these cements depend on clinker and slag fineness. Fineness of the latter ought to be 4000- 5000 m^2/Kg Blaine, in spite of the high energy consumption required by the grinding process. Slag grinding can be made easier by means of intergrinding of 5- 10% clinker, which improves also particle size distribution of the product.

In order to improve the properties of conventional slag cement and develop a high quality binder, the use of ultra- highly pulverized blast- furnace slag (Blaine fineness 850 m^2/Kg) up to 70-80% cement replacement has been suggested (84). A very dense and uniform structure of the hydrated paste and superior characteristics with high- strength concrete, having more than 100 Mpa as compared to plain Portland cement high- strength concrete, have been observed. Strength development, especially at early stage and setting time of Portland blast-furnace slag cement can be improved (85) by means of increasing the fineness of slag, but flow, heat of hydration and drying shrinkage are adversely influenced. By adding 2-5% of super fine limestone powder to Portland blast-furnace slag cement, strength development, except compressive strength, at later ages was largely improved. Setting time, strength after autoclave curing and drying shrinkage were also improved by limestone. The use of high - range water- reducing admixtures allows less bleeding, and the noticeable improvement of the resistance to acid and sulphate attack, as well other characteristics, can be attributed to the densification and to the reduced amount of calcium hydroxide caused by hydration of slag. Additional use of semi-crushed granulated blast- furnace slag, added as fine aggregate to the ultra-high pulverized fraction, improves durability of concrete and lowers heat of hydration and, of course, strengths.

Blast-furnace slag may be used to replace the major portion of cementitious materials when the early strength is not the most important prerequisite. However early strengths may be achieved by further grinding of the slag, high temperature curing, or using low water- cement + slag ratio, whenever appropriate. Early demoulding may significantly reduce the strength of slag/cement mortars and excessive amount of alkalis appears to favour flash setting. Curing temperature can significantly increase strength at early ages, but when curing temperature exceeds 80°C unfavourable effects on strength have been recorded. Finally, slag tends to make the pores finer, increasing durability of mortars exposed to adverse environment.

As regards cementitious property in particular, slags activated with water glass or sodium carbonate showed a significant influence of curing conditions on the flexural strength (86), without substantial variation of compressive strength of slag/sand mortars. The flexural strength decrease, observed in mortar samples transferred from water to air of 65% RH, has been attributed to the formation of microcracks, owing to the release of large quantities of water content by the gel-like slag hydration products. The change of gel volume produces microcracks in the hardened paste, reflecting mainly on flexural strength. Suitable fineness, proper slag/sand ratio and curing conditions proved to reduce volume changes and consequently microcracks formation.

In the Federal Republic of Germany, too, is produced a blast-furnace trass cement in two compositions: 15% wt. trass, 30% blast-furnace slag, 55% Portland cement clinker; or 20% wt. trass, 50% blast-furnace slag, 30% clinker (87). Improved workability, low heat of hydration, long-term strength development of up to 70%, watertightness, high resistance to chemical attack, are the characteristics indicated.

3.3. Condensed silica fume

The production technology of microsilica and the development of its use as addition, particularly in concrete, have been the object of many investigations (88). Microsilica consists essentially of vitrified silica (100% glass), and because of its reactivity can generally replace three to four times its

weight of Portland cement, mantaining equal compressive strength. It is to be noted that just as all pulverized fuel ashes are not suitable for use in concrete, not all microsilica is suitable (89) and sources and types must be carefully controlled. Different types of condensed silica fume have revealed that the material is essentially vitreous. A diffuse halo peak corresponding to the strongest peak of crystobalite has been identified via X-ray diffraction (53).

Typical nitrogen adsorption surface area for condensed silica fume, ground granulated blast-furnace slag and fly ash, are of the order: 17.000 to 20.000 m^2/kg; 400 to 600 m^2/kg; 300-350 m^2/kg, respectively (53). An experimental apparatus that allows amorphous silica powders with specific surface of 136 m2/g to be produced, has been also set up (90).

Inclusion of microsilica in cement systems is regarded as a way of accelerating the hydration process during early hours. Addition of microsilica has the effect of accelerating the reaction of C_3S. Microsilica itself is consumed during hydration and an increased amount of polymer calcium silicate hydrates is formed (91). The increased rate of cement hydration has been observed (92) when microsilica exists still as chemically inert filler, suggesting a possible effect of submicroscopic particles of silica fume as nucleation sites, so enhancing precipitation of hydration products. Evidence of pozzolanic reaction has been also revealed within three days, irrespective of the water to - binder ratio used (between 0.40 and 0.56), and of the cement used (Portland and blast-furnace cement). In both cases, chemisorption from the liquid phase of OH^-, Ca^{+2}, K^+ and Na^+ ions during early days of hydration is believed to be preceeded, at a relatively high pH, by attack of microsilica by OH^- ions.

From the scientifical and technological point of view great importance is due to the orientation of calcium hydroxide crystals at the interfacial zone betwwen cement paste and inserts (aggregates, fillers, reinforcements). SEM examination (93) showed that silica fume tends to affect the pattern of crystallization and degree of orientation of $Ca(OH)_2$ crystals at the aggregate surface during the first few days of cement hydration, because of the tendency of the crystals to nucleate and grow on the fine particles. In the silica fume blended mortars, calcium hydroxide disappeared from the aggregate by 28 days hydration. With 5% cement replacement, the preferential orientation of calcium hydroxide crystals in the transition zone is reduced with hydration progress and a denser hydration product is formed, accounting for the important role of pozzolanic reaction between lime and silica fume in the strenthening of the transition zone. Studies on the effects of the mineral additions on the interfacial zone cement/aggregate pointed out that fly ashes and slag significantly decreases the degree of orientation of $Ca(OH)_2$ crystals, particularly in the case of slag- bearing cement paste, influencing durability and mechanical properties of concrete. The addition of fly ashes or slag seems to suppress precipitation of $Ca(OH)_2$ crystals in the interfacial zone and restrict ettringite formation in the limited zone within 10μm from interface (94), favourably influencing resistance of the interfacial zone against aggressive agents supplied from the surrounding.

In cement paste-limestone combination, calcium carboaluminate is formed in the interfacial zone, in which its formation is increased by the addition of fly ashes or slag. Hydroxide crystals with preferred orientation have been also observed at the interface steel-cement silica fume bearing pastes, even at a high level of cement replacement (95).

Investigations on Portland cement - silica fume mortars gave evidence of a definite influence of the sand-matrix interface on pore size distribution, porosity and mechanical strength, emphasizing that properties of blended pastes appear to be quite different from those of blended mortars (96). The discontinuous pores formed, attributable to the subsequent consumption by silica fume of calcium hydroxide crystals deposited at the interface of inclusions, showed to be more numerous and large than those in pastes of the same water to cement and silica fume content, owing to interface effects. This consideration could explain the improvement of frost resistance of silica fume mortars and concretes owing to the presence of those pores which act in the same way as air entrained bubbles. SEM observation on silica fume-lime crystals mixture (97) gave evidence of the existence of large voids corresponding to the initial $Ca(OH)_2$ crystals sites, not refilled by any further precipitation after 28 days hardening. The coarse pore family in the 1-2μm size range observed in hydrated silica

fume mortars could be originated in such a way. Large amounts of silica fume significantly increase also drying shrinkage, whereas freeze-thaw resistance is improved (96). Silica fume, particularly at the longest period of curing, increase porosity and the compressive strength of pastes, due to the low lime content, whereas Young's modulus of elasticity falls, owing to the formation of a low-density dispersed hydrate product of low CaO/SiO_2 (98). Silica fume was found to decrease permeability, which appears not to be particularly dependent upon the amount added (99). It has been found that compressive strength on mortars reaches a maximum with 8% wt. silica fume (100), decreasing, particularly at early age of hydration, because of porosity rises. Mortars with more than 5% wt silica fume have shown good resistance to sulphates, buckling to a lesser extent than normal sulphate-resistant mortars, due to the lack of gypsum and the presence of small amount of ettringite. It has been proved (101) that silica fume addition increases compressive strength of mortars, enabling, in turn, an increase in the fly ashes addition.

As regards the common introduction of condensed silica fume in high strength concrete as partial replacement of the cement , it has been pointed out that these by products act in concrete as reactive pozzolan and as filler (102). Enhancement of compressive strength of ultrafine mineral admixtures: silica fume or fine alumina powder in pastes and mortars prepared with a Portland cement, has been attributed to an action as filler and it has been emphasized that associated with a superplasticizer they have shown an equal reducing effect. The difference in the pozzolanic reactivity levels led to tne conclusion that the influence of pozzolanic reaction on compressive strength is negligible (103). When silica fume is employed as mineral addition, the proper use of superfluidifiers appears to be well appropriate.

3.4. True pozzolans and volcanic tuffs

The making of hydraulic binders using natural pozzolans dates back from ancient times. The preparation of mortars made with lime and volcanic sand of the ancient Thera (the Island of Santorin) is attributed to the Phoenicians (104). Water cisterns plastered with hydraulic mortars have been found at Jerusalem, dating back to the time of king Solomon (10th century B.C.).

In today's cement production their use is increasing in those countries which possess only limited sources of industrial, hydraulic - active mineral additions. Experiences with production, application and performance of pozzolan cement concrete in Chile from the very beginning to the present time, have indicated that the long-term performance of Portland - natural pozzolan concretes is, at least, the equivalent of Portland cement concretes (105). Chilean experience with economic and efficient use of country's natural resources has encouraged other countries in Latin America. Recently, Portland - pozzolan cements in Colombia and Equador were introduced in the market.

Natural pozzolans are incoherent pyroclastic sialitic products. Consist mainly of silica and alumina which give them acid character and great affinity for lime, as well as alkalis and are essentially vitreous products. Finely subdivided and bubbly elements with large internal surface area characterize true pozzolans. The crystalline phases are somewhat limited and strictly depend on the type of magma from which pozzolans originated. Phlegraean volcanic areas (near Naples) originated alkali - trachytic pyroclasts, in which sanidine and to a lesser extent augite, are the main crystalline phases, distributed in the abundant vitreous mass. Pozzolans originate only from volcanic eruption having had an explosive course, so that the violent ejection of melted magma into the atmosphere causes the rapid quenching and the glassy state (106). Gases accompanying the explosion account for the bubbly shape (Fig.2) and the wide specific surface area of the pyroclast.

Eruptions having a non-explosive course originate only volcanic ashes, which, being cooled rather slowly, show fewer and no bubbly vitreous fragments, thus being much less reactive towards lime. Silicate glasses, because of their high free energy content, are particularly reactive in moist environment, so that under the diagenetic action of groundwaters, undergo - according to the conditions - zeolitization, feldspartization, argillization phenomena, responsible for the cementing of the incoherent original vitroclasts. Low-alkaline environments favour in fact zeolitization processes (107), through a superficial or exogeneous alteration, but not atmospheric, named: diagenesis.

Lithoidal volcanic tuffs are therefore the zeolitized counterparts of the true pozzolans, including Rhenish trass (108), the oldest known one and a wide series of tuffs available in Central southern Italy, particularly in the volcanic districts of Latium, Campania, Potenza, Caserta (109).

Microscopical examination of thin sections of these tuffs reveals the rocks to consist of a nearly isotropic matrix of diffused crypto-crystalline zeolites, which surround crystalline fragments of other minerals. Very small zeolite crystals are often recognizable in the small cavities of the rocks, too. Zeolite content is in the range 50-80% wt. Neapolitan yellow tuff, for instance, the zeolitized counterpart of the phlegraean pozzolan, appears to be highly homogeneous, rich in fibrous and bubbly fragments of pumices and crystals of plagioclase and light-green pyroxene. The yellowish, nearly isotropic matrix, consists mostly of phillipsite (Fig.3) or chabazite (Fig.4).

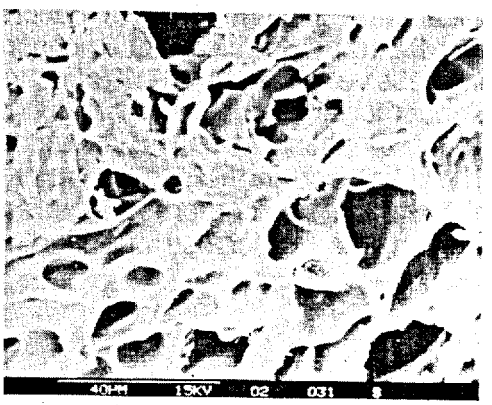

Fig.2. Glass fragment of Phlegraean pozzolan, showing a vacuolated morphology.



Fig. 3. Aggregate of needle-shaped phillipsite crystals diffused in the ground mass of Neapolitan yellow tuff.



Fig. 4. Aggregate of rhombohedral chabazite crystals diffused in the zeolitized facies of Companian grey tuff.

Pre-ground volcanic tuffs have tendency to combine with lime to an extent at least similar, if not greater, than that of pozzolans originated from the same magma (110), and this is not unexpected if one remembers the particular structure of porous solids characterizing zeolite minerals. Owing to the channels and pores running across the whole solid, lime attack is at least as easy as that of the bubbly glass. Hydration products are, of course, similar (111).

In Italy, lithoidal tuffs are not yet employed in the manufacture of blended cements, owing to the availability of large deposits of the incoherent counterparts, though tuff-cements are to be classified in all respects as pozzolanic cements. It is to be noted however that the advantage due to the incoherence of the pozzolans is more apparent than effective, since consumption for the grinding operation does not differ very much for both products, owing to the fine - grained texture of the lithoidal counterpart. 8-10 Kwh/ton are in fact needed for grinding either a tuff or a pozzolan, in comparison with 30 Kwh/ton for Portland clinker, energy consumption for drying either the tuff or the pozzolan being similar, too, (200-250 Kcal/kg) (112). On the contrary, "trass-zemente" have a very old and worthwhile tradition.

Fig.5 quotes compressive strength values of ISO-Rilem mortars manufactured with blended cements prepared with the same clinker (Blaine fineness 370 m^2/kg) and amount ranging from 10 to 40% of phlegraean pozzolan or neapolitan yellow tuff, respectively, ground until a residue of 13% remains on a 32μm sieve. One can see that portland-tuff-cement shows values higher than that of portland - pozzolan - cement, particularly at longer ages.

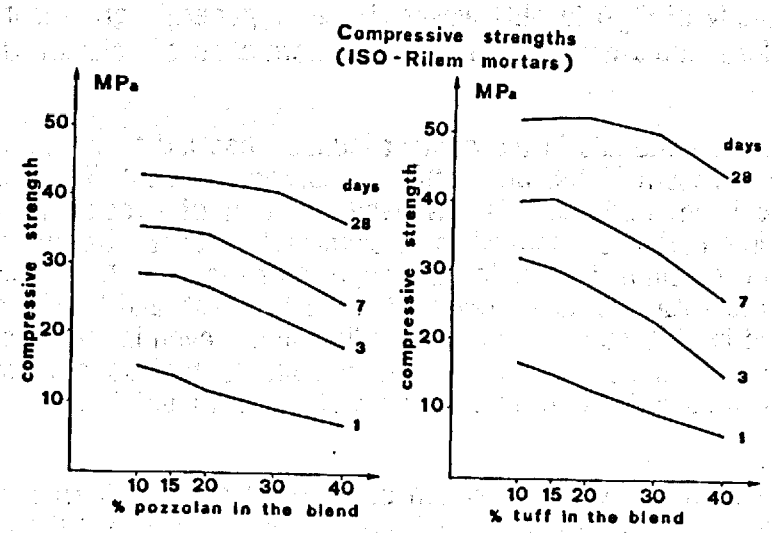

Fig. 5. Compressive strength development of ISO-RILEM mortars, as a function of mineral addition content and curing duration. a, Portland-pozzolan cement; b, Portland-tuff cement.

The synthesis of framework silicates such as zeolites or feldspathoids has been suggested as a practicable way to prepare geopolymeric compounds, constituting the blended geopolymer-lime (113). Fabrication involves calcination at 700°C for limestone dolomite and kaolinitic soils. Addition of Na_2CO_3 or K_2CO_3 and also silica, produces NaOH and KOH which react strongly with calcined kaolin, yielding a geopolymeric binder of the analcime type. Geopolymer chemistry, when associated with Portland cement, is claimed to yield cementitious material with remarkable properties, such as ultrarapid strength gain, natural sulphate and freeze-thaw resistance and foreseeable long-term stability; though such characteristics are still waiting for the test of a long practical employment. Synthetic geopolymers and geopolymeric matrix have also been suggested as a material suitable for immobilizing hazardous elemental wastes (114).

As regards burnt clay, a simple and cheap binder has been prepared mixing two parts of dolomite calcined at 950°C and three parts of clay burnt at 750°C, ground to the same fineness. Process appears to be advisable for small factories and binder can be employed for plain constructions (115).

3.5. Limestone filler

A current proposal in ASTM Committee C-1 on cement would allow up to 5% limestone to be interground with clinker into Portland cement. The proponents claim a significant saving of energy during production, without a degradation in quality and cite improvements in some cement and concrete characteristics. The opponents claim that limestone acts merely as an adulterant and that strengths are reduced (116). Carbonate addition to normal Portland cement to a maximum of 5% is already allowed in some countries (117) and Canadian Standards Association is now considering the possibility of extending carbonate addition also to high-early strength Portland cement, mainly used in precast and prestressed concrete. Preliminary investigations have shown that carbonate addition contribute to compressive strength development of heat-cured concrete made with such a cement , without detrimental effects either to length change or to freezing and thawing resistance.

It is known that limestone additions to cement may have several functions: completion of the granulometric curve of deficient fine grain cement; obstruction of capillar pores, hampering water

percolation; variation of the rheological parameters of the slurries; interaction with hydration process. It is well-founded to suppose that optimum amount of carbonate addition varies depending on the composition of the clinker, particularly of C_3A level.However, there is general agreement that limestone is not a pozzolan and therefore would not be involved in the formation of calcium silicate hydrates.

The search for less costly alternative materials in the cement industry has led to the proposal for partial substitution of limestone for gypsum in the production of Portland cement. There is, of course, agreement that solubility of calcium carbonate is low, whereas that of gypsum is much greater. The formation of a stable calcium carboaluminate when calcium carbonate is introduced in a system containing large quantities of calcium aluminate, although more slowly than calcium sulphoaluminate, is also known. Powdered X-ray diffraction revealed (118) that high and low forms of calcium carboaluminate can be observed in all systems incorporating limestone, even in the presence of gypsum and X-ray diffraction analysis has been suggested as a suitable technique to follow calcium carboaluminate and calciumsulphoaluminate formation, as well gypsum uptake in cement systems.

Investigations on rheological properties and water retention capacity of cement slurries made with cement and up to 15% wt limestone with high $CaCO_3$ content, allowed one to point out (119) that the variations in the yield point and plastic viscosity account for the "lubricity power" of the amount of particles below 10μm, increased by the relatively greater grindability of limestone, without appreciable changes in water retention value.

As regards gypsum addition, experimental investigations - though limited to materials and methods - gave evidence (120) that the optimum SO_3 content of the blend decreases with limestone amount. This influence has been attributed mainly to limestone effect on the particle size distribution of cement and perhaps to the reaction calcium carbonate/calcium aluminate, too. Results allowed one to reach the conclusion that addition of limestone ground together with the clinker lowers strength performance of cement, even at optimum SO_3 content at all addition level and fineness. Addition of interground of blended limestone in Portland cement can also adversely affect drying shrinkage. Additional steps are therefore recommended in order to amend such a disadvantage.

It has been emphasized (121) that Portland cement with a high C_3A content (type III ASTM) can react readily during hydration with carbonates, forming significant amount of calcium carboaluminates with beneficial effects on strength development and resistance to sulphate attack, but it is not so for Portland cement with normal C_3A content (type II ASTM, max 8%). In this case only minor and delayed reactions with carbonate were observed, suggesting that for these cements limestone additions act mostly as relatively inert diluents, so that potential negative effects could outweigh any positive results. The possibility of extending carbonate additions also to cements for sulphate resistance and moderate heat of hydration, has been evaluated according to ASTM C452 Specification (potential expansion of Portland cement mortars exposed to sulphate) and ASTM C1012 Specification (developed for the evaluation of blended cements) (122). In the range of C_3A content 7.3 to 10.3%, SO_3 from 2.93 to 3.80 and calcium carbonate levels up to 5%, sulphate resistance appeared to be unaffected by carbonate additions and primarily influenced by C_3A content. Neither carbonate additions showed consistent effect on heat of hydration and sulphate resistance of Portland cement (122).

Investigations on the assessment criteria for the suitability of limestone for producing Portland limestone cement and the effects on the working characteristics, as well on durability, allowed one to infer (123) that the high proportion of fine particles in the mixture widen the particle size distribution, in comparison with plain Portland cement, reducing the water demand and improving concrete consistency. Only a mere action of inert has been attributed to the filler, emphasizing that an increased fineness of the clinker fraction offset the loss in standard strength due to dilution and that a concrete manufactured with blended cements containing 20% limestone filler, with more than 75% wt

$CaCO_3$ of suitable chemical and mineralogical characteristics, reaches the same strength level as a Portland cement of the same class, with frost resistance sufficiently high.

One can see that there are still differences in opinions and experimental evidence of limestone addition to Portland clinker requires further consideration.

3.6. LD Steel work slag

It is formed during the production of steel which involves the removal of impurities such as carbon, silicon, manganese, phosphorus, from pig iron. Steel slags may be rich in phosphate or in calcium and contain metastable dicalcium silicate. Main chemical components, are therefore CaO, SiO_2, Al_2O_3, FeO, Fe_2O_3, MgO, MnO, P_2O_5 and free - CaO. Mineralogical composition depends mainly on chemical composition, which varies with steelmaking processes.

At the present, steelwork slags are classified in terms of basicity ratio

$$\frac{CaO}{SiO_2+P_2O_5}$$

which appears to correlate well with cementing properties (124). High basicity ratios favour in general slags activity. Composition fluctuates significantly. The urgent problem to be solved for use in cement production is therefore how to evaluate cementing properties, select proper proportioning, and ensure constancy in the processing technology. In general, steelwork slag positively reacts with water but possesses weak hydraulicity, that is why it is necessary to investigate its possible activation. Sodium hydroxide proved to be an accelerator for hydraulic reactions, especially in the beginning, though with changes in composition and morphology (125).

Possibilities of using LD slag in combination with granulated blast-furnace slag as a partial Portland cement clinker replacement, has been analysed. In view of the importance of the problem and the variability of chemical and mineralogical composition, it has been suggested studying possible utilization case by case (126). In a blastfurnace slag cement the substitution - at a rate of about 10%- of blastfurnace slag for steel slag, reasonably typical of major Italian industrial production, resulted (126) in the following modifications: slight reduction in the amount of water for blends of standard consistency; slight acceleration of initial set and delay of the final one; decrease of whiteness of the blend; slight lowering in strength progress, acceptable at longer age. Application possibilities and limits of LD slag cement have been investigated with reference to sulphate resistance, too (127). Cements prepared blending 70% ordinary Portland cement and 30% steel slag, showed a relatively short hardening period: about six months, but in part low final strength, higher capillarity pore volume than Portland cement, variable $Ca(OH)_2$ content, low sulphate resistance. The reduced performance might be assigned rather to the arising texture of hydrated phases, than to a chemical incompatibility. The addition of steel slag and granulated blast-furnace slag to Portland cement showed a distinct improvement in sulphate resistance and acceptable final strength values, though longer hardening period. Free lime content of LD slag did not appear to cause unsoundness of blended mortars.

Steel slag containing more than 10% alumina have been obtained by a mixed technique (128) combining the addition of CAMFLUX in the converter and the treatment of the liquid slag in the slag pot by oxygen injection and the addition of bauxite and aluminium scrap. Such a slag, mixed with Portland cement, behaved like the best blast-furnace slag presently used for Portland cement blends.

Ultra-fine wastes, by-products of iron alloys manufacture, have been suggested (129) as concrete constituents. Added in proper ratios, such wastes appear to reduce cement consumption and improve strength and durability of reinforced concrete structures.

3.7. Non ferrous slags

Preliminary investigation on the application of slag produced in the smelting of copper, zinc, lead, nickel and tin, indicate that some solid wastes from metal industry have "pozzolanic" properties (130) and might be useful as partial substitutes for cement and for aggregates in concrete. Lead slag is an industrial by product which does not present large numbers of utilization, giving rise to progressive deterioration of the environment. Encouraging results were reached through an investigation (131) on durability of mortar samples manufactured with 30% ground lead slag to Portland cement. Mechanical tests performed on mortars previously plunged in aggressive solution, gave evidence of a durability higher than that of reference: Spain Standard cements: Portland with high early strength (class type I 45 A) or Portland with high sulphate resistance (class type II-S/Z). Advantages on production expenses due to the low cost of the by-product have been emphasized.

A slag from the Zaire cobalt industry with 40% SiO_2, 39.7% CaO, 9.5% Al_2O3, 6.8% MgO, supplied medium strength binders by addition of lime or ordinary Portland cement clinker in small amount (132). Hydration can be accelerated by addition of sodium sulphate. Applications such as pavement and road are suggested, but long-term durability of cobalt slag cement needs to be assessed.

Granulated phosphorus slag is a by-product in the production of yellow phosphorus, that mainly consists of CaO and SiO_2, with a CaO/SiO_2 ratio between 0.8 and 1.2. Glass content is more than 95%. It also contains less than 5% Al_2O_3 and a certain amount of phosphates. It has been pointed out (133) that phosphorus slag can be activated by cement clinker, cement clinker and Na_2SO_4, water glass and that its hydraulic activity is lower than that of blast-furnace slag at early stage. Maximum dosage is 30%, otherwise setting time becomes too long and the early strength noticeably decreases. Addition of 4% Na_2SO_4 may significantly improve early strength of Portland phosphorus slag cement blends. After 8 months strength has been found higher than that of Portland - blast-furnace slag cement. Hydration products are mainly: dense C-S-H gel with low CaO/SiO_2 ratio. No crystalline compounds were detected. Electrothermophosphorus slags can be used as mineralizer in cement raw mix compositions, too.

3.8. Non ferrous metallurgy by-products

Alumina production wastes have been suggested as active additive to cements. Nepheline slurry (73) is a leaching product of nepheline-limestone cakes and its chemical composition shows an intermediate position between blast-furnace slags and Portland cement clinker. Main chemical components are CaO and SiO_2 (about 85%) with a molar ratio 2:1. Most important phase is β-C_2S, content of which varies from 55 to 85%. Maximum admissible content of slurry in cement appears to be up to 15%, reduction of strength values becoming evident with 30-50% addition. Soluble alkalis in the slurry reduce both strengths and setting time and the particle aggregation suggests a careful choice of the grinding process.

Bauxite caked slurries can be used also as active addition. A special feature is both the high content of iron oxides (red mud) and the large range of dispersion. Main phase components are C_2S, magnetite and perowskite. Soluble alkalis promote degradation of engineering properties of the resultant cement.

3.9. Other by-products

The possible use as a "pozzolan" of a processed sedimentary rock-consisting mainly of a mixture of montmorillonite and siliceous diatom skeletons in the form of amorphous opal, resulting from production of Moler bricks-has been investigated (134), evaluating the requirements for fineness, chemical composition, water soluble alkalis content, pozzolanic activity and prevention of alkali silica reaction. Finely granulated calcined Moler showed to be an excellent "pozzolan" for use in concrete, comparable to a microsilica.

Rice husk is an abudant product in some countries and has reactive characteristics after burning, due to silica content (135). Investigations on the effect of burning temperature on reactivity (136) pointed out that heating rate, burning period and ambient furnace conditions, affect ashes quality. Experiments on pastes at a cement replacement level of 0 up to 20%, revealed that rice husk ashes accelerate strength development and ultimate strength, heat of hydration varying inversely with water/cement ratio and bleeding inversely with ashes content (135). Water retaining effect of ashes and increased quantity of C-S-H gel filling the space previously occupied by free water, appear to be the major parameters influencing strength and physical properties.

A lime reactivity index has been suggested as a reliable parameter for evaluating the amount of reactive silica present in rice husk ashes burnt for a period of 1 to 30 hours between 400 and 900°C (137). Palm bunch wastes, too, have been investigated as addition to Portland clinker (138).

4. ASSESSMENT OF REACTIVITY OF MINERAL ADDITIONS.

Other methods have recently been proposed in addition to the traditional ones. A spectrophotometric method has been suggested (139) for assessing the quality of "pozzolans" for blended cement. Boiling of "pozzolan" samples for 3 min. in 100 ml 0.5 N NaOH dissolves reactive glassy silica and small amounts of other constituents, without dissolving non-pozzolanic matters. A good correlation has been postulated between adsorbance values of "pozzolans" and "pozzolan" reactivity index Ps, in the place of lime-"pozzolan" mortar strength, to characterize the pozzolanic properties of a product, derived by

$$Ps = \frac{\text{lime-pozzolana mortars strength}}{330\ (Kg/cm^2)}$$

where 330 is the limit strength value of the Portland cement at 28 days, according to the Specification of the Bureau of Indian Standards. Increasing and decreasing Ps indicate better and worse pozzolan quality, respectively. The following classification has been obtained:

Tab.III

CLASSIFICATION	POOR	GOOD	EXCELLENT
Absorbance	0.0-0.34	0.34-0.52	>0,52
"Pozzolan" reactivity index	0.0-0.12	0.12-0.18	>0.18

"Pozzolans" of absorbance value < 0.34 or lime-"pozzolan" index 0.12 should not be used for Portland cement manufacture.

An indirect method (140) for determining the pozzolanic activity, suitable for natural products, allowing one to classify the sample in two minutes, is based on the decrease of conductivity of a saturated calcium hydroxide solution, in which 5 g of natural product has been added. Variation in conductivity (mS/cm) less than 0.4 identifies a non pozzolanic matter; between 0.4-1.2 its pozzolanicity is variable; with pozzolanicity > 1.2 behaviour is good. Another conductometric technique based on the determination of the electric conductivity of a solution of 200 mg of pozzolans in HF 0.2 M after 30 min at 25°C, has been proposed (141). The result is related to the amount of active silica and showed good correlation with the strength development of a lime- pozzolan mortar.

It is helpful to remember at this point that cementitious properties of ground granulated blast-furnace slags can be evaluated on mortars by "ASTM C989 Slag Activity tests with Portland cement".

Strength of a 50:50% blend of slag and a reference Portland cement is compared with that of the plain Portland. The test requires adjustment of water addition, to get a mortar flow of 110±5%, so an indication of water requirement of the specific product is also obtained. Slag activity index %=(SP/P)x100, where SP= average compressive strength of slag- reference cement mortar cubes at designated ages (MPa) and P= average compressive strength of reference cement mortar cubes, was found to correlate best with specific surface of the slag (142). A method utilizing both thermal and alkali activation to accelerate strength development of ground slag-sand mortars has been proposed (143) in order to evaluate slag hydraulicity, except cementitious slag is used in place of Portland cement. Rapidity and freeing from the influence of different Portland cements appear to be the advantages of such a method, reputed suitable when ground granulated blast-furnace slag is used as a separate cement to be added at the concrete mixer.

It has been suggested that shape of the particle size distribution of the slag might have an influence on how the strength contribution from the slag will develop with time and such a contribution was found to be highly correlated with the specific surface of the slag, irrespective the way of grinding.

The effects of fly ashes as a substitute for cement are characterized by their activity: the ratio of the compressive strengths of mortars of concretes with fly ashes to that of the control mortars of concrete without fly ashes. Specimens are stored in water at either + 20°C or + 40°C, the last for estimating activity over a larger period (59). Equations covering the combined effect of fly ashes characteristics and ordinary Portland cement composition have been presented (144), capable of a rapid evaluation of activity index at different curing ages.

5. POZZOLANIC REACTION.

Evolution of fly ash-calcium hydroxide reaction by time has been investigated on selected samples from Spanish Power Station, without previous treatment (sieving or grinding) (145). Compositional differences of C-S-H, in comparison with plain Portland cement, concern the lower C/S ratios and the higher amount of alkalis retained (4). X-ray diffraction after the treatment with lime gave evidence of the formation of: calcium aluminate hydrate (C_4AH_{13}) as well as carbonate ($C_4A\overline{C}H_{11}$ and monosulphate $C_3A.C\overline{S}.H_{12}$). Evidence of formation of other hydrated aluminates C_xAH_y and $CA\overline{C}H$ has been achieved, too. The presence of the main peak of calcite hid C-S-H and none of the samples showed traces of ettringite.

As concerns the mechanism of the pozzolanic reaction, two steps have been suggested (146): the first involves the precipitation of $Ca(OH)_2$ at the active sites of fuel ashes particles and the second, the attack of the glassy phase of the particles by the $Ca(OH)_2$ mass formed. It is well known that the reaction of fly ashes in cement only starts significantly after an incubation period, during which ashes behave more or less as an inert material, acting as a precipitation nucleus for $Ca(OH)_2$ and C-S-H gel, originating from the cement hydration. After the initiation of the pozzolanic reaction of fly ashes, the cement paste becomes increasingly denser. A strong dependency of the breaking down of the glass phase on the alkalinity of pore water- which increases strongly only after some days - has been suggested as an explanation of the incubation period (147). The precipitation of reaction products of the cement on fly ash particles prevents moreover the early breaking down of the glass network, so that glass attack is supported only by high pH values of pore water. A lower early strength is therefore to be expected in the case of cements with a lower pH development, as in the case of the blended ones. Cement ratio and temperature affect, of course, pozzolanic reaction.

Pozzolanic reactivity increases by optimization in the fine particle range, both for the enlargement of the potential reaction surface and for the enrichment of chemically reactive constituents (69). Particles shape appears to be a further factor governing water-reducing effect: the more closely the particle shape approximates to an optimum spherical conformation, the more favourable appears the effect on workability. An unfavourable particles shape decreases the improvement of rheological properties due to increased fineness, which however improves the solid

structure of hardening mortars, leading to an increase in the early strength. Strength development and expansion were found to be strongly influenced by deposits present on the surface of pulverized fly ashes, which affects reaction mechanism. Removal of these surface deposits by acid treatment resulted in fact in a considerable reduction in the expansion of high temperature cured pulverized fuel ashes-lime materials and a much earlier commencement of strength development. Expansion has been attributed to ettringite decomposition, rather than to its formation (148).

5.1. Evaluation of the degree of hydration

The reaction between cement and water is measured by means of the determination of the degree of hydration. Loss on ignition is often used for evaluating the hydration progress in Portland cements. Selective dissolving methods are used for determining the degree of hydration of blended cements. The principle of this method is based on the fact that clinker phases, their hydrates and the fraction of reacted addition are largely dissolved, whereas the fraction of unreacted addition remains as a residue. Experimental investigations (149) showed that the selective dissolution method using a pycric acid-methanol-water solution, is suitable to remove reacted cementitious products and leave a residue of unhydrated "pozzolans", such a fly ash and silica fume when mixed with cement, enhabling their quantitative determination at various ages of hydration. An improved procedure - compared to that reported in the 1982 CEN draft, based on the extraction of cement with an alkaline ethylene diamine tetracetic acid solution - is claimed to give much more precise determination of the clinker content, especially in cement containing slag (150). This procedure makes use of a buffered solution containing a fixed volume of diethylamine, in place of a variable volume of sodium hydroxide, adjusted to give a specified starting pH value. The formula:

$$C = [1.1\ (94\text{-}F)\text{-}R\text{-}A\ ]\%$$

where F= insoluble fraction; R= $1.813 \times SO_3$; A= $2.273 \times CO_2$, is claimed to provide a close estimation of the clinker content of composite cements, calculated from single determination of insoluble fraction in diethylamine reagent and SO_3 and CO_2 contents.

The extent to which the dissolving methods are applicable for determining the conversion of granulated blast-furnace slag in hydrated slag cements, has been also investigated (151). Considering that the pycric acid methods appear not to give quantifiable results, because of the partial solubility of alkali aluminosilicate glasses, slag hydration has been quantified by extraction with methanolic salicylic acid and the hydration of Portland cement fraction in the blended cement has been described on the basis of chemically bound water.

Assuming that fly ashes, slags, natural pozzolans etc., both in cements and in concretes, invalidate the analytical determination of Portland cement in a hardened concrete containing one of these additions, because of interferences caused by the presence of soluble silica, a procedure based on two parallel chemical analyses on soluble fractions obtained from the same homogeneized sample of hardened concrete and a design of a graphical procedure have been described for identifying the nature of the mineral addition present in the sample and determining its content (152). IR-spectroscopy has also been suggested for determining the ash content of a blended cement, provided that raw materials are available (153).

5.2. Hydration

The chemistry of hydration of cements forms the subject of specific themes under monogram III-0. So that only a short account will be given here (theme II-A).

5.2.1. Clinker.- The possible interaction in the combined hydration of pure clinker minerals (C_3S, C_3A, C_4AF), synthesized from suitable blends, has been thoroughly investigated (154). The progress of C_3S hydration appears to be only little affected by the simultaneous presence of C_3A and C_4AF, both with and without gypsum. Only large amounts of C_3A accelerate C_3S hydration. The joined presence of C_3S changes very little the progress of C_3A hydration. Only large amounts of C_3S depress early C_3A hydration. Gypsum addition significantly depresses the initial progress of C_3A

hydration. C_4AF hydration is considerably retarded in the presence of C_3S, only in the initial stage. Setting time of C_3S-C_3A pastes becomes shorter with the increase of C_3A, whereas that of C_3A-C_4AF pastes is delayed as C_4AF content increases. The joined presence of gypsum appears to significantly abate setting time variations due to C_3A or C_4AF addition to C_3S. In a semi-logarithmic scale and between 1 and 90 days, pure C_3S exhibits a nearly linear strength development. C_3S replacement by C_3A increases strength at early ages, whereas at long ages and with large C_3A amounts, strength may even decline after having reached a maximum. At any ages C_3S replacement by C_4AF decreases strength, the more as C_4AF increases. Data obtained (154) are summarized in Fig. 6.

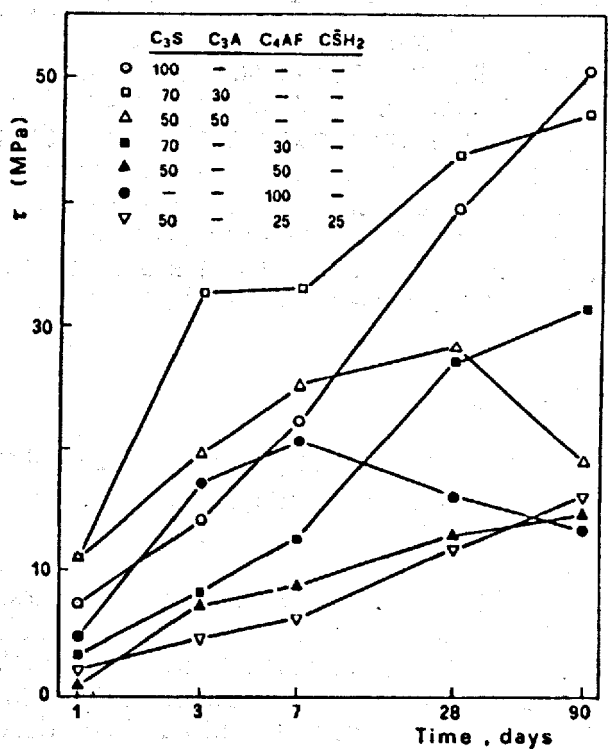

Fig. 6. Compressive strength development of blends of clinker components.

5.2.2. Additions - Strength development and ultimate strength of blended cements depend - besides the clinker quality and fineness - mainly on the inherent hydraulicity and amount of individual additions.

In contrast with silica fume, cement setting is commonly retarded by fly ashes addition. Usually, the retard is higher for high-calcium than for low-calcium fly ashes, though the overall reaction is greater in the first case. However, in both cases, unreacted particles have been picked out in the hydration products, even at later ages, more abudant, of course, when low-calcium fly ashes are used. A good quality fly ash enhances hydration of cement at early ages, thereby contributing to an increase in strength. At early ages the contribution made by the pozzolanic reaction appears to be not significant and becomes apparent only after about 14 days of continuous curing. Enhancement is thought to be due to the presence of sub-micron particles in fuel ash acting as nucleation sites on to which hydrates could form (155). The consequence of this view is that the addition of fine particulate material to a Portland cement could impart an influence on the hydration of cement with which it is blended and would therefore not act just as a simple filler. Such material might be inert or have latent hydraulic properties.

Examination of homogeneous mixtures of five parts by mass Portland cement and one of rutile (titanium dioxide) allowed one to reach the conclusion (156) that such a non-hydraulic filler significantly enhances the hydration of Portland cement, accompanied by an increase in the quantity of bound water and Portlandite. This observation supports the view that at early ages the pozzolanicity of a fine pulverized fuel ash might be attributed, in part, to the enhanced hydration induced by "a particle size effect", owing to the presence of fine particles of filler, which provide additional nucleation sites. The repercussion of the presence of a fine, inert filler on water demand and setting time are, of course, to be considered, too (157).

Blending 5% pulverized fuel ash, slag, kaolinite or illite, were found to have no significant effect on the time of appearance of the main heat evolution peak of ordinary Portland cement. However, calcite additions have been found to accelerate, in some cases, and retard in other case evolution peak (158).

Blending the same Portland cement with fine hydraulic matters, such as fuel ash or blast-furnace slag, respectively, their reactivity has been attributed (159) to the association of two factors: "a particle size effect", because of the larger specific surface than that of the cement and a inherent hydraulicity of the secondary component.

Comparative investigations on calcium hydroxide content of blast-furnace slag cement containing 70% slag and ordinary Portland cement pastes, as a function of hydration length, showed (160) that after 28 days Portland cement contains about 20% lime, whereas blast-furnace slag only about 4%. On the contrary, the depletion of unhydrated slag fraction in blast-furnace slag cement is slower than that of unhydrated clinker fraction in Portland cement. After one year, about 50% slag remains still unhydrated, against about 18% clinker.

The rates of reaction of mineral additions blended with Portland cement tend to be lower than those of Portland cement of the same fineness. The handicap can be abated in the stage of the manufacture of the cement or in that of the curing, to ensure suitability performance, including strength development. However, hydration rate, mechanism and microstructural development of blended cements are a complex process and hydration behaviour of mineral additions requires further consideration.

5.3. Hydration products

A solid water theory (161) conceives the hydraulic hardening of cement as a process by virtue of which very fine silica is permanently bonded together by solidifying water. Cement becomes solid and remains solid owing to a silicification. Part of the liquid water becomes a component of C-S-H phase. Concrete in fact first loses its pore water and then its structural water by evaporation. The force involved in the hardening process can reliably be designated as "hygroscopic suction force". Transition from deformable moist or wet fresh concrete to solid and dry hardened concrete with its lighter colour, can be characterized by a "solid water model".

The blended mineral additions all react with water, or with water and calcium hydroxide, to form as major products calcium silicate hydrates and calcium aluminate hydrates, rather similar to those produced by the reactions of Portland cement with water, though, as would be expected, there is considerably less CH and rates of reaction are not necessarily the same. Hydration process and products both of Portland (162) and of blended cement (4) have been already reviewed with full particulars, emphasizing also the differences in C-S-H chemical composition, concerning not only the lower CaO/SiO_2 ratios, but also the higher alkalis retained in their hydration products.

Advanced facilities allowed one to note (163) that in hardened cement pastes, C/S molar ratio of C-S-H decreased with the increase in blending component and that, amount of replacement being the same, such an effect was the most remarkable for silica fume, very remarkable for fly ashes and remarkable for slag. The mean C/S ratio of C-S-H formed in ordinary, slag (40%), fly ashes (40%) and silica fume (10%) cement pastes, was 1.7, 1.6, 1.2, 1.4, respectively. The amount of aluminium increased in the low C/S C-S-H. Magnesium transferred by the clinker to the pore solution, accumulated at the external rim of C-S-H surrounding unhydrated alite. Magnesium in slag did not migrate, remaining at the same position as in the original slag grains. Iron also hardly migrated into hydration products. Sodium supplied by the clinker was homogeneously distributed in the paste; potassium, particularly in ordinary cement pastes, was condensed in C-S-H surrounding unhydrated alite and hydrated compounds around interstitial phase. Especially in fly ash and silica fume cement pastes, potassium tended to be fixed in low C/S C-S-H, neoformed by pozzolanic reaction.

Investigation on structure pointed out (164) that both an increase in the temperature of formation and the addition of silica fume, increased the degree of silicate polymerization in the C-S-H produced by hydration of alite. The formation of linear chain silicates and the absence of any cross-linking appeared consistent with data collected.

The presence of aluminate-ferrite-monosubstituted (AFm) and related phases such as strätlingite (C_2AH_8) and hydrotalcite (a Mg-equivalent of AFm phase) in slag cement products is known (165). Reactions of natural pozzolans, synthetic glasses, blast furnace slag glasses, zeolite minerals, with saturated lime solution, in suspensions at ordinary temperature, allowed one to point out (166) that in all cases substantial amounts of CaO were removed from the solution. X-ray diffraction analysis showed that C-S-H and one or more hydrated aluminate phases had been formed. In many cases, the C-S-H was more specifically C-S-H (I). Except with the slag glasses, the aluminate phase most often present was strätlingite. In absence of this phase, C_4AH_{13}, $C_4A\bar{C}H_{11}$ or hydrogarnet have been detected, suggesting the hypothesis that high concentrations of SiO_2 and Al_2O_3, arising through the presence of alkalis, favour strätlingite formation, whereas high concetrations of CaO and Al_2O_3, hydrogarnet formation. C_4AH_{13} was formed from glasses high in SiO_2 and low in Al_2O_3.

The excellent performance of the pre-ground counterparts of the natural pozzolans: the zeolitic tuffs, in partial replacement of Portland clinker, is attributable mainly to the destruction of their aluminosilicate framework in the alkaline environment (167). Owing to the peculiar crystalline structure of porous solids, zeolite minerals offer to the attack of alkaline solution a specific surface area wider than that of the bubbly pozzolanic glass, favouring a more rapid formation of similar hydration products. The presence of pores and channels moving across the zeolite minerals, reasonably favours the alkaline attack.

6. POROSITY-STRENGTH RELATIONSHIP.

Strength, permeability, and durability of cementitious materials are strongly influenced by pore structure (168). Porosity appears to be the main factor determining the strength properties of cement pastes (169). Mineral additions may significantly affect pore size distribution and related properties: in particular, permeability. Although the role of pore volume, size distribution and shape has long been recognized, the experimental techniques used for measuring these parameters are still subject of controversy, though measurements can be properly corrected by means of suitable procedures (170). The quantitative evaluation of their influence still presents some uncertanties and as a result phenomena of technological importance, such as strength and durability, are not yet completely understood.

Mercury intrusion investigations allowed one to point out (171) a difference between the pore structure in plain cement paste and that formed in concrete, the latter being more porous and with pores of larger diameters. Pastes that form in mortars showed a pore structure more like that in concrete than in plain paste. In cement pastes total porosity appears to be controlled by the water/solid volume ratio, but the pore size distribution generally diminishes in mature blended materials compared with ordinary Portland cement paste, reducing ionic diffusion rates and permeability (172).

The relation between total porosity, generally expressed as a volume fraction of pores, and strength has been examined by a number of investigators, suggesting a variety of more or less satisfactory equations. Considering that porous structure is strongly influenced by curing temperature, compressive strength has been correlated with pore size distribution using a parameter containing the volume fraction of pores X_V, the mean distribution radius rm and the characteristic strength Rc as a function of curing temperature, incorporated into the expression: (173)

$$x = R_c \frac{(1 - X_V)}{\sqrt{r\ m}}$$

Experimental results on blast-furnace compacts-activated with lime, gypsum or Portland cement showed that compressive strength is related to total porosity by means of an exponential law.

The close relationship between pore structure and strength of cement based composites has been attributed to the fact that both these properties depend decisively on the volume, kind and other parameters of the neo-formed hydration products (174). A connection between the parameters

governing pore structure and the volume, type and binding properties of the hydration products, has been suggested as a feasible way to collect information on the binding capacity of a cement, through the investigation of the structure of the micropores present in the hardened system. The following formula has been suggested (174) between the compression strength of hardened cement pastes and their pore structure:

$$S = K \frac{\sqrt{P_0 - P}}{w/c \cdot P}$$

where Po is the porosity of the system after the mixing with water and P, the porosity occurring after a determined curing period, in the course of the formation of hydration products. $P = Po - \Delta Vhp$ where ΔVhp corresponds to the variation of volume of the solid phase, owing to the formation of hydration products.

Many investigators have reported that in normally - cured cement pastes, the inclusion of slag shifts the pore size distribution from coaser to finer pores. Since the presence of large capillary pores is believed to be responsible for high permeability and low strength of hardened cement paste, such a physical modification seems to play a more important role in improving strength and durability of slag-cement products (53). High levels of slag substitution for Portland cement usually diminish the pore size, thereby increasing the durability, as reflected in chloride diffusion and related properties (75). Experimental results on slag (about 80%) clinker (about 20%) mortars (175), pointed out that the decrease of total porosity with the progress of hydration appears essentially from the reduction of larger pores volume (R>500 Å), whereas the volume of smaller pores (37 - 500 Å) remains partially constant. The diminution of larger pores volume was more important for the slag cement than for the Portland cement mortars. Total porosities being equal, larger pores volume or hydraulic radius of slag cement mortars, was smaller than that of Portland cement mortars. For a given porosity, pores radius increased with the decrease of water cement ratio. The presence of limestone filler (19.6%) in a Portland cement prepared with the same clinker, yielded a change of pore size distribution of the mortars. The amount of smaller pores volume, compared to that of larger ones, increased with age more rapidly than for ordinary Portland cement mortars.

To sum up, effective ways for increasing mechanical strength of cement pastes appear to be still the lowering both of total porosity and of pore size dimensions. Mechanical strength increases with reduction of capillary porosity, which is in turn progressively filled with hydration products and can be lowered by reducing water/cement ratio. Porosity can be also lowered by filling the pores with ultrafine particles. for instance: silica fume, associated with a water - reducing agent.

7. DURABILITY.

Good concrete is one of the most durable of building materials, as we can infer from the contributions given by the major Organizations which have been and are active in the field (176). Durability, stability and mechanical strength of cement paste, mortar or concrete are closely related to each other.

It is well known that durability - in conformity with the environmental conditions - depends on the type of cement used and on the concrete components, but, at the same time, on the water cement ratio and on the compactness of the structures. In recent times, increasing attention has been addressed to durability of concretes (177), as evidencied by the number of specific Symposia appointed (178) and takes a step forward the belief that cement would preferably be characterized primarily on the basis of its effect on the performance of concrete in the actual environmental conditions, and only secondarily on chemical composition, without relaxing, of course, those prescriptive requirements, which lie on the safe side (179). In addition to the type of cement and aggregate, the quality of concrete depends, of course, on the mix design and the workmanship involved in making, placing and curing.

The most common causes of deterioration are associated to porosity and permeability (180) which favour aggressive ions penetration, or to the course of chemical reaction. Permeability controls the physical and chemical process of degradation, caused by the action of water movement, i.e. permeability to aggressive water determines the rate of deterioration (181). Nevertheless it is not incompatible, that ions diffusivity might be influenced also by cement composition. Penetration of ions such as chloride and sulphate includes at the same time chemical reactions and diffusivity (182). Really, using the steady-state (thin disc) technique (183), total and free chloride measurements have indicated that the effective diffusivity of chloride in sulphate resisting Portland cement, was larger than that in ordinary Portland cement, whereas increasing slag content of an ordinary Portland - blast furnace slag-cement, diffusivity progressively decreased. The higher chloride-binding capacity of slag cement resulted in much lower proportions of free chloride in the pore solution. Results of accelerated corrosion monitoring tests showed (184) that a high C_3A content (about 9.5%) has a beneficial effect on reinforcement corrosion resistance performance of concrete structures, attributable to a superior chloride complexing ability of the cement, resulting in the formation of insoluble calcium chloro aluminate compound. However, great caution is to be used when comparing the behaviour of cements of different type, since many and various can be the factors affecting the result. Carbonation resistance, for example, has been sometimes observed to be higher in Portland cement concretes than in those made from blast-furnace or from pozzolanic cements. It is to be borne in mind however that concretes having the same strength and water/cement ratio, do not necessarily carbonate at the same rate. This is true also for another drawback: the cracking. Data collected on blended cement concretes revealed in fact (185) that their long-term durability was at least the equal of ordinary Portland cement concretes under service conditions.

There is general agreement that blended cements are to be preferred with regard to sulphate environments or when alkali-aggregate reactive materials are used, though it has been emphasized (186) that blended cement systems, particularly those with slag, may approach a steady state more slowly than ordinary Portland cement. Completeness of accelerating effect of thermal curing is still questioned. It is generally accepted also that C_3A in a Portland cement is the main components that leads to sulphate attack in a sulphate environment, but although the expansion is usually high when C_3A is high, there is often no simple relationship between C_3A content and expansion. It has been pointed out (187) that if SO_3 content in a cement is considered in conjunction with C_3A content, there is often a better relationship and when C_3A is high and SO_3 is also relatively high, there appears to be less expansion in some cases, but even so there are many instances where this is not true. Moreover, alkali content of a cement should also be kept in mind, when considering correlations between C_3A and SO_3 content and expansion. The latter can be prevented or at least minimized increasing to a certain level both SO_3 and alkali content (187).

With regard to the mechanism, degradation by sulphate attack involves three processes: - diffusion of sulphate ions into matrix, controlled by porosity and permeability (8); - reactions between sulphate ions and certain constituents of hydrated cement, to form expansive compounds; - cracking of matrix leading to strength loss and disintegration.Low - C_3A Portland cements (188) (type II and V ASTM Standard cements) and low water-cement ratios are still recommended precautions in order to minimize sulphate expansion.

Enhancement of Portland cement durability, due to mineral additions, is to be attributed to many factors: - reduction of matrix permeability, owing to pore size refinement produced by pozzolanic reaction and, consequently, decrease of the diffusion rate of aggressive ions; - removal of CH formed during calcium silicates hydration; - unfavourable conditions to ettringite formation; - fine filler effect caused by the physical presence of the addition; - C_3A reduction, owing to the replacement for the addition.

Recommended methods for testing potential sulphate resistance of blended cements are based on evaluation of changes in mechanical strength or expansion of cement pastes or mortars immersed in sulphate solution or submitted to percolation tests. A systematic investigation, in standardized conditions, on the effects of percolation by magnesium sulphate, or magnesium chloride solutions of

the same normality, through cylindrical mortar samples of Portland and blended cements, respectively, normally cured, allowed one to point out (189) that magnesium sulphate exhibits higher aggressiveness than magnesium chloride solution. Percolation by magnesium sulphate solution may cause even the crumbling of the sample. The strong sulphate attack considerably influences mechanical strength. In the severe conditions chosen, Portland, pozzolan and blast-furnace cements, demonstrated to be all liable to sulphate attack, although blended cements, particularly high slag blast-furnace cement, suffered the attack to a slightly lower extent, owing to reduction of pore size, too (190). Strength decrease of mortars ranged between 20-40% according to cement type.

Flexural strength development appears to be closely related to sulphate resistance of blended cement and crack time associated with the capacity of strength development for a same cement type (191). Cement pastes manufactured with Portland cement and 15% wt silica fume, water/cement ratio 0.3, showed (192) that such an addition improves resistance to sodium sulphate, but lowers that to magnesium sulphate. Accelerating tests of Portland and Portland - fly ash cement mortar cubes showed (193) that incorporation of fly ashes decreases the rate of sodium sulphate solution attack, owing to the refinement of pore sizes of the paste and to the formation of AFm, rather than that of AFt phase. The increased chemical resistance of mortar and concrete incorporating more than 50% slag is attributable (181) mainly to the process of pore refinement which is associated with the pozzolanic reactions involving the removal of $Ca(OH)_2$.

Much more complex is the problem of selecting a type of cement suitable for use in volcanic areas (194). A series of blended cements prepared with "pozzolanic" or blast-furnace slag additions, exposed to the action of fumarole exhalations for two years, demonstrated inability to suffer the strong attack of carbon dioxide and hydrogen sulphide, mixed with super-heated steam. Reliable and appropriate procedures to safeguard the structures are to be examined case by case under such severe conditions.

Investigations on the effect of unhydrated clinker reserve fraction on the development of mechanical and chemical resistance of hardened pastes, prepared with ordinary Portland cement, or blast-furnace cement containing 50% granulated slag, allowed one to point out (195) that the optimum value of the hydration ratio of the binder in a paste for Portland and blast-furnace slag cement concretes, in contact with sulphate solutions like groundwaters (pH 5-8) ranges between 0.5-0.6. Approximately the same contribution has been attributed to the hydrated products pertaining to the clinker or to the slag components, suggesting a correction of the granulometric and mineral composition in cements for corrosion-resistant works.

Interest in the use of active additions to control alkali - silica reaction has led to a number of International Conferences and investigations. Identification of alkali-silica products in concrete can be performed staining them with uranyl ions, adsorbed only on the gel - like products and not on cement hydration products (196).

A suitable method for reducing the risk of cracking no doubt is clinker replacement for active additions. Blending agents contain considerable quantities of total alkalis which are initially bound within the glassy matrix and can be released (197) into the pore liquid. It is therefore important to elucidate the balance between their release as the glass reacts with the cement pore liquid and their incorporation into the hydration products (198). Alkalis decrease the Ca/Si ratio of C-S-H gel phase, formed by the pozzolanic reaction, thereby improving its potential uptake for alkali (199). Blast-furnace slag, pulverized fuel ash, natural pozzolans, pre-ground volcanic tuffs, silica fume, respectively, successfully abate expansion, provided that each of these blending agents is properly characterized and added in appropriate amount. Fig.7 shows that the expansion of Portland cement mortars can be minimized by replacement for pozzolanic additions ranging between 20-40%, whereas the same result has been attained with cement containing 60-70% granulated blast-furnace slag (200). Tests have been performed according to ASTM Specification C441-81 and, with reference to curing, according to ASTM C227-81. To minimize alkali - aggregate expansion, therefore, selection of type and amount of addition must be strictly correlated not only with the type of construction and the actual environmental conditions, but also with the influence of each addition on the strength properties

of the resultant cement.It has been hypothesized that a major mechanism of expansion reduction is an increase in the effective SiO_2/Na_2O ratio to values in excess of the pessimum value (201). The greater the deviation of this ratio from the pessimum value, the less appears to be expansion, the effectiveness of the replacements being: precipitated silica > pulverized fuel ash > granulated blast-furnace slag.

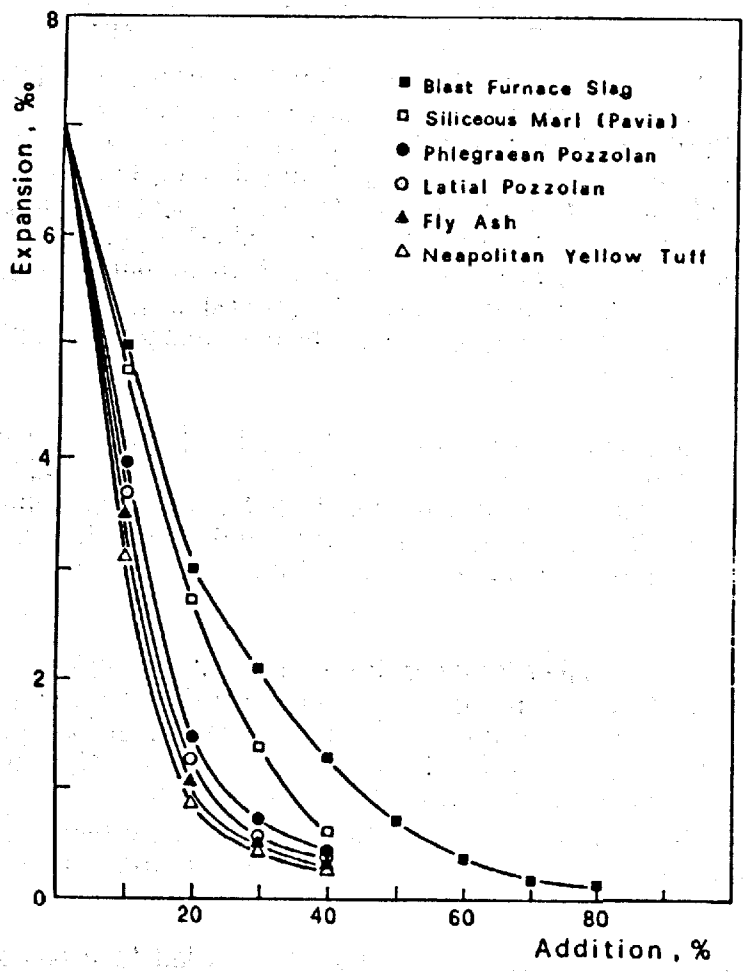

Fig. 7. Alkali-aggregate reaction. Expansion of mortar bars after two years, as a function of type and amount of addition.

It has been observed that pulverized fuel ash and granulated blastfurnace slag, when used as a partial replacement for a high alkali cement, act primarily as alkali diluters, whereas microsilica, owing to its ultra-fine particles, actually promotes the alkali - silica reaction while the mixture is still in a fresh state (202).

It is to be noted that particular interest in preventing alkali - silica reaction is shown, too, by the use of the zeolitized counterparts of the true pozzolans: the pre-ground lithoidal volcanic tuffs, as replacement of Portland clinker. Portland - zeolite - cements (167) minimize, in fact, expansion better than Portland - pozzolan - cements, exhibiting slightly higher compressive strength, too. Moreover, improved results can be reached using volcanic tuffs, previously activated by thermal treatment, at temperatures of incipient collapse of the prevailing zeolitic framework. Fig. 8 and 9.

The excellent performance of zeolitized counterparts of the true pozzolans is likely to be attributable to the higher reactivity of the porous solids. Zeolite minerals in fact offer to the attack of alkaline solution a specific surface area wider than that of the bubbly pozzolanic glass, in this way enhancing the neoformation of hydrated phases. A more rapid and almost exhaustive Si-O-Si bond break, procured by lime solution, is responsible for a likewise more rapid neoformation of abudant, low basic, amorphous hydrated calcium silicate, which enhances strength progress and, at the same time, incorporates remarkable amount of alkalis, otherwise available for fostering the dangerous expansion reaction. The further expansion minimization supplied by the previous activation process of zeolitic tuffs - a thermal treatment rather ineffectual for the unzeolitized counterparts - can be reasonably attributed to: - the formation of free bonds at the surface of the solid after evolution of the bound water from pores and channels of the zeolite minerals; - a sort of mobilization of the chemical constituents of the rock, the framework having collapsed; - a wide specific surface area induced in the neoformed amorphous system by the originary crystalline structure of porous solid (203). In the presence of alkali reactive aggregate, zeolitic additions allow therefore the utilization of clinkers with alkali content highly exceeding the

Na_2O eq. 0.6% limit of ASTM Specification, according to the advances in clinker processing technology.

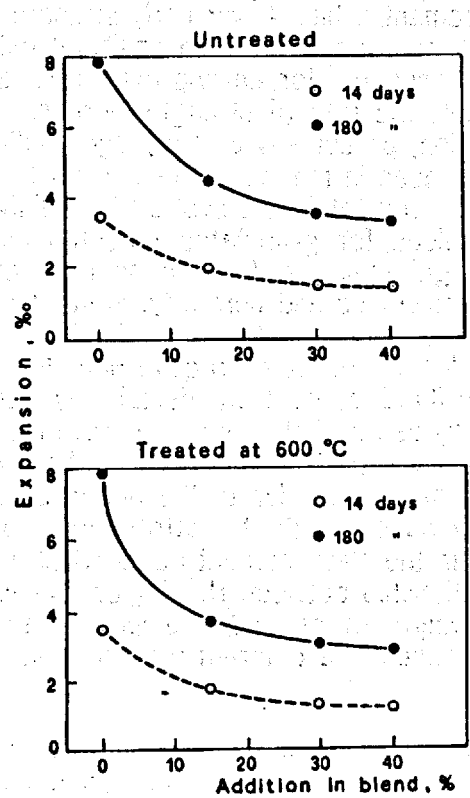

Fig. 8. Alkali-aggregate expansion. Effect of partial replacement of Portland clinker for phlegraean pozzolan, activated or not.

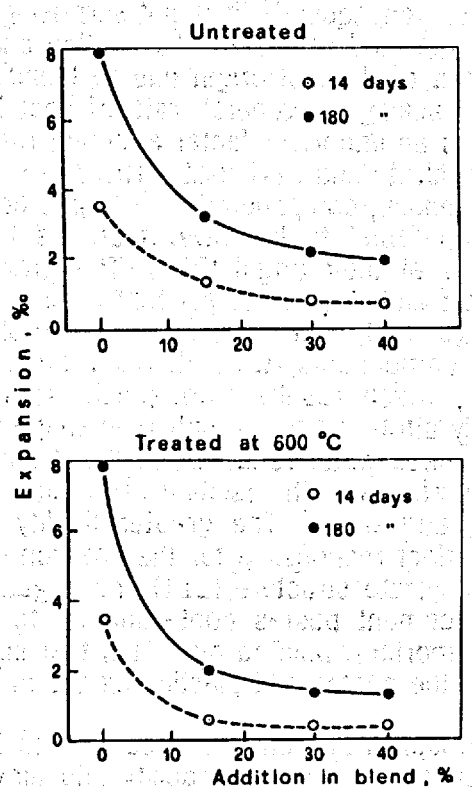

Fig. 9. Alkali-aggregate expansion. Effect of partial replacement of Portland clinker for pre-ground Neapolitan yellow tuff, activated or not.

With reference to the incorporation of alkali hydroxides within a well defined C-S-H phase, it has been suggested (204) that the amount of bound alkali depends upon alkali concentration, composition of C-S-H phase, ionic radius of alkali, additional incorporated cations like Al^{+3} and temperature formation of C-S-H phase. Alkalis are incorporated within the interlayer of the C-S-H phase mostly by neutralizing SiOH-groups. Amount of alkali hydroxide incorporable increases with decreasing CaO/SiO_2 mole ratio.

However, it is recommended to establish effectiveness of mineral additions in preventing damage due to alkali - silica reaction (205) or at least, submit the aggregates to potential reactivity quick chemical test. (206). Alkali - silica reactivity (207) could be detected by suspending a mixture of CaO and the aggregate tested in a saturated KCl solution mantained at 70°C, for 24 hours. The OH^- ion concentration is then compared to that of a control suspension: a mixture of quartz aggregate and CaO. The difference in the OH^- ion concentration is a measure of alkali - silica reactivity of the aggregate. As concerns the possible restoration of the structures injured by alkali-aggregate reaction, their availability to further expansion can be evaluated (208) by measuring, at established dates of expiry, the expansion of concrete samples stored in a saturated chloride solution at 50°C. Reference point is the expansion of companion samples stored in wet sand at the same temperature.

8. SOME EFFECTS OF MINERAL ADDITIONS ON MAIN TECHNICAL PROPERTIES OF CEMENT.

Strength development is somewhat connected with the corrosion rate of particle surface of blending components under the action of lime released during clinker grain hydration, or of the activators. Consequently, it is not surprising that blended cement exhibit lower early strength, longer setting times and rate of heat evolution and require longer curing periods. The ability of mitigating phenomena of thermal origin due to blending components accounts for an improved resistance to thermal cracking. In general, rate of heat liberation parallels the rate of strength increase, though fineness is an important factor affecting rate of heat evolution, particularly at early ages, influencing also placeability and workability. There are, of course, differences in the rate of heat evolution of the various blending components. At all ages heat evolution rates and total heat evolved by the fly ashes have been found to be lower than the corresponding values for granulated blast-furnace slag, regardless of their origin (209). The greater quantity of gel phase and the denser structure of hardened blended cements account for improved chemical resistance and durability. Water-demand of cement generally increases as clinker replacement increases, but by introducing finely- dispersed blending components, water-demand can be reduced. Reduction of water requirement for flow of concrete, which results from partial replacement of Portland cement by certain fly ashes, is commonly attributed to the spherical shape of many of the fly ash particles. An alternative hypothesis (210) ascribes water reduction to the adsorption of very fine ash particles on portion of the cement particle surfaces, with resulting dispersion of the cement particles similar to the action of organic-reducing admixtures. The greater fluidity imparted by fly ashes might be attributed also to a diluition effect responsible for the creation of smaller units in the fresh cement paste which interrupt the agglomerate structure (211). Investigations on the relationship between rheological behaviour of Portland cement pastes containing up to 70% slag by weight of cement and workability of the resultant mortars, pointed out (212) that slag fineness influences in a different way the consistency, stiffening the pastes and plasticizing the mortars.

It is known that effects of cement on freeze-thaw resistance depend on the degree to which its characteristics affect permeability and air-void system of concrete. Blending components tend, in general, to lower frost resistance at early ages. Their influence is however to be investigated case by case. Shrinkage, segregation and bleeding of concrete at a given slump are normally reduced when introducing blending components.

Reinforcement corrosion depends upon detrimental components, especially sulphur compounds. Recently it has been pointed out (213) that the passive layer thickness on reinforcement rises more rapidly in concrete manufactured with blast-furnace slag cements, than in those manufactured with ordinary Portland cements, owing to the way in which the film is originated, favouring an easier passivation. However, selection and proper use of cement types have been fully investigated by ACI Committee 225, 1985 (188).

9. STANDARDS FOR SUPPLEMENTARY CEMENTING MATERIALS.

The Standard Specifications for mineral admixtures in concrete have been thoroughly reviewed (214). First of all it has been pointed out that standards covering the use of natural pozzolans, fly ashes, granulated slag and silica fume are prescriptive, rather than performance-based and that the critical examination of chemical and physical requirements shows that many requirements in the current standards are unnecessary. For quality assurance and uniformity of the product, fineness, ignition loss and activity index appear to qualify for testing and control on a mandatory basis, other requirements depending on the specific material and on the conditions of its use. The development of a single document containing separate specifications for natural pozzolan, fly ashes, granulated blast-furnace slag and silica fume has been closely examined and considered possible, whereas, in addition to chemical and physical requirements, the testing methods appear still to need careful check. The major needs for improvement occur in fact in the physical testing area (215). Moreover, to give an early indication of strength performance, it would be desiderable to adjust an effective fineness test in the micron and sub-micron range.

A critical review of the main standard Specifications concerning the use of fly ashes in concrete, allowed to assess (216) that there is no general agreement about the fly ash parameters to be controlled, except for carbon content and fineness. One of the more complete Standard Specifications appears to be the ASTM C-618. Neverthless, it appears inadequate to control a great number of chemical and physical parameters of fly ashes, without assessing strict relationships with the engineering properties of concrete.

10. CONCLUDING REMARKS.

An effort has been made to summarize the main present-day useful knowledge that share both in the manufacture and performance of a blended cement of good quality and in its proper use. Attention has been paid to the combination of factors required for preparing an optimum clinker, taking into account also the technological and ecological implications. The importance of a full characterization of individual mineral additions is pointed out, in connection not only with their origin and chemical composition, but also with fineness and particles size distribution, emphasizing the belief that strength development and ultimate strength of blended cements, besides clinker quality, fineness and curing (217), mainly depend on the inherent hydraulicity and amount of individual addition. Assessment criteria for estimating reactivity of additions are examined in connection with Specifications for quality assurance and uniformity, pointing out the opportunity of a fair compromise between compositional and performance - based Standards (218).

As concerns technical behaviour, due attention is paid to the most common causes of deterioration, emphasizing the role of the mineral additions on pores structure refinement, too, and consequently on durability of mortars and concretes. Data collected ought to be a useful guide to the proper utilization of blended cements with reference to the characteristics of the works to be realized in a plurality of environmental conditions.

No doubt, blended cements will play a fundamental role in cement industry also in the near future, not only from energy saving angle, but also for inherent properties: first of all durability and for advantages as the industrial wastes utilization, preventing soil and water contamination. New ideas are of course expected, concerning not only the manufacture of high-strength cements, but also that of low-energy consuming multicomponent cements and finely-dispersed multicomponent cements. Activation processes of mineral additions, reactive belite cement, alinite cement (chlorine - substituted C_3S phase in Portland cement) (219), are important fields of further investigation. The suitability of blended cements for the manufacture of: advanced fibre-reinforced cement-based composites, densified systems containing homogeneously arranged ultra-fine particles, macro defect free cements; the role of the additives in setting and hardening of blended cements; the optimization of the utilization of industrial wastes in blended cements manufacture, are all important fields of investigation for the years to come, though not at all exhaustive of the huge area of pure and applied reseach in cement and concrete science and technology.

REFERENCES.

(1) Bucchi R. Outlines on additions and composite cements. Point of view of Industry. 8th Int. Congr. Chem. Cement. 8th I.C.C.C. Principal Report, I, 185 (1986).
(2) Regourd M. Caracteristiques et activation des produits d'addition. 8th I.C. C. C. Principal Report, I, 200 (1986).
(3) Calleja J. Future trends in the research of the structure, properties and behaviour of blended cements. 8th I. C.C.C.Principal Report, I. 233 (1986).
(4) Uchikawa H. Effect of blending components on hydration and structure formations . 8th I.C.C.C.Principal Report, I, 249 (1986).
(5) Aguanell M., Baragano J., Gonzales V., Lopez R., Martinez J.I., Perez J., Puig J., Rezola J.Industrial investigation on energy saving in the blended cements. Silicates Ind., 50, 9-10, 119 (1985).

(6) Massazza F., The role of the additions to cement in the concrete durability. Cemento, 84, 4, 359 (1987).
(7) Springenschmid R., Breitenbücher R. Are low-heat cement the most favourable cement for the prevention of cracks due to heat of hydration? Beton + Fert-Tech. 11, 704 (1986).
(8) Hughes D.C. Sulphate resistance of OPC, OPC/Fly ash and SRPC pastes: pore structure and permeability. Cem. Concr. Res., 15, 6, 1003 (1985).
(9) Newmann K., Blended cements or concrete mixer blends- Which does the concrete producer prefer? Proc. Second CANMET/ACI Int. Conf. Fly Ash, Madrid, Malhotra Ed., 2, SP 91-78, 1589 (1986).
(10) Cement Standards of the World. Cembureau. The European Cement Association (1985) .
(11) Schaefer H. U. Assessment of raw materials for the cement industry. World Cem. 18, 7, 273, 282, (1987) .
(12) Dreizler I., Schaefer H. U. Chemical fraction analyzing for evaluating the heterogeneity of raw meals. Third NCB Int. Seminar Cem. Build. Materials. New Dehli, January (1991).
Petrasinovic-Stojkanovic L., Duric M. Predicting a compressive strength of Portland cement and optimizing its raw mixture composition. Cem. Concr. Res., 20, 3, 484 (1990).
(13) Brüggemann H., Brentrup L. Beziehungen zwishen der Zementfestigkeit und chemisch-mineralogischen parametern des klinkers. Zem-Kalk-Gips, 43, 1, 30 (1990).
(14) Strunge J., Knöfel D. , Dreizler I. Einfluss der Alkalien und des Schwefels auf die Zement-eigenschaften. IV. Zusammenfassende Betrachtungen. Zem-Kalk-Gips, 43, 4, 199 (1990).
(15) Kouznetsova T.V.. Influence des facteurs differents sur la composition de phase et les proprietes du clinker. 8th I.C. C. C. II, 249 (1986).
(16) Kouznetsova T.V., Akimov W. G., Panjuskin W. N. Reaktions fähigkeit der Mineralien von Portland-Zement klinker. Silikattech., 37, 4, 125 (1986).
(17) Kasselouris V., Ftikos C. , Parissakis G. On the hydration of MgO in cement pastes hydrated up to eight years . Cem. Concr. Res., 15, 5, 758 (1985).
(18) Mohan L., Ghosh S.N. Magnesia in cement. Cemento, 85, 1, 43 (1988).
(19) Schierloh U. Auswirkungen der Kalksteinqualität auf den Sinterprozess. Tonind. Zeit., 109, 9, 670, (1985).
- Tsimas S., Tsivilis S., Moutsatsou A. Upgrading of limestone for cement and lime industries. Zem.-Kalk-Gips Int. Ed. B. 43, 12, 601 (1990).
(20) Chatterjee A. K., Page C.H. Industrial application of mineralisers for improved clinker burning. Illustrative case studies. Cem. Res. Inst. India, III, 192 (1984).
(21) Ellerbrock H. G., Sprung S.,Kuhlmann K. Korngrössenverteilung und Eigenschaften von Zement. III. Einflusse des Mahlprozesses. Zem-Kalk-Gips, 43, 1, 13 (1990).
(22) Maki I. Processing conditions of Portland clinker and fine textures of alite. Cemento, 85, 2, 89 (1988).
- Chromy S., Maki I. Influenza della velocità di riscaldamento sulla cinetica di formazione del clinker di Portland. Cemento, 88, 1, 19 (1991).
(23) Scheuer A. Assessment of the mode of operation of clinker coolers and the effect on the clinker properties. Zem-Kalk-Gips, 41, 3, 113 (1988).
(24) Kakali G., Kasselouri V., Parissakis G. Investigation of the effect of Mo, Nb, W , and Zr oxides on the formation of Portland cement clinker. Cem. Concr. Res., 20 , 131, (1990).
(25) Sychev M.M. Verfahren zur Steigerung der Klinker und Zement-Aktivität. Tsement, 7, 14 (1985).
(26) Kurdowski W. Chemistry and mineralogy of cement clinker. In: Cement and Concrete Science and Technology. S.N. Gosh Ed., I, Part. 1, 201-236. ABI Book Pvt. Ltd. New Dehli (1991).
(27) Hassaan M. Y., Eissa N. A. Applications of Mössbauer spectroscopy in cement studies. Bull. Am. Ceram. Soc., 66, 12, 1747 (1987).
(28) Tagnit Hamou A., Sarkar S.L. The influence of varying sulphur content on the microstructure of commercial clinkers and the properties of cement. World Cem. 21, 9, 389 (1990).
(29) Gies A., Knöfel D. Influence of alkalis on the composition of belite - rich cement clinkers and the technological properties of the resulting cement. Cem. Concr. Res., 16, 411 (1986); 17, 2, 317 (1987).
(30) Kurdowski W. Alkalien in Klinkerbildungsverfahren. Cem. Wapno Gips, 4, 74 (1986).

(31) Kreft W. Alkali-und Schwefelverdampfung in Zementöfen in Gegenwart hoher Chloreinmahmen. Zem-Kalk-Gips, 8, 418 (1985).
(32) Seidel G. Kohlequalität, Sinterzonenzustand Betriebsergebnisse bei Zementdrehöfen. Zem-Kalk-Gips, 38, 6, 289 (1985).
(33) Locher F.W. Entwicklung des Umweltschutzes in der Zementindustrie. Zem-Kalk-Gips, 42, 3, 120 (1989).
- Best available technologies not entailing excessive costs (BAT) for the production of cement. Ciments, Betons, Platres, Chaux, 788, 1, 29 (1991).
(34) Rosemann H. Einfluss der Brennstoffart und des Einsatzorts auf Energieverbrauch, Betriebsverhalten und Emission von Drehofenanlagen. Zem-Kalk-Gips, 41, 5, 231 (1988).
(35) Scheuer A. Nichtkatalytische Reduction des NO mit NH3 beim Zement-brennen. Zem-Kalk-Gips, 43, 1, 1, (1990).
(36) Kreft W. Ökologische Gesichtspunkte zur Zementherstellung - Umweltorientierte Technologieanwendung als Beitrag zum Klimatschutz. Zem.-Kalk-Gips, 43, 3, 153 (1990).
(37) Sprung S. Spurenelemente - Anreicherung und Minderungsmassnah-men. Zem-Kalk-Gips, 41, 5, 251 (1988).
- Kuhlmann K., Kirchartz B., Rechenberg W., Bachmann G. Probenahme von Spurenbestandteilen in Rein-gas von Zementdrehrohrofen. Zem-Kalk-Gips Int. 44, 5, 209 (1991).
(38) Gu Z.Z., Zhou B.W., Yue M.L., Tang T.F., Wang W.J. Effect of cement composition on the strength contribution of fly ash. 8th I.C.C.C., IV, 150 (1986).
(39) Frigione G., Sersale R., The influence of the chemical composition of the clinker on the strength properties of blast-furnace slag cement. Cem. Concr. Res., 15, 159 (1985).
(40) Baragano Coronas J.R. Cementos con adiciones activas. Cemento Hormigon, 652, 181 (1988).
(41) Gustaw K., Roszczynialski W., Liburna J. Die bestimmung des richtigen Gipszusatzes für Zemente mit verschiedenem C3A-Gehalt, auf Grundlage einer Studie der jeweiligen Hydrationverlaufe. Cement Wapno Gips, 6, 139 (1986).
(42) Tang F.J., Gartner E.M. Influence of sulphate source on Portland cement hydration. Advances Cement Res., 1, 2, 67 (1988).
(43) Sersale R., Frigione G. Portland and blast-furnace slag cements: a comparative investigation. Proc. Second Beijing Int. Symp. Cem. Concr. 4, 280 (1989).
(44) Frigione G., Sersale R., Gypsum content and strength development, as a fucntion of curing temperature, in Portland and blast-furnace slag cement mortars. Materials Eng. 1, 3, 855 (1990).
(45) Sersale R., Cioffi R., Frigione G., Zenone F. Relationship between gypsum content, porosity and strength in cement. I. Effect of SO3 content on the physical microstructure of Portland cement mortars. Cem. Concr. Res., 21, 120 (1991).
- Sersale R., Cioffi R., Frigione G., Zenone F. SO3 content of Portland and blended cements. Porosity and behaviour of the resultant mortars. Proc. of this Int. Congress.
(46) Babatschev G.N. Portlandzement ohne Gips. Baustoffindustrie, 33, 2, 41 (1990).
(47) Soroka I. Effect of phosphogypsum on properties of Portland cement. Am. Ceram. Soc. Bull., 1502 (1984).
(48) Olmez H., Erdem E. The effect of phosphogypsum on the setting and mechanical properties of Portland cement and trass cement. Cem. Concr. Res., 19, 3, 377 (1989).
(49) Goldshtein L.Y.A. Cement production from industrial by products. (Wastes). Utilization, 2, Stroiizdat, Leningrad (1985).
(50) Montanaro L., Negro A., Regourd M. Action de CaCO3, CaSO4 et CaSO4.2H2O sur l'hydratation de C3S. Cem. Concr. Res., 18, 3, 431 (1988).
(51) Campitelli V.C., Florindo Maria C. The influence of limestone additions on optimum sulphur trioxide content in Portland cement. Carbonate additions to cement. Klieger/Hooton Eds. ASTM STP 1064, 30. Philadelphia (1988).
(52) RILEM Final Report on Siliceous by- products for use in concrete. Matèr. Constr. 21, 121, 69 (1988).
(53) Mehta P.K. Pozzolanic and cementitious by- products in concrete. Another look. ACI SP- 114-1, 1, (1989).
(54) Philleo R.E. Slag or other supplementary materials? ACI SP 114-58, 1197 (1989).
(55) Diamond S. Particle morphologies in fly ash. Cem. Concr. Res., 16, 4, 569 (1986).

(56) Valenti G.L.,Cioffi R., Sersale R., Chemical and physical properties of fly ashes and influence on the mechanical performance of the resultant cement mortars. Cemento, 83, 4, 565, (1986).
- Valenti G.L., Cioffi R., Sersale R., Production and utilization of fly ash in Italy. ACI-SP 91-35, 741 (1986).
(57) Bernshausen H. Pfa in blended cement-its production and application. World Cem., June, 250 (1988).
- Slanicka S. The influence of fly ash fineness on the strength of concrete. Cem. Concr. Res., 21, 2-3, 285 (1991).
(58) Mehta P. K. Influence of fly ash characteristics on the strength of Porland- fly ash mixtures. Cem. Concr. Res., 15, 4, 669 (1985).
(59) RILEM Draft Recommendations. Use of fly ash in building. Test methods for determining the properties of fly ash and fly ash for use in building materials. Materials Structures, 22, 299 (1989).
(60) Chinchon J. S., Lopez Soler A., Rovira J., Yague A., Vazquez E. Dètermination de la phase vitreuse dans les cendres volantes par diffraction X. Bull. Liaison Lab. Ponts et Ch., 147, 37 (1987).
(61) Van Roode M., Douglas E., Hemmings R.T. X ray diffraction measurement of glass content in fly ash and slag. Cem. Concr. Res., 17, 2, 183 (1987).
(62) Giergiczny Z., Werynska A. Influence of fineness of fly ashes on their hydraulic activity. ACI SP114-4, 97 (1989).
(63) Matkovic B., Grzèta B., Paljevic M., Rogic V., Dasovic D., Dimic D. Hydrated fly ash with SiO2 fume and/or Portland cement addition. Reactions in pastes and strength development in mortars. Cem. Concr. Res., 20, 3, 475 (1990).
(64) Materials Research Society Symposium Proc. Vol.113. Fly ash and coal conversion by-products: Characterization, Utilization and Disposal IV. Mc. Carthy, Glasser, Roy, Hemmings Eds. (1988).
(65) Mc. Carthy G. X-ray powder diffraction for studying the minaralogy of fly ash. Proc. Mat. Res. Soc. Symposium Boston, 75 (1988).
(66) Kilgour C. L., Diamond S. The internal structure of low-calcium fly ash. Proc. Mat. Res. Soc. Symp. Boston, 65 (1988).
(67) Lu S., Ludwig U. Zur Bewertung der Eigenschaften von Steinkohlen flugaschen.Zem- Kalk- Gips, 42, 7 (1989).
- Carles- Gibergues A., Vaquier A. Influence du broyage sur la réactivité d'une cendre volante. Cim. Béton. Rev. Mat. Constr. 1, 752, 46 (1985).
(68) Frias M., Luxan M.P., Sanchez de Rojas M.I., Garcia N. Granulometric analysis of fly ashes by laser diffraction. Adv. Cem. Res., 3, 10, 47 (1990).
(69) Schiessl P., Härdtl. R. The change of mortar properties as result of fly ash processing. Third CANMET/ACI Int. Conf. Supplementary papers, 277 (1989).
(70) Ferrari F., Frigione G. Utilizzazioni delle ceneri volanti in cementeria. Preventivo frazionamento granulometrico. ENEL. Rassegna Tecnica Problemi Energia Elettrica, 8, 4, 2 (1988).
(71) Chinchon J.S., Lopez-Soler A, Sanchez Reyes A., Ginjaume M., Varquez E., Yague A. Quantification of fly ash in cements and mortars by means of gamma spectrometry. Cem. Concr. Res., 19, 2, 173 (1989).
(72) Douglas E., Zerbino R., Characterization of granulated and pelletized blast- furnace slag. Cem. Concr. Res, 16, 5, 622 (1986).
(73) Goldshtein L.Y.A. Cement production from industrial by-products. Utilization. 1. Stroiizdat, Leningrad. Skoe Otdelenie (1985).
(74) Wu X.,Jiang W., Roy D.M. Early activation and properties of slag cement. Cem. Concr. Res., 20, 6, 961 (1990).
(75) Roy D.M. Hydration, microstructure and chloride diffusion of slag- cement pastes and mortars. ACI SP 114-61, 1265 (1989).
(76) Runzhang Y., Qiong Gao., Shixi O. Study on structure and latent hydraulic activity of slag and its activation mechanism. Silicates Ind., 53, 3-4, 55 (1988).
(77) Douglas E., Brandstetr J. A preliminary study on the alkali activation of ground granulated blast-furnace slag. Cem. Concr. Res., 20, 5, 746 (1990).
(78) Teoreanu I. The interaction mechanism of blast- furnace slag with water. The role of activating agents. Cemento, 88, 2, 91 (1991).
(79) Dutta D.K., Borthakur P.C. Activation of low- lime high alumina granulated blast- furnace slag by anhydrite. Cem. Concr. Res., 20, 5, 711 (1990).

(80) EL- Hemaly S.A.S., Galal A.F., Mosalamy F.H., EL- Didamony H. Activation of granulated blast-furnace slag by waste sulphate ash. Silicates Ind. 52, 1-2, 9 (1987).
(81) Tashiro C., Yoshimoto T. Effect of sodium compounds on the strength and microstructure development on blast- furnace slag cement mortars. ACI SP 114-63, 1307 (1989).
(82) Blunk G., Brand J., Kollo H., Ludwig U., Zum Einfluss der Korngrossenverteilung von Huttensand und Klinker auf die Eigenschaften von Hochofenzementen. Zem- Kalk- Gips, 41, 12, 616 (1988).
(83) Opoczky L., Verdes S. Eine Mahltechnologie für die Herstellung hochfester Zemente mit hohem Schlackengehalt. Epitoanyag, 38, 8, 225 (1986).
(84) Numata S., Koide Y., Shimobayashi S. Properties of ultra- highy pulverized granulated blast-furnace slag- Portland cement blends. ACI SP 91- 66, 1341 (1986).
(85) Harada H., Shizawa M., Kotani H. Influence of super fine granulated blast-furnace slag and limestone on the properties of Portland blast-furnace slag cement. Rev. 40th General Meeting Cement Assoc. Japan, 67 (1986).
(86) Malolepszy J., Deja J. The influence of curing conditions on the mechanical properties of alkali activated slag binders. Silicates Ind., 53, 11-12, 179 (1988).
(87) Friede H., Blast-furnace trass cement - starting material for concrete with special properties. Betonwerk+Fert-Tech., 6, 385 (1986).
(88) Bradley-Williams T.S. The production of microsilica. Concrete, 20, 8, 17 (1986).
- FIP. Condensed silica fume in concrete. State of art. Thomas Telford Ed., (1988).
(89) Tixier R., Carles-Gibergues A., Grandet J. Influence de l'adjonction d'une fumée de silice condensée riche en carbone sur le comportment mécanique du liant cendres volantes-chaux. Annales Inst. Tech. Bat. Trav. Pub., 476, 118 (1989). Materiaux 71.
(90) Schulz G., Drost H., Mach R., Klotz H.D. Suhrke K.D. Erzeugung feindispersen SiO2-pulvers mit hilfe eines Kapazitivgekoppelten HF-Plasmas. Silikattechnik, 40, 6, 199 (1989).
(91) Hjorth J., Skibsted J., Jakobsen H.J. 29Si MASNMR studies of Portland cement components and effects of microsilica on the hydration reaction. Cem. Concr. Res., 18, 5, 789 (1988).
(92) Larbi J.A., Fraay L.A., Bijen J.M.J.M. The chemistry of pore fluid silica fume-blended cement systems. Cem. Concr. Res., 20, 4, 506 (1990).
(93) Larbi J.A., Bijen J.M.J.M. Orientation of calcium hydroxide at the Portland cement paste-aggregate interface in mortars in the presence of silica fume: a contribution. Cem. Concr. Res., 20, 3, 461 (1990).
(94) Saito M., Kawamura M. Effect of fly ash and slag on the interfacial zone between cement and aggregate. ACI SP 114-32, 669 (1989).
(95) Monteiro P.J.M., Gjorv O.E., Mehta P.K. Effect of condensed silica fume on the steel cement paste transition zone. Cem. Concr. Res., 19, 1, 114 (1989).
(96) Feldman R.F., Cheng-yi H. Properties of Portland cement-silica fume pastes. I. Porosity and surface properties. Cem. Concr. Res., 15, 5, 765 (1985).
(97) Buil M., Delage P. Some further evidence on a specific effect of silica fume on the pore structure of Portland cement mortars. Cem. Concr. Res., 17, 1, 65 (1987).
(98) Feldman R.F. , Cheng-yi H. Properties of Portland cement-silica fume pastes. II. Mechanical properties. Cem. Concr. Res., 15, 6, 1943 (1985).
(99) Banthia N., Mindess S. Water permeability of cement paste. Cem. Concr. Res., 19, 5, 727 (1989).
(100) Tkalcec E., Zelic J. Der Einfluss amorpher Kieselsäure-Kiesielsäurerauch auf die Eigenschaften von Portlandzementmortel. Zem.-Kalk-Gips, 40, 11, 574 (1987).
(101) Giergiczny Z. Influence of silica fume on properties of fly ash cements. Proc. 2nd Int. Symp. Cem. Concr. Beijing, 4, 24, 8 (1989).
(102) Radjy F.F., Bogen T., Sellevold E.J. Loeland K.E. "A review of experiences with condensed silica fume slag and natural pozzolans in concrete. ACI SP-91, 1135 (1986).
(103) Carles-Gibergues A., Ollivier J.P., Hanna B. Ultrafine admixtures in high strength pastes and mortars. ACI SP-114-53, 1101 (1989).
(104) Sersale R. Lime: the first in time among the justly named binding materials. Atti Acc. Pontaniana, 40, 257 (1991).
- Malinowski R., Garfinkel Y. Prehistory of concrete. Concrete Int., 62 March (1991).
(105) Downey P., Dratva T. 30 years experience with natural pozzolans in Chile. Proc. Third CANMET/ACI Int. Conf. Supplementary Papers, 795 (1989).

(106) Sersale R. Genesi e costituzione del tufo giallo napoletano. Rend. Acc. Sc. Fis. e Mat., Napoli, 4, 25 (1958).
(107) Sersale R. Ricerche sulla zeolitizzazione dei vetri vulcanici per trattamento idrotermale. 1a Herschelite da vetro ricavato attraverso fusione di roccia sanidica. Rend. Acc. Sci. Fis. Mat., Napoli, 4, 26 (1959).
(108) Sersale R., Analogie costituzionali fra il "trass" renano ed il tufo giallo napoletano. Ind. Ital. Cemento, 24, 5 (1959).
(109) Sersale R. Occurrence and uses of zeolites in Italy. In: Natural Zeolite. Occurrence, properties, use. Sand, Mumpton Eds. Pergamon Press, N.Y., 285 (1978).
(110) Sersale R., Frigione G. Natural zeolites as constituents of blended cements. Chimica Industria, 67, 4, 177 (1985).
(111) R. Sersale. Sull'attività "pozzolanica" delle zeoliti. Nota I. Reattività dell'herschelite con soluzione di idrossido di calcio. Rend. Acc. Sc. Fis. e Mat., Napoli, 4, 27 (1960).
(112) Sersale R. Le zeoliti naturali quali sostituti delle pozzolane nella produzione dei cementi pozzolanici. Atti Acc. Pontaniana, 36, 243 (1988).
(113) Davidovits J. Ancient and modern concretes: What is the real difference? Concrete Int., 23, Dec. (1987).
(114) Davidovits J., Comrie D.C., Paterson J.H., Ritcey D.J. Geopolymeric concretes for environmental protection. Concrete Int., 30, July (1990).
(115) Vo Dinh Luong, Henning O. Einfachherzustellende puzzolanische Bindebaustoffel. Wiss. Z. Hochsch. Archit. Bauwes. 33, 3, 170 (1987).
(116) Mayfield L.L. Limestone additions to Portland cement. An old controversy revisited. Carbonate Additions to Cement. Klieger/Hooton Eds. ASTM STP 1064, 3, Philadelphia (1990).
(117) Bedard C., Bergeron M. The effect of steam curing on high-early strength Portland cement containing carbonate addition. Carbonate Additions to Cement. Klieger/Hooton Eds., STP 1064, 51, Philadelphia (1990).
(118) Ingram K., Poslusny M., Daugherty K., Rowe W. Carboaluminate reactions as influenced by limestone additions. Carbonate Additions to Cement. Klieger/Hooton Eds. ASTM STP 1064, 14. Philadelphia (1990).
(119) Neto C.S., Campitelli V.C. The influence of limestone additions on the rheological properties and water retention value of Portland cement slurries. Carbonate Additions to Cement. Klieger/Hooton Eds., ASTM STP 1064, 24. Philadelphia (1990).
(120) Adams L.D., Race R.M. Effect of limestone additions upon drying shrinkage of Portland cement mortars. Carbonate Additions to Cement. Klieger/Hooton Eds., ASTM STP 1064, 41. Philadelphia (1990).
(121) Klemm W.A., Adams L.D. An investigation of the formation of carboaluminates. Carbonate Additions to Cement. Klieger/Hooton Eds., ASTM STP 1064, 60, Philadelphia (1990).
(122) Hooton R.D. Effects of carbonate additions on heat of hydration and sulphate resistance of Portland cement. Carbonate Additions to Cement. Klieger/Hooton Eds., ASTM STP 1064, 73. Philadelphia (1990).
(123) Sprung S., Siebel E. Beurteilung der Eignung von Kalkstein zur Herstellung von Portland Kalksteinzement (PKZ). Zem-Kalk-Gips Int., 44, 1, 1 (1991).
(124) Zhu G., Sun S., Wu G., Hu J. Quality of steelmaking slag and assessing method for its cementing property. Proc. 2nd Int. Symposium on Cement and Concrete. Beijing, 2, 295 (1989).
(125) Duda A. Hydraulic reactions of LD steelwork slag. Cem. Concr. Res., 19, 5, 793 (1989).
(126) Sersale R., Amicarelli V., Frigione G., Ubbriaco P. Characterization and potential uses of a steel slag. Silicates Ind., 51, 11-12, 163 (1986).
(127) Duda A. Aspects of sulphate resistance of steel slag cement. Cem. Concr. Res., 17, 3, 373 (1987).
(128) Hamman M., Pazdej R., Sorrentino F.P., George M., Verschaeve M. Etude du traitment du laitier d'acierie à l'oxygene en vue de son utilization en cimenterie. Commission des Communautés Européennes. Rapport Final. Luxembourg (1985).
(129) Bartakov V.G., Kaprieov S.S., Ivanov F.M., Sheinfeld A.V. Evaluation of ultra-fine wastes from metallurgical processes as additives in concrete. Soviet Journ. Concr. reinf. concr. 5, 1, 82 (1991).
(130) Douglas E., Mainwaring P.R. Hydration and pozzolanic actvity of non ferrous slag. Amer. Ceram .Bull., 64, 5, 700 (1985).

(131) Roxan Arroyo P. Durabilité d'un ciment avec addition d'un laitier de plomb. Proc. Second CANMET/ACI Int. Conf. Durability Concr. Montreal. Supplementary Papers, 125 (1991).
- Roxan Arroyo P. Estudio de las propriedades de la escoria de plomo para su empleo como aditivo en cementos. Cemento-Hormigon 62, 689, 17 (1990).
(132) Moukwa M. Cobalt furnace slag: a latent hydraulic binder. Cem. Concr. Res., 20, 2, 253 (1990).
(133) Caijum S., Xiuren T., Yinyu L. Studies on the activation of phosphorus slag. Third CANMET/ACI Int. Conf. Supplementary Papers, 656 (1989).
(134) Johansson S., Andersen P.J. Pozzolanic activity of calcined Moler clay. Cem. Concr. Res., 20, 3, 447 (1990).
(135) Hwang C.L., Wu D.S. Properties of cement paste containing rice husk. ACI SP 114-35, 733 (1989).
(136) Kapur P.C. Production of reactive bio-silica from the combustion of rice husk in a tube-in basket burner. Powder Techn. 44, 1, 63 (1985)
(137) James J., Subba Rao M. Reactivity of rice husk. Cem. Concr. Res., 16, 3, 296 (1986).
- James J., Subba Rao M. Characterization of silica in rice husk ash. Amer. Ceram. Soc. Bull., 85, 8, 1177 (1986).
- James J., Subba Rao.M. Hydration of rice husk ash-lime pastes. Cemento, 84, 4, 383 (1987).
- James J., Subba Rao.M. Optimization of ash-lime ratio for rice husk ash-lime cement. Cemento, 85, 2, 101 (1988).
(138) Adepegba D. Pozzolanic activity of palm bunch wastes. Mat. Constr., 22, 129, 220 (1989).
(139) Surawa M.S., Joshi S.N. Estimating reactivity of pozzolanic materials by a spectrophometric method. Adv. Cem. Res., 3, 10, 81 (1990).
(140) Luxan M.P., Madruga F., Saavedra J. Rapid evaluation of pozzolanic activity of natural products by conductivity measurement. Cem. Concr. Res., 19, 1, 63 (1988).
(141) Surana M.S., Joshi S.N. Conductometric technique for estimating the activity of pozzolanic materials.Indian Concr. Journ., 64, 2, 89 (1990).
(142) Osbaek B. Ground granulated blast- furnace slag grinding methods, particle size distribution and properties. ACI SP 114- 60, 1239 (1989).
(143) Hogan F.J., Rose J.H. ASTM Specification for ground iron blast-furnace slag: its development, use and future. ACI SP 91-76, 2, 1551 (1986).
(144) Zhangzhao G., Baowei Z., Meilong Y., Changfu T., Weijun W. The pozzolanic activity index of fly ash. Proc. 2nd Int. Symp. Cem. Concr. Beijing, 4, 224 (1989).
(145) Luxan M.P., Sanchez M.I., Frias M. Investigation on the fly ash-calcium hydroxide reactions. Cem. Concr. Res., 19, 1, 69 (1989).
(146) Tenoutasse N., Marion A.M. Characterization of Belgian fly ashes and their behaviour in cement paste. ACI SP 91-2, 1, 51 (1986).
(147) Fraay A.L.A., Bijen J.M., de Haan Y.M. The reaction of fly ash in concrete. A critical examination. Cem. Concr. Res., 19, 2, 235 (1989).
(148) Wild S., Hadi M., Leng Ward G. Expansion mechanisms and cementation in cured PFA - lime composites. Part. I. Development of mechanical strength and expansion. Part. II. Microstructural development, cementation and reaction mechanisms. Adv. Cem. Res., 3, 10, 55, 63 (1990).
(149) Li S., Roy D.M., Kumar A. Quantitative determination of pozzolanas in hydrated systems of cement or Ca(OH)2 with fly ash or silica fume. Cem. Concr. Res., 15, 6, 1079 (1985).
(150) Erntroy H.C. Bestimmung des Klinkeranteils in Mischzementen. Zem-Kalk-Gips, 40, 5, 270 (1987).
- European Committee for Standardization. Methods for testing cement. Quantitative determination of constituents. pr EN 196-4, Brussels, (1982).
(151) Stark J., Ludwig H.M., Müller A. Zur Bestimmung des Hydratationsgrades von Schlackenzementen. Zem. Kalk Gips, 43, 11, 557 (1990).
(152) Gomà F. The chemical analysis of hardened concrete containing fly ashes, slags, natural pozzolans, etc.Proc. Third CANMET/ACI Int. Conf. Supplementary Papers 828 (1989).
(153) Myohl P. Bestimmung des Aschegehalts in Zumahlstoffzement mit Hilf der Infrarot-Spektroscopie. Silikat Techn., 37, 9, 307(1986).
(154) Locher D., Older I. Interaction phenomena in the combined hydration of clinker minerals. Cemento, 86, 1, 25 (1989).

(155) Dalziel J.A., Gutteridge W.A. Techn. Report 560. Cem. Concr. Associat., Slough (1986).
(156) Gutteridge W.A., Dalziel J.A. Filler cement: the effect of the secondary component on the hydration of Portland cement. Part I. A fine non-hydraulic filler. Cem. Concr. Res., 20, 5, 778 (1990).
(157) Ramachandran V.S., Zhang-chun-mei. Influence of CaCO3 on hydration and microstructural characteristcs of tricalcium silicate. Cemento, 84, 1, 75 (1987).
- Chatterji S. Discussion on Ramachandran and Zhang-chun-mei paper.
(158) Barker A.P. Conduction calorimetric studies of cement containing 5% additions. Cem. Concr. Res., 20, 2, 219 (1990).
(159) Gutteridge W.A., Dalziel J.A. Filler cement: the effect of the secondary component of the hydration of Portland cement. Part. II. Fine hydraulic binders. Cem. Concr. Res., 20, 6, 853 (1990).
(160) Frigione G., Nastro A. Effect of triethanolamine on properties and hydration of blast-furnace slag cement. Cemento, 81, 2, 53 (1984).
(161) Keil F. Vereinfachte Deutung der hydraulischen Erhärtung von Zement. Die Festwasser-Theorie. Zem-Kalk-Gips, 38, 8, 451 (1985).
(162) Taylor H.F.W. Chemistry of cement hydration. 8th I.C.C.C. Principal Report I, 82 (1986).
- Mehta P.K. Hardened cement paste. Microstructure and its relationship to properties. 8th I.C.C.C. Principal Report, I, 113 (1986).
- Diamond S., The microstructure of cement paste in concrete. 8th I.C.C.C. Principal Report. I, 122 (1986).
(163) Uchikawa H., Uchida S., Hanehara S. Element distribution on the polished surface of hardened cement pastes estimated by EPMA ultra high speed wide area multianalyser. Cemento, 84, 2, 117 (1987).
(164) Young J.F. Investigations of calcium silicate hydrate structure using silicon-29 nuclear magnetic resonance spectroscopy. Journ. Am. Ceram. Soc., 71, 3, C-118 (1988).
(165) Roy D.M., Sonnenthal E., Prave R. Hydrotalcite observed in mortars exposed to sulphate solution. Cem. Concr. Res., 15, 914 (1985).
- Barker A.P. An electron optical examination of zoning in blast-furnace slag hydrates. Part. I. Slag cement pastes at early age. Adv. Cem. Res., 2, 8, 171 (1989).
(166) Sersale R., Giordano Orsini P. Hydrated phases after reaction of lime with "pozzolanic" materials or with blast-furnace slags. Proc. 5th I.S.C.C., 4, Tokyo, 114 (1969).
(167) Sersale R., Frigione G. Portland-zeolite-cement for minimizing alkali-aggregate expansion. Cem. Concr. Res., 17, 40 (1987).
(168) Schiessl P. Durability of concrete structures. Cem. Hormig, 58, 642, 472 (1987).
(169) Rössler M., Odler I. Investigations on the relationship between porosity, structure and strength of hydrated Portland cement pastes. I. Effect of porosity. Cem. Concr. Res., 15, 2, 320 (1985).
(170) Uchikawa H., Uchida S., Hanehara S. Measuring method of pore structure in hardened cement paste, mortar and concrete. Cemento, 88, 2, 67 (1991).
(171) Winslow D., Liu D. The pore structure of paste in concrete. Cem. Concr. Res., 20, 2, 227 (1990).
(172) Kumar A., Komarneni S., Roy D.M. Diffusion of Cs+ and Cl- through sealing materials. Cem. Concr. Res., 17, 1, 153 (1987).
(173) Atzeni C., Massidda L., Sanna U. Porosity-strength relations in blast-furnace slag compacts. Silicates Ind., 53, 7-8, 117 (1988).
(174) Jambor J. Pore structure and strength development of cement composites. Cem. Concr. Res., 20, 948 (1990).
(175) Shi-Ping J., Grandet J. Evolution comparée des porosités des mortiers de ciment au laitier et des mortiers de ciment Portland. Cem. Concr. Res., 19, 3, 487 (1989).
(176) Wright J.R. Frohnsdorff G. Durability of building materials: durability research in the United States and the influence of RILEM on durability research. Mat. Constr., 18, 105, 705 (1985).
(177) Volzhenskii A.V. Effect of fineness of cement and water/cement ratio on the durability of hardened cement and concrete. Soviet Journ. Concr. Reinf. Concr. 5, 1, 7 (1991).
(178) Malhotra V. Ed. CANMET/ACI. Durability of concrete. Second Int. Conf. Montreal (1991).
(179) Wischers G. Performance as a criterion for the standardization of cement and concrete. Betonwerk+Fert.-Tech, 3, 51 (1990).
(180) Negro A., Montanaro L. Sulla durabilità del calcestruzzo. Cemento, 86, 1, 11 (1989).

(181) Douglas E. Blast-furnace slag cement mortar and concrete: durability aspects. Supplementary Cementing Materials for concrete. Malhotra Ed. SP86-8E, 337 (1986).
(182) Buenfeld N.R., Newman. Examination of three methods for studying ion diffusion in cement pastes, mortars and concrete. Materials Structures, 20, 115, 3 (1987).
- Feldman R.F., Beaudoin J.J., Philipose K.E. Effect of cement blends on chloride and sulphate ion diffusion in concrete. Cemento, 88, 1, 3 (1991).
(183) Decter M.H., Short N.R., Page C.L., Higgins D.D. Chloride ion penetration into blended cement pastes and concretes. ACI SP 1/14-68, 1399 (1989).
(184) Rasheeduzzafar, Al-Saadoun S.S., Al-Gahtani A.S., Dakhil F.H. Effect of tricalcium aluminate content of cement on corrosion of reinforcing steel in concrete - Cem. Concr. Res., 20, 5, 723 (1990).
(185) Roper H., Kirkby G., Baweja D. Long-term durability of blended cement concretes in structures.ACI SP91-22, 1, 463 (1986).
(186) Luke K., Glasser F.P. Internal chemical evolution of the constitution of blended cements. Cem. Concr. Res., 18, 3, 495 (1988).
(187) Van Aardt J.H.P., Visser S. Influence of alkali on the sulphate resistance of ordinary Portland cement mortars. Cem. Concr. Res., 15, 3, 485 (1985).
(188) Guide to selection and use of hydraulic cements. ACI Mat. Journ., 901,. Nov.-Dec. (1985).
- El-Sayed H.A., Amin A.M. Resistance of pastes of different cements to sulphate attack and simultaneous effects on the corrosion behaviour of embedded reinforcement. Cemento, 84, 3, 261 (1987).
(189) Frigione G., Sersale R. The action of some aggressive solutions on Portland, pozzolanic and blast furnace slag cement mortars. Cem. Concr. Res., 19, 885 (1989).
(190) Sersale R., Cioffi R., Frigione G. Influenza della temperatura di stagionatura sull'attacco solfatico di cemento Portland e d'altoforno. Memorie Convegno AITEC "La durabilità delle opere in calcestruzzo", 155, Padova (1987).
(191) Irassar E.F. Sulphate resistance of blended cement. Prediction and relation with flexural strength. Cem. Concr. Res., 20, 2, 209 (1990).
(192) Cohen M.D., Bentur A. Durability of Portland cement - silica fume pastes in magnesium sulphate and sodium sulphate solution. ACI Mat. Journ., 85, 3, 148 (1988).
(193) Cabrera J.G., Plowman C. The mechanism and rate of attack of sodium sulphate solution on cement and cement-pfa pastes. Adv. Cem. Res., 1, 3, 171 (1988).
(194) Sersale R., Frigione G. The influence of fumarole exhalations on the behaviour of concrete in volcanic areas. Proc. First Int. Rilem Congress. Durability of construction Materials. III. Maso J.C. Ed. Chapman Hall, 1139 (1987).
(195) Mchedlov - Petrossyan O.P., Chernyavsky V.L. On the function of the clinker fund in the formation of cement materials properties. Cemento, 87, 4, 228 (1990).
(196) Natesaiyer K.C., Hover K.C. Further study of an in-situ identification method for alkali-silica reaction products in concrete. Cem. Concr. Res., 19, 5, 770 (1989).
(197) Barlow D.F., Jackson P.J. The release of alkalis from pulverized - fuel ashes and ground granulated blast-furnace slags in the presence of Portland cements. Cem. Concr. Res., 18, 2, 235 (1988).
(198) Canham I., Page C.L., Nixon P.J. Aspects of the pore solution chemistry of blended cements related to the control of alkali silica reaction. Cem. Concr. Res., 17, 5, 839 (1987).
(199) Glasser F.P., Luke K., Angus M.J. Modification of cement pore fluid composition by pozzolanic additives. Cem. Concr. Res., 18, 2, 165 (1988).
(200) Sersale R., Frigione G. On the minimization of the alkali - aggregate reaction. Influence of pozzolans, powdered volcanic tuff, blast-furnace slag and fly ash. Proc. 7th Int. Conf. on Alkali - Aggregate reaction. P.E. Grattan - Bellew Ed.Ottawa, Canada (1986).
(201) Zhang X., Groves G.W. The beneficial effect of pozzolanas in suppressing the alkali-silica reaction. Adv. Cem. Res., 3, 9, 15 (1990).
(202) Hobbs D.W. Alkali - silica reaction in concrete. Thomas Telford Ltd., London (1988).
(203) Sersale R., Frigione G., Blended cements: an effective utilization of natural zeolites. Rend. Acc. Sc. Fis. e Mat., Napoli. The volcanoclastic rocks of Campania (Southern Italy). Special Issue. Liguori Ed. 307 (1987).

(204) Stade H. On the reaction of C-S-H - di, poly - with alkali hydroxides. Cem. Concr. Res., 19, 5, 802 (1989).
(205) Ranc R., Sorrentino D., Cariou B. Réactions silico-alcalines. Mise au point de methodes fiables. Annales Inst. Tech. Bat. Trav. Pub. Essais et Measures. 480, 106 (1990).
(206) ASTM. Standard test method for potential reactivity of cement aggregate combination (mortar-bar method). Annual Book of ASTM Standards. ASTM, 1986, Part 14: Concrete and mineral admixtures, C-227-81, 157-162.
(207) Chatterji S., Jensen A.D. Simple chemical test method for the detection of alkali - silica reactivity of aggregates. Cem. Concr. Res., 18, 4, 654 (1988).
- Strunge H., Chatterji, S., Jensen A.D. Studies of alkali-silica reaction: Part 8. Correlation between mortar-bar expansion and values. Cem. Concr. Res., 21, 1, 61 (1991).
- Larbi J.A., Hudec P.P. A study of alkali-aggregate reaction in concrete: measurement and prevention. Cem. Concr. Res., 20, 1, 73 (1990).
(208) Strunge H., Chatterji S., Jensen A.D. Estimation of residual expansion capacity of concrete structures due to alkali-silica reaction. Cemento, 88, 3, 158 (1991).
(209) Douglas E, Elola A., Malhotra V.M. Characterization, conduction calorimetry, microstructure and properties of ground granulated blast-furnace slags and fly ashes. Proc. Third CANMET/ACI Int. Conf. Supplementary Papers, 618 (1989).
(210) Helmuth R.A. Water-reducing properties of fly ash in cement pastes, mortars and concretes: causes and test methods. ACI SP-91, 723 (1986).
(211) Roy D.M. Fly ash and silica fume chemistry and hydration. ACI SP-114-5, 1, 117 (1989).
(212) Atzeni C., Massidda L., Sanna U. Relationship between rheology and workability of cement mixes containing blast-furnace slag. Silicates Ind., 51, 1-2, 5 (1986).
(213) Arpaia M., Pernice P., Costantini A. A low frequency impedence study of steel concrete interface. Mat. Chem. Phys., 24, 525 (1990).
(214) Mehta P.K. Standard Specification for mineral admixtures - an overview. ACI SP-91-30, 637 (1986).
(215) Butler W. B. A review of some existing Standards for supplementary cementing materials and possible deficiences in them. Proc. Third CANMET/ACI Int. Conf. Supplementary Papers, 811 (1989).
(216) Valenti G.L., Puccio M., Sersale R. Utilization of fly ash in concrete: the foreign Standard Specifications and the situation in Italy. Materials Eng., 1, 3, 873 (1990).
(217) Thomas M.D.A. The effect of curing on the hydration and pore structure of hardened cement paste containing pulverized fuel ash. Adv. Cem. Res., 2, 8, 181 (1989).
(218) Philleo R.E. Recent development in Pozzolan Specification. Proc. Second Int. Conf. on Fly ash. Supplementary Papers. n. 27, 1 (1986).
(219) Ftikos Ch., Georgiades A., Philippou Th..Preparation and hydration study of alinite cement. Cem. Concr. Res., 21, 6, 1129 (1991).

Mehrkomponentenzement, Mahlen, Oberfläche, Stoffeigenschaft

BLENDED CEMENTS

J B Udachkin

Corporation "Building Materials of Russia", MOSCOW

BLENDED CEMENTS

"Cement is a valuable semi-product for builders, since its properties display themselves differently after technological treatment under construction conditions" [1].

As a rule, mass cement production proceeds with an excessive clinker potential. To provide adequate building and engineering properties of cement one should make corrections in its composition by combining clinker binder and mineral additives, optimizing clinker activity by7 mineral additives as well as by dispersivity of the ingredients. Of great importance are in this case small correcting additives (crents etc.) which regulate the setting and hardening time, shrinkage indices and the final product strength.

All these problems are solved in the world practice by means of blended cements.

Blended cements have been known for a long time. Production of pozzolanic cements was started in Italy in 1929. Cements with granulated blast furnace slag are pgroduced in Germany, France, Luxemburg, Belgium and other countries for more than half a century.

As formulated by R. Bukki, blended cements are those, which contain less than 95% portland cement clinker (main component) and various quantities of one-two additives (secondary components) [2].

It is only in 20 standards of 24 countries out of 64 that the production of blended cements is not provided. The main producers of blended cement are CIS, China, India, Cembureau-countries: Spain, Italy, Greece.

A detailed study of blended cement properties has shown the possibility of reducing considerably the quantity of clinker used for cement production in order to reduce power consumption.

For this purpose the research organizations of CIS have carried out investigations aimed at developing the blended cements with 30 — 50% clinker content. The cements thus obtained possess a high activity and preserve their basic building-engineering properties. Such cements were obtained making use of active silica-containing additives.

Of course, the technology of blended cement production directly depends on the characteristics of mineral additives.

Taking into account the classification of industrial silicate wastes, suggested by P. K. Metha [3] and R. Sersale [4], (Table 2), a number of Ukrainian institutes have carried out investigations on using natural and technogenic silicate wastes (pozzolana, tuffs, diatomites, wastes of mining, metallurgical and power industries).

Technological investigations were accompanied by geological survey and evaluations which finally enabled to compile a regional cadastre of silica-containing raw materials as a guide for designers and consumer-plants.

The most typical representatives of silica-containing raw materials have been divided into three groups.

I group — especially active materials. These are mainly technogenic products of pyrogenous nature (acc. to Eiler). The most typical examples of this group are: fly dust of ferrosilicium production (OPF), siliceous wastes of superphosphate production etc.

2 group — active materials with an increased content of amorphous SiO_2 and unit surface of

300 — 400 m^2/kg. This group is represented by the milled volcanites of liparite type with SiO_2 content of more than 60%, broken quartz glass etc.

3 group — traditional mineral additives in the form of a clean quartz sand, fly-ash of thermal power stations (TPS) and other known materials the activity of which increases after their milling together with clinker.

Table 1

Group of material	Name of material	Contents		Hydraulic activity	
		SiO_2 %	Glass phase	$S_{unit}=300$ m^2/kg	additional milling to $S_{unit}=400$ m^2/kg
1.	Fly-ash of ferrosilicium production (unit surface $S_{unit}=2000$ m^2/kg	90	84		$A_h=127.2$*
2.	Liparite Beregovsky (Ukraine)	72	63	12.5	24.3
	Broken quartz glass, milled	86	75	36	80
	Zeolites Sopernitskiye (Ukraine)	80	65	24	60
3.	Silicate sand	98	8.5	3.2	7.6
	Fly-ash of Kurakhovskaya TPS (Ukraine)	48	48	5.8	12.6

*) A_h = OPF − 2,5 m^2/g

Table 1 gives basic characteristics of silica-containing additives. We draw your attention to the methods of determining the hydraulic activity A_h of materials.

This characteristic feature is evaluated according to the quantity (mg) of CaO, absorbed by I g of silica-containing material with a different unit surface: standard — 300 m^2/kg and up to 400 m^2/kg, obtained by additional milling of the additive in a laboratory-type vibrating mill.

As to fine-dispersed materials with the initial unit surface of more than 400 m^2/kg, these have been studied without any additional milling.

However, we are not completely satisfied with the accepted methods of activity determination and share the opinion of the scientists (including Prof. Sersale) who think that the most objective evaluation of the activity may be obtained in case of testing the additives in concrete. In this connection the data on A_h should be considered as relative values and it is reasonable to draw the conclusions on the technology on the basis of an additional tests provided for additives in concrete.

The data given in Table 1 show that even a small additional milling of a component in a vibrating mill will increase its activity twice and proves the efficiency of obtaining blended binders by means of a combined milling of clinker and mineral additive.

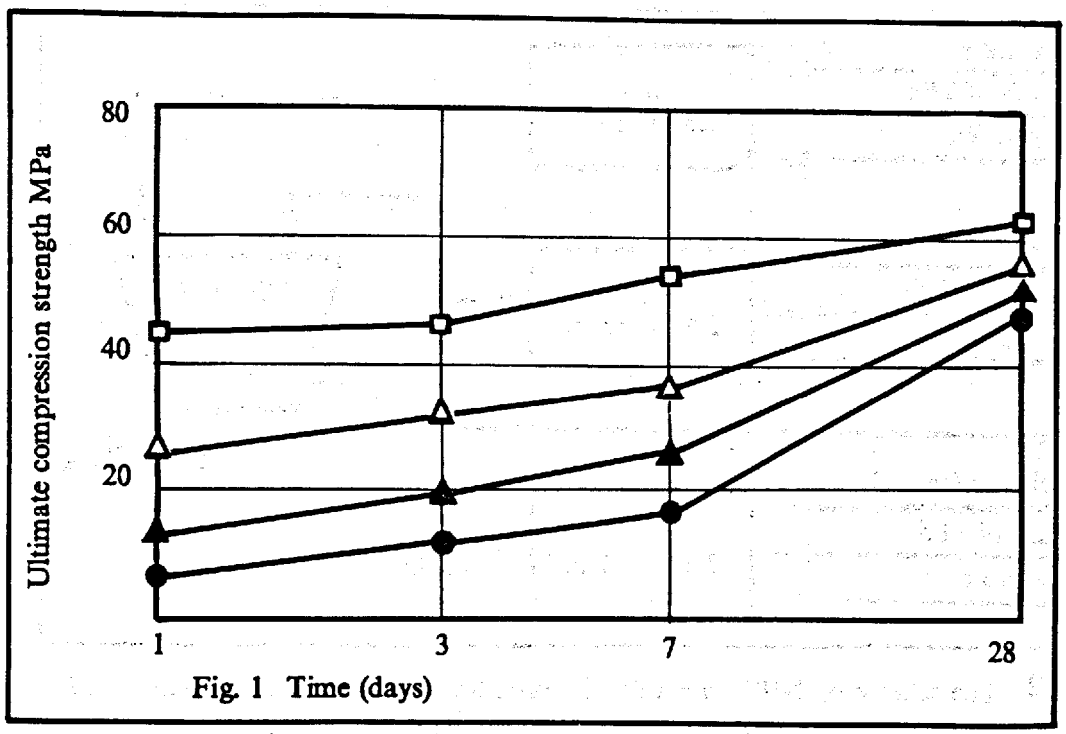

Fig. 1 Time (days)

● — control concrete with portland cement
▲ — concrete based on blended cement (clinker + broken quartz glass)
△ — clinker + broken glass with a repeated grinding up to the unit surface 400 m^2/kg
□ — concrete based on blended cement (clinker + sand + OPF)

Fig. 1 shows the results of standard tests for hardening of concretes prepared of biended cement and an active additive.

The problems of heat evolution during hydration have been studied at Kharkovsky civil engineering institute in the laboratory headed by Prof. Usherov — Marshak.

It has been found that the activity of the siliceous component is in direct proportion to the amount of hydration heat.

The higher is the component activity, the more intensive is heat evolution.

Blended cements based on fly ash of thermal power stations

The optimum version in respect to the rational consumption of the resources is the increase of cement production without the provision of additional capacities by adding to the blended cement composition a considerable amount of mineral additives (up to 70%) of technogenic origin and additional powder cement milling to the unit surface of 400 — 500 m^2/kg. In this case the active clinker material is utilized more completely at the stage of its hydrolysis and hydration. The production of the blended cement may be provided through the use of modern milling technology: closed cycle, two-stage milling, classification (separation) of the milling product etc.

NIITsement has worked out an efficient technological scheme of cement milling with pneumomechanical cement separation.

This scheme has been erected and is used at Angarsky cement-mining integrated works, since this works can use dry fly-ash of the local thermal power station (TPS) as a mineral additive (fig 2).

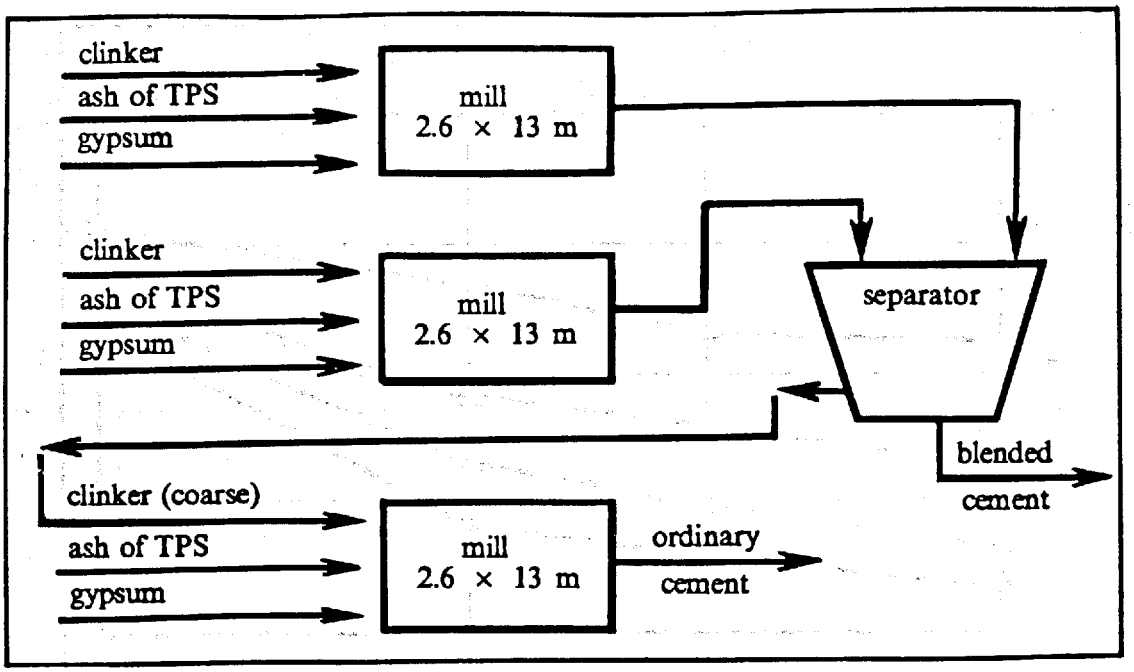

Fig. 2 The scheme by NIITsement for the production of a blended cement based on fly-ash of TPS at Angarsky cement-mining works

The choice of technological schemes for blended cement production has been predetermined by conducting industrial tests at a particular plant and finding the criteria for the development of general concepts and new-generation equipment.

Fig. 3 schows the results of hardening tests for blended cement which contains 50% of clinker, 47% of ash and 3% of gypsum as compared with ordinary cement. Further tests of blended cement in concrete have shown that it is possible to save up to 50% of clinker material per cu. m. of concrete and products. In this case the products had the required physical and mechanical characteristics and possessed a sufficient durability (tests by "NIIZhB").

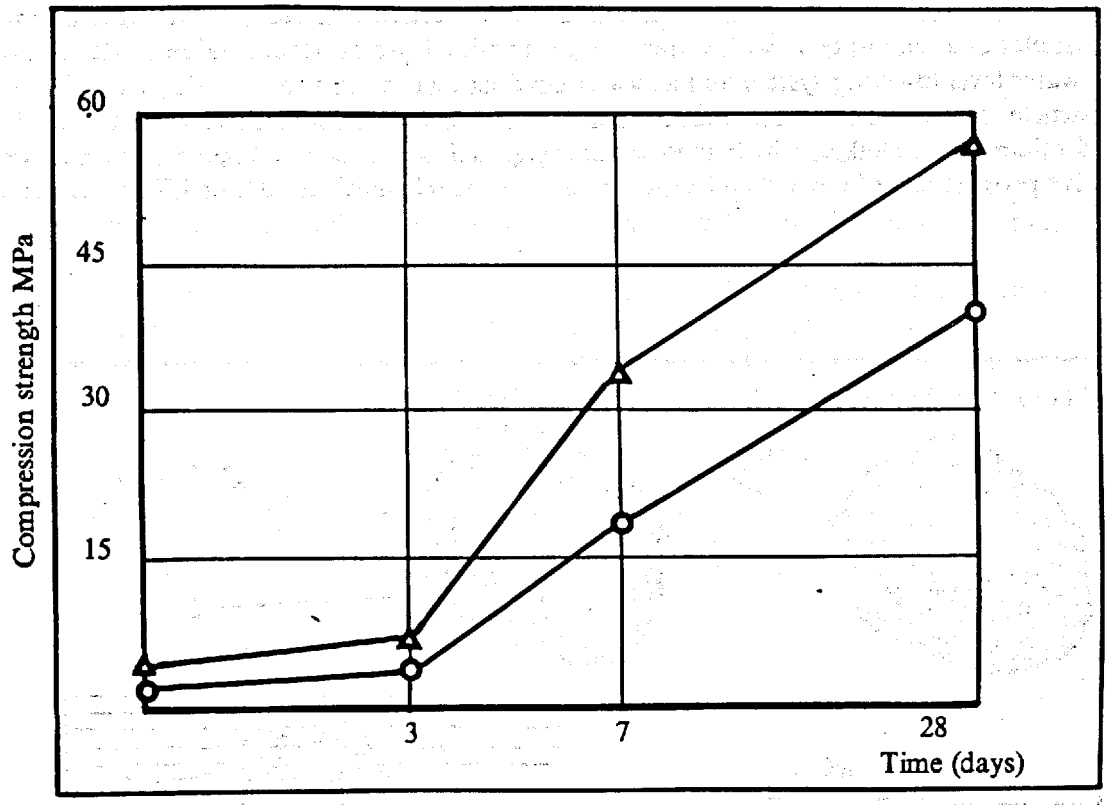

Fig. 3

The common disadvantage of fine-milled cements is their increased water demand. This feature has induced to the development of low water demand cements (table 2) [5 — 8].

Table 2.

Category	Cement type	Content, mass %				Quartz sand %	Superplasticizer, dry %
		Clinker K	Granulated b. f. slag S	Natur, pozzol., fly-ash Z	Dust F	P	C
I	Portland cement	$95 \leqslant K \leqslant 100$	$0 \leqslant S$	—	$F \leqslant 5$	—	—
II	Slag Portland cement	$65 \leqslant K \leqslant 90$	$10 \leqslant S \leqslant 35$	$0 \leqslant Z$	$F \leqslant 5$	—	—
II	Pozzolanic Portland cement	$65 \leqslant K \leqslant 90$	$0 \leqslant S \leqslant 5$	$10 \leqslant Z \leqslant 35$	$0 \leqslant F \leqslant 5$	—	—
II	Blended Portland cement	$65 \leqslant K \leqslant 88$	$6 \leqslant S \leqslant 29$	$6 \leqslant Z \leqslant 29$	$0 \leqslant F \leqslant 5$	—	—
III	Cement with granulated slag	$20 \leqslant K \leqslant 64$	$35 \leqslant S \leqslant 80$	$0 \leqslant Z$	$F \leqslant 5$	—	—
IV	Pozzolanic cement	$K \geqslant 60$	$0 \leqslant S \leqslant 5$	$40 \geqslant Z$	$0 \leqslant F \leqslant 5$	—	—
V	Fine-milled and blended cements (with or without organic additive)						
	— fine-milled	$K \geqslant 50$	$S = 0$	$Z \geqslant 50$	—	—	—
	— low water demand binder (LWDB)	$K \geqslant 30$	$25 > S > 10$	—	—	$45 \geqslant P \geqslant 20$	$C \leqslant 3$
		$K = 30$	—	—	—	$P = 70$	—

Blended cement of low water demand is a hydratically active material in which the hollows of clinker particles that tend to react with water, are filled with a layer of water-retaining additive, which acts as a water level lowering system and as water conducting channels to the defective points of the clinker particle. The water-retaining additive penetrates into the defective clinker cavities during its combined milling with clinker, which predetermines special conditions of binder milling as well as quantitative proportions of clinker and organic additive. A schematic model of LWDB is shown in Fig. 4

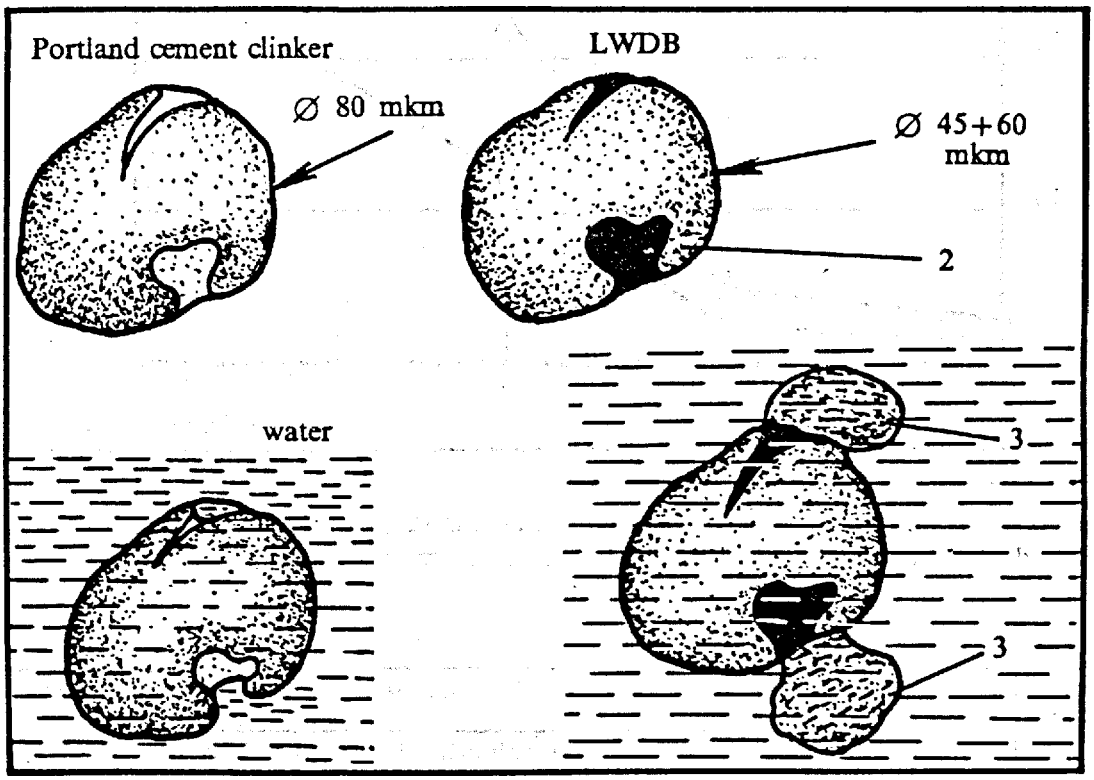

Fig. 4. 1. The most active defective points of clinker grain.
2. Organic additive at defective grain points.
3. Hydration products.

The programme of blended cement use in CIS

The possibility of obtaining high-strength binders with cement clinker consumption of 50 and even 30% has been laid to the basis of the programme concept of the Corporation "Building materials of Russia" aimed at providing the individual and low-rise housing construction with materials produced at quick-mountable and mobile small-capacity plants with the use of modern blended cement production technologies.

Programme concept: the cost of building materials makes the greater part of the construction costs. The excessive centralization of production makes it dependent on raw material sources, power and transport. The building materials, produced from the local raw materials at small enterprises are the cheapest ones. Such materials are:

— local binding materials;
— leight-weight wall blocks;

— cement-sand tile;
— facing tile for inside and outside wall finishing used with fine-milled binder.

Basic technological demands:

— technology simplicity and equipment reliability;
— the enterprise is a complex one and provides the production of blended cement, binding materials, wall blocks (or cast-in-situ housing), roofing materials;
— enterprise capacity is designed for the consumer market located within the range of 60 km. Certain enterprise facilities are mobile and rearrangable;
— the construction period of an enterprise is from 3 to 18 months with the exception of blended cement production, where construction periods may be increased;
— ecological protection of the enterprise meets the international requirements;
— the raw material base is local, including industrial, power or secondary raw material wastes.

The list of technologies and equipment.

The technologies provide for scientific and technical developments which include "know-how".

1. Production of Portland cement clinker at a mini-cement plant of 30 to 70 thou.t clinker a year capacity, Fig 5

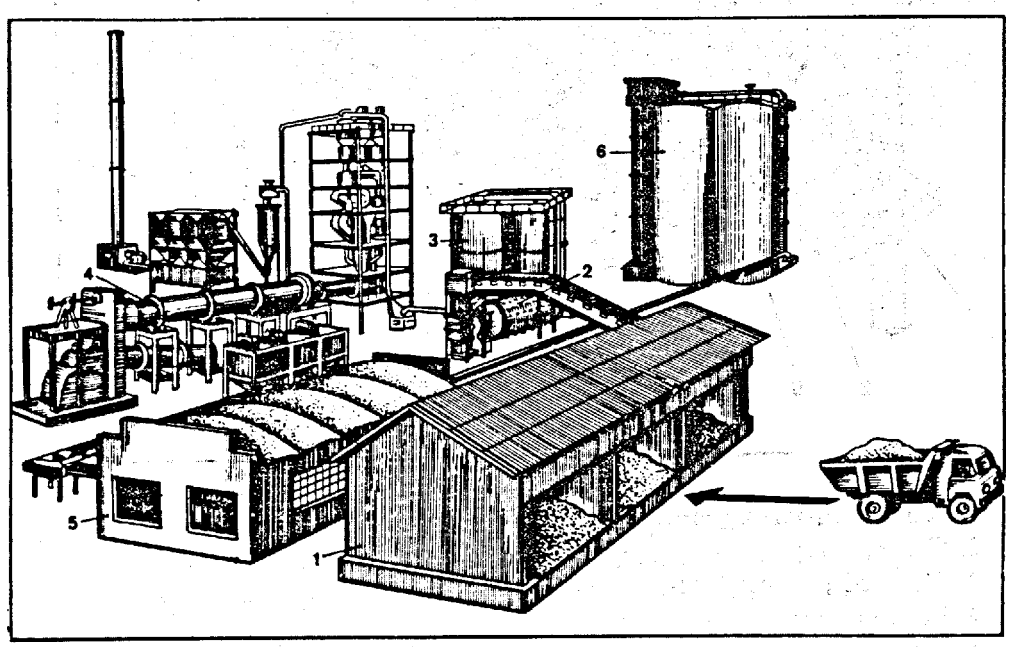

Fig. 5 1. Joint raw material and additives storage;
2. Raw material processing department;
3. Charge blending department;
4. Calcination department;
5. Cement milling department;
6. Finished product storage and shipment department.

2. Production of blended cements and dry mixes at complete milling plants of 10; 25 and 350 thou.t. blended cement a year capacity, Fig 6; Fig 7.

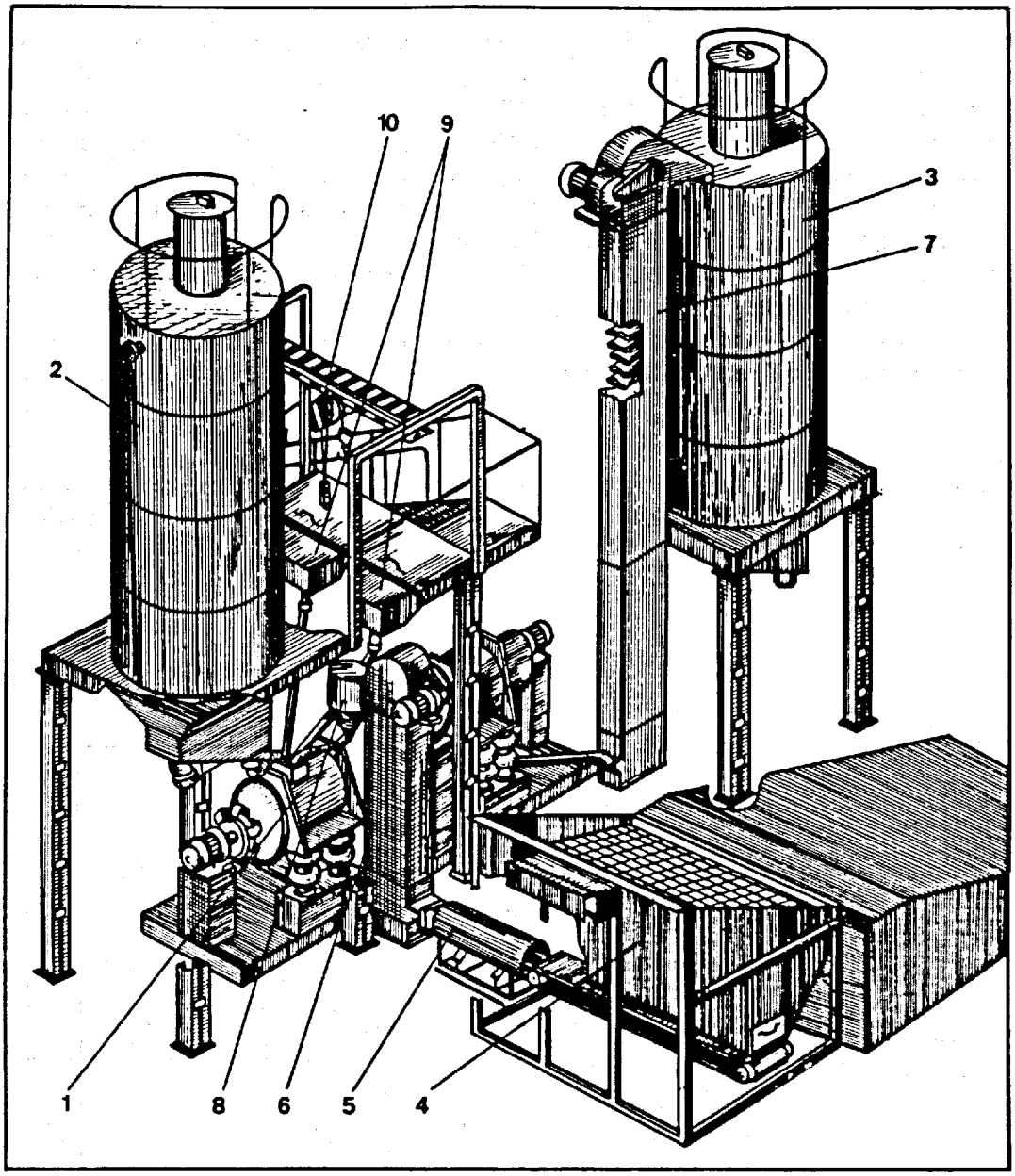

Fig. 6 1. Self-synchronizing vibrating mill;
2. Cement bin;
3. Finished product bin;
4. Feeding bin;
5. Vibrating drier;
6, 7. Elevator;
8. Accumulator;
9. Vibrating batcher;
10. Electric hoist.

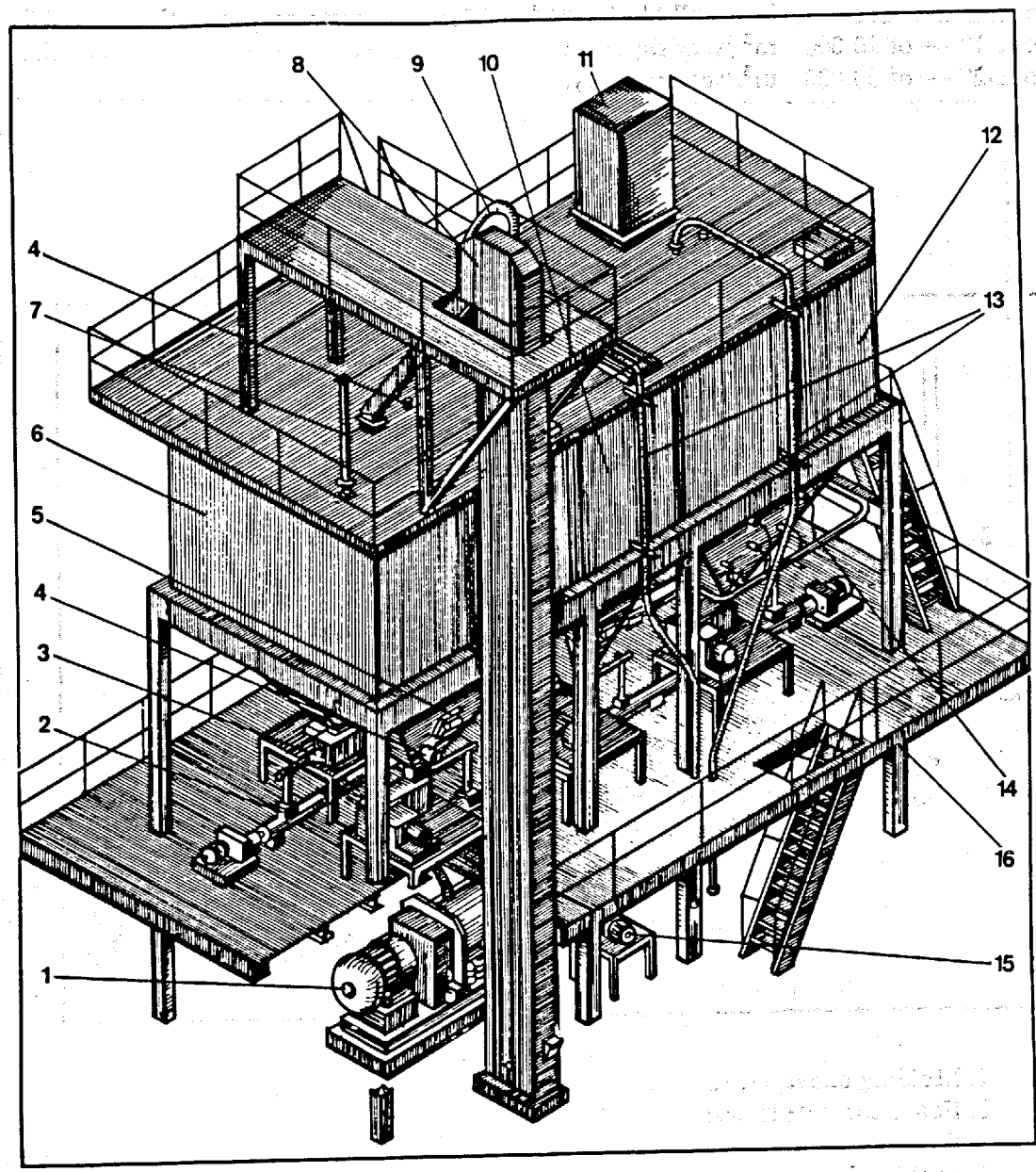

Fig. 7. 1. Vibrating mill;
2. Screw conveyer;
3. Screw feeder;
4. Winged level gauge;
5. Electric vibrator;
6. Dry sand bin;
7. Dust precipitator;
8. Elevator;
9. Shaped return bend;
10. Additives bin;
11. Hose filter;
12. Cement bin;
13. Cement and additive supply system;
14. Aerating arch breaking device;
15. Screw conveyer;
16. Metal structure.

3. Production of non-autoclave wall blocks made of foam concrete on production lines (Fig 8):
"Siblock-1" — of 20 000 m^3./year capacity;
"Siblock-2" — of 50 000 m^3./year capacity.

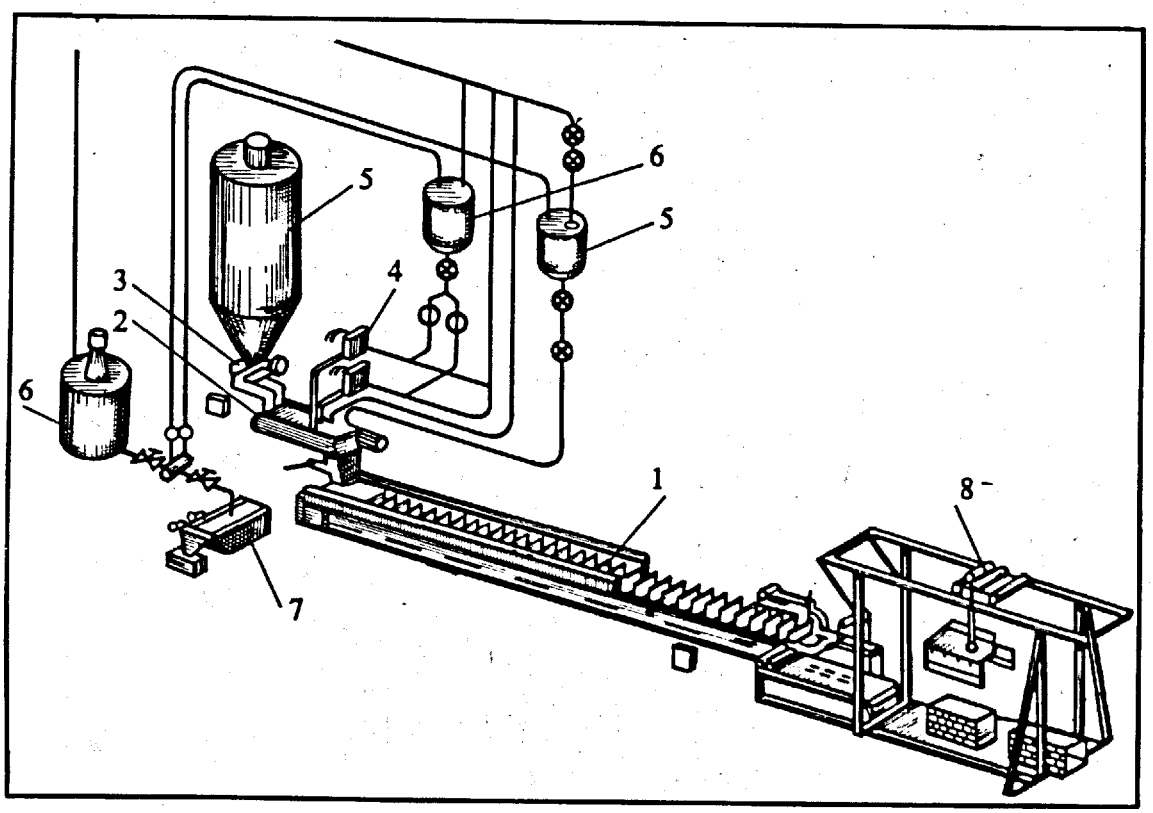

Fig. 8. 1. Molding conveyer;
2. Foam concrete mixer;
3. Batcher;
4. Turbine foam generator;
5. 6. Tanks;
7. Discharge tank;
8. Automatic placer.

4. Production of roofing materials — cement-sand roof tile, including the colour one, on production lines of 50 and 150 thou. sq. m. /year capacity, Fig 9.

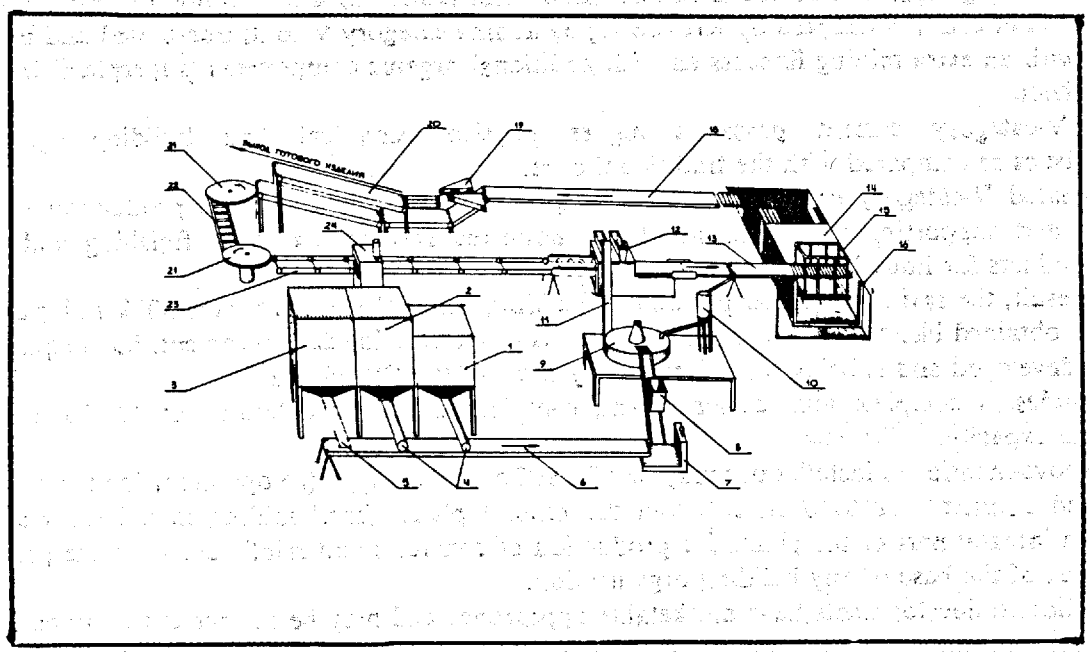

Fig. 9 CEMENT-SAND TILE PRODUCTION LINE.

1. Pigment bin;
2. Cement bin;
3. Sand bin;
4. Screw feeders;
5. belt feeder;
6. Collecting conveyer;
7. Platform balance;
8. Skip hoist;
9. Mixer;
10. water metering tank;
11. belt conveyer;
12. tile molding machine;
13. End conveyer;
14. Sliding roller table;
15. Rack;
16. Hoist;
17. Steam curing chamber;
18. Hoisting conveyer;
19. Tile from tray separation point;
20. Two-level conveyer;
21. Turning table;
22. Roller table-spacer;
23. Accumulating conveyer;
24. Tray lubrication device.

5. Cast-in-situ housing — on a movable continuous concreting plant "Monolit" of 3;6 m^3./h /capacity and with the use of foam concrete.

6. Production of other building products for low-rise housing.

The first sampies of the equipment presented were a success, they have a complete technical form and are put to series production.

In 1992, in accordance with the signed agreements the corporation "Building materials of Russia" will submit to the customers 19 lines for production of wall blocks, 24 milling units, 15 lines for production of cement-sand roof tile, 2 mini-cement plants and other equipment to be erected.

The corporation "Building materials of Russia" supplies the equipment both for complex plants on building material production and for separate technological lines.

Conclusions

1. The investigations carried out in CIS during the last years, prove the necessity of extending the classification of cements adopted by RILEM [5] by adding category V to it: fine-milled and blended cements with an extra milling fineness an with additional organic components (superplasticizers) or without them.

The V-category cement possesses higher physico-mechanical and building-engineering characteristics as compared with the traditional ones.

2. Blended V-category cements represent a specific raw material for the production of wall materials and supporting cast-insitu structures, non-fired roofing materials, finishing and other silicate products for housebuilding purposes.

As a result, the saving of clinker per unit of building material volume makes 30% and more.

3. The obtained blended V-category cement needs new technological equipment. Such equipment has been developed and is being manufactured by some of the CIS plants.

It includes: a complete mini cement plant, complete milling installations of 10, 25 and 350 thou.t/year capacity.

The above-mentioned installations may be of a self-contained type (to operate using the supplied clinker and additives) or to operate within the cement plant. Small milling installations should become an integral part of the plants for production of concretes and reinforced concrete products or be a part of the base of any building organization.

All indicated developments have marketable appearance and may be proposed to any customer via the corporation "Building materials of Russia" or Engineering Academy of the Russian Federation.

References

1. Shestoperov S. V. The ways of solving cement saving problems. A collection of scientific papers by MADI "Motor transport & road construction", 1980, Moscow.

2. Bukki R. Additives and blended cements from industrial point of view. A special report. The 8-th International Congress on cement chemistry, 1986, Rio-de-Janeiro.

3. Metha P. K. Pozzolanic and cementitious by-products as mineral admixtures for concrete. A critical review. Proceedings, CANMET/ACJ I-st International Conference ACJ Publ. SP-79, Montebello, 1983.

4. Sersale R. Aspects of the Chemistry of Additions. Advances in Cement Technology / Ed. by S. N. Gosh-Oxford: Pergamon Press, 1983.

5. Babajev Sh. T., Bąchlykov N. F., Goldina I. Ja. High-strength cement compositions based on low water demand binders. Journ. "Building Materials" No. 10, 1990.

The proceedings of the 8-th All-Union scientific & tech. conference on cement chemistry and technology.

6. Babajev Sh. T., Bashlykov N. F., Sorokin Ju. V., Dmitrijev A. M., Judovich B. E., Tarnarutsky G. M. Basic properties of concrete mixes and concretes based on low water demand binders.

7. Tarnarutsky G. M., Levin L. I., Babajev Sh. T. et al. Dry, complex-type modi fiers used to obtain low water demand binders.

8. Judovich B. E., Tarnarutsky G. M., Bukreeva T. V. et al. Mechanical and chemical activation and hydration of low water demand binders.

9. Cembureau (European Cement Association). Technical Newsletter TN I/1985, 28-th January, Paris.

Specific Theme II B

Developments in Non-portland Cements

Zement, Bindemittel, Zementbestandteil, Tonerde Zement, Quellzement, Eisenportlandzement, Alit, Belit, Phosphatzement, Sonderzement,

DEVELOPMENT IN NON-PORTLAND CEMENTS

Su Muzhen
China Building Materials Academy, Beijing, CHINA

W Kurdowski
Mining and Metallurgy Academy, Krakow, POLAND

and

F Sorrentino
Lafarge Coppee Recherche, FRANCE

ABSTRACT

The driving force for the development of non Portland cements comes from the need to fulfil the requirements of the customers for uses where ordinary Portland cement itself or with moderate additions is unsatisfactory. To this, must be added the need to satisfy environmental constraints and the ever present necessity to minimize the manufacturing costs.

In this work we describe the tendencies of these developments, based on the existing literature and the on-going experimental works from the authors. The most important feature of these special cements is the wide range of chemical and engineering properties covered and the difficulty to be exhaustive in this area.
The choice has thus been oriented to the binders which are the most widely developed. Among these cements, high-alumina cements, expansive cements, alumino or ferro sulfate cements are already produced industrialy in large amount (more than one million tons a year). Some others are still under development or at the semi-industrial stage.

The research made on these special cements which often utilizes the same concepts and techniques used for Portland cement, are therefore applicable to both fields and these add to these add to the pool of knowledge of boths types of cement.

1 – INTRODUCTION

This paper deals with the development of Non-Portland Cements. It is not a review of literature, already presented at this congress but an attempt to sort out the main directions of research and development in the area of special cements ; new results will also be presented, many of them coming from China where special cements are well developed. These binders find applications in fields where Portland cements or mixtures of Portland cement with moderate quantities of additives are unsatisfactory.

They cover very wide range of applications, from the well known fast setting or hardening cements, to lunar concrete(1) or incinerated waste stabilisers, through dental cements, magnesia-phosphate cements (2), to oil well cements or "alkali-activated aluminosilicate binders" (3).. Useful information can be found in progress reviews which have been recently published (4 /5/6/7/8/9/10/11).

The creation of any kind of new cement is driven by the need of civil engineering, in the light of the development of the national economies and the respect for environmental constraints. In the process of worldwide industrialization, the advance of cement industry is often impeded by its high energy consumption. The cement developers have been conducting serious researches on the process technology and the equipment for cement production in order to reduce the energy consumption ; consequently, many new kinds of dry process kiln emerged, in the most advanced of which, the clinker heat consumption is as low as 650-700 kcal/Kg. In addition various new sorts of vertical mills and other efficient comminution equipment decrease the electricity consumption for powder-milling to a great extent. Breakthroughs have been made in the development of new processes and equipment. In the recent decades, cement chemists turned their attention to the effects of energy conservation by changing the physico-chemical process of clinker formation and mineral composition.

They have been focusing their effort on creating new kinds of cements, centering round such aspects as energy conservation, multifunction and improvement of concrete durability (12). Accordingly, the objective of energy saving has, by a large margin been achieved and new fields for clinker formation and hydration of cement have been opened up, which provided new theories for the structure of hardened cement paste and exploited new applications for cement, a traditional building material. On the other hand, the possibility of using increasing quantities of waste leads to new types of cements different from Portland cements (13)

In this paper we have choosen to discuss those Non- Portland Cements which are already well developed, mainly since 1985 or have great hope of being developed in the near future. Our approach has been to classify cements by chemical or mineralogical systems instead of applications.
The content will be schematically :

FORMATION OF NON PORTLAND CEMENT. Thermodynamic and kinetic
MECHANISM OF HYDRATION
MICROSTRUCTURE
PERFORMANCES AND USES

The systems are :

$CaO-SiO_2-Al_2O_3$ (belite cements, glass cements, alcali activated slag or silico-aluminate cements)
$CaO-SiO_2-Al_2O_3-CaX_2$ (X being F-for the fluoro-aluminate cements or X being Cl-for the alinite cements)
$CaO-SiO_2-Al_2O_3-SO_3$ (sulpho-aluminate cements)
$CaO-SiO_2-Al_2O_3-SO_3-CaF_2$ (belite or alite sulpho-aluminate cements)
$CaO-SiO_2-Al_2O_3-Fe_2O_3$ (high-alumina cements, ferro-alumina cements)
$CaO-SiO_2-Al_2O_3-Fe_2O_3-SO_3$ (sulpho-aluminate, sulpho ferro-aluminate cements)
Phosphate cements (calcium or magnesium phosphates cements)

2 - FORMATION OF NON-PORTLAND CEMENTS.
Thermodynamic and Kinetics Mechanism

2.1 - $CaO-SiO_2-Al_2O_3$

2.1.1 - <u>Crystallised compounds</u> - This system, represented schematically in figure N°1, covers many hydraulic systems : synthetic crystallised products such as super-white cement {1}, belite clinker {2}, high-alumina cement for refractory application {3}, by-products such as slag {4}, glass cement {5}, high-alumina amorphous products{6} and binders obtained by mixing natural or artificial pozzolanas or coal fly ash with lime {7}.

FIGURE N°1

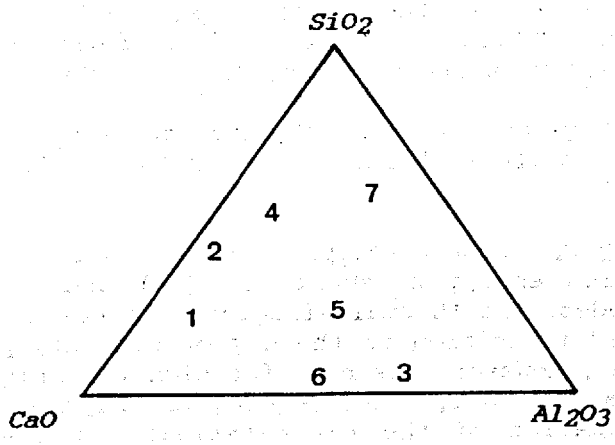

- A thermodynamic model allows prediction of the possible reactions and their extent during the sintering of mixtures of the system $CaO/Al_2O_3/SiO_2$, and thus the choice of operating conditions (14). The thermal balance in an industrial process can be accurately calculated from the enthalpy of formation of calcium aluminates, silicates and silico-aluminates which have been obtained by means of high-temperature conduction calorimetry and the technique of dissolution in lead metaborate (15). The results are :

$CaO + SiO_2$	--------->	$CaSiO_3$	$\Delta H = -87$ kj
$2\,CaO + SiO_2$	--------->	Ca_2SiO_4	$\Delta H = -119$ kj
$3CaO + 2SiO_2$	--------->	$Ca_3Si_2O_7$	$\Delta H = -206$ kj
$3CaO + SiO_2$	--------->	Ca_3SiO_5	$\Delta H = -124$ kj
$3CaO + Al_2O_3$	--------->	$Ca_3Al_2O_6$	$\Delta H = +19$ kj
$12CaO + 7Al_2O_3$	--------->	$Ca_{12}Al_{14}O_{33}$	$\Delta H = -199$ kj
$CaO + Al_2O_3$	--------->	$CaAl_2O_4$	$\Delta H = -7,9$ kj
$CaO + 2Al_2O_3$	--------->	$CaAl_4O_7$	$\Delta H = -14,3$ kj
$CaO + 6Al_2O_3$	--------->	$CaAl_{12}O_{19}$	$\Delta H = -47$ kj
$Al_2O_3 + SiO_2$	--------->	$Al_6Si_2O_{13}$	$\Delta H = +7,8$ kj
$CaO + Al_2O_3 + 2SiO_2$	--------->	$CaAl_2Si_2O_8$	$\Delta H = -87$ kj
$2CaO + Al_2O_3 + SiO_2$	--------->	$Ca_2Al_2Si_2O_7$	$\Delta H = -129,8$ kj

The quasi binary system $CaO-Al_2O_3$ has been calculated from thermodynamic data (16) but the $C_{12}A_7$ phase is not included in the main optimization since it has been shown not to be stable in the anhydrous $CaO-Al_2O_3$ system (17). The liquid phase is described by a simple two-sublattice subregular solution model, with Ca^{2+} and Al^{3+} as cationic and O^{2-} as anionic species.

The kinetics of the solid phase reactions, occurring for $C_{12}A_7$, CA and CA_2 during the production of clinker of high alumina cement by sintering, follow the Arrhenius type relation (18).

$\ln K_{C12A7} = -6008,3013/T°K - 12,7853$

$\ln K_{CA} = -11376,1840/T°K - 7,1797$

$\ln K_{CA2} = -22567,8080/T°K + 2,9290$

The mechanism of formation of CA is controled in the first stage by the mechanism of surface reaction, passing afterwards to a diffusional mechanism ; the activation energy is given as 72,4/74,0 Kcal/moles which is somewhat different from the preceding values (19). When sintered compacts of CaO and Al_2O_3 are put in contact with each other at temperatures higher than 1100°, Ca^{2+} diffuses into the Al_2O_3 to form calcium aluminate according to the sequence $C/C_3A/C_{12}A_7/CA/CA_2/CA_6/A$ with the relative concentrations $C_{12}A_7 > C_3A > CA_6 > CA_2 = CA$. The composition and the particle size of the starting material influence these constants (20).The formation of CA_2 occurs from the diffusion of alumina into CA by a phase boundary reaction and the activation energy is 33.40 $Kc.Mole^{-1}$ (21).
The difficulty of obtaining the same sort of data for $C_{12}A_7$ relates to the change of stoechiometry during its preparation, by absorption or desorption of water or oxygen (22/23).

2.1.2 - <u>Belite cements</u> - The development of C_2S/belite- based clinker has been motivated by its low energy consumption (24) and a better durability. During the past few decades, the thermal efficiency of cement kilns has improved markedly by the completed transition to the dry or semi dry process and the use of suspension preheaters ; however, the need for high temperature (1450°C) in the present process limits the scope for energy savings as does the energy requirement for decarbonation of the raw materials. If the process could be operated at lower temperature than those presently in use, energy requirement could, in general, be reduced but this may require the dependence of strengths on dicalcium rather than tricalcium silicate. Several papers are known in the literature concerning the preparation of dicalcium silicate of a high hydraulic activity, quickly reacting with water (25/26).In these papers two directions can be distinguished.

a) synthesis of dicalcium silicate at low temperature (27)
b) stabilization by admixtures of the high temperature polymorph.

Both methods allowed production of dicalcium silicate giving the mortars of a relatively high strength. However the results of these researches did not lead to important industrial application. A separate trend represents the experiments, the goal of which was to obtain active belite clinkers, namely by rapid quenching of this material from temperature of clinkerisation (28/29).

- Belite clinkers and cements have been produced by the Polish cement industry for a long time (30). The industrial experience shows that belite cements of good properties can be produced from chalky and marly raw materials, giving clinker of high silica ratio. These raw materials are very plastic, giving a slurry containing 75% of grains under 5 µm. The burning of these raw materials with low LSF can proceed at low temperature of about 1350°C and the obtained clinker has a high porosity of about 19%.

The content of free lime is less than 1% and the liter weight is 1150g/l. These clinkers are relatively easy to grind. Their chemical characteristics are as follow : LSF about 0.8 SR about 3.5 and AR 3.2. The mineralogical composition is 35/45 alite, 35/45% belite, so the sum of calcium silicate is 80% and C_3A 9/10%, C_4AF 7/8%. Microstructure of these clinkers is very fine. Alite and belite crystals are below 20µm with the medium value of about 10µm. Belite phase is composed of two types of crystals (figure N°2):

FIGURE N°2
Crystals of belite in belite-cement (x 800)

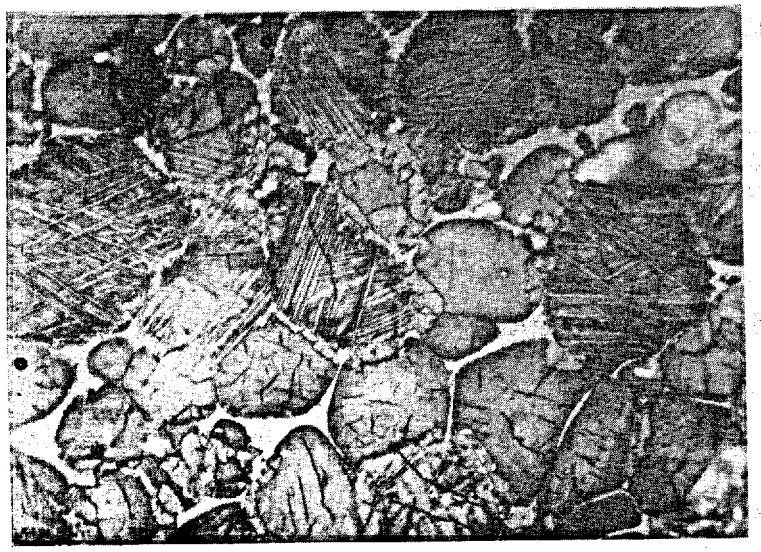

typical belite type 1 with two sets of striations and belite type III without striations. The latter crystals show numerous microcracks, probably of thermal origin. This type of belite corresponds to the presence of αC_2S phase, proved by X ray diffraction, in which the content of minor elements is greater, especially of Al_2O_3 (table N° 1).

TABLE N°1

Compound	Al2O3	Fe2O3	Na2O	K2O	MgO	TiO2
Belite I	1,44	0,50	0,05	0,66	0,40	0,30
Belite III	3,19	0,50	0,08	0,93	0,30	0,40

For the quality of a cement, the most important criterium is the silica content. Belite clinkers can be obtained from raw materials other than chalk and marl but then the burning process is much more difficult.
Good belite cements can also be obtained when 4-5% of BaO is added to the raw materials. In such clinker, baryum monoaluminate is present and the concentration of BaO in belite is about 1,5%.

2.1.3 - <u>Glass cements</u> - In the lower part of the $CaO-SiO_2-Al_2O_3$ phase diagram the hydraulicity is developed by crystallised compounds mainly C_3S, C_2S and CA, C_3A, $C_{12}A_7$.

In the upper part of the diagram, crystallised products do not develop hydraulic bonds and it is necessary to produce a disorganised structure to obtain any significant hydration.
For example, gehlenite (C_2AS), which crystallises in high-alumina cements and in blast furnace slags, is hydraulically inert. Glass of the gehlenite composition, found in granulated blast furnace slags, can be hydrated in the presence of activators such as alkalis, calcium hydroxyde or sulfate or in hydrothermal conditions (31/32/33). Without activators there is little significant hydraulic activity. Studies on the hydraulic properties of glass in the system $CaO-Al_2O_3-SiO_2$ show that a composition near gehlenite is the most reactive(34). Industrially, the maximum strengths have been produced with artificial "slags" whose composition is close to the gehlenite composition (35).

In 1985, J.F. MacDowell (36/37) was able to produce at laboratory scale a cement based on CaO, Al_2O_3, SiO_2 glasses which hydrate without activators and develop interesting mechanical properties.

A large composition range of glass cements is produced by melting a mixture of pure oxydes at 1650°, followed by rapid quenching by pouring the melt between water cooled rollers or into water.

The quenched glass is then crushed and ball-milled to the final fineness and used as a cements. Modifications of the setting and hardening properties have also been obtained by a change in the degree of crystallinity of calcium aluminate phases.

Amorphous calcium aluminate along the line $C_{12}A_7$ /CA have been prepared and studied (38/39/40). These glass are obtained by melting the stoechiometric mixture at high temperature (>1600° C) and a rapid quenching.
Comparing to the high-silica containing glass cements whose properties have been largely studied, very little or contradictory results are found in the field of amorphous high-alumina compounds.

2.2 - CaO-SiO2-Al2O3-CaX2 (X being F- or Cl-)

2.2.1 - CaF_2 System - The main phases in the fluoroaluminate clinker area are C_3S, C_2S, and $C_{11}A_7.CaF_2$. In this system, the introduction of F-modifies the phase assemblage, reacts with calcium aluminate compounds and also is favourable to the formation of C_2S. The research by Liu Baoyuan and Chen Yimin (41/42) showed that α-C_2S begins to form at about 800°C and a non-active mineral, 2 $C_2S.CaF_2$, forms at 900°C not directly from CaO, SiO2 and CaF_2 but according to the sequence:

$$4\ CaO+2SiO_2 + CaF_2 \xrightarrow{800°C} (2\ \alpha'\text{-}C_2S)+CaF_2 \xrightarrow{900°C} 2C_2S.CaF_2$$

- The mineral is stable within a broad temperature range of 900-1040 °C. When the temperature keeps rising, $2C_2S.CaF_2$ decomposes incongruently into CaO and liquid phase.

When the temperature reaches 1100 °C, an other transitional mineral is obtained : $C_{11}S_4.CaF_2$. Due to the volatilization of fluorine at higher temperature, the molecular formula of this mineral is not well defined at the present time. From the available data, it must be close to $C_{11}S_4.CaF_2$. Its stability temperature ranges from about 1100° to 1150°. Above 1150 °C incongruent melting occurs and the mineral decomposes into $C_3S(F)$, (alite containing F -) and a liquid phase. Since $C_{11}S_4.CaF_2$ reacts directly and forms $C_3S(F)$, the temperature required is 300-400°C lower than for the synthesis of C_3S by means of pure chemical reagents and 150-230°C lower than the formation of alite in clinker of conventional Portland cement. The maximum solid state solubility of fluorine in C_3S has been found to be 1.5% at 1350 °C (43).

In the system containing Al_2O_3, $C_{11}A_7$ CaF_2 forms primarily. The formation temperature of this mineral is 1100°C and its stability temperature range is from 1100° to 1300°C. When exceeding 1300°C, it decomposes into C_3A. In industrial production, the burning temperature has a narrow range, usually between 1250-1300°C
By varying the ratio of limestone, alumina and fluorine, two types of fluoroaluminate cement clinker can be provided having the following mineral composition :

Type Mineralogical composition of the clinker

	C11A7 . CaF2	C2S	C3S
I	65 - 75	25 - 15	little
II	20 - 30	< 15	50 - 60

The fluoroaluminate cement made from type 1 clinker is the commercially available product on the market .

2.2.2 - $CaO\text{-}SiO_2\text{-}Al_2O_3\text{-}CaCl_2$ - This system is particularly important because it leads to the production of alinite cements. The alinite phase can be formulated as 3(0.875 CaO 0.070 MgO 0.055 $CaCl_2$) (0.885 SiO_2 0.115 Al_2O_3) (44) but substitutions can occur and, specificaly, bromide alinites have been evidenced (45/46). Magnesia seems to have a stabilizing effect on the alinite and calcium chlorides (47).

- Calcium chloride is a very strong mineraliser and several intermediate phases are formed during heating of the raw mixture (48/49/50/51). Many fundamental researches have been carried out in this complex system (52/53/54/55). At about 680°C, calcium chloro-silicate is formed, which decomposes at 900°C to $Ca_2\{SiO\}_4$ and free lime. The process of belite formation is thus very accelerated. In the CO_2 rich atmosphere, which is typical for any cement kiln, spurrite phase is formed as intermediate phase. It is stable between 700°C and 960°C.

In this four-components system $C_{11}A_7.CaCl_2$ is also quicky formed at about 700°C which, as in the previous case, is linked with the appearance of the liquid phase in the mixture $CaCl_2$-$CaCO_3$-CaO. The phase $C_{11}A_7.CaCl_2$ is stable in a relatively large range of temperature, even up to 1350°C, depending on the partial pressure of chlorides in the gaseous atmosphere coexisting with the sample. This is the reason why in alinite cements the aluminous phase is always present (49). In industrial mixes, the alinite phase is formed at about 1150°C and begins to decompose at about 1300°C. The decomposition becomes very quick at about 1400°C (56).

The chloroaluminate is more stable than alinite, and even at 1400°C, when the concentration of the latter is quickly diminishing, the quantity of $C_{11}A_7$ $CaCl_2$ remains, practicaly the same. The addition of chloride to raw mixes accelerates the process of clinker formation and makes it possible to lower the temperature of clinkering by about 150°C. It represents a lowering of energy consumption by about 450/650 Kj/kg of clinker. Simultaneously, the evaporation of chlorine, which increases above 1200°C, requires a by-pass of 100 per cent of the gases as well as recovering of the chlorine from the gaseous phase.

The loses of energy linked with these operations practically cancel the advantages resulting from the reduction of the clinkering temperature.
The interest in alinite cements must be found more in their properties than in the energy consumption saving during their manufacture.

2.3 - CaO-SiO_2-Al_2O_3-Fe_2O_3

Most of the research carried out in the field of the manufacturing of high alumina cements aims at an improvement of the quality of the product by better process control. Different processes have been experimented with shaft, rotary, electric kiln.etc...(57/58/59/60/61/62) and the results concerning the relations between the manufacturing conditions and the mineralogy and the quality of the product are of a great interest (63/64).

When the high-alumina cement is made by fusion, the atmosphere and rate of cooling influence strongly the phase composition(65/66/67). In air and at a fast cooling rate, small intergrown crystals form, more Fe^{3+} enters the monocalcium aluminate crystal. Its formula, determined by EDAX is :

$Ca_{1,00}\ Al_{1,867}Fe_{0,124}Si_{0,006}O_4$ for a fast cooling and

$Ca_{1,00}\ Al_{1,925}Fe_{0,063}Si_{0,007}O_4$ for a slow cooling rate.

Figure N°3 shows the percentage of Fe versus Al contents of the solid solution of monocalcium aluminate. The points lie close to the ideal line (Fe + Al)/Ca=2) but two distinct populations are noted depending on the cooling rate ; fast-cooled monoaluminate (black points) having higher levels of iron substitution than the slower cooled (open squares).

FIGURE N° 3

Composition of monocalcium aluminate Fe versus Al contents of the solid solution

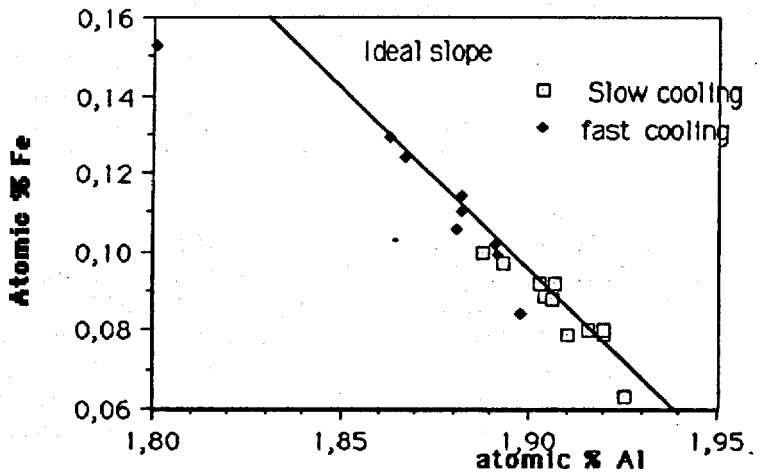

A fast cooling rate increases the quantity of silicon entering the calcium aluminoferrite : its formula is $Ca_{1.74}\ Al_{1,21}Fe_{0,75}Si_{0,15}O_5$ and $Ca_{203},Al_{1,13}Fe_{0,84}Si_{0\ 003}O_5$, respectively, for a fast an slow cooling rate.
There is a little change in the C_2S and $C_{12}A_7$ formulas which are, on average :

$Ca_{1,96}\ Al_{0,013}Fe_{0,015}Si_{0,99}O_4$ and

$Ca_{11,55}\ Al_{13,46}Fe_{0,71}S_{0,09}O_{33}$

The gehlenite phase has been detected to have an important silica deficiency according to the following formula.

$Ca_{3,929}\ Al_{4,007}Fe_{0,495}Si_{1,658}O_{14}$ (slow cooling) and :

$Ca_{3,95}\ Al_{3,83}Fe_{0,92}Si_{1,46}O_{14}$ (fast cooling).

This silicon deficiency must be taken into account during the calculation of phase percentage by the so called "modified Yamaguchi" method as it is described in several papers (68/69). The other methods developed (X ray diffraction, image analysis) are unable to account for this phenomenon (70/71/72).
In reducing conditions, intergrowth structures form at fast cooling while porphyric textures develop upon slow cooling. Under these conditions, the fields of $C_{12}A_7$ and C_2S expand and those of CA and ferrite are reduced. Pleochroite phase (also called fibres) is found as the primary phase for silica-rich compositions for FeO>5%. Under strongly reducing conditions it disappears and is largely replaced by $C_{12}A_7$. The formation of pleochroite leads to decrease in the monocalcium aluminate content of the cement. The composition of pleochroite is variable and two typical formulae are as follows :

$Ca_{20,87}Al_{25,46}Fe_{3,91}Si_{1,53}O_{68}$

$Ca_{19,64}Al_{25,37}Fe_{3,80}Si_{2,30}O_{68}$

Under reducing conditions, the solid solution lies between C_2AS and C_5A_3 and between C_2AS and CA_2 in air, C_2S transforms into the gamma form when silica content is higher than 4%. Its average composition is (slow cooling rate).

$Ca_{2,003}Al_{0,011}Fe_{0,0211}Si_{0,974}O_4$.

FeO is found as wustite, or in pleochroite and spinel. Different types of phase assemblage are found when the cooling is fast, showing a large departure from equilibrium conditions.

2.4 - $CaO-SiO_2-Al_2O_3-SO_3$

In this system emphasis of our discussion is laid on the sulpho-aluminate clinker zone with main mineral composition of $C_4A_3\bar{S}$-C_2S, with possible presence of calcium aluminates (73/74/75/76).

Decomposition temperature of $CaCO_3$ in the system is no higher than 900°C, under which CaO, SiO_2, and Al_2O_3 react first and combine as calcium silicate, calcium aluminate and C_2AS. When the temperature of the system reaches 1000°C, $CaSO_4$ starts to react with C_2AS and forms $C_4A_3\bar{S}$ and α' C_2S, decreasing the content of C_2AS continuously. At the temperature of 1100°C, CaO reacts partially with SiO2 and forms α' C_2S. Some of the CaO, Al_2O_3 and $CaSO_4$ react to form $C_4A_3\bar{S}$; free lime content decreases considerably.

When temperature reaches 1200°C, C_2AS and free lime disappear completly and a second transitional phase of $2C_2S.CaSO_4$ forms, which is non-hydraulic and cannot be formed by direct reaction of CaO, SiO_2 and $CaSO_4$ but by α' C_2S reaction with $CaSO_4$ at 1200°. Above 1298°C, the mineral again decomposes into α C_2S and $CaSO_4$. Therefore, the stabilizing temperature range of the mineral is quite narrow (1200°/1298°C). When this transitional mineral exists in clinker, it appears to be of light green color. In order to avoid its occurrance, the calcination temperaure of the fluoroaluminate cement clinker should be kept at a temperature higher than 1300°C. In industrial production of the cement when limestone, alunite and gypsum are used as raw materials, the fluoroaluminate cement clinker calcined under 1350°±50°C, has the mineral composition ranges of $C_4A_3\bar{S}$,75/55% and C_2S 35/15%. The clinker is primarily formed by solid state reaction. Therefore, it is loose and porous, and weights only 700 to 850g/l, containing about 30% fine particles of 1 to 3 mm diameter. The clinker grindability is excellent. The enthalpy of formation of $C_4A_3\bar{S}$ has been determined by a direct measurement through conduction drop calorimetry (77) : the endothermal value of 443 j/g has been found for the enthalpy of formation of $C_4A_3\bar{S}$ from pure oxides and calcium sulfate. In the system, the C_2S crystal pattern is rather complicated. In the industrial clinker, the majority of the crystals appears in the form of α C_2S and a small proportion of β: $C_4A_3\bar{S}$ crystallises in hexagonal tabular. The structure of - C4A3$\bar{S}$ ($Ca_4\{Al_6O_{12}\}(SO_4)$) belongs to the sodalite type structure, while the calcium silicosulphate $Ca_5(SiO_4)(SO_4)$ is orthorhombic and iso-structural with the mineral silicocarnotite (78). Their crystal size is usually fine (less than 5 microns), therefore a high hydraulic activity must be expected.

FIGURE N°4

The hexagonal tabular C4A3$\bar{S}$ produced in dry process kiln.

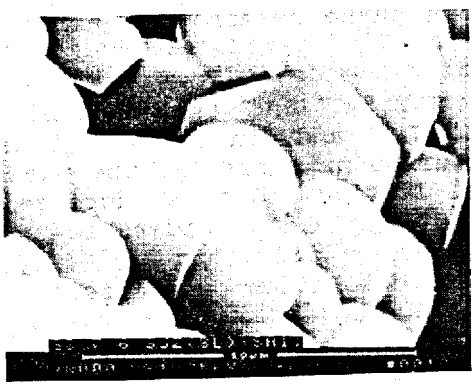

FIGURE N°5

C2S produced in dry process kiln

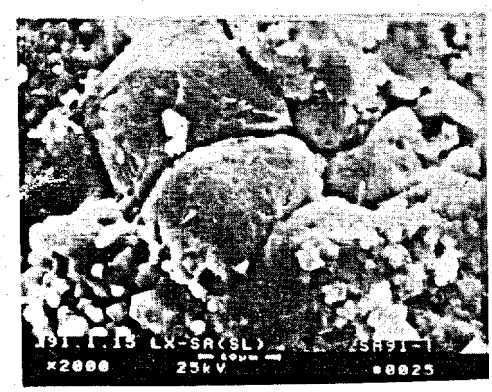

2.5 - $CaO-SiO_2-Al_2O_3-Fe_2O_3-SO_3$

In this pentanary system, the emphasis of the discussion lies in aluminoferrite cement clinker area composed mainly of $C_4A_3\bar{S}$, C_6AF_2 and alpha C_2S. Since the report by Mehta (79) concerning high ferrite cement and especially after the industrialised production of the high performance high-aluminoferrite cement in China in 1982, the ferrite phase has arisen great interest (80/81/82/83). The ferrite phase formed by reaction of the solid phase is clearly distinctive from the ferrite phase crystallised from the interstitial melt of ordinary Portland cement in that the former has high hydraulic activity. After the 7th international Conference on Cement Chemistry, research on the ferrite phases has been carried out in the following areas.

1) Formation of $C_2F-C_6A_2F$ solid solution system and determination of thermodynamics and structural data of the major ferrite phase minerals.

2) $C_2F-C_6A_2F$ solid solution system formation process and its mechanism. (84/85/86/87).
When the temperature increases, Al. dissolves into the ferrite phase by substituting iron (88).
The compounds CF and C_2F are easily formed at lower temperature (1040°C and 1220°C), and their formation is accompanied by exothermic reactions. When the Al/Fe ratio was greater than 0,32, Al dissolved into ferrite phase and first formed C_6AF_2, then C_4AF and finally C_6A_2F. Therefore some scientists claimed that the C_6AF_2 was the initial high temperature ferrite phase according to the sequence :

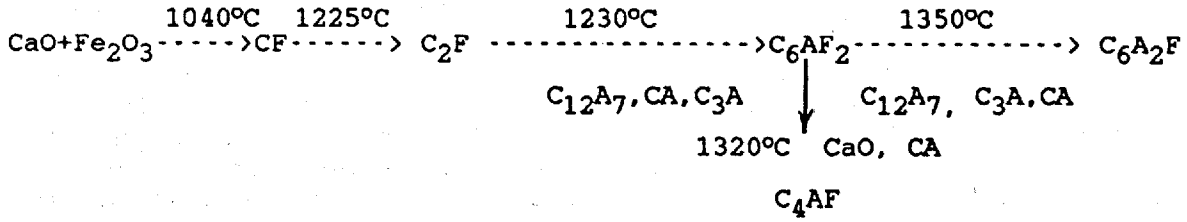

The relationship between spacing and composition has been studied by several researchers (89) and the main X ray peaks have been determined for C_6AF_2

3) Effect of minor elements such as MgO, TiO_2 and SO_3 on ferrite phase solid solution and on its characteristics.
Guo et al (88) studied the solid solution of TiO_2, MgO, SO_3, and SiO_2 and demonstrated that along with the growth of TiO_2, the solid solution reactivity of the ferrite phase grew too. Moreover, the optimal condition was observed at 2% solid solution. MgO behaves the same way, with a maximum solubility of about 5%. MgO is an inert component in all phases assemblages of the sub-system $CaO-CA-C_2S-C_4AF-KS$ - MgO. Above 1030°, only two stable relevant seven phase assemblages exist : 1) $CaO-C_4AF-C_4A_3\bar{S}-C_2S-C\bar{S}$-MgO-liq and
2) $CaO-C_3A-C_4AF-C_4A_3\bar{S}-C_2S$-MgO-liq (90).
The solid solution of Ti in C_2F might reach 2,5%, and the mechanism of substitution was that $2Fe^{2+}$ was substituted by 2 Ti^{4+} and, in the same time O^{2-} ions were replenished. The Ti^{4+} substitution occurred primarily at the place of octahedrons which resulted in defects of crystal lattice and thus increased its activity. In C_6AF_2, the solid soluble quantity of MgO was considerable and was basically substituted Ca^{2+} and, sometimes, Al^{3+} and Fe^{3+}. Si^{4+} and Mn^{4+} only substitute Al^{3+} and Fe^{3+}. The impact of S and Si solid solution on characteristics of ferrite was not obvious.(91).

The ferrite phase acts as a host and scavenger for many elements such as titanium and manganese ; the limit of solid solution of Mn in C_4AF lies in the range 7,9 (by electron microscope) and 6,67 / 7 % Mn by (X-ray diffraction) (92).

From Mössbauer spectroscopy it is shown that Si^{4+} plays a dominant part in altering the Fe^{3+} spin state from the original spin in the pure ferrite and could be responsible for the change in the reactivity of the ferrite (93) The most obvious difference in the mineral $C_4A_3\bar{S}$ between the system with and without Fe_2O_3 lies in the fact that there is more Fe solid solutions in the latter. Almost 20 -30% of Al was substituted by Fe. The industrially produced aluminoferrite cement clinker which uses limestone, ferro-bauxite and gypsum as raw materials, or waste slag of similar composition have very similar formation processes as that of sulpho-aluminate cement clinker. It is only the introduction of Fe_2O_3 that lowers the decomposition temperature of $2C_2S.CaSO_4$ to 1230°C.

Therefore, the calcination temperature range for aluminoferrite cement clinker can be lowered to 1300 ± 50°C with the mineral composition of the clinker as $C_4A_3\bar{S}$ 35-55%, C_2S 15-30% and C_6AF_2 45-15%. According to Kapralic et al (90), $C_4A_3\bar{S}$ is not compatible with C_3S. At temperature below 1180°C C_3S reacts with $C_4A_3\bar{S}$ to give $C_2S+C_3A+C_5S_2\bar{S}$. Above 1180°, the phase association $C_4A_3\bar{S}+C_2S+$ CaO is stable. To obtain good mechanical properties, it is necessary to mix the clinker containing $C_4A_3\bar{S}$ with anhydride and Portland cement (94). Under some conditions(presence of fluorine as mineralizers) it is possible to produce F- doped alite and $C_4A_3\bar{S}$ (13).

2.6 - $CaO-SiO_2-Al_2O_3-Fe_2O_3-SO_3-CaF_2$

In this hexanary system we lay our amphasis on alite-calcium sulpho aluminate cement clinker area composed mainly of minerals of C_3S, C_2S, $C_4A_3\bar{S}$, C_4AF and a small quantity of $C_{11}A_7.CaF_2$ or C_3A. Since F and S in the system coexist the temperature of the liquid phases occurrance in the system is 150°-200°C lower than that in the conventional Portland cement clinker. According to Li Xiuying and others (95), the liquid phase in the system occurred at 1200°C which therefore, facilitated the coexistence of the two minerals C_3S and $C_4A_3\bar{S}$. This is in agreement with other researchers (96/97) who found a liquid phase at 1180° whose the composition is 54 % CaO, 3% $Al2O_3$ 3%, 11% SiO_2, 4% CaF_2, 24% $CaSO_4$. In this system SiO_2 reacts with to CaO to form C_3S and C_2S ; the proportion of the two was determined by alkalinity coefficient:

$$K = \frac{C-0,55A-1,05.F-0,7(S+Ti)}{2,85}$$

In the system, in addition to F^-, certain amount of $\bar{S}$ also solid dissolved in C_3S. According to Ye Qing (43), the maximum solid solution of S in C_3S is 2.4%. The report also showed that, when the added amount of CaF_2 was 1%, 2%, and 3%, the amounts of solid solution of $CaSO_4$ are respectively 4%, 4% and 1%. Hence, the solid solution of F and S was restricted by each other. But the crystalline transformation was basically dependent on the added amount of CaF_2. When the CaF_2 added is 1% and the added $CaSO_4$ varies from 0% to 8%, C_3S solid solution crystal lattice was always T111. But when the added amount of CaF_2 was 2% without any $CaSO_4$ added, C_3S was of R type. When the added amount of $CaSO_4$ varies from 1% to 4%, the crystal lattice is M11 and when it exceeded 4% the lattice became T111, which at the same time showed that the solution of $\bar{S}$ gave rise to calcium ion vacancies thus reducing the symetry of the C_3S crystal.

In the same way as C_3S, alite simultaneously dissolves F- and $\bar{S}$ in which F- also played the predominant role. Alite was of M11 type, but when the added CaF_2 was 0,5% it became M111 type and when the added amount was equal or larger than 2%, it became of R type. When only 1% $CaSO_4$ was added, alite was M11, and when the added amount was equal or larger than 2% the M1 type was formed. When CaF_2 added was 2% and $CaSO_4$ was within the limiting quantity (3%) the alite was of R type.

In the system, four alumina containing minerals are formed : $C_4A_3\bar{S}$, C_4AF, $C_{11}A_7.CaF_2$ or C_3A. In this system $C_{11}A_7.CaF_2$ and C_3A did generally not coexist. At the temperature of 1300°C or over $C_{11}A_7.CaF_2$ disappears and C_3A emerges. Based on the free energy variation

determination of C_4AF, $C_4A_3\overline{S}$, and $C_{11}A_7$. CaF_2 (98), it was shown that the reaction sequence of CaF_2, $CaSO_4$ with Fe_2O_3 and CaO with Al_2O_3 was $CaF_2 > CaSO_4 > Fe_2O_3$. $C_{11}A_7.CaF_2$ forms first, followed by $C_4A_3\overline{S}$ while $CaSO_4$ inhibits the formation of C_4AF and CaF_2 inhibits the formation of both the $C_4A_3\overline{S}$ and C_4AF. The proportion of $C_4A_3\overline{S}$ to $C_{11}A_7$. CaF_2 was dependent upon the ratio of S/F. In order to obtain the desired phase assemblages, the quantity of CaF_2 addition must be carrefuly controled. During heating, at 800°C α' C_2S begins to form, at 900°C $2C_2S.CaF_2$ and a new quaternary compound $3C_2S.3CaSO_4.CaF_2$ emerges.

The transitional mineral could be formed by reaction of oxides directly at 900°C ; its stability temperature range was 900°C/1200°C. At 1100°C, they formed $C_{11}A_7$. CaF_2 and at 1150°/1200°C, $C_4A_3\overline{S}$ and ferrite phase were formed (41). At 1200°C, $3C_2S.3CaSO_4.CaF_2$ melts incongruently into liquid and lime. Although it could not directly form alite, it could lower the temperature of liquid phase formation in the system by 150°C-200°C compared to the conventional Portland cement. When calcined in the temperature range of 1300$^{\pm}$ 40°C, the alite sulphoaluminate cement clinker had the mineral composition of C_3S 30/55% C_2S 30/40% $C_4A_3\overline{S}$ 5-20% and C_4AF 5-10%. This theoretical study supports the use of mineralizers (86).

2.7 - Phosphates cements

2.7.1 - Magnesium phosphates - Originating from phosphate bonded refractories and certain kinds of dental cements, magnesium phosphate cements exhibit fast setting and high early strengths .Such cement are formed by combining a powder mixture (MgO, ZnO or aluminosilicate glasses) and a liquid (e.g phosphoric acid). The reaction of MgO with phosphoric acid is strongly exothermal and produces soluble hydrates, but its reaction with other acids leads to rapid formation of hard, insoluble products. One of the first known compositions satisfying requirement of the construction industry such as, workability and setting time, high compressive strength or protection of the reinforcement was obtained by mixing dead-burned magnesia with water-soluble polyphosphate and water soluble $NH_4H_2PO_4$. When sodium tripolyphosphate is added, workable paste is formed and setting occurs after 10 to 15 minutes.

2.7.2 - Calcium phosphate cements - This type of cement is obtained by mixing tetracalcium phoshate and dicalcium phosphate dihydrate, or tetracalcium phosphate and dicalcium phosphate anhydrate. Tetracalcium phosphate, which is not commercially available at present may be prepared by heating an equimolar mixture of dicalcium phosphate anhydrate and $CaCO_3$ to 1500°C for 24 hours. After grinding,this cement is mixed with a dilute phosphoric acid solution. Modification of the properties is obtained by adding components such as hydroxyapatites or calcium fluoride. Their setting properties and biocompatibility makes these cements useful in many applications in dentistry and bone surgery (99/100).

3 – CHEMISTRY OF HYDRATION OF NPC

3.1 - $CaO-SiO_2-Al_2O_3$

In this chapter, we treat the hydration of crystallised and amorphous aluminates and silico-aluminates in the system $CaO-Al_2O_3-SiO_2$. This includes special binders such as glass cements, activated slags, pouzzolanic, geopolymer and belite cements. The stability relationships between the liquid phase in contact with the hydrates show that, at high pH, the hydrates which precipitate are C-S-H, C_4AH_{13}, alumina gel, and silica gel. The solubility curve changes with pH and the final liquid composition can be calculated from thermodynamic models (101). The presence of small amount MgO does not change fundamentally the phase assemblages in the system $CaO-Al_2O_3-SiO_2$ (102).

3.1.1 - Cristallised aluminates - The results concerning the hydration of calcium aluminates (C_5A_3,(103), CA, (104/105/106/107108/109), CA_2, (110/111),) or the mixtures of

calcium aluminates are well established and do not differ greatly from one author to the other. Small differences in the morphology and the kinetics of formation of the hydrates can be due to the complexity of the hydration of calcium aluminates.

- These reactions depend on many factors such as conditions of synthesis, small deviations from theoretical chemical composition, grinding process, value of the water/solid ratio, and temperature.
The setting time of high aluminate cements increases above 2°C to reach a maximum at 28° C then shortens very quickly above this temperature. Hydration of pure CA presents a similar setting behavior at 28°-29°C, which seems to coincide with the disappearance of CAH_{10} above the temperature : it has been said that this effect was due to difficult nucleation of C_2AH_8.

Hydration of pure $C_{12}A_7$ is accelerated with temperature, the retardation effect is completly avoided in this case and the hydrates formed at any temperature under 35°-40°C are mainly C_2AH_8 with a very short nucleation period if any. These results prove that C_2AH_8 presents neither difficult nucleation nor retarded setting time at any temperature when it precipitates congruently from a solution, and cannot be taken as an explanation of the retardation at 28°C. The mechanism of retardation between 20° and 29°C can be described as a more and more difficult nucleation with temperature until it becomes nearly impossible above 29°C when C_2AH_8 precipitates uncongruently from a solution. The formation of gel phase acts as a slowing barrier to further dissolution / precipitation. The combination of C_2AH_8 and AH_3 presents a difficult nucleation and slows the growing of nuclei, while temperature acts as an accelerator. When this reaction becomes the predominant one the setting time accelerates very quickly (112/113/114/115/116). Commercial cements behave slightly differently from pure CA because they contain certain amount of $C_{12}A_7$ in different proportions : some containing more $C_{12}A_7$ than other precipitate higher proportions of C_2AH_8.

3.1.2 - Belite cements - The hydration of belite cement is not fundamentaly different from that of Portland cement and the main hydration products are the same. Belite cements hydrate and harden more slowly, and less portlandite is produced during the hydration. The differences occuring between the cements are due to the polymorphic forms of the belite (117) and to the other phases present with the belite.

- Comparison between 3 cements containing 28%, 38% and 57% C_2S and, respectively 45%, 35%, 16% C_3S show that the hydration rate at early age is driven by the hydration of C_3S. From 2 to 7 days the hydration rate is increased as the C_2S content increases and, more specifically, as the proportion of alpha and α' C_2S become higher. After 28 days, the hydration progresses with the same rate. As can be expected, the portlandite content of the cement paste normaly decrease when the % of C_2S increases. In the described experiments, for the hydrated cement rich in C_3S, most of the sulphates are in the form of ettringite, while for those rich in C_2S a part of ettringite is transformed into monosulpho-aluminate (118). In other experiments, the less favourable workability of the belite cement than from alite cements has be explained by the increased formation of ettringite due to the lower alkalinity of the solution. This lower alkalinity leads to stronger formation of short and long prismatic ettringites throughout the solvent phase due to the increased solubility of the aluminate ions (119).

3.1.3 - Glass cements -
Amorphous calcium aluminate : The properties of the calcium aluminates are dependant on their composition and the degree of crystallinity produced during manufacturing.

- Concerning the composition, rapid setting is associated with cements rich in $C_{12}A_7$ and C_3A which dissolve rapidly, and quickly exceed the solubility of the C_2AH_8 hydrate (120). Initial hydration behavior of calcium aluminate is greatly influenced by SiO_2 as a minor component : the rate of hydration of calcium silicates decreases when the silica content in the sample increases (121).

According to Nakagawa et al (121), amorphous $C_{12}A_7$ hydrates immediately after contact with water and sets in 3 to 5 seconds, which is faster compared to cristallised $C_{12}A_7$. The degree of hydration is 24% at 15 seconds after addition of water, followed by gradual reaction, reaching 62% at 30 minutes.
In contrast, based on the analysis of CaO and Al_2O_3 concentrations in the liquid phase, Hisashi et al (40) reported that the setting of glassy $C_{12}A_7$ was slower than that of crystallised $C_{12}A_7$.

During the hydration of amorphous and crystallised mixtures of CA and $C_{12}A_7$ the presence of amorphous or microcrystalline portion inhibits the hydration, or has no strong effect after 6 hours in the case of calcium aluminate having a CaO/Al_2O_3 ratio between 1/1 and 12/7 (122). The time of large precipitation of the hydrates, determined from conductivity evolution, decreases when $C_{12}A_7$ amount in the anhydrous sample increases.

The pseudo-amorphous samples give the same result, except for pure $C_{12}A_7$. For pure CA and $C_{12}A_7$, the time of precipitation of the hydrates is extended when the product are pseudo-amorphous : this is in agrement with Hisashi's work. The existence of small quantity of glass phase, whose composition is not the same as the main crystal, contributes largely to the hydration at the beginning. The quick hydration tendency of glass-containing cements can be explained by the presence of reactive microcristalline matrix which is absent in sintered cement but could be present in small quantity in slowly cooled melted sample.

Calcium alumino silicates : The hydration kinetics and hydrated products depend on the initial composition. From the conductivity curve and the hydrated phases it is shown that there are two distinct families of cements, one giving hydrogarnet ($Ca_3Al_2(SiO_4)_3$-$Ca_3Al_2(H_4O_4)_3$ (123) and the other gehlenite hydrate $2CaO\text{-}Al_2O_3\text{-}SiO_2\text{-}8H_2O$ (124) .Glass cements leading to hydrogarnet as main hydration product have very short setting time and low to moderate mechanical strengths (125/126). The conductivity of the solution, in contact with these cements increases up to a maximum and decreases to reach a plateau, directly or in two steps. During the increase of conductivity, we detect small quantity of gehlenite hydrate in the solid ; the decrease corresponds to a large precipitation of hydrogarnet ; the bound water increases. The silica content of the solution is negligible.

The cements leading to a gehlenite hydrate give practical setting times and high strengths, but have a thermal stability lower than hydrogarnet cements.In the case of cements giving gehlenite hydrate the solution contains appreciable amounts of silica.

3.1.4 - <u>Activated slag</u> - The reactivity of industrial slags is relatively poor at ambient temperature. Therefore to produce cement, activation is necessary and the best activators are sodium hydroxyde or carbonate and , in some cases , sodium silicate. The amount of addition of activators is relatively high, typical, addition is 5% of the slag weight. Sodium hydroxide is the strongest activator but in some cases, the addition of sodium carbonate is favorable. The latter gives very good results when the slag is rich in MgO, i.e when the composition of the glass lies near akermanite (127).

- The main component of slag paste is C-S-H phase and among the magnesium constituents, hydrotalcite. In more basic slags also gehlenite hydrate is present (128/129). In the case of Na_2CO_3 activation, $CaCO_3$ is precipitated (figure 6). The elevation of temperature above 100°C leads to the transformation of C-S-H phase into tobermorite and gyrolite. In small quantities also hydrated calcium sodium silicate pectolite is formed (figure 7) and, occasionally, analcite can also be found. The sodium ions introduced with activator only in small extend form stable hydrates, namely pectolite and analcite.

FIGURE N°6

Na_2CO_3 activated slag ($CaCO_3$) (x 3000)

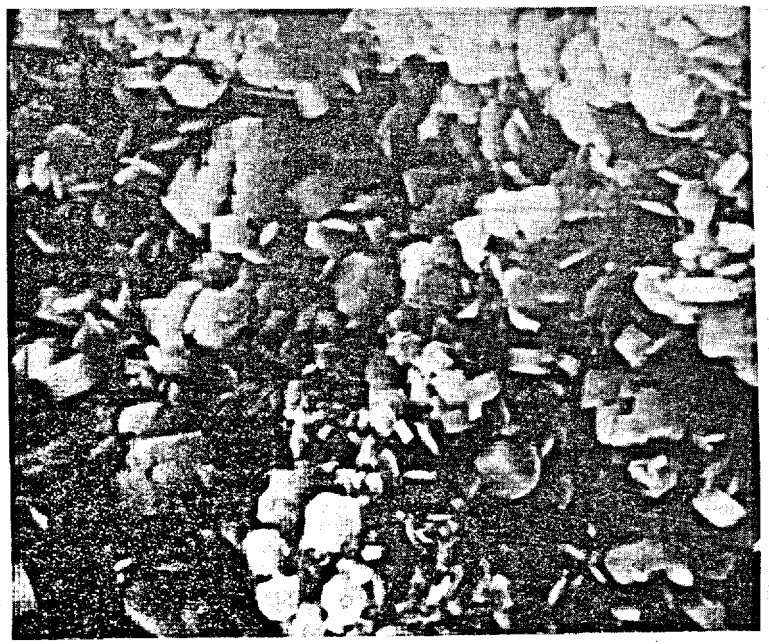

FIGURE N°7

Tobermorite and hydrated CA/Na silicate pectolite (x 2000)

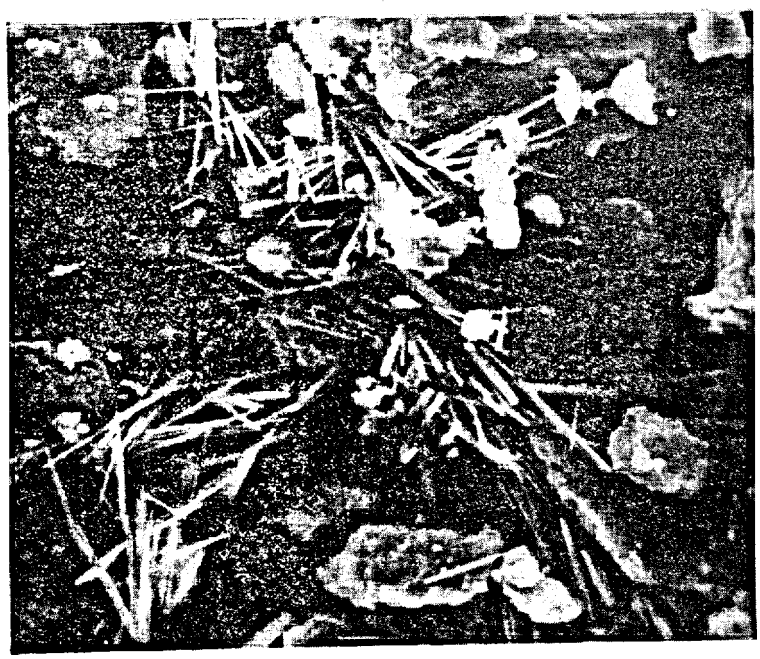

In the major part they enter into C-S-H phase solid solution. A large part of sodium, about 50% after five years of storage, is water soluble and easily leaves the mortar giving efflorescence. The slag paste has much greater gel porosity and smaller capillary porosity (table N°2). Gel porosity is substantially greater than that of Portland cement. Also, the greater gel content causes a high shrinkage of the mortar. The shrinkage is 50% to 100% greater than that of Portland cement but, for steam cured mortars, is comparable to Portland cement (130).

The primary field of application of slag concretes is in the highly corrosive environments. Slags concretes are very durable in sulphates and chlorides solutions, even of high concentration and in presence of magnesium cations (131).

Table N°2

Porosity of cement pastes after 28 days (W/C =0.3)

King of porosity	Type of cement	
	slag+5% Na2CO3	OPC
Total	25%	26%
Capillary (2000/10 nm)	11%	16%
Gel (>10 nm)	15%	9%

3.1.5 - Pozzolanic cements - Much attention has been paid to the structural properties or "bonding ability" of the gehlenite hydrate compared to the hydrogarnet solid solution. Hydrogarnets, and gehlenite hydrate are obtained separatly or together in many hydraulic system, for example in mixture of lime and natural or artificial pozzolanas (132/133/134), blast furnace slags, hydrothermally treated lime and silica/alumina containing materials (135), mixtures of high alumina cements and blast furnace slag (136), hydration of calcium aluminosilicate glass cements, etc ....

- The reactions of thermally activated kaolin and lime produce mainly "C-S-H" hydrogarnet (C_3AH_6), and gehlenite hydrate (C_2ASH_8). The thermochemistry of the hydration of these system shows similarities with Portland cements hydration. Both systems are characterized by rather large heat evolution during the first 24 hours (137). The gehlenite hydrate content increases when the lime content increases up to 20%, remains constant between 20 and 30%, decreases for higher lime content and disappears when the lime content is higher than 60%.

When the temperature rises (from 50°C to 100° C), the gehlenite hydrate reacts with hydrated lime to give hydrogarnet. According to Zampieri(138), the "C-S-H" and hydrated gehlenite appear as the principal phases responsible for the mechanical strength of the calcined clay and calcium hydroxyde mixture. In contrast, Pera et al. (139), find a correlation between the "CSH" only and the mechanical strengths: the presence of CH decrease the strength.

Mixtures of silico-aluminate compounds with alkali hardeners develop early strengths and good thermal stability ; the hydrated products of these binders also called "geopolymeric binders" are claimed to have similar characteristics to natural rock-forming minerals such as zeolite, felspatoids and feldspars (140/141/142/ 143/ 144).

3.2 - $CaO-SiO_2-Al_2O_3-CaX_2$ (X being halogenide Cl- or F-)

We discuss here the hydration of calcium silicate and its derivatives like C_3S (alite), C_2S (belite) containing certain amount of minor elements and alinite. The features of the system lie in the fact that the major hydrated products are C-S-H gel and CH crystal. Due to the different C/S ratio of the unhydrated minerals and different kinds of solid soluble impurities, their hydration rate composition of hydrated products, C/S ratio, and morphology are different (145).

When pure C_3S was compared with C_3S containing F (the added amount of CaF_2 was 1% and 2%), the fluorine contained C_3S has a shorter induction period and higher reactivity than pure C_3S (146). When F content reaches the limit of solid solution, the hydration rate during the acceleration period was low. The same result is obtained by the degree of hydration and $Ca(OH)_2$ content measurement.

The samples with added 1-3,5% CaF_2 have the highest degree of hydration. The effect of F is different for alite and pure C_3S. When the added amount of CaF_2 ranges from 0,5 to 3.5%, the induction period last more than 36 hours.

This illustrates that the initial hydration activity was poor when F-alite was contained. The initial degree of hydration was lower for F-alite than pure alite.

The C_3S containing S had a higher initial hydration activity than pure C_3S. When the $CaSO_4$ content is 1%, 1 to 3%, 3 to 4.5%, the exothermicity of the doped C_3S hydration increases respectively by 1.25 cal/g.h,1.32 cal/g.h and 0.12 cal/g.h. Therefore, the relationship between the solid solution of S in C_3S and the hydration activity of (S)C_3S is not clear. For 4.5% of $CaSO_4$ in alite, the heat released during the first 36 hours of hydration was 16.9 cal/g higher than that in pure alite.

The sample containing 4.5% $CaSiO_4$ had a similar or somewhat lesser degree of hydration and $Ca(OH)_2$ but higher strengths than pure alite. The hydration activity tests of C_3S containing F and S show that the sample containing 1% CaF_2 and 3% CaSO4 had higher hydration heat than that of pure C_3S, while the degree of hydration and $Ca(OH)_2$ content were higher than for pure C_3S at the initial stage and approximately the same at 28 days.

The hydration activity of alite containing F and S had slow initial rate of hydration and longer induction period (about 10 hours), but the hydration reaction after the induction period was normal. The degrees of hydration at one and three days were low, but were close to that of pure alite at 7 and 28 days. The initial hydraulic property of F and S containing alite are improved with the increase of S content and becomes best when 1% of CaF_2 and 3% of $CaSO_4$ were added.

Hydration rate of alinite phase seems to be higher than that of alite. Alinite hydration rate also affects that of β C_2S, reducing it especially at early ages. Liberated $Ca(OH)_2$ during hydration of alinite cement is lower than that of Portland cement. The presence of chloroaluminate favors dissociation of ettringite and formation of secondary gypsum (145).

The fast hydration of alinite produces rapid hardening cements, however the limiting factor of larger application of this binder is its high chlorine content. The chloride ions can form the solid solution in C-S-H phase in a rather limited degree but, the majority of chlorine will be present in the paste as Friedel 's salt ($Ca_2Al(OH)_6$) $Cl.2H_2O$. The utilization of alinite cements must be therefore limited to special cases, especially for placing concrete in cold areas (e.g., in the permafrost regions).

3.3 - CaO-SiO2-Al2O3-Fe2O3

3.3.1 - <u>High-alumina cements</u> - Although some detail have still to be understood, the main characteristics of the hydration of high-alumina cements are well established. The main directions of development in high-alumina cements involve the change of the hydrated system compatibility with slags, carbonate, or finely divided silica, and the modifications of the properties of the cements by additives or by changes in the curing process (147/148).

- During the hydration of high-alumina cement, the strengths first decrease due to the transformation between CAH_{10} and C_2AH_8 into hydrogarnet and later increase again : the reason for the strengths recovery could be the hydration of the remaining CA or the cristallisation of C_2ASH_8 which is formed as a minor compounds. The addition of calcium carbonate to form carbo-aluminate is the proposed way to modify the hydration of high-alumina cement (149/150/151)and to increase its sulfate resistance (152).

The addition of calcium silicates-containing compounds such as C_3S, C_2S, (Portland cement) or C-S-H, to high-alumina cements increases the quantity of gehlenite hydrate but the effect on the strength evolution and the durability of the final products requires more studies (153/154). Gehlenite hydrate can also be produced by adding microsilica, but the transformation into C_3AH_6 occurs at a

temperature higher than 70°C (155). Instead of adding Portland cement or fine silica, slag addition has been tried : gehlenite hydrate is the main hydrated product of mixtures obtained by addition of granulated blast furnace slag to Fondu, or Secar aluminous cement, or to pure calcium aluminates such as $C_{12}A_7$ or CA. For a neat paste of 50% Fondu / 50% blast furnace slags (cured at W/C=0,3 at 40°), the hydrogarnet phase produced initialy tends to diminish after 28 days.

According to Majumdar and al (156/157/158/159/160/161), the formation of crystalline C_2ASH_8 at the expense of calcium aluminate hydrates is the main factor in the elimination of progressive strength loss in high-alumina cement /Slag concrete. The mechanism of interaction between high-alumina cement and blast furnace slag has been studied on simpler systems such as CA/slag or $C_{12}A_7$ /slag. When a mixture of CA and blast furnace slag is in contact with water, CA reacts first giving CAH_{10} or C_2AH_8. The slag activated by calcium ions reacts more slowly. At 20°, the slag hydration produces hydrogarnet phase, while at 40°C, the main hydrated product is gehlenite hydrate : this result contrasts with the observation on $C_{12}A_7$ mixture in which lime /alumina ratio leads to the formation of large quantity of C_3AH_6 at 40°C. Granulated slags are usualy activated by soda, calcium sulfate or lime (often Portlandite coming from the Portland cement hydration) : "C-S-H" gel, ettringite, C_4AH_x, hydrogarnet and gehlenite hydrate are formed. If the calcium content of the slag is low and the ratio $Al_2O_3/SiO_2<1$, the gehlenite hydrate will form preferentially : addition of lime will lead to the formation of hydrogarnet.

The addition of admixtures modifies the the set of high-alumina cements. From microcalorimetry mesurements it has been demonstrated that foreign cations with a ratio of electrical charge/ionic radius higher than 27 nm modify the nature of the nucleation process. The hydration process of both CA and high-alumina cement is quite different from that of C_3S and Portland cement for which the precipitation of metallic hydroxide does not promote any acceleration of the hydration kinetics due to formation of a protective layer on the anhydrous phases (162). The use of a superplasticizer (sulphonated naphtalene formaldehyde condensate) and a lithium salt as an accelerator has been a solution proposed to reduce the w/c and thus the rate of conversion : nevertheless, the use of large quantity of superplasticizer reduces strengths (163/164/165/166/167/ 168).
Thermal treatment is an other way to modify the properties of the cement. Autoclaving increases the flexural strengths and suppresses the microcracking (169).

3.3.2 - <u>Iron rich cements</u> - The hydration of the C_2F-C_6A_2F solid solution system has been reported by Guo Yong et al (170). When water is added to C_2F, semi colloid or colloid C_4FH_{13} and FH_3 are formed. The solid solution series C_6AF_2-C_6A_2F hydrates into $C_3(A,F)H_6$, $C_4(A,F)H_{13}$ and FH3 or AH3. With increasing Al/Fe ratio of the initial alumino-ferrite the amount of $C_3(AF)H_6$ increases and at the same time, the $C_4(AF)H_{13}$ and FH_3 decreases and the Al/Fe ratio in hydrated products (except C_2F) increased (171). The hydration rate sequence of the ferrite phases agrees with the previously published work (172). The minor elements Ti^{4+}, Mg^{2+} and S^{6+} have improved the hydration activity of C_6AF_2 and other ferrite phases to various degrees.

3.4 - $CaO-SiO_2-Al_2O_3-Fe_2O_3-SO_3$

This system includes the hydration of C_3A, $C_{12}A_7$, CA, CA_2, C_6A_2F, C_6AF_2 solid solution, $C_4(A,F)_3S$, $C_{12}A_7$. CaF_2, $C_{11}A_7$.$CaCl_2$ in the presence of calcium sulfate. The common feature of this system is their similar hydrated products, AFt, AFm, FH_3 and Friedel salt. The ratio AFt to AFm is determined by the added amount of calcium sulfate and its form. The rate of AFt formation, its quantity in the hydration of high alumina cement and calcium sulphate mixes also depends on the added amount of sulfate and its form. For example, hemihydrate reduces hydration shrinkage but implies its use in large quantity close to the point beyond which

cracks appear in the structure and the highest mechanical strengths are obtained with anhydrite (173/174/175).

The formation of AFt phase through a dissolution precipitation mechanism seems the most likely. The conditions of the formation of AFt and AFm and the relationship between the nucleation rate, the crystal growth and the ionic concentration in SO_4^{2-} and Ca^{2+} have been studied from thermodynamic model (176). The results are in agreement with the interpretation of the thermodynamic calculation of the solubility curves in the system $CaO-Al_2O_3-CaSO_4-H_2O$ or in more complex systems (177/178).

Experimentaly, the solubility curves, the conditions of ettringite formation have been determined with $C_{12}A_7-CaSO_4-H_2O$ as initial material and confirm the results previously found and calculated from theoretical models (179/180/181/182). The relation betwen the rate of ettringite formation and the expansion of cement is fundamental for the industrial application of this phenomenon (183). A good expansive cement should assure proper balance between expansion strain and mechanical properties of the concrete : the rate and magnitude of expansion strain that develops in the concrete depends on the kinetics of ettringite formation and the ability of concrete to accomodate to growth of ettringite. During the hydration of $C_4A_3\bar{S}$, the kinetics of formation of the hydrated product follow the Avrami Jerofejev relationship which describes hydration processs through ionic diffusion in water solution and nucleation of products on the interface, followed by crystal growth when the nuclei achieve their critical dimension after induction period (184/185/186). AFt has complicated configurations which was determined by the pH value of liquid phase, environment and space for crystallisation. When pH value is over 13, more fine needle-like AFt is formed. When the pH value is lower, cylindrical AFt particles are formed preferentially. The results obtained by Li Shaozheng et al (187) showed that AFt exists in three forms : one is AFt of crystal size and crystal structure, most of which was described as above, but when there is higher concentration of liquid phase SO_4^{2-} and wide space, the form could be of a hexagonal tube as illustrated in figure 8. Its performance in the hardened cement paste has yet to be clarified.

FIGURE N° 8
Hexagonal tube AFt in hardened paste



The second was an AFt of colloidal size (below nanometer) and crystalline structure. In hardened sulpho-aluminate cement paste, this kind of AFt was hard to be observed by scanning electron microscope, but could be clearly detected by X ray. Amorphous particles whose the composition is close to that of AFt can also be observed by means of DTA or energy spectrum analysis.

Regarding the composition of AFt in five hardened cement pastes with and normal water/cement ratio, large differences in chemical composition occur (181). In AFt, 4,34 wgt % of Fe_2O_3 and 1,95 wgt% of SiO_2 can be dissolved, thus reducing the unit cell coefficient a from 11.2 nm to 11.7nm respectively, and c axis from 21.49 nm to 21.44 nm and 21.38 nm respectively. The result of study of AFt in hardened aluminoferrite cement paste has shown that about 25% of Al_2O_3 could be substituted by Fe_2O_3 (187).

Concerning the stability of AFt phase, two issues are here involved : thermal stability and resistance to carbonation. Tang Mingshu calculated, from thermodynamic data that the dehydration and decomposition temperature of AFt was 122.6°C that of pure AFm was 146°C (188). In their study of thermal stability of sulpho-aluminate concrete, LiDedong et al found that, at the temperature of 100-300°C the X-ray lines of AFt dislocate, at 400-500°C AFt becomes amorphous and, at 600°C, it decomposes into $C_4A_3\overline{S}$,$CaSO_4$, $C_{12}A_7$ (189).

It is well known that AFt is easily carbonated, but the intermediate phases formed during thisprocess are rather·complicated and require more researches. Zhang Feipeng calculated the temperature of transformation into calcium aluminocarbonate was 60°C(190). The low porosity and the high resistance to carbonation which have been observed in hardened sulpho-aluminate and ferroaluminate cement paste can be due to compactness of amorphous product developed during the hydration(171). The effect of two expansives sources (ettringite and brucite) can be cumulated to produce appropriate expansion and low porosity in the hardened cement pastes(191).

3.5 - Phosphates Cements

The mixture between MgO and soluble phosphates such sodium or ammonium phosphates rapidly develops strength. During the hydration reaction struvite ($MgNH_4PO_4$, $6H_2O$) is formed and seems to be responsible for the strength. The setting time depends on the the characteristics of the initial compounds and specially on the quality of MgO and its fineness. In the cases where the setting time was too short, sodium tetraborate can be used as set retarder (192).

By mixing an equimolar quantity of $Ca_4(PO_4)_2O$ and $CaHPO_4,2H_2O$ or $Ca_4(PO_4)_2O$ and $CaHPO_4$ and water, or dilute phosphoric acid solution a hardening time of few minutes is obtained. The development of hydroxyapatite $Ca_5(PO_4)_3OH$ through a dissolution repreciptation process is the basis of the hardening reaction of the calcium phosphate cements. The hydration mechanism can be described by the solubility curves and the solubility product value.

The only product formed is $Ca_5(PO_4)_3OH$ and the reaction is completed at 4 hours at which time compressive strengths range between 20 and 40 MPa. The factors that effect the compressive strengths are the crystallinity of the hydroxyapatite nuclei and the particle size of the initial phosphates.

4 - MICROSTRUCTURE OF NPC CEMENTS

The microstructure of the cement is the necessary link to understand the relationship between the engineering properties and behavior of individual phases. The development of the microstructure with time during the hydration of Portland cement, its relationship between microstructure and engineering properties have been widely studied, which is not the case for special cements. The same concepts as for Portland cement could be applied, provided that we obtain sufficient quantity of information on the system (porosity, structures of the pores, the amount and crystallinity of the hydrates)

4.1 - $CaO-SiO_2-Al_2O_3$

4.1.1 - Crystallised compounds - During the hydration of CA, microcrystallised CAH_{10} is formed. When CAH_{10} is sufficiently well crystallised, it forms networks of interlocking prisms, individually about 1µm long and 0.1µm wide. These prisms are barely resolved in backcsattered electron image (Scanning electron microscopy). X ray microanalyses of regions of these networks gave Ca/Al ratios usually above the theoretical value of 0.5 (typically around 0.7) (193).)
C_2AH_8, hexagonal, crystallised in well formed plates, seen on edge in polished sections and typically about 1µm thick and 20-30µm across.

C_3AH_6 was characteristically observed as aggregates of equidimensional nodules, individually about 0.2µm in diameter. X ray microanalyses of such aggregates gave Ca/Al ratios of 1.2, 1.3, with total of 60-70% and up to 4% of SiO_2. The composition and morphology suggest that the nodules were C_3AH_6.
AH_3 was generally observed as apparently structureless regions of low and uniform grey level which could be readily identified by X ray microanalysis.

During the hydration of low-iron, high-alumina cement an "inner" product replacing CA is observed in many pastes samples. It is apparently structureless and gave Ca/Al ratios of 1.2/1.3 and analysis around 70% ; the inner product retains all the CaO and part of the Al_2O_3 the rest of which is expelled : the nature of this inner product is uncertain (poorly crystalline or amorphous). Studies by transmission electron microscopy show that the paste consists of crystalline components bonded by an amorphous hydrate gel based on aluminate, but containing significant amount of calcium (194). The morphology of the hydrated products change with the curing temperature (195).

At 5°C, CA dissolved and CAH_{10} precipitated, leaving empty space where the CA previously existed. As reaction proceeds, this process is accompanied by one in which an inner product is formed : this product has a Ca/Al ratio of 1.2-1.3. It was not detected by XRD and is either amorphous or poorly crystaline, in the latter case probably a mixture of C_3AH_6 and AH_3. The factor favouring its formation could be a local increase of temperature (193).
The backscattered electron images showed that after 6 hours, the microstructure consists of partly reacted grains in a matrix of CAH_{10} prisms with large open pores. CAH_{10} was also observed as hollow shells surroundings voids a few micrometres in size which may have been formed by the complete hydration of small grains.

With longer hydration times the amount of CAH_{10} increased and it could be seen that more of the cement had reacted. The 7 day old paste showed a particularly marked change in microstructure with distance from a edge of the specimen. In the outermost millimeter, very little porosity was detectable : further in, the microstructure was much more open and its motled texture suggested that conversion to C_3AH_6 and AH_3 could have occurred : XRD showed CAH_{10} as the only detectable product in any of the specimen examined (193).

According to Scrivener et al., the SEM evidence is compatible with the hypothesis that temperature increases within this specimen caused increased reaction and partial or complete conversion, but the XRD evidence suggests that any products other than CAH_{10} are of low crystallinity or small in amount or both (193).
At 40°C, for the samples hydrated for 4 hours the microstructure had changed markedly. It contained highly porous regions some 100-200 µm in size separated by regions that were relatively dense. The space previously occupied by water consisted mainly of fine nodules probably of C_3AH_6 but too small for analysis, embedded in a matrix of AH_3 : large plates of C_2AH_8 were observed. The fine nodules formed arrays, sometimes mixed with residual C_2AH_8 plates : this suggested that C_3AH_6 had formed locally from reaction of the C_2AH_8. A considerable amount of inner product was observed, mainly replacing the CA.

By 7 days almost all the CA had reacted leaving AH_3 interdispersed with regions of brighter material which was sometime nodular, sometimes platey and sometime intermediate between the two : X ray microanalysis suggested that most of these bright areas were of C_3AH_6 though some analysis indicated that some C_2AH_8 remained. In the case of high alumina cement, plates of strätlingite were observed : some plates consisted partly of C_2AH_8 and partly of strätlingite which had possibly formed from the C_2AH_8 by reaction with silicate ions. XRD confirmed that nearly all the the CA and a substantial proportion of the gehlenite had reacted and showed the major products to be C_3AH_6 an AH_3, with some strätlingite.

In the case of macro defect free high-alumina cement (196), electron diffraction data show unusual elongated crystals of hydrogarnets which grow near CA_2 particles. TEM micrographs show areas with the granular appearing structure whose the pore size are about 100 nm (197).

4.1.2 - **Glass cements** - During the hydration of glass cements, gehlenite hydrate or hydrogarnet precipitate, depending on the initial composition of the cement. Gehlenite hydrate develops a microstructure which seems more favorable to the mechanical strength than hydrogarnets.
Gehlenite hydrate reacts with lime to give hydrogarnet, following the reaction :

$$C_2ASH_8 + 2\ Ca(OH)_2 + 3H_2O \dashrightarrow C_3AH_6 + C\text{-}S\text{-}H$$

Depending on the temperature (at lower temperature) another type of reaction can occur :

$$C_2ASH_8 + 3\ Ca(OH)_2 + 3H_2O \dashrightarrow C_4AH_{13} + C\text{-}S\text{-}H$$

These two types of reaction are linked, and in agreement with the thermodynamic data.

$$C_3AH_6 + Ca(OH)_2 + 6H_2O \dashleftarrow\dashrightarrow C_4AH_{13}$$

- In the systems C_3A/H_2O or CA/H_2O, the hexagonal phases are thermodynamically the most stable, within a range 25°C to 50°C and at temperature above 50°C to 75°C the cubic calcium aluminate precipitates. In presence of, C_3S, C_2S or microsilica gehlenite hydrate is the the major hydration product of the mixture and no hydrogarnet is found.

On the other hand a mixture of C_2S alumina gel, hydrated lime and β C_2S produces C_2ASH_8 : alumina gel reacts with CH to give C_2AH_8 and C_4AH_{10} and then these react with C-S-H produced during the C_2S hydration to give C_2ASH_8. According to Midgley (153), CAH_{10} reacts with the hydration product of C_2S to form C_2ASH_8 while C_3AH_6 will not. During the hydration of mixtures of CA and colloidal silica, it can be seen by DTA that the hexagonal phases CAH_{10} and C_2AH_8 decrease to give C_2ASH_8, but simultaneously, the peaks of AH_3 and alumina gel decrease, involving a consumption of these phases (198). As opposed to the hexagonal phases CAH_{10} or C_2AH_8 which transform into hydrogarnet, alumina gel or AH_3 is released according to the well known reactions

$$3CAH_{10} \dashrightarrow C_3AH_6 + 2AH_3 + 18H_2O \quad \text{or} \quad 3C_2AH_8 \dashrightarrow 2\ C_3AH_6 + AH_3 + 9H_2O$$

These reactions cannot explain the decrease of alumina phases. This decrease can be explained only if a phase having a calcium alumina ratio higher than 2 (for C_2ASH_8) reacts with alumina : hydrogarnet could be this phase, in spite of the fact that we do not see a decrease of the peak of C_3AH_6 by DTA. Another type of alumina consumming reaction could be assumed :

$$C_2AH_8 + CSH + AH_3 + 3H_2O \dashrightarrow 2\ C_2ASH_8 \text{ or}$$

$$C_2AH_8 + AH_3 + 3H_2O \xrightarrow{\text{in presence of [C] and [S] solution}} 2\ C_2ASH_8$$

During the hydration of binders such as pozzolanas and lime, slag, mixtures of slag, microsilica and high alumina cement, unstable hydrates precipitate first and transform into more stable system : hydrogarnet, C-S-H, gehlenite hydrate. The rate of the transformation depends on the temperature and the proportion of the hydrate at equilibrium depends on the starting composition.

In contrast, the hydration of calcium alumino-silicate glass cements produces rapidly and directly a mixture of hydrogarnet and gehlenite hydrate whose the proportion depends also on the composition of the starting glass (199).

The evolution of the hydration (studied by XRD and DTA) shows that the equilibrium between hydrogarnet and gehlenite hydrate remains stable during 3 years at temperature lower than 50/60°C.

The morphology of the hydrate paste (studied by SEM) shows that the system of structures obtained directly (case of glass cement) is different from those obtained by a transformation from unstable to stable hydrates : the stable structure obtained directly is probably more favourable than a structure which comes from a transformation. The stability with curing temperature of hydrogarnet and gehlenite hydrate and their influence on the mechanical strengths needs to be quantified.

4.2 - $CaO-Al_2O_3-SiO_2-CaX_2$ (X being halogenides Cl-, F-)

The main difference in the hydration products observed by XRD between alinite and Portland cement pastes is the presence of calcium chloro aluminate in the former. From SEM it is shown that the C-S-H morphology of alinite phase differs from that of alite. C-S-H produced from alinite is mostly presented in a spongy morphology. The existence of a lot of chloroaluminates on the C-S-H crystals surfaces reveals that most of the chloride contained in the alinite phase is diffused out the formed gel (145)

4.3 - $CaO-SiO_2-Al_2O_3-Fe_2O_3$

The microstructure of two years old mixtures of high-alumina cement and granulated slags revealed that all crystalline components of the high alumina cement has been consummed by this age. The major hydration products is C_2ASH_8, and two distinct mainly amorphous gels : an outer gel product occupying the space originally filled by water and an inner gel product occupying space created by slag reaction (200).

In the system calcium aluminate-siliceous aggregates, the cracks propagation occurs through the paste. In the case of aluminous-calcareous aggregate, the process is intergranular at the beginning of hydration and becomes transgranular after few months. The transitional layer formed at the interface between a calc.reous aggregate and aluminous cement paste , changes with time and develops a zone rich in hydrated carboaluminate which is form by epitaxic growth on calcium carbonate (201/202).

The morphology of the hydrates are modified by the presence of minor elements dissolved into the ferrite phase. Ti^{4+} reduces the size of the $C_3(AF)H_6$ crystals, whilst Mg^{2+} changes particles of $C_3(AF)H_6$ into flake-like shapes which when surimposed become flower-like structures. After the S^{6+} has been dissolved, $C_3(AF)H_6$ appears as curled flakes again in flower-like forms.

Zhang Liang (203) reported the microstructure of high strength crushed stone concrete made of alumino ferrite cement and pointed out that the alumino-ferrite blend cement composed of the cement clinker, 20% fly ash and 10% silica fume had an optimized particles size distribution and also that, the water/cement ratio can be lowered to below 0.2.

Therefore, by using conventionnal concrete making techniques the total porosity of concrete might drop to about 7,5% and the size of the pores to less than 500 nm. The interfaces formed between the hardened cement paste, the limestone coarse aggregates and the sand fine aggregate were very similar to that of hardened cement paste in terms of their structure and composition. When the fly ash reacts with the cement, the products formed are C-S-H, amorphous AH_3 and AFt crystals.

The compressive and flexural strengths of this "crushed stone concrete" could reach as high as 140 MPa and 20 MPa respectively. Moreover, the interface was no longer the weak area of the concrete. In the broken concrete, most of the fracturing cracks pass through the aggregates.

4.4 - $CaO-SiO_2-Al_2O_3-Fe_2O_3-SO_3$

The addition of $CaSO_4$ considerably affects the microstructure of $\bar{C}_4A_3S-C_2S-CaSO_4-H_2O$ system cement pastes. The microstructure of varied hydrated cement pastes, and the interface between the paste and aggregates have been studied in the case of sulpho-aluminate cements (204/205/206). The results showed that when the amount of gypsum was zero, $C_4A_3\bar{S}$ hydrated rather slowly and the degree of hydration at 1 day was 30% forming only 5 % of crystaline AFt. At 3 days, the degree of hydration increased up to 65% then slowed down and finally reached 75% at 28 days.

The quantity of AFt was then 12%. These results suggest that the amount of SO_4^{2-} was not sufficient. The products of hydration were primarily amorphous gel, poorly crystallized AFt and AFm and AH_3 gel etc. The ratio of crystal to gel of hydrated products was small in the hardened cement paste. The great amount of colloids makes the hydrated cement compact. Consequently, the 28 day total porosity was only about 13% and the majority of the pores were gel types whose size equal or smaller than 3000 nm. When 5 to 45% gypsum are added, the rate of $C_4A_3\bar{S}$ hydration increased greatly and at one day, the degree of $C_4A_3\bar{S}$ hydration was close to 70% and AFt crystal 20%. The results indicated that at the early stage of hydration, the gypsum was in the saturated state, but was exhausted with the continuation of the hydration in the system with small amounts (5 to 15% gypsum), and the increasing rate of crystalline AFt slowed down. As a result, the AFt crystal amount during the period 3 to 28 days was only 2 to 3% higher than that of one day. When the amount of gypsum was more than 25% (25 to 45%) residual gypsum occurred, therefore the hydration had taken place in conditions of saturated $CaSO_4$. At that time, the amount of AFt crystal increased with the increase of gypsum and the margin of AFt increment enlarged with the prolongation of age. As gypsum was added, then the ratio of crystal to gel in the hydration products changed and increased with the gypsum increment.

In the $C_4A_3\bar{S}-C_2S-CaSO_4-H_2O$ system, C_2S hydrates slower than that $C_4A_3\bar{S}$. Provided residual gypsum exists in the system, the hydration of C_2S takes place because the sulfate and aluminate ions released during the hydration of $C_4A_3\bar{S}$ and $CaSO_4 . 2H_2O$ combine with the calcium ions from C_2S to form AFt phase.

Therefore, the existence of $C_4A_3\bar{S}$ and $CaSO_4 . 2H_2O$ in large amounts accelerates the hydration of C_2S.
The results showed that the pore structure of hydrated cement with various added amounts of gypsum has the following characteristics :

1) the total porosity increases with the gypsum content, but the difference was not larger than 20 /30% at 28 days. The total porosity was much less than that of the hydrated early strength Portland cement with 0% gypsum.

2) the majority of the pore was less than 4000 nm and the proportion of pores larger than 1000 nm was low.

3) in terms of pore shapes, most of them were ink bottle like so the determination of the pore structure by mercury porosimeter would lead to large error. The decrease pressure curve of pressure porosimeter showed ink bottle-like pores accounted for 30-40% (207/208).

Li ShaoZheng et al (187) also studied the interface between limestone and hardened sulpho-aluminate cement with 0 to 45% addition of gypsum and found a great difference in their interface. The interface of pure clinker with 0% of gypsum is quite a thin layer of alumina gel, followed by AFt crystal and a little $Ca(OH)_2$. The whole thickness of the interface is about 50μm.

It was observed that AFt and $CaSO_4$, 2 H_2O crystals concentrated at the interface between limestone and hardened paste with 10 to 15% gypsum but it was not found that the crystal arranged in preferred orientation. The size of AFt crystal on the interface was large (figure 9), then the transition zone of the paste itself became small and the whole layer of interface was some 50µm thick. At the interface of expanding cement with 25% gypsum, there are large and rough AFt crystal arranged like chrysanthemums and colloidal AH_3 layer covering over the crystals. With the increase of gypsum amount, the chrysanthemum-like arranged AFt increased (figure 10).

The interface of self-stressing cement with more than 45% gypsum, almost all of the crystals were the chrysanthemum like arranged AFt. Under controled condition, the interface layer became much thinner (30-40 µm), crystal size much smaller and interface area structure more compact.

FIGURE 9
Loose interface structure
and compact paste

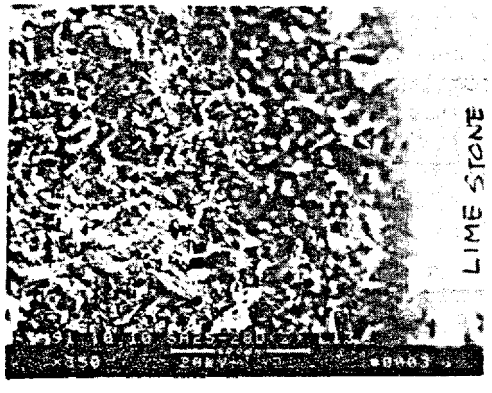

FIGURE 10
The chrysanthemum-like arranged AFt
in the interface between self stressing
cement and limestone paste



The interface between low-alkali sulpho-aluminate cement mortar and alkali resistant fibre is formed by a amorphous $Zr(OH)_4$ which polymerises on the glass fibre surface, forming a compact layer and thus raising the corrosion resistance of the glass fibre. In the case of the Portland cement, $Ca(OH)_2$ crystallises at the interface, on the side of the glass fibre, while in the case of sulpho-aluminate cement, the interface is formed by AFt. This interface forms early, has a compact structure, thus preventing ions from diffusing between the glass fibre and cement. Alleviation of the corrosion of the fibre glass extends the service life of glass reinforced products made from low-alkali cement and alkali resistant glass fibres.

4.5 - Phosphates cements

From SEM studies the early hydrated calcium phosphates cements show amorphous materials consisted of small petal like crystals : these appear to be responsible for the setting. The amount and crystallinity of materials present at the interparticle spaces increased with time and in fully set samples the paste consist of mostly rod-like crystal with a smaller amount of platy crystals.

The main mineral formed during the hydration of magnesium phosphate cement is struvite. The change in the morphology of struvite crystals is associated with increased amount of water or incorporation of sodium tripolyphosphate or borax : in a system optimized in retarder and water content, the struvite is the dominant hydrate and it crystallises in fine needles (209/210).

5 – PERFORMANCE AND USES OF NPC

This chapter, which takes into account more the use and engineering properties than the chemistry of cement is written in the sense of a justification of the development of the Non-Portland-Cement.

The confidence in which these special cements fill the requirements of the customer must involve an estimation of the durability and an understanding of the properties.

5.1 - $CaO-SiO_2-Al_2O_3$

5.1.1 - Belite cements - The interest in the development of belite cements lies in the low energy consumption and the expected high durability due the low $Ca(OH)_2$ content released during the hydration (211). Because of Its low setting time and strength development it can be used succesfully as a road foundation.

- Table N°3 shows the compressive strength of industrial belite cement obtained from different raw materials (212) .

TABLE N°3
Compressive strengths in MPa of mortars from belite cements (300 Kg/m3)

Sample (Raw material) (Process)	Clinker			Strengths of mortar (after days)			
	LSF	SM	AM	3	7	28	90
A (chalk /wet)	0,79	3,6	2,2	18	30	49	59
B (chalk, wet)	0,80	3,0	2,3	18	29	44	53
B (chalk , wet)	0,80	2,3	0,9	10	17	35	51
C (triassic / Semi dry)	0,79	3,0	1,7	19	23	37	49
D (jurassic/ Semi wet)	0,83	2,4	2,8	26	37	48	nd

5.1.2 - Alkali activated slags or aluminosilicates - The addition of sodium silicate (water glass) permits regulation of the setting time of the cement and a relatively shorter setting time is typical when modulus of water glass (n=Si/Na) is low. For example the setting time with NaOH activation is about 100 to 240 minutes for the initial set and about 420 min for the final setting time whereas, for water glass these time are 30 to 90 and 180 min respectively depending on the slag fineness (213). Also with the water glass activation, high initial strengths are frequently met.

- The compressive strength of the slag mortar with NaOH addition is about 20 to 40 MPa after 28 days when curing temperature is 20°C and 35 to 80 MPa for water glass activation, again depending on the fineness of the slag. The best results are given by steam curing. At the temperature of 80°C the mortar strength can be 50 to 100 MPa immediatly after curing.

The strength of slag mortars increases progressively with time for NaOH and Na_2CO_3 addition. For example after 15 years it is 2.5 time greater than after 28 days. However water glass activation gives only a very small increases of strength (214). Hydraulic compositions based on activated slag and water soluble polymer can develop a bending strength of several hundred MPa under favorable conditions of curing (215).

Alkali activated silicates (also called geopolymeric cements) develop mortar strengths of 25 MPa, 35 MPa, 60 MPa and 100 MPa respectively at 2 hours, 3 hours, 1 and 7 days. This type of cement could find application for road pavements, pavements repairs, airport pavements and in most applications where rapid strength gain is needed. The poor reliability due to the quantity of alkali content of the cement is one of the reason of the slow development of this type of binders.

5.1.3 - Glass cements - The setting time of glass cement, leading after hydration to pure gehlenite hydrate is too long to have useful applications (1 to 3 days) in spite of the quality of the matrix (dense and strong with very low porosity). By decreasing the silica content of the glass, it is possible to obtain a pastes containing hydrogarnet and gehlenite hydrate with an initial set of 1-2 hours, final set 3-4 hours and developing about 100 MPa at 4 hours. These cement paste have a lower porosity than Portland cement and the quality required for a good highway and bridge deck material (216).

5.2 - $CaO-Al_2O_3-SiO_2-CaX_2$

5.2.1 - Alinite cements ($CaCl_2$) - The strength development of alinite cements is not significantly affected, up to 90 days by the quantity of gypsum added (from 4 to 8 % SO_3). It is also shown that W/C ratio affects strength development remarkably. As measured by the standard consistency test, alinite cement requires lower W/C ratio than Portland cement. Even at lower chloride content the strength of alinite cement is comparable to this of traditional cements (145). Because of the release of chloride ions during the hydration, this cement may not be steel reinforced and could find applications in permafrost regions.

5.2.2 - Fluoroaluminate Cement (CaF_2) - Ground from fluoroaluminate clinker with the composition of $C_{11}A_7.CaF_2$ or C_3S and $C_{11}A_7.CaF_2$ added with slag and anhydrate, this cement was put into industrial production in 1975. According to the report by Shen Meifei (217), the cement contains large amount of $C_{11}A_7.CaF_2$, its hydration is very fast. The setting time is from a few minutes to over ten minutes, so it is necessary to add retarders before use. Its features are high early strength, the 4 hour strengths can be as high as 5.4 MPa.
Due to its good behavior under low and negative temperatures, the cement is used for sand forming cement and rush repair or rapid construction works.

5.3 - $CaO-SiO_2-Al_2O_3-Fe_2O_3$

High-alumina cement obtained by melting is largely used worldwide for refractories applications, building and construction. The problem of reliability has been particularly studied from experimental tests and understanding the phenomena. According to C.M George (218/219/220), "conversion" is the normal and predictible route by which the material reaches its stable long term characteristics and the unique advantage of this cement is that the long term performance potential can be attained (and exceeded temporarily) within a few hours of placing the concrete under standard curing conditions (221). Among others advantages of these cements we mention the ability of calcium aluminate hydrates to absorb foreign ions,as well as their thermal stability. Its good sulfate resistance has been recognized on concrete buried after 15 years into sulfate rich soils (222/223/224/225/226/227). In chloride solution,a protective layer is formed at the surface of the cements blocks : this coating is composed by brucite and basic magnesium chloride. Densification of the microstructure have a positive effect on the stability of the cement stored in corrosive solution (228).

5.4 - $CaO-SiO_2-Al_2O_3-SO_3$

5.4.1 - Belite sulpho-aluminates cements - These cement are produced by intergrinding sulpho-aluminate cement clinker composed primarily of minerals $C_4A_3\overline{S}$ and C_2S and a certain amount of dihydrate gypsum or anhydrite. By means of

altering the amount of anhydrite added we can obtain quick-hardening, expanding, self stressing and low alkali series of cements. The industrial production of these cement was started in China in 1974. At present there are a dozen cement mills producing such kind of cement with a total annual output of 500000 tonnes. The cement has the following performance characteristics :

1) Excellent strengths, 3 days compressive strengths which may reach 90 MPa, and 10 MPa in bending strength

2) Good anti seepage properties. Under the hydraulic pressure of 3 MPa, the maximum seepage height are only 7 cm with concrete of different mix, and in most cases than 1 cm (cement consumption of 270-500 kg/m^3)

3) Good frost resistance : the freezing-thawing tests show, a good resistance after 50 cycles of freezing and thawing

4) Excellent corrosion resistance, especially to SO_4^{2-}, Mg^{2+} Cl^- and their compound salts

5) Good behaviour at low temperature. It is sufficient to put cover on the cement series or its products in ambient temperature of 0,-10°C, the strength can grow to 80% of the designed grade in 3/7 days. While in temperature of 0,-20°C, a certain amount of anti freezing admixture shall be added and 80% of the designed strengths can be achieved within 3 days.

6) Regulated expansion. The free expansion can be regulated in the range of 0.5-2%. Self stressing value is high, the magnitude can reach 6.0 MPa within 28 days, the stabilizing period is short (28 days) and may have a good durability.

5.4.2 - **Alite sulpho-aluminate Calcium Cement (HCA)** - The cement is made of alite sulpho-aluminate calcium clinker, with addition of some blended materials gypsum and ground together. Its industrial production started in China in 1985. By adjusting the added quantity of gypsum, altering the gypsum variety and added amount of blended material (over 30%), as well as changing kinds of the blended materials such as slag, fly ash and red mud, quick hardening cements and various modified portland cement can be produced (73).

- The cement has moderate setting time and much higher strength than conventional Portland cement or blended cements its 28-day compressive strength can reach as high as 50-65MPa and the flexural strength 8-9 MPa. It also has good anti seepage properties, good micro expansion (its 28 days percentage of free expansion is less than 0,4%) and good wear resistance.

The cement is suitable for use in underground projects, seepage resistant, crack prevention items road construction and for concrete products like telegraph wire poles, railway sleepers etc...

5.5 - $CaO-SiO_2-Al_2O_3-Fe_2O_3-SO_3$

The cement series, which includes the Ferro-aluminate Cement series, is produced by intergrinding a mixture of aluminoferrite clinker composed mainly of calcium aluminoferrite, anhydrous sulpho-aluminate calcium and dicalcium silicate limestone and anhydrite. A regulated addition of gypsum can produce quick-hardening and expanding and self-stressing cement series. Such a cement series has been produced industrially in China since 1982 and at present the total output is 100000 tons per year (229/230/231).

The performance features of the cement are basically similar to those of the sulpho-aluminate cement. It has excellent strength, the 3 day compressive strength can reach 80 MPa and bending strength 10 MPa. It has eliminated the shortcomings inherent in sulpho-aluminate cement surface dusting. Hydration produces large amount of iron gel that endows the cement with excellent anti-abrasive and sea water resistent properties. It has better corrosion resistance than that of the sulpho-aluminate cement especially to compound salts containing SO_4^{2-} and Cl^- and $(NH_4)_2SO_4$ which is incomparable to any other kinds of cement. It has been shown shows that aluminoferrite cement does not have alkali aggregate reaction and moreover, can form a passivation film on steel reinforcement that is very favourable to protecting the reinforcement from corrosion (188) .

The engineering properties of sulpho and ferro-aluminate cements are quite similar and therefore their applications are also identical. Quick hardening sulpho and ferro-aluminate cements are mainly used in
1) Winter construction in China's North, North East and North West areas as well as in constructional work in the Antartic.
2) Rush repair and rapid construction . The quick hardening ferro-aluminate cement is especialy suitable for harbour engineering, where work must be completed before a next tide coming or for rush repair of taxi way in airport and highway surfaces.
3) Corrosion resistance projects especially for construction on salina and some chemical plants.
4) Refill of high water level lane side of coal mining, because its technical features match those of the commercially available products.

Sulpho and ferro-aluminate cements expanding cements are primarily adopted for leakage and seepage prevention projects, especially for those underground or semi- underground projects in localities close to the seaside, as well as for waterproof layers of rigid roofing. It is also good for leakage and seepage uses in mines and tunnels.

Sulpho and ferro-aluminate self stressing cements are used for making pressure water, petroleum and gas pipeline of 100-800mm diameter.
Low-alkali sulpho-aluminate cements are used mainly for compounding with alkali resistant glass fibre to make glass reinforced cement products as internal and external wall panels, decorative corrugated roofs granary and GRC architectural short pieces (203/204).

5.6 - Phosphate cements

Magnesia phosphate cements exhibit fast setting and high early strengths and find applications for rapid repairs to damaged concrete Calcium phosphate cement produces, during hydration, hydroxyapatite, the principal mineral in teeth and bones and thus because of the apatite nature of the set cement it is highly compatible with soft and hard tissues. The combination of self setting and high biocompatibility makes calcium phosphates cements unique biomaterials.

6 – CONCLUSIONS

The Non-Portland cements described in this paper have common features : the diversity of their application, the low energy consumption in their manufacture, the possibility to solve environmental problems by using wastes and by-products. Among the special applications, the use in cold weather, in rush repair construction, for waste stabilisation, or as biomaterials are only few examples. Among other advantages, the blending of special cements must be mentioned. It is possible to manufacture with the same clinker different cements with different properties and applications by modifying the quality and quantity of the additions (e.g. gypsum, slag , ...).

This can bring about for the enterprises strong vitality and broad horizons for product development. At the same time it opens up a better path for mass industrial wastes utilization and comprehensive usage of mineral ressources.
In spite of numerous advantages, the development of Non-Portland is impeded by the availability raw material and the difficulties for the customers to break away from old traditional ways of using conventional cement.

The new directions of future development will be concentrated in the diversification of raw material sources for the manufacture of special cement such as industrial waste, chemical gypsum, high SiO_2, bauxite and high MgO limestone which are abundant, low Ca containing minerals and in the optimization of the burning process to lower the heat consumption in their production.

Concerning cement hydration, the impact of industrial wastes and additives on hardening of special cements will be studied so as to explore possibilities of using blended materials in larger percentages (30/70%) to manufacture special blend cements. Concerning the aspects of hardened cement paste microstructure, emphasis will be laid on pore structure of concrete made of special blend cements, its interface effects and crystal/gel ratio, on theoretical models in order to optimize structural enginering properties of the concrete and its durability. With concentrated efforts by the cement developers all over the world, a great leap forward will be launched for expansion of cement variety. The new special cements will prove their worth in manufacture and utilization, contending with the traditional Portland cement which has history of 160 years of production.

Acknowledgements :

I wish to express my thanks to Dr Jan Skalny for helpful discussions and advices during the writing of this manuscript. I am grateful to R. Montgomery for translating this manuscript, with much skill and patience.

7 – REFERENCES

Some references are quoted as confidential or internal reports. They corresponds mainly to thesis or on going experiments and can be obtained directly from the authors.

1) Kaden, R.A. : "Lunar concrete", American Concrete Institute, 1991, SP 125.
2) Sharp, J.H., Winbow, H.D. : "Magnesia-Phosphate Cements", Cement Progress Research, 1990, 233-263.
3) Davidovits, J. : "Liant geopolymérique fluoro-alumino-silicate et procédé d'obtention", French Patent 1990, N° 90 02854.
4) Scheetz, A.G., Landers, A.G., Odler, I., Jennings, H. : "Specialty cements with advanced properties", Material Research Society, Boston, 1989, vol 179.
5) Mohan, L. : "Advances in some special and newer cements", in Cement and concrete science & technology vol 1 part 1 edited by S.N. Gosh, 1991, 252-308.
6) Manghabhai, R.J. : "Calcium aluminate cements", July 1991, Proceedings of the International Symposium London 9-11, ed E.F.N Spon.
7) Kurdowski, W., George, C.M., Sorrentino, F.P. : "Special cements", Principal paper, 8th International Congress on the Chemistry Cement Rio de Janeiro 1986 vol 1, 297-304.
8) Kurdowski, W., Sorrentino, F.P. : "Special cements", in Structure and Performance of cements edt P. Barnes 1983, 471-555.
9) Wan Yanmou., Su Muzhen. : "The feature of new kinds of cement and their development trend in China", Cement 1990, 3 , 15 pages.
10) Wan Yanmou., Jun'an D., Su Muzhen. : "An investigation into cement CaO-SiO2-Al2O3-Fe2O3 system", 1986, 8th International Conference on the Chemistry of Cement, Rio, 2, 300-305.
11) Gartner, E.M., Myers, D.F. : "New cements and Novel Cement Matrices", "Advances in cementitious materials", ceramic transactions, American ceramic Society, 1990, 621-642.
12) Stark, J., Müller, A. : "International development trends in low energy cements", Zement-Kalk-Gips 1988, 4, 88, 162-165.
13) Odler, I. : "The possibilities of increasing SO3 content in cement", Advances in cement manufacture and use, Engineering Foundation conferences 1988, 303-310.
14) Djuric, M., al. : "Computerized thermodynamic analysis of reactions during sintering of CaO-Al2O3-SiO2 system", Cement Concrete Research, 1992, 22, 139-148.
15) Ayed, F. "Contribution à l'étude des phénoménes thermiques lors de la clinkérisation de crus de ciments Portland", Ph D. thesis 1991 Université de Provence, Marseille, France.

16) Hallstedt, B. "Assessment of the CaO-Al2O3 system". Journal of American Ceramic Society, 1990, 75, 1, 15-23.
17) Nurse R.W., al. "The CaO-Al2O3 System in a moisture free atmosphere", Transaction of British Ceramic Society 1965, 64, 409-418.
18) Pitak, N.V., al. : "Kinetics of the solid phase reactions occuring during the production of clinker of a high alumina cement by sintering", Ogneupory 1988, 8, 3-6.
19) Scian, A.N., al. : "High alumina cements. Study of CA formation", 1) Stoechiometric mechanism. Cement Concrete Research 1987, 17, 2,198-204. 2) Kinetics. ibid. 1987,17, 4, 525-531.
20) Packter, A. : "The kinetics of heterogeneous K alumina calcium oxide powder reaction to form calcium aluminates : composition and particles size effects", Silicates Industriels 1986, 7/8, 109-113.
21) Ali M.N., al : "Kinetics and diffusion studies in CA2 formation", Cement Concrete Research 1989, 19, 1, 47-52.
22) Derdacka Grzymek, A., al. : "Scanning electron microscope observation of polymorphic transitions occuring on a C12A7 surface under electron beam action", Journal of material Sciences 1989, 24, 1, 355-358.
23) Togan, D., al. : "The crystallisation kinetics of 12CaO-7Al2O3 glass", Thermochemica Acta 1989, 149, 387-391.
24) Stark, J., al. : "Manufacture of active belite cement with regards to the reduction of energy consumption", Il cemento 1987, 3, 239-250.
25) Suzuki K., al : "Hydration and strengths of alpha, alpha prime and beta dicalcium silicates stabilized with Na-Al, K-Al, Na-Fe and K-Fe", 7 th International Conference on Chemistry of Cement Paris 1980, 2, 47-51.
26) Suzuki, K., al. : Semento Gitutsu nempo, 1978, 32-37.
27) Struillou., al. "Synthesis at about 750° and properties of a sulphated beta C2S", International Conference on Chemistry of Cement Paris 1980, 3, 75-80.
28) Stark, J., al. : "Existence conditions of an hydraulic active belite cement", Zement Kalk Gips 1981, 34, 9, 476-481.
29) Müller, A., al. : "Present position in developing an active belite cement", Zement Kalk Gips 1985, 38, 303-304.
30) Kurdowski, W., al. : Beijing Inter Symp on Cement and concrete, China Academic Publishers 1985, 4.
31) Keil, F., al. : "Hydraulic Properties of basic glasses with the gehlenite and akermanite composition", Zement Kalk Gips, 1958, 11, 137-143.
32) Locher, F.W. : "Hydraulic properties and hydration of glasses of the system CaO-Al2O3-SiO2", 4 th international congress of the chemistry of cement Washington 1960, 267-271.
33) Malopetzi, J., al. : "Effect of additions on the hydration process of vitrified gehlenite", Cement Wapno Gips 1987, 40, 6, 114-118, 1987, 40, 7, 136-140.
34) Dron, R.: "Structure et réactivité des laitiers vitreux", PH.D. Thesis Paris VI 1984.
35) Trief, V. : "Method for producing a hydraulic binder in powder form", U.S.P N° 2819172 7/01/1953.
36) Mac Dowell, J.F. : "CaO/Al2O3/SiO2 hydraulic cements" U.S.P N°4605443 12/08/1986.
37) Mac Dowell, J.F. : "Hydrogarnet gehlenite hydrate cements from CaO/Al2O3/SiO2 glasses", 8 th International Congress Chemistry of cement (RiO), 1986,423-428.
38) Nakagawa, K., al.: "A study of hydration of amorphous calcium aluminate by selective dissolution analysis", Cement Concrete Research, 1990, 20, 655-661.
39) Nakagawa, K., al. : "Influences of glass contents and chemical composition on the very early hydration of amorphous calcium aluminate", Gypsum Lime, 1991, 231, 10-15.
40) Hisashi, O., al.: Journal of Ceramic Society Japan, 1979, vol 87, 400-404.
41) Liu Baoyuan., al. : "High temperature XRD research on several transitional phases during the formation of Portland cement clinker in the presence of CaF2 and CaSO4", Journal of the Chinese Ceramic society, 1981, vol 9, N°4, 456-462.
42) Chen Yiming., al. : "A phase of calcium fluosilicate and the relationship between its and C3S formation", Tian Tiang University, (China), 1985 MSc degree.
43) Xue Jungan., Yie Qin. : "Crystal chemistry Research on C3S solid solution containing ions of fluorine and sulphur", Journal of the Chinese ceramic society, 1989, 17, 2, 97-104.

44) Massazza, F., Gilliotti C. : "Contribution to the alinite knowledge", Il cemento 1982, 80 2, 101-106.
45) Kurdowski, W.:"Bromide alinite", Cement Concrete Research, 1989, 19, 657-661.
46) Kurdowski, W., Moryc U. : "Once more about bromide alinite" Cement Concrete Research, 1989, 19, 657-661.
47) Lampe F.Ket., al. : "Synthesis crystal structure and properties of a New magnesium monosilicates chloride Ca8Mg,(SiO4)4Cl2) Cement Concrete Research 1986, 16, 624-632.
48) Garbacik, A. : "Acceleration of the formation of dicalcium silicate by the addition of calcium chloride", Ph D thesis Academy of mining and metallurgy Krakow 1982.
49) Kurdowski, W., Garbacik A.: "Transitory phases in the synthesis of dicalcium siicate in the presence of calcium chloride", Polish Academy of science Kracow Ceramika 1980, N° 30, 47-52.
50) Kurdowski, W., Garbacik A.: "Calcium chloride utilization in clinker burning", 7 th International conference on cement chemistry, 1980, vol 4, 702-706.
51) Yao Daixi., Tong Daimo. : "Research on silicate clinker calcined at low temperature with a mineralizer composed of calcium chloride and calcium sulphate", Wuhan Polytechnic College (China), Master of science, 1991.
52) Su Muzhen. : "Research on the formation of phases in the CaO-SiO2-CaCL2 system", Bulletin of the Chinese Silicate Society, 1982, 1, 2.
53) Chen Yangmin., Ye Ruilun. : "Phase diagram of CaSiO4-CaCl2 system", Wuhan Polytechnic College (China), Master of science 1991.
54) Wu Bolin., Ye Ruilin. : "Crystal structure of high temperature type of CaSiO4. CaCl2", Wuhan Polytechnic College (China), Master of science 1991.
55) Mingyauan Chen., Yi Fang. : "The chemical composition and crystal parameters of calcium chlorosulfo silicate", Cement Concrete Research, 1989, 19, 184-188.
56) Lampe F.V., al. : "Synthesis, structure and thermal decomposition of alinite", Cement Concrete Research 1986, 16, 4, 505-510.
57) Pozun, A.: "Operating experience in the production of high alumina cement", Zement Kalk Gips, 1988, 9, 344-346.
58) Kvyatkovskii O.V., al. :"Burning clinker for high alumina cement in a rotary kiln" Refractories", 1987, 28,5/6, 333-334.
59) Sorokin, I.N., al. : "Production of high alumina cement clinker by fusion in an electric furnace", Ogneupory, 1984, 5, 293-295.
60) Sawkow, J.: "High alumina cements based on calcium aluminate clinker with different phase compositions and sintering degrees", ref 6, 27-38.
61) Sokolov, A.N., Kvyatkovsii, O.V. : "Preparation of the charge and firing in a shaft kiln of high alumina clinker", Refractories, 1986, 27, 9-10, 588-591.
62) Bakalkin, A.P., PitakN.V.: "Experience with producing high alumina cement by calcination in a shaft kiln", Refractories, 1986, 27, 9-10, 592-594.
63) Venkateswaran, D., al. : "Microstructure of high purity high alumina cement clinkers and its effect on cement properties", Proceeding of the 13 th international conference on cement microscopy, Tampa Florida 8-11 april 1991, 71-85.
64) Chakraborty, I.N., Narayanan, S., al. : "Effect of morphology on the hydration characteristics of high alumina cements", ref 6, 17-26.
65) Sourie, A., Glasser F.P. : "New study of the mineralogy of high alumina clinker", International Symposium London 9-11 July 1990.
66) Sourie, A., Glasser F.P. : "Studies of the mineralogy of high alumina cement clinkers", British Ceramic Transaction J . 1991, 90, 71-76.
67) Sourie, A.: "Mineralogy of aluminous cements and their reactivity", Ph.D thesis Aberdeen University 1991.
68) Taylor, H.F.W.: "Modification of the Bogue calculation", Advances in Cement Research 1989, 6, 73-77.
69) Sorrentino, F.: "Comparison of methods for quantitative determination of phases in high alumina cement clinker", International Symposium on High Alumina cements, London 9-11 July 1990.
70) Pekarek, D. : "Rapid semi quantitative XRD of HAC", Silikaty, 1988, 32, 3, 267-271.
71) Marciano, E., Da Cunha Munos, F.A. : "Characterization and quantitative determination of calcium aluminate clinker phases through reflected light microscopy", 11th International Conference on Cement Microscopy New Orleans (USA), 1989, 1-15.
72) Capelle, M., Capmas A., Chaix, J.M. : "Characterization of phases in an aluminous cement by image analysis", 11th Conference on Cement Microscopy New Orleans (USA), 1989, 15-129.

73) Wang Yanmou., Su Muzhen. : "Summarization of Special Aluminate cement", Cement, 1987, 5, 6.
74) Ikeda, K. : "Cements along the join C4A3$\bar{S}$-C2S", 7th International Conference on the Chemistry of cement, Paris 1980 vol II, III - 31 bis III - 36.
75) Mubhatkal, G.A., Chatterjee, A.K., al. : "Non alite cement from calcium sulfoaluminate clinker, optimization for high strength and low temperature application Intern. conference on chemistry of cement", Rio (Brazil) 1986, 4, 364-370.
76) Viswanathan, V.N., Raina, S.J., Chatterjee, A.K. : "An exploratory investigation on Porsal cement", World cement technology 1978, 9, 109-118.
77) Ayed, F., Lehoux, P., Sorrentino, F. : "Calcium sulfoaluminate formation", 14 International conference cement microscopy, Costa Mesa, California 5-9 April 1992,325-332.
78) Hanic, F., Havlica., al. : "Crystal chemistry and thermodynamics of the sulfate compounds", Ca2Al16O12)SO4 and Ca5(SiO4)2(SO4) British Ceramic Transaction Journal, 1986, 85, 52-57.
79) Mehta, P.K.: "High Iron oxide hydraulic Cement", July 19, USP N° 4036657, 1977.
80) Wang Yanmou., Su Muzhen., Deng Junan. : "Success in industrialized Production of ferro aluminate cement", Institute of building materials Beijing (China), 1982, 4.
81) Wang Yanmou., Su Muzhen., Deng Junan. : "Study of ferroaluminate cement", Cement, 1982, 8 -15.
82) Wang Yanmou., Su Muzhen., Deng Junan., LiDedong. : "Research on mineralogical composition of cement", in quinary system of CaO-SiO2-Fe2O3-SO3" Journal of silicate, 1982, 10, 4, 369-376.
83) Guo Yong., Deng Junan Su Muzhen., Wang Yanmou. : "Investigation in mechanism of ferric phase formation in ferro aluminate cement" journal of silicate, 1988, 16, 6-11.
84) Mackenzie, K.J.D., Alasti, H. : "Formation kinetics of Portland Cement Clinker phases, Part 2 : Tetracalcium Aluminoferrite", Transaction of British Ceramic Society, 1978, 77, 5, 162-167.
85) Fan Aoming, Zhong Jinyu. : "Study of forming process of calcium ferroaluminate and some effecting factors", Research institut of building materials Beijing (China) 1988.
86) Xue Jungan., Li Xuiying., al. : "The effect of adding F-, S- on the law of aluminoferrous phase formation", Journal of Silicate, 1985, 13-17.
87) Tikhonov, V.A., al. : "Special high ferriginous cement", Proceedings of 6th international conference on the chemistry of cement vol 2, 1974, III, 4, N° 161.
88) Guo Yong., Wang Yanmou., Su Muzhen., Deng Junan. : "Research on characteristics of hydration of ferric phase in ferro aluminate cement", journal of silicate, 1989, 17, 4, 296-301.
89) Newkirk, T.F., Thwaite, R.D. : "Pseudoternary system calcium oxide-monocalcium aluminate, (CaO.Al2O3), dicalcium Ferrite (2CaO.Fe2O3)" journal of Research of the National Bureau of Standards, 1958, 61 4, 233-243.
90) Kapralik, I., Hanic, F. :"Phase changes in the system CaO-Al2O3-SiO2-Fe2O3-MgO-CaSO4-K2SO4, in air up to 1300° referred to sulfo aluminate clinker", Transaction of the British ceramic Society 1986, 85, 131-136.
91) Kimura, S., Muan, Z.A. : American mineralogist, 1971, 56, 1332.
92) Puertas, F., Glasser, F.P. : "Modification of the ferrite phase in cements by manganese substitution", Advances in Cement Research vol 1, N°1 31-34.
93) Zeng Yanwei., Yang Nanru. : "A comparative study of the ferrite phase in high iron cements with the pure C2AxF1-x by Mössbauer spectroscopy", Cement concrete Research 1991, 21, 31-37.
94) Kunbargi, H. : "Very early setting ultra high early strength cement", US patent N° 4957556, Sep. 18, 1990.
95) Li Xuiying., al. : "Study of alite sulphoaluminate cement", Journal of silicates (China) 1990, 16, 6, 557-564.
96) Palomo, A., Blanco-varela, M.T.,Vasquez T. : "Microstructure found in the solidification of compositions of the system CaO/Al2O3/Fe2O3 and its variations by the presence of CaF2", Silicates Industriels, 1988, 1, 2 21/31.
97) Blanco-Varala, M.T., Vazquez, T., Palomo, A. : "A study of a new liquid phase to obtain low energy cements", Cement Concrete Research 1986, 16, 97-104.
98) Lu Ping. : "Formation of C4AF, C4A3$\bar{S}$ and C11A7CaF2 and their early hydration", Journal of silicate (China), 1985, 13, 3-6.
99) Chow, L.C., Takagi, S., Constantino, P.D.: "Self setting calcium phosphate cements", in ref. 4, 1989 vol 179, 3-25.
100) Xie, L., Monroe, E.A.: "Calcium phosphate dental cements", in ref. 4, 1989 vol 179, 25-41.

101) Nishikawa, T., Suzuki, K., Ito, S.: "Formation of hydrates in the system CaO-Al2O3-SiO2-H2O at high PH", Il cemento, 1985, 4, 185-194.
102) Kapralik, I., Stevula, I. , Hanic F. : "Hydration and hydraulic properties of the phase in the System CaO-Al2O3-H2O referred to high Alumina Cements", Cement Concrete Research, 1989, 19, 519-526.
103) Brisi, C., Lucco Borlera, M., al. : "Hydration of C5A3", Cement Concrete Research, 1986, 16, 2, 156-160.
104) Fujii, K., al., "Kinetics of hydration of monocalcium aluminate", J. American Ceramic Society, 1986, 4, 361-364.
105) Fournier, A.A., Lecompte, J.P., al. : "Hydratation de l'aluminate monocalcique, Influence des écarts de composition" Cement Concrete Research, 1985, 15, 1, 151-158.
106) Fournier, A.A., J.P, Lecompte., al. : "Hydratation de l'aluminate monocalcique role du broyage", Cement Concrete Research 1985, 15, 2, 269-275.
107) Mascolo, G., Marroccoli, M. : "A study on the reactivity of C4A, n-H2O with aqueous solutions", Cement Concrete Research , 1986, 16, 5, 679-684.
108) Ball, M.C., al. : "Surface composition of anhydrous monocalcium aluminate", J. Materials Science 1988, 3, 4, 1431-1435.
109) Bachiorini, A., al. : "Hydratation du CA amorphe, orthorhombique et monoclinique", Ciments, bétons Platres Chaux, 1986, 760, 172-174.
110) Ohta, M., Kimura, T., Yanagida H. : "The early stage of hydration of CA2", J. Ceramic Society Japan, 1988, 96, 1, 36-40.
111) Zaldat, G.L., Kukuj, S.M. : "Hydration kinetics and activity of CA2", Ogneupory, 1987, 54, 18-21, Refractories 1987, 28, 5/6, 313-317.
112) Capmas, A., Sorrentino, D., Damidot, D. : "Effect of temperature on setting time of calcium aluminate cements", ref 6, 65-81.
113) Rettel, A., al. : "On the hydration of CA at various temperature" British Ceramic Transactions. J. 1985, 84, 25-28.
114) Bushnel-Watson, S.M., Sharp, J.M. : "The effect of temperature upon the setting behavior of refractory calcium aluminate cements", Cement Concrete Research 1986, 16, 6, 875-884.
115) Edmonds, R.N., Majumdar, A.J. : "The hydration of Secar 71 Aluminous Cement at different temperatures", Cement Concrete Research, 1989, 19, 289-294.
116) Murat, M.,al. : "Etude par calorimétrie isotherme de l'influence de la température sur la réaction d'hydratation de l'aluminate monocalcique", Comptes rendus de l'académie des sciences de Paris (France) 1980, 291, 113-115.
117) Chen Yimin., Shi Liping. : "On hydration of dopped beta C2S 8 th Conference on cement", chemistry and technology CCCP 1991.
118) Ftikos, Ch., al. : "Preparation and hydration study of rich C2S cements", Cement and Concrete Research 1990, 20, 934-940.
119) Bei; R., Ludwig, U. : "Hydraulic reactivity of belite-rich Portland cements", Zement Kalk Gips 1990, 10, 90, 506-510.
120) Menetrier-Sorrentino, D., al. : "The setting and hardening characteristics of calcium aluminate cements : studies of the systems C12A7-C3A, and C12A7-CA", 8th International Congress on the Chemistry Cement, Rio de Janeiro, 1986, vol 4, 334-338.
121) Nakagawa, K., al. : "Mechanism of fast hydration and hardening of amorphous calcium aluminate and anhydrite" Gypsum and lime 1989, 218,12-17.
122) Menetrier-Sorrentino, D., al. : "Hydration of amorphous and crystallised compounds based on monocalcium aluminates", UNITECR, Aachen, sept 1991, 267-271.
123) Shoji, T. : " Ca3Al2(SiO4)3- Ca3Al2(H4O4)3 series garnet , composition and stability" Journ. Mineral Soc. Jap.1974 , 259-272 .
124) Kuzel, H.J. : "Crystallographic data and thermal decomposition of synthetic gehlenite hydrate 2CaO-Al2O3-SiO2-8H2O" N. Jahrbuch f. Mineralogie Monatshefte 1976 , 320-325 .
125) MacDowell, J.F.,Sorrentino, F. : "Hydration mechanism of gehlenite glass cements" Advances in Cement Research 1990,3,12,143-152
126) MacDowell, J.F : "Stratlingite and hydrogarnet from calcium alumino silicate glass cements", Fall MRS meeting Boston 1989.
127) Malolepsszy, J. : "Hydration and properties of slag paste", Ceramika 53 Krakow 1989, Zeszyty Naukowe AGH
128) Teoreanu, I., Puri, A.:"Erhärtungsmechanismus und Hydrattphasen im System Gehlenit-Wasserglas-Wasser", Zement Kalk Gips, 1984, 8, 427-31 .
129) Teoreanu, I., Georgescu, M. : "Chemical studies and X ray analysis of the hydration of vitreous gehlenite in the presence of activators" Bulletin of the polytechnic institute of Bucharest 1970, 32, 6, 1-8

130) Malolepsszy J. Deja J. unpublished data.
131) Kurdowski, W., Malolepsszy, J. 2d Inter Seminar : "Durability of concrete, Aspects of admixtures", Gothesburg 1989, 77-82
132) Murat, M., Comel, C. : "Hydration reaction and hardening of calcined clays and related minerals III - influence of calcination process of kaolinite on mechanical strengths of hardened metakaolinite", Cement and Concrete Research, 1983,13 ,5 ,631-7 .
133) Prince, W., Perami, R.: "Conditions de formation préférentielle de géhlénite hydratée dans les liants de kaolin activée et de chaux", Comptes rendus de l'Académie des sciences, Paris, 1989, t. 309, Série II, 49-52 .
134) Prince, W. : "Etude de la réactivité de matériaux naturels activés par voie thermique ou mécanique en vue de leur utilisation comme liant", Ph. D thesis, Paul Sabatier University, Toulouse (France), 1987.
135) Midgley, H.G, Chopra, S.K. : "Hydrothermal reactions between lime and aggregates fines", Magazine of concrete Research, 1960, 2, 35, 73-81.
136) Majumdar, A.J., et al : "Hydration of mixtures of "Ciment Fondu" Aluminous cement in presence of granulated blastfurnace slag", Cement and Concrete Research, 1990, 20, 197-208.
137) De Silva, P.S., Glasser, F.P : "Hydration of cements based on metakaolin thermochemistry", Advances in cement research 1990, 3, 12 167-177
138) Zampieri, V.A. : "Mineralogical and microstructure of reaction products in metakaolinite-lime 12th mixtures", International Conference on cements microscopie Vancouver 1990, 79-96
139) Pera. J, al. : "Effet pouzzolanique du métakaolin. Corrélation entre le développement des résistances mécaniques et la nature des hydrates formés", Comptes rendus de l'Académie des sciences, 1984, Paris, t. 299, Série II, 18, 1251-54.
140) Malone, P.G., al. : "Potential applications of alkali-activated aluminosilicate binders in military operations", U.S. army Corps of engineers reports GL 85 15 Washington D.C. 1985.
141) Heitzman, R.F., Gravitt, B.B., Sawyer, J.L. : "Cements composition curable at low temperatures", US patent N° 4842649, Jun. 27, 1989.
142) Davidovits, J. : "Geopolymers of the first generation : Siliface-process", First europeen conference on soft mineralurgy. Geopolymer 1988, vol 1, 49-67.
143) Davidovits, J., "Mineral polymers and methods of making them", US patent N° 439386, sep 14, 1982 "Synthetic mineral polymer compound of the silicoalumintes family and preparation process", U.S. Patent N° 4472199, sep. 18, 1984.
144) Tanjin building materials research Institute : supplementary report on alkali waste cement clinker sintered with oil. Unpublished report 1982.
145) Ftikos, Ch., Georgiades, A., Philipou, Th. : "Preparation and hydration study of alinite cement", Cement concrete Research 1991, 21, 1129-1136.
146) Yie Qing., Liu Baoyan., Xue Jungan. : "Study of hydraulicity of tricalcium silicate solid solution containing fluorine and sulphur", journal of silicate, 1989, 3, 1, 230-239.
147) Afshar, A.B., Mccarter, W.J. : "Early hydration characteristics of aluminous cement" J. Mater. Sci. Letters 1985, 4, 7, 851/854.
148) Greenslade, D.J., al. : "The use of nuclear magnetic resonnance (NMR) in the study of high alumina cement hydration", ref 6, 81-95.
149) Beylouni, M.F. : "Fillerisation du ciment alumineux ; étude de l'influence des conditions thermiques d'hydratation", PH.D Thesis INSA Toulouse 1988.
150) Perez, M. : "Effect of CaCO3 added to high alumina cement mortar subjected to elevated temperature curing and carbonation", Cement Concrete Research 1984, 14, 1-10.
151) Fentiman, C. : "Hydration of carboaluminous cement at different temperatures", Cement Concrete Research 1985, 15, 4, 622-630.
152) Piasta, W.G. : "The effect of limestone fillers on sulphate resistance of high alumina cements composites", ref 6, 241-256.
153) Midgley, H.G., Rao, P.B. : "Formation of Strâtlingite in relation to the hydration of high alumina cement" Cement and Concrete Research, 8, 1978, 168-172.
154) Rao,P.B., Viswanathan, V.N. : "Chemistry of arresting strength retrogression in structural high-alumina cements" 7 th Int Congress Chemistry of cement (Paris), 1980, 5, 51-55.
155) Bentsen, S et al : "Effects of microsilica on conversion of high alumina cement", ref 6, 294-319.
156) Edmonds, R.N, Majumdar, A.J : "The hydration of mixture of monocalcium aluminate and blastfurnace Slag" Cement concrete research, 1989, 19, 779-782.

157) Majumdar, A.J.,et al : "Hydration of mixtures of C12A7 and granulated blastfurnace slag" Cement and Concrete Research,1989, 19, 848 -856.
158) Majumdar, A.J., et al : "Hydration of SECAR 71 Aluminous cement in presence of granulated blastfurnace slag" Cement and Concrete Research, 1990, 2, 7-14.
159) Majumdar, A.J.et al : "Hydration of calcium aluminates in presence of granulated blastfurnace slags" ref 6, 259-272.
160) Majumdar, A.J. : "Cement compositions" European Patent application N° 0312323, 12 / 10 1989.
161) Fentiman, C. et al : "The effect of curing conditions on the hydration and strengths development in fondu slag", ref.6, 272-282.
162) Murat, M., El H. Sadok : "Role of foreign cations in solution on the hydration kinetics of high alumina cement", ref 6, 155-166.
163) Gill, S.M. et al : "The influence of superplasticizing admixture", ref 6, 127-141.
164) Yamazaki, K. et al : "Surface state of calcium monoaluminate in the presence of phosphoric acid solution", J. Mater. Sci. Letters, 1987, 6, 4,471-473.
165) Sharp, J.H. et al : "The effect of admixtures on the hydration of refractory calcium aluminate cements", ref 6, 127-141.
166) Teoreanu, I. et al : "The influence of some organic admixture on refractory aluminous hydration", Il Cemento, 1986, 3, 191-198.
167) Teoreanu, et al : "Refractory concretes based on aluminous cement and chromic anhydrite and sodium tripolyphosphate admixtures" Verre, 1987, 1, 2, 160-170.
168) Currell, R., al. : "The acceleration and retardation of Set High Alumina Cement by additives", Cement Concrete Research 1987, 7, 420-432.
169) Sarandily, A., Baggott, R. : "Effects of autoclaving on the strength of hardened calcium aluminate cements" ref 6, 353-362.
170) Wang Yanmou., Guo Yu., Su Muzhen. : "Investigation in ferric phase in ferroaluminate cement", Institut of Building Material, Beijing (China) Master of sciences 1987.
171) Su Muzhen., Chen Yimin., Shi iping., Deng Jun'an., Liu Xizaoxin. : "The application of thermal analysis and conduct ion calorimetry on the formation and hydration of calcium aluminoferrite", The 5th Confeence on calorimetry and thermal analysis, Zakopane, (Poland) 1991.
172) De Keyser, W.L., Tenoutasse, N. : "The hydration of the ferrite phase of cements", International symposium on chemistry of cement Tokyo 1968 Paper 2-120, 379-385.
173) Bayoux, J.P., al. : "Study of the hydration properties of aluminous cement and calcium sulphate mixes", ref 6, 320-334.
174) Brooks, S.A., Sharp, J.H. : "Ettringite-based cements", ref 6, 335-350.
175) Banfill P.F.G. "The effect of sulphate on the hydration of high alumina cement", Cement Concrete Research, 1986, 16, 602-604.
176) Lu Ping. : "Tentative research on mechanism of Aft formation", Symposium on ettringite, China silicate society 1982.
177) Beau, D. : "Action de CO2, SO4, sur les aluminates de calcium hydratés à l'équilibre de solubilité" Ph.D. thesis, Universite de Bourgogne, France 1990.
178) Atkins, M., al. : "Solubility data for cement hydrate phases", Department of the environment HMIP report N° DoE/HMIP/RR/91/0.32, 1991.
179) Zhong Baiqiang., Yang Nanru., Dong Pan., Wang juan. : "Conditions for AFt phase Formation and stabilizing" Symposium on ettringite 1982.
180) Xue Jungan. : "Formation, stabilization and expansion of ettringite phase", Journal of silicate, 1983, 11, 2-10.
181) Liu Baoyan., Xue Jungan. : "Ettringite in hardened cement Paste", Symposium on ettringite 1982.
182) Xi Yaozhong. : "Accurate determination on date of X-ray Powder of hydrated calcium high sulphoaluminate and calcium", journal of silicate, 1988, 6, 16-18.
183) Cohen, M.D., Mobasher, B.: "Effects of sulfate and expansive clinker contents on expansion time of expansive cement paste", Cement Concrete Research 1991, 21, 147-157.
184) Hanic, F., al. : "Mechanism of hydration reactions in the system C4A3$\bar{S}$-CS-CaO-H2O , referred to hydration of sulfoaluminate cements", Cement Concrete Research 1989, 19, 671-682.
185) Kapralik, I., Hanic, F. : "Phase relation in the subsystem C4A3$\bar{S}$-CSH2-CH-H of the system CaO-Al2O3-CS-H2O referred to hydration of sulphoaluminate cement", Cement Concrete Research 1989, 19, 89-102.

186) Feng Xuiji., liao Guanglin. : "Probe into the structure of 3CaO3Al2O3 CaSO4 and its rate of hydration", Journal of Wuhan Polytechnic University 1991.
187) Li Shaozheng., Wang Yanmou., SuMuzhen. : "Research on interface between hardened sulphoaluminate cement pastes aggregate postgraduate division, Wuhan Polytechnic University 1990.
188) Tang Mingsu. : "A thermodynamic estimation of decomposition temperature of sulphoaluminate and carboaluminate", symposium on ettringite 1982.
189) Li Dedong., Den Junan. : "Study of thermal stability of ettringite in hardened sulphoaluminate cement paste", Confidential report 1982.
190) Zhang Feipeng. : "Primary Investigation in formation of minerals like ettringite and thermodynamics and their transformation", Symposium on ettringite 1982.
191) Lou Zonghan., Wang Yuqing., al. : "Double expanding cement for dam and the principle of minimum energy of expansion", Proceeding of Beijing 2d International congress on cement and concrete 1989.
192) Zurz, A., Odler, I., Dettki, B. : "Investigations on phosphate cements", hardening at room temperature ref 4, 83-88.
193) Scrivener, K.L., Taylor, H.F.W.: "Microstructural development in pastes of a calcium aluminate cement", ref 6, 41-51.
194) Poon, C.S., Groves, G.W. : "TEM observations of high alumina cement paste", J. mater Sci. letters 1988, 7, 3, 243-241.
195) Gessner, W. et al, "On the change of microstructure during the hydration of monocalcium aluminate at 20° and 50°C", ref 6, 96-110.
196) Sinclair, W., Groves, G.W. : "The microstructure of high strength cement pastes" in.: "Very high strength cement-based materials" edt by Young F, Material research society, 1989, 39-44.
197) Castano, V.M., al. : "Transmission electron microscope studies on hydrated calcium aluminate cements", 8th Intern. conf.cement microscopy, 1986, 118-131.
198) Seltveit, A., al. : "Microstructural aspects of microsilica-blended high alumina castables", Ceram. Eng. Proceed, 1986, 7, 1-2, 243-260.
199) MacDowell, J.F., al. : " Hydrogarnet-gehlenite hydrate in glass cements", Proceeding of the 13th international conference on cement microscopy 131-146, Tampa Florida 8-11 april 1991.
200) Richardson, I.G., Groves, G.M. : "The microstructure of blastfurnace slag/ high alumina cement pastes", ref 6, 282-293.
201) Bachiorini, A., Murat, M. : "Evolution microstructurale des composites du systeme ciment alumineux granulats calcaires 1) mode de propagation de la fissure Cement Concrete research 1987, 17, 2, 242-248, 2) Influence sur la porosité et les résistances mécaniques Cement", Concrete research 1987, 17, 3, 397-403.
202) Bachiorini, A., al.: "Microstructural disorder and calcium carbonate reactivity with monocalcium aluminate during hydration", Mater. Chem. Phys. 1986, 14, 1, 1-46.
203) Zhang Liang., Wang Yanmou., Su-Muzhen., Deng Junan. : "Study of high strength concrete made from blend ferro-aluminate cement" Master degree China Building Materials Academy 1981.
204) Wang Yanmou., Yang Renhe., SuMuzhen. : "Hydration Characteristic of sulpho-aluminate cement and quantitative investigation in its hardened cement", Confidential report 1991.
205) SuMuzhen., Yang Renhe., Li Shaozheng., Wu Zongdao., Deng Juan., Liu Baoyuan "Study of interface between hardened sulphoaluminate cement paste and limes-tone", Confidential report 1991.
206) Lu Yonghua Wang Yanmou., Su Muzhen. : "Study of the Interface between hardened sulphoaluminate cement paste and limestone", Confidential report 1991.
207) Feng Xuiji., Long Shizong. : "Research of Positron annihilation and hydra-tion" Cement concrete research 1987 , 17, 532-538.
208) Yei Mingxun., Wang Fao., Xue Jungan., Xu Wenia. : "Liquid phases in pores and voids in hardened cement paste" Master degree 1982.
209) Abdelrazig, B.E.I., Sharp, J.H., El-Jazairi. : "The microstructure and mechanical properties of mortars made from Magnesia-Phosphate cements", Cement and Concrete Research 1989, 19, 247-258.
210) Popovics, S., Rajendran, N., Penko, M. : "Rapid hardening cements for repair of concrete" ACI materials journal 1987, 84, 64-73.
211) Rajczyk, K., Kurdowski, W., Werynski; : "Cement Wapno Gips", : under Press
212) Malolepsszy, J., Deja, J., Cement wapno Gips ; 1983, 10-11.

213) Malolepsszy, J., Deja, J., Cement wapno gips 1984, 5.
214) Malolepsszy, J., Deja, J., 10th int Baustoff and Silicattagung vol 2 Weimar 1988, 198-201.
215) Kiomoto, M., al. : "Hydraulic compositions and high strength composite material", European Patent N° 431503 A2 Dec 1990.
216) MacDowell, J.F., Chowdhury, A. : "Quick setting high early strength glass-based cements for rapid highway repair" Transportation research board meeting,;1990, paper N° CB023, 7-12,1.
217) Sheng Meifei, Deng Zhongyan et al : "Study of paper, high early strength aluminate cement" Confidential report, 1991.
218) George, C.M.: "Manufacture and performance of aluminous cement : a new perspective" ref 6, 181-207.
219) George, C.M., Racher R.P.: "Fondu and Secar cements. Refractory and non refractory uses" Industr. Minerals, suppl., 1986, 26-34.
220) George, C.M,. Racher, R.P."Process control and quality assurance of calcium aluminate cement" Ceram. Eng. Sci. Proc.1988, 9, 1-2, 91/104.
221) Collins, R.J., Gut,t W. : "Research on long term properties of HAC concrete" Concr. Res. 1988, 145, 195-208.
222) Crammond, N.J.: "Long term performance of high alumina cement concrete in sulphate-bearing environments" ref 6, 208-221.
223) Piasta, J., Sawicz, Z., Piasta, W.G : "Durability of high alumina cement pastes with mineral additions in water sulfate environment" Cement concrete research 1989, 19, 103-113.
224) Piasta J. : "Sulfate corrosion of high alumina cement pastes" Proc . of 1V National conference on mechanics and technology of composite materials, 1985, 740-743.
225) Sawicz Z.et al : "Durability of HAC concretes with limestone in water and sulphate environment" 4th Int. Conf. Durability 1987, 733-740.
226) Griffiths, D.L. et al : "Calorimetric studies on high alumina cement in the presence of chloride, sulphate and seawater solutions" ref 6, 167-178.
227) Bayoux, J.P. et al : "Acidic corrosion of high alumina cement" ref 6. 239-240.
228) Kurdowski, W. et al : "Behavior of high alumina cement in chloride solutions", ref 6, 222-229.
229) China Building Material Academy Tianjin : "Research Institute of building Materials", Research report, 1989.
230) Cement institute, China building material academy : "Study of quick setting and rapid hardening cement for rush repair" Internal Technical Paper, 1978.
231) SuMuzhen, Yang Renhe, Li Shaozheng, et al : "The microstructure of hardened sulpho-aluminate cement pastes", Internal report, 1991.

Specific Theme II C

Cementitious Systems Including DSP, CBC, etc

Zement, Chemie, Stoffeigenschaft, Korngröße, Feuchtigkeit,
2 SW: Macrodefect-free

ADVANCED CEMENT SYSTEMS, INCLUDING CBC, DSP, MDF

Della M Roy

Materials Research Laboratory
The Pennsylvania State University, USA

SUMMARY

New developments in the making of very strong and high performance cementitious materials are discussed. These include CBC (chemically bonded ceramics) which is a generic term describing ceramic-like materials formed by chemical reactions at ordinary temperatures. Innovations in chemistry, as well as processing, are responsible for the major improvements. Pressure densification to yield ultra-high strength materials is briefly discussed, and the formation of macrodefect-free (MDF) cements utilizing different compositions and high-shear polymer processing methods. Calcium aluminate MDF cements have yielded bending strengths of up to 300 MPa, but they still require some improvement in moisture resistance. DSP cements (densified systems containing homogeneously arranged ultra-fine particles) combine dense packing with suitable chemistry to produce cast materials with compressive strengths as high as 300-500 MPa when cured hydrothermally. Alkali-activated cements, which generate very early high strength materials are also discussed. They have much potential because of the development of a working strength in about four hours, and also have relatively low porosity. Finally, potential applications of generic CBCs are summarized.

INTRODUCTION

Recent developments in the making of very strong, or otherwise high performance, cementitious materials have been the result of new innovations in composition and processing. These new developments have led to some tenfold enhancements in the properties of such materials, which result in performance approaching that of many traditional ceramics or modern composites (1). The term chemically bonded ceramics (CBC) was coined (2) to designate a group of ceramic-like materials in which the consolidation takes place by means of chemical reactions which occur at low temperatures; this term will be used extensively in this paper. Two parameters distinguish CBCs from traditional ceramics: (i) their bonding is not achieved by thermally stimulated diffusion; and (ii) their bonding is achieved at or near room temperature. Best known examples are the many kinds of cements, phosphate bonded materials, dental cements and, in nature, bones, teeth, and skeletons of invertebrates (3). The bonding in such CBCs is a mixture of ionic, covalent, and van der Waals bonding, with ionic and covalent bonds dominating; while in traditional cement hydration products, van der Waals and hydrogen bonding dominate. The term CBC is a broadly generic term, and therefore includes many of the newer high-performance cementitious materials (4) such as DSP (5) and MDF cements, as well as the relatively new alkali-activated cements and their hydration products. For the purpose of this Symposium, the subject will be restricted to advanced cementitious materials with compositions largely deriving from portland cement materials.

The materials within these new families of CBCs follow the general rules of behavior of cementitious materials in certain respects: The solidification of cement with water to yield normal hardened cement pastes takes place with little volume change. When high-density cement particles are mixed with low density water, they react to form a solid hydration product consisting of solids of intermediate density and interspersed residual porosity. The strength of hardened cement paste increases as the ratio of water to cement (w/c) is reduced (6). Because the residual porosity, its distribution, and the excess uncombined molecular water are responsible for most of the limitations on the properties of conventional hardened cement paste (7, 8), many attempts have been made to reduce the amount of water used in processing. However, there is a practical limit if the mixture is to remain workable. The situation has changed beginning in about 1970, as new approaches have led to the development of more advanced cement matrix composites (1). Major advances have taken place in the following areas: (i) the formation of specially densified or warm-pressed, ultra-high strength cement pastes that have properties approximating those of fired ceramics (8); (ii) the modification of the chemical composition of the cement (9); (iii) the formation of strong macrodefect-free (MDF) cements prepared by special processing (10, 11) and (iv) the design and manufacture of a variety of cement-based composites. In this treatment, we shall limit the latter composite concept to include only the use of fine particle cementitious components (5). Finally, (v) the family of alkali-activated (12) or geopolymeric (13a,b) cementitious materials contains high performance, very early high-strength cementitious materials.

Furthermore, such advances have begun to result in applications in a number of diverse areas, ranging from very specialized exotic materials to bulk concrete to waste management (both hazardous and nuclear). In this paper, we discuss some of the advances within the families of calcium aluminosilicate and largely portland cement (PC)-based CBCs.

Pressure Densification and Warm Pressing

For decades uncertainties existed regarding the theoretical strength of hydrated cement paste, or the strength a cement paste could achieve if it could approach the theoretical density. The bonds limiting the strength of cement paste are normally thought to be weak van der Waals forces. However, one might expect materials prepared under conditions involving dissolution and diffusion reactions which result in a dense interlocking microstructure to be somewhat stronger. Before 1970, the potential strength of cement paste at theoretical density (possibly related to Powers "intrinsic

strength") (7) had never been approached, because considerable porosity (20 to 30% or more total porosity) always remained after complete hydration of the cement. Following this, research resulted in achieving very high strengths by "warm pressing" (applying heat and pressure simultaneously) of cement pastes (8). Some modest increases in strength were achieved by application of pressure alone (13c), which increased the compaction and decreased the porosity. Strengths, an order of magnitude higher than those of normal cement pastes, were achieved by warm pressing different types of cements, such as portland varieties, calcium aluminate cements, and individual cement compounds. Compressive strengths (σ_c) up to 650 MPa (compared to the more typical 30 MPa) tensile strength (σ_T) up to 68 MPa, and values of Young's modulus (E) up to 40 GPa were attained. These dense cementitious materials are microcomposites consisting of about 50% residual anhydrous phases surrounded by interstitial hydrous calcium silicates and aluminates of both crystalline and noncrystalline varieties. Enormous increases in strength resulted from the removal of most of the porosity and the generation of very homogeneous, fine, microstructures with porosities as low as about 1.7%. Micrometer-sized flaws were visible occasionally in the microstructure, for example, along residual grain boundaries.

Several phenomena were apparent as a result of these studies . In contrast to the situation in normal cement dehydration, the densification and strength generation mechanisms were believed to result from the following typical reaction sequence; (i) rapid initial compaction; (ii) an abbreviated induction period as temperature began to rise,with minimal hydration; (iii) a rapid hydration period, during which hydration products (very fine particles) are mechanically rearranged as they are formed and fill intergranular positions; and (iv) final stages of hydration, densification, and microstructure development. The dense structures formed were partially the result of a bimodal particle size distribution which developed during processing (14) and better filled the space. The fine hydrated crystallites which formed around residual anhydrous cores and consolidated under the applied stress were welded into a monolithic mass. Occasional selvages of hydration products integral to the anhydrous grains, which penetrate into the interstitial matrix microstructure, generated a dense, well-bonded product.

Particle Size Effects

In addition to the above consideration, the importance of at least bimodal particle size distribution has been further demonstrated through the deliberate incorporation of a second phase of fine colloidal size particles. When properly dispersed, the fine material filled interstices,which apparently decreased the flaw size. The addition of colloidal alumina or silica markedly enhanced the tensile strength, which increased with the proportion of colloidal material added (14). The highest tensile strength (68 MPa) was measured immediately after warm pressing a material that had a composition of 88% cement, 3.6% colloidal solids, and 8.4% water. Additional studies might be expected to optimize the processing and further increase the strength.

The above-reported strength represented a 50% increase over that of an equivalent material formed without added colloidal particles. Further improvements commonly occurred after curing such materials from 1 to 28 days, which allowed additional hydration and pore filling. Remarkable strength enhancement was produced by the incorporation of such fine particles in materials prepared even at lower pressures (15-18). Other investigators have demonstrated that addition of small amounts of fine particles (colloidal or near colloidal) improved the rheological properties and densification in normal ceramic processing (19). These enormous increases in strength with warm-pressed cement pastes demonstrated that very strong ceramic-like materials could be made at or near room temperature with the CBC process.

MACRODEFECT-FREE CEMENTS

General

Although the warm-pressed cements, discussed in the previous section, were successful, they were not easy to produce in large amounts due to the high pressures used for optimization. The engineering of a new class of high-strength materials (the so-called macrodefect-free (MDF) cements) was another innovation, pursued originally by Birchall and co-workers at Imperial Chemical Industries and Oxford University (20-24). MDF refers to the absence of relatively large voids or defects which are usually present in conventionally mixed cement pastes because of entrapped air and inadequate dispersion. Such voids and defects limit the strength that can be achieved by acting as stress concentrators (20-24). In the MDF process, 4 to 7% of one of several water-soluble polymers (such as hydroxypropylmethyl cellulose, polyacrylamide, or hydrolyzed polyvinylacetate) is added as a rheological aid to permit cement to be mixed with very small amounts of water. Subsequent high-shear mixing produces a plastic, cohesive mixture which can be shaped by extrusion or other forming technique and which sets in times ranging from minutes to hours. The highest strength materials have been prepared with calcium aluminate cements, which harden rapidly, although portland cements have been used less successfully. Besides being a processing aid, the polymer constituent appears to be a significant structural component. Control of the particle size distribution (for optimum particle packing) was also considered important for generating strength. A final processing stage, in which entrapped air is removed by applying modest pressure (~5 MPa), resulted in a paste that is free of large defects. The mechanical properties of MDF cements are remarkable as compared with those of normal cements, and easily fit within the category of CBCs. Materials prepared with different compositions and additional processing steps achieved even higher strengths, as, for example, a calcium aluminate cement mixture, that was press-molded (at ~5 MPa) to remove bubbles and heated at 80°C. A volume decrease of 9% occurred, which could be the result of the polymer shrinkage. This reflected a collapse of the colloidal porosity. Very low porosities were achieved (<1%) (23) at considerably lower pressures than in earlier warm-pressing studies (5, 14), as well as flexural strength of ~ 150 MPa, a compressive strength of ~300 MPa, and a Young's modulus of 50 GPa.

The original explanation of the enhancement of strength in this new class of materials was the reduction of flaw sizes via the use of energy intensive processing. Figure 1 gives a summary comparing the strength, toughness and stiffness of MDF materials with other engineering materials (1, 25). Figure 2 compares with the flexural strengths observed (23) in, a) normal portland cement paste, b) portland cement based MDF and, c) calcium aluminate cement-based MDF as a function of flaw size. As is suggested by Figure 2, and has been reported elsewhere, MDF materials prepared from calcium aluminate cements have flexural strengths approximately twice those of MDF materials prepared from portland cements. Young and co-workers (26) have reported that strengths of approximately 300 MPa for calcium aluminate systems and 150 MPa for portland cement systems seem to be the upper limits for these materials. The offset of the curves for the portland MDF, as compared to the ordinary portland cement paste at the same flaw sizes is interesting. This suggests that the higher strengths observed in these systems are not due simply to a reduction in the flaw sizes and that the polymer phase may be contributing significantly to strength development.

The term, macrodefect-free, should not be interpreted as implying pore-free systems. Figure 3 summarizes the flexural strengths and porosity of a number of MDF materials prepared using a variety of cements, polymers and processing techniques. Porosities (by mercury porosimetry) of up to twenty percent are not unusual for MDF materials prepared from portland cements (MDF-PC); however, for MDF materials prepared using calcium aluminates (MDF-CA) much lower porosities (1-5%) are typically observed.

Other investigations (27) have shown that while low porosities may not always be achieved the maximum flaw sizes in these systems are reduced and are in the range of 10-100 micrometers.

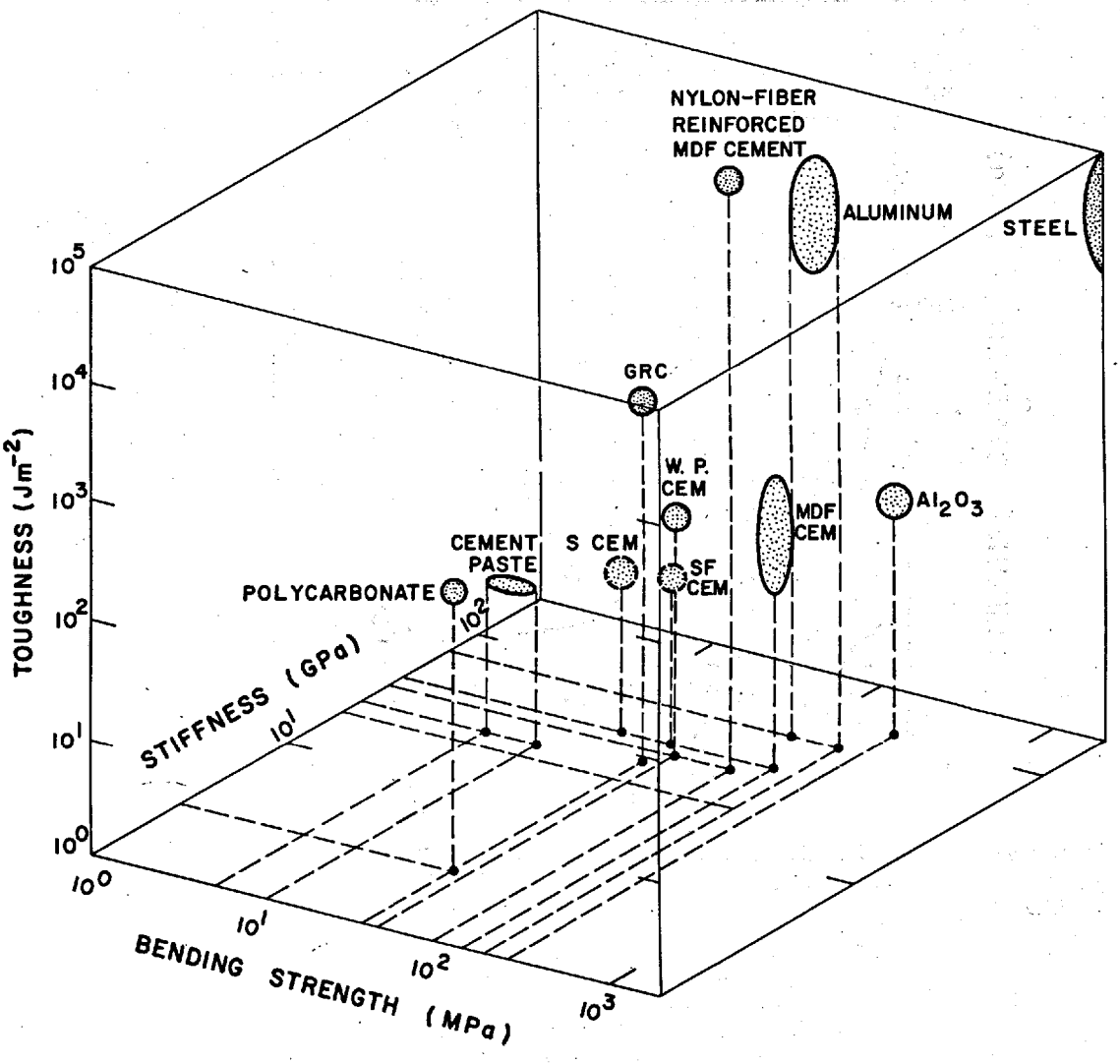

Figure 1. Strength, toughness, and stiffness of conventional cement paste and modified cement composites as compared with plastics, alumina, aluminum and steel. Abbreviations: CEM, cement; S, slag; SF, silica fume; WP, warm pressed; GRC, glass-reinforced; MDF, macrodefect-free [Adapted from (1, 25)].

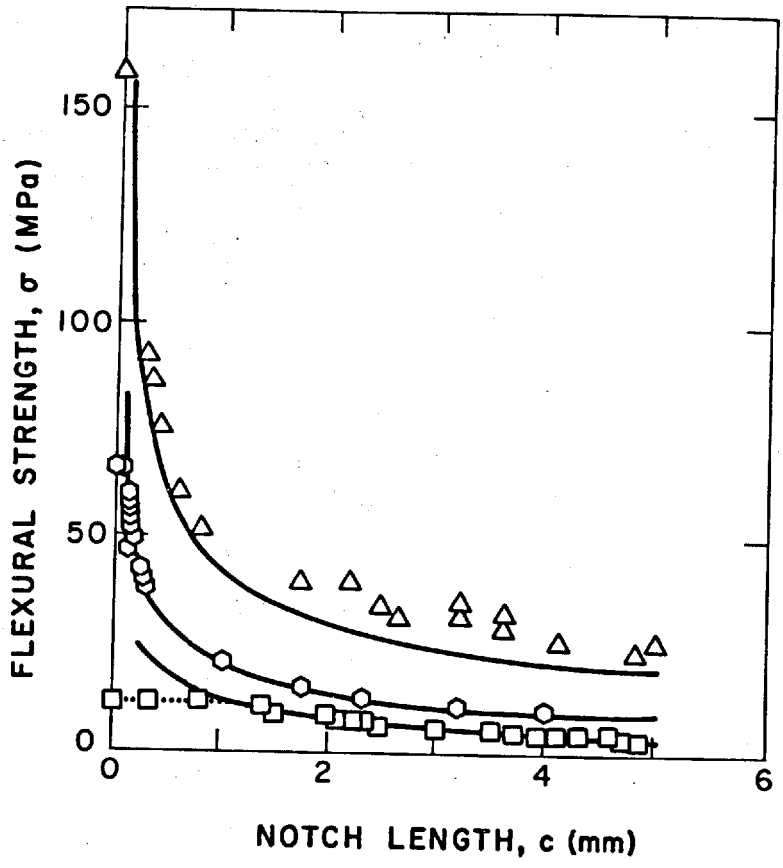

Figure 2. Notched beam test of the flexural strength of cement pastes. Curves are theoretical fits to the data. Bottom curve (squares) normal portland cement paste, middle curve (hexagons), portland MDF; upper curve (triangles), calcium aluminate MDF (20).

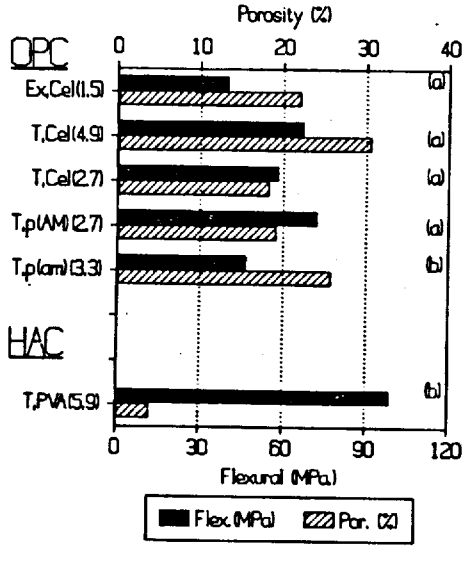

Figure 3. Porosities (as determined by mercury porosimetry) and flexural strengths for a number of MDF materials [top, Poon, (3); bottom, Alford (11)].

Li et al. (32) contrasted the behavior of an inert filler, corundum (plus lime) with that of cement in preparing MDF materials. They investigated the flexural strengths in corundum, polyacrylamide, lime and water mixtures and reported flexural strengths in excess of 80 MPa, only slightly lower than MDF cements prepared in a comparable manner. In contrast, simply replacing portland cement with ground quartz (36) does not produce a MDF cement body with typical MDF cement characteristics.

Influence of Moisture

The detrimental influence of moisture on MDF cement is now well established, and has been reported in several studies. The importance of the final drying step at 80°C in calcium aluminate MDF cements is to remove all traces of moisture and provide high strength. Table 1 contrasts the effect of wet and dry exposure conditions on the strength of portland and aluminate MDF cements.

Table 1. Effect of post-curing exposure to moisture on properties of MDF cements.

Cement/Poly Combination	Polymer wt.%	Moist Curing Conditions	σ_{flex} (MPa) Dry	Wet	Immersion Period	Linear Expans. (%)	Ref.
OPC Polyac	6	–	47	15	1d/20°C	0.4	34
				32	7d/20°C	0.4	34
	6	3d/40°C	72	26	1d/20°C	0.3	34
				37	7d/20°C	0.3	34
	8	3d/40°C	85	20	1d/20°C	1.7	34
				18	7d/20°C	1.9	34
CAC/PVA	7	10mn/80°C	164	49	3d/70°C	2.3	33
				82	28d/20°C	0.9	33

after Young (26); Polyac = polyacrylamide; CAC = calcium aluminate cement

In fact, many investigators (26, 27) have reported on the persistent problem of the effect of moisture on the mechanical properties of MDF. When exposed to moisture the flexural strengths of MDF materials may be decreased to 20-40% of oven dry strengths (4 hours at 80°C). When an MDF material is exposed to moisture, the polymer phase, which may constitute up to 30% on a volume basis, swells and softens. Uchiyama (29) investigated the effect of repeated wet-dry cycling on the flexural strengths of MDF-PC. He observed that the wet strengths increased with repeated cycling while the dry strengths remain more or less constant. Others (30) have reported that for MDF-CA the loss in strength is often permanent and upon redrying, the MDF-CA will never regain its original dry strength. Park et al. (31) investigated the effect of acetone-water mixtures on the flexural strengths observed in MDF-PC. Their results are shown in Figure 4. They found that when even a small amount of moisture was present in the mixtures, the strengths were drastically reduced and that the loss in strength was accompanied by a swelling of the MDF-PC.

The polymer influences hydration (37, 38) and, in turn, is influenced by hydration. The hydration of calcium aluminate cement is significantly retarded by the presence of PVA. At high concentrations, the course of hydration is significantly altered by the PVA and particularly noticeable is an enhanced heat evolution at early times. Ions released by the cement were proposed by Rodger et al. (37) to be central to the formation of an MDF cement.

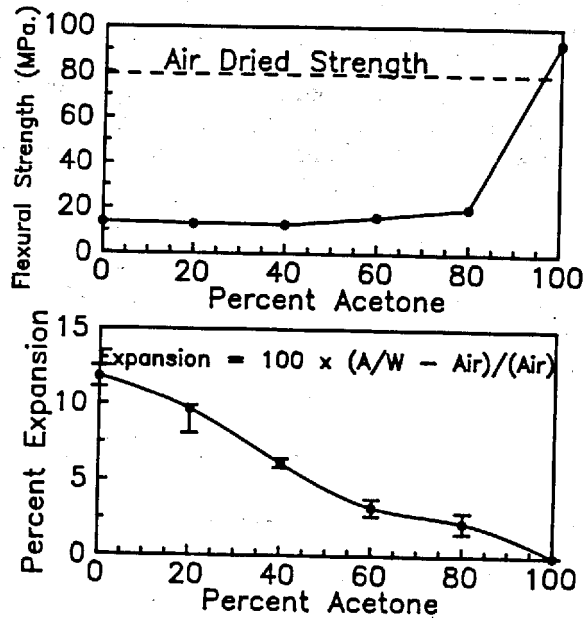

Figure 4. The effect of acetone-water mixtures on the flexural strengths observed in MDF-PC (portland cement) (31).

Metal Cross-Linked Polymer Gels

The properties and characteristics of metal cross-linked polymer gels have been investigated by many researchers (32, 39, 40). According to Tanaka (40), the characteristics of a metal cross-linked polymer gel that determine its behavior are: 1) rubber elasticity; 2) polymer - polymer affinity and, 3) hydrogen-ion pressure.

The rubber elasticity of a polymer is the resistance that a polymer chain offers to either compression or stretching. According to Tanaka, (40) for a polymer chain at equilibrium, the ends of the chain will be separated by a distance equal to the square root of the number of segments multiplied by the length of a segment.

The second characteristic of a polymer gel, its polymer-polymer affinity is the result of interactions between the polymer chains and the solvent. Depending on the electrical properties of the polymer molecules and the solvent, the forces may be either attractive or repulsive. Since these forces are rather short range forces, the mean separation distance between the polymer chains is important. For instance, as a gel shrinks and more and more polymer molecules come into close contact the attractive forces increase; conversely, as the gel expands, at some point the individual molecules will lose contact and these forces will become less important.

The final characteristic of a polymer gel, its hydrogen ion "pressure" is the result of ionization of the polymer network which releases positively charged ions into the gel fluid. The location of these positively charged ions is restricted to the immediate vicinity of the polymer and the resulting effect is much like that of gas in a confined vessel.

These three characteristics of properties of a gel will, in large part, determine its behavior where exposed to a variety of environments. One example was studied of three polyacrylamide gels exposed to water/acetone mixtures of different compositions. As the acetone concentration in the solvent phase is increased, the gels shrink; an abrupt transition occurs at approximately 42% acetone, resulting in a collapse of the gel structure. According to Tanaka (40) at the highest levels of hydrolysis (where approximately 25% of the side groups have been converted) the volumes may change as much as 350 times. These transitions may also be brought about by changes in pH and temperature.

In summary, distinct transitions in the volumes of metal cross-linked polymer gels may be caused by changes in temperature, pH, and solvent characteristics. These transitions may involve large changes in volume and are reversible.

Gel Reactions

Earlier, we discussed heat released by the reaction of MDF calcium aluminate - PVA mixtures. Maes (41) studied the heat released during the polymerization of polyacrylamide gels in the presence of various alkaline and alkaline earth hydroxide solutions, finding that these reactions were always exothermic and occurred at relatively short times. The heat released was not significantly affected by additions of $Ca(OH)_2$, while NaOH strongly retarded the reactions when the pH exceeded approximately 12.5.

Others have examined the hydration of the cementitious portions of MDF materials. Dunstar and Parsonage used trimethylsilation extractions to study the hydration of some OPC-MDF materials, (42) and observed that there were few or no polynuclear silicate species present in the OPC-MDF materials. Rodger et al. (37) used Infrared spectroscopy to examine the molecular interactions in MDF materials, suggesting that a calcium acetate forms as the result of the interactions between PVA and Secar 71. Maes (41) examined the Raman spectra of polyacrylamide gels containing Na or Ca hydroxide and concluded that Ca^+ formed real cross-links while Na^+ forms no permanent cross-links or chain entanglements; differences in the viscoelastic behavior of the gels that were observed were dependent on the cross-linking ion (41).

Additional Moisture Sensitivity Measures and Other Properties-Moisture sensitivity can be eliminated by burning out the PVA from the hardened cement at 500°C and then impregnating the porous body with various polymers (43). The use of novolac epoxies raises the useful service temperature to 350°C, whereas with the original PVA, the thermal limit is in the range 100-120°C. Other approaches included developing water-resistant MDF cement (44) by incorporating an isocycanate compound to cross-link the PVA molecules through urethane bonding. Russell et al. (27) have generated improvement in water resistance of MDF (PVA-CA) cements by silane treatment, while boric acid and Quilon L were less successful in promoting enhanced cross-linking.

Dielectric properties of MDF cements have been investigated by a number of authors (45, 28, 26) with a view of applications for electronic substrates. Dielectric constants as low as 5.3 (26) were achieved in CA/PVA MDF cements filled with silica, while use of hollow microspheres in sintered CA/PVA composites resulted in a dielectric constant below 3 (45).

Summary

In summary, it is clear that the role of the polymer phase in MDF materials is not simply that of a rheological aid. The polymer phases interact with the cementitious phases by a variety of means. It seems that many of the properties and characteristics of MDF materials are heavily influenced by the metal cross-linked polymer gels. In many respects MDF materials are perhaps better described as filled polymers as opposed to cementitious systems. However, there is ample evidence that the cementitious portion of these materials contributes to their behavior. It seems reasonable that the inorganic portion of these composites forms a semi-rigid network around which the metal cross-linked polymer gel forms. Thus, the final composite shares many of the properties and characteristics of metal cross-linked organic polymer systems and inorganic cementitious systems in a single material (35). Advances in controlling hygroscopicity have been achieved, but much work remains to be done. Nevertheless, the risks attendant in developing applications for these novel materials are rapidly diminishing. The next few years should see a further gradual introduction of components made from MDF cements into the market place.

DSP AND OTHER DENSELY-PACKED SYSTEMS

General

New materials termed DSP (Densified Systems containing homogeneously arranged, ultra-fine Particles) were first elucidated in detail by Bache. (5) These materials evolved from a history of exploration of the utilization of ultra-fine silica fume, mostly in Scandinavia. (46-49). In actual context, the densely-packed particles are normally portland cement, and the ultra-fine particles silica fume. The "new" class of materials is defined as materials with a matrix comprising, or formed from, 1) densely packed particles of a size ranging from 0.5 to 100 μ, and 2) homogeneously arranged, ultra-fine particles ranging in size from about 50Å to 0.5 μ, arranged in the spaces between the larger particles. The shaping of the fresh material is typically performed from a viscous mass in a low stress field achieved by eliminating the locking effect of surface forces between adjacent particles by means of dispersing agents.

The combination of densely packed cement and silica fume was found to be fortuitous for a combination of reasons (5):

1) The silica particles are smaller than even the finest cement produced by grinding, and are, therefore, more conducive to dense packing into the spaces between the cement particles.

2) The silica particles, being formed by condensation from gas phase, are spherical in shape (unlike crushed cement particles, which are angular), promoting dense packing.

3) The particles are chemically less reactive than cement, which eliminates the problem of too rapid hardening encountered with very fine cement; in addition, the silica is likely to ensure the formation of a coherent structural skeleton between the cement particles, resulting in a fine, dense micro-structure (very fine cement is likely to dissolve too quickly for this purpose).

Finally, the effect of dispersing agents on the dispersion of cement + silica fume in water is essential for the achievement of the dense structure of the paste, i.e., low water requirement.

The formation of a typical DSP in represented in Figure 5, in contrast with usual portland cement pastes. Numerous investigators have contributed to the understanding of the effects of fine particles in densely-packed cementitious materials, including (14-18, 32, 46-58). Many have described the physical effects, including Cohen et al. (61) who calculated that for a 15% silica fume replacement of cement, there are approximately 2,000,000 particles of silica fume for each grain of portland cement in a concrete mixture. In fact, very impressive properties can be achieved when silica fume (also called condensed silica fume or microsilica) is substituted for portland cement in amounts ranging up to 25%. Concretes containing 5 to 15% silica fume have high compressive strengths (up to and above 100 MPa), flexural strengths (up to 12 MPa), and Young's moduli (up to 34 GPa), and also have very low permeabilities to water (10^{-9} μm^2). The microstructure of the critical interfacial zone between cement paste and the aggregates in concrete is more dense and uniform than when conventional pastes are used, and the bond between paste and other embedded materials such as aggregates and fibers appears to be improved.

The most striking results, however, have been found with silica fume-substituted pastes, and DSP systems. Compressive strengths of up to 270 MPa or higher with Young's moduli up to 80 GPa were achieved in preparations with up to 20 to 25% silica fume at a water to solids (w/s) ratio of 0.12 to 0.22 through mechanical compaction. A dense but fairly fluid paste is formed by the combination and chemical dispersion of particles that have dissimilar size ranges. No major air voids remain in products that are processed properly, as hydration proceeds, and only a few small

"capillary" pores exist. Shrinkage upon drying of the cement hydration product is limited, and the residual cement grain cores act as a strong internal filler or "microaggregate."

Dense silica fume-based cementitious composites are used to resist severe mechanical erosion in impeller screws for moving coal and fly ash and in flooring to industrial area (36).

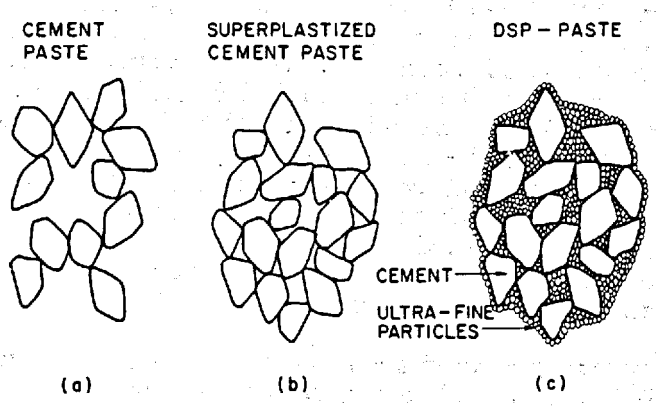

Figure 5. Packing of DSP (silica fume) pastes. (a) flocculated ordinary cement pastes; (b) better packing achieved with dispersant (superplasticizer)); (c) cement, silica fume, and superplasticizer. [Adapted from (5)].

Another version is commercially available as a tooling and molding material in applications where vacuum tightness or mirror finishes are required. The latter material (Table 2, last column) retains a compressive strength of ~300 MPa up to about 500°C and ~200 MPa at about 700°C.

Silica Fume Hydration Reactions

As indicated above, silica fume particles, when properly dispersed, fill the interstices of the fresh cement paste structure, where they are available to react with the alkali hydroxide and $Ca(OH)_2$ liberated by the hydrating portland cement, forming insoluble C-S-H. When used in proportions to replace up to 10% of cement, it significantly reduces bleeding and segregation of the mixtures, and

Table 2. Comparison of mechanical properties of cement particle composites; MDF, Warm-pressed, and Several DSP Type Materials.

Cement particle composite	σ_T (MPa)	σ_F (MPa)	E (GPa)	σ_c* (MPa)
1. Ordinary cement	~5	6	15	40
2. MDF cement		40-150	35-50	100-300
3. Warm-pressed dense-fume mortar	68		27-41	300-650
4. Slag mortar	81-20†		48	180
5. Steam cured 82-11††			50	250
6. Steel aggregate steam-cured mortar•		28	49	250-350
7. Chopped steel, fiber high temp. steam-cured DSP/CBC*		75		500

* Flexural strength. †See (54); †† See (55); • See (93) and * See (91 and 92)

may be used in higher proportions. Aqueous slurries of silica fume may be prepared without superplasticizing admixtures, but the resulting cementitious mixtures usually require higher w/c ratios. Because of their very high surface area, early reaction of the fume takes place with the alkaline cement pore solution.

Since silica fume contains particles as fine as 0.1 μm or less and has high surface energy, it partially dissolves in saturated $Ca(OH)_2$ solution in a time as early as 5 to 15 minutes, and a SiO_2-rich hydrate is deposited in layers or films on the silica fume particles. C-S-H having a C/S ratio of about 1 has been reported to form at 20°C in 24 hours after mixing with water and at 38°C in only 6 hours [Grutzeck et al., (66)]. The reaction of silica fume with $Ca(OH)_2$ is affected by the specific surface area, and the surface energy. Typically, the C-S-H produced has a lower C/S ratio than that of cement. Since C-S-H with a C/S ratio of less than 0.8 is considered to be thermodynamically unstable, calcium silicate hydrate once produced is converted to a C-S-H variety having the lower limit of C/S, which coexists with excess silica containing very little calcium. This lower C/S ratio tends to be confirmed in reports of Taylor (63). Diamond (68), Glasser (69) and Roy (70) have described the changing composition of pore solutions with longer time periods, which reflect the hydration processes occurring beyond the early ages.

Despite the early rapid reaction, much silica fume remains for later slow reaction. For example, Li et al. (64, 65) showed from selective dissolution experiments that, while much SF is reacted in a SF-OPC mixture at 7 days, considerable unreacted SF remains. The early heat of hydration of silica fume-containing mixtures is frequently equivalent to that of high-early-strength cement, although the rate at which heat is liberated depends upon the proportions, and the w/c ratio. The basic cement hydration process is, of course, an exothermic process; hydration reaction begins immediately upon mixing with water, and is affected by gypsum or other additives incorporated as a set regulator which is added to the clinker during grinding, or other set regulator added in mixing the paste.

The heat of hydration, measured by isothermal calorimetry is shown to increase by addition of silica fume when referred to amount of cement (63b, 64b, 84). See Figure 6.

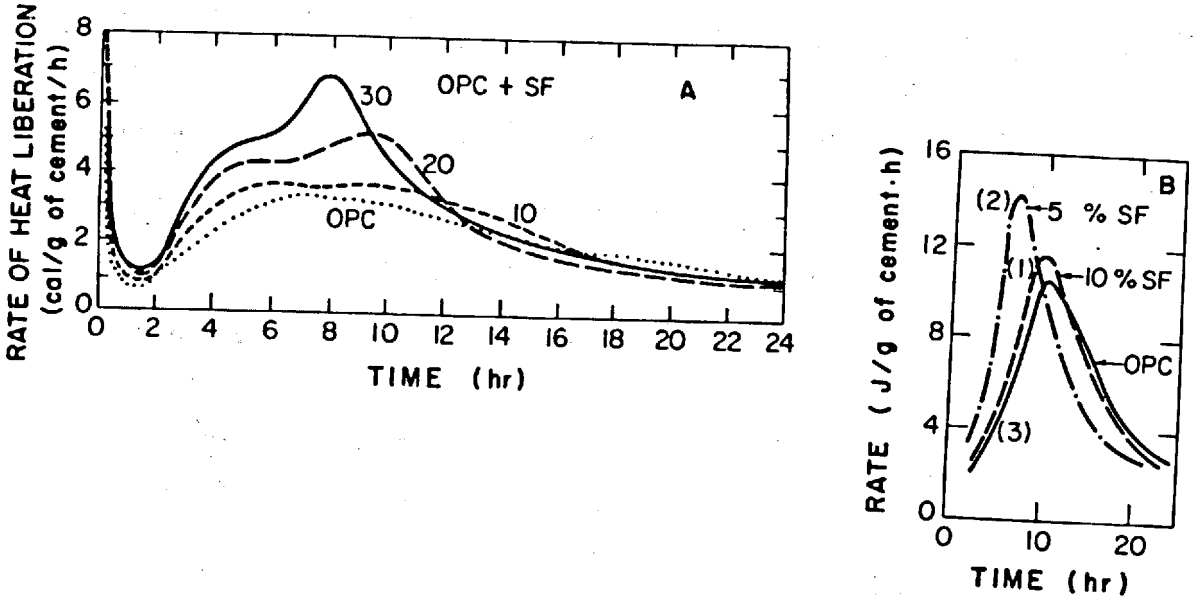

6. Heat evolution curves of the hydration of cement with silica fume; (a) with 0, 10, 20, and 30, percent silica fume (84); (b) with 0 and 10% silica fume, and 5% ultra-fine aerosil (64b).

The degree of reaction of silica fume was reported to vary (63b). Additional insight into the hydration recently has been gained by using AC electrical conductivity and dielectric permittivity measurements (85, 86) as illustrated in Fig. 7.

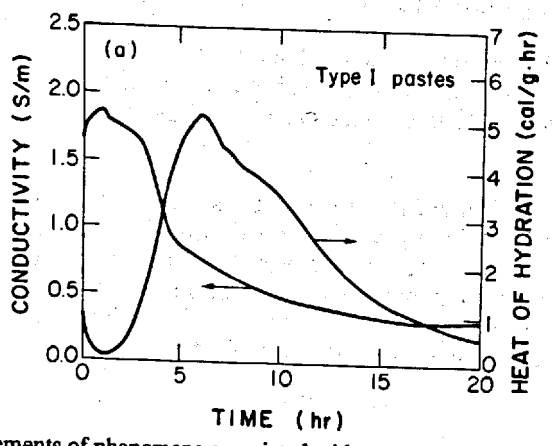

Figure 7. Comparable measurements of phenomena associated with rate of hydration; heat of hydration by isothermal calorimetry, and AC electrical conductivity (85, 86).

Using selective dissolution procedures, Li and Roy (64) have found in cement-SF mixtures that half of the silica fume (with 10% SF-90% cement) was hydrated in one day, and two-thirds during the first three days, although thereafter the hydration proceeded slowly. Between 28 and 90 days, additional hydration took place. They also found in C_3S - SF mixtures that approximately equal total reaction (of C_3S + SF) occurs with C/S ratios of 1.5 to 0.83 by using selective dissolution methods. Sun, et al. (60) found lower percentage reaction at one day when higher percentages SF were used. Khayat and Aitcin (81) have recently reviewed the application of silica fume in preparing high strength concrete, in which the DSP principle is used. Justnes et al. (82) and Sellevold and Justnes (83) have described characterization of silica fume - substituted cement binders with substitution of up to 16% silica fume, and water/binder ratios as low as 0.20. They suggested the degree of hydration is best analyzed when considering w/c, rather than w/(C+S) ratios.

The fume particles surround each cement grain, densifying the matrix, filling the voids with strong hydration products, and improve the bonding with aggregates (71-73), and reinforcing materials such as glass fiber. Silica fume by reacting with alkali also affords a protection against the alkali-aggregate type reaction occurring between a cement pore solution and glass fiber (74, 75).

Particle Packing

Bache (5) early emphasized the importance of dense packing which is the essential feature of DSP-materials. The new materials combine very densely-packed cement particles, ultra-fine (silica) particles in the spaces between the cement particles and, normally, densely arranged fibres and/or aggregates. Others (5, 14, 54, 76) showed that the influence of even a very small percentage of fine particles is very significant. The packing of particle systems in which surface forces are insignificant (e.g. cement-size particles) is independent of the absolute particle size, depending only on the shape of the particles, the relative size distribution and the mechanical placing of the particles, i.e. the kinematics. This means that regular packing of equal spheres results in the same volume fraction of solids (for example, 0.52 for cubic packing and 0.74 for hexagonal packing), irrespective of the absolute size of the spheres.

PC-based computer codes have been developed which can be used to adequately predict the dry packing behavior of the components in cementitious systems. This allows the optimization of

both the individual components of cementitious formulations and the mixture of components in the formulation to provide maximal packing thus minimizing unwanted and unnecessary porosity (77).

As modified and implemented, the Toufar/Aim (78-80) model of dry particle packing has been verified as adequately modeling the dry packing of mixtures of powder, each with a different size distribution. Typically, three different size distribution materials may be mixed. Furthermore, the characterization of the size distribution can be modeled by a commonly used procedure described by Rosin-Rammler (78). Input to this PC-based algorithm consists of the experimentally determined tap density of each component and the characteristic diameter of the distribution as described by D' in the Rosin-Rammler fitting equation.

The results of applying this algorithm to concrete systems has provided the mathematical basis for formulating concrete mixtures which were developed through field experience in the practice of concrete placement. Its applications should prove useful in monitoring the quality of concretes in the design stages and to adjust the components of the formulation to maximize performance. It may also be applied to the optimization of compaction of fine materials, such as the DSP systems. Figure 8 shows an example of the calculated maximum density of 3 fine materials, including silica fume, using this method (77).

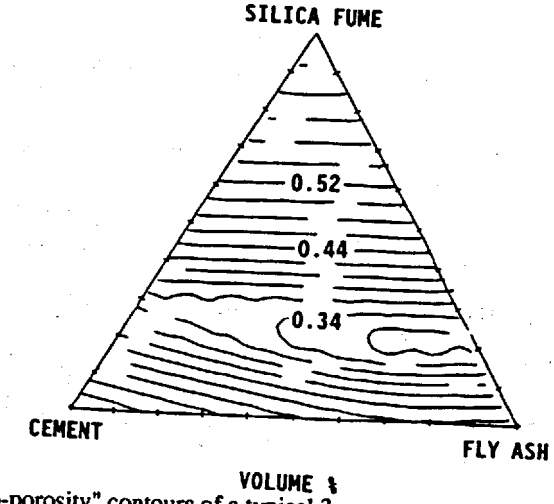

Figure 8. Calculated "iso-porosity" contours of a typical 3-components system of cement-fly ash-silica fume (77).

Discussion

In summary, the hydration reactions in DSP cement pastes are responsible for the fine microstructural development. These complex reactions involve phase solubility, accelerating and retarding effects of a multiphase, multi-particle material, and surface effects at the solid-liquid interface. Particle packing due to dispersion of the ultra-fine silica fume particles between the cement particles is extremely important for developing strength. The initial degree of dispersion of cement and fume in the paste strongly influences the development of final hardened paste microstructure. Adequately dispersed silica fume, due to its ultra-fine particle size can fill the intergranular interstices and produce a denser paste structure, reflected in a very high strength.

Both physical and chemical characteristics influence the hydration kinetics. Silica fume ordinarily accelerates the early portland cement hydration, largely because of its very high surface area, accelerating and increasing the heat development resembling a high early strength cement. Fume also disperses the hydration product, provides for deposition of C-S-H, and thereby fills the pore interstices with fine hydration products. Its optimal use is with superplasticizers to minimize the water demand and adequately disperse the fine particles. Dense products with fine pore size (87, 88), very low permeability (87, 89), and low ionic diffusivity (90) commonly are the result. Despite the rapid early hydration, much silica fume remains unreacted until a later stage (63, 64).

The mechanical properties of some high-strength DSP-type materials have been summarized earlier in Table 2 (numbers 4-7) and compared with normal cement paste, MDF cement paste and warm-pressed materials.

ALKALI-ACTIVATED CBC/CEMENTITIOUS MATERIALS

General

The use of blended cements in applications where rapid setting times and early strength development are required has often been hindered by their relatively slow rates of reaction. Alkali additions used for many years to activate the latent capabilities of certain pozzolanic materials have recently come to increasing attention. The F-cements of Finland (12a) and related (94) cements constitute areas where this technique has currently been employed. These materials typically require approximately 30% less water than conventional cements resulting in lower total porosities. The CaO/SiO_2 (C/S) ratio is adjusted such that there is no free calcium hydroxide remaining in the hydrated material. Two main disadvantages are longer mixing times and smaller batch sizes, due to stickiness and special handling requirements because of the highly alkaline nature of the activators. The activators used in these materials may be divided into three classes (94): 1) caustic alkalis; 2) non-silicate salts of weak acids; and 3) silicate salts. Recent work suggests that it may be possible to utilize other, perhaps less alkaline, materials such as high alumina cements (38, 98) and aluminum sulfates (38) as activators for slags. Dosages are in the range of 3-10% of NaOH, as Na_2O are utilized with dosages in the range 3-6%, giving optimum strength development (94). The hydration of the slag generally requires the breaking of bonds and dissolution of the three-dimensional network structure of the glass. The network contains interlinked SiO_4 and AlO_4 tetrahedra and AlO_6 octahedra which are attacked by the OH in a high pH environment. When the pH of the liquid phase is kept at approximately 12 and sulfate ions coexist, a well-crystalized calcium sulfo-aluminate can be produced (38). The alkalis present may react with the aluminosilicate portion of the slag, forming hydro-aluminosilicates (94, 97) that are zeolitic in nature and have the general formula:

$$R_2O{\cdot}Al_2O_3{\cdot}xSiO_2{\cdot}nH_2O$$

With normal short-term curing, x will be approximately 2, while with longer curing times or steam curing, x will be in the range of $2 \leq x \leq 3$ and with long-term steam curing x will approach 4. Under normal curing conditions, the reaction products will be mostly noncrystalline; however, with long curing times, especially at elevated temperatures or autoclave conditions, calcium silicate hydrate (C-S-H) phases with some short-range order or possibly some crystalline reaction products belonging to the zeolite group may be formed. Combination, with conventional hydraulic cements, of one or more of the class of latent hydraulic materials (i.e., fly ash, blast furnace slags, silica fumes, etc.) with a small amount of activator can lead to materials with enhanced durability and/or strengths.

Recently, new hydraulic compositions have been developed, combining many of these advances into a new type of cement. One type of composition is that commercially available under the trade name, Pyrament*, which is the outgrowth of work by Davidovits (13a) and others (13b) on alkali-activated aluminosilicate materials originally inspired by studies of ancient building materials. The new formulations are very early high strength cements which combine rapid strength development with relatively high later strength. Silica fume, in common with its role in DSP cements, has been found to be a particularly useful component in materials we have studied (12b, 96, 98).

Strength Development and Reactivity

Typical strength development data are shown in Table 3 (12b). We and others have developed dense, low water/cement ratio formulations, employing alkali activation to shorten the

setting times and increase the rate of strength development. The results of characterization of these materials using hydration calorimetry, SEM, x-ray diffraction, and mechanical property techniques show that the properties developed early do not deteriorate, but continue to be enhanced with time. These materials have been prepared employing both normal and high-shear mixing MDF processing (99).

Table 3. Compressive strengths (MPa) for three alkali-activated cements cured at 25°C, at W/C = 0.25 (standard deviation in parentheses.

Time	Portland Type III	Alkali Activated		
		Pyrament	P-14	P-15
5 hours	not set	23.4(0.4)	23.3(0.4)	29.1(0.6)
1 day	83.5(2.8)	47.0(0.9)	64.7(2.9)	63.9(1.0)
3 days	91.0(8.7)	59.1(1.6)	60.1(1.2)	--
7 days	109.9(8.3)	69.5(0.6)	77.3(9.9)	--
14 days	122.4(4.6)	78.6(1.4)	92.4(5.5)	--
21 days	118.3(13.1)	82.5(3.3)	93.0(1.6)	71.0(10)
28 days	107.1(10.1)	84.6(2.0)	75.2(4.9)	92.3(0.8)

Blast furnace slag cement (BFSC), a blend of glassy slag and portland cement, has been found to be superior to PC with respect to its contribution to the properties and performance of concrete at later ages, especially to the durability. However, on the negative side, are the disadvantages of somewhat lower early strength and longer setting time of BFSC. Various activators such as sodium sulfate and potassium aluminum sulfate and the alkalis were used as major activators in recent studies (95). Other additives investigated include superplasticizers (SP), aluminate, or high alumina cement (HAC) (100). The results of these studies confirmed that each of these activators or additives increases the reactivity, under proper conditions. Furthermore, the results of the studies showed that the synergetic effects due to the combination of additives are frequently greater than when they are used singly, increasing early age compressive strength and shortening the setting time. Combinations of additives were clearly found to be more effective than a single one; two optimum ternary combinations were 1) Na_2SO_4, KAl sulfate, and SP, and 2) Na_2SO_4, HAC, and SP (95).

Studies have also been undertaken to discern the reactions taking place during the hydration of various types of hydraulic cements, including alkali-activated materials (101). Figure 9 contains the results of analysis of the solutions extracted by centrifuging pastes with W/C = 1.0 at early times ($\leq$ 5 hours) for Type I, III, and Pyrament pastes. The high initial concentrations of aluminum found in Figure 9 for the Pyrament paste most likely are the result of the ability of the potassium (and the associated counter ions) to activate the aluminosilicate pozzolans present in the Pyrament formulation. (99).

Figures 10-11 show the (1) rate of temperature rise in and (2) the temperatures attained in a typical concrete formulation (Figure 10) compared with a Pyrament-based formulation (Figure 11) cured under adiabatic conditions. One of the attractive features in utilizing industrial by-products in cement and concrete formulations is the ability to control the rate of heat evolution during the setting process. Comparison of Figures 10 and 11 reveals that the maximum temperature reached in the pozzolan-rich Pyrament-based composition was only approximately 10°C higher than the composition based on Type I cement, notwithstanding the rapid setting characteristics of the blended material. Figure 11 reveals at least two distinct peaks on the rate of heat evolution curve, consistent with microstructural studies which suggest that an alkali-rich phase forms first and may be at least partially responsible for the rapid setting of these materials. The second peak tends to correspond to more

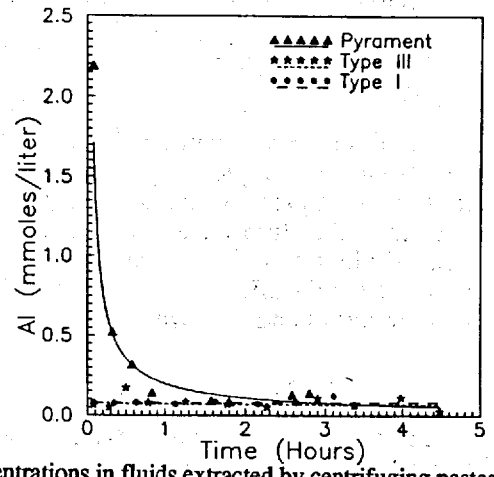

Figure 9. Aluminum concentrations in fluids extracted by centrifuging pastes of Type I, Type III, and Pyrament cements with a W/C = 1.0 at early times.

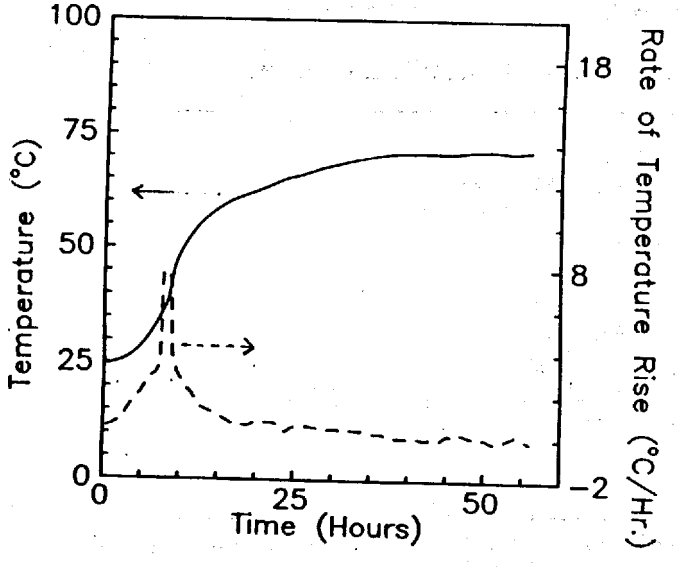

Figure 10. Rate of temperature rise and temperature attained in typical Type I cement concrete (99).

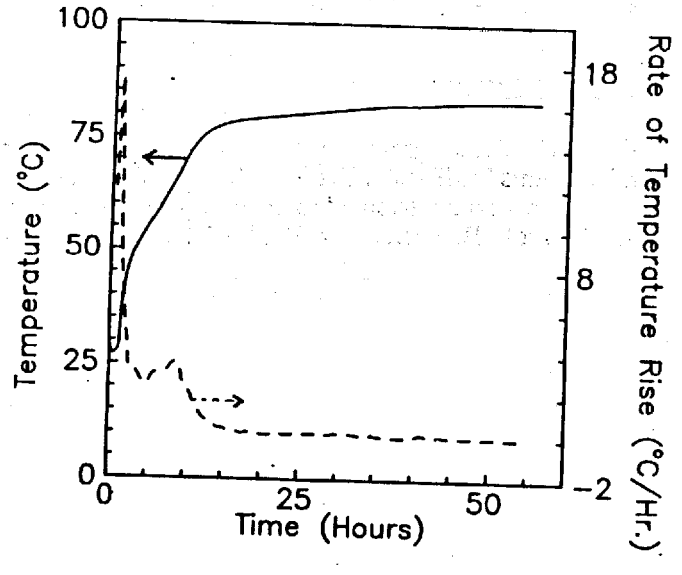

Figure 11. Rate of temperature rise and temperature attained in lower W/C ratio Pyrament cement concrete (99).

conventional hydration processes, leading to the development of the relatively high ultimate strengths observed in these materials.

Discussion

The results of these studies overall describe a very promising new class of materials. They show that it is possible to combine the advantages of rapid strength development by alkali activation with high ultimate strength, by control of particle packing and chemistry in a single formulation of blended cements containing fly ash, slag and silica fume. More research will be required to fully optimize these materials and characterize the long-term behavior of these materials. One unknown aspect is the long-term behavior, with respect to the effect of the somewhat higher alkali levels characterized in these materials on their properties and performance.

CONCLUSIONS

Major advances have been made in several properties of advanced cement/chemically bonded ceramics (CBC) materials of widely ranging compositions having much potential in modern technology. After a general discussion of progressive developments, in this paper, we have focused on very strong high density materials of the pressed, MDF, DSP, and alkali-activated varieties. A number of key properties have been investigated, and very high strengths have been attained. Certain of these materials are already being used in novel applications, which include, but are not limited to, those depending on chemical properties. Examples of potential applications are given below:

Table 4. Potential Applications of CBCs and Their Composites

- Acoustics
- Cryogenics
- Tooling, molding materials, machine beds
- Armor/impact resistance
- Electro-magnetic radiation screening
- Electronic packaging
- Fire-resistant application
- Erosion-resistant materials/stilling basin
- Rapid repair materials; road overlays
- Boards, panels, claddings; machinable components; permanent forms
- Hazardous waste management

The challenge remains to better understand the mechanisms involved in generating strength and toughness, the effects of compositional and microstructural modifications, and the range of methods and parameters which control the properties of such composites. Other investigations should emphasize the prediction of long-term durablity. Such knowledge will open further horizons in the field of synthesis of new cementitious materials.

ACKNOWLEDGEMENTS

The author gratefully acknowledges the support of the U. S. National Science Foundation under Grants DMR-88-12824 and MSM-87-18111, and numerous present and former associates at Penn State who contributed to portions of the research described, including Drs. M. R. Silsbee, M. W. Grutzeck, B. E. Scheetz, P. H. Licastro, M. Perez-Pena, A. Kumar, and G. R. Gouda.

REFERENCES

1. Roy, D. M.: "New Strong Cement Materials: Chemically Bonded Ceramics", Science, Feb. 6, 1987, 651-658.

2. Roy, Rustum: Workshop on Chemically Bonded Ceramics, The Pennsylvania State University, Materials Research Laboratory, 1984.

3 (a) Roy, Rustum: Personal Communication 1980.
(b) Somiya, S.: **Chap. 1: Ceramics: Definitions.** Advanced Technical Ceramics, S. Somiya, Ed., Academic Press, Japan, 1989, p. 9.

4. Roy, D. M.: "Advances in Cements/Chemically Bonded Ceramics", **Ceramics: Toward the 21st Century, The Ceramic Society of Japan, Centennial International Symposium,** 1991, p. 535-551.

5. (a) Bache, H. H.: "Densified Cement/Ultra-Fine Particle-Based Materials," presented at the **Second International Conference on Superplasticizers in Concrete,** Ottawa, Ontario, June 10-12, 1981; Aalborg Portland, Aalborg, Denmark, 35 p.
(b) Bache, H. H.: "Compact Reinforced Composite Basic Principles", CBL Rapport No. 41, Aalborg Portland, Aalborg, Denmark, 1987, 87 p.

6. Feret, B.: Bull. Soc. Encour. Ind. Natl., Paris, 1897, **2**, p. 1604.

7. Powers, T. C.: **Proceedings of the 4th International Symposium on the Chemistry of Concrete** (Washington DC, 1960), Natl. Bur. Stand. (U.S.) Monogr. No. 43 (Nat. Bur. Stand., Washington DC) 1962, **2**, p. 557.

8. Roy, D. M., G. R. Gouda, and A. Bobrowsky: **Cem. Concr. Res.** 1972, **2** p. 313; ibid. 1973, **3**, p. 807; ibid. 1975, **5**, p.153; G. R. Gouda and D. M. Roy, ibid. 551.

9. (a) Yudenfreund, M., I. Odler, and S. Brunauer: Cem. Concr. Res., 1972, 2, p. 313; M. Yudenfreund, K. M. Hanna, J. Skalny, I. Odler and S. Brunauer, ibid., 731.
(b) Roy, D. M., Ed. V. M. Malhotra: Am. Concr. Inst. SP-114, 1989, **1**, p. 117-138.
(c) Roy, D. M., Ed. V. M. Malhotra: Am. Concr. Inst. SP-114, 1989, **2**, p. 1265-1281.

10. Birchall, J. D., A. J. Howard and K. Kendall: "Flexural Strength and Porosity of Cements," **Nature,** 1981, **289**, p. 388-390.

11. (a) Birchall, A. J. Howard and K. Kendall: "Strong Hydraulic Cements," Proc. Br. Ceram. Soc., 1982, **32**, p. 256.
(b) Alford, N. McN.: "A Theoretical Argument for the Existence of High Strength Cement Pastes," Cem. Concr. Res., 1981, **11**, p. 605.

12. (a) Forss, B.: **Alkalis in Concrete,** Copenhagen, Denmark, 1983, p. 101-104.
(b) Roy, D. M., M. R. Silsbee and D.Wolfe-Confer: "New Rapid-Setting Alkali-Activated Cement Composition," **MRS Proc.,** 1990, **v.179**, p. 203-220, Eds. B. E. Scheetz and A. Landers.

13 (a) Davidovits, J.: "Ancient and Modern Concretes: What is the Real Difference?", Concr. Intl., 1987, p. 23-35.
(b) U. S. Patent No. 4,642,137, 1987. Heitsmann, R. F., M. Fitzgerald and J. L. Sawyer.
(c) L'Hermite, R., and M. Valenta: **Ann. Inst. Tech. Baltim. Trav. Publics No. 6,** 1937, p. 23; C. D. Lawrence, **Research Report 19,** Cement and Concrete Association, London, 1969.

14. Gouda, G. R.: Ph.D. Thesis. Pennsylvania State University, 1975.

15. Oyefesobi, S. O. and D. M. Roy: Cem. Concr. Res. **7**, 1977, p. 165.

16. Oyefesobi, S. O.: Ph.D. Thesis. Pensylvania State University, 1976.

16. Oyefesobi, S. O.: Ph.D. Thesis. Pensylvania State University, 1976.

17. Roy, D. M., B. E. Scheetz, M. W. Grutzeck, A. K. Sarkar, S. D. Atkinson: **Proceedings of the International Symposium of Ceramics in Nuclear Waste Management**, T. D. Chikalla and J. M. Mendel, Eds., American Ceramic Society, Columbus, Ohio, 1979, p. 136.

18. Grutzeck, M. W., B. E. Scheetz, E. L. White, D. M. Roy: **Borehole and Shaft Plugging Proceedings** (meeting jointly sponsored by the Organization for Economic Cooperation and Development and USDOE, Columbus, OH, 7 to 9, May, 1980 and Organization for Economic Cooperation and Development, Paris, 1980, p. 353.

19. Phelps, G. W. and M. G. McLaren: "Ceramic Processing Before Firing", Wiley, New York, 1978.

20. Birchall, J. D., A. J. Howard, K. Kendall, **Nature**, London, 1981, 289, p. 388.

21. _____, **Proc. Br. Ceram. Soc.**, 1982, 32, p. 256.

22. Hirsch, P. et al., Eds.: Technology in the 1990s: Developments in Hydraulic Cements, Royal Society, London, 1983.

23. Kendall, K., A. J. Howard, J. D. Birchall: ibid., p. 139.

24. Birchall, J. D.: ibid., p. 31.

25. Birchall, J. D. and Kelly, A., Sci. Amer. 248, 104, May 1983.

26. Young, J. F.: "Macrodefect-free Cement: A Review", **Mat. Res. Soc. Symp. Proc. v. 179**, 1991, p. 101-122.

27. Russell, P., J. Shunkwiler, M. Berg and J. F. Young: "Moisture Resistance of Macrodefect-Free Cement", **Ceramic Transactions**, Ed., S. Mindess, 1991, v. 16, p. 501-519.

28. Silsbee, M. R., D. M. Roy and M. Perez-Pena: **Mat. Res. Soc. Symp. Proc.**, Ed. Scheetz, et al., 1991, v. 179, p. 145-156.

29. Uchiyama, Masahiko: "Assessment of and Modeling the Mechanical Behavior of Macro-Defect-Free Cementitious Materials," M.S. Thesis, The Pennsylvania State University, 1989.

30. Titchell, I.: J. Mater. Sci., 1991, 26 [5], p. 1199-204.

31. Park, C. K., M. R. Silsbee and D. M. Roy: "Fiber-CBC Composites," presented at The Science Behind Materials Synthesis, Materials Research Laboratory, University Park, PA, 6/10/90.

32. Li, H., M. R. Silsbee and D. M. Roy: "Effect of Particle Size Distributions on Properties of High Strength Cementitious Composites," presented at the **92nd Annual Meeting of the American Ceramic Society**, 1991, manuscript in preparation.

33. Poon, C. S., L. E. Wassell and G. W. Groves: **Trans. Brit. Ceram. Soc.**, 1987, v. 86, p. 58-62; **Mater. Sci. Technol.**, April, 1988, p. 993-6.

34. Poon, C. S. and G. W. Grove: **J. Mater. Sci.**, 1988, v. 23, p. 657-670.

35. Silsbee, M. R. and D. M. Roy: "The Chemistry of MDF Materials," Eng. Found. Conf., Potosi, Mo., 1991, in press.

36. ralkner, R. F.: M.S. Thesis, Univ. Illinois, 1989.

37. Rodger, S. A., W. Sinclair, G. W. Groves, S. A. Brooks and D. D. Double: **Mater. Res. Soc. Symp. Proc.**, 1985, v. 42, p. 45-51; J. Mater. Sci., 1985, v. 20, p. 2853-60.

38. Edmonds, R. N. and A. J. Majumdar: **J. Mater. Sci.**, 1989, v. 24, p. 3813-18.

39. Menjivar, J. A.: "Use of Gelation Theory to Characterize Metal Crosslinked Polymer Gels," in **Water Soluble Polymers, Beauty and Performance**, Advances in Chemistry Series, Am. Chem. Soc., Glass Ed., 1986, v. 213, p. 299-312.

40. Tanaka, T.: **Sci. Am.**, 1981, v. 244 [1] p.124-38.

41. Maes, K. B.: "Characterization and Use in Gel Casting Systems of Different Polyacrylamide Admixtures," M.S. Thesis, The Pennsylvania State University, 1991.

42. Dunstar, A. M. and J. R. Parsonage: "A Trimethylsilyation Study of the Silicate Anion Distribution of Portland Cement," **Cem. Con. Res.**, 1988, v. 18, p. 758-762.

43. Chandrashekhar, G. V. and M. W. Shafer: **J. Mater. Sci.**, 1989, v. 24, p. 3353-3355.

44. Japan Patent No. 35735/87, 1987: Kataoka, N., H. Igarashi and M. Ohshima; Europ. Patent Appl. No. 0280971 A1, 1988.

45. Sliva, Paul: Ph.D. Thesis, The Pennsylvania State University, 1985.

46. Tratteberg, A.: "Waste Materials in the Construction Industry," Cement and Concrete Research Institute, Norwegian Institute of Technology, Trondheim, Norway, 1977.

47. Asgeirsson, H. and G. Gudmundsson: **Cem. Concr. Res.**, 1979, v. 9, p. 249.

48. Hjorth, L. in Hirsch, P. et al., Eds: Technology in the 1990s: Developments in Hydraulic Cements, Royal Society, London, 1983, p. 167.

49. Radjy, F. F., T. Bogen, E. J. Sellevold, R. E. Loeland: **Proceedings of the First International Conference on the Use of Fly Ash, Silica Fume, Slag and Other Mineral By-Products in Concrete**, (meeting sponsored jointly by the Canadian Center for Mineral and Energy Technology and the American Concrete Institute) (ACI Publ. SP-79, American Concrete Institute, Detroit, 1983) p. 1135.

50. Aitcin, P.-C., C. Bedard, M. Plumat, G. Haddal: **Mat. Res. Soc. Proc. v. 42**, Pittsburgh, Ed. J. F.Young, 1985, p. 201.

51. Diamond, S., **ibid.**, p. 233.

52. Wise, S. et al., **ibid.**, p. 253.

53. Malhotra, V. M., Ed.: **Proceedings of the First International Conference on the use of Fly Ash, Silica Fume, Slag and Other Mineral By-Products in Concrete**, (meeting sponsored jointly by the Canadian Center for Mineral and Energy Technology and the American Concrete Institute), (ACI Publ. SP-79, American Concrete Institute, Detroit, 1983); a) D. M. Roy and K. M Parker, **ibid**, p. 397; b) M. W. Grutzeck, S. D. Atkinson, D. M. Roy, **ibid**, p. 643; c) A. Kumar and D. M. Roy, **J. Am. Ceram. Soc.**, 1986, 64, p. 356; d) D. M. Roy, A. Kumar and J. P. Rhodes, **Fly Ash, Silica Fume, Slag and Natural Pozzolans in Concrete**, V. M. Malhotra, Ed. (ACI, Detroit, 1986), p. 1423.

54. Nakagawa, D., D. M. Roy, E. L. White: Advances in Ceramics, 8, **Nuclear Waste Management**, G. G. Wicks and W. A. Ross, eds. (American Ceramic Society, Columbus, Ohio, 1984, p. 710.

55. Roy, D. M. and G. M. Idorn: Very High Strength Concrete-Based Materials, **Mater. Res. Soc. Symp. Proc. v. 42**, J. F. Young, Ed., Materials Research Society, Pittsburgh, 1985, p. 133.

56. Roy, D. M., Z. Nakagawa, B. E. Scheetz, E. L. White: **Ibid.**, p. 245.

57. Aitcin, P.-C., P. Pinsonneault, D. M. Roy: **Bull. Am. Ceram. Soc.**, 1984, 63, p. 1487.

58. Grutzeck, M. W., D. M. Roy and D. Wolfe-Confer: **Proceedings of the 4th International Cement Microscopy Association Meeting**, Las Vegas, 1982 (International Cement Microscopy Association, TX, p. 193.

59. Bach, T.: **Ceramic Transactions v. 16**, 1991, p. 67-102.

60. Sun, G., P. Lu, Stouse, and J. F. Young: **Ceramic Transactions**, 1991, v. 16; p. 381-304.

61. Cohen, M. D., J. Olek and W. L. Dolch: **Cem. Concr. Res.**, 1990, v. 20, p. 103-119.

62. (a) Park, C. K., M. R. Silsbee and D. M. Roy: **Mat. Res. Soc. Symp. Proc.**, 1991, v. 211, p. 239-246, eds. S. Mindess and J. Skalny, Mat. Res. Soc., Pittsburgh.
(b) Silsbee, M. R., D. Wolfe-Confer and D. M. Roy: **Mat. Res. Soc. Symp. Proc.**, 1991, v. 211, p. 231-238.

63. Taylor, H. F. W.: "Chemistry of Cement Hydration, **Proc. 8th Intl. Conf. on the Chemistry of Cement**, Rio de Janeiro, 1986, paper 2.1, v. 1, p. 82-110.

64. (a) Li, S., D. M. Roy and A. Kumar: "Quantitative Determination of Pozzolanas in Hydrated Systems of Cement or $Ca(OH)_2$ with Fly Ash or Silica Fume," Cem. Concr. Res., 1985, v. 15, 1079-1086.
(b) Uchikawa, H., Proc. 8th Intl. Cong. on the Chemistry of Cement, Rio de Janeiro, 1986, v. 1, p. 249-280 (paper 3.2).

65. Li, S., D. M. Roy: "Preparation and Characterization of High and Low CaO/SiO_2 Ratio 'Pure' C-S-H for Chemically Bonded Ceramics," J. Mat. Res. Vol., 1988, 3 [2], p. 380-386.

66. Grutzeck, M. W., D. M. Roy and D. Wolfe-Confer: "Mechanism of Hydration of Portland Cement Composites Containing Ferrosilicon Dust," **Proc. 4th Intl. Cement Microscopy Assn. Mtg.**, Las Vegas, Intl. Cem. Micr. Assn., Duncanville, TX, 1982, A3-202.

67. Grutzeck, M. W. S. D. Atkinson, D. M. Roy: "Mechanism of Hydration of Conendsed Silica Fume in Calcium Hydroxide Solutions," **Proc. CANMET/ACI First Intl. Conf. on the Use of Fly Ash, Silica Fume, Slag and Other Mineral By-products in Concrete**, 1983, Vol. II, Ed. V. M. Malhotra, ACI, Detroit, ACISP-79, p. 643-664.

68. Diamond, S.: "Effects of Microsilica (Silica Fume) on the Pore Solution Chemistry of Cement Pastes," **J. Am. Ceram. Soc.**, 1982, v. 66, C82-C84.

69. Glasser, F. P., S. Diamond and D. M. Roy: "Hydration Reactions in Cement Pastes Incorporating Fly Ash and other Pozzolanic Materials," **Mat. Res. Soc. Proc.**, 1987, v. 86, p. 139-158.

70. (a) Roy, D. M.: "Mechanisms of Cement Paste Degradation Due to Chemical and Physical Factors," **Proc. 8th Intl. Congr. Chem. Cement**, Brazil V. I, 1986, p. 362-380.
(b) Roy, D. M.: "Hydration of Blended Cements Containing Slag, Fly Ash, or Silica Fume," Institute of Concrete Technology, Coventry, U. K., 1987.

71. Mindess, S.: "Bonding in Cementitious Composites: How important is it?", **MRS Symposium Proceedings**, 1988, v. 114, p. 3-10.

72. Malhotra, V. M., V. S. Ramachandran, R. F. Feldman, and P. C. Aitcin: **Condensed Silica Fume in Concrete**, CRC Press, Inc., 1987, Chapt. 4, p. 29-51.

73. Detwiler, R. J., P. J. M Monteiro, H. R. Werk and Z. Zengqiu: "Texture of Calcium Hydroxide Near the Cement Paste-Aggregate Interface", **Cement and Concrete Research**, 1988, v. 18, p. 823-829.

74. Diamond, S., ed.: **Proc. Durability of Glass Fiber Reinforced Concrete Symposium**, Prestressed Concr. Inst., Chicago, Illinois, 1986.

75. Kumar, A. and D. M. Roy: "Microstructure of Glass Fiber/Cement Paste Interface in Admixture Blended Portland Cement Pastes," **Proceedings, Durability of Glass Fiber Reinforced Concrete Symposium**, Ed., S. Diamond, Prestressed Concrete Institute, Chicago, Illinois, 1986a, p. 147-156.

76. Nelson, J. A. and J. F. Young: **Cem. Concr. Res.**, 1977, v. 7, p 277-282.

77. Scheetz, B. E., S. A. Sabol, R. I. A. Malek, P. J. Andersen, V. Johansen, P. D. Cady and D. M. Roy: "Effect of Packing on Concrete Properties Optimization," presented at TRB, January, 1991.

78. Aim, R. B. and P. Le Goff: "Powder Technology", 1967-68, v. 1, p. 281-290.

79. Toufar, W., M: Born and E. Klose: **Freiberger Forschungsheft**, A 558 VEB Deutscher Verlag fuer Gundstoffindustrie, 1967.

80. Toufar, W., E. Klose and M. Born: **Aufberitungs-technik**, 1977, 11.

81. Khayat, K. H. and P.-C. Aitcin: "Silica Fume in Concrete - An Overview," American Concrete Institute, Detroit, MI, 1993, ACI SP-132a, v. 2, p. 835-872.

82. Justnes, H., E. J. Selevold and G. Lundevahl: "High Strength Concrete Binders, Part A, American Concrete Institute, Detroit, MI, 1993, ACI SP-132a, v. 2, p. 873-890.

83. Sellevold, E. J. and H. Justnes: "High Strength Concrete Binders, Part B", ACI SP-132a, v. 2, p. 891-902.

84. Cheng-Yi, H. and R. F. Feldman: "Hydration Reaction in Portland Cement-Silica Fume Blends," **Cem. Concr. Res.**, 1985, v. 15 (4), p. 585-592.

85. Perez-Pena, M., D. M. Roy and F. D. Tamas: "Influence of Chemical Composition and Inorganic Admixtures on the Electrical Conductivity of Hydrating Cement Pastes," **J. Mat. Res.**, 1989, v. 4 (1), p. 215-223.

86. Perez-Pena, M.: **Electrical Conductivity and Dielectric Studies of Hydraulic Cements**, Ph.D. Thesis,The Pennsylvania State University, 1986.

87. (a) Roy, D. M.: "Fly Ash and Silica Fume Chemistry and Hydration," **Concrete Workshop '88, Supplementary Papers**, Sydney, Australia, Ed., W. G. Ryan, 1988, p. 1-20.
(b) Roy, D. M: "Fly Ash and Silica Fume Chemistry and Hydration," **Third Intl. Conf. on the Use of Fly Ash, Silica Fume, Slag, and Natural Pozzolans in Concrete**, Trondheim, Norway, Ed. V. M. Malhotra, Am. Concr. Inst., Detroit, MI, 1989, 1, p. 117-138.

88. Touse, S. A., and T. A. Bier, C. A. Knepfler, J. F. Young, B. Francis, and L. Richard: **Mater. Res. Soc. Symp. Proc. v. 137**, 1989, 449-56.

89. Banthia, N. and S. Mindess: **MRS Symp. Proc. v. 137**, 1989, p. 173-8.

90. Kumar, A., S. Komarneni and D. M. Roy: "Diffusion of Cs^+ and Cl^- Through Sealing Materials", **Cem. Concr. Res.**, 1987, v. 17, p. 153-160.

91. Wise, S. and R. K. Jones: "High Temperature Processes and Applications of Silica-Modified Portland Cement CBC Composites", **MRS Symp. Proc. v. 179**, 1991, p. 89-100.

92. Wise, S., K. Jones, C. Herzfeld and D. Double: **MRS Symp. Proc. v. 114**, 1987, p. 197-204.

93. Wise, S., J. Satkowski, B. Scheetz, J. Rizer, M. MacKenzie and D. Double: **MRS Symp. Proc. v. 42**, 1985, p. 251-263.

94. Talling, B. and J. Brandstettr: "Present State and Future of Alkali-Activated Slag Concretes," **Fly Ash, Silica Fume, Slag and Natural Pozzlons in Concrete**, Proceedings Third International Conference, Trondheim, Norway, ACI, 1989.

95. Xuequan, Wu, W. Jiang and D. M. Roy: "Early Activation and Properties of Slag Cement", **Cem. Concr. Res.**, 1990, v. 20, p. 961-74.

96. Silsbee, M., R. I. A. Malek and D. M. Roy: **Vol 4 of the Proceedings of the 8th International Conference on The Chemistry of Cement**, Financiadora de Estudos e Projectos, Rio de Janeiro, 1986, p. 263-269.

97. Kaushal, S., D. M. Roy and P. H. Licastro: "Heat of Hydration and Characterization of Reaction Products of Adiabatically Cured Fly Ash and Slag Mixtures," in Fly Ash and Coal Conversion By-Products: Characterization, Utilization and Disposal II, Mat. Res. Soc. Symp. Proc., Eds. R. T. Hemmings, E. E. Berry, G. J. Berry and F. P. Glasser, **MRS Proc., v. 65, Pittsburgh**, 1989, p. 87-97.

98. Silsbee, M. R., D. Wolfe-Confer and D. M. Roy: "Fiber Reinforced Alkali Activated Blended Cement Materials," **Fiber Reinforced Cementitious Materials**, MRS, Eds. S. Mindess and J. P. Skalny, 1992, in press.

99. Roy, D. M. and M. R. Silsbee: "Alkali-Activated Materials: An Overview", MRS, 1991 (in press).

100. Majumdar, A. J., R. N. Edmonds and B. Singh, **Cem. Concr. Res.**, 1990, v. 20, p. 7-14.

GENERIC THEME III

CHEMISTRY OF HYDRATION OF CEMENTS AND CEMENTITIOUS SYSTEMS

CHEMISTRY OF HYDRATION OF CEMENTS AND CEMENTITIOUS SYSTEMS

Franco Massazza
Italcementi SpA, Bergamo, ITALY

and

Masaki Daïmon
Tokyo Institute of Technology, Tokyo, JAPAN

1. INTRODUCTION

"Hydration" is a chemical process taking place between the cement compounds and water. Hydration has both physical and mechanical effects and influences therefore the engineering properties of cement, i.e. rheology of fresh paste, setting and hardening, creep, heat evolution, microstructure, durability, etc.

Fig. 1 exemplifies the changes caused by hydration in the water-cement system and at the same time shows that the different test methods used to measure the chemical and physical variations of the system are also useful for monitoring cement hydration.

The hydration degree of three portland cements, for instance, has been recently correlated with some parameters (non-evaporable water, chemical shrinkage, heat of hydration) thus obtaining almost linear correlations, similar yet different for each cement (1). It is reasonable to assume that the differences would have been greater if the tests had been extended to blended cements or mortars and concretes.

The lack of general correlations applicable to all types of cement is due to the fact that the hydration process is affected by many parameters that depend on the chemical and mineralogical composition of the cements and the ambient conditions in which the reactions occur (see fig. 2).

Theoretically, the potential reactivity of cement compounds can be examined in terms of crystal chemistry, by considering the stability of simmetry at Ca-ion sites.

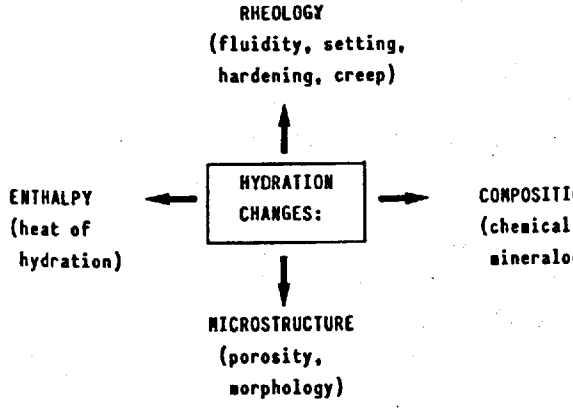

FIG. 1: Changes induced in the cement water-system by hydration

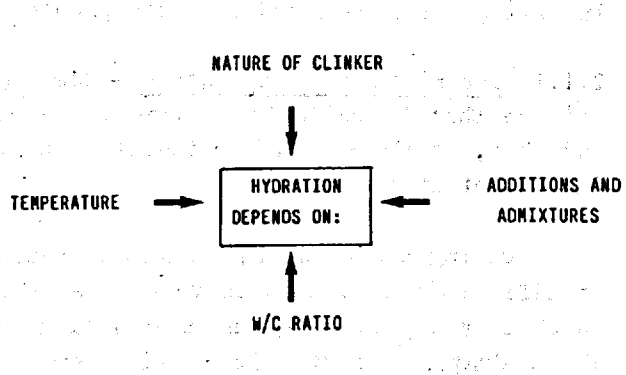

FIG. 2: Parameters influencing cement hydration

The lattice energy and electric potential of polymorphs of C_2S (2) and doped C_3S (3), could be used for predicting the reactivity of compounds by the intensity and direction of the electric field on Ca positions (4)(2), but the crystal chemistry-based approaches are insufficient in order to know the practical hydration mechanism of cements.

All these difficulties also explain why the numerous efforts made to develop mathematical models designed to assess the different properties of the pastes and concretes have not yet led to acceptable general results. The argument of modelling will not be dealt with in this paper, but it is felt appropriate to mention these important pioneering studies (from 5 to 27).

2. THE HYDRATION OF CEMENT COMPONENTS

The hydration of cements and their components is a complex phenomenon which depends on the characteristics of the reactive phases (chemical composition, crystalline structure, fineness, thermal history, etc.) as well as on the environmental conditions (water/solid ratio, chemical species dissolved or dispersed in the water, temperature, etc.).

Owing to the number of variables involved, the modelling of the hydration process is a problem that does not lend itself to easy solution. In any case the amount of test data that is being acquired and the theories that are being proposed to account for them are progressively dispelling doubts and converging on simpler and more consistent models.

This optimism is based in particular on actual progress that has been made, since the 8th Int. Congress on the Chemistry of Cement, in the knowledge of the chemistry of hydration reactions of individual cement components and of the structure of hydration products. Cement properties, including applicational or engineering ones, are the outcome of all the complex reactions that involve the various phases forming the cement-water system. However, the study of simpler systems is preparatory and indispensable to carry out any research on cements.

2.1 The Hydration of C_3S

As in the past, special attention has been devoted since the Rio Congress to the hydration of alite and pure C_3S owing to the prominent role played by this compound in fixing the cement and concrete properties.

2.1.1 The Kinetics of hydration - NMR (Nuclear Magnetic Resonance) has allowed to observe that hydration commences as soon as C_3S comes into contact with water (28) and that, at the end of the induction period, the silicate has undergone hydration to the extent of about 2% (29).

During the first 15 minutes of hydration, i.e. before the induction period, the specific surface increases reaches a peak and then diminishes rapidly. This peak is matched by a peak in the heat evolution curve as well (30) (31) (see fig. 3).
The hydration of C_3S is usually studied in pastes since it is felt that this condition, which is similar to that under which the cement is used, is closer to real ones than highly diluted suspensions. By contrast, some recent works (32)(33)(34) have

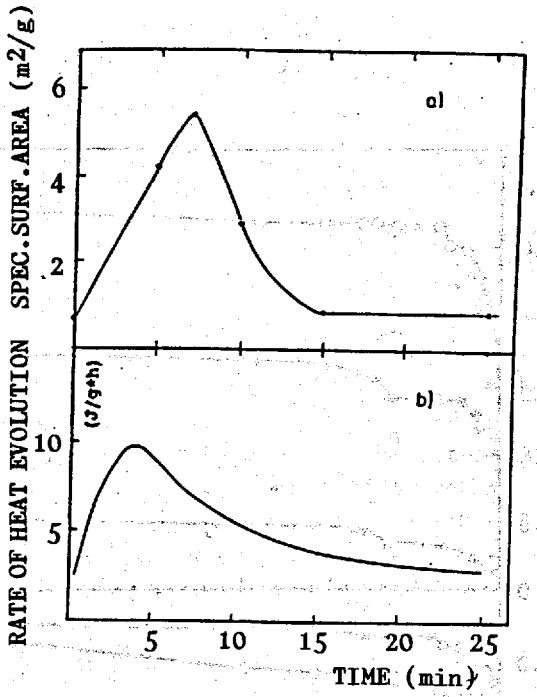

FIG. 3: Specific surface area (a) and rate of heat evolution (b) of C_3S

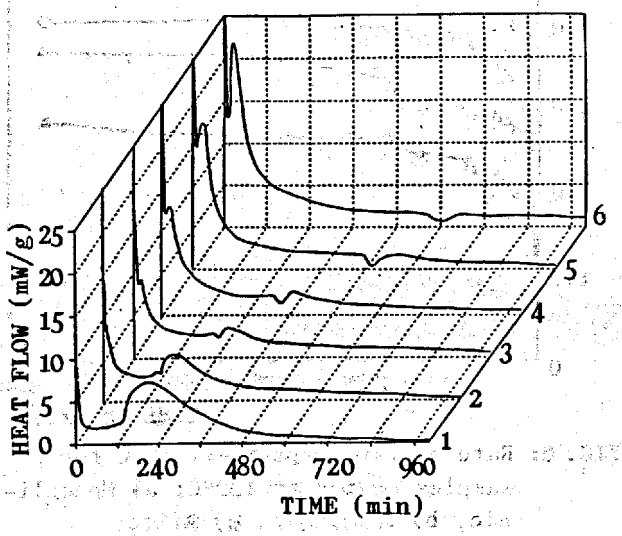

FIG. 4: Rate of heat evolution curves of C_3S at different w/c ratios

w/c = 5(1); 10(2); 15(3); 20(4); 40(5); 50(6)

shown that by operating with suspensions, phenomena can be stressed that cannot be observed in the pastes.

In pastes with a w/C3S ratio ≥ 10, the heat evolution curve shows 3 exothermal peaks and 1 endothermal peak (33) (see fig. 4)(34). With w/C_3S ratios ≤ 5, the latter does not appear and the curve has the typical pattern of C_3S pastes. It is interesting to observe that the experimental demonstration of the existence of this exothermal peak matches the exothermicity postulated, based on thermodynamic considerations, by (35).

The beginning of the endothermal peak matches the abrupt decrease in the electric conductivity of the suspension due to the beginning of the precipitation of portlandite. Position in time and intensity of the peaks depend on the w/C_3S ratio.

The dissolution of C_3S is immediate, and the same applies for the precipitation of the CSH which begins 1-3 minutes after contact with water. As shown by fig. 5 (34), the formation of C-S-H is fast and begins whatever the C_2S/C_3S ratio as soon as (SiO_2) achieves a concentration of (1.7) mmol/kg and (Ca^{++}) 5.5 mmol/kg.

A contribution to the knowledge of the alite hydration process is also given by a study of the C_3S+ water vapour reactions (36). The C_3S absorbs water from the environment increasingly with time (up to 2750 hours) and to a variable degree depending on its structure (monocline, tricline, alite), the activation temperature (120°C and 950°C) and the temperature at which absorption takes place. The water absorption curve (see fig. 6) (36) shows the presence of various hydration

stages occurring at different times and depending on the temperature at which absorption takes place. During periods of hydration stasis it may be assumed that the surface is entirely covered by hydration products and that the surface forces are saturated with water molecules. The stasis might be due either to the impermeability of the layer or to the passivation of the surface (36)(37).

Reaction kinetics depends on many factors and many papers were devoted to study their influence.

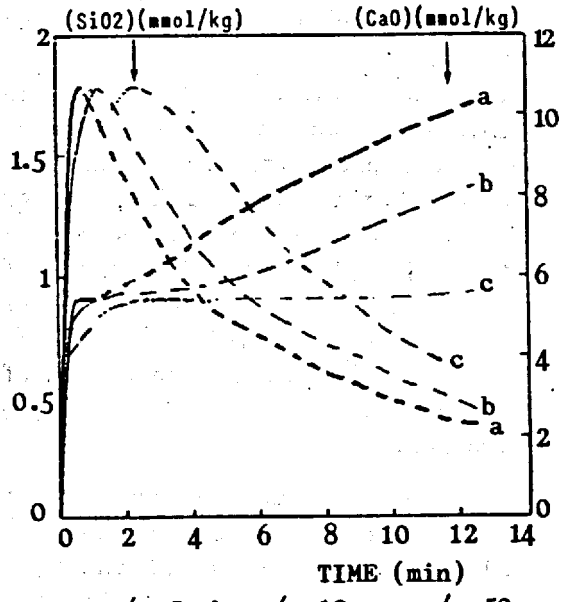

FIG. 5: Evolution of (CaO) and (SiO_2) versus hydration time

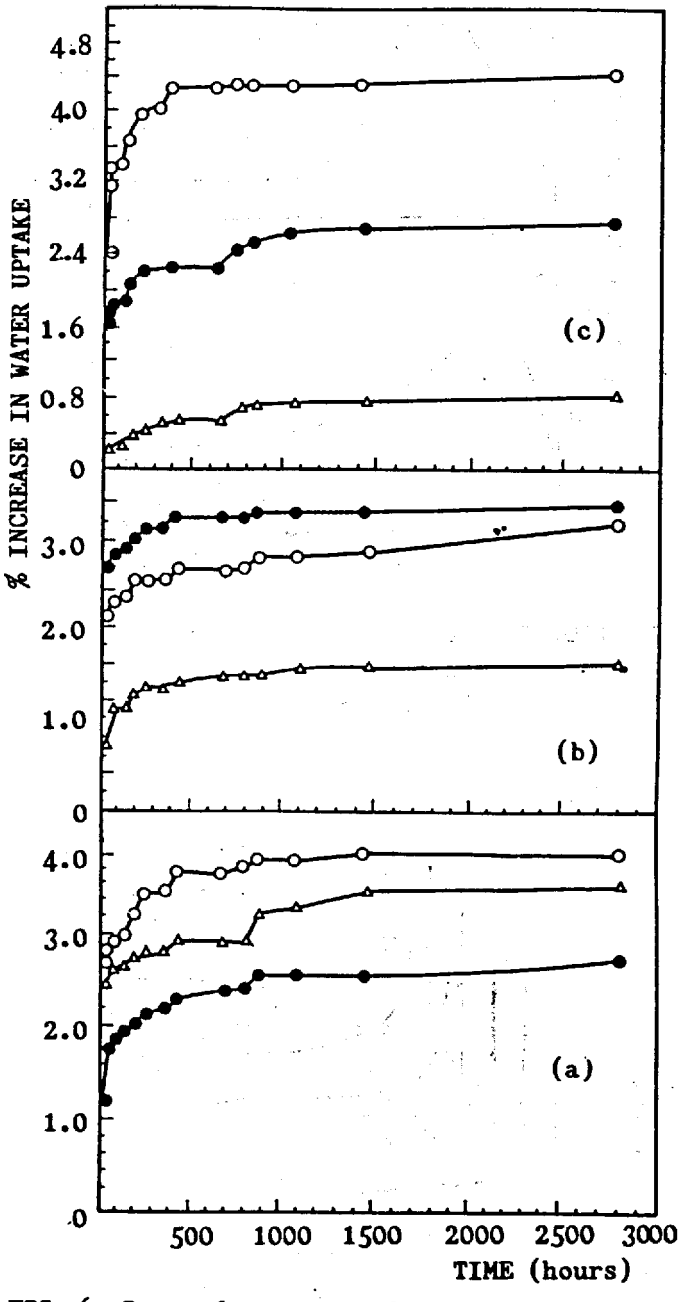

FIG. 6: Rate of water uptake at 10°C for C_3S samples heated at 120°C: a) Monoclinic, b) Triclinic, c) Alite; (o) C_3S_{-1} (•) C_3S_{-2} (Δ) C_3S_{-3}

* As is known, the rate of hydration, and consequently the extent of hydration of the C_3S, increases, under equal ageing, as the water/solid ratio increases (38)(39). Also the porosity of the hydration products increases with the

water/solid ratio (38).

* A temperature increase accelerates the hydration of alite. In particular, the initial heat evolution rate is increased (the 2nd heat peak is shifted towards lower hydration times and becomes more intense), total heat developed in the first 24 hours increases, the induction period becomes shorter.
  The analysis of the results suggests that the acceleratory period corresponds to a process controlled by nucleation and growth of the crystals and may be expressed by a modified Avrami equation. The subsequent deceleratory period, instead, is a phenomenon controlled by the diffusion which obeys to Jander's equation (40).
* The presence of "doping" elements in the lattice modifies alite hydration quantitatively even though it does not change its prominent features. The heat evolution curve shows that the presence of Na_2O and K_2O in the lattice of C_3S (and C_3A) accelerates hydration (41) inasmuch as the induction period is reduced and the 2nd peak advanced. It should be noted that C_3S doped with alkalis hydrates faster than doped alite (42). The heat evolution rate increases with increasing Al contents (43), which corresponds to the acceleration of setting as pointed out earlier. Synthetic alite containing 2% of ZnO hardens faster than zinc-free silicate, while fluorite-containing alite hardens more slowly (44). For equal contents of CaF_2, the reactivity of C_3S diminishes as the firing temperature is increased (45).
  Generally speaking, the introduction of cations in the C_3S lattice (Mg^{2+}, Ba^{2+}, Cd^{2+}, Al^{3+}, Ni^{2+}, Fe^{3+}, Ti^{4+}) accelerates the hydration of tricalcium silicate (46).
  The difference in behaviour between pure compounds and variously doped compounds also has practical consequences. This is particularly apparent when comparing the hydration rates of C_3S and C_2S, alite and belite, since, at least under considerably humid conditions, belite combines water faster than alite, while C_2S combines it more slowly than C_3S (47).
* Also heavy water, D_2O, slightly affects the hydration of C_3S by slowing it down, with an effect that grows with the D_2O/H_2O ratio. The total heat developed at the end of the second peak of the heat evolution rate, instead, is approximately the same (roughly 250 $J.g^{-1}$) (48).

The trend of C_3S hydration also depends on the presence of other substances in the C_3S-water system. The influence of these materials may be chemical, physical, chemico-physical and mixed. The chemical interference is especially marked, but the other actions are perceivable and measurable as well.

The sensitivity of the C_3S to the hydration environment is also noticed with regard to the phases which are habitual constituents of clinker and of hydrated pastes.

* In the first 20 minutes after mixing, alite and belite mixes with 75:25, 50:50 and 25:75 ratios show a greater heat development rate not only than that of belite, but also than that of alite, which, as is well-known, hydrates faster. After 6 hours the heat development rate increases with the alite content, but after 24 hours the alite hydration behaviour is not different from that of the 75:25 mix. This means that as far as hydration is concerned, there is no benefit in exceeding an alite/belite ratio of 3:1. The thermal data are confirmed by the values of combined water (49).
  The hydration of C_3S, expressed by the hydration degree, is only slightly speeded up by the presence of C_3A, unless the ratio between the two compounds achieves the 50:50 value. In any case, the presence of gypsum normalizes the behaviour

of the different mixes. Also C_4AF does not affect the progress of hydration of C_3S to an appreciable degree (50) and the slight speeding up observed may be ascribed to a physical rather than a chemical action.

* The addition of ettringite to C_3S accelerates the hydration of the silicate, probably because it increases the number of active sites on which the nucleation of C-S-H takes place. The sulphoaluminate, however, does not change the growth simmetry of the nucleation centers and the morphology of the resulting phases (51).

The presence of electrolites in the mixing water affects the hydration of C_3S.

* As is known, CO_2 dissolves in water forming the highly reactive anion HCO_3^-. For this reason CO_2 lowers the concentration of Ca^{++} and accordingly increases that of SiO_2 present in the solution (52). As a result, the hydration rate of C_3S may become so fast as to cause the induction period to disappear.
Likewise, small quantities of $NaHCO_3$ (0.67%) slow down the hydration of C_3S while Na_2CO_3 (1.7%) speeds it up (53). NaOH solutions slow down the hydration of tricalcium silicate when they are weakly alkaline (0.05 n) and accelerate it when they are more highly concentrated (0.5-2.0 n) (54). As (OH^-) increases, the solubility of Ca^{++} is lowered and the precipitation of $Ca(OH)_2$ is favoured (55). The solubility of the silica increases accordingly (54).
$CaCl_2$, $Ca(HCOO)_2$, Na_2CO_3, $TlCO_3$ accelerate the hydration of C_3S, even if with decreasing efficacy. After 24 hours the hydration degree of C_3S doubles in the presence of CaCl, passing from 40 to 80%. The cynetic values follow the Jander's equation $K.t = [1-(1-\alpha)^{1/3}]^2$ and this means that the hydration is a diffusion-controlled process (56).
The addition of gypsum puts forward the heat flow peak and increases slightly the amount of heat developed over the first 24 hours (57).
The initial hydration of C_3S is delayed by Mn, Ni and Cu salts (2-4%), but after 28 days the influence of the additives is not longer noticeable (58).

The hydration of C_3S is accelerated or slowed down by the presence of admixtures.

* Lactic acid (1%) not only anticipates and raises the second peak of the heat evolution curve, but also causes a marked peak to appear after 30 minutes of hydration and suppresses the induction period. The acceleration observed in the first 24 hours is also revealed by a considerable increase in the amount of non-evaporable water, free lime and therefore of the hydration degree (59).
The acceleration caused by lactic acid is ascribed to the formation of an eminently fibrous C-S-H which, owing to its structure, apparently does not hinder the penetration of water into the anhydrous core of the C_3S (59).
The acceleration caused by the sodium formiate (1M solution) is connected with the formation of an initial C-S-H featuring a comparatively low c/s ratio and high specific surface (60).
The interference of the admixtures is highest at the early stages of hydration, i.e., when a rapid evolution of the solid and of the aqueous phases takes place. The retarding effect of citric acid on the hydration of C_3S becomes lower the more delayed the addition (31).

The presence of materials considered inert modifies the course of the hydration of C_3S with such results as to induce one to feel that the expression "inert" is rarely true.

* A typical example is given by $CaCO_3$ which, when added to C_3S, increases the

hydration rate with an effect that is so much stronger, the greater its content and fineness (61)(62)(63)(64). No doubts appear to be cast on this conclusion since it has been generally proved by the results achieved by different test methods. In the first 2 days, as a matter of fact, when calcite is present, the content of $Ca(OH)_2$ and of evaporable water increase, while the residual C_3S content diminishes. In the first 24 hours the hydration heat increases (65)(61), and the curve of the Ca^{++} concentration in the pore solution reaches the peak earlier (61).

The TG analysis of $C_3S+C\bar{C}+H$ pastes has in turn pointed out that after 3 days of hydration the peak, due to decarbonation of the $CaCO_3$ dimishises (see fig. 7) (61). Since the phenomenon is all the more marked the smaller the size of the $CaCO_3$ particles, it may be inferred that a part of the calcite is incorporated in the C-S-H phase. As a result, the C/S ratio of the C-S-H increases (61)(66).

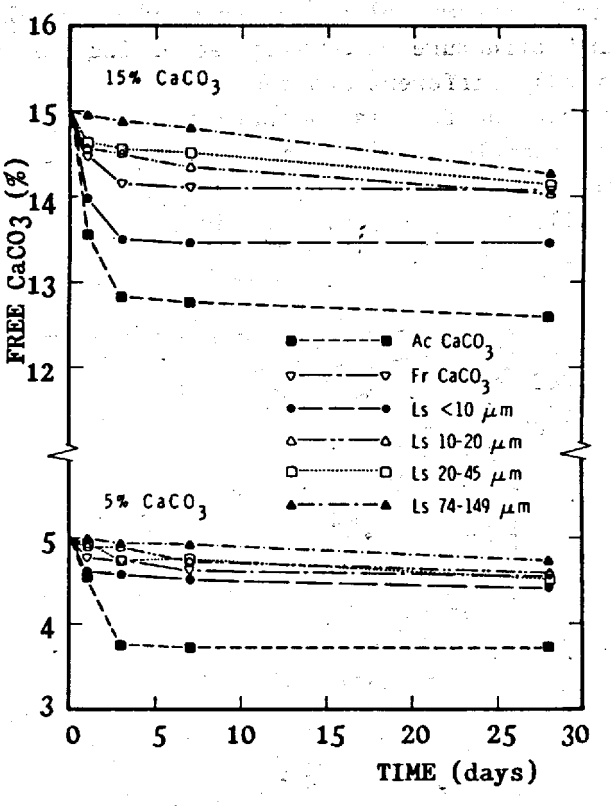

FIG. 7: Free $CaCO_3$ remaining in C_3S pastes at different times of hydration

According to other Authors, instead, a basic calcium carbonate forms at the interface between $CaCO_3$ and C-S-H, which strengthens the interface bonds and improves the mechanical properties of the hardened paste (64). From this point of view, therefore, it can not be said that the $CaCO_3$ added to the C_3S or to the cement is a truly inert material.

* Also the addition of finely divided silica accelerates the hydration of C_3S, but in this case one cannot neglect the acid character of the material which underlies its pozzolanic activity. The action of the silica is revealed by a considerable change of the heat evolution rate curve. In particular, there is a reduction of the induction period (from 180 to 90 minutes) and the highest peak is shifted from 660 to 280 minutes. The acceleration seems to be independent of the fineness of the silica, while the pozzolanic reaction, which develops later on, is strongly dependent on the fineness (67). Other Authors have reported, however, that acceleration occurs without reducing the induction period (68). If the accelerating effect of the fine silica particles on the early hydration of C_3S is evident, the reasons behind it are not very clear because:

a) the acceleration is observed before the pozzolanic reaction is revealed
b) the addition of other fine materials to the C_3S has no effect (α-alumina, titania, graphite), a retarding down effect (γ-alumina) or in any case

modest effects (clays).

The latter circumstance would seem to show that acceleration of hydration is not due to a general increase of the nucleation of the hydrates, promoted by the extreme fineness of the colloidal silica, but must be ascribed to a solution chemical effect which is established in a very short time. This effect might be a reduction of the potential of the Ca^{++} ion in the solution or an increase of the concentration of silicate ions (67).

2.1.2 Phase Relationships - After the Congress of Rio de Janeiro others attempts were made to determine the composition and structure of silicate hydrates. The results of such research did not provide a final answer to all queries, but they did give an important contribution to an improved knowledge of calcium silicate hydrates and of their phase relations. These studies tried, in particular, to verify whether CSH is a single phase, having a composition and structure that vary according to ambient conditions, or forms a family of structurally different compounds.

* The idea that C-S-H may present more than one form is no novelty, and has had its advocates in the past. It has been recently proposed again on the basis of a critical analysis of new and old test results concerning the composition of the liquid in contact with the calcium silicate hydrates. A study revealed (69) that all pairs of SiO_2 and CaO concentration values present in the aqueous contact solution are distributed along two separate curves irrespectively of the procedure followed in preparing C-S-H (see fig. 8). The points of curve A chiefly come from reactions between CaO and silicic acid, or have been obtained with similar procedures, while those of curve B all come from the hydration of C_3S and therefore from specimens that were likely to contain C_3S that was not yet hydrated. The existence of two separate curves thus supports the assumption that more than one form of C-S-H may form during the hydration of C_3S, each featuring a specific composition and structure (69). Curve A might be associated with C-S-H (I), a form structurally correlated to tobermorite, while curve B might be a mixture of "tobermorite-like" and "jennite-like" (69). Both

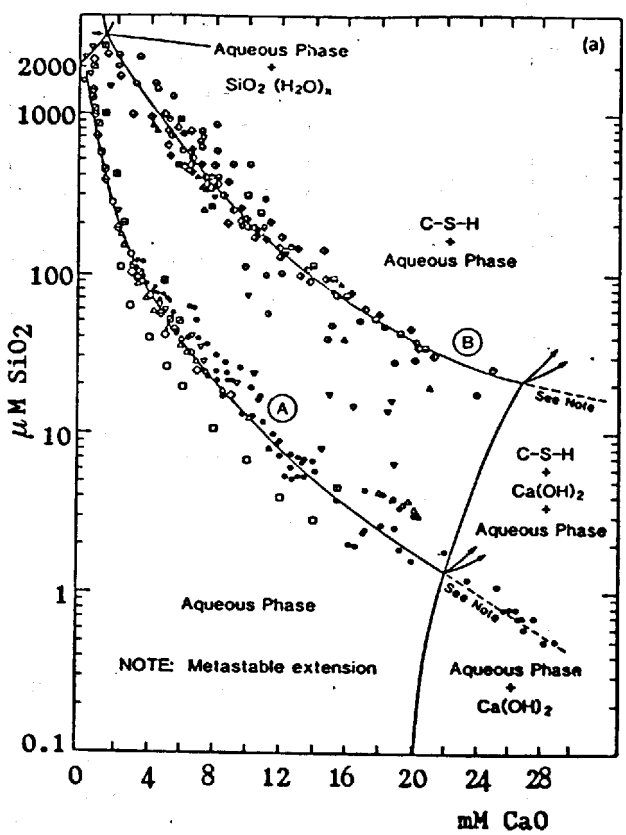

FIG. 8: Plot of concentrations of the components SiO_2 versus CaO in aqueous phase

curves represent metastable equilibria and the formation of the two types of silicate hydrate might be due to their formation conditions (concentration gradients, pH, etc.) while the transformation into more stable phases (such as the one corresponding to curve A or awfillite) might be intrinsically slow (69).

* The existence of two separate C-S-H phases has been postulated also as a result of a survey of the literature and studies carried out on C_3S suspensions subjected to hydration in excess water (a/s=500), but with a preset pH ranging from 8 to 12. The results collected would show that the composition of C-S-H depends on the pH rather than on the length of the reaction (70).

This same conclusion has been reached by letting CaO, SiO_2 (silica fume) and water with water/solid ratios = 11, 25 and 200 react for two years (71). The analysis of the solid phases and of the aqueous solution have made it possible to plot the chart of fig. 9, where the C/S mol ratio of the solid is expressed as a function of the pH of the solution.

The figure closely matches figs. 1 and 2 shown by Steinour in the London Symposium (72) where the C/S ratio in the solid was expressed as a function of the CaO concentration in the solution. The vertical portion of the curve at pH=9.9 represents an invariance: to the left, silica hydrate, containing a few mol% of calcium oxide, and a CSH with C/S 0.65 coexist; on the right, the rise in pH is attended by an increase of the C/S ratio of the solid phase which reveals that the system is no longer invariant (71). The final portion of the curve, which is markedly vertical, reveals the presence of a second CSH and consequently the existence of a second invariance where two CSH phases with C/S phases equal to 1.0 and 1.1 respectively coexist (71).

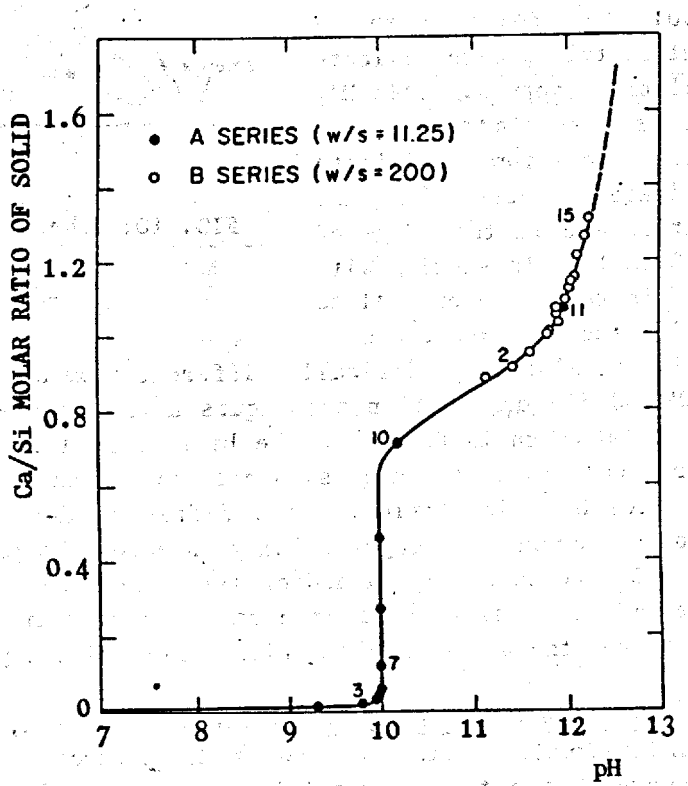

FIG. 9: Ca/Si molar ratio of the solid plotted as a function of the pH of the solution phase

The MAS NMR spectra of the solid hydrates have confirmed the analytical data and made it possible to characterise three different solid species:

1) lime-rich C-S-H (C/S = 1.1-1.3), which is formed at pH=12, has two peaks that show the prevalence of dimeric groups and/or final groups (Q^1) and lower quantities of silica tetrahedra (Q^2).
2) silica-rich C-S-H with C/S = 0.71-0.91 has one single peak, characteristic of secondary unbranched chains of silica tetrahedra (Q^2).
3) silica gel, which contains small quantities of Ca, has two peaks that are

characteristic of tertiary (Q^3) and quaternary (Q^4) networks.

These test results, jointly with others taken from literature, have made it possible to plot the phase relations shown in fig. 10 (71). The graph proposed is merely indicative and not in scale, being an interpretation of several test results.

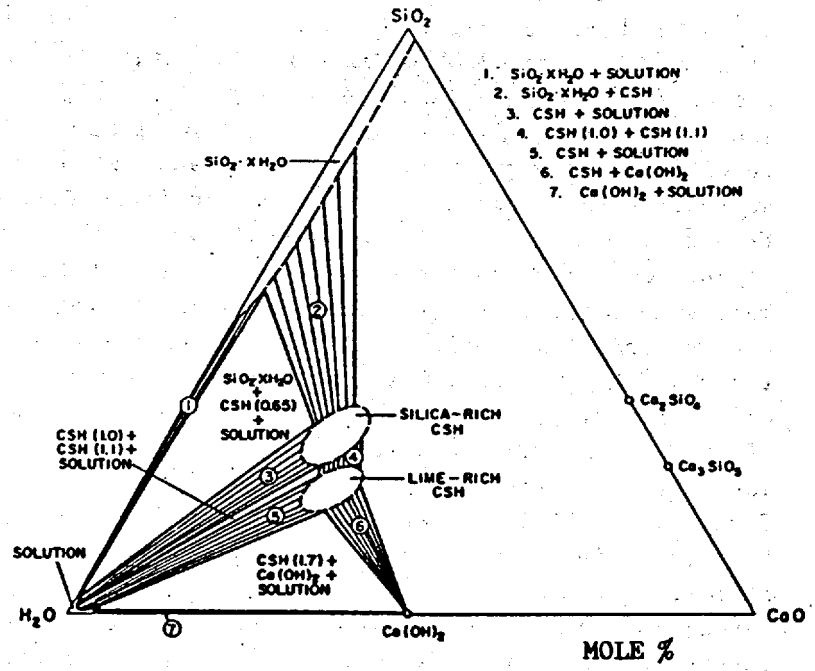

FIG. 10: Schematic representation of proposed room-temperature phase relations in the system $CaO-SiO_2-H_2O$

* By letting a calcium hydroxide solution (approx. 0.01 M) react with a tetracetyl orthosilicate solution (approx. 0.444 M), it is possible to synthetize calcium silicate hydrates, whose C/S mol ratios are in the range of 0.2 to 1.4. In samples with C/S in the range of 0.41 to 0.78 they form a phase which is also morphologically different from ordinary C-S-H and silica gel (73).
* TEM and SEM diffraction techniques have revealed that the structural polymorphism of C-S-H which is formed in the hydration of C_3S is greater than that revealed by more traditional techniques. A gel phase and four crystalline phases, α, β, γ and δ, have been identified, which differ by d-spacings (see table 1) (74) and the growing degrees of crystallinity. Needle-like particles of C-S-H, radially grown from C_3S (both of type 1 and of type 2), are the main product of hydration. They are formed in situ, while the other polymorphic phases with sheet-like morphology form from the solution along with portlandite crystals (74).

2.1.3 The Structure of C-S-H - The composition, structure and morphology of portlandite, which with C-S-H forms the products of hydration of C_3S, are fairly well known, while those of calcium silicate hydrate are much less so owing to the extremely small size and low crystallinity of the hydrated phases. For this reason the matter is still being investigated and although considerable progress has been made in the past few years, the data are still partly incomplete and contradictory.

* Several experimental results have led to the assumption that the majority of layers forming the C-S-H structure are made up of imperfect jennite layers ($Ca_9Si_6O_{32}H_{22}$) and, to a lower extent, of layers of 1.4 nm tobermorite ($Ca_5Si_6O_{26}H_{18}$). Octahedral Ca-O layers would be similar to those to be found in the layer structures of the two minerals, but these would be distorted and would lack many of their silicate tetrahedra. In support of this structural model speaks the fact that C-S-H has a fairly high proportion of pentameric anions units and that jennite-type material with 5 anionic units has a C/S ratio of 1.8, approximately the same as that of the gel (75).
* Based on X-ray diffraction data, the assumption has been made that the structure

of C-S-H in cement pastes is similar to that of portlandite, albeit with a slightly distorted unit cell (see fig. 11). In this model some of the Ca ions would be replaced by Si ions in octahedral positions or by octahedral voids. The smaller size of the Si ions would account for their relative mobility, which would allow them to oscillate or migrate between adjacent lattice positions and therefore be strongly polarized in an electric field. The dielectric constant of the (dry) cement paste is over 500, that is to say, higher than 80 found for ice and water (76).

* It is generally acknowledged that C-S-H has a layered two-dimensional structure, however direct evidence of this type of structure has been provided only in recent times.

In order to contribute to overcoming these structural uncertainties, a number of different calcium silicate hydrates with C/S ratio in the range of 0.8 to 1.9 have been prepared, making use of a particular technique. An aqueous solution of $Ca(OH)_2$ is made react with a hexane solution containing $(C_2H_5O)_4Si$. Since the two solutions

TABLE 1: Lattice constants or d-spacings and morphological appearance of C-S-H phases observed during the first 14 days of the hydration of C_3S by TEM diffraction techniques

phase	lattice constants or d-spacings	morpological appearance
gel-like phase	diffuse rings with d ≈ 2.94 Å and d ≈ 1.10 Å	vermicular-like, quasi crystalline size ≤ 1 µm
α-CSH	a = 10.1 Å b = 7.8 Å	from C_3S grains radial grown type 1 : needle-like type 2 : sword-like (higher degree of crystallinty) size ≤ 1 µm
β-CSH	a = 9,75 Å b = 6.85 Å	i)sheet-like particles, often conglomerated ii)epitaxial intergrowth with portlandite and/or γ- and δ-CSH size ≈ 1 µm
γ - CSH	a = 10.55 Å b = 7.29 Å	epitaxially grown together with β-CSH and/or portlandite and δ-CSH
δ - CSH	a = 11.2 Å b = 8.0 Å	epitaxially grown together with portlandite, β- and γ-CSH

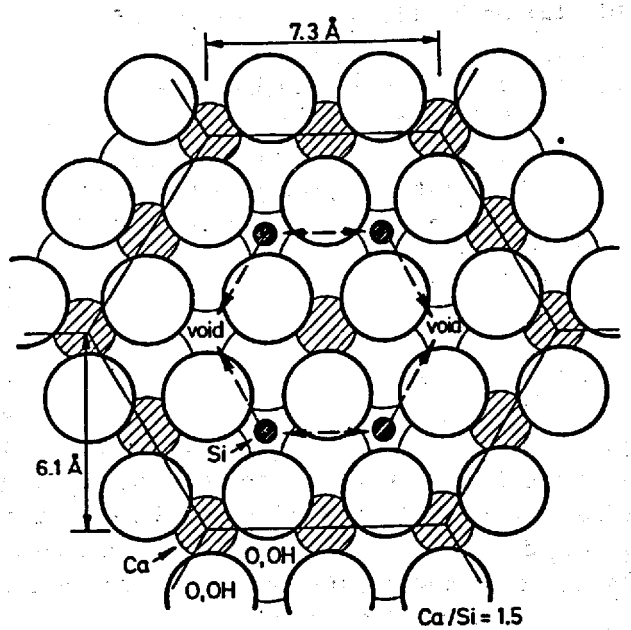

FIG. 11: Suggested structure of C-S-H gel in cement paste

do not mix the reaction products thus form at the solution- solution interface. The material which is formed is collected with a grid and inspected under the electronic microscope. The results obtained show that the composition of the calcium silicate hydrates as well as their structural order depend on the conditions that prevail in the two reacting systems. In particular, saturated solutions of $Ca(OH)_2$ typically produce amorphous hydrates, while less highly concentrated solutions produce hydrates with a greater structural order.
On examining these preparations under a high-resolution TEM, the molecular structure of (C-S-H) has been observed and photographed. It shows to be formed almost exclusively of 1 nm-thick curved sheets, extended over 10^2-10^6 nm^2, and a few double sheets measuring approx. 2 nm in thickness. This basic structure applies both to amorphous hydrates and to micro-crystalline ones, whose C/S ratio is in the range 0.9 to 1.75.
Data collected suggest that the hydrates are formed of protonated polyhedral CaO_x sheets sandwiched between short-chain silicate groups (fig. 12). This structure does not depend on the special preparation procedure of the silicate hydrates, since also the C-S-H prepared according to the usual technique, namely, from the reaction between $Ca(OH)_2$ and SiO_2, and which at lower magnification showed a fibrous microstructure, proved to be made of sheets consisting of up to 6 sandwiched layers stretching from 10^2 to 10^3 nm (77).

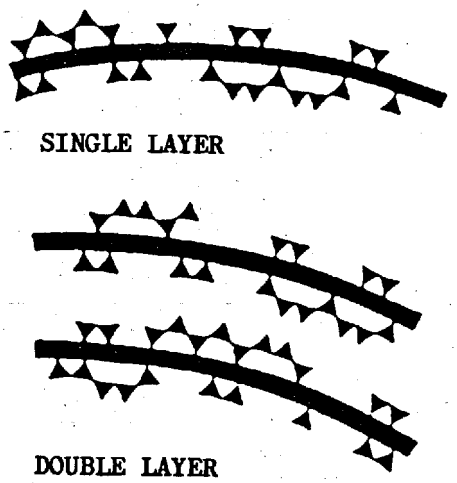

FIG. 12: Schematic representation of the layer-like structure of calcium silicate hydrate. Triangles are silicate tetrahedra and the core sheet consists of protonated CaO_x polyhedra

2.1.4 The composition of C-S-H - At the Congress of Rio de Janeiro it was finally established that the degree of polymerization of the silicate anion that makes up the C-S-H depends on several factors, such as time, environment conditions, presence of pozzolanic materials, etc. The polymerization degree achieved by silicate hydrates during hydration by evolution of the silicate units forming C_3S may be investigated according to different analytical techniques, such as the molybdate reaction, trimethylsililation and paper-chromatography, but all have strong limits.

A technique which has recently come up in the determination of the polymerization degree is Nuclear Magnetic Resonance (NMR), since the chemical shifts of the resonance of the ^{29}Si nuclei in silicates are dependent on the degree of condensation of the silicate tetrahedra. This method does not show the same limits

as earlier methods since, for example, the joint use of CP (cross polarization) and non-CP NMR makes it easy to distinguish the protonated, i.e., the hydrated silicate units, from the anhydrous ones. NMR thus makes it possible to measure the hydration degree of C_3S pastes.

* It has been observed that after 24 hours the peak intensity Q^0 corresponding to the tetrahedra that form the anhydrous C_3S has dropped by 40% and that at the same time considerable amounts of dimer (peak Q^1) and small amounts of trimer (peak Q^2) have formed (68).
  CP-MAS NMR tests have revealed that during early hydration the C-S-H that forms also contains hydrated monomeric silicate units Q^0. The quantity of this species is however low (2%) and remains unchanged at least up to 24 hours (78). Q^0 for a long as anhydrous C_3S is present, but not observed in synthetic C-S-H (28). After 28 days of hydration, the average length of the silicates chain is 2.6 and the C/S ratio ≈ 1.7 (68).
* The anionic structure of C-S-H changes as hydration progresses. Solid-state NMR has revealed that during the induction period, C-S-H contains exclusively monomeric units, while in the first 24 hours it prevalently contains dimeric units and becomes rich in polymeric units only in subsequent periods (78). The end of the induction period corresponds to the beginning of the formation of dimeric species which prevail in the acceleratory period (79), while silicate species with a longer chain are formed in the deceleratory period (29). The rate of formation of the trimer increases slowly. This means that as the C_3S hydration proceeds, the number of final units of the silicate chains diminishes and that of the intermediate units increases (see tab. 2), namely as the paste ages, the simpler units condense to give higher polymeric units (78). This fact may be accounted for in two ways: the formation of monomeric C-S-H stops and the stability of the hydrate is such as to prevent its polymerization, or else it forms continuously, but as continuously it is transformed into dimeric or polymeric units.
  The consequence of polymerization should be a lowering of the C/S ratio, but since this does not in fact occur, the gel structure should incorporate additional Ca^{++} and OH^- ions (78).

The condensation degree of anions appears to be determined by the conditions under which the C-S-H is formed.

TABLE 2: ^{29}Si solid state NMR results from a series of C_3S samples

Time of Hydration	Distribution of silicate sites (%)		
	anhydrous	end units in silicate chains	middle units in silicate chains
12 hours	89	11	-
1 day	68	30	2
7 days	48	43	9
14 days	33	52	15
1 month	30	53	17
3 months	18	62	20
6 months	14	65	21
1 year	10	55	35
2 years	6	52	42
26 years	0	42	58

* As a matter of fact, the lime-richer C-S-H formed at pH ≥ 12 is prevalently made up of dimeric groups (Q^1) and shorter chains (Q^1 end units and Q^2 middle units), while the one poorer in lime (C/S=0.71-0.42), which is formed at pH ≤ 10, is chiefly made up of comparatively long silica tetrahedra chains (Q^2 middle units) (71) (tab. 3).
* The initial formation of the monomeric species should be due to the favourable water-rich, low-pH environment (29). The importance of the environment on the degree of polymerization has been ascertained by comparing the polymerization degree of gel-like calcium silicate hydrates prepared by reaction between CaO silicic acid and water, with those obtained in the hydration of the C_3S of portland cement.

TABLE 3: Observed ^{29}Si chemical shifts (ppm) as a function of c/s ratio of solids

Mixture	C/S	Q^1	Q^2	Q^3	Q^4
A3	0.02			−100.7	−114.5
A7	0.12		−85.0	−100.7	−114.7
A10	0.71		−85.0		
B2	0.91		−86.8		
A11	1.07	−79.2	−85.8		
B15	1.31	−80.4	−86.6		

The synthetic gels kept humid prove to be chiefly made up of dimeric silicate units, but the young gels situated in environments with low humidity (10, 30 and 50% R.H.), polymerize mainly forming linear pentameric silicates. Gels which have undergone extensive wet curing better withstand polymerization due to drying (80). Unlike synthetic gels, C_3S and portland cements show higher degrees of polymerization because they contain octomers and oligomers. This difference in behaviour may be due to a local drying of freshly formed CSH due to the request for water by the adjacent, still unhydrated C_3S (80).
The degree of polymerisation increases with increasing temperature however after a 78-day hydration there vas no evidence of cross linking groups (81).

The different composition of the polymeric chains could explain, at least in part, the differences in the properties of "inner" and "outer" calcium silicate hydrates formed by the hydration of C_3S (80).

The presence of other compounds can modify the degree of polymerization of silicate anions.

* As an example alkalis favour the depolymerization of silicate hydrates increasingly with their concentration and with the succession KOH, NaOH, LiOH (82). In the presence of CO_2, the quantities of dimer and trimer formed are less than in CO_2-free air (79).
* The presence of finely divided silica modifies the process of polymerization, because the lowering of peak Q^0 and the rise of peaks Q^1 and Q^2 undergo considerable acceleration. In addition, after 8 days, while peak Q^2 continues to grow, Q^1 begins to diminish. Of course peak Q^4, which corresponds to silica, diminishes in time as the pozzolanic reaction proceeds. In the presence of silica the average length of the silicate chain reaches 3.6 and the C/S ratio drops to 1.5 (68). The addition of SiO_2 gel modified with 1-10% of Fe_2O_3 increases the polymerization of silicate anions of C-S-H (83).

Variability of C/S ratio was already been mentioned: it depends on many factors which

cannot be easily analysed since they often operate on microlevel.

* The composition of the hydrated phases that form in the first minutes of the hydration is very different (C/S=1) from that obtained at the end of the acceleratory period (C/S=1.6) as well as from that observed in an intermediate stage (2.1-2.5) (30).
* When one considers the composition of C-S-H, one usually privileges the C/S ratio and neglects the content of bound water. It is clear, instead, that water has an important role in the formation and stability of the silicate hydrates.
  The water content of C-S-H obtained by hydration of the C_3S depends on the relative humidity. It goes from $C_{1.7}-S-H_4$ for silicate hydrate kept in environment with 90% R.H. and $C_{1.7}-S-H_{1.2}$ for D-dried silicate. This affects the density, which increases from 1.85-1.90 to 2.39 g/cm^3, accordingly. The calculations thus indicate that if under conditions of quasi-saturation the C-S-H has an S/H ratio of 4, the complete hydration C_3S requires a w/c ratio of 0.42, i.e., higher than that found by Powers (84).
* The hydration of C_3S in the presence of colloidal silica decreases the basicity of C-S-H (85). C/S ratio is ~ 1.4-1.5, with an S/H ratio of 3.8 in nearly saturated condition which drops to Si/H = 1 under D-drying conditions (84).

The presence of foreign elements in the C_3S or the hydration water does not fail to affect the C-S-H composition.

* It is a known fact that C-S-H may incorporate alkaline hydroxides. The quantity of M^+ fixed increases as the concentration in the solution increases and as the molar ratio C/S diminishes from 2 to 0.8, as the temperature of formation of the C-S-H drops from 150°C to 20°C and as the cation radius diminishes ($K^+ < Na^+ < Li^+$). The quantity of alkaline hydroxides that may be incorporated is reduced by the simultaneous presence in the C-S-H lattice of Al, coming both from the C_3S and from the solution (86). The aluminium is to be found in the C-S-H both in tetrahedral and in octahedral coordination and the $Al^{(4)}/Al^{(6)}$ ratio diminishes as the C/S ratio increases (87).
  The incorporation of Na^+ in C-S-H consequently modifies the C/S ratio, which drops from 1.77 (in water) to 1.5 (in 0.8 M NaOH solution). An N/S ratio = 0.5 corresponds to the latter value (55). Furthermore it has been found that a minor C/S ratio is associated with a higher degree of C-S-H crystallization (88).

2.1.5 The Morphology of Hydration Products - Ion-beam thinned sections examined by TEM (Transmissione Electron Microscopy) have made it possible to obtain precise information on the microscopic structure of hardened C_3S pastes.

* The relicts of unhydrated C_3S appear enveloped by a homogeneous gel which represents an inner product formed within the boundaries of the original grains of C_3S. The regions formed by this gel are connected by an outer product, generally fibrillar or perhaps lamellar, in any event being considerably more porous (89)(39). The C/S ratio of these products does not appear to depend on the morphology of the gel (89)(78). However, as mentioned earlier, the fibrillar aspect of the C-H-S would derive from the adhesion of some thin elementary lamellae (77).
* Alongside the C-S-H, there are to be found portlandite crystals, comparatively large and imperfect, and if the pastes are not protected by the CO_2 present in the air, also crystals of calcite (diam. 0.1 µm). Since calcite is present only in the "outer product", it is natural to assume that its formation occurs by precipitation from the solution (89).

* The interface between inner and outer C-S-H appears weaker than the CH/C-S-H interface, since the fractures tend to pass between the two types of C-S-H (39)(61).
* TEM research has revealed that C_3S hydration leads to the formation of 5 different forms of calcium silicate hydrate (74). The essential morphological differences are the following:
  - gel-like C-S-H surrounding still anhydrous C_3S grains
  - α-C-S-H, which projects radially from the gel-like C-S-H. The 1st type is needle-like, the 2nd type (more crystalline) is sword-like
  - ß-C-S-H, formed by sheet-like particles. It often shows epitaxial growth with CH, γ-C-S-H and σ-C-S-H. It is formed in solution.
  - γ-C-S-H, it is observed only in epitaxial growths with CH and ß-C-S-H,
  - σ-C-S-H, it is observed only in epitaxial growths with ß, and γ-C-S-H and portlandite 2).

  It is known that the C/S mol ratio of calcium silicate hydrates depends on the w/c ratio and on the method of determination. The existence of calcium silicate hydrates which have grown epitaxially with portlandite might justify the variability of the C/S ratio encountered by many researchers.

The presence of other materials in C_3S pastes may modify the morphology of hydration products.

* Portlandite is normally present under the form of regular and comparatively large crystals, but in C_3S pastes containing calcite as addition it appears under the form of more numerous, smaller and more irregular crystals which have precipitated around the $CaCO_3$ grains.
* In pastes containing C_3S and $CaCO_3$, C-H-S is present both in the form of inner and of outer product, which cover not yet hydrated C_3S, and of a fibrous precipitate on $CaCO_3$ particles. This means that these act as crystallization nuclei (61).
  The fact that C-S-H forms on $CaCO_3$ particles also means that the silicate ion may migrate comparatively far and that the calcium silicate hydrate is formed not only on site but also elsewhere, through a process of dissolution and precipitation.
* When C_3S paste is cast on a polished marble surface, some structural differences on it become evident. The quantity of portlandite diminishes as the distance from the interface increases, its crystals located close to separation surfaces are preferably oriented with their C-axis perpendicular to the interface, the C-S-H located close to the interface has a C/S mol ratio being higher than in the bulk paste, where it ranges between 1.5 and 2.0. This fact is ascribed to CH closely intermixed with the C-S-H phase (90).
* The microstructure of calcium silicate hydrates that form from the hydration of C_3S is not qualitatively modified by the presence of fly ash, but the C/S ratio of both the inner and the outer products is lowered. The latter may moreover contain elements coming from the fly ash. A layer of C-S-H of course forms around the fly ash particles as a reaction-product (91).
  In fly ashes, however, there are particles which are inert or almost inert, chiefly consisting of crystalline minerals, and active particles, consisting of vitreous spheres. The electronic transmission microscope (TEM) shows that the particles of the first type are simply covered by a rim of C-S-H having a thickness of 0.5 µm and formed by the precipitation of ions coming from the hydration of the C_3S. The C/S ratio of this C-S-H is 1.4±0.1 and contains foreign elements in a very low concentration (71). It is evident that these particles have

merely acted as preferential precipitation sites.
Fly ash particles of the 2nd type are, instead, attacked by alkaline solution which, after a year of ageing, has dissolved them in full or in part depending on their diameters. When these particles are still visible, they appear covered with a dense outer rim of C-S-H and fibrillar C-S-H which extends radially from the particle (91)(92).
The rims which precipitated within the original boundary of particles of fly ash as well as the fibrillar radial gel have a C/S ratio = 1.4±0,1 and contain appreciable quantities of other elements (Al, Fe and K), obviously coming from the fly ashes (92). In the regions underneath the initial perimeter of the fly ash particles, also a hydrogarnet phase with approximate composition $C_{12}A_3FS_4H_{16}$ can be found (91).
With the time the gel's C/S ratio in the outer areas gradually diminishes (92).
* The C/S ratio of C-S-H obtained in the presence of silica fume is lower (1.2) than that measured with C_3S alone (1.6)(67). Electronic transmission microscopy of ion-beam thinned samples has made it possible to observe products with a greater difference in composition. More precisely, while the inner product which is formed by hydration of the pure C_3S has a C/S ratio of 1.68±0.07, that formed in the presence of microsilica only attains a value of 1,60±0.15. However, in microsilica-containing specimens, it is also possible to observe areas where the C/S ratio is equal to 0.92±0.09. The overall c/s ratio of calcium silicate hydrate diminishes as the pozzolanic reaction proceeds and more of the silica reacts (68).

2.1.6 Porosity - The porosity of C_3S and cement paste consists of the so-called capillary pores, where transport phenomena occur, and of the gel pores of which they form an essential structural element.
Pore distribution in hardened alite is shown on table 4 (93).

TABLE 4: Volume fraction porosity in hardened alite*

	Age (days)			
	1	3	10	28 and 203
Degree of hydration (%)	22	30	50	83
Volumetric measurement of porosity (%)	10	14	23	22
d < 50 nm	3	5	8	9
d < 5 nm	51	44	34	27
d > 50 nm	55	44	38†	31†
Image analysis of impregnated porosity (%)				
Calculated vol % porosity within C-S-H:	56	54	54	44
if include all pores d < 50 nm	30	29	29	23
if include only pores d < 5 nm				
Density of C-S-H if pores are included and filled with H_2O (kg m^{-3})	1960	1990	2040	2060
Density of C-S-H excluding all pores (kg m^{-3})	2375 ± 70 (all ages)			

*Values taken from an average of four micrographs.
†Value takes into account large dense regions which account for 12% of area at 10 days and 26% of area at 28 days.

Pores having >50 nm diameter may be impregnated with resin, while those with <50 nm diameter are not. These may be considered to be formed by the porosity of the gel and that of small capillary pores. Table 4 shows that such porosity does not change after 10 days, although the hydration degree increases. This fact may be ascribed to the disappearance, owing to ageing of the gel, of some of the pores, to filling of a part of the pores with the products of further reaction, to the formation, at longer ages, of small-pore hydrated products. The capillary porosity always diminishes (93).

The specific surface of the products of hydration of C_3S, in addition to the conventional methods of gas absorption and mercury penetration may be performed via NMR. By applying this method to pastes made up with a w/C_3S ratio = 0.4 and aged up to one year it has been shown that the hydration degree achieves 90% after 25 days. The hydration degree continues to increase while the specific surface diminishes (94).

For equal hydration degrees of the C_3S, the addition of very fine calcium carbonate diminishes the density and increases the porosity of the paste (66).

2.1.7 The Hydration Mechanism of C_3S-Studies carried out to interpret the hydration mechanism of C_3S were based on both traditional and innovative investigation techniques. Data collected have made it possible to reach general conclusions, although many details have not yet been focussed accurately owing to the complexity of the hydration phenomenon and its sensitivity to ambient conditions.

* Hydration of C_3S in the first 40 minutes may be described as a process that chiefly takes place on the solid-liquid interface. The first reaction products are formed immediately after the contact between C_3S and water, are calcium-poor (C/S=1) because they release more lime than silica to the solution, and they have a large specific surface. These two parameters vary quickly in time and the calcium content of hydrates increases while the specific surface diminishes. As a consequence also the permeability diminishes (95). The induction period begins at the time the early C-S-H is transformed into a little-permeable and Ca-rich layer which, after 10-20 minutes of hydration, attains a C/S ratio of 2.0-2.5 (30).
* In contact with water, the C_3S dissolves non- stoichiometrically. Ca^{++} is far more soluble than Si and therefore leaves a layer of silica hydrate on the C_3S grains without changing the appearance of the crystals. When the concentration of SiO_2 exceeds certain values (approx. 60-70 mg/l), nucleation centres are formed consisting of low-basicity Ca silicate hydrates (cfr 30) on which the calcium silicate hydrates grow. The dissolution of CaO is however slowed down by the increase of concentration of Ca^{++}. The formation of nucleation centres of $Ca(OH)_2$ upsets the metastable equilibrium which was at the origin of the induction period, the concentration of Ca^{++} diminishes, further CaO passes into the solution, the induction is over.
  With this model the end of the induction period corresponds to the formation of portlandite (96), although it has also been found that it is not the nucleation of portlandite crystals that controls the induction period.
* The formation of the five different forms of C-S-H (74) would take place at different times and under different conditions. The C_3S is initially covered by gelatinous C-S-H which transforms into a more ordered ß-C-S-H formed by changed particles. The ß-phase is present either alone or under the form of epitaxic growth together with γ-C-S-H and portlandite, while the δ phase is epitaxially associated with ß-C-S-H, γ-C-S-H, and portlandite (74).

* An early hydration mechanism of C_3S in aqueous suspension which has been more recently proposed is based on the assumption of the existence of two types of calcium silicate hydrate (69) and of strong gradients of concentration around the grains (97). It may be summed up as follows:
  a) The water attacks the C_3S and the interface solution loses H^+ ions and gains Ca^{++} and OH^- ions.
  b) A fine-grained C-S-H precipitates on the C_3S particles. This initial hydrate, which is stable at low pH (< 11.5) and metastable at high pH (pH > 11.15), forms a barrier that slows down the progress of hydration which is therefore controlled by diffusion.
  c) Water and Ca^{++} cross this barrier in the opposite direction, modifying the local microenvironmental conditions and making it easier for new hydrated materials to form at the solid- hydrate interface.
  d) When the bulk solution becomes sufficiently oversaturated, another stable, pH dependent C-S-H is formed. If the pH ≤ 11.5, it is morphologically the same as the surface one. If the pH exceeds 11.5, a coarse-grained reticulated second-stage C-S-H is formed.
  e) The second hydrate catalyses the conversion in situ of the early hydrate into a more permeable silicate.
  f) The induction period starts with the precipitation of little-permeable early hydrates and ends when the second- stage hydrate starts to form (97).
* The hydration of the paste of C_3S obviously takes place under different conditions compared with suspensions, however the mechanism which has been proposed has several points of contact with the former.
  This model too is based on the assumption that hydration of the C_3S depends on the ambient conditions under which the reactive species are to be found, since the situation of the surface of C_3S initially exposed to the bulk solution, differs from that of the inner layers, protected and screened by the hydrated product which have already formed (29).
  This model is set up as follows:
  a. The first hydrated phase that forms is made up of monomeric species.
  b. This species is formed preferentially because the C_3S is in a water-rich, low-pH environment.
  c. It is likely that this species is formed prevalently, if not exclusively, on the surface of C_3S grains.
  d. It may be deduced that the hydration delay may be ascribed to a barrier action performed by the initial C-S-H formed by monomeric forms (cfr 97).
  e. The anhydrous C_3S underneath the first layer is however surrounded by C-S-H where the water has a high pH and the concentration in silicate and calcium ions is far higher than in the bulk solution: these conditions promote the formation of dimeric species.
  f. The end of the induction period and beginning of acceleration of the hydration correspond to the onset of the dimeric species (29).
* The decelaration which hydration undergoes as the temperature drops may also be due to another fact. The density of the products of hydration is higher at 5°C than at 20°C (40), and therefore ionic species and water would have greater difficulty at low temperatures to cross the barriers formed by early C-S-H.
* The barrier which during the induction period halts, though for the time only, the hydration might be different in nature from the merely physical one due to the formation of little-permeable layers of early C-S-H. The determination of the zeta potential of alite particles dispersed either in water or in a 10^{-3}M

solution of $Ca(OH)_2$ has made it clear that they possess a positive charge, possibly due to an adsorption on Ca^{++} ions. This positive charge might be an impediment to the continuation of the hydration and give origin to the induction period (40). The addition of a superplasticiser (Melment) causes the zeta potential of the particles (40) to turn negative and should therefore induce acceleration of the hydration, while it is known that such an admixture in fact delays hydration (98).

* The course of the early hydration is strongly conditioned by the environment and especially by the presence of other substances that could interfere with the dissolution of Ca^{++} ions. For this reason the hydration delay is always greater the faster the growth in concentration of Ca^{++} (30).
The hydration of C_3S proceeds after the induction period following a uniform mechanism and the changes in reaction rate would depend on the greater or lesser penetrability of the reaction products covering the surface of the C_3S by the ions. After about 10 hours of hydration, the C/S ratio achieves a value of 1.6 and the volume of the pores of the hydration products (radius $\leq$ 5 mm) which had peaked after 5 hours, drops suddenly to a steady level after approximately 15 hours (95).
* The products which form by evaporation of the liquid expressed by the pastes cured for seven days differ from the hydration products of the C_3S, and this would lead one to suppose that the hydration of C_3S follows a topochemical mechanism (99).
* Although it is generally acknowledged that around partially hydrated alite C-S-H is present under the forms of an "outer" and an "inner" product, it has not yet been finally established if the border between the two types of C-S-H corresponds or not with the initial border of the alite grain.

These two assumptions are schematically represented in fig. 13 (100). On the left, the boundary between "inner" and "outer" product corresponds to the original perimeter of the alite particle on the right, the "middle product" formed starting from the 3rd day of hydration turns out to overlap the original perimeter of the alite. Subsequently a "late product" is formed (indicatively after 10 days). The border between "middle" and "late" product is sharp.

The Authors (100) have other important remarks to make:

a) sometimes a gap between the outer and inner products can be seen, which can be filled in with resin.

b) C-S-H adjacent to the large capillaries is loosely consolidated

c) the small C-S-H particles appear to lack an alite core even after one day of

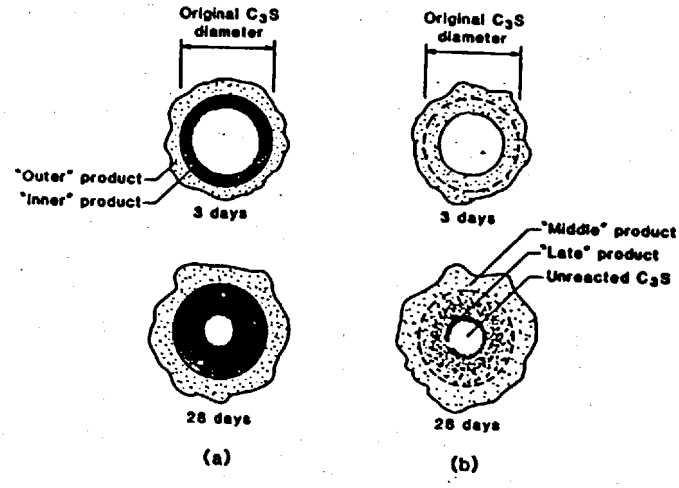

FIG. 13: Schematic representations for two types of hydration phenomena

hydration.
These results can be explained as follows: aa) the gaps are likely due to shrinkage arising from drying of the specimens; bb) close to large water-filled capillaries the calcium silicate hydrate was able to develop without restraints and compactness is therefore low; cc) the C-S-H particles without alite core may have been formed a way from the alite through a process of dissolution and precipitation, as proved by the deposit of calcium silicate hydrate on the particles of calcite or fly ashes.
The boundary of the outer product cannot represent rigorously the original alite surface because unavoidably in the early hydration phases, the surface alite layers are transformed into hydrated phases, but it may represent the form of the alite grain between 3 and 10 days (100), the more so in so far as the thickness of the outer product (1-4 μm) does not change in time (100).

* Also the study of hydration in diluted suspensions is useful for an understanding of the hydration mechanism. The four thermal effects observed when hydrating diluted suspensions of C_3S (32)(33)(34) may be interpreted with a model which undergoes the following reactions:
1) congruent dissolution of C_3S
2) supersaturation of SiO_2 and starting of C-S-H saturation
3) oversaturation of Ca^{++} and precipitation of the portlandite.
The hydration depends on the rates v_1, v_2, v_3 with which the above mentioned reactions occur and on the w/C_3S ratio. The kinetics may in any case be broken down into 5 steps in which the reactions become progressively simultaneous

a) 1)
b) 1) + 2) $(v_2 > v_1)$
c) 1) + 2) $(v_2 \simeq v_1)$
d) 1) + 2) + 3) $(v_3 > v_2 > v_1)$
e) 1) + 2) + 3) $(v_3 = v_2 = v_1)$

The hydration reactions of C_3S which take place in the paste and in suspension are similar, but the relevant extent and duration depend on the dilution and consequently on the concentration of the lime in solution: from a kinetic point of view the C-S-H precipitation is limiting reaction, while after that it is the diffusion that governs hydration (34).
An accurate critical analysis of the types of C_3S hydration mechanics is reported in (101) together with a summary of the basic principles of nucleation, dissolution and growth of the crystals, diffusion, adsorption and change of phase.

In conclusion the experimental data collected on the hydration of C_3S up to now have allowed to propose mechanisms which appear to be consistent on the whole, and it is likely that it will shortly be possible to formulate a single model that accounts for most of the test results.

2.2 The Hydration of C_2S

The hydration of dicalcium silicate arouses less interest than tricalcium silicate, although it is one of the basic components of portland clinker-based cements. There is no lack of investigations on the matter, however, also in relation to the production of belitic cements, so called this way because rich in belite.

* Electric conductivity measurements of β-C_2S in water excess have shown that

hydration takes place through dissolution and precipitation processes. In hydration, C_2S behaves like a weak electrolyte, while C_3S behaves like a strong electrolyte. The slowness of hydration of ß-C_2S may be interpreted on the basis of the prevalent formation of an ion pair $[Ca(H_2O)_5OH]^+$ and $[Ca(H_2O)_3OH.H_2SiO_4]^-$ (102).

* The amplitude of the early peak of hydration heat flow observed in the first 30 minutes is approximately identical for the three different forms, α-, ß- and γ-of C_2S and it is similar to that of C_3S. The curves that represent the variation of concentration of Ca^{++} and of SiO_2 in the solution, instead, are different. From this fact one might infer that the primary reaction layer formed on the surface of the different forms of C_2S has different compositions (103).
* The hydration of the different species of C_2S is accelerated by the removal of Ca^{++} ions from the solution and slowed down by the lime already present in the pore solution. The latter behaviour might account for the fact that when C_3S and C_2S are hydrated together, the former hydrates faster and the latter more slowly (103). It may be remembered in this context that mixtures of alite and belite in ratios 75/25, 50/50 and 25/75 have higher hydration rates than alite alone (49).
* Generally speaking, the hydration rate of C_2S is adversely affected by the presence of doping elements in solid solution (104). For instance, the addition of Na to ß-C_2S diminishes the hydraulic activity of the calcium silicate probably because it preferably concentrates on the grain surfaces and causes the free energy of the crystal boundary to diminish (105). The effects of course vary according to the element because it has been seen that the rate of hydration drops when passing from the impurity formed by B+K to B+Al, B+Fe, that is to say, with the reduction of the concentration of current carriers (106). It is not unlikely, however, that the effect of doping elements is indirect. It has been observed, as a matter of fact, that the hydration rate is higher the smaller the size and the greater the microstress of the crystals, but these two parameters depend on the doping element as well (107).

  As regards the degree of condensation of the silicate anion, the hydration degree being equal, C_2S gives less dimer and more polymer than C_3S (108).

2.3 The Hydration of C_3A

The hydration of C_3A is an important phase in the overall hydration of the cement, because it has considerable effects on setting and early hardening. The hydration of C_3A is far more strongly affected by environment conditions than that of C_3S and in particular by the presence of other substances with which it can react.

A knowledge of the role played by the different factors is thus essential to interpreting and, possibly, modelling cement hydration.

* The method itself of preparing C_3A, by changing as it does the chemical characteristics of C_3A, modifies its hydration process. For instance, C_3A containing a small quantity of SiO_2, molten and quenched, hydrates much more slowly than the aluminate prepared with pure materials and synthetized by firing in the solid state. After 10 days the hydration is not yet complete and the C_3AH_6 grows very slowly (109).
* It is a known fact that industrial clinkers and their phases contain such accessory elements as Na_2O, K_2O, SO_3 and Cl coming from raw materials, fuel and the lining of the kilns. When C_3A is synthetized in the presence of these elements, changes in its crystal lattice and the formation of other phases occur.

In particular, while Na_2O dissolves in the lattice of C_3A, K_2O and SO_3 give rise to potassium sulphate or double salts that coat the C_3A crystals in part or in full. The consequences to hydration as a result of the presence of these elements on hydration also vary: the increase of concentration of Na_2O in the C_3A up to the solid saturation limit has a favourable effect on hydration, while the increase of the other accessory elements decreases the hydraulic activity of C_3A (110).

* The very presence of C_3S and $Ca(OH)_2$ changes considerably the course of hydration of C_3A since the two compounds reduce the solubility of Al, and increase the pH (111).
* The transformation of more or less strongly carbonated hexagonal aluminate into cubic hydrogarnet depends on environmental conditions and in particular on the Ca^{++} concentration of the solution. It is favoured by the conditions of lime saturation, lack of aluminium and high temperature (111).
* In clinker-based cement, hydration of C_3A always takes place in the presence of gypsum and this accounts for the constant interest shown in the C_3A-$CaSO_4.2H_2O$-H_2O system. In dispersions of C_3A and gypsum in water excess, the early concentration of SO_4^{2-} depends on the quantity of gypsum present. It remains unchanged for fifteen minutes, after which it starts diminishing as ettringite begins to form. The monosulphate becomes the prevalent phase by effect of the conversion of the ettringite, which reacts with the uncombined C_3A. In any cases the presence of monosulphate can be observed in the early hydration stages. The concentration of Al in the solution follows a reverse trend since it is kept low by the presence of the sulphate ion and increases as the gypsum is consumed while ettringite is formed (112).

  In the system C_3A-$CaSO_4.\frac{1}{2}HO_2$ - H_2O, hemihydrate converts rapidly to gypsum. Ettringite formation can be observed already ten minutes after mixing. Both reactions are temperature dependent (101).
* In diluted C_3A-$CaSO_4.2H_2O$ solutions, the formation of ettringite, monosulphate and calcium hydrate depend in a complex manner on the concentration of sodium hydroxide present and on time. The sodium hydroxide depresses the formation of ettringite and initially accelerates that of calcium hydroxide, but lowers it after approximately 3 hours. The saturation concentration of SO_4^{2-} increases as the content of alkali increases, but in any case, it quickly drops after some time, depending on the concentration of NaOH. The alkalis favour the formation of hexagonal aluminate hydrate and monosulphate (38).
* Also metal salts interfere with the hydration of tricalcium aluminate. A typical case is that of $CaCl_2$, which accelerates hydration of C_3A while it slows down that of C_4AF (113), but also $MnCl_2$, $NiCl_2$ and $CaCO_3$ modify the trend of the reaction between C_3A, $CaSO_4.2H_2O$ and water to a different extent, which depends, however, also on the C_3A:$CaSO_4$ ratio (114).
* Another cause of change in the C_3A hydration is the presence of admixtures. The interaction between the admixtures and the C_3A or its hydrated derivatives is used to advantage to modify the engineering characteristics of cement, such as rheology, setting and hardening rates, etc.

  Melamine-formaldehyde sulphonate slows down hydration of C_3A-gypsum mixes, delays the conversion of ettringite into monosulphate and modifies the morphology of the reaction products. In pure pastes ettringite shows larger crystals, while in pastes with the admixture it tends to maintain amorphous structures, probably precursors of ettringite, or favours the formation of fibrous ettringite (115). The addition of triethanolamine accelerates the conversion in monosulphate. The

presence of Na in the lattice of C_3A and lime in the mixing water increase and decrease, rispectively, the reactions (116).

* C_3A hydration is also enhanced by substances that used to be considered inert. In the presence of $CaCO_3$, the heat evolution rate peak, located at approx. 10 min., is not shifted but its height is increased to an extent that depends heavily on the content of $CaCO_3$. The reaction leads to the formation of calcium carboaluminate and its solid solution, and this accounts for the fact that in the presence of large quantities of $CaCO_3$, the formation of C_3AH_6 is considerably delayed, or eventually it does not occur (117).

Also the formation of ettringite by reaction of the C_3A and gypsum is accelerated by the addition of $CaCO_3$ (117). Calcium carbonate favours the conversion of ettringite into monosulphate (117).

* The hydration of C_3A in the presence of other compounds is complicated by the fact that hydrated products are often made up of solid solutions. For instance, between $C_3A.Ca(OH_2).xH_2O$ and $C_3A.CaSO_4.yH_2O$ there is a limited solubility that changes with the temperature. In addition, the first compound decomposes at temperatures exceeding 30°C, forming $C_3A.6H_2O$ and CH (118).

Therefore, in order to account for the phenomena observed during hydration both of pure species and of variously doped ones, as well as of cement , phase relations must be established without misunderstandings. A study concerning phase relations existing at 22°C among C_3A, $CaSO_4.2H_2O$, $CaCO_3$ and $Ca(OH)_2$ has made it possible to clear up a number of controversial points. The results of this study are summarized in the diagram on fig. 21. The details of the diagram that have been evidenced are: the partial solubility of $C_3A.Ca(OH)_2.18H_2O$ in $C_3A.CaSO_4.14H_2O$ and the stability, ascertained at least up to one year, of $C_3A.Ca(OH)_2.18H_2O$ which does not transform into $C_3A.6H_2O$ or of $C_3A.CaSO_4.14H_2O$ which does not transform into $C_3A.3CaSO_4.32H_2O$, as well as the field of coexistence of pairs of phases like ettringite with monosulphate, of hemicarbonate ($C_3A.\frac{1}{2}\ CaCO_3\ \frac{1}{2}\ Ca(OH)_2\ 11{,}5\ H_2O$) with monocarbonate ($C_3A.CaCO_3.11H_2O$) (119).

In other words, the presence of CO_2 in the $C_3A+CaSO_4.2H_2O+H_2O$ system, whether coming from the atmosphere or from the added calcite, modifies the mineralogical composition of the pastes. For instance, in the $C_3A:CaO:CaSO_4.2H_2O=1:1:1$, at first ettringite forms, then, when the gypsum is consumed, it is transformed into a monosulphate.

Anyway if the above mix is added with 2/3 M of $CaCO_3$, the monosulphate does not form and, at the end of a series of reactions, trisulphate and monocarbonate are shown to coexist according to the overall reaction.

$$3CaO+3C_3A+3CaSO_4.2H_2O+2/3CaCO_3+48H_2O \longrightarrow$$
$$\longrightarrow C_3A.3CaSO_4.32H_2O+2(C_3A.CaCO_3+11H_2O)+3Ca(OH)_2 \qquad 1)$$

Of course with different ratios different results are achieved that may be explained by fig. 14, but what counts is to point out that the failure of the trisulphate to be transformed into monosulphate - as is often observed in cements - is due to the presence of CO_2 in the paste (120).

The variability of the composition of aluminate hydrates depends on the presence of other compounds in the liquid phase or in any case in the mix with C_3A, but is chiefly due to the fact that interlayer OH^- can be easily exchanged with several anions.

This ease in forming complex salts is also observed by attacking suspensions

of $C_3A.Ca(OH)_2.12H_2O$ with different salts. OH^- can be replaced by many anions, with rate of exchange depending on the type of anion (121).

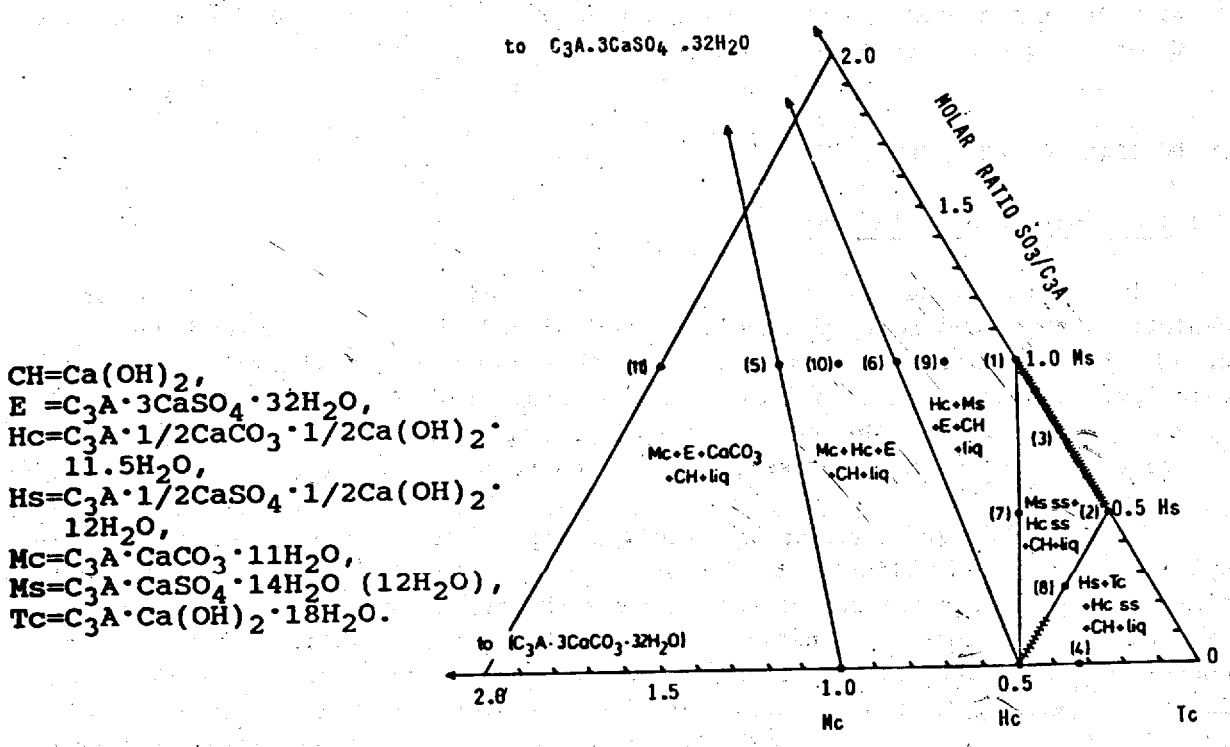

$CH=Ca(OH)_2$,
$E=C_3A\cdot 3CaSO_4\cdot 32H_2O$,
$Hc=C_3A\cdot 1/2CaCO_3\cdot 1/2Ca(OH)_2\cdot 11.5H_2O$,
$Hs=C_3A\cdot 1/2CaSO_4\cdot 1/2Ca(OH)_2\cdot 12H_2O$,
$Mc=C_3A\cdot CaCO_3\cdot 11H_2O$,
$Ms=C_3A\cdot CaSO_4\cdot 14H_2O$ $(12H_2O)$,
$Tc=C_3A\cdot Ca(OH)_2\cdot 18H_2O$.

FIG. 14: Phase assemblage stable in the system $C_3A.Ca(OH)_2.18H_2O$–$C_3A.3CaSO_4.32H_2O$–$C_3A.3CaCO_3.32H_2O$ at 22°C.
Solid solutions are indicated by hachured lines.

2.4 The Hydration of C_4AF

Of the main compounds of clinker, C_4AF is the least thoroughly investigated, but its presence cannot fail to affect the hydration of the other cement compounds. The dispersion of aluminoferrite, in a gypsum-saturated solution with a C_4AF/Sol. ratio of 1/100, shows a rapid dissolution of Ca^{++}, SO_4^{2-}, OH^- and Al^{3+}, whose concentrations achieve about 19, 15, 6 and 0.3 mmol/l respectively in a few minutes. These figures drop markedly within the first 5 hours. The solution proves practically iron-free.
The hydrated products that form initially in the presence of SO_4^{2-} are rich in C_2AH_8 or alumina gel, comparatively poor in calcium and almost totally lacking sulphate. At a later stage the alumina gel or C_2AH_8 react with SO_4^{2-} and Ca^{2+} giving AFt while $[Ca^{2+}]$ and $[SO_4^{2-}]$ in the solution diminish. In a third stage $[Ca^{2+}]$ and $[SO_4^{2-}]$ diminish in a constant ratio. Since the AFt phase is iron-free, it must be considered ettringite together with this compound, an amorphous iron- rich phase, likely to contain Ca is formed.
In the presence of gypsum and lime, instead, during the first five hours, the concentrations of Ca^{2+} and SO_4^{2-} become very little lower, that of OH^- grows slightly, Al remains at the mmol/l level.

The presence of $Ca(OH)_2$ in solution reduces the reaction rate of C_4AF but does not modify the composition of AFt (65).
In the presence of C_3S the hydration of C_4AF is initially slowed down and then accelerated. The products of hydration are C-S-H, CH, $C_3(A,F)H_6$. The hydration of C_4AF in the presence of C_3S and $CaSO_4.2H_2O$ leads instead to the formation of C-S-H, CH and AFt (50).

3. PORTLAND CEMENT HYDRATION

3.1 The Kinetics of Hydration

The progress of hydration may be followed and recorded by measuring the evolution of the chemical, physical, mechanical and electrical properties of the paste or of the concrete with time. One can thus measure the changes in composition, enthalpy, ultrasonic pulse velocity, volume and, of course, consistency and strength of the pastes. During the early stage of hydration also the electrical parameters change and may therefore be taken, in addition to the above, to monitor the process.

Since each parameter being recorded depends on the same event, namely, on hydration, there is little to be wondered at that there may be considerable similarities between the curves that express the evolution of the different properties as a function of time. For instance, there is a close correlation between calorimetric curves, ultrasonic pulse velocity curves, and penetrometric curves. At the end of the induction period, that is to say, at the beginning of the hydration acceleration period, the ultrasonic pulse velocity rises sharply and the paste's resistance to penetration starts to increase marking the beginning of setting. The 2nd peak which one observes in the calorimetric curve marks instead the end of the setting time (122).

The ultrasonic pulse velocity curve may be broken down into three stages, characterized, respectively, by almost steady, almost linearly growing and steady rate. Its course reflects the changes of the structure and of the elastic properties of the hydrating pastes. The ultrasonic pulse velocity increase with in time as well as with decreasing the w/c ratio (123).

Although enthalpic, along with penetrometric methods, are the most widespread in the study of cement hydration, a technique has been recently set up that makes it possible to measure and record accurately the changes in volume of the solid phases in the cement pastes (83).

In a closed system the entropy variation due to chemical reactions may be written in the form

$$T\Delta S = \Delta W_{irr} + \Delta Q_r \qquad 2)$$

where Δ_R is the heat of reaction with a negative algebraic sign and W_{irr} is the irreversible work due to the change of volume. The equation shows that the reaction kinetics may be correctly described only if the heat of hydration and the volume work are recorded simultaneously.

In spontaneous reactions ΔS must be ≥ 0. Since the heat of hydration of the hydrated compounds is always positive, ΔQR is negative and therefore Wirr must be positive, that is to say, a reduction in volume must be observed. In fact, for all cement compounds, the difference in volume between hydrated and reagent products is always negative and this means that in C-S-H, for instance, bond energies are higher than in the original product. Figs. 15 and 16 (35) show two curves that indicate the total volume variation and its derivative. As one can see, they are similar to the curves obtained by measuring the heat of hydration, including the initial horizontal line that corresponds to the induction period.

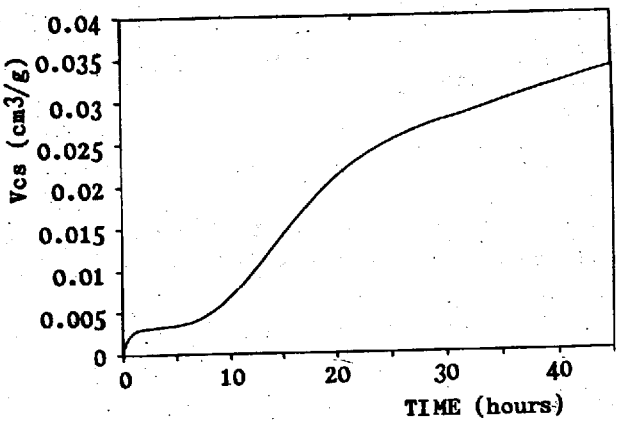

FIG. 15: Typical volume change during cement hydration

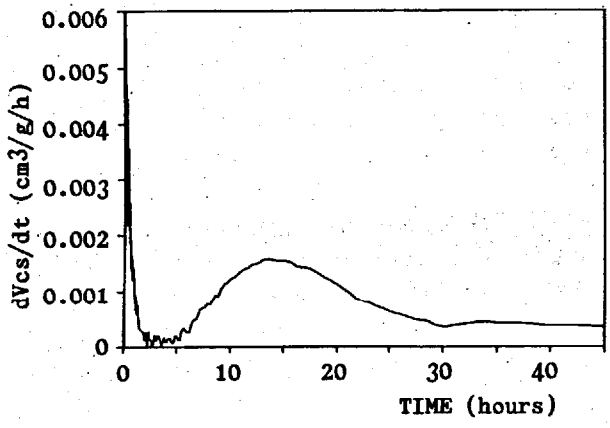

FIG. 16: Volume change velocity during cement hydration

However, fig. 17 shows that not all cements have the same behaviour during early hydration. The S-type curve shows a volume increase and this means that ΔW_{irr} is negative. As a consequence, according to equation 1), the reaction must be endothermic. This circumstance concerns the early period of hydration, since when crystallization starts a volume shrinkage always occurs (35). Literature does not mention cases of early hydration stages showing heat absorption, except for the case of diluted suspensions of C_3S (34) and it is therefore likely that the contradiction is only apparent and due to the fact that a multiplicity of reactions, with possible overlapping of effects, occur during early hydration. It

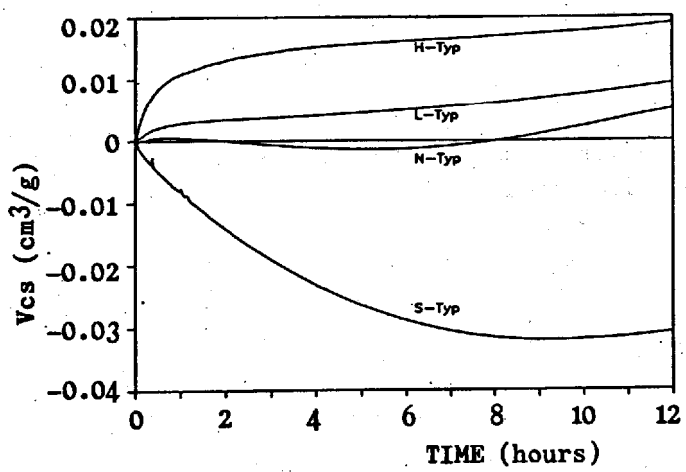

FIG. 17: Different types of volume change during cement hydration

may happen that a reaction with a strong volume increase is weakly exothermic, while a simultaneous reaction with volume reduction develops strong hydration heat. On the whole, therefore, one could have an expansion and a positive hydration heat.

During the first 48 hours of hydration, the volume of the paste changes and the curve that represents the volume change rate shows a peak at about 10 hours, whose intensity depends on the type of cement. The peak, which denotes a chemical shrinkage, achieves its maximum approximately to match the peak of the heat evolution curve (124).

The values of the cement paste's dielectric constant and resistivity depend on the frequency and the relevant curves are modified quantitatively although they remain essentially similar (125). Over approximately 5 hours the dielectric constant rises steeply and then diminishes. The paste's resistivity diminishes in the initial first 50 minutes and increases slightly in the next 50-150. Between 150 and 250 minutes resistivity increases a little, between 250 and 300 min does not increase and then grows with an inflexion at about 550 minutes (125).

The dielectric constant values depend on the charges present in the water-cement system and in particular on the mobile unbound ones, in the bulk solution, and on the electrostatically bound ones present in the double diffuse layer, gel and grain surface layer. The polarization of these surface charges may induce considerable dipole moments giving high dielectric constants (126).

Approximately five hours after mixing the resistivity of the portland cement pastes begins to increase rapidly because the amount of free water diminishes. For the same reason there is a considerable increase in resistivity when the w/c ratio diminishes, but only a slight one when the frequency is increased from 100 Hz to 300 KHz. Electric conduction is the sum of ion conduction, through continuous water-fille capillaries, and surface conduction, through the adsorbed gel water. A high value of PFE(°), the frequency term effect, indicates that the paste has a high percentage of blocked capillaries, a high gel-space ratio and a low permeability. There is a good correlation between the PFE and gel-space ratio (126).

3.2 Factors affecting the hydration

The kinetics of cement hydration depends on a number of factors that may be correlated both to the nature of the cement and to the environment in which the reactions occur.

* The rate of hydration of the cement chiefly depends on that of its individual components and is therefore governed by C_3S and C_3A which hydrate more quickly than C_2S and C_4AF (127).

(°) $PFE = \frac{\varrho_o - \varrho_{ac}}{\varrho_o} \times 100$

where ϱ_o is the resistivity at low frequencies (100 Hz) and ϱ_{ac} is the resistivity at high frequencies (300 KHz).

The decreasing basicity of clinker is accompanied by a decrease in the early heat evolution rate and an increase in 28-day strength (128).
In the case of belitic cements, an important role is also played by the cooling rate of the clinker which influences the phase transformations of C_2S and therefore the contents of the phases which are hydraulically the most active (129).

* The hydration degree of the main phases varies with time to a different extent from cement to cement (130). This depends on the chemical and mineralogical differences existing between the phases and the differences existing in the environment where hydration occurs.The minor elements contained in the clinker, by modifying the composition and the structure of the different phases, affect the progress of hydration (131) and consequently, as in the case of C_4AF, the reaction differs from that of the corresponding pure compound (132).
The firing conditions, i.e., rate of heating and temperature of firing, affect the hydration of the cements since they influences the characteristics of the clinker components. With a slower heating rate, the alite crystals are larger and its hydration is slower at first, faster later. The small alite crystals behave instead in the opposite way. In the case of belite, the greater hydration rate is obtained when the crystals are comparatively large (133).
Also the grain size distribution influences the hydration and properties of the pastes. Fine-grained cements ($\lesssim$ 20 μm) hydrate faster than coarse-grained ones ($\gtrsim$ 63 μm) and give pastes with lower porosity and higher flexural and compressive strengths. This result is obtained only if the w/c ratios are the same, but if the comparison is made with equal consistencies, the properties of finer cements, which have a higher water demand, grow worse. Practically speaking, optimal values, both of the microstructure and of the physical and mechanical properties, are achieved when the cements have intermediate finenesses ($\lesssim$ 40 μm) (134).
As a consequence of the large number of factors that take part in the hydration, every cement forms a case apart, at least from a quantitative viewpoint.
* The hydration degree of the cement and of its constituents increases with the temperature, but the effect on belite hydration is far higher than that observed on other clinker components (135).
* The influence of gypsum on cement hydration and the fact that the strength increases with its content up to a maximum value (optimum) beyond which it decreases is a well known fact. The reason for this strength increase is not yet known, but it does not appear to depend on the density of the products of hydration or on differences in pore distribution (136). The optimum value may be established by determining, besides strength, the hydration heat or the quantity of ettringite formed (137).
When clinker phases contain potassium, the effectiveness of hydration control by gypsum diminishes and the consistency of the pastes in the early stages of hydration increases (138).

The deceleration of the hydration, however, also depends on the form in which the sulphate is to be found: gypsum, semi-hydrate, anhydrite, aphthitalite ($3K_2SO_4.Na_2SO_4$), Ca-langbeinite ($2CaSO_4.K_2SO_4$), syngenite ($CaSO_4.K_2SO_4.H_2O$). In the first 30 minutes the least effective action is performed by the aphthitalite, the most powerful by calcium langbeinite and syngenite. The behaviour changes after 30 minutes.
The consumption rate of C_3A depends on the preparation of the mix of C_3A as it is higher when the gypsum is interground rather than with mixed with the clinker (139).

Phosphogypsum is an abundant by-product of the production of phosphoric acid, however, its use in the cement industry is limited by the fact that the impurities it contains, derivatives of phosphoric acid, interfere with the clinker's normal hydration, increasing setting time and considerably reducing the flexural strength of the pastes. The compressive strength, instead, makes up for the initial delay after 14 days and may exceed even that of samples with natural gypsum (140).
Some gypsums coming from chemical synthesis interfere with the cement hydration since they slow down setting owing to the organic substances they contain (141).
The hydration of Portland cement is only slightly accelerated by the increase in the gypsum content, but is strongly delayed when the optimum is exceeded. The effect depends on the cement's specific surface, but in any case the mechanical strength changes linearly with the water combined, i.e., it depends closely on the hydration degree (142).

* According to some studies (143), water treated magnetically at 3,000 S for 0.1-0.3 sec would promote hydration reactions and the thickening of the texture of the cement paste. The water, containing 0.5-2% of Fe_3O_4 (on cement basis) would increase the concrete's strength by 6-8% (144). It has also been reported that cement pastes mixed with low w/c ratios (0.27) and with plasticizer, after activating for 120 minutes with positive or positive+negative polarization, exceed 80 MPa at 28 days (145).

* Careful curing mainly means storing the pastes in an environment with a high relative humidity. Figure 18 shows that if curing takes place under 100% R.H. conditions, the alite achieves an 80% hydration degree after 14 days and 95% after 90 days. If the R.H. is 60%, instead, the hydration degree only goes up to 65% after 14 days and the value remains unchanged at least for 40 days. The effect of the humidity is even stronger for C_2S. C_3A and C_4AF have behaviours which are similar to C_3S and C_2S respectively (146).

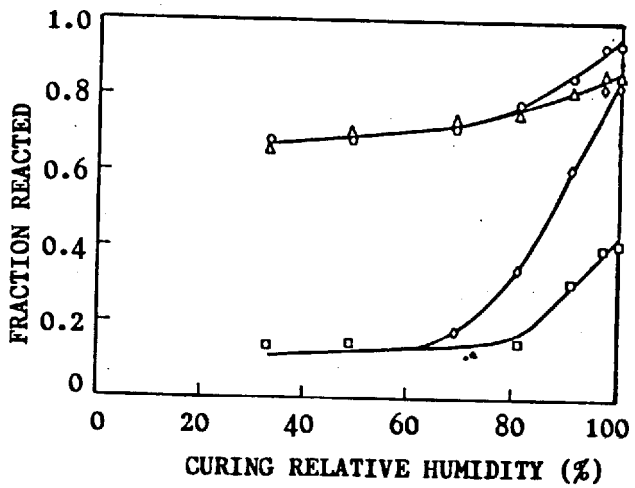

FIG. 18: Alite and belite hydration against curing relative humidity:
(△) alite, 14 d; (○) alite, 90 d;
(□) belite, 14 d; (◇) belite, 90 d

* The addition of fine materials to portland cement accelerates the hydration of the Portland cements and of its constituents. This effect is produced both by such inert powders as rutile (147) and by active powders such as slag, fly ashes and silica fume (148).
* It is known that the rise in temperature accelerates the hardening of cements at least up to 55°C (149). At higher temperatures, the compressive strength Rc of the pastes diminishes, while the Rc/porosity ratio does not change (150).

As the temperature increases the hydration degree always keeps increasing, but the bound water and the free lime present are maximum between 50 and 70°C. This is interpreted assuming that the temperature increase leads to the formation of hydrates with increasing lime content and diminishing water content. A temperature increase accelerates gypsum consumption but makes the AFt phase instable (150). The heating may be obtained using high-frequency waves for 15-40 minutes. The induction period is abbreviated but with regard to hydration degree and compressive strength, no difference is observed after 11-12 hours between the samples treated with microwaves and those cured under standard conditions (151).

* Electrolites present in the solution, whatever their origin, interfere with cement hydration. Some are added to the cement intentionally and should therefore be considered admixtures. The hydration of portland cement in an 0.5-1.0 M NaOH solution does not change the nature of hydration products but only their kinetics of formation. Under these conditions, the gypsum consumption rate and the ettringite formation rate increase, as the formation rates of C-S-H and portlandite do. If however the concentration of NaOH exceeds 2.0 M, the formation of the sulphoaluminates is delayed and a sodium-substituted monosulphate is formed rather than ettringite (152). Sodium silicate delays the hydration of the Al bearing phases, but if also Na_2HPO_4 is present, the hydration is accelerated (153).
Owing to its high electrolite content, sea water modifies the course of hydration observed when using fresh water, such as drinking water, river water and underground water. At the beginning of hydration the sea water causes the precipitation of gypsum and subsequently the reduction of the quantity of portlandite (154). The precipitation of gypsum is observed already 2 minutes after mixing with sea water (155).
Compared with drinking water the other waters give the same products of hydration but they generally modify setting times and strength (156).

Cement and concrete admixtures consist of inorganic and organic compounds and may be simple or complex. Their action may be chemical, physical or chemico-physical. In this paper of course only the action exercised on the cement hydration process is considered.
The admixtures influence the progress of hydration considerably because they modify: a) the content of bound water; b) the content of free lime; c) the content of ettringite; d) the content of residual gypsum; e) the hydration degree; f) the heat evolution rate; g) the volume of the solids; h) the rheology; i) the setting and the hardening.

* $CaCl_2$ accelerate the hydration of C_3S and C_3A and modifies a)b)c). The bound water increases against that contained in the chloride-free pastes probably because a slightly water-richer C-S-H is formed. Portlandite diminishes most likely due to a higher C/S ratio of the C-S-H (157). The addition of electrolites such as $CaCl_2$ accelerates the dissolution of the cement minerals owing to an increase of the H bonds between the liquid phase and the solid phases of the water-cement system (158). Among the chlorides, the strongest accelerating action is induced by the trivalent ions Al^{3+}, Fe^{3+}, Cr^{3+} (159). The influence of the alkaline and alkaline-earth halogenides may be expressed by the equation $CCP = r_c/r_a \cdot \Delta X_{av}$, where CCP is a chemical crystal parameter, and r_c and r_a are the radii of the cation and the anion respectively and ΔX_{av} is the difference of electronegativities (160).

Other salts, such as $NaNO_3$ and NaSCN, give results similar to $CaCl_2$ when compared on equal molar bases (161).
When Cl^-, NO_3^- and NO_2^- are added to portland cement mortars, their concentrations in the pore solution diminish quickly in the first 24 hours and then more slowly. After 14 days the concentration has diminished by 65%, 75% and 70% respectively. The submersion of the mortar samples in a 3% solution of NaCl immediately boosts the concentration of Cl^- in the pores, but it starts at once to diminish again (162). The ion concentration in the pores diminishes progressively although the free water diminishes with time. This means that a part of the ions is incorporated in the hydrated phases.

* The addition of 2% of $NaNO_3$ and of $Ca(HCOO)_2$ suppresses the destructive effects of freezing when the cement is hydrated at -10°C, but also modifies the progress of hydration. Indeed, the contents of portlandite, of calcium aluminate hydrates, of the complex salt $C_3A.Ca(NO_3)_2.10H_2O$ and of calcium silicate hydrate increase (163).

* Phenol, catechol and pyrogallol slow down, in increasing order of strength, the final setting of white cement. All three, but above all the last two, diminish the hydration degree measured by the residual content of C_3S, the portlandite content and the content of non-evaporable water. In the first 5 hours the three phenols reduce, with growing effect, the initial concentration of Ca^{++}, OH^+ and K^+ in that order (164). N-ligninsulphonate and melamine are used as water reducers, but they also have a delaying effect on the hydration of C_3S and C_3A. Saccharose instead only depresses the hydration of C_3S, but not that of C_3A (157) as the quantity of ettringite which forms increases (161).
The delaying effect of melment is shown by the reduction in content of free lime and the lower degree of C_3S hydration; in any case, pastes with admixture have a strength exceeding that of the control pastes (165) already after 24 hours.
The delaying action performed by the ligninsulphonate is stressed by the heat evolution rate curve whose peak is so much more delayed the higher the admixture content (166). In this context it is pointed out that the variations of the heat evolved (167)(168) and of the paste rheology (166) do not depend only on the admixture, since identical admixtures have different effects with different cements.

* In considering the effectiveness of admixtures, it is often forgotten that their action depends heavily on the cement with which they are used (168)(167). An example is provided by three different admixtures used with two different cements (A) and (B) for class G oil wells (168). $CaCl_2$ accelerates the hydration of cement A to a limited extent, bringing forward and increasing slightly the 2nd peak of the heat flow curve, while brings forward and increases considerably the peak of cement B. $CaCl_2$ lowers the saturation factor of Ca^{++} in the pore solution of cement A, leaves unchanged that of cement B. A superplasticizer (polynaphthalene sulphonate) slightly enhances the 2nd peak of cement A's heat evolution, delays that of cement B. The saturation factor of Ca^{++} remains unchanged in cement A, grows at first in B.
The retarder calcium glucoheptonate shifts the second peak from 8 to 12 hours for cement A and from 8 to 40 hours for cement B. The saturation factor is unchanged in cement A, while it diminishes considerably in B. These data show how difficult it is to evaluate the behaviour of an admixture according to tests conducted merely using a single cement.

* α-hydroxy carboxylic acids are retarders, but citric acid and lactic acid deviate from this behaviour. Citric acid is known as a retarder, but in concentrations below 0.1% it behaves like an accelerator (169). Lactic acid, unlike other α-hydroxy carboxylic acids, is a setting accelerator and its action is revealed by the increase of non-evaporable water and of the heat of hydration and the growth of the first peak of the heat evolution curve due to aluminates (170).

Admixtures stress volume changes in the early stages of hydration. For instance, accelerators increase early shrinkage while retarding agents increase swelling (see figs. 19 and 20). However, the effects also depend on the content and type of cement, and the specific action of a given admixture must therefore be tested with each specific cement (171).

* There is a weak correlation between slowing down of the hydration and sorption of the organic retarding agents on the cement. This means that the molecules of the admixtures do not act through the formation of a protective layer on clinker particles. It is thus more likely that the slowing down of the hydration caused by the admixture is due to a reduction of the permeability of the hydrated phase that forms as soon as water comes in contact with the cement or to the poisoning of the growth of portlandite nuclei (172) (173).

The effectiveness of admixtures also depends on the temperature as well as, of course, on their nature. At 20°C, $CaCl_2$ brings forward and raises the 2nd peak and reduces the induction period as its content increases (up to 1 mol/l = 4.9% of the cement). At 5°C there is no longer a sequential response to the increase of $CaCl_2$ and the greatest acceleration is obtained when the concentration achieves 0.3 mol/l. The presence of shoulders in the heat evolution curve with 0.5 and 1.0 mol solutions of

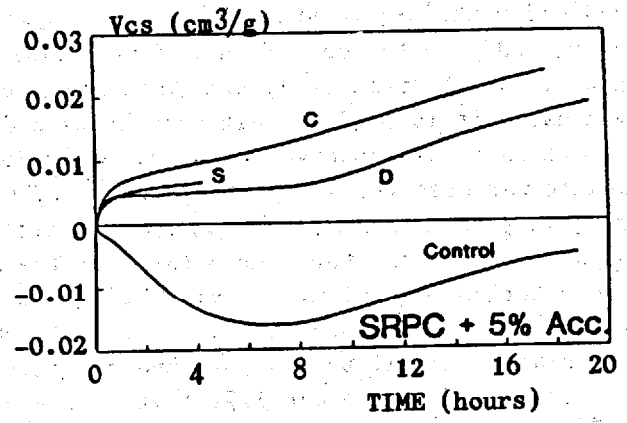

FIG. 19: Volume change with 5% accelerators. Control = SRPC cement

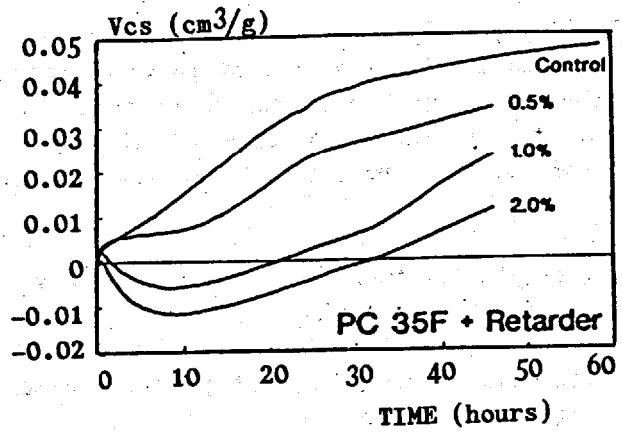

FIG. 20: Volume change with retarder. Control = 35F OPC

$CaCl_2$ suggests that the reactions that occur at 10°C are different from those that occurring at 20°C.
At 20°C the maximum effect is observed with $Ca(HCOO)_2$ at the 0.3 M concentration, but in any case its effectiveness is less than that of $CaCl_2$. At 5-0.1 M and 0.3 M the solutions show an accelerating effect, whereas those at 0.5-1.0 M show a retarding effect (174).

3.3 Structure and composition of the hydrated portland cement pastes

3.3.1 - The hydrated phases - Polished slices of synthetic clinker have been soaked in a $Ca(OH)_2$ and $CaSO_4$ saturated solution containing 0.2 mole/litre of KOH and have been examined under the SEM to study the formation of hydrated phases on the surfaces under non-restricted growth conditions. The phases recognized were hydrated calcium aluminates, AFt (ettringite), AFm (monosulphate) and C-S-H. Considering the type of specimen used, it is evident that the phases had formed by topochemical reaction. The first hydrated phases observed were calcium aluminates, and not sulphoaluminates. No portlandite was observed among the products of hydration, which evidently precipitated far from the clinker surface (175). The tests do not of course exclude that the other hydrated phases form, even far from the clinker surface, through a dissolution and precipitation mechanism. The variability of C-S-H composition is also observed at microscopic level, since the C/S ratio of the calcium silicate hydrate diminishes as the distance from alite and portlandite increases. Indeed, while the average C/S ratio of the cement paste was 1.7, that in the proximity of alite and portlandite rose to 2 (176).

During the cement hydration the polymerization degree of the silica increases with time, but less quickly than observed in C_3S and C_2S. The extent of polymerization depends on other factors as well, including the composition of the liquid phase, since it is greater with distilled water and lesser when (SiO_4) is substituted with (SO_4) and (AlO_4)(177).

The sensitivity of C-S-H to ambient conditions is confirmed by the formation of oligomers with a higher degree of polycondensation, when the hardening of the cement and of the C_3S occurs under deformation (178). When the cement contains alkalis and magnesium, the infrared spectrum of the hydrated pastes shows changes that are interpreted as the result of variations in composition and structures of C-S-H (179).

Trimethylsililation is useful to analyse the structure of cement silicate hydrates, but the preparation of the polyorganosiloxanes may lead to side reactions if the Lentz method is followed, and thus it is preferable to follow Tamas' modified method (180). The composition of portland cement pastes becomes stable with time because the compositions of inner and outer hydrates of modern portland cement pastes are the same as those to be found in cement pastes hydrated for 136 years (181).

A fundamental component of the hydrated phases is water, but the problem of the exact determination of the bound water is a hard one to solve since a part of the bound water is relatively labile and goes lost under severe drying conditions. This is the case with the interlayer water of C-S-H and structural water of ettringite.
The problem has been set aside in the past by considering not so much the bound

water as the so-called non-evaporable water which remains at 23°C when the water pressure is kept at 5.10^{-4} Torr. Starting from the composition of the single hydrated phases and from the relevant quantities in which they are present in the cement, it has been calculated that the bound water in fully hydrated cements is approximately 30% of the calcined mass, and not 22% as calculated with D-drying. The first value corresponds to the quantity of water which remains in pastes dried at 18°C and 11% R.H. (182).

A relation between the C/S ratio and the strength of the paste has not yet been found, most likely because of the heterogeneous nature of the paste at microscopic level. For instance, the C-S-H adjacent to the still unhydrated cement grains which formed at 50°C is more compact and stronger than that formed at 5°C. However, since the C-S-H which precipitates at 50° in the interstices between the cement grains is more porous than that formed at 5°C, the strength of cements cured at 50°C is less than that of cements cured at 5°C, which have a more uniform structure (183).

In ordinary portland cements, the SO_3/C_3A mol ratio varies between 0.7 and 1.2 and the final product of C_3A hydration should therefore be monosulphate or one of its solid solutions. Often, however, even several years later, only ettringite is found. The failure to transform from tri to monosulphate is due to the CO_2 coming from outside or contained in the paste as calcite, that reacts with the C_3A, untransformed into ettringite, forming monocarboaluminate and hemicarboaluminate. When CO_2 is absent, the ettringite is transformed, as expected, into monosulphate (120). On the other hand the quantity of ettringite in hardened cements is often higher than calculated according to the SO_4^{2-} content, because it may be replaced by the anions CO_3^{2-} and OH^- in its lattice (184).

* The cement paste may react with the aggregates forming compounds that are not observed in the hardened portland cement pastes. Disregarding pathological cases such as the silica alkali reaction, C_3S and portland cement react with marble surfaces to obtain a basic calcium hydrate carbonate $CaCHO_3$-$Ca(OH)_2$-H_2O of variable composition (185).
  Two further reactions may take place at the marble-cement paste interface: a) attack of the calcite by the alkaline pore solution and precipitation of the calcium hydroxide b) formation of carboaluminate $3CaO.Al_2O_3.CaCO_3.11H_2O$ and of the hemicarbonate $3CaO.Al_2O_3.\frac{1}{2}CaCO_3.12H_2O$.
  The presence of carboaluminates in the rock-paste interface appears to improve the interface bond, but the comparatively large and oriented portlandite crystals that precipitate by effect of reaction a) weaken it (186) .

3.3.2 The pore solution - The pore solution of the cement pastes has a strong ion force and contains significant quantities of complex ions. The electric conductivity of cement paste, which releases a lot of ions as soon as it comes into contact with water, is therefore higher than that of C_3S pastes (187).

* The pore solution quickly becomes oversaturated with regard to gypsum and portlandite. In the case of gypsum the supersaturation diminishes rapidly and after 20 minutes is little higher than 1, while in the case of sodium and potassium sulphates it remains considerably above 1. In any case, the gypsum saturation factor remains constant throughout the period of latency.
* The saturation curve of portlandite depends on the type of sulphate used. The curve

maximum of $[Ca^{++}]$ does not coincide with the end of the induction period (188).

* In the pore solution of the portland cement pastes and in the cement mixes containing slag, fly ash, silica fume, the alkaline ions prevail by far over the Ca^{++} ions, but each time the concentration of the alkalis diminishes $[Ca^{++}]$ increases. The other elements are always present in very small quantities (see table 5) (189).

TABLE 5: Data for the pore waters (ion concentrations in mg/l)

	SPP	CPA	SRP	MP	ALP	FAP	SIP
Volume[a]	8	4	9	9	7	8	4
Age[b]	10	4	9	10	10	10	10
w/c	0.5	0.36	0.5	0.5	0.5	0.5	0.35
Na	1500	1800	600	3200	4200	1600	300
K	6300	5700	600	6000	100	7500	700
Ca	90	20	470	50	1	15	130
Mg	0.2	0.1	0.2	0.1	0.06	0.15	0.1
Al	5	30	5	5	2800	15	5
Si	6	6	6	6	6	6	6
Fe	0.5	0.5	0.5	0.5	0.9	0.7	0.5
I_{calc}[c]	0.23	0.22	0.04	0.29	0.18	0.26	0.03
Eh[d]	139	-196	84	-377	131	106	134
pH	13.4	13.2	13.1	13.5	13.3	13.4	12.4

[a] Volume of pore water pressed from 0.2 kg solid, ml
[b] Age of cement paste sample before pore water pressing and analysis, months
[c] Calculated according to $I = 0.5 \Sigma C_i Z_i^2$, M
[d] in mV

The pH of the pore solution increases rapidly after mixing up to a peak value which is achieved so much the faster, the lower the w/c ratio (190). For a time, the composition of the pore solution does not represent a system in equilibrium, not only due to supersaturation in Ca^{++}, but also to the presence of other ions in the solution. For example $[SO_4^{2-}]$ also depends on $[OH^-]$. Only when hydration has advanced and the SO_4^{2-} ions have almost all been removed from the solution does the Fratini relation which links $[Ca^{++}]$ to $[OH^-]$ remain valid (191).

* The complexity of equilibriums or pseudo-equilibriums existing in the pore solution is increased by the presence of polymeric additions. For instance, 5-15% of a styrene-acrylate (SA) and a polyinylidene chloride (PVDC) lower the concentration of OH^- ions, while the addition of a styrene-acrilate modified with silane (SA+c.a.) increases it. All three polymers lower the concentration of Ca^{++} and increase that of Na^+ and, slightly, K^+ and interfere with that of SO_4^{2-} (192).

3.3.3 The microstructure - By applying a special liquid air cooling technique, the cement pastes may be observed under the SEM immediately after mixing. Five minutes later the portland cement particles are more or less agglomerated and the average thickness of the water film around the particles is 3 μm instead of 9 μm as appears from the calculation. After the induction period, in addition to the ettringite, also the C-S-H starts to precipitate and the cement particles start to agglomerate by effect of the bonds formed by the calcium silicate hydrate. At the end of setting, the C-S-H deposited at the points of contact between the cement particles forms a three-dimensional network (193).

As the hydration progresses, the particles weld together, and the unhydrated alite appears covered by C-S-H. This compound appears formed by an inner and an outer product whose boundary is clearly distinguishable, as the latter has a comparatively more porous texture (194). The TEM makes it possible to distinguish the areas of the inner product and of the fibrillar outer product together with large CH crystals and small AFm crystals (195).

The inner product has a C/S ratio of 1.5 ± 0.15 and is generally lacking Al, S and K. The outer product formed by a fibrillar gel has a different and a slightly more variable composition (C/S = 1.6 ± 0.2) and is frequently contaminated by Al, K and S. Sometimes a further component is present: hydrotalcite (195).

The presence of the so-called duplex film on the particles of aggregate formed by a continuous layer of portlandite backed up by a layer of C-S-H is still controversial since other papers report that only C-S-H has been observed. However, the surface of the cement matrix left uncovered by the pull-out of the aggregate grains was shown to be formed by portlandite (196). On the other hand the duplex film has never been observed in mortars prepared with different types of aggregate, and coating of C-S-H observed on the sand grains is similar to that observed on fly ash particles blended with C_3S. The morphology of the paste suggests that the precipitation of calcium silicate hydrate probably takes place during early hydration. The C/S ratio of the coating has normal values. The CH has been seen close to the interface, but rarely in contact with the aggregate (197).

* In the presence of superplasticizers the dispersion degree of cement is initially very high and therefore the early phases of hydration occur without bridges and agglomerations forming (193).
  Ligninsulphonate has a dispersing action comparable to that of naphthalene sulphonate condensate with formaldehyde, but it accelerates the formation of ettringite (193).

* When casting the cement paste on a marble surface a film of portlandite on the aggregate can be observed whose crystals have an orientation index that diminishes at increasing distances from the interface (198). A high orientation index means that the planes (001) of the CH are preferably parallel to the surface of the aggregate and this fact is accounted for by the thermodynamic principle of minimum energy (199).
  The orientation of portlandite, expressed by I(001)/I(101) XRD peak intensity ratio, depends on several factors. The orientation index is higher with quartz than with marble when the surface of the aggregate is smooth rather than rough, and tends to zero as the distance from the interface increases also when the silica fume content increases (199).
  The addition of melamine sulphonate resin to the cement reduces the ratio of

peaks I(001)/I(101), whereas the addition of naphthalene sulphonate resin does not cause any changes (200). The ratio diminishes also with time and the w/c ratio. The latter circumstance induces one to feel that the higher value of I(001)/I(101) encountered at the cement/aggregate interface as compared to the paste may also be due to different causes than that of an oriented growth of portlandite crystals for example to changes of CH morphology (200).
Diminishing the thickness of the transition zone and the formation of the compound $3CaO.Al_2O_3.CaCO_3.11\ H_2O$, as a consequence of the reaction between marble and cement paste, increases the strength of the bond between paste and aggregate (198).

The existence of an orientation index appears to be in contrast with what we said earlier on the absence of portlandite on the sand grains (197), but it must be remembered that composites consisting of an ordinary mortar cannot be compared with composites obtained by casting the cement paste on a piece of smooth and fairly large aggregate. The latter do not represent very well the true structure of mortars and concretes, especially with regard to the concentration and orientation of the phases. By completely wrappings a piece of aggregate in cement paste a macrostructure more similar to that of actual concrete is obtained (201).
With this configuration it has been seen that the farther one gets from the surface of the aggregate, the more the quantity of anhydrous material increases, while the quantity of portlandite diminishes only slightly, and the porosity diminishes considerably. In any case, the difference only involves the first 30-40 μm (201).

* The reduction of the w/c ratio makes it possible to prepare high-strength concretes (R_c > 100 MPa) as a result of reduced porosity and greater compactness; however, also the microstructure is affected since portlandite crystals have smaller dimensions, the C-S-H has lower crystallinity and contains a larger number of foreign ions (202).

* Around the entrained air voids, the paste forms a shell that is distinguishable from the bulk paste because of its greater density and alkali content. One may in fact assume that the greater stability of the void observed with the increasing content of alkalis in the cement may be linked to this localization of Na^+ and K^+ around the voids (203).

* Also accelerating admixtures such as $CaCl_2$ and $Ca(HCOO)_2$ can modify the morphology of the hydrated pastes (174).

3.3.4 Porosity - Porosity can be considered an intrinsic constituent of the cement paste which influences all the properties of concrete, from strength to durability. Porosity and pore size distribution depend, sometimes in a very complex manner, on a number of factors.

* The overall porosity of portland cement pastes made up with high w/c ratios (0.8-1.0) ceases to diminish after three (and perhaps two) days of hydration, while at lower ratios (0.4-0.6) it continues to diminish at least up to ages exceeding 60 days. Under the former conditions, the linear relationship between overall porosity and strength, which on the contrary continues to grow, no longer prevails. At the same time the capillary porosity diminishes and that of the gel

increases (see fig. 21) (171) thus the relationship between capillary porosity and strength still exists. As regards the BET specific surface and strength, pastes being considerably rich in water and pastes with a lower w/c ratio show the same dependence on the hydration degree (204).

* Gypsum affects not only compressive strength, shrinkage and expansion in autoclave, but also the structure of the hydrated products and of the pores (205). Cement pastes mixed with the same quantity of water and having the same hydration degree, but cured at different temperatures and for different times have different porosities. Namely, the overall porosity is the greater the higher the curing temperature. Here the difference chiefly regards the volume of the larger pores (206).

* The influence of the addition of electrolites on cement hydration also involves the porosity of mortar and of concrete which, for instance, becomes greater in the presence of NaOH (207). The cement paste of concrete and mortar is more porous than that of the plain paste and the difference increases with time (208).

* Paste curing at low relative humidity causes the relative volumes of pores with diameter ≤ 37 nm to diminish, since the reaction that leads to the formation of the gel

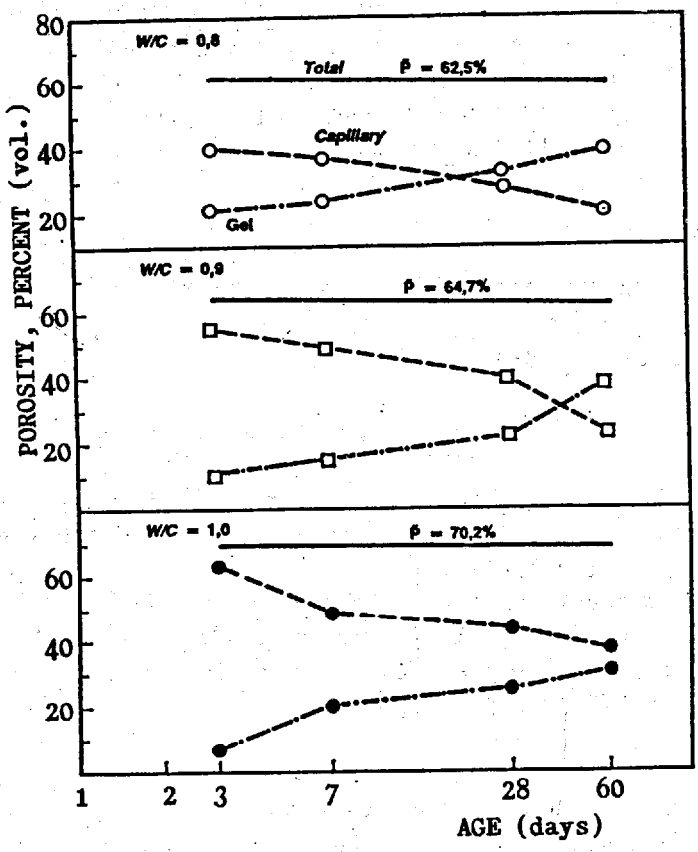

FIG. 21: Porosity versus age in pastes with different w/c ratios

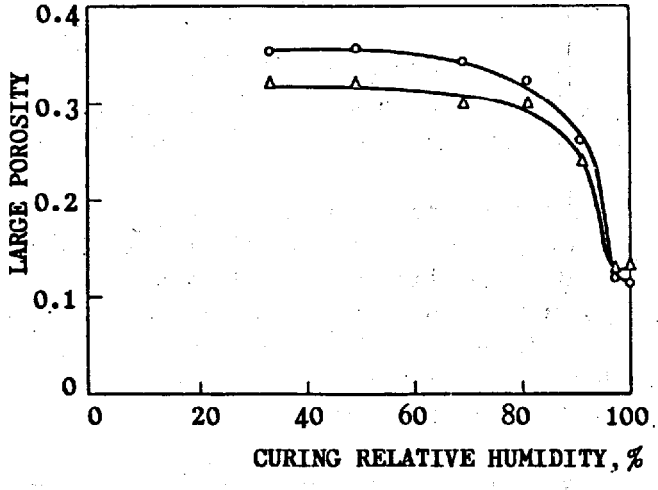

FIG. 22: Large porosity (pore width > 37 nm) against curing relative humidity: (Δ) 14 days; (o) 90 days

is prevented, but causes the macroporosity, i.e. that concerning pores (≥ 37 nm), to increase threefold (see fig. 22). The test results show that when the vapor pressure of the water in the capillary pores drops below 80%, the hydration is substantially reduced. To summarize, the water available at low humidity is chiefly adsorbed in the smaller pores and does not contribute much to the hydration process (146). The implications for the durability of the concrete are obvious.

4. THE HYDRATION OF CEMENTS CONTAINING BLASTFURNACE SLAGS

4.1 Slag hydration

As is known, slags are used for producing binders which however require to be activated with alkaline compounds in order to reveal their hydraulicity. By adding a sodium silicate solution, and using low w/c ratios, it is possible to obtain compressive strengths after 28 days that exceed even those of an ordinary portland cement. Unfortunately, up to 7 days the specimens have hardened so little that they cannot be submitted to the strength test. The addition of small quantities of portland cement, lime and sodium sulphate modifies this situation and enables the slag to achieve, already after 1 day, strengths that are comparable with those of portland cement (209).

The presence of minor elements in the slag activated with NaOH modifies its heat evolution curve. Some elements have a favourable action, but the TiO_2 is particularly unfavourable in so far as it delays and reduces the evolution of heat and strength (210) when slag hydrates under adiabatic conditions. Activation with $Ca(OH)_2$ and $CaSO_4.2H_2O$ follows a complex process. For example at seven days the temperature grows with the growing $Ca(OH)_2$ content, but if also $CaSO_4.2H_2O$ is added, the curves show a steep minimum which is so much greater the higher the SO_3 content (211).

4.2 Kinetics of the hydration of cements containing slag

The slowness of hydration of slags influences the hydration rate of slag cements. As a rule these have a rather slow early hardening but after 28 days' curing can achieve and exceed strengths of the reference cement.

The replacement of a part of the portland cement with slags lowers the hydration heat measured with the isothermal calorimeter but less than does the replacement with the same quantity of ground sand. This difference might mean that slag plays a role in cement hydration already in the early hours after mixing. The heat of hydration depends on the nature of the slag and on its fineness, but since the 2nd peak of the heat evolution rate is shifted forward, one must assume that the slag also accelerates the hydration of the clinker (212).

Slag modifies the heat evolution curve also from a qualitative viewpoint since its causes a 3rd peak to appear which cannot be ascribed to the clinker hydration (185).

The slag content begins to diminish after two days of hydration, but remains fairly high even after a year. The grinding fineness affects the hydration of

the slag to a greater extent than it does the hydration of clinker (213). Slag, is shown to be hydrated to a 40% extent after 28 days. This activity is followed by a period of latency which lasts for about five months. The reaction starts up again but, about one year after mixing, stops for at least another year (214). The step occurs although a part of the slag is still unreacted after one year (215). Raising the temperature accelerates hydration of the slag (table 6) (214).

By curing slag cement pastes under adiabatic conditions for three days the curve of the variation of temperature shows 5 peaks of different intensity depending on the SO_3 content (216).
Concluding, all these test evidences lead one to suppose that the slag hydration process is more complex than is commonly supposed.

TABLE 6: BSF hydrated (on ign. wt.%) in blended cements

Curing Temp. °C	curing time (months) 0.5	1	3	6	12	24
25	-	42	40	40	62	62
40	49	46	51	61	61	-
55	54	53	55	60	-	-

4.3 Structure and composition of cement pastes containing slag

4.3.1 The Hydrated phases - The hydrated phases observed in pastes containing slag, cured at 25°C for 90 days are the same as present in plain portland cement pastes, including calcite, although in different proportions (217). However, alongside common compounds, AFm, CH, CSH, also hydrotalcite, gehlenite and massaite have been observed (218). The phases formed by the hydration of slag incorporate a part of free calcium hydroxide, since the portlandite begins to diminish already after 2 days (213). For this reason the $Ca(OH)_2$ content of the cements containing 30% of slag is slightly but systematically lower than that calculated by diluting the portland cement with the same quantity of inert material (219).

By increasing the slag content the C/S and C/S+A ratios of the C-S-H diminish significantly while the Al content in the calcium silicate hydrate increases (215)(194). On a microscopic level, the C-S-H formed by hydration of the slags has a C/S ratio = 1.6, which diminishes as its Al content increases (194).
In slag cements the C/S ratio of the C-S-H close to the as yet unhydrated alite is 1.9, but it drops quickly down to 1.6 as one moves away from the anhydrous grain.

4.3.2 The pore solution - Slag contributes to the total concent of alkalis in the pore solution (220). Replacing 60-70% of the clinker with slag reduces considerably the $[OH^-]$ in the pore solution but does not modify the pH to any great extent. In the presence of slag the Na^+ concentration in the pore solution increases although the slag lacks sodium, while that of K^+ diminishes. This behaviour is noticed between 20 and 55°C and does not appear to change at least during the 24 months of curing (218). The slag also diminishes the $[Ca^{++}]$, which naturally tends to decrease with time.

At 20°C the concentration of SO_4^{--} remains unchanged if a part of the clinker is replaced with slag, but at 55°C the concentration of the sulphate proves higher than that of the reference cement paste and the gap grows considerably as curing proceeds (218).

4.3.3 Microstructure - With blended cements the dispersion of the particles in water is higher than observed in Portland cements, the average thickness of the water round the particles being 1.5-2.0 μm with 50% of rough slag and approx. 1 μm with 25% of fine slag. In any case, the thickness of the water film round the slag particles is greater than observed round the clinker grains (193).

4.3.4 Porosity - The porosity of slag cements diminishes in time, but is so much higher the greater the slag content (215) and therefore it is always greater than that of the reference portland cement (217).

Porosity being equal, the specific surface of the paste appears to be little affected by the slag/clinker ratio (215). Slag also modifies the distribution of the pores and in slag cements the percentage of finer pores is higher than in portland cements.

5. THE HYDRATION OF CEMENTS CONTAINING POZZOLANA

Pozzolanas are materials without hydraulic properties but are capable of hardening as a consequence of their reaction with calcium hydroxide and water. The family comprises both natural materials, which have been used for thousands of years, and artificial materials, such as fly ashes, silica fume, burnt clay, of more recent use.The family of the pozzolanas includes materials of widely varying composition, but all of them very rich in silica.

Among the fly ashes it is necessary to distinguish the silico-aluminous ones which, being poor in lime and rich in vitreous phases, behave like typical natural pozzolanas, from the calcareous ones which, as they contain hydraulic components, may even harden without adding lime from outside (221).

Pozzolana-containing cements are obtained by an intimate blend of portland cement and pozzolana. The portland clinker, by hydrating, supplies the necessary lime for the pozzolanic reaction to take place.

5.1 Kinetics of the Hydration of Cements Containing Pozzolanas

It is a known fact that the pozzolanic reaction generally becomes perceivable only several days after mixing and in any case after the hydration of the clinker has progressed considerably. The reaction rate however varies depending on the material and if fly ashes show a reaction only after a week, silica fume shows signe of reaction after less than one day (222). In any case, the presence of the pozzolana affects the hydration of the clinker after a very short time. By replacing 10% of a portland cement with a very active tufa, the alite hydration is accelerated (223). Replacing 20-40% of the portland cement with fly ashes delays, instead, the appearance of the 2nd peak in the heat evolution curve, but makes it higher (224).

The cement's overall heat of hydration diminishes the more so the greater the replacement of the portland cement with silico-aluminous fly ashes. With calcareous fly ashes, instead, the hydration heat may be higher than the reference cement owing to the free lime and anhydrite content (225).

* As is known, excellent artificial pozzolanas are obtained by burning clays. In blends of portland cement and burnt clay the bound water diminishes as the percentage of pozzolana increases. For all mixes, hydration, measured by the value of the bound water, does not vary sequentially with the rise of the firing temperature (226).

* The addition of 5-10% of silica fume to portland cement increases the heat of hydration since it accelerates the hydration of C_3S. During the first three days the hydration of the C_3A appears instead to be fairly delayed (227).
Microsilica increases the initial heat evolution rate, but since it practically does not react in the early hours, it may be inferred that at the beginning its particles act like nucleation centres for the clinker's hydration products (228).
The microsilica added to the portland cement is consumed by the lime which forms progressively and for this reason it may be observed under the TEM after 28 days only if it is present in appreciable quantities, i.e., exceeding 15% (229).
In portland cements the kinetics of hydration may be monitored by the increase of non-evaporable water, but with cements containing silica fume this is impossible, since the evaporable water diminishes between 90 and 550 days even if the pozzolanic reaction continues (222).

The different influence of the type of pozzolanic additions on the early hydration of portland cements has been recently summarized as follows (230). In the first 4 hours the natural pozzolanas and microsilica increase the 2nd peak of the heat evolution rate and therefore accelerate the clinker hydration. Fly ashes cause an increase of the 2nd peak but delay its appearance, that is they extend the induction period since they contain unburnt organic products that delay hydration of alite. For this reason combustion of the compounds causes the heat delay do disappear (230).

5.2 Structure and composition of the pozzolana-containing cement paste

5.2.1 The hydrated phases - The hydrated phases found in pastes of pozzolana-containing cements are essentially the same as those present in portland cement pastes, at least as long as the overall composition of the two types of cement does not differ too much. In cements with fly ashes CSH, CH and AFm and hydrogarnet are formed (195). AFm may sometimes lack, while an unknown phase and vaterite ($CaCO_3$) may be present (218).
The C/S molar ratio of C-S-H of cements containing 40% of fly ash is 1.2 on the average, but in the proximity of alite the ratio is higher. With 10% of microsilica the average C/S ratio is 1.4, i.e. higher than that of fly ash (194). The result might be explained by the fact that the ash-containing cement has an overall C/S ratio which is lower than cement containing silica fume.
A high microsilica content (30%) gives rise to a C-S-H with a very low C/S molar ratio, which achieves 1.1 on the surface of the clinker particles and drops to 0.68 as far from these particles (231). In other cases, with an undefined but probably lower clinker/microsilica ratio the C/S proved to be 0.80-0.18 (232).
In cements containing microsilica the dimerization process, expressed by the h_2/h_1 ratio of the peaks height of the dimer and of the monomer, increase with time. It is only slightly higher than that of the portland cement before 55 days (233) and the same after 250 days (234).

5.2.2 The pore solution - The composition of the pore solution is changed since a part of the clinker is replaced by pozzolana material (220). This may combine portlandite and may contribute to increasing or decreasing the overall alkali content, for example by lowering the C/S ratio of C-S-H and thus increase its capacity to fix the alkalis.

* Fly ashes diminish the concentration of Ca^{++} and OH^{-} in the pore solution (218) but the drop is less than that caused by the replacement with sand (235). Changes in the composition of the pore solution caused by fly ashes are variable and they depend on their alkali contents and on the type of the alkali containing compound (218).
  This variability has been observed in 30-70 mixes of two fly ashes with a portland cement. One was much richer in alkalis than the cement, the other moderately richer (218)(236).

  The concentrations of Na^{+} and K^{+} in the pore solution grow for 14 days both in the case of portland cement and in the case of blended cements (236). After 14 days the concentrations stabilize. The first ash causes $[Na^{+}]$ to increase and the second to diminish as against the concentration to be found in the portland cement paste. Also $[K^{+}]$ depends on the initial potassium content in the ash, but is always lower than that observed with plain portland cement (218). The variability in the behaviour of the alkalis of fly ashes may be ascribed to the presence of easily soluble alkalis in addition to alkalis rooted in the vitreous matrix of the fly ashes (218).

* Microsilica considerably reduces $[Na^{+}]$ and $[K^{+}]$ of the pore solution, with 16% replacement hydration, the pH does not drop below 12.7 (222) or 12.8 (219) after 550 days of hydration. By increasing the microsilica contents up to 20% the pH decreases only slightly (237)(189). Minor changes occur also when the Na_2O equivalent content changes (219).

  Microsilica is considerably more reactive than other common pozzolanic materials and therefore it controls the alkalis in the solution more effectively. In any case, with or without fly ash, the concentration of Na^{+} and K^{+} in the solution increases with time (236).
  Microsilica present to the extent of 20% in a cement accelerates early dissolution of OH^{-}, K^{+} and Na^{++}. The concentrations of the three ions attains a peak after 5-10 hours, but then they decline rapidly. This fact suggests that the alkalis are partly incorporated in the solide hydrated phases (228)(see fig. 23).
  The reduction of the concentration of alkalis (Me^{+}) is attended by an increase of $[Ca^{++}]$.

5.2.3 Microstructure - Already after 7 days of hydration shells formed by radial growth of C-S-H and ettringite appear on the fly ash particles. Since fly ashes react later, these shells are probably formed by precipitation of the products of hydration of the clinker + gypsum (224). In other words, at the beginning of hydration the particles of fly ash supply preferential sites for precipitation of C-S-H (224). In cements with fly ash the boundary between inner and outer C-S-H normally found around non-hydrated alite is not always clear. Probably a recrystallization of internal C-S-H occurs which, initially with a higher C/S ratio, subsequently turns into a product with a lower C/S ratio (194).

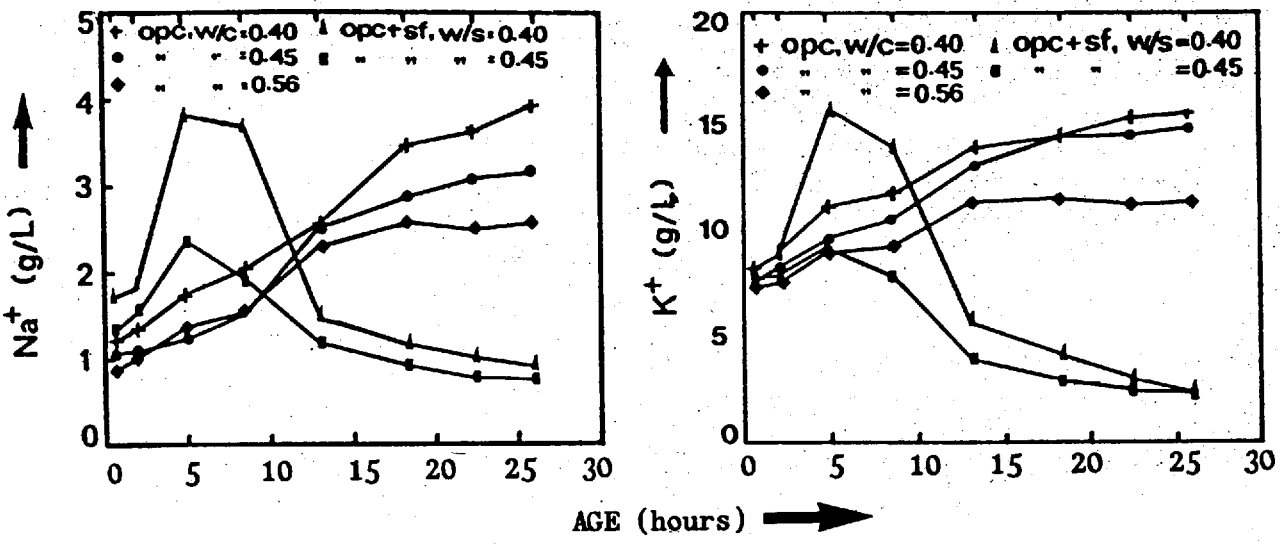

FIG. 23: Na^+ and K^+ concentrations of pore solution of pastes

In pastes containing fly ash one can observe inner and outer product around the still unhydrated clinker particles; the outer product having its typical fibrillar appearance. Their composition depends on the clinker/fly ash ratio and on the w/c ratio. The C/S mol ratio is lower than that found in pure portland cement and ranges between 1.49-1.56 and 1.45-1.5 respectively for the inner and outer product (195). After 17-30 months of hydration, the fly ash particles are covered with a radial fibrillar layer of C-S-H formed within the original boundaries of the particle and due to the pozzolanic reaction (195).

* While in portland cements the interface zone between the sand and the paste has a microstructure which differs from that of the bulk paste, in the cements containing microsilica (15%) it appears homogeneous and thick like the bulk paste and of course without the presence of massive CH rims or of gaps.
This different microstructure might be the result of suppressing the bleeding and of the silica fume particles' capacity to fill the space next to the surface of the sand grains (196).
High-strength concretes can be are obtained with high cement content (450-500 kg/m^3) and very low w/c ratios (0.33). Replacing the portland cement with 15% of silica fume lowers the porosity and increases the compressive strength, but does not modify the quantity of unhydrated cement in the transition zone. Here the

quantity of portlandite is practically the same as the cement matrix (238).

5.2.4 Porosity - The presence of pozzolanas modifies also the paste porosity.

* The pore structure of a mature paste containing fly ash is more discontinuous and finer than that of the reference portland cement pastes. This circumstance is ascribed to changes in reaction rate of the different cement phases caused by the availability of suitable nucleation sites (224).

The overall porosity of the cement paste containing fly ash is higher than that of the reference cement (224), but the threshold value, the maximum continuous diameter and the frequency of the corresponding pores are lower than those of control portland cements (239).

The porosity of the cements containing microsilica increases linearly with increasing contents of the admixture as, if one wants to keep the consistency constant, the w/c ratio increases (229). In any case also when w/c ratio is the same, the paste porosity of cement containing microsilica is higher than the porosity of the control paste (238).

Of course if w/c ratio is drastically reduced with considerable concentrations of superplasticizers, the microsilica particles may reduce the overall porosity (232). By increasing the silica fume content the overall porosity of the paste diminishes after one day of hydration as the dimensions of the pores do (199).

The pore distribution of hardened mortars shifts towards smaller pores when cement containg silica fume (30%). The overall porosity decreases with time and the structure of the micropores becomes uneven and thus the effective coefficient of diffusion of Cl^- becomes smaller (231).

CONCLUSIONS

In the years that have elapsed between the congress held in Rio de Janeiro and the one of New Delhi, cement hydration has been the object of several studies which have considered the reactions concerning clinker components, portland cement and blended cements.

Progress made in a better knowledge of the complex problem of hydration is considerable and significant. These successful results have been obtained by resorting to recent and advanced testing techniques, but also to well-tried, more traditional techniques. Test results gathered in the past have been reviewed, analysed and interpreted in the light of the latest acquisitions.

The new investigation techniques which have yielded important test results are Nuclear Magnetic Resonance and Transmission Electron Microscopy (TEM), the latter adquately assisted by the preparatory technique of Ion Beam Thinned Sections.

Observations by TEM have revealed that C-S-H basically consists of fine sheets formed by a narrow protonated CaOx layer sandwiched between two layers of SiOx. Each elementary sheet has a thickness of 1 nm and an area of 10^2-10^6 nm^2. Depending on the conditions of formation, the C-S-H may be formed by an association of 4 to 6 sheets. These sheets have been photographed by means of HRTEM. This structure may account for the variability in composition of the C-S-H, but needs of course to be compared with

other test results and especially with those provided by the NMR regarding the degree of condensation of the silicate anions.

The NMR has proved to be an important means of investigation not only in establishing the polymerization degree of the silicate ions of C-S-H, but also in defining equilibria existing in the $CaO-SiO_2-H_2O$ system. As regards this system, test results agree on the existence of two silicate hydrates with distinct though variable C/S ratio. The composition of C-S-H appears to depend heavily on its conditions of formation, such as concentrations in the liquid phase, pH, the presence of other ions, temperature, etc.

Also the more traditional techniques, however, have contributed considerably to research: SEM, TGA, TDA, for instance, have made it possible to explain some apparent incongruities observed in the relations between trisulphate and monosulphate. SEM appears to have settled the vexed issue between topochemical reactions and through solution by showing that both can take place.

Studies on hydration have been preferably focussed on simpler systems than those formed by cement, but there is no doubt that studies on C_3S, C_3S+slag, C_3S+fly ashes or microsilica have led to results that shed light on cement hydration.

The study of the hydration of individual cement constituents is an approach which is necessary but not sufficient to interpret events that depend on the hydration of cement.

In fact, hydration takes place under conditions that are quite different from laboratory conditions and it must therefore be studied in real systems as well, i.e., in mortars and concretes (146). One must also consider that cement is not synonymous with portland cement and that every type of blended cement is a case to be studied apart from all others.

Concluding, the results of studies carried out on the hydration of cement and of the systems connected with it have shown a remarkable progress and it is doubtless that the fall-out on cement applications will be considerable.

REFERENCES

1) PARROTT, L.J., GEIKER, M.; GUTTERIDGE, W.A.; KILLOH, D., "Monitoring Portland Cement Hydration: Comparison of Methods", Cem. Concr. Res. 1990, 20 (6), 919-26

2) TSURUMI, T.; KONDOH, T.; SAGA, K.A.; DAIMON, M., "Crystal Structure and Reactivity of Ca3Si05 Solid Solution", CAJ Proc. of Cem. & Concr. No. 44, (Tokyo, 1990), 62-7

3) ONO, Y., "Hydraulic Activity and Equilibrium Vapour Pressure of Clinker Compounds", CAJ Proc. of Cem. & Concr. No. 44, (Tokyo, 1990), 24-9

4) TSURUMI, T.; ASAGA, K.; DAIMON, M.; "Electrostatic Potential Calculation of Ca2Si02", CAJ Proc. of Cem. & Concr. No. 43, (Tokyo, 1989), 2-7

5) BERNES, U.R. "Modelling Porewater Chemistry in Hydrated Portland Cement", Symp. on Scientific Basis for Nuclear Waste Management X, (Boston, 1986), MRS Symp. vol. 84, Mat. Res. Soc., Pittsburgh, 319-30

6) BEZJAK, A., "An Extension of the Dispersion Model for the Hydration of Portland Cement", Cem. Concr. Res. 1986, 16 (2), 260-4

7) BEZJAK, A., "Nuclei Growth Model in Kinetic Analysis of Cement Hydration", Cem. Concr. Res. 1986, 16 (4), 605-9

8) BROWN, P.W., "Effects of Particle Size Distribution on the Kinetics of Hydration of Tricalcium Silicate", J. Am. Ceram. Soc., 1989, 72 (10), 8129-32

9) COHEN, R.D.; COHEN, M.D., "Kinetics of Depletion of a Population of Hydrating Cement Particles", J. Mat. Sci. 1987, 22, 2032-6

10) COHEN, M.D.; COHEN, R.D., "Modelling of the Hydration of Tricalcium Silicate", J. Mat. Sci. 1988, 23, 3816-20

11) GARTNER, E.M.; Jennings, H.M., "Thermodynamics of Calcium Silicate Hydrates and their Solutions", J. Am. Ceram. Soc. 1987, 70 (10), 743-9

12) GLASSER, F.P.; LACHOWSKI, E.E., MACPHEE, D.E.; "Compositional Model for Calcium Silicate Hydrate (C-S-H) Gels, their Solubilities, and Free Energies of Formation", J. Am. Ceram. Soc. 1987, 70 (7), 481-5

13) GLASSER, F.P.; MACPHEE, D.E., LACHOWSKI, E.E.; "Modelling Approach to the Prediction of Equilibrium Phase Distribution in Slag-Cement Blends and their Solubility Properties", Symp. on Scientific Basis for Nuclear Waste Management XI, (Boston, Nov. 30-Dec. 3, 1987), MRS Symp. vol. 112, Mat. Res. Soc. Pittsburgh, 3-12

14) JENNINGS, H.M.; JOHNSON, S.K., "Simulation of Microstructure Development During the Hydraton of a Cement Compound", J. Am. Ceram. Soc. 1986, 69 (1), 790-5

15) JENNINGS, H.M., "Towards Computer-Based Microstructure Models for Cement-Based Systems", Symp. on Microstructural Development During Hydration of Cement (Boston, Dec. 2-4, 1986), MRS Symp. vol. 85, Mat. Res. Soc., Pittsburgh, 291-300

16) KATSURA, O.; YOSHINO, T.; KAMADA, E., "A Model Describing Strength Development of Concrete Considering Porosity and Hydration of Cement", CAJ Proc. of Cement and Concrete No. 44, 1990, 324-9

17) KOROBOV, A.I.; URZHENKO, A.M.; USHEROV,MARSHAK, A.V., "Mathematical Models for Thermokinetic Analysis of the Hydration of Binders", Tsement 1987, (11), 15-17

18) PARROTT, L.J., "Modeling of Hydration Reactions and Concrete Properties", Materials Science of Concrete I, Ed. by Skalny, The Am. Ceram. Soc., Westerville, 1989, 181-995

19) PLECAS, I.B., PERIC, A.D.; DRIJACA, J.D.; KOSTADINOVIC, A.M., "Mathematical Modeling of Physico-Chemical Characteristics of Concrete in Immobilization of Radioactive Waste", Cem. Concr. Res. 1991, 21 (5), 941-6

20) POMMERSHEIM, J.M., "Effect of Particle Size Distribution on Hydration Kinetics", MRS Symp. on Microstructural Development During Hydration of Cement (Boston, Dec. 2-4, 1986), MRS Symp. vol. 85, Mat. Res. Soc., Pittsburgh, 301-6

21) POMMERSHEIM, J.; CHANG, J., "Kinetics of Hydration of Tricalcium Aluminate", Cem. Concr. Res. 1986, 16 (3), 440-50

22) POMMERSHEIM, J.; CHANG, J., "Kinetics of Hydration of Tricalcium Aluminate in the Presence of Gypsum", Cem. Concr. Res. 1988, 18 (6), 911-22

23) POPOVICS, S., "Model for the Quantitative Description of the Kinetics of Hardening of Portland Cements", Cem. Concr. Res. 1987, 17 (5), 821-38

24) "Mathematical Modeling of Hydration of Cement", Mat. Constr. 1986, (110), 137-47

25) SCHLUSSLER, K.-H., KASSNER, B.; SESSNER, R.; PETKE, M., "Die Hydratationskinetic von Zement - Messung und mathematische Modellierung", Silikattechnik 1989, (5), 162-5

26) SCHLUSSLER, K.H., "Mathematical Modeling of the Kinetics of Binder Hardening", Cem. Concr. Res. 1986, 16 (2), 215-26

27) VOLLET, D.R.; CRAIEVICH, A.F., "Alternative Model for the Fine Porous Structure in Hydrated Tricalcium Silicate", Advances in Cement Research 1988, 1 (2), 107-11

28) RASSEM, R.; ZANNI-THEVENEAU, H.; VERNET, C.; HEIDEMMANN, D.; GRIMMER, A.R.; BARRET, P.; NONAT, A.; BERTRANDIE, D.; DAMIDOT, D., "An NMR Investigation of C_3S Hydration in Pastes and in Stirred Diluted Suspensions", 1st Int. Workshop on Hydration and Setting (Dijon, July 1991), pp. 5

29) RODGER, S.A.; GROVES, G.W.; CLAYDEN, N.J.; DOBSON, C.M., "Hydration of Tricalcium Silicate Followed by 29SiNMR with Cross-Polarization", J. Am. Ceram. Soc. 1988, 71 (2), 91-6

30) TRETTIN, R.; WIEKER, W., "Zur Hydratation von Trikalziumsilikat I. Ursachen der Induktionsperiode", Silikattechnik 1986, (3), 75-8

31) TRETTIN, R.; SATAVA, V.; WIEKER, W., "Studies on Physico-Chemical Changes in Time of Initial Setting of C_3S", 1st Int. Workshop on Hydration and Setting (Dijon, July 1991), pp. 5

32) BARRET, P.; BERTRANDIE, D., "Fundamental Hydration Kinetic Features of the Major Cement Constituents: Tricalcium Silicate (Ca3Si05) and ß-Dicalcium Silicate (ß-Ca_2SiO_4), J. Chim. Phys. Phys.-Chim.Biol. 1986, 83 (11-12), 765-75

33) DAMIDOT, D.; NONAT, A.; BARRET, P., "Kinetics of Tricalcium Silicate Hydration in Diluted Suspensions by Microcalorimetric Measurements", J. Am. Cer. Soc. 1990, 73 (11), 3319-22

34) DAMIDOT, D.; NONAT, A., "Investigations of the C2S Hydration Process During the First Hours", 1st Int. Workshop on Hydration and Setting (Dijon, July 1991), pp.7

35) PAULINI, P., "Kinetic Reaction Measurements in Cement Hydration with the Immersion Weighing Method", Zem. Kalk Gips 1988, (10), 525-31

36) HANAFI, S.; EL-SHAFEI, G.M.S.; PHILIP, CH.A.; SELIM, S.A., "Vapour Phase Hydration and Water Uptake of C_3S in Relation to Structure and Texture", Il Cemento 1989 (2), 105-20

37) HANAFI, S.; EL SHAFEI, G.M.S.; SELIM, S.A., "Hydration of Alite from the Vapour Phase-Structural and Textural Characteristics", Il Cemento 1988, (4), 283-96

38) GHORAB, H.Y.; ABOU EL FETOUH, S.H., "The Role of Sodium Hydroxide in the System C_3A-$CaSO_4$-H_2O at 30°C", Symp. on Microstructural Development During Hydration of Cement (Boston, Dec. 2-4, 1986), MRS Symp. vol. 85, Mat. Res. Soc., Pittsburgh, 255-60

39) GROVES, G.W., "TEM Studies of Cement Hydration", Symp. on Microstructural Development During Hydration of Cement (Boston, Dec. 2-4, 1986), MRS Symp. vol. 85, Mat. Res. Soc., Pittsburgh, 3-12

40) LUDWIG, U.; SINGH, N.B., "Kinetics and Mechanism of Alite Hydration", Zem. Kalk Gips 1986, (12), 688-92

41) MUELLER, W.; VOLKE, K., "Untersuchungen zur Alkalibindung im technischen C3S (Alit) und C3A (Aluminat)", Silikattechnik 1988, (4), 113-4

42) WACHTLER, H.-J.; USCHOLD, T.; MUELLER, W.; VOLKE, K., "Uber den Einfluss brennstoffbedingter Akzessorien auf die Hydratation des Trikalziumsilikats und Alits", Silikattechnik 1987, (7), 234-7

43) NOCUN-WCZELIK, W.; TRYBALSKA, B., "The Studies of Al-Doped Tricalcium Silicate Hydration", J. Thermal Anal. 1987, 32, 1719-22

44) BURGER, D.; LUDWIG, U., "Zur Reaktivitat von im Niedrigtemperaturbereich hergestellten Kalziumsilikaten", Silikattechnik 1986, (4), 131-3

45) ODLER, I.; ABDUL-MAULA, S., "Hydration Reactions in the System CaO-SiO_2-CaF_2", J. Am. Ceram. Soc. 1987, 70 (1), 39-42

46) KUSNEZOVA, T.W.; AKIMOV, W.G.; PANJUSKIN, W.N., "Reaktionsfahigkeit der Mineralien von Portlandzementklinker", Silikattechnik 1986, (4), 125-7

47) ONO, Y., "Hydraulic Activity and Equilibrium Vapour Presure of Clinker Compounds", Caj Proc. Cem. & Concr. 1990, (44), 24-9

48) KING, T.C.; DOBSON, C.M.; RODGER, S.A., "Hydration of Tricalcium Silicate with D_2O", J. Mat. Sci. Lett. 1988, (7) 861-3

49) ZIEMER, B.; OLIEW, G., "Zur gemeinsamen Hydratation von Alit und Belit", Silikattechnik 1986, (5), 171-2

50) LOCHER, D.; ODLER, I., "Interaction Phenomena in the Combined Hydration of CLinker Minerals", Il Cemento 1989, (1), 25-36

51) NIKONOVA, N.S.; MATYUKHINA, O.N.; MITYUSHIN, V.V.; NESTERINA, E.M., "Kinetics of heat Release in Hydration of Tricalcium Silicate in the Presence of Ettringite", Izv. Vyssh. Uchebn. Zaved. Khim. Tekhnol 1989, 32 (9), 77-80

52) OH, H.K.; CHOI, S.H., "Early Hydration of Tricalcium Silicate: I", Yoop Hakhoechi 1986, 23 (5), 35-40

53) USHIYAMA, H., "Early-stage Hydration of the Alite-carbonate-water System as Studied by ESCA", Semento Gijutsu Nenpo 1986, (40), 36-8

54) STADELMANN, C.; WIEKER, W., "Uber die Wirkung von Alkalilaugen auf die Hydratation von Trikalziumsilikat (C_3S)", Silikattechnik 1986, (7), 226-9

55) MACPHEE, D.E.; LUKE, K.; GLASSER, F.P.; LACHOWSKI, E.E., "Solubility and Aging of Calcium Silicate Hydrates in Alkaline Solutions at 25°C", J. Am. Ceram. Soc. 1989, 72 (4), 646-54

56) SINGH, N.B.; PRABHA SINGH, S., "Hydration of Tricalcium Silicate", 1st Int. Workshop on Hydration and Setting (Dijon, July 1991), pp. 4

57) MONTANARO, L.; NEGRO, A.; REGOURD, M., "Action de $CaCO_3$, $CaSO_4$ et $CaSO_4 \cdot 2H_2O$ sur l'hydratation de C_3S", Cem. Concr. Res. 1988, 18 (3), 431-7

58) WANG, T.; LUO, Z.; TIAN, Q., "Low-temperature Rapid-Sintering Cement Clinker with Complex Mineralizers", Huanan Gongxueyuan Xuebao 1985, 13 (1), 41-51

59) SINGH, N.B.; SARVAHI, R., "Effect of Lactic Acid on the Hydration of C_3S", Il Cemento 1991, (4), 197-210

60) STADELMANN, C.; TRETTIN, R.; WIEKER, W.; RAMM, M., "Surface Studies on Tricalcium Silicate Hydrated in Sodium Salt Solutions", Il Cemento 1987, (4), 331-6

61) RAMACHANDRAN, V.S.; ZHANG CHUN-MEI, "Dependence of Fineness of Calcium Carbonate on the Hydration Behaviour of Tricalcium Silicate", Durability of Building Materials 1986, (4), 45-66

62) RAMACHANDRAN, V.S., "Thermal Analysis of Cement Components Hydrated in the Presence of Calcium Carbonate", Thermochimica Acta 1988, 127, 385-94

63) ZHANG, C.; RAMACHANDRAN, V.S., "Effect of Calcium Carbonate as a fine Aggregate on the Hydration of Tricalcium Silicate", Guisuanyan Xuebao 1988, 16 (2), 110-7

64) LU, PING; LU, SHUBIAO, "Effect of Calcium Carbonate on the Hydration of C_3S", Guisuanyan Xuebao 1987, 15 (4), 289-94

65) BROWN, P.W., "Early Hydration of Tetracalcium Aluminoferrite in Gypsum and Lime-Gypsum Solutions", J. Am. Ceram. Soc. 1987, 70 (7), 493-6

66) RAMACHANDRAN, V.S.; CHUN-MEI, Z., "Influence of CaCO3 on Hydration and Microstructural Characteristics of Tricalcium Silicate", Il Cemento 1986, (3), 129-52

67) BEEDLE, S.S.; GROVES, ,G.W.; RODGER, S.A., "The Effect of Fine Pozzolanic and Other Particles on the Hydration of C_3S", Adv. Cem. Res. 1989, 2 (5), 3-8

68) DOBSON, C.M.; GOBERDHAN, D.G.C.; RAMSAY, J.D.F.; RODGER, S.A., "29Si MAS NMR Study of the Hydration of Tricalcium Silicate in the Presence of Finely Divided Silica", J. Mat. Sci. 1988, (23), 4108-14

69) JENNINGS, H.M., "Aqueous Solubility Relationships for Two Types of Calcium Silcate Hydrate", J. Am. Ceram. Soc. 1986, 69 (8), 614-8

70) RAMACHANDRAN, A.R.; GRUTZECK, M.W., "Microstructural Development During Suspension Hydration of Tricalcium Silicate "Floating" and Fixed pH Conditions", Symp. on Microstructural Development During Hydration of Cement (Boston, Dec. 2-4, 1986), MRS Symp. vol. 85, Mat. Res. Soc., Pittsburgh, 33-8

71) GRUTZECK, M.; BENESI, A.; FANNING, B., "Silicon-29 Magic Angle Spinning Nuclear Magnetic Resonance Study of Calcium Silicate Hydrates", J. Am. Ceram. Soc. 1989, 72 (4), 665-8

72) Proc. of the 3rd Int. Symp. on The Chemistry of Cement (London, September 15-20, 1952), C.A.C.A., London

73) SUZUKI, K.; NISHIKAWA, T.; HAYASHI, T., "Characterization of Lox-Lime C-S-H", CAJ Review No. 42 (Tokyo, 1988), 34-7

74) MELZER, R.; EBERHARD, E., "Phase Identification During Early and Middle Hydration of Tricalciumsilicate (Ca_3SiO_5)", Cem. Concr. Res. 1989, 19 (3) 411-22

75) TAYLOR, H.F.W., "Proposed Structure for Calcium Silicate Hydrate Gel", J. Am. Ceram. Soc. 1986, 69 (6), 464-7

76) GRUDEMO, A., "The Crypto-crystalline Structure of C-S-H Gel in Cement Pastes Inferences from X-Ray Diffraction and Dielectric Capacitivity Data", Cem. Concr. Res. 1987, 17 (4), 673-80

77) HENDERSON, E.; BAILEY, J.E., "Sheet-like Structure of Calcium Silicate Hydrates", J. Mat. Sci. 1988, 23, 501-8

78) RODGER, S.A.; GROVES, G.W.; CLAYDEN, N.J.; DOBSON, C.M., "A Study of Tricalcium Silicate Hydration from very Early to very Late Stages", Symp. on Microstructural Development During Hydration of Cement (Boston, Dec. 2-4, 1986), MRS Symp. vol. 85, Mat. Res. Soc., Pittsburgh, 13-20

79) OH, H.K.; CHOI, S.H., "Early Hydration of Tricalcium Silicate: II", Yoop Hakhoechi 1987, 24 (2), 133-8

80) MACPHEE, D.E.; LACHOWSKI, E.E.; GLASSER, F.P., "Polymerization effects in C-S-H: Implications for Portland Cement Hydration", Adv. Cem. Res. 1988, 1 (3), 131-7

81) YOUNG, J.F., "Investigations of Calcium Silicate Hydrate Structure Using Silicon-29 Nuclear Magnetic Resonance Spectroscopy", J. Am. Ceram. Soc. 1988, 71 (3), C118-C120

82) NIKONOVA, N.S.; TIKHOMIROVA, I.N.; CHEKUNOVA, E.V.; MITYUSHIN, V.V., "Effects of Alkalies on the Degree of Polymerization of Silicon-oxygen Anions of Calcium Silicate Hydrates", Zh. Prikl. Khim. 1989, 62 (10), 2237-40

83) KUZNETSOVA, T.V.; DOBRONRAVOVA, L.A.; SOVETNIKOVA, N.K., "Effect of a Modified Silica-Containing Additive on the Hardening of Cement Systems", Zh. Prikl. Khim. (Leningrad), 1987, 60 (10), 2351-4

84) YOUNG, J.F.; HANSEN, W., "Volume Relationships for C-S-H formation Based on Hydration Stoichiometries" MRS Symp. on Microstructural Development During Hydration of Cement (Boston, Dec. 2-4, 1986), MRS Symp. vol. 85, Mat. Res. Soc., Pittsburgh, 313-22

85) KRAMAR, L.Ya.; TROFIMOV, B.Ya.; TALISMAN, L.S.; IVANOV, F.M.; KOLBASOV, V.M., "Effect of Microsilica Addition on Alite Hydration and the Sulfate Resistance of Cement Stone", Tsement 1989, (6), 14-7

86) STADE, H., "On the Reaction of C-S-H(di,poly) with Alkali Hydroxides", Cem. Concr. Res. 1989, 19 (5), 802-10

87) STADE, H.; MULLER, D., "On the Corrosion of Al in Ill-crystallized C-S-H Phases formed by Hydration of Tricalcium Silicate and by Precipitation Reactions at Ambient Temperature", Cem. Concr. Res. 1987, 17 (4), 553-61

88) YUAN, R.; TAN, D., "Study of the Surface Characteristics of Hydrated Calcium Silicates", Guisuanyan Xuebao 1988, 16 (6), 489-93

89) GROVES, G.W.; LE SUEUR, P.J.; SINCLAIR, W., "Transmission Electron Microscopy and Microanalitycal Studies of Ion-Beam- Thinned Sections of Tricalcium Silicate Paste", J. Am. Ceram. Soc. 1986, 69 (4), 353-6

90) YUAN, C.Z.; ODLER, I., "The Interfacial Zone between Marble and Tricalcium Silicate Paste", Cem. Concr. Res. 1987, 17 (5), 784-92

91) RODGER, S.A.; GROVES, G.W., "The Microstructure of Tricalcium Silicate/ Pulverized-Fuel ash Blended Cement Pastes", Adv. Cem. Res. 1988, 1 (2), 84-91

92) RODGER, S.A.; GROVES, G.W., "Electron Microscopical Studies of Tricalciumsilicate - Fly Ash Blended Pastes", MRS Symp. on Fly-Ash and Coal Conversion bY-Products: Characterization, Utilization and Disposal IV (Boston, Dec. 1-3, 1987), MRS Symp. vol. 113, Mat. Res. Soc., Pittsburgh, 117-8

93) JENNINGS, H.M.; PARROTT, L.J., "Microstructural Analysis of Hardened Alite Paste: I", J. Mat. Sci. 1986, 21, 4048-52

94) MAGGION, R.; TINET, D.; LEVITZ, P.; VAN DAMME, H.; FAUGERE, A.M., "Microtextural Evolution of CSH Pastes During Hydration", 1st Int. Workshop on Hydration and Setting (Dijon, July 1991), pp. 6

95) TRETTIN, R.; WIEKER, W., "Hydration of Tricalcium Silicate: II - Course of Hydration after the Induction Period", Silikattechnik 1986, (11), 363-6

96) BOBROV, B.S., "Initial Hydration of Tricalcium Silicate", Zh. Prikl. Khim. 1987, 60 (10), 2231-5

97) GRÜTZECK M.W.; RAMACHANDRAN, A.R., "An Integration of Tricalcium Silicate Hydration Models in Light of Recent Data", Cem. Concr. Res. 1987, 17 (1), 164-70

98) SINGH, N.B.; PRABHA SINGH, S., "Lattice Defects and the Effect of Melment on the Hydration of Alite", J. Mat. Sci. 1987, 22, 2751-8

99) GOLDSCHMIDT A., "Hydration Mechanism of the C_3S with the Application of the Slow Evaporation Technique in its Liquid Phase", Cem. Concr. Res. 1986, 16 (4), 472-80

100) JENNINGS, H.M.; PARROTT, L.J., "Microstructural Analysis of Hydrated Alite Paste: II", J. Mat. Sci. 1986, 21, 4053-9

101) GARTNER, E.M.; GAIDIS, J.M., "Hydration Mechanisms: I", Materials Science of Concrete I, 1989, 95-125, Ed. by Skalny, J.P., The Am. Ceram. Soc., Westerville

102) HELMY, F.M.; SHEBL, F.A.; SUMMAN, A.M., "Identification of Ion Pair in ß-Dicalcium Silicate-Water System at 25°", Chem.-Ztg. 1988, 112 (6), 207-9

103) TRETTIN, R.; OLIEW, G.; STADELMANN, C.; WIEKER, W., "Very Early Hydration of Dicalcium Silicate-polymorphs", Cem. Concr. Res. 1991, 21 (5), 757-64

104) RINALDI, D.; VALENTI, G.L., "Influence of Some Mineralizers on Syntesis and Hydration of Beta-dicalcium Silicate", J. Mat. Sci. Lett. 1986, (5), 620-2

105) XIUJI, F.; SHIZONG, L.; DEXUN, S., "Research of Positron Annihilation and Hydration of Doped ß-C_2S", Cem. Concr. Res. 1987, 17 (4), 532-8

106) KUZNETSOVA, T.V.; OSOKIN, A.P.; AKIMOV, V.G.; KUDRYAVTSEV, A.B.; PANYUSHKIN, V.N.; SELEZNEVA, O.Yu., "Reactivity of Calcium Silicates" Zh. Prikl. Khim. 1986, 59 (4), 945-8

107) FENG, X.; WANG, L.; LONG, S.; SUN, W., "Relation Between Size of Doped ß-C_2S Cristals and Activity of Hydration", Guisuanyan Xuebao 1988, 16 (6), 552-6

108) TAMAS, F.D.; KUZNETSOVA, T.V.; CHEKUNOVA, E.V.; NIKONOVA, N.S., "Polycondensation of Silicon-oxygen Anions in the Hardening of Pastes from Alite and ß-belite", Tsement 1988, (3), 18-9

109) TSUYUKI, N.; OTAKE, H.; TSUGIO, M.; KASAI, J., "Physical Properties and Hydration of Tricalcium Aluminate ($3CaO.Al_2O_3$) Quenched After Fusion" Yogyo Kyokaishi 1986, 94 (7), 636-43

110) WACHTLER, H.-J.; USCHOLD, T.; GATZ, E.; SPANN, F., "Uber den Einfluss brennstoffbedingter Akzessorien auf die Hydratation des Trikalziumaluminats", Silikattechnik 1986, (4), 127-31

111) GHORAB, H.Y; ABOU EL FETOUH, S.H.; AHMED, H.M., "New Aspect for the Hydration Reaction of Tricalcium Aluminate in Presence of Alite", Zem. Kalk Gips 1988, (12), 624-7

112) GHORAB. H.Y.; ABOU EL FETOUH, S.H., "Effect of Gypsum Additions on the Hydration of Tricalcium Aluminate at 30°C", Egypt. J. Chem. 1986, 29 (3), 265-73

113) KLYUSOV, A.A., "Effect of Chlorides on the Hydration Rate and Thermophysical Properties of Stone from Calcium Aluminate (3CaO.Al2O3) and Calcium aluminoferrate (4CaO.Al2O3.Fe2O3)", Izv. Akad. Nauk SSSR, Neorg. Mater. 1986, 22 (12), 2043-6

114) SYCHEV, M.M.; LUKINA, L.G.; STEPANOVA, I.N.; SVATOVSKAYA, L.V., "Effect of Additives on Simultaneous Hydration of Tricalcium Aluminate and Gypsum", Zh. Prikl. Khim. 1989, 62 (1), 75-9

115) YILMAZ, V.T.; GLASSER, F.P., "Early Hydration of Tricalcium Aluminate-Gypsum Mixtures in the Presence of Sulphonated Melamine Formaldehyde Superplasticizer", Cem. Concr. Res. 1991, 21 (5), 765-76

116) PAURI M.; COLLEPARDI, M., "The Effect of Ethanolamines on the C3A Hydration in the Presence of Gypsum", Il Cemento 1987, (2), 131-40

117) RAMACHANDRAN, V.S.; ZHANG CHUN-MEI, "Hydration Kinetics and Microstructural Development in the $3CaO.Al_2O_3$-$CaSO_4.2H_2O$-$CaCO_3$-H_2O System", Mat. Constr. 1986, 19 (114), 437-44

118) POELLMANN, H., "Solid Solution in the System $3CaO.Al_2O_3.CaSO_4.aq$-$3CaO.Al_2O_3.ca(OH)_2.aq$-H_2O at 25°C, 45°C, 60°C, 80°C", Neues Jahrb. Mineral., Abh. 1989, 161 (1), 27-40

119) KUZEL, H.-J.; POELLMANN, H., "Hydration of C3A in the Presence of $Ca(OH)_2$, $CaSO_4.2H_2O$ and $CaCO_3$", Cem. Concr. Res. 1991, 21 (5), 885-95

120) KUZEL, H.-J.; MEYER, H.W., "Effect of CO2 on the Hydration of Pastes", 1st Int. Workshop on Hydration and Setting (Dijon, July 1991), pp. 7

121) MASCOLO, G.; MARROCCOLI, M., "A Study of the Reactivity of C4A.nH2O with Aqueous Solutions", Cem. Concr. Res. 1986, 16 (5), 679-84

122) HWANG, C.L.; SHEN, D.H., "A Study of the Hydration Mechanism of Portland Cement", Proc. Natl. Sci. Counc. Repub. China, Part A: Phys. Sci. Eng. 1988, 12 (4), 275-83

123) KIM, H.C.; YOON, S.S., "Ultrasonic Measurements during Early-Stage Hydration of Ordinary Portland Cement", J. Mat. Sci. 1988, 23, 611-6

124) GOTO', S.; DAIMON, M., "An Apparatus for Measurement of Chemical Shrinkage", CAJ Proc. of Cem. & Concr. No. 43 (Tokyo, 1989), 30-5

125) McCARTER, W.J.; AFSHAR, A.B., "Monitoring the Early Hydration Mechanisms of Hydraulic Cement", J. Mat. Sci. 1988, 23, 488-96

126) McCARTER, W.J., "Gel Formation during Early Hydration", Cem. Concr. Res. 1987, 17 (1), 55-64

127) ISHIZAKI, M.; ASAGA, K.; DAIMON, M.; TAKAHASHI, S., "Measurement of the Reaction Ratio of each Compound in the Hydration of Portland Cement", Semento Gijutsu Nenpo 1988, (42), 40-3

128) KRAPLYA, A.F.; KNYAZEVA, T.M. "Increase of the Activity of Portland Cement and Low-Basicity Clinkers", Tsement 1988, (5), 21-2

129) VON LAMPE, F.; ALTRICHTER, B.; MUELLER, A., "Correlation of Auxiliary Components in Belite with Cooling Rate, Crystallographic Modification, and Hydraulic Properties", Silikattechnik 1986, (7), 238-43

130) ISHIZAKI, M.; ASAGA, K.; DAIMON, M.; TAKAHASHI, S., "Measurement of Reaction Ratio of Each Compound in the Hydration Process of Portland Cement", CAJ Review No. 42 (Tokyo, 1988), 38-41

131) IKABATA, T.; HONDA, M.; YOSHIDA, H., "Effect of Solid Solution of Minor Components in Alite and Belite on Hydration Properties of Cement", Semento Gijutsu Nenpo 1988, (42), 24-7

132) HANZE, D.; LAHAJNAR, G.; DIMIC, D.; HANZEL, D.; LASIC, D., "A Study of Two Yugoslav Cements by Moessbauer Spectroscopy of Iron-57", Vestn. Slov. Kem. Drus. 1986, 33, 147-50

133) KRAMAR, L.Ya.; TROFIMOV, B.Ya.; TALISMAN, L.S.; IVANOV, F.M.; KOLBASOV, V.M., "Effect of Microsilica Addition on Alite Hydration and the Sulfate Resistance of Cement Stone", Tsement 1989, (6), 14-7

134) DANKOVA, M.; HOFFMANN, O.; CERNY, K.,"Effect of the Particle Size Distribution of Cement on the Properties of Cement Pastes", Silikaty 1987, 31 (1), 33-42

135) KONISHI, K.; ASAGA, K.; TSURUMI, T.; DAIMON, M., "Effect of Heating Rate on the Hydration of Each Compound of Portland Cement at 80°C", CAJ Proc. of Cem. & Concr. No. 44 (Tokyo, 1990), 68-73

136) SOROKA, I.; ABAYNEH, M., "Effect of Gypsum on Properties and Internal Structure of PC Paste", Cem. Concr. Res. 1986, 16 (4), 495-504

137) GUSTAW, K.; ROSZCZYNIALSKI, W.; LIBURA, J., "Determination of the Proper Amount of Gypsum Addition to Cements with Different C_3A (Tricalcium Aluminate) Contents on the Basis of Hydration Studies", Cem.-Wapno-Gips 1986, (6), 139-40

138) GRZESZCZYK, S., "The Influence of the Early Stage of Hydration of Cement Pastes on their Consistency and Strength",

139) TANG, F.J.; GARTNER, E.M., "Influence of Sulphate Source on Portland Cement Hydration", Adv. Cem. Res. 1988, 1 (2), 67-74

140) OLMEZ, H.; ERDEM, E., "The effects of Phosphogypsum on the Setting and Mechanical Properties of Portland Cement and Trass Cement", Cem. Concr. Res. 1989, 19 (3), 377-84

141) BLAHA, J.; HANUSOVA, H.; JEDLICKA, J., "Control of Cement Setting by using Synthetic Gypsum", Stavivo 1988, 66 (2), 51-4

142) SOROKA, I.; ABAYNEH, M., "Effect of Gypsum on Properties and Internal Structure of PC Paste", Cem. Concr. Res. 1986, 16 (4), 495-504

143) HIROTSUGU, Y.; TOMOYA, Y.; KIYOMI, N.; TAKEO, I.; AKIHIRO, S., "Effect of Magnetic Treatment of Water on Compressive Strength of Cement Mortar", Semento Konkuriito 1986, (468), 36-40

144) ARENKO, L.N.; REZNICHENKO, I.P., "Magnetic Water Treatment in Concrete Manufacture", Stroit. Mater. Konstr. 1987, (4), 34-5

145) MATVIENKO, V.A.; SYCHEV, M.M., "Activation of the Hardening of Cement Paste by Polarization", Tsement 1987, (8), 7-8

146) PATEL, R.G.; KILLOH, D.C.; PARROTT, L.J.; GUTTERIDGE, W.A., "Influence of Curing at different Relative Humidities upon Compound Reactions and Porosity in Portland Cement Paste", Mat. Constr. 1988, (21), 192-7

147) GUTTERIDGE, W.A.; DALZIEL, J.A., "Filler Cement: the Effect of the Secondary Component on the Hydration of Portland Cement - Part 1: A Fine non-Hydraulic Filler", Cem. Concr. Res. 1990, 20 (5), 778-82

148) GUTTERIDGE, W.A.; DALZIEL, J.A., "Filler Cement: the Effect of the Secondary Component on the Hydration of Portland Cement - Part 2: Fine Hydraulic Binders", Cem. Concr. Res. 1990, 20 (6), 853-61

149) PARRY-JONES, G.; AL-TAYYIB, A.J.; AL-DULAIJAN, S.U.; AL-MANA, A.I., "^{29}Si MAS-NMR Hydration and Compressive Strength Study in Cement Paste", Cem. Concr. Res. 1989, 19 (2), 228-34

150) ODLER, I.; ABDUL-MAULA, S.; ZHONGYA, L., "Effect of Hydration Temperature on Cement Paste Structure", Symp. on Microstructural Development During Hydration of Cement (Boston, Dec. 2-4, 1986), MRS Symp. vol. 85, Mat. Res. Soc., Pittsburgh, 139-44

151) HUTCHISON, R.G.; CHANG, J.T.; JENNINGS, H.M.; BRODWIN, M.E., "Thermal Acceleration of Portland Cement Mortars with Microwave Energy", Cem. Concr. Res. 1991, 21 (5), 795-9

152) WAY, S.J.; SHAYAN, A., "Early Hydration of a Portland Cement in Water and Sodium Hydroxide Solutions: Composition of Solutions and Nature of Solid Phases", Cem. Concr. Res. 1989, 19 (5), 759-69

153) LUGININA, I.G.; PUTRENKO, M.A., "Hydration of Cement with Sodium Silicate and Phosphate Additives", Tsement 1987, (1), 16-7

154) GHORAB, H.Y.; HILAL, M.S.; KISHAR, E.A., "Effect of Mixing and Curing Waters on the Behaviour of Cement Pastes and Concrete - Part I: Microstructure of Cement Pastes" Cem. Concr. Res. 1989, 19 (6), 868-78

155) GHORAB, H.Y.; HILAL, M.S.; KISHAR, E.A., "Effect of Mixing and Curing Waters on the Behaviour of Cement Pastes and Concrete: I", Cem. Concr. Res. 1989, 19 (6), 868-78

156) GHORAB, H.Y.; HILAL, M.S.; ANTAR, A., "Effect of Mixing and Curing Waters on the Behaviour of Cement Pastes and Concrete - Part 2: Properties of Cement Paste and Concrete", Cem. Concr. Res. 1990, 20 (1), 69-72

157) ODLER, I.; ABDUL-MAULA, S., "Effect of Chemical Admixtures on Portland Cement Hydration", Cem. Conc. Aggr. 1987, 9, 38-43

158) MARKOSOV, Yu.A., "Current Aspect of the Mechanism of the Effect of Electrolytes on Hydration of Cement", Zh. Prikl. Khim. (Leningrad) 1987, 60 (1), 201-4

159) BERDOV, G.I.; MADZAEVA, O.S.; BURUCHENKO, A.E.; LINNIK, S.I., "Interactions of Clinker Minerals with Aqueous Chloride Solutions", Izv. VUZOV, Stroit. Arkhit. 1987, (10), 59-63

160) DOROSHENKO, Yu.M.; MARKOSOV, Yu.A., "Relation between Cement Hydration Rate and Some Crystal Chemical Parameters of Electrolyte Additives", Zh. Prikl. Khim. (Leningrad) 1987, 60 (4), 955-7

161) ABDELRAZIG, B.E.I.; BONNER, D.G.; NOWELL, D.V., "Estimation of the Degree of Hydration in Modified Ordinary Portland Cement Pastes by Differential Scanning Calorimetry", Thermochimica Acta 1989, 145, 203-17

162) CORBO, J.; FARAZAM, H. "Influence of Three Commonly used Inorganic Compounds on Pore Solution Chemistry and their Possible Implications to the Corrosion of Steel in Concrete", ACI Mat. J. 1989, 498-502

163) SLANICKA, S.; JANOTKA, I.; FRTALOVA, D.; STEVULA, L., "The Effect of $Ca(HCOO)_2$ and $NaNO_3$ on the Hydration of Portland Cement at -10°C", Silikaty 1988, 32, 331-42

164) SINGH, N.B.; SINGH, S.P.; SARVEHI, R., "Effect of Phenols on the Hydration of Portland Cement", Adv. Cem. Res. 1989, 2 (6), 43-8

165) SINGH, N.B.; SINGH, A.K.; "Effect of Melment on the Hydration of White Portland Cement", Cem. Concr. Res. 1989, 19 (4), 547-53

166) NAWA, T.; EGUCHI, H., "Effect of Alkali Sulfate on Rheological Behaviour of Cement Paste", CAJ Review No. 42 (Tokyo, 1988), 50-3

167) UCHIDA, S.; OKAMURA, T.; TAKEHIRO, M.; UCHIKAWA, H., "Influence of Characters of Cement on Fluidity of Fresh Cement Paste and Mortar with Organic Additives", CAJ Proc. of Cem. & Concr. No. 44 (Tokyo, 1990), 86-91

168) VIDICK, B.; FLETCHER, P.; MICHAUX, M., "Evolution at Early Hydration Times of the Chemical Composition of Liquid Phase of Oil-Well Cement Pastes with and without Additives - Part II", Cem. Concr. Res. 1989, 19 (4), 567-78

169) SINGH, N.B.; SINGH, A.K.; SINGH, S.P., "Effect of Citric Acid on the Hydration of Portland Cement", Cem. Concr. Res. 1986, 16 (6), 911-20

170) SINGH, N.B.; SINGH, S.P.; SINGH, A.K., "Effect of Lactic Acid on the Hydration of Portland Cement", Cem. Concr. Res. 1986, 16 (4), 545-53

171) PAULINI, P., "Reaction Mechanisms of Concrete Admixtures", Cem. Concr. Res. 1990, 20 (6), 910-8

172) BANFILL, P.F.G.; SAUNDERS, D.C., "The Relationship between the Sorption of Organic Compounds on Cement and the Retardation of Hydration", Cem. Concr. Res. 1986, 16 (3), 399-410

173) BANFILL, P.F.G., "Precipitation of Calcium Hydroxide in the Presence of Organic Compounds", J. Mat. Sci. Lett. 1986, 5 (1), 33-4

174) LOTA, J.S.; SCRIVENER, K.L.; PRATT, P.L., "Effects of Accelerator Additives upon Microstructural Developments in Class G Oilwell Cement Hydration at Low and Ordinary Temperatures", Proc. of 12th Int. Conf. on Cement Microscopy (Vancouver, April 2-6, 1990), 201-17

175) PEIMING, W.; ODLER, I., "Progress of Hydration as Determined by SEM on Polished Clinker Surfaces", Proc. of the 12th Int. Conf. on Cement Microscopy (Vancouver, April 2-6, 1990), 382-402

176) TAKEMOTO, K.; UCHIKAWA, H., "Hydration of Pozzolanic Cement", 7th Int. Congress on the Chemistry of Cement (Paris, 1980), vol. I, IV-2/1-2/29

177) NIKONOVA, S.N.; MASHIR, T.N.; SMIRNOVA, M.N.; ZHELTOVA, G.V., "Structure of Silicate Anions of Calcium Silicate Hydrates", Inst.-Mosk. Khim.-Tekhnol. Inst. im. D.I. Mendeleeva 1986, 412, 80-91

178) INOZEMTSEV, Yu.P.; NIKOL'SKAYA, S.I., "Effect of Hardening on Polycondensation Characteristics of Calcium Silicate Hydrates in Hydration of Portland Cement Clinker", Zh. Prikl. Khim. 1988, 61 (10), 2235-7

179) HASSAAN, M.Y.; ABDEL-HAKEEM, N., "Study of Anhydrous and Hydrated Portland Cement containing Alkali Ions by Infrared Spectroscopy", J. Mat. Sci. Lett. 1989, 8, 578-80

180) DUNSTER, A.M.; PARSONAGE, J.R.; VIDGEON, E.A., "Silicate Anion Analysis in Portland Cement Pastes", Mat. Sci.& Technol. 1989, 5, 708-13

181) RAYMENT, D.L., "The Electron Microprobe Analysis of the C-S-H phases in a 136 Year Old Cement Paste", Cem. Concr. Res. 1986, 16 (3), 341-4

182) TAYLOR, H.F.W. "Bound Water in Cement Pastes and its Significance for Pore Solution Compositions", Symp. on Microstructural Development During Hydration of Cement (Boston, Dec. 2-4, 1986), MRS Symp. vol. 85, 47-54

183) KJELLSEN, K.O.; DETWILER, R.J.; GJORV, O.E., "Backscattered Electron Imaging of Cement Pastes Hydrated at Different Temperatures", Cem. Concr. Res. 1990, 20 (2), 308-11

184) POELLMANN, H.; KUZEL, H.-J.; WENDA, R., "Solid Solution of Ettringites: I - Incorporation of OH^- and CO_{32} in $3CaO.Al_2O3.3CaSO_4.32H_2O$", Cem. Concr. Res. 1990, 20 (6), 941-7

185) MONTEIRO, P.J.M.; MEHTA, P.K., "Interaction between Carbonate Rock and Cement Paste", Cem. Concr. Res. 1986, 16 (2), 127-34

186) YUAN C.Z.; GUO W.J., "Bond between Marble and Cement Paste", Cem. Concr. Res. 1987, 17 (4), 544-52

187) NONAT, A.; MUTIN, J.C., "From Hydration to Setting", 1st Int. Workshop on Hydration and Setting (Dijon, July 1991), pp. 11

188) MICHAUX, M.; FLETCHER, P.; VIDICK, B., "Evolution at Early Hydration Times of the Chemical Composition of Liquid Phase of Oil-Well Cement Pastes with and without Additives - Part I", Cem. Concr. Res. 1989, 19 (3), 443-56

189) ANDERSSON, K.; ALLARD, B.; BENGTSSON, M.; MAGNUSSON, B., "Chemical Composition of Cement Pore Solutions", Cem. Concr. Res. 1989, 19 (3), 327-32

190) CHERNYKH, V.F.; OGURTSOVA, O.S.; KUPRIYANOV, I.V. "A pH-metric Study of Hydration of Portland Cement", Izv. VUZOV, Stroit. Arkhit. 1987, (11), 66-9

191) MORAGUES, A.; MACIAS, A.; ANDRADE, C., "Equilibria of the Chemical Composition of the Concrete Pore Solution. Part I: Comparative Study of Synthetic and Extracted Solutions", Cem. Concr. Res. 1987, 17 (2), 173-82

192) LARBI, J.A.; BIJEN, J.M.J.M., "Interaction of Polymers with Portland Cement during Hydration: a Study of the Chemistry of the Pore Solution of Polymer-Modified Cement Systems", Cem. Concr. Res. 1990, 20 (1), 139-47

193) UCHIKAWA, H.; UCHIDA, S.; HANEHARA, S., "Flocculation Structure of Fresh Cement Paste Determined by Sample Freezing-Back Scattered Electron Image Method", Il Cemento 1987, (1), 3-22

194) UCHIKAWA, H.; UCHIDA, S.; HANEHARA, S., "Element Distribution on the Polished Surface of Hardened Cement Pastes Estimated by EPMA with Ultra High Speed Wide Area Multianalyser", Il Cemento 1987, (2), 117-30

195) RODGER, S.A.; GROVES, G.W., "Electron Microscopy Study of Ordinary Portland Cement-Pulverized Fuel Ash Blended Pastes", J. Am. Ceram. Soc. 1989, 72 (6), 1037-9

196) BENTUR, A.; COHEN, M.D., "Effect of Condensed Silica Fume on the Microstructure of the Interfacial Zone in Portland Cement Mortars", J. Am. Ceram. Soc. 1987, 70 (10), 738-43

197) ZHANG, X.; GROVES, G.W.; RODGER, S.A., "The Microstructure of Cement Aggregate Interfaces", Symp. on Bonding in Cementitious Composites (Boston, Dec. 2-4, 1987), MRS Symp. vol. 114, Mat. Res. Soc., Pittsburgh, 89-95

198) WANG, J.; ZHIYAN, C., "Microstructure and Strengthening of the Interface between Marble and Hardened Cement Pastes", Guisuanyan Xuebao 1986, 14 (3), 275-84

199) JIA, W., "Mechanism of Orientation of $Ca(OH)_2$ Crystals in Interface Layer between Paste and Aggregate in Systems containing Silica Fume", Symp. on Bonding in Cementitious Composites (Boston, Dec. 2-4, 1987), MRS Symp. vol. 114, Mat. Res. Soc., Pittsburgh, 127-32

200) ZURZ, A.; ODLER, I. "XRD Studies of Portlandite Present in Hydrated Portland Cement Paste", Adv. Cem. Res. 1987, 1 (1), 27-30

201) SCRIVENER, K.L.; GARTNER, E.M., "Microstructural Gradients in Cement Paste around Aggregate Particles", Symp. on Bonding in Cementitious Composites (Boston, Dec. 2-4, 1987), MRS Symp. vol. 114, Mat. Res. Soc., Pittsburgh, 77-85

202) SARKAR. S.L.; AITCIN, P.-C., "Comparative Study of the Microstructures of Normal and Very High-Strength Concretes", Cem., Concr. Aggr., 1987, 9, 57-64

203) PIGEON, M.; PLANTE, P., "Study of Cement Paste Microstructure Around Air Voids: Influence and Distribution of Soluble Alkalies", Cem. Concr. Res. 1990, 20 (5), 803-14

204) SOROKA, I.; BAUM, H., "Cement Pastes with High Water/Cement Ratio"emento", Il Cemento 1986, (1), 3-12

205) HWANG, C.L.; LIN, R.Y., "Effect of Gypsum on the Microstructure of Cement Pastes", Ts'ai Liao K'o Hsueh 1986, 18A (2), 60-9

206) KJELLSEN, K.O.; DETWILER, R.J.; GJORV, O.E., "Pore Structure of Plain Cement Pastes Hydrated at Different Temperatures", Cem. Concr. Res. 1990, 20 (6), 927-33

207) KAZUSUKE, K.; MORIE, O.; KENJI, N.; YUUICHI, U., "Effect of Alkalis on Micropore Structure of Concrete", Seisan Kenkyu 1988, 40 (7), 344-5

208) WINSLOW, D.; LIU, D., "The Pore Structure of Paste in Concrete", Cem. Concr. Res. 1990, 20 (2), 227-35

209) DOUGLAS, E.; BRANDSTETR, J., "A Preliminary Study on the Alkali Activation of Ground Granulated Blast-Furnace Slag", Cem. Concr. Res. 1990, 20 (5), 746-56

210) AIMOTO, T.; SHIZAWA, M.; IDE, W., "Influence of Various Elements on the Structure and Hydraulic Activity of Blast-Furnace Slag", CAJ Review No. 42 (Tokyo, 1988), 66-7

211) KATO, K.; MATUZAKI, S.; SAWAKI, S.; FUKAYA, Y., "Effects of Calcium Hydroxide and Gypsum on Hydration Reaction of Blast Furnace Slag Under Adiabatic Condition", CAJ Proc. of Cem. & Concr. No. 44 (Tokyo, 1990), 92-7

212) DOUGLAS, E.; ZERBINO, R., "Characterization of Granulated and Pelletized Blast Furnace Slag", Cem. Concr. Res. 1986, 16 (5), 662-70

213) HINRICHS, W.; ODLER, I., "Investigation of the Hydration of Portland Blastfurnace Slag Cement: Hydration Kinetics", Adv. Cem. Res. 1989, 2 (5), 9-13

214) LUKE, K.; GLASSER, E.P., "Internal Chemical Evolution of the Constitution of Blended Cements", Cem. Concr. Res. 1988, 18 (4), 495-502

215) ODLER, I.; HINRICHS, W., "Investigation of the Hydration of Portland Blastfurnace Slag Cement: Composition, Structure and Properties of the Hydrated Material", Adv. Cem. Res. 1989, 2 (5), 15-20

216) KATO, K.; SAWAKI, S.; FUKAYA, Y., "Effect of Gypsum on Adiabatic Temperature Rise of Slag Cement", CAJ Proc. of Cem. & Concr. No. 43 (Tokyo, 1989), 72-7

217) WU, X.; JIANG, W.; ROY, D.M., "Early Activation and Properties of Slag Cement", Cem. Concr. Res. 1990, 20 (6), 961-74

218) LUKE, K.; GLASSER, F.P., "Time and temperature dependent changes in the internal constitution of blended cements", Il Cemento 1988, (3), 179-92

219) RASHEEDUZZAFAR & EHTESHAM HUSSAIN, S., "Effect of Microsilica and Blast Furnace Slag on Pore Solution Composition and Alkali-Silica Reaction", Cem. Concr. Comp., 1991, 13, 219-25

220) BARLOW, D.F.; JACKSON, P.J., "The Release of Alkalis from Pulverized-fuel Ashes and Ground Granulated Blastfurnace Slags in the Presence of Portland Cements", Cem. Concr. Res. 1988, 18 (2), 235-48

221) MARSH, B.K.; DAY, R.L., "Pozzolanic and Cementitious Reactions of Fly Ash in Blended Cement Pastes", Cem. Concr. Res. 1988, 18 (2), 301-10

222) ZHANG, M.-H.; GJORV, O.E., "Effect of Silica Fume on Cement Hydration in Low Porosity Cement Pastes", Cem. Concr. Res. 1991, 21 (5), 800-8

223) DUQUE FERNANDEZ, G.L.; LLOPIZ, J.C.; RUBIO FRIAS, E., "Hidration of Tricalcium Silicate in Blended Cements Manufactured with Cuban Tuffs", Materiales de Construccion 1989, 39 (213), 5-10

224) COOK, D.J.; CAO, H.T., "An Investigation of the Pore Structure in Fly Ash/OPC Blends", Proc. of the 1st Int. RILEM Congress on Pore Structure and Materials Properties, vol. 1, Chapman and Hall, 69-76

225) TOKYAY, M., "Effects of Three Turkish Fly Ashes on the Heat of Hydration of PC-FA Pastes", Cem. Concr. Res. 1988, 18 (6), 957-60

226) GALAL, A.F.; HEKAL, E.E.; NOAIMI, K.KH.AL.; ABO-EL-ENEIN, S.A., "Hydraulic Reactivity and Microstructure of Artificial Pozzolana-lime Pastes", Proc. of 11th Int. Conf. on Cement Microscopy (New Orleans, April 1989)

227) DUREKOVIC, A., "Activity of Alite and Tricalcium Aluminate during Hydration in Cement Pastes with the Addition of Silica Fume", Cement 1988, 27 (1), 3-6

228) LARBI, J.A.; FRAAY, A.L.A.; BIJEN, J.M.J.M., "The Chemistry of the Pore Fluid of Silica Fume-Blended Cement Systems", Cem. Concr. Res. 1990, 20 (4), 506-16

229) TKALCEC, E.; ZELIC, J., "Influence of Amorphous Silica (Silica Dust) on the Properties of Portland Cement Mortars", Zem. Kalk Gips 1987, 11, 574-9

230) MASSAZZA, F., "Microstruture of Puzzolanic Cements", 1st Int. Workshop on Hydration and Setting (Dijon, July 1991)

231) KAIZAKI, K.; MINO, I.; SAKAI, E., "Microstructure and Phase Composition of Hardened Ultrahigh-Strength Cement", Semento Gijutsu Nenpo 1987, (41), 54-7

232) SINCLAIR, W.; GROVES, G.W., "The Microstructure of Portland Cement-Silica Fume Pastes", J. Mat. Sci. Lett. 1986, 5 (1), 101-2

233) DUREKOVIC, A.; POPOVIC, K., "The Influence of Silica Fume on the Mono/di Silicate anion Ratio during the Hydration of CSF-containing Ccement Paste", Cem. Concr. Res. 1987, 17 (1), 108-14

234) DUREKOVIC, A., "Silicate Anions Polymerization in the Pastes of OPC and of OPC-Silica Fume Blends during Hydration and after Action of Leaching Attack - Part I: Study by Use of Direct TMS Method", Cem. Concr. Res. 1988, 18 (2), 185-92

235) FRAAY, A.L.A.; BIJEN, J.M.; DE HAAN, Y.M., "The Reaction of Fly Ash in Concrete. A Critical Examination", Cem. Concr. Res. 1989, 19 (2), 235-246

236) GLASSER, F.P.; LUKE, K.; ANGUS, M.J., "Modification of Cement Pore Fluid Compositions by Pozzolanic Additives", Cem. Concr. Res. 1988, 18 (2), 165-78

237) POELLMANN, H., "Sem-, X-Ray and Thermoanalytical Studies on Hydration Products of Tricalciumaluminate in the Presence Sulphate-, Carbonate-, and Hydroxide Anions" Proc. of the 9th Int. Conf. on Cement Microscopy (Reno, April 5-9, 1987) 1987, 426-45

238) BENTUR, A.; GOLDMAN, A.; COHEN, M.D., "The Contribution of the Transition Zone to the Strength of High Quality Silica Fume Concretes", Symp. on Bonding in Cementitious Composites (Boston, dec. 2-4, 1987), MRS Symp. vol. 114, Mat. Res. Soc., Pittsburgh, 97-103

239) COSTA, U.; MASSAZZA, F., "Remarks on the Determination of the Pore Distribution of Portland and Pozzolanic Cement Pastes", 1st Int. Rilem Congress "Pore "From Materials Science to Construction Materials Engineering" (Versailles, Sept. 1987), vol. 1, 159-66

Specific Theme III A

Advances in Hydration of Cements at Low, Ambient and Elevated Temperatures

ADVANCES IN HYDRATION AT LOW, AMBIENT AND ELEVATED TEMPERATURES

K L Scrivener
Department of Materials, Imperial College of Science, Technology and Medicine, UK

and

W Wieker
Zentrum Für Anorganische Polymere, GERMANY

SUMMARY - Advances in the hydration of Portland cement are reviewed. The thermodynamics and mechanisms of hydration of the silicate and interstitial phases at ambient temperatures are considered, including discussion of the way in which the hydration of these phases is modified in Portland cement. The effects of temperature on the hydration of cement in the range 5 to 100°C and the reactions which occur in heat treated pastes, mortars and concretes on subsequent curing at room tempertaure are reviewed.

ZUSAMMENFASSUNG - Die Fortschritte bei der Hydratation von Portlandzement werden rezensiert. Es werden die Thermodynamik und die Mechanismen der Hydratation von Silikat-, Aluminat- und Ferritphasen bei Umgebungstemperatur betrachtet. Ebenso wird der Weg, wie diese Phasen in Portlandzement modifiziert werden, diskutiert. Der Einfluß der Temperatur auf die Hydratation von Zement im Bereich von 5 bis 100°C und die Reaktionen, die in hitzebehandelten Pasten, Mörtel und Beton während der Nachbehandlung bei Raumtemperatur vorkommen, werden rezensiert.

1. INTRODUCTION

The purpose of this paper is to review work relating to the hydration of cementitious compounds, primarily since the 8th International Congress in Rio de Janeiro in 1986. At that Congress Taylor gave an excellent summary of investigations into the chemistry of cement hydration up to that time [1]. Since the Rio conference Taylor has produced a more comprehensive review with the publication of "Cement Chemistry" [2]. Other collected works published in the last six years relevant to hydration include the proceedings of a Materials Research Society Symposium, "Microstructural Development During the Hydration of Cement" [3], and the first two volumes of "The Materials Science of Concrete" [4].

The subject matter encompassed by this paper includes consideration of the effect of temperature on hydration. Very little cement paste in 'real' concrete will have reacted isothermally at 20-25°C. However, there has been comparatively little recent work on hydration outside this 'ambient' range and this area was not specifically reviewed at the Rio conference. It has thus been necessary to include discussion of earlier papers in this section.

The rationale for the structure of the paper has been to present, as far as possible, a cohesive picture of recent advances in the state of knowledge on hydration rather than to give an exhaustive account of all the work which has been published on the subject. The clinker minerals are considered in two groups: the silicates, C_3S and C_2S; and the interstitial phases, aluminate and ferrite. For each group the reaction of the individual phases with water are considered first. However, in cement paste the phases are intimately mixed within polymoneralic grains as shown in Figure 1.. So the way in which the reaction of each group of phases is modified in cement is discussed. The effect of temperature is considered in the context of cement as a whole although some of the work referred to has involved study of individual phases.



Figure 1.
Distribution of clinker phases within poly-mineralic grains in Portland cement.
(bse image in the SEM)

Space, time or inclusion in other principal reports have meant that it has not been possible to cover a number of related topics in this paper, these include: the effect of chemical admixtures and mineral additives on hydration; pore structures resulting from hydration; the structure of the hydration products notably C-S-H; and the hydration of calcium aluminate and other non Portland cements.

2. SILICATE PHASES

The silicate phases, C_3S and C_2S, together constitute some 70-90% of Portland cement. The major product from the hydration of these phases, C-S-H, is principally responsible for the development of mechanical strength and for the durability of concrete. It is therefore not surprising that the reactions of these phases, and in particular C_3S, have received more attention than those of the interstitial phases. Over the years many mechanisms have been proposed to explain the hydration of C_3S. These have recently been comprehensively reviewed by Taylor [2] and by Gartner and Gadis [5].

2.1. Thermodynamic Aspects of the $CaO-SiO_2-H_2O$ System

In the last few years there has been an increasing awareness of the relevance of phase equilibrium studies to the interpretation of the reaction mechanisms of C_3S (and indeed cement as a whole) [e.g. 6,7,8,9,10]. Figure 2. shows a simplified schematic version of the $CaO-SiO_2-H_2O$ phase diagram (derived from 6,7,11). This Figure is not drawn to scale as in reality the solubility curves for amorphous silica, C-S-H, and calcium hydroxide lie very close to the H_2O corner of the phase diagram. Jennings has demonstrated [12] that experimental results for the concentrations of SiO_2 and CaO measured in solution lie on two distinct curves. The solubility of C-S-H formed from soluble salts appears to lie at lower concentrations indicating that this C-S-H (denoted C-S-H(s)) has a lower free energy and is therefore more stable. Solutions from hydrating C_3S or in contact with C-S-H formed by precipitation from solutions of $Ca(OH)_2$ and silicic acid contain higher concentrations of lime and silica indicating the existence of a metastable C-S-H, denoted C-S-H(m).

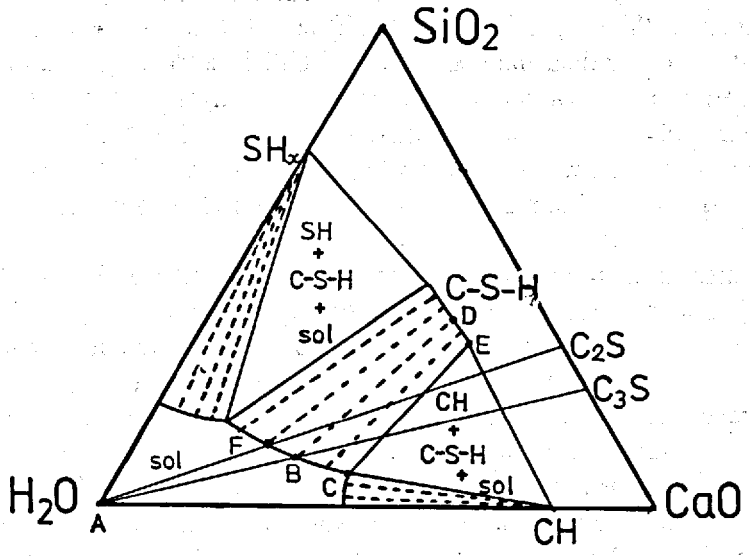

Figure 2 - Schematic phase diagram for the $CaO-SiO_2-H_2O$ system. NOT TO SCALE

Despite these complications the quasi equilibrium hydration sequence of C_3S can be described in terms of the phase diagram as follows:

a) C_3S dissolves congruently with the composition of the solution following line **AB**.
b) At point **B**, when the composition of the solution reaches the phase boundary between solution alone and solution plus C-S-H, the solution is saturated with respect to C-S-H, C_3S will continue to dissolve until the solution is sufficiently supersaturated for C-S-H to nucleate;
c) Once C-S-H has nucleated the concentration of the solution will fall back to the C-S-H solubility curve. C_3S continues to dissolve and form further C-S-H so that the composition of liquid follows line **BC** and composition of solid follows line **DE** (i.e. the C/S ratio of the solid should increase);
d) When the composition of the liquid reaches point **C** it is saturated with respect to calcium hydroxide as well as C-S-H, but again a level of supersaturation is necessary for the formation of stable nuclei. Once calcium hydroxide has nucleated the composition of the liquid should return to point **C**.
e) Calcium hydroxide and C-S-H (of the composition at point **E**) continue to form as further C_3S dissolves.

Broadly speaking this hydration sequence appears to be in agreement with experimental observations. However, the mechanisms which control the kinetics of hydration are less clearly established.

2.2. Kinetics and Mechanisms of C_3S Hydration

The hydration of C_3S is usually considered in five stages, based on the rate of heat evolution or the degree of reaction of C_3S.

Stage 1 *Initial Reaction* - C_3S starts to react immediately upon contact with water with a corresponding initial peak in the rate of heat evolution.
Stage 2 *Induction Period* - The rate of reaction declines and remains low for 0-2 hours.
Stage 3 *Acceleratory Period* - The rate of reaction increases rapidly.
Stage 4 *Decelerator Period* - The rate of reaction declines.
Stage 5 *Slow Continuing Reaction* - The reaction continues steadily at a slowly decreasing rate. (sometimes combined with Stage 4).

2.2.1. Initial Reaction - During the initial reaction C_3S starts to dissolve and the concentrations of calcium oxide and silica (calcium hydroxide and silicates) in solution increase rapidly. At the water to cement ratios found in pastes (<1) this period of initial reaction is extremely short (a few seconds). Because of the very short duration of this stage, it has been difficult to establish whether the dissolution of C_3S is congruent. Barret et al [13,14] studied the dissolution of C_3S in a flowing solution. They found the dissolution to be congruent after the solvation of the first atomic layer. Damidot and Nonat [15,16] studied the early hydration of C_3S at a very wide range of w/c ratios (0.5 to 5000) and found the initial dissolution to be almost congruent. At w/c $>$ 3000 all the C_3S dissolved during this initial stage with no induction period, so an enthalpy of dissolution could be calculated as 132 $\pm$15 kJ/mol (at 25°C).

Congruent dissolution would appear to be contradicted by ESCA observation of the change in C/S ratio of the surface layers of C_3S during the early stages of hydration [17,18]. These show a drop in C/S ratio to a minimum of 2.2-2.5 during the first 5 seconds of hydration followed by an increase back to a C/S ratio close to 3. However, these results are explained by Barret et al [13,14] as a consequence of the protonation of the surface layer. This results in the dissolution of two thirds of the Ca ions in the first atomic layer of the C_3S prior to dissolution of silicates. ESCA studies of cements and synthetic compounds by Ball [19,20] indicate that the outer layers of C_3S and C_2S are already depleted of calcium in the unhydrated state. If this is the case an initial rise in the C/S ratio of the surface would be observed, which would correspond to dissolution of these disrupted surface layers to expose the bulk material with the stoichiometric ratio of C/S. New work by Trettin et al [21,22,23] has determined the C/S ratio by ESCA and the specific surface area by Krypton adsorption during the early hydration of C_3S. The ESCA measurements are in good agreement with earlier determinations and it is found that the initial drop in C/S ratio corresponds to an increase in surface area from about 0.7 to 1.6 m^2/g. The subsequent rise in C/S ratio corresponds to a fall in the specific surface area back to about 1.1 m^2/g. They interpret these results as indicating the early formation of a product with a high C/S ratio ($\sim$3) which initially has a high surface which then decreases. However, the findings on specific surface area could possibly be interpreted by the dissolution model described by Barret, if the initial protonation of the surface and dissolution of calcium leads to a roughening of the surface and effective increase in surface area.

2.2.2. Induction Period - Many workers have proposed the formation of a barrier layer on the C_3S surface as the cause of the induction period. The work of Damidot and Nonat [15] showed that the initial period of congruent C_3S dissolution ends when the critical concentrations of 5.5 m*M* of CaO and 1.7 m*M* SiO_2 in solution are reached, irrespective of the w/c ratio (Figure 3.). Thereafter, the concentration of silica in solution falls while that of lime remains constant for a period before starting to rise again. This indicates the

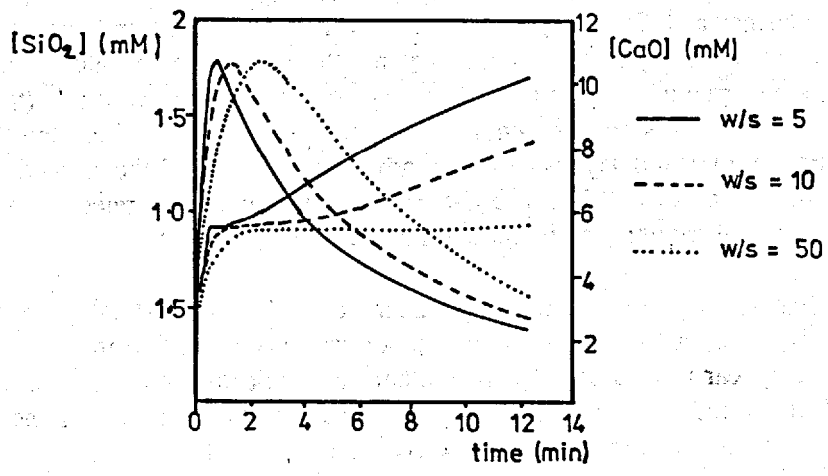

Figure 3 - Evolution of [CaO] and [SiO2] versus hydration time for C_3S hydrated at different w/s ratios. From [15]

precipitation of C-S-H with a low C/S ratio (~1.0) at a critical level of supersaturation (as previously identified by Ménétrier [24]). Once C-S-H starts to precipitate, the concentrations in solution move back towards the equilibrium solubility curve for C-S-H(m). The precipitation of C-S-H on the surface of the C_3S slows down but does not prevent the continued dissolution of C_3S. However, the equilibrium between the coating of C-S-H and the solution now controls the concentrations of lime and silica in the solution as found by Brown et al [25]. Consequently C-S-H should continue to form throughout the induction period. Experimental evidence of the continued slow formation of product throughout the induction period has been reported. Roger at al [26,27] noted the increase in monomeric silicate groups associated with early product by ^{29}Si NMR and Miljkovic et al [28] noted an increase in the amount of loosely bound water associated with hydration products by hydrogen NMR.

If the reaction is controlled by the concentration of the solution, the amount of product formed during the induction period will increase with increasing w/c ratio. Damidot and Nonat [15] confirmed that this happens and showed that for w/c ratios from 3000 down to 2000 all the C_3S is consumed during this stage of the reaction. This enabled an enthalpy of precipitation for the C-S-H formed initially to be estimated at 25 ± 10 kJ/mol (in good agreement with theoretical values). Several earlier studies also noted the effect of w/c ratio on the amount of reaction occurring in the induction period. Brown et al [24] observed that an increasing proportion of C_3S was reacted during the induction period as the w/c ratio was increased. Groves [29] reviewed the literature on the formation of C-S-H during the early stages of hydration of C_3S and noted that reports of large amounts of product all related to the use of high w/c ratios, while studies of hydration at lower w/c (typical of paste) reported much less product. His own work at w/c ratios of 0.5 and 50 confirmed this observation.

The effect of this initial precipitation of C-S-H(m) on the kinetics of hydration appears to be in restricting, but not preventing, the further dissolution of C_3S. As noted by Gartner and Gadis [5] in unretarded pastes, the duration of the induction period is very short. The action of retarders can be explained in terms of their effect on the structure of the early C-S-H. Changes in the structure may on the one hand affect the permeability of the C-S-H(m) layer on the C_3S surface or alternatively inhibit the transformation of C-S-H(m) to a more permeable form of C-S-H [5,30].

2.2.3. End of the Induction Period - The end of the induction period is marked by a rapid increase in the rate of hydration. This occurs around the time that the formation of calcium hydroxide is first noted but the two events may not be coincident. There are two possibilities for the process which leads to the increase in reaction rate seen at the end of the induction period:

a) There is a change in the structure of the C-S-H layer, possibly from C-S-H(m) to C-S-H(s), so that it ceases to restrict the dissolution of C_3S;

b) Calcium hydroxide precipitates, facilitating rapid growth of both product phases.

Gartner and Gadis [5] evaluate the available evidence and firmly conclude that the former is the case. Amongst the arguments advanced against the nucleation of calcium hydroxide being rate determining are: that the degree of supersaturation with respect to calcium hydroxide (taking account of all the activities of all species present) is not high enough for homogeneous nucleation; and that additions of calcium hydroxide to hydrating pastes delay rather than advance the end of the induction period. They also note that the transformation of C-S-H(m) to C-S-H(s) would involve the rejection of small amounts of calcium hydroxide which might trigger the precipitation of calcium hydroxide.

Studies at high w/c ratios by Damidot and Nonat [15,16] appear to support this conclusion. These clearly show that the increase in reaction rate occurs *before* the precipitation of calcium hydroxide, which would appear to be a consequence rather than the cause of the end of the induction period. They equate the end of the induction period with a change in the permeability of the C-S-H layer which occurs when the concentration of lime in solution exceeds about 22 m*M*.

Several recent discussions of hydration mechanisms [e.g. 10,31] have referred back to earlier studies of the variation in C/S ratio of C-S-H with lime concentration [23,32,33,34,35]. These show the C/S ratio is relatively constant between 1 and 20 m*M*, but then increases sharply (Figure 4.). Gartner and Jennings [10] have calculated theoretical curves for C/S ratio against lime concentration for the metastable, C-S-H(m), and stable, C-S-H(s). These intersect at a CaO concentration of 19m*M* and a C/S ratio of 1.7 (Figure 4). The similarity between the critical CaO concentration at the end of the induction period, found experimentally by Damidot and Nonat [15,16], and that calculated theoretically for a possible transition between C-S-H(m) and C-S-H(s), supports the hypothesis that there is a causal link between a change in structure of the C-S-H and the ending of the induction period. Grutzeck and Ramachandran [36] have proposed that the pH of the aqueous phase determines the stability of C-S-H(s) relative to C-S-H(m), but Gartner and Gadis [5] argue that the pH is merely a consequence of the calcium and alkali ions in solution.

Other experimental evidence points to the occurrence of a structural change in C-S-H at the end of the induction period. NMR studies of silicate polymerisation show the appearance of dimers [25,26]. Ramachandran and Grutzeck [37] note a distinct change of C-S-H from a homogeneous gel to a reticulated foil-like morphology with pH, and associate this with the uptake of calcium by the gel. A similar change in morphology has been noted around the end of the induction period by many workers [e.g. 17]. Trettin et al [22] note a sharp increase in the specific surface area of the product which is consistent with the findings of Ramachandran and Grutzeck. It seems unlikely that any change in the structure and hence permeability of the C-S-H layer is caused by an osmotic rupture of a membrane.

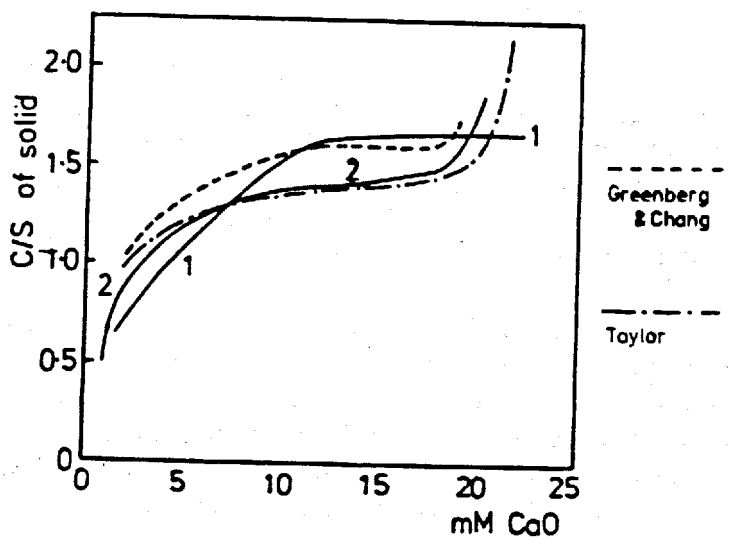

Figure 4 -
$CaO:SiO_2$ ratio of C-S-H vs CaO concentration. Showing curves 1 & 2 calculated by Gartner and Jennings and experimental curves from refs 33 and 34. From [10]

There remain a few details of the reaction which would appear to confute the appearance of C-S-H(s) as the reason for the end of the induction period. First it might be expected that the composition of solutions taken from pastes after the end of the induction period should lie on the C-S-H(s) solubility curve. Very little data on solution compositions in the later stages of hydration has been reported, but there does not appear to be a sudden change in the compositions of solution. However, McPhee et al [38] found that solutions from C_3S hydrated at a high w/c approached those in contact with C-S-H made from solution after ageing for 182 days (when it was assumed no more C_3S was present). Several authors have suggested that any remaining C_3S will continue to be covered by a thin layer of C-S-H(m) and that this phase will continue to control the solution composition until all C_3S is consumed or until a sufficiently thick layer of hydrates has formed to isolate the pore solution from the effect of the C_3S. Jennings [39] reports that the compositions of pore solutions from cement pastes tend to approach the C-S-H(s) curve after several days hydration.

The other factor, somewhat at odds with the appearance of C-S-H(s), is the C/S ratio reported for C-S-H in pastes of C_3S. Most recent studies tend to agree on a value of around 1.7 for this ratio for pastes of a variety of ages up to 26 years [26,28,40] and 1.61 - 1.65 in a 136 year old concrete [41]. However, thermodynamic studies indicate that the maximum C/S ratio for C-S-H formed from soluble salts is around 1.4 [37]. Again it is possible that the higher C/S ratio is due to the fact that during the hydration of C_3S, C-S-H(s) is forming from C-S-H(m) and that kinetic factors do not favour the rejection of calcium necessary to bring the C/S ratio down to the equilibrium level. This might explain the observations that some of the calcium in C-S-H is more readily 'leachable' than the remainder [42]. It is also interesting to note that analyses of C-S-H in Roman concretes [43] give C/S ratios of around 1.3 - 1.4 (within the range predicted for C-S-H(s)) although these lower values may be due to the presence of pozzolanic materials and the original C/S ratio is unknown.

2.2.4. Acceleratory Period - The main feature of this stage is that the reaction appears to be auto catalytic. Gartner and Gadis [5] proposed that the rate was proportional to the surface area of C-S-H and found a good fit of this model to experimental data. They also note that accelerators appear to have more effect on the rate of reaction during the acceleratory period than on the length of the induction period. This can be explained as an effect on the rate of growth of C-S-H.

Damidot and Nonat [15] found that the there was relatively little increase in the rate of reaction during this stage at high water to cement ratios. They proposed that the rate in this stage was determined by the number of nuclei available. At high water to cement ratios larger amounts of C-S-H form during the induction period so at the end of the induction period there are already many nuclei from which renewed growth can occur. In this case the rate of reaction is rapid at the beginning of this stage, but does not increase dramatically thereafter. At low water to cement ratios, very little product is formed prior to the end of the induction period so there are relatively few nuclei available from which further growth can occur. When the induction period ends, more nuclei then form and the rate of reaction accelerates.

Microstructurally the main feature of the acceleratory period is the appearance of C-S-H with a morphology variously described as sheets or foils or fibrillar. Jennings [44] has pointed out that if the C-S-H which forms during this stage is C-S-H(s) it will be growing into a solution which is supersaturated with respect to it, which would explain these dispersed morphologies.

2.2.5. Deceleratory Period - There has been much less study of the mechanisms which operate during this period than for earlier stages of the reaction. However, there is also fairly general agreement that this period of the reaction marks a transition from chemical control to diffusion control of the reaction. Knudsen [45,46] and Bezjak [47,48], consider the downturn in reaction rate to be attributable, at least in part, to the depletion of small particles which have completely hydrated. Cohen and Cohen [49,50] have recently also

developed a model showing a switch from an acceleratory period to a deceleratory one, based on the particle size distribution of the cement.

2.2.6. Slow Continuing Reaction - It is worth emphasising that all the preceding stages of hydration usually occur within the first day or so of reaction and that at the end of the deceleratory period the degree of reaction may only be 50% or less. By this point the paste has set and a rigid three dimensional structure has been established, but it is the subsequent hydration which is responsible for much of the reduction in porosity and increase in strength. Despite this there has been little study of the mechanisms operating during this period. Brown et al [51] point out the difficulty in developing kinetic models due to the lack of accurate data for the latter stages of hydration available in the literature.

This period is often combined with the preceding deceleratory period, but several factors indicate that different mechanisms operate in this stage. In calorimetry curves the rate of heat evolution levels off, showing a distinct change of slope. Kinetic analysis of alite hydration by Bezjak [48] identified three periods of hydration (corresponding to stages 3,4, and 5), between which the kinetic control of the overall hydration process changes.

Microstructural studies indicate that, during this period, a portion of the C-S-H forms within the boundaries of the original grains as 'inner' product. This product has a homogeneous appearance and in TEM studies is seen to be quite distinct from outer product [29]. Taylor has proposed that this inner product may be formed by a solid state mechanism [52], in which Ca^{2+} and Si^{4+} move outwards and H^+ inwards. The rate controlling process for this mechanism would be the migration of silicon.

Alongside the formation of inner product, outer product C-S-H and calcium hydroxide must continue to form in the remaining pore space. Kinetic analysis by Bezjak [48] suggests that the reaction rate is limited by the growth of the outer product. If this is the case it might be that the progressive reduction in the amount of available space in which the outer product can grow is the rate limiting factor.

2.3. Hydration of C_2S

In the field of C_2S hydration only a small number of papers have been published since the Rio conference. The existing state of knowledge has been reviewed by RILEM committee 68-MMH [53] and by Taylor [2]

2.3.1. Effect of Polymorphism on Reactivity - In contrast to C_3S, the different polymorphs of C_2S (α, α', β and γ) vary widely in their reactivity. Much work has been concerned with explaining these differences and in trying to prepare more reactive forms of C_2S. Tsurumi et al [54] calculated the electric field intensity at each lattice point in the γ, β, α' modifications. They found it difficult to explain the hydration activity differences by the total lattice energies, but they observed strong electric fields on special calcium positions in the β and α'-C_2S. The difference in electric field intensity between γ and the other C_2S polymorphs they believe to be the origin of the variation in the hydration activity. Their argument for this is that the strong electric fields make the calcium/proton exchange or the moveability of the calcium ions easy during the early stages of hydration.

The preparation of a γ-C_2S under autoclave conditions is reported by Mitsuda et al [55]. Starting from calcium oxide and silica or from β-C_2S they got γ-C_2S samples slightly differing in their cell parameters. The γ-C_2S sample synthesized from β-C_2S showed a loss of ignition of 5-6 wt% due to dehydration. If this sample is heated to 500°C and no higher it rehydrates reversibly on cooling. At present, it is not known if the water content of this form of γ-C_2S is only absorbed or bound by a chemical reaction producing $\equiv$SiOH groups and $(CaOH)^+$ cations. The formation of a γ-C_2S containing some water by an autoclave reaction at

180°C was also confirmed by Choi et al [56], but they have not investigated in which way the water is bound in this substance either.

A new form (β*-belite) of β-C_2S which was obtained by Lampe et al [57] from a raw meal of medium alkali- and aluminium-oxide content by very rapid quenching ($\sim 5 \times 10^4$ K min^{-1}) from 1450°C to room temperature. The authors found that this β*-belite reacts much more intensively with water than the normal β-belite. The heat of hydration evolved, i.e. 120 J/g after 72 hours, is nearly double that produced by a normal β-belite. The compressive strength of $1 \times 1 \times 1$ cm cubes of β*-belite pastes (6% gypsum, water/belite = 0.6) after 90 day hardening at room temperature was 21.8 MPa while that of normal β-belite was only 8.3 MPa. Corresponding results were also obtained using $4 \times 4 \times 16$ cm test bars.

Gartner and Jennings [10] calculated the chemical potential of the different polymorphs of C_2S in the presence of liquid water from the thermodynamic data of Spencer [58], along with the chemical potential curves for C-S-H(m) and C-S-H(s). The potential of γ-C_2S was almost indistinguishable from that of C-S-H(m) which would explain the inertness of γ-C_2S in water.

2.3.2. Mechanism of C_2S Hydration - The hydration of the reactive polymorphs of C_2S is slower than that of C_3S, but appears to be mechanistically similar [59]. According to the phase diagram of the CaO-SiO_2-H_2O system (Figure 1), C_2S would dissolve congruently until the solution intercepts, the C-S-H + solution phase boundary at **F**. The first C-S-H to form would have a slightly lower C/S ratio than in the case of C_3S and the portion of the curve **FC** over which the composition of the solution changes before reaching the triple point is longer. Thus even if C_2S had the same chemical potential as C_3S a slightly longer induction period would be expected.

Tong et al [60,61,62] studied the hydration of β-C_2S by NMR using cross-polarisation (CP) and magic angle spinning (MAS). They identified stages similar to those observed during the hydration of C_3S - detecting monomeric silicate species during the induction period and later the formation of dimers. Comparison of the hydration of β-C_2S, C_3S and retarded C_3S indicated that basically the same products were formed in all three cases, but that those formed from C_2S and retarded C_3S showed more signs of ordering and contained higher molecular weight silicate anions.

Trettin et al [63] investigated the hydration of the α', β and γ-C_2S by very sensitive Krypton adsorption, Figure 3. For γ as well as for β and α'-C_2S an alternating increase and decrease of the specific surface area was observed during the first 30 minutes of hydration (Figure 5.). As with the corresponding results from C_3S hydration, these changes were attributed to the formation and transformation of C-S-H phases on the surface of the different C_2S modifications. Unexpectedly, γ-C_2S, despite its low overall reactivity, showed the same behaviour, suggesting that the reaction products formed in this case might inhibit further hydration. ESCA measurements on the hydration of γ and β-C_2S (Figure 6.) showed that there is a decrease in the Ca/Si ratio of the surface directly after contact with water indicating that there is indeed a chemical reaction with water at the surface of γ-C_2S. Results similar to those of Ménétrier et al [64] were obtained for β-C_2S.

Trettin et al also studied the effect of different water to C_2S ratios on the development of the specific surface area of β-C_2S (Figure 7.). At w/s = 0.5 alternating increases and decreases were observed in the first 30 minutes, but at w/s = 5 only an initial increase followed by a decrease to a constant value is seen. This effect confirms that the changes in specific surface area are connected with reactions at the surface. These findings may also indicate a similar effect of water to solid ratio on the kinetics of hydration of C_2S to that observed by Damidot and Nonat for C_3S hydration.

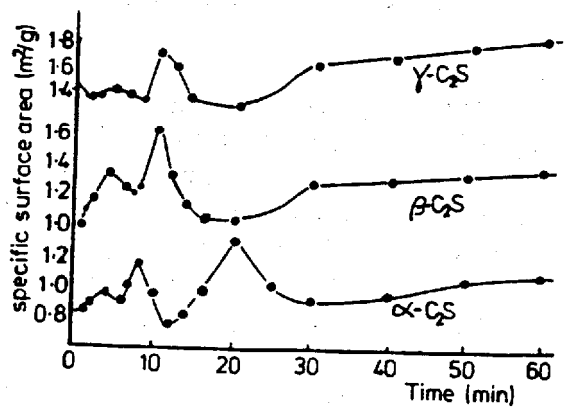

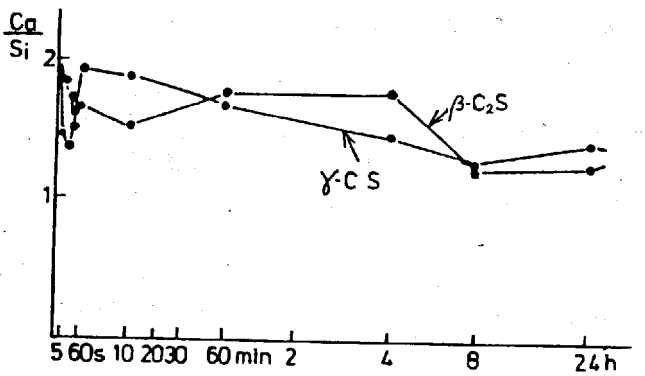

Figure 5. (above left)
Change of specific surface area of hydrating C_2S polymorphs. [61]

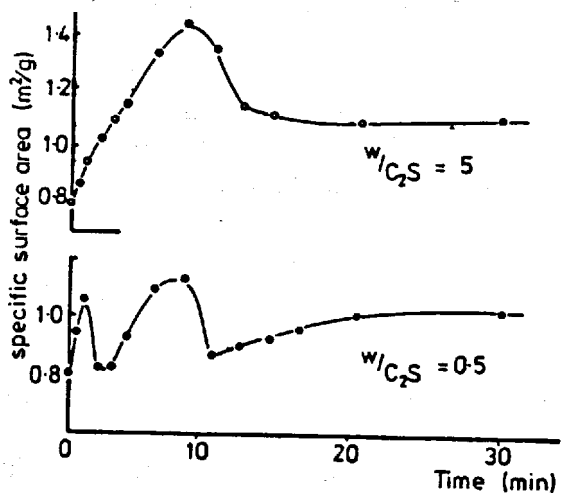

Figure 6. (above)
ESCA measurements of Ca/Si ratio at the surface of hydrating C_2S polymorphs. [61]

Figure 7. (left)
Influence of water/solid ratio on the change of specific surface area of hydrating β-C_2S. [61]

2.3.3. Microstructure of C_2S Hydration - Little new work has been reported regarding the microstructure of C_2S hydrated alone. However observations of belite grains in cement paste by Scrivener [65,66] indicates that reaction occurs preferentially along the boundaries of the twin planes (Figure 8.). The morphology of the twin lamellae are preserved in fully reacted relics of belite in old pastes, supporting the proposition that hydration in the latter stages may occur by a solid state mechanism [67,68].

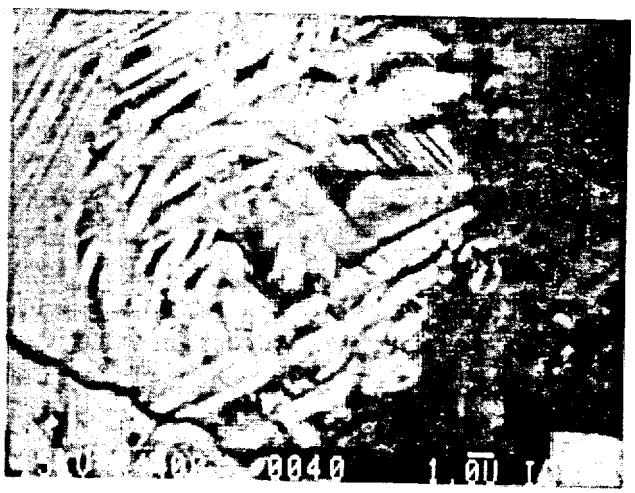

Figure 8.
Preferential reaction of a belite particle in a mature cement paste (bse image in the SEM)

2.4. Reactions of the Silicate Phases in Portland Cement

The heat output curves from C_3S and cement (Figure x) are very similar. The additional peaks (3 and 4) which appear in the curve for cement can positively be identified with reactions of the interstitial phases (see Section 3.4). The mechanism of C_3S hydration in cement would therefore appear to be similar to that of C_3S alone. Jennings reports [39] that concentrations of CaO and SiO_2 measured in pore solutions from cement paste lie on the same curve as that derived from studies of C_3S hydration.

It is well known that polymorphic changes, the presence of other elements in solid solution and the burning and cooling conditions can all affect the reactivity of C_3S or alite. For example the effect of Al content in C_3S recently reported by Nocun-Wczelik and Trybalska [69]. These factors appear to be more significant in determining the rate at which alite reacts in cement than the presence of the other clinker phases.

Studies on physical mixtures of C_3S and C_3A by Locher and Odler [70] showed that the rate of hydration of C_3S was only altered in the presence of an equal weight of C_3A with no added gypsum. Many studies of alite/belite mixtures show belite hydration accelerated by alite. However, there appears to be little affect by belite on the hydration of alite, when they are combined in proportions typically found in Portland cement. An extensive study of laboratory-made Portland cements by Abdul-Maula and Odler [71], showed that the fraction of C_3S hydrated was almost unchanged when the proportions of C_3S and the other clinker phases were varied over a wide range of compositions. In contrast, Uchikawa et al [72] found that the hydration of C_3S in cements was accelerated by increased content of C_3A. Bezjak [73] found that the hydration of alite in a mixture of 90% alite and 10% C3A was more rapid than in pure alite although there was very little difference in the rate of alite hydration between two clinkers with similar alite but different C_3A contents (3 and 9% by XRD). It is probable that these apparently contradictory findings may result from a number of experimental differences, e.g. particle size distribution, and chemical compositions of the materials used.

It has, however, been shown that the hydration of alite is significantly accelerated by the presence of gypsum [e.g. 74]. This finding has recently been confirmed by Montanaro et al [75]. Acceleration is also observed in the presence of aphthitalite ($K_3N\overline{S}_4$) [60]

The principal difference between the hydration of C_3S alone and that of alite in cement is the way in which the C-S-H product is distributed in the microstructure. When C_3S is hydrated alone the product forms around and *in contact* with the reacting grains. In contrast the C-S-H product formed in cement is observed to form shells separated from the underlying grain and in some cases hollow shells (often called 'Hadley grains') (Figure 9.). Examination of the microstructure of a mixture of monomineralic grains of C_3S and C_3A (75% C_3S, 25% C_3A, + 5% hemihydrate) [76] indicates that in this case separated shells are



Figure 9.
Microstructure of cement paste hydrated for one day showing separated shell of hydration product and hollow shells or 'Hadley' grains. (bse image)

only formed around the grains of C_3A and that the product around the C_3S grains remains in contact with the surface (Figure 10.). The reasons for this phenomenon are not clear. It has been suggested [77] that a gelatinous product of high water content initially forms of the surface of the grains in the presence of alumina. Such a product has not been observed directly and is assumed to disappear on drying.



Figure 10.
Microstructure of C_3S, C_3A, hemihydrate mixture at one day showing hydration product in contact with C_3S grains and well separated from C_3A grains. [74,75].
(bse image)

The width of the gaps between shell and anhydrous grain appear to increase with time during the acceleratory stage of hydration. At two hours it is just visible, by 5 hours it is quite distinct and about 0.05 - 0.1 μm wide, increasing to about 1 μm at 12 hours and 2 μm or more after 18 hours. This increase in width suggests that ionic species from the dissolution of the clinker phases migrate through the shell and precipitate as product on the outside. This may be because the higher concentrations of certain ions (e.g. dissolved alumina species) inhibit the precipitation of C-S-H. The width of the gaps are very uneven, owing to the polymineralic nature of cement grains. After the first day or so the size of the gap decreases again as C-S-H is deposited on the inside of the shell. When the grains are large enough to continue hydrating ($> \sim 15$ μm) the separation between shell and core will disappear after about 2 weeks hydration.

3. INTERSTITIAL PHASES

While the hydration of the silicate phases dominate the setting, hardening and subsequent properties of cement paste, that of the interstitial phases plays an important role, both in their own right and in modifying the hydration of the silicate phases. In Portland cement the presence of the interstitial phases is particularly important in two respects:

a) in determining the early rheological properties of pastes, particularly in the presence of admixtures and

b) in determining the dimensional stability of pastes which are exposed to a source of sulphate ions or which have experienced elevated temperatures during curing.

Since the Congress at Rio, two excellent reviews of the hydration of the interstitial phases have been published [78,79].

3.1. Thermodynamic Aspects

As with the silicate phases, there has been a renewed interest recently in phase equilibria related to the reaction of the aluminate and ferrite phases. However, the greater complexity of the systems concerned has impeded the representation and use of phase diagrams in this area. In cement the interstitial phases react in the presence of calcium sulphate and lime. Thus the simplest system relevant to the hydration of cement

consists of four components, $CaO-Al_2O_3-CaSO_4-H_2O$ and cannot be simply represented in two dimensions. Consideration of reactions involving Fe_2O_3 introduces another component. The situation is further complicated by alkali metal ions, Na^+ and K^+, invariably present in commercial cements, which are known to affect the reaction of the interstitial phases.

Brown [6,7] has reconsidered the data on the $CaO-Al_2O_3-CaSO_4-H_2O$ system originally reported by Jones [80,81] and by D'Ans and Eick [82,83]. Several important points emerge from these studies.

a) In the presence of water the AFm phase, calcium monosulpho-aluminate, $C_3A.C\overline{S}.12H_2O$ is only metastable with respect to ettringite and C_3AH_6 at 20-25 °C. This has recently been confirmed by Atkins et al [84]. During hydration, the continued reaction of C_3A after the depletion of sulphate provides the thermodynamic driving force for formation of monosulphate at the expense of ettringite.
b) Gibbsite, γ-AH_3 is reluctant to crystalise and instead an amorphous alumina gel is precipitated. This gel forms over a wide range of solution compositions. The composition of the gel itself is unclear but it contains significant quantities of calcium and sulphate.
c) The sulphate concentration of the solution at the invariant point where ettringite, monosulphate and calcium hydroxide are in metastable equilibrium with solution is very low, equivalent to 0.0294 m*M* of $CaSO_4$. Thus ettringite will continue to form in preference to monosulphate until all solid forms of sulphate are exhausted.

In addition, consideration of phase compatibility in the $CaO-Al_2O_3-CaSO_4-H_2O$ system and requirements of local equilibria indicate that ettringite should not be formed in direct contact with anhydrous C_3A. Rather AFm phases and their solid solutions would be expected to exist in the interfacial region between C_3A and ettringite [78]. The presence of small amounts of these phases during the hydration of C_3A has been reported by several authors [85,86,87]

3.2. Kinetics of C_3A Hydration

The basic reactions of C_3A with water in the presence of calcium sulphate are well established. Initially ettringite (AFt) is formed:

$$C_3A + 3C\overline{S}.H_2 + 26H \rightarrow C_3A.(C\overline{S})_3.H_{32} \qquad (1)$$

When the supply of sulphate is exhausted C_3A reacts with the ettringite already formed to give calcium alumino monosulphate:

$$2C_3A + C_3A.(C\overline{S})_3.H_{32} + 4H \rightarrow 3C_3A.C\overline{S}.H_{12} \qquad (2)$$

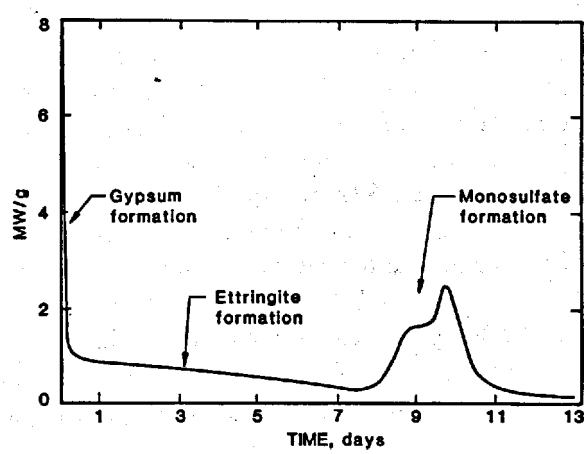

Figure 11.
Heat evolution curve for the hydration of equimolar proportions of C_3A and hemihydrate in a saturated calcium hydroxide solution at 25°C. From [78]

A heat evolution curve for the hydration of C_3A with hemihydrate is shown in Figure 11.. The initially high rate of heat evolution is mainly due to the formation of gypsum from hemihydrate. Thereafter, the rate of heat evolution arising from the formation of ettringite gradually declines. After about 7 days the rate of heat evolution increases rapidly as monosulphate starts to be formed.

Many theories have been advanced regarding the mechanism responsible for the reduction in reaction rate during the formation of ettringite. These have been comprehensively reviewed (e.g. 2,78,79) and will not be discussed in detail again here, however, there are a few points are worth making.

First, as outlined above, the requirements of local equilibria predict that several other phases may exist in the interfacial region between anhydrous C_3A and ettringite; small quantities of AFm phase have been reported experimentally [85,86,87]. Scrivener [74,75], observed C_3A hydrated for 10 minutes in the environmental cell of a high voltage transmission electron microscope. Small rods, probably of ettringite, were observed outside a region of filmy, possibly amorphous product (Figure 12.).

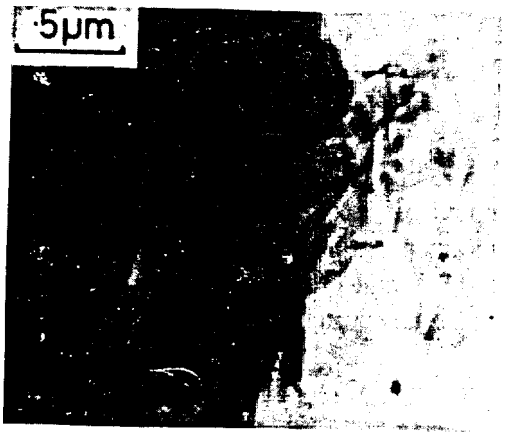

Figure 12.
Microstructure of C_3A with calicium sulphate after 10 minutes hydration observed in an evironmental cell in a high voltage electron microscope without prior drying. The surface of the C_3A on the left and small rods of ettringite are begining to form on the right. Between the two filmy and possibly amorphous phases can be observed [74,75]

Secondly, the fairly gradual decrease in reaction rate seen during the formation of ettringite is very different to the dramatic drop in rate seen at the start of the induction period in the hydration of C_3S. Thus, it may be inferred that the products forming in the case of C_3A are more permeable than the initial C-S-H formed during the hydration of C_3S.

Many workers have reported that the growth of ettringite is controlled by a diffusion process [e.g. 88,89,90,91]. Brown and LaCroix [90] carried out an analysis of the kinetics of ettringite formation at 5, 25 and 41°C. They analysed their data with three different models and were able to calculate an activation energy near 1 kcal/mol for one model. This value clearly suggests diffusion control, in contrast to the value of 12 kcal/mol reported by Tenoutasse [88] which is more typical of a chemically controlled reaction.

The time at which the formation of monosulphate begins depends mainly on the amount of sulphate present, but will also be affected by the reactivity and particle size distribution of the C_3A. The sulphate to alumina ratios in Portland cement typically range between 0.5 and 1 [92]. From calorimetry curves published in the literature the time at which the formation of monosulphate starts, for this S/A range, varies from 16 hours for an $\overline{S}/A$ ratio of 0.52 (w/s=1, CH:C_3A=1.2(molar)) [79] to over 7 days for $\overline{S}/A$ = 1 (w/s = 0.68, saturated CH solution) [78]. Additions of calcium hydroxide are also reported to delay the onset of monosulphate formation, but this effect appears to be fairly small [78]. For any one preparation of C_3A a relationship $T=k(\%gypsum)^2$ has been reported [89]. Once reaction (2) starts it proceeds fairly rapidly and often produces a double peak in heat evolution curves [78]. There is little reported regarding the kinetics of monosulphate formation. However, Pommersheim and Chang [91] found that a model based on diffusion through a thinning ettringite layer gave a good fit to experimental results.

3.3. Hydration of the Ferrite Phase

The composition of the ferrite phase in Portland cements varies over a wide range of composition based on the solid solution series $Ca_2Fe_{(2-x)}Al_xO_5$ (where x ranges from 0 to 0.65) but also containing appreciable amounts of magnesium, silicon and titanium substituted for the iron [1,2,78]. Most work on the hydration of the ferrite phase alone or in the presence of gypsum or lime has used the compound C_4AF. The extent to which these studies can be applied to the reaction of the ferrite phase in cement is questionable.

The hydration of C_4AF is usually considered to parallel that of C_3A with the formation of a phases analogous to ettringite (generalised as AFt) and then a monosulphate phase (AFm) after the depletion of sulphate. There is, however, controversy as to the extent to which iron enters the AFt and AFm product phases. The reactions given below identify the possible extremes of behaviour with iron either being totally excluded from (3a,4a) or fully incorporated in (3b,4b) the AFt and AFm products:

$$C_4AF + 3C\overline{S}H_2 + 30H \rightarrow C_3A.(C\overline{S})_3.H_{32} + \{FH_3\} + CH \quad \textbf{(3a)}$$

$$C_4AF + 6C\overline{S}H_2 + 2CH + 50H \rightarrow C_6AF.(C\overline{S})_6.H_{64} \quad \textbf{(3b)}$$

$$2C_4AF + C_3A.(C\overline{S})_3.H_{32} + 12H \rightarrow 3C_3A.C\overline{S}.H_{12} + 2\{FH_3\} + 2CH \quad \textbf{(4a)}$$

$$2C_4AF + 2C_3A.(C\overline{S})_3.H_{32} + 4CH + 4H \rightarrow 2C_9A_2F.(C\overline{S})_3.H_{36} \quad \textbf{(4a)}$$

(where $\{FH_3\}$ represents products containing excess iron and not a specific compound)

Taylor and Brown et al [2,78] have reviewed earlier evidence on this matter. While it is clear that iron substituted AFt and AFm phases do exist, the products formed during the hydration of C_4AF are generally reported to have much lower A/F ratios than C_4AF, or not to contain iron at all. This deficiency of iron is probably due to the low mobility of species containing Fe^{3+} in alkaline solutions. Although the presence of lime might at first sight appear to facilitate the incorporation of iron into the AFt and AFm, it may also increase the alkalinity of the solution and so decrease the mobility of the Fe^{3+}. The iron not incorporated into the sulpho-aluminate phases is usually considered to form an amorphous iron hydroxide, which may also contain calcium, but such a compound has not yet been directly identified and characterised.

Two pieces of work reported recently support this view. Brown studied the compositions of solutions in contact with C_4AF and gypsum or gypsum-lime mixtures [93]. From his results, he suggests: that alumina gel or C_2AH_8 precedes the formation of AFt during the hydration of C_4AF; that this AFt product contains little or no iron; and that an iron-rich gel also forms. In a recent presentation, Gartner and Myers [94] indicated that the hydration of C_4AF was significantly modified in the presence of higher tertiary alkanolamines, which are thought to complex Fe^{3+}. An extra heat peak was observed, after that associated with the formation of monosulphate. Extra phases, thought to be hydroxyaluminoferrites, were identified by XRD. It was suggested that after the depletion of gypsum the mobility of the Fe^{3+} was increased through the formation of complexes with the tertiary alkanolamines so that Fe^{3+} could be incorporated into AFm phases. The presence of these additives in cement pastes leads to significant strength increases.

The kinetics of the hydration of the ferrite phases have received very little attention. It is generally assumed that the rate of hydration is slower than that of C_3A, but anecdotal evidence suggests that the reactivity of different preparations is highly variable. Recent work by Beaudoin and Ramachandran [95] compared the hydration and strength gain in pastes of each of the four major clinker minerals, all having

similar particle size distributions. It was found that the C_4AF pastes had the highest strengths for hydration times up to ten days. This suggests that C_4AF may be as, if not more, reactive than any of the other phases in cement. Scrivener [77] examined the hydration of C_4AF and observed copious amount of AFt after as little as 10 mintues hydration. Qualitatively the development of microstructure during the early stages of hydration of C_4AF did not appear different to that of C_3A.

3.4. Hydration of Interstitial Phases in Portland Cement

During the hydration of Portland cement both AFt and AFm phases form, indicating that the overall pattern of reaction is not too dissimilar to that observed in simpler systems. During the early hydration of oilwell cements (containing little or no C_3A) AFt is also observed, that indicating the hydration of the ferrite phase is occuring. Taylor ([2] pg 201) cites evidence for the presence of hydrogarnet in portland cement pastes, but concludes that this is a minor product. In mature pastes quantities of ettringite and monosulphate appear to co-exist. Ettringite is usually dispersed as small needle-like crystals throughout the paste, but under moist conditions it may recrystallize as large agglomerates of crystals in pores, air voids and cracks. Monosulphate appears to be much more intimately mixed with the C-S-H, possibly on the scale of individual crystal layers [1,2] and this might further inhibit the conversion of this metastable product to ettringite and hydrogarnet.

As remarked earlier, calorimetry curves from cement, such as that shown in Figure 13, exhibit several further peaks after the intial peak on addition of water, in contrast to the single further peak seen during the hydration of alite. The third peak which appears as a small shoulder on the main heat evolution peak in Figure 13. (labelled 3), is often ascribed to the formation of monosulphate after the depletion of gypsum. However, parallel microstrucutral studies [77,96] on the same cement, clearly show that this peak corresponds to a regrowth of ettringite in the paste (Figure 14.). Monosulphate is first observed in the microstructure after about 2 days and its formation, in this cement is probably associated with the weak fourth peak (4 in Fig. 13.).

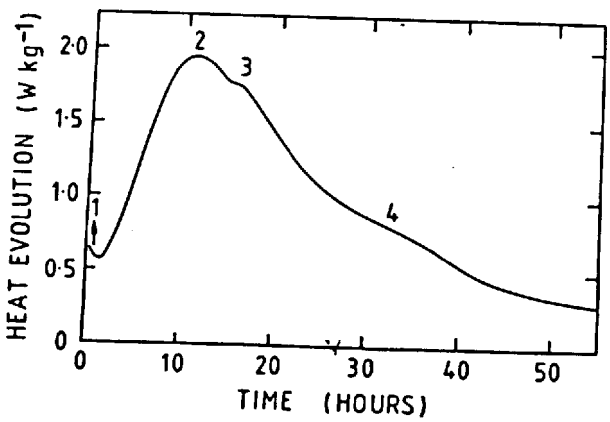

Figure 13.
Rate of heat evolution at 20°C for a typical Portland cement. [77,96]

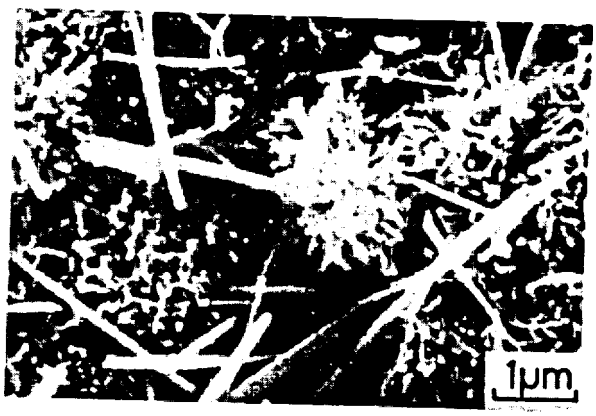

Figure 14.
Microstructure of same cement paste after 18 hours. [77]
(fracture surface in SEM)

Some of the other calorimetry curves reported in the literature, show a much stronger third peak. An example can be seen in the classic work of Lerch [97], some of which is illustrated in Figure 15. This more pronouced type of peak does, indeed appear to correlate with the appearance of monosulphate.

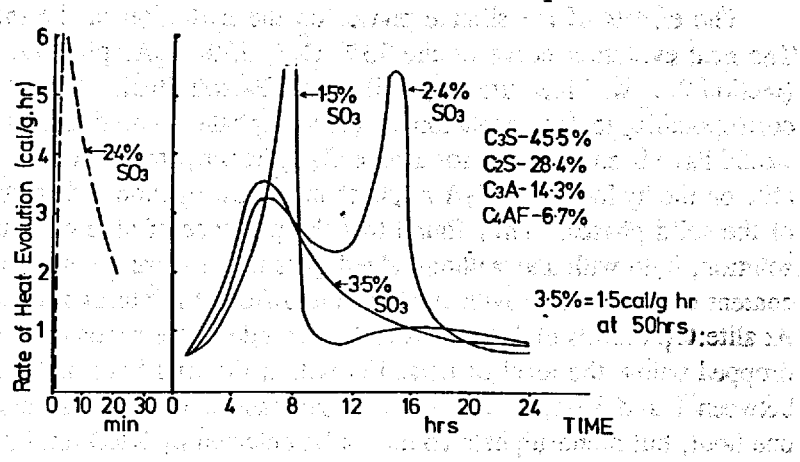

Figure 15.
Calorimetry curves from Lerch [97], illustrating the effect of gypsum and the type of third heat peak observed when the formation of monosulphate starts during the first day of hydration.

These differences in behaviour for different cements pose two questions:

a) What is the effective alumina content of cement available to form sulpho-aluminate phases during the early stages of hydration?
b) How does the presence of the silicate phases affect the hydration of the interstitial phases?

Before discussing these questions in more detail it is worth pointing out how the compositions of Portland cements have tended to change over the last fifty years of so. The cements used by Lerch generally had lower alite contents (by Bogue ~45%) and tended to have lower alkai sulphate contents than modern cements [92]. The $\overline{S}/A$ ratios of the cements studied by Lerch ranged from 0.5 to 1, whil the $\overline{S}/A$ ratios of modern cement tend towards the top of or above this range. The cement described above studied by Scrivener [77] and Pratt and Ghose [96], had a Bogue C_3S contents of 59%, C_3A of 8.5% and an $\overline{S}/A$ ratio just over 1.

Condsidering the typical $\overline{S}/A$ range of cements (0.5 to 1), if the alumina in cement were availiable to react in the same way as in pure C_3A and the hydration was unaffected by the presence of the silicate phases, one would expect to observe times for the start of the monosulphate reaction in cements ranging from about 16 hours to several days. However, the effective alumina content of the cement will depend on several factors:

a) The amounts, and alumina contents, of the clinker phases. Alumina in C_3A and in alite should be readily available. That in the ferrite phase may be available initally, but may be restricted later if gelatinous iron-rich phases form at the surface. That in the belite phase may not be available until later in the hydration process.
b) The reactivity of the interstitial phases which may vary with their compositions and with the burning and cooling conditions of the clinker.
c) The distribution of the interstitial phases in the anhydrous cement grains, which will depend on the microstructure of the clinker and the way the clinker fractures during grinding. The work of Lerch [97] showed that the fineness of the cement affected the quantity of aluminate pahses available for early reaction and so the quantity of gypsum required for proper retardation. A preliminary study by Scrivener [98] indicated that the proportions of the interstitial phases on the surface of cement grains may differ from their proportions in the bulk.

At present very little is known about the effects and relative importance of these factors, reflecting a lack of work on the characterisation of the microstructure of anhydrous cement and its effect on hydration. However, the work of Locher [99,100] indicates that the amount of C_3A reacting in the first hour of hydra-

tion may vary widely between cements and the work of Tang and Gartner indicates that the precise nature of the sulphate source in cements may also significantly affect the early reactivity of the aluminate phase [101].

The effects of the silicate phases on the hydration of the interstitial phases is also poorly understood. The heat evolution curve of the 75% C_3S, 25% C_3A, plus 5% hemihydrate mixture described previously (section 2.4) was measured by Killoh and Parrott [102]. This mixture had a $\overline{S}/A$ ratio of 0.37 and a peak corresponding to the formation of monosulphate occured after 48 hours hydration, significantly later than would have been expected for a pure C_3A, hemihydrate mixture. Ghorab et al[103,104] studied the effects of alite on the hydration of C_3A in phase mixtures, by monitoring the composition of the liquid phase and XRD of the solid phases. They found that the presence of alite dramatically supressed the amount of alumina in solution, both with and without added gypsum. Figure 16. shows their results for the variation in aluminium content of the solution with time for the different mixtures studied in the presence of gypsum ($\overline{S}/A = 1.5$). At alite:C_3A ratios of 1:1 and 10:1 (either side of the ratios in cement), the amount of aluminium in solution dropped below the level of detection within the first hour and aluminium did not reappear in solution until between 1 and 3 days. The level of sulphate in solution had also dropped below the level of detection by one hour, but monosulphate could not be detected by XRD until 3 days.

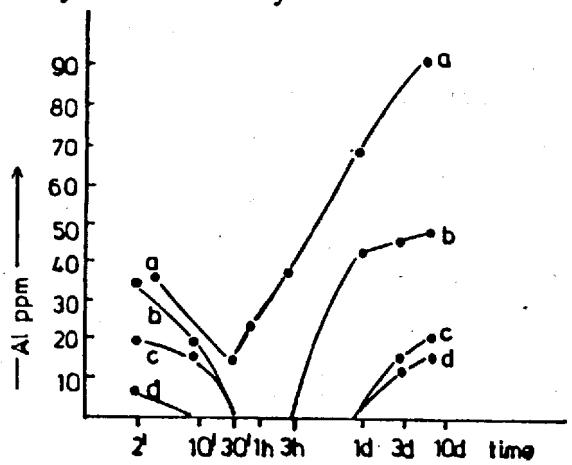

Figure 16.
Variation in aluminium content of solution, for the hydration of :
a) 1:1.5 C_3A:gypsum
b) 0.1:1:1.5 alite:C_3A:gypsum
c) 1:1:1.5 alite:C_3A:gypsum
d) 10:1:1.5 alite:C_3A:gypsum
From [104]

Very few detailed pore solution studies from the early hydration of cement have been reported. The early work of Lawrence [105] is widely referred to and this shows the concentration of sulphate in solution drops to near zero at about 16 hours. This work was carried out on cements with a $\overline{S}/A$ ratio of around 0.5 and a Bogue composition similar to the cements used by Lerch [106]. More recent work by Wieker and Herr [107] shown in Figure 17, shows similar phenomena. As shown by this work and by that of Gartner et al [108], a steady state of gypsum and calcium hydroxide saturation of the solution is acheived within the first hour. This situation persists until the sulphate level drops when the sources of sulphate in the paste are exhausted. As shown in Figure 17., the concentration of calcium hydroxide in solution then starts to rise to balance the Na^+ and K^+ cations.

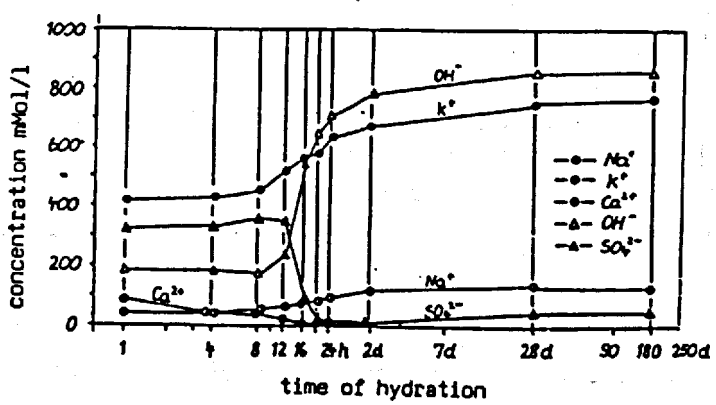

Figure 17.
Composition of the pore solutions from Portland cement hydrated at 20°C. From [107]

In cement pastes, Locher et al [100] observed rapid formation of ettringite during the first few minutes, but negligible further consumption of C_3A between 5 minutes and 4 to 6 hours. After this 'dormant' period the reaction of C_3A was observed to resume, with the formation of ettringite until the gypsum was exhausted. This corresponds to the microstructural observations of Scrivener [76,77], in pastes hydrated for one hour many small rods of ettringite were seen scattered across the surface of the grains. However the rods did not cover the surface of the grains and would appear unlikely to be responsible for any significant retardation of the hydration of the interstitial phases. Little increase in the amount of ettringite was observed during the next few hours until the secondary growth, described above, at around 12-18 hours. Richartz [109] studied cements with different alkali and sulphate contents and observed a strong increase in the reaction rate of C_3A after about 16 hours. Tang and Gartner [107] studied the early hydration of clinker with different addtions of sulphate. For those mixtures with $\overline{S}/A$ ratios comparable to commercial cements (and for some of those with lower $\overline{S}/A$ ratios) no monosulphate was detected by XRD at 24 hours.

From the above, it appears that the evidence regarding the pattern of reaction of the interstitial phases during the early stages of hydration is somewhat confused. The presence of alite certainly appears to suppress the initial reaction to form AFt. When the reaction recommences either monosulphate may start to form or a renewed growth of ettringite may occur first. The course the reaction takes may depend on the details of the composition of the cement and in particular the $\overline{S}/A$ ratio. At present, it must be concluded that the details of the interaction between the interstitial and silicate phases are not well understood.

4. EFFECT OF TEMPERATURE

The curing of concrete between room temperature and 100°C is widespread in the production of prefabricated components, e.g. panels for house construction, railway sleepers and prestressed high pressure water supply tubes. In practice, several types of heat treatment are used. The most common is the introduction of low pressure steam into the environment surrounding the concrete, but there are also cases where infrared radiation, electric current or microwave devices are used. Normally heat treatment is followed by moist curing at ordinary temperatures. Furthermore the hydration of cement, especially in very massive constructions such as dams, occurs at elevated temperatures because of the accumulation of the heat of hydration within the concrete due to its relatively low heat conductivity. Hydration at elevated temperatures also plays an important role in hot climates. In spite of the importance of hydration at elevated temperatures, the number of papers published since the Rio Congress concerned with this subject is very limited. However, earlier reviews do exist in the literature [110,111,112,113].

4.1. General Effect of Temperature on the Hydration and Maturity Relationships

The most noticeable effect of temperature is to increase the rate of hydration. This can be seen clearly from calorimetry curves, Figure 18. [114]. As the temperature increases, the main peak of the heat evolution curves is shifted to shorter reaction times. The pattern of peaks also changes implying that the reactions of the different phases are affected in different ways.

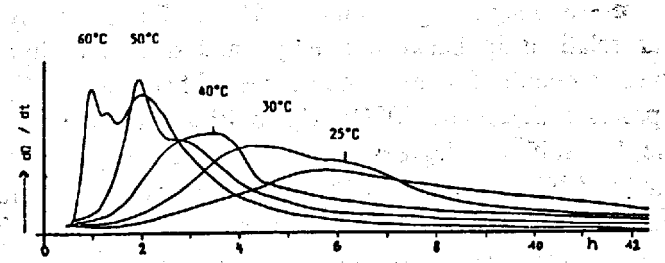

Figure 18.
Calorimetric curves for the hydration of Portland cement at elevated temperatures.

The increase in rate with temperature is a consequence of the thermodynamics of the reaction. The change in rate with temperature can be used to calculate the apparent activation energy of hydration. Kjellsen and Detwiler [115] have calculated activation energies for Portland cement at different degrees of hydration. At low degrees of hydration (20 - 30%) they calculated a comparatively high activation energy indicating a chemically controlled reaction. The apparent activation energy decreased with increasing degree of hydration, suggesting a shift to diffusion control. The initial values of activation energy and the decreasing trend with hydration are in broad agreement with earlier work reported by Copeland and Kantro [116], however the values reported around 60 and 70% hydration are much lower. These differences may be attributable to differences in w/c ratios, composition and particle size distribution of the cements used.

From an engineering viewpoint it is desirable to be able to calculate an approximate strength, or maturity, based on the thermal history of curing. The simplest maturity relationships based on the work of Saul [117] assume a linear increase in the rate of reaction with increase of the reaction temperature above some datum temperature below which the hydration effectively ceases (usually taken to be around -10 to -12°C). This model has been widely used and reasonable agreement with experimental results has been reported. However Carino et al [118,119] failed to find a unique strength-maturity relationship based on this model for concretes cured at temperatures between 5 and 43°C. Deviations were especially acute for differences in temperature of early age curing.

Thermodynamics indicates that the relationship between rate of reaction and temperature should be more correctly described by the Arrhenius equation incorporating an exponential expression:

e.g. $$R_T = R_0 e^{-\alpha/T}$$

where R_T is the rate of reaction at temperature T and R_0 and α are constants.

Freiesleben Hansen and Pedersen [120] have developed a more sophisticated maturity model based on this approach, which uses constants derived from the adiabatic heat curve of an individual cement. This model has been shown to give good agreement with experiment and has been used as part of the quality control process for several engineering projects in Denmark. Regourd and Gautier also adopted the Arrhenius approach to predict the short term strength of heat treated concrete [121,122].

Even a strength-maturity relationship based on the Arrhenius equation assumes that strength is a unique function of the degree of hydration for a given cement regardless of the temperature at which hydration occurs. This may be true for moderate degrees of elevated temperature curing up to about 40°C, or perhaps 60°C. However several workers have reported that the ultimate strengths developed by cement pastes cured at higher temperatures are less than those of pastes cured at room temperature. Lower ultimate strengths have been attributed to: coarser porosity which may be due to less efficacious arrangement of the hydration products; restriction of the degree of hydration; or modification of the reaction mechanism of the interstitial phases (discussed below). Parry-Jones et al [123,124,125] studied the hydration of cement pastes and mortars hydrated at temperatures between 20 and 80°C up to 31 days. They calculated the degree of hydration of the pastes from ^{29}Si magic-angle-spinning NMR. For pastes hydrated between 20 and 55°C, there was a unique linear relationship between strength and degree of hydration, but pastes hydrated at 80°C had markedly lower strengths for the same degree of hydration. Kjellsen et al [126] studied the hydration and strength of pastes at 5, 20 and 50°C. Up to 40% hydration the strength of pastes hydrated at 5 and 50°C was the same, but at higher degrees of hydration the strengths of the pastes hydrated at 50°C was lower than those hydrated at 5°C. For pastes where the temperature of hydration was switched from 5 to 50°C or vice versa after 30% hydration, the temperature at which the latter part of hydration occurred (beyond 30%) appeared to have most effect on strength.

4.2. Effect of Temperature on Reaction Mechanisms and Microstructure

4.2.1. Silicate Phases - Increases in temperature up to 100°C appear to have little effect on the reaction mechanisms of the silicate phases. The reaction products are calcium hydroxide and amorphous calcium silicate hydrate with little evidence for the formation of crystalline calcium silicate hydrates. However studies indicate some effect of temperature on the structure and distribution of these phases. As the hydration temperature is increased, microscopical studies indicate that calcium hydroxide becomes more interspersed with the C-S-H. This can be explained by the decrease in solubility of calcium hydroxide with temperature, so that higher temperatures will favour nucleation of this phase. Conversely, pastes hydrated below ambient temperatures contain large masses of calcium hydroxide with a well-developed morphology of large plates elongated along the basal plane [126,127], Figure 19.

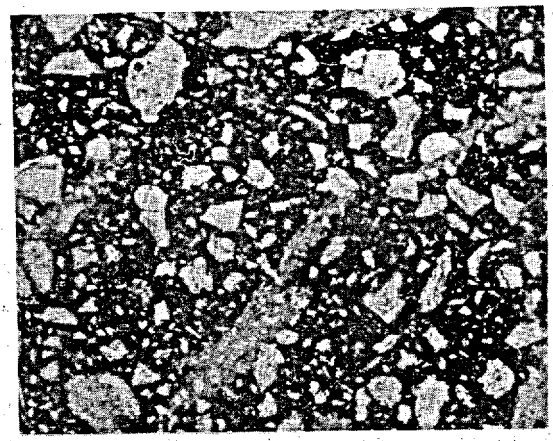

Figure 19.
Microstructure of paste hydrated at 5°C, showing well developed morphology of the calcium hydroxide crystals

The effects of temperature on the structure of C-S-H are not clear. Several workers found that the degree of polymerization of the C-S-H, as measured by trimethylsilation, increases with the temperature of hydration [128,129,130]. The degree of polymerisation cannot be measured directly by NMR, but can be inferred from the ratio of Q^2 (middle units of chains) to Q^1 (end units). In Figure 20. the Q^2:Q^1 ratios from the results of Al-Dulaijan et al [125] are plotted against degree of hydration for pastes hydrated at different temperatures. It can be seen that this ratio increases with temperature for equivalent degrees of hydration. The slope of the line through each group of points which related to a single temperature of hydration also increases with temperature indicating that the rate of polymerisation increases slightly with increasing temperature.

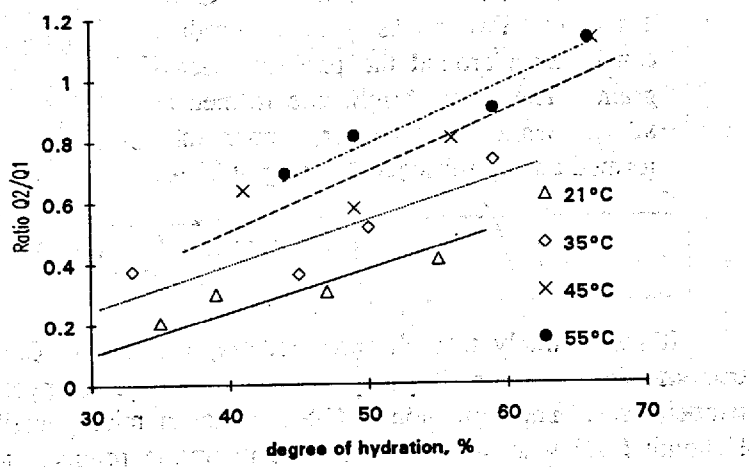

Figure 20.
Ratio Q^2/Q^1 for pastes hydrated at different temperatures at different degrees of hydration from the results of Al-Dulaijan et al [125].

The influence of temperature on the C/S ratio of the C-S-H phase has been investigated by several authors by calculation of the degree of reaction and the amount of calcium hydroxide formed. The results are conflicting, possibly due to the large experimental errors inherent in this method, particularly at low degrees of hydration, but tend to indicate that the C/S ratio increases [2]. Odler et al [131] suggest that

increases in the C/S ratio are found from studies on Portland cement and constant or decreasing values found for C_3S pastes. They found no change in C/S ratio up to 75°C for cement pastes, but an increase for pastes hydrated at 95°C. An increased degree of polymerisation should result in a decreased C/S ratio. On the other hand, the instability of ettringite and monosulphate at higher temperatures in cement pastes (discussed below) would lead to the incorporation of more calcium in the C-S-H structure from the reaction of the interstitial phases. These competing effects could explain some of the discrepancies between reported results for cement and C_3S. In particular Odler et al [131] only detected an increase in the C/S ratio at temperatures where the aluminate hydrates were unstable.

In microscopical studies Regourd and Gautier [121] noted that outer C-S-H formed at 80°C had a much more fibrous morphology, similar to that seen in pastes hydrated with calcium chloride accelerators. The effects of temperature on C-S-H are especially evident in the rims of 'inner' product around the larger cement grains observed in backscattered electron images. Kjellsen et al [126,132] observed that the rims in pastes hydrated at 40°C were brighter than those in pastes hydrated at 5 or 20°C. Scrivener [133] examined pastes hydrated initially at 80°C and then at 20°C and observed two zones of inner product in the rims (Figure 21.). The outer part of the rim, formed at the higher temperature is brighter than the inner part which formed subsequently at the lower temperature. Several factors may be responsible for the brighter appearance of C-S-H formed at higher temperatures: an increase in average atomic number, due to an increase in the C/S ratio, a decrease in the water content or both; or a decrease in the microporosity of the product. Preliminary energy dispersive X-ray analysis indicated a difference in the analysis totals for the light and dark product, indicating a decrease in the water content or in the microporosity of the C-S-H formed at higher temperatures. The decrease in bound water contents noted by Odler et al [131] for pastes hydrated at higher temperatures is consistent with decreased interlayer water in the C-S-H. There may also be a slight increase in the C/S ratio of the product formed, but the inherent variability of the C-S-H makes this difficult to determine. Crumbie et al [134] found a C/S ratio of 2.4 for pastes hydrated at 80°C and one of 2.1 for pastes hydrated at 25°C. However, Uchikawa [135] reports C/S ratios of 2.03 and 1.90 for pastes hydrated at 20 and 45°C respectively.



Figure 21.
Microstructure of paste heat treated at 80°C and then cured in water at 20°C for 4 months. Two zones of inner product can be seen around the partialy reacted grain. The outer, bright one formed at 80°C, while the darker, inner one formed during subsequent curing at 20°C.

It seems likely that all three factors, increase in C/S ratio, decrease in bound water content and decrease in microporosity may contribute to the changes in observed in C-S-H formed at elevated temperatures. The formation of C-S-H of lower microporosity is consistent with the views of Verbeck and Helmuth [136] who suggested that the hydration products formed at higher temperatures are less evenly distributed and that a product layer of low permeability forms around the hydrating grains, inhibiting further hydration. It is apparent that more work is necessary to determine the precise effects of temperature on the C-S-H structure.

4.2.2. Interstitial Phases - In contrast to the silicate phases the reaction mechanism of the interstitial phases changes dramatically at elevated temperatures. Somewhere between 60°C and 80°C ettringite becomes unstable with respect to monosulphate and calcium sulphate. This means that any ettringite already formed will decompose and that further reaction of C_3A will lead directly to the formation of monosulphate. At still higher temperatures (approaching 100°C) monosulphate also becomes unstable and hydrogarnet phases (C_3AH_6) may form directly. The exact temperatures at which ettringite and monosulphate become unstable is not clear. Pure ettringite in the presence of liquid water is stable up to at least 90°C [137] although at ordinary humidities it will start to dehydrate at 50°C [2,138].

It has also been found that the stability of ettringite also decreases with increasing pH [139]. Hampson and Bailey [140] stated that ettringite was not stable in a 0.25 M NaOH solution at 25°C and converts to monosulphate. Ghorab and Kishar [141] investigated the stability of ettringite in sodium hydroxide solutions at 30, 60 and 100°C. With increasing temperature and concentration of sodium hydroxide the concentration of aluminium and sulphate in solution after one day increases dramatically. The decomposition of ettringite resulted in the formation of crystalline calcium hydroxide and sulphate free AFm phases and, at 100°C, hydrogarnet.

With regard to the stability of ettringite in cement pastes, Ludwig and Co-workers have published many papers related to elevated temperature curing of pastes, mortars and concretes [138,142,143,144,145]. These indicate that the amount of ettringite formed during hydration is significantly reduced at temperatures of 70°C and above and that even at 60°C ettringite tends to be replaced by monosulphate. Sylla [146] found that the ettringite content in cement pastes starts to decrease after about 3 hours hydration at 60°C and has almost completely disappeared by this time at 80°C, Figure 22. However at both temperatures, ettringite was formed initially. Odler et al [131] found that ettringite was rapidly replaced by monosulphate at 75°C and that monosulphate itself disappeared after curing for more than one day at 95°C. Wieker and Herr [107] noted reductions in the amount of ettringite formed in pastes heat treated at 70°C or above. Earlier studies indicated that pastes cured at temperatures close to 100°C contained little or no crystalline aluminate phases [147,148]. However, Taylor reports the formation of hydrogarnet in a cement paste moist cured at 90°C for 2 months [149]. The breakdown of the crystalline hydrated calcium alumino sulphates will also contribute to the reduction in bound water content relative to the degree of hydration noted by Odler et al [131].

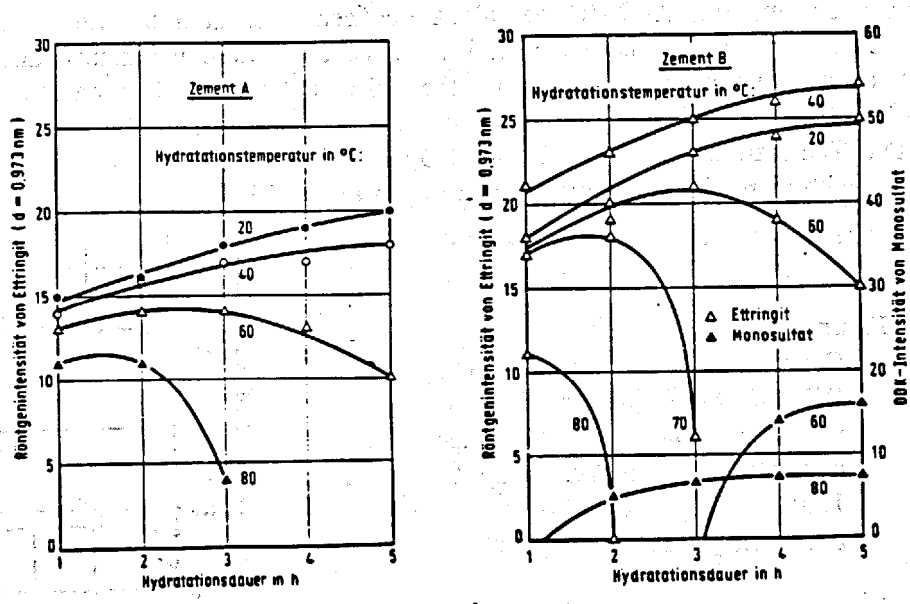

Figure 22.
The development of ettringite (a) and ettringite and monosulphate (b) in pastes hydrated at different temperatures. From Sylla [146]

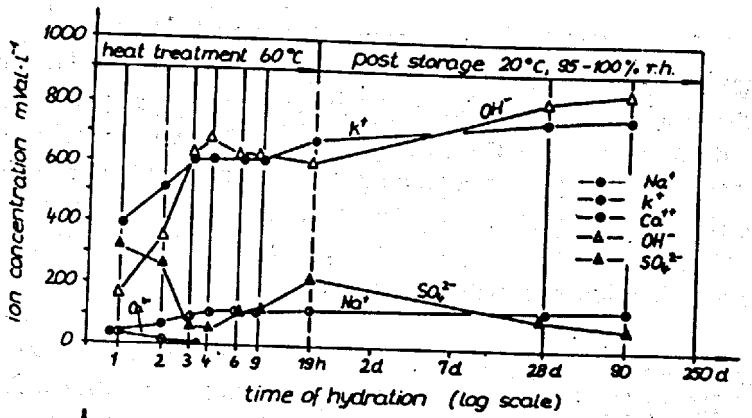

Figure 23.
Composition of the pore solutions from Portland cement hydrated at 60°C. From [107]

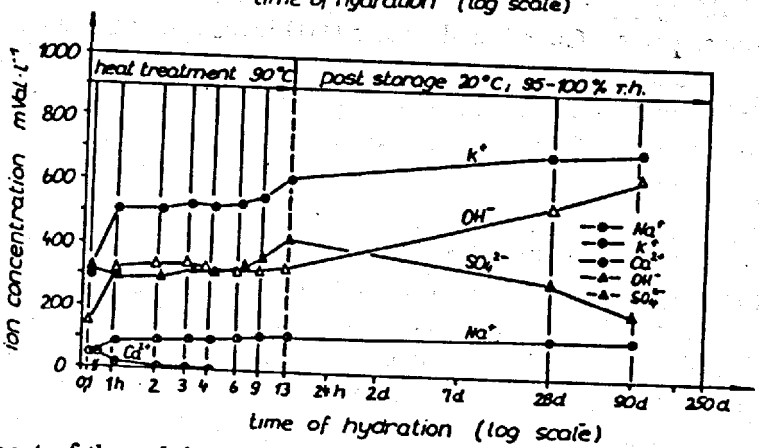

Figure 24.
Composition of the pore solutions from Portland cement hydrated at 90°C. From [107]

As the hydration temperature increases, most of the sulphate and alumina released by the decomposition of ettringite appears to become incorporated into the C-S-H gel, but some is present as monosulphate and the concentration of sulphate ions in the pore solution also increases. The results of Wieker and Herr [107,150] on the composition of pore solutions squeeezed from pastes hydrated at 60°C (Figure 23.) and 90°C (Figure 24.) demonstrate this effect. At 60°C the sulphate concentration after 1 hour is similar to that found in the paste hydrated at 20°C (Figure 17.), but this falls rapidly due to the accelerated formation of ettringite and then monosulphate, as also shown by Sylla [143] (Figure 22.). However, after about 6 hours the concentration of sulphate starts to increase again up to the end of the heat treatment as the sulpho aluminate phases decompose. At 90°C the sulphate concentration after one hour is also similar to that observed at 20°C, but no decrease is observed, instead the concentration remains fairly constant throughout the heat treatment with some increase towards the end of the period. In both cases, as with the paste hydrated at 20°C, it is clear that the composition of the pore solution is dominated by the alkali metal ions, K^+ and Na^+. These are balanced by OH^- and SO_4^{2-}. The balance between these two anions moves to higher SO_4^{2-} levels with increasing temperature as shown in Figure 25.

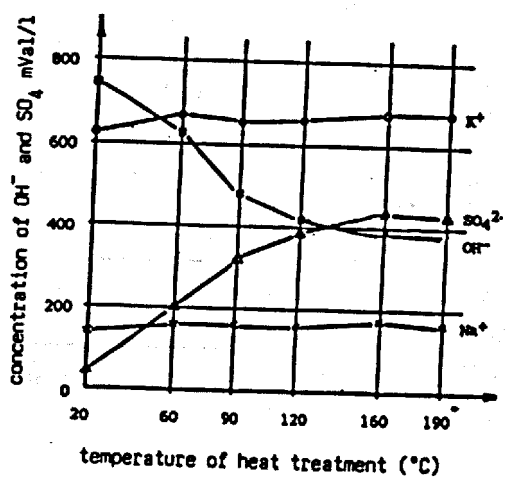

Figure 25.
Concentrations of K^+, Na^+, OH^- and SO_4^{2-} ions in the pore solutions from cement pastes hydrated at temperatures up to 190°C for °C × hours of treatment = 1150. From [150]

Figure 25. indicates that the concentration of SO_4^{2-} ions continues to increase above 100°C, at which temperature all the sulpho-aluminate phases should have decomposed. Therefore, it appears that this increase is not only due to the decomposition of the sulpho-aluminate phases, but also a result of a shift to the right of the equilibrium between alkali hydoxide, calcium sulphate compounds, alkali sulphate and calcium hydroxide with increasing temperature:

$$\{CaSO_4\}_{(s)} + 2Me^+_{(aq)} + 2OH^-_{(aq)} \leftrightarrows Ca(OH)_{2(s)} + 2Me^+_{(aq)} + SO_4^{2-}{}_{(aq)}$$

(where $\{CaSO_4\}_{(s)}$ represents sulphate in AFt, AFm, gypsum and C-S-H phases and Me = Na or K)

4.2.3. Changes Occuring in Heat Treated Pastes on Subsequent Storage at Room Temperature - Most studies of pastes cured at elevated temperatures, and subsequently cured in moist conditions at room temperature, indicate that ettringite reforms [107,142,143,144,145,146,150]. This process is referred to as 'secondary' or 'delayed' ettringite formation. However, ettringite reformation was not observed by Buck [151]. Figure 26. shows the DTA traces of pastes subjected to different heat treatments and then stored in water for 3 months. These indicate that the reformation of ettringite is substantially complete by one month.

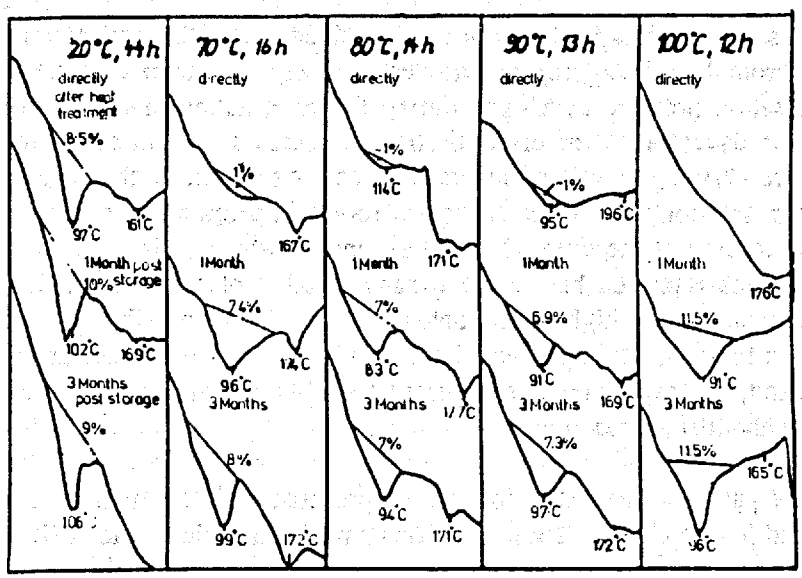

Figure 26. DTA curves of Portland cement directly after hydration at elevated temperatures and after one and 3 months showing the thermal decomposition and reformation of ettringite. From [107]

Pastes heat treated at 80°C were studied by Scrivener and Taylor [152] in the SEM; very few discrete areas of ettringite could be observed after 35 days curing at room temperature. However after 4 months the ettringite had further recrystallised and was clearly visible in pores throughout the pastes (Figure 27.).

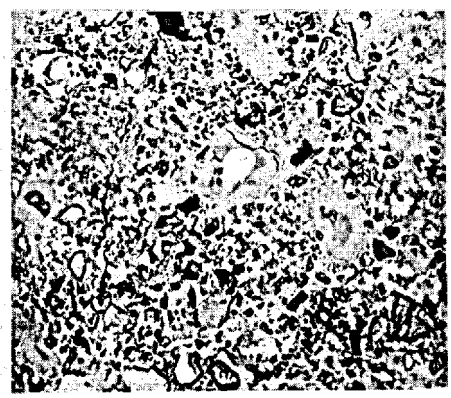

Figure 27. Microstructure of paste heat treated at 80°C and then cured under water for 4 months.

Heinz and Ludwig [142,143,144,145] and Wieker and Herr [107,150] and Lawrence et al [153] have all shown that mortars heat treated and then stored in water expand. Expansion curves from the work of Wieker and Herr are shown in Figure 28. The expansion starts earlier, the higher the temperature of heat treatment. Once started the expansion increases relatively rapidly reaching values of up to 6 mm/m. The mechanism of stress build up appears to be unclear at present.

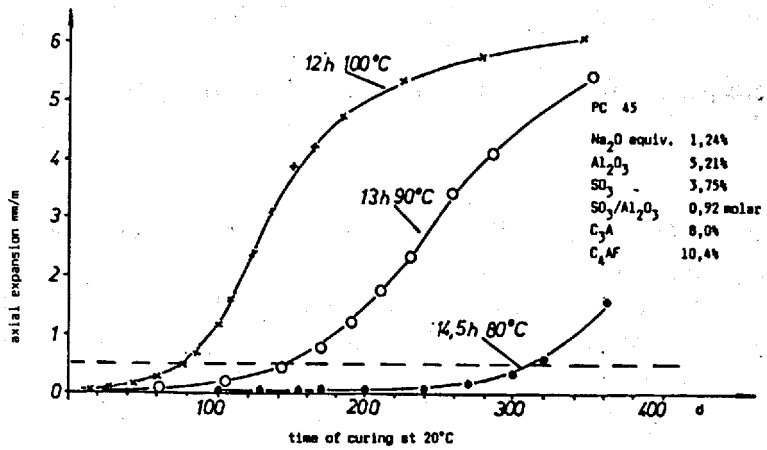

Figure 28.
Expansions of mortar bars from Portland cement treated at 100°C, 90°C and 80°C with time of subsequent curing at 20°C under moist conditions. From [107].

In thin sections of expanded mortars examined under the optical microscope, bands of ettringite are observed surrounding the aggregate particles. Ludwig and Heinz [142,143,144,145] attribute the expansion to the crystallisation pressure developed during the reformation of ettringite at the paste/aggregate interface. However, the development of crystallisation pressures sufficient to overcome the strength of the mortar, would require very high levels of supersaturation. As shown by the pore solution studies, the concentration of sulphate in solution declines on storage at room temperature, so sufficiently high levels of supersaturation are unlikely to exist at the time when the expansions are occuring. In addition, it is observed that most of the ettringite has reformed before the expansion takes place. As the decomposition of ettringite is most severe in cements with a high alkali content, it may also be possible that alkali silica reaction contributes to the expansion process, but expansions have also been observed in mortars made with unreactive quartz. On the other hand, the expansion is suppressed by additions of reactive silica [143,154], which are known to suppress the alkali silica reaction.

Over the past few years deterioration of precast concrete structures cured at elevated temperatures has been reported [e.g. 153,155]. These problems have been attributed to ASR, inadequate precuring before heat treatment, or to the reformation of ettringite. However, in many cases the cause of deterioration is unclear and more study of the durability aspects of concrete subject to hydration at elevated temperatures is needed.

5. CONCLUDING REMARKS

In writing this paper, the difficulty in drawing a cohesive picture of the hydration process from the diverse array of published results has become apparent. Results which at first appear contradictory turn out on closer inspection to have been carried out under different experimental conditions or with different starting materials. Comparison between results is hampered by lack of characterisation of starting materials: determination of the amounts of the phases present; their compositions; and their spatial distribtutions both within and between the different cement grains.

The consequences of making comparison between dissimilar starting materials and experimental conditions are vividly illustrated by the recent paper by Beaudoin and Ramachandran [95]. It has always been assumed that C_4AF contributes relatively little to the strength of Portland cement based on the early

work of Bogue and Lerch, that pastes of C_4AF hydrated alone showed very low strength development. However, comparison of this phase with the other clinker phases using materials of the same particle size distributions by Beaudoin and Ramachandran, found that C_4AF actually showed the highest strength gains up to 10 days.

Portland cement is a complex system and it is usually assumed that equilibrium conditions do not exist during hydration. However, it seems to be emerging that the solution phase quickly establishes a quasi-equilibrium with the solid phases after the addition of water and that phase equilibria can be of use in intrepreting the sequence of hydration reactions. In the future, the use of computers for manipulating and visualising data should facilitate the use of thermodynamics to study reactions in complex cement systems.

Many more studies of pore solution compositions are being made. However, it is important that the solid phases are also studied in conjunction with the liquid phase, and that the interactions between different ionic species within the liquid phases are considered. This latter problem has been dealt with in several recent publications [8,108,156,157]. In addition, it has been questioned whether the compositions of solutions squeezed from cement pastes are in fact representative of the liquid phase within the paste [158]. Thermodynamic approaches have also been used as a tool to predict the performance of cement in the very long term [e.g. 159].

Kinetic studies and other forms of mathematical modelling such as that developed by Bentz and Garboczi [e.g. 160], will have an increasing role to play in illuminating hydration mechanisms. However, these modelling approaches can only bear fruit if they can be verified against a sufficient body of experimental data. Many theoretical models are still being tested on data relating to cements produced more than 30 years ago, which differ significantly from modern cements. The work of Parrott et al [161] also illustrates that different methods of measuring the degree of hydration may not always give the same answers. The lack of rigourous data examining the effect of: hydrating cements of the same composition under different conditions; cements of the same composition but different particle size distribution; and cements of the same particle size distribution but of different compositions was emphasised by Taylor in his review for the Rio conference [1]. The situation appears to have improved little over the last few years.

The establishment of a data base of experimental results which will have a significant impact on advancing our understanding of hydration will probably necessitate more collaboration and cooperation between researchers. No one experimental technique, be it, electron microscopy, pore solution chemistry, NMR, or calorimetry, is sufficient to provide all the information needed and it is unlikely that the expertise, manpower, equipment or finance, will be available for all these studies to be carried out by one group of researchers.

6. REFERENCES

1. Taylor, H.F.W.: "Chemistry of Cement Hydration". **Proc. 8th Int. Cong. Chemistry of Cement, Rio de Janeiro, Brazil,** 1986. **Vol I,** 82-110.
2. Taylor, H.F.W.: **Cement Chemistry,** Academic Press, 1990.
3. Materials Research Society Symposia Proceedings, **Vol 85, Microstructural Development During Hydration of Cement,** ed Leslie J. Struble & P.W. Brown, 1987.
4. **The Materials Science of Concrete,** Vol I, ed J.P. Skalny, 1989; Vol II, ed J.P. Skalny & S. Mindess, 1991; American Ceramic Society.
5. Gartner, E.M. and Gadis, J.M.: **Hydration Mechanisms I.** The Materials Science of Concrete, Vol I, ed J.P. Skalny, American Ceramic Society, 1989, p95-126.

6. Brown, P.W.: "The Implications of Phase Equilibria on Hydration in the Tricalcium Silicate-Water and the Tricalcium Aluminate-Gypsum-Water Systems", **Proc. 8th Int. Cong. Chemistry of Cement, Rio de Janeiro, Brazil,** 1986. **Vol III,** 231-238.
7. Brown, P.W.: **Phase Equilibria and Cement Hydration.** The Materials Science of Concrete, Vol I, ed J.P. Skalny, American Ceramic Society, 1989, p73-94.
8. Gartner, E.M. and Skalny, J.P.: "Computation of solubility relationships for Hydrating Cement Systems", **Proc. 8th Int .Cong. Chemistry of Cement, Rio de Janeiro, Brazil,** 1986. **Vol III,** 244-250.
9. Glasser, F.P.; Lachowski, E.E. and McPhee, D.E.: "Compositional Model for Calcium Silicate Hydrate (C-S-H) Gels, Their Solubilities, and Free Energies of Formation". J. Am. Ceram. Soc., 1987, **70**(7), 481-485.
10. Gartner, E.M. and Jennings, H.M.: "Thermodynamics of Calcium Silicate Hydrates and Their Solutions". J. Am. Ceram. Soc., 1987, **70**(10), 743-749.
11. Taylor, H.F.W.; Barret, P.; Brown, P.W.; Double, D.D.; Frohnsdorff, G.; Johansen, V.; Menetrier-Sorrentino, D.; Odler, I.; Parrott, L.J.; Pommersheim, J.M.; Regourd, M. and Young, J.F.; RILEM Committee 68-MMH, Task Group 3: 'The Hydration of Tricalcium Silicate', Mater. Construct., 1984, **17**, 475.
12. Jennings, H.M.: "Aqueous Solubility Relationships for Two Types of Calcium Silicate Hydrate". J. Am. Ceram. Soc., 1986, **69**(8), 614-618.
13. Barret, P.; Ménétrier, D. and Bertrandie, D.: "Mechanism of C_3S Dissolution and Problem of the Congruency in the Very Initial Period and Later On". Cem. Concr. Res., 1983, **13**(5), 728-738.
14. Barret, P.: "Hydration Mechanism of Calcium Silicates (C_3S, C_2S) Cement Compounds, Through the General Concepts of the Reactivity of Solids". **Proc. 8th Int. Cong. Chemistry of Cement, Rio de Janeiro, Brazil,** 1986. **Vol III,** 86-92.
15. Damidot, D. and Nonat, A.: "Investigation of the C_3S Hydration Process During the First Hours". **Proc. 1st Int. Workshop on Hydration and Setting, Dijon, France,** 1991.
16. Damidot, D., Nonat, A. and Barret, P.: "Kinetics of Tricalcium Silicate Hydration in Diluted Suspensions by Microcalorimetric Measurements". J. Am. Ceram. Soc., 1990, **73**(11), 3319-3322.
17. Ménétrier, D., Jawed, I.; Sun, T.S. and Skalny, J.P.: "ESCA and SEM Studies on Early C_3S Hydration". Cem. Concr. Res., 1979, **9**(4), 473-482.
18. Regourd, M.;,Thomassin, J.H., Baillif, P. and Touray, J.C.: "Study of the Early Hydration of Ca_3SiO_5 by X-ray Photoelectron Spectrometry". Cem. Concr. Res., 1980, **10**(2), 223-230.
19. Ball, M.C., Simmons, R.E. and Sutherland, I.: "Surface Compositions of Anhydrous Calcium Silicates". Proc. Brit. Ceram. Soc., 1984, **35**, 1-10.
20. Ball, M.C. and Simmons, R.E.: "Surface Composition of Anhydrous Portland Cements". Cem. Concr. Res., 1988, **18**(1), 29-34.
21. Stadelmann, C.; Trettin, R. and Wieker, W.: "Studies of the Hydration of Ca_3SiO_5 by ESCA and Krypton Adsorption Measurements". Cem. Concr. Res., 1985, **15**(1), 145-150.
22. Trettin, R. and Weiker, W.: "Zur Hydration von Trikalziumsilikat. I. Ursachen der Induktionsperiode". Silikattechnik, 1986, **37**(3), 75-78.
23. Trettin, R.; Satava, V. and Wieker, W.: "Studies on Physico-Chemical Changes in Time of Initial Setting of C_3S". **Proc. 1st Int. Workshop on Hydration and Setting, Dijon, France,** 1991.
24. Ménétrier, D.: **Contribution à l'étude cinétique de la période initiale d'hydration du silicate tricalcique, constituant principal du ciment portland.** PhD Thesis, University of Bourgogne, Dijon, France, 1977.
25. Brown, P.W., Franz, E., Frohnsdorff, G. and Taylor, H.F.W.: "Analyses of the Aqueous Phase During Early C_3S Hydration". Cem. Concr. Res., 1984, **14**(2), 257-262.
26. Roger, S.A., Groves, G.W., Clayden, N.J. and Dobson, C.M.: "Hydration of Tricalcium Silicate Followed by ^{29}Si NMR with cross-polarization". J. Am. Ceram. Soc., 1988, **71**(2), 91-96.

27. Roger, S.A.; Groves, G.W.; Clayden, N.J. and Dobson, C.M.: "A Study of Tricalcium Silicate Hydration from Very Early to Very Late Stages". Materials Research Society Symposia Proceedings, Vol 85, **Microstructural Development During Hydration of Cement**, ed Leslie J. Struble and P.W. Brown, 1987, 13-20.
28. Miljkovic,L.; Lasic, D.; MacTavish, J.C.; Pintar, M.M.; Blinc, R. and Lahajnar, G.: "NMR studies of Hydrating Cement: a Spin-Spin Relaxation Study of the Early Hydration Stage". Cem. Concr. Res., 1988, **18**(6), 951-956.
29. Groves, G.W.: "TEM Studies of Cement Hydration" Materials Research Society Symposia Proceedings, Vol 85, **Microstructural Development During Hydration of Cement**, ed Leslie J. Struble and P.W. Brown, 1987, 3-12.
30. Jennings, H.M.; Taleb, H.; Frohnsdorff, G. and Clifton, J.R.: "Interpretation of the Effects of Retarding Admixtures on Pastes of C_3S, C_3A plus Gypsum, and Portland Cement". **Proc. 8th Int. Cong. Chemistry of Cement, Rio de Janeiro, Brazil,** 1986. **Vol III**, 239-243.
31. Barret, P. and Bertrandie, D.: "Fundamental Hydration Kinetic Features of the Major Cement Constituents: Ca_3SiO_5 and βCa_2SiO_4", J. Chim. Phys., 1986, **83**(11/12), 765-775.
32. Flint, E.P. and Wells, L.S.: " ". J. Res. Nat. Bur. Stand., 1934, **12**, 751.
33. Taylor, H.F.W.: "Hydrated Calcium Silicates, Part I. Compound Formation at Ordinary Temperatures". J. Chem. Soc., 1950, 3682-3690.
34. Greenberg, S.A. and Chang, T.N.: "Investigation of the Colloidal Hydrated Calcium Silicates: II Solubility Relationships in the Calcium Oxide-Silica-Water System at 25°C". J. Phys. Chem., 1965, **69**(1), 182-188.
35. Kalousek, G.L.: Discussion in **Proc. 3rd Int. Symp. Chem. Cem.,** 1954, 296-311.
36. Grutzeck, M.W. and Ramachandran, A.R.: "An Integration of Tricalcium Silicate Hydration Models in Light of Recent Data". Cem. Concr. Res., 1987, **17**(1), 164-170.
37. Ramachandran, A.R. and Grutzeck, M.W.: "Microstructural Development During Suspension Hydration of Tricalcium Silicate under Fixed pH Conditions". Materials Research Society Symposia Proceedings, Vol 85, **Microstructural Development During Hydration of Cement**, ed Leslie J. Struble and P.W. Brown, 1987, 33-38.
38. McPhee, D.E.; Luke, K.; Glasser, F.P. and Lachowski, E.E.: "Solubility and Aging of Calcium Silicate Hydrates in Alkaline Solutions at 25°C". J. Am. Ceram. Soc., 1989, **72**(4), 646-654.
39. Jennings, H.M.: "The Physical and Chemical Development of Calcium Silicate Hydrate During the Setting and Hardening of Portland Cement", **Proc. 1st Int. Workshop on Hydration and Setting, Dijon, France,** 1991.
40. Taylor, H.F.W and Newbury, D.E.: "Calcium hydroxide Distribution and Calcium Silicate Hydrate Composition in tricalcium Silicate and β-Dicalcium Silicate Pastes". Cem. Concr. Res., 1984, **14**(1), 93-98.
41. Rayment, D.L.: "The Electron Microprobe Analysis of the C-S-H Phase in a 136 Year Old Concrete". Cem. Concr. Res., 1986, **16**(3), 341-344.
42. Shebl, F.A., Helmy, F.M. and Ludwig, U.: "A New Approach on the Hydration Mechanism of Tricalcium Silicate". Cem. Concr. Res., 1985, **15**(4), 747-757.
43. Rayment, D.L. and Pettifer, K.: "Examination of Durable Concrete from Hadrian's Wall". Mat. Sci. Tech., 1987, **3**, 997-1004.
44. Jennings, H.M.: "Comments on the Mechanism of C_3S Hydration". **Advances in Cement Manufacture and Use,** Proc. Eng. Foundation Conf., Potosi, U.S.A., ed. E.M. Gartner, 1989, 79-88.
45. Knudsen, T.: "The Dispersion Model for Hydration of Portland Cement I - General Concepts". Cem. Concr. Res., 1984, **14**(5), 622-30.
46. Knudsen, T.: "The Dispersion Model for Hydration of Portland Cement II - The Influence of Fineness": **Proc. 8th Int. Cong. Chemistry of Cement, Rio de Janeiro, Brazil,** 1986. **Vol III**, 369-374.
47. Bezjak, A.: "An Extension of the Dispersion Model for the Hydration of Portland Cement". Cem. Concr. Res., 1986, **16**(2), 260-264.

48. Bezak, A.: "A New approach to Mathematical Modelling of Nucleation and Growth in Kinetic Analysis of Cement Hydration". **Advances in Cement Manufacture and Use**, Proc. Eng. Foundation Conf., Potosi, U.S.A., ed. E.M. Gartner, 1989, 57-66.
49. Cohen, R.D. and Cohen, M.D.: "Kinetics of Depletion of a Population of Hydrating Cement particles". J.Mat. Sci., 1987, **22**, 2032-2036.
50. Cohen, M.D. and Cohen, R.D.: "Modelling of the Hydration of Tricalcium Silicate". J. Mat. Sci., 1988, **23**, 3816-3820.
51. Brown, P.W.; Pommersheim, J. and Frohnsdorff, G.: "A Kinetic Model for the Hydration of Tricalcium Silicate". Cem. Concr. Res., 1985, **15**(1), 35-41.
52. Taylor, H.F.W., "The Reaction of Cement Compounds with Water". Mater. Sci. Monogr., 1985, **28A**(Reactivity of Solids Part A), 39.
53. Young, J.F., :"The Hydration of Dicalcium Silicate". Mat. Construct., 1987, **20**(119),
54. Tsurumi, T.; Asaga, K. and Daimon, M.: "Calculation of the Electrostatic Potential of Calcium Silicate Ca_2SiO_4". Semento Konkurito Ronbunshu, 1989, **43**, 2-7.
55. Mitsuda, T. and Toraya, H.: "Hydrothermally Formed Gamma Calciumsilicate Ca_2SiO_4 Cellparameters and Thermogravimetry". Kanyu Hokoku-Asahi Garasu Kogyo Gitutsu Shoreikai, 1987, **50**, 65-8, 49-5.
56. Choi, S.H.; Sasaki, M.; Asaga, M. and Daimon, M.: "Hydration in the Early Stage of Calciumsilicate b Ca_2SO_4 Under Hydrothermal Conditions". Semento Gijutsu Nanpo, 1984, **38**, 46.
57. Lampe, F. and Seydel, R.: "On a New Form of β-Belite". Cem. Concr. Res., 1989, **19**, 509.
58. Spencer, P.J.: "The Thermodynamic Properties of Silicates". N.P.L. Report Chem, 1973, **21**, National Physics Laboratory, Teddington, U.K.
59. Skalny, J.P. and Young, J.F.:"Mechanisms of Portland Cement Hydration". **Proc. 7th Int. Cong. Chemistry of Cements, Paris, France,** 1980, **vol I**, 1/4 -1/45.
60. Tong, Y.; Tu, H. and Fei, L.: "CP/MAS NMR Studies of the Initial Hydration Processes of Activated and Ordinary Beta-Dicalcium Silicates". Cem. Concr. Res., 1990, **20**(6), 986-991.
61. Tong, Y.; Tu, H. and Fei, L.: "Hydration Process of Beta-Dicalcium Silicate Followed by MAS and CP/MAS Nuclear Magnetic Resonance". Cem. Concr. Res., 1991, **21**(2/3), 355-358.
62. Tong, Y.; Tu, H. and Fei, L.: "Comparison Between the Hydration Processes of Tricalcium Silicate and Beta-Dicalcium Silicate". Cem. Concr. Res., 1991, **21**(4), 509-514.
63. Trettin, R.; Oliew, G.; Stadelmann, C. and Wieker, W.: "Very Early Hydration of Dicalciumsilicate Polymorphs". Cem. Concr. Res., 1991, **21**(5), 757.
64. Ménétrier, D.; Jawed, I.; Sun, T.S. and Skalny, J.P.: "Surface Studies of Hydrated β-C_2S". Cem. Concr. Res., 1980, **10**(4), 425.
65. Scrivener, K.L.: **The Microstructure of Concrete,** The Materials Science of Concrete, Vol I, ed J.P. Skalny, American Ceramic Society, 1989, p127-161.
66. Scrivener, K.L.: "A Study of the Microstructure of Two Old Cement Pastes". **Proc. 8th Int. Cong. Chemistry of Cement, Rio de Janeiro, Brazil,** 1986. **Vol III**, 389-93.
67. McConnell, J.D.C.: "The Hydration of Larnite and Bredigite and the Properties of the Resulting Gelatinous Mineral Plomberite". Mineral. Mag., 1955, **30**, 672-80.
68. Funk, H.: "Two Different Ways of Hydration in the Reaction of b-Ca2SiO4 with Water at 25 to 120°C". **Proc. 4th Int. Symp. Chemistry of Cement, Washington, U.S.A.,** 1962, **Vol. I**, 291-295.
69. Nocun-Wczelik, W. and Trybalska, B.: "The Studies of Al-Doped Tricalcium Silicate Hydration". J. Therm. Anal., 1987, **32**, 1719-1722.
70. Locher, D. and Odler, I.: "Interaction Phenomena in the Combined Hydration of Clinker Minerals", Cemento 1989, (1), 25-36.
71. Abdul-Maula, S. and Odler, I.: "Effect of Oxidic Composition on Hydration and Strength Development of Laboratory-Made Portland Cements". World Cement, June 1982, 218-222.
72. Uchikawa, H.; Uchida, S. and Shirasaka, T.: "Influence of Chemical Moduli of Raw Mixture on Burning Degree, Character of Clinker, Hydration Characteristics, and Property of Cement". Semento Gijutsu Nenpo, 1988, (42), 28-31 (in Japanese, Chem. Abs. **111**(10):83089v).

73. Bezjak, A.; Jelenic, I.; Mlakar, V. and Panovic, A.: "A Kinetic Study of Alite Hydration". **Proc. 7th Int. Cong. Chem. Cement, Paris, France,** 1980, **Vol-II,** II-111-116.
74. Ménétrier, D.; Jawed, I. and Skalny, J.P.: "Effect of Gypsum on C_3S Hydration". Cem. Concr. Res., 1980, **10**(5), 697-702.
75. Montanaro, L.; Negro, A. and Regourd, M.: "Action de $CaCO_3$, $CaSO_4$ et $CaSO_4.2H_2O$ sur l'Hydration de C_3S". Cem. Concr. Res., 1988, **18**(3), 431-437.
76. Scrivener, K.L. and Pratt, P.L.: "Microstructural Studies of the Hydration of C_3A and C_4AF Independently and in Cement Paste". Brit. Ceram. Proc., 1984, **36**, 207-220.
77. Scrivener, K.L. "The Development of Microstructure during the Hydration of Portland Cement". PhD Thesis, University of London, 1984.
78. RILEM Committee 68-MMH, Task Group 3: "The Hydration of Tricalcium Aluminate and Tetracalcium Ferrite in the Presence of Calcium Sulphate", Mater. Construct., 1986, **19**(110), 137-147.
79. Gadis, J.M. and Gartner, E.M.: **Hydration Mechanisms II.** Materials Science of Concrete II, ed J. Skalny and S. Mindess, American Ceramic Society, Westerville, OH, 1991, 9-40.
80. Jones, F.E.: "The Quaternary System $CaO-Al_2O_3-CaSO_4-H_2O$ at 25°C", Trans Faraday Soc., 1939, **35**, 1484.
81. Jones, F.E.: "The Quaternary System $CaO-Al_2O_3-CaSO_4-H_2O$ at 25°C; Equilibria with Crystalline $Al_2O_3.3H_2O$, Alumina Gel, and Solid Solutions", J.Phys. Chem., 1944, **48**, 311.
82. D'Ans, J. and Eick, H.: "Das System $CaO-Al_2O_3-CaSO_4-H_2O$ bei 20°C und das Erharten der Tonerdezemente", Zem. Kalk. Gips, 1953, **6**, 197.
83. D'Ans, J. and Eick, H.: "Das System $CaO-Al_2O_3-CaSO_4-H_2O$ bei 20°C", Zem. Kalk. Gips, 1953, **6**, 302-311.
84. Atkins, M.; Macphee, D.; Kindness, A. and Glasser, F.P.: "Solubility Properties of Ternary and Quaternary Compounds in the $CaO-Al_2O_3-SO_4-H_2O$ System". Cem. Concr. Res., 1991, **21**(6), 991-998.
85. Collepardi, M.; Baldini, G. and Pauri, M.: "Retardation of Tricalcium Aluminate Hydration by Calcium Sulphate". J. Am. Ceram. Soc., 1979, **62**, 33-35.
86. Schweite, H.E.; Ludwig, U. and Jager, P.: "Investigations in the System $3CaO.Al_2O_3-CaSO_4-H_2O$", Highway Research Board, Special Report 90, 1966, 353-366.
87. Chatterji, S.: "Mechanism of Retardation of C_3A: A Critical Evaluation". **Proc. 7th Int. Cong. Chem. Cement, Paris, France,** 1980, **Vol-IV**, 465-470.
88. Tenoutasse, N.: "The Hydration Mechanism of C_3A and C_3S in the Presence of Calcium Chloride and Calcium Sulphate". **Proc. 5th Int. Symp. Chemistry of Cement, Tokyo, Japan,** 1968, **Vol II**, 372-378.
89. Mori, H. and Minegishi, K.: "The Effect of Temperature on the Early Hydration of the System $3CaO.Al_2O_3-CaSO_4.2H_2O-Ca(OH)_2-H_2O$" **Proc. 5th Int. Symp. Chemistry of Cement, Tokyo, Japan,** 1968, **Vol II**, 349-361.
90. Brown, P.W. and LaCroix, P.: "The Kinetics of Ettringite Formation". Cem. Concr. Res., 1989, **19**(6), 879-884.
91. Pommersheim, J. and Chang, J.: "Kinetics of Hydration of Tricalcium Aluminate in the Presence of Gypsum". Cem. Concr. Res., 1988, **18**(6), 911-922.
92. Kanare, H.M. and Gartner, E.M.: "Optimum Sulphate in Portland Cement". pp 213-251 in Cements Research Progress, 1984, ed J.F. Young, American Ceramic Society, Westerville, Ohio.
93. Brown, P.W.: "Early Hydration of Tetracalcium Aluminoferrite in Gypsum and Lime-Gypsum Solutions". J. Am. Ceram. Soc.,1987, **70**(7), 493-496.
94. Gartner, E. and Myers, D.: "Influence of the Ferrite Phase on Cement Strength Development", presented at Am. Ceram. Soc. meeting 1991, submitted to J. Am. Ceram. Soc.
95. Beaudoin, J.J. and Ramachandran, V.S.: "A New Perspective on the Hydration Characteristics of Cement Pastes". Cem. Concr. Res., 1992, **22**(4), 689-694.
96. Pratt, P.L. and Ghose, A.: "Electron Microscopy Studies of Portland Cement Microstructure during Setting and Hardening". Phil. Trans. R. Soc. Lond., 1983, **A310**, 93-103.

97. Lerch, W.: "The Influence of gypsum on the Hydration Reactions of Portland Cement". Proc. ASTM., 1946, **46**, 1252.
98. Scrivener, K.L.: "The Microstructure of Anhydrous Cement and its Effect on Hydration". MRS.
99. Locher, F.W., Richartz, W. and Sprung, S.: "Setting of cement, Part I: Reaction and Development of Structure". Zement-Kalk-Gips, 1976, **29**, 435-442.
100. Locher, F.W., Richartz, W. and Sprung, S.: "Setting of cement, Part I: Effect of Adding Calcium Sulphate". Zement-Kalk-Gips, 1980, **33**(6), 271-277 (english translation **33**(8), 150-153).
101. Tang, F.J. and Gartner, E.M.: "Influence of Sulphate Source on Portland Cement Hydration", Adv. Cem. Res., 1988, **1**(2), 67-74.
102. Parrott, L.J. and Killoh, D: unpublished results.
103. Ghorab, H.Y., Abou El Fetou, S.H. and Ahmed, H.M.: "New aspect for the hydration reaction of tricalicium aluminate in presence of alite". Zement-Kalk-Gips, 1988, **41**(12), 624-627.
104. Ghorab, H.Y. and Ahmed, H.M.: "The liquid-solid interaction in pure systems of Portland cement. Part II: The effect of alite on the hydration reaction of C3A with gypsum, also in the presence of lime". Zement-Kalk-Gips, 1990, **43**(1), 34-37.
105. Lawrence, C.D.: "Changes in the composition of the aqueous phase during hydration of cement paste and suspensions". Highways Research Board, Special Report, **90**, 1966, 378-391.
106. Lawrence, D.L.: private communication.
107. Weiker, W. and Herr, R.: "Zu Einigen Problem der Chemie des Portlandzements". Z. Chemie, 1989, **29**(9), 321-327
108. Gartner, E.M., Tang, F.J., Weiss, S.J.: "Saturation factors for Calcium Hydroxide and Calcium Sulphate in Fresh Portland Cement Pastes". J. Am. Ceram. Soc., 1985, **68**(12), 667-673.
109. Richartz, W.: "Einfluß des K2O-Gehalts and des Sulfatisierrungsgrada auf Erstarren und Erhärten des Zements". Zement-Kalk-Gips, 1986, **39**, 678.
110. Budnikow, P.P. and Erschler, E.Ya.: "Studies of the Process of Cement Hardening in the Course of Low-Pressure Steam Curing of Concrete", Proc. on the Structure of Portland Cement Paste and Concrete, Sp. Rpt. 90, Highways Res. Board, Washington, 1966, 431-446.
111. Butt, Yu.M.; Kolbasov, V.M. and Timashev, V.V.: "High Temperature Curing of Concrete under Atmospheric Pressure", **Proc. 5th Int. Symp. Chemistry of Cement, Tokyo, Japan,** 1968, **Vol 3**, 437-471.
112. Idorn, G.M.: "Hydration of Portland Cement Paste at High Temperature under Atmospheric Pressure", **Proc. 5th Int. Symp. Chemistry of Cement, Tokyo, Japan,** 1968, **Vol 3**, 411-428.
113. Vernuat, M.:"Effect of Elevated Temperatures and Pressures on the Hydration and Hardening of Cement". **Proc. 6th Int. Symp. Chemistry of Cement, Moscow, USSR,** 1976, **Vol 2**(2), 109.
114. Oliew, G. and Schüttauf, St.:Betontechnik, 1980, **3**, 483.
115. Kjellsen, K.O. and Detwiler, R.J.: "Reaction Kinetics of Portland Cement Mortars Hydrated at Different Temperatures". Cem. Concr. Res., 1992, **22**(1), 112-120.
116. Copeland, L.E. and Kantro, D.L.: "The Hydration of Portland Cement". **Proc. 5th Int. Symp. Chemistry of Cement, Tokyo, Japan,** 1968, **Vol 2**, 387-421.
117. Saul, A.G.A.: "Principles Underlying the Steam Curing of Concrete at Atmospheric Pressure". Mag. Conc. Res., March 1951, 2(6) ,127-135.
118. Carino, N.J.; Lew, H.S. and Voltz, C.K.: "Early Age Temperature Effects on Concrete Strength Prediction by the Maturity Method". J. A.C.I., March-April 1983, 93-101.
119. Carino, N.J. & Lew, H.S.: "Temperature Effects on Strength-Maturity Relations of Mortar". J. A.C.I., May-June 1983, 177-182.
120. Freiesleben Hansen, P. and Pedersen, E.J.: **Basis for Planning and Monitoring of Concrete Curing Processes,** Appendix 2, The Concrete of the Farø Bridges, ed H.H. Gotfredsen, K.R. Henriksen, F. Meyer, G.M. Idorn, The Danish Ministry of Transport, Copenhagen, Denmark, 1985, pp 105-119.
121. Regourd, M. and Gauthier, E.: "Comportement des Ciments Soumis au Durcissement Accéléré". Beton, 1980, **387**, 83-96.

122. Gauthier, E. and Regourd, M.: "Le Durcissement du Beton en Fonction de la Température". **Proc. RILEM Conf., Concrete at Early Ages**, Paris, France, 1982, **Vol I**, 145-150.
123. Parry-Jones, G.; Al-Tayyib, A-H.J. and Al-Mana, A.I.: "Evaluation of Degree of Hydration in Concrete using ^{29}Si Magic Angle Spinning NMR in Solids". Cem. Concr. Res., 1988, **18**(2), 229-234.
124. Parry-Jones, G.;.Al-Tayyib, A-H.J.; Al-Dulaijan, S.U. and Al-Mana, A.I.: "^{29}Si MAS-NMR Hydration and Compressive Strength Studies in Cement Paste". Cem. Concr. Res., 1989, **19**(), 228-234.
125. Al-Dulaijan, S.U.; Parry-Jones, G.; Al-Tayyib, A-H.J. and Al-Mana, A.I.: "^{29}Si Magic-Angle-Spinning Nuclear Magnetic Resonance Study of Hydrated Cement Paste and Mortar". J. Am. Ceram. Soc., 1990, **73**(3), 739-739.
126. Kjellsen, K.O.; Detwiler, R.J. and Gjorv, O.D.: "Development of Microstructures in Plain Cement Pastes Hydrated at Different Temperatures". Cem. Concr. Res., 1991, **21**(1), 179-189.
127. Lota, J.S.:
128. Bentur, A.; Berger, R.L.; Lawrence, F.V.; Milestone, N.B. and Mindess, S.: "". J. Am. Ceram. Soc., 1979, **62**, 362.
129. Stade, H.; Wieker, W. and Garzo, G.: "Anionzusammensetzung der Hydratationsprodukte des Tricalciumsilicats". Z. Anorg. Allg. Chem., 1983, **500**, 123.
130. Hirljac, J.; Wu, Z-Q. and Young, J.F.: "Silicate Polymerization During the Hydration of Alite". Cem. Concr. Res., 1983, **13**(6), 877-886.
131. Odler, I.; Abdul-Maula, S. and Zhongya, Lu.: "Effect of Hydration Temperature on Cement Paste Structure". Materials Research Society Symposia Proceedings, Vol 85, **Microstructural Development During Hydration of Cement**, ed Leslie J. Struble and P.W. Brown, 1987, 139-144.
132. Kjellsen, K.O.; Detwiler, R.J. and Gjorv, O.D.: "Backscattered Electron Imaging of Cement Pastes Hydrated at Different Temperatures". Cem. Concr. Res., 1990, **20**(2), 308-311.
133. Scrivener, K.L.: "The Effect of Heat Treatment on Inner Product C-S-H". submitted to Cem. Concr. Res.
134. Crumbie, A.K.; Taylor, H.F.W. and Pratt, P.L.: "The Significance of Thermal History for Offshore Grouts" This proceedings.
135. Uchikawa, H.: J. Res. Onoda Cement Company, 1986, **38**, 1.
136. Verbeck, G.J. and Helmuth, R.H.: "Structures and Physical Properties of Cement Paste". **Proc. 5th Int. Symp. Chemistry of Cement, Tokyo, Japan,** 1968, **Vol III**, 1-31.
137. Ogawa, K. and Roy, D.M.: "C_4A_3S Hydration Ettringite Formation, and its Expansion Mechanism: I. Expansion; Ettringite Stability". Cem. Concr. Res., 1981, **11**(5/6), 741-750.
138. Ghorab, H.Y.; Heinz, D.; Ludwig, U.; Meskendahl, T. and Wolter, A.: "On the Stability of Calcium Aluminate Sulphate Hydrates in Pure Systems and in Cements". **Proc. 7th Int. Cong. Chem. Cements, Paris, France,** 1980, **Vol-IV**, 496-503.
139. Gabrisová, A., Havlica, J. and Sahu, S.: "Stability of Calcium Sulpho-Aluminate Hydrates in Water Solutions with Various pH values". Cem. Concr. Res., 1991, **21**(6), 1023-1027
140. Hampson, C.J. and Bailey, J.E.: "On the Structure of some Precipitated Calcium Alumino-Sulphate Hydrates", J.Mat. Sci., 1983, **18**, 402.
141. Ghorab, H.Y. and Kishar, E.A.: "Stability of calcium sulphoaluminate hydrates in aqueous solutions". **Proc. 8th Int.Cong.Chemistry of Cement, Rio de Janciro, Brazil,** 1986. **Vol V**, 105.
142. Ghorab, H.Y. and Ludwig, U.: "Modellversuche zur Klärung von Schadensursachen an wärmebehandelten Betonfertigteilen, Teil I: Zur Stabilität von Monophasen and Ettringite". Tonindustrie-Zeitung (Facherichte), 1981, **105**(9), 634-640.
143. Heinz, D.; Ludwig, U and Nasr, R.: "Modellversuche zur Klärung von Schadensursachen an wärmebehandelten Betonfertigteilen, Teil II: Wärmebehandlung von Mörteln und Späte Ettringitbildung". Tonindustrie-Zeitung (Facherichte), 1982, **106**(3), 78-83.

144. Heinz, D. and Ludwig, U.: " Mechanisms of Subsequent Ettringite Formation in Mortars and Concretes After Heat Treatment". **Proc. 8th Int.Cong.Chemistry of Cement, Rio de Janeiro, Brazil,** 1986. **Vol V**, 189-194.
145. Heinz, D. and Ludwig, U.: " Mechanisms of Secondary Ettringite Formation in Mortars and Concrete Subjected to Heat Treatment". **Concrete Durability**, Mather Symposium, ACI SP100-105, 1987, 2059.
146. Sylla, H.-M.: "Reaktionen im Zementstein durch Warmebehendlung". Beton, 1988, **38**, 449-454.
147. Kalousek, G.L. and Adams, M.: "". J. Am. Conc. Inst. (Proc), 1951, **48**, 77.
148. Aitken, A. and Taylor, H.F.W.: "" **Proc. 4th. Int. Symp. Chem., Washington, U.S.A.,** 1960, **Vol 1**, 285-290.
149. Taylor, H.F.W. unpublished data, 1989, cited pg 363 in Ref 2.
150. Wieker, W. and Herr, R.: "On the Composition of Pore Solutions Squeezed from Autoclaved Cement Pastes" **Proc. 1st Int. Workshop on Hydration and Setting, Dijon, France,** 1991.
151. Buck, A.D.: "". **Proc. 8th Int.Cong.Chemistry of Cement, Rio de Janeiro, Brazil,** 1986. **Vol III**, 417.
152. Scrivener, K.L. and Taylor, H.F.W. to be published.
153. Lawrence, C.D., Dalziel, J.A. and Hobbs, D.W.: "Sulphate Attack Arising from Delayed Ettringite Formation". Interim Technical Note, **12**, Brit. Cem. Ass., 1990.
154. Weiker. W. and Herr, R.: unpublished results.
155. Tepponen, P., Eriksson, B.E.: "Damage in Concrete Railway Sleepers in Finland". Nordic Concr. Res. Oslo, 1987, **6**, 199.
156. Reardon, E.J.: "An Ion Interaction Model for the Determination of Chemical Equilibria in Cement/Water Systems". Cem. Concr. Res., 1990, **20**(2), 175-192.
157. Brown, P.W. and Shi, D.: "A Model for the Variations in Solution Chemistry During Tricalcium Silicate Hydration". Adv. Cem. Res., 1991/92, **4**(1), 17-27.
158. Chatterji, S.: "On the Relevance of Expresses Liquid Analyis to the Chemical Processes Occurring in a Cement Paste". Cem. Concr. Res., 1991, **21**(2/3), 269-272.
159. Glasser et al: Am Ceram Soc, 1987, **70**(7), 481-485.
160. Bentz, D.P. and Garboczi, E.J.: " Percolation of Phases in a Three-Dimensional Cement Paste Microstructural Model". Cem. Concr. Res., **21**(2/3), 325-344.
161. Parrott, L.J.; Geiker, M.; Gutteridge, W.G. and Killoh, D.: "Monitoring Portland Cement Hydration: Comparison of Methods". Cem. Concr. Res., 1990, **20**(6), 919-926.

Specific Theme III C

Structural Models for Hydrated Cement Pastes

THE STRUCTURE OF HARDENED CEMENT PASTE

J J Beaudoin
Institute for Research in Construction, National Research Council, CANADA

and

P W Brown
Materials Research Laboratory, The Pennsylvania State University, USA

Abstract

Microstructural characteristics of hardening cement paste are reviewed in the context of structural modelling.

Spatial relationships between anhydrous silicates and calcium silicate hydrate are considered. Structures of non-silicate phases are also discussed. Models of C-S-H structure are critically examined in terms of advances made since 1986. Evaluation of cement paste structural parameters relevant to modelling processes includes: development of descriptors for paste-aggregate interface properties; comparison of silica gel and C-S-H structure; determination of compositional and porosity differences in presence and absence of admixtures; numerical simulations of paste structure; pore structure modelling; pore structure characterization using solvent replacement, mercury intrusion porosimetry and A.C. impedance spectroscopy. The paper provides an integrated assessment of recent progress in the development and evaluation of concepts central to the description of hydrated cement paste. More than 200 references are reviewed.

INTRODUCTION

In this review we consider the structure of hardening cement paste. Structure in this context relates to the spatial relationships among the residual anhydrous phases, the hydrates formed and the aggregate. Of necessity, structure is considered on both the nanometer and the micrometer levels. In a general sense, hydration involves the progression by which a mechanical mixture of reactive and inert solid particles is replaced by a more-or-less continuous matrix of hydration products. This hydration product matrix is not compositionally homogeneous, varies in density and contains porosity. It is the spatial relationships between the hydration products and their anhydrous precursors that influences both the rate of hydration and the development of properties. Initially, we consider the spatial relationships between the anhydrous silicates and calcium silicate hydrate. Structures of non-silicate phases are also discussed. The development of a more comprehensive understanding of the processes by which C-S-H fills the space originally occupied by water is a topic of continuing interest.

Models for C-S-H structure are critically considered with emphasis on empirical and theoretical advances made since 1986. The C-S-H structure is briefly compared with the structure of silica gel; the dimensional changes of these gels on drying are also compared. The structure of the interphase between the bulk paste and the aggregate differs from the paste structure. Compositional differences and differences in porosity and their modification by chemical and mineral admixtures are discussed in detail.

Computer models to describe various aspects of microstructure continue to be developed. Models relating kinetics and microstructure, models for the microstructure of the interfacial zone, and models for the pore structure are considered.

Recent advances in the investigation of pore structure are considered at length because of importance in determining properties. The characteristics of the pore structure obtained are typically dependent on the measurement technique used. Both mercury intrusion porosimetry (MIP) and solvent replacement are discussed as are specimen preparation techniques. A.C. Impedence spectroscopy has been applied to characterize paste and paste-aggregate interfaces and this technique is reviewed.

THE SPATIAL RELATIONSHIPS OF CALCIUM SILICATE HYDRATE WITH ITS PARENT PHASES

Perhaps the single most important feature which affects the hydration and property development in portland cement is the spatial relationship between hydrated and anhydrous silicate phases. Interposition of hydrates between residual anhydrous phases and the aqueous phase has a significant effect on further hydration. Distribution of hydrates throughout the original water-filled space, and particularly their ability to form interconnections between hydrate rims of adjacent particles, has much to do with property development. The rate of hydration and property development are strongly dependent on manner in which C-S-H is distributed. Continuing studies have been carried out to resolve two major issues: the origin of the induction and acceleratory periods and the manner and extent of transport between the hydrolyzing surfaces of the calcium silicates and the remaining water-filled space.

Work along several avenues has contributed to the further understanding of these issues. These studies have accumulated additional evidence by electron optical techniques, kinetic analyses, crystal-chemical arguments and phase studies. One impetus for these studies was provided by Taylor [1, 2] who suggested that inner product C-S-H formed during C_3S hydration occurs *in situ*. According to the arguments developed, the number of oxygens per unit volume remain essentially constant for C_3S, C_2S and C-S-H. Thus, hydration need only involve transport of calcium, silicate species, and protons. Groves [3] pursued this approach and observed that jennite contains only 5% fewer Si atoms per unit volume than does C_3S. Thus, in the absence of porosity in the inner product, relatively little transport of silica would need occur.

There is, however, inner product porosity through which transport processes are occurring. Gartner and Gaidis [4] comprehensively reviewed the mechanisms controlling

hydration reaching the general conclusion that the rate of hydration of tricalcium silicate is limited by silica transport. Tricalcium silicate hydration was described as occurring in 5 stages: initial reaction, induction period, acceleratory period, deceleratory period, and final slow reaction. Initial reaction was envisioned as resulting in the formation of a small amount of C-S-H which acts as a barrier layer and causing the onset of the induction period. Apparently, a unified view of the processes that result in the onset of the acceleratory period, whether CH precipitation or nucleation and growth of a new C-S-H, has not emerged. Reflecting the decrease in the research emphasis on hydration kinetics, little new information pertinent to this appears to have been published. It is generally accepted that the rate of hydration in the acceleratory period is controlled by the rate of C-S-H formation. Two factors were pointed out that could lead to the post acceleratory period. These are diffusion limitation due to C-S-H accretion around the C_3S grains or lack of space for formation of outer product. The period of final slow reaction is an extension of the post acceleratory period. In an analysis of the hydration kinetics of two C_3S preparation with different fineness, Brown [5] observed that early hydration was controlled by the fineness to which the C_3S had been ground. Both the rate of hydration and the extent of hydration achieved were dependent on surface area. Kinetics in the post-acceleratory period was independent of fineness.

As Gartner and Gaidis discuss, the prevailing view is that the onset of the induction period is due to the formation of a barrier layer which is disrupted at the onset of the acceleratory period. This remains conceptually appealing in that it provides a mechanism by which the effects of species in the aqueous phase can modify the properties of such a layer and thereby influence the rate of early hydration. However, none of the work described has yet resulted in a model adequate to explain the absolute rates of hydration in terms of the rates of transport of the various species involved.

Groves and colleagues [6-8] described the analogous microstructural changes in C-S-H during cement hydration. Early hydration at w/c = 0.5 did not appear to result in a barrier layer. As Groves has pointed out, one of the difficulties in refining hydration mechanisms is that when a sample is observed by electron optical means, either the sample preparation procedure or the observation process itself affects the condition of the specimen. While traditional SEM analyses have concentrated on readily observed outer product, TEM analyses tend to resolve C-S-H in transverse section allowing an assessment of the variability in inner product. Apparently, the latter does not vary greatly and may be characterized as homogeneous, finely grained and lacking obvious channels through which transport occurs. In accord with the TEM observations of Groves, Yang et al [9] used small angle x-ray scattering and observed the porosity in the size range from 1 to 30 nm increased with increasing w/c ratio at 28 days. The most probable pore size was found to be 4-5 nm and did not vary with w/c, age or the presence of silica fume. Being such raises the question as to the mechanism by which silica in particular can be transported to form outer product. In an admittedly highly speculative publication Grudemo [10] suggested a structural model for C-S-H which bears a relationship to that of CH and further suggests such a structure could result in a high silicon mobility. An indirect assessment of the rate of transport through inner product C-S-H was obtained by Groves et al [11] in a study of cement carbonation. The C/S ratio of inner product C-S-H was found to decrease from 1.7 to 1.3 after only one hour of carbonation. Thus, one hour is adequate to cause the redistribution of approximately 25% of the calcium present suggesting the relative ease of transport. It was also observed that initial carbonation of outer product C-S-H occurs without great morphological change. Only after a longer period of carbonation are masses of calcium carbonate crystals observed.

MODELS FOR CALCIUM SILICATE HYDRATE STRUCTURE

The structure of the silicate phases in hydrated portland cement paste has not been fully resolved. Classical methods of structural investigation eg. x-ray diffraction have not been successful due to the pseudo-amorphous nature of these hydrates. Evaluation of structural models has historically relied on postulates based on indirect experimental evidence. Engineering behavior of hardened paste has been explained by application of particular physico-chemical or mechanical aspects of the particular model advanced. The inherent validity of a structural model of cement paste rests on its ability to explain the widest range of

phenomenological and experimental evidence. Research activity on the development of structural models in the period 1986-1992 has been limited. The most recent linkage of structural compatibility with extensive experimental observation was provided by Taylor (12-14). The Taylor rationalization is similar in concept to that previously described by Feldman (15). The Taylor and Feldman models appear to be supported by the largest body of experimental evidence. The cardinal features of these primarily layered silicate models will be discussed on a comparative basis with earlier models featuring predominantly non-layered micro (gel)-porous C-S-H continua. Comment on the major experimental strategies will be given.

Taylor Model:

Taylor [12] further developed a model for C-S-H by considering it to be structurally related to both jennite, $[Ca_8(Si_3O_9H)_2(OH)_8]Ca\cdot 6H_2O$, and 1.4 nm tobermorite, $[Ca_4(Si_3O_9H)_2]Ca\cdot 8H_2O$. The primary postulate is that C-S-H gel is a layered mixture of jennite and 1.4 nm tobermorite modified by the omission of a substantial portion of the bridging tetrahedra. Missing bridging tetrahedra result in finite chains containing 2, 5, 8 ...., 3n-1 tetrahedra. This is in agreement with silica polymerization results for C-S-H gel in C_3S, alite and cement pastes [16]. The concept of missing tetrahedra is also a feature of the Feldman model although there are no mineralogical analogs described (figure 1). By eliminating bridging tetrahedra C/S ranging from 0.83 to 1.25 for tobermorite and from 1.5 to 2.25 for jennite can be attained, figure 2. This variability in C/S ratio with hydration can be accounted for by the initial formation tobermorite dimers and their eventual conversion to jennite-like pentamers.

Time dependent variations in Ca/Si ratio are easily explained by the Taylor model. The ratio is a function of chain length or silicate anion size and mixture proportions of jennite and tobermorite. The hypothesis suggests that a mixture of both mineral types exists at early ages with predominantly jennite forming at later ages. The extreme values of Ca/Si ratio for jennite and tobermorite are cited as 1.5 to 2.25 and 0.83 to 1.25 respectively. Several pieces of experimental evidence give credence to the model. These include H_2O/Ca ratios, densities, TGA, and analytical electron microscopy. H_2O/Ca ratios obtained at 11% RH (a datum point delineating the separation of pore water and constitutional, interlayer and adsorbed water) lie between that of jennite and 1.4 nm tobermorite. Densities for C-S-H gel are comparable to those obtained for minerals with similar H_2O/Ca ratios. X-ray diffraction spectra for C-S-H generally reveal two diffuse bands suggesting the presence of Ca-O layers as an integral part of a disordered structure broadly resembling those of either jennite or tobermorite. Electron optical evidence provided by Copeland, Grudemo and others is compatible with structures assigned to jennite, tobermorite or a binary mixture of the two minerals [17, 18].

Argument related to the state of water in portland cement paste has provided much of the basis for structural modelling. Taylor has demonstrated that the bound water (excluding non-evaporable water) content of cement paste calculated from the amounts and composition of the individual hydrated phases is about 32% of the ignited weight [13]. This is equivalent to the amount retained on equilibration at 11% RH consistent with the results of Feldman [19]. The definition excludes water held in micropores and large pores and the results suggest that perhaps micropores comprise an insignificant part of the gel structure below 11% RH as water loss is accounted for primarily by interlayer and adsorbed species.

Several investigations of the ternary $CaO\text{-}SiO_2\text{-}H_2O$ system are relevant to view that the variability in C/S ratio during hydration can be accounted for by the conversion of first formed tobermorite to jennite. Brown et al [20] established a solubility curve for C-S-H and the composition of the C-S-H-CH invariant point. Although only a single solubility curve was observed in that study, based on a comprehensive survey of the literature Jennings [21] observed that the solubility data for C-S-H tended to group along two curves, figure 3. The C-S-H curve exhibiting the lower solubility was interpreted as that for C-S-H(I). The higher solubility curve was interpreted as that for the jennite-like C-S-H of Taylor. While there was no disagreement about the validity of the data, Barrett and Bertandie [22] disagreed with this interpretation suggesting instead that the higher solubility curve is fact that for a protonated interfacial layer of composition C_3SH_x. One difficulty in reconciling these findings is that

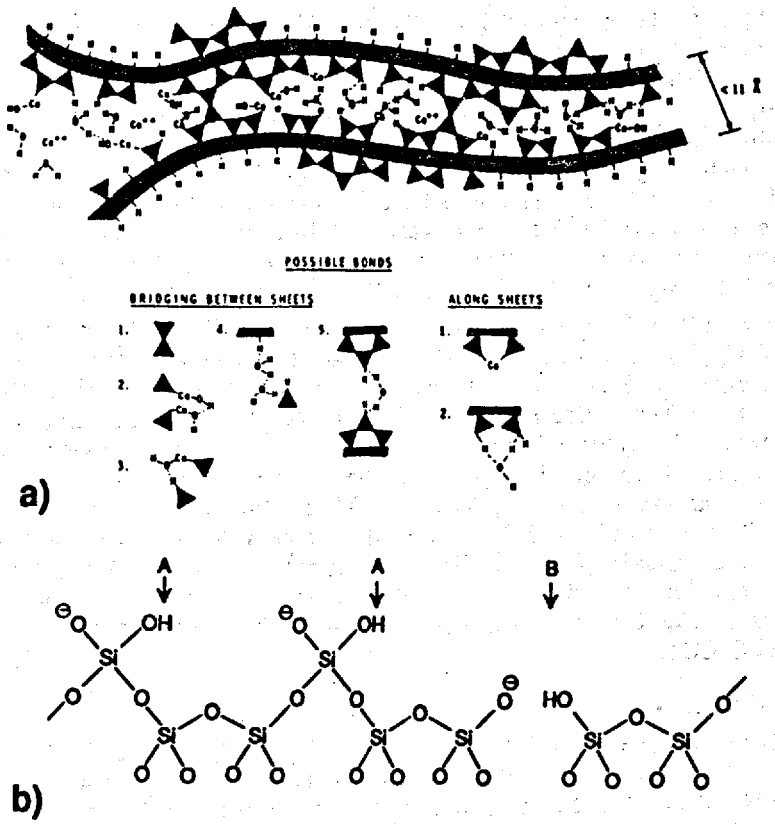

Figure 1 (a) Representation of C-S-H gel structure after Feldman, illustrating bonds between and along sheets and polymerization of silicate chains [15].
(b) Representation of features of C-S-H gel structure after Taylor [12]. Silicate chain of the type present in jennite and 1.4 nm tobermorite showing the probable positions of the H atoms (marked A) and suggested modification (at B) by the omission of a bridging tetrahedron.

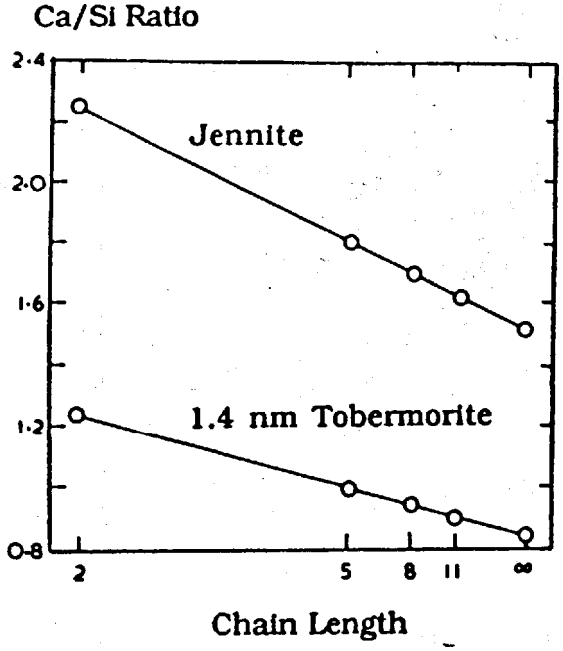

Figure 2 Calculated Ca/Si ratio plotted against a function of chain length for jennite and 1.4 nm tobermorite structures modified by omission of bridging tetrahedra [12].

Taylor indicates that it is a jennite-like C-S-H which is in equilibrium with CH while the tobermorite-like material is that in equilibrium with hydrous silica. figure 2 also shows excluded compositions suggesting that C-S-H is not be a single phase over the range of C/S ratios from 0.83 to 1.67. Thus, if the solubility curves observed by Jennings are related to those of a tobermorite-like and a jennite-like C-S-H, an invariant point between them is required. Such a point has been indirectly observed by Grutzeck et al [23]. In measuring the equilibrium pH values attained in mixtures of CH and silica, it was noted that there are two pH values (10 and 11.9) at which the C/S ratio of the solid varies, figure 4. If it is assumed that two solids are present when these constant pH values are attained, these points represent invariant points in the $CaO\text{-}SiO_2\text{-}H_2O$ ternary system. The presence of more than a single solid in equilibrium with the solutions at these pH values was suggested by ^{29}Si NMR. The invariant point at pH 10 was interpreted as involving a silica-rich C-S-H. That at 11.9 was interpreted as involving silica-rich C-S-H and lime-rich C-S-H. The invariant point involving lime-rich C-S-H and CH was not attained in this study. The silica-rich C-S-H was reported to exist over a range of C/S ratios from 0.65 to 1.0 while the lime-rich material exists at C/S ratios between 1.1 and 1.3. Although the latter was interpreted to be jennite-like, the range of C/S ratios exhibited are closer to those of tobermorite as shown in figure 2. Thus, the results recently developed favor the existence of more than a single C-S-H. Indeed a recent TEM study has actually suggested the existence of 4 Types of C-S-H [24]. Unlike the morphology distinctions defined by Diamond [25], these types are reported to differ in both morphological and unit cell. However, in commenting on this work, Groves [26] suggested that three of the types reported could actually be CaO, $Ca(OH)_2$ and $CaCO_3$.

Feldman-Sereda (F-S) Model:

The F-S model describes C-S-H as a layered, poorly crystallized, malformed tobermorite-like material [27]. The relevant states of water described include interlayer, adsorbed and bulk pore water. Intercalation processes occur over the entire humidity range. Interlayer water contributes to the structural response of the system; it is part of the structure. It is postulated that gel pores do not exist ie. interlayer space is not part of the pore system. Porosity is determined by displacement with fluids (eg. isoproponal, nitrogen, helium) that do not penetrate interlayer positions.

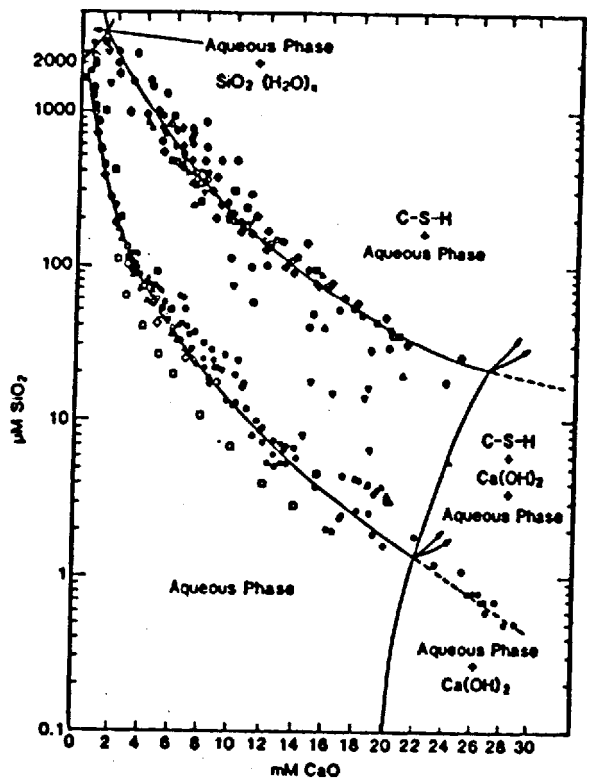

Figure 3 Phase diagram indicating the solubilities of two types of C-S-H [21].

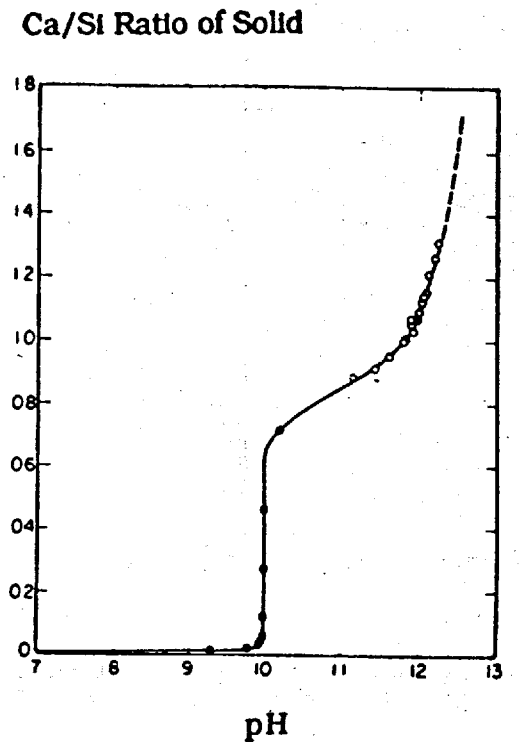

Figure 4 C/S molar ratio of the solid plotted as a function of the pH of the coexisting solution phase. Two invariances exist in the system, one at pH 10.0 and possibly one at 11.9.

Evidence for the existence of interlayer water in the C-S-H structure is extensive. It includes deduction based on: sorption (length-weight change and engineering parameter isotherms), x-ray, density, helium diffusion, NMR, low range x-ray scattering, quasi-elastic neutron scattering and thermal analysis measurements.

Sorption experiments are particularly relevant. Length and weight change isotherms obtained by Feldman exhibit massive primary and secondary hysteresis and the existence of scanning loops. The implication of this hysteresis is profound. Implicit in the application of adsorption theory to isotherm data obtained for cement paste is that it is representative of a thermodynamically reversible adsorbate-adsorbent system. The validity of this type of analysis (via a classical approach) is then highly questionable for the cement paste system. Isotherms exhibiting large primary and secondary hysteresis (for hydrated cement or C_3S paste) have also been observed by Powers, Helmuth, Daimon and Skoblenskaya, figure 5 [28-31]. Powers also observed the existence of scanning loops and reported that adsorption phenomena could not be fully understood until the loops were adequately interpreted [28]. His analysis was, however, based on the application of classical adsorption theory to all isotherm data. Weight and length change isotherms for C_3S pastes reported by Helmuth exhibited both primary and secondary hysteresis [29]. The data was very similar to that obtained by Feldman. Daimon published weight-change isotherms for C_3S paste and CH free - C_3S paste [30]. These isotherms also exhibited complete hysteresis.

Feldman separated the isotherm into reversible and irreversible components and applied adsorption theory to the reversible isotherm [32]. Surface area determinations were in agreement with those obtained by N_2 adsorption methods. The C-S-H structure was considered to stabilize through desorption along a scanning loop. Weight gain along the loop represented true adsorption; water surface areas were equivalent to those obtained with N_2 adsorbate. Application of thermodynamic theory developed by Flood and Heyding [33] to length change data along typical scanning loops gave approximately constant values of a parameter βK, the product of solid compressibility and a structure factor [34]. This supports the assumption that material properties are essentially constant on the segment of each scanning curve used to construct the reversible isotherm.

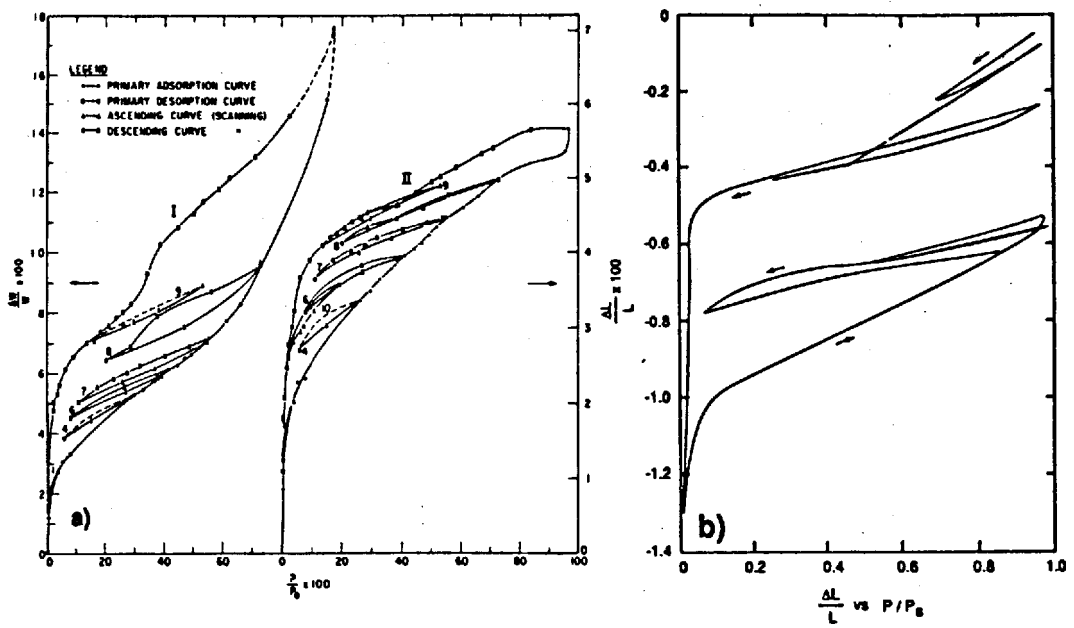

Figure 5 (a) Weight and length change isotherms of portland cement paste depicting scanning loops and large primary and secondary hysteresis [32].
(b) Length change isotherm of C_3S paste showing similar features to the isotherm for portland cement paste [29].

The question of whether water could re-enter the layered structure after D-drying (equilibration at the vapor pressure of dry ice, -79°C) was addressed by several experiments including drying more severe than D-drying. Low angle x-ray scattering measurements indicated that surface areas including interlayer surfaces were regenerated after rewetting from the D-dried position [35]. Penetration of interlayer space with helium after rewetting indicated water re-entered the structure. Density values for the intercalate were comparable with those obtained on first drying. Helium gas was able to flow into vacated interlayer positions as water was removed incrementally. This permitted systematic estimation of volumes associated with interlayer space, density of interlayer water and collapse of structure associated with its removal [36].

Differential thermal analysis conducted under controlled humidity revealed the existence of two low temperature endothermic peaks (65-80 and 90-105°C). The peaks grow simultaneously as humidity increases along the ascending branch of the adsorption isotherm. Desorption to the 11% RH datum from various positions along the ascending branch clearly indicates that the 11% RH position is not unique. The 90-105°C peak grows larger as the RH on adsorption increases. The 65-80°C peak is always reduced to a very small size on return to 11% RH. These results show that the two peaks can distinguish interlayer water from adsorbed water on the free surface. Interlayer water re-enters D-dried hydrated C_3S and portland cement paste over the entire humidity range and conventional surface area calculations based on water sorption are not valid [37]. It is noted that earlier DTA work by Wittmann did not reveal two discernible low temperature peaks possibly due to less exacting humidity control and conditioning procedures [38]. Irreversible volume change due to drying and wetting is arguably due to aging effects resulting from exit and entry of interlayer water. Layering processes involve translation of C-S-H sheets, creation and elimination of interlayer positions. The Bangham effect triggered by the thermodynamics of adsorption is operative but accounts for only a small fraction of the total volume change. Creep is analogous to shrinkage and involves mechanisms other than mass transport diffusion controlled processes. These might include non-linear particulate sliding, shearing and other processes related to ageing including silica polymerization effects.

The F-S model can be used to explain the humidity dependence of the mechanical properties of hardened cement paste, eg. strength and modulus of elasticity. Water uptake from

the D-dried state weakens the paste; modulus of elasticity however increases. Strength decrease is attributed to attenuation and rupture of Si-O-Si bonds to form silanol groups -Si-OH, OH-Si-. Increase in modulus of elasticity, particularly at higher humidities is attributed to the stiffening effect of the intercalation process. The stiffening effect can also be predicted from application of Flood and Heyding's theory of solid compressibility [33].

Daimon Model

The model developed by Daimon and co-workers essentially recognizes two kinds of gel pores - a wider inter gel pore and a smaller intra gel pore [30]. This model is very similar to the Feldman and Taylor representations. The distinction lies in the introduction of an intercrystallite micropore (intragel type) in addition to the interlayer space described by Feldman.

The primary evidence is obtained from water sorption experiments on C_3S and CH free C_3S pastes which exhibited large primary and secondary hysteresis. Evidence was provided for the existence of scanning loops and the view that the resorption branch represents the true pore structure. It was suggested that during resorption (after D-drying) the solid phase undergoes structural changes. This was attributed to penetration of water into micropores and subsequent swelling. It was suggested that interlayer packing was very disordered. This is a major departure from the Feldman model which attributes a large part of the length change to interlayer penetration. No length change mechanism was described and the role of interlayer water was not discussed.

These investigations noted that extraction of CH from paste remarkably increases the observed volume of small pores suggesting that sorption is hindered by CH. It is possible however that CH particle size itself can be of this order and its removal may create new space. The earlier postulation by Bernal that interlayer water in C-S-H could leave and return reversibly appears unlikely given the irreversible nature of the water isotherm [39].

Wittmann Model:

This structural model referred to as the Munich model views cement paste as a microporous xerogel [40]. Water interactions with the paste are considered to comply with classical adsorbate-adsorbent behavior. Length change in the 0 to 40% RH region is described as primarily Bangham and considered proportional to the change in surface free energy of the solid adsorbent accompanying adsorption. NMR evidence is cited to support the view that water adsorbed in the monolayer behaves as a two-dimensional Van-der-Waals gas [38]. The sorbed water is bound as interlayer water and hydrate water only at higher humidities.

Water enters interlayer space at higher humidities because the solid has been conditioned by the expansion process at lower humidities. This is a major difference between this model and the others. Later evidence showed that water in the interlayers of hydrated C_3S paste exchanges with the surrounding atmosphere over the whole humidity range [41].

The inability of thermal analysis to differentiate types of hydrate water is cited as evidence that no significant consumption of hydrate water is taken up during adsorption. The implication in application of adsorption theory is that perturbation of the solid is not sufficient to invalidate application of reversible thermodynamics. The sorption hysteresis effects observed by others are not explained and not considered sufficient to invalidate the approach. Structural changes do not involve intercalation processes in the adsorption region of the isotherm. Adsorbates such as nitrogen and alcohol yield the surface area of dried paste since they cause no significant structural alterations during sorption.

Relative strength of cement paste exposed to different humidities was shown to be linearly dependent on the change in surface energy [42]. Strength decrease with humidity is attributed to weakening resulting from swelling due to adsorption. Swelling is a consequence of disjoining pressure at high humidities. It overcomes other bonding forces holding the gel particles together. The strength of these forces is reduced and the particles glide apart with respect to each other. This mechanism cannot account for the increase in cement paste solid volume occurring under constant applied stress. It is also incompatible with the observation that strength is not greatly reduced from 50 to 100% RH and modulus of elasticity increases

greatly over this range.

Application of the model to descriptions of volume change based on thermally activated processes does not recognize movements occurring in the solid phase as a source of creep deformation. Activation energies determined by application of models recognizing that creep means alteration of solid structure yield values of activation energy varying from 25 to 110 kcal/mole in comparison with values of 5 to 40 kcal/mole suggested by Wittmann [43].

Powers and Brownyard Model:

This model based on extensive water vapor sorption studies describes cement paste as a body composed of gel particles (approximately 1000 nm in diameter) separated by a water film up to 60 nm thick [28]. The solid to solid distance between particles is about 180 nm. Gel pores have entrances less than 40 nm in diameter. The cement paste system is considered as an ideal absorbent. It comprises unreacted cement, hydration product and capillary pores. Evaporable water resides in gel pores contained within the hydration product and capillary pores. The hydration product is considered to contain a fixed amount of non-evaporable water and an intrinsic gel porosity of 28% independent of water-cement ratio and degree of hydration. It was deduced that a minimum water/cement ratio of 0.38 was required for complete hydration. This was dictated by the differences in specific volume of the hydration products and the reactants and the relative constancy of the total paste-volume on hydration. Mature pastes with water-cement ratio <0.38 contain virtually no capillary pores and space is inadequate for complete hydration.

The particles are held together mainly by van der Waal's forces. Swelling is explained by individual particles separating due to layers of water molecules between them. Some chemical bonds between the particles are postulated to explain the limited swelling nature of the materials but the location and function of these bonds is not clear. Creep is the result of water being squeezed out from between the particles during the application of stress. Shrinkage is attributed to mass transport and moisture loss due to free energy gradients.

In a later refinement of the model the concept of disjoining pressure due to hindered adsorption in narrow places between solid bodies was introduced [44]. Disjoining pressure on solid surfaces is required to establish equilibrium with the pressure in the adsorbed layer and water in areas of restricted adsorption between particles. The hindered adsorbed water is described as load bearing. Mass transport results when an external force or change in humidity causes a change in equilibrium of the system. This theory cannot explain weight gain and subsequent creep of paste specimens re-wet while under load [45]. Wittmann's creep results are also at odds with this theory [46]. Creep rate increases only after exposure of D-dried specimens to humidities above 45% RH. It was argued that there is no justification in assuming irreversible creep is due to viscous or plastic flow of the solid structure. Activation energies greater than 100 kcal/mole reported by Day would appear to be in opposition to this argument [43]. Bazant in a further refinement of Powers model argued in support of the disjoining pressure concept using diffusion theory applied to paste systems considered under thermodynamic equilibrium [47]. The chemical potential for water was expressed as:

$$d\mu_w = -SdT + \Gamma_w^{-1}\, d\Pi_w - P_w\Gamma_w^{-1}\, dl + \frac{\partial \mu}{\partial \xi}\, d\xi$$

where l is the half-thickness of the adsorbed layer, Π_w is the spreading pressure (Bangham effect), Γ the surface concentration (subscripts w and s for water and CH solids respectively) and $\xi = \Gamma_s/\Gamma_s + \Gamma_w$. S and T are entropy and temperature respectively. It is assumed that dl and $d\xi$ are negligible. The assumption that the dl term is negligible is not valid as creep results in solid volume increases and creation of new interlayer space by movement of sheets in certain specific sites. Creep strain at specific sites is substantial although overall creep strain is low. The diffusion of water molecules may be the rate-controlling process only at very early ages even though creep is very sensitive to humidity and water content.

Brunauer's investigations of complete pore structure analysis involved techniques of micropore analysis applied to the Powers model [48, 49]. Brunauer employed micropore (MP) analysis of C-S-H based on the studies of deBoer and co-workers [50]. The MP-method makes use

of v_t - t curves obtained for non-porous adsorbents. The volume of adsorbate in the liquid film v_t should be a linear function of the film thickness, t. Estimation of the hydraulic radius of a group of pores, surface area and total pore volume is made using v_t - t curves and water vapor sorption data. Cement paste surface areas of about 200 m^2/g are obtained using water vapor as adsorbate. This is cited as being in agreement with areas determined by low angle x-ray scattering data [35].

The MP-method does not recognize structural changes to the cement paste adsorbent that occur on adsorption of water vapor. The v_t - t curves for cement paste are constructed from isotherms which are assumed to be reversible in the adsorption region. The t curve data is obtained from isotherms on non-porous adsorbents assumed to be applicable to cement systems. This is in conflict with models proposed by Taylor, Feldman and Daimon. It is also in conflict with full water vapor isotherm data published by Powers and Helmuth.

COMPARISON WITH MODELS FOR SILICA GEL STRUCTURES

The sol-gel process has features in common with the cement hydration process in that both occur by precipitation reactions and both result in the formation of condensed silicates of colloidal dimensions. In the sol-gel process, alkoxides are hydrolyzed and then condensed [51]. These processes are illustrated in the following example using tetramethoxysilane (TMOS):

$$Si(OCH_3)4 + nH_2O \Rightarrow HOSi(OCH_3)(4-n) + nCH_3OH.$$

Continued hydrolysis results in the formation of hydrous silica species. These will undergo condensation reactions. This may be represented as follows:

$$HOSi(OCH_3)(4-n) + HOSi(OCH_3)(4-n) \Rightarrow (CH_3O)(4-n)SiOSi(OCH_3)(4-n) + H_2O.$$

In the hydration of the silicate phases in cement, calcium ions, hydroxyl ions and silicate species enter solution then precipitate. Subsequently, the silicates condense resulting in the formation of dimers in the short term with the eventual formation of higher polymers.

One interesting phenomenon observed during the drying of silica gels is that of syneresis. Syneresis involves the contraction of the gel network with the expulsion of pore liquid. Syneresis is observed in organic gels and small changes in temperature or in the composition of the pore fluid may result in reversible dimensional changes of 2 orders of magnitude. Syneresis in inorganic gels results in smaller changes in volume (~15%) and is irreversible. The basis for the phenomenon is condensation of M-OH groups with the formation of M-O-M bonds and water. The reduction of the liquid-solid interfacial areas of these gels has been suggested as the driving force for syneresis [52]. Although silica gels and calcium silicate hydrate form under very different conditions, both have very high specific surface areas [53]. Syneresis of silica gels involves dimensional changes in linear structure (chains). The process has been modelled by assuming the solid to be intersecting right cylinders [54]. As the networks form, the kinetics of the process and the attendant dimensional changes are both reduced. Dimensional changes due to irreversible drying shrinkage of cement pastes are much smaller than those in silica gels [55]. However, the nano-scale connectivity is higher in C-S-H. Hansen [56] recently reviewed the various mechanisms reported to produce drying shrinkage in cement paste and similar mechanisms appear to apply to both cements and silica gels. Recognizing this similarity, Ferraris and Wittmann further treated cement paste as a zerogel and have developed a model for the capillary forces involved in interparticle interactions [57]. Thus, the similarity in the phenomena between inorganic gels and hardening cement pastes suggest that the theoretical developments in modelling behavior in silica and like inorganic gels may be useful in developing a more comprehensive understanding of the dimensional changes in cement-based materials.

Calculating the structures of gels formed by sol-gel processing is also an area of interest. Similar calculations may provide a means to further define the nanostructures of C-S-H. For example Garofalini [58] has used molecular orbital and molecular dynamic calculations to describe the process by which silicate polymerization occurs. Molecular orbital calculations have modeled the structures of bulk silicates [59]. Evaluation of the effects of cations have also

been carried out to calculate the structural changes caused by the presence of cations on amorphous silicates [60, 61].

STRUCTURES OF NON-SILICATE PHASES IN CEMENT

The spatial distributions of the non-silicate are well established. Calcium hydroxide tends to form as sheafs of hexagonal plates at locations remote from the alite and belite surfaces. A structureless layer calcium aluminosulfate hydrate may form on the available surfaces in the first minutes of hydration. However, ettringite principally forms in association with the interstitial phases. While it has long been held that an ettringite layer serves as a diffusion barrier controlling the hydration of C_3A, analysis of the phase behavior in the quaternary system $CaO\text{-}Al_2O_3\text{-}CaSO_4\text{-}H_2O$ suggests that the formation of alumina gel near the C_3A surface may be responsible for controlling its hydration [62]. The decomposition of ettringite eventually results with its intimate intermixing with C-S-H. Early studies [63, 64] indicate that the size of the AFm regions are smaller than about 2 μm. For this reason AFm phases are not discerned in mature cement pastes. Taylor summarized evidence obtained using a variety of analytical methods to suggest that C-S-H is cement paste is relatively free of aluminum iron and sulfate [65]. Rather these are intermixed or interstratified with C-S-H on on a fine scale, possibly on an atomic scale. Taylor also reports that layers of $Mg(OH)_2$ and hyrdotalcite may also be admixed with C-S-H in a similar manner. Using TEM, Rodger and Groves [66] confirmed that inner product C-S-H is essentially pure. As would be expected, there was no evidence for the presence of AFm as a second phase. Compared to inner product, the outer product C-S-H was compositionally more variable and some areas showed the presence of aluminum and sulfur. Small, sulfate deficient AFm crystals were also observed. Occasional regions containing needles of a hydrotalcite-like phase and a poorly crystallized hydrogarnet-like material of approximate composition: $C_3A_{0.3}F_{0.3}SiH_x$ were observed. In a study of the hydration a cement containing 10% MgO it was reported that the magnesium silicate hydrate cerolite was identified [67].

COMPUTER MODELS OF MICROSTRUCTURE

Computer models developed to emulate microstructure tend to fall into three generic categories. One such category includes models which simulate the spatial distributions of anhydrous phases and hydration products. However, little appears to have been published in this area in the last several years.

A second class of models are those which simulate some aspect of hydration or microstructure. Bezjak [68] modified the Avrami equation to account for the growth of outer and inner product thus further developing the relationships between hydration kinetics and microstructure. According to the Avrami equation

$$d\alpha/dt = nkt^{(n-1)}(1-\alpha)$$

Bezjak introduced a surface area term to the Avrami equation by the use of an effective radius to define the surface where hydration product is forming. This leads to

$$[1 - (1-\beta\alpha)^{1/3}]^{1/n} = k\beta t/R^M$$

for inner product growth, where the term β has been introduced to account for hollow shell formation. For outer growth

$$[1 - (1-v\alpha)^{1/3}]^{1/n} = kvt/R^M$$

where n is the volume ratio of inner to outer product. Bentz and Garboczi [69, 70] have recently developed a microstructural model for C_3S hydration which relates degree of hydration, connectivity and transport through the paste. Extension of the model includes consideration of the effects of mineral admixtures and preliminary extensions to cement pastes. The basis for this model is percolation theory. Percolation theory was applied to phase transitions [71]. In percolation theory, the development of a critical property, such a electrical conductivity, continuous porosity, impermeability, etc., is associated with the development of a critical structure. The development of a critical structure, such as an interconnected network of pores which bridge a specimen is probabilistically based.

The third category of models which have been developed are those which consider the physical aspects of microstructural development by use of equations to relate strength gain,

porosity, etc to measurable parameters such as composition and fineness. Parrott developed a model to predict the degree of hydration of constituents in cement, heat evolution, bound water, porosity, and properties based on a variety of input parameters. These include cement composition, fineness, curing temperature and curing condition. [72, 73].

A model developed by Osbaeck emphasizes the relationship between hydration characteristics, porosity and property development [74]. The following equation was developed to relate porosity to hydration characteristics:

$$p = [(w/c) - (\Delta v_i f_i \alpha_i)]/[(w/c) + 1/\rho_c]$$

where w/c is the water-to-cement ratio, Δv_i are the specific volume increases with hydration of the various phases present, f_i are the fractions of the anhydrous phases, α_i are the fractional degrees of reaction of these phases, and ρ_c is the density of the cement. Using this expression for porosity and calculating the compressive strength using the expression: $\alpha = \alpha_o \exp(-kp)$, where α_o is the strength at full density, provides the correlation shown in figure 6.

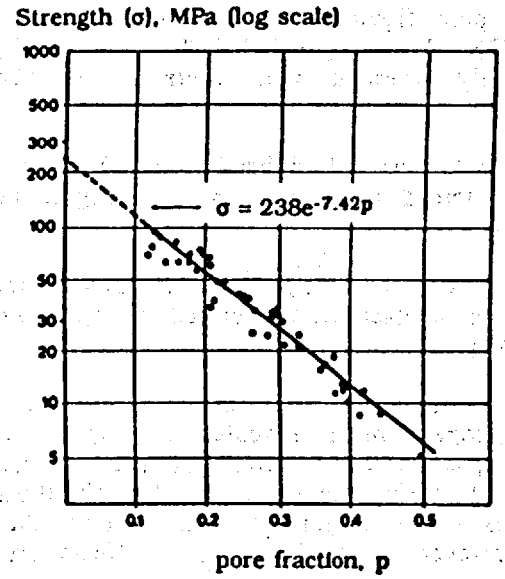

Figure 6 Relationship between compressive strength of cement paste and porosity after Osbaeck [74].

STRUCTURE OF THE CEMENT PASTE - AGGREGATE INTERFACE

Structural models for bulk hydrated cement paste are generally not representative of microstructure at the cement paste - aggregate interface. A distinct region with a nominal thickness of 50 μm has been described by several workers and is referred to as the transition zone [75, 76]. There is varied opinion about the conditions of formation, composition, crystallite orientation and pore structure of the transition zone. Earlier descriptions of the transition zone have been re-examined carefully by several investigators [77-80]. The majority of these workers have identified the following components of this region: a thin layer of CH parallel to the aggregate surface; a small amount of large unhydrated cement grains; hollow shell hydration grains; pores; a layer of CH oriented perpendicular to the aggregate surface; a low proportion of C-S-H and ettringite.

Considerable new evidence for the existence of a duplex film, consisting of a 0.5 μm thick layer of CH and a 0.5 μm layer of C-S-H next to the aggregate surface has been reported since the 8th International Congress. Others have not been able to identify the film [81]. The orientation of subsequent layers of CH in the transition zone has also been critically examined. The effect of additives, admixtures, cement and aggregate type on transition zone properties

was reported. New developments based on transition zone modification have resulted in improved physico-chemical performance of cement-based high performance materials [81-84]. Physical and computer modelling provided new insight into processes affecting transition zone formation and development. An analysis of recent research on the structure of the cement paste - aggregate interface as it relates to the above topics follows.

CH in the Transition Zone

A layer of oriented CH crystals at the paste-aggregate interface has been described by several workers. The XRD method of Grandet and Olivier has been the principle technique used to determine the degree of orientation of these crystals [85]. It is based on the postulate that CH peak intensity ratio $I(001)/I(101)$ in bulk paste = 0.74. Differences in the ratio within the transition zone are ascribed to preferred orientation. This concept was challenged by Zürz and Odler who found that the ratio was not constant and varied with hydration time, water-solids ratio and superplasticizer addition [86]. It was suggested that the existence of a high peak intensity ratio at the interface was possibly due to the water-cement ratio effect. Differences in peak intensity ratio were also found to be dependent on the type of superplasticizer used eg. naphthalene sulphonate resin decreased the peak intensity ratio.

Detwiler and Monteiro utilized a pole figure goniometer in order to validate inferences based on the standard XRD technique [87]. It was concluded that calcium hydroxide crystals at the paste-aggregate interface are strongly oriented with their c-axis perpendicular to the interface.

A method adopted by Yuan et al makes use of diffraction line rocking curve analysis [88]. Greater precision than the standard XRD method is claimed; relative degree of CH orientation in the transition zone is shown to be similar.

Grazing incidence x-ray scattering was used by Monteiro and Ostertag to give more precise information on the thin interfacial contact film ascribed to CH [89]. No broadening associated with amorphous material was observed.

In contrast to the above, back scattered electron imaging techniques applied to specimens fabricated with a single aggregate piece revealed no significant increase in CH content near the interface [90]. The apparent contradiction of these observations with those reported by others may be the result of preferential fracture through those weaker areas in the transition zone where CH is present in larger cavities around the aggregate. The specimens used may be inappropriate, however, as mixing process effects are not modelled.

Other workers have reported difficulties in the detection of a duplex film at the aggregate-paste interface. Zhang et al reported in their TEM studies that C-S-H gel, not CH, is in many cases in intimate contact with the aggregate surface [80]. No evidence was found for the nucleation of CH on aggregate particle surfaces. Formation of the C-S-H layer appeared to be independent of aggregate particle composition. In C_3S - aggregate mortars this layer consists exclusively of C-S-H with a normal Ca/Si ratio at least at early ages. The layer may contain AF_t or AFm phases in portland cement systems.

A possible explanation for the lack of a duplex film or a predominance of CH at the interface itself may be attributed to the small particle size of the aggregate (50-12 μm). It has been demonstrated in other work that aggregate size is related to the size of the transition zone [91]. It is argued that nucleation of C-S-H before CH is compatible with the solubility of silicate and calcium in the early stages of hydration. Silicate concentration begins to decrease while the calcium concentration increases. Orientation of CH crystals at the interface is likely a growth rather than a nucleation effect as the long and narrow high water-cement ratio zone favors continued growth of plates oriented parallel to the interface. Interface fracture is likely to occur through the less dense cement matrix. Examination of the fracture surface on the cement paste side may indicate the presence of more CH than the true interface contains.

Jia employed a minimum energy principle to explain CH orientation effects at aggregate interfaces [92]. The minimum energy state occurs with the (001) plane of the crystal parallel to the aggregate surface. Cement particles away from the interface interfere with the orientation of CH crystals which decreases with distance from the aggregate surface.

Effect of Mineral Additives on Transition Zone Microstructure

Several workers have noted that mineral additives affect the microstructure at the paste-aggregate interface [93-98]. Larbi et al noted that silica fume tends to affect the pattern of crystallization and degree of orientation of CH crystals during the first few days of hydration [93]. The duplex film apparently is not present. This was attributed to the tendency of CH crystals to nucleate and grow on the silica fume particles on the aggregate surface. Mehta and Monteiro observed transition zones with smaller and less preferentially oriented CH crystals when using mineral additives such as silica fume, granulated blast-furnace slag and fly ash [94].

Improvement in transition zone characteristics through use of these pozzolanic and cementitious admixtures was attributed to processes of pore and grain refinement. These involve permeability reduction; initiation of nucleation processes and diminution of CH crystal size; pozzolanic activity; CH reduction and system densification [95]. In contrast to the above, back scattered electron imaging techniques applied to cement systems containing silica fume indicate that silica fume has only a slight effect on the interfacial microstructure [96]. The single aggregate specimens used, however, do not model mixing effects in concrete manufacture. Lack of calcium hydroxide is attributed to infilling of the porous interface region with a porous C-S-H gel produced by the rapid hydration of the relatively small silica fume particles which tend to collect there.

Bentur et al refer to strengthening of concrete containing silica fume as due to formation of a much denser transition zone possibly due to reduced bleeding and better packing of the bimodal cementitious particles [97]. Their conclusions are based on observations that strength enhancement due to silica fume addition occurs in concretes and not in pastes, all systems prepared at the same effective water-cement ratio. This strengthening effect due to silica fume addition is corroborated by the work of Sarkar et al who observed that in non-silica fume concretes, hydrated lime and ettringite are found primarily at the interface while in silica fume concretes only C-S-H is observed [98]. The C-S-H is in direct contact with the aggregates. Jia infers that small particles of silica fume in the interface layer interfere with the orientation of CH crystals [92]. The crystals no longer grow on the surface of the aggregate with plane (001) parallel to the aggregate; they grow on the surface of silica fume particles. This is the principal reason why the orientation index of $Ca(OH)_2$ crystals decreases with the addition of silica fume.

Blast furnace slag addition results in reduction of porosity, CH, and anhydrous cement at the interface and within the transition zone [99-101]. Exposure of slag concrete to sea water reduces chloride concentration at the interface. Calcium hydroxide at the interface is, however, not completely depleted. This is compatible with improved durability of slag concrete in sea water.

Monteiro et al detected the presence of a CH film at the steel-cement paste interface for levels of silica fume replacement up to 16% [95]. The dominant effect that occurs throughout the transition zone is the densification of the structure behind the CH film. The porosity of the transition zone is reduced. Similar observations were made by Bentur and Cohen who argued that the absence of a massive CH layer in mortars containing silica fume was due to reduced bleeding and the ability of the silica fume particles to more efficiently fill the space in the vicinity of the sand grain surface than bigger cement particles [102].

The transition zone composition is different with Type K expansive cement or limestone aggregate [103, 104]. Evidence of chemical interaction between paste and limestone aggregate at ages greater than 56 days was reported. Improved strength due to grain refinement was attributed to formation of a basic calcium carbonate hydrate. The formation of a continuous hydroxide film and preferentially oriented crystals did not occur with the use of Type K cement. A large amount of ettringite and randomly oriented calcium hydroxide forms.

Superior mechanical performance of Type K concrete is attributed to improved transition zone properties.

Transition Zone Pore Structure Revealed by Backscattered Electron Imaging

Backscattered electron imaging and quantitative image analysis methods have been used to effectively characterize transition zone pore structure [77, 90, 96, 105]. The techniques permit estimation of porosity, amount of andryous material and CH with distance from the aggregate surface. No significant increase in CH contact was found near the interface as described earlier. Porosity, however, increases near the interface; the content of anhydrous grains decreases. Observations related to porosity generally acknowledge dramatic increase in volume concentration of pores as the interface is approached. Porosity drops to a relatively constant level after about 30 μm (figure 7). This is ascribed to the following: lack of anhydrous material near the interface; hydration of small particles in the region to form hollow hydration shells. There were no significant differences in porosity distribution of systems containing silica fume compared to plain paste systems.

Transition Zone Modification

Interface and transition zone modification techniques can be used to increase aggregate-paste bond and enhance composite strength. One method involves treatment of aggregate surfaces to produce a hydraulically reactive layer or coating. Several types of

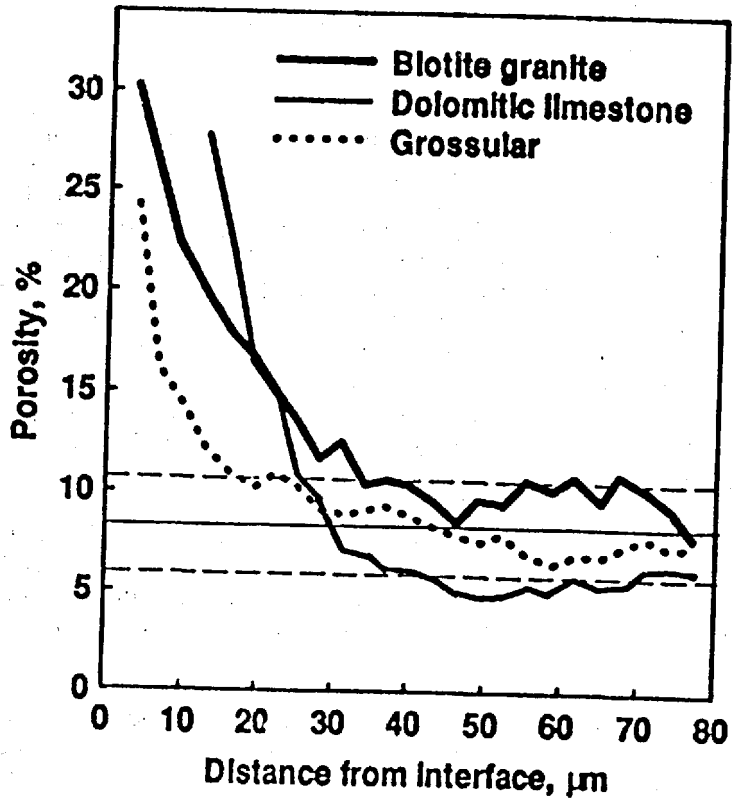

Figure 7 Variation in porosity with distance from the aggregate interface. Solid horizontal lines indicate the average quantity of each component from 24 fields well away from the interface. Dashed lines indicate variation between these fields [77].

treatment have been investigated. Wu et al coated aggregates with a water glass-calcium chloride solution [83]. Bond strength between aggregate and cement paste was increased. Porosity, average pore size, volume of large pores, electrical conductivity and degree of CH orientation were decreased. Large oriented portlandite crystals within the transition zone disappeared and the density of the region increased.

Yang et al utilized corundum particles (pre-treated to form a hydraulically active surface layer) to optimize transition zone properties [81, 82]. Carborundum particles (0.15-0.75 mm) mixed with $CaCO_3$ powder and a small amount of calcium sulfate and water were calcined at 1400° C and slowly cooled to ambient. A layer of hydraulic minerals consisting primarily of

$C_4A_3\bar{S}$ and $C_{12}A_7$ forms on the surface. A very dense transition zone forms in mortars prepared with the treated aggregate. Compressive and flexural strength and corrosion resistance of mortar are substantially increased.

Ping and Beaudoin applied a 10-30 μm layer of silica fume to aggregate surfaces to enhance transition zone microstructure [84]. During the hydration process the interfacial zone composed initially of silica fume is gradually densified due to pozzolanic reaction between silica fume and calcium hydroxide. An interfacial zone more dense than the bulk paste forms after about three to four days of hydration. The character of the interfacial zone composed of silica fume and products of pozzolanic reaction appears not to be significantly affected by aggregate type and w/c ratio.

Sugama treated sillimanite-based hollow microspheres with a $Ca(OH)_2$ saturated solution at temperatures up to 200°C [106]. It was found that the epitaxial layers precipitated by interactions between hot alkali and the sphere surface play an important role in developing cement paste-microsphere interfacial bonds and in enhancing the extent of hydration of the cement matrix. The major constituents of the epitaxial layer seem to be $CaO\text{-}Al_2O_3\text{-}SiO_2\text{-}H_2O$ and $CaO\text{-}SiO_2\text{-}H_2O$ systems.

Transition Zone Development — Physical and Computer Modelling

Electrical conductivity models for concrete were used to develop characteristic parameters describing transition zone development at cement-paste aggregate interfaces [107-111]. The apparent electrical conductivity of mortar or concrete was expressed as follows:

$$\sigma = \sigma_a \psi_a + \sigma_p \psi_p + \sigma_f \psi_f$$

Where σ, ψ are electrical conductivity and area fraction and a,p,f are subscripts referring to aggregate, cement paste and interface regions. A parameter, θ, a descriptor of microstructural change in the interfacial region was derived.

$$\theta = \delta (\psi_{ps} - \psi_{fs}) \sigma_f$$

Where δ, is the transition zone thickness and ψ_s the total area fraction of the solid components in the specimen section. If $\theta > 0$ or $\sigma_f > \sigma_p$ or $\psi_{ps} > \psi_{fs}$ interfacial microstructure is less dense than that of the bulk paste. When $\theta < 0$ or $\sigma_f < \sigma_p$ or $\psi_{ps} < \psi_{fs}$ the interfacial microstructure is more dense than that of the bulk paste.

Further analysis and experimentation led to the following conclusions. The formation rate of the interfacial zone is higher than that of the bulk paste. θ is to a first approximation independent of w/c ratio. θ appears to be independent of the type of aggregate used. This result suggests that non-porous, inert or slightly reactive aggregate may have similar effects on formation of the interfacial zone. A model featuring a water film on a non-porous aggregate surface and a layer of source cement particles adjacent to the film led to the following expression for θ:

$$\theta = \frac{\delta_w \sigma_f}{1 + (w/c)\rho_c} \left[\lambda_c (1-m) + \lambda_{ge} \eta_{ge} m + \lambda_{CH} \eta_{CH} m \right]$$

where δ_w is thickness of the water film on the aggregate surface at mixing, ρ_c is the density of cement, m is the degree of hydration of cement, and λ, η are constants related to the geometries of solid phases, such as unhydrated cement particles, C-S-H gel and $Ca(OH)_2$. θ, the thickness of the water film on the aggregate surface and thickness of the transition zone generally decreases with aggregate size. θ eventually becomes negative when small limestone particles are used as aggregate. This indicates that the transition zone is denser than the bulk paste and

suggests the possibility of chemical interaction. This supports the conclusions of Mehta and Monteiro [94].

The θ parameter appears to be a convenient descriptor revealing the following information about the cement paste aggregate interface: the process of formation and development of microstructure; chemical interaction between aggregate and cement paste.

Garboczi and Bentz reported results of digital image based simulation models of the interfacial zone [112]. They simulated a dissolution-diffusion-reaction-like cycle of hydrating cement particles packed around a simple non-reactive aggregate particle. Features seen experimentally such as increased porosity and CH content in the interfacial zone were accurately reproduced by an algorithmic growth model.

Transition zone characteristics are explained in terms of a one-sided growth mechanism and traditional particle packing concepts. CH clusters very near the aggregates have their growth limited on that side by the presence of the aggregates itself. The one-sided growth effect is due to the fact that non-reactive aggregate does not supply dissolved species. This effect contributes to higher porosity in the interfacial zone but to a lesser extent than the initial particle placement effect. The effects were separated by eliminating inefficient particle packing due to the aggregate edge. Simulations clearly revealed a small increase in transition zone porosity due solely to the one-sided growth effect. Aggregate edge effects are dominant in the 5-50 μm range. One sided growth contributes to transition zone microstructure within 5 μm of the aggregate surface.

PORE STRUCTURES

Measurement Techniques

Mercury Porosimetry and Solvent Replacement - Mercury intrusion porosimetry provides an important means by which the pore structures of cement pastes are determined. However, porosity measurement and pore structure determination of hardened cement paste are subject to large variation [113] and the results obtained tend to show a significant dependence on specimen preparation. The hydrated cement-water system is moisture sensitive, microporous, and thermodynamically unstable. Cement paste microstructure is sensitive to changes in temperature, humidity and stress. Mercury intrusion porosimetry is not only subject to the limitation inherent in cement systems but also to possible misinterpretation resulting from exclusion of pore structure damage effects [114]. Sample preparation for intrusion experimentation necessarily involves removal of pore fluid. Solvent replacement techniques wherein pore water is replaced with organic fluid eg. methanol have been investigated as possible means of stabilizing microstructure for pore structure evaluation by mercury intrusion and other methods [115-128] Work since 1986 has focused on identification and clarification of the limitations affecting these techniques to optimize test procedures and improve interpretation of results. A critical review of this research follows.

A study [129] in which oven drying and freeze drying of cement pastes with W/S ratios of 0.6, 0.4 and 0.2 were employed indicated major differences in pore volume depending on the drying technique used. The pore volumes observed in freeze-dried specimens was lower than those in oven dried specimens and the differences increased with decreasing W/S ratio. The drying process itself introduces stresses which coarsen the pore structure. Kumar and Roy [130] evaluated post-freeze drying desiccation on pore structure. They observed that further desiccation has minimal effect on the pore structure of cement and slag-cement pastes. In addition to variability associated with sample preparation, establishing the variability in pore structure depending on the presence of aggregate is essential in understanding transport properties in concrete, Winslow and Liu [131]. It was determined that the pore structures of cement paste and the paste fraction of concrete are different. Paste in concrete is more porous than is cement paste and the additional porosity occurs in pores having relatively large diameters. These differences are illustrated in figure 8 when both are hydrated at a W/C ratio of 0.45. The paste fraction of mortar was found to be have a pore structure which is closer to that of the paste in concrete than it is to cement paste.

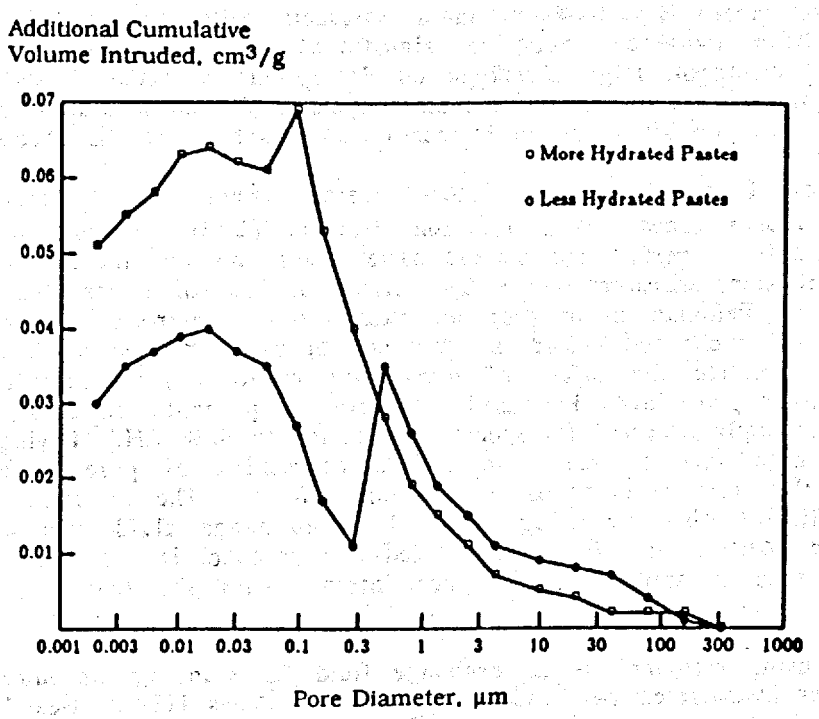

Figure 8 Additional cumulative volume intruded in the paste fraction of concrete relative to plain cement paste [131].

Abdel-Jawed and Hansen measured porosity by gas adsorption and mercury intrusion and concluded that neither technique is adequate by itself to measure porosity [132]. However, they report that the total pore volume of cement may be assessed by combining the results obtained by the two techniques. In spite of its various limitations Winslow concluded that MIP continues to be a useful technique and that it is amenable to modifications which will extend its utility [133].

A comparative study by Day and Marsh [115] evaluated porosity measurement of cement paste (with and without silica fume, fly ash) by mercury intrusion; resaturation with methanol, propanol and water; propanol and methanol exchange. Methanol and propanol resaturation gave equivalent porosity values. Alcohol porosity was, however, significantly less than water porosity. This was interpreted as the inability of alcohol to enter interlayer space. The largest differences were observed with flyash and silica fume paste that contained a greater volume concentration of C-S-H and proportionately more interlayer space. Alcohol resaturation and mercury intrusion also gave similar results. Alcohol exchange porosities unlike resaturation values are similar to water porosities.

In the saturated state distance between C-S-H layers is greatest and they are more receptive to intercalation processes involving alcohol exchange. These authors argued that drying from the solvent replaced condition had a greater effect on structural stabilization and hence increased suitability for mercury intrusion experiments.

A considerably greater pore volume in the size range <20 µm is obtained by mercury intrusion methods compared to values obtained by nitrogen sorption. The ratio of the pore volume measured by nitrogen sorption for blended cement pastes varies from 0.19 to 0.32; for plain pastes to 0.45-0.59. This was attributed to pore structure damage during mercury intrusion.

Elucidation of factors affecting solvent exchange was provided by Feldman [116, 117]. Solvent exchange with methanol resulted in up to 0.1 % expansion of water-saturated cement paste specimens; propanol exchange produced large shrinkages, up to 0.14%. Methanol exchange of water-saturated porous glass had little or no effect on its dimensions. This

strongly suggested the possibility that methanol interacts with components of hydrated portland cement. Other evidence including significant decreases in Young's modulus following immersion in methanol, large shrinkage on desorption of methanol and increases in surface area due to various treatments with methanol suggest that methanol penetrates the layered structure of the calcium silicates and increases the separation of the sheets.

Counter-diffusion of propanol into water-saturated cement paste yielded diffusion coefficients similar to those obtained for chloride ion diffusion, ($D=5x10^{-12}$ to $2x10^{-11}$ m^2/s). It was felt that propanol did not perturb the cement paste solids and was therefore an acceptable fluid for diffusion coefficient measurements. The effect of internal stress due to predrying was also investigated by Feldman using propanol exchange of water-saturated cement paste. The diffusivity of propanol exchanged, water saturated cement paste predried to 75, 42 and 11% RH was determined to isolate the effect of drying on microstructural modification [117]. Predrying and resaturation procedures increased the rate of propanol diffusion through the paste. Maximum rate generally occurred for specimens predried to 42% RH. Drying at 42% RH accelerates ageing of high surface area material and coarsening of pore structure due to compressive stress on the solid resulting from meniscus effects. The influence of predrying on the diffusion coefficient obtained using propanol as exchange fluid was less than for methanol exchange by a factor of 4. It was concluded that propanol is better than methanol as an exchange fluid because it apparently does not interact with the hydration products of portland cement.

The validity of using methanol as an exchange fluid for studying the microstructure of cement paste was further investigated by Beaudoin [118] and Thomas [119]. Beaudoin presented evidence for a methanol-calcium hydroxide reaction based on several techniques including IR spectroscopy, surface area, length change, conduction calorimetry, DTA and TGA. Similarities between the reaction products and $Ca(OCH_3)$ were detected by these techniques. Surface area of $Ca(OH)_2$ samples, for example, increased by a factor of 2.5. Thomas reported there was no evidence of a reaction between methanol and cement paste or calcium hydroxide and concluded that solvent exchange techniques are suitable precursors for pore structure determinations. It was also stated that the solvents were most probably strongly adsorbed in concert with the work of Taylor and Turner [120] and that apparent reactions occurred during thermal analyses. Differences in the IR and XRD spectra obtained by Thomas and Beaudoin for $Ca(OH)_2$ may be due to differences in sample preparation. Samples prepared by Beaudoin were porous bodies obtained by compaction at pressures of 350 and 650 MPa. Calcium hydroxide crystals in cement paste are strained. Reaction with methanol may be stress induced.

Several pre-treatment methods for preparation of cement paste for mercury intrusion measurements were investigated by Feldman and Beaudoin [121]. Specimens were predried before intrusion measurements using several procedures including solvent replacement with methanol, evacuation and/or heating for various periods and conditioning at 11% RH. Second mercury intrusions were also performed to investigate the effects of first intrusion. It was concluded that it is not possible to obtain an actual pore size distribution of cement paste by mercury intrusion because of its sensitivity to stress. A brief review of the pertinent evidence for this statement is given. Mercury intrusion and reintrusion curves are presented in figure 9 for two cement paste specimens (w/c = 0.60). Both specimens were solvent exchanged with methanol. Large differences between the first and second intrusion curves are evident. Coarsening of the pore structure is exhibited. The pore structure changes that occur during first intrusion are a result of solvent exchange [122]. The primary curve does not represent a true pore size distribution since some features in the curve are due to these changes. Other treatments had similar effects. Storage of specimens at 11% RH for 30 days followed by vacuum drying also resulted in considerable pore coarsening. This is probably due to compressive stress (over an extended period of time at 11% RH) imposed by water menisci present in small capillaries. The effect was, however, not pronounced as that due to the solvent exchange pretreatment.

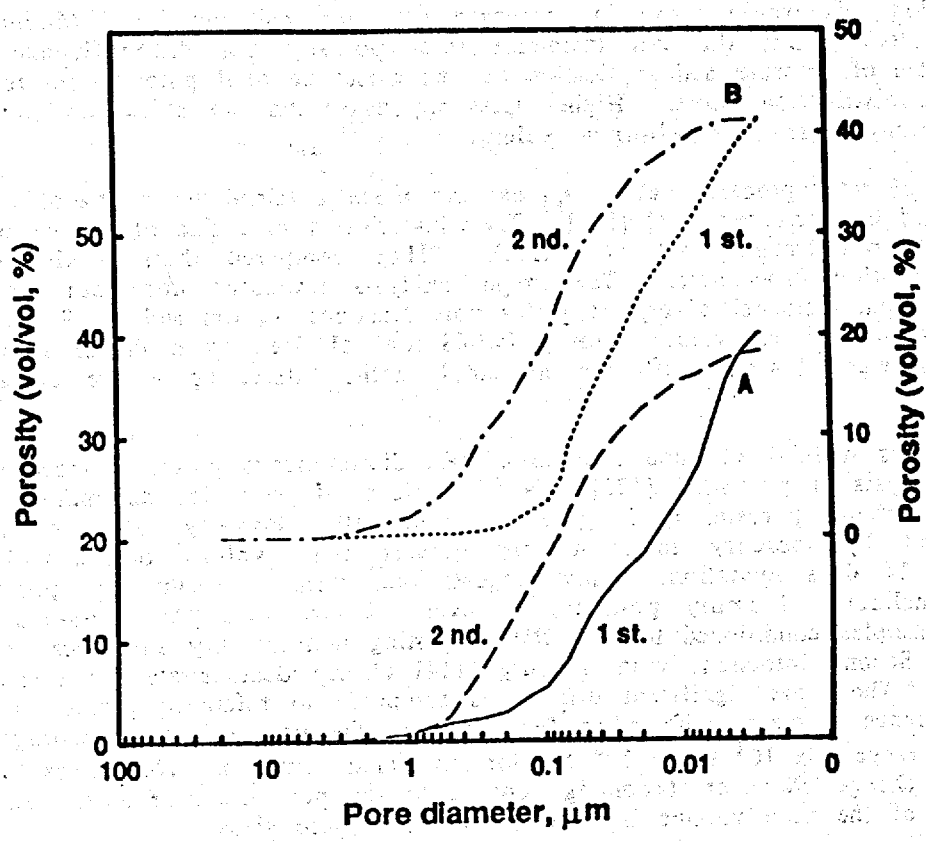

Figure 9 First and second mercury intrusion of portland cement paste specimens (w/c = 0.60) solvent exchanged with methanol. Specimens vacuum treated for 2 hours followed by twenty hours of vacuum plus heat at 100°C. Mercury removed by heat at 135°C for 408 h (Specimen A) and 624 h (Specimen B) [121].

Solvent replacement by methanol increased the threshold pore diameter of the pore size distribution curve by changing surface characteristics of the solid cement hydrate. No evidence of this effect occurring with isopropanol was observed. Solvent replacement allows removal of water without major stress application. Subsequent evacuation times and temperature of heating are relatively unimportant to the resultant pore size distribution. The major factor affecting the pore size distribution of the solid appears to be stress. Sources of stress make it impossible to obtain a true pore size distribution. Relative changes to pore structure however, can be monitored by mercury intrusion techniques. Isopropanol exchange followed by immediate evacuation and heating appears to least affect the original pore structure.

Day utilized propanol exchange data to define two microstructure parameters relevant to durability [123]. The 'offset' and 'slope' of the linear portion of the exchange (%) versus $(time)^{1/2}$ curve are the terms used to obtain correlations with water, oxygen and chloride permeability of various cement pastes. The 'offset' term is the displacement between the linear portion of the exchange curve and a parallel line through the origin. The objective of this work (in progress) is to develop a simple 'permeability indicator' test for some practical situations. This work appears to be complimentary to Feldman's correlation of chloride and isopropanol diffusivity [117].

Other limitations in mercury intrusion testing are reported by Hearn and Hooton [124]. They investigated sample mass and dimension effects on mercury intrusion results. Specimens were propanol exchanged and vacuum dried to constant weight. They observed that a reduction of sample mass results in a decrease of total porosity. The possibility of incomplete drying of larger samples was dismissed as a reason for this apparent anomaly. The argument

advanced was that this would result in decreased not increased porosity. Minimum sample dimensions up to 6.5 μm did not influence total porosity but did influence pore size distribution. Rates of pressure and application had no effect on total porosity but resulted in a shift of the size distribution curve. Higher rates apparently did not allow sufficient time for mercury penetration to reach equilibrium values.

Estimates of total porosity values approaching those obtained by methanol displacement have been obtained by Scrivener et al [125]. They investigated pore size of cement pastes using Backscattered Electron Image Analysis (BEIA). They compared their results with those obtained by adsorption procedures. The image analysis technique does not resolve pores smaller than 500 mm; methanol adsorption yields pore fractions >4 μm and >36.8 μm. Porosity obtained by BEIA was plotted versus porosity (>36.8 μm) obtained by methanol adsorption. A linear correlation was obtained with the methanol method detecting a greater amount. of porosity.

Cement pastes with silica fume addition contain discontinuous pores. Evidence based on pore structure analysis is presented [122]. A comparison of porosities determined by helium pycnometry and mercury porosimetry is given in figure 10. Porosity values of silica fume pastes determined by mercury intrusion are greater than values obtained by helium pycnometry after 14 days hydration. This suggests that mercury breaks into pores that are inaccessible to helium. Mercury porosity, however, is less than that obtained by water displacement on samples conditioned to 11% RH suggesting that mercury still does not enter all the micropores. Second intrusions with mercury [114] clearly demonstrate the effect of silica fume, figure 11. There are significant differences compared to reference pastes without silica fume. The difference increases with silica fume content, the pore volume becoming greater in the pore diameter range 3 x 10^1 to 3 x 10^4 nm for the second intrusion. The curves for 10% and 30% silica fume change character, becoming concave to the pore diameter axis. In general a higher proportion of the pore volume is intruded at higher pore sizes.

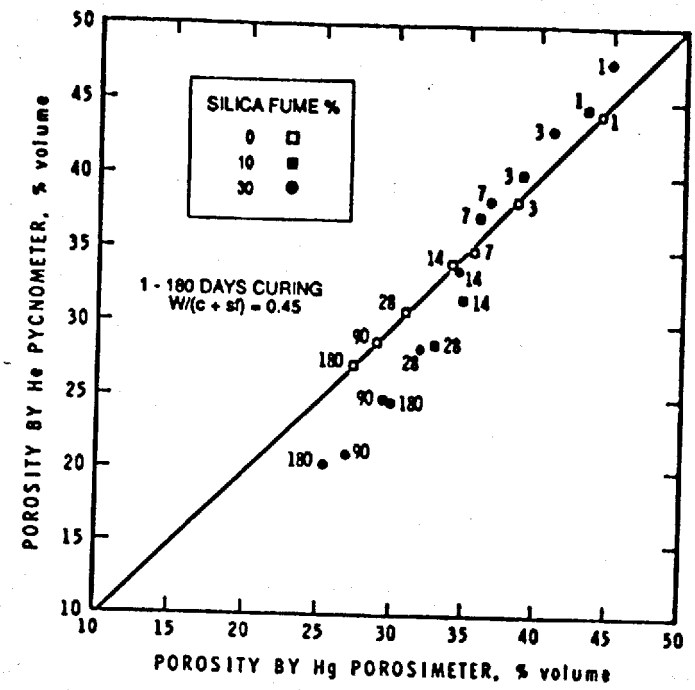

Figure 10 Comparison of porosities determined by helium pyncnometry and mercury porosimetry on cement paste specimens containing silica fume, water/cement and silica fume = 0.45 [122].

Changes in pore distribution curves for mortar blends containing silica fume are more marked than those in paste blends 134-136]. This is especially true for the variations in the large pore-size range caused by the formation of discontinuous pores, due partly to the

removal of lime accumulated at the sand-paste interface and partly to the reaction of lime with silica fume within the matrix. First and second intrusions of mortars containing varying amounts of silica sand and 10% silica fume are plotted in figure 12. Comparison of these results with those of equivalent pastes shows that most of the changes between first and second intrusion occur for the mortar blend in the size range between 10^3 - 10^4 μm. Increase in volume in the higher range is greater for mortar specimens. Hystereses between the two curves increases with sand/cement ratio up to 2.0. Beyond this it decreases because specimens with sand/cement ratios of 2.25 and 3.0 already have relatively high pore volumes in the coarse ranges on first intrusion as well as larger pore volumes in the finer ranges.

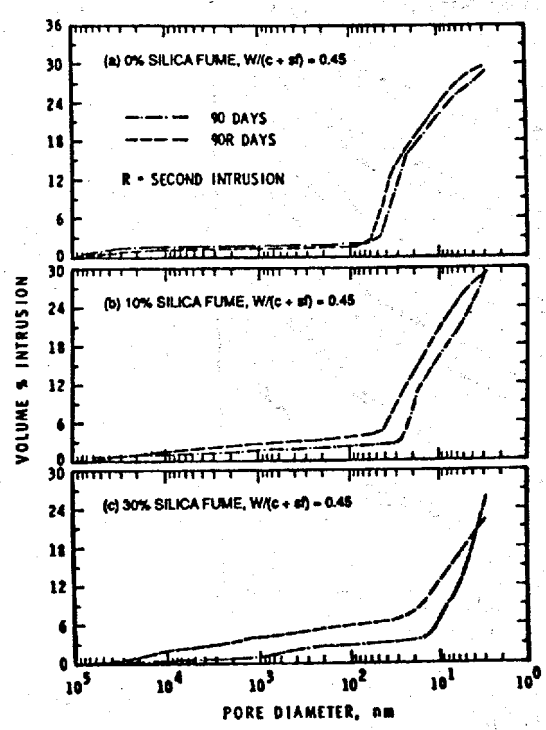

Figure 11 Pore size distribution curves of cement paste with different silica fume contents - first and second intrusions with mercury [114].

It is apparent that accurate determination of cement paste pore structure by any method is complex. Most techniques including mercury porosimetry are linked with microstructural change due to water removal. Solvent exchange methods do not appear to have resolved this problem. Interpretation of pore volume - size curves obtained with first intrusion mercury porosimetry data is moot.

Pore Casts - One method by which the distribution of larger porosity can be determined is through pore casting. In this method the porosity is filled with an epoxy or with a monomer which is then polymerized and the original inorganic material is dissolved away. While this method is relatively common in geology [137], it does not seem to have been exploited to any degree in the analyses of porosity in cements. One exception is an analysis of the porosity developed in C_3S [138]. Rather, the observation of porosity in cement pastes has been largely confined to optical observations carried out on thin sections or to electron optical observations on polished sections [139]. Methods for observing, analyzing and modelling the porosity in geological materials is relatively advanced [140, 141] and has become a useful tool in predicting the movement of fluids through the porosity in these materials.

Direct Observation - Pratt [142] reviewed the state-of-the-art in microstructural investigation. In discussing these techniques it was pointed out that observations of fracture surfaces suffer several disadvantages. The observations are confined to regions of weakness as they are

performed on specimens crushed to fine powders. As a consequence of the latter, the larger context of microstructural relationships may be lost. Finally, the spatial relationships between anhydrous phases and their hydrates are not readily observed. Because of the requirement for specimen thinning, TEM images routinely show hydration products in transverse section and a number of such studies have already described.

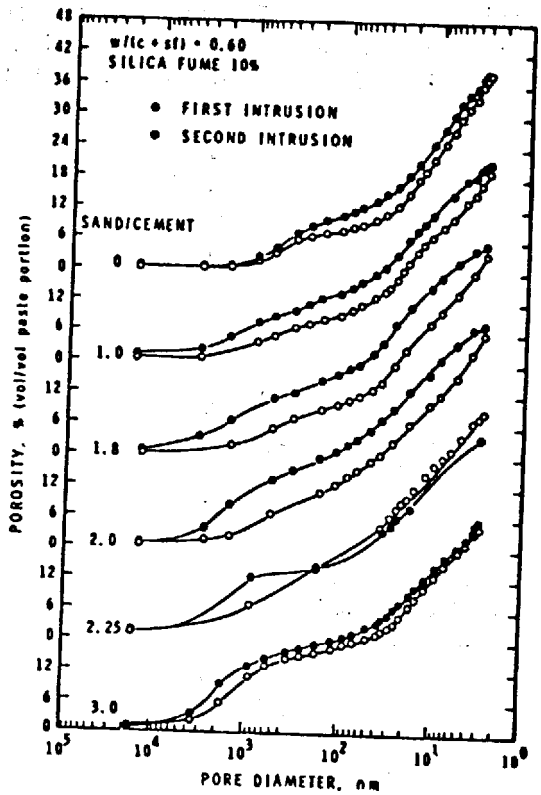

Figure 12 Pore size distribution curves of cement mortars - first and second intrusions with mercury [134].

A significant advance in the ability to relate variations in microstructure and other parameters such as the degree of hydration has been realized by carrying out analyses on polished sections using backscattered electrons [143-145]. One particular advantage to this technique is that it allows the observation of the microstructure in context. Microstructural observation can be combined with compositional analyses to obtain compositionally-dependent spatial relationships. The size distributions of various microstructural features can also be determined. These include the areas of anhydrous cement phases, C-S-H, CH and porosity [125].

Because porosity can be directly observed by this method it allows comparison with porosity determined by other means. The hydration products which formed at 5 and 50°C were compared by Kjellsen et al [146] through observation of polished sections. Comparison of gray levels indicated that hydration shells can be readily discriminated at 50°C. Kjellsen et al compared the sizes of pores observed by backscattered images and those determined by mercury intrusion porosimetry [147]. Increasing the curing temperature from 5 to 50°C resulted in increased porosity in the 20-100 nm range as determined by MIP. Porosity in the 250-1,250 nm range was observed to increase when analyses were carried out on polished sections. Patel, et al measured the porosity of blended cements by methanol adsorption, methanol exchange and by image analysis of microstructures obtained by BSE [148]. Their findings indicted a good correlation between the methods. However, it has been pointed out that care must be exercised when attempting to analyze porosity by electron microscopy [149].

A.C. Impedance Spectroscopy - Characterization of cement paste systems using low frequency electrical measurements is well known. Complex impedance spectra (IS) for hydrating cement pastes however, have been obtained only recently [150-153]. These results cast doubt as to the

the validity of low frequency measurements. The plotting techniques (IS) can be used to separate the electrical response into two distinct regions — one relating to electrode - cement paste interface processes and the other to bulk cement paste effects. Several authors have indicated the limitations of fixed frequency electrical measurements and the apparent advantages of A.C. impedance spectroscopy [154]. The technique permits the monitoring of microstructural evolution in cement pastes through the development of equivalent circuit models. Plots of the complex plane (imaginary impedance versus real component impedance) for portland cement paste are generally characterized by a low frequency arc and one or more high, frequency arcs [151]. The low frequency arc is ascribed to electrode effects; the high frequency arc to pore structure and microstructure effects. A typical frequency scan covers the range 10mHz-15MHz, although frequencies greater than 50MHz have been employed. Discussion in this section focuses on the development of equivalent circuit models for hydrating cement and cement-silica fume pastes.

McCarter and Brousseau have proposed the model depicted in figure 13, [151]. The model consists of three circuit elements in series. Electrode effects are represented by a parallel combination of resistor, R_{ct} and a frequency dependent capacitor, C_{dl}. R_{ct} represents the charge transfer resistance and C_{dl} double layer capacitance at the electrode/cement paste interface. A Warburg impedance element, W, is included to account for slow ionic diffusion effects at the electrode interface at ultra low frequencies. The bulk paste behavior is represented by a similar RC circuit element in seres with a resistance R_e. R_e accounts for the fact that the complex plot does not pass through the origin at high frequencies.

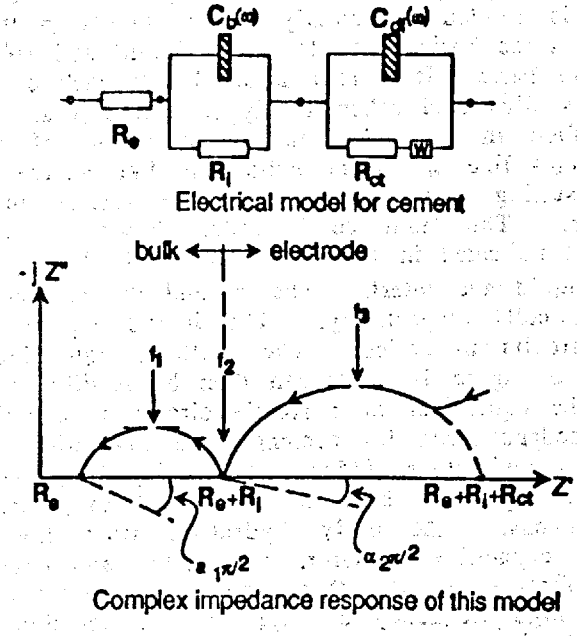

Figure 13 An electrical model for cement paste and its complex impedance response [151].

It was apparent that some model parameters were related to the hydration process. Analysis of results led to the following observations: Complex arc radii increase with extent of hydration; complex arcs are semi-circles with centres below the real axis; centre depression can be modeled by introduction of a non-Debye capacitive element into the equivalent circuit; the frequency at which the low and high frequency arcs have a common intercept with the real axis and the characteristic frequency of the high frequency arc decrease with increasing degree of hydration.

Scuderi et al utilized a similar equivalent circuit model to describe the electrical response of hydrating cement paste [152]. The model incorporates an additional circuit

element to account for a second high frequency arc. It differs from the McCarter-Brousseau model in that the capacitators in the "bulk paste" circuit elements are not frequency dependent. It was noted by these authors that the same impedance spectrum can be explained by a variety of different equivalent circuits. They concluded that additional information is required to determine the equivalent circuit that best represents the actual situation. This was best obtained through additional microstructural characterization.

The work of Scuderi and coworkers indicates that silica fume additions to cement paste result in a proportional increase in sample resistance [154]. The resistance increases at a faster rate than controls without silica fume due to accelerated development of a fine pore structure and decreasing pore fluid conductivity. They concluded that resistance minima in previously reported results for portland cement paste appears to be the result of a microstructural variation, not a pore fluid phenomena. Conductivity experiments with pore fluids obtained by high pressure extraction from pastes containing silica fume provided evidence to support the view that high frequency arc characteristics reflect microstructural change. The conductivity of the pore fluids changed by a factor of only 3 to 4 times during the test hydration period. Conductivity of the bulk paste changed by 2 to 3 orders of magnitude during the same period. Microstructural change appears to be much more dominant than pore fluid chemistry in contributing to sharp increases in resistive characteristics of the paste.

Ping et al [155] developed a new equivalent circuit model to investigate the mechanism of hydration of portland cement paste, from 48 to 380 h. The proposed equivalent circuit was chosen so that its RC parameters would physically represent microstructural elements of the cement paste. A layer model of hydrating portland cement paste was used for equivalent circuit simulations. The specimen is divided horizontally into m layers in the direction of the electric field. It is postulated that three basic elements: solid, liquid and solid-liquid interfacial phases exist in each layer of cement paste. It is also assumed that each divided layer contains "solid liquid interface unit cells" as illustrated schematically in figure 14a. The ionic charges align themselves along the interface in parallel with the direction of the electric field. Similarly, the induced opposite charges line up in the solid side like charge planes, parallel to the solid-liquid interface. The resulting separation of charges simulates an electric capacitor capable of storing electric charge. The "unit cell" model shown in figure 14a can be represented by an equivalent circuit indicated in figure 14b in which the R_s, R_l, R_{int} and C_{int} terms are the resistance of solid, liquid and interface phases, and the capacitance of the solid-liquid interface for a single "unit cell" respectively. The impedance of the layer can be expressed by n unit equivalent circuits in series. The multiple equivalent circuit can be simplified into the circuit displayed in figure 14c. It can then be readily shown that the total impedance of a cement paste can be equivalent to a simple circuit as exhibited in figure 15. Plots in the complex plane of impedance data for cement paste (hydration time 48-380h) are quite similar to those reported by other authors [151]. The delayed appearance of the high frequency arc is evidence that the capacitive behavior is related to microstructure changes during the cement hydration process. At early hydration time the rigidity of the microstructure is too low to detect capacitive behavior. Simulated and experimental data for each hydration time plotted in the form of log (mod) vs log (freq) exhibit excellent agreement in the frequency range where the high frequency arc appears. Conclusions drawn from the modelling process include the following. The significant decrease in free water content during early hydration causes a rapid increase in $R_{t\ (s+l)}$. The solid resistance mainly contributes to $R_{t(s+l)}$ in the later stages of the hydration process. The growth in diameter of the high frequency arc is directly related to the increase in the number of interfaces. Different impedance properties of the interface are derived from both solid and liquid phases during the hydration process. The terms $R_{(int)}$ and $C_{t(int)}$ are highly dependent on the interface microstructure. They can be used to characterize qualitatively the degree of hydration and extent of microstructural change of cement paste.

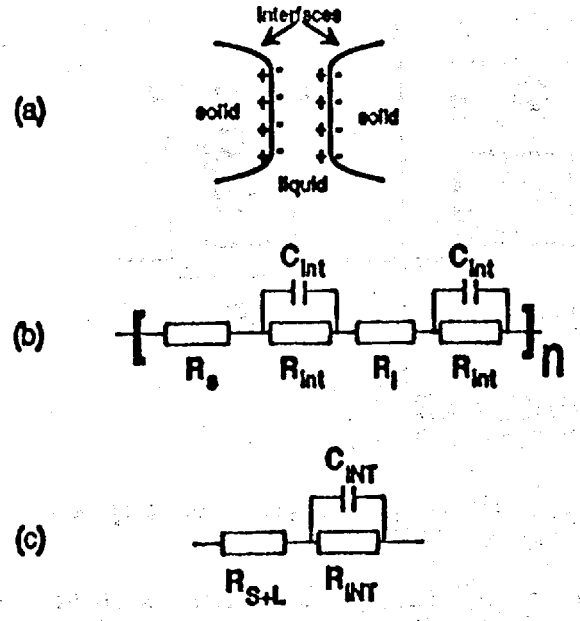

Figure 14 (a) Schematic of the "solid-liquid interface unit cell" model for cement paste.
(b) The corresponding equivalent circuit for a single layer of cement paste.
(c) Simplified equivalent circuit for one layer of cement paste [155].

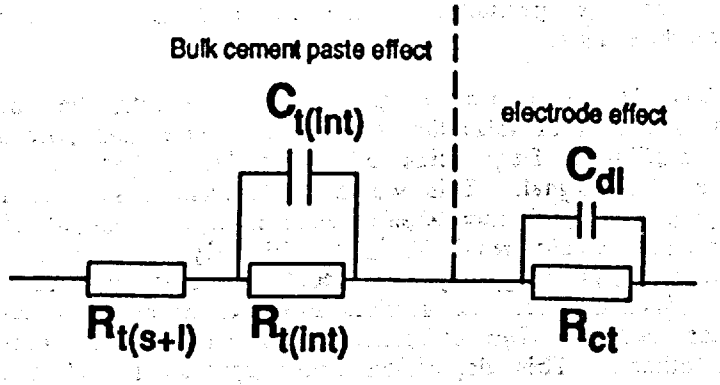

Figure 15 A modified equivalent circuit for hydrating cement paste [155].

Ping et al demonstrated that impedance measurement is very sensitive to changes in hydration kinetics and microstructure development due to the presence of silica fume [156]. A modified equivalent circuit containing a frequency dependent resistance element was proposed to model hydration of these microporous systems (figure 16). The subscripts of the RC terms refer to solid, liquid and interface characteristics as described above. The frequency dependent resistance, $R_{t(int)} = \omega/B$ where ω is the angle frequency and B is the real constant.

AC impedance behavior of cement paste containing 5,10, and 15% silica fume (W/C + sf = 0.35) was determined at hydration times of 48 to 380h. The cement-silica fume pastes show the early appearance of a high frequency arc associated with bulk cement effects, rapid growth of the high frequency arc at later hydration times. The early appearance of the high frequency arc indicates rapid formation of the cement paste pore structure. These results are similar to those obtained by Scuderi et al. [154].

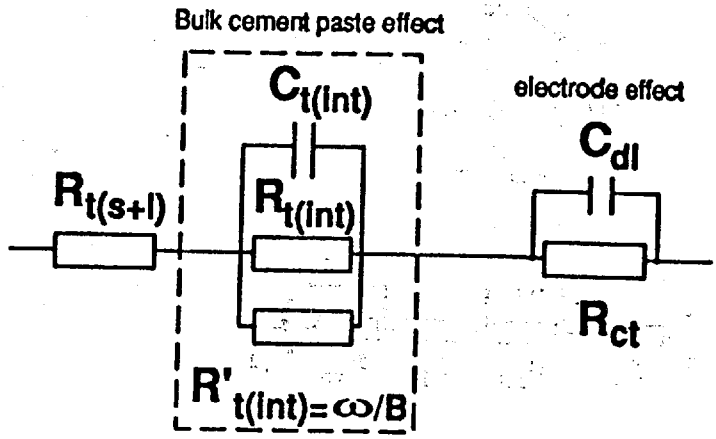

Figure 16 A modified equivalent circuit for cement paste including a new frequency dependent element [156].

A plot of log (modulus) vs. log (freq) demonstrates excellent agreement between the model simulation and experimental data. The extent of hydration is manifested by the growth of the bulk arc diameter, and hence the solid-liquid interfacial resistance $R_{t(int)}$. There is a linear correlation between R_t (int) and hydration time for cement paste containing 0, 5, 10 and 15% silica fume. The slopes are proportionate to the amount of silica fume. Rapid decreases in solid-liquid interfacial capacitance are associated with microstructure formation and large pore in-filling. Silica fume addition reduces the capacitance values. Lower values of capacitance correspond to increased density of the matrix and small pore size. Ions in solution adsorb on the solid surface inside the saturated micropore and function as micro-capacitors. Ions and water molecules oscillate under the electrical field and their relaxation times are significantly less because of the geometric limitation and the chemical and physical interactions among the adsorbed ions.

Depression of the high frequency arc in the impedance spectra has been explained by McCarter [150] in terms of a spread of relaxation times. Pore size and pore surface chemistry, however, could limit the oscillation frequencies of the hydrated ions and water molecules which respond to the applied A.C. signal. This would result from a stronger ion-ion interaction in small pores. A broad pore size distribution would result in a wide spread of relaxation times. A narrow pore size distribution would result in a significantly reduced spread of relaxation times. Less depression of the high frequency arc would be observed. The depression angle decreases rapidly at early hydration times and reaches a relatively constant angle at 140 h for specimens with silica fume added. The reference sample (0% silica fume) has a larger depression angle than the others. This depression angle appears to relate to the pore size distribution. A wider spread of pore diameters can be associated with a larger depression angle. This observation appears to be consistent with the pore size distributions observed for control pastes (0% silica fume) and those containing varying amounts of silica fume. It is concluded that RC parameters, $R_{t(s+l)}$, $R_{t(int)}$, $C_{(int)}$, and the depression angle, α, can be used to describe the extent of hydration and microstructure development in a cement paste.

Models For Pore Structure

Porosity is an important materials consideration affecting a number of engineering disciplines. Periera, Rice and Skalny reviewed a number of porosity models emphasizing those related to chemical engineering, figure 17 [157]. One of these may have particular relevance to cements in that it considers the effects of macroscopic pores between microporous particles. Porosity in cements should be considered at two levels because the fine pores in the inner products are likely to strongly affect hydration rates while having a minimal effect on bulk transport. Depending on the technique used, the porosity observed may be of one type or the other. TEM studies typically investigate the fine porosity likely to influence hydration kinetics [158] while optical or BSE observations carried out on polished sections reveal porosity

affecting mass transport. Roy [159] recently reviewed the relationships between porosity, transport and microstructure suggesting the following relationship between porosity and diffusion:

$$D = C_1 P^{(rC_2C_3)}$$

where D is the ratio of the theoretical-to-effective diffusion rates, P is the porosity, r is median pore radius and C_1, C_2, C_3 are constants.

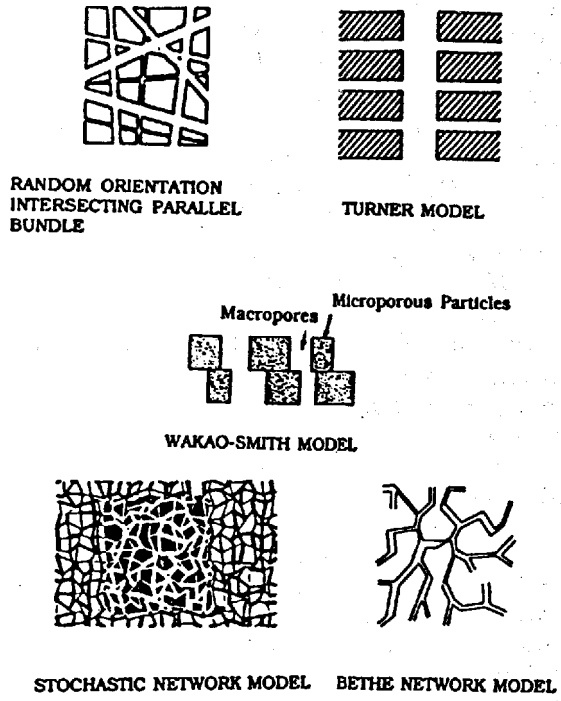

Figure 17 Various porosity models with chemical engineering application [157].

Shi and colleagues [160-162] developed a model for the pore size distributions in cements by building on a concept first developed by Diamond and Dolch [163]. Because of the range of sizes intruded by mercury, pores which principally affect mass transport and those which principally affect hydration kinetics may both be intruded. Using a technique to deconvolute MIP curves, three lognormal subdistributions can be generated. The central distribution includes pores in the size range of capillary porosity while the finest distribution extends down to the size of gel pores.

Among the models for porosity are those relating it to other physical properties. Jambor recently reiterated that a close relationship exists between pore structure and strength [164]. Several publications describing models for porosity and porosity-strength relationships have appeared. Tang developed a network model for the structures of porous materials [165]. Compressive strengths were calculated based on the model developed. Calculated strengths compared favorable with empirically determined values. One study [166] related the capillary porosity in cement paste to the compressive strength using a modified Ryskewitch equation [167]. In a series of publications Odler and colleagues [168-170] investigated the relationships between the pore structures of cement pastes and the strengths developed. Effects of varying the surface area and the proportions of C_3A, C_4AF and gypsum on pore volume and strength were determined. It was established that the slopes of strength-porosity curves decrease with increasing C_3A content when the C_3S and C_2S contents were held constant. Sersale et al [171] in studying the effects of gypsum on cement properties observed that an SO_3 content between 2 and 3.5% promotes the refinement in pore structure and affects the compressive strength accordingly. These results support observations of Odler and Röβler that pores smaller than about 10 nm do not have a major effect on reducing the compressive strength. However, the

results of Sersale et al are in contrast to those of an earlier study in which variation in SO_3 was reported not to influence the pore size distribution [172].

In a series of three papers [173-175] Odler and Köster explored structural development in fully hydrated C_3S and cement pastes. In comparing the effects of hydration at 20 and 90°C, they found that the bound water and the chemical shrinkage were lower at 90°C, whereas the density of the hydrates was higher. They also observed that the water bound for complete hydration at 20°C showed a dependence on the original w/c ratio. Significantly, this effect was observed in both cement and C_3S pastes. Observation in the latter suggests the density of C-S-H to depend on the original w/c ratio. In evaluating the development of pore structure at 20°C, it was observed that pore size distributions obtained by nitrogen adsorption and mercury intrusion are not in good agreement. The pore volume filled by nitrogen was found to be lower than that which was mercury filled. C_3S and cement pastes showed significantly different pore size distributions and the pores intruded by mercury after d-drying were lower than the total porosities. However, the volume of inaccessible pores in C_3S differed from those in cement. In a further investigation of C_3S and cement pastes cured at 20 and 90°C it was observed that the BET surface areas determined by water vapor adsorption are relatively independent of w/c ratio and hydration temperature. This BET surface area does not differ greatly between C_3S and cement. BET specific surfaces determined by nitrogen are lower than those for water vapor. The permeabilities of undried pastes increase greatly with increasing porosity and permeabilities of cement and C_3S pastes at equal porosities are similar. Vidick compared the adsorption of nitrogen, argon, and krypton [176]. Comparing nitrogen and argon adsorption in detail, the nitrogen specific surface areas were observed to be about 5 times those of argon for hydrated cement and for hydrated aluminoferrites.

In addition to varying with temperature and composition, the pore structure of cement paste also has been observed to vary depending on the relative humidity during curing [177]. As would be expected curing at RH below 95% limited hydration and gel porosity increased with increasing hydration. Curing at RH below 80% resulted in a much coarser pore structure and the diameters of the large pores were observed to be three times larger than when curing was carried out under conditions of saturation. This illustrates the role of transport in refining the pore structure of pastes. Because large pores are more likely to empty first, the mechanism by which they would become partially infilled with hydration product is precluded.

THE EFFECT OF ADDITIVES AND ADMIXTURES ON CEMENT PASTE MODEL PARAMETERS

Admixture (additive) interaction with portland cement and cement phases can affect composition, pore structure, and morphology of the hydrated constituents of portland cement paste [178-82]. Changes in C-S-H stoichiometry and surface area and modification of CH in the presence of admixtures (particularly superplasticizers) are factors to be considered in determining model parameters. This section reviews contributions in the admixture (additive) area since the 8th International Congress with specific reference to work that provides relevant input to concepts of structural modelling. The review is divided into three sections: calcium hydroxide, supplementary cementing materials, polymer modification and miscellaneous admixtures.

Calcium Hydroxide:

Calcium hydroxide is a major constituent of portland cement paste which contains about 20-25% by volume. Yilmaz and Glasser [183, 184], Barker et al [185] and Inokawa et al [186] reported work on interactions between calcium hydroxide and superplasticizer. Sulphonated Melamine Formaldehyde (SMF) was observed to affect both morphology and crystallite size. Control samples generally exhibited a pseudo-hexagonal prismatic morphology. Morphology resulting from 1% SMF addition changed to well-shaped flattened pseudo-hexagonal plates with occasional growth spirals visible on surfaces normal to the c-axis. At higher SMF concentrations (e.g. 2%) CH crystals were very thin and irregular consisting of numerous stacked plates. Na, Cl and S were incorporated into the CH structure. It was suggested (based on IR data) that a chemical complex forms between CH and SMF by an intercalation process [183]. Further work by Yilmaz and Glasser generally confirmed that the mean size of the CH crystallites was reduced and the crystal habit changed from blocky to platy [184]. It was also

observed that ettringite crystallizes in coarser laths with SMF than it does without. X-ray line broadening was observed but no significant changes in the lattice parameters of CH were detected. The results of Barker et al [185] are essentially in agreement with those of Yilmaz and Glasser including substitution for Ca^{2+} or OH^- within the crystal structure. Their results were generally descriptive of the influence of several plasticizers containing the SO_3Na group. Yilmaz and Glasser attribute the interaction, however, to more than chemisorption to an ettringite precursor. Desorption and crystallization of ettringite and a slow denaturation reaction occurs resulting in precipitation of a chemically altered form of SMF. It is clear that further work is required to predict the behavior of admixture modified cement paste based on structural models.

Supplementary Cementing Materials:

Additions of silica fume, fly ash and more recently finely divided calcium carbonate have been shown to modify the structure and properties of C-S-H [179, 182, 186-191].

Groves and Rodger employed analytical transmission electron microscopy to characterize microstructure developed in hydrating C_3S and portland cement systems containing microsilica [189]. In C_3S pastes silica particles were observed embedded in C-S-H gel giving the appearance of excellent bonding between the two phases. The C-S-H gel had foil-like morphology. The silica was described as having the appearance of hydrous silica of equilibrium composition.

The inner product C-S-H within original C_3S grains had a similar morphology to outer product C-S-H. Inner product C-S-H gels had Ca/Si ratio values of about 0.8. Outer product C-S-H in portland cement-silica fume pastes had slightly lower Ca/Si ratios ie., about 0.66. Solid state NMR results indicated that the silicate chain length is approximately 8.5 for both C_3S and portland cement systems.

Alkali addition (in the form of KOH) had little effect on the microstructure of C_3S paste. In portland cement-silica fume pastes isolated regions of low calcium and high alkali content with distinctive morphology were detected. In C_3S pastes incorporation of NaOH increased early strength up to 7 days hydration [192]. Subsequent strengths were diminished relative to control pastes. There was, however, a larger volume concentration of fine pores in NaOH treated C_3S pastes. Strength generally increases with amount of fine pores. Decreased strength of alkali treated C_3S paste is attributed to a coarser microstructure and poor interparticle bonding.

Fly ash did not significantly affect the morphology of hydration products of C_3S [187]. The Ca/Si ratio of the C-S-H was, however, reduced in all areas. Morphology after one year of hydration is described as follows: hydrogarnet shells formed within reacted zones of fly ash particles; radially fibrillar C-S-H within reacted zones and shells of dense C-S-H. C-S-H formation is described as occurring immediately outside the flyash particle surface and subsequent to later shell formation within the reacted zone by rhythmic precipitation. The Ca/Si ratio of the outer and inner product was similar averaging between 1.4 and 1.5. Microanalysis revealed that the composition of inner and outer product is affected by the presence of fly ash.

The Ca/Si ratio (2 weeks hydration) of the inner product is about 1.56 when fly ash is present, otherwise about 1.70. At one year the ratios are about 1.45 and 1.60 respectively. The inner product in blended pastes is free of other elements (in addition to Ca and Si) whereas the outer product may contain many trace elements, in particular substantial concentrations of potassium.

Portland cement-fly ash systems and C_3S-fly ash systems react in a similar way [189]. The fly ash particles form radially fibrillar gel and hydrogarnet phases. In addition regions of small particles of poorly crystalline iron-containing material exist intermixed with C-S-H and hydrotalcite type needles. These regions may originate from C_4AF interstitial phases in cement clinker. The microstructure of the inner and outer products is not significantly different than

that for C_3S-fly ash system.

The microstructure of cement paste is altered by both fine aggregate particles and silica fume, either alone or in combination. Feldman has determined that pores with diameters in the range (0.18-0.97) $x10^3$ nm form at the fine aggregate particle-cement paste interface [193]. Interface porosity in this size range is increased considerably in presence of silica fume. A significant proportion of the pores are discontinuous. In cement paste containing silica fume and fine aggregate particles a larger coarse pore fraction than in control paste exists contrary to many published reports. The large apparent increase in fine pore structure observed on first intrusion with mercury is really due to penetration of large but relatively discontinuous pores at higher pressures in the mercury intrusion experiment.

Silica polymerization determinations of cement pastes indicate that silica fume addition increases the proportion of higher mers [194,195]. Leaching of these pastes with ammonium nitrate reduces the amount of CaO and increases SiO_2 and R_2O_3 [196]. The degree of polymerization of the silica anions is increased [194-196].

Cement containing calcium carbonate is becoming more widespread in North America and Europe [190, 191]. Much work prior to the 8th Congress focused on interaction of $CaCO_3$ with aluminate phases in cement. Reference here concentrates on the C_3S phase as it is more relevant to development of models for cement paste. Calcium carbonate is not an inert filler in C_3S and portland cement systems. Reference C_3S pastes (at 28 days hydration) can be generally described as containing parallel hexagonal plates of calcium hydroxide and fibrous particles of various size. The fibrous particles are much smaller with 5% addition of calcium carbonate. At the 15% calcium carbonate level the microstructure exhibits no fibrous features and shows only occasional evidence of hexagonal plates. The surface gives the appearance of a densely consolidated network. The structure in the samples containing 15% calcium carbonate contains a greater proportion of fine pores than does the controls.

Other model parameters in the C_3S-CaO_3 system are noteworthy. Plots of degree of hydration versus porosity and density are distinct for control pastes and those containing calcium carbonate. At a particular degree of hydration pastes with no calcium carbonate addition have lower porosity values. It appears that calcium carbonate particles act as nuclei for growth of C-S-H. C-S-H formed on calcium carbonate surfaces may incorporate some carbonate. Nucleation on the surface of C_3S could result in accelerated C_3S hydration. Ramachandran concluded that in the presence of $CaCO_3$ silicate ions can migrate farther from the confines of the C_3S phase and grow as C-S-H on the $CaCO_3$ particles [191]. This is in addition to existing as inner and outer products. The Ca/Si ratio is modified to slightly higher values in C_3S paste containing $CaCO_3$: Values of about 1.95 at 15% $CaCO_3$ content compared to 1.85 for control pastes were reported.

Polymers and Miscellaneous Admixtures:

Pore structure of cement paste is influenced by addition of waste dispersible polymers (e.g. styrene butadiene and ethylene vinyl acetate) and polymer emulsions [197-199]. Generally polymer latices reduce porosity in the large pore region (diameter >0.4 μm) and increase porosity in the finer pore regions (diameter <150 nm) [197, 198]. Total porosity decreases with increase in polymer-cement ratio.

Work on insitu polymerization of vinyl sulphonate in cement pastes and mortars indicates that system porosities are approximately equal when polymer is present [199]. This is attributed to the accumulation of polymer at the interface. Excess porosity present in controls without polymer is eliminated. In addition the presence of silica fume changes the nature of the polymer phase which becomes continuous, cracks less, and forms a better bond with the matrix.

Pigeon and Laplante reported a concentration of soluble alkalies around the periphery of entrained air voids and attributed void stability with alkali content to this phenomena [200]. The microstructure of cement paste around the air voids did not appear to be significantly influenced.

The effect of organic sodium salts on microstructure of C_3S pastes was reported by Stadelmann et al [201]. An accelerator, sodium formate had the general effect of lowering the Ca/Si ratio of C-S-H and increasing the specific surface area. Sodium propionate, a retarder, is described as contributing to formation of a surface layer (on C_3S particles) with a high Ca/Si ratio and small specific surface area. The layer is considered to be a low permeability barrier. Na is incorporated into the surface layers until the Ca/Na ratio of these layers has attained an equilibrium value.

Dunster and Parsonage determined that saccharide retarders apparently do not alter the silicate anion distribution of C-S-H at a given degree of hydration in spite of altered hydration kinetics [202].

It is apparent that microstructural descriptions suitable for modelling the structure of hydrated cement paste vary with the additive type and each admixture system. Considerable progress, however, has been made since 1986 in delineating factors controlling various cement admixture interactions, particularly those involving superplasticizers and cement phases.

ACKNOWLEDGEMENTS

J.J. Beaudoin gratefully acknowledges the support of the Natural Sciences and Engineering Research Council of Canada through the Network of Centres of Excellence program. J.J. Beaudoin would also like to acknowledge Dr. V.S. Ramachandran, IRC Distinguished Researcher, for discussions and assistance related to the use of chemical admixtures.

P.W. Brown gratefully acknowledges the support of the US Air Force Office of Scientific Research, Aerospace Sciences Directorate in conducting this work.

REFERENCES

1. Taylor, H.F.W.: "The Reactivity of Cement Compounds With Water," Proc.10th Intl. Sym. React. Solids," Dijon, Elsevier, Amsterdam,1984.
2. Taylor, H.F.W.: "Some Aspects of Cement Hydration Mechanisms," 95-8 in Research on the Manufacture and Use of Cements, G. Frohnsdorff Ed., Engr. Fnd, NY, 1986.
3. Groves, G.W.: "TEM Studies of Cement Hydration," 3-20 in Microstructural Development During Hydration of Cement, L.J. Struble and P.W. Brown, Eds., MRS Pittsburgh, 1987.
4. Gartner, E. and Gaidis, J.: "Hydration Mechanisms, I," 95-125 in The Materials Science of Concrete-I, J.P. Skalny, Ed, Am. Ceram. Soc., Westerville, 1989.
5. Brown, P.W.: " Effects of Particle Size Distribution on the Kinetics of Hydration of Tricalcium Silicate, J. Am. Ceram. Soc., 1989, 72, 1829-32.
6. Groves, G.W.: "TEM Studies of Cement Hydration," 3-20 in Microstructural Development During Hydration of Cement, L.J. Struble and P.W. Brown, Eds, MRS Pittsburgh, 1987.
7. Rodger, S.A. and Groves, G.W.: "Electron Microscopy Study of Ordinary Portland Cement and Ordinary Portland Cement-Pulverized Fuel Ash Blended Pastes," J. Am. Ceram. Soc., 1989, 72, 1037-39.
8. Richardson, I.G., Rodger, S.A. and Groves, G.W.: "The Microstructure of ggbfa/OPC Hardened Cement Pastes and Some Effects of Leaching," 63-74 in Scientific Basis for Nuclear Waste Management XIII, V.M. Oversby and P.W. Brown, Eds, MRS Pittsburgh, 1990.
9. Yang, R., Liu, B. and Wu, Z.: "Study on the Pore Structure of Hardened Cement by SAXS," Cem. Concr. Res., 1990, 20, 385-93.
10. Grudemo, A.: "The Crypo-crystalline Structure of C-S-H Gel in Cement Pastes. Inferences from X-ray Diffraction and Dielectric Capacitivity Data," Cem. Concr. Res., 1987, 17, 673-80.
11. Groves, G.W., Brough, A., Richardson, I.G. and Dobson, C.: "Progressive Changes in the Structure of Hardened C_3S Cement Pastes due to Carbonation," J. Am. Ceram. Soc., 1991, 74, 2891-96.

12. Taylor, H.F.W.: "Proposed Structure for Calcium Silicate Hydrate Gel", J. Amer. Cer. Soc., 1986, 69 (6), 464-467.
13. Taylor, H.F.W.: "Hardened Cement Pastes: Models of Structure" in Cement Chemistry, Academic Press, London, 1990, pp 475.
14. Taylor, H.F.W.: "Bound Water in Cement Pastes and Its Significance for Pore Solution Compositions", Proc. Mat. Res. Soc. Symp. on Microstructural Development During Hydration of Cement, 1987, Vol. 85, 47-54.
15. Feldman, R.F.: "Bond Formation" in Concrete Science, Heyden & Son Ltd., London, 1981, pp 427.
16. Lachowski, E.E.: "Trimethyl silylation as a Tool for the Study of Cement Pastes (1) Comparison of Methods on Derivatisation", Cem. Concr. Res., 1979, 9 (1), 111-114.
17. Copeland, L.E., Boder, E., Chang, T.N. and Weise, C.H.: "Reactions of Tobermorite Gel with Aluminates, Ferrites and Sulfates", J. PCA Res. Dev. Lab., 1967, 9 (1), 61-74.
18. Grudemo, A.: "Electron Microscopy of Portland Cement Pastes", Chapter 9 in The Chemistry of Cements, Vol. 1, Ed. H.F.W. Taylor, Academic Press London, 1964.
19. Feldman, R.F. and Ramachandran, V.S.: "A Study of the State of Water and Stoichiometry of Bottle Hydrated Ca_3SiO_5", Cem. Concr. Res., 1974, 4 (2), 155-166.
20. Brown, P.W., Franz, E., Frohnsdorff, G. and Taylor, H.F.W.: "Analysis of the Aqueous Phase During Early C3S Hydration," Cem. Concr. Res., 1984, 14, 257-62.
21. Jennings, H.: "Aqueous Solubility Relationships for Two Types of Calcium Silicate Hydrate," J. Am. Ceram. Soc., 1986, 69, 614-18.
22. Barrett, P. and Bertandie, D.: "Comment on "Aqueous Solubility Relationships for Two Type of Calcium Silicate Hydrate," J. Am. Cer. Soc., 1988, 71, C113-15.
23. Grutzeck, M., Benesi, A. and Fanning, B.: "Silicon-29 Magic Angle Spinning Nuclear Magnetic Resonance Study of Calcium Silicate Hydrates," J. Am. Ceram. Soc., 1989, 72, 665-68.
24. Melzer, R. and Berhard, E.: "Phase Identification During Early and Middle Hydration of Tricalciumsilicate (Ca_3SiO_5)," Cem. Concr. Res., 1989, 19, 411-22.
25. Diamond, S.: "Hydraulic Cement Pastes: Their Structures and Properties," CCA, Wexham Springs, Slough, 1976.
26. Groves, G.W.: A Discussion of the Paper "Phase Identification During Early and Middle Hydration of Tricalciumsilicate (Ca_3SiO_5)," Cem. Concr. Res., 1990, 20, 315-6.
27. Feldman, R.F. and Sereda, P.J.: "A New Model for Hydrated Portland Cement and Its Practical Implications", Eng. J., 1970, 53 (8-9), 53-59.
28. Powers, T.C. and Brownyard, T.L.: "Studies of the Physical Properties of Hardened Portland Cement Paste", Bull. 22, Portland Cement Assoc., 1948, 276-287.
29. Helmuth, R.A.: "Dimensional Changes and Water Adsorption of Hydrated Portland Cement and Tricalcium Silicate", MSc. Thesis, Illinois Institute of Technology, 1965, pp 61.
30. Daimon, M., Abo-el-enein, A., Hosaka, G., Goto, S. and Kondo, R.: "Pore Structure of Calcium Silicate Hydrate in Hydrated Tricalcium Silicate", J. Amer. Ceram. Soc., 1977, 60 (3-4), 110-114.
31. Skoblinskaya, N.N.: "Problems of Creep and Shrinkage of Concrete", Proc. 2nd All Union Conference in Erevan, 1974, pp 175-184.
32. Feldman, R.F.: "Sorption and Length Change Isotherms of Methanol and Water on Hydrated Portland Cement", V. Int. Symp. Chem. Cem., 1968, Vol. 3, pp 53-66.
33. Flood, E.A. and Heyding, R.H.: " Stresses and Strains in Adsorbent Adsorbate Systems" Can. J. Chem. 1954, 32, 660.
34. Beaudoin, J.J. and Feldman, R.F.: "Stresses and Strains in the Hardened Cement Paste-Water System", Cem. Concr. Res. 1984, 14 (2), 231-237.
35. Winslow, D. and Diamond, S.: "Specific Surface of Hardened Portland Cement Paste as Determined by Small-Angle X-ray Scattering", J. Amer. Ceram. Soc. 1974, 57 (5), 193-197.
36. Feldman, R.F.: "The Flow of Helium into the Interlayer Spaces of Hydrated Portland Cement Paste", Cem. Concr. Res. 1971, 1 (3), 285-300.
37. Feldman, R.F. and Ramachandran, V.S.: "Differentiation of Interlayer and Adsorbed Water in Hydrated Portland Cement by Thermal Analysis", Cem. Concr. Res. 1971, 1 (6), 607-620.
38. Englert, G. and Wittmann, F.: "Water in Hardened Cement Paste", Mat. et Const. 1968, 1 (6), 535-546.

39. Bernal, J.D.: "The Structures of Cement Hydration Compounds", Proc. III Int. Symp. Cem. Chem. London, 1954, 216-236.
40. Wittmann, F.: "Surface Tension Shrinkage and Strength of Hardened Paste", Mat. et Const., 1968, 1 (6), 547-552.
41. Englert, G. and Wittmann, F.: "Beitrag Zum Studium der Wasserverteilung in hydratisiertein Tricalciumsilikat als Funktion des Feuchtigkeitsgehaltes", Mater. Sci. Eng. 1971, 7, 125-133.
42. Setzer, M.J. and Wittmann, F.: "Surface Energy and Mechanical Behaviour of Hardened Cement Paste", Appl. Phys. 1974, 3, 403-409.
43. Day, R.L. and Gamble, B.R.: "The Effect of Changes in Structure on the Actuation Energy for the Creep of Concrete", Cem. Concr. Res. 1983, 13 (4), 529-540.
44. Powers, T.C.: "The Thermodynamics of Volume Change and Creep", Mat. et Const., 1968, 1 (6), 487-507.
45. Hannant, D.J.: "The Mechanism of Creep in Concrete", Mater. et Const., 1968, 1 (5), 403-410.
46. Wittmann, F.: "Einflub des Feuchtigkeitsgehaltes auf das Kriechen des Zementsteines" Rheol. Acta, 1970, 9, 282-287.
47. Bazant, Z.: "Constitutive Equation for Concrete Creep and Shrinkage Based on Thermodynamics of Multiphase Systems", Mater. et Const. 1970, 3 (13), 3-36.
48. Brunauer, S.: "Pore Structure Analysis by Water-Vapor Adsorption IV. Analysis of Hydrated Portland Cement Pastes of Low Porosity",
49. Brunauer, S.: "Pore Structure Analysis by Water-Vapor Adsorption III. Analysis of Hydrated Calcium Silicates and Portland Cements",
50. Lippens, B.C., Linsen, B.G., and de Boer, J.H.: "Studies in Pore Systems and Catalysis:The Adsorption of Nitrogen Apparatus and Calculation", J. Catalysis, 1964, 3, 32-37.
51. Brinker, C.J. and Scherer, G.W.: Sol-Gel Science, Academic Press, NY 1990.
52. Scherer, G.W.: "Drying of Gels I. General Theory," J. Non-Cryst. Solids 87, 199-225, 1986.
53. Shamrikov, V.M., et al: Soviet J. Colloids, 1984, 46 (3) 544-46, Engl. Trans., Quoted in Brinker and Scherer.
54. Scherer, G.W.: " Sintering of Low Temperature Glasses-I. Theory," J. Am. Ceram. Soc. 1977, 60, 236-39.
55. Verbeck, G. and Helmuth, R.A.: "Structures and physical properties of cement pastes,", 1968, 5th ICCC, III, 1-31.
56. Hansen, W.: "Drying Shrinkage Mechanisms in Portland Cement Paste," J. Am. Ceram. Soc. 1987, 70, 323-28.
57. Ferraris, C.F. and Wittmann, F.H.: "Shrinkage Mechanism of Hardened Cement Paste," Cem. Concr. Res. 1987, 17, 453-64.
58. Garofalini, S.H.: "Simulation of the Sol-Gel Process,"16-27 in Sol-Gel Technology for Thin Films, Fibers, Preforms, Electronics and Specialty Shapes, Lisa Klein, Ed. Noyes, 1987.
59. Gibbs, G.V.: "Molecules for Models, Bonding in Silicates," Am. Min. 1982, 67, 421-50; M. O'Keeffe, B. Domenges, and G.V. Gibbs, "Ab Initio Molecular Orbital Calculation on Phosphates: Comparison with Silicates," J. Phys. Chem. 1985, 89, 2304-09.
60. Geisinger, K.L., Gibbs, G.V. and Navrotsky, A.: "A Molecular Orbital Study of Bond Length and Angle Variations in Framework Structures," Phys. Chem. Min. 1985, 11, 266-83.
61. de Jong, B.H.W.S., Keefer, K.D., Brown, G.E. and Taylor, C.M.: "Polymerization of silicate and aluminate tetrahedra in glasses, melts and aqueous solutions-III. Local silicon envrionments and interal nucleation in silicate glasses," Geochim. Cosmochim. Acta, 1981, 45, 1291-1308.
62. Brown, P.W.: "Phase Equilibria and Cement Hydration," 73-93 in The Materials Science of Concrete-I, J.P. Skalny, Ed., Am. Ceram. Soc., Westerville, 1989.
63. Lachowski, E.E., Mohan, K., Taylor, H.F.W. and Moore, A.E.: "Analytical Electron Microscope Study of Cement Pastes: II, Pastes of Portland Cements and Clinkers," J. Am. Ceram. Soc. 1980, 63, 447-53.
64. Taylor, H.F.W. and Newbury, D.E.: "An Electron Microprobe Study of a Mature Cement Paste," Cem. Concr. Res. 1984, 14, 565-73.
65. Taylor, H.F.W.: "Do Cements Contain C-S-H Gels?" 295-302 in Advances in Cement Manufacture and Use, E. Gartner, Ed., Eng. Fnd, NY, 1988.

66. Rodger, S.A. and Groves, G.W.: "Electron Microscopy Study of Ordinary Portland Cement and Ordinary Portland Cement-Pulverized Fuel Ash Blended Pastes," J. Am. Ceram. Soc. 1989, 72, 1037-39.
67. Kasselouri, V. and Ftikos, C.H.: "A longterm study of MgO hydration in cement pastes," Matls. Struct. 1989, 22, 121-24.
68. Bezjak, A.: "A New Approach to Mathematical Modeling of Nucleation and Growth in Kinetic Analysis of Cement Hydration," 57-66 in Advances in Cement Manufacture and Use, E. Gartner, Ed., Eng. Fnd, NY, 1988.
69. Bentz, D.P. and Garboczi, E.: "A Digitized Simulation Model for Microstructural Development," 211-26 in Advances in Cementitious Materials, S. Mindess, Ed., Am. Cer. Soc., 1991.
70. Garboczi, E.: "Percolation of Phases in a Three-Dimensional Cement Paste Microstructural Model," Cem. Concr. Res. 1991, 21, 325-44.
71. Ziman, J.M.: 370-86 in Models of Disorder, Cambridge Univ. Press, 1979.
72. Parrott, L.J.: "Modelling the Development of Microstructure," 43-73 in Research on the Manufacture and Use of Cements, G. Frohnsdorff Ed., Engr. Fnd, NY, 1986.
73. Parrott, L.J.: "Modeling of Hydration Reactions and Concrete Properties," 181-95 in Materials Science of Concrete-I, J.P. Skalny, Ed., Am. Ceram. Soc., Westerville, 1989.
74. Osbaeck, B.: "Modelling the Strength of Cement Paste and Concrete," 75-86 in Research on the Manufacture and Use of Cements, G. Frohnsdorff Ed., Engr. Fnd, NY, 1986.
75. Struble, L.: "Mircrostructure and Fracture At the Cement-Paste Aggregate Interface" Proc. Mat. Res. Soc. 1988, 114, 11-20.
76. Diamond, S.: "The Microstructures of Cement Paste in Concrete" Proc. 8th International Congr. Chem. Cem. 1986, I, 122-147.
77. Scrivener, K.L. and Gartner, E.M.: "Microstructural Gradients In Cement Paste Around Aggregate Particles", Proc Mat. Res. Soc. 1988, 114, 77-85.
78. Older, I., and Zurz, A.: "Structure And Bond Strength of Cement —Aggregate Interfaces" Proc. Mat Res. Soc. 1988, 114, 21-27.
79. Bentur, A.: "Interfaces In Fibre-Reinforced Cements" Proc. Mat. Res. Soc. Symp. 1988, 114, 133-144.
80. Zhang, X., Groves, G.W. and Rodger, S.A.: "The Microstructure of Cement Aggregate Interfaces" Proc. Mat. Res. Soc. 1988, 114, 89-96.
81. Yang, S., Xu, Z., Ping, X. and Mingshu, T.: "A New Method of Enhancing Cement-Aggregate Interfaces "I Ideal Aggregate And Its Effects on Interfacial Microstructures". In Press.
82. Yang, S., Xu, Z., Ping, X. and Mingshu, T.: " A New Method of Enhancing Cement-Aggregate Interfaces II Mechanical Properties and Sulphate Attack Resistance of Mortar". In press.
83. Wu, X., Li, D., and Mingshu, T.: "Modification of the Interfacial Zone Between Aggregate and Cement Paste" Proc. Mat. Res. Soc., 1988, 114 35-40.
84. Ping, X. and Beaudoin, J.J.: "Modification of Transition Zone Microstructure—Silica Fume Coating On Aggregate Surfaces", Cem. Concr. Res. In press.
85. Grandet, J., and Ollivier, J.P.: " Orientation des Hydrates Au Contact des Granulats", Proc. 7th Int. Congr. Chem. Cem., 1980, Vol. III, pp VII 63-68.
86. Zürz, A. and Odler, I.: "XRD Studies of Portlandite Present in Hydrated Portland Cement Paste" Advances in Cement Research, 1987, 1, (1), 27-30.
87. Detwiler, R.J. and Monteiro, P.J.M.: "Texture of Calcium Hydroxide Near the Cement Paste-Aggregate Interface", Cem. Concr. Res., 1988, 18 (5), 823-829.
88. Yuan, C.Z., Wei Min and Jiang Lin: "Determination of Preferred Orientation Degree of Portlandite By Using Rocking Curve of Diffraction Line, " Mater. et Const., 1988, 21, 329-335.
89. Monteiro, P.J.M. and Ostertag, C.P.: "Analysis of The Aggregate-Cement Paste Interface Using Grazing Incidence X-ray Scattering", Cem. Concr. Res. 1989, 19, (6), 987-988.
90. Scrivener, K.L., Bentur, A. and Pratt, P.L.: "Quantitative Characterization of the Transition Zone in High Strength Concretes", Advances in Cem. Res., 1988, 1, (4), 230-239.
91. Ping, X. and Beaudoin, J.J.: "Effects of Aggregate Size On Transition Zone Properties At the Portland Cement Paste Interface", Cem. Concr. Res., 1991, 21 (6), 999-1005.

92. Jia, W.: "Mechanisms of Orientation of Ca $(OH)_2$ Crystals In The Interface Layer Between Paste and Aggregate In Systems Containing Silica Fume", Proc, Mat. Res. Soc. Symp. 1988, 114, 127-132.
93. Larbi, J.A. and Bijen, J.M.: "Orientation of Calcium Hydroxide at the Portland Cement Paste-Aggregate Interface in Mortars in the Presence of Silica Fume, A Contribution" Cem. Concr. Res., 1990, 20 (3).
94. Mehta, P.K. and Monteiro, P.J.M.: "Effects of Aggregate Cement and Mineral Admixtures on the Microstructure of the Transition Zone", Proc. Mat. Res Soc. 1988, 114, 65-75.
95. Monterio, P.J.M. and Mehta, P.K.: "The Transition Zone Between Aggregate and Type K Expansive Cement" Cem. Concr. Res. 1986, 16 (1), 111-114.
96. Scrivener, K.L., Crumbie, A.K. and Pratt, P.L.: "A Study of the Interfacial Region Between Cement Paste and Aggregate in Concrete" Proc. Mat. Res. Soc. 1988, 114, 87-88.
97. Bentur, A., Goldman, A. and Cohen, M.: "The Contribution of the Transition Zone to the Strength of High Quality Silica Fume Concretes" Proc. Mat. Res. Soc. 1988, 114, 97-103.
98. Sarkar, S., Diatta, Y. and Aiticin, P.C.: "Microstructural Study of Aggregate/Hydrated Paste Interface In Very High Strength River Gravel Concretes," Proc. Mat. Res. Soc. 1988, 114, 111-116.
99. Saito, M. and Kawamura, M.: "Effect of Fly Ash and Slag on the Interfacial Zone Between Cement and Aggregate, " Amer. Concr. Inst. SP114, 1989, 669-688.
100. Onabolu, O. and Pratt, P.L.: "The Effect of Blast Furnace Slag on the Microstructure of the Cement Paste/Steel Interface", Proc. Mat. Res. Soc. Symp. 1988, 114, 255-261.
101. Detwiler, R., Krishnan, K. and Mehta, P.K.: "Effect of Granulated Blast Furnace Slag On the Transition Zone in Concrete", Amer. Concr. Inst. SP-100, 63-72.
102. Bentur, A. and Cohen, M.D.: "Effects of Condensed Silica Fume on the Microstructure of the Interfacial Zone in Portland Cement Mortars", J. Amer. Ceram. Soc. 1987, 70, (10), 738-743.
103. Monterio, P.J.M. and Mehta, P.K.: "The Transition Zone Between Aggregate and Type K Expansive Cement", Cem. Concr. Res. 1986, 16 (1), 111-114.
104. Monteiro, P.J.M. and Mehta, P.K.: "Interaction Between Carbonate Rock and Cement Paste", Cem. Concr. Res. 1986, 16 (2) 127-134.
105. Zhang, M.H., Gjoerv, O.E.: "Backscattered Electron Imaging Studies On the Interfacial Zone Between High-Strength Lightweight Aggregate and Cement Paste", Adv. Cem. Res., 1989, 2 (8), 141-146.
106. Sugama, T.: "The Effects of Ca $(OH)_2$ -Treated Ceramic Microspheres on the Mechanical Properties of High Temperature Lightweight Cement Composites, " Proc. Mat. Res. Soc. Symp. 1988, 114, 301-306.
107. Ping, X., Beaudoin, J.J. and Brousseau, R.: "Flat Aggregate—Portland Cement Paste Interfaces" I Electrical Conductiviity Models, Cem. Conc. Res. 1991, 21 (4), 515-522.
108. Ping, X., Beaudoin, J.J. and Brousseau, R.: "Flat Aggregate-Portland Cement Paste Interfaces II Transition Zone Formation" Cem. Concr. Res. 1991, 21 (5), 718-726.
109. Ping, X., Mingshu, T.: "Effects of Portland Cement Paste-Aggregate Interface on Electrical Conductivity and Chemical Corrosion Resistance of Mortar", Cemento, 1988, 85 (1), 33-42.
110. Ping, X. and Beaudoin, J.J.: "Effects of Transition Zone Microstructure on Bond Strength of Aggregate - Portland Cement Paste Interfaces", Cem. Concr. Res. In press.
111. Ping, X. and Beaudoin, J.J.: "Characterization of Cement-Aggregate Interfaces By Electrical Conductivity Methods" Proc. Engineering Foundation Conference July 1989, American Chemical Soc. In press.
112. Garboczi, E.J. and Bentz, D.P.: "Digital Simulation of the Aggregate - Cement Paste Interfacial Zone in Concrete," J. Mater. Res. 1991, 6(1), 196-201.
113. Parrott, L.: "Measurement and Modeling of Porosity In Drying Cement Paste", Proc. Mat. Res. Soc. 1987, 85, 91-104.
114. Feldman, R.F. and Huang Cheng-yi: "Properties of Portland Cement — Silica Fume Pastes I. Porosity and Surface Properties, Cem. Concr. Res. 1985, 15 (5), 765-774.
115. Day, R.L. and Marsh, B.K.: "Measurement of Porosity in Blended Cement Pastes, "Cem. Concr. Res., 1988, 18 (1), 63-73.
116. Feldman, R.F.: "Effect of Predrying on Rate of Water Replacement from Cement Paste by Propan-2-ol", Il Cemento 1988, 85 (3), 193-202.
117. Feldman, R.F.: "Diffusion Measurements In Cement Paste By Water Replacement Using Propan-2-ol", Cem. Concr. Res., 1987, 17 (4).

118. Beaudoin, J.J.: "Validity of Using Methanol for Studying the Microstructure of Cement Paste", Mater. Struct., 1987, 20, 27-31.
119. Thomas, M.D.A.: "The Suitability of Solvent Exchange Techniques for Studying The Pore Structure of Hardened Cement Paste", Adv. Cem. Res. 2 (5), 29-34.
120. Taylor, H.F.W. and Turner, A.B.: "Reactions of Tricalcium Silicate Pastes with Organic Liquids", Cem. Concr. Res., 1987, 17 (4), 613-623.
121. Feldman, R.F. and Beaudoin, J.J.: "Pretreatment of Hardened Hydrated Cement Pastes for Mecury Intrusion Measurements", Cem. Concr. Res. 1991, 21, (43) 297-308.
122. Feldman, R.F.: "Microstructure Investigation of Cements and Mortars Containing Condensed Silica Fume", Proc. Int. Workshop on Cond. Silica Fume in Conc., CANMET, Montreal, May, 1987, pp 1-9.
123. Day, R.L.: "Rate of Solvent Exchange As a Measure of the Permeability of Mortar" Paper presented to ASTM Task Group on Permeability, ASTM Subcommittee C09.03-12, San Diego CA, December 1991.
124. Hearn, N. and Hooton, R.D.: "Sample Mass and Dimension Effects on Mercury Intrusion Porosimetry Results", Cem. Concr. Res. In press, 1992.
125. Scrivener, K.L., Patel, H.H., Pratt, P.L. and Parrott, L.J.: "Analysis of Phases in Cement Paste Using Backscattered Electron Images, Methanol Adsorption and Thermo-gravimetric Analysis", Proc. Matls. Res. Soc. 1985, 67-76.
126. Parrott, L.J.: "Effect of Drying History Upon the Exchange of Pore Water With Methanol and Upon Subsequent Methanol Sorption Behavior in Hydrated Alite Paste", Cem. Concr. Res. 1981, 11 (5), 651-658.
127. Marsh, B.K.: "The Effect of Solvent Replacement Upon the Pore Structure Characteristics of Portland Cement Paste", Proc. RILEM/CNR Symp. Principles and Application of Pore Structural Characterization, Milan, 1983. Arrowsmith, Bristol, 1985, 365-374.
128. Day, R.L.: "Reactions Between Methanol and Portland Cement Paste", Cem. Concr. Res., 1981, 11 (3), 341-349.
129. Moukwa, M. and Aïtcin, P.C.: "The Effect of Drying on Cement Pastes Pore Structure as Determined by Mercury Porosimetry," Cem. Concr. Res. 1988, 18, 745-52.
130. Kumar, A. and Roy, D.: "The Effect of Desiccation on the Porosity and Pore Structure of Freeze Dried Hardened Portland and Slag-Blended Pastes," Cem. Concr. Res. 1986, 16, 74-8.
131. Winslow, D. and Lin, D.: "The Pore Structure of Paste in Concrete", Cem. Concr. Res., 1990, 20, 227-235.
132. Abdel-Jawed, Y. and Hansen, W.: "Pore Structures of Hydrated Cement Determined by Mercury Porosimetry and Nitrogen Sorption Techniques," 105-18 in Pore Structure and Permeability of Cementitious Materials, L. Roberts and J.P. Skalny, Eds. MRS, 1989, Vol. 137.
133. Winslow, D.: "Some experimental Possibilities with Mercury Intrusion Porosimetry," 93-103 in Pore Structure and Permeability of Cementitious Materials, L. Roberts and J.P. Skalny, Eds. MRS, 1989, Vol. 137.
134. Feldman, R.F.: "Influence of Condensed Silica Fume and Sand/Cement Ratio on Pore Structure and Frost Resistance of Portland Cement Mortars", Proc. 2nd Int. Conf. on Fly Ash Silicate Fume Slag, and Natural Pozzolans in Concrete, Madrid 1986, (Amer. Concr. Inst. SP 91-47, 2, 973-989).
135. Feldman, R.F.: "The Effect of Sand/Cement Ratio and Silica Fume on the Microstructure of Mortars", Cem. Concr. Res. 1986, 10, 31-39.
136. Feldman, R.F.: "Dependence of the Durability of Mortars on Sand/Cement Ratio and Micro-Silica Addition" Durability of Build. Matls., 1986, 4 (2), 137-149.
137. Straley, C. and Minnis, M.M.: "Epoxy Rock Replicas for Microtoming," J. Sed. Petro. 1983, 53, 667-69.
138. Parrott, L., Patel, R., Kiloh, D. and Jennings, H.: "Effect of Age on Diffusion in Hydrated Alite Cement," J. Am. Ceram. Soc. 1984, 67, 233-37.
139. Kjellsen, K.O., Detwiler, R.J. and Gjorv, O.E.: "Pore Structure of Plain Cement Pastes Hydrated at Different Temperatures," Cem. Concr. Res. 1990, 20, 927-33.
140. Lin, C. and Hamasaki, J.: "Pore Geometry: A New System for Quantitative Analysis and 3-D Display," J. Sed. Petro., 1983, 53, 670-72.
141. Lin, C., Pirie, G. and Trimmer, D.A.: "Low Permeability Rocks: Laboratory Measurements and Three-Dimensional Microstructural Analysis," J. Geophys. Res. 1986, 91, 2173-81.

142. Pratt, P.L.: "Current Developments in Cement and Concrete Microstructures," 107-16 in Research on the Manufacture and Use of Cements, G. Frohnsdorff Ed., Engr. Fnd, NY, 1986.
143. Scrivener, K.L. and Pratt, P.L.: "Backscattered Electron Images of Polished Cement Section in the Scanning Electron Microscope," 6th ICCM, Albuquerque NM, 145-55, 1984.
144. Scrivener, K.L. and Pratt, P.L.: "The Characterization and Quantification of Cement and Concrete Microstructures," 61-8 Proc. 1st RILEM Congress, Versailles, 1987.
145. Scrivener, K.: "The Use of Backscattered Electron Microscopy and Image Analysis to Study the Porosity of Cement Paste," 129-140 in Pore Structure and Permeability of Cementitious Materials, L. Roberts and J.P. Skalny, Eds. MRS, 1989, Vol. 137.
146. Kjellsen, K.O., Detwiler,R.J. and Gjorv, O.E.: "Backscattered Electron Imaging of Cement Pastes Hydrated at Different Temperatures," Cem. Concr. Res. 1990, 20, 308-11.
147. Kjellsen, K.O., Detwiler, R.J. and Gjorv, O.E.: "Pore Structure of Plain Cement Pastes Hydrated at Different Temperatures," Cem. Concr. Res. 1990, 20, 927-33.
148. Patel, H.H., Pratt, P.L. and Parrott, L.J.: "Porosity in the Microstructure of Blended Cements Containing Fly Ash, 381-90 in in Pore Structure and Permeability of Cementitious Materials, L. Roberts and J.P. Skalny, Eds. MRS, 1989, Vol. 137.
149. Rubin, G.C. and Shafer, M.W.: "Stereo-TEM Imaginf of Sol-Gel Glass Surfaces," 207-12 in Better Ceramics Through Chemistry-II, 1986.
150. McCarter, W.J., Garvin, S. and Bouzid N.: "Impedance Measurements on Cement Paste" J. Matl. Sci. Letters, 1988, 7, 1056-1057.
151. McCarter, W.J. and Brousseau, R.: "The A.C. Response of Hardened Cement Paste", Cem. Concr. Res. 1990, 20 (6), 891-900.
152. Scuderi, C.A., Mason, T.O. and Jennings, H.M.: "Impedance Spectra of Hydrating Cement Pastes", J. Matls. Sci. 1991, 26, 349-353.
153. Brantervik, K., Nilasson, G.A.: "Circuit Models for Cement Based Materials Obtained From Impedance Spectroscopy". 1991, 21 (4), 496-508.
154. Scuderi, C.A.: Private Communication.
155. Ping, G., Ping, X., Beaudoin, J.J. and Brousseau, R.: "A.C. Impedance Spectroscopy I - A New Equivalent Circuit Model for Hydrated Cement Paste", Cem. Concr. Res., submitted for publication.
156. Ping, G., Ping, X., Beaudoin, J.J. and Brousseau, R.: "A.C. Impedance Spectroscopy II Microstructural Characterization of Hydrating Cement- Silica Fume Systems", Cem. Concr. Res. In press.
157. Periera, C.J., Rice, R. and Skalny, J.P.: "Pore Structure and its Relationship to Properties of Materials," 3-21 in Pore Structure and Permeability of Cementitious Materials, L. Roberts and J.P. Skalny, Eds. MRS, 1989, Vol. 137.
158. Richardson, I. et al: "The Porosity and Pore Structure of Hydrated Cement Pastes as Revealed by Electron Microscopy Techniques," 313-23 in Pore Structure and Permeability of Cementitious Materials, L. Roberts and J.P. Skalny, Eds. MRS, 1989, Vol. 137.
159. Roy, D.M.: "Relationships Between Permeability, Porosity, Diffusion and Microstructure of Cement Pastes Mortar, and Concrete at Different Temperatures," 179-89 in Pore Structure and Permeability of Cementitious Materials, L. Roberts and J.P. Skalny, Eds. MRS, 1989, Vol. 137.
160. Shi, D., Brown, P. and Kurtz, S.: "A Model for the Distribution of Pore Sizes in Cement Paste," 23-34 in Pore Structure and Permeability of Cementitious Materials, L. Roberts and J.P. Skalny, Eds. MRS, 1989, Vol. 137.
161. Shi, D., Ma, W. and Brown, P.: "Lognormal Simulation of Pore Evolution During Cement and Mortar Hardening," 143-48 in Scientific Basis for Nuclear Waste Management XIII, V.M. Oversby and P.W. Brown, Eds, MRS Pittsburgh, 1990.
162. Shi, D., Brown, P.W. and Ma, W.: "Lognormal Simulation of Pore Size Distribution in Cementitious Materials," J. Am. Ceram. Soc. 1991, 74, 1861-67.
163. Diamond, S. and Dolch, W.: "Generalized Lognormal Distribution of Pore Sizes in Hydrated Cement Paste," J. Coll. Interface Sci. 1972, 38, 234-44.
164. Jambor, J.: "Pore Structure and Strength Development of Cement Composites, Cem. Concr. Res. 1990, 20, 948-54.
165. Luping, T.: "A Study of the Quantitative Relationship Between Strength and Pore-Size Distribution of Porous Materials," Cem. Concr. Res. 1986, 16, 87-96.

166. Granju, J.L. and Grandet, J.: "Relationship Between the Hydration State and the Compressive Strength of Hardened Cement Pastes," Cem. Concr. Res. 1989, 19 579-85.
167. Ryskewitch, E.: "Compresssion Strength of Porous Sintered Alumina and Zirconia," J. Am. Ceram. Soc. 1953, 36, 65.
168. Röβler, M. and Odler, I.: "Investigations on the Relationships Between Porosity, Structure, and Strength of Portland Cement Pastes, I. Effect of Porosity," Cem. Concr. Res. 1985, 15 (2), 321-30.
169. Odler, I and Röβler, M.: "Investigations on the Relationship Between Porosity Structure and Strength of Hydrated Portland Cement Pastes II. Effect of Pore Structure and of Degree of Hydration," Cem. Concr. Res. 1985, 15, 401-10.
170. Odler, I. and Abdul-Maula, S.: "Investigations on the Relationship Between Porosity Structure and Strength of Hydrated Portland Cement Pastes III. Effect of Clinker Composition and Gypsum Addition," Cem. Concr. Res. 1987, 17, 22-30.
171. Sersale, R., Cioffi, R., Frigione, G. and Zenone, F.: "Relationship Between Gypsum Content, Porosity, and Strength in Cement. I. Effect of SO_3 on the Physical Microstructure of Portland Cement Mortars," Cem. Concr. Res. 1991. 21, 120-27.
172. Soroka, I. and Abayneh, M.: "Effect of Gypsum on Properties and Internal Structure of PC Paste," Cem. Concr. Res. 1986, 16, 495-504.
173. Köster, H. and Odler, I.: "Investigation on the Structure of Fully Hydrated Portland Cement and Tricalcium Silicate Pastes. I. Bound Water Chemical Shrinkage and Density of Hydrates," Cem. Concr. Res. 1986 16, 207-14.
174. Odler, I. and Köster, H.: "Investigation on the Structure of Fully Hydrated Portland Cement and Tricalcium Silicate Pastes. II. Total Porosity and Pore Size Distribution," Cem. Concr. Res. 1986, 16, 893-901.
175. Odler, I. and Köster, H.: "Investigation on the Structure of Fully Hydrated Portland Cement and Tricalcium Silicate Pastes. III. Specific Surface Area and Permeability," Cem. Concr. Res. 1991, 21, 975-82.
176. Vidick, B.: "Specific Surface Area Determination by Gas Adsorption: Influence of the Adsorbate," Cem. Concr. Res. 1987, 17, 845-7.
177. Patel, R.G., Killoh, D.C., Parrott, L.J. and Gutterage, W.A.: "Influence of curing at different relative humidities upon compound reactions and porosity in Portland cement paste," Matls, Struct. 1988, 21, 192-97.
178. Levchenko, A., Ambartsumyan, P., Verzhanovskaya, E.B. and Kaminskii: "Influence of the Composition of Retarding Admixtures on the Hydration of Cement and Microstructural Development of Cement Stone", Tsement, 1989, No. 10, 15-17.
179. Tenoutasse, N. and Marion, J.: "Influence of by-products on the porosity of hydrated portland cement" in Materials Science to Construction Materials Engineering. Proc. First International RILEM Congress, Versailles, Chapman and Hall, London and New York 1987, 3 vols., pp 33-40. (Ed: Maso)
180. Bier, Th. A.: "Influence of type of cement and curing on carbonation progress and pore structure of hydrated portland cement pastes (Ed: Struble and Brown: Microstructural development during hydration of cement, Materials Res. Soc Symp Proc., 1987, Vol 85 Materials Res Soc., Pittsburg.
181. Aitcin, P.C., Sarkar S. and Diatta: "Microstructural study of different types of very high strength concretes", ibid, pp 261-272.
182. Kumar, A. and Roy, D.M.: "Pore structure studies of high early strength portland cements containing silica fume", Trans Indian Ceram Soc., 1988, 47, 11-15.
183. Yilmaz, V.T. and Glasser, F.P.: "Crystallization of Calcium Hydroxide in the Presence of Sulphonated Melamine Formaldehyde Superplasticizer", J. Matls. Sci., Letters, 1991, 16, 712-715.
184. Yilmaz, V.T. and Glasser, F.P.: "Crystallization of Calcium Hydroxide in the presence of Sulphonated Melamine Formaldehyde Superplasticizer ", J. Matls. Sci., Letters, 1991, 16, 712-715.
185. Barker, A.P., Brett, N.H. and Sharp, J.H.: "Influence of Organic Additives on the morphology and X-ray diffraction line profiles of synthetic calcium hydroxide", J. Mat. Sci. 1987, 22, 3253-3260.
186. Inokawa, H., Takahashi, K. and Uchida, K.: "Analysis of calcium hydroxide and calcium aluminate hydrate formed in the presence of superplasticizer", Zairyo, 1987, 36, 617-623.

187. Rodger, S.A. and Groves, G.W.: "The microstructure of tricalcium silicate pulverized fuel ash blended cement pastes", Adv. Cement Res., 1988, 1, 84-91.
188. Zhang and Gjorv, O.E.: "Effect of Silica fume on pore structure and chloride diffusivity of low porosity cement paste", Cem. Conc. Res., 1991, 21, 1006-1015.
189. Groves, G.W. and Rodger, S.A.: "The hydration of C_3S and ordinary portland cement with relatively large additions of microsilica", Adv. Cem. Res. 1989, 2 (8), 135-140.
190. Ramachandran, V.S. and Zhang, Chun-Mei: "Dependence of fineness of calcium carbonate on the hydration behavior of tricalcium silicate", Durability of Mater., 1986, 4, 45-66.
191. Ramachandran, V.S. and Zhang, Chun-Mei: "Influence of $CaCO_3$ on hydration and microstructural characteristics of tricalcium silicate", Il Cemento, 1986, 83, 129-152.
192. Ramachandran, V.S., Sarkar, S. and Beaudoin, J.J., and Aimin, X.: "Physico-chemical investigations of the effect of NaOH on the hydration of $3CaO.SiO_2$.", Il Cemento. In press.
193. Feldman, R.F.: "Effect of sand/cement ratio and silica fume on the microstructure of mortars", Cem. Conc. Res., 1986, 16 (1), 31-39.
194. Durekovic, A. and Tkalcec, E.: "Cement pastes of low water solid ratio: An Investigation of the polymerization of silicate ions in the presence of superplasticizer and silica fume", Cem. Conc. Res., 1991, 21, 1015-1023.
195. Durekovic, A.: "Silicate anions polymerization in the paste of OPC and of OPC-silica fume blends during hydration and after action of leaching attack-Case of direct TMS method, Part 1", Cem. Conc. Res., 1988, 18, 185-193.
196. Durekovic, A and Popovic, K.: "Effect of ammonium nitrate solution on the structure and strength properties of cement pastes containing sil fume", Adv., Cem. Res., 1988, 1 (3), 138-146.
197. Ohama, Y., et al.: "Pore size distribution and oxygen diffusion resistance of polymer-modified mortars", Cem. Conc. Res., 1991, 21, 309-316.
198. Larbi, J.A. and Bijen, J.M.: "Interface between polymer-modified cement paste and aggregate", Cem. Conc. Res., 1990, 21, 983-990.
199. Bentur, A. et al.: "The effect of insitu polymerization on the chloride diffusion and microstructure of polymer-modified portland cement pastes and mortars", Adv. Cem. Res., 1990, 3 (9), 1-9.
200. Pigeon, M. and Plante, P.: "Study of cement paste microstructure around air voids: Influence on distribution of soluble alkalis", Cem. Concr. Res., 1990, 20, 803-815.
201. Stadelman, C., Trettin, R., Wieker, W. and Ramm, M.: "Surface studies of tricalcium silicate hydrated in sodium salt solutions", Il Cemento, 1987, 84 (4), 331-335.
202. Dunster, A.M. and Personagem, J.R.: "A study of the effects of saccharide and retarders on the polymerization using trimethyl silylation", Advances. Cem. Res. 1988, 1(4), 215-220.

Specific Theme III D

Effect of Admixtures

EFFECT OF ADMIXTURES

Mario Collepardi
Department of Materials Science, University of Ancona, ITALY

and

V S Ramachandran
Institute for Research in Construction, National Research Council, CANADA

Synopsis: The paper is divided into two parts.

The first part of the report is devoted to the discussion on the theoretical research carried out to understand the mechanisms of the superplasticizer action on the fuidizing effect, hydration, microstructure and durability aspects of cement mixes. Dispersion, adsorption and electrical repulsion effects have been examined by taking into account two main factors affecting these phenomena: *a*) type of polymer including chemical nature, molecular weight, monomer content, etc; *b*) type of cement, including mineralogical composition, form of calcium sulfate, amount of alkali sulfate, mineral additions, etc.

In the second part of the paper major advances made in the field of admixtures, with special reference to their practical implications are reviewed. The discussion include: the synthesis of admixtures, the development of new admixtures, use of admixtures in new applications and their effect on concrete properties in the fresh and hardened state. The review discusses the following: 1) Accelerators 2) Water Reducers 3) Superplasticizers 4) Retarders 5) Air-Entraining Agents 6) Polymer-Modified Mortars and Concrete 7)Activators for Slags 8)Admixtures to Reduce Alkali-Aggregate Expansion 9)Underwater Concreting 10)Re-Use of Returned Concrete 11)Antifreezing and 12)Corrosion Inhibitors.

I. EFFECT OF SUPERPLASTICIZERS ON THE PHYSICO-CHEMICAL CHARACTERISTICS OF CEMENT

1. INTRODUCTION

This report reviews publications in the area of cement and concrete admixtures mainly published after the last International Congress on the Chemistry of Cement, held in 1986. After this Congress exhaustive reviews (1-4) and Conference Proceedings (5, 6) specifically devoted to admixtures have been published.

Admixtures will be examined separately in two distinct Parts: Part I substantially deals with the effect of superplasticizers on the physico-chemical characteristics of cement pastes. Part II deals with the development of traditional admixtures (accelerators, water-reducers, superplasticizers, etc.) as well as of new admixtures (activators for slags, corrosion inhibitors, products for re-use of returned concrete, etc.). Each part is treated independently of the other with respect to discussion, references, tables and figures.

2. SUPERPLASTICIZERS

In the last twenty years, the admixture that has received the greatest interest in terms of research and development is high-range water reducers or superplasticizers. Even after the last International Conference held in 1986 superplasticizing admixtures dominate the admixture literature. This is due to the fact that superplasticizers provide important advantages to concrete from both technological and economical aspect of view.

In the first section of this report only the most used types of superplasticizers based substantially on condensed sulfonated melamine formaldehyde type (SMF) or sulfonated naphthalene formaldehyde type (SNF) will be examined in some detail. Developments of new superplasticizers, as well as other chemical admixtures are examined in Part II of the report.

3. TECHNICAL AND ECONOMIC ADVANTAGES OF USING SUPERPLASTICIZERS

Successful applications of superplasticized ready mixed concrete include the Channel Tunnel (7), concrete platforms in the North Sea (8), dry dock underwater concrete placement (9), and high-rise buildings with high strength concrete (10-12).

The technical and economical advantages of using superplasticized concrete for the manufacture of precast elements have also been examined (13-15). These include high rates of concrete placement, increased productivity by decreasing demoulding cycles, reduced cement contents to achieve a given strength and improved properties of hardened concrete. Also the technical advantages provided by superplasticizers in steam curing of concrete in precast plants have been studied widely(16-19).

The use of superplasticizers has been studied to solve specific problems in concrete technology such as pumping (9), underwater placing (9, 20), slip forming (21, 22) manufacture of paving concrete (23) as well as in special cement grout injections (24, 25).

In a feasibility study on the concrete production in areas remote from gravel deposits, it has been found that the replacement of natural aggregates by crushed stone allows a more economical concrete production provided that superplasticizers are used (26). The economical advantages of using superplasticizers to reduce the cement content and therefore the cost of concrete have been examined widely (27-29).

4. STUDIES ON THE MECHANISMS

The practical advantages of using superplasticizers justify and explain why increasing efforts are devoted to theoretical research to understand the mechanism of the action of these chemical admixtures on the fuidifying effect on cement/concrete mixes.

Skalny (30) has examined the role of superplasticizers on the thickness and quality of cement paste layer between aggregates, and concluded that there is need for a new approach in studying the rheology of cement mixes including cement pastes, mortars and concretes.

Some studies have been devoted to find a relationship between the physico-chemical characterization of naphthalene and melamine based superplasticizers and their action on the fuidizing effect of cement paste.They include emission and infrared spectography (31),thermal analysis (DTA/DTG) and Fourier transform infrared spectroscopy (32) which have been used to characterize commercial samples of superplasticizers. A more practical approach for a quick assessment of the relative effectiveness of various superplasticizers is based on deflocculation and vibratory compaction tests (33) or fluidity tests by using special mixing apparatus (34). All the above mentioned tests are useful to check the conformity of a supplied admixture and to verify the constancy of properties of a given superplasticizer.

The mechanism action of superplasticizers on the properties of cement pastes is a quite a complex problem since the influence of a superplasticizer depends on many parameters such as:

- chemical nature of superplasticizer;
- average molecular weight and its distribution;
- actual dosage (dry basis) and method of addition of admixtures;
- type of cement including fineness, mineralogical composition, alkali and sulfate contents;
- gypsum form (dihydrate/hemihydrate);

These data are not always available in published papers. Therefore sometimes it is difficult to explain contradictory results obtained by different authors when apparently the same experimental conditions have been used.

4.1 DISPERSION, ADSORPTION AND ELECTRICAL REPULSION

Even with the above mentioned limits, the available data as summarized by Ramachandran (35) indicate that the fluidizing effect of superplasticizers is basically related to the three following physico-chemical phenomena: dispersion, adsorption, and electrical repulsion (zeta potential).

Large and irregular agglomerates of cement particles predominate in a cement paste. The addition of superplasticizers causes dispersion into smaller agglomerates or even individual cement particles. The relationship between the dispersing effect and the improvement in the fluidity of the water-solid suspension finds applications in systems other than cementitious mixes.

The dispersing effect of superplasticizers is generally ascribed to the development of the same electrostatic (negative) charges on the cement particles as determined by the electrokinetic or zeta potential. In other words, attractive forces existing among cement particles suspended in water cause agglomeration, and these attractive forces can be neutralized by adsorption of anionic polymers, such as SNF or SMF, on the surface of cement particles.

At first glance the amount of adsorption of superplasticizers could be associated with a change in zeta potential and therefore with a dispersing effect, as shown in Fig. 1. Proper intepretation of these data requires additional information.

Both adsorption and zeta potential increase by increasing the superplasticizer dosage (Fig. 1) with the same type of superplasticizer and cement and the same method of addition (36). This does not necessarily mean that higher zeta potential and therefore more effective dispersion is always associated with higher adsorption of superplasticizers on the surface of cement particles. Basile et al. (37), for instance, have found (Table 1) that by using 0.4% of the same dry SNF polymer, the fluidizing effect, as determined by the minislump test, is quite different for two cement brands (A and B) even with substantially the same amount of adsorption of superplasticizer (about 80% of the original polymer). They have ascribed this difference in

behaviour of the same cement with the same superplasticizer to the different state of the calcium sulfate present in portland cement, i.e., dihydrate in cement A and hemihydrate in cement B.

TABLE1: ZETA POTENTIAL, ADSORPTION AND FLUIDITY (MINISLUMP) OF CEMENT PASTES (w/c = 0,35) IN THE PRESENCE OF SNF (0.4% AS DRY POLYMER) WITH TWO CEMENT BRANDS (37)

CEMENT BRAND	ZETA POTENTIAL (mV)	ADSORPTION (% ORIGINAL POLYMER)	MINISLUMP (cm^2)
A	- 23.5	80	188
B	- 20.4	83	87

4.2 TYPE OF POLYMER AND ITS EFFECTS

Andersen et al. (38) have found that although the adsorption of SNF is higher than that of SMF and PSS (sulfonated polystyrene), the zeta potential of PSS-treated cement has a larger negative value than that of SMF or SNF cement suspension (Fig. 2). Again, these results indicate that the polymer which is most effectively adsorbed is not necessarily the one that gives the largest negative zeta potential. These data, however, cannot be considered as a potential evaluation of the fluidizing effect of the three polymers (SNF, SMF and PSS) since rheological measurements of the cement mixes with and without polymers were not available. On the other hand, the molecular weight (MW) of the three polymers were quite different (15000, 19000 and 70000 for SNF, SMF and PSS respectively) and therefore the different zeta potential or adsorption characteristics cannot be ascribed directly and only to the different chemical nature of the polymers.

The influence of the molecular weight (MW) of the polymer on the zeta potential, adsorption and viscosity of the cement mixes strongly depends on the chemical nature of the superplasticizer, the MW range investigated and how the MW is expressed (weight or number average). Ferrari et al. (39), for instance, have found that commercial SNF- based superplasticizers exerted the best fluidizing effect in the MW range 6000-8000 (weight average), but at higher range the effect decreased when C_3A rich cements were used. Cements that were rich in C_4AF did not show this drop at higher molecular weight.

Andersen et al. (40) have studied the effect of the MW (4000-70000 weight average) of PSS superplasticizers on zeta potential and have found that the higher the molecular weight of the polymer, the better is the dispersion of the cement (in terms of zeta potential) (Fig. 3). However no viscosity measurement has been carried out to confirm the assumed relationship between large negative zeta potential and high fluidizing effect. This assumption does not agree with other results obtained by Biagini et al. (41) indicating that too much of high MW (over 50000 average weight) of PSS causes a decrease in the fluidizing effect. This drop at higher MW of PSS could be due to flocculation of solid particles caused by a bridge-effect of a single long-chain polymer molecule adsorbed on different cement grains.

The study of the effect of the MW of SMF superplasticizer on the adsorption on cement particles has led to contradictory results. Cunnigham et al. (42) found that higher molecular weight fractions of SMF preferentially adsorb onto the cement particles. These data do not confirm those of Sebok (43) who concluded in the adsorption of SMF polymer that all molecular weight fractions adsorb similarly.

The complex relationship between adsorption, zeta potential and molecular weight on one hand, and the fluidizing effect on the other, has been extensively examined by Basile et al. (44). They have studied the performances of the same SNF condensate but reacted for different periods of polymerization time: 2, 4, 10 and 14 hrs. The four polymers have been characterized by MW (number average), the monomer content and the GPC chromatograms. Apparently the higher the molecular weight of the polymer, the better is the fluidizing effect. However, the increase in the MW is accompanied by the reduction in the monomer content. Therefore it is difficult to conclude whether the increase in fluidizing effect is caused by the MW increase

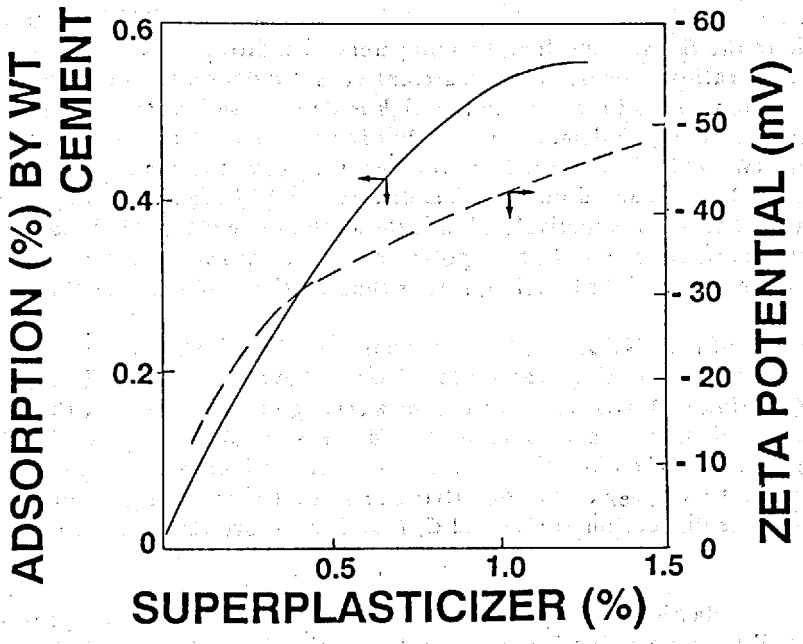

Fig. 1. Adsorption and zeta potential as a function of superplasticizer dosage (36)

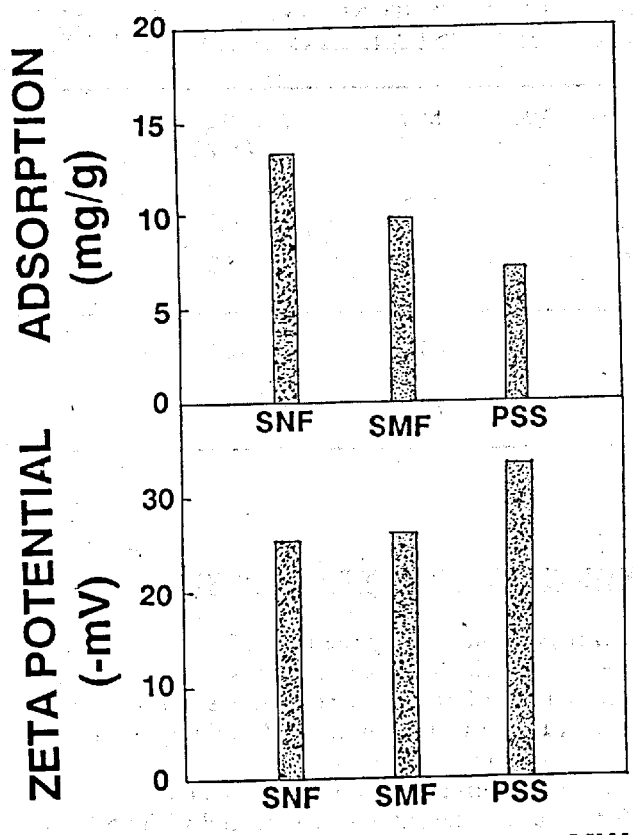

Fig. 2. Effect of superplasticizer with different MW (weight average) based on SNF (MW = 15000), SMF (19000) nad PSS (70000) on zeta potential and adsorption; admixture 1% in water (38)

or the monomer reduction. In order to evaluate which of the two parameters (MW or monomer content) plays the more important role in the fluidizing effect, two polymers with different MW and monomer content have been treated by the ultrafiltration process. This treatment causes a decrease in the content of monomer and low molecular weigth fraction, and an increase in the high molecular weight fraction (Fig. 4). Table 2 shows the effect of treated and untreated polymers on the fluidizing effect: after ultrafiltration, even if the two polymers have different MW (435 and 735 number average), they have the same fluidizing effect (185 cm^2 as minislump). Moreover, the 14-hr-reacted polymer has different MW (number average) before and after the ultrafiltration process (635 and 735 respectively), but it shows the same effect (185 cm^2 as minislump). These data would indicate that the effectiveness of a SNF polymer as a superplasticizer depends more on the content of monomer and lower molecular weight fraction, rather than on the MW value of the polymer.

A better fluidizing effect of the SNF superplasticizer has been found when it is added to cement paste or concrete a few minutes after the mixing water (45). This behaviour has also been confirmed for SMF superplasticizer (35). Addition with mixing water causes a strong incorporation of the superplasticizer into the C_3A-gypsum system, leaving only small amounts for dispersion of C_3S and C_2S. This agrees with the viscosity increase of the cement mix when the ettringite content is increased (46, 47). With late addition, superplasticizer is adsorbed to a lower extent on ettringite so that there is a greater amount of polymer in the aqueous phase to promote dispersion of C_3S and C_2S, and therefore fluidize the cement mix to a greater extent.

Delayed addition of superplasticizers appears to be more effective even in the presence of silica fume, creating a greater workability and a reduction in slump loss with mixing time (48-50).

TABLE 2: EFFECT OF MW (MOLECULAR WEIGHT, NUMBER AVERAGE) OF SNF POLYMERS BEFORE AND AFTER ULTRAFILTRATION ON THE FLUIDITY OF CEMENT PASTE (44)

ULTRAFILTRATION	CONDENSATION TIME (hr)	MW	MINISLUMP (cm^2)
Before	4	290	75
	14	635	185
After	4	435	185
	14	735	185

4.3 TYPE OF PORTLAND CEMENT AND PERFORMANCE

The fluidizing effect of superplasticizer is influenced by the type of cement used.

Hanna et al. (34) have examined the properties of cement grouts with SNF superplasticizer and have confirmed (47 , 51) that the C_3A content and the fineness of cement are among the most important factors: the higher the C_3A content and the cement fineness, the lower the fluidizing effect.

Basile et al. (44) have found that cements manufactured with the same clinker, but with different forms of calcium sulfate as set regulators, perform much differently when treated with SNF polymer: in the presence of calcium sulfate dihydrate, the fluidizing effect is much more significant than with hemihydrate. Table 3 indicates that by using two different clinker sources (A and B) the fluidizing effect of a SNF based superplasticizer on the Portland cement paste is more effective when gypsum in the form of dihydrate is used instead of hemihydrate, even though the zeta potential and the polymer adsorption are almost equal for the cement. These results have been confirmed by Nawa et al. (52) who found that in the presence of SNF superplasticizer cement pastes are much more fluid when dihydrate is used instead of hemihydrate. However,

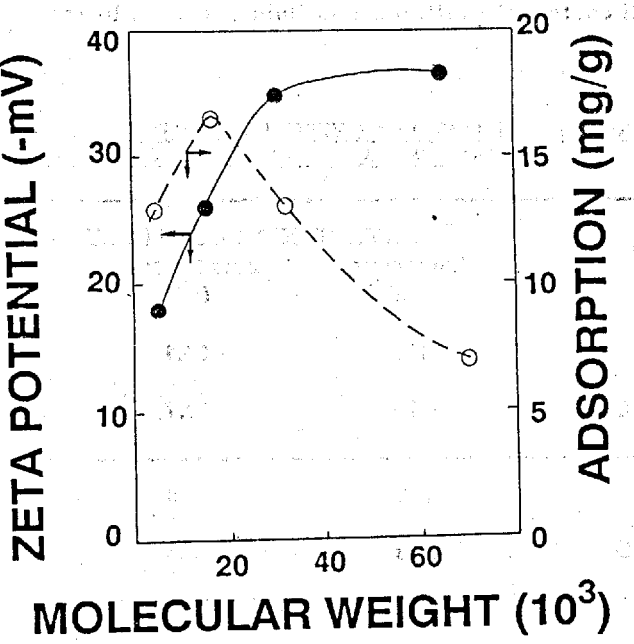

Fig. 3. Adsorption and zeta potential in cement pastes (w/c = 2) versus MW (weight average) of PSS (40)

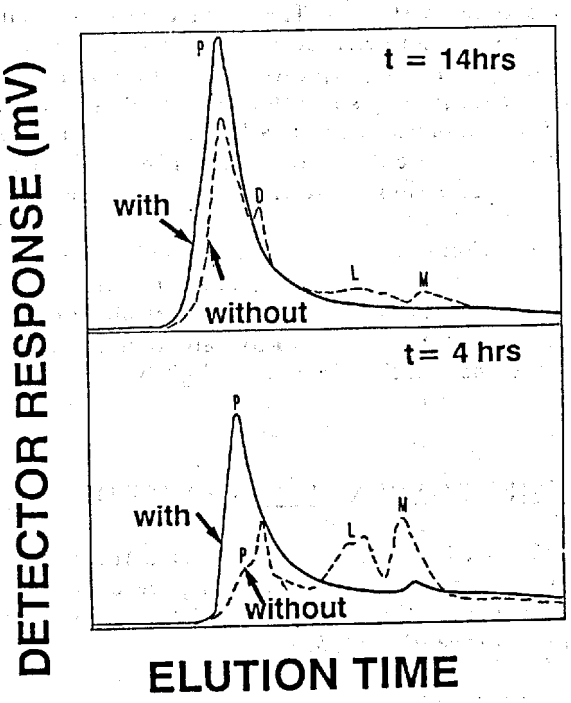

Fig. 4. GPC chromatograms of superplasticizer samples condensed for 4 hours and 14 hours without and with ultrafiltration. P = polymer; D = disulfonate; M = monomer; L = low molecular weight fraction (44)

for a cement with very low alkali content the difference in fluidity caused by the two calcium sulfate forms is negligible.

TABLE 3: INFLUENCE OF THE FORM OF GYPSUM AS SET REGULATOR ON THE CHARACTERISTICS OF SUPERPLASTICIZED CEMENT PASTES (37)

CLINKER SOURCE	GYPSUM FORM	EFFECT OF 0.4% SNF POLUMER ON: Minislump (cm^2)	Zeta Potential (mV)	Adsorption (% of original polymer)
A	$CaSO_4 \cdot 2H_2O$	175	- 24.1	82
A	$CaSO_4 \cdot 1/2\ H_2O$	79	- 23.7	82
B	$CaSO_4 \cdot 2H_2O$	189	- 23.2	82
B	$CaSO_4 \cdot 1/2\ H_2O$	83	- 22.4	82

Nawa et al. (52) have found that with calcium sulfate in the form of anhydrite as a set regulator, the fluidity of superplasticized cement paste lies between the values obtained with dihydrate and hemihydrate, except that in a cement with very low alkali content the fluidity is much lower.

Nawa et al. (52) have examined the complex influence of the water soluble alkali sulfate of the cement on the fluidizing effect of the SNF - based superplasticizer. They have confirmed that SNF, as well as SMF as found by Ramachandran (35), adsorb on C_3A and C_4AF more quickly and selectively than on C_3S and C_2S. In the presence of alkali sulfate the adsorption of superplasticizer on C_3A and C_4AF is inhibited, leading to increased adsorption on C_3S and C_2S. Consequently since the silicate phase adsorbs a much lower amount of polymer than the aluminate phase does, an increase in the alkali content of the cement causes a reduction in the total amount of polymer adsorbed on cement and this results in a higher amount of polymer in the aqueous phase to promote dispersion and reduction of the viscosity of the cement paste (Fig. 5).

However, according to Nawa et al. (52), excessive amount of alkali sulfate compresses the electric double layer causing a small increase in viscosity of the cement paste. These results would indicate that there is an optimum alkali sulfate content with respect to the fluidity of superplasticized cement paste (52, 53). Figure 5 shows that by increasing the amount of Na_2SO_4 added to a low alkali content cement, the viscosity of the superplasticized cement paste first decreases and then increases slightly.

4.4 PORTLAND CEMENT HYDRATION AND MICROSTRUCTURE

It is well known that SNF and SMF based superplasticizers retard the hydration of pure C_3A and in particular that of pure C_3S. However, in cement or a mixture of pure components, the C_3S hydration is retarded to a lower extent because the superplasticizer is adsorbed mainly by the C_3A phase (51). This has been confirmed by the data obtained more recently (54, 55).

Pistilli and Smith (56) have found that SNF produces higher one day strength than does SMF. In apparent agreement with these results, Regourd (55) has found that SMF acts as a stronger retarder than SNF. However, these data with SMF and SNF based superplasticizers may not necessarily contain polymers with the same MW, monomer content and MW distribution. Therefore, it is not surprising that these results do not agree with other data generally indicating that SMF is less retarding than SNF (57). For the same reason Pistilli and Smith (56) found that SMF is less effective than SNF as a water reducer, whereas Andersen et al. (38), on the basis of zeta potential measurements, concluded otherwise. Different MW characteristics could explain these contradictory results.

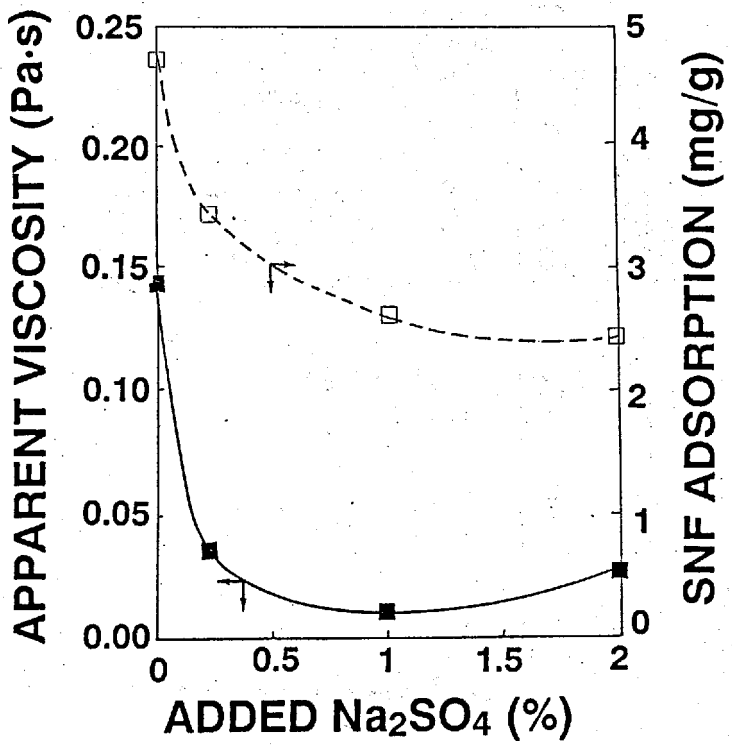

Fig. 5. Effect of Na_2SO_4 addition on SNF polymer adsorption and viscosity of the cement paste (52)

The retarding effect of SNF superplasticizer at the normal dosage (0.4% as dry polymer by weight of cement) has been confirmed by Basile et al. (44) for laboratory portland cements containing calcium sulfate in the form of pure dihydrate. However, no retardation has been found for the corresponding cements containing pure hemihydrate as the set regulator. Commercial cements containing both forms of calcium sulfate should show an intermediate performance depending on the dihydrate/hemihydrate ratio.

The effect of the form of calcium sulfate on the retardation of cement hydration caused by superplasticizer is quite complex, because the effect also depends on the amount of water soluble alkali sulfate present in cement. The effect of superplasticizer on the time of the appearance of the second maximum heat peak, corresponding to the C_3S hydration, in the conduction calorimetric curve has been studied (52). For cements with high alkali sulfate content (Fig. 6), the retardation caused by superplasticizer at normal dosage (1%) with respect to the control mix is significant when dihydrate and in particular anhydrite is used, whereas the retardation is negligible in the presence of hemihydrate unless very high dosages of the superplasticizer are used. For low alkali sulfate cements (Fig. 7), independently of the calcium sulfate form present as a set regulator, there is no substantial retardation unless high a dosage of superplasticizer ($>$ 1%) is used. Therefore, for a given form of calcium sulfate, there is a tendency for retarding effect of SNF to increase with the increase in the alkali sulfate content of cement.

According to the mechanism proposed by Nawa et al. (52), alkali sulfate in cement inhibits adsorption of SNF on the aluminate phase, permitting a larger amount of superplasticizer to be adsorbed on the silicate phases and causing a more significant retardation of C_3S and C_2S hydration.

Apparently the alkali ions present in sodium-based SNF superplasticizer do not have the same retarding effect as that of alkali sulfates in cement. Matsukawa and Diamond (58) have found that addition of sodium-based SNF superplasticizer results in a higher concentration of sodium in the cement paste pore solution, with a partial compensation for the potassium ions released by cement (lower in the presence of the superplasticizer). Fukaya and Kato (59) have found that alkali ions in superplasticizer adsorb on *C-S-H* but

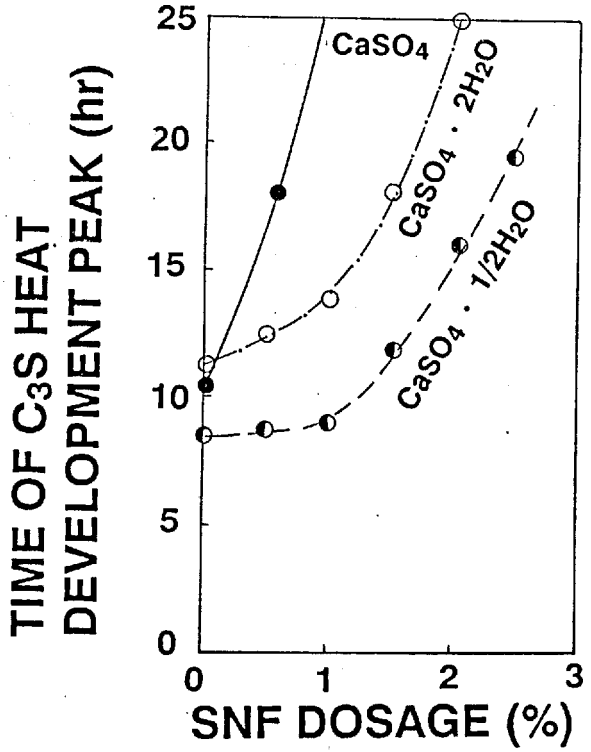

Fig. 6. Effect of SNF on the C_3S hydration rate in high alkali Portland cement with different forms of calcium as set regulators (52)

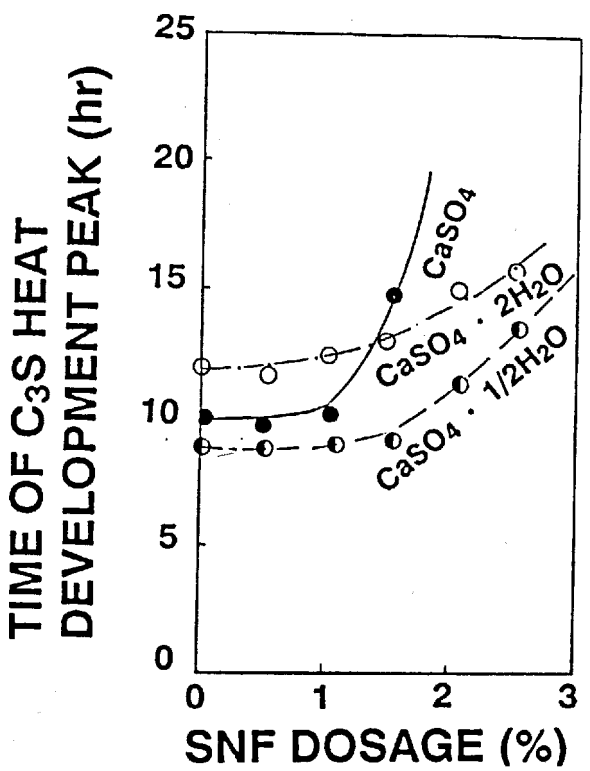

Fig. 7. Effect of SNF on the C_3S hydration rate in low alkali Portland cement with different forms of calcium as set regulators (52)

not on ettringite, and the adsorption of these ions do not affect the admixture adsorption. On the other hand, they have found that calcium ions in the superplasticizer adsorb on both *C-S-H* and ettringite and increase the adsorption of admixture. This could explain why calcium-based SNF is more retarding than the corresponding sodium-based SNF superplasticizer (60).

A limited amount of work has been carried out on the microstructure of superplasticized cement pastes. Only a few papers on the microstructure of pure C_3S or C_3A - $CaSO_4 \cdot 2H_2O$ system with and without superplasticizer have been published (51). In more recent articles the influence of SNF-based superplasticizer on the microstructure of *C-S-H* and *C-A-F* phases has been examined (35, 61). It has been found that a denser structure in cement paste is formed in the presence of superplasticizers.

4.5 BLENDED PORTLAND CEMENTS AND HIGH-ALUMINA CEMENT

The influence of superplasticizers on portland cement in the presence of silica fume, fly ash and slag has been extensively studied in recent years and several symposia (62-64) have been devoted to this specific subject. However, the greater part of the papers concerns engineering properties, whereas only few publications deal with mechanism aspects.

Diamond and Struble (65) studied the adsorption of superplasticizer on silica fume. They have found that in cement pastes where silica fume replaced 10% by weight of cement, the adsorption of superplasticizer is increased, although silica fume by itself adsorbed a negligible amount of superplasticizer. However, the adsorption of superplasticizer on the surface of the ingredients replacing portland cement could be affected by *pH*, chemical composition and ionic strength of the aqueous solution. All these parameters strongly change when adsorption is measured in the presence or in the absence of portland cement. Pierre et al. (66), for instance, have found that the adsorption of SNF polymer in $CaCO_3$ aqueous dispersions is increased by reducing the *pH* and increasing the ionic strength.

Ollivier et al. (67) studied the influence of superplasticizer in the presence of silica fume on the orientation of portlandite crystals as well as ettringite crystallization at the interfacial zone between cement paste and aggregate. They also found (68) that calcium silicate hydration is accelerated initially by the presence of silica fume and superplasticizer, whereas it is known that the early hydration of silicates is retarded by the presence of superplasticizer (51).

Collepardi et al. (57, 69, 70) studied the effect of SNF or SMF superplasticizers on the properties of Type I and Type III portland cement mixes in the presence of fly ash or silica fume. They found that in general SNF appears to be more effective than SMF as a water reducer and retarder. However, the retarding effect of SNF and SMF is reduced in the presence of silica fume. Even fly ash reduces retardation provided that a Type III portland cement is used. Due to the higher C_3S content and higher fineness, the hydration of this type of cement produces a larger amount of $Ca(OH)_2$ which is available for the pozzolanic reaction with silica fume or fly ash to form *C-S-H* which increases strength.

It has been found (71) that in the presence of blast-furnace slag replacing portland cement up to 85%, superplasticizers appear to be more effective, thus confirming previous results (51).

It is well known that SNF or SMF-based superplasticizers perform poorly when used for high alumina cement mixes. They retard the calcium aluminate hydration and at 180 days the strength of superplasticized and control mixes are comparable (51). Gill et al. (72) found that the retardation effect could be overcome by the simultaneous use of superplasticizer and lithium salts which act as accelerators. Banfill et al. (73) studied whether the sulfate in superplasticizers affected the hydration of high alumina cement. Sulfate is considered to be a retarder for this cement. They however found that at the dosage of superplasticizer normally used, the sulfate was not able to retard the hydration of high alumina cement.

5. DURABILITY OF SUPERPLASTICIZED CEMENT MIXES

Freezing and thawing effects, sulfate attack and chloride penetration are the most aggressive effects on concrete structures. In general, when superplasticizers are used to reduce the *w/c* ratio, a denser microstructure with lower capillary porosity in the cement paste is obtained, so that a concrete with higher

durability, and with a higher strength, results. However, use of superplasticizer per se does not necessarily make concrete resist aggressive action in the absence of air-entraining agent or mineral addition.

5.1 FREEZING AND THAWING EFFECTS

Air bubbles provide concrete ability to resist the undesirable effects of freezing and thawing. Adequate frost resistance requires that the spacing factor should not exceed 200 μm. In superplasticized cement mixes this value is exceeded. Mac Innis and Racic (74) found that SNF and SMF superplasticizers, added 40 min after batching and mixing, cause a significant drop in air volume and specific surface, and increase in the spacing factor in hardened concrete. The change in the spacing factor and void system caused by superplasticizers with or without silica fume has been confirmed (75-77).

In spite of the increased spacing factor, the freeze-thaw durability of superplasticized concrete tested according to ASTM Standard C-666 in general is not impaired (35). Previous work (78) has shown that superplasticizer mortars exhibit good frost resistance in spite of a spacing factor in excess of 200 μm and reduced porosity with respect to the reference mortar without air-entraining agent (Table 4). These results show that the spacing factor limitations stipulated for air-entraining concrete may not be valid for superplasticized mortars and concretes (35).

TABLE 4: EFFECT OF SUPERPLASTICIZER ON SPACING FACTOR AND POROSITY (78)

MORTAR	SPACING FACTOR (μm)	POROSITY INCREASE (% WITH RESPECT TO THE REFERENCE MORTAR)
reference mortar (without admixture)	790	—
mortar + air entrainment	280	246
mortar + air entrainment + 0.75% superplasticizer	330	194
mortar + air entrainment + 1.5% superplasticizer	430	105

However, conflicting results (79-81) on the frost resistance tests for superplasticized concrete have been reported, thus confirming some unexplained exceptions previously reported (82, 83). Petrographic data would indicate that in the failed specimens the entrained air bubble is too large, with the spacing factor exceeding a value of 200 μm.

5.2 SULFATE ATTACK

Ettringite ($C_3A \cdot 3CaSO_4 \quad 32H_2O$) and/or thaumasite ($CaSO_4 \cdot CaCO_3 \cdot CaSiO_3 \cdot 15H_2O$) can be formed by sulfate attack of cement mixes. Thaumasite formation is favoured by low temperatures (0-5°C) and high relative humidities (>90%).

The resistance of concrete to sulfate attack (monitored by determining changes in weight, length and dynamic modulus of elasticity) is improved by reducing the w/c ratio. Therefore when superplasticizers are

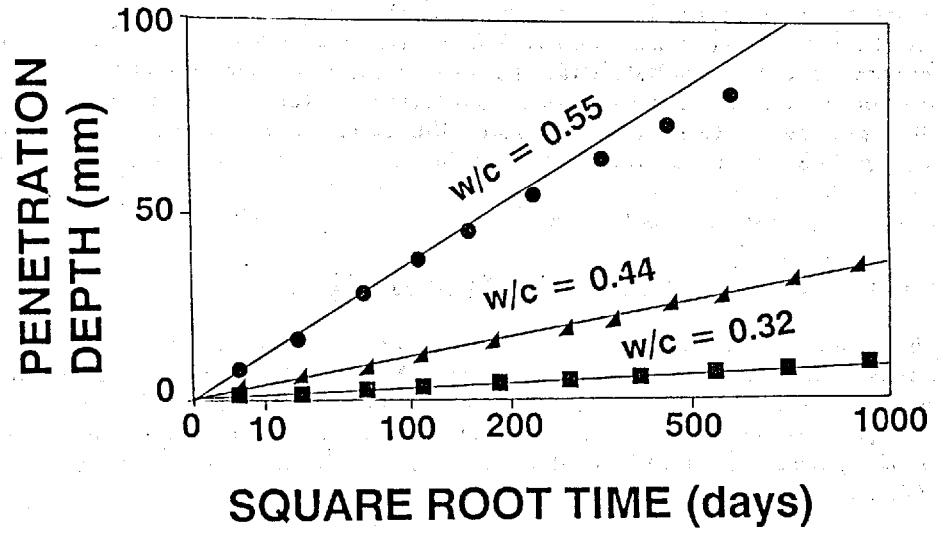

Fig. 8. Chloride penetration depth versus time. Curing time before exposure to 10% $CaCl_2$ aqueous solution: 28 days, (87).

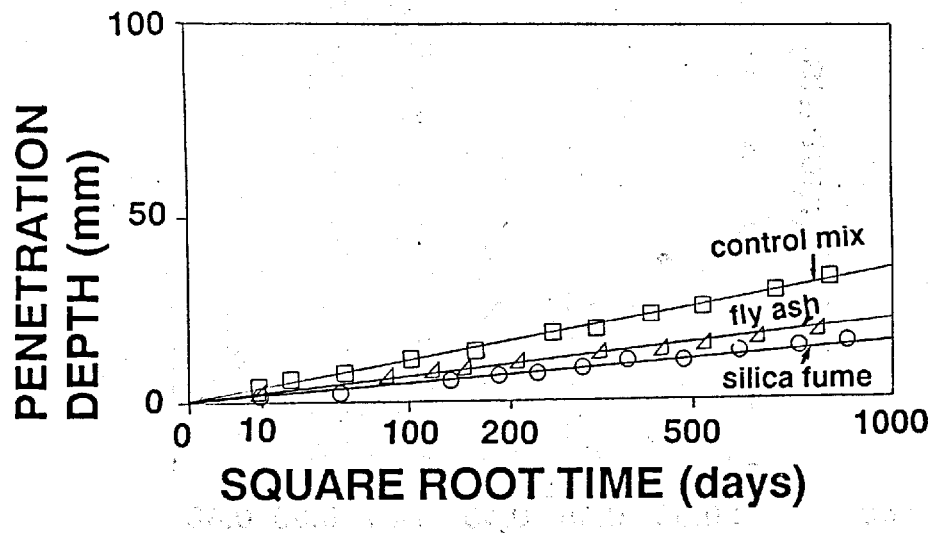

Fig. 9. Effect of fly ash or silica fume addition on chloride penetration of concrete with w/c = 0.44. Curing time before exposure to 10% $CaCl_2$ aqueous solution: 28 days, (87)

used to increase workability without reducing the *w/c* ratio, the resistance of superplasticized concretes is comparable to that of the reference mixes (35, 84). When the admixtures are used to reduce the *w/c* ratio, superplasticized concrete resists the sulfate attack better than the reference mixes (9, 85).

Collepardi (86) found that at hygrothermal conditions favorable for the formation of thaumasite, a *w/c* ratio lower than 0.40 is required to produce concretes able to resist the sulfate attack: in such a case a relatively higher dosage (0.8% as dry polymer) of superplasticizer is required to produce a sulfate resistant concrete.

5.3 CHLORIDE PENETRATION

It well known that chloride salts penetrating concrete cover can promote corrosion of rebars. This can occur in reinforced concrete structures exposed to deicing agents ($NaCl$ or $CaCl_2$) or sea water. By reducing the *w/c* ratio through the use of superplasticizers, chloride diffusion through the concrete cover can be significantly reduced (Fig. 8) and steel corrosion in reinforced concrete structures can be avoided (87). A combined addition of superplasticizer and fly ash or silica fume (87) further reduces the chloride diffusion through concrete (Fig. 9).

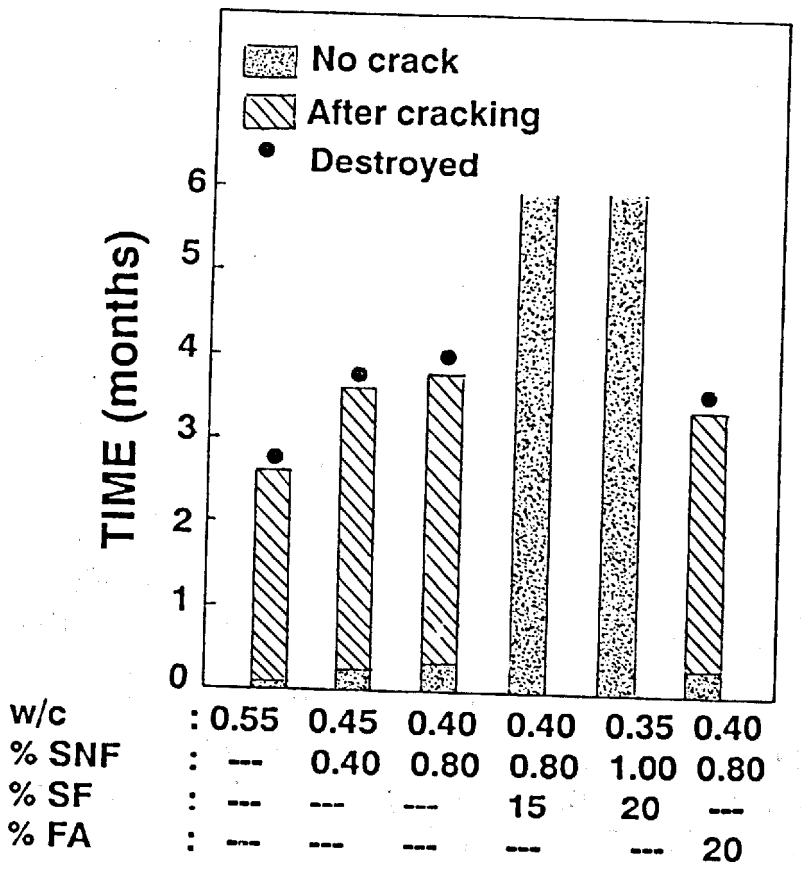

Fig. 10 Calcium chloride attack: time of cracks appearance and full deterioration as a function of concrete composition. Silica Fume (SF) or fly ash (FA) have also been used to replace cement (86)

For a long time chloride was considered to be an aggressive agent only for steel reinforcement but not for concrete. However, more recent data indicate that $CaCl_2$ and $NaCl$ may severely attack concrete, in addition to causing rebar corrosion. Chatterji (88) found that chloride, in the form of 30% $CaCl_2$ aqueous solution, can also attack concrete very quickly provided the temperature is lower than 20°C and preferably 5°C. Monosi et al. (89) found that the "Chatterji effect" occurs even with 10% $CaCl_2$ aqueous solution and at a temperature higher than 20°C, although lower temperatures, such as 5°C, create the most severe conditions for the $CaCl_2$ attack. According to these authors the action of $CaCl_2$ used as de-icing agent has been masked for a long period of time by another concurrent deteriorating mechanism, that is the freezing-thawing effect.

Monosi and Collepardi have found (90) that $3CaO \cdot CaCl_2 \cdot 15H_2O$ is the main salt responsible of the deterioration caused by $CaCl_2$. The product forms by reaction of penetrating $CaCl_2$ in concrete with $Ca(OH)_2$ which is present in the cement paste. Collepardi (86) found that the combined addition of superplasticizer and silica fume (15-20%) produces durable concrete that resists the very severe attack of $CaCl_2$, because of the reduction in both chloride diffusion and the amount of free lime. Superplasticizer alone or a combination of superplasticizer and fly ash (20%) is not able to produce concrete that is able to resist the aggressive action by $CaCl_2$ (Fig. 10).

Chatterji (91) found that exposure of concrete to a 10% $NaCl$ aqueuos solution accelerates the alkali-aggregate reaction. This has been confirmed by Collepardi (86) who has found that concretes containing non-reactive aggregate and which are able to perform quite well for a long time even in combination with an alkali rich cement, become very reactive when exposed to a 10% $NaCl$ aqueous solution. The addition of superplasticizer alone does not substantially improve the durability to the alkali-aggregate reaction when tested in the presence of $NaCl$. Addition of fly ash or silica fume plus superplasticizer allows concrete specimens to perform very well in the presence of $NaCl$.

6. CONCLUSIONS

The mechanism of action of superplasticizers on the fluidizing effect of cement mixes has been investigated extensively in terms of the dispersion, adsorption and electrical-repulsion effects. This approach appears to be still useful at least for the simplest cement mix system (cement paste). However, there is apparently some contradiction between the results reported in the literature because some aspects, such as polymer type and cement type, are not always clearly described. For instance, superplasticizers with the same chemical polymer (SNF or SMF) may perform quite differently depending on the molecular weight distribution, monomer content, etc. of the polymer. On the other hand, the same superplasticizer may have different fluidizing effect depending on the form of calcium sulfate used as a set regulator or the amount of alkali sulfate present in the clinker. Therefore more attention should be directed to the characterization of polymer and cement used for solving the mechanism of the action of superplasticizer.

Concrete durability (in terms of resistance to freezing-thawing effects, sulfate attack and chloride penetration) is improved by using superplasticizers. However, they should be used in combination with an air-entraining agent to produce frost-resistant concretes, and with silica fume when exposed to $CaCl_2$ de-icing salts.

REFERENCES

(1) Factor, D.F., Fack, S.M., Kinney, F.D., Lupyan, D.A., and McFarland, M.A., "Admixtures", Chapter 6 in "*Cement Research Progress 1986*", pg 139-185.

(2) Factor, D.F., Kinney, F.D., Lupyan, D.A., Nelson C.M., and McFarland, M.A., "Admixtures", Chapter 6 in "*Cement Research Progress 1987*", pg 95-136.

(3) Harris, R.L., Kinney, F.D., Lupyan, D.A., McFarland, M.A., Nelson, C.M, Siebert, E.J., Wolff, A.R., and Young, A.M., "Admixtures", Chapter 6 in "*Cement Research Progress 1988*", pg 147-199.

(4) Kinney, F.D., McFarland, M.A., Siebert, E.J., and Viacers, J.M., "Admixtures", Chapter 6 in "*Cement Research Progress* 1989".

(5) Third CANMET/ACI Intern. Conf. on "*Superplasticizers and other chemical admixtures in concrete*", Ottawa 1989, Ed. V.M. Malhotra, ACI, Detroit, Michigan, 1989.

(6) Proceedings of the Intern. RILEM Symp. on "*Admixtures for Concrete, Improvement of Properties*", Barcelona 1990, Ed. E. Vasquez, Chapman and Hall, London, 1990.

(7) Harmant, J., Jensen, P., and Poitevin, P.,"Channel tunnel Concrete:a 120 year durability challenge", *Proceedings of IX European Ready Mixed Concrete Organization Congress*, Stavanger, Norway, 1989, pg 504-577.

(8) Moksnes, J., "Concrete platforms in the North Sea two decades of experience with high strength concrete",*Proceedings of IX European Ready Mixed Concrete Organization Congress*, Stavanger, Norway, 1989, pg 578-594.

(9) Collepardi, M., Khurana, R., and Valente, M., "Conctruction of a Dry Dock Using Tremie Superplasticized Concrete", pg 471-492 in ref. (5).

(10) Hideshima, S., Moriya, Y., and Takada, M., "The Applications of High-Range AE Water-Reducing Admixture for High-Strength Concrete. Dealing with RC Skyscrapers Built with Structural Hi-Strength Concrete", *Proc. Japn.Congr. Mater.Res.* 3199-101, 1988.

(11) Tomatsuri, K., Koroha, K., and Namiki, S., "Application of High-Strength Concrete to High-Rise Building", *Tasei Technical Research Report*, 20 105-108, Technical Research Inst., Tokyo, Japan, 1897.

(12) Anthony, W.R., and Steiner, P.J., "Concrete High-Rises Offer Many Cost Advantages", *Concr. Constr.*33 (5), pg 453-456, 1988.

(13) Kern, A., and Reichert, J., "Technical and Economical Advantages of Superplasticizers in Precast Concrete Plants", *Betonwerk Fertigteil Tech.*, 53 (11), pg 769-774, 1987.

(14) Ianescu, I., Ianescu, E., Cracium, I., and Popa, Z., "New Aspects of the Use of Superplasticizers in the Technology of Concrete and Precast Structures", *Mater. Constr.*, 18(4), pg 235-240. 246, 1988.

(15) Mladova, M.V., and Bibik, M.S., "Economy of Cement with the Use of Superplasticizer S-3 (Experience of Precast Steel-Reinforced Concrete-Manufacturing Plants of Belorussia)", *Beton Zhelezobeton*, Moscow, (4), pg 11-13, 1989.

(16) Carette, G.G., Malhotra, V.M., Bedard, C., De Benedictis, V,. and Plumat, M., "Development of Heat-Curing Cycles for Portland Cement-Fly Ash Concrete for the Precast Industry", *CANMET/ACI Inter.Conf. on "Fly Ash, Silica fume, Slag and Natural Pozzolans in Concrete"*, Ottawa 1986, Ed. V.M. Malhotra, ACI, Detroit, Michighan, vol. I, pg 249-272, 1986.

(17) Kropp, J., Seeberg, J., and Hilsdorf, H.K., "Chemical and Physical Properties of Cement Paste and Concrete Containing Fly Ash After Hydrothermal Exposure",*CANMET/ACI Inter.Conf. on "Fly Ash, Silica fume, Slag and Natural Pozzolans in Concrete"*, Ottawa 1986, Ed. V.M. Malhotra, ACI, Detroit, Michighan, vol. I, pg 201-218, 1986.

(18) Bach, T., "Autoclaved Cement Based Products Containing Fly Ash", *CANMET/ACI Inter.Conf. on "Fly Ash, Silica fume, Slag and Natural Pozzolans in Concrete"*, Ottawa 1986, Ed. V.M. Malhotra, ACI, Detroit, Michighan, vol. I, pg 291-312, 1986.

(19) Mantegazza, G., Ciatti, G.,and Bolzoni, A., "Durable ready-mixed concrete for pre-stressed steam cured beams", *Proceedings of IX European Ready Mixed Concrete Organization Congress* , Stavanger, Norway, 1989, pg 436-452.

(20) Kawakami, M., Wada, S., and Sukukawa, K., "Effects of Chemical Admixtures on Colloidal Underwater Concrete", pg 493-516 in ref. (5).

(21) Tjugum, O.M., "The Challenge of the Concrete and the Ready mixed Concrete Industry in the Offshore Market", *Proceedings of IX European Ready Mixed Concrete Organization Congress* , Stavanger, Norway, 1989, pg 701-707.

(22) Ronneberg, H., "Use of Chemical Admixtures in Concrete Platforms", pg 517-533 in ref. (5).

(23) Baessgen, W., "Paving Concrete With Superplasticizers-Use and Experience in the GDR", *Zem. Beton (Vienna)*, 33(4), pg 192-196, 1988.

(24) Gray, M.N., and Keil, L.D., "Field Trials of Superplasticized Grout at AECL's Underground Research Laboratory", pg 605-616 in ref. (5).

(25) Onofrei, M.N., and Gray, M.N., "Adsorption Studies of S-Labelled Superplasticizer in Cement-Based Grout", pg 645-660 in ref. (5).

(26) Schaeper, M., "Concrete Made with Coarse and Fine Crushed Aggregates. A Feasability Study", *Betonwerk Fertigteil Tech.*, 53(11), pg 757-763, 1987.

(27) Markaryan, T.G., Sarkisyan, R.R., Asaturyan, V.S., and Avetikyan, V.A., "Ways to Decrease Cement Comsumption in Construction", *Prom-st., Stroit., Arkhit. Arm.*, (12), pg 50-52, 1987.

(28) Matracka, E.,and Wirpsza, Z., "Effect of Sulfomethylated Melamine Formaldehyde Resin on the Properties of Concretes. Part II.", *Cem.Wapno-Gips*, (4-5), pg 81-83, 1987.

(29) Danielsen, S.W., "Aggregate Technology for Ready Mix Concrete", *Proceedings of IX European Ready Mixed Concrete Organization Congress*, Stavanger, Norway, 1989, pg 616-627.

(30) Skalny, J., "Some Comments on Concrete Workability", Invited Lecture for the *Int. Symp. on Admixtures for Concrete, Improvement of Properties*, RILEM, Barcelona, 1990.

(31) Verhasselt, A. , and Ista, E., "Chemical Characterization of Plasticizers and Superplasticizers", pg. 99-116 in ref. (5).

(32) Khorami,J., and Aitcin, P.C., "Physiochemical Characterization of Superplasticizers", pg 117-131 in ref. (5).

(33) Verhasselt, A., and Pairon, J., "Rapid Methods of Distinguishing Plasticizer from Superplasticizer And Assessing Superplasticizer Dosage", pg 133-155 in ref. (5).

(34) Hanna, E., Luke, K., Perraton, D., and Aitcin, P.C., "Rheological Behavior of Portland Cement In the Presence of a Superplasticizer", pg 171-188 in ref. (5).

(35) Ramachandran, V.S., "Use of Superplasticizer in Concrete", *Il Cemento*, 84, pg 273-298, 1987.

(36) Collepardi, M., Corradi, M., Baldini, G., and Pauri, M., "Influence of Sulfonate Naphtalene on the Fluidity of Cement Paste", *VII Int. Congr. on Chemistry of Cements, Paris*, vol. III, pg 20-25, 1980.

(37) Basile, F., Biagini, S., Ferrari, G., and Collepardi, M., "Effect of the gypsum state in industrial cements on the action of superplasticizers", *Cem. Concr. Res.*, 17, pg 715-722, 1987.

(38) Andersen, P.J., Roy, D.M., and Gaidis, J.M., "The Effects of Adsorption of Superplasticizers on the Surface of Cement", *Cem. Concr.Res.*, 17, pg 805-813, 1987.

(39) Ferrari, G., Basile, F., Dal Bo, A., and Mantoni, A., "The Influence of Molecular Weight of Beta Naphthalene Sulfonate-Based Polymers on the Rheological Properties of Cement Mixes", *Il Cemento*, 83, pg 445-454, 1986.

(40) Andersen, P.J., Roy, D.M., and Gaidis, J.M., "The Effect of Superplasticizer Molecular Weight on its Adsorption on, and Dispersion of Cement", *Cem. Concre. Res.*, 18, pg 980-986, 1988.

(41) Biagini, S., Ferrari, G., Maniscalco, V., Casolaro, M., Tanzi, M.C., and Rusconi, L., "Sulfonated Polystyrene as Superplasticizer", *Il Cemento*, 79, pg 345-354, 1982.

(42) Cunnigham, J.C., Dury, B.L., and Gregory, T., "Adsorption Characteristics of Sulfonated Melamin e Formaldehyde Condensates by High Performance Size Exclusion Chromatography", *Cem. Concr. Res.*, 19(6), pg 919-928, 1989.

(43) Sebok, T., "The effects of the Molar Parameters of Sulfonated Melamine and Formaldehyde Polycondensates on Mortar Properties", *Proc. 8th International Congress on the Chemistry of Cement, Theme 2, Vol. III, pg 34-39, 1986.*

(44) Basile, F., Biagini, S., Ferrari, G., and Collepardi, "Influence of Different Sulfonated Naphthalen e Polymers on the Fluidity of Cement Paste", pg 209-220 in ref. (5).

(45) Collepardi, M., Corradi, M., and Valente, M., "Influence of Polymerization of Sulfonated Naphthalene Condensate and its Interaction with Cement", *Amer.Concr. Inst.* Sp-68, pg 485-498, 1981.

(46) Nawa, T., and Eguchi, H., "Effect of Type of Calcium Sulfate on Fluidity of Cement Paste", *Sem. Gijtsu Nenpo*, (41), pg 46-49, 1987.

(47) Burk,A.A., Gaidis, J.M., and Rosenberg, A.M., "Adsorption of naphthalene-based superplasticizers on different cements", presented at the *II Inter. Conf. on Superplasticizer in Concrete*, Ottawa, 23, 1981.

(48) Mangialardi, T., and Paolini, A.E., "Workability of Superplasticized Microsilica-Portland Cement Concretes", Cem. Concr. Res., 18(3), pg 351-362, 1988.

(49) Paiellere, A.M., Serrano, J.J., and Grimaldi, M., "Influence of dosage and addition method of superplasticizers on the workability retention of high strength concrete with and without silica fume", pg 63-79 in ref. (6).

(50) Saada, R., Barrioulet, M., and Leygrand, C.,"Influence of Plasticizers on the Rheological Characteristics on Cement Pastes Containing Fillers", pg 80-93 in ref. (6).

(51) Ramachandran, V.S., and Malhotra, V.M., "Superplasticizers", Chapter 4 in Concrete Admixtures Handbook, Properties, Science and Technology, Ed. V.S. Ramachandran, Noyes Publications, Park Ridge, New Jersey, USA, pg 211-268, 1984.

(52) Nawa, T., Eguchi, H., and Fukaya, Y., "Effect of Alkali Sulfate on the Rheological Behavior of Cement Paste Containing a Superplasticizer", pg 405-424, in ref. (5).

(53) Nawa, T., and Eguchi, H., "Effect of an Alkali Sulfate on Rheological Behavior of Cement Paste", Sem. Gijutsu Nenpo, (42), pg 52-55,1988.

(54) Singh , N.B., and Singh, P.S., "Lattice Defects and the Effect of Melment on the Hydration of Alite ", J. Mater. Sci, 22(8), pg 2751-2758, 1987.

(55) Regourd, M., "A Review of the Use of Proton Magnetic Resonance to Study Superplasticizers", Mater. Res. Soc. Symp. Proc. (Microstruct. Dev. Hydration Cem.), 85, pg 245-254, Paris, France, 1987.

(56) Shiiba, H., and Honda, S., "Experimental Research on a New Type of Admixture for use in Concrete, Part II, Principal Properties of Superplasticized Concrete", Fukuota Daigaku Kogaku Shuho, 36, pg 77-86, 1986.

(57) Collepardi, M., Monosi, S., and Valente, M., "Optimization of Superplasticizer Type and Dosage in Fly Ash and Silica Fume Concretes", pg 425-443, in ref. (5).

(58) Matsukawa, K., and Diamond, S., "Quantitative Study of Naphthalene Sulfonated Effects on Cement Paste Pore Solution Chemistry", Advances in Cement Materials Vol. 16, pg 41-54, Editors L. Robert and S. Mindess, Am.Cer. Soc., Westville, OH, 1991

(59) Fukaya, Y.,and Kato, K.,"Adsorption of Superplasticizers on CSH(I) and Ettringite", Proc. 8th Inter. Congr. on the Chemistry of Cement, Theme 2, Vol III pg142-147, 1986

(60) Collepardi, M., unpublished results.

(61) Inokawa, H.,Takahashi, K., and Uchida, K., "Analysis of Calcium Slicate Hydrates and Calcium Aluminate Hydrates formed in the Presence of a Superplasticizer", Zairyo, 36, 495, pg 617-623, 1987.

(62) Proceedings of the Second Intern. Conf. on Fly Ash, Silica Fume, slag and Natural Pozzolans in Concrete , Ed. V.M. Malhotra, CANMET/ACI, Madrid, 1986.

(63) Supplementary Cementing Materials for Concrete, Ed. V.M. Malhotra, CANMET/ACI, Madrid, 1986.

(64) Third CANMET/ACI Inter. Conf. on Fly Ash Silica Fume, Slag & Natural Pozzolans In Concrete, Ed. Malhotra, Trondheim, Norway, 1989.

(64a) Malhotra, V.M., Ramachandran, V.S., Feldman, R.F., and Aitcin, P.C., "Condensed Silica Fume in Concrete", CRC Press, pg 221, 1987.

(65) Diamond, S., and Struble, L.J., "Interaction Between Naphthalene Sulfonate and Silica Fume in Portland Cement Pastes", Mater. Res. Soc. Symp. Proc., 114 (Bonding Cem. Compos.) pg 117-126, 1988.

(66) Pierre, A., Lamarchi, J.M., Mercier, R., and Foissy, A., "Adsorption d'un fluidifiant du ciment sur le carbonate de calcium", Cem.Concr. Res., 19, pg 692-702, 1989.

(67) Ollivier, J.P., Grandet, J., and Hanna, B., "Effect of Superplasticizer and Reactive Condensed Silica Fume on the Mortar-Coarse Aggregate Bond", Congr. Int. Quim. Cimento, [An], 8th, 4, pg 204-209, 1986.

(68) Park, S.B., and Go, Y.S., "An Experimental Study of the Rheological Properties of Superplasticized Cement Paste", Normunjip-Ch'ungnam Taehakkyo Sanop Kisul Yan-Guso, 2(1), pg 10-15, 1987.

(69) Collepardi, M., Monosi, S., Pauri, M., Biagini, S., and Alverà, I., "The Influence of Superplasticizer Type and Dosage on the Compressive Strength of Portland Cement Concrete in the Presence of Fly Ash", pg 168-174 in ref. (6).

(70) Collepardi, M., Moriconi, G., Pauri, M., Biagini, S., and Alverà, I., "Superplastized Silica Fume High-Strength Concretes", pg 175-182 in ref. (6).

(71) Nishibayashi, S., Yoshino, A., Hideshima, S., Takada, M., and Chikada, T., "A Study on Superplasticized Concrete Containing High Volumes of Blast-Furnace Slag", pg 445-455 in ref. (5).

(72) Gill, S.M., Banfill, P.F.G., and El-Jazairi, B., "The Effect of Superplasticizers on the Hydration of Aluminous Cement", Proc. 8th. Inter. Congr. on the Chemistry of Cement, Theme III, Vol. IV, pg 322 -327, 1986.

(73) Banfill, P.F.G., "The Effect of Sulfate on the Hydration of High Alumina Cement", Cem.Concr. Res., 16(4), pg 602-604, 1986.

(74) MacInnis, C., and Racic, D., "Effect of Superplasticizers on the Entrained Air-Void System in Concrete", Cem.Concr.Res., 16, pg 345-352, 1986.

(75) "Resistance of High-Strength Concrete to Freezing and Thawing", Concr. Constr., 33(3), pg 346-347, 1988.

(76) Pigeon, M., Gagne, R., and Foy, C., "Critical Air-Void Spacing Factors for Low Water-Cement Ratio Concretes with and without Condensed Silica Fume", Cem.Concr. Res., 17(6), pg 896-906, 1987.

(77) Balaguru, P., and Ramakrishnan, V., "Chloride Permeability and Air-Void Characteristics of Concrete Containing High Range Water Reducing Admixtures", Cem. Concr. Res. 18(3), pg 401-414, 1988.

(78) Litvan, G.G., "Air Entrainment in the Presence of Superplasticizers", Am. Concr. Inst. J., 80, pg 326-331, 1983.

(79) Dhir, R., Dransfield, J., and Tham, K., "Durability of Concrete with a Superplasticizing Admixture", Proc. Katherine and Bryant Mather International Conference, 2 , pg 741-764, 1987.

(80) Robson, G., "Durability of High Strength Concrete Containing a High Range Water Reducer", Proc. Katherine and Bryant Mather International Conference, 2 , pg 765-780, 1987.

(81) Korla, J., and Zajc, A., "Frost and Frost-Deicing-Salt Resistance of Concretes Containing Superplasticizers", Zem.Beton (Vienna), 34(2), pg 65-66, 1989.

(82) Ghosh, R.S., and Malhotra, V.M., "Use of Superplasticizers as Water Reducers", CANMET Div. Report MPR/MRL pg 78-189 (J), CANMET, Ottawa, 1978.

(83) Mather, B., "Tests of High range Water-Reducing Admixtures", Superplasticizers in Concrete, Publication SP-62, pg 157-166, ACI, Detroit, Michigan, USA, 1979.

(84) Brooks, J.J., Wainwright, P.J., and Neville, A.M., "Time Dependent Properties of Concrete Containing Mighty Admixtures", Superplasticizers in Concrete Publication SP-62, pg 293-314, ACI, Detroit, Michigan, USA, 1979.

(85) Collepardi, M., and Corradi, M., "Influence of Naphthalene-Sulfonated Polymer Based Superplasticizers on the Strength of Ordinary and Lightweight Concretes", Superplasticizers in Concrete Publication SP-62, pg 315-336, ACI, Detroit, Michigan, USA, 1979.

(86) Collepardi, M., "Effects of Chemical Admixtures on Concrete Durability", Invited Lecture for the Int. Symp. on "Admixtures for Concrete, Improvement of properties, RILEM, Barcelona, 1990.

(87) Collepardi, M., and Monosi, S., "Low porosity and early durability concrete", Proceedings of the I Inter. Congr. on Pore Structure and Construction Materials Porperties, Paris, Chapman and Hall, Vol.I, pg 9-16, 1987.

(88) Chatterji, S., and Jensen, A.D., "Studies of the Mechanism of Calcium Chloride Attack on Portland cement Concrete", Nordisk Beton, 19, pg 5-6, 1975.

(89) Monosi, S., Alverà, I., and Collepardi, M., "Chemical attack of Calcium Chloride on the Portland Cement Paste", Il Cemento, 86, pg 97-104, 1989.

(90) Monosi. S., and Collepardi, M., "Research on 3CaO *CaCl2 · 15H2O identified in Concrete Damaged by CaCl2 Attack", Il Cemento, 87, pg 3-8, 1990*

(91) Chatterji, S., "An Accelerated Method for the Detection of Alkali-Aggregate Reactivities of Aggregates", Cem.Concr. Res., 8, pg 647-650, 1978.

II. DEVELOPMENTS IN ADMIXTURES

1. INTRODUCTION

An admixture, according to the American Concrete Institute (ACI) document 116R and ASTM C 125 is a material other than water, aggregate, hydraulic cement, and fiber reinforcement, used as an ingredient of concrete or mortar, and added to the batch immediately before or during its mixing. Chemical admixtures are not defined but include accelerators, retarders, water retarders, superplasticizers, etc. The ACI committee report entitled "Chemical Admixtures for Concrete" includes among others, air-entraining admixtures, pumping aids, coloring admixtures, alkali-aggregate expansion reducing admixtures and others. In this review chemical admixtures are defined as those exclusive of mineral admixtures. Most of the chemical admixtures are used in small quantities and are water soluble or emulsified systems. A brief account of the important developments that have taken place in the last 5 years is emphasized. It is not meant to be an exhaustive survey but merely a review of the trends in the development of chemical admixtures. Significant advances have particularly been made in the production and application of superplasticizers. Important developments are foreseen in such admixtures as lignosulfonates, accelerators, air-entraining admixtures, alkali-aggregate expansion reducing admixtures, admixtures for underwater concreting, polymer-modified and macrodefect free systems, activators and stabilizers for reuse of returned concrete, activators for slags, corrosion inhibitors, etc. The review lays emphasis on the improvements in water reduction, dispersion, workability, strength development, durability, etc in concrete containing the chemical admixtures.

TABLE 1: YEARLY STATISTICS ON PATENTED FORMULATIONS

Year	Accelerators	Superplasticizers		AE Agents	Multi-Func. Adm.	
		Water Reducers	Retarders	Polymer Mod.Cem.		
1985	7	14	14	2	1	1	4
1986	4	12	4	-	2	29	13
1987	9	30	7	-	11	27	15
1988	3	22	26	1	11	49	21
1989	37	24	38	8	4	15	116
Total	60	102	89	11	29	121	169

There is constant interest in the development of novel admixtures, as evidenced by the number of patents taken each year. In Table 1 above the number of patents taken in the years 1985-1989 are given. The year refers to the year in which the patents were reported in the Chemical Abstracts (CA).

2. ACCELERATING ADMIXTURES

A large amount of data is available on the use of calcium chloride as accelerator in concrete (1). The presence of chloride ions in concrete however, tends to increase the potential for corrosion of the embedded steel and hence there has been continued interest to develop an alternative to calcium chloride that

accelerates cement hydration but does not promote corrosion of steel. Soluble salts such as bromides, fluorides, carbonates, thiocyanates, nitrates, nitrites, thiosulfates, silicates, aluminates and alkali hydroxides are known to accelerate the setting of cement. Organic compounds such as triethanolamine and formates also act as accelerators. Commercial non-chloride accelerators contain a combination of admixtures and their short and long term effects on concrete are yet to be completely assessed.

Rear and Chin (2) tested 3 commercially available non-chloride admixtures for their effect on early strength development of concretes with five ASTM Type I and Type I/II cements, two ASTM class F fly ashes and two ASTM C fly ashes. The three accelerators studied were Ca-nitrite, Ca-nitrate and Na-thiocyanate. At 22°C with the Ca-nitrite and Na-thiocyanate admixtures the one day strength of concrete increased by 128-144% and the 7 day strength by 109-131%. Not much improvement resulted with Ca-nitrate. At 10°C however, all the admixtures promoted higher strengths with respect to the reference concrete at 1 day and 7 days. In class C fly ash concrete containing three types of cements, the Ca-nitrite based admixture promoted strength in two of them. In class F fly ash concrete two cements showed higher strengths at 1 day and all cements showed higher strengths at 7 days with respect to the reference concrete containing no calcium nitrite. At 28 days generally calcium nitrite enhances the strengths of concrete containing all the 3 cements.

Brook et al (3) have described the effect of a new non-chloride accelerating admixture on concrete containing a fly ash (called class CF) in which the *CaO* content was 5-15%. The setting, strength and other characteristics of the concrete were investigated at 21xC and 10xC. The accelerator shortened the setting times by 80-180 min and increased the compressive strengths at 3, 7 and 28 days. For example, the 3-day strength of the plain concrete was about 24 MPa and that containing an accelerator dosage of 2.8L/100 kg of cement, had a strength of about 31 MPa. The corresponding values at 28 days were 41.4 and 44.8 MPa. Although the flexural strength at 3 days was higher for concrete with the accelerator, the 7 and 28 day strengths were only equal to those of the plain concrete. There was no deleterious effect of the accelerator on shrinkage and air void characteristics. The accelerator had also beneficial effects on concrete made with class F and C fly ashes.

Many other non-chlorides have been studied for their action on the hydration and strength development in cements, mortars and concrete. Kuroda et al (4) found acceleration of setting and strength development using a multicomponent Calcium nitrite-Calcium rhodonate-triethanolamine admixture in concrete. Triethanolamine was found to be an accelerator for the slag cement (5). A water soluble organic material of the carboxylic acid-type was investigated for its effect on cement, mortar and concrete by Popovics (6). At a dosage of 2% the 3 and 7 day-strengths increased in comparison with the reference mortars. Sodium molybdate as well molybdenum oxides have also been found to be accelerators for cement but they are not as efficient as calcium chloride (7,8).

3. LIGNOSULFONATE-BASED WATER REDUCERS

In concrete applications lignosulfonate admixtures are used widely as normal water reducers. At a dosage of 0.05-0.1% they reduce the water requirement by 6-10%. Because of the relatively lower price of lignosulfonates there has been continued interest in developing a superplasticizer based on lignosulfonates. Attempts have been made to develop a synthetic superplasticizer based only on lignosulfonates. Rixom and Waddicor (9) prepared various types of lignosulfonates and studied their effect on concrete slump and water requirement. The significance of molecular weight, cationic species, degree of sulfonation and carbohydrate contents on initial set, workability and strength characteristics of concrete was studied. It was concluded that increase in molecular weight of lignosulfonate resulted in a more workable concrete, retardation of initial set and a slight reduction in compressive strength at 24h. Increase in sulfonation did not affect workability or entrained air but it reduced the setting time. It was also found that sodium lignosulfonate was a better plasticizer than calcium lignosulfonate. Generally increased amounts of sugars in lignosulfonate resulted in longer setting times. A comparison of the effects of lignosulfonate, melamine sulfonate and naphthalene sulfonate admixtures was made. Sodium lignosulfonate was found to be a more effective plasticizer than others. The slump retention was also higher with sodium lignosulfonate. Table 2 illustrates the effect of three admixtures when used at double the normal dosage (9). When lignosulfonate is used at a lower dosage, it decreases early strengths and prolongs the setting times. Incorporation of an accelerator decreases the setting time and increases the compressive strength. At a normal dosage with the accelerator setting time of concrete was 7.5 hrs and the 24 hr compressive strength was 12.6 MPa (9).

TABLE 2: INITIAL SET AND COMPRESSIVE STRENGTH OF CONCRETE CONTAINING SUPERPLASTICIZERS

Admixture	Dosage (30% w/w)	W/C	Initial Set (h)	24h Comp Str MPa
Reference	-	0.65	5.50	10.3
Melamine-based	2.67	0.65	7.75	11.2
Naphth-based	2.00	0.65	9.25	11.35
Na-Lignosulf	1.50	0.65	12.50	6.0
Na Lignosulf + Accelerator	1.50	0.65	11.50	9.8

Ronnberg (10) has described the properties of concrete containing a lignosulfonate with low sugar contents. The plasticity was almost the same as with other superplasticizers. When it was used as a water reducer, the air content, and setting time were not different fron those using other superplasticizers. When lignosulfonate was used to increase the slump of concrete the setting time was increased. Recently Bialski and Nayak (11) attempted to synthesize a lignosulfonate for use as a superplasticizer. Spent liquor was subjected to heat treatment to reduce sugar content. The resultant product was subjected to ultrafiltration to remove low molecular weight materials including sugars. The molecular weight of the products was in the range 20,000 to 50,000. Several properties of the lignosulfonates and their effect on mortars were determined. The properties studied on cement and mortar included viscosity, flow characteristics, setting times, water reduction and compressive strength. Of the many lignosulfonates studied five preparations imparted better mortar flow characteristics than those with a melamine-based superplasticizer. Although a tailored lignosulfonate may qualify as a superplasticizer several problems associated with its use have to be solved. Many lignosulfonates may foam when used in mortars and increase the air entrainment. The setting times are generally increased. If the dosages of normal superplasticizer and those of lignosulfonates are kept low the compressive strength of concrete will have lower strengths. The use of defoamers and accelerators in lignosulfonate could offset some of the disadvantages mentioned above. Caution should be excercised in the selection of defoamers as some of them affect the aggregate-cement bond.

4. SUPERPLASTICIZERS

Synthesis

A novel four step process has been developed for the synthesis of a sulfonated melamine formaldehyde. Over 20 superplasticizers were prepared by this process and the workability and mechanical properties of concrete incorporating them has been studied (12).

Table 3 shows the relative water reducing capabilities of three superplasticizers at a slump of 50 mm (12). A significant increase in water reduction occurs with the synthesized admixtures at lower dosages. It was also observed that the synthesized admixtures were effective in increasing the slump of concrete. For example, to obtain a slump of 200 mm, 1.3% commercial superplasticizer was required but the same value can be obtained with 1% of the newly synthesized superplasticizer. Slump retention, as well as strength was also greater with the synthesized admixture. At 28 days the strength of a neat mortar, that with 3% commercial superplasticizer and 3% synthesized admixture was 30, 28 and 34 MPa, respectively.

TABLE 3: RELATIVE WATER REDUCING CAPABILITIES OF SUPERPLASTICIZERS AT DIFFERENT DOSAGES

Dosage (%) =	1	2	3	4	5
			Water Redn (%)		
Commercial	9	19	29	36	38
Synthesized I	13	25	35	38	41
Synthesized II	13	24	34	37	40

Collepardi and coworkers (13, 14) synthesized 20 naphthalene sulfonated formaldehyde samples of different degrees of polymerization. Both adsorption and zeta potential values of these admixtures increased with the molecular weight, up to a particular value. Strength of mortars increased with the degree of polymerization. A plot of the monomer content vs minislump of cement paste showed a steady decrease in values as the monomer content increased, the minislump values being 175 and 25 cm^2 at monomer contents of 10 and 100%, respectively.

Ferrari and others (15) found that sulfonated naphthalene-based superplasticizers exerted the best fluidizing effect in the molecular weight range 6000-8000 (weight average) but at higher range the effect decreased. These cements were rich in C_3A. Cements that were rich in C_4AF did not show this drop at higher molecular weights.

Heavily Dosed Superplasticizer Systems

Important benefits result in certain concrete systems by using higher than normal dosage of superplasticizers. In an investigation of the possibility of using high volume fly ashes in concrete, Langley and co-workers (16) succeeded in making durable fly ash concrete comprising 50-60% class F fly ash (of the total cementitious material) low unit water content equal to w/c 0.35, and a superplasticizer content of up to 7.9 L/m^3. Although the early strength gain of control mixes containing no fly ash was higher than that with fly ash, a significant gain in strength for the fly ash concrete occurred from 7 to 28 days. For example, the mixture with 150 kg/m^3 cement and 190 kg/m^3 fly ash showed a strength of 25.8, 46.1 and 61.8 MPa at 7, 28 and 91 days and the reference concrete without fly ash had a strength of 38.7, 47.2 and 51.3 MPa, respectively. In spite of relatively low cement factor, the fly ash concrete showed desirable mechanical properties, satisfactory freeze thaw resistance and low permeability to chloride ions.

Fly ashes are incorporated into concrete to counter the expansion caused by alkali aggregate reactions. Alasali and Malhotra (17) studied the effect of higher than normal additions of fly ash (50-60%) in concrete (by using higher than normal dosages of superplasticizer) and determined the inhibiting effect of this concrete to alkali aggregate expansion. For example, the reference concrete containing alkali and exposed to normal sodium hydroxide at 80°C for 275 days showed an expansion of 0.409% whereas that containing fly ash and alkali exhibited an expansion of only 0.083%.

Mine tailing dumps and some rock outcrops are susceptible to attack by penetrating rain and surface water. The leachates that result from this action may be potentially toxic and cause environmental and health problems. A new capping technology, using high volume fly ash shotcrete has been suggested (18). The use of superplasticizer and excess air entraining agent permits production of high volume blast furnace slag. In the work of Nishibayashi et al (19), concrete containing 85% slag was used. Regardless of the percentage of the slag used the compressive strength of superplasticized concrete was almost equal to that of the control concrete. The initial setting time was unaffected but the final setting time increased as the amount of slag increased (19).

Slump Loss

Superplasticizers are known to increase the initial slump of concrete considerably. This increase however, is only transient because it is generally not maintained beyond about 30-60 min. One method is to add the superplasticizer at the point of discharge. There are some problems associated with this approach. Several other methods can be adopted to control slump loss. They include adding a higher than normal dosage of superplasticizer, redosing the superplasticizer at different intervals of time or by including some type of retarder in the formulation. Continued interest is evident from the research carried out on various methods of controlling slump loss. A few of the recent developments are discussed.

The effectiveness of superplasticizer is related to its concentration in the liquid phase. The concentration of superplasticizer decreases considerably, especially through strong adsorption in the early periods of hydration of cement. Fujiu et al (20) have developed a polymeric dispersant which by itself is insoluble but under the alkaline environment during cement hydration forms a product which has a superplasticizing effect. Thus by this time-delay mechanism the admixture is capable of maintaining the slump for a longer period. The polymer precursor has ester, acid chlorides, amides, and acid anhydrides as functional groups.

A new slump retaining admixture (Mighty 2000) has been reported. It is based on polymers. It consists of a naphthalene sulfonate based superplasticizer and a reactive polymer. Concrete with this admixture exhibits better slump retention characteristics than the reference concrete containing only the naphthalene-based superplasticizer. For example, at 90 min the slump values using the new formulation and that containing only naphthalene sulfonate formaldehyde are about 20 and 14 cm respectively (21).This superplasticizer was successfully used in a housing project (22).

Several types of polycarboxylic acid dispersants have been examined for their effect on slump increase and slump retention. Both the initial slump values and slump retention times were found to increase by the use of polycarboxylic acids at a level of 0.12% by weight of cement. The optimum molecular weight of the superplasticizer was found to be 10,000 (23). In general, this admixture in comparison with the naphthalene-type superplasticizer, imparted lower bleeding, higher slump and slump retention but the concrete had higher air content and longer setting times.

Ramachandran and co-workers (24) investigated the effect of different dosages of various latexes on the slump of superplasticized concrete. The styrene-butadiene (P_1) latex was most effective in controlling the slump loss in a melamine formaldehyde-based (S_1) superplasticized concrete. The initial slump increased further when 2% latex was added to concrete containing 0.3% superplasticizer. Fig.1 compares the slump retention characteristics of concrete containing 0.3%S1, 0.3%S_1 + 1% or 2% P_1. The concrete containing no P_1 has a steep rate of slump loss, attaining a value of about 5 cm at 4 h. By adding 1 and 2% P_1 to 0.3% S_1 the slump retention at 4 h is relatively higher than that without P_1, being about 8 cm and 14 cm, respectively.

Ultra High Strength Concrete

Normal weight structural concrete members have strengths between 23.5 and 35.2MPa. Utilization of superplasticizers enables field placed concrete to attain strengths of 60 MPa (25). Ultra high strength concrete defined as that having compressive strengths from 68 to 124 MPa and a flexural strength of 14 MPa may be fabricated at a water/cement of 0.22. In silica fume concrete, addition of superplasticizer decreases the water requirement, thus increasing the strength. The pozzolanic action of the highly reactive silica fume also contributes to concrete strength. Further enhancement of strength is achieved using a high cement factor and stronger aggregates. With 593 kg/m^3 ASTM Type I cement, 119 kg/m^3 silica fume ($W/C = 0.22$, slump 11.9 cm) a strength of 111.4 MPa at 28 days and 124 MPa at 128 days may be achieved(26)

Mitsui and coworkers (27) have carried out a comprehensive investigation on the production of high strength silica fume concrete utilizing an admixture consisting of a sulfonated naphthalene formaldehyde and a copolymer with a functional sulfonic and carboxylic group. In Fig. 2 (27) the strength developmentat 28 days for concrete made at different water/cement + silica fume (W/C + SF) is given. Maximum strength is developed at 20% SF (SF 20).

Several other reports confirm that superplasticized silica fume concrete develops very high strengths. Aitcin and Riad obtained a strength of 85.9 MPa at a W/C 0.21 (28). Malhotra (29) found that concrete containing 3.89% naphthalene based-superplasticizer (42% solids) and containing 8% silica fume and

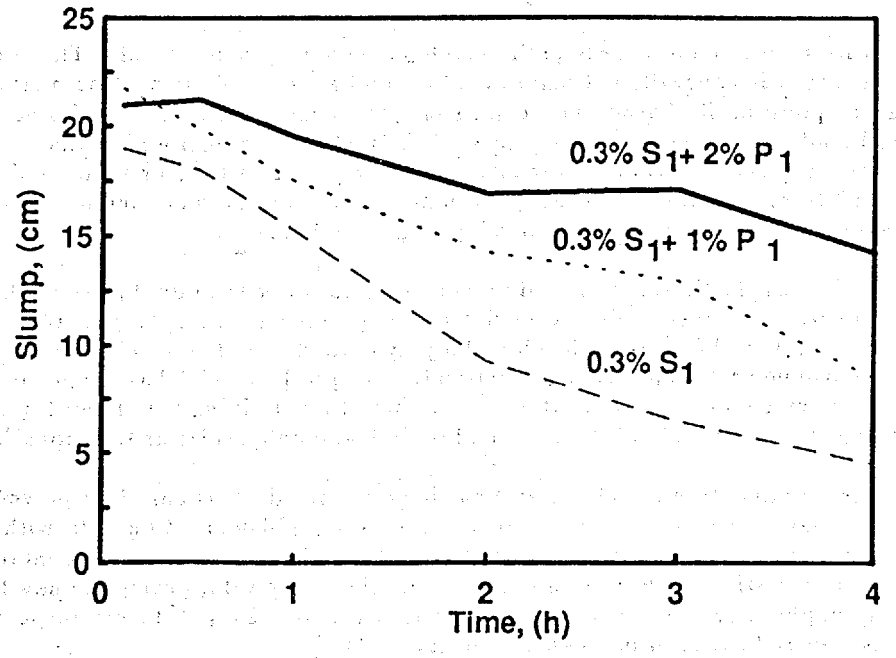

Fig. 1. Effect of commercial superplasticizer and polymer on slump.

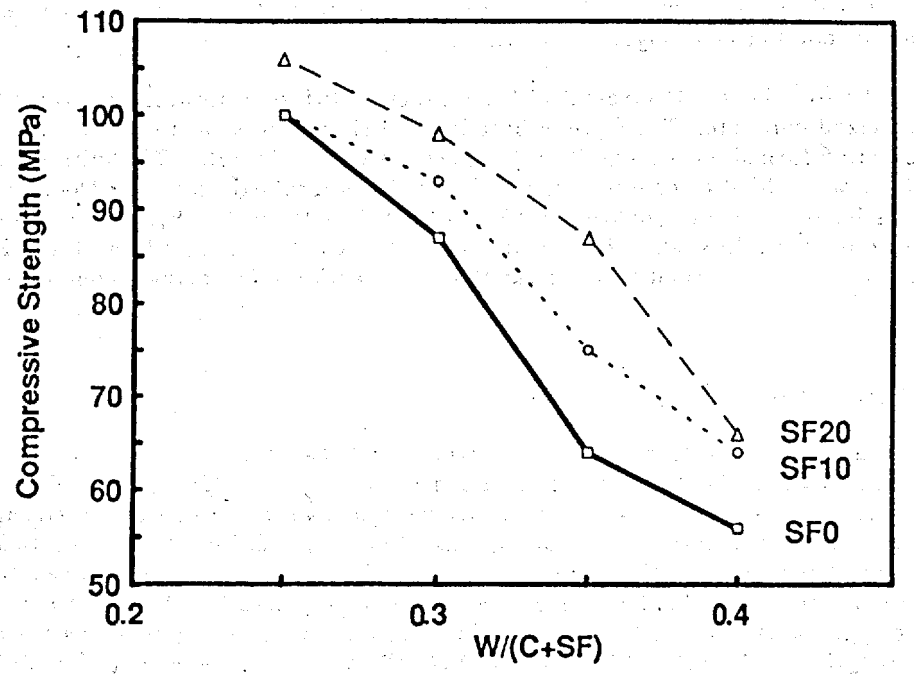

Fig. 2. Effect of silica fume on compressive strength development.

fabricated at a $W/C = 0.25$ developed a strength of 74.2 MPa and 89.9 MPa at 28 and 91 days, respectively. The mix containing 8% silica fume and 20% slag exhibited a strength of 95.8 MPa.

Strengths of about 100 MPa were obtained by Collepardi et al (30) in concrete (slump of 20 cm) containing 10-20% silica fume, 2.4% superplasticizer and 400 kg/m of cement. Strengths of the order of 80 MPa have been reported in concrete containing portland cement, sand, zeolite and admixtures such as triethanolamine and a superplasticizer (31). Mortars of compressive strength greater than 170 MPa have been obtained with portland cement, fine aggregates such as silica sand, silica fume, stainless steel particles, high purity silica and superplasticizer, by curing them at high temperatures (32).

5. RETARDERS

Not much new work has been reported on retarders, although some work has been carried out on the use of 'extended' or 'super' retarders for special applications. Two reviews have been published on super retarders and their general applications (32a, 32b). Use of super retarders to improve the construction joints has been described by Shiiba and Honda (32c). Some work has been carried out on binary retarding systems for attaining best performance. For example, a combination of Ca and *Zn* gluconate or *ZnO* and *Ca* gluconate has been found to yield better results than when either one of them is used (32d). A patent refers to a retarder containing humic acid and sulfonic acid groups (33) and another containing amino acids or their alkali metal salts or alkaline earth metal salts imparted good fluidity and strength characteristics to concrete (34). Urea has been suggested as a good retarder in another recent patent (35). Lignosulfonates have a retarding action. In one formulation, an alkalized sulfite liquor was mixed with ethylene oxide-propylene oxide copolymer to extend the setting time of cements by 2 1/2 to 5 hrs (36). In cementing well applications, *Ca* lignosulfonate in combination with potassium pentaborate and alkanolamine titanium chelates produced a good retarding action (37). Extended set retarders are produced by a mixture of phenol carboxylates with an alkali such as *NaOH* or saccharides. The setting times vary between 2 and 10 days (38, 39).

Other retarders include phenol polymer pretreated with formaldehyde and monomethyl urea (40), hydroxymated polyacrylamide homopolymer or copolymer (0.01%) (41), and waste syrups from pentaerythritol (42).

6. AIR-ENTRAINING AGENTS

The general method of counteracting freezing and thawing attack on concrete is to use air-entraining admixtures. Factors such as variability in the material, mixing, placing methods, and temperature may make it difficult to adjust the required amount of air with the right bubble size and spacing. It is also not easy to adjust the air in blended cements, superplasticized concrete, and high strength concretes. Whiting and Stark (43) have listed 23 factors that affect air entrainment.

The problems associated with the use of air entraining agents are largely circumvented by adding preformed bubble reservoirs in the form of porous particles. In one method hollow plastic microspheres with diameters between 10 and 60 fm were added to concrete at 1% dosage by Summer (44). Vanhanen (45) confirmed some of the findings of Sommer using 0.3, 0.6, 0.9 and 1.2% microspheres by weight of cement. Recently Litvan (46) demonstrated that porous particles made with fired clay bricks, diatomaceous earth, vermiculite, pumice and perlite can be added to concrete to increase its frost resistance. These results show that concretes containing porous particles are generally more durable than the plain concrete. The expansion and dynamic modulii of elasticity of concrete specimens exposed to different number of cycles of freezing and thawing cycles indicated that concrete containing higher concentrations of particulates showed high freezing and thawing resistance even after exposure to 350-400 cycles. The plain reference concrete (containing no air-entrainment) failed after 60 cycles at a $w/c = 0.60$ and that fabricated at a w/c of 0.56 failed after 300 cycles, using ASTM C-666 procedure B.

In fly ash concrete proper air-entrainment becomes difficult if the ash contains variable amounts of carbon. Novel air-entraining agents have been produced which function by preferential adsorption of polar species into the sites of carbon, leaving the air-entraining agent to function normally (47).

Several new air-entraining agents known variously as Micro Air, Stable Air or Catexol have been introduced. The claims include superiority over vinsol resin in terms of more evenly spaced air bubbles,

stable air content, increased resistance to freeze thaw action, reduced permeability, reduced segregation and bleeding, improved plasticity and workability. Some field data indicate that final air contents have higher than designed air contents. In their study of Micro Air, Wegel et al (48) found that the air content depends on the mixing time. The air content increased rapidly during the first 20 mins of mixing and then remained stable. It was concluded that results obtained after mixing for 20 mins was representative of final air content than a test made at 15 mins.

7. POLYMER-MODIFIED MORTAR AND CONCRETE

Polymer-modified mortars and concretes are used as construction materials for finishing and repair purposes. They are widely used for bridge deck overlays and patching, and also as adhesives, anticorrosive liners, decorative coatings and integral waterproofers. It is estimated that annually 1.2 million sq metres of bridge decks are overlayed with polymer-modified concrete (49). The polymers are usually added to the mixing water just as other chemical admixtures, at a dosage of 5-20% by weight of cement. There is evidence that interactions occur between polymers and hydrating cement (50, 51). Polymers influence the setting, bleeding, workability, hydration and mechanical properties of cement. There is continued interest to develop polymer-based admixtures for various new applications in concrete.

The polymers consist of latices, liquid resins and those that are water soluble. The latices are more widely used than others. The major types of latices (dispersed suspensions of solid polymer microparticles in water) comprise styrene butadiene (SBR), ethylene-vinyl acetate (EVA), polyacrylic ester (PAE) and epoxy resin (EP).

Ohama, et al (52) have developed a highly durable concrete using polymer dispersions containing 0.5% alkyl silane. Polymer-modified mortars may be used for repairs but they harden slowly, so that their application on substrates with flowing or leaking water is not very effective. An ultrarapid hardening shotcrete (URH) has been developed which contains magnesium acrylate in combination with sodium persulfate and sodium ascorbate (53).

Significant increases in compressive strengths in concrete are possible utilizing polymer admixtures. Adequate strength increases are achieved using an epoxy resin, in combination with a superplasticizer or an accelerator. Fig.3 compares the rate of strength development in a control concrete, epoxy-modified concrete and epoxy-modified concrete with a superplasticizer (54). The possibility of increasing the ductility of concrete by incorporating a mixture of natural rubber latex and a superplasticizer has been examined (55).

Extension of workability, superior bonding strength and increased ratio of bonding: compressive strength have been demonstrated in a polymer-modified mortar containing an acrylic latex and a superlasticizer (56).

The corrosion inhibiting properties of styrene-butadiene latex, ethylene-vinyl acetate emulsion and polyacrylic ester mortars in which rebar was embedded; showed that these systems provided superior corrosion resistance to steel (57).

8. ACTIVATOR ADMIXTURES FOR SLAGS

The activation of granulated blast furnace slag in slag concrete is generally based on the alkalis released from the hydration of portland cement. Use of slag as a cement without portland cement has advantages. Because the strength development of slag by itself occurs at a slower rate than that of portland cement, much attention has been directed to a study of the activation of slag containing no cement. Activators are of three types. viz, caustic alkalis (*Na, K* or *Li* hydroxide) non-silicate salts of weak acids (R_2CO_3, R_2SO_3, R_2S or RF; $R = Na$, K or Li) and silicate salts of type $(R_2O)(n).SiO_2$. All three types are used for basic slags but for neutral or acid slags non-silicate salts of weak acids are not recommended.

The types of activators used include sodium hydroxide, sodium carbonate, F-activator produced in Finland (contains $NaOH$, Na_2CO_3 and lignosulfonate) sodium silicate, sodium sulfate, potassium sulfate, lime and their combinations. For better workability and low water requirements admixtures such as lignosulfonates, gluconates and superplasticizers have also been added with activators. The rate of hydration of slags is enhanced using finely ground slag and higher temperatures. The degree to which the slag is activated depends not only on the type and amount of the activator, temperature and fineness but also on the chemical

composition and glass content of slag. In view of this the best activator suggested for a particular slag may not be applicable for another slag.

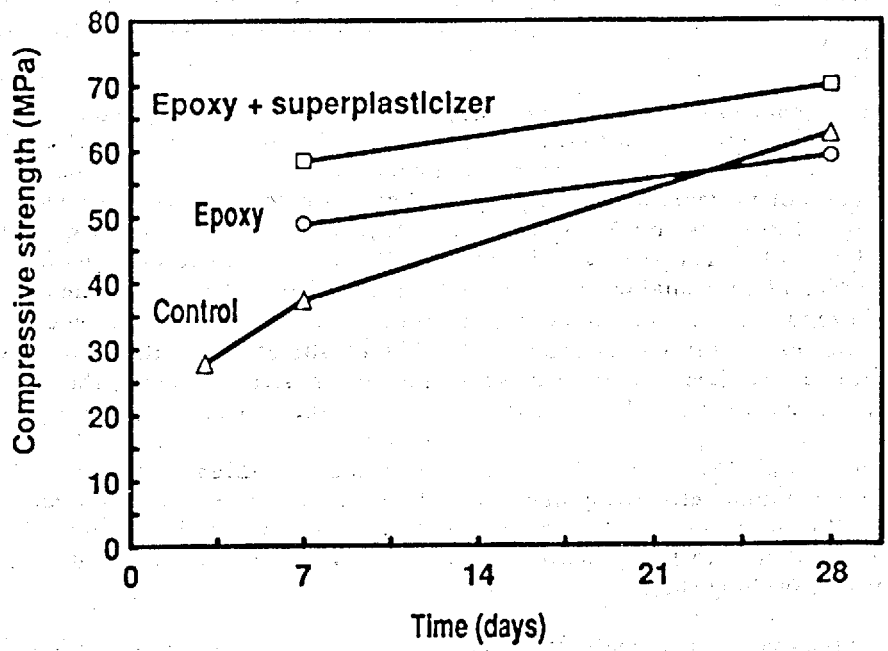

Fig. 3. Compressive strengths in epoxy-modified concretes.

With F concrete, (Finnish formulated concrete) using alkali activators, Byfors et al (58) concluded that best strengths are obtained with 2% $NaOH$ + 2% Na_2CO_3. Talling (59) achieved optimum strengths in slag-mortars with sodium silicate activators containing 3-6% Na_2O. Gjorv (60) studied the alkali activator in combination with the Finnish formulation 'F on physical and mechanical properties of slags of different Blaine surface areas, and at different temperatures. With a Blaine surface area of 640m^2/kg, strength (at 24 h) attained a value of 22.6 MPa. A review of alkali-activators was published by Talling and Brandstetr (61). The strength development in a normally cured slag mortar containing sodium silicate of M_S = 2 (SiO_2/Na_2O ratio) and made at a water/slag of 0.32-0.35, was reported to be 10-20 MPa at 8 h, 30-42 MPa at 1 day, and 55-85 MPa at 28 days. Further increase in strength occurred at higher temperatures.

In a comprehensive investigation, using pastes and mortars, Andersson et al (62) evaluated the activation of slags using $NaOH$, Na_2CO_3 and water glass of general composition, Na_2O (n). SiO_2, where n varied between 0.9 and 3.35. At 28 days sodium silicate-activated slag had strength in excess of 50 MPa, whereas the reference concrete showed a strength of about 40 MPa. Shrinkage values (at 231 days) of activated mortars were generally higher, the values being in the range 0.093 - 0.22% compared to 0.068 for the reference mortar.

Although there are several advantages of using activated slags there are some problems associated with their use viz, quick setting, sticky consistency, efflorescence effects, increased alkali-aggregate expansion, higher carbonation, irritation to the skin by the use of some activators, and higher costs. Much more work needs to be done on activators for resolving some of the apparently contradictory results reported in the literature.

9. ALKALI-AGGREGATE EXPANSION REDUCING ADMIXTURES

One of the well known methods of reducing the expansion of concrete caused by alkali-aggregate reaction is to incorporate pozzolans in the mix. The possibility of using chemicals to reduce expansion was first

suggested in the early 50's. The materials that have been studied include salts of lithium, barium and sodium, proteinaceous air-entraining agents, aluminum powder, copper sulfate, water reducing and set retarding agents. The expansion of concrete containing reactive limestone aggregate could be reduced by adding lithium and ferric chloride (63). Any chemical that is used should not only reduce expansion but also not adversely affect other concrete properties such as setting times, mechanical characteristics and durability. Because of limited laboratory data no recommended practices have been formulated pertaining to the use of these admixtures (64).

There has been a resurgence of interest in the development of a chemical to reduce the expansion caused by alkali-aggregate reaction. Ohama et al (65) investigated the effect of sodium silicofluoride, alkyl alkoxy silane, lithium carbonate, lithium fluoride, styrene-butadiene rubber latex and lithium hydroxide on the expansion of mortar containing cement with 2% equivalent Na_2O. Compressive strength measurements were also carried out. In Fig.4 the expansion results are plotted (65). The reference mortar without the chemical shows an expansion of 48×10^{-4}. The expansion is only 26×10^{-4} with 0.5% sodium silicofluoride. This was attributed to the formation of an insoluble compound with strong siloxane linkages. The alkyl alkoxy silane is also very effective in reducing the expansion of the reference mortar by 95%. Lithium compounds reduce expansion, but to a lesser extent than other compounds. The results of the relative compressive strengths indicate that the mortar with sodium silicofluoride shows the highest strength, being about 50% higher than that of the reference. The addition of other admixtures did not result in changes in strength.

The work by Sakaguchi et al (66) on the effect of lithium carbonate, lithium nitrite and lithium hydroxide showed that all these compounds effectively decreased the expansion due to alkali-silica reactions. Fog example, at a $LiOH.H_2O$ dosage of 0.65% the expansion reduced from about 0.25% to 0.1%. The effect of lithium compounds is attributed to the formation of lithium silicate that dissolves at the surface of the aggregate without causing swelling (66).

A method of treating the reactive aggregate before making concrete or treating the hardened concrete with calcium phosphate has been proposed as a method of countering the alkali-silica expansion (67).

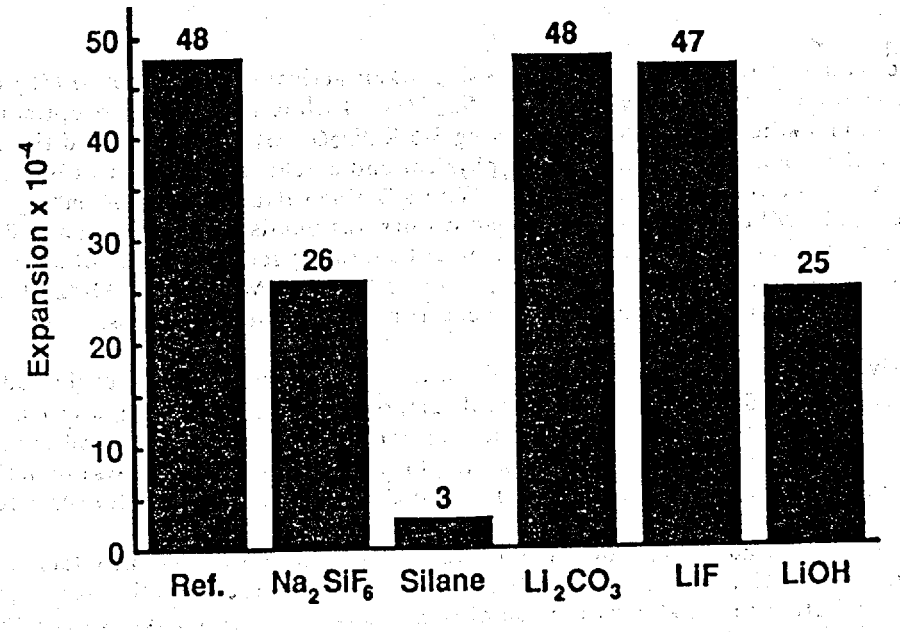

Fig. 4. Effect of chemicals (0.5%) on alkali-aggregate expansion.

10. UNDERWATER CONCRETING

Dewatering of hydraulic structures for repair is difficult and expensive. Recent advances in cohesion-inducing admixtures have allowed placement of concrete under water without the use of conventional tremies. The concrete is cohesive enough to allow limited exposure to the water, yet has good mobility to move underwater with little loss of cement. Such cohesion inducing admixtures are referred to as antiwashout admixtures (AWA's).

Most AWA's are composed of water soluble cellulose ethers or water soluble acrylic-type polymers as the main component (68).The action of admixtures is to increase the viscosity of water in the mix. This results in an increased thixotropy of the concrete and an improved resistance to segregation. Dosage of the admixture ranges from 1-1.5% by weight of the water in the mix and it is frequently used in combination with a superplasticiser (69). The magnitude of the effect produced is dependent on the admixture dosage and the molecular weight of the main component. It is usually discharged into the mixer at the same time as the other materials.

Typical applications of AWA is in the production of nondispersible colloidal underwater concrete. Minimum *w/c* ranges from 0.36 - 0.40. Cement and fine aggregate contents are usually higher than corresponding mixes placed on land. Silica fume may be used in conjunction with a superplasticizer or conventional water reducers to reduce segregation. Often it is difficult to adjust the mixture proportions to achieve desired design parameters for all properties of concrete. Consequently the properties of colloidal underwater concrete are controlled by the addition of three chemical admixtures. The key to a non-dispersible concrete with self levelling characteristics is the successful optimization of the AWA with the superplasticizer used to increase the slump.

Laboratory and field evaluation of non-dispersible concretes has been carried out to study the effect of various combinations of water reducers and supersplasticizers (68-71). Conventional lignosulfonate and hydroxy carboxylic acid water reducers and naphthalene formaldehydesulfonate (NFS) and melamine formaldehyde sulfonate (MFS)-based superplasticizers were used in these studies. The Tatterstal two point workability test and wash out test were used to evaluate the mix characteristics. Best results were obtained with lignosulfonates and MFS. The NFS superplasticizers produced erratic results in flowability and cohesion (69). Other work has centered on the use of auxillary agents to reduce the amount of polymer used in the concrete for cost reduction purposes (72). This agent reportedly reacts with the polymer in the AWA to increase the apparent molecular weight of the polymer thereby improving its cohesion inducing properties. It has also been found that with very high fineness slag (13200cm^2/g), concrete with good segregation and strength characteristics can be made (73).

11. ADMIXTURES FOR RE-USE OF RETURNED CONCRETE

Every year millions of m^3 of the ready mixed concrete produced are returned for disposal in dump sites. There are now increasing environmental concerns and restrictions regulating the disposal of returned plastic concrete. The Environment Protection Agency classifies both returned plastic concrete and truck wash water as hazardous waste. Consequently, the conventional methods of disposal have become redundant, and disposal of plastic concrete is now a major problem for the ready-mixed concrete industry (74).

In an effort to assist concrete producers, to comply with new environmental regulations, admixture manufacturers have developed a cost effective alternative to disposal. The technique keeps concrete plastic for longer periods making possible its storage and later use. The system uses two non-chloride admixtures (stabilizer and activator), which alternately suspend and reactivate cement hydration. In this system a stabilizer coats cement particles to suspend hydration and interacts with hydration products that are in solution. Depending on the dosage, the mix can be maintained in an de-activated state for hours or days. An activator is then used to remove the coating, allowing hydration to proceed. The admixture system may be used the same day during long hauls, long waiting periods as a consequence of pump, truck or equipment breakdown, thus permitting the reuse of aged plastic concrete. Overnight/weekend stabilization of both returned plastic concrete and truck wash water for reuse as part of the mix batched the next day, is another important application.

The stabilizer is usually used at a dosage ranging from 0.325-8.47 L/100 kg of cementitious materials. Dosage is influenced by a number of factors including, (a) mix proportioning, (b) elapsed time between

batching and stabilizing, (c) average ambient temperatures, (d) quantity of reclaimed concrete and (e) desired time of stabilization. The activator dosage range is 0.65-0.98 L/100 kg of cementitious material and is also governed by most of the factors influencing the stabilizer dosage. Unlike conventional retarders, the stabilizer can be used at high dosages without the attendent adverse effects such as flash set and poor strength development characteristics resulting from the use of normal retarders (75).

The stabilizer may consist of carboxylic acids and phosphorus-containing organic acid salts. The mechanism of action of the stabilizer admixture is thought to be related to the inhibition of *CSH* and *CH* nucleation.

Manufacturers claim that the admixture has been tested for its effect on setting, air entrainment, freezing-thawing resistance, mixes containing fly ash and slag, flexural and compressive strengths, length change, susceptibility to cracking and corrosion and creep. The reported field and lab data show that no adverse effects are produced by the admixtures on these properties.

12. ANTIFREEZING ADMIXTURES

Accelerating admixtures such as calcium chloride are used in cold weather concreting. A significant increase in the early strength development at normal and low temperature enables reduction in the curing and protection periods necessary to achieve specific strengths in concrete. Calcium chloride cannot be considered an antifreezing admixture. For example, at a dosage of 2% and a water:cement ratio of 0.50 the freezing point of water is lowered by about 1.4°C which is negligible from practical considerations.

Antifreezing admixtures are capable of depressing the freezing point of water in concrete considerably so that their use is of practical significance. Antifreezing admixtures are used in the USSR at temperatures as low as -30°C (63).

The mode of action of the antifreezing admixture is a) to lower the freezing point of water in concrete and act as either a weak accelerator or retarder of setting and hardening. The admixtures that are used for this purpose include sodium nitrite, sodium chloride, weak electrolytes and organic compounds such as high molecular weight alcohols and carbamide, or b) to accelerate significantly the setting and hardening with good antifreezing action. In this group belong chemicals such as calcium chloride, sodium chloride, sodium nitrite, calcium nitrite-calcium nitrate and urea.

The Russian literature contains a significant amount of information on antifreezing admixtures (1). Only recently has some interest been evident from other sources. The RILEM committee recognizes antifreezing admixtures for cold weather concreting (76). It also includes cautions to be taken in the use of these admixtures. Generally, larger dosages of antifreezing admixtures are used compared to chemical admixtures. For example, with 8% sodium nitrite 50% of water will still be in the liquid state in concrete at a temperature of -15°C. In Table 4 (76) the strengths (as a percentage of designed strength) are given for concrete cured at -5°C and containing sodium nitrite (*SN*), calcium nitrite-nitrate-chloride (*CNNC*), and calcium chloride-calcium nitrate (*CC+SC*). The binary admixture addition at lower dosages imparts higher strengths than when used singly.

TABLE 4: STRENGTH GAIN IN CONCRETE CONTAINING ANTIFREEZING ADMIXTURES

Admixture	Amount (%)	Percent of designed strength		
		7 days	28 days	90 days
CNNC	3-5	40	80	100
CC + SC	2-3	35	80	100
SN	4-6	30	80	90

In Finland premixed dry mix mortars containing antifreezing admixtures are marketed. They can be used even at D15°C and are specially applicable for joints and repair purposes (77). Fig. 5 shows the strength development in mortars with this product at -5, -15 and 20°C. Even higher strengths are achieved at -15°C beyond 28 days of curing(77)

It has also been shown that with the antifreezing admixtures the strength of concrete with ordinary cement may exceed that obtained with the rapid hardening cement, containing no admixture (78). Brook et al (79) have described an admixture called ATA, a non-chloride admixture that is non-corrosive, water reducing and set accelerating. With this admixture (10% solids) ice formation at -6.7°C can be prevented. In another publication Scanlon and Ryan (80) have provided data on a new freeze-protection admixture. This admixture accelerates set time and accelerates strength development at sub-zero temperatures. A non-freezing admixture has also been reported in the Japanese literature (81). Concrete containing this admixture when cured at -10°C showed strengths of 14, 75, 165 and 213 kg/mm^2 at 3, 7, 14 and 28 days respectively and the corresponding values for untreated concrete were 2, 3, 4 and 6 kg/mm^2. Continued interest in antifreezing admixtures is evident from other recent publications on potash-lignosulfonate-sodium tetraborate (82), potassium carbonate-lignosulfonate (83), nitrite-nitrate-alkali (84) and polyamine-lime-alumina cement-potash (85).

Much more information has to be collected before these admixtures can be used widely. Antifreezing admixtures are expensive especially as they are used in higher dosages. The hardening rate is sometimes too slow, the accelerating rates may be affected by plasticizers, and compatibility with other normal admixtures as well as their effect on long term durability has to be established for each mix and curing regime.

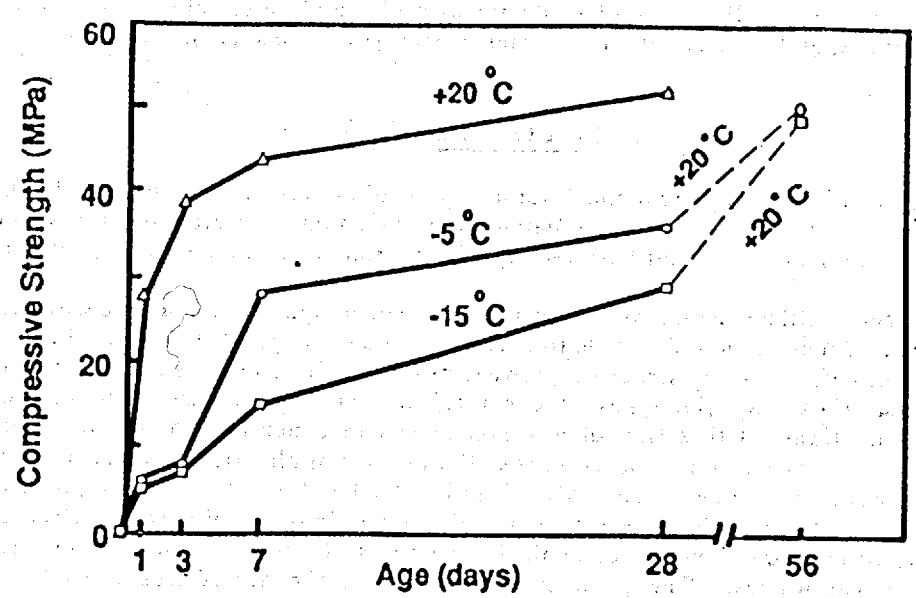

Fig. 5. Strength development of dry-mix mortar at low temperature.

13. CORROSION INHIBITORS

Corrosion of steel in concrete is enhanced in the presence of chlorides added in excess as an admixture and through the permeation of de-icing salts. Corrosion inhibiting admixtures are added in small amounts to check, decrease or prevent corrosion of the re-inforcement.

A number of reports have dealt with the use of nitrite-based inhibitors. Alonso et al (86) have suggested that in order to protect steel from corrosion due to carbonation, nitrite at a dosage of 3% should be used. Although Ca-nitrite is known to be a good inhibitor the dosage at which it should be used for effectiveness depends on the concentration of the chloride. At 2% calcium nitrite, and 391 kg/m^3 cement, corrosion will be initiated if chloride ion per cu. metre exceeds 0.6-1.2 kg (87). Recent work on the use of sodium nitrite on the corrosion of concrete exposed to sea water has shown that in cracked concrete corrosion actually increases with this inhibitor (88). Sodium nitrite is also reported to be deleterious to strength development, to cause efflorescence and also expansion due to alkali-aggregate expansion.

Mixed inhibitor systems have a good potential for use in reinforced concrete. A mixture of Ca-nitrite and Na-molybdate effectively protects steel from corrosion. For eg., $Ca(NO_2)_2$: Na-molybdate in the ratio of 1:11 is more effective than Ca-nitrite (89). The feasibility of injecting synergistic inhibitors has been tried to protect steel in concrete (90). The compounds found to be effective included tetramethyl phosphonium nitrite, tetraethyl phosphonium nitrite, tetrabutyl phosphonium nitrite and tetraphenyl phosphonium nitrite.

Attempts have been made to develop formulations that accelerate hardening of concrete and also act as corrosion inhibitors. They include: a mixture of calcium chloride, sodium nitrite, gypsum and calcium lignosulfonate (91), triply bonded diol (eg. 2 butyne-1, 4-diol) (92), iron salts (93), a complex mixture of Na-silicate, $NaOH$, $NaNO_3$, Na-lignosulfonate, triethanolamine and Bu_3PO_4 (94), aqueous solutions of monosaccharides with CH_2OH groups and Zn ions (95, 96), a mixture of hydroxy-carboxylic acid and saccharide with a styrene butadiene co-polymer latex as well a high fatty acid salt (97, 98), and a mixture thiocyanate, thiosulfate, and a water soluble polymer or methyl cellulose (99).

14. CONCLUSIONS

There has been a continuous activity in the development of admixtures as evidenced by published literature and patents. In the year 1985-1989 nearly 600 patents were taken on concrete admixtures and the enormous interest in their development is evident from an impressive number of 242 patents reported in 1989.

In construction, there will be an increasing demand for the development of concrete with high performance characteristics. Such concrete should be able to perform adequately against hostile environments when used in ocean sea floor tunnels, off-shore structures, sewage pipes, and in structures exposed to hazard chemicals and radioactive materials. Special types of concrete have also to be developed for repairs, and for infrastructural applications. Utilization of waste materials in concrete and solidification of hazardous materials in concrete will also require special mixes. For all such applications utilization of novel admixture combinations will have to be developed. Multifunctional admixtures for various purposes, in which a combination of admixtures would be necessary will be developed in the coming years. Greater attention will be directed to the production of more economical admixtures utilizing new techniques and raw materials derived from chemical wastes. The production of some of the admixtures presently used, such as lignosulfonates may pose environmental concerns; hence new methods will have to be devised to synthesize them or alternative admixtures have to be developed. Although non-chloride admixtures are being used presently they are not as efficient as calcium chloride. Therefore there is a great need to develop an admixture as efficient as calcium chloride. Efforts will continue in the field of advanced cement systems to produce materials of very high strengths and for such systems novel admixtures will have to be developed. The antifreezing admixtures are not popularly used in North America. Some work has been carried out on these admixtures and it can be foreseen that more attention will be directed towards the production of these admixtures in the future. Also more work will be carried out to develop economical admixture combinations for the re-use of returned concrete in the ready-mixed concrete plants. Although research has shown that some chemicals retard the alkali-aggregate expansion reaction, much more long term work will have to carried out before they will be applied in practice. Interesting work has been done on the activation of slags using admixtures but a more exhaustive work has to be carried out in North America for large scale applications. Corrosion inhibitors are being used to counteract the corrosion of the reinforcement. The long term corrosion aspects and also the possibility of using dual inhibitors are expected to receive more attention in the coming years. Improved properties are obtained by the use of polymers in concrete and further

improvements and the possibility of new applications will be sought by using novel types of polymers in combination with other admixtures. Extended set retarders have been used for various purposes, such as in hot weather concreting, in concretes containing large amounts of cement, for long hauls, in large pours and for preventing cold joints. Work is expected to be carried out on the development of more efficient retarders that will not have any adverse effects on concrete.

15. REFERENCES

1. Ramachandran,V.S., "Calcium Chloride in Concrete", Applied Science, UK., 1976, pp 216.

2. Rear,K., and Chin,D., "Non-Chloride Accelerating Admixtures for Early Compressive Strength", Concrete International, Vol 12, 1990, pp 55-58.

3. Brook,J.W., Beckley, R.A., and Farzam, H., "A Non-Chloride Accelerating Admixture for Class CF Fly Ash". Concrete International, Vol 12, 1990, pp 51-54.

4. Kuroda, T., Goto,T., and Koboyashi, S., "Chloride-Free and Alkali Metal- Free Type Accelerator", Conc. Ass. Japan Rev., 1986, pp 194-197.

5. Tachihata, S., Kotani, H., and Joe,Y., "The Effect of Triethanolamine on the Hydration Mechanism and Strength Development of Slag Cement"., Silic. Ind., Vol 49, 1984, pp 107-112.

6. Popovics, S., "Strength-Increasing Effects of a Chloride-Free Accelerator", Am.Concr. Inst., SP102, 1987, pp 79-106.

7. Thomas, N.L., and Egan, P.J., "Assessment of Sodium Molybdate as an Accelerator of Cement Hydration and Setting", Adv. Cement Res., Vol 2, 1989, pp 89-98.

8. Fischer, H.C., "Molybdenum Trioxide - An Acceleratorof Portland Cement", Cem. Conc. and Aggregates, Vol 12, 1990, pp 53-55.

9. Rixom, M.R., and Waddicor, J., "Role of Lignosulfonates as Superplasticizers", International Conf. on Developments in the Use of Superplasticizers, Amer. Concr. Instt., SP-68, 1981, pp359-379.

10. Ronneberg, H., "The Use of Admixtures in Advanced Concrete Technology", ERMCO 89 Congress, The European Cement Association, 1989, pp 686-700.

11. Bialski, A.M. and Nayak, K.V. (Private Communication).

12. Lahallh, S.M., Absl-Halabl, and Ali, A.M., "Effect of Polymerization Conditions of Sulfonated Melamine Formaldehyde Superplasticizers on concrete", Cement and Conc. Res., Vol 18, 1988, pp 513-531.

13. Collepardi, M., Corradi, M., and Valente, M., "Influence of Sulfonated Naphthalene Condensate and its Interaction with Cement", Developments in the Use of Superplasticizers, Amer.Conc.Inst., SP-68, 1981, pp 485-498 (Editor: V.M.Malhotra).

14. Basile, F., Biagini, S., Ferrari, G., and Collepardi, M.,"Use of Different Sulfonated Naphthalene Polymers on the Fluidity of Cement Paste", Third Intl.Conf. on Superplasticisers and Other Admixture-sin Concrete, Amer.Conc.Inst. SP-119, pp209-220 (Editor: V.M.Malhotra).

15. Ferrari, G., Basile, F., Dal Bo, A., and Mantoni, A., "The Influence of Molecular Weight of Beta Naphthalene Sulfonate-Based Polymers on the Rheological Properties of Cement Mixes"., Il. Cemento., Vol 83, 1986, pp 445-454.

16. Langley, W.S., Carette, G. C., and Malhotra, V.M., "Structural Concrete Icorporating High Volume of ASTM Class F Fly Ash", ACI Materials J., Vol 86, 1989, pp 507-514.

17. Alasali, M.M., and Malhotra, V.M., "Role of High Volume Fly Ash Concrete in Controlling Expansion Due to Alkali-Aggregate Reaction"., Mineral Sci. Lab., CANMET Rept., MSL 89-66, 1989, pp 14.

18. Malhotra, V.M., Carrette, A., Bilodeau, A., and Dibble, D., "Fibre-Reinforced High Volume Fly Ash Shotcrete for Controlling Aggressive Leachates from Exposed Rock Surfaces and Mine tailings", CANMET Rept. MSL.89-70, 1989, pp 14.

19. Shibayashi, S., Yoshino,A., Hideshima, S., Takada, M., and Chikada, T., "A Study on Superplasticized Concrete Containing High Volumes of Blast-Furnace Slag"., Proc. III Intl. Conf. on Superplasticizers and Other Admixtures in Concrete, ACI Publicaton, SP-119, 1989, pp445-455 (Editor: V.M.Malhotra).

20. Fujiu, A., Tanaka, H., and Iizuka, M., "Slump Control by Reactive Polymer Dispersant", Rev. 39th General Meeting, Cement Assen, Japan, 1985, pp 72-73.

21. Fukuda, M., Mizunuma,T., Izumi, T., Iizuka,M., and M. Hisaka," Slump Control and Properties With a New Superplasticizer, I, Proc. International RILEM Symp., Barcelona, 1990, pp 10-19.

22. Yamakawa,C., Kishtiani,K., Fukushi,I., and Kuroha, K., " Slump Control and Properties of Concrete With a New Superplasticizer", II, Ibid, pp94-105.

23. Iizuka, M., Fujiu,A., and Yamamuna,M., "Molecular Structures and Properties of a Newly Developed Poly carboxylic Acid Type Superplasticizer"., Rev. 39th Gen. Meeting, Cem.Assen., Japan, 1985, pp 78-79.

24. Ramachandran,V.S., Beaudoin,J.J., and Shihua, Z., "Control of Slump Loss in Superplasticized Concrete", Mater. & Structures, Vol 22, 1989, pp 107-111.

25. Murata, J., Kawai, T., and Kokubu, K., "Studies on the Utilization of Water-Reduced High Strength Concrete for Monorail Piers", Amer. Concr.Inst. Publication SP-68, 1981, pp 41-60 (Editor:V.M. Malhotra).

26. Wolsiefer, J., "Ultra High Strength Field Placeable Concrete With Silica Fume Admixture", Concr. International, Vol 6, 1984, pp 25-31.

27. Mitsui, K., Kasami, H., Yoshioka, Y., and Kinoshita, M., "Properties of High Strength Concrete With Silica Fume Using High Range Water Reducer of Slump Retaining Type", " Superplasticizers and Other Admixtures", Amer. Concr. Inst., SP-119, 1989, pp 79-97.

28. Aitcin, P.C., and Riad, N., "Curing Temperature and Very High Strength Concrete", Concr. International, Vol 10, 1988, pp 69-72.

29. Malhotra, V.M., "Ternary Cementitious Systems for Producing High Strength Concrete", CANMET Rept. MSL-90-22, 1990, pp 15.

30. Collepardi, M., Monosi, S., and Valente, M., "Optimization of Superplasticizer Type and Dosage of Fly Ash and Silica Fume Concretes", Superplasticizers and Other Admixtures in Concrete", Amer. Concr. Inst., SP-119, 1989, pp 425-4

31. Feng, N.Q., Li, G.Z., and Zang, X.W., " High Strength and Flowing Concrete With a Zeolitic Mineral Admixture", Cem. Concr. Aggregates, Vol 12, 1990, pp 61-69.

32. Ohama, Y., Demura, K., and Lin, Z., " Development of Superhigh Strength Mortars Using Silica Fume", Concrete for the Nineties, Intl. Conf. on the Use of Fly Ash, Slag, Silica Fume and Other Materials in Concrete, New South Wales, Australia, 1990, pp 12.

32a. Shiiba., H., " Super Retarders for Concrete", Konkurito Kogaku, Vol 26, 1988, pp50-54.

32b. K.Ho., and T.Takeuchi, " Application of the Super Retarders", Sement KonKurito, Vol. 471, 1986, pp31-37.

32c. H. Shiiba, and S. Honda., " Effects of Super Retarding Admixtures on Concrete Construction Joints Under Various Conditions", Fukuoka Daigaku Kogaku Shuho, Vol. 39, 1987, pp93-102.
32d.F.Shirsu., and T. Iwabuchi, " Effects of Binary Retarding Admixtures on Setting and Strength of Mortar", Sem. Gijutsu Nenpo., Vol 41, 1987, pp74-77.

33. Admixture for Cement, CA., Vol 102, 208403, 1985.

34. Mortar Compositions, CA., Vol 104, 154681, 154686, 154687, 212158, 212159, 212160, 212162, 1986.

35. Polymer Concrete, CA., Vol 105, 44397, 1986.

36. Polymer Concrete Mix, CA., Vol 105, 98883, 1986.

37. Carbonation Inhibitors for Concrete, CA., Vol 105, 28852, 1986.

38. Process for the Production of Building or Construction Materials, CA., Vol 107, 182333, 1987.

39. Polymer Cement Composition, CA., Vol 107, 82839, 1987.

40. Coating Materials for Wall or Roofing Materials, CA., Vol 107, 63838, 1987.

41. Polymer Cement Mortar Panels with High Strength and Heat Resistance, CA., Vol 106, 161705, 1987.

42. Protective Coating Compositions for Building Materials and Construction Structures, CA., Vol 107, 120194, 1987.

43. Whiting, D., and Stark, D., "Control of Air Content in Concrete", NCHRP Rept. No.258., Trans. Res. Board, Washington, May 1983, pp 84.

44. Sommer, H.,"A New Method of Making Concrete Resistant to Frost and De-Icing Salts", Betonwerk Fertigteit-Technick, Vol 9, 1978, pp 476-484.

45. Vanhanen, A., "Air-Entraining Agents for Frost Resistance of Concrete", Lab. Report No. 73, Tech. Res. Centre , Finland, 1980, pp73.

46. Litvan, G.G., and Sereda, P.J., "Particulate Admixture for Enhanced Freeze-Thaw Resistance of Concrete", Cement and Concrete Research, Vol 8, 1978, pp 53-60.

47. Hoarty, J.T. and L. Hodgkinson," Improved Air Entraining Agents for Use in Concrete Containing Pulverised Fuel Ashes", Admixtures for Concrete, Proc. International RILEM Symp., Barcelona, Chapman & Hall, 1990, pp449-459.

48. T.A. Weigel, J.P.Mohsen and D.J. Hagerty, " A Study of Some Aspects of Micro Air As Air Entraining Admixture in Fly Ash Concrete", Ibid, 1990, pp578-582.

49. Ohama, Y., "Current State and Trend on Concrete-Polymer Composites", Intl. Meeting on Advanced Materials, Mats. Res. Soc., Vol 13, 1989, pp 79-97.

50. Chandra, S., and Flodin, P., "Interactions of Polymers and Organic Admixtures on Portland Cement Hydration", Cem. Conc. Res., Vol 17, 1987, pp875-890.

51. Ramachandran, V.S., "Admixture and Addition Interactions in the Cement-Water System", Il. Cemento, Vol 83, 1986, pp 13-38.

52. Ohama, T., Demura, K., Satoh, Y., Tachibana, K., and Miyazaki, Y., "Development of Admixtures for Highly Durable Concrete", Proc. 3rd Intl. Conf. on Superplasticizers and Other Admixtures in Concrete, Ottawa, Canada, Amer. Conc. Inst., SP-119, 1989, pp 321-339 (Editor: V.M.Malhotra).

53. Amano, T., Ohama, Y., Takemoto, T., and Takeuchi, Y., "Development of Ultrarapid Hardening Polymer-Modified Shotcrete Using Metal Acrylate", Proc. 1st Japan Intl. SAMPE Symposium, Chiba, 1989, pp 1564-1569.

54. Popovics, S., "Modification of Portland Cement Concrete with Epoxy as Admixtures", Polymer Concrete, Uses, Materials and Properties, Amer. Concr. Inst., Detroit, SP-89, 1985, pp207-229.

55. Nagaraj,T.S., Sundara Raja Iyengar, K.T., and Kameshwara Rao, B., "Superplasticized Natural Rubber Latex Modified Concretes", Cem. Conc. Res., Vol 18, 1988, pp 138-144.

56. Atzeni, C., Mantegazza, Massida, L., and Sanna, U., "Combined Effect of Superplasticizer and Acrylic Latex on Cement Mortars With and Without Silica Fume"., Proc. 3rd Conf. Superplasticizers and Other Admixtures in Concrete", Amer. Conc. Inst. , SP-119, 1989, pp 457-470.

57. Y. Ohama, K. Demura., and T. Ono., " Corosion Ihibiting Property of Polymer-Modified Mortars and Polymer Mortars and Method for Its Evaluation", Proc. 6th International Conf., Shanghai, China, International Academic Publishers, Beijing, 1990, pp 806-811.

58. Byfors, K., Klingstedt, G., Lehtonen, H.P., and Romben, L. "Durability of Concrete Made With Alkali-Activated Slag", 3rd Intl. Conf. on Fly Ash, Silica Fume, Slag and Natural Pozzolans in Concrete, Amer. Conc. Inst. SP-114, 1989, pp 1429-1444 (Editor: V.M.Malhotra).

59. Talling, B., "Effect of Curing Conditions on Alkali-Activated Slags", Ibid, 1989, pp 1485-1500.

60. Gjorv, O.E., "Alkali Acivation of Norwegian Blast Furnace Slag", Ibid, 1989, pp 1501-1517.

61. Talling, B., and Brandstetr, J., "Present State and Future of Alkali-Activated Slag Concretes", Ibid, 1989, pp 1519-1545.

62. Andersson, H., Gram, H.E., Malolepszy, J., and Deja, J., "Alkali-Activated Slag", Swedish Cem. and Concr. Res. Inst., No. 1-88, 1988, pp104.

63. Ramachandran, V.S., "Concrete Admixtures Handbook", Noyes Publications, New Jersey, USA, 1984, pp 626.

64. "Chemical Admixtures for Concrete", ACI Committee 212, 1990, pp 31.

65. Ohama, Y., Demura, K., and Kakegawa, M., "Inhibiting Alkali-Aggregate Reaction With Chemical Admixture", 8th Intl Conf. on Alkali-Aggregate Reaction, Kyoto, Japan, 1989, pp 253-258.

66. Sakaguchi, Y., Takakura, M., Kitagawa, A., Hori, T., Tomosawa, F., and Abe, M., "The Inhibiting Effect of Lithium Compounds on Alkali-Silica Reaction", Ibid, 1989, pp 229-234.

67. Hudec, P.P., and Larbi, J.A., "Chemical Treatments and Additives to Minimize Alkali Reactivity", Ibid, 1989, pp 193-198.

68. Nagataki, S., "Antiwashout Admixtures for Underwater Concrete", RILEM Committee TC 84-AAC, May 1989, pp8.

69. Saucier, K.L., and Neeley, B.D., "Antiwashout Admixtures for Underwater Concrete". Concr. International, Vol 9, 1987, pp 42-47.

70. Anderson, J.M., "Remote Controlled Hydrocrete", Concrete, Vol 17, 1983, pp 12-15.

71. Kawakami, M., et al., "Effects of Chemical Admixtures on Colloidal Underwater Concrete", ACI SP-119, Proc. III International Conf. on Superplasticizers", Ottawa, Canada, 1989, pp 493-516 (Editor: V.M.Malhotra).

72. Sakuta,M., Yoshioka, Y., and Kaya, T., "Use of Acryyl- Type Polymer as Admixture for Underwater Concrete", ACI SP-89, ACI, Detroit, 1985, pp 261-278.

73. M. Hara, K. Sato, M.Sakamoto, and T. Hatsuzaki., " Admixing Effect of High Fineness Slag on the Properties of Underwater Concrete, Proc. International RILEM Symp. "Admixtures for Concrete", Barcelona, Spain, Chapman & Hall, 1990, pp440-448.

74. Anon, "Chemical System Puts Hydration for Hours or Even Days", Concrete Constrn., Vol 33, 1988, pp 316-319.

75. Anon, "Delvo System", Res. and Development, Dept. Master Builders Technologies, 1988, pp 24.

76. Kukko, H., and Koskinen, I., "RILEM Recommendations for Concreting in Cold Weather" , Tech. Res. Center of Finland., Res. Notes 827, 1988, pp 52.

77. Kivekas, L., and Leivo, M., "Research and Use of Antifreeze Admixtures in Finland", III Intl. RILEM Symp. on Winter Concreting, Espoo, Finland, 1985, pp 208-222.

78. Kivekas, L., Huovinen, S., and Leivo, M., "Concrete Under Arctic Conditions". Tech. Res. Centre., Report No. 343, Espoo, Finland, 1985, pp 53.

79. Brook, J.W., and Ryan, R.J., "A Year-Round Accelerating Admixture", III Intern. Conf. on Superplasticizers and Other Admixtures in Concrete, Amer.Conc. Inst., SP 119, 1989, pp 535-555 (Editor:V.M.Malhotra).

80. Scanlon, J.M., and Ryan, R.J., "Accelerating Admixtures for Cold Weather Concreting", Concrete Construction, Vol 35, 1990, pp 287-288, 292, 293.

81. Takada, M., Umezawa, K., Ohashi, T., and Watanabe, H., "Rationalization of Cold Weather Concreting Using Non-Freezing Agent", Workshop on Low Temperature Effects on Concrete, Sapparo, Hokkaido, Japan, 1988, pp 168-191.

82. Lagoida, A.V., and Rubanov, A.V., "Potash-Based Complex Antifreeze Additive", Beton Zhelezobeton, No. 2, 1988, pp 21-23.

83. Shpynova, L.G., Sanitskii, M.A., and Shiiko, O.Ya, "Gypsum-Free Portland Cement With a Potash Additive for Winter Concreting", Beton Zhelezobeton, No. 3, 1988, pp 21-23.

84. Piterskii, A., "Catalyst-Manufacturing Waste as an Antifreeze Additive for Concrete', Beton Zhelezobeton, No. 6, 1986, pp 22-23.

85. Sheikin, A., Dobshits, L., and Solomatov, V., "Cement", Otkrytiya, Izobret, Vol 8, 1986, pp130; Chem. Abstr., Vol 104, 1986, 212143.

86. Alonso, C, Acha, M., and Andrade, C., " Inhibiting Effect of Nitrites on the Corrosion of Rebars Embedded in Carbonated Concrete", Proc. RILEM Symp. on Admixtures for Concrete, Barcelona, Chapman & Hall, London, pp219-228, 1990.

87. Berke, N.S. and A. Rosenberg, "Calcium Nitrate Corrosion Inhibitor in Concrete", Ibid, pp251-268.

88. Collepardi, M., Fratesi R., Moriconi G., Coppola L. and Corradetti C., " Use of Nitrite Salt as Corrosion Inhibitor Admixture in Reinforced Concrete Structures Immersed in Sea Water", Ibid, pp279-288.

89. B.B. Hope and A.K.C. Ip., "Effect of Ca-Nitrite and Sodium Molybdate on Corrosion Inhibition of Steel in Simulated Concrete Environment", Ibid. pp299-306.

90. M.F. Asaro, A.T. Gaynor and S. Hettiarachchi, " Electrochemical Chloride Removal and Protection of Concrete Bridge Components", Strategic Highway Res. Program., Washington, D.C., 1990, pp53.

91. Anticorrosive Setting Accelerator for Concrete, CA., Vol 109, 175437, 1988.

92. Admixtures for Concrete Compositions to Accelerate Setting and Hardening, CA., Vol 109, 1152421, 1988.

93. Admixtures for Mortar and Concrete, CA., Vol 107, 82841, 1987.

94. Corrosion Prevention of Galvanized Members, CA., Vol 106, 54933, 1987.

95. Corrosion Prevention and Adhesion Improvement of Galvanized Steel Members, CA., Vol 106, 54934, 1987.

96. Rust Preventing Composition for Steel Reinforcement, CA., Vol 104, 94218, 1986.

97. Corrosion Prevention of Steel Reinforcement concrete Structures in the Inshore, CA., Vol 104, 94218, 1986.

98. Steel Reinforced Cement Mortar and Concrete, CA., Vol 105, 28859, 1986.

99. Hydroxylated Polymers as Additives for Retarding Setting Rate of Hydraulic Cement Compositions, CA., Vol 110, 198224, 1989.

GENERIC THEME IV

PERFORMANCE AND DURABILITY OF CONCRETE AND CEMENT SYSTEMS

PERFORMANCE AND DURABILITY OF CONCRETE SYSTEMS

P K Mehta
University of California, Berkeley, USA

P Schiessl and M Raupach
Technical University, Aachen, GERMANY

1 INTRODUCTION

The principal object of this report is to present a summary of the literature, published during the period 1987 to 1991, on damage to cement and concrete products by phenomena that have deleterious effects on their service life. A reduction in the engineering properties of concrete, such as strength, elastic modulus and durability can occur due to a variety of chemical and physical causes that are fully described in textbooks and reports on the subject (1-3). To limit the scope of this paper, not all durability problems are covered here. Only the phenomena known to be responsible for most of the damage to existing concrete structures, are selected for the purpose of this review, namely carbonation, sulfate attack, alkali-aggregate reactions, frost action, and corrosion of reinforcing steel.

A recent review of fifty years of research and experience with concrete by one of the authors (4) showed that, in spite of major achievements in science and technology of cement and concrete, many serious cases of deterioration even with relatively young concrete structures continue to take place. According to the generally accepted state-of-the-art, water seems to be at the heart of most of the physical and chemical causes underlying the deterioration of concrete structures. In well-proportioned (i.e., low water-to-cementitious ratio) and well-cured concretes, the amount of free water present is usually insufficient to cause any major durability problems. Therefore, water must penetrate from outside before any significant damage can occur. The property, popularly known as the permeability of concrete, determines the ease with which water or other harmful fluids can penetrate into the interior of concrete. Many of the durability problems can be attributed to poor construction practices resulting in permeable concrete.

However, there are recently reported cases where, in spite of the use of recommended construction practice and materials meeting standard specifications, concrete structures have suffered deterioration. It should be the purpose of ongoing research to prevent such occurrences. Regrettably, from a review of the current publications in the field of concrete durability it appears that not much effort is being spent by the researchers on grasping the complexity of durability- related problems, especially in regard to development of relevant test methods and specifications. For example, it is well known that, in practice, the deterioration of concrete is seldom due to a single cause. Structures with deterioration so advanced as to attract attention, usually show that more than one deleterious phenomenon is at work. The physical and chemical causes of deterioration and their effects are often mutually reinforcing. Thus the results from short-term laboratory tests, involving the evaluation of one deleterious phenomenon at a time, cannot be meaningfully integrated to predict the behavior of a structure subjected to two or more types of attacks occurring simultaneously. To solve the durability-related problems, more research is needed toward integration of the present knowledge.

For each of the five topics which form the subject of this report, namely carbonation, sulfate attack, alkali-aggregate reactions, frost action and corrosion of steel in concrete, the authors have made introductory remarks on the state-of-the-art before presenting brief summaries of selected papers, published during the 1987-1991 period. Each of the five sections ends with a summary of its own; these summaries are in addition to the overall conclusion at the end of the report.

The authors would like to point out that even within the limited scope of concrete durability topics chosen by the authors, the number of publications during the period under review (1987-91) are so numerous that it is impossible to present a comprehensive report of all the published literature. For instance, for the year 1987 alone, Struble (5) cited 638 references drawn from three conference proceedings and various journal articles on durability, published during the year. For the purposes of this review we have selected the papers which, in our judgement,

represent major areas of current research interest. In this task, there is no doubt that many contributions deserving attention may have escaped our notice, for which we would like to render a sincere apology to the authors.

2 CARBONATION

Introduction

Carbonation of concrete with atmospheric CO_2 occurs at a rapid rate at 50 to 65% relative humidity and is accelerated by open pore structure. Consequently, excessive carbonation of portland or blended portland cement products is generally a problem only when the water/cementitious ratio is high and/or the curing is insufficient. The carbonation reaction involving the transformation of CH to calcium carbonate has the most negative free energy change; however, if given adequate access to CO_2, all cement hydration products including ettringite and C-S-H would carbonate.

A reduction in the alkalinity of the cement paste is obviously one of the manifestation of a carbonated concrete. This can be a serious problem in the depassivation and corrosion of steel in reinforced concrete structures. Limited carbonation of the surface layer of concrete, however, is known to seal the pores by forming calcium carbonate, which may have the effect of reducing the permeability and increasing the strength of the carbonated layer. Continued carbonation causes the transformation of calcium carbonate into bicarbonate, which leaches out thus increasing the porosity. Highly carbonated concrete, therefore, is more porous and permeable. This has a detrimental effect on the strength, and also reduces the durability of the product to other types of physical and chemical attacks.

Recent Studies

From an analysis of samples obtained from a 36 years old concrete column, Parrott and Killoh (6) concluded that **outdoor exposure** was more severe on the basis of depth of fully carbonated concrete. However, when partial carbonation was taken into consideration, **indoor exposure** was more severe than the outdoor exposure. Observations over 16 years of exposure (204) showed that the relation of carbonation depths of storage conditions "laboratory" (20 °C/65 % r. h.) : "outdoor sheltered from rain" : "outdoor not sheltered" was in the range of 1 : 0.7 : 0.2. Additionally it was shown that the rate of carbonation for structures not sheltered from rain was lower than according to the square root time law especially at older ages. Bakker (205) showed that the carbonation rate of outdoor concretes is dominantly influenced by the wetting and drying properties of the concrete under the given environment. Kobayashi and Uno (7,8) investigated the effect of alkali content of cement on the rate of carbonation and reported an increasing rate with increasing alkali in cement. Also, the effect was greatly enhanced by the migration of the pore solution.

Ying-yu and Qui-dong (9) investigated the mechanism of carbonation of cement mortars and the dependence of carbonation on pore size. Since the gaseous-phase carbonation process is a chemical reaction controlled by diffusion, the authors suggest **prediction of the carbonation coefficient** by the equation, $a_1(2C_1/kP)^{1/2}$, where C_1 is the partial pressure of CO_2 and P is porosity. The carbonating sample was divided into three areas--the carbonated area, the carbonating area and the uncarbonated area, and a set of differential equations were used to describe the diffusion process in each area. The authors found that pores with radii above 320 A increased the carbonation coefficient greatly. Regarding the mechanism of carbonation it is concluded that there are some active sites on the pore walls. When carbonation occurs, $CaCO_3$ first nucleates on these sites. Hydration products near

the pore dissolve continuously to furnish Ca^{++} ions to the liquid phase from which the ions migrate to the $CaCO_3$ nucleating site, where the crystal growth takes place.

Schubert (10) reported the **carbonation behavior of mortars and concretes containing different types of cements and fly ashes.** Effect of various parameters on the depth of carbonation, the carbonation rate, and compressive strength was investigated for laboratory storage conditions (20°C, 65% relative humidity) for up to 10 years. The author found an inverse linear relationship, $(1/\sqrt{f_c})$, between the carbonation rate and the 28-day compressive strength. For specimens with similar compressive strength, no significant differences in the carbonation behavior were found between concretes and mortars with or without fly ash as long as cements with normal CaO content were used, the cement content was not too low (i.e. < 240 kg/m^3), and the fly ash content was not too high (i.e. < 30% by weight of blended cement). Cements with unusually low lime contents (i.e. 70% slag cement) showed increase in carbonation rates. Additionally it was found by Bier (206) that high amounts of slag (> 50 %) in the cement may lead to a coarser pore structure due to carbonation as compared to uncarbonated concrete made from these cements. Carbonation depths of mortar specimens moist-cured for 28 days were much smaller than the 7-d moist-cured specimens. From a similar study Ohga and Nagataki (11) confirmed that concrete with fly ash is more affected by initial curing period in water than concrete without fly ash. The authors claim that carbonation depths of concrete both with and without fly ash can be predicted by an equation obtained from an accelerated test. The equation is expressed by the 28-day compressive strength of concrete. Kokubu and Nagataki (12) reported similar results from a 20 years old field test. According to the authors, these test results have been incorporated into the Japanese standard specification for concrete cover. For fly ash concretes with 7 days of standard moist curing, Ho and Lewis (13) found that carbonation depth depended mainly on the water/cement, not water/binder ratio regardless of the mix constituents used in their study. Also, the results from a survey and existing structures in Australia showed that with comparable 28-day strength, binder content and water/binder ratio, portland cement-fly ash concretes showed lower resistance to carbonation than neat portland cement concretes.

Dhir et al. (14) studied the effect of 28-day concrete strength on depth of carbonation in 20 years, using an accelerated test method. Both normal and a **superplasticized concrete** showed similar trend with regard to the effect of concrete strength on carbonation; namely with increasing strength the depth of carbonation was reduced proportionately. However, for a given strength level, it was found that the superplasticized concrete always had a lower depth of carbonation than the corresponding normal concrete. For instance, with 40 MPa strength level, the normal concrete showed 15 mm depth of carbonation against 10 mm for the superplasticized concrete. Interestingly, 60 and 70-MPa superplasticized concretes showed negligible carbonation in 20 years in the accelerated test. Malhotra et al. (15) reported that a superplasticized, high-volume fly ash concrete containing 56% fly ash by weight of the cementitious material, even with 30 MPa compressive strength at 28-day showed only 3 mm carbonation in one year and 7 mm in five years in the laboratory air (50 ± 5% relative humidity).

Oye and Justnes (16) investigated the carbonation resistance of **latex-modified cement mortars** and reported that, contrary to a general improvement in other properties, the carbonation resistance of latex modified mortars showed no significant improvement when compared to unmodified mortars. In fact, some of the epoxy-modified systems performed very poorly in the carbonation resistance test. It seems that CO_2 diffusion in the polymer-modified cement mortar occurred through channels in the cement paste which are found between three- dimensional network of the polymer phase.

Sakuta et al. (17) discussed **methods to reduce the rate of carbonation** in concrete. It was found that the addition of amino alcohol and glycol ether derivatives was effective in controlling carbonation. Amino alcohol derivatives used for desulfurization and deoxidization during petroleum refining, also possess the ability to absorb atmospheric CO_2 and slow down the rate of surface carbonation of concrete. The use of a water-insoluble glycol ether derivative, which is an efficient anti-foaming agent, reduced the size of air bubbles in concrete and made it less permeable. This slowed down the progress of carbonation considerably. The authors proposed that the carbonation of concrete can be effectively controlled by the use of low water-cement ratio, the two derivates discussed by them and by thorough curing of concrete after placement. Aimin and Chandra (18) investigated the effect of acrylic polymer additions on the rate of carbonation of portland cement paste. Increasing the polymer loading reduced the porosity and water absorption of the cement paste. However, this increased the rate of carbonation which was maximum at 10 to 15% polymer loading and decreased thereafter.

Lach (19) reported that in Czechoslovakia, a part of a hall built with **high alumina cement** concrete collapsed unexpectedly. Analysis of the deteriorated concrete showed that it had lost most of the original strength due to conversion and subsequent carbonation of the cement hydration product, CAH_{10}. The author believes that gibbsite (AH_3) and calcite ($CaCO_3$), which are the products of conversion and carbonation of CAH_{10}, possess only a slight cementing property.

Discussing the Italian experience with **cements containing natural pozzolans**, Massazza and Oberti (20) reported that the carbonation depths with pozzolanic cements were similar to that of portland cements provided that concretes having similar strengths were compared. The carbonation behavior of blended cements was inferior to portland cement only when the moist- curing period is too short. With prolonged moist curing, there was usually a reversal of the behavior. The existence of a correlation between strength and depth of carbonation did not seem surprising to the authors since both strength and permeability depend on the porosity of concrete. While carbonation affected the porous and permeable concretes negatively (i.e., high carbonation depths are recorded), it affected the dense and strong concretes favorably since their porosity and permeability are greatly reduced.

Paillere et al. (21) investigated the effect of freezing and thawing cycles on air-entrained concrete containing fly ash or slag. With increase F-T cycles carbonation depths were increased. Whereas the presence of entrained air improved the resistance to freezing and thawing cycles, it did not help against the penetration of CO_2; in fact, it enhanced the carbonation depths. Portland cements containing up to 29% Class F fly ash or blastfurnace slag showed similar behavior to carbonation as neat portland cements; at increasing levels of cement replacement, the carbonation of concrete was enhanced.

Bijen and van Selst (22) compared the carbonation resistance of normal portland cement concrete with **portland blast-furnace slag cement concrete**, when a part of the cement was replaced by fly ash. Due to the lower alkalinity of the portland blast-furnace slag cement paste, the fly ash does not show significant pozzolanic activity with this cement. As expected, therefore, the carbonation rate of concrete made with portland blast-furnace slag cement containing the fly ash was found to be higher than the corresponding concrete made with normal portland cement and the fly ash. Bijen et al. (23) reported earlier that substantial differences in carbonation rate between portland cement concrete and portland blastfurnace slag cement concrete that was observed in the laboratory curing at 20°C and 65% R.H. was not observed with outdoor exposure tests.

From field tests and actual structures where the concrete contained different levels of ground blastfurnace slag as cement replacement material, Osborne (24)

concluded that the two main factors influencing the depth of carbonation were the level of cement replaced by slag and the environmental conditions around the concrete. Carbonation depths were greater for higher slag contents when the concrete was in a sheltered or dry climate. As the cement content was increased from 350 to 450 kg/m^3 and slag replacement level was reduced from 70 to 40%, both the carbonation depth and the permeability of concrete were substantially reduced.

Sakai et al. (25) compared the carbonation characteristics of a **Type K expansive cement concrete** with ordinary portland cement concrete from a 22-years old building in Niigata Prefecture, Japan. From the core samples, the compressive strength and the carbonation depths of the two concretes, both made with 0.57 water-to-cement ratio, were found to be similar and of the order of about 58 MPa and 12 mm, respectively. Mineralogical analysis of the carbonated material confirmed that C-S-H was decomposed to calcite and silica gel, whereas the AFt (ettringite) phase in the expansive cement concrete decomposed to calcite, gypsum, and $Al(OH)_3$ gel. The authors observed that the decomposition rate of AFt by carbonation was somewhat slower than that of C-S-H.

Strohbauch and Kuzel (26) studied the mechanism of damage due to ettringite formation in heat-treated precast concrete products exposed to carbonation (weathering). In the first stage of carbonation, a partial conversion of the monosulfate hydrate resulted in the formation of $C_4A \cdot \frac{1}{2}CO_2 \cdot 12H_2O$ and gypsum. Gypsum reacted with the still unconverted monosulfate hydrate to form ettringite. In the second stage of carbonation, $C_4A \cdot CO_2 \cdot 11H_2O$ formed and, finally, all the hydration products decomposed to form the stable phases, $CaCO_3$, $Al(OH)_3$, and gypsum.

Nagataki et al. (27) investigated the carbonation behavior of mortars covering the range of mix proportions and consistencies that are commonly employed in ferrocement construction. According to the results, carbonation can present a serious problem for **ferrocement structures** unless proper measures are taken during the design and construction. The rate of carbonation increased with decreasing cement content and increasing water-to-cement ratio of the mix. Prolonged moist-curing was the most effective, surface coating with emulsion paints were moderately effective, and white-washing with lime was the least effective measure against carbonation. Based on the test results, the authors have proposed equations, which can be used to predict long-term carbonation depths.

Summary

Carbonation of concrete can be a problem in areas where the concentration of CO_2 is high (urban and industrial environments) and relative humidity is moderate (50-60%). Only porous and permeable concrete products made with low cement content, high water-to- cementitious ratio, and inadequately moist-cured tend to suffer from serious carbonation. A limited carbonation of the surface layer of concrete should not be a cause for concern because it would make the surface layer more impermeable and somewhat stronger. A high degree of carbonation due to highly increased CO_2-levels of the ambient air will have the effect of increasing the porosity and permeability of concrete, thus reducing the strength and durability. High amounts of blending agents may as well lead to increased porosity and permeability after carbonation at normal CO_2-levels. Reduction in the alkalinity of cement paste by carbonation is a factor in destroying the passive film on the reinforcing steel, which is the first step in steel corrosion. However corrosion risk is only given for sufficiently high relative humidity of the ambient air (> 90 % r. h. at 20 °C) that means outdoor conditions. There is sufficient evidence that deleterious carbonation should not be a problem with properly cured and low water-to-cementitious ratio products, such as superplasticized concretes with or without mineral admixtures.

3 SULFATE ATTACK

Introduction

The term, sulfate attack, is generally used to describe the deterioration of concrete as a result of physical-chemical interactions between the minerals in hydrated portland cement paste and sulfate ions from the environment. Soils containing sulfates of calcium, sodium, potassium, and magnesium are the primary source of sulfate ions in groundwaters. Since the solubility of gypsum at ambient temperatures is rather low (1400 mg/l SO_4) a high sulfate content in water is generally indicative of the presence of magnesium and/or alkali sulfates. The severity of the sulfate attack depends not only on the sulfate content of the attacking solution but also on the other cations and anions present. There is high potential for sulfate attack when the sulfate concentration exceeds 1500 mg/l. In combination with hydrogen, magnesium, ammonium, chloride, nitrate and carbonate ions, the sulfate ion attack is more severe. Thus effluents from ammonium sulfate fertilizer production, drainage water from heavily fertilized soils, and ashes as well as gaseous products from the combustion of high-sulfur fuels are among the sources of sulfates that have proven harmful to concrete.

The sulfate attack on concrete is known to manifest itself in the form of expansion, cracking, loss of mass and/or disintegration. Expansion and cracking is generally associated with the formation of ettringite which forms as a product of the chemical reaction between sulfate ions and the hydration products present in high-C_3A portland cement pastes:

$$C_3A \cdot C\bar{S} \cdot H_{18} + 2CH + 2\bar{S} + 12H$$

$$C_4AH_{19} + 2CH + 3\bar{S} + 11H \rightarrow C_6A\bar{S}_3H_{32}$$

The mechanism by which ettringite formation causes expansion is a subject of controversy. Two of the several hypotheses that have been proposed to explain the development of pressure are the crystal growth of ettringite and the water adsorption by ettringite when it is poorly crystalline. Several researchers including Hamson et al. (28) have confirmed that at high pH ($\geq$ 12.5) conditions typical of hydrated portland cement pastes, the crystal structure of ettringite is disordered and the crystal size is very small, when compared to the ettringite formed at lower pH values ($<$ 11.5).

In addition to ettringite, cement products subjected to prolonged attack by aggressive sulfate solutions, such as $MgSO_4$, generally contain gypsum which forms as a result of progressive decomposition of calcium hydroxide and calcium silicate hydrates:

$$Ca(OH)_2 + MgSO_4 + 2H_2O \rightarrow CaSO_4 \cdot 2H_2O + Mg(OH)_2$$

$$3CaO{\cdot}2SiO_2 - 3H_2O + 3MgSO_4 + 8H_2O \rightarrow 3(CaSO_4 \cdot 2H_2O) + 3Mg(OH)_2 + 2SiO_2 \cdot H_2O$$

The decomposition of the main constituents of hydrate portland cement paste by the chemical reactions shown above, leads to a reduction of stiffness and strength, with eventual transformation of the material into a mushy or noncohesive mass.

In general, cement replacement with pozzolans or slag improves the resistance of portland cement mortar and concrete to sulfate attack. Again, the mechanisms by which this improvement occurs, are not fully understood. Also, for a variety of reasons there is dissatisfaction with accelerated laboratory tests that are recommended by ASTM and other standard organizations for evaluation of sulfate

resistance of cements. In the absence of dependable test methods and specifications, it is difficult to predict accurately the field performance of a concrete subjected to sulfate attack. In a comprehensive review of sulfate attack, Lawrence (29) has discussed a broad range of issues, such as type of sulfate solutions, chemical reactions, effect of cement types and mix design, and codes.

Recent Studies

According to Dunstan (30), **the effect of fly ash type** on the sulfate resistance of concrete, containing 15 - 25% fly ash by weight of cement can be predicted from the R-Value calculated from chemical analysis of the fly ash [R = (% CaO-5)/% Fe_2O_3]. The lower the R-Value, the greater the sulfate resistance. On the basis of his laboratory tests, the author proposed that fly ash with R-Values lower than 3.0 should improve the sulfate resistance of concretes over that of reference concrete using the same cement but no fly ash. However, investigations by Hooton (31), Manz et al. (32), and Mehta (33) gave results which did not confirm the validity of Dunstan's R-Value hypothesis. Mehta's work included five bituminous, three lignite, and eight subbituminous coal fly ashes with R-Value in the -0.01 to 4.5 range. Using a Type I portland cement (11% C_3A) for reference and an accelerate test for sulfate resistance, the author reported that all three lignite fly ashes of his study, with about 4.0 R-Value, gave excellent sulfate resistance. On the other hand, a subbituminous ash with about 1.2 R-Value and two bituminous ashes with -0.1 or less R-Value reduced the sulfate resistance significantly. From mineralogical analyses of the fly ashes and the hydrated cement pastes containing the fly ashes it was discovered that lignite fly ashes containing very high content of soluble sulfates helped to form ettringite rapidly in the hydrated cement pastes. No further ettringite formation occurred when these pastes were subsequently exposed to attack by a sulfate solution. Therefore, in spite of their high R-Values, the lignite fly ashes improved the sulfate resistance of the high C_3A cement rather than reducing it. On the other hand, some subbituminous fly ashes, in spite of lower calcium contents and therefore low R-Values, contained high amounts of reactive alumina, which resulted in large ettringite formation and expansion upon sulfate exposure of hydrated cement pastes. The author concluded that the sulfate resisting behavior of blended cements containing fly ash depended on the cement-fly ash interaction products of the hydrated system prior to the sulfate exposure, rather than any arbitrary factor based on the chemistry of fly ash alone.

Fraay et al. (34) reported that the fineness of fly ash rather its chemical composition had more influence on the sulfate resistance of portland cement and portland slag cement mortars. Seven different fly ashes were used, with 20% cement replacement by weight and 0.45 or 0.50 water-to-cementitious ratio. In the 5-months immersion test in a 4% Na_2SO_4 solution, the sulfate content and the pH of the solution were maintained at a constant level by titration with a standard H_2SO_4 solution. The authors concluded that the strength and porosity of the mortar, which was directly influenced by the fineness of the fly ash, exercised more effect on the sulfate resistance behavior than the C_3A content of the cement.

Wong and Poole (35) confirmed that the fineness of pozzolans correlated strongly with sulfate-generated expansion. According to the authors, the inverse relationship between the fineness and the rate of expansion is plausible because finer pozzolans react more rapidly to reduce the permeability which would inhibit the ettringite formation due to unavailability of sulfate ions from the immersion solution. In general, when tested with ASTM Standard Method C 1012, portland-pozzolans cements were found to perform as well as the ASTM Type II cements and, in some cases, the ASTM Type V cements. Also, the test results showed that, contrary to the assumption made by some researchers, there was no evidence that high-calcium fly ash (ASTM Class C) caused poorer resistance to sulfate attack in portland cement-fly ash systems.

Hooton and Emery (36) reported the results of up to 10 years of exposure of concrete specimens made with blended **portland-blast furnace slag cements.** Ground, pelletized slags from Canadian sources were used for this study. These slags contain an unusually low content of alumina (8 to 9% Al_2O_3) which is believed to be responsible for the test result, showing that only 45 percent by mass replacement of a high-C_3A (12.3%) portland with slag was sufficient to give equivalent or better sulfate resistance, as compared to a sulfate-resisting portland cement (ASTM Type V). In fact, concretes with 45 to 72% slag used as cement replacement, did not exhibit any deterioration after 10.5 years exposure to 3000 mg/l sulfate solutions (either sodium or magnesium sulfate). On the contrary, all concretes made with portland cements, containing from 3.5 to 12.3% C_3A, showed various degrees of deterioration. The improved resistance to sulfate attack by portland-slag cements, containing more than 50% slag, is attributed more to the reduction of permeability than to the dilution effect. Osborne (37) reported the results of an investigation on the sulfate resistance of portland-blastfurnace slag cement concretes. At 70% cement replacement level, combinations of high-C_3A portland cements (C_3A contents 9 to 12%) and ground granulated or pelletized blastfurnace slag, with alumina contents less than 14%, produced cements that were as good in sulfate resistance as low-C_3A portland cements (such as the British SRPC or ASTM Type V). The author emphasized the importance of curing regime to which concrete is subjected prior to immersion in aggressive sulfate environment. The most significant finding was the beneficial effect derived from pre-curing in air at 20°C at 65% R.H.. It seems that the surface carbonation of concrete prior to sulfate exposure reduced the degree of sulfate attack considerably.

In recent years, there have been reports from several countries (38-40) that **precast concrete products** (panels and railway sleepers) produced by low-pressure steam curing have cracked and lost strength on weathering. Heinz and Ludwig (41,42) have proposed an interesting theory involving secondary ettringite formation as a possible mechanism to explain this type of damage. According to the authors, at curing temperatures of 75°C and above, the calcium sulfoaluminate hydrate phases are not stable. The aluminate and sulfate ions get adsorbed on the C-S-H gel, however subsequently during weathering these ions become available to form ettringite at the interfacial zone between aggregate and cement paste, and this leads to expansion and strength loss. Deteriorated concrete from a tunnel lining of a hydroelectric power plant in Italy was analyzed by Berra and Baronio (43). The authors' found the presence of large quantities of thaumasite, $CaSiO_3 \cdot CaCO_3 \cdot CaSO_4 \cdot 15H_2O$. It was concluded that in a high humidity, high CO_2 and low temperature (5°C) environment, ettringite must have decomposed to form thaumasite.

Piasta et al. (44) investigated the **effect of aggregate type** on sulfate resistance of mortars and concretes. Portland cement mortars containing crushed limestone sand showed a higher resistance to sulfate attack in Na_2SO_4 solution than mortars with quartz sand. The difference was attributed to the preferential formation of calcium carbo aluminate hydrate instead of ettringite. However, in the case of concrete mixtures, the degree of detrimental sulfate attack was not dependent on aggregate mineralogy but on the porosity of the coarse aggregate. The highest sulfate resistance was found with concrete containing a granite as coarse aggregate, and the lowest sulfate resistance was found with concrete containing a porous limestone as coarse aggregate. In a study on the effect of sustained loading on sulfate attack, the authors (45) found that due to development of microcracking the attack was enhanced with sustained loads at high stress-strength ratio (0.65). Concrete with a limestone aggregate performed better than the concrete with a granite aggregate. In another test, the authors (46) found that the durability of a high-alumina cement paste to sulfate attack was improved by the addition of limestone powder.

An unusual case of sulfate attack, where particles of the aggregate were the source of sulfate ions is reported by Stark (47). Subbase for an airfield runway consisted of slag aggregate stabilized with portland cement. The materials were analyzed when abnormal expansion and heaving of the base occurred. Sulfate-bearing minerals, such as gypsum, ettringite, and thaumasite were found in the voids of slag particles. Deterioration of the base concrete was observed only when gypsum, which is soluble, was the principal sulfate mineral in the slag aggregate. Areas of the base, which contained ettringite and thaumasite as the principal sulfate bearing minerals in the slag aggregate, remained free from sulfate expansion. Since both ettringite and thaumasite are relatively insoluble, the authors believe that due to inadequate supply of sulfate ions in solution, the cement paste was not attacked.

Almeida (48) investigated the **sulfate resistance of high-strength concretes** (60-110 MPa compressive strength) to soaking and drying cycles in a sodium sulfate solution. Concrete mixtures were tested with or without the presence of a superplasticizing agent, and pozzolanic additions of several types (e.g. silica fume, fly ash, and volcanic ash). The author concluded that the physical effect of reduction of porosity and capillary absorption resulting from the use of the superplasticizing agent was much more important in the sulfate resistance of concrete than the chemical effect of CH reduction by the pozzolanic reaction.

Cohen and Bentur (49) reported the results of attack from magnesium and sodium sulfate solutions on 0.3 water-to-cementitious ratio cement pastes made with ASTM Type I or V portland cement and with or without 15% cement replacement with silica fume. In the 10% Na_2SO_4 solution (5.64% SO_3), the sulfate attack manifested itself mainly in the form of expansion, with practically no effect on strength and mass change. In 140 days of exposure, Type I portland cement (10.5% C_3A) paste showed considerable expansion (approx. 0.8%), however, Type V cement (2.2% C_3A) paste showed relatively low expansion (0.3%). With 15% silica fume replacement, both cements showed only a little expansion. In the 8.5% $MgSO_4$ solution (4.5% SO_3), the sulfate attack manifested mainly in the form of loss of strength and mass, and there was not much difference in the sulfate resistance behavior between Type I and Type V cements, with or without silica fume replacement. In fact, the addition of silica fume increased the strength and mass loss by a factor of 5 to 10, irrespective of the cement type. Confirming earlier finding of Mehta (50), the authors proposed that C-S-H, whether formed by portland cement hydration or by pozzolanic reaction, is simply not resistant to attack by certain sulfate solutions, such as magnesium sulfate, ammonium sulfate, and sulfuric acid.

Using Mehta's accelerated test, Rasheeduzzafar et al. (51) investigated the effect of cement composition on sulfate resistance. Cement paste specimens made with a blended cement containing 80% Type I portland cement (14% C_3A) and 20% silica fume, showed better resistance to exposure in a 5% Na_2SO_4 solution (held at a constant pH of 6.4) than similar specimens made with a Type V portland cement (1.9% C_3A). At the same water-to-cementitious ratio (0.5), the specimens made with neat Type I portland cement were completely destroyed in 200 days. Mineralogical studies revealed that, in addition to the C_3A content of the cement, the C_3S/C_2S ratio had a significant effect on the sulfate resistance. For instance, the compressive strength data showed that deterioration from 150 days of sulfate attack on Type I cement was 2.5 times when the C_3S-to-C_2S ratio was 7.88 and the C_3A content was 11.9 as compared to the cement with 2.57 C_3S-to-C_2S ratio and 9.3% C_3A content. According to the authors, cements with high C_3S-to-C_2S ratios tend to liberate more calcium hydroxide which, on a continued exposure to the sulfate solution, is converted to gypsum; and the formation of gypsum is associated with reduction in strength. In fact, a Type V cement, in spite of very low C_3A content (1.88%), showed significant deterioration in the sulfate solution, because of high ratio (5.28) between C_3S and C_2S.

Using a Type I and a Type V portland cement, Attigobe and Rizkalla (52) investigated the behavior of 5-6,000 psi concrete mixtures exposed to a 1% **sulfuric acid solution.** In the 70-days immersion test, no significant effects of the cement type on expansion or weight loss of concrete specimens were observed. Wet-dry cycles of exposure to sulfate attack increased the degree of concrete deterioration, which can be expected from the increase in permeability due to microcracking. Interestingly, an air-entrained concrete mixture (6% air) showed negligible weight loss in the 70-days exposure to sulfuric acid solution, as compared to about 15% weight loss by a similar concrete mixture which contained no air. If hydraulic pressure due to swelling of ettringite by water sorption is the primary cause of expansion, it is possible that entrained air provides a mechanism for the pressure relief.

Fattuhi and Hughes (53,54) presented two reports describing the effect of sulfuric acid concentration (1, 2, or 3 percent) on mortar and concrete cubes, using weight loss as the criterion for deterioration. Not only the weight loss increased with increasing acid concentration but also with increasing cement content at a given acid concentration. Reduction of the water-to-cement ratio through the use of a superplasticizer resulted in a reduction of the weight loss, especially with concentrations below 2%. The authors, therefore, concluded that the generally recommended practice of using a relatively high cement content for concrete subjected to sulfate attack will produce an adverse effect if the attacking agent happens to be a sulfuric acid solution of 1% or more concentration. Earlier Kong and Orbison (55) arrived at the same conclusion that concretes containing high cement contents are more vulnerable to deterioration by sulfuric acid attack. ASTM Type I portland cement concrete cylinders of 3000 to 9000 psi (20 to 60 MPa) strength were exposed to solutions of 2, 3, 4, and 5 pH (simulating acid rain composition the solutions were prepared by mixing sulfuric and nitric acids in a two-to-one ratio). Weight loss was used as the deterioration criterion in a 90-days immersion test. The high-strength specimens, those with compressive strength of 7000 psi (48 MPa) and above, experienced more weight loss and at a higher rate, when compared to ordinary concretes of 3000 psi (20 MPa) and 4000 psi (27 MPa) compressive strength. For some unexplained reason, the 9000 psi (60 MPa) concrete produced a greater surface deterioration and a greater weight loss in the pH 3 solution than the pH 2 solution. In a discussion on the paper, Hime (56) attempted to explain this anomaly by suggesting that with decreasing pH, gypsum--a product of the reaction between cement paste and sulfuric acid, will become insoluble in a concentrated sulfuric acid solution and form a protective surface coating, preventing further attack.

Using a **chemical model**, Reardon (57) simulated the phase changes that occur with the progressive addition of sulfate (in the form of sulfuric acid) to a mixture containing C_4AH_{13}, CH, and C-S-H. With decreasing pH, in the range 12 to 12.5 first CH and C_4AH_{13} dissolve and ettringite is formed. Later, in the 11.6 to 10.6 pH range, gypsum is formed. Ettringite begins to decompose at 10.6 pH, and C-S-H decomposes at 8.8 pH. This data satisfactorily explains why the sulfate attack is associated with loss of strength or mass in seawater and in solutions of magnesium or ammonium sulfate, which tend to reduce the pH of the pore fluid in hydrated portland cement paste. It also explains why the presence of acidic ions, such as carbonate or chloride, tends to increase the severity of sulfate attack. More recent work by Gabrisova et al. (58) on the stability of monosulfate and ettringite in solutions of various pH (using the potentiometric method) showed that the limiting pH values for the disappearance of ettringite and monosulfate hydrate were 10.7 and 11.6, respectively. Only gypsum was stable below pH 10. It is to be noted that Reardon's model also predicts an overall decrease in the Ca/Si ratio of C-S-H from 2.12 at a pH of 12.5, to a Ca/Si ratio of 0.5 at a pH of 8.8, below which the C-S-H will decompose to form silica gel. Thus changes in the C-S-H composition when the pH drops below 12.5 and its eventual decomposition, have obvious implications to the sulfate deterioration phenomena involving loss of strength and adhesion in cement products,

which is frequently the case in field structures subjected to sulfate attack. Since the Ca/Si ratio of the C-S-H in the hydrated pastes of portland-blast furnace slag cements or portland-pozzolan cement is much lower than neat portland cements, Reardon's model also gives another reason why the former cements can be expected to show more resistance to attack by sulfate and other acidic solutions.

Only a few investigations are reported on the effect of simultaneous presence of SO_2 and CO_2 on cement products. Scholl and Knoffel (59) reported that sulphation of the surface resulted in the formation of a gypsum crust approximately 0.5 mm thick in 90 days whereas carbonation reached up to 6 mm depth. Only soaking in water removed the gypsum crust. Chandra (60) confirmed a significant increase in carbonation in the presence of SO_2. Harrison (61) reported that up to 3% chloride (as calcium or sodium salt in mixing water) by weight of cement added to ordinary or sulfate-resisting portland cement had little effect on the sulfate resistance of concretes exposed to 0.35% SO_3 (magnesium or sodium sulfate solution). However, in strong sulfate solutions (1.5% SO_3) calcium chloride additions to concrete substantially increased the rate of sulfate attack on ordinary portland cement concrete, and to a lesser extent on sulfate-resisting portland cement concrete.

Ouyang et al. (62) investigated sulfate attack on mortars, using phosphogypsum as an internal source of sulfate ions (similar to ASTM C 452 test method for sulfate resistance). With a given proportion of phosphogypsum, both the expansion in prisms and the loss of compressive strength in mortar cubes specimens were higher when the authors used a portland cement with 8.8% C_3A, as compared to cements with 7.0 or 4.4% C_3A. Based on the results, a progressive fracture model for internal sulfate attack in cement-based products containing phosphogypsum is proposed. The constitutive equation describing the model contains terms representing loss of intrinsic strength of C-S-H in the presence of sulfate ions, and subsequent damage due to sulfate expansion. The authors claim that the model can be used to predict the compressive strength of mortars containing phosphogypsum. In a subsequent report Ouyang (63) presented a general model for sulfate attack from which the compressive properties, such as compressive strength, elastic modulus, and stress-strain behavior can be predicted from expansion values obtained with 25 by 25 by 285 mm mortar prisms exposed to a mixed solution of sodium and magnesium sulfate (ASTM standard C 1012 test). The author defined a damage variable as a function of Powers' gel-space ratio. For sulfate attack, the additional damage was introduced as a function of the expansion of mortar specimens. Expansion limits for sulfate attack computed by this model are reported to agree with the expansion limits proposed for the ASTM C 1012 test.

- **Mechanisms:** On the basis of a laboratory study, Odler and Gasser (64) concluded that the overall **mechanism of expansion from ettringite formation** in hardened cement pastes appears to involve local stresses due either to topochemical formation or to oriented growth of ettringite crystals. An uptake of water from the environment is not essential for expansion, although the expansion increased significantly under wet conditions. This, according to the authors, may be due to the simultaneous occurrence of the phenomena of swelling and osmotic pressure.

Generally, in the case of sulfate attack, a reference to topochemical reaction resulting in the formation of ettringite implies a solid state reaction between C_3A and sulfate ions. In practice, the ettringite formation in sulfate on concrete takes place as a consequence of interaction between the penetrating sulfate ions and the hydration products of C_3A, such as $C_4AS{\cdot}H_{18}$ or C_4AH_{19}. In a subsequent review paper by Odler and Jawed (65), the topochemical reaction mechanism is extended to include the hydration products of C_3A as the primary reactants. Also, it is not so much the "topochemical" reaction in its classical sense but the oriented crystal growth of ettringite in a system with pores full of water (i.e., an open-pore system in contact

with an outside source of water) which, according to the authors, is the principal cause of expansion.

From a review of many case histories of field structures subjected to long-term sulfate exposure, Mehta (66) reported that in most cases the loss of adhesion and strength, rather than expansion and cracking, were the primary manifestations of sulfate attack. Mineralogical analyses of deteriorated concrete specimens invariably showed that the loss of adhesion and strength was associated with the decomposition of the principal products of cement hydration, i.e. C-S-H and CH. The author, therefore, proposed that a comprehensive theory integrating the effect of sulfate attack on all constituents of hydrated cement paste is more relevant to field practice than individual theories explaining this phenomenon from the expansion of ettringite alone.

In a recent review paper on sulfate attack on concrete, Cohen and Mather (67) suggested that lack of understanding the mechanism of sulfate attack on portland cement concrete has limited the confidence that can be placed in, and hence the reliability of existing standards tests and models to predict the performance and service life of concrete subjected to sulfate attack. The authors have identified the numerous fundamental questions that have remained unanswered after decades of research and need to be answered clearly by future research. Specifically, some of the questions are: consequences of gypsum and ettringite formation; correlation between morphology and amount of ettringite formed and expansion; causes, effects, and mechanics of delayed expansion, loss of mass, loss of strength, and elastic modulus; establishing appropriate methods of accelerating sulfate attack and failure criteria; effect of sulfate solution type and concentration on the sulfate attack mechanism; validity of using paste as a representative model for concrete.

Summary

From the results of recent investigations it can be concluded that, for improved resistance to sulfate attack, a reduction in the porosity and consequently the coefficient of permeability, is more important than modifications in the chemistry of portland cement. Reduction in permeability seems to be the principal mechanism by which mineral admixtures, such as fly ash, ground blastfurnace slag and silica fume exercise a beneficial influence on the sulfate resisting behavior of concrete. This also satisfactorily explains why very low water-to-cementitious; ratio (superplasticized) concretes with or without mineral admixtures, irrespective of the chemistry of portland cement used, show excellent resistance to moderate conditions of sulfate attack.

With strongly acidic sulfate solutions (such as those containing more than 1% H_2SO_4, acid rain, and sewage water) recent research shows that even superplasticized concrete containing highly active mineral admixtures (viz. silica fume) will not be sufficiently resistant to sulfate attack. This is because no hydration product of portland cement including C-S-H (regardless of the C/S ratio) is stable below the pH 8.8. (Note that C-S-H is also the main product of the pozzolanic reaction). For the same reason concretes containing superplasticizing and pozzolanic admixtures have not shown satisfactory performance on exposure to strong sulfate solutions of magnesium or ammonium, because these solutions tend to lower the pH of the cement paste. Obviously, under these conditions even the use of a high cement content fails to prevent an acidic type of sulfate attack. For sulfuric acid attack, researchers recommend the use of low cement content and calcareous sand or additives which can form stable carboaluminate hydrates.

Most studies on mechanisms of sulfate attack and factors influencing the phenomenon, fail to consider the effect of the environmental pH on main constituents

of the cement paste. Lack of pH control in laboratory experiments has prevented a proper understanding of the mechanisms underlying sulfate attack and, therefore, the development of reliable methods for the evaluation and prediction of sulfate resistance of cement products.

In the pH range 12.5 to 12, calcium hydroxide, calcium monosulfate hydrate and aluminate hydrates, dissolve in a sulfate solution from which ettringite precipitates out. Next, gypsum precipitates out in the pH range 11.6 to 10.6; below pH 10.6, ettringite is no longer stable and will start decomposing. At the same time note that with the lowering of the pH below 12.5, the C-S- H phase is also subjected to cycles of dissolution and reprecipitation (Ca/Si ratio is 2.12 at pH 12.5, and 0.5 at pH 8.8) which continue until it is no longer stable at or below pH 8.8. All the foregoing chemical changes in a hardened portland cement product must be taken into consideration when attempting to understand their physical manifestations, such as expansion, cracking, and loss of strength or mass.

On the basis of differences in morphology and internal crystal structure and from direct scanning electron micrographic observations, there is little doubt that the transformation of hydration products of portland cement into ettringite and gypsum occurs by through-solution reactions. There is no experimental data in the published literature regarding the effects of dissolution of original hydration products on the physical properties of the cement paste, however, it is not difficult to imagine that, with the gradual lowering of pH, repeated cycles of dissolution, supersaturation, and reprecipitation of minerals will result in changes of porosity, elastic modulus, strength and adhesiveness which, eventually, will have an adverse effect on dimensional stability. The scenario depicted here is probably the real cause of sulfate-generated deteriorations in concrete, rather than the formation of ettringite alone, which is one of the effects and probably not the principal cause of sulfate deterioration. Note that it is not the intention of the author to suggest, for instance, that the swelling of poorly crystalline minerals under certain ionic conditions and/or crystal growth, have no role to play in the sulfate attack. What is being proposed here is that a broader and more comprehensive view of the problem (compared to the fragmented views taken in the past) is necessary before future research is able to answer the fundamental questions raised by Cohen and Mather (67). And until this happens, there will be no real progress in the development of meaningful test methods and predictive models for evaluation of sulfate resisting behavior of cement products.

Finally, in regard to sulfate attack, the validity of predictive model is seriously jeopardized by the fact that almost no data exist on the combined effect of sulfate with other anions which are almost invariably present in natural environments. For instance, Chandra (60) found an acceleration in the deterioration when concrete specimens were exposed to a mixture of dilute sulfuric and nitric acids (pH 3), simulating acid rain. One of his tests showed that there was a significant increase in the depth of carbonation when only a trace of sulfur dioxide was mixed with CO_2. Note that, from the standpoint of durability, this is contrary to the experience when the surface carbonation occurs **prior to the sulfate exposure** (37). Predictive models for service life or concrete in a given environment, depend on extrapolations based on simplifications and generalizations that may not be applicable to field practice.

4 ALKALI-AGGREGATE REACTIONS

Introduction

Chemical reactions between aggregates containing certain reactive constituents and alkalies and hydroxyl ions released by the hydration of cement can have a

deleterious effect on concrete. The reaction that has received greatest attention is the alkali-silica reaction (ASR), which involves rocks and minerals containing reactive forms of silica. Expansion and cracking, leading to loss of strength, elasticity, and durability are among the physical manifestations of ASR.

Since the discovery in 1940 of ASR-generated expansion in concrete by Stanton in California, the phenomenon is now known to be worldwide and has been a subject of several international conferences. The Proceedings of the Seventh International Conference on the Alkali-Aggregate Reaction (1987) contain national reviews of the problem by researchers from Australia (68), Canada (69-72), China (73), India (74), Italy (75), Japan (76), New Zealand (77), Poland (78), United Kingdom (79), and Yugoslavia (80). Case histories of affected structures are also reported by Mullick (81), Ono (82), Kobayashi et al. (83), Samarin (84), Shayan (85), and Shayan and Quick (86).

ACI Committee 201 (87) has compiled a list of deleterious forms of siliceous constituents that may be present in aggregates. Amorphous silica (e.g. opal), microcrystalline and poorly crystalline silica (e.g. Chalcedony), fractured or strained quartz and glassy silica (e.g. andesitic and rhyolitic glasses) are among the commonly known alkali-reactive forms of silica. Depending on the alkali content of cement and the water-to-cement ratio, the pH of the liquid phase in a hydrated portland cement may be 13 and above. Minerals containing silica with a disordered structure would not remain stable in such a strongly alkaline solution. Depending on the degree of disorder, porosity, particle size, and temperature, the depolymerization of silica structure (i.e. dissolution of O-Si-O bonds) will gradually occur, followed by adsorption of the alkali-metal cations on newly created surface of the reaction product. When in contact with water, the alkali- silicate gels swell by sorption of water through osmosis. The hydraulic pressure so developed is believed to cause expansion and cracking of the affected aggregate particle, and subsequently the cement paste matrix surrounding it.

Later, researchers discovered that aggregates derived from other siliceous rocks, such as phyllites, greywackes, and argillites were also prone to the ASR-type of expansive behavior. In the 1960's, the alkali-carbonate reaction involving certain argillaceous dolomitic limestones was also found to exhibit the deleterious expansion characteristics similar to the ASR. In this case, it was proposed that the dedolomitization reaction in a high-pH solution caused the expansion.

Since deleterious expansion from alkali-aggregate reactions in field concretes takes years to develop, considerable research effort has been spent on development of accelerated laboratory tests to evaluate potentially deleterious aggregates. The validity of these methods has been a subject of much controversy in the published literature. Also, it is well known that mineral admixtures, such as natural pozzolans, fly ash, silica fume, and ground granulated blastfurnace slag, when used as partial cement replacement in concrete, can be effective in suppressing the ASR expansion. The mechanisms by which this is achieved are not yet fully resolved, and conflicting results with these admixtures are often reported in the published literature.

Recent Studies

Effect of Mineral Admixtures: Hobbs (88,89) has shown that the **effectiveness of fly ash and slags** in preventing expansion due to ASR varies widely and, in fact, the use of some fly ashes and slag may not reduce the risk of deleterious expansion (i.e. expansion greater than 0.05%). With the help of an extensive literature review and some additional tests, the author questioned the popularly held views that fly ash and slag either contribute little alkali to the ASR or only the water-soluble

alkali. When a fly ash or slag is being considered as a potential replacement for a high-alkali cement to reduce the risk of deleterious expansion, the author recommends that either (1) the usefulness of a particular fly ash or slag for suppressing the ASR expansion be established by a test in which a natural reactive aggregate is used in concrete specimens stored under moist conditions at 20°C; or, (2) if tests are not possible, the "effective" alkali content of the particular fly ash be taken as one-sixth of its total alkali content, and that of the particular slag as one-half of its acid-soluble alkali content. Using three different fly ashes, four natural pozzolans, and three different slags with wide ranging alkali contents, Kollek (90) reported an experimental study the results of which essentially confirmed the findings of Hobbs. According to the author, for purposes of ASR expansion, if the effective alkalies derived from portland cement are taken as 100%, then the contribution of effective alkali from fly ash or natural pozzolan should be taken as 17%, and from blastfurnace slag as 50% of the total alkali present in these mineral admixtures.

From a comparison of the British, American, and other methods of evaluating the contribution of alkali from fly ash or slag to be incorporated into a portland cement concrete, Barlow and Jackson (91) concluded that the available alkali contents varied widely with the type of method used for the evaluation. Factors influencing the amount of alkali released include temperature, composition of portland cement, and fly ash-to-cement ratio. Using 14 Class F fly ashes from Japan and crushed andesite as reactive aggregate, Kobayashi et al. (92) reported that at 20% or higher levels of cement replacement, there was little expansion in mortar bars even after 6 months. The expansion controlling ability of a fly ash was found to be directly related to the SiO_2 content of the fly ash and the alkali content of the cement. However, with Class C fly ash, Lee (93) discovered that replacement of 15% high-alkali cement with the fly ash or up to 40% low-alkali cement with fly ash produced greater expansions than without any fly ash. Maximum expansions were observed when the Na_2O/SiO_2 ratio of the cementitious material was at a critical value, which varied with the fly ash composition.

Durand et al. (94) used a siliceous limestone, a dolomitic limestone, and an argillite aggregate from Canadian sources to test the effectiveness of two fly ashes, a slag, and a silica fume in controlling the ASR expansion. The authors found that the role and the efficiency of mineral admixtures varied according to the type of alkali aggregate combination involved. Thus, a mineral admixture that efficiently counteracted one type of alkali-aggregate reaction could be quite inefficient for reducing another type of alkali-aggregate reactivity. In another test, Durand et al. (95), used silica fume additions to investigate the relationship between pore solution characteristics and expansion in mortar and concrete prisms containing a high-alkali cement and an alkali-reactive siliceous limestone aggregate. With increasing amounts of silica fume (5 to 15% by weight of cement), there was a corresponding decrease in the concentration of Na^+, K^+, and OH^- ions in the pore solutions. Similarly, the Na and K content of CSH of the hydrated cement paste also increased with increasing silica fume additions. Due to these effects the ratios of expansion in both mortar and concrete prisms were reduced sufficiently at 5% level of silica fume addition. However, with very reactive aggregates the authors recommend that it would be safe to use 10% silica fume. Using the aggregates from Durant et al.'s study (94) as well as pyrex glass, which is the standard reactive aggregate in the ASTM C 441, Soles et al. (96) investigated the effectiveness of various mineral admixtures in controlling the alkali-aggregate reactivity. Concrete expansion tests showed that most mineral admixtures used in the investigation were ineffective in suppressing the expansion with the dolomitic limestone. Slag and diatomite (but not silica fume) were notable in reducing the expansion with this type of aggregate.

Yamamoto et al. (97) found that both granulated and air-cooled blastfurnace slag are effective in preventing the excessive expansion due to ASR. Using ASTM Method C

289, the authors attempted to explain the differences in the reaction behavior between fly ash and slag when exposed to a NaOH solution. Oberholster and Davies (98) reported the results of 4-6 years of an outdoor exposure test to establish the influence of granulated blastfurnace slag, fly ash, calcined shale, and silica fume admixtures on the expansion of concrete made with a high-alkali cement and a reactive-quartz aggregate. With a moderate cement content in concrete (approximately 4 kg/m^3 alkali), replacement of the cement by 15% calcined shale or 5% silica fume was not effective in preventing the expansion to reach a deleterious level (0.05%), whereas 15% replacement by an approved fly ash was found to be effective. With a high cement content in concrete (approximately 5 kg/m^3 alkali), the replacement of cement by either 50% ground granulated blastfurnace slag or 10% silica fume appeared to be effective in preventing the deleterious expansion.

Long-term exposure (up to 14 years) studies by Bhatty and Greening (99) of blended cements made from high-alkali portland cements and Class F fly ashes or calcined shales showed that as much as 95% of the total alkali was retained in the hydration products of blended cement pastes compared to only 15% retention in portland cement paste. Also, it was found that the lower the amount of leachable alkali from the paste, the less likely the deleterious expansion of concrete. In other words, more alkali tie-up in the C-S-H produced a more stable system with respect to deleterious alkali-aggregate reaction.

Perry et al. (100) investigated twelve Canadian fly ashes in regard to their effectiveness in suppressing the ASR in a modified ASTM C 227 test. It was confirmed that the expansion was suppressed less effectively by high-alkali fly ashes. Also, with most fly ashes at least 30% cement replacement with fly ash was needed to obtain a reasonable degree of reduction in expansion. The data did not support the theory that high-calcium fly ashes are less effective in reducing expansion.

Robert (101) suggested that fly ash is a "delayer" rather than a "permanent inhibitor" of the ASR expansion. Like other investigators, the author confirmed from his experimental work that 30 to 45% cement replacement with fly ash was needed to successfully delay the onset of ASR. Since fly ash did not seem to be very effective in suppressing the ASR expansion with highly reactive aggregates, such as Beltane opal and Pyrex glass, the author recommends that in practice it should be used with mildly reactive aggregates only.

With Belgian fly ashes Tenoutasse and Marion (102) observed a high-potassium binding capacity of one of the hydration products in the portland cement-fly ash system. The authors proposed that the formation of this non-expansive product may be responsible for reducing or inhibiting the ASR expansion. The authors (103) drew the same conclusion from the study of a system containing silica fume. It is proposed that the expansive properties of silicate gels are related to their potassium content, and that the mineral admixtures help by increasing the potassium binding capacity of the silica gel.

Using both ASTM Class F and Class C fly ashes, Farbiarz and Carrasquillo (104) investigated the effectiveness of 17 to 62 volume percent cement replacement on the expansion of ASTM C 227 mortar prisms. The authors found that, in general, low-calcium fly ashes were more effective in reducing the ASR expansion than high-calcium fly ashes, and that the effectiveness of a fly ash was reduced directly with an increase in its alkali content. Also, the effectiveness in reducing the ASR expansion increased with increasing levels of cement replacement with fly ash. However, with fly ashes containing more than 1.5% alkalies there was a pessimum limit below which no beneficial effect was achieved. According to the author, this pessimum limit is an inherent property of each fly ash.

Nagataki et al. (105) reported the results of the evaluation of eight fly ashes for controlling ASR using Pyrex glass as the reactive aggregate. The authors found that the mortar bar expansions were independent of the alkali content of the fly ash but were influenced by the cement replacement ratio and glass content, as well as by the particle size of the fly ash. ASR expansions could be reduced by using higher replacement ratios, a fine fly ash, and fly ashes containing more glass content. It is suggested that expansion of mortars containing fly ash can be predicted by using an equation which contains the mean particle diameter and the amount of non-crystalline SiO_2 of the fly ash, and the cement replacement ratio.

Swamy and Al-Asali (106) reported that the addition of fly ash as a cement replacement material can be very effective in reducing the ASR expansion substantially, both at ambient and higher temperatures (40°C). However, even at the 50% replacement level, the ASR expansion cannot be fully eliminated. Blastfurnace slag, on the other hand, behaved differently because it decomposed at high temperatures quite easily and the alkali released from the slag decomposition contributed to the ASR. The authors also reported that the reductions in the elastic modulus and flexural strength in concrete, as a result of ASR expansion, were much higher than the reduction in compressive strength.

In regard to the effectiveness of a fly ash in reducing hydroxyl ion concentrations of pore solutions in hydrated cement pastes, Nixon and Page (107) list three factors which, in order of relative importance, are as follows: the alkali content of the portland cement, the reactivity of the fly ash, and the alkali content of the ash. With low-alkali portland cement (below 0.6% Na_2O) none of the fly ashes tested by the authors were effective. However, with higher-alkali cements all the ashes were able to reduce the hydroxyl ion concentration significantly and the differences between them were minor. It seems that, when the concentration of ions in the pore solution is low, the release of alkalies is favored. However, if the alkali content of the cement is high and the corresponding ionic concentration of the pore solution is also high, the release of alkali ions from the ash is hindered and the hydration products of the ash can incorporate sufficient alkali and hydroxyl ions to reduce their concentration in the solution. Another important observation made by the authors from their data is that fly ashes needed a minimum of 28 days to have a significant effect on the pore solution chemistry. This is the same timescale as far the pozzolanic reaction and gives a strong pointer to the pozzolanic reaction being the mechanism by which the alkalies and hydroxyl ion concentrations are reduced in the pore solution. Many of the conflicting test results on the effectiveness of fly ashes in reducing the ASR expansion, using the ASTM C 441 method and fourteen-day performance criterion, can be explained in the light of above observations by Page and Nixon. The authors also reported that, in contrast to fly ashes, granulated blastfurnace slag acts more as a diluent and some slags are not even effective as diluents.

Research by Carrasquillo and Snow (108) confirmed the findings of Nixon and Page that the effectiveness of a fly ash in reducing damage due to alkali-aggregate reaction was dependent on the available alkali contents of the cement and fly ash, and the cement-to-fly ash replacement ratio. The calcium content of the fly ash did not show any significant effect on alkali-aggregate expansion with natural reactive aggregates. When the available alkali content of a fly ash was less than 1.5%, its beneficial effect in preventing ASR expansion increased with increasing cement replacement, regardless of the class of fly ash, alkali content of cement, and reactivity of the aggregate. However, when the available alkali content of the fly ash was greater than 1.5%, a minimum cement replacement level was indicated below which the fly ash caused expansions larger than mortar mixtures containing no fly ash. Above this "pessimum limit" the fly ash caused smaller expansions. The authors, therefore, propose that, when using fly ash to control deleterious ASR

expansion in concrete, a minimum percentage of cement replacement, rather than a maximum allowable alkali content of fly ash, should be specified.

In a study reported by Thomas et al. (109), concrete beams containing 20 or 30% fly ash showed little expansion and no cracking after seven years of outdoor exposure, and petrographic examination showed no evidence of damage due to ASR. Alkali-silica gel was present at some sites, but was not associated with any cracking. On the other hand, concretes containing either no fly ash or only 5% fly ash exhibited considerable expansion and cracking, which was diagnosed by petrographic examination to be due to ASR. Electron probe microanalysis of hydration products around alite grains showed the average Ca/Si ratio to be 1.94 and 1.57 for portland cement concrete and fly ash concrete, respectively. In addition, the potassium content of the hydration product around alite was four times higher in the fly ash concrete than the portland cement concrete. The authors suggest that the lower quantity of available calcium in the fly ash concrete and the increased potassium-binding capacity of the C-S-H present in the fly ash concrete may have been responsible for suppression of the damaging expansion due to ASR.

Al-Asali and Malhotra (110) reported the results of research which was undertaken to address the concern that alkalies released from the use of a high-alkali fly ash (3.16% K_2O, 0.54% Na_2O) may cause deleterious expansion in superplasticized concrete incorporating **high volumes of fly ash** (58% fly ash by weight of the total cementitious material). The reference concrete was made with a high-alkali ASTM Type I portland cement (1.38% K_2O, 0.24% Na_2O) and a reactive limestone aggregate. In an accelerated test, concrete prisms without fly ash, when immersed in 1 normal NaOH or KOH for 275 days, showed about 0.3% expansion, whereas those with fly ash showed insignificant expansion.

Kawamura et al. (111) investigated the effectiveness of four different types of **silica fume** in preventing the ASR expansion, using mortar specimens containing opal as a reactive aggregate. At a silica fume content of 5 percent by weight of cement, the addition of any of the four types of silica fume increased the expansion. At 10 percent cement replacement level, one of the additives was able to reduce the expansion considerably, two of the additives increased the expansion, and the fourth did not make any difference. At 15% replacement level, all but one of the additives completely suppressed the ASR expansion. The preventive ability of a silica fume additive did not correlate with the pozzolanic activity. Although the addition of silica fume reduced the alkali ion concentration in pore solutions to considerably lower levels, it seems to the authors that other factors than mere reduction in alkalinity are responsible for alkali-related expansions in mortars containing silica fume. Swamy (112) also investigated the effectiveness of silica fume in reducing the ASR expansion. Unlike the experience of other researchers, especially involving the reactive aggregates in Iceland, the author found that 10% cement replacement by silica fume was inadequate in controlling the ASR expansion of a portland cement concrete containing fused silica as the reactive aggregate in the presence of external alkalies and chloride ions. However, 30% silica fume replacement was found to be adequate. The author concluded that with a given amount of silica fume, the effectiveness in controlling the expansion varies with the type of reactive aggregate present.

Walters and Jones (113) investigated the effect of **metakaolin** (calcined kaolin) on ASR expansion using concrete prisms containing 35% reactive aggregate (chert/flint) by weight of the total aggregate. The prisms were stored in a moist environment at 38°C and the expansions were monitored over a period of 18 months. Without metakaolin, the prisms expanded by 0.45% after 6-9 months. Expansions were reduced to less than 0.01% when 10-15 wt. % cement was replaced by metakaolin. The authors suggest that a thorough mixing of metakaolin with cement before mixing with

aggregates and water is essential to prevent local variations in the portland cement-to- metakaolin ratio throughout the concrete mass.

Mechanism of Expansion: In a series of reports, Chatterji et al. (114-117) noted that a 3N alkali hydroxide solution caused less expansion due to ASR than a 3N alkali salt solution. The results also showed the expansion due to ASR is not directly proportional to the degree of chemical reaction. The results are consistent with a mechanism of ASR expansion proposed by the authors. Practical implications of the proposed mechanism are discussed in the context of long dormant period, sources of alkalies, relative aggressivity of sodium and potassium, and relationship between the degree of chemical reaction and expansion. The authors also described a simple chemical test method for the detection of alkali-silica reactivity of aggregates.

Kawamura et al. (118) investigated the effect of NaCl immersion on ASR in mortars containing fly ash. Hydroxyl ions within the mortar moved outward to the immersion solution and expansion occurred only when OH^- ion concentration in the pore solution exceeded a critical value, 300 m mol/l. Once the ASR is initiated above the critical OH^- concentration, it is Cl^- ions from the surrounding solution which seem to catalyze the reaction. According to the authors, solid CH in the interfacial zone around reactive aggregate particles plays a role in maintaining a high OH^- concentration in pore solutions, i.e. it acts as a buffer to cope with the reduction of OH^- ion concentration brought about by the consumption of OH^- by the ongoing ASR within reactive aggregate particles in the presence of Cl^- ions.

Bachiorrini and Montanaro (119) pointed out that as low as 1-4% microinclusions of disordered silica minerals in **calcareous aggregates** may be sufficient to cause the alkali-silica reaction because even in highly compact rocks the residual porosity is large enough to permit penetration of the alkaline solution to disordered-silica microinclusions. The alkali-silica gel found within the aggregate exerted a breaking action on the aggregate, the extent of which depend on the shape and size of channels of flow. Collins and Bareham (120) investigated porous natural aggregate or lightweight aggregate for **ASR expansion.** Very much reduced expansions were found when these aggregates replaced a dense limestone in mix containing a reactive sand. The authors discussed the results in terms of aggregate absorption, concrete porosity, and potential reactivity of porous aggregates. Test Methods and Their Relevance: Davies and Oberholster (121) showed that the NBRI (South Africa) accelerated test can be successfully used to screen different mineral admixtures for their effectiveness in preventing the deleterious expansion due to ASR. The test is simple and can be completed within 14 days. In a subsequent report (122) the authors stated that the ASR reaction products from this test are similar in composition to those found in field structures affected by the reaction. The procedure was also used with success by Shayan et al. (123). Hudec and Larbi (124) described a modified version of the NBRI methods which, in the opinion of the authors, is more suitable for rapid evaluation of both siliceous and carbonate alkali-reactive rocks.

Durand and Berard (125) reported that the composition of the gel found in the veins within a reactive limestone aggregate from Montreal, Quebec, was fairly constant and corresponded to 51% SiO_2, 12% CaO, 8% K_2O, 6% Na_2O and 2% FeO, the remainder being water of hydration. The authors suggest that the uniform composition of gel permits its analysis to be used as a means of diagnosing alkali-aggregate reactivity in concrete structure. According to De Ceukelair (126) the average composition of globular rosettes formed as a result of ASR in concrete products in Australia, Belgium, Canada, and South Africa has been reported to correspond to $2K_2O{\cdot}6CaO{\cdot}18SiO_2{\cdot}12H_2O$. This composition is close to the natural mineral rhodesite which is a precursor of chert. As most of the chemical reactions in nature are reversible, one can suppose that when chert is attacked by alkali hydroxides, a rhodesite-like material can be the result.

Commenting on the limitations of laboratory data from ASR expansion tests, Swamy and Al-Asali (127) stated that much of the published data may not be directly useful to the engineer who wishes to understand the influence of the development of such reactions on the engineering behavior of concrete structures. There are three possible reasons for this. **First**, much of the published information in the literature relates to mortar rather than concrete. Mortars have very high cement contents that are not generally used in practice in concrete construction. Also, using the same cement, the same cement content, and the same reactive aggregate, the mortar bar expansions at twenty-eight days and at three months were found to be almost twice as much as in comparable concrete. This is probably due to the higher degree of restraint in concrete due to the presence of coarse aggregate. **Second**, much of the published information is based on the use of Pyrex glass or Beltane opal as a reactive aggregate, whereas with most of the reactive aggregate used in practice the expansions are lower. The authors found that expansions in concrete were similar to those found in construction practice when fused silica was used as a reactive aggregate in laboratory tests. **Third**, the influence of alkali was found to be dependent on the sources of alkalies. When all the alkali present in the system was derived from cement, an alkalinity content of 3 to 4 kg/m^3 appeared to represent a critical limit, above and below which there was either a dramatic increase or a decrease in expansion. Above this threshold value, increases in alkalinity whether from the cement or other sources, seemed to increase the expansion dramatically.

In a subsequent report Swamy and Al-Asali (128) discussed the relationship between the ASTM C 227 expansion limits (at three and six months) and engineering properties of concrete affected by ASR. Their results showed that different reactive aggregates affected the engineering properties at different rates, and that the properties most affected by ASR were flexural/tensile strength and elastic modulus. The authors pointed out that these properties are important in engineering design and are significant in relation to cracking and deflection of flexural members as well as durability of all concrete members. At 0.1% expansion in the ASTM C 227 test (which is the six-month specification limit for deleterious ASR expansion), concrete with fused silica aggregate lost nearly 50% flexural strength and about 20% elastic stiffness, whereas concrete with opaline aggregate lost nearly 40% elastic modulus. At this expansion level, the loss in compressive strength remained low, at about 10%. Both dynamic modulus of elasticity and pulse velocity measurements showed significant losses due to ASR at a very early age when no expansion was indicated. Questioning the ASTM C 227 expansion limits, the authors state:

"Since losses in engineering properties do not occur at the same rate or in proportion to expansion undergone by the concrete, and since expansion can be excessive or deleterious without evidence of cracking, depending on the function of the concrete element, **it is difficult to see how single values of critical limits can be applicable to all situations.**"

Further, according to Swamy (129), the ASTM C 441 test method of evaluating the effectiveness of pozzolanic and other mineral admixtures in controlling ASR expansion has also several drawbacks. For instance, the use of Pyrex glass as a standard reactive aggregate is questionable because it is not a good representative of natural reactive aggregates. Furthermore, in a laboratory study the performance criteria (i.e. more than 75% reduction in expansion at fourteen days) were met with a silica fume at a 10% cement replacement level. However, the specimens continued to expand after fourteen days and eventually cracked. The test is also found to be inadequate when an external source of alkalies is present.

Courtier (130) reviewed the problems underlying the **engineering assessment of structures affected with alkali-aggregate reaction.** The author cautions that assessments would concentrate on the overall behavior of the structures and not be over-concerned with cores. It is argued that the evaluation of restrained expansion

characteristics should be the dominant parameter of interest. Tordoff (131) reported on the engineering assessment of 16-year old prestressed concrete bridges suffering from ASR. According to the author, "As the assessment progressed the author became increasingly aware that research into ASR has concentrated on petrography, chemistry, and microstructure of concrete. Insufficient research has been carried out to assess the structural consequences of ASR and no work has been carried out on concrete members which are truly representative of the prototype. From the evidence available it was concluded that the bridges have not been weakened by ASR and that there is no reason to suspect that durability will be a greater problem than in other typical bridges in similar locations.

From the results of an international, interlaboratory test program involving the use of the ASTM C 227 mortar prism method for determining the potential reactivity of aggregates, Oberholtser (132) concluded that the ASTM C 227 criteria for distinguishing between deleterious and innocuous aggregates does not apply to reactive quartz-bearing aggregates. Also, the test results were found to be highly sensitive to the precise control of relative humidity inside the storage containers.

Knudsen (133) used chemical shrinkage caused by the reaction between sand particles and a sodium hydroxide solution at 50°C as a measure for evaluating the potential alkali reactivity of sands. It is claimed that this method, in one day, is able to give results that are similar to an eight-week standard test. Tang et al. (134) used a rapid autoclave test to evaluate the potential ASR activity of a number of aggregates from China. The authors report that their test is satisfactory for preliminary screening purposes of a large number of aggregates and gives results that are comparable to the ASTM C 277 and C 289 methods. Results from a similar autoclave test are reported by Nishibayashi et al. (135). Mortar bars containing 1.5% total Na_2O and precured for 24 hours after casting were exposed for five hours to 0.15 MPa pressure in an autoclave. The level of expansion obtained was claimed to be similar to the one obtained by eighteen months of storage at 40°C and 100% relative humidity. A slight variation of the method is reported by Tamura (136), who used two days of precuring of mortar bars containing 2.5% Na_2O, followed by two hours of exposure to boiling water under pressure (111°C). Cracking behavior due to ASR was evaluated from changes in ultrasonic pulse velocity and dynamic modulus values. Yoshioka et al. (137) reported the expansion data from an accelerated method used for evaluating the reactivity of aggregate, which involved immersion of mortar bars in a 1N NaOH solution at 80°C for 24 hours. A good correlation was reported between the results of this method and the standard mortar bar expansion test.

Baronio et al. (138) used infrared spectroscopy to develop a correlation between the microcrystalline disorder coefficient (C_d) and potential alkali reactivity of siliceous aggregates. Fifteen concrete cores from ASR deteriorated structures located in different parts of the world were examined. From C_d values and petrographic examination, it was concluded that aggregates having less than 120 C_d were not reactive, aggregates with C_d values between 120 and 200 (such as strained quartz) would take a long time to react, aggregates with C_d values between 200 and 300 (such as fine chert) would react in a relatively short period, and those with C_d greater than 300 (such as vitreous silica chalcedony) would react rather rapidly. With the degree of disorder increasing to $C_d > 450$, the aggregate begins to behave as a pozzolan and the deleterious effects of ASR are minimized. The authors suggest that more research should be undertaken to confirm the validity of these types of rapid and simple techniques for forecasting the reactivity of siliceous aggregates.

Alkali-Carbonate Reaction: Hugenberg (139) reported the case of deleterious expansion due to alkali-carbonate reaction in the forty year old Center Hill Dam (Tennessee). The reaction was identified by a combination of field and laboratory tests. According to the author, the expansion due to the reaction is causing the structure to move in the longitudinal direction, which resulted in binding of the

spillway gates and closure of the expansion joints at the bridge spans. Shortening of the spillway gates and bridge spans in 1985 was found to be necessary in order to maintain operational capability. The mineralogical composition of most of the aggregate shows calcite, dolomite, and quartz, with some feldspars and clays. In the ASTM C 586 test for potential alkali reactivity of carbonate rocks, aggregates from two of the five cores met or exceeded the 0.1% expansion limit, although this limit was reached much later than the 84 days prescribed by the performance specification.

Tang et al. (140) investigated the mechanism of alkali-carbonate reaction from the microstructure of a reactive carbonate rock, characterized by a distribution of rhombic crystals of dolomite in a matrix of clay and fine-grained calcite. It is proposed that water, alkalies, and hydroxyl ions penetrated the aggregate through the clay network and reacted with the dolomite crystals. The entry of these ions and molecules in restricted spaces caused expansion. The expansion can also be generated by the rearrangement of the products of dolomitization reaction. Other causes which contribute to expansion are water imbibition by dry clay and osmotic pressure from differences in ionic concentration.

Structural Effects of Alkali-Aggregate Reactions: Mullick and Samuel (141) described the microstructure of the ASR product from concrete cores of 25-30 year old dams. In one case, the reactive aggregate consisted of quartzite river pebbles containing chert and chalcedony. In the other case a biotite-granite crushed rock aggregate was used in which 50 to 80% quartz grains were strained and no other metastable silica minerals were present. In the case of quartzite aggregate, white deposits of the amorphous gel were found in the cracks and voids in the concretes, whereas in the case of strained quartz, dark reaction rims around the aggregate particles were predominant but deposits of alkali-silica gel were not so frequent. In both cases, however, the external manifestations of the ASR were typical map-cracking, long horizontal cracks, malfunctioning of sluice gates, and misalignment of crane gantries and power-generating machinery.

The structural effects of alkali-aggregate reaction on more than 100 reinforced concrete structures were discussed by Wood et al. (142). It is reported that, in inadequately reinforced members (viz. 0.9% area of steel), sufficient force can be generated by the reaction to yield the steel or cause delamination failure between the reinforcement and the reactive concrete. Interestingly, the authors found that with some reactive aggregates the magnitude of expansion was four times at 13°C, compared to that at 38°C (the temperature commonly used in laboratory tests). Also, the authors confirmed that the engineering effects of alkali-aggregate reaction are highly sensitive to the type and size range of the reactive aggregate particles, and that the characteristics of alkali-aggregate reaction cannot be generalized.

Figg (143) presented an analysis of practical effects of ASR expansion on concrete structures. According to the author, the surface cracking pattern resulting from an internally expanding concrete depended on the internal and external restraints and other constraints, which generally account for the differences in modes of cracking among plain, reinforced, and prestressed concretes. To diagnose that ASR is responsible for cracking, it is important to remember that ASR-generated cracking must originate from the aggregate and that it is a time- dependent and a slow phenomenon which takes many years. The author also observed that maximum expansion due to ASR occurred at a lower temperature than the temperature for maximum rate of expansion.

ASR expansion in five 40-60 year old concrete dams located in the southwestern United States was investigated by Stark and DePuy (144). In most cases the expansions were attributed to the use of high-alkali cements and cryptocrystalline-to-glassy volcanic aggregates of andesitic-to- rhyolitic composition. From field measurements of the relative humidity of concrete, the authors found that atmospheric

drying had reduced the RH values to below the threshold level for expansive reactivity only within several inches of the exposed concrete surfaces. Most of the concrete in the interior contained enough moisture to permit the alkali-silica reaction and the associated expansion. However, the progress of expansion either stopped completely or slowed down considerably due to the depletion of alkalies. It was confirmed that, in field structures, the physical manifestations of ASR are variable and they include pattern- or map-cracking, longitudinal cracking, pinching at joints, and misalignment or movement of affected members. Map-cracking is generally the combined result of internal expansion due to ASR and other volume changes from intermittent cycles of wetting and drying near exposed concrete surfaces. Longitudinal cracks typically occurred in beams and columns. Cracks were generally shallow (extending only a few inches into the concrete) and ranged from hairline width to several centimeters across. The authors observed that cracks occurred mainly in unconstrained portions of the structures, such as at the top of the dams (rather than at the bottom), and unrestrained joints. They caution that pattern-cracking should not be used as a diagnostic test for ASR since these types of cracks may also occur from shrinkage. Unreinforced structures exposed to the sun (surface drying conditions) frequently showed map-cracking associated with ASR. It is possible that the drying shrinkage cracks, by providing direct access of external water to an ASR-affected concrete interior, can become instrumental in increasing the expansion and further cracking. In a subsequent report Stark (145) showed that RH values greater than 80%, referenced to 21-24°C, are sufficient to support expansive ASR activity. Ordinary concrete structures in arid desert climates and not in direct contact with external moisture may exhibit RH levels sufficiently low to prevent expansive ASR activity. However, as discussed in the previous report, mass concretes even in dry climates will retain sufficient moisture in the interior to sustain ASR expansion for prolonged periods of time.

Summary

In the words of Peter Smith (146), **rocks which may have been happy in one environment for many millions of years may not take kindly to a new one as concrete aggregate. Since it is too late to reform the rocks, all we can do is try our best to make concrete kinder.** The use of low-alkali portland cements has been known to be one way to make the concrete system kinder to alkali-reactive aggregates. The use of mineral admixtures, such as natural pozzolans, fly ash, slags and silica fume, is another method. A large number of recent publications on deleterious expansions caused by alkali-aggregate reactions have dealt with the use of mineral admixtures in suppressing the expansion. It is clear that, due to a variety of interacting factors, no general predictions can be made in regard to the effectiveness of a particular mineral admixture in controlling the potentially deleterious expansion from a cement-aggregate combination. For example, the effectiveness of a mineral admixture depends not only on its proportion in the concrete mixture but also on its reactivity, which is greatly influenced by the cement composition and as well as environmental temperature and humidity conditions. Frequently, the test conditions and the cement used for evaluating a mineral admixture in accelerated laboratory tests are not the same as in the field concrete. Neither the mechanisms of expansion for all alkali- reactive aggregates nor the mechanisms by which each mineral admixture is able to suppress the alkali-aggregate expansion with a particular aggregate, are the same. Therefore, the results from a standard laboratory test using a standard reactive aggregate may not be generally applicable to all reactive aggregates.

There is overwhelming evidence that too much effort is being wasted on time-consuming accelerated tests, the results from which have no direct bearing on the performance of concrete in the field. Simple and rapid methods, such as infrared spectroscopy for evaluation of siliceous aggregates (138), represent a development

which is in the right direction. It is questionable whether it is worth spending so much time and money on tests whose outcome often leads to concerns and measures that may not have been necessary. Investigators, who have considerable experience with structures alleged to be suffering from alkali-aggregate reactivity point out that evidence of these reactions can be found in most field structures, but only a few suffer any significant damage. In spite of the reaction, expansion will not occur unless sufficient moisture is present in the environment. Expansions such as those from swelling of gels may be beneficial to concrete rather than harmful, provided that they occur under conditions of adequate restraint. According to Idorn (147), in properly reinforced concrete structures cracking and loss of structural reliability is unlikely. High expansions and unacceptable levels of cracking and deterioration of concrete containing alkali-reactive aggregates occur in field concretes due to the combined effects of alkali-aggregate reaction, corrosion of reinforcing steel, and cycles of heating- cooling, wetting-drying, and freezing-thawing. It is obvious that the synergetic effects of these interacting phenomena are too complex to be predicted from simple laboratory tests.

5 FREEZING AND THAWING

Introduction

When a concrete element is exposed to cycles of F-T (freezing and thawing), two types of damage are known to occur: internal cracking and surface scaling. Scaling is greatly enhanced in the presence of deicer salts, such as NaCl and $CaCl_2$, and in cold climates it is probably the most serious problem with concrete pavements. Generally, the mechanism underlying F-T damage involves the expansion of cement paste due to a combination of hydraulic and osmotic pressures generated by internal moisture movement. That is why a high degree of saturation is necessary before a cement paste can expand and crack on freezing. A highly porous and permeable cement paste that can get readily resaturated, would obviously be more vulnerable to F-T damage. Thus the microporosity of the cement paste, which is controlled by the water-to-cementitious ratio and the degree of cement hydration, plays an important role in determining the frost resistance of concrete. Also, with normal concrete mixtures it is well known that possible damage due to F-T attack can be prevented by incorporating within the cement paste system closely-spaced air voids for providing pressure relief. The use of certain microporous aggregates in concrete is also known to be the cause of cracking on exposure to F-T cycles.

Summarizing the state-of-the-art with respect to frost and scaling resistance of concrete, Mather (148) said that concrete will be immune to frost action with or without the use of deicing chemicals, **if it remains below critical saturation.** Critical saturation happens when practically all (over 91%) the capillary pores (i.e., pores large enough to hold freezable water) are full of water. A critically saturated concrete will continue to be immune to frost action as long as the aggregate and the cement paste are frost resistant. The aggregate will be frost resistant if its porosity is low or if it is not critically saturated; the cement paste will be frost resistant if it is mature when frozen (i.e., if the freezable water is not large) and if the air void system is proper (i.e. bubble spacing factor is 0.2 mm or less).

During the last decade, there has been considerable research and development on new products, such as high-strength concrete and roller-compacted concrete. Naturally, long-term durability of these products must be assured before their large scale application. In this section a brief review of recent publications on the effect of freezing and thawing cycles on high-strength concrete, roller-compacted concrete, and concretes containing fly ash or slag is presented. Miscellaneous reports of general interest are reviewed separately. A summary of the state-of-the-

art, both the major advancements of the 1987-91 period and the gaps in the area of F-T damage, is presented at the end.

Recent Publications

High-Strength Concrete: With the advent of superplasticizing admixtures, it is possible to produce highly workable concrete mixtures with water-to-cementitious ratios considerably lower than 0.4 and 28-day compressive strengths considerably higher than 40 MPa. Microstructural improvements resulting from the use of superplasticizers, highly active mineral admixtures, such as silica fume, and good quality aggregates have made possible the commercial production of concretes with up to 120 MPa compressive strength. The porosity and permeability of the cement paste in high-strength concrete is very low and, consequently, there is little or no freezable water. Using low-temperature calorimetry, Hammer and Sellevold (149) indeed confirmed that there was no freezable water in the well-cured concrete mixtures made with 0.45 water-to-cementitious ratio. Also, due to the presence of very fine and disconnected pores in the cement paste microstructure it seems that, in practice, wetting and drying cycles should have less influence on the degree of saturation of high-strength concrete as compared to normal concrete.

Sellevold (150) used a variety of methods to investigate the F-T and salt scaling resistance of superplasticized concrete mixtures containing silica fume. With dosages below 15% silica fume by weight of cement, the F-T and salt scaling resistance was increased over a wide range of water- to-cementitious ratios. In fact, the author observed that silica fume addition improved the frost resisting behavior of concrete more than the strength improvement. In the 0.35 to 0.55 water-to- cementitious ratio range, the use of high dosages of silica fume (20 to 30%) showed some evidence of reduction in frost resistance, however with very high strength mixtures (less than 0.3 water-cementitious ratio) the silica fume concretes were frost resistant **even without air entrainment.** Pettersson (151) reported that by using silica fume although it was possible to produce concretes almost impermeable even to chloride ions, this did not guarantee a high resistance to salt scaling because a different damage mechanism is at work when products with fine pore structure (such as those containing silica fume) are exposed to the action of deicer chemicals.

Seibel (152) investigated the influence of air-void characteristics and F-T resistance of superplasticized concretes containing melamine or naphthalene sulfonates. According to the author, the number of voids with diameter less than 0.3 mm decreased whereas those with larger than 0.5 mm diameter increased and the bubble spacing factor also increased. Therefore, even with sufficient air contents, the F-T durability might be impaired. Pigeon et al. (153) found that the critical air void spacing factor was 0.4 mm with a 60-MPa concrete (0.3 water/cement ratio). Using the same materials, Foy et al. (154) found that, with 0.25 water/cementitious ratio, the critical spacing factor was 0.75 mm. Since these spacing factors can be generally found in normal concrete mixture containing no air-entraining agent and since the F-T durability was found to be satisfactory, this shows that with high-strength concrete deliberate entrainment of air is not essential for F-T protection. However, in Hammer and Sellevold's tests (149), some 91 MPa and 115 MPa non-air-entrained concrete specimens were damaged by F-T cycles. Since there was little freezable water in these concretes, the authors suggested that the deterioration was probably caused by the differences in the coefficients of thermal expansion between the cement paste and the aggregate. Similarly, Pigeon et al. (155) in one of their tests noted that a 82-MPa non-air- entrained concrete, with an air-void spacing factor of about 0.7 mm, was not fully frost resistant.

Whiting (156) investigated the durability to freezing and thawing cycles, both with and without deicer salts, of superplasticized concrete mixtures of 40, 55, and 70 MPa nominal strength. Air entrainment varied from zero, 3-4%, 4-6%, and 7-9%. Two curing regimes were employed: a 28-days moist curing and a 7-days moist curing followed by 21 days of air curing. At the end of the curing cycle, the specimens were tested for resistance to 300 cycles of freezing and thawing in water or in 4% solution of calcium chloride. All non-air-entrained concrete mixtures performed poorly, i.e. failed in less than 300 cycles of freezing and thawing in water irrespective of their original strength or type of curing. All air-entrained concrete mixtures performed satisfactorily in 300 cycles of freezing and thawing in water. In regard to salt scaling, all non-air-entrained concrete mixtures showed severe scaling within 50 cycles of the test. However, the 40 MPa air- entrained concrete performed satisfactorily. Both the 55 MPa and the 70 MPa concretes, irrespective of the air content or type of curing, showed severe salt scaling within the 300-cycles test period. Whiting and Schmitt (157) also investigated statistical models relating the degree of surface scaling to various parameters. A three-parameter linear model incorporating the spacing factor, water-to-cement ratio, and alteration of near-surface air voids was found to yield the highest level of correlation with observed scaling.

Robson (158) reported the results of freezing and thawing tests on two high-strength concrete mixtures, 40 MPa and 55 MPa. The test specimens were cured for 14 days before exposure to freezing and thawing cycles in ethylene glycol (ASTM Test Method C 666, Procedure A). Even with adequate air entrainment (4-10%), the presence of a superplastizing admixture in concrete changed the air void system markedly. The bubble size and bubble spacing factors were significantly increased, and the specific surface of the air void system was reduced to well below the minimum requirement for adequate frost resistance (i.e. 600 $in.^2/in.^3$). Consequently, the concrete mixtures gave a very low durability factor in the ASTM C 666 test. In contrast, the use of a normal water-reducing admixture in combination with a compatible air-entraining agent gave an acceptable air void system at 6% air content (i.e. approx. 700 $in.^2/in.^3$ specific surface, and 0.18 mm bubble spacing factor). The F-T durability of this concrete mixture was found to be satisfactory.

With superplasticized high-strength concrete mixtures, **using a different method of test for durability to freezing and thawing,** Dhir et al. (159) arrived at a conclusion which was not in conformity with the findings of other researchers. The test specimens, 80 x 80 x 300 mm prisms, were subjected to freezing and thawing cycles in which the temperatures employed were similar to those specified in ASTM C 666, however the failure criteria used was linear expansion exceeding 0.3%. For acceptable frost resistance according to this test a normal concrete mixture, without a superplasticizer and without air entrainment, required 60 MPa cube-strength at 28-day with approximately 500 kg/m^3 cement content and 0.49 water-to-cement ratio. The authors concluded that the superplasticized high-strength concrete possesses greater durability to freezing and thawing cycles, even without air entrainment.

Malhotra (160) reported the results of an extensive series of freezing and thawing tests (ASTM C 666) on both non-air-entrained and air-entrained concretes, with and without silica fume, on superplasticized concrete mixtures. Water-to-cementitious ratios of 0.25, 0.30, and 0.35 were used. The silica fume content was either 10 or 20% by mass of the total cementitious material. The 28-day compressive strengths for non-air-entrained concrete ranged form 51 to 72 MPa without silica fume, and from 61 to 87 MPa with silica fume. The non-air-entrained showed very low durability factors in the ASTM C 666 test. With about 7% air content, the spacing factors as well as the durability factors were satisfactory in control mixtures without silica fume. However, with low water/cement ratio mixtures containing silica fume, it was difficult to entrain adequate air to achieve the required minimum spacing for satisfactory frost resistance.

Commenting on the results of frost resistance tests with low water/cement ratio concrete mixtures containing high range (superplasticizing) water-reducing admixtures and silica fume, Philleo (161) concluded that the test method, not the concrete, appears to be the source of the problem. The ASTM C 666 test method exposes the specimens to freezing at an intermediate level of maturity, with no opportunity for drying by loss of water to the surroundings prior to the test and exposes them to very rapid freezing cycles that are rarely encountered in field practice. According to the author, while this test may be useful in evaluating the frost resistance of young and saturated concretes exposed to severe frost conditions, the resistance of well-cured concretes to more typical exposures might better be assessed by altering the specimen curing requirements in the ASTM C 666 test method or by replacing the test with a more realistic one, such as ASTM C 671. On theoretical grounds also it seems that a high-strength concrete, even without entrained air, should be durable to freezing and thawing action. Philleo proposed that superplasticizers do not alter the fundamental characteristics of the hydrated cement paste; they merely help to extend traditional concrete technology to a range of water/cement ratios that were formerly impractical. The addition of silica fume does alter the pore structure in the sense that more of the pore volume is found in very fine pores in which water cannot freeze at temperatures ordinarily encountered in field practice.

In two comprehensive reports (162, 163), Pigeon and his associates described a procedure to assess the stability of the air-void characteristics in superplasticized concretes and recommended a method to produce a stable air-void spacing factor from a given concrete mixture and its constituent materials. According to the authors, the production of a superplasticized concrete mixture with satisfactory air voids system of F-T protection is fairly simple, however with a given superplasticizer the spacing factor stability during concrete transportation is dependent on the composition of cement and the type of air entraining admixture. Preliminary results show that the content of soluble alkalies in cement is one of the parameters that can influence the stability of the air-void system. The use of an air-entraining agent derived from a synthetic detergent yielded a more stable air-void system. In further reports on air-void stability (164-166), Pigeon and his associates described the effect of variables on air-void characteristics of good quality concrete (0.45 water-to-cement ratio). The variables investigated included silica fume, superplasticizers, retempering, temperature, and type of field tests. It was concluded that addition of up to 10% silica fume by weight of cement did not influence the stability of the spacing factor. Superplasticizers can destabilize the air-void system significantly (especially when used in large dosages), and the phenomenon appeared to depend on the problem of chemical compatibility of the superplasticizer with other admixtures and cement. Retempering of concrete with water to increase slump by 50 mm did not influence the spacing factor, however retempering with an air- entraining agent increased the air content and reduced the spacing factor. The temperature of the concrete mix did not seem to influence the spacing reactor. In regard to relevant field tests, for routine verification of air-void characteristics the authors recommended casting specimens after 60 minutes of concrete mixing to see if the air-void system is adequately maintained during transportation. A performance index is proposed to simplify understanding and to estimate the overall quality of any given air-void system.

Petersson (167) investigated the effect of superplasticizing admixtures on **deicer salt scaling resistance** of air-entrained concrete mixtures, with cement content not exceeding 400 kg/m³ and a minimum compressive strength of 45 MPa. The durability to salt scaling was better when the air-entraining agent was used alone. This is because in combination with the superplasticizer the air-void system was less stable. In superplasticized concretes, a significant amount of the entrained air was lost on consolidation of concrete by vibration, thus, coarsening the air-void system. A separate investigation in Germany by Ranisch and Rootasy (168) confirmed the results of Petersson's study. It seems that the combination of some air-

entraining and superplasticizing agents lead to a marked increase in the size of air voids, and the larger voids the more readily they are driven out of concrete on vibration. In this regard, Berntsson (169) reported that the use of a new, cereal-based, air-entraining agent may provide a solution to the problem. This air-entraining agent is a powdered material insoluble in water but soluble at the high pH in a portland cement paste. When added to cement in amount of 0.04 to 0.10% by weight of cement, it provided 5 to 6% air in the form of a stable air-void system which remained undisturbed when a superplasticizing admixture was subsequently added. Even after transportation and pumping, the reported loss in air content was low.

Deicer salt scaling resistance of high strength concretes was also reported by two other research teams (170,171), with similar results. In Canada, Gagne et al. (170) used 60-90 MPa superplasticized concretes both with and without air entrainment (a low and a high spacing factor). All the specimens were subjected to 150 daily cycles of freezing and thawing in NaCl solution in accordance with ASTM C 672. The results showed that **non-air-entrained concretes**, with or without silica fume (water/cementitious ratio of 0.30), possessed very good resistance to deicer scaling. For the concretes made with ASTM Type III portland cement, the length of curing period made no difference to the scaling resistance. The non-air-entrained concretes made with a Type 1 portland cement with silica fume also showed good scaling resistance after a 24- hours curing period but, in this case, a higher durability was obtained with a longer (7-28 days) curing period. Interestingly, the authors found that the use of air entrainment somewhat reduced the scaling resistance of the high-strength concrete, rather than causing an improvement, probably due to saturation of the air voids near the exposed surface. In Finland, Kukko and Matala (171) investigated the freeze-thaw resistance (using a method similar to ASTM C 666, Procedure B), and salt scaling resistance of high-strength 660-100 MPa) concretes in saturated NaCl solution (freezing at -15°C and thawing at +20°C, with each cycle taking 24 hours). To investigate the effect of aging, some tests were performed on specimens exposed to wetting and drying cycles for one year. On the basis of their test results, the authors concluded that durable high-strength concretes can be produced, **without air-entrainment**, when the strength of concrete exceeds 80 MPa and the water/cementitious ratio was lower than 0.30-0.32. Compared to blends of a rapid hardening portland cement with silica fume (5-6%) or fly ash (25%), blended slag cement (33% slag) and a slow-hardening portland cement gave lower values of scaling resistance. The aging procedure did not adversely affect the freeze-thaw or scaling resistance of high-strength concretes made with the rapid hardening portland cement with or without silica fume or fly ash, but the blended slag cement showed very low resistance to salt scaling after aging.

Preliminary results from a round-robin test program involving five Nordic laboratories has confirmed that, as with F-T durability, **the salt-scaling durability of very high strength concrete is excellent, even without the use of entrained air.** According to Sellvold (172) a 115-MPa non-air- entrained concrete mixture (with 10% silica fume and 0.27 water-to-cementitious ratio) showed minimal salt scaling in the 140-cycles test regardless of drying-rewetting pretreatment or salt concentration on the surface of test specimens. On the other hand, **air-entrained concrete mixtures with the 33-56 MPa strength range** (0.55 water-to-cementitious ratio and with or without the presence of 7% silica fume) showed poor resistance to salt scaling. At the intermediate strength levels (47-66 MPa), with 0.45 water-to-cementitious ratio and with or without 7% silica fume, the salt scaling was acceptable in air-entrained concrete mixtures.

Whiting and Burg (173) investigated the freeze-thaw durability of high-strength (59 to 73 MPa), air-entrained (5% air), **lightweight** (1920 to 2080 kg/m^3 density), **concretes made with expanded shale aggregates.** Test methods included exposure to 300 cycles of the ASTM C 666, Procedure A (six cycles per day of alternately lowering the

temperature from 4.4°C to -17.8°C, and raising it from -17.8°C to 4.4°C), and a "spectral" procedure specially formulated to simulate the climatic conditions to which a marine structure in the arctic is exposed (60 rapid freeze-thaw cycles in artificial seawater). Under the ASTM standard freezing and thawing test, the concretes showed outstanding performance. However, under the simulated arctic offshore conditions, on prolonged exposure significant damage was caused. The authors concluded that durability of high-strength, lightweight aggregate concrete is a strong function of cumulative freezing and thawing cycles and moisture content of the concrete (with saturation of aggregates prior to test leading to premature failure). In general, moisture content must be fairly high (11-13% oven-dry weight) for failure to be initiated. Such high levels of moisture content can be achieved due to microcracking after a large number of freezing and thawing cycles or by the use of aggregates with high moisture content in the initial concrete mixture.

In several reports Morgan (174-177) has presented a comprehensive review of the F-T durability of steel and polypropylene **fiber-reinforced shotcretes** made with both wet and dry-mix processes. It is shown that both steel and high volume polypropylene fiber-reinforced wet-mix shotcretes can be made F-T durable, provided the shotcrete contains 8-10% entrained air with a proper air-void system. In the dry-mix shotcrete process, it was not possible to achieve effective air entrainment; in spite of this, properly designed and applied steel fiber-reinforced dry-mix shotcrete can be made durable to F-T cycles although it is difficult to achieve this in practice. However, non-air-entrained fiber-reinforced wet-mix shotcrete deteriorated rapidly in the ASTM C 666 test. Again, the significance of adequate curing, followed by drying prior to the exposure of a shotcrete to freezing, is strongly recommended for F-T durability.

Roller-Compacted Concrete: Roller-compacted concrete (RCC) is a zero-slump, low cement- content concrete which is quite attractive for mass concrete applications because of high production rates and associated cost savings. Since it is not possible to entrain air in lean and dry concrete mixtures, the durability of RCC to freezing and thawing is considered poor, and much research effort has been devoted recently to improve the freeze-thaw durability of RCC. Dolen (178) reported that in **workable concrete mixtures**, with Vebe consistency of 5 to 35 seconds, it is possible to entrain 2 to 3% air, which is sufficient to improve the freeze-thaw durability significantly. As a result of air entrainment, a reduction in the water content of a concrete mixture is possible, which has the effect of increasing the compressive strength and consequently the freeze-thaw durability of concrete. Marchand et al. (179) investigated the salt-scaling resistance of RCC mixtures using the ASTM C 672 test method. The authors reported that it is extremely difficult to entrain air in this type of concrete even if fairly large dosages of air- entraining agent are employed and mixing time is increased. However, without the use of an air-entraining admixture, it was possible to produce a scaling-resistant RCC when either 7% silica fume or 20% fly ash by weight of cement were used as additives. It is recommended that due to lack of spherical air bubbles in dry concrete mixtures, ASTM C 457 should not be used for investigation of RCC. No relationship was found between the air-void spacing factor and frost resistance of RCC mixtures.

Based on U.S. Army Corps of Engineers experience since 1978, Liu (180) concluded that RCC, when properly designed and constructed, is not inferior to conventional concrete. Although because of the lack of intentionally entrained air, RCC performs rather poorly in the ASTM C 666 test for freeze-thaw resistance, the field performance up to ten years has been satisfactory for RCC in dams and pavements subjected to natural freezing and thawing conditions. The satisfactory field performance is due probably to the fact that existing RCC structures are not critically saturated. The author recommends that, until the long-term durability of RCC to freezing and thawing is well established, it is desirable to use conventional

air-entrained concrete facing elements to protect RCC from possible deterioration by freezing and thawing cycles.

Concrete Containing Fly Ash or Slag: Klieger and Gebler (181) investigated the influence of fly ash type on resistance of air-entrained concretes exposed to 300 cycles of freezing and thawing in water as well as in a 4% NaCl solution. Although the majority of concretes of this study produced relatively stable air-void systems and showed satisfactory frost resistance, the volume of entrained air during intermittent agitation over a 90-minute period was affected by the fly ash composition. Generally, the air content of concretes containing ASTM Class C fly ashes was more uniform than those containing Class F fly ashes. This happened primarily because the Class C fly ashes had a lower content of carbon and other organic matter which required the use of higher dosages of air-entraining admixtures. Concretes with fly ashes requiring high dosages of air-entraining admixtures generally exhibited poor retention of air on agitation. The authors also investigated the effect of curing temperatures on resistance to freezing and thawing. Air- entrained concretes, with or without fly ash, that were moist-cured at 23°C, generally showed good resistance to freezing and thawing cycles. However, those cured at low temperature (5°C) showed slightly less resitance with Class F fly ash than with Class C fly ash. The deicer scaling (i.e. freezing and thawing in 4% NaCl) of the air-entrained concretes was more aggressive than freezing and thawing in water. In general, air-entrained concretes without fly ash performed better than air-entrained concretes with fly ash, regardless of the type of fly ash and the type of curing provided.

Rodway (182) used five fly ashes with widely varying lime content, at 25% cement replacement level in concrete mixtures. The hardened concretes contained satisfactory air-void systems from the standpoint of F-T resistance regardless of the lime content of fly ash. Johnston (183) investigated the freeze-thaw durability of relatively lean concrete mixtures containing up to 42% Class C fly ash or up to 15% silica fume by weight of cement, with 0.53-0.88 water/cementitious ratios. Procedure A of the ASTM C 666 test method was used to determine the durability factor in 300 freeze-thaw cycles and ASTM C 672 was used to assess the resistance to salt scaling. Replacement of cement by fly ash did not reduce the durability factor of concrete in the ASTM C 666 freeze-thaw test provided that the water/cementitious ratio was less than 0.53 and the air-void spacing factor was less than 0.25 mm. The fly ash concretes, which performed well in the ASTM C 666 test, did not give satisfactory scaling resistance in the ASTM C 672 despite their low water/cementitious ratio (0.53) and adequate spacing factor. Replacement of cement by silica fume did not reduce the durability factor in the ASTM C 666 freeze-thaw test even with water/cementitious ratios of up to 0.88 provided that the dosage of the air-entraining admixture was increased to achieve satisfactory air-void spacing factor. As with the fly ash concretes, salt scaling was severe with high water/cementitious ratio (0.88) in silica fume concretes although it seemed that satisfactory performance was possible at a slightly lower water/cementitious ratio of 0.7, which is much higher than the recommended 0.45 for scaling resistance of concretes without silica fume.

Bilodeau et al. (184) investigated the influence of fly ash on salt scaling behavior of air- entrained concrete samples cured under different conditions. ASTM Class F fly ash, 20 and 30% cement replacement by mass, was used with water-to-cementitious ratios of 0.35, 0.45, and 0.55. After one-day moist curing, some of the concrete slabs were covered with a curing compound while others continued to be moist-cured until required for testing at the end of a specified curing period. Some of the slabs were air-dried before subjecting them to freezing and thawing in a 4% $CaCl_2$ solution in accordance with the ASTM C 672 test method. The data showed that, in general, all fly ash concretes performed well in the scaling test, irrespective of the fly ash content, water/cementitious ratio, and curing

conditions. The majority of the specimens showed slight-to- moderate scaling with the mass loss less than the acceptance limit of 0.80 kg/m^2. The authors attribute the satisfactory performance to an adequate air-void system in all cases. Only some moist-cured concretes gave higher-than-acceptable mass loss in the scaling test. Membrane curing seemed to improve somewhat the durability of concrete, especially the fly ash concrete, under the combined action of freezing and thawing and deicer scaling.

Recently, the development of a superplasticized (low water/cementitious ratio) concrete containing 56% fly ash by weight of the total cementitious material has been reported. Malhotra et al. (185) investigated the durability aspects of this new material including the resistance to freezing and thawing cycles (ASTM C 666, Procedure A) and salt scaling (ASTM C 672). With 154 kg/m^3 cement content, 212 kg/m^3 fly ash content (ASTM Class F), 0.33 water/cementitious ratio, and 4.3% air content (0.22 to 0.25 mm spacing factor), durability factors exceeding 90 were obtained in 300 cycles of freezing and thawing in water. However, in the deicing salt scaling test, the high-volume fly ash concrete performed poorly. The authors, therefore, do not recommend the use of this type of concrete where it is to be exposed to repeated applications of deicing chemicals.

Gunter et al. (186) described a laboratory investigation on the resistance of concrete specimens to freezing and thawing cycles in a saturated NaCl solution. The concretes were made with portland cement and portland-blast furnace slag cements of varying slag content (30-75% slag). Different water/cement ratios, air contents, and curing regimes were investigated. Resistance to deicer scaling was evaluated with two different test methods, one similar to ASTM C 672, and the other a more severe test which is proposed by the German Concrete Association (DBV). According to the test, the percent loss in volume to the freeze-thaw cycle of concrete cubes is measured for 70 days under storage in saturated NaCl at 15°C for 8 hours, followed by storage in water at 20°C for 16 hours. Since the pore structure of the hydrated cement paste, together with the air-void system, are the governing factors for the freeze-thaw and deicer sealing resistance of concrete, the authors confirmed that the parameters influencing the pore structure (such as the water/cement ratio, slag content of cement, duration of curing and carbonation) also influenced the durability of concrete to frost action. Air-entrained portland cement concretes, especially with low water/cement ratio, needed only a short curing period to give a pore structure that was sufficiently dense to impart high resistance to concrete exposed to freezing-thawing and deicer scaling cycles. Carbonation of portland cement concretes resulted in a denser microstructure (finer pores) which improved the durability under severe exposure conditions. In regard to concretes made with portland-blast furnace slag cements, when the slag content of the cement was high and the specimens were cured well, the microstructure was very dense. Therefore, the specimens did not become critically saturated for long periods of exposure to freeze-thaw cycles and, with 4 to 5% air content, showed good durability to the DBV test. Contrary to the experience with portland cement concretes, the carbonation of portland-blast furnace slag cement concretes resulted in a coarser pore structure which increased the amount of freezable water and caused a severe reduction in durability.

Miscellaneous Reports: Buck (187) proposed a new definition of critical dilation for use in the ASTM Method C 671. Using the new definition, only a single cycle of freezing is needed to determine whether or not a concrete is frost resistant. Rashed et al. (188) investigated the microstructure of the air-void systems in concrete using low-temperature scanning electron microscopy and freeze drying. Gunnink et al. (189) demonstrated the use of conductometric phase transition porosimetry to monitor changes in the pore structure of concrete exposed to freezing and thawing cycles. The authors proposed that these changes can be used to study the damage mechanisms and to evaluate the freeze-thaw durability of concrete. Bager and

Sellevold (190,191) reported the use of low-temperature scanning calorimetry to measure ice formation in hardened cement paste. The authors found that the drying shrinkage of cement paste caused an increase in the volume and continuity of large pores, with a corresponding decrease in fine pores. This effect increased with decreasing relative humidity from 100 to 58%, below which the effect remained constant. Also, the changes in the pore structure caused by drying are irreversible. Since an increase in the size and continuity of large pores will have the effect of increasing the permeability and the degree of critical saturation of surface layer in concrete, the implication of this phenomenon to salt scaling effects should be obvious. From microstructural studies Pigeon and Regourd (192) reported that cycles of freezing and thawing tend to dissolve CH and perhaps also the sulfoaluminates present in the hydrated cement paste. This has the effect of creating large voids, thus increasing the porosity and permeability of a system to a point when it becomes more vulnerable to freeze-thaw damage.

Yamato et al. (193) presented the results of accelerated freezing and thawing tests on non-air-entrained and air-entrained concretes (0.55 water/cementitious ratio) containing 0.1, 0.3, 0.5, 1.0, 3.0, 5.0, and 7.0% NaCl. The durability to cycles of freezing and thawing was tested in both water and seawater according to the ASTM C 666, Procedure A. The results showed that the freezing-thawing resistance in both water and seawater decreased with increasing chloride content above 0.3% NaCl. The air-entrained concrete containing less than 0.3% NaCl showed good resistance. However, air-entrained concretes containing more than 0.5% NaCl did not perform satisfactorily.

Balaguru et al. (194) used up to 900 cycles of the ASTM C 666, Procedure A to investigate the freeze-thaw durability of non-air-entrained concrete mixtures containing different amounts of a liquid epoxy monomer with a curing agent (0.2 to 0.6 polymer-cement ratio). When the polymer-cement ratio was greater than 0.4, the non-air-entrained concrete was able to withstand the 900 cycles of freezing and thawing without significant damage. However, the specimens containing no polymer or 0.2 and 0.3 polymer-cement ratio disintegrated in 300 cycles of freezing and thawing.

Bjegovic et al. (195) discussed the theoretical aspects of concrete resistance to cycles of freeze-thaw and deicer chemicals attack. It is shown that differences in the constituent materials of concrete mixtures and concreting practice can result in widely different concrete types. Since the environmental exposure conditions also vary widely, the authors concluded that no single test method is universally applicable to all concrete types and environmental conditions. Based on a comprehensive survey of world methods for testing the resistance of concrete to freeze-thaw cycles and deicer chemicals, the authors recommend that the measurement of concrete dilation during the freezing period is a reliable indicator of frost resistance.

Pigeon et al. (196) investigated the effect of silica fume content (5 and 10% by weight of cement) on the freeze-thaw and deicer salt-scaling durability of air-entrained concrete mixtures. Although silica fume concretes were found to be somewhat more susceptible to scaling in the ASTM C 672 test, the performance with or without silica fume was not signficantly different as long as the silica fume content was low (up to 10% by weight of cement), the air void spacing factor was correct, the water/cementitious ratio was low, and the specimens were adequately cured before the test. The authors observed that the critical spacing factor concept for freeze-thaw durability (i.e. internal cracking of concrete) is not applicable to surface scaling, which can never be completely prevented, and, therefore, very low spacing factors offer no special advantage. It was suggested that various tests, including field tests, are needed to properly assess the freeze- thaw durability of a concrete. One single test can only yield incomplete information, not only because concrete is a complex material and freeze-thaw conditions are highly variable, but also because

surface scaling and internal cracking are two distinctly different manifestations of distress due to frost action.

Sturrup et al. (197) reviewed Ontario Hydro's experience in predicting the freeze-thaw durability of concrete by comparing the results from 28 years of outdoor exposure studies and accelerated laboratory tests on companion specimens. From the test results the authors concluded that laboratory freezing and thawing tests are frequently unreliable in predicting the potential durability of concrete. In the outdoor exposure tests, equal deterioration was recorded with a lower water/cementitious ratio (0.5-0.6) non-air-entrained concrete and an air-entrained concrete with a higher water/cementitious ratio (0.8). In contrast, by the ASTM C 666, Procedure A test method, a non-air-entrained concrete with a 0.5 water/cementitious ratio showed much less durability than an air-entrained concrete with a water/cementitious ratio of 1.0. While the benefits of air entrainment are obvious, the authors concluded that Procedure A tends to overemphasize these benefits in contrast to non-air-entrained concepts. Thus, overmagnification or poor reproduction of the exposure conditions in accelerated laboratory tests can lead to misleading results. Results from field tests are far more reliable, although time-consuming. In field tests, the exposure conditions may also not be duplicated exactly, but they are more closely simulated than in the accelerated laboratory tests.

Among the few papers which discuss damage mechanisms due to freezing and thawing is a report by Vanderhorst and Janssen (198) on the factors affecting the severity of freezing-thawing environments. The authors contend that the severity of cooling rate, which controls the damage mechanisms, varies with material properties, moisture conditions, and salt exposure. Therefore, laboratory freezing and thawing tests should be used with extreme caution for predicting the field performance because differences in specimen and environmental conditions can lead to drastically different cooling rates and different damage mechanisms. This is especially important with the development of new high-performance concretes which may have material characteristics that are significantly different from concretes that have been used in the past to develop the current body of knowledge concerning the resistnace of concrete to freeze-thaw environments.

To assess the freeze-thaw durability of concrete under arctic conditions, Moukwa et al. (199) reported that the ASTM C 666, Procedure A test method is not reliable. According to the authors, this test was designed to produce internal damage to concrete from expansion. Under arctic conditions, however, surface effects can play an important role in the mechanisms of deterioration.

New Admixtures: There were three interesting reports about the use of new admixtures to improve the freeze-thaw resistance of concrete. Aavik and Chandra (200) investigated the use of a natural polymer protein which is non-air-entraining but which improved the durability of concrete to freeze-thaw cycles and salt scaling. Speculating on the reasons for the positive influence of the polymer on concrete, the authors suggest the following possibilities: (a) carboxylate ions of the polymer dispersion react with calcium ions to form an insoluble complex of calcium, thus preventing the formation of the deleterious double salt, $Ca(OH)_2 \cdot CaCl_2 \cdot xH_2O$; (b) the polymer dispersion dries to form a hydrophobic film which reduces water adsorption by the concrete; or (c) polymer films hinder the propagation of microcracks. Gutmann (201) reported the use of a new air-entraining agent, a methyl ester derivative of cocamide diethanolamine, which offers many advantages over the conventional products by producing very small, spherical, and stable air voids in cement pastes. Test results indicate that, as a result of a more uniform and stable air-void system, the mix-water requirement is reduced, and consequently the compressive strength is increased by 10 to 25%. The author also reported a 400% increase in freeze-thaw durability when compared to conventional air-entraining

agents. Sugiyama et al. (202) reported the use of a glycol ether as a concrete admixture which reduced the drying shrinkage and also improved the durability to freezing and thawing cycles. Using the ASTM C 666, Procedure A, very high durability factors were obtained in 300 freeze-thaw cycles with non-air-entrained concrete mixtures (0.6 water/cementitious ratio) containing 2% or 4% ethylene glycol by weight of cement, provided that the specimens were air-dried for at least two days prior to the beginning of the freeze-thaw testing. The drying process reduced the degree of saturation to 80% or less, which might have been a factor in the improved resistance to frost action. Although the total air content of the concrete mixtures was low (< 1%), the authors noted that the number of air bubbles present was considerably large because, in the presence of glycol ether (which is an anti- foaming surfactant), the size of the bubbles was extremely small (150 μm).

Summary

At present, air entrainment is the only accepted method to produce concrete that is durable when subjected to cycles of freezing and thawing. During the 1980's the advent of superplasticizing and highly active pozzolanic admixtures, such as silica fume, has made the commercial production of very high-strength concrete mixtures, in the 60 to 120 MPa range, which are reported to be frost-resistant even without air entrainment. The cement paste in very high-strength concrete contains very fine and discontinuous pores. Consequently, the permeability is very low and there is little or no freezable water present. Also, as compared to normal concrete, very high-strength concrete is less prone to microcracking and resaturation when exposed to weathering (i.e. ambient conditions of wetting and drying, and heating and cooling). However, the performance of very high-strength concrete in accelerated laboratory tests for evaluation of freeze-thaw resistance, has not always been satisfactory. Most researchers believe that the problem is not with the material but lies with the test methods that are unusually severe, such as the ASTM C 666. In a few cases, a large difference in the coefficients of thermal expansion between the cement paste and the aggregate may have caused unacceptable levels of freeze-thaw damage in the test. However, researchers have concluded that the severity of cooling rate controls the damage mechanisms, which vary with the material properties and the moisture condition of the concrete. Vanderhorst and Janssen (198) caution that this is especially important with the new high-performance concretes which have material characteristics significantly different from normal concretes since the current body of knowledge (including the methods of testing) on frost resistance was developed for application to normal concrete only. Even with normal concrete, Sturrup et al. (197) found a poor correlation between long-term field exposure tests and the accelerated laboratory test (ASTM C 666). Obviously, the results from the accelerated laboratory freeze-thaw tests such as ASTM C 666, cannot be used for predicting the field performance of concrete. Also, there is an urgency for development of better test methods and specifications for different concrete types and environmental conditions.

6 INGRESS OF CHLORIDES

Introduction

Chlorides may be present in the fresh mix or may penetrate into the hardened concrete. Due to the deleterious effect of chlorides on the corrosion protection of the reinforcement, the chloride content of the mix is limited to values below 0.4 % in relation to cement in almost all countries or standards. During use of the structures, chlorides may penetrate into the concrete from various sources. The most important of these are sea water, de-icing salts and PVC fires. De-icing salts in particular have caused tremendous damage to bridges in various countries.

Chlorides penetrate into the concrete as ions within partly or completely water-filled pores. They are partially bound by chemical or physical means within the cement matrix.

Unlike carbonation penetration, chloride penetration is not associated with a reaction front. On the contrary, a chloride profile with a chloride content decreasing from the the concrete surface to the interior is usually found.

Where chlorides penetrate into hardened concrete, two basic transport mechanisms are involved:

- pure chloride ion diffusion
- chloride transport combined with water transport.

When assessing the penetration of chlorides into the concrete and the associated risk of reinforcement corrosion, it is necessary to differentiate between two basic influencing parameters:

- the diffusion resistance of the concrete to ingress by chlorides; this diffusion resistance depends primarily on the pore size distribution of the concrete;

- the binding capacity of the concrete with respect to chloride ions (physical and chemical binding). This binding capacity influences both the penetration rate and the ratio of bound to free chloride ions in the pore water.

The binding capacity of concrete is particularly influential, since the risk of corrosion at the reinforcement is determined solely by the free chlorides in the pore water. Consequently, free chlorides in the pore water or the ratio of bound to free chlorides are the decisive factor in judging the reinforcement corrosion risk.

Both pure chloride diffusion and chloride transport via water transport can be described according to Fick's diffusion laws, using physical terms. Fick's first diffusion law governs stationary water diffusion through a structural element; all non-stationary processes are described by Fick's second diffusion law.

A knowledge of diffusion coefficients is necessary in order to calculate penetration depth using Fick's diffusion laws. The diffusion coefficients may be determined in a number of ways. Real diffusion coefficients which do not include the binding capacity, as described in (207) are measured after the binding processes within the specimen have been completed and when a constant quantity of chlorides per unit time is diffusing through the specimen. Fig. 1 shows a test set-up for this type of test to measure the real diffusion coefficient. Another frequently-used method relies on calculation of the diffusion coefficient from a measured chloride profile of the concrete after a defined period of chloride attack, using Fick's second diffusion law. This approach yields the effective diffusion coefficient D_{eff}. The effective diffusion coefficient D_{eff} incorporates the binding capacity of chlorides for concrete. As a result, the D_{real} and D_{eff} diffusion coefficients for a particular concrete may differ, necessitating different procedures for the calculation of penetration depths with these diffusion coefficients. If D_{real} is employed, the chloride concentration of the environment is taken as the chloride content of the attacking solution. However, the formula for Fick's second diffusion law must contain the binding capacity of the concrete, which is incorporated in the diffusion coefficient D_{eff}. In this case, therefore, the chloride content of the concrete surface layer has to be taken as the chloride concentration of the attacking environment. This procedure has been used in (214). The literature often fails to draw a clear distinction between these two procedures.

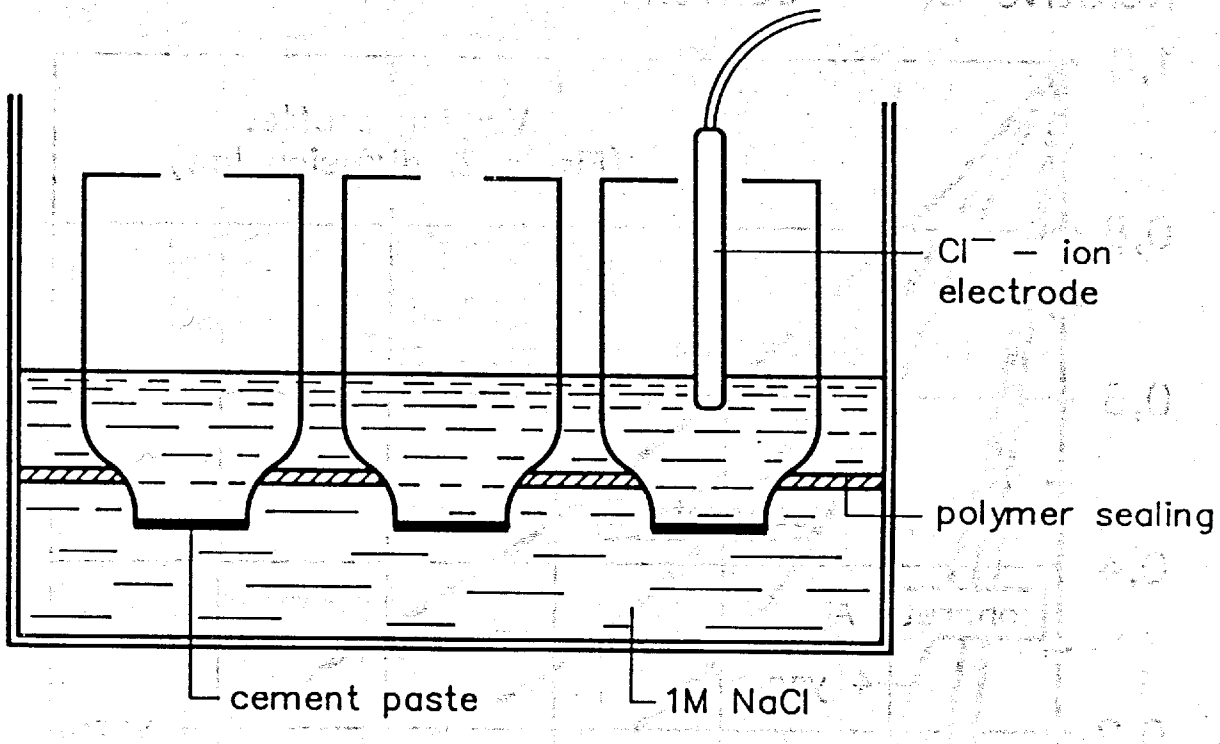

Fig. 1: Test set-up for the determination of chloride diffusion coefficients D_{real} of cement paste specimens (207)

Recent Studies

In various investigations, ingress of chlorides into the hardened concrete is described as a process of pure chloride diffusion. Smolzyk's studies (208) may be taken as an example (see Fig. 2).

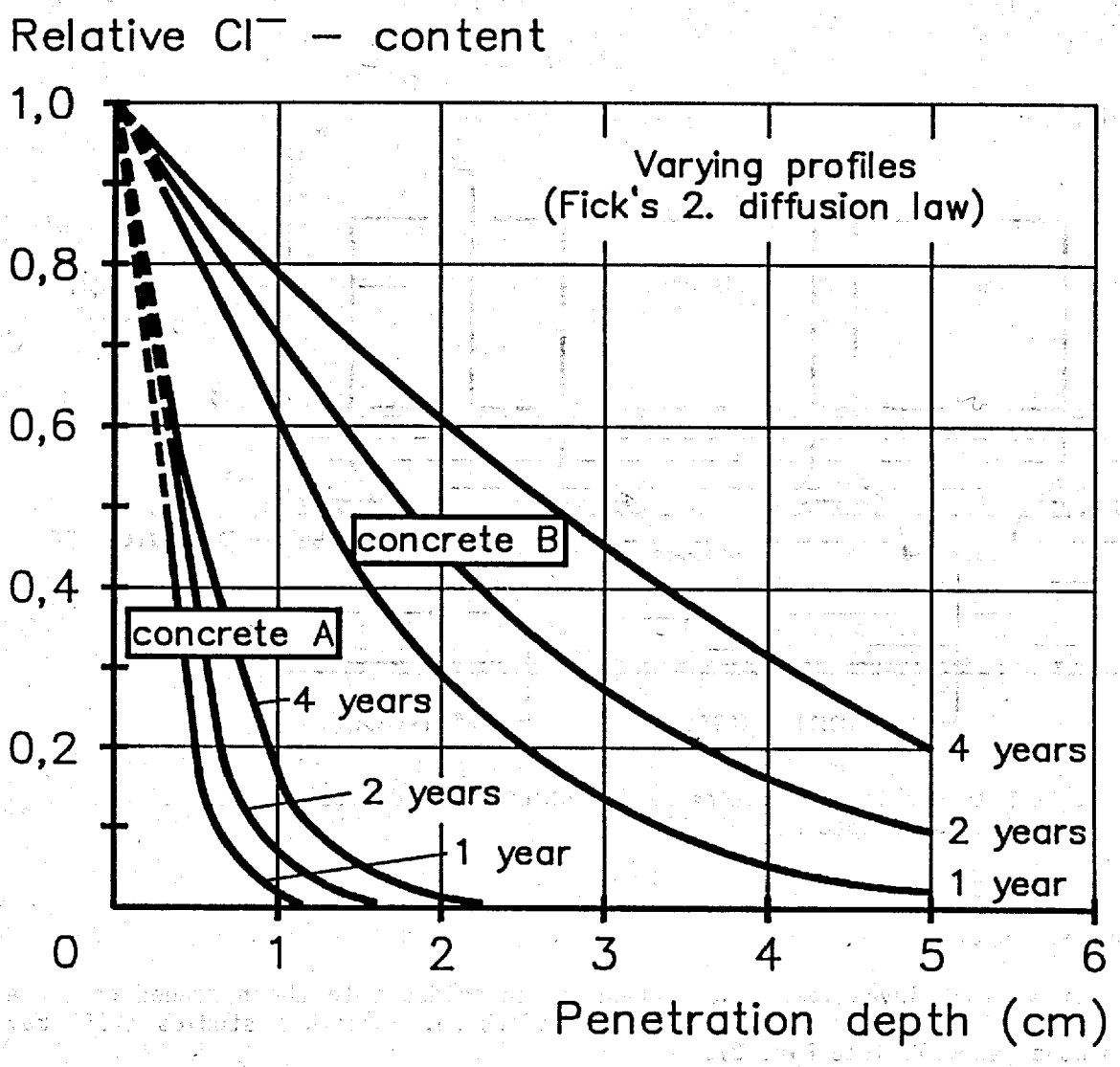

Fig. 2: Chloride profiles calculated using Fick's second law (208)

Taking real practical conditions into account, chloride ingress is virtually always combined with water transport in the form of both capillary suction and evaporation. Lawatsch and Volkwein (209) investigated the ingress of chlorides in combination with water vapour diffusion in and against the direction of water vapour diffusion. The results in Fig. 3 indicate clearly that large quantities of chloride have penetrated into the concrete in the direction of water vapour diffusion, whereas virtually no chloride penetration has occurred in the opposite direction.

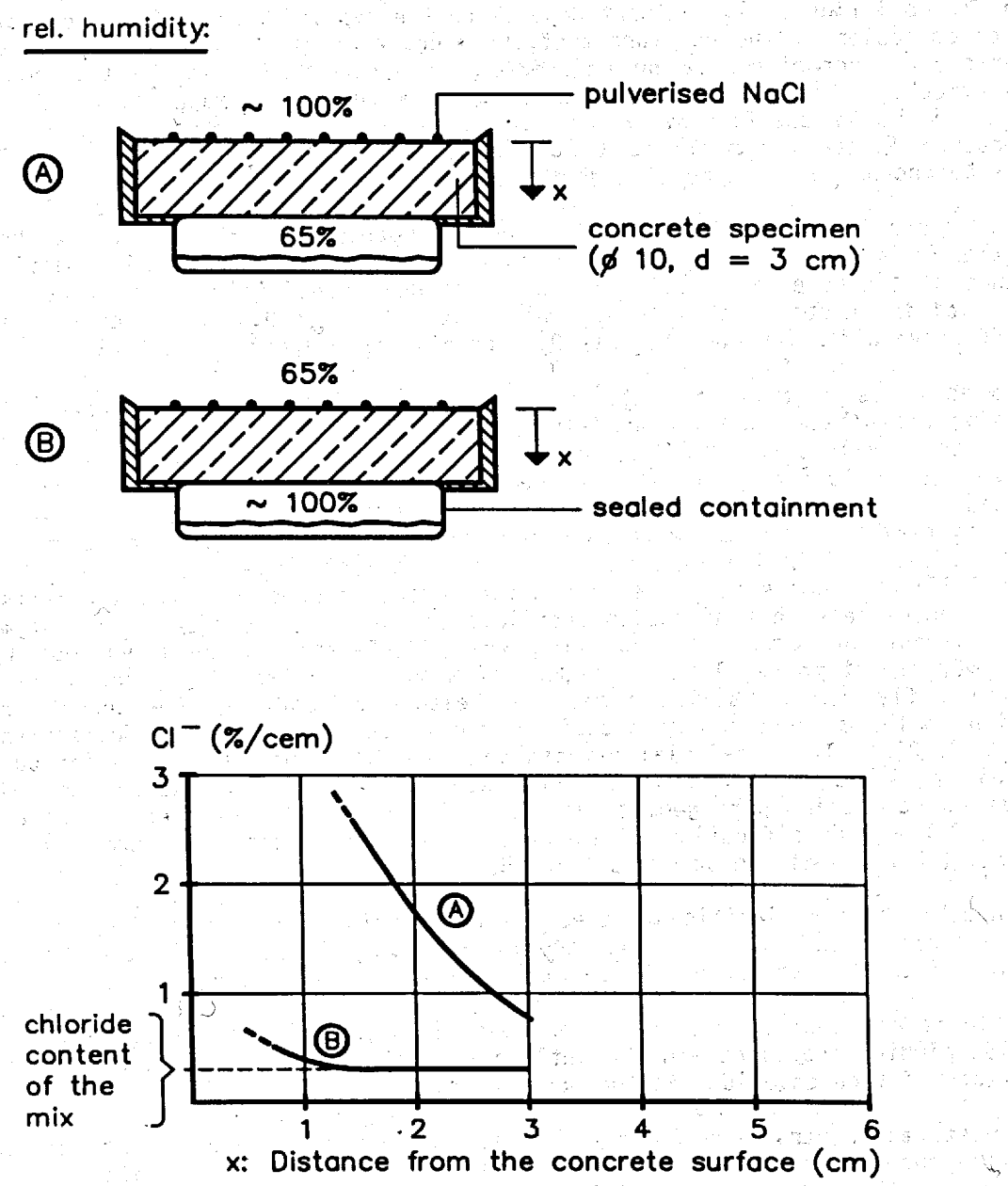

Fig. 3: Influence of water transport on chloride penetration of concrete (209)

A similar effect is well-known in the case of concrete structures where one side of a section is in contact with chloride-containing water and a second side is dry; high chloride concentrations may then accumulate on the dry side, due to evaporation (210, 211).

Chloride content and penetration depth are highly dependent on **microclimatic conditions** at the concrete surface. Chloride content usually reaches its highest values in the splash water zone (210, 212...214). Apart from humidity conditions, the **type of salt** is of importance. Real chloride diffusion coefficients D_{real} are about 50 % higher if $CaCl_2$ as opposed to NaCl solutions are applied (235). The binding capacity of the concrete is, however, higher in the case of $CaCl_2$ as compared to NaCl attack (e.g. 236). These effects exert opposing influences on chloride penetration

depth. Which influence is dominant depends on the type of cement. With respect to the risk of corrosion at the reinforcement, however, account must be taken of the higher percentage of corrosion-relevant chlorides in the pore water with NaCl as compared to $CaCl_2$ attack. Another important influencing parameter is the **temperature.** An increase in the diffusion coefficient of between 50 % and 150 % has been measured for a temperature increase from 15 °C to 30 °C (235) or from 20 °C to 50 °C (237), both values depending on the type of cement and the age of the concrete.

Another important parameter is **concrete composition.** Various researchers have investigated the influence of the **water/cement ratio** on the chloride diffusion resistance of concrete. Frey (216) measured diffusion coefficients for almost all cements used in Europe. With water/cement ratios of 0.4 : 0.6, he observed ratios for the effective diffusion coefficients D_{eff} ranging from about 1 : 2 to 1 : 4.

Much more decisive than the water/cement ratio is the **type of cement.** The lowest diffusion resistances are measured for sulphate-resistant portland cements with low C_3A contents. Values for the D_{eff} diffusion coefficient range from $D_{eff} = 115 \cdot 10^{-9}$ to $D_{eff} = 60 \cdot 10^{-9}$ cm^2/s at a water/cement ratio of w/c = 0.5. Values for ordinary portland cement lay between $D_{eff} = 10 \cdot 10^{-9}$ and $D_{eff} = 2 \cdot 10^{-9}$ cm^2/s. The highest diffusion resistance is encountered with slag cements with a slag content exceeding 65 %. D_{eff} diffusion coefficients of between $D_{eff} = 2 \cdot 10^{-9}$ and $D_{eff} = 0.3 \cdot 10^{-9}$ cm^2/s have been found for concretes made with these cements. These results demonstrate that diffusion coefficients for a single type of cement may differ by almost one order of magnitude, while differences between various types of cement may amount to nearly three orders of magnitude. Like slags, pozzolana such as pulverized fly ash or silica fume, used either as part of the cement or as an addition to the concrete, have a positive influence on chloride diffusion resistance (217, 218, 233). The beneficial effects of these blending agents are not due solely to their positive influence on the concrete pore size distribution. As additional influences, differing pore geometries (219), ion exchange processes at the pore surfaces (220) and densification of the interface layer aggregate matrix by hydration products (221) are all reported as being decisive.

Another highly significant aspect is the **binding capacity** of the concrete. This binding capacity is time-dependent, and is decisively influenced by the type and composition of the binder and by the duration and form of chloride attack.

In recent years, various authors described the time-dependent development of chloride binding processes and the influence of cement type and chloride type on the percentage of free chlorides in the pore water.

Most researchers have found that, with respect to time-dependent chloride binding, the quantity of bound chlorides decreases with time. Most of the chlorides are bound within the first few days (222...224). Fig. 4 details some typical time-dependent chloride binding processes and time-dependent chloride contents in pore water.

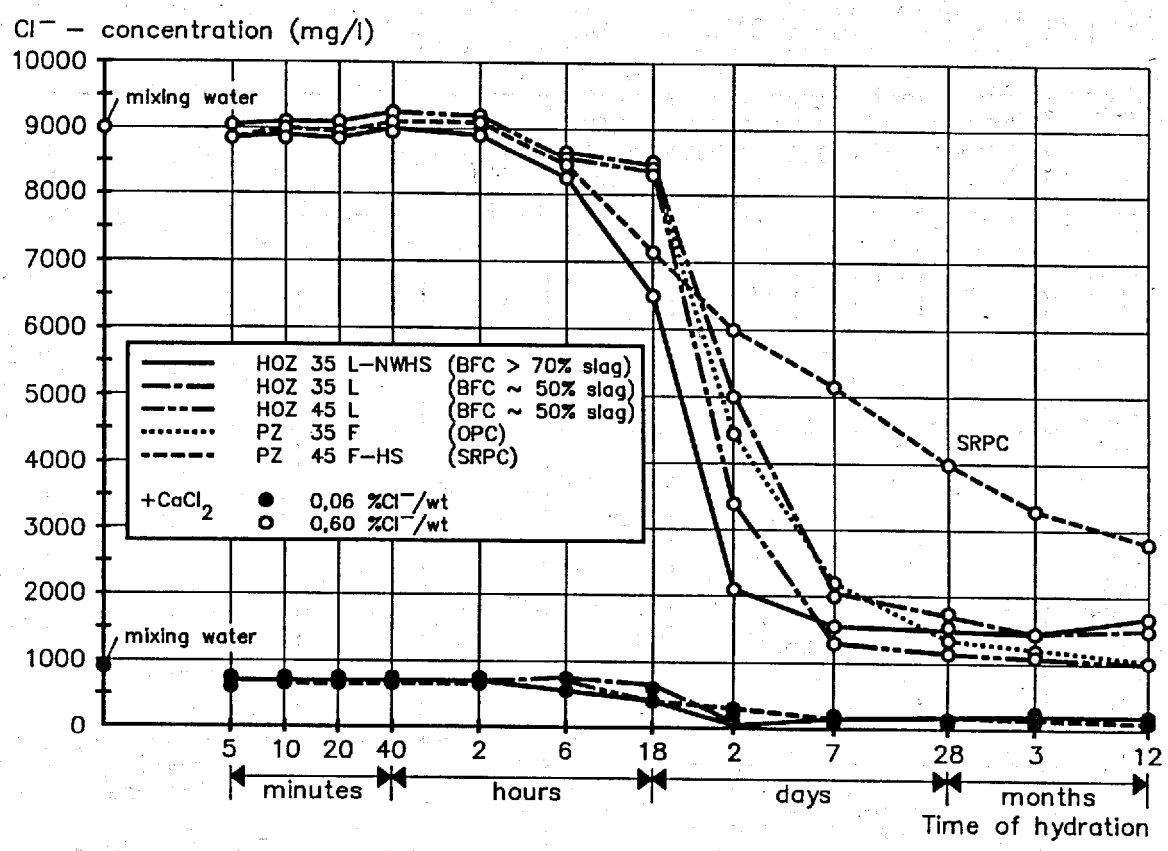

Fig. 4: Time-dependent chloride contents of pore water in cement paste according to (225)

According to (222, 225, 226), far less of the chloride is corrosion-active when chlorides are added to the mix rather than attacking the hardened concrete. The explanation is that chlorides added to the mix are chemically bound within hydration products during the hydration process.

More recent investigations (224) indicate that in the case of $CaCl_2$ attack on hardened concrete, there is virtually no difference in the amount of bound chlorides as compared to chlorides added to the mix. However, there are different findings if NaCl solutions are applied to concrete (see Fig. 5). If the total chloride content is less than 1.4 % in relation to the cement weight, only negligibly more chlorides are bound when added to the mixing water than in the case of chloride attack after 28 days hydration. If chloride content exceeds 1.4 %, many more chlorides can be bound if they penetrate into the hardened concrete rather than being added to the mix. According to (224), this phenomenon may be attributed to the simultaneous diffusion of OH^--ions from the concrete when chlorides penetrate it. This effectively lowers the pH value of the pore water and increases chloride binding capacity.

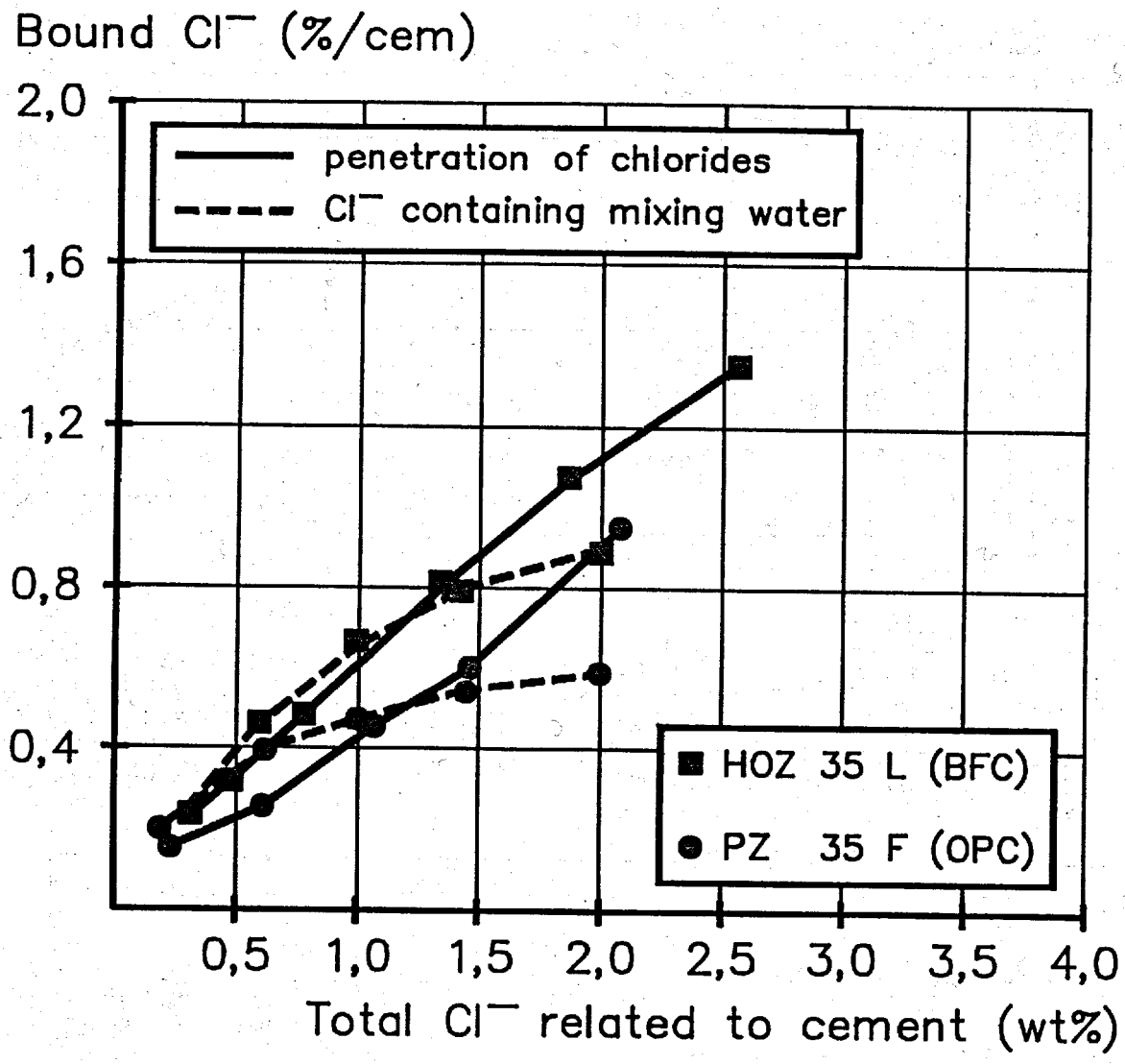

Fig. 5: Influence of chloride source (added to the mix or penetrating the hardened concrete) on chloride binding after 28 days (224)

These tests also show that the amount of bound and free chlorides is of the same order of magnitude both for chlorides added to the mix and those penetrating the hardened concrete.

Investigations reported in (222, 223, 227) have shown that the amount of bound chlorides in relation to total chloride content varies inversely with increasing chloride content. This means that there is a more than proportional increase in the percentage of free chlorides in the pore water as the chloride content of the concrete rises (see Fig. 6).

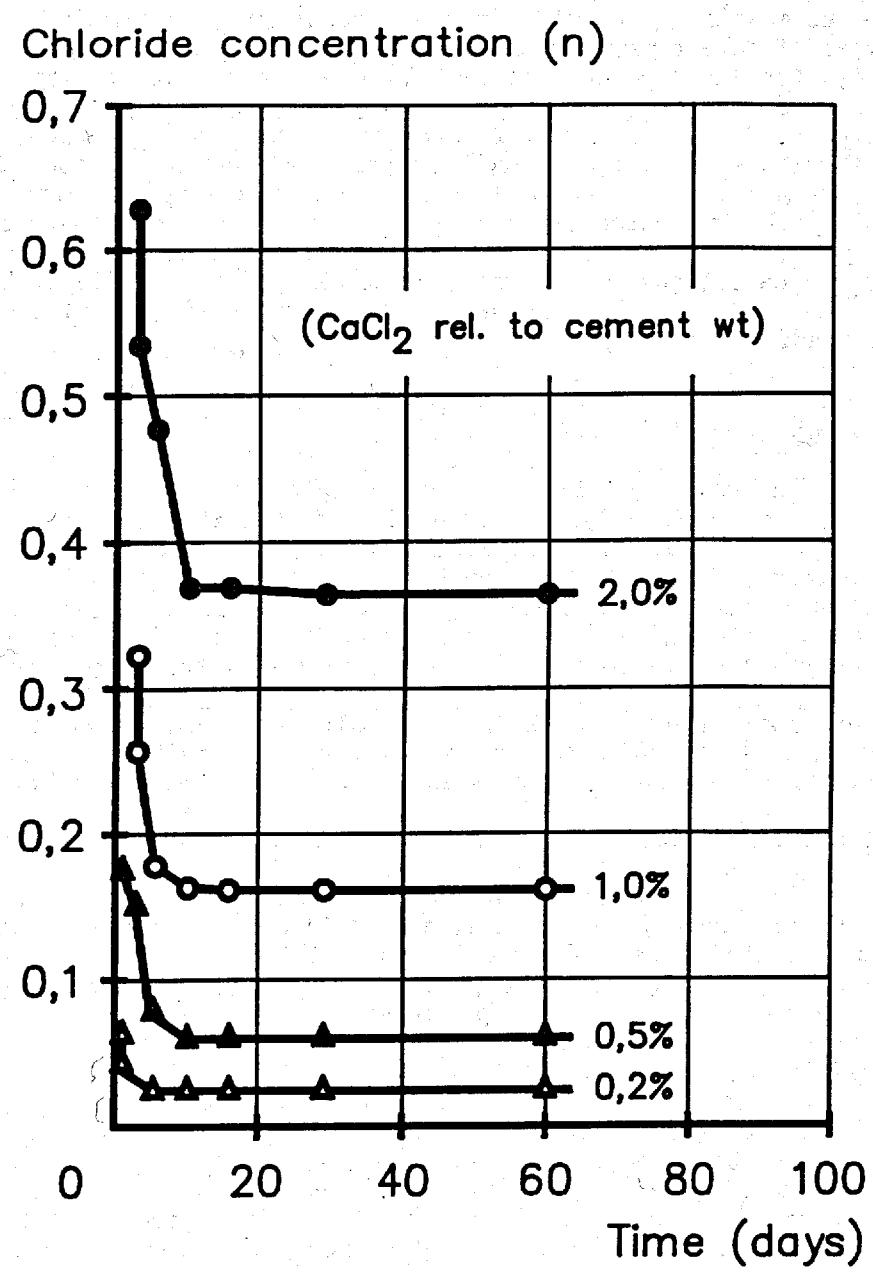

Fig. 6: Chloride concentration of pore water as a function of the amount of chlorides added, according to (227)

Since Friedel's investigations (228), chlorides are known to be bound in the presence of C_3A as so-called Friedel salt:

$$C_3A \cdot CaCl_2 \cdot 10\ H_2O \text{ (Friedel salt).}$$

Various studies with cements containing differing amounts of C_3A, especially with sulphate-resistant portland cements having low C_3A contents, have revealed that the chloride binding capacity of the cement paste increases with rising C_3A content (e.g. 222, 229).

There are contradictory results in the literature concerning the comparative binding capacities of cement pastes made from portland or slag cement and fly-ash cement respectively. Results reported in (222, 231) indicate that portland cement concretes are able to bind more chlorides than slag or fly-ash cement concretes. However, results presented in (229, 230, 224) are controversial. This may be attributed to the different methods of investigation employed. Portland cement concretes exhibit a lower binding capacity in chemical analysis of expressed pore water. With other methods, such as chloride extraction using, for example, ethyl alcohol (231) or measurement of the concentration of a chloride solution brought into contact with pulverized hardened cement paste, portland cement has proved capable of binding more chlorides than other cements. The reasons for these conflicting results have not yet been fully explained.

Results describing the influence of silica fume additions to the concrete are similarly contradictory (230, 231).

No final conclusion can yet be drawn on the influence of the **type of cement** on **chloride binding capacity**. Briefly, it may be stated that the C_3A content of the cement is not the sole parameter influencing the chloride binding capacity of the cement. On the contrary, all hydration products appear to be capable of binding a greater or smaller amount of chlorides by physical or chemical means. Other researchers regard both the pH value of the pore water and the fineness of the cement as important influences on the chloride binding capacity of hardened cement (230).

Both concrete carbonation (e.g. 232) and simultaneous sulphate attack (e.g. 229) reduce the binding capacity of chlorides and may release initially bound chlorides into the pore water, increasing the corrosion-relevant chloride content.

Some test results indicate that the rate of penetration of chlorides into concrete increases with growing **aggregate size** (234). An increase in maximum aggregate size from 8 to 16 mm has been shown to entail a rise in the surface-area chloride content of the concrete by a factor of 2.1, and an increase in maximum aggregate size from 8 to 32 mm to entail a rise in chloride content by a factor of 3. These results are due to the decisive influence which the interface layer between the aggregates and the hardened cement paste has on most transport mechanisms. It is now accepted that transport mechanisms are decisively affected by the structure of the interface layer (e.g. 238). Zimbelmann (239) has developed a model of the interface layer. According to this model, a contact layer some 2 to 3 µm thick is built up at the aggregate surface. This contact layer is composed chiefly of $Ca(OH)_2$ crystals. Between the contact layer and the cement paste is a roughly 20 µm thick intermediate layer formed of needle- and plate-like hydrates of the cements. The decisive influence of the aggregate/cement interface layer means that diffusion coefficients calculated from tests with cement paste specimens are not directly transferable to concrete.

The **curing of concrete** ensures adequate hydration by preventing the concrete from drying out. An increasing degree of hydration leads to a decisive decrease in the chloride diffusion coefficients (235, 240). Resistance to chloride penetration can hence be improved dramatically by good as opposed to bad curing. This effect has been demonstrated in a number of test series. One of such series consisted of exposure tests in the splash water zone close to a motorway in the vicinity of Düsseldorf (241). It is evident from Fig. 7 that more chlorides penetrated more deeply into the concrete on one-day-cured concrete specimens than on a similar specimen cured for seven days.

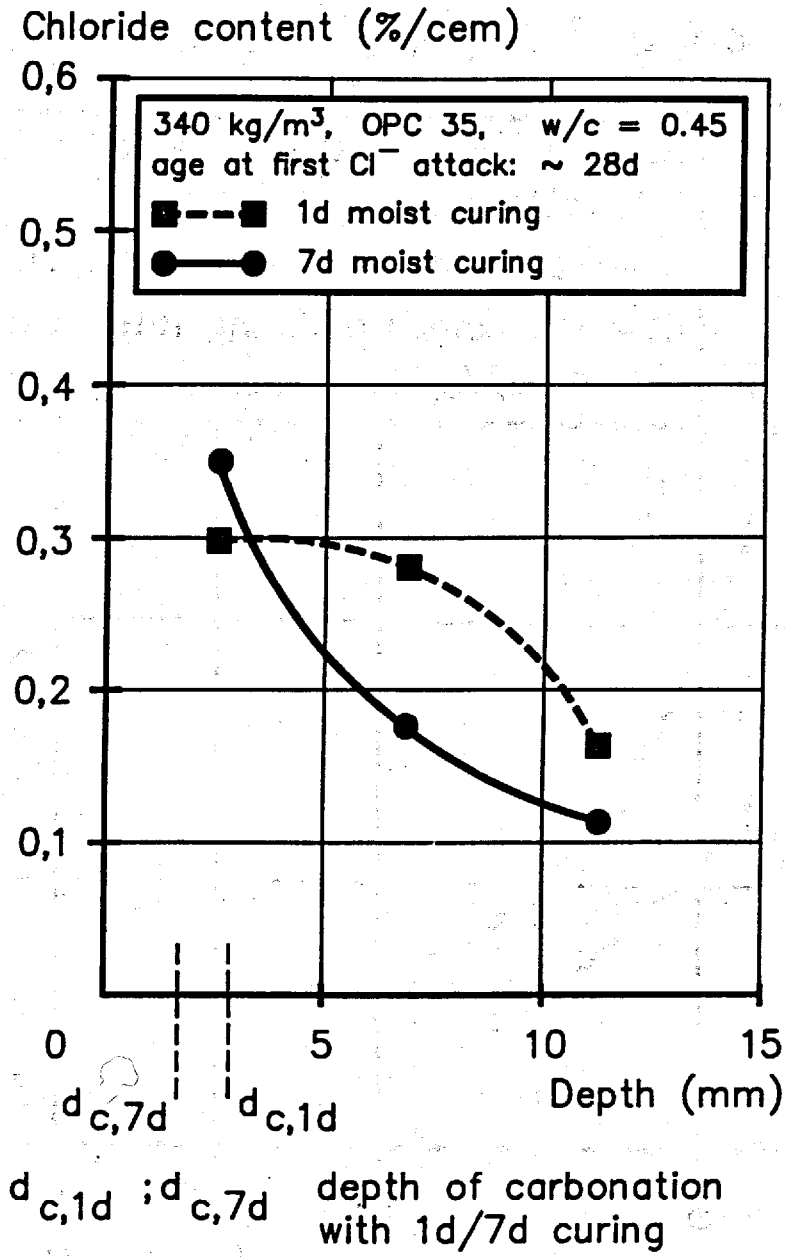

Fig. 7: Influence of duration of curing on the penetration of chlorides according to (241)

Another very important parameter affecting resistance to the penetration of chlorides is the age of the concrete when chloride attack first commences. Fig. 8 shows further chloride profiles measured on concrete specimens from the exposure tests noted above. These specimens have been exposed for one winter period. Results clearly indicate that the chloride contents of specimens exposed in the spring and subjected to chloride attack in the following winter are substantially lower than those of specimens produced and exposed immediately before the winter period. This effect may be attributed to the substantially higher degree of hydration in the case of the specimens produced and exposed in the spring.

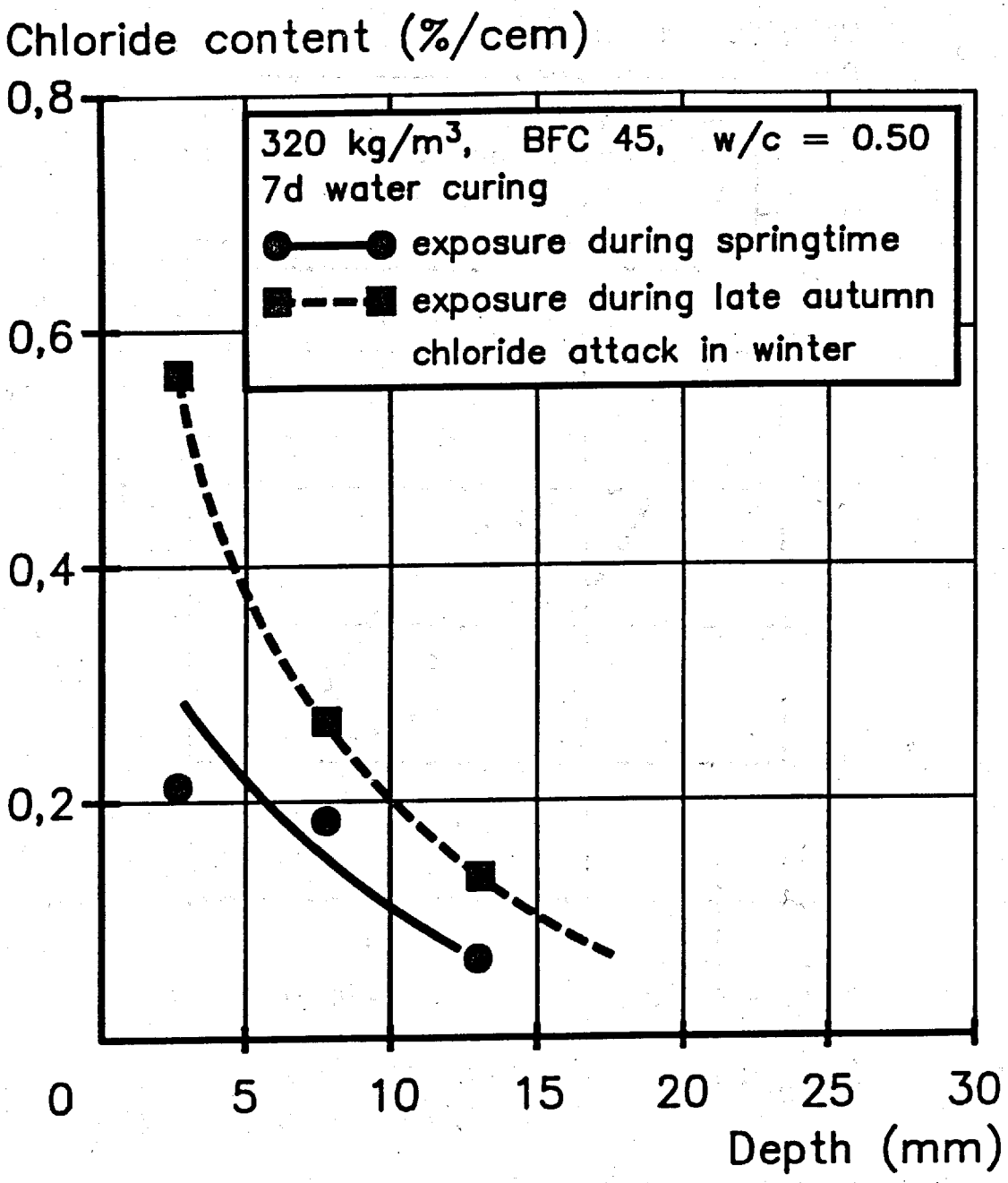

Fig. 8: Influence of concrete age at first chloride attack, according to (241)

The results of this research also indicate that the influence of concrete age when chloride attack first begins completely outweighs the influence of moisture curing duration (between 1 and 7 days).

Summary

The ingress of chlorides into hardened concrete is decisively dependent on and influenced by water transport mechanisms. Substantially greater amounts of chlorides may ingress into the hardened concrete via water transport mechanisms than via pure chloride ion diffusion.

The rate of penetration depends both on the diffusion resistance of the concrete and on its binding capacity. Studies often fail to discriminate between these two influencing factors, which are combined in an effective diffusion coefficient D_{eff}. In assessing research results, it is necessary to take into account whether or not the reported diffusion coefficients include the binding capacity of the concrete.
The composition of the binder is much more decisive for the penetration resistance of concrete than the amount of cement used and the water/cement ratio.

The transport mechanisms for penetration of chlorides into hardened concrete are generally located in the interface layer between aggregates and hardened cement pastes. It is therefore impossible to transfer results for pure cement paste specimens directly to concrete. Hydration processes at older ages have a more or less decisive influence on the pore structure in the region of these interface layers, depending on the type of cement. Resistance to the ingress of chlorides may therefore increase considerably even at older ages on a scale of months or years.

7 CRITICAL CHLORIDE CONTENT

Introduction

In principle two definitions of "critical chloride content" are conceivable:

A) A critical chloride content at which depassivation of the steel surface commences, whether or not this leads to visible corrosion damage at the concrete surface.

B) A critical chloride content which in course of time leads to a corrosion phenomenon classified as damage.

Critical chloride content may be considerably higher according to Definition B) than to Definition A), because corrosion damage occurs only if, in addition to depassivation of the steel surface, other conditions conducive to a correspondingly accelerated rate of corrosion (e.g. oxygen supply, humidity) are fulfilled.

In the literature, the term "critical chloride content" is used to connote the chloride content described by Definition A) (e.g. 242), generally in laboratory tests, while in assessing the durability of existing structures it is also sometimes used to mean the damage-initiating chloride content B) (243). This ambiguity must be borne in mind when reading the literature, to guard against misinterpretation.

It is evident from current knowledge that critical chloride content is not a fixed vale but is dependent both on the quality of the concrete cover and on environmental conditions. Fig. 9 presents this relationship in qualitative terms (244). The much-criticized chloride content of 0.4 % in relation to the cement content was arrived at through research into the chloride binding capacity of concrete (245), and generally is on the safe side. Under certain conditions, much higher chloride contents may be uncritical, as discussed in more detail below.

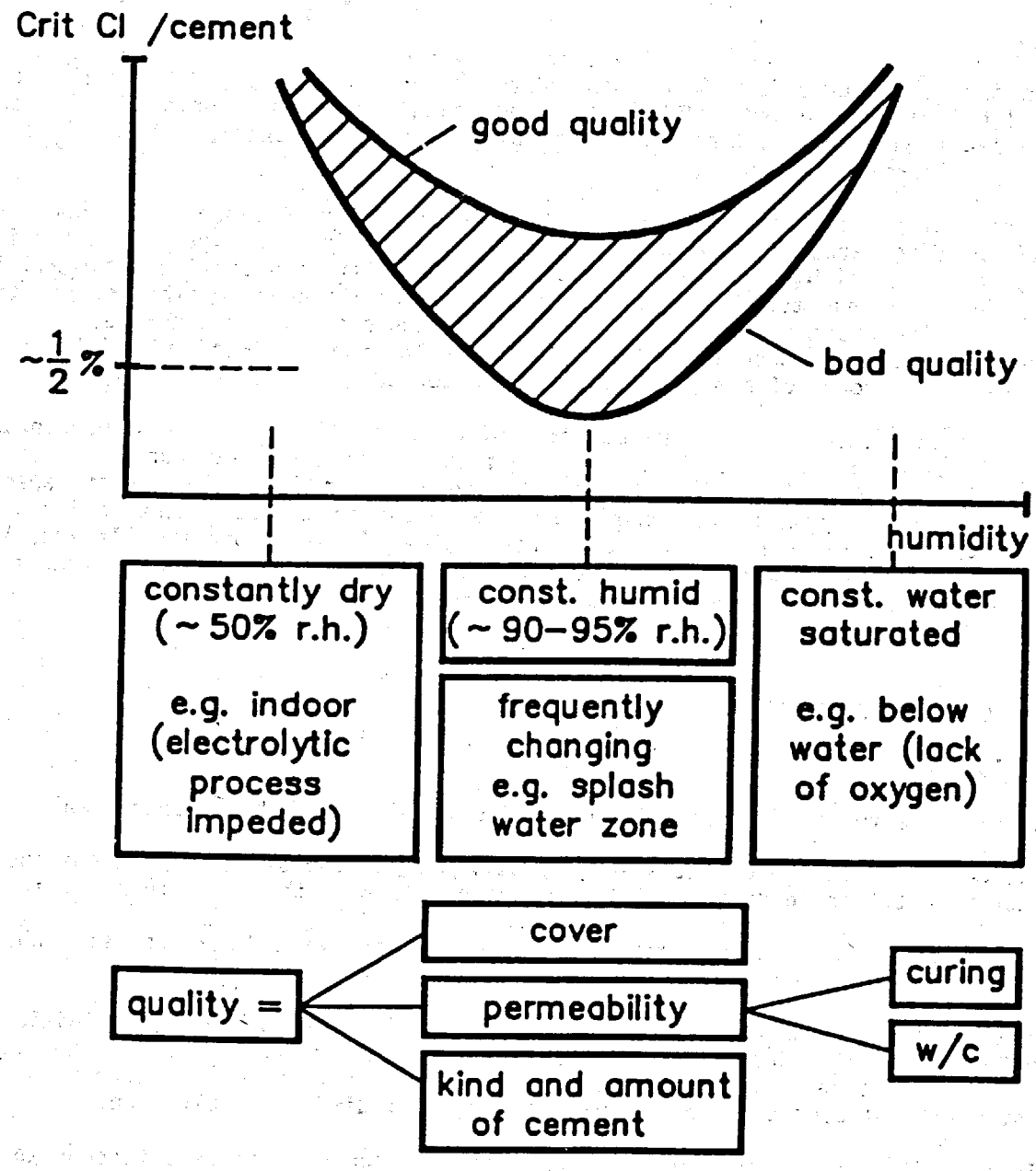

Fig. 9: Influence of concrete cover and environmental conditions on critical chloride content according to (244)

In order to assess the critical chloride content, is not sufficient merely to determine the chloride binding capacity, since all the other ions present in the pore solution, especially the OH^- ions, also affect critical chloride content.

Recent Studies

Owing to the great practical importance of critical chloride content in assessing the durability of reinforced concrete components, there are numerous studies, based on three different test principles:

(A) Electrochemical testing of steel in artificial pore solutions;

(B) Electrochemical tests on mortar-sheathed steels in specific solutions;

(C) Tests on reinforced concrete specimens (without applying an external current).

In method (A), a counter-electrode is used to apply an external current or voltage to steel specimens in aqueous solutions, usually with a high pH value and a defined admixture of chloride, and the resulting voltage or current is measured. The measured voltage-current curves can be used to assess whether the steel is in an active, corrodable state or in a passive state in specific potential ranges.

Studies of this kind have shown that critical chloride content is decisively dependent on the pH value and composition of the solution and on the supply of oxygen to the steel surface (e.g. 246...251). Depending on test conditions, critical chloride contents between 10.6 (248) and 35000 ppm (247) were determined.

Tests according to method (B), with mortar-sheathed steels and external currents or voltages, enable the effects of concrete composition to be taken into account. Critical chloride contents ranging from 0.3 to 1.1 % in relation to cement content have been determined in a series of studies using different concrete compositions and test conditions (e.g. 252...256). An exception is the critical chloride content for steel in high alumina cement, which was some 3.1 % in (252).

A useful practical method (C) is to test reinforced concrete structures without applying an external current or voltage. A fundamental distinction must be drawn between visual assessment of the corrosion state (e.g. 257) and electrochemical tests. Electrochemical test methods may be further sub-divided into potential measuring methods, whose usefulness is confined to determining status (active or passive) without yielding absolute values for the corrosion rate (e.g. 258), and cell current measurements, where, given a suitable test set-up, readings are directly proportional to the corrosion rate (e.g. 259...263).

Chloride contents determined with the aid of this practical method and by assessing existing structures are between 0.4 and 2.2 % (e.g. 262...265). Two exceptions are results in (242) and (266): in (242), steel corrosion was already observable at 0.2 % chloride content. (266) reports that a beam with a 1.5 cm concrete cover and excellent concrete quality exhibited no corrosion phenomena when exposed to chlorides, despite a chloride content of 5 %; this was, however, due to the protective cathodic effect of severe corrosion on a nearby reinforcement.

Summary

The studies show that the critical chloride content, as noted above, is not a fixed value but is dependent both on environmental conditions and on concrete quality.

The influence of the decisive parameters on critical chloride content in reinforced concrete has already been indicated in Fig. 9. More precise conclusions cannot be drawn at present, as individual relationships are extremely complex and no corresponding research results are available. Whereas virtually no corrosion of the reinforcement can take place in permanently dry or permanently water-saturated concrete, the lowest critical chloride contents are found in permanently moist or varying environmental conditions. Given good concrete cover and quality, which can essentially be ensured by a low w/c ratio and good curing of the concrete, the critical chloride content may be much higher than with a poor quality concrete cover.

Critical chloride contents for existing structures can therefore be determined only for specific cases, taking all decisive influencing parameters into account.

8 CORROSION OF STEEL IN CONCRETE

Introduction

Reinforcement corrosion visible with the naked eye is the outward manifestation of the effects of a number of small corrosion cells on the steel surface (e.g. 267).

A corrosion cell is essentially a short-circuited battery consisting of a metallically and electrolytically connected anode and cathode. Unlike the process in a rechargeable battery, the corrosion process is not, however, reversible. The voltage of a corrosion cell is set up through differences in potential on the steel surface. The differences in potential needed for corrosion of the reinforcement may be caused by overlapping local differences in the chemical composition of the concrete, differing aeration conditions, inhomogeneities in the steel surface or uneven coating of the steel surface with corrosion products. In the case of concrete-covered steel, there are always differences in potential.

Cells where the differences in potential result from the combination of different metals are referred to as "contact cells", cells with differing concentrations of certain components in the electrolyte, in this case the pore solution of the concrete, are termed "concentration cells" and cells with differing levels of oxygen admission to the steel surface are known as "aeration cells" (251).

The **corrosion process** takes place in two sub-processes, as outlined in Fig. 10:

- At the **anode**, iron ions go into solution, separating from the electrons. They are converted into rust products in further reactions.
- At the cathode, electrons, water and oxygen are converted into hydroxyl ions.

These hydroxyl ions transport the negative charge in the electrolyte through the electrical field created between the anode and the cathode, in the direction of the anode. Near the anode, they react with the steel ions in solution. Depending on moisture and aeration conditions, this intermediate product may continue to react, producing the final corrosion products.

Individual processes are in fact much more complicated. The RILEM Report (60-CSC) (268) indicates the state of knowledge in this field.

In order for the corrosion process to take place, a number of preconditions for the **anodic and cathodic sub-process** and for the electrolytic process must be satisfied simultaneously.

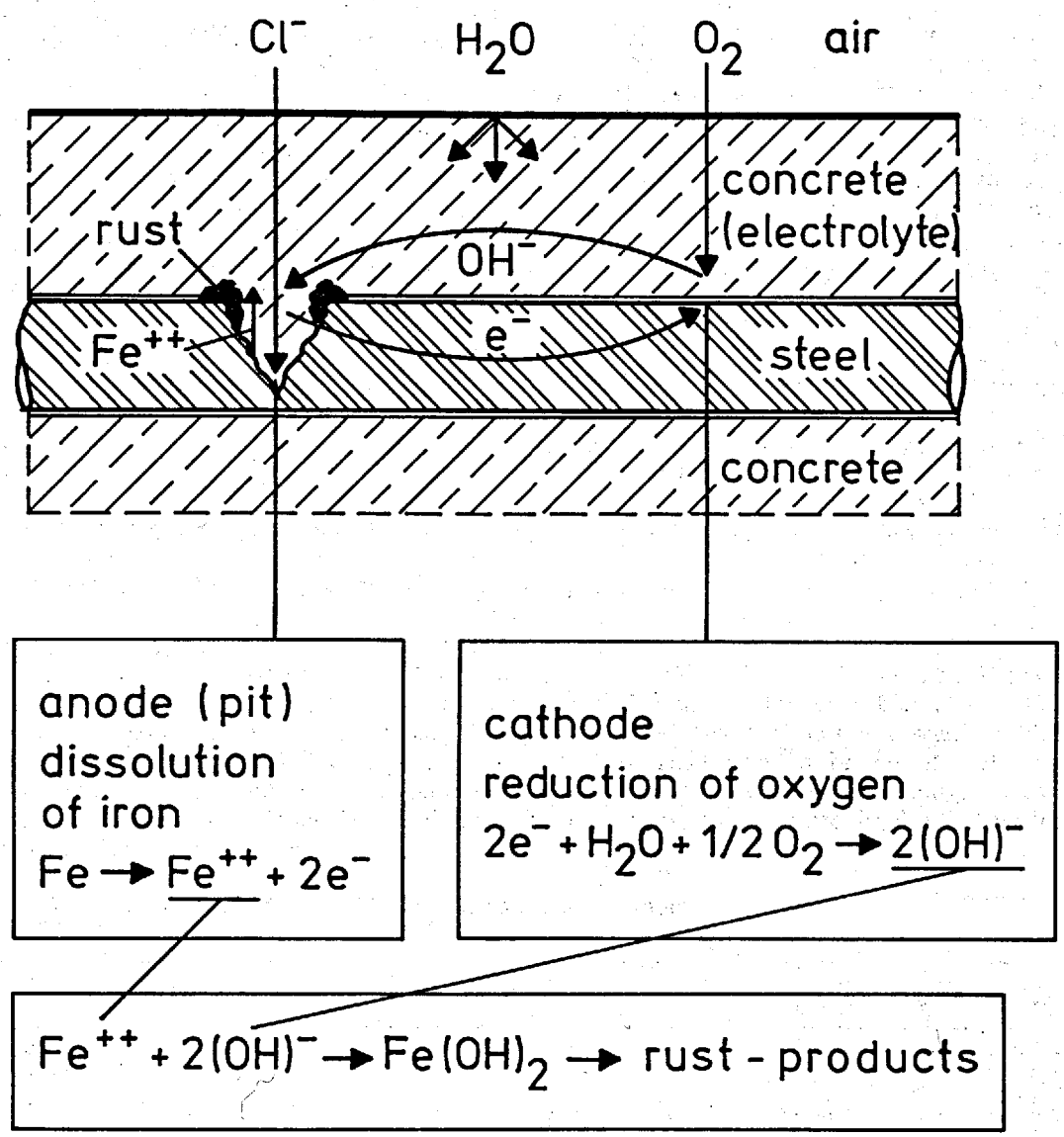

Fig. 10: Diagram showing chloride-induced corrosion of steel in concrete schematically

- As already noted, there must be differences in potential. The preconditions for sufficiently large differences in potential are, however, virtually always met, and in the case of chloride-induced corrosion these may be several 100 mV (e.g. 269...274).

- Anodic and cathodic surface zones of the steel must be electrically and electrolytically connected, i.e. a flow of electrons and ions between them must be possible (e.g. 274).

The metallic connection necessary for an electron flow from the anode to the cathode is provided by the reinforcement system in the reinforced concrete. The electrolytic connection is represented by the concrete. This must, however, be sufficiently moist, since otherwise there can be virtually no migration of ions. In dry interior spaces, for example, the electrolytic conductivity of the concrete is too low to permit corrosion of the reinforcement, even if the carbonation front reaches the reinforcement, leading to loss of alkaline protection.

- Anodic solution of ion must be possible due to depassivation of the steel surface. The cathodic sub-process can, however, take place even in zones with a passive steel surface.

- Sufficient oxygen must be available at the cathode. There must be continuous diffusion of oxygen from the surface of the concrete to the steel surface acting as the cathode. There is therefore practically no risk of corrosion to reinforced steel components which are permanently immersed in deep water.

If all conditions for corrosion are fulfilled simultaneously, the reinforcement will corrode. If only one of the conditions can be eliminated, corrosion can be prevented or brought to a stop. Fundamental repair principles may be inferred from this knowledge (275).

Corrosion phenomena may be externally sub-divided into uniform corrosion and local pitting. Pitting may be understood as a form of corrosion in which crater-shaped hollows undermining the surface or appearing in the form of needles occur without any removal outside the pitting locations points themselves.

Uniform corrosion is generally caused by carbonation of the concrete over a wide area (276) or uniformly very high chloride contents in the vicinity of the steel. This leads to the formation of so-called microcells, consisting of pairs of immediately adjacent anodes and cathodes. These are microscopic in size, so that externally they appear to produce uniform removal of the steel.

Pitting generally results from chloride-induced corrosion. In this case, so-called macrocells are formed, with the pits acting as the anodes and the neighbouring sections of the reinforcement as cathodes. Anodes and cathodes are not necessarily adjacent; they may well be situated at a considerable distance from one another. (271) reports a macrocorrosion cell on a supporting wall in which anodes and cathodes were several metres apart.

The removal rates in macrocells are generally much greater than in microcell corrosion, as the anodes of macrocells are usually very small in relation to the cathodes, leading to high current densities and hence high corrosion rates. The potential size of a macrocorrosion cell is determined largely by the electrolytic conductivity of the concrete, i.e. by its water content, and by the permeability and chemical composition of the pore solution in the concrete. In dry or extremely dense concretes, macrocorrosion cells remain localized. Macrocells may, however, also occur where there is carbonation of the concrete over a wide area, with uneven moisture distribution or aeration, or in zones with localized depassivation, e.g. in cracks or gravel pockets. Here again, corrosion rates higher than those encountered with uniform corrosion of the reinforcement may be expected.

Recent Studies

Owing to the variety of corrosion mechanisms concerned, the following section will first deal with corrosion caused by carbonation of the concrete, then passing to a consideration of chloride-induced corrosion of the steel in the concrete.

Very few studies of the **corrosion rate of steel in carbonated concrete** have been published in the literature. Research on old concrete structures indicates, however, that the corrosion rate in normally moist concrete which has been carbonated throughout will be lower than in unprotected steel specimens with generalized corrosion removal (277).

(246) includes a presentation of research into the dependence of the corrosion rate in carbonation-induced corrosion on atmospheric humidity at the concrete surface. Steel rods with a length of roughly 16 mm and a diameter of 10 mm were sheathed in an approximately 3.5 mm thick layer of mortar and wetted with 1 Vol.-% CO_2, so that the specimens were carbonated throughout after a period of about 2 months. After a 2-year test period, the weight losses of the steel were measured and the mean corrosion rates calculated. Results may be summarized as follows:

- Corrosion rates decrease over time.
- There was no significant corrosion at below 80 % relative atmospheric humidity.
- Maximum corrosion rates occurred at a relative atmospheric humidity of 95 %.
- The maximum corrosion rate was approximately 60 µm per year, with much lower mean corrosion rates.

In (278) it was also noted that corrosion due to carbonation is strongly dependent on the **distribution of water content** in the concrete. It is inferred from results of water content measurements that only low corrosion rates occur from a concrete cover of 15 mm upwards on structures exposed to weathering. In (279), however, larger corrosion rates were measured with a concrete cover of 20 mm exposed to water than with a concrete cover of 10 mm. Further research is necessary in order to clarify this problem.

Only a few results are available on the **influence of concrete composition** on the corrosion rate of steel in carbonated concrete. In (280), it was observed that removal by corrosion following identical storage was greater in the case of blast-furnace cement concretes than for fly-ash-containing concretes or portland cement concretes. On the other hand, no significant influence of curing or the w/c ratio was detected.

(276) similarly describes research into the corrosion behaviour of reinforcement in carbonated concrete. Polarization resistance measurements on reinforced mortar specimens carbonated rapidly in a chamber with raised CO_2 content showed that the corrosion rate is strongly dependent on ambient humidity, but only negligibly dependent on cement type (see Fig. 11). Additional tests are again necessary to elucidate the problem. Although corrosion due to carbonation of the concrete generally takes place more slowly than chloride-induced carbonation, the current state of, for example, balconies or facade elements with concrete covering layers of inadequate quality demonstrates that the corrosion of reinforcement due to carbonation of the concrete may well lead to substantial damage.

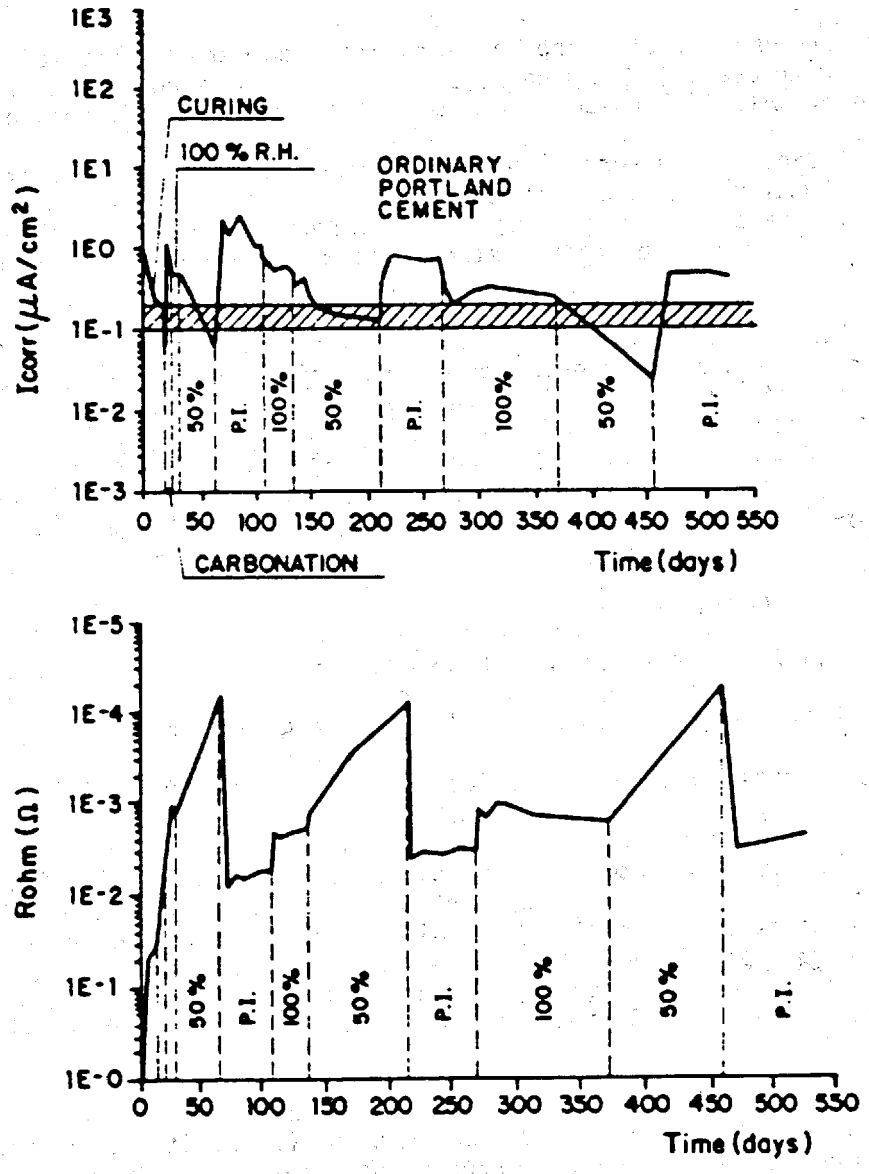

Fig. 11: Evolution of I_{corr} and ohmic resistance with time for steel bars embedded in carbonated mortar held at different ambient relative humidities according to (276)

There are many more publications relating to **chloride-induced corrosion** of the reinforcement than to carbonation-induced corrosion. The following section will first describe research into the influence of **concrete composition** and then studies of the influence of **environmental conditions** on the rate of chloride-induced corrosion.

As expected, the **chloride content** in the concrete at the steel surface has a decisive influence on the corrosion rate. If the chloride content rises above a critical, corrosion-initiating value, there will be a roughly linear increase in the corrosion rate with the chloride content (242, 262, 281). An increase in chloride content from 1 to 2 % in relation to cement content led to approximate tripling of the corrosion rate in (262) (see Fig. 12).

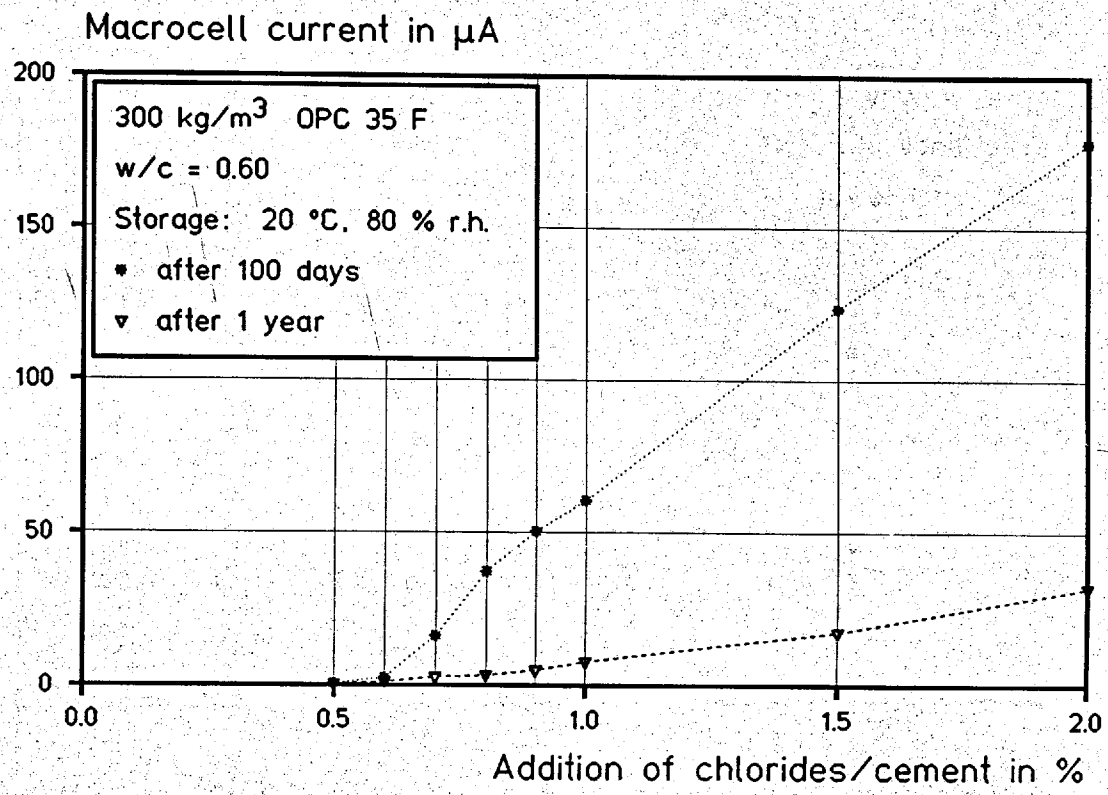

Fig. 12: Influence of the chloride content of the concrete on the corrosion rate of concrete corrosion cells according to (262)

The influence of the **salt type** was studied in (282). It was found that the corrosion rates for addition of NaCl or $CaCl_2$ with identical chloride content of the concrete, i.e. differing amounts of salt, were roughly the same. Where chloride is added to concrete, the type of cation (Na, Ca) is hence of only subsidiary importance. Since, however, according to (235), the type of cation influences the penetration of chlorides into the concrete, it is not clear at present whether the influence of salt type in cases where chlorides penetrate into the concrete from the surface is also negligible.

Research into the influence on the corrosion behaviour of the steel using polarization resistance measurements revealed that the corrosion rate is lower for a **blast-furnace cement** than for a portland cement with identical concrete composition (283, 284). Cell current measurements on concrete corrosion cells confirmed this result; at an addition of 2 % chloride in relation to cement content, the corrosion rate decreased substantially with increasing blast-furnace slag content (262). One reason for this influence is the significant rise in the eletrolytic resistance of the concrete, also measured in (262) (see Fig. 13).

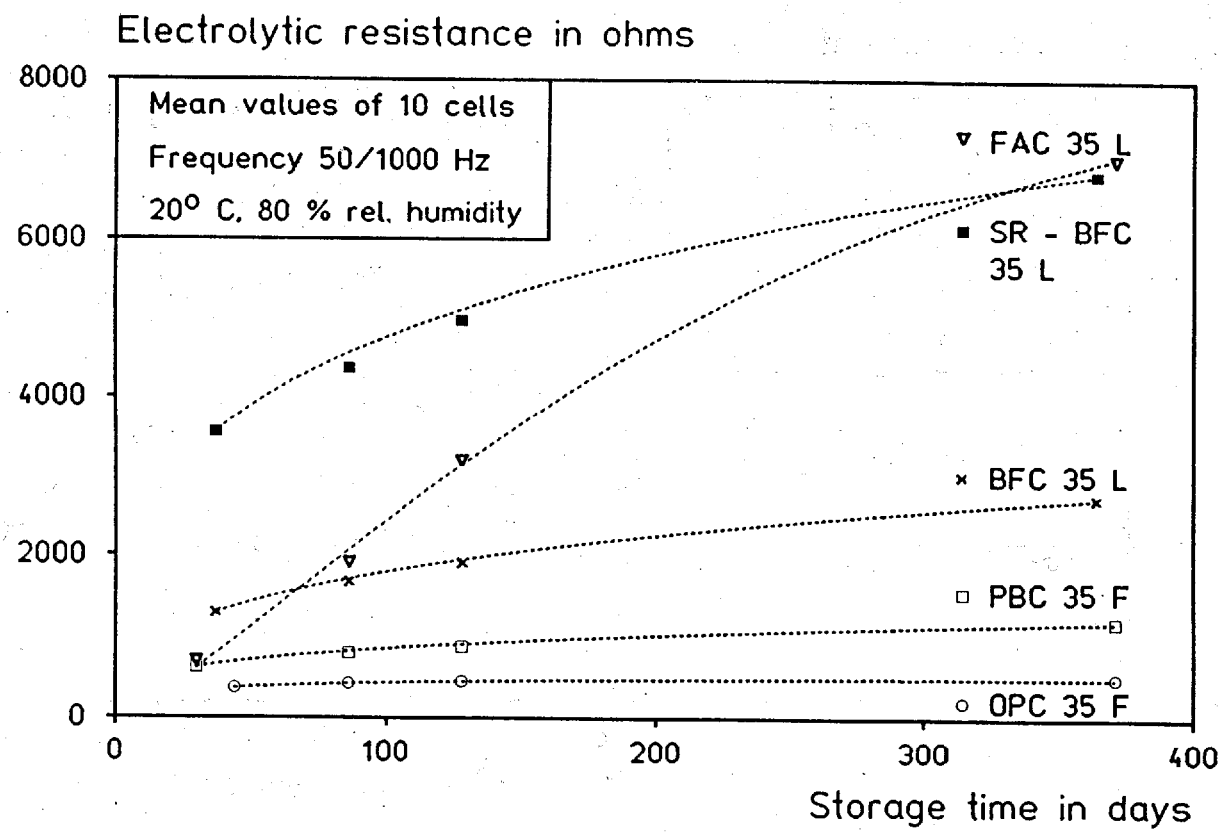

Fig. 13: Influence of blast-furnace slag and fly-ash on the electrolytic resistance of the concrete of corrosion cells according to (291)

Measurement of polarization resistances on electrodes sheathed in hardened cement revealed that the corrosion rate with a **fly-ash cement** was also lower than that with a portland cement from the same clinker (284).

The same result was found for concrete specimens in (262). Owing to the slow pozzolanic reaction, when a fly-ash cement with 26 % fly ash was employed, electrolytic resistance increased over the course of one year to roughly the same level as for a rich blast-furnace cement with 74 % blast-furnace-slag (see Fig. 13). Apart from electrolytic resistance, however, the anodic polarization resistance probably also played a decisive part, while cathodic polarization resistance is influenced only slightly by concrete composition (285). Further research is necessary into the influence of concrete composition on the anodic reaction rate (chloride supply to the pits, removal of corrosion products, etc.).

The use of **silica fume** as a concrete agent generally reduces the permeability of the pore structure, especially if accompanied by the usual addition of plasticizing agents (e.g. 286). Sample tests carried out in (287) on steels embedded in hardened cement paste with various silica fume contents showed that the corrosion rate rises with increasing silica fume content. However, tests with concrete corrosion cells described in (262) revealed exactly the opposite relationship. In this case, despite addition of 2 % to the concrete in relation to cement content, the corrosion rate was shown to fall so rapidly over a period a few months following laying of the concrete, that only negligibly low removal rates were measured for a silica fume addition of

20 %. In comparison with portland cement concrete without added silica fume, the electrolytic resistance of the concrete rose by a factor of 40. With extremely high silica fume contents, high corrosion probabilities are therefore impossible, due alone to the low electrical conductivity of the concrete. Corrosion behaviour is, however, substantially improved even with smaller silica fume contents (288).

Apart from the influencing parameters already discussed above, the **C_3A content** of the cement plays a decisive role. As already noted, chloride binding capacity is significantly influenced by C_3A content. The C_3A content does not, however, influence the electrolytic resistance of the concrete to such a decisive extent as the use of blast-furnace cement, fly ash or silica fume (289, 290). As is to be expected from the discussion of chlordie binding capacity, the corrosion rate of the steel decreases substantially with increasing C_3A content of the cement (258, 284, 291). Under simultaneous chloride and sulphate attack, the use of, for example, blast-furnace cement rich in blast-furnace slag is therefore to be preferred to the use of low C_3A cement.

Chloride-induced corrosion is also influenced by the water/cement ratio, the aggregate, concrete cover and curing. Exposure tests (257) and cell current measurements (292) have shown that the corrosion rate falls with a decreasing **water/cement ratio**, a phenomenon which may be attributed to the known reduction in the permeability of the concrete.

As part of investigations into the influence of cement type, (285) set up two corrosion cells with the same water/cement ratio of 0.5 and different aggregate particle-size distribution curves. In order to ensure roughly identical consistencies, a water content of 150 kg/m^3 at 32 mm and 180 kg/m^3 at 16 mm maximum particle size was selected.

A comparison of the cell currents revealed that, irrespective of the type of cement, higher corrosion rates were in each case measured for the corrosion cells with a maximum aggregate particle size of 32 mm, although this had a lower hardened cement paste content. This result may possibly be attributable to interface effects between the aggregate particles (see chapter 7), which permit rapid material transport along the phase boundary between the aggregate and the hardened cement paste at large granulometries. Further research is necessary in order to achieve final clarification of these effects.

During the aging tests described in (257), it was observed that corrosion through chloride penetration decreased significantly with increasing **concrete cover**. This may be due partly to the clear reduction in chloride content with chloride penetration from the surface which is empirically known to occur as the concrete cover increases. Where chloride is added to the mixing water, i.e. with uniformly distributed chloride content, it was, however, also noted that the corrosion rate falls significantly with increasing concrete cover (285). The causes of this behaviour have not yet been established. Anode aeration may play a decisive role.

No research results describing the influence of **curing** on the rate of chloride-induced corrosion are currently available. Since, however, the permeability of concrete in the surface zone is generally known to decrease with increasing curing age, it may be assumed that well-cured concretes will perform better than poorly-cured concretes when subjected to chloride-induced reinforcement corrosion.

In addition to concrete cover and the properties of the concrete, the durability of reinforced concrete structures is also substantially influenced by microclimatic conditions, i.e. temperature and humidity.

The considerable influence of **temperature** on the corrosion rate of the reinforcement is, for example, apparent from the fact that corrosion damage due to corrosion of the reinforcement occurs much sooner in hotter regions than in zones with a temperate climate (e.g. 293, 294). According to (281, 295), the corrosion reaction rate basically increases with rising temperature, the influence of temperature being governed by the Arrhenius equation, i.e. by an exponential relationship between the corrosion rate and the temperature:

$$I_e = \frac{I_o}{e^{a(1/T-1/T_o)}}$$

where

I_e corrosion rate (cell current) at temperature T
I_o corrosion rate at temperature T_o
T, T_o absolute temperatures in K
a constant in K

If the corrosion rate (cell currents) is known under otherwise identical conditions but at least two different temperatures, the **a** constant can be calculated. This equation is, however, valid provided that the same sub-step in the corrosion process determines the corrosion rate throughout the temperature range under consideration. If this condition is not satisfied, the relationship between the temperature and the corrosion rate cannot be described by a single constant, but requires the superimposition of a number of constants.

As already noted in publication (282), an increase in the storage temperature of the corrosion cells from 15 to 20 °C resulted in an average 1.5-fold rise in the cell currents of eight specimens at an age of 75 d, if the values for corrosion cells with 0.5 and 0.6 % chloride addition/cement content are left out of account due to their low corrosion rates. The average water content of the concrete in these corrosion cells was still relatively high, as drying occurred solely via the top surface of the concrete. The **a** constants for these conditions were determined as 6955 K, indicating an approximate doubling of the corrosion rate for a temperature rise of 10 °C.

Sample tests were also performed on macrocells, using a piece of reinforcing steel as the anode and a platinum-coated titanium rod as the cathode, with a concrete cover of 12 mm (296). The temperature was increased in stages from 20 to 60 °C, and the influence of temperature determined, the **a** constants exhibiting differing values as a function of storage humidity, as shown in Fig. 14.

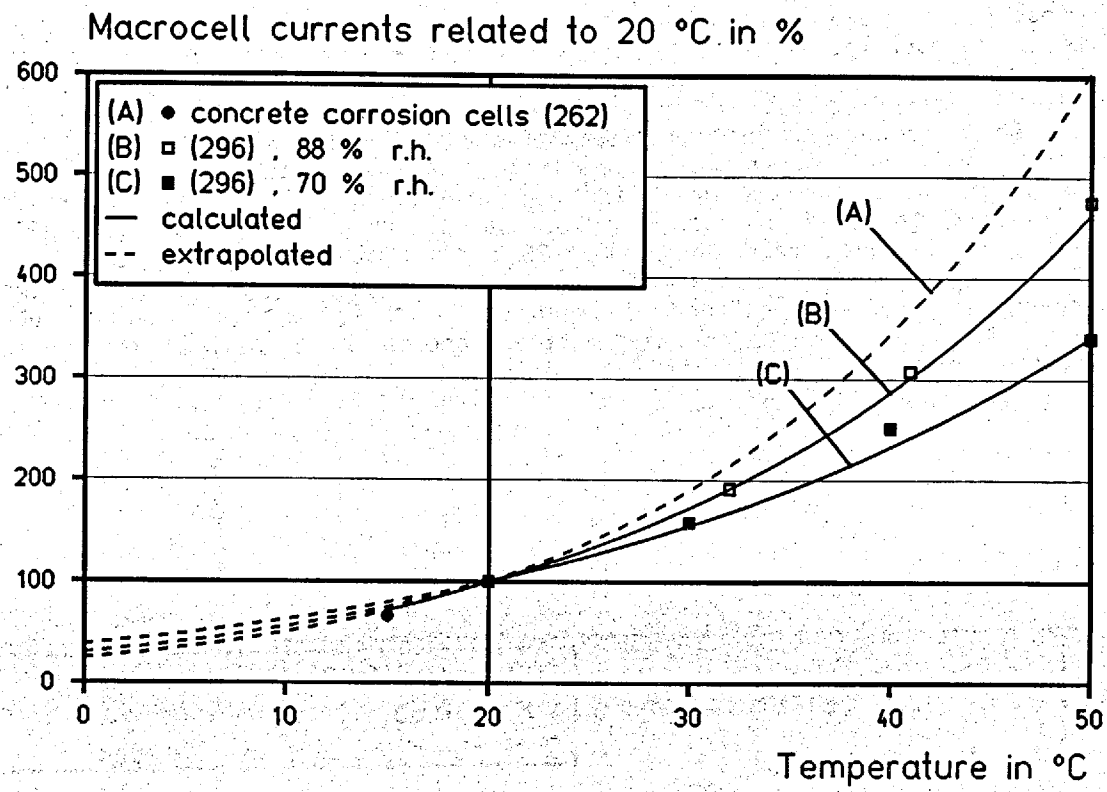

Fig. 14: Influence of temperature on the corrosion rate measured as macrocell current at concrete corrosions cells according to (285)

Since the **a** constants are a direct measure of the temperature-dependence of the corrosion rate, the temperature influence appears to decrease with falling humidity, though this needs to be established conclusively in further studies.

Fundamentally, the influence of temperature should not be assessed without taking into account the water content of the concrete. Leaving aside the case of permanent water saturation of the concrete, a temperature rise invariably leads to drying out of the concrete, as demonstrated in (297) on the basis of sorption isotherms at different temperatures. This drying leads in turn to a reduction in the electrolytic conductivity of the concrete and hence to decreasing corrosion rates.

Unfavourable environmental conditions consequently prevail at high temperatures and simultaneously high water content of the concrete. Depending on humidity conditions, the influence of temperature on the corrosion rate according to the Arrhenius equation may be estimated as approximately 4000 to 7000 K.

As expected, studies of the influence of **humidity** on the corrosion rate revealed that, like carbonation-induced corrosion, chloride-induced corrosion increases substantially with rising humidity (e.g. 262). However, water saturation of the concrete at the steel surfaces results in an oxygen deficit, restricting corrosion rates to negligibly low values where concrete is submerged for long periods (234, 246, 298...305). Once the residual oxygen in the concrete has been used up, these corrosion rates are determined solely by the oxygen diffusion resistance of the concrete cover and the oxygen supply in the water at the concrete surface.

In (285), cathodic potentiostatic tests were conducted on reinforced steel specimens, using different concretes and concrete covers and at varying atmospheric

humidities. Tests showed that the cathodic reaction rate was almost exactly as high at extreme atmospheric humidities approaching the saturation point as at 65 % relative humidity. An oxygen deficit, expressed in a reduced cathodic oxygen reduction rate, was observed only after several weeks of **immersion** of the specimens (see Fig. 15). The time between initial immersion and the appearance of an oxygen deficit depends on the concrete cover, concrete quality and intensity of corrosion, since the concrete at the steel surface must first be water-saturated throughout, and the residual oxygen at the steel surface must then be used up. For concretes generally used in practice and concrete covers exceeding 25 mm, a period of several weeks is necessary (285). This means that an important influence of oxygen diffusion via the concrete cover is virtually confined to exceptional cases, e.g. permanently submerged structures. As a rule, the corrosion rate therefore increases with rising atmospheric humidity or wetting of the concrete.

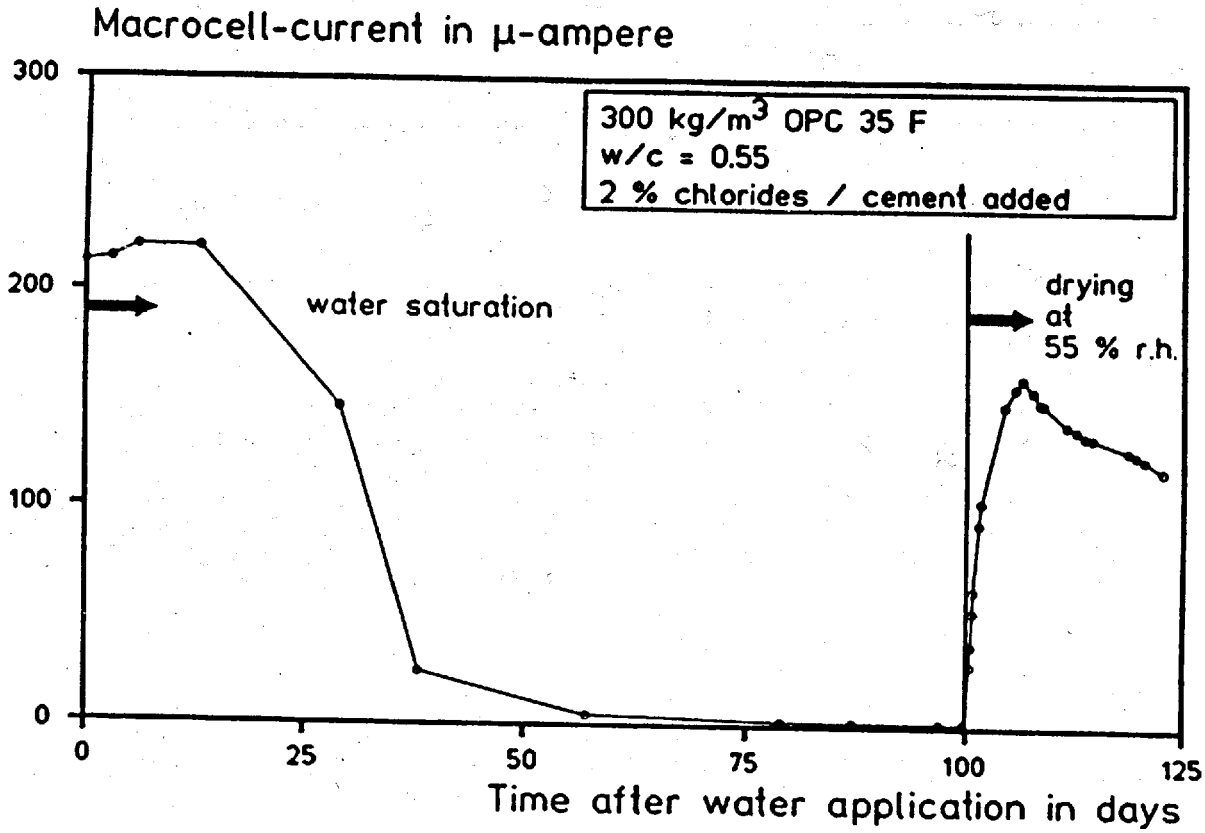

Fig. 15: Influence of the water content of the concrete on the corrosion rate of concrete corrosion cells according to (262)

Recent reports on the **corrosion of reinforcement in crack zones** are already available (234, 306). Attention here will therefore be confined to the essential interrelationships.

Whereas in uncracked concrete a good quality concrete covering layer will generally prevent depassivation of the reinforcement, prevention is practically impossible in crack zones, since both the carbonation front and the chlorides penetrate much more rapidly into the crack zone than elsewhere (303, 306, 307). The capillary suction capacity of the cracks plays an important role in the penetration of chlorides.

The corrosion mechanism in the crack zone is of decisive significance for the corrosion rate of the reinforcement. Generally different fundamental mechanisms for corrosion phenomena in crack zones are conceivable. In (305, 308...313), cell current and voltage measurements on cracked reinforced steel beams exposed to chloride attack clearly demonstrated that large macrocells are formed under certain conditions. The reinforcement in the crack zone acts as an anode, the reinforcement between the cracks up to a distance of several decimetres as a cathode, often leading to extremely high measured corrosion rates in the crack zone.

Although the corrosion rate increased with increasing crack width, global steel removal rates were in fact considerably more dependent on concrete cover and composition than on crack width. Fig. 16 illustrates this relationship. It shows the losses in mass determined by cell current measurements on, cracked reinforced concrete beams at various crack widths, water/cement ratios and concrete covers according to (313) exposed to chlorides in defined intervals. The influence of concrete cover is also confirmed in (314).

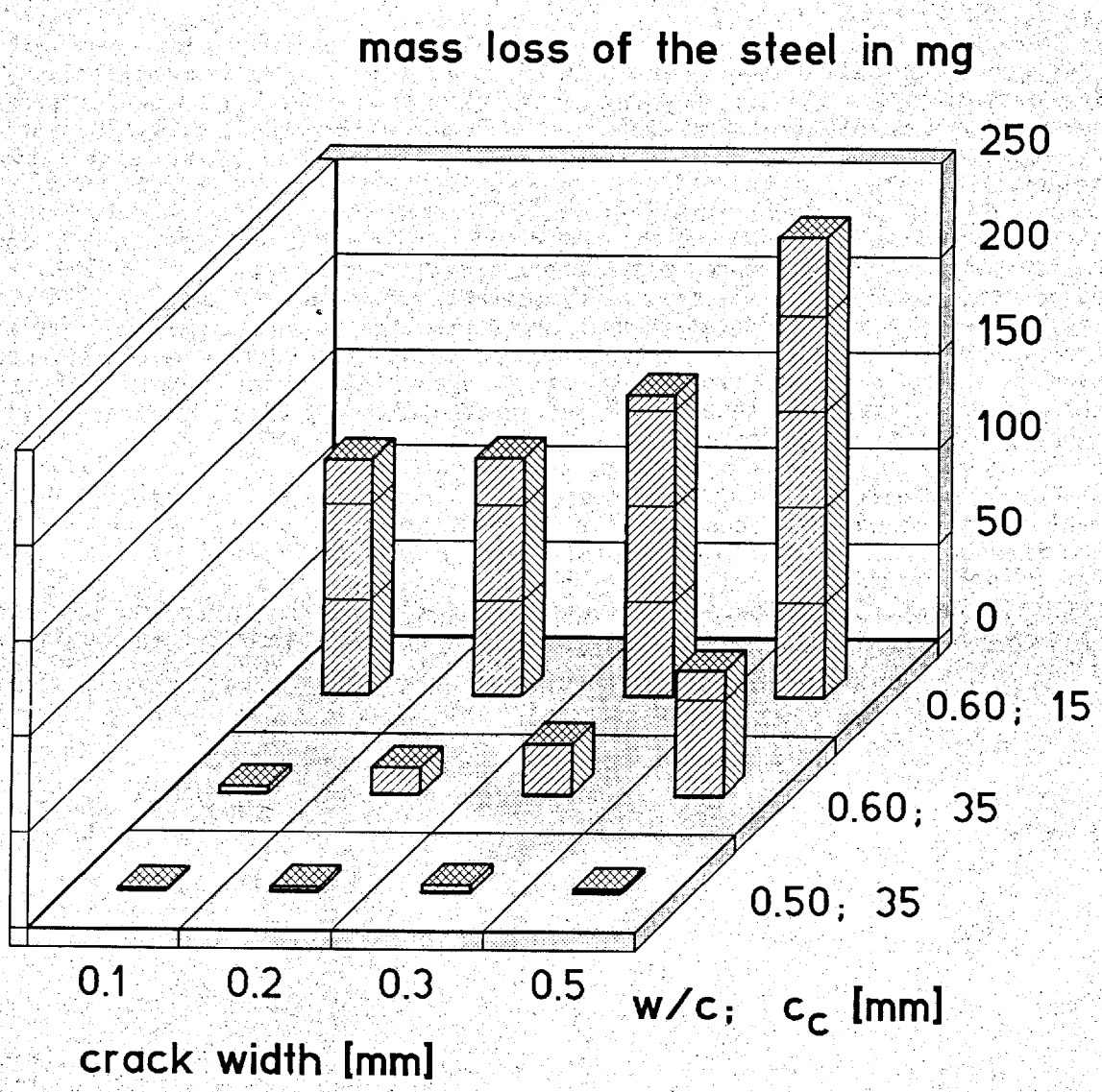

Fig. 16: Mass losses of the reinforcement in the area of a crack after cyclic chloride application according to (313)

These relationships do not, however, apply to permanently submerged reinforced concrete components. In (311), it was found that crack widths of up to 0.6 mm do not lead to corrosion damage where the cracks run parallel to the reinforcement, whereas even 1 mm wide cracks which cross the reinforcement are a hazard. These results are due to the oxygen deficit, and do not apply to the alternate immersion zone (305, 310).

It is agreed that the quality of the concrete covering layer is the dominant influencing variable for the corrosion rate in the crack zone. This is, however, true only of crack widths up to about 0.4 mm. With larger cracks, which do not generally occur if the relevant regulations for the dimensioning of reinforced concrete components are observed, crack width is also of decisive importance, since a different corrosion mechanism is dominant for crack widths of this order (306).

Summary

A simplified summary of results on the corrosion of steel in concrete indicates that the corrosion rate can be reduced by means of the following modifications:

- decreasing chloride content,
- increasing curing time,
- increasing blast-furnace slag content (BFC, SR-BFC),
- increasing fly-ash content
- increasing silica fume content,
- increasing C_3A content of the cement,
- decreasing water/cement ratio,
- increasing concrete cover,
- decreasing temperature,
- decreasing constant relative humidity and
- increasing dryness of the concrete.

Despite numerous publications on the corrosion of steel in concrete, quantification of the effects of the influencing parameters is virtually impossible, since the relationships concerned are extremely complex and since additional geometrical influencing variables (steel diameter, degree of reinforcement, etc.) are significant. In consequence, it is basically impossible to transfer the results of corrosion studies to any given geometrical conditions (272, 273, 285, 292).

9 ELECTROCHEMICAL CORROSION TEST METHODS

Introduction

In recent years, electrochemical test methods have predominated in investigations of the mechanisms and effects of the decisive factors influencing the corrosion of steel in concrete. The following section surveys the significant new developments in such methods.

Recent Studies

The **potential measurement method** has been used widely in recent years to pinpoint localized corrosion in reinforced concrete structures, due doubtless in part to its simplicity.

Using a high-resistance voltmeter, an electrochemical potential difference can be measured between steel in concrete and a reference electrode placed on the concrete surface (see Fig. 17). In principle, the probability of corrosion increases with more negative potential values, allowing critical points to be localized. This method was developed in the course of assessment work which had become necessary on

the state of the reinforcement on de-icing-salt-damaged bridges in the USA during the nineteen-sixties (315...319).

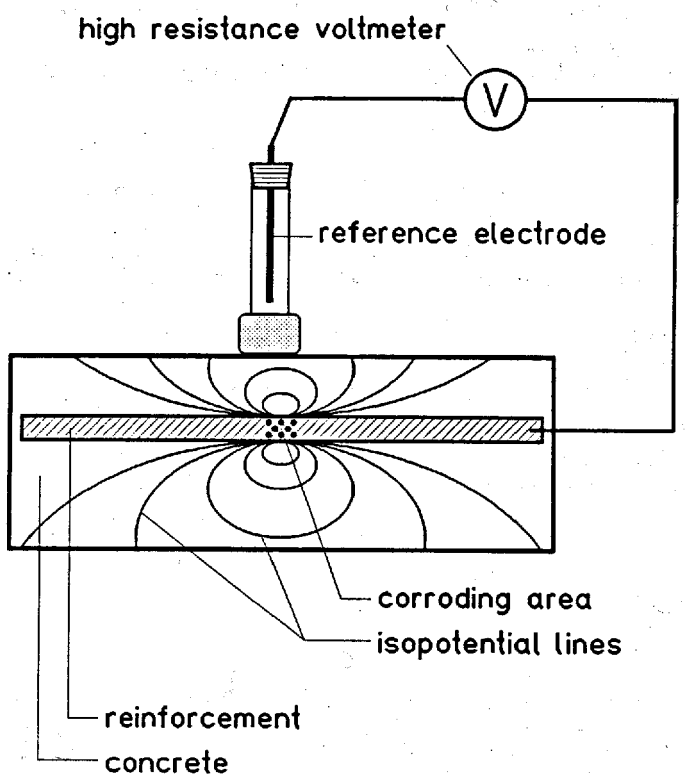

Fig. 17: Schematic representation of the set-up for potential measurements

On the basis of these studies, the ASTM C 876-91 regulation, containing criteria for assessing potential readings, was formulated in the USA. More recent findings indicate, however, that these limiting values cannot be applied to any given component conditions, i.e. that potentials must be judged individually depending on the conditions prevailing at the structure (320...329).

A sophistication of this method of measurement is the **galvanostatic anodic pulse measurement** method (324, 327, 330...332). A counter-electrode placed on the concrete surface is used to polarize the reinforcement briefly by means of an anodic current pulse, and the change in potential over time is registered via a reference electrode (Fig. 18). An additional switch-off measurement can also be used largely to determine and eliminate the influence of the electrolytic resistance of the concrete.

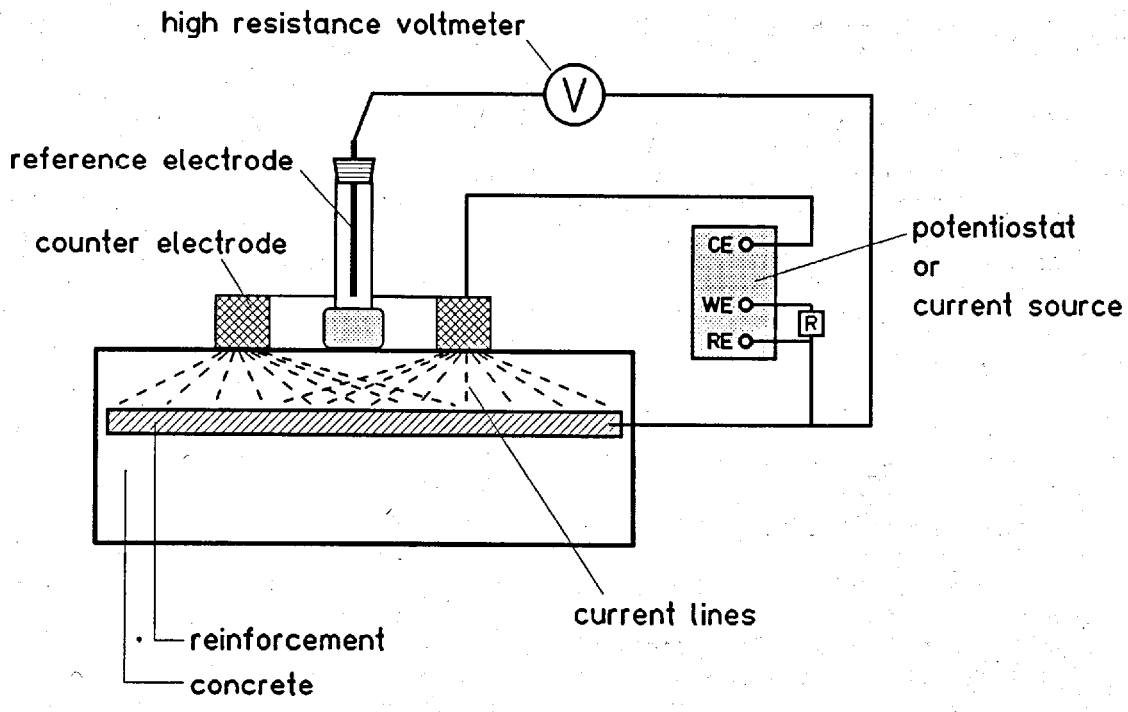

Fig. 18: Schematic representation of the set-up for anodic pulse measurements

Whereas the information provided by potential measurements is confined to the probability of reinforcement corrosion, **current measurements** can be used for the direct determination of current corrosion rates due to cell formation. Cell current measurements are employed in many different fields (302, 333...336). In reinforced concrete, this method is also increasingly chosen for laboratory studies (see ASTM G 01.14 and 246, 305, 309, 337...345)

On a specially-constructed specimen with locally separated anodic and cathodic zones of the steel surface, the cell current between the two electrodes is proportional to the corrosion rate, in accordance with Faraday's laws (so-called concrete corrosion cells, (e.g. 274, 291). So-called corrosion monitoring cells based on laboratory studies with concrete corrosion cells have now been developed; cell current measurements with these cells can be used to determine the risk of corrosion to the reinforcement as a function of time and depth (345a). **Corrosion monitoring cells** of this type can be employed in new structures in corrosive environments, to monitor the effectiveness of repair measures, or to assess the corrosion behaviour of existing structures.

So-called **electrochemical noise** occurs due to the activity of the oxide layer on the surface of the steel. This is in dynamic equilibrium, with a continuous alternation between depassivation and repassivation (346), causing low-frequency fluctuations in the free corrosion potential, in the microvolt range. By measuring the free corrosion potential with a voltmeter with a very high input resistance (> 10 GΩ) and suitable resolution, it is possible to differentiate between actively corroding and passive zones respectively, on the basis of their different levels of voltage fluctuation (347). Detailed interpretative criteria can then be formulated by mathematical analysis of the frequency spectrum. As yet, there are only a few results documenting the use of this technique on reinforced concrete structures. Apart from the problem of the large volumes of data required and the analytical effort involved

(348), the role played by other sources also liable to cause noise in larger structures is not yet clear (349).

Through slight polarization of an electrode in the order of the corrosion potential, e.g. about ±10 mV, it is possible to determine the **linear polarization resistance** R_p as the ratio of voltage change to current change. This describes the gradient of the voltage-current curve near the corrosion potential.

According to research reported in (350), the corrosion rate of the electrode concerned can then be calculated from

$$I = B/R_p$$

where

I	corrosion current
B	constant according to (350)
R_p	linear polarization resistance.

According to (349, 351), the constant **B** ranges from 13 to 52 mV, depending on the properties of the corrosion system under investigation, and must be determined individually in each case. The principles and application limits of this method are described in (351). An essential precondition for the determination of the corrosion rate is the presence of a homogeneous mixed electrode, of the kind which frequently be assumed to exist where there is wide-area carbonation of the concrete towards the steel surface. The informativeness of the corrosion currents measured in this way is, however, limited in cases of chloride-induced macrocell corrosion.

Using this method, many studies have been made in recent years, both on reinforced concrete specimens in the laboratory and in situ on structures. Results show a very good correlation between the corrosion rates of reinforced laboratory specimens and the corrosion current calculated from the polarization resistance under certain conditions (e.g. 349), whereas interpretation of the measured data from in situ tests is far more difficult (352). The method is currently being sophisticated (353).

The methods noted below are generally confined to laboratory studies, as they require defined constraints and a considerable amount of equipment.

Electrochemical reaction rates are generally dependent on potential: in anodic **polarization** (change in potential towards more positive values through the application of external current), anodic sub-reactions are accelerated and cathodic sub-reactions decelerated. In cathodic polarization the situation is reversed.

In order to determine the rates of various electrochemical reactions at defined potentials, the **potentiostatic test** adjusts the potential of the working electrode concerned in elation to a reference electrode to a specified desired potential by means of a potentiostat (e.g. 255). The resulting current flowing between the working electrode and a supplementary counter-electrode is used as a measure of the rate of the corresponding reaction or reactions (see ASTM G 5-87).

If a voltage-current curve is such that small changes in potential lead to large changes in current, **galvanostatic tests** are more effective. A specified desired current is set up between the working electrode and counter-electrode with the aid of a constant current source, and the potential of the working electrode measured (e.g. 252).

Where it is necessary to determine the behaviour of an electrode over wide ranges rather than for specific potentials or currents, **voltage-current curves** can be

recorded. Under certain conditions, the corrosion rate of the steel surface under consideration can theoretically be determined by interpreting the measured anodic and cathodic branches of static voltage-current curves, although in practice only approximate values can be obtained (e.g. 272).

It is fundamentally possible to distinguish between static, quasi-static and non-static voltage-current curves:

- **voltage-current curves for static conditions** can be determined by correlating results from a number of static tests, a technique which is particularly effective where long periods must elapse before static conditions are attained at certain potentials or currents.

- If polarization of the working electrode concerned takes place at a constant rate, so slowly that virtually constant static conditions prevail, curves are described as **quasi-static voltage-current curves.**

- **Non-static voltage-current curves** occur when specimens are polarized so rapidly that static conditions cannot arise. Such curves do not permit direct inferences on reaction rates, but provide insights into the reaction mechanisms involved.

In recent years, many results of **impedance measurements** on reinforced concrete specimens have been published (354...359). The intensive research activity in this field is due partly to the ability of impedance measurements both to furnish information on the corrosion rate and to identify the step in the corrosion process which determines the corrosion rate.

Apart from references in the above-listed literature, the principles of the method are described in (360...364). The steel surfaces under consideration are polarized slightly, generally using sinusoidal alternating voltages at various frequencies, and the resulting current/time curves are measured and evaluated. Equivalent circuits consisting of resistors and capacitors are assumed for the corrosion process, and the size of the individual components determined, allowing inferences as to the corrosion mechanism under defined constraints.

Summary

Apart from traditional aging tests, a number of electrochemical test methods allowing investigation of reinforcement corrosion are currently available. Some of these permit continuous determination of the corrosion rate, i.e. changes over time due to temperature and humidity fiuctuations or as a result of hydration or increased chloride content. They also enable differentiated conclusions to be drawn on the corrosion process mechanism and the decisive influencing parameters.

10 CONCLUDING REMARKS

Corrosion of reinforcement, frost action, carbonation, alkali-aggregate reactions, and sulfate attack are the major causes which adversely influence the durability of concrete structures. From a review of selected publications during the 1987-91 period, the authors have come to the following conclusions:

1. There are many interesting reports on durability of concrete products containing superplasticizing admixture and mineral admixtures, such as silica fume and fly ash. Except carbonation, all the damaging phenomena mentioned above involve expansion and cracking, which is controlled by the coefficient of permeability of

concrete because water from an external source is invariably needed to promote the physical-chemical phenomena underlying expansion. The low water-to-cementitious ratio, made possible by the use of superplasticizers and/or mineral admixtures, helps to reduce the coefficient of permeability. Therefore, concrete mixtures containing these materials generally perform well in the durability tests.

2. A lot of research effort is going into the development of laboratory tests and specifications for evaluation of concrete-making materials from standpoint of their individual contribution to the durability of concrete under certain conditions. Since it is not possible to simulate the field service conditions by accelerated laboratory tests and since most of the durability problems in the field occur as a result of two or more attack types occurring simultaneously, these laboratory tests serve only a limited purpose.

3. In his review of durability publications during the period 1974-79, Calleja (203) made the following observation, which is also valid for the period of this review:

   In the field of durability as well as in many other fields of cement and concrete research, most of the research work runs around the same themes, using the same methods, applying the same ideas, and arriving repeatedly almost always at the same partial, and not decisive conclusions. To solve the durability-related problems, we need to divert more resources towards integration of our present knowledge into a holistic understanding of the durability issue.

11 REFERENCES

1. F. M. Lea, The Chemistry of Cement and Concrete, Chemical Publishing Company, 1971.

2. P. K. Mehta, Concrete: Structure, Properties and Materials, Prentice Hall Inc., 1986.

3. ACI Committee 201 Report, Guide to Durable Concrete, ACI Mat. Jour., V. 88, No. 5, pp. 544-82, 1991.

4. P. K. Mehta, in Durability of Concrete, ed: V. M. Malhotra, ACI, SP-126, pp. 1-32, 1991.

5. L. Struble, Cement Research Progress, ed: P. W. Brown, Am. Ceram. Soc., pp. 157-238, 1989.

6. L. J. Parratt and D. C. Killoh, Cement and Concrete Research, V. 19, No. 4, pp. 649-56, 1989.

7. K. Kobayashi and Y. Uno, Cement and Concrete Research, V. 19, No. 5, pp. 821-26, 1989.

8. K. Kobayashi and Y. Uno, Cement and Concrete Research, V. 20, No. 4, pp. 619-22, 1990.

9. L. Ying-yu and W. Qui-dong, in Concrete Durability, ed: J.M. Scanlon, ACI, SP 100, pp. 1915-43, 1987.

10. P. Schubert, Cement and Concrete Research, V. 19, No. 4, pp. 1945-62, 1987.

11. H. Ohga and S. Nagataki, ACI, SP-114, ed: V.M. Malhotra, pp. 275-94, 1989.

12. M. Kokubu and S. Nagataki, in Concrete Durability, ed: J.M. Scanlon, pp. 315-29, 1989.

13. D. W. S. Ho and R. K. Lewis, Cement and Concrete Research, V. 17, No. 3, pp. 489-504, 1987.

14. R. Dhir, K. Tham, and J. Dransfield, Cement and Concrete Research, V. 19, No. 4, pp. 741-64, 1987.

15. V. M. Malhotra, G. G. Carrette, A. Bilodeau, and V. Sivasundaram, in Durability of Concrete, ed: V. M. Malhotra, ACI, SP 126, pp. 65-82, 1991.

16. B.A. Oye and H. Justnes, in Concrete Durability, ed: J.M. Scanlon, ACI, SP 100, pp. 1031- 1046, 1991.

17. M. Sakuta, T. Urano, I. Izumi, M. Sugiyama, and K. Tanaka, in Concrete Durability, ed: J. M. Scanlon, ACI, SP-100, pp. 1963-77, 1987.

18. X. Aimin and S. Chandra, Jour. Cement Composites, V. 10, No. 1, pp. 49-51, 1988.

19. V. Lach, in Concrete Durability, ed: J. M. Scanlon, ACI, SP-100, pp. 1903-14, 1987.

20. F. Massazza and G. Oberti, in Durability of Concrete, ed: V. M. Malhotra, ACI, Sp 126, pp. 1259-84, 1991.

21. A. M. Paillera, M. Raverdy, and G. Grimaldi, ACI, SP-91, pp. 541-62, 1986.

22. J. Bijen and R. van Selst, ibid, pp. 1001-30.

23. J. Bijen, G. van der Wegen, and R. van Selst, Cement and Concrete Research, V. 19, No. 4, pp. 645-68, 1989.

24. G. J. Osborne, Cement and Concrete Research, V. 19, No. 4, pp. 1209-38, 1989.

25. E. Sakai, K. Kosuge, S. Teramura, and K. Nakagawa, in Durability of Concrete, ed: V. M. Malhotra, ACI, SP-126, pp. 989-1000, 1991.

26. G. Strohbauch and H. J. Kuzel, Zement Kalk Gips, V. 41, No. 7, pp. 358-60, 1988.

27. S. Nagataki, M. A. Mansur, and H. Ohga, ACI Mat. Jour., V. 85, No. 1, pp. 17-25, 1988.

28. C. J. Hamson and J. E Bailey, J. Mat. Science, V. 18, p. 402, 1983.

29. C. D. Lawrence, Mag. Concrete Research, V. 42, No. 153, pp. 249-64, 1990.

30. E. Dunstan, in Concrete Durability, ed: J. M. Scanlon, ACI, SP 100, pp. 2027-36, 1987.

31. R. D. Hooton, ACI, SP-91, pp. 333-46, 1986.

32. O. E. Manz, ibid, pp. 347-66, 1986.

33. P. K. Mehta, Jour. ACI, Proc., V. 83, No. 6, pp. 994-1000, 1986.

34. A. Fraay, A. Reigersman and J. de Pee, in Concrete Durability, ed: J. M. Scanlon, ACI, SP-100, pp. 2041-58, 1987.

35. G. Wong and T. Poole, in Concrete Durability, ed: J. M. Scanlon, ACI, SP-100, pp. 2121- 34, 1987.

36. R. D. Hooton and J. J. Emery, ACI Mat. J., V. 87, No. 6, pp. 547-55, 1990.

37. G. J. Osborne, in Durability of Concrete, ed: V. M. Malhotra, ACI, SP-126, pp. 1047-71, 1991.

38. H. M. Sylla, Beton, V. 38, pp. 449-54, 1988.

39. U. Neck, ibid, pp. 438-39, 1988.

40. D. Tepponen and B.E. Ericksson, Nordic Concrete Research, No. 6, pp. 199-209, 1987.

41 .D. Heinz and U. Ludwig, in Concrete Durability, ed: J. M. Scanlon, ACI, SP-100, pp. 2059-71, 1987.

42. D. Heinz and U. Ludwig, Concrete Precasting Plant and Tech., VII, pp. 56-61, 1989.

43. M. Berra and G. Baronio, in Concrete Durability, ed: J. M. Scanlon, ACI, SP-100, pp. 2073-89, 1987.

44. J. Piasta, W. Piasta, and Z. Sawicz, in Concrete Durability, ed: J. M. Scanlon, ACI, SP- 100, pp. 2153-70, 1987.

45. J. Piasta, W. Piasta and Z. Sawicz, Cem. and Concrete Research, V. 19, No. 2, pp. 216-27, 1989.

46. J. Piasta, W. Piasta and Z. Sawicz, in Concrete Durability, ed: J. M. Scanlon, ACI, SP-100, V. 19, No. 1, pp. 103-13, 1989.

47. D. Stark, in Concrete Durability, ed: J. M. Scanlon, ACI, SP-100, pp. 2091-2102, 1987.

48. I. R. de Almeida, in Durability of Concrete, ed: V. M. Malhotra, ACI, SP-126, pp. 1073- 92, 1991.

49. M. D. Cohen and A. Bentur, ACI Mat. J., V. 85, No. 3, pp. 148-57, 1988.

50. P. K. Mehta, Cement and Concrete Research, V. 15, No. 6, pp. 969-78, 1985.

51. Rasheeduzzafar, F. H. Dakhil, A. S. Al-Gahtani, S. S. Al-Saadoun and M. A. Bader, ACI Mat. J., V. 87, No. 2, pp. 114-22, 1990.

52. L. K. Attigobe and S. H. Rizkalla, ACI Mat. J., V. 85, No. 6, pp. 481-88, 1988.

53. N. I. Fattuhi and B. P. Hughes, Cement and Concrete Research, V. 18, No. 4, pp. 545-53, 1988.

54. N. I. Fattuhi and B. P. Hughes, ACI Mat. J., V. 85, No. 6, pp. 512-18, 1988.

55. H. L. Kong and J. G. Orbison, ibid., V. 84, No. 2, pp. 110-16, 1987.

56. W. G. Hime, ibid., V. 85, No. 1, pp. 62-63, 1988.

57. R. J. Reardon, Cement and Concrete Research, V. 20, No. 1, pp. 175-92, 1990.

58. A. Gabrisova, J. Havlica and S. Sahu, Cement and Concrete Research, V. 21, No. 6, 1991.

59. E. Scholl and D. Knoffel, ibid., No. 1, pp. 127-36, 1991.

60. S. Chandra, Swedish Council for Building Materials Research, Stockholm, Report No. D- 6, 1990.

61. W. H. Harrison, Mag. Concrete Research, V. 42, No. 152, pp. 113-26, 1990.

62. C. Ouyang, W. Suaris and W. F. Chang, ACI Mat. J., V. 85, No. 2, pp. 82-89, 1988.

63. C. Ouyang, Cement, Concrete, and Aggregates J., V. 11, No. 2, pp. 92-99, 1989.

64. I. Odler and M. Gasser, J. Am. Ceram. Soc., V. 71, No. 11, pp. 1015-20, 1988.

65. I. Older and I. Jawed, Material Science of Concrete, V. 2, Ed. J. P. Skalny, Am. Ceram. Soc., 1991.

66. P. K. Mehta, Material Science of Concrete, V. 3, Ed. J. P. Skalny, Am. Ceram. Soc., 1992.

67. M. D. Cohen and B. Matter, ACI Mat. J., V. 88, No. 1, pp. 62-69, 1991.

68. A. Shayan, R. Diggins, D. F. Richie and P. Westgate, Proc. 7th Intl. Conf. on Alkali- Aggregate Reactions, ed. P. E. Grattan-Bellew, National Research Council, Ottawa, Canada, pp. 247-52, 1987.

69. C. A. Rogers, ibid., pp. 5-9, 1987.

70. P. Albert and S. Raphael, Proc. 7th Intl. Conf. on Alkali-Aggregate Reactions, ed. P. E. Grattan-Belleue, National Research Council, Ottawa, Canada, pp. 10-16, 1987.

71. E. R. Magni, C. A. Rogers, and P. E. Grattan-Bellew, ibid., pp. 17-21, 1987.

72. B. Fournier, M. A. Berube, and D. Vezina, ibid., pp. 23-29, 1987.

73. H. Y. Xu and M. Chen, ibid., pp. 253-57, 1987.

74. H. C. Visvesvaraya, C. Rajkamar, and A. K. Mullick, ibid., pp. 188-92, 1987.

75. M. Bera and G. Baronio, ibid., pp. 231-36, 1987.

76. K. Okada, ibid., pp. 216-20, 1987.

77. D. A. St. John, ibid., pp. 237-241, 1987.

78. B. Penkala, ibid., pp. 221-25, 1987.

79. W. J. French, ibid., pp. 226-30, 1987.

80. S. Cmilijamic and M. Ravmovic, ibid., pp. 242-46, 1987.

81. A. K. Mullick, Cement and Concrete Composites, V. 10, No. 4, pp. 225-32, 1988.

82. K. Ono, ibid., pp. 247-59, 1988.

83. K. Kobayashi, S. Inoue, T. Yamasaki and K. Nakano, ibid., pp. 233-40, 1988.

84. A. Samarin, ibid., pp. 241-46, 1988.

85. A. Shayan, ibid., pp. 259-66, 1988.

86. A. Shayan and G. W. Quick, ibid., pp. 209-14, 1988.

87. ACI Committee 201 Report, Guide to Durable Concrete, ACI Mat. Jour., V. 88, No. 5, pp. 544-82, 1991.

88. D. W. Hobbs, Mag. Concrete Research, V. 38, No. 137, pp. 191-205, 1986.

89. D. W. Hobbs, Alkali-Silica Reaction in Concrete, Thomas Telford Ltd., 1988.

90. J. J. Kollek, Cement and Concrete Research, V. 20, No. 4, pp. 373-402, 1989.

91. D. F. Barlow and D. J. Jackson, ibid., V. 18, No. 2, pp. 235-48, 1988.

92. S. Kobayashi, Y. Hozumi, T. Nakano, and T. Yanagida, ibid., V. 20, No. 4, pp. 403-16, 1989.

93. C. Lee, ibid., V. 20, No. 4, pp. 417-30, 1989.

94. B. Durand, J. Berard, and J. A. Soles, Proc. 7th Intl. Conf. on Alkali-Aggregate Reactions, ed. P. E. Grattan-Balleue, National Research Council, Ottawa, Canada, pp. 30-35, 1987.

95. B. Durand, J. Berard, R. Roux and J. A. Soles, Cement and Concrete Research, V. 20, pp. 419-28, 1990.

96. J. A. Soles, V. M. Malhotra and R. W. Suderman, Proc. 7th Intl. Conf. on Alkali-Aggregate Reactions, ed. P. E. Grattan-Ballew, National Research Council, Ottawa, Canada, pp. 79-82, 1987.

97. C. Yamamoto, M. Makita, Y. Moriyama and S. Numata, ibid., pp. 49-52, 1987:

98. R. E. Oberholster and G. Davies, ibid., pp. 60-65, 1987.

99. M. Bhatty and N. Greening, ibid., 1987.

100. C. Perry, R. L. Day, R. C. Joshi, B. W. Langan and J. E. Gillot, ibid., pp. 93-97, 1987.

101. M. Robert, ibid., pp. 98-103, 1987.

102. N. Tenoutasse and A. M. Marion, ibid., pp. 44-48, 1987.

103. N. Tenoutasse and A. M. Marion, ibid., pp. 71-75, 1987.

104. J. Farbiarz and R. Carrasquillo, ibid., pp. 1787, 1987.

105. S. Nagataki, H. Ohga and T. Inoue, in Durability of Concrete, ed: V. M. Malhotra, ACI, SP-126, pp. 955-72, 1991.

106. R. N. Swamy and A. Asali, Swedish Council for Building Materials Research, Report No. D-1, p. 145, 1988.

107. P. J. Nixon and C. L. Page, in Concrete Durability, ed: J. M. Scanlon, ACI, SP 100, p. 1849, 1987.

108. R. Carrasquillo and P. Snow, ACI Materials Jour., V. 84, No. 4, pp. 299-305, 1987.

109. M. D. A. Thomas, P. J. Nixon, and K. Pettifer, in Durability of Concrete, ed: V.M. Malhotra, ACI, SP-126, pp. 919-40, 1987.

110. A. Asali and V. M. Malhotra, ACI Materials Jour., V. 88, No. 2, pp. 159-162, 1991.

111. M. Kawamura, K. Takemoto, and S. Hasaba, in Concrete Durability, ed: J. M. Scanlon, ACI, SP-100, p. 1809, 1987.

112. R. N. Swamy, Swedish Council for Building Research, Report No. D-6, 1989.

113. G. V. Walters and T. R. Jones, in Durability of Concrete, ed: V. M. Malhotra, ACI, SP- 126, pp. 941-53, 1991.

114. S. Chatterji, N. Thaulow and A. D. Jensen, Cement and Concrete Research, V. 16, p. 246, 1986.

115. S. Chatterji, N. Thaulow, and A.D. Jensen, ibid., V. 17, pp. 777-83, 1987.

116. S. Chatterji, N. Thaulow, and A.D. Jensen, ibid., V. 18, pp. 363-66, 1988.

117. S. Chatterji, N. Thaulow, and A.D. Jensen, ibid., V. 18, pp. 654-56, 1988.

118. M. Kawamura, K. Takemoto, and N. Terashima, Mag. Concrete Research, V. 40, No. 144, pp. 163-51, 1988.

119. A. Bachiorrini and L. Montanaro, Cement and Concrete Research, V. 18, pp. 731-38, 1988.

120. R. J. Collins and P. D. Bareham, ibid., V. 17, pp. 89-96, 1987.

121. G. Davies and R.E. Oberholster, ibid., V. 17, pp. 97-107, 1987.

122. G. Davies and R.E. Oberholster, ibid., V. 18, pp. 621-35, 1988.

123. A. Shayan, R. G. Diggins, J. Ivanusec and P. C. Westgate, ibid., V. 18, pp. 843-51, 1988.

124. R. P. Hudac and J. A. Larbi, ibid., V. 19, pp. 905-12, 1989.

125. B. Durand and J. Berard, Mat. and Structures, V. 20, No. 115, pp. 39-43, 1987.

126. L. De Ceukelair, ibid., V. 24, pp. 169-71, 1991.

127. R. N. Swamy and A. Asali, ACI Mat. Jour., V. 85, pp. 33-40, 1988.

128. R. N. Swamy and A. Asali, ibid., p. 367, 1988.

129. R. N. Swamy, Swedish Council for Building Research, Report No. D-6, 1989.

130. R. H. Courtier, Cement and Concrete Composites, V. 12, pp. 191-201, 1990.

131. M. A. Tordoff, ibid., pp. 203-10, 1990.

132. R. E. Oberholster, Proc. 7th Intl. Conf. on Alkali-Aggregate Reactions, ed. P.E. Grattan- Ballew, National Research Council, Ottawa, Canada, p. 368, 1987.

133. T. Knudsen, ibid., pp. 289-93, 1987.

134. M. Tang, S. Han, S. Zhan, M. Yuan, Y. Ye and Y. Lu, ibid., pp. 294-98, 1987.

135. S. Nishibayashi, K. Yamura and H. Matsushita, ibid., pp. 299-303, 1987.

136. H. Tamura, ibid., pp. 304-308, 1987.

137. Y. Yoshiko, H. Kasami, S. Ohno and Y. Shinozaki, ibid., pp. 314-18, 1987.

138. G. Baronio, M. Berra, A. Bachiorrini, A. Delmastro and L. Montanaro, ibid., pp. 309-13, 1987.

139. T. Hugenberg, in Concrete Durability, ed: J.M. Scanlon, ACI, SP 100, p. 1889, 1987.

140. Mi Tang, Z. Liu and S. Han, Proc. 7th Intl. Conf. on Alkali-Aggregate Reactions, ed. P.E. Grattan-Ballew, National Research Council, Ottawa, Canada, pp. 275-79, 1987.

141. A. K. Mullick and P. Samuel, ibid., pp. 381-85, 1987.

142. J. G. M. Wood, J. S. Young and D. E. Ward, ibid., pp. 157-61, 1987.

143. J. Figg, ibid., pp. 152-56, 1987.

144. D. Stark and DePuy, in Concrete Durability, ed: J. M. Scanlon, ACI, SP 100, 1987.

145. D. Stark, in Durability of Concrete, ed: V.M. Malhotra, ACI, SP 126, p. 973, 1991.

146. P. Smith, Proc. 7th Intl. Conf. on Alkali-Aggregate Reactions, ed. P.E. Grattan-Ballew, National Research Council, Ottawa, Canada, 1987.

147. G. Idorn, Proc. Gerwick Symp. on Durability of Concrete in Marine Environment, ed. P. K. Mehta, University of California at Berkeley, 1989.

148. B. Mather, Swedish Council for Building Research, Report D-1, p. 159, 1988.

149. T. A. Hammer and E. J. Sellevold, ACI SP-126, p. 17, 1990. 150.E. J. Sellevold, Swedish Council for Building Research, Report D1:1988, p. 173, 1988.

151. P. E. Pettersson, ibid., pp. 179-189, 1988.

152. E. Seibel, ACI SP-119, pp. 297-320, 1989.

153. M. Pigeon, R. Gagne and C. Foy, Cement and Concrete Research, V. 17, pp. 896-906, 1987.

154. C. Foy, M. Pigeon and N. Banthia, ibid., V. 18, pp. 604-14, 1988.

155. M. Pigeon, R. Gagne and P. C. Aitcin, ibid., V. 21, pp. 844-852, 1991.

156. D. Whiting, in Concrete Durability, ed: J.M. Scanlon, ACI, SP 100, pp. 169-86, 1987.

157. D. Whiting and J. Schmitt, ACI SP-119, pp. 343-60, 1989.

158. G. Robson, ibid., pp. 765-80, 1987.

159. R. Dhir, K. Tham and J. Dransfield, ibid., pp. 741-64, 1987.

160. V. M. Malhotra, K. E. Paintor and A. Bilodeau, ASTM J. Cement, Concrete, and Aggregates, V. 19, No. 2, pp. 65-79, 1987.

161. R. Philleo, in Concrete Durability, ed: J. M. Scanlon, ACI, SP-100, pp. 819-842, 1987.

162. M. Pigeon, P. Plante and M. Plante, ACI Mat. J., V. 86, No. 5, pp. 482-90, 1989.

163. P. Plante, M. Pigeon and F. Saucier, ibid., No. 6, pp. 581-89, 1989.

164. F. Saucier, M. Pigeon and P. Plante, ibid., V. 87, No. 1, pp. 3-11, 1990.

165. M. Pigeon, F. Saucier and P. Plante, ibid., V. 87, No. 3, pp. 252-59, 1990.

166. F. Saucier, M. Pigeon and G. Cameron, ibid., V. 88, No. 1, pp. 25-36, 1991.

167. P. Petersson, Swedish Council for Building Research, D9:1989, pp. 161-69, 1989.

168. E. H. Ramisch and F. S. Rostasy, ibid., pp. 170-78, 1989.

169. L. Berntsson, ibid., pp. 18-22, 1989.

170. R. Gagne, M. Pigeon and P. C. Aitcin, in Durability of Concrete, ed: V. M. Malhotra, ACI, SP-126, pp. 185-200, 1991.

171. H. Kukko and S. Matala, in Durability of Concrete, ed: V.M. Malhotra, ACI, SP 126, pp. 229-48, 1991.

172. E. J. Sellevold, Swedish Council for Building Research, D9:1989, pp. 215-17, 1989.

173. D. Whiting and R. Burg, in Durability of Concrete, ed: V. M. Malhotra, ACI, SP-126, pp. 83-100, 1991.

174. D. R. Morgan, ibid., pp. 901-918, 1991.

175. D. R. Morgan, Concrete International, V. 11, No. 8, pp. 86-93, 1989.

176. D. R. Morgan, A. J. Kirkness and N. McAskill, ASTM J. Cement, Concrete, and Aggregates, V. 10, No. 2, pp. 96-102, 1988.

177. D. R. Morgan, Concrete International, V. 10, No. 1, pp. 24-30, 1988.

178. T. P. Dolen, in Durability of Concrete, ed: V. M. Malhotra, ACI, SP 126, pp. 101-114, 1991.

179. J. Marchand, J. Boisvert, M. Pigeon and H. L. Isabelle, in Durability of Concrete, ed: V. M. Malhotra, ACI, SP-126, pp. 131-54, 1991.

180. T. C. Liu, in Durability of Concrete, ed: V. M. Malhotra, ACI, SP-126, pp. 155-68, 1991.

181. P. Klieger and S. Gebler, in Concrete Durability, ed: J. M. Scanlon, ACI, SP-100, pp. 1043-69, 1987.

182. L. E. Rodway, Cement, Concrete and Aggregates J., ASTM, V. 10, No. 1, pp. 35-38, 1988.

183. C. Johnston, in Concrete Durability, ed: J. M. Scanlon, ACI, SP-100, pp. 1183-1204, 1987.

184. A. Bilodeau, G. G. Carette, V. M. Malhotra and W. S. Langley, in Durability of Concrete, ed: V. M. Malhotra, ACI, SP-126, pp. 201-28, 1991.

185. V. M. Malhotra, G. G. Carette, A. Bilodeau and V. Sivasundram, ibid, pp. 65-82, 1991.

186. M. Gunther, Th. Bier and H. Hilsdorf, in Concrete Durability, ed: J. M. Scanlon, ACI, SP- 100, pp. 877-900, 1987.

187. A. D. Buck, Cement, Concrete, and Aggregates J., ASTM, V. 10, No. 1, pp. 48-49, 1988.

188. A. I. Rashed and R. B. Williamson, J. Mat. Res., V. 6, No. 9, pp. 2004-12, 1991.

189. A. M. Gunnink in Concrete Durability, ed: J. M. Scanlon, ACI, SP-100, 1987.

190. D. H. Bager and E. J. Sellevold, Cement and Concrete Research, V. 17, No. 1, pp. 1-11, 1987.

191. D. H. Bager and E. J. Sellevold, ibid., V. 17, No. 6, pp. 1010-11, 1987.

192. M. Pigeon and M. Regourd, Durability of Building Materials, V. 4, No. 1, pp. 1-19, 1986.

193. T. Yamamoto, Y. Emoto and M. Sweda, in Concrete Durability, ed: J. M. Scanlon, ACI, SP-100, pp. 901-18, 1987. 194.P. Balaguru, M. Ukadike and E. Nawy, ibid., pp. 863-76, 1987.

195. D. Bjegovic, D. Mikulic and V. Ukraincik, ibid., pp. 947-972, 1987.

196. M. Pigeon, R. Gagne and P. C. Aitcin, Cement and Concrete Research, Vol. 21, pp. 844- 52, 1991.

197. V. Sturrup, R. Hooton, P. Mukherjee, and T. Carmichael, in Concrete Durability, ed: J.M. Scanlon, ACI, SP-100, pp. 1121-54, 1987.

198. N. M. Yanderhorst and D. J. Janssen, ACI SP-122, pp. 181-200, 1990.

199. M. Moukwa, P. C. Aitcin, M. Pigeon and H. Hornain, ACI Mat. Jour., V. 86, No. 4, pp. 360-66, 1989.

200. J. Aavik and S. Chandra, Swedish Council for Building Res., D1:1988, pp. 233-234, 1988.

201. P. Gutman, ACI Mat. Jour., V. 85, No. 5, p. 361-66, 1988.

202. M. Sugiyama, K. Tanaka, M. Sakuta and T. Urano, in Concrete Durability, ed: J.M. Scanlon, ACI, SP 100, pp. 1103-20, 1987.

203. J. Calleja, Seventh International Congress on the Chemistry of Cements, Paris, 1980.

204. H.-J. Wierig. Die Carbonatisierung des Betons. In: Naturstein-Industrie (DNI) 22 (1986), no. 5, pp. 26, 28-35

205. R. Bakker. Measures of Protection. In: Corrosion of Steel in Concrete : Report of the Technical Committee 60-CSC RILEM (1988), pp. 22-55 (Schiessl, P. (ED.)). London : Chapman and Hall.

206. Th. A., Bier. Karbonatisierung und Realkalisierung von Zementstein und Beton. Karlsruhe : Institut für Massivbau und Baustofftechnologie (1988) No. 4

207. C. M. Hansson and B. Sorensen. The Influence of Cement Fineness on Chloride Diffusion and Chloride Binding in Hardened Cement Paste. In: Nordic Concrete Research 6 (1987), pp. 57-62

208. H.-G. Smolczyk. Stand der Kenntnis über Chloriddiffusion im Beton. In: Betonwerk + Fertigteiltechnik 50 (1984), No. 12, pp. 837-843

209. K.-H. Lawatsch and A. Volkwein and Institut für Bauingenieurwesen II. Eindringen von Chloriden in Abhängigkeit von der Feuchte (Chloriddiffusion). München : Institut für Bauingenieurwesen II der TU München, 1984. - Forschungsbericht No. 3123

210. Concrete in the Oceans ; Cement and Concrete Association ; C&CA ; BCA: Marine Durability Survey of the Tongue Sands Tower. Wexham Springs : Cement and Concrete Association, BCA. - In: Technical Report 5 (1980)

211. Dyckerhoff & Widmann AG: Chlorideindringung : Vergleich Zeitraffer- und Langzeittest. München : Dyckerhoff & Widmann AG, 1983 - In: Spätschäden an Spannbetonbauteilen, Bericht No. 45/19

212. K. Wesche and G. Neroth. Eindringen von Chloriden und Karbonatisierung des Betons im Sprühnebelbereich von Straßen. Bonn-Bad Godesberg : Bundesminister für Verkehr, Abteilung Straßenbau: - In: Forschung Straßenbau und Straßenverkehrstechnik (1982), No. 370, pp. 1-21

213. ACI-SP 65: Performance of Concrete in Marine Environment (1980), Detroit

214. L. Uji and Y. Matsuoka and T. Maruya. Formulation of an equation for surface chloride content of concrete due to penetration of chloride. In: Corrosion of Reinforcement in Concrete. London : Elsevier Applied Science. SCI Society of Chemical Industry (1990), pp. 258-267

215. R. Frey. Untersuchung des Wanderungsmechanismus und Ermittlung der Kenngrößen von Streusalz-Chlorid in Betonen. In: TIZ-International Powder & Bulk Magazine 115 (1991), No. 10

216. Ch. Jägermann. Effect of water-cement ratio and curing on chloride penetration into concrete exposed to mediterranean sea climate. In: ACI Material Journal, July-August 1990

217. Y. Efes, Y. ; R. Rankers. Zum Einfluß der Zementart auf die Chlorid-Diffusion im Beton : Untersuchungen nach einer Chloridlagerungsdauer von 24 Monaten. Aachen : Institut für Bauforschung der RWTH Aachen, 1985. - Forschungsbericht No. F 176

218. M. Thomas and J. D. Matthews and C. A. Haynes. Chloride diffusion and reinforcement corrosion in marine exposed concretes containing pulverised fuel ash. In: Corrosion of Reinforcement in Concrete. London : Elsevier Applied Science. SCI Society of Chemical Industry (1990), pp. 198-212

219. R. F. M. Bakker. Permeability of blended cement concretes. Detroit : American Concrete Institute, ACI SP-79. - In: Proceedings of the CANMET/ACI First International Conference of the Use of Fly Ash, Silica Fume, Slag and other Mineral By-Products in Concrete. Vol. 1 (1983), pp. 589-605

220. R. F. M. Bakker and W. J. M. Thomasen. Diffusienelheid van Inonen in Beton. In: Cement 29 (1977), No. 9, pp. 419-421

221. R. Zimbelmann. A method for strengthening the bond between cement stone and aggregates. In: Cement and Concrete Research 17 (1987), No. 4, pp. 651-660

222. G. Neroth ; Institut für Bauforschung (ibac): Zur Bindung von Chlorid im Zementstein. Wiesbaden : Bauverlag, 1985 - In: Baustoffe '85, pp. 140-147

223. J. Tritthart ; TVFA der Technischen Universität Graz: Chloridinduzierte Betonstahlkorrosion - Zur Zusammensetzung der Porenlösung von erhärtetem Zement. Graz : Technische Versuchs- und Forschungsanstalt für Festigkeits- und Materialprüfung der Technischen Universität Graz, 1987

224. P. Gunkel. Die Bindung von Chlorid im Zementstein und die Zusammensetzung chloridhaltiger Porenlösungen. In: Beton-Informationen 29 (1989), No. 1, pp. 3-11

225. H.-G. Smolczyk. Flüssigkeit in den Poren des Betons - Zusammensetzung und Transportvorgänge in der flüssigen Phase des Zementsteins. In: Beton-Informationen 24 (1984), No. 1, pp. 3-11

226. H. Kupfer and H. H. Müller and A. Rauen. Corrosion Activity of Chloride Added to Fresh Concrete or Penetrated into Hardened Concrete. Karlsruhe : Institut für Massivbau und Baustofftechnologie, 1988. - In: Dauerhaftigkeit nichtmetallischer anorganischer Baustoffe : Abschlußkolloquium des Forschungsschwerpunktprogrammes der DFG, Karlsruhe 4./5. Oktober 1988, pp. 47-53

227. S. Diamond. Chloride Concentrations in Concrete Pore Solutions Resulting from Calcium and Sodium Chloride Admixtures. In: Cement, Concrete and Aggregates, Baltimore 8 (1986), No. 2, pp. 97-102

228. M. G. Friedel. Sur un Chloro-Aluminate de Calium Hydrate se Maclant Par Compression. In: Bulletin de Mineralogie 20 (1987), pp. 122-136

229. W. R. Holden and C. L. Page and N. R. Short. The Influence of Chlorides and Sulphates on Durability. Chichester, England : Ellis Horwood Limited, 1983 - In: Corrosion of Reinforcement in Concrete Construction : Meeting Held in Londong, England on 13-15 June 1983, (Crane, A.P. (ED)), pp. 143-150

230. K. Byfors and C. M. Hansson and J. Tritthart. Pore Solution Expression as a Method to Determine the Influence of Mineral Additives on Chloride Binding. In: Cement and Concrete Research 16 (1986), No. 5, pp. 760-770

231. C. L. Page and O. Vennesland. Pore Solution Composition and Chloride Binding Capacity of Silica-Fume Cement Pastes. In: Materiaux et Construction 16 (1983), No. 91, pp. 19-25

232. O. A. Kayyali and M. N. Haque. Effect of Carbonation on the Chloride Concentration in Pore Solution of Mortars and Without Fly Ash. In: Cement and Concrete Research 18 (1988), No. 4, pp. 636-648

233. O. E. Gjørv. Effect of Condensed Silica Fume on the Electrolytic Conditions in Concrete. Trondheim : The Norwegian Institute of Technology, 1986

234. G. Rehm and U. Nürnberger and B. Neubert. Chloridkorrosion von Stahl in gerissenem Beton : A Bisheriger Kenntnisstand : B Untersuchungen an der 30 Jahre alten Westmole in Helgoland : C Auslagerung gerissener, mit unverzinkten und feuerverzinkten Stählen bewehrten Stahlbetonbalken auf Helgoland. Berlin : Beuth. - In: Schriftenreihe des Deutschen Ausschusses für Stahlbeton (1988), No. 390, pp. 43-144A

235. H. A. Brodersen. Zur Abhängigkeit der Transportvorgänge verschiedener Ionen im Beton von Struktur und Zusammensetzung des Zementsteins. Dissertation an der Fakultät für Bauwesen der RWTH Aachen, 1982

236. J. Tritthart. Zum Einfluß des Kations der Chloridverbindung und des Gipsgehaltes von Zement auf die Chloridkonzentration der Porenlösung. In: Zement und Beton 32 (1987), No. 4, pp. 157-159

237. C. M. Hansson and H. Strunge and J. B. Markussen and T. Forlund. The Effect of Cement Type on the Diffusion of Chloride. In: Nordic Concrete Research 4 (1985), pp. 70-80

238. O. A. Kayyali. Porosity of Concrete in Relation to the Nature of the Paste-Aggregate Interface. In: Materiaux et Constructions 20 (1987), No. 115, pp. 19-26

239. R. Zimbelmann. A Contribution to the Problem of Cement Aggregate Bond. In: Cement and Concrete Research 15 (1985), No. 5, pp. 801-808

240. P. Rechberger. Elektrochemische Bestimmung von Chloriddiffusionskoeffizienten in Beton. In: Zement-Kalk-Gips 38 (1985), No. 11, pp. 679-684

241. J. Weber. Penetration of Chlorides into Concrete on the Normal Exposure Conditions. Karlsruhe : Institut für Massivbau und Baustofftechnologie, 1988. - In: Dauerhaftigkeit nichtmetallischer anorganischer Baustoffe : Abschlußkolloquium des Forschungsschwerpunktprogrammes der DFG, Karlsruhe 4./5. Oktober 1988, pp. 55-60

242. Y. P. Virmani ; K. C. Clear ; T. J. Pasko. Federal Highway Administration: Time-To-Corrosion of Reinforcing Steel in Concrete Slabs. Washington : Federal Highway Administration, 1983

243. W. Lukas. Zusammenhang zwischen Chloridgehalt im Beton und Korrosion in schlaffer Bewehrung an österreichischen Brücken und Betonfahrbahnbrücken. In: Betonwerk und Fertigteil-Technik 51 (1985), no. 11, pp. 730-734

244. Bundesanstalt für Straßenwesen - BAST. Sachstandsbericht der Projektgruppe der Bundesanstalt für Straßenwesen: Schutzwirkung des Brückenbetons gegen Bewehrungskorrosion, insbesondere bei Tausalzeinwirkung. Bergisch Gladbach : Bundesanstalt für Straßenwesen, 1988

245. W. Richartz. Die Bindung von Chlorid bei der Zementerhärtung. In: Zement-Kalk-Gips 58 (1969), no. 10, pp. 447-456

246. K. Tuutti. Corrosion of Steel in Concrete. Stockholm : Swedish Cement and Concrete Research Institute. - In: CBI Research (1982), no. FO 4:82

247. H. A. Berman. Sodium Chloride, Corrosion of Reinforcing Steel, and the PH of Calzium Hydroxide Solution. In: Journal of the American Concrete Institute 72 (1975), no. 4, pp. 150-157

248. H.-J. Engell ; N. D. Stolica. Untersuchungen über Lochfrass an passiven Elektroden aus unlegiertem Stahl in chlorionenhaltiger Schwefelsäure. In: Archiv für das Eisenhüttenwesen 30 (1959), no. 4, pp. 239-248

249. D. A. Hausmann. Steel Corrosion in Concrete - How does it occur? In: Materials Protection, Houston 6 (1967), Nov. 1967, pp. 19-23

250. A. Bäumel. Die Auswirkung von Kalziumchlorid auf das Korrosionsverhalten von Stahl in Beton. In: Beton 10 (1960), no. 6, pp. 256-259

251. V. K. Gouda. Corrosion and Corrosion Inhibition of Reinforcing Steel - I: Immersed in Alkaline Solutions. In: Britisch Corrosion Journal 5 (1970), no. 5, pp. 198-203

252. A. Bäumel. Die Auswirkung von Betonzusatzmitteln auf das Korrosionsverhalten von Stahl in Beton. In: Zement-Kalk-Gips 12 (1959), no. 7, pp. 294-305

253. W. Manns ; W. R. Eichler. Zur korrosionsfördernden Wirkung von thiocyanathaltigen Betonzusatzmitteln. In: Betonwerk + Fertigteil-Technik 48 (1982, no. 3, pp. 154-162

254. H. Kaesche. Untersuchungen über die Korrosion unlegierter Stähle in Kalziumhydroxydlösung und in feuchtem Beton. In: Archiv für das Eisenhüttenwesen 36 (1965), no. 12, pp. 911...

255. P. Rechberger. Elektromechanische Modellversuche zur Frage der chloridinduzierten Betonstahlkorrosion. In: Zement-Kalk-Gips 36 (1983), no. 10, pp. 582-590

256. C. E. Locke ; S. Siman ; ASTM STP 713 ; ASTM. Electrochemistry of Reinforcing Steel in Salt-Contaminated Concrete. Philadelphia, PA. : American Society for Testing and Materials, 1980. - In: Corrosion of Steel in Concrete -ASTM STP 713 pp. 3-16

257. E. Atimtay ; M. Ferguson. Early Chloride Corrosion of Reinforced Concrete - a Test Report. In: Materials Performance 13 (1974), no. 12, pp. 18-21

258. Rasheeduzzafar ; S. S. Al-Saadoun ; A. S. Al-Gahtani ; F. H. Dakhil. Effect of Tricalcium Aluminate Content of Cement on Corrosion of Reinforcing Steel in Concrete. In: Cement and Concrete Research 20 (1990), no. 5, pp. 723-738

259. ASTM G01.14. Proposed Test for Evaluation of Corrosion Inhibitors in Reinforced Concrete. (Edition January 1988)

260. J. Holm. Comparison of the Corrosion Potential of Calcium Chloride and a Calcium Nitrate Based Non-Chloride Accelerator - A Macrocell Corrosion Approach. Detroit : American Concrete Institute, 1987. - In: Corrosion, Concrete and Chlorides (ACI SP-102), pp. 35-48

261. J. Gulikers. Beeinflussung der Korrosion der Bewehrung durch örtliche Instandsetzungsarbeiten (Orig. engl.). Zürich : Internationale Vereinigung für Brückenbau und Hochbau, ETH-Hoenggerberg, 1989 - In: Iabse Symposium, Lisbon, 1989, Sept. 6-8 "Dauerhaftigkeit von Bauwerken" pp. 151-156

262. P. Schießl ; M. Raupach. Influence of Concrete Composition and Microclimate on the Critical Chloride Content in Concrete. London : Elsevier, 1990 - In: Corrosion of Reinforcement in Concrete, International Symposium, Wishaw, Warwickshire, UK, 21-24 May, pp. 49-58

263. Wiss, Janney, Elstner Association. Corrosion Protection Tests on Reinforced Concrete Treated with Chem-Trete BSM40 Silane Sealer for Dynamit Nobel of America Inc. Rockleigh, New Jersey WJE No. 840168 June 1986. Chicago : Wiss, Janney, Elstner Association, 1986

264. K. C. Clear ; Federal Highway Administration - FHWA. Evaluation of Portland Cement Concrete for Permanent Bridge Deck Repair. Washington : Federal Highway Administration, 1974 Report no. FHWA-RD-74-5

265. J. Tomek ; F. Vavrin. Zur Frage der Stahlkorrosion im Beton durch Calziumchlorid. In: Zement-Kalk-Gips 14 (1961), no. 3, pp. 108-112

266. G. Hartl. Korrosionsschutz der Betonstahlbewehrung bei Tausalzeinwirkung - Einfluß der Rißbreite - Auswertung der 0,5-, 1,0- und 1,5-Jahrestermine für die Balken mit w/z = 0,50 und 3,5 cm Betonüberdeckung. Wien : Forschungsinstitut des Vereins der österreichischen Zementfabrikanten, 1983

267. U. R. Evans ; E. Pietsch. Korrosion, Passivität und Oberflächenschutz von Metallen. Berlin : Springer, 1939

268. P. Schießl ; RILEM ; Technical Committee 60-CSC. Corrosion of Steel in Concrete. New York : Champman and Hall, 1988 (RILEM Report)

269. H.-J. Abel ; C.-L. Kruse. Untersuchung über die Auswirkung der Elementbildung zwischen Stahl in Beton und Stahl in Erdböden. In: Werkstoffe und Korrosion 33 (1982), pp. 89-93

270. ACI 222R-85 ; Journal of the ACI. Corrosion of Metals in Concrete. In: Journal of the ACI 82 (1985), no. 1, pp. 3-32

271. H. Laase ; W. Stichel. Stützwandsanierung in Berlin : Spezielle Aspekte der Korrosion an der Rückwand. In: Bautechnik 60 (1983), no. 4, pp. 124-129

272. J. Noeggerath. Zur Makroelementkorrosion von Stahl in Beton : Potential- und Stromverteilung in Abhängigkeit verschiedener Einflußgrößen. Dissertation an der eidgenössischen Technischen Hochschule Zuerich, 1990

273. C. C. Naish ; A. Harker ; R. F. A. Carney. Concrete Inspection: Interpretation of Potential and Resistivity Measurements. London : Elsevier, 1990 - In: Corrosion of Reinforcement in Concrete, International Symposium, Wishaw, Warwickshire, UK, 21-23 May 1990, pp. 314-322

274. P. Schießl ; M. Raupach. Macrocell Steel Corrosion in Concrete Caused by Chlorides. Montreal : CANMET/ACI, 1991 - In: Second CANMET/ACI International Conference on Durability of Concrete, (Malhotra, V. M. (ED)), pp. 565-583

275. Deutscher Ausschuß für Stahlbeton - DAfSt. Richtlinie "Schutz und Instandsetzung von Betonbauteilen"

276. C. Alonso ; C. Andrade ; J. A. Gonzalez. Relation Between Resistivity and Corrosion Rate of Reinforcement in Carbonated Mortar made with Several Cement Types. In: Cement and Concrete Research 18 (1988), no. 5, pp. 687-698

277. G. Rehm ; H. L. Moll. Beobachtungen an alten Stahlbetonbauteilen hinsichtlich Carbonatisierung des Betons und Rostbildung an der Bewehrung. Berlin : Ernst. - In: Schriftenreihe des Deutschen Ausschuß für Stahlbeton (1965), no. 170, pp. 1-22

278. R. F. M. Bakker ; CUR. Carbonatatie, Corrosie en Vocht. Gouda : CUR, 1990 - CUR Rapport 90-3

279. P. Schießl ; M. Raupach. Der Einfluß wasserdichter, dampfdurchlässiger Beschichtungen auf die Korrosionsgeschwindigkeit bei karbonatisiertem Stahlbeton. Aachen : Institut für Bauforschung, 1991. - Forschungsbericht no. F 290

280. L. J. Parrott. Carbonation, Corrosion and Standardization. London : E.&F.N.Spon, 1990 - In: Protection of Concrete Proceedings of the International Conference held at the University of Dundee, Scotland, UK, on 11-13 Sept. 1990, pp. 1009-1023

281. B. B. Hope ; IP, A.K.C. Chloride Corrosion Threshold in Concrete. In: ACI Materials Journal 84 (1987), no. 4, pp. 306-314

282. P. Schießl ; M. Raupach. Einfluß der Betonzusammensetzung und der Umgebungsbedingungen auf die chloridinduzierte Korrosion von Stahl in Beton: Ergebnisse von Untersuchungen mit Betonkorrosionszellen. In: Betoninformationen 30 (1990, no. 4, pp. 43-54

283. B. B. Hope ; IP, A.K.C. Corrosion of Steel in Concrete made with Slag Cement. In: ACI Materials Jounal 84 (1987), no. 6, pp. 525-531

284. C. L. Page ; N. R. Short ; W. R. Holden. The Influence of Different Cements on Chlorideinduced Corrosion of Reinforcing Steel. In: Cement and Concrete Research 16 (1986), no. 1, pp. 79-86

285. M. Raupach. Chloride-Induced Macrocell Corrosion of Steel in Concrete. Aachen : Technische Hochschule, Fachbereich 3, Dissertation, 1991 (will be published 1992)

286. Ch. Alfes. Hochfeste verformungsarme Betone mit Silikastaub. In: Betonwerk + Fertigteil-Technik 55 (1989), no. 11, pp. 62-66, 68-71

287. C. L. Page ; J. Havdahl. Electrochemical Monitoring of Corrosion of Steel in Microsilica Cement Pastes. In: Materiaux et Conctruction 18 (1985), no. 103, pp. 41-47

288. J. T. Wolsiefer. Silica Fume Concrete: A Solution to Steel Reinforcement Corrosion in Concrete. Detroit : American Concrete Institute, ACI SP-126, 1991 - In: Durability of Concrete Second International Conference Montreal, Canada 1991, Vol. I, pp. 527-558

289. N. R. Buenfeld ; J. R. Newmann. Permeability of Marine Concrete. London : Marine Concrete, Papers for the International Conference on Concrete in the Marine Environment, 22-24 Sept. 1986

290. I. L. H. Hansson ; C. M. Hansson. Electrical Resistivity Measurements of Portland Cement Based Materials. In: Cement and Concrete Research 13 (1983), no. 5, pp. 675-683

291. P. Schießl ; M. Raupach. Influence of the Type of Cement on the Corrosion Behaviour of Steel in Concrete. New Delhi : National Council for Cement and Building Materials, 1992 - In: 9th International Congress on the Chemistry of Cement, New Delhi, 23-28 Nov. 1992, 6 pages

292. P. Schießl ; M. Schwarzkopf. Chloridinduzierte Korrosion von Stahl in Beton. Herrn Professor Dr.-Ing. Herbert Kupfer zum 60. Geburtstag 1987 gewidmet. In: Betonwerk und Fertigteil-Technik, Wiesbaden 52 (1986), no. 10, pp. 626-635

293. S. Rostam. International Codes of Practice with Particular Reference to Durability; Can Durability be Codified?. Bahrain : BSE, 1987 - In: Deterioration and Repair of Reinforced Concrete in the Arabian Gulf; Proceedings of the 2nd International Conference, 11.-13. Oct. 1987, Vol. 2, pp. 135-159

294. K. W. Treadaway. A Review of Comparative Performance of Reinforced Concrete in UK and Arabian Gulf Conditions. Bahrain : BSE, 1985 - In: Deterioration and Repair of Reinforced Concrete in the Arabian Gulf; Proceedings of the 1st International Conference, 26-29 Oct. 1985, Vol. 1, pp. 301-308

295. E. Heitz ; Kreysa. Grundlagen der technischen Elektrochemie - Erweiterte Fassung eines Dechema-Experimentalkursus. 2. Aufl. Weinheim : Verlag Chemie, 1980

296. M. Raupach ; C. Jaegermann. Untersuchungen zum Einfluss der Temperatur auf die Korrosionsgeschwindigkeit von Stahl in Beton. (will be published in 1992)

297. J. Hundt ; A. Wagner. Sorptionsuntersuchungen am Zementstein, Zementmörtel und Beton. Berlin : Ernst & Sohn. - In: Schriftenreihe des Deutschen Ausschuß für Stahlbeton (1978), no. 297, pp. 25-39

298. Z. P. Bazant. Physical Model for Steel Corrosion in Concrete Sea Structures - Theory and Application. In: Journal of the Structural Division 105,2 (1979), no. ST6, pp. 1137-1153, pp. 1155-1166

299. O. E. Gjorv ; O. Vennesland ; A. H. S. El-Busaidy ; Corrosion '76 ; Nace. Diffusion of Dissolved Oxygen Through Concrete. In: NACA Corrosion '76, 22-26 March 1976. Houston, Texas : Paper 17

300. R. B. Polder ; TNO ; IBBC ; Institute for Building Materials and Structures. Electrochemical Investigations into the Corrosion of Concrete Reinforcement in the Splash Zone - Revised Version. Delft : TNO Institute for Building Materials and Structures -IBBC-, 1989 - Projectnumber 61.5.3610. - Presented at the 9th European Congress on Corrosion 2-6 Oct. 1989 Utrecht, The Netherlands, 22 pages

301. C. L. Page. Basic Principles of Corrosion. London : Chapman and Hall, 1988 - In: Corrosion of Steel in Concrete: Report of the Technical Committee 60-CSC RILEM (Schießl, P. (ED.)), pp. 3-21

302. W. Schwenk. Elektrochemische und Korrosionschemische Untersuchungen an unlegiertem Stahl in Zementmörtel. In: 3R International 26 (1989), no. 10, pp. 666-668

303. P. Schießl. Zur Frage der zulässigen Rißbreite und der erforderlichen Betondekkung im Stahlbetonbau unter besonderer Berücksichtigung der Karbonatisierung des Betons. Berlin : Ernst & Sohn. - In: Schriftenreihe des Deutschen Ausschuß für Stahlbeton (1976), no. 255, München, Technische Universität, Dissertation, 1976

304. W. Schwenk. Korrosionsgefährdung und Schutzmaßnahmen bei Elementbildung zwischen erdverlegten Rohren und Behältern aus unterschiedlichen Metallen. In: GWF-Gas/Erdgas 113 (1972), no. 11, pp. 546-550

305. N. J. M. Wilkins ; P. F. Lawrence ; Concrete in the Oceans ; C&CA ; BCA. Fundamental Research Mechanisms of Corrosion of Steel Reinforcements in Concrete Immersed in Sea-Water. Wexham Springs : Cement and Concrete Association; BCA, 1980 In: Concrete in the Oceans Technical Report (1980), no. 5

306. P. Schießl. Einfluß von Rissen auf die Dauerhaftigkeit von Stahlbeton- und Spannbetonbauteilen. Berlin : Ernst & Sohn. - In: Schriftenreihe des Deutschen Ausschuß für Stahlbeton (1986), no. 370, pp. 10-52

307. G. Hartl ; W. Lukas. Untersuchung zur Chlorideindringung in Beton und zum Einfluß von Rissen auf die chloridinduzierte Korrosion der Bewehrung. In: Betonwerk und Fertigteil-Technik 53 (1987), no. 7, pp. 497-506

308. K. Okada ; T. Miyagawa. Chloride Corrosion of Reinforcing Steel in Cracked Concrete. Detroit, Michigan : American Concrete Institute, 1980 (ACI SP-65) In: Performance of Concrete in Marine Environment, pp. 237-254

309. T. Migagawa. Early Chloride Corrosion of Reinforcing Steel in Concrete. Dissertation at the Kyoto University, Japan, School of Civil Engineering, 1985

310. M. Makita ; Y. Mori ; K. Katawaki. Marine Corrosions Behavior of Reinforced Concrete Exposed at Rokyo Bay. Detroit, Michigan : American Concrete Institute, 1980 (ACI SP-65) In: Performance of Concrete in Marine Environment, pp. 271-290

311. N. J. M. Wilkins ; J. A. Stillwell. The Corrosion of Steel Reinforcement in cracked Concrete Exposed to Seawater Immersion. London : Marine Concrete, Papers for the International Conference on Concrete in the Marine Environment, 22-24 Sept. 1986

312. G. Grimaldi ; P. Brevet ; G. Pannier ; A. Raharinaivo. Factors Influencing Electrode Potential of Steel in Concrete. In: British Corrosion Journal 21 (1986), no. 1, pp. 55-62

313. P. Schießl ; M. Raupach. Untersuchungen zum Mechanismus der Bewehrungskorrosion im Bereich von Rissen. Berlin : Ernst & Sohn, 1990 - In: Baustofftechnische Einflüsse auf Konstruktionen. Zum 60. Geburtstag von Hubert K. Hilsdorf, pp. 583-599

314. K. Suzuki ; Y. Ohno ; S. Srisompong. Experimental Study on Internal Cracking of Partially Prestressed Concrete Flexural Members Part 1: Examination of Double Injection Technique; Part 2: Internal Cracking Characteristics. In: Journal of Structural and Construction Engineering (1985), no. 356, pp. 24-31, no. 365, pp. 9-17

315. J. W. Figg ; A. F. Marsden ; Concrete in the Oceans ; C&CA ; BCA. Development of Inspection Techniques for Reinforced Concrete : A State of the art Survey of Electrical Potential and Resistivity Measurements for use above Water Level. London : Her Majesty's Stationery Office ; Department of Energy. - In: Concrete in the Oceans Technical Report (1985), no. 10 = Offshore Technology Report OTH 84 205

316. D. G. Manning ; J. Ryell. Decision Criteria for the Rehabilitation of Concrete Bridge Decks. In: Transportation Research Record 762 (1982), pp. 1-9

317. R. F. Stratfull. Half Cell Potentials and the Corrosion of Steel in Concrete. State of California : Materials and Research Department, Research Paper CA-HY-MR-5166-7-72-T2, Interim Report PB 218-70, Department of Public Works, 1972

318. J. R. Daveer van. Techniques for Evaluating Reinforced Concrete Bridge Decks. In: Journal of the ACI 72 (1975), no. 6, pp. 697-704

319. P. Vassie. Reinforcement Corrosion and the Durability of Concrete Bridges. In: Corrosion Prevention & Control (1985), June, pp. 43-49

320. H. Arup. Electrochemical Monitoring of the Corrosion State of Steel in Concrete. Bahrain : BSE, 1985 - In: Deterioration and Repair of Reinforced Concrete in the Arabian Gulf ; Proceedings of the 1st International Conference 26-29 Oct. 1985, Vol. 1, pp. 485-493

321. A. F. Baker. Potential Mapping Techniques. London : Global Corrosion Consultants -GCC-, 1986. - In: Corrosion in Concrete Monitoring, Surveying and Control by Cathodic Protection London, 13th May 1986, pp. 3.1-3.21

322. B. Elsener ; S. Müller ; M. Suter ; H. Bohni. Potential Survey of Reinforced Concrete Structures Theory and Practice. Lyon : Centre d'Actualisation Scientifique et Technique -CAST-, 1988 - In: Proceedings of the International Conference Measurements and Testing in Civil Engineering, Vol 1, pp. 227-236

323. G. Grimaldi ; P. Brevet ; G. Pannier ; A. Raharinaivo. Factors Influencing Electrode Potential of Steel in Concrete. In: British Corrosion Journal 21 (1986), No. 1, pp. 55-62

324. B. Isecke. Potentialmessung zur Ermittlung von Bewehrungskorrosion. Darmstadt : Freunde des Instituts für Massivbau E.V., 1990 - In: Darmstädter Massivbau-Seminar 4 (1990), 10 pages

325. R. Müller. Dem Rost im Stahlbeton auf der Spur. In: Bautenschutz Bausanierung 10 (1987), no. 3, pp. (131-(134)

326. H. Marquart ; E. Sziesielski. Anwendung der elektrochemischen Potentialdifferenzmessung zum zerstörungsfreien Auffinden korrodierender Bewehrung im Hochbau. Berlin : Institut für Baukonstruktionen und Festigkeit ; Fachgebiet Allgemeiner Ingenieurbau der Technischen Universität Berlin, 1987

327. K. Menzel, H. Preusker. Potentialmessung: Eine Methode zur zerstörungsfreien Feststellung von Korrosion an der Bewehrung. In: Bauingenieur 64 (1989), no. 4, pp. 181-186

328. J. V. Sharp ; J. W. Figg ; M. B. Leeming. The Assessment of Corrosion of the Reinforcement in Marine Concrete by Electrochemical and other Methods. Detroit : American Concrete Institute, 1988 ACI SP-109 In: Concrete in Marine Environment Proceedings of the Second International Conference St. Andrews By-The-Sea, Canada, Aug. 1988, pp. 105-125

329. J. Tritthart ; H. Geymayer. Zerstörungsfreies Auffinden von Korrosionszonen der Bewehrung : Anwendung der Potentialdifferenzmessung. In: Beton 31 (1981), no. 6, pp. 237-240

330. H. Boehni ; B. Elsener. Früherkennung von Bewehrungskorrosion : Potentialfeldmessung und galvanostatische Impulstechnik. Berlin : DGZFP ; BAM. In: Vorträge und Plakatberichte Internationales Symposium zerstörungsfreie Prüfung im Bauwesen Diagnose Substanzerhaltung Qualitätssicherung, DGZFP Berichtsband 21 (1991), Vol. 1, pp. 101-122

331. B. Elsener ; S. Müller ; M. Suter ; H. Boehni. Corrosion Monitoring of Steel in Concrete - Theory and Practice. London : Elsevier, 1990 - In: Corrosion of Reinforcement in Concrete, International Symposium, Wishaw, Warwickshire, UK, 21-24 May 1990, pp. 348-357

332. H. Hildebrand ; W. Schwenk. Potential- und Polarisationsmessungen an Korrosionselementen. In: Werkstoffe und Korrosion, Weinheim 23 (1972). no. 5, pp. 364-370

333. A. Martini ; S. Mennenoeh. Über die Ausbildung von Makroelementen an Spundbohlen in Meerwasser. In: Stahl und Eisen 101 (1981), no. 1, pp. 79-85

334. J. Postlethwaite. Direct Measurement of the Corrosion Current for Oxygen-Reduction Corrosion. Philadelphia : American Society for Testing and Materials, ASTM STP 727, 1981 In: Electrochemical Corrosion Testing, pp. 290-302

335. A. M. Shams El DIN ; S. M. Abd El Haleem ; J. M. Abd El Kader. Studies on the Pitting Corrosion of Zinc in Aqueous Solutions II: Measurement of Pitting Corrosion Currents Operating under Natural Conditions. In: Journal Electronical Chemistry 65 (1975), pp. 335-349

336. B. Tsujino ; S. Miyase. On Ratio on Anode to Cathode for Iron in Neutral Solution. In: Corrosion 37 (1981), no. 9, pp. 541-545

337. A. W. Deeby. Development of a Corrosion Cell for the Study of the Influence of Environment and Concrete Properties in Corrosion. Australia : The Institution of Engineers, 1985 - In: Concrete 85 Conference "The Performance of Concrete and Masonry Structures", Bisbane 23-25 Oct. 1985, pp. 118-123

338. J. A. Gonzalez ; S. Feliu ; M. L. Escudero ; C. Andrade ; A. Macias. Relative Influence of Galvanic Macrocells and Local Microcells in the Corrosions of Reinforced Concrete Structures. Lyon : Centre D'Actualisation Scientifique et Technique -CAST-, 1988 - In: Proceedings of the International Conference Measurements and Testing in Civil Engineering, Vol. 1, pp. 237-249

339. J. J. W. Gulikers ; J. G. M. Mier van. The Effect of Patch Repairs on the Corrosion of Steel Reinforcement in Concrete. Montreal : CANMET/ACI, 1991 - In: Second CANMET/ACI International Conference on Durability of Concrete, pp. 445-460

340. F. Hunkeler. Kathodischer Schutz : Wissensstand, Einsatzmöglichkeiten und Einsatzgrenzen. Zuerich : Schweizerischer Ingenieur- und Architekten-Verein, 1988. - In: Korrosion und Korrosionsschutz. Teil 2: Schutz- und Sanierungsmethoden von Stahlbetonbauwerken, Studientagung März 1988 in Zürich, pp. 27-42

341. J. Holm. Comparison of the Corrosion Potential of Calcium Chloride and a Calcium nitrate Based Non-Chloride Accelerator - A Macrocell Corrosion Approach. Detroit : American Concrete Institute, 1987. - In: Corrosion, Concrete and Chlorides (ACI SP-102), pp. 35-48

342. R. W. Lambe ; M. J. Humphrey ; T. F. Watkins. Development of Materials for Repair and Protection of Reinforced Concrete. London : Elsevier, 1990 - In: Corrosion of Reinforcement in Concrete, International Symposium, Wishaw, Warwickshire, UK, 21-24 May 1990, pp. 471-485

343. V. I. Novgorodskii. Corrosion of the Steel Reinforcement in Cracked Concrete. In: Journal of Applied Chemistry of the USSR 40,1 (1967), no. 3, pp. 543-547

344. K. Suzuki ; Y. Ohno ; S. Praparntanatorn ; H. Tamura. Macrocell Corrosion Mechanism of Steel in Concrete. In: Journal of Structural and Construction Engineering (1990, no. 407, pp. 1-9

345. A. Volkwein. Anstriche als Korrosionsschutz der Bewehrung bei Sanierungen? Esslingen : Technische Akademie Esslingen, 1986 - In: 2. Internationales Kolloquium : Werkstoffwissenschaften und Bausanierung, pp. 707-715

345a P. Schießl ; M. Raupach. Monitoring System for the Corrosion Risk for Steel in Concrete. In: Concrete International (1992), no. 7

346. S. G. McKenzie. Techniques for Monitoring Corrosion of Steel in Concrete. London : Global Corrosion Consultants -GCC-, 1986. - In: Corrosion in Concrete Monitoring, Surveying and Control by Cathodic Protection London, 13th May 1986, pp. 4.1-4.25

347. K. Hladky ; J. L. Dawson. The Measurement of Localized Corrosion using Electro-Chemical Noise. In: Corrosion Science 21 (1981), no. 4, pp. 317-322

348. J. L. Dawson ; D. G. John ; M. I. Jafar ; K. Hladky ; L. Sherwood. Electrochemical Methods for the Inspection and Monitoring of Corrosion of Reinforcing Steel in Concrete. London : Elsevier, 1990 - In: Corrosion of Reinforcement in Concrete, International Symposium, Wishaw, Warwickshire, UK, 21-24 May 1990, pp. 358-371

349. C. Andrade. Monitoring Techniques. London : Chapman and Hall, 1988 - In: Corrosion of Steel in Concrete : Report of the Technical Committee 60-CSC RILEM (Schießl, P. (ED.)), pp. 79-95

350. M. Stern ; W. Schwenk. Arbeitsgruppe "Grundlagen der Anwendung physikalisch-chemischer Korrosionsprüfmethoden" der europäischen Föderation Korrosion. In: Werkstoffe und Korrosion 27 (1976), pp. 241-245

352. E. Escalante. Effectiveness of Potential Measurements for Estimating Corrosion of Steel in Concrete. London : Elsevier, 1990 - In: Corrosion of Reinforcement in Concrete, International Symposium, Wishaw, Warwickshire, UK, 21-24 May 1990, pp. 281-292

353. S. Feliu ; J. A. Gonzalez ; C. Andrade ; I. RZ-Maribona. Errors Introduced by the Guard Ring Device in the On-Site Measurement of Rebar Corrosion Rates. London : Elsevier, 1990 - In: Corrosion of Reinforcement in Concrete, International Symposium, Wishaw, Warwickshire, UK, 21-24 May 1990, pp. 293-302

354. S. Feliu ; J. A. Gonzalez ; C. Andrade ; V. Feliu. The Determination of the Corrosion Rate of Steel in Concrete by a Non-Stationary Method. In: Corrosion Sience 26 (1986), no. 11, pp. 961-970

355. J. L. Dawson ; L. M. Callow ; K. Hladky ; J. A. Richardson. Electrochemical Impedance Measurements Applied to the Corrosion of Reinforcing Steel in Concrete. In: Proceedings of Corrosion 78, NACE, Texas, March 1978, pp. 125/1-125/19

356. B. B. Hope ; J. A. Page ; A. K. C. Ip. Corrosion Rates of Steel in Concrete. In: Cement and Concrete Research 16 (1986), no. 5, pp. 771-781

357. K. Matsuoka. Monitoring of Corrosion of Reinforcing Bar in Concrete. Houston : National Association of Corrosion Engineers, 1987 - In: Corrosion of Metals in Concrete; Proceedings of the Corrosion / 87 Symposium on Corrosion of Metals in Concrete, pp. 42-48

358. J. Noeggerath ; H. Boehni. Investigations on Active/Passive-Macroelements for the Local Corrosion of Steel in Concrete. In: Materials Science Forum Vol. 44&45 (1989), pp. 357-374

359. A. A. Sagues. Evaluation of Corrosion Rate by Electrochemical Impedance in a System with Multiple Polarization Effects. In: NACE Corrosion '89, Paper 25

360. I. Epelboin ; C. Gabrielli ; M. Keddam ; H. Takenouti. Alternating-Current Impedance Measurements Applied to Corrosion Studies and Corrosion-Rate Determination. Philadelphia : American Society for Testing and Materials, ASTM STP 727, 1981. In: Electrochemical Corrosion Testing, pp. 150-166

361. S. Haruyama ; T. Tsuru. A Corrosion Monitor Based on Impedance Method. Philadelphia : American Society for Testing and Materials, ASTM STP 727, 1981. In: Electrochemical Corrosion Testing, pp. 167-186

362. K. Hladky ; L. M. Callow ; L. J. Dawson. Corrosion Rates from Impedance Measurements: An Introduction. In: British Corrosion Journal 15 (1980), no. 1, pp. 20-25

363. S. G. Millard ; K. R. Gowers ; J. S. Gill. Reinforcement Corrosion Assessment using Linear Polarization Techniques. In: Proceedings of the ACI International Conference on Evaluation and Rehabilitation of Concrete Structures and Innovations in Design, Dec. 3-6, 1991, Hong Kong, 28 pages

364. D. D. MacDonald ; M. C. H. McKubre. Electrochemical Impedance Techniques in Corrosion Science. Philadelphia : American Society for Testing and Materials, ASTM STP 727, 1981. In: Electrochemical Corrosion Testing, pp. 110-149

Specific Theme IV B

Cement-aggregate Compatibility and Structure Property Relationship Including Modelling

CEMENT-AGGREGATE COMPATIBILITY AND STRUCTURE PROPERTY RELATIONSHIPS INCLUDING MODELLING

H M Jennings and Y Xi
Civil Engineering and Materials Science Engineering
North-western University, Evanston, USA

ABSTRACT

The role of aggregate, and its interface with cement paste, is discussed with a view toward establishing models that relate structure to properties. Both short (nm) and long (mm) range structure must be considered.

The short range structure of the interface depends not only on the physical distribution of the various phases, but also on moisture content and reactivity of aggregate. Changes that occur on drying, i.e. shrinkage, may alter the structure which, in turn, feeds back to alter further drying and shrinkage. The interaction is dynamic, even without further hydration of cement paste, and the dynamic characteristic must be considered in order to fully understand and model its contribution to properties.

Microstructure and properties are two subjects which have been pursued somewhat separately. This review discusses both disciplines with a view toward finding common research goals in the future. Finally, comment is made on possible chemical reactions which may occur between aggregate and cement paste.

简介一般讨论了骨料、骨料与水泥基之间界面对材料性能的影响，侧重于建立模型来描述结构与性能之间的关系，包括微观结构(nm)与宏观结构(mm)的影响。

界面的微观结构不仅取决于各相的合理分布，取决于含水量及骨料与基材之间的反应能力。干燥引起的收缩可以改变结构，而这种改变反过来又影响干燥和收缩。因此，即使不考虑水化进程，结构与性能之间的互相影响也是动态的。所以必须考虑动态特征才能全面理解和建立骨料及界面对材性的影响。

微观结构和宏观性能一直是两个被分别研究的课题。本文从另一个角度来讨论这两个课题：即寻找把它们联系起来的共同研究目标。最后，本文评价了骨料与基材之间可能产生的化学反应。

INTRODUCTION

"Cement aggregate compatibility" may be studied from at least three points of view: 1) Microstructure, 2) Influence of processing and chemistry, including long term cement-paste aggregate interaction 3) Properties including strength, toughness and shrinkage. In all three cases the interface, sometimes called the transition zone, and sometimes the bond, is the region of interest and will be the focus of discussion in this paper. It is a region that greatly influences the bulk properties of concrete.

Concrete is a composite material composed of several phases including various hydration products, pores, unreacted cement, and both fine and coarse aggregate. In the simplest sense concrete may be considered to be aggregate bound together by cement paste. Many properties are controlled by the bond between paste and aggregate and, therefore, it has been studied extensively. Perhaps the most important feature of the zone is the relatively high porosity compared to the bulk paste. High porosity means that the zone has poor properties such as low strength, and high permeability. These interfaces are typically zones of weakness and, since a crack follows the path of least resistance, the interface is important to strength, toughness, and other properties.

Because the bond is distributed throughout the volume, in other words it has a long range structure, it may be argued that essentially all of the engineering properties of concrete are influenced strongly by the bond. Thus, both the microstructure of the bond (short range structure) and the macrostructure of its distribution throughout the volume of concrete (long range structure) are important. This review emphasizes both of these characteristics with a view towards establishing quantitative relationships to properties.

One of the least understood, but most important aspects of the cement paste aggregate region is chemical compatibility. If the two materials are not compatible than they may react-- the so called alkali aggregate reaction. This is a topic that is poorly understood from a mechanistic point of view, and, therefore, the reaction has not been modelled, and detailed relationships to properties have not been established. This review will comment only briefly on an approach to modeling the reaction.

MICROSTRUCTURE OF CEMENT PASTE-AGGREGATE INTERFACE

The interface has been studied extensively (Barnes, 1978, 1979; Monteiro, 1985; Monteiro and Mehta, 1985; Monteiro and Ostertag, 1989; Scrivener and Gartner, 1988; Xie, 1992; and Monteiro and Mehta, 1986). Essentially all aspects of the microstructure of the interface, such as the distribution of anhydrous grains, CH crystals, and porosity, vary with distance from the surface of the aggregate particle into the bulk paste as shown in Fig. 1(a) (Scrivener and Gartner, 1988). The porosity at the surface of aggregate, for example, may be three times higher than that in the bulk paste. The properties of the interface, therefore, are significantly different from those of the paste away from the interface, as shown schematically in Fig. 1(b) (Zimbelmann, 1985).

The thickness of interfacial region is often measured to be about 40-50 μm. Furthermore, for a typical well proportioned concrete, the mean spacing between aggregate particles is only 75-100 μm (Diamond et al, 1932; Mindess, 1988), thus, a large fraction of cement paste belongs to interface zone, only a small part bulk cement paste exist.

Although the microstructure of the interface has been much studied, its macrostructure has received relatively little attention. As defined here, the macrostructure is the long range structure associated with the size, volume fraction, and distribution of the aggregate, or, more precisely, the surface of the aggregate. In many respects the macrostructure must be considered to be at least as important as the microstructure. As already mentioned, the distance between aggregate particles in concrete is often

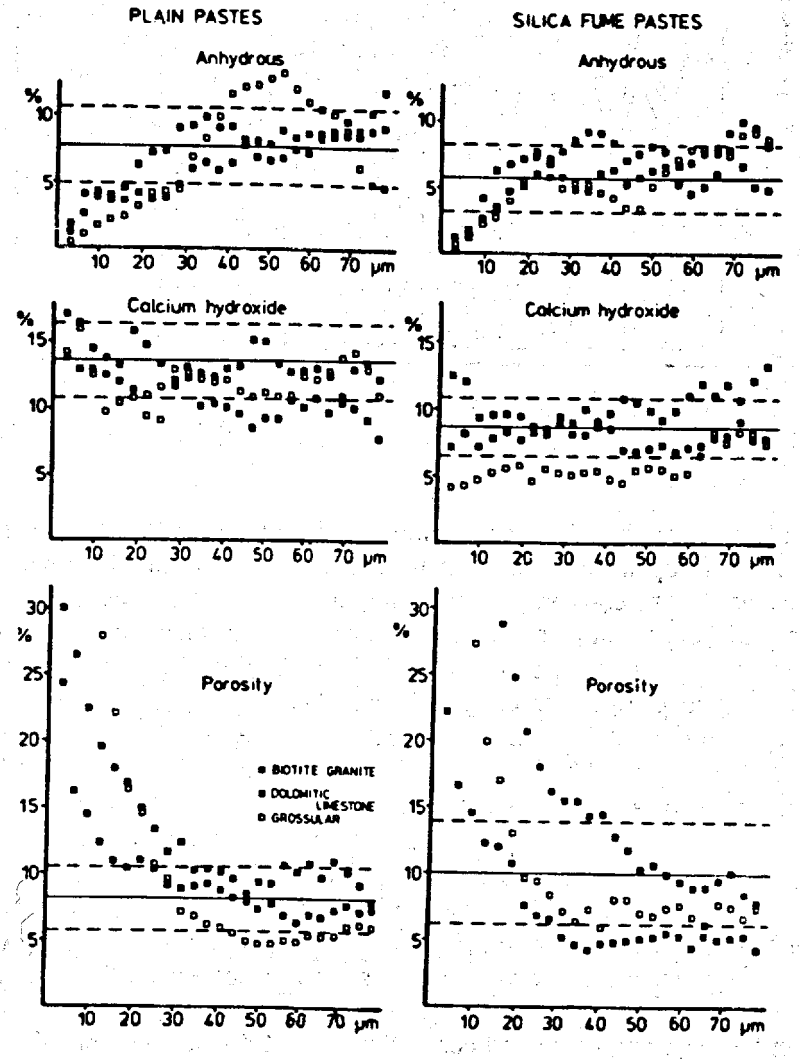

Fig. 1(a) Variation in the amounts of anhydrous material and CH and of porosity with distance from the aggregate interface (Scrivener and Gartner, 1988).

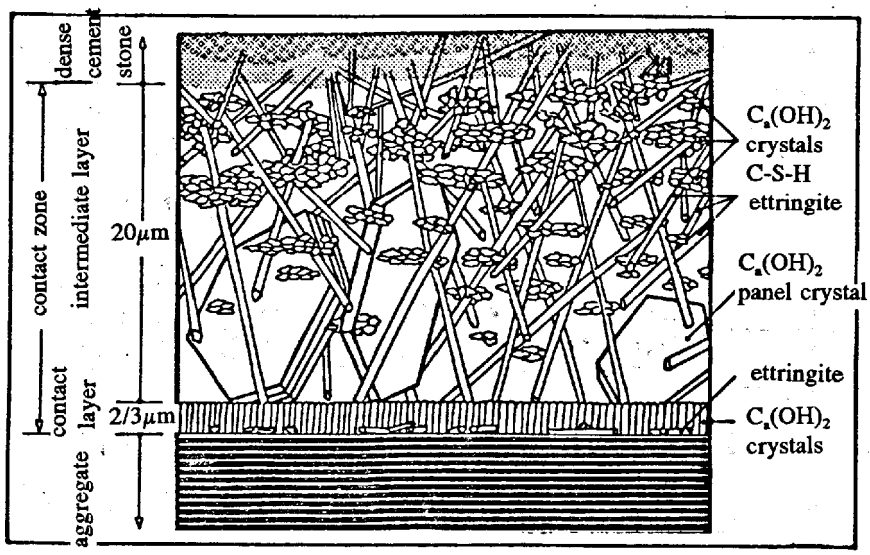

Fig. 1 (b) Schematic view of interfacial zone (Zimberlmann, 1985).

sufficiently small that all of the region where aggregates are close together has the structure of a transition zone. Thus, a "closed" and "open" interface has been defined (Pope and Jennings, 1992) where the structure of the interface may not be constant, for example, the structure between closely spaced aggregate, may contain more pores, CH and Hadley grains than the normal transition zone (Pope and Jennings, 1992) This "closed" interface may be particularly damaging to bulk properties. The long distance structure might be thought of as an entangled cellular structure. There also may be gravitational effects that cause variation in structure between top and bottom of aggregate. In other words bleeding may cause the zone to be somewhat larger at the bottom of aggregate particles than it is at the top, as has been observed for grouts with high water:cement ratios (Helal and Krizek, 1992).

The strength of the bond is related to the strength of mortar and concrete, but only qualitative correlations have thus far been suggested. The surface of aggregate is also important. Different aggregates consume different amounts of water, and even with the same kind of aggregate, the thickness of the water layer on the aggregate surface will have a significant effect on the formation of interfacial bonding (Xie, 1992). Furthermore, the surface condition of aggregate is important, the rougher surface providing better contact between aggregate and cement matrix. Chemical compositions of the aggregate influences the bond because if the aggregate reacts with surrounding cement matrix, then the interfacial bonding increases considerably. More research in this area should lead to improved concrete.

Although the long range structure of the interface has not been studied explicitly, there is some information that has been presented in a variety of different studies. In particular, the size, shape, and volume fraction of aggregate is related directly to the distribution of the associated interface and it has also been related to several bulk properties. Both short and long range structures must be considered in order to relate the bond to properties.

An often neglected aspect of the structure of the bond between paste and aggregate is the influence of moisture content, and moisture gradients. This review will address explicitly the influence of moisture on properties and, therefore, the influence of moisture on structure will be suggested.

RELATIONSHIP BETWEEN INTERFACE AND BULK SHRINKAGE

An important property that is controlled by the transport of moisture is bulk shrinkage or drying shrinkage. Aggregate is (to a first approximation) a non-shrinking filler, which has a restraining influence on bulk shrinkage. Both the short and long range structures are important. Indeed, all of the components of cement aggregate compatibility are important to shrinkage, i.e. aggregate, interface and paste.

(1). Bulk shrinkage of cement paste

Water to cement ratio of cement paste is a dominant parameter that has a very strong effect on shrinkage. High water to cement ratio, generally, results in high shrinkage. Cement composition, or the type of cement, also has the effect on cement paste shrinkage. Tests on pastes made from individual cement compounds have shown that C_3A shows large volume change, while C_3S exhibits relatively little microstructural change (Carlson, 1939). However, the evidence from recent (Environmental Scanning Electron Microscope) tests (Bergstrom et al, 1992) show that C_3S has also a large shrinkage deformation as shown in Fig. 2. Shrinkage is measured by applying an image intensity matching technique (Xi et al, 1992). Fig. 2 shows the displacements of six points in Fig. 3, in which a specimen is dried from R.H. = 50% to R.H. = 30%. From Fig. 2, for instance, the shrinkage strain between points A and F are about 0.02%. This is a very large shrinkage strain, an order of magnitude larger than the shrinkage at macro-scale.

(2). Cement paste shrinkage at the interface

More recent research using the Environmental Scanning Electron Microscope (Sujata et. al, 1992) has investigated the shrinkage in the interfacial zone of large aggregate (5mm). Fig. 4 shows the trend of the displacement as a function of distance from the aggregate surface. The slope of the data represents the intensity of deformation (strain). It is clear that the slope in the near field is larger than that in the far field, which means the cement matrix shrinks more in the near field than in the far field.

Fig. 5 shows the result from a mortar specimen, where the distance between surfaces of the two observed sand particles is about 120 micrometers. Fig. 5 also shows the results from a sand particle surface to the mid-point between adjacent particles. There is no far field displacement. One can see that the slope is kept almost a constant, which means that the inter-particle cement matrix shrinks almost uniformly.

Thus, the structure of the aggregate and its distribution is very important to shrinkage. The results indicate the dependence of shrinkage of the interfacial zone, on the size of aggregate, and the distance between aggregates.

(3). Aggregate Type

If the aggregate does not shrink, the restraining effect will be maximum. However, if the aggregate shrinks the same as cement paste, there will be no restraining effect. Commonly used aggregate are between these extremes and may be classified into three types (Carlson, 1939):

(A). High shrinkage aggregate: hornblende, pyroxene, marble, and sandstone,
(B). Low shrinkage aggregate: limestone, quartz, glass, feldspar, and dolomite,
(C). Intermediate Shrinkage: granite.

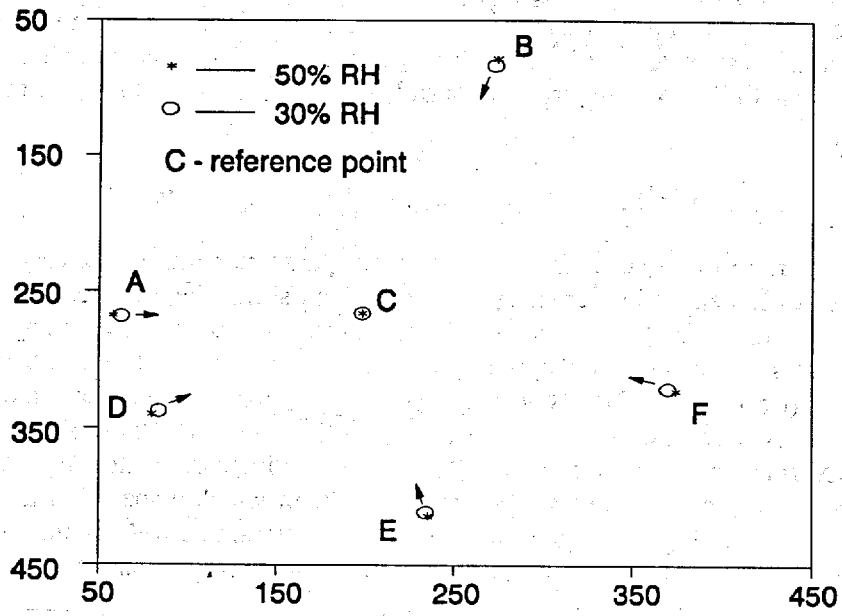

Fig. 2 Shrinkage of C_3S (Vectors at each point represent displacement with respect to point C)

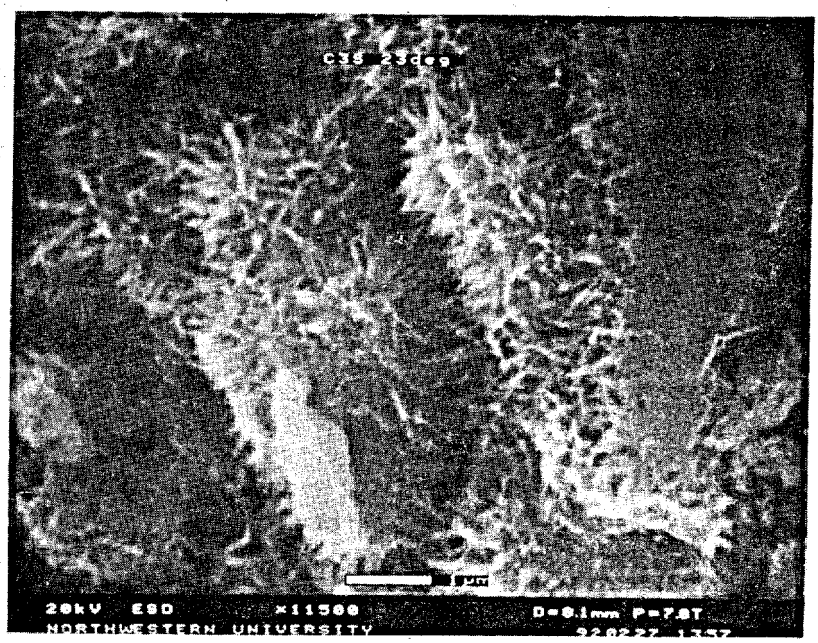

Fig. 3 ESEM image of C_3S paste image, R.H. = 30%, w/c = 0.5, t = 7 days.

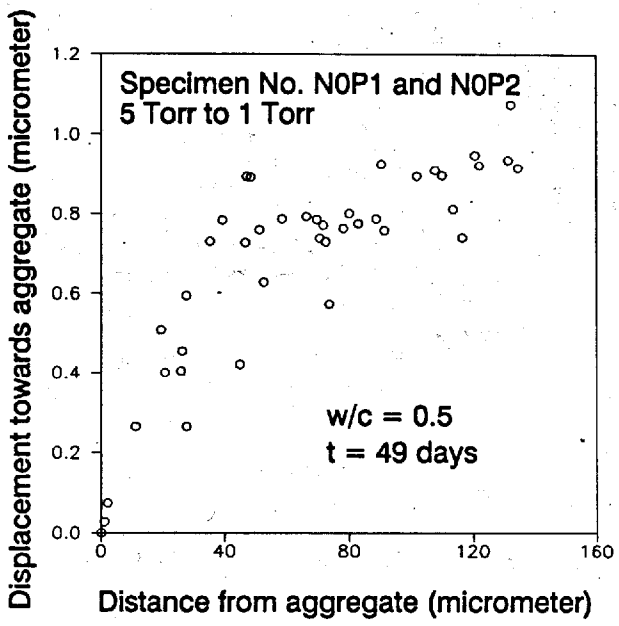

Fig. 4 Cement paste deformation in two aggregates specimen

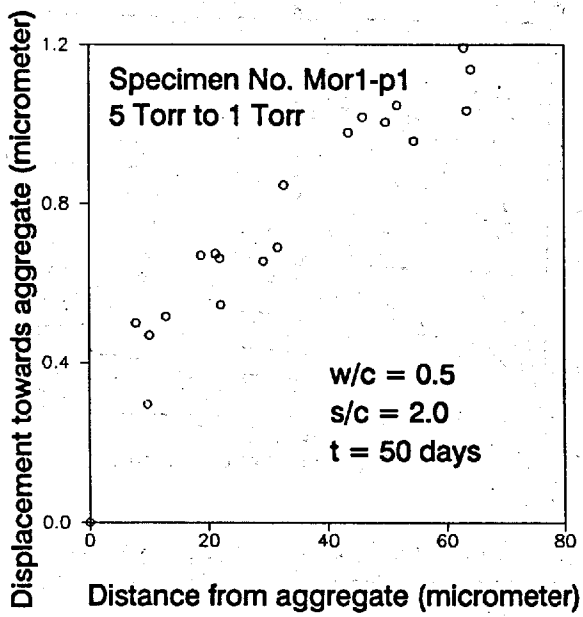

Fig. 5 cement paste deformation in mortar specimen

The structure of the interface, as shown in Fig. 1, and discussed above, has been determined mainly from dried specimens in an SEM. This structure may well depend on the shrinkage of aggregate as well as that of cement paste.

The ratio of elastic moduli is defined as E_a/E_c, where E_a and E_c are elastic moduli of aggregate and cement paste, respectively. The higher the ratio the lower is the shrinkage.

The ratio of Poisson's ratio is defined as ν_a/ν_c, where ν_a and ν_c are the Poisson's ratios of aggregate and cement paste, respectively, exhibits the same effect as the ratio of elastic modulus, that is, the higher the ratio the lower is the shrinkage.

(4). <u>The content and size distribution of aggregate</u>

High aggregate content leads to low shrinkage of concrete. This is a basic observation from test results as shown in Fig. 6(a). Concrete made with very little aggregate shrinks almost the same as cement paste, while the concrete made with very little cement content exhibits almost no shrinkage.

In general, the larger the maximum size of aggregate the smaller is the shrinkage (see Fig. 6(b)). As long as the maximum size of aggregate and consistency of concrete are not varied, the gradation of aggregate does not have much of an effect on the shrinkage.

RELATIONSHIP BETWEEN BOND AND STRENGTH OF CONCRETE

One way of studying the influence of the bond is to alter the bond and measure a bulk property. Methods for improving the bond include the addition of silica fume to reduce porosity (Zimbelmann, 1985, 1987; Jia, 1988), the addition of certain agents to arrange CH crystals in random orientation (as opposed to oriented crystals) and the coating of aggregate to promote chemical reaction with the matrix (Monteiro,

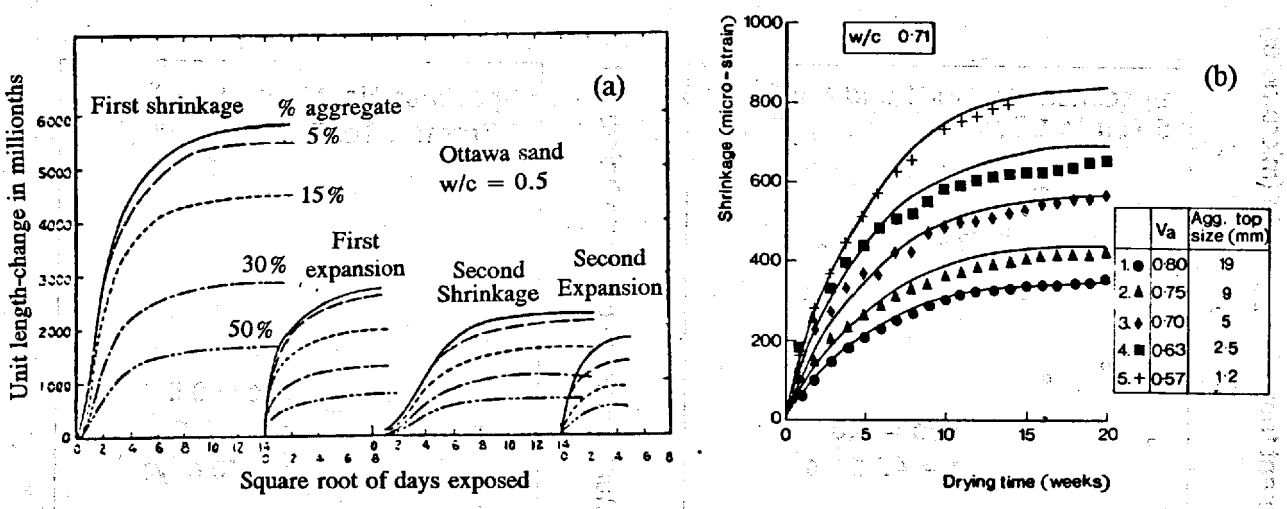

Fig. 6 (a) Shrinkage at various aggregate content (w/c = 0.5) (Pickett, 1965), and (b) the effect of aggregate size on shrinkage (Hobbs, 1974).

1985). All of these methods improve the strength of concrete.

The suggestion has been made that a thinner zone is a stronger zone. (Zimbelmann, 1985; Xie, 1992). Tenside has been added to reduce the surface tension of water, and consequently diminish the thickness of water film on aggregate, and thus has led to improved strength.

Aggregate push-out tests (Shah and Li, 1992) (as discussed in the next section) show that strength of the bond is increased by coating the aggregate with a slurry of the cement plus silica fume. This results in the bulk surface fracture energy of the interface increasing by about 10 times. It is also shown that coating the aggregate with a slurry of cement without silica fume, about an hour before mixing the concrete, can improve interface behavior, but the mechanism is not clearly understood yet.

The bond is not a static structure, but rather it develops with time, and it changes with applied stress and with change in the environment. The difference between the mechanical properties of the aggregate and cement matrix causes stress concentrations, which leads to cracking in the interfacial zone when stress is applied and when shrinkage due to drying occurs. One question is: Does microcracking remain in concrete at the equilibrium state of moisture, and if so, what is the effect of these cracks on strength? Certainly, the structure and properties of the interface are a function of moisture content.

Considering the first part of the question, large cracks have been observed everywhere in concrete during drying (Hsu et al, 1963a,b,c; Slate and Olsefsk, 1963; Backstrom, 1955; Forrester, 1968; Ringot, 1987; Sicard et al, 1992). Saito (1991) put strain gages inside aggregate and observed the shrinkage strain during drying. The results show that strain within aggregate changes little with time. Comparing this with the large shrinkage in the surrounding matrix, therefore, it can be inferred that some microcracks, or something equivalent, have formed around aggregate particles. However, other evidence shows that these drying shrinkage cracks will close up when internal moisture distribution reaches an equilibrium (Hwang and Young, 1984; Day and Illston, 1983; and Day, Cuffaro, and Illston, 1984).

The combined influence of shrinkage and cracking is not understood qauntitatively. For example, moisture gradient, and associated shrinkage, is a size dependent problem since moisture diffusion is size dependent. Different conclusions have been drawn based on different test data. Hsu (1963a) used specimens with cylinder dimension 4" x 8" and dried for only 3 days, while Hwang (1984) used thin specimen of 2 mm thick and dried for 6 days. The existence of microcracking at equilibrium is important for determining unrestrained shrinkage of concrete. In other words, microcracking is a mechanism that apparently reduces shrinkage and if this effect cannot be excluded then the measured shrinkage will be an apparent behavior, but not a real material property (Chatterji, 1976). The influence of microcracking must be understood quantitatively. Furthermore, the extent of microcracking is related to aggregate content.

The effect of these interfacial drying cracks on load carrying capacity is important. Once again, experimental evidence from different researchers has not been completely consistent. Observations of Hsu et al (1963a,b,c) and recent results on surface cracking of fiber reinforced cement paste by moire interferometry technique (Shah and Shao, 1992) have shown that cracks due to loading usually initiate from existing surface shrinkage cracks, which means the failure process starts from shrinkage cracks, and thus shrinkage cracks decrease material strength. Therefore, in order to understand failure mechanisms of concrete, shrinkage cracks prior to loading must be understood. Some other test results that support this idea are from Eden and Bailey (1984), and Alexander (1959). However, in the same report Hsu et al (1963c) found that drying reduces tensile strength but increases compressive strength. Eden and Bailey (1984) reported that drying decreases flexural strength of ordinary portland cement paste.

In contrast to the above, Wittmann (1973) reported test data that show the effects called "drying-strengthening and "wetting-weakening", which means that drying increases cement paste strength. Wittmann (1968) also explained the physical background of the phenomena. The wetting process decreases surface tension, surface energy, which according to Griffith equation, reduces the ultimate stress, and consequently, the strength is reduced. Supporting evidence has been published by Pihlajavaara (1965, 1974), Sereda (1966) and Rostasy and Budelmann (1986).

Thus, the structure of the interface depends on drying and this, in turn, influences strength. Drying itself is a very complicated process, depending on age, composition, size, and shape. For example, the direction in which moisture is removed controls the orientation of shrinkage microcracking, and thus gives various effects on strength. Structure influences drying and drying influences structure, and both influence strength. There are no quantitative relationships between the structure of the bond and strength. Perhaps the main obstacle has been the absence of a quantitative description of bond.

RELATIONSHIP BETWEEN INTERFACE AND FRACTURE TOUGHNESS

Interest has been heightened recently in the fracture properties of the interface. This section will discuss some of the methods and results relevant to the toughness of the bond. Toughness of the bond is a property which may be measured directly.

The bond region is thin and, as discussed above, the structure varies across the interfacial region. This implies variable properties across the interfacial region and the question must be asked: What is a representative property? Frequently, a test fails to measure a property of the bond because failure occurs somewhere else. Tests designed to measure a property of the bond often "force" failure to occur in the bond region, but satisfying this criteria is very qualitative.

Forcing failure to occur at the bond is usually accomplished by deep grooving, or the introduction of a large flaw. Under these conditions, the distinction between strength and toughness is blurred. In other words, strength is controlled by flaws and the introduction of a large "artificial" flaw, or notch, means that toughness, or the material's resistance to the extension of a flaw, is being measured. Attempts

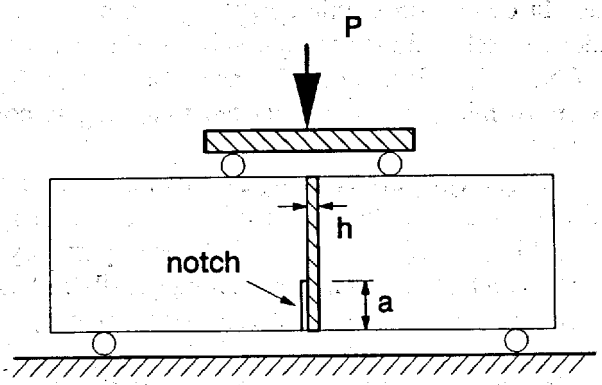

(a) Four-point-bending specimen

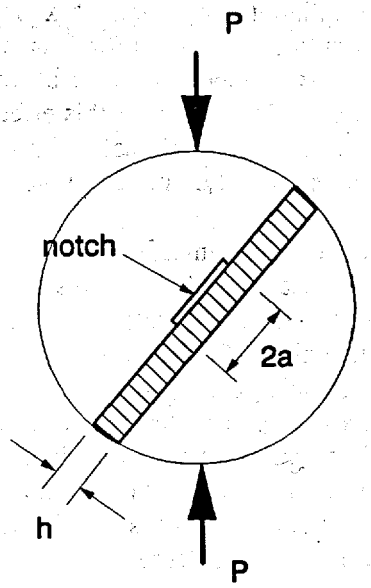

(b) Brazilian disk specimen

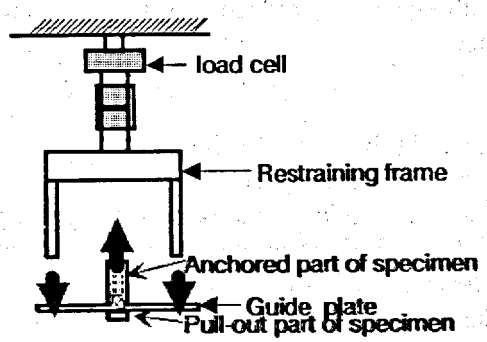

(c). Pull-out test

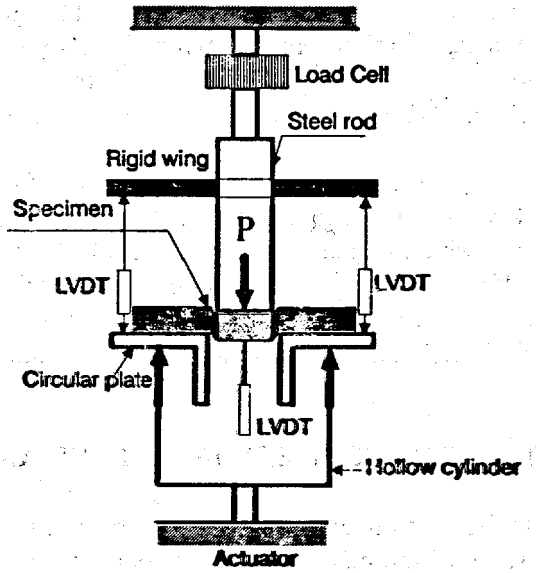

(d). Push-out test.

Fig. 7 Four commonly used experimental setup for interfacial mechanical behavior.

to measure tensile and shear strengths, and toughness under various loads are frequently reported. This is a topic of current research.

It should be noted that testing frequently involves idealized specimen geometries. It follows that the structure of the bond may be different in an idealized test than it is in a commercial concrete. For example, the bond may depend on mixing at the interface, and, therefore, casting cement paste against a flat surface may produce a different result than mixing aggregate in a large concrete mixer. Indeed, mixing is known to alter the transition zone (Pope and Jennings, 1992).

The fracture toughness of the interface, in general, has been studied by Williams (1959), who shows that a crack follows a characteristic oscillating stress singularity. Rice (1988) has developed the complete form of the near tip field at an interface by an analytic function. To determine the fracture toughness of the interface, particularly for concrete, four currently used experimental setups are used as shown in Fig. 7. Fig. 7(a) and 7(b) (Hillemeier and Hilsdorf, 1977; Buyukozturk and Lee, 1992) show sandwich specimens with a notch in the bond. If the thickness of the sandwich layer is small compared to the length of the notch, (and to all other relevant in-plane lengths) the interface stress intensity factor, K, and the stress intensity factors for a homogeneous matrix material, K_I (mode I) and K_{II} (mode II), can be related (Suo and Hutchinson, 1989):

$$K\, h^{i\epsilon} = p\, |K^{\infty}|\, e^{i\psi}$$

$$p = \sqrt{\frac{1-\alpha}{1-\beta^2}}, \qquad \psi = \phi + \omega(\alpha,\beta), \qquad \phi = \tan^{-1}\left(\frac{K_{II}}{K_I}\right) \tag{1}$$

where $i = (-1)^{1/2}$, α and β are Dundurs constants, which are the function of elastic modulus and Poisson's ratio of matrix and aggregate, $|h^{i\epsilon}| = 1$, $K^{\infty} = K_I + iK_{II}$; ω is a certain function of α and β, ϵ is the oscillation index depending on β. ϕ is the phase angle of K^{∞}, which is the direction of the traction vector loaded at far field. Physically, Eq. 1 means that the complex interface stress intensity factor combination, $Kh^{i\epsilon}$, has a magnitude scaled by a factor p and phase angle shifted by ω with respect to K^{∞}. For example, a mode I specimen with a sandwich layer ($\phi = 0$) will not be "mode I" at the interface crack tip but with a phase angle, $\psi = \omega$. Thus, ψ measures the relative proportion of mode II to mode I on the interface, and ω reflects the shift in the relative proportion in the applied remote field to that in the interface field.

Eq. 1 is important because K can not be determined directly, but K_I and K_{II} can be determined from a specimen made of homogeneous matrix material. The energy release rate G is related to K

$$G = \frac{(1/E_1 + 1/E_2)}{2\cosh^2 \pi\epsilon} |K|^2 \tag{2}$$

By using Eqs. 1 and 2, fracture toughness of a mortar/granite interface (mortar is considered a homogenous matrix) has been determined by Buyukozturk and Lee (1992) and shown in Fig. 8. It is seen clearly that fracture toughness is dependent on the elastic parameters of each components of the composite.

The mechanical behavior of the bond is being studied by push out tests similar to those used to study fibers in ceramics. The experimental setup is shown in Fig. 7(c, d) (Li et al, 1991). Again, the fracture toughness and strength of the bond are not measured directly, and a model has been developed

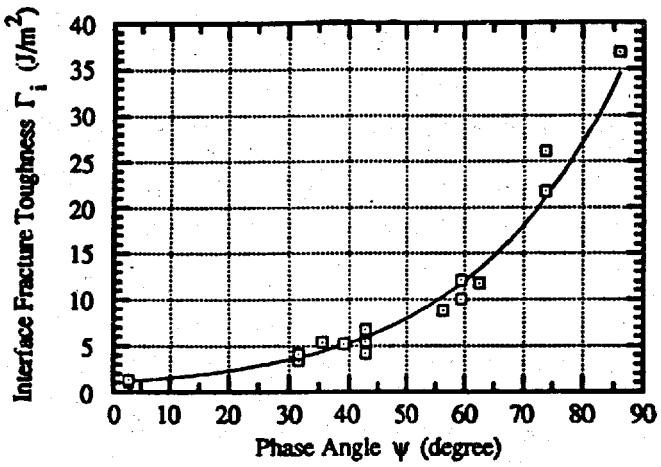

Fig. 8 Fracture toughness curve for the mortar/granite interfaces (Buyukozturk and Lee, 1992).

to relate measurable experimental quantities to mechanical properties. Therefore, mechanical parameters of the interface are dependent on the theoretical models. Shah et al (1992; Stang et al 1990; Li et al, 1991) established a model based on the equilibrium equation of a partly debonded fiber and a shear-slip relation as shown in Fig. 9. Contrary to the fracture mechanics approach, the maximum stress at the crack tip is q_y rather than a stress singularity, and the sliding surface behind the crack tip (type II crack) has the frictional shear force q_f instead of a traction free crack. For a given geometry and material, q_f, q_y, and the energy release rate, Γ, can be determined by maximum load, P_{max}, and the slip displacement corresponding to P_{max}. These three parameters have been expressed explicitly as a function of fiber elastic modulus, E_f , and ω, $\omega = (k/E_fA_f)^{1/2}$, where k is the slope of shear force and slip displacement curve (see Fig. 9), A_f is the sectional area of the fiber. k can be determined from the initial slope of the experimental load-slip displacement curve, and thus the interaction between the two materials is summed into ω.

Tables 1 and 2 show the parameters for fiber pull-out tests and aggregate push-out tests with the effects of specimen length, water to cement ratio, and various coatings. As mentioned previously, the coating treatment increases all of the parameters significantly (see Table 2 row 5). One can see from Tables 1 and 2, and Fig. 8 that many parameters influence the bond. In order to understand the parameters that control the bond, there is a need to go one step further, for instance, it is necessary to study the relationship of k to the microstructure quantitatively.

THE EFFECT OF AGGREGATE ON TRANSPORT PROPERTIES

In general, the addition of aggregate controls the rate of moisture transport in mortars and concretes. This is typically attributed to the high porosity near the aggregate surface. However, like strength, transport properties of the interface are not measured directly, but rather, the influence of aggregate on average transport properties has been studied.

Transport behavior can be characterized partly by moisture capacity, which is the reciprocal of the slope of desorption (or adsorption) isotherm curves. Gleysteen and Kalousek (1955) carried out adsorption tests on concrete and found the surface area of the cement paste within concrete (excluding aggregate) is about 100 m^2/g (water as adsorbat), much lower than the surface area of pure cement paste (about

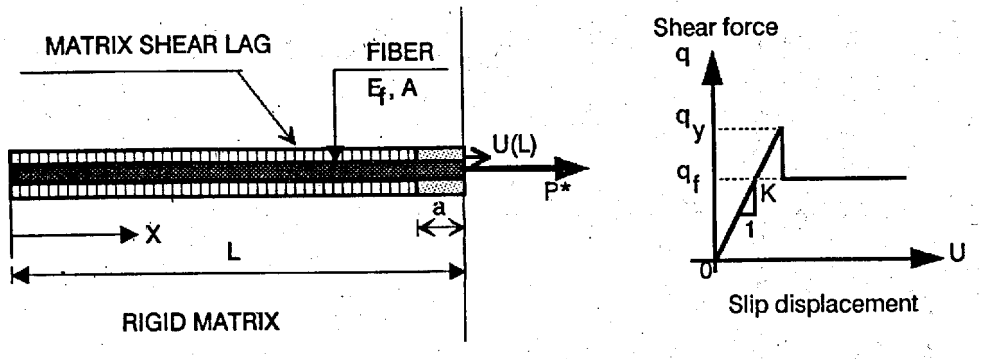

Fig. 9 Theoretical model and constitutive relationship for interface (Stang et al, 1990).

Table 1 Test results for stell fiber specimens (Li et al, 1991)

Curing	L	P_{max}	τ_y	τ_f	Γ
Days	mm	N	Mpa	Mpa	N/m
28	10.3	247	2.74	1.97	17.2
	12.9	245	2.35	1.42	17.7
14	7.2	80.1	1.12	1.05	2.01
	11.4	97.9	0.90	0.79	2.54
	12.0	134.2	1.18	1.05	4.81
	25.4	150.0	0.78	0.43	6.86

Table 2 Test results for aggregate-cement specimen with 28-day curing (Li, et al, 1991)

No.	Comments	ω (1/m)	τ_y (MPa)	τ_f (MPa)	Γ (N/m)
1	w/c=.35, cement matrix no coating, limestone	20.30	4.07	3.98	4.74
2	w/c=.65, cement matrix no coating, limestone	19.09	3.76	3.73	2.01
3	w/c=.35, cement matrix no coating, granite	13.09	3.33	3.26	3.67
4	w/c=.35, 10% SF matrix no coating, limestone	23.02	5.88	5.71	9.64
5	w/c=.35, 10% SF matrix C+SF coating, limestone	27.36	11.44	10.34	59.02

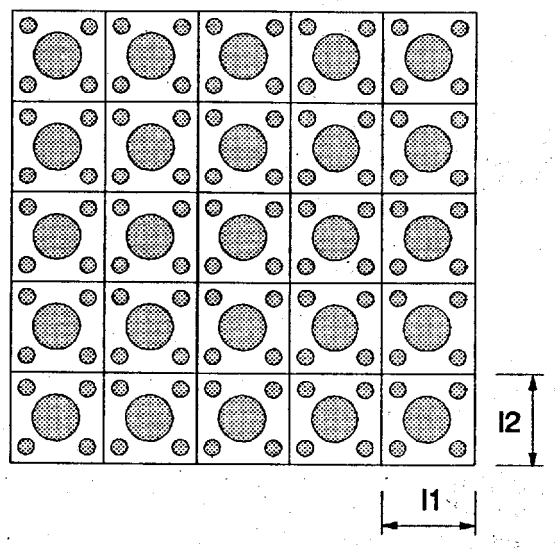

Fig. 10 Two dimensional spatially periodic porous medium with unit cell lattice l1 and l2

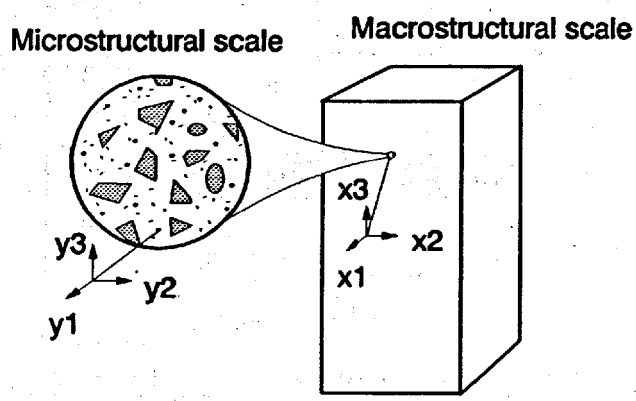

Fig. 11 Microscopic and macroscopic scales

200m^2/g). This may result from an altered structure of C-S-H in the interfacial zone. Their results also show the shape of the adsorption isotherm is type II according to the BET classification (Brunauer et al, 1940; Brunauer, 1943), similar with that of pure cement paste. However, the detailed test data were not provided, and therefore the analysis of moisture capacity can not be carried out.

To consider the effect of aggregate on transport behavior, Saito (1991) and Aroni et al (1967) studied the shrinkage of light weight concrete as a limiting case. They show that shrinkage of concrete made from light weight aggregate is much lower than that from regular weight aggregate, which implies that the presence of water in pores of aggregate changes the rate of moisture transport and the profile of the gradient of moisture.

As for theoretical analysis of transport behavior, it is generally agreed that transport properties can be modelled by a diffusion equation

$$\frac{\partial H}{\partial t} = \frac{\partial}{\partial x_i} C(x) \frac{\partial H}{\partial x_j} \qquad (3)$$

where H could be relative humidity, temperature or other concentration field. This equation is only valid for a homogeneous system. Thus, for concrete, the determination of the diffusion coefficient, C(x), in Eq. 3 is the main issue. One method is to consider concrete as a homogeneous material at the macroscopic level, and the heterogeneous behavior at the microscopic level is ignored. The coefficients can be obtained as effective or bulk values by fitting the diffusion equation with bulk test data (Bazant, Xi, and Molina, 1992; Wittmann et al, 1989; Daian, 1988, 1989). The coefficient C(x) has also been considered a function of the concentration of water C(H) (Bazant and Najjar, 1972), and thus Eq. 3 becomes a nonlinear equation. Although this is a commonly used method, the obtained coefficient can only be related to average bulk behavior, and, therefore, to average microstructure. As is true for strength and toughness, the direct prediction of transport properties is not possible because of the large number of variables that influence the microstructure. In particular, the bond strongly influences transport properties and this

influence must be studied further.

The heterogenous microstructure can be handled in two ways, 1) the averaging method and 2) the multi-scale method. The average method was originally used by Whitaker (1967), Slattery (1967), and Ryan et al (1980) to deal with the ongoing chemical reaction between aggregate and matrix. Bear and Bachmat (1984) described in detail the spatial averaging methods in 2D, 3D and the relationship between them. However, the multi-scale method is more rigorous, and has been developed by Saez et al (1989), Jerauld and Salter (1990), and Chang (1982) to deal with microscopic heterogeneity, particularly for the porous medium with periodic microstructural features (Fig. 10). By perturbation and convergence analysis (Bensoussan et al, 1978; Keller, 1977; Keller, 1980) Eq. 3 becomes

$$\frac{\partial H_0}{\partial t} = A_{ij} \frac{\partial^2 H_0}{\partial x_i \, \partial x_j} \tag{4}$$

This equation has the same form as Eq. 3, however, the coefficients A_{ij} are different

$$A_{ii} = \frac{1}{Y} \int_Y C\left(1+\frac{\partial \phi^i}{\partial y_i}\right) dY \qquad i = 1,2,3$$

$$A_{ij} = \frac{1}{Y} \int_Y C\left(\frac{\partial \phi^j}{\partial y_i}\right) dY \qquad i \neq j \tag{5}$$

where functions ϕ^i can be determined from the microstructure of one unit cell (Fig. 10), Y in Eq. 5 is the domain of one unit cell

$$\frac{\partial}{\partial y_i} C(y) \frac{\partial \phi^j}{\partial y_i} = -\frac{\partial C}{\partial y_j} \tag{6}$$

The coordinate x in Eq. 4 is macroscopic, and the coordinate y in Eqs. 5 and 6 is microscopic as shown in Fig. 11, this is why the method is called the multi-scale method. The dependencies of the diffusion coefficient on packing density, particle shape and particle spatial distribution are reflected in the differential equation, Eq. 6. Using this method, the macrostructural behavior is connected mathematically with microstructural features. Up to now, Eq. 6 has been solved analytically for only very simple cases, thus for most practical cases, a numerical solution is necessary. It has not, as yet, been applied to concrete.

MACROSCOPIC MODELS OF ELASTICITY, STRENGTH AND SHRINKAGE

As discussed in the introduction, the long range structure of the bond is important, and depends on the quantity, size, and size distribution of the aggregate. Although the long range structure has not been studied as an independent variable, there have been indirect studies. There have been, basically, three ways to predict the influence of aggregate on mechanical properties of concrete. One is based on elasticity and composite theory, the second is an empirical formulation from the observation of available test data, and the third is finite element simulation.

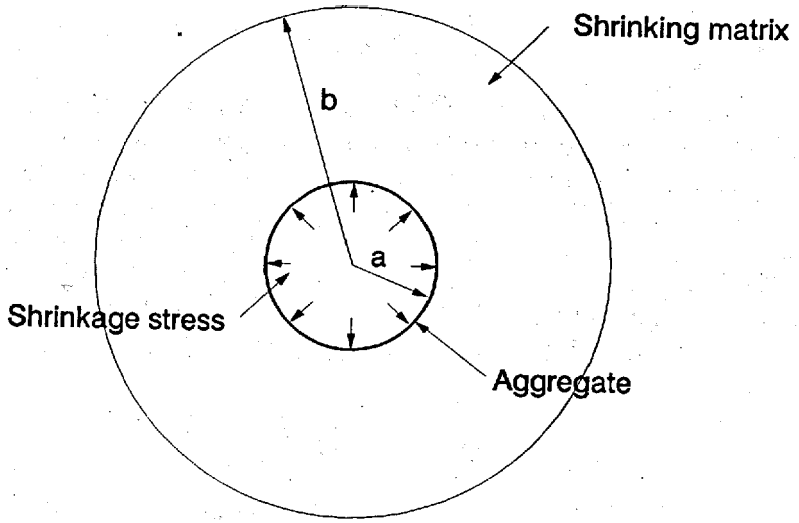

Fig. 12 Nonshrinking circular aggregate embedded in shrinking matrix

Composite model

Concrete may be idealized as a two-phase elastic composite material. Pickett (1956) and Hansen-Nielsen (1965) considered the restraining effect of a small spherical particle (aggregate) embedded in a infinitely large elastic body (concrete), which is assumed to be homogeneous as shown in Fig. 12. The following equation can be obtained (Pickett, 1956)

$$S=S_0(1-g)^{\alpha} \tag{7}$$

$$\alpha=\frac{3(1-\nu)}{1+\nu+2(1-2\nu_a)\frac{E}{E_a}} \tag{8}$$

in which g is aggregate volume fraction, S is the shrinkage of concrete, and S_0 is the shrinkage of cement matrix, E and ν are the elastic modulus and Poisson's ratio of the composite. Eq. 7 is based on the assumption that E and α are independent of g, and also that there is no interaction between embedded particles. Based on Pickett's test result (Pickett, 1956), parameter $\alpha = 1.7$.

The elastic modulus of concrete is a function of g. Hence, Hansen first developed a relationship between E and g (Hansen, 1958).

$$E=\frac{1}{\frac{(1-g)}{E_c}+\frac{g}{E_a}} \qquad \text{for} \quad E_a>E_c \tag{9}$$

$$E=(1-g)E_c + gE_a \qquad \text{for} \quad E_a < E_c \tag{10}$$

These relationships may be used to produce a more complicated model for concrete shrinkage (Hansen and Nielsen, 1965).

An important part of these analyse is the characterization of E by g. Values for the two phases, aggregate and cement matrix, may be combined in many different ways. Fig. 13 shows three different combinations of the two phases at a given g. Fig. 13a is a serial coupling that leads to Eq. 10, which is the lower bound of E, and Fig. 13b is a parallel coupling that results in Eq. 9, which is the upper bound. Although the Hansen-Nielsen model includes the elastic modulus of aggregate, the effect is not significant because, usually, $E_a > E_c$, Eq. 10 is used, which corresponds to the lower bound.

Hansen (1960) extended the concept of composite materials to the cement paste phase alone. The unhydrated grains are considered as aggregate in a matrix of products of hydration, the latter, in turn, consists of soft capillary pores in a hard matrix of cement gel. Thus, the modulus of elasticity of hydrated cement paste is given by

$$\frac{1}{E_{cp}} = \frac{V_{uc}}{E_{uc}} + \frac{V_{hc}}{V_{cg}E_{cg}} \tag{11}$$

where V is volume fraction, and the subscripts refer to cp = cement paste, uc = unhydrated grains, hc

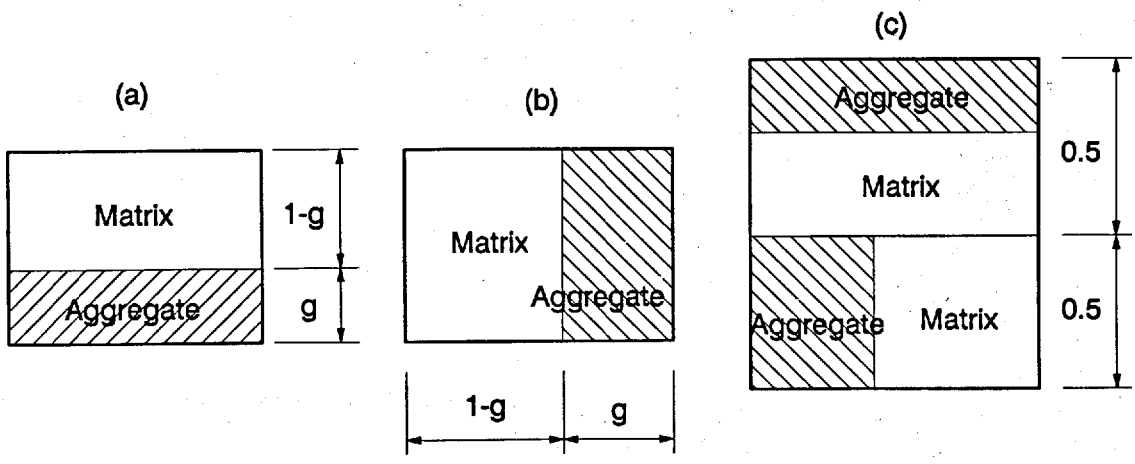

Fig. 13 (a) Serial coupling of the two phases, (b) Parallel coupling of the two phases, and (c) Geometric mean of serial and parallel coupling

= hydrated cement (without unhydrated grains, including capillary pores), and cg = cement gel (including gel pores).

The third combination referred to in Fig. 13c is a compromise between (a) and (b). Hansen-Almudaiheem (Hansen and Almudaiheem, 1987; Hansen, 1987) incorporated the relationship of E and g developed by Hirsch (Hirsch, 1962), which is the geometric mean of the lower and upper bounds and is shown schematically in Fig. 13c (Dougill, 1962). Because case c is a combination of case a and case b, the model predicts that the elastic modulus of aggregate is much more significant than the other two models, about four times higher than the Hansen-Nielsen model. The model also considers the unhydrated grains to be nonshrinking particles, which allows the effect of hydration on shrinkage to be included. However, these models have not been compared to experimental results. Other models of this kind in the literature are from Fulton (1961), Christian and Patten (1968), Cribb (1968), Hobbs (1969), and C&CA model (Hobbs, 1969).

(2). Empirical Models

Since the real spatial distribution of dispersed aggregates inside concrete is highly random, and the working mechanism of the restraining effect is not completely understood, some numerical trends may be obtained directly from test results.

Bazant and co-workers (1991, 1992) developed an empirical formula for shrinkage. A large amount of test data, totalling 173 data sets, have been collected since 1978 and a comprehensive data-base has been established. Based upon these data an empirical formula relating the effect of composition to shrinkage was developed (Bazant, Kim, and Panula, 1991). Ultimate concrete shrinkage, $\epsilon_{s\infty}$, is expressed as a linear function of aggregate volume fraction g.

$$\epsilon_{s\infty} \propto f_{sh}\ (\ t,\ t',\ h,\ K_s)(1-g) \qquad (12)$$

where f_{sh} is a function of age, t, drying time, t', relative humidity, h, and shape factor, K_s. Eq. 12 and

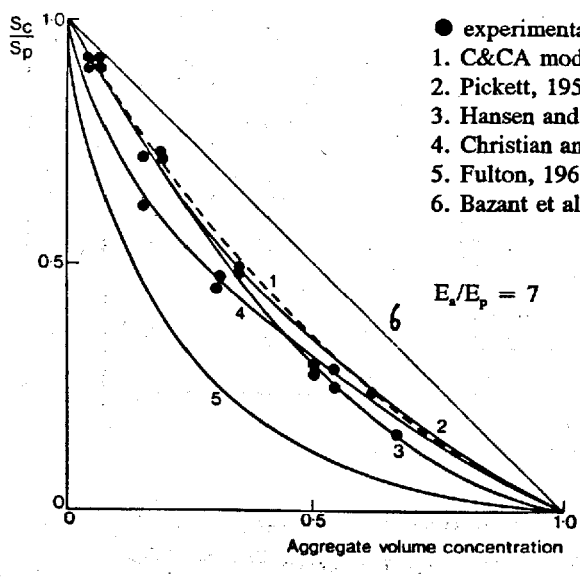

● experimental, Pickett, 1956
1. C&CA model, Hobbs, 1969
2. Pickett, 1956
3. Hansen and Nielson, 1965
4. Christian and Patten, 1968
5. Fulton, 1961
6. Bazant et al, 1992

Fig. 14 Comparisons of the models and test data.

Eq. 7 give different trends for the effect of aggregate, Eq. 7 is a power function, while Eq. 12 is a linear function. Eq. 12 covers a broad range of aggregate effect, a/c ratio (by weight) is between 2.81 - 10.7, where $a=a_g+s$, a_g is gravel content, and s is sand content, c is cement content.

Fig. 14 shows various model results and test results, where $E_a/E_c = 7$. The sensitivity analysis of the parameters in some of those models can be seen in Hobbs (1974). The accuracy of the models and the sensitivity of the effective parameters involved in the prediction of shrinkage by elasticity and composite theory depend mainly on the relation between E and g, which is a classic problem in micromechanics. The extensive discussions on such general topics the reader may be refereed to Mura (1987), and Baker (1959).

(3). Finite Element Models

The structure of concrete is in many respects random, thus, all of the constitutive relations are a reflection of the average behavior of the structure. For instance, when the various combinations of cement matrix and aggregate are modelled by composite theory, they are just simplified descriptions of the mean value of the distribution. Instead of averaged behavior, concrete may be simulated as a random finite element system composed of many different elements for aggregate, sand, and cement matrix.

Bazant and Tabarra (1989) simulated concrete by a random particle system in 2D (see Fig. 15(a)). All of the particles are simplified as circles with three or four prescribed sizes. Two adjacent circular particles are assumed to interact only in the axial direction, thus the connections between the particles form a random truss system (see Fig. 15(b)). Assumptions are that the aggregate is elastic and the matrix is nonlinear inelastic. The model simulates realistically the spread of cracking, and predicts correct macroscopic nominal strength.

Wittmann (1986) and Zaitzev and Wittmann (1981) generated a random system for "numerical concrete." In this system the locations of the particles and also the sizes and the shapes of the particles are random. "Numerical concrete" is first generated and then the whole material is divided into three different parts, aggregate, cement matrix, and interface between matrix and aggregate. The elements for these three parts are assigned to different material properties. This model predicts strength.

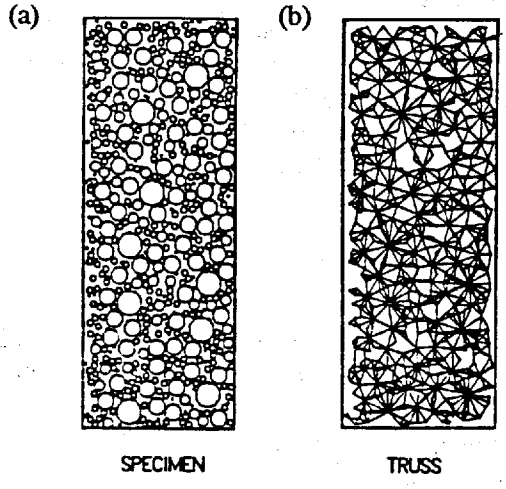

Fig. 15 (a) Random particle model

(b) random truss system

(Bazant and Tabarra, 1989).

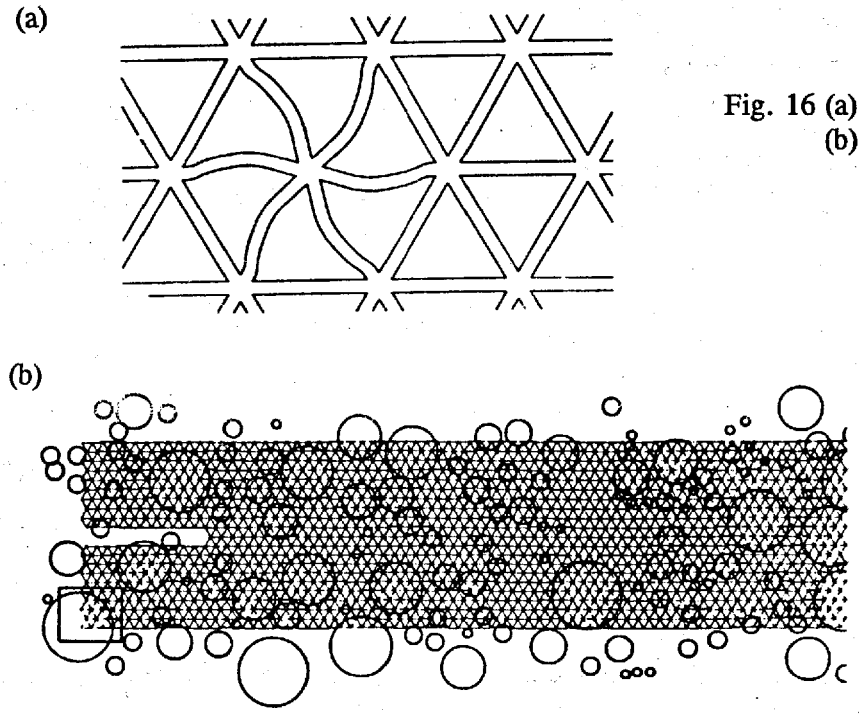

Fig. 16 (a) Triangular lattice
(b) Generated particle structure with triangular lattice system projected on it.
(Schlangen and van Mier, 1991).

Schlangen and van Mier (1991) developed a simulation method which is composed of two different systems, one is a triangular lattice of linear elastic beam elements as shown in Fig. 16(a), another is a random grain or particle system to simulate aggregate. When the grain structure is generated, the triangular lattice is projected on top of it, and different beam strengths and stiffnesses are assigned to the respective beam elements (see Fig. 16(b)). The nonlinear behavior of the bulk material is introduced through the fracture of beam elements, in other words, a beam element is removed from the mesh as soon as the combination of normal force and bending moment in the element exceeds a certain value. This model predicts strength.

The heterogeneity of concrete can be introduced by a lattice system. Rossi and Richer (1987), Herrmann (1988), and Termonia & Meakin (1986) developed models that specify certain distributions of the strength and stiffness of the lattice system. These models are very useful for analyzing the heterogeneous behavior of cement paste. The elastic lattice models have some advantages over conventional nonlinear finite element models. For example, the procedure is extremely simple, and the lattice structure incorporates the growth of complex and realistic crack patterns.

ALKALI AGGREGATE REACTION

The subject of cement aggregate compatibility is one that should also include chemical effects. Indeed, chemical reactions at the interface will effect both the structure and properties of concrete and, once again, no one characteristic of the system is independent. For example, chemical reaction may cause cracking which, in turn, will influence transport, which in turn, will influence shrinkage, etc...

Alkali aggregate reaction is not well understood and, models are simply not available. Some aggregates are fairly reactive and a disruptive gel is formed.

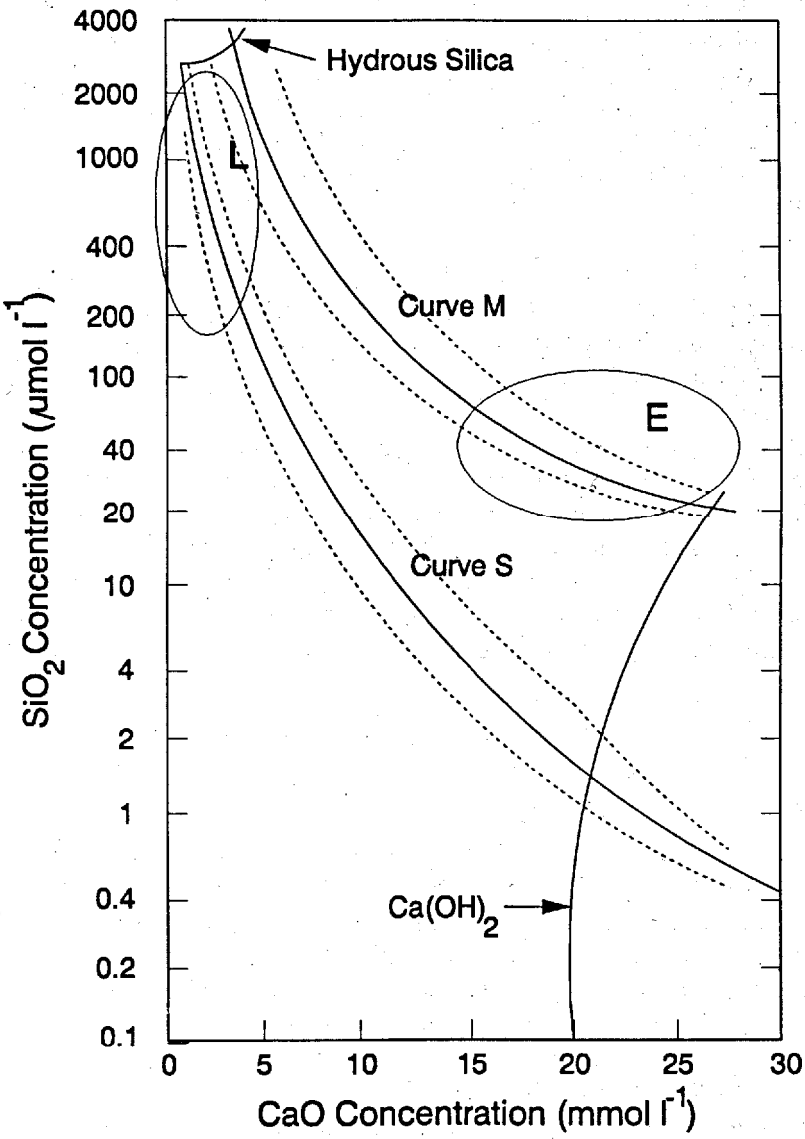

Fig. 17 Concentration data for C-S-H based on the results of many investigations. broken lines give an indication of the scatter of the data. Points cluster in region E at early ages and points cluster in region L at later ages for typical portland cement pastes.

Recent research (Jennings, 1986; Jennings and Christensen, 1992; Christensen et. al, 1992; Kelzenberg et. al, 1992a,b) has shown that the chemistry of the aqueous phase can be understood in terms of a collection of complex phase diagrams, and that the $CaO-SiO_2-H_2O$ system can be studied independently from the $CaO-Al_2O_3-CaSO_4-H_2O$ system. A phase diagram approach may provide a new angle on rationalizing the complex chemistry between aggregate and cement paste. For example, the $CaO-SiO_2-H_2O$ subsystem has been studied extensively for cement pastes, Fig. 17. Data from the aqueous phase typically lies in a region near the upper curve, C-S-H (M), (region E) during the first several hours of reaction and near the upper left region of the lower (region L) C-S-H (S) (region L) curve thereafter. It is important to note that the upper left region of this diagram has not been studied in detail, but that there is a phase region for $SiO_2 \bullet (H_2O)n$. This is a hydrous gel.

The presence of aggregate can move points along the two curves both at early ages and at later ages. Our results show that points move both above and below the C-S-H (M) curve during the early age, depending on aggregate type and mixing technique. This indicates that aggregate can influence the reaction, even during the first minutes and hours.

In mature pastes the concentrations of CaO drops to about $3x10^{-3}$ M. According to Diamond (1983) the concentration of CaO falls to less than $1x10^{-3}$ M after six months. However, no research has been carried out to investigate the influence of aggregate on the aqueous phase of mature specimens. Furthermore, because of the common ion effect, high alkali could further suppress the concentration of CaO. If this is the case, high alkali will tend to push the solution into a region in equilibrium with silica gel, and this could be a problem. Since gel phases may be mapped as part of phase diagrams, both for the silicates and for the aluminates, this approach could place an understanding of alkali aggregate reactions on a more rational footing.

SUMMARY

The properties of concrete are a function of its structure. Perhaps the three most important components are 1) Paste 2) Aggregate and 3) Interface. To some extent the influence of these three components have been studied and the results reported in the literature. However, concrete has a structure that ranges in size from sub-nanometer to hundreds of millimeters. The bond region has both short range and long range structure. Short range is the interfacial region and long range is the structure, surface area, distribution, connectedness and other properties of the aggregate surface itself. Both the structure and chemistry of the paste and the aggregate are important. A complete description of properties, based on microstructure, requires the summation of characteristics that range several orders of magnitude in size. In other words, both short range and long range structure must be considered. This is, perhaps, the major challenge facing the materials science of concrete.

This review is a somewhat arbitrary discussion on how some characteristics of these components of the microstructure combine to influence properties. One outstanding observation is that many properties interact. For example, shrinkage may cause cracking, which in turn affects permeability, and both of these influence strength and toughness. The region between cement-paste and aggregate, or the bond, is perhaps where these interactions combine most strongly, and this is the meaning of cement aggregate compatibility in this paper.

Important properties have been modelled mainly without consideration of microstructure. In particular, aggregate and the bond are not considered explicitly. A few models that attempt to connect the microstructure of aggregate to properties have been discussed. These models do not account for the interface between aggregate and paste.

Finally, the chemical characteristics of aggregate must be considered so that predictive models for

their stability in the environment of cement paste can be developed. The authors think that a thermodynamic-phase diagram approach will be necessary in order to accomplish this task.

ACKNOWLEDGMENTS

Financial supports under DOE Grant DE-FG02-91ER45460, NSF grant # DMR-8808432-01 Center for Advanced Cement-Based Materials, and Concrete Technology Corporation is gratefully acknowledged.

REFERENCES

Alexander, K.M., and Wardlaw, J., (1959) "Effect of Powdered Minerals and Fine Aggregate on the Drying Shrinkage of Portland Cement Paste", Journal of ACI, 55(12), June, 1303-1316.

Alexander, K.M., (1959) "Errors Caused by Partial Drying of Hardened Portland Cement during Testing", Nature, Vol. 183, March, 885-886.

Argon, A.S., (1972a) "Fracture of Composites", in Treatise on Material Science and Technology, Ed. by Herman, H., Academic Press, New York, 79-114.

Argon, A.S., (1972b) "Statistical Aspects of Fracture", in Composite Materials: Fracture and Fatigue, 5, Ed. by Broutman L.J., and Krock, R.H., Academic Press, New York, 153-190.

Aroni, S., and Polivka, M., (1967) "Effect of Expanded shale Aggregate on Properties of Expansive-Cement Concrete", RILEM Symposium on Lightweight Aggregate Concretes, Budapest, March, 475-502.

Backstrom, J.E., and Burrows, R.W., (1955) "Observations on the Resistance of Concrete to Freezing and Thawing", Journal of ACI, Vol. 51, p. 352.

Baker, A.L.L., (1959) "An Analysis of Deformation and Failure Characteristics of Concrete", Magazine of Concrete Research, 11(33), Nov., 119-128.

Barnes, B.D., Diamond, S., and Dolch, W.L., (1978) "The Contact Zone Between Portland Cement Paste and Glass 'Aggregate' Surfaces", Cement and Concrete Research, 8, 233-244.

Barnes, B.D., Diamond, S., and Dolch, W.L., (1979) "Micromorphology of the Interfacial Zone Around Aggregates in Portland Cement Mortar", Journal of The American Ceramic Society, 62(1), Jan. - Feb., 22-24.

Bazant, Z.P., Kim, J.K., Panula, L., (1991) "Improved Prediction Model for Time-dependent Deformations of Concrete: Part I - Shrinkage", Materials and Structures, RILEM, Paris, 24, 327-345.

Bazant, Z.P., and Najjar, L.J., (1972) "Nonlinear Water Diffusion in Nonsaturated Concrete", Materials and Constructions, (RILEM, Paris), 5(25), 3-20.

Bazant, Z.P., Panula, L., Kim, J.K., and Xi, Y., (1992) "Improved Prediction Model for Time-dependent Deformations of Concrete: Part VI - Simplified Code-Type Formulation", Materials and Structures, RILEM, Paris (in press).

Bazant, Z.P., Xi, Y., and Molina, L., (1992) "Drying of Cementitious Materials, Part II. Theoretical Modelling", to be submitted.

Bear, J., and Bachmat, Y. (1984) "Transport Phenomena in Porous Media - Basic Equations", Fundamentals of Transport Phenomena in Porous Media, Ed. Bear, J., and Corapcioglu, M.Y., Martinus Nijhoff Publishers, Dordrecht/Boston/Lancaster, 3-61.

Bensoussan, A., Lions, J.-L., and Papanicolaou, G., (1978) "Asymptotic Analysis for Periodic Structures", North-Holland Publishing, Amsterdam.

Bergstrom, T.B., Sujata, K., Xi, Y., and Jennings H.M. (1992) "Quantitative Microanalysis of Shrinking Cement Paste, Part II. ESEM Results", to be submitted to J. Amer. Ceram. Soc.

Brunauer, S., (1943) "The Adsorption of Gases and Vapors", 1, Princeton University Press

Brunauer, S., Deming, L.S., Deming, W.E., and Teller, E. (1940) "On a Theory of the Van der Waals Adsorption of Gases", J. Amer, Chem. Soc., 62, July, 1723-1732.

Buyukozturk, O., and Lee, K.M., (1992) "Interface Fracture Mechanics of Concrete Composites", Proceedings of the First International Conference on Fracture Mechanics of Concrete Structures, Ed. Bazant, Z.P., June, Breckenridge, Colorado.

Carlson, R.W., (1935) "The Chemistry and Physics of Concrete Shrinkage", Proceedings, ASTM, Vol. 35, Part II, p.370.

Carlson, R.W., (1939) "Drying Shrinkage of Concrete as Affected by Many Factors", Proceedings, ASTM, Vol. 38, Part II, 419-440.

Chang, H.C., (1982) "Multi-Scale Analysis of Effective Transport in Periodic Heterogeneous Media", Chem. Eng. Commun., 15, 83-91.

Chatterji, S., (1976) "Drying Shrinkage of Cement Paste and Concrete" A Reappraisal of the Measurement Technique and its Significance", Cement and Concrete Research, Vol. 6, 145-148.

Christensen, B.J., Shimokogawa, K. and Jennings, H.M., (1992) "Phase Equilibria of the Calcium-Silicate-Hydrate System in Mature Portland Cements, Part II: Influence of Curing Temperature," J. Amer. Ceram. Soc. accepted for publication.

Christian, B.H., and Patten, B.J.F., (1968) "Multiple Aspects of Concrete Drying Shrinkage", Civil Engineering Transactions, Institution of Engineers, Australia, Vol. 2, Oct., 229-236.

Cribb, J.L., (1968) "Shrinkage and Thermal Expansion of a Two Phase Material", Nature (London), Nov., 576-577.

Daian, J-F., (1988) "Condensation and Isothermal Water Transfer in cement Mortar: Part I - Pore Size Distribution, Equilibrium Water Condensation and Imbibition", Transport in Porous Media, 3, 563-589.

Daian, J-F., (1989) "Condensation and Isothermal Water Transfer in cement Mortar: Part I - Transient Condensation of Water Vapor", Transport in Porous Media, 4, 1-16.

Day, R.L., Cuffaro, P., and Illston, J.M., (1984) "The Effect of Rate of Drying on the Drying Creep of Hardened Cement Paste", Cement and Concrete Research, 14, 329-338.

Day, R.L., and Illston, J.M., (1983) "The Effect of Rate of Drying on the Drying/Wetting Behavior of Hardened Cement Paste", Cement and Concrete Research, 13, 7-17.

de Haas, G.D., Kreijger, P.C., Niel, E.M.M.G., Slagter, J.C., Stein, H.N., Theissing, E.M., and van Wallendael, M., (1975) "The Shrinkage of Hardening Cement Paste and Mortar", Cement and Concrete Research, 5, 295-320.

Diamond, S., Mindess, S., and Lovell, J., (1982) in Colloque Internationale, Liaisons Pates de Cement Materiaux Associes, C42-C46.

Diamond, S.,(1983) "Effects of Microsilica (Silica Fume) on Pore-Solution Chemistry of Cement Pastes," J. Amer. Ceram. Soc., 66, No. 5, May, 311-388.

Dougill, J.W. (1962) Discussion of "Modulus of Elasticity of Concrete Affected by Elastic Moduli of Cement Paste Matrix and Aggregate", by T.J. Hirsch, Journal of ACI, Sept., 59(9), 1363-1365.

Eden, N.B., and Bailey, J.E., (1984) "On the Factors Affecting Strength of Portland Cement", Journal of Material Science, 19, 150-158.

Feldman, R.F. (1971), Highway Research Record, 8, p. 370.

Forrester, J.A., (1968) "The Structure of Concrete", Cement and Concrete Association, London, p. 157.

Fulton, F.S., (1961) "A Co-ordinated Approach to the Shrinkage Testing of Concretes and Mortars", Magazine of Concrete Research, 13(39), Nov., 133-140.

Gleysteen, L.F., and Kalousek, G.L., (1955) "Simplified Method for the Determination of Apparent Surface Area of Concrete Products", Journal of ACI, Jan., 437-446.

Gupta, V., Argon, A.S., and Cornie, J.A., (1989) "Interfaces with Controlled Toughness as Mechanical Fuses to Isolate Fibres from Damage", J. Mater. Sci., 24, 2031-2040.

Gupta, V., Argon, A.S., and Cornie, J.A., (1990) "Interface Problems in Metal Matrix Composites", Proc. of the American Soc. for Composites, Fifth Technical Conference, June 12-14, East Lansing, Michigan.

Gutteridge, W.A., and Parrott, L.J., (1976) "A Study of the Changes in Weight, Length and Interplanar Spacing Induced by Drying and Rewetting Synthetic CSH(I)", Cement and Concrete Research, 6, 357-366.

Hansen, W., (1987) "Constitutive Model for Predicting Ultimate Drying Shrinkage of Concrete", Journal of the American Ceramic Society, 70(5), 329-332.

Hansen, W., and Almudaiheem, J.A. (1987) "Ultimate Drying Shrinkage of Concrete - Influence of Major Parameters", ACI Materials Journal, May-June, 217-223.

Hansen, T.C., (1960) "Creep and Stress Relaxation of Concrete", Proc. No. 31, Swedish Cement and Concrete Research Institute: Stockholm, 112 pp.

Hansen, T.C., and Nielsen, K.E.C. (1965) "Influence of Aggregate Properties on Concrete Shrinkage", Journal of ACI, 62(7), July, 783-793.

Helal, M., and Krizek, R. (1992) "Preferred Orientation of Pore Structure in Cement - Grouted Sand", Proceedings of the ASCE Conf. on Grouting, Soil Improvement and Geo-Synthetics, Geochemical Special Publication 30, Vol. I, Ed. Borden, R., Holtz, R., and Juran, I., New York, New York, 526-540.

Herrmann, H.J. (1988) "Introduction to Modern Ideas on Fracture Patterns", Random Fluctuations and Pattern Growth: Experiments and Models, Ed. Stanley, H.E., and Ostrowsky, N., Kluwer Academic, Dordrecht, 149-160.

Hillemeier, B., and Hilsdorf, H.K., (1977) "Fracture Mechanics Studies on Concrete Compounds", Cement and Concrete Research, 7, 523-535.

Hirsch, T.J. (1962) "Molulus of Elasticity of Concrete Affected by Elastic Moduli of Cement Paste Matrix and Aggregate", Journal of ACI, March, 59(3), 427-452.

Hobbs, D.W. (1969) "Bulk Modulus, Shrinkage, Thermal Expansion of a Two Phase Material", Nature (London), Vol. 222, May, 849-851.

Hobbs, D.W. (1971) "The Dependence of the Bulk Modulus, Young's Modulus, Creep, Shrinkage and Thermal Expansion of Concrete Upon Aggregate Volume Concentration", Materials and Structures/Research and Testing (Paris), 4(20), Mar.-Apr., 107-120.

Hobbs, D.W., (1974) "Influence of Aggregate Restraint on the Shrinkage of Concrete", Journal of ACI, Sept., 445-450.

Hsu, T.T.C., Slate, F.O., Sturman, G.M., and Winter, G., (1963a) "Microcracking of Plain Concrete and the Shape of the Stress-Strain Curve", Journal of ACI, Vol. 60, Feb., 209-224.

Hsu, T.T.C., (1963b) "Mathematical Analysis of Shrinkage Stresses in a Model of Hardened Concrete", Journal of ACI, Vol. 60, March, 371-389.

Hsu, T.T.C., and Slate, F.O., (1963c) "Tensile Bond Strength Between Aggregate and Cement Paste or Mortar", Journal of ACI, Vol. 60, April, 465-485.

Hwang, C.L., and Young, J.F., (1984) "Drying Shrinkage of Portland Cement Pastes, I. Microcracking during Drying", Cement and Concrete Research, 14, 585-594.

Jennings, H.M., (1986) "Aqueous Solubility Relationships for Two Types of Calcium Silicate Hydrate," J. Amer. Ceram. Soc., 69, 614-618.

Jennings, H.M., and Christensen, B.J., (1992) "Phase Equilibria of the Calcium-Silicate-Hydrate System in Mature Portland Cements, Part I: Neat Pastes and Pastes Containing Selected Admixtures," J. Amer. Ceram. Soc.. accepted for publication.

Jerauld, G.R., and Salter, S.J., (1990) "The Effect of Pore-Structure on Hysteresis in Relative Permeability and Capillary Pressure: Pore-Level Modelling", Transport in Porous Media, 5, 103-151.

Jia, W., (1988) "Mechanism of Orientation of $C_a(OH)_2$ Crystals in Interface Layer Between Paste and Aggregate in Systems Containing Silica Fume", Mat. Res. Soc. Symp. Proc., Vol. 114, 127-132.

Keller, J.B. (1977) "Effective Behavior of Heterogeneous Media", Statistical Mechanics and Statistical Methods in Theory and Application, Ed. Landman, U., Plenum Press, New York and London, 631-644.

Keller, J.B. (1980) "Darcy's Law for Flow in Porous Media and the Two-Space Method", Nonlinear Partial Differential Equations in Engineering and Applied Science, Ed. Sternberg, R.L., Kalinowski, A.J., and Papadakis, J.S., Marcel Dekker, Inc., New York and Basel, 429-443.

Kelzenberg, T., Claridge, M., and Jennings, H.M., (1992a) "Aqueous Phase Chemistry of Portland Cement at Early Ages Part I: Pastes," J. Amer. Ceram. Soc. in preparation.

Kelzenberg, T., Claridge, M., and Jennings, H.M., (1992b) "Aqueous Phase Chemistry of Portland Cement at Early Ages Part II: Mortars," J. Amer. Ceram.Soc. in preparation.

L'Hermite, R.G., (1960) "Volume Changes of Concrete", Proceedings of 4th International Symposium on Chemistry of Cement, US Department of Commerce, National Bureau of Standards, Monograph 43, Vol. II, Washington, 659-694.

Li, Z., Mobasher, B., and Shah, S.P., (1991) "Characterization of Interfacial Properties in Fiber-Reinforced Cementitious Composites", J. Amer. Ceram. Soc., 74(9), 2156 - 2164.

Mills, R.H., (1985) "Mass Transfer of Water Vapor through Concrete", Cement and Concrete Research, 15, 74-82.

Mindess, S. (1988) "Bonding in Cementitious Composites: How Important is It?", Mat. Res. Soc., Symp. Proc., Vol. 114, 3-10.

Monteiro, P.J.M., (1985) "Microstructure of Concrete and its Influence on the Mechanical Properties", Ph.D Dissertation, University of California, Berkeley.

Monteiro, P.J.M., and Andrade, W.P., (1987) "Analysis of the Rock-Cement Paste Bond Using Probabilistic Treatment of Brittle Strength", Cement and Concrete Research, 17, 919-926.

Monteiro, P.J.M., Maso, J.C., and Ollivier, J.P., (1985) "The Aggregate-Mortar Interface", Cement and Concrete Research, 15, 953-958.

Monteiro, P.J.M., and Mehta, P.K., (1985) "Ettringite Formation on the Aggregate-Cement Paste Interface", Cement and Concrete Research, 15, 378-380.

Monteiro, P.J.M., and Mehta, P.K., (1986) "The Transition Zone Between Aggregate and Type K Expansive Cement", Cement and Concrete Research, 16, 111-114.

Monteiro, P.J.M., and Ostertag, C.P., (1989) "Analysis of the Aggregate-Cement Paste Interface Using Grazing Incidence X-ray Scattering", Cement and Concrete Research, 19, 987-988.

Mura, T., (1987) "Micromechanics of Defects in Solids", Martinus Nijhoff Publishers, Dordrecht.

Odler, I., and Skalny, J., (1973) "Pore Structure of Hydrated Calcium Silicates - Analysis of a Synthetic Tobermorite", Journal of Colloid and Interface Science, 42(2), Feb., 291-297.

Parrott, L.J., (1986) "Discussion of Chapter 1: Mechanisms and Their Mathematical Descriptions", Proceedings of 4th RILEM Int. Symp. on Creep and Shrinkage of Concrete: Mathematical Modelling, Aug. 26-29, Ed. Bazant, Z.P., Northwestern University, Evanston, Illinois, 459-467.

Pickett, G. (1956) "Effect of Aggregate on Shrinkage of Concrete and a Hypothesis Concerning Shrinkage", 27(5), Jan., 581-590.

Pihlajavaara, S.E., (1965) "Main Features and Methods of Investigation of Drying and Related Phenomena", Valtion Tek. Tutkimuslaitos, Julk, No. 100, 142 pp.

Pihlajavaara, S.E., (1974) "A Review of Some of the Main Results of a Research on the Ageing Phenomena of Concrete: Effect of Moisture Conditions on Strength, Shrinkage and Creep of Mature Concrete", Cement and Concrete Research, 4, 671-771.

Pope, A.W., and Jennings, H.M., (1992) "The Influence of Mixing on the Microstructure of Cement Paste/Aggregate Interfacial Zone and on Strength of Mortar", Journal of Materials Science, in press.

Rice, J.R. (1988) "Elastic Fracture Mechanics Concepts for Interfacial Cracks", Journal of Applied Mechanics, Transactions of the ASCE, 55, March, 98-103.

Ringot, E., Ollivier, J.P., and Maso, J.C., (1987) "Characterization of Initial State of Concrete with Regard to Microcracking", Cement and Concrete Research, 17, 411-419.

Rossi, P., and Richer, S., (1987) "Numerical Modelling of Concrete Cracking Based on a Stochastic Approach", Materials and Structures, RILEM, Paris, 20, 334-339.

Rostasy, F.S., and Budelmann, H., (1986) "Strength and Deformation of Concrete with Variable Content of Moisture at Elevated Temperature up to 90°C", Cement and Concrete Research, 16, 353-362.

Ryan, D., Carbonell, R.G., and Whitaker, S. (1980) "Effective Diffusivities for Catalyst Pellets under Reactive Conditions", Chemical Engineering Science, 35, 10-16.

Saito, M., Kawamura, M., and Arakawa, S., (1991) "Role of Aggregate in the Shrinkage of Ordinary Portland and Expansive Cement Concrete", Cement and Concrete Composites, 13, 115-121.

Saez, A.E., Otero, C.J., and Rusinek, I., (1989) "The Effective Homogeneous Behavior of Heterogeneous Porous Media", Transport in Porous Media, 4, 213-238.

Schlangen, E., and van Mier, J.G.M., (1991) "Experimental and Numerical Analysis of Micromechanism of Fracture of Cement-based Composite", Progress in Concrete Research, Annual Report, Delft University of Technology, Vol. 2, 45-70.

Scrivener, K.L., and Gartner, E.M., (1988) "Microstructural Gradients in Cement Paste around Aggregate Particles", Mat. Res. Soc. Symp. Proc., Vol. 114, 77-85.

Sereda, P.J., Feldman, R.F., and Swenson, E.G., (1966) "Effect of Sorbed Water on Some Mechanical Properties of Hydrated Cement Pastes and Compacts", Highw. Res. Bd., Spec. Rep., No. 90, 58-73.

Shah, S.P., and Li, Z., (1992) "Bond Properties in Fiber-Cement and Aggregate-Cement Paste Interfaces", Proc. of First Int. Conf. on Fracture Mechanics of Concrete Structures, Ed. Bazant, Z.P., Breckenridge, Colorado, U.S.A., 1-5 June, Elsevier; England.

Shah, S.P., and Shao, Y., (1992), Private communication in Northwestern University, Evanston, IL.

Sicard, V., Francois, R., Ringot, E., and Pons, G., (1992) "Influence of Creep and Shrinkage on Cracking in High Strength Concrete", Cement and Concrete Research, 22, 159-168.

Slate, F.O., and Olsefsk, S., (1963) "X-rays for Study of Internal Structure and Microcracking of Concrete", Journal of ACI, Vol. 60, May, 575-587.

Slattery, J.C. (1967) "Flow of Viscoelastic Fluids Through Porous Media", AIChE Journal, 13(6), Nov.,

1066-1071.

Smith, R.H., Bayliss, P., Gamble, B.R., and Mills, R.H., (1972) "Crystallographic Investigation of CSH(I) ", Cement and Concrete Research, 2(5), Sept., 559-566.

Stang, H., Li, Z., and shah, S.P., (1990) "Pullout Problem: Stress versus Fracture Mechanical Approach", J. of Engineering Mechanics, 116(10), October, 2136-2150.

Sujata, K., Xi, Y., and Jennings, H.M., (1992) "Cement Past Shrinkage in Interface Zone", to be submitted to J. Amer. Ceram. Soc.

Suo, Z., and Hutchinson, J.W., (1989) "Sandwich Test Specimens for Measuring Interface Crack Toughness", Materials Sci. and Engrg., A107, 135-143.

Termonia, Y., and Meakin, P. (1986) "Formation of Fractal Cracks in a Kinetic Fracture Model", Nature, 320, 429-431.

Whitaker, S., (1967) "Diffusion and Dispersion in Porous Media", AIChE Journal, 13(3), May, 420-427.

Williams, M.L. (1959) "The Stresses Around a Fault or Crack in Dissimilar Media", Bull. Seismol. Soc. America., 49, 199-204.

Wittmann, F.H., (1968) "Surface Tension, Shrinkage and Strength of Hardened Cement Paste", Material and Constructions, (RILEM, Paris), 1(6), 547-552.

Wittmann, F.H., (1973) "Interaction of Hardened Cement Paste and Water", Journal of The American Ceramic Society, August, 56(8), 409-415.

Wittmann, F.H., (1986) "Mechanisms of Creep and Shrinkage - Further Viewpoints", Proceedings of 4th RILEM Int. Symp. on Creep and Shrinkage of Concrete: Mathematical Modelling, Aug. 26-29, Ed. Bazant, Z.P., Northwestern University, Evanston, Illinois, 469-476.

Wittmann, X., Sadouki, H., and Wittmann, F.H., (1989) "Numerical Evaluation of Drying Test Data", Proc. of 10th SMIRT, Q, 71-79.

Xi, Y., Bergstrom, T.B., and Jennings, H.M., (1992) "Quantitative Microanalysis of Shrinking Cement Paste, Part I. Quantitative Analysis", to be submitted to J. Amer. ceram. Soc.

Xie, P., and Beaudoin, J.J., (1992) "Effects of Transition Zone Microstructure on Bond Strength of Aggregate-Portland Cement Paste Interfaces", Cement and Concrete Research, 22, 23-26.

Zaitsev, Y.B. and Wittmann, F.H. (1981) "Simulation of Crack Propagation and Failure of Concrete", Materials and Constructions, (RILEM, Paris), 14(83), 357-365.

Zhang, M.H., and Gjorv, O.E., (1990) "Microstructure of The Interfacial Zone Between Lightweight Aggregate and Cement Paste", Cement and Concrete Research, 20, 610-618.

Zimbelmann, R., (1985) "A Contribution to the Problem of Cement-Aggregate Bond", Cement and Concrete Research, 15, 801-808.

Zimbelmann, R., (1987) "A Method for Strengthening the Bond Between Cement Stone and Aggregate", Cement and Concrete Research, 17, 651-660.

Specific Theme IV C

Physico-chemical, Biological and Thermal Degradation Including Environmental Effects

PHYSICO-CHEMICAL, BIOLOGICAL AND THERMAL DEGRADATION INCLUDING ENVIRONMENTAL EFFECTS

A K Mullick
National Council for Cement and Building Materials, New Delhi, INDIA

and

Satish Chandra
Chalmers University of Technology, SWEDEN

SUMMARY

Performance of cements is now being increasingly expressed in terms of durability of concrete constructions. This report reviews the recent published literatures, which reveal that although adequate knowledge is now available about the various aspects of durability of concrete, there are many instances of failures in service. The basic mechanisms involved and case studies of in-service behaviour related to corrosion of reinforcements, sulphate and seawater attack and carbonation are discussed. Newer areas of concern include concrete in industrial environments and degradation due to biological agencies and atmospheric pollution. A "System's" approach to durability is suggested which enables a holistic treatment of the concrete structure with the environment. Importance of making concrete impermeable with appropriate cement systems and additives like pozzolana, slag, condensed silica fume and inert fillers are discussed.

RESUME

La performance des ciments s'exprime de plus en plus, ces jours-ci, en fonction de la durabilité des constructions en béton. Le présent rapport passe en revue la documentation récemment publiée qui révèle que bien qu'on ait maintenant une connaissance suffisante des divers aspects de la durabilité du béton, les cas de rupture en service sont nombreux. Les mécanismes fondamentaux en jeu et les études de cas de comportement en service relatives à la corrosion des armatures, à l'attaque par les sulphates et par l'eau de mer et à la carbonatation sont discutés. Les nouveaux domaines d'intérêt comprennent le béton dans les environnements industriels et la dégradation dûe aux agents biologiques et à la pollution atmosphérique. Une approche à la durabilité par la théorie des systèmes est proposée, ce qui permet un traitement holistique de l'ouvrage en béton avec l'environnement. L'importance de rendre le béton impermeable utilisant des systèmes de ciment appropriés et d'additifs tels que la pozzolane, le laitier, les vapeurs condensées de silice et les charges inertes est discutée.

1 INTRODUCTION

Like many other engineering materials, the load-carrying capacity in terms of strength has long been regarded as the cardinal property of concrete. As a result, developmental efforts from the very beginning have concentrated on properties of concrete in terms of its strength, elastic and non-elastic deformations, and the constitutive relationship in stress-strain-time system. These properties were explained in terms of the microstructural features of cement paste and behaviour of concrete as a composite system, which provided impetus for further refinements. Over the years, it has, however, been noticed that this structural material was really not 'inert' during service and often got affected either by the service environment to which it was exposed or physico-chemical causes due to reasons residing within. As a result, performance of concrete started being expressed increasingly in terms of its durability so as to ensure satisfactory service life of concrete structures.

The emphasis on durability along with strength properties for characterising a material like concrete, which is sensitive not only to load, external and internal stresses and strains, but also to the environment, could be considered as a rational and satisfactory step. What was not so satisfactory, however, was the manner in which the concern on durability of concrete became important, in view of innumerable instances of unsatisfactory performance in service (1, 2).

This concern has coincided with voluminous research on various aspects of durability of concrete throughout the world for more than 50 years now. It is somewhat disquieting that there seem to be more problems in making concrete of adequate durability now, than in the past. Ben Gerwick had said "tremendous strides have been made in the understanding of durability in corrosive environments, yet it still remains the foremost problem facing structural concrete used today" (3). In the words of Neville, "It is tempting to ask why, after all these years of research there are still so many problems with the durability of concrete. Possibly, there are even more problems these days than, say, fifty years ago" (1).

Many answers to this dilemma have been offered in terms of changing properties of cement as manufactured at present in modern cement plants, the level of workmanship and quality assurance in construction practices, limitations of the specifications both in characterising the service environment as well as in terms of primary emphasis on strength aspects, with durability often being a by-product, and many others (1, 4). However, a few other developments also merit consideration. The first and the foremost is the diversity of usage of cement concrete in constructions. For example, concrete in the tidal zone of a marine structure exposed to freezing weather which can be considered as 'one of the most aggressive exposures, a concrete can routinely experience' (5). Such applications have grown with the use of concrete for oil platforms and other offshore structures. Economic development often brings in its wake rapid boom in construction activities. Concrete constructions in the Middle East and Gulf areas have often shown signs of rapid deterioration within a short span of ten to fifteen years. The environment is considered to be extremely aggressive, characterised by high temperature-humidity regimes combined with severe ground and ambient salinity. The constructions are continuously exposed to frequent and persistent winds charged with sea water and sea salts. High ambient temperatures accelerate both the chemical attack and physical deterioration (6). Problems of bridge deck deterioration in North America due to use of de-iceing salts or failures of concrete structures due to corrosion of reinforcements in concrete built with calcium chloride as an accelerator in UK are examples where aggressive conditions were inadvertently created by the user. Certain effluents, fumes and salts in chemical industries can

prove to be extremely aggressive to normal structural concrete without external protection (7). Concrete can neither be expected to be immune from deterioration due to environmental pollution caused by industrial activities throughout the world (8). A host of concrete aggregates which would prove to be innocuous by the specifications and tests prevalent in the 40s and 50s are now shown to be alkali-reactive, albeit at a slower rate (9). The problem of durability of concrete has to be viewed in the context of such changing service environments, limitations of specifications in many cases and lack of adherence to basic requirements of sound engineering practice.

1.1 Systems Approach

Distress in concrete structures due to inadequate durability would, more often than not, have involved some chemical reactions. The mechanisms of attack of concrete due to various chemical ions and salts, arrived at essentially on the basis of laboratory investigations, are well documented (10, 11). The in-situ behaviour of concrete, however, is more complex, which cannot be fully simulated in the laboratory. In service environment, a number of chemical agencies could be combined. For example, sea water contains both sulphates and chlorides of various cations; the soil or ground water in many situations entrain more than one type of salt. The behaviour of the structure is made more complicated by a number of physical and mechanical causes which can promote and accelerate deleterious reactions due to the chemical agencies. A typical situation is what Rasheeduzzafar and Dakhil (6) had described of the high chloride-sulphate environment in the Gulf areas, as under :

"Even a superficial analysis of the inspection survey of deteriorated structures provide positive indications of the fact that the total deterioration is hardly a simple arithmetic summation of the deteriorations caused by each of the operative causal factors individually. Disintegration due to one factor initiates and sometimes accelerates another form of attack and the total deterioration is cumulative in a complex way. It is to be emphasized at the outset that this interactive situation and the cross-correlation of the deterioration data considerably complicate a quantitative understanding of the deterioration problem in the Gulf area".

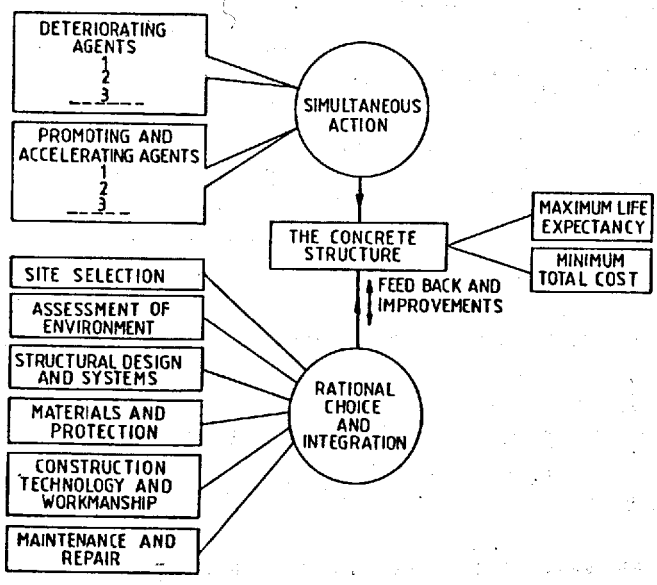

Fig 1
System of Durability of Concrete Structures (12)

The current approach of durability of concrete structures is one of a 'System' (12). In such a System's approach to durability of concrete, the deterioration is seen to be due to a number of causative factors; in addition, there are promoting and accelerating factors as described above. Accordingly, specifications for durable concrete structures are through appropriate site selection and assessment of the environment, adequate structural design and structural systems, use of appropriate concrete materials, construction technology and workmanship, and timely maintenance and repair. Such a system is depicted in Fig 1.

The approach is essentially in line with what Valenta had suggested more than two decades ago (13). Such a System's approach enables one to take a holistic view of the structure and its interaction with the environment so as to lead to satisfactory durability.

2 THE SCOPE

A general definition of durability of concrete is 'its capability to maintain satisfactory performance along with desired safety during its stipulated life under the anticipated service environments'. In a more specific way, durability may be defined as 'the resistance of cement and concrete to either internal or external, physical, physico-chemical or chemical actions. The chemical, physico-chemical and physical actions are so interlinked together in practice that it is neither possible nor prudent to consider any of them in isolation, neglecting the others' (10). In a recent review, Mehta has pointed out what an enormous task it would be to review all the research done on performance of cements and durability of concrete, covering such a broad specturm (4). The scope of the present Report has, therefore, to be optimally chosen. It has accordingly been attempted to concentrate on the key areas of concern. What are those key areas?

In Fig 2 is reproduced, what Hoff has described as 'the most aggressive exposure a concrete can routinely experience' in marine and offshore structures (5). The deterioration of concrete in such a case is primarily due to corrosion of steel reinforcements, cracking due to freezing and thawing, physical abrasion, and chemical decomposition of hydrated cement and chemical attack on concrete - carbonation and sulphate attack. In the severe chloride-sulphate environment of the Middle East, the main mechanisms of deterioration are again corrosion of reinforcements, sulphate attack, salt weathering, shrinkage and early thermal movements (6). Mehta has identified corrosion of reinforcing steel, frost action in cold climate and physico-chemical effects in aggressive environments as the major causes of concrete deterioration today (4). In petro-chemical and fertilizer industries, the deterioration is mainly due to action of ammonium salts, HCl, H_2SO_4 and other weak acids, urea, and sulphur dioxide combined with other agents which function as promoting and accelerating factors (7). Clearly, these are, thus, common causes of deterioration, which can help in identifying the key areas of concern for the present Review.

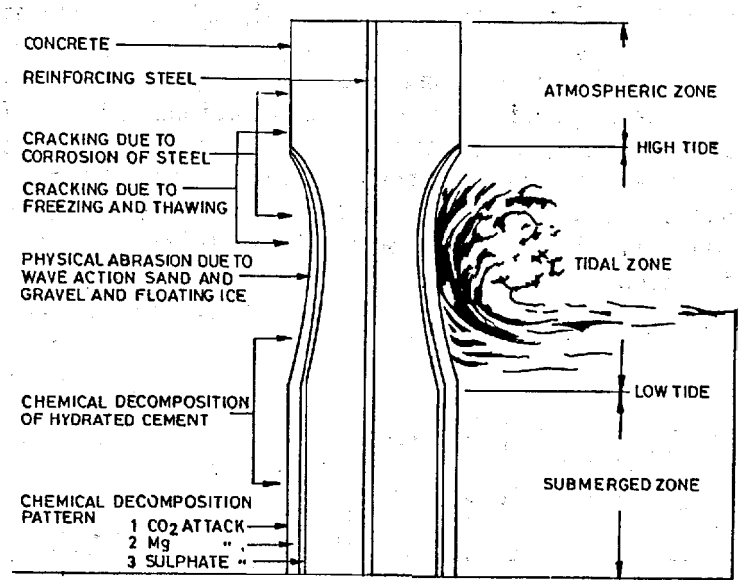

Fig 2
Deterioration of a Concrete Structure in Seawater (2)

Five major durability conferences were held since the 8th Congress on the Chemistry of Cement in Rio de Jeneiro (14, 15, 16, 17, 18). The summary of the analyses of the subject of papers presented in these is shown in Fig 3, from which it will appear that corrosion of reinforcements, sulphate and sea water attack, carbonation,

and physical causes like freezing and thawing, thermal effects and abrasion were the major areas. Papers on deterioration of concrete structures in industrial environments were presented mostly in technical journals.

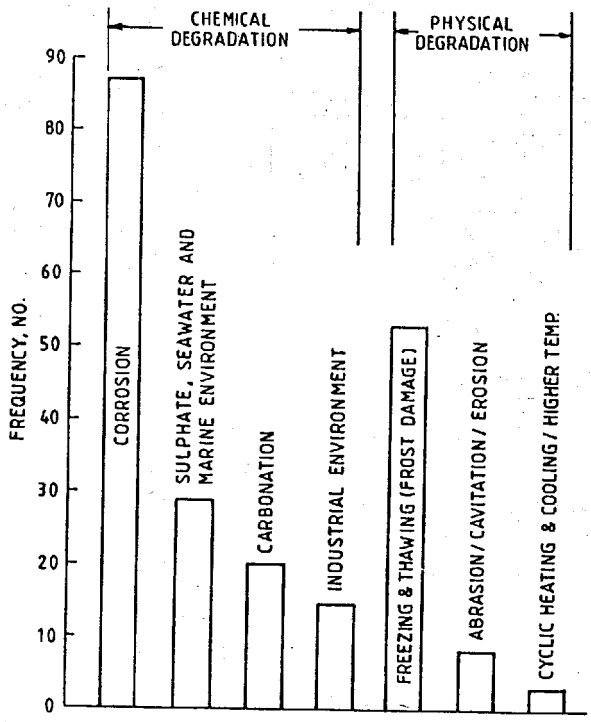

Fig 3
Subjects of Papers Presented in the last five Durability Conferences

The above analyses also brought out the following salient trends in the reported literature :

(i) Although adequate knowledge is available about the mechanisms of actions of various deleterious agencies on concrete, there are many instances of failures in service, so much so that concrete cannot be considered as a material which is maintenance-free and where no repair would be required.

(ii) There is an increasing number of case studies on in-service behaviour of concrete reported, in addition to conventional laboratory research.

(iii) Major instances of durability problems are related to corrosion of reinforcements, sulphate and sea water attack, carbonation, and in cold climates, freezing and thawing.

(iv) Newer areas of concern include concrete in industrial environments and degradation due to biological agencies and atmospheric pollution.

(v) Hot and humid climate accelerates the degradation phenomenon. Ambient service conditions are, therefore, important considerations in design and specifications, especially in the tropics.

(vi) Considerable information is available on the performance and durability of cement systems with additives like pozzolana, slag, condensed silica fume and even inert fillers, mostly under laboratory tests.

Subsequent Sections in this Review Report would address to the salient developments as mentioned above. The subject of Alkali-Aggregate Reaction (AAR) has been covered exclusively in two International Conferences during the intervening years (19, 20) and another is being planned almost simultaneously with this Congress (21). The subject of alkali-aggregate reaction would, therefore, not be dealt with in any great detail in this Report.

3 THE BASIC MECHANISMS - COMMON PHYSICO-CHEMICAL EFFECTS

3.1 Corrosion of Reinforcement

Corrosion of steel is an electrochemical phenomenon which can be separated into an anode process and a cathode process (Fig 4):

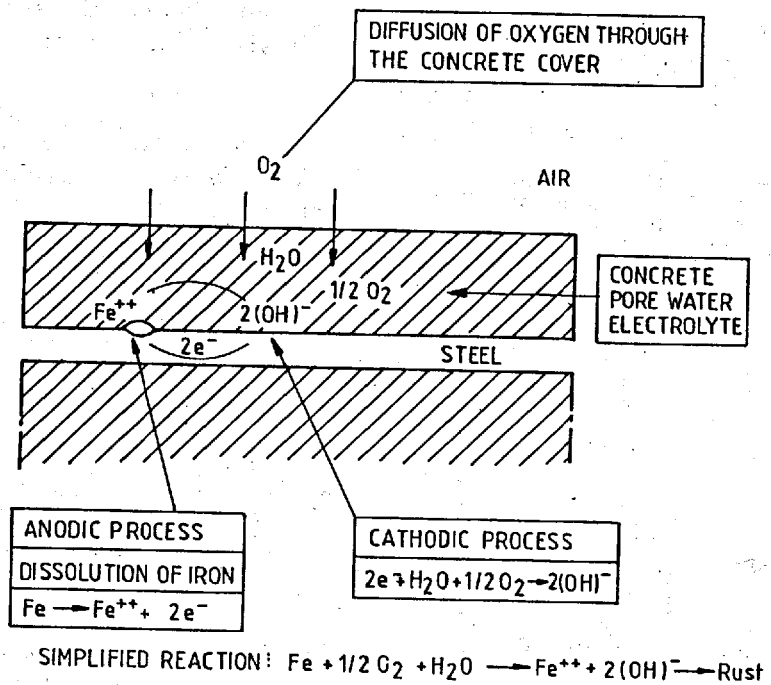

Fig 4
Corrosion of Steel in Concrete - A Simplified Model

Anode : (metallic iron) $Fe \dashrightarrow 2e^- + Fe^{2+}$ .... (1)

Cathode : $\frac{1}{2}O_2 + H_2O + 2e^- \dashrightarrow 2(OH)^-$ .... (2)

and the corrosion undergone by steel is due to combination of iron and (OH^-) ions;

$Fe + \frac{1}{2}O_2 + H_2O \dashrightarrow Fe^{2+} + 2(OH) \rightarrow$ iron hydroxides (rust) .... (3)

The oxygen dissolved in water enhances corrosion when the pH is in between 4 and 10. For pH more than 10, reaction (3) takes the form :

$2Fe^{2+} + 3H_2O \dashrightarrow Fe_2O_3 + 6H^+ + 2e^-$ .... (4)

$3Fe^{2+} + 4H_2O \dashrightarrow Fe_3O_4 + 8H^+ + 2e^-$ .... (5)

For transformation of metallic iron to rust, iron must be available in a metallic (Fe) state at the surface of reinforcing steel; oxygen and moisture must be available for the cathode process; and the electrical resistivity of concrete must be low to facilitate the electron flow in the metal from anodic to cathodic areas.

Mehta points out that in reinforced concrete, with adequate cover of good quality concrete, none of the three conditions listed above may be met during the service life (4). There exists an adherent surface film of iron oxides or γ- FeO.OH (lepidocrocite), which usually protects (passivates) the underlying metallic iron. This protective film is thermodynamically stable above pH 11 and the pH range of hydrated portland cement paste is 12.5 to 13.0. The depassivation of steel would require, first, the decomposition and removal of the crystalline calcium hydroxide (in the proximity of the reinforcement) and, second, the destruction of the protective iron oxide film present on the surface of metallic iron. Aggressive waters containing

high concentrations of CO_2, sulphate, or chlorides will react with calcium hydroxide and form leachable products (such as, calcium bicarbonate, calcium sulphate, and calcium chloride). With portland cement paste, chlorides can also form products, such as $C_3A.CaCl_2.H_2O$, and $Ca(OH)_2.CaCl_2.H_2O$. These products will, however, decompose and release the chloride ions in the case of sulphate or CO_2 attack, which does happen with many natural waters. Once the crystalline calcium hydroxide has been removed from the vicinity of reinforcing steel, the pH of the pore solution drops below 11 and the iron oxide film loses its protection (4). For instance, in the presence of chlorides, a basic iron chloride, $3Fe(OH)_2.FeCl_2$, is formed (22) which later decomposes to produce akaganeite (β -FeO.OH).

The mechanism of expansion in concrete due to rust formation has been explained by Mehta (4). He has pointed out that depending on the environmental pH at the anode, ferrous ions may be associated with more or less hydroxyl ions :

$$\underset{(pH\ 7)}{Fe(OH)^+} \rightleftharpoons Fe(OH)_2 \rightleftharpoons \underset{(pH\ 14)}{Fe(OH)_3} \qquad \ldots\ (6)$$

Compared to metallic iron, the hydroxides of iron are more voluminous and their formation is accompanied by expansive pressures. Similar to expansion of cryptocrystalline ettringite in sulphate attack or expansion of silica gel in alkali-aggregate reaction, the gel-like iron hydroxides formed as a result of steel corrosion can imbibe water and swell under certain conditions. Acidic conditions (such as those when hydroxyl ions have been replaced by chloride, sulphate or bicarbonate) weaken the hardened cement paste, and the paste thus weakened can expand and crack from the development of hydraulic pressure via gel swelling. This explains the field observation that the corrosion of reinforcing steel is usually accelerated not only in the presence of chlorides but also sulphates, and CO_2 (4).

The above description brings out the interaction of oxygen, water and chloride ions, both as the agencies responsible for corrosion of reinforcement and the agencies responsible for destroying the passivity around the reinforcement in concrete provided by the alkaline environment. In practice, the interaction between these parameters is quite intense. The nature of the cation at the same chloride level is important. For example, $CaCl_2$ addition creates a more open pore structure allowing an easier diffusion and reduction in pH of the pore solution. Compared to that, alkali chlorides (NaCl and KCl) enhances the porosity to a lower extent and in general increase the pH of pore solution. Therefore, calcium chloride is considered to be more deleterious than NaCl or KCl (23). The diffusion coefficient of chloride ions itself depends upon the cation and decreases in the following order :

$$MgCl_2 > CaCl_2 > KCl > NaCl$$

The effect of carbonation in lowering the alkalinity in concrete and promoting corrosion of reinforcement will be discussed later. Recent tests have shown that there is an interactive effect of carbonation and chloride ion ingress leading to much more rapid corrosion than where the two phenomenon would have occurred independently, provided the presence of high chloride ion concentration did not lower the rate of carbonation (24). The presence of oxygen and water are both necessary for corrosion process to take place, but the degree of saturation of oxygen in water decreases in the presence of chloride ion. This could be a reason of lack of corrosion of steel reinforcement even in the presence of high chlorides concentration as noticed sometimes (25). On the other hand, it has also been noticed that under certain conditions where oxygen supply was negligible, even then the rate of corrosion was considerable in

presence of sufficient chloride ions. It would seem that some alternative cathodic process could take place which does not require oxygen diffusion (26). The existence of crevices at the steel/concrete interface affording relatively low pH environments, is presented as a possible explanation for corrosion without reduction of oxygen. The process is postulated as follows :

(a) Generation of differential aeration cells in crevices where oxygen is consumed.

(b) Migration of Cl^- into crevices offsetting free Fe^{2+} ions and acidification of crevices due to hydrolysis of the resultant compounds.

(c) Destruction of passivity with the progressive acidification and increase in Cl^- concentration.

(d) Corrosion continues due to cyclic catalytic mechanism.

Presence of oxygen is necessary to initiate this process only, and Cl^- is required to cause acidification (26).

$$\begin{array}{ccc} & Fe^{2+} + 2Cl^- + \uparrow H_2 & \\ Fe \nearrow & & \searrow \\ & 2HCl + Fe(OH)_2 \xleftarrow{2H_2O} FeCl_2 & \end{array} \qquad \ldots\ (7)$$

From engineering standpoint, two types of situations are necessary to be considered. The steel reinforcements, being well protected in the alkaline medium in concrete, would take a certain amount of chloride ion to be present in order that corrosion can take place. On the other hand, if the passivity is destroyed because of one reason or the other, and the pH of concrete is lowered below a certain threshold value, all that is needed for corrosion to take place is oxygen and water, and presence of chlorides is not necessary. Concrete constructions, in order to be durable, have to ensure that the limiting amount of chloride ions is not exceeded in concrete and neither the pH value of concrete is lowered below the threshold value. Practical limits of tolerable chloride ion concentration and limiting pH value are best arrived at by in-service record of concretes.

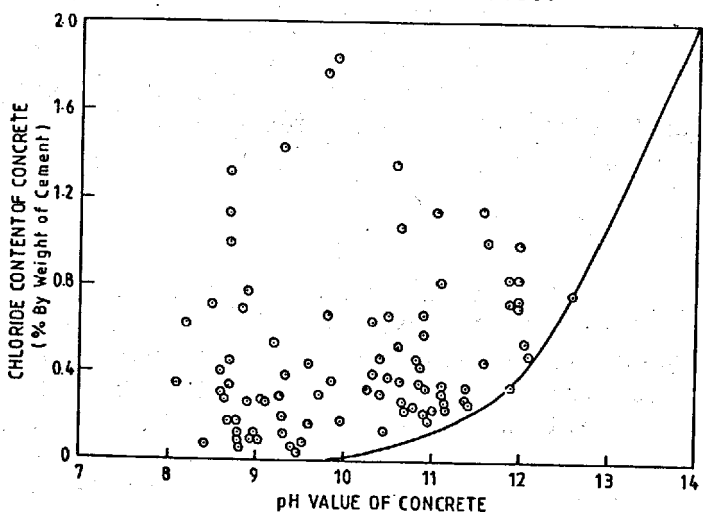

Fig 5
Interaction Diagram of pH Value and Chloride Content in Corrosion-damaged Concrete

From a large number of field data on concrete structures in India which had undergone distress due to corrosion of reinforcement, it has been found that whenever the pH value of the cover concrete was below 10, either due to carbonation or inadequate cement content or leaching, corrosion of reinforcement had invariably taken place irrespective of the presence of Cl^- ions or otherwise (Fig 5) (27). On the other hand, for concrete structures of average quality and having pH value of 11.5 and above, a limiting chloride ion content of the order of 0.15 percent by weight of cement was found to be required for the onset of corrosion (Fig 6).

For typical concrete mixes, this could correspond to 0.6 to 0.8 kg of chloride ions (Cl^-) per cubic metre of concrete. Field studies of concrete constructions from the Gulf areas have been reported where chloride concentration of 0.6 kg/m³ to about 3.75 kg/m³ has been measured (6, 28).

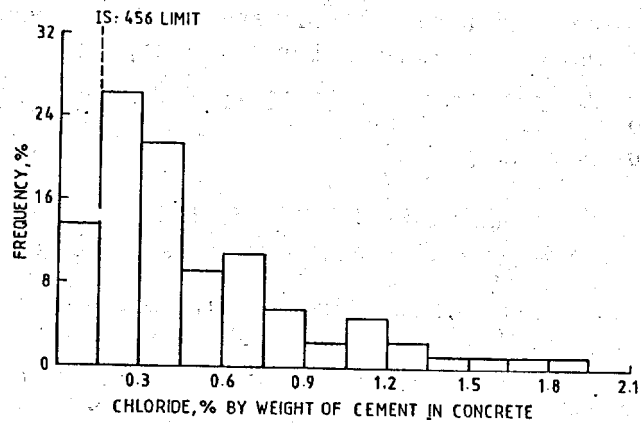

Fig 6
Distribution of Chloride Content in Corrosion-damaged Concrete (27)

3.2 Attack by Sulphate and Sea Water

The nature of attack of sulphate solutions on the hydrated cement systems is guided by the more or less basic character of the hydration products of cements. It implies the possibility of an acid attack at a pH below a certain value. On the other hand, a base exchange may take place between $Ca(OH)_2$ and salts of cations, eg, magnesium salts, giving weaker and/or less soluble hydroxides and anions forming soluble calcium salts. Finally, more complex attack is possible by interaction of hydrated aluminates and ferrites from the cement with the sulphates. According to Calleja, the main mechanisms causing sulphate attack can be identified as follows (10):

1) formation of sulphoaluminates (ettringite)

$$C_3A + CH + 12\,H \longrightarrow C_4AH_{13} \quad \ldots\ (8)$$

and

$$C_4AH_{13} + 3\,C\bar{S}\,H_2 + 14\,H \longrightarrow C_3A(C\bar{S})_3H_{32} + CH \quad \ldots\ (8\text{-}A)$$

leading to

$$C_3A + 3\,C\bar{S}\,H_2 + 26\,H \longrightarrow C_3A(C\bar{S})_3H_{32} \quad \ldots\ (9)$$

2) formation of gypsum

$$N\bar{S} + CH + 2\,H \longrightarrow NH + C\bar{S}\,H_2 \quad \ldots\ (10)$$

the acidic nature of sulphate attack causes surface deterioration by softening without expansion;

3) When alkali sulphate concentration is high and conditions are favourable, formation of alkali sulphate crystals takes place; for instance :

$$N\bar{S} + 10\,H \longrightarrow N\bar{S}\,H_{10} \text{ (mirabilite)}, \quad \ldots\ (11)$$

contributing to surface deterioration by spalling and splitting;

4) In the case of magnesium sulphate, formation of brucite and gypsum takes place :

$$M\bar{S} + CH + 2\,H \longrightarrow MH + C\bar{S}\,H_2 \quad \ldots\ (12)$$

both contributing to deterioration;

5) formation of hydrated silica (in the case of magnesium sulphate) with simultaneous formation of gypsum and brucite, which can be schematically expressed as :

$$CSH + M\bar{S} + H \longrightarrow MH + C\bar{S}.H_2 + SH \quad \ldots\ (13)$$

Attack on hydrated cement systems by sea water is characterised by the presence of both chloride and sulphate ions, which influence the corresponding effect of individual cause. For instance, the intensity and extent of attack by sea water is in most cases found to be less severe than what should be expected corresponding to the concentration of SO_4^{2-} ion or that of $MgSO_4$ solution, if present in individual sulphate solutions.

According to Calleja (10), the most general, wide ranging and complete attack by sea water on hydrated cement is characterised :

a) by elimination of calcium, either by solution or substitution for magnesium (cation exchange), leaching of portlandite CH, formation of brucite MH or transformation of the $C_xS_yH_z$ type of calcium silicate hydrates into the more complex $C_x.M_x.S_y.H_z$. magnesium type of compounds (29);

b) by formation of secondary dense expansive ettringite through reaction of sulphates with CH;

c) by (subsequent) strong carbonation converting ettringite into thaumasite when the temperature is lower (0 - 5°C). However, thaumasite need not only be carbonated ettringite. It can also form by reaction of CSH with sulphate and carbonate ions when water is available for transport, eg, sulphate water containing CO_2 (30).

d) by crystallization of gypsum;

e) by formation of $C_3A.CaCl_2.H_{10}$ which initially prevents the immediate formation of ettringite, but being unstable in the presence of sulphates finally tends to form ettringite;

f) by penetration of Cl^- ions in tobermoritic gels.

In addition, physical factors like temperature, frost action, mechanical causes like erosion, alternating tidal and wave action etc and effects of carbonation, salt crystallisation are superimposed on the above chemical actions, making the whole process of action of sea water on hydrated cement quite complex.

A number of case studies have been reported in deterioration of concrete under marine environment and in the Middle East and Gulf environment, where more than one mechanism, ie, sulphate attack and carbonation, in addition to corrosion of reinforcements, were predominant mechanisms of deterioration (2, 6, 31). Sulphate attack in concrete has also been reported in connection with attack due to sulphuric acid, either in industrial environment or due to acid rain. These will be discussed in latter sections. Occurrence of distress to certain steam-cured concrete components have been reported and ascribed to formation of thaumasite and ettringite. Initially, a few hair-line cracks formed, which gradually increased in number. In the course of time, the cracks widened until finally the components had to be taken out and replaced. Microscopic, radiographic and microfluorescence analytical examinations showed needle-shaped crystals in cracks and around aggregates which were similar to ettringite in their morphology, but also contained silicic acid in addition to aluminium. This finding indicated a second formation of mixed crystal bonds between ettringite and thaumasite which led to swelling effects in cracks - that previously occurred in the micro range, as well as to destabilization (32). Occurrence of thaumasite has also been reported in case of bridges in Sweden (8).

In another reported case of deterioration in concrete tunnel linings due

to calcium sulphate dissolved in water and under low temperature service conditions (4 - 6°C), presence of thaumasite and calcite were detected without any ettringite content (Fig 7) (33). The pH value of water was 6.5 owing to presence of free CO_2. The silica needed for the formation of thaumasite was probably supplied by alteration of mica and feldspar present in the aggregate as well as alteration of CSH phase.

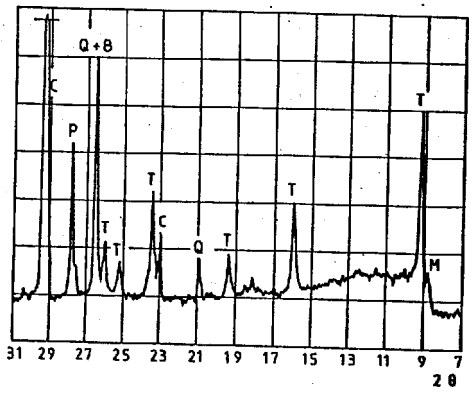

Fig 7
X-ray Diffraction Analysis of the Powdery Material present in the Deteriorated Concrete (33)
(B = Biotite, C = Calcite, M = Muscovite, P = Plagioclase, Q = Quartz, T = Thaumasite)

Limestone aggregates have been reported to significantly restrain development of sulphate attack in comparison to granite. It is due to formation of monocarboaluminate from limestone and aluminate phases. This phase reduces the amount of aluminates available for sulphate attack as well as creates a strong chemical bond between cement paste and limestone aggregates (34).

3.3 Carbonation

CO_2 in air or dissolved in water is known to react with hydrated cement systems. The phase most susceptible to carbonation is calcium hydroxide. But other products of cement hydration can also be affected to some extent by carbonation, being decomposed to form finally calcium carbonates and hydrated silica, alumina and ferric oxide, as ultimate products of a total carbonation. For example, total carbonation of tobermorite gels can lead to decomposition into calcite and amorphous silica (10) :

$$C_3S_2H_3 + 3\,\bar{C} \longrightarrow 3\,C\bar{C} + 2S + 3H \qquad \ldots\ (14)$$

In a 22 years old construction, products of carbonation of hydrated cement included carbonated CSH gel having calcite phases together with amorphous silica gel and calcium silicate hydrate of low C/S ratio along with portlandite which was still present (Fig 8) (35).

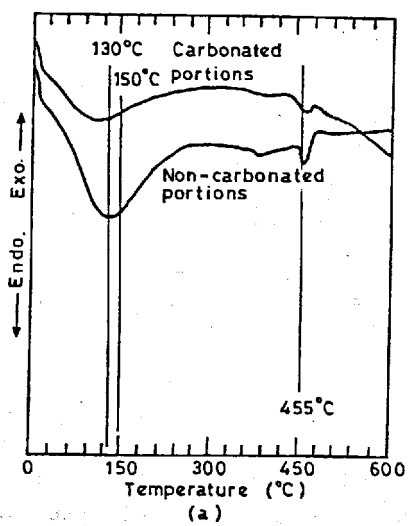

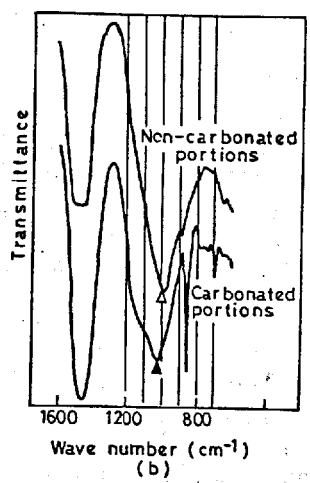

Fig 8
(a) DCS Curves, and (b) FT-IR Spectra of Hydration Products Separated by Heavy Media showing Effects of Carbonation (35)

This seems to indicate that CO_2 reacts with hydrated calcium silicates as well as on portlandite, according to

$$C_3S \xrightarrow[H]{\text{hydration}} \begin{matrix} CSH \\ CH \end{matrix} \xrightarrow[\bar{C}]{\text{Carbonation}} \begin{matrix} C\bar{C} \\ CH \\ S\ (gel) \end{matrix} \quad \ldots\ (15)$$

As a product of carbonation, calcium carbonte may appear as mixtures of vaterite; calcite and/or aragonite in different proportions (36). Hydrated alumina, firstly amorphous, is transformed afterwards into bayerite and finally into gibbsite. Gypsum may also appear together with aragonite, as a result of carbonation of calcium solfoaluminates (10).

'Pure' waters contain a certain amount of total dissolved CO_2 depending upon the ambient condition. A part of this CO_2 is fixed as calcium-bicarbonate - $Ca(HCO_3)_2$ and the remaining part is available as 'free' CO_2. Again, part of this 'free' CO_2 is required for the stabilization of the carbonate-bicarbonate equilibrium in the reaction

$$Ca\,CO_3 + CO_2 + H_2O \rightleftharpoons Ca\,(HCO_3)_2 \quad \ldots\ (16)$$

and the amount of CO_2 which is in excess of this quantity has been called 'aggressive' CO_2, which may attack and dissolve calcium carbonate (4, 10).

As far as ambient conditions influencing atmospheric carbonation are concerned, relative humidity is very important. Carbonation proceeds at high rates for RH values between 50 and 75%, being much slower for RH between 75 and 100% or 0 and 45%. The reason is that at humidity values higher than 75% the capillary pores in hydrated cement are filled with water and CO_2 must first dissolve and then diffuse to penetrate, which is much slower; Humidity values lower than 45% retard the process, probably because at such lower values water has not the liquid characteristics corresponding to ordinary water for dissolving either $Ca(OH)_2$ or CO_2 (10).

Kobayashi and Uno have pointed out the importance of pH value of the pore solution in concrete on the rate of carbonation (37). According to their investigations, pH value is dependent upon the amount of alkali salts and higher the pH value, the higher will be the rate of carbonation. They have pointed out that if the rate of carbonation in cement concrete structures constructed in Japan after the 60s have been markedly higher, it is because of increase in the alkali content in the cements produced by modern process of cement manufacture.

Much of attention on carbonation of concrete has been in relation to lowering of the alkalinity (pH value) of concrete which affects the protection available to steel reinforcement against corrosion. The reason of lowering of pH value of pore solution in concrete due to carbonation is because of depletion of $Ca(OH)_2$. The pH value of the pore solution of concrete which has not been carbonated is maintained in a range of 12.5 or more by the calcium hydroxide dissolved. However, with penetration and reaction of CO_2, the pH is decreased and, in the carbonated portion, can become close to 8.3 (37).

Of late, attention has also been focussed on the somewhat beneficial effects of carbonation in rendering greater impermeability to the outer skin of concrete. Carbonation of hydrated cement paste takes place mainly on the pore surface. There are some active sites on the pore walls; only on those sites can $CaCO_3$ nucleate and grow and Ca^{2+} ions migrate and gather near the pore. Owing to transportation and

redistribution of minerals, carbonation leads to certain changes in the pore size distribution. There is a net decrease in the pore sizes and pore volume (38, 39). There is always an optimum size (radius) of the pores where carbonation and precipitation of calcite is preferred because pores smaller than these may lack adequate nucleation sites and also may get blocked due to calcite being deposited near its openings (38). The decrease in porosity is more manifest on smaller pores having radius 630 A° and below in case of ordinary portland cement mortar, and those with radius below 320 A°. in case of cement incorporating flyash (39). Such pore modifications may be beneficial in preventing ingress of harmful chemicals from outside. Osborne has shown the effect of carbonation in improving sulphate resistance of concretes (40). While limited carbonation of hydrated portland cement paste will be impermeability-improving, because of formation of insoluble calcium carbonate which plugs up the pores, excessive carbonation in the presence of aggressive CO_2 will be impermeability-reducing, because of the formation of calcium bi-carbonate which is soluble and can be leached away and widen the existing pores and micro-cracks (4).

Lach (41) has reported the failure of concrete structures built with high alumina cement where the cause of deterioration was found to be decrease in concrete strength brought about by conversion and carbonation of high alumina cement concrete according to the equation :

$$3\ CAH_{10} \xrightarrow{\text{conversion}} C_3AH_6 + 2\ AH_3 + 18\ H$$

$$\xrightarrow{\text{carbonation}} 3CaCO_3 + 2\ AH_3 + 21\ H \qquad \ldots\ (17)$$

or, in simplified manner, $CAH_{10} \longrightarrow CaCO_3 + AH_3 + 7\ H$ $\ldots\ (18)$

4 CHEMICAL REACTIONS AND PHYSICAL EFFECTS INVOLVING AGGREGATES

Constituents of certain aggregates can undergo chemical changes or react with the cement-water system in such a way as to cause deterioration to concrete. The most well-known phenomenon of alkali-aggregate reaction (AAR) involving alkalis primarily from the cement and the reactive constituents in certain aggregates, is not being discussed in this report in any great detail. However, there are other instances of deleterious chemical reactions, probably involving oxidation of ferrous iron, pyrites or marcasite, which can cause deterioration of concrete (42).

Distress to a ten-year old concrete hospital floor slab in the form of severe blistering over an extensive area of the floor, resulting in unevenness of the floor and rupturing of the vinyl tiles has been reported (43). The aggregates used in the concrete contained a considerable amount of pyrite (FeS_2) where blistering had occurred. Iron sulphide, including pyrite, are unstable in the presence of oxygen and moisture and oxidize to produce sulphuric acid and iron sulphate as follows :

$$2FeS_2 + 7O_2 + 2H_2O \longrightarrow 2FeSO_4 + 2H_2SO_4 \qquad \ldots\ (19)$$

After the oxidation of pyrite started, the resulting H_2SO_4 first attacked the aggregate minerals and the surrounding mortar, and then attacked the portion of vinyl tile in contact with the affected aggregate with the result that the portion of the tile lost its resilience and became brittle. It may be noted that, with the limited amount of moisture available in the concrete environment, the H_2SO_4 resulting from pyrite oxidation must have been highly concentrated and detrimental to the surrounding material.

Reaction of H_2SO_4 with the mortar in the form of acid as well as sulphate attack (reactions 20 and 21 below) neutralised the cementing agents of the mortar and the resulting gypsum caused a volume increase that was probably the start of blister formation and produced expansive forces on the vinyl tile :

$$Ca(OH)_2 + H_2SO_4 \longrightarrow CaSO_4.2H_2O \quad \ldots\ (20)$$

$$2\ Ca_{1.5}SiO_{3.5}nH_2O + 3H_2SO_4 \longrightarrow 3(CaSO_4.2H_2O) + 2SiO_2 + (2n-3)H_2O \quad \ldots\ (21)$$

At the same time, acid reacted with other mineral components of the aggregate to form complex sulphates such as jarosite, halotrichite, and exerted expansive forces on the tiles. A rust-like boundary was observed around the reaction zone which was probably formed according to reactions (22) and (23) below, from the iron sulphate formed in reaction (19) :

$$FeSO_4 + Ca(OH)_2 + 2H_2O \longrightarrow CaSO_4.2H_2O + Fe(OH)_2 \quad \ldots\ (22)$$

$$2Fe(OH)_2 + H_2O + \tfrac{1}{2}O_2 \longrightarrow 2\ Fe(OH)_3 \quad \ldots\ (23)$$

Pyrite aggregates within the concrete were not affected due to complete protection by the mortar and a general sulphate attack was not observed (43).

The presence of jarosite as a product of deterioration in concrete has been observed only scarcely. A case study of the deterioration in a Belgian bridge reveals the formation of jarosite, caused by the oxidation of a rare type of aggregate - 'black' pyritic sandstone consisting of essentially two minerals : quartz and pyrite (44). The geological occurrence of the observed pyritic sandstone, as a single layer or as a constituent of a larger unit, has not been reported in Belgium before. The most striking symptoms of deterioration were the staining of the concrete surface and the evolution of popouts in the bridge piers. The deterioration mechanism in the case of the popouts is related to the massive formation of gypsum and jarosite in the boundary zone between the black sandstone aggregate and the cement paste in the concrete surface layer. The rust products were also present, but there are two reasons why they were not considered responsible for the expansion damage. Firstly, a portion of the Fe^{3+}- ions are built in the jarosite structure which means a reduction of the potential of rust formation. Secondly, the expansive rust products are formed in the porous structure of the black sandstone (44).

Distress to swimming pools constructed 15 years ago in the South of Sweden has been reported (45). Concrete placed at the back of the glazed tiles lining appeared porous and became brownish when in contact with water. Many translucent and opaque fibres and white particles were observed under a stereomicroscope, spreading over the whole surface of the concrete, and, in spots, a white precipitate also was observed. From the data of the various laboratory analyses, it was concluded that the deterioration of the concrete was caused by a combination of interacting factors, possibly involving alteration of feldspar, dissolution of iron sulphide (pyrite), and aggressive action of sulphates and alkalis.

Oxidation of pyrite led to increased quantities of sulphates in the water. The porosity of the concrete and the flow of such water led to deterioration due to the aggressive action of sulphate. In addition, mineralogical analyses revealed conversion of potassium feldspar, as per a complicated mechanism. When potassium feldspar comes in contact with water (pH > 10), it reacts and produces free alkalis and a residium of aluminium and silicon. Occurrence of alkali-silica reaction was also noticed (45).

Shrinkage and thermal expansion properties of certain aggregates can cause distress to concrete. Lea had reported instances of dolorites, basalts, sandstones, limestones, mudstones and other aggregates in which the shrinkage on drying was large enough to cause distress to concrete (42). The large difference in coefficients of thermal expansion of concrete constituents may include stresses that are capable of cracking the hardened concrete, particularly when exposed to conditions of large temperature variations (46). In addition, carbonate rocks can be thermally non-homogenous and non-isotropic. This is reflected in the data on thermal expansion of Australian limestone aggregates as reporated by Orchard (47); Fig 9 reproduced from Ref 47 shows the expansion with increase in temperature as curvilinear in case of limestone, so much so that in one case the increase in expansion from 80° to 90° C was 11 times the expansion with increase in temperature from 20° to 30°C. In addition, there is an appreciable residual expansion when the limestone is heated from 20° to 90°C and then cooled to 20°C (Fig 9).

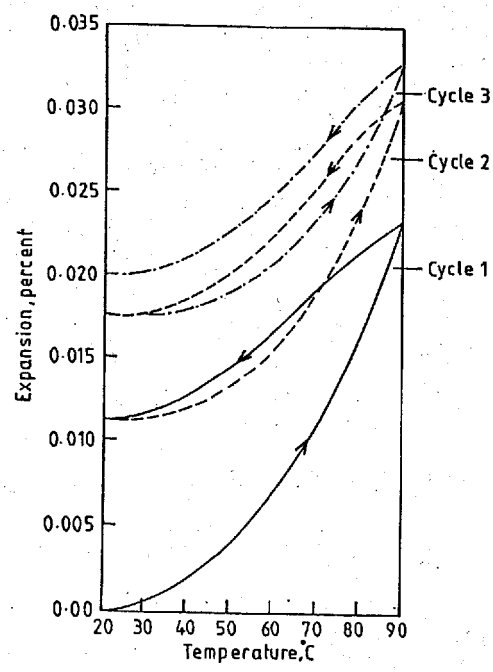

Fig 9
Typical Thermal Expansion of Limestone Aggregate (47)

Limestone rock, the commonly available source of coarse aggregates in the Arabian Gulf, has a low coefficient of thermal expansion as compared to that of hardened cement paste. For every 10°C change in temperature, tensile stresses of the order of 10 to 20 kg/cm^2 can develop, corresponding to coefficients of thermal expansion of 5 x 10^6/°C for aggregates and 15 x 10^6/°C for hardened cement paste. Due to large daily temperature change (15 to 25°C) in the Arabian Gulf, these stresses may equal or exceed the tensile strength of concrete, leading to the development of cracks. The cracks may or may not be structurally dangerous, but once they develop, the ingress of aggressive elements can give rise to other deterioration mechanisms (48). Failure of two concrete bridges within ten years in Yugoslavia, which used limestone aggregates causing such thermal incompatibility with the cement paste system have been reported (46). Distress to concrete foundations in a super thermal power station in India, which used limestone aggregates having thermal non-homogeneity and thermal anisotropy of the nature of Fig 9, has been noticed. The ambient temperature in the turbine hall can vary from 42° to 61°C and a thermal gradient upto 10°C between the opposite horizontal faces of the foundation blocks was measured, which can give rise to thermal stresses large enough to cause cracking (49).

5 CONCRETE IN INDUSTRIAL ENVIRONMENT

With rapid industrialization, concrete is finding increased use in the construction of industrial structures for various chemical, fertilizer and energy related projects. An important consideration governing the performance of such industrial structures is the durability of concrete in the man-made environment to which these are exposed. Implicit faith in the durability of concrete construction under normal conditions of usage, eg, housing or institutional buildings, quite often makes the engineer complacent while dealing with industrial structures, which need special care and protection. The mechanisms of deterioration in each case have to be arrived at, taking into account the corrosiveness of the chemical agencies, operating

temperatures and pressures, ambient atmospheric conditions and facilities for ventilation of fumes, drainage of effluents etc. Laboratory tests cannot simulate the conditions; and field observations have to be relied upon to provide valuable inputs.

Results of Condition Survey of a large number of industrial concrete structures built over the last 30 years in India have been reported (7). Table 1 lists the principal chemical agencies responsible for deterioration and types of distress noticed.

Table 1

Summary of the data on Concrete Structures
in Fertilizer Plants, Oil Refineries and Petro-chemical Industries

Sl No	Structural system	Time of appearance of symptom, years	Causative factor	Original protective treatment	Symptoms
1	Tower	8	Urea (fumes and solution)	nil	Spalling and corrosion of reinforcement
2	Tower	15	Urea (fumes and solution)	Epoxy paint	Horizontal and vertical cracks
3	Storage yard	10	Urea (solid)	nil	Cracking and spalling of concrete and corrosion of reinforcement
4	Frame building	12	Ammonium chloride	nil	Cracking and spalling of concrete
5	Frame building	5	Ammonium nitrate	nil	Heavy Cracking and spalling of concrete
6	Frame building	5	Sulphuric acid	nil	Swelling and spalling of concrete
7	Frame building	18	SO_2	nil	Spalling of concrete + corrosion of reinforacement
8	RCC tank	5	HCl NaOH	Acid resistant brick lining	Lining damaged
9	RCC floor	10	3% Sodium hypo-chloride	Brick lining	Lining damaged
10	RCC tank	5	Acetic/ Formic acid	nil	Spalling of concrete and corrosion of reinforcement

It was found that, in the absence of additional protective coating, the onset of distress in majority of the cases was within the first five years. Subsequent repairs including provision of protective treatment were not successful because of limitations in neutralising the effects of chemical salt and ions already entrenched inside the concrete (7).

The most widely used fertilizers are nitrogen-based and amongst them ammonium nitrate is predominant. Ammonium nitrate fertilizer contains 75% NH_4NO_3 and 25% $CaCO_3$ as filler. In case of deterioration of concrete in an ammonium nitrate plant in a fertilizer factory, the basic reactions involved are postulated as below (50, 51) :

(i) reaction between nitrate ion and the lime liberated by cement hydration, to form the highly soluble calcium nitrate

$$Ca(OH)_2 + 2NH_4NO_3 + 4H_2O \longrightarrow Ca(NO_3)_2.4H_2O + 2NH_4OH \quad \ldots. (24)$$

(ii) reaction between calcium aluminate hydrate and the calcium nitrate from equation (24) to form hydrates of calcium nitroaluminate

$$4CaO\ Al_2O_3.6H_2O + Ca(NO_3)_2.4H_2O + H_2O \longrightarrow 3\ CaO.Al_2O_3.Ca(NO_3)_2.10H_2O + Ca(OH)_2 \quad \ldots. (25)$$

which can be identified with the help of DTA (Fig 10) and XRD (Fig 11) techniques (27, 50).

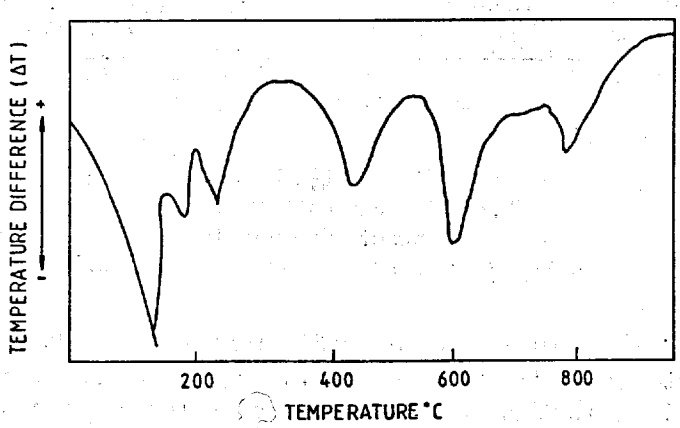

Fig 10
DTA of Concrete Deteriorated by NH_4NO_3 Solution (50)

Ammonium hydroxide formed in the reactions dissociates and releases ammonia gas. The formation of calcium nitro-aluminate hydrate results in considerable increase in solid volume leading to expansions and disruption of the hardened concrete. Wherever leaching is likely to take place, the highly soluble calcium salts are washed away leaving voids behind (7).

In the investigation to determine the corrosive effect of ammonium nitrate-based fertilisers on cement concretes, it was found that in the aqueous soluitions of NH_4NO_3, there was a continuous increase in the NO_3 concentration and decrease in the NH_4 concentration (51). While the decrease in NH_4 concentration may be explained as a result of conversion to volatile NH_3 gas, the increase in NO_3 concentration was attributed to a bacterial nitrification. The autotrophic bacteria nitrosomonas and nitrobacteria multiply in a medium having a pH value between 7 and 10 in the presence of $CaCO_3$, which is a source of CO_2. The ammonium nitrate fertilizer in the aqueous solution and the alkalinity of the solution provide a suitable medium. By this process, the NH_4^+ ions are converted to NO_3^- :

$$NH_4^+ + 3/2\ O_2 \longrightarrow NO_2^- + 2H^+ + H_2O \quad \ldots. (26)$$

$$NO_2^- + \tfrac{1}{2}\ O_2 \longrightarrow NO_3^- \quad \ldots. (27)$$

Thus, the medium is automatically enriched in terms of NO_3^- ions, and becomes more corrosive. This is the reason that NH_4NO_3 is more corrosive than other nitrates (51).

In another case study relating to reinforced concrete construction housing open tanks containing hydro-chloric acid and other chemicals like lime, borax, phosphate etc showed severe deterioration of concrete (7). The process involved heating of the acid baths and the environment abounded in acid vapours producing a severe aggressive environment around the concrete elements. The corrosion caused by HCl vapours resulted in pitting of concrete surface. HCl is a strong acid and its charged H^+ ions are extremely mobile and highly reactive. HCl attacks hardened concrete through dissolution process and reacts with the readily soluble compounds of hardened cement paste leading to leaching of components, particularly of $Ca(OH)_2$. The hardened concrete thus loses its strength owing to the dissolution of hardened cement paste components and destruction of the hydrosilicate matrix. These were evident from XRD studies on concrete samples (7).

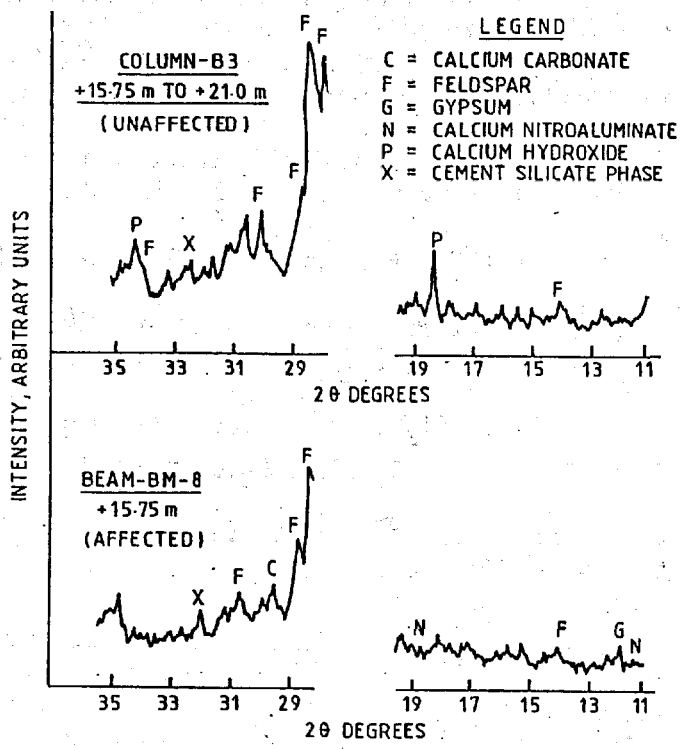

Fig 11
Typical X-ray Diffractograms of Concrete Samples from Ammonium Nitrate Plant Building (27)

Chandra describes HCl attack as a reaction which occurs in layers forming different distinct zones (52). The mixtures of hydroxides formed during hydrolysis circumvents undamaged concrete in a layer form. This layer is very hard and dark brown in colour. Concrete will be further damaged after dissolution of this hydroxide zone. In this zone, there is a precipitation of Mn and Fe compounds, which gives a very dark matrix around the mineral grains. It can also be a Fe-Si complex (Iddingsite). A tendency of rim formation around the aggregates, which can be of aluminium silicates, have also been noticed in the thin section analysis. This creates intense swelling. In the zone next to this hydroxide layer, no iron precipitates could be noticed, due to the formation of soluble iron chlorides. However rim formation around the aggregates is clearly seen here also. Besides, there are indications of expansive double salt formation with C_3A (Friedel salt).

The effect of sulphuric acid attack on cement paste and concrete has been studied both in the context of industrial environment and as generated by bacteria in concrete sewage systems (53, 54). Concrete is susceptible to attack by sulphuric acid produced from either sewage or sulphur dioxide present in the atmosphere of industrial cities. This attack is due to the high alkalinity of portland cement concrete. Sulphuric acid is particularly corrosive due to the sulphate ion participating in sulphate attack, in addition to the dissolution caused by the hydrogen ion. Sulphuric acid forms calcium sulphate with $Ca(OH)_2$ and ettringite with calcium aluminates which are very expansive salts. It creates cracking and concrete disintegrates due to the pressure produced during the formation of these salts. When tested in laboratory, the concrete test samples become white in H_2SO_4solution. It is due to the formation of above mentioned salts, which are white in colour. In one

investigation it was noticed that the generally accepted requirement of using a relatively high cement content in concrete mixes produced a negative effect, when the concrete was subjected to sulphuric acid solutions of high concentrations, and deterioration of concrete was greater, higher the cement content (54).

6 BIOLOGICAL DEGRADATION OF CONCRETE

Beyond the generally recognised chemical and physico-chemical factors, the degradation of concrete is also caused by biological factors as well. The biological components referred as "air spora" which include bacteria, spores of fungi, spores of mosses, terrestrical and epiphytic algae, fragments of lichen and pollen are such factors. Bacteria and fungal spores are in abundance. The process of bacterial growth conditions are briefly described below.

Most of the intra-cellular reactions responsible for bacterial growth take place in an acqueous environment. It makes water or water films, which is needed for the growth of most of the "air spora", whereas filamentous fungi and lichens are known to extract moisture from the air (55). All fungi, like most bacteria, are heterotrophs, which means that they require organic substances both for energy and growth. It has been found that the condensation of respiratory exhalation, cigarette smoke or fingerprints on inert, clean surface can promote germination and growth of fungal spores, which indicates that the dust and dirt present on the construction surfaces can offer enough organic substances for certain fungal growth. Autotrophs, on the other hand, are those which do not require any supply of organic substances. They can use CO_2 as source for carbon. Some of them are photo-autotrophs, which acquire energy from sunlight, others are chemo-autotrophs (chemo-litotrophs), which derive energy from inorganic substances by oxidizing them.

Cyanobacteria (also known as blue green algae) are photo-autotrophs. These are self sufficient organisms. They can build both CO_2, N_2 into organic molecules. They are free living or constitute the algae components which in symbiosis with a fungal partner composes a lichen. Mosses and true algae also are photo-autotrophs.

Microbial sulphur cycle has been reported by Jorgensen (56). The aerobic sulphur bacteria are very diverse. These thiobacilli obtains energy from the oxidation of inorganic sulphur compounds and carbon from CO_2. These range from true autotrophs (chemolitotrophs) to pure heterotrophs. They also include mixotrophs, which, depending upon the environmental conditions, can grow as an autotroph or as a heterotroph. The derivation of energy from the oxidation of reduced sulphur by thiobacilli occurs as follows :

$$H_2S \dashrightarrow SO_3^{2-} \dashrightarrow SO_4^{2-} \qquad \ldots\ldots (28)$$

$$S_2O_3^{2-} \dashrightarrow S_4O_6^{2-} \qquad \ldots\ldots (29)$$

Increased activity of sulphur bacteria has been observed in the supply of organic substrates accumulated in cracks and fissures where restricted evoperation also promotes growth. In such cases, where metabolically produced organic acids are the active agents, the deterioration is biogenic. If the concentration of sulphur is high, e.g., in highly polluted areas, biological deterioration decreases and chemical corrosion proceeds. But in the less polluted areas having lower concentration of sulphurous gases, biological deterioration will dominate.

The bacteria present in soils and water may either promote the formation of sulphate or may have a sulphate reducing action. In sewage the environment is prone to growth of microorganism which are detrimental to concrete structures. Two types of bacteria are involved in bacterial action on sanitary sewers : first those which inhabit liquid (anaerobic bacteria) and can reduce sulphur-containing substances to hydrogen sulphide gas; and second, those which inhabit the damp but aerated walls (aerobic bacteria) and can oxidise the hydrogen sulphide to sulphuric acid (57, 58). Sulphuric acid so formed reacts with concrete producing gypsum and ettringite. The deterioration of concrete in the unsubmerged parts of the walls in the sewage lift station in an Arabian Gulf country was attributed to high H_2S emission from the sewage due to oxygen deficiency and increased anaerobic bacterial activity in the sewage (58). In this case, typical environmental conditions were high humidity (RH = 100%) and high atmospheric and sewage temperature (more than 30°C). H_2S released from the sewage was absorbed by the moisture film on the unsubmerged sewer structures where it is converted to sulphuric acid in the presence of aerobic bacteria (Thiobacilli), leading to severe deterioration of concrete.

In another case, the degree of concrete deterioration of concrete pipes could be correlated with the number and type of thiobacilli present (59). Extensive deterioration was observed at the crown of reinforced and asbestos concrete pipes, where the most acidophilic group of thiobacilli were present in large numbers. Areas of lesser deterioration were somewhat acidic, with a combination of different sulphur-oxidising thiobacilli present. Areas that did not appear to be deteriorated were populated with the least acidophilic group of thiobacilli (59).

The organic growth of 'mold' algae and lichen can develop on concrete surface. The conducive conditions are dampness, water and reduced pH of concrete. These growths, apart from their unsighty appearance and functional problems, can cause surface damage to concrete largely by the acids formed by them.

Micro-organisms occur in buildings from the time of construction or are introduced in the building as a background flora. These are transformed from low level field flora to the high levels of selective bacteria by the supply of moisture. Some times when the ventilation in well-insulated houses is not appropriate, indoor humidity increases, and bacteria are transported to the building. Micro-organisms through their secondary metabolism can produce strongly irritating compounds both with or without odour, like high moleculer weight alcohols, organic acids, ketones etc. Many of these compounds are highly volatile and can penetrate through the wall, roof and floor. It results in unpleasant indoor odour. This odour increases with the use of plasticizers containing formaldehydes (60).

In Sweden, self-levelling compounds containing Caesin, are used to produce smooth and horizontal surfaces. A number of instances of damages in such floor after a few years have been reported. Compounds like caesin or other proteins in high humid atmosphere can create discolouration of floors, bad odour etc. In an analysis of the degraded concrete containing caesin, it is shown that the clostridia isolated are alkali-tolerant (61). Thus the caesin is attacked even at high pH in the concrete.

In various food processing industries, the environment is often saturated with micro-organisms. In bakery industries, the hydroscopic flour dust and existing temperature and humidity conditions cause the growth of fungus. Similarly in dairy, the generation of metabolic products of micro-organisms produced are acids such as citric, oxalic, acetic and maleic acids which have been found to cause surface crumbling of plaster and destruction of walls. Apart from bio-degradation involving sewage

or fermentation of foodstuffs, investigators have found a variety of bacteria associated with concrete structures exposed to these conditions. These bacteria may produce ammonia, hydrogen sulphide, nitrogen and nitric acid and butyric acid.

During fermentation of proteins a series of very odourous products can be produced, eg, ammonia, methane gas, volatile organic acid such as butryic acid, hydrogen sulphide and amines. Presence of volatile organic acids and amines have been substantiated in the analysis of degraded concrete whereas in the undamaged concrete only the presence of acetic acid could be detected. It is further reported that the alkalinity of the material, pH 12-13, in combination with humidity, makes the proteins unstable, resulting in the formation of ammonia at about 75% RH and bad odour above 90% RH.

Degradation of concrete may also take place due to biological actions by iron organisms. These bacteria exist on the products of weathering of iron or manganese containing rocks, in ferrous soils or in iron water mains. The iron organism found in large number in the ground water seeping through the construction joints of the walls in an underground construction may be taken as an example. As soon as this water becomes exposed to air at the internal surface of concrete, stains of bacteria develop, adhering as a brown mass to concrete. Under these cultures, spalling of concrete occurs due to carbon dioxide resulting from the physiological activity of these bacteria.

Several cases of floor heavings due to chemico-microbiological effect have been reported (62). In one case, physical and chemical changes were observed to have taken place in the foundation rock, which was black shale. On minerological analysis of the samples of shale, the presence of quartz, gypsum (colourless crystals), small amounts of jarosite, $KFe_3(SO_4)_2\ (OH)_6$ (yellowish brown deposit) and pyrite was detected. The unaltered zone at a depth of 120-180 cm, did not show the presence of gypsum or jarosite; only pyrite, calcite, illite and quartz were present. The pH value in the altered zone was 2.2 - 4.5 and had micro-organisms of the Ferrobacillus-Thiobacillus group. These observations have suggested that the weathering of pyrite was a chemical-microbiological process (62).

In coal mines oxidation can occur in the presence of autotrophic bacteria. Energy for bacterial growth is supplemented by the oxidation of inorganic compounds in the presence of oxygen from air. Ramachandran et al (63) have explained the main reactions involved in the oxidation of pyrite :

$$FeS_2 + 2H_2O + 5\ O_2 \dashrightarrow FeSO_4 + 2H_2SO_4 \quad \ldots\ (30)$$

$$4FeSO_4 + O_2 + 2H_2SO_4 \dashrightarrow 2Fe_2\ (SO_4)_3 + 2H_2O \quad \ldots\ (31)$$

$$7Fe_2(SO_4)_3 + FeS_2 + 8H_2O \dashrightarrow 15FeSO_4 + 8H_2SO_4 \quad \ldots\ (32)$$

Equation (30) is chemical in nature but may be assisted by autotrophic bacteria. Equation (31) seems to be entirely due to the bacteria as it cannot proceed chemically in acid solution. The oxidation of pyrite (equation 32) can occur by the reaction of ferric sulphate in autotrophs. Shale is calcarious. Gypsum can also be formed by the reaction of $CaCO_3$ with H_2SO_4. These create heaving because the molar volume of the reaction products are much higher than the reactants. For example, increase of molar volume when pyrite transforms to jarosite is 115% whereas calcite transformation to gypsum results in 103% increase in molar volume (63). Similar sulphate attack in contact with alum shale have been reported (64).

7 DETERIORATION DUE TO ATMOSPHERIC POLLUTION

Most building materials are subjected to deteriorating attack through the combined action of a number of meteorological and chemico-atmospheric factors. Practical observations and systematic studies have shown that the rate of such deterioration is always higher in polluted urban and industrial atmospheres than in clean rural atmosphere (65). One requirement for the rate and extent of such deterioration being significant is that the surface of the material must be wet. The total deterioration effect during a certain period is, therefore, determined by the time of wetness, concentration of air pollutants and temperature. Temperature has a complex effect on atmospheric deterioration. On the one hand, the chemical processes can be thermally activated, on the other, rising temperature can cause the moisture films to dry out faster, which means a shorter time of wetness.

The air contains pollutants basically in three states - gas, solid particles and substances dissolved in water droplets or in a liquid film on the surface of the solid particles. SO_2, NO_x, CO_2 and chlorides are most significant pollutants. Out of these, nitrous oxides were long believed to be virtually insignificant in so far as atmospheric degradation was concerned. In recent years, however, laboratory tests have shown that SO_2 and NO_2 can produce a strong synergistic effect. The following reaction

$$SO_2 + NO_2 + H_2O \dashrightarrow H_2SO_4 + NO \qquad \ldots\ (33)$$

causes corrosion to accelerate, for example, in cupreous materials (65).

SO_2, NO, NO_2, CO_2 which constitute major part of the pollutant gases form secondary pollutants under the influence of sunlight, temperature and humidity with other pollutants. These compounds are

Gas phase	SO_2, SO_3, NO_2, HNO_3, HCl, organic acids, O_3
Aerosols	H_2SO_3, NH_4HSO_4, $(NH_4)_3$, $H(SO_4)_2$, $(NH_4)_2SO_4$, NaCl
Rain water ions	H^+, NH_4^+, HSO_3, SO_4, NO_2^-, NO_3, HCO_3.

These are quite reactive and may be detrimental to cement concretes (8).

During the past three decades, acid precipitation (acid rains) has become relatively widespread over large part of Europe and North America. Precipitation having pH levels between 4 and 4.5 have recently been detected (66). The acidification is primarily due to nitric and sulphuric acids - SO_x and NO_x in the atmosphere reacts with water to form sulphuric and nitric acid respectively. During continual tests on the roof of buildings in Sweden, pH of rain water was found to vary between 3.0 - 4.5 (8).

Influence of pollutant gases on concrete and mortar has not been researched very much. Chandra (8) has done some studies to analyse the deteriorated concrete from different environmental conditions and to see the resistance of mortar and concrete exposed to different gases and acids in the laboratory. The investigations revealed that in dry environment, pollutants specially sulphates interact with $Ca(OH)_2$ and calcium aluminate hydrate, producing gypsum and ettringite. These salts crystallise

and develop microcracks and, due to the microcracks formation, CO_2 penetration becomes a lot easier. It neutralises the concrete and reduces the passivity. Thus corrosion of reinforcing steel occurs. Analysis of some of the concrete from bridges have shown the presence of monosulphate hydrate, partially carbonated-aluminate, chloro-aluminate, calcium hydroxide chloride, gypsum, ettringite etc (8). The presence of gypsum, ettringite, monosulphate are the clear evidence of sulphate attack, whereas chloro-aluminates and hydroxide chlorides show chloride attack, possibly due to the use of deicing salts in the winter time. At some places thaumasite was also detected (8).

In laboratory tests when concrete cubes were exposed to CO_2 and CO_2 + SO_2 atmosphere in gas chamber, it was noticed that SO_2 accelerated carbonation. The actual mechanism is not clear, but it is known that the tobermorite and calcium aluminate hydrate are unstable in SO_2 when the partial pressure of SO_2 exceeds $10^{-58.2}$ atm (8).

Similarly, in a specially designed test, concrete was exposed to (SO_2 + NO_x) gases in an air-tight box for 16 hours, 2 hours wetting and 6 hours drying cycle. The results showed the synergetic effect of the pollutant gases, moisture and temperature variation on concrete deterioration.

Tests to simulate deterioration of concrete due to acid precipitation has been reported (67). Concrete specimens with design compressive strength varying from 3000 to 9000 psi (21 to 63 N/mm^2) were exposed to acidic solutions prepared by adding concentrated sulphuric and nitric acids to distilled water in a 2:1 ratio so as to have four solutions having pH levels of 2, 3, 4 and 5. The response of the specimens to the simulated acid precipitation solution varied with pH level of the solution and the strength of concrete mix. As expected, loss of specimen surface material generally increased with increasing acidity of the simulated acid precipitation solution. In addition, all acidic solutions produced discoloration of the specimens. However in general, concretes of higher design strength experienced greater deterioration (67).

8 ROLE OF CEMENT SYSTEMS AND ADDITIVES

The requirements of chemical compositions and physical properties vary in different types of cement. Among the chemical characteristics of cement, which influence the durability of concrete are its C_3A and alkali contents and, to some extent, C_3S content (42). Limits of chloride ions in the cement are also now being introduced in some national standards. C_3A content is important from the point of view of sulphate attack and resistance to corrosion of reinforcement. In general, C_3A content less than 5% is preferred for limiting the chances of sulphate attack, whereas higher C_3A content favours fixation of chloride ions in the pore solutions with the formation of chloro-aluminates and resistance to corrosion of reinforcement is, therefore, believed to increase with increase in C_3A content. Such fixation of chlorides by C_3A could be temporary in presence of sulphates (10) and a compromise solution for cement specification is to limit C_3A to about 8% or lower for use in marine conditions. Different crystalline forms of C_3A in the cement - cubic, orthorohmbic and tetragonal - are reported to react differently with sea water. While cubic C_3A gives more ettringite, gypsum and brucite, tetragonal form enhances the formation of MSH in the cement paste more than the other two forms (68).

Importance of alkali content in cement from the point of view of alkali-aggregate reaction is obvious and need no elaboration. In addition, Kobayashi and Uni have pointed out that pH of pore solution in concrete which depends on the amount

of alkali in cement, is a factor governing the rate of carbonation of concrete and that this rate is higher, higher the pH value (37). Increasing amount of C_3S in cement results in increased proportion of calcium hydroxide $Ca(OH)_2$ in the hydration product, which is undesirable from the point of view of both leaching and sulphate attack. In the sulphate or sea water attack containing magnesium sulphate, Mg- salts replace the calcium of the hydrated silicate system CSH to a varying but a considerable degree (10). For a given C_3A content, attack of this type is known to increase with the amount of C_3S in the cement.

Chemical composition and physical characteristics of cement can also influence the durability of concrete by physico-mechanical interactions. Greater fineness and/or higher C_3S and C_3A contents give rise to increased heat of hydration, which may cause thermal cracking, thereby enabling ingress of harmful chemicals from the environment. In addition, these tend to increase the early age strength of concrete - at least up to 28 days. As was pointed out earlier, this is one aspect in the modern day cements which is believed to have made profound influence on the durability of concrete. Both Neville and Mehta argued that modern day cements with higher strength characteristics, primarily because of increase in the proportion of C_3S and fineness, enable a leaner concrete mix using less cement and a higher water-cement ratio to result in the same 28 day strength of concrete specified in the design (1, 4). As a typical example, it has been cited that with the present-day UK cements, a cement content of about 320 kg/m^3 and a water-cement ratio of 0.54 would suffice for resulting in a 30 MPa concrete, compared to cement content of 405 kg/m^3 and water-cement ratio of 0.43, that would have been required in the fifties (69). Such a concrete will have lower density and a higher permeability than before, which can undergo carbonation much more rapidly and allow the passage of moisture and oxygen more rapidly than the concrete of the earlier years. This enhances the risk of corrosion of reinforcements in the concrete (1).

In the UK cements, the range of C_3S was reported to be 54 to 63% in 1984, compared to 15 to 48% in the period 1914 to 1922; the mean 7 days strength of cement increased from 20 N/mm^2 before 1950 to 32 N/mm^2 in 1984 and concomittant increase in the heat of hydration (69). Similar decadal surveys in case of Indian cements have, however, brought out that the average level of strength and fineness of cement produced have remained essentially constant, although there has been substantial increase in the amount of cement produced during the period. This is because, while on the one hand Indian cement industry improved its manufacturing process, operational practices as well as plant and machinery, on the other, it had to encounter depleting reserves of good quality limestone and also had to use coal as fuel, of increasing ash content (70).

Results of alkali content in the cement produced in UK in the same period as well as in India are reported (69, 70) and summarised in Figs 12 and 13. It will appear that in both the cases, the proportion of cement having total alkalis (as Na_2O equivalent) up to 0.6% has come down, essentially because of predominance of dry process cement plants, which employ recirculation of waste gases in the system for energy conservation, thereby giving rise to concentraion of alkalis, sulphates and chlorides. Periodic surveys also reveal that the chloride content in the cements manufactured in India were not always negligible, and it has led to stipulation of a limit of total chloride ions content in the cement as 0.05% in the Indian Standard Specifications for use in prestressed concrete and important RCC structures.

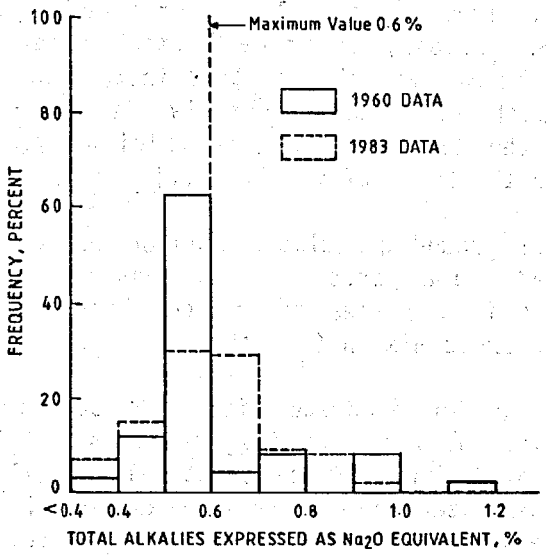

Fig 12
Alkalis in British Cements (69)

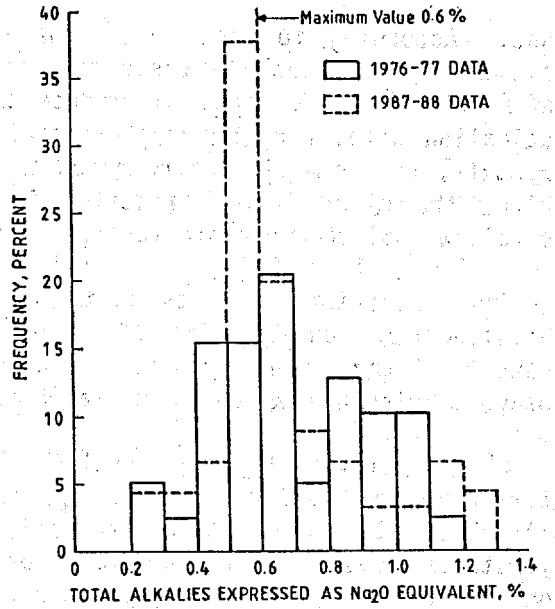

Fig 13
Alkalis in Indian Cements (70)

8.1 Blended Cements and Use of Mineral Admixtures and Fillers

One of the main uses of cements incorporating various natural and artificial pozzolans, slags or condensed silica fume, has been to improve the durability of the concrete. These additives can either be blended or interground with cement clinker, to result in a blended or composite cement, which are called with appropriate nomenclature (portland pozzolana cements, portland slag cements, pozzolanic cements, slag cements, etc), or can be incorporated in the concrete mixer at the time of mixing cement, water and aggregates. Large amount of data is now available on the performance of such cement systems specially under laboratory tests. The general conclusion would be that addition of pozzolans, slags or condensed silica fume would improve the durability of concrete in terms of resistance to leaching, carbonation, sulphate attack, diffusion of chloride ions, and reducing alkali-silica reaction.

The basic mechanism in case of incorporation of pozzolans is the reaction with $Ca(OH)_2$ forming further CSH products of lower C/S ratio. A part of the reaction product forms in situ and a part by the effect of dissolution, transport and precipitation phenomenon (71). The hydration products, which precipitate in the capillary pores formed earlier, may not be adequate to fill them up completely, but would be sufficient to block the path and provide discontinuity of flow in the pore structure. It has also been shown that the pozzolana addition also transforms bigger pores to finer pores. Consequently, the porosity of the blended cement paste is higher than the portland cement, but their permeability becomes lower (71). The beneficial action in reducing leaching of lime as well as preventing sulphate attack originates due to fixation of $Ca(OH)_2$ with the formation of more complex hydrates, or to the higher protective action on the susceptible alumina compounds exerted by the impervious films of different calcium silicate hydrates with lower C/S and A/S ratios (42). Pore modifications and decrease in the impermeability results in retardation of the ingress of aggressive agents. It has been suggested that the resultant decrease in the permeability of concrete is also due to the effect of these additives on the transition

zone. According to Mehta (72) the pozzolan particles act to reduce the thickness of the transition zone via several mechanisms. First, the inclusion of fine particles in a concrete mix tends to reduce bleeding. Second, the fine particles serve as nucleation sites for the crystallization of calcium hydroxide so that instead of large crystals, the formation of numerous small crystals of random orientation is encouraged. Third, the slow chemical reaction involving the transformation of calcium hydroxide to calcium silicate hydrate further reduces the thickness of the transition zone.

Beneficial effects on the addition of ground granulated slag on the sulphate resistance of concrete has also been observed. The performance depends on the C_3A content of the cement and the alumina content in the slag on the one hand, and the dosage of slag and water-cement ratio in the concrete mix on the other.

Improvement in the sulphate resistance of concrete with slag addition is attributed to the reduction in C_3A content with increase in slag addition and lower S/A ratio. It provides more protective impervious films of different calcium silicate hydrates. It also helps retention of lime from leaching. More abundant gels, lower ionic diffusion, particularly that of SO^{2-} ions through the paste of lower penetrability and higher impermeability and decrease in the formation of ettringite are the other factors. According to another hypothesis, lack of calcium hydroxide in hydrated pastes of pozzolanic or slag cements give rise to the formation of non-colloidal and non-expansive ettringite (73). It may be due to the lack of double-layer type interparticle repulsion, which is otherwise produced by a large water absorption.

In an exhaustive investigation, Osborne has reported that for blends of medium C_3A portland cement (9%) or of ground glassy slags with low to medium alumina levels (Al_2O_3 = 7.5 to 11.5%), 70% replacement levels of slags for OPC are likely to give good sulphate resistance properties (40). If the C_3A in cement or alumina in slag are higher, the slag content may have to be higher. It was emphasised that the sulphate resistance is however not solely dependant on the type of cement, the cement content and the water-cement ratio, but the method of manufacture, curing conditions and mode of exposure are also prominant factors. In particular, Osborne's tests significantly reported the beneficial effects that was derived from curing concrete specimens in air at 20°C and 65% relative humidity. The effectiveness of 20 days air curing was clearly demonstrated which was ascribed to the fact that carbonation render impermeability to the concrete and result in pore blocking (40).

Beneficial effects of using mineral admixtures in improving resistance to corrosion of reinforcements have been reported. Li and Roy reported that fly ash blended cement has a high potential to prevent diffusion of chloride ions (74). The optimum proportion of cement : fly ash found in their study was 60:40 percent (by weight). It was due, on the one hand, to the clogging of pores by gel produced from pozzolanic reaction; and to the tortuosity, and the action of multivalent cations on chloride-ion diffusion in the pore solution, on the other.

In another investigation, the long-term corrosion resisting characteristics of concretes made with two different flyashes, a natural pozzolans, a blast furnace slag cement, and a preblended portland flyash cement were evaluated (75). Specimens were immersed in 5% sodium chloride solution for a period of more than five years and the corrosion activity was evaluated by monitoring half-cell potentials and measuring the corrosion rate of embeded steel using linear polarisation resistance technique. It was found that the corrosion rates of reinforcing steel in pozzolanic cements and blast furnace slag cement concrete were lower than in plain cement concrete; the rating of different cement systems being depicted in Fig 14 (75).

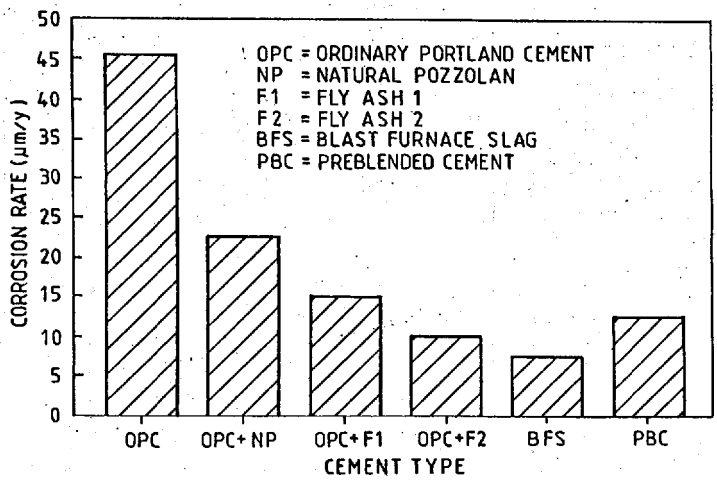

Fig 14
Corrosion Rate of Reinforcement Bars in Plain, Pozzolan and Slag Cement Concretes (75)

Massazza has reported the performance of pozzolanic cements which are being commercially manufactured in Italy and used in concrete constructions for a long time (71). In such pozzolanic cements, the amount of pozzolana added is sufficient to combine with all the calcium hydroxide released during hydration of the OPC and would be required to satisfy the pozzolanicity test. In general, the pozzolana content in such pozzolanic cement would be higher than in portland pozzolana cements where the fixed proportions of pozzolana are blended or interground with OPC clinker. The durability of concrete in terms of resistance to diffusion of air and water, sulphate and sea water attack and diffusion of chloride ions were in general better than ordinary portland cement concrete (71). Proper moist curing is necessary for deriving the beneficial effects. After adequate moist curing, the oxygen permeability is reduced and so are the chances of corrosion of reinforcement bars (Table 2).

Table 2

Coefficients for Diffusion of Chloride Ion into Cement Pastes (71)

Sample	D ($cm^2\ s^{-1} \times 10^3$)	Temp (°C)
Portland cement paste	1.23	10
	2.51	25
	4.85	40
Pozzolona cement paste	0.83	10
	0.90	25
	0.97	40
Portland cement paste (RHPC)	19.20	20
	13.20	30
	28.30	50
Fly ash cement (22% PFA)	9.20	20
	11.60	30
	13.70	50
SRPC	15.10	20
	19.30	30
	37.00	50

Resistance to penetration of chloride ion was greater in case of cements containing pozzolana than the portland cement, because the former are able to immobilise greater quantities of Cl^- in aluminates and silicates than in case of the corresponding ordinary

portland cement and the diffusion of Cl^- in pozzolanic cement is considerably slower (Fig 15). After adequate moist curing, for concretes compared on the basis of having equal strength, the extent of carbonation was the same, whereas in case of inadequate curing, carbonation of pozzolanic cement concrete was found to be higher (71). Hence it is important that concretes made with pozzolanic cements receive moist curing for longer period than when made with ordinary portland cement.

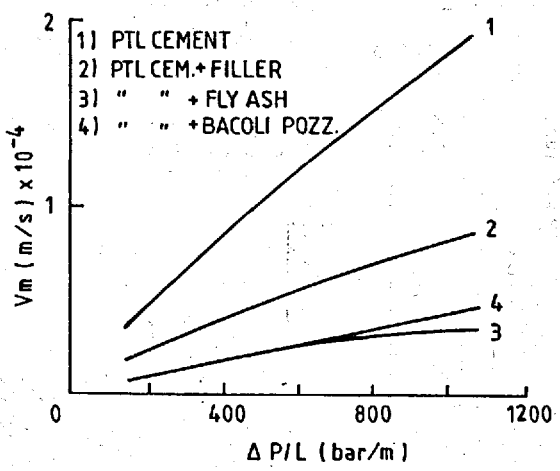

Fig 15
Air Permeability of Pastes made with Portland and Pozzolanic Cements, Cured for 7 months (71)

The proportion of portland blast furnace slag cement commercially manufactured in many European countries is substantially high; in the Netherlands, for example, it comprises 60% of the total production and contains 65 to 75% ground granulated slag by weight. Investigations on the effect of incorporation of flyash on such portland blast furnace slag cement was reported (76). While the rate of carbonation in case of ordinary portland cement and portland blast furnace slag cements were found to be comparable, incorporation of 25% flyash either in OPC or in portland slag cement increased the rate of carbonation, the difference being very substantial in the latter case (Fig 16).

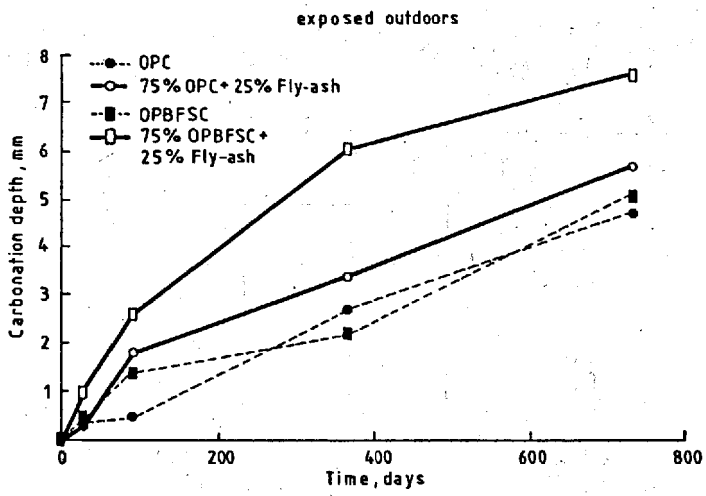

Fig 16
Carbonation in Concrete made with OPC and OPBFSC and Effect of 25% Replacement by Flyash (7 days water cured 20°C, outdoor exposure) (76)

This was primarily because flyash in portland blast furnace slag cement could not cause any significant pozzolanic activity. Hobbs has also reported increased carbonation in concretes containing fly ash cured for 24 hours (77). This emphasises the need of adequate and prolonged moist curing to derive the advantages of addition of pozzolans, slags or condensed silica fume. Addition of natural pozzolans up to 30% has been found to decrease the durability of concrete against ammonium nitrate (51).

Use of large volume of flyashes for making structural concrete of higher strength grades have been extensively reported by Malhotra and his co-workers (78). Typical high volume flyash concrete contain about 150 kg/m³ of cement and ASTM class F flyash content is about 210 kg/m³, ie, 56 - 58% by weight of the total cementious materials. The water to cementitious material ratio is kept about 0.32 with the use of superplasticisers and required air entrainment is achieved by use of AEA. Satisfactory durability of such concretes in terms of significant resistance to freezing and thawing, chloride ion diffusion, carbonation and alleviation of alkali-silica reaction has been reported (78). The excellent durability characteristics would primarily be due to use of low W/C+F ratio. Resistance to deiceing salt scaling was however not satisfactory.

Use of condensed silica fume in concrete started with the development of high strength concrete. Improved durability of concrete due to incorporation of condensed silica fume has also been extensively reported (18, 20). Largest attention has, for obvious reasons, been towards resistance to corrosion of steel reinforcement. It is now held that incorporation of condensed silica fume of the order of 10 to 12% or more by weight of cement offers 'good' to 'excellent' corrosion resistance. The beneficial effects are ascribed to increase in impermeability of concrete because of resulting dense micro-structure and decrease in porosity. Use of condensed silica fume significantly lowers the permeability of concrete to prevent ingress of chloride ions to the level of reinforcing bars and simultaneously increases the electrical resistance of concrete to corrosion currents each by an order of magnitude (79, 80). Acting as a 'super' pozzolana of high reactivity, incorporation of condensed silica fume lowers the rate of carbonation and increases resistance to sulphate attack in the same manner as fly ash and other pozzolans do (80). Simultaneous addition of fly ash along with condensed silica fumes also helps in improving corrosion resistance. However, the beneficial effects are realised only when the percentage of condensed silica fume is 10% or more. Lower dosages of condensed silica fumes and/or using higher water-cement ratio (0.5 or more) may not necessarily result in better performance (79). Similarly the need of adequate concrete cover to the reinforcement when exposed to aggressisve environment has to be ensured much in the same way as concrete without any condensed silica fume incorporated.

Attention has been focussed whether because of dense micro-structure and decrease in porosity, incorporation of condensed silica fume would improve the freeze-thaw resistance. In one investigation it has been reported that high strength (80 MPa) concrete having a low water-cement ratio (0.3 to 0.32) may have satisfactory freeze-thaw resistance (ASTM C-666, Procedure B) even without any air-entrainment (81). Contradictory results have been reported in another investigation wherein it was found that incorporation of 20% condensed silica fume resulted in poorer freeze-thaw resistance even when air-entrainment has been used (82). Typical results in another series of investigations are shown in Fig 17, wherein, with increasing condensed silica fume content the durability factor decreased in super-plasticised air-entrained concretes, but the general level of durability still remained satisfactory (83).

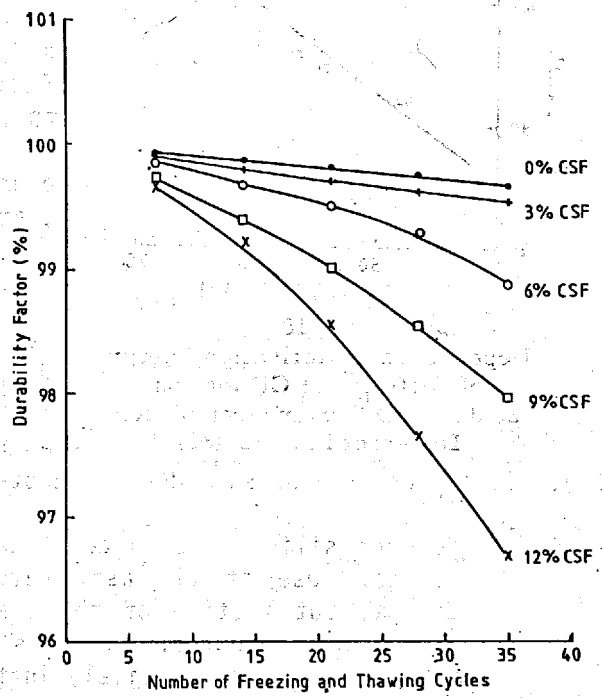

Fig 17
Durability Factors for
Air-entrained Concretes
with Varying CSF Contents (83)

Paillere et al have also reported that condensed silica fume content of less than 10% with corresponding reduction in cement content did not lead to any significant improvement in resistance of mortars to sea water attack. In addition, moist curing for at least the first seven days was essential for satisfactory durability when condensed silica fume is incorporated. A curing time of only 48 hours was found to be highly detrimental in terms of subsequent performance in sea water (84). In another investigation, addition of condensed

silica fume was found to improve the compressive strength of concrete upon exposure to ammonium nitrate solution due to benevolent pore modifications. Durability was also improved due to increase in degree of polymerisation of silica anions, caused by reduction in CaO, both as a result of pozzolanic reaction and nitrate attack (85).

In addition to these cementitious additives discussed above, considerable attention is now focussed on incorporation of inert fillers in cement which are permitted in many European Codes (86). Ranc et al have reported on the considerable experience gained in France with such types of cements which have been prevalent for quite some time (87). It is reported that when comparison is made between cements with or without such inert fillers, but having comparable strength range, the durability properties are more or less similar. This is explained by the fact that with incorporation of fillers or inert additives and yet to achieve the same strength range, cement clinker fraction has to be ground finer, thereby resulting in comparable hydration rate and total porosities. In a comparative evaluation of 5 filler cements of Strength Grade 45, with 15 and 30% calcareous fillers, 10 and 25% silicious fillers and 15% blast furnace slag compared to two ordinary portland cement of similar strength grades it was found that after four years, the extent of carbonation in case of all the cements were generally of the same order and cements with fillers provided the same protection against carbonation as OPC of the same strength class (87). Similar freeze-thaw resistance was obtained with such filler cements by incorporation of air entraining agents so as to entrain 4-5% of correctly distributed air (L^- = 200 to 300μm). The activation energies for the diffusion of chloride ions depended essentially on the mortar strength of the binder and not on the type of binder (Fig 18). Resistance to sea water was more related to the C_3A content in the cement and as long as the C_3A content in the cement was not greater than 6.6%, presence of calcareous filler in a cement did not affect its sea-water resistance (87). On the other hand, it has been stipulated that the addition of ground limestone (3 to 5%) to portland cement can indeed increase its sulphate resistance, the beneficial effect being more prevalent in cements with higher C_3A content, eg, ASTM Type I, and less in ASTM Type II cements (88).

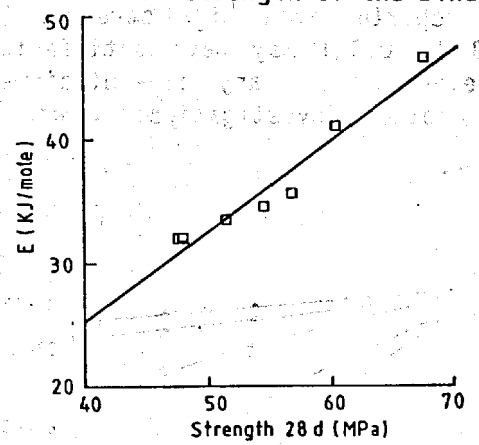

Fig 18
Dependence of Activation Energy of Diffusion of Cl^- ions on 28 days ISO Mortar Strength for Different Binders (87)

Considerable attention naturally has also been focussed on the role of cementitious additives like flyash, pozzolans, slags and silica fumes, on alleviating alkali-aggregate reactions. Results of such investigations have been extensively reported and would not be highlighted here (20, 21). Consensus can be summed up as quoted in Ref 89 :

> "Use of silica fume in adequate dosage appears to reliably prevent damage. Use of fly ash, natural pozzolan and slag may prevent damage, but testing of the specific material is usually necessary to ensure favourable results in practice since some materials of this type are relatively ineffective or indeed hazardous."

In particular, Hobbs has drawn attention that fly ash and natural pozzolans have not always been too effective in preventing cracking and expansion due to ASR (89). In view of considerable variation in the characteristics of pozzolans or slags, any generalisation would be difficult. This is more so in view of the role played

by the alkalis present in the pozzolans and the slags. Results also depend upon the level of alkalis present in the portland cement and the percentage replacement or substitution made (89). Mullick et al (90) had pointed out that the uncertainty in case of commercially manufactured portland pozzolana cement or portland slag cement could indeed be higher in the sense that samples of pozzolana or slags interground with the cement clinker at the cement plant may not be available for evaluation or determination of its alkali content, or even the exact dosages incorporated in the commercial production may not be known. Notwithstanding these, tests carried out with cements commercially produced in India have clearly shown the beneficial effect of alleviating ASR expansion in mortar bar tests even when the dosages of incorporation of pozzolans (average 15%) or slags (average 50%) in the blended cements were lower than what is considered optimum (Fig 19).

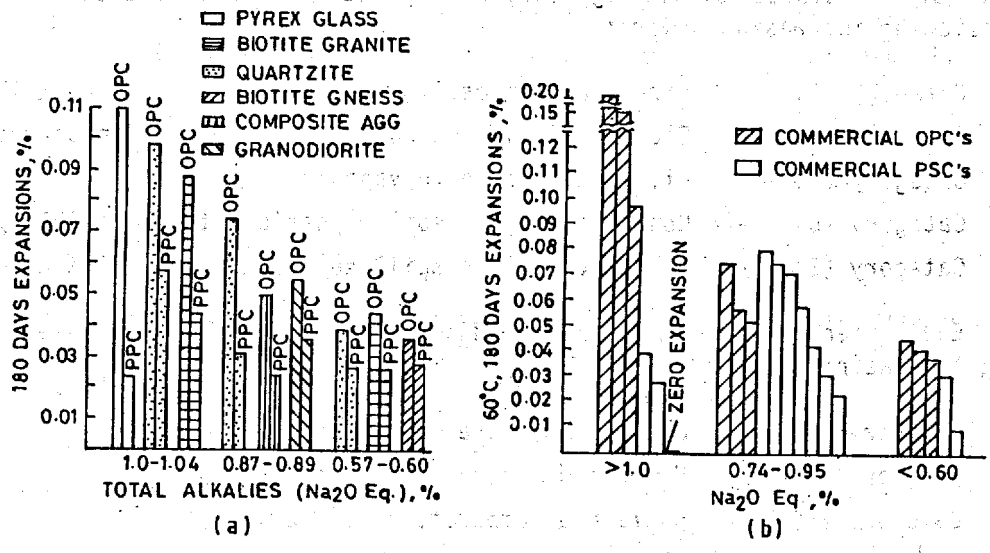

Fig 19
Performance of Commercial (a) PPC and (b) PSC Samples as compared to OPC in Alleviating ASR (90)

9 MAKING CONCRETE DURABLE - CONCLUDING REMARKS

In a State of the Art Review of the performance and durability of concrete systems, it is customary to discuss the mechanisms of various degradation processes and also highlight case studies of deterioration of concrete in service in support of the mechanisms proposed. However, these should not distract us from the fact that there is a very large number of concrete structures built all over the world which are rendering satisfactory service in different environments. Adequate knowledge now exists for characterising the service environments of concrete in terms of potential mechanisms of deterioration and the basic requirements to counteract them. In spite of considerable instances of failure of concrete structures because of 'durability problems', one may like to conclude on an optimistic note that concretes can be made durable by adopting the following basic steps :

(i) **Characterise Environment in Totality** - A "Systems" approach to durability was advocated earlier. One notable feature of such a Systems approach is that it enables a holistic view of the structure and its interaction with the environment. This means designing the structure for the environment per se, and not the chemical agencies of deterioration in isolation. In other words, a structure will be designed

for exposure to marine environment and not separately for chlorides, sulphates, and freezing and thawing; or alternately, a structure should be designed for use in the Arabian Gulf environment characterised by severe ground and ambient salinity and high temperature humidity regimes and the synergetic effects of the operative causal factors (6).

(ii) **Determine Severity of Environment** - Within the broad spectrum of the temperature-humidity regime and the chemical nature of the deteriorating agencies, the ease with which these can come in contact with or penetrate into concrete becomes important. Rate of deterioration would thus depend upon the aggressiveness of exposure as well as environmental conditions. The concepts can be explained in terms of what has been suggested for concrete structures in industrial environment (7). The exposure conditions of structures to the aggressive agencies can be graded for their severity in the following increasing order :

Category (A) - Air-borne aggressive substances
Category (B) - Close proximity to operations; deposition of dust
Category (C) - Risk of exposure to vapours
Category (D) - Contamination in soil + possibility of capillary action
Category (E) - Direct contact + spillage + mechanical action.

Environmental conditions can similarly be graded for their severity in the following increasing order :

Category (a) - Dry and moderate temperature
Category (b) - Humid and moderate temperature
Category (c) - Humid and temperature 60°C or more
Category (d) - Alternate wetting and drying, moderate temperature
Category (e) - Alternate wetting and drying temperature 60°C more

The interaction of exposure conditions and ambient environment which ultimately determines the severity of attack, is depicted in Fig 20. Depending upon the gradation of exposure conditions (A) to (E) and environment conditions (a) to (e), the service environment in turn is classified into five interactive categories (1) to (5) of increasing severity, where, (1) is the least severe and (5) the most severe combination. The type of chemical salts and ions superimposed on this space shown in Fig 20 define the service environment, for which the specifications for construction are to be evolved (7).

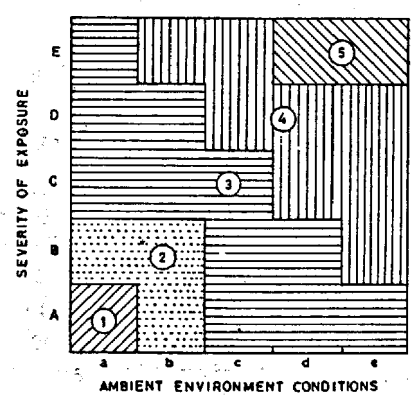

Fig 20
Classification as per Exposure-Environment Interaction (7)

(iii) **Making Concrete Impermeable** - Since the presence of harmful salts and ions can originate from contaminated natural aggregates or impure mixing water (91),

special care has to be taken in the choice of concrete making materials so as to limit the amount of harmful agencies, eg, chlorite and sulphate ions in the fresh concrete. Once this is done, what is required is to prevent ingress of ions and salts from outside, which can be done by making concrete as impermeable as possible. According to Pomeroy , the most durable concretes are those with the lowest permeabilities and he considers all other factors as secondary to this (92). Since presence of moisture is necessary for the various chemical attacks to take place, which lead to expansion and cracking (4), a low water-cement ratio helps, in addition to reducing the permeability of concrete. Specifying adequate cement content and low water-cement ratio in the mix, use of superplasticisers and cementitious additives like pozzolans, slags or condensed silica fume prove useful. The emphasis can be exemplified by quoting the following specifications for prestressed concrete piles for Naval piers (5) ;

> "The cement to be used should be ASTM C 150 Type II, low alkali, with a tricalcium aluminate (C_3A) content of 6 to 10 percent. Alkalis as Na_2O shall be less than 0.60. Mineral admixture additions shall be used at a minimum rate of 15 percent by weight of cement for flyash or a minimum rate of 5 percent by weight of cement for silica fume. The concrete will have a minimum cement content of 600 lbs/cu yd (360 kg/m^3), a maximum water cement ratio of 0.40 by weight and have 5 to 8 percent entrained air."

Specifications in many other countries for concrete in aggressive environment follow similar lines (93). Wherever required, protective coatings, paints or barriers may have to be additionally provided (7).

(iv) **Workmanship and Design Details** - Proper workmanship in concrete making, its placing, compaction, and curing are essential as are a number of structural design details in the form of thickness of cover, detailing of reinforcements to limit the stresses at the level of reinforcements, or limiting the crack width. These are outside the scope of the present Congress on Chemistry of Cement. It is interesting to note that the specifications for structural concrete in various countries incorporate more or less similar provisions (93).

In conclusion, one would like to recall what Katharine and Bryant Mather (94) had stated :

> "The message we have decided to leave with you at this time is (a) that concrete need not deteriorate and (b) that knowledge exists by the use of which concrete can be caused to exist in any of the environments of service for which it may be reasonably proposed with tolerable degradation during its intended service life, if precautions to limit degradation appropriate to the environmental severity are taken."

ACKNOWLEDGEMENT

The first author (AKM) acknowledges the help of his colleagues Mr R C Wason, Dr M M Ali, Dr George Samuel and Mr N Subramanian, in the preparation of this Report.

REFERENCES

1. Neville, A. : "Why we have Concrete Durability Problems". Proc, **Concrete Durability, Katharine and Bryant Mather International Conference,** Pub, SP-100, Vol.1, American Concrete Institute, Detroit, Michigan, USA, 1987, p 21-30.

2. Mehta, P.K. : "Durability of Concrete in a Marine Environment - A Review". Proc, **International Conference on Performance of Concrete in a Marine Environment,** Pub, SP-65, American Concrete Institute, Detroit, Michigan, USA, 1980, p 1-20.

3. Gerwick, B.C. : "Pressing Needs and Future Opportunities in Durability of Concrete in Marine Environment". Proc, **Ben Gerwick Symposium on International Experience with Durability of Concrete in Marine Environment,** University of California at Berkeley, Ed. P.K. Mehta, 1989, p 1-5.

4. Mehta, P.K. : "Durability of Concrete - Fifty Years of Progress". Proc, **Second CANMET/ACI International Conference on Durability of Concrete,** Pub, SP-126, Vol.I, American Concrete Institute, Detroit, Michigan, USA, 1991, p 1-32.

5. Hoff, G.C. : "Durability of Offshore and Marine Concrete Structures". **Ibid,** p 33-64.

6. Rasheeduzzafar and Fahd, H. Dakhil. : "Field Studies on the Durability of Concrete Construction in a High Chloride-Sulphate Environment". International Journal for Housing Science and its Applications, 1980, 4(3), 203-232.

7. Mullick, A.K., Rajkumar, C & Jain, N.K. : "Performance of Concrete Structures in Industrial Environment". Proc, Second **CANMET/ACI International Conference on Durability of Concrete,** Pub, SP-126, Vol.I, American Concrete Institute, Detroit, Michigan, USA, 1991, p 577-597.

8. Satish Chandra. : **Influence of Pollution on Mortar and Concrete.** Doc. D6:1990, Swedish Council for Building Research, 83 p.

9. Mullick, A.K. : Alkali Silica Reaction - Indian Experience, Alkali-Silica Reaction in Concrete. Ed. R.N. Swamy, Blackie and Son Ltd, London, U.K., 1992, p 307-333.

10. Calleja, J. : "Durability", Principal Report on Sub-theme VII-2, **International Congress on the Chemistry of Cement, 7th,** Paris, France, 1980, Vol.I, p VII-2/1-48.

11. Regourd, M. : "Durability, Physico-chemical and Biological Processes Related to Concrete". **CEB-RILEM International Workshop** - Durability of Concrete Structures (Ed. Steen Rostam), Copenhagen, Denmark, 1983, p 49-71.

12. Mullick, A.K. : "Systems Approach to Durability of Concrete". Souvenir, **ING/IABSE Seminar on Pile Foundations, Corrosion, Detailing and Ground Anchors,** Madras, India, 1979, p 65-71.

13. Valenta Oldrich. : "Durability of Concrete". Principal Paper, Session III-2, Proc, **International Symposium on the Chemistry of Cement,** 5th, Tokyo, Japan, 1968, Vol.III, p 193-228.

14. **Concrete Durability, Katharine and Bryant Mather International Conference.** Pub, SP-100, Vols 1 & 2, American Concrete Institute, Detroit, Michigan, U.S.A., 1987, 2179 p.

15. **International Conference on Durability of Building Materials and Components, 4th,** Singapore, 1988.

16. **Paul Klieger Symposium on Performance of Concrete.** Pub, SP-122, American Concrete Institute. Detroit, Michigan, U.S.A., 1990.

17. **International Conference on Durability of Building Materials and Components, 5th,** London, U.K., 1990.

18. **CANMET/ACI International Conference on Durability of Concrete, 2nd,** Pub, SP-126, Vols. I & II, American Concrete Institute, Detroit, Michigan, USA, 1991, 1361 p.

19. **International Conference on Alkali Aggregate Reaction, 7th,** Ottawa, Canada, 1986.

20. **International Conference on Alkali Aggregate Reaction, 8th,** Kyoto, Japan, 1989.

21. **International Conference on Alkali Aggregate Reaction, 9th,** London, U.K., 1992.

22. Figg, J. : Salt, Sulfate, Rust and other chemical Effects, Proc, **Ben Gerwick Symposium on International Experience with Durability of Concrete in Marine Environment,** University of California at Berkeley, Ed. P.K. Mehta, 1989, p 49-69.

23. Hansson, C.M., Frolund Th., and Markussen, J.B. : "The Effect of Chloride Cation type on the Corrosion of Steel in Concrete by Chloride Salts". Cement and Concrete Research, 1985, 15, p 65-73.

24. Roper, H. & Baweja, D. : "Carbonation-Chloride Interactions and Their Influence on Corrosion Rates of Steel in Concrete". Proc, **Second CANMET/ACI International Conference on Durability of Concrete,** Pub, SP-126, Vol.I, American Concrete Institute, Detroit, Michigan, USA, 1991, p 295-315.

25. Durekovic, A. and Calogovic, V. : "Investigation of Concrete from a Bridge Support After 11 years of Exposure to Seawater". **Ibid,** p 627-642.

26. Gonzalez, J.A., Molina, A., Otero, E. and Lopez, W. : "Role of Oxygen Diffusion on Mechanism of Steel Corrosion in Concrete", Magazine of Concrete Research, 1990, 42 (150), 23-27.

27. Mullick, A.K. and Rajkumar, C. : "Multi-disciplinary Investigation of Distress to Concrete Constructions", **Third International Conference on Concrete Technology for Developing Countries,** Tripoli, Libya, 1992.

28. Rasheeduzzafar, Fahd H. Dakhil and Ahmed S. Gahtani. : "Corrosion of Reinforcement in Concrete Structures in the Middle East". Concrete International : Design & Construction, ACI, 1985, 7(9), 48-55.

29. Regourd, M. : Ann ITBTP, No 329, 1975, p 86-102.

30. Bensted, J. : "Thaumasite - A Deterioration Product of Hardened Cement Structures". Il Cemento, Jan-March 1988, 1, 3-10.

31. El-Sayed, H.A., A B D El-Wahed, M.G. and Ali, A.H. : "Some Aspects of the Corrosion of Reinforcing Steel in Concrete in Marine Atmospheres". Durability of Building Materials, July 1987, 5(1), 13-25.

32. Sylla Heinz-Martin. : "Reactions in Hardened Cement Paste Under Heat Treatment" (in German). Beton (Dusseldorf), Nov 1988, 38(11), 449-454.

33. Berra, M. and Baronio, G. : "Thaumasite in Deteriorated Concretes in the Presence of Sulfates". Proc, **Concrete Durability, Katharine and Bryant Mather International Conference,** Pub, SP-100, Vol.2, American Concrete Institute, Detroit, Michigan, USA, 1987, p 2073-2089.

34. Piasta, W.G., Sawicz, Z. and Piasta, J. : "Sulphate Durability of Concretes under Constant Sustained Loads". Cement and Concrete Research, 1989, 19(2), 216-227.

35. Sakai, E., Kosuge, K., Teramura, S. and Nakagawa, K. : "Carbonation of Expansive Concrete and Change of Hydration Products". Proc, **Second CANMET/ACI International Conference on Durability of Concrete,** Pub SP-126, Vol.II, American Concrete Institute, Detroit, Michigan, USA, 1991, p 989-999.

36. Slegers, P.A. and Rouxhet, P.G. : "Carbonation of the Hydration Products of Tricalcium Silicate". Cement and Concrete Research, 1976, 6(3), 381-388.

37. Kobayashi, K. and Uno, Y. : "Mechanism of Carbonation of Concrete". **Concrete Library of JSCE,** December 1990, No.16, p 139-151.

38. Dewaele, P.J., Reardon, E.J. and Dayal, R. : "Permiability and Porosity Changes Associated with Cement Grout Carbonation". Cement and Concrete Research, 1991, 21(4), 441-453.

39. Ying-yu, L. and Qui-dong, W. : "The Mechanism of Carbonation of Mortars and the Dependence of Carbonation on Pore Structure". Proc, **Concrete Durability, Katharine and Bryant Mather International Conference,** Pub, SP-100, Vol.2, American Concrete Institute, Detroit, Michigan, USA, 1987, p 1915-1943.

40. Osborne, G.J. : "The Sulphate Resistance of Portland and Blastfurnace Slag Cement Concretes". Proc, **Second CANMET/ACI International Conference on Durability of Concrete,** Pub, SP-126, Vol.II, American Concrete Institute, Detroit, Michigan, USA, 1991, p 1047-1071.

41. Lach, V. : "The Deterioration of Alumina Cement Concrete". Proc, **Concrete Durability, Katharine and Bryant Mather International Conference,** Pub SP-100, Vol.2, American Concrete Institute, Detroit, Michigan, USA, 1987, p.1903-1914.

42. Lea, F.M. : **The Chemistry of Cement and Concrete.** 3rd ed. London, Edward Arnold, 1970.

43. Shayan, A. : "Deterioration of a Concrete Surface due to Oxidation of Pyrite contained in Pyritic Aggregates". Cement and Concrete Research, September 1988, 18(5), 723--730.

44. Ceukelaire, L.De. : "Concrete Surface Deterioration due to the Expansion by the Formation of Jarosite". Cement and Concrete Research, July 1991, 21(4), 563-574.

45. Satish Chandra and Leif Berntsson. : "Deterioration of Concrete Swimming Pools in the South of Sweden". ACI Materials Journal, Nov-Dec 1988, 85(6), 489-494.

46. Srdjan D. Venecenin. : "Thermal Incompatibility of Concrete Components and Thermal Properties of Carbonation Rocks". ACI Materials Journal, Nov-Dec, 1990, 87(6), 602-607.

47. Orchard, D.F. : **Concrete Technology** : 3rd ed. Applied Science Publishers, Vol.3 Properties and Testing of Aggregates, 1976, 113 p.

48. Al-Tayyib, A.J. and Khan, M.S. : "Concrete Deterioration Problems in the Arabian Gulf - A Review". Durability of Building Materials, 1987, 4, 287-298.

49. National Council for Cement and Building Materials, Assessment of Concrete in Boiler Feed Pump Foundation of Korba Super Thermal Power Plant, Unpublished Project Report, CDI-SP-560, Aug 1992.

50. Dinesh Mohan and Mohan Rai. : "Deterioration of Concrete in Fertiliser Factories". Proc, **1st International Conference, Durability of Building Materials and Components,** Ed. P.J. Sareda & C.G. Litvan, ASTM Spl Tech Pub 691, 1980, p 388-396.

51. Suheyl Akman, M. and Metin Yildirim. : "Loss of Durability of Concrete made from Portland Cement blended with Natural Pozzolana due to Ammonium Nitrate". Durability of Building Materials, 1987, 4, 357-369.

52. Satish Chandra. : "Hydrochloric Acid Attack on Cement Mortar - An analytical study". Cement and Concrete Research, 1988, 18(2), 193-203.

53. Attiogbe, E.K. and Rizkalla, S.H. : "Response of Concrete to Sulphuric Acid Attack". ACI Materials Journal, Nov-Dec 1988, 85(6), 481-488.

54. Fattuhi, N.I. and Hughes, B.P. : "The Performance of Cement Paste and Concrete subjected to Sulphuric Acid Attack". Cement and Concrete Research, 1988, 18(4), 545-553.

55. "Air Pollution and Conservation - Safeguarding our Architectural Heritage", **Introductory Information on Interdisciplinary Symposium,** Rome, October 15-17, Ed. J. Rosvall, Swedish Institute for Classical Studies in Rome, 1986, p 1-43.

56. Jorgensen, B. : **The Microbial Sulphur Cycle, Microbial Geochemistry,** Ed. W.E. Krumbein, 1983.

57. Pluym-Berkhout, J.M., Mijnsbergen, J. and Polder, R.B. : "Biogenic Sulphuric Acid Corrosion on Concrete in Pipes" (in Dutch). Cement ('s Hertogenbasch), 1989, 41(9), 16-20.

58. Saricimen, H., Maslehuddin, M. and Shamim, M. : "Case Study of Deterioration of Concrete in Sewage Environment in an Arabian Gulf Country". Durability of Building Materials, 1987, 5(2), 145-154.

59. Kulpa Charles, F. and Baker Cassandra, J. : "Involvement of Sulphur-oxidising Bacteria in Concrete Deterioration". Proc, **Paul Kleiger Symposium on Performance of Concrete,** Pub, SP-122, American Concrete Institute, Detroit, Michigan, USA, 1990, p 313-322.

60. Strom, G., Palmgren, U., Wessen, B., Hellstrom, B., and Kumlin, A. : "The Sick Building Syndrome - An effect of microbial growth in building construction". Proc, **International Conference on Indoor Air-Quality and Climate, 5th,** Toronto, Canada, 1990.

61. Karlsson, S. and Albertsson, A.C. : "The biodegradation of a biopolymeric additive in building materials". RILEM, Materials and Structures, 1990, 23(7), 352-357.

62. Penner, E., Gillott, J.E., and Eden, W.J. : "Investigation of Heave in Billings Shale by Minerological and Biochemical methods". Canadian Geotechnical Journal, 1970, 7, 333-338.

63. Ramachandran, V.S., Feldman, R.F. and Beaudoin, J.J. : **Concrete Science, Treatise on Current Research.** Ed. Heyden & Son Ltd., London, U.K., 1981.

64. Moum, J. and Rosenquist, I.T. : "Sulphate Attack on Concrete in the Oslo Region". Proceedings, American Concrete Institute, 1960, 56, 257 p.

65. CIB : "Feedback from Practice of Durability Data, Appendix, Examples of Field Investigations". CIB Working Commission W 80 and RILEM Technical Committee 100-TSL, CIB Report Publication 128.

66. Liken, G.E. : "Acid Precipitation : Our Understanding of the Problem". Proc, **Conference on Emerging Environmental Problems - Acid Precipitation,** EPA-902/9-75-001, US EPA, Region 2, New York, 1975, p 45-75.

67. Kong, H.L. and Orbison, J.G. : "Concrete Deterioration due to Acid Precipitation". ACI Materials Journal, 1987, 84(2), 110-116.

68. Schramli, W. : "An Attempt to Assess Beneficial and Detrimental Effects of Aluminates in Cement on Concrete Performance, Part I". World Cement Technology, 1978, 2, 35-42.

69. Concrete Society, "Changes in the Properties of Ordinary Portland Cement and their effects on Concrete". Tech Rep. No 29, Concrete Society, U.K., October 1987, 30 p.

70. Visvesvaraya, H.C. & Mullick, A.K. : "Quality of Cements in India - Results of Three Decadal Surveys". ASTM Special Tech Pub, STP 961, Ed. E. Farkas & P. Kilieger, 1988, p 66-79.

71. Massazza, F. : "Pozzolanic Cements : An Answer to Durability Problems". Proc, **NCB International Seminar on Cement and Building Materials, 3rd,** New Delhi, India, 1991, Vol. 4, p VIII-13-27.

72. Mehta, P.K. : "Influence of Pozzolanic Admixtures on the Transition Zone in Concrete". **International Seminar on Industrial Byproducts and Durability of Concrete,** Gothenburg, Sweden, 1986.

73. Mehta, P.K. : "Mechanisms of Expansion Associated with Ettringite Formation". Cement and Concrete Research, 1973, 3(1), 1-6.

74. Shiqun, Li and Della M. Roy. : "Investigations of Relation between Porosity, Pore Structure and Cl^- Diffusion of Flyash and Blended Cement Pastes". Cement and Concrete Research, 1986, 16, 749-759.

75. Maslehuddin, M., Al Mana, A.I., Saricimen, H., and Shamim, M. : "Corrosion of Reinforcing Steel in Concrete Containing Slag or Pozzolans". ASTM, Cement, Concrete and Aggregates, Summer 1990, 12(1), 24-31.

76. Bijen, J. and Van Seist, R. : "Effects of Flyash on carbonation of concrete with portland blast furnace slag cement". Proc, **Second CANMET/ACI International Conference on Durability of Concrete,** Pub, SP-126, Vol.II, American Concrete Institute, Detroit, Michigan, USA, 1991, p 1001-1030.

77. Hobbs, D.W. : "Carbonation in presence of pfa". Magazine of Concrete Research, 1988, 40(143), 69-76.

78. Malhotra, V.M., Carette, G.G., Bilodreau, A., and Sivasundaram, V. : "Some aspects of durability of high volume ASTM Class F (low-calcium) flyash concrete". Proc, **Second CANMET/ACI International Conference on Durability of Concrete,** Pub, SP-126, Vol.I, American Concrete Institute, Detroit, Michigan, USA, 1991, p 65-82.

79. Berke, N.S., Scali, M.J., Regan, J.C., and Shen, D.F. : "Longterm corrosion resistance of steel in silica fume and/or flyash containing concretes". **Ibid,** p 393422.

80. Anqi, L., Baoyu, L., Guoping, H., Yeibo, C., and Guolian, S. : "Study on corrosion prevention in reinforced concrete containing condensed silica fume and its application". **Ibid,** p 499-509.

81. Kukko, H. and Matala, S. : "Effect of composition and aging on the frost resistance of high-strength concrete". **Ibid,** p 229-248.

82. Galeota, D., Giammatteo, M.M., Marino, R., and Volva, V. : "Freezing and thawing resistance of non-air-entrained and air-entrained concretes containing a high percentage of condensed silica fume". **Ibid,** p 249-261.

83. Sabir, B.B. and Kouyiali, K. : "Freeze-thaw durability of air-entrained CSF concrete". Cement and Concrete Composites, 1991, 13, 203208.

84. Paillere, A.M., Platret, G., Roussel, P., and Gawsewitch, J. : "Influence of curing time on behaviour in seawater of high strength mortar with silica fume". Proc, **Second CANMET/ACI International Conference on Durability of Concrete,** Pub, SP-126, Vol.I, American Concrete Institute, Detroit, Michigan, USA, 1991, p 559-576.

85. Durekovic, A. and Popovic, K. : "Effect of ammonium nitrate solution on the structure and strength of cement pastes containing silica fume". Advances in Cement Research, 1988, 1(3), 138-145.

86. Fauveau, P. : "Filler-composite cement : An energy saving product". Proc, **NCB International Seminar on Cement and Building Materials, 3rd,** New Delhi, India, 1991, Vol. 3, p VII-125-140.

87. Ranc, R., Moranville M - Regourd, Cochet, G., and Chaudouard, G. : "Durability of cements with fillers". Proc, **Second CANMET/ACI International Conference on Durability of Concrete,** Pub, SP-126, Vol.II, American Concrete Institute, Detroit, Michigan, USA, 1991, p 1239-1257.

88. Ingram, K.D. and Daugherty, K.E. : "A review of limestone additions to portland cement and concrete". Cement and Concrete Composites, 1991, 13, 165-170.

89. Hobbs, D.W. : "Effect of mineral and chemical admixtures on alkali-aggregate reaction". Proc, **International Conference on Alkali-Aggregate Reaction, 8th,** Kyoto, Japan, 1989, p 173-186.

90. Mullick, A.K. and Wason, R.C. : "Performance of commercial blended cements and their role in alleviating ASR". Proc, **International Seminar on Durability of Concrete, Aspects of Admixtures and Industrial By-products, 2nd,** Gothenburg, Sweden, June 1989, p 138-148.

91. Nanni Antonio and Lista Walter L. : "Concrete cracking in coastal areas : Problems and solutions". Concrete International, Design & Construction, ACI, 1988, 10(12), 67-72.

92. Pomeroy, D. : "Concrete Durability : From basic research to practical reality". Proc, **Concrete Durability, Katherine and Bryant Mather International Conference,** Pub SP-100, Vol.1, American Concrete Institute, Detroit, Michigan, USA, 1987, p 111-130.

93. Mullick, A.K., Wason, R.C., and Rajeev Kumar. : "State of the Art : Behaviour of concrete under seawater and in marine environment". Special Report No 10, IRC Highway Research Board, New Delhi, India, 1989, 79 p.

94. K & B Mather. : "Reflections on Concrete durability and on international conferences on concrete durability". Proc, **Concrete Durability, Katherine and Bryant Mather International Conference,** Pub, SP-100, Vol.1, American Concrete Institute, Detroit, Michigan, USA, 1987, p 1-9.

-:-:-:-

Specific Theme IV D

Special Concrete and Cement Composites

FIBRE REINFORCED CEMENT — THIN SHEETS

A J Majumdar
Building Research Establishment, UK

SUMMARY

The current state-of-the art in fibre reinforced cement (FRC) thin sheets is reviewed with particular reference to materials already in use. The strength properties of cement composites reinforced by different types of fibres are described, and long-term results are given wherever possible. Some phenomenological aspects of fibre reinforcement of cement are briefly considered together with the manufacturing methods used in the production of FRC thin sheets. The possible mechanisms for the reduction of strength properties with time observed in the case of some FRC materials are discussed. A summary of the commercial applications of various FRC thin sheet materials to date is given and comments are made about their future prospects.

RESUME

La technologie de pointe relative aux feuilles minces en ciment renforcé de fibres (CRF) est passée en revue, surtout en ce qui concerne les matériaux qui sont déjà d'usage. L'auteur décrit les propriétés de la résistance des composés de ciment renforcés de divers types de fibres et il en donne les résultats à long terme en tout cas que c'est possible. Certains aspects phénoménologiques due renforcement fibreux de ciment sont examinés brièvement ainsi que les méthodes de fabrication utilisées pour la production des feuilles minces CRF. Les mécanismes possibles de la réduction avec le temps des propriétés de la résistance observée chez certains matériaux CRF sont traités. Les applications commerciales jusqui'ici de divers matériaux pour les feuilles minces CRF sont résumées et des observations sont faites au sujet des perspectives d'avenir de ceux-là.

FIBRE REINFORCED CEMENT - THIN SHEETS

by A J Majumdar

1. INTRODUCTION

All heterogeneous materials are composites by definition. The scope of this definition has recently been extended to include solids where heterogeneity is detectable only at the sub-micron level and the term 'nano-composites' has been coined to describe these materials (1). Inorganic hydraulic cements consist of different chemical compounds or phases separated by interfaces and are, therefore, composite materials, and have been treated as such (2). When sand and aggregate are added to cement to produce the practical materials, mortar and concrete widely used in construction, the degree of complexity in the composite structure is greatly increased. However, it is still possible to derive constitutive relationships for cement mortar and concrete using composite principles (3). Further complexities are introduced when fibres are incorporated in these materials to enhance their tensile strength and impact resistance. In discussing the properties of fibre reinforced cement and concrete (FRC) it is customary to treat these materials as two-phase systems - fibre and matrix - and ignore the composite nature of the matrix itself.

The idea of reinforcing brittle materials by fibres to improve their integrity and toughness has been known to man from the dawn of civilisation and cement composites reinforced by various asbestiform fibres have been in regular use for at least a century. The renewed interest in FRC materials over the past three decades or so owes its origin to various factors. Firstly, very many different types of fibre became commercially available during this period, and rapid progress was made in the science and technology of composite materials. It was soon appreciated that an inorganic construction material, that is light but strong and tough, and is mouldable, could now be produced. Extensive research using glass as the reinforcing fibre, first in the former USSR and then elsewhere, has demonstrated that many of the fabrication techniques developed in the fibre reinforced plastics (FRP) industry can be easily adapted to manufacture products from cement-based materials. Secondly, it became apparent during this period that many of the important properties of concrete can be significantly improved by the addition of small pieces of steel wire. Work with other fibres that are alternative to steel soon followed. Thirdly, it has now become clear that nearly all asbestos cement (AC) products, widely used in the construction industry, will have to be replaced in the coming years because of the health hazards of asbestos. New FRC materials have already been developed to satisfy this social need. For the developing countries, the possibilities of using indigenous, natural vegetable fibres in cement-based composites say, as roofing sheets are very attractive.

Various types of FRC materials are in use throughout the world today and they cover a wide range of applications. This review concentrates on those that are produced in the form of thin sheets and preference is given to composites that have achieved a degree of acceptance by the user. The performance and durability aspects are discussed and some idea is given of the likely future developments in this field, in research as well as in applications.

2. THE MATRIX PHASE

In most of the applications of the new FRC materials to date the proportions of the fibre reinforcement in the composite have been small, 10% by volume or less. The matrix is, therefore, very important in the development of composite properties and the durability of the material.

Various types of hydraulic cement - for example, Portland, high-alumina, supersulphated, regulated set, etc and blended cements of various kinds - are used in the construction industry, and in principle FRC products can be made from any of them. However as Portland cements are by far the most important among inorganic cements,

accounting for more than 90% of the world production of cements, nearly all FRC products use this type of cement as the matrix at the present time. In recent years the use of blended cements has grown. In these, a part of the Portland cement (PC) is replaced by a pozzolanic material such as pulverised fuel ash (pfa), ground granulated blastfurnace slag (ggbs), microsilica (silica fume) or metakaolin. Neat cement pastes are very rarely used in the production of FRC thin sheets. A quantity of sand and/or other fillers up to about half the weight of cement is usually added for reducing shrinkage.

For glass fibre reinforced cement (grc), the high alkalinity of PC matrices poses a difficult problem from the point of view of long-term durability and special cements with reduced alkalinity have been developed. One such cement manufactured by Chichibu Cement Company in Japan consists mainly of calcium silicates $3CaO.SiO_2$ and $2CaO.SiO_2$, calcium aluminosulphate $3CaO.3Al_2O_3.CaSO_4$, calcium sulphate $CaSO_4$ and water quenched blastfurnace slag (4). On hydration, the major products are calcium silicate hydrates (C-S-H) and ettringite $3CaO.Al_2O_3.3CaSO_4.32H_2O$. Similar cements are now available elsewhere also (5,6).

The composition of the solution present in the pores of the matrix phase in FRC materials and especially its OH^- ion concentration have important bearings on the properties of nearly all FRC materials, particularly those reinforced by glass, steel, natural fibres such as sisal and even some organic polymer fibres. In recent years a considerable amount of data has been collected on liquids 'expressed' from solid cement paste or concrete by the technique first used by Longuet (7). These results refer mainly to Portland or blended Portland cements. OH^- concentrations in pore solutions expressed from ordinary PC and some blended cements are given in Table 1 and Figure 1. More recent observations have been summarised by Taylor (10).

Table 1 Hydroxyl ion concentration in cement paste pore solution (Reference 8)

% Na_2O equivalent		wt% addition	water ratio solids	Storage time (days)	OH^- ion concentration (m mol/l)
Cement	Addition				
0.67	-	-	0.45	28	604.0
				365	661.7
	pfa			28	331.1
0.67	3.37	40	0.45	365	319.6
	slag			28	466.4
0.67	0.97	40	0.45	365	505.8
	slag			28	341.1
0.67	0.97	60	0.45	365	358.9

Alternative but less relevant methods of assessing cement alkalinity consist of suspending the ground cement paste in a known quantity of water or making a cement slurry with a very high w/c and keeping it stirred for a long period of time. The results from the analysis of the solution phase in one series of experiments are shown in Table 2. Ca^{++} ion concentration near the fibre is important, particularly if the reinforcement is in the form of fibre bundles (as is the case with glass), and this may control the extent of precipitation of solid $Ca(OH)_2$ inside the fibre bundle.

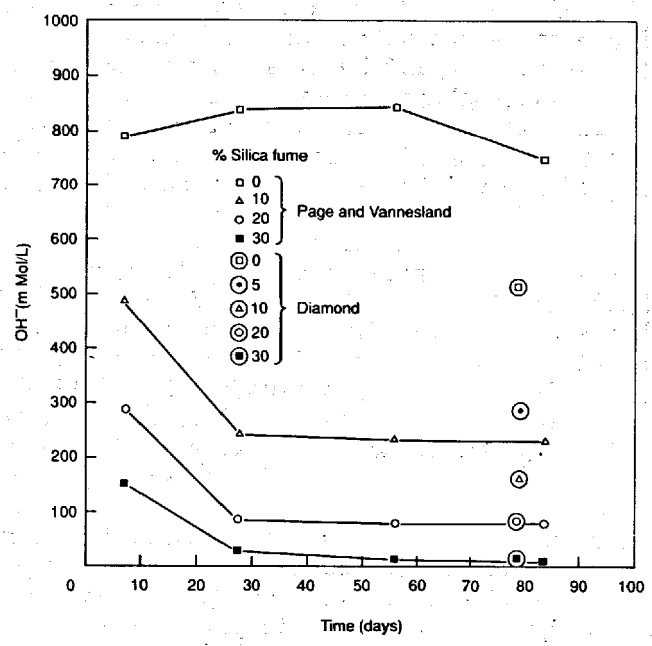

Figure 1. Change in hydroxyl ion concentration with time and proportion of silica fume (Reference 9)

Table 2 Composition of the aqueous phase in contact with various cements (Reference 11)

g/litre	Portland cement	60% Portland cement + 40% pfa	60% Portland cement + 40% pozzolana*	High-alumia cement
Ca^{2+}	0.71	0.53	0.51	0.16
Na^{+}	0.24	0.33	0.28	0.06
K^{+}	0.57	0.56	0.54	0.30
Alkalinity as (OH^{-})	1.04	0.95	0.87	0.67
pH	12.07	12.65	12.60	12.05

*Italian pozzolana from Naples

The use of admixtures of various kinds and superplasticisers is now widespread in concrete technology and in many FRC products these admixtures are used extensively for air entrainment, water reduction, workability and shrinkage control.

One of the interesting cement-based materials to emerge in the last decade is the macrodefect-free or MDF cement. It is a polymer modified cement, processed in a certain way to produce flexural strengths of the order of 150 MPa or more. Attempts to improve the toughness of this novel material by fibre incorporation have been made (12) and are continuing. Other matrices relevant for this review are autoclaved lime (or cement) plus silica mixtures and gypsum plaster.

3. FIBRE PROPERTIES

Various different types of fibres have been used in the past twenty years to reinforce cement and concrete. These can be classified into six groups:
a) crystalline mineral fibres such as chrysotile asbestos b) silicate glass fibres c) ceramic fibres such as carbon and alumina d) synthetic organic polymer fibre such as polypropylene e) natural vegetable fibres, unprocessed such as sisal or refined such

as cellulose (wood) pulp and f) metal fibres such as those made from different types of steel. The use of animal fibres such as horse hair to reinforce gypsum plaster was prevalent in Europe in earlier times but there is little interest in them at present as viable alternatives have been found. Typical properties of a few fibres that are currently being used as reinforcement in various commercial FRC products are listed in Table 3. Similar data on other fibres of interest to FRC can be found elsewhere, for instance, in Hodgson (13) and in Bentur & Mindess (14). Brief descriptions of some of these fibres follow.

Table 3 Fibre Properties

Fibre	Diameter (μm)	Maximum length (mm)	Sp.Gr.	Young's modulus (GPa)	Tensile strength (MPa)	Elongation at break (%)	Poisson's ratio	Coefficient of thermal expansion †
Chrysotile (white asbestos)	0.02 - 0.4	<40	2.55	164	3100	2 - 3	0.3	-
E-glass filament	8 - 15	c	2.53	75.5	3600	~2	0.25	5
AR glass filament	8 - 15	c	2.68	70	~3000	~2	0.22	7.5
Mineral Wool	<3 - 25	>100		68 - 98	540 - 980	-	-	-
Carbon fibres (from PAN)	7 - 9.7	c	1.75 - 1.95	250 - 390	200 - 2700	0.5 - 1.0	0.35	[-0.1 - 1.2 (parallel) 7 - 12 (radial)]
" " (from pitch)	18	c	1.60	30 - 32	600 - 750	2.0 - 2.4	-	
Polypropylene filament	50 - 500	c	0.9	1 - 8	400 - 750	18	0.29 - 0.46	86
" fibrillated	20 - 200	c	"	"	"	8		
Polyethylene	5 - 100	c	0.95	Up to 31.5	700 - 2600	10	-	-
Polyvinyl alcohol	12 - 25	c	1.3	Up to 36	1000 - 1600	3.5 - 6	-	-
Acrylic	13 - 104	c	1.18	14 - 19.5	400 - 1000	6 - 11	-	-
Aramid	10 - 15	c	1.39 - 1.45	69 - 125	2800 - 3600	2.2 - 4.4	0.32	Slightly negative
Nylon (Type 242)	>4	c	1.14	Up to 4	750 - 900	13.5	0.4	29
Wood fibre (Kraft pulp)	20 - 120	0.5 - 5	1.5	4 - 71	500 - 900	-	-	-
Sisal	5 - 50	1200	1.48	13 - 26	300 - 800	3 - 5	-	-
Jute	100 - 200	3000	1.03	26 - 32	250 - 350	1.5 - 1.9		
Steel	5 - 500	c	7.84	200	500 - 2000	0.5 - 3.5	0.3	11

c = continuous † (10^{-6}/°C)

3.1 Crystalline mineral fibre

By far the most successful fibre that has been used as reinforcement for cement is asbestos. Asbestos is a general name for several variations of naturally occurring crystalline fibrous silicate minerals which possess a rather unique range of physical and chemical properties. By far the most abundant mineral is chrysotile ($3MgO.2SiO_2.2H_2O$) or white asbestos, a member of the serpentine group. Chrysotile constitutes more than 90% of the world asbestos reserves and is the predominant fibre in asbestos cement products. The reinforcement in AC products is in the form of fibre bundles with tensile strength in the range of 300-1800 MPa. Individual filaments have much higher strengths, >3000 MPa, and electron microscope examination indicates that they are tubular (15) which may partly account for their affinity for cement. The fibres resist well the severe mechanical attrition received during processing and the strong, long-term alkalinity of the cement matrix.

Asbestiform fibres are significant hazards to health. All commercially produced asbestos can cause asbestosis and bronchial cancers (16). A cancer of the lining of the lung, mesothelioma, is believed to be caused by inhalation of asbestos and some forms of stomach cancer are also attributed to the mineral. For these reasons there is general agreement that the use of asbestos in construction should be phased out as soon as practicable.

Other crystalline minerals having a fibrous habit that have found use in reinforced cement products are wollastonite and xonotlite (13). Although not fibrous, mica has also been used (17) to achieve benefits. In general it can be said that crystalline mineral fibres are durable in a cement matrix.

3.2 Silicate glass fibres

Although fibres made from inorganic silicate glasses have been used very successfully for more than fifty years to reinforce plastics and resin matrices, their application in highly alkaline cement-based materials has always been looked upon with a degree of suspicion. Such concerns stem from the fact that silicate glasses can probably never be made totally alkali-resistant (18,19). Biryukovich and co-workers (20) produced cement composites based on E-glass and A-glass fibres nearly three decades ago. In the late 1960's Majumdar and Ryder (21) demonstrated that glass fibres more suitable than E- or A-glass fibres for cement reinforcement can be produced from compositions containing large amounts of zirconia. Such glass fibres are now known as alkali-resistant (AR) glass fibres. During the last twenty years or so numerous patents have been granted to many AR glass fibre compositions but only a few were ever commercially produced. Majumdar and Laws (22) have recently reviewed the current position. If the sol-gel method of producing glass fibres (23) becomes viable one may expect to see novel compositions for new AR-glass fibres.

One of the most interesting developments in the AR glass fibre field in recent years has been the innovation of an 'inhibitive coating' (24,25) for the fibre surface. Such coatings, often based on derivatives of trihydroxy organic compounds such as pyrogallol, are believed to retard the hydration of cement in the close neighbourhood of the fibre.

Continuous glass fibre is manufactured in the form of strands comprising, typically, 204 filaments. The tensile strength of glass fibre strands, usually in the range of 1700-2200 MPa, is lower than that of the corresponding filament (Table 3). It is thought at the present time that such glass fibres with diameters usually greater than 12 μm are not hazardous to health.

Mineral wool and glass wool comprise the largest volume of man-made mineral fibre (MMMF) and are widely used in insulation. The mineral wools include slag wool and rockwool, the former made from blastfurnace slags and the latter from crushed igneous rocks such as basalt. Most mineral wool fibres have poor alkali resistance and hence are not suitable for reinforcing cementitious matrices. Some improvements in alkali-resistance of these wool products can be made by including some zirconia in their composition (26). Some mineral wool products have shown excellent filtration properties when incorporated in conventional asbestos cement mixes. The length and diameter of mineral wool fibres cannot be controlled as effectively as in the case of continuous glass filaments and hence there is some general concern about the possible health hazards of MMMF and guidelines have been issued in some countries about their use (27).

3.3 Ceramic fibres

Carbon fibres were developed primarily for their high strength and stiffness properties for applications in the hi-tech industries such as aerospace. At the present time high performance carbon fibre made from textile fibres still remain rather expensive, a factor which is limiting its use in the building industry.

Relatively inexpensive fibres made from pitch look more attractive. Some pitch-based fibres have usually much reduced properties (Table 3) compared to high performance fibres but in recent years fibres with high strength and high modulus have been produced from coal tar pitch (28).

Carbon fibre has a unique fibrous structure closely related to the starting material. Such a texture allows the fibre to develop good frictional bond with the matrix. The fibre may also be surface treated in a suitable way to provide better bonding with particular matrices. Because of the extreme inertness of carbon and the strength and stiffness of the C-C covalent bond carbon fibres provide excellent reinforcement in aggressive environments such as cements. They are stable in inert conditions to temperatures exceeding 2500°C, but they will oxidise slowly in air at temperatures above 500°C (13).

A list of other ceramic fibres of interest will include mullite, alumina and zirconia fibres, silicon carbide and silicon nitride. These fibres are used mainly in high temperature products and not for cement reinforcement at the present time.

3.4 Synthetic organic fibre

A number of synthetic organic fibres has been proposed as reinforcement for cement and in the replacement of asbestos in asbestos cement (AC) products such fibres are finding increasing use. In his pioneering research on the use of synthetic polymer fibres to reinforce cement and concrete, Goldfein (29) used polypropylene (PP) monofilaments, but in recent years more interest has been shown to the use of PP in the form of a fibrillated network. As a material polypropylene is hydrophobic and does not bond well with cement but the fibrils in the fibrillated tape are extremely fine and the reinforcement network is believed to produce a fair mechanical bond (30). A high tensile PP fibre of rectangular shape produced by mechanically splitting an extruded tape and sold under the trademark 'Krenit' has been developed in Denmark (31). Only a few attempts have been made to use the other common olefin, polyethylene, to reinforce cement and concrete (32).

The synthetic fibre that has found most favour in Europe so far as a replacement for asbestos in typical AC products such as corrugated sheets and roofing slates is polyvinyl alcohol (PVAL). PVAl is hydrophillic and is therefore suitable as reinforcement in cement products but it cannot be satisfactorily mixed in as the sole fibrous component and the use of other secondary fibres or cellulose pulp as the carrier is found to be necessary. Highly drawn PVAl fibres for specific use in reinforced cement products have been developed. Split fibres from polyacrylonitrile film have strengthening properties similar to those of fibrillated PP and these are considered suitable for reinforcing cement-based matrices. A kaolin loaded acrylic fibre has been developed in Japan for this purpose (13).

Although fibres made from aliphatic amides, eg nylon, have been in existence for several decades, their use as reinforcement for cement and concrete has been studied mainly at the academic level so far. The aromatic polyamides (aramids) are more recent innovations and some of the several varieties now on the market have been tried out as cement reinforcement. These fibres have very good chemical and abrasion resistance, and they burn with difficulty.

Small amounts (0.1-0.2 vol %) of synthetic fibres with high aspect ratios have been used in FRC materials to reduce the effect of early drying and plastic shrinkage cracking. The use of PP towards this end is well known; acrylic and polyester fibres can also be used for this purpose. Polyester fibres are hydrophobic and encounter difficulties in bonding with cement.

Like asbestos and glass, synthetic fibres can be offered in various forms of reinforcement from monofilament and fibrillated network to woven cloth and this feature adds to the attraction of these fibres. By adopting manufacturing conditions such as

hot-stretching the structure of polymer can be manipulated to give high Young's modulus but quoted values of ultra high modulus are often strain rate dependent. Fibrillated networks are usually strong only in one direction.

Although the short- and medium-term durability results have been satisfactory, the very long-term viability of the synthetic fibres as reinforcement in cement still needs to be established (13). Moisture is known to have a degradating effect on PP over a long term. Polyolefins are also sensitive to O_2 and UV radiation. The most critical feature of the synthetic fibres in building applications is associated with their melting points, which are invariably low, and their flammability. There must be some doubt about the fire resistance of FRC based on synthetic organic polymer fibres.

3.5 Natural fibres

3.5.1 Unprocessed fibres - Natural fibres are available in reasonably large quantities in many countries and represent a renewable resource. In the last decade or two FRC materials containing fibres such as sisal, jute, coir and elephant grass have found applications in a number of industrially developing countries, for example Kenya and Peru (33). The list of other unprocessed natural fibres that have received attention includes flax, sugarcane, bagasse, waterreed, plantain, palm, bamboo and a few others. The properties of some of these fibres are given in Table 3. In general these fibres are light, their specific gravity being in the range 1-1.3 and hence they have reasonably high specific strength and stiffness. However, they absorb water readily and moisture has a great influence on the mechanical properties of unprocessed natural fibres, wet conditions inducing an increase in failure strain and a reduction in modulus of elasticity.

It is with respect to chemical durability in the alkaline cementitious matrix that natural vegetable fibres are particularly vulnerable. The hemicellulose and lignin constituents of these fibres are attacked by the alkali (34) and the fibres may also be susceptible to fungal and bacterial decomposition (35) and to insect attack. Furthermore they are combustible. In most cases the properties of natural plant fibres vary greatly from batch to batch. Fibres containing appreciable amounts of sugar and other carbohydrates may affect the development of properties in the cement matrix (36).

3.5.2 Processed fibre - Among the natural fibres used in a cementitious matrix, those derived from wood have been found to be particularly important. Wood pulp is the source of cellulose fibre, and in recent years cellulose fibre has emerged as a complete replacement for asbestos in fibre reinforced cement products, an advance made possible through the development of high quality fibre and the use of an autoclave curing process. Cellulose pulp is used in many FRC sheet manufacturing processes to retain cement.

Wood pulps are produced from both coniferous soft woods with high lignin contents or deciduous hardwoods with a somewhat lower lignin content. The preparation of the pulp is achieved by mechanical or chemical methods, often using elevated temperatures. In Australasia, where most developments in cellulose reinforced cements were made, Montesey Pine (pinus radiata) which gives good quality long cellulose fibres is the preferred source and the current trend is towards pulps produced by the chemical Kraft process, preferably bleached. The diameter of refined cellulose fibres lies in the 20-60 μm range for hardwood and 30-120 μm for soft wood. The corresponding lengths are in the range 0.5-3.0 mm and 2.0-4.5 mm respectively (37). Cellulose fibres have higher strain capacity than asbestos, the exact value depending on temperature and humidity.

Refined cellulose contains very little lignin and is, therefore, far more durable in alkaline environments than vegetable fibres such as sisal. However, some of the drawbacks of the latter type of fibres mentioned in the previous section apply to cellulose also. But, because of their low cost, wood and other cellulose fibres will remain attractive.

3.6 Metal fibres - Short lengths of steel fibres of various shapes having aspect ratios usually in the range 30-100 are used as reinforcement in many concrete products at the present time. Fibres made from carbon, low carbon and stainless steel have been used in these applications. Attempts have been made to use these reinforcements in thin sheets, but with limited success.

Some interest has been shown in recent years (38) in the potential of ribbons made from metallic glass (ie extremely rapidly cooled amorphous metallic alloys) as reinforcement for cement and concrete. The compositions of metallic glasses vary widely; ribbons made from alloys containing Fe, Cr, P, C and Sr having tensile strength of the order of 2500 MPa and very good corrosion resistance are considered suitable (39). Typically these ribbons are 1-2 mm wide and 20-30 μm thick; they may be made in lengths from 15-60 mm. Experiments with some metallic glass ribbons have shown that they are more alkali resistant than AR glass fibres.

4. MANUFACTURING METHODS

Many fibre cement composites in the form of thin sheets are now produced commercially using well known industrial methods. Asbestos cement replacement products containing PVAl, cellulose, glass, acrylic, polypropylene and some other fibres have been produced by the Hatschek (40) process. It has also been demonstrated that other AC production methods such as Magnani or Manville can also be employed successfully for some of these fibres, eg glass (41).

Some of the fibres that are being employed in place of asbestos in FRC sheet products, eg PVAl, do not retain cement particles very well in dilute slurries used, for instance, in the Hatschek method. It has been found advantageous to use small amounts of cellulose pulp to overcome this problem (13). Pulps of synthetic organic polymer or short fibres of polymers such as polyethylene or acrylic are also effective in this respect.

The technology for producing FRC sheets containing polyolefin fibres commercially by the adaptation of the Netcem process (42) has been developed (43). For glass reinforced cement sheets the spray method remains the most popular and with de-watering this technique produces the strongest sheets with minimum anisotropy (44,45). A variation of the technique is used for the production of a general purpose grc building board. The spray process can also handle a premixed fibre cement slurry.

Fibre nets or 'crenettes' are now available for several fibres such as glass, carbon and synthetic polymer fibres. The use of carbon and aramid fibre nets in repairing structural concrete components has aroused considerable interest (46). The incorporation of glass 'tissue' in plasterboards has been another interesting recent development (47). Mats of natural vegetable fibres such as sisal or coir have been incorporated in the cement mortar sheets (33) by the 'lay-up' method to provide roofing slates in a number of developing countries.

Short fibres of various kind have been incorporated into the cement mortar or concrete mix by the pre-mix methods. True (44) has given a detailed account of these methods as used at present for manufacturing grc products. In principle other fibres can be treated in a similar way although some adjustments usually need to be made. In thin walled concrete, eg tunnel linings, short steel fibres are easily incorporated by adapting the normal shotcreting techniques. It is also possible to produce thin sheets from short steel fibres and mortar using the spray method (48). Bentur and Mindess (14) have recently reviewed the fabrication methods used in the production of FRC in general terms.

For economic and practical reasons several man-made fibres including carbon and aramid are produced as bundles and it has been found difficult to disperse the fibres in the chopped bundles uniformly in the cementitious matrix. A proper dispersion of fibres is particularly important in the case of expensive fibres such as carbon. Ando

et al (28) have recently reported that their high performance carbon fibres made from coal-tar pitch disperse quickly and uniformly in the cement without the use of any special type of mixer.

The use of undirectional reinforcement in FRC sheets is rare, although its advantages are well known and well illustrated in the work of Aveston et al (49) and of Briggs et al (50) with carbon fibres. Very recently in the manufacture of corrugated asbestos-free roofing sheets continuous AR glass fibres have been used undirectionally in selective places (51). In a small scale operation continuous AR glass fibres were used in fabricating fenceposts (52).

The quality of FRC products where the proportion of fibre is rather small depends very strongly on the amount of fibre incorporated and its length and orientation. The quality also depends on the uniformity of fibre distribution in the matrix and how well the latter has been compacted around the fibre to provide an intimate bond. During the production of grc sheet materials some of these quality control parameters are monitored by continuously checking the fibre consumption from the weight loss in the roving and the mortar pump output. Very often a test piece is made which is similar in all operational respects to the product. The fibre content of the composite is determined routinely from samples taken out from this test piece by the wash-out method (53). Ashley (54) has described a method of estimating the glass content in grc containing AR glass fibres based on the determination of zirconium by X-ray fluorescence. For industrial products such as AC sheets and slates or their replacement FRC equivalents quality control procedures are stipulated in standards.

It is more difficult to accurately evaluate the orientation and distribution of fibres in a FRC product. For young grc products some idea of these parameters can be obtained by a technique first studied by Hibbert (55) which utilises the fibre-optic characteristics of glass fibres and in contact prints of grc sections glass fibres are easily seen. Steel wire in concrete or mortar can be seen in a suitably taken X-ray photograph (56).

5. COMPOSITE PROPERTIES

5.A Phenomenological aspects - Fracture processes in FRC materials have to be rationalised, as far as possible, with their stress-strain behaviour under different forms of loading. In this respect most attention has been paid to the behaviour of cement composites in tension. Broadly speaking, three different types of tensile stress-strain curves are obtained with these materials, as shown in Figure 2. The principles governing the behaviour depicted schematically in curves A and B are now well understood. Curve C, representative of asbestos cement, is a special case. Different approaches seem to be necessary to accurately describe the various salient points in the three curves in Figure 2. A resumé of these ideas is not given here and the reader is referred to the recent excellent book by Bentur and Mindess (14) for a critical appraisal of the current position. Table 4, taken from Bentur and Mindess, lists the principal concepts and their topicality.

Currently there is considerable interest in the application of non-linear fracture mechanics to account for the observed behaviour of FRC materials, particularly those exhibiting post-cracking ductility. Concepts such as the crack-mouth opening displacement, R-curve analysis, the fictitious crack model and others that assume the existence of a 'process zone' of discontinuous cracks in front of the advancing crack, are being applied increasingly to FRC materials. Many recent developments in this field are discussed in Shah (57). The R-Curve approach has been used by Mai (58) to characterise the fracture behaviour of asbestos cement (Fig 2, curve C). The tensile and bending strengths of AC materials have also been analysed using composite principles and mixture rules (59,60).

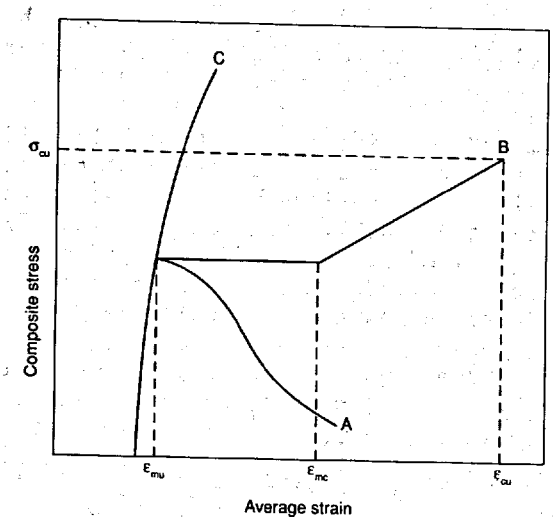

Figure 2. Theoretical tensile stress-strain curves for different types of fibre cement composites

Table 4 Phenomenological description of the salient features of the tensile stress-strain curve (Reference 14)

Tensile Property	Concept
Initial modulus of elasticity, E_c	Composite materials - rule of mixtures
First crack stress (matrix crack stress), σ_{mu}	Composite materials - rule of mixtures. Linear elastic fracture mechanics (LEFM) - spacing factor
First cracking strain (matrix cracking strain), ε_{mu}	Energy balance
Strain at the termination of multiple cracking, ε_{mc}	Multiple cracking
Ultimate composite strain, ε_{cu}	Aveston-Cooper-Kelly (ACK) model - multiple cracking
Ultimate composite strength, σ_{cu}	Composite materials

In this review of rather limited scope, only a few of the phenomenological issues of interest in design and hence applications of FRC materials are discussed below, albeit very briefly.

5.A.1 Critical volume and critical length of fibres - The difference between the theoretical curves A and B in Figure 2 arises because in the former case there are not enough fibres in the composite to support the load after the matrix cracks at its ultimate failure strain ε_{mu}. In this case the composite fails by single fracture. Curve B is typical of composites that show multiple fracture of the matrix. The fibre volume fraction that marks the transition from single to multiple fracture is the critical fibre volume $V_{f,crit}$.

For composites containing short fibres the concept of a critical length parameter l_c, defined as the minimum fibre length required for the fibre to reach its fracture stress, is equally important. Length effects in FRC materials, both in the

pre-cracking and post-cracking states of the composite, have been discussed by many authors, among them Krenchel (61) and Laws (62). Bentur and Mindess (14) have reviewed these contributions in a comprehensive manner.

For any given fibre cement composite system the critical fibre volume, $V_{f,crit}$, depends on both the length and orientation efficiency of the fibres. Calculated values of $V_{f,crit}$ for continuous aligned composites having steel, glass or polypropylene reinforcements are in the range 0.3-0.8%. But for practical FRC composites having a random two- or three-dimensional dispersion of discontinuous fibres, appropriate 'efficiency factors' need to be introduced in the calculations and much higher values of $V_{f,crit}$, ~1-3% range result. Hannant et al (63) have given estimates for the 'Netcem' material and grc. These values are, of course, subject to the uncertainties about the numerical values of the bond strength and of the efficiency factors that apply to a particular type of cement composite system. Bentur and Mindess (14) have plotted (Fig 3) calculated values of $V_{f,crit}$ against aspect ratio (l/d) for short fibres, showing the effect of fibre/matrix bond strength and fibre orientation. For any given FRC system $V_{f,crit}$ is lower in flexure than in tension.

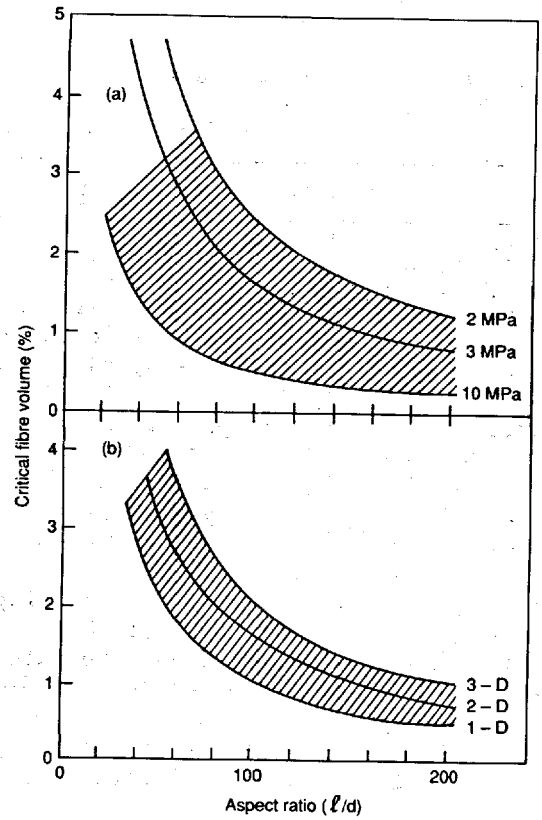

Figure 3. Plots of calculated critical fibre volume, $V_{f(crit)}$ versus aspect ratio l/d for short fibres: (a) composites with different fibre-matrix bond strenth τ_{fu}, with σ_{mu} = 3 MPa and random 2-dimensional fibre array; and (b) composites of different fibre orientations, with σ_{mu} = 5 MPa and τ_{fu} = 3 MPa (Reference 14)

Hannant (64) has recently re-emphasised the point that as $V_{f,crit} = \sigma_c/\sigma_{fu}$, an increase in σ_c, the composite cracking stress or a decrease in σ_{fu}, the ultimate tensile strength of the fibre will increase $V_{f,crit}$. In FRC containing fibrillated PP nets, Hannant reports an increase in $V_{f,crit}$ from 2.9% to 4.8% after 10 years of natural weather due to an increase in σ_c alone. For glass reinforced cement under similar weathering conditions an increase in σ_c would occur but in this case a substantial decrease in σ_{fu}has also been recorded (65,66). For such composites a

significant increase in $V_{f,crit}$ on weathering is, therefore, to be expected. If the fibre volume fraction in the composite is less than this increased $V_{f,crit}$ value (due to ageing), the composite will fail in the single fracture mode when stressed. Tensile rather than flexural tests are more likely to identify this embrittlement in marginal cases.

5.A.2 Stress and strain at matrix cracking - Increases in the cracking stress and strain of the matrix as a consequence of fibre incorporation are expected on theoretical grounds. Figure 4 shows the predictions of the matrix cracking strain from three different models (63) for inclusion of fibrillated PP in cements and compares these with the experimental results. For many FRC materials, eg glass reinforced cement, the bend-over point (BOP) where gross multiple cracking begins (67) is easier to determine in the tensile stress-strain diagram than the onset of matrix cracking. Shah and co-workers (68,69) have confirmed, by using a variety of techniques, that isolated microcracks form in the matrix long before the BOP is reached. They have estimated the BOP stress in several FRC materials by subtracting the contribution of the fibre from the composite response using the law of mixtures. In one case, that of a continuous aligned composite containing 13.4 vol % of PP fibre, a value of 15 MPa was obtained for the matrix cracking strength (or BOP stress) whereas the tensile strength of the plain matrix was only 4 MPa. More recently Ouyang and Shah (70) have attempted to describe similar 'matrix toughening' observed by others in composites made from high-strength cements by the R-curve analysis.

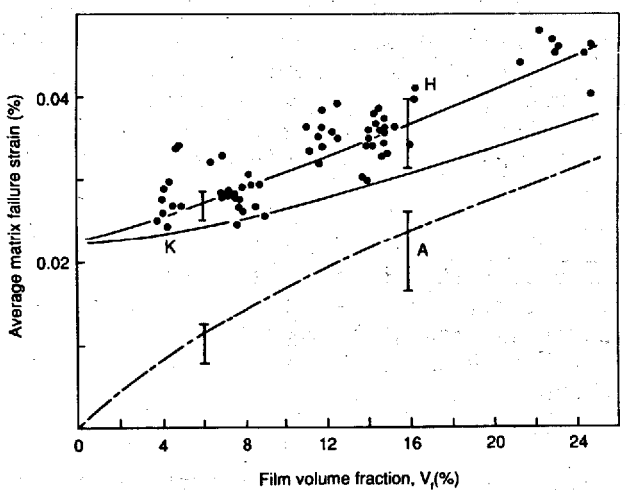

Figure 4. Relation between average matrix cracking strain and film volume fraction of a composite containing fibrillated polypropylene (Reference 63)

When the fibre 'spacing' is less than the Griffith flaw size, in many FRC composites a sizeable stress is developed in the fibre at matrix cracking according to Hannant et al (63). For glass fibres in cement they calculated that for such fibres stress can be of the order of 300 MPa which is much greater than 28 MPa, the value of $E_f \varepsilon_{mu}$ for $\varepsilon_{mu} = 4 \times 10^{-4}$.

5.A.3 Bond strength - The nature and the strength of the bond between the fibre and the matrix is one of the key parameters that governs the properties of all FRC materials. When the composite is loaded, the stress transfer across the fibre/matrix interface is effected predominantly by elastic shear forces up to the point of the first crack stress, σ_c. On further loading, debonding becomes common and the process controlling stress transfer becomes one of frictional slip. The transition from one mode of stress transfer to the other is gradual and is completed when the shear forces at the interface due to loading exceed what Bentur and Mindess (14) have described as the 'adhesional shear bond strength'. They describe the other type of bond as 'frictional shear bond'. Detailed analyses of pull-out traces have been made by

various authors including Bartos (71), Laws (72), Grey (73) and most recently by Li et al (74).

There is still some uncertainty about the bond strength values to be used in designing with FRC. Kelly (75) is of the view that a good idea of the bond strength can be had from crack-spacings seen in multiply cracked aligned composites and work in several fibre reinforced cement systems (14) seems to confirm this view. For short fibre composites where fibre pull-out plays a most significant role in fracture there are difficulties in taking this approach.

Bentur and Mindess (14) and Li et al (74) have reviewed the bond strength determinations of many recent studies involving various type of fibres. They report, from pull-out experiments on steel fibre in cements, a range of 3-100 MPa for adhesional shear bond strength and 1-20 MPa for the frictional bond. For PP, the corresponding quoted values are 0.5-1.0 MPa and 0-0.33 MPa respectively. Uncertainties about bond strength values are translated to computed values of composite properties. The effect of an increase in bond strength from 0.2 to 0.8 MPa on the average matrix failure strain in composites containing fibrillated polypropylene net is illustrated in Figure 4 by vertical bars. It is seen that the effect is not negligible. Li et al (74) have given other examples. For polymer fibres the predicted effect of 'Poisson contraction' in debonding and rupturing the composite (76) has not been seen in practice (77).

For reinforcements that are manufactured in the form of bundles, eg glass, carbon and asbestos, or are non-cylindrical in shape the determination of bond strength poses a special problem. A bond strength value in the range 1-5 MPa has been measured for glass fibre strands in cement. Li et al (74) have reported a higher bond strength between AR glass fibres and cement at 55°C than at 20°C. The addition of styrene butadiene rubber latex produced a stronger bond in carbon fibre composites studied by Soroushian et al (78).

5.A.4 Microstructure at the interface - Microstructural studies of the interface in fibre cement composites indicate that different features are prominent with different fibres. In the case of steel wire, there is very good evidence (79) that a 'transition zone' rich in $Ca(OH)_2$ crystals is present between the fibre surface and the bulk matrix. The transition zone, which may extend to tens of microns from the fibre surface, may harbour the weakest interfacial link. According to Tabor (80) the poor inter-layer adhesion in $Ca(OH)_2$ may be the limiting factor.

For fibre bundles, eg glass, a different microstructure predominates. $Ca(OH)_2$ crystals and other products of cement hydration precipitate inside the strands and bond the individual filaments. Akers and Garrett (60) found no evidence of the $Ca(OH)_2$ rich zone in the matrix near the fibre bundle in asbestos cement. It is assumed generally from microstructural evidence that fibre/matrix bond strength increases when fibre bundles are filled up with cement hydration products. The densification of the interface apparently has little effect on the strength of the bond in Netcem (81).

5.A.5 Bending properties and MOR/UTS ratio - For FRC materials that show multiple cracking of the matrix, calculation of the bending strength (modulus of rupture, MOR) from the elastic beam theory is inappropriate. However, as these materials are frequently subjected to flexural loading and are usually tested in bending, it is useful to have some idea of the bending to tensile strength ratio prevailing in these materials. Aveston et al (49) have developed constitutive relations for the MOR and the MOR/UTS ratio based on the ACK model. Their theoretical upper limiting value of 3 for the MOR/UTS ratio is somewhat higher than 2.44 predicted by Hannant (82) and the range 1.9-2.6 found experimentally for some FRC materials (14). Further theoretical work in this area has been carried out by Laws (83).

It is generally agreed that for FRC materials that fail after multiple cracking, the UTS is given by $\eta\sigma_f V_f$, when η is an efficiency factor and there is no contribution

from the matrix. But experimental work from several sources (50,84) suggests that a mixture rule might apply for the bending strength. Laws (83) has put forward the view that these results can be interpreted in terms of the ACK model (85) also using the relation between MOR and UTS.

5.A.6 Work to Break - The response to tensile stresses as seen in the tensile stress-strain diagrams of FRC materials (Fig 2) perhaps provides the most informative picture of the fracture processes in these materials. Hibbert and Hannant (86) had expressed the view some time ago that the area under the tensile stress-strain curve up to fibre failure, when expressed as energy per unit volume of material, is the most appropriate parameter to describe the energy absorbing capacity of FRC materials. For continuous aligned FRC, Hibbert and Hannant calculated the theoretical energy to be 1036 kJ/m^3 for fibrillated PP and 250 kJ/m^3 for steel wire for composites having 10 vol% of fibre. Aramid fibres gave greater than 3000 kJ/m^3 as the amount of energy absorbed. In these examples the contribution from multiple cracking is only a small proportion of the total energy expended and the predominant contribution is the elastic strain energy of the fibre. The 'toughness index' proposition described by Henager (87) is based on similar ideas but the area under a portion of the load-deflection curve of the composite provides a measure of the energy absorption in this case. An up-to-date account of research in this area is given in Bentur and Mindess (14).

Theoretical relationships have been derived for the energy to break short fibre composites where the fibres are much longer than the critical length (88). In this case some fibres would break at composite failure strain and others will pull out and both processes need to be taken into account in calculating the total energy to break the composite. Following Kelly (89), Bentur and Mindess (14) have re-emphasised that in short fibre composites the pull-out work is at its maximum when the length of the fibre equals critical length. As the length increases more fibres break rather than pull out, improving strength efficiency but at the expense of the 'toughness'. A notion of a critical bond strength has been introduced for short fibre composites.

5.A.7 Synergy in FRC materials - In earlier studies on FRC materials containing mixture of fibres (90,91) the issue of any synergistic effect was not seriously addressed. This has now been done by Xu and Hannant (92) in their work on cement composites containing mixtures of PP and glass fibres. Both tensile and flexural test results show improvement in properties that is greater than the sum of the contributions from individual fibre types. It was observed that in the presence of fibrillated PP nets having a large strain capacity glass fibres maintained maximum load at higher deflections than would be possible on their own. The use of the fibre mixture produced composites with a higher LOP (in bending) and improved flexural properties in the post-cracking regime compared to their individual composites. It is interesting to note that a mixture of PP net, continuous glass fibre rovings and chopped glass fibre strands is used commercially in Italy in the manufacture of corrugated sheeting.

5.B PROPERTIES OF INDIVIDUAL FRC COMPOSITES

5.B.1 From Crystalline Fibres

5.B.1.1 Asbestos cement - Although the health hazards of asbestos are well documented (16) and several countries have taken positive steps to eliminate the use of asbestos in buildings and construction, the volume of AC production globally still remains very high at possibly tens of millions of tonnes. One reason for this is the cheapness and abundance of this natural fibre. But there are important technical reasons also. Asbestiform minerals, chrysotile in particular, combine exceedingly well with cement to produce a wet flat which has the right plasticity and strength so it can be moulded easily into corrugated sheets, pipes and other products. Secondly, the technology, which is capital intensive, is well established and there are some ninety countries in the world where AC products are made (13).

A good formulation for AC sheets and pipes will have 12-14% of chrysotile asbestos. More hazardous amphibole asbestos has been phased out in many countries in the manufacture of pressure pipes, for instance.

Properties of the AC material in various applications are governed by national and international standards and these are undergoing substantial revision at the present time (93) to accommodate the alternative non-asbestos FRC products. For AC products Hodgson (13) stipulates that the transverse loading or flexural strength of flat or corrugated sheet must not be less than 15.7 MPa. Most manufacturers will exceed this minimum in their product to provide an overall safety factor of 1.3 to 1.4. Pressure pipes should have a circumferential tensile strength of at least 22.5 MPa. The density of the AC products has to be strictly controlled so that water absorption does not exceed 25% in sheets or 20% in pipes.

The mechanical properties of AC have been studied by many authors among them Mai (58) Allen (59) and Akers and Garrett (60). Akers and Garrett concluded that the strength of the composite could be accounted for without any matrix contribution whereas Mai included such a contribution in his study. From microstructural studies (60) it appears that failure in AC takes place via fibre pull-out, although as the reinforcement is in the form of bundles of very fine fibrils, the pull-out process is rather complex. Single fibre pull-out tests have indicated that the pull-out bond strength is in the range 0.8 to 2.4 MPa (14).

In use AC sheets have sometimes lasted sixty years or more. On weathering an increase in the bending strength but a decrease in impact toughness has been observed (94).

5.B.2 From Silicate Glass Fibres

5.B.2.1 Glass Fibre Reinforced Cement (GRC) - Following the work of Biryukovich and co-workers in Russia (20) and that in England in the late sixties and early seventies at BRE and Pilkingtons (22) glass fibre reinforced cement (grc) has emerged as an interesting constructional material of considerable versatility. The grc industry is now well established. At the present time alkali-resistant (AR) glass fibres containing fairly large proportions of ZrO_2 constitute the principal fibre-type used in the industry although in specially polymer modified cement matrices borosilicate E-glass fibres have also found commercial applications.

The mechanical properties of grc made from the first generation AR fibre (CemFIL) up to 20 years and that from second generation fibre (CemFIL 2) provided with an inhibitive coating up to 10 years have been published. These studies included investigation of the effect of pozzolanas such as pulverised fuel ash, granulated blastfurnace slag and microsilica, of lightweight aggregates such as pfa 'cemospheres' and of various polymer dispersions on the properties of grc made from Portland cement. Grc made from non-Portland cements were also studied. In these composites a nearly 2-dimensional random distribution of short fibres (34-38 mm) amounting to ~ 4 vol% of the composite was obtained by using the spray-dewatering production technique. Long-term results on E-glass reinforced polymer modified Portland cement prepared in a similar way are also now available (95). A detailed review of the findings of these studies is not given here as they are discussed in full in the recent book by Bentur and Mindess (14) and in the monograph by Majumdar and Laws (22).

The 28-day properties of spray-dewatered grc made from the first generation AR fibre are as follows: MOR 35-40 MPa, LOP 19-17 MPa, UTS 14-17 MPa, strain at failure ~ 1.0%, BOP 9-10 MPa, Young's modulus 20-25 GPa and Izod impact strength 17-31 kJ/m^2. If kept in relatively dry air (40% rh), these properties do not change very much up to 20 years but in a wet environment, the strength properties show a substantial reduction. In particular the tensile failure strain is reduced to very low values, 0.02-0.04%, in course of a few years rendering the material essentially brittle. The matrix controlled properties, e.g. the Young's modulus, LOP (in bending) and BOP values

show an increase however. When the second generation fibres with inhibitive coatings are used, the extent of reduction in properties is much smaller after equivalent times, for instance the failure strain value after nine years of weathering at BRE is in the range 0.4-0.5%, but stable values might not have been reached. Several authors have studied the microstructural changes that attend changes in grc properties in various environments (14,22).

For vibration-cast premix grc used commercially and having a sand:cement ratio of 0.5:1 and w/c of 0.33, the initial mean property values are as follows (45): compressive strength 40-60 MPa, MOR 10-14 MPa, LOP 5-8 MPa, UTS 4-7 MPa, strain to failure 0.1-0.2% and impact strength 8-14 kJ/m^2. Some changes in these values on long-term weathering are to be expected.

Predictions have been made about the very long-term strength of grc from accelerated ageing tests by immersing the material in hot water at various temperatures (96,97). A comparison of the predicted and real time bending strength for spray-dewatered grc is shown in Figure 5 (98). The predictions are based on an Arrhenius-type relationship.

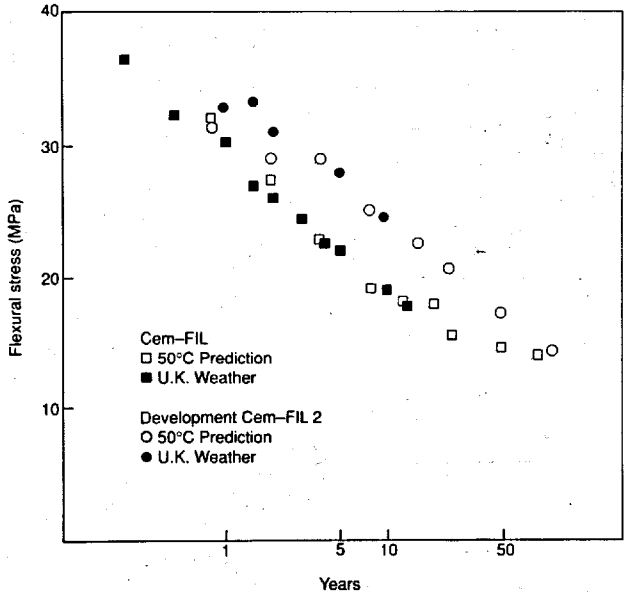

Figure 5. Comparison between weathering results and predictions from accelerated ageing of grc (Reference 98)

Although some reduction in grc properties with age can be tolerated, if allowed for in design, in many grc applications it would be desirable if there is no decrease in properties. Research has been carried out in the past few years to achieve this end. The strategies employed are based on the use of 1) highly efficient pozzolanas together with a suitable polymer dispersion and 2) special cements with or without mineral admixtures. Considerable work has been done with silica fume as the mineral admixture in Portland cement to be used in grc (14,22) and more recently metakaolin has come into prominence (99). Special cements that have been developed for grc contain sulphoaluminates as a main constituent. The Chichibu cement (4)contains a proportion of granulated slag also whereas the recently announced product from Blue Circle in the UK (6) metakaolin is the preferred admixture. The new cements produce little or no $Ca(OH)_2$ and the pH of the pore solution is probably below 11 at all times (5). Composites made from these cements show less shrinkage on drying.

Hyashi et al (100) have described the properties of grc made from Chichibu cement and AR glass fibres. Almost no reduction in the bending strength of the composite was seen up to 56 days under water at 70°C. The corresponding failure strain value also

remained at their start level (~ 0.8%) after the exposure. Another interesting observation was that even when the moderately alkaline sulphoaluminate cement was used with E-glass fibres, the composites were degraded fairly rapidly at elevated temperature.

Figure 6 compares the flexural properties of grc made from 'calcrete', the new sulphoaluminate cement from UK (6) with those of grc from Portland cement, both using AR glass fibres. The accelerated test results for the new cement composites are encouraging. Similar promising results have been seen with sulphoaluminate cement made in China (5).

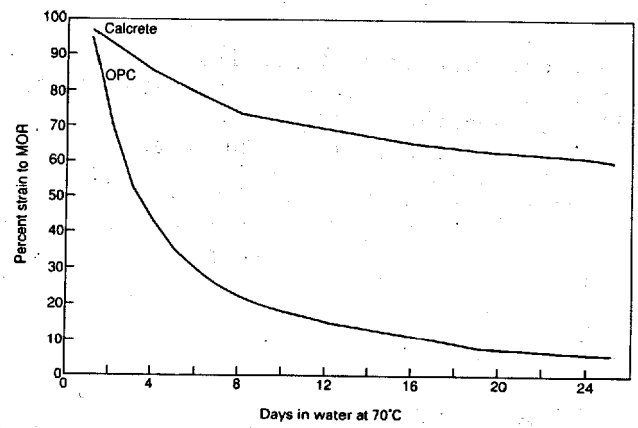

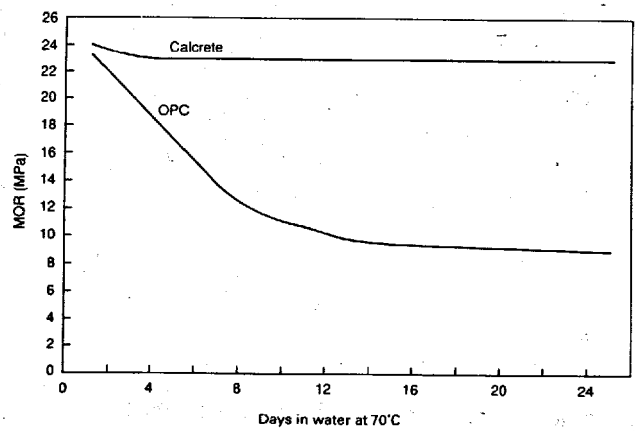

Figure 6. Flexural properties of sprayed up grc made from calcrete (Reference 6)

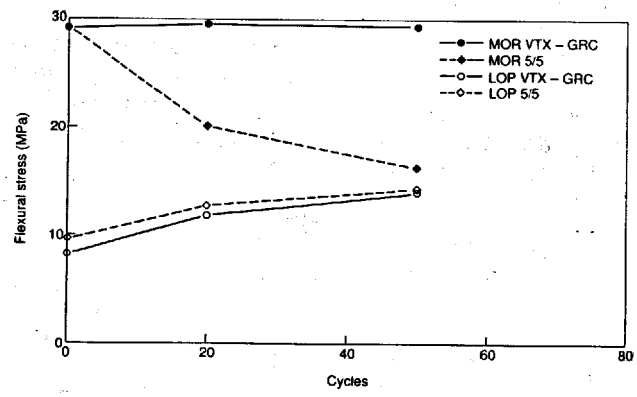

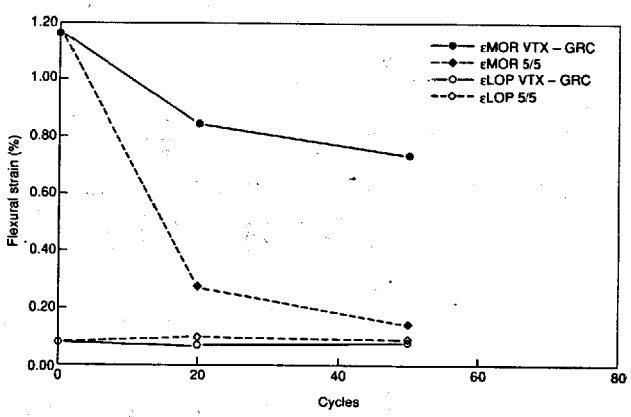

Figure 7. Flexural properties of VTX-grc after cyclic wet and dry tests (Reference 99)

As the hot water test does not show any reduction in flexural strength of grc made from some of these new cementitious mixes, the long term strength of the composite cannot be predicted using the relationships developed by Proctor et al (97). New tests are being developed for this purpose. Bijen (95) and Thiery et al (99) have used a cyclic wet and dry test and the latter authors have employed a cyclic freeze thaw test also to assess their grc products made from AR glass fibres and modified Portland cement. The results from the cyclic wet-dry tests on grc specimens prepared by Thiery et al using a matrix of PC plus metakaolin and polymer are shown in Figure 7. The results are compared with those of grc from the so called 5/5 mix (5 wt% of AR fibre plus 5 vol% of acrylic polymer in Portland cement). Toughness values for the new VTX composite after the test were also encouraging as well as the results from the cyclic freeze-thaw tests. Further results on the durability of the VTX-grc have recently been published by Soukatchoff and Ridd (101). In particular, the authors stress that the strain capacity of the new composite remains at a very high level after accelerated ageing tests in hot water kept at 30°, 50° and 60°C, after cyclic wet-dry and

freeze-thaw tests and after extended carbonation. The value of the failure strains in bending were of the order of 0.8% after 72 days in water at 60°C and greater than 0.6% after 2 years at 30°C. The authors estimate that the results at 30°C corresponds to 40 years' weathering. Accelerated carbonation produced an increase in the bending strength.

Thiery et al (99) have pointed out that the addition of metakaolin does not seem to be effective when E-glass fibres are used as reinforcement for grc. The Glass Reinforced Cement Association (GRCA) have recently summarised (102) the current views about the long-term durability of various types of grc including the new formulations discussed above.

5.B.2.1.1 Durability and Glass/Cement Interaction - Until recently the hot water test (97,103) was used exclusively in the assessment of grc durability. From the published results of these tests and long-term natural weathering data (22) it can be concluded that grc made from first generation AR glass fibres and Portland cement on its own or modified by mineral admixtures such as pfa and ggbs or polymer dispersions such as acrylics will show a reduction in some mechanical properties in the long-term when used in wet conditions. GRC made from high-alumina and supersulphated cements may perform better in some situations. Composites made from E-glass fibre will follow a similar trend, but probably at a much enhanced rate. The use of the second generation AR fibre (e.g. Cem FIL 2) produces more durable cement composites but some loss in strength is still expected in the longer term. The use of this fibre in high-alumina cement has given encouraging results.

The newer grc's made from formulations based on mixtures of sulphoaluminate cement and mineral admixtures or Portland cements modified by metakaolin and polymers have given very promising results in accelerated ageing tests. However, the natural weathering results on these composites over long periods of time are not available yet. Until these and results from field trials in different parts of the world are available one cannot be completely certain about the long-term durability of grc.

Given that grc, even those made from AR glass fibres has a durability problem, a special conference to address this issue was arranged by the Prestressed Concrete Institute of the USA in 1985, and the proceedings (See ref 98) of this conference reflect the divergent views that exist today on the subject of glass/cement interactions in grc.

Broadly speaking, two main mechanisms have been identified for the reduction of grc properties with time, especially in wet environments: 1) a progressive reduction in the strength of the reinforcement caused by hydroxyl ion attack on the glass and 2) precipitation inside the fibre strand of cement hydration products, mainly $Ca(OH)_2$ crystals, which transforms the flexible reinforcement into a monolithic, rigid one via strong interfilament bonding. A detailed analysis of these hypotheses is given in Bentur and Mindess (14) and Majumdar and Laws (22), and only a few comments are given below. The promising results obtained recently with the new cementive mixtures can be explained by both models.

It is acknowledged by most of the investigators that chemical interactions between the highly alkaline cement pore solution and AR-glass fibres at high temperatures will reduce the strength of the fibre. Whether the same can be said about reactions at room temperature remains controversial. A reduction in the strength of the glass fibre reinforcement, together with an increase in the matrix cracking strength with time brought about by progressive hydration of cement in wet environment, will have the effect of increasing the critical fibre content, $V_{f,crit}$ required for multiple fracture in grc. Hannant et al (63) have calculated that for aligned grc containing AR glass fibres, $V_{f,crit}$ may be 1% at 28 days and 2% after 10 years in natural weathering. The corresponding values for spray-dewatered grc having short fibres are 3.5% at 28 days and more than 7.4% after 10 years.

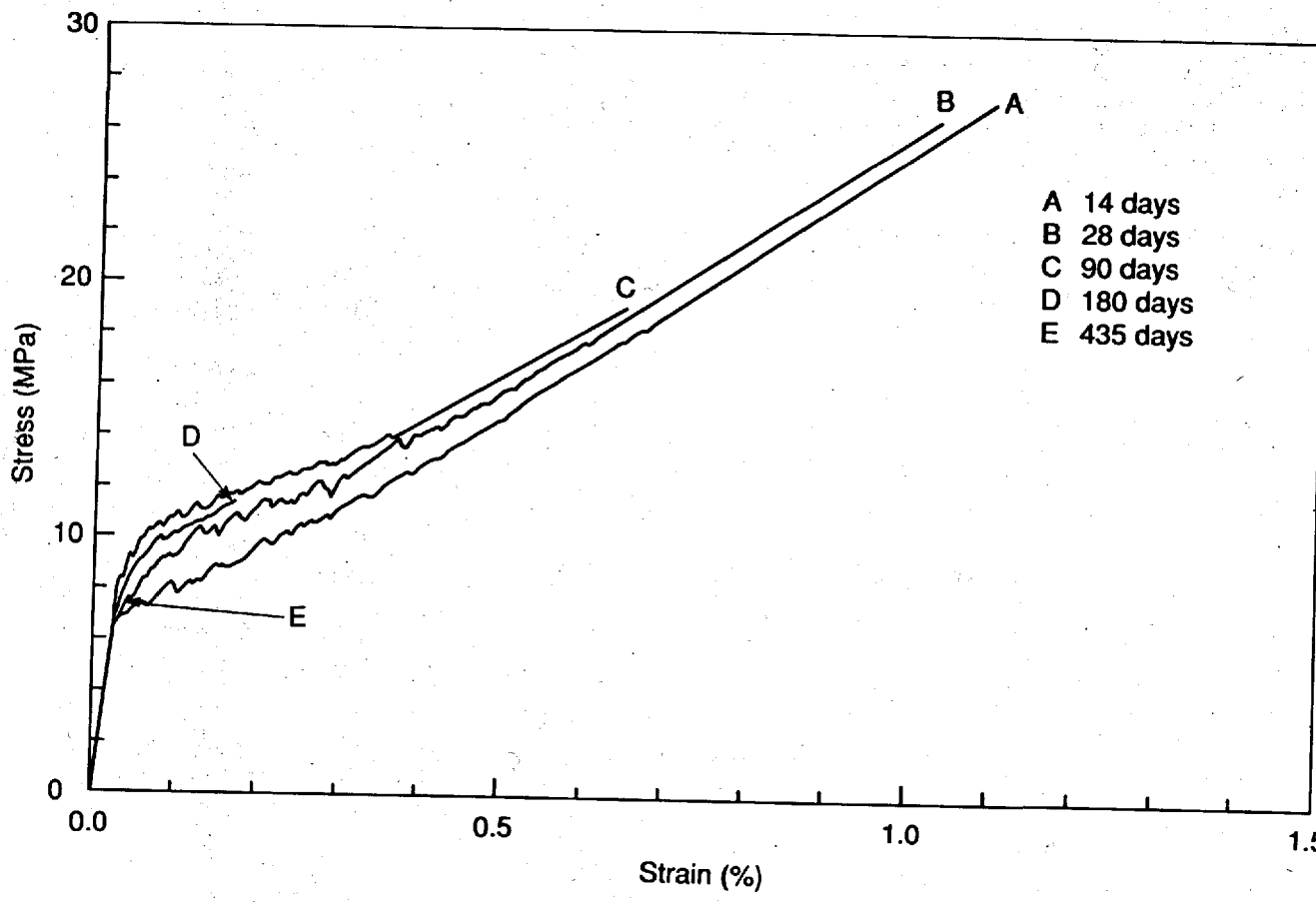

Figure 8. Tensile stress-strain diagram of aligned grc, stored in water at 19°C

Recently Walton (104) has measured the tensile strength of continuous aligned grc composites containing ~ 3 vol% first generation CemFIL AR glass fibres kept under water at 19°C over a period of several months. His tensile stress-strain diagrams at various ages including some new results are given in Figure 8. After 435 days very little if any multiple fracture was seen, the composite failing at a stress of 7.3 MPa. The starting strand strength was 1064 MPa, much lower than that of a freshly manufactured strand. Assuming that the ACK model is applicable to grc, the tensile stress-strain diagrams in Figure 8 can only be explained by assuming significant reductions in fibre stress and strain with time. The branching of matrix cracks as observed by Bentur and Diamond (105) were not seen in great abundance and although this would have put an extra flexural strain on those fibres that are intersected at an angle, its magnitude probably would not be very large. Any increase in the fibre matrix bond will probably reduce this strain due to reduction in the crack width. In practical grc composites where short fibres are distributed in the matrix in random 2 or 3 dimensions, a significant proportion of the fibres will meet the advancing cracks at an angle and the flexural strain imposed on them may be substantial and if they can not bend freely rupture may follow (106).

Another mechanism, rather different from those described above, has been advocated by Yilmaz et al very recently (107) for the degradation processes in grc. These authors suggest that continuous chemical corrosion of AR fibres in the cement matrix produces a hollow fibre in the limit and crystallisation of $Ca(OH)_2$ crystals adjacent to the fibre leads to accelerated local attack at the point of contact. The latter process termed 'notching' effectively reduces the mean length of the fibres. An 'onion-skin' effect has been seen when uncoated AR glass filaments were subjected to hot NaOH solutions (22) and penetration of the glass fibre surface by $Ca(OH)_2$ crystals

has also been seen occasionally but so far these processes have not been thought to be the main failure mechanisms in grc composites under ambient conditions. Fibre surfaces from weathered and wet-stored grc composites of different descriptions have been examined by various authors and although gross surface damage has been reported (14), to the best of the writer's knowledge 'hollow fibres' of the kind described by Yilmaz et al have not been identified as a key feature of aged grc microstructure.

The work of Yilmaz et al records the extent of chemical interaction that takes place between the cement matrix and the AR fibre, particularly at 55°C, over periods of time up to one year. There is evidence of much inter-diffusion of ions. Whether these chemical processes create flaws on the fibre surface at 20°C and thus effect a reduction in fibre strength is not clear. Obviously, further work in this area will be necessary to confirm these observations and assess their relevance in the use of grc.

5.B.2.2 Glass Fibre Reinforced Gypsum (grg) - In many countries boards made from gypsum plaster contain a proportion of glass fibre to provide reinforcement and integrity in fire. A relatively new product in the UK (47) uses glass fibre 'tissue' as surface reinforcement. Grg has been used in many one-off applications in the UK but an industry to exploit the properties of this material has not developed. The essential features of the glass reinforced gypsum are well known (108).

5.B.3 From Ceramic Fibres

5.B.3.1 Carbon Fibre Reinforced Cement - Because of the extremely good mechanical properties and chemical inertness of carbon fibres, a considerable amount of work has been done on cement composites reinforced by carbon fibres, beginning in the early seventies. The interest has been sustained with the introduction of commercial products in Japan. It has been recognised that as the high strength, high modulus fibres (Table 3) still remain very expensive for the construction industry, maximum utilisation of their reinforcing potential is desirable and this is leading to applications where continuous aligned or mat reinforcement is feasible (46).

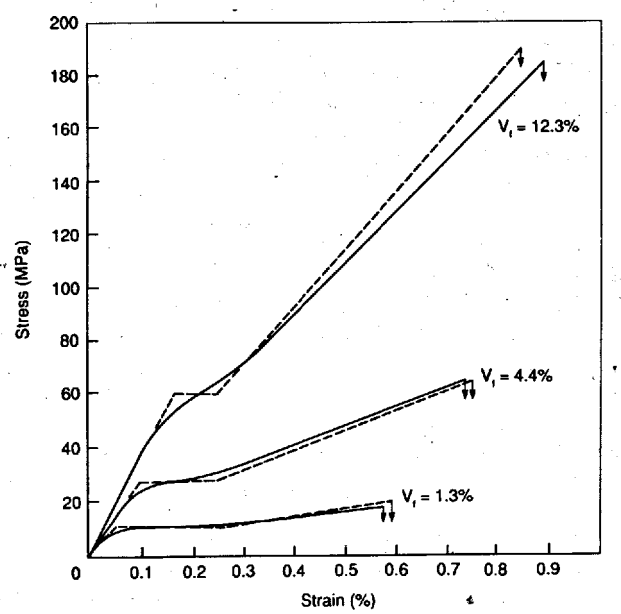

Figure 9. Tensile stress-strain diagrams for continuous carbon-fibre reinforced cement. Full lines are the experimental curves, broken lines are the curves predicted by the ACK theory (Reference 49)

Early work on the properties carbon fibre reinforced cement has been reviewed recently by Bentur and Mindess (14). Tensile stress-strain curves of continuous,

aligned composites due to Aveston et al (49) are shown in Figure 9 as they seemingly validate the ACK model so precisely. High strength fibres can be formed into a tape using polyvinyl acetate (109) to produce aligned composites. More recent work has concentrated on the use of less expensive fibres made from pitch. Composites made from pitch fibres employ short fibres, and are usually produced by premixing and casting techniques. Uniform dispersion of the reinforcement as individual filaments is difficult in these cases but by using fibres, 3-10 mm in length, reasonable success has been claimed for fibre volumes up to 5% (14). Nishioka et al (110) have studied the reinforcing capability of pitch based carbon fibres with tensile strength in the range 440-764 MPa and Young's modulus in the range 26.6-32.4 GPa. They have concluded that for composites made by premix and casting, the tensile strength of the fibre should be in excess of 640 MPa. At 3 vol% fibre addition, MOR values up to ~ 26 MPa were obtained with the stronger fibres. They also point out that during the production process a significant proportion of the short carbon filaments are mechanically degraded and may break, and that such considerations affect the composite fracture mechanisms. Both pull out and fracture of fibres have been seen in failed carbon fibre reinforced cement composites. Soroushian et al (78) have studied the properties of polymer modified carbon fibre reinforced cement mortars.

Akihama et al (111) have compared the properties of cement composites made from pitch-based carbon fibres with those reinforced by high-strength fibres made from acrylics. Using premixed and cast composites having V_f up to 5.5% they found that the strength of the composites having the high strength fibre was always higher but the difference was less than expected from the differences in fibre strength. One interesting aspect of their work was the use of an autoclave treatment (180°C, 5 hours), which produced composites which were slightly stronger than the air-cured material. Polymer impregnation of the autoclaved material produced composites with substantially higher strength. By measuring the pull-out lengths from a large number of broken tensile specimens the authors were able to calculate the 'efficiency factors' and thus compare their results with theoretical predictions.

Pitch fibres stronger than those mentioned above have been produced in Japan recently employing coal-tar as the starting material. Short lengths of these fibres, ~ 17 μm in diameter and having tensile strength of ~ 1600 MPa and Young's modulus of ~ 180 GPa can be incorporated in the cementitious matrix using ordinary concrete mixers. At 2 vol% addition, a flexural strength of the order of 14 MPa was found experimentally for the composite, and it has been claimed that this is nearly double that of composites made from the low-strength pitch fibre (46).

Information on the extent to which short carbon fibres improve the impact resistance of the brittle cement matrix is rather scarce. Akihama et al (111) reported a value of the order of 2000 microstrain as the tensile failure strain for an autoclaved composite containing 5.3% pitch fibre and this value was substantially reduced after polymer impregnation. Banthia and Sheng (112) have recently published load-deflection traces of cement composites containing various proportions of 6 mm long carbon fibre made from pitch. Only for the composite containing greater than 3 vol% fibre was the area under the load-deflection curve conspicuously large indicating good toughness. A reduction in toughness has been observed in carbon fibre composites made with low w/c ratios or when pressing has been applied. It has been suggested that densification of the matrix in these cases might have produced an increase in the bond strength leading to fibre fracture rather than pull-out. Bond strength values in the range 0.8 to 2.5 MPa have been reported by various investigators, and calculated critical fibre length for pitch based carbon fibre of diameter 10-20 μm has been estimated to lie in the range 0.6-2 mm (14).

One of the most attractive features of carbon fibre reinforced cement is their excellent durability in various environments. Short fibre composites (28,46) made by using the new fibre produced from coal tar have shown no reduction in bending strength after ageing in hot water (85°C), exposure to accelerated conditions in a weatherometer, and to salt water sprays. Similar promising results have been reported

after 300 cycles of freeze thaw. The drying shrinkage of autoclaved composites is greatly reduced, the extent of reduction increasing with the amount of fibre used. Carbon fibres are reactive towards acids such as sulphuric and nitric but in the cement composites they seem to retain their strengthening power when placed in acid environments (112), at least in the short term.

5.B.4 From Synthetic Organic Polymer Fibres - Among the synthetic organic polymer fibres two are occupying important positions at the present time in commercially produced asbestos cement replacement materials. These are polyvinyl alcohol (PVAl) and polypropylene (PP). High modulus acrylic fibres have also been used as primary reinforcement in some of these products.

5.B.4.1 Polypropylene reinforced cement - Both single filaments that are mechanically split from extruded tape and fibrillated networks of PP film either as continuous or short mat forms are now used as replacement for asbestos in reinforced thin sheets.

With these reinforcements flexural strength of the order of 30 MPa can be easily obtained at high fibre volume fractions, say 10%. The toughness of the PP composite has been compared by Hibbert and Hannant (86) with other FRC thin sheet materials and has been found to be excellent. The high energy absorption in PP composites is, however, obtained at large deflections and this may not be acceptable in some applications. PP reinforced cements have also low first crack stress and strain and are not particularly resistant to fire. The latter problem has been addressed to a certain extent by the application of anti-oxidant coatings on the fibre. For improving the first crack properties incorporation of a relatively small amount of glass yarn has been found to be helpful. Such a composite ('Retiver') having flexural strengths of the order of 45-50 MPa has been introduced to the market recently. Xu and Hannant (92) have studied the mechanical properties of this type of composite.

The tensile stress-strain of an unaxial FRC composite made from high-tenacity PP split fibre roving is shown in Figure 10 from Krenchel and Shah (113). Acoustic emission studies indicated high activity in the section A-B-C but practically none in C-D. The fibre content was 10% by volume.

Figure 11, due to Hannant and Zonsvald (42), shows the tensile stress-strain and bending load deflection curves of a FRC composite reinforced by 5.7 vol% of fibrillated PP mat. Vittone (114) has published strength data on the Netcem material containing various proportions of fibre. As fibrillated PP mats have strong fibres aligned in one direction only, in commercial Netcem products care should be taken to place a number of mats in a perpendicular direction also to reduce anisotropy.

Reported bond strength values for PP fibre reinforcements in cement range from 0.12-3.45 MPa (14). It is claimed (113) that by special treatments of the fibre surface, even higher bond strengths can be achieved. Hannant (81) has recently reported that the bond strength between cement and polypropylene as calculated from crack spacing of 'Netcem' composites is of the order of 0.4 MPa and this value apparently did not change up to 10 years when the composite was kept in different environments.

5.B.4.1.1 Durability - The ten-year results reported by Hannant (81) show that in weathered specimens the fibre strength remained almost unaffected over this period (Fig 12). The composite stress-strain curves were significantly different in different environments, those kept under water at 20°C over the entire period showing the smoothest curves. For this storage condition, surprisingly there was no change in the cracking stress of the matrix and the 10-year stress-strain curve was very similar to that seen after one month. The excellent toughness of the material was retained up to 10 years.

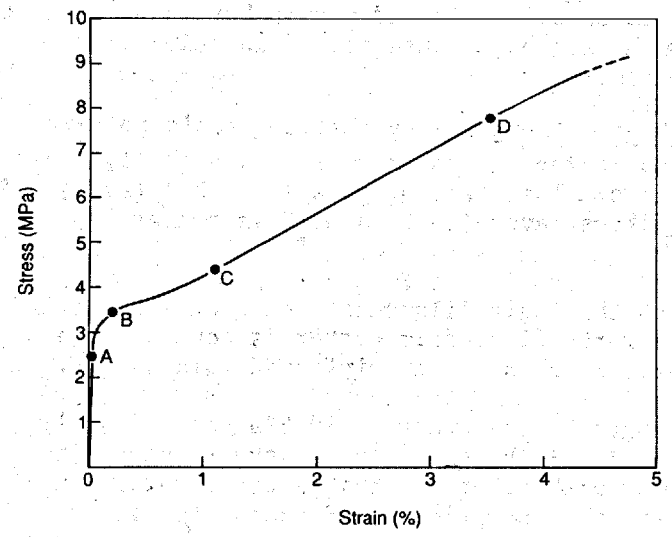

Figure 10. Stress-strain curve from uniaxial tension test on pp-roving-reinforced cement (longitudinal fibre orientation, V_f = 10%, w/c = 0.36) (Reference 113)

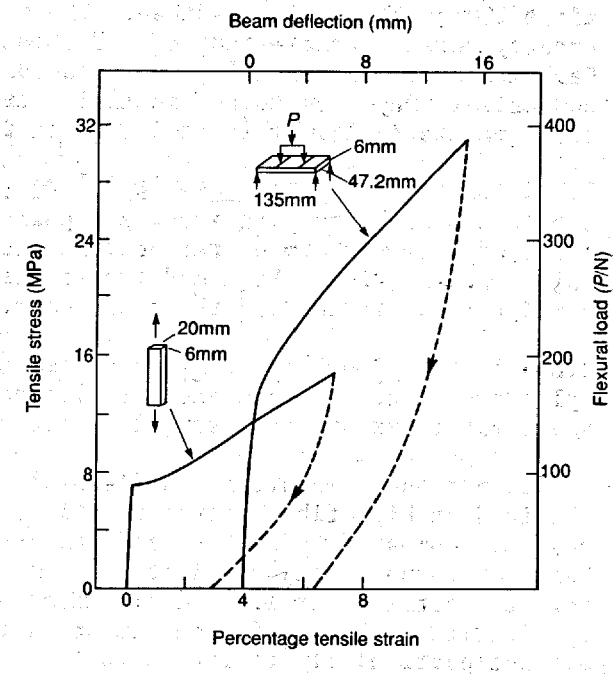

Figure 11. Tensile stress-strain curve and load-deflection curve in flexure for a composite containing 5.7% by volume of fibrillated film networks parallel to direction of stress (Reference 42)

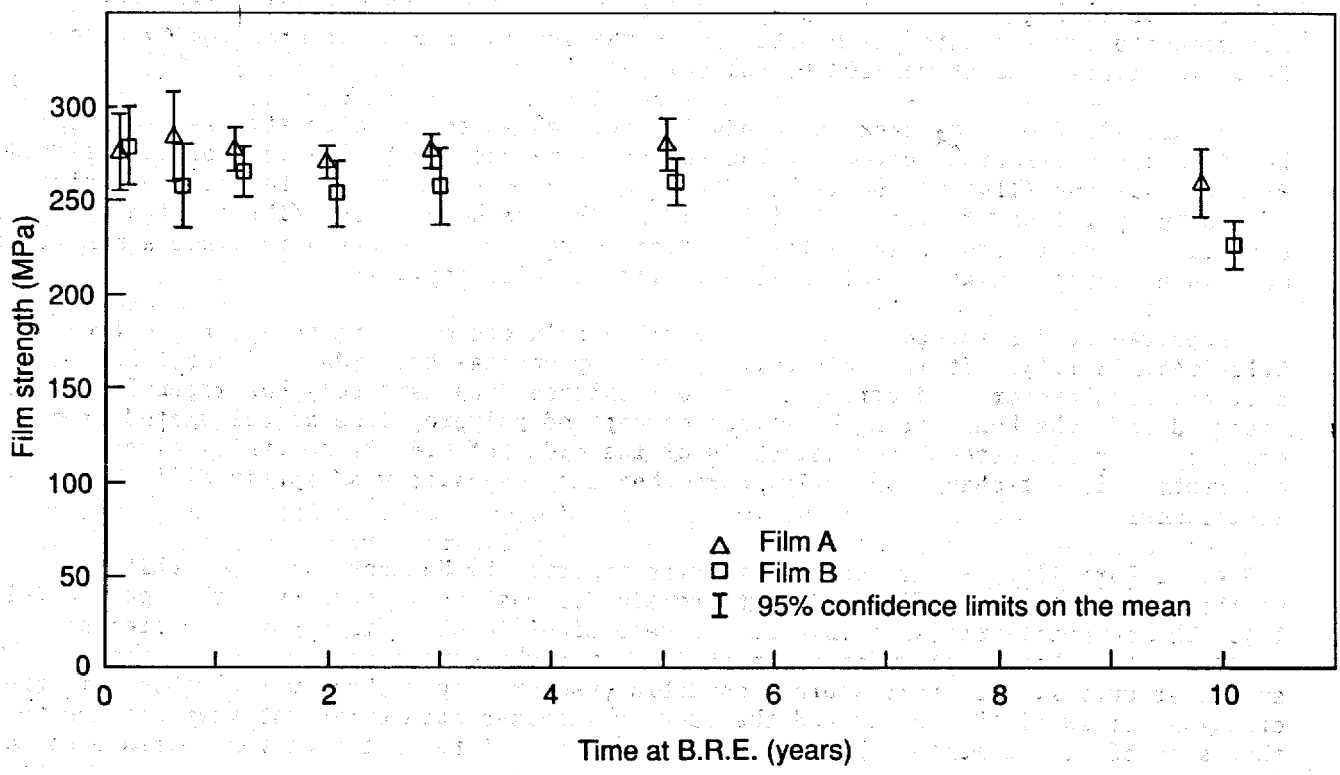

Figure 12. The effect of natural weathering for up to 10 years on the film strength (Reference 81)

The above result would suggest that under ambient conditions PP reinforced cement is expected to perform satisfactorily over a long period of time in agreement with earlier predictions from accelerated tests (90). Krenchel and Shah (113) reported a decrease of ~ 30% in the strength of their high-tenacity PP fibre after four years at 90°C. Fibre strength loss at high temperature has also been reported by Mai et al (115). In the presence of air Gardiner et al (116) observed significant reductions in strength when PP fibres and their composites were kept at high temperatures, up to 140°C over longish periods of time, presumably due to oxidation of the fibre. From the results they predicted a service life of at least 25 years for the FRC material. The effect of UV radiation on the fibre is not thought to be significant in composites where the fibres are protected by cement (42).

5.B.4.2 Polyvinyl alcohol fibre reinforced cement - Information on the properties of FRC materials containing PVAl fibres is still very limited. Hikasa and Genba (117) have claimed that cement composites containing only 3% PVAl fibre together with an amount of wood pulp and manufactured by the Hatschek process can develop nearly 50 MPa flexural strength, higher than that of conventional AC product. The modulus of the PVAl composite is somewhat lower, however. Akers et al (118) have reported a much lower flexural strength, in the range 17-23 MPa, for a series of composites containing PVAl fibres.

The long-term properties of commercial PVAl reinforced cement in the form of corrugated and flat sheets and roofing slates are being studied at BRE (119). A selection of our findings are given in Table 5. Obviously, the initial strength of the material is selected to meet the requirements of the standards for the different types of products but it is worth noting that the new FRC materials are much weaker in bending than the corresponding AC products; for instance, a batch of asbestos cement slates gave MOR values of 45.5 and 26.8 MPa respectively for the longitudinal and transverse samples. Like AC products the new composites gave higher strength values when dry than wet.

Table 5 Properties of PVAl Fibre Reinforced Cement

Curing conditions	Test conditions	Property	Slates L	Slates T	Corrugated sheets
Stored to constant weight at 20°C and 65% rh	dry (65% rh)	MOR (MPa)	27.1	17.4	21.2
		LOP (MPa)	21.4	16.4	9.6
		UTS (MPa)	11.5	9.2	8.1
		Failure strain (%)	0.05	0.04	0.12
		E (GPa)	26.2	24.5	13.9
7 days in water at 20°C	wet	MOR (MPa)	20.7	12.8	21.8
		LOP (MPa)	12.4	11.5	10.5
		UTS (MPa)	7.7	5.8	7.5
		Failure strain (%)	0.23	0.03	-
		E (GPa)	22.4	21.9	15.8
5 years in natural weather at Garston, England	dry (65% rh)	MOR (MPa)	25.3	22.2	23.5
		LOP (MPa)	25.3	22.2	22.0
		UTS (MPa)	10.6	7.6	9.3
		Failure strain (%)	0.03	0.03	0.07
		E (GPa)	32.3	30.3	20.1
"	wet	MOR (MPa)	21.4	-	20.5
		LOP (MPa)	21.3	-	15.0
Accelerated ageing in water at 50°C	wet	MOR (MPa)	21.2	16.4	20.1
		LOP (MPa)	14.2	15.6	11.3
		UTS (MPa)	9.7	6.3	7.3
		Failure strain (%)	0.04	0.03	0.10
		E (GPa)	26.0	25.3	21.0
			(after 180 days)		(after 365 days)

L = longitudinal, T - transverse

5.B.4.2.1 Durability - Akers et al (118) have reported on the properties of several PVAl composites after a few years of natural weathering in Switzerland. They observed that in all cases the flexural strength of the composite increased with age. Hikasa and Genba (117) reported a reduction in toughness of nearly 50% after only one year's weathering. From Table 5 it can be seen that curing in hot water at 50°C over long periods has not produced any reduction in strength of the PVAl-reinforced product but at 80°C significant reductions have been seen after five years (119). Akers et al (118) have also observed reductions in the strength of PVAl fibres, and cement composites made from them, if they are exposed to alkalis and heated under cyclic wet and dry conditions. X-ray diffraction studies of PVAl fibres extracted from aged composites indicated some differences in structure from the unaged material. Microstructural studies (120) indicate that whereas in young composites failure is caused by the pull-out of fibres, with age the mechanism changes predominantly to one of fibre fracture.

5.B.4.3 Acrylic Fibre reinforced cement - High strength acrylic fibres with Young's modulus in the range 14-25 GPa have been developed for cement reinforcement (14). Some commercial AC replacement products sold in Europe a few years ago definitely contained a proportion of the acrylic fibre as primary reinforcement but whether this practice is continuing at the present time is not certain. Acrylic fibres are reported to form good bonds with cement, values up to 4 MPa have been recorded (121). Flexural strength values of ~ 25 MPa can be achieved in composites made by the Hatschek process with fibre addition of ~ 2% plus the processing fibre (122), and in laboratory experiments (123) it has been shown that an increase in the acrylic fibre content can lead to a significant improvement in the toughness of the composite.

Data on the long term properties of cement composites containing acrylic fibres are rather scarce. From the results on the fibre alone (14) it would appear that a combination of high-alkalinity and temperature rise may reduce the strength of the fibre, and hence that of the composite.

5.B.4.4 Aramid fibre reinforced cement - Aramid fibres such as 'kevlar' reinforce the cement matrix efficiently and as the decomposition points of these polymers (~ 400°C) are appreciably higher than the melting points of PP or PVAl, cement composites made from the aramid fibres have obvious advantages at high temperatures. However, the fibres still remain expensive and not many thin sheet applications other than in structural repairs are known to the author.

The mechanical properties of cement composites containing aramid fibres were investigated by Walton and Majumdar (124) many years ago and by Ohgishi et al (125) and Akihama et al (126) among others more recently. The durability of the aramid in the cement matrix has been reported to be very good although some doubts still exist as to the very long term alkali resistance (14). The composites can be autoclaved. Using several mineral admixtures such as microsilica in their matrix Akihama et al found that best results were obtained when the autoclaving was done at 140°C. Such a treatment reduced the drying shrinkage of the composite very substantially when compared to the air-cured material.

Wang et al (127) found that the bond between aramid fibre and cement can be reasonably strong ~ 2.75 MPa or even higher, 4.5 MPa, for some fibres. As the fibres are manufactured in the form of bundles, uniform distribution of the reinforcing filament in the matrix is not easy and further work in this area is warranted. Because of the high strength of the fibre/matrix bond individual fibre pull out is not significant in the failure of aramid FRC. Bundle splitting, bundle shearing and fibre fracture are the more important mechanisms.

5.B.5 From Natural Plant Fibre - In the past two decades considerable efforts have been made in assessing the potential of natural vegetable plant fibres as reinforcements for cement and concrete. International conferences have been held under the auspices of organisations such as RILEM (128), and at least one edited text on the

subject is also now available (129). A critical appraisal of developments in this field can be found in Bentur and Mindess (14).

5.B.5.1 Unprocessed Plant Fibre Reinforced Cement - With most unprocessed fibres, improvements in the strength properties of the matrix that can be achieved with practical fibre volumes are modest. Hussin and Zakaria (130) have studied the properties of flat and corrugated sheets containing up to 6% of coconut fibres, 37-250 mm in length. Using w/c of 0.35 and vibration casting they recorded an MOR value of over 6 MPa at 28 days for flat sheets having 3 and 4 vol % fibre; corrugated sheets which were pressed gave nearly twice this value at 4% fibre addition. Paramasivan et al (131) have reported much higher values for their corrugated sheets made from coconut fibres. Using 25 mm long fibres and applying a pressure of 152 kN/m^2 they obtained an MOR value of 22 MPa for the composite containing 3% fibre. Using special manufacturing techniques Majumdar and Walton (104) obtained bending strength values of the order of 16 MPa for 3.9% sisal reinforced cement sheet where the fibres lay in a two-dimensional random orientation. Mansur and Aziz (132) have studied the effect of fibre length and content on the mechanical properties of cements reinforced with jute fibres.

The introduction of natural plant fibres in the cement matrix can increase the impact toughness of the material considerably, depending on the length of fibre used and its amount in the composite. This is one of the main benefits of adding fibres, and areas under load deflection diagrams of these composites are nearly always several times larger than that of the control. Using Izod pendulum methods Majumdar and Walton (104) report an impact strength of 18.3 kJ/m^2 for composites containing 3.9% of sisal fibre which compares well with impact strengths of other fibre cement composites discussed in this review.

Interest in sisal fibre reinforced gypsum continues (133).

5.B.5.1.1 Durability - The long-term durability of cement composites reinforced by unprocessed natural plant fibres remains questionable. Natural weathering over a short time has been found to produce a loss in strength and toughness in sisal FRC (34). The absorption of large amounts of water by most of the natural fibres produces swelling in the composite and they degrade in the wet-dry cycles although this is not always reflected in a reduction of strength or toughness. Chemical degradation of the fibre in the alkaline cement environment through dissolution of the alkali soluble components in the fibre and depolymerisation of others is a more potent mechanism. Lewis and Mirihaglia (35) have measured the effect of alkali attack on the strength of various natural fibres, and Gram (34) has discussed the underlying mechanisms in great detail with respect to sisal fibres but his observations are probably valid for most of the unprocessed fibres. The degradation of the fibre, whatever the cause, and the volume changes attendant on wetting and drying affect the interfacial properties of the composite and lead to reduced strength and toughness. When the reinforcement is in the form of bundles, precipitation of cement hydrates inside the bundle might affect the toughness of the composite adversely as discussed in a previous section.

Attempts have been made to improve the performance of vegetable fibres in cements by applying coatings of suitable water-repellent substances such as formic and stearic acid (34) but the improvements have not been very marked. Canovas et al (134) have experimented with sisal fibre reinforcement impregnated with various substances including natural resin. There is some evidence that if blended cements are used, particularly the ones containing large amounts of microsilica, the retention of strength in sisal FRC over the long term is improved. Again the rate of precipitation of $Ca(OH)_2$ inside the reinforcement is an important consideration here.

5.B.5.2 Processed Plant Fibre Reinforced Cement - Refined cellulose derived from wood by a pulping process, described by some (135) as wood fibre, has been found to be the most cost-effective replacement of asbestos in products such as corrugated sheets for roofing and cladding and general purpose building board. For a considerable time it

has been used as a partial asbestos substitute in AC products made by the Hatschek process which can handle cellulose pulp with relative ease. Nearly all but the most recent work has been reviewed by Bentur and Mindess (14).

The cellulose reinforced FRC products are based either on Portland cement or a calcium silicate matrix produced when PC plus silica or lime plus silica mixtures (containing the cellulose pulp) are autoclaved at temperatures around 180°C. For air-cured composites Coutts and Warden (136) reported a flexural strength of the order of 30 MPa at 8 wt % fibre addition and it is now recognised that a flexural strength in excess of 20 MPa can be easily achieved by adding say 10% by mass of refined cellulose to a cementitious matrix. Compared to asbestos cement the cellulose reinforced product shows a higher strain capacity (137).

The effect of differences in the manufacturing methods used in the production of cellulose pulp and its subsequent refining on the properties of the composites has been studied in some detail by Coutts and his colleagues (37,138). In general, pulps produced by the chemical process (Kraft) seem to provide the most efficient strength reinforcement but sometimes at the expense of impact toughness. Further refining by mechanical means accentuates this difference. Attempts have been made to relate these observations to the physical and chemical nature of the refined fibre, its length and geometry and to the strength of the bond it forms with the matrix. SEM photos of the fracture surfaces of composites tend to show that when high tensile or flexural strength is achieved fibre fracture is the predominant failure mechanism whereas good impact toughness is associated with fibre pull-out. Mai et al (139) have demonstrated that if Kraft pulp is bleached, the autoclaved FRC material shows an improvement in flexural strength and modulus of elasticity compared to the composites containing the unbleached reinforcement, but again the impact toughness is impaired due to bleaching of the fibre. The use of 'coupling agents' to improve bonding, on the other hand, has not been particularly effective in increasing the tensile or bending strength (140).

The effect of matrix composition, ie Portland cement or autoclaved calcium silicates, on the properties of the cellulose FRC materials has been studied by Coutts and his colleagues (136,141) and by Akers and Studinka (142). Vinson and Daniel (143) have studied the properties of cement composites reinforced with cellulose derived from high-density summerwood. A fibrillated version of the same fibre was found to be very efficient as a processing fibre.

Even refined cellulose or wood fibres absorb a large quantity of moisture and this factor affects the strength properties of composites in a significant way. An increase in the moisture content produces a decrease in the elastic modulus and flexural strength of the composite but an increase in impact toughness. These changes are greater in magnitude than similar effects in asbestos cement and microstructural studies tend to support the hypothesis that failure of cellulose FRC materials under wet conditions is mainly due to fibre pull-out indicating a weaker interfacial bond than in the dry state. Soroushian and Marikusite (135) have made a statistical analysis of the various factors involved in producing moisture effects on cellulose pulp FRC properties.

Commercial FRC sheetings produced by the Hatschek process show considerable anisotropy in properties and cellulose pulp reinforced materials are no exception. Some idea of the extent of this anisotropy can be obtained from the results given in Table 6.

Coutts (144) has recently reported on the properties of gypsum plaster products reinforced by waste paper fibres. Sheets prepared by the slurry/dewatering technique gave bending strengths of ~ 17 MPa at fibre addition of 10% by mass.

5.B.5.2.1 Durability - The effects of natural and accelerated weathering on the changes in the mechanical properties of cellulose-pulp FRC composites have been studied by Akers and Studinka (142) and their results on the naturally cured material are shown in

Table 6 Properties of Cellulose Reinforced Autoclaved Calcium Silicate

Curing conditions	Test conditions	Property	Flat sheets L	Flat sheets T	Corrugated sheets
Stored to constant weight at 20°C and 65% rh	dry (65% rh)	MOR (MPa)	34.9	19.1	30.9
		LOP (MPa)	29.4	19.0	21.2
		UTS (MPa)	23.9	14.8	19.0
		Failure strain (%)	0.14	0.09	0.14
		E (GPa)	21.5	18.4	14.4
7 days in water at 20°C	wet	MOR (MPa)	26.2	13.3	23.3
		LOP (MPa>)	18.9	12.6	12.3
		UTS (MPa)	-	-	10.7
		Failure strain (%)	-	-	0.12
		E (GPa)	-	-	13
5 years in natural weather at Garston, England	dry (65% rh)	MOR (MPa)	37.2	23.8	29.3
		LOP (MPa)	29.9	23.8	28.7
		UTS (MPa)	21.5	15.2	20.0
		Failure strain (%)	0.12	0.09	0.10
		E (GPa)	21.3	18.0	16.2
	wet	MOR (MPa)	26.5	15.1	24.7
		LOP (MPa)	17.7	13.4	19.0
		UTS (MPa)	13.7	6.7	11.3
		Failure strain (%)	0.10	0.05	0.09
		E (GPa)	19.2	15.3	12.9
Accelerated ageing in water at 50°C for 1 year	wet	MOR (MPa)			27.0
		LOP (MPa)			18.2
		UTS (MPa)			11.3
		Failure strain (%)			0.12
		E (GPa)			14.9

L - longitudinal, T - transverse

Table 7. A selection of results from the current study at BRE on the autoclaved material is shown in Table 6.

Table 7 Properties of the naturally cured cellulose fibre cement products exposed to various ageing tests (Reference 142)

Type of ageing	Flexural strength N/mm^2	E-modulus kN/mm^2	Tensile strength N/mm^2	Strain at failure %	CO_2 content %	DP (fibre)	Density kg/m^3
Non-aged	16.4 ±0.9	10.9 ±1.3	7.0 ±0.2	2.80 ±0.70	1.65 ±0.12	581 ±60	1770 ±20
Accelerated aged 3 months ambient environment	12.3 ±1.1	14.8 ±1.2	2.6 ±0.9	0.04 ±0.01	4.85 ±0.16	430 ±50	1780 ±10
Accelerated aged 3 months CO_2 rich environment	23.9 ±2.2	18.9 ±1.4	7.2 ±1.3	0.05 ±0.01	6.71 ±0.05	435 ±80	1800 ±10
Natural weathering	25.1 ±1.6	18.0 ±0.9	7.4 ±0.9	0.05 ±0.01	9.72 ±0.10	491 ±50	1830 ±40

It can be seen from Tables 6 and 7 that on natural weathering the strength of both types of cellulose FRC materials increase whereas the failure strain values are

reduced, very sharply in the case of the room-temperature cured material. Considerable improvements in the flexural strength and elastic modulus of the material cured at ambient temperature followed after placing in a CO_2 rich environment. It can be seen also, from Table 6 that the hot water test did not produce any reduction in the mechanical properties of the autoclaved FRC product, confirming the earlier observations of Sharman and Vautier (145). Accelerated tests based on wetting and drying, on the other hand, show degradation of properties (142). Part of this degradation may be due to moisture movement in the matrix itself, the cement matrix composites showing greater reduction in properties than the autoclaved FRC.

Detailed microstructural studies with the SEM by Bentur and Akers (146) have revealed hollowness in the cellulose fibre after cyclic wetting and drying and 'petrification' (mineralisation) after treatment in a CO_2-rich environment. These features contribute to the property changes mentioned earlier. No evidence has been found, however, of the presence of a $Ca(OH)_2$-rich zone near the fibre in cellulose pulp FRC materials or in AC products they have been developed to replace.

In spite of the reasonable durability results obtained in the laboratory, examination of the cellulose FRC products in the field in the UK has revealed signs of distress in many instances on weathering (147). Warping and curling and delamination have been seen in earlier flat sheets and longitudinal cracks in the corrugated products. Most wood-cement particle boards, where the reinforcement is in the form of wood chips, show some loss in strength on long-term weathering (148). A combined effect of alkaline hydrolysis of the non-cellulosic component and volume changes associated with wetting and drying may be the underlying causes.

5.B.6 From metallic fibres - Thin sheets of cement mortar reinforced by steel fibre have been produced by spray or hand lay-up methods using a wire mesh. Commercial building panels have also been produced (48). At the present time there is not a great deal of user interest in these materials and steel fibres remain the principal candidate for reinforcement of bulk concrete.

An interesting new development is the emergence of metallic glass ribbons. Initial results as reinforcements for cement have been encouraging (39).

6. APPLICATIONS AND FUTURE PROSPECTS

In many parts of the world asbestos cement products continue to be used as roofing and cladding panels, slates and in pipes. Alternative products have been developed in many cases but it is proving difficult to replace pressure pipes with other FRC products. Several countries in the industrially developed world have decided to phase out the use of asbestos products in the building industry as soon as practicable and this trend is expected to be followed by other nations.

Over the last two decades or more the glass fibre cement industry has pioneered the use of thin sheet grc products in many new areas - architectural cladding, permanent formwork, agricultural structures, decorative panels, fire resistant partitions and doors, box elements and moulded products of various descriptions, small and often mobile buildings etc. The composite material has been used successfully in the construction of domestic housing and in the refurbishment of old buildings. In addition, the feasibility of making various AC products in grc has been amply demonstrated. In these and other applications, the mouldability of grc and its light weight are the most attractive features and every year new applications are added to the list. So far, the applications of grc have been seriously limited by concerns over the long-term durability of the material, but as mentioned earlier in this review promising results have recently been obtained with some new matrix formulations. Hopefully, these composites will prove to be more durable in external exposure than their predecessors.

The use of synthetic organic polymer fibres in thin sheet applications has steadily grown over the years but except in the field of AC replacement products where polyvinyl alcohol, polypropylene and acrylic fibres hold dominant positions, these fibres have not made the expected impact in the construction materials field yet. In principle many of the applications of grc mentioned above are suitable for synthetic polymer fibre FRC materials also. Chemical inertness is the most important asset of these fibres which is counterbalanced by low melting points and low modulii of elasticity. Considerable success has been achieved in increasing the stiffness of these fibres and in making them more resistant to oxidation and degradation by ultraviolet and no doubt these efforts will continue. Use of PP fibres in conjunction with glass has produced composites with better mechanical properties than with PP alone and this trend may be followed with other fibres. More generally, it is already clear that in the production of thin sheet FRC materials by processes such as the Hatschek, mixtures of fibres need to be used, if only for operational reasons. Synthetic polymer fibres have a role to play in this area as secondary or processing fibre.

High strength, high modulus aramid and carbon fibres have excellent properties and are eminently suitable as reinforcements for cements but their price still remains too high for exploitation in FRC. The fibres from pitch are far less expensive and offer hope, particularly as the properties of the fibres have progressively improved. It has been adequately demonstrated that thin sheet FRC made from the pitch fibre is a durable material and can be used in many of the applications mentioned earlier for grc. Further work will still be needed to develop fabrication methods that can utilise the properties of these fibres more efficiently.

The use of natural plant fibres in the unprocessed state will probably remain in the low-cost housing area in the developing countries for the time being. A two-room house with a natural plant fibre reinforced cement roof and costing only £100 was exhibited at the Ideal Home Exhibition in London in 1991 (149). The roof designed by the Intermediate Technology Development Group cost only £40. Considerable improvement in the weatherability of FRC materials made from these fibres will be required if wider applications are desired. With cellulose pulp, perhaps the present uses in the AC replacement area exploit the properties of the material most advantageously. Excessive moisture absorption or flammability of the fibre remains its main disadvantage while considering new applications.

There is, at present, a considerable amount of interest in the very strong cements produced by special techniques incorporating microsilica or polymers. Although strong, these materials remain brittle and some, e.g. the MDF cement, are sensitive towards exposure to moisture. It has been amply demonstrated that the toughness of these materials can be improved substantially by the addition of suitable fibres. Attempts are being made to improve the water resistance of MDF cements; the use of an organosilane coupling agent has given promising results (150). In the fullness of time these materials should find applications in the construction industry, perhaps as structural elements. Otherwise, for the present time the use of FRC thin sheets will remain mainly in the non— or semi-structural applications. In special structural repairs, however, strong and chemically resistant fibres have possibilities.

7. ACKNOWLEDGEMENT

The author wishes to thank P.L. Walton for his help in preparing this paper. This paper is published by kind permission of the Chief Executive, Building Research Establishment.

8. REFERENCES

1. Roy, R. : "Ceramics by the solution-sol-gel route." Science, 1987, 238, 1664-1669.

2. Hansen, T.C. : "Theories of multiphase materials applied to concrete, cement mortar and cement paste." **IC International Conference on The Structure of Concrete and its Behaviour under Load, London, UK** 1968, 16-23.
3. Hobbs, D.W. : "The Strength and deformation of concrete under short-term loading; a review". **Cement and Concrete Association Technical Report,** no. 42-484, London, UK, 1973, 27 p.
4. Tanaka, M. & Uchida, I.: "Application of the calcium silicates - $C_4A_3\overline{S}$ - slag type cement to GRC." **International Symposium on Cement and Concrete, Beijing, China** 1985, Abstracts, 171-172.
5. Shen Rongxi : "Research and development of some new fibre reinforced cement composites in China." **International RILEM Symposium on Developments in Fibre Reinforced Cement and Concrete, 3rd, Sheffield,UK.** 1986, V2.
6. Gartshore, G.C. Kempster, E. & Tallentire, A.G. : "A new high durability cement for grc products." **GRCA Congress, 8th Biennial, Maastricht, The Netherlands** 1991, 3-11.
7. Longuet, P, Burglen, I. & Zelwer, A.: "The Liquid phase of hydrated cement." Revue des Matériaux et Construction, 1973, **676**,35-41.
8. Canham, I., Page, C.L. & Nixon, P.J. : "Aspect of the pore solution chemistry of blended cements related to the control of alkali-silica reaction" Cement and Concrete Research, 1987, **17**, 839-844.
9. Page, C.L. & Vennesland, O.: "Pore solution composition and chloride binding capacity of silica-fume cement pastes." Materials and Structures : Research and Testing, 1983,**16**, 19-25.
10. Taylor, H.F.W. : **Cement Chemistry,** London, Academic Press, 1990, 475 p.
11. Majumdar,A.J. & Nurse, R.W.: "Glass fibre reinforced cement." Materials Science and Engineering, 1974, **15**, 107-127.
12. Birchall, J.D. "Cement in the context of new materials for an energy-expensive future." Philosophical Transactions Royal Society, London, 1983, **A310**, 31-42.
13. Hodgson, A.A. : **Alternatives to Asbestos and Asbestos Products.** 2nd ed. Crowthorne, Anjalena Publications, 1987, 284 p.
14. Bentur, A. & Mindess, S. : **Fibre Reinforced Cementitious Composites.** London, Elsivier Applied Science, 1990, 449 p.
15. Hodgson, A.A. : "Fibrous Silicates." **Royal Institute of Chemistry, London,** 1966, 46p.
16. Health and Safety Commission, UK. : **Report of the Advisory Committee on Asbestos.** London, HMSO, 1979, **V1** 100p, **V2** 103 p.
17. Beaudoin, J.J. : "Effect of mica surface treatment on mechanical properties of mica-flake-reinforced cement composites." Cement and Concrete Research, 1985, **15**,637-644.
18. Dimbleby, V. & Turner, W.E.S. : "The relationship between chemical composition and the resistance of glasses to the action of chemical agents. Part 1." Journal Society Glass Technology, 1926, **10**, 304-358.
19. Paul, A. : **Chemical Durability of Glass.** Chemistry of Glasses, 2nd ed London, Chapman and Hall, 1982, p 179-218.
20. Biryukovich, K.L., Biryukovich, Yu L. Biryukovich, D.L. : **Glass Fibre Reinforced Cement.** Kiev, Budivelnik, 1964. Translatioin No. 12., Civil Engineering Research Association, London, UK, 1965, 41 p.
21. Majumdar, A.J. & Ryder, J.F. : "Glass fibre reinforcement of cement products." Glass Technology, 1968, **9**, 78-84.
22. Majumdar, A.J. & Laws, V. : **Glass Fibre Reinforced Cement,** London, BSP Professional Books, 1991, 197 p.
23. Shin, W.S. : "Recent developments in alkali-resistant fibres at the Battelle Institute." **International GRC Congress, Paris, France** 1981, 359-374.
24. Proctor, B.A. : "The development and technology of AR fibres for cement reinforcement."**PCI Symposium on Durability of Glass Fibre Reinforced Concrete, Chicago, USA.** 1985, 64-77.
25. Ohta, H., Yanagisawa, O., Mukaiyama, T., Ohigashi, T. & Takeda, R. : "New AR-glass fibre - AR-Fibre-Super." **GRCA Congress 5th Biennial,Darmstadt, Germany** 1985, 37-43.

26. Li Chuanhe, Yicong Zou, Haolin Hou & Changman Yue. : "Reseárch on titaniferrous alkali-resistant slag wool fibre cement." **International RILEM Symposium on Developments in Fibre Reinforced cement and concrete, 3rd, Sheffield, U.K. 1986, V2.**
27. Health and Safety Executive : "Main-made mineral fibres." Guidance Note EH46, London, HMSO, 1990, 8 p.
28. Ando, T., Sakai, H., Takahasi, K. Hoshijima, T., Awata, M. & Oka, S. : "Fabrication and properties of a new carbon fibre reinforced cement product." **ACI Symposium on Thin-Section Fibre Reinforced Concrete and Ferrocement, Atlanta and San Diego, USA, 1989.** ACI, SP-124, 1990, 39-60.
29. Goldfien, S. : "Fibrous reinforcement for Portland cement." Modern Pastics, 1965, 4, 156-159.
30. Hannant, D.J., Zonsveld, J.J. & Hughes, D.C. : "Polypropylene film in cement based materials." Composites, 1978, 9, 83-88.
31. Krenchel, H. & Jensen H.W.: "Organic fibres for reinforcement of cement and concrete." **Concrete Society Symposium on Fibrous Concrete, London, UK.** 1980, Construction Press, 87-98.
32. Bijen, J. & Geurts, E.: "Sheets and pipes incorporating polymer film material in a cement matrix." Ibid, 194-202.
33. Schilderman, T. : "From research to dissemination of fibre concrete roofing technology."**International RILEM Symposium on Vegetable Plants and Their Fibres as Building Materials, 2nd, Salvador, Brazil,** 1990, Chapman and Hall, 204-213.
34. Gram, H.E. : "Durability studies on natural organic fibres in concrete." **International RILEM Symposium on Developments in Fibre Reinforced Cement and Concrete, 3rd, Sheffield, U.K., 1986, V2.**
35. Lewis, G. & Mirihagalia, P. : "Natural vegetable fibres as reinforcement in cement sheets." Magazine Concrete Research, 1979, 31, 104-108.
36. Cabrera, J.G. & Nwaubani, S.O. : "Experimental methods for the preparation of palm fruit and other natural fibres for use in reinforced cement Composites." **International RILEM Symposium on Vegetable Plants and Their Fibres as Building Materials, 2nd, Salvador, Brazil,** 1990, Chapman and Hall, 29-35.
37. Campbell, M.D. & Coutts, R.S.P. "Wood fibre reinforced cement composites." Journal Materials Science, 1980, 15, 1962-1970.
38. Argon, A.S., Hawkins, G.W. & Kuo, H.Y.: "Reinforcement of mortar with Metglas fibres" Journal Materials Science, 1977, 14, 1707-1716.
39. de Guillebon, B. & Sohm, J.M. : "Metallic glass ribbons - a new fibre for concrete reinforcement." **International RILEM Symposium on Developments in Fibre Reinforced Cement and Concrete 3rd, Sheffield, UK,** 1986. **V1.**
40. Ryder, J.F. : "Applications of fibre cement." **International RILEM Symposium on Fibre Reinforced Cement and Concrete, London, U.K.** 1975, Construction Press, 23-35.
41. Smith, J.W. : "The replacement of asbestos cement by GRC". Composites, 1982, 13, 161-163.
42. Hannant, D.J. & Zonsveld, J.J. : "Polyolefin fibrous networks in cement matrices for low cost sheeting." Philosophical Transactions Royal Society London, 1980, A294, 591-597.
43. Vittone, A. : "Industrial development of reinforcement of cement based products with fibrillated polypropylene networks as replacement of asbestos." **International RILEM Symposium on Developments in Fibre Reinforced Cement and Concrete, 3rd, Sheffield, UK, 1986, V2.**
44. True, G. : **GRC Production and Uses.** London, Palladian Publications, 1986, 104 p.
45. PB : "CemFIL GRC Technical Data." Pilkington Brothers PLC, St. Helens, U.K. 1985.
46. MKC : "Technical Information Sheet." Mitsubishi Kasei Corporation, Tokyo, Japan, 1991.
47. EG : "Glass Rock GRG Board." British Gypsum Limited, Loughborough, UK, 1991.
48. Marsden, W.A. : "The diversifying applications of steel fibre reinforced concrete in Australia." **International RILEM Symposium on Developments in Fibre Reinforced Cement and Concrete, 3rd, Sheffield, U.K. 1986, V2.**
49. Aveston, J., Mercer, R.A. & Sillwood, J.M. : "Fibre reinforced cements - Scientific foundations for specifications." **NPL Conference on Composites - Standards, Testing and Design." Teddington, U.K.** 1974, IPC Science and Technology Press, 93-103.

50. Briggs, A., Bowen, D.H. & Kollek, J. : "Mechanical properties and durability of carbon-fibre-reinforced cement composites." **International Carbon Fibre Conference on Carbon Fibres - Their Place in Modern Technology, 2nd, London, UK.** 1974, The Plastics Institute, P 8.
51. Pachow, V. : "Facades made from glass fibre reinforced cement," **GRCA Congress, 5th Biennial, Maastricht, The Netherlands, 1989, 131-142.**
52. Majumdar, A.J., Singh, B, & Evans, T.J. : "Glass fibre reinforced supersulphated cement" Composites, 1981, 12, 177-183.
53. Ward, D. & Proctor, B.A. : "Quality control test methods for glass fibre reinforced cement." **International RILEM Symposium on Testing and Test Methods of Fibre cement composites, 2nd, Sheffield, U.K.** 1978, Construction Press, 35-44.
54. Ashley, D.G. : "Measurement of glass content in fibre cement composites by x-ray flourescence analysis. Ibid, 265-274.
55. Hibbert, A.P. : "A method for assessing the quantity and distribution of glass fibre in an opaque matrix." Journal Materials Science Letters 1974, 9, 512-514.
56. Skarendahl, A. : "Precast and sprayed steel fibre concrete." **Concrete Society Symposium on Fibrous Concrete, London, U.K. 1980,** Construction Press, 115-127.
57. Shah, S.P. (ed) : **Application of Fracture Mechanics to Cementitious Composites.** Dordrecht, The Netherlands, Martinus Nijhoff, 1985, 715 p.
58. Mai, Y.W. : "Strength and fracture properties of asbestos cement mortar composites." Journal Materials Science, 1979, 14, 2091 - 2102.
59. Allen, H.G. : "Tensile properties of seven asbestos cements." Composites, 1971, 2, 98-103.
60. Akers, S.A.S. & Garrett, G.G. : "Observations and predictions of fracture in asbestos cement composites". Journal Materials Science, 1983, 18, 2209 - 2214.
61. Krenchel, H. : **Fibre Reinforcement.** Copenhagen, Akademisk Forlag, 1964, 159 p.
62. Laws, V. : "The efficiency of fibrous reinforcement of brittle matrices". Journal Physics D. Applied Physics, 1971, 4, 1737 - 1746.
63. Hannant, D.J., Hughes, D.C. & Kelly, A. : "Toughening of cement and other brittle solids with fibres." Philosophical Transactions Royal Society London 1983, **A310,** 175-190.
64. Hannant, D.H. : "The effect of changes in matrix properties with time on the measured and predicted long term properties of fibre reinforced cement." **International CANMET/ACI Conference on Durability of Concrete, 2nd, Montreal, Canada,** 1991, ACI SP-26. V II, 783-797.
65. West, J.M. & Majumdar A.J. : "Strength of glass fibres in cement environment." Journal Materials Science Letters, 1982, 1, 214-216.
66. Proctor, B.A. : "The stress-strain behaviour of glass fibre reinforced cement composites." Journal Materials Science, 1986, 21, 2441-2448.
67. Proctor B.A., Oakley, D.R. & Wichers, W. : "Tensile Stress/Strain characteristics of glass fibre reinforced cement." **NPL Conference on Composites - Standards, Testing and Design, Teddington, U.K.** 1974, IPC Science and Technology Press, 106-107.
68. Mobasher, B., Stang, H. & Shah, S.P. : "Microcraking in fibre reinforced concrete." Cement and Concrete Research, 1990, 20, 665-676.
69. Mobasher, B. Ouyang, C. & Shah, S.P. : "Modelling of fibre toughening in cementitious materials using an R-curve approach." International Journal Fracture, 1991, 50, 199-219.
70. Ouyang, C. & Shah, S.P. : "Toughening of high strength cementitious matrix reinforced by discontinuous short fibres." To appear in Cement and Concrete Research, 1992.
71. Bartos, P. : "Review Paper : bond in fibre reinforced cements and concretes." International Journal Cement Composites and Lightweight Concrete, 1981, 3, 159-177.
72. Laws, V. : "Micromechanical aspects of fibre-cement bond." Composites, 1982, 13, 145-151.
73. Gray, R.J. : "Analysis of the effect of embedded fibre length on fibre debonding and pull-out from an elastic matrix Parts 1 and 2." Journal Materials Science, 1984, 19, 861-870 and 1680-1691.
74. Li, Z., Mobasher, B. & Shah, S.P. : "Characterization of interfacial properties in fibre reinforced cementitious composites." Journal American Ceramic Society, 1991, 74, 2156-2164.

75. Kelly, A.: "Fibre reinforced cement in context." **MRS Symposium on Advances in cement-matrix composites, Boston, USA,** 1980, 3-16.
76. Kelly, A. & Zweben, C. : "Poisson contraction in aligned fibre composites showing pull-out." Journal Materials Science, 1976, **11,** 582-587.
77. Baggott, P. & Gandhi, D. : "Multipile cracking in aligned polypropylene fibre reinforced cement composites." Journal Materials Science, 1981, **16,** 65-74.
78. Soroushian, P., Aouadi, F. & Nagi, M. : "Latex modified carbon fibre Reinforced mortar". ACI Materials Journal, 1991, **88,** 11-18.
79. Bentur, A., Diamond, S. & Mindess, S. : "Cracking processes in steel fibre reinforced cement paste." Cement and Concrete Research, 1985, **15,** 331-342.
80. Tabor, D. : **Principles of Adhesion-Bonding in Cement and Concrete.** Adhesion problems in The Recycling of Concrete, ed by P.C. Kreijger, New York, Plenum Press, 1980, 63-90.
81. Hannant, D.J. : "Durability of cement sheets reinforced with fibrillated polypropylene networks : 10 year results." Magazine Concrete Research, 1991, **43,** 257-264.
82. Hannant, D.J. : **Fibre Cements and Fibre Concretes.** Chicester, John Wiley, 1978, 219 p.
83. Laws, V. : "On the mixture rule for strength of fibre reinforced cement." Journal Materials Science Letters, 1983, **2,** 527-531.
84. Swamy, R. N. & Mangat, P.S. : "A theory for the flexural strength of steel fibre reinforced concrete." Cement and Concrete Research, 1974, **4,** 313-325.
85. Aveston, J., Cooper G.A. & Kelly, A. : "Single and multiple fracture." **NPL Conference on The Properties of Fibre Composites, Teddington, UK,** IPC Science and Technology Press, 1971, 15-26.
86. Hibbert, A.P. & Hannant, D.J. : "Toughness of cement composites containing polypropylene films compared with other fibres." Composites, 1982, **13,** 393-399.
87. Heneger, C.H. : "Steel fibrous concrete - a review of testing procedures." **Concrete Society Symposium on Fibrous Concrete, London, U.K.** 1980, Construction Press 16-28.
88. Majumdar A.J. & Laws, V. : "Composite materials based on cement matrices" Philosophical Transactions Royal Society London, 1983, **A310,** 191-202.
89. Kelly, A. : "Interface effects and the work of fracture of a fibrous composite." Proceedings Royal Society London, 1970, **A319,** 95-116.
90. Walton, P.L. & Majumdar, A.J. : "Cement based composites with mixtures of different types of fibres." Composites, 1975, **6,** 209-216.
91. Kobayashi, K. & Cho, R. : "Flexural Characteristics of steel fibre and polythene fibre hybrid-reinforced concrete." Composites, 1982, **13,** 164-168.
92. Xu, Guodong & Hannant, D.J. : "Synergistic interaction between fibrillated polypropylene networks and glass fibre in a cement-based composite." Cement and Concrete Composites, 1991, **13,** 95-108.
93. CEN : pr EN 492-1991: "Fibre-cement slates and their fittings."; pr EN 494-1991 : "Fibre-cement profiled sheets and fittings." Draft European Standards. European Committee for Standardisation, Brussels, Belgium, 26 p and 45 p.
94. Jones, F. E. : "Weathering tests on asbestos - cement roofing materials." **Building Research Technical Paper no. 29,** London, HMSO, 1947, 38 p.
95. Bijen, J. : "Improved quality grc by polymer modification." **GRCA Congress, 7th, Biennial, Maastricht, The Netherlands,** 1989, 95-106.
96. Litherland, K.L., Oakley, D.R. & Proctor, B.A. : "The use of accelerated ageing procedures to predict the long-term strength of GRC composites." Cement and Concrete Research, 1989, **11,** 455-466.
97. Proctor, B.A., Oakley, D.R. & Litherland, K.L. : "Developments in the assessment and performance of GRC over 10 years." Composites, 1982, **13,** 173-179.
98. Litherland, K.L. : "Test methods for evaluating the long-term behaviour of grc." **PCI Symposium on Durability of Glass Fibre Reinforced Concrete, Chicago, USA,** 1985, 210-221.
99. Thiery, J., Vautrin, A. & Francois-Brazier, J. : "High durability glass-fibre reinforced modified cementitious matrix." **MRS Symposium on Fibre Reinforced Cementitious Materials, Boston, USA,** 1990, 79-91.

100. Hayashi, M., Sato, S. & Fuji, H. : "Some ways to improve durability of grc." **PCI Symposium on Durability of Glass Fibre Reinforced Concrete, Chicago, USA**, 1985, 270-284.
101. Soukatchoff, P. & Ridd, P.J. : "High durability glass fibre reinforced cement using a modified cementitious matrix." **GRCA Congress, 8th, Biennial, Maastricht, The Netherlands**, 1991, 45-60.
102. GRCA : "New matrix blends for enhanced long-term ductility in glass fibre reinforced cement composites." GRCA News Special Supplement, August 1991, Glass Fibre Reinforced Cement Association, Wigan, UK, 4 p.
103. BSI : "Draft standard specification for sprayed non-polymer glass reinforced cladding for external use" British Standards Institute, London, UK, No 90/13434, 1991; 13 p.
104. Majumdar, A.J. & Walton, P.L. : "Durability of fibre cement composites." **International CANMET/ACI Conference on Durability of Concrete, 2nd, Montreal, Canada**, 1991. ACI SP-126, V II, 745-771.
105. Bentur, A. & Diamond, S. : "Fracture of glass fibre reinforced cement" Cement and Concrete Research, 1984,. **14**, 31-42.
106. Stucke, M.S. & Majumdar, A.J. : "Microstructure of glassfibre reinforced cement composites." Journal Materials Science, 1976, **11**, 1019-1030.
107. Yilmaz, V.T., Lachowski E.E. & Glasser, F.P. : "Chemical and microstructural changes at alkali-resistant glass fibre-cement interfaces." To appear in Journal American Ceramic Society, 1992.
108. Ali, M.A. & Grimmer, F.J. : "Mechanical properties of glass fibre reinforced gypsum." Journal Materials Science, 1969, **4**, 389-395.
109. Brown, A.D. & Hufford, H.H. : "The structural properties of cement plates reinforced with carbon fibre/PVA prepreg." **International RILEM Symposium on Developments in Fibre Reinforced Cement and Concrete, 3rd, Sheffield, U.K.**, 1986, **V1**.
110. Nishioka, K., Yamakawa, S. & Shirakawa, K. : "Properties and applications of carbon fibre reinforced cement composites." Ibid, **V1**.
111. Akihama, S., Swenaga, T., Nakagawa, H. & Suzuki, K. : "Influences of fibre strength and polymer impregnation on the mechanical properties of carbon fibre reinforced cement composites." Ibid, **V1**.
112. Banthia, N. & Sheng, J. : "Durability of carbon fibre reinforced cement in acidic environments." **International CANMET/ACI Conference on Durability of Concrete, Montreal, Canada**, 1991, ACI SP-126, V II, 837-850.
113. Krenchel, H. & Shah, S.P, : "Synthetic fibre for tough and durable concrete." **International RILEM Symposium on Developments in Fibre Reinforced Cement and Concrete, 3rd, Sheffield, U.K.** 1986, **V1**.
114. Vittone, A. "Reinforcement of cement based products with fibrillated polymeric networks". Paper presented at the **ACI Fall Convention, Baltimore, USA**, November 1986, Cited in Reference 14.
115. Mai, Y.M., Andonian, R. & Cottrell, B. : "Thermal degradation of polypropylene fibres in cement." International Journal Cement Composites and Lightweight Concrete, 1980, **4**, 149-156.
116. Gardiner, G.M., Keating, J. & Hannant, D.J. : "Accelerated ageing of cement sheets containing polypropylene networks." Journal Materials Science, 1985, **20**, 3574-3580.
117. Hikasa, J. & Genba, T. : "Replacement for asbestos in reinforced cement products - 'Kuralon' PVA fibres, properties, structure." Paper presented at the **International Man-made Fibres Congress, Austrian Chemical Institute, Dornbirn, Austria**, September, 1986, Cited in Reference 14.
118. Akers, S.A.S., Studinka, J.B., Meier, P., Dobb, M.G., Johnson, D.J. & Hikasa, J. : "Long term durability of PVA reinforcing fibres in a cement matrix." International Journal Cement Composites and Lightweight Concrete, 1989, **11**, 79-91.
119. West, J.M. & Majumdar, A.J. : "Durability of non-asbestos fibre reinforced cement" **Building Research Establishment**, 1991, IP 1/91, 4 p.
120. Tait, R.B. & Akers, S.A.S., : Micromechanical Studies of fresh and weathered fibre cement composites." International Journal Cement Composites and Lightweight Concrete, 1989, **11**, 125-131.

121. Hahne, H., Karl, S. & Warner, J.D. : "Properties of polyacrylonitrile fibre reinforced concrete." **ACI Symposium on Fibre Reinforced Concrete Properties and Applications, Baltimore, USA,** 1986 and San Antonio, USA, 1987, ACI SP-105, 211-223.
122. Gale, D.M. : "Cement reinforcement with man-made fibres." Paper presented at the **International Man-made Fibres Congress, The Austrian Chemical Society, Dornbirn, Austria,**September 1986. Cited in Reference 14.
123. Odler, I. : "Structure and mechanical properties of Portland cement - polyacrylonitrile fibre composites." **MRS Symposium on Bonding in Cementitious Composites, Boston, USA,** 1988, **144,** 153-158.
124. Walton, P.L. & Majumdar, A.J. : "Properties of cement composites reinforced with Kevlar fibres." Journal Materials Science, 1978, 13, 1075-1083.
125. Ohgishi, S., Ono, H. & Tanahashi, I. : "Mechanical properties of cement mortar pastes reinforced by polyamide fibres." Transactiona Japan Concrete Institute, 1984, **6,** 309-315.
126. Akihama, S., Nakagawa, H. Tukada, T. & Yamaguchi, M. : "Experimental study on aramid fibre reinforced cement composites 'AFRC' - mechanical properties of AFRC with short fibres." **International RILEM Symposium on Developments in Fibre Reinforced Cement and Concrete, 3rd, Sheffield, U.K.** 1986, **V1.**
127. (a) Wang, Y., Backer, S. & Li, V.C. : "An experimental study of the synthetic fibre reinforced cementitious composites." Journal Materials Science, 1987, 22, 4281-4291.
(b) Wang, Y., Li, V.C. & Backer S. : "Tensile failure mechanisms in synthetic fibre reinforced mortar." Ibid, 1991, **26,** 6565-6575.
128. Sobral, H.S. (ed) : "Vegetable plants and their fibres as building materials." **International RILEM Symposium, 2nd, Salvador, Brazil,** 1990, Chapman & Hall, 374 p.
129. Swamy, R.N. (ed) **Natural Fibre Reinforced Cement and Concrete. Concrete Technology and Design, V5.** Glasgow, U.K., Blackie and Sons, 1988, 304 p.
130. Hussain, M.W. & Zakaria, F. : "Prospects for coconut fibre reinforced thin cement sheets in the Malaysian Construction Industry." Reference 128, 77-86.
131. Paramasivan, P., Nathan, G.K. & Das Gupta, N.C. : "Coconut fibre reinforced corrugated slabs." International Journal Cement Composites and Lightweight Concrete, 1984, 6, 19-28.
132. Mansur, M.A. & Aziz, M.A. : "A study of jute fibre reinforced cement composite." Ibid, 1982, 4, 75-82.
133. Mattone, R. : "Comparison between gypsum panels reinforced with vegetable fibres: their behaviour in bending and under impact." Reference 128, 120-129.
134. Canovas, M.F., Kawiche, G.M. & Salva, N.H. : "Possible ways of preventing deterioration of vegetable fibres in cement mortars." Reference 128, 120-129.
135. Soroushian, P. & Marikunta, S. : "Effects of moisture content on mechanical properties of wood fibre reinforced cement." Reference 128, 39-49.
136. Coutts, R.S.P. & Warden, P.G. : "Air cured wood pulp fibre cement composites." Journal Materials Science, 1985, 4, 117-119.
137. Fordos, Z. & Tram, B. : "Natural fibres as reinforcement in cement based composites." **International RILEM Symposium on Developments in Fibre Reinforced Cement and Concrete, 3rd, Sheffield, U.K.** 1986, **V2,**
138. Davies, G.W., Campbell, M.D. & Coutts, R.S.P. : "A SEM study of woodfibre reinforced cement composite." Holzforschung, 1981, 35, 201-204.
139. Mai, Y.W., Hakeem, M.I. & Cotterell, B. : "Effects of water and bleaching on the mechanical properties of cellulose fibre cements. Journal Materials Science, 1983, 18, 2156-2162.
140. Coutts, R.S.P. & Campbell, M.D. : Coupling agents in wood fibre reinforced cement composites." Composites, 1979, 10, 228-232.
141. Coutts, R.S.P. : "Autoclaved beaten wooden fibre reinforced cement composites." Composites, 1984, 15, 139-143.
142. Akers, S.A.S. & Studinka, J.B. : "Ageing behaviour of cellulose fibre cement composites in natural weathering and accelerated tests." International Journal Cement Composites and lightweight concrete, 1989, 11, 93-97.
143. Vinson, K.D. & Daniel, J.I. : "Specialty cellulose fibres for cement reinforcement." **ACI Symposium on Thin-Section Fibre Reinforced Concrete and Ferrocement, Atlanta and San Diego, USA,** 1989, ACI SP-124, 1990, 1-18.

144. Coutts, R.S.P. : "Wastepaper fibres in plaster products." Journal Materials Science Letters, 1991, 10, 77-78.
145. Sharman, W.R. & Vautier, B.P. : "Durability Studies on wood fibre reinforced cement sheet" **International RILEM Symposium on Developments in Fibre Reinforced Cement and Concrete, Sheffield, U.K.**, 1986, V2.
146. Bentur, A. & Akers, S.A.S. : (a) "The microstructure and ageing of cellulose reinforced cement composites cured in a normal environment." (b) "The microstructure of ageing of cellulose fibre reinforced autoclaved cement composites." International Journal Cement Composites and Lightweight Concrete, 1989, **11**, (a) 99-109 ; (b) 111-115.
147. West, J. : Private Communication, BRE, 1991.
148. Dinwoodie, H.M. & Paxton, B.H. : Cement bonded particleboard - a technical assessment. **Building Research Establishment**, 1992, Information Paper (in press).
149. de Groot P.: "A roof over your head for £100." New Scientist, 23 March 1991, p 26.
150. Russell, P.P., Shunkwiler, J., Berg, M & Young J.F. : "Moisture resistance of macrodefect-free cement." **NIST/ACerS Conference on Advances in Cementitious Materials, Gaithersberg, USA**, 1990, Ceramic Transactions, 1991, **16**, 501-519.

EFFECT OF FIBERS-MATRIX INTERACTION ON CONCRETE STRENGTH

Surendra P Shah and Chengsheng Ouyang

NSF Center for Science and Technology of Advanced Cement Based Materials
North-western University, Evanston, USA

ABSTRACT

Many of the current applications of fiber reinforced concrete involve the use of fibers ranging up to 1% by volume of concrete. It is usually assumed that fibers with this amount do not influence the tensile strength of a matrix, and only after the matrix has cracked, do fibers contribute by bridging the crack. Recently, with a variety of fabrication techniques it is possible to incorporate up to 15% of fibers by volume into concrete. With such a large volume of fibers, some evidence presented in this paper indicates that fibers seem to substantially increase the inherent tensile strength of matrices.

INTRODUCTION

Portland cement concrete is a relatively brittle material with a rather low tensile strength. This deficiency of concrete can be overcome for example, by reinforcing concrete with small diameter fibers. These fibers can be glass, steel or synthetic fibers. Most of the current applications with fiber reinforced concrete involve the use of fibers ranging up to 1% by volume of concrete. It is usually assumed that fibers do not influence the tensile strength of the matrix, and only after the matrix has cracked, do fibers contribute by bridging the cracks[1].

Recently, with a variety of processing techniques, it is possible to incorporate up to 15% fibers by volume into concrete. Fibers in such large quantities seem to fundamentally alter the nature of a cement-based matrix. If this is so, then it is important to understand under what conditions such a beneficial interaction can occur so that one can design composites to promote such interaction. To examine this question, in this paper the results of tests conducted on specimens with different fibers are first analyzed. A fracture mechanics (R-curve) approach is then proposed to simulate such fiber matrix interaction.

THE SPACING CONCEPT AND THE TENSILE STRENGTH

The current interest in fiber reinforced concrete can be at least partially traced to a simulating research reported by Romualdi and Batson[2]. They assumed that fracture strength of concrete in tension can be predicted by Griffith's criterion:

$$\sigma_c^2 = \frac{G_c E}{(1-\mu^2)\pi a} \tag{1}$$

where σ_c is the average tensile stress at failure, G_c is the critical strain energy release rate, E is the modulus of elasticity, μ is the Poisson's ratio, and a is half the length of the critical crack.

They pointed out that reducing the spacing between wires decreases the length of the critical crack at fracture and thus should significantly increase the tensile strength of concrete. Their theoretical prediction is shown in Fig. 1. To support their theoretical argument Romualdi and Batson conducted tests on mortar beams reinforced with small diameter wires. The volume of wires was kept the same in their test, but the spacing between these wires was varied. From their results they concluded that below about 10 mm (0.4 in.) spacing, the ultimate resisting moment of the beam was influenced by spacing (see Fig. 2). However Broms and Shah[3] point out that to vary the spacing and to maintain the same volume of steel, Romualdi and Batson used different diameters for different spacings. For smaller spacings, wires with smaller diameters and with much higher yield strength were used. Taking this effect into account, Broms and Shah recalculated the ultimate resisting moments for beams (Fig. 3). These results indicated that there is no effect of spacing on the ultimate strength of beams.

It is noted that Romualdi and Batson assumed in their theoretical prediction that: (1) the critical crack length is equal to the spacing between wires, (2) the value of G_c is the value at crack initiation, and (3) the bond between fibers and matrix is perfect. These assumptions are incorrect.

Several studies have been conducted where strain at first cracking has been carefully measured. Based on these tests it is now generally accepted that fibers do not significantly enhance the first cracking stress of cement-based matrices reinforced with small fiber volume fraction (Fig. 4)[4].

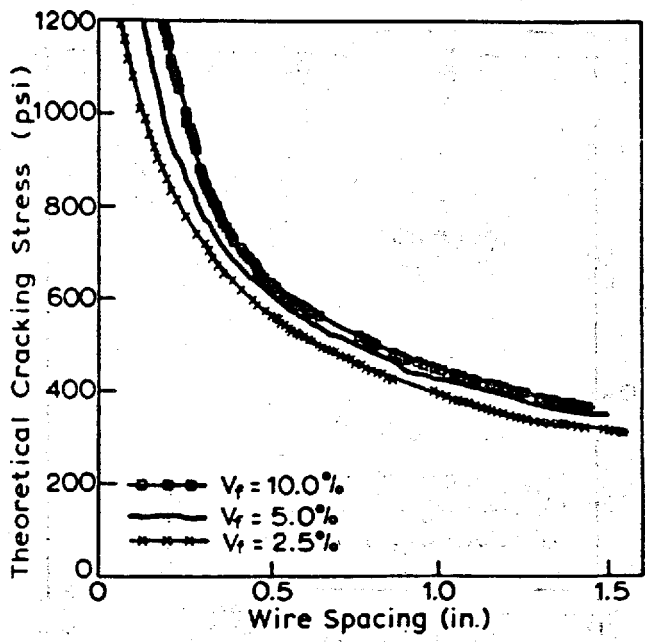

Fig. 1 Theoretical prediction for the effect of spacing of wires

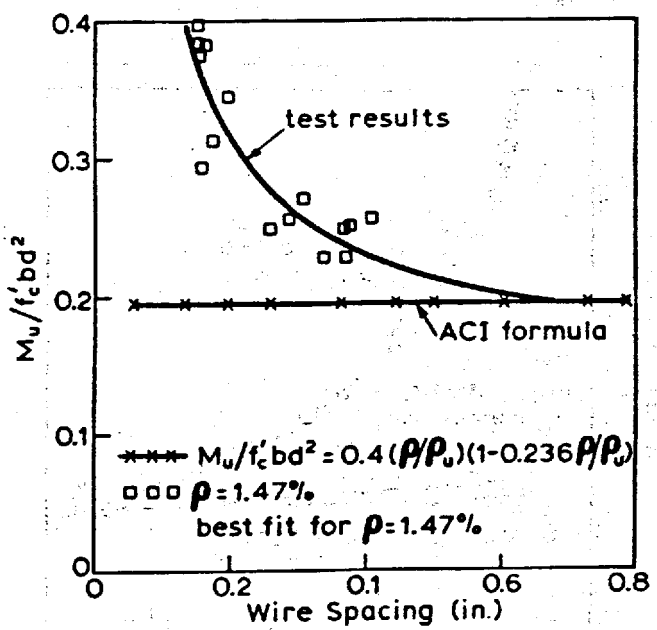

Fig. 2 Relationship between ultimate strength and wire spacing from Romualdi and Batson, where M_u = moment at ultimate load, f'_c = concrete ultimate strength, b = width of beam, ρ = percentage of reinforcement, $\rho_u = 0.4f'_c/f_y$, and f_y = yield strength of wires

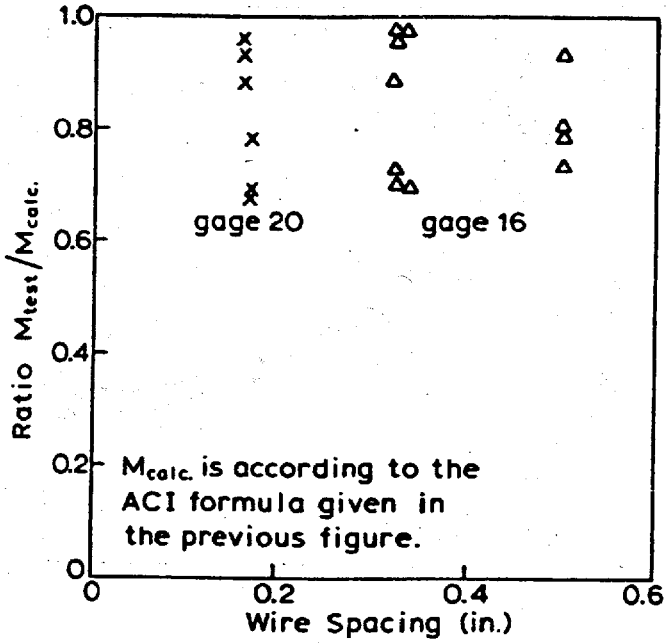

Fig. 3 Relationship between ultimate strength and wire spacing from Broms and Shah

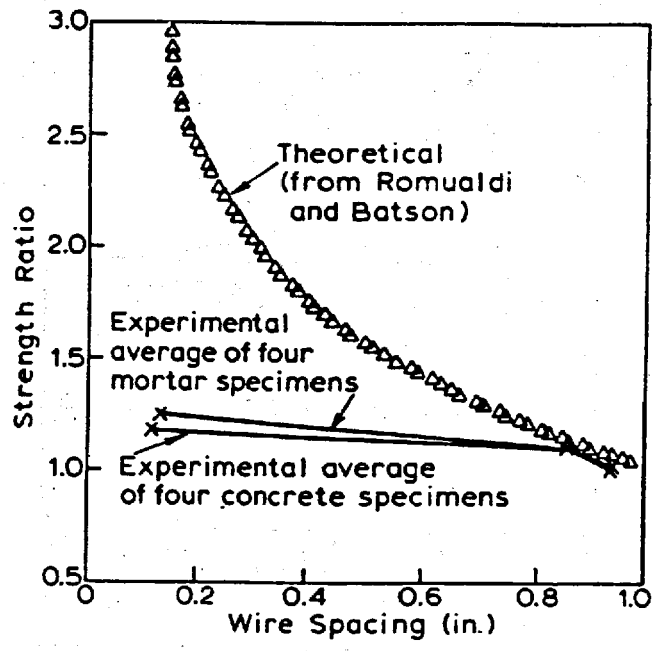

Fig. 4 Effect of spacing of reinforcement on cracking strength of concrete from Shah and Rangan

It should be noted that even if fibers or closely spaced wires do not change the first cracking stress, it does not necessarily mean that the tensile strength of the matrix is not influenced by the presence of fibers. This is because crack initiation in cement-based matrices does not always lead to critical crack propagation. In general, for these quasi-brittle materials, crack initiation is followed by stable crack propagation. Thus the maximum load is usually attained only after a substantial, precritical stable crack growth has occurred. It is likely that fiber can influence this stable crack growth and consequently the tensile strength of the matrix. This possibility is examined for different fiber in the subsequent sections of this paper.

EXPERIMENTAL OBSERVATIONS

(1) Test with Glass Fibers

Specimens reinforced with uniaxial, continuous glass fibers were manufactured[5]. The uniaxial tensile specimens were 178 mm long and 25 mm wide, while the thickness varied from 4 to 5 mm. Each glass fiber strand had 204 filaments and 1% by volume of fibers required 30 strands.

Two series of specimens were made: one with epoxy matrix and the other with cement matrix. For each series, the volume fraction of fibers were varied from 0 to 10%. Uniaxial tensile tests were conducted in a closed-loop test facility. Displacement recorded by two LVDT's with a gage length of 76 mm was used as a control. The tensile load-elongation responses of glass fiber reinforced epoxy specimens are shown in Fig. 5. Because of the difficulty in conducting the tensile test of glass fibers, the modulus of elasticity of glass fibers was obtained from Fig. 5 by assuming that the composite response is linear and plotting the slope of the curve. The values of composite stiffness (E_c) are plotted for different volume fraction of fiber (V_f) in Fig. 6. The value of the modulus of elasticity of glass fibers (E_f) obtained in this manner compare favorably with those reported by other researchers[6]. Knowing the modulus of elasticity of the glass fibers, the contribution of the epoxy matrix for each set of the specimens containing different volume fractions of fibers can be calculated. The calculated stress strain curves of the epoxy matrix are shown in Fig. 7. It can be seen that the contribution (in term of the tensile stresses) of the reinforced epoxy matrix is the same regardless of the volume of fibers. In addition, the calculated stress strain curves of the plain epoxy obtained from composite response match quite well with the independently measured curve of the plain epoxy matrix.

Using the same procedure, the contribution of cement matrix was calculated and is shown in Fig. 8. Unlike epoxy matrix, the stress-strain response of cement matrix depends on the volume of fiber. It was observed that when the composite stress strain curve deviated from linearity, the contribution of the matrix was maximum. This point is often called the bend-over-point (BOP). To calculate the matrix contribution, it was assumed that glass fibers response is linear with the modulus of elasticity as determined from the previously described tests with the epoxy matrix. Further, it was assumed that the elongation of fibers is the same as that of the specimen as measured with the gage length of 75 mm. After matrix cracking, the fibers may not be strained uniformly all along the gage length. Thus the strain values referred to here is valid only on the average sense. It is not necessary to assume that the fibers or the matrix respond linearly for applying the rule of mixtures. It is, however, necessary to assume that the overall displacements of the fibers and the matrix are the same. It is noted that the penetration of cement matrix within the glass fiber strands was not as uniform as that of epoxy matrix. Thus the contribution of cement matrix shown in Fig. 8 is perhaps underestimated. This procedure has been applied to cement-based matrices reinforced by different fibers to obtain matrix contributions as described in the following sections.

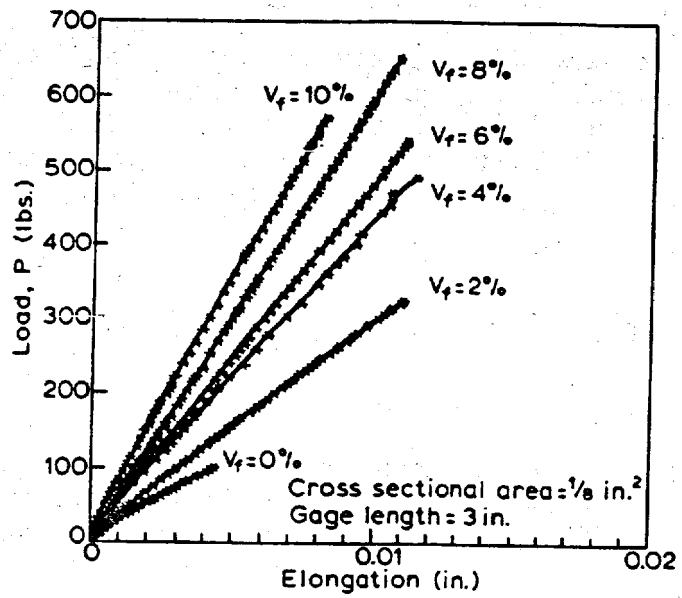

Fig. 5 Tensile load elongation response of glass fiber epoxy matrix composites with varying volume fractions of fibers

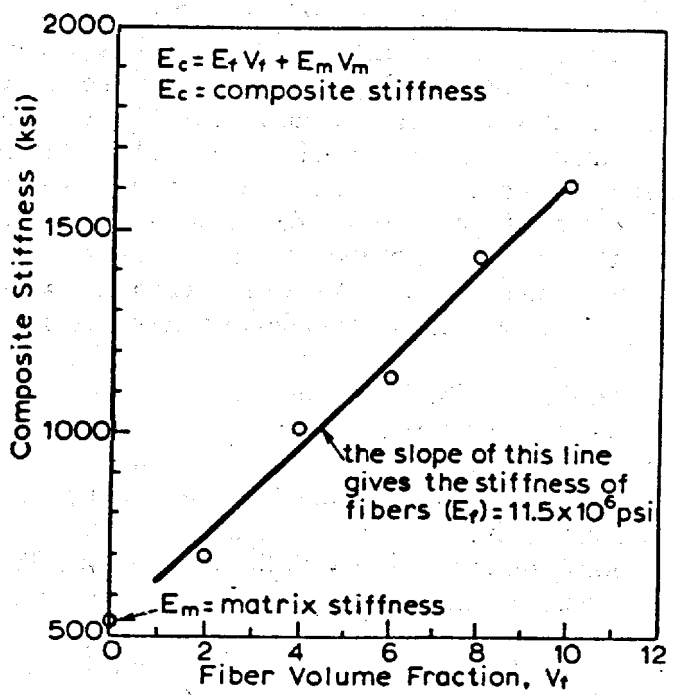

Fig. 6 Composite stiffness as a function of the fiber volume fraction

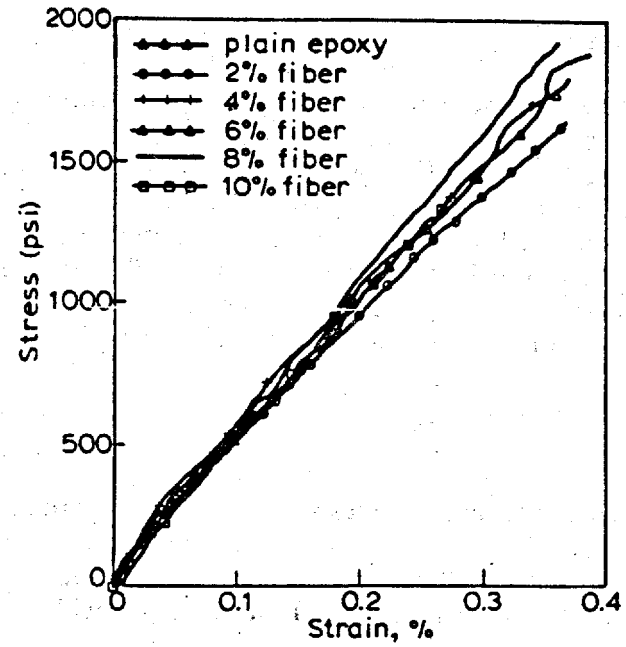

Fig. 7 Stress-strain response of the epoxy matrix computed from the composite response using the rule of mixtures

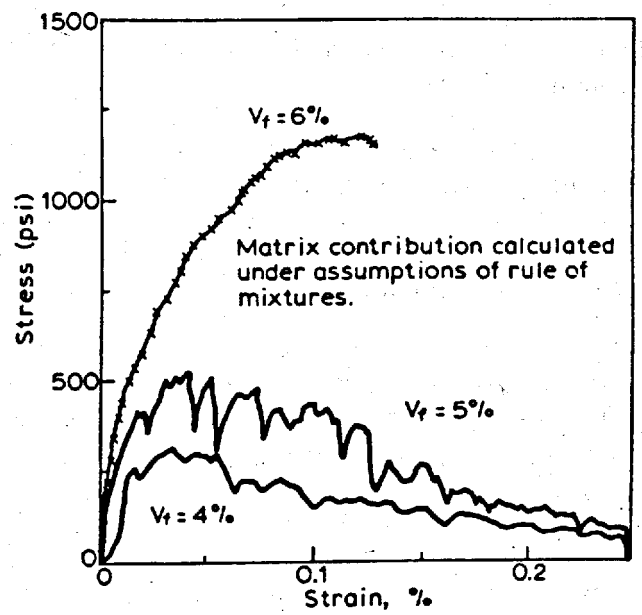

Fig. 8 Stress-strain response for cement matrix computed from the overall composite response

(2) Tests with Polypropylene Fibers

Mobasher, Stang and Shah[7] conducted uniaxial tensile test on cement-based matrices reinforced with fibrillated continuous, uniaxial polypropylene fibers. The dog-bone specimens with the cross sectional area of 16x10 mm were tested. The tensile stress-strain curves of cement-based matrices reinforced with 8.7% and 13.4% volume fractions of are shown in Fig. 9. The contribution of the matrix (shown in the inset) was obtained by subtracting the contribution of fibers from the composite response using the law of mixtures as previously described. The tensile strength of the cement-based matrix reinforced with 13.4% by volume of fibers is approximately 15 MPa, and it is remarkable that even at an average strain of 2%, the matrix contributes a tensile stress of about 8 MPa.

(3) Tests with Steel Fibers

Somayaji and Shah[8] conducted uniaxial tensile tests on cement mortar reinforced with steel wires. Specimens tested were 305x25.4x9.5 mm. Continuous steel wires of diameter 1.19 mm were used as reinforcement. The matrix stresses at the BOP obtained from their results are shown in Fig. 10 for different fiber volume fractions. The matrix stress at BOP increases with increasing fiber volume fraction.

Banthia and Sheng[9] tested a high strength mortar reinforced by discontinuous, short steel fibers. The high strength mortar matrix consisted of portland cement, silica fume, aggregate, and superplasticizer. The steel fibers used had an average diameter of 0.025 mm and an average length of 3 mm. Three-point bend beams with dimensions of 19 x 19 x 150 mm were tested (clear span of the beam = 130 mm). The contribution of matrix in terms of the load resisted by the matrix is plotted as the function of fiber volume fraction in Fig. 11.

The above results on cement-based matrices reinforced by continuous and discontinuous glass, polypropylene or steel fibers indicate the evidence that the use of high volume fraction (greater than 2% by volume) of fibers seems to fundamentally alter the tension-weak nature of concrete. As a result, the inherent tensile strength and strain capacity of the matrix itself is significantly enhanced. The use of high volume fraction of fiber may lead to produce a new class of cement-based materials.

This beneficial interaction between fibers and quasi-brittle matrices has been studied using fluorescent microscopy and laser holography at ACBM Center[7][10]. Some of the results of these studies are indicated in Fig. 12. It was observed that microcracks in the matrix prior to BOP (point A) are few and uniformly distributed. Some of these microcracks localized into macrocraks at the BOP (point B). The presence of fibers can delay this localization phenomenon thus increasing the tensile strength of the matrix. The spacing of the localized band of macrocrack was observed to decrease beyond the BOP (point C). The spacing of cracks reaches minimum at point D. Beyond this saturation point, it can be assumed that the matrix contribution is essentially constant, but not necessarily negligible. Note that for low volume of fibers, the tensile strength of the matrix at the BOP may not be significantly different than that of plain matrix and the stress-strain response of the composite beyond the BOP may be characterized by strain softening rather than hardening as observed for high volume fraction of fibers.

The desirable interaction between fibers and matrix described above will obviously depend on type, length, diameter and volume fraction of fibers, properties of matrix and the bond characterization of interface. To optimize these variable parameters theoretical modeling is essential. We have

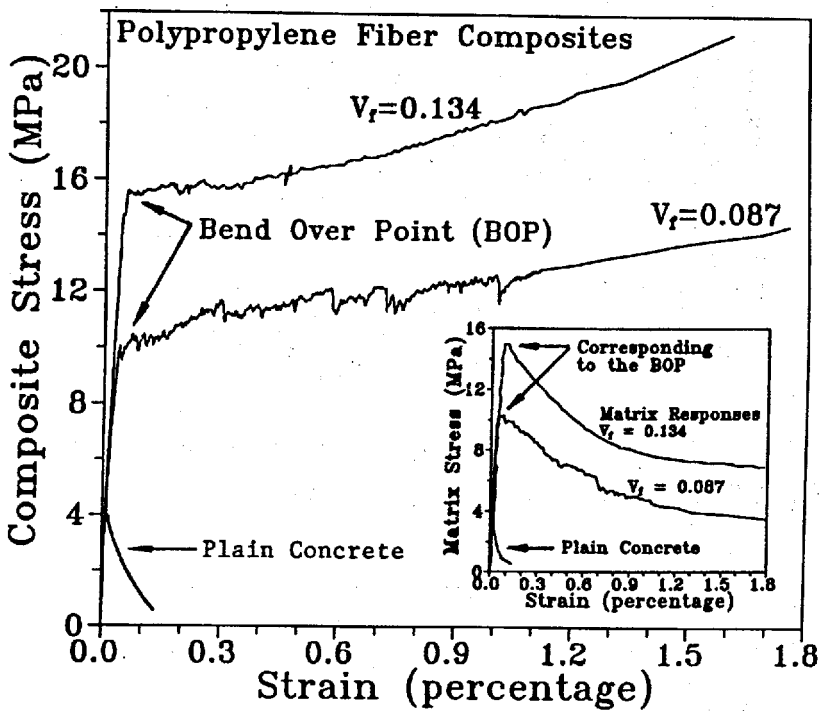

Fig. 9 Stress-strain response of the composite material plotted for two-volume fraction fibers. Computed response of the matrix phase is also shown in the inset

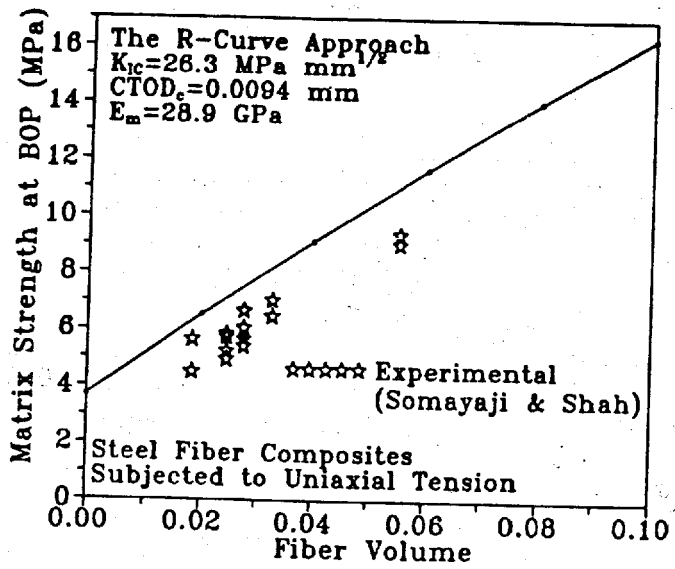

Fig. 10 Matrix strength at the BOP for steel fiber reinforced cement-based composites

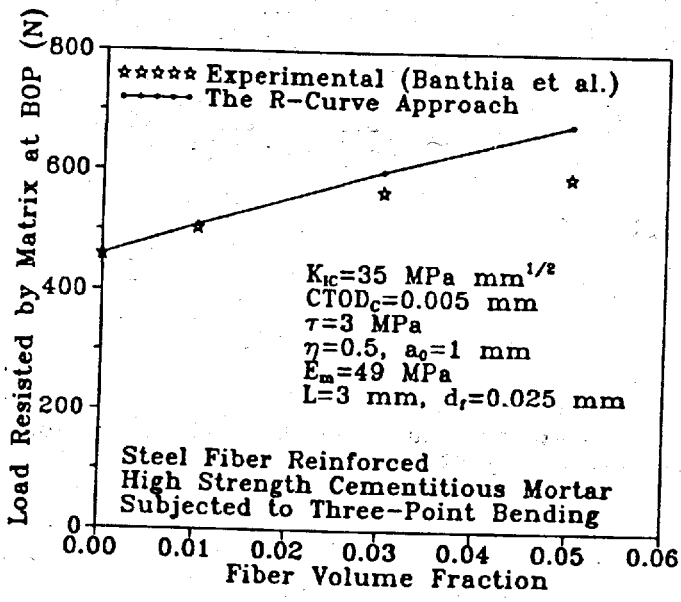

Fig. 11 Load resisted by matrix at the BOP for high strength cementitious mortar reinforced by discontinuous, short steel fibers

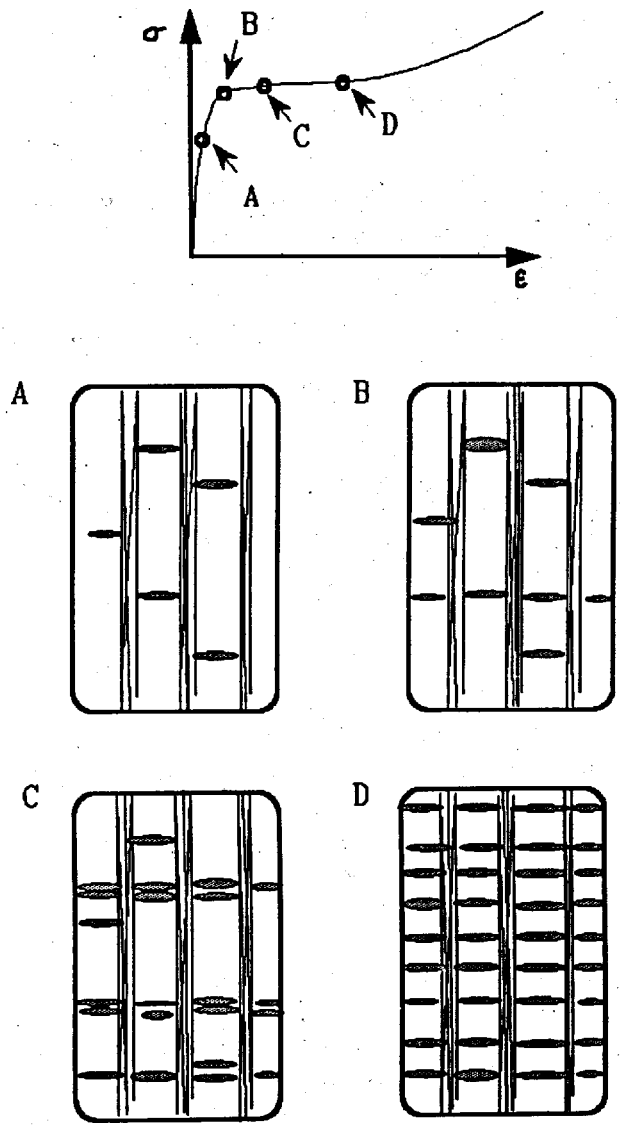

Fig. 12 Stages of cracks in cement-based fiber reinforced composites

summarized some available approaches in Reference 11.[11] An R-curve approach to predict the enhanced tensile strength of cementitious matrix and developed at ACBM Center is described below.

R-CURVE APPROACH FOR PREDICTING MATRIX RESPONSE AT THE BOP

As indicating in Fig. 12B, since only a single macrocrack penetrates whole cross section of the specimen at the BOP, a fracture mechanics approach can be used to model fracture response at the BOP.

When load is applied to a specimen with an initial crack of size a_0, it produces strain energy (U). The rate of strain energy with respect to crack length (a) is denoted by G and is termed as the strain energy release rate. On the other hand, the crack propagation at the crack tip needs to consume some energy (W). Rate of change of this with respect to crack length (a) is denoted by R and is termed as the fracture resistance. The crack propagates when the following condition is satisfied:

$$G = R \tag{2}$$

For a brittle material such as glass, R is a material constant which may referred as to G_c (or equivalently K_c), and propagation of the initial flaw means catastrophic failure of the specimen. However in cementitious materials, due to the existence of crack arrest mechanisms such as aggregate bridging and microcrack shielding, the crack steadily propagates until a second condition is also satisfied (see Fig. 13):

$$\frac{\partial G}{\partial a} = \frac{\partial R}{\partial a} \tag{3}$$

The crack length which simultaneously satisfies conditions (2) and (3) is the critical crack length and is denoted as a_c. Therefore two quantities, G_c and a_c, should be known in order to model failure of cementitious materials, where G_c is the value of G at $a = a_c$. Many studies have indicated that the value of a_c depends not only on material properties, but also on geometry of the specimen and size of the initial flaw[12][13]. Jenq and Shah[14] proposed to use the critical crack tip opening displacement ($CTOD_C$), rather than a_c, to describe fracture of cementitious materials. According to their two parameter fracture model, fracture properties of cementitious materials can be obtained from two constants: the critical stress intensity factor, K_{IC} [$K_{IC} = (EG_c)^{1/2}$, E being Young's modulus of the material], and $CTOD_C$. They found that both K_{IC} and $CTOD_C$ are material properties, which can be determined from a single notch beam test[15]. By using the two parameters Ouyang, Mobasher and Shah[16][17] have derived a general R-curve formulation from the basic definitions of the R-curve given in Eqs. (2) and (3) for quasi-brittle materials. The approximate formulation of the R-curve is given in the following equation:

$$\begin{aligned} R &= \beta\psi(a-a_0)^{d_2} \\ \psi &= 1-\left[\frac{d_2-(\alpha-1)/\alpha}{d_1-(\alpha-1)/\alpha}\right]\left(\frac{\alpha a_0-a_0}{a-a_0}\right)^{d_2-d_1} \\ d_{1,2} &= \frac{1}{2}+\frac{\alpha-1}{\alpha}\pm\left[\frac{1}{4}+\frac{\alpha-1}{\alpha}-\left(\frac{\alpha-1}{\alpha}\right)^2\right]^{\frac{1}{2}} \end{aligned} \tag{4}$$

where $\alpha = a_c/a_0$, and β is a constant to be determined. The values of α and β can be obtained from

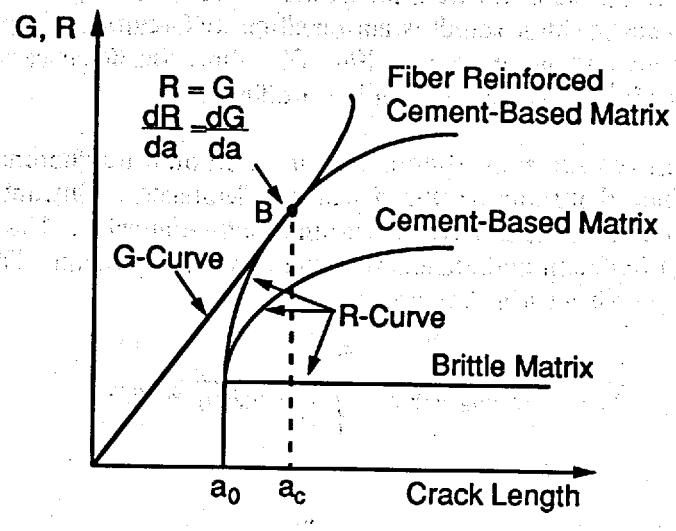

(a) R-curve behavior of different matrices

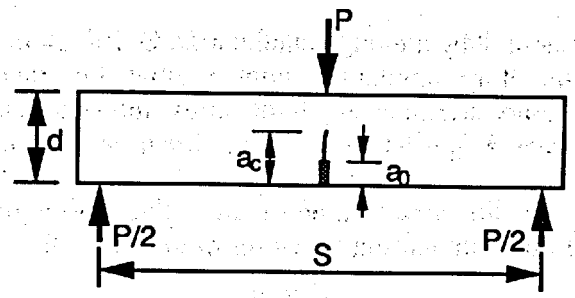

(b) Three-point bend beam

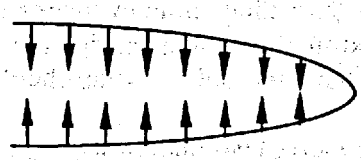

(c) Modeling of fiber bridging by a closing pressure

Fig. 13 Toughening of cementitious matrix due to fiber reinforceementt

the conditions: $K_I = K_{IC}$ and $CTOD = CTOD_C$, where K_I and CTOD are the stress intensity factor and the crack tip opening displacement respectively, resulting from the applied force. Both K_I and CTOD can be obtained from a linear elastic fracture mechanics (LEFM) handbook[18]. The R-curve determined from Eq. (4) can be interpreted as an envelope of G-curves of specimens with different sizes but the same initial flaw and geometry (see Fig. 13). Once the R-curve is known for a material with a certain geometry, its fracture response can be predicted.

For cementitious matrices with fiber reinforcement, additional toughening due to fiber bridging should be considered when determining the R-curve. Mobasher, Ouyang and Shah[19][20] have recently extended their R-curve to fracture of fiber reinforced composites. The presence of fibers can reduce both the stress intensity factor and the crack tip opening displacement. Therefore, the instability conditions (the BOP) for matrices with fiber reinforcement are:

$$K_{IC} = K_I^m(\sigma_{mf}, a_c) - \int_0^{a_c} p(x, a_c) K_I^F(x, a_c) dx \tag{5}$$

$$CTOD_c = CTOD_m(\sigma_{mf}, a_c, a_0) - \int_{a_0}^{a_c} p(x, a_c) Q(\sigma_{mf}, a_c, a_0) dx \tag{6}$$

where σ_{mf} is the stress at BOP resisted by the toughened matrix, Q is the Green's function for the crack closure at point a_0 due to a unit force applied at point x along the crack length, p is the closure pressure at a point x along the crack face, and K^F_I is the stress intensity due to a unit load applied at the point x along the crack surface. K^m_I, $CTOD_m$, K_I^F and Q can be obtained based on LEFM[18].

An experimental fiber-pull out slip curve can be served as the closing pressure. Alternatively, the following expression may be used as the closing pressure up to the BOP:

$$p = \frac{\eta \tau V_f Lu}{d_f u_0} \tag{7}$$

where η is the fiber efficiency factor depending on many factors such as the fiber orientation and the fiber length, τ is the average bond strength of fiber-matrix interface, V_f is the fiber volume fraction, L is the fiber length, d_f is the fiber diameter, and u_0 is the fiber slip at the maximum pull-out load.

After determining the closing pressure, two unknowns, σ_{mf} and a_c, can be obtained from Eqs. (5) and (6). Parameters α and β can then be determined, and mechanical response of matrices reinforced by fibers can be predicted.

Comparisons between theoretical and experimental results are also given in Fig. 9 for the continuous glass fiber composites, in Fig. 10 for the continuous steel fiber composites, and in Fig. 11 for discontinuous, short steel fiber composites. It is found that the proposed R-curve approach match quite well with the experimental results.

Park, Lee and Lim[21] reported their experimental results on high strength cementitious paste reinforced with discontinuous, short carbon fibers. The high strength cement paste consisted of portland cement, silica powder, and superplasticizer. The pitch based carbon fiber, with the length of 3 mm and the diameter of 14.5 micron, was used. Dog-bone specimens with a cross sectional dimension

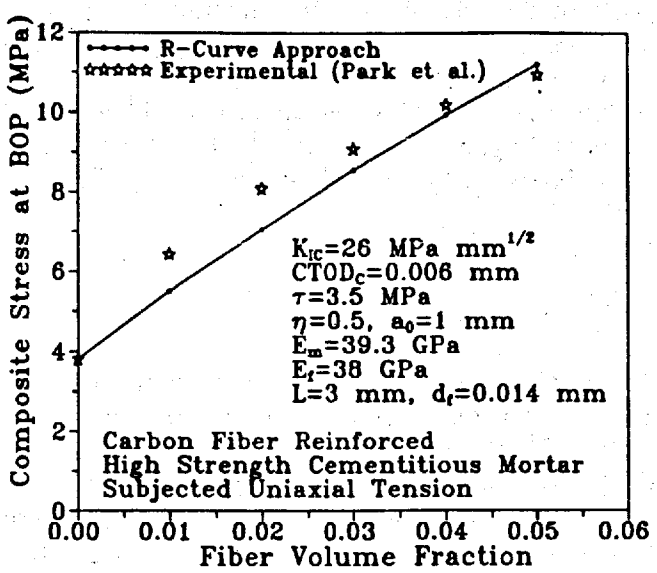

Fig.14 Theoretical and experimental comparison for high strength cementitious mortar reinforced with carbon fibers subjected to unaxial tension

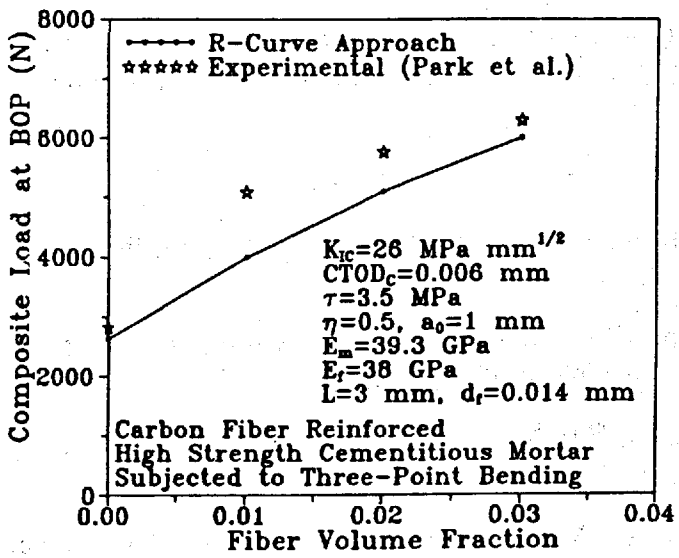

Fig. 15 Theoretical and experimental comparison for high strength cementitious mortar reinforced with carbon fibers subjected to three-point bending

of 30 x 12 mm, and beams with dimensions of 40 x 40 x 160 mm were cast. The dog-bone specimens were tested under uniaxial tension, whereas the beams were tested in three-point bending. The specimens were tested after 7-day curing in an autoclave. Both theoretical and experimental composite loads for different fiber volume fractions are depicted in Figs. 14 and 15 for the uniaxial tension specimen and the three-point bend beam, respectively[20]. It is noteworthy that by using the same material properties the proposed R-curve approach is capable of predicting the fracture responses of different geometries.

CONCLUSIONS

Toughening of cementitious matrices reinforced by continuous and discontinuous steel, glass, polypropylene or carbon fibers has been studied. It is found that when a cement-based matrix reinforced with not greater than 1% fibers, the fibers almost do not influence the tensile strength of the matrix, and only after the matrix crack, do the fibers contribute by bridging the cracks. However, when a cement-based matrix reinforced with greater than 2% fibers, the interaction between the fibers and the matrix seems to fundamentally enhance the inherent tensile strength and strain capacity of the matrix. Such beneficial interaction may lead to produce a new class of cement-based materials.

An R-curve approach has been proposed to simulate fracture behavior of toughened matrices. The proposed R-curve can reasonably well describe the matrix toughening due to fiber reinforcement.

ACKNOWLEDGEMENTS

The support from NSF Center for Science and Technology of Advanced Cement-Based Materials (ACBM) Grant #DMR-8808432, and NSF Grant MSM-8906937 is gratefully appreciated.

REFERENCES

1. Shah, S. P.: "Do Fibers Increase The Tensile Strength of Cement-Based Matrix?" ACI Materials Journal, 1991, 88 (6), 595-602.

2. Romualdi, J. P., and Batson, G. P.: "Mechanics of Crack Arrest in Concrete". Journal of Engineering Mechanics Division, ASCE, 1963, 63, 147-168.

3. Broms, B., and Shah, S. P.: "Mechanics of Crack Arrest in Concrete". Discussion, Journal of Engineering Mechanics, ASCE, 1964, 90, 167-173.

4. Shah, S. P., and Naaman, B. V.: "Mechanical Properties of Glass and Steel Fiber Reinforced Mortar". ACI Journal, 1976, 73, 50-53.

5. Mobasher, B., and Shah, S. P.: **Interaction between Fibers and Cement Matrix in Glass Fibers Reinforced Concrete.** Thin-Section Fiber Reinforced Concrete and Ferrocement, ed J. Danniel and S. P. Shah. American Concrete Institute, Detroit, 1990, SP-124, p. 136-150.

6. Oakley, D. R., and Proctor, B. A.: **Tensile Stress-Strain Behavior of Glass Fiber Reinforced Cement and Concrete.** Fiber Reinforced Cement & Concrete, RILEM Symposium, ed by A. Neville. The Construction Press LTD, 1975, p. 347-360.

7. Mobasher, B., Stang, H., and Shah, S. P.: "Microcrack in Fiber Reinforced Concrete". Cement and Concrete Research, 1990, 20, 665-676.

8. Somayaji, S, and Shah, S. P.: "Bond Stress vs. Slip Relationship and Cracking Response of Tension Members". ACI Journal, 1981, 78, 217-225.

9. Banthia, N., and Sheng, J.: "Strength and Toughness of Cement Mortars Reinforced with Micro-Fibers of Carbon, Steel and Polypropylene". **Proceedings of 2nd Canadian Symposium on Cement and Concrete**, 1991.

10. Mobasher, B., Castro-Montero, A., and Shah, S. P.: "A Study of Fracture in Fiber Reinforced Cement-Based Composites Using Laser Holographic Interferometry". Experimental Mechanics, 1990, 30, 286-294.

11. Shah, S. P., and Ouyang, C.: "Mechanical Behavior of Fiber-Reinforced Cement-Based Composites". Journal of the American Ceramic Society, 1991, 74 (11), 2727-2738, 2947-2953.

12. Jenq, Y.-S., and Shah, S. P.: "Fracture Toughness Criterion for Concrete". Engineering Fracture Mechanics, 1985, 21, 1055-1069.

13. Bazant, Z. P., and Kazemi, M. T.: "Determination of Fracture Properties from Size Effect Tests". International Journal of Fracture, 1990, 44 (111), 111-131.

14. Jenq, Y.-S., and Shah, S. P.: "A Two Parameter Fracture Model for Concrete". Journal of Engineering Mechanics, 1985, 111, 1227-1241.

15. RILEM Committee on Fracture Mechanics of Concrete: "Determination of Fracture Parameters (K^s_{IC} and $CTOD_C$) of Plain Concrete Using Three-Point Bend Tests," Materials and Structures, 1990, 23, 457-460.

16. Ouyang, C., Mobasher, B., and Shah, S.P.: "An R-Curve Approach for Fracture of Quasi-Brittle Materials". Engineering Fracture Mechanics, 1990, 37, 901-916.

17. Ouyang, C., and Shah, S. P.: "Geometry Dependent R-Curve for Quasi-Brittle Materials". Journal of the American Ceramic Society, 1991, 74 (11), 2831-2836.

18. Tada, H., Paris, P. C., and Irwin, G. R., **The Stress Analysis of Cracks Handbook**, 2nd Ed., Paris Productions, St. Louis, U.S.A., 1985.

19. Mobasher, B., Ouyang, C., and Shah, S. P.: "Modeling of Fiber Toughening in Cementitious Materials Using an R-Curve Approach". International Journal of Fracture, 1991, 57, 199-219.

20. Ouyang, C. and Shah, S. P.: "Toughening of High Strength Cementitious Matrix Reinforced by Discontinuous Short Fibers". Cement and Concrete Research, 1992, in press.

21. Park, S. B., Lee, B. I., and Lim, Y. S.: "Experimental Study on the Engineering Properties of Carbon Fiber Reinforced Cement Composites". Cement and Concrete Research, 1991, 21, 589-600.

POSTER THEME

ADVANCES IN PHYSICO-CHEMICAL EVALUATION CHARACTERISATION AND QUALITY CONTROL TECHNIQUES AND SYSTEMS

State of the Art Report

by

Hiroshi Uchikawa

ADVANCES IN PHYSICO-CHEMICAL CHARACTERIZATION AND QUALITY CONTROL TECHNIQUES FOR CEMENT AND CONCRETE

Hiroshi Uchikawa

Prof. Dr. Eng., Executive Director
Research and Development
ONODA Cement Co, Ltd, JAPAN

CONTENTS

1. INTRODUCTION ---------- 797

2. DEFINITION OF TERMS ---------- 797

3. ADVANCED CHARACTERIZATION TECHNIQUE ---------- 799

3.1 Outline of Characterization Technique ---------- 799

3.2 Advanced Characterization Technique in Bulk and Macroscopic Region ---------- 799

3.2.1 Composition ---------- 799

(1) Absorptiometry ---------- 799
(2) Atomic absorption spectrometry ---------- 801
(3) Emission spectrometry ---------- 803
(4) Polarography ---------- 803
(5) Chromatography ---------- 804
(6) X-ray fluorescence analysis ---------- 805
(7) Mass analysis ---------- 805
(8) Activation analysis ---------- 806

3.2.2 Structure ---------- 806

(1) XPS(ESCA) ---------- 806
(2) NMR ---------- 809
(3) ESR ---------- 811
(4) Thermal analysis ---------- 812
(5) SFC ---------- 813
(6) Determination of pore structure ---------- 813
(a) Measurement of gel pore space ---------- 815
(b) Measurement of capillary pore space ---------- 816
(c) Air void ---------- 816

3.3 Advanced Characterization Techniques of Surface and Microscopic Region ---------- 819

(1) SEM and FESEM ---------- 819
(2) ESEM ---------- 822
(3) TEM and AEM ---------- 825
(4) CMA/EPMA ---------- 828
(5) AES and μ-AES ---------- 833
(6) Microfocus x-ray diffractometer ---------- 840
(7) Extended x-ray absorption fine structure (EXAFS) ---------- 842
(8) SIMS ---------- 842
(9) STM and AFM ---------- 845
(10) Microscopic Fourier transform infrared spectrophotometer ---------- 847
(11) Microwave scanning electron spin resonance microscope ---------- 849
(12) Differential interference microscope ---------- 850

3.4 Image Processing ---------- 851

4. DEVELOPMENT OF NEW QUALITY CONTROL TECHNIQUE ---- 855

4.1 Evaluation and Control of Rheological Properties and Setting of Cement ---- 855

4.1.1 Relationship between Characters of Clinker and Fluidity and Setting of Cement ---- 855

(1) Setting of cement from the viewpoint of rheology and chemical reaction ---- 855
(2) Relationship between Morphology of C3Ass and C4AFss in clinker and fluidity of cement ---- 856
(3) Relationship between etching characteristics of polished surface of clinker and setting of cement ---- 856
(4) Relationship between heat of hydration and fluidity and setting of cement ---- 857
(5) Relationship between morphology of interstitial phase in clinker, etching characters of clinker and heat of hydration of cement, and manufacturing conditions of cement ---- 858

4.1.2 Control of Fluidity and Setting of Cement ---- 858

4.2 Evaluation and Control of Strength of Cement ---- 861

4.2.1 Relationship between Characters of Clinker and Strength of Cement ---- 861

(1) Process of hydration of cement and development of strength ---- 861
(2) Relationship between optical properties of clinker mineral and strength of cement ---- 861
(3) Relationships between trace and minor components in clinker mineral and burning degree of clinker and strength ---- 864
(4) Relationships of optical properties of clinker, trace and minor component in clinker mineral and burning degree with manufacturing conditions ---- 865

4.2.2 Control of Strength of Cement ---- 865

4.3 Evaluation and Control of Grindability of Clinker ---- 867

4.3.1 Relationship between Characters of Clinker and its Grindability ---- 867

(1) Evaluation of grindability of clinker ---- 867
(2) Relationship between pore structure of clinker and its grindability ---- 868
(3) Relationship between optical properties of clinker minerals and its grindability ---- 870

4.3.2 Control of Grindability of Clinker ---- 871

5. SUMMARY ---- 874

REFERENCES ---- 876

1.INTRODUCTION

For estimating the production process of mineral compounds in clinker, the production reaction conditions including temperature and atmosphere, and burnability, fineness and uniformity of raw materials, it is necessary to know the characters including texture of clinker, types and contents of clinker minerals, composition, type, content and distribution of minor and trace element in clinker minerals, size of crystal, optical properties, crystallinity, distribution of clinker minerals, pore size distribution and porosity of clinker.

The hydration process of cement and the characters of hydrate produced as well as the unhydrated cement particles and aggregate are closely related to the flocculated and hardened structures of concrete and the development of physical properties of concrete.

The characterization of clinker, cement, and hydrate and concrete system is, therefore, indispensable for the material design of cement and the development of high-performance and multifunctional cement and a guide for giving the control function of hydration reaction and structure formation and the intelligent function to cement and concrete to develop desirable properties(**1**).

Conventional techniques have been mainly aimed at the characterization of materials in bulk and macroscopic region using various chemical analyses, infrared spectrophotemetry, nuclear magnetic resonance spectroscopy, thermal analysis, optical microscopy and powder x-ray diffractometry to determine the mean structure, estimate the state of bonding, identify the minerals, observe the surface structure and determine the structure of material.

With the advance of electronic, control and image processing technologies, the establishment of the correlation in the material between the characters and the properties and the need for the precise and reliable production and quality control systems, the characterization techniques are shifting to the microscopic region aiming at the elucidation of the surface characters more closely related to the properties of mineral.

Meanwhile, the advanced characterization and evaluation techniques give the basic data to choose the conditions suited for producing cement and concrete with specified quality and desirable properties and play an important role in the establishment of the quality control system.

This paper outlines the report of all researches presented since 1986 when 8th International Congress on the Chemistry of Cement was held in Rio de Janeiro and describes the characterization of clinker, cement, and hydrate and concrete systems, the evaluation method of properties and the current technical level of quality control system with new knowledge.

2. DEFINITION OF TERMS

"Composition" and "structure" are used for characterizing "matter". The composition includes mean chemical and ionic composition, mineral composition, compound composition, and chemical, mineral and ionic compositions of each compound. The structure includes electronic and band structures in the order of magnitude of atom; coordinate structure, lattice defect and solid solution structure in the order of magnitude of crystal structure; mosaic structure, crystallite and twin structure in the order of magnitude of polycrystalline structure and agglomeration structure including crystal, amorphous substance and pore

The composition and structure in such a broad sense are defined as "character".

Each matter has its own properties including strength, conductivity, refractivity, magnetism, mass, expansibility and elasticity. "Properties" are the nature and the chemical quantity inherent in the matter, which are recognized by reacting to other matter or energy. Properties completely depend upon the composition and structure of the matter.

"Characterization" is to elucidate and express the character of matter.

Let c_i = individual character, p_i = individual property, C = all characters, P = all properties, m = composition and n = structure,

$$p_i = f_i (m_1, m_2, ..., n_1, n_2, ...) = f_i (m_j, n_j)$$
$$= f_i (m \& n) = f_i (C) \quad \text{---------- 2.1)}$$

Individual property is related to all properties through f_i. Also the following formula exists:

$$P = \Sigma p_i = \Sigma f_i (m_j, n_j) = F (m_j, n_j) = F (C) \quad \text{---------- 2.2)}$$

All properties are related to all characters through F. Expressing some characters by C' or (m' & n'),

$$p_i \cong f_i (m' \& n') = f_i (C') \quad \text{---------- 2.3)}$$
$$P \neq F (m' \& n') \quad \text{---------- 2.4)}$$

The formulas of **2.3)** and **2.4)** reveal that all properties are unable to be related to some characters though some properties are related approximately to some characters.

It is generally impossible, though desirable, to elucidate all characters of matter and to relate characters to individual or all properties of it. Partial characterization to approximately relate some characters to some specified properties is, therefore, widely applied to the knowledge of property in the field of materials science.

"Reaction" is a change of character with time and "state" is an equilibrium state of character. Science to determine the correspondences of f and F in the formulas of **2.1)** through **2.4)** on the fixed characters to clarified properties is called the "theory of the properties ".

An aggregation of matter with some performance is defined as "material".

"Performance" is some properties of matter or material incarnated in the form applicable to a certain purpose. "Evaluation" is to judge the applicability of matter or material to the purpose using quantified property or performance of it. "Matter design" is to determine the characters of matter required for incarnating some predetermined properties and the matter design for the specified-performance material forming the body with a certain purpose is defined as "material design".

It is, therefore, able to considerably accurately estimate the specified properties by the partial characterization of some characters closely related to the specified properties. When something unusual is noticed in the specified properties, it is also able to restore the properties by modifying the character related to unusual properties by examining some characters concerned. The concept is widely used in quality control of the production of materials.

"Quality" is a general term for the character, property or performance of material or product. Although the quality should be indicated by the property or performance, it can be comprehensively indicated by some characters instead of the property or performance when it is difficult or it takes a long time to determine them.

"Quality control" is to keep the quality constant or improve it using appropriate tools, methods and systems to most economically manufacture the material or product with quality meeting the requirements of customers.

Quality control is usually carried out by clarifying the relationship in the material or product between the character and the property, quantitatively determining the effect of each character on the property, analyzing and measuring some effective characters, controlling the

characters based on the data obtained and maintaining the properties within a constant range or improving them.

A new characterization technique, the principle for statistically treating the measurements, and computer and artificial intelligence for the data processing and the feedback or feedforward of data to the production process are being applied to the higher degree quality control.

3. ADVANCED CHARACTERIZATION TECHNIQUE

3.1 Outline of Characterization Technique

Clinker, hydrated cement and concrete are multi-component heterogeneous systems composed of components and their textures widely ranging from orders of magnitude of nm to cm. The regions for characterization of clinker, cement, hydrate and concrete are classified into the textural, particulate and atomic levels according to the size. The characters of those levels by the compositions and structures are shown in **Table 1.**

The characterization techniques corresponding to the characters described in **Table 1** are classified the separation, composition analysis, shape observation, state analysis and structural analysis as shown in **Fig. 1.**

Macrocharacters are the characters of the matters or materials in the macro region shown in **Table 1** and they are indicated in most cases as mean compositions and structures in bulk in the whole range. Microcharacters are the characters of the composition and structure in the micro region such as in a local place, on the surface and in the direction of depth.

3.2 Advanced Characterization Technique in Bulk and Macroscopic Region

3.2.1 Composition

Since the characterization in bulk and macroscopic region is frequently aimed at determining the mean composition and mean structure, the sample is generally decomposed into an analyzable or measurable form and the analytical methods range from wet chemical analysis to large-scale instrumental analysis according to the nature and properties of sample, the shape, kinds and contents of coexisting components, the quantity of sample and the required accuracy. The main analytical methods of chemical composition are shown in **Table 2.**

Chemical analysis including gravimetric and volumetric analyses and x-ray fluorescence analysis are used for determining the main components, and emission spectroscopic photometry as well as absorptiometry and atomic absorption spectrometry is used for the trace components. Since the analyzable limit requirement of the target elements and the accuracy requirement of data have been increasingly exacting, great efforts are being spent to improve the sensitivity and selectivity of those techniques.

(1) Absorptiometry

The absorptiometry including flow injection analysis (FIA)(2), stopped flow analysis and high performance liquid chromatography (HPLC) in addition to conventional analyses are being developed in many divergences as the important detecting technique for the flow spectrophotometrical system. Highly sensitive thermal lens spectrophotometry and photoacoustic analysis for analyzing feeble absorption, high sensitive higher order differential method for separating overlapped absorption peaks, determining the shoulder of peak and eliminating the background, rapid scanning method, multiple wavelength photometry using a diode array detector and two wavelength spectrometry contribute to the progress of absorptiometry.

Highly sensitive organic reagents with molar absorptivity exceeding 10^5 of chelate reagents

including porphyrin, azo, hydrazone, crown and oxime compounds, ion-associating reagents, reagents coexisting with surfactants have been steadily developed. Moreover, absorptiometric systems including the collective concentration using a membrane filter and the preconcentration system using ion-exchange resin as the collection medium have been developed to improve the sensitivity and selectivity of absorptiometry.

Table 1 The character and the region of characterization of clinker, cement, hydrated cement and concrete

		Micro region: Atomic level (< 10nm)	Micro region: Particle level (10nm - 100 μm)	Macro region: Texture level (100 μm <)
Clinker and Cement	Structure	Crystal structure, Coordination number, Lattice defect, Super lattice, Surface structure	Morphology and texture of clinker mineral, Zonal structure, Lamellar structure, Twin crystal, Inner mineral, Morphology and texture of blending component, Morphology and kind of gypsum	Distribution and deposited texture of clinker mineral, Pore structure, Eutectic structure
	Composition	Incorporation site of element, Compositional change in the direction of depth from surface	Element distribution in clinker mineral, Amount of incorporated element, Density	Mean chemical composition, Mean mineralogical composition, Pore volume, Mean denisty, Kind and amount of blending component
Hydrated cement	Structure	Crystal structure, Coordination number, Condensation degree of anion, Lattice defect, Super lattice, Surface structure, Gel pore structure	Morphology of hydrates, Specific surface area, Twin crystal, Capillary pore structure	Flocculation structure, Hardened structure, Distribution of hydrates, Air void
	Composition	Incorporation site of element, Compositional change in the direction of depth from surface	Composition of hydrates, Element distribution in hydrates, Density	Mean chemical composition, Mean mineralogical composition, Pore volume, Mean denisity
Concrete	Structure	Adsorption structure of organic admixture	Transition zone between cement paste and aggregate, Element distribution in unhydrated cement, hydrates, blending component and aggregate	Distribution of cement, hydrates aggregate, air void and reinforcing material
	Composition		Amount of hydrates, Amount of $Ca(OH)_2$	Amount of cement, Coarse aggregate/fine aggregate ratio Amount of aggregate, Amount of blending component, Mean degree of hydartion, Element distribution Amount of admixture

Since a highly sensitive detector with the full scale of absorbance of 0.005 has been developed, a substance contained in the sample at the level of ppb can be directly determined combining with a reagent with a molar absorptivity of tens thousands. The detector is applied also to the multi-component determination method.

(2) Atomic absorption spectrometry

Even a small quantity of sample can be sensitively determined by the furnace atomic absorption photometry using an electric furnace such as a graphite furnace atomizer (GFA) and a metal-heating furnace for atomizing a target compound. Various improvements of the furnace design including the material, the inside wall surface of furnace, the introduction of sample, the temperature distribution in the furnace, the atomization reaction

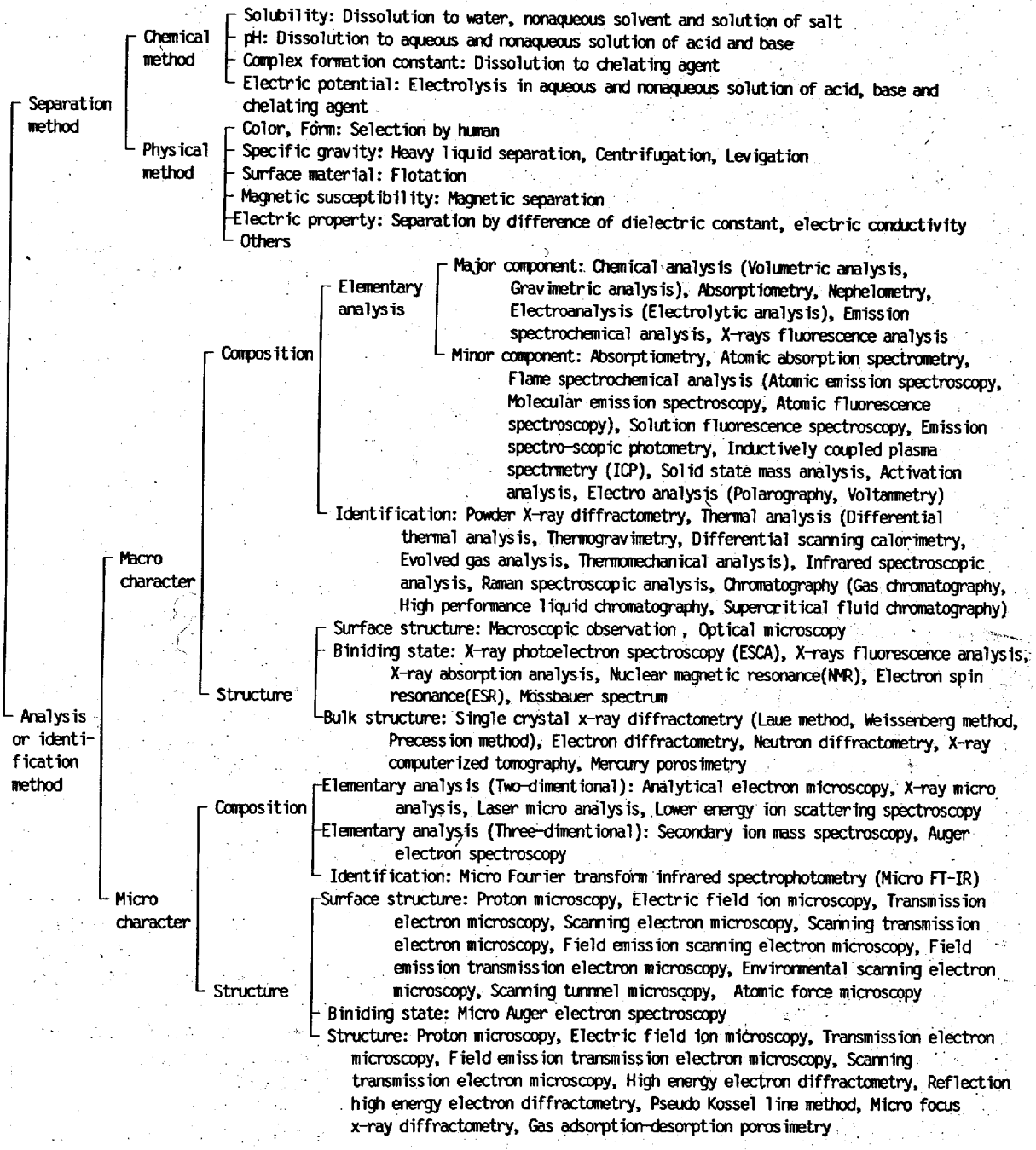

Fig. 1 Classification of characterization method

and the chemical interference and its elimination have been investigated. The temperature distribution in the furnace has become possible to be temporally and spatially uniformed by using a two-step atomizer equipped with GFA called the integrated contact cuvette with many contact points of electrode(3). The chemical interference can be eliminated by the matrix modification(4). A matrix modifier of palladium is sometimes added to the sample at the ashing stage to produce a thermally stable compound when the target component is volatile and to accelerate the vaporization or atomization when the target component may lower the atomization efficiency due to the production of oxide or carbide. The platform method(5) using a platform made of tantalum or graphite has been developed to improve the sensitivity. The atomic absorption photometry using the stabilized temperature platform furnace (STPF) combined with the matrix modification excellent in sensitivity, accuracy, interference and applicability to the analysis of actual sample is spreading.

Table 2 Comparison of various methods for chemical composition analysis

Method		Basic theory	Objective component	Sample	Sensitivity	Precision(%)	Factors affecting sensitivity
Chemical analysis		Titlation Gravimetry	Main Minor	Liq.(D)	10^{-5}mol	0.01-0.1	Analytical method, Purity of agent
Absorptiometric method		Photo adsorption	Minor	Liq.(D)	5×10^{-4} - 0.1ppm	5-10	Measurement condition, Coexisting element
Polarography		Current-voltage Characteristic	Minor	Liq.(D)	1×10^{-4} - 0.1ppm	5-10	Volume measurement
Flame photometry	Atomic spectroscopy	Emission Spectrum	Minor	Liq.(D)	2×10^{-3} - 0.1ppm	1-10	Structure of burner, Fluctuation of emission spectrum, Noise
	Atomic absorption	Absorption Spectrum	Minor	Liq.(D)	1×10^{-3} - 0.1ppm	1-10	Structure of burner and nebulizer
Emission spectrophotometry	Spark excitation	Emission Spectrum	Minor	Sol.(D)	0.1-100 ppm	5-10	Temperature change in plasma discharge, Self-adsorption, Gas
	Inductively coupled plasma spectrometry	Emission Spectrum	Minor	Liq.(D)	0.1-100 ppm	1-5	Structure of nebulizer and plasma dischanging tube
X-ray fluorescence analysis		Characteristic x-ray	Main Minor	Sol. and Liq.(N)	0.1- 100 ppm	0.01-0.1 5-10	Intensity of incident X-ray, Sensitivity of detector, White X-ray
Solid mass spectrograph		Mass-charge Ratio	Minor	Sol.(D)	0.1-100 ppm	Semi-quantitative	Method of excitation and detection
Neutron activation analysis		α-ray, β-ray γ-ray	Minor	Sol.(N)	10^{-3} - 10^{-8} ppm	2-10	Condition of irradiation, Kind of nuclei

Note, Liq.: Liquid, Sol.: Solid, D: Destruction, N: Nondestruction

In the flame atomic absorption spectrometry, the on-line preconcentration and the separation of matrix directly connected to FIA(6) and the optimization of atomic absorption spectrometry system using FIA(7) including parameters such as the suction rate of nebulizer and the flow rate of carrier have gained attention. The flame atomic absorption spectrometry is sometimes used as the detector of HPLC(8) for the chemical to determine elements by the states and as the absolute determination(9) without using the standards.

Glow discharge sputtering which is expected to be applied to advanced ceramics and high-temperature superconductor as well as metallic sample is highlighted as a new light source (10). An atomic absorption multi-element analyzer is being developed.

(3) Emission spectrometry

Emission spectrometry is an atomic emission spectrometry using spark discharge, arc discharge and inductively coupled plasma (ICP) as the excited light source. The emission spectrometry including ICP emission spectrometry is applied to the analysis of actual sample in various areas these days.

Since the introduction efficiency of the sample into plasma strongly affects the detection limit and accuracy in the ICP emission spectrometry, supersonic wave nebulizer, recycling nebulizer, thermospray and the Babington-type nebulizer for solution containing a salt at high concentration as well as conventional nebulizer are investigated. The slurry method(11) for injecting a sprayed water suspension of the fine powder samples of minerals and clay into ICP is also investigated. In addition to them, the electrothermal vaporization method(12) for introducing microliters of the sample solution vaporized by electrical heating in a graphite tube or on a tantalum or tungsten boat into ICP and the methods using spark discharge and laser ablation (13) to introduce the powder or solid sample into ICP receive considerable attention. Separation and concentration of a target component, removal of matrix components and chemical speciation are being investigated by combining FIA(14), HPLC(15) and ion chromatography (IC)(16) with ICP.

Prototypes of argon ICP(17) and helium ICP(18) using a torch of laminar flow formed by introducing the cooling gas and plasma gas from the circumference of the torch to the center have been fabricated to improve the detection limit. The helium ICP is expected to be a highly sensitive analysis for halogen elements with high excitation energy.

The photodiode array detector as the spectrophotometric multi-channel two dimensional detector is investigated to more efficiently use the multi-element analysis regarded as a special feature of the emission spectrometry(19)(20). Data processing on the spectral interference including near or overlapped spectral lines is computerized.

In addition, a continuous spray introduction method of aerosol has been developed for the microwave induced plasma emission spectrometry using plasma as the excited light source. The glow discharge tube is investigated gaining attention from the point of view of the direct analysis of solid and the solid surface characterization.

ICP-mass spectrometric analysis has so high sensitivity that it is characterized by the simultaneous determination of many microelements without the operations of separation and concentration of co-existing elements(21). The ICP-mass spectrometric analysis has been, therefore, increasingly used in recent years.

(4) Polarography

The incipient hanging mercury drop electrode (HMDE) is of the type using mercury drops supplied from the dropping mercury electrode (DME) to the tip of a platinum wire enclosed in a glass tube. At present, a micrometer type HMDE is used. Since a constant quantity of mercury is pushed out from a capillary tube with a piston or plunger moved by a micrometer screw in this type of HMDE, reproducibility is high and maintenance and management are easy. Recently , a static mercury drop electrode (SMDE) having the characteristics of both DME and HMDE has been developed. A mercury drop is almost instantaneously hung,

thereby improving the reproducibility of mercury drop.

Stepped wave semi-derivative and -integral polarography has been developed and a computerized polarography is being investigated. In this new rapid, high-sensitivity, high-resolving power polarography, stepped voltage is applied to the work electrode and the semi-derivative or semi-integral of the current sampled while the effect of charged current is decreased is plotted versus the potential.

The computer simulation of electrode reaction, the automatic control of electrochemical measurement and the on-line data processing will be applied to the detector of FIA(22).

(5) Chromatography

Chromatography is roughly classified into gas chromatography (GC), high performance liquid chromatography (HPLC) and supercritical fluid chromatography (SFC) according to the states of mobile phase.

GC is steadily used as the capillary GC. The determination accuracy of the split injection of sample is improved by using an autosampler injecting the sample for a period as short as 0.1 seconds. The loss of a component in the sample can be decreased and microanalysis can be made by applying the injection method to a cold-on-column. The sensitivity of GC is enhanced by injecting the sample as much as tens microliters into a capillary column. In the thermal cracking capillary GC useful for the characterization of polymers, quantitative microanalysis of low-boiling substance can be made by a newly developed thermal desorption apparatus based on the dynamic head space method.

A thick film wide pore capillary column is suitable for GC/MS and GC/FT-IR to determine trace and volatile components. High-molecular weight components have become possible to be analyzed by the development of high-temperature resistant capillary column(23).

An ultraviolet ray absorbing detector with long light path, a non-radiative electron capture detector utilizing energy generated by microwave induced discharge in helium and a detector combining a microwave induced plasma emission spectrometer with a photodiode array monitor(24) have been developed to improve the sensitivity and selectivity of detector. Combination of GC with other analytical methods including the GC/FT-IR/MS(25) and LC/GC(26) systems are putting high-separation, high-sensitivity capillary columns to practical use.

Since a high-pressure, infinite feeding, constant flow rate, non-pulsating feed pump is required for HPLC, various types of pumps are commercially available. Although a septum sample injector has been used for HPLC so far, a bubble injector is widely used at present. An injector weighing the sample with a perforated disc and injecting it by rotating the disc has been developed for micro-HPLC using a small-diameter column to prevent the peak width from widening. In the computer-based HPLC system, the stable base line is obtained by the temperature gradient analysis programming the temperature of column oven.

An ultraviolet-visible detector, differential refractive index detector and fluorescence detector are usually used for HPLC. In order to obtain the qualitative information on the peak and improve the sensitivity, selectivity and flexibility of detection, MS, NMR, FT-IR, ultraviolet detector, Raman spectrophotometer, ESR, electrochemical detector, detectors utilizing radioactivity, chemical emission and laser, ICP, rotary power detector, dielectric gas detector, flame detector and flow potential detector are being investigated.

Computerization is tried not only to the application to the data processing but also to the data transmission to a host computer as a part of laboratory automation regarding HPLC with integrator as a terminal analytical system. Fast-HPLC has recently been developed to shorten the analyzing time maintaining the separating power constant by reducing the particle size of filler as small as 3 to 5μm and cutting down the column length.

Highly sensitive ion chromatography has recently been developed by connecting a background-eliminating column to the outlet of the separating column in series in the ion-exchange chromatograph to remove acidic or basic material used as the eluting agent in the form of water or transform it into lower-conductivity material, thereby feeding only target ion specimens to the conductometric cell. This ion chromatography is widely used.

(6) X-ray fluorescence analysis

Although x-ray fluorescence analysis has made great technical progress in the data processing and the improvement of operability based on the computerization, the analytical method and instrument have been only partially improved.

In the simultaneous multi-element analyzer, the counting linearity is extended to 3200 Kcps by improving the counting circuit. In the sequence analyzer, the x-ray intensity is increased by shortening the x-ray path length and any component ranging from trace to main components can be analyzed under the same excitation conditions by installing an absorber for controlling the amount of x-ray at a perfect integral ratio at any wavelength. As a result, a hybrid analyzer using a goniometer and a fixed monochromator has been developed for qualitative and quantitative analyses. An artificial multilayer film with high reflection intensity has been developed as a spectral element in the analysis in the long wavelength x-ray region **(27)**.

Since synchrotron orbital radiation (SOR) is characterized by the wavelength region, intensity, directivity and polarization characteristics unlike conventional radiation source, microanalysis, microscopic analysis, surface analysis and state analysis are being developed using SOR as the exciting radiation source **(28)**.

The correction method of matrix effect to improve the reliability of quantitative analysis includes the correction factor method and the fundamental parameter (FP) method. The accuracy of determination of the correction factor method is improved by the improvement of the accuracy of measurement of x-ray fluorescence intensity and the using of many standard samples, and the fundamental parameter method is improved by the improvement of reliability of various data used. The FP method is becoming the main unroutine correction method by investigating the fundamental constants and wavelength integral and utilizing a high-accuracy minicomputer.

An automatic bead sample-preparing machine incorporated into the on-line analytical system is spread for raw materials analysis in most cement manufacturing plant**(29)**.

(7) Mass analysis

Mass analysis is made in such a way that the sample is ionized and the produced ions are separated according to the mass during the passing through the magnetic field and detected. Accordingly, the molecular weight of the sample can be accurately, sensitively, rapidly determined, the elementary composition can be easily determined and the isotopes can be distinguished from each other**(30)**.

Using a new soft ionization method, especially the fast atom bombardment (FAB) method using fast argon atoms instead of the primary ion and the collision activated dissociation(CAD) method for conducting mass analysis of fragment ions decomposed by the collision of ions coming from the ion source to a collision chamber installed between the ion source and the electric field, a mine of information can be obtained and even a mixture can be analyzed. A computer with a molecular weight of 20,000 or more can be analyzed by the newly developed FAB method.

The secondary electron multifier is now almost used as the detector in such a way that the ionic current amplified with a DC-amplifier is visualized on a cathode ray tube, recorded and processed with a pen-recorder or a computer. A time-of-flight (TOF) type detector is used for determining a compound with a molecular weight as high as 10,000 or more and an ion-

cyclotron resonance type detector is used for improving the resolving power.

High-resolving power, high-sensitivity, rapid analysis of a mixture can be made by combining the soft ionization method with link-scanning or MS/MS. Although a volatile mixture sample is analyzed by GC/MS, a non-volatile one is expected to be analyzed by LC/MS, and instruments based on the thermospray, electronspray and Frit-FAB methods have recently been put to practical use.

(8) Activation analysis

Activation analysis is widely used as an elemental analysis characterized by both radiochemical activation analysis and instrumental activation analysis. The fundamental issues including the principle and procedure have not been progressed and the radiation detectors and data processing techniques have been limited to diversification. The radio-chemical activation analysis is a microanalysis superior in the sensitivity and accuracy **(31)** and the instrumental activation analysis provides the information on the concentrations of many elements only by counting γ-rays with a germanium semi-conductor detector after activation.

Solvent extraction, ion-exchange and precipitation methods and a method vaporizing the hydrogenated sample and collecting it are used for preconcentration before activation to determine an element by separating chemical specimens of the element with different valences from each other and separating an inorganic compound from an organic compound **(32)**. Derivative activation analysis **(33)** is being studied to produce a measurable activated compound when a radioactive nuclide and a γ-ray emitting nuclide are hardly produced from the target element or compound.

Since a high-resolving power germanium semi-conductor detector has been developed, the instrumental neutron activated analysis (INAA) for detecting and determining many elements without chemical separation is mainly used at present as the activation analysis**(34)**. A correction method of the counting loss of γ-rays at high counting rate and an elimination method of piled up pulse have been proposed for INNA. Programs for more accurately determining the peak area from the γ-ray spectrum have been developed. A program coping with special measurements including the analysis considering the self-absorption affecting the γ-ray measurement in a low-energy region and the spectral difference method for reducing the Compton background effect in the analysis of very short life nuclide have been developed.

Since prompt gamma radiation analysis capturing neutrons is characterized by the independence of the characteristics of nuclei produced unlike the conventional thermal neutron activation analysis, this analysis is used for the on-line analysis of bulk sample utilizing the high permeability of neutron and γ-ray.

3.2.2 Structure

Analysis of interatomic and intermolecular bindings and that between atom and molecule, structural analysis and the tracing of reaction have been actively made by the x-ray photoelectron spectroscopy, nuclear magnetic resonance spectroscopy, electron spin resonance spectroscopy and supercritical fluid chromatography in recent years.

Since the pore structure in clinker, hydrate and concrete are closely related to their physical properties, the combined method of the gas adsorption method, the mercury intrusion method, the optical microscope - image processing method, the x-ray CT - image processing method for determining total pore distribution in concrete have been proposed.

(1) XPS(ESCA)

X-ray photoelectron spectroscopy detects kinetic energy of photoelectrons emitted from the sample irradiated with soft x-rays under a pressure as low as 10^{-8} Torr with an electronic energy analyzer to identify the elements from the difference of the kinetic energy distributions and conduct the state analysis.

The apparatus used for this analysis is called x-ray photoelectron spectroscope (XPS). X-ray photoelectron spectroscopy may be, therefore, called electron spectroscopy for chemical analysis (ESCA) and is suitable for the surface analysis of a material because photoelectrons are emitted only from the surface layer approximately 1nm deep. Soft x-rays with a narrow proper width such as MgKα and AlKα converged into hundreds microns through a collimator are used as the primary x-rays. Kinetic energy of photoelectrons emitted from the sample is measured with a hemispherical electrostatic analyzer shown in **Fig. 2**. The kinetic energy of photoelectrons is a difference between the energy of incident x-rays and the bond energy of electrons in a solid, ranging from zero to 1500eV as shown in **Fig. 3**. Since the bond energy depends upon the element and its state of chemical bonding, the state of chemical bonding can be determined by measuring the shift of the peak of energy as well as identification of element. XPS is suitable for analyzing all the elements except hydrogen because x-rays are used as the exciting source, though the spatial resolving power is not so high.

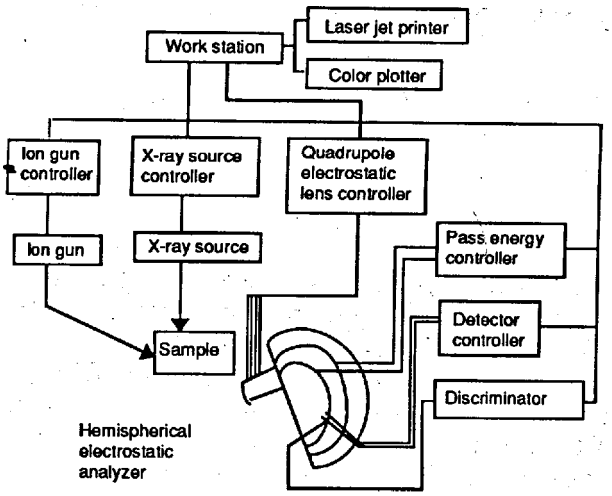

Schematic explanation

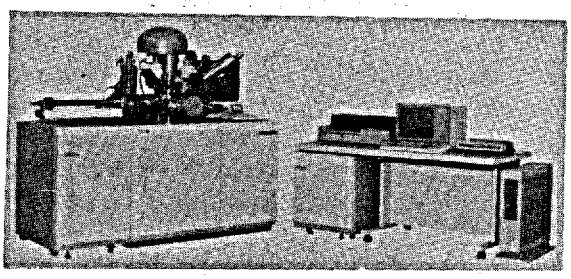

Fig. 2

X-ray photoelectron spectroscope (XPS: ESCA) and its block diagram (JEOL JPS-9000MC)

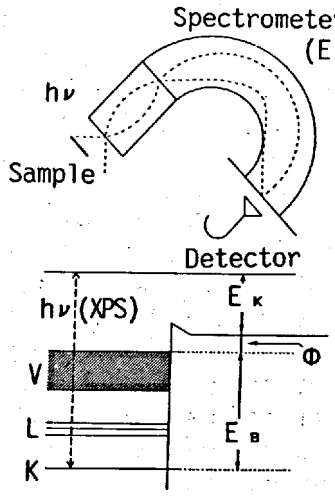

$E_B = h\nu - E_K - \Phi$

E_B : Bond energy of electron
E_K : Kinetic energy of photoelectron emitted from sample
$h\nu$: Energy from x-ray source
Φ : Work function

V : Valence band

Fig. 3

Kinetic energy of photoelectron

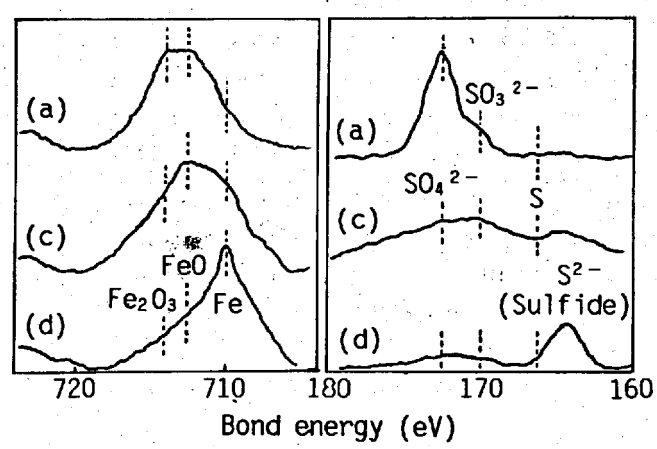

Burning atmosphere
(a): Oxidizing, (c): Slightly reducing,
(d): Reducing

Fig. 4

Photo electron spectra of Fe and S in clinker burnt under various atmospheres (Uchikawa et al; (42))

In the cement and concrete field, a series of studies **(35)(36)(37)** was made for tracing the change of surface composition of cement compounds just after mixing with water in the first half of the 1980s. Since Rio de Janeiro Congress, the x-ray photoelectron spectroscopy (XPS) has been applied to the inference of the mechanism of alkali erosion from the behaviors of Zr^{4+}, Si^{4+}, Ca^{2+} and Na^{+} determined by the analysis of the surface of alkali-resistant glass fiber**(38)(39)**, the pursuit of the erosion process**(40)** and the evaluation of the erosion rate**(41)** as a part of the research on the durability of zirconia-containing alkali-resistant glass fiber for GRC.

The example applied to determine the existing state of iron and sulfur in clinker burnt in various atmospheres from the peak shift in XPS is shown in **Fig 4(42)**. The condition (a), (b), (c) and (d) correspond to that in the oxidizing, very slightly reducing, slightly reducing and reducing atmospheres, respectively. The result was compared with the peak profile of iron compounds with different oxidation numbers and it was found that Fe in the clinkers burnt in (a) and (c) is mainly trivalent and bivalent, respectively. Fe in (d) is metallic iron. When diameter of x-ray probe by XPS is decreased to 50 μm to determine oxidizing number of Fe in alite, S/N ratio of x-ray photoelectron becomes small because of decrease of content of Fe in alite but oxidizing number of Fe in alite in each clinker is the same as in the clinker burnt under various condition. Fe^{3+} produced by burning clinker in the oxidizing atmosphere substitute for Si^{4+} in alite, while Fe^{2+} produced by burning clinker in the reducing atmosphere substitute for Ca^{2+} in alite. Since the latter substitution takes place more readily than the former one from the view point of the structure and the balance of electric charge in alite, and the weight ratio of Fe_2O_3 /FeO is 2.23, it is considered that the content of Fe in terms of Fe_2O_3 is higher in the reducing atmosphere. State of S in clinker in (a) and (c) is 6-valent SO_4^{2-} and 4-valent SO_3^{2-}, respectively. Sulfur substitutes for silicon and exists dominantly in belite under oxidizing atmosphere and the content of S in the interstitial phase increases and that in belite decreases as the burning atmosphere shifts from the oxidizing atmosphere to the reducing one. The hexavalent S is reduced into bivalent S in (d) and the bivalent S is distributed in the form of CaS in the interstitial phase.

(2)NMR

Spinning energy given to a material with magnetic moment in a magnetostatic field is diverged by the Zeeman effect and quantized in the direction of magnetic field. Resonance adsorption occurs by irradiating the material with electromagnetic waves having energy corresponding to the splitting width. The nuclear magnetic resonance (NMR) method is based on the magnetic resonance adsorption by irradiating an atomic nucleus having nuclear magnetic moment with radio waves. The electron spin resonance (ESR) method is also based on the principle similar to NMR by irradiating lone pair electrons with microwaves. The resonance conditions in NMR and ESR are expressed by the following formulas **3.1)** and **3.2)**, respectively:

$$\Delta E = h\nu = h\gamma H_0/2\pi \quad \text{---------- 3.1)}$$

$$\Delta E = h\nu = g\beta H_0/2\pi \quad \text{---------- 3.2)}$$

Where ΔE = energy difference between levels, h = Planck constant, ν = resonance frequency, γ = gyromagnetic ratio, H_0 = intensity of external magnetic field, g = spectroscopic splitting factor, and β = Bohr magneton.

NMR determines the molecular structure including the state of electrons in the vicinity of nucleus, types of bonding atomic group, state of bonding, distance between spins and direction of spin by the chemical shift depending upon the variation of the electron densities in the vicinity of nucleus according to the properties of atom including polarization and the properties of molecule including ring current and by the spin-spin interaction (J-coupling) caused by being shielded from the external magnetic field by the adjacent nuclei with magnetic moment. Information on rotation, vibration and translation of molecule can be acquired by determining the relaxation mechanism including the inversion recovery technique measuring the spin-lattice relaxation time, T_1, by observing the transverse magnetization caused by the irradiation with the 90°-pulse (pulse rotating the magnetizing vector of nuclear spin oriented by the external magnetic field by 90°) τ seconds after irradiating with 180°-pulse and by the spin echo technique measuring the spin-spin relaxation time, T_2, by observing the spin echo caused by irradiating with the 180°-pulse τ seconds after irradiating with the 90°-pulse. NMR includes the continuous wave (CW)-NMR and Fourier transformation (FT)-NMR or pulse-NMR. CW-NMR determines the resonance absorption sweeping the external magnetic field of the frequency of radio wave used for irradiation. FT-NMR produces the spectrum of the frequency region by the Fourier transformation of the free induction decay signal generated by the irradiation with a short but high-power radio wave. Although the sensitivity of NMR is much lower than those of infrared and ultraviolet spectrophotometries, the FT-NMR method has so high sensitivity by integration that the NMR signal of elements of low isotopic abundance can be easily obtained. The market share of the apparatus based on FT-NMR is, therefore, extremely higher.

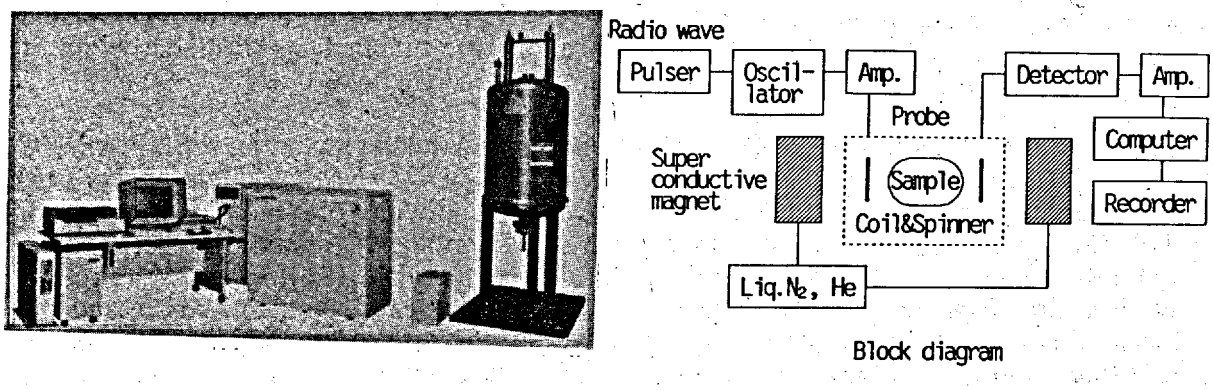

Fig. 5 Nuclear magnetic resonance spectrometer and its block diagram (JEOL JNM-GSX500)

A uniform, strong magnetic field is required for improving the resolving power of NMR. The resonance frequency of ^{1}H of the initial apparatus was approximately 40MHz. At the end of the 1960s, it was increased up to 100MHz. The intensity of magnetic field has been remarkably increased by the development of superconducting magnet up to 500 to 600MHz. The increased strength of magnetic field, improved probe and progress of computer have recently made the determination of ^{27}Al and ^{29}Si as well as ^{1}H and ^{13}C in solid possible. ^{43}Ca will be determined by NMR in the near future.

Although all the elements can be theoretically determined by NMR, practically the elements including ^{1}H and ^{13}C in the organic materials are mainly analyzed. NMR has hardly been applied to solid inorganic materials so far because these materials have so large anisotropy of chemical shift and so large interactions of dipole-dipole and quadrupole-quadrupole that no high-resolving power spectrum with narrow half-width can be obtained. NMR is being rapidly applied to the solid inorganic materials due to the progress of technologies including 1) dipolar decoupling, 2) cross polarization and 3) magic angle spinning. Dipolar decoupling is used for eliminating the interaction between ^{1}H and a different nucleus, one of the dipole-dipole interactions. Since the intensity of the dipole-dipole interaction in solid is as high as tens kHz which is remarkably larger than that of the spin-spin interaction in liquid, hundreds watts is required for eliminating the dipole-dipole interaction. The techniques including the combined rotation and multiple pulse spectroscopy (CRAMPS)**(43)** described later are required for eliminating the interaction between same type nuclei observed in the analysis of ^{1}H and ^{19}F of high isotopic abundance.

The sensitivity of solid-NMR lower than that of liquid-NMR is improved by one of the double resonance methods transferring the magnetization from ^{1}H to the nucleus to be analyzed through the dipole-dipole interaction by the irradiation with the electromagnetic waves resonant with ^{1}H. This is the cross polarization which increased the sensitivities of ^{13}C and ^{15}N by approximately 4- and 10-times, respectively, in the analysis of solid materials. Since the relaxation time of ^{1}H is relatively short, the waiting time of the pulse irradiation for integration can be shortened, so a signal with high S/N ratio can be taken up in a short period.

The anisotropy of chemical shift caused by the variation of resonance frequency according to the difference in the directions between the external magnetic field and the molecule can be eliminated by rotating the sample tilted at 54.7° (magic angle) to the external magnetic field at a rate of thousands Hz. The dipole-dipole interaction between the same type nuclei can be eliminated by rotating the sample at a rate as high as 10 to 20kHz without CRAMPS in ^{1}H- and ^{19}F-NMR**(44)**. The strength of signal is, however, distorted by increasing the rotating rate too much. The double rotation method rotating the sample at the magic angle and 30.6° and the dynamic angle spinning method periodically switching the rotation axis or continuously varying it with time between 37.4° and 79.2° has been studied**(45)**. Such improved high-resolving power solid-NMR is applied to the analysis of the structure of silicate ion in unhydrate and hydrate in the cement and concrete field.

Nuclear magnetic resonance (NMR) is used for analyzing nuclei including ^{29}Si, ^{27}Al, ^{13}C and ^{1}H in the cement and concrete field. The studies of ^{29}Si-NMR include papers **(46)** **(47)** presenting the relationship between the spectral band width of clinker constituents or clinker minerals and the crystal system, a paper **(48)** describing the relationship between the hydraulic reactivities and the chemical shift, papers**(49)(50)(51)(52)** presenting the relationships between the polycondensation degree of silicate anion in hydrate and the chemical shift, a paper **(53)** presenting the relationships between the absorption-spectral intensities of Q_0, Q_1 and Q_2, the hydration rates and the compressive strengths, and a paper **(54)** describing the change of the form of silicate anion by carbonation. The studies of ^{27}Al-NMR include papers **(55)(56)** presenting the change of the coordination number of Al in hydrate during the hydration process and the estimation of hydration rate. The studies of ^{13}C-NMR include a paper **(57)** describing the inference of the cause of retardation of hydration

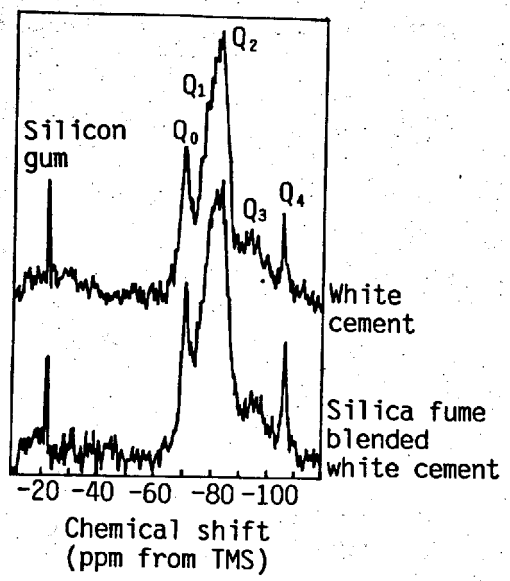

Fig. 6

^{29}Si-MAS-NMR spectra of hydrated white cement mortar and silica fume blended white cement mortar cured by autoclave (Uchikawa et al; (63))

by sucrose(saccharose). The studies of ^{1}H-NMR include papers**(58)(59)** presenting the pursuit of the behaviors of organic admixtures used for the hydration of cement and the estimation of hydration rate at the early stage of hydration, a paper **(60)** describing the estimation of the hydration mechanism of alite at the initial stage, a paper **(61)** presenting the state analysis of water by measuring the relaxation time, T_2, of ^{1}H, and a paper**(62)** describing the inference of porosity in hardened cement paste from the measurements of the relaxation time of ^{1}H in pore solution.

The following study contains the data obtained by solid high-resolving power FT-NMR which suggest the silicate anion structure of C-S-H. The result of autoclaved hardened mortar of white portland cement and silica fume-blended white portland cement analyzed by ^{29}Si-MAS-NMR spectrometer are shown in **Fig. 6(63)**. The gated decoupling method irradiating ^{1}H for decoupling only during the observation was used instead of the cross polarization method to get a sufficiently intense signal from a silicate anion without ^{1}H. The structure unit of silicate anion, that is, SiO_4^{4-} monomer, the end, middle and branched moieties of chain and the network chain have their respective chemical shift values, Q_0, Q_1, Q_2, Q_3 and Q_4, respectively, in the NMR spectrum as shown in **Fig. 6**. Their contents are determined from the peak intensity of Q_1, Q_2 and Q_3 corresponding to the silicate anion in C-S-H produced. Q_0 corresponds to unhydrated calcium silicate and Q_4 corresponds to quartz in fine aggregate and unreacted silica fume. The peak intensity ratio of Q_1/Q_2 depends upon whether silica fume is added or not. It is predicted from the peak of Q_3 that C-S-H contains the double chain structure. Relatively large peak width and peak resolution of Q_1 and Q_2 are attributed to the effects of the bonds of Qn-Ca and Qn-H_2O, the bond angle of Si-O-Si and the bond length of Si-O on the field state of silicon nucleus. Accordingly, new knowledge for elucidating the relationship between the characters of cement and the physical properties of mortar and concrete is being acquired.

(3)ESR

ESR identifies the paramagnetic species with lone pair electrons and estimates the valence of metal ion, electron state, spin state, density distribution of spin, symmetricalness of coordination of ligand and crystal structure by determining the variation of the resonance magnetic field intensity according to the shift of g-factor (corresponding to the chemical shift in NMR) caused by the interaction of the magnetic moment of electron derived from the orbital electron with the electron spin oriented in the external magnetic field and the split of peak of hyperfine structure (corresponding to the spin-spin interaction in NMR) affected by the adjacent nuclei with magnetic moment. Information on the interaction of paramagnetism center with the surrounding environment, exchange speed, rotary diffusion and translation can be acquired by determining the relaxation mechanism from the pattern and width of the

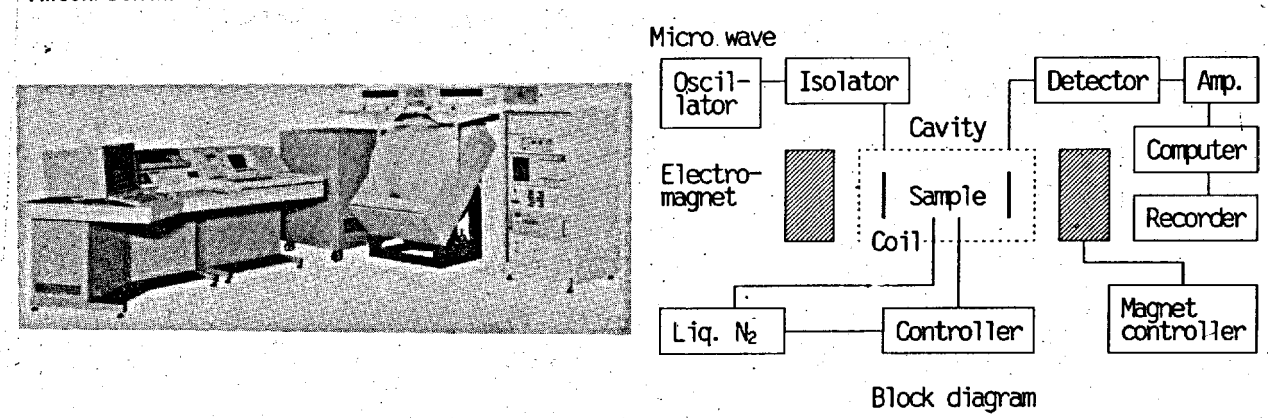

Fig. 7 Electron spin resonance spectrometer and its block diagram (JEOL JES-RE3X)

spectrum. ESR has been applied so far to the analysis of the location and coordination state of metal irons adsorbed onto the surface of clay materials in the inorganic chemistry.

The studies on the applications of electron spin resonance (ESR) to the cement and concrete field include a paper **(64)** presenting the determination of transition metal elements such as Fe^{3+} and Mn^{2+} by the charge numbers and the relationship between the content of transition metal and the lightness of white cement paste, a paper **(65)** describing the relationship between the number of lattice defects caused by incorporation of small quantities of Fe, Cu and Ni in C_3S, alite and belite, and the hydration reactivity, a paper **(66)** presenting the confirmation of the substitution of Mn for the tricalcium aluminate phase, a paper **(67)** presenting the crystal structure of C_3A, a paper **(68)** presenting the analysis of surface composition of C_3A, and a paper **(69)** presenting the crystal structure analysis of β-C_2S.

ESR has, however, been applied to a few researches, because the sample substances hardly contain lone pair electron and the interpretation of spectrum is too difficult to obtain useful information. It is expected that the technique for providing the sample with ESR activity will be developed and the interpretation technique of spectrum and its application will be systemized so that even average chemists will be able to apply ESR to the analysis for specified purposes. **Fig. 7** illustrates the apparatuses and block diagrams of ESR.

(4) Thermal analysis

Application of a microcomputer to the analysis of reaction rate by differential scanning calorimetry (DSC), the data processing with a dynamic thermal instrumental analysis requiring complicated calculation and the precision calibration of differential scanning calorimeter spreads and the thermal analyzer is being improved.

A differential thermal analyzer with the stable base line at high temperature has been fabricated on an experimental basis for studying the phase transformation of crystal and data by differential thermal analysis (DTA) have been obtained within the pressure variation of 0.1 MPa under a pressure up to 200 MPa **(70)**. A differential thermal analyzer using gas-firing **(71)** used in the high temperature region up to 3100°C has been fabricated on an experimental basis and the temperature is controlled by the optical technique. A apparatus for thermogravimetric analyzer has been improved so that the analysis can be made even in special atmosphere. A horizontal differential type thermogravimetric analyzer has been fabricated on an experimental basis for eliminating the apparent change of thermogravimetric curve by the thermal molecular flow (TMF) effect and the reaction of limestone and dolomite with SO_2 at high temperature has been investigated using a high-pressure type thermogravimetric analyzer.

A solid electrolyte gas sensor is used as a selective detector in a combined system of thermogravimetry-evolved gas analysis (TG-EGA). The phase transformation of the

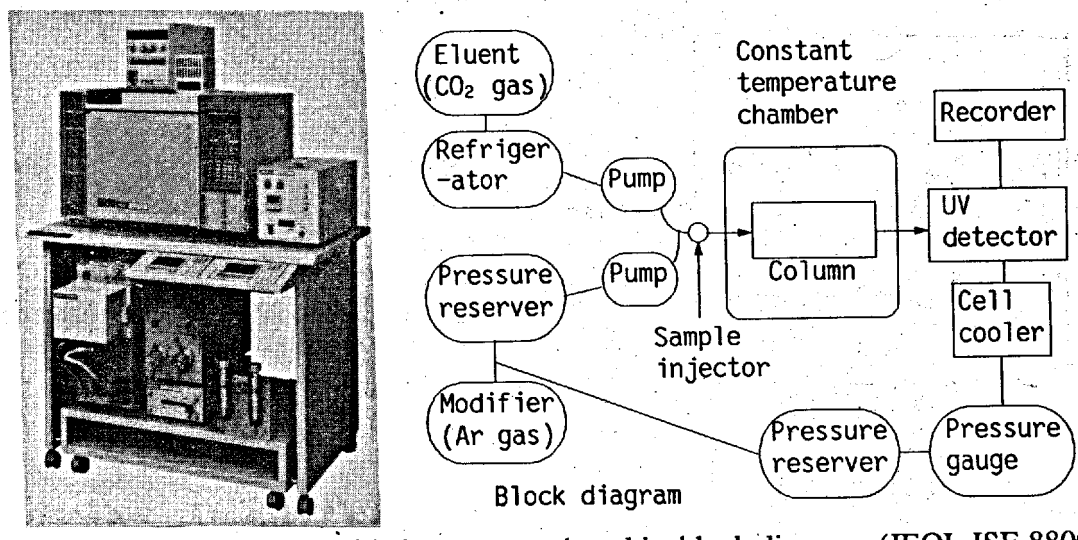

Fig. 8 Supercritical fluid chromatograph and its block diagram (JEOL JSF-8800)

ferromagnetic material is used as the standard substance for calibrating the temperature of thermogravimetric analyzer and it is supplied from ICTA (International Confederation for Thermal Analysis) - NBS. Temperature calibration is accurately made by connecting a balance to a weight with the thermometric substance.

An analyzer combining TG with GC, FT-IR and MS is being investigated **(72)** and it is expected as a characterization technique of high polymer materials.

(5) SFC

Supercritical fluid chromatography (SFC) uses a supercritical fluid produced by compressing gas up to high density at temperature and a pressure exceeding the critical points as the eluent. Although CO_2 containing a small quantity of an organic solvent as the modifier is generally used, hexane and some sort of gas such as Xe and N_2O can be also used depending upon the purposes. SFC unites the performances of gas chromatography (GC) and high performance liquid chromatography (HPLC). Thermally unstable and non-volatile materials which cannot be analyzed by GC can be analyzed by SFC because the effluent containing a modifier has high solubility at low temperature. High-resolving power separation and analysis can be made in a short time with a longer column with larger theoretical plate number using a low viscosity fluid than in HPLC because the viscosity of eluent is approximately one-tenth that of liquid with the same density and the diffusion coefficient of it is ten-times that of the liquid. **Fig. 8** illustrates a photograph and block diagram of SFC.

The application example measuring the condensation degree of silicate anion in C-S-H produced in the ternary component blended cement composed of portland cement, blast furnace slag and fly ash hardened paste is shown in **Fig. 9(73)**. Since the trimethylsylylated silicate polymer derivative composed of tetramer or higher polymers is non-volatile, it cannot be analyzed by conventional gas chromatography. Although the molecular weight distribution in the sample can be obtained by high performance liquid chromatography, it cannot be eluted into fractions by the condensation degrees **(74)**. Since silicate polymer derivatives up to heptamer can be clearly eluted by SFC, the variation of the condensation degree of silicate anion in C-S-H according to the progress of hydration can be traced in detail. SFC is, therefore, expected to be a useful technique to relate the structural change of silicate polymer derivatives to the physical properties of mortar and concrete.

(6) Determination of pore structure

Since the pore structure in hardened concrete is closely related to the physical properties including strength and durability **(75)(76)(77)**, it is indispensable to accurately determine the pore structure including pore size distribution and porosity for estimating and evaluating the physical properties of hardened concrete.

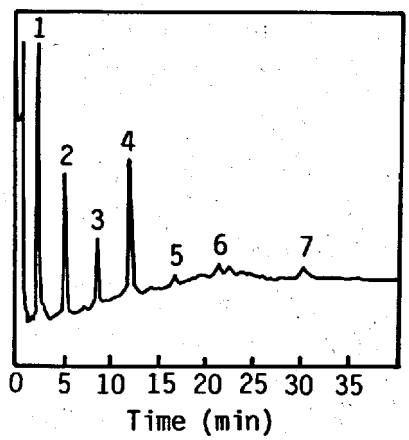

Fig. 9

Supercritical fluid chromatogram of hydrated ternary components blended cement composed of slag, fly ash and portland cement treated by TMS (Uchikawa et al; (73))

The pore in hardened concrete comprises water and air void. The water void includes the pore space filled with water produced by bleeding on the undersurface of aggregate, capillary pore space remaining unfilled with the hydrates between solid components in hardened cement paste and gel pore space corresponding to the space of C-S-H interlayers. The air void includes the entrapped air in mixing concrete and the entrained air introduced by the air entraining (AE) agent. Some aggregate contains pore space.

The size of pore space in hardened concrete rages from 1 nm to 10 mm or 10^7 as shown in **Fig. 10** and the shape of it is diversified. It is considered that the hydraulic radii of gel and capillary pore spaces are 3 nm or less and 3 nm to 2 μm, respectively. As mentioned later, pore spaces 2 to 30 μm in radius hardly exist in hardened concrete. The radius of air voids is 30 μm or more and that of entrapped air is 10 mm or more in maximum. The size of pore space is expressed by the platy pore diameter, d, cylindrical pore radius, r, and hydraulic radius, r_h. The relationship among them is expressed by the following formula applies for those values:

$$d = r = 2r_h \quad \text{---------- 3.3)}$$

The measuring method of pore size distribution includes the liquid substitution method, gas adsorption-desorption method, mercury intrusion porosimetry, optical and electron microscopy and x-ray small angle scattered method. The accurately measurable pore size range varies according to the principle.

The NMR method has recently gained attention as the measuring method of pore size distribution. This method is based on the principle that the relaxation time of pore solution approximately 40nm away from the interface between pore and solid is shorter than that of free pore solution because the former pore solution is restrained by the surface of material. The NMR-relaxation method **(78)** is characterized by requiring no drying of the sample and accurately measuring the pore size distribution because the method is hardly affected by the shape of pore. The studies at the initial stage include a study on the variation of the relaxation of proton in pore solution according to the hydration, measurement of the variation of specific surface area according to the hydration from the relaxation time and a study revealing by analyzing a simple system of silica sintered from fine particles with uniform pore distribution that the NMR method is more accurate than the mercury intrusion porosimetry **(79)**. There is a method for determining the pore size distribution in a system with uneven pore size and its uneven pore size distribution from the relationship between the specific surface area and the pore size distribution making the inverse Laplace transformation of the measurements of free induction decay (FID) caused by the pulse sequence applying a three-dimensional "diffusion cell model" expressed in the diffusion length, approximately 1μm, of water in the measuring time of NMR to the independent cell **(80)**. It will be possible to analyze the three-dimensional pore structure by combining the NMR-relaxation

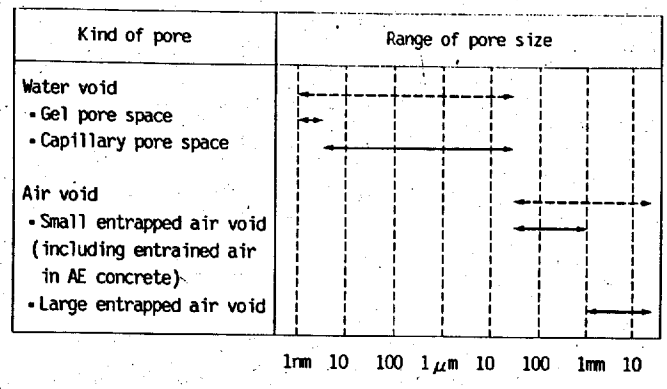

Fig. 10 Pore size in hardened concrete

with the NMR imaging **(78)**.

It is expected to apply the NMR-relaxation method for determining the pore size distribution to the cement and concrete research. It is necessary, however, to further study the problems that the relaxation time is affected by the alkaline pore solution and that the maximum measurable limit of pore size is as large as 10μm.

The pore size distribution in hardened concrete is so wide that it is unable to determine it using a single apparatus and method. Accordingly, the total pore space in hardened concrete has not been determined so far. However, all the pore size distribution and volume of pore space including gel pore space, capillary pore space, air void of 30μm to 1 mm in diameter and large air void of 1 mm or more in diameter have been determined by combining the nitrogen adsorption-desorption method, the mercury intrusion porosimetry, the optical microscopy and the x-ray CT method **(81)**.

(a) Measurement of gel pore space

The measuring method of pore space with small diameter includes the gas adsorption-desorption method**(82)**, the mercury intrusion porosimetry **(76)**, the scanning electron microscopy (SEM)**(83)** and the small angle x-ray scattering method**(84)**. The gas adsorption-desorption method is, however, most suitable for measuring the gel pore space.

The pore diameter can be obtained from the following formula in the gas adsorption-desorption method;

$$d = (-4\gamma V \cos\theta)/(\rho RT \ln(P/P_o)) \quad \text{----------} \quad \textbf{3.4)}$$

where γ: surface tension of adsorbing medium,
d: diameter of platy pore space where adsorption and desorption take place
θ: angle of contact (usually zero),
V: adsorptive capacity of adsorption medium,
R: gas constant,
ρ: density of adsorption medium,
P/P_o: relative vapor pressure,
T: absolute temperature.

The volume of pore space is apt to be overestimated using water vapor as the adsorption medium **(85)** and the measuring operation is complicated. Nitrogen is, therefore, used instead of water vapor as the adsorption medium because the operation is simplified and the reproducibility is improved in an automatic apparatus. Typical cumulative pore volume and pore size distribution (dV/dd) in cement paste are shown in **Fig. 11(81)**. Symmetric peaks are observed at 2 nm. The peak become higher with the advance of age. This pore is, therefore, corresponds to gel pore space derived from the production of C-S-H.

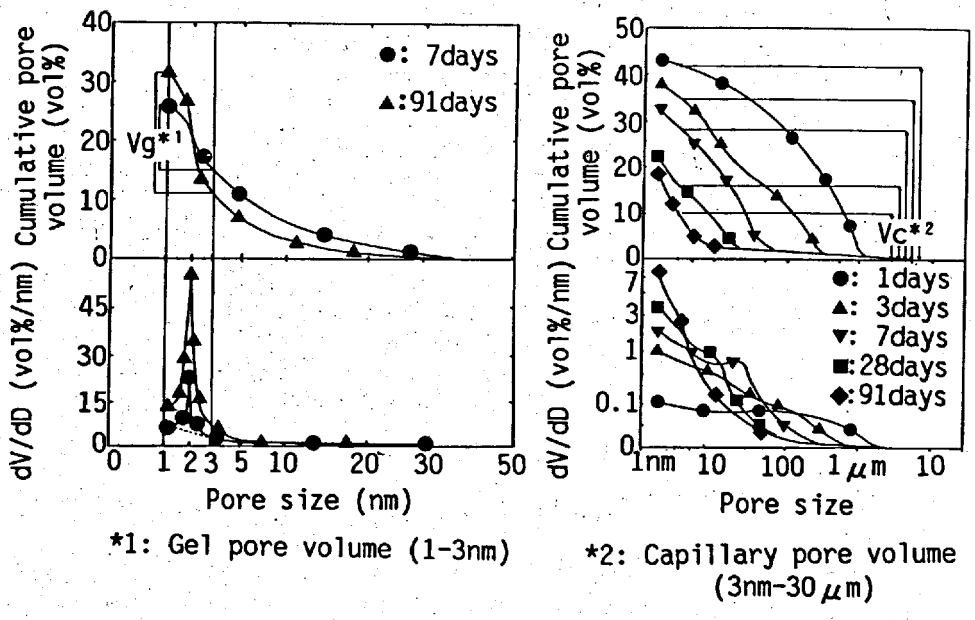

Fig. 11 Cumulative pore volume and pore size distribution of hardened cement paste measured by nitrogen gas adsorption-desorption method and mercury porosimetry (Uchikawa et al; (81))

(b) Measurement of capillary pore space

The mercury intrusion porosimetry is widely used for determining the capillary pore space. The method adopts a penetration curve of mercury vapor to estimate the pore size distribution. The relationship between the pore diameter and the external pressure is expressed by the following formula:

$$d = -2\gamma \cos\theta / P \quad \text{---------- 3.5)}$$

where d: diameter of platy pore space, γ = surface tension of mercury,
θ: angle of contact between mercury and sample, and P = external pressure

Since a new type apparatus uses the maximum compression pressure of mercury vapor as high as approximately 4300 atm, the pore diameter ranging from several nanometers to several tens microns can be measured. The operation of this apparatus is simple and its accuracy is high though it is necessary for interpreting the data to take into consideration whether or not the pore has the shape easily introducing mercury vapor and whether or not the sample is deformed by high-pressure mercury vapor.

Fig. 11(81) shows an example of the results of cumulative pore space and pore size distribution of hardened cement paste.

(c) Air void

Air void in hardened concrete includes mainly the entrapped air in the mixing of concrete and the entrained air artificially introduced by the AE agent. The air voids disappear when the pressure difference between the inside and outside pressures reaches 10% or higher of the inside pressure.

Assuming that the external pressure is to be atmospheric pressure and the surface tension, γ, of mixing water is to be 45 to 73 dyne/cm taking the addition of the admixtures into consideration, the minimum diameter of air void has to be approximately 30 to 40 μm from the following formula and air voids of 30 μm or less in diameter hardly exist in hardened concrete:

$$\Delta P = 4\gamma/d \qquad \text{3.6)}$$

where ΔP = pressure difference between inside and outside of air void
γ = surface tension of water, and
d = diameter of air void.

The size distribution and volume of pore space of the air voids as small as 30 μm to 1 mm in diameter are determined by taking many visual fields of microphotographs and making the image processing. The x-ray CT method followed by the image processing is used for determining those values of the air void as large as 1 mm or more in diameter. The relationship between the field number and the coefficient of variation of the volume of air voids is shown in **Fig. 12(81)**. Tomograms of concrete taken by the x-ray CT method and part of a section of concrete and apparatus are shown in **Fig. 13(81)** and **Fig. 14(81)**, respectively. Some measuring conditions of air voids are shown in **Table 3(81)**.

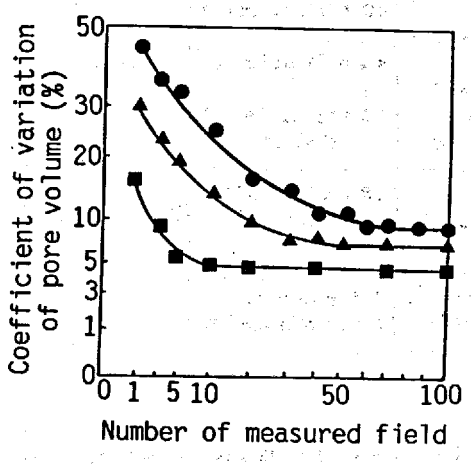

Pore size
●: 30-80 μm (measured by OM and IP)
▲: 80 μm-1mm (measured by OM and IP)
■: > 1mm (measured by X-CT and IP)

Fig. 12

Relationship between number of measured fields and coefficient of variation of pore volume of hardened cement paste, mortar and concrete measured by optical microscopy (OM) and x-ray computerized tomography (x-ray CT) and image processing (IP) (Uchikawa et al; (81))

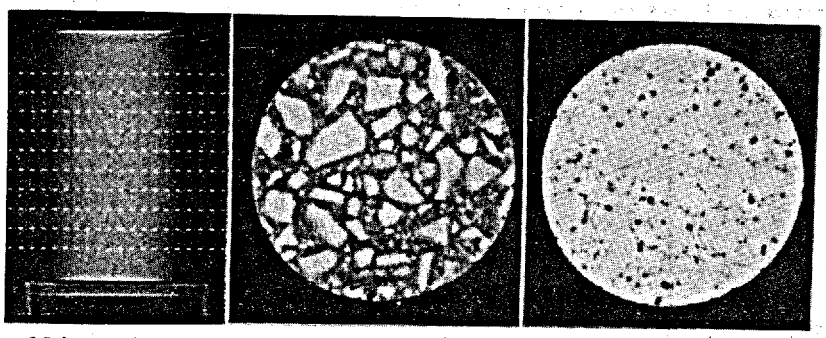

Fig. 13

Cross section of hardened concrete specimens by x-ray computerized tomography (Uchikawa et al; (81))

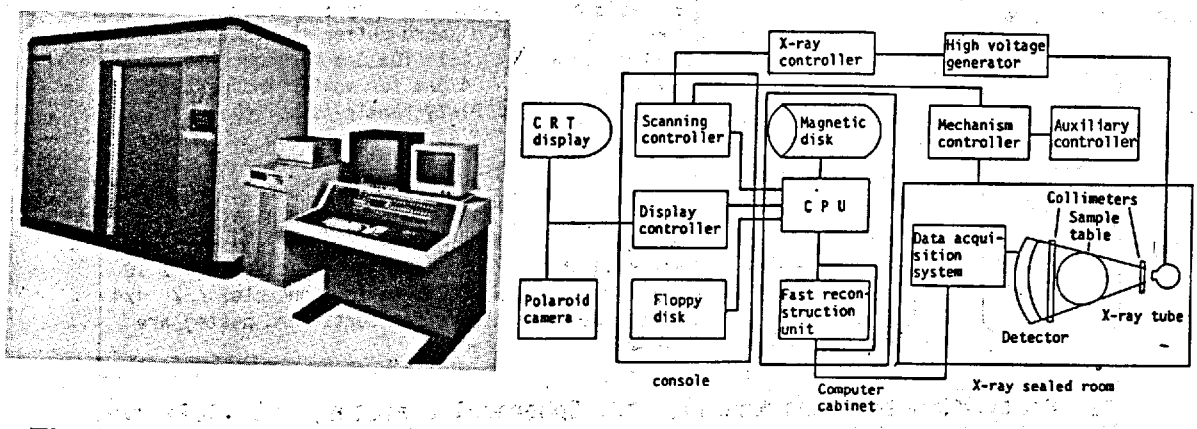

Fig. 14 Middle-energy industrial x-ray CT scanner (TOSHIBA TOSCANER-23200)

Table 3 Sample preparation and conditions of measurement of pore structure in hardened concrete (Uchikawa et al; (81))

No.	Pore	Measuring range	Method	Sample state	Sample size	Relative deviation*3
1	Gel pore space	1-3nm *1	Nitrogen gas adsorption-desorption method (B.J.H.method)	a (ground to grain <2.5mm)	Cement paste 2g Mortar 5g Concrete 10g	<10%
2	Capillary pore space	3nm-30μm *1	Mercury porosimetry	a	Cement paste 10g Mortar 10g Concrete 20g	<5%
3	Small entrapped air (entrained air)	30μm-1mm *2	Optical microscopy and image processing	b-1: Concrete b-2: Cement paste, Mortar	70 fields(70mm²) for magnification of x30 50 fields(48cm²) for that of x3	<10%
4	Large entrapped air	>1mm *2	X-ray computerized tomography and image processing	c-1: Concrete c-2: Cement paste, Mortar	10 fields(780cm²) for concrete 10 fields(160cm²) for cement paste and mortar	<5%
5	Total pore volume	cement paste: 1+2+3+4 mortar : 1+2+3+4 (1+2+3+4-3') concrete : 1+2+3+4 (1+2+3+4-3') [Capillary pore space of 200nm to 30μm (3') measured by mercury porosimetry is apt to contain small entrapped air volume as ink-bottle type void. When volume of air void is 1/4 or more of total water void, total pore volume is value of 1+2+3+4-3']				

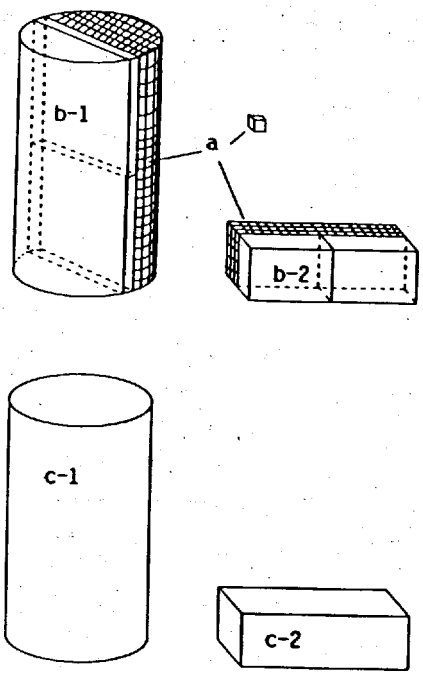

Measurement	Sample preparation
Gel pore space and capillary pore space	①Specimen is cut by diamond cutter to 0.5cm cubic sized samples(a). ②Small sized samples(a) are immersed in acetone, repeatedly. ③They are dried by D-drying method and mixed uniformly.
Air void of 1mm or less (entrained air void)	①Specimens is sectioned by diamond cutter to platy sample (b-1: 10x10cm for concrete, b-2: 4x8cm for mortar and paste). ②Platy sample is polished with #240, #400 and #800 SiC powder. ③The surface of sample is smeared with mixture of burnishing Al_2O_3 powder and liquid paraffin.
Air void of 1mm or more (entrapped air void)	Non-destructive specimens (c-1 10 φ x 20ℓ cm for concrete, c-2 4x4 x16 cm for mortar and paste) are used.

*1: Platy diameter (thickness), *2: Spherical diameter, *3: Relative deviation (error) of measurement

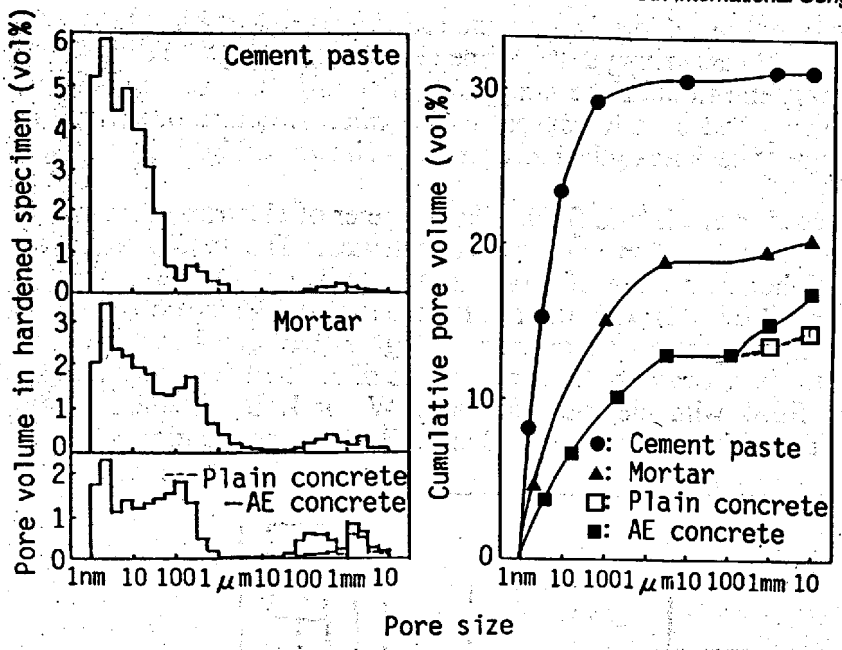

Fig. 15

Pore size distribution and cumulative pore volume of hardened cement paste, mortar and concrete (Uchikawa et al; (81))

It is indispensable in the optical microscopy to select the suitable magnification, the range of visual field and the number of measured field according to the size of air voids. The data processing by the x-ray CT is substantially the same as the optical microscopy. The optimum size of visual field and the optimum number of measured fields are 10cm in diameter and ten in number, respectively.

Fig. 15(81) shows the volume of air voids and the distribution (dV/dd) in cement paste, mortar and concrete.

3.3 Advanced Characterization Techniques of Surface and Microscopic Region

The characterization of surface and microscopic region is being improved by the sophisticated sample treatment, improvement of two- and three-dimentional resolving power, development of new apparatus based on new ideas, improved accuracy of measurement by new technique, simultaneous acquisition of diversified information, data processing by computer and artificial intelligence, and development of image processing system.

These examples are cryostat system for cooling the sample in electron microscopic observation and diffraction, special deposition apparatus by ion sputtering, ion thinning, field emission scanning electron microscope, transmission electron microscope, micro Auger electron spectroscope, microfocus x-ray diffractometer, environmental scanning electron microscope, scanning tunnel microscope, atomic force microscope, protection of insulating sample from charging by sample inclination method, multi analysis by morphological observation, composition analysis and electron diffraction, simultaneous acquisition of diversified information with combination of two or more instruments, correction of atomic number effect, absorption effect, fluorescence effect and element distribution display by contents in electron probe microanalyzer, and quantitative expression of crystal shape by image processing.

(1) SEM and FESEM

A sample is irradiated with electron beams accelerated by specified voltage to convert the input energy of electron into characteristic x-rays, continuous x-rays, back scattered electrons, secondary electrons, Auger electrons, light and sample current by the interaction with the sample material. When the sample is thin, part of electron beam penetrates it.

Electrons with relatively high energy reflected or scattered from the sample are called back scattered electrons and those of approximately 50eV or less are called secondary electrons.

Energy of the back scattered electrons depends upon the atomic number, while that of the secondary electrons varies sensibly according to the shape of surface, crystalline orientation and electric potential and magnetic field of the sample. A scanning electron microscope (SEM) is based upon this theory and used for observing the microstructure of surface of material. The measuring range of each analytical instrument is shown in **Fig. 16.**

Electron beam can be converged in an electric field. The diameter of electron beam can be converged as small as approximately 10nm with the latest device. The spatial resolving power of electron beam is higher than those of x-rays and ionic beam. A field emission scanning electron microscope (FESEM) with the field emission type electron emitter is characterized by high emissivity of electron, a luminance as high as 10^9A/cm^2 sr, a diameter of radiation source as small as approximately 3nm and a range of emitted energy as narrow as 0.3eV or 1/3 to 1/5 that in SEM with electric gun using W or LaB_6 filament (**Fig. 17**). Since even low accelerating voltage can be applied to FESEM, the penetration depth of

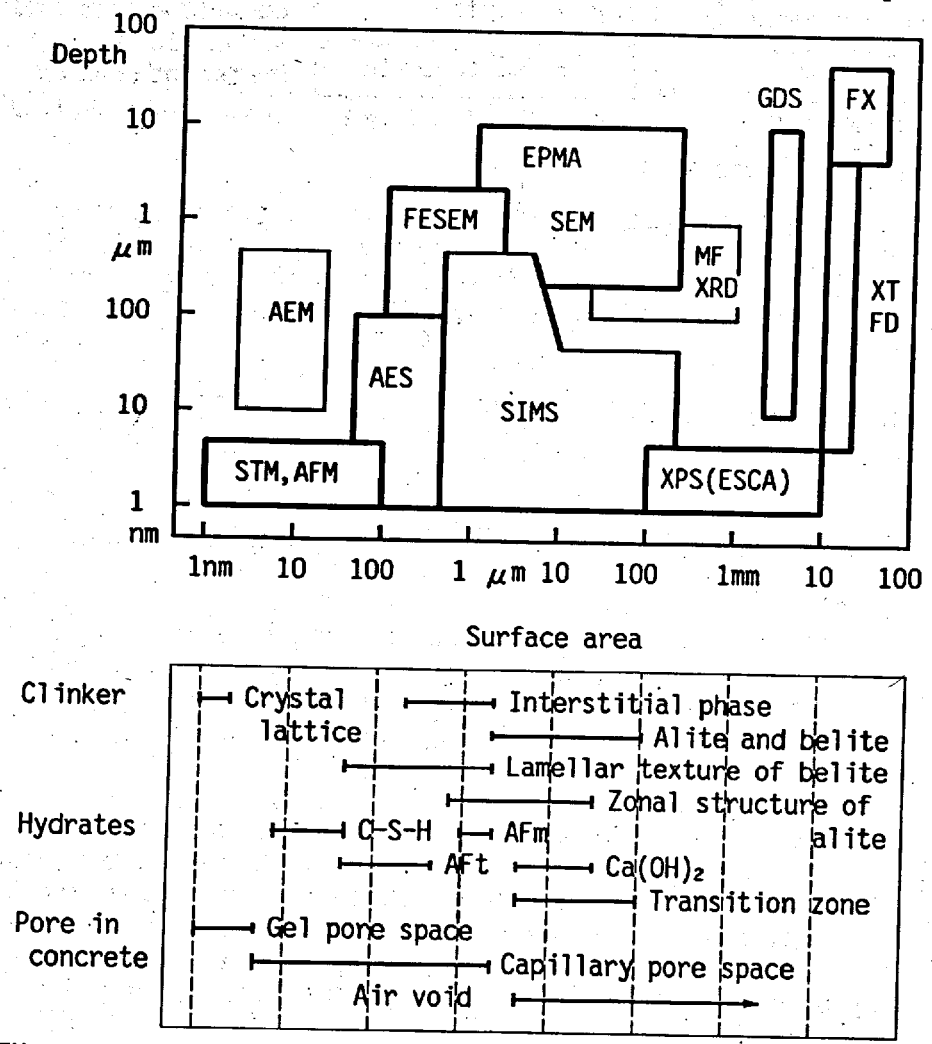

AEM: Analytical Transmission Electron Microscope, STM: Scanning Tunnel Microscope, AFM: Atomic Force Microscope, AES: Auger Electron Spectroscope, FESEM: Field Emission Scanning Electron Microscope, EPMA: Electron Probe Micro Analyzer, SIMS: Secondary Ion Mass Spectroscope, XPS(ESCA): X-ray Photoelectron Spectroscope, MFXRD: Micro Focus X-ray Diffractometer, GDS: Glow Discharge Spectrometer, XTFD: X-ray Thin Film Diffractometer, FX: Fluorescent X-ray Spectrometer

Fig. 16 Measuring range of each surface and local characterization instruments

electron beams into the sample is as small as 10nm to microns compared with 100nm to 10μm in SEM to which an accelerating voltage as high as 10 to 20kV is applied. A several-times higher contrast image and good resolution are, therefore, able to be obtained using FESEM. Since the angle of aperture can be increased by setting the sample in the objective lens of in-lens FESEM, the magnification and resolving power can be augmented as high as of 0.7nm compared with the ordinary FESEM.

Fig. 18(86) illustrates a back scattered electron image of lamellar structure in clinker belite by in-lens FESEM. The image of belite obtained by the in-lens FESEM gives two sets of lamellas crossing each other at 60°. The image enlarged by higher magnification gives the lamella composed of different structures. The bright part is a lamella 0.5 to 1.0 μm thick composed of oriented secondary lamellas 0.1μm or less thick, while the dark part is a lamella 0.1 to 0.4μm thick.

The secondary electron images before and after etching the surface of clinker with a water for 30 seconds by in-lens FESEM are shown in **Fig. 19(87)**. The particles existing on the surfaces of alite and belite before etching are contaminants. Holes 10nm in diameter from where elements are dissolved are made after etching more on the alite crystal than on the belite crystal. The general structure of them is regarded as a network considering from the roughness of surface. The surface structure of C_4AF phase is not so much changed by etching.

For observing microstructure enlarged by tens of thousands, a thin layer of a specified conductive material can be deposited on the sample using a depositing apparatus shown in **Fig. 20** without directly irradiating the sample with plasma ions or electrons to prevent the sample from damaging.

Also a cryosystem cooled with liquid nitrogen has been developed for preventing the sample from damaging by increased temperature derived from the irradiation with electron

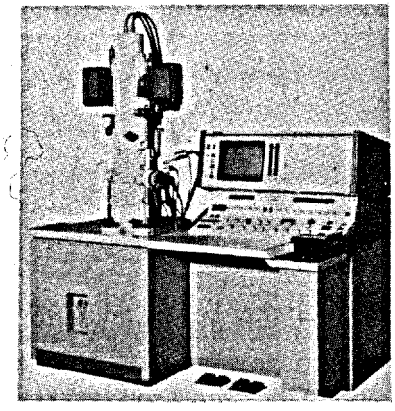

Fig. 17

In-lens type field emission scanning electron microscope (JEOL JSM-890)

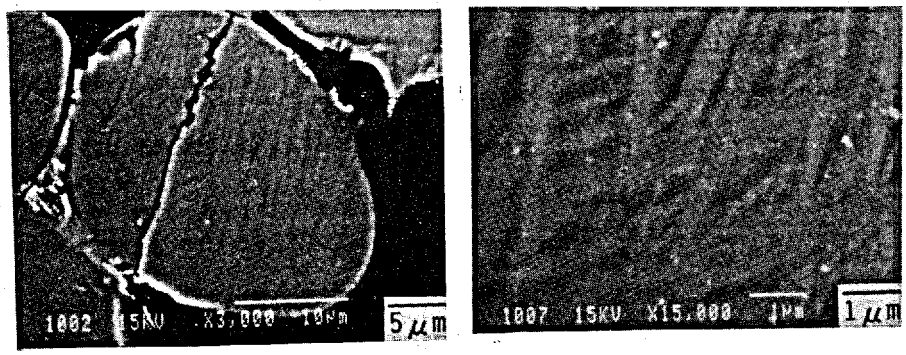

Fig. 18 Back scattered electron image of clinker belite observed by in-lens type EFSEM (Uchikawa et al; (86))

beams. Since the sample chamber of the cryosystem can be kept very low atomic pressure, the highly resolved image of sample can be observed. Cryosystem can be used for observing such a sample that its texture and structure is changed by the evaporation of water in the evacuated sample chamber as it is by freezing the sample.

Applications of the cryosystem to the cement and concrete field began with a study **(88)** on the comparison of the flocculation structure of blended cement at the initial hydration with that of ordinary portland cement. The system has recently been used for observing a secondary electron image of the fracture surface of hardened mortar under various drying conditions. A paper **(89)** presents that the breaking of the bonding of aggregate with paste and the cracking in paste caused by drying are affected by the curing conditions before drying and related to the kinds and morphology of C-S-H.

(2) ESEM

Environmental scanning electron microscope (ESEM) is an instrument for observing the secondary electron image and back scattered electron image and analysing the chemical composition under the low vacuum as low as 20Torr (mmHg) **(90)**. Considering from the operating condition and resolving power , ESEM is characterized by the applicability to the gap between the optical microscope and the SEM and TEM and by directly observing and analysing the sample as it is.

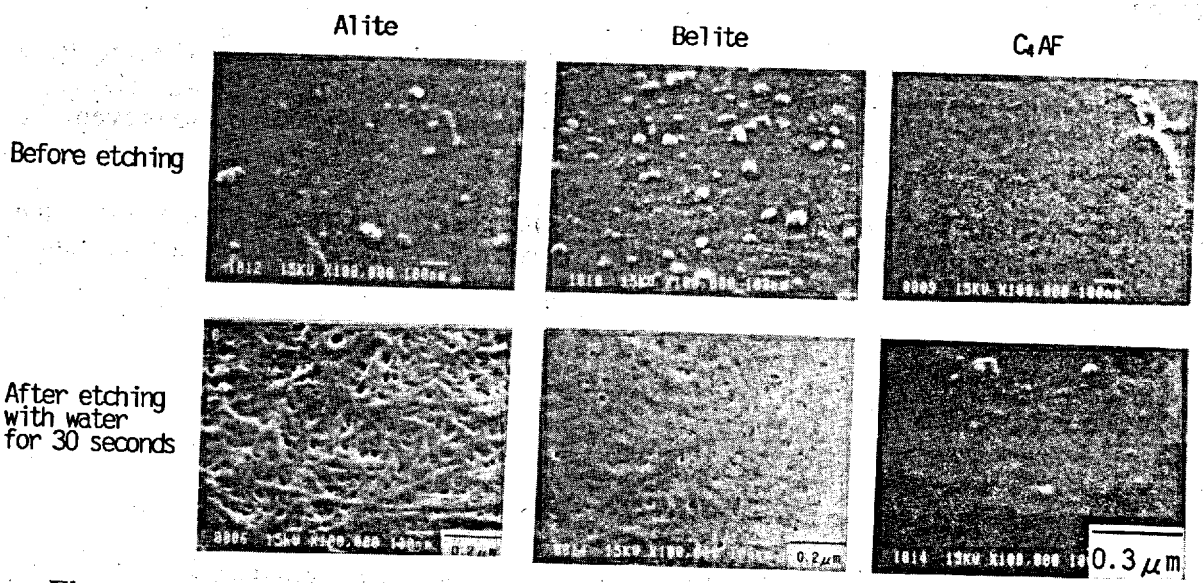

Fig. 19 Secondary electron image of the surface of clinker before and after etching (Uchikawa et al; (87))

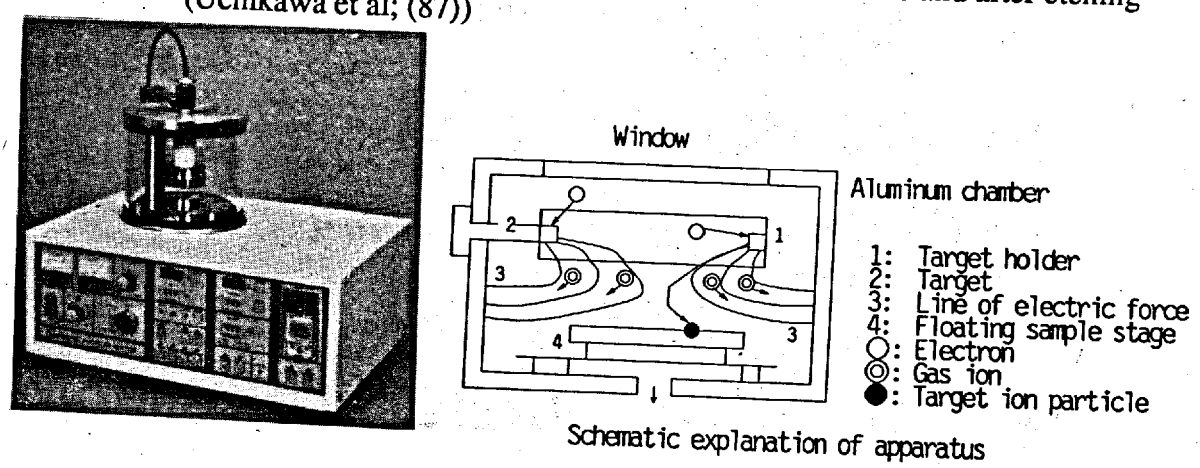

Fig. 20 Depositing apparatus for sample preparation (HITACHI EP-1030)

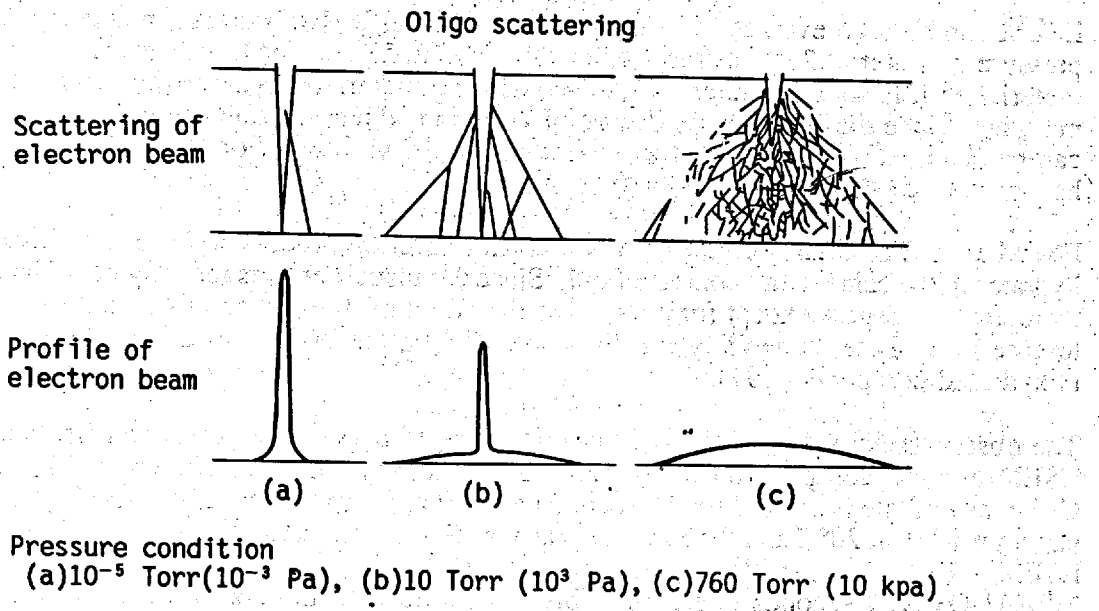

Fig. 21 Schematic explanation of scattering of electron beam under various pressures

Electron beam is scattered by the atmospheric gas under low vacuum. The probability of the scattering depends upon the accelerating voltage,type of atmospheric gas, gas pressure and working distance. When the gas pressure in the sample chamber is as high as atmospheric pressure, the electrons are scattered as shown in **Fig. 21(c)**, so neither the electron beam nor the high-resolving power secondary electron can be obtained. Meanwhile, the Oligo scattering of electrons are observed under the pressure of the sample chamber as low as 10Torr because tens percent of the electron can be reach the sample without collision with the gas molecules and the average number of collisions of an electron with the gas molecules is 2 to 3 times or less. The diameter of electron beam is 30nm nearly equal to that under high vacuum and the current of electron beam is 10 to 20% of that under high vacuum. Since the scattered electrons are distributed from the electron beam in a skirt shape as shown in **Fig. 21(b)** and most of them form direct current component, a high-resolving power secondary electron image can be obtained in the same way as SEM.

In SEM, the secondary electrons are amplified with a photomultiplier while ESEM uses the atmospheric gas as the amplifying medium of secondary electrons. Secondary electrons with energy as low as several electron volts emitted from the sample surface ionize the gas molecules colliding with them according to the reaction of $M + e \rightarrow M^+ + 2e$, thereby one more electron is emitted adding an emitted electron. The emitted electron collides with the gas molecules and the reaction repeatedly occurs. Since the secondary electrons successively emitted by this process are amplified and collected around the electrode, the secondary electrons are detected as current with a secondary electron detector (SE detector). Since part of gas molecules positively ionized by the collision with the secondary electrons is neutralized with charged electrons on the sample surface, charge-up is restrained. Even though the sample is an insulating material, it is unnecessary to treat the sample by deposition.

An energy dispersive x-ray spectrometer is used for the chemical analysis of sample due to low intensity of characteristic x-rays. The absorption of x-rays by gas molecules such as water vapor is negligible except in the case of measuring light elements such as oxygen even under pressure of 20Torr. Two pressure-controlling apertures are installed for connecting the electron gun and lens-barrel kept at a reduced pressure as low as approximately 10^{-6} Torr and the sample chamber kept at pressure as high as 20Torr. ESEM is shown in **Fig. 22.**

ESEM can be used even under the pressure as high as 20Torr corresponding to the vapor pressure of water at 20°C as mentioned before so that it is useful for directly observing a material as it is such as water- and oil-containing materials, hydrates and gas-generating material. Since the atmosphere, degree of vacuum and temperature of the sample chamber can be changed, the reaction process of the sample with water or gas and the change by heating can be observed without delay.

ESEM is applied mainly to the observation of hydration process and the identification of hydrates in the cement and concrete field. Since the instrument has recently been developed, there are few papers except for presenting the effect of the stirring of cement paste on the texture of hydrate, especially the thickness of hydrate layer formed on the surface of unhydrated components(**91**).

The observational result of the hydration process of C_3A in the presence of anhydrite by ESEM and the composition of hydrate determined by EDX are shown in **Fig. 23(42)**. C_3A was hydrated at 20°C for 10 seconds and 10 minutes under 12Torr(mmHg) of water vapor pressure at 20°C and the pressure was immediately decreased to 3Torr to observe it by ESEM. The mixing ratio of anhydrite and C_3A was fixed to 1.0 as molar ratio of SO_3/Al_2O_3. Ten seconds later, fine fibrous hydrate with the composition similar to the theoretical composition of monosulfate hydrate composed of 36.0% of CaO, 16.4% of Al_2O_3 and 12.9% of SO_3 was produced on the surface of C_3A particles. Ten minutes later, a large amount of needle-shaped hydrate was produced on the surface of C_3A particles. The results of composition analysis by EDX indicated that the composition of needle-shaped hydrate was the same as the theoretical composition of ettringite composed of 26.8% of CaO,

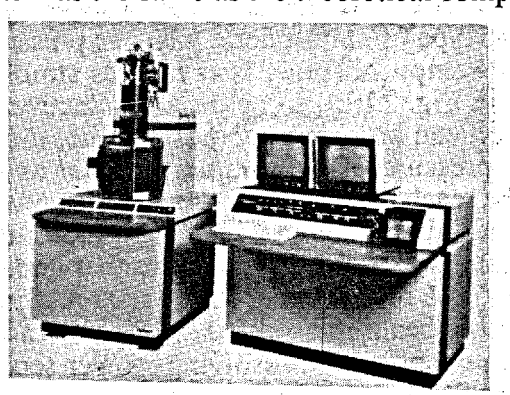

Fig. 22

Environmental scanning electron microscope (ESEM) (Electro Scan Co., ESEM-20)

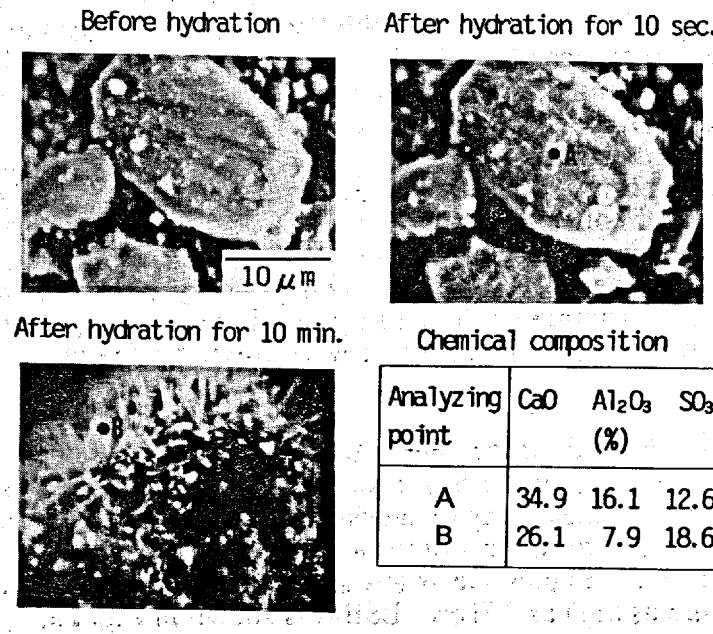

Chemical composition

Analyzing point	CaO	Al_2O_3	SO_3
	(%)		
A	34.9	16.1	12.6
B	26.1	7.9	18.6

Fig. 23

Secondary electron image of C_3A before and after hydration in the presence of anhydrite by ESEM (Uchikawa et al; (42))

8.1% of Al_2O_3 and 19.1% of SO_3. As mentioned before, ESEM is a useful tool for directly observing the hydration process and identifying the reaction product.

(3) TEM and AEM

A transmission electron microscope (TEM) is used for observing an image obtained by electrons penetrating the sample. An analytical electron microscope (AEM) is used for observing and analyzing a thin sample as a device with spatial resolving power augmented by sharply converged electron beams to reduce the matrix effect of the material in the vicinity of the measuring position.

The resolving power, σ, of electron microscope depends upon the coefficient of spherical aberration, Cs, and the acceleration voltage, E. The following formula **3.7)** exists between those values **(92)**:

$$\sigma = 0.65Cs^{1/4} \times (12.26/E^{1/2})^{3/4} \quad \text{---------- 3.7)}$$

The resolving power is, therefore, able to be improved by increasing the accelerating voltage. The resolving power of a latest electron microscope as shown in **Fig. 24** is improved up to 0.22nm by applying 200kV.

TEM is used for observing an image obtained by electron beam penetrating a relatively thin sample. A constant-phase contrast is formed on the image by the interference of the waves of electron beam scattered at the time when penetrating the sample. A lattice image of crystal similar to the atomic configuration can be obtained by adjusting the direction of incidence of electron beam to the same direction as the zone axis of crystal so that the Bragg's reflection takes place around it. In addition to the conventional morphological observation and electron diffraction method, the direct observation of a lattice image has been made possible by improving the resolving power. TEM is, therefore, of utility value.

The point resolving power of field emission transmission electron microscope (FETEM) is enhanced by the improved chromatic aberration derived from the high luminance of electron gun and narrow energy distribution of electron beam. Since inelastic scattered electrons making the image flat are hardly emitted because of high coherent beam, a sharp image can be obtained in a wide field of vision.

For fully displaying the performance of high-resolving power TEM, it is necessary to pay close attention to the preparation of sample. Even such a bulky sample as clinker can be thinned to tens nanometers by the ion thinning method **(93)** utilizing the ion sputtering to observe the lattice image. A method for minimizing the damage of sample and preventing

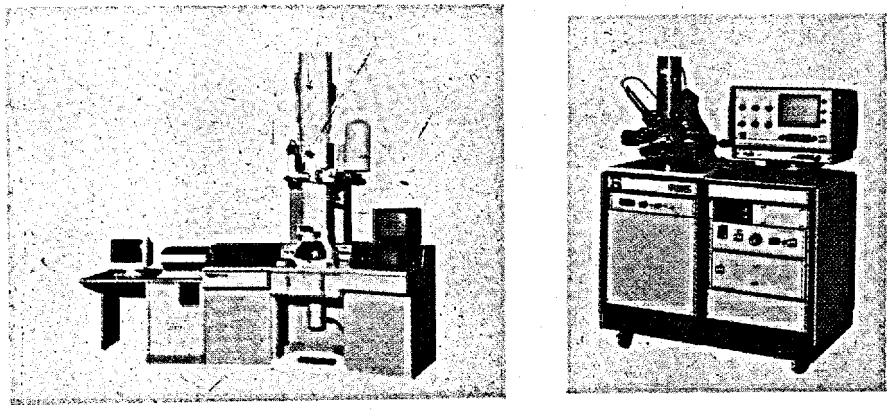

Fig. 24 Analytical transmission electron microscope (ATEM) (JEOL JEM-3010) and ion thinning apparatus (GATAN Inc., Model 645 PIMS™)

the selective etching has been developed for preparing a thin sample by the ion thinning method, which has been recently used in addition to the replica and powder methods for TEM. The sample preparation by grinding with a dimple grinder followed by ion thinning is effective due to a short time of preparation(94).

The transmission image and electron diffraction pattern of each phase in belite determined by TEM are shown in **Fig. 25(86)**. The bright part in SEM corresponding to dark part in TEM and dark part in SEM corresponding to bright part in TEM show the diffraction patterns of ß- and α-forms, respectively. It is considered that the bright part is produced by the transformation of the α-form into the α'_L-form successively into the ß-form. This agrees with the before-mentioned observational result shown in **Fig. 18(86)** that the bright part is composed of fine secondary lamellas. The result of electron diffraction is supported by this fact. Minor and trace components are contained more in the bright parts than in the dark part.

The structural study by the lattice image observation includes a paper(95) describing that the Jeffery's structure is observed as the lattice image of monoclinic alite in the actual space and a paper(96) reporting the observation of the lattice image in an interfacial region nanometers in MDF cement paste.

Photographs of the lattice images of tobermorite regarded as similar to that of calcium silicate hydrate in cement paste and those of C-S-H are shown in **Fig. 26(97)**. Lattice image of the alite and the α-form of belite in clinker are shown in **Fig. 27(42)** using sample prepared by the ion thinning method and the multi-slice method. A twinning structure crossing each other at approximately 60° regarded as the production by the transformation from trigonal from to monoclinic form is observed in the lattice image of alite.

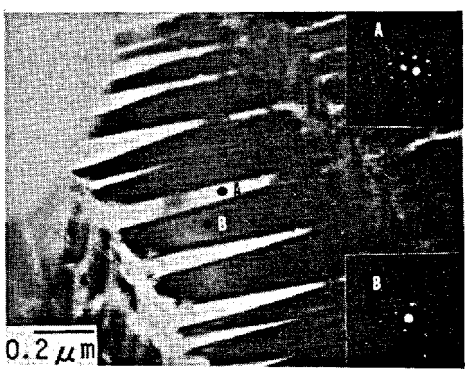

Transmission electron image and electron diffraction pattern of lamellar structure in clinker belite

Point	Amount of minor element (%) MgO	SO_3	Al_2O_3	Fe_2O_3	Na_2O	K_2O	Transformation
A	0.40	0.71	1.84	1.75	0.18	1.13	α
B	0.37	0.29	1.63	0.79	0.15	1.05	β

Fig. 25 Lamellar structure in clinker belite and it local composition determined by AEM (Uchikawa et al; (86))

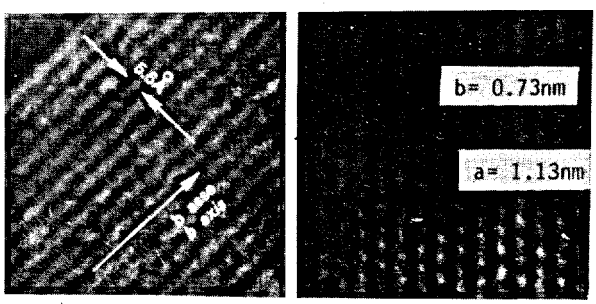

Fig. 26

Lattice image of C-S-H and tobermorite (Uchikawa et al; (97))

The lattice image varies according to the focus of beam in the apparatus as shown in **Fig. 28.** High-level crystallographic knowledge is therefore, generally required for identifying the lattice image corresponding to the crystal structure. Recently, however, the lattice image can be easily interpreted by the multi-slice method in which the lattice image is obtained by simulating a model inputting the data including crystal structure, observation direction, thickness of sample, accelerating voltage and spherical aberration of the objective lens to a computer**(98).**

EPMA is widely used for the elemental analysis in a microscopic region. AEM has higher spatial resolving power than EPMA. The sample for AEM is limited to a thin sample so that electrons converged into an electron beam 10nm in diameter penetrate the sample before diffusing. Accordingly, the characteristic x-rays emitted from a microscopic region in the thin sample are so weak that energy dispersive x-ray spectrometer with including a semiconductor detector is substituted for the analyzing crystal. Electron energy loss spectroscopy (EELS) for obtaining the energy loss spectrum showing the difference in energy between the inelastic scattered electron and the incident electron beam is used for analyzing lighter elements. Since the probability of emission of characteristic x-rays and inelastic scattering electrons increase with the increase of the luminance of electron beam, the analytical precision of FETEM is remarkably improved.

The analytical electron microscopy (AEM) is mainly used for analyzing the local composition of hydrate in the cement and concrete field**(99).** A paper **(100)** presents that the outer C-S-H has a lot of pores, while the inner C-S-H has a fine, homogeneous structure, though both hydrates have the same composition, and a paper **(95)** describes that the C/S ratio of each hydrate was determined within a range of accuracy of 0.1% with an AEM of voltage as high as 200 KeV provided with an energy-dispersive spectrometer taking off X-ray at a large angle. Although applications of AEM to clinker minerals are few because the sample has to be thinned, there is a paper **(97)** reporting that a local field of the lamellar structure of

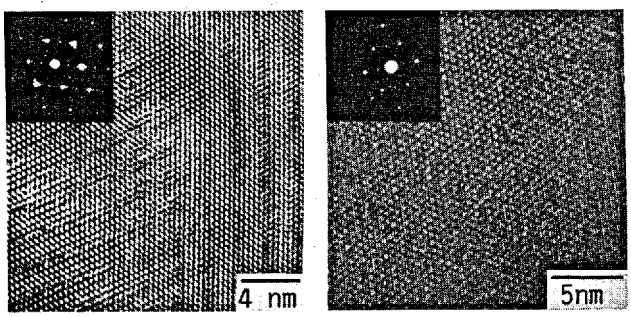

Lattice image of clinker alite with twinning

Lattice image of α-form clinker belite

Fig. 27

Lattice image of clinker alite and clinker belite (Uchikawa et al; (42))

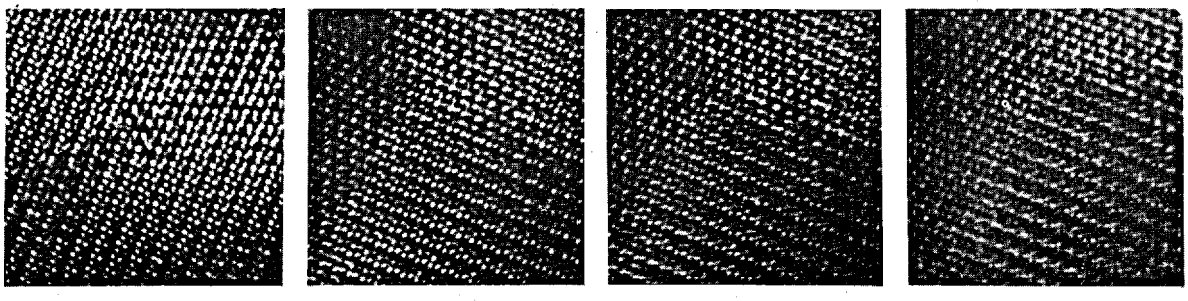

Fig. 28 Variation of lattice image of clinker alite according to focusing condition

belite in clinker obtained by the electron diffraction was analyzed by AEM. AEM is also applied to the elemental analysis in microscopic region for confirming the incorporation of Mg, Si and Fe in an ettringite **(101)** and determining the C-S-H composition **(99)**. More reliable result will be obtained by the spread of FETEM and the development of data processing system in near future.

(4) CMA/EPMA

Electron probe micro analysis is a method for detecting and quantitatively analyzing the elements existing in a small region by amplifying, spectrally diffracting the characteristic x-rays emitted from the sample irradiated with electron beam. The elemental analysis in a large region can be made by scanning the electron beam. Depending upon the accelerating voltage of electron beam, the analytical region is approximately 1μm and 100nm to 1μm in SEM type and FESEM type, respectively.

A computer-aided electron probe microanalyzer (CMA/EPMA) incorporating a high-speed wide-area multi-channel analyzer and a computer into EPMA as shown in **Fig. 29** has recently been developed. CMA/EPMA is applied to the composition analysis for a region from several micrometer square to 10 centimeter square by scanning the electron beam on the sample surface, continuously analyzing the points close to each other, processing the data and correcting the atomic number effect (Z), the absorption effect (A) and fluorescence effect (F). The concentration or concentration ratio of the elements is displayed in colors.

Some researches on cement and concrete using CMA/EPMA have been reported in Japan and UK since the data of slag **(75)** and hardened cement paste **(75)** were disclosed at Rio de Janeiro congress. CMA/EPMA is widely used for studying the zonal structure of alite **(42)(86)**, the lamellar structure of belite **(86)**, the structures of hardened paste **(89)** and hardened mortar **(102)**, and the distribution of alkali in hardened concrete **(103)(104)** using a two-dimensional presentation of the distribution and content of each element in a space from a microscopic region of 1μm^2 to 10 cm^2 of the sample.

Fig. 30 is the optical micrographs of a polished thin section of cement clinker product showing the zonal structure of alite **(87)**. Micrograph a) and b) were taken through an open polar and a cross-polar, respectively, and micrograph c) was obtained by observing thin section etched with a 0.01% NH_4Cl solution for thirty seconds with a reflection microscope. Micrograph b) reveals that the birefringence in peripheral part and inner parts of clinker alite are as high as 0.006 and as low as 0.004, respectively. The inner part is more easily etched and the boundary line between the different birefringence in the transmission-microscopic image coincides with the boundary line between the different color tones in the reflection microscopic image.

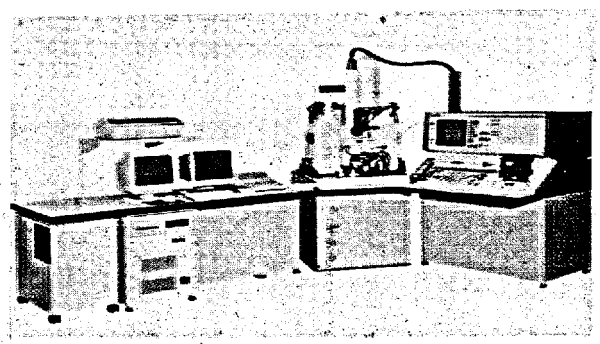

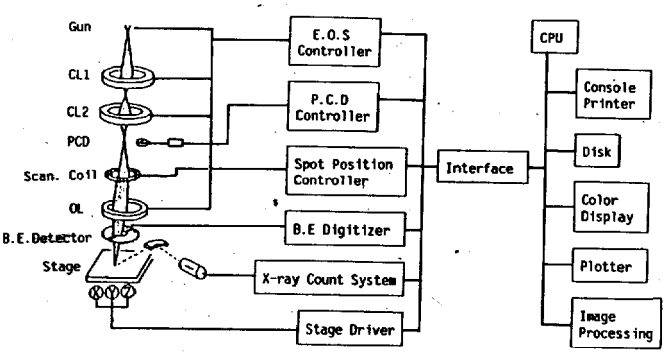

Block Diagram

CL: Condenser lens, PCD: Probe current detector, OL: Objective lens, B.E.:Back scattered electron, E.O.S.: Electron optical system, CPU: Central processing unit

Fig. 29 Computer-aided electron probe microanalyzer (CMA/EPMA) and its block diagram (JEOL JXA-8621MX)



Fig. 30

Transmitted and reflected light micrograph of clinker alite with zonal structure (Uchikawa et al; (86))

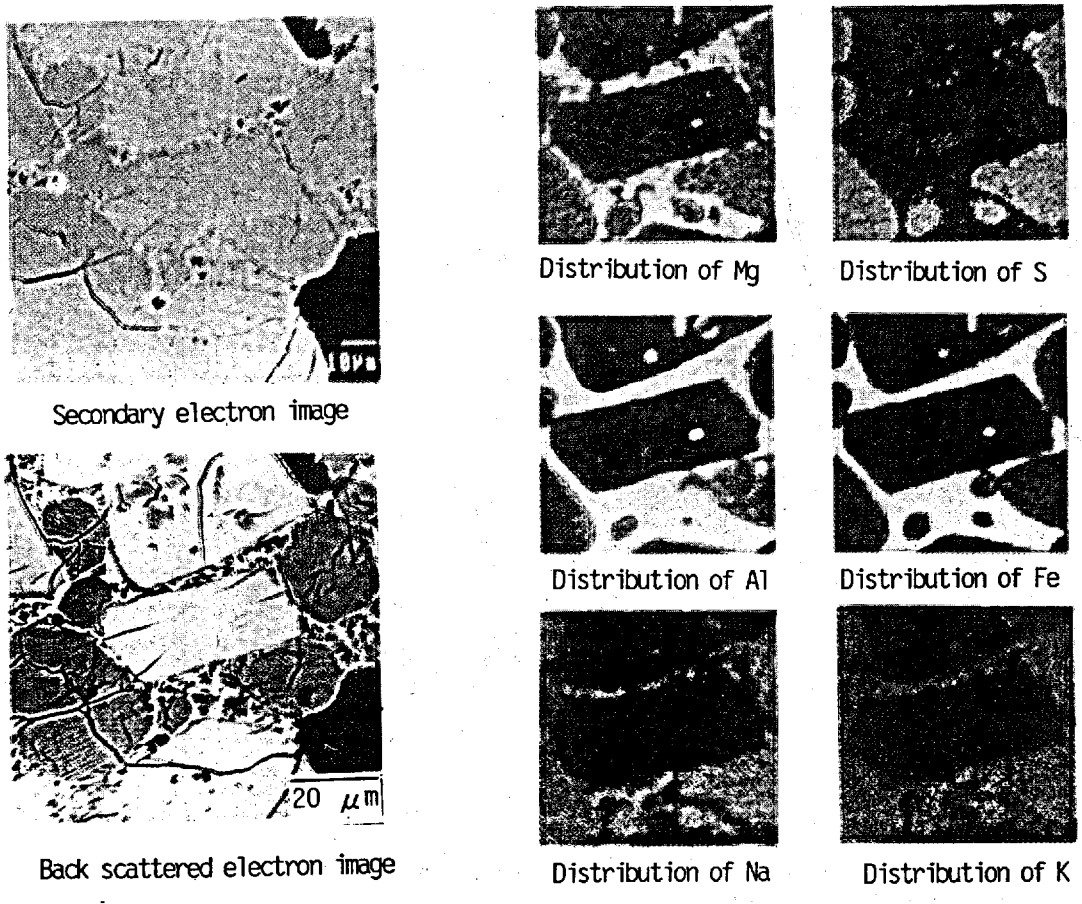

Explanation of color representing the oxide content (%)

Color	MgO	SO_3	Al_2O_3	Fe_2O_3	Na_2O	K_2O	Color	MgO	SO_3	Al_2O_3	Fe_2O_3	Na_2O	K_2O
White	>5.0	>4.0	>5.0	>5.0	>2.0	>2.0	Green	0.6	0.6	1.9	1.8	0.6	0.6
Pink	2.0	2.0	3.5	3.0	1.5	1.5	Sky blue	0.4	0.4	0.9	1.2	0.4	0.4
Red	1.0	1.0	2.3	2.5	1.0	1.0	Blue	0.2	0.3	0.7	0.7	0.2	0.2
Yellow	0.7	0.8	2.0	2.3	0.8	0.8	Black	<0.1	<0.1	<0.5	<0.3	<0.1	<0.1

Fig. 31 Secondary and back scattered electron image and x-ray image map of Mg, S, Al, Fe, Na and K of clinker alite with zonal structure (Uchikawa et al; (86))

Fig. 31 shows the secondary electron image and back scattered electron image of the zonal structure of clinker alite and the distributions of MgO, SO_3, Fe_2O_3, Al_2O_3, Na_2O and K_2O in it obtained by CMA/EPMA. Although MgO is uniformly distributed in the alite crystal, Al_2O_3, Fe_2O_3,SO_3, Na_2O and K_2O are densely distributed in the inner part of alite crystal, coinciding with the division of zonal structure by the boundary lines. The average contents of the components in the inner and peripheral parts of the zonal structure were determined ten times each by the point analysis and calculated by the Bence and Albee method as shown in **Table 4.**

The other example is on the effect of burning atmosphere on the distribution of minor components in clinker minerals **(42). Fig. 32 and 33** show the back scattered electron image and x-ray image maps of minor constituents in clinker burnt under various condition described before and chemical composition of clinker mineral in it . From these data, it is concluded that the content of aluminum in terms of Al_2O_3 in alite decreases and that in belite increases with shifting from the oxidizing atmosphere to the reducing atmosphere, though that in interstitial phase is not so much changed. The change of the content of Al shifts from the peripheral part to the inner part of alite and belite particles.

Table 4 Chemical composition determined by EPMA and birefringence of each part of zonal structure of clinker alite (Uchikawa et al; (86))

Analyzing point	Chemical composition (%)									Biref -ringence
	SiO_2	Al_2O_3	Fe_2O_3	CaO	MgO	SO_3	Na_2O	K_2O	Total	
Inner part	25.12	0.93	0.82	72.45	1.20	0.10	0.25	0.18	101.05	0.004
Peripheral part	24.09	0.71	0.58	73.76	1.11	0.07	0.21	0.10	100.63	0.006

Measuring condition of EPMA:
Accelerating voltage = 15kV, Probe current = 3 x10^{-8} A

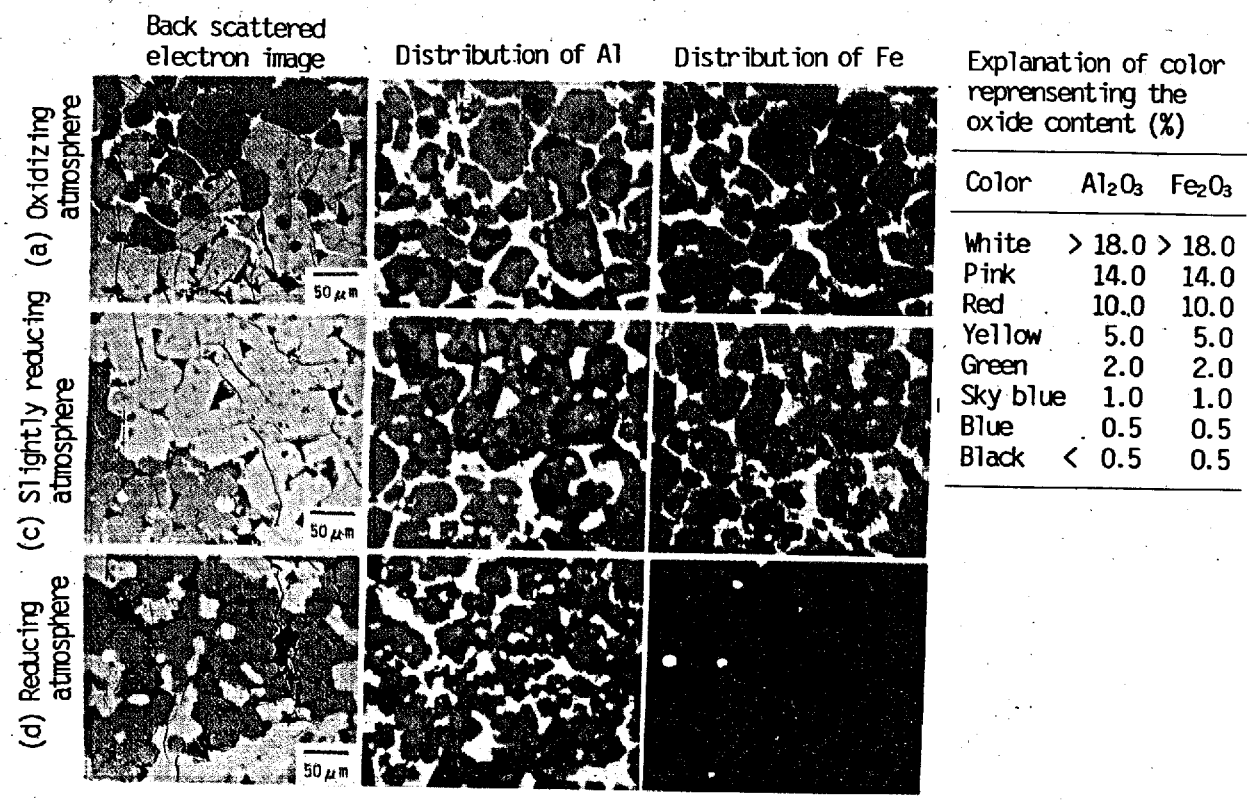

Fig. 32 Back scattered electron image and x-ray image map of Al and Fe burnt under oxidizing, slightly reducing and reducing atmospheres (Uchikawa et al; (42))

Although the content of iron in terms of Fe_2O_3 in alite remarkably increases up to the maximum in (c), it is almost eliminated from alite in (d), remaining in interstitial phase as white spots of metallic iron. The behavior of Fe in belite is similar to that in alite though that is not so conspicuous as this. In the interstitial phase, the content of Fe decreases with raising the level of reducing atmosphere and quite a large amount of C_4AF transforms into C_3A in (c), which increases to occupy the interstitial phase in (d).

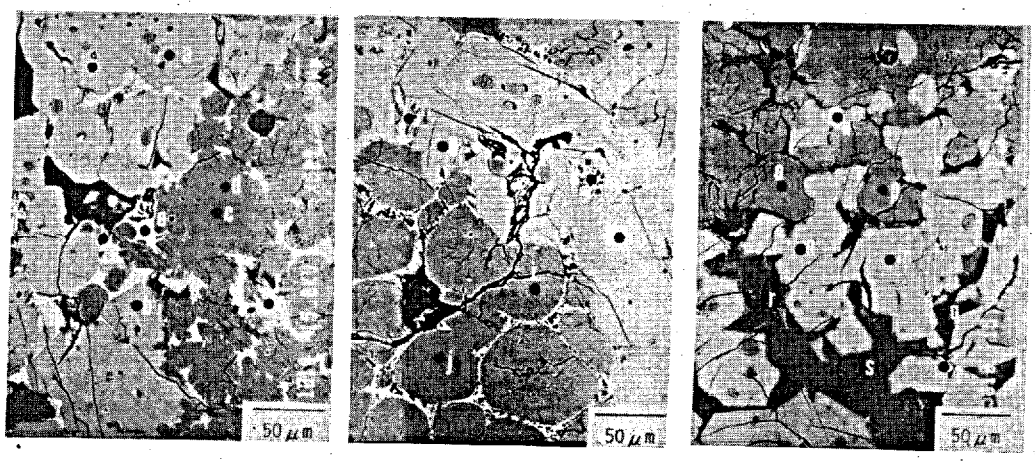

(a) Oxidizing atmosphere (c) Slightly reducing atmosphere (d) Reducing atmosphere

Chemical composition of clinker burnt under various atmospheres determined by EPMA

B.C.*1	Point	Phase *2	Chemical Composition (%) CaO	SiO_2	Al_2O_3	Fe_2O_3	MgO	SO_3	Na_2O	K_2O	Total	a/f *3	a+f *4
(a)	a	A	74.10	25.23	0.97	0.57	1.14	0.08	0.03	0.02	102.14	1.70	1.54
	b	A	73.61	24.54	1.16	0.71	1.15	0.16	0.25	0.09	101.67	1.63	1.87
	c	B	66.81	34.26	0.32	0.43	0.31	0.09	0.28	0.36	102.86	0.78	0.75
	d	B	66.90	34.48	0.46	0.53	0.28	0.06	0.20	0.41	103.32	0.87	0.99
	e	I	48.95	3.01	22.89	20.15	3.46	0.19	0.11	0.27	99.03		
	f	I	48.82	3.23	20.87	21.86	3.43	0.00	0.26	0.00	98.47		
(c)	g	A	73.34	25.00	1.01	1.38	1.18	0.02	0.00	0.00	101.93	0.73	2.39
	h	A	72.33	25.19	1.53	1.38	1.20	0.04	0.05	0.00	101.72	1.11	2.91
	i	B	66.70	32.02	1.42	0.56	0.44	0.02	0.08	0.03	101.27	2.54	1.98
	j	B	66.53	31.79	1.59	0.72	0.35	0.02	0.03	0.05	101.08	2.21	2.31
	k	I	52.06	4.08	27.61	6.57	10.56	0.00	0.03	0.00	100.91		
	l	I	57.12	3.68	30.58	4.79	4.73	0.23	0.10	0.01	101.24		
(d)	m	A	73.69	25.92	0.73	0.00	1.45	0.04	0.03	0.02	101.88	-	0.73
	n	A	73.84	25.63	0.78	0.04	1.49	0.04	0.05	0.00	101.87	-	0.82
	o	B	66.75	32.73	1.68	0.02	0.67	0.11	0.03	0.17	102.16	-	1.70
	p	B	66.83	32.48	2.14	0.05	0.41	0.18	0.00	0.15	102.24	-	2.19
	q	I	60.25	4.95	34.23	0.01	1.90	0.06	0.08	0.09	101.57		
	r	I	60.34	4.60	32.59	0.00	2.24	4.17	0.12	0.11	104.17		
	s	I	45.80	4.88	38.99	0.15	8.94	4.89	0.04	0.18	103.87		
	t	Fe	0.76	0.05	0.02	148.8	0.00	0.00	0.08	0.00	-		
	u	Fe	1.55	0.07	0.02	148.6	0.00	0.00	0.02	0.00	-		

*1; B.C.: Burning condition, (a): Oxidizing atmosphere, (c): Slightly reducing atmosphere, (d) Reducing atmosphere, *2; A: Alite, B: Belite, I: Interstitial phase, Fe: Metalic iron, *3: Weight ratio of Al_2O_3 to Fe_2O_3, *4: Sum of Al_2O_3 and Fe_2O_3

Fig. 33 Back scattered electron image of clinker burnt under various atmosphere (Uchikawa et al; (42))

The contents of magnesium in terms of MgO in alite and belite slightly increase as the burning atmosphere shifts from the oxidizing atmospheres to the reducing one. The distribution of Mg is uneven in interstitial phase almost composed of C_3A in (c) and (d).

The content of sulfur in terms of SO_3 increases in interstitial phase as the burning atmosphere shifts from oxidation to the reducing and the distribution of sulfur in interstitial phase become uneven in condition (c) and (d).

Deposition of $Ca(OH)_2$ on the surface of aggregate in concrete and formation of transition zone obtained by CMA/EPMA(**105**)(**106**), and variation in the composition of the hydrate in the vicinity of pozzolana and cement particles obtained by FESEM type EPMA (**107**) are shown in **Fig. 34** and **35**, respectively.



Back scattered electron image



Secondary electron image showing transition zone of concrete

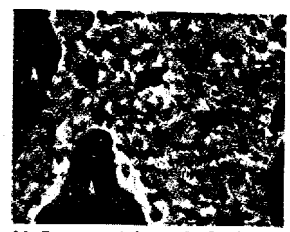

Molar ratio of Ca/Si

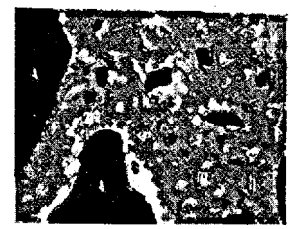

Distribution of Ca

Explanation of color representing the molar ratio and oxide content

Color	Molar ratio Ca/Si	CaO (%)
White	> 3.5	> 75.0
Pink	3.0	70.0
Red	2.5	65.0
Yellow	1.8	60.0
Green	1.6	50.0
Sky blue	1.4	40.0
Blue	1.2	20.0
Black	< 1.2	< 20.0

A: Aggregate, c: $Ca(OH)_2$, h: C-S-H, m: Monosulfate hydrate, u: Unhydrated cement particle (alite, belite and interstitial phase)

Fig. 34 Transition zone around aggregate in hardened concrete determined by CMA/EPMA (Uchikawa et al; (106))

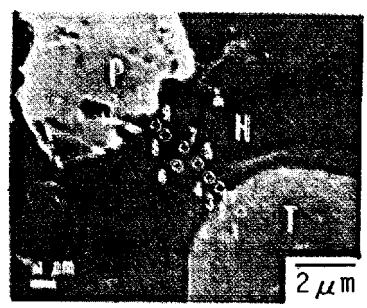

Secondary electron image

P: Pozzolana, H: Hydrate, U: Unhydrate (Alite)

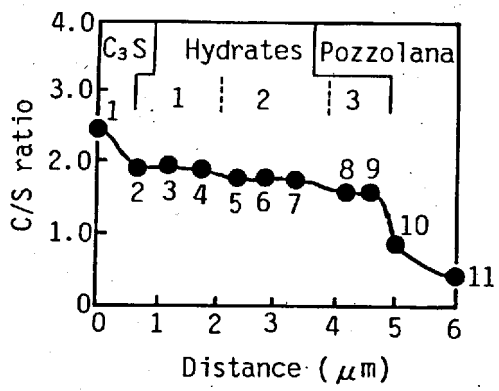

Fig. 35 Variation in composition of C-S-H between pozzolana and unhydrated grains (Uchikawa et al; (107))

(5) AES and μ-AES

When electron beam irradiates the sample, an electron on the L_2(2p)-shell is emitted through an intermediate process called the Auger process in such a way that an electron on the L_1(2s)-shell transfers to a vacancy on the K(1s)-shell and energy corresponding to the difference is given to the electron on the L_2(2p)-shell as shown **Fig. 36**. The method that specifies the elements in the sample by measuring the kinetic energy (E_K-$2E_L$) of the emitted electron and quantitatively analyze their content is called Auger electron spectroscopy and the apparatus used for this is called Auger Electron Spectroscope (AES). The energy level of the Auger electron is so low that it is measured under a vacuum as high as 10^{-8}Torr using an electron energy analyzer (EEA).

Auger microprobe electron spectroscopy obtaining a secondary electron image and an Auger image having a plane resolving power of 50nm or better has recently been developed by scanning the electron beam converged into the order of several nanometers. The device is called an Auger microprobe electron spectroscope (μ-AES) as shown in **Fig. 37**.

Since emitted energy is as low as 40 to 2000eV as shown in **Fig. 38**, the depth from which energy can be released is nanometers or less or 1/1000 that for the characteristic x-rays. μ-AES is characterized by having the potential to analyze the elements contained in a microscopic region of the surface. The S/N ratio of Auger electron is so small that energy of electron is often expressed by differential coefficient of energy.

The sample for μ-AES is generally limited to a conductive material. Recently, however, even an insulator providing no correct Auger electron spectrum due to charge-up has been able to be a sample for μ-AES by a newly developed sample inclination method. Current of primary electron beams, Ip, is the sum total of back scattered electrons, Ib, secondary electron, Is, Auger electron, Ia and absorbed current, Iab. The absorbed current is nearly equal to zero in an insulating material, then Ip > Ib + Is + Ia. Electrons corresponding to Iab are, therefore, charged up and released, whereupon a noise produced by them interferes with the measurements. Since Is is much larger than Ib and Ia, the sum total of Is, Ib and Ia can be equalized to Ip by increasing Is. The measurement is, therefore, able to be released from the interference of the noise by improving the emission efficiency of secondary electron, δ. Meanwhile, δ depends upon the accelerating voltage of primary electron beam, Ep, angle of incident electron beam, (θ), and the type of sample material. The emission efficiency of secondary electron, δ_θ, for the angle of incidence, θ, of sample is expressed by the following formula **3.8)**:

$$\delta_\theta = (1/\cos\theta) \times \delta(0) \quad \text{---------- 3.8)}$$

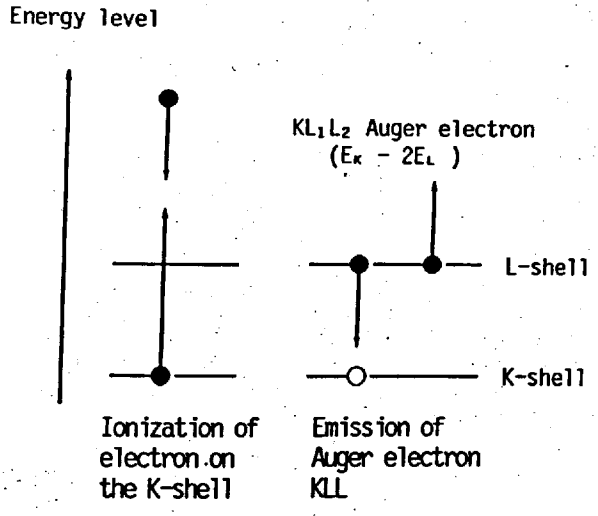

Fig. 36

Emission process of Auger electron

Where $\delta(0)$ = emission efficiency of secondary electron at θ of zero. $\delta(0)$ near an accelerating voltage of 5kV of the primary electron beam at the measurement of Auger electron spectrum is 0.3 to 0.5. Substituting 0.3 for $\delta(0)$ and 1 for δ_θ in Equation **3.8**), θ is given as 72.5°. The resolving power decreases with the increase of θ. The angle of inclination of sample was, therefore, fixed to 75°.

The two-dimensional distribution of element in the direction of depth can be determined by combining the sample inclination method with the ion-sputtering method. And the two-dimensional concentration distribution can be determined at a resolving power of 50nm, though the resolving power of EPMA is 500 to 1000nm, by incorporating the data processing and system control functions in the same way as for CMA/EPMA. The result is shown in **Fig. 39**.

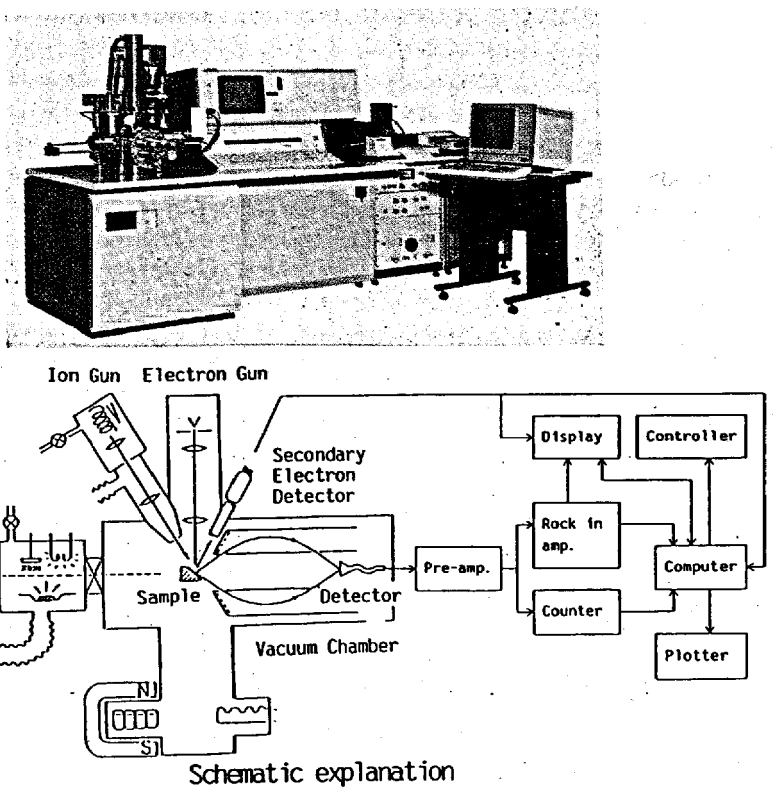

Fig. 37 Auger electron spectroscope and its explanation (JEOL JAMP-7100E)

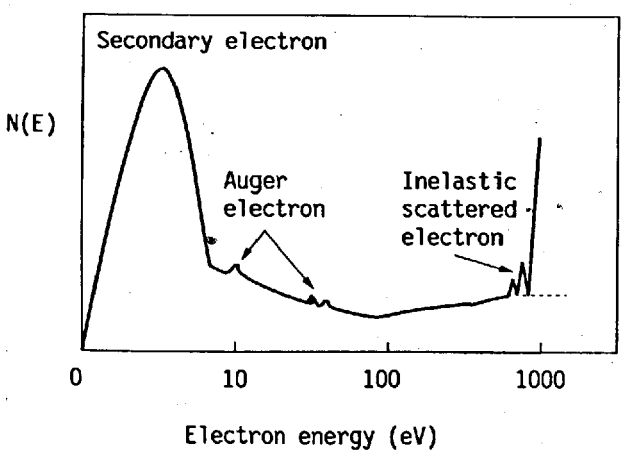

Fig. 38

Energy of electron and number of electron emitted (N(E))

Though Auger electron spectroscope (AES) is used for analyzing the surface composition of a material, applications to the cement and concrete field are few. Papers on the applications of AES include a paper **(108)** presenting that the bonding state of C_3S, $C_{12}A_7$, CA and CA_2 can be estimated from the symmetricalness of Auger spectra of Ca, O and Al, and a paper**(109)** suggesting from the analytical result in the direction of depth of the passive layer on the reinforcement in concrete that Ca^{2+} penetrates the passive layer when pore solution is the saturated solution of $Ca(OH)_2$, while it stays on the surface of passive layer when Na is contained in the pore solution.

An attempt has been done to measure the change of surface composition of clinker minerals toward the depth with time in initial stage of hydration by AES**(87)**. The change of composition in the direction of depth from the surface of alite and belite crystals according to the dipping time in water is shown in **Fig. 40(87)**. Sizes of alite and belite crystal are within a range from 10 to 40μm. AES is appropriate for determining the element distribution in the direction of depth from the surface, because the analytical region of surface by AES is

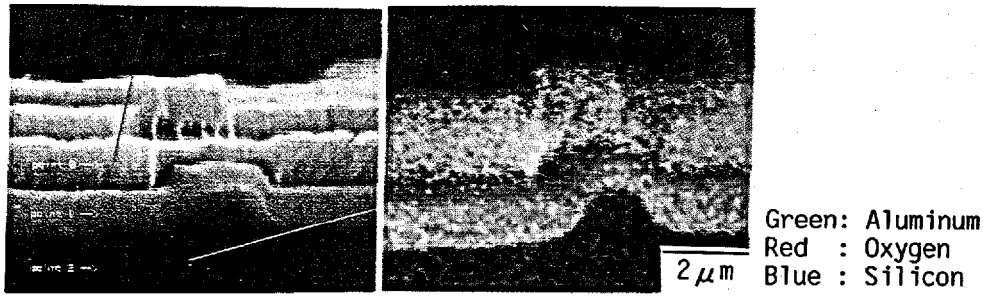

Fig. 39 Electron distribution map of the cross section of semi-conductor device determined by Auger electron spectroscope (courtesy of JEOL)

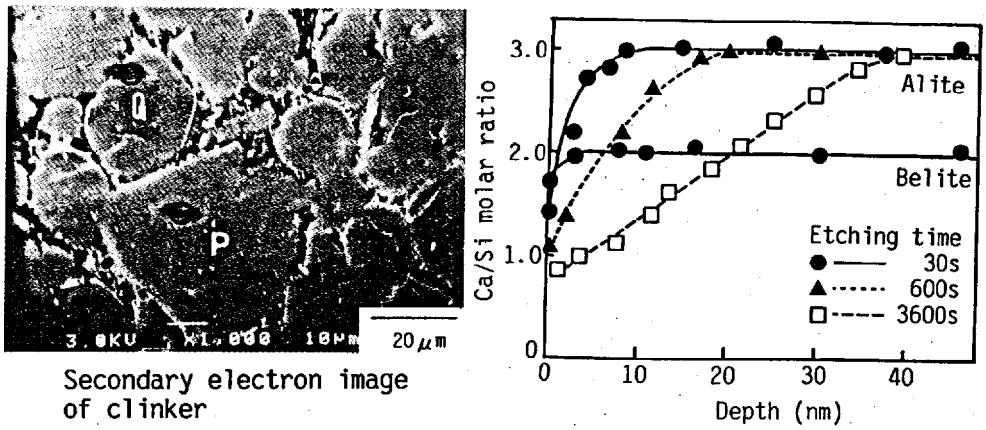

Measuring condition of AES

Accelerate voltage: 3.0 kV, Porbe current: 1.98×10^{-7} A,
Pressure: 4.4×10^{-2} Pa, Time constant: 0.1 second,
Ion gun voltage: 3.00 kV, Sputtering rate: 2.5 nm/min

Fig. 40 Change of Ca/Si molar ratio toward the direction perpendicular to surface after water etching determined by AES (Uchikawa et al; (87))

100nm to 1 μm in the cross wide direction and ion-sputtering can be applied to AES. The analytical positions are the center of alite and belite shown in the secondary electron image. The C/S molar ratio in the surface layer and depths of 3 and 8nm from the alite surface etched for thirty seconds are approximately 1.3, 2.1 and 3.0, respectively. Ca ions in alite are selectively dissolved at the beginning of hydration. As mentioned before, the position showing the theoretical value of C/S ratio of alite is 8nm deep. The depth coincides with the distance between the peak and the trough on the surface of approximately 11nm by AFM described later in **Fig. 58(87)**. The C/S ratios in the surface layer of belite and at a depth of 3nm from it are 1.6 and 2, respectively. The result indicated that the hydration reactivity of belite is lower than that of alite because Ca ions are dissolved at the beginning of hydration less from shallower part in belite than in alite.

Next example is the results of the studies on the adsorptive behavior of organic admixtures to each cement mineral at the initial stage of cement hydration. Carbon and sulfur, main components of organic admixture, and calcium, one of main components of clinker minerals, were analyzed by AES in the direction of the depth from the surface of adsorbed layer. The sample was prepared in such a way that the polished surface of clinker was dipped in a practical concentration of 2.5% aqueous solution of β–naphtalenesulfonic acid-based admixture or that of 0.2% aqueous solution of lignin sulfonic acid-based admixture for thirty seconds. The diameter of the incident electron beam at the measurement by AES is estimated to be 1μm.

Analytical points by AES are shown on the secondary electron image photographs of **Fig. 41** and the changes of the concentrations of carbon, sulfur and calcium in adsorbed layer on alite and on interstitial phase are shown in **Fig. 42**.

As shown in the left figure of the sample dipped in the aqueous solution of β–naphtalenesulfonic acid-based admixture, the concentration of carbon in adsorbed layer on alite was as high as about 70. It sharply decreased with the increase of the depth and it went down to about half of the concentration of the surface of the adsorbed layer at the depth of 20 nm from its surface, reaching the constant value equal to the back ground level at the depth of approximately 50nm. The concentration of calcium increased with the increase of the depth, reaching the constant value at the depth of 50nm, though its concentration on the surface of the adsorbed layer was as low 2 or 3. In the case of the sample dipped in the aqueous solution of lignin sulfonic acid-based admixture, the concentration of carbon on the surface of the adsorbed layer was about 80 which was higher than that in the sample dipped in the aqueous solution of β–naphtalenesulfonic acid-based admixture and it went down to no more than approximately three quarters the concentration of the surface of the adsorbed layer at the depth of 20nm. The concentration of carbon decreased, however, sharply at the depth exceeding 60nm, reaching zero at the depth of about 100nm. Calcium was hardly detected on the surface of the adsorbed layer and the concentration of it increased with the decrease of the concentration of carbon.

As shown in the right figure of **Fig. 42** of the sample dipped in the aqueous solution of β–naphtalenesulfonic acid-based admixture, the concentration of carbon in adsorbed layer on interstitial phase went down to about half of the concentration of the surface of the adsorbed layer at the depth of 40nm and decreased slowly at the depth exceeding 40nm, reaching the constant value equal to the background level at the depth of approximately 300nm. The concentration of calcium increased slowly with the increase of the depth, reaching the constant value at approximately 300nm. In the case of the sample dipped into the aqueous solution of lignin sulfonic acid-based admixture, the changes of the concentrations were more remarkable in carbon, sulfur and calcium than those in the sample dipped into the aqueous solution of β–naphtalenesulfonic acid-based admixture. The concentration of carbon on the surface of the adsorbed layer went down sharply one fifth the concentration of the surface of the adsorbed layer at the depth of 60nm and decreased slowly at the depth exceeding 60nm, reaching zero at the depth of about 200nm. The concentration of calcium increased slowly with the increase of the depth, reaching the constant value at approximately 200nm. Although these organic admixtures are adsorbed physically near the surface of the

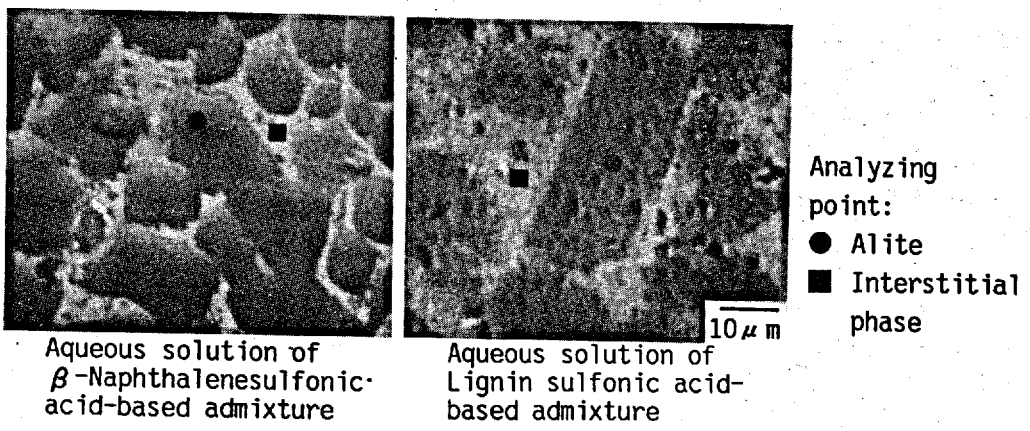

Fig. 41 Secondary electron image and analyzing points by AES of polished surface of clinker dipped in aqueous solution of organic admixture

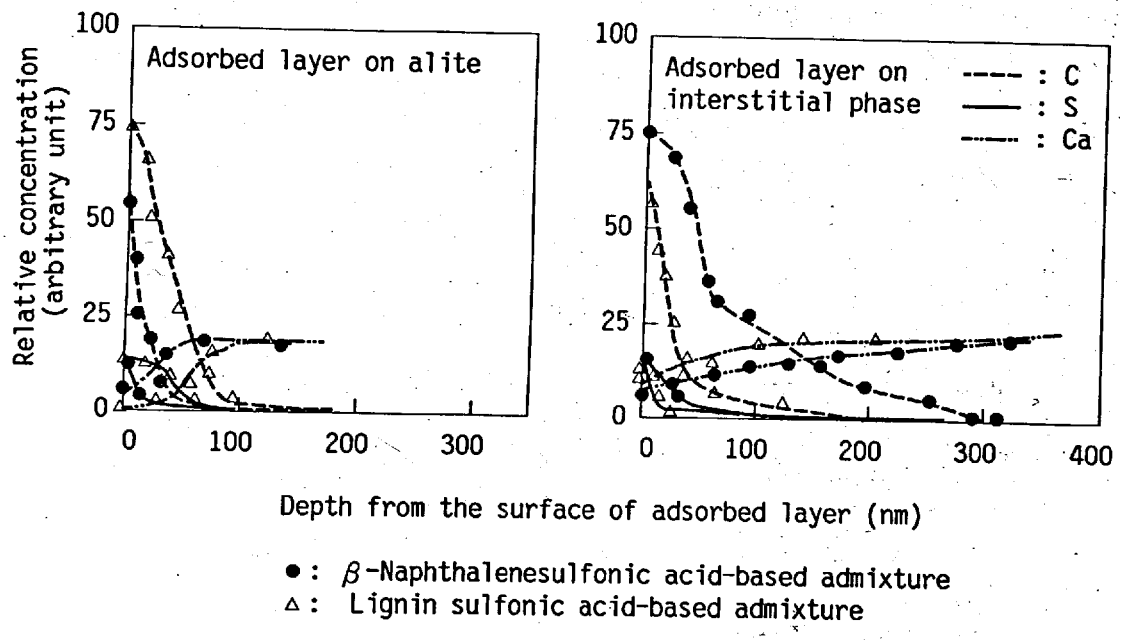

Fig. 42 Changes of carbon, sulfur and calcium concentration in the adsorbed layer toward clinker surface determined by AES

1) Dipped in a water

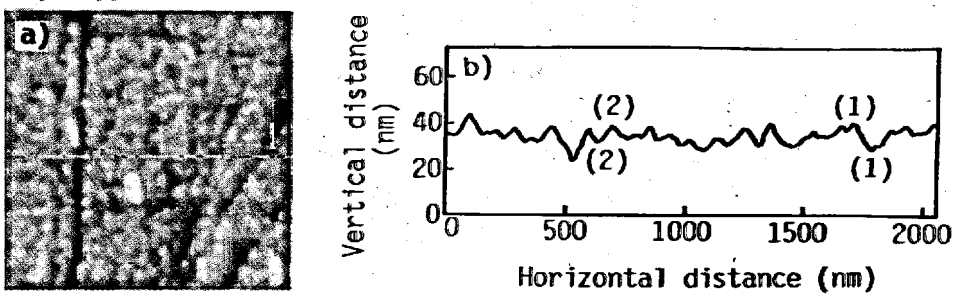

	(1)	(2)
Horizontal distance [nm]	71.41	51.01
Vertical distance [nm]	12.45	7.07
Angle [deg]	9.89	7.90

2) Dipped in an aqueous solution of β-naphthalenesulfonic acid-based admixture

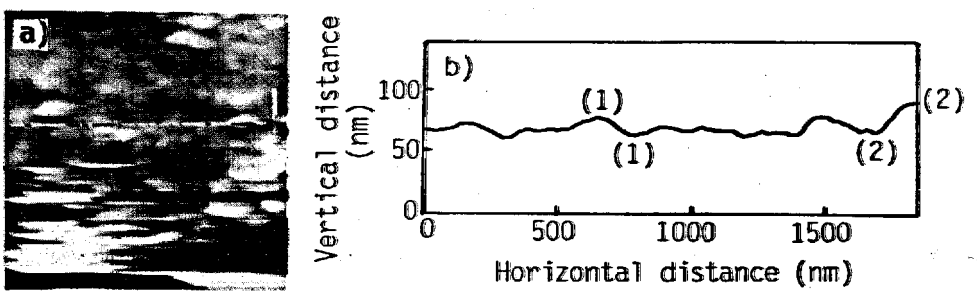

	(1)	(2)
Horizontal distance [nm]	127.11	118.03
Vertical distance [nm]	17.11	27.57
Angle [deg]	7.67	13.15

3) Dipped in an aqueous solution of lignin sulfonic acid-based admixture

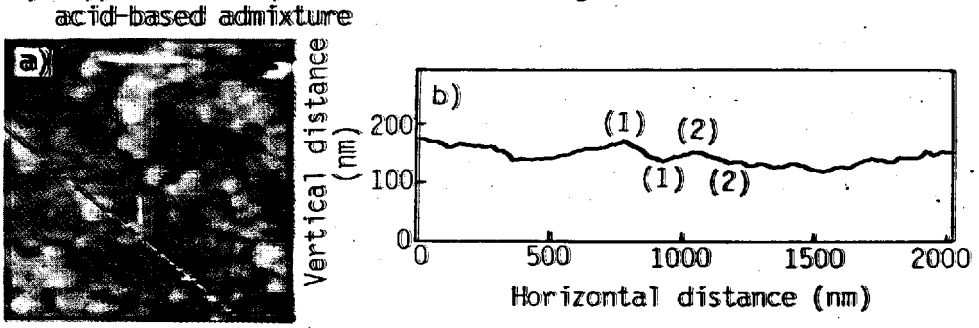

	(1)	(2)
Horizontal distance [nm]	138.00	118.88
Vertical distance [nm]	35.60	21.76
Angle [deg]	14.46	10.37

a): AFM image, b): Surface profile of line I shown in a)

Fig. 43 AFM image and roughness of the surface of clinker alite after dipping in aqueous solution

adsorbed layer, it is inferred that they are fixed on the surface of clinker mineral by chemisorption accompanying with the change of the chemical composition in the adsorbed layer toward the surface of clinker mineral.

As shown in **Fig. 42**, organic admixtures is adsorbed preferably more on interstitial phase than on alite and the preferred adsorption is remarkable in β–naphtalenesulfonic acid-based admixture. The thickness of adsorbed layer on alite is thicker in lignin sulfonic acid-based admixture and that on interstitial phase is thicker in β–naphtalenesulfonic acid-based admixture.

The surface roughened by dipping the polished clinker in the aqueous solutions of both admixtures were determined by AFM. The results are shown in **Table 5** and **Fig. 43**. The distance between the peak and the trough on the surface and the distance between peaks were increased by the existence of the admixtures. Schematic explanation of physically adsorptive and chemically adsorptive state of β–naphtalenesulfonic acid- and lignin sulfonic acid-based admixtures estimated from the above-mentioned results is shown in **Fig. 44**.

Table 5 Roughness of the surface of clinker alite after dipping the aqueous solution determined by AFM

Solution	Distance between peaks (vertical)	Distance between the peak and the trough (Horizontal)
Water	100 nm	10 nm
Aqueous solution of β-Naphthalene-sulfonic acid-based admixture	250 nm	20 nm
Aqueous solution of lignin sulfonic acid-based admixture	250 nm	30 nm

Dipping time: 30 sec

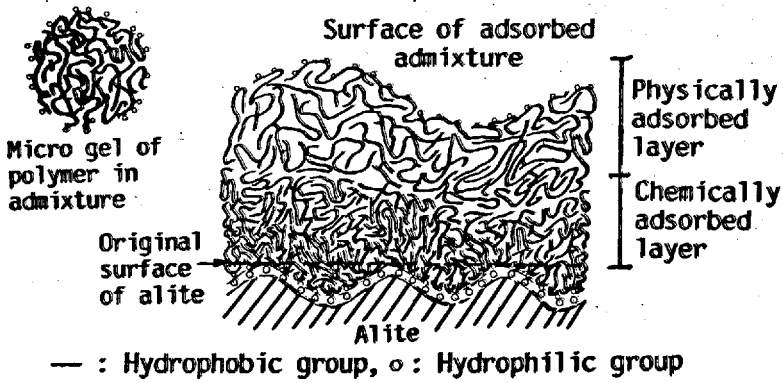

Fig. 44 Schematic explanation of adsorption of organic admixture on clinker mineral

(6) Microfocus x-ray diffractometer

Microfocus x-ray diffractometer is an instrument for obtaining structural information of a microscopic region of a sample by taking x-rays in a spot of 1 mm by 1 mm and converging the x-rays into a size of tens microns in diameter with a collimater, while the conventional x-ray diffractometer has a line x-ray source of hundreds microns by 10 mm. The microfocus x-ray diffractometer is illustrated in **Fig. 45**. Since the number of crystallite required for the diffraction is too small for the microfocus x-ray diffractometer, the x-ray diffracted from the microscopic region is uniformalized and the intensity of the diffracted x-ray is augmented by the triaxial (ω, χ and ϕ) rotation and fluctuation of the sample using a system to prevent

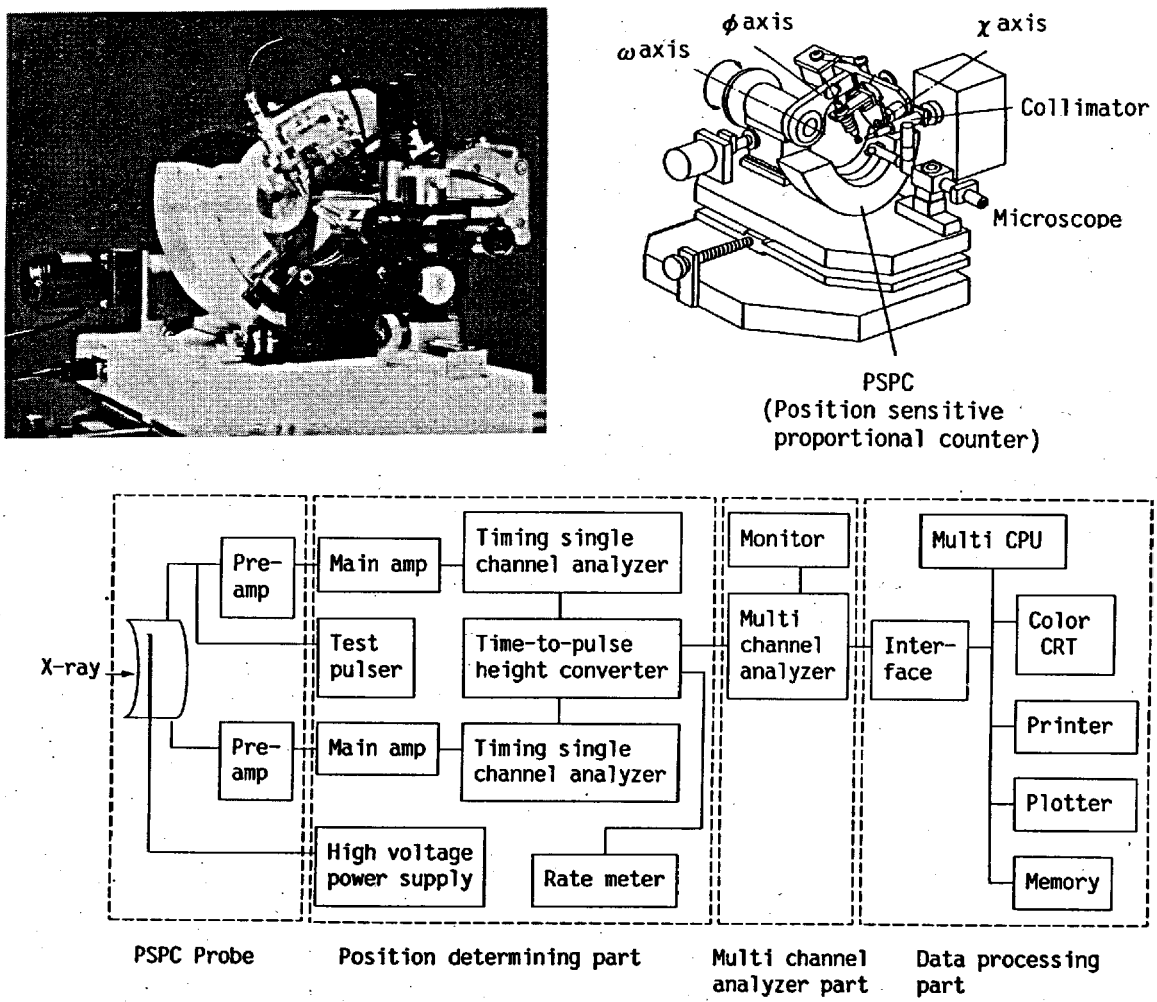

Fig. 45 Microfocus x-ray diffractometer and its block diagram (Rigaku Co. PSPC/MDG system)

the Debye-Scherer ring from discontinuity. A high-power x-ray source of 10 to 18 kW is used and a curved position sensitive proportional counter (PSPC) of 80 mm in radius shown is used to integrate as well as detect the x-ray diffracted from the sample for improving the S/N ratio. PSPC has a metal core wire and a delay line in it and is filled with PR gas. The incidence point of diffracted x-ray is determined by measuring the time difference because the voltage pulse caused on the metal core wire by the incident x-ray does not appear simultaneously at the both ends of the delay line. Although the spatial resolving power is 0.2°(2θ) which is lower by two orders of magnitude than that of the conventional x-ray diffractometer, the measuring range is as wide as 0 to 150° (2θ), so even higher-angle diffracted lines can be measured. Measurements of the position and intensity of diffracted x-ray using PSPC and the data processing system are shown in **Fig. 45**. The triaxial fluctuation effect using the powder and the single crystal of silicon oxide is shown in **Fig. 46**, and that of fine extraneous matter of 60 μm by 100 μm in an aluminum alloy is shown in **Fig. 47**.

A x-ray diffraction pattern of the zonal structure of alite in cement clinker is shown in **Fig. 48(86)**. Considering with the results of CMA/EPMA, the diffraction pattern of the zonal structure of M_1 phase and that of the peripheral region of M_3 phase are different from each other.

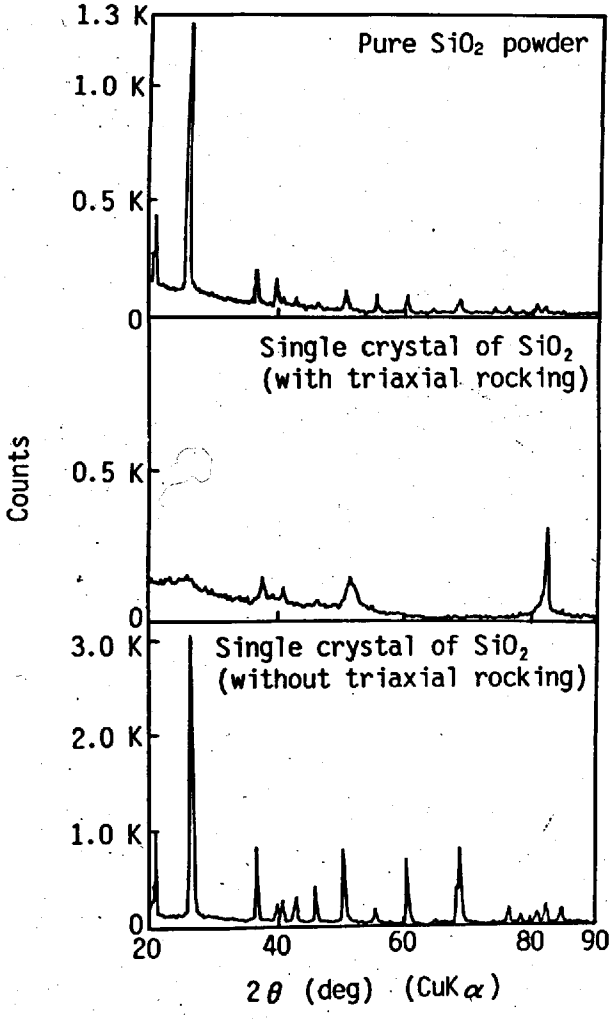

Fig. 46 X-ray diffraction profile of quartz in rock determined by microfocus x-ray diffractometer (courtesy of Rigaku Co.)

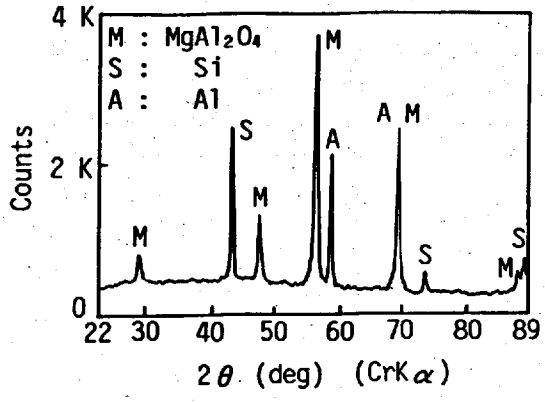

Fig. 47 X-ray diffraction profile of inclusion of $MgAl_2O_3$ in aluminum alloy

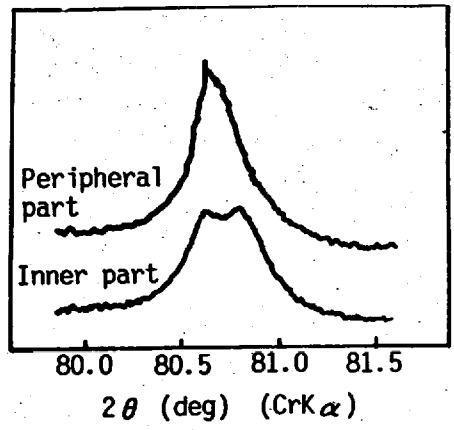

Fig. 48 X-ray diffraction profile of inner and peripheral part of clinker alite with zonal structure determined by microfocus diffractometer (Uchikawa et al; (87))

(7) Extended x-ray absorption fine structure (EXAFS)

Ordinary solid and liquid have fine structure of x-ray absorption changing from the x-ray absorption edge to the higher energy side of approximately 1000 eV as shown in **Fig. 49**. The region from the x-ray absorption edge to approximately 50 eV and that from 50 to 1000 eV are called the x-ray absorption near edge structure (XANES) and extended x-ray absorption fine structure (EXAFS), respectively. Photoelectrons coming out by the excitation of inner shell are scattered by surrounding atoms during the propagation of spherical wave of photoelectrons through the solid and the modulated spherical wave gives fine fluctuating structure in the absorption spectrum. Although the steric configuration of atoms surrounding the x-ray absorbing atoms and the state density of conducting material can be determined by the analysis of XANES, the analysis is so complicated because XANES appears as the result of the interference effect caused by the multiple scattering between the x-ray absorbing atoms and the surrounding atoms that a structural model is required. It is inferred from the resolving power of monochromator and the absorption of x-ray in air that only the atoms having the adsorption edge in a range from 5 to 25 eV such as titanium or higher atoms can be measured in XANES. The distance between an x-ray absorbing atom and a surrounding atom and the coordination number and the types of x-ray absorbing atoms can be determined by the analysis of EXAFS. High-luminance synchrotron orbital radiation (SOR) or high-power x-ray is used as the x-ray source. An EXAFS apparatus using a rotating anode type x-ray source is shown in **Fig. 50**.

EXAFS is widely used for the structural study of multicomponent glass. If lighter atoms can be determined by evacuating the passage of x-ray or filling with helium, EXAFS will be applied to the cement and concrete field.

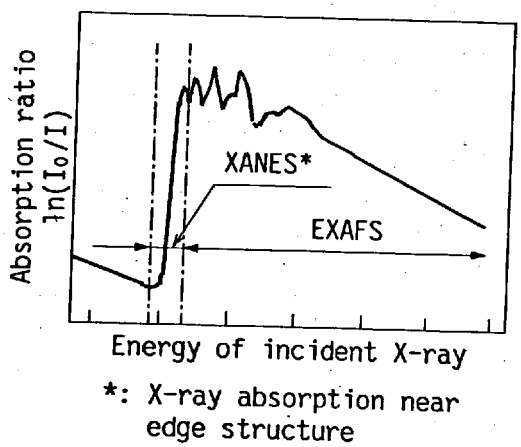

Fig. 49 X-ray energy and x-ray absorption near absorption edge

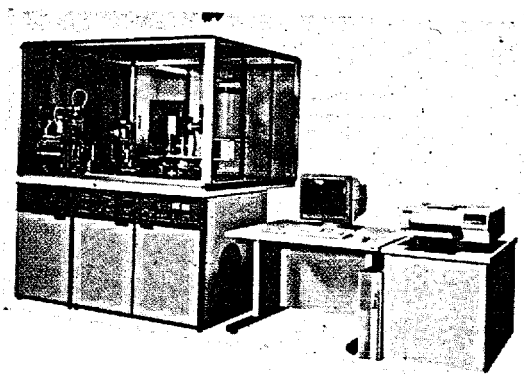

Fig. 50 Extended x-ray absorption fine structure analyzer (EXAFS) (Rigaku Co.)

(8) SIMS

Low-penetrability ionic beam with sputtering function is used for determining the element distribution on the surface and in the direction of depth of a solid. Neutral atoms and molecules, x-rays, secondary ions and secondary electrons are emitted from the surface of a solid sample irradiated with high-energy ions. Secondary ion mass spectroscopy (SIMS) is a method for analyzing the composition of a sample using the secondary ions among them. An ion microprobe mass analyzer (IMMA) is an instrument for analyzing the microscopic region of surface and has the function of observing the two-dimensional element distribution of the surface of the sample by irradiating with the ionic beam converged into hundreds namometers.

When a sample is irradiated with the ionic beam such as O_2^+, Ar^+ and Cs^+ of 10 to 20keV, the atoms in the sample are given kinetic energy by the collision of ions. When the kinetic energy is sufficiently larger than a potential barrier in the material of sample, the atoms move in the sample colliding with other atoms and finally the atoms in the surface layer are driven out as the secondary ions as shown in **Fig. 51.**

The secondary ions driven out are separated and detected with mass spectrometer and the elements contained in the sample are both qualitatively and quantitatively analyzed by SIMS as shown in **Fig. 52**. The area of the measuring region for SIMS is hundreds nanometers to hundreds microns lying between those for AES and ESCA. The two-dimensional information of the surface layer of 1 to tens nanometers in depth can be obtained. Even a small quantity of 100ppm to 0.1ppb of any element can be analyzed. The sample is inclined to the direction of incident ionic beam at 45°. The secondary ions emitted from the sample by sputtering are detected. Since the sample is eroded conically, the secondary ions emitted from the rim of the hollow eroded conically make the measurement inaccurate. The area masking **(110)** or electronic aperture **(111)** method combining a restricted field lens and a restricted field slit is used for analyzing a sample in the direction of depth so that only the secondary ion emitted from the center of sputtered area are detected. An ion gun is selected considering the elements to be analyzed and the measuring region. Since the mass analysis has a small background and a large dynamic range, it is suitable for the microanalysis, but inapplicable to the state analysis.

Charging-up in the analysis of an insulating material is prevented by covering with electron conductive layer on the surface except measuring region and blowing the vapor of indium only upon the measuring region to form an electron bombardment-induced conductive layer **(112)** or neutralizing the charge by the thermionic irradiation method or the negative ionic beam **(113)**.

The application of SIMS to the cement and concrete field began to be reported in the first half of the 1980s. Papers published since then include a paper**(114)** inferring from the comparison of the average composition in bulk with the surface composition determined by SIMS that Fe, K and alkali are concentrated on the surface of high-early-strength portland cement, blast fuenance cement and hydrated high early strength portland cement respectively, a paper**(115)** presenting the determination of the capability of ordinary cement to fix Co, Ce and Sr by SIMS together with other analyses and the existing state of those atoms in hydrated cement, respectively, a paper **(116)** describing the limit of qualitative analysis of admixtures due to the structural factors and the possibility of quantitative analysis, and a paper **(117)** presenting by analyzing the interface between quartz and cement paste in

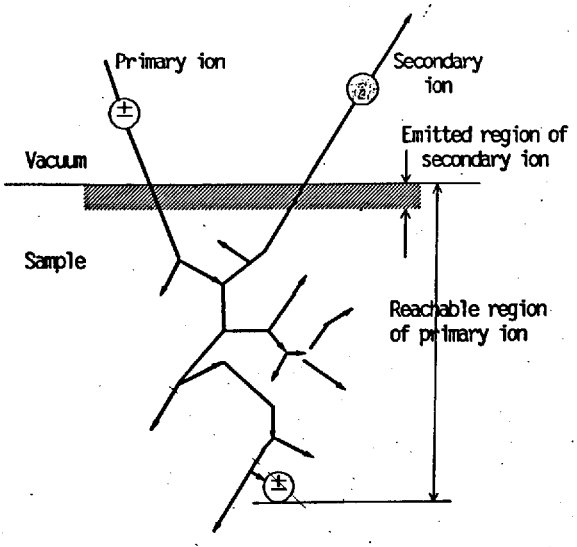

Fig. 51

Interaction between incident ion and solid sample

mortar prepared by using quartz as aggregate left to stand in SO_2 gas of the concentration of 5% that Si is concentrated in the paste at a depth of submicrons from the interface and so Na is decreased.

The analytical result of alite in clinker by SIMS using Cs^+ and O_2^+ as the primary ion source is shown in **Fig. 53(42)**. The result indicates that alite contains trace elements including F, Ti, P, Co and Zn as well as minor elements including Mg, S, Na and K. The location and name of the cement manufacturing plant can be estimated from the kind and contents of those trace elements contained in each clinker mineral.

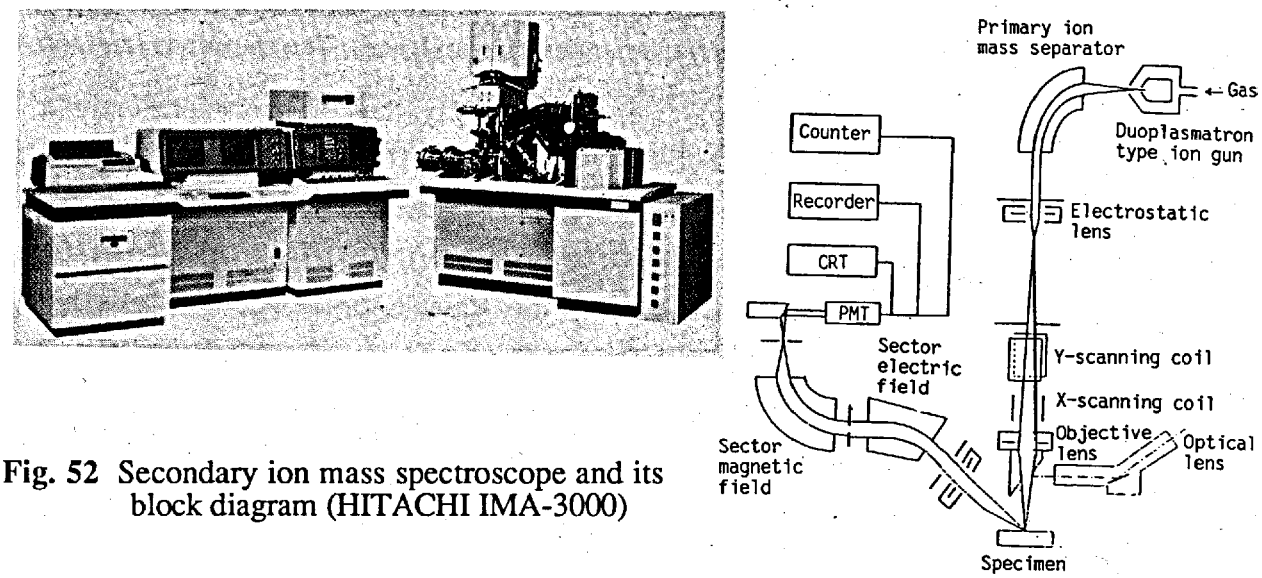

Fig. 52 Secondary ion mass spectroscope and its block diagram (HITACHI IMA-3000)

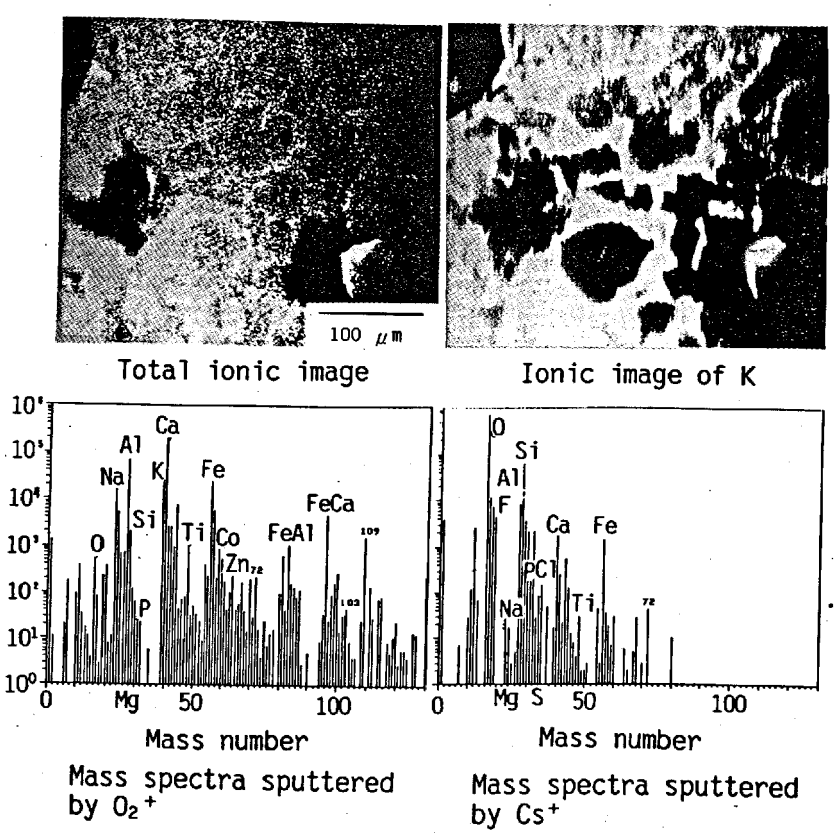

Fig. 53 Ionic image and mass spectra of cement clinker determined by SIMS (Uchikawa et al; (42))

(9) STM and AFM

When a voltage of approximately several volts is applied to a gap of approximately 1nm between a needle and a conductive sample, electric current passes through the gap by the tunnel effect in the inverse proportion to the gap distance. An image showing the roughness of surface of sample at the atomic level is, therefore, able to be obtained by scanning the surface with the needle keeping the tunnel current constant(**118**). A microscope utilizing this theory is called a scanning tunnel microscope (STM) shown in **Fig. 54** and **55**. A microscope substituting the atomic force between the probe and the sample for the tunnel current is called an atomic force microscope (AFM) shown in **Fig. 56**. A method for identifying an element from the relationship between the tunnel current and the voltage is called scanning tunnel electron spectroscopy. A combined instrument of STM with SIMS or XPS is being developed for determining the structure and composition of the surface layer at the same time. It is expected to be a useful tool for characterizing a material.

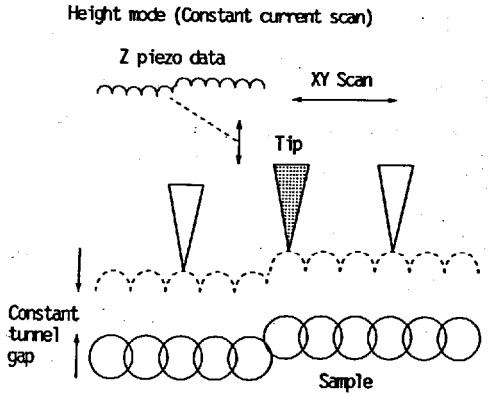

Fig. 54

Theoretical diagram of scanning tunnel microscope

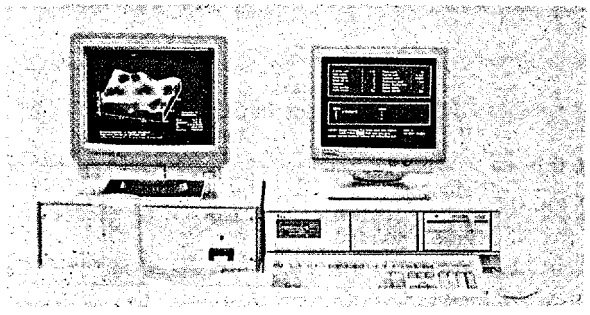

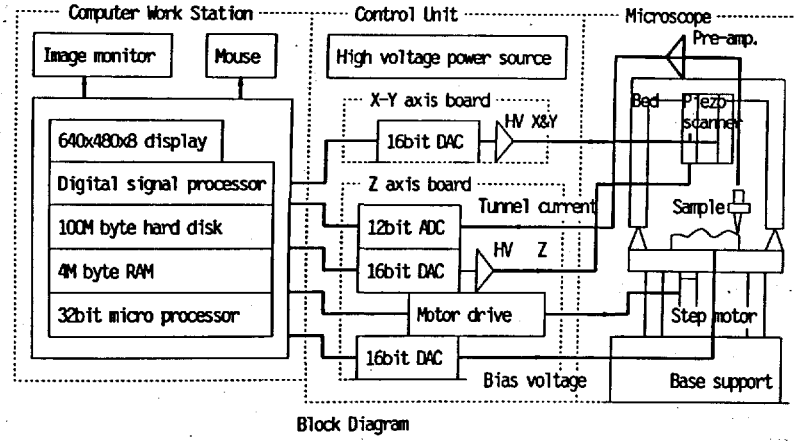

DAC: Digital-analog converter, ADC: Analog-digital converter,
RAM: Random access memory, HV: High voltage

Fig. 55 Scanning tunnel microscope and its block diagram (Digital Instruments Co., Nano scope AFM)

Various improvement have been made on STM developed at Zurich Research Laboratories of IBM in 1982 and started to be put to practical use. Tungsten, platinum and an platinum iridium alloy are used for the needle probe. It is most important for obtaining the accurate data to keep the probe by removing impurities deposited on it during the measurement and to improve the reliability.

STM is characterized by having enough resolving power as high as 0.1nm in the vertical direction and 0.01nm for the vacuum type STM for obtaining a real image of each atom. Attention has been paid to STM as a tool for the final fine processing (atomic manipulation) of a material as well as for the characterization of it. STM is, therefore, developed to fine machining of a material at the level from the magnitude of an atom to an order of nanometer using phenomena such as electric field evaporation, movement of atom by adsorption, surface reaction of gas and mechanical cutting.

AFM is operated in such a way that the surface of sample is scanned with the probe controlling a piezoelectric element so as to keep the repulsive force between the atoms at the tip of probe and those in the sample constant. An image of the surface structure of sample can be obtained by the signal sent from the piezoelectric element. AFM is useful for observing the surface structure of an insulating material such as clinker minerals and hydrates in cement and concrete.

The AFM images of the surfaces of alite before and after dipping in water for thirty seconds are shown in **Fig. 57(87)**. The smooth surface before dipping has a roughness as well as approximately 1 to 2nm and fine scratches at intervals of approximately 50nm regarded to be abraded with abrasion grains of 0.05 μm in average diameter. The roughness of surface after

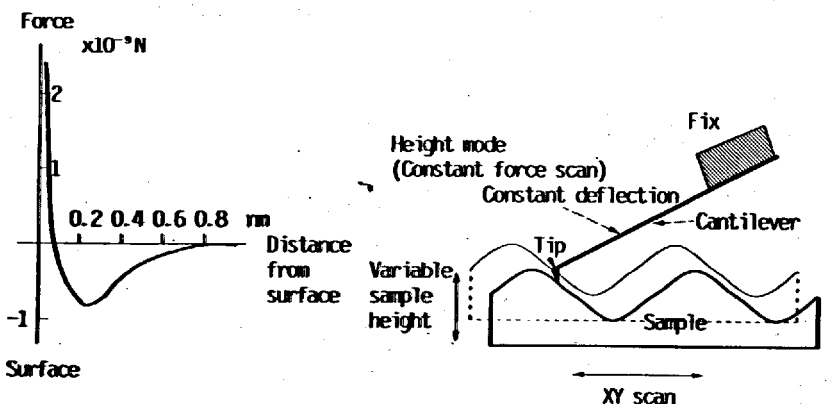

Fig. 56 Theoretical diagram of Atomic Force Microscope

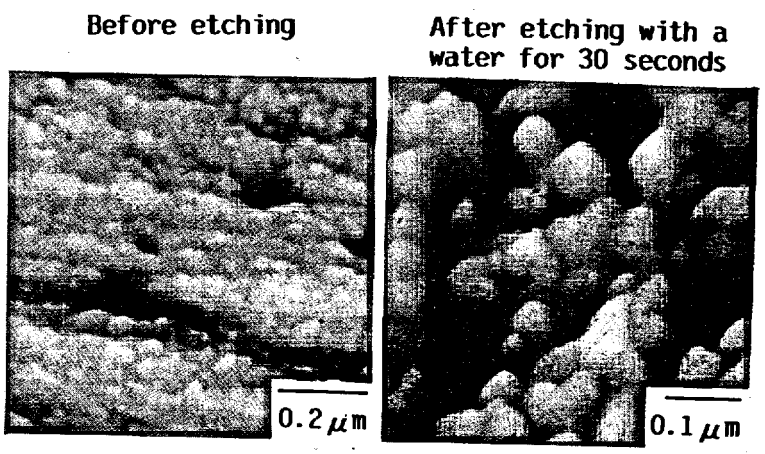

Fig. 57

AFM image of clinker alite surface before and after etching with water
(Uchikawa et al; (87))

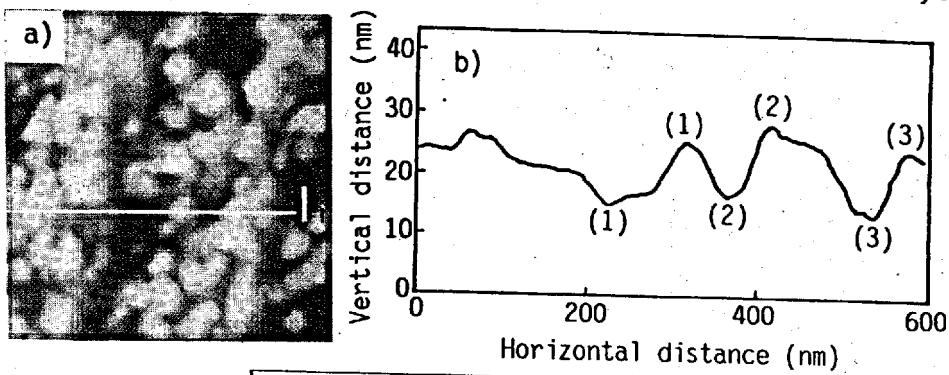

a) AFM image,
b) Surface profile of line I shown in a)

	(1)	(2)	(3)
Horizontal distance [nm]	93.00	57.00	36.00
Vertical distance [nm]	10.34	11.55	10.29
Angle [deg]	6.35	11.45	15.96

Fig. 58 Roughness of the surface of clinker alite etched with a water for 30 seconds determined by AFM (Uchikawa et al; (87))

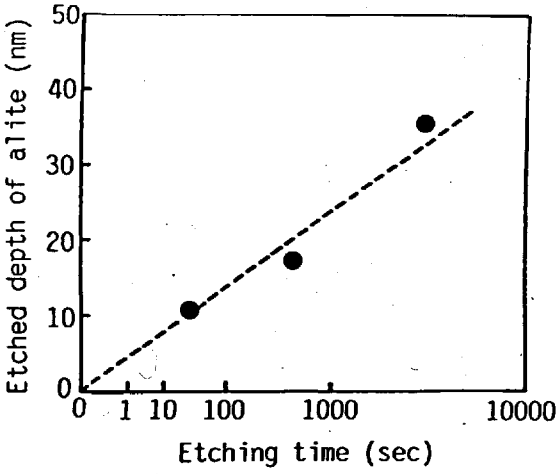

Fig. 59

Relationship between etching time and etched depth of clinker alite (Uchikawa et al; (87))

etching is enlarged by the dissolution of elements and the distance between peaks is approximately 100nm. The smoothness of the surface determined in an accuracy of 0.1nm in the direction of depth is shown in **Fig. 58(87)**. The distance between the peak and the trough on the surface of alite is 10.3 to 11.5nm. Assuming that the distance corresponds to the size of an alite crystal dissolved, four unit cells with the c-axis 2.5nm long are leached out from the surface in the direction of c-axis. The distance is increased to 18.5 and 39.4 nm by increasing the dipping time to 600 to 3600 seconds, respectively. The distance is proportional to the 1/4 power of the dipping time as shown in **Fig. 59(87)**.

STM and AFM require no evacuated environment unlike the electron microscopes and it can be operated even in the atmosphere, gas and water. STM and AFM are, therefore, expected to spread in the future.

(10) Microscopic Fourier transform infrared spectrophotometer

The microscopic Fourier transform infrared spectrophotometer is a FT-IR equipped with a transmission or reflection microscope with lenses for infrared ray and the spatial resolving power is approximately 10 μm. Chemical compounds are, therefore, able to be identified with it. The wavenumber used for the identification ranges from 5500 to 450 cm^{-1}.

The wavenumber accuracy and the maximum resolving power are 0.01 cm^{-1} and 1 cm^{-1}, respectively. Using a sample stage which can be driven at intervals of 10 μm, a sample with dimensions of 50 mm by 50 mm by 0.5 mm can be analyzed and mapped. The microscopic FT-IR and the measurements of spherical particles of aluminum are shown in **Fig. 60** and **61**, respectively. Since pulverized crystal with ionic chemical bonds is strongly affected by the anti-polarization field, the position and shape of absorption band extremely vary according to the shape and diameter of particles and the refractive index of dispersing medium. A circuit with an organic film printed on a silicon wafer and the absorbance distribution determined by microscopic FT-IR with the movable sample stage are shown in **Fig. 62.**

Applications of FT-IR to the cement and concrete field include the identification of low - calcium C-S-H by the shift of absorption peak(**119**). It is expected that new knowledge will be obtained by determining the infrared absorption spectrum of microscopic region and the two-dimensional distribution of absorbance with the microscopic FT-IR .

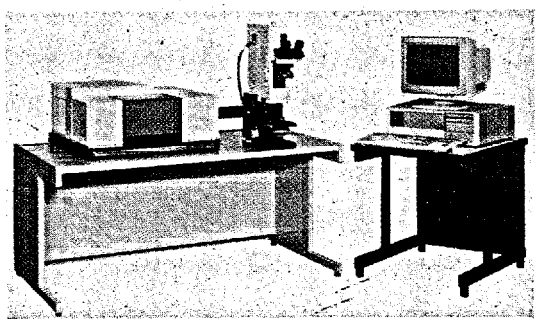

Fig. 60

Microscopic Fourier transform infrared spectrophotometer (Microscopic FT-IR) (JEOL RFX-4000)

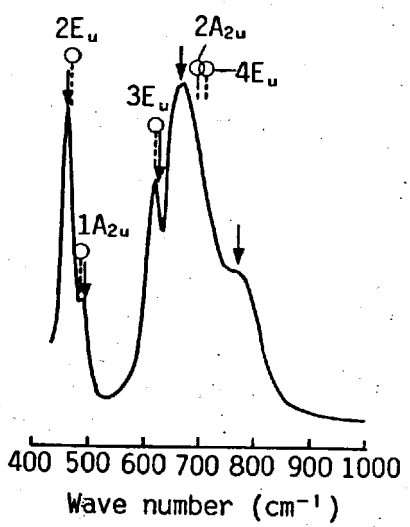

↓ : Measured peak position
○ : Caluculated peak position

Fig. 62

A mosaic like display of circuit with an organic film printed on a silicon wafer by the absorbance distribution determined by microscopic FT-IR with the movable sample stage (courtesy of JEOL)

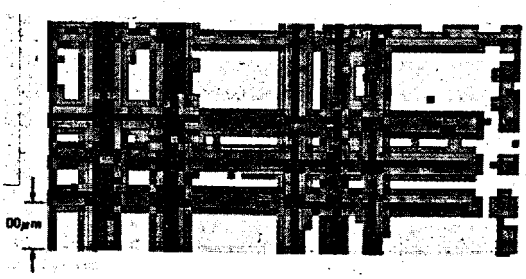

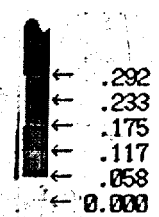

Fig. 61

IR spectrum of α-alumina powder of 0.75μm(KBr method)

(11) Microwave scanning electron spin resonance microscope

A two-dimensional electron spin resonance (ESR) pattern of a specified region can be obtained by ESR-CT using gradient magnetic field. A similar pattern to that obtained scanning a fixed sample with microwave beams can be obtained by mechanically scanning the sample with the X-Y stage and irradiating the microscopic region of sample with converged microwave beams. Microwave scanning ESR microscope uses the latter technique. The diagram of the microwave scanning ESR microscope is shown in **Fig. 63**. A microscopic region on the sample is irradiated with converged microwave leaking through a hole of a cavity resonator shown in **Fig. 64**. A normal ESR spectrometer (JOEL RE-1X) is used for the microwave generator and a small movable permanent magnet with high magnetic field (NEOMAX: Nd-B-Fe) is used as the external magnet surrounding the cavity. The magnetic field is modulated with another coil outside the cavity resonator. The distributions of nitrogen center in diamond and of signal intensity of ESR are shown in **Fig. 65(120)**.

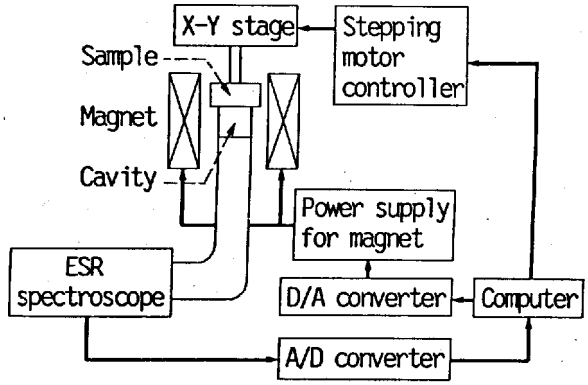

Fig. 63 Block diagram of microwave scanning electron spin resonance (ESR-CT) microscope

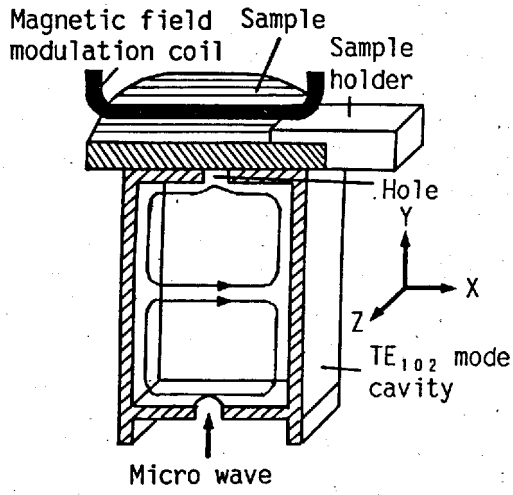

Fig. 64 Microwave leaking and sample stage of ESR-CT

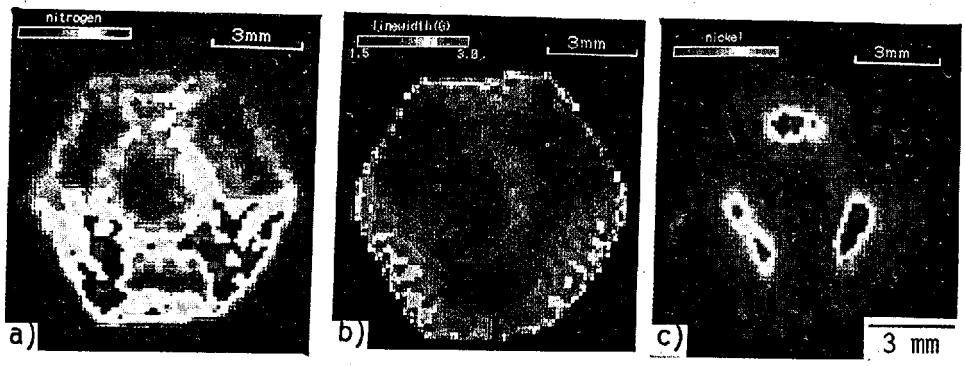

a) Concentration distribution of nitrogen center in diamond crystal
b) Mapping image of the line width of nitrogen center
c) ESR signal intensity distribution of nickel measured at 77 K

Fig. 65 ESR-CT image of nitrogen in diamond (Furusawa et al; (120))

(12) Differential interference microscope

In the differential interference microscope(DIM), the sample is irradiated with two perpendicularly crossing polarized lights different in phase and the phase difference of the polarized waves interfere with each other in an analyzer to produce a stereoscopic image as shown in a photograph on the right side of **Fig. 66**, while a plane image is provided by irradiating with normal light or polarized light in one direction as shown in a photograph on the left side of **Fig. 66**. Roughness at the levels of atom and molecule on the surface of sample can be determined at a resolving powers of 100nm using transmitted or reflected light. As shown in **Fig. 67**, a 1/2 λ-plate and the sample are placed between a pair of uniaxial crystal plates along the light path in DIM to obtain an interference light through the uniaxial crystal plate(ii). The phase difference is expressed by the following formula:

$$\text{Phase difference} = \partial\delta/\partial\xi \cdot \Delta\xi \qquad 3.9)$$

where δ = phase, and ξ = light path length.

The phase difference is, therefore, proportional to the phase gradient ($\partial\delta/\partial\xi$). The roughness of the stereoscopic image is adjusted by controlling the phase difference putting in and out the uniaxial crystal plate(i) shown in **Fig. 67**. Although DIM is superior to the phase contrast microscope in the point that even a large phase difference can be measured due to no halo, it is a shortcoming that the unevenness cannot be determined independently because the phase difference is used.

There are many researches on the stepwise observations of crystal growth using DIM. An example of the observation of a twinning plane of cubic boron nitride grown up to 3mm in diameter is shown in **Fig. 68(121)**.

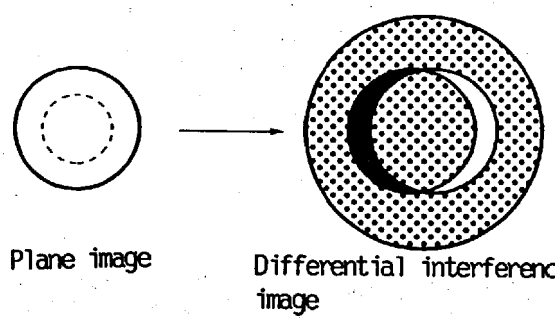

Fig. 66

Image explaining the difference between differential interference microscope and optical microscope

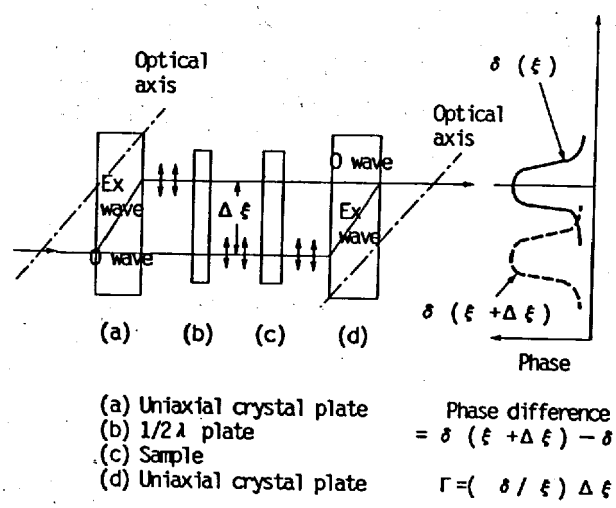

Fig. 67

Diagnostic diagram of differential interference microscope

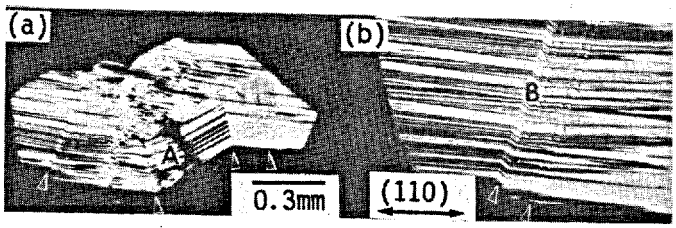

Surface microtopograph of (113) face or m_1 of the crystal and (b) the enlargement of lower left side of (a)

Fig. 68

DIM image of twinning plane of cubic boron nitride (Kagamida et al; (121))

3.4 Image Processing

For getting full performance of characterization instrument, it is extremely important to visually image the numerical data obtained by up-to-date instruments or numerically formulate the image obtained by visualizing apparatus. The typical numerically formulation process of image obtained by measuring apparatus is as follows : a two-dimensional image is divided into pixels in the x and y direction ; analog information including color tone and brightness of each pixel is digitized to input to memory ; the original image is transformed into numerical value including area, length and shape factor by numerical value matrix ; and the numerical value are outputted. The system comprises an imaging device, analytical computer, displaying device and system control computer as shown in **Fig. 69**.

Although a charge-coupled device (CCD) type television camera and three primary color-television camera are mainly used as the imaging device, a device directly processing the inputted image signal is being spread at present. Since some analytical computers have the image memory as large as 16 M byte, these computers are able to display two images of 2048 x 2048 pixels x 16bits each. Image of 1024 x 1024 pixels is, however, enough for usual uses. Although the analytical memory is displayed and processed either by a monochrome image or by a binary image depending upon the purpose, it is also able to be partially displayed by these methods. The binary image is obtained by displaying each pixel in 256 gradations of concentrations of black and white and three primary color (red, green and blue), brightness, hue and purity, which are formed by displaying two parts of each element divided with the threshold value as unity and zero, respectively. Only a pattern required is, therefore, able to be displayed by using the selected appropriate threshold value. Rapid processing of data can be attained by paralleled processing a local region with two or more digital data processors or by installing processors for exclusive use of binary image and rapid Fourier transform. Various softwares have been developed for determining diversified images. Since it takes only 30μsecond for processing a pixel, the number and shape parameters of particle can be usually determined less than several to tens seconds. The processed image is transmitted from the analytical computer to the displaying device through a mixer.

A high-accuracy, high-fineness 16 to 20 inch CRT is used as the displaying device. The size of monochrome and color image are usually 1 and 3 M byte, respectively and these images can be stored in a floppy disk, magneto-optical disk or VTR. Since the system can be rapidly and simply processed by the interactive operation of a mouse, it can be easily analyzed.

Imagé analysis is widely applied to the analysis of shape and particle size distribution of cement or aggregate, the determination of reactive minerals in aggregate, the analysis of texture and pore structure in clinker and hardened specimens, and the diagnosis of a structure combined with the nondestructive inspection.

In the image analysis of shape and particle size distribution of cement and aggregate, there are examples of the determination of the type of aggregate from the shape factor obtained by processing video camera image, the determination of particle size distribution of cement by measuring the shape and size of particles from microphotographs and counting the number

of particle in a visual field with counter (122), and the estimation of alkali-aggregate reactivity by binarizing the red to brown colored volcanic glass under open-polar and determining the glass phase from the area of it (123)(124).

In the composition analysis of hardened specimens, there are examples of the determination of quantity of cement and aggregate by making a thin section of concrete and processing the transmission-microscopic image (125), the determination of the quantity of spherical fly ash by counting the number of particles in a specified particle range in a two-dimensional image and deducting the number of irregular clinker particles from it (126), and the development of the soft ware to determine automatically the compositions of many element distribution images obtained by CMA/EPMA for concrete sample (127).

Although there was the attempt to determine rapidly the air void diameter distribution and the air void spacing factor by making the image processing of a photograph of cut surface of hardened concrete so far, the determination of various size of pores ranging 0.05μm in the minimum diameter using a back scattered electron image of cement paste (128), the determination of hydrates and unhydrates and large void by processing a back scattered electron image of the transition zone in concrete (129)(130)(131)(132) and the determination of void and pore size distribution from gel pore to air void of centimeters in diameter by combining the image analysis of x-ray CT and optical microscopy with the mercury intrusion porosimetry and gas adsorption methods(81) have recently been reported.

The diagnosis of a construction structure is made by the image processing of fine crack photographed using x-ray. An automatic crack determination system for diagraming the numerical data of the position, width and length of crack has been developed.

The temperature distribution on the surface of concrete is determined by image processing of infrared photograph to detect the voids and flaws inside the concrete (133)(134), and estimate the stress distribution caused by internal heat (135)(136) and the corrosion of reinforcement (137). A technique for observing the flaws of concrete by the imaging the propagation of ultrasonic wave is reported (138).

The example of image processing applied to the quantifiction of morphological change of interstitial phase caused by quenching is shown after. The back scattered electron image of the polished surface of clinker quenched from various temperature are shown in Fig. 70(42). C_4AF phase in clinker quenched From 1400°C is eutectic needle crystals, while C_3A and C_4AF are deposited separately between alite and belite in clinker quenched from 1200°C.

A binary image of C_4AF transformed from BEI is shown in Fig. 70. A dimensionless value, T, showing the number of projection of a figure is expressed by the following formula 3.10):

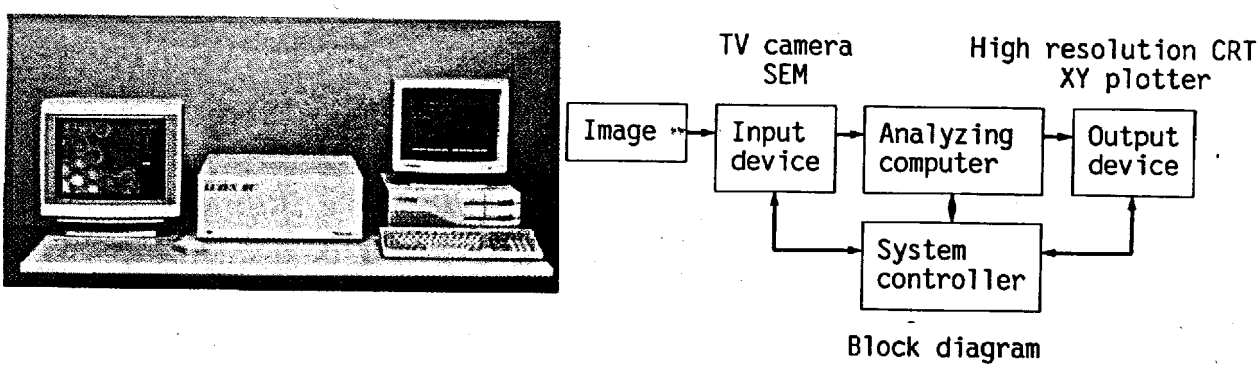

Fig. 69 Image processor and its block diagram (NIRECO Co., Ltd (Japan) LUZEX IIIU)

$$T = (L^2/A)/4 \quad \text{---------- 3.10)}$$

Where L = length of circumference of figure and A = area of figure. T indicates the shape of C_4AF. When T equals to 1, the figure is a circle. When the value of T of figure are the same as each other, these figure are similar.

The mean value and standard deviation of nine measurements of T for the clinker quenched from 1400°C are 1669 and 1485, respectively, while those of fourteen measurements of it for the clinker quenched from 1200°C are 293 and 70.6, respectively. Thus the morphology of interstitial phase in clinker quenched at different temperature can be quantitatively expressed. It is expected that the image processing will be widely used for quantification of the distribution of the elements as well as the size and shape of composing materials and pores in cement and concrete.

The following is the example of the determination of the composition of low heat blended cement composed of moderate heat portland cement, blastfurnace slag and fly ash. The blended cement is sieved through as AJS screen with an opening of 20 to 30μm to make the particle size range of each component constant and it is confirmed that the composition of cement passing through the screen is the same as that of original blended cement. Open-polar and cross-polar microphotographs of the cement passing through the screen taken through a polarizing microscope provided with a sensitive color plate are shown in **Fig. 71.** Fly ash is nearly spherical, and moderate heat portland cement and blastfurnace slag are angular. Both blastfurnace slag and fly ash are vitreous and non-birefringent, and the color of them is the

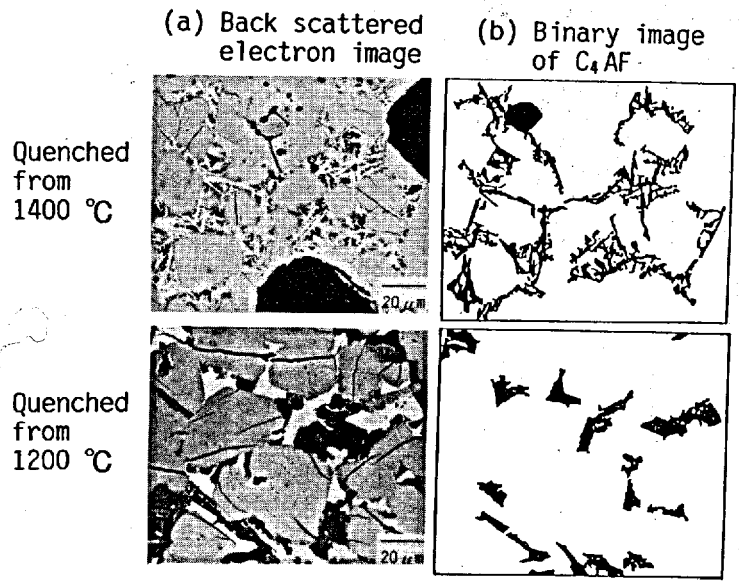

The value of T which indicates the shape of C_4AF in each clinker

	T	Standard deviation
Quenched from 1400℃	1669	1485
Quenched from 1200℃	273	70.6

$T = (L^2/A)/4\pi$
L = Length of circumference of figure
A = Area of figure

Fig. 70 Back scattered electron image of clinker quenched from 1400 and 1200°C and binary image of C_4AF (Uchikawa et al; (42))

same as that of sensitive color plate. Since alite and belite are birefringent, the cement particles containing them are blue and yellow, respectively. The components are, therefore, able to be determined by the optical properties.

The two dimensional shape of each particle observed is expressed by the following formula **3.11)** for a dimensionless figure, S, showing the circularity of particle:

$$S = [\pi (L/2)^2] / A \times 100 \quad \text{---------- 3.11)}$$

Where L = maximum length and A = area

S is 100 for the circular particle and S is larger than 100 for the non-circular particle. The histogram of the shape factor of blended cement particles is shown in **Fig. 72.** The measurement is made by observing approximately 10,000 particles in each field of view. The mean values and standard deviations of S for moderate heat portland cement and blastfurnace slag particle are 165.9 and 56.6, and 234.2 and 98.3, respectively, while those values for fly ash particles are 111.8 and 6.3, respectively. Thus, the value of S for the former is larger than 120, while that for the latter is 100 to 120. The particles showing S below 120 may be identified as fly ash and those showing 120 or more of S may be identified as moderate heat portland cement and blastfurnace slag. Moderate heat portland cement particle is discriminate by the binarization of the shade depth of the three primary colors of reds, green and blue.

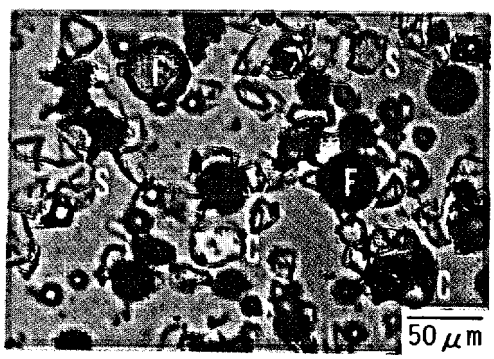

C: Moderate heat portland cement
S: Blastfurnace slag
F: Fly ash

Fig. 71 Micrograph of ternary blended cement by crossed polar

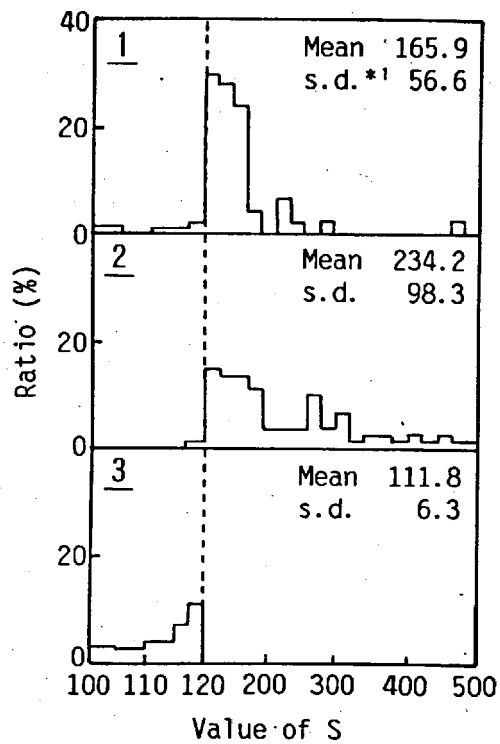

1: Moderate heat portland cement
2: Blastfurnace slag
3: Fly ash

*1: Standard deviation

Fig. 72 Histogram of the shape factor of the components of blended cement particles

Table 6 Content of each blending component in ternary blended cement determined by optical microscope with image processing

	Number of particle	Mixing ratio (%) Measured	Designed
MPC*1	2765	31.0	30.0
Slag *2	4843	49.2	50.0
Fly ash	2349	19.8	20.0

*1: Moderate heat portland cement
*2: Blastfurnace slag

The range of sensitive color is R 72, B 78 and G 90. The number of particle of fly ash determined from the shape factor and that of cement from the color tone and the mixing ratio of those components determined from the multiplying the number of particles by specific gravity. The number of particles is shown in **Table 6**. The number of blastfurnace slag is determined by deducting those of moderate heat portland cement and fly ash from the total number of particles. The accuracy of this method is nearly plus or minus 1% for measuring approximately 10,000 particles.

4. DEVELOPMENT OF NEW QUALITY CONTROL TECHNIQUE

4.1 Evaluation and Control of Fluidity and Setting of Cement

4.1.1 Relationship between Characters of Clinker and Fluidity and Setting of Cement

(1) Setting of cement from the viewpoint of rheology and chemical reaction

When cement paste prepared by mixing cement with a proper amount of water is left as it is, the viscosity of it increases with the time and finally it is hardened. The viscosity of cement paste increases sharply at the beginning, slowly in the middle and then sharply again at the last stage as shown in **Fig. 73**. The initial and final setting of cement paste correspond to the specified periods on the change of viscosity, which are defined using the values of penetration resistance expressed by the resistance to penetration of needle specified by standard under constant load into cement paste prepared by mixing with water so as to give the standard consistency.

The increase of viscosity in cement paste at the beginning is mainly attributed to the formation of a three-dimensional skeletal network structure composed of gypsum produced by the hydration of hemihydrate contained in cement and ettringite ($C_3A \cdot 3CaSO_4 \cdot 32H_2O$) produced by the hydration of tricalcium aluminate solid solution (C_3Ass) and ferrite solid solution (C_4AFss) contained in cement. The stationary increase of viscosity in the middle is attributed to the decrease of supply of Ca^{2+} to the liquid phase because the surface of cement particles is covered with prismatic crystals and calcium silicate hydrate (C-S-H) produced at the beginning, so the transfer of water mentioned above and ions is controlled by the diffusion through the hydrate layers. When the concentration of Ca^{2+} in the liquid phase reaches the saturation ratio of $Ca(OH)_2$ (see *Note 1*) depending upon the hydration temperature, water is brought into contact with newly developed surfaces of cement particles by the rapid deposition of C-S-H around the crystalline nuclei produced before (the delayed nucleation theory), the unbalanced concentrations of ions existing in and outside the protective layer of hydrate around the unhydrated cement particles and the breaking of the protective layer of hydrate by the sharp increase of osmotic pressure (the protective layer theory). The viscosity of cement paste increases sharply again by vigorous production of C-S-H(**138**) as mentioned before. In the normal setting, the viscosity value corresponding to initial and final setting is gained during the vigorous hydration process of C-S-H(**139**).

Note 1: Saturation ratio is defined as the ratio of the actual solubility product determined from $[Ca^{2+}][OH^-]^2$ contained in the liquid phase to the theoretical solubility product of $Ca(OH)_2$ taking the ionic strength of various ions contained in the liquid phase into consideration. When the saturation ratio is equal to 1 and larger than 1, the solution is defined as a saturated solution and a supersaturated solution, respectively.

According to the classification of the initial hydration process of cement by the author based on the heat evolution curve (**75**), the period related to the fluidity of concrete corresponding to Stage I, setting corresponding to Stage II, strength development corresponding to Stage III or later.

(2) Relationship between morphology of C_3Ass and C_4AFss in clinker and fluidity of cement

Ettringite is produced by the before-mentioned vigorous hydration just after the mixing with water and by the continuous hydration of the interstitial phase during Stage I. The size, morphology, amount and deposition place of ettringite are closely related to the change of fluidity of cement paste with time. When kinds and amount of free lime, calcium sulfate and alkali sulfate are constant, the rate of hydration of interstitial phase depend mainly upon the morphology and crystallinity of it.

The morphology of interstitial phase is affected by the cooling temperature and rate of cooling of clinker. By quenching interstitial phase at high temperature, needle-shaped crystals of C_4AFss are arborescently deposited forming a eutectic structure as shown in **Fig. 70**. By slowly cooling it at lower temperature, however, C_3Ass and C_4AFss are segregated in such a manner that the shape factor T decreases and the size and crystallinity of crystals increase. The slowly cooled interstitial phase has higher reaction rate of hydration. A large amount of ettringite with smaller diameter of prismatic crystal and higher aspect ratio is formed at the beginning of hydration and is earlier transformed to monosulfate hydrate in case of slowly cooled interstitial phase which leads to lower mortar flow, larger change of it and lower fluidity **(138)**. Using clinkers with different texture of interstitial phase and the same amounts of free lime and alkali sulfate, cement with the same specific surface area, particle size distribution and added amount of gypsum was prepared. The relationship between the variation of mortar flow of the cement and the shape factor of C_4AF is shown in **Fig 74.**

(3) Relationship between etching characteristics of polished surface of clinker and setting of cement

An example of reflection optical micrograph of clinker is shown in **Fig. 75**. The color of alite in clinker is turned to brown by etching and darkening with etching time. The color of belite is hardly changed by etching. The C_3A phase is easily soluble in the interstitial phase and show stronger contrast with C_4AF with the increase of etching time. The color of spherical particles of free lime is turned to various colors by etching.

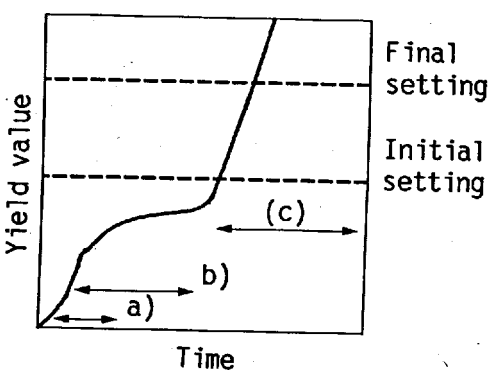

a) Formation of gypsum from hemihydrate
b) Formation of ettringite
c) Formation of C-S-H

Fig. 73

Schematic diagram explaining the change of yield value of fresh cement paste (Uchikawa et al; (138))

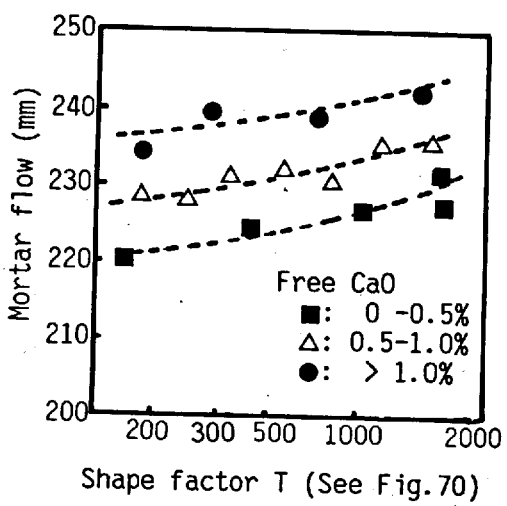

Fig. 74

Relationship between shape factor of C_4AFss and mortar flow

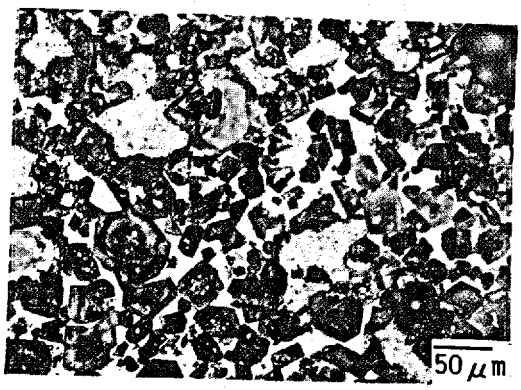

Fig. 75

Reflected light micrograph of clinker etched by 0.01% NH_4Cl aq. for 30 seconds

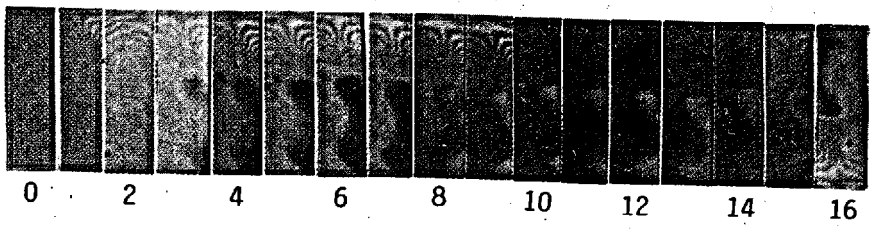

Fig. 76 Color change of alite etched by 0.01% NH_4Cl aq.

Since the color change of the surface of clinker minerals by etching is attributed to the combination of the interference of light passing through different light paths according to the roughness of surface caused by etching and the different transmitting rates of light through the etched surface layer. The rougher the surface is, the stronger the interference color becomes.

The relationship between the dipping time of clinker in a most popular 0.01%-aqueous solution of ammonium chloride for etching and the change of colors or interference color numbers of alite observed with a reflecting microscope is illustrated in **Fig. 76**. Using the difference of the reactivity of each clinker mineral with the etching agent, therefore, the reactivities of hydration of clinker minerals at the initial and early stages of hydration can be estimated by the color change by etching. Using distilled water as the etching agent, the etching depth is changed by the ions dissolved from the sample to water in a long etching time. It is necessary, therefore, to use a less influential solution such as a 0.01%-aqueous solution of ammonium chloride instead of water and convert the data into those for water.

The relationship between the average interference color number of alite in clinker manufactured in different plants and the initial setting time is shown in **Fig. 77(86)**. Setting is largely affected by the quantity of free lime in clinker. When the content of free lime is classified into three groups, less than 0.5%, 0.5 to 1.0% and more than 1.0%, it becomes clear that the more the clinker is easily etched, the shorter the setting time is. The initial setting time is shortened by approximately 40 minutes when the content of free lime is increased by 0.5%. The same relationship applies to the final setting.

(4) Relationship between heat of hydration and fluidity and setting of cement

The cumulative heat of hydration of cement paste within half an hour in Stage I is related to the mortar flow as shown in **Fig. 78**. The fluidity of fresh mortar and concrete can be estimated from the measurements of the heat of hydration. The cumulative heat of hydration of cement paste up to 2 hours in Stage II is related to the setting time of cement paste as shown in **Fig. 79**. The setting time can be estimated from the measurements of the cumulative heat of hydration.

(5) Relationship between morphology of interstitial phase in clinker, etching characters of clinker and heat of hydration of cement, and manufacturing conditions of cement

The fluidity of cement paste, mortar and concrete in Stage I varies according to the reactivity of hydration including the morphology and crystallinity of interstitial phase. The setting is related to the hydration rate of alite in Stage II. Both fluidity and setting can be evaluated by the quantitative determination of the morphology of interstitial phase and the interference color change of etched alite and by the cumulative heat of hydration of cement paste up to 30 minutes and two hours after the mixing water with cement as well.

The morphology of interstitial phase in clinker mainly depends upon the temperature of clinker at the outlet of kiln and the cooling efficiency of cooler. Although the eutectic point, T_2, of C_3A and C_4AF in the pure system is 1338°C, it is decreased by approximately 100°C due to the impurities and burning atmosphere in the actual burning process of clinker. T_2 is, therefore, decreased to the temperature ranging from 1200 to 1250°C in which the morphology of interstitial phase is changed during quenching. As shown in **Fig. 70**, C_4AFss is arborescently deposited forming a eutectic structure by cooling the clinker at a temperature of 1250°C or higher, while C_3Ass and C_4AFss are conspicuously segregated as the cooling temperature of clinker is decreased under 1200°C. Although the eutectic structure remains unchanged at a cooling rate of 100°C/min. or higher, the shape of C_4AFss became strip-shaped with larger diameter at a cooling rate lower than 100°C/min. and it is conspicuously segregated at that of 30°C/min. or lower. Although C_3Ass remarkably decreases in the coexistence of MgO, C_3Ass is increased though decreasing C_4AFss because Fe is incorporated into calcium silicate phase and deposited as α-Fe under the reducing atmosphere.

The more alite incorporates trace and minor components, the smaller and the more compressed crystal shapes and the lower temperature stable polymorph, the more the alite in clinker is easily etched and the deeper the interference color is turned. Alite is more easily etched in the manufacturing process of clinker with the increase of heating rate, the decrease of burning temperature, the coarsening of the particles of raw materials and the burning atmosphere approaching to reducing. Using clinkers with different morphology of interstitial phase and different interference colors of etched alite, the cumulative heat of hydration up to 30 minutes and two hours after mixing of water with cement were determined. The relationships between these cumulative heat of hydration and the mortar flow and setting time are shown in **Fig. 80**. The cumulative heat of hydration up to 30 minutes after mixing of water with cement correlates with the mortar flow and that up to two hours after mixing of water with cement correlates with the setting time. The accuracy of the evaluating of the fluidity and setting time of cement is expected to be improved by determining the cumulative heat of hydration value together with the variations of the morphology of interstitial phase and of the interference color of etched alite.

4.1.2 Control of Fluidity and Setting of Cement

The characters of cement affecting the fluidity and setting include the potential compound composition, contents of free lime, hemihydrate and alkali sulfate and the fineness and so on. When these characters are almost constant, the fluidity and setting of cement can be simply controlled by determining the morphology of interstitial phase, the interference color change of etched alite and the cumulative heat of hydration. An example of diagram to control the fluidity and setting of cement is illustrated in **Fig. 81**.

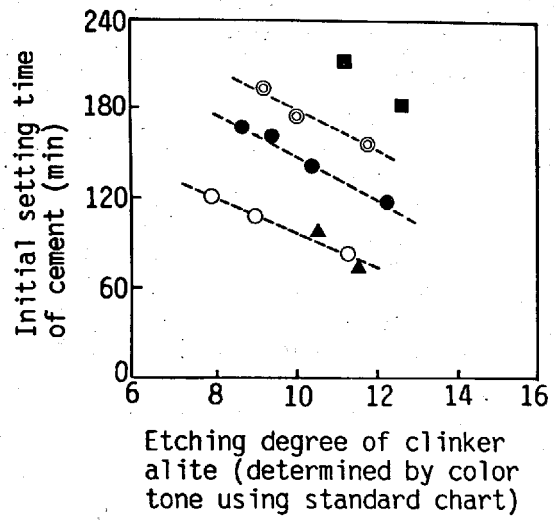

■: Ordinary portland cement (Free CaO: 0-0.5%)
●: Ordinary portland cement (Free CaO: 0.5-1.0%)
▲: Ordinary portland cement (Free CaO: 1.0-1.5%)
○: High early strength portland cement (Free CaO: 0.5-1.0%)
◎: Moderate heat portland cement (Free CaO: 0.5-1.0%)

Fig. 77 Relationship between the etching degree of clinker alite and the initial setting time of cement (Uchikawa et al; (87))

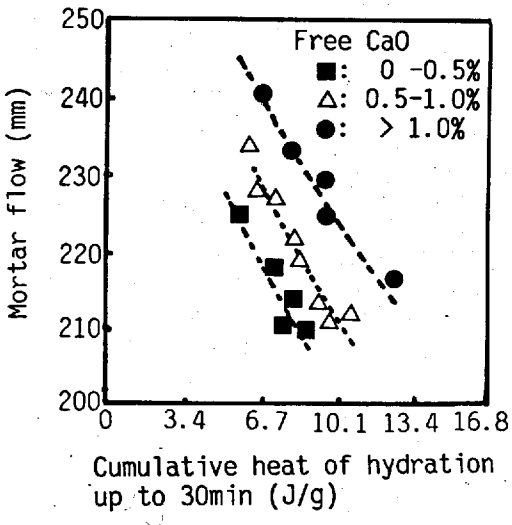

Fig. 78 Relationship between cumulative heat of hydration up to 30 minutes and mortar flow (Ordinary portland cement)

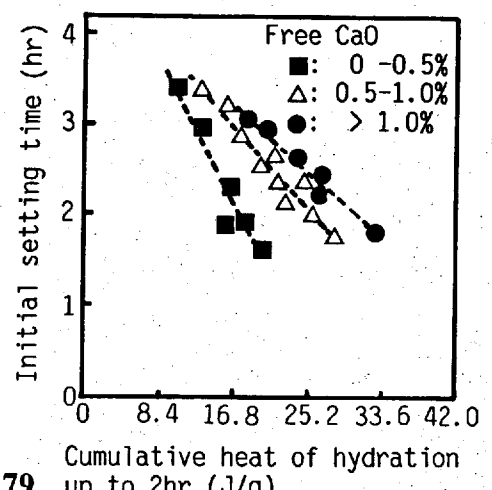

Fig. 79 Relationship between cumulative heat of hydration up to 2 hours and initial setting time of cement paste (Ordinary portland cement)

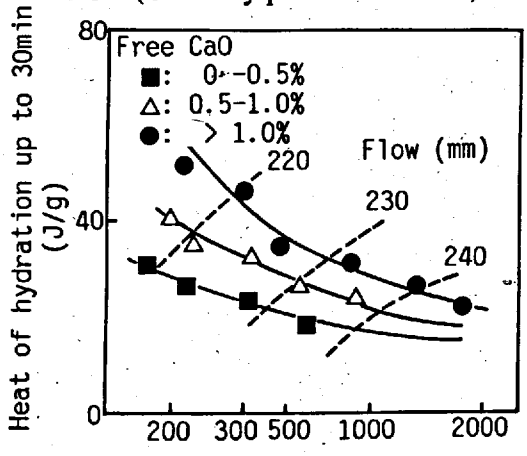

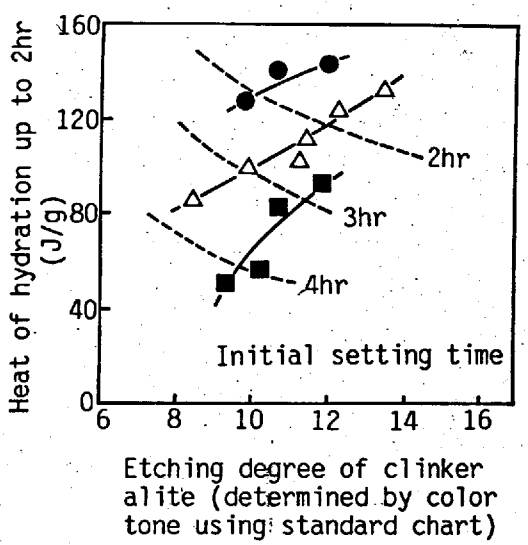

Fig. 80 Relationship between shape factor of interstitial phase, etching degree of alite, heat of hydration and fluidity (Ordinary portland cement)

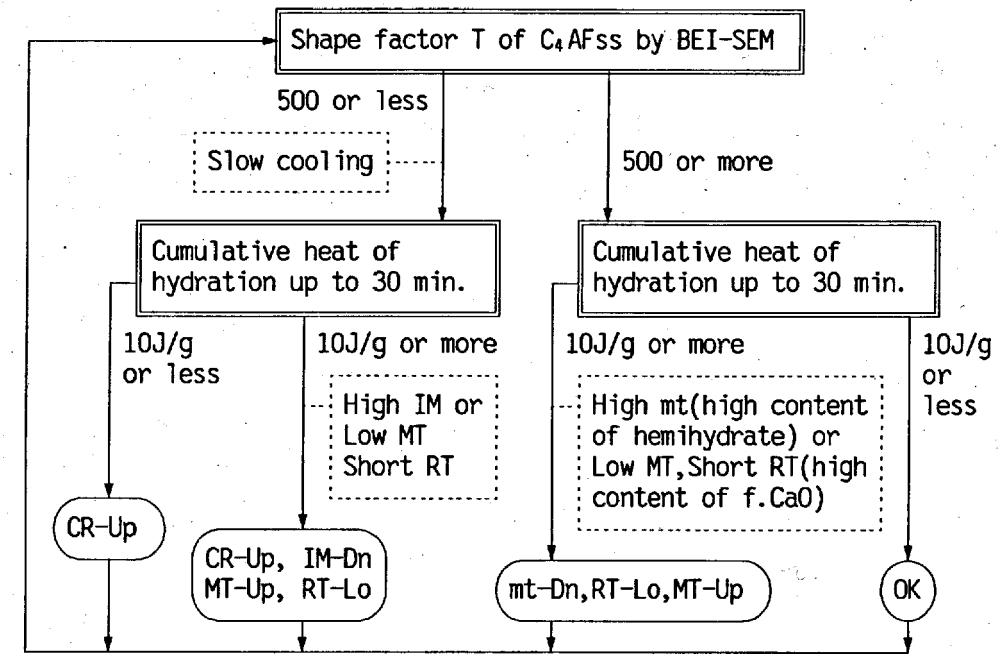

An example of the diagram to control the fluidity

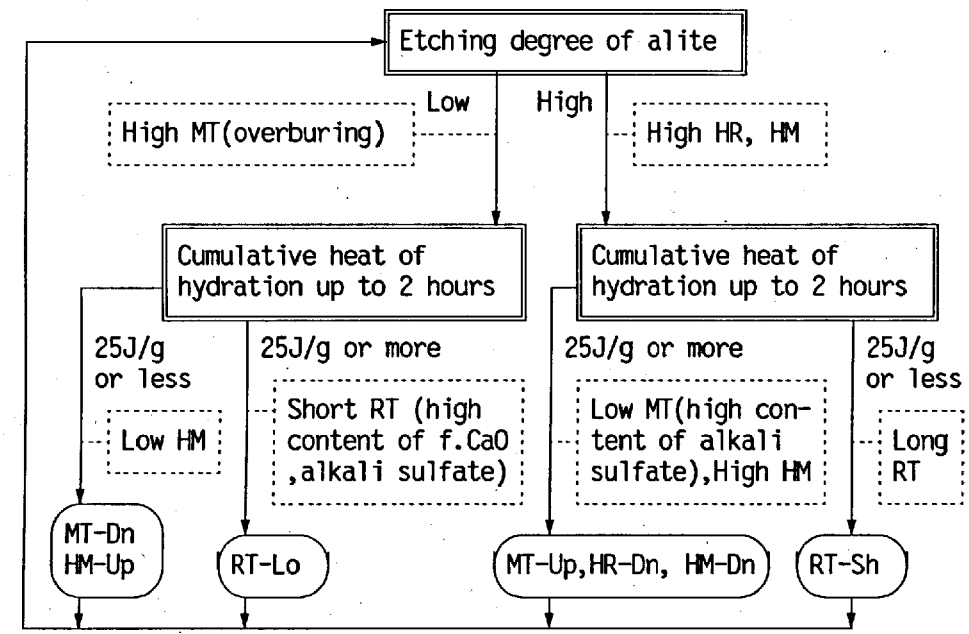

An example of the diagram to control the setting time

Note : Measurement : Action, : Reason

HR: Heating rate, MT: Maximum temperature of clinker burning, RT: Retention time at sintering temperature, CR: Cooling rate of clinker, HM: Hydraulic modulus of raw materials, IM: Iron Modulus, mt: Temperature of cement mill, Up: Up, Dn: Down, Lo: Long, Sh: Short

Fig. 81 An example of the diagram to control the fluidity and the setting time of cement

4.2 Evaluation and Control of Strength of Cement

4.2.1 Relationship between Characters of Clinker and Strength of Cement

(1) Process of hydration of cement and development of strength

When concrete is prepared by mixing, water films are formed around the unhydrated cement particles. Hydrate produced on the surface of cement particles and aggregates and deposited in the free space bridged the gap among the cement particles and between cement particles and aggregates into relatively coarse flocculation structure as the hydration process described in 4, 1.1(1) proceeds. Since the volume of cement hydrates is approximately twice the sum of the volumes of unhydrated cement particles and water, the decreasing volume of unhydrated cement particles cause by the hydration is compensated, the free space occupied previously by water is filled up and the structure of hardened concrete is formed with lead the development of strength. This process corresponds to the Stage III and after during hydration. When the aggregate has sufficient strength, the strength of concrete depends upon the strength of hardened cement paste and the bonding strength between cement paste and the aggregate. Although the strength of hardened cement paste is closely related to the coagulation energy of hydration products, the actual strength is 1/10 to 1/10,000 of the strength calculated from the coagulation energy. This discrepancy is caused by the pore structure, porosity, pore size distribution and shape of pore. The actual strength is closely correlated to porosity of hardened specimens and the volume of pore with a certain range in size. The strength is sometimes remarkably decreased by the stress concentrated on the specified pores and the specified shape of pore**(106)**.

The compressive strength of cement paste is closely correlated to the volume of pores of 3 nm to 2 μm and those of mortar and concrete with the W/C ratio of approximately 0.40 or more are closely related to the volume of pores of 50 nm to 2 μm. The voids 50nm to 2 μm in diameter are distributed partially in the transition zone around the aggregate, which shows the structure of transition zone affects the strengths of mortar and concrete. The compressive strength, σ, of ordinary cement concrete with the W/C ratio of 0.4 to 0.6 can be expressed by the following formula **4.1)(105)**:

$$V_{50\text{-}2} = 0.08A^2 - 0.645A + 5.550 \quad \text{---------- 4.1)}$$
$$A = 13.04 - 1.1815(T)^{0.5} + 0.107Vp$$
$$\sigma = 690 - 17.2Vp$$

where $V_{50\text{-}2}$ = Volume of pores of 50 nm to 2 μm, Vp = Volume of cement paste part, and T = age.

The strength depends upon the pore structure of hardened specimens and the pore structure depends upon the volume of water space, namely, the W/C ratio and volume of pore, that is, the type, shape and production of hydrates. It is, therefore, necessary for controlling the strength development to control the fluidity of cement particles and the hydration reactivities of clinker minerals. Cement mainly composed of nearly spherical belite with less reduction of the early fluidity at the early stage due to the late hydration **(140)** and preparation of spherical cement particles is being developed. The control method of the hydration of clinker minerals is described hereafter.

(2) Relationship between optical properties of clinker mineral and strength of cement

For obtaining high-strength, it is necessary to keep the hydration reactivities of alite and belite high at and after stage III. It is generally said that the clinker minerals with high hydration reactivity include clinker minerals having the metastable high-temperature transformation at normal temperature, the low-temperature transformation coexisting with the high-temperature transformation remaining unchanged due to incomplete transformation, a low crystallinity with many defects due to irregular atomic configuration, and supersaturated state at normal temperature due to insufficient deposition of the elements incorporated at high temperature.

C_3S has seven types of temperature polymorphs. Alite in ordinary portland cement clinker has M_3- and M_1-phase with similar crystal structure and these phases exist sometimes forming a zonal structure in a single crystal of alite. The birefringence of alite crystal with zonal structure is 0.005 and 0.0025 in the peripheral part and inner part of the alite, respectively **(141)**. The M_1-phase is transformed into the M_3-phase at 940°C **(142)**. C_2S has five types of temperature polymorphs. Although belite in ordinary clinker usually exists as β-phase (B:0.020), the α-phase (B:0.010) sometimes coexists with the β-phase. The strength of cement increases with the increase of the average birefringence of alite or portion of M_3-phase keeping the optical properties other than birefringence constant, while that of cement increases with the decrease of the average birefringence of belite or the portion of α-phase. It is generally difficult to measure the birefringence of belite because it becomes yellow or dark yellow by the deposition of colored trace components including iron at cooling. The color change is, however, related to the coexisting ratio of α-phase in belite. Since the sizes of alite and belite are inversely proportional and proportional to the strength of mortar at the age of 28 days, the strength of mortar of 28 days can be estimated using four parameters as shown in **Table 7(143)** including size and birefringence of alite and size and color of belite determined with a optical microscope. The relationship between the estimated strength and the measured strength is illustrated in **Fig. 82(143)**.

Table 7 Relationship between the burning condition, hydration reactivity and optical properties of alite and belite (Ono; (143))

Hydration reactivity	Excellent(+)	Good(vv)	Average(v)	Poor(-)
Burning rate	Quick ←			→ Slow
Size of alite (μm)	15-20	20-30	(25)30-40	40-60(120)
Maximum temperature	High ←			→ Low
Birefringence of alite	0.010-0.008	0.007-0.006	0.006-0.005	0.005-0.002
Burning time	Long ←			→ Short
Size of belite (μm)	(20)25-40(60)	(15)20-25	(10)15-20	5-10
Cooling rate	Quick ←			→ Slow
Color of belite	Clear(C)	Faint yellow(fY)	Yellow(Y)	Amber(A)

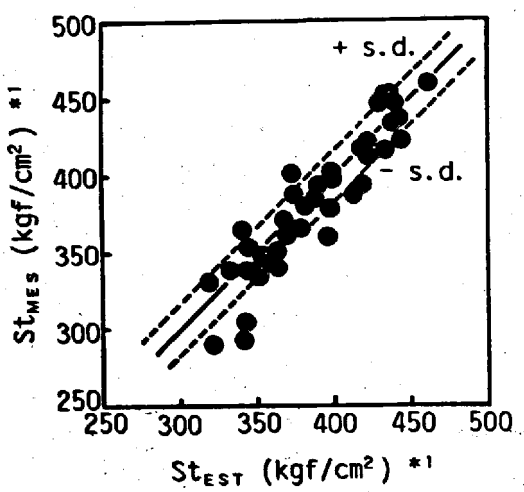

*1: St_{EST} : Estimated compressive strength of JIS mortar at 28days

St_{MES} : Measured compressive strength of JIS mortar at 28days

Fig. 82

Microscopical estimation of JIS mortar strength from table 6 (Ono; (143))

The strength of mortar at and after the age of 28 days varies by as much as 30% at the highest according to the hydration reactivity of belite. The characteristic polymorphous texture of belite observed through a optical microscope is composed of the following three types: Type I with a structure containing groups of lines crossing each other at 60° in the round crystal; Type II with a structure containing a group of lines parallel to each other in the crystal; and Type III showing irregularly shaped crystals. The lamellar structure in type I is produced in the transformation of $\alpha \rightarrow \alpha'_H \rightarrow \beta$ and it is often observed in the quenched clinker. The lamellar structure of type II is produced in the transformation of the α'_L-phase to the β-phase. Type III includes type IIIa comprising ellipsoidal crystals and type IIIb with radial projection around the ellipsoidal crystals (42). Type III is produced by slowly cooling at 1200°C or under the clinker burnt at low temperature and it is mainly composed of β-phase. The radial projections of type IIIb is composed of a peritectic which is formed by the remelting of part of α-phase followed by the deposition of α'-phase on the surface of α-phase. The back scattered electron image of belite of types I, IIIa and IIIb are shown in **Fig. 83**. Since the belite of type IIIb is relatively uniform with the deposits is concentrated on a limited part, it does not turn dark yellow and can not be distinguished from quick quenched belite by a optical microscopy. Estimation of mortar strength at the age of 28 days by optical microscopy with compensation of type of belite determined by back scattered electron image is shown in **Fig. 84**. Although the strength of mortar containing belite of type IIIa is lower than that of mortar containing belite of type I at the ages of 28 days or more, those of mortars containing belite of type IIIa and IIIb are not so much different each other. The accuracy of the estimation of strength is further improved by adding the observation of the structure of belite to those four microscopic observational factors mentioned above.

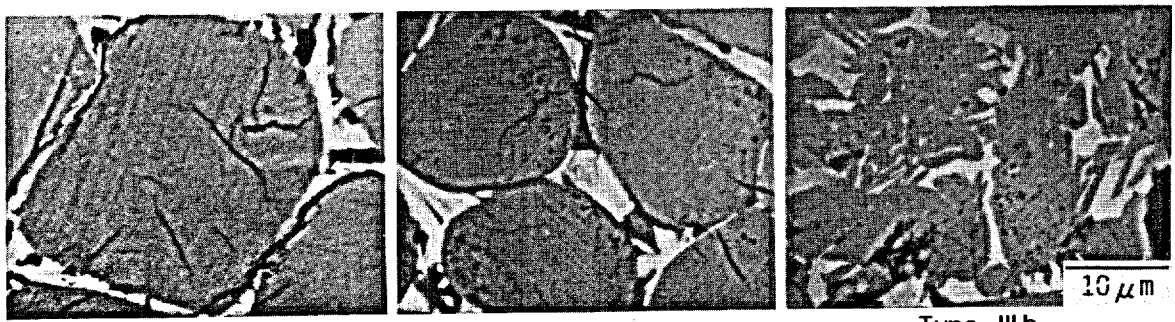

Fig. 83 Types of belite in clinker

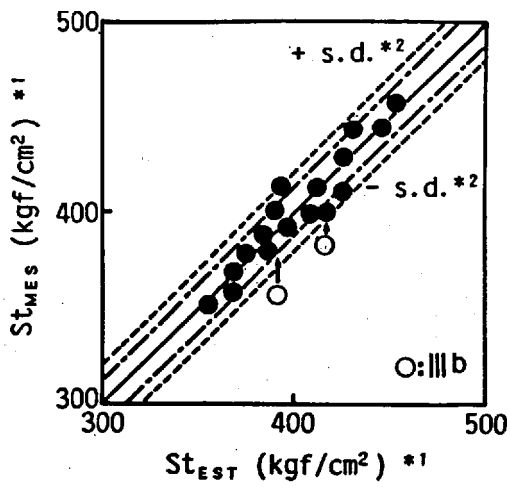

*1: St_{EST} : Estimated compressive strength of JIS mortar at 28days
St_{MES} : Measured compressive strength of JIS mortar at 28days

*2: ------ : Standard deviation
------ : Standard deviation after correction

Fig. 84

Relationship between measured and estimated 28 days strength by modified belite compensation method.

(3) Relationships between trace and minor components in clinker mineral and burning degree of clinker and strength

The relationships between the trace and minor components in alite obtained by burning the same raw materials and the strength is shown in **Table 8**. The less the amount of incorporated impurities in clinker alite, the higher the strength of mortar at the ages of 3, 7 and 28 days are. It is able to estimate the compressive strength of mortar at 28 days by determining the ratio of specified components in the clinker minerals because the strength is related to the Al_2O_3/Fe_2O_3 ratio in alite and burning atmosphere as shown in **Fig. 85.**

The burning degree of clinker has been determined so far by the liter weight method which is widely used for determining the degree of sintering reaction in the process of clinker formation together with the determination of the content of free lime. The porosity and pore size in clinker decrease with the proceeding of the sintering reaction. These changes correspond to the increase of the liter weight of clinker. The relationships between liter weight of clinker, pore volume of 1 to 20μm and 1μm or less in clinkers, and their mortar strength is shown in **Fig. 86.** The strength of clinker increases with the increase of the liter weight of clinker and pore volume of 1 μm or less (up to 1.2 of liter weight) and of 1 to 20μm.

Table 8 Chemical composition of alite in clinker determined by EPMA and its mortar strength of cement prepared from same lot clinker

	Chemical composition of alite in clinker (%)								Compressive strength (JIS R 5201) (kgf/cm²)		
	CaO	SiO_2	Al_2O_3	Fe_2O_3	MgO	SO_3	Na_2O	K_2O	3days	7days	28days
a	70.22	24.94	0.78	0.52	0.64	0.07	0.17	0.20	185	275	435
b	71.43	25.10	1.06	0.71	0.85	0.11	0.22	0.23	155	245	395
c	71.36	24.52	1.12	0.72	0.88	0.13	0.26	0.27	125	210	360

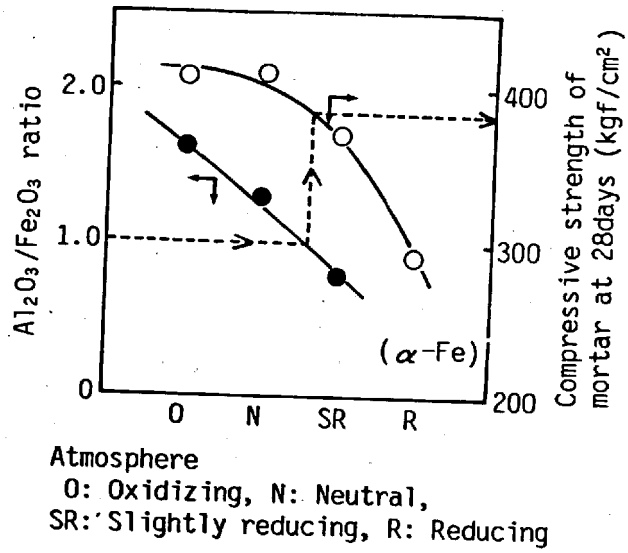

Fig. 85

Relationship between Al_2O_3/Fe_2O_3 of alite in clinker, burning condition and mortar strength (JIS R5201)

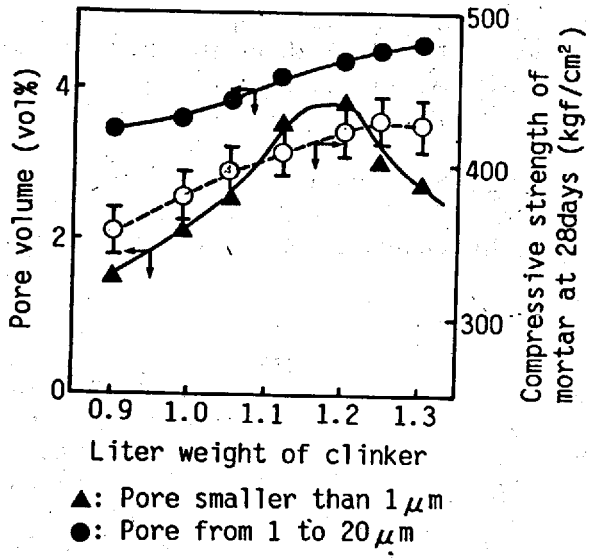

Fig. 86

Relationship between liter weight and pore structure of clinker and mortar strength (JIS R5201)

(4) Relationships of optical properties of clinker, minor component in clinker mineral and burning degree and manufacturing conditions

The optical properties of alite and belite in clinker depend upon the thermal history of raw materials in the kiln. Alite is formed at 1250°C or high from free CaO and C_2S. Rapidly heating in that temperature range using short flame, the crystal size of alite is decreased because the number of nuclei is increased and its growing rate is high. On the contrary, the crystal size is increased by slow heating. Since the content of M_3 phase in burnt alite increases with the increase of the temperature of burning zone, alite with high birefringent is produced.

Crystals of belite grow remarkably in α-phase. The crystal grows large and the amount of incorporated of trace and minor components increase with the increase of the retention time at 1425°C or higher. The transformation temperature of α-phase to α'_H-phase is decreased by the impurities to approximately 1300°C or under. The contents of the impurities in belite or the ratio of α-phase developing mores strength at normal temperature to β-phase depends upon the cooling rate in that temperature range. The content of the transparent α-phase developing more strength increases, therefore, with the increase of the cooling rate. Meanwhile, the strength of clinker is decreased by type IIIa and IIIb of belite produced with the decrease of cooling rate in that temperature range.

The strength of clinker is not well developed in the reducing atmosphere in burning because the content of triclinic form in alite increases and part of belite is converted into γ-phase. Size of alite is decreased, the pore volume of smaller than 1μm in alite is increased and that of pore larger than 20μm is decreased by the rapid heating, while the viscosity of liquid phase and the total pore volume are decreased by the burning at the high temperature. The pore volume of larger than 20μm is gradually decreased by extending the retention time at high temperature and pore volume of smaller than 1μm is increased by the cracking caused by thermal contraction by the quenching of clinker.

4.2.2 Control of Strength of Cement

The characters of cement affecting its strength include chemical and mineralogical composition and fineness. In the case of those changes are small, the strength of cement depends upon the temperature transformations, crystallinity, size and shape of alite and belite. Consequently, the strength of cement can be estimated and controlled by determining

the optical properties of clinker minerals with a polarizing microscope, observing the shape of belite using back scattered electron image (BEI-SEM), determining the content of incorporated elements in clinker minerals by EPMA, and analyzing the pore structure in clinker with a mercury intrusion porosimeter or combined use of these.

An example of the control procedure of the strength of cement is shown in **Fig. 87**. Cement developing high strength can be manufactured by rapid heating and rapid cooling the clinker under the oxidizing atmosphere and burning it at high temperature for a long retention time in the burning zone.

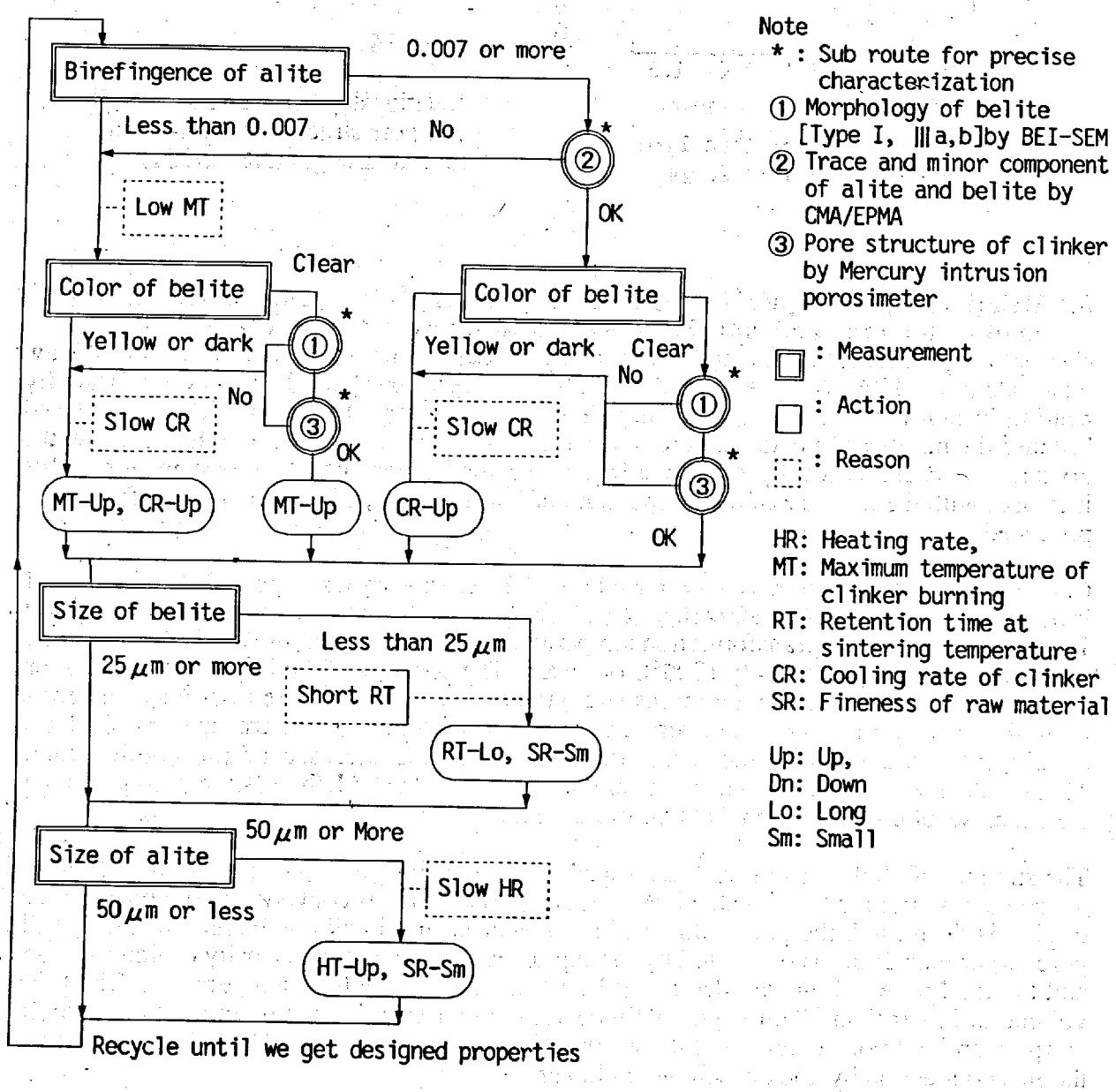

Fig. 87 An example of the diagram to control the strength of hydrated cement

4.3 Evaluation and Control of Grindability of Clinker

4.3.1 Relationship between Characters of Clinker and its Grindability

(1) Evaluation of grindability of clinker

Improvement of the grindability of cement clinker as well as for the development of high-performance grinding and separating facilities is important for the improvement of quality of cement and the reduction of power cost.

The grindability is usually expressed by the time or electric power required for grinding a given material into particles smaller than a specified size using a specified mill. The work index method is expressed by grinding raw materials in a ball mill with the standard dimensions and evaluating the grindability of it from size passing 80% of the ground product and the electric power consumption. The hardgrove method is expressed by evaluating the grindability in such a way that a material powder of 590 to 1190 μm is ground in a specified ball-bearing mill and the ground product passing through a screen with the opening of 74 μm is weighed. The operating work index method is described as indicating the grindability of clinker by measuring the electric power required for grinding it into particles with specified fineness in a mill used in the plant. Some papers **(144)** indicate that the work index and hardgrove method are inadequate for the evaluation of grindability of clinker because the opening of the screen used for evaluations relatively large for the finely ground clinker particles.

The relationship between the time required for grinding clinker using a test mill and the specific surface area of ground product is shown in **Fig. 88(144)**. The figure reveals that the grindability varies in the coarse grinding and fine grinding processes into which the grindability is classified at the specific surface area of approximately 1500 cm^2/g. Assuming that the material to be ground is divided as cubic as shown in **Fig. 89**, energy required for grinding is exponentially increased as the grinding proceeds. Accordingly, studies **(145)** for evaluating the grindability by classifying grinding into stages of coarse grinding, fine grinding and agglomeration of fine particles have been reported.

Since the obtained results for grindability vary according to the type of mill, the grinding time and the measuring method of fineness, the indices often cannot be used for estimating the amount of ground product and the electric power consumption in the plant mill. The operating work index method is inadequate for evaluating the grindability of clinker itself because the size and amount of the grinding medium and the structure of mill affect the amount of ground product and the electric power consumption. To overcome these difficulties, a new quality control technique for evaluating the grindability by determining the characters of clinker is spreading these days.

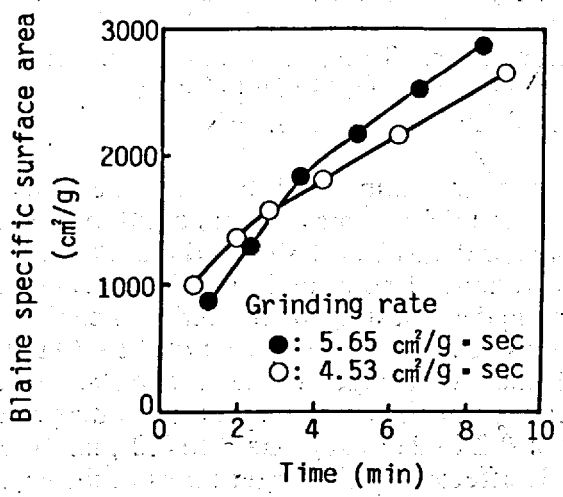

Fig. 88

Grinding time and specific surface area of clinker (Butt et al; (144))

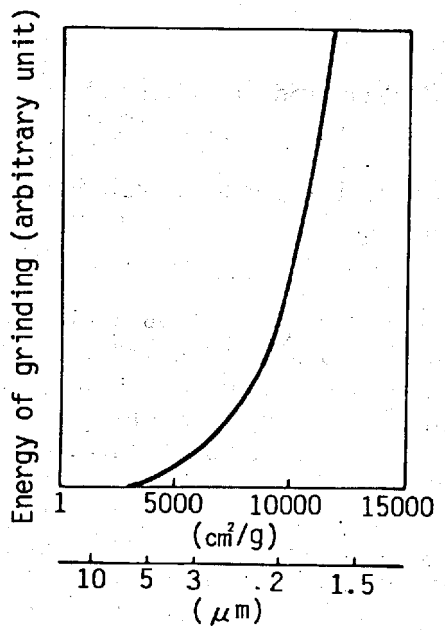

Fig. 89

Relationship between specific surface area, mean particle size and energy of grinding

(2) Relationship between pore structure of clinker and its grindability

The fracture strength of the material free from defects and pores is equal to the force required for separating the atoms in crystal, between crystals and at grain boundary from each other. Meanwhile, the fracture strength of the porous material depends upon the defects and pores in it rather than bonding force of atoms in crystal and bonding force between crystal or at grain boundary. Since clinker has a volume of porosity of approximately 20%, the fracture strength of it mainly depends upon the pore structure including volume, size, shape and pore size distribution. The distortion, structural defect and strength of clinker mineral itself (interatomic bonding force in the crystal) are related to the fracture strength of clinker at the final stage of grinding when the porosity of clinker particles approaches zero. Pore structure of clinker manufactured in a rotary kiln equipped with suspension preheater is roughly classified into three groups: (a) a total pore volume (V) more than 21 vol.% and a ratio of the volume of pore of 1 to 20 μm to that of pore of 20 μm or larger (R) less than 0.4; (b) V of 16 to 21 vol.% and R of 0.4 to 0.7, and (c) V less than 16% and R more than 0.7. **Fig.90** reveals that (c) has relatively large size of pores and disuniform distribution of them, (b) has almost round-shaped pore and almost uniform distribution of them, and (a) comprises large deformed and small pores. **Fig. 91** shows the pore size distribution in clinker. Pore of 20 μm or more are air void entrapped between the minerals during the forming process of clinker minerals **(144)**. Pores of 1 to 20 μm are mainly formed as a result of filling the larger pores with the movable molten liquid phase and depositing interstitial phase during the forming process of clinker. Pores smaller than 1 μm comprise the pores and cracks at the grain boundary or in the crystal of clinker minerals generated by the shrinkage or transformation of clinker minerals during the cooling. Thus, the pores in clinker vary according to the characters of raw meals and burning conditions **(146)(147)**. The pore size affecting the grindability of clinker varies as the grinding process proceeds.

In the grinding of clinker in a ball mill, there are relationships **(144)** between the grinding rate at the first stage, r_1, and the second stage, r_2, and the volume of pores of 20 to 250 μm, V_I, that of pores of 2 to 20 μm, V_{II}, that of pores of 0.2 to 2 μm, V_{III}, and that of pores of 0.008 to 0.2 μm, V_{IV}, as shown in **Fig. 92**. The volume of pores of 20 to 250 μm is closely correlated with the grinding rate at the beginning in the first stage where lumps of clinker are coarse ground into particles composed of groups of crystals, while that of 2 to 20 μm is closely correlated with the grinding rate in the whole first stage. In the second stage where clinker is ground into the crystals or fractured crystals of clinker minerals, the grinding rate is closely correlated with the volumes of pores of 0.2 to 2 μm and 0.008 to 0.2 μm. These results indicate that the grinding rate is strongly affected by the larger pores in the coarse grinding process and the smaller pores in the fine grinding process, and the grindability of

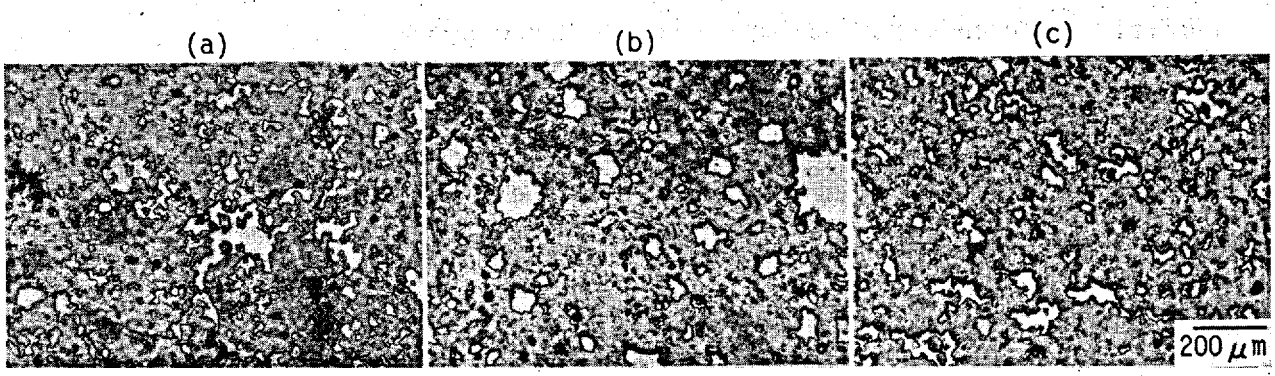

Fig. 90 Shape and distribution of pore in clinker

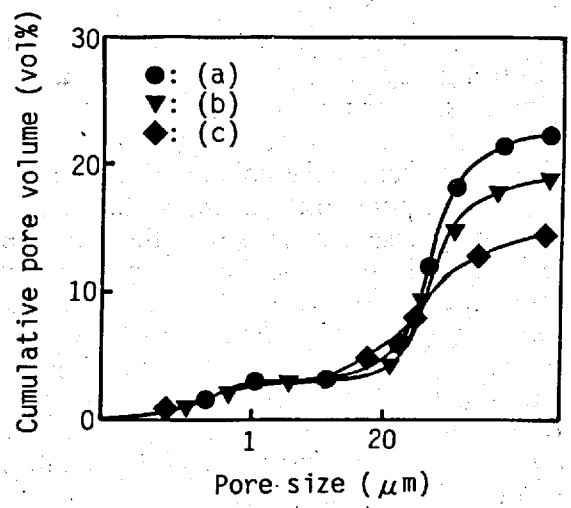

Fig. 91 Pore size distribution of clinker (Uchikawa et al; (147))

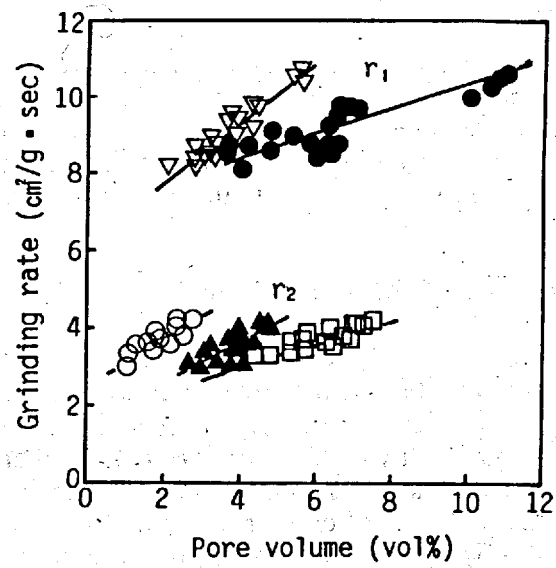

	Range of pore diameter	Pore volume
●:	20-250 μm	V_1
▽:	2-20 μm	V_2
○:	0.2-2 μm	V_3
▲:	0.008-0.2 μm	V_4
□:	0.008-2 μm	V_4

r_1 : Grinding rate at the first stage

r_2 : Grinding rate at the second stage

Fig. 92

Relationship between pore size, volume and grinding rate of clinker
(Butt et al; (144))

clinker hardly depends upon the shape and distribution of pores.

The relationships of the burning conditions of clinker with the optical properties, pore structure and grindability are summarized in **Table 9**. As the heating rate increases, alite is rapidly formed, the size of it decreases, the volume of pores smaller than 1 μm increases, that of pores larger than 20 μm decreased and the ratio of the former to the latter increases. The viscosity of liquid phase decreases with the increase of temperature and the total pore volume decreases with the increase of the maximum burning temperature because the pores are filled with the movable liquid phase and the volume of pore of 1 to 20 μm increases by deposition of interstitial phase. The volume of pores larger than 20 μm gradually decreases with the increase of retention time, resulting in the decrease of the ratio of the volume of pores larger than 20 μm to the total pore volume. Since cracking is caused by the contraction of clinker minerals and fine interstitial phase is deposited with the increase of cooling rate, the volume of pores of 1 to 20 μm decreases while that of pores smaller than 1 μm increases.

The relationship between the chemical composition of the raw materials and the pore structure under the constant burning degree is also shown in **Table 9**. The total pore volume, especially volume of pores smaller than 1 μm, increases with the increase of HM. Although the volume of pores smaller than 1 μm increases while that of pores larger than 20 μm decreases with the decrease of SM because the volume of the liquid phase increases, the decrease of SM hardly affects the total pore volume. Since the amount of C_4AF increases and the melting temperature of liquid phase decreases with the decrease of IM, clinker is so easily burnt that the total pore volume decreases while volume of pores smaller than 1 μm increases and reaches the maximum at 1.4 of IM with the largest amount of liquid phase at 1338°C. Although the total pore volume and volume of pores larger than 20 μm increase with the increase of SO_3, the volume of pores smaller than 1 μm decreases, thereby improving the grindability in coarse size and lowering the grindability in fine size. Since the total pore volume and the volume of pores larger than 20 μm decrease and that of pores smaller than 1 μm increases with the increase of MgO, the grindability in coarse size is lowered while the grindability of fine size is improved.

Although the total pore volume remains unchanged even though the particle size of raw meal is reduced, the volume of pores smaller than 1 μm increases **(147)**, thereby improving the grindability in fine size.

The effect of the type of finish mill on the pore structure is mentioned hereafter. Clinker with less total pore volume and more volume of pores smaller than 1 μm is easily ground by impact grinding using a ball mill. Clinker with moderate total pore volume and more volume of pores smaller than 1 μm is easily ground by press grinding in a vertical mill and that with less total pore volume and more volume of pores smaller than 1 μm is easily ground by hybrid system with roller press and ball mill.

(3) Relationship between optical properties of clinker minerals and its grindability

Among the clinker minerals, the grindabilities of alite and belite are high and low, respectively, and that of the interstitial phase lies between them. It is known that the grindabilities of alite and belite are improved as the size of alite becomes smaller and that of belite becomes larger, but belite turned to deep yellow by deposits on it or clustered crystals of belite is hardly ground. It is being tried to estimate the grindability of clinker from the optical properties including birefringence and color tone of clinker minerals for the quality control. An example is shown in **Fig. 93(145)**. The figure reveals that the grindability using the Blaine specific surface area estimated by optical microscopy is closely correlated with the measured values. Since the optical properties of clinker minerals are closely related to the thermal history in the forming process of clinker in the same manner as the pore

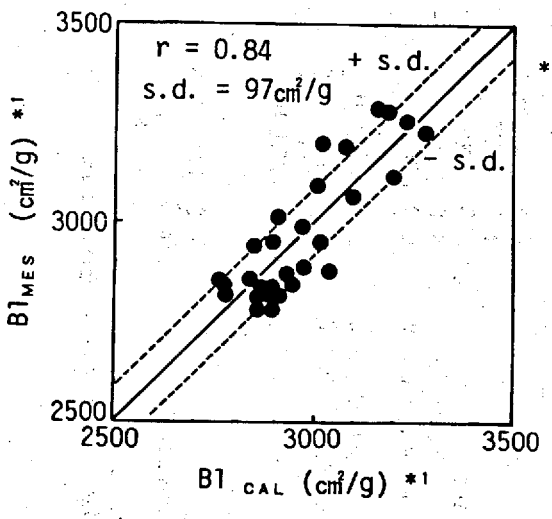

*1 Bl_{CAL} : Calculated value of Blaine specific surface area
= 1513+171xAS+167xAB+417xBS-153xBC
AS : Size of alite (μm)
AB : Birefringence of alite
BS : Size of belite (μm)
BC : Color of belite

Bl_{MES} : Measured value of Blaine specific surface area

Fig. 93

Estimation of grindability of clinker by optical properties (Kawamura et al; (145))

structure as shown in **Table 9**, the grindability of clinker can be more accurately estimated by combining the determination of pore structure with that of optical properties.

4.3.2 Control of Grindability of Clinker

As mentioned before, the grindability of clinker depends upon the burning conditions of clinker, the chemical composition and particle size of raw meal and the type of grinding mill. Conditions appropriate for producing clinker with the optimum pore structure and optical properties in a given mill are, therefore, able to be fixed. Since the chemical composition of raw meal can be hardly changed according to the type of cement and the quality standards, the grindability of clinker is first controlled by changing the burning conditions flexible in the changing conditions and then the chemical composition of raw meal if necessary. The burning conditions are controlled in such a way that the pore structure of clinker sampled at constant interval is determined with a mercury intrusion porosimeter and measured values are referred to the items shown in **Table 9**. The measures for improving the grindability of clinker by optimizing the pore structure are generally coincide with those for improving the quality of clinker described in **4.1**.

Measurements for controlling the grindability of clinker and the measures based on them are shown in a diagram of **Fig. 94**.

Table 9 Relationship between burning condition and raw materials blending, pore structure, and optical properties of clinker

Condition	Direction of change	Appeared phenomena		Change in character of clinker: Alite	Belite	Interstitial phase	Pore structure: Volume	Proportion
Burning condition								
Heating rate	⇨ Rapid	Nuclei number of A	⇧ Increase	Size ⇩ Small			L,M ⇧	L/N ⇧
				Shape ⇧ Compressed			N ⇩	Decrease
Maximum temperature	⇨ High	Amount of I	⇧ Increase		Size ⇧ Large		T ⇩	
		Viscosity of I	⇩ Decrease	Amount of M, ⇧		Homogenities of chemical	M ⇧	Increase
		Crystal growth of A and B	⇧ Remarkable	Birefringence ⇧		compositon ⇧ Up		
Retention time	⇨ Long	Crystal growth of B	⇧ Remarkable		Size ⇧ Large		N ⇩	N/T ⇩
					Cluster rate ⇩ Decrease			
Cooling rate	⇨ Rapid	Thermal crack in A and B	⇧ Increase		Color ⇧ Clear	Shape facter T ⇧	L ⇧	L/M ⇩
		Polymorph of B	⇧ High temp. mod.		Type III ⇩ Decrease		M ⇩	
		Eutectic texture of I	⇩ Fine					
Burning atomsphere	⇨ Reducing	Segregation of metalic Iron	⇧ Remarkable	Decomposition ⇧	Size ⇧	Amount of C_3A ⇧	M,N ⇧	L/M ⇩
		Incorpolation of Fe in A	⇧ Increase	Triclinic ⇧	Remarkable		L ⇩	
Raw material								
HM	2.05 → 2.13	Amount of A	⇧ Increase	Amount ⇧	Amount ⇩		T,L,M ⇧	L/N,L/M ⇧
		Nuclei number of A	⇧ Increase	Size ⇩			N ⇩	N/T ⇩
SM	2.1 → 2.7	Amount of I	⇩ Decrease		Shape ⇩ Compressed		L ⇩	N/T ⇧
						Amount ⇩	N ⇧	
IM	1.3% → 1.8%	C_3A/C_4AF	⇧ Increase			Amount of C_3A ⇧	L ⇧	L/N ⇩ N/T ⇧
		Al_2O_3/Fe_2O_3 in A and B	⇧ Increase					
MgO	0.5% → 2.0%	Amount of M_3 in A	⇧ Increase	Amount of M, ⇧		Amount of C_3A ⇩	L ⇧	L/N,L/M ⇧
		Al_2O_3/Fe_2O_3 in C_4AF	⇧ Increase			Al_2O_3/Fe_2O_3 in C_4AF ⇧	N ⇩	N/T ⇩
SO_3	0.2% → 1.0%	Nuclei number of A	⇩ Decrease	Size ⇧			L ⇩	L/N ⇩
Na_2O, K_2O	0.4% → 1.0%	Incorpolation of alkali in A and B	⇧ Increase		Size ⇧		N,T ⇧	N/T,L/M ⇧
		Melting point of I	⇩ Down					
Fineness		Number of grain in	⇧ Increase	Distribution of size ⇧	Wide		T ⇧	L/T ⇩
88μm residue	10.0% → 30.0%	cluster of A and B			Cluster rate ⇧ Increase		L ⇩	
		Homogeneities of chemical composition	⇩ Down					

Note: A: Alite, B: Belite, I: Interstitial phase, T: Total pore volume, L: Pore volume of 1μm or less, M: Pore volume of 1μm to 20μm, N: Pore volume of 20μm or more

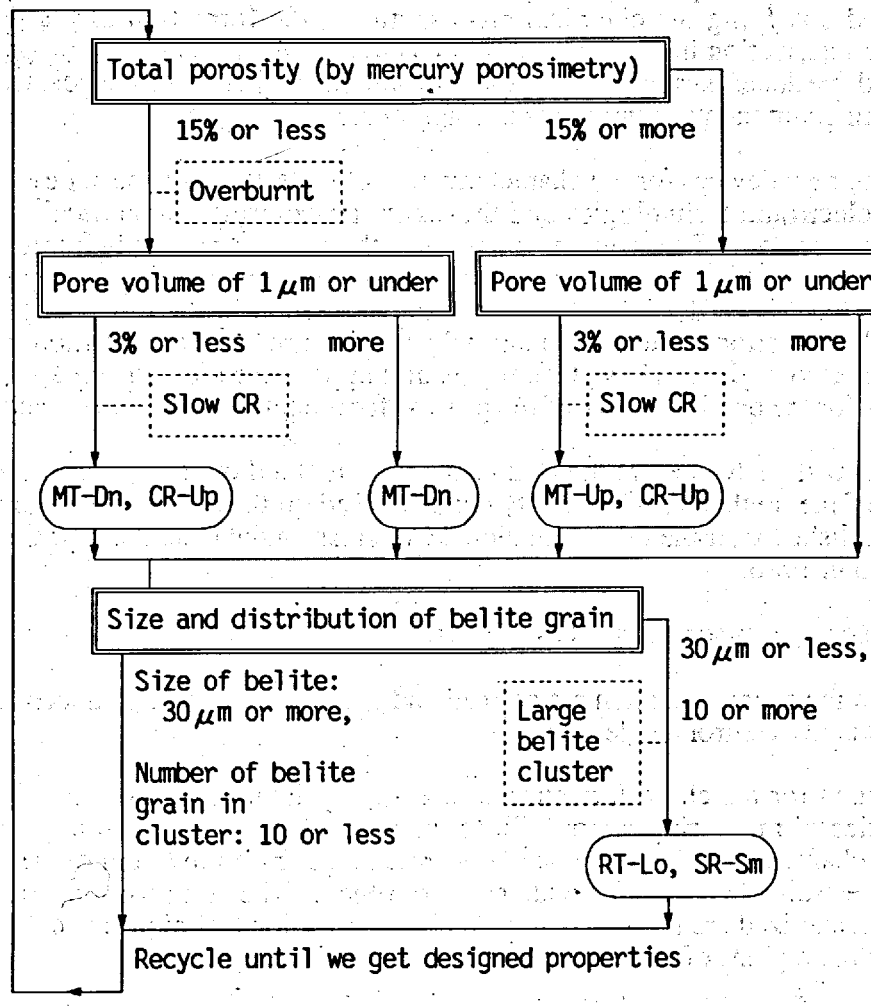

Note : Measurement, : Action, : Reason

CR: Cooling rate of clinker, MT: Maximum temperature at burning, RT: Retention time at sintering temperature, SR: Fineness of raw material, Up: Up, Dn: Down, Lo: Long, Sm: Small

Fig. 94 An example of the diagram to control the grindability of clinker

5. SUMMARY

In order to establish a high-precision quality control system of the process for manufacturing cement from the selection of raw materials to the cement product and develop high-performance multifunctional cement meeting the diversified requirements, it is indispensable to know the relationship between the characters and properties of cement clinker, cement paste, mortar and concrete by interpreting the abundant information on forming process of clinker itself and clarifying the chemical process during the formation of hardened body through the characterization in higher level of the cement clinker, its hydration product and flocculation and hardened structure composed of unhydrated cement particles, hydration product, blending components, admixtures and aggregate.

Meanwhile, some new devices for the characterization of materials have been developed with the advance of electronic technologies and the computer-controlled analytical instruments have spread. The accuracy of measurement has been, therefore, remarkably improved. With the progress of data and image processings, various sample preparation apparatuses suitable for any research have been developed for the characterization in the micro region, on the surface and in the direction of depth of material as well as the characterization of the bulk material in the macro region. Those techniques and apparatuses have been applied to the analytical means for the quality control of the process for manufacturing cement and concrete.

This paper presents the advances in the characterization method of cement and concrete and the application of the methods to the quality control based on the new knowledge presented on the papers published after the 8th International Congress on the Chemistry of Cement held in Rio de Janeiro in 1986.

The content of the paper is summarized as follows:

(1) The terms on the characterization are defined and the significance of characterization and the meaning of quality control are described.

(2) It is important for the characterization to use appropriate techniques according to the object and the size of measuring region. Since the sizes of the component and structure of the object to be characterized in cement and concrete range from nm to cm of 10^7, there are diverse techniques suitable for such a wide range of object. The composition, structure and texture to be characterized are presented and the characterization techniques suitable for them are classified by the regions of object.

(3) Among the characterization techniques of average composition and structure of bulk material in macro region, recent progresses in the analysis techniques for composition of absorptiometry, atomic absorption spectrophotometry, emission photometry, polarography, chromatography, x-ray fluorescent spectroscopy, mass spectrometry and radio activation analysis are reviewed.

The time required for the analysis and measurement is being shortened and the accuracy and precision of the measurement together with the detection limit are being improved by the concentration and collection of a component to be determined by pretreating the sample, the elimination of matrix effect, the introduction of software for correcting measured data by computer, the development of correcting software based on the theory such as fundamental parameter method in x-ray fluorescent analysis, the improvement of hardwares including detector for improving the sensitivity and the use of highly sensitive reagent, the development and introduction of new sample-feeding method, sample transporting method and exciting method, the development of on-stream and on-line analyses, and the development of the multiple and simultaneous data acquisition system by combining with other analytical and measurement techniques.

(4) X-ray photoelectron spectroscopy, nuclear magnetic resonance spectroscopy, electron spin resonance spectroscopy, supercritical fluid chromatography and void and pore structure analysis over a wide area are applied to the characterization of cement and concrete in the field of the structural analysis of macro region.

The x-ray photoelectron spectroscopy has been firmly established as the method of state analysis for elements in material by the improvement of the sensitivity of energy analyzer. The nuclear magnetic resonance spectroscopy has been applied rapidly to the analysis of inorganic solid material, the determination of the bonding of H, C, Al and Si in various hydrates, the clarification of the relationship between the estimated condensation degree and structure of silicate anion and the physical properties, and the estimation of porosity of hardened cement paste in keeping with the improvement of the intensity of magnetic field and the establishment of the technologies for dipolar decoupling, cross polarization and magic angle spinning of sample. The electron spin resonance spectroscopy has recently begun spreading for elucidating the relationships of the electron shell structure and structural defect with the physical properties. Since a microcomputer is applied to thermal analysis to easily calibrate the analytical instrument and easily process the data, the analysis can be used for determining the dynamic thermal change and accurately determining the chemical and thermal changes and the phase transformation at ultrahigh temperature under high pressure in various gas atmospheres. Since the theoretical plate number for separation in supercritical fluid chromatography characterized by high solubility, low viscosity and high diffusivity at low temperature is remarkably increased, it is used for analyzing the structure of silicate anion in C-S-H using together with the trimethylsilylation method. The whole void and pore size distribution and porosity in concrete can be determined by void and pore structure analyses over a wide area combining the gas adsorption, mercury intrusion and microscopic observation / image processing methods and x-ray computerized tomography to clarify the relationship in concrete between the void and pore structure and the physical properties including strength and durability.

(5) Characterization of the surface and micro region is making a new development by the advanced sample preparation, improved two- and three-dimensional resolving powers, newly developed devices based on new ideas, improved accuracy and precision of measurement by new techniques, simultaneous acquisition of diverse information, and development of data processing and image processing systems with computer and artificial intelligence.

Those new techniques include the cryostat system in obtaining the electron microscopic image and electron diffraction, special deposition apparatus and ion thinning, field emission scanning electron microscope and transmission electron microscope, micro Auger electron spectroscope, microfocus x-ray diffractometer, environmental scanning electron microscope, scanning tunnel microscope, atomic force microscope, prevention of insulator sample from charging by sample inclination method, simultaneous analysis including morphological observation, composition analysis and electron diffraction, simultaneous acquisition of diverse information by combining several analytical instruments, correction of atomic number effect, absorption effect and fluorescent effect, mapping of element distribution by content in electron probe microanalysis, and quantification of crystal shape by image processing.

Applications of those techniques to cement and concrete include the observation of the first- and second-order lamellar structures of belite caused by the phase transformation by in-lens FESEM, observation of the change of surface structures of alite and belite caused by hydration, observation of the forming process of calcium aluminosulfate hydrates and their composition analysis by ESEM, observation of the lattice images of alite and belite by TEM, observation of electron diffraction images of lamellar parts in belite by TEM, composition analysis of the inner and peripheral parts of the zonal structure of alite, tracing of the composition change of clinker minerals in various burning atmospheres and composition analysis of transition zone in concrete by CMA/EPMA, analysis of surface composition of clinker minerals in the direction of depth in the initial hydration by AES, determination of the

crystal transformation in the inner and peripheral parts of zonal structures of alite by microfocus x-ray diffractometer, observation of the dissolved state of elements from the surface of clinker minerals in the initial hydration and investigation of action mechanism of superplasticizer in the hydration of cement by AFM ,and quantification of shape of interstitial phases in clinker and determination of the amounts of admixtures in blended cement by microscopic observation / image processing.

(6) Those advanced characterization techniques are applicable to the data acquisition for quality control in the manufacturing of cement as well as the research on cement and concrete as material science.

Applications of the new idea and the advanced characterization techniques to quality control include the control of the fluidity of cement by changing the cooling rate of clinker based upon the quantitative expression of the morphology of C_3Ass and C_4AFss by microscopic observation / image processing and researches on the relationship between the morphology and crystallinity of C_3Ass and C_4AFss and the fluidity and on the relationship between the shape and crystallinity of C_3Ass and C_4AFss and the cooling rate of clinker; the control of setting time of cement by changing the conditions of burning and cooling of clinker based upon the scaling of the color change of etched alite with reflecting microscope and researches on the relationship between the color of etched alite and the setting time of cement and on the relationship between the color change of etched alite and the conditions of burning and cooling of clinker; the control of the strength development of cement by changing the conditions of burning and cooling of clinker based upon the optical microscopic observation of the sizes, color and optical properties of clinker minerals and researches on the relationship between the four optical parameters of clinker minerals including the size, birefringence of alite and the size, color tone of belite and the strength of mortar and on the relationship between the four optical parameters and the condition of burning and cooling of clinker; and the control of the grindability of clinker by changing the conditions of burning and cooling of clinker based upon the determination of the pore structure of clinker with mercury intrusion porosimeter and the researches on the relationship in clinker between the pore structure and the grindability and on the relationship in clinker between the pore structure and the conditions of burning and cooling.

REFERENCES

1) H. UCHIKAWA (1991). "The Way to the Creation of High-performance, Multi-functional Cement", Cement & Concrete (in Japanese) (535) 112-118.
2) K. OGUMA (1988). "Flow Injection Analysis: Its Application to Inorganic Analysis", Bunseki (in Japanese) 14(1) 75-80.
3) E. LUNDBERG, W. FRECH and J.M. HARNLY (1988). "Simultaneous Multi-Element Analysis by Continuum Source Atomic Absorption Spectrometry with a Spatially and Temporally Isothermal Graphite Furnace", J. Anal. At. Spectrom. 3 (12) 1115-1119.
4) D.L. TSALEV, V.I. SLAVEYKOVA and P.B. MANDJUKOV (1990). "Chemical Modification in Graphite-furnace Atomic Absorption Spectrometry", Spectrochim. Acta. Rev. 13(3) 225-274.
5) B.V. L' VOV, V.G. NIKOLAEV, A.V. NOVICHIKHIN and L.K. POLZIK (1988). "Effect of Platform Material on Sample Vaporization Rate in Graphite Furnace Atomic Absorption Spectrometry", Spectrochim. Acta. 43B 1141-1146.
6) J.F. TYSON (1988). "Atomic Spectrometry and Flow Injection Analysis: A Synergic Combination", Anal. Chim. Acta. 214 57-75.
7) Z. FANG, B.WELZT (1989). "Optimisation of Experimental Parameters for Flow Injection Flame Atomic Absorption Spectrometry", J. Anal. At. Spectrom. 4(2) 83 -89.
8) L. EBDON, J.I.G. ALONSO, S. HILL and A. HOPKINS (1988). "Versatile Computer Controlled Interface System for Directly Coupled High - Performance Liquid Chromatography - Flame Atomic Absorption Spectrometry", ibid

3 395-399.
9) B. MAGYAR, K. IKRENYI and E. BERTALAN (1990). "Standardless Flame Atomic Absorption Spectrometry : Problems Involved in the Determination of Aluminum", Spectrochim. Acta. 45B(10) 1139-1150.
10) D.S. GOUGH, P. HANNAFORD and R.M. LOWE (1989). "Studies of Sputtering Atomizers for Atomic Absorption Spectroscopy", Anal. Chem. 61 1652 -1655.
11) L. EBDON, M.E. FOULKES and S. HILL (1990). "Direct Atomic Spectrometric Analysis by Slurry Atomization Part 9. Fundamental Studies of Refractory Samples" J. Anal. At. Spectrom. 5(2) 67-73.
12) H. NICKEL, M. REISCH and M. MAZURKIEWICZ (1989). "Investigation of Alumina-based Ceramic Materials Using ICP-OES with External Electrothermal Vaporization", Fresenius Z Anal.Chem. (335) 631-636.
13) T. MOCHIZUKI, A. SAKASHITA, T. AKIYOSHI and H. IWATA (1989). "Direct Analysis of Steels by Inductively Coupled Plasma Emission Spectrometry with a Q-Switched Neodymium: YAG Laser", Anal. Sci. 5 535-538.
14) J.F. TYSON (1990). "Atomic Spectrometric Detectors for Flow-Injection Analysis", Anal. Chim. Acta (234) 3-12.
15) J.A. TIELROOY, P.H.M. VIEESCHHOUWER, J.C.KRAAK and F.J.M.J.MAESSEN (1988). "Determination of Rare-earth Elements by High -Performance Liquid Chromatography/Inductively-Coupled Plasma/Atomic Emission Spectrometry", ibid (207) 149-159.
16) S.B. ROYCHOWDHURY and J.A. KOROPCHAK (1990). "Thermospray Enhanced Inductively Coupled Plasma Atomic Emission Spectroscopy Detection for liquid Chromatography", Anal. Chem. 62(5) 484-489.
17) A. MONTASER, R.H. CLIFFORD, S.A. SINEX and S.G. CAPAR (1989). "Atomic Emission Spectrometric Detection Limits and Noise Power Spectra of Argon Inductively Coupled Plasma Discharges Formed With Laminar- and Tangential-flow Torches", J. Anal. At. Spectrom. 4(5) 499-503.
18) H. TAN, S. CHAN and A. MONTASER (1988). "Laminar-Flow Torch for Helium Inductively Coupled Plasma Spectrometry", Anal. Chem. 60(22) 2542 -2544.
19) K.C. LEPLA and G. HORLICK (1989). "Photodiode Array Systems for Inductively Coupled Plasma-Atomic Emission Spectrometry", Appl. Spectrosc. 43 (7) 1187-1195., K.C. LEPLA and G. HORLICK (1990). "Data Processing Techniques for Improved Spectrochemical Measurements with Photodiode Array Spectrometers", ibid 44(8) 1259-1269.
20) K.R. BRUSHWYLER, N. FURUTA and G.M. HIEFTJE (1990). "Use of a Spectrally Segmented Photodiode-Array Spectrometer for Inductively Coupled Plasma Atomic-Emission Spectroscopy - Examination of Procedures for the Evaluation of Detection Limits - ", Talanta 37(1) 23-32.
21) J. TAKAHASHI (1990). "Inductively Coupled Plasma Mass Spectrometry", Bunseki (in Japanese) 16(2) 104-113.
22) Z. KOWALSKI and W. KUBIAK (1984). "Linear-Sweep Voltammetry at a Dropping Mercury Electrode in Continuous Flow Systems", Anal. Chim. Acta, (159) 129-137.
23) S.R. LIPSKY and M.L. DUFFY (1986). "High Temperature Gas Chromatography: The Development of New Aluminum Clad Flexible Fused Silica Glass Capillary Columns Coated with Thermostable Nonpolar Phases : Part 1", J. High. Resolution Chromatography & Chromatography Communications 9 376-382.
24) Y. TAKIGAWA, T. HANAI and J. HUBERT (1986). "Microwave-Induced Plasma Emission Spectrophotometer Combined with a Photodiode Array Monitor for Capillary Column Gas Chromatography", ibid 9 698-702.
25) E.S. OLSON and J.W. DIEHL (1987). "Serially Interfaced Gas Chromatography/Fourier Transform Infrared Spectrometer/Ion Trap Mass Spectrometer System", Anal. Chem. 59 443-448.
26) I.L. DAVIES, K.E. MARKIDES, M. L. LEE, M.W. RAYNOR and K.D. BARTLE (1989). "Applications of Coupled LC-GC - A Review -", J. High Resolution

Chromatography 12 193-207.
27) T. ARAI (1986). "Recent Developments of Instrumental and Analytical Techniques in X-Ray Fluorescence Analysis", Advances in X-ray Chemical Analysis (in Japanese) 17 189-206
28) A. IIDA (1990). "The Application of Synchrotron Radiation to Analytical Chemistry", Bunseki (in Japanese) 16(9) 692-698.
29) H. TAKEMICHI, K. ICHISAWA and H. MARUYAMA (1988). "Application of X-ray Fluorescence Analysis with Automatic Bead Sampler for Cement Raw Material", Production Symposium of CAJ 46 64-67.
30) M. TSUCHIYA (1988). "Mass Spectrometry", Bunseki (in Japanese) 14(9) 628 -638
31) K. TOMURA (1989). "Progress in Activation Analysis Involving Preconcentration and Radiochemical Separation", Bunseki (in Japanese) 15(5) 360-366.
32) W.M. MOK, N.K. SHAH and C.M. WAI (1986). "Extraction of Arsenic(III) and Arsenic(V) from Natural Waters for Neutron Activation Analysis", Anal. Chem. 58 110-113.
33) W.D. EHMANN, R.C. YOUNG, D.W. KOPPENAAL, W.C. JONES and M.N. PRASAD (1987). "Derivative Techniques in Activation Analysis", J. Radioanal. Nucl. Chem, Articles 112(1) 71-87.
34) S. HIRAI (1987). "Instrumental Neutron Activation Analysis", Bunseki (in Japanese) 13(9) 636-641.
35) I. JAWED, D. MENETRIER and J. SKALNY (1980). "Early Hydration of Calcium Silicates: Surface Phenomena", 7th. Int. Congr. Chem. Cem. (Paris) 2 182-187.
36) M. REGOURD, J.H. THOMASSIN, P. BAILLIF and J.C. TOURA (1980). "X-ray Photoelectron Spectrometry Investigation of the Early Stages of C_3S Hydration - the Role of NaF Admixture", 7th. Int. Congr. Chem. Cem. 2 123-128.
37) P. BARRET, D. MENETRIER and D. BERTRANDIE (1983). "Mechanism of C_3S Dissolution and Problem of the Congruency in the Very Initial Period and Later on ", Cem. Concr. Res. 13 728-738.
38) N. KOSHIZAKI (1988). "Interfacial Analysis between Zirconia-containing Glass and Cement by X-ray Photoelectron Spectroscopy", J. Mat. Sci. Lett. 7 1190-1192.
39) S. LIHUA, Y. MENGCHU (1989). "Analysis of Glass Surface States in the Na_2O-SiO_2-ZrO_2-TiO_2 System", J. Non-Crysts. Solids 112 413-418.
40) N. KOSHIZAKI (1986). "XPS Analysis on Initial Alkali Corrosion Process of ZrO_2 Containing Glass", Yôgyô Kyôkai-shi 94(5) 521-527.
41) N. KOSHIZAKI, H. TAKAYANAGI and K. KENMOCHI (1987). "Interfacial Analysis between Zirconia Containing Glass and Various Alkaline Media by X-ray Photoelectron Spectroscopy", Non-cryst. Solids 95/96 1111-1118.
42) H. UCHIKAWA and S. HANEHARA (1991). "Advances in the Characterization of Cement Clinker", Eng. Found. Conf. 'Advance in the Production and Utilization of Cement-based Materials' at Trout Lodge, Potosi, Missouri, ; Now Printing
43) R.K. HARRIS, P. JACKSON, L.H. MERWIN and B.J. SAY (1988). "Perspective in High-resolution Solid-state Nuclear Magnetic Resonance, with Emphasis on Combined Rotation and Multiple-pulse Spectroscopy", J. Chem. Soc., Faraday Trnas.1 84 3649-3672.
44) S.F. DEC, R.A. WIND, G.E. MACIEL and F.E. ANTHONIO (1986). "High -Speed Magic-Angle Spinning", J. Mag. Res. 70 355-359.
45) A. SAMOSON, E. LIPPMAA and A. PINES (1988). "High resolution solid-state N.M.R. Averaging of Second-order Effects by Means of a Double-rotor", Molecular Physics 65 1013-1018.
46) A-R GRIMMER and von F. LAMP (1984). "Hochauflösende ^{29}Si-NMR an festen Silikaten Polymorphie von Beliten", Silikattechnik 35(9) 273-276.
47) A-R GRIMMER and von F. LAMP (1985). "High-resolution Solid-state ^{29}Si-NMR of Polymorphs of Ca_2SiO_4", Cem. Con. Res. 15 467-473.
48) Von F. LAMP (1989). "Über die Abhängigkeit der hydraulischen Aktivität von kalziumsilikaten von Eigenschaften ihres Kristallitters", Baustoffindustrie 32(3)

71-75.
49) E.T. LIPPMAA, M. MÄGI, A. SAMOSON, G. ENGELHARDT and A.R. GRIMMER (1980). "Structural Studies of Silicates by Solid-State High-Resolution ^{29}Si NMR", J. Am. Chem. Soc. 102 4889-4893.
50) E.T. LIPPMAA, M. MÄGI and M. TARMAK (1982). "A High Resolution ^{29}Si-NMR Study of the Hydration of Tricalciumsilicate", Cem. Con. Res. 12 597-602.
51) W. WIEKER, A.R. GRIMMER, A. WINKLER, M. MÄGI, M. TARMAK, E. T. LIPPMAA (1982). "Solid-state High-resolution ^{29}Si NMR Spectroscopy of Synthetic 14Å, 11Å and 9Å Tobermorites", Cem. Con. Res. 12 333-339.
52) J. F. YOUNG (1988). "Investigation of Calcium Silicate Hydrate Structure Using Silicon-29 Nuclear Magnetic Resonance Spectroscopy" J. Am. Ceram. Soc. 71 C118-C120.
53) G. PARRY-JONES, A.J. AL-TAYYIB, S.U. AL-DULAOIJAN and A.I. AL-MANA (1989). "^{29}Si MAS- NMR Hydration and Compressive Strength Study in Cement Paste", Cem. Con. Res. 19 228-234.
54) G.W. GROVES, A. BROUGH, I.G. RICHARDSON, C.M. DOBSON (1991). "Progressive Changes in the Structure of Hardened C_3S Cement Pastes due to Carbonation", submitted to J. Am. Ceram. Soc.
55) T. LUONG, H. MAYER, H. ECKERT and T. I. NOVINSON (1989). "In Situ ^{27}Al NMR Studies of Cement Hydration: The Effect of Lithium-Containing Setting Accelerators", ibid 72(11) 2136-2141.
56) S. KOMARNENI, R. Roy and D. M. Roy (1985). "Al-Substituted Tobermorite - The Coordination of Aluminum as Revealed by Solid-State ^{27}Al Magic Angle Spinning (MAS) NMR ", Cem. Con. Res. 15 723-728.
57) N.L. THOMAS and J.D. BIRCHALL (1983). "The Retarding Action of Sugars on Cement Hydration", ibid 13 (6) 830-842.
58) L. MILJKOVIC, J.C. MACTAVISH, J. JIAN and M.M. PINTAR (1986). "NMR Study of Sluggish Hydration of Superplasticized White Cement", ibid 16(6) 864-870.
59) M. LETELLIER, H.V. DAMME, B. MORTUREUX and M. REGOURD (1986). "Mechanism of the Action of Superplasticizers Studied by the Proton NMR", Proc. 8th Int. Congr. Chem. Cem. (Rio de Janeiro) III 93-100.
60) D.D. LASIC, M.M. PINTAR and R. BLINC (1988). "Are Proton NMR Observations Supportive of the Osmotic Model of Cement Hydration?", Philosophical Magazine Letters 58(5) 227-232.
61) R.F. FELDMAN (1989). "The Porosity and Pore Structure of Hydrated Portland Cement Paste", Mat. Res. Soc. Symp. Proc. (Boston) 137 59-73.
62) S. DIAMOND (1989). "Methodologies of Psd Measurements in Hcp: Postulates, Peculiarities, and Problems", ibid (Boston) 137 83-89.
63) H. UCHIKAWA, T. OKAMURA and M. TAKEHIRO (1992). "Relationship between the Structure and Polycondensation Degree of Silicate Ion of C-S-H Estimated by FT-NMR, GPC and SFC and the strength of mortar", submitted to communication paper of 9ICCC in New Delhi.
64) H.UCHIKAWA (1984). "Materials Design of Cement", Bul. Ceram. Soc. Japan 19(5) 394-403.
65) T.W. KUSNEZOWA, W.G. AKIMOW and W.N. PANJUSKIN (1986). "Reaktionsfauhigkeit der Mineralien von Portlandzementklinker", Silikattechnik 37(4) 125-127.
66) F. PUERTAS, J. SORIA, M.A.T. BLANC, O-VÁRELA and T. VAZQUEZ (1988). "Modification on the Tricalcium Aluminate Phase in Cements by Manganese Substitution", Cem. Con. Res. 18 837-842.
67) M.C. BALL, C.M. MARSH and M.C.R. SYMONS (1987). "Electron Spin Resonance and Thermoluminescence of Tricalcium Aluminate, $Ca_3Al_2O_6$", J. Mat. Sci. 22(11) 4121-4124.
68) M.C. BALL, C.M. MARSH, R.E. SIMMONS, I. SUTHERLAND and M.C.R. SYMONS. "Surface Composition of Anhydrous Monocalcium Aluminate, $CaAl_2O_4$", ibid 23 1431-1435.
69) M.C. BALL, C.M. MARSH and M.C.R. CYMONS (1990). "Thermoluminescence

and ESR of Boron-Stabilized β-Dicaicium Silicate", ibid 25(1A) 325-327.
70) M. OGUNI, O. YAMAMURA, T. MATSUNO and H. SUGA (1982). "Construction of an Apparatus for Differential Thermal Analysis under Constant High Pressure", NETSUSOKUTEI 9(4) 135-139.
71) O. KNOTEK, E. LUGSCHEIDER, H. REIMANN and H.G. SASSE (1981). "Hochtemperatur-Differential Thermoanalyzse mit Optischer Tempertarmessung", METAL 35(2) 130-132.
72) J. CHIU (1986). Applied Polymer Analysis and Characterization 1, Edited by Mitchell J. Jr. (Carl Hanser Verlag, Munchen).
73) H. UCHIKAWA, S. UCHIDA and T. OKAMURA (1991). "Role of Fly Ash on the Hydration and Structure Formation of Ternary Components Blended Cement Composed of Blastfurnace Slag, Fly and Portland Cement", Proceeding of Shanghai 1991 Ash Utilization Conference 2 65-1 - 65-14.
74) H. UCHIKAWA and R. FURUTA (1981). "Hydration of C_3A-Pozzolana Paste Estimated by Trimethylsilylation", Cem. Con. Res. 11 65-78.
75) H.UCHIKAWA (1986). "Effect of Blending Components on Hydration and Structure Formation", 8th International Congress on the Chemistry of Cement I 249-280.
76) R.F. FELDMAN (1986). "Pore Structure, Permeability and Diffusivity as Related to Durability ", ibid I 336-356.
77) P.K. MEHTA (1986). "Concrete (structure, properties, and materials)", Prentice-Hall, INC., U.S.A.
78) W.P. HALPERIN, F. D'ORGAZIO, S. BHATTACHARJA and J.C. TARCZON (1989). "Magnetic Resonance Relaxation Analysis of Porous Media; in Molecular Dynamics in Resticted Geometries - Edited by J.Klafter and J.M.Drake -" Wildy New York 311-349.
79) S.M. DOUGLAS, E.H. TERRY, P.G. GALLEGOS and L.S. DOROTHY (1987). "Pore Structure Analysis via NMR, Mercury Porosimetry, and Dynamic Methods", Adv. in Ceram. 21 779-791.
80) S. BHATTACHARJA, F. D'ORGAZIO, J.C. TARCZON and W.P. HALPERIN (1989). "Internal Structure of Porous Silica: A Model System for Characterization by Nuclear Magnetic Resonance", J. Am. Ceram. Soc. 72(11) 2126-2130.
81) H. UCHIKAWA, S. UCHIDA and S. HANEHARA (1991). "Measuring Method of Pore Structure in Hardened Cement Paste, Mortar and Concrete" il Cemento 88 67-90.
82) F.G.R. GIMBLETT, C.D.LAWRENCE and K.S.W. SING (1989). "Sorption Studies of the Microstructure of Hydrated Cement", Langmuir 5(5) 1217-1222.
83) L.J. PARROTT, R.G. PATEL, D.C. KILLOH and H.M. JENNINGS (1984). "Effect of Age on Diffusion in Hydrated Alite Cement", J. Am. Ceram. Soc. 67(4) 233-237.
84) D.N. WINSLOW and S. DIAMOND (1974). "Specific Surface of Hardened Portland Cement Paste as Determined by Small-Angle X-Ray Scattering" ibid 57 193-197.
85) A. BENTUR (1980). "The Pore Structure of Hydrated Cementitious Compounds of Different Chemical Composition", ibid 63 381-386.
86) H. UCHIKAWA, S. HANEHARA and T. SHIRASAKA (1992). "Relationship between Zonal Structure in Alite, Lamellar Texture in Belite and their Production Process, Composition and Crystal Structure", submitted to Communication Paper of 9th ICCC in New Delhi.
87) H. UCHIKAWA, S. HANEHARA and D. SAWAKI (1992). "Observation of the Change of Composition and Surface Structure of Alite and Estimation of Hydration Reactivity of Etching", submitted to communication papers of 9th ICCC in New Delhi.
88) H. UCHIKAWA, S. UCHIDA and S. HANEHARA (1987). "Flocculation Structure of Fresh Cement Paste Determined by Sample Freezing-Back Scattered Electron Image Method", il cement 84 2-22.
89) H. UCHIKAWA, S. HANEHARA and D. SAWAKI (1991). "Structural Change of Hardened Mortar by Drying", 3rd. NCB Int. Sem. on Cem. and Build. Mater. 4 VIII 1-12.
90) G.D. DANILATOS (1988). "Foundation of Environmental Scanning Electron Microscopy", Advances in Electronics and Electron Physics, 7 109-250.

91) D.A. LANGE, K.SUJATA and H. M. JENNINGS (1991). "Observations of wet cement using electron microscopy", Ultramicroscopy 37 234-238.
92) J.C.H. SPENCE (1981). "Experimental High-Resolution Electron Microscopy", Clarendon Press, Oxford.
93) G.W. GROVES (1981). "Portland Cement Clinker viewed by Transmission Electron Microscopy", J. Mater. Sci. 16 1063-1070.
94) D.G. IVEY and M. NEUWIRTH (1989). "A Technique for Preparing TEM Specimens from Cementitious Materials", Cem. Con. Res. 19(4) 642-648.
95) K.URABE and M. OOYANAGI (1991). "TEM Microstructure of A Clinker Mineral", CAJ Proceedings of Cement and Concrete 45 14-17.
96) J.F. YOUNG (1991). "Microstructural Development in Very High Strength Cement Pastes", 1st. Int. Workshop, July 3-5 (DIJION - France).
97) H. UCHIKAWA, S. UCHIDA and Y. MIHARA (1978). " Characterization of Hydrated Ultra Rapid Hardening Cement Pastes" il Cemento 75(2) 59-70.
98) S. HORIUCHI and Y. MATSUI (1983). "Crystal Structure image by High-Resolution Transmission Microscopy", Journal of the Crystallographic Society of Japan 25 3-20.
99) J.A. GARD, K. MOHAN and H.F.W. TAYLOR (1980). "Analytical Electron Microscopy of Cement Pastes: I, Tricalcium Silicate Pastes", J. Am. Ceram. Soc. 63(5-6) 336-337.
100) S.A. RODGER and G.W. GROVES (1989). "Electron Microscopy Study of Ordinary Portland Cement and Ordinary Portland Cement - Pulverized Fuel Ash Blended Pastes", J. Am. Ceram. Soc. 72(6) 1037-1039.
101) E.E. LACHOWSKI, K. MOHAN, H.F.W. TAYLOR and A.E. MOORE (1980). "Analytical Electron Microscopy of Cement Pastes: II, Pastes of Portland Cements and Clinkers", J. Am. Ceram. Soc. 63 447-452.
102) K. KOBAYASHI, R. SHIRAKI and T. MASAKI (1988). "Concentration Gradient of Alkalis in Concrete Members - Analysis by Electron Probe Micro-analyzer", Rep. of Inst. of Ind. Sci. Univ. of Tokyo 40(8) 403-406.
103) H. UCHIKAWA, S. UCHIDA and S. HANEHARA (1989). "Relationship between Structure and Penetrability of Na Ion in Hardened Blended Cement Paste, Mortar and Concrete", 8th. Int. Conf. on Alk. Agg. Rea. 1 121-128.
104) H. UCHIKAWA, S. HANEHARA and D. SAWAKI (1991). "Influence of Water Cement Ratio on the Ionic Penetrability of Blended Cement Paste, Mortar and Concrete", Second CANMET/ACI International Conference on Durability of Concrete, Supplementary papers I 525-544.
105) H. UCHIKAWA, S. UCHIDA and S. HANEHARA (1989). "Researches on the Composition and structure of Hardened Cement Paste, Mortar and Concrete Related to Their Performance", 2nd Beijing Int. Symp. Cem. Conc. 1 314-330.
106) H. UCHIKAWA (1988). "Similarities and Discrepancies of Hardened Cement Paste, Mortar and Concrete from the standpoints of Composition and Structure", Eng. Found. Conf. 'Advances in Cement Manufacture and Use' at Trout Lodge, Potosi, Missouri, 1 271-294.
107) K. OGAWA, H. UCHIKAWA, K. TAKEMOTO and I. YASUI (1980). "The Mechanism of the Hydration in the System C_3S-Pozzolana", Cem. Con. Res. 10 683-696.
108) B.S. IVANOV, N.A. KOZYREKVA and I.I. SELEVA (1988). "Ozh Spektralvnyi Ainliz Mineradov Tsemontogo Klinkera", Zh. Prikl. Khim., 61(6) 1295-1300.
109) J.R. GANCEDO, C. ALONSO, C. ANDRADE and M. GRACIA (1989). "AES Study of the Passive Layer Formed on Iron in Saturated $Ca(OH)_2$ Solution", Corrosion, 45(12) 976-977.
110) H. TAMURA, Y. IKEBE, H. SUMIYA, H. TOITA, H. IWAMOTO, H. HIROSE and H. SHICHI (1990). "Development of New Field Limiting Method for SIMS", Hitachi Scientific Instrument News 33(1) 3073-3077.
111) Y. GOOSHI, H. MAEDA and K.SATO (1986). "Spectroscopy by Ion Excitation and its Application", Gakkai-Shuppan-Center, Japan.
112) Y. IKEBE, H. IWAMOTO, H. TOITA and H. TAMURA (1989). "SIMS Analysis of Insulating Materials Using EBIC", Surface Science (in Japanese) 10 345-351.

113) H. TAMURA (1983). "Analysis of Insulating Materials by Negative Ion Microprobe", J. Vacuum Soc. Japan 26 179-188.
114) W. GERHARD and E. NAGELE (1983). "The Hydration of Cement Studied by Secondary Ion Mass Spectrometry (SIMS)", Cem. Con. Res. 13 849-859.
115) J.M. LAMEILLE, G. GOUTIERE, J-C. PETIT and M. REGOURD (1987). "Retention of Cobalt, Cesium, and Strontium in the Hydrates of C_3S, C_3A, and Gypsum" J. Am. Ceram. Soc. 70(8) 604-614.
116) E. NAGELE and U. SCHNEIDER (1985). "Analysis of Surfactants Adsorbed on Cement Using Secondary Ion Mass Spectrometry (SIMS)", Cem. Con. Res. 15 1022-1026.
117) E. HOKE, G. EDER and M. GRASSBAUR (1983). "Analytical Electron Microscopy for Interface Characterization - Corrosion of Concrete", Microchim. Acta 1 307-313.
118) G. BINNING, H. ROHRER, C.H. GERBER, E. WEIBEL (1982). "Vacuum Tunneling", Physica 109&110B 2075-2077.
119) K. SUZUKI, N. NISHIKAWA and T. HAYASHI (1988). "Characterization of Low Lime C-S-H" Semento Gijyutsu Nenpo (in Japanese) 42 34-37.
120) M. FURUSAWA and M. IKEYA (1990). "Distribution of Nitrogen and Nickel in a Synthetic Diamond Crystal Observed with Scanning ESR Imaging", J. Phys. Soc. Jpn. 59 2340-2343.
121) M.KAGAMIDA, H. KANDA, M.AKAISHI, A.NUKUI and T. OSAWA (1990). "Crystal Growth of Cubic Boron Nitride Using Li_3BN_2 Solvent and Morphology of the Growth Crystal", Science and technology of new diamond, KTK Scientific Publishers.
122) H.G. BARTH, S-T.SUN and R.M. NICKOL (1987). "Particle Size Analysis", Anal. Chem. 59(12) 142R-162R.
123) R. SHIRAKI, K. KOBAYASHI and A. MARU (1988). "Application of Analytical Instruments to Rock Including Reactive Minerals", Annual Meeting of Japan society of Civil Engineers 43 206-207.
124) R. SHIRAKI and K. KOBAYASHI (1989). "Quality and Quantity Determinations of Reactive Substances in Volcanic Rocks", 8th. Int. Conf. on Alk. Agg. Rea. (Kyoto) 1 567-572.
125) Y. EFES (1988). "Determination of the Composition of Hardened Concrete by Image Analysis", Betonwerk Fertigteil-Tech 54(11) 86-91.
126) R.E. FERRELL and A.W. DREW(1988). "Quantification of Fly Ash in Concrete by Image Analysis Techniques: A Preliminary Investigation", Mat. Res. Soc. Symp. Proc 136 99-106.
127) D. SHI (1988). "An Automatic Quantitative Image Analysis System for Cement and Concrete Research", Publ. Am. Concr. Inst. SP-106 139-157.
128) K.L. SCRIVENER (1989). "The Use of Backscattered Electron Microscopy and Analysis to Study the Porosity of Cement Paste", Mat. Res. Soc. Symp. Proc 137 129-140.
129) K.L. SCRIVENER and P.L. PRATT (1988). "Quantitative Characterization of the Transition Zone in High Strength Concretes", Adv. Cem. Res. 1(4) 230-237.
130) K.L. SCRIVENER, A.K.CRUMBEI and P.L. PRATT (1988). "A study of the Interfacial Region between Cement Paste and Aggregate in Concrete", Mat. Res. Soc. Symp. Proc. 114 87-88.
131) K.L. SCRIVENER and E.M. GARTNER (1988). "Microstructural Gradients in Cement Paste around Aggregate Particles", ibid 114 77-85.
132) L. STRUBLE (1988). "Microstructure and Fracture at the Cement Paste-Aggregate Interface", ibid 114 11-20.
133) N. YANAI (1989). "Thermal interpretation concrete inner on property", J. Remote Sensing Soc. Japan 9 49-50.
134) T. SAKUDA, F. MACHIDA, Y. TACHIBANA and Y. KAZIKAWA (1988). "Thermographic Inspection Test of RC Slab Defect", J. Japan. Soc. Non-destructive Inspection 37 (9A) 867-868.
135) N. YANAI and T. TAKEUCHI (1989). "Temperature Characteristics of Concrete which has Received Compressive Stress", CAJ Proseedings of Cement and

Concrete 43 286-291.
136) N. YANAI and T. TAKEUCHI (1988). "Research on Surface Temperature Distribution when Prestress is Introduced in Prestress Concrete", Semento Gijyutsu nenpo (in Japanese) 42 511-514.
137) H. IMA, H. YAMADA and Y. ISHIBASHI (1988). "Measurement of Corrosion Area in RC by Means of Heat Radiation", Fall meeting 1988 of the Institute of Electronics, Information and Communication Engineers (in Japanese) D-1 127.
138) H. UCHIKAWA, S. UCHIDA, K. OGAWA and S. HANEHARA (1984). "Influence of $CaSO_4 \cdot 2H_2O$, $CaSO_4 \cdot 1/2H_2O$ and $CaSO_4$ on the initial hydration of clinker having different burning degree", Cem. and Con. Res. 14 645- 656.
139) H. UCHIKAWA, K. OGAWA and S. UCHIDA (1985). "Influence of Character of Clinker on the Early Hydration Process and Rheological Property of Cement Paste", Cem. Con. Res. 15 561-572.
140) H. UCHIKAWA (1990). "The Future for Cement/Concrete in Japan - the Way to the Prosperity of Japanese Cement Industry through Self-renewal", Onoda Pacific Conference in Sydney - Australia 2 Uchikawa-1 - 77.
141) I. MAKI and K. GOTO (1982). "Factors Influencing the Phase Constitution on Alite in Portland Cement Clinker", Cem. Con. Res. 12 301-308.
142) S. CHROMY (1967). "High-Temperature Microscopic Investigation of Tricalcium silicate and Dicalcium silicate phases in portland cement clinker", J. Am. Ceram. Soc. 50 677-681.
143) Y. ONO (1980). "Microscopical Estimation of Burning Condition and Quality of Clinker", Proc. 7th Int. Cong. Chem. Cem. 2 I-206-211.
144) J. M. BUTT, V. M. KOIBASOV and G. A. MEINIEKIJ (1974). "The Interrelation between Pore Structure and Grindability of Clinker from Various Burning Condition and Cooling Process", Zement-Kalk-Gips 27 27-32.
145) S. KAWAMURA, T. AIZAWA, S. HANEHARA and Y. KUBOTA (1982). "Estimation of Grindability of Clinker by Optical Microscopy", Semento Gijyutsu Nenpo (in Japanese) 36 89-92
146) S. UCHIDA, T. SHIRASAKA, S. HASHIMOTO and H. UCHIKAWA (1990). "Influence of Kind and Raw Materials and Burning Condition on Pore Structure of Burnt Clinker", CAJ Proceedings of Cement and Concrete, 44 30-35.
147) S. UCHIDA, T. SHIRASAKA, H. HIRAO and H. UCHIKAWA (1991). "Influence of Major and Minor Chemical Constituents of Raw Meal on Pore Structure of Burnt Clinker", CAJ Proceedings of Cement and Concrete, 45 46-51.

AUTHOR INDEX
(Volume I)

A

Ahluwalia, S C — 83

B

Beaudoin, J J — 485
Boikova, A I — 3
Brown, P W — 485

C

Chandra, S — 695
Chatterjee, A K — 177
Chengsheng Ouyang — 775
Collepardi, M — 529

D

Daimon, M — 383
Della, M Roy — 357
Delort, M — 155

G

Glasser, F P — 125

J

Jennings, H M — 663

K

Kouznetsova, T V — 49
Kurdowski, W — 317

M

Majumdar, A J — 737
Massazza, F — 383
Mehta, P K — 571
Moir, G K — 125
Moranville-Regourd, M — 3
Mullick, A K — 695

N

Narang, K C — 213

P

Page, C H — 83

R

Ramachandran, V S — 529
Raupach, M — 571

S

Schiessl, P — 571
Scrivener, K L — 449
Sersale, R — 261
Shah, S P — 775
Sorrentino, F — 317
Sprung, S — 155
Su Muzhen — 317

U

Uchikawa, H — 794
Udachkin, J B — 303

V

Vagn, Johansen — 49

W

Wieker, W — 449

X

Xi Y — 663

9th International Congress on the Chemistry of Cement New Delhi, India, 1992

VOLUME II

COMMUNICATION PAPERS — THEME I

NATIONAL COUNCIL FOR CEMENT AND BUILDING MATERIALS
NEW DELHI

9th International Congress on the Chemistry of Cement New Delhi, India, 1992

COMMUNICATION PAPERS

Volume II

CHEMISTRY, STRUCTURE, PROPERTIES AND QUALITY OF CLINKER

Organised by

NATIONAL COUNCIL FOR CEMENT AND BUILDING MATERIALS
NEW DELHI

Co-sponsored by :

Department of Scientific & Industrial Research
Ministry of Science & Technology
Govt. of India

Cement Manufacturers' Association, India

The India Cements Ltd

J K Cement Works

Madras Cements Ltd

Narmada Cement Co Ltd

Orissa Cement Ltd

This volume is a part of six-volume series of the Congress Papers.
Title of each volume is given below :

I—Congress Reports
II—Communication Papers—Theme I
III—Communication Papers—Theme II
IV—Communication Papers—Theme III
V—Communication Papers—Theme IV
VI—Reports on Special Panel Discussions and Poster Papers

Published by :
National Council for Cement and Building Materials (NCB)
M-10 South Extension Part II New Delhi 110 049 INDIA

No Part of this publication be reproduced without the written permission of the Publishers.

The views expressed in the technical papers printed in this publication are those of authors and not necessarily of the Publishers.

Printed in India by Tara Art Press, New Delhi

PREFACE

Commencing with a one-day meeting in London on 14 January 1918 arranged by the Faraday Society, to discuss "The setting of cements and plasters", which is taken as the first Symposium to deal solely with the chemistry of cement, the subsequent International Symposia and Congresses on the Chemistry of Cement have been held in Stockholm (1938), London (1952), Washington DC (1960), Tokyo (1968), Moscow (1974), Paris (1980) and Rio de Jenairo (1986). At the conclusion of the Rio Congress, it was decided that the next Congress will be held in India. Accordingly, the 9th International Congress on the Chemistry of Cement is being held in New Delhi, India, from 23 to 28 November 1992.

The preparatory and organisational work for this 9th Congress was commenced immediately after the 8th Congress. To start with, all the participants in the previous two Congresses and a large number of individuals and organisations interested in the subject of the Congress were contacted through an extensively worked out and widely distributed Questionnaire. The response was most encouraging. The responses were carefully analysed and the directions which would meet the views of the largest number of participants towards advancing the cement sciences were determined. Based on these findings the first Bulletin was issued in August 1988, providing the necessary preliminary information on the Congress and outlining its scope and essential organisational aspects.

The objectives of the Congress were set to advance the knowledge of chemistry of cements with emphasis on application of this knowledge in both the manufacturing aspects and utilization of cements in practice. Within this broad scope, the thrust was on tracking the scientific progress made in the field since the last Congress, assessing the status of exploitation of the results by the industry and the society, and mapping of the new frontiers of knowledge.

The overall organisation of the Congress was governed by a National Organising Committee which was responsible for all organisational aspects including financial arrangements. Taking into account the suggestions received from various quarters, the International Scientific Committee consisting of 67 experts from 39 countries all over the world was formed which was responsible to finalise : (a) the themes and sub-themes of the Congress, (b) procedures for inviting, receiving and reviewing of papers, (c) selection of authors for general and special reports, and (d) the system for conduct of the proceedings of the sessions and other related scientific and technical matters.

The International Scientific Committee held two meetings in New Delhi in November 1989 and in January 1991. In addition, informal meetings were held with representative groups in Seoul, Tokyo, Paris, Washington DC and Montreal. The International Scientific Committee finalised the Generic and Specific Themes of the Congress. It was decided that for each Generic Theme, there shall be one Principal Review Paper, which shall cover the progress achieved in the area of the Generic Theme between the two Congresses. For each Specific Theme, there shall be one Congress Paper highlighting trends of research and realisation of the results in the industry in the areas related to the Specific Theme. Under each Specific Theme, in addition to the invited Congress Papers, there shall also be Communication Papers. Both the principal review papers as well as the Congress papers were to be presented by the invited experts identified after deliberations of the International Scientific Committee.

Preliminary Abstracts of communication papers were solicited through the Second Bulletin in May 1991. 537 Abstracts were received which were scrutinised by a panel of Indian experts and 513 were short-listed. Authors were requested to send full manuscripts of the paper for detailed review and acceptance for publication and presentation. As many as 412 communication papers from 40 countries were received which were reviewed by a panel of international experts. As a result, 346 communication papers belonging to the four themes of the Congress were finally

accepted for presentation and publication. These were in addition to 21 State-of-the-Art Congress Reports received from invited authors; reports on two Specific themes could not be had because the authors selected expressed their inability at a late stage, making replacement difficult.

In addition to the papers on deliberative thematic sessions, a poster session is being organised on "Advances in Physico-Chemical Evaluation, Characterisation and Quality Control Techniques and Systems" for Clinkers, Particulate Cements, Hydrated Systems and Concrete Systems. The State-of-the-Art Report would be presented by an invited expert and 24 contributions made in the form of posters will be presented during the Congress. In addition, Special Panel Discussions are being organised to survey the newer frontiers of knowledge in the areas of computerisation in cement science and concrete systems; resource economy in cement and concrete making; and cement in hazardous waste management.

The proceedings in six Volumes contain all the above contributions received for the Congress. This **Volume II** contains **Communication Papers on the Generic Theme "Chemistry, Structrure, Properties and Quality of Clinker".**

A novel feature of the 9th Congress will be that, in addition to the normal sessions as in the earlier Congresses, there will be three sessions to bring out the technological and techno-ecnomic impact of the scientific advances on the industry. These are intended to provide a better appreciation of the implications of the scientific advances specially on the process control machinery and related industries as well as on operational aspects related especially to energy conservation and environmental improvement. Texts of these Special Lectures will be published in Volume VII of the Proceedings to be brought out after the Congress, along with the texts of Addresses at the Inaugural and Concluding Sessions and List of nearly 550 delegates from 42 countries who are expected to attend the Congress.

I am grateful to the members of the International Scientific Committee for their whole-hearted co-operation, to those who reviewed the Abstracts, and to the International Panel of Reviewers of Manuscripts for providing very useful technical and editorial comments on the communication papers. The co-operation of the authors in accepting and implementing the reviewers' suggestions and revising their manuscripts accordingly is greatly appreciated. Thanks are also due to those authors whose communication papers could not be accepted essentially because the contributions did not fit in with the themes of the Congress and not because of any technical deficiency. We recommend that the authors have those papers published elsewhere.

The unstinted efforts put in by my colleagues in the National Council for Cement and Building Materials in all aspects of organising this Congress, is thankfully acknowledged.

A K Mullick
Chairman
International Scientific Committee
9th International Congress
on the Chemistry of Cement

New Delhi
14 September 1992

GENERIC THEME I

CHEMISTRY STRUCTURE PROPERTIES AND QUALITY OF CLINKER

EXPLANATORY NOTES

The following symbols, which have been universally recognised by cement chemists for formulating more complex compounds, are used interchangeably with the respective oxide formulae throughout this volume :

A	:	Al_2O_3	K	:	K_2O
C	:	CaO	M	:	MgO
$\bar{C}$	:	CO_2	N	:	Na_2O
CH	:	$Ca(OH)_2$	P	:	P_2O_5
F	:	Fe_2O_3	S	:	SiO_2
H	:	H_2O	$\bar{S}$	:	SO_3

Commonly used abbreviations of more general nature are as follows :

DTA	—	differential thermal analysis
EPMA	—	electron probe micro analysis
IR	—	infrared
NMR	—	nuclear magnetic resonance
RH	—	relative humidity
w/c	—	water-cement ratio
XRD	—	X-ray diffraction
SEM	—	scanning electron microscope
EDAX	—	energy dispersive analysis of X-rays

CONTENTS

Volume II

SPECIFIC THEME I-A : Clinker Formation Including New Processes

1. Relationship Between Zonal Structure in Alite, Lamellar Texture in Belite and their Production Process, Composition and Crystal Structure 3
Hiroshi Uchikawa, Shunsuke Hanehara and Tokuhiko Shirasaka

2. Phase Composition Formation of Portland Cement Clinker and Alite Formation Kinetics 10
B S Albats, Yu R Krivoborodov and V P Ryazin

3. Crystal Structure Analysis of Major Constituent Phases in Ordinary Portland Cement 17
Masaki Daimon, Yoshinobu Hirano,Takaaki Tsurumi and Kiyoshi Asaga

4. Growth of Hydraulic Activity of Portland Cement Clinker as a Result of Using of Precalcining 23
B Weryñski and L Janecka

5. Negative Effect of Alkali on Burning and Properties of Portland Cement Clinker and its Improving Measures 29
Shan-ba Wang and Yuankui Chen

6. Research on Forming Mechanism of Portland Cement Clinker under Different Burning Conditions 36
Ji Shang Xing and Xu Fengjuan

7. Optimal Parameters of Clinker Formation in a Rotary Kiln 43
G B Yegorov, I E Alexandrov and A M Turetski

8. The Decomposition of Alite in Portland Cement Clinker 49
Shunni Liu and Zongshou Lin

9. Role of Clinker Liquid in Promoting the Clinkerisation and its Impact on Clinker Morphology and Microstructure 56
S C Ahluwalia, R K Goswami and T V Kouznetsova

10. Acceleration of the Clinker Formation Process 62
P F Rumyantsev and N T Erofeeva

11. Trace Element Balances in Kiln System of a Few Indian Cement Plants 67
N A Krishnan, V K Gore, S A Khadilkar, R V Hargave, C H Page and A K Chatterjee

12. Phase Transformations when Synthesizing Clinkers Produced of Technogeneous Raw Materials 74
I S Akhmetov and O A Miryuk

13. Studies on Rapid Burning Temperature, Time and Raw Meal Modulus Range in Portland Cement 81
Hu Shuguang

14. The Structure and Properties of Low-CaO Contained Clinker 88
T V Kouznetsova, A P Osokin, V G Akimov and V N Panyuskin

15. Research on the Chemical Composition and Microstructures of Sulpho-Aluminate Cement Clinker 94
Su Muzhen, Deng Junan, Wu Zongdao and Liu Xiaoxin

16. Formation and Solid State Properties of β-Dicalcium Silicate 101
N B Singh, S P Singh and A K Shukla

17. Orthosilicate Compositions in $CaO-SrO-BaO-SiO_2$ System and Their Water Reactivity 107
Ion Teoreanu and Ecaterina Andronescu

18. Effect of Increased Magnesium Oxide Contents and Mixture Basicity Upon Clinker Phases 114
I G Luginina, A I Boykova and O I Fomichova

19. Development of Alumino-Belitic Coloured Clinkers 118
S Laxmi, Lata Mohan, P S Sharma and A K Dhawan

20. The Effect of the Combustion of Coal Mixed with Limestone on the Burning Process of Clinker 125
Wang Yuping, Huang Wenxi, Jiang Youxing and Ye Qiaoming

21. Effect of Thermal Treatment on the Reactivity of Clinker Minerals Produced from Vertical Shaft Klin 132
K Raina and R Bhargava

22. A Study on Improving Heat Transfer Between Gas and Solid in Suspended State — A New Material Sealing and Dispersion Device 139
Xia Youming, Cheng Jingxiang and Huang Wenxi

23. Morphology and Microstructure Features of Clinker from Vertical Shaft Kiln 146
S C Ahluwalia and K Raina

24. The Study and Application on High-Quality Cement Clinker Calcining with Low Heat Consumption in Shaft Kiln 153
Z G Qin

25. Mechanoactivation of Portland Cement Raw Mixes 160
L M Sulimenko

26. The Study on the Formation of Portland Cement Clinker in Low-Temperature and a Rapid Heating-up Burning Process 164
Huang Wenxi, Lu Zhongyuan and Xu Guangliang

27. Development of Radiation-Thermal Technology of Cement Manufacture 171
I G Abramson, A F Vaisman, R M Kapralova and N G Fadeyeva

28. Evaluation of Radiation Synthesized Clinker 177
S K Handoo, George Samual, R K Goswami, I G Abramson and Yu V Nikiforov

29. Kinetics of the Radiation-Thermal C_2S Synthesis 183
G B Yegorov, B K Kanimov and G V Shkatova

30. Clinkerisation Through Melting — A New Approach 190
S A Khadilkar, P G Lele, C H Page and A K Chatterjee

31. Peculiarities of the Process of Cement Clinker Formation by Changing the Interaction Sequence of Reacting Components 196
V D Barbanyagre, V M Shamshurov and T I Timoshenko

32. Low Temperature Reducing-Oxidative Technology for Portland Cement Production 201
P P Lerke

33. Physical and Chemical Peculiarities of a New Low-Energy-Consuming Technology for Portland Cement Production 205
P P Lerke

34. Thermal Treatment of Cement Raw Materials Through Intensive Heat Exchange 210
A B Ryzhik, M V Kougiya and A V Alexandrov

SPECIFIC THEME I-B : Effect of Low Grade Fuels, Combustible Wastes and Non-traditional Raw Materials

35. The Reduction of Dioxin in Connection with the Use of Waste-Derived Fuels in the Cement Industry 217
Richard Bolwerk

36. Effects of Using Rice Husk and its Ash as Fuel and Raw Material Component Respectively in Cement Manufacture 224
S P Ghosh, K Mohan and R K Gandhi

37. Complete Substitution of Natural Raw Materials by Shale Industry Waste at Cement Plant Reconstruction 232
A K loganson, M V Kougiya and L S Fraiman

38. Conservation of Raw Material Through Use of Industrial Wastes in Cement Manufacture 238
V K Gore, S A Khadilkar, P G Lele, C H Page and A K Chatterjee

39. Safety and Ecological Problems in Burning Energy-Saving Raw Materials 245
A B Ryzhik, A K loganson, L S Fraiman and A V Alexandrov

40. Studies of Belite Cement From Barium Containing By-product 250
K Rajczyk and W Nocuń-Wczelik

41. Formation of C_3S in the Mixtures Containing Different Silicate Raw Materials 255
Kurdowski Wieslaw and Deja Jan

42. New Data on Raw Mixes Burning in Dry-Process Kilns on the Basis of an Artificial Clayish Component 261
A I Zdorov and V L Bershtein

43. An Impact of Non-traditional Raw Materials on the Formation and Properties of Clinker 265
M A Akhmedov, A A Mukhamedbaev, M T Artykbaev, Z S Salimov and A P Fiodorov

44. Studies on Producing Portland Cement with Tailings of Molybdenum-Iron Ore 271
Pan Yi Zhou

45. Experiences in Use of Industrial By-product Sludge for Cement Manufacture by SOL-Gel Technology 278
V Varadarajan, C H Thombare, S A Borkar, C H Page and A K Chatterjee

SPECIFIC THEME I-C : Effect of the Use of Mineralisers, Modifiers and Activators

46. Thermal Behaviour of Mineralized Portland Cement Raw Meal 287
F Ayed, R Castanet and F P Sorrentino

47. Sintering Mechanism of Portland Cement Clinker with Energy-Saving and Early-Strength 294
Wang Xinrong, Zhu Jiaoqun, Xian Yafang and Wang Shanba

48. Role of Mineralizers in Alite Formation in a Rice Husk Ash - $CaCO_3$ Raw Mix 301
K C Misra and P C Borthakur

49. Quality Improvement in Clinker Using Mineralisers/Activators 308
A K Parashar, V K Mathur, Shree Gopal and S K Handoo

50. Formation of Low Temperature Portland Cement Clinker by Using Non-traditional Aluminosilicate Rock and Mineralizer 315
Sanjaasuren Radnaasediin

51. Effect of SO_3 on Mineral Formation and Properties of Clinkers 322
Su Dagen, Chen Weiqing, Huang Qixiu, Mai Huo and Zheng Liqiang

52. The Influence of SO_3 in $C_2A_xF_{1-x}-C_{11}A_7CaF_2-C_2S$ System on Formation of $C_{11}A_7CaF_2$ 329
Yang Yurong, Huang Wenxi, Qian Guangren and Qi Yangyong

53. Effect of Sulphate on the Reaction of C_3S Formation 335
H M Cheong, S H Choi, K S Han and J D Jaung

54. Effect of Fluorite-Gypsum Composite Mineralizer on the Microstructure and Properties of Portland Cement Clinker Phase 342
Ye Qing, Kong Jianmin and Liu Baoyuan

55. Evaluation of an Optimum Percentage Addition of Fluorspar in White Cement Raw Mix Containing 4% SO_3 351
H U Shah and Zafar Iqbal

56. Influence of $\bar{F}$ on Crystalline Structure of C_3S 358
Shanba Wang and Zhonghui Zhow

57. Effect of Fluorine-Bearing Limestone on Clinker Quality 365
G Goswami, B N Mohapatra and J D Panda

58. The Effect of ZnO on Burning of Portland Cement Clinker in Rapid Heating-Up Burning 372
Xu Guangliang, Huang Wenxi, Lu Zhongyuan and Qian Guangren

59. The Effect of Calcium Fluorosulpho-Silicate on Formation of Calcium Silicate 379
Huang Wenxi, Xu Guangliang and Lu Zhongyuan

60. The Effect of the Composite Mineralizers of CaF_2, $CaSO_4$ and ZnO on the Formation of the Portland Cement Clinker in a Rapid Heating-Up Burning 386
Lu Zhongyuan, Huang Wenxi and Xu Guangliang

61. Research and Application of Composite Mineralizer in Rotary Kiln 393
Li Peiquan, Liu Changfa, Su Muzhen, Lu Baoshan, Li Guangmin, Ge Wenmin and Chen Yongfan

62. Active Belite Cement 399
Ingo Mielke, Anette Müller and Jochen Stark

63. Lithium as Intensifier in the Formation of Dicalcium Silicate Phase 406
V K Mathur, R S Gupta and S C Ahluwalia

64. Effect of SO_3 and MgO on Phase Relations and Crystal Chemical State of Phases in Belite-Aluminoferrite Clinkers 413
A I Boikova, O I Fomicheva and L V Grishchenko

65. Role of Manganese on the Kinetics of Formation and Hydration of C_3S Phase 420
Ram Prakash, S C Ahluwalia, N K Katyal and V K Mathur

66. Burning Cement Clinker from the Raw Meal Using Barite and Fluorspar as a Combined Additive 427
Xu Xianyu, Yang Liqun and Chen Jian

67. Application Feasibility of a Calcination Catalyst in Cement Manufacture — A Case Study 434
S A Khadilkar, P G Lele, C H Page and A K Chatterjee

68. Activators for Accelerated Calcination 440
S Laxmi, A K Ailawadi and M M Ali

Specific Theme I-A

Clinker Formation Including New Processes

RELATIONSHIP BETWEEN ZONAL STRUCTURE IN ALITE, LAMELLAR TEXTURE IN BELITE AND THEIR PRODUCTION PROCESS, COMPOSITION AND CRYSTAL STRUCTURE

Hiroshi Uchikawa*, Shunsuke Hanehara and Tokuhiko Shirasaka****

**Executive Director, Research and Development, Onoda Cement Co Ltd, JAPAN*
***Central Research Laboratory, Onoda Cement Co Ltd, JAPAN*

SUMMARY

The relationship between the zonal structure and composition and crystal structure of alite, and the relationship between lamellar structure and composition and transformation of belite were investigated by using a synthesized clinker from the plant raw mix at various temperatures and the cement clinker product with CMA/EPMA, microfocus X-ray diffractometer, in-lens FESEM, ion-thinning method and AEM. The composition, birefringence and hydration reactivity of alite differ with the zoned region in the zonal structure. The peripheral part of alite crystal with high-birefringence is M_3, while the inner part with low-birefringence is M_1. The content of minor components in the high-temperature stable transformation(M_3) is less than that in the low-temperature stable transformation(M_1). From the electron diffraction pattern of restricted area, analysis of micro area and back scattered electron image, the lamellar texture of belite is confirmed to be produced at the time when the α -phase transforms into the α'_H -phase and further transforms into the ß -phase. The minor components are more contained in the α -phase than in the ß -phase.

Résumé

La relation entre structure zonale, composition et structure cristalline d'alite, et la relation entre les lamellas et la composition et la transformation de belite ont été examinées par les scories sythétiques d'un mélange cru prélevé en usine à diverses témpératures, et des scories de ciment, en utilisant des méthodes CMA/EPMA, diffractomètre de rayons X en microfoyer, dans-lentille FESEM, une méthode d'amincissement ionique et AEM. La composition, la biréfringence et la réactivité d'hydration diffèrent selon la région zonée dans la structure zonale. La zone périphérique du cristal d'alite de haute biréfringence est M_3, alors que la partie interne de faible biréfringence est M_1. La composition en composants secondaires dans la transformation stable de haute-température(M_3) est moindre que celle relative à la transformation stable de basse-température(M_1). D'après électronogramme d'aire restreinte, analyse de microaire et imagerie électronique rétrodiffusé, il est constaté que la texture lamellaire de belite est produit lorsque la phase se transforme en phase α'_H puis en phase ß. Les composants secondaires sont plus abondants dans la phase α que dans la phase ß.

1. INTRODUCTION

The zonal structure of alite with different color tone by etching and birefringence happened to be produced under a particular burning conditions. The optical microscope image of belite in cement clinker includes the type I composed of groups of lines crossing each other at 60° in a circular crystal, the type II composed of a group of parallel lines and the type III composed of irregularly shaped crystals.

In this study, the zonal structure of alite using a raw material mix taken from the plant and cement clinker product as the sample was examined by transmission and reflection optical microscope, CMA/EPMA and a microfocus x-ray diffractometer to determine the zonal structure of alite crystal and the relationship between the zonal structure, composition and crystal structure. The lamellar structure of belite in cement clinker was also investigated by in-lens FESEM and AEM with ion-thinning method to determine the relationship between the lamellar structure, composition and crystal transformation.

2. EXPERIMENT

2.1 Sample

Cement clinker product in which alite has the zonal structure and belite has the type I lamellar structure was used. Its chemical composition and optical properties of clinker minerals are shown in **Table 1**. The same raw material mix was burnt to clinker at 1450-1600°C using electric furnace and examined.

2.2 Analysis of the zonal structure of alite

In the polished thin section of cement clinker product containing alite crystal with zonal structure was observed by transmission and reflection optical microscope and the elements distribution including Al_2O_3, Fe_2O_3, MgO, SO_3, Na_2O, K_2O in the same area was measured by CMA/EPMA(1). Composition of the inner and peripheral part in zonal structure was determined by EPMA using Bence and Albee method. Crystal system of alite was identified by microfocus x-ray diffractometer (20μmϕ) equipped with high power x-ray generator (18kVA). As for the clinker burnt at different temperature using electric furnace, the contents of minor elements incorporated in alite were determined by EPMA.

2.3 Analysis of lamellar structure of belite

In the polished sample of cement clinker product, the lamellar structure of belite was observed from back scattered electron image obtained by in-lens FESEM. The composition and electron diffraction pattern of each lamella in belite was determined by AEM using a thin section approximately 10nm thick by the ion-thinning method.

3. RESULTS AND DISCUSSIONS

3.1 Composition and structure of alite with zonal structure

The alite has the zonal structure with different color tone by etching and birefringence varying with crystallization conditions and production process. It is known that the birefringence in the peripheral part of crystal is higher, while that in the inner part is lower. Chromy inferred from the result of the observation with a high-temperature microscope that the inner part of crystal is the biaxial triclinic phase with the birefringence of 0.0025, while the peripheral part of it is the uniaxial rhombohedral phase or the monoclinic phase akin to that

Table 1 Characters of clinker

Chemical composition (%)									free	Optical properties			
SiO_2	Al_2O_3	Fe_2O_3	CaO	MgO	SO_3	Na_2O	K_2O	total	lime	AS*1	AB *2	BS *3	BC*4
22.0	5.0	3.2	65.5	1.6	0.6	0.17	0.46	98.5	0.5%	30-40(60)	0.006	20-30(40)	fY(C)

*1: size of alite (μm), *2: birefringence of alite, *3: size of belite (μm),
*4: color of belite

phase with the birefringence of 0.005(2). He confirmed also that the low-birefringence phase transforms into the high-birefringence phase at 940°C. According to study by Maki et al, the peripheral and inner parts of the zonal structure are composed of M_3 and M_1 phases, respectively(3). However, no demonstrative study on the conditions and mechanism of the production of zonal structure of alite has been made and no data directly indicating the structure and composition of each part of the zonal structure has been published so far. The authors have examined the zonal structure of alite by up-to-date instruments mentioned above with combination of conventional instruments.

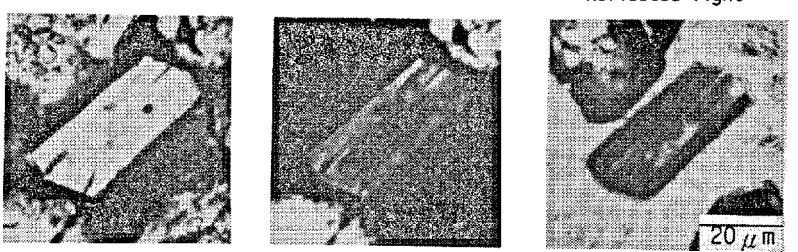

Fig. 1 Transmitted and reflected light micrograph of clinker alite with zonal structure

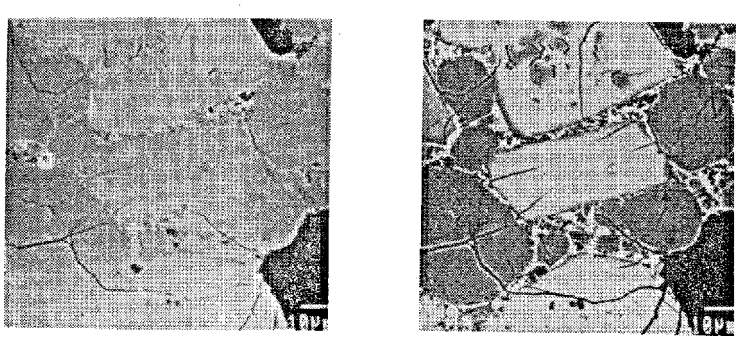

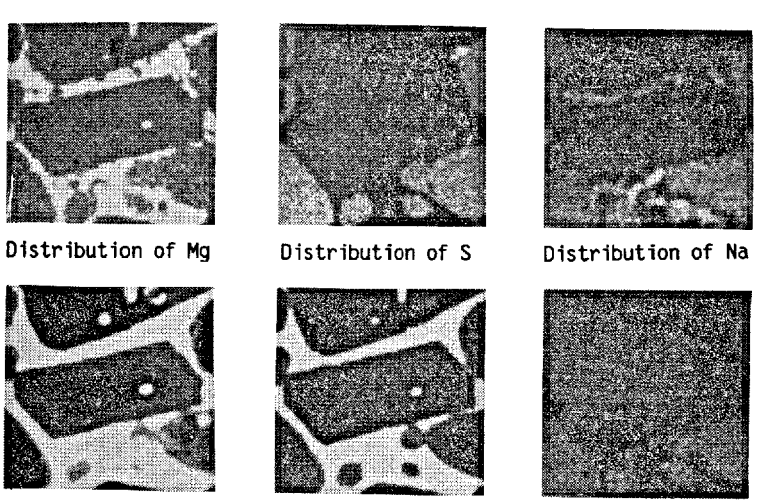

Explanation of tone representing the oxide contnent (%)

Tone	MgO	SO_3	Al_2O_3
W.	>5.0	>4.0	>5.0
Lgr.	≒0.2	≒1.0	≒0.7
Gra.	≒1.2	≒0.2	—
Bk.	<0.1	<0.1	≒0.9
Tone	**Fe_2O_3**	**Na_2O**	**K_2O**
W.	>5.0	>2.0	>2.0
Lgr.	≒0.8	≒0.4	≒0.2
Gra.	—	—	—
Bk.	≒0.6	≒0.2	<0.1

W. : White
Lgr.: Light gray
Gra.: Gray
Bk. : Black

Measuring condition of CMA/EPMA:
Accelerating voltage = 15kV,
Probe current = 7 x10 $^{-8}$ A

Fig. 2

Secondary and back scattered electron image and x-ray image map of Mg, S, Al, Fe, Na and K of clinker alite with zonal structure

Optical micrographs of a polished thin section of cement clinker product are shown in **Fig. 1.** Micrograph a) and b) were taken through an open-polar and a cross-polar with a transmission optical microscope, respectively, and micrograph c) was obtained by observing thin section etched with a 0.01% NH_4Cl aqueous solution for 30 seconds with a reflection optical microscope. Micrograph b) reveals that the birefringence in the peripheral part and inner parts of clinker alite are as high as 0.006 and as low as 0.004, respectively. The inner part is more easily etched and the boundary line between the different birefringence in the transmission-microscopic image coincides with the boundary between the different color tones in the reflection-microscopic image.

Fig. 2 shows the secondary electron image and back scattered electron image of the zonal structure of clinker alite and the distribution of MgO, SO_3, Fe_2O_3, Al_2O_3, Na_2O, K_2O in it obtained by CMA/EPMA. Although MgO is uniformly distributed in the alite crystal, Al_2O_3, Fe_2O_3, SO_3, Na_2O and K_2O are densely distributed in the inner part of it, coinciding with the division of zonal structure by the boundary lines. The average contents of the components in the inner and peripheral parts of the zonal structure were determined ten times each point analysis and calculated by the Bence and Albee method as shown in **Table 2.**

The result of each phase in zonal alite determined by microfocus x-ray diffractometry is shown in **Fig. 3.** The figure reveals that the peripheral part showing high birefringence is a monoclinic phase of M_3 akin to trigonal, while the inner part showing low birefringence is a monoclinic phase of M_1. Compared with **Fig. 2,** amount of minor and trace components are contained less in the high-temperature stable transformation of the alite in the cement clinker product than in the low-temperature stable transformation, unlike results by Woermann et al(4) using a sample prepared from pure chemicals. From the result of the measurement of heat evolution curve at initial hydration, higher hydration reactivity of low-temperature transformation of M_1 than high-temperature stable transformation of M_3 is confirmed(5). This supports that high-temperature stable transformation of the alite with less amounts of minor and trace components has higher hydration reactivity in the cement clinker product.

Table 2 Chemical composition determined by EPMA and birefringence of each part of zonal structure or clinker alite

Analyzing point	Chemical composition (%) SiO_2	Al_2O_3	Fe_2O_3	CaO	MgO	SO_3	Na_2O	K_2O	total	Biref -ringence
Inner part	25.12	0.93	0.82	72.45	1.20	0.10	0.25	0.18	101.05	0.004
Peripheral part	24.09	0.71	0.58	73.76	1.11	0.07	0.21	0.10	100.63	0.006

Measuring condition of EPMA:
Accelerating voltage = 15kV, Probe current = 3 $\times 10^{-8}$ A

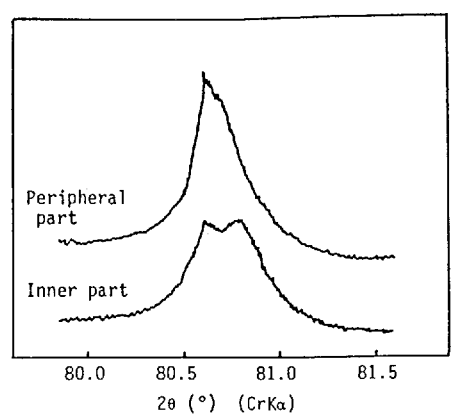

Fig. 3

X-ray diffraction profile of inner and peripheral part of clinker alite with zonal structure (X-ray power: 18kVA)

Table 3 Composition determined by EPMA and birefringence of alite burnt under various temperature

B.T. °C*1	Chemical composition (%) SiO_2	Al_2O_3	Fe_2O_3	CaO	MgO	SO_3	Na_2O	K_2O	total	Birefringence
1600	24.09	0.74	0.57	73.76	1.05	0.12	0.21	0.05	100.59	0.007
1550	25.06	0.76	0.60	73.29	1.18	0.08	0.22	0.06	101.25	0.006
1500	25.10	0.79	0.68	73.10	1.21	0.09	0.24	0.07	101.28	0.005
1450	25.40	0.83	0.79	72.78	1.25	0.13	0.25	0.08	101.51	0.004-5
Cl*2	21.97	5.03	3.21	65.46	1.6.	0.58	0.17	0.46	98.52	

*1: B.T.: Burning temperature, *2: Clinker
Measuring condition of EPMA:
Accelerating voltage = 15kV, Probe current = 3 x10^{-8} A

The average composition and average birefringence of alite in the clinker prepared by burning a raw material mix taken from the plant at various temperatures in an electric furnace are shown in **Table 3**. The composition of the clinker was determined by averaging out the measurements at twenty analyzing points in different field of view using CMA/EPMA. The composition obtained by chemical analysis of bulk clinker is listed in **Table 3** for reference. The table shows that the contents of Al_2O_3, Fe_2O_3, MgO, Na_2O and K_2O decrease with the increase of burning temperature, though the content of SO_3 is low independent of burning temperature. This is opposite to the results of a preceding researcher(6) that the contents of solid solutions in C_3S of the sample prepared from pure chemicals increase with the increase of burning temperature. Assuming that crystals with birefringence of 0.004 or more are monoclinic, the contents of solid solutions including MgO, Al_2O_3, Fe_2O_3, Na_2O and K_2O in the monoclinic alite will decrease with the increase of burning temperature. These results mentioned above explain that a inner part in alite with low temperature stable transformation rich in minor and trace element is produced initially at lower temperature and secondary peripheral part grows around inner part at higher temperature.

3.2 Structure and composition of belite with lamellar texture

The transmission optical microscopic image of belite in cement clinker includes the type I composed of groups of lines crossing each other at 60° in a circular crystal, the type II composed of a group of parallel lines and the type III composed of irregularly shaped crystals(7). There are constant thickness lamellas in type I and type II belite and the dark parts in the cross section observed in SEM appeared as lines in optical microscope as described later. Belite has five transformations - α(trigonal) form, α'_H and α'_L (orthorhombic) form, ß (monoclinic) form and γ (orthorhombic) form in order of temperature level. The lamella in type I belite is produced in such a way that the α -form is transformed into the α'_H -form by cooling the clinker from the α -form stable temperature and [101] of the α'_H -form (Pcmn) structurally equivalent to [102] of the α -form ($P3_1c$) develops in six directions in belite crystal. By cooling the clinker up to normal temperature, type I belite transforms into a mixture of the α -and ß -forms at a mixing ratio depending upon the cooling rate. The lamella in type II belite observed through an open-polar is composed of the stacking structure of [100] of the ß-form ($P2_1/n$) topotaxicially developed from [010] of the α'_L -form ($Pna2_1$) when the α'_L -form transforms into the ß-form. In the microscopic image of type II belite almost composed of the ß-form obtained through a cross-polar, the continuous twin structure parallel to the lamella is observed in the z-direction(8). Belite often turns yellow because Fe_2O_3 is deposited at the time when the α -form transforms into the α' -form with limited solubility of Fe_2O_3.

No data on the relationship between the microscopic structure and the composition are, however, available. Although some papers present the transformation of belite crystal inferred from the microscopic observation(7), no paper identifying the polymorphs of belite lamellas directly using crystallographic experimental data has been reported. The authors have observed the lamellar structure from an clearer back scattered electron image obtained by in-lens FESEM than by conventional SEM, determined the composition of each lamella in clinker belite by AEM using a sample approximately 10nm thick by ion-thinning method and directly identified the lamellar structure by electron diffraction. **Fig. 4** illustrates a back scattered electron image of lamellar structure in clinker belite by in-lens FESEM. Since the angle of aperture can be increased by setting the sample in the objective lens of in-lens FESEM, the magnification and resolving power can be argued as high as of 0.7nm compared with the ordinary FESEM. The image of belite obtained by the in-lens FESEM gives two sets of

lamellas crossing each other at 60°. The image enlarged by higher magnification gives the lamella composed of different structures. The bright part is a lamella 0.5 to 1.0μm thick composed of oriented secondary lamellas 0.1μm or less thick, while the dark part is a lamella 0.1 to 0.4μm thick.

The transmission image and electron diffraction pattern of each phase in belite determined by AEM is shown in **Fig. 5**. The bright part in SEM corresponding to dark part in AEM and dark part in SEM corresponding to bright part in AEM show the diffraction patterns of ß - and α -forms, respectively.

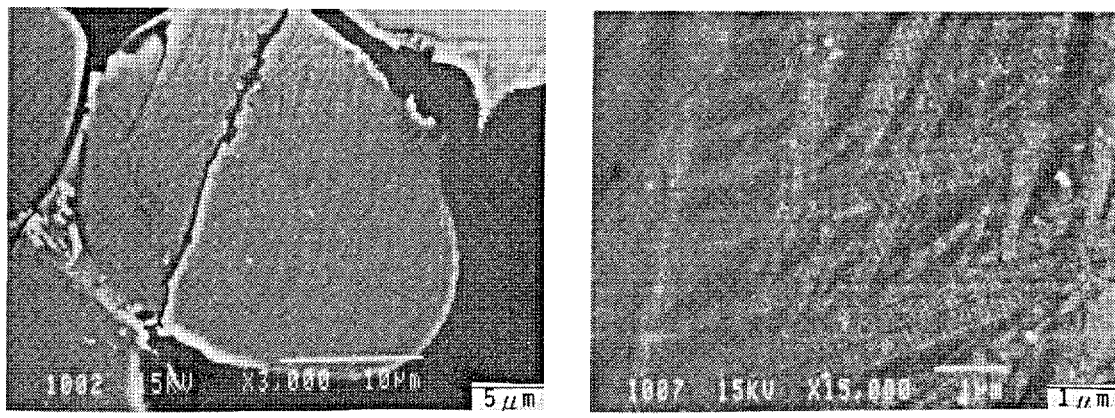

Fig. 4 Back scattered electron image of clinker belite observed by in-lens FESEM

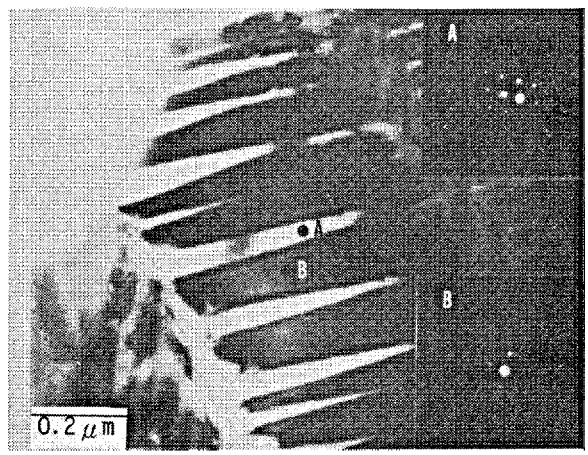

Fig. 5

Transmission electron image and electron diffraction pattern of lamellar structure in clinker belite

Table 4 Local point composition determined by AEM in lamellar structure

part	Amount of minor element (%) MgO	SO_3	Al_2O_3	Fe_2O_3	Na_2O	K_2O	transformation
A	0.40	0.71	1.84	1.75	0.18	1.13	α
B	0.37	0.29	1.63	0.79	0.15	1.05	β

Measuring condition of AEM:
Accelerating voltage = 200kV, Probe current = 3×10^{-11}A

It is considered that the bright part in SEM is produced by the transformation of the α -from into the α'_L-form successively into the ß-form. This agrees with the above-mentioned observational result that the bright part is composed of fine secondary lamellas. The result of electron diffraction is supported by this fact. Minor and trace components are contained more in the dark parts in SEM than in the bright part as shown in **Table 4.**

4. CONCLUSIONS

1) Zoned region observed by transmission light microscope coincides with that observed by reflected light. Minor elements distribution obtained by CMA/EPMA in the same area also coincides with the division of zonal structure by the boundary lines. Inner part of alite with low birefringence is identified by microfocus x-ray diffraction as M_1, while peripheral part with high birefringence is M_3. The content of minor components in M_3 is less than that in M_1 unlike the result of the study by preceding researchers.

2) The image of belite by in-lens FESEM shows two sets of lamellas crossing each other at 60°. The bright part is a lamella 0.5 to 1.0μm thick composed of oriented secondary lamellas 0.1μm or less thick, while the dark part is a lamella 0.1 to 0.4μm thick. The bright part contains less minor elements than dark part. The former phase shows monoclinic electron diffraction pattern of ß-form and the latter shows the trigonal pattern of α-form.

REFERENCES

1. Uchikawa, H., Uchida, S. and Hanehara, S.: "Element Distribution on the Polished Surface of Hardened Cement Paste Estimated by EPMA with High Speed Wide Area Multianalyser", Il Cement, 1987, 84, 117-129

2. Chromy, S.: "High-Temperature Microscopic Investigation of Tricalcium Silicate and Dicalcium Silicate Phase in Portland Cement Clinker", Journal of American Ceramic Society, 1967, 50(12), 677-681

3. Maki, I. and Goto, K.: "Factors Influencing the Phase Constitution of Alite in Portland Cement Clinker", Cement and Concrete Research, 1982, 12(3), 301-308

4. Woermann, E., Eysel, W. and Hahn, Th.: "Chemical and Structural Investigations of Solid Solutions of Tricalcium Silicate, Part 5", Zement-Kalk-Gips, 1969, 22, 414-422

5. Uchikawa, H., Hanehara, S. and Sawaki D.: "Observation of the Change of Composition and Surface Structure of Alite Crystal and Estimation of Hydration Reactivity by Etching", submitted to Supplementary Paper for **9th International Congress on the Chemistry of Cement, New Delhi, India** 1989.

6. Insley, H. and McMurdie, H.F.: "Minor Constituents in Portland Cement Clinker", Journal of Research of the National Bureau of Standard, 1938, 20(2), 173-184

7. Ono, Y., Kawamura, S. and Soda, Y.: "Microscopic Observations of Alite and Belite and Hydraulic Strength of Cement", **Proceeding of 5th International Symposium on the Chemistry of Cement, Tokyo, Japan** 1968, **VI**, 275-284

PHASE COMPOSITION FORMATION OF PORTLAND CEMENT CLINKER AND ALITE FORMATION KINETICS

B S Albats, Yu R Krivoborodov and V P Ryazin

NIICement, Moscow, RUSSIA

SUMMARY

In the formation of portland cement clinker phases, a great role belongs, apart from the previously known factors, to the ionic sxchange between the melt and the superficial layer of alite crystals according to the relationship : $Ca^{2+} \rightleftharpoons Al^{3+}(Fe^{3+})$. Its directions causes the cyclicity or continuity of alite formation. The ionic exchange nature depends on the synthesis conditions and the raw mix composition.

При формировании фаз портландцементного клинкера наряду с известными факторами большая роль принадлежит ионному обмену между расплавом и поверхностным слоем кристаллов алита по схеме $Ca^{2+} \rightleftharpoons Al^{3+}(Fe^{3+})$, направленность которого обусловливает цикличность или непрерывность алитообразования. Характер ионного обмена зависит от условий синтеза и состава сырьевой смеси.

INTRODUCTION

By means of microprobe X-ray phase analysis (XRA), infra-red spectroscopy (IRS) and petrographic methods, investigations were made on the changes in the amount, composition and structure of clinker phases during sintering of commercial raw mixes (Table 1) at a heating rate of 5 and 20°C/min.

Table 1 Source raw mixes

No of mixes	LOI	SiO_2	Al_2O_3	Fe_2O_3	CaO	MgO	SO_3	Na_2O	K_2O	TiO_2
1	33.23	12.9	3.69	2.61	42.69	2.38	1.44	0.22	0.63	0.13
2	34.12	13.18	4.16	2.66	43.66	1.09	0.24	0.25	0.43	0.17
3	33.8	13.7	3.83	3.80	42.85	0.6	0.17	0.56	0.69	0.17

Clinker phase composition formation is strongly influenced by a number of external factors depending on synthesis conditions, and internal factors such as the composition of source raw mixes.

RESULTS AND DISCUSSIONS

Irrespective of synthesis conditions, alite is predominantly formed in melt areas with a relatively acidic composition having a propensity for dissolving the belite. The SiO_2 content of the internal layers of alite crystals is 0.5 to 1.5 % by mass higher than that of the surface layers (Table 2). Alite formation in sintering at a heating rate of 5°C/min occurs cyclically. As the alite content goes down by 4 to 10 % by mass, the belite amount also decreases by 2 to 5 % by mass. Concurrently, the combined content of aluminate and alumoferrite is reduced by 0.5 to 3 % by mass. The total amount of crystalline phases detected by XRA is lowered and stands at 80 to 85 % by mass.

The SiO_2 concentration of the alumoferrite phase goes up by 0.6 to 0.8 % by mass. Between 1,350 to 1,400 °C, Ca^{2+} ions from the melt replace Al^{3+} ions and, to a lesser extent, Fe^{3+} and Mg^{2+} ions prevailing in the surface layers of alite. This occurs as a result of the capture of impurities by the rapidly growing (2.5 to 3 µm/min within the interval of 1.350 to 1.375 °C) alite crystals. Simultaneously, part of

Table 2 Chemical composition (% by mass) of silicate phases in the process of their formation (alite crystal size 10x30 mm; A - crystal average, S - in the surface layer up to 4 mm thick, I - in the internal layer).

Heating temp., °C and rate, °C/min	Phase (content, % by mass)	Crystal portion	CaO	SiO_2	Al_2O_3	Fe_2O_3	MgO	K_2O	TiO_2	Cr_2O_3	SO_3	C/S (molar ratio)
1,350	Alite	A	67.06	23.88	3.16	2.21	1.45	0.18	0.23	0.49	0.36	3.01
____	(45)	S	66.34	22.95	4.46	3.04	1.45	0.19	0.25	0.48	0.38	3.10
5		I	67.77	24.81	1.87	1.39	1.46	0.18	0.22	0.51	0.35	2.93
	Belite(36)	A	61.26	30.06	2.91	1.77	0.87	0.22	0.41	0.62	1.60	2.18
1,375	Alite	A	71.10	24.14	1.27	1.09	1.18	0.17	0.27	0.26	0.26	3.16
____	(49)	S	70.80	23.70	1.27	1.20	1.18	0.17	0.27	0.26	0.26	3.20
5		I	71.30	24.40	1.27	1.00	1.18	0.17	0.27	0.26	0.26	3.10
	Belite(28)	A	63.00	29.50	2.86	1.78	0.66	0.17	0.27	0.37	1.06	2.26
1,400	Alite	A	71.20	23.65	1.90	1.55	1.54	0.21	0.27	0.25	0.31	3.23
____	(51)	S	71.06	23.19	2.18	1.69	1.27	0.23	0.28	0.25	0.32	3.29
5		I	71.34	24.10	1.62	1.41	1.80	0.18	0.26	0.24	0.28	3.18
	Belite(26)	A	62.46	32.94	2.39	1.55	0.65	-	0.33	-	0.71	2.02
1,425	Alite	A	69.07	24.31	2.01	1.64	1.48	0.58	0.28	0.50	0.63	3.05
____	(44)	S	68.80	23.55	2.51	2.09	1.38	0.55	0.27	0.48	0.63	3.14
5		I	69.29	24.92	1.63	1.22	1.57	0.61	0.33	0.51	0.64	2.98
	Belite(24)	A	62.19	30.26	2.30	1.89	0.53	0.93	0.44	0.44	1.03	2.21
1,350	Alite	A	66.94	25.38	2.42	1.61	1.5	-	0.25	0.36	-	2.81
____	(45)	S	66.61	24.92	2.97	1.87	1.58	-	0.25	0.32	-	2.86
20		I	67.17	26.78	2.03	1.45	1.44	-	0.25	0.38	-	2.77
	Belite(30)	A	61.77	30.34	2.30	2.00	1.65	-	0.36	0.57	0.25	2.18
1,375	Alite	A	69.00	24.31	1.92	1.54	1.35	0.22	0.25	0.88	0.39	3.04
____	(46)	S	69.14	23.90	1.99	1.51	1.4	0.17	0.21	0.88	0.37	3.09
20		I	68.70	25.14	1.81	1.62	1.27	0.34	0.29	0.88	0.43	2.93
	Belite(27)	A	63.93	29.86	2.18	1.85	0.61	-	0.29	0.51	-	2.29
1,400	Alite	A	70.01	24.22	2.20	1.62	1.63	-	0.24	0.67	-	3.11
____	(50)	S	69.62	23.86	2.54	1.92	1.63	-	0.26	0.65	-	3.14
20		I	70.56	24.72	1.72	1.21	1.63	-	0.21	0.71	-	3.06
	Belite(24)	A	62.94	30.08	2.33	1.79	1.38	-	0.30	0.41	1.18	2.25
1,425	Alite	A	70.69	23.84	2.15	1.63	1.32	-	0.27	0.30	0.28	3.20
____	(50)	S	70.47	23.45	2.49	1.72	1.36	-	0.27	0.28	0.30	3.25
20		I	71.20	24.78	1.32	1.20	1.23	-	0.27	0.34	0.25	3.08
	Belite(23)	A	62.42	29.87	3.26	2.25	0.60	0.22	0.38	0.37	1.10	2.24

belite crystals that have failed to dissolve are also blocked. The alumoferrite phase composition is shifted to become more aluminate-rich. The C/S ratio in the surface layers of alite crystals thus increases from 3.1 to 3.29, which makes its crystal lattice more susceptible to impurities. Beginning with 1,400 ^{o}C, the heating rate beeng 5°C/min, the ionic replacement nature changes from $3Ca^{2+}_{melt} \longrightarrow 2Al^{3+}(Fe^{3+})_{cryst.}$ to the reverse, and C/S decreases (see Table 2). As the concentration of Al_2O_3 predominantly involved in the ionic exchange reaches 2.5% by mass in the alite surface layer, the mineral disintegrates, which is clearly evidenced under the electron microscope. Belite blocked by alite crystals dissolves, saturating the melt by new Ca^{2+} ions. When the Ca^{2+} ion whose radius equals 1.04 A is replaced by small-sized Al^{3+} (0.57 Å) and Fe^{3+} (0.8 Å) ions, there occurs a compression of the alite lattice. Deformations caused by this are intensified even more by the chande in the coordination of aluminium and iron atoms from octahedral $(MeO_6)^{9-}$ to tetrahedral $(MeO_4)^{5-}$,which in the long run brinds about alite destruction.

The distribution of impurities in the volume of alite crystals is not uniform. Fine crystals (10 x 30 μm) are distinguished from coarser ones (60 x 100 μm) at any burning temperature through a higher C/S ratio and a greater content of impurities (3.01 to 3.23 and 4.5 to 8% by mass versus 2.84 to 3.06 and 5.4 to 6.45% by mass respectively). Irrespective of the chemical composition of source mixes, their dispersity, burning temperature and crystal sizes, their surface layer has a higher C/S ratio, and a greater content of impurity oxides, mainly through Al_2O_3 and Fe_2O_3. The combined content of impurities at different sintering temperatures attained 4.61 to 10.25% in surface layers and 4.19 to 6.51% in internal layers.

Belite crystals are more uniform in composition than alite crystals. In all micrivolumes of the crystals examined, C/S is higher than the stoichiometric (2.0) and amounts to 2.02 to 2.26 at different burning temperatures. The impurity content of belite at different burning temperatures varies within the limits of 5.63 to 8.4%, and is on the average higher than that of alite.

Microvolumes corresponding to the composition of calcium aluminate can be characterized as $C_{4.41}S_{0.63}A_{0.35}M_{0.18}F_{0.08}S_{0.03}K$ which is similar to the composition of calcium aluminate in commercial

clinkers (1). Only a SiO_2 excess of 2% by mass (approximately) and an enhanced K_2O content are observable.

Alite from rapid burning has somewhat lower absolute values of C/S, both in the surface and internal layers. In these alites, the C/S continually rises with temperature. The trend of oxide concentration variation layer-wise is preserved, irrespective of the heating rate.

The combined content of impurities fluctuates, depending on the temperature within the limits of 6.42 to 7% in the surface layer and 4.61 to 6.64% in the internal layer. The composition of rapidly burnt alite is considerably more uniform than that of slow burning. The diffusion direction of Ca^{2+} ions from the melt into alite remains unchanged. There is no ionic exchang of the type $Me^{3+}_{melt} \longrightarrow Ca^{2+}_{cryst.}$, where Me^{3+} is an element with a smaller ionic radius than that of Ca^{2+}, i.e. the alite lattice does not experience a compressive stress.

As in the case of slow heating, belite is noted for a higher content of impurities compared to alite (Table 2). The aluminium and iron oxides content is close to or slightly exceeds the same parameters in alite; the MgO content is as a rule lower. The C/S ratio at any temperature is higher than the stoichiometric 2.18 to 2.29 (Table 2). Compared to slow heating, belite of rapid heating has a higher C/S ratio and a greater conter content of impurities.

The minimum impurity content of silicate phases corresponds to their compositions close to the stoichiometric. While C/S changes from 3 to 3.3, the impurity volume in alite grows within the limits of 4 to 7 and 4.5 to 12% by mass, depending on the burning temperature and the heating rate.

Whatever the clinker synthesis conditions may be, the impurity content of silicate phases goes up with the growth of MgO in them. Magnesium ions replace calcium ions and are incorporated in voids. The Mg-O bond has a lower energy than Ca-O has: 119.45 Kcal and 128.55 Kcal respectively (2). The ionic radius of magnesium (0.74 Å) is smaller than that of calcium (1.04 Å). Hence, the incorporation of magnesium into the alite lattice makes it more susceptible for the incorporation of impurities capable of stabilizing crystal energetics.

For alite containing MgO within the limits of 0.06 to 1%, and alite comprising MgO within the range of 0.8 to 2%, bends in curves are typical at 0.5 to 0.6 and 1.4 to 1.5% MgO respectively. In excess of the said values, the combined amount of impurities in alite grows drastically. This is apparently brought about by a structural rearrangement of alite, namely T_I-T_{II} and T-M_I transitions (3).

A greater Mg^{2+} content of the AF phase at initial temperatures, whereby Mg^{2+} substitutes as a rule for Al^{3+} and Fe^{3+} or enters the lattice voids, contributes to a certain "loosening" of the lattice, particularly when there is a higher SiO_2 content of the AF phase. The following exchange arrangement implementation is probable: $2(Al,Fe)^{3+} \rightleftharpoons Si^{4+} + Mg^{2+}$, involving enhanced parameters of the unit cell and lattice constant of C_6A_2F (4).

An analysis of alite formation kinetics as exemplified by a large number of commercial raw mixes during liquid-phase sintering within the range of 1,320 to 1,440°C has revealed the presence of anomalous areas caused by a retardation of the dissolution stage of belite and calcium oxide and by the assimilation of the latter. Instead of the classical exponential or sigmoid curves describing the variation of the reaction rate constant versus temperature (5), This dependence was characterized by a saw-shaped curve for most of the mixes. For those mixes in which the coarse fractions are enriched in silica, the process rate constants, especially in the initial stage of liquid-phase sintering (1,320 to 1,350°C), practically do not change, which indicates a prolonged induction period brought about, in particular, by low-active belite inheriting the nature of the silica component.

Areas with a reaction rate constant going down when the temperature rises within the limits of 15 to 30°C indicate that it is not appropriate to evaluate the alite formation process during these periods on the basis of CaO_{free} assimilation. In this case, alite formation is constrained by the diffusion of small-sized ions (with an ionic radius smaller than that of Ca^{2+}) from the melt into the surface layer of alite crystals, the latter (primarily aluminium) replacing calcium ions in octahedral positions. The activation energy is several times higher than values usually characterizing the various stages of alite formation or the process as a whole (6).

CONCLUSION

Anomalous areas can be eliminated through a rational combination of melt activity (amount, composition, properties) and the proper condition of the solid phases dissolving (belite and calcium oxide). An increased amount of the melt, its low viscosity and a relatively high surface tension, which ensure a good penetrating power of the melt and a wetting of the solid surfaces, coupled with the newly-formed crystals of belite and CaO, all promote a speedy dissolution of these phases and an accelerated nucleation of alite. The subsequent slow growth of alite crystals under conditions of a virtually permanent oversaturation of the melt with calcium ions ensures a quicker alite formation and an enhanced alite output in the finished clinker.

REFERENCES

1. Boikova A.I.:"Chemical composition of raw materials as the main factor responsible for the compaction, structure and properties of clinker phases". **8th International Congress on the Chemistry of Cement. Rio de Janeiro**, 1986, vol.1, p.19-33.

2. Woermann,E., Eisel,W and Hahn,T.:"Polymorphism and solid solutions of the ferrite phase." **Proceedings of the 5th International Symposium on the Chemistry of Cement. Tokyo**, 1968, pt.1, p.54.

3. Maki,I.:"Relationship of processing parameters to clinker properties; influence of minor components". **8th International Congress on the Chemistry of Cement. Rio de Janeiro**, 1986, vol.1, p.34-47.

4. Butt,Yu.M. and Timashev,V.V.: **Portland cement.** Moscow, "Stroyizdat" Publishers, 1974, 325 p. (in Russian).

5. Budnikov,P.P. and Ginstling,A.M.: **Reaction in blends of solid substances.** Moscow,"Stroyizdat" Publishers, 1971, 486 p. (in Russian).

6. Timashev,V.V.:"The kinetics of clinker formation. The structure and composition of clinker and its phases". **7th International Congress on Chemistry of Cement. Paris**, 1980, vol.1, p.1-3/1-20.

CRYSTAL STRUCTURE ANALYSIS OF MAJOR CONSTITUENT PHASES IN ORDINARY PORTLAND CEMENT

Masaki Daimon*, Yoshinobu Hirano, Takaaki Tsurumi* and Kiyoshi Asaga*****

**Department of Inorganic Materials, Faculty of Engineering*
Tokyo Institute of Technology
***R&D Center Cement Division, Ube Industries, Ltd*
****Faculty of Engineering, The Nishi Tokyo University*
JAPAN

ABSTRACT

The alite, belite and ferrite phases were separated from the ordinary portland cement (OPC) or its clinker and the characterization of these phases was carried out.

The alite separated from the OPC consisted of only M3 phase in XRD measurement. The belite in the OPC consisted of α and β -phase. The crystal structure of the β -phase was refined by Rietveld method. Though the structure was basically consistent with that obtained for single crystal of β -Ca_2SiO_4 [1], there was some differences in the lattice parameters and Si-O bonding distances between them. The texture of the belite was observed with optical microscope, SEM and TEM. The observations indicated that the belite belonged to the type I and had twin lamellae,about 20-25nm in size. As for the lattice parameters of the ferrite phase, it was found that all the parameters were smaller than those of pure C_4AF [2].

エーライト、ビーライト、フェライト相を普通ポルトランドセメント（クリンカー）から分離し、それぞれの相についてキャラクタリゼーションを実施した。

分離したエーライトの粉末X線測定を行ったところ、M_3相のみが確認された。ビーライトは、α，βの2相から成り、主要構成相であるβ相の結晶構造については、リートベルト法によって、精密化を行った。その結果、単結晶ビーライト[1]と比較し、格子定数、Si－O結合距離に若干の違いがあるものの基本的には同じであることが確認された。また、光学顕微鏡、SEM、TEMによって、TypeI型のビーライトが観察され、大きさ20～25nmの集片双晶ラメラも観察された。フェライト相は、斜方晶系で、格子定数が、純粋なC_4AF[2]のものより小さいことが確認された。

INTRODUCTION

The major constituent phases of the ordinary portland cement (OPC) are alite, belite, aluminate and ferrite phases. As the hydration property of the OPC is mainly determined by the characters of the four constituent phases, it is necessary to know the characters of the phases, such as chemical compositions, crystal structures and textures, in order to control the quality of the OPC. The chemical composition of each phase in the clinker has been analysed so far, and the results were summarized in ref. [3]. The crystal structure of each phase has been refined by using single crystal specimens synthesized from pure chemical regents [2)4)5)6)]. However, the crystal structure of each constituent phase in the clinker may be different from that determined for single crystals, because the chemical composition and the crystal growth condition are totally different between them.

In the present study, we separated the constituent phases from the OPC or clinker and analysed them from the crystallographic point of view. Especially for the belite, we refined the crystal structure by Rietveld method and observed the texture with optical microscope, SEM and TEM. The belite is important for the strength development at longer periods. Some researchers have been studied the belite in the clinker and indicated from XRD measurements that the polymorph of belite was β -form. Y.Ono [7] separated the belite from the clinker though it included a small amount of other phases, and detected 20-30% of α -form by XRD measurements. However, the study of the crystal structure and microscopic texture of the belite have not been done so far because of the difficulty in separation of pure belite from the OPC or clinker. We used a chemical method combined with separation process with heavy liquids, and succeeded to obtain pure belite and other constituent phases except for the aluminate phase. This report includes some new results obtained by the characterization mainly on the belite phase.

EXPERIMENTAL

Separation and characterization of constituent phases

The belite was separated from the OPC (chemical composition determined in the present study is shown in Table 1 by the following procedure. The OPC was first ground with a vibration mill. The ground powder (0.9g) was treated in the solution (30ml) containing KOH (8%) and sucrose (8%) at 85 ℃ for 5 min in order to dissolve the interstitial phase and gypsum in the OPC. The belite phase was separated from resulting mixture of silicate phase using heavy liquid whose specific gravity was 3.22. The texture of belite obtained was observed by means of optical microscope, SEM with EDX and TEM.

Table 1 Chemical Compositions of OPC, alite, belite and interstitial phases(%).

	OPC	Alite	Belite	Interstitial phase
ig. loss	1.0	1.6	0.8	1.1
insol.	0.0	–	–	–
SiO_2	21.8	24.2	31.3	4.5
Al_2O_3	4.9	1.6	1.2	25.1
Fe_2O_3	2.9	1.0	1.4	13.2
CaO	64.0	68.8	62.8	49.9
MgO	1.7	1.6	1.0	2.1
SO_3	2.2	0.0	0.1	0.1
Na_2O	0.2	0.1	0.2	1.0
K_2O	0.6	0.1	0.5	1.2
TiO_2	0.2	0.1	0.2	0.7
MnO	0.1	0.1	0.1	0.5
P_2O_5	0.3	0.3	0.4	0.1
f.CaO	0.6	–	–	–

The alite phase was

separated from the mixture of silicate phase by taking out the impurity phase (belite) whose densities are larger than 3.17 or less than 3.00. The interstitial phase was first tried to be separated from the OPC, but it was difficult to avoid the remaining of gypsum in the obtained powder. Therefore, the interstitial phase was separated form the clinker of OPC by dissolving silicate phases by a salicylic acid - methanol method. The clinker was first ground with a vibration mill. The ground powder (0.5g) was treated in the methanol solution (120ml) containing salicylic acid (18g) at 20 ℃ for 6 hrs. In order to obtained the pure ferrite phase, the powder of interstitial phase (0.5g) was subsequently treated in the mixed solution of nitric acid (7vol%) and methanol (93wt%) at 20 ℃ for 30 min. to dissolve the aluminate phase.

The resulting powders were analysed by XRD to confirm the performance of each separation process. And, chemical compositions of belite, alite and interstitial phase were determined.

Crystal structure refinement

The crystal structure refinements were carried out for the belite and alite using Rietveld method (program Rietan [8]). The XRD intensity data were corrected by step scanning from 10 to 90 ° in 2 θ (Cu K α). The interval of each step was 0.02 ° and the intensity was measured for 20 sec in each step. The trial structure for the refinement of the belite was that reported by S.Udagawa et al. [1] The crystal structure of alite were tried to refine.

RESULTS AND DISCUSSION

XRD pattern and chemical composition

Figure 1 shows the XRD patterns of the OPC, alite, belite, interstitial phase, and ferrite. It is verified from XRD patterns that the pure alite, belite and ferrite could be separated from the OPC or the clinker. The XRD pattern of alite indicates that the alite consists of only M3 phase. In the belite, the shoulder of XRD peak at 2 θ =33.0 ° and the peak at 2 θ =46.6 ° clearly indicated the formation of α -phase. The aluminate phase consists of only orthorhombic phase, and the ferrite phase consists of orthorhombic phase.

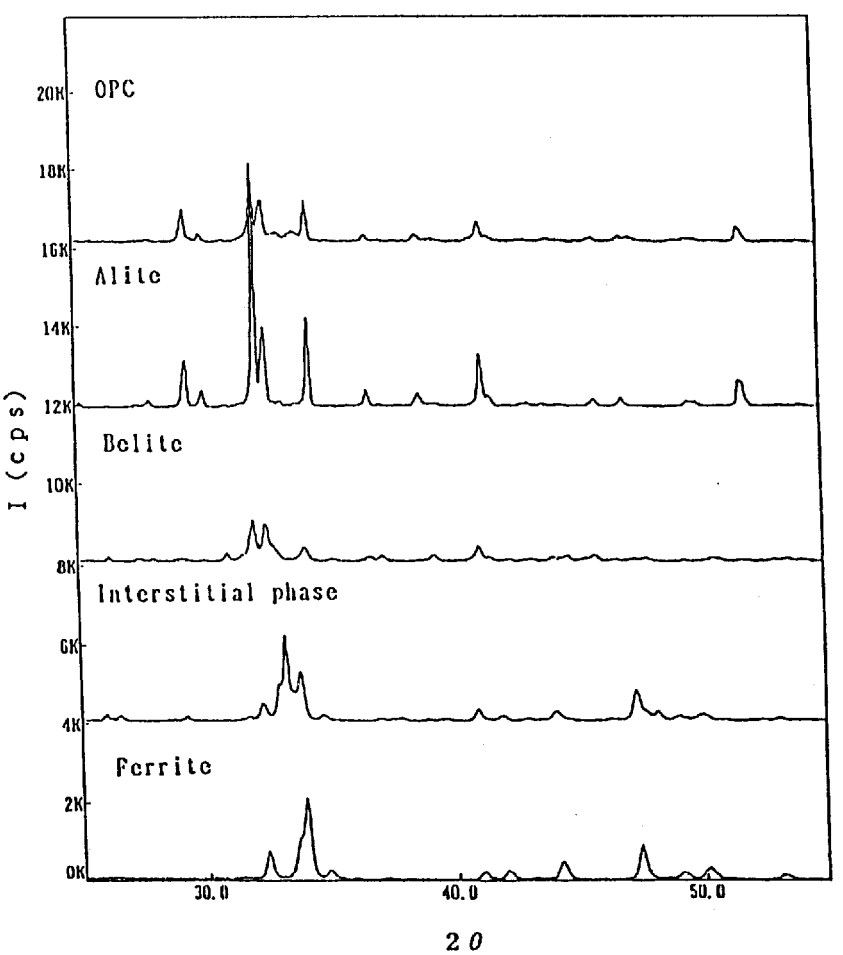

Fig. 1 XRD patterns of the OPC, alite, belite, interstitial phase, and ferrite.

Table 2 Lattice parameters of alite, belite and ferrite.

	a(A)	b(A)	c(A)	α	β	γ
Alite(M_3)	12.2422	7.0452	24.9677	90°	90.100°	90°
Belite(β)	5.5041	6.7622	9.3281	90°	94.172°	90 °
Ferrite	5.5405	14.5856	5.3474	90°	90°	90°

Chemical compositions of OPC, alite, belite and interstitial phase are listed in Table 1. Lattice parameters of alite, belite and ferrite are listed in Table 2. The total contents of impurity oxides obtained in the alite and belite were 4.9% and 5.1% respectively. The content in the alite is a little larger than that reported [3]. The MgO content (1.6%) in the alite seem to be enough to stabilize the M3 phase [9], which is consistent with the result of XRD measurement. As for the lattice parameters of the ferrite phase, all the parameters were smaller than those of pure C4AF [2].

Texture of Belite

Figure 2 shows a optical microscopic photograph of the belite separated from the OPC. A few kinds of belite crystals with different morphology were observed. The crystals were light yellow, yellowish brown or clear and from 20 to 30 μ m in mean dimension. As for the striated structure, some sets of parallel striation or those crossing with about 60 ° were observed. The belite crystals observed in the present study basically belong to Type I [10], and twin lamellae due to α' to β transition were not observed under the optical microscope. Some lamellae in the crystals with the crossing striations did not transmit light when the stage was rotated in cross polarized observation. This may indicate the formation of α -phase in lamella structure.

Figure 3 shows a SEM photograph of a belite crystal. The skeleton structure is clearly observed on the photograph. The width of each lamella is about 1.0 μ m. The chemical compositions analyzed by EDX at two different positions in Figure 4 (a and b) were shown in Table 3. It was found that the content of impurities such as Al, Fe, Mg at position (a) was larger than that analyzed at position (b). This may indicate that the

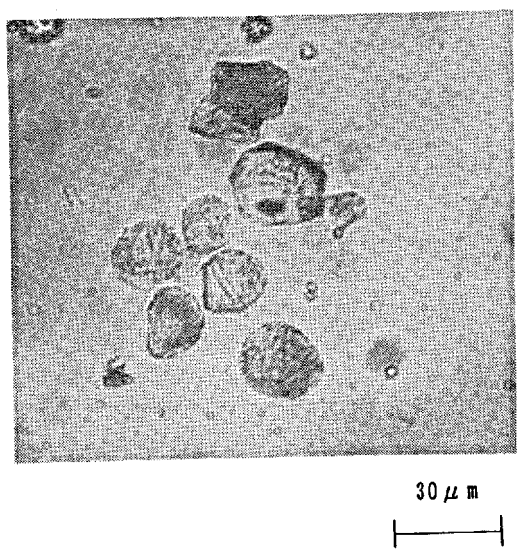

Fig. 2 Optical microscopic photograph of belite

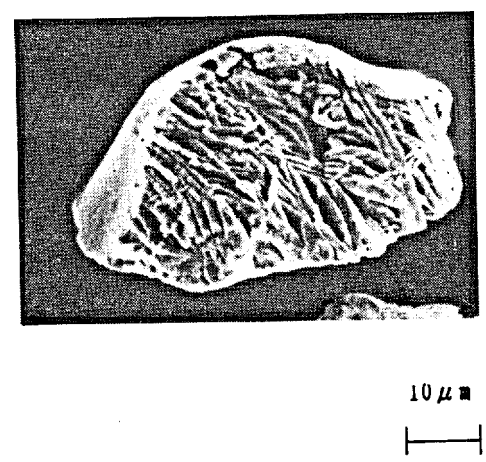

Fig. 3 SEM photograph of belite

Table 3 Composition of belite grain

	Compositions(At %)	
	(a)	(b)
Mg	2.60	1.01
Al	2.07	1.67
Si	25.60	29.53
K	0.97	1.02
Ca	67.71	66.30
Fe	1.06	0.48
Total	100.00	100.00

segregation of impurities occurred around the interface of lamellae during cooling process and/or phase transformation form α to α' and β -phase. The α -phase also remained around the interface of lamellae.

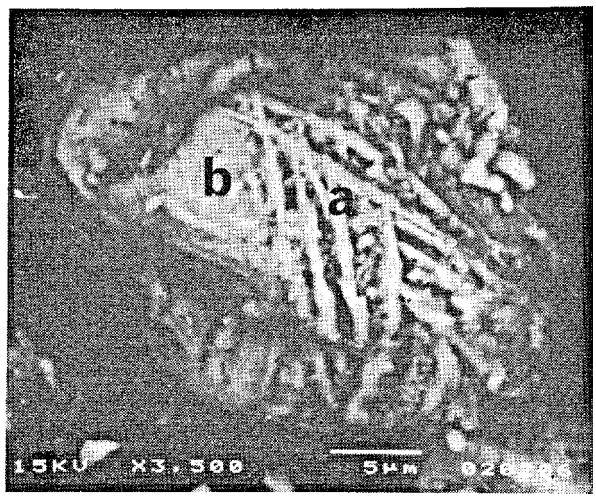

Fig. 4 SEM photograph of belite

Figure 5 shows a TEM photograph of the belite. Twins along [100] * direction of β -phase were clearly observed. The width of each twin lamellae was found to be 20 to 25nm. The domain structure of α -phase was not found in spite of high magnitude and high resolution observations.

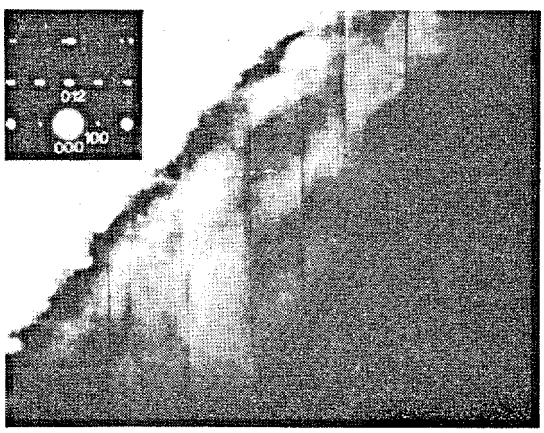

Fig. 5 [021] TEM image demonstrating the (1 0 0) twins in belite.

Crystal Structure of Belite

The crystal structure of belite was first refined by assuming that the belite consisted of pure β -phase. The reliable factor (R-factor) at this stage was 1.41%. In the next stage, the refinement of crystal structure was carried out as a 2 phase mixture of α and β -phase. The final R-factor obtained was 1.26%. The atomic parameters refined were listed in Table 4. These parameters were almost same as that reported by S.Udagawa et al.[1]. By comparing lattice parameters (Table 2) with reported values of single crystals stabilized by 1.6wt% of Al_2O_3, it is verified that the a-parameter decreases, c-parameter increases and β -angle decreases to 90° in the belite in the OPC. The interatomic distances between cations and anions are listed in

Table 4 Atomic parameters of β-Ca_2SiO_4

Phase	Atomic	X	Y	Z
β	Ca(1)	0.230	0.342	0.431
	Ca(2)	0.228	-0.001	0.294
	Si	0.270	-0.220	0.415
	O (1)	0.218	0.009	0.442
	O (2)	0.029	-0.325	0.369
	O (3)	0.460	-0.260	0.316
	O (4)	0.325	-0.318	-0.422

β-Ca_2SiO_4 a=5.5041, b=6.7622, c=9.3281A
β=94.172° , R-factor=1.26%

Table 5. The impurities incorporated in Ca sites may be K, Na and Mg, but the distribution of these ions could not be determined. The comparison of Ca-O distances with reported values however indicates that the substitution of these ions affect the Ca(1)-O distances rather than Ca(2)-O distances. Moreover, it was found that the Si-O distances were larger than those reported. This result is attributable to that the small P ions replace Si in belite in the OPC or the content of large Al ions is less than the that reported.

Table 5 Interatomic distances of β-Ca_2SiO_4

SiO_4 tetrahedron			
Si-O1	1.5994		
O2	1.5359		
O3	1.4697		
O4	1.6701		
mean	1.569		
$Ca(1)O_{10}$ polyhedron		$Ca(2)O_8$ polyhedron	
Ca1-O1	2.2581A	Ca2-O1	2.4600A
O2	3.3774	O1*	2.7258
O3	2.5591	O2	2.4690
O4	3.0558	O3	2.4599
O2*	2.4330	O4	2.5268
O3*	2.8606	O2*	2.6821
O4*	2.4615	O3*	2.4806
O2'	2.5570	O4*	2.3976
O3'	3.1910		
O4'	2.7062		
mean	2.746		2.525

CONCLUSIONS

The alite, belite and ferrite phases were separated from the OPC or clinker and the characterization of these phases was carried out. The results obtained were summarized as follows.

1) The pure alite, belite, interstitial phase and ferrite could be separated by the method combining chemical process and separation process using heavy liquids.

2) The alite separated from the OPC contained larger amount of impurities than that reported previously and consisted of only M3 phase in XRD measurement.

3) The belite in the OPC consisted of α and β -phase. The crystal structure of the β -phase was almost consistent with the results for single crystal, but there was some differences in the lattice parameters and Si-O bonding distances between them. The texture of the belite indicated that the belite belonged to the type I and had twin lamellae about 20-25nm in size along [100] * direction.

ACKNOWLEDGMENTS

The authors are grateful to Dr.Y. Yano and Mr.H.Kato for TEM observation and valuable discussion.

REFERENCES

(1) S.Udagawa, K.Urabe, T.Yano,: "Stabilization Mechanism of Polymorphisms of Ca_2SiO_4", CAJ Review of the 34th General Meeting, 1980, 37-39.

(2) A.A.Colville and S.Geller,: "The Crystal Structure of Brownmillerite, Ca_2FeAlO_5", Acta.Cryst., 1971, B27, 2311-2315.

(3) H.F.W.Taylor, Cement Chemistry, Academic Press Inc., San Diego, CA, 1990

(4) F.Nishi, Y.Takeuchi,: "Tricalicium silicate $Ca_3[SiO_4]$: The monoclinic superstructure", Zeitschrift fur Kristallographie, 1985, 172, 297-314.

(5) S.Udagawa, K.Urabe,: "The Crystal Structures of the Modifications of Ca_2SiO_4 and their Phase Transformations", CAJ Review of the 32nd General Metting, 1978, 31-33.

(6) P.Mondal, J.W.Jeffery,: "The Crystal Structure of Tricalcium Aluminate, $Ca_3Al_2O_6$", Acta Cryst., 1975, B31, 689-697.

(7) Y.Ono, Ph.D.thesis, Univ.Tokyo, 1963

(8) F.Izumi,:"Xsen oyobi Tyuseishikaisetuzukei no Rietveldkaisekishisutemu", Journal of the Crystalloraphic Society of Japan, 1985, 27, 23-31

(9) I.Maki, K.Goto,: "Phase Idetification of Alite in Portland Cement Clinker", Cem. Concr. Res. 1982, 12, 93-100.

(10)G.Yamaguchi, Y.Ono,: "Microscopic Studies on the Textures of Belite in Portland Cement Clinker", CAJ Review of the 16th General Metting, 1962, 32-34.

GROWTH OF HYDRAULIC ACTIVITY OF PORTLAND CEMENT CLINKER AS A RESULT OF USING OF PRECALCINING

B Weryński and L Janecka

Institute of Mineral Building Materials
Opole, POLAND

SUMMARY

The investigations of the effect of precalcining in a dry method kiln system with 4-stage cyclone preheater on the clinkering process and clinker properties are presented. The intensification of industrial burning process by rising the degree of raw materials decarbonation in fluidized bed causes an increase in hydraulic activity of clinker as compared with clinkers burnt with a conventional method. It is connected mainly with disordering of crystalline structure of transient phases during clinkering, as well as with disordering of clinker phases. An advantageous effect of precalcination, finding expression in reduction of the variations of clinker quality (litre weight, free CaO content) and in the increase of the mortar strength after 28 days of hardening has been stated.

ZUSAMMENFASSUNG

Im Aufsatz wurde der Einfluss der Vorkalzinierung in einer Brennanlage mit vierstufigem Wärmetauscher auf den Klinkerbildungsprozess und die Eigenschaften des Klinkers dargestellt. Die Intensivierung des industriellen Brenn - prozesses durch eine Erhöhung des Decarbonisierungsgrades im Schwebezustand steigert die hydraulische Aktivität des Klinkers im Vergleich zum klassischen Verfahren. Das ist hauptsächlich mit dem störenden Einfluss auf die Kristallstruktur der Übergangsphasen während der Klinkerbildung und der Klinkerphasen verbunden. Es konnte festgestellt werden, dass eine Vorkalzinierung die Klinkerqualitätsschwankungen verringert und die 28 - Tagefestigkeit erhöht.

INTRODUCTION

The development of research in the field of cement chemistry and the improvement of test engineering in 1970–1980 allowed to extend considerably the knowledge on the clinkering process under industrial conditions.However in view of a complexity of chemical reactions and phase changes occuring in the burning process, this problem is still the object of numerous scientific works. It is manifested in many papers. Considerable number of the papers deal with investigations of burning process in the modern kiln installations, where the formation of clinker runs in preheating and calcining zones at reduced time.

Many investigators call attention to advantageous influence of rapid preheating of raw materials on the clinkering process and the properties of clinker.

The reactivity of materials " in statu nascendi " is considered to be of special importance. It is connected with particle dimensions and lattice defects of the forming phases and with occuring in the same time of calcium carbonate dissociation and clay minerals decomposition. Fine, with defected structure oxide crystals formed on these conditions mutually react very intensively which leads to the major clinker minerals formation.

Although the most of tests were carried out under laboratory conditions it should be stated, that a rapid heating of raw materials is possible, in some range, under industrial conditions, when the precalcination of raw meal will be realized in fluidized bed in outer heat exchangers and then the calcined material, in great part in active state, is introduced to high-temperature zone of kiln, where the real process of Portland cement clinker formation occurs. The intensification of the preheating and precalcining processes causes a change in conditions of essential sintering process and it has some influence on the properties of obtained clinker. In particular it was stated, that the rate of raw meal preheating influences the rate of alite and belite crystallization, the porosity and the texture of clinker. It is connected mainly with disordering of crystalline structure of transient phases during clinkering, as well as with disordering of clinker phases.

INVESTIGATIONS

The tests were made in cement plant with the kilns ϕ 5,75 x 92 m with 4-degree cyclone heat exchanger and output of 3500 tpd. The kilns were equipped additionally with precalcining systems. The tests were carried out at the time of industrial working of two kilns : one of them worked in existing system and the second - with precalcination. Both the kilns were fed with the same raw meal / LSF of meal = 98,5 _ 104,5 / and fired with the same pulverized coal.

In the period of the testing 38 parameters of kiln operation have been recorded with frequency of 7 min. by means of a computer system. The specimens of raw meal and clinker have been taken for carrying out detailed quality control.

In the framework of identifying tests the measurements of material movement in the kiln have been carried out using tracermethod at which the radioactive isotopes were introduced into the material.

The tests revealed that as a result of using of precalcining the burning process was much stable, which became visible in smaller fluctuations of

examined parameters of kiln operation, expressed by standard deviation.

A regression analysis carried out for a few series of measurements showed, that there was a close dependence between the amount of fired coal in additional burner and the basic parameters of kiln operation, which was manifested by high coefficients of mutual and multiple correlation of about 0,8 - 0,9. Moreover it was stated that in consequence of using of precalcining the conditions of clinker burning have been modified as a result of the differences in temperature distribution in the kiln and traveling speed of material.

An installation of additional burner at the cold end of the kiln, in which about 20 % of fuel was combusted, caused a displacement of decarbonation process in cyclone exchangers. As a result the calcining zone in the kiln has been found to be shorter and the high-temperature zone to be spread out and shifted in the direction of cold end of the kiln. The cooling zone with precalcining has been extended but in consequence the conditions of clinker cooling have been modified slightly for the reason of shorter residence time of material in the zone which is connected notably with improvement of transport properties of better granulated material.

On the base of radioisotope studies it was stated, that the using of precalcining influenced the increase in the traveling speed of material. It caused considerable shortening of the time of passage of the raw mix through the kiln. The time of passage of material through the decalcining zone was shortened most of all. In this zone the material greatly scarified owing to intensive evolution of CO_2 was characterized by higher mobility than that in the conventional process. The sintering and cooling zones were affected in lower degree nevertheless the acceleration of the material movement was observed also, which probably was caused by better granulation of the material. The overall residence time of the material in the kiln was shortened by about 30 %. The average residence time of material in respective sections of kiln installation is presented in Fig. 1. The tests in industrial scale were complemented with laboratory tests.

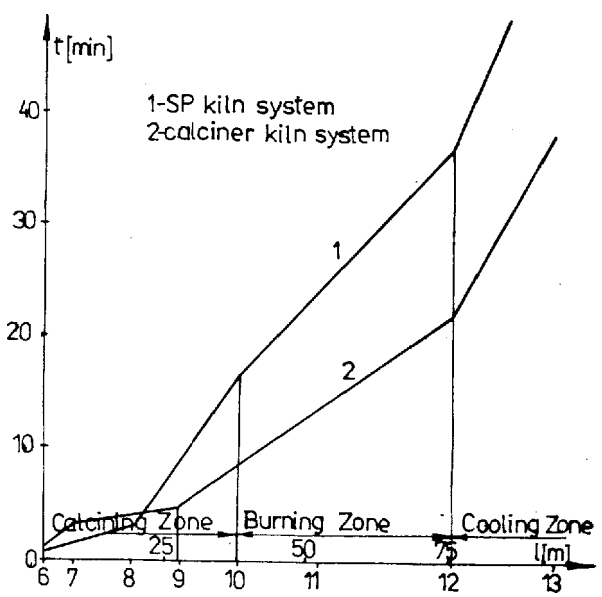

Fig. 1

DISCUSSION

The tests have shown, that in consequence of using of precalcining the conditions of clinker were varied as a result of differences in temperature distribution in the kiln and in the velocity of material movement.

The reduction of calcining zone, the extention of high-temperature and

cooling zones as well as the increase of the traveling speed of material in the kiln, what is observed particularly in the section between input and high-temperature zones, created advantageous conditions for the reactions occuring in the burning material. It is reflected in the properties of obtained clinker. Using of precalcining exerted an emphatic influence on reducing of free CaO content of the clinker regardless of type of burning meal. The changes of free CaO content are given in Fig. 2.

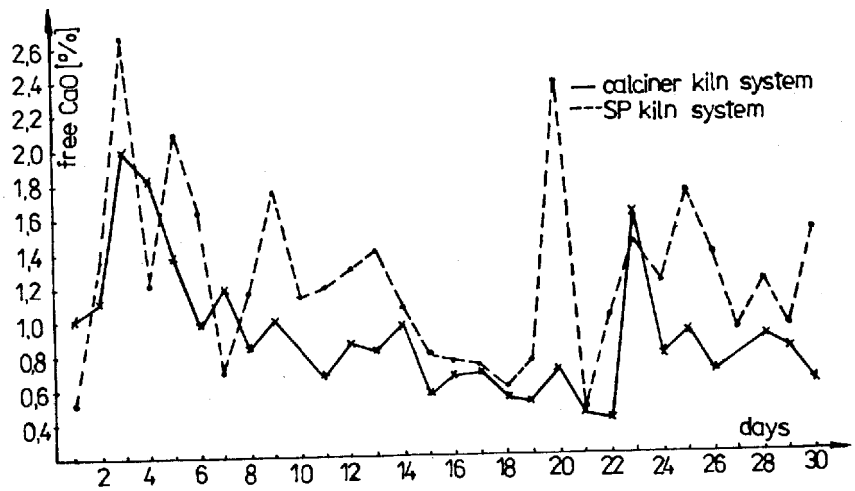

The strength of clinker obtained from the kiln with precalcining is higher than that of conventionally burnt clinker average about 15 % .

The rate of hydration was determined by differential thermal analysis. It was stated, that the rate of hydration of clinker specimens burnt in the kiln with precalcining is higher also. These differences in the strength and in the rate of hydration may be elucidated by microscopic characteristics and phase composition of the clinker.

The structure of the clinker from the kiln with precalcining is moderately-crystalline. For the clinkers burnt in the kiln with precalcining there are characteristic a loose structure and a great porosity. Micro-cracks and intercrystalline pores joined for void systems make a possibility of advanced penetration of water into material during hydration which in consequence accelerates this process. Fig. 3.

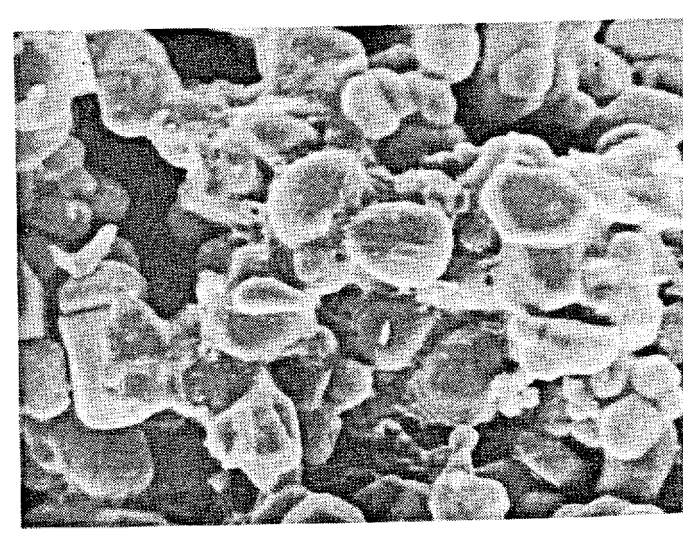

X-ray micro-analysis doesn't show essential differences in character of arrangement of Si, Al and Mg in clinkers burnt conventionally and with precalcining. On the other hand the tests have shown a higher concentration of potassium in belite areas of the clinkers from the kiln with precalcining. Probably in defected structure of clinker from the kiln with precalcining the potassium ion has found advantageous conditions for enter crystal lattice of belite phase. Fig. 4. May be, in the case of clinker burnt in the kiln with precalcining a atabilizing action of potassium ion made that beside of β-C_2S some amounts of α'-C_2S modification have remained, which is considered by many authors as advantageous effect from point of view of reactivity of belite phase. Microareas of belite are given in Fig. 5.

Quantitative determinations of phase composition by microscopic method have manifested somewhat higher alite content of clinkers burnt in the kiln with precalcining.

A higher alite content of clinker burnt in the kiln with precalcining has been confirmed by comparative estimation of alite content by X-ray method. The laboratory tests have confirmed the supposition about the predominant influence of initial period of burning on the formation of advantageous micro-structure, texture and phase composition of obtained clinker, from the point of view of hydration properties. On this base it was stated, that microscopic observations of laboratory clinkers had differed slightly from that of industrial clinkers. It is glaring, considering the different conditions of clinkering in laboratory kiln. Nevertheless the clinkers from accelerated burning process show some characteristics of industrial clinker obtained in the kiln with precalcining :

- a loose, porous micro-structure with great amount of micro-cracks,
- superiority of moderately-granular structure without distinct evidences of recrystallization of clinker minerals,
- somewhat higher alite content than that of clinkers from conventional

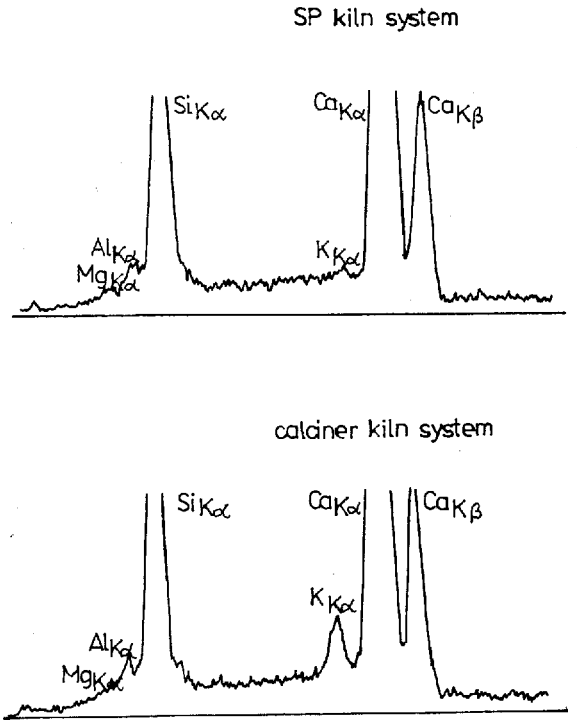

Fig. 4

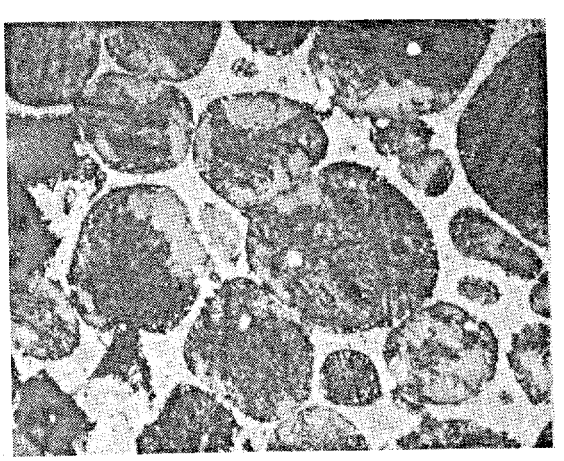

Fig. 5

burning process.

All these characteristics, according to earlier considerations, act positively on the properties of clinkers.

To sum up one should emphasize that using precalcining in rotary kiln provokes essential changes in burning conditions which influence advantageously the clinkering process and the properties of obtained clinker. Both laboratory and industrial tests have shown, that the initial period exerts the greatest influence on the quality of obtained clinker. Considerable shortening of the time of approach of burning material to high-temperature zones has favoured the using of its high reactivity and has influenced the acceleration of clinkering process and obtaining of the clinker with advantageous phase composition and crystal structure.

REFERENCES

1. Ono Y. , Kawamura S. , Soda Y. : Proc. of the Fifth Int. Symp. on the Chemistry of Cement, Tokyo 1968, (I), 275-281. (Pub. : The Cement Association of Japan, Tokyo 1969)

2. Phillipp O. , Schrader R. : Sestoj Mezd. Kongress po Chimii Cementa, Moskva 1974, Strojizdat, Moskva 1976, (I), 207-211.

3. Sprung S. : 7-th Intern. Congress on the Chemistry of Cement, Paris 1980, (I-1.2), 1-15.

4. Ono M. , Nagasima N. : Sestoj Mezd. Kongress po Chimii Cementa, Moskva 1974, Strojizdat, Moskva 1976, (I), 170-173.

5. Ranga Rao M.V. , Kamal Kumar : 7-th Intern. Congress on the Chemistry of Cement, Paris 1980, (II-1), 119-123.

6. Guinier A. , Regourd M. : Sestoj Mezd. Kongress po Chimii Cementa, Moskva 1974, Strojizdat, Moskva 1976, (I), 25-51.

7. Timasev V.V. : Izbrannye trudy. Sintez i gidratacija vjazuscich materialov, Nauka, Moskva 1986.

8. Tsuboi T. , Ogawa T. : Zement - Kalk - Gips, 6, 1972, 292-294.

9. Volkonski B.V. , Saudakas L.G. , Krapla A.F. , Bernstein P. : 7-th Intern. Congress on the Chemistry of Cement, Paris 1980, (II-1), 17-19.

10. Kristmann M. : Mineralogische und mineralchemische Untersuchungen, Portlandzement - Klinker, HOLDERBANK Management und Beratung AG, Basel 1977.

NEGATIVE EFFECT OF ALKALI ON BURNING AND PROPERTIES OF PORTLAND CEMENT CLINKER AND ITS IMPROVING MEASURES

Shan-ba Wang and Yuankui Chen

Wuhan University of Technology, Wuhan, P R CHINA

SUMMARY

The negative effect of alkali on the burning and properties of portland clinker and its improving measures have been studied by measuring f-CaO,setting time, strength, XRD, petrometry as well as chemical analysis. Results show that the main negative effect of alkali lies in increasing the melt viscosity and forming $RC_{23}S_{12}$ instead of C_2S to hinder the formation of C_3S. Adding CaF_2+$CaSO_4$ or CaF_2+$BaSO_4$ can improve the quality of high-alkali clinker more remarkably than that of sulphate added solely, especially at lower LSF and lower IM. But further study is needed to clarify the relationship between retarding setting and lower PH value of liquid phase in contact with the paste of cement clinker doped with CaF_2.

摘　　要

用测量**f-CaO**,凝结时间和强度以及**XRD**，岩相分析，化学分析等方法研究了碱对硅酸盐水泥熟料煅烧和性能的有害作用及其改善措施。结果表明，碱的有害作用主要在于提高液相粘度和形成$RC_{23}S_{12}$,从而阻碍C_3S形成,掺CaF_2+$CaSO_4$或CaF_2+$BaSO_4$比单掺$CaSO_4$更能改善高碱熟料的质量,特别是在低**LSF**和低**IM** 时更明显。掺CaF_2煅烧的高碱熟料凝结时间延缓而浆体液相**PH**值比未掺者低。两者之间的关系有待更进一步研究

INTRODUCTION

Alkalies (K_2O,Na_2O) lead to obviously negative effects on the burning and properties of Portland clinker, such as higher clinkering temperatuer, rapid setting and strength decreasing at later ages. J.Strunge and D.Knofel[2] studied the influence of alkalies and sulphur on the properties of cement. It has been also investigated that using florite and gypsum mineralizer improves the quality of high-alkali clinker by some investigators in China[1][3].But the investigations are less on mechanism of alkali's negative effect and of improvement.A report is present here on the formation and properties of high-alkali clinker as well as relative mechanism.

EXPERIMENTS

All materials are from cement plant except chemical agent K_2CO_3, Na_2CO_3, CaF_2 and $CaSO_4 \cdot 2H_2O$.Two types of experiment were performed. One, the effects of sulphate, LSF and IM;another, the effects of CaF_2,$CaSO_4$and the alkali content.94-96% of raw mix and 95-97% of clinker are less 0.08mm. All samples are burnt at 1360-1450 ℃ for 1h. Gypsum is added for retardation of cement.

First, physical properties and compressive strength of each clinker sample are determined, then the mineral composition, crystal structure and hydrated property of high-alkali clinker produced at various condition are studied by chemical analysis, XRD, petrographic analysis and by determining PH value as well as chemical composition of liquid phase in the paste. Chemical composition of industrial materials is listed in Table 1.

Table 1 Chemical composition of materials (wt%)

materials	Loss	SiO_2	Al_2O_3	Fe_2O_3	CaO	MgO	SO_3	BaO
Limestone	41.66	2.48	1.07	0.56	53.08	0.48	/	/
Clay	6.45	69.52	14.22	6.84	1.01	0.61	/	/
Iron	1.21	9.18	5.24	65.12	8.34	2.66	/	/
Gypsum	/	/	/	/	/	/	32.35	/
Barite	/	/	/	/	0.70	0.08	32.48	62.11

RESULTS

Effects of Sulphate, LSF and IM:

First, effect and optimalizing content of $CaSO_4$ in clinkers are studied. XRD results show that alkalies react preferentially with sulphur to form R_2SO_4 rather than combination with C_2S and C_3A. However, exceeding sulphur not only lead to strength drop but also rapid setting because of forming syngenite. The optimal SO_3 content is 0.6-1.0 of SO_3/K_2O+Na_2O mol ratio in clinker. This is in agreement with that of other investigators[1]. For the study of effect of LSF and IM, the alkali content of clinkers are fixed at 2.30% (Na_2O=0.3%) and SO_3/R_2O=1.0, LSF is in the order of 86, 90, 94, 97 for S-1 to S-4,(SM=2.0, IM=1.30); IM, 0.60, 1.0, 1.30, 1.58 for S-5 to S-8, (LSF=94, SM=2.0). All samples are heated at 1360 ℃ for 1h, the results are showed in Table 2, Fig 1,2, 3, 4.

Table 2: Properties of the samples S-1 to S-8

Sample No		S-1	S-2	S-3	S-4	S-5	S-6	S-7	S-8
f-CaO conten, %		0.38	2.89	2.56	4.93	0.85	2.01	2.56	6.78
normal consistency, %		0.25	0.25	0.23	0.27	0.23	0.24	0.23	0.28
settingtime (h:min)	initial	0:55	2:35	2:16	1:20	4:15	3:05	2:35	1:10
	final	2:02	4:40	3:25	2:55	6:30	4:47	4:40	2:28

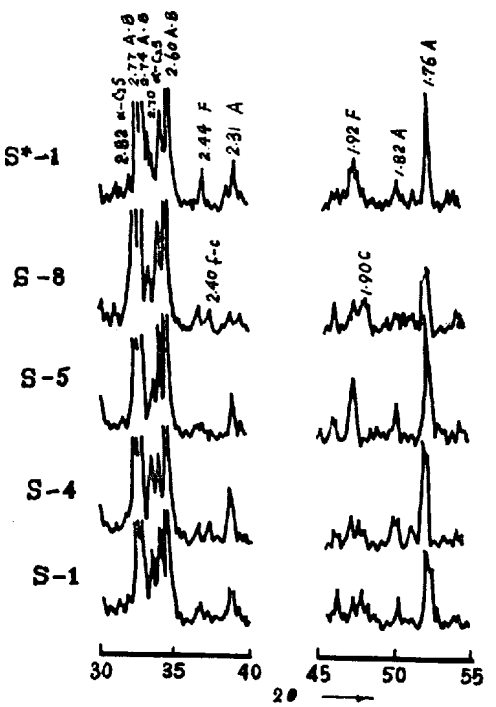

Fig.1 XRD diagrams of samples S-1, S-4, S-5, S-8, S*-1

When LSF was 90 and 94, the clinker's properties are all normal, but obviouse change takes place in sample S-1(LSF: 86) and S-4 (LSF:97). F-CaO content of S-4 is increased up to 4.93% and strength dropped, but f-CaO content of S-1 is only 0.38%, strength at all ages are on a par with the samples LSF being 90 and 94. XRD of the samples show a same tendency. It might be found a stronger f-CaO peak (2.40A) in S-4 (Fig,1) and more sharp, stronger peaks of Alite as well as minute peak of f-CaO in S-1, indicating more perfect crystal of alite in S-1.All of above prove that higher alkali and higher LSF clinker are difficult to clinkering especially at lower temperature; but in the clinker of lower LSF, there is a little f-CaO and perfect Alite crystal. Besides. C_2S might be activated by alkali and sulphur. When useing CaF_2 and barite instead of $CaSO_4$ in S*-1. (SO_3/R_2O=0.38 SO_3/F^-=0.81), the result shows the highest strength lower free lime among the samples.

XRD show α-C_2S(2.70A,2.82A) present in clinker (Fig.1). Hence, a high alkali belite -rich clinker with higher strength can be produced by adding CaF_2+$BaSO_4$ composited mineralizer.

As LSF:94, SM:2.0, IM is dropped to 1.30 and to 0.60 from 1.58, f-CaO is decreased from 6.75% to 2.55% and 0.85%, respectively, the soundness as well as strength is also improved, especially S-5(IM:0.60). Even slow cooling, the physical properties and strength of the sample with lower IM(S*-5, Composition same as S-5) are similar to that of S-5. Oppositely, high aluminous sample S-8 has a rapid setting, higher normal consistency and severe strength decrease at later age. Observing XRD (Fig.1), Alite peak(1.76A) of S-8 was more weaker and C_3A peak(1.91A) appeared obvously tripartition, but in S-5's crystals develop much better than that of S-8. Particularly, essential change occuurs in interstitial phase of both, mainly C_3A in S-8, C_4AF and C_6AF_2 in S-5(Fig.4).

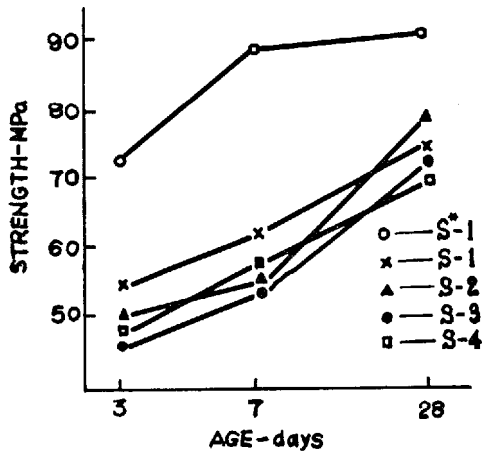

Fig.2 Relationship between compressive strength and LSF

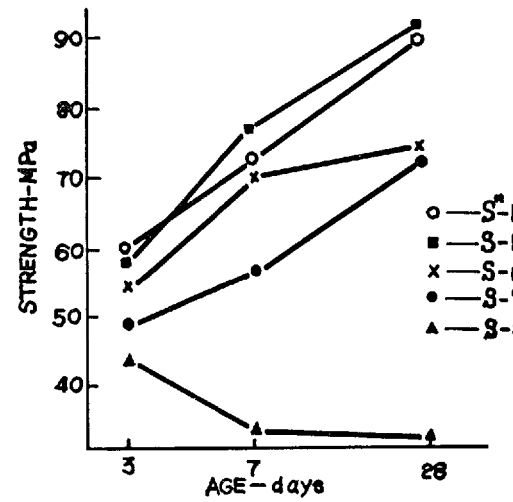

Fig.3 Relationship between compressive strength and IM

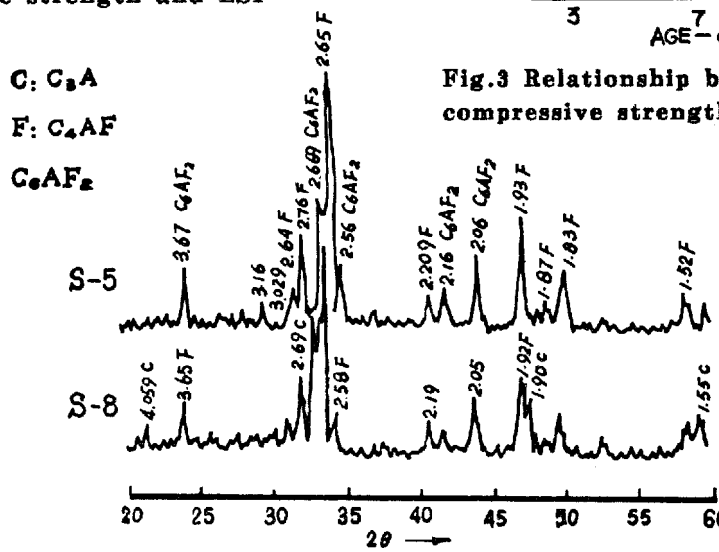

Fig.4 XRD diagrams of interstitial phase of S-5, S-8

Effects of CaF_2 and $CaSO_4 \cdot 2H_2O$

Control samples (group A) are added alkalies solely, samples(group B) are added CaF_2 and $CaSO_4 \cdot 2H_2O$ with same alkali content as group A. Group A are clinkered at 1450℃ for 1h and group B, 1400℃ for 1h, target clinker LSF:93, SM:2.53, IM: 1. 62. The results are presented in Table 3, Fig 5.6.

Table 3: Properties of samples Group A and B:

Sample NO	K_2O in clinker (%)	Na_2O in clinker (%)	SO_3 R_2O	F^- in clnker (%)	f-CaO (%)	normal consistency (%)	setting time (h:min) initial	final
A-0	0. 77	0. 30	0	/	2. 76	0. 27	1:45	3:45
A-1	1. 91	0. 30	0	/	3. 25	0. 30	2:15	3:35
A-2	2. 71	0. 30	0	/	3. 04	0. 30	1:30	3:20
B-0	0. 77	0. 30	1. 92	0. 64	0. 51	0. 25	3:40	5:02
B-1	1. 91	0. 30	1. 00	0. 64	0. 09	0. 26	3:55	5:20
B-2	2. 71	0. 30	0. 68	0. 64	2. 40	0. 27	1:49	3:00
B-4	1. 91	0. 30	1. 00	/	2. 76	0. 25	2:25	3:40

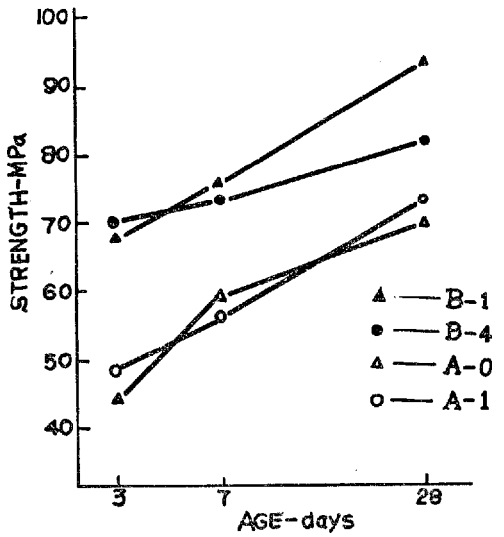

Fig.5 Effect of alkali contents on compressive strength.

It can be found that the properties of gruop A are worse than that of group B, although the sintering temperature is higher than that of group B. After CaF_2 and $CaSO_4$ added, samples of group B are remarkablly retarded in setting time, their strength at 7 days have canght up with that of group A at 28 days,(Table 3), (Fig.5). This means that the effect of CaF_2+$CaSO_4$ is much better than that of $CaSO_4$ added solely. Same in group B, compared with B-4, f- CaO of B-1 is decreased from 2. 78% to 0. 08% and strength is increased by 15 Mpa.

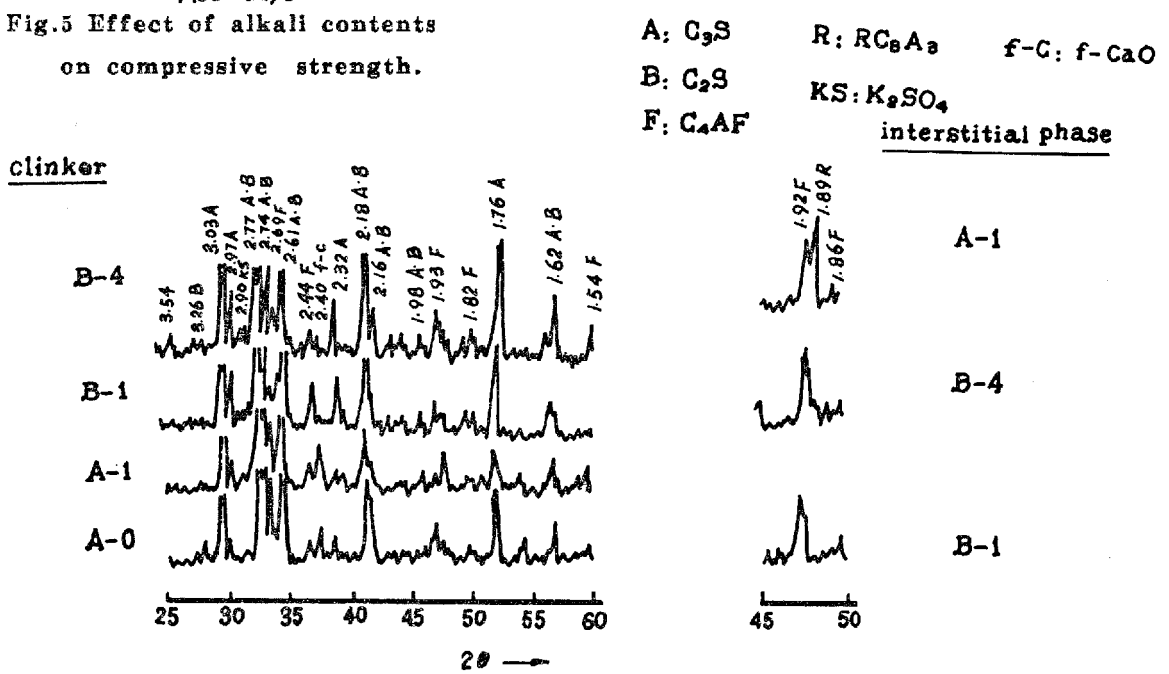

Fig.6 XRD diagrams of clinker and interstitial phase of A-0, A-1, B-1, B-4.

XRD(Fig.6) show stronger peaks of RC_8A_3 and f-CaO and weaker peak of Alite with increasing of alkali in group A, group B have more sharp peaks except f-CaO and K_2SO_4 (2.90A). But the crystal in B-4 is somewhat imperfect, the reason might be that SO_3 promoted forming big C_3S crystal and hindered absorbing f-CaO. Petrographic analysis of sample A-1, B-1 and B-4 tell us that there are many well-developed Alite crystals with 15-30μ of uniform grain size, a few C_2S and the interstitial phases are mainly glass in B-1, the grain size of Alite in B-4 is not uniform, from 10μ to 40μ or more, larger C_2S crystal nest,more dark intersititial phase. Especially in A-1, there are many belite crystals having intersection twin, imperfect Alite and RC_8A_3 solid solution characterized by prismatic dark interstitial phase.

Fig 7 and 8 show the K_2O, CaO, SO_3 concentrations and PH values in liquid phase in

contact with A-1, B-1 and B-4. From Fig 7, it can be found that concentrations of K_2O and SO_3 in liquid phases of samples (B-1,B-4) doped with $CaSO_4$ are all higher than that of control sample A-1 and maximum concentrations all occur at 4h, as well as SO_3/R_2O mol ratios are about 1. These results indicate indirectly that in the clinkers doped with $CaSO_4$ are present in the form of R_2SO_4 which coincides with the results of XRD and petrographic study. Lower concentration of K_2O in sampse A-1 seem to imply K_2O present in $RC_{23}S_{12}$ which releases K_2O into solution slowly because of lower hydration rate of $RC_{23}S_{12}$.

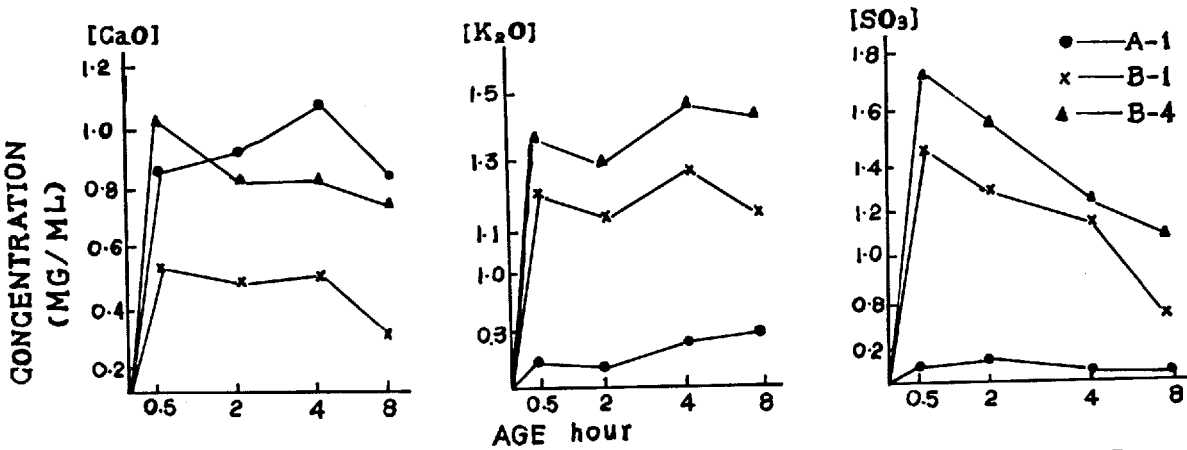

Fig.7 CaO, K_2O, SO_3 concentrations in liquid phase of pastes of A-1, B-1,B-4.

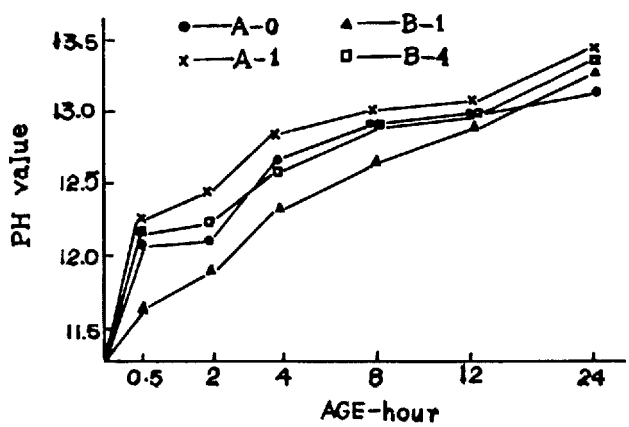

Fig.8 PH value in liquid phase of pastes of A-0, A-1, B-1, B-4

The lowest PH value of liquid phase of sample B-1 doped with CaF_2+$CaSO_4$ until 12h is showed in Fig. 8. As mentioned above, sample B-1 has the longest setting time among all samples studied. Is the longest seting time of B -1 associated with it's lowest PH value? Is the lowest PH value associated with the addition of CaF_2 ? The answer is "yes". But further study is still needed.

The Negative Effect of Alkali and Improving Mechanism of $CaF_2 \cdot CaSO_4$ and Lower IM

Why does alkali has a negative effect on the burning and properties of portland cement Clinker? A well-known view point has been proposed by Y.M. Butt and V.V. Timashev[4] that alkali increase remarkablly the melt viscosity, but people seem not to pay attention to it enough. Our results evident in both case adding CaF_2 and $CaSO_4$ or lowing IM that all can drop viscosity of the melt drastically and then promote the formation and perfect of Alite. Therefore, alkali increasing the viscosity of the melt is a important cause of it's negative effect.

The addition of $CaSO_4$ will change R_2O to R_2SO_4 and drop melt viscosity to help

C_3S formation, but exceeding SO_3 will hinder the forming of C_3S if existing Al_2O_3 and form $K_2SO_4 \cdot CaSO_4 \cdot H_2O$ causing rapid setting of the paste. When CaF_2+$CaSO_4$ added, a excellent effect has been obtained. Beause CaF_2 lowers the temperature the melt occurs and drops the melt viscosity too. Also it promotes the formation and development as well as homogeneous size and distribution of C_3S crystls. Besides CaF_2 leads more Al_2O_3 solved in ferrite avoiding to form C_3A. The high improvment on the properties of high-alkali clinker is of combined effect of CaF_2 and $CaSO_4$.

Lower IM has same effect as CaF_2 for high-alkali clinder because of lower melt viscosity and promoting C_3S formation too. At the same time, higher quantity of iron convertes the C_3A to alumino-ferrite solid solution. All of these lead to setting retarding and strength increasing.

CONCLUSION

$CaSO_4$ may improve the quality of high alkali clinkler. The effect of CaF_2+$CaSO_4$ is much better than that of $CaSO_4$ added alone.

Fe_2O_3 also improves the burning and properties of high alkali clinker. A high alkali belite-rich clinker with higher strength can be produced from a raw meal with lower LSF and lower IM.

For clinkers doped with CaF_2, pH value of liquid phase decreases a lot at first several hours and cement setting is retarded obvously. Is there any relationship between both? What is the cause? Further study is needed.

The negative effects of alkali on the burning and properties of Portland clinker lies in increasing the melt viscosity and forming $RC_{23}S_{12}$ instead of C_3S to hinder the formation of C_3S, hence all measures dropping viscosity of the melt such as adding CaF_2, $CaSO_4$, deceasing IM etc can improve the burning and quality of high-alkali clinker remarkablly.

REFERENCES

1. J · Strunge, D · knofel, "Influence of alkalies and sulphur on the properties of cement", Z · K · G, 1985. vol 38.3.150-158, 8.441-450,1986, vol 39, 7, 380-385, 8.451-456.

2. Jianqin Hu, Jiazhi Yang, "Influence of alkalies on the hydration of Portland cement with complex mineralizer", Journal of the Chinese silicate society, 1987, 15(6), 495-502.

3. Changfa Liu, Paquan Li, " Improving quality with high-alkali clinker by affixing compounded gypsum and fluorite admixture in raw mix", CHINA CEMENT TODAY, 1990. 1, 27-41.

4. Y · M · Butt, V.V.Timashev, "The mechanism of Clinker formation processes and the modification of its structure," 6th, ICCC, Moscow,(Chinese version) vol 1, 233-279.

RESEARCH ON FORMING MECHANISM OF PORTLAND CEMENT CLINKER UNDER DIFFERENT BURNING CONDITIONS

Ji Shang Xing and Xu Fengjuan

Department of Material Engineering, Wuhan University of Technology
Wuhan, Hubei, P R CHINA

SUMMARY

In present paper the formation mechanism of silicate minerals in clinker under different burning conditions was studied with XRD.SEM-EPMA.chemical analysis etc.The results show that under rapid burning the formation mechanism of silicate mineral may be different from that under ordinary burning.Under rapid burning the silicate minerals in clinker are formed more easily which promote the formation of clinker at lower temperature.

摘 要

本文运用XRD、SEM-EPMA、化学分析等方法研究了不同煅烧条件下硅酸盐水泥熟料中硅酸盐矿物的形成机理。结果表明，在快速煅烧条件下，熟料中硅酸盐矿物形成机理与普通煅烧条件下不一样，在快烧条件下，熟料中硅酸盐矿物较易形成，这可使熟料烧成温度较低。

INTRODUCTION

In general it is considered that during the burning of portland cement clinker C_2S in the clinker is formed at 800～1250℃ by solid reaction,then C_3S,is formed by solid-liquid reaction after melt had formed above 1250℃.It is necessary to maintain a higher temperature of about 1450℃ so that the C_2S formed can combine CaO to form C_3S quickly and the clinker can be burnt faster.Recently it has been proposed that the portland cement clinker can be burnt under lower temperature of about 1300℃ with rapid burning method and some studies point out (1) that under rapid burning condition the clinker melt may appear easilier at lower temperature and the viscosity of the melt may be lower which can promote the formation of clinker at lower temperature.But,as is well known,the mainbody in clinker is silicate minerals and it is most difficult to form C_3S during the burning of clinker.In view of this fact,to research the formation mechanism of clinker under rapid burning,it is important to study the formation mechanism of silicate minerals under different burning conditions.We think that under rapid burning condition the solid reaction may be negligible and the solid-liquid reaction may be dominant because of the earlier occurrence of clinker melt.So under this condition will any changes take place in the formation mechanism of silicate minerals in clinker?The following are the results of our research.

EXPERIMENTS AND RESULTS

1.Comparison of Different Burning Methods

The raw meal was prepared from industrial raw materials and its moduli values are listed as below: LSF=0.92 SM=2.1 IM=1.2

The raw meal prepared was pressed into ϕ 25×1mm sample disks and an electric furnace was used.In rapid burning test,the rate of temperature rise of sample disks was high and the samples could attain the burning temperature within a short time of about 110 sec.We determined the rate of temperature rise by a special method.Shown in Table 1.When rapid burnt

Table 1 The Rate of Temperature Rise of Disks

Temperature of sample disks (℃)	800	900	1000	1100	1200	1250	1310
Time of the temperature rise(sec.)	6	9	13	21	40	60	110

for 17 sec.at 1310℃(the temperature of samples can attain about 1050℃) the clinker melt formed (2),and ,after burning for 45 min.at 1310℃ the f-CaO in the sample disks was reduced to 1.41%.It indicated that the sample disks had clinkered.But,in ordinary burning test the temperature of the sample disks was raised at 5～10℃/min.(as with commercial manufacture) and after burning for 45min.at 1310℃ the sample disks contained about 7.5% f-CaO.So it had to be burnt at 1450℃ under ordinary burning condition.

2.XRD Determination

The phase composition of the ordinary burnt samples at different temperature and rapid burnt were determined by XRD.The results are shown in Fig.1 and Fig.2.We can see from Fig.1 that the reaction process of ordinary burning corresponds to the results of F.M.Lea (3).But Fig.2 shows that when the sample was burnt for 17sec.(the clinker melt had formed) the C_3S in sample disks had begun to form but the amount of C_2S was still low.In the XRD spectra of the rapid burnt samples for 20 sec.and 1 min.the height of the peaks of the C_3S is lower than that rapid burnt for 20～45 min.and the height of the XRD peaks of C_3S increased with the continuity of burning during this period.In the meantime the height of the peaks of CaO in samples reduced.It shows that the amount of C_3S increased and the f-CaO reduced during this period.This continued till the clinker was formed.From Fig.2 we can see that in the sample rapid burnt for 45 min.the f-CaO had disappeared and there was a large amount of C_3S formed.The height of the peaks of the SiO_2 in samples reduced fast after the clinker melt

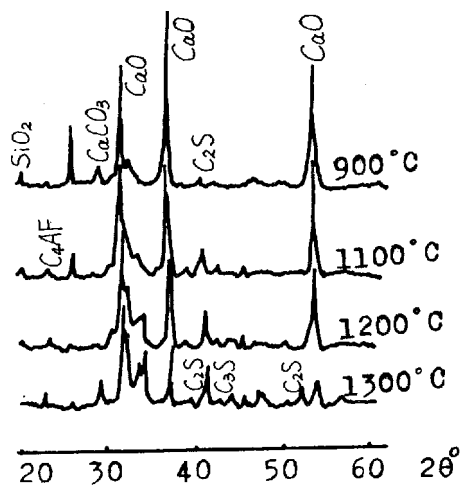

Fig.1 XRD pattern of the samples ordinary burnt at different temperature

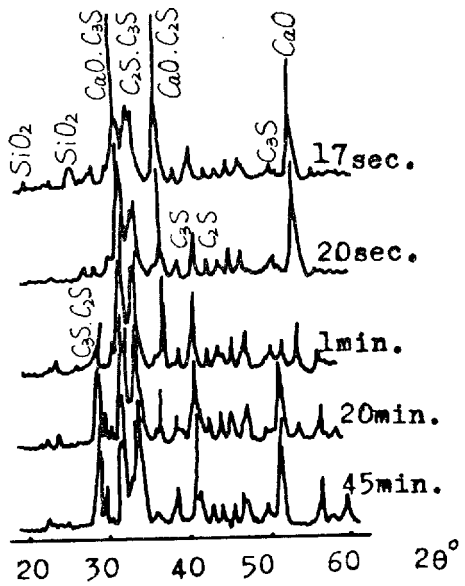

Fig.2 XRD pattern of the samples rapid burnt

formation at 17sec. and when rapid burning for 20sec. the peaks of the SiO_2 disappeared. It can show that there was no residual crystalline SiO_2 in samples when it was burnt for 20sec.

The slow scan of 0.5°/min. of XRD was used to determine semi-quantitatively the amount of C_3S and C_2S in samples rapid burnt for different times up to 1310℃. These amounts are expressed by the areas of the XRD peaks. The results are shown in Fig.3. The curve 1 indicates

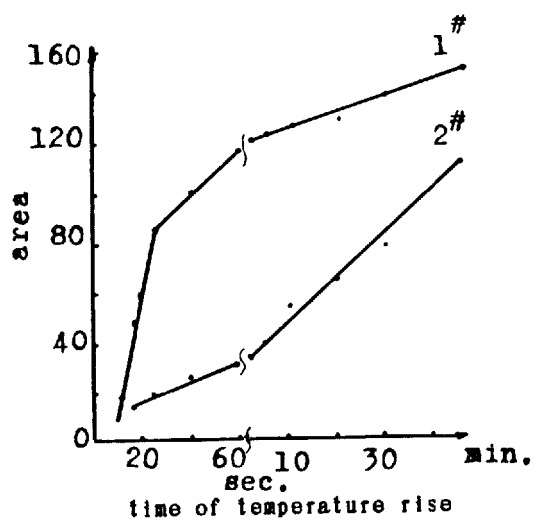

Fig.3 The relationship between the areas of peaks and the burning times(burnt at 1310℃)

the increase of the area of the C_3S and C_2S overlap peak(2θ 41.5°) with rapid burning, and curve 2 indicates that of C_3S(2θ 51.8°) with the burning time. The slope of the curves indicates the increase rate of the areas. In fact they indicate the increase rate of the total amount of C_3S and C_2S as well as the amount of C_3S respectively. Form Fig.3 we see that

the slope of curve 1 is greater than that of curve 2 within the initial 2 min.of burning.It indicates that during this period the increase rate in the total amount of C_3S and C_2S was larger than that of C_3S.So we can conclude that during this period the amount of C_3S increased and the C_2S increased too.Especially within the initial 25 sec.of burning the slope of curve 1 is more greater than that of curve 2. It indicates that the amount of C_2S increased faster with the increase of C_3S.After 2 min.burning the slope of curve 1 began to reduce and was smaller than that of curve 2 till the end of rapid burning.It means that the increase rate of C_3S exceeded that of the total amount of C_3S and C_2S during this period,i.e.the amount of C_2S reduced with the increase of C_3S during this period.

3.Extraction and Chemical Analysis

We quenched the rapid burnt samples and the ordinary burnt one and extracted these samples with 1:5 salicylic acid methanol solution (4).The silicate minerals could be dissolved and the remainder which were fusion agent minerals mainly were chemically analyzed. Because of quenching the samples the high temperature melt could become glass and could be retained.So by analyzing the remains we can understand roughly the composition of high temperature melt.The results of chemical analysis are shown in Table 2. From table 2 we see

Table 2 The Chemical Analysis Results of SAM Remainder(%)

No	Samples	SiO_2	Fe_2O_3	Al_2O_3	CaO	MgO
1	Rapid Burnt for 17 sec.	34.42	9.38	9.60	36.18	3.56
2	Rapid Burnt for 40 sec.	12.97	18.25	17.82	37.32	7.07
3	Rapid Burnt for 1 min.	9.36	19.74	18.83	38.24	8.48
4	Rapid Burnt for 2 min.	3.80	20.33	19.12	40.65	9.92
5	Rapid Burnt for 5 min.	2.97	20.90	20.19	40.44	10.70
6	Ordinary Burnt to 1310℃	1.64	19.72	21.60	41.74	10.08
7	Ordinary Burnt to 1420℃	2.95	19.80	19.92	43.25	9.04

that the amount of SiO_2 in samples of No.6,No.7 is small.The reason is that in ordinary burning process the SiO_2 reacts with CaO to form C_2S by solid reaction first and then some C_2S combines with CaO to form C_3S by solid-liquid reaction.So in the high temperature melt the SiO_2 exists as C_2S and C_3S mainly and the uncombined SiO_2 is small.But in the melt rapid burnt for 17 sec,40 sec.and 1 min.there was more SiO_2 and the amounts were 34.42%,12.97% and 9.36% respectively.The SiO_2 didn't reduce to below 3.0% in the rapid burning process until 5min.rapid burning.It can be considered that in rapid burning process the solid reaction time was very short (<17sec.) and the solid reaction products were few,the SiO_2 dissociated from raw meal could not form more C_2S by solid reaction during the short period.Because of the high activity of dissociated SiO_2 it could fuse largely into the melt to form amorphous SiO_2.Thus,although the fusion amount was large,in XRD pattern of the sample rapid burnt for 20 sec.there were not peaks of SiO_2.

4.Research of SEM and EPMA

Fig.4,5,6 and Table 3 are the results of SEM and EPMA.Fig.4 shows that in the ordinary burnt quenched samples there were many particles which were different in shape and size. Table 3 shows that these particles are C_2S and CaO mainly.For example ,the CaO/SiO_2 ratio in particle "a"(No.1)is 1.81,so it is C_2S,but particle "b"(No.2),CaO is 88.74%,so it is CaO. Since under ordinary burning condition the clinker must be formed at about 1450℃ and at 1310℃ the C_2S formed by solid reaction could not combine with CaO quickly to form more C_3S,



Fig.4 SEM photo of quenched sample ordinary burnt to 1310℃

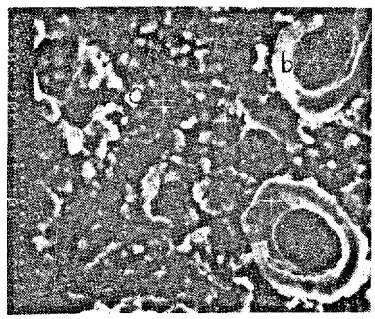

Fig.5 SEM photo of quenched sample rapid burnt for 40sec.



Fig.6 SEM photo of quenched sample rapid burnt for 2min.

Table 3 EPMA Results(%)

No	Determined regions	MgO	Al_2O_3	SiO_2	CaO	Fe_2O_3
1	"a" in Sample Ordinary Burnt to 1310℃	0.00	0.00	35.56	64.00	0.00
2	"b" in Sample Ordinary Burnt to 1310℃	2.60	1.62	1.39	88.74	5.09
3	"a" in Sample Rapid Burnt for 40 sec.	1.52	2.37	40.18	53.9	0.36
4	"b" in Sample Rapid Burnt for 40 sec.		0.70	15.82	69.71	3.91
5	"c" in Sample Rapid Burnt for 40 sec.	1.20	8.06	17.26	57.31	15.93
6	"a" in Sample Rapid Burnt for 2 min.	0.00	0.52	17.97	78.63	2.00
7	"b" in Sample Rapid Burnt for 2 min.	6.35	17.92	12.58	43.07	20.07

the C_2S and CaO remained in the samples.Fig.5,6 show that there were many round particles in the samples rapid burnt for 40 sec.and 2 min.The results in Table 3 show that these round particles consisted of CaO and SiO_2 mainly and the amounts of Al_2O_3,Fe_2O_3,MgO were low in them(No.3,4,6),but they were neither C_2S nor C_3S because the CaO/SiO_2 ratios were neither 1.87 nor 2.8 but were different in different parts of particles.For example the CaO/SiO_2 ratios of the determined regions of No.3,4,6 were 1.34,4.35 and 4.37 respectively.Apart from these round particles the rest of samples might be the melt because the amounts of Al_2O_3,Fe_2O_3 were high as No.5,7 of Table 3.The results of SEM and EPMA indicate that more C_3S and C_2S can not form at the initial stage of rapid burning.This corresponds to the XRD results. It should be pointed out that the results of EPMA and XRD all show that at the initial stage of rapid burning the amount of C_2S in samples was lower and EPMA shows again that there were more round particles which consist of CaO and SiO_2 but their CaO/SiO_2 ratios were different

in samples during this stage.

DISCUSSION

On the basis of our experiments we can see that when the clinker melt formed in samples rapid burnt for 17 sec.the amount of C_2S was lower but the C_3S had begun to form.During initial 2 min.of rapid burning the C_3S and C_2S all increased and after burning 2 min.the C_3S increased continuously but the C_2S reduced gradually.During the initial stage of rapid burning more C_3S and C_2S could not form.The SiO_2 dissociated from raw meal could fuse into the melt quickly and exist mainly as amorphous SiO_2.In the high temperature melt there were more round particles which consisted of CaO and SiO_2 but their CaO/SiO_2 ratios were different.We think these round particles may be the united granules of SiO_4^{4-} and Ca^{2+} mainly.According to above results we can conclude that under rapid burning conditions the formation mechanism of silicate minerals in clinker could be different from that of ordinary burning conditions.Because the solid reaction time was very short in rapid burning process the more solid reaction product-C_2S could not be formed.Then during the period of solid-liquid reaction the C_2S could be formed continuously.As it is known that under ordinary burning condition the SiO_2 and CaO react to form C_2S first,then the C_2S fuses into the melt above 1250℃ and combines with CaO to form C_3S.But under rapid burning the formation of C_3S could be distinct.

According to our results we propose a new formation mechanism of silicate minerals in clinker:When rapid burning to the fusion point (about 1050℃)more clinker melt form and the unreacted SiO_2,CaO could fuse into the melt,the Ca^{2+} and SiO_4^{4-} fused in melt diffuse and unite into granules.Within these united granules the CaO and SiO_2 could react to form C_3S and C_2S directly.We have known that in the structure of C_3S,C_2S the $[SiO_4]$ quadridentate is an island structure,all $[SiO_4]$ quadridentates are separated by $[CaO_x]$ polyhedrons and the vertex angle of $[SiO_4]$ quadridentates are not connected to each other.The O^{2-} situated in the vertex angle of $[SiO_4]$ does not coordinate with other SiO_4^{4-} and its unsaturated bond can coordinate with a Ca^{2+}ion.So the $[SiO_4]$ quadridentates are connected by Ca^{2+}ion in the crystal structure of C_3S,C_2S. The numbers of Ca^{2+} connected with $[SiO_4]$ are different with the difference of the CaO/SiO_2 ratio.Thus the C_3S and C_2S could be formed.In the united granules in the initial stage of rapid burning the diffusion of Ca^{2+} and Si^{4-} is not proportional.In some regions in which the ratio of CaO/SiO_2 reaches the CaO/SiO_2 ratio of C_3S the C_3S could be formed directly by solid-liquid reaction of SiO_4^{4-} and Ca^{2+}.In other regions the SiO_4^{4-} is surrounded by less Ca^{2+} and the amount of Ca^{2+} is not enough to form C_3S,the C_2S is formed.Within this period the C_3S and C_2S all increase.As the raw meal is prepared in proportion and the CaO/SiO_2 ratio in raw meal is proportion the diffusion of Ca^{2+} and SiO_4^{4-} could trend towards an equilibrium with the progress of rapid burning and the CaO/SiO_2 ratio in the united granules could be readjusted.The C_2S formed would combine with the surplus CaO to form C_3S and readjust its crystal structure,so that the C_3S increases continuously and the C_2S,CaO reduce in the meantime.These reactions proceed until the all surplus CaO is combined.

As above discussion has shown that by rapid burning process the solid reaction could hardly proceed and the clinker was formed by solid-liquid reaction.Thus the formation of silicate minerals is easier than that under ordinary burning.It can promote the formation of clinker at lower temperature.

CONCLUSIONS

The belowing conclusions can be drawn from above results and discussion: Under rapid burning condition the melt appear quickly at lower temperature,so the silicate minerals in clinker are formed by solid-liquid reaction instead of solid reaction first and then solid-liquid reaction as in ordinary burning.The forming mechanism of silicate minerals in clinker under rapid burning may be different from that under ordinary burning.We bring up a new mechanism in this paper,that is:The clinker melt appear quickly(when rapid burnt for 17 sec. at 1310℃)——→CaO,SiO_2 fuse into the melt——→Ca^{2+},SiO_4^{4-} diffuse and unite into granules in the melt——→The silicate minerals are formed by solid-liquid reaction in the united granules ——→ The CaO/SiO_2 ratio readjusts in the united granules and the structure of calcium silicate

readjusts too——→The C_3S increases and the C_2S reduces until the all f-CaO is combined——→ The reactions are finished.In above way the silicate minerals in clinker are formed more easily which can promote the formation of clinker at lower temperature.

REFERENCE

1.2. Huang Wenxi.Ji Shangxing et al:"A study of the liquid phase in rapid heating-up burning of cement clinker". International Symposium of Cement and Concrete,2nd,Beijing,China 1989,V1,230-237.

3. Lea,F.M.:The chemistry of cement and concrete".2nd ed.London,Edward Arnold,1956,116p.

4. Feng Mingfen:"The research of the chemical phase extraction method of the clinker containing CaF_2 and $CaSO_4$".Annual Meeting of Cement Committee of Chinese Silicate Society,2nd,Changsha,China 1984,315～319.

OPTIMAL PARAMETERS OF CLINKER FORMATION IN A ROTARY KILN

G B Yegorov, I E Alexandrov and A M Turetski

Institute of Transport Engineers
St Petersburg, RUSSIA
Cement Works "Kunda Cement"
Kunda, ESTONIA

SUMMARY

This paper presents results of laboratory investigation in the formation of the most essential parameters of portland cement clinker, including its activity, under the influence of clinker liquid characteristics (its content, viscosity and surface tension). The quantitative description of these influences allows to close the system of models that are necessary for the optimum control of a cement rotary kiln.

АННОТАЦИЯ

В лабораторных условиях изучено воздействие характеристик клинкерной жидкости (ее количества, вязкости и поверхностного натяжения) на основные свойства портландцементного клинкера, включая его активность. Количественное описание полученных взаимосвязей позволяет замкнуть систему математических моделей, необходимых для оптимизации управления вращающейся печью цементного производства.

INTRODUCTION

It has long been noted that when a rotary kiln produces well granulated clinker, the coating in the sintering zone is also good and the clinker has sufficiently hight hydraulic activity (quality). Dusting of clinker as well as lumping in the kiln involves the formation of clinker rings on the lining and deterioration of the clinker quality.

EXPERIMENTAL

Special experiments were conducted on a rotary kiln ø 0.5 x 7.0 m with continuous γ-isotopic measurements of the coating layer thickness. The study of the interrelation of the clinker crystallographic and granulometric characteristics in a rotary kiln, of the coating layer thickness in its sintering zone and the quality (strength) of resulting clinker has allowed to see that between all these parameters and the characteristics of the clinker liquid phase (its content L and mobility η) there are extreme interrelations with fairly closely coinciding maxima.

The variation of portland cement clinker strength with practically equal degree of certainty (at the level of r=0.9) can be described using the correlations of clinker phases (1), variation of the medium-weighted Gibbs potential (2) or the alite phase content and crystallographic features (3,4). The latter in turn are greatly determinated by the content and correlation of fluxing minerals and, correspondingly, by the content and properties of the liquid phase of clinker.

Fig.1 shows the variation of three characteristics - the maximum size of alite crystals $C_{99}^{C_3S}$(3), the mass thickness of the coating layer ρd (5) and the content of large fractions in clinker N_9 (6) at the variations of content L, viscosity η and surface tension σ of the clinker liquid in clinkers (1). The N_9 characteristic was chosen as a summary content of clincer fractions larger than a certain characteristic dimension (in our case 9 mm) known to transform the most probable size of each of 22 clinkers (1,5). The joint discussion of interrelations represented in the Fig.1 permi ts to state the following.

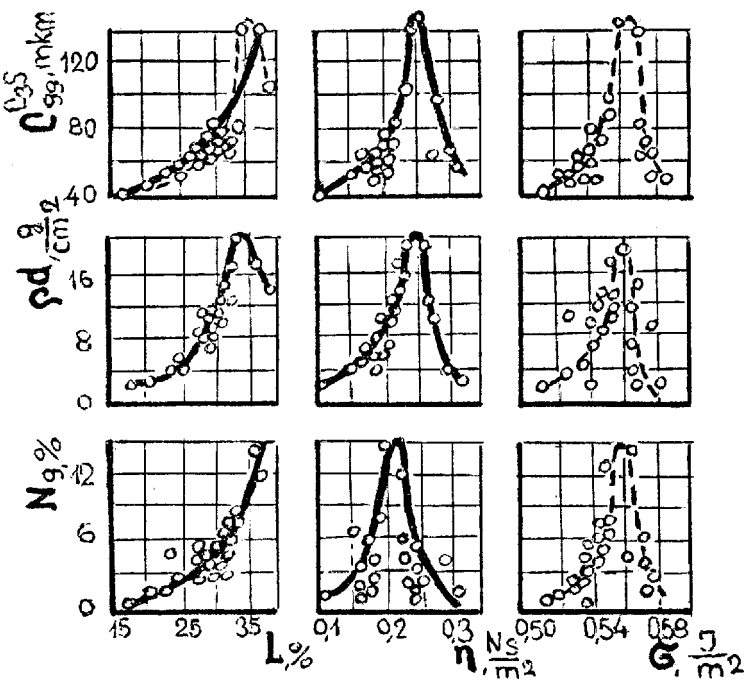

Fig.1 Interrelation between the characteristics L, η and σ of the clinker liquid phase, the maximum size of alite crystals $C_{99}^{C_3S}$ in it, the mass thickness of the coating layer ρd and the content of large granules in clinker N_9.

RESULTS AND DISCUSSIONS

When the content of liquid phase L in clinker is increased from 15 to about 25%, there occurs some minor increase of both the alite crystals in the clinker and of granules of fairly small dust-like clinker; in the sintering zone accumulates a thin and not very stable coating layer which is obviously insufficient for proper protection of the refractory lining. The solid phases skeleton and the porous space of clinker are maintained the liquid sufficiently strongly.

When the L content is over 25%, a part of the clinker liquid phase acquires the possibility to segregate and move towards the refractory brick, thus greatly increasing its bond with the coating. Up to L=32-35% there is observed a rapid growth of alite crystals (on account of the combining of small crystals into larger blocks) up to the dimensions that are optimum from the standpoint of the cement strength (3). The mass thickness of the coating layer grows just as rapidly, the coating itself becomes denser and more stable. Clinker produced in the kiln is

of normal size with a small content of minor fractions. Operation of the kiln becomes stable.

When L increased over 34-35%, the stability of the sintering zone operation is decreased. The size of the clinker granules keeps on growing and there appear lumps. A large clinker liquid content causes segregation of the growing alite crystals and prevents their combination into large blocks (4); there is observed decrease of size of alite crystals, causing variations of the clinker quality. The coating loses its stability, mass thickness of the layer decreases - in different clinkers there is observed either "flow" of coating or its falling together with the lumps of clinker stuck to it. It can be supposed that at L>34-35% there develops a situation when the joining of clinker and refractory material and clinker-clinker in the coating is insufficient for detaining in the upper arch of sintering zone all the mass of the formed coating layer together with the lumps stuck to it. This tends to decrease the coating layer thickness in the highest temperatures zone on the one hand, and to form some clinker rings in the furthest and the nearest parts of sintering zone on the other.

The influence of the clinker liquid viscosity on the crystal structure of alite has a most obvious extreme character. There is the range of η values that corresponds to a considerably larger alite crystallisation than in the case of greater or smaller mobility of the clinker liquid phase. It can be assumed that in a liquid of limited mobility the drawing together and block formation is difficult for small crystals. On the contrary, in an excessively mobile liquid the formation of crystal nucleating centres is intensified but the stage of their growth is prevented by the insufficiency of crystallizing matter. Only a definite, relatively narrow range of η values creates most favourable conditions for an intense increase of crystal size.

The relations between viscosity η of the clinker liquid, the thickness of the coating layer ρd and the size of clinker granules N_9 also have a definite character. Without going into a sufficiently complicated description of the physico-chemical mechanics of heterogenous systems at varying phase compositions and temperatures, we

shall merely point out the obvious role of the wetting and surface tension phenomena whose quantitative roles is still to be established. The marginal angles of wetting in our experiments were not determined, the range of variations in the assessment of surface tension (4,5) was small, the variation of σ itself in the discussed range of temperatures is automodal to the variation of η. Thus these dependences are still to be reliably interpreted.

CONCLUSIONS

It is obvious that the majority of most essential parameters of portland cement clinker, including its activity, is formed in the sintering zone of a rotary kiln under the influence of the same characteristics of clinker liquid and has the form of the same interrelations that are probably inherent to the pelletizing of solid-liquid mixtures at variable temperatures. In our opinion, a characteristic feature here is the extreme character of these interrelations which permits to define a certain range of physico-chemical parameters that are optimal from the quality of clinker, its granulometric composition, and characteristics of the clinker coating. The quantitative description of these interrelations allows to close the system of models that are necessary for the optimum control of cement rotary kiln.

REFERENCES

1. Yegorov, G.B., Belov, L.V. etc.: "Mathematic Models of Portland Cement Hydraulic Activity", Cement, 1975, 3, 18-19.

2. Yegorov, G.B., Kapralova, R.M. etc.: "Comparison of Strenght Values with Gibbs Thermodynamic Potentials of Portland Cement Clinker Hydratation", Cement, 1987, 8, 11-12.

3. Okorokov, S.D., Yegorov, G.B. etc.: "Correlations between the Composition, Structure and Strength of Portland Cement Clinker", Cement, 1975, 6, 8-10.

4. Yegorov, G.B., Sytshev, M.M. etc.: "A Trend in the Portland Cement Crystallic Structure Control", Cement, 1981, 7, 11-13.

5. Yegorov, G.B., Bojkov V.A. etc.: "A Trend in the Coating Layer Depth Control in the Sintering Zone of a Rotary Kiln", Cement, 1990, 3, 16-18.

6. Yegorov, G.B., Turetski A.M. etc.: "Clinker Formation in the Sintering Zone of a Rotary Kiln", Cement, 1991, 5-6, 44-47.

THE DECOMPOSITION OF ALITE IN PORTLAND CEMENT CLINKER

Shunni Liu and Zongshou Lin

Department of Materials Engineering, Wuhan University of Technology
Wuhan, Hubei, P R CHINA

SUMMARY

The decomposition speed and mechanism of alite in portland cement clinker are studied by means of optical microscopy, EPMA, XRD and chemical analysis. The results show that alite in portland cement clinker decomposes at the maximum speed when the temperature is at 1025°—1175°C. It takes about 40 hours for the alite in clinker burnt in the rotary kiln to completely decomposes at 1175°C, and about 68 hours for the alite burnt in RSP—kiln. The presence of CaF_2 or $CaSO_4$ greatly affects the decomposition speed of alite, the former resists alite to decompose but the latter accelerate it and enable alite to decompose completely within 6 hours or less.

INTRODUCTION

As we know, alite is the major strength mineral in portland cement clinker. Its proportion contained in the clinker largely influences the quality of cement clinker. Many authors[1],[2],[3] have done a lot of studies on the formation and the stability of alite as well as the effect of different additives on the formation of alite. But when the temperature is lower than 1250°C, alite is a metastable phase, therefore its decomposition is a energe release process. As mineralizrs are widely used, it is important to study the influence of different additives on the decomposition rate and temperature of alite.

EXPERIMENTAL

The cement clinkers used in experiments are listed as follows. The chemical compositions of samples A1, A2 and A3 are shown in Tab. 1.

Tab. 1 The chemical composition of clinker A1, A2 and A3 (%)

samples	SiO_2	Al_2O_3	Fe_2O_3	CaO	MgO	SO_3	F-Cao
A1	20.00	4.95	4.96	66.78	1.62		2.46
A2	19.48	5.44	4.69	64.57	1.80	1.38	3.87
A3	23.03	5.79	3.90	65.54	0.71		0.32

A4 — the clinker made from A1 + 1.0%(wt) CaF_2 which are together ground and burnt at 1350°C for 1 hour.

A5 — the clinker made from A1 + 1.0%(wt) CaF_2 + 2.0%(wt) SO_3 which are treated in the same way as A4.

A6, A7, A8 — the clinker made respectively from A1 + 1.0%(wt)SO_3, A1 + 2.0%(wt) SO_3 and A1 + 3.0%(wt) SO_3 which are treated the same way.

In experiment, SO_3 is introduced into the raw meal as $CaSO_4$. Analytically pure grade CaF_2 and $CaSO_4$ were used. The free-CaO content was measured by chemical analysis.

RESULTS AND DISCUSSIONS

1. The decomposition temperature of alite in different clinkers

There are different formation condition of alite, such as different clinkering temperature, different ways of the existence of additives. Therefore the decomposition speed and temperature of alite in different clinkers are also not the same. This has been proved by experimental results. In the

experiment, clinker A1, A2, A3, A4, A5 and A7 are respectively placed in a platinum crucible with a platinum cover and heated to different temperature for one hour. Then the clinker is taken out and the free-CaO content measured. The results are shown as fig. 1.

From fig. 1, it was seen that normal alite existing in clinker A1 and A3 has the maximum decomposition speed when the temperature is at about 1175°C, and 1025°C for the alite existing in A5 with only CaF_2 additive. The alite in clinker A6 with SO_3 additive decomposes very quickly and the temperature corresponding to the maximum decomposition speed is about 1150°C. More interesting, the temperature corresponding to the maximum decomposition speed of alite in clinker A2 and A7 with the composite mineralizers CaF_2 +SO_3 is about 1050°C 1100°C, between the decomposition temperature of alite in A5 and that in A6. From the experimental results it can also be concluded that the decomposition speed and temperature depends largely on the crystalline condition and active state of alite. The temperature corresponding to the maximum decomposition speed of alite is not fixed but varies with the clinker composition. The temperature corresponding to the maximum decomposition speed is lower in the alite in the clinker with CaF_2 additive, because CaF_2 can make the alite decompose at a lower temperature.

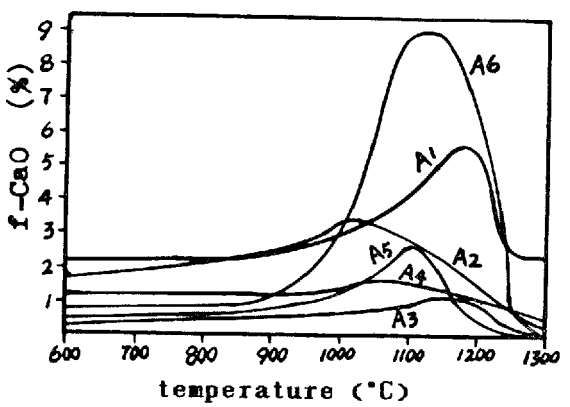

Fig. 1 Effect of temperature on f - CaO

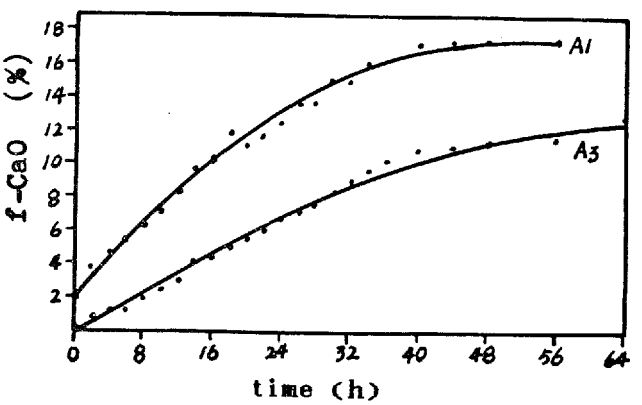

Fig. 2 Relations of F-CaO with time

2. The new method of measuring the alite content

In this experiment, the content of alite in clinker A1 and A3 was measured by optical microscopy. The results are shown in table 2.

Because alite in clinker A1 and A3 has the maximum decomposition speed when heated to 1175°C, these were placed in a platinum crucible with cover and heated to 1175° for different lengths of time. Part of the clinker was

Tab. 2 The quantitative results of alite in clinker A1 and A3

sample	alite%(wt)	belite%(wt)	interphase%(wt)
A1	63.78	5.46	30.76
A3	50.34	31.17	18.49

taken out and the free-CaO content measured. The results are shown in fig. 2.

From fig. 2 it can be seen that the f-CaO content in the rotary kiln clinker A1 is almost constant when it is heated for about 40 hours, but the RSP-kiln clinker A3 needs about 58 hours to keep a constant f-CaO value. The stable f-CaO content may mean that the alite in the clinker has been completely decomposed. To confirm it, the clinker A1 heated for 45 hours at 1175°C and A3 for 60 hours were tested by means of XRD. The characteristic peaks of C_3S are not detected, therefore it may be assumed that alite in A1 and A3 heated for 45 and 60 hours has decomposed completely. Every clinker has its initial f-CaO value which can be labelled (f-CaO)o. When heated, the f-CaO content in clinker will vary with heat time and tend to a stable value which is labelled (f-CaO)s. The difference of (f-CaO)s and (f-CaO)o is (f-CaO)*. Considering the (f-CaO)* value comes from the decomposition of alite, the content of alite in clinker therefore can be calculated as table 3.

Table 3 the alite content at different times

sample	(f-CaO)o%	(f-CaO)s%	(f-CaO)*%	C_3S=4.07(f-CaO)*%
A1	2.10	17.70	15.60	63.49
A2	0.30	12.53	12.23	49.78

Comparing the results of table 3 with table 2, it was seen that the alite content obtained by means of heat decomposition (see table 3) is very close to that measured by the optical microscopy (see table 2). Therefore it is probable that the heat decomposition of alite can be used as a new practical quantitative method for alite determination. But because alite existing in clinker is a solid solution which has differnt chemical composition from pure C_3S, the method using (f-CaO)* value to calculate the content of alite still has a certain error. The estimate of this error band needs further studies and experiments.

3. The influence of additive on the decomposition speed of alite

Clinkers A4, A5, A6, A7 and A8 were also placed in a platinum crucial with cover and heated at 1100°C for different times. At a certain point the clinkers are taken out and the f-CaO content measured. The relations of f-CaO

content with heating time are shown as fig. 3.

Fig. 3 shows that alite existing in clinker with only CaF_2 additive (clinker A4) has a very slow decomposition speed. When heated for 18 hours, the (f-CaO)* value of the clinker is less than 1.0%. Therefore CaF_2 can largely decreace the decomposition speed of alite. The XRD analysis of the clinker A4 heated for 18 hours shows that there is no new phases such as $C_3S \cdot CaF_2$ formed. This fact indicats that the effect of CaF_2 additive to decrease the decomposition speed of alite is mainly due to the function of F^- ion solution. When F^- is introuduced into the C_3S crystal, F^- ion can partly replace O^{2-} ion. Because one O^{2-} ion needs two F^- to balance the electrovalence, there are more interstitial F^- ions (F_i^-) to form. In the replacement process, the cavity in the structure of C_3S is narrowed and the diffusion rate of Ca^{2+} ion slows down, therefore the decomposition speed of alite is largely decreased.

From fig. 3 it can also be seen that SO_3 additive will largely increase the decomposition speed. It only takes about 6 hours to decompose completely the alite of clinker with only SO_3 at 1100°C. The XRD analysis of clinker A6, A7 and A8 heated for 6 hours at 1100°C shows that there is no new phase e.g. $C_3S \cdot CaSO_4$ formed and the characteristic peak of C_3S is absent. The above results prove that the alite solutinzing SO_3 has a very high decomposition speed. The function of SO_3 to accelerate the decomposition of alite can be explained from the structure of C_3S crystal. When SO_3 is introduced into the C_3S crystal, $(SO_4)^{2-}$ may replace $(SiO_4)^{4-}$ or S^{2-} ion replace

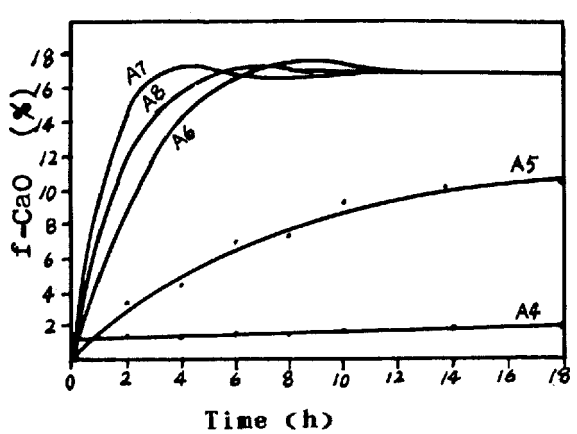

Fig.3 The relations of the content of F-CaO with time

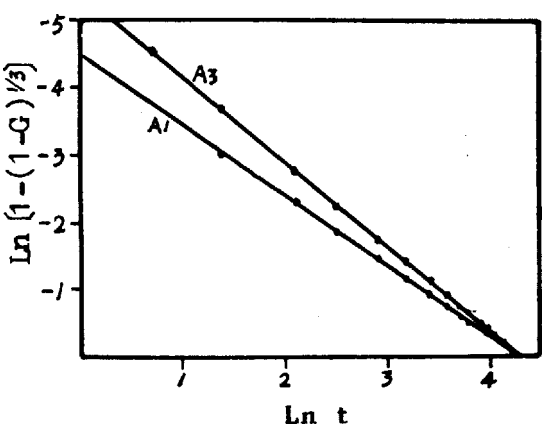

Fig.4 The decomposition dynamics curve of clinker A1 and A3

Ca^{2+} ion. Because the space for $(SO_4)^{2-}$ and S^{2-} is smaller than ($SO_4)^{2-}$

and Ca^{2+} ion, and on the other hand, $(SO_4)^{2-}$ can not exist as interstitial ions, to balance the electrovalence in structure, a vacancy of Ca^{2+} may form. The results of this replacement tends to expand the cavity in the structure of C_2S and accelerate the diffusion of Ca^{2+} ion. this is why the decomposition speed of alite with SO_3 additive is accelerated. But more interesting, when CaF_2 is present together with SO_3, the function of SO_3 to accelerate the decomposition of alite tends to disappear. This can be seen from the results of clinker A5 in fig. 3. The decomposition speed of alite in clinker A5 is far lesser than that of clinker A6, A7 or A8 but greater than A4.

4. The decomposition of alite

By means of optical microscopy and EPMA, the decomposition process of alite in clinker A1 and A3 was observed. Very small Cao crystal can be seen in the frame of alite crystal in clinker A1 heated for 4 hours. When A1 is heated for 12 hours, more small CaO crystals can still be observed and the frame of alite still keep a sharp outline. But when A1 is heated for 24 hours or more, CaO crystals can still be observed but the frame of alite tends to blur. Because alite in clinker A3 crystallizes better than alite in A1, it must be heated for 12 hours so that the very small CaO crystals can be observed with the optical microscope. Therefore alite in clinker A3 has smaller decomposition speed than clinker A1. That is to say, the diffusion and crystallization of CaO has a very important effect on the decomposition of alite. In fact, the decomposition speed of alite depends largely on the diffusion rate of CaO. It can be confirmed from Jander's dynamics equations. The dynamic relations of clinker A1 and A3 are shown as Fig. 4. In fig. 4, G means the decomposition rate of alite in clinker.

$$G = \frac{(C_2S)t}{(C_2S)o} = \frac{4.07\,[(CaO)t-(CaO)o]}{(C_2S)o}$$

(CaO)t: f-CaO content at a specific time and can be got from fig. 2.

(CaO)o: the initial f-CaO value and listed in table 3.

$(C_2S)o$: the true alite content of clinker which can be calculated from the data of table 2 and table 3.

$(C_2S)o$ of A1=0.5(63.78+63.49)%=63.64%

$(C_2S)o$ of A3=0.5(50.34+49.78)%=50.06%

CONCLUSIONS

1. Alite obtained in different ways has different decomposition temperature and speed. The temperature corresponding to the maximum decomposition speed of alite varies from 1025°C～1175°C.

2. Additives have very important effect on the decomposition of alite. CaF_2 resists alite to decompose, but SO_3 accelerates the decomposition of alite to such an extent that alite can be completely decomposed within 6 hours or less.

3. It is probable that the heat decomposition of alite can be used to quantity the content of alite in a clinker.

4. The decomposition speed of alite depends largely on the diffusion and crystallization rate of CaO. The additive such as SO_3 tends to expand the cavity in the structure of C_3S and makes CaO diffuse faster, therefore accelerate the decomposition of alite.

REFERENCE

1. U. LUDWIG, A. WOLTER 7 the inter. cong. on the chem. of cement " The formation and stability of C_3S and alite"
2. KLEMM, W.A. AND JAWED, Proc. 7th intl. congress chem. cem. paris (1980) "Mineralizers and fluxes in the clinkering process"
3. CHRISTENSEN, N.H. AND JOHANSEN, V. 7th intl. congress chem. cement "Mineralizers and Fluxes in the clinkering process:"

ROLE OF CLINKER LIQUID IN PROMOTING THE CLINKERISATION AND ITS IMPACT ON CLINKER MORPHOLOGY AND MICROSTRUCTURE

S C Ahluwalia*, R K Goswami* and T V Kouznetsova**

**National Council for Cement and Building Materials*
New Delhi, INDIA
***Mendeleev Institute of Chemical Technology*
Moscow, RUSSIA

SUMMARY

Cement raw mixes integrated with coal ash, covering a wide range of composition and clinker liquid were investigated for the role of clinker liquid in promoting the clinkerisation of the raw mixes and its impact on clinker morphology and microstructure. The amount and composition of liquid phase in clinker was determined by chemical composition of raw mix and the firing temperatures. Two important properties of the melt phase i.e. surface tension (σ) and viscosity (η), which control the shrinkage, porosity, pore sizes and crystal growth of the clinker phases were determined experimentally.

It was observed that σ/η ratio had a significant relationship with the burning of cement raw mixes and a range has been suggested for optimum burning. The clinkers prepared under laboratory conditions were studied for free lime, morphology and microstructure. The role of liquid phase in development of microstructure has been discussed, but study does not permit any conclusion to be drawn on this aspect.

INTRODUCTION

The outcome of sintering process of portland cement clinker in a rotary kiln is determined by a set of thermodynamic and physico-chemical parameters. While the thermodynamic parameters are specific to a particular kiln system, the role of physico-chemical parameters in promoting clinkerisation can be generalised to some extent. According to the theory of sintering process in the presence of liquid phase, three stages of consolidation process corresponding to viscous flow of liquid, dissolution-precipitation and sintering in the solid phase exist. These three stages of sintering are reached with the start of sintering zone, movement in the sintering zone and towards the end of sintering zone. The process of clinkerisation can be intensified by lowering the viscosity of melt in first stage and by maximising dissolution-precipitation in second stage. The third stage corresponds to solid state sintering and grain growth where the balance of forces is an important factor. Several publications (1-6) have treated the subject by various angles and established the role of melt phase properties. Certain views on development of microstructures and role of liquid phase properties are being put forward herein.

EXPERIMENTAL

1. Selection of Raw Materials

Raw meal from four plants located in different parts of country were selected for this study. The raw meals were so chosen as to represent wide variation with respect to alkalies, sulfate and calcium oxide content.

2. Measurement of Liquid Phase Properties

Amount and composition of liquid phase at various temperatures was calculated by using relevant phase diagrams. The melts of desired composition were then synthesized by using pure oxides. Viscosity of these melts was measured by a high temperature rotary viscometer. The surface tension was measured by the gas bubble formation method.

3. Microscopic Examination

Raw meal samples integrated with coal ash were fired at 1450°C for 20 minutes in electrical furnace and were air quenched. Polished sections of the resultant clinker were examined by polarizing microscope while the fractured surfaces were subjected to scanning electron microscopic examination.

RESULTS AND DISCUSSIONS

TABLE 1

CHEMICAL COMPOSITION OF KILN FEEDS

Sl.No.	LOI%	SiO_2%	Al_2O_3%	Fe_2O_3%	CaO%	MgO%	SO_3%	K_2O%	Na_2O%
1	36.13	13.62	2.82	2.03	43.51	1.32	-	0.21	0.16
2	36.52	11.69	2.26	1.59	43.90	3.13	0.05	0.62	0.21
3	36.25	12.26	2.26	2.57	42.57	2.72	0.25	0.57	0.21
4	35.18	10.96	2.44	1.82	45.77	2.65	-	0.33	0.33

The calculated amount and composition of liquid along with experimentally measured values of the viscosity and surface tension of the synthesized liquid phase at various temperatures in different samples are reported in **Table 2.** It is observed that the amount of liquid phase increases by about 1.5% as the temperature is raised from 1350°C to 1450°C. In other words more than 90% of liquid is already available at 1350°C. It is found that the value of surface tension decreases marginally (by ∽15%) on raising the temperature by 100°C but the viscosity decreases exponentially (to ∽10%) in the same temperature range. These values suggest that the liquid phase is highly viscous at 1350°C and therefore, does not facilitate first stage of sintering i.e. rearrangement of particles. The condition improves at 1400°C and viscosity takes a still lower value at 1450°C. A further increase in temperature is not considered desirable as a lower value of surface tension will result in decrease of driving forces of agglomeration process. These observations are completely in line with observations recorded during burnability studies. It was found that free CaO values, which are normally high at 1350°C change slightly at 1400°C but sharply come down to < 0.5% at 1450°C. On the basis of shrinkage rate analysis Timashev (1) has also concluded that the nature of sintering process changes from rearrangement to dissolution at 1450°C and the second stage i.e. dissolution prevails thereafter.

Scanning electron micrographs of the four clinkers are presented in Fig.1 (a,b,c,d). The clinker No.1 shows uniform development of phases,

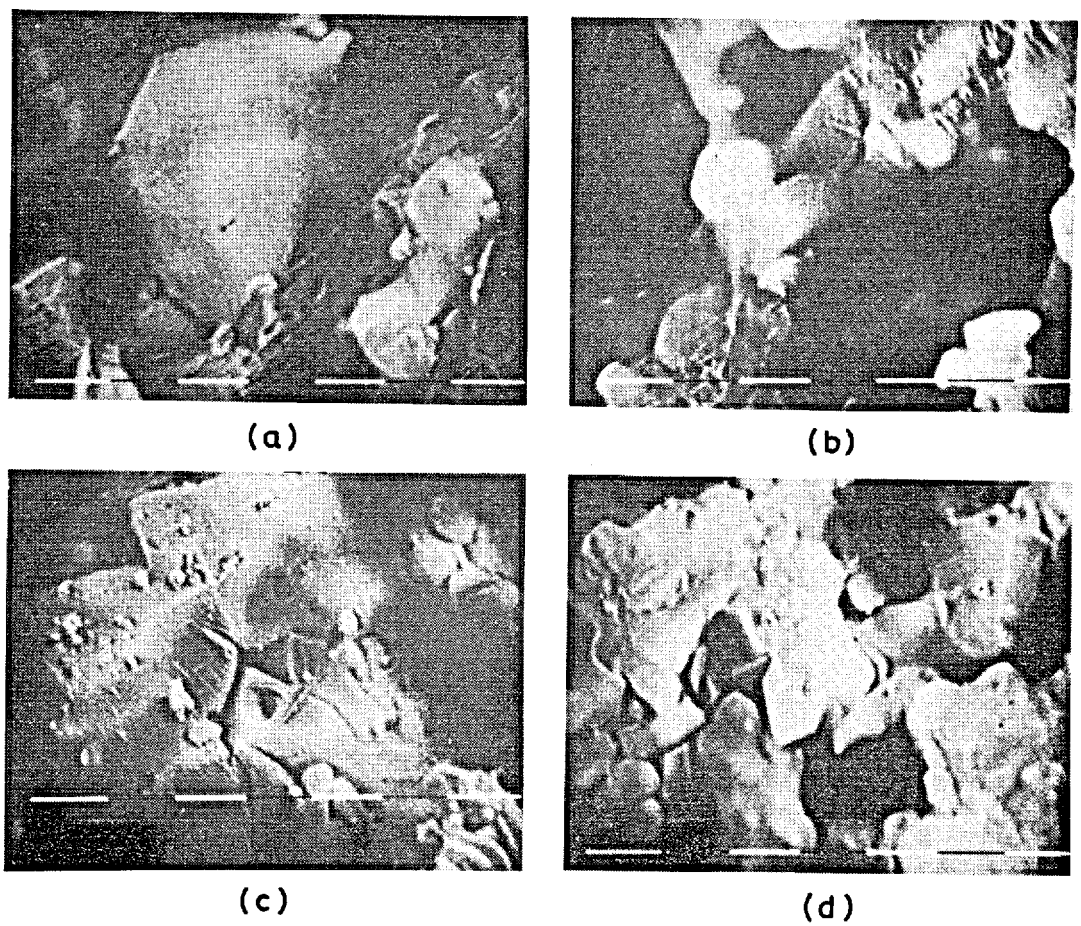

FIG.1 : SCANNING ELECTRON MICROGRAPHS OF CLINKERS (- 10 μm)

TABLE 2

QUANTITY, COMPOSITION AND PROPERTIES OF CLINKER LIQUID PHASE

Clinker No.	Temperature °C	Amount,%	SiO_2%	Al_2O_3%	Fe_2O_3%	CaO%	MgO%	SO_3%	K_2O%	Na_2O%	Viscosity Pa S^{-1} (η)	Surface tension n/m (σ)	σ/η
	1350	26.30	6.62	18.38	18.71	49.86	5.02	-	0.80	0.61	0.445	0.490	1.10
1	1400	27.44	7.38	18.12	17.74	50.60	4.81	-	0.77	0.58	0.085	0.468	5.50
	1450	27.91	7.54	17.84	17.77	50.80	4.79	-	0.75	0.57	0.040	0.420	10.50
	1350	25.04	5.92	18.96	16.79	48.97	6.00	0.02	2.48	0.84	0.440	0.488	1.10
2	1400	26.40	6.78	16.81	16.46	50.61	6.00	0.10	2.35	0.80	0.105	0.450	4.28
	1450	27.08	6.90	17.08	15.93	50.83	6.00	0.18	2.30	0.78	0.055	0.428	7.78
	1350	27.47	6.08	17.74	17.88	46.56	6.00	0.91	2.07	0.76	0.425	0.488	1.14
3	1400	28.93	6.55	16.66	18.11	49.12	6.00	0.86	1.97	0.73	0.115	0.452	3.93
	1450	29.40	6.79	16.94	17.51	49.26	6.00	0.85	1.94	0.71	0.025	0.402	16.08
	1350	26.12	5.80	19.43	15.13	51.12	6.00	-	1.26	1.26	0.375	0.470	1.25
4	1400	28.08	6.12	19.20	14.98	51.34	6.00	-	1.18	1.18	0.075	0.450	6.00
	1450	28.78	6.20	19.12	14.78	51.60	6.00	-	1.15	1.15	0.035	0.412	11.77

average size about 35-40 μm and homogeneous texture. The microstructures of clinker No.2 (Fig.1 b) are characterised by very large pores and smaller grain sizes (15-20 μm). The texture is not homogeneous. Fig.1 c of clinker No.3 shows very large grains with a small number of pores non-uniformly distributed. The grain sizes in Fig.1 d (of clinker No.4) show wide variation. The pores in this clinker are of medium size and uniformly distributed. Also, the grains are very densely packed.

The data on liquid phase properties σ and η presented in **Table 2** has been examined with reference to the typical microstructural features reported above. In case of clinker No.2 there are very large pores, surrounded by closely packed grains of smaller sizes. This sample also shows maximum values of surface tension as well as that of viscosity. With a highly viscous melt phase, having poor flow, it is expected that long range transport of material will not be possible resulting in such inhomogenities. Such a melt, with associated high value of surface tension, will have more predominently capillary action preferentially filling up the micropores. Such conditions may not be favourable for growth of large crystals (Fig. 1 b). Another extreme case is represented by clinker No.3 where viscosity as well as surface tension of the melt are minimum. It can be argued that this melt has better flow properties but poor capillary action. Thus the large pores will be filled by flowing melt but micropores will be left unfilled. The conditions are more than favourable for long range transport of material and growth of much larger crystals. The cases represented by clinker No.1 and 4 have intermediate values of these parameters and as such are showing intermediate microstructural features approaching to almost ideal case. Clinker No.4, however, shows larger variation in grain sizes.

Development of microstructures is closely linked to the third stage of sintering process i.e. the solid state sintering, which is arrived at during cooling. In a comprehensive treatment of the process, Timashev (1) expresses the predominent particle size as:

$$R = \frac{\sigma}{\eta \cdot \frac{dl/lo}{d\tau}} \; f(\psi)$$

where $f(\psi)$ is a complex trigonometrical function characterising liquid volume and $(dl/lo)/d\tau$ is shrinkage rate. The value of these two functions can be considered to be approximately constant during this phase of sintering (4), then the predominent particle size, which corresponds to sizes of growing grains in this controlled experiment varies proportionately with σ/η. The observations reported above, about the grain sizes of clinker 2 and 3 are thus in accordance with this treatment.

CONCLUSION

Intensification of clinkerisation process can be achieved by lowering the melt phase viscosity, which promotes dissolution and subsequent precipitation. Surface tension of the melt phase is required to be maintained at higher level, which may otherwise adversely affect the sintering process. Moreover, the ratio of surface tension to viscosity (σ/η) plays an important part in the development of microstructural features of the clinker. It is generally observed that the value of σ/η between 10 and 12 helps in proper burning and also develops optimum microstructural features in clinker.

ACKNOWLEDGEMENT

The results presented here are part of the studies related to role of minor components in affecting the liquid phase properties and kinetics of clinkerisation being conducted jointly at National Council for Cement and Building Materials, New Delhi and Mendeleev Institute of Chemical Technology, Moscow, Russia. The results are being published with the permission of Dr A K Mullick, Director General of NCB.

REFERENCES

1. Timashev, V.V. & Albats, B.S. : " The Process of liquid phase sintering of portland cement clinker" **The VI International Congress on the Chemistry of Cement**, Moscow 1974, V.I, 165-170.

2. Zozulya, P.V., Upolovnikov, A.B., & Wachtler H.J. : "On the composition of the liquid phase of portland cement clinker" **The VI International Congress on the Chemistry of Cement**, Moscow, 1974, V.I, 162-165.

3. Subin, V.I. : "Investigation into consolidation of portland cement clinker" **The VI International Congress on the Chemistry of Cement**, Moscow, 1974, V.I, 173-177.

4. Kouznetsova, T.V. : Private Communication, National Council for Cement and Building Materials, New Delhi, India.

5. Bucchi, R : "Influence of the nature and preparation of raw materials on the reactivity of raw mix, Principal Report", **The 7th International Congress on the Chemistry of Cement**, Paris 1980, V.I, I-1/3 - 1/43.

6. Timashev, V.V. : "The Kinetics of clinker formation : The structure and composition of clinker and its phases. Principal Report", **7th International Congress on the Chemistry of Cement**, Paris 1980, Vol.I, I-3/1 - 3/20.

ACCELERATION OF THE CLINKER FORMATION PROCESS

P F Rumyantsev and N T Erofeeva

Institute of Silicate Chemistry of the Russian Academy of Sciences
St Petersburg, RUSSIA

SUMMARY

This paper deals with the study of the possibility of acceleration of the clinker formation process in Portland cement by substituting the aluminosilicate component of the raw mix (clay) for compositions providing the obtaining of the liquid phase at temperatures which are lower compared to the conventional ones. As such compositions, two low-melting eutectique were chosen in the $CaO-SiO_2-Al_2O_3$ system.

Исследовалась возможность ускорения процесса клинкерообразования портландцемента заменой алюмосиликатного компонента сырьевой смеси (глины) на составы, обеспечивающие получение жидкой фазы при более низких, чем традиционные, температурах. В качестве таких составов были выбраны две низкоплавкие эвтектики в системе $CaO-SiO_2-Al_2O_3$.

INTRODUCTION

To decrease the firing temperature of clinker it is necessary to accelerate the physical-chemical processes of clinker formation.This effect can be attained by decreasing the temperature of the liquid phase formation. To this purpose, at the grinding stage impurities promoting the earlier appearance of the liquid phase (1,2) were added to the raw mix or low-melting components were used as the raw mix (3,4).

We studied the possibility of acceleration of the clinker formation process in Portland cement by substituting the aluminosilicate component of the raw mix (clay) for compositions providing the obtaining of the liquid phase at lower temperatures compared to the firing temperature of the conventional raw mix. As such compositions we chose two eutectiques in the $CaO-SiO_2-Al_2O_3$ system with melting temperatures of 1265°C (I) and 1170°C (II).

EXPERIMENTAL

Two the eutectiques composed of pure oxides and $CaCO_3$ were preheated until the full binding of the initial oxides was reached.Then six various raw mixes were prepared. Three of them were used to obtain a Portland cement clinker with LSF=0.88: one mix without the eutectique (1) and the other two with the indicated eutectiques (2)and (3).Then three more mixes were prepared in an analogous way (LSF=0.88) which contained ferrous oxide in the limits of the existing standards (4-6) The mixes were fired to 1400°C, the change of the quantity of free calcium oxide being controlled.

RESULTS AND DISCUSSIONS

Mixtures with components of eutectique composition contained a significantly lower quantity of free calcium oxide within the whole temperature region thah the mixture without the eutectique(Figs.1 and 2). The indicated difference was determined to be 15-20% at temperatures of 1150-1300°C and 20-25% at 1350-1400°C. At 1150-1200°C in mixtures containing ferrous oxide the formation of CF and C_2F is possible, and this can be the reason of a considerable decrease of the free calcium oxide content compared to analogous mixtures without ferrous oxide (Figs.3and 4).

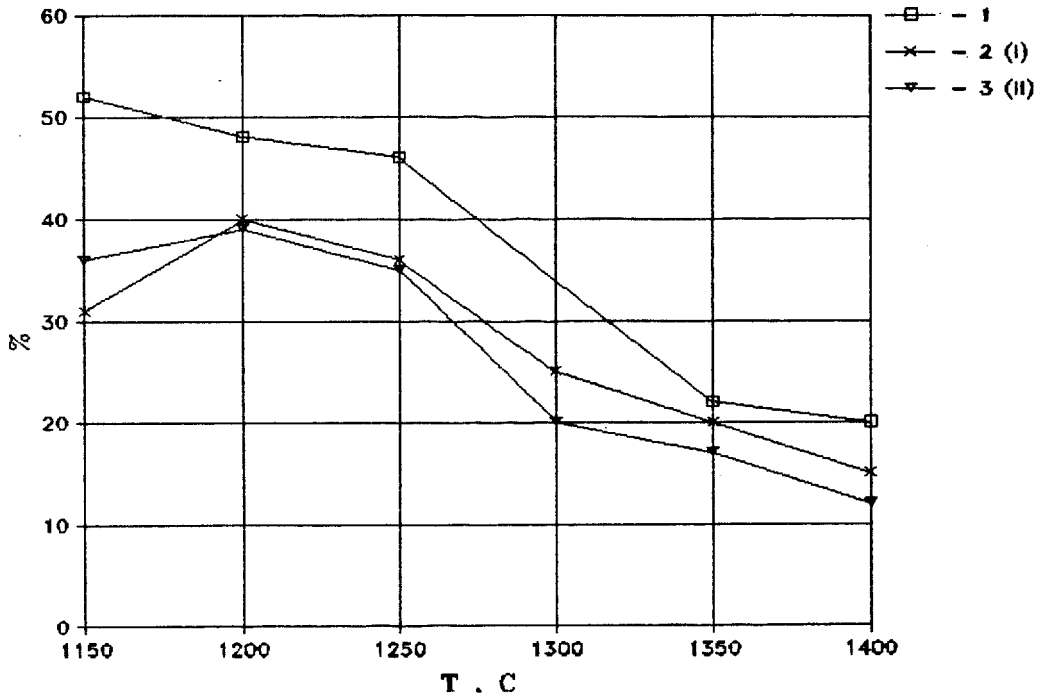

Fig.1 Dependences of the free calcium oxide content on the firing temperature: 1 - raw mix without the eutectique; 2 - raw mix with eutectique I; 3 - raw mix with eutectique II.

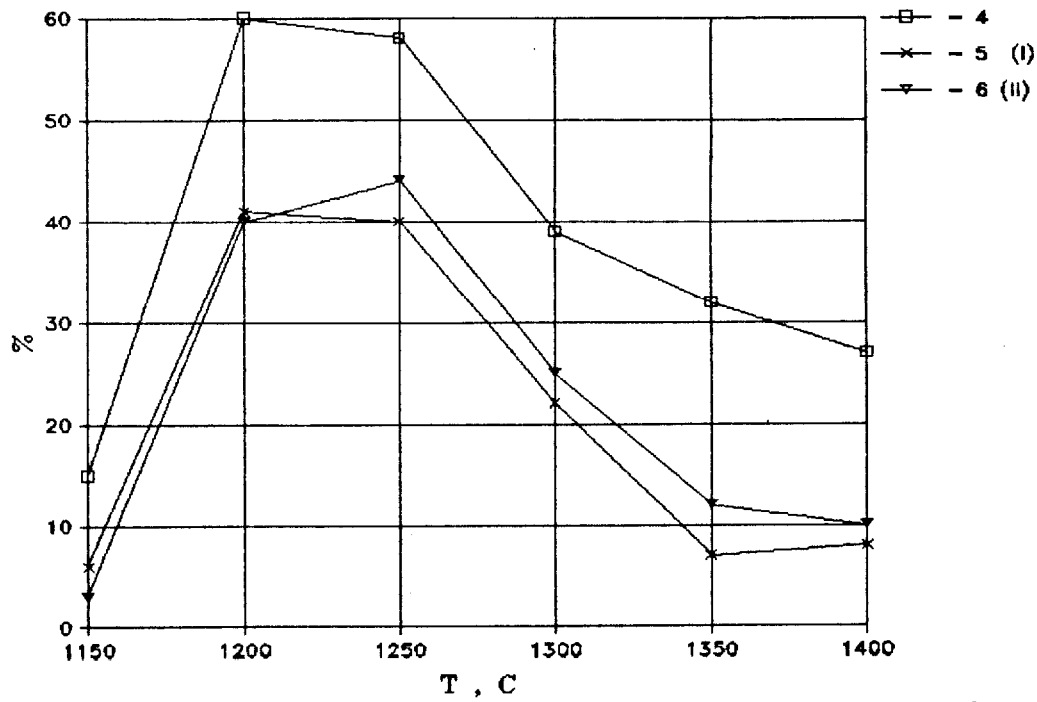

Fig. 2 Dependences of the free calcium oxide content on the firing temperature (all raw mixes contain ferrouse oxide) : 4 - rawmix without the eutectique; 5 - raw mix with eutectique I; 6 -raw mix with eutectique II.

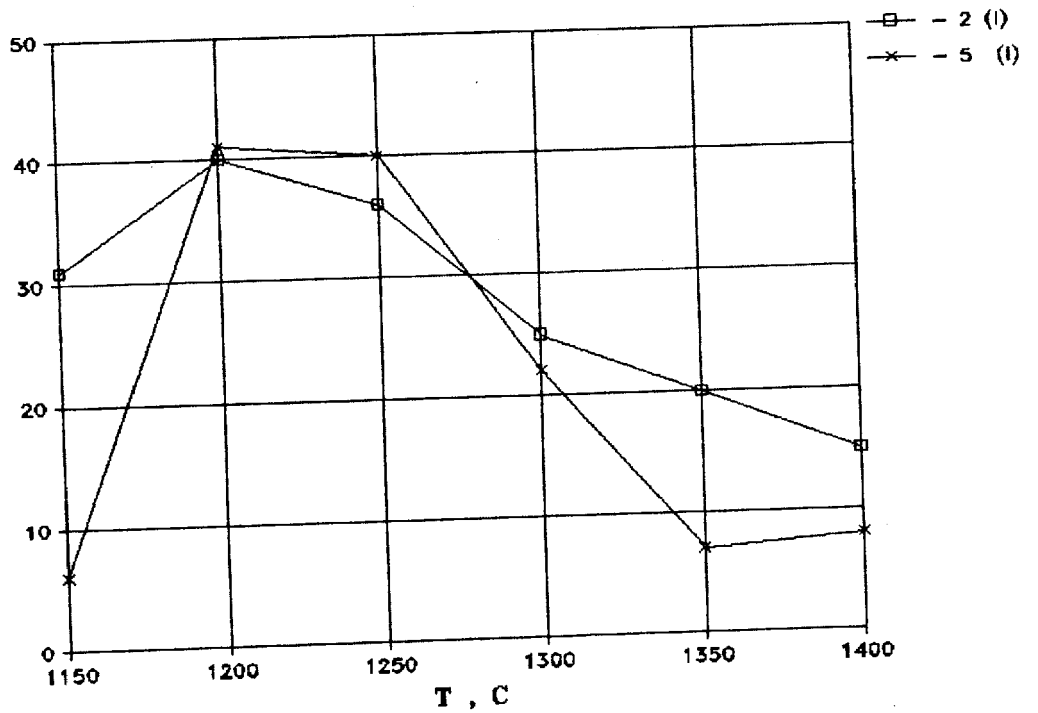

Fig.3 Dependences of the free calcium oxide content on the firing temperature: 2 (I) - raw mix with the eutectique I; 5 (I) - raw mix containing ferrous oxide and eutectique I;

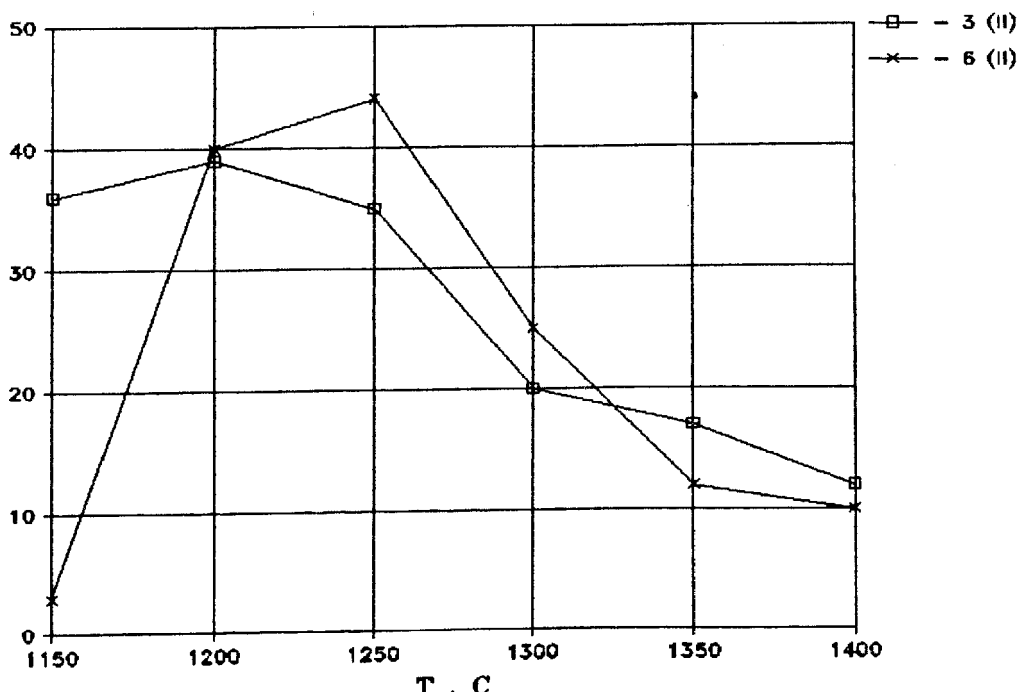

Fig.4 Dependences of the free calcium oxide content on the firing temperature: 3 (II) - raw mix with the eutectique II; 6(II) - raw mix containing ferrous oxide and eutectique II;

The quantity of free calcium oxide in clinkers with eutectiques(Fig. 2) at 1400°C is three times as low as in compositionswithout eutectiques.

CONCLUSIONS AND RECOMMENDATIONS

The earlier appearance of the clinker liquid phase accelerates the clinker formation process. The results obtained in this work opennew possibilities for a decrease of firing temperature of Portland cement clinker by substituting the clay by rocks, slags or ashes whose chemical composition calculated for the 100% amount of three main oxides (CaO, SiO_2, Al_2O_3) is eutectique or near-eutectique. In thiscase the effect of a decrease in firing temperature will be reducedwith deviation from the eutectique composition.

In addition, the impurities contained in the aluminosilicate component of the raw mix will strengthen the positive effect but they should be present in such quantities that theircontent in clinker could not exceed the existing limits.

REFERENCES

1. N.A.Toropov.: "Cement Chemistry", Promstroiizdat, Moscow, 1956, 184 -186.

2. B.V.Volkonsky, P.F. Konovalov and S.D.Makashev.: "Mineralizers in Cement Industry", Stroiizdat, Moscow, 1964, 199.

3. A.A.Pashchenko, E.A.Myasnikova, A.A.Myasnikov et al.:"Cements Made from Bazaltoids", Naukova Dumka, Kiev, 1983, 192.

4. R.Saanzasuren.:"Portland cement clinker synthesized at low temperatures and its properties", Collection of papers Building Materials Made from Side Commercial Products, Leningrad, 1988, 81-84.

TRACE ELEMENT BALANCES IN KILN SYSTEM OF A FEW INDIAN CEMENT PLANTS

N A Krishnan, V K Gore, S A Khadilkar, R V Hargave, C H Page and A K Chatterjee

Research and Consultancy Directorate
The Associated Cement Cos Ltd
Thane, INDIA

SUMMARY

The raw materials, additives and fuels used in cement manufacture contain the trace elements in varying concentrations. Some of the trace elements are volatile and they are observed to show a cyclic phenomenon in cement kiln systems. The extent of concentration of the volatile trace elements in such cycles, being influenced by nature of trace element, type of process, material/gas flow parameters in kiln system and characteristics of kiln feed/clinker/fuel, along with burning conditions in the kiln. Thus influenced by these parameters, the different trace elements get incorporated in clinker, electrostatic precipitator dust at varying levels, or partly escape to the environment.

In the present paper, an attempt has been made through evaluation of circuit samples to establish the balances of the trace elements in dry, wet, semi wet and semi dry processes of a few selected cement plants in India. Based on the data generated, the paper explains the behaviour of the trace elements in cement kiln systems.

INTRODUCTION

The natural raw materials, additives, fuel used in cement clinker production contain various concentrations of trace elements, some of which may affect the environment. Depending on the physico-chemical characteristics, high temperature employed in the clinkering process and other operating parameters of rotary kiln system, these elements get incorporated in the clinker in varying concentrations, or form volatile cycles. This paper attempts to study mass balances of some trace elements in process materials of six plants of THE ASSOCIATED CEMENT COMPANIES LTD., which employ different kinds of processes namely, dry process, wet process, semi-dry process and semi-wet process.

MASS BALANCE INVESTIGATIONS OF TRACE ELEMENTS IN CEMENT PLANTS

BASIC APPROACH

Mass balances of trace elements in cement plants have been attempted through evaluation of process input and process output samples. Periodic samples of Raw Meal (without kiln dust) and coal (inputs), clinker and kiln dust (outputs) were collected over a period of 48 hours, and representative average samples were taken for evaluation of the trace element concentrations. Taking into consideration the mass flow rates of raw meal, coal, kiln dust and clinker, the total inputs and total outputs of trace elements were computed. The deficit in the trace elements would be representative of the behaviour of the elements in the kiln system. In order to have an overview of the trace elements levels in the raw materials, the raw material and correctives used by each plant were also analysed for these trace elements.

The mass balance investigations were carried out on the following cement plants in the country.

PLANT-A, PLANT-B and PLANT-C are dry process plants with suspension preheater and precalciner systems, and PLANT-D is a wet process plant. The nature of kiln dust of PLANT-D is siliceous and due to this, there is limitation in recirculation of dust in the system. PLANT-E is a semi wet process plant with suspension preheater and precalciner system. PLANT-F is a semi dry process plant with lepol system (Grate precalciner kiln).

Thus, except for PLANT-D, the kilndust is recirculated to the kiln system in all the plants.

ANALYSIS PROCEDURE

Representative average samples of raw materials, raw meal, kiln dust, clinker and coal were analysed for some of the trace elements namely, Barium, Strontium, Chromium, Manganese, Cobalt, Nickel, Copper, Zinc, Cadmium, Antimony, Arsenic and Lead. The determination was carried out by Atomic Absorption and Colorimetric techniques. The raw materials and process materials excepting coal under study were treated with a mixture of nitric acid and hydrofluoric acid to effect complete dissolution of the materials. Coal samples were first incinerated at a low temperature to destroy the carbon matrix and then treated with the mixture of acids as above.

Various trace elements in solution were determined using the Atomic Absorption Spectrophotometer (IL.951, Double-Beam, Double Channel of Instrumentation Laboratory). With standard conditions presented in Table-1.

TABLE-1 STANDARD CONDITIONS FOR ATOMIC ABSORPTION ANALYSIS

S.No.	Element	Flame	Analytical Wavelength (nm)
1.	Copper (Cu)	Air - C_2H_2	324.8
2.	Barium (Ba)	N_2O - C_2H_2	455.4*
3.	Strontium (Sr)	Air - C_2H_2	460.7
4.	Manganese (Mn)	Air - C_2H_2	279.5
5.	Chromium (Cr)	Air - C_2H_2	357.9
6.	Cobalt (Co)	Air - C_2H_2	240.7
7.	Nickel (Ni)	Air - C_2H_2)	341.5
8.	Zinc (Zn)	Air - C_2H_2	213.9
9.	Cadmium (Cd)	Air - C_2H_2	228.8
10.	Antimony (Sb)	Air - C_2H_2	206.8
11.	Lead (Pb)	Air - C_2H_2	283.3

* To avoid molecular absorption by Ca-OH Bonds, this ion line was selected.

Arsenic was determined by a preliminary separation as Arsine (AsH_3) and by molybdenum blue colorimetric method using a Spectrophotometer (Cary-219 of Varian) at 840 nm.

EVALUATION OF TRACE ELEMENTS

The trace element analysis of limestone, corrective materials, coal and kiln dust was carried out by the analysis procedure. The analytical data is presented in Table-2.

Taking into account the mass flow rates of raw meal, coal, clinker and kiln dust for each cement plant and based on the concentrations of trace elements in these materials, the total inputs, outputs and deficit in trace element concentration was computed for each cement plant under study, which is given in Table-3.

The concentrations of trace elements in Raw Meal and kiln dust on loss free basis for each plant is presented in Table-4, and the △ concentration (kilndust-Raw Meal) of trace elements is presented in Fig.1.

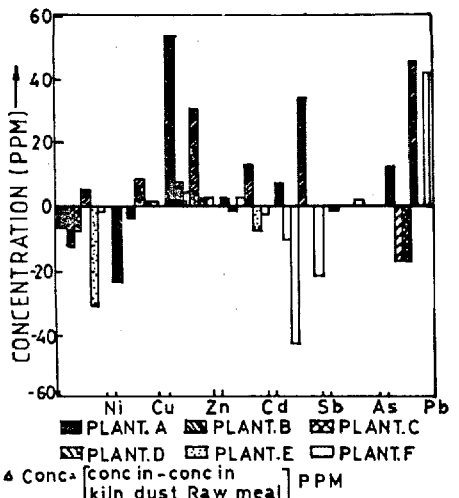

FIG.1 △-CONCENTRATION OF TRACE ELEMENTS.

TABLE-2 TRACE ELEMENT CONCENTRATION IN RAW MATERIALS, COAL AND KILN DUST

	Plant	Ba	Sr	Cr	Mn	Co	Ni	Cu	Zn	Cd	Sb	As	Pb
A	Limestone	1295	315	16	350	20	22	7	27	12	50	-	<10
	Laterite	<100	<10	540	234	33	772	8	73	9	40	-	15
	Iron Ore	<100	<10	9	760	25	41	12	25	8	45	-	<10
	Coal	140	<10	58	95	14	33	28	26	<10	30	4.0	<10
	Kiln Dust	135	192	25	42	16	22	12	46	11	60	<0.5	16
B	Limestone	<100	17	<10	135	10	<20	5	10	<10	25	-	<10
	Shale	<100	10	55	490	22	31	20	54	<10	25	-	20
	Iron Ore	<100	12	33	105	38	80	8	25	10	40	-	<10
	Coal	<100	<10	52	180	12	24	24	30	<10	26	4.0	<10
	Kiln Dust	<100	12	14	280	10	<20	14	19	<10	25	<0.5	<10
C	Limestone	<100	82	25	295	14	<20	9	24	8	52	-	<10
	Clay	<100	19	108	1174	35	82	65	52	9	20	-	20
	Iron Ore	<100	<10	50	131	14	20	15	25	10	31	-	<10
	Coal	<100	<10	61	175	13	28	25	32	<10	43	1.0	<10
	Kiln Dust	<100	48	9	237	10	<20	10	39	12	27	<0.5	<10
D	Limestone	<100	385	13	16	12	<20	8	25	10	83	-	<10
	Laterite	<100	<10	345	121	75	120	131	85	7	78	-	49
	Coal	<100	<10	37	90	11	22	24	26	<10	20	4.4	<10
	Kiln Dust	<100	10	38	30	22	31	20	54	14	122	1.7	46
E	Limestone	695	89	21	377	11	<20	9	39	11	35	-	<10
	Basalt	<100	<10	3640	245	30	1020	149	131	11	76	-	<10
	Iron Ore	<100	<10	115	295	23	48	28	57	11	76	-	<10
	Coal	112	<10	69	230	11	39	23	46	<10	30	1.0	<10
	Kiln Dust	690	118	53	625	13	35	24	51	7	43	<0.5	<10
F	Limestone-1	<100	94	20	400	14	20	4	20	10	96	-	<10
	Limestone-2	<100	833	22	309	12	14	6	22	9	104	-	<10
	Coal	<100	<10	47	170	11	28	26	45	<10	30	4.2	30
	Kiln Dust	<100	100	27	361	15	20	8	25	9	96	0.5	47

TABLE : 3 MASS BALANCES OF TRACE ELEMENTS IN DIFFERENT CEMENT PLANTS

Trace Element	PLANT - A			PLANT - B			PLANT - C			PLANT - D			PLANT - E			PLANT - F		
	I	O	I - O	I	O	I - O	I	O	I - O	I	O	I - O	I	O	I - O	I	O	I - O
Ba	1840	1860	- 20	36,	38	-2	100,6	99.4	+1.2	55	54.5	+0.5	987	990	-3	88	85	+ 3,0
Sr	443	440	+ 3	25	26	- 1	121.2	122.0	- 0.8	538	540	- 2.0	145	150	- 5.0	13.8	140	- 2.0
Cr	40.7	41.5	- 0.8	24.2	25	- 0.8	47.4	48.9	- 1.5	48	48.6	- 0.6	189	190	- 1.0	71	69	+ 2.0
Mn	524	540	- 16	212	210	+ 2.0	477.5	476.0	+ 1.5	65	66.2	- 1.2	560	562	- 2,0	701	700	+ 1.0
Co	31.2	31.0	+ 0.2	18.4	18.4	Nil	22.8	29.0	- 0.2	38.7	39.0	- 0.3	18.0	20.0	- 2.0	30	30	Nil
Mn	36.4	51.0	- 14.6	37.8	38.0	- 0.2	34.9	45.0	- 10.1	41.5	57.0	- 15.5	75.5	75.8	- 0.3	49	58	- 9.0
Cu	15	17	- 2	10.7	18.2	- 7.5	18.9	20.0	- 1.1	26.4	26.7	- 0.3	20.5	23.0	- 2.5	28.5	28.0	+ 0.5
Zn	42.8	49.5	- 6.7	19.3	38.6	- 19.3	40.0	45.9	- 5.9	48.7	48.0	+ 0.7	64.0	71.0	- 7.0	67.5	103	- 35,5
Cd	17.0	18.5	- 1.5	15.2	18.0	- 2.8	12.2	21.2	- 9.0	15.0	20.0	- 5.0	53.8	59.0	- 5.2	23.0	34.0	- 11.0
Sb	75.8	137	- 61.2	43.9	102.5	- 58.6	78.1	153.7	- 75.6	127	147.5	- 20.5	30.1	118	- 87.9	172	190	- 18
As	2.0	2.4	- 0.4	1.2	1.2	Nil	0.6	0.8	- 0.2	0.8	0.9	- 0.1	0.8	0.8	Nil	1.1	1.1	Nil
Pb	18.6	59.0	-40.4	10.8	22.0	- 11.2	28.9	57	- 28.1	15	46.0	- 31.0	21.0	56.0	- 35.0	46	62	- 16

I - Input O - Output

TABLE : 4 - LOSS FREE BASIS TRACE ELEMENT CONCENTRATIONS IN RAW MEAL & KILN DUST

	PLANT - A		PLANT - B		PLANT - C		PLANT - D		PLANT - E		PLANT - F	
	RM	KD	RM	KD	RM	KD	RM	KD	RM	KD	RM	KD
Ba	1962	180	28.1	13.3	95.3	95.0	60.1	60.0	1048	920	76.9	60.0
Sr.	476.6	256	25.9	16.0	124.6	64.0	582.0	475.3	134.7	157.3	140	133.3
Cr.	36.9	33.3	20.5	18.6	42.9	12.0	35.9	50.6	199.0	70.6	32.3	36.0
Mn.	552.8	576.4	208.4	373.3	491.0	316	30.5	40.0	581.4	833	57,38	490
Co.	31.9	21.3	18.4	13.30	22.8	13.3	37.2	29.3	18.1	17.3	21.5	20
Ni	35.3	29.3	38.9	26.6	33.9	26.7	35.6	41.3	78.3	46.6	26.1	26.6
Cu	42.8	18.8	18.9	18.7	16.9	13.3	17.8	26.6	30.9	32.0	9.7	10.7
Zn.	18.3	71.9	17.5	25.3	38.8	42.7	41.6	72	65.5	68.0	30.8	33.3
Cd.	14,4	17.0	15.3	13.3	13.1	16.0	5.9	18.7	17.3	9.3	15.4	12.0
Sb.	77.8	85.0	44.4	33.3	79.5	36.0	129.3	162.7	57.3	57.3	150.7	128.0
As.	1.7	0.78	0.93	0.7	0.8	0.7	0.8	2.2	1.2	0.7	0.8	0.7
Pb.	13.0	25.0	30.9	13.3	30.9	13.3	16.4	61.3	20.9	30.9	21.5	62.7

BEHAVIOUR OF TRACE ELEMENTS

a) Barium, Strontium, Chromium, Manganese and Cobalt

The total input and output concentrations of Ba, Sr, Cr, Mn and Co presented in Table-3 illustrates that there is no increase in levels of these elements in the outputs which indicates negligible volatility of these elements in the clinkerisation process. The concentrations of these elements in kilndust is relatively lower as compared to the raw meal.

b) Nickel and Copper

The computed total input and outputs of Nickel given in Table-3 shows that Nickel concentration in the outputs is observed to be more in all the plants except Plant-E (Semi wet process) and Plant-F (Semi dry process). In plants A,B,C (Dry process), the concentrations of Nickel is lower in kiln dust, while in the kiln dust of plant-D (wet process), its concentration is higher than the raw meal. As reported by a number of co-workers, the volatility of Nickel is associated with presence of chloride. Although chloride levels in a dry-process plant are at quite low level, formation of internal cycles even at that low levels of chlorides is feasible. (Ref.1,2,3). While in the wet process plant-D, the carry over of the volatile Nickel compounds to the kiln dust is relatively more. In plant-E (semi-wet process) and plant-F (semi dry process) the Nickel inputs match very well with outputs indicating very low volatility of this element in these plants.

Copper also indicate increased levels in the outputs in all the plants under study. Except for plant-D (wet process), the concentration of this element in the kiln dust is low. As already studied by S.Sprung et al (Ref. 1,2,3,4), the volatile compounds of the element may be establishing an internal cycles in the kiln/preheater region and so the carry over of copper to the kiln dust is relatively low.

c) Zinc, Cadmium

Enrichment of Zinc is observed in the output of all the plants, except plant-D (wet process) where due to the nature of dust, it is not recirculated). This indication of internal cycleof zinc in the kiln system is not only restricted to kiln/preheater system but even the kiln dust is observed to be richer in the element. (Ref.1).In plant-D the kiln dust is observed to contain relatively higher concentration of this element as compared to other plants. Due to the siliceous nature of the kilndust, it is not possible to recirculate the dust back to the kiln system, as a result of which the build up of concentration of this element in plant-D is less.

Cadmium also shows a similar enrichment in the outputs in all the plants. However, in kiln dust of plants, A, B, E and F, the cadmium concentrations are slightly lower than the raw meal. As cadmium is known to exhibit somewhat higher volatility, it is found to increase in outputs, however depending on the degree of condensation of cadmium compounds, variation of its concentration (Ref.3) in kiln dust is expected.

d) Arsenic, Antimony and Lead

The p-block elements, Arsenic, Antimony and Lead show a very high degree of volatility, with the concentrations of these elements in the external cycle (outputs) being considerably higher than the inputs.

Earlier studies (Ref.5) have shown that high levels of incorporation of Arsenic and Antimony in clinker is attributable to the formation of calcium arsenates and calcium antimonates respectively and the mechanism of formation of these compounds is linked with presence of excess of CaO, oxidising kiln atmosphere and elevated temperature of cement kilns. The data presented in this paper regarding the mass balance of these elements is also in tune with the observed and reported trends.

As regards the behaviour of lead, the data presented in this paper reveals that the lead concentrations in all the plants is more in outputs and only in plant-D (wet process) and plant-F (semi-dry process with grate calciner system) its concentrations in the kiln dust is found to be much higher as compared to the Dry process plants, (Plant A, B, C) and Semi-wet process plant. (Plant-E) similar observations have also been reported on the behaviour of lead in cement kiln systems. (Ref. 1 & 4).

CONCLUSIONS

The mass balance investigations of some of the trace elements in different processes of cement manufacture presented in this paper reveal that -

i) Ba, Sr, Cr, Mn and Co are more or less balanced in inputs and outputs, indicating less possibility of these elements forming internal cycles. This phenomenon has been observed in materials from dry process, wet process, semi-wet and semi dry processes under study.

ii) Nickel internal cycles are more pronounced in dry process plants than in semi-dry and semi wet processes, while copper illustrates increase in concentrations in output material of all processes, except in wet process plant without recirculation of kiln dust, where the carry over of these elements to the dust is more.

iii) The zinc and cadmium internal cycles are not restricted only to kiln/preheater system but their carry over to kiln dust is also observed, with zinc concentrations being more than cadmium in kiln dust.

iv) The extent of enrichment of Arsenic, Antimony and Lead in the material outputs is relatively more as compared to other trace elements in all processes under study.

Further studies are being carried out to evaluate the extent of internal cycles of the trace elements in different types of kiln preheater systems, by analysing the preheater samples at different periods of kiln running time, the findings of which would be published.

REFERENCES

1. S.Sprung, G.Kirchner & W. Rechenberg. "Reactions of Poorly volatile trace elements in cement clinker burning". ZKG No. 10/84, Pg. 513-518.

2. G.Kirchner. "Reactions of cadmium in the clinker burning process". ZKG No.9/85. Pg. 535-539.

3. S.Sprung. "Trace elements - Concentration build up and measures for reduction. ZKG No.5/88. Pg. 251-257.

4. G.Kirchner. "Behaviour of heavy metals during cement clinker burning". ZKG No.10/86. Pg. 555-557.

5. W.Wesweiler and W.Kremar. "Arsenic and Antimony balances of cement kiln plants with grate preheater. ZKG. No. 3/89. Pg. 133-135.

PHASE TRANSFORMATIONS WHEN SYNTHESIZING CLINKERS PRODUCED OF TECHNOGENEOUS RAW MATERIALS

I S Akhmetov and O A Mlryuk

Rudny Industrial Institute
Republic of KAZAKHSTAN

SUMMARY

Interactions of calcium carbonate when burning with separate minerals of technogeneous cement raw materials (CMS_2, C_3AS_3, NAS_6) are investigated. The technology of formation of C_6A_4 MS-phase from oxide mix is studied. We defined the influence of CaF_2, $CaSO_4$, Na_2CO_3 on these processes. Schemes of interactions are given together with diagrams of changing the phases content. We present data on hydration and solidification of C_6A_4MS-phase.

РЕФЕРАТ

Исследованы взаимодействия при обжиге карбоната кальция с отдельными минералами техногенного цементного сырья (CMS_2, C_3AS_3 , NAS_6). Изучен характер образования фазы C_6A_4MS из смеси оксидов. Установлено влияние добавок CaF_2, $CaSO_4$, Na_2CO_3 на эти процессы. Представлены схемы взаимодействий, диаграмма изменения содержания фаз. Приведены данные о гидратации и твердении фазы C_6A_4MS.

INTRODUCTION

The use of technogeneous materials in cement production complicates substance composition of the raw mixes.Such mixes are characterized by the structure of minerals and variety of admixtures. Optimum mineral compositions would enable to govern the phaseformation and influence the properties of clinkers. Therefore it is necessary to have an idea of the role of each mineral in process of clinkers formation.

Most of technogeneous materials contain minerals diopside, grossularie, albite. Thermal conversion of these minerals are described in the published works (1,2,3). However, interaction of minerals and calcium carbonate and influence of catalytic and modifying additions on such conversion are investigated insufficiently. The presented paper deals with this very problem.

C_6A_4MS-phase (Q-phase) is a component of high-alumina cement derived from the raw containing silica and magnesium admixtures. Many researchers refer to hydration activity of C_6A_4MS-phase (3,4). For that reason the presence of Q-phase in cement is considered to be undesirable. The results of investigation of Q-phase formation in different raw mixes and its hydration properties are given in this paper.

EXPERIMENTAL

The investigation of thermal interactions between some minerals allows to imagine the mechanism of phase-forming in multicomponent cement raw mixes. Transformations are studied which occur in burning the raw mixes including calcite and one of the minerals of technogeneous silicate raw materials. We defined the influence of catalytic and modifying additions on such transformations. Raw mixes (Lime Saturation Factor LSF=0,70...0,75) were prepared from pregrinded components. Mixes for C_6A_4MS-phase synthesis were obtained from the chemical agents ($CaCO_3$, Al_2O_3, MgO, SiO_2). The choice of sorts of additions is conditioned by their catalytic and modifying action as well as by their wide spreading in technogeneous raw material. The quantity of additions introduced was 5 percent beyond 100 percent of mass. Mixes were homogeneous and mould into briquettes (D=H=10 mm), then burnt in a kiln. Isothermal curing was 20 minutes. Clinkers underwent air cooling. Thermal interactions schemes are given below, they are composed on basis of data of Differential Thermal Analysis (DTA) and X-Ray Diffraction analysis.

Hydraulic properties of C_6A_4MS-phase synthesized from oxides under the temperature (T) of 1300°C were investigated.For comparison monophase cements from CA and $C_{12}A_7$ were used. Tests on strength of cements were carried out. Samples 1x1x6 cm were made of plastic paste (cement/water). Samples were kept in water under the T=18...25°C.

RESULTS AND DISCUSSIONS

Calcite : diopside ($CaCO_3$: CMS_2 - 62:38, mass%)

General mass of CMS_2 is transformed into C_2MS_2 and C_3MS_2 ($850<T<1250^oC$). Simultaneously decomposition of CMS_2 ($950<T<1250^oC$) takes place:

$$CMS_2 + 3C \rightarrow 2C_2S + M \quad (1)$$

Temperature raising (1250...1300°C) all reactions of CaO with silicates result in the formation of C_2S and MgO. When introducing CaF_2 , decarbonization of $CaCO_3$ is accelerated by appearance of eutectic melt ("-"810°C, Fig.1). This process is accompanied by isolation of active CaO which is favourable to the reaction of substitution 1 when $750<T<1150^oC$. As a result highcalcium phases C_2MS_2 and C_3MS_2 don't appear. Low temperature C_2S form $2(C_2S)CaCO_3$. Exothermal reactions of synthesis $2(C_2S)CaF_2$ and $C_{11}S_4CaF_2$ smooth out the effect of dissociation $2(C_2S)CaCO_3$("-"870...915°C).The phase $2(C_2S)CaF_2$ is stable till temperature is 950°C. Incongruent melt of $C_{11}S_4CaF_2$ is indicated at 1150°C. Clinker ($T=1350^oC$) contains C_2S, C_3S, MgO, CaF_2.

Calcite : grossularie ($CaCO_3$: C_3AS_3 - 58:42, mass%)

Changes in the burnt mix may be divided into 3 stages. Stage I - till $T=1050^oC$:

$$C_3AS_3 + 3C \rightarrow C_2AS + 2C_2S \quad (2)$$

$$2C_2S + CaCO_3 \rightarrow 2(C_2S)CaCO_3 \quad (3)$$

Under $T>1000^oC$ $2(C_2S)CaCO_3$ decomposes .Stage II - $T=1150...1250^oC$:

$$2C_3AS_3 \rightarrow C_2AS + 3CS + CAS_2 \quad (4)$$

Stage III - $T=1230...1400^oC$. Phases isolated in the reaction 4 are saturated by CaO until C_2S and C_3A are formed. In a mix containing CaF_2 due to high activity of C_3AS_3 the following interactions are possible:

$$2C_3AS_3 + CaCO_3 \rightarrow 2(C_2S)CaCO_3 + 2CAS_2 , \quad T=750...850^oC \quad (5)$$

$$C_3AS_3 + 6C \rightarrow C_3A + 3C_2S , \quad T=750...1150^oC \quad (6)$$

$$C_3AS_3 \rightarrow CAS_2 + C_2S , \quad T=1150^oC \quad (7)$$

No helenite in the burnt mix. Under $T=950^oC$ C_3A is transformed into $C_{11}A_7CaF_2$ (5). Decomposition of carbonates and formation of silicates fluoride takes place as well as in a raw mix containing diopside (Fig.1). Concentration of CaO is not large, that is why content of CAS_2 decreases slightly ($T=1150...1350^oC$). Addition $CaSO_4$ reacts with C_2S and C_2AS isolated in the reaction 2. In the first case $2(C_2S)C\bar{S}$ is formed, which is decomposed under $T>1150^oC$. Second reaction proceeds in such a way :



Fig.1 Fragments of DTA of raw mixes containing diopside 1 and grossularie 2

$3C_2AS + 3C + C\bar{S} \rightarrow 3(CA)C\bar{S} + 3C_2S$ (8)

Clinker (T=1300°C) contains C_2S and $3(CA)C\bar{S}$. In joint of CaF_2 and $CaSO_4$ into a mix, thermal stability of $2(C_2S)C\bar{S}$ reduces onto 100°C. Due to primary and advantageous forming of $C_{11}A_7CaF_2$ concentration of $3(CA)C\bar{S}$ reduces, $CaSO_4$ keeps in a clinker. Cooling of clinkers containing fluoride from T=1150°C and higher is accompanied by inversion $\beta \rightarrow \gamma$ - C_2S. Partial transition of $\beta \rightarrow \gamma$ - C_2S is characteristic of clinkers containing no additions on the basis of CMS_2 , C_3AS_3 .

Calcite : albite ($CaCO_3$: NAS_6 - 75:25, mass%)

First, CAS, CS, C_2S, NA are formed. Melting of NAS_6 (T=1120°C) favours an increase of reactionary ability of a mix. Content of C_2S, NA increases, CAS_2 , C_2AS, NS appear. The following interactions precede the formation of N_2AS_2 , CA (T=1200°C) :

$CAS_2 + 2NA + C \rightarrow N_2AS_2 + 2CA$ (9)

$CAS_2 + 2NS + 3C \rightarrow N_2AS_2 + 2C_2S$ (10)

Burning of a mix under T>1250°C is accompanied by transformations :

$N_2AS_2 + 5C \rightarrow 2C_2S + CA + 2N$ (11)

$CA + 2C \rightarrow C_3A$ (12)

An isolated Na_2O dissolves in C_2S, as a result we observe a partial transition $\beta \rightarrow \alpha'$- C_2S. Preference of dissolving Na_2O in C_2S, and not in C_3A is predetermined by late forming of C_3A. When $CaSO_4$ is added into a mix, decarbonization of $CaCO_3$ is prolonged because of the forming $Na_2Ca(CO_3)_2$:

$NA + CaSO_4 \rightarrow Na_2SO_4 + CA$ (13)

$CaCO_3 + Na_2SO_4 \rightarrow CaSO_4 + Na_2Ca(CO_3)_2$ (14)

$Na_2Ca(CO_3)_2$ is decomposed under T=1000...1050°C. On the basis of CA there $3(CA)C\bar{S}$ is formed (T>900°C). In the course of the reaction of CS and Na_2O we get NCS. After melting NAS_6 we observe intensive isolation of C_2S. An exothermal process takes place under T=1100...1160°C :

$3(CA)C\bar{S} + NCS \rightarrow NA + 2CA + C_2S + CS$ (15)

The phase of $CaSO_4$ reacts with C_2S and NA and there are formed $2(C_2S)C\bar{S}$ and Na_2SO_4 correspondingly. The greater part of Na_2SO_4 is sublimated. Clinker synthesized under T=1300°C contains β- C_2S, $C_{12}A_7$, CA, C_3A. As far as an addition of $CaSO_4$ absorbed the alkali, the dissolving of Na_2O in the clinker's phases is very insignificant. Concentration of CaO in melted clinker is higher at the expense of adding $CaSO_4$ and prevailing of aluminates with low basicity.

Stechiometric mix for getting a Q-phase

According to the data of X-Ray Diffraction analysis we defined changes in the composition and content of phases in clinkers, as well as the influence of additions on transformations in a mix (Fig.2). Appearance of C_6A_4MS in a stechiometric mix is preceeded by formation of calcium aluminates with different basicity, C_2AS , C_2S. Main portion of C_6A_4MS is formed under T=1250...1300°C, after liquid phase appears. When burning a mix the following interactions are possible :

$C_2AS + C \rightarrow C_2S + CA$ (16)

$C_{12}A_7 + 5A \rightarrow 12CA$ (17)

$$4CA + C_2S + M \rightarrow C_6A_4MS \qquad (18)$$

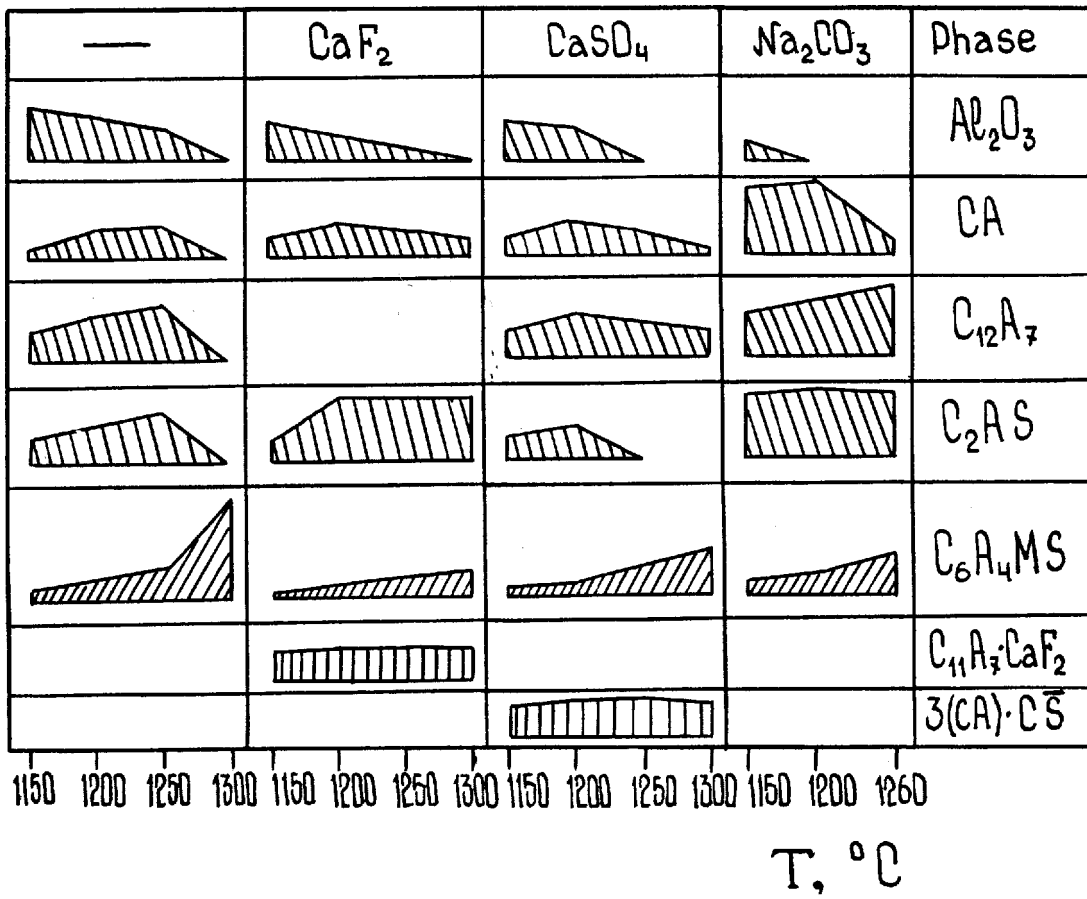

Fig.2 The change of alumina phases content subject to composition and temperature of mix burning

Transformations in a mix are more varied than in a given scheme. Formation of C_6A_4MS is probable on the basis of unstable phase C_5A_3 which can dissolve magnesium and silicon (6). C_3A is observed in a clinker under T=1200...1250°C, later it turns into CA or C_5A_3 . Consequently, all possible ways of formation C_6A_4MS are supposed to bring an appearance of solid solution on the basis of calcium aluminates together with silica and magnet-containing phases. Under T=1380...1400°C Q-phase is incongruently melting with an isolation of CA. It is coordinated with the data (3). When introducing additions into a mix we see that stechiometrum of reacting phases is broken and concentration of C_6A_4MS reduces. Outflow of CaO into highbasic aluminates stipulates conservation of C_2AS in clinkers of mixes with CaF_2 , Na_2CO_3 . Addition of Na_2CO_3 intensifies the formation of C_6A_4MS at low temperatures.

Cement stone on the basis of Q-phase hardens intensively not at an early stage only but further on during a long time as well (table).

Table

Phase	Blaine, m^2/kg	Water/ Cement	Compressive Strength, kg/cm² age per day			
			1	3	28	360
CA	280	0,30	630	740	1010	910
$C_{12}A_7$	280	0,50	370	420	350	200
C_6A_4MS	300	0,28	520	600	900	1240

Peculiarities of Q-phase hydration : smooth crystallisation of calcium hydroaluminates; higher stability of hexagonal hydrates; plenty of colloidal combinations during a long hydration period; varied speed and crystallization degree of component gel parts. The mentioned fact of high hydraulic activity of Q-phase contradicts the noted data (3, 4). It should be taken into account that C_6A_4MS is a multicomponent solid solution with a vacillating content of components, whose properties considerably depend upon the condition of burning and cooling.

CONCLUSIONS AND RECOMMENDATIONS

Participation of minerals of technogeneous raw materials in the process of forming clinkers is accompanied by complication of composition of intermediate compounds and by deflection from usual schemes of reactions between components, as well as by modificational transformations of clinker's phases. It is determined that: an addition CaF_2 in a mixture of $CaCO_3$ and CMS_2 prevents an emergence of intermediate phases of C_2MS_2 , C_3MS_2 , and in a mixture of $CaCO_3$ and C_3AS_3 it is an obstacle for C_2AS to appear. When combining CaF_2 and $CaSO_4$ in a mixture of $CaCO_3$ and C_3AS_3 thermal stability of $2(C_2S)C\bar{S}$ reduces, an emergence of $3(CA)C\bar{S}$ slows down. The clinker synthesized from $CaCO_3$ and NAS_6 mix under the temperature of 1300°C contains C_3A , β- and α'- C_2S. An addition of $CaSO_4$ into a mixture of $CaCO_3$ and NAS_6 prevents the formation of α'- C_2S and it results in a slowing down of saturation of calcium aluminates with lime. The formation of C_6A_4MS is preceded by an appearance of CA, $C_{12}A_7$, C_3A, C_2AS, C_2S and their subsequent varied transformations with the participation of CaO, MgO, Al_2O_3 . When adding CaF_2 , $CaSO_4$ into a mixture expected to form C_6A_4MS, first and foremost $C_{11}A_7CaF_2$, $3(CA)C\bar{S}$ emerge; and if this mixture contains Na_2CO_3 then $C_{12}A_7$ appears. In a burning mixture with Na_2CO_3 the stability of C_2AS is raised. Fixed character of interactions allows to regulate reactionary ability of raw mixes and composition and modification of clinker's phases. According to indices of hydraulic activity C_6A_4MS-phase is approximate to CA-phase.

ACKNOWLEDGEMENTS

Much of the cement tests were carried out by the Belgorod Technological Institute of Building Materials (Russia). The authors would like to thank Professor I G Luginina who lent her careful help, advice and invaluable assistance in the preparation of this paper.

REFERENCES

1. Morey, G.W.:"Phase Equilibrium Relations of the Common Rock-Forming Oxides Except Water". London, Washington, US Gov.print.off., 1964, 159 p.

2. Eitel, W.:"The Physical Chemistry of the Silicates". The University of Chicago Press, 1954, 1055 p.

3. Berezhnoi, A.S.:"Multicomponent Alkali Oxide Systems". Kiev, Naukova Dumka, 1988, 200 p.

4. Kuznetsova, T.V. and Talaber, I.:"Alumina Cement". Moscow, Stroiizdat, 1988, 272 p.

5. Chattergy, A.K.:"Stability of Three-Calcium Aluminate in the System of Calcium Oxide - Aluminium Oxide - Fluor-Spar". YI-th International Congress on Chemistry of Cement, Moscow, Stroiizdat, 1976, V1, p 91-95.

6. Butt, Yu.M. and Timashev, V.V.:"Portlandcement". Moscow, Stroiizdat, 1974, 328 p.

STUDIES ON RAPID BURNING TEMPERATURE, TIME AND RAW MEAL MODULUS RANGE IN PORTLAND CEMENT

Hu Shuguang

Department of Materials Engineering
Wuhan University of Technology, Wuhan, P R CHINA

SUMMARY

The optimal temperature and time of duration for the rapid burning of portland cement clinker in the reactor based on a tube oven controlled under the different temperature from 1280 ℃ to 1400℃ has been investigated, the raw meal modulus range suitting to the rapid burning process has been studied. The influences of two different methods for the burning process of clinker were discussed. The experimental results showed that portland cement clinkers could be burnt with a shorter burning time and a lower burning temperature by taking rapid burning technique. According to the experiment results and the analyses of mathematics method, the relation formula between burning time and temperature was deduced and raw modulus range stuitting to rapid burning technique was suggested.

摘　　要

本文研究了硅酸盐水泥熟料在一种特制管式电阻炉中，温度范围从１２８０℃～１４００℃在快速煅 烧条件下烧成温度与烧成时间的关系，对适用于这种工艺方法的生料率值进行了分析，同时也讨论了快速 与常规两种煅烧方法之间的差异。研究结果表明，采用快速烧成工艺，可以使硅酸盐水泥在较低的温度下用较 短的时间烧成。根据实验结果和数学方法分析，导出了最佳烧成温度范围；烧成温度与烧成时间的关系， 同时也提出了适合于快速烧成工艺的生料率值范围。

INTRODUCTION

The feature of rapid burning is that the speed of temperature rise is much faster than that of common burning method during burning process.Some studies snowed, when raw meals of cement were burnt at very high heating ratio, dehydration of clay raw material, decomposition of limestone, appearance of liquid phase and reaction of solid phase took place nearly in the same time. In this case, various reactants are in highly active state, the activition energy of carbonate decomposition and cement clinker formation are decreased effectively [1-4]. Under this condition, cement clinker can be burnt at a lower burning temperature and a shorter burning time. In reacent years, several of industral tests of rapid burning technique have been performerd [5], more and more people expect that this kind of saving-energy technology in cement manufacture can be realized in the near future.

Although some research work of rapid burning has been carried out, the results about practical test and technology data have not been reported as yet. In this paper, we investigated the relation between burning temperature and time in the certain temperature range, discussed the raw meal modulus range suitting to rapid burning technique in portland cement by using a special rapid burning reactor.

EXPERIMENTAL

The special rapid burning reactor was equipped based on a tube oven, an auxiliary platform with a preheating tube was linked with the oven door. A steady and adjustabe temperature field can be formed in the middle area of the oven because of the exact temperature control and the operation of opening oven door. In the experiment, we easily know that the distribution of the temperature field according to the certain controlled temperature, and we can also determined the ratio of temperature rise by controlling the speed of sending sample in the oven tube. The test samples were loaded in a little platinum boat. The scehmatic of the designed reator and the temperature field distribution is shown in Fig.1.

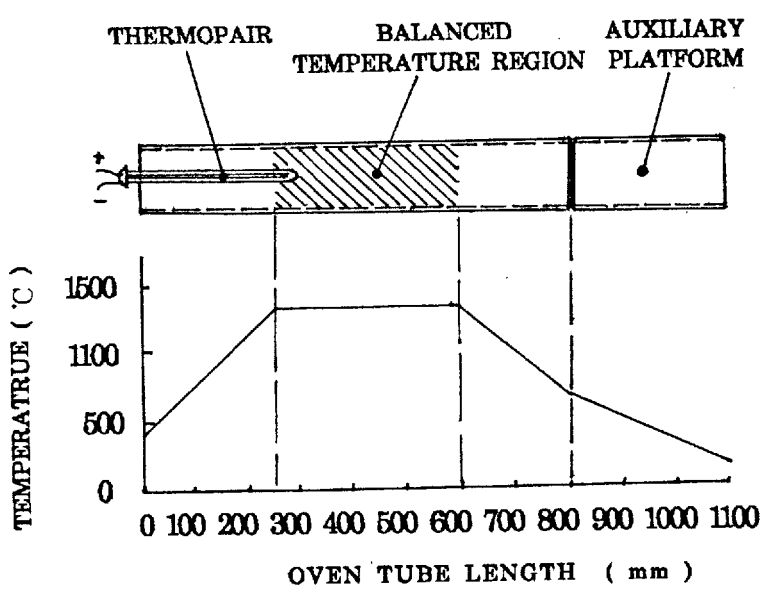

Fig. 1 Schematic of the reactor and temperature field distribution

The cement meals were prepared by ordinary commercial raw materials, which were grinded to Blain specific surface 320m²/Kg. In order to get the raw meals be heated at a rapid speed of temperature rise, meawhile, the liquid-solid phase reaction take place successfully, we compressed the samples into thin pieces of $\phi 30 \times 0.5$-1.0 mm under the pressure of 20 MPa. All burnt samples were puenched in air.

RESULTS AND DISCUSSION

Burning Temperature and Time

Rapid burning method can decrease burning temperature and short burning time, but the detail experiment result have not been reported by now. As we know, the burning temperature of portland cement is about 1450℃, and the burning time is more than two hours from raw meal to clinker in a rotary kiln. In the experiment, the burning temperature range from 1280℃ to 1400℃ and the corresponding burning time were studied. The burnt clinkers were examined by the method of F-CaO testing of absolute alcohol-glycerine and lithofacies analysis. The chemical compositions of the test meal samples are in Table 1.

Chemical composition of the raw meal sample Table 1

sample	CaO	SiO_2	Al_2O_3	Fe_2O_3	I.L	Σ	KH	SM	IM
1	42.93	14.00	3.16	2.15	35.47	97.71	0.94	2.64	1.47
2	44.13	14.50	3.74	2.77	34.05	99.21	0.91	2.23	1.35
3	41.77	14.06	3.60	3.65	35.72	98.60	0.88	1.94	0.98

Note: KH- $(CaO-1.65Al_2O_3-0.35Fe_2O_3)/2.8SiO_2$
SM- $SiO_2/(Al_2O_3+Fe_2O_3)$
IM- Al_2O_3/Fe_2O_3
I.L- ignition loss

The samples in Table 1 were respectively burnt at the temperature rise ratio of 600℃/min under the differnt burnt temperature from 1280℃to 1400℃. Table 2 are the experiment results (the average value of three samples). As a consequence of the selecting results in Table 2., we obtained the dotting line in Fig.2, it describes the relation between burning temperature and time. Seeing the dotting line, we found that burning time is reduced with the increasing of burning temperature, but the variation trend is obviously different in various temperature region. According to the variation feature of the dotting line in Fig.2, we can divided it into three sections to discuss.

Section AB is in low temperature region, The variation of burning time is much great with the change of temperature. Section CD belongs to high temperature region, the variation of time is smooth with the chang of temperature. Section BC is considered as a transition region between section AB and section CD. In region AB, T<1300℃, the formation condition of main clinker mineral (calcium silicate) is difficult. Seen from the appearance, these clinkers were loose and light colour because of the inadequacy of burning time. Therefore, the burning time is rather long in Table 2, e.g. the sample was burnt at 1290℃ for 250 minutes had still more than 5% F-CaO. The results tell us that portland cement is very difficult to be burnt below 1300℃ even if rapid burning technique is used.

Burnability of clinker in different burning temperature and time Table 2

temp (℃)	experiment results										select results	
	time (min)	F-CaO (%)	time (min)	F-CaO (%)	time (min)	F-CaO (%)	time (min)	F-CaO (%)	time (min)	F-CaO (%)	time (min)	F-CaO (%)
1280	50	11.03	80	10.72	150	8.80	180	7.66	250	7.73	250	7.73
1290	90	9.25	120	8.53	210	6.30	240	3.61	250	3.53	250	3.50
1295	45	7.32	60	5.18	90	4.72	120	3.91	150	3.08	150	3.50
1300	35	5.49	45	3.32	50	2.29	55	1.50	60	1.45	55	1.50
1310	30	2.09	33	1.75	35	1.60	36	1.40	35	1.34	36	1.40
1320	24	2.31	26	2.15	27	1.86	28	1.45	35	1.05	28	1.45
1330	20	2.75	21	1.96	22	1.82	24	1.33	25	1.35	24	1.33
1340	18	2.72	19	2.14	20	1.85	21	1.41	25	0.96	21	1.41
1350	14	2.57	16	1.66	18	1.43	20	1.40	22	1.06	18	1.43
1360	10	2.25	15	2.10	16	1.67	17	1.50	20	1.04	17	1.50
1370	10	2.25	12	1.96	14	1.83	15	1.45	17	1.37	15	1.45
1380	9	2.17	10	2.10	11	1.84	13	1.44	14	1.27	13	1.44
1400	6	3.14	8	2.21	10	1.42	12	1.34	15	1.13	10	1.42

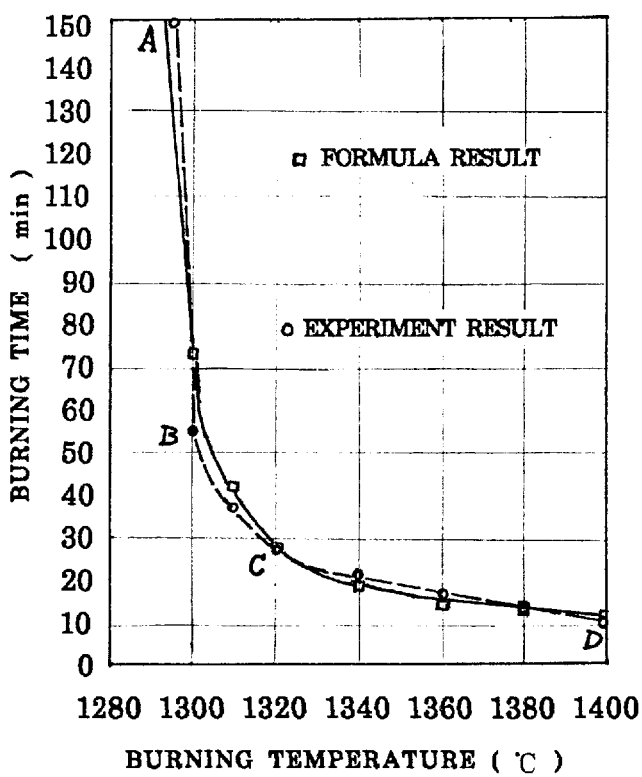

Fig. 2 The relation curve of burning time and temperature

At T=1300℃, the burning time of clinker needs about 50 minutes, but the burning time will be increased greatly if the burning temperature only drop a little, e.g. drop only 5 ℃ from 1300 ℃ to 1295 ℃, the burning time will increase tiwce. That is to say, that T = 1300 ℃ is the critical point of rapid burning. According to these results, we should design a higher temperature than 1300 ℃ in rapid burning technique, because it is very possible that some areas produce a temperature fluctuation in a kiln due to various reasons in practical prodution, which fluctuation will certainly influence the quality of clinker if it is not noticed.

Point C in Fig. 2 is 1320 ℃, the correponding burning time is 28 minutes. As comparing with point B, point C is 20 ℃ higher, but its burning time reduces a half. In section CD, the variation of the burning time with the temperature is smooth. So it is easily to be controlled when the burning temperature is in this region. As mentioned above resuls, we consider that burning temperature should be selected in section CD. On the other hand, the burning time can't be too short because of the need of stabilizing control and practical production.

We handled the experiment results in Table 2 with mathematics method and obtained the relation formula of burning time and temperature as follows:

$$t = 6.8242\ EXP\ [\ 71.5780/(T-1270)\ ]$$

here, t--burning time (min)

T--burning temperature (℃)

By the formula, we have the theory curve in Fig. 2 (the full line). The result showed that the formula has a good correlation. Considering the feature of rapid burning and the stability of production control, we suggest the burning temperature should be between 1320℃ to 1360℃.

Suitable Raw Meal Moduli

The range of raw meal compositions suitting to rapid burning in portland cement have been discussed.The raw meal modulus range of common burning technology in protland cement are KH: 0.82-0.94, SM: 1.7-2.7, IM: 0.9-1.7. We took the orthogonal testing method of three factors and four gradations to design the experiment scheme, which are KH=0.88, 0.90, 0.92, 0.94; SM = 2.0, 2.2, 2.4, 2.6; IM = 1.0, 1.2, 1.4, 1. 6. We designed the burning temperature 1320℃ and burning time 28.5 minutes according to the above study result. Table 3 is the experiment scheme and results. The results of grade different analysis are in Fig. 3. The results of common burning method as comparing (simulating rotary kiln,ratio of temperature rise 600℃/hr.) is in Fig. 4.

Raw meal scheme and experiment results Table 3

sample	KH	SM	IM	F-CaO(%)	F1	F2	F
1	0.88	2.04	0.99	0.39	9.22	5.0	14.22
2	0.88	2.11	1.18	0.00	10.00	5.0	15.00
3	0.89	2.35	1.41	0.57	8.86	4.5	13.36
4	0.87	2.67	1.51	1.17	7.66	4.0	11.66
5	0.89	2.02	1.15	0.98	8.04	4.5	12.54
6	0.90	2.10	1.07	1.58	6.84	4.5	11.34
7	0.92	2.15	1.54	1.26	7.48	3.5	10.98
8	0.90	2.60	1.30	1.65	6.70	4.5	11.20
9	0.92	2.15	1.32	1.93	6.14	3.0	9.14
10	0.92	2.28	1.52	1.80	6.40	3.0	9.40
11	0.92	2.44	1.00	2.12	5.76	5.0	10.76
12	0.92	2.67	1.24	1.35	7.30	5.0	12.30
13	0.94	2.22	1.51	3.61	2.78	4.5	7.28
14	0.94	2.28	1.38	2.74	4.60	4.0	8.60
15	0.94	2.30	1.32	3.24	3.52	4.0	7.52
16	0.94	2.51	1.05	3.12	3.76	4.0	7.76

In Fig.3, the sequence of effect extent to three moduli is KH>IM>SM (R_{KH}=23.06, R_{SM} =0.80, R_{IM}=8.04 here, $R_X=X_{Max}-X_{Min}$), the optimal result is KH=0.88, SM= 2. 20, IM= 1. 2. Comparing to Fig. 4, we found that the changing trend of KH is the same in two methods basicly, and F increases with decreasing of KH, but the variation extent of rapid burning is stronger than that of common burning. SM is very smooth and IM have the optimal value in Fig 3, but they are different in Fig. 4. Analyzing the above results, we suggest that raw meal modulus suitting rapid burning technique should be lower KH, higher SM and

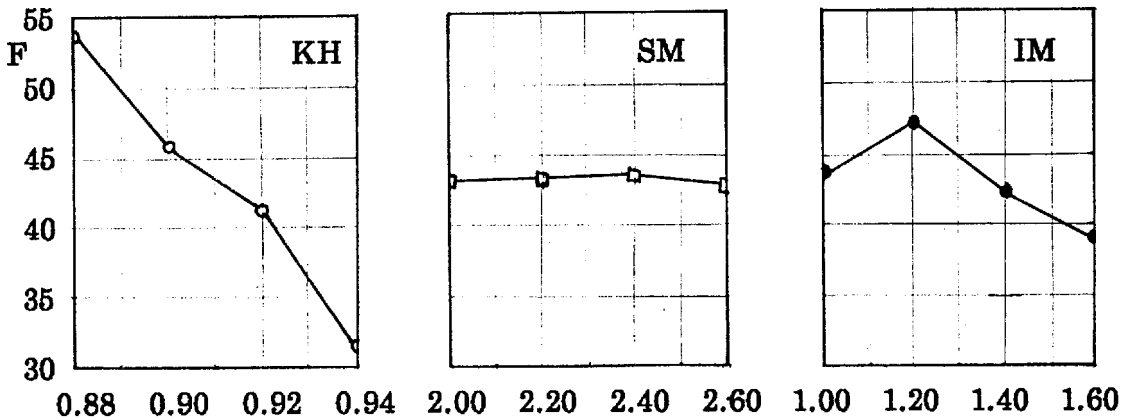

Fig. 3 The grade different analyses of the rapid burning method

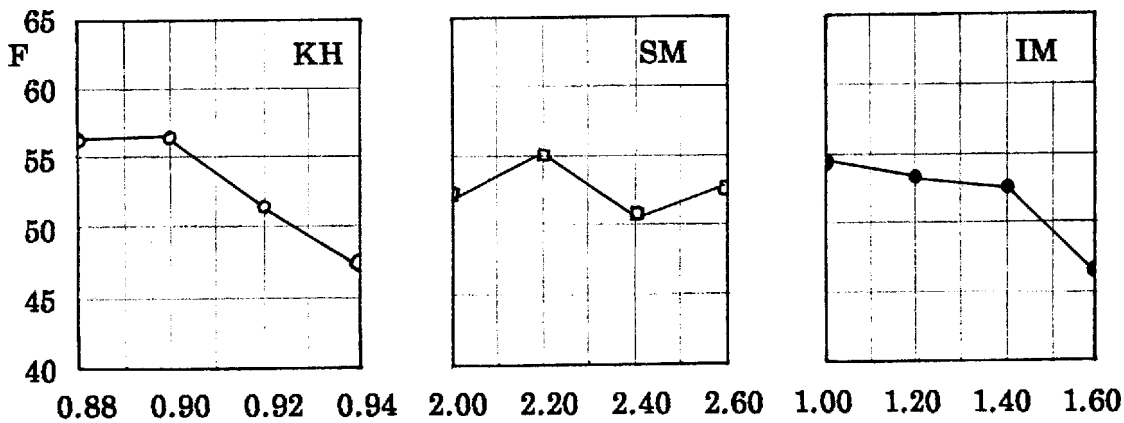

Fig. 4 The grade different analyses of the odinary burning method

moderate IM. In Fig. 4, KH=0.90 is the optimal point, but the result in Fig. 3 seems to show that KH should be taken a lower value. We know that low KH indicates high dicalcium silicate content in cement clinker, that is to say, rapid burning technique can suit to the cement of higher dicalcium silicate content.

In Fig. 3, the influence of SM is the samllest in three factors to rapid burning. SM governs the proportion of silicate mineral and fluxing mineral in clinker, and it also indicates the amount of liquid phase in burning process. We know, in the formation process of cement clinker,the main action of fluxing is to lower burning temperature and accelarate the solid phase reaction under the condition of existing liquid-solid phase. By the ordinary viewpoint, the more fluxing mineral is, the more favourable reaction will be, but there exists not this relation in rapid burning process from by experiment result, which reveals the different of the formation mechanism of clinker minerals in two method.

Our study results [6] showed that a lot of small size Belites formed early state contain with more impurties and defects, these Belites have higher reaction activity in the formation process of Alite. Meanwhile, the liquid phase formed simultanecusly in rapid

burning has some character which is very useful to the formation of calcium silicate. Considering clinker quality and practical production, we suggest that raw meal modulus range should take KH:0.88-0.90, SM>2.4 and moderate IM.

CONCLUSION

1. Portland cement clinker can be burnt by using rapid burning technique with a lower burning temperature and a shorter burning time, which has the significant effect of energy conserving in cement manufacture.

2. The relation between burning time and temperature in rapid burning is given as follows:

$$t = 6.8242 \text{ EXP } [71.5780/ (T-1270)]$$

Considering the feature of the rapid burning and the stability of production control, we suggest that burning temperature region should be in 1320℃ to 1360℃.

3. The raw meal modulus rang suitting to the rapid burning technique is lower KH, moderate IM, higher and changable SM. Considering clinker quality and practical production, we suggest that this range take KH:0.88 to 0.90, SM.2.4 and moderate IM.

REFERENCES

1. Alimmary, S. A. et al., "Burnbility of Cement Raw Materials at Rapid Calcination Condition", Cem. Concr. Res., 1980, Vol. 10, 739-745
2. Phillip, O. " Einflub des Aufheizverhaltens auf den Garbrand von ZementRklinker", Silikattechnik, 1973, H. 8/9, 265-268
3. Joseph, H. F. et al., "The Effect of Heating Rate upon the Coupling Complex Reactions", Thermochimica Acto, 1980, Vol. 37, 225-231
4. Huang Wenxi et al.,"Effect of Different Burning Process on Mechanism of Portland Cement Clinker Formation", Beijing Inter. Cem. Concr. Sym., 1985, P 29
5. Wang xie et al., "A New Method of Burning Cement Clinker -Study on the Suspending and Ebullient Burning Method", J.of Wuhan Building Material College, 1982, Vol.8, No.3, 267-274
6. Hu Shuguang,"Studies on the Formation Mechanism of Calcium Silicate in Rapid Burning at Low Temperature (M. D. Thesis) Wuhan University of Technology, 1984

THE STRUCTURE AND PROPERTIES OF LOW-CaO CONTAINED CLINKER

T V Kuznetsova, A P Osokin, V G Akimov and V N Panyuskin

Mendeleev Institute of Chemical Technology
Moscow, RUSSIA

SUMMARY

This paper presents results of the investigation of the content, structure and hydration activity of clinkers (LSF = 0.70 - 0.85; SR = 2.2 - 3.3; AR = 0.6-1.2), obtained by roasting the raw material on the base of limestone, lay and cinders. The carried out study showed the expediency of application of thermochemical activation of processes for mineralformation in the technology of highly active low-base clinkers. The fuel economy at the roasting of such low-base clinkers at 1300-1350°C is 10-20% in comparison with the highly - base clinkers.

INTRODUCTION

One of the ways to cut down energy consumption at cement production by 10-20% is the conversion of the industry to the production of belite clinkers of higher activity. Due to the selection of the corresponding roasting and cooling regimes of the material, belite is activized to such an extent, that it becomes possible to overcome the slow growth of strength, which is characteristic of the mineral. At the production of low-base clinkers the process should be aimed to obtain not only highly active solid solution on the base of β -, α' - and α -C_2S, but to enhance the reactivity of a multiphase system in general.

EXPERIMENTAL

The investigation of the content, structure and hydration activity of clinkers, obtained by roasting the raw material (LSF = 0.70 - 0.85; SR = 2.2 - 3.3; AR = 0.6 - 1.2) on the base of limestone, clay and cinders, was carried out with different catalyzers which were contained in waste products at the temperature of 1350-1450°C. The application of marl allows to lower the temperature by 100°C.

The evaluation of the character of clinker mineral formation as well as of the products of their hydration was carried out with the help of optic and screen electron microscopy, phase X-ray analysis and X-ray spectral analysis, IR-spectroscopy. The hydration activity of the cement at W/S = 0.4 was stadied at an X-ray diffractometer, and the strength of the hardened block with plaster (3% SO_3) was determined with the help of a tensile-testing machine. The calculation of energy consumption for clinker forming was carried out taking into account the value of heat effect for the solution of the clinker and the raw material in HF. The solution was conducted in a thermostatic unit of an adiabatic calorimeter at temperature of 25°C at the solid-ligwid ratio 1:2000.

RESULTS AND DISCUSSION

The application of waste products influences positively the processes for mineral forming during clinker roasting. From the viewpoint of flaw formation in calcium silicate crystals, which are solid solutions, the ions of additives, differring significantly in dimensions and charges from the ions Ca^{2+} and Si^{4+}, are the most preferable and in this case the effect on the anion sublattice shows the

best result. In this connection it is recommended to use waste products containing phosphorous, chromium, sulfur and titanium compounds as modifying additives. The introduction of carbon in the composition of the raw material mixture enables thermochemical activation of the process for mineral formation (Fig.1), because local parts appear during its combustion at temperature 2145-2160°C just before the decarbonization of the bulk of the limestone (300-700°C). It results in the increase of non-stoichiometry in the composition of the main minerals, contained in the Portland cement clinkers, and also in the formation of solid solution with impurity elements. Microelements, introduced in the structure of such crystals, increase the defectiveness of their structure by several factors. In the fields of non-stoichiometric composition of alite and belite the concentration of free charge carries increases by 45-70 and 40-150 times respectively, and the density of dislocations at local parts of crystals is higher than the mean value by a factor of $10-10^3$. The mineralogic composition of clinkers experimentally found, doesn't always correspond to the calculated data. At the values of LSF 0.67-0.75 the deviation from the theoretical values in the direction of the increase in the alite quantity and decrease in the belite quantity is observed; at LSF 0.80-0.85 the contradictory phenomenon is observed. At calculations the relationship between the carbon and the additive concentrations in the composition of the raw material should be taken into account. For the clinkers containing sulfuric compounds as a mineralizer (Table 1) the largest deviation is determined at $C/SO_3 = 0.3$. The application of wastes containing, phosphorus, chromium and manganese changes the numeric value of this relationship, but it doesn't influence the nature

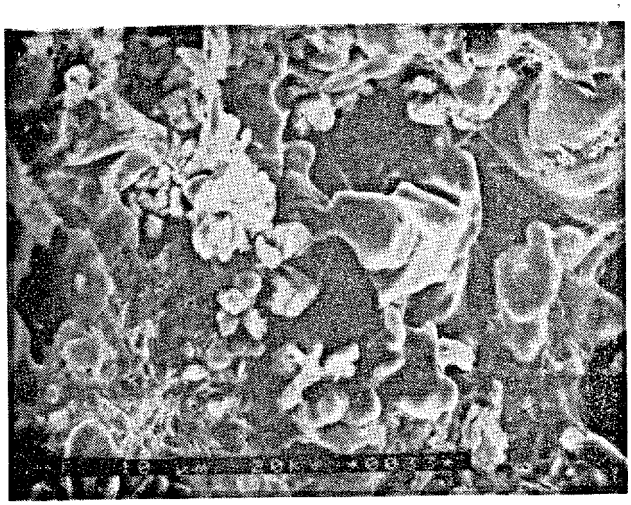

Fig.1 The microstructure of the low-base clinker, synthesized at 1350°C with the use of carbon-containing additive.

of the determined regularity. The mineralogic composition of clinkers, synthesized at temperature 1350 and 1400°C, is identical. The drop in the roasting temperature to 1200°C didn't allow to obtain qualitative caked clinkers.

Table 1 The mineralogic composition of the clinker

N	LSF	C/SO_3	Concentration, %		
			alite	belite	calcium aluminates and aluminoferrites
1	0.70	0.0	12	59	30
2	0.69	0.3	20	48	30
3	0.68	0.6	15	53	28
4	0.67	0.9	14	54	32
5	0.76	0.0	27	46	28
6	0.75	0.3	25	43	31
7	0.74	0.6	20	47	31
8	0.72	0.9	18	49	31
9	0.80	0.0	31	38	31
10	0.79	0.3	28	38	33
11	0.77	0.6	26	40	33
12	0.76	0.9	24	43	32

In all clinkers the mixture of triclinic and monoclinic modification is stabilized. In the centre of most crystals of monoclinic modification ($CaO/SiO_2 > 3.0$) the M_{1a} form of alite is determined, and on the border ($CaO/SiO_2 < 3.0$) the M_{1b} form of alite is determined. Belite is stabilized for the most part in the β -form. But some quantity of α' - and α - C_2S is formed. The increase in the rate of cooling of the clinker from 200 to 5000°C/min causes the growth of concentration of the high temperature belite modification, and the crystals of calcium silicate are characterized by a wide range of areas of nonstoichiometric composition. The reactivity of alite and belite of nonstoichiometric composition increases by 15-20%, and the strength of the hardened block grow by 2.0 - 7.0 MPa.

The introduction of the optimum quantity of the additive (C/SO_3 =

0.3-0.6) into the composition of the raw material mixture results in the maximum growth of its hydration activity because of the increase in the structure defectiveness of the main minerals. The degree of hydration of the silicate components (alite + belite) can reach 50-65% (28 days), and the strength at compression of samples increases by 8-31% in comparison with standard values (Table 2) resulting from the lowering of their porosity, and foming low-base calcium hydrosilicates.

Table 2 Hydration activity of minerals and clinkers

N	The degree of hydration, %					Compression strength, MPa	
	alite	belite		silicates			
	Time of hardening (in days)						
	1	1	28	1	28	1	28
1	50	4	20	14	37	4.7	36.2
2	62	4	38	21	56	7.0	60.2
3	80	4	24	21	41	4.8	48.3
4	50	4	12	14	31	4.5	40.7
5	50	4	27	21	52	6.9	50.9
6	58	9	30	27	57	9.0	67.9
7	62	4	28	21	53	7.0	61.8
8	74	4	27	22	47	6.4	48.1
9	58	9	35	31	60	9.7	58.7
10	58	9	42	31	65	14.0	85.0
11	57	9	37	28	62	11.0	67.0
12	67	14	29	33	54	8.4	46.9

As it is obvious from the study, the value of heat effect of clinker formation, depending on LSF value, is 1900-1910 and 1510-1690 KJ/kg for ordinary alite and for synthesized low-base clinkers respectively. The fuel economy at roasting of belite clinkers is determined as 10-20% in comparison with the alite one. The deviation from the stoichiometric composition of alite, caused by the irregular distribution of main and admixture ions in the mineral structure, leads to a significant change in the energy content of the substance. 665 and 710 KJ/kg respectively is consumed to from calcium silicates with CaO/SiO_2 = 2.8 and 3.2, and that is by 13 and 6 % lower than for the mineral with CaO/SiO_2 = 3.0; and their reactivity surpasses the standard values. The lower quantity of energy is consumed at the formation of highly active belites and calcium aluminates, but the enthalpy values

for their formation are almost similar: 720-728 and 732-784 KJ/kg respectively.

CONCLUSIONS

Thus the carried out study showed the expediency of application of thermochemical activation of processes for mineralformation in the technology of highly active low-base clinkers. The use of wasre products with carbon-containing components in the composition of the raw material mixture allows to increase the strength of a cement block by 8-31%, resulting in the formation of clinkers minerals with zonal structure of crystals, characterized by the elevated reactivity during the interaction with water. The fuel economy at the roasting of such low-base clinkers at 1300-1350°C is 10-20% in comparison with the highly-base clinkers.

RESEARCH ON THE CHEMICAL COMPOSITION AND MICROSTRUCTURES OF SULPHO-ALUMINATE CEMENT CLINKER

Su Muzhen, Deng Junan, Wu Zongdao and Liu Xiaoxin

China Building Materials Academy
Beijing, P R CHINA

ABSTRCT

The industrial sulpho–aluminate cement clinker, using lime stone, bauxite and anhydrite as raw materials and sintered at 1300℃, can be featured as small sparse and porous particles. The mineral composition, microstructure and constituents of the main mineral $C_4A_3\bar{S}$ in the clinker which was produced by different processes (in an ordinary dry–process rotary kiln, the kiln with shaft preheater and with reinforced suspension preheater) and on the different Al_2O_3 / SiO_2 ratios in bauxite were investigated by means of SEM / EDAX. The results show that in the industrial SAC clinker that formed at non–equilibrium condition, $C_4A_3\bar{S}$ is not a compound with fixed composition but a solid solution of which constituents can be continuously changed in relatively larger scales and there is the substitution of different kinds of hetero–ions in it.

〔摘　要〕

用天然石灰石、铝矾土和石膏为原料，在1300℃煅烧而成的硫铝酸盐水泥熟料，具有结粒细小且多孔的特点。本文采用SEM / EDAX研究了干法中空窑、预热器窑（SP）和RSP窑等不同煅烧工艺和不同Al / Si比的铝矾土原料对熟料矿物组成，显微结构和主要矿物$C_4A_3\bar{S}$组成的影响。研究结果表明，在非平衡状态下形成的工业熟料，其$C_4A_3\bar{S}$矿物不是一种具有固定成分的化合物，而是成分在较大范围内连续变化的固溶体。同时存在多种异离子的取代。

INTRODUCTION

In 1974, China Building Materials Academy (CBMA) was succeed in industrial trail–production of sulpho–aluminate cement (SAC) using natural lime stone, bauxite and anhydrite as raw materials. The production process adopted include the ordinary dry–process rotary kiln (DPR), the kiln with shaft preheater (SP) and with reinforced suspension preheater (RSP). The main mineral composition for the clinker is $C_4A_3\bar{S}$ 55–75%, α–C_2S 15–25% and few free $CaSO_4$, CT and ferrite phases.

In its applications, it was found that the SAC produced by different processes and used different bauxite as raw materials will cuase the different performances. The effects, therefore, was studied of bauxites with different Al_2O_3 / SiO_2 ratios and different types of kiln on the mineral compositions, microstructures of SAC clinker and its $C_4A_3\bar{S}$ compositions. Through this study, the more rational mineral composition for the clinker and the mechanism of the hetero–ions was established, the performances of the SAC could be improved further.

SAMPLING AND TESTING

1.Sampling for studying on the clinker formation process in kiln

To research the clinker formation process in DPR kiln, the samples were respectively taken along a 1.0+21m kiln at the sites from the head to 1,2,3,4,5,8,12,15,19 meter and nine samples were taken altogether. Each sample was tested by means of chemical analysis and XRD and the related raw mix was investigated by DTA, the results are shown in Fig.1 and 2.

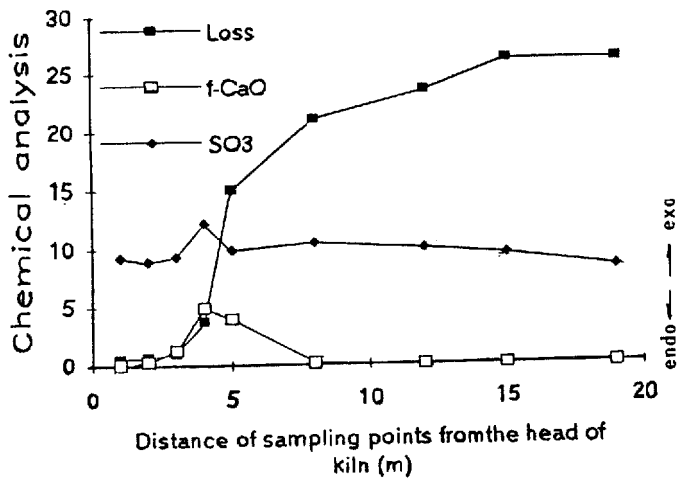

Fig.1 Chemical Analysis of Materials in Kiln

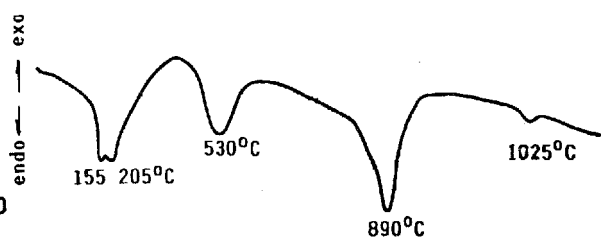

Fig.2 DTA curve for raw mix

2.Sampling on different SAC clinker

For studying on the effects of different bauxites and kilns on the microstructures and phases compositions of clinker, the samples were chosen from four representative plants which are Lengshuitan (LST), Maomin (MM), Tianjin (TJ) and Luanxian (LX). These plants respectively stand for three kinds of process related with different types of kiln: DPR kiln for LST and TJ, SP kiln for LX and RSP kiln for MM plant. The samples also stand for two kinds of bauxite according to different Al_2O_3 / SiO_2 ratios and fuels used (MM–dead oil, others–soft

coal). The liter weights for all the samples vary from 650 to 850 g / l. The chemical analysis of the raw mixes and fuels are shown in Table 1.

Table 1. Chemical analysis of the raw materials and fuels in 4 plants

Plant	Type of kiln	Raw materials Boux.	Lime	Anhy.	Coal ash (%)			Clinker (%)			
		A / S	C	SO_3	S	A	Ash	$C_4A_3\bar{S}$	C_2S	A / S	C / A
MM	RSP	24.13	53.17	50.45	0.00	0.00	0.00	83	6	2.70	0.84
LX	SP	3.73	49.07	51.01	46.58	17.48	14.04	57	31	2.45	1.44
TJ	DPR	4.99	51.11	50.45	47.47	16.00	15.00	57	27	2.52	1.37
LST	DPR	13.14	52.06	53.08	57.04	23.04	16.24	71	18	2.59	1.08

3.Preparation of different clinker samples for SEM / EDAX test

Two kinds of sample were prepared respectively for micro–morphology and oxide analysis.

a.For micro–morphology analysis— Break the clinker specimen into two pieces and choose a relatively smooth unpolished section as a tested surface.

b.For oxide analysis— Crush the specimens into smaller particles with diameter of 2–3 mm, then put them in a mold and pour epoxy into it to form. Polish the specimens with absolute ethanol consequently. Spray carbon conducting–layer on the tested surfaces of the two kinds of samples by a DMX–220A coater. A KYKY–1000B scanning electronic microscope was employed for investigating the micro–structure and morphology of SAC clinker, a TN–SERIES II X–ray energy spectrometer for oxide analysis.

RESULTS AND DISCUSSION

1.The formation mechanism for industrial SAC clinker

Through the comprehensive analysis on Fig.1, 2 and XRD results, the chemical reaction process of industrial clinker formation along the kiln are expounded as follows:

The dehydration and decomposition of bauxite have taken place at 7–10 m from the head of the kiln and the reaction temperature is around 530℃. About 900℃, a great quantity of $CaCO_3$ is decomposited (at 4–6 m place) and the generated CaO is reacted immediately with α–SiO_2 and Al_2O_3 from decomposited bauxite into a transitional phase C_2AS. By reason of that, there is no great amount of free CaO founded in Fig.1. Thereafter, the amount of C_2AS was continuously increased as materials inch into the higher temperature zone of the kiln. C_2AS reacted with $CaSO_4$ into $C_4A_3\bar{S}$ and α–C_2S when temperature reached 1000℃. $C_4A_3\bar{S}$ could also be formed directly from CaO, Al_2O_3 and $CaSO_4$ as temperature went up consequently. CaO and SiO_2 compounded into β–C_2S above 1100℃, which decreases free CaO in a great quantity (at 2–3 m place). The transitional phase C_2AS and free CaO were vanished when temperature reached 1250℃ (at 1–2 m place) and α–C_2S reacted with $CaSO_4$, at same time, into a new transitional phase—$2C_2S \cdot CaSO_4$ which will be decomposited back into α–C_2S and free $CaSO_4$ as sintering temperature went over 1280℃. At this moment, the amount of $C_4A_3\bar{S}$ and C_2S will hit their tops and it is successful in sintering the SAC clinker.

It must be point out that in the tetra-system of $CaO-Al_2O_3-SiO_2-SO_3$, no matter how much CaO present, SiO_2 reacts with CaO only into C_2S but C_3S as the quantity of $CaSO_4$ is over 4% in the system. The surplus CaO only present as free CaO.

For different bauxite adopted as raw material, the varying scales for the phase composition of SAC clinker are that: $C_4A_3\overline{S}$ 55–75% and C_2S 15–35%.

2.Microstructure of SAC clinker

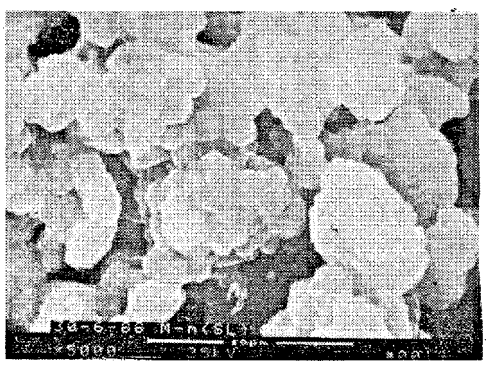

Fig.3 Micromorphology of $C_4A_3\overline{S}$ in MM clinker

SEM / EDAX was employed to investigate the aforementioned clinkers from those four plants. The morphologies of the clinker phases were shown and the effects of various production processes on the morphologies would be seen in Fig.3,4,5 and 6. Because of the faster rotary speed of RSP kiln and, therefore, the shorter remaining time in kiln, the microstructures of this kinds of clinker (see Fig.3) was in granular accumulation. The crystal size for $C_4A_3\overline{S}$ was comparatively samller ($<2\mu$) and its appearance looked irregular. This kind of clinker has a higher hydrating rate.

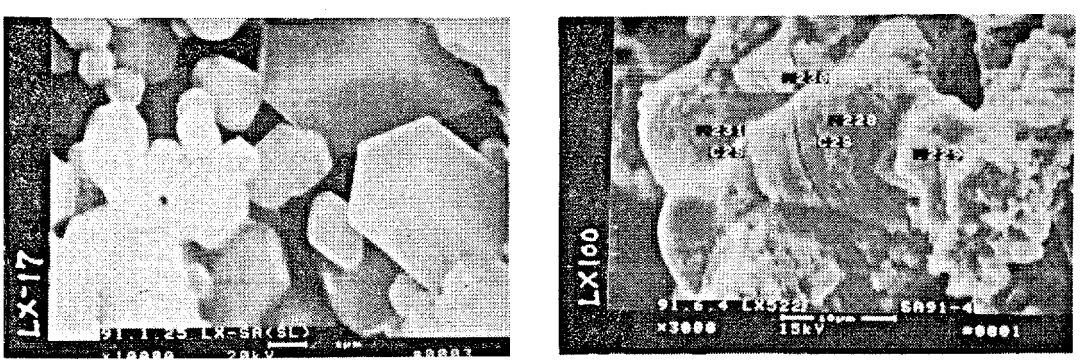

(a) (b)

Fig.4 Micromorphologies of $C_4A_3\overline{S}$ (a) and C_2S (b) in LX clinker

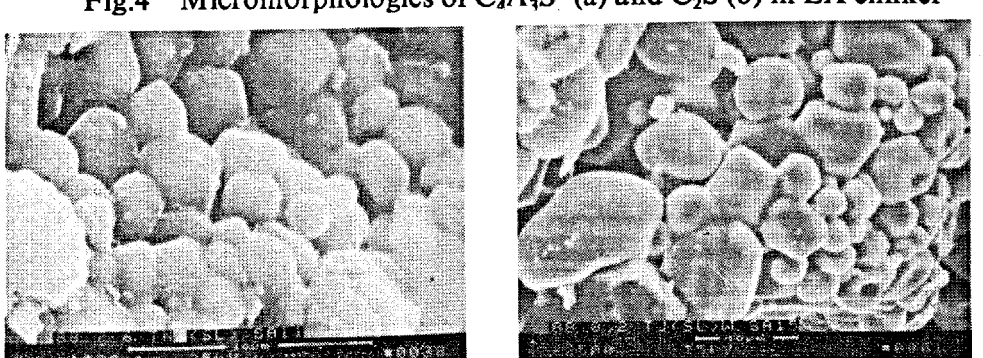

(a) (b)

Fig.5 Micromorphologies of $C_4A_3\overline{S}$ (a) and C_2S (b) in TJ clinker

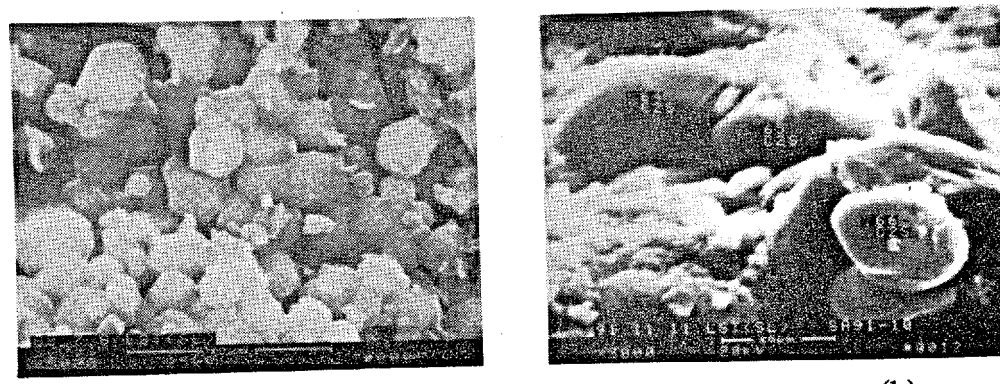

(a) (b)

Fig.6 Micromorphologies of $C_4A_3\bar{S}$ (a) and (b) in LST clinker

For the clinker sintered in SP kiln, since the raw mix was preheated well, the $C_4A_3\bar{S}$ crystal appearance showed regulated with hexagonal plate and tetragonal polycylinder shapes, and its crystal sizes (around 2–5μ) were bigger than that of the one produced in RSP kiln. The clinker of SP kiln hydrated relatively slower than the one of RSP kiln but performed a higher physical strength at later stage. As far as the clinker produced in DPR kiln was concerned (see Fig.5 and 6), it was packed up in a layer and granular structure. Most of $C_4A_3\bar{S}$ crystals in this kind of clinker were in hexagonal or tetragonal plates and short–polycylinder shapes, and their sizes were also around 2–5μ.

C_2S phase in all the clinkers takes roughly a spherical shape. According to EDAX analysis, C_2S twins usually with crystal $C_4A_3\bar{S}$ and the variation in its size is greater.



Fig.7 Micromorphology of alkali–contained phase in SAC clinker

Since a small amount of K_2O and Na_2O included in the bauxite, some alkali–contained phases, which are primarily the matchstick shaped crystals, can be found in SAC clinkers (Fig.7). The composition for the alkali–contained hases (EDAX results) as follow:

CaO	Al_2O_3	SO_3	K_2O	SiO_2	Fe_2O_3	TiO_2	MgO
50.81	13.28	20.02	8.83	3.41	2.60	1.05	0.15

3.Research on the chemical composition of $C_4A_3\bar{S}$ phase in industrial clinkers

C_4A_3S phases, that in the clinkers produced at the four above–mentioned cement plants, were investigated in this study by means of EDAX in order to decide the effects of the bauxites with different Al_2O_3 / SiO_2 ratios and different types of rotary kiln on the chemical composition of C_4A_3S phase.

The statistical results are shown in Table 2 and Fig.8. In the industrial clinker, C_4A_3S is not a chemical compound with a fixed composition but a solid solution of which components can be changed continuously in relatively larger scales. Also several hetero–ion substitutions were found in it.

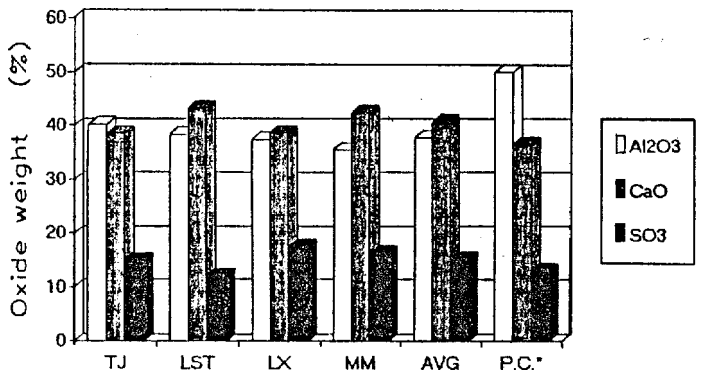

Fig.8 Oxides analysis for the industrial C_4A_3S phase

Table 2. Oxide Analysis for $C_4A_3\bar{S}$ from the Four Plants

	TJ	LST	LX	MM	AVG	P.C.*
Al_2O_3	40.22	38.31	37.47	35.47	37.83	50.12
CaO	38.56	43.33	38.70	42.47	40.83	36.76
SO_3	14.90	11.91	17.45	16.26	15.13	13.12
SiO_2	3.12	2.80	3.19	2.98	3.02	0.00
Fe_2O_3	1.60	1.28	1.39	0.60	1.22	0.00
TiO_2	0.61	1.15	0.64	0.54	0.74	0.00
MgO	0.53	0.68	0.63	0.79	0.66	0.00
K_2O	0.51	0.61	0.75	0.69	0.64	0.00
SUM	100.05	100.07	100.07	100.07	100.07	100.00

* Ideal crystal of $C_4A_3\bar{S}$

Comparing with its ideal crystal composition, the industrial C_4A_3S has a quite lower percentage of Al_2O_3 but a little higher for the components of CaO and SO_3. The variation of Al_2O_3 is related to the different bauxites used in raw mixes (see Table 1 and 2). For the clinkers from the two plants (MM and LST) on higher Al_2O_3 / SiO_2 ratio of the bauxite, there were over 65% of C_4A_3S (test point), according to the results of EDAX, in which Al_2O_3 content was around 40–50% (this value was relatively close to the content in ideal $C_4A_3\bar{S}$ crystal). The other 35% C_4A_3S only have 30–40% of Al_2O_3 content. But for the clinkers from the other two plants (LX and TJ), which had lower Al_2O_3 / SiO_2 ratios, the Al_2O_3 content in over 50% of C_4A_3S; was less than 35%. In general, the higher Al_2O_3 content in bauxite, the higher it in industrial $C_4A_3\bar{S}$; but even in the case that Al_2O_3 content reached up to 76.48% in bauxite (MM plant), the content in industrial C_4AS was still lower than the one on its ideal crystal. The content of SO_3 in industrial C_4A_3S is changed with different type of rotary kiln. For the kilns with preheater (SP or RSP), the volatilized SO_3 is easier to be absorbed back by raw mix, the content of SO_3 in industrial $C_4A_3\bar{S}$ is a little higher than that in its ideal form, but for the kiln with no preheater, the SO_3 content is lower than or close to the ideal value.

The substitution of hetero–ions in C_4A_3S is mainly that Ca replaced by Mg and Al by Si, Fe and Ti.

CONCLUSIONS

1. The SAC clinker can be produced at relatively lower sintering temperature – 1300℃ and has remarkable burnability. The conventional color of clinker is light grey which changed with the variation of Fe content in raw mix. The clinker can be featured as small sparse and porous particles and its liter–weights variated between 650–850 g / l.

2. There are some obvious differences in the morphologies and microstructures of SAC clinkers sintered in the different types of rotary kiln. The morphology for the mineral phases of the clinker produced in SP kiln was more regular than the other two and the microstructure had a higher distinctness. The outline of the one produced in RSP kiln was the most irregular, its crystal size was extreme fine ($<2\mu$) and it was granular packing in a layer.

3. The industrial $C_4A_3\bar{S}$ phase formed in a non–equilibrium condition is not a compound with fixed composition but a solid solution of which components (espcially CaO) can be continuously changed in a relatively large scale. The variation rules are that: 1) CaO content is decided by the proportion of raw mix.; 2) the percentage of Al_2O_3 depended on the quality of bauxite and higher bauxite content produced higher $C_4A_3\bar{S}$; 3) the percentage of SO_3 is losed to its ideal value and variated with the different clinker production processes.

4. The hetero–ions substitution will occur in the industrial C_4A_3S that produced by substitution of Ca by Mg, Al by Si, Fe and Ti.

5. It was found that a match–stick shaped alkali–contained phase was formed when few K_2O was introduced by bauxite. The clinker will fast set and expand when the content of this phase exceeds a certain amount.

REFERENCES

1. Wang Yanmou, Su Muzhen, Deng Junan et al.: "A Study on Mineral Composition of Cement in the Quin–system of $CaO–Al_2O_3–SiO_2–Fe_2O_3–SO_3$", Journal of Chinese Silicate Society, 1982, 10(4), p369.

2. Wang Yanmou and Su Muzhen: "The features of the new kind of special cement and its further developmental tendency", 1990, 3.

3. Deng Junan, Ge Wenmin, Su Muzhen et al.: "Sulfoaluminate cement series", 6th International Symposium on Chemistry of Cement, 1980.

4. Liu Baoyuan et al.: "Study of the internidiums formed at low temperature by high–temperature XRD", Journal of Chinese Silicate Society, 1981, 9(4), p456.

FORMATION AND SOLID STATE PROPERTIES OF β-DICALCIUM SILICATE

N B Singh, S P Singh and A K Shukla

Chemistry Department, University of Gorakhpur
Gorakhpur, INDIA

SUMMARY

In an attempt to conserve energy, dicalcium silicate, an important constituent of portland cement has been prepared from different component mixes. These were sintered at different temperatures. The kinetic data was found to obey Jander's equation. From the rate constant values activation energies were calculated for $CaCO_3 + SiO_2$ system together with entropy of activation, activation enthalpy and free energy of activation. It is found that the activated state is more ordered indicating that during the course of reaction only slight rearrangement in the crystal lattice occurs. The overall results have indicated that $Ca(NO_3)_2 + SiO_2$ system is the most reactive system amongst those studied.

Hydration studies of β-C_2S formed under different conditions were made at 28 days by measuring free lime and non-evaporable water content. It is proposed that extent of hydration is related to the defects present in the structure.

INTRODUCTION

β-Dicalcium silicate hydrates similar to tricalcium silicate although at a much lower velocity. Thus, it does not play an important role during the early strength development. However, late strength is controlled by the hydration of β-C_2S phase in portland cement. Further, β-C_2S can be prepared comparatively at a much lower temperature compared to C_3S and hence if a portland cement can be made with a high content of highly reactive β-C_2S, it would be more economical. Also according to Murdoch and Blackledge (1), cements in which a high proportion of C_2S is formed, have relatively high resistance to chemical attack, relatively low drying shrinkage and hence are more durable.

One important step in this direction is to synthesize β-C_2S at lower temperatures by using different mineralizers and dopants (2).

β-dicalcium silicate is generally prepared by heating a stoichiometric mixture (2:1) of CaO and SiO_2 at around 1450°C. It is well known that freshly prepared CaO has high surface area and is more reactive. For this reason different compounds giving CaO on decomposition have been chosen for the preparation of β-C_2S. In the present paper we will discuss the kinetics of β-C_2S formation from different component mixes. Hydration studies of β-C_2S are also discussed.

EXPERIMENTAL

Materials

Calcium carbonate, calcium nitrate, calcium acetate, calcium oxalate and (calcium nitrate + ammonium nitrate)$_{eutectic}$ were mixed with silica (aerosil) to prepare different reaction mixtures. All chemicals were of AR grade.

Method

Stoichiometric mixtures of the following systems in the ratio of 2:1 (with reference to CaO) were made :

(1) $CaCO_3 + SiO_2$, (2) $Ca(NO_3)_2 + SiO_2$, (3) $Ca(COOCH_3)_2 + SiO_2$,

(4) $CaC_2O_4 + SiO_2$ and (5) $[CaNO_3 + NH_4NO_3]_{eutectic} + SiO_2$

Mixtures were made homogeneous by adding isopropyl alcohol under constant magnetic stirring. The excess isopropyl alcohol was evaporated and the reaction mixtures were pelletized in the form of pellets having diameter 1.5 cm and heights between 1.0 - 1.5 cm. These pellets were then fired in a muffle furnace at different temperatures (1100° - 1400°C) for different intervals of time. Few pellets were prepared in presence of mineralizers also. After each firing the samples were rapidly cooled in air and ground into fine powder and allowed to pass through 100 mesh sieves. Percent free lime of the fired samples were determined by modified Franke extraction method (3) and from this the extent of reaction was calculated. The β-C_2S formed in different reaction mixtures were also characterized by X-ray diffraction. Electrical conductivity of solid pellet of β-C_2S was also determined.

Different β-C_2S prepared were subjected to hydration (w/s = 1.0) for 28 days. The hydration was stopped and free lime and non-evaporable water content determined.

RESULTS AND DISCUSSIONS

Reactions in number of reacting systems have been studied at different temperatures (1100° - 1400°C). Following calcium salts were used to obtain CaO: $CaCO_3$, $Ca(NO_3)_2$, $Ca(COOCH_3)_2$, CaC_2O_4 and $[Ca(NO_3)_2 + NH_4NO_3]_{eutectic}$. There was hardly any difference between $Ca(NO_3)_2$ and eutectic mixture. In all the cases calcium salts decomposed to give CaO, which ultimately reacted with SiO_2 in stoichiometric ratio to give β-C_2S. Among all the reactions, the kinetics of the following reaction was studied in detail :

$$2CaCO_3 + SiO_2 \longrightarrow 2CaO.SiO_2 + 2CO_2$$

The kinetic data obeys Jander's equation (4) -

$$[1-(1-\alpha)^{1/3}]^2 = kt \qquad \ldots.(1)$$

where, α is the extent of reaction at any time t and k is the rate constant. When 2 log $[1-(1-\alpha)^{1/3}]$ is plotted against log t, straight lines (Fig. 1) are obtained.

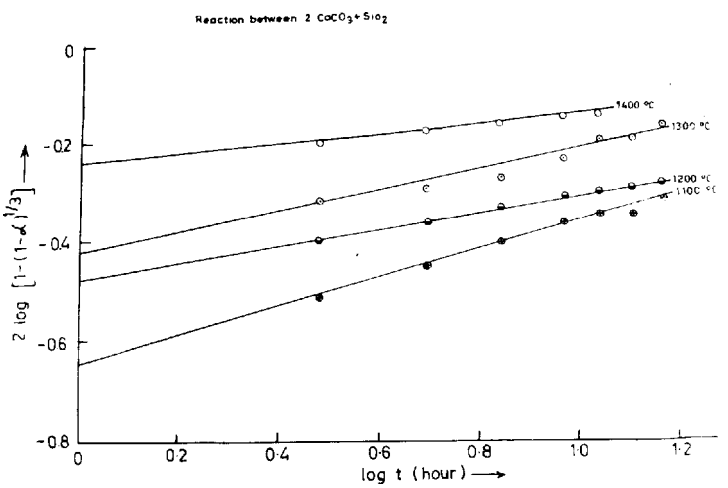

Fig. 1. Test of Jander's equation for the reaction $2CaCO_3 + SiO_2$ at different temperatures

From the slope of the lines, the values of k were calculated and are given in Table 1.

Table 1

Kinetic parameter for the reaction
$2CaCO_3 + SiO_2 \longrightarrow 2CaO.SiO_2 + 2CO_2$

S.No.	Temp. (°C)	k ($hour^{-1}$)	E (J/mole)	ΔG^* (J/mole)	ΔH^* (J/mole)	ΔS^* (J/mole)
1	1100	0.23	58800	370561	47384	-235
2	1200	0.33		393814	46553	-236
3	1300	0.38		419601	45722	-238
4	1400	0.58		441371	44890	-237

When log k is plotted against 1/T, straight line is obtained (Fig. 2) showing that Arrhenius equation is obeyed -

$$k = Ae^{-E/RT} \qquad ....(2)$$

where, E is the energy of activation, R is gas constant, A is constant and T is the temperature in degrees absolute.

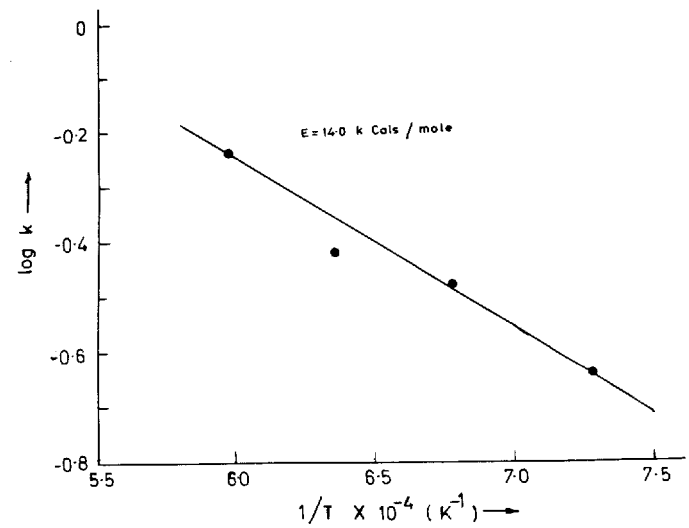

Fig. 2. Arrhenius plot for the reaction between $CaCO_3$ and SiO_2

The value of energy of activation is found to be 58.8 kJ/mole. The value is lower than the values reported by other researchers (4). The reason for this difference may be due to difference in the reactivity of SiO_2 and the surface area of CaO produced.

From the energy of activation value, the thermodynamic parameters such as activation enthalpy, free energy of activation and entropy of activation have also been calculated and are given in Table 1. The negative value of entropy of activation suggests that the activated state is more ordered as given below -

$$2\,CaO_2 + SiO_2 \rightleftharpoons (2CaO.SiO_2)^* \longrightarrow \beta\text{-}2CaO.SiO_2$$

Activated state
(more ordered)

The extent of reactions for all the systems at 1100°C and 1200°C are given in Table 2.

From the table it is clear that the reactivity of $Ca(NO_3)_2$ with SiO_2 is highest and lowest for the calcium oxalate system. It appears that calcium oxalate does not form C_2S at this temperature. The extent of reactions for the other systems are in the following sequence -

$$Ca(NO_3)_2 + SiO_2 > CaCO_3 + SiO_2 > Ca(COOCH_3)_2 + SiO_2 > CaC_2O_4 + SiO_2$$

Table 2

Extent of reactions

S.No.	Reaction Systems	Extent of reaction, α (%) after 3 hours	
		1100°C	1200°C
1.	$CaCO_3 + SiO_2$	91.1	94.9
2.	$Ca(NO_3)_2 + SiO_2$	93.9	95.8
3.	$Ca(COOCH_3)_2 + SiO_2$	82.4	83.4
4.	$CaC_2O_4 + SiO_2$	76.5	74.4
5.	$[Ca(NO_3)_2 + NH_4NO_3]_{eutectic} + SiO_2$	94.0	95.1

The difference in reactivity may be due to difference in the process of decomposition of calcium salts and the effect of gaseous atmosphere during decomposition. The different calcium salts decompose in the following manner -

$$CaCO_3 \longrightarrow CaO + CO_2$$
$$Ca(NO_3)_2 \longrightarrow CaO + 2NO_2 + 2NO + 2O_2$$
$$Ca(COOCH_3)_2 \longrightarrow CaO + 3H_2O + 4C$$
$$CaC_2O_4 \longrightarrow CaO + CO_2 + CO$$

It appears that the activity of CaO produced is significantly affected by the gaseous atmosphere.

Effect of different mineralizers (2.0 wt. %) on the formation of β-C_2S was also studied and is found that NaF is most effective for the $Ca(NO_3)_2 + SiO_2$ system at 1100°C. The order of the effectiveness of the mineralizers are as -

$$NaF > KF > CaF_2$$

It is possible to prepare β-C_2S of better quality at lower temperature by using suitable reacting system and mineralizer.

Electrical conductivity measurements of solid pellets show that β-C_2S behaves as a semiconducting material and contains defects. The electrical conductivity values for different β-C_2S obtained from different component mixes are different but the nature of variation is almost similar. This simply indicates that concentration of defects is different in different samples.

Free lime and non-evaporable water contents of some β-C_2S hydrated at 28 days are given in Table 3. These values are the measure of the extent of hydration and from the table it is clear that the extent of hydration is different for β-C_2S prepared under different conditions.The W_n value for β-C_2S obtained from the following reactions

$$Ca(NO_3)_2 + SiO_2 \xrightarrow[15\ h]{1200°C} \beta\text{-}C_2S$$
$$CaCO_3 + SiO_2 + NaF \xrightarrow[15\ h]{1200°C} \beta\text{-}C_2S$$

are quite high and the values can be further increased. However, unless the data for the entire systems are obtained, it is difficult to make a general remark.

Table 3

%Free lime and % Non-evaporable water content of some β-C_2S samples prepared at 1200°C (heating duration = 15 h) and hydrated for 28 days.

S.No.	Reaction System	% Free lime	% W_n
1	$Ca(NO_3)_2 + SiO_2$	2.5	6.9
2	$CaCO_3 + SiO_2$	1.9	4.7
3	$CaCO_3 + SiO_2 + NaF$ (2.0%)	4.9	9.2
4	$CaCO_3 + SiO_2 + KF$ (2.0%)	3.0	4.7
5	$CaCO_3 + SiO_2 + CaF_2$ (2.0%)	1.9	3.8

The difference in reactivity may be due to

1) Difference in the nature and concentration of defects in β-C_2S. Experiments have shown that β-C_2S contains defects (5) and the nature and concentration can be changed under different conditions.

2) Difference in surface activity. Surface activity may be higher or lower depending upon the nature of

   (i) gaseous atmosphere
   (ii) mineralizers

Thus it can be concluded that β-C_2S can be made reactive by choosing suitable conditions of its preparation.

ACKNOWLEDGEMENTS

The authors are thankful to Professor S. Giri, Head, Chemistry Department, Gorakhpur University, for providing the necessary laboratory facilities. S. Prabha Singh gratefully acknowledges CSIR, New Delhi for the award of Research Associateship and A.K. Shukla ia grateful to UGC, New Delhi for Financial support.

REFERENCES

1. Murdoch, L.J. and Blackedge, G.F., **Concrete Materials and practice**, Edward Arnold (Publishers) Ltd., London, 1968, 398 p.

2. Weisweiler, W., Osen, F.J. and Hofer, H., Cem.Concr.Res. 1988,18 , 55.

3. Jander, W., Anorg. Allg. Chem., 1927, 168 1-2, 1-30.

4. Mathur, V.K., Goswami, R.K. and Sharma, K.M., **NCB International Seminar on Cement and Building Materials, 3rd, New Delhi, India 1991, V4**, VIII-37.

5. Maycock, J.N. and McCarty Jr., M., Cem. Concr. Res., 1973, 3, 701.

ORTHOSILICATE COMPOSITIONS IN CaO - SrO - BaO - SiO_2 SYSTEM AND THEIR WATER REACTIVITY

Ion Teoreanu and Ecaterina Andronescu

Polytechnical Institute Bucharest
ROUMANIA

SUMMARY

Calcium orthosilicate, an important component of portland cement clinker, reacts with water, slowly. But, it is also possible to form in the portland cement clinkers, some more active orthosilicate phases by the partial substitution of the Ca2+ ions with the more basic alkaline-earth ions : Sr2+ and Ba2+.

The present study reports majore contributions in respect of phase relations at subsolidus temperatures in the 2CaO.SiO2 - 2SrO.SiO2-2BaO.SiO2 system, as also,the chemical process mechanism in solid phase between mixtures of the system. In addition, the reactivity of the enriched orthosilicate compositions is characterised by the data obtained, whereas conform the aforementioned hypothesis of the work.

L'ortosilicate de calcium - important composant du clinker de ciment portland -a une lente interaction avec l'eau. La formation, dans les clinkers de silicate, des phases ortosilicatiques plus actives est possible aussi par la voie de la substitution partielle du ion Ca2+ par des ions alcalins - terreux plus basiques : Sr2+ et Ba2+.

Dans l'étude ci-présente on apporte d'importantes contributions en ce qui concerne les relations de phases à des températures sous-solidous, dans le même que mécanismes de réaction en phase solide, correspondant aux mélanges du système. On y caractérise, en même temps, l'activité des compositions ortosilicates afferentes, les informations obtenues confirmant l'hypothèse de travail mentionnée en haut.

INTRODUCTION

Calcium orthosilicate - an important component of portland cement clinker - reacts slowly with water. The reaction, is one of hydrolysis. The hydrolysis process of salts derived from strong basis and weak acids, calcium orthosilicate being one such salt,is to be expected be in proportional direct relation with the original basis, keeping during the reaction time, the same anion and the same basis oxide / acid oxide, ratio.

For measuring the reactivity of these salts with water,it was suggested, in the previous work / 1;2 /, to determine the ion potential of the component cations.The rate of hydrolysis leaves inversely,with the ion potential.

Having the same anion and same MeO/SiO2 ratio,besides of course similar electron configuration of the cations, the alkaline earth orthosilicates-calcium, strontium and barium-could be expected have a water reactivity in the order:2CaO.SiO2<2SrO.SiO2< 2BaO.SiO2

Consequently, it should be possible to form, in the portland cement clinkers, some more active orthosilicate phases by the substitution of Ca2+ ions with the more basic alkaline earth ions (having smaller ion potential values : 1.88/Ca2+/>1.57/Sr2+/>1.40/ Ba2+/). For this reason, research on phase relations,reaction mechanism in solidus phase and reactivity of orthosilicate compositions in the oxide system CaO-SrO-BaO-SiO2, has a special interest, in cement chemistry.

As regards the calcium and barium orthosilicate binary system detailed information is available on their phase relations and reaction mechanism in solidus phase /3-7/ as well as their water reactivity /5,8,9/.

Multiple isomorphous relations are to be found in this system both with ß and α' structure of calcium orthosilicate (having 2.5% mol 2BaO.SiO2 and 7.5% mol 2BaO.SiO2 and with barium orthosilicate structure having 2.5% mol 2CaO.SiO2).

It must also be pointed out that the system has solidus solutions inside itself "T" with hexagonal structure(Ba1.5Ca0.5 SiO4-Ba1.2Ca0.8SiO4/3-5/) and "X" having orthorombic structure (Ba0.48Ca1.52SiO4).It is possible that,at high temperatures, the solidus solutions "T", "X" and α'C2S form a single phase. In the binary system Sr2SiO4-Ba2SiO4 phasal thermal equilibrium relations are well known, also.

The smaller difference between the Ba2+and Sr2+radii leads to larger fields of isomorphism /10/. However, not much data are available on the phase relations in the third binary system Ca2SiO4-Sr2SiO4, through analogy, large isomorphous fields can be expected to appear because of the quasi similarity between the dimensions of Sr2+ and Ca2+ radii. In this work both the system Ca2SiO4-Sr2SiO4 and the enriched calcium orthosilicate zone of the ternary system Ca2SiO4-Sr2SiO4-Ba2SiO4 have been analysed from the standpoint of the phase nature and the relations between them.Also are analysed the chemical process mechanism at subsolidus temperature and the water reactivity of the synthesized compositions.

EXPERIMENTAL

Four binary compositions in the system 2CaO.SiO2-2SrO.SiO2and three ternary orthosilicate compositions were chosen to be analysed. All these are shown in Table 1. For synthesizing the above mentioned compositions high purity CaCO3, BaCO3,SrCO3 and reactive SiO2 were used. After measuring and suitable homogenisation, the pasttilles of these compositions were thermally treated at 900...1500°C, for 1...3 hours.

Table 1

Sample no.	Oxide compositions, % mass.				Mineralogical compositions % mass.		
	CaO	SrO	BaO	SiO2	C2S	Sr2S	B2S
1	13.03	62.09	-	24.88	30	60	-
2	26.047	46.567	-	27.386	40	60	-
3	39.07	31.045	-	29.885	60	40	-
4	52.093	15.552	-	32.385	80	20	-
5	52.093	7.761	8.361	31.785	80	10	10
6	45.581	7.761	10.721	29.937	70	10	20
7	45.581	15.522	8.361	30.536	70	20	10

After each of the considered thermal treatment,the compositions were analysed by means of X ray diffraction to evaluate the phase composition evolution of the system, phasal nature and relations.

Water reactivity of the synthesized compositions for different treatment conditions was determined by establishing the values of PH of water suspensions (1/50), after 1 hour of mixing with water.

The solide powders utilised were of compatible granulometric conditions.

RESULTS AND DISCUSSION

X-ray diffractometry of products from the thermal treatment of binary compositions 2SrO.SiO2-2CaO.SiO2 at 900°C reveals the formation of orthosilicates besides, presence of unreacted reactants. There are, initially, two orthosilicate phases of calcium and strontium having deformed structure.

The system evolution points to the forming of single phase, having α'L structure - the calcium orthosilicate, the proportion and the crystallinity of this type of solid solutions increasing with the temperature of the synthesis. At 1400°C α'L C2Sss is the single constituent phase of the thermal treated composition.

Depending on the composition, in some characteristic planes, at these temperatures, when the composition have a single phase - α'L-C2Sss - the crystals there are developed, especially along the /222/ planes. Similar conclusions can be drawn, practically, for mixtures 5-7, also, placed in the ternary system C2S-Sr2S-B2S (C=CaO; Sr=SrO; B=BaO) near the C2S point. Even in this case, the interaction process begins at low temperature, when are in the equilibrium, having a single phase of type α'L - C2Sss.

With due regard both to the published data on the binary C2S-B2S, and the above mentioned results for the ternary C2S-Sr2S-B2S, a large miscibility field in the solid state is assumed. Fig. 1 gives a subsolidus equilibrium diagram for the ternary system examined.

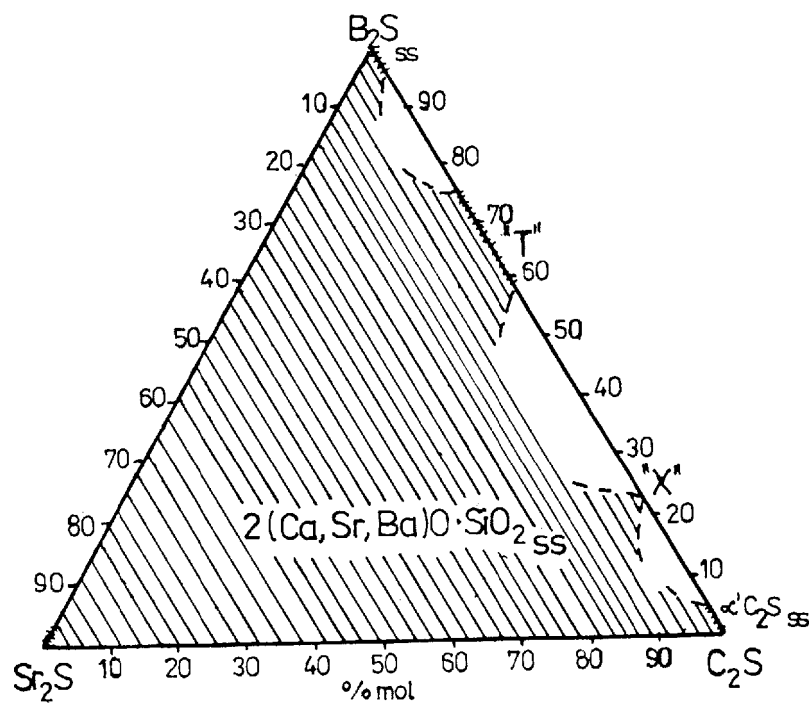

Fig.1 Subsolidus diagram of the ternary system solid solutions field

The results obtained on the reactivity with water of the synthesized substances in terms of the pH values of their suspensions, were studied vis-a-vis their composition and thermal treatment temperature. An increased reactivity indicates that the hydrolysing process is more intense. This could be manifest by a higher pH of the suspension for the same contact time with the water.

Since all the synthesized substances are of orthosilicate character, the differences between them being only in the nature and proportion of the component alkaline earth ions, their structural - compositional peculiarities were correlated with the medium ionic potential of the alkaline earth ions. The ionic potential was defined by the z/r ratio (z=2,the number of oxidation of alkaline earth ion and r=its ionic radius).

The curves in Fig. 2 were thus obtained. Examination of these curves gives us an idea about the evident diminution of the intensity of the hydrolysis process (of pH value) with the increase in ionic potential, for the same treatment temperature.

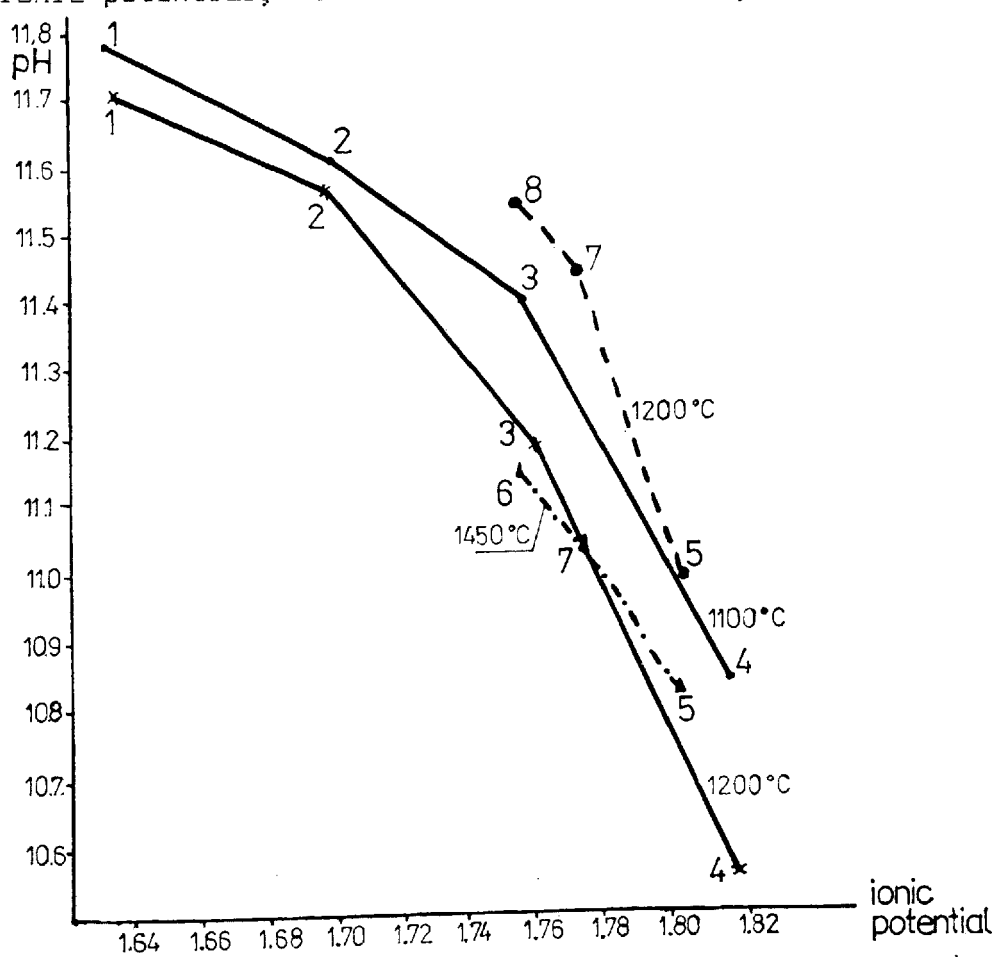

Fig. 2 Dependence of pH % orthosilicate phase suspensions with medium ionic potential for alkaline - earth ions for different thermal treatment temperature.

This dependence is manifest by the equivalent values of medium ionic potential at the same treatment temperature for the ternary compositions (with Ca2+,Sr2+ and Ba2+) as against the binary compositions (with Ca2+ and Sr2+).

The conclusion can be drawn for compositions 1...4, treated at 1200°C. In the binary compositions having calcium and strontium, the partial replacement of calcium ions with strontium ions, leads to a disturbance in the equillibrium of the intensity of alkaline earth ions ligand with the ligand of silicate structure (Me-O) and a weakening of those in direct proportion with the Sr2+ ion value.

The effect mentioned is more pronounced in the ternary compositions where the Ca2+ ions are substituted by Sr2+ and Ba2+ to the same degree. In addition, the nonhomogeneity in distribution of the intensity of Me-O ligands is increased, having favourable consequences on the hydrolysis process of the orthosilicate phases synthesized.

Phase structures synthesized at low temperatures, present more "birth" deficiencies, wich conferred on these structures a higher reactivity with increase in the temperature, to a certain value, these deficiencies will be "corrected" and the resulting phases will consequently have a low water reactivity.

Thus one can understand why more reactive orthosilicate phases were obtained at a lower temperature, under the given treatment conditions.

Thus, it is possible to obtain active clinkers from calcium silicate cement of a lower degree of lime saturation (with lower proportion of potential tricalcium silicate) by partial substitution of Ca2+ with Sr2+ and Ba2+, even in relatively small proportions. The stable ternary orthosilicate phases are preponderent in such clinkers and give them a satisfactory activity. In addition these clinkers could be burnt at relativity lower temperatures.

CONCLUSIONS

In the orthosilicate system 2CaO.SiO2-2SrO.SiO2 phase field,of ternary solid solutions has been established.

This field has a zone near the point 2CaO.SiO2 - system's component, which holds great interest portland cement chemistry.The behaviour with water of these high calcium ternary solid solutions, where the Ca2+ ion was partially substituted with Sr2+ and Ba2+ ions, shows the possibility of active orthosilicate phases and, consequently, of some silicate clinkers with low degree of lime saturation and satisfactory activity.

REFERENCES :

1. I. Teoreanu - Rev. Roum. Chim. 17(7) 1211 (1972)
2. I. Teoreanu - Binders technology, Bucharest, Ed. tech. 1975
3. J. Czechowski - Interceram 39(3) 28 (1990)
4. C. Brisi - Ind. Ital. Cem. 33, 937 (1963)
5. B. Matkovic - J. Am. Ceram. Soc. 69, 132 (1986)
6. V. V. Volkov - Stroi. Mat. Silik. Prom. 10(12) (1977)
7. I. Teoreanu; E. Andronescu; M. Enoescu; "Ternary solide solutions in the system CaO-BaO-SiO2", 3-th Congress chemie Bucharest, 1988
8. A. Braniski - Zement - Kalk - Gips 21,91 (1968)
9. I. Teoreanu; E. Andronescu : "Le comportament dans le procesus de durcissment des certaines compositions dans sisteme 3CaO.SiO2-2CaO.SiO2-2BaO.SiO2" 7-th int. Congr.Chem.Cem.Rio de Janeiro,1986
10. J.M. Fields Jr. ; P.S.Dear; J.J. Bourn Jr ; J. Am. Ceram. Soc. 55 (12) 585, (1972)

EFFECT OF INCREASED MAGNESIUM OXIDE CONTENTS AND MIXTURE BASICITY UPON CLINKER PHASES

I G Luginina, A I Boykova and O I Fomichova

Technological Institute of Building Materials, Belgorod
Institute of Silicate Chemistry, St Petersburg, RUSSIA

SUMMARY

A comparison of seven industrial clinkers with different basicities (KH) and magnesium oxide contents has been carried out. The solubility limit of magnesium oxide in clinker phases has been established. Decrease in basicity of raw meal increases isomorphous alite content. Brediglte has been found in high magnesia clinkers besides larnite.

РЕФЕРАТ

Проведено сравнение семи промышленных клинкеров с разной концентрацией оксида магния и основностью (КН). Установлен предел растворимости оксида магния в фазах клинкера. Понижение основности сырьевой смеси увеличивает изоморфную емкость алита. В высокомагнезиальных клинкерах наряду с ларнитом обнаружен бредигит.

In the study of distribution of admixtures in the different phases of cement clinker the effect of raw mix basicity (KH) and presence of a most typical admixture - magnesium oxide is an interesting aspect.

Clinkers from seven cement works with different MgO contents (0.4 - 5.2% mass) and different basicities - KH 0.89 - 0.97 (Table 1) were used for analysis.

These had been obtained from the natural limestone and clays, excepting clinker 5 wherein ash was used instead of clay, and clinker 4 wherein clay was replaced with marl. The raw components were remarkable for their consistent chemical composition.

Admixed oxides content in the clinker phases was determined with the help of "Camelax" electron probe microanalyser.

Table 1. Chemical composition of the clinkers used

Clinker No.	KH	% mass						
		MgO	SiO_2	Al_2O_3	Fe_2O_3	CaO	R_2O	SO_3
1	0.97	0.4	21.5	4.5	3.8	67.7	1.4	-
2	0.96	0.4	22.1	4.4	4.1	68.3	0.9	-
3	0.92	2.6	20.9	5.4	4.5	64.5	0.9	0.2
4	0.95	2.8	21.2	4.2	3.8	64.9	0.8	0.2
5	0.89	4.1	21.3	5.2	3.8	63.2	0.7	0.3
6	0.89	5.2	21.6	4.7	4.0	62.7	1.1	-
7	0.89	1.3	21.8	5.5	4.7	65.1	0.8	-

The following general correlations were found to exist, as revealed by phase analyses, arising from magnesium oxide. Increase in MgO concentration is accompanied by a steady increase of its content in alite and aluminoferrites. While it reached 1.9% in alite, it was 3.3% mass in aluminoferrite.

With increase in mix basicity MgO's ability to be retained in the alite crystal lattice decreases.

The probability of MgO dissolving in belite increases with its concentration. Raw mix batches containing sulphate ion provide the most favourable conditions of MgO isomorphic substitution in belite, since sulphate ion facilitates oxide dissolving in belite.

Hence, magnesium oxide content increases in all the clinker phases with increased dolomitization of limestones used in making portland cement. But when a certain limit, which is characteristic for each phase is crossed, any more oxide is accompanied by periclase crystallization.

Chemical composition of limestone has a certain effect on the overall admixtures content in alite: the less admixture in the source calcium carbonate, the less admixture in alite for the same or very nearly same basicity values of raw mixes.

Alite isomorphic ability to absorb more admixed atoms into its crystal lattice is more evident with lower KH. Nevertheless, silicon dioxide concentration is unaltered despite the higher acidity of caking material. The rest of acid oxides content - aluminium, iron, sulphur (if this oxide is present in the raw material or in the fuel) in alite increases. The ability of alite to absorb acid and alkaline (potassium oxide, for example) admixtures is more evident with lower raw meal basicity.

A remarkable feature of high magnesia industrial clinkers is the presence of two belite modifications: larnite and bredigite - α' - C_2S - high-temperature form, which is able to incorporate more admixtures into its crystal lattice compared to larnite. Spectral analysis detected increased concentration of admixtures in this belite phase, especially potassium oxide. Belite of industrial clinkers, despite limited magnesium oxide content, is able to incorporate potassium and sodium alkali oxides into its crystal lattice. Belite isomorphic capacity for alkali element oxides, unlike alite isomorphic capacity, does not depend on KH value; the limiting factor here is evidently the concentration of alkali containing admixtures and sulphur.

Increase in raw mix basicity (KH) impedes magnesium oxide deposition in the crystal lattice of calcium aluminoferrite.

Fe oxide concentration increases up to a certain level, but with increase in MgO admixture begins to reduce. CaO content is the most stable and does not depend upon changes in KH and MgO quantities, if KH values are high enough. Decrease in KH is naturally accompanied by a decrease of oxide in aluminoferrite. It is accompanied by increase of aluminium oxide in aluminoferrite. With the formation of more MgO saturated aluminoferrite phase in magnesium containing clinkers, the oxide concentration increases from 0.9 to 2.4 - 3.3% mass. While examining changes in aluminoferrites content with change in KH values and magnesium oxide concentration, it should be noted that the oxide content in the raw mix is a limiting value. Increase in magnesium oxide concentration leads to simultaneous phase enrichment with aluminium oxide. The literature on the subject points to a pronounced effect of burning temperature upon aluminium oxide content, but according to our analyses temperature is of minor importance.

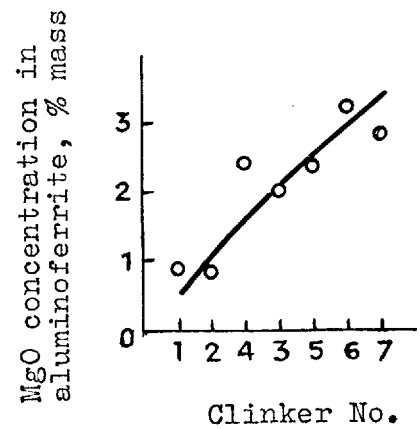

Fig. 1 MgO content in aluminoferrite

Decrease of clinker basicity at high magnesium oxide concentration in raw mix is accompanied by an increase of MgO isomorphic substitution ability in aluminoferrite as well as aluminium oxide content in this phase.

A definite relation between magnesium oxide content and aluminium

oxide in the aluminoferrite crystal lattice is not established yet. Aluminium oxide content in aluminoferrite changed slightly, not showing substantial effect of magnesium oxide concentration, KH or increase in burning temperature.

Tricalcium aluminate crystal lattice is remarkable for its high alkali oxides content, especially potassium oxide. Neither KH value nor increasing magnesium oxide concentration in the raw meal affect K_2O content in C_3A. Lowering of basicity leads to increase in Al_2O_3 concentration in the phase, but aluminium oxide is considerably lesser than it is necessary to consider the phase as being in conformity with its stoihiometry: Al_2O_3 is 5.5 - 6% and CaO is 3 - 5.5% mass less at low basicity. At the **same time** tricalcium aluminate is saturated with Fe and Si acid oxides, with the total content of these oxides in C_3A crystal lattice decreasing with decrease in KH.

At relatively limited MgO content in belite, increase of its concentration in the raw meal does not affect the quantity of calcium oxide in the phase. The factor determining CaO concentration in belite is basicity (KH) of the raw mix. The higher the KH value, the higher the oxide content in C_2S. Characteristically, the most saturated calcium oxide phases - tricalcium silicate and tricalcium aluminate, as a rule, do not increase their calcium oxide concentration in the crystal lattice as KH increases, the CaO content in the phase stays rather stable, unlike the less calcium oxide saturated phases - belite and aluminoferrite, in which the CaO content depends directly on changes in KH. Low basicity phases respond considerably stronger to CaO concentration compared to high basicity ones.

DEVELOPMENT OF ALUMINO-BELITIC COLOURED CLINKERS

S Laxmi, Lata Mohan, P S Sharma and A K Dhawan

National Council for Cement and Building Materials
New Delhi, INDIA

SUMMARY

Blue and pink coloured clinkers have been prepared by incorporation of suitable chromophores Co^{2+}, Fe^{3+}, Zr^{4+} (2 - 5 percent) and a combination of gypsum and CaF_2 mineralizers in alumino-belitic compositions at 1210 - 1330° C and 1050 - 1120° C respectively under controlled heating and cooling schedules. Laboratory clinkers thus prepared have been evaluated for their strength development, mineralogical and colour characteristics.

XRD, SEM and optical microscopic studies indicated the presence of β-C_2S, aluminates (CA and CA_2), gehlenite, sulphoaluminate, chromophore-bearing silicate and aluminate phases.

The performance of the blue clinker was comparable to that of OPC, but the compressive strength obtained at various ages for pink clinkers is somewhat lower. Diffuse reflectance spectra (DRS) measured in the range 300-1000 nm showed that the intensity of colour was not affected for both pink and blue cements even after hydration.

INTRODUCTION

Incorporation of ion chromophores like Fe^{3+}, Fe^{2+}, Ti^{4+}, Cr^{3+}, Mn^{4+}, Co^{2+}, etc in clinker compositions is known to affect the colour of clinker produced due to phenomena based on either idiochromatism or allochromatism. So far clinkers of yellow, green, emerald green, dark blue, green, yellow brown, brownish, violet tint and black colours have been reported with suitable chromophores. Various factors which determine nature of colour generation include the nature and quantity of ion chromophore, mineralogical composition, microstructure of clinker and the burning and cooling schedule. In this regard clinkers based on Ordinary Portland Cement and alumino - belite compositions have been reported (1, 2, 3).

Present studies report detailed investigations with respect to the preparation of alumino-belite blue and pink laboratory clinkers through identification of suitable chromophores, optimization of chromophore concentration, mineral composition, burning and cooling schedules, microstructure, performance and colour characteristics.

EXPERIMENTAL

Clinkers of blue and pink colours were prepared using natural raw materials including limestone, clay, bauxite and quartzite sand with gypsum and calcium fluoride as mineralizer. Raw mix components for blue clinker were weighed as per the designed values of LSF 0.5-1.1, SM 0.3-0.99, AM 55-95, chromophore 1.5 - 4.5 percent for raw mixes RC-11, RC-11a, B-V and blended. Raw meal with $\sim$12 percent residue on 170 mesh sieve was then nodulized with 12-15 percent moisture to give nodules (1 cm dia). Dry nodules were fired in an electric furnace at a temperature of 1200-1300° C with a retention time of 30-45 minutes. Clinkers thus obtained were cooled under controlled conditions.

Three raw mixes for pink clinkers were designed with design parameters LSF 0.47 - 0.74, SM 0.40 - 0.52, AM 3.20 - 4.24, and combinations of iron and zirconium as the chromophore at 2.0 - 4.0 percent. Raw meal nodules corresponding to raw mixes were fired in an electric furnace at 1080 - 1120° C with a retention time of 20-35 minutes. Clinkers were cooled under controlled conditions.

RESULTS AND DISCUSSION

Extensive studies (4) on various parameters like chromophoric ion, chromophore concentration, mineralogical composition of clinkers, burning and cooling schedules have resulted into optimization of above parameters for blue and pink clinkers.

Blue Clinkers :

Stable blue coloured clinkers were obtained in alumino - belite compositions (Table 1) using Co_3O_4 as chromophore. Incorporation of a combination of gypsum and CaF_2 as a mineralizer in the raw mix resulted in lowering in clinkerization temperature and better colour stability. All the clinkers corresponding to design B-V, RC-11, RC-11a were stable and low in free lime. Generation of blue colour in the clinkers is mainly due to formation of cobalt silicate (Co_2SiO_4) and cobalt aluminate ($CoO.Al_2O_3$). The generation of the blue colour was largely affected by the presence of calcium, magnesium and alkalies. Investigations (4) showed that for generation of blue colour the CaO content should be maintained < 45-48%, Mgo content < 2% and alkalies < 0.8%.

TABLE 1

Chemical Composition of Pink (PC-1) and Blue (RC-11a) Clinkers

S. No.	Sample No.	Constituent (Percent) SiO_2	Fe_2O_3	Al_2O_3	CaO	MgO	R_2O	Co_3O_4	ZrO_2	F^-	$\overline{S}$
1.	PC-1	13.32	6.75	26.88	42.21	0.25	0.35	--	3.3	0.48	6.01
2.	RC-11a	13.69	0.40	36.90	42.02	0.50	0.25	1.58	--	0.56	3.41

XRD studies have indicated presence of β-C_2S and aluminate phases (CA and CA_2), gehlenite, sulphoaluminate and cobalt bearing silicate and aluminate phases. The XRD pattern of blue clinker RC-11a is presented in Figure 1.

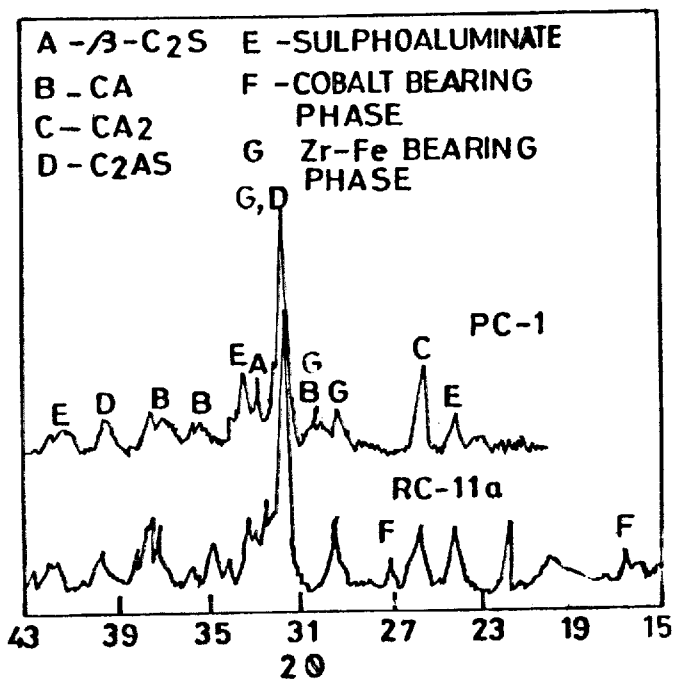

Fig 1 X-Ray diffractograms of pink and blue clinkers

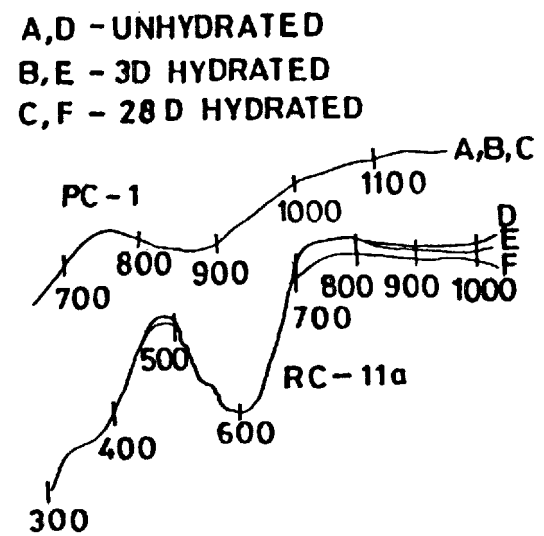

Fig 2 Diffuse reflactance spectra of unhydrated and hydrated pink and blue clinkers

DRS of blue cement and that of hydrated samples at 3 and 28 days is presented in Figure 2. The variation in the intensity of peaks of hydrated samples is not significant, indicating that the intensity of the blue colour is not affected by hydration. The high colour stability has been attributed (5) to the hydraulic inertness of the colour phases.

Microscopic studies have revealed that the clinkers are highly porous with the development of micro to cryptocrystalline phases. Development of belite and prismatic irregular grains of monocalcium aluminate were observed (Plates I and II).

SEM studies have indicated that the clinkers have fine grained, loose and highly porous matrix. Hexagonal rods of sulphoaluminate, belite and prismatic monocalcium aluminate crystals have been observed together with deposition of certain precipitates (Plates III and IV). However from microscopy alone it is difficult to identify the coloured phases.

Physical characteristics of clinkers RC-11, RC-11a and B-V were evaluated at a Blaine's fineness of $\sim$425 m^2/kg and the results are presented in Table 2.

Pink Clinkers:

All the clinkers corresponding to designs PC-1, PC-2 and PC-3 (Table 1) were stable and low in free lime indicating completion of the clinkerization reaction.

XRD studies indicated the presence of β-C_2S, aluminates (CA and CA_2), gehlenite and sulphoaluminate phases. Certain aluminate and silicate based phases incorporating iron-zirconium have also been observed. The XRD pattern of pink clinker PC-1 is shown in Figure 1.

Microscopic studies have revealed that the clinkers are highly porous with development of micro to cryptocrystalline phases (Plate V). Development of belite was observed. Microstructural features are similar to alumino-belitic clinkers.

SEM studies have revealed that the clinkers have fine grained, loose and a highly porous matrix. Hexagonal rods of sulphoaluminate, belite and prismatic monocalcium aluminate crystals have been observed alongwith deposition of certain precipitates (Plates VI and VII).

Clinkers corresponding to the designs PC-1, PC-2, PC-3 were evaluated and the setting time and strength characteristics are presented in Table 2.

DRS of pink cement and that of hydrated samples at 3 and 28 days is presented in Figure 2. The variation in the intensity of peaks of hydrated and unhydrated samples is not significant indicating that the colour is not affected during hydration.

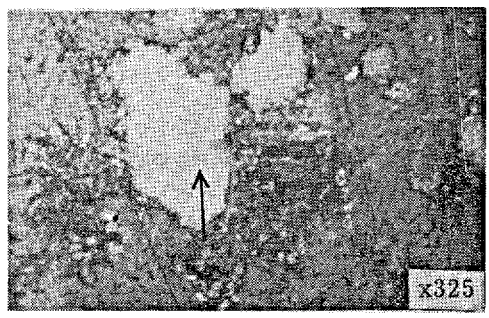

PLATE I DEVELOPMENT β-C_2S

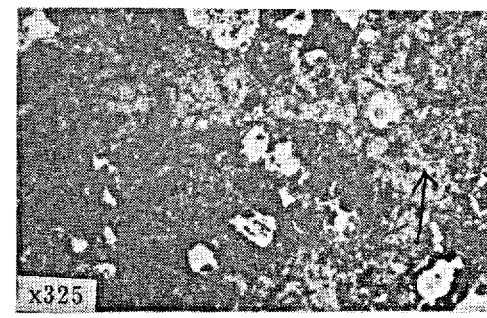

PLATE II PRISMATIC IRREGULAR GRAINS OF CA

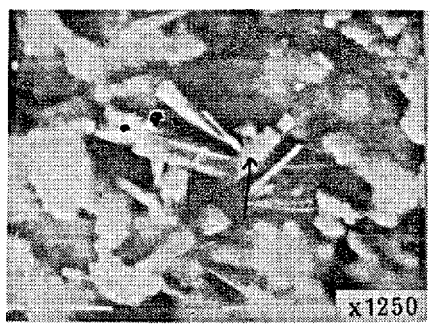

PLATE III SULPHOALUMINATE WITH β-C_2S

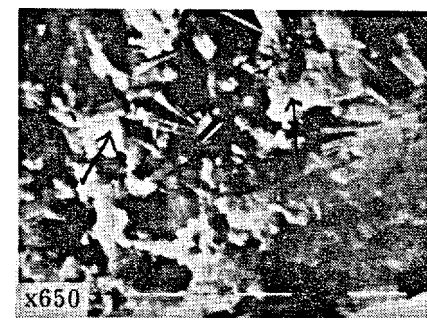

PLATE IV β-C_2S WITH PRECIPITATES

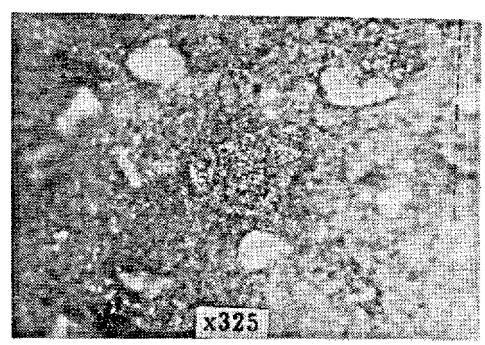

PLATE V MICRO TO CRYPTOCRYSTALLINE PHASES

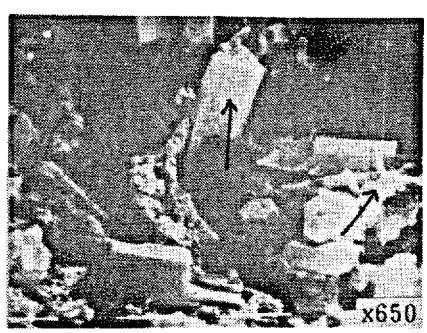

PLATE VI SULPHOALUMINATE WITH β-C2S

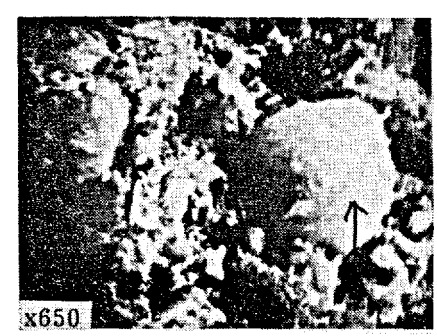

PLATE VII BELITE CLUSTERS

TABLE 2

Physical Characteristics of Blue and Pink Clinkers from Raw Materials

Sl. No.	Sample Code/ Characteristic	RC-11	RC-11(a)	B-V	PC-1	PC-2	PC-3
1.	Blaines fineness (m^2/kg)/ % Retention on 45 μm Sieve	405	425	268	26.0	28.8	23.5
2.	Setting time, minutes						
	Initial	45	12	35	15	--	--
	Final	145	45	130	25	--	--
3.	Compressive Strength (N/mm^2)* (25 mm cubes)						
	3 days	12.7	19.1	12.9	13.9	8.9	7.4
	7 days	--	25.8	14.7	15.2	10.0	9.0
	28 days	27.7	30.8	17.0	15.7	12.2	10.5

*Cured at $27\pm2^{o}C$ under water

CONCLUSIONS

It is possible to generate blue and pink colours in alumino-belitic clinker compositions by incorporation of Co_3O_4 and combination of zirconium and iron with and without mineralizers in the temperature range 1050-1330° C. Both the clinkers have similar microstructural features and good colour stability. Performance characteristics are satisfactory. The salient features of this technology include lower fuel consumption due to lower temperature of clinkerization by 100-400° C as compared to OPC. Further, the technology is cheaper vis-a-vis technology of pigment addition to white cement for making coloured cements.

ACKNOWLEDGEMENT

The authors have freely drawn upon completed R&D work/status reports. The paper is being published with the permission of the Director General, National Council for Cement and Building Materials, New Delhi, India.

References

1. Bozhenove, P I and Holopova, L I : " Coloured Portland Cement Clinker". Tsement, 1965, 31 (6), 9-10.

2. Zokharov L A : " Alumina - Belite Cement". The VIth International Congress on the Chemistry of Cement, Moscow, September 1974.

3. Brovkov, A S and Shestrakova O P : " Production of Coloured and White Siliceous Portland Cement", Vim, Kiv, Politeck, Inst. Ser. Khim Meschinobuduv Tekhrol 1977, 14, 78-80

4. NCB : " Development of Technology for Light Decorative Coloured Clinkers", R & D Report, National Council for Cement and Building Materials, New Delhi, 1986.

5. V. I. Turchaninov, "Preparation and properties of coloured Alumino-Belite Cements", Izv. Vyssh. Uchebn. Zaved , Khim. Tekhnol.,25(4), 458-60(1982).

THE EFFECT OF THE COMBUSTION OF COAL MIXED WITH LIMESTONE ON THE BURNING PROCESS OF CLINKER

Wang Yuping*, Huang Wenxi**, Jiang Youxing* and Ye Qiaoming*

*Sichuan Institute of Building Materials, Sichuan, P R CHINA
**Chengdu Design & Research Institute of Building Materials Industry, Sichuan, P R CHINA

ABSTRACT

This paper studies the regularity of the combustion of coal mixed with limestone and it find that this kind of combustion can lead to not only the improvement in the quality of the clinker and its inner homogeneity, but also the fully utilization of the energy given by the burning process. Experiments indicate that abut 5-10% of energy can be saved when the preparation of raw materials is suitable.

摘　　要

本文研究了煤与石灰混合后燃烧的规律，这种燃烧不仅可改善熟料的质量及其内部均匀性，还可更完全利用燃烧所放出的热能．试验表明若掺量合适可节能5-10%.

1. INTRODUCTION

On the burning process of clinker, the coal ash after the coal combustion is almost fully precipitated in the raw meal that come from the kiln end and forme the cement clinker. Because the composition of the coal ash closely resemble the one of clay, the preparation of raw materials is made in high lime saturation coefficient to ensure suitable clinker composition. That causes the clinker to have a poor burnabilty. Generally, the ash's precipitating takes place on the surface of the kiln charge (material being burned), so that the coal ash precipitating in the raw meal is not distributed. If the CaO content in the coal ash is increased and closely resembles the raw meal's, the uneven distribution of the coal ash in the clinker will not occur. So the raw meal will have a low lime saturation factor and the clinker will have a good burnability. This paper has studied the effect of the combustion of coal mixed with limestone on the burning process of clinker. It has been found that this kind combustion not only improves the inner homogeneity of the clinker, but also has a high heat efficiency on the burning process, and the decomposition rate of $CaCO_3$ and the other chemical reactions in the pulverzed coal are improved.

2. EXPERIMENT

In the clinker manufacture, if the coal mixed with some limestone, the flame of coal may be changed. In particular, the coal releases heat and flame temperature may be affected. This papers will study those changes. In the experiment, there are four kinds of raw coals that are chosen. The coal ash composition and the industry analysis of the coals are shown in Table 1, 2, the limestone composition is shown in Table 2 too.

Table 1 the industry analysis of the coals

Coal-No.	W_r	V_r	C_r	A_r
1	2.44	12.62	52.71	32.23
2	2.15	22.11	43.14	32.60
3	1.00	28.67	50.63	19.70
4	0.82	25.26	42.01	31.91

Table 2 the composition of the coal ash and limestone

coal-No.	SiO_2	Al_2O_3	Fe_2O_3	CaO	MgO	SO_3	TiO_2	Loss
1	50.50	26.03	13.89	2.47	1.72	3.37		
2	59.30	28.29	5.11	0.90	3.22	1.20		
3	44.80	32.72	9.79	5.87	1.93		2.03	
4	40.20	30.81	16.42	3.51	1.80		1.43	
limestone	2.61	2.17	0.60	52.20	0.52			41.40

The experiment is divided into two parts, one is the heat release measure in different limestone content. The oxygen bomb calorimeter is adopted. Another part is combustion experiment. First, the mixed coal powder is injected into a furnace which has a certain temperature range, then, collect the product of combustion and analyses its mineral by X-ray diffration method. In the experiments, the environment temperature is controlled in 20±2℃ and the relative air humidity in 85± 5%.

There are three steps in the experiment. First is the coal powder preparation: After being dried, the coal is ground into powder; the limestone is ground also. Then, weigh the coal and

limestone accurately according to the proportion defined in advance, and mix the coal and limestone system homogeneously. Second is the calorific value measurement: Using the oxygen bomb calorimeter, we measure the heat release of the mixture system. Third is the combustion experiment: The combustion experiment furnace has been made by ourselves, its chamber is 65mm in diameter and 600mm in height. The ash is collected by a cyclone collector. At a certain temperature, the coal powder is injected into furnace chamber and has a complete combustion.

3. THE RESULTS OF EXPERIMENT

3.1 The heat value of coal

In the experiment, the heat value (or the caloric value) of coal is the heat evolution per unit pure coal. In other words, it is the heat effect of the mixed system which have 1 kg pure coal and some limestone. The heat value of the four kinds coal are shown in Fig. 1A, B, C. From the Fig. 1, the law of the coal calorie value for the coal mixed with some limestone is distinguished. As in the fig. 1, the results vary with the kinds of the coal, coal NO- 1 has a maximum caloric value when the limestone content is about in 0.15-0.25kg- limestone/kg- coal; and the maximum caloric value of coal NO-3 is about 0.10kg-limestone/kg- coal. No- 2 was about 0.05kg -limestone/kg-coal; and No-4 sample caloric value is higher than raw coal when limestone content less than 0.35kg -limestone/kg-coal. Although, their highest releasing heat is in defferent limestone content. The majority of the coals has the same rule in the heat effect change, all kinds of coal have a peak value on the releasing heat, and , if the contents of limestone is increased continuously, the caloric value of the mixed coal will decrease

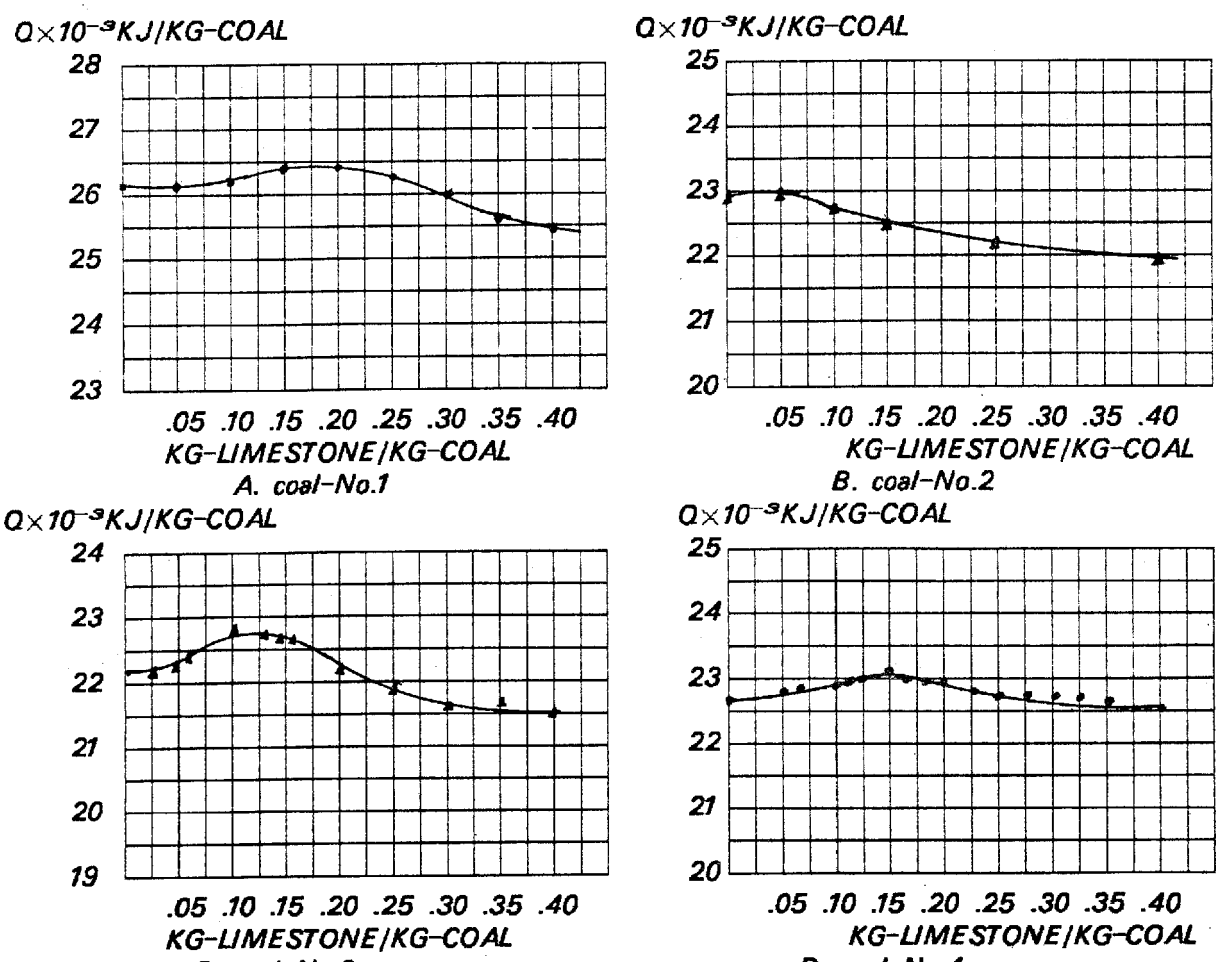

Fig.1 the effect of the heat value in mixed system

3.2 The reactions in the coal ash

When the coal is mixed with some limestones, the coal ash chemical composition is changed, and its chemical property is also changed. On the combustion process, the carbon and other combustive materials supply a large number of heating and form a high temperature flame. The high temperature brings about the decomposition of the $CaCO_3$, and the other chemical reactions take place simultaneously. The main effect factors in the decomposition of the $CaCO_3$ as well as other reactions are temperature, ash compositions, reaction surrounding , reaction time et. In this case, many conditions are not easy to be changed, but the combustion temperature and ash composition could be changed. In the different temperature range, the decomposition rate of $CaCO_3$ was different. The higher the combustion temperature, the more rapid the decomposition rate of $CaCO_3$. In 1200℃ (furnace temperature), the CaCO3 decomposing ratio in the mixed coal could attain 75% in 1 second. When the temperature reach 1300℃, its decomposing ratio could attain to 98. 6% in same time. As the burning temperature come up to about 1350 ℃ , the decomposition almost fulfilling(>99%). Table 3 is the results of the decomposition ratio changing with combustion

Table 3 The results of the decomposition ratio of the calcium carbonates

temperature℃	1100	1200	1300	1400
decomposition ratio %	73.2	75.0	98.6	99.7

temperature. Also, the temperature can cause important effect on the other reactions. During the combustion, some other minerals will be formed, in 1100℃ -1200℃, it is very easy to form C_2AS in the system. When the temperature is over 1200℃, the contents of C_2AS will decrease in the ash, and the silicate mineral can be formed. From the experiments, we find that the CaO, C_2S, C_3S, CA, CS, CA, CS, A_3S_2 $C_{11}A_7$, C_2AS are formed in the product of combustion, and, if the coal contains some sulphide, the $C_2A_3\bar{S}$ will be found in the ash.

4. THE DISCUSSION AND THEORY CALCULATION

If we consider only on the amounts of limestone in the coal, the limestone mixed with coal can cause an endothermic reaction increases and the absorption heat increases with the amounts of limestone. This is not comprehensive. In fact, the quantity of releasing heat of the coal could be divided into two parts. One is caused by the part of combustibles in the coal(carbon, the organic substance...), another is caused by the reaction occurring in the ash. When the amounts of ash is smaller, the effect of reaction in the ash is not notable. For the low heat value coal, the ash amount is in high proportion, so, the effect of reaction in ash can not be neglected. Supposing the quantity of heat of the combustible parts in the coal does not change, the main effect factor of the release heat quantity of the coal is the reactions in the ash. As stated above, the reactions are related to the compositions of ash, the combustion temperature, the surrounding of the reactions and reaction time. If those conditions are adjusted, we could have a best use results to attain minimum consumption on the burning process.

4.1 The reaction model of combustion

In industry, the combustion time is fixed for a certain furnace, the combustion temperature and the composition of coal as well as other condition can be changed. Generally, in the clinker manufacture, the flame temperature is maintained in certain range. In order to improve the overall thermal efficiency of the kiln system, changing the coal composition is feasible. The coal mix with some limeston is a better method. This method has two advantages, one is that the chemical reaction in the ash will have an optimum condition, some minerals can be formed, another is that the $CaCO_3$ calcining heat in the coal could be saved. Of course, if the endothermic reaction in the

coal is too much, the combustion temperature will be affected, and that in turn, it will act the reactions in the coal combustion. Also, the production of the reaction will be changed. From the results of the x-ray analysis, the following reactions can be supposed:

$$C + O_2 \longrightarrow CO_2 \qquad S + O_2 \longrightarrow SO_2$$
$$CO + O_2 \longrightarrow CO_2 \qquad 2H_2 + O_2 \longrightarrow 2H_2O$$
$$CaCO_3 \longrightarrow CaO + CO_2 \qquad CaCO_3 + SiO_2 \longrightarrow CS + CO_2$$
$$2CaCO_3 + SiO_2 \longrightarrow C_2S + 2CO_2 \qquad 3CaCO_3 + SiO_2 \longrightarrow C_3S + 3CO_2$$
$$CaCO_3 + Al_2O_3 \longrightarrow CA + CO_2 \qquad 11CaCO_3 + 7Al_2O_3 \longrightarrow C_{11}A_7 + 11CO_2$$
$$CaO + SiO_2 \longrightarrow CS \qquad C + CaCO_3 \longrightarrow CaO + 2CO$$
$$2CaO + SiO_2 \longrightarrow C_2S \qquad 3CaO + 2SiO_2 \longrightarrow C_3S_2$$
$$CS + CaO \longrightarrow C_2S \qquad C_2S + CaO \longrightarrow C_3S$$
$$3CaO + SiO_2 \longrightarrow C_3S \qquad 2SiO_2 + 3Al_2O_3 \longrightarrow A_3S_2$$
$$2CaO + Al_2O_3 + SiO_2 \longrightarrow C_2AS \qquad 4CaO + 3Al_2O_3 + SO_3 \longrightarrow C_4A_3\bar{S}$$

According to the reaction conditions and the composition, some of those reactions may be strong or weak and some glassy phase may be formed. But above reactions have taken place truely.

At present, it is difficult to ascertain the definite path of the reaction. Because of the very short reacting time, the rapid heat transfer and the violent irreversible reactions, [3] But, we can find out: The heating up rate of the coal particle could come up to 10^4 -10^6℃/s[1] in the furnace(or in the flame), the time of the combustion was only about 1-5 second, the combustion temperature can come up to 1300℃ or higher[2], the alkalinity of ash will be increased, the decomposition reactions and combination are different from the pure raw coal. These shall make a remarkable influence on the chemistry reaction in ash of system, it will cause the mass transfer much faster, the reaction activation energy decreased and so on. This is a very complicated system. For convenience sake, the combustion model of the coal-limestone mixture system can indicate as Fig. 3. In the system, there are three parts. One is the raw materials of combustion - - - coal, limestone and air. Next is the production of combustion--- the ash, gas and release heat. Third is the reaction unit----various chemistry reactions in the system.

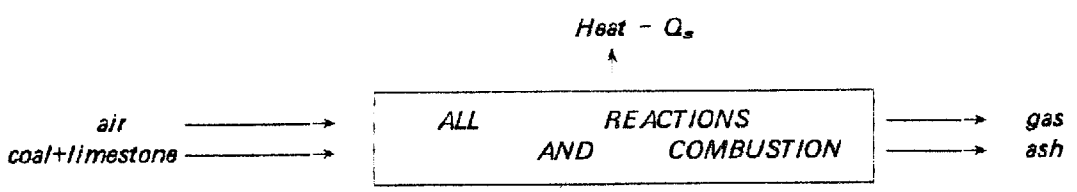

Fig. 2 combustion model of the coal mixed with the limestone system

4.2 The calculation heating efficiency for the coal+limeston mixture system

Rapidly rising temperature can increase the decomposition rate of carbonate and decrease the quantity of heat consumption of the decomposition. When the decomposition temperature is at 1300C, the CaCO3 calicining heat will decrease from 175.06 mj/mol to 145kj/mol[4] Also, the rapid heating-up burning process will cause $CaCO_3$ directly react with other oxide. Furthermore, this case could lead to the decomposition of $CaCO_3$ more quickly and every reaction would coincide. According to the law of thermodynamics and above model, we could calculate the heating efficiency of the mixture system. Fig. 3 is the calculated results for two kinds of coal mixed with some limestones. The results prove that the quantity of the heat can not be ignored because of the reaction in ash; and the results also show that the suitable composition in the ash is favorable to exothermic heat-releasing of the mixed coal system. Changing the ash composition of the coal could obtain an optimum or maximum heat evolution.

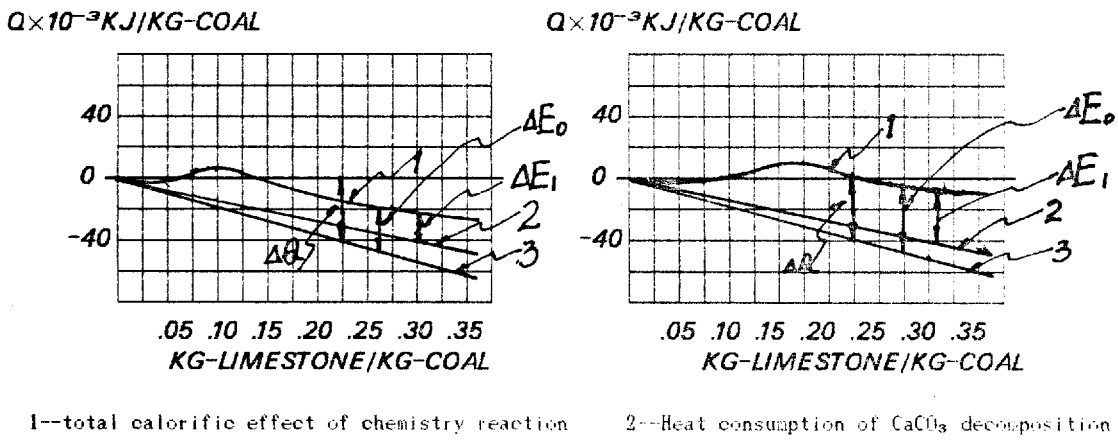

Fig.3 The colorific effect calculated value of the coal mixed with limestone

In fig. 3, The curve-1 stands for the overall thermal effect of the coal mixture system, curve-2 represents the $CaCO_3$ calcining heat in the combustion, and the curve-3 means the calcining heat ($\triangle Q$) in the normal condition. While, $\triangle E_0$ indicates the saved energy of the mixture system, $\triangle E_1$ is refereed to as the chemical reaction release heat in the mixture system, and $\triangle Q$ is the convention calculate value for the amount of limestone in the system.

In the burning process of the cement clinker, if the coal is mixed with the limestone, the $CaCO_3$ content in fuel (coal) will be increased. but the heat consumption of the CaCO3 decomposition could be compensated by the excess release heat ($\triangle E_1$) in the system, because some part of $CaCO_3$ is in fuel and the $CaCO_3$ calcining heat of raw meal can be deceased(the $CaCO_3$ contents decrease). Therefore, The overall thermal efficiency on the burning process of clinker will be improved.. In addition, the decomposed CaO in this combustion process will be more active, because it has more crystal defects and in a shorter-time decomposition. It makes the clinker synthesize more easy. On the other side, we have made a lower KH in the raw meal, and the kiln feed could be increased. This could lead to the increase of the clinker output of the kiln.

As the above analyses, for the normal rotary kiln (dry process or wet process), and normal kind of coal, the amounts of the limestone mixed with coal at about 0.2-0.3kg/kg, the clinker output for the rotary kiln will increase by a factor of 3.75-7.5%, and, the heat consumption of the clinker will be saved 5-10%. Furthermore, if the coal ash composition is as same as raw meal, the clinker output will increase 10% more then one in normal condition.

5. THE REALIZATION OF THE METHOD

The coal mixed with some limestone is a favorable method for saving energy. This method realization must be settled on the basis of the clinker burning condition —— the coal kinds, calorific power, the ash composition , and the combustion equipments ets. The process includes two steps. First, we can detect the suitable CaO content in the coal (generally from experiment), and, according to the compositions of the mixture coal ash, calculate the raw meal composition and prepare it. Second, make the limestone mix with coal in the coal mill (feeding with coal together on the mill head), and using this pulverzed coal normally on the clinker burning process.

Although, this method is not used in practice, some evidences have proved that is to be available. KY cement plant employs the lignite [contain chalk layer ($CaCO_3$)] which has high contents of CaO (29-47%) in ash and low quantity of heat (only 12450kj/kg) to mix with bitumineus

coal and even use the lignite directly on the burning process of clinker. In this case, the $CaCO_3$ contents is about 12-16% in the pulverzed coal, it has not harmful effect on the burning process, and the lower grade limestone has been utilized, the quality of clinker has been improved. Some results of production are shown in Table 5. In Table 5, the heat consumption of the clinker in the specific condition come down about 5 -8%. It is evident that the project is useful and practical.

Table 5 Produced information of KY cement plant in comparison with same plant(wet process)

plant	KY	KM	YD	DT
strength of clinker (MPa)	62.17	61.8	61.78	57.7
heat consumption (kj/kg)	5983.11	6292.37	6282.15	6501.27

information of 1988

6. CONCLUSION

(1). There is a best range of the limestone content mixed with coal on the burning process which can release maximum quantity of heat.

(2). When the coal is mixed with limestone, the decomposition rate of calcium carbonate in the pulverzed coal will be increased. As the burning temperature come up to about 1350 ℃, the decomposition fulfilling time will be in 1 second.

(3). If this method is used in industry, it could improve the quality of the clinker and the clinker output of the kiln will be increased 3.75-7.5%, and also, the heat consumption of clinker could be saved about 5-10%.

REFERENCE

1. M.A.Field etl. Combustion of Pulverised Coal Institute of Energy, 1983, p164-196

2. N.A.Chigier, Combustion and application of Coal, 1981.2, p.78-90

3. S.R.De Groot , Non-equilibrium Thermodynamics 1962, p.198-240

4. Huang Wenxi etc., Tha Approach on Heat Econorany of a New Type of Set Burned Portland Cement Clinker Suspended Fluidized Clcainer, Journal Of Sichuan Institute of Building Materials, No.2, 1987, p.2-10

EFFECT OF THERMAL TREATMENT ON THE REACTIVITY OF CLINKER MINERALS PRODUCED FROM VERTICAL SHAFT KILN

K Raina and R Bhargava

National Council for Cement and Building Materials
New Delhi, INDIA

SUMMARY

Thermal treatment of cement raw mix is known to have a profound impact on the reactivity of clinker minerals and therefore its performance. Since nearly 4 percent of cement produced in India is from Vertical Shaft Kiln (VSK) technology using the black meal process where the thermal treatment both in terms of clinkerization and cooling is significantly different from the rotary kiln. Investigations were undertaken to study the relative reactivity of clinker minerals under the pyroprocessing conditions available in VSK and rotary kiln. Laboratory clinkers were also prepared under controlled conditions for comparative studies. The clinkers were investigated using X-ray diffraction, scanning electron microscopic and optical microscopic techniques. The cements prepared from these clinkers were subjected to strength determination and hydration studies. VSK and laboratory fired clinkers prepared under similar burning and cooling conditions are porous with the bulk density (litre weight) in the range of 900 - 1100 g/l and had similar performance characteristics, whereas rotary kiln clinkers were dense with bulk density (litre weight) 1310 g/l having large crystals. The initial rate of strength development was low for rotary kiln clinkers.

INTRODUCTION

There are nearly 134 vertical shaft kiln based cement plants currently running in the country and 90 more are in various stages of implementation. Total production of cement from these kilns is nearly 2 million tonnes constituting 4.0 percent of the total cement production. Vertical shaft kilns are usually using black meal process (1,2) where raw materials and fuel usually low volatile coal or coke breeze a by-product from steel plants are interground dry to a fine powder and nodulised. In the technology developed and commercialized by NCB the nodules are then fed into VSK through a specially designed revolving feeder(3). The mechanism of clinker burning (4,5) is different in VSK as each nodules is burning in its own environment due to integrated fuel in the raw meal. The thermal treatment in VSK is different as the sintering is normally completed within the conical portion which is specially designed to accommodate for shrinkage of nodules. The various zones of reactions starting from top of the kiln are, the drying zone, the calcining zone, the sintering zone and the cooling zone. The lower 2/3 portion of the kiln is the cooling zone and clinker takes 6-7 hr to pass through various kiln zone resulting in the slow cooling of the clinker, which exchanges heat with the combustion air and cools down from 1450°C to $\sim$ 70°C.

Since the heating and cooling schedules have significant influence on the reactivity of clinker minerals investigations were taken up to study the impact of thermal treatment on the hydration of clinker minerals produced from VSK and rotary kiln. Investigations were also conducted on the laboratory prepared clinker under simulated conditions of burning and cooling.

The clinker minerals were studied for their mineralogical and morphological features using XRD, SEM and optical microscopic techniques. Reactivity of these minerals were also studied by using DTA/TGA of hydrated samples.

EXPERIMENTAL

Two plant clinkers one each from VSK and rotary kiln using the same raw materials were collected. Raw meal nodules of VSK plant were also collected and dried in an oven at 105°C for 2 hrs. These dried nodules were fired in an electric furnace at 1450°C, with a retention period of 20 minutes. Clinkers thus obtained were air cooled at ambient temperature. The three clinkers, laboratory clinker (CL-L), VSK Plant clinker (CL-V) and rotary kiln clinker (CL-R) were analysed for elemental composition using volumetric cum gravimetic method. Free lime (CaOf) was determined by extraction method. To determine the crystal size, shape and stabilization of mineral phases following methods were used:

a) Microscopic studies were carried out on polished sections by fixing the clinker in araldite under vaccum. These sections were examined under reflected light using Carlziess Amplivol Polorizing microscope.

b) SEM studies were carried out on fractured clinker samples using Philips model (ST) CM 301 G scanning electron microscope.

c) X-ray diffraction studies were conducted on powdered samples using D-Max, Rigaku, Japan diffractometer.

The clinkers CL-L, CL-V and CL-R were ground in a ball mill to a fineness of 320±5 m^2/kg with gypsum to maintain a level of 1.75 percent SO_3. The resultant cements OPC-L, OPC-V and OPC-R obtained from CL-L, CL-V and CL-R respectively were evaluated for performance characterisation. Bulk density (litre weight) and bond work index were also determined as per the standard procedures.

Cement samples OPC-L, OPC-V and OPC-R were also studied for the degree of hydration. The hydration reaction was arrested at the ages of 1, 4 & 8 h by washing with acetone and dried under vaccum for 2 h. Thermal studies of these samples were carried out using Mettler Thermal Analyser TA-1 system .

RESULTS AND DISCUSSIONS

The elemental analyses of clinkers CL-L, CL-V and CL-R are presented in **Table 1.** Free lime occurs mostly in the light yellow coloured nodules of clinker which are generated due to large nodule size, interrupted operation of kiln and undue exposure of red hot nodules to atmosphere at the feed end of the kiln. The laboratory clinker has the lowest free lime, followed by the rotary kiln clinker and the VSK clinker in that order. This is expected in view of the burning and cooling conditions and the LSF of these clinkers.

Optical microscopic studies conducted on CL-L, CL-V and CL-R and mineral phases determined **(Table 2)** which compare favourably with the mineral composition as obtained by Bogue's equation. The granulometric results indicate the average crystal size as well as grain size variation of C_3S and C_2S for clinker CL-R is the highest followed by CL-L and CL-V.

The optical micrographs (Plate 1,2,3) show the distribution of crystals. In CL-L and CL-V the distribution of phases is more homogeneous, whereas in CL-R the belite occurs in clusters with sharp edges of alite. In case of CL-V distorted phase formation is observed. The clinkers CL-L and CL-V are highly porous which is expected in view of the black meal process and in line with the low bulk density (litre weight) of such clinkers.

TABLE 1

ELEMENTAL ANALYSIS OF CLINKER SAMPLES

Sl No.	Sample No.	LOI%	SiO_2%	Fe_2O_3%	Al_2O_3%	CaO%	MgO%	CaO_f%	SM	AM	LSF
1	CL-L	1.56	20.98	4.49	6.46	63.92	2.45	1.01	1.91	1.44	0.92
2	CL-V	1.98	20.36	4.71	6.63	63.56	2.15	2.11	1.80	1.40	0.94
3	CL-R	1.00	21.80	3.60	7.01	65.01	2.20	1.50	2.07	1.94	0.92

TABLE 2

MINERAL ANALYSIS OF CLINKER SAMPLES BY BOGUE'S EQUATION AND OPTICAL MICROSCOPY

Sl No.	Sample No.	Phase present	Quantity % Bogue	OM	Granulometry (m) Min	Max	Av.
1	CL-L	C_3S	50.91	51	5	25	18
		C_2S	21.74	29	5	25	20
		C_3A	9.52				
		C_4AF	13.66	21	-	-	-
2	CL-V	C_3S	52.70	50	5	35	25
		C_2S	18.64	30	5	30	21
		C_3A	9.60				
		C_4AF	14.33	20	-	-	-
3	CL-R	C_3S	46.76	45	8	90	39
		C_2S	27.22	37	7	42	25
		C_3A	12.31				
		C_4AF	10.95	17	-	-	-

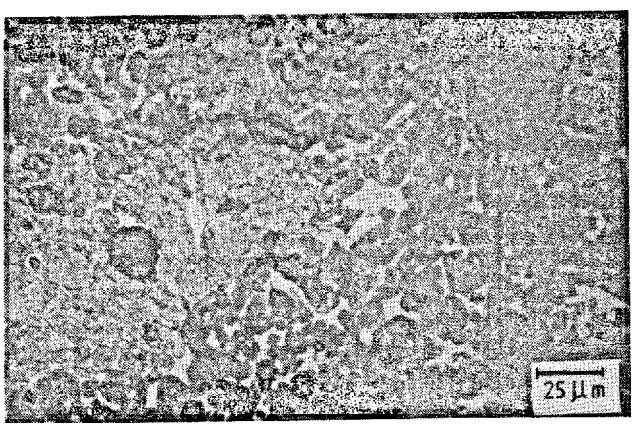

Plate 1 : Optical Micrograph of laboratory clinker

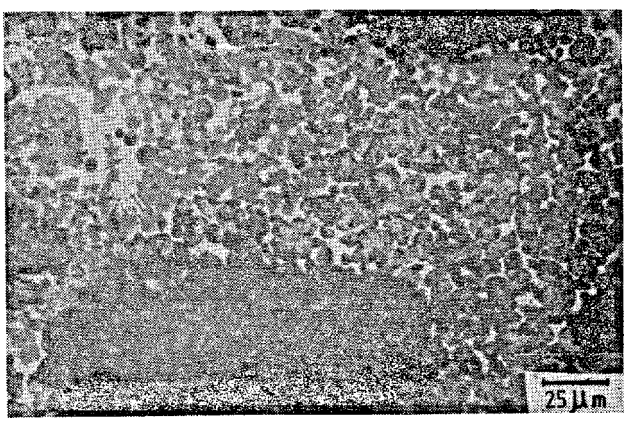

Plate 2 : Optical Micrograph of VSK Clinker



Plate 3 : Optical Micrograph of rotary clinker

The scanning electron micrographs of clinker CL-L, CL-V and CL-R are presented in Plates 4,5 and 6 respectively. The distribution of phases in CL-L and CL-V are more uniform as compared to CL-R. Sharp edges of alite phases are observed in clinker CL-R.

X-ray diffraction studies of clinkers CL-L, CL-V and CL-R revealed the presence of all major phases i.e. C_3S, C_2S, C_3A and C_4AF **(Fig.1)**. The percentage of alite phase is comparable in CL-L and

CL-V and more as compared to CL-R. This may be attributed to uniform burning of raw mix due to interground fuel. No polymorphs are observed in all the three clinkers except β C_2S.

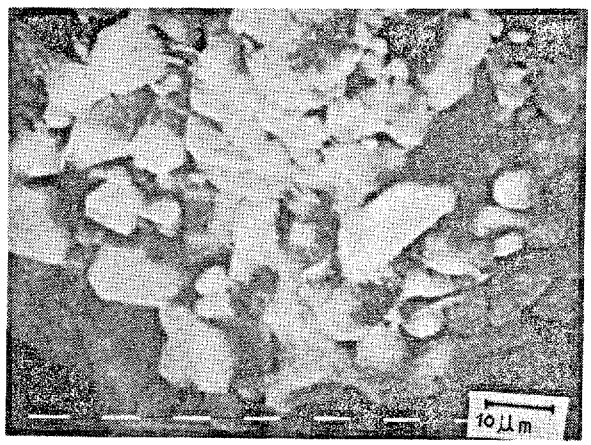

Plate 4: SEM of laboratory burnt clinker

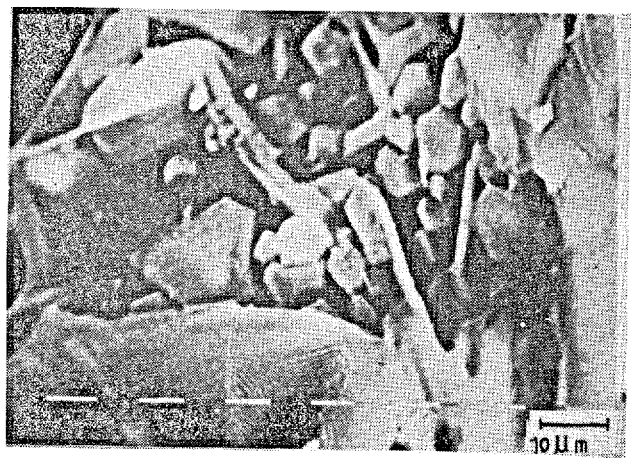

Plate 5: SEM of VSK-plant clinker

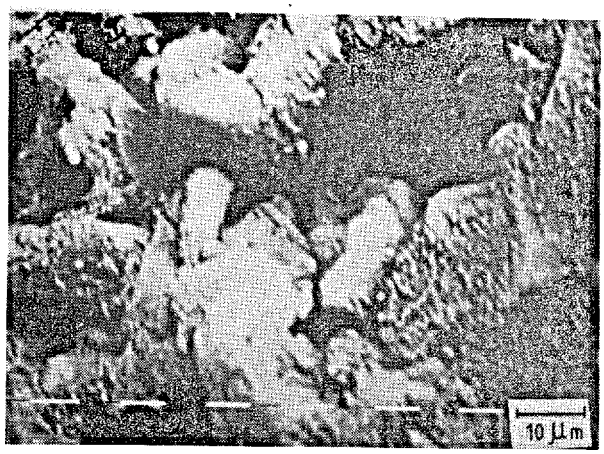

Plate 6 : SEM of rotary clinker

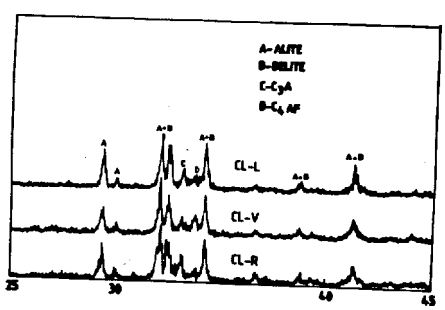

Fig 1 : X-ray diffraction of clinkers

The bulk density (litre weight) of clinker samples has been determined by taking the sized fraction of clinker between 6-10 mm. The Bond's work index was also determined. Bulk density (litre weight) and Bond's index are given in **Table 3.**

TABLE 3

HARDNESS OF CLINKER PRODUCE FROM DIFFERENT PROCESSES

Clinker	Grindability (g/rev)	Bond's Work Index (kWh/t)	Bulk Density (Clinker Litre Weight) (g/l)
CL-V	1.15 - 1.25	11.00 - 11.50	1100
CL-R	1.00	14.00 - 14.50	1310

The results indicate that the clinker produced from vertical shaft kiln is more soft as compared to the rotary kiln clinker because of the porous nature due to the interground supply of fuel for pyroprocessing (6). This difference in bond work index results in 20 percent saving in grinding energy for clinkers produced in VSK. The strength determination results presented in **Table 4,** indicate that CL-L and CL-V has comparable strengths at all ages and are higher than those obtained for CL-R. The reactivity of clinkers prepared in VSK and laboratory is more as compared to rotary kiln clinker.

TABLE 4

COMPRESSIVE STRENGTH OF ORIDINARY PORILAND CEMENT SAMPLES

Sl No.	Sample No.	Fineness (m^2/kg)	Compressive trength (N/mm^2) 3d	7d	28d
1	OPC-L	315	33.0	41.0	51.0
2	OPC-V	320	32.0	40.5	51.5
3	OPC-R	325	24.0	32.0	49.0

Hydration Studies

The thermograms of hydrated cement pastes at 1, 4 and 8 h are presented in **Fig.2.** The thermograms show usual endothermal peaks related to dehydration of hydrated phases at $\sim$ 115°C and of $Ca(OH)_2$ at $\cap$ 475°C. The exotherm at $\sim$ 170°C and 180°C at 1 hr and 4 hr for OPC-R is associated with gypsum dehydration. The release of $Ca(OH)_2$ is minimum for OPC-R as compared to OPC-L and OPC-V at early ages. This was further confirmed by x-ray diffraction analysis. The losses due to C-S-H phase were determined and found to be 5.8, 4.0 and 2.2 for 1 h samples, 6.9, 5.2 and 5.0 for 4 h samples and 12.5, 10.5 and 12.5 for 8 h for OPC-L, OPC-V and OPC-R respectively.

The area under unreacted C_3S calculated from x-ray diffractograms were plotted with respect to the age of hydration (Fig 3). The cement prepared from rotary clinker (OPC-R) has the highest amount of unreacted C_3S followed by laboratory clinker (OPC-L) cement and the VSK clinker cement (OPC-V).

The results indicate that the reaction rate is lower in case of rotary plant made cement.

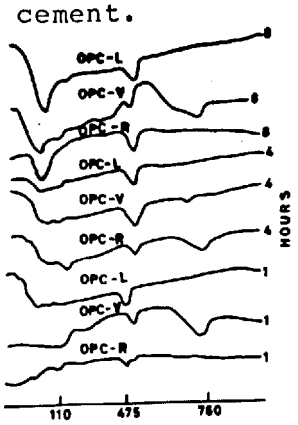

Fig.2 : Thermograms of Hydrated Cement Pastes

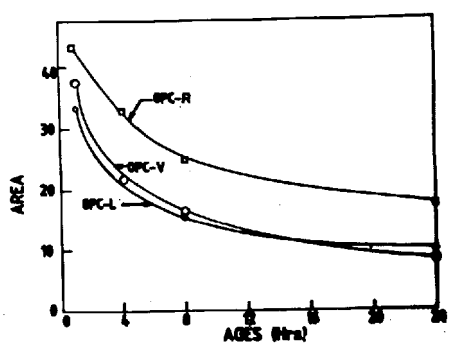

Fig.3 : Unreacted C_3S at Different ages

CONCLUSIONS

(1) The present investigations have revealed that the vertical shaft kiln clinker varies in chemical composition, microstructure and morphology from those prepared in rotary kiln.

(2) The rotary clinkers are dense with large crystal size compared to the clinkers obtained from VSK plant. The porous nature of VSK clinker results in low bulk density (litre weight) and low bond index, which in turn reduces the grinding energy to the extend of 20 percent

(3) The compressive strength data shows that early age strengths are higher in VSK clinker compared to rotary clinker.

(4) The DTA/TGA studies on hydrated samples also revealed that the formation of C-S-H in VSK prepared clinker is higher than rotary kiln clinker. Similarly the XRD studies have indicated the unreacted cement phases are more in rotary kiln clinkers at all ages than clinkers from VSK plant.

(5) The thermal treatment of cement raw mixes has profound effect on reactivity of clinker minerals.

ACKNOWLEDGEMENTS

The authors have freely drawn up data available as an outcome of projects of National Council for Cement and Building Materials, New Delhi. This paper is being presented with the permission of Director-General of the Council.

REFERENCES

1 Spone, E.:"Cement Shaft Kiln of Today." Zement-Kalk-Gips, Germany, **11**(7), 1958, 285-290.

2 Narjes, A.:"What is the present position of shaft kiln." Zement Kalk Gips, Germany, (9), 1960, 409-418.

3 Jain, V.K., Rao,D.B.N., Gupta, S.K. and Singh, D.K.: "Technology of mini cement plant.", **Proceedings of Naional Seminar of Mini Cement Plants, New Delhi, India**, 1982, 41-53.

4 Kono, H.: "An analysis of the reaction zone of shaft kilns." Zement-Kalk-Gips,1965,**29**(2),101-106.

5 Locher, F. W.:"Effect of clinker manufacture on the properties of cement." Zement-Kalk-Gips,1975,**28**(7), 265-272.

6 Samuel,G., Subba Rao,V.V and Chopra,S.K.: "Influence of the burning process on the morphology and microstructure of Indian cement clinkers." **Proceedings of the Sixth International Conference on Cement Microscopy, Texas, USA**, 1984, 20.

A STUDY ON IMPROVING HEAT TRANSFER BETWEEN GAS AND SOLID IN SUSPENDED STATE—A NEW MATERIAL SEALING AND DISPERSION DEVICE

Xia Youming*, Cheng Jingxiang* and Huang Wenxi**

*Sichuan Institute of Building Materials, Mianyang, P R CHINA
**Chengdu Design & Research Institute of Building Materials Industry, Sichuan, P R CHINA

ABSTRACT

A new material sealing and dispersion device, substituting for flap-valves, is introduced. The paper discusses methods of saving total energy consumption by improving system heat transfer efficiency and reducing system pressure loss after adopting the new device.

摘　　要

取代传统的旋风筒闪动阀。本文介绍了采用一种新型料封分散装置，对改善旋风预热器系统传热效率，降低系统总压力损失的节能效果。

1. INTRODUCTION

With the advent of suspension preheater kiln, the way of heat transfer between gas and solid has undergone radical changes. The heat transfer area and rate greatly increase because of the sufficient contact between the suspended materials and the gas. The experiments[1] [2] [3] show that the heat transfer for well dispersed raw meal in pipeline would occur within 0.1 second, with gas-solid temperature difference ΔTa less than 30℃ after heat transfer. However ΔTa may reach as high as 150 ℃ for incompletely dispersed material. Calculations show that exhaust gas temperature will increase by 6-8℃ and raw meal temperature decrease by 9 -10℃, while ΔTa increases by 10℃. It is therefore clear that the quality of dispersion of material in pipeline immediately affects the thermal efficiency and the heat consumption of clinker. A lot of work for improving the dispersion of material in pipeline was done in theory and design [1] [4] [5] . Some dispersion devices were used, but the effect is not very good. And because of using the flap- valve for controlling air leakage in the dipleg of cyclone, two problems appear. Firstly, it is difficult to ensure good sealing at the point of flap-valve, so interior and exterior air leakage of system results. In this case, it is possible not only to increase heat consumption of exhaust gas, but also intensify internal recirculation of raw meal, affecting the heat transfer efficiency. Secondly, when the valve flaps, the material in dipleg enters the up- pipeline in large batches, resulting in difficulty to disperse. And when the gas velocity is not large enough, the material may not suspended but descend into the next cyclone, causing system 'short -circuit' and deteriorating the heat transfer.

Therefore, in order to decrease air leakage, raise the separation efficiency of cyclone and increase heat transfer surface area between gaseous and solid phases, a new material sealing and dispersion device for energy saving has been developed. The new device substituting for flap-valves is also considered to intensify battering and dispersing of the material by air, enable the material to uniformly enter the up- pipeline and get dispersed. This paper discusses the methods of saving heat and power consumption by improving system heat transfer efficiency and reducing system pressure loss adopting the new device.

2. EFFECT OF THE NEW DEVICE ON HEAT TRANSFER BETWEEN GAS AND SOLID

It is reported [6] that particles larger than 100 μm can be dispersed singly by battering of gas flow, and particles surface in gas flow can be calculated as heat transfer area. However, in the case of particles below 100 μm, it is easy for them to coalesce and form larger sized particle. But unlike a big particle dispersed singly, collected particles usually are coalescence of several small particles, too. The particle coalescence affects the heat transfer between gas and solid. In order to futher define the heat transfer mechanism and apply it to an industrial design, a study was carried out to see the difference in heat transfer when adopting the new device and without any devices, at all.

The elementary test flowchart is shown in Fig. 1. The material used in the experiment is the raw meal for manufacturing portland cement in a cement plant. The particle size distribution is given in Table 1. The gas flow velocity is 12 m/s and solid-gas feed ratio is 0.48-1.08 kg/Nm³.

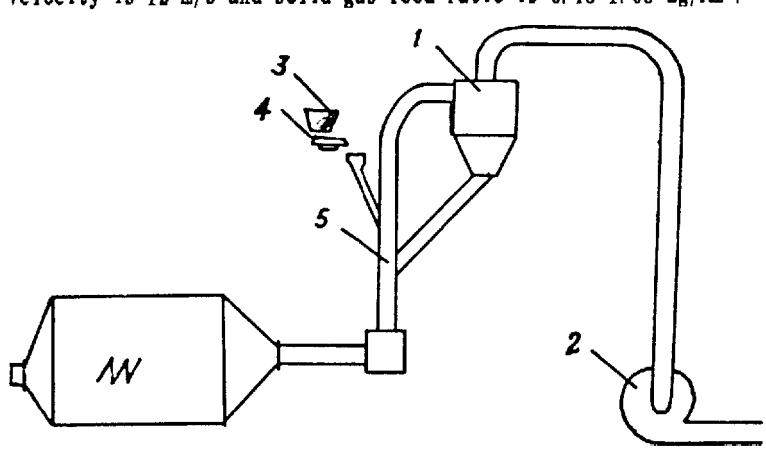

Fig. 1. Test flowchart

Table 1 Particle size distribution of raw meal

Particle size, μm	> 80	60-80	40-60	20-40	<20
Percent, wt %	1.42	13.25	22.60	31.27	21.46

characteristic diameter : 43 μm

The experimental results, obtained with the new device and without the new device under various conditions, are given in Table 2

Table 2 Calculated heat transfer data under various conditions

	Without any dispersion device					With the new device				
Initial gas temp, ℃	225	225	225	225	225	210	210	210	210	210
Initial material temp, ℃	28	28	28	28	28	28	28	28	28	28
Solid gas ratio, kg/Nm³	0.48	0.59	0.71	0.84	0.98	0.53	0.67	0.80	0.92	1.08
Final gas temp, ℃	175.0	169.6	161.6	153.7	146.6	160.0	154.2	148.4	142.0	134.0
Final material temp, ℃	145.0	137.3	127.9	119.2	109.0	142.7	135.3	127.6	121.0	111.6

Heat absorbed by the material in pipeline can be calculated as follows:

$$Q=G \cdot Cm \cdot \Delta Tm \qquad (1)$$

where Q denotes the heat absorbed by the material, G is the material feed rate, Cm is the specific heat of the material and ΔTm is temperature difference of materials. Heat transfer efficiency between gas and solid is calculated according to the following formula:

$$\eta = Q/Qo \qquad (2)$$

where η is heat transfer efficiency, Qo is maximum heat absorbed by material in theory. The heat transfer area per kilogram of raw meal can be calculated from the formula:

$$Q_{g-s}=h \cdot \Delta T \cdot Fm \cdot V \cdot C \qquad (3)$$

where Q_{g-s} denotes the heat transfer from gas to materials, h is heat transfer coefficient between gas and solid which is basically a constant under the operating condition and can be calculated with the aid of equation $Nu=1.13\ Re^{0.5}$, ΔT is logarithmic mean temperature difference between gas and solids, Fm is heat transfer area per kilogram of raw meal, V is volume of heat transfer unit and C is solid-gas feed ratio. The results are given in Table 3 , and shown in Fig. 2, Fig. 3, Fig. 4 and Fig. 5.

Table 3. Calculated data of heat transfer under various conditions

		Without any dispersion device					With the new device				
Solid gas ratio	kg/Nm³	0.48	0.59	0.71	0.84	0.98	0.53	0.67	0.80	0.92	1.08
ΔTa	℃	30.0	32.3	33.7	34.5	36.6	17.8	18.4	20.8	21.0	22.4
Q	kj/s	6.77	7.79	8.69	9.27	9.62	7.64	9.00	9.94	10.65	11.37
η	%	82.63	80.60	78.79	76.64	72.71	93.20	91.40	90.30	89.29	86.84
Fm	m²/kg	12.54	11.18	10.01	9.08	8.0	15.08	13.93	12.45	11.48	10.52

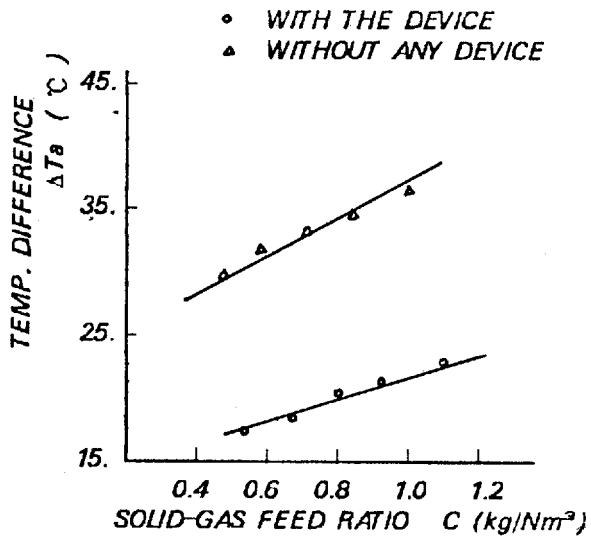

FIG. 2. Temp. difference characters

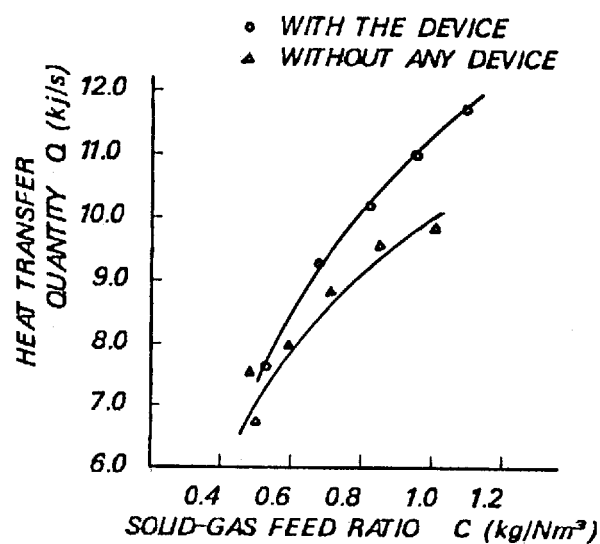

FIG. 3. Heat transfer quantity characters

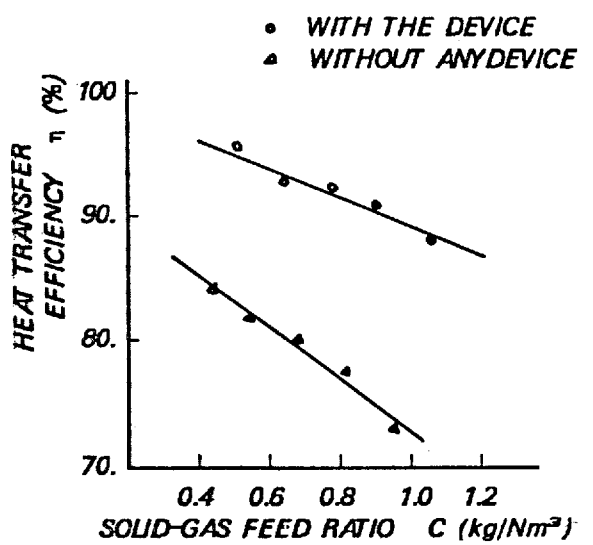

FIG. 4 Heat transfer efficiency characters

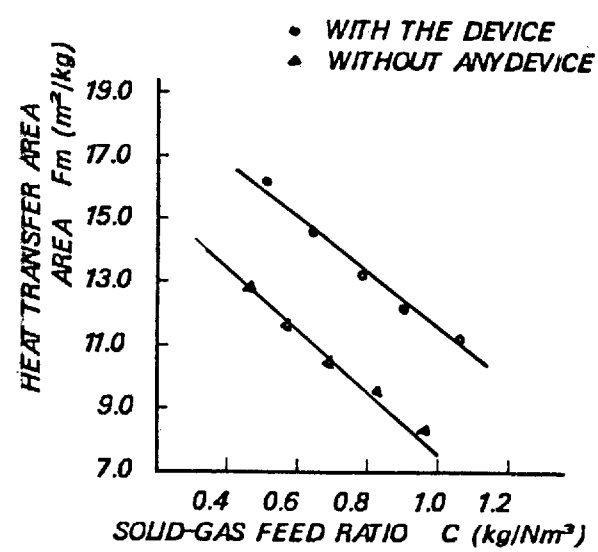

FIG. 5 Heat transfer area characters

The temperature difference of gas and solid after heat transfer, are shown in Fig. 2. It shows temperature changes from 30.0-36.6℃ without any dispersion device to 17.3-22.4℃ with the new device. Thus an reduction of about 40% was achieved by adopting the new device. Fig. 2 also shows that solid-gas feed ratio affects the temperature difference in that it increases with increase of the ratio. In other words, it is disadvantageous for heat transfer effect of system to increase the ratio. This is because increase in this ratio makes it difficult for materials to be dispersed in gas. But with adopting the new device, the relating between temperature difference and the ratio changes in that the temperature difference gradient decreased remarkably with increase of the ratio.

Fig. 3 shows the relationship of heat absorbed by materials per unit time with the solid-gas feed ratio. The heat, for the ratio of 0.5-1.0 kg/Nm³, increases from about 7.0 to 9.7 kj/s without the new device to 7.3 -11.1 kj/s with the new device. Heat exchange was enhanced to the extent of 4.3% and 14.4 % at the respective ratios of 0.5 kg/Nm³ and 1.0 kg/Nm³. It indicates that the new device has an advantageous influence on heat

transfer at high ratio. Fig. 4 shows the relationship between heat transfer efficiency η and the solid- gas feed ratio with and without the new device. The efficiency η decreases with increase in the ratio in both cases, but with different gradients, having a decreasing rate of 19.6 % and 11.0 % per unit ratio without the new device and with the new device respectively. The efficiency η increases from about 82.63-72.71% to 93.20 -86.84%, compared to the case without the new device, the efficiency η adopting the new device increases from about 13.2 % to 20.9 % for the ratios of 0.5 kg/Nm^3 and 1.0 kg/Nm^3 respectively. Fig. 5 shows the relationship between heat transfer area and solid-gas feed ratio. The heat transfer area decreases with the increase of ratio, thus showing a similar behaviour as in Fig. 4, but with different gradients, too. Comparing with the case without the new device, the area Fm increases from 12. 54-8.04 m^2/kg to 15.08-10.52 m^2/kg. Thus an increase of 25-30 % is observed, which is very large.

It can be seen from the above that, after adopting the new device, the heat transfer between gas and solid in pipeline was intensified remarkably, the heat transfer area increases obviously, too, and the temperature difference ΔTa reduces correspondingly. So the heat absorbed by the materials and heat transfer efficiency η of the system increases enormously. And to overcome the difficulty when materials are dispersed at higher ratio, it is significant to adopt the new device for visibly improving the heat transfer effect between gas and solid .

The concentration field in pipeline is also measured for further studying the mechanism of the new device on improving heat transfer. The concentration distribution of a section is similar in both cases no matter whether the new device is used or not, for the same gas flow velocity and concentration, but the pulse height of concentration is intensified remarkably after adopting the new device for a constant point. This is the case for the fluid flow phenomenon in pipeline. The irregular high frequency pulse of velocity at a point in the field causes surely the pulse of concentration at the same point. So the material and gas can contact and mix sufficiently and heat transfer effect is intensified, too. On the cold-state model, we observed that the material entering the pipeline in large batches can not be dispersed sufficiently and may sink in the pipe when the new device is not be used, whereas after adopting the new device, the material enters the circular section in which gas flow velocity is high, and gets dispersed uniformly. It also indicates why the new device improves the heat transfer.

3. PRESSURE LOSS IN THE NEW DEVICE.

3.1 Gas flow velocity in pipeline

In the process of production, friction and collision between the particles themselves, and between the particles and the pipe wall, irregular gas velocity distribution in the pipeline with valve and bend, gravitational influence and so on exist in the system, so the practical gas velocity must be much more than the theoretical suspension velocity. And the velocity affects not only the heat transfer between gas and solid, but also the total pressure loss of the system. In general, the higher the velocity , the more uniform the material is dispersed and the higher the pressure loss. When the velocity is too low, sinking of materials and bad fluid pattern may occur in the pipeline. Therefore, it is very important to determine the optimum velocity. And for reducing the friction and the pressure loss in system, a relatively low velocity is adopted usually. The relationship between the solid-gas feed ratio C with critical Frouds number at which materials does not sink was given by W. Barth, et al in experiment [7], [8].

$$C = a\,[Frc/10]^b \qquad (4)$$

where a and b are constants, Frc is critical Frouds number.

On the experiment condition, the gas flow velocity for suspending and dispersing materials at the various solid-gas feed ratios is researched in detail. The result shows the velocity is only 7.8 m/s and 10.8 m/s respectively the ratio of 0.51 kg/Nm^3 and 1.08 kg/Nm^3. Comparing the general design value of gas flow velocity , the velocity in pipeline has a large reduction. Taking the system of UNSP developed by Ube for

example [9] [10], the total pressure loss of the system is about 5870 Pa, where about 3260 Pa caused by 5-stage preheater, 980 Pa by the precalcinator and kiln, and 1630 Pa by the pipeline and bends (up to 27.7 % of the total pressure loss). When the velocity decreases from 16-17 m/s to 12 m/s adopted in practical design, the pressure loss of the pipeline and bend will decrease from 1630 Pa to about 865 Pa. The total pressure loss also reduces to about 6105 Pa with a reducing percent of about 14.1 %. And the proportion of the pressure loss by pipeline and bend decreases from 27.7% to 16.9%, too. It shows that the new device plays the important role of ensuring suspension and dispersion of materials at low gas flow velocity, so that the pressure loss of system and power consumption reduces remarkably.

3.2 Partial pressure loss caused by the new device.

The pressure loss caused by a body in gas flow, besides friction resistance, has a kind of loss named as pressure difference loss, which has little relation with the body surface area but the shape of a body. Fig.6 gives a group of bodies with equal pressure loss [12]. It is unimaginable only according to friction loss.

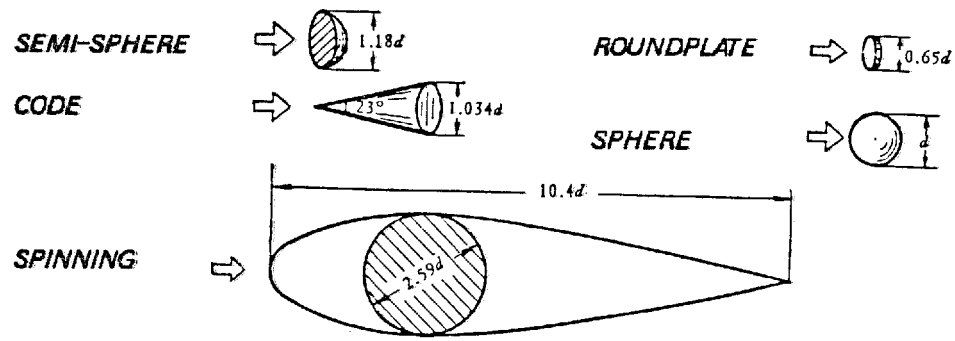

FIG. 6. Size comparison of a group of body with equal loss

Comparing the dispersion device having been used in industry, the new device is designed with a dripping structure. The pressure loss can be calculated relying on experiments for calculating the loss.

$$\Delta P = 1/2 \cdot Cd \cdot \rho \cdot W^2 \qquad (5)$$

where Cd is resistance coefficient, ρ is the density of fluid, W is the gas flow velocity. The result is given in Table 4.

Table 4. Pressure loss and resistance cofficient adopting the new device

Gas flow velocity m/s	8	10	12	14	16
Pressure loss Pa	21.6	30.4	38.2	49.0	62.7
Resist. coef. Cd	5.5	5.0	4.3	4.1	4.0

The result shows that pressure difference loss increases with increase of gas flow velocity, whereas the resistance coefficient Cd decreases with increase of gas flow velocity. The reason is that the sharp mixed effect of turbulence at high Reynolds number causes the detaching point of fluid flow move back, and the detaching region behind the device becomes narrow.

As already analysed above, the new material sealing and dispersion device has better dispersion function, it ensures that the gas flow velocity in the pipeline is lower than that of the usual industry design level, the pressure loss in the 5-stage precalcinater system decreases by 12.1-16.1%, and because of the suitable shape of new device structure, the partial pressure loss is only 21.6-62.8Pa. It will be of great practical value in theory and industry design.

4. CONCLUSIONS

4.1 The new device reported improves the suspension and dispersion of materials in pipeline and intensifies turbulent mix and heat transfer between gas and solid phases. The temperature difference Δ Ta reduces from 30.0-36.6℃ to 17.3-22.4℃, heat transfer efficiency increases 13.2 % and 20.9 % and heat exchange quantity increases 4.3 % and 14.4 % respectively to the solid-gas feed ratio of 0.51 kg/Nm^3 and 1.08 kg/Nm^3, after adopting the new device. And it is remarkable for the new device to improve heat transfer at high ratio, specially.

4.2 Using the new device, the velocity in pipeline can be decreased to 7.8-10.3 m/s, and the total pressure loss can reduce by about 12.1-16.1%, whereas the practical pressure loss Of new device is only 21.6 -62.8 Pa for adopting a suitable shape and structure.

REFERENCE

1. Huang Wenxi, et al.: 'On heat transfer between gaseous and solid phase in the suspended and fluidized states', Journal of Wuhan Institute of Building Materials, 1984, 1(1), 33-43.

2. Xu Delong, et al.: 'The characteristics of momentum and heat transfer between gas and particles in a transport bed', Fluidization 84. conf. Papers China-Japan Symp., Beijing, Chain. 445-455.

3. Huang Wenxi, et al.: 'The study on thermal character in rotary kiln with precalciners', 1987, (2), Cement, 3-9. (in Chinese).

4. K·P·Yen, et al.: 'Anew attemp at modifying the RSP kiln', World Cement, 1988, (3), 94-99.

5. Shen Wei, et al. Cement Technology, to be published by Publishing House of Wuhan Industry University.

6. Dept.. of Chemical Enginerring, Chengdu Science and Technology University, The Design Date in Chemical Enginerring Prinicple, 1983.6, 25-33.

7. W·Barth, : 'Stromungsvorgange bein transport von festteilchen und flussigkeisteichen in gasen mit besonderer berucksichtigung der vorgange bei pheumatischer forderung', Chem. Ing. Tech., 1958, 30(3), p. 171.

8. W·Barth,: ' Physikalische und wirtchaftliche problem des transport von festteichen in flussigkeiten und gasen ', Chem. Ing. Tech., 1960, 32, p. 161.

9. S·Saski, et al., Z-K-G, 1986, (7), p. 407-409.

10. Ube new suspension preheat system. Firmeninformation Ube Industries 1985. 3. 500m.

11. Li Yiqi, et al., fluid kinetic base, science press, 1983.10, 163-170. (in Chinese).

MORPHOLOGY AND MICROSTRUCTURE FEATURES OF CLINKER FROM VERTICAL SHAFT KILN

S C Ahluwalia and K Raina

National Council for Cement and Building Materials
New Delhi, INDIA

SUMMARY

Clinker obtained from the burning of cement raw mix made by Vertical Shaft Kiln technology (VSK) has certain characteristic mineralogical and morphological features. These are significantly different from those of the clinkers obtained from processing of raw mix in rotary kilns. This is primarily due to the preparation of the raw meal in which the fuel is interground and specific pyroprocessing technique applied. The raw mix design in VSK is significantly different from the raw mix design for a rotary kiln. This, coupled with the process of making the black meal and the burning and cooling conditions obtained in VSK imparts chracteristic distribution of the clinker minerals and morphological and microstructural features. Since these form important parameters for defining the clinker quality, a study was undertaken to investigate the VSK clinkers for establishing a correlation between these parameters and clinker quality.

Clinker samples from various VSK plants were studied for their mineralogical, morphological and microstructural features using XRD, SEM and optical microscopic techniques and compared with the clinkers prepared in the laboratory. The clinkers obtained from VSK process normally have lower clinker litre weight and higher free lime (CaO_f). These distinctive features of the two clinkers have been highlighted.

INTRODUCTION

Vertical shaft kiln (VSK) technology for the manufacture of OPC is well established (1,2) and widely practised in India and China. It has proved highly useful in exploiting small deposits of limestone and helps spread plants more evenly to promote local production and consumption without putting strain on the transportation system.

Vertical shaft kiln technology (VSK) can be based on the coal slurry process (3) and black meal process (4-5). However all the plants in India are based on the black meal process (6). In this process raw material and fuel, usually low volatile coal or coke breeze, a by-product from steel plants, are interground to a fine powder, formed into nodules of 6 - 8 mm size and burnt in VSK. As the material passes down the kiln, it is dried, heated, burnt and cooled in the same shaft.

The mechanism of clinker burning is different in VSK as each nodule burns in its own environment, hence making it a different pyro-processing technique, which involves different thermal treatment compared to the rotary kiln burning due to the presence of intergrated fuel in raw meal.

Clinker samples from six VSK plants were collected and studied for their mineralogical, morphological and microstructural features using XRD, SEM and optical microscopic techniques. Clinkers were also prepared in the laboratory from the plant raw mix nodules under controlled conditions and comparative study has been reported in this paper.

EXPERIMENTAL

Six VSK cement plants were selected for the study and the raw mix nodules and corresponding clinker samples were collected from the plants.

The raw meal nodules from the six plants were fired in a laboratory high temperature furnace at 1450°C with a retention time of 20 minutes. The nodules were introduced in the furnace at ambient temperature and heated to 1450°C at the rate of 10°C/min. The clinker were taken out of the furnace and allowed to cool to room temperature. Physical and chemical characteristics of the plant and laboratory clinker were determined as per Indian standard methods.

a/ Microcopic studies were carried out on polished sections using Carl-zeiss Amplivol polarizing microscope with a magnification range of x 260.

b/ SEM studies were carried out on fractured clinker samples, using Philips CM 301 scanning electron microscope, using gold for coating the sample.

c/ X-ray diffraction studies were conducted on powered samples using D-Max, X-ray diffractometer, Rigaku, Japan.

RESULT AND DISCUSSION

Twelve raw meal samples from six VSK plants were characterised for elemental composition **(Table 1)** and the various modulii values calculated. The potential phase composition by the Bogue's method is

TABLE 1
ELEMENTAL ANALYSIS AND MODULI VALUES OF CLINKERS

Clinker Sample		Chemical Composition						Modulii Values		
		LOI%	SiO_2%	Fe_2O_3%	Al_2O_3%	CaO%	MgO%	SM	AM	LSF
1	CLP-1	1.98	20.36	4.71	6.63	63.56	2.15	1.79	1.4	0.93
	CLL-1	0.65	21.67	4.97	5.98	62.92	2.45	1.81	1.4	0.90
2	CLP-2	1.56	20.98	4.49	6.46	63.79	1.83	1.88	1.66	0.90
	CLL-2	0.89	20.59	5.76	7.26	63.12	1.33	1.79	1.08	0.89
3	CLP-3	1.35	21.81	4.76	6.81	64.26	0.88	1.88	1.43	0.88
	CLL-3	0.34	21.91	4.79	6.79	64.41	1.08	1.89	1.41	0.88
4	CLP-4	0.57	22.70	4.25	6.41	64.10	2.15	2.12	1.51	0.86
	CLL-4	0.34	22.79	4.70	6.55	64.07	2.00	2.13	1.52	0.87
5	CLP-5	3.09	23.43	5.42	6.45	60.13	2.10	1.97	1.19	0.80
	CLL-5	0.98	21.22	4.67	7.11	62.75	2.77	1.02	1.19	0.81
6	CLP-6	1.00	21.29	5.98	7.04	62.03	1.43	1.93	1.21	0.88
	CLL-6	0.69	21.18	5.84	6.74	62.73	1.87	1.93	1.24	0.88

also presented along with mineralogical composition by optical microscopy, the mineral size, free lime and clinker litre weight are presented in **(Table 2)**. The raw meals selected present a wide variation in both the elemental and mineral composition. The silica modules (SM) varies in the range 1.79 to 2.13 which makes these raw mixes easy to burn, compared to rotary kiln raw mixes which have SM value normally in the range 2.2 - 2.6.

TABLE 2
MINERAL COMPOSITION OF CLINKER INCLUDING FREE LIME AND LITRE WEIGHT

Clinker sample		MINERALOGICAL COMPOSITION							GRANULOMETRY (μm)				Free Lime (%)	Clinker Litre Wt (g/l)
		Bouges Equation (%)				Optical Microscopy (%)			C_3S range	Average	C_2S range	Average		
		C_3S	C_2S	C_3A	C_4AF	C_3S	C_2S	Interstatical matter (%)						
1	CLP-1	52.71	18.63	9.6	14.33	50	30	20	8-90	25	5-36	20	2.61	1150
	CLL-1	45.56	27.77	10.00	15.12	51	29	21	5-36	22	5-36	18	1.01	1100
2	CLP-2	43.66	27.21	12.77	13.66	41	38	19	5-40	25	5-45	20	2.60	1145
	CLL-2	46.62	26.73	6.84	17.52	47	33	20	5-25	18	5-25	18	1.15	1110
3	CLP-3	43.26	29.90	10.00	14.48	45	36	19	5-42	20	5-39	24	2.35	1000
	CLL-3	43.19	30.24	9.88	14.57	46	34	20	5-30	20	5-28	18	1.56	975
4	CLP-4	23.77	49.25	7.92	16.49	30	48	21	5-30	20	5-26	18	3.10	1030
	CLL-4	27.49	46.41	7.77	16.03	32	49	19	5-28	18	5-25	16	3.77	1000
5	CLP-5	41.09	34.10	9.79	12.93	40	42	18	5-50	21	5-35	25	1.22	1100
	CLL-5	42.04	31.62	8.75	13.08	47	34	19	6-30	20	5-25	15	1.28	1100
6	CLP-6	42.99	28.61	7.57	15.15	44	36	20	5-45	28	5-44	27	0.43	1150
	CLL-6	43.77	28.57	7.91	15.03	52	38	20	5-42	18	5-24	12	0.46	1100

The main three burnability parameters i e, loss on ignition (LOI), free lime (CaO_f) and clinker litre weight show variation from the rotary kiln clinker values generally obtained. They range from 0.69 ⊢ 3.57% and 0.43 ⊢ 3.77% respectively. The higher value in both the cases is indicative of incomplete decomposition/reaction. Litre weight of the clinkers obtained by both plant and laboratory are in the range 975⊢1150 g/l which is lower compared to rotary kiln clinker values which generally lie in the range 1250 ⊢ 1350 g/l. Low clinker litre weight values are due to the pores produced by burning of the intergrated fuel used for black meal process.

The mineral composition by optical microscopy shows the percentage of alite is in the range 30⊢52% and belite in the range 29⊢49%. These values are comparable to those obtained by Bogue's method. When SM is more than 2.1 the raw mix becomes hard to burn for VSK which is also indicated by low alite content values high LOI and free lime values (Table 1 & 2).

Optical Microscopy Studies

Micrographs of laboratory VSK burnt clinkers are highly porous **(Plate IA)**. Alite crystals are well developed, brown in colour and have sharp boundaries. It is observed that the pores are normally surrounded by alite crystals which may have been formed by burning of coal generating localised heat. This results in higher local temperature and alite formation. Inclusions of belite in alite are common. Belite crystals are rounded and the average belite grain size varies in the range 12 - 18 μm and alite grain size in the range 18 ⊢ 22 μm.

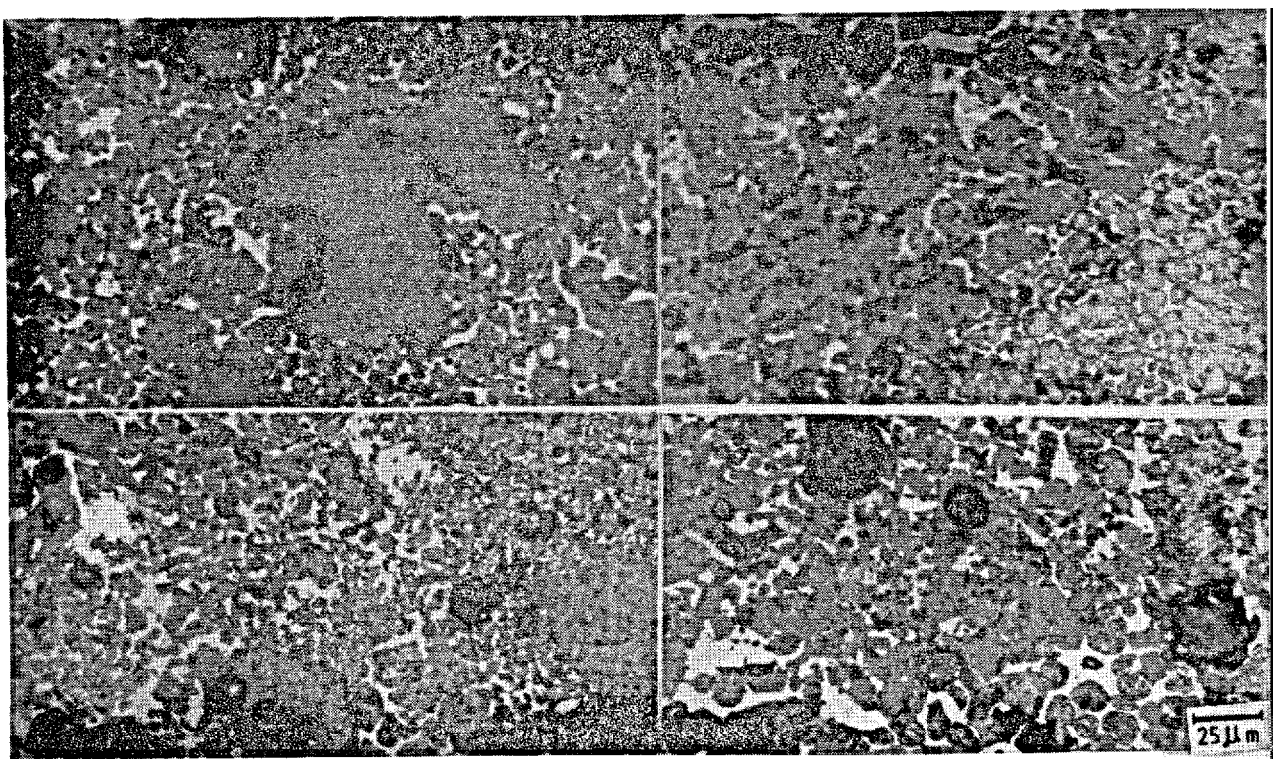

(A) LABORATORY CLINKER **(B) CRI⊢MVSK CLINKER**

PLATE 1 : OPTICAL MICROGRAMS OF CLINKERS

Plant burnt VSK clinker **(Plate IB)** shows that the clinkers are porous having moderate to well developed phases. Alite is prismatic to polygonal in shape. Pores are surrounded by either alite or belite crystals or by both. In some cases, alite grains occur as inclusions with belite grains. Belite grains are generally rounded to oval in shape. The average belite grain size varies in the range 20 - 27 μm and alite grain size varies in the range 20 - 28 μm. The variation in crystal sizes between laboratory and plant clinker is due to slow cooling conditions in the VSK.

SEM Studies

SEM studies of laboratory burnt clinker **(Plate 2A)** and CRI-MVSK plant clinker **(Plate 2B)** indicates that the clinker is porous in nature both at macro and micro levels. Alite grains are well formed with sharp edges. The results are generally in line with those of optical microscopy.

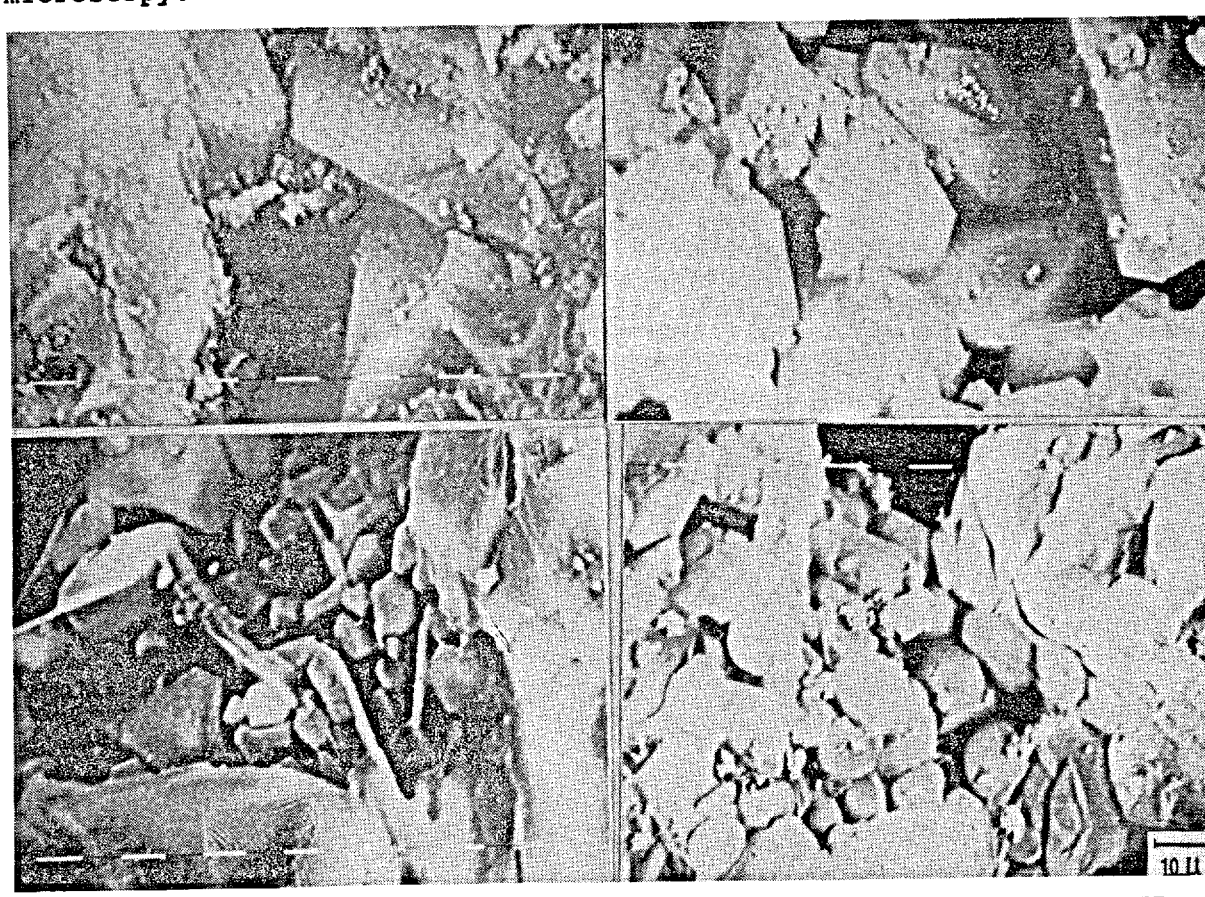

(A) LABORATORY CLINKER **(B) CRI-MVSK CLINKER**

PLATE 2 : SEM OF CLINKERS

XRD Studies

X-ray diffraction studies on clinkers produced in laboratory and CRI MVSK plants have indicated presence of all major clinker phases i.e, C_3S, C_2S, C_3A, C_4AF **(Fig 1)**. The percentage of alite phase is abundant in *CRI-MVSK clinker.

Performance characteristics of the plant clinker (Table 3) indicates that despite the relative high free lime and IR and low litre weight, the quality of cement produced is quite good in terms of early as well as 28 days strengths. All the cements passed soundness test as per IS:269-1968, except one, CLP-4, which was subject to areation as per IS:269-1968. This was due to high SM of raw mix which on burning produced high free lime (6) and low litre weight clinker (Table 2).

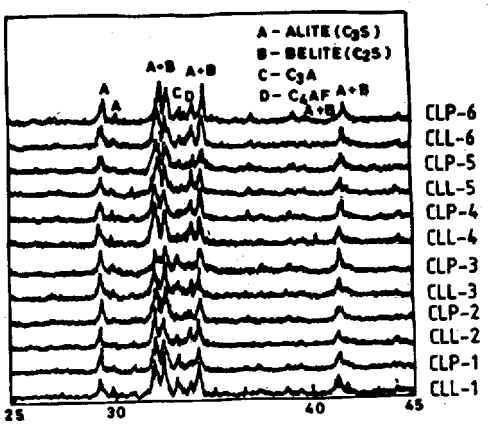

Fig 1 : XRD OF PLANT AND LABORATORY BURNT CLINKERS

TABLE 3
PHYSICAL DATA OF CEMENT OBTAINED FROM CRI-MVSK PLANTS

Plant	Fineness cm_2/g	Compressive Strength 3d	7d	28d	Soundness Auto-clave %	Le chatlier mm
			Kg/cm^2			
CLP-1	3199	330	405	515	0.5	7
CLP-2	3396	210	290	400	0.21	6
CLP-3	3250	220	305	425	0.1	2
CLP-4	3300	200	220	385	0.9	4*
CLP-5	3101	300	380	500	0.9	3
CLP-6	3205	310	395	515	0.6	2

* after aeration

CONCLUSION

Manufacture of cement in vertical shaft kiln by black meal process produces clinker having high and variable value of LOI and free lime indicating incomplete decomposition/reaction in some cases. Silica modulus plays an important role in burnability and governs the mineral phases formed, free lime and LOI of the clinker and is partly responsible for some of the morphological and mineralogical characteristics influencing both sintering and cooling characteristics of the VSK clinkers. The clinker is porous in nature which is due to the inter-ground fuel in raw meal. The pores are normally surrounded by alite crystals indicating the presence of coal particles which on burning generate localised heat and result in high local temperature. Alite and belite grains are well developed and sharp. Data of optical microscopy is supported by SEM and XRD studies. Physical data of cements produced by VSK clinker is showing high strength.

ACKNOWLEDGEMENTS

The authors have freely drawn up data available as an outcome of projects of NCB. This paper is being published with the permission of Director General of National Council for Cement and Building Materials, New Delhi.

REFERENCE

1 "Country paper on the mini cement industry in India". **Asia - Pacific region, Mini Cement Plant Workshop, Beijing, China,** 1984.

2 Jain, V.K., Rao, D.B.N., Gupta, S.K. and Singh, D.K.: "Technology of Mini Cement Plant", **Proceedings of CRI, National Seminar on Mini Cement Plants New Delhi, India,** 1982, 41-53.

3 Gottlieb, S and Swamy, R.K.: "A New Vertical Kiln Cement Plant in India", **Proceedings of CRI, National Seminar on Mini Cement Plants, New Delhi, India,** 1982, 69-70.

4 Spone E.:"Cement Shaft Kiln of today". Zement-Kalk-Gips, Germany, 1958, **11**(7), 285-290.

5 Rao, A.V.S., Imran, M and Raina, K.:"Plants Trials with Alternate Fuels in CRI-MVSK Plants". **Third NCB International Seminar on Cement and Building Materials, New Delhi, India,** 1990, **Vl,** TS-I, 90-103.

6 Locher,F.W.: "Effect of clinker manufacture on the properties of cement". Zement-Kalk-Gips, 1975, **28**(7), 215-272.

THE STUDY AND APPLICATION ON HIGH-QUALITY CEMENT CLINKER CALCINING WITH LOW HEAT CONSUMPTION IN SHAFT KILN

Z G Qin

Cement Research Institute
China Building Materials Academy, P R CHINA

SUMMARY

This paper presents the study on calcination ability of shaft kiln by production practice. We successfully produced high-quality clinker from black raw meal with low heat consumption by using rapid calcination mothed in plants. From the experiments in laboratory, we find out the saving energy mechanium from black raw meal using rapid calcination method. It proved the method used in plants was fit for objective law.

本文介绍了通过生产实践对立窑煅烧能力的研究．采用全黑生料快烧方法在工厂成功的用低热耗烧成高质量熟料．试验室试验发现了全黑生料快速煅烧的节能机理．这证明生产上所用方法符合客观规律．

INTRODUCTION

In China, there are thousands of cement manufacturing plants using shaft kiln. It is common practice in most of these plants to calcine Portland cement clinker with a heat consumption over 800kcal / kg.Study on how to decrease the consumption of coal is not only the need of technology progress, promoting profits in plants, but also the measure of decreasing the output of CO_2 and protecting environment.

Over the last decade, we made a thorough study of shaft kiln calcining ability. We pursued the small nodulized black raw meal rapid calcination method by using new mineralizers and high lime saturation factor. In Ying Dian Jie Cement Plant, Zhe Jiang Province, we have produced high-quality clinker, whose 28-day compressive strength is 62.5MPa(625kg / cm^2), the heat consumption was as low as 625kcal / kg or so. In palnts we have reached stable production and obtained obvious economical profits.

THE PROBE ON CLINKER WITH HEAT CONSUMPTION AND CHOICE OF CALCINATION METHODS

In 1977, we calcined clinker with 800kcal / kg, measured the temperature of kiln, it was 1600℃ or so. This indicated that the shaft kiln has the ability of calcination[1]. In 1984, we found that the clinker which KH was 0.83～0.84, can be successfully calcined with 580～600kcal / kg[2]. Based on the study, we think that: if the liquid exists, the clinker which KH = 1 can be calcined with the increase of 50kcal / kg.

In oredr to obtain high-quality clinker, we used the black raw meal process in which all coal was ground with the raw meal. Generally speaking, the heat consumption in this method is high. Why could we produce high-quality clinker from black raw meal with low heat consumption using rapid calcination method in plants? From a study on the different formation mechanisms of clinker from raw meals with different coal contents and calcination methods, we can find out the reason[3].

THE CLINKER FORMATION PROCESS FROM COAL-CONTAINING RAW MEAL

In order to study the calcination mechanism of clinker from coal-containing raw meal we prepared the raw meal samples with deifferent heat contents (by using the ordinary raw meal which has not coal, coal and coal ash). The composition (especially KH)of clinker from these samples was entirely the same.The heat content of these samples was respectively similar to the needed heat of raw meal which does not have coal (white raw meal)J1, preheating and dewater J2, theoretical heat consumption J3, precalcination kiln J4,shaft kiln J5,dry process rotaty kiln J6 and wet process rotaty kiln J7.The clinker after calcination were respectively named J1C, J2C, J3C, J4C, J5C, J6C, J7C. The compositions of the raw meals are shown in Table 1.

Table 1 Compositions of raw meal

Name	J1	J2	J3	J4	J5	J6	J7
Heat carried with raw meal,kcal / kg.cl	0	225	450	675	900	1125	1350
Heat carried with raw meal, kJ / kg.cl	0	940.5	1881	2821.5	3762	4702.5	5643
Coal needed,g	0	3.96	7.92	11.88	15.84	19.80	23.75
Coal ash in coal,g	0	0.92	1.85	2.77	3.69	4.62	5.54
Coal ash of addition,g	5.54	4.62	3.69	2.77	1.85	0.92	0
White raw meal,g	146.1						

These samples were heated to different temperatures by two calcination methods,ie rapid calcination and slow calcination. Then we monitored and analysed the changes in the process of calcination.

1 DTA

Rapid rise of temperautre in DTA curve indicated that: the decomposition temperature of $CaCO_3$ in the raw meal decreased at first, then increased with the increase in heat carried with raw meal, and the decomposition temperature of J4 was the lowest. It showed that the decomposition was accelerated when raw meal brought heat to kiln, but the combustion of extra coal induced reaction, absorbed heat, so hindered the process of decomposition. The results agreed with the experimental results in precalciner stated by reference[4].

2 Burnability

Clinker was made by calcining nodulized raw meal and then we measured ignition Loss, F.C (fCaO) and calculated transformation rates α of CaO.

$$\alpha = \frac{CaO - (F.C + \frac{56}{44} Loss) \times \frac{100}{100 - Loss}}{CaO} \qquad (1)$$

CaO: burned basic value of total CaO in clinker after calcination, here 66.99

F.C: free CaO content in clinker. It showed the non-combination CaO content after decomposition of the limestone in the raw meal.

Loss: ignition loss of clinker after calcination, it showed the non-decomposition CaO content.

α: combination of two factors It showed the CaO content which was transformed into clinker mineral.

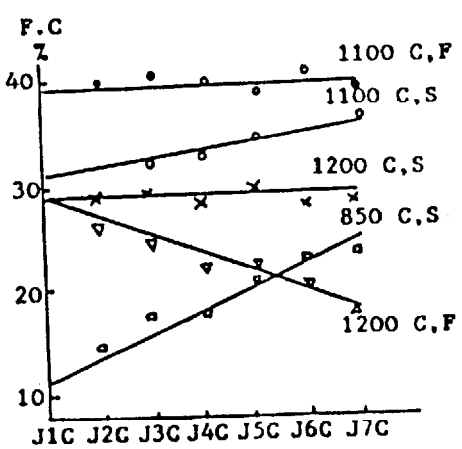

Fig.1 The F.C of clinker

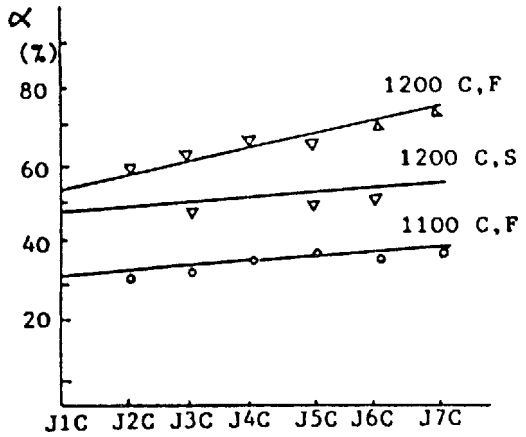

Fig.2 The α of clinker

The results of F.C and α of clinker indicated that the increase of coal content in raw meal promoted the decomposition of limestone. When using rapid calcilation method, the α valuc increased apparently. It indicated that activity of CaO increased, and transformation of clinker became faster. It was most obvious at 1200℃, F.

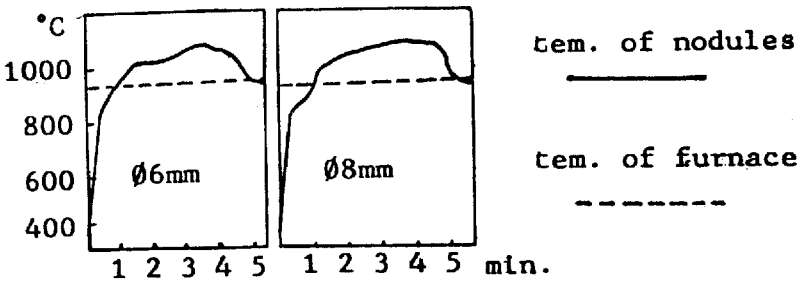

Fig.3 The tem. of black raw meal nodules in burning

Adding coal was the basic condition for rapid calcination (it facilitated rapid calcination) Rapid calcination took advantage of the effect of coal combustion, and the ash from burning combined with active CaO after decomposition for clinker formation.

Rapid calcination of black raw meal promoted combination also because black raw meal was a kind of fuel .The temperature which was attained in the process of calcination was higher than the furnace temperature. As shown in Fig3 the temperature rise curve of coal–containing raw meal within a short time of burning was higher than furnace temperature.

3 Formation kinetics of clinker with the rapid calcination method

We rapidly calcined J1, J4, J7 at different temperatures, and maintained the temperature constant for different times. We calculated the value of calcined clinker using formula[1]and then calculated f(α) using several kinds of kinetics equation, entering the data in the form: $f(\alpha)=Kt+L$. In here, K is the rate of reaction, t is time of revention temperature and L is the intercept of line. We chose the best kinetics mechanism from theK value of samples which corresponded to the best controlling mechanism. We drew Figs 4 of LnK−1 / T (T is the absolute temperature) using Arrhenius equation. The slope of the line was the activation for energy formation of clinker mineral, as shown in Fig.4.

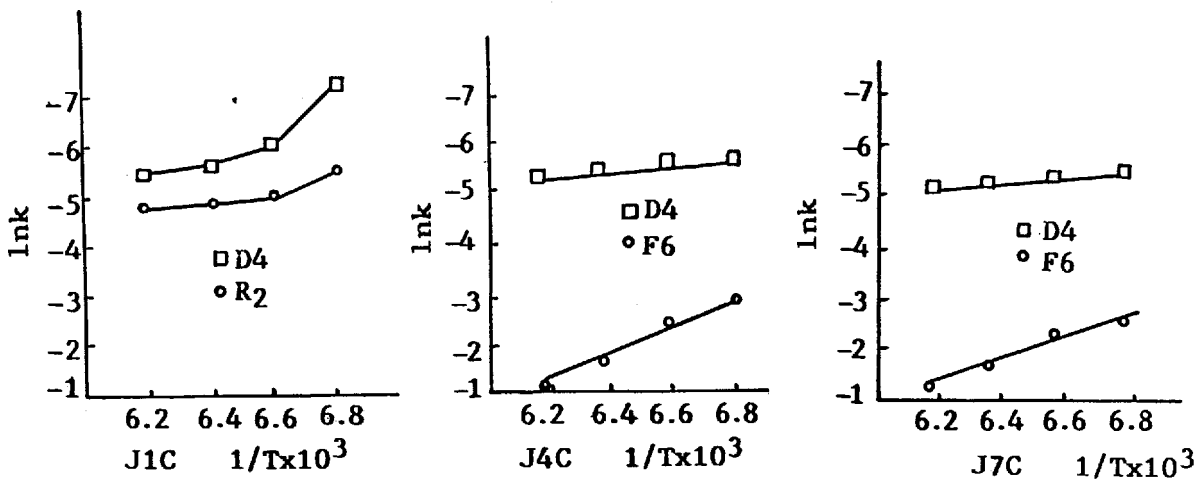

Fig.4 The Figure of lnK-1/T of J1C, J4C, J7C calculating the activation energy of clinker formation

In Fig4, we can see the different controlling mechanisms of JIC (clinker was calcined from white raw meal) from two lines with different slopes in LnK−1 / T. It indicated that JIC at 1200℃ was still in solid diffusion and at 1250℃ it became liquid, then behaved as liquid diffusion. We took 3 points in high temperature to calculate the activation energy of formation of C_3S. The results were 123KJ / mol using D4, and 50 KJ / mol using R2. The kinetics mechanism of formation was that at high temperature, CaO and C_2S dissolved into liquid to form $Ca^{++}$and SiO_4^{4-}. $Ca^{++}$and SiO_4^{4-} diffused to the liquid–C_3S, interface and by surface diffusion C_3S was produced. Crystal grew larger. This process mainly was composed of the diffusion of Ca in liquid and reaction of surface chemistry (diffusion of SiO_4^{4-}depended on that of Ca^{++}), as shown in Fig5.

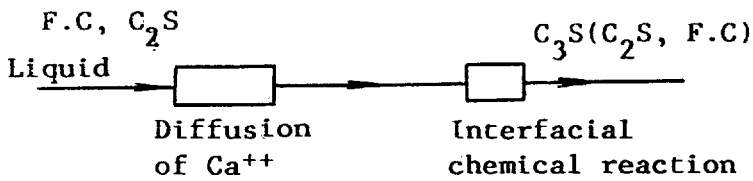

Fig.5 Schematic diagram of clinker formation from white raw meal

The difficult factor (high activation energy) would be the rate controlling factor. By calculation we knew that the energy activation of Ca^{++}diffuison (123 kJ / mol) was higher than that of surface chemistry reaction (50 kJ / mol). So the Ca^{++} diffusion of JIC in liquid was in accordance with Ginstling equation and is the kinetics controlling mechanism of C_3S formation. In the LnK−1 / T Fig. collinearity of 4 points of J4C, J7C was very good. It indicated that formation of liquid was at 1200℃, when black raw meal was calcined . The result from of calculation J4C activation energy was 47kJ / mol using D4 and 224 kj / mol using F6.The result from of calculation J7C activation energy was 128kJ / mol using D4,and 55.8kJ / mol using F6. Both diffusion and nucleus formation and growth can became the kinetics controlling mechanism of clinker mineral. C_3S formation could procced throuyh two routes. The first was liquid diffusion of Ca and crystalline deposit on C_3−liquid Sinter surface; the second was nucleus formation and growth in liquid. This is shown in Fig.6

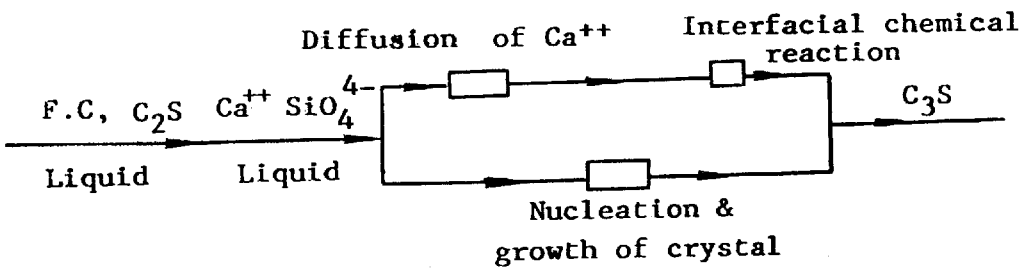

Fig.6 Schematic diagram of clinker formation from black raw meal

The one (its activation energy was low) which easily formed the clinker mineral became the kinetics controlling mechanism. Based on calculation, J4C was also controlled by diffusion, it accorded with Ginstling equation, the activation energy of C_3S formation was 47kJ / mol. J7C was mainly controlled by nucleaus formation and growth, the activation energy of C_3S formation was 55.8kJ / mol. From this, we can see that the activation energy of clinker formation of black raw meal decreased largely, and the activation energy of clinker formed from J7C was higher than that from J4C, which could be related to the reduciing enviorment.

4 The character of formation of clinker mineral

The kinetics study indicated that the activation energy of clinker mineral formation decreased when coal−containing raw meal was calcined and the mechanism and temperature of clinker formation had changed. Comparing the X−ray diffraction pattern of J1C with that of J7C when rapid calcination taking, we knew: at 1100℃, J7C produced $2C_2S$. $CaCO_3$, but J1C did not. Based on the view of W.Weisweiler, $2C_2S \cdot CaCO_3$was formed by combining $-C_2S$ with calcite, so we can say that $CaCO_3$in coal−containing raw meal participated in the formation of clinker mineral. At 1200℃, $2C_2S$. $CaCO_3$decomposed: $2C_2S$. $CaCO_3 \rightarrow 2C_2S+CaO+CO_2$, C_3S was formed, but there was not C_3S in J1C.

Due to the high reactivity of CaO from decomposition of $2C_2S.CaCO_3$, it can rapidly combine to form $C_3A.C_4AF$ and so on. When rapid calcination was taking place, before it grew up, the temperature reached

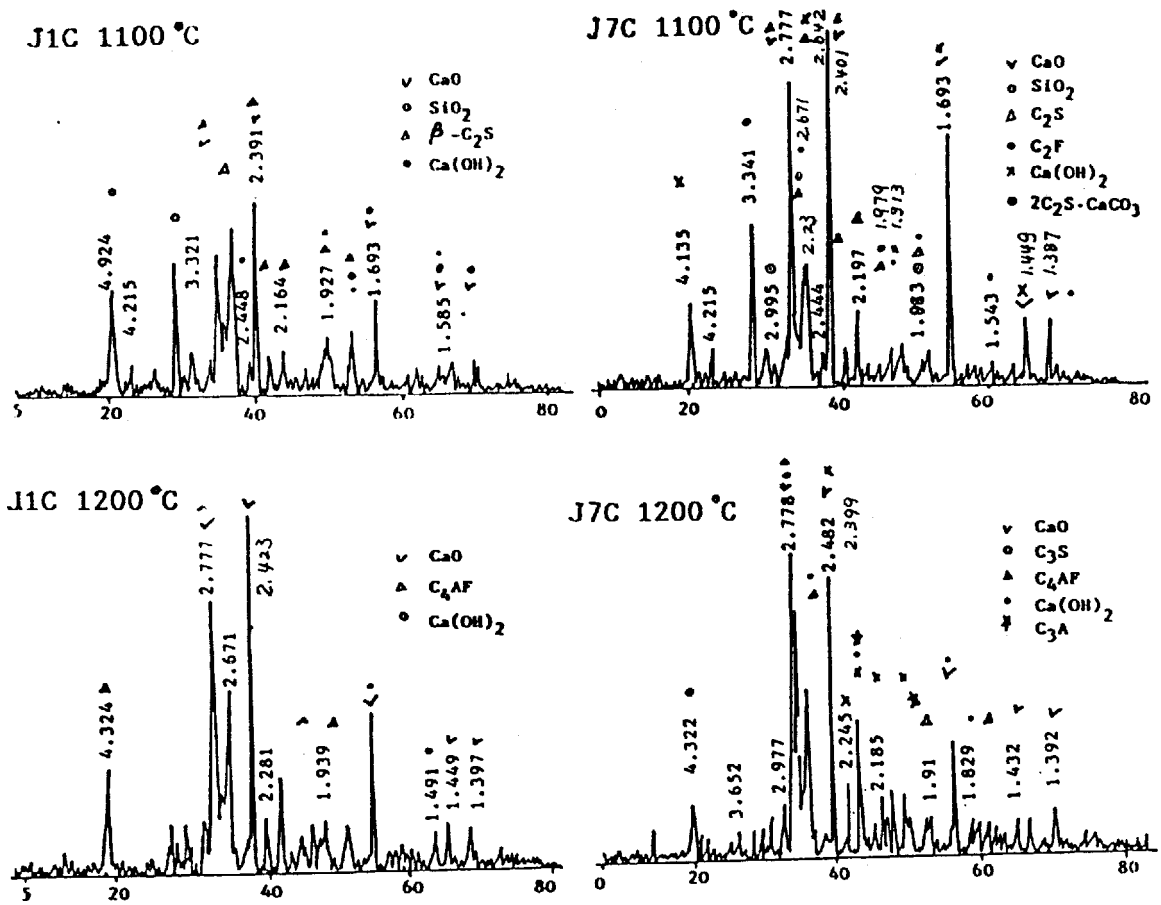

Fig.7 XRD diagram of clinker from rapid calcination

higher so micro–crystal of solvent mineral was formed. Due to the high vapour pressure of such micro–crystal, low melting point and high solubility, it melts at low temperature. When clinker was calcined from black raw meal, it advanced the appearance of the melting phase and promoted clinker formation. From Fig7, we knew that C_2F in J7C at 1100℃ was changed into C_4AF at 1200℃. Based on the calculation made by T.K Chatteriec, this kind of change took place only with the help of liquid phase this also verified that liquid phase was formed in advance, when black raw meal was rapidly calcined. Fig8 is scan energy pattern of Alite crystal in clinker rapidly calcined from raw meal J6, we can know that the main composition in solid–solution of Alite crystal were Fe and Al, so the intermediate phase was less in clinker formed from coal–containing raw meal, this agreed with the resultes of the rock facies study.

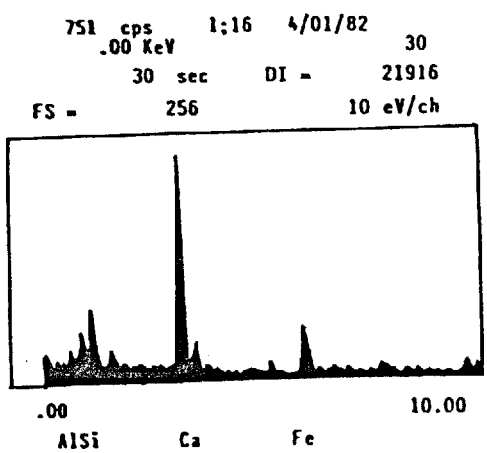

Fig. 8 EDS diagram of J6C clinker from rapid calcination

CALCINATION MECHANISM OF BLACK RAW MEAL

1. The combustion of coal in black raw meal nodules produced high temperature, so the combustion and heat transfer occurred at the same time, and the decomposition of carbonate in raw meal was accelerated.

2. Rapid calcination enabled the fuel not to burn at low temperature and enter high temperature state, so that CaO of high activity from decomposition combined rapidly with SiO_2, Al_2O_3in clay and coal ash to form clinker mineral. So rapid calcination utilized the effect of fuel in black raw meal to full degree.

3. When black raw meal was calcined, liquid had already been formed at 1200℃, and so it accelerated the formation of C_3S. In plants, by adding new mineralizers to decrease the temperature of liquid formation, the temperature range of C_3S calcination was further widened to increase the quantity of C_3S and guarantee the utilization of rapid calcination. But f.CaO was not very high.

4. When black raw meal was calcined, both diffusion and nucleus formation and growth controlled the formation of C_3S, which of the two was prominent depended on the amount of heat carried with raw meal. The activation energy of C_3S formation from black raw meal was lower than that from white raw meal. But when more heat was brought to the kiln, the activation energy increased again. In plants, the dust from kiln separated by dust separator was added to raw meal uniformly. There were some decomposed raw meal particles and a litthe clinker in the dust from the kiln.The latter acts as the nucleus of crystal, hence increased the proportion of nucleus formation and growth, which was beneficial to clinker formation.

5. In the laboratory, the heat carried with raw meal was over 900kcal / kg, reducing atmosphere was formed to produce reducing meal. So more heat carried with raw meal was harmful to calcination and quality of clinker. In plants, however we controlled this to be below 675kcal / kg, it was in the region of lower activation energy of C_3S formation.

Based on these results we think the calcination method used in plants was fit for objective law. When we calcined high quality clinker with low heat consumption, technical and economic effects were achieved.

ACKNOWLEDGEMENTS

"Study on The Formation Process of Clinker From Raw Meal Containing Coal Powder" was accomplished by graduate Y.S.Cao with direction of Professer M.S.Tong assistant Prof. X.H. Chui and help from senior engineers H,Zhou. P.Gao. Engineers S.Y.Fu.,E.S.Chui, C.J. Yu.,Y.Lon,G.C.Sien did a lot of about producing high-quality clinker with low heat consumption in plant. I greatly appriciate the help from all of them.

REFERENCE

1.Qin, Z.G. "Clinker With High Lime Saturation Factor can also be Burnt in Shaft Kiln,"in Chinese. Cement, 1982.8.

2.Qin.Z.G: "Production of Special Cement in the Cement Plant with Shaft Kiln", in Chinese. The Proceedings of The Third Annual Meeting on Cement Sponsored by The Cement Committee of The Chinese Ceramic Socicty, (1986).

3.Cao Y.S., Chui X.H., Zhou H., Gao P., Qin Z.G., Tang M.S.:"Study on The Formation Process of Clinker From Raw Meal Containing Coal Powder." in Chinese. China Building Materials Science & Technology. 1992.2.

4.Gu D.G: "Mathematic Models for The Series of (SLC), Precalcinator 1990.2.

5.Huang W.X. Qiy.y. "A Kinetics Study on Formation of Clinkes in Rapid Rising-Temperature-An Inquiry Probe on Kinetics Mechanism of Formation of Clinker Minerals at Different Rising-Temperature Rate. in Chinese.

MECHANOACTIVATION OF PORTLAND CEMENT RAW MIXES

L M Sullmenko

Moscow Institute of Public Utilities and Civil Engineering
Moscow, RUSSIA

Summary

The possibilities for mechanoactivation of portland cement raw mixes in comminution machinery of various type are presented. A comminution process specifies structural and chemical parameters of materials comminuted and their chemical activity. The most effective dispensers for cement raw mixes are mills of impact–attrition type of loading. The optimal mode of mechanoactivation ensures a lower temperature of burning and higher quality of clinker

Показаны возможности механоактивации портландцементных сырьевых смесей в измельчителях различного типа. Способ измельчения определяет структурно–химические параметры измельчаемых материалов, их химическую активность. Наиболее эффективными диспергаторами цементных сырьевых смесей являются мельницы с ударно–сдвиговым характером нагружения. Выбор оптимального режима механоактивации обеспечивает снижение температуры обжига и повышение качества клинкера.

The mechanical energy directly perceived by the molecular structure of a solid body belongs to the most efficient vehicles of catalytically acting upon the chemical transformations of materials. The principal act of the mechanical processing of materials is a constant interaction of particles with one another and with the tools of comminution. The difference in kinetic energy before and after such an interaction is consumed in heating up the material treated and the grinding media charge, for disintegrating the particles, as well as for boosting their energy as a result of structural, phase and other transformations. The materials surface growth is associated with the release of free energy according to this relationship:

$$dE=\sigma dS,$$

where dE stands for the total change of material surface free energy (J),
σ – surface tension (J/m^2), and
dS – surface change (m^2).

Because of this, mechanoactivation is sometimes identified with the growth in the surface area of the system treated. Experimental findings, howewer, contradict such a viewpoint.

Mechanoactivation of cement raw blends and model materials (calcite and quartz) was accomplished by: slow impact with attrition (a ball mill), intensive impact with attrition (a planetary mill), attrition with crushing (a roller mill), fast multiple impact against a macrosurface (a disintegrator), fast mutual collision of particles (a jet mill).

It was demonstrated that, in addition to a rise in the surface energy, a growth in the internal energy arising from a higher concentration of structure defects and stressed states plays a far greater role in the energy accumulation of the material comminuted. It is these phenomena that underline mechanoactivation, which may promote the effectiveness of the subsequent technological operations, or mechanochemical reactions occurring directly in the process of mechanically treating the matherial.

Mechanochemical effects by a number of researchers have been registered in comminuted cement raw materials (1). The occurrence of a precalcining reaction during the splitting of natural calcite monocrystals with release of $\sim 2 \cdot 10^{13}$ molecules of CO_2 per cm^2 of newly formed surface has been pointed out. Several other studies (2,3) have confirmed quartz amorphization, transition of α–quarts into β–quarts and β–cristobalite. Howewer, the comparatively poor chemical activity of cement raw materials and the relatively low intensity of their mechanical treatment in conventional grinding units restrict the possibilities of mechanochemical interaction in cement raw mixes.

In the letter, as a rule, we deal with the mechanoactivation phenomenon, which represents but one of the stages in the comminution process. One can single out three comminution stages occurring consecutively: destruction of aggregates, secondary sintering and mechanochemical activation. In the first two stages the energy applied to the materials under disintegration is spent on destroying the aggregates of particles, while in the activation stage it is spent on creation of their defect structure. Mechanoactivation process, as a rule, is accompanied by a significant increase in the specific surface of the material, whereas in certain types of comminution machinery there may even occur its reduction (see Table 1). Thus, grinding a cement raw mix in a ball mill for 1 to 4 hours is accompanied by a consistent decrease of its specific surface.

Quantitative estimation when exactly the activation begins remains debatable. The opinion of Ye.L.Goldenberg and S.V.Pavlov (4) in this regard deserves serious attention. According to Pavlov, it coincides with the viscous–brittle transition, i.e. a switch–over from brittle destruction of particles to their plastic deformation. Such a transition becomes feasible only when a definite size (r) of particles is reached. If r exceeds the size corresponding to the viscous–brittle transition point (r^*), destruction take place;if r is less than r^*, plastic flow will result. When the condition $r<r^*$ is satisfied, it signifies the end of dispersion and the start of mechanoactivation.

At the same time, the beginning of activation also depends on the energy intensity of the comminution machinery. It is obvious that the power applied to the material comminuted can be varied both through impact energy E and frequency w_k. It is also clear from the standpoint of energy intensity that the two are far from being equivalent. By raising w_k, we only vary the same scale, attaining purely quantitative effects. But if we increase E, the particles will undergo great stresses during impacts, which may engender qualitatively novel processes.

The most efficient dispersers and activators for materials with a higher hardness, which bulk of cement raw materials are, are equipment with an impact–shear nature o loading (in the present instance, planetary mills). The size of the microcrystallite blocks of solid bodies produced in them is 2 to 4 times smaller, and the magnitude of microdeformations is respectively larger than those in other comminution machinery (see Table 2). It is notable that, as grinding processes in a ball mill, the material is sintered at the micro–level as well. In 4 hours, the size of microcrystallite blocks is larger by an order of magnitude than in 1 hour of grinding.

While the change in size of microcrystallite blocks corresponds sufficiently exactly to the specific surface growth, no such dependence is observable regarding micro–deformations. Moreover, with one and the same comminution technique, deformations may grow in one crystallographic direction and diminish in another.

Table 1. Effect of duration of comminution on specific surface area of cement raw mixes

Mill type	Specific surface, $m^2/kg \cdot 10^3$ (by BET) Grinding duration								
	Minutes					Hours			
	2	5	10	15	20	1	2	3	4
Ball	–	–	–	–	–	28.5	24.7	22.3	20.7
Planetary	–	22.0	23.2	23.4	22.3	–	–	–	–
Roller	21.1	24.8	24.3	26.4	–	–	–	–	–

Table 2. Effect of mechanoactivation on the size of microcrystallites (D) and deformations (ε) of calcite and quartz crystal lattices

S. No.	Mill type	S*, m^2/kg	Calcite		Quartz	
			D, Å	ε, %	D, Å	ε, %
1.	Ball	350	1,720	0.143	5,640	0.147
2.	Ball	550	20,220	0.048	43,420	0.081
3.	Roller	520	9,850	0.05	5,040	0.089
4.	Roller	1,105	7,330	0.136	7,230	0.102
5.	Planetary	1,090	1,090	0.188	24,020	0.07
6.	Planetary	1,170	750	0.236	2,810	0.117
7.	Jet	380	82,330	0.016	33,850	0.069
8.	Jet	870	930	0.186	4,980	0.09
9.	Disintegrator	360	9,080	0.054	7,130	0.09
10.	Disintegrator	1,020	1,480	0.144	5,110	0.035

*Blain's

Taking into account the multistaged nature of cement manufacturing process as well as the subsequent hardening cement paste, it is important to estimate the extent and limits to which the mechanoactivated effects could be foreserved in the later stages of processing the mixes. It has been established that materials which are burnt preserve the structural perculiarities entailed by the technique of their mechanoactivation. An enhanced deformation degree of the crystal lattice of the source minerals brings about their great deformation during burning as well.

For a constant surface area of raw mixes, the clinkering dynamics depends on the technique of their mechanoactivation. No universal mechanoactivation method has been found. Accordingly, the advantages of different techniques of mechanoactivating manifest themselves at different stages of the subsequent technological processing of the raw mixes.

The precalcining reaction is accelerated in the course of intensive impact–attrition comminution. For the same specific surface area, raw mixes produced in a planetary mill have energy almost twice as low as those ground in a ball mill (82.4 and 156.7 kJ/mole respectively). Likewise, quick–impact comminution raises the activation energy of material due to the limited amount of finely dispersed fraction in it.

Solid–phase synthesis within a temperature range up to 1,000 ^{0}C is intensified in the course of impact–attrition comminution in conventional ball mills. In mixes of quick–impact comminution, 55% CaO is fixed at 1,000 ^{0}C, while in mixes of impact–attrition grinding, it is already 70 to 30%. At higher temperatures, howewer, the process is retarded, the orthosilicate formed recrystallizes, which later tells negatively on alite synthesis.

Liquid–phase sintering is intensified in mixes subjected to the most intensive comminution techniques. Raising the intensity of mechanoactivation enables CaO assimilation to be speeded up 1.5 to 2–fold. Quick–impact activation with a maximum impact–delivering rate of 250 m/sec makes it possible to achieve a complete clinker formation within 10 min at 1,300 ^{0}C already.

Mixes of quick–impact comminution yielded the densest fine–grained clinker, uniform in structure and containing an enhanced amount of alite (see Table 3).

The structural peculiarities of clinkers from mechanoactivated mixes affect their grindability. To produce cement with a specific area of 300 m^2/kg based on clinkers obtained from raw mixes mechanoactivated in a roller, ball, planetary, jet mill and a disintegrator, 6, 5, 4, 4 and 3 minutes were required, respectively for grinding.

Table 3. Influence of mechanoactivation technique of raw mixes on clinker mineralogical composition (burning temperature 1,450 ^{0}C)

S. No.	Mill type	Specific surface area, m^2/kg (BET)	Content of clinker minerals, mass %			
			C_3S	C_2S	C_3A	C_4AF
1.	Ball	20.7	58	19	3.5	14.7
2.	Roller	22.0	55	27	3.2	14.0
3.	Planetary	21.1	56	25	6.0	13.0
4.	Jet	17.5	65	14	5.0	16.0
5.	Disintegrator	16.1	63	15	3.4	15.0

One can also trace the influence of mechanoactivation of raw mixes even at the hardening stage of cement stone distinctly enough, especially during the initial period of hardening. In particular, at age of 2 hours the strength of cement based on clinkers out of raw mixes of jet and disintegrator comminution is twice as low, and at the age of 10 hours thrice a slow compared to cements from clinkers ground in a ball mill. As hardening progresses, howewer, these differences gradually even out.

REFERENCES

1. Fox, P.G. and Soria–Ruiz, J.: J. Proc. Soc., 1970,(317), 79–90.
2. Khodakov, G.S.: Fine comminution of building materials. Moscow, Stroyizdat, 1972,239 p.
3. Schrader, R., Hoffman, B. and Pläntzer, H.: Zement – Kalk – Gips, 1970, (5), 194–199.
4. Goldenberg, Ye.L. and Pavlov, S.V.: Theses of reports for the 11th All–Union symposium on the mechanochemistry and mechanoemission of solid bodies, Chernigov, Russia 1990, V11, 120–121 (in Russian).

THE STUDY ON THE FORMATION OF PORTLAND CEMENT CLINKER IN LOW-TEMPERATURE AND A RAPID HEATING-UP BURNING PROCESS

Huang Wenxl*, Lu Zhongyuan** and Xu Guanglang**

*Chengdu Design & Research Institute of Building Materials Industry, Sichuan, P R CHINA
**Sichuan Institute of Building Materials, Sichuan, P R CHINA

SUMMARY

The authors have studied the mechanism of Portland cement clinker formation in rapid heating-up burning process (800℃/min)without any mineralizers and with the composite mineralizers of CaF_2,$CaSO_4$ and ZnO by using Positron Annihilation, Mossbauer Spectrometer and High Temperature Microscope etc. The study has proved that Portland cement clinker could been formed at about 1300℃ without any mineralizers and about 1050℃ with the composite mineralizers of CaF_2,$CaSO_4$ and ZnO.

摘 要

应用正电子湮没、穆斯堡尔谱和高温显微镜等，在快速加热煅烧过程中（800℃/min），作者研究了掺和不掺CaF_2、$CaSO_4$和ZnO复和矿化剂时波特兰水泥的形成机理。研究表明，掺和不掺上述复和矿化剂时波特兰水泥熟料分别在大约1050℃和1300℃形成。

INTRODUCTION

Generally, portland cement clinker can be formed when the raw meal is sintered above 1450℃. However, such high temperatures affect greatly the output and quality of the cement, and furthermore it consumes great energy. According to statistics, cement industry is one of consuming maximum energy. The total energy consumped thermal energy account for more 70~80%. Therefore, low-temperature burning clinker is one of the are as for study that is attracting increasing attention. One method of lovering the temperature of clinker burning is to add mineralizers to the raw meal. Many such studies have been conducted[1, 2, 3,4]. Research results shoved that mineralizers could lover the initial temperature of liquid phase formation by 50~150℃ in the formation process of clinker, increase the speed of the liquid phase formation, improve the properties of the liquid phase. Intermediate transition phatses of $3C_3S \cdot CaF_2$ and $3C_2S \cdot 3CaSO_4 \cdot CaF_2$ etc are also formed. Decomposition of these intermediate transition phases could aids C_3S formation at lovtemperature. Another method of obtaining lovtemperature burning clinker is to heat the raw meal to the sintering temperature under an extremely high temperature gradient in an extremely short time —heating activation. M. F. Chebfcor, B. C. Rangnekar, O.Phillipp[5,6,2]et al had carried out similar studies. They considered that heating activation could accelerate clinker formation. The effect of mineralizers on the formation of clinker in rapid burning has been discussed in other papers[10, 11, 12,] . The authors have studied relatively systematically and comprehensively the mechanism of clinker formation in a rapid heating-up burning process (rapid burning for short) with the composite mineralizers of CaF_2, $CaSO_4$ and ZnO, as well as without any mineralizers by using the methods of Thermodynamical Analysis (TA for short), High Temperature Microscope (HTM for short) , Mossbauer Spectrometer(MS for short) , DTA-TG of Infrared Rapid Heating Type(DTA-TGIRHT for short) , Positron Annihilation(PA for short)etc. The results shoved that the clinker could be formed respectively at 1050℃ and 1300℃ in rapid burning with and without the composite mineralizers of CaF_2,$CaSO_4$,ZnO.

THE EFFECT OF RAPID BURNING ON THE FORMATION OF PORTLAND CEMENT CLINKER

1. The effect of rapid burning on the decarbonation and the activities of CaO

Table 1. Chemical composition of raw meal(drying Wt%)

SiO_2	Al_2O_3	TiO_2	Fe_2O_3	CaO	MgO	R_2O	SO_3	LOI
13.6	2.97	0.19	2.37	43.11	1.00	0.61	0.22	35.76

Table 2. Relation between activation energy E with Φ

samples	$CaCO_3$		cement raw meal					
Φ (℃/min)	10	600	10	80	200	300	600	800
E(kj/mol)	198.16	135.78	173.79	146.66	143.27	133.01	117.90	75.70

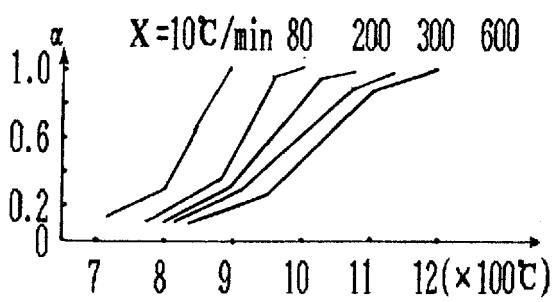

Fig.1.1 Decomposition curves of raw meal under various Φ

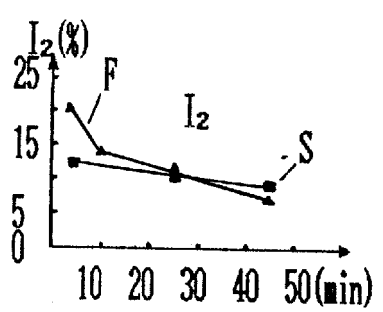

Fig.1.2.A relation of intensity I_2 of τ_2 with retention time in CaO crystal by PA

Samples are prepared from general industrial raw materials and AR grade $CaCO_3$. The chemical composition of raw meal is given in Table 1. The samples were heated to 1300℃ from room temperature at the heating-up rate of Φ =10~800℃/min. and then cooled. Experiments were conducted using DTA-TG-IRHT. Experimental results are given in Table 2 and Fig.1.1.It can be seen from Table 2 that when Φ =10 ℃/min, the decomposition activation energy of $CaCO_3$ in AR grade and cement raw meal are respectively 198·16 and 173·79 KJ/mol. This basically agrees with the value of E=176~188 KJ/mol reported earlier.This shows DTA-TG to be a good experimental technique and the calculating method used to be appropriate too. Decomposition activation energy decreased with increasing heating-up rate (Table 2) . By carrying out the regression analysis, the decomposition activation energy of raw meal and heating rate in region Φ =10~800 ℃/min,the linear equation:$E=165.71 - 0.1024\Phi$ is obtained.The correlation coefficient is equal to 0.911. This indicates that linearity is remarkable. It can be seen from decomposition formula, $dE/d\Phi = -0.1024$, namely decreasing activation energy 10.24KJ/mol with increasing heating-up speed 100℃/min,when Φ =800℃/min, activation energy decrease by 81. 92 KJ/mol. decomposition rate of $CaCO_3$ increases remarkably with decreasing activation energy . It can be seen from Fig.1.1 that when the heating-up rate is increased,the decomposition curves of $CaCO_3$ move to a higher temperature region, that is to say the decomposition temperature of $CaCO_3$ becomes higher. When Φ is increased from 10℃/min to 600℃/min , starting decomposition temperature of $CaCO_3$ increases from less than 700℃ to about 800℃, complete decomposition temperature of $CaCO_3$ increases from about 890℃ to about 1200℃ .The relations of crystal size obtained by XRD and defect amount of nascent state CaO obtained by PA in rapid and normal burning with the retention time are given in Table 3 and Fig.1.2.

In rapid burning,the size of CaO crystal formed is smaller,It is only a few hundred angstroms at the starting time, but in normal burning it is higher,say more than one thousand and three hundreds angstroms in the same retention time (for example at 1300℃, 2 minutes) , the latter is ten times larger than the former (Table 3) , Whether in rapid or normal burning .the crystals grow with increasing burning time,but do so more rapidly in rapid burning (Table 3) . It indicates that nascent state CaO "aging"is more rapid. Because of CaO crystal defects, such as holes, micro cavities, displacements, etc, attract violently positrons, making the intensity I_2 of length age component τ_2 increases. Therefore, crystal defects concentration increases with I_2 value.It can be seen in Fig.1.2 that whether in rapid or normal burning , I_2 values decrease with the increasing burning time. It indicates that the CaO crystal defect concentration decreases . It can be seen that the nascent state CaO crystal defect concentration in rapid burning at 1300℃ is higher than under any other conditions .

2.Hydration activity of rapid burning β -C_2S

Experiment results can be seen in Tables 4, 5 and Fig.1.3. It can be seen in Table 5 that the β -C_2S crystal size obtained by XED in rapid burning is smaller than that of normal burning and micro-stress (e^2) obtained by XRD is higher than that of normal burning.In Fig 1.3, the hydration rate of β -C_2S from rapid burning is more rapid than that of normal burning, especially the combined water of FB1 (3.16%) at early age(3days)hydrate is over six times higher than NB(0.52%). The combined water of β -C_2S at the same

Table 3. Size (Å) of CaO crystal (220) surface in rapid and normal burning

Burning mode	1300℃,2min	1300℃,3min	1300℃,10min	1300℃,25min
Rapid	138	507	1248	1941
Normal	1329	1381	1504	2052

Table 4 Synthetic condition of β -C_2S

	FB1	FB2	FB3	NB
Φ (℃/min)	over 800	over 800	over 800	5
Temp.(℃)	1400	1450	1400	1400
Time(min)	20	20	45	720
f-CaO(%)	0.36	0.01	0.02	0.36

Table 5.Crystal size(Å) and microstress$\langle e^2 \rangle$ of β -C_2S

No.	FB1	FB2	FB3	NB
(Å)	476	699	986	1199
$\langle e^2 \rangle \times 10^3$	1.94	1.22	1.18	1.13

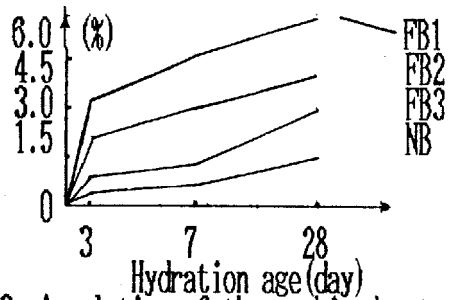

Fig 1.3. A relation of the combined water(%) of β -C_2S with hydration age

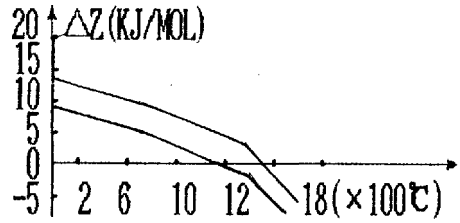

Fig 1.4. A relation of ΔZ-T in $CaO+C_2S=C_3S$ system

age changed as follows in rapid burning condition: FB1>FB2>FB3(Fig.1.3). The microcrystal size changed as following : FB1<FB2<FB3.The micro-stress changed as FB1>FB2>FB3(Table 5).It can be seen that when burning temperatures are the same,the hydration activities of β -C_2S decrease with increasing retention time.When the retention time is the same, the hydration activities of β -C_2S decrease with increasing burning temperature.The latter results were in agreement with the conclusion of A.A.paschenko[7].

3. Effects of heating-up rate on the formation process of C_2S ,C_3S and clinker

The three reaction systems from which C_3S and C_2S can be formed are as follows:

i CaO--C_2S system $CaO + C_2S = C_3S$ (1-1)

ii CaO--SiO_2 system $2CaO + SiO_2 = C_2S$ (1-2)

$3CaO + SiO_2 = C_3S$ (1-3)

iii $CaCO_3$-CaO-SiO_2 system $CaCO_3 = CaO + CO_2$ (1-4)

$2CaCO_3 + SiO_2 = C_2S + 2CO_2$ (1-5)

$3CaCO_3 + SiO_2 = C_3S + 3CO_2$ (1-6)

From the three systems above, U.Ludvig[8] et al had got the ΔZ-T relation figure of system(i). Obviously, even though at high-temperature in system(i),the formation of C_3S is not easy.V.I.Basushkii[9] had discussed the reaction possibility of system(ii) and system (iii) when T> 1160 K(Fig 1.5).Except that CaO and SiO_2 could form C_2S and C_3S, $CaCO_3$ and SiO_2 could form C_3S and C_2S too.But he considered when T> 1160K, $CaCO_3$ has been decomposed, $CaCO_3$-CaO-SiO_2 system could not exist,only CaO-SiO_2 system could exist. Thereby the decomposition temperature of $CaCO_3$ increase in rapid burning (Fig 1.1) , and there is not enough time for $CaCO_3$ to decompose totally so exist in high temperature.That is why When T>1160K,CaO-$CaCO_3$ -SiO_2 system can exist. From chemical thermodynamical analysis,we calculated the free energy of formation of C_2S and C_3S in CaO-$CaCO_3$-SiO_2 system when T> 1160K. The results can be seen in Fig 1.5 as dotted line. According to Fig 1.5,compare system(ii)with system(iii)as following:

At 1300℃ (1573K) system(ii):

ΔZC_2S =-142 KJ/mol,

ΔZC_3S =-128 KJ/mol.

At 1300℃ (1573k),system(iii):

ΔZC_2S =-257 KJ/mol,

ΔZC_3S =-300 KJ /mol.

From above ΔZ value comparsion can be seen that when T > 1160K, the posibility of $CaCO_3$ reacting directly with SiO_2 to form C_2S and C_3S is maximum. in CaO_3-CaO-SiO_2 system,and then CaO reacting with SiO_2. The posibility of CaO reacting with C_2S to form C_3S is minimum. From the above results it can be proved that when T> 1160K,the following reactions are likely to take place:

Table. 6. ε and f-CaO of various retention times at 1300℃ in rapid and normal burning

	t(min)	0	5	30	45
normal	f-CaO	14.18	9.10	5.35	2.64
	ε	0.7887	0.8644	0.9203	0.9607
rapid	f-CaO	35.02	6.80	3.09	2.03
	ε	0.3189	0.8849	0.9540	0.9698

$2CaCO_3 + SiO_2 = C_2S + 2CO_2$, $3CaCO_3+SiO_2 =C_3S + 3CO_2$

The rav meal sample as in Table 1 is made into the pellets of Φ 20mm × 0.5mm under pressure,then placed quickly in a tube type high temperature furnace under 1300℃. The interal between the time the samples were placed at the furnace center to the time there temperature reached 1300℃ (1 minute) was regarded as

Table 7. The process of minerals formation in rapid burning at 1300℃

	heating-up process				normal burning process					
t,(min)	0	1/6	1/2	1	1	2	3	5	30	45
SiO_2	+++	+++	++	+	-	-	-	-	-	-
$CaCO_3$	+++	+++	++	+	+	-	-	-	-	-
CaO	-	-	++	++	+	+	+	+	+	+
C_2S	-	-	+	++	++	++	++	++	++	++
C_3S	-	-	-	-	++	++	++	++	+++	+++
C_4AF	-	-	+	+	+	+	+	+	+	+
C_3A	-	-	-	+	+	+	+	+	+	+

(*:+++ = a large amounts, ++ = middle amounts, + = a little, - = nil.)

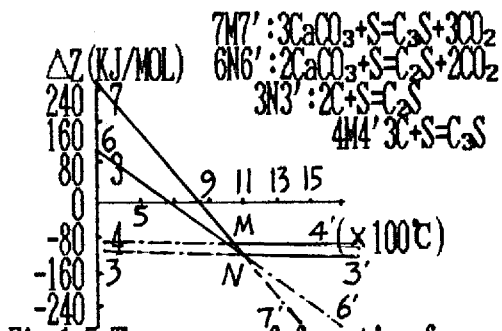

Fig.1-5 The curves of formation free energy of C_2S and C_3S in various system.

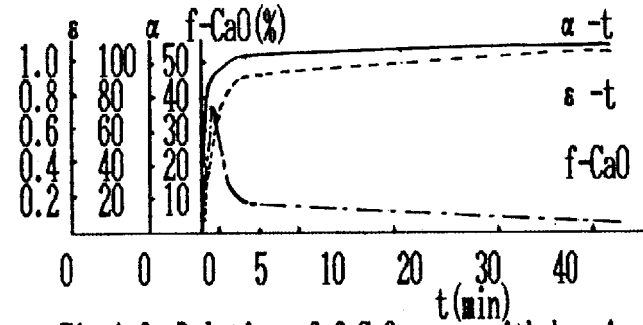

Fig.1-6. Relation of f-CaO, ε, α with burning time in rapid burning at 1300℃

the heating-up process of raw meal. Then starting from the time the samples reached the furnace temperature,through the retention period 0~45 minutes,up to the time the samples was quickly taken out of the furnace for cooling quickly was regarded as burning process. The samples were tested by XRD, microscope,etc.Experimental results are shown in Tables 6 and 7, and Fig.1.6.

It can be seen from Table 7 the when the heating-up process has taken place for one minute to 1300℃ (namely retention temperature starting),the decomposition of $CaCO_3$ is not complete, but considerable C_2S, C_3A and C_4AF have been formed. However when the temperature was held for one minute at 1300℃,even though the decomposition of $CaCO_3$ is still not completed,apart from C_3A and C_4AF,a lots of C_2S and C_3S have been formed too. This indicates that $CaCO_3$-CaO-SiO_2 system existed at 1300℃, and there was a possibility of $CaCO_3$ directly taking part in reactiones of silicates formation. It is shown in Fig.1-6 that the raw meal is sintered directly at 1300℃, once the heating-up process is completed (that is temperature of the raw meals reach the furnace temperature) , $CaCO_3$ is decomposed sharply to near 80%,f-CaO increases sharply to maximum, the reaction rate ε of CaO is near one-third. Through such a short decomposition process,a lots of C_3S, C_2S, C_3A and C_4AF are being formed continuously by nascent state CaO.When the temperature is held for one minute, f-CaO decreases to 14.4%, the reaction rate ε of CaO is near three fourths. It indicates that the reaction rate is much higher in the starting minute when the temperature of rapid heating-up reaches to 1300℃. The reaction rate ε increases 41.97% in one minute. It can be seen from Table 7 that the retention temperature for 0 to 1 minute respectively , C_3S and C_2S minerals have been formed obviously. Judging from the external appearance of clinker, the sintered samples for which temperature is retained for one minute are black, and are difficult to grind, which indicate that abundant liquid-phase had been formed.Our research results[14]have shown that rapid burning caused a change in the coordination number of Al^{3+} and Fe^{3+} in clinker,the coordination number of some of the Al^{3+} and Fe^{3+} ions could be changed from four to six, forming more loose structures,lowering liquid-phase viscosity,decreasing liquid phase appearance temperature by about 200℃. When t >1 minute,f-CaO decreased gradually,the reaction rate ε of CaO increased slowly, the XRD characteristic peak of C_2S and C_3S increased gradually. Therefore, in

Table 8. Physical properties of cement clinker from rapid burning without any mineralizers

Sintering temp. (℃)	Comp.str.(MPa)			Bending str.(MPa			Setting time(h:min)	
	3d	7d	28d	3d	7d	28d	Initial	Finial
1310℃	31.7	47.0	64.5	6.2	7.4	9.0	2:14	4:07
1290℃	32.1	47.1	66.8	6.5	7.4	9.0	1:52	2:43
1300℃	34.2	51.9	67.8	7.0	8.1	9.2	1:38	2:35

the starting 2 minutes rapid burning (heating-up for 1 minute, retention temperature for 1 minute) , not only did $CaCO_3$ decompose rapidly and nearly completed, but also the nascent state CaO started compounding reaction sharply, this made the reaction rate s of CaO and the reaction speed reached a higher level. After reaction process through starting several minutes , CaO decreased constantly and considerable C_3S was formed. It can be seen from Table 7 that when t>5 minutes, comparing normal burning clinker with rapid burning, even though the former heating-up process is increased for more than two hours, the f-CaO content of the former is higher than that of the latter while heating-up to 1300℃, f-CaO content for normal-burn sample is only 14. 18%, which after 30 minutes, is still 5.53%,decreasing only 8.83%, whereas when rapid-burning,f-CaO content decreases from 53.02% to 3.09% for the some period.Therefore the rate of minerals formation in rapid burning is much higher than that in normal burning. The grades of clinker formed in rapid burning at 1300℃ have arrived at over 625#(shown in Table 8) . To sum up ,the mechanisms of the clinker sintered rapidly at low-temperature are that the raw meal is heated to sintering temperature in an extremely short time in rapid burning, resulting in a great decrease of the activation energy of $CaCO_3$ dissociation and clinker formation, increasing the dissociation temperature of $CaCO_3$, and $CaCO_3$ may directly react with SiO_2 to form C_2S and C_3S,accelerating the formation of C_3S;In rapid burning the number of crystal defect of the nascent state CaO and C_2S are increased,the crystal structure is more loose,crystal size is smaller,increasing the chemical reaction activities of CaO with C_2S. Al^{3+} ions and Fe^{3+} ions in the liquid phase transform partly from closepacking 4-fold coodination sites into loose 6-fold coordination sites, decreasing the temperature of liquid phase appearance in clinker by about 200℃, greatly reducing liquid phase viscosity, accelerating the diffusion speed of the particles. In rapid burning , all the kinds of process occur such as : decomposition of $CaCO_3$, solid- phase reactions, liquid-phase formation, C_2S and C_3S, etc,minerals formations ,etc,tend to overlap ,the activities of the various components be come into full play, the aging opportunity of the nascent state be decreased, thereby accelerate C_3S formation.

THE FORMATION PROCESS OF PORTLAND CEMENT CLINKER WITH COMPOSITE MINERALIZERS IN RAPID BURNING

The chemical compositions of the raw meal used in experiment can be seen in Table 9. The experiment results as shown Table 10. It can be seen from Table 10 that when it is heated rapidly to 1050℃ (t= 1 minute), C_4AF, β -C_2S, $C_{11}A_7 \cdot CaF_2$ and f-CaO were formed.When t=2 minutes intermediate transition phase $3C_3S \cdot CaF_2$ appeared,and a little C_3S was formed,the decomposition of $CaCO_3$ is yet not completed,but f-CaO content reached at maximum values of 14.28%, f-CaO maximum content was much lower than that in normal burning clinker process (f- CaO=20~30%) in general composite mineralizers. On the one hand it indicated that the formation speed of clinker minerals was more rapid in rapid burning process.On the other hand it indicated that $CaCO_3$ may take part directly in the formation reaction of C_3S and C_2S. When t=3 minutes, $CaCO_3$ decomposition is completed, $3C_3S \cdot CaF_2$ contents increased, f-CaO contents decreased, C_3S contents increased a little.When t=5 minutes,$3C_3S \cdot CaF_2$ contents decreased greatly,C_3S contents increased rapidly, and f-CaO contents decreased continually. When t> =10 minutes, $3C_3S \cdot CaF_2$ decomposition reaction have completed ,C_3S contents increased continually,and f-CaO contents decreased further.The $3C_3S \cdot CaF_2$ existed at 800~1000℃ in rapid burning and have decomposed vastly into C_3S at 1050℃ [10],making a lot of C_3S form at about 1050℃.

Portland cement clinker can be formed at relatively low temperatures with the help of the composite mineralizers of CaF_2, $CaSO_4$ and ZnO, this is so mainly because lots of $3C_3S \cdot CaF_2$ can be formed at low-temperature (800~1050℃) and the decomposition of the intermediate transition phase $3C_3S \cdot CaF_2$ forms C_3S at 1000~1050℃ along with the function of CaF_2,$CaSO_4$,ZnO and heating activation,making the temperature of liquid phase appearance and liquid phase viscosity be greatly reduced , in this case, the C_3S formation temperature is decreased,the formation speed of C_3S is increased,accelerated the formation of C_3S.Gutt[4] et al agreed with this conclusion. Secondly rapid burning makes chemical reactions at all stages of clinker burning tend to overlap practically. As a result, the reaction minerals in the formation process

Table 9. The chemical composition of raw meals (sintering Wt%)

No	Al_2O_3	Fe_2O_3	SiO_2	CaO	MgO	F,SO_3,ZnO
1	4.61	4.98	18.7	62.1	2.49	suitable
2	4.95	5.64	19.3	62.5	2.06	suitable

Table 10. Formation of minerals at 1050℃

t(min)	1	2	3	5	10	15	30	45
$CaCO_3$	+	+	-	-	-	-	-	-
CaO	++	+++	++	++	+	+	+	+
C_4AF	+	+	+	+	+	+	+	+
C_2S	+	++	++	++	++	++	+	+
C_3S	-	+	+	++	+++	+++	+++	+++
$C_{11}A_7 \cdot CaF_2$	+	+	+	+	+	+	+	-
$3C_3S \cdot CaF_2$	-	+	++	+	+	-	-	-

of clinker minerals are put into a highly reactive state, the reaction activation energy is decreased,the clinker formation rate is accelerated greatly and the burning temperature is reduced, so much to the portland cement clinker can be formed at about 1050℃.

CONCLUSIONS

Portland cement clinker can be formed at 1300℃ and 1050℃ respectively in a rapid heating-up process without any mineralizers and with the composite mineralizers of CaF_2, $CaSO_4$ and ZnO. The decomposition temperature of $CaCO_3$ increases with increasing the rate of heating-up.In rapid burning,the crystal defect amounts of nascent state CaO is higher, crystal structure is more loose, CaO crystal size is smaller, and CaO crystal has high activity;the crystal size of β -C_2S is smaller,the crystal free energy is higher,the hydrate activity is higher; it decreaseds liquid-phase formation temperature and liquid-phase viscosity, increases the diffusion rate of the particles greatly, decreases the possibility of "aging" of CaO, C_2S, SiO_2 etc before reaction.In a rapid heating-up burning process,portland cement clinker can be formed at a relatively low temperature. This has been explained as due to the processes of clinker formation tending to overlap,thus putting the reaction minerals in the formation process of clinker minerals under a highly reactive state, decreasing activation energy of clinker forming, accelerating greatly the clinker forming rate and lowering the burning temperature.Howerer when F^-,SO_3 and ZnO are introduced into the raw meal,a large amount of intermediate transition phase $3C_3S \cdot CaF_2$ is formed, which melts at 800~1050℃, thus accelerating portland cement clinker formation.

REFERENCES

1. W.Gutt,R.W.Nurse. 6th ICCC(1),p128-134.(China)
2. O.Phillipp,R.Schrader,6th ICCC(1),p386-393.(China)
3. Wang Tiandi,Journal of South China University of Technology,1985,1. p41-51.(China)
4. W.Gutt,M.A.smith,Trans.Brit.Ceram.Soc.66,557(1967),67,487(1968),69,125(1970).
5. М.Х.чебуков,В.А.ньячев. 6th ICCC(I),p342-347.(China)
6. B.C.Rangnekar,V.RG.Srinivasan,V.N.Pai,6th ICCC(I),p365-370.(China)
7. А.А.Пащенко,Е.А.Старчевская,6th ICCC (I),p371-376.(China)
8. U.Ludwig, A.Wolter. 7th Iccc.p109~115 (china)
9. В.И.Багушкин. 《Silicate Thermodynamics》.(China)
10. Lu Zhongyuan,Huang Wenxi,Xu Guangliang, 9th ICCC,New Delhi,India.
11. Huang Wenxi,Xu Guangliang,Lu Zhongyuan,9th ICCC,New Delhi,India.
12. Xu Guangliang,Huang Wenxi,Lu Zhongyuan,9th ICCC,New Delhi,India.
13. T.K.chatter jee etal ,Silicate Industry,XLV(4--5)81(9)171(1980)
14. Huang Wenxi,Ye Qiaoming et al 2ND ISCC Beijing,China Vol.1.p203

DEVELOPMENT OF RADIATION-THERMAL TECHNOLOGY OF CEMENT MANUFACTURE

I G Abramson, A F Valsman, R M Kapralova and N G Fadeyeva

Design and Research Institute of Cement Industry "Giprocement"
St Petersburg, RUSSIA

SUMMARY

This paper presents fundamentals of radiation-thermal (RT) method of cement clinker production which is based on the use of a powerful beam of accelerated electrons as a power source. Results obtained at an experimental plant as to properties of RT-clinkers, chemical-and-technological relationships of RT-clinker formation, as well as to special production equipment are systematized. It is shown that RT-method offers promise for production of super-refractory, electrotechnical and other kinds of special cements.

РЕЗЮМЕ

В представленной работе изложены основы радиационно-термического (РТ) способа получения цементного клинкера, при котором в качестве источника энергии используется мощный пучок ускоренных электронов. Систематизированы результаты, полученные на экспериментальной установке, относительно свойств РТ-клинкеров, химико-технологических взаимосвязей РТ-клинкерообразования, а также специального технологического оборудования. Показана перспективность РТ-способа для получения особоогнеупорных, электротехнических и других видов специальных цементов.

INTRODUCTION

The radiation-thermal (RT) method of cement clinker production based on the use of powerful beams of accelerated electrons as a power source has been proposed in seventies (1). Despite of remote prospects for commercial implementation (mainly, due to insufficient power of accelerators available and a relatively high cost price of power generated by them) the development of the cement technology on the basis of the RT-method was stimulated by the energy and ecological situation as well as by the branch demand for the cement production intensification. The radiation-thermal method ensures practically unlimited power concentration, its introduction into the material volume (for a depth of the electron path) and as a consequence, heating of raw materials up to the clinker formation temperatures in seconds under conditions approximating the adiabatic.

At the initial, laboratory, stage of works kinetic features of RT-clinker formation were studied on up to 20 kW accelerators, as well as main interrelations between the clinker chemical-and-mineralogical composition and structure, power parameters of the clinker formation process and quality of cement obtained (2,3). Reveal of effect of radiation (overthermal) activation of solid-phase interaction in the clinker formation should be related to the main outcomes of these works. This activation - along with the realization of the known advantages of the "rapid burning"-intensifies drastically the process as a whole.

EXPERIMENTAL

For the further development of the RT-technology of cements and other power-intensive products an experimental plant was built in Novosibirsk on the basis of a ЭЛВ-6 commercial accelerator with the electron beam power up to 100 kW (4).

A number of designs of radiation-thermal apparatus (RTA) for clinker production in the electron beam have been tested at this plant. It has been shown experimentally that conveyor designs with material moving perpendicularly to the linear-swept beam do not ensure clinker homogeneity and require surplus (by 50% and more) power consumption. Shaft-conveyor and, particularly, shaft designs of RTA proved to be much effective. They provide for material particle transfer from the surface deep into the radiation zone and, as a result, obtaining a product more homogeneous in properties at minimum power consumption. As applied to the shaft devices, the problems of uniform distribution of raw material and electron flows over the radiation zone surface are solved, interaction of the chemically-active clinker obtained with RTA structural elements is excluded, ozone generation is practically eliminated.

RESULTS AND DISCUSSIONS

Investigations of sequence and progress of mineral formation at raw mix radiation did not reveal any significant anomalies in the mineralogical composition of clinkers and intermediate products as against the traditional thermal burning. The differencies are observed only in kinetics of the processes which results from different heating rates. At high radiation intensities and, respectively, heating rates the RT-clinker formation processes are shifted to the area of higher temperatures. The temperature shift is observed more distinctly at heating ra-

tes above 50 K/s though under conditions of the radiation-thermal treatment it is less than at a similar variation in the heating rate in case of the rapid thermal burning. The material holding at the maximum temperature after completion of radiation practically always promotes the more complete running of the clinker formation processes. On the other hand, the high-speed clinker cooling after this holding completely eliminates such unpleasant phenomenon as alite decomposition.

Conditions of high-rate heating of raw mix by electron beam with subsequent (for some minutes) material holding at a high temperature followed by rapid clinker cooling after its grinding are realized effectively in shaft RT-apparatus. Therewith, the heating rate is determined by the electron beam current density, and the holding time - by the height of the clinker block formed in the shaft.

In studying chemical-and-technological relationships of the RT-clinker formation at the shaft-type apparatus it has been confirmed that limit of free lime content in RT-clinkers safe from the point of view of soundness is 3.0-3.5%. At the same time, clinker with f-CaO of 1.7%, burnt in the kiln, did not withstand the soundness test. Clinkers with f-CaO content up to 2.5-3.0% feature, as a rule, high strength (45 - 59 MPa after 28 days of hardening). The low-lime clinkers with KH (LSF) = = 0.83-0.86 have a higher hydraulic activity at the age of 28 days (46--53 MPa) and a good rate of the strength gain at the early stages. Comparison studies of strength characteristics of clinkers obtained from one and the same raw mix in the rotary kiln and by the RT-method and containing similar amounts of f-CaO have shown that the activity of the latters at all hardening ages exceeds (by 5-15 MPa) the activity of clinkers from the rotary kiln.

Revealed in laboratory experiments phenomenon of "overirradiation" characterized by decrease in RT-clinkers activity with appearance at microsections of melt zones with large acicular crystals of alite measuring up to 200 μm and more takes place for clinkers produced in a shaft-type apparatus. At the same time, the decrease in activity is observed when a major part of the section area has a structure of "melted" clinker, and the maximum size of alite crystals may be as high as 700 μm and more. Thus, traces of alite decomposition and its solution in the intermediate material as well as secondary belite are fixed sometimes.

The relationship between the clinker activity and their free lime content has an extremal nature with maximum of activity being observed at different f-CaO content according to the absorbed dose power. The activity decrease observed at f-CaO content of 1.8% (for the dose power P = 60 kGr/s) and f-CaO = 0.8% (for P = 110 kGr/s) is in good correlation with the petrography data in compliance with which these samples have every indications of clinker "overirradiation".

The interrelation between the activity of RT-clinkers obtained at the experimental plant and their alite content is linear and rather strong for clinkers having no signs of "overirradiation". With increase in alite content (up to KH (LSF) = 0.95) activity of these clinkers increases by 10-20 MPa at all hardening ages. With occurrence of "overirradiation" adversely affecting both the energy and strength characteristics the influence of the chemical and mineralogical composition on

clinker activities decreases sharply.

Experience gained at the experimental plant was drawn on in designing a demonstration process line on the basis of the USSR most powerful commercial accelerator "Fakel" with a design power of electron beam up to 500 kW and electron energy up to 1 MeV. The line comprises: RT-apparatus of a shaft type with a capacity of up to 400 kg/hr, three-stage suspension preheater, roll crusher for clinker block, cooler as well as equipment for raw mix and finished product conveying. The line erection is suspended because of financial difficulties.

It has been shown experimentally that the use of electron beams for carrying out the high-temperature synthesis of ceramic compounds, abrasives, special glasses, catalysts and so on has good prospects for future. Economically effective production of complex oxide materials forming the basis for obtaining ceramics with unique characteristics has been organized at the experimental plant.

One of the promising directions is the use of the radiation-thermal treatment for obtaining super-refractory, electrotechnical and a number of other kinds of special cements for synthesis of which temperatures higher than for production of ordinary portland cement are required and heavy demands are placed on the product purity.

Thus working out of the radiation-thermal method of cement clinker manufacture has stimulated the development of a new effective direction in high-temperature inorganic technology allowing for obtaining various materials hard-to-synthesize by other methods.

CONCLUSIONS AND RECOMMENDATIONS

A radically new, radiation-thermal method of cement manufacture has been developed and tested at an experimental plant. The advantages of the RT-technology based on it are as follows:

- complete obviation of the process need for a natural organic fuel;
- improvement in cement strength and special properties;
- substantial reduction of dust formation and hazardous gas emissions into the atmosphere;
- considerable decrease in equipment metal intensity and size, as well as in operation area;
- possibility of producing a valuable by-product, i.e. high-concentration carbon dioxide.

It is rather difficult to conduct a thorough economic comparison between cement manufacture by the RT-method and by the up-to-date dry process. Laying the investment aspects aside, we will try to assess the part of the operating expenses which is accounted for by power costs. It is the major portion of the operating expenses.

Calculations show that with a beam power utilization factor equal to 75-80% which is achievable for RTA of a shaft type, and the same (75-80%) clinker and CO_2 heat content utilization degree, specific energy consumption (only power in the RT-technology) will make up 900 kWhr/

/t cl. = 3240 kJ/kg cl. When compared to a dry process kiln with specific fuel consumption of 125 kg ref.fuel/t cl. = 3666 kJ/kg cl. and specific power consumption of 40 kWhr/t cl. = 144 kJ/kg cl., the physical saving in the power consumption in case of the RT-technology will be 570 kJ/kg cl. But at present the share of thermal power stations in electric energy generation is rather high, even if different in different countries. And the above physical saving in power consumption with the RT-technology can turn for a national economy on the whole into overconsumption of fuel as compared to the dry process technology.

Based on the above values of specific power consumption and on the thermal power station efficiency of 40%, the share η of thermal power stations in the electric energy balance, at which the RT-technology will become economically competitive, could be determined from the equation below:

$$\frac{(3240 - 144)\eta}{0.4} = 3666 \text{ kJ/kg cl.}$$

We obtain $\eta = 47.3\%$. Thus, with all the advantages listed above the RT-technology of ordinary cement types will become competitive in relation to the up-to-date dry production process there and then, where and when the share of thermal power stations in the electric energy generation is below 50%. Because of this, it is advisable to orientate the first pilot plants towards manufacture of expensive special cements by RT-method.

However, in ecological respect the RT-technology even today, if it were mastered under commercial conditions, would be beyond compare. It should be borne in mind that year after year the environmental control requirements on industrial production will become more stringent resulting in respective increase in expenditures for environmental protection measures as well as in a higher product cost. One of global problems consists in suppression of the hothouse effect caused by increased carbon dioxide generation. This is responsible for tendencies towards restrained introduction of new thermal power stations and fuel-consuming productions.

Due to these factors the RT cement technology can be asked for as an inevitable alternative to the classical one in the approaching twenty first century.

ACKNOWLEDGEMENTS

The authors would like to record their thanks to the participants of experimental work, employees of Engineering-technological Center PTT S N Fadeyev, S Ye Petrov, M G Golkovsky, A I Korchagin, as well as to Dr. Yu V Nikiforov, deputy director of Giprocement, Prof. G B Yegorov, Prof. A N Skrinsky, director of the Institute of Nuclear Physics in Novosibirsk, Dr. G A Spiridonov, deputy director, Profs. R A Salimov and V L Auslender, chiefs of laboratories, for their permanent assistance and discussion of results.

REFERENCES

1. Abramson, I.G., Volkonsky, B.V., Danushevsky, S.I. et al.: "Radiatsionno-khimichesky sposob polucheniya tsementnogo klinkera" ("Radiation-chemical method of cement clinker production"), Tsement, 1976, (9), 6-7.

2. Abramson, I.G., Vaisman, A.F., Voronin, A.P. et al.: "Osobennosti formirovaniya i teknicheskikh svoistv portlandtsementnogo klinkera v mostchnykh potokakh uskorennykh elektronov" ("Features of portland cement clinker formation and technical properties under powerful flows of accelerated electrons"). Zhurnal fizicheskoi khimii, 1984, 58(5), 1100-1103.

3. Yegorov, G.B., Vaisman, A.F., Kapralova, R.M. et al.: "Issledovaniya protsessa klinkeroobrazovaniya v potokakh uskorennykh elektronov" ("Investigation of clinker formation process in flows of accelerated electrons"), Tsement, 1982, (1), 14-18.

4. Abramson, I.G., Vaisman, A.F., Kapralova, R.M. et al.: "Experimentalnaya ustanovka dlya issledovaniya i tekhnologicheskoi otrabotki radiatsionno-termicheskikh protsessov na baze uskoritelya ЭЛВ-6" ("Experimental plant for study and technological development of radiation-thermal processes on the basis of ЭЛВ-6 accelerator"), Vth All-Union Conference on Industrial Application of Charged Particles Accelerators, Moscow, 1985, 72-73.

EVALUATION OF RADIATION SYNTHESIZED CLINKER

S K Handoo*, George Samuel*, R K Goswami*, I G Abramson** and Yu V Nikiforov**

*National Council for Cement and Building Materials
New Delhi, INDIA
**Giprocement, St Petersburg, RUSSIA

SUMMARY

An attempt has been made to study the possibility of cement clinker synthesis from two industrial raw mixes, one from a hard to dissociate dolomitic limestone and the other having higher reactivity. Clinkers from these mixes were produced using an electron beam from an ELB-6 accelerator in a shaft type radiation thermal apparatus. The results of physico-chemical tests on these clinkers show a rather high 28-d strength and a good rate of strength development at an early age. Petrographic and X-ray phase analyses of different clinker samples reveal them to be of improved quality. Hydration studies indicate a similar behaviour to that of a conventional cement. It is concluded that the radiation-thermal method can be successfully employed to obtain high quality clinker even from less reactive raw mixes.

INTRODUCTION

The developments in the field of high temperature mineral processing by electron beam accelerators have led to the successful radiation synthesis of cement clinker (1-3) besides many other applications. It has now been established that at an absorbed dose power of 20-40 Mrads complete clinkerization of a cement raw mix is achieved in a few seconds compared to about 40 minutes in a modern dry process plant (4, 5).

The studies reveal that cements produced from radiation synthesized clinker achieve strengths which are higher than those from cements with comparable phase composition but prepared by the normal process (6). Keeping in view the typical features of this technology complete elimination of natural fuel, reduction in dust generation and emission, reduction in dimensions and specific amount of metal per unit capacity, high quality cement produced, it is likely to be a futuristic technology for cement manufacture especially for special cements requiring very fine process control (7).

The present paper reports investigations carried out on two industrial raw mixes, one hard and the other a soft to burn, processed by radiation synthesis. The resulting clinkers/cements have been evaluated for phase composition, granulometry and physical properties.

EXPERIMENTAL

Selection of Raw Materials

Two industrial raw mixes, one based on less reactive, coarse grained, dolomitic limestone and the other having high reactivity because of carbide sludge ($\backsim$30%) were selected for the studies. The raw mixes were mixed with coal ash equivalent to actual ash absorption in order to bring the overall composition close to actual clinker composition.

Mineralogical Characterisation

X-ray diffraction analysis of the materials was carried out on DPOH-3 X-ray Diffractometer and DTA/TGA was performed on Q-1500 Derivatograph.

Clinkerisation

The powdered raw mix was clinkerized by using 100 KW electron beam accelerator (ELB-6) at the pilot plant facility of Giprocement at Novosibirsk (Russia). The clinker was produced in a shaft type radiation thermal apparatus, in batches of about 4 kgs by irradiating the raw mix for about 10 seconds. The beam current was 30 mA, average current density 40 $\mu A/cm^2$, the electron energy 1.2 Mev and the power of absorbed dose 8-9 Mrad/s. While the present experiment was carried out in a batch process, it is possible to produce 11-12 tph of clinker in a continuous process by using electrom beam accelerator of 10 MW (8). Actual thermal efficiency of the process can be established only after such full scale trials.

Evaluation of Clinker and Cement Properties

Clinker morphology and microstructure were studied using Zeiss polarising microscope and Philips EM-301 electron microscope. Semi quantitative estimation of major clinker phases was performed by XRD and

microscopic study. Clinkers were ground with 5% gypsum and physical properties of resultant cement were determined according to IS:4031 and GOST 310-76

RESULTS AND DISCUSSION

The chemical analysis of two raw mixes (Table 1) show that the mix RM-2 has a lower LOI value. The reason for this becomes clear with the consideration of XRD analysis (Fig. 1), which shows this mix containing high amount of portlandite, dissociating at 520°C (DTA, Fig.2). As the

Table 1

Chemical Composition of Raw Mixes and Clinkers

Raw Meal/ Clinker	LOI %	CaO %	SiO_2 %	Al_2O_3 %	Fe_2O_3 %	MgO %	CaO_f %	Residue % on 80 µm	200 µm
RM-1	34.26	41.34	14.24	3.01	2.60	3.10	-	9.0	0.5
RM-2	31.35	45.21	14.60	4.14	1.50	2.01	-	2.0	0.08
Cl-1	-	62.50	21.60	4.71	4.95	4.83	0.60	-	-
Cl-2	-	65.92	21.80	6.08	2.41	3.12	0.71	-	-

CaO_f = Free lime

lime liberated from the dissociation of portlandite is known to be more reactive than the lime liberated by dissociation of calcite, this mix can be categorised as soft burning. On the other hand, the mix RM-1 contains difficult to dissociate dolomite and less reactive α-quartz (XRD, Fig.1). Petrographic examination shows that the limestone is very coarse grained, average size of calcite and quartz being about 800-900 µm, with maximum grain sizes going upto 1200 µm. Such a material poses multiferious problem in processing i.e in grinding as well as in burning of the material.

Clinkerisation was achieved by irradiation of the material to high energy (1.2 Mev) beam of electrons in ELB-6 electron accelerator. In this process, the material temperature is raised to clinkerisation in a matter of few seconds and the process is normally over in 8-10 seconds. Experiencing the difficulties in burning of RM-1 initially, the material temperature

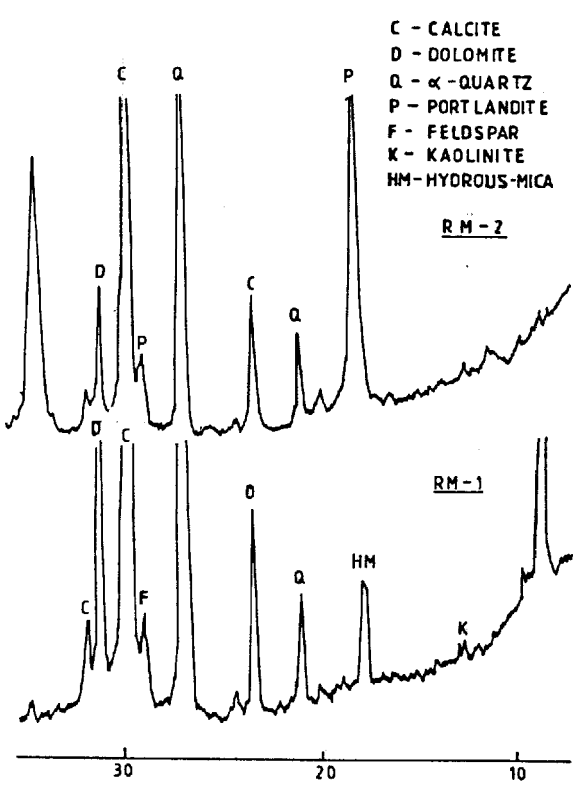

Fig 1 X-Ray Diffractogram of Raw Mixes RM-1 and RM-2

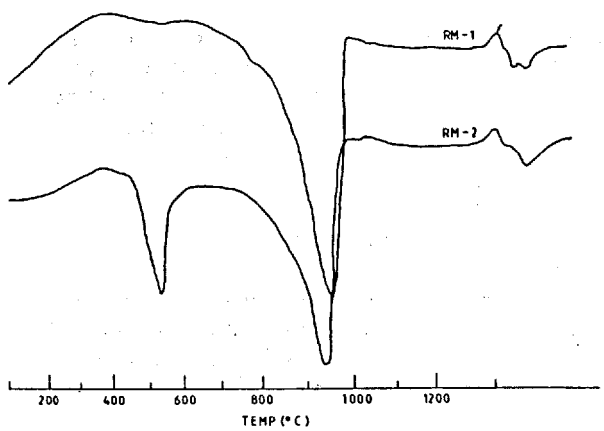

Fig 2 DTA Curves of Raw Mixes RM-1 and RM-2

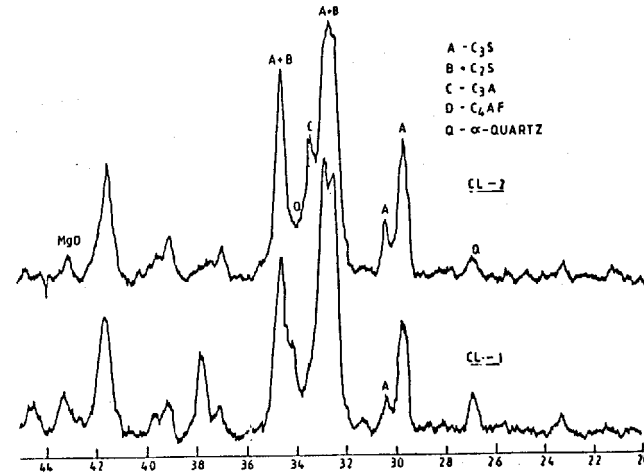

Fig 3 X-Ray Diffractogram of Clinkers CL-1 and CL-2

was raised upto 1600°C. This resulted in the formation of excess melt and facilitated clinkerisation. However, the macro-inhomogenities, like areas of excessive melt content were noticed in the processed material on visual examination. Chemical and XRD analysis (Table 1, Fig.3) of the clinkers revealed completion of clinkerisation and adequate development of clinker phases. Semi-quantitative estimation of phases by XRD and microscopy are in good agreement (Table 2). The average grain sizes of alite and belite are slightly on the low side, which made the phases hydraulically more active.

Table 2

Semi-quantitative Estimation of Clinker Phases

Clinker	Optical Microscopy			XRD			
	Alite (%)	Belite (%)	Interstitial Matter (%)	Alite (%)	Belite (%)	C_3A (%)	C_4AF (%)
Cl-1 (RM-1)	49 (13 μm)	31 (10 μm)	20	52	30	4	11
Cl-2 (RM-2)	55 (16 μm)	25 (12 μm)	20	57	23	8	5

Scanning electron micrographs of the two clinkers show (Fig.4) very well developed and uniformly distributed silicate phases. The alite has sharp grain boundaries and rhombohedral shapes. Elongated lathe shaped grains of alite are noticed sparingly, particularly in the areas of high melt content. Belite grains are seen with characteristic round shapes and striations indicating higher temperature of clinkerisation. The grain size distribution falls in the close range of 10-15 μm. These microstructural features are at a variance with the other industrial clinkers, which normally have alite in distorted hexagonal shapes and belite shapes are undefined.

Table 3

Physical Properties of Cement

Cement	W/C ratio	Fineness cm^2/g	Compressive Strength (kg/cm^2) 3-days	7-days	28-days
CEM-1 (C1-1)	0.4	3300	300	360	470
CEM-2 (C1-2)	0.4	3200	238	360	476

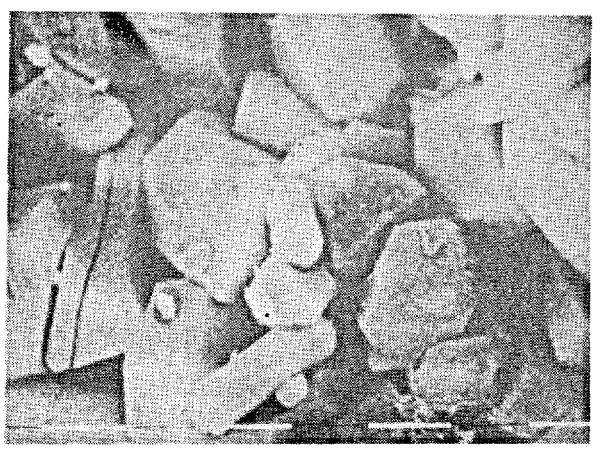

(a)

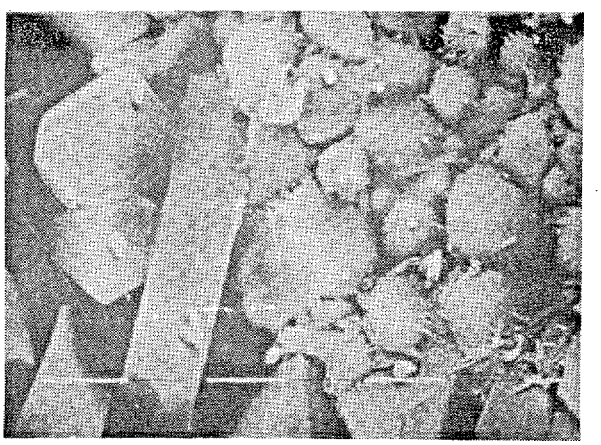

(b)

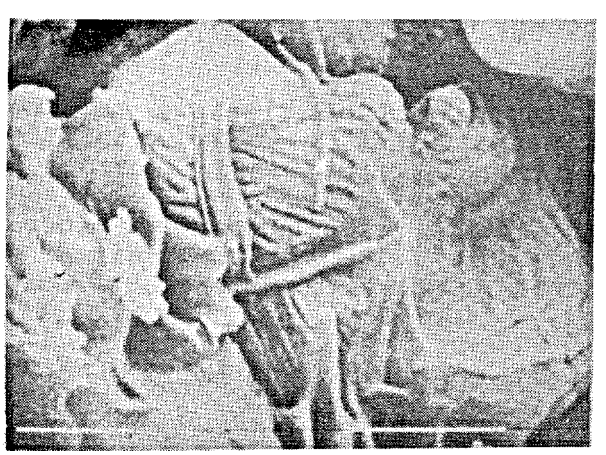

(c)

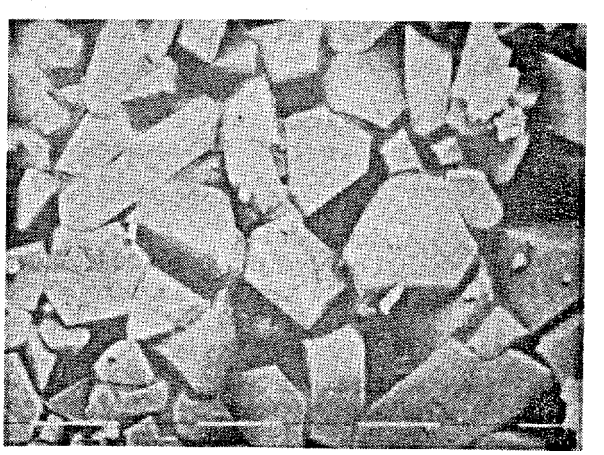

(d)

Fig.4 Scanning Electron Micrographs of Radiation Synthesized Clinkers Showing :

a : Well formed alites (bar 10 μm)
b : Elongated Alites and a Belite Cluster (bar 10 μm)
c : Twinning of Belite (bar 10 μm)
d : Well formed Alites (bar 10 μm) of different sizes

Physical characteristics of the cements made by these clinkers are reported in table 3. The values of compressive strength at various ages are on higher side of those for normally prepared cements of comparable phase composition. The cements have also passed the soundness test.

CONCLUSIONS

The investigations carried out reveal that radiation thermal method makes it possible to obtain high quality clinkers even from hard burning raw mixes based on coarse grained dolomitic limestones.

The physico-mechanical properties of the clinkers produced by shaft type radiation thermal system show that these gain higher early strength and also have rather high 28-day strength.

ACKNOWLEDGEMENT

The authors have freely drawn upon completed R&D work/status reports of NCB. The authors are thankful to Director General NCB for permitting to publish this paper. The authors are also thankful to Director and Mr A F Vaisman of Giprocement, for extending necessary co-operation to process the raw mixes.

REFERENCES

1 US Patent 4178219 Dec. 1979. Method for producing mineral binder.

2 I G Abramson, et.al.: "Peculiarities of formation and technical properties of portland cement clinker obtained in powerful beam of accelerated electrons". Jour. Phy. Chem., USSR Accad. of Sc., 1984, 38(5), 1100-09 .

3 I G Abramson, et.al.: "Clinker formation in high energy flux of accelerated electrons", **7th Int. Cong. Chem. of Cem. Paris**, 1980, V II, 26-28.

4 I G Abramson, et.al.: "Study of properties of clinkers obtained from Indian raw mixtures at experimental plant 'clinker' with ELB-6 Electron Accelerator", 1989, (Giprocement, unpublished report).

5 S K Handoo and R K Goswami : "Application of electro beam process technology for production of cement". **Indo USSR Seminar on Industrial Application of Electron Accelerators, BARC, Bombay,** 1988, V II, 118-126.

6 S J Raina and R K Goswami: Report on tour to USSR, 1987 (NCB unpublished report).

7 S J Raina, R K Goswami and G Samuel: "Radiation synthesis of cement clinker". **Proceedings of 2nd NCB International Seminar on Cement and Building Materials,** 1989, V II, TS V, 45-53.

8 S K Handoo and G Samuel : Report on tour to USSR, 1988 (NCB, unpublished report).

KINETICS OF THE RADIATION-THERMAL C_2S SYNTHESIS

G B Yegorov, B K Kanimov and G V Shkatova

Petersburg Institute of Transport Engineers
Moskovsky, St Petersburg, RUSSIA

SUMMARY

This paper presents results of laboratory investigation in the radiation-thermal synthesis of calcium orthosilicate. Investigations have shown that the diffusionally controlled kinetics of C_2S synthesis under radiation-thermal conditions upon the action of electronic radiation includes three activation mechanisms: thermal, radiation-thermal and one connected with the polymorphic transformations of the reaction product.

АННОТАЦИЯ

Представлены результаты лабораторного исследования радиационно-термического синтеза ортосиликата кальция. Показано, что диффузионно контролируемая кинетика синтеза C_2S в радиационно-термических условиях под действием ускоренных электронов включает в себя три механизма активации: термический, радиационно-термический и связанный с полиморфными превращениями продукта реакции.

INTRODUCTION

The rate of C_2S synthesis from corresponding oxides is limited by the calcium ions transportation through a layer of the reaction products and can be described by the equation

$$d\alpha/dT=K_1(\alpha)K_2(T). \quad (1)$$

The constant of action $K_1(\alpha)$ is connected with the morphology of the mixture. The temperature constant $K_2(T)$ for a diffusionally controlled solid phase reaction (DCSR) has the sense of a parameter determining the defect concentration C of the ionic subsystem in the layer of reaction products. At thermal synthesis (1), according to the Bolzman distribution, will appear as

$$d\alpha/dT=K_1(\alpha)C_T(T,E_d), \quad (2)$$

where E_d is the activation energy of defect formation. Under radiation-thermal conditions (electronic radiation of P>10kGr/s, temperature T>1000K) the defect generation will be determined both by thermal and radiation-thermal (RT) defect formation which supposes a superthermodynamic defect generation in the result of interaction between the radiational and thermal excitations. The concentration of energetic disequilibriums as a function of the kinetic energy E_o of a primary electron to a certain level E is determined by the degradational spectrum Z(E). Thermal excitations in the range of energies from kT to E_d are discribed by the Bolzman distribution $f(E_d,T)$. The probability of the defect formation at a temperature T can be found from the densities convolution of these functions

$$P(E)=i\int_{kT}^{E_d} Z'(E_d-E)f'(E)dE, \quad (3)$$

where "i" is the electron beam density related to the field of the maximum absorbtion of the radiation energy.

The probability of the defect formation according to the RT mechanism is comparable to the thermal one and even exceeds it in the

field close to E_d, is lineary connected with the electron beam density "i" and correspondingly with the power of dose at the obvious P=iZ(E). The closeness of the energetics RT defect formation to the thermal one supposes a higher stability of defects comparably with the low-temperature radiational ones (1). Therefore under RT-conditions the defect concentration will be the sum of point defects of thermal and radiation-thermal nature $[C_T(T,E_d)+C_{RT}(T,P,E_d)]$, while the function of the reaction rate (1) will appear as

$$d\alpha/dT=K_1(\alpha)[C_T(T,E_d)+C_{RT}(T,P,E_d)] \quad (4)$$

or by the electron beam density

$$d\alpha/dT=K_1(\alpha)[C_T(T,E_d)+iC_{RT}(E_d,T,Z\ (E)] \quad (5)$$

at E_0=const the reaction rate will be found to be linearly connected with the radiation intensity.

Kinetics of C_2S synthesis is also connected with another sourse of defect generation - polymorphism of the product layer. Evidently the defect concentration at the moment of polymorphic transformation C_p is at its maximum, and is connected mainly with its intensity in the temperature and time coordinates and is proportional to its depth α_p. In the temperature coordinates the defect formation will be the function of the passage rate of polymorphic transformation temperature interval ΔT_p and the period of the existence of defective structure

$$C_p=dN_p/dT=q\alpha_p/\Delta T_p, \quad (6)$$

where q=dT/dt is the heating rate. Assuming that the polymorphic transformation in the layer of the reaction product will be complited during the time of synthesis, i.e. α_p=1, the rate of DCSR under RT conditions at the heating regime will be

$$d\alpha/dT=K_1(\alpha)[C_T(T,E_d)+iC_{RT}(T,Z\ (E),E_d)+C_p(q,\Delta T_p)]. \quad (7)$$

Evidently q P and the latter member under thermal conditions depends on the heating rate, in RT conditions on the strength of the absorbed dose.

EXPERIMENTAL

According to the above, the kinetics of RT synthesis C_2S in a nonisothermal regime should be characterised by linear dependence of the reaction rate on the intensity of radiation (5); at $d\alpha/dT$=const by sharp activation of interaction (7) within temperatures of polymorphic transformations of the reaction product (β-α'-C_2S at 1160°C, α'-α-C_2S at 1420°C); by some decrease of relation $d\alpha/dT$ with the increase of the strength of dose. The latter is connected with the thermal effects of polymorphic transformations and the reaction itself, in the result of which there appear in the kinetics of the exothermal RT synthesis effects inherent in a thermal process.

Hence follow the requirements for the methodical assurance of experiments on the investigation of the kinetics of RT synthese of C_2S: constant registration of the transformation degree and temperature in the specimen with time resolution not less than 30-40% and 200°C per second. For these purposes there were specially developed instruments and methodics of dilatometric registration of the transformation degree of C_2S by the changes of linear dimension of specimen (1). A reliable diffusional control of the reaction was ensured by the large size (30-40 mm) of the covered component - crystobalite - and small size (2-6 mm) of calcium oxide.

RESULTS AND DISCUSSIONS

Nonisothermal kinetics of the RT synthesis of C_2S at P=120 kGr/s is shown in Fig.1, its approximation of the Coates-Redfern function in Fig.2. There is twice traced the division of ourves into two parts, one of which is independent of temperature, while the other depends on it. The first part corresponds to the synthesis activated by polymorphic transformations according to (7) at temperatures 1150-1180°C and 1400-1450°C. The second part, in the intervals between these temperatures, corresponds to the radiation-thermal synthesis where the reaction rate according to (5) linearly depends on the strength of dose(Fig.3). The thermal component determines the decrease of relation $d\alpha/dT$ with the increase of the heating rate for greater depth of interaction (Fig.1 a). The exothermal nature

of the reaction of the polymorphic transformation causes a self-heating of the specimen and results in the decrease of the radiational part of energy in the specimen heating and in the decrease of the relations "strenght of dose-temperature" and "radiative-thermal - thermal defect concentration". The self-heating also causes the prevalence of thermal mechanism in the diffusional mass transplantation; under RT conditions $d\alpha/dT=const$, since according to (5) the defect generation is proportional to the intensity of radiation.

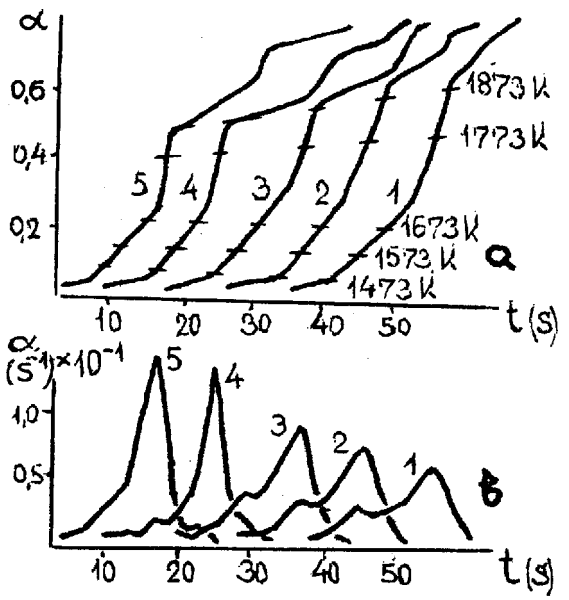

Fig.1. Nonisothermal kinetics of the C_2S synthesis (a) and its rate (b) at the stregth of absorbed doses (kGr/s) : 1-40, 2-64, 3-80, 4-104 and 5-120 kGr/s.

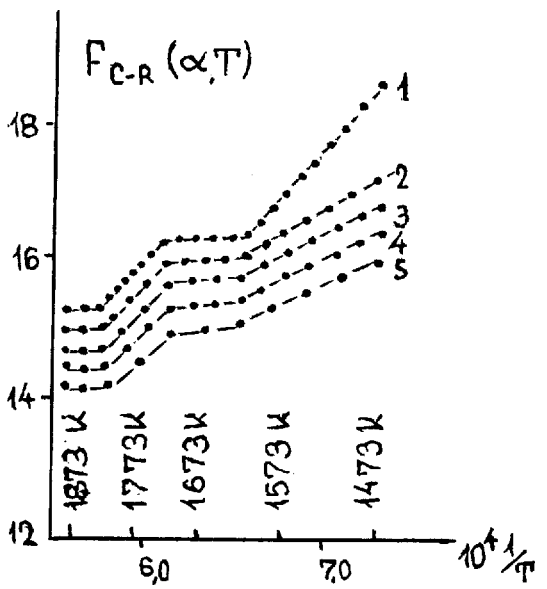

Fig.2. Approximation by the Coates-Redfern function of the kinetics of C_2S synthesis at the same strength of absorbed doses.

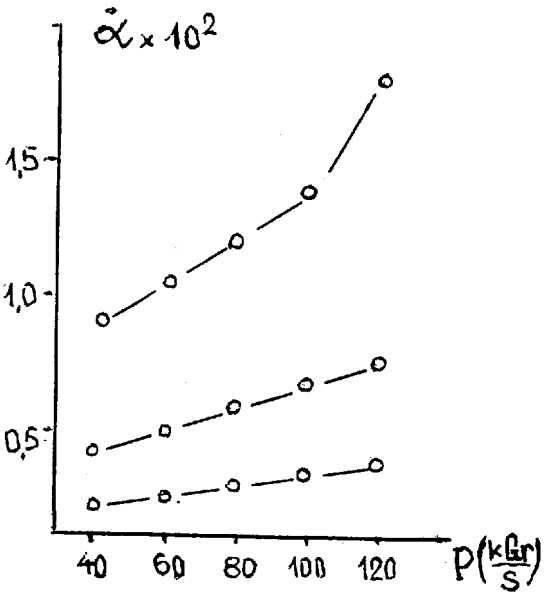

Fig.3. The dependence of C_2S synthesis rate on the strength of the absorbed dose at T=1573K (1), 1673K (2) and 1773K (3).

CONCLUSION

Thus it can be stated that the diffusionally controlled kinetics of C_2S synthesis under radiative-thermal conditions upon the actions of electronic radiation actually includes three activation mechanisms: thermal, radiative-thermal and one connected with the polymorphic transformations of the reaction product.

The influense of radiational action is determined by the mechanism of radiational-thermal defect formation which, in the coordinates of time, is manifested in the linear dependence of reaction rate on the strength of dose, while in the temperature coordinates - in the decrease of activation energy of the reaction. The formation of point defects by this mechanism is connected with the interactions of the excitation of ionic sobsystem of the solid body lattice of radiational and thermal nature in the temperature region of effective thermal defect formation.

The accelerating of interaction at the moment of polymorphic transformation is connected with the increase, dependent of the heating rate, of the point defect concentration in the layer of reaction product and the increase of diffusional mass transfer. The value of activation is determined by the physico-chemical characteristics of polymorphic transformation. At this stage of reaction the radiational influence on the kinetics of synthesis is negligible.

In the temperature intervals between polymorphic transformation the rate of interaction is determined by the strength of the absorbed dose, while the equiponderous in temperature the degree of transformation at low values does not depend on the intensity of radiation. At deep interaction and great strength of dose there is manifested the thermal mechanism of mass transport in the form of characteristics decrease of the transformation degree with the increase of the heating rate (strength of the dose). The size of decrease is determined by the value of exothermal reaction effect and of polymorphic transformation.

REFERENCES

1. Boldyrev, V.V., Kanimov, B.K. etc.: "Radiation-thermal activation of diffusion controlled solid phase reactions", The Transactions Ac.Sc.USSR, Siberian Dep., Chemical Sc.ser., 1988, 6, 3-9.

CLINKERISATION THROUGH MELTING—A NEW APPROACH

S A Khadilkar, P G Lele, C H Page and A K Chatterjee

Research and Consultancy Directorate
The Associated Cement Cos Ltd
Thane, INDIA

SUMMARY

The technological status for the cement is a fast changing one, where innovations in both software and hardware are being made in order to achieve an overall reduction in capital and operating costs. In this perspective, The Research and Consultancy Directorate of The Associated Cement Cos.Ltd., has carried out investigative studies to evaluate the feasibility of adopting the melting process for clinkerisation purposes.

In this technique, the secondary crushed raw materials without further grinding and homogenisation are taken for clinkerisation. The secondary crushed size of raw materials (4.0 - 6.0 mm) were taken in appropriate proportions of the cement raw mix and melted in an induction furnace. The melted product (the clinkerised mass) obtained was evaluated for its chemical properties, mineralogical phase - assemblage and its hydraulic characteristics.

While developing this technique, clinkers were produced from different raw material and correctives in use at various cement plants in our country. The paper presents the characterisation of these clinkers and further attempts to evaluate the feasibility aspects of this new technique.

INTRODUCTION

In tune with the global trend of achieving reduction in power/energy costs, The Research and Development Division of ACC - RCD, Thane, India, had carried out a number of investigative studies to evaluate the feasibility of some innovative approaches in cement manufacture. "The clinkerisation through melting" was one of such projects which had shown substantial potential towards achieving the objective of reduced capital and operating costs in cement manufacture.

This paper discusses the melting technique and presents the chemico-mineralogical, physico-mechanical and hydraulic characteristics of the clinkers produced. The paper also attempts to evaluate the feasibility aspects of the new technique and gives the possible merits of this approach.

EXPERIMENTAL WORK

Technique Adopted

In this technique, the secondary crushed raw materials of size range 4-6 mm,without further grinding and homogenisation were taken in appropriate proportions of a cement raw mix and melted in the graphite crucible (backed up with magnesia lining) of an induction furnace at a temperature range of 1700°C - 1800°C. The molten clinkerised mass was maintained in the molten condition for 15-20 minutes and then tapped out in a clay graphite crucible (air quenching) and cooled with compressed air. For aqueous quenching, the molten clinkerised mass was cooled in cold water.

RAW MIX AND MELT PREPARATION

Seven raw mixes (Raw Mix-1 to Raw Mix-7) were prepared by using different limestone and correctives. The chemical composition of raw materials used is given in TABLE 1

TABLE - 1 CHEMICAL COMPOSITION OF RAW MATERIALS

Raw Materials	SiO_2	Al_2O_3	Fe_2O_3	CaO	MgO	LOI	Na_2O	K_2O	SO_3	Cl	TiO_2	Total Carbonate	Free Silica
Limestone-A	14.2	3.4	2.1	42.8	1.3	34.7	0.21	0.80	0.1	0.01	0.2	77.5	7.1
Limestone-B	14.2	3.4	1.9	42.9	1.4	34.6	0.21	0.90	0.1	0.01	0.2	77.9	8.3
Limestone-C	10.0	4.0	1.4	44.9	2.1	37.0	0.09	1.20	0.1	0.01	0.3	81.0	5.8
Limestone-D	7.4	2.6	1.0	48.0	1.0	39.2	0.02	0.51	0.1	0.01	0.2	85.3	3.8
Limestone-E	14.2	3.5	1.7	42.3	1.8	34.9	0.21	0.91	0.1	0.01	0.2	77.5	7.4
Limestone-F	17.8	3.8	2.3	37.9	2.6	33.4	0.11	0.93	0.3	0.01	0.3	70.6	11.2
Limestone-G	1.6	0.7	0.2	53.8	0.3	43.1	0.02	0.03	0.2	0.01	0.2	97.0	-
Limestone-H	11.2	2.5	2.0	43.8	2.1	36.8	0.11	0.74	0.3	0.01	0.2	82.0	6.9
Limestone floatation rejects	59.8	4.6	1.1	18.2	1.0	13.8	0.37	1.0	0.1	-	-	32.5	-
Sandstone	85.6	5.7	1.9	0.7	0.4	1.2	0.52	3.0	0.2	0.01	0.2	-	78.5
Quartzite	98.5	0.7	0.1	0.1	0.1	0.2	0.04	0.18	0.1	0.01	-	-	97.5
Bauxite	17.4	40.3	16.8	1.2	0.4	22.8	0.02	0.04	-	-	-	-	-
Laterite	16.5	10.4	52.8	4.0	0.6	14.1	-	-	-	-	-	-	-
Iron Ore	-	-	90.0	-	-	-	-	-	-	-	-	-	-
Basalt	45.4	16.2	14.5	9.4	1.8	2.6	0.9	1.2	0.2	-	0.4	-	-

conditions in the clinkers were very much different from the targeted values (TABLE 3). The free lime in clinkers was observed to be in the range of 5.0-6.2%. The XRD patterns of these clinkers (Fig.1) indicate differences in mineral phase assemblage, peak intensities and position as compared to the clinkers produced by sintering route. One of the causes reported (Ref.2) for such observed changes in XRD pattern are due to the

TABLE 3 - CHEMICAL COMPOSITION OF CLINKERS PRODUCED BY MELTING TECHNIQUE

	SiO_2	Al_2O_3	Fe_2O_3	CaO	MgO	Free CaO	LSF	M_s	M_A	Potential Phases C_3S	C_2S	C_3A	C_4AF	Liquid at 1450°C	Bond Grindability Index Kwh/Sh.T
Clinker-1	22.8	6.5	0.1	62.1	8.0	5.0	0.82	3.45	65.0	15.1	54.0	17.1	0.3	21.7	12.4
Clinker-2	23.8	5.5	0.1	65.0	4.9	6.2	0.860	4.25	55.0	21.1	52.3	14.4	0.3	18.7	12.0
Clinker-3	25.8	6.1	0.2	66.2	1.2	5.4	0.804	4.1	30.5	9.9	66.5	15.8	0.6	20.8	12.4
Clinker-4	24.2	7.0	0.2	66.7	1.3	5.5	0.840	3.36	35.0	17.6	56.1	18.2	0.6	23.5	12.4
Clinker-5 Air & Aqueous quenched	23.5	6.5	0.2	64.6	4.6	5.5	0.840	3.51	32.5	17.8	54.0	16.9	0.6	22.0	12.0
Clinker-6	23.2	6.1	0.1	66.9	2.9	6.0	0.891	3.74	61.0	30.2	43.7	16.0	0.3	20.5	12.0
Clinker-7 Air & Aqueous quenched	23.3	6.3	0.1	65.5	4.2	5.6	0.866	3.64	63.0	24.0	48.7	16.5	0.3	21.0	12.0

change in chemistry of alite under the reaction conditions, where in Al^{+3} enters the crystal lattice of alite with or without MgO. Similar changes in XRD pattern was observed in this study., The microstructural evaluation of the clinkers indicate that the air quenched clinkers have a much coarser crystal size of alite and belite as compared to aqueous quenched clinkers (Fig.2A & 2B).



Fig.2A :Air quenched clinkers showing coarser alite (X 640)

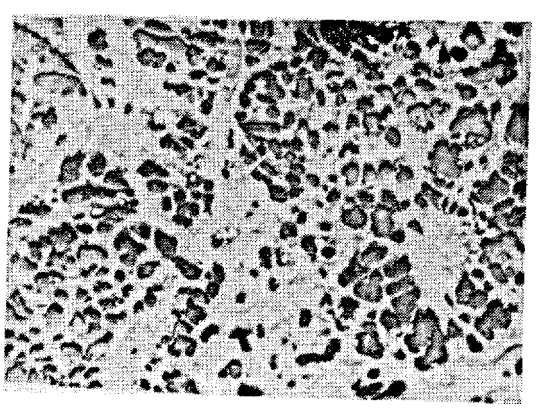

Fig.2B : Aqueous quenched clinkers with fine grained alite(X 256)

In the air cooled clinkers the alite crystals are formed of larger size, with cellular structure, with the interstices filled with eutectic mixture of finer alite and aluminates. The alite and belite crystals appear to be oriented in the direction of flow of the clinker melt. (Fig.3). The microstructural observation also reveal the presence of metallic iron in small amounts. (Fig.4). The microstructural features of these clinkers are very much different from the clinkers produced from conventional route. (Ref.2)

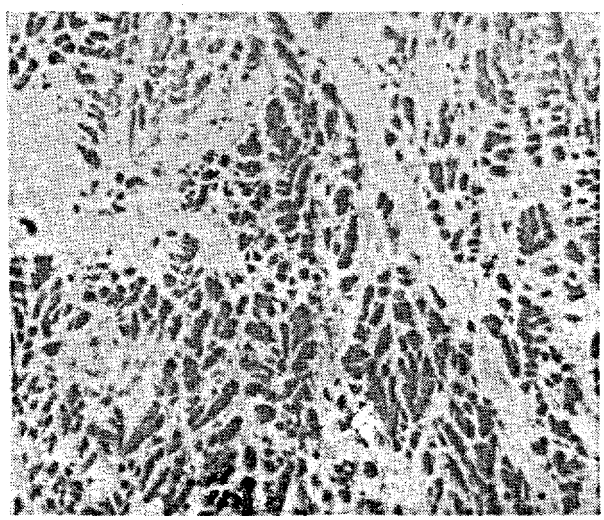

Fig.3: Cellular structure of alite with flow oriented alite & belite(X 256)

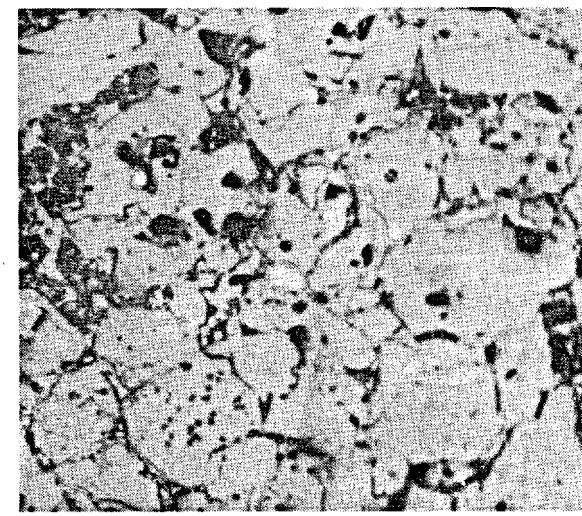

Fig.4: Clinker microstructure showing presence of metallic iron(X 640)

The physical tests of Lab-ground cements, presented in TABLE-4, indicate that the cements show cold expansion of 0.2 - 0.3%. This type of cold expansion is generally observed in cementitious materials used in shrinkage compensation grouts. In these cements, the cold expansion could be attributed to the relatively high free lime and also may be linked with the generation of acetylene gas during hydration of these cements. However, in aerated cements, liberation of acetylene gas was not observed during hydration.

TABLE - 4 COMPRESSIVE STRENGTHS OF LAB-GROUND CEMENTS WITH AND WITHOUT AERATION

Property	Cm-1		Cm-2		Cm-3		Cm-4		Cm-5		Cm-6		Cm-7		Cm-5 (Water quenched Clks)		Cm-7	
	A	B	A	B	A	B	A	B	A	B	A	B	A	B	A	B	A	B
Compressive Strength (kg/cm^2)																		
1 D	35	110	100	160	40	110	45	130	40	130	100	170	80	160	35	100	100	130
3 D	100	195	160	235	100	210	135	200	100	210	185	270	150	235	95	165	165	220
7 D	140	225	210	270	140	210	160	240	135	245	230	320	210	275	165	275	225	310
Cold Expansion in cements without Aeration	0.2		0.2		0.24		0.23		0.30		0.25		0.30		0.2		0.3	

A : Cements without Aeration B: Cements with Aeration

The compressive strengths of the cements prepared from clinkers with potential C_3S less than 20% i.e. CM-1, CM-3, CM-4 and CM-5 (without aeration) at 1-day, 3-days, and 7-days are observed to be in the range of 35-40 kg/cm^2, 100-135 kg/cm^2 and 140-160 kg/cm^2 respectively, while the compressive strengths of cements prepared from clinkers with potential C_3S more than 20% i.e. CM-2, CM-6 and CM-7 (without aeration) for the three ages are observed to be in the range of 80-100 kg/cm^2, 150-185 kg/cm^2 and 210-230 kg/cm^2 respectively.

It was observed that on exposure to atmosphere (aeration) the cements lose their cold expansion property. The aerated cements show improved compressive strengths. In aerated cements, CM-1, CM-3, CM-4 and CM-5 (from clinkers of low C_3S), the compressive strengths, at 1-day, 3-days and 7-days are in the range of 110-130 kg/cm^2, 195-210 kg/cm^2 and 225-245 kg/cm^2 respectively while in the cements CM-2, CM-6 and CM-7, (from clinkers with higher potential C_3S) the compressive strengths at three ages are in the range of 160-170 kg/cm^2, 235-270 kg/cm^2 and 270-320 kg/cm^2 respectively.

The aerated as well as non-aerated cements prepared from water quenched clinkers show relatively higher strengths as compared to the cements prepared from air quenched clinkers.

The strength characteristics after aeration indicates improved hydraulic property even at lower C_3S conditions in the clinkers produced by the melting technique. Further understanding of microstructural features of these clinker melts and its correlation with the hydraulic characteristics is under investigation and may indicate the possible reason for observed results.

CONCLUSIONS

Studies carried out so far by melting technique for producing cementitious materials appears feasible, and few preliminary conclusions can be made as follows:

i) It is possible to use secondary crushed raw mixes of size range 4-6 mm.

ii) Characteristic larger crystals of alite and belite compared to the conventional sintered route.

REFERENCES

1. Iwao Maki, Koji Nakagawa, Kiyoko Hiraiwa, Toru Nonami. "Characterisation of fluorine bearing alite in rapid hardening high strength cement clinker manufactured by fusion". iL Cemento Vol-4, 1984, pp. 165-173.

2. Iwao Maki, "Growth instability and crystaline textures of Alite in Cement Clinker". iL Cemento, Vol-4, 1984, pp. 165-173.

PECULIARITIES OF THE PROCESS OF CEMENT CLINKER FORMATION BY CHANGING THE INTERACTION SEQUENCE OF REACTING COMPONENTS

V D Barbanyagre, V M Shamshurov and T I Timoshenko

Technological Institute of Building Materials
Belgorod, RUSSIA

SUMMARY

Different interaction sequences of alumina, silica, calcium and ferric oxides in their pure form has been studied and modelled. Fifteen variants were obtained and examined. Kinetics of the process, phase composition of the intermediate and final products of firing, clinker structure, the strength of cement stone were studied in our research. The following specific features were established: the possibility to add the whole amount of silica into the melt which increases its amount twice. and lowers the melting temperature to 1130-1180°C and finishes the clinker sintering at 1300°C; the area of the high-based aluminate and silicon solid melts formed on matrix the composition of which is like tricalcium ferrite; the conditions of formation the most hydraulic active phases of cement clinker increasing the strength of cement stone in 1,5-2 times; the possibility to put into practice some variants by using natural raw materials and existing equipment in industrial scale.

АННОТАЦИЯ

На смеси из чистых оксидов кальция, кремния, алюминия и железа смоделирована различная последовательность их взаимодействия. Получено и исследовано 15 вариантов. Изучались кинетика процесса, фазовый состав промежуточных и конечных продуктов обжига, структура клинкера, прочность цементного камня.

Установлено: возможность введения всего кремнезема в расплав с увеличением количества расплава в 2 раза, снижением температуры плавления до 1130-1180°С и завершением спекания клинкера при 1300°С; область образования высокоосновных алюминатных и силикатных твердых растворов на матрице, близкой по составу к трехкальциевому ферриту; условия формирования наиболее гидравлически активных фаз цементного клинкера, повышающих прочность цементного камня в 1,5-2 раза; возможность реализации некоторых вариантов на природном сырье в промышленном масштабе на существующем оборудовании.

INTRODUCTION

It is difficult to explain the fact that at present the influence of tens of admixtures on cement properties and the process of its formation is studied in detail while the mutual influence of the four main oxides on each other remains practically unknown.

EXPERIMENTAL

This paper deals with the attempt to model all possible variants of interaction sequence of reacting components on the basis of pure oxides by heating the cement raw material mixtures. At the same time the interaction of two and three oxides in all possible combinations was accomplished by preliminary firing. Then all the remaining components were added during reheating. Fifteen variants of varying interaction sequence of four oxides have been studied (Table I).

TABLE I.

Variants of Mixtures	Preheated Composition		Components of Remixing
	Type	Composition	
I	two-component	6%Al_2O_3+5%Fe_2O_3	67%CaO+22%SiO_2
2	" "	22%SiO_2 +6%Al_2O_3	67%CaO+5%Fe_2O_3
3	" "	22%SiO_2 +5%Fe_2O_3	67%CaO+6%Al_2O_3
4	three-component	22%SiO_2 +6%Al_2O_3+ 5%Fe_2O_3	67%CaO
5	two-component	67%CaO +5%Fe_2O_3	22%SiO_2+6%Al_2O_3
6	" "	67%CaO +6%Al_2O_3	22%SiO_2+5%Fe_2O_3
7	" "	67%CaO +22%SiO_2	6%Al_2O_3+5%Fe_2O_3
8	three-component	67%CaO +6%Al_2O_3+ 5%Fe_2O_3	22%SiO_2
9	four-component	I7%CaO +6%Al_2O_3+ 22%SiO_2 +5%Fe_2O_3	50%CaO
I0	four-component	67%CaO +22%SiO_2+ 6%Al_2O_3 +5%Fe_2O_3	
II	three-component	67%CaO +22%SiO_2+ 6%Al_2O_3	5%Fe_2O_3
I2	" "	67%CaO +22%SiO_2+ 5%Fe_2O_3	6%Al_2O_3
I3	two-component		mixture I + mixture 7
I4	" "		mixture 2 + mixture 5
I5	" "		mixture 3 + mixture 6

Variant IO presents the raw material mixture taken for the comparison. It was obtained by common method, i.e. by the simultaneous mixing of the initial constituents. In preheated and remixed compositions the oxides have the same proportions as in mixture IO, therefore the chemical composition of the fired ultimate products are similar.

To avoid hydration of calcium oxide grinding and mixture averaging were made in dehydrated ethyl alcohol. In our research X-ray phase, chemical petrographic and physico-mechanical methods of analyses were used.

RESULTS AND DISCUSSIONS

According to Table I fourteen preheated mixtures consisting of two, three and four components were synthesized and examined. It was stated that the following changes had occured, i.e. mutual solid solution of Al_2O_3 and Fe_2O_3 (variant I), ferric-containing mullite and crystobalite were formed (variant 3,4). The formation of the high-based solution unknown before was discovered when heating the mixtures of calcium, alumina and ferric oxides (variant 8), exept aluminates and alumoferrites the composition of which is well-known. The composition of this solid solution is $C_3(A_{0.1}F_{0.9})$ I I I. The formation of one more unknown high-based ferrite phase of limited composition $C_3(S_{0.33}F_{0.67})$ was observed while firing calcium and ferric oxides with silicon oxides (variant I2).

In mixture 9 ferric-containing gehlenite and pseudovollactonite were being synthesized during heating and the low-temperature melt (below I200°C) has been obtained. The amount of the melt formed due to dissolution of the whole amount of silicon oxide is two times as large as the amount of the melt produced by conventional firing technique. The peculiarities, mentioned above, provide the base for the development of the new, so-called two-batch technology, which allows to carry out the process of clinker sintering at the temperature not above I300°C with the fuel saving II-23% I 2 I.

Thus, preliminary firing of the studied compositions gives rise to the formation of the definite chemical combinations and solid solutions of interacting phases. Their influence on the rate of the following reactions, composition, structure and properties of definite phases was being studied in the process of reheating and interaction of the mixtures remixed by the remaining components.

Intencities and interplane space of diffraction peaks in the X-ray patterns of synthesized phases and the amount of non-assimilated calcium oxide and crystobalite in the fired products are critical for estimation the interaction degree of reacting components. The least assimilation of CaO is observed in mixture IO. Preliminary thermal treatment of initial oxides in all studied compositions accelerates the CaO assimilation, i.e. it promotes chemical activation of the components by accelerating diffusion processes and, as a result, the acceleration of chemical interaction occurs.

During the process of preheat treatment chemical activation of the constituents of cement raw material mixtures depends, mainly, on the selected method of preliminary treatment. Therefore, preliminary interaction of alumina and ferric oxides occuring, as stated above, due to the formation of the solid solutions on the base of both phases is the

least desirable variant because it gives the lowest assimilation of calcium oxide. Similar effect causes the preliminary interaction of alumina and calcium oxides (variant 6).

Variants 2,3,4 show the importance of silica component activated by alumina oxide (variant 2), ferric oxide (variant 3) and by both once and once (variant 4). In the process of sintering the mixture prepared according to variant I5 chemical activation is much higher than in variant I4, therefore preliminary interaction of ferric oxide with silica and alumina oxide with calcium oxide but not vice verca is more preferable.

The preliminary interaction of initial oxides in studied variants results in the changes occuring not only in kinetics but in the composition of minerals and subsequence of their formation. So firing of silica with ferric oxides promotes the formation of larger amount of low-temperature melt containing high content of silicon discribed in two-batch technology I 2 I. This explains the higher activity of mixture in variant 4.

According to the structure and hydraulic activity variant 8 appeared to be the optimum one, in which aluminate and alumoferrite phases were formed first and then silicon minerals I 3 I were obtained by subsequent remixing of silica. Clinker microstructure is notable for fine, uniform and very clear crystallization of minerals without any mutual phase inclusions.

Hydraulic activity of clinkers ground with 4 per cent of gypsum in small specimens prepared from cement paste containing 25 per cent of water is shown in Table 2.

TABLE 2

Variants of clinkers	Specific surface, m^2/kg	Compressive strength, Mla, at the age	
		3 days	28 days
I	370	84,5	I43,8
2	360	68,I	I07,2
3	330	88,2	I33,8
4	3I0	88,9	I44,4
5	280	50,0	I38,7
6	360	73,3	I59,4
7	280	82,I	I32,9
8	330	I26,2	I75,2
9	350	57,9	I23,7
I0	3I0	67,3	98,6
II	300	78,5	I29,8
I2	330	77,3	I72,I
I3	280	99,8	I26,3
I4	3I0	84,2	I33,7
I5	320	82,0	I48,9

Preliminary thermal treatment of reacting constituents in different combinations influences substantially on the clinker activity. The compressive strength of cement stone at the age of 72 hours is changing from 50 to I26 Mla, i.e. more than in two times. At the age of 28 days the wide range of strength is observed too. It ranges in the limit of 98,6-I75,2 Mla at high absolute value exceeding the clinker activity obtained by common technology almost in two times when all components are subjected to simultaneous thermal treatment (variant I0). Clinkers of variants 8,I2,6 and 4 exhibited the highest hydraulic activity.

Naturally, not all these four variants investigated in our research can be used at the cement plants because of the dificiency of corresponding component in its pure form. Variants8,9 and 4, however, present definite practical interest.

CONCLUSIONS

I.Preliminary interaction of initial constituents in combinations involved allows sufficiently to change sequence and rate of chemical reactions, synthesis of minerals and, as a consiquence, to control the structure and hydraulic activity of clinker phase.

2.The results obtained in our experiments having modelling character allow to find technological methods of cement clinker formation ensuring fuel saving (variant 9), higher quality of cement (variant 8) or combination of these factors (variant 4).

3.The established regularities can be used both for improvement of existing technology of clinker sintering and for the development of the new methods of cement production.

4.There exists the principle possibility to realize some variants (4,8,9,I2) using natural raw materials in production scale and the equipment in general use.

REFERENCES

I. Барбанягрэ В.Д., Шамшуров В.М. Превращение алюмоферритных фаз и свойства клинкера //Труды НИИЦемента.-М., I988.-Вып.97.-С.62-67.

2. Барбанягрэ В.Д., Шамшуров В.М., Киринкина О.А., Тимошенко Т.И. Спекание портландцементного клинкера методом двухшихтовой технологии //Сб.трудов "Совершенствование химии и технологии строительных материалов".-М.,I984.-С.9I-98.

3. А.С. СССР I447772 С 04 В 7/36.- Способ получения портландцементного клинкера.-Б.И.-I988.-№48.

LOW TEMPERATURE REDUCING-OXIDATIVE TECHNOLOGY FOR PORTLAND CEMENT PRODUCTION

P P Lerke

The Kazakh Institute of Chemical Technology, Chimkent
Republic of KAZAKHSTAN

SUMMARY

We worked out the main technological parameters and physical and chemical principles of the clinker process control in the conditions of redox for highalite Portland cement production using low temperature technology. Conventional raw material components both in the ground form and in the form of crushed stone 0-30mm size are used for this technology realization. It is worthy to mention that firing temperature reduction is attained without the use of mineralizers (CaCl2, CaF_2, etc;). We also worked out the constructive decisions of low temperature technology realization which allows to reduce the firing temperature to I200 - I300°C i.e. by I50 - 200°C and to increase the furnace productivity and to reduce fuel consumption by 20 - 30 %. The peculiarities of clinkering are studed by means of physical and chemical methods.

АННОТАЦИЯ

Разработаны основные технологические параметры и физико-химические принципы управления процессами клинкерообразования в восстановительно-окислительных условиях для получения высокоалитового портландцемента по низкотемпературной технологии. Для реализации этой технологии используются традиционные сырьевые компоненты как в молотом виде, так и в виде щебня фракции 0-30 мм. Следует отметить, что снижение температуры обжига достигается без применения минерализаторов (CaCI2, CaF_2 и т.д.). Разработаны конструктивные решения реализации разработанной низкотемпературной технологии, которая позволит снизить температуру обжига до I200-I300°C, т.е. на I50-250°C, что позволит, как следствие, повысить производительность печи и снизить расход топлива на 20-30%.

Используя физико-химические методы исследований изучены особенности процессов клинкерообразования.

INTRODUCTION

Power and ecological problems in the world make specialists work out new less power-consuming Portland cement production methods. In the Portland cement production process special role belongs to firing as it makes about 47% of all production expences and 71% of fuel-power consumption.

At present we can single out three trends of cement production to achieve fuel economy while clinker firing:
- hydraulic active belite cement;
- supphomineral cement;
- cement obtained using oxide-salt melt technology.

In the first two trends alite is formed in little quantities or is absent in the obtaining of cement clinker, but in the third trend chlorine-containing analogue of alite is formed through oxide - salt melt obtained at the temperature about 1100°C.

The reduction of melt formation temperature from 1300 to 1100°C is the basis for the temperature reduction of the synthesis of high-basic mineral - alite. Using this principal we worked out theoretical basis of the reducing-oxidative synthesis of high-alite Portland cement clinker at 1200 - 1250°C with use of conventional raw material mixtures without mineralizing admixtures and fluxes.

EXPERIMENTAL

Experiments proved the possibility of mineral-formation process control depending on reducing - oxidative firing conditions where temperature reduction of Portland cement clinker firing to 1200-1250°C owing to oxide melt formation with melting temperature 1100 - 1150°C is attained using the conventional raw material mixture. It is worthy to mention that firing coditions make it possible to use conventional initial raw materials without their preliminary grinding to 10 mm size, i.e. to realize low temperature (1200-1500°C) firing crushed stone technology using basalt rocks. It became possible due to the temperature reduction of the clinker melt formation and due to the increase of mobility of anion complexes and cations as a result of electronic modification of the crystal structure and the associates of silicoxigen tetrahedrons in the clinker melt.

The essence of electronic modification is as follows: under the influence of the reducing agent (R - C,CO,H_2) the partial pressure of oxygen in the system reduces and is accompanied by ion reduction of transitional metals from the highest degree of oxydation (Fe^{3+}, Mn^{4+}) to the lowest degree of oxydation (Fe^{2+}, Mn^{2+}). The ions of iron and manganese, occupying the position in the crystal lattice in the lowest degree of oxidation under the crystal field influence, can be electron donors. This can be explained by small transition energy of the electron from twovalent ions of the transitional metals into the condition zone under the influence of the crystal field of silicon and oxygen ions which is characterized by high electronegativeness. As a result there appears the possibility of a free electron adsorbtion on the silicoxygen tetrahedrons. Therefore, highmobile silicon - electronic-oxygen tetrahedrons are formed according to the following scheme:

$$R + SiO_4^{4-} \xrightarrow{+e} SiO_3^{4-} + RO$$

$$R + SiO_3^{4-} \xrightarrow{+e} SiO_2^{4-} + RO$$

As follows from the reactions suggested above lass complex and large anions (SiO_3^{4-}, SiO_2^{4-}) which have higher mobility in the melt are formed and their presence in the crystal lattice of the silica - containing component as a result of the vacant space extension must increase the diffusion rate of cations (Ca^{2+} and Fe^{2+}) deep into their crystal lattice. The silicon-electronic-oxygen tetrahedro formation is one of the main reasons of clinker melt temperature decrease.

The stated above theoretical conceptions about the reasons of low temperature melt formation and the increase of the reaction ability of raw materials as a result of electronic modification are based upon the typical properties of the electron. A tendency to the reaction of addition not only to cations, anions and free radicals but also to the neutralmolecules which leads to anion-radicals, for example, to anion- radicals of the simplest non-organic molecules $O_2 \xrightarrow{+e} O_2$, is typical to the electron in general. Thus, a free electron is, as a matter of fact, the simplest of anion-radicals. The wave nature of the electron specifically affects its chemical behaviour. Many reactions of electronic transfer do not obey the laws of chemical kinetics. In particular the rate of electronic transfer reaction doesn't depend on temperature and as a result on the potential barrier value, i.e. doesn't obey Arrhenius equation. In other words, the electron due to its wave properties doesn't climb to the top of the tunnel (the tunnel effect). The tunnel transfer reactions, as the calculations show, begin long before the real physical collision of the reacting particles. It is stated that while conducting a reaction between K and I_2 the electron transfer from K-atom to I- molecule takes place at a distance 6-8 Å in vapours and 20 Å - in solutions and in the melt. That's why the reactions of this type, known as " harpoon", can proceed in dielectrics as well to which calcium silicates with donor element admixtures refer (I).

In the low temperature technology the presence of reducing medium promotes the proceeding of the electronic transfer reaction in the silicate systems with donor element admixtures. This explained by the f a c t that under the influence of the reducing agents the reduction of oxygen partial pressure in the system which is accompanied by the formation of anion oxygen vacancies (V_x^{2-}) takes place. Lack of anions leads to the appearance of donor levels as ionization energy of surplus cations (in the metal positions) is little. Heterovalent substitution of Ca^{2+} ion position by Fe^{3+} also promotes donor cations appearance. In this case a spare third valent electron which doesn't take part in two valent lattice bonds is under the influence of the periodic lattice field and coulomb oxygen ion field. This electron has to occupy higher level as its bond with the nucleus weakened. That's why imparting slight energy to this electron (often at room temperature) it breakes off its orbit and passes into the conduction zone.

In the confirmation of the stated above we can cite thermodynamic analysis. From the refference book of thermodynamic values it follows that free energy of formation (G°_{298}) of hydrogen atoms from their molecules from 203.07 and 231.53 kj/mol respectively. This value of free energy must be approximately equal to the energy of paired electron formation at the transfer of the electron from donor to Si-ion as a result of oxygen vacancies formation in its nearest environment under the action of

reducing medium. The energy of electron going out in the conduction zone for three valent iron and manganese will be not more than 2.2 - 2.5 electron-volts. Therefore, since free electron formation energy from threevalent ions of iron and manganese is less than of paired electron formation thermodynamically electronic modification of the silicate material structure is possible. Portland cement produced according to the low temperature reducing - oxidative technology in contrast to low temperature salt technology possesses all the advantages in the constructional-technological properties of Portland cement produced according to the existed technology.

RESULTS AND DISCUSSIONS

Theoretically based and experimentally proved is the possibility of Portland cement clinker synthesis at I200 - I250°C owing to the reducing-oxidative firing, when oxide clinker melt is formed with melting temperature II00 - II5I°C.

Temperature reduction of clinker melt and the increase of diffusion rate of ions are mainly attained by the electronic modification following which more compact and mobile anions SiO_3^{4-} and SiO_2^{4-} are formed instead of lowmobile anions SiO_4^{4-}. This will make possible to ensure Portland clinker synthesis both from the grinded mixtures and by using crushed stone I0 mm size as the initial raw material.

CONCLUSIONS

I. Theoretically based is the possibility of high reaction capability siliconelectronic -oxygen tetrahedrons of SiO_3^{4-} and SiO_2^{4-} which promote the formation of low-temperature clinker melt at II00 - II50°C.
2. Experimentally proved is the electronic - modified oxide clinker melt formation which provides the reduction of alite in clinker formation temperature from I450°C to I200-I250°C, i.e. by 200-250°C.
3. High diffusion capability of electronic-modified silicon oxygen tetrahedrons makes it possible to use the crushed stone I0 mm size as the initial raw material.

REFERENCES

I. Yeletsky, A.V.: " When Argon is Similar to Potassium ", Chemistry and Life, I982, N I0, p 30-34.

PHYSICAL AND CHEMICAL PECULIARITIES OF A NEW LOW-ENERGY-CONSUMING TECHNOLOGY FOR PORTLAND CEMENT PRODUCTION

P P Lerke

The Kazakh Institute of Chemical Technology, Chimkent
Republic of KAZAKHSTAN

SUMMARY

Theoretically base and experimentally proved the optimum parameters of the raw material mixture fractional content make it possible to decrease the melting temperature of clinker melt and to increase its quantitative content owing to substantial increase of SiO_2 portion turned into a primary clinker melt as well as to ensure the directed mineralization both of hard - phase reactions and reactions through clinker melt using a less power-consuming scheme. In particular, according to our technology belite formation takes place advantageously through a clinker melt; alite synthesis takes place advantageously not after $2CaOSiO_2$ formation and its interaction with CaO through a clinker melt but by means of a direct synthesis from a clinker melt during its interaction with CaO. Clinker hydraulic activity increases as a result of stabilization of a more hydraulically active alite modification. Other than that permanent dust escape from the furnace is reduced by 25-30%, the raw material mill capacity increases by 2.5-4 times and the specific power expenditure for raw material grinding is reduced by 2.5 - 4 times.

АННОТАЦИЯ

Теоретически обоснованные и экспериментально подтвержденные оптимальные параметры фракционного состава сырьевой смеси позволяют снизить температуру плавления клинкерного расплава и увеличить его количественное содержание за счет существенного увеличения доли SiO_2, перешедшего в первичный клинкерный расплав, а также обеспечить направленное минералообразование как твердофазовых реакций, так и реакций через клинкерный расплав по менее энергоемкой схеме. В частности, по разработанной технологии образование белита происходит преимущественно не путем твердофазовых реакций при 900-1300°С, а через клинкерный расплав, синтез алита происходит преимущественно не после образования $2CaO \cdot SiO_2$ и взаимодействия его с CaO через клинкерный расплав, а путем прямого синтеза из клинкерного расплава при взаимодействии его с CaO. Повышается гидравлическая активность клинкера в результате стабилизации более гидравлически активной модификации алита. Снижается пылевынос из печи на 25-50%.

INTRODUCTION

Portland cement production is a high-energy-consuming one in which a portion of power expenditure for raw material grinding makes approximately two thirds of energy resourses in general. That's why the reduction of energy consumption for Portland cement production process, particularly raw material grinding, is one of the main tasks of the cement industry. Conditionally, the clinker formation process depending on the phase quantity may be divided into two stages: mineral synthesis of Portland clinker by means of hard-phase reactions in the first stage and through the clinker melt in the second stage. For the Portland cement clinker quality increase which is defined by the completeness of CaO assimilation and for energy consumption reduction for its production it is advisible to intensify the mineralization reactions both by means of hard-phase interaction and through the clinker melt simultaneously. At the same time it is known that mineralization rate through a liquid phase is by 4 orders (approximately by I0000 times) higher than through a hard phase and therefore is less energy-consuming.

An important factor of mineral synthesis through the melt is that mineralization rate little depends on hard phase particle size of ion remove from adsorbtion (border) layer of the melt by which itis saturated as a result of crystal phase solution. In this respect it is advisible to work out the physical and chemical principles of mineralization process control in such a way that, as a result of the directed intermediate clinker mineral synthesis, the clinker melt quantity increases and as a consequence the clinker mineral formation takes place advantageously not by means of hard-phase interactions but through the melt using raw material mixture without addition of fluxes and mineralizers.

EXPERIMENTAL

The worked out theoretical concepts and the laboratory researches conducted on this base showed that optimization of fractional raw material content is such a trend. The new technology is based on the fact, that: hard-phase reactions are ensured by the presence of particles less than 80 mkm;
- diffusion of CaO^{2+} ions from the dissolving crystal CaO faces to crystal C_3S growth zones in the limiting alite synthesis stage through the clinker melt;
- rankinite and wollastonite have least melting temperature in the system "CaO - SiO_2".

The result analysis of the reactionary tendency of raw material mixtures of traditional and optimized fractional content showed that a higher CaO-free content up to I300°C and the maximum CaO-free content shift in the direction of high temperatures by 80-I00°C is characteristic to the mixture with the optimized granulometric content of the limestone component. Other than that it is worthy to mention that the firing products of the raw material mixture of the optimized granulometric content at I300°C find themselves more clinkered and at I450°C have a less quantity of the residual CaO. This testifies to the earlier eutectic melt appearance and its quantity increase which is proved by the results of the electroconductivity determination depending on the heating temperature. The results of the X-ray-phase analysis showed that during the firing of raw material mixture of optimized fractional content at II00 - I250°C there exists a primary formation of low-base silicates (C_3S_2 and CS) which in the bynary system CaO - SiO_2 have the lowest melting tempe-

rature since they correspond to eutectic content.

In this respect we can consider that low- base silicates (CS and C_3S_2) turn into the clinker melt equally with C_3A and C_4AF. These conclusions are confirmed by electronic sonde analysis data according to which the clinker melt appearance at I300°C an intermediate phase of firing products of raw material mixture of optimized fractional content has a higher silica content in comparison with the firing products of the raw materials of a traditional grinding. Stoichiometric content of the intermediate phase with the clinker melt appearance at I300°C and belite stated at the same temperature in the samples of raw material mixtures of traditional and optimized fractional content is shown in Table I.

TABLE I. Electronic sonde mineral analysis after raw material mixture firing at I300°C.

Stoichiometric content in mols									
CaO	Al_2O_3	Fe_2O_3	SiO_2	Na_2O	K_2O	MgO	P_2O_5	SO_3	TiO_2
Raw material mixture of traditional grinding:									
intermediate phase									
7.79	0.85I	I.00	I.259	0.0243	0.0077	0.2333	0.033	0.02I4	0.0522
belite									
2.53	0.056I	0.0303	I.0	0.007I	0.0033	0.0II4	-	0.0I54	0.0073
Raw material mixture of optimized fractional content:									
intermediate phase									
5.76	I.I8	I.0	I.439	0.055	0.II2	0.5505	0.0048	0.03I9	0.0642
belite									
2.25	0.02I8	0.0I58	I.0	0.0073	0.0045	0.0III	-	0.0096	0.004I

It is worthy to mention that the belite phase formed at I300°C in the samples of raw material mixture of optimized fractional content is less oversaturated in respect of CaO and has a lower content of impurity oxides Al_2O_3, Fe_2O_3, MgO, SO_3, TiO_2. The lowered basement of the belite phase of raw material mixture of optimized fractional content is explained by the clinker melt formation at I300°C of the lowered basement. The impurity oxide content reduction in belite is caused by the fact that the belite phase during the firing of raw material mixture of the optimized grinding in contrast to the traditional one is formed mainly through the clinker melt. This is agreed with the law of cocrystallization of phases and impurities, according to which the impurity content is reduced during the crystallization of the phase from the melt.

With the temperature increase to I400°C and higher the impurity oxides content in the alite and belite phases in the synthesis products of the optimized and traditional grinding becomes equal. More than that, an intermediate phase basement and that of the formed clinker minerals also become equal. It should be noted that at the last firing stage, irrespe-

ctive of the nature of the initial raw materials in the firing products of raw material mixtures of optimized fractional content in comparison with those of traditional grinding the impurity MgO content in alite, unlike other impurities, doesn't decrease but increases.

Thus, regardless of the existing notions according to X-ray-phase analysis a high-temperature rhombohedric alite modification (and not low--temperature monowedge-like one) is stated in alite with MgO content increases. This allows to increase the Portland cement clinker hydraulic activity with Mg content increase and to enlarge the raw material base owing to the use of raw materials with a higher MgO content. Thus, the results prove the supposition about the possibility to work out the technology of the directed Portland cement clinker synthesis using a power profitable scheme. The clinker quality synthesized of raw material mixtures of different fractional content was determined by means of petrographic analysis. The results obtained showed that alite content in the clinker on the basis of the optimized fractional composition of the limestone component is higher by 7-I0% and their microstructure is notable for a more clear crystallization.

The industrial tests and introduction results showed that with the using of the raw material mixture of the optimized fractional composition of the limestone component the specific energy expenditure for the raw material grinding and the expenditure of grinding bodies are reduced by 2.5 - 4 times, the raw material mill capacity increases by 2.5-4 times and the noise level decreases by 2-3 times. According to the wet production method the flowability increases and the raw material slime moisture decrease were observed. At equal flowability the moisture of a limestone slime of the optimized content is reduced by 6-8%. This is explained by the fact that the adsorbed water quantity is reduced with the decrease of the specific surface of the grinding material. Probably, this idea as well as the gross clinker melt quantity increase and the silicate synthesis using a power profitable scheme make it possible to reduce the power consumption for raw material mixture firing by I0-I5% and to increase the furnace capacity by 7-I0%. Dust escape from the furnace judging by the tests before the filters is reduced by 25-50%.

To study physical and chemical properties of the clinker-based cements, produced using the low-energy-consuming and conventional technologies, the clinker samples were ground together with 5% of gypsum to the specific surface formation of3000 sm^2/g. The results of physical mechanical tests showed that the compression strength of the samples 4x4xI6sm formed on the clinker basis of the raw material mixture of the optimized fractional composition was not reduced in comparison with the clinkers produced using the traditional technology. At present the new energy-saving technology is introduced into industrial production.

RESULTS AND DISCUSSIONS

The new low-energy-consuming technology for Portland cement production was worked out on the basis of experimental researches as well as new theoretical ideas of the possibility of clinker formation processes intensification in the liquid - phase sintering stage owing to directed synthesis of intermediate clinker minerals in the solid - phase sintering stage, which proved the correctness of the suggested theoretical grounds. The main idea of it is in the selection of the raw material optimal frac-

tional content, which ensures a sharp reduction (2.5 - 4 times) of energy consumption for raw material grinding, the increase of grinding bodies productivity (2.5-4 times), the reduction of dust escape from the furnace by 20-50% and the Portland cement clinker synthesis using less power-consuming schemes. The theoretical ideas are proved by a great number of phisico-chemical researches done. The new low-energy-consuming technology which permits to increase the raw material basis for Portland cement manufacture has already been tested and introduced into industrial production.

CONCLUSIONS

The fractional raw material content optimization made the directed synthesis of clinker minerals in the stage of hard-phase reactions possible, which owing to the formation of CSand C_3S_2instead of C_2S permits to increase clinker melt with improved properties (reduced melting temperature, viscosity and surface tension) and as a result to intensify alite and-belite formation process in the stage of solid-phase sintering.

The alite formation according to the new low-energy-consuming technology takes place not owing to belite reaction with CaO through clinker melt, but rather to less energy-consuming scheme by means of direct CaO reaction with clinker melt. The belite substantial part synthesis takes place to its melt crystallization after the belite basement was oversaturated.

The redistribution of the silicate minerals impurity oxide into the intermediate phase is the result of silicate synthesis mainly through the higher melt quantity with improved properties according to the new technology. Clinker microstructure has more clear crystallization and the alite content is increased by 7-10% as a result of the reduction of belite oversaturation with CaO.

The new Low-energy-cosuming technology will reduce the energy expenditure for the raw material grinding and the expenditure of grinding bodies by 2.5-4 times, the noise level by 2 - 3 times, dust escape from the furnace by 25-50%, fuel consumption by 10-15%, slime wetness by 5-7%.. Other than that it will increase the grinding bodies productivity by 2.5-4 times.

THERMAL TREATMENT OF CEMENT RAW MATERIALS THROUGH INTENSIVE HEAT EXCHANGE

A B Ryzhik, M V Kouglya and A V Alexandrov

Design and Research Institute of Cement Industry "Giprocement"
St Petersburg, RUSSIA

SUMMARY

This paper deals with features of clinker formation reactions occurring at shock heating in a vortex type reactor. It is found that in spite of the short residence time of the raw material in the reaction chamber, these reactions are practically complete, and the burnt product comprises the clinker mineral conglomerates. The basic possibility of producing cement clinker when absorbing calcium chloride by raw mix from a vapour-drip flow is substantiated. It is shown that the changes taking place in the calcium chloride bearing raw material are deeper in a rapid burning regime than in the traditional mixes.

РЕЗЮМЕ

Обсуждаются особенности протекания реакции клинкерообразования при ударном нагреве в реакторе вихревого типа. Установлено, что, несмотря на малую длительность пребывания сырьевого материала в реакционной камере, эти реакции практически завершаются и продукт обжига представляет собой конгломераты клинкерных минералов. Обоснована принципиальная возможность получения клинкера при адсорбции сырьевой смесью хлорида кальция из паро-капельного потока. Показано, что при быстром обжиге в кальцийхлорсодержащем материале происходят более глубокие изменения, чем в традиционных смесях.

INTRODUCTION

Drastic intensification of interphase heat exchange can be obtained from treatment of raw materials in the fluidized state. However, the inhomogeneity of the solid phase concentration field as well as formation of coatings on the heat exchanger walls lower the system efficiency and impede safe operation. To avoid this a pilot-commercial reactor (1) was developed at the Institute of Giprocement. It is based on the laws of a stabilized vortex flow with a central outlet where a gas-dynamic repulsion of the solid phase from walls occurs (2).

EXPERIMENTAL

A vortex reaction chamber (Fig.1) in which a gas swirling device is mounted forms the basis of the burning plant. By this means, the chamber is divided into two zones - a reaction (working) one where the process of cement clinker sintering takes place and a buffer one where the combustion of a gaseous fuel is organized. Fuel and air burn within the buffer zone, and the combustion products are introduced through the gas swirling device into the working zone of the reaction chamber. The exit gas is directed through the chamber throat to a cyclone type preheater. The powdered raw material is pneumatically conveyed to the cyclone preheater after which it enters the reaction zone of the vortex chamber through openings in the top cover. The burnt product is directed to the clinker cooler through the chamber bottom.

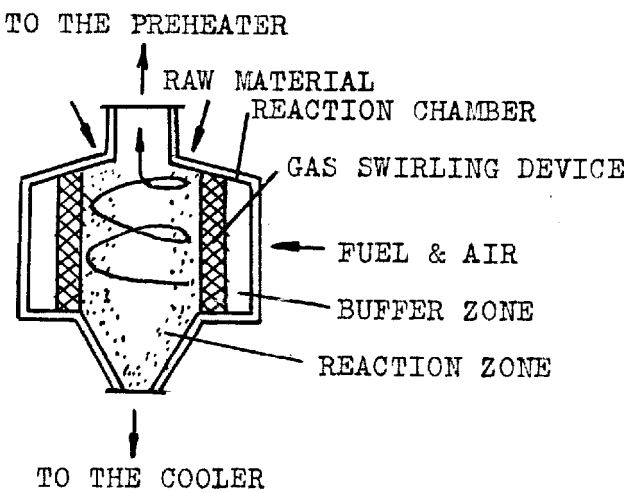

Fig 1 Scheme of Vortex Reactor

Raw mix was calcined to the extent of 40.73% in the preliminary tests. The experiments were carried out with natural associations of argillaceous and carbonaceous components (marls of the Novorossiisk deposit) mixed with cinders (Table 1). The burning was conducted at a temperature of 1400° C. The capacity was 1430 kg/hr, the particle residence time in the reaction chamber did not exceed 1 s.

RESULTS AND DISCUSSIONS

The burnt product was a fine-grained agglomerated material of dark shades from dark-grey to black with a slightly higher grain size as compared to the raw mix. The agglomerates had an almost spherical shape and reached up to 600μm in size (the maximum size of the raw mix particles did not exceed 200μm).

The burnt product was subjected to mechanical tests and physico-chemical studies including chemical, XRD and microscopic analyses, determination of hydration characteristics in the presence of 5% gypsum and identification of hydrate phases after curing of the specimens in a microcalorimeter during one day. The microscopic and XRD analyses showed that the burnt product contained the main clinker minerals in

Table 1. Chemical Composition and Fineness Characteristics of Raw Materials and Burnt Products

Components	Value, %					
	Marl		Cinders	Raw mix	Partly calcined product	Burnt product
	High	Low				
Oxides						
SiO_2	14.80	23.10	-	15.34	17.34	22.65
Al_2O_3	2.29	4.34	-	2.45	3.19	4.10
Fe_2O_3	1.17	1.64	74.65	2.45	3.21	4.60
CaO	45.06	36.96	-	43.54	50.01	62.87
LOI	32.00	30.00	-	31.27	23.59	3.53
f-CaO	-	-	-	-	-	4.98
Moduli						
KH (LSF)	0.98	0.45	-	0.90	0.90	0.86
n (silica)	4.28	3.86	-	3.13	2.71	2.6
p (alumina)	1.96	2.65	-	1.00	0.99	0.89
Fineness Sieve residues, %						
0.2 (72 mesh)	6.6	7.6	-	6.8	10.75	65.0
0.08 (200 mesh)	22.4	23.8	-	14.3	32.1	93.0

the ratios characteristic of portland cement clinker, but its distinguishing feature was a rather high content of uncombined calcium oxide, free CaO, in a fine-crystalline state. Curves of total heat evolution Q and its rate $dQ/d\tau$ on interaction of the product obtained with water, in the presence of 5% gypsum (Fig.2) are also typical of portland cement clinker because of the presence of two maxima in the heat evolution rate curve. The first peak is caused by the hydration of the clinker aluminate minerals and uncombined calcium oxide, and the second one is due to the hydration of the silicate minerals. Only a fair margin for the first and second peaks on the heat evolution rate curve support the results of the XRD, chemical and microscopic analyses as regards the low content of calcium aluminates and alite in the sample of the low-lime clinker investigated.

The mechanical tests conducted on cement prepared from the burnt product however showed that in spite of the phase-mineralogical composition and hydration kinetics being typical of the portland cement clinker, production of a commercially feasable cement was handicapped due to the higher f-CaO content.

To decrease the detrimental effect of uncombined calcium oxide, cements were prepared with 10% pozzolanic additives, i.e. tripoli or amorphous silica of very high fineness from a ferrosilicon production. These compositions withstood the soundness tests, and their strength characteristics after 90 days of hardening were not below 40.0 MPa.

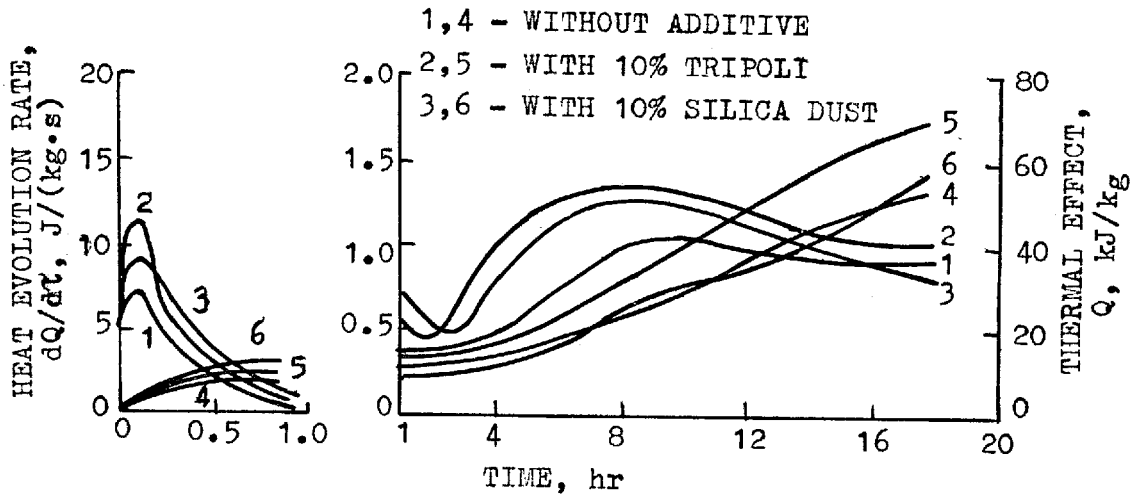

Fig 2 Heat evolution rate (1-3) and thermal effect (4-6) of interaction between the burnt product and water in the presence of 5% gypsum

The heat evolution during the first day of hydration for the cements with these additives did not differ markedly from ordinary portland cement, as shown in Fig.2. Microscopic analysis showed the presence of new hydrate phases of tobermorite type in the hydration products of the specimens extracted from the microcalorimeter. Formation of these new hydrate phases could be cause of increase in the cement stone strength. The greatest silicate hydrates content was found in the specimen containing microsilica.

The influence of the vapour-and-gas atmosphere on the phase composition of the burnt products was also studied. These experiments were conducted in conjunction with the energy-saving low-temperature process of clinkerisation in the presence of chloride salts which has been in practice on a large scale in the last few years (3,4). The positive effect in these cases is achieved due to the formation of stable silicate structures characterized by mixed unions in the chlorine-bearing atmosphere at lower (by 300-350°C) temperatures as compared to conventional portland cement technology. The quality of the burnt product is regulated by the presence of chlorine in the structure of the crystal lattice thus producing new clinker minerals (alinite, in particular). Thus the thermal treatment of a raw mix under conditions of shock heating practically excluding the possibility of sublimation of the chlorine-containing compounds is of special interest.

This series of experiments was also conducted with a precalcined raw mix as described in Table 1. Calcium chloride solution of 28.4% concentration (density 1270 kg/m^3) was injected with the help of the swirl burner into the outlet gas duct of the reaction chamber which ensured spraying of the raw mix particles with calcium chloride-contain-

ing vapour-drip mixture. The solid phase and solution mass ratio was maintained in the range of 1/0.227 at a calcium chloride content of 6% in the raw meal. The burning was performed at 1100°C, i.e. at a temperature which is typical for formation of the alinite clinker in rotary kiln. A product was obtained with LOI of 2.45%, f-CaO content 0.22% and Cl^- 6.27%. The following phases were identified in it (in the order of decreasing content): alinite, spurrite C2S.CaCO3; chlorosilicate $2C_2S$. .CaCl2; carbonate chloride $CaCO_3.2CaCl_2$; f-CaO; SiO_2; $CaCO_3$.

In shock heating the fine-grained suspended raw material reacts with the calcium chloride in the gaseous phase thus resulting in large changes of the solid phase with calcium chloride absorption prevailing over its sublimation. In spite of the high percentages of the associated chloride and alinite, primary intermediate phases are present in the clinker in the form of the calcium carbonate chloride and chlorosilicate. Small amounts of f-CaO, silica and undissociated calcite also remain . This indicates an inadequate degree of the initial raw material transformation under the action of chlorine, which in turn is possibly connected with a relatively low temperature and a short residence time of the particles in the reaction chamber.

CONCLUSIONS AND RECOMMENDATIONS

By burning in the vortex reactor a product with characteristics similar to cement clinker was obtained. The experiments conducted supported the principle of the interphase heat exchange intensification to form the basis of the experimental plant, thus fulfilling the prerequisites for development of full-scale commercial high-capacity plants. For a steady production of alinite clinkers it is necessary to optimize the parameters of the burning process in the vortex reactor.

REFERENCES

1. USSR certificate of authorship No.1035387, 19 March 1982 "Ustroistvo dlya teplovoi obrabotki vysokodispersnogo materiala" ("A device for thermal treatment of fine-grained material").

2. Ryzhik, A.B. and Nelidov, V.A.: "Gazodinamicheskiye osobennosti reaktora-dekarbonizatora s vikhrevym stokom" ("Gas-dynamic features of calcining reactor with vortex flow with central outlet"). Trudy NIItsementa, 1984, 67, 32-41.

3. Bikbau, M.Ya.: "Novoye nauchnoye napravleniye v khimii i tekhnologii tsementa" ("A new scientific direction in the cement chemistry and technology"). Chimkent, Kasakhsky chimiko-tekhnologichesky institut, 1983, 114 p.

4. Nudelman, B.I.: "Kinetika nizkotemperaturnogo klinkeroobrazovaniya" ("Kinetics of low-temperature clinker formation"). VNIIESM, Promyshlennost stroitelnykh materialov. Ser.1. Tsementnaya promyshlennost, 1985, 2, 52 p.

Specific Theme I-B

Effect of Low Grade Fuels, Combustible Wastes and Non-traditional Raw Materials

THE REDUCTION OF DIOXIN IN CONNECTION WITH THE USE OF WASTE-DERIVED FUELS IN THE CEMENT INDUSTRY

Richard Bolwerk

The President of the Administrative District of Münster
Münster, GERMANY

SUMMARY

Due to many tests and constant operations it appeared in the past that a modern cement plant is to a high degree suitable for the use of multifarious residual products. The conditions of the cement burning process - high temperatures, sufficient retention times, oxidizing atmosphere - in connection with an optimized process, security and observation technology guarantee that the emissions of dioxin and furan are below the limit values of 0,1 TEQ/cubic meter (TEQ = toxicological equivalent) in force in Germany.

ZUSAMMENFASSUNG

Wie sich in der Vergangenheit aufgrund vieler Versuche und Dauereinsätze gezeigt hat, ist ein modernes Zementwerk in besonderem Maße geeignet, die vielfältigen Reststoffe umweltverträglich zu verwerten. Die Bedingungen des Zementbrennprozesses - hohe Temperaturen, ausreichende Verweilzeiten, oxydierende Atmosphäre - in Verbindung mit einer optimierten Verfahrens-, Sicherheits- und Überwachungstechnik stellen sicher, daß die Emissionen an Dioxinen und Furanen unterhalb der in Deutschland geltenden Grenzwerte von 0,1 mg TEQ/Kubikmeter liegen.

INTRODUCTION

For the burning of cement clinker mainly rotary kilns with cyclone preheaters and clinker coolers are used in Germany. The raw meal is fed at the top step of the cyclone system and gets into the rotary tube with a temperature of about 800° Celcius. In the sintering zone, the hotest part of the kiln, the combustibles are heated up to 1450° C. With gas temperatures of 1200° - 2000°C (Figure 3), the retention times of the gases come to 3 - 5 seconds according to the length of the kiln (Figure 4). The conditions as well as the oxidizing atmosphere which is necessary for the quality of the products, permit the use of fuel substitutes or other materials over the primary side of the rotary kiln if special conditions are considered.

USE OF WASTE-DERIVED FUELS

The part of sulphur, halegonides and heavy metals often rises proportionally when waste-derived fuels are used. Therefore it has to be taken care that the trace elements from the waste-derived fuels will not be an additional load for the environment. Waste products which can be used industrially, are among others waste oils, solvents, old tyres, rubber chips, household and industrial refuse as well as residues from concentration flue-gas cleaning processes. Herewith it has turned out that even dangerous stuff like PCB, PCDD is used increasingly.

The elements fed to the kiln with raw materials, waste-derived materials and fuels are important as far as their steam-pressure is concerned. Some of them have a low steam pressure or they make compounds which show a low steam pressure, too. Therefore attention has to be especially paid to the concentration of Na, K, CL and S, the operationallly disturbing elements, as well as to the elements Zn, Pb, Cd, Tl and Hg, which are important for the emission.

Because most of the time the materials which are fed bring chlorine into the kiln, the elements Zn, Pb, Cd, Tl and Hg can always find Cl to react with. Therefore the elements will probably be found in chlorine-compounds. Due to their low steam-pressure such elements tend to build circulations. Basically the circulation depends on the quantity of elements which are fed. It is only possible to influence this by a strict selction of the materials fed. Consequently it is important to clear up how much the quantity of elements will differ from the quantity of elements from the different kinds of coal respectively from other materials burnt today. It is also important to get to know in which way these concentrations differ within the old range.

In various plants in Germany waste-derived materials have already been used by now. Concerning the heavy-metals, they could be compared with other known fuels or materials. Or they have been restricted by new established decrees. The new limit values can be compared with the old ones. But it is still necessary to remove the operationally disturbing chlorids from the kiln system in order to avoid accumulations and stoppings in the lower cyclone part and to guarantee an equal operation of the kiln. For this reason the installation of a by-pass is generally necessary. The concept is to seperate parts of the gas flows at the kiln inlet to achieve already here a fractionation of the seperated gas-dust-mixture. The by-pass ventilator has got a correspondingly high range of regulation. So a dust quantity can be seperated which is, with regard to the polutants, equivalent to the waste quantity.

It has to be thought about carefully how the raw material and the heat of the by-pass flows can be tied up in the whole production process of a cement plant, because a new waste production has to be avoided. By-pass gases can be used for drying, meal and dust flows can be added at the grinding of the cement. The quality of the cement lays down the permissible quantities. It is even possible to use them in connection with the production of mortar, respectively extra mortar.

CONDITIONS OF BURNING

In comparison to the high temperature part of the rotary kiln, the conditions in the calcinator are less favourable for the burning of halogenized hydrocarbons. Carefull observations have to be made if materials with potential emission danger shall be used in the calcinator. Due to the experiences made it is guaranteed that especially the chlorinated stuff will be destroyed and rendered harmless in the high-temperature part of the kiln. Constant operation of the kiln and constant conditions concerning the use of waste-derived fuels are essential preconditions for low PCDD/PCDF emissions:

- The process of burning has to be surveyed constantly by the means of modern process technology.
- Waste materials have to be under constant arrival control and have to be pre-homogenized in a large-scaled way. Liquids have to be taken continously,too.
- The main analysis parameters of the waste materials (heating value, chemical compound etc.) have to be entered quasi continously into the process control.
- The "Aufgabelanze" (an especially for this purpose produced kind of kiln spear) has to be constructed the way that the waste-derived fuels can be injected centrally and the ignition takes place in the front of flames of the main fuel.
- The regulation aggregates have to permit an addition independant from the waste-derived fuels.
- The waste-derived fuels must be fed only with a trouble-free, continous operation in the range of the normal efficiency.

CONTROL OF SECURE BURNING

With the previous licenses concerning the use of waste-derived fuels, an ingenious security-system was prescribed which allows a permanent control. It cuts the feeding of the waste-derived fuels if:

1) the gas temperature at the kiln inlet goes beyond 800° C,
2) the gas temperature at the kiln outlet goes below 1250° C,
3) the content of carbonmonoxid (Vol %) goes beyond the values stipulated in an experiment,
4) inadmissble differences at the comparison of the nominal and actual values turn out at the coal scales,
5) the raw-meal quantity fed goes below 75 % of the possibly fed quantity,
6) an underpressure at the exhaust blast goes below a value stipulated in an experiment,
7) the electrostatic precipitator fails,
8) the exhaust ventilator fails,
9) the burner fails or
10) the dust content goes beyond 50 mg/cubic meter.

To stipulate definitely the limit values in the 10 - points - security - chain, a calibration of the temperature sensors in advance at the kiln in- and outlet is necessary. This has to be done under variation of the normal efficiency. Therewith the measuring points have to be evaluated. As a conclusion from these results, the optimal range can be stipulated. The optimal range is the range, within the burning of waste-derived fuels can be permitted. Also the necessary limit values for the control temperatures arise.

The following facts have to be measured and noted continously to characterize the operational conditions:

> oxygen (O2), carbon monoxid (CO), carbon dioxide (CO2), total carbon C, dust, temperature of the clinker at the kiln outlet, temperature of the kiln exhausts at the kiln inlet, underpressure at the exhaust blast, sulphur dioxide (SO2) and natrogen oxide

Due to the measurement series the following polutants will additionally be found in the exhausts:

> heavy metals (PB, Zn, Cd, As, Ni, Tl, Cr, Be Hg, V, Se, Te), Cl-, F-, PCDD/PCDF, PAH, PCB, PCP, HKW

To determine the total concentration of PCDD/PCDF, the concentrations of the following individual PCB-isomers determined in the exhaust have to be multiplied with the equivalent factor and have to be summed up. As limitation a sum value due to the equivalents of 0,1 ng TEQ/cubic meter is valid.

toxicological equivalent		equivalent factor
2,3,7,8	Tetrachlordibenzodioxin (TCDD)	1
1,2,3,7,8	Pentachlordibenzodioxin (PeCDD)	0,5
1,2,3,4,7,8	Hexachlordibenzodioxin (HxCDD)	0,1
1,2,3,7,8,9	Hexachlordibenzodioxin (HxCDD)	0,1
1,2,3,6,7,8	Hexachlordibenzodioxin (HxCDD)	0,1
1,2,3,4,6,7,8	Heptachlordibenzodioxin (HpCDD)	0,01
	Octachlordibenzodioxin (OCDD)	0,001
2,3,7,8	Tetrachlordibenzofuran (TCDF)	0,1
2,3,4,7,8	Pentachlordibenzofuran (PeCDF)	0,5
1,2,3,7,8	Pentachlordibenzofuran (PeCDF)	0,05
1,2,3,4,7,8	Hexachlordibenzofuran (HxCDF)	0,1
1,2,3,7,8,9	Hexachlordibenzofuran (HxCDF)	0,1
1,2,3,6,7,8	Hexachlordibenzofuran (HxCDF)	0,1
2,3,4,6,7,8	Hexachlordibenzofuran (HxCDF)	0,1
1,2,3,4,6,7,8	Heptachlordibenzofuran (HpCDF)	0,001
1,2,3,4,7,8,9	Heptachlordibenzofuran (HpCDF)	0,001
	Octachlordibenzofuran (OCDF)	0,001

JUDGEMENT OF THE ENVIRONMENTAL LOAD

Existing measuring results concerning the use of alternative combustibles have proofed that the polutants will be burnt safely if the liquids are screened and the solid waste-derived fuels (for example polychlorinated hydrocarbons) are spread in the gas flow. With regard to the emissions of PCDD and PCDF, the exhaust values of the cement rotary kilns can only be achieved in other burning processes by the means of large-scale after-cleaning equipments. They are about a ten-potency below the equivalent value of < 0,1 ng TEQ/cubic meter in force in Germany. This means 0,01 ng/cubic meter, which speaks for an efficient burning process. Furthermore there could not be prooved any PCB, PCDD and PCDF in the fire-proofed case of a rotary kiln. The measuring results show that the concentrations of all other polutants (for example chlorbenzols, chlorphenols, PAH = polychlorinated aromatic hydrogen and so on) have not been provable or they have been far below the limit values of the TA-Luft (Technical Rules for Air Pollution Prevention) in force in Germany.

For the control of emissions a severe surveillance concept has been established. This concept consists of returning single measurements, continous measurements and emission surveilling calculators with severe evaluation methods. So the plants are surveilled exactly and detailled with regard to the observance of the prescriptions. Concerning the decrees, the concentration of flue gas, for example, has to be between 10 - 20 mg/cubic meter during continous operation. Therewith it is guaranteed that the concentration will be far below the existing limit value of 50 mg/cubic meter in order to assure the observance of the official orders.

Also the low limit values of trace elments from the kiln exhausts should be noticed. The feed of special materials containing heavy metals has been limited and, what is even more important, process engineering measures make it possible that also accumulations of heavy metals in kilns are interrupted. So the limit values of TA-Luft (Technical Rules for Air Pollution Prevention) for inorganic, dusty materials are kept within a wide security-range. Results from various measurements have proofed this. Consequently the emission of halogenized hydrocarbons are today well to the fore.

The present experiences have been made when old oils, solvents, prepared household refuse (BRAM and Eco-Brig = fuel from refuse through comminution, screening and classifying) fed over the primary side of the kiln as well as tyres, rubber chips, mineral soil containing oil, residues from construction works and so on fed over the secundary side of the kiln were used. They have shown that the cement rotary kilns can be used more safely, more ecologically beneficial and more economically. The dioxin can be reduced by the means of a strictly surveilled operation of the kiln combined with further technical regulation security facilities and adequate supervision of the emissions. With these aspects the cement industry is able to fulfil an essential contribution to the use of the low-priced alternative materials.

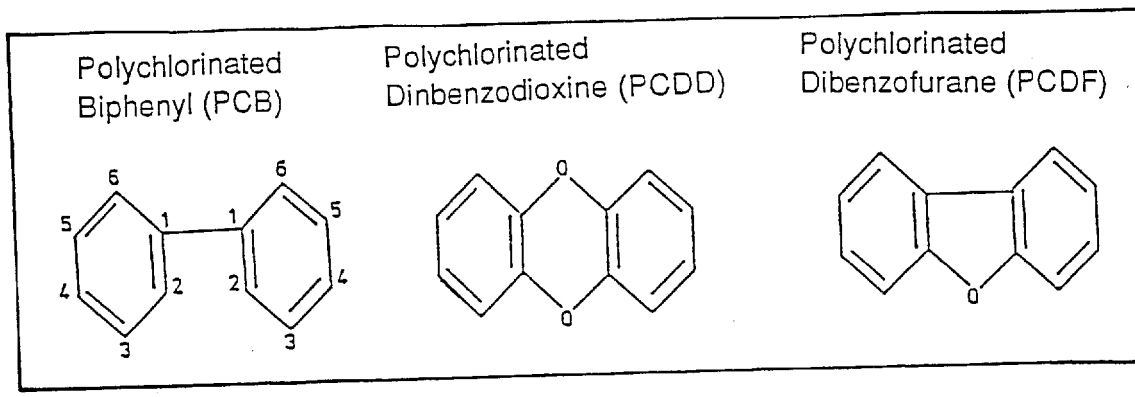

Figure 1: Fundamental structure of PCB, PCDD, PCDF

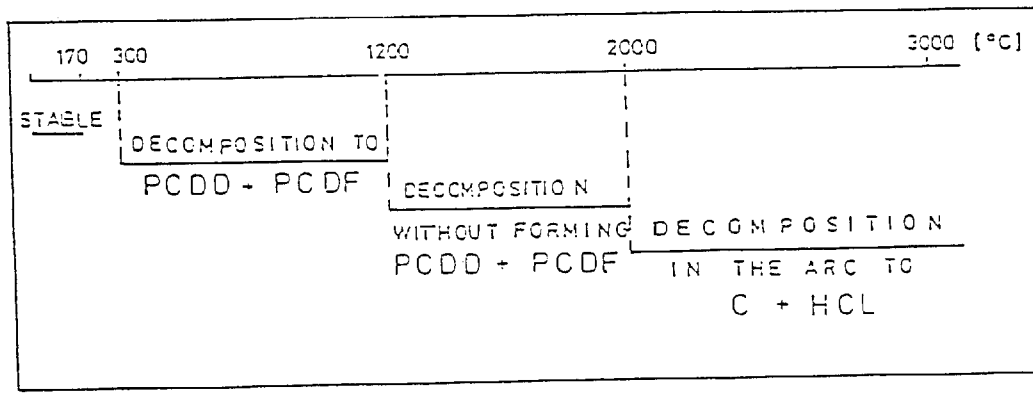

Figure 2: Thermal decomposition of PCB (G. Krogbeumer, 1988)

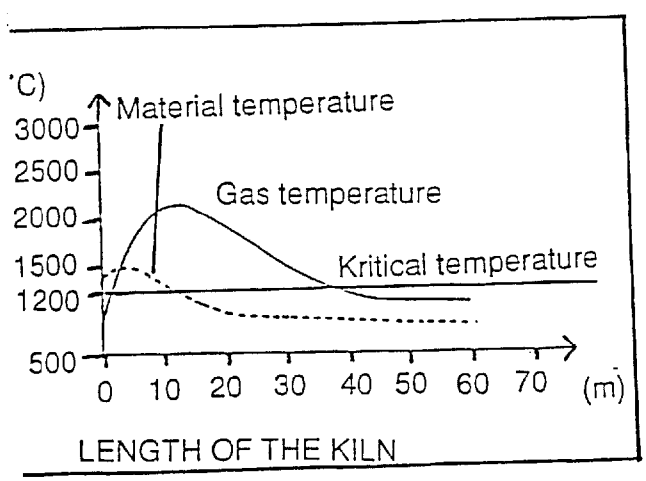

Figure 3: Gas and material temperatures along the rotary kiln

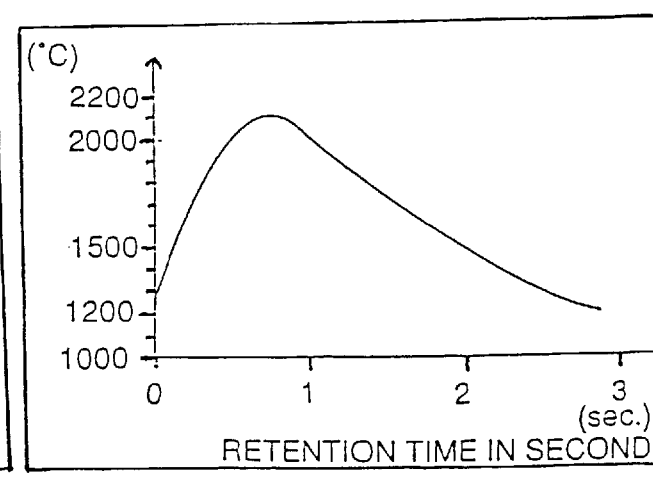

Figure 4: Retention time at temperatures above 1200°C

PUBLICATIONS

Krogbeumker, G.: "Safety arrangements for the auxiliary combustion of waste oils containing PCB in rotary cement kilns", **Cement-Lime-Gipsum 41** (1988), copy 9, p. 188 - 192

Krogbeumker, G.: "Thermal use of old-oils containing PCB with the production of cement", **Technische Überwachung 3** (1990), p. 236 - 240

Maury, H. D.; Pavenstedt: "Primary and secondary fuels in clinker burning", **Cement-Lime-Gipsum 42** (1989), copy 2, p. 90 - 93

Maury, H. D.; Pavenstedt: "Chlorine bypass for increasing the fuel input from refuse in clinker burning", **Cement-Lime-Gipsum 41** (1988), copy 11, p. 540 - 543

VDI Guideline 2094 (september 1085), Emission Control Cement Works

Schimpf, W. A.: "Destruction of Pesticides and Chemical Waste by Means of a Cement Kiln", **Pesticide Management and Integrated Pest Management in Southeast Asia**, 1988 (edited by P. D. Teng and KL. Heong), College Park: Consortium for International Crop Protection, pp. 423 - 432

Bolwerk, R.: "Feasibility study for the use of plan-protective agents in cement plants in Morocco", **Deutsche Gesellschaft für Technische Zusammenarbeit (GTZ)**, october 1991

Bolwerk, R.: "Experiences regarding pollution control problems in connection with production of cement", **Proceeding of the seventh world clean air congress 1986**, Sydney

Bolwerk, R.: "Combustibles and industrial waste products in the cement industry", **Proceeding of the 9th world clean air congress 1992**, Montreal

EFFECTS OF USING RICE HUSK AND ITS ASH AS FUEL AND RAW MATERIAL COMPONENT RESPECTIVELY IN CEMENT MANUFACTURE

S P Ghosh, K Mohan and R K Gandhi

Cement Corporation of India Limited, New Delhi, INDIA

SUMMARY

Rice husk, a locally abundant agricultural waste has been used as a partial substitute (5-20%) of high ash coal in 3 dry process suspension preheater kilns of different capacities in different parts of India. Significant economy in fuel consumption, as well as improvement in clinker quality and cement strength was noted in most cases. Besides, use of rick husk ash as an alternative to sandstone in a raw mix containing a high grade limestone in one plant eased the burnability problem and also expansion and strength development problems of cement. Inspite of the mentioned advantages, scope of continuous large scale use of rick-husk and its ash in the production stream are beset with problems of its handling, intergrinding, blending and homogenisation with coal or kiln feed and requires specific remedial measures.

DIE FOLGEN DER VERWENDUNG VON REISSCHALE UND SEINE ASHCE WIE BRENNMATERIAL UND CRUNDSTOFFENBESTANDTEIL IN DER ZEMENTEN HERSTELLUNG

S P GHOSH, K MOHAN und R K GANDHI

ZUSAMMENFASSUNG

Reisschale, ein Landwirtschaftlicher Abfall, der örtlich in grossen Umfang zu erhalten ist wie ein Partiellerersatz (5 bis.20.p) des Hochaschenkohls in drei trockenprozess suspension vorheizer kilns mit verschiedenen Inhalten in verschiedenen Zonen Indiens verwendet. Bedeutsame ökonomie in Brennstoffen verbrauch als auch Verbesserung in der Qualität von Klinker und Zement wurde in meisten Fälen festgestellt. Ausserdem der verbrauch des Reischallenasches als eine Alternative zum Sandstein in einer Rohmischung mit einer Hochwertigenkalkstein in einer Anlage erleicherte des Problem der Brennbarkeit des Kiln speises und auch löste die Probleme der Ausdehnung und Entwicklung der Festigkeit des Zements. Trotz des gennanten Vorteils, die Möglichkeit des ununterbrochenen Verbrauchs in grossen Ausmassen von Reisschale und seine Asche in der Herstellungs verlauf ist mit Probleme von seiner Hand habung, Zwischeneinmahlung, Mischung und Homogenisierung mit der Kohle order Kilnspeise verbunden und braucht spezifische abhelfende Massnahmen.

INTRODUCTION

Consequent upon the invention of rice husk based cement (1) considerable investigations had been carried out in different countries on use of rice husk as cement or binding material in constructions (2-6). The primary objective of these investigations is the use of a locally and abundantly available low-cost agricultural waste as a pozzolanic additive to cement or binder for local constructional purposes. Use of rice husk and its ash in the cement manufacturing process as fuel and raw material component respectively has a different set of objectives, namely, (1) substitution of high ash and low calorific value of coal by locally available low-cost agricultural waste of similar or higher fuel value, (2) energy conservation and cost reduction in clinker making and (3) improvement in quality of clinker and cement. This article summarizes the results from plant trials and industrial production of ordinary portland cement with use of rice husk as partial substitute of coal and rice husk ash as a raw material component.

THEORETICAL CONSIDERATIONS

Comparisons between proximate analysis of high ash coal and rice husk from different parts of India (7) and between chemical compositions of their ashes indicate the theoretical prerequisites for the use of the latter (Table-1). Rice husk has almost the double the volatile content and nearly half the ash content than high ash coal, its useful heat value is approximately 200 k.cal/kg higher than such coal. Since, rice husk contains about 70% combustibles, its heat value will be appreciated if used in combination with coal. However, because of higher volatiles content, even 5% substitution of coal by rice husk will increase the volatiles in kiln gases by 0.5 to 1%. Keeping 5% margin for allowable fluctuations in kiln volatiles content, theoretically upto 20% rice husk can be used as substitute fuel. Ash content (20%) of rice husk, though much lower in amount than ash content (35%) of coal, however, the silica in rice husk is known to occur in silico-organic or amorphous form and is, therefore, more reactive than predominantly free silica in coal ash. Balancing of kiln feed raw meal with respect to ash absorption from pulverized fuel and clinker quality will permit 15 to 20% rice husk substitution. Different limitations in rice husk use are also imposed by process and operational parameters of individual plants and are discussed separately.

Table-1 : Comparison between proximate and chemico-mineralogical characteristics of high ash coal and rice husk.

Fuel	Proximate Analysis (%)				Calorific value	Chemical composition(%)					Mineralogy
	Internal Moisture	Volatiles	Fixed Carbon	Ash	K.cal/kg	LOI	SiO_2	Al_2O_3	Fe_2O_3	CaO	Free silica(%) and source
Coal (High Ash)	2.8-5.4	22.4 29.8	32.5 38.8	29.8 42.6	2750 4000	0.6 0.8	60.3 64.2	20.6 23.2	5.0 6.5	2.8 4.2	55-60, clay minerals, α-quartz, chert, feldspar, mica minerals.
Average	4.0	27.0	34.0	35.0	3500						
Rice husk	4.2-6.2	58 62	12 18	18 22	3500 4000	4.8 7.5	78 90	3.0 4.5	2.0 3.0	0.2 1.2	Nil, organic compounds, amorphous silica.
Average	4.6	60.0	15.5	20	3750						

CASE STUDIES

A. As substitute for high ash coal

Case-1 - Upto 6% rice husk has been used as partial substitute for high ash coal for a difficulty burnable (burnability factor of Peray-135.6) raw mix in a 1200 tpd SP-kiln in south India. The plant has to use run-of-mine limestone containing about 12% SiO_2 and 45.5% CaO. wherein about 10.5% of SiO_2 is contributed by chert (an amorphous mineral phase of SiO_2). Because of poor grindability of such limestone, the raw meal grinds coarser, and the residue on + 170 mesh sieve tends to be higher (16 to 20%). With increase in coal ash content, the kiln feed burnability decreases inspite of switching over to less siliceous additives, e.g. bauxite and iron ore in place of laterite in the raw mix. Coal was substituted by 2.5% and then 5% rice husk in the pulverized fuel. Their respective fuel characteristics do not show any difference in the fuel value but rice husk has lower ash and higher volatiles content. The effects of substitution on clinker composition and properties of resultant OPC are summarized in **Table-2.** It is evident that even with increase in coal ash content from 34-36% to 38-40%, its substitution by upto 6% rice husk has enabled to maintain the quality of clinker and cement or even to marginally improve them.

Discussions - The specific gravity of high ash coal is 0.94 to 1.06 and that of rice husk is 0.02 to 0.03. For proper mixing, the husk is thoroughly mixed with coal before feeding to coal hopper to avoid seggregation of husk in the table feeder. Very uniform feed rate from fine coal weigh feeder is required for maintaining uniform flame length and constant CO concentration at kiln outlet for proper burning of kiln feed. Finer grinding of kiln feed (12-13% residue on + 170 and 1% on + 72) and of pulverized coal (12% on + 170 and 2% on + 72) has been found to improve the burning condition and clinker quality, as routine grinding of coal + rice husk leaves higher residue (20-27% on + 170 and 3 to 6% on + 72). However, finer ground coal + husk blend increases the power consumption by 8 to 12 kwh/tonne of cement.

Table-2 : Clinker and Cement quality with partial substitution of Coal by rice husk in a 1200 tpd plant with 4 stage SP.

Clinker characteristics:

	LOI%	SiO_2%	Al_2O_3%	Fe_2O_3%	CaO%	Pulverized Coal				
						Ash%	UHV K.Cal./kg	Residue +170	Residue + 72	
Kiln feed	35.9-36.5	11.4-12.4	3.3-3.5	1.8-2.2	44.6-45.2	35-36	3200-3350	16-20	1.2-3.4	
Coal ash	-	64.2	20.6	6.5	4.0					
						C_3S%	C_2S%	C_3A%	C_4AF	Liquid
Clinker-I (with 6.5% coal ash absorption)	0.2 0.4	21.7 22.7	5.1 7.2	3.2 4.2	64.7 65.6	45 55	20 28	8 10	10 12	26 28
Clinker-II (2.5% rice husk substitution of 37-38% ash coal).	0.15	22.4	6.1	3.5	65.0	48	28	10	10.5	27.3
Clinker-III (6% rice husk substitution of 36 to 40% ash coal	-	22.0	6.2	4.1	65.9	54	23	9.5	12.5	29

OPC Characteristics (Average) : Table-2 ...contd..

	Specific surface cm^2/gm(Av.)	Setting time(min.) Initial	Final	Expansion(Average) Le Chatelier (mm)	Auto Clave(%)	Compressive Strength Average (kg/cm^2) 3days	7days	28days
OPC-I	2750	75	155	5.6	0.4	250	330	400
OPC-II	2750	65	140	3.5	0.2	255	325	410
OPC-III	2750	55	130	4.0	0.3	295	380	450

Case-2 - Extent of energy economy and cost benefit parameters from upto 20% substitution of high ash coal by rice husk has been established from industrial use of the latter in a 1200 tpd 4-stage SP Kiln plant in central India. The plant uses marginal grade limestone with no additive but high ash (27-38.5%) coal. Substitution of coal by upto 10% husk contributed 1% economy in coal consumption, 5% economy in fuel cost/tonne and no significant change in clinker or cement quality. About 20% substitution contributed 2% reduction in coal consumption, 9.75% economy in fuel cost/tonne and 8.5% total saving in fuel bill. However, clinker quality showed deterioration and required blending with better quality clinker for manufacturing OPC of specified quality. It has been found that finer grinding of coal + 20% husk mix (12% residue on + 170 mesh instead of 19-25%) improves the clinker quality to the required level (as per Clinker-I in Table-3) at the cost of additional 12-14 kwh/tonne power consumption. The fuel characteristics of rice husk and coal, compositional characteristics of kiln feed and clinker and physical properties of resultant OPC are summarized in **Table-3.**

Discussions - The test results indicate that relatively low lime content of kiln feed and low calorific value of coal contributing to relatively low strength development of OPC can be remedied by substituting coal by 10% rice husk. Higher reactivity of silica in husk is found to improve clinkerization. However, because of poor grindability of husk, its larger use (20%) leads to deterioration in burnability of kiln feed, as is evident from high free lime content of clinker. The inhomogeneity in fineness of the mixed fuel also leads to varying CO concentration in the kiln outlet.

Table-3 : Characteristics of kiln feed, fuel, clinker and cement with partial substitution of coal by rice husk in a 1200 tpd plant with 4 stage SP.

Fuel characteristics (Average) :

Fuel	Proximate Analysis (%) Internal Moisture	Volatiles	Fixed Carbon	Ash	Useful heat value K.cal/kg	Chemico-mineralogical composition of ash (%) LOI	SiO_2	Al_2O_3	Fe_2O_3	CaO	Fineness of ground fuel + 170	+ 72
Coal (Av.)	4.75	24.25	38.5	32.5	3700	-	57.5	28.7	8.75	2.0	22	3.4
Rice husk	4.64	62	12.5	20.5	3750	4.2	88.2	3.1	2.1	0.6	38	9.5

Clinker characteristics (Average) :

	Chemical Composition(%)						Free	Mineral phases (%)				Liquid
	LOI	SiO_2	Al_2O_3	Fe_2O_3	CaO	SO_3	lime(%)	C_3S	C_2S	C_3A	C_4AF	(%)
Kiln feed	35.3	10.3	4.0	2.3	41.7	-	-	-	-	-	-	-
Clinker-I (without rice husk)	0.3	20.2	7.6	4.2	61.3	0.45	2-3.5	40	27.5	13	13	37.7
Clinker-II (10% rice husk)	0.1	21.5	6.9	3.9	63.75	0.42	1.5-2	47	26	11.5	12	34.7
Clinker-III (20% rice husk)	0.5	22.3	6.5	3.7	61.5	0.44	2-4	34.5	38	11	11	32.5

OPC Characteristics (average) :

	Gypsum(%) added	Specific surface cm^2/gm	Setting time(mm)		Expansion (Av.)		Compressive strength Average (kg/cm^2)		
			In.	Final	Le Chatelier(mm)	Auto clave(%)	3days	7days	28days
OPC-I	6	2700-2850	100	225	3.0	0.8	210	305	410
OPC-II	6	2700-2850	70	160	2.2	0.4	265	355	425
OPC-III	6	2700-2850	140	290	2.8	0.7	195	275	360

Case-3 - Fixing the high lime content in kiln feed on account of high grade run-of-mine limestone (CaO 49.8-52.6%, SiO_2 3.4 to 4.2%) had been the primary objective in partial substitution of relatively high ash (35-38%) coal by rice husk (2-5%), besides reduction in coal consumption and fuel cost. Higher ash content of coal involves increased coal consumption for maintaining required burning zone temperature or more retention time of the high lime feed in burning zone for proper clinkerization resulting in lower clinker output at higher cost. Use of upto 5% rice husk pulverized with coal had significantly improved the burnability (inspite of decrease in clinker melt content) and also the quality of clinker and cement. The operational results are summarized in **Table-4.**

Table-4 : Improvement in clinker and cement quality quality with partial substitution of coal by rice husk in a 600 tpd plant with 4 stage SP.

Fuel Characteristics :

Fuel type	Proximate Analysis(%)		Useful heat value (K.Cal/kg.)	Chemical composition of Ash				
	Internal Moisture	Ash		LOI	SiO_2	Al_2O_3	Fe_2O_3	CaO
Coal	4.8-5.4	31.8-39.3	2750-3800					
Average	5.1	35.5	3250	0.6	60.4	23.2	6.3	3.2

Fuel type	Proximate Analysis(%)		Useful heat value (K.Cal/kg.)	Chemical composition of Ash				
	Internal Moisture	Ash		LOI	SiO_2	Al_2O_3	Fe_2O_3	CaO
Rice husk average.	4.6	22.5	4000	6.5	78.6	3.5	2.5	0.5
Coal with 5% husk.	5.06	34.7	3300	6.0	61.5	21.9	5.9	3.0

Clinker characteristics :

	LOI(%)	SiO_2(%)	Al_2O_3(%)	Fe_2O_3(%)	CaO(%)	Free lime(%)	Phase composition (%)				
							C_3S	C_2S	C_3A	C_4AF	Liquid
Kiln feed	35.0-36.1	12.1-13.9	2.6-3.8	1.7-2.8	44.2-45.2	-	-	-	-	-	
Clinker-I (control)	0.7-1.2	22.0-23.6	6.0-6.6	4.7-5.5	61.8-62.4	1.8-2.2	26-28	48-51	7-8	13.5-15	32.2
Clinker-II (5% coal substituted by rice husk)	0.5-1.0	21.8-23.8	5-7	3.7-5	62.6-63.8	1.0-1.5	35-40	40-45	7-8.6	13-14	29.7

OPC Characteristics :

	Specific cm^2/gm	Setting time (min)		Expansion Le Chatelier	Compressive strength (Average)		
		Initial	Final		3 days	7 days	28 days
OPC-I	3200-3300	100	200	4.8 mm	200	280	340
OPC-II	3200-3300	90	165	3.2 mm	230	335	425

B. As a Raw Mix Component :

An equally effective device for improving clinkerization of high lime bearing kiln feed in the same plant had been replacement of siliceous sand in raw mix by rice husk ash. Incidentally, locally available rice husk ash has almost similar chemical composition as impure sand, but only 5 to 10% of total silica is in free state in comparison to 85-90% in impure sand, as illustrated by a typical analysis below:-

Chemical Composition

Material	TC(%)	LOI(%)	SiO_2(%)	Al_2O_3(%)	Fe_2O_3(%)	CaO(%)	MgO(%)	Na_2O+K_2O	Free silica (%)
Impure sand	2.0	1.20	78.0	4.0	2.2	1.0	0.94	1.40	68.5
Rice husk ash	1.0	6.50	78.6	3.5	2.5	0.5	0.50	-	6.8

Use of rice husk ash was found to be more advantageous in view of its better reactivity in the clinkerization process, as well as, its abundant availability in the vicinity of the plant as a waste from calcium carbide and precipitated calcium carbonate manufacturing industries. The improvements in clinker and cement quality with gradual substitution of sand by rice husk are illustrated in **Table-5.**

Table-5 : Improvement in Clinker quality and Cement properties by increased replacement of sand by rice husk ash.

	Raw Mix with shale, sand(7%) and iron ore	Sand in Raw Mix replaced by 50% rice husk ash(3.5%)	Sand fully replaced by rice husk ash(7%)
Clinker Composition (%)			
LOI	0.7	0.5	0.65
SiO_2	23.0	22.68	21.60
Al_2O_3	5,9	6.0	6.30
CaO	63.21	63.81	63.81
MgO	1.20	1.10	1.05
Free lime	upto 3.64	upto 2.08	upto 1.6
C_3S	36	40	47
C_2S	38	35	26
Compressive strength of Cement (kg/cm^2)			
3 days	200	230	245
7 days	275	295	315
28 days	380	410	420

The free lime content in clinker reduced from 3.64% in the initial clinker (without rice husk ash) to 1.6% in the variety containing 7% rice husk. The tricalcium silicate content correspondingly increased from 36% to 47%.

Significant differences have been noted in the microstructural features, morphology and actual mineral phase composition of the three clinker types. The clinker without rice husk ash shows predominant microinhomogeneity with alite and belite occurring mostly in separate clusters (Fig.1). Both these phases are mostly anhedral in form with indistinct grain boundaries. Alite grains rarely exceed 35 μm in dimension and are mostly irregular in shape, constituting 30-35% of the mineral assemblage : belite constitutes 50-55%. The clinker with 50% substitution of sand by rice husk ash (3.5%) shows better morphology and lesser microinhomogeneity. Alite grains are subhedral, tabular to prismatic in form and attain upto 45-50 μm in dimension (Fig.2). Belite grains are anhedral to subhedral, rounded in form and often shows twinning or concentric zoning. This may be explained to be due to belite formation from two sources of silica, viz. less reactive silica from sand and highly reactive silica from rice husk ash. This clinker contains about 40% alite and 30 to 35% belite. The clinker with total substitution of sand by rice husk ash in raw mix shows still better morphology and much less microinhomogeneity. Alite and belite are evenly distributed with the interstitial phases (Fig.3). Alite grains are well formed with distinct boundaries, both prizmatic and pseudohexagonal varieties are common. The size of alite varies from 30 to 120 m, the average being 60 to 70 μm; belite grains do not show zoning or twinning, are hexagenal to tabular in form and with distinct grain boundaries. Alite constitutes 45 to 50% and belite 20 to 25% of the clinker.

Higher than 7% rice husk addition was found to increase the free lime content in clinker under the same residence time (kiln speed) and firing condition (burning zone temp.)-schedule and was not persued. Besides, addition of larger quantity of husk ash created jamming of chutes and diaphragms in the raw mill circuit due to seggregation requiring its frequent stoppages. Its uniform blending in the silos also required more intensive and prolonged stirring than conventional raw mix causing thereby lesser utilization of blending silo capacity.

The cited examples clearly demonstrate that depending upon process and operational parameters in individual plants specific quantity of rice husk or its ash can be used as substitute fuel or raw mix component.

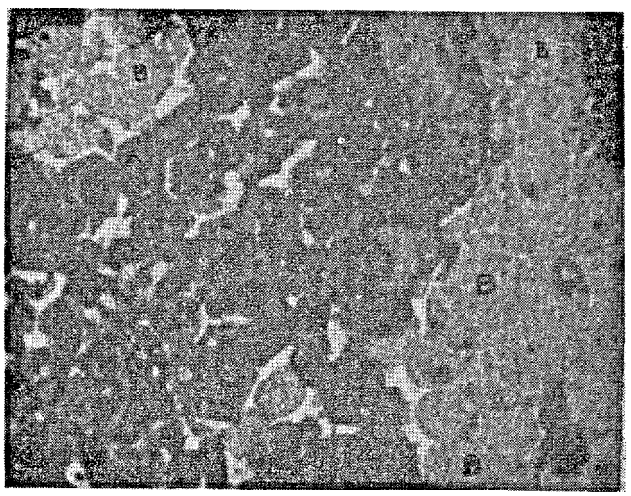

Fig.1 - Microphotograph of clinker without rice husk addition. Predominant micro-inhomogeneity and separate clustering of alite(A) and belite(B) is notable. Polarized light X 125



Fig.2 - Microphotograph of clinker with 3.5% rice husk addition in raw meal. Less uneven distribution of alite(A) and belite(B), zoning in belite grains and better morphology of alite are notable. Polarized light, X 125



Fig.3 - Microphograph of clinker with 7% rice husk addition in raw meal (sand totally excluded). Even distribution of alite(A) andinterstitial phases(I) and less frequent belite(B) are notable. Polarized light, X 125

ACKNOWLEDGEMENT

The work described here has been carried out as a part of the measures taken by the Cement Corporation of India in utilization of wastes for fuel economy in Cement manufacture and this paper is published with the permission of Director(Operations).

REFERENCES :

1. Mehta,P.K.and Pitt,N.: Resource Recovery and Conservation,1976,2, 23.
2. "CRI Rice Husk Ash Masonary Binder Cement-RHAM". CRI Technology Digest,New Delhi,India, July,1982, 8 p.
3. Vimal,O.P.: "Rice Husk - Raw Material for silica - based units". Indian Ceramics, 1982, 25(1), 10-15.
4. Khan, M.H.,Mohan, K and Taylor, H.F.W.: "Pastes of tricalcium silicate with rice husk ash". Cement and Concrete Research, 1985, 15(1), 89-92.
5. Adhikary, A.C.,Ahmed, A., Khorsed Alam, A.K.M.: "Study of production of rice husk ash cement". NCB International Seminar on Pragmatic Strategies and Modernisation, 1st, New Delhi, India 1987, V3, 31-39.
6. Boateng, A.A. and Skeete, D.A. : "Incineration of rice husk for use as a cementitious material". Cement and Concrete Research, 1990, 20, 795-802.
7. Grover, P.D.: Bio-mass thermo-chemical characterization. Indian Institute of Technology, New Delhi,1989.

COMPLETE SUBSTITUTION OF NATURAL RAW MATERIALS BY SHALE INDUSTRY WASTE AT CEMENT PLANT RECONSTRUCTION

A K Ioganson, M V Kouglya and L S Fraiman

Design and Research Institute of Cement Industry "Giprocement"
St Petersburg, RUSSIA

SUMMARY

This paper presents results of investigations of waste formed in mining and processing of oil shales - kukersites carried out for the purpose of their utilization in cement manufacture. The experiments were performed under laboratory, pilot and commercial scale conditions. They showed that on the basis of technogenous materials not mixing them with natural and corrective additives it is possible to obtain two-component mixtures in burning of which clinker of at least 40 MPa strength at the age of 28 days is produced. Thus the fuel and power savings are achieved. The investigations conducted allow for development of a new flow sheet of cement production with the use of technogenous waste including crusher-drier for a damp ash, precalciner for limestone waste and bypass system. The cement plant under reconstruction is situated at the area of the oil shale deposit.

РЕЗЮМЕ

В работе представлены результаты исследования отходов, образующихся при добыче и переработке горючих сланцев-кукерситов, с целью их использования в производстве цемента. Эксперименты проводились в лабораторных, полузаводских и заводских условиях. Показано, что на основе техногенных отходов без подшихтовки природными и корректирующими добавками можно получить двухкомпонентные смеси, при обжиге которых получается клинкер с 28-суточной прочностью не ниже 40,0 МПа. При этом наблюдается экономия топлива и электроэнергии. Выполненные исследования позволили разработать новую технологическую схему производства цемента с использованием техногенных отходов, включающую дробилку-сушилку для влажной золы, декарбонизатор для известняка-отхода и систему байпаса. Реконструируемый цементный завод расположен в районе месторождения горючих сланцев.

INTRODUCTION

Over a number of years the authors conducted detailed investiga - tions on the utilization of wastes resulting from mining and processing of oil shales-kukersites in cement production. In view of lack of competitive aluminosilicate materials at the plant to be reconstructed, it is mainly intended to use ash-and-slag waste formed in combustion of oil shales at the thermal power station. The mass of fresh ash products is made up of ash and slags washed off the furnaces by water (hydraulic removal ash) and of multicyclone ash which is in the main also discharged to the common hydraulic transport system to the ash dump. Waste from thermochemical processing of shales (gas generating station ash and compartment furnace semicoke ("koksik") used at the cement plant were also studied. It was proposed to use the oil shales rock mass dressing waste as the carbonaceous raw material. This limestone waste contains 3-10 % kerogen. Possibilities of clinker production by burning the rock mass representing a pack of alternating beds of shale and limestone were also under investigation.

EXPERIMENTAL

The chemical composition and physical characteristics of the waste are given in Table 1. The phase-mineralogical composition is presented in Fig.1.

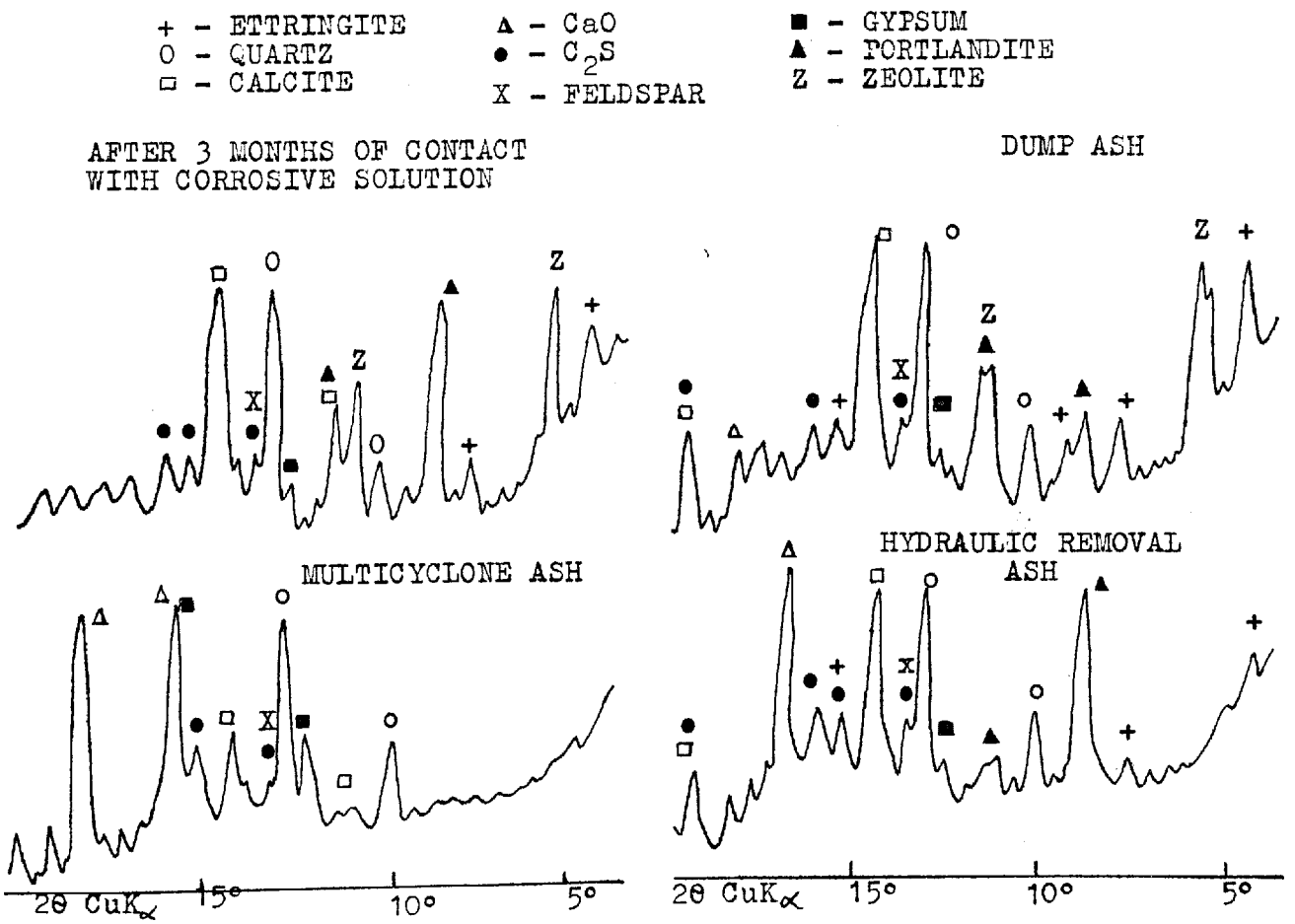

Fig.1. X-ray diffractograms of ash

Table 1. Chemical Composition and Physical Characteristics of Oil Shale Processing Waste

Waste		Multicyclone ash: Initial	Multicyclone ash: After 3 months of contact with corrosive solution	Hydraulic removal ash	Gas generating station ash	Dump ash	"Koksik"	Limestone waste	Three-bed rock mass	Four-bed rock mass
Content of oxides on ignited sample basis, %	SiO_2	33.18	31.21	34.30	36.49	28.06	38.15	11.83	21.37	19.71
	Al_2O_3	8.61	8.62	9.18	10.24	7.64	9.25	2.83	5.98	4.84
	Fe_2O_3	5.07	5.58	4.64	3.96	5.00	4.46	2.00	3.26	3.11
	CaO	41.50	42.54	40.06	35.70	48.85	34.50	69.32	58.61	60.51
	MgO	3.77	4.76	3.60	3.06	3.74	3.57	2.16	3.80	-
	SO_3	3.19	2.92	3.91	5.60	3.74	5.62	2.10	3.82	-
	K_2O	3.62	3.21	3.65	4.69	2.61	-	-	2.90	-
	Na_2O	0.13	0.20	0.13	-	0.09	3.26	1.39	0.13	-
	TiO_2	0.60	0.38	0.61	0.50	0.52	0.51	-	0.34	-
	Cl-	0.29	-	0.10	0.55	0.05	0.05	0.04	0.35	-
	Total	99.96	99.42	100.18	100.29	100.28	100.28	100.0	100.21	-
Moisture content, %		0.5	-	60	40	42	-	3.4	-	-
Bulk density, g/cm^3		-	-	-	-	-	-	2.3	-	-
Bulk mass, g/cm^3		1.26	-	-	1.0	0.83	-	1.30	-	-
Flowability		high	-	medium	medium	low	-	medium	-	-
Fusibility temperature	Fusion	1280	-	1280	-	1330	-	-	-	-
	Liquid--molten state	1310	-	1310	1440	1360	-	-	-	-

The physicochemical analysis of the multicyclone ash was found to be in agreement with the results of earlier works (1), the bulk of ash being made up of spherical glassy particles with refractive index close to that for the melilite glass. Areas of belite crystallization also occur. Crystalline quartz, calcite and calcium oxide are present in the sample. The hydraulic removal ash contains fine-grained material apart from the glassy particles. Besides quartz and calcite, one can also see here portlandite and ettringite. Microscopic studies of dump ash samples indicated glassy particles and fine cementing formations. Besides the reflections mentioned above there are rather high reflections in the area of $2\theta = 5 \div 20°$ in the X-ray diffractograms. Detailed analysis of the materials used at the cement plant showed that calcite, quartz and CaO are contained in "koksik". The gas generating station ash is composed of fine-grained material comprising calcite, quartz, ettringite and gypsum.

An understanding of the crystalline phase genesis under conditions of conveying and storing waste ash greatly help for a more precise identification. To this end special experiments were conducted on contact between a solid substance and a liquid solution. For approximation to actual conditions fuel slag pulp filtrate was chosen as dispersion medium. The filtrate is characterized by pH values in excess of 8 and oxide content in mg/l as follows: SiO_2 - 0.3; CaO - 1470; SO_3 - 486; K_2O- - 890; Na_2O - 20.8; Cl^- - 330. Decrease in gross SiO_2 content in the sample I after 3 months of contacting with alkaline-salt solution (see Table 1) points to the silica-oxygen bond breaking and peptization. At the same time, under strained conditions new hydrate phases are formed which intergrow and fasten the ash particles. The data of physicochemical analysis of solid residues showed that for 2 wecks of interaction a new hydrate phase, i.e. ettringite was formed in the multicyclone ash samples, and after 3 months there appeared reflections of a phase with d/n = 7.8 and 4.7 A° (Fig.1). In the case of hydraulic removal and gas generating station ash this phase was observed even after 2 weeks of leaching action. The nature of specimen dehydration shows that this phase is a finely-porous material in which the hydrate water is gradually removed from narrow channels when heated. This can be materials of the zeolite type.

In the preparation of raw materials for use as part of raw mixes, their behaviour in heating is very important. To study this, different representative samples of waste ash, as well as the limestone-waste and its mixes were subjected to thermal analysis. Burning trials of raw mixes with the dump ash and limestone-waste under pilot plant conditions demonstrated the possibility of producing clinker of mark 400. Microscopic investigations showed that the clinker obtained was characterized by a high porosity. It had a glomeroblastic unequigranular structure with a medium crystallization. Alite is present as grains of 5-70 μm size. Belite is constituted by 30-35 μm grains with notched edges. The interstitial phase is differentiated in aluminoferrite and the aluminate constituents.

RESULTS AND DISCUSSION

It can be seen from Table 1 that proceeding from the formulation the aluminosilicate component can not come entirely from the freshly formed ash because of its high content of alkalies and chloride. It is necessary to use the dump ash the content of harmful admixtures in which is considerably reduced by virtue of washing-out. The dump ash is cha - racterized by the highest fusion temperature. Lower fusion temperature of multicyclone and hydraulic removal ash is the result of their high

alkali-sulfate admixture contents. Since the dump ash contains new formations with a developed specific surface, a great quantity of water is immobilized within the structure. In this case, water retained by specimens of dump ash has various forms of bond with the ash solid frame. It is to be found in macropores (40-45%), micropores (25-30%), in adsorbed (25-30%) and structurally-bound states (3%) at the total initial moisture content up to 50%. This offers some difficulties when drying the ash. At the same time, considering the features of the cement plant reconstruction flow sheet according to which the aluminosilicate component is fed to the suspension preheater system, it should be noted that for a more effective lowering of the exit gas temperature it is necessary to aim at the greatest possible ash moisture content. Because of this the main limitation on the moisture content is the dump ash transportability through available materials handling systems and its caking (consolidation) in silos. Preliminary experiments showed that material with a moisture content above 10% sticks together, whereas at 7-10% it has a sufficient flowability. The data obtained show that the ash species in their passage through suspension preheater system retain their mobility over the whole temperature range. Further the dump ash is preferred to the "fresh" waste ash.

Besides the waste from oil shale combustion in heat-and-power station, in the cement plant use is made of secondary products from initial rock processing in the form of semicoke ("koksik") and gas generating station ash. The cement plant in question used freshly removed "koksik" as part of the raw mix for 20 years. Occasionally, gas generating station ash was used instead of "koksik". In the case, despite of high alkalies content of these wastes, cements of strength characteristics of at least 40.0 MPa at the age of 28 days were obtained under industrial conditions.

Alternative modes of utilizing rock mass in the cement industry were also studied. Compounds of 3 and 4 beds of shale and limestone were tested, their chemical composition is given in Table 1. As the thermal investigations showed, the physicochemical transformations taking place at burning of the mined rock mass are similar to those at heating of laboratory raw mixes prepared from limestone and mineral residues of shales, except for a more intense heat evolution at the burning-out of the organic constituents of the combustible rock. When burning natural rock mass too, the clinker obtained had a 28-day strength of not below 40 MPa.

CONCLUSIONS

The physicochemical studies conducted for evaluation of phase mineralogical composition, pyrophoric and physical properties of the mineral residues from oil shale processing, as well as the thermal behaviour of the cement raw mixes incorporating them showed the possibility of using these materials as raw mix components for producing cement of at least 400 mark.

The results of the laboratory and pilot scale studies are applied in the design of the plant reconstruction.

REFERENCES

1. Epik, I.P.: "Vliyaniye mineralnoi chasti slantsev na usloviya ra-

boty kotloagregata" ("The effect of shale mineral part on the ope - rating conditions of a boiler unit"). Est. gos. izd., Tallinn, 1961, 249p.

CONSERVATION OF RAW MATERIAL THROUGH USE OF INDUSTRIAL WASTES IN CEMENT MANUFACTURE

V K Gore, S A Khadilkar, P G Lele, C H Page and A K Chatterjee

Research and Consultancy Directorate
The Associated Cement Cos Ltd
Thane, INDIA

SUMMARY

Industrialisation and increased usage of natural resources, as well as the generation and disposal of the industrial wastes, has resulted in serious ecological and environmental imbalance. In tune with global emphasis on conservation of natural resources and cleaner environment, the Research and Consultancy Directorate of The Associated Cement Cos.Ltd. have undertaken a number of investigative studies on potential applications of industrial wastes in manufacture of cement and building materials.

The case studies presented in this paper discuss the use of some major industrial wastes like lime sludges, fly ash, slags, red mud, fluoride wastes, etc. in cement manufacture. The characterisation of these industrial wastes, their compatibility with the kiln feed and quality of clinker produced has been illustrated in the case studies. Derived benefits on the plant scale, with the usage of some of these industrial wastes have also been discussed.

INTRODUCTION

Rapid industrialisation has resulted into dwindling of non-renewable natural resources. Furthermore, many industries are generating tonnes and tonnes of solid waste material which is posing threat to the environment. Therefore for maintaining socio-economic balance, minimisation of waste generation and effective utilisation of waste generated has gained prime importance.

The main objective of this paper is to share the experience gained and the benefits derived from waste utilisation in authors' plants. It can be seen that many types of industrial waste which are hitherto less unknown can be usefully utilised in cement industry. If cement industry promotes the increased waste utilisation, the main objective of this paper is fulfilled.

AVAILABILITY OF INDUSTRIAL WASTES

Some of the major industrial wastes in India, which are of specific interest to cement industry, their source, availability and typical composition is presented in Table - 1.

TABLE - 1 MAJOR INDUSTRIAL WASTES, SORUCE, AVAILABILITY AND COMPOSITION

TYPE OF WASTE	LIME RICH				FLUORIDE BEARING		SUITABLE AS CORRECTIVE		
AVAILABILITY (Million Tonnes)	4.0				1.0		72.5		
SOURCE INDUSTRY	Paper Pulp	Sugar	Calcium Carbide	Ammon. Ferti-liser	Fluoride Cheml.	Fluorspar Mines	Thermal Power Station	Alumi-nium	Steel
TYPICAL COMPOSITION	Sludge	Sludge	Sludge	Sludge	Effluent Sludge	Mine Rejects	Fly Ash	Red Mud	Slags
% SiO_2	8.3	3.6	4.1	6.4	6.0	67.6	60.4	9.2	30.9
% Al_2O_3	1.3	2.9	2.0	0.3	2.6	4.7	23.5	22.8	23.5
% Fe_2O_3	0.8	0.6	0.4	0.3	1.2	5.7	5.7	46.4	1.2
% CaO	47.8	34.5	50.6	47.5	53.8	10.7	1.8	2.7	28.5
% MgO	1.5	1.0	0.5	0.5	1.1	0.8	0.6	0.7	11.6
% LOI	38.8	50.3	32.4	36.8	16.0	3.1	4.6	13.5	0.4
% Na_2O	1.4		0.02	0.02	0.68	0.16	0.08	4.74	0.2
% K_2O	0.2		0.02	0.01	0.03	1.9	1.37	0.11	0.68
% SO_3	0.4		6.3	6.3	-	0.3	0.4		
% Cl			0.23	0.02	-	0.03	<0.01		
% P_2O_5			0.1	2.4	-	0.2	0.2		0.2
% F				1.26	27.3	5.4	-		-

Thus, it can be seen that industrial wastes can be classified into three main categories:

Lime rich wastes

Calcareous sludges from paper, sugar and calcium carbide industry are grouped here. These materials, by virtue of their higher CaO content can be a potential source of CaO, especially where the limestone quality is inferior with respect to CaO content. Utilisation of these type of materials can replace scarce and expensive high grade limestone.(2)

Fluoride bearing wastes

Waste materials from Fertilizer, Fluorine Chemicals and Fluorspar industries are grouped here. These materials contain Fluoride as one of the constituent which is a potential pollutant and thereby these materials create problem of disposal.

Mineralising nature of Fluorides can be advantageously exploited by cement industry for improving the reactivity of the cement raw mix.

Materials suitable as correctives

Waste materials such as steel slags, fly ash and red mud are covered in this group. Although presently most of these materials are being used for making blended cement, unconventional use of theirs as a corrective material can also be thought of.

WASTE UTILISATION - PROSPECTS AND PROBLEMS

Physical proximity of a cement plant to the source of industrial waste mentioned earlier need not be the sole deciding factor for utilisation.

A decision of waste utilisation needs to be taken, based upon the following few major aspects:

- Extent of availability on sustained basis for the waste.
- compositional compatibility of raw materials and waste.
- Type of process employed and production capacity.
- Infrastructural facilities for handling and storing of the waste materials.

Due to very nature of its generation, waste material is not a uniform material. Some of the major constraints which are to be given a closer attention are listed below:

- Wide variation in composition, not only from different source but within the single given source.
- High moisture content, sticky nature and higher fineness levels.
- Handling and feeding problems associated with waste material.

WASTE UTILISATION - CASE STUDIES

Authors have attempted the utilisation of various industrial wastes in many operating cement plants. Data of the raw materials and the waste material utilised alongwith the observed benefits is presented in Table - 2.

TABLE 2 : WASTE UTILISATION DERIVED BENEFITS

Case No.	Raw Materials	Chemical Composition (% Oxide)								% Used		Derived Benefits
		SiO_2	Al_2O_3	Fe_2O_3	CaO	LOI	Eq. Na_2O	SO_3	F	N	M	
1.	Limestone	11.9	3.0	1,2	45.1	35.1		0.0		99.0	94.0	High clinker LSF could be maintained.
	Iron Ore	2.0	1.8	90.0	0.5	2.0				1.0	1.0	Helped in balancing alkali/ sulphate ratio.
	Paper sludge	8.0	1.3	0.8	47.8	38.8	1.53	0.4		0.0	5.0	Increased Raw Mill Output
2.	Limestone	12.0	3.1	2.0	44.7	35.7				99.5	89.5	Conservation of limestone deposits
	Blue Dust	1.2	6.6	91.5	0.2	0.3				0.5	0.5	Increased Raw Mill Output
	Sugar Sludge	3.6	2.9	0.6	34.5	50.3				0.0	10.0	Better coatability characteristics of clinker meet
3.	Limestone(1)	16.1	3.3	0.9	43.2	35.3				68.0	60.0	Improved clinker quality
	Limestone(2)	9.4	2.2	0.9	47.4	38.5				26.0	29.0	Cost reduction
	Limestone(3)	3.5	1.0	0.1	53.0	41.9				5.0	-	Increased Raw Mill Output
	Iron Ore	5.2	2.0	90.0	0.6	1.6	-	-	-	1.0	10.0	
	Fertilizer sludge	6.4	0.3	0.3	47.5	36.8	0.02	6.3	1.3		1.0	
4.	Limestone	10.6	2.2	2.1	46.2	37.6	0.15	<0.1	-	96.0	92.1	Improved burnability of kilnfeed even at higher sieve residues
	Clay (1)	39.9	8.6	6.5	18.3	22.6	1.06	-	-	2.0	6.9	Saving Heat Energy
	Clay (2)	17.5	27.8	32.0	0.2	18.2	0.15	-	-	2.0	-	Better granulometry/
	CaF_2 Sludge	6.0	2.6	1.2	53.8	16.0	0.70	-	27.3	-	1.0	grindability of clinker
5.	Calcareous sand	2.9	0.5	0.3	5.4	42.8				84.0	94.0	Fly ash acted as slurry thinner
	Clay	58.5	15.4	6.8	1.4	9.9				15.0	9.0	Reduction in KF slurry moisture (3%)
	Iron Ore	4.1	1.4	93.0	0.6	1.4				1.0	1.0	Improved burnability of Kiln feed
	Fly ash	60.4	23.5	5.7	1.8	4.6				0.0	6.0	10% increase in kiln output Saving of 100 Kcal/kg cl. in Heat energy
6.	Limestone (1)	19.1	1.2	0.9	43.4	34.2	0.24	0.23		38.0	38.0	Optimum sulphate modulus could be achieved
	Limestone (2)	8.9	1.1	1.0	49.3	38.8	0.21			56.5	56.0	
	Bauxite	17.4	41.3	16.8	1.2	22.8	0.05			4.5	3.5	Use of iron ore could be avoided
	Iron Ore	2.2	1.3	90.4	0.5	4.3				1.0		
	Red Mud	9.2	22.8	46.4	2.7	13.5	4.81				2.5	Reduced tendency of undesired build ups

N = Normal Raw Mix

M = Mix with industrial waste

Some of the case studies of waste utilisation along with the derived benefits are discussed below.

Calcareous Paper Sludge

It mainly consists of calcium carbonate, unreacted calcium hydroxide along with impurities of alkalies. In the final stage of disposal from paper industry, it is in the form of wet cake (% H_2O 20-40%), having 80% particles below 20 micron size.

In a dry process plant (Class-1) marginal quality of limestone with respect to CaO content (CaO 4.5%) coupled with higher ash and sulphur content, inferior clinker quality, especially the LSF was the main area of concern.

After Laboratory Evaluations, plant trial was conducted by replacing 5% of the limestone with paper sludge (on dry basis).

Following benefits were observed :

- Higher clinker LSF could be maintained which was not feasible earlier with high ash coal.
- High Alkali content of paper sludge (1.5%) helped in balancing the SO_3 contribution at high sulphur coal.
- Tendency of undesirable build ups in kiln system was found to be minimised.

The modulii of Raw mix with and without paper sludge utilisation are tabulated below:

Raw Meal	LSF	SM	AM	MSO_3
Without paper sludge	1.15	2.31	1.43	1.33
With paper sludge	1.18	2.37	1.45	1.01

Very fine nature of paper sludge increased the Raw Mix output by about 7%.

Fertilizer sludge containing Fluoride mineraliser

Ammonium sulphate plant produces a by product sludge which is mainly made of calcium carbonate. It contains impurities of sulphate (6.3%) and Fluorides (1.2%). Major constituent of interest is the Fluoride, which can be advantageously utilised as a mineraliser for improving the reactivity of the raw mix.

A wet process plant having siliceous and marginal limestone deposits was dependent upon the availability of high grade limestones. Increasing scarcity and cost of purchased high grade limestone was affecting the profitability of cement manufacture.

Moreover, in order to maintain clinker quality at desirable level, consumption of purchased limestone could not be lowered down.

Utilisation of fertilizer sludge was attempted in this plant. The limiting proportion of the sludge utilisation, mainly due to the SO_3 concentration present in it, was around 10%. (Case-3).

Plant trial conducted using 10% sludge in the raw mix showed following benefits:

1. Use of costly high grade limestone could be curtailed by around 6%.

2. Even at lower LSF values of the clinker, due to mineralising nature of Fluorides, the strength development of cement was at desired level. Improvement in micro-structure of clinker can be seen from Fig.1 and 2.

3. Finer particle size distribution of sludge helped in increasing the Raw Mill Output substantially.

PHOTOMICROGRAPHS OF CLINKER

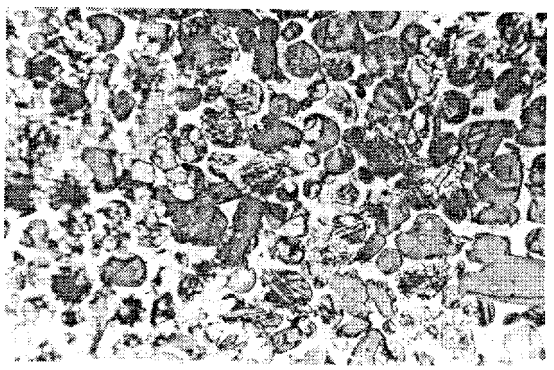

Fig.1 Without Mineraliser

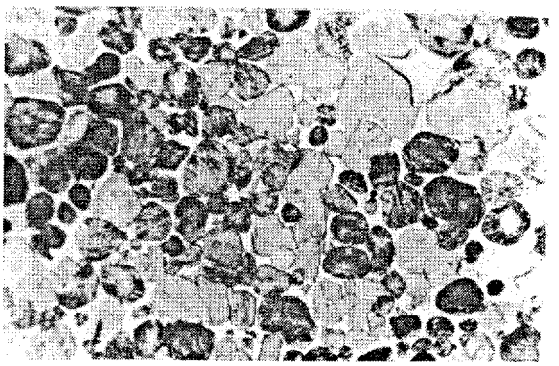

Fig.2 With Mineraliser

Fly Ash

The various physico-chemical details of fly ash available from thermal power plants need not be explained as it is widely being used in manufacture of Portland Pozzolana cement.

Unlike present use, case study presented here utilises the fly ash as a raw meal constituent. (1)

In a wet process plant case, if the kiln feed slurry moisture was required to be maintained at around 43% for proper pumpability. The main responsible factor for the said phenomenon was the very high plastic nature of the clay used as a raw meal component.

Although available slurry thinners could bring down the moisture requirement, their use was cost prohibitive.

Therefore, plant trial was attempted replacing 7% of the clay with fly ash, having more or less similar chemical composition as that of clay. (Case-5).

The Fig.4 shows the rheological behaviour of kiln feed slurry with and without fly ash utilisation.

Following benefits could be obtained:

1. Reduction in kiln feed slurry moisture from 43% to 40%

2. Improved burnability of kiln feed resulted into 10% increase in the clinker production along with saving of about 10 Kcal/kg clinker in heat system.(Fig.3).

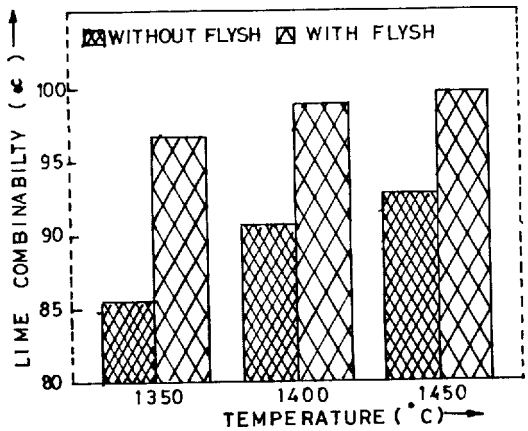

Fig.3 Burnability of raw mixes

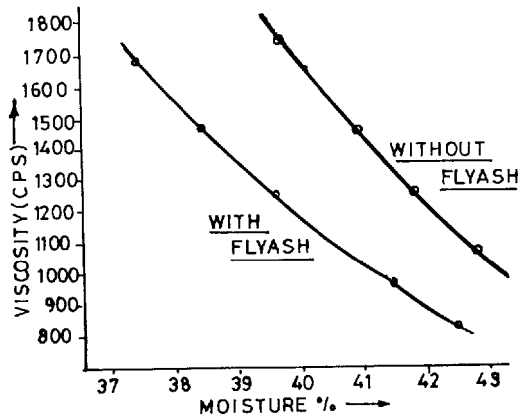

Fig.4 Rheological characteristics of kilnfeed slurry

CONCLUSIONS

Case studies exemplified in this paper establishes the usefulness of few industrial wastes for cement manufacture.

Waste sludges from paper/sugar plants can suitably replace scarce and costly high grade limestone or in some cases may even extend plant/quarry life in India.

Solid wastes like fly ash from thermal power plants can also be used as a reactive siliceous corrective for replacing clay component in the raw mix.

Due to presence of Fluoride in the wastes from Ammonium Sulphate/Phosphate plants or effluents from fluorine chemical industry, they can be used as a potential source of mineraliser for improving the reactivity of the mix.

Nevertheless, increased thrust needs to be given for utilising ever increasing quantities of industrial wastes, for ultimate objective of conservation of natural resources and minimisation of adverse environmental impact.

The endeavour of generating wealth from waste can only be achieved through continued and positive interaction amongst producers and the prospective users of industrial waste.

REFERENCES

1. D.Ghosh, C.H.Page and A.K.Chatterjee." Potentials of cost reduction in raw meal preparation systems in running plants." AFCM 8th Technical Symposium on cost reduction in cement industry. 4-6 March 1987 Code-11

2. Pritam Vachani ; " Utilisation of Waste Lime Sludge for manufacture of Cement" World Cement Technology, January/February 1981.

SAFETY AND ECOLOGICAL PROBLEMS IN BURNING ENERGY-SAVING RAW MATERIALS

A B Ryzhik, A K Ioganson, L S Fraiman and A V Alexandrov

Design and Research Institute of Cement Industry "Giprocement"
St Petersburg, RUSSIA

SUMMARY

The results of fire- and explosion-proof, as well as ecologically acceptable burning of cement raw mixes using fuel-bearing additives of different origins are summarized. The spark ignition in electrostatic precipitators is found to be the most likely trigger of combustion (explosion) of kiln waste gas containing volatiles. A theory is proposed with due consideration of the practical conditions of ignition. It is pointed out that emission into atmosphere of toxic volatiles which are not burnt out would give rise to ecological problems.

РЕЗЮМЕ

Обобщаются результаты пожаровзрывобезопасных и экологически чистых обжигов цементных сырьевых смесей на основе топливосодержащих добавок различного происхождения. Установлено, что наиболее вероятным механизмом инициирования горения (взрыва) отходящих печных газов, содержащих летучие, является искровое зажигание в электрофильтрах. Предложена теория и исследованы практические условия воспламенения. Экологические проблемы, обусловленные выбросом в атмосферу невыгоревших токсичных летучих, рассматриваются в качестве альтернативы процессу воспламенения.

INTRODUCTION

When burning cement raw mixes with fuel-bearing additives intensive liberation of combustible volatiles occurs in low-temperature zones with oxygen concentrations excluding ignition. Electrostatic precipitators are the most probable location of volatiles ignition (explosion) since it is here that the most favourable conditions for air in-leakage are realized with the added presence of a powerful source of ignition in the form of spark and corona discharges whose temperature can be around 2000°C (1). Granting that no ignition of the toxic volatiles has taken place, the alternative course of venting them into the atmosphere presents ecological problems.

In this context, a design-and-analysis method for evaluating the fire and explosion hazard of clinker production process was developed in Giprocement for the first time (2,3). Further to the foregoing, the present work deals with the features of utilizing waste fuels in cement clinker production. One of them is a kerogen-bearing raw material which is burnt in a ⌀ 4x60 m dry process suspension preheater kiln at the Slantsevsky cement plant. The other is a raw material containing waste coal from the "Artyom" colliery burnt in a ⌀ 5x185 m wet process kiln at the Karachayevo-Cherkessky plant.

THEORY

The gas mixture consisting of the combustibles, oxygen and inert constituents was considered as noninflammable if even one of the following conditions characterized by three dimensionless criteria is met:

- Content of combustibles in the mixture, φ_r, is below the lower concentration limit of the explosive range, φ_H :

$$K_H = 4\varphi_r / \varphi_H \leqslant 1 \qquad (1)$$

where 4 is safety factor for a homogeneous mixture with an ignition source, (2).

- Oxygen concentration in mixture with inhibitor, φ_{O2B} , is less than the minimum explosive oxygen content, $\varphi_{O2\varphi}$:

$$K_{O2} = \varphi_{O_2B} / (1.2\,\varphi_{O_2\varphi} - 4.2) \leqslant 1 \qquad (2)$$

where 1.2 and 4.2 are safety factors (2).

- Inhibitor content, $\varphi_{\varphi B}$, in the air mixture exceeds the minimum inhibiting concentration, φ_φ

$$K_\varphi = \varphi_{\varphi B} / 1.2\,\varphi_\varphi \leqslant 1 \qquad (3)$$

The characteristics $\varphi_{O2\varphi}$, φ_φ were determined by the procedure of Giprocement. Calculation of φ_H in the development of earlier publications (2,3) involved the use of a method based on determination of φ_H of the mixture of combustibles with inhibitors in air

$$\varphi_{H\varphi} = 100/(1 + \vartheta_t) \qquad (4)$$

Number of air moles in this equation falling on 1 mole of the source mixture is determined from the expression

$$\vartheta_t = \left(\vartheta_t^r - \frac{\sum_{j=1}^{m} \varphi_{\varphi rj} \cdot C_j}{\sum_{\kappa=1}^{n} \varphi_{r\varphi\kappa}}\right) \cdot \frac{\sum_{\kappa=1}^{n} \varphi_{r\varphi\kappa}}{100} \qquad (5)$$

where $\varphi_{r\varphi k}$ is content of the k-th combustible component in the mix with inhibitors (less air); $\varphi_{\varphi rj}$ is content of the j-th inhibitor in the mix with combustibles (less air); c_j is inhibition factor. Number of air moles falling on 1 mole of the mixture combustible part makes up:

$$\varphi_{\delta}^{r} = 100 / \varphi_{HB} - 1 \qquad (6)$$

By this means φ_H of combustibles mix in the inhibitor-bearing air is equal to:

$$\varphi_H = \varphi_{H\varphi} \cdot \varphi_{r\varphi} / 100 \qquad (7)$$

To ensure the balance conditions of volatiles burning-out in the kiln by oxidizer the oxygen content in the waste gases should be increased as against its amount determined only by the fuel consumption and in the end - by the excess air factor α_n at the kiln outlet. The value of the new excess air factor α_Λ should remain unchanged (similar to the case of the fuel consumption increase), but calculating on the resultant combustibles mix (fuel + volatiles). It means that the apparent value α_Λ (in relation to fuel only) will be equal to:

$$\alpha_\Lambda = \alpha_n \ (1+10^{-4}GMN/Q\,\rho_\Lambda), \qquad (8)$$

where G is capacity of the kiln unit; M,N is percentage of waste coal in the raw mix and of volatiles in waste coal, respectively; Q is gas fuel consumption; ρ_Λ is volatiles density.

Apparently, the last balance condition is necessary but not sufficient for the volatiles to burn-out since the process of material transfer and the kinetic features of the reactions are not taken into consideration in it.

RESULTS AND DISCUSSION

On the basis of data of gas analysis at the kiln outlet when burning the raw mix without waste coal the excess air factor α_Λ was computed as well as the new waste gas composition duly taking into account the composition of volatiles which remain without burning-out in the limiting case (in accordance with the assumption made). Composition of the gases in the electrostatic precipitator was determined proceeding from the conditions of their dilution by air. The entire of calculations were performed on computer.

The critical conditions of ignition

$$K_H = 1; \quad K_{O_2} = 1; \quad K_\varphi = 1 \qquad (9)$$

were computed by a method of iterations in relation to the excess air factor α_Σ in electrostatic precipitators and the volatiles concentration in the raw mix.

$$\delta^{\circ} = MN/100 \qquad (10)$$

As initial data use was made of the results of commercial tests from plants which do not use fuel-bearing additives:

	Slantsevsky plant	Karachaevo-Cherkessky plant
Kiln capacity, kg clinker/hr	31500	73000
Type of fuel	Coal/shale mix (60/40)	Gas

Fuel consumption, kg/hr	8060	
Nm^3/hr		13350
Composition of dry waste gas at the kiln outlet, % vol.		
CO_2	17.7	22.5
O_2	4.3	2.6
N_2	78.0	74.9
CO, CH_4, H_2	0	0
Excess air factor $\alpha_п$ at the kiln outlet	1.20	1.15
LOI, % mass	33.5	34.5
Raw material (slurry) moisture content, % mass	0	39
Volatiles content in waste, % mass	1-10	6-44
Gas temperature in the electrostatic precipitator, °C	250	250

The composition of volatiles from shale was as follows:,% vol.: CO_2 - 23.4; H_2S - 14.6; H_2 - 5.3; CO - 8.9; N_2 - 6.4; C_nH_{2n+2} - 31.7 (including CH_4 - 12.5; C_2H_6 - 10.6; C_3H_8 - 6.5; C_4H_{10} - 1.7; C_5H_{12}-0.6); C_nH_{2n} - 9.73 (including C_2H_4 - 2.60; C_3H_6 - 4.30; C_4H_8 - 2.10; C_5H_{10} - 0.73). The composition of volatiles from coal was taken as H_2/CH_4 = 50/50.

With the critical ignition conditions met the raw mix volatiles content δ and excess air factor in the electrostatic precipitators $\alpha_э$ were as follows: for the Slantsevsky plant - 2.4%; 2.03; for the Karachayevo-Cherkessky plant - 3.2%; 2.32. With decreasing δ and $\alpha_э$ the burning process becomes fire and explosion hazardous. When critical conditions for δ are met, the content of waste in the raw mix can vary over a wide range depending on the volatiles content of the waste.

Achievement of critical values of $\alpha_э$ appears to present no technical difficulties. It is different with δ . So, for the Slantsevsky plant the critical condition δ = 2.4% can not be fulfilled stably because of sharp changes of the volatiles content in the limestone waste which makes it impossible to conduct burning according to the traditional flow sheet.

The ecological calculations performed for the Slantsevsky plant kiln without calciner showed that atmospheric emissions of hydrocarbons (on carbon basis) and hydrogen sulphide formed at gasification of kerogen amount, respectively, to 112 and 56 g/s (3541 and 1760 t/year). Such an emission is many times over the permissible limit and thus results in air pollution. Presence of hydrogen sulphide in the waste gas inevitably involves small amounts of extremely toxic shale phenols the permissible limits for which are very low ($\sim$ 0.007 mg/m^3). Besides, sanitary conditions of the kiln plant operation are also impaired due to emission of carbon monoxide in amount of 25 g/s ($\sim$780 t/year).

CONCLUSIONS AND RECOMMENDATIONS

In order to ensure fire- and explosion-proof conditions of burning of kerogen-bearing raw material at the Slantsevsky cement plant and to eliminate hazardous emissions, the suspension preheater there is being modernized with installation of a calcining reactor. The new technology provides for feeding the limestone-waste directly to the calciner where the volatile combustible components should completely burn out. For the Karachayevo-Cherkessky plant, fulfilment of the critical condition $\delta = 3.2\%$ is rather practicable because of the low proportion of the waste coal in the raw mix wherein it is only an additive and has no more than a slight influence on the basic process parameters.

REFERENCES

1. Meek, J. and Craggs, J.D.: "Electrical break-down in gases", Oxford, Cla rendon Press, 1953, 486 p.

2. Ioganson, A.K., Ryzhik, A.B. and Fraiman, L.S.: "Ispolzovanie toplivosoderzhashchikh otkhodov dlya polucheniya tsementnogo klinkera" ("Utilisation of fuel-bearing waste for cement clinker production") VNIIESM, Moscow, 1990, 44 p.

3. Ryzhik, A.B. and Alexandrov, A.V.: "Vosplamenyaemost i toksichnost pechnykh gazov pri obzhige tsementnykh syryevykh smesei s toplivosoderzhashchimi dobavkami". ("Inflammability and toxicity of kiln gases at burning of cement raw mixes with fuel- bearing additives"). Tsement, 1991, (5-6), 84-86.

STUDIES OF BELITE CEMENT FROM BARIUM CONTAINING BY-PRODUCT

K Rajczyk* and W Nocuń-Wczelik**

*Institute of Mineral Building Materials, Opole, POLAND
**University of Mining and Metallurgy, Kraków, POLAND

SUMMARY

The investigation of the barium containing wastes utilization in the portland cement clinker production have been carried out with aim to reduce the temperature of burning and to improve the properties of belite phase. The results have shown that the activation of belite could be realized by Ba addition. Simultaneously a reduction of heat consumption on clinker burning was determined.

RÉSUMÉ

On a étudié la synthèse de clinker à haute teneur de bélite en utilisant le matérial secondaire contenant Ba en vue d`abaisser la témperature de la cuisson, ainsi que d`accélérer l`hydratation de bélite. A partir de clinkers on a preparé des ciments de bon qualité, c`est à dire avec le degagement de chaleur et la résistance méchanique suffisante.

INTRODUCTION

The modification of the ordinary portland cement clinker composition towards the belite phase content increase is one way of the energy consumption lowering in the portland cement production [1-4]. However, the reactivity of belite to water is much more lower than that of alite. Therefore, the studies on the activation of this phase to water have been carried out [5]. The researches of more economic techologies are strongly connected with the natural environment protection by the management of different wastes and by-products. The production of cements is one of the best examples illustrating the problem. In the presented work the results of the investigations on the barium containing wastes utilization in the portland cement clinker production are shown. These wastes were introduced with aim to reduce the temperature of burning and to improve the properties of belite phase.

The extensive studies of the barium addition on the synthesis and properties of clinker minerals were carried out by Kurdowski [6] and showed the positive influence of BaO addition on the sintering of clinker and the properties of clinker phases at the optimum BaO content, depending on the assumed phase composition. The materials containing BaO were used in the production of OPC 45 cement and rapid hardening cement [7]. Cements with lowered LSF were studied by Sytchev[8]. Addition of $BaSO_4$ and $CaSO_4$ to the raw mixture resulted in the active α'-C_2S modification formation [9]. The effect of barium depends strongly on the chemical and phase composition of Ba containing waste material used as a component of the raw mixture [9].

EXPERIMENTAL

The mixtures containing limestone and clay were prepared at different LSF values, 0.9, 0.85, 0.7 respectively. Some amount of ash from the bituminous coal combustion was also added. The Ba containing waste material from BaS production was added as 1% by mass of dry raw mixture. The chemical compositions of limestone, clay and Ba containing material is as presented below:
BaS: 2-7%, $BaCO_3$+$BaSiO_4$: 20-30%, $BaSO_4$: 5-40%, SiO_2: 4-10%, Fe_2O_3: 2-5%, Al_2O_3: 1-7%, CaO: 2-4%.

The mixture at LSF=0.90 was heated at 1450°C, the other mixtures - at 1350°C in a laboratory furnace. The clinkers thus obtained were subjected to the microscopic observations under SEM , to the microanalytical and XRD studies and, finally, used in cement preparation. The cements were tested using the standard methods and studied by use of microcalorimetry and other thermoanalytical technics. The raw mixtures were subjected to the high temperature microcalorimetric measurements and DTA studies.

RESULTS

The DTA curves of the clinkerization are shown in Fig.1 and the calculated enthalpies of processes occurring on heating are listed in Tab.1. Mixture 1 is the reference sample with LSF=0.90, mixture 2 is the sample containing 1% Ba-bearing admixture and having lowered LSF=0.85.In Fig.1 the endothermic peaks attributed to the clayey minerals decomposition at 120°, 550° and 770°C are seen. The calcium carbonate decomposition begins at 860°C with the peak maximum at 950°C. At 1230°C the exothermic peak corresponding to the reaction between CaO and acid oxides as well as the effect of the melt formation appear. As it results from the DTA curve, the clinkerization process in the Ba containing mixture is completed at 1350°C, i.e. at lower temperature that in the case

of traditional OPC clinker formation (mixture 2).

TABLE 1.

Heat consumption during the clinkerization process.

Temperature range (^{o}C)	Heat consumption in J/g mixture 1 (reference)	mixture 2 (with Ba)
20 - 400	394	393
400 - 600	243	233
600 - 800	471	489
800 - 1100	1649	1658
1100 - 1350	628	586
1350 - 1450	253	285
Total enthalpy at 20-1450°C Enthalpy of clinkerization	3637 (to 1450°C)	3246 (to 1350°C)

As it results from the XRD studies, the clinkers synthesized at lower LSF exhibit higher belite phase content and the peak corresponding to d=2.54Å desappears. On the other side the new peak corresponding to d=2.84Å which can be attributed to the α' - C S_2 phase can be detected. One can also notice that the splitting of the 2.74 and 2.76Å peaks does not occur. This "smoothing" of peaks may result from the formation of solid solution of Ba in C_2S.

The observation under SEM were carried out with aim to visualize the differencies in the belite and aluminate morphology in the presence of barium. In Fig.1 the belite grains in the clinkers of lower LSF are shown. The interstitial aluminate phase linking the belite grains is strongly modified but the effect of Ba on the belite grains is less pronounced. In Fig.2 the X-ray microanalysis data for the polished section of belite clinker are shown. The higher concentrations of BaO in the belite and aluminate phase can be easily seen.

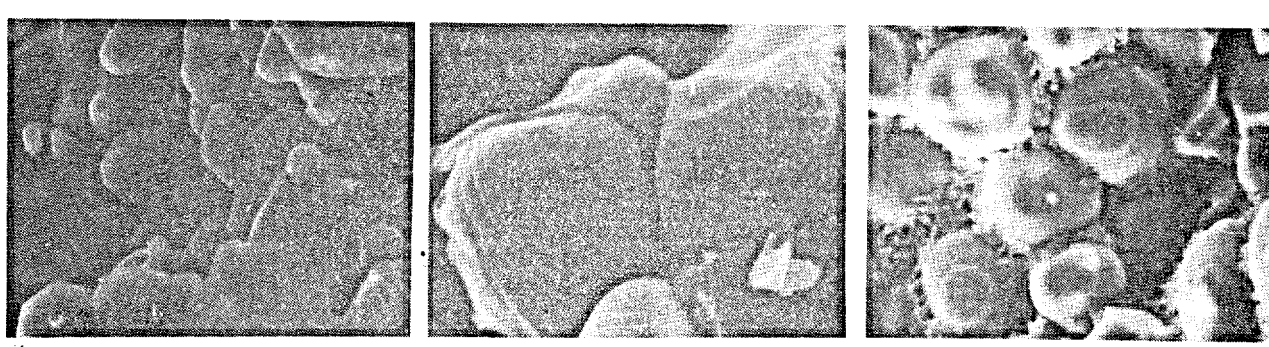

a/ b/ c/

FIGURE 1. SEM micrographs of belite clinkers with Ba.
a/ - LSF=0.85, 0.5% BaO; b/, c/ - LSF=0.70, 0.5% BaO.

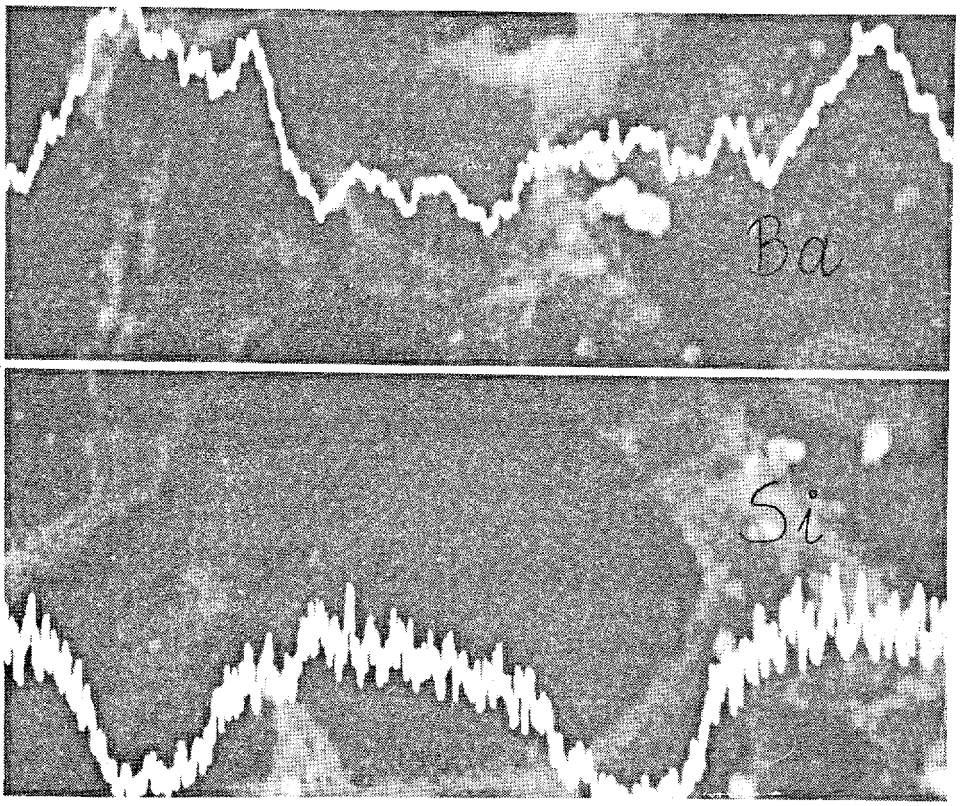

FIGURE 2. Concentration of Ba and Si in belite clinker (LSF=0.85).

The clinkers were ground to the specific surface 300 m^2/g with 5% gypsum. The standard ISO bars were subsequently prepared: the results of the compressive and flexural strength tests are given in Table 2.

TABLE 2.

Compressive and flexural strength of belite cements.

LSF	BaO content	Flexural strength			Compressive strength		
		3d	7d	28d	3d	7d	28d
0.90	-	5.9	7.0	7.1	33.0	46.2	58.1
0.90	0.5	6.0	7.0	7.0	33.5	46.8	59.9
0.70	-	2.3	3.2	5.1	7.6	12.6	15.6
0.70	0.5	3.0	4.2	6.7	10.0	22.0	22.0

The cements were also subjected to the microcalorimetric measurements and studies of the hydration products by thermoanalytical methods. The microcalorimetric curves are shown in Fig.3. As the Ba containing addition is introduced to the clinker, the hydraulic activity of material decreases in relation to the "classic" OPC, but it is much more higher than in the case of the belite clinker without any activator.

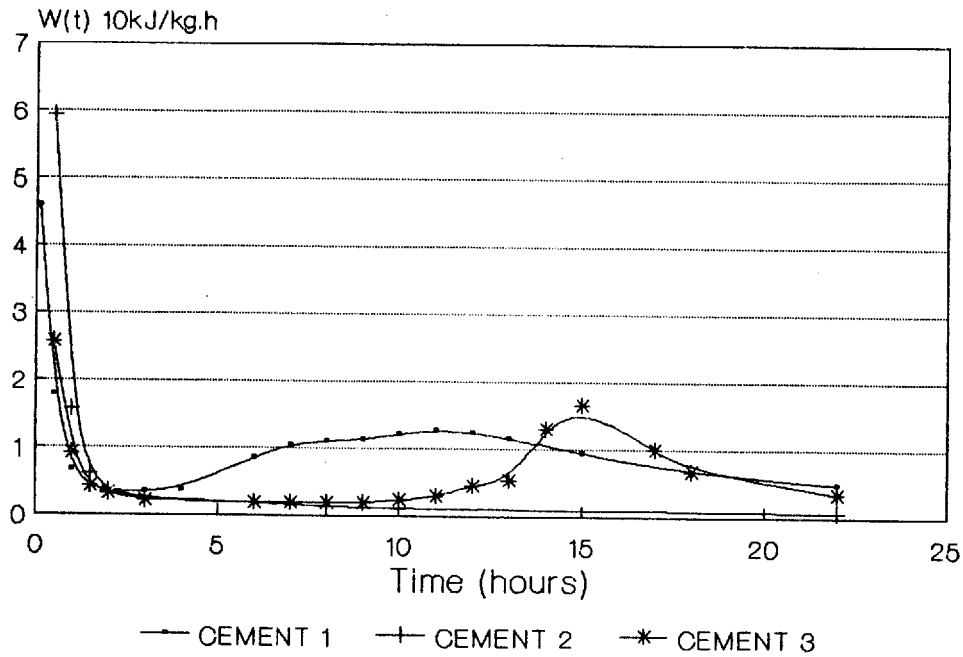

FIGURE 3. Microcalorimetric curves of cements with different clinkers.
1 - reference OPC clinker (Q=269 kJ/kg),
2 - clinker with high belite content (Q=107 kJ/kg),
3 - clinker with high belite content (LSF=0.70) modified by barium (Q=188 kJ/kg).

DISCUSSION

As it results from the data presented above, it is possible to produce the active clinker at the lower heat consumption and higher belite content. The activation process of the belite phase can be realized by use of barium containing waste material. Ba is incorporated not only by the belite phase but also by the aluminate one and strongly modifies their properties. As a consequence, the compressive strength increase in the case of clinker with LSF=0.90 is observed and the satisfying results are obtained also for the clinker with LSF=0.70 and doped with barium.

The studies of the clinkerization process by the high temperature calorimetry allow to calculate the difference in the heat consumed when the phase composition is modified by Ba toward the belite content increase. This difference is established as about 400 J/g. The studies of the heat evolution process during the reaction with water confirmed the positive effect of barium on the hydraulic activity of clinker.

REFERENCES

1. Meric, J.P.: Ciment, Béton, Plâtre et Chaux, 1987, 87(1), 19-22.
2. Stark, J. and Müller, A.: Proc. of 10th IBAUSIL, Weimar 1988, 160.
3. Peukert, J. and Peukert, S.: Cement, Wapno, Gips, 1984
4. Sytchev, M.M.: Cement, 1983, 5.
5. Gawlicki, M. and Nocuń, W.: Cement, Wapno, Gips, 1979, 32/46, 81.
6. Kurdowski, W.: Prace Komisji Ceramicznej PAN, Kraków, 1972
7. Gigova, L.F.: Proc. of 10th IBAUSIL, Weimar 1988, 216.
8. Sytchev, M.M.: Zour.Prikl.Chimii, 1987, 60(2).
9. Sulejmenov, A.T.: **Cementing Materials from Wastes**, Moscov, 1986.

FORMATION OF C_3S IN THE MIXTURES CONTAINING DIFFERENT SILICATE RAW MATERIALS

Kurdowski Wieslaw and Deja Jan

Academy of Mining and Metallurgy, Cracow, POLAND

SUMMARY

In order to explain the influence of different silica containing components on the tricalcium silicate formation the samples were prepared by mixing CaO and the following materials: silica gel, quartz, silica glass, synthetic glass corresponding to the formula "$CaO \cdot 2SiO_2$", α- and β- wollastonite, rankinite, γ-dicalcium silicate. The markedly higher free CaO contents and subsequently lower tricalcium silicate contents are found in the samples with different forms of silica. In the mixtures with "$CaO \cdot 2SiO_2$" and CaO the substantial tricalcium silicate content increase was evidenced in the first stage of reaction but the reaction rate clearly decreased with time. Comparing the results for the wollastonite polymorphs one can notice the higher $3CaO \cdot SiO_2$ contents for the samples with β- wollastonite. The similar course of C_3S formation can be observed in the mixtures with rankinite.

RESUME

On a étudié la synthèse de silicate tricalcique à partir de CaO et différents composants silicieux: gel de silice, quartz, verre de silice, verre de composition "$CaO \cdot 2SiO_2$", α et β- wollastonite, rankinite, γ-silicate bicalcique. La plus haute teneur en CaO et la basse teneur en silicate tricalcique a été établie dans les échantillons contenants différents formes de silice. La vitesse de la synthèse dans les mélanges de CaO et verre "$CaO \cdot 2SiO_2$" augmentait dans la période initiale mais aprés la réaction décélérait. La teneur en $3CaO \cdot SiO_2$ dans les mélanges de β-wollastonite et CaO est plus haute que dans les échantillons de α phase. La formation de $3CaO \cdot SiO_2$ dans les mélanges de CaO et rankinite va avec la même vitesse.

1. Introduction.

The reactions of the calcium silicates formation, specially those occurring during the portland cement clinker burning are the subject of numerous investigations [1-7]. The calcium silicate synthesis is a typical solid state reaction with the formation of intermediate products on the interface between the reacting oxides. The further reaction proceeds through the relatively slower diffusion, which is the rate limiting stage of all the process.

In order to explain the influence of different silica containing components on the tricalcium silicate formation the samples were prepared by mixing CaO and the following materials: silica gel, quartz, silica glass, synthetic glass corresponding to the formula "$CaO \cdot 2SiO_2$ ", ß-wollastonite, α-wollastonite, rankinite, γ-dicalcium silicate.

2. Characteristics of materials.

The calcium silicate components mentioned above were synthesized from the analytically pure calcium carbonate and silica gel. The mixtures at proper CaO : SiO_2 ratio were ground in the laboratory ball mills with in 24h, pelletized and heated in the superkanthal furnace. The samples after heating and cooling were ground in the laboratory agate mills to the fineness below 60 μm. The products were controlled by XRD. The uncombined CaO content determined in all the samples by Franke method did not exceed 0,2 %. The other materials, such as CaO, silica gel, quartz and vitreous SiO_2 were analytically pure.

2.1. Preparation of mixtures for $3CaO \cdot SiO_2$ synthesis.

The calcium silicates (γ-$2CaO \cdot SiO_2$, $3CaO \cdot 2SiO_2$, α and ß-wollastonite, "$CaO \cdot 2SiO_2$"), quartz, silica glass and silica gel were classified using the separator to obtain the $20 \div 40 \mu$m fraction. The 5-10 μm fraction was separated from the CaO sample. These components were dried to the constant weight at 378K and stored in closed containers over the silica gel (to avoid the water adsorption). The CaO sample was heated at 873 K for 1 h before the storage in the hermetic container. The mixtures at $CaO/SiO_2 = 3$ were subsequently prepared and homogenized within 24 h in the hermetic containers. The composition of mixtures was controlled by chemical analysis.

2.2. Synthesis of the tricalcium silicate.

The pelletized mixtures were heated in the superkanthal furnace at the following temperatures: 1623K, 1673 K, 1773 K. The pellets were prepared as follows: 3,0 g of samples were subjected to the 100 MPa pressure within 30 s in a mould of 18 mm in diameter. The pellets were stored in desiccator over the silica gel and placed in Pt crucibles just before heating. The heating was carried out within 5 to 480 min. The

heating and cooled samples were ground in the agate mills to the fineness below 60 μm and stored in the hermetic glassy containers.

3. Methods of reaction progress evaluation.

Because of the limited usefulness of the QXRD and thermal methods to the precise quantitative evaluation of the phase composition the free CaO determination was applied as the main method. The two former techniques were used as the auxiliary methods to semi - quantitative $3CaO \cdot SiO_2$ and other phases identification.

4. Results.

The uncombined CaO contents in the samples were determined by Franke method and then a content of tricalcium silicate was calculated. The calculated tricalcium silicate contents as a function of time and temperature are presented in Fig.1. At it results from the data thus presented, different sources of silica show different reactivity toward the lime in the tricalcium silicate synthesis. As one could expect, the rise of reaction temperature brings about the reaction rate increase. Irrespectively of the rise of temperature, the markedly higher free CaO contents and subsequently lower tricalcium silicate contents are found in the samples with different forms of silica. In this set of samples the highest free CaO contents are evidenced for those containing silica gel. The silica glass and quartz show the similar reactivity to CaO. Slightly higher results are found for the samples with quartz. In the mixtures with "$CaO \cdot 2SiO_2$" and CaO the substantial tricalcium silicate content increase was evidenced in the first stage of reaction (5-10 min), but the reaction rate clearly decreased with time. Comparing the results for the wollastonite polymorphs one can easily notice the higher $3CaO \cdot SiO_2$ contents for the samples with ß-wollastonite. After the 480 min. heating at 1773 K the mixtures with ß-wollastonite show $3CaO \cdot SiO_2$ content 99%.

The similar course of the $3CaO \cdot SiO_2$ formation can be observed in the mixtures with rankinite. The higher free CaO contents are found at the beginning but after a time (120-480 min), the quick free CaO content decrease is observed and the results are quite similar to those for ß-wollastonite.

The lowest uncombined CaO values have been determined in the mixtures with γ-$2CaO \cdot SiO_2$ + CaO. As early as after the 15 min. heating at 1773 K the free CaO content is only 8.54% and lowers quickly with time. It was shown that after the 420 min. reaction at 1773 K there was no free CaO practically and only $3CaO \cdot SiO_2$ was present in the sample. However, regarding the results for γ-$2CaO \cdot SiO_2$, which can be assumed as a standard, one should take into account that the uncombined CaO content in the initial γ-$2CaO \cdot SiO_2$ + CaO mixture is the lowest from all the samples and equal only 24.56%.

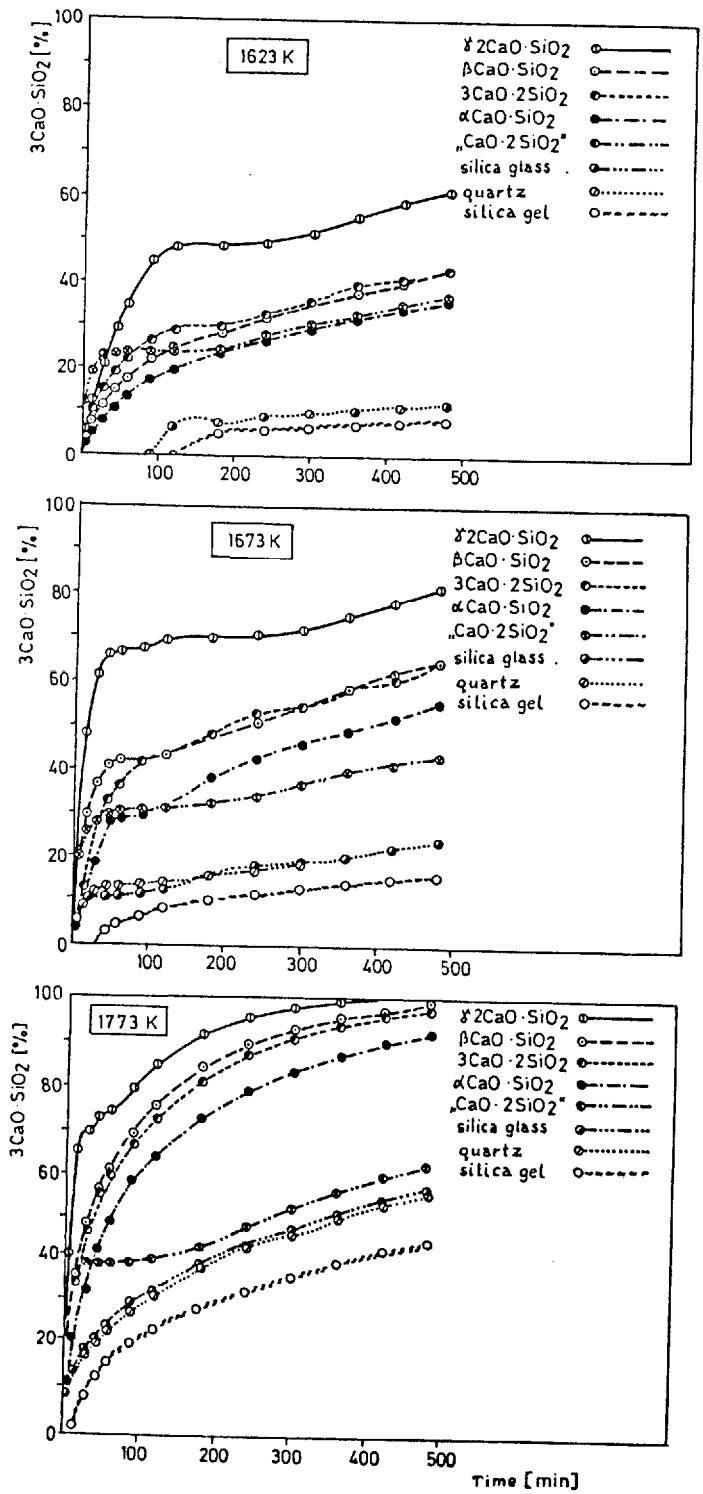

Fig.1. $3CaO \cdot SiO_2$ contents versus time and temperature.

The quantitative evaluation of the kinetics by the free CaO determination can be supported by the QXRD measurements. The highest $3CaO \cdot SiO_2$ contents are found for the mixtures with γ-$2CaO \cdot SiO_2$, lower for rankinite, α, ß-$CaO \cdot SiO_2$ and the lowest for the initial mixtures with silica gel.
The substantial phase composition differences between the samples are clearly visible on the XRD patterns. As early as after 5 min. reaction at 1673 K there is no SiO_2 bearing reactants.

In all the samples, except of those with γ-$2CaO \cdot SiO_2$, the formation of large amount of γ-$2CaO \cdot SiO_2$ phase is observed during cooling (d= 3.01; 2.89; 2.75; 2.73; 1.76). The γ-$2CaO \cdot SiO_2$ content decreases with increasing time of heating and the ß-$2CaO \cdot SiO_2$ content increases simultaneously (d=3.05; 2.78; 2.75). In the mixture γ-$2CaO \cdot SiO_2$ + CaO the stabilization of the ß polymorph takes place and only this mixture does not reveal the self disintegration.

The differences of the phase composition are also confirmed in DTA studies. The results of DTA measurements are presented in Fig.2.

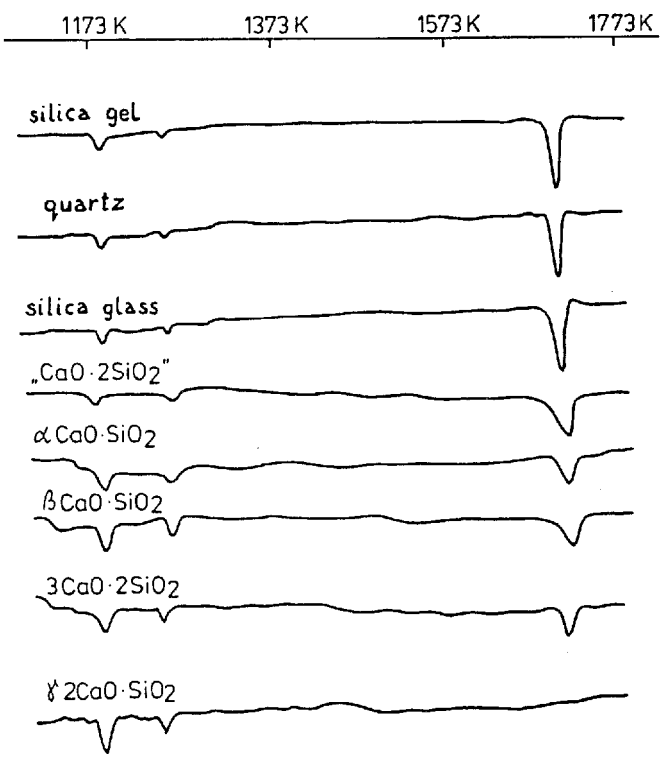

Fig.2. DTA curves of samples heated at 1673K (CaO/SiO_2 = 3).

On the DTA curves of samples heated for 480 min. at 1673 K the weak endothermic peaks at 1173 - 1178 K and 1223 - 1231 K attributed to the tricalcium silicate transitions are visible. The endothermic peak about 1703 K corresponding to $\alpha'_H \rightarrow \alpha$ $2CaO \cdot SiO_2$ is also marked. The areas of peaks indicate that the highest $3CaO \cdot SiO_2$ amount was formed in the mixture γ-$2CaO \cdot SiO_2$ + CaO (the peak of $2CaO \cdot SiO_2$ transition is negligible; the largest peaks correspond to $3CaO \cdot SiO_2$ transition). The lowest reactivity of the silica gel + CaO mixture has been also thus evidenced.

5. Conclusions.

The results show that the crystalline structure of the silicate raw materials is an important factor influenced the $3CaO \cdot SiO_2$ formation. The highest $3CaO \cdot SiO_2$ contents have been detected in the mixtures with γ-$2CaO \cdot SiO_2$ (orthosilicate) and CaO. The use of raw materials containing condensed silicate anions (rankinite, α, ß wollastonite) reduces the rate of tricalcium silicate formation. The different reactivity of the ß- and α- wollastonite results from the different structure and consequently from the higher activation energy of Ca^{2+} diffusion in α- $CaO \cdot SiO_2$ [8]. The significantly lower tricalcium silicate contents are found in the samples with different forms of silica i.e. silica gel, quartz, silica glass (skeleton structure).

6. References.

1. Hild K., Tromel G., Z.Anorg.Allg.Chemie, 215, 333 (1933).
2. Jander W., Hoffmann E., Z.Anorg.Allg.Chemie, 218,211 (1934).
3. De Keyser, Bull.Soc.Chim.Belg., 62, 235 (1953).
4. Kurdowski W., Silicates Industr., 30, 500-506, (1965).
5. Gebauer J., Fitzer E., Zement-Kalk-Gips, 22, 402 (1969).
6. Weisweiler W., Osen E.J., Eck J.,Hofer H., Cem.Concr.Res., 16, 283 (1986).
7. Weisweiler W.,Osen E.J.,Eck J., Cem.Concr.Res.,18, 55(1988).
8. Lindner R., Z.Phys. Chemie, 6, 129 (1956).

NEW DATA ON RAW MIXES BURNING IN DRY-PROCESS KILNS ON THE BASIS OF AN ARTIFICIAL CLAYISH COMPONENT

A I Zdorov and V L Bershtein

NPKO Yuzhgiprocement, Kharkov, UKRAINE

SUMMARY

There are considered the theoretical questions of designing of raw mixes compositions,containing complex additives of industrial by-products. At laboratorial and industrial level there have been proved the advantage of mixes with artificial clayish component over traditional ones as far as reduction of fuel consumption for clinker burning in dry-process kilns and increase of clinker activity are concerned.

АННОТАЦИЯ

Рассмотрены теоретические вопросы проектирования сырьевых смесей, содержащих комплексные добавки промышленных техногенных продуктов. На лабораторном и промышленном уровне доказаны преимущества смесей с искусственным глинистым компонентом над традиционными смесями в части снижения расхода топлива на обжиг клинкера в печах сухого способа производства и увеличения активности клинкера.

INTRODUCTION

Development and improvement of dry process production don't eliminate the task of further intensification of Portland cement clinker burning processes at the expense of chemical engineering techniques.The most perspective one is the use of industrial by-products and industrial wastes in raw mix composition.Last years this problem acquires ecological essence not only in connection with environment pollution control, but also with inevitable worsening of quarrying conditions and natural raw materials quality accompanying cement production growth.

Long-term observation of high-capacity dry-process kilns operation indicates the presence of at least three interrelated parameters,such as kiln output,fuel consumption for clinker burning,and clinker strength characteristics.These parameters can be significantly improved due to raw mix mineral composition optimization.Two last parameters have been accentuated in our investigations.Working hypothesis consists in observing the principle of correspondence of Portland cement raw mix pyrophysical properties to clinker burning peculiarities in dry-process kilns,in particular,to material heat processing in suspension preheaters.Laboratory complex investigations have shown that the most unfavourable raw mix component is high-aluminate clay - a wide-spread component in dry-process technology.Authors' early works carried out at Lipetsk cement plant,where high-aluminate clay was substituted by granulated blast-furnace slag,resulted in 5-8 MPa increase of Portland cement clinker activity and 10-12 percent decrease of fuel consumption for its burning.

Early appearance of melt due to presence of slag promotes integration of mix particles into conglomerates,which results in improvement of conditions for their chemical interaction in preparing zones and clinker granules formation.At the same time,insignificant content of fusing agents in raw mix composition and low probability of their contact with clinker intermediate phases limit possibilities of the method indicated.Authors suppose that further development of this method is in using complex compounds,added to a raw mix,on the basis of industrial by-products capable of substitution for natural clay completely or as maximally as possible.

EXPERIMENTAL

Considering that industrial by-products percentage in raw mix composition is high enough the decisive factor is the availability of main Portland cement clinker oxides in the mix,otherwise there can arise problems with clinker production of set composition.Thus the development of optimum complex compounds comes to a limited number of constitution diagrams.Undoubtedly,it is preferable to work with tetracomponent constitution diagram $CaO-Al_2O_3-SiO_2-Fe_2O_3$.However,now we have no rather reliable data concerning this diagram for the whole ferric oxide cross-sections range.A zone of compositions approaching Portland cement clinker ones may be regarded as having been studied,but these compositions are characterized by high melting point.In this connection,analysis has been carried out on ternary constitution diagrams which made calculation results conventional to some extent and required their correction during experimental investigations on actual materials.

There have been investigated 17 kinds of industrial by-products

divided into 4 main groups according to the predominance at least of one of oxides in them.It was foreseen that raw mix composition shouldn't contain two representatives of one group.Thus maximum quantity of industrial by-products was limited to four ones but in most cases we have received results with a ternary additive.

After preliminary investigations taking into account technological factors and calculation results of raw mixes with $CaCO_3$ basic carbonate component we have chosen 6 kinds of wide-spread industrial by-products namely granulated blast-furnace slags (GBFS),ash-slag wastes (ASW),coal preparation wastes (CPW),worked-out moulding sands (WMS),converter slags (CS) and ore dust (OD).

Experimental investigations for selection of the most fusible additives were based on the experiment specially developed by the authors (simplex planning) and simplified but rather reliable technique for refractoriness determination of compositions to be investigated.This technique allows fixing both the temperature of samples softening beginning, that is characterized by appearance of drop melts,and evaluation of their viscosity.These data are of great importance in connection with the concept being developed and concerning the influence of raw mix pyrophysical properties on clinker formation process.

Authors have received results of experimental determination for melting points of boundary compositions of the matrix.With their help 12 binary diagrams of refractoriness and 10 ternary ones have been plotted.These diagrams are universal and can be used for any raw situation regardless carbonate component chemical composition.

Mathematical analysis allowed us in each diagram to determine zones of compositions where melt appeared at 1160-1180 °C.In a number of cases zones of minimum melting points adjoin the GBFS-ASW binary system.The availability of the minimum in this diagram agrees well with analysis data of $CaO-Al_2O_3-SiO_2$ ternary constitution diagram where the line,connecting these products compositions,passes through the invariant point. In diagrams with GBFS and ASW there are wide-spread compositions zones where melt appeares at temperature lower than 1200 °C.Smooth character of melting point change is of great importance for providing for controllability of preparing raw mix of preset chemical composition.

There are such zones of optimum compositions practically in all diagrams investigated.Not analysing all refractoriness diagrams plotted, which is the theme of a separate work,it is possible to conclude that the aim of development of chemical engineering techniques for burning process intensification can be achieved on the basis of artificial clayish component manufacture from industrial by-products.

The advantage of such raw mixes over conventional ones was fixed while investigating kinetics of free calciumoxide combining.Reacting capacity of model mixes on the basis of industrial by-products optimum compounds which completely substitute for clayish component is higher in the whole temperature range.Especially this is revealed at 1450 °C.The most advantageous results have been received using GBFS,ASW,CS and CPW.

Authors have the experience of commercial checking the method developed for clinker burning intensification in 5m and 7m dia. dry-process

kilns.Complex additive on the basis of GBFS-ASW-OD industrial by-products was prepared at Rezina cement plant.It allowed complete exception of high-aluminate clay from the use and half cutting ordinary clay use. Long-term commercial tests have shown the highest values for Portland cement clinker activity and kiln output in cement industry.During tests a decrease in equivalent fuel consumption for 1 t clinker burning amounted 18-25 kg and sometimes 30 kg.In some periods of time heat consumption reached 3,250-3,300 kJ/kg of clinker.

During the tests carried out at Lipetsk cement plant the clayish component was completely substituted by GBFS-ASW-CS complex compound of industrial by-products.In this case a decrease in fuel consumption was somewhat lower because the standard mix,which was burned,contained granulated blast-furnace slag.Equivalent fuel consumption reached 112 kg per 1 t of clinker.

The fact that in all cases at carrying out industrial investigations there is observed improvement of quality indicies of Portland cement clinker,is quite important.The content of dust fractions (less than 1 mm) in clinker has more than twice reduced. The size of alit crystals in the main mass has reduced from 40-70 mkm to 10-30 mkm. In some periods of time this has provided for the clinker activity increase by 5-10 MPa.

CONCLUSIONS AND RECOMMENDATIONS

The investigations carried out have shown that the trend connected with use of complex compositions of industrial by-products introduced into raw mix composition as clayish component,at dry process of cement production,are perspective.In the institute "Yuzhgiprocement" this work finds its reflection in introducing results received into new cement plants designs.

ACKNOWLEDGEMENTS

This paper is based on the results of long-term investigations, carried out in the laboratory of process intensification of Yuzhgiprocement.The authors appreciate the help of their colleagues,M Babich, E Degtyar, V Demenko and M Zlatocrylov in carrying out experimental investigations and introducing the work results into the industry.

AN IMPACT OF NON-TRADITIONAL RAW MATERIALS ON THE FORMATION AND PROPERTIES OF CLINKER

M A Akhmedov, A A Mukhamedbaev, M T Artykbaev
Z S Salimov and A P Flodorov

The Institute of Chemistry, Academy of Sciences
Tashkent, UZBEKISTAN

SUMMARY

Recently in development of the cement production in the USSR and abroad the use of various non-traditional raw by-materials is of great importance.

This work adduces data on an impact of a non-traditional raw material, the over-burden rock ef coal mining - secondary kaolin clays - as the alumosilicate part of the raw mixture, on the formation and properties of clinker. The examinations proved that the reactions of mineral formation of clinker ran faster in such mixture, a compared to a raw mixture of a traditional natural raw material. The amorphous substance, being in metastabile state and formed after dehydratation and a failure of the crystallic lattice of the mineral of Kaolinite, is of the highest capability for Interacting with calcium carbonate, intensifying its dissociation and facilitating the processes of formation of silicates, aluminates, alumoferrites and calcium ferrites.

В работе приводятся данные о влиянии нетрадиционного сырья, вскрышных пород угледобычи-вторичных каолиновых глин в качестве алюмосиликатной части сырьевой смеси, на формирование и свойства клинкера. Как показали исследования, реакции минералообразования клинкера в такой смеси протекают быстрее, чем при сырьевой смеси из традиционного природного сырья. Находящееся в метастабильном состоянии аморфное вещество, образовавшееся после дегидратации и разрушения кристаллической решетки минералов каолинита, обладает наивысшей способностью к взаимодействию с карбонатом кальция, интенсифицируя его диссоциацию и облегчая процессы образования силикатов, алюминатов, алюмоферритов и ферритов кальция.

It is known that in the Middle Asia limestone and loess loam is mainly used as a traditional material for production of clinker, and pyrite cinder is used as the correcting addition.

Recently in development of the cement production in the USSR and abroad the use of various non-traditional raw by-materials is great importance.

The physical and chemical processes, available in firing the cement clinker, greatly depend on chemical-mineralogical and substance composition of raw constituents and mixtures, as well as on used by-products and industrial waste (1-4).

The dissociation reactions, taking place during temperature transformations, the dehydratation ones, accompanied with a change of the inner structure and the chemical relation of a material as well as a failure of the crystallic lattices of minerals and an amorphization of the substance are of a particular importance in the revealing of reactivity of a raw mixturo.

Kinetics of the reaction of dissociation of calcium carbonates, which are the basic source of calcium oxide in a raw mixture, mainly depends on their form, a structure of minerals, a crystallinity, a dispersivity of the crystals as well as on an availability of admixtures in the form of solid solutions. This substantially impacts on temperature limits of dissociation of carbonates and on formation of CaO in the most active state.

A reactivity of a raw mixture also depends on structure and thermal strength of the crystal lattice of argillaceous, alumosilicate and by- raw constituents.

The data on an impact of the non-traditional raw material - the over-burden rocks of coal mining (secondary kaolin clays) as the alumosilicato part of a raw mixture on the formation and properties of clinker are adduced in the work. Samples of kaolin clays from various bays, benches and stakes of the coal stripping "Angrensky" ware taken for an examination of the secondary kaolin clays and a determination of the possibility of their use as the raw constituents in production of cement.

A petrographic analysis of the kaolin clay indicated that the rock consisted of a rather fine-disperse constituent (mainly kaolinite with a small admixture of the minerals of the group of hydrous micas and gallauzite. The argillaceous fraction contained approximately 86% of kaolinate and 14% of hydrous mica. The aleurite admixture made not more than 2-3% and consisted of quartz grains, having maximal size 0.05 mm. The highly-disperse argillaceous particles sized 0.0005 mm and the dustous ones - 0.005-0.05 mm.

After an examination of the granulometric composition of the loess loam and the kaolin clays it has been determined that the concentration of the fractions sized less than 0.001 mm in the kaolin clay was three times as more than in the loess loam, that is, particles of argillaceous minerals were of a greater fineness in the active state than in the loess loam. The concentration of undesirable large particles (0.05-0.5 mm) was lower. This feature contributes to its value when using them as a raw constituent. Hence, the addition of the non-traditional raw material - kaolin clay - caused the enriching and an even distribution of fine fractions in the whole mass of raw mixtures. This fact, in its turn, facilitatesthoe proceeding of an interaction of oxides at relatively low temperature.

Data of a thermographical analysis of the kaolin clays indicated a presence of kaolinite in them, which is characterized by the endothermal effect at 450-580° C, caused by dehydratation of kaolinite.

The process of dehydration of kaolinite during firing took place slowly and ended at the temperature 700-800° C. The exotermal effect at the temperature 990-1100° C and higher characterized the proceeding of a discomposition of kaolinite to metokaolinite and the beginning of the formation of mullite,at later under an increase of the temperature, to separate oxides Al_2O_3 and SiO_2, which were in a more active form. The oxides accelerated the mineral-formation processes at low temperature, interacting with the constituents of fired material (4,5,6).

At roentgenograms of the kaolin clays diffraction maximums, poculiar to kaolinite - d = 4.43; 2.58; 1.49 Å and quartz - d = 4.27; 3.35; 2.45; 2.23; 2.13; 1.98; 1.81; 1.66 and 1.54 Å could be observed.

A chemical composition of secondary kaolin clays are adduced in Table 1.

Table 1. A chemical composition of the kaolin clays

Campling site	Calcination losses (%)	Concentration of oxides (%)					
		SiO_2	Al_2O_3	Fe_2O_3	CaO	MgO	R_2O
Bench 6,stake 11	10.80	51.84	29.20	3.91	0.56	0.48	0.64
Bench 7,stake 12	11.48	50.66	30.91	2.63	1.45	0.68	1.13
Bench 7,stake 11	12.51	55.70	25.71	1.35	0.34	0.52	0.71
Bench 8,stake 11	10.82	59.28	27.30	0.96	0.73	0.08	0.84
Bench 9,stake 4-5	10.20	61.51	26.20	0.72	0.95	0.08	0.92
Bench 10,stake 6	10.10	61.59	25.38	1.01	0.16	0.33	0.86

The table showes that kaolin clays, sampled in various sites, differ by concentration of SiO_2, AI_2O_3, CaO and Fe_2O_3. The chemical composition varied in the following limits: (mass %) SiO_2 = 50.7-61.6; AI_2O_3=25.4-31.0; Fe_2O_3=0.72-3.91; CaO = 1.16-1.45.

Limestone, loess and cinders were used for the examinations (the materials were in use at the "Akhangarantsement" production association). A chemical composition of testing materials is adduced in Table 2.

The data in Table 2 show that the loess loams were heterogenous by concentration of SiO_2, AI_2O_3 and much R_2O.

Table 2. A chemical composition of raw constituents.

Constituents	Calcination losses (%)	Concentration of oxides (%)						
		SiO_2	AI_2O_3	Fe_2O_3	CaO	MgO	R_2O	SO_3
Limestone	41.22	3.39	1.37	1.59	52.54	0.32	0.16	-
Looss	13.23	51.59	12.03	1.07	12.17	2.40	3.84	-
Cinders	2.28	3.10	1.21	77.41	2.97	1.52	0.46	4.51

Mesh analyses of the loess indicated that tho rosidual in the mesh (900 holes/cm^2) fluctuated within 0.30-6.0 %, and in some samples (sandstons) the figure reached 40-50%, and the fraction (0.01 mm) equalled 51.28%. The loess contained a great amount of large inclusions which exceeded the tolerance limits by the grammlometric composition. A partial substitution of the loess to the non-traditional raw material - secondary kaolin clays, has been considered for an ehhancement of quality of the argillaceous constituent.

By data of the chemical analysis three- and four-constituent mixtures were made, observing the following parametres SC = 0.90-0.93; n = = 1.76-2.19; p = 0.92-1.37. In the four-constituent raw mixture the loess was by 25-60% substituted with kaolin clay. A substance composition and modules of the raw mixtures are presented in Table 3.

Table 3. A substance composition of the raw mixtures
(mass %)

Samples	Composition of mixtures (%)				Modules		
	lime-stone	loess	kaolin	cinders	SC	n	p
1	76.54	21.46	-	2.00	0.93	2.18	0.92
2	77.20	12.40	8.40	2.00	0.93	1.76	1.31
3	77.80	12.00	8.20	2.00	0.93	1.93	1.37
4	78.00	12.00	8.00	2.00	0.93	1.99	1.34
5	75.99	22.01	-	2.00	0.90	2.19	0.99
6.	76.00	18.00	4.00	2.00	0.92	1.99	1.14
7.	76.00	17.50	4.50	2.00	0.90	2.07	1.19

The raw mixtures were composed in accordance with the following scheme: 2 and 6 with an addition of kaolin from the bay 6, 3 and 7 from the bay 8, and 4 with an addition from the bay 9. All these mixtures were subject to full chemical analysis.

The prepared raw mixtures were fired in a laboratory furnace with platinum resistance. Kinetics of assimilation of lime was examined at the temperature range 1100-1450 °C with a 30-minute standing.

The results of definition of the free lime indicated that all varieties of the kaolin clays contributed to an increase in reactivity of the raw mixture, beginning from 1200°C. At 1400° C the concentration of the free lime made 0.2-1.0 %, and the check one - 1.30 %. At 1450°C in the kaolin-containing mixtures a full assimilation of lime took place. An inerease in SC caused less difficulties, than an increase in the argillaceous module. Henco, the positive influence of kaolin clay assumea an expediency of an introduction of 5-8% (mass) to the raw charge.

On the basis of laboratory examinations at the "Akhangarantsement" production association industrial trials of the raw mixtures with a concentration of the kaolin clays from 5 to 8% (mass) have been conducted: A four-constituent charge with composition (% mass): limestone - 76.82, loess - 16.93, kaolin - 4.77 and pyrite cinders - 1.48, has been prepared. The slurry was prepared without any change in production technology. The obtained slurry was characterized by the following parametres: humidity: 42.40-44.60 %; titre : 76.15-77.25 %; SC : 0.92-0.93; n - 2.24-2.50; p - 1.04-1.33.

When using the kaolin clays as a constituent of the raw mixture the quantity of dust removal and cocaentration of carbonic acid in the off-gases did not change. A considerable improvement of formation and preservation of the coating in the zone sintering has been actually fixed.

The petrographic examinations of the clinkers of trial set at gringed samples indicated a distinct crystallization of the minerals.Rarely the crystals of alite with partial failures could be observed. Sizes of alite ranged within 5-40 mcm, and belite - 5-30 mcm. The intermediate phase had acicular and prismatic inclusions, as compared to ordinary clinkers.

By results of the chemical analysis of concentration of the free lime in the sinters, the non-combined lime was present in the clinkers in the quantity of 0.18-0.32 %. Examinations of industrially grinded cements for a definition of the time of setting, fineness of grinding, specific surface, the cone spread and strength of the samples in the age of 3-28 days of hardening, have been conducted. The results are adduced in

the Table 4.

Table 4. The strength indicators of cements

Setting (h-min)		Specific surface	Cone spread	Ultimate strength (MPa)			
beginning	end	(cm^2/g)		bending		compression	
				3	28	3	28
2-35	3-45	3300	114	4.8	6.7	29.0	48.4
3-05	4-25	3050	114	5.5	7.4	29.2	55.3
3-10	4-15	3160	115	5.5	7.3	28.6	57.9
2-25	4-25	3010	115	5.6	7.2	30.5	52.7
2-35	4-15	2960	114	5.2	7.2	28.2	54.7
2-45	4-20	2880	114	5.4	6.9	30.9	53.7
3-25	4-45	3100	115	5.0	7.4	29.1	56.6
3-15	4-25	2970	112	5.5	7.1	28.9	55.0

According to the data the specific surface of the kaolin-containing cements made 2880-3160 cm^2/g. The strength under compression for the 28th day of hardening equalled 52.7-57.9 MPa, that is the minimal mark of the cements "500". Samples from the chek cement under specific surface 3300 cm^2/g had the strength 48.4 MPa. The cements by time of setting, fineness of grinding and an evenness of a change of the volume corresponded to the requirements of the GOST (all-union state standard)

Results of indistrial trials indicated a possibility of use of the non-traditional raw material - oversanded high-disperse kaolin clays - as a raw constituent in the firing of portland-cement clinker.

BIBLIOGRAPHY

1. Butt Yu.M., Timashev V.V. Portland-cement clinker. Moscow, 1967.
2. Sychov M.M. Technological properties of raw cement charges.
3. Kravchenko I.V., Vlasova M.T., Yudovich B.E. High-strength and super-rapid-setting cements. Moscow, 1971.
4. Akhmedov M.A., Mukhamedbaev A.A., Ashirova D.A., Menapova R.A., Fiodorov A.P., Kiseliova O.D. Use of kaolin clays as a raw constituent. "Tsement", 1989. - Nr.11.
5. Toporov N.A. Chemistry of cements. Moscow, 1956.
6. Tashpulatov Yu.T. Portland-cement brick. Tashkent, 1958.

STUDIES ON PRODUCING PORTLAND CEMENT WITH TAILINGS OF MOLYBDENUM-IRON ORE

Pan Yi Zhou

Zhejiang Building Materials Scientific Research Institute
Hangzhou, P R CHINA

SUMMARY

The effect of molybdenum-iron ore tailings on producing portland cement and the mechanism of influence of molybdenum on clinker formation in particular have been studied by XRD, SEM and chemical analysis. MoO_3 can promote the combination of cement clinker and this may be attributed to the change of the melt properties through reduction of viscosity and surface tension of the melt, and accelerating rate of C_3S formation. The distribution of molybdenum in various phases of clinker indicates that it is mostly dissolved in the interstitial phase and least in the silicate phase. The amount of molybdenum dissolved in alite and belite are relatively close. But in interstitial phase, molybdenum may concentrate in ferrite phase.

摘　要

本文应用XRD、SEM和化学分析等方法，对利用钼铁矿尾矿作为原料烧制水泥进行了研究，并着重探讨了MoO_3对水泥熟料形成的作用机理。结果表明钼可通过改变熟料形成过程中的融体性质如降低液相粘度和表面张力来加速C_3S形成和游离氧化钙的吸收，促进熟料烧成。钼在熟料各相中的分布规律为主要固溶在中间相，少量固溶在硅酸盐相中。在硅酸三钙和硅酸二钙中的固溶量相接近，而在中间相中钼富集在铁酸盐相中。

INTRODUCTION

The scope for utilizing tailings of minerals to produce Portland cement has recently widened owing to the necessity to utilize wastes and exploit new raw material resources. The tailings of molybdenum-iron ore in the Zhejiang province in China are solid wasts discharged from dressing molybdenum concentrate and iron concentrate, and consist mainly of silicon, iron, calcium and aluminium oxide and various trace elements. If the tailings are used to produce cement,would the trace elements (particularly molybdenum) present affect the clinker formation? Would the molybdenum inhibit the formation of tricalcium silicate or change the mineral composition in clinker? How does the molybdenum increase the free lime and decrease the strength of clinker? These problems are not clear from already published data(1-6). In order to investigate the mechanism of the influence of Mo on clinker formation, we have carried out many studies on the properties and mineral compositions of clinkers using XRD, microscopic techniques in the laboratory. The results indicated the feasibility to produce common Portland cement using tailings containing Mo which act as a mineralizer and could substitute certain raw materials. Subsequently, further studies have been carried out for understanding the role of the tailings in cement clinker formation and determining the parameters for manufacture of cement, this was followed by a trial industral manufacture in a cement plant.

EXPERIMENTAL

Materials and Methods

Compositions of tailings of molybdenum-iron ore (Table 1)

Table 1 Composition of tailings(%)

name	Loss	SiO_2	Fe_2O_3	Al_2O_3	TiO_2	CaO	MgO	SO_2
tailings	0.30~4.00	37.00~44.00	15.00~19.00	6.00~8.50	0.50~1.00	21.00~24.50	4.00~8.00	2.00~5.00

Spectral analysis of tailings of molybdenum-iron ore.(Table 2)

Table 2 Spectral analysis of tailings Unit: ppm

Ba X×10²	Be X×10	Pb X×10	Sn X×10	Ga X×10	Ni X×10	Mo X×10	V X×10	Cu X×10	Yb X×10	Zn X×10²	Co X×10	Y X×10
1.5	<1	2	<1	<1	1.5	50	<1	20	<1	5	4	1.5

Raw mixes for the experimental work were divided into two groups.In one group, natural limestone,clay and iron powder were mixed with the appropriate amount of MoO_3 or molybdenum concentrate. The other group was composed of limestone, clay and the tailings of molybdenum-iron ore instead of iron powder and mineraliser.

Raw materials were ground into powder separately. The raw mixes were proportioned according to the designed ingredients and mixed throughly in a honogenizer and made into cylinders 20mm in diameter and 30mm in height. After drying, the samples were placed in refractory dishes in electric furnace and preheated at the chosen temperature for a certain time interval and cooled in air. Free lime in the sintered samples was determined by using glycerin-alcohol

solution and mineral compositions were determined by XRD. Morphological features and sizes of crystals and distribution of molybdenum in the clinkers were observed by reflected light microscopy and scanning electron microscopy.

Clinkers were fired at 1350°C for one hour and gypsum (3% w/w) were respectively ground in a ceramic mill for 40min. Keeping w/c 0.3 in all the cases, the mortar compressive strengths were measured on 20×20×20mm specimens.

RESULTS AND DISCUSSION

1. Effect of molybdenum on burnability of raw mix

Results of burnability of raw mix by adding molybdate in various proportions are illustrated in Figure 1. The free lime of sintered samples in the presence or absence of Mo are similar below 1200°C. At the burning temperature of 1200°C the free lime content of the sinters containing Mo reduce remarkably and the extent of reduction was inversely proportionate to the amount of Mo added. The free lime of sinter in the absence of Mo decreases obviously until the temperature reaches at 1300°C and is higher than that of clinker with Mo in the temperature range of 1200°C~1350°C.

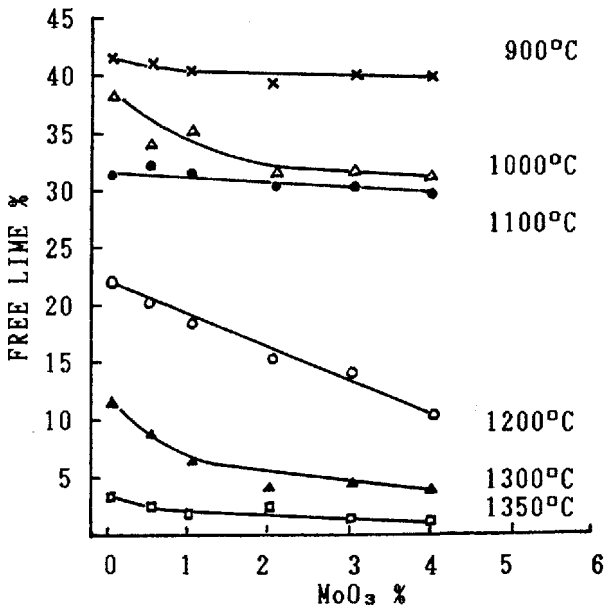

Fig.1 Influence of MoO_3 on burnability of raw mix

In the absence of mineralizer the temperature of initial liquid fromation when burning raw mix is 1260°C~1280°C in most cases. At or above this temperature, reaction in the solid-solid phase gets converted to solid-liquid or liquid-liquid phase during the clinkering process, which significantly accelerates the rate of transport of ions and favours absorption of the free lime and formation of C_3S in clinkerization process.

The above results indicated that addition of MoO_3 was found quite effective because it could lower the temperature of initial liquid formation during the clinkering process, decrease the viscosity and surface tension of the liqiud phase and improve the burnability of raw mixes.

2. Effect of MoO_3 on clinker mineral composition

In order to investigate the action of MoO_3 on mineralogical compositions and size of crystals of the clinker phase, petrographic tests of clinkers containing added MoO_3 are carried out vis-a-vis control samples without MoO_3.After sinters are polished and etched with 1%HNO_3 alcohol solution on its surface, there many tiny holes are observed on the surface of clinker in the absence of MoO_3 under reflected light microscopy and the crystals of C_3S are small with irregular shapes. But clinkers containing MoO_3 have denser structure and are mainly made up of C_3S with regular and plank-like shape and well formed crystals and also contain a lot of white interstitial phases found in clinker simultaneously. Addition of MoO_3 as observed from the mineral analysis has no adverse effects on C_3S formation, and this has further been corroborated by XRD analysis of the same sample.

There are quite a lot of differences between the XRD patterns of clinkers with and without MoO_3.The main peaks of tricalcium silicate and dicalcium silicate of clinker containing MoO_3 rise obviously and the peaks of aluminoferrite rise as well and turn to the direction of C_6A_2F. On the other hand, different peaks are not found for the aluminate phase. It indicates that MoO_3 dissolves in the interstitial phase and the influence is more pronounced on aluminoferrite. The problem of whether Mo would cause the formation of new minerals or not needs further study.

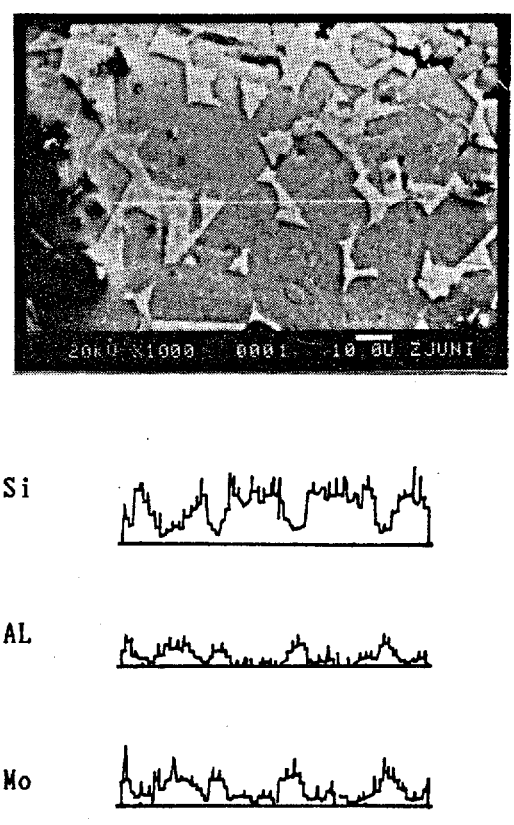

Fig.2 SEM photo and corresponding linear energy spectrum

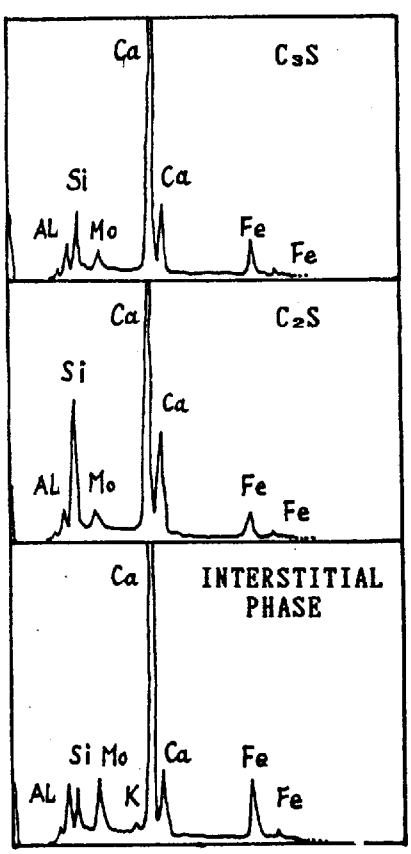

Fig.3 The point energy spectrum curves of clinker with Mo

3. Distribution of molybdenum in various phases of clinker

In order to investigate the solid-solubility and distribution of Mo in the minerals of clinkers, the samples were subjected to SEM and EPMA (Fig2,3). It shows significantly that curves of Si are higher in tricalcium silicate crystals and lower in the interstitial phase. On the contrary, curves of Al show opposite results. The curves of Mo are similar to those of Al. It is further supported by the point energy spectrum analysis that Mo is mainly dissolved in the interstitial phase. The following qualitative and quantitative concepts are obtained in micro-area energy spectrum analysis and XRD. Mo exists in a relatively minor amount and is similar to the dissolved content of iron and alumina in silicate, and this is considered as a solid solution form. There are similar contents of solid solution in dicalcium silicate and tricalcium silicate. However, a major part of the Mo dissolves in the interstitial phases and concentrates in the aluminoferrite phase.

4. Eeffect of MoO_3 on the strength of clinker

Table 3 shows the results of clinker mortar strength tests. Compared with the clinker sample without Mo, samples mixed with Mo exhibit better strength increase at early ages (3 days) at 0.5~3 % MoO_3 addition. The strength of clinker mixed with 2% MoO_3 reaches a maximum and 0.5 % MoO_3 addition in clinker is considered as optimum with high compressive strength measured at 28 days. The strength of cement reduced markedly when MoO_3content exceeded this particular dose in clinker. An increase in strength at early ages in the presence of MoO_3 may be attributed to Mo changing the characteristics of the melt at high temperature and accelerating the formation of C_3S at the same time. When the amounts of MoO_3 added to the raw mixes are high (> 2%) adverse effects on the ultimate strength of clinker are observed probably due to modification of the aluminoferrite crystalline form and formation of a new mineral.

Table 3 Compressive strengths of clinkers with different amounts of MoO_3

Dosage	Compressive strengths, MPa		
(%)	3 days	7 days	28 days
0	30.30	57.05	80.91
0.5	35.34	65.16	82.73
2.0	37.52	55.73	80.02
3.0	35.11	58.21	67.27

5. Eeffect of molybdenum-iron ore tailings

Addition of molybdenum-iron ore tailings or together with mineralizer provide significantly improves the burnability and clinker quality. Burnability experiments of raw mixes performed in presence of tailings of molybdenum-iron ore and other mineralizers prove the effect of compound mineralizers and tailings on the clinkering of cement raw mixes to be in following order: fluorite+tailings > fluorite alone > tailings alone > no mineralizers. Fluorite and tailings in combination acts as a complex mineralizing agent, producing excellent results due to combination of CaF_2 with trace elements (such as molybdenum in tailings). Thus a composite mineralizer is formed which lovers the temperature of phase transition of solid-liquid phase and reduces the viscosity and surface tension of the liquid phase during the clinkering process and accelerates the rate of ion mobility in liquid and significantly increases the rate of C_3S formation.

In addition, chemical compounds of F^-,S^{2-} form an intermediate transition phase so as to improve the formation of alite and facilitate clinkerization (7,8).

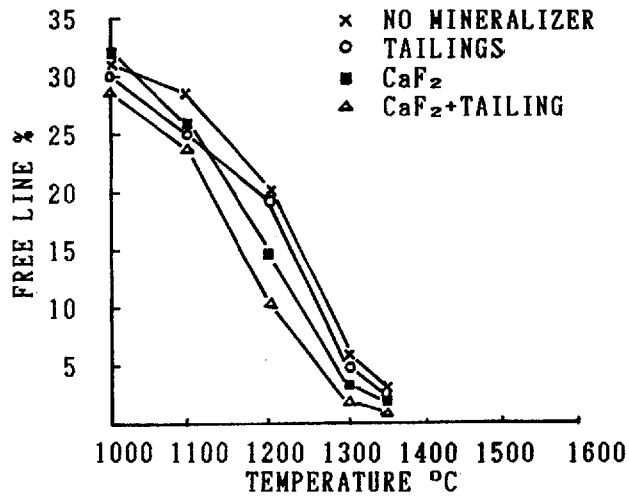

Fig.4 Influence of tailings on burnability of raw mix

6. Trial industrial production

Based on the results of our laboratory experiments, an industrial production was carried out in two shaft kilns of a plant, for six months and excellent results were obtained.

Parameters selected : KH=0.93~0.97
N=2.0 ± 0.2
P=0.8~1.2

To sum up , use of tailings in cement manufacture facilitates formation of clinker. Its effect is obvious in improving early age as well as ultimate strengths. It is found to markedly increase kiln output and quality of clinker as manpower requirement has decreased by the improved working of kiln. An increase in kiln output of mean 13.33% corresponded to the coal saving at mean 5.1% and free lime contents also decreased. Besides, raw mixes with the tailings of molybdenum-iron ore are not only considered as a substitute for all ferrous materials and parts of natural mineral of limestone and clay , but also acts as mineralizers instead of mineral gypsum and it has showed significant effect on the output, quality and cost of cement manufacture.

CONCLUSIONS

1. MoO_3 promotes the combination of cement clinker and this may be attributed to the change of the melt properties through reduction of viscosity and suface tension of the melt, and accelerating rate of C_3S formation and increasing absorption of free lime.

2. The distribution of molybdenum in various phases of clinker indicates that it is mostly dissolved in the interstitial phase and least in the silicate phase. The amount of molybdenum dissolved in alite and belite are relatively close. But in interstitial phase, molybdenum may concentrate in ferrite phase.

3. The compressive strengths of the clinker are related to the proportion of the MoO_3addition. Maximum of strength can be achieved when the level of molybdenum

is 0.5% in the clinker.

4. The results of the industrial production experiments indicated that the use of tailings of molybdenum-iron ore to produce Portland cement can not only promote the burnability of raw meal and achieve fuel savings, but also improve the formation of clinker and the quality of cement.

REFERENCES

1. TIMACHEV.V.V.Proc 7th Int. Cong. Chem. Cement, Paris.V.1, I.3/1 (1980).

2. FIERENS P, VERHAEGEN J.P. Cen. Concr. Res.,5,233,(1975).

3. TASHIRO C, Proc. 7th Int. Cong. Chem. Cement, Paris V.2,II,37(1980).

4. A.i.BOIKOVA, Dr. Chem, Sc. 8th Int,Cong, Chem, Cement. Rio de Janeiro, V.1, 19 (1986)

5. F.M.Lea. "The Chemistry of Cement and Concrete" London, E. Arnold Ltd, Third Edition, (1970)

6. G.Kakali, V.Kasselouri, Cem, Concr. Res., Vol.20 PP.131-138, (1990).

7. G.K.Moiv, "Mineralised high alite Cement" World Cement VoL 13. PP.374-382, (1982).

8. KUMAR, S.S. and KATARIA, S.S. Oplimization of burning characteristics of raw meal for fuel economy by special mineraliser, World Cement Technology, Vol.12, No.4. PP 279-285. (1981).

EXPERIENCES IN USE OF INDUSTRIAL BY-PRODUCT SLUDGE FOR CEMENT MANUFACTURE BY SOL-GEL TECHNOLOGY

V Varadarajan, C H Thombare, S A Borkar, C H Page and A K Chatterjee

Research & Consultancy Directorate
The Associated Cement Companies Ltd
Thane, INDIA

SUMMARY

Apart from the development of sol-gel technology for advanced materials (1-5), it has also been studied in the system CaO - Al_2O_3 - SiO_2 for production of super-white cement in the R & D division of The Associated Cement Cos.Ltd. As an extension to the above, work was undertaken to study compatibility of various industrial by-product sludges as one of the raw materials for low temperature clinkerisation by sol-gel technique.

The synthesis, the features of sol-gel technology developed and adopted, optimisation of process parameters have been discussed in the paper. The characterisation of gels, sintering characteristics, microstructural features of clinker obtained and physical properties of cement produced are also highlighted.

INTRODUCTION

Studies carried out in the system CaO - Al_2O_3 - SiO_2 modified by fluorine have established the technical feasibility of producing super white cement with very high reflectance and high compressive strength levels by a sol-gel route at temperatures of 1200°C, primarily in the chemical system CaO - SiO_2 - Al_2O_3 containing fluoride based mineraliser (6). In order to improve the economic viability the use of by-product sludges as a source of lime and adopting an aqueous sol-gel route, has been studied for the manufacture of conventional cement. The present paper highlights some of the salient findings of this investigations.

EXPERIMENTAL WORK

By-product lime sludge from fertilizer, paper and carbide industries were selected. The lime sludges were characterised for their physical and chemical properties. Based on characteristics of the sludge, experiments were designed to optimize gel formation parameters. The typical gel characteristics with various sludges and their utilization is indicated in Table-I.

TABLE - I

Typical Gel Characteristics

	Fertiliser	Paper	Carbide
Solid Content (g/L)	150	190	255
Viscosity(c.p.) of Gel	2700	2800	2750
Acid catalyst (g mol/L of gel)	0.003	0.003	0.003
Gelation time (hrs)	3	3	2
pH of Gel	11	12	11.5
% of Sludge	30	37	78

The proportion of raw materials and fluoride based mineraliser was designed to achieve targeted sinter composition. In the case of raw mix with paper and fertilizer sludges hydrated lime was used as corrective. The procedure used for gel preparation is as follows:

Nitric acid (1:1) was added to a mixture of desired composition of dilute solution of silica-sol, aluminium nitrate and fluoride based mineraliser under constant stirring. To the above reaction mixture lime sludge and hydrated lime (corrective) was added and the mixture stirred for 2-3 hours. The gel so obtained was dried in an oven at temperature of 110-120°C for a period of 10-12 hours. The dried gels were pelletised and sintered.

CHARACTERISATION OF MATERIALS

1) Properties of Sludges

TABLE-II Physical and Chemical properties of Sludges

Physical Parameters	Fertilizer	Paper	Carbide
Specific gravity	3.33	2.6	3.03
Particle size (%)			
45 microns	90	98	98
10 microns	47	77	65
d_{50} microns	11	5	6

Chemical Parameters	Fertilizer	Paper	Carbide
SiO_2	8.1	4.4	4.6
Al_2O_3	2.6	1.0	1.2
Fe_2O_3	0.4	0.5	0.3
CaO	45.8	40.1	55.6
MgO	1.0	2.2	0.2
SO_3	2.2	0.4	0.6
Na_2O	0.31	0.49	0.01
K_2O	0.12	0.05	0.01
Fluoride	0.6	-	-
P_2O_5	0.6	0.05	0.05
LOI	38.3	50.7	37.4
Σ Impurities	3.9	1.0	0.6

2) Infrared Spectrophotometry

The infrared spectrophotometric studies were carried out for dried gels and IR-spectra are given in Fig. 1(a), (b), (c).

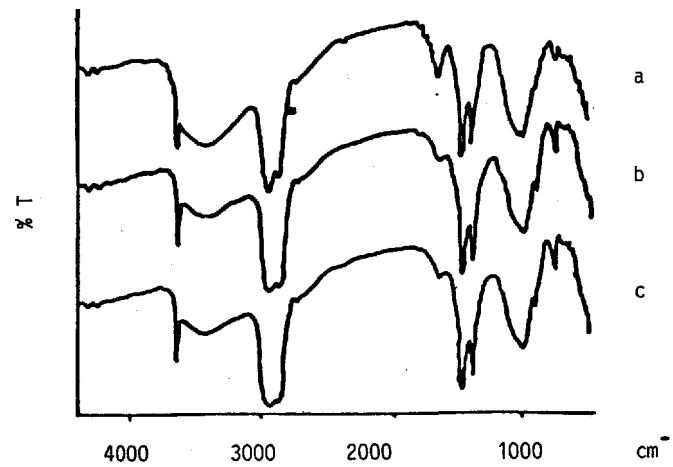

Fig.1 - IR Spectra of dried gel obtained from
a) Fertilizer b) Paper c) Carbide sludges

3) Differential Thermal Analysis/Thermo Gravimetric Analysis

The differential thermal analysis (DTA) and thermo gravimetric analysis (TGA) of dried gel sample was carried out on a Mettler Thermoanalyser in a nitrogen atmosphere at a flow rate of 40 ml/min and heating rate of 8°C/min from room temperature to 1400°C.

4) Scanning Electron Microscopy

The gel was dried at 110-120°C and characterisation was carried out of the dried gel by Scanning Electron Microscopy and the photomicrographs are shown in plate - 1, 2, 3 respectively.

SEM OF DRIED GELS

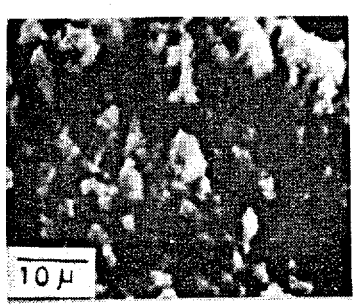

Plate 1
With fertilizer sludge

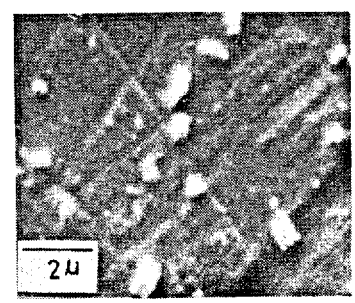

Plate 2
With paper sludge

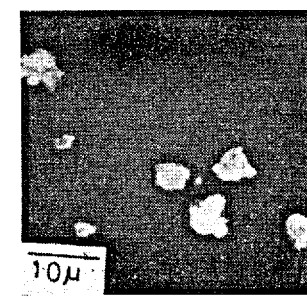

Plate 3
with carbide sludge

5) Chemical Analysis of Sinters

The chemical composition of sintered products (1200-1225°C) is given in Table III

TABLE III

Chemical Composition of Sinters

	Fertilizer %	Paper %	Carbide %
SiO_2	29.6	28.2	28.2
Al_2O_3	1.6	1.6	2.0
Fe_2O_3	0.4	0.4	0.3
CaO	65.8	67.2	67.9
MgO	0.8	1.8	0.6
Na_2O	0.15	0.37	0.01
K_2O	0.06	0.04	0.01
SO_3	1.1	0.3	0.7
Fluoride	0.1	0.1	0.1
P_2O_5	0.3	0.04	0.07
f CaO	1.0	1.4	0.6
CaO/SiO_2 (Molar)	2.38	2.54	2.58
Σ Impurities	1.8	0.6	0.9

6) Lime Combinability

The lime combinability of the raw mix (dried gel) at 1200°C is given in Table IV.

TABLE IV - Lime Combinability at various Temperatures

Lime Source	Free CaO at °C 1000	1100	1200	Lime Combinability %	Phases found at 1200°C
Fertilizer	11.9	9.0	1.0	98.5	C_3S, β C_2S, C_3A
Paper	13.8	6.5	1.4	97.9	C_3S, β C_2S, C_3A
Carbide	6.5	2.0	0.6	99.1	C_3S, β C_2S, C_3A

7) X-Ray Diffraction

The X-Ray diffraction patterns of various phases was obtained by a SIEMENS X-Ray Diffractometer using Cu-Kα radiation and scanning range 15-60° (2 θ). Fig.2. The XRD scan carried out between 51-52° (2 θ) are depicted in Fig.3.

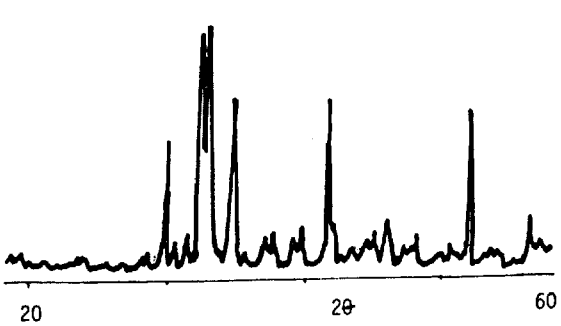

Fig.2a) XRD Pattern of Fertilizer Sludge Sinter

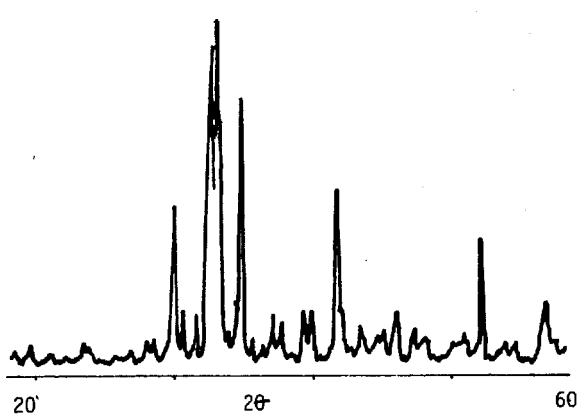

Fig.2a) XRD Pattern of Paper Sludge Sinter

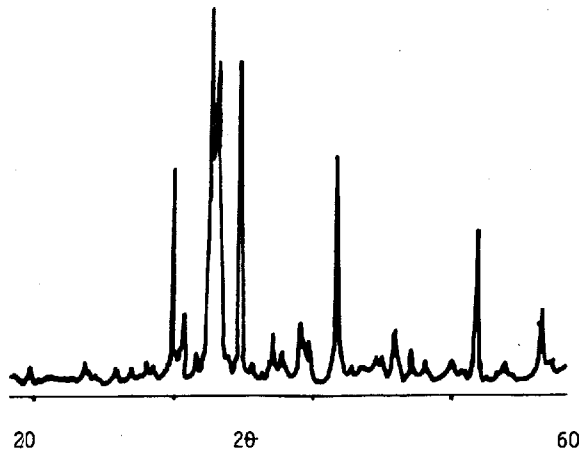

Fig.2 c) XRD Pattern of Carbide Sludge Sinter

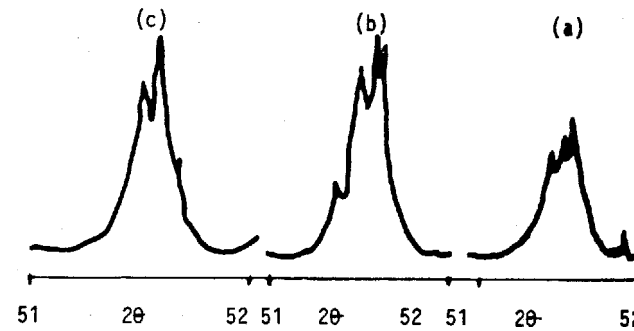

Fig.3 XRD scan 51-52° (2θ)
a) Fertilizer Sludge Sinter
b) Paper Sludge Sinter
c) Carbide Sludge Sinter

8) Scanning Electron Microscopy

Microstructural features of sinters were obtained by Scanning Electron Microscopy. Plate 4, 5 and 6 illustrate the microstructure of sinters of fertilizer, paper and carbide sludge respectively.

SEM OF SINTERS

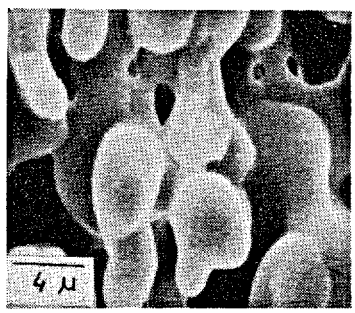

Plate - 4
With Fertilizer Sludge

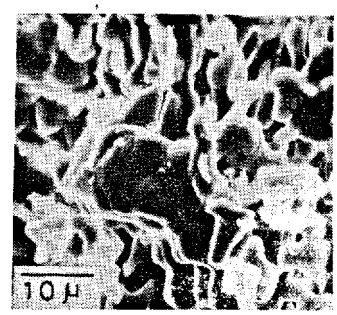

Plate - 5
With Paper Sludge

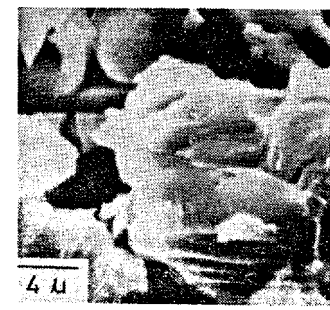

Plate - 6
With Carbide Sludge

9) Physical Testing of Cements

The cement obtained by intergrinding of sinters and required quantities of gypsum to control SO_3 levels, was evaluated for physical properties in accordance with the relevant Indian Standard Test procedures. The results are given in Table-V.

TABLE-V Physical Properties of Cement

	Fertilizer	Paper	Carbide
Specific Surface (cm^2/g)	4000	3800	4100
Standard consistency (%)	26.3	27.3	27.0
Setting Time (Min)			
Initial	290	220	150
Final	390	270	200
Expansion (Soundness)			
Le-Chatelier (mm)	0.5	0.5	0.5
Autoclave (%)	0.02	0.02	0.03
Comp.strength (kg/cm^2) (1:3 Mortar, 27°C)			
1 day	140	230	330
3 days	270	320	425
7 days	370	390	570
28 days	580	520	670

RESULTS AND DISCUSSION

The chemical composition of lime sludges (Table-II) indicates variations in the lime content (74-89% on loss free basis) and total impurities (1.0-6.3% on loss free basis). The fertilizer sludge was coarser than the other two sludges viz. paper and carbide.

The rheological studies of various gels indicate that to maintain same viscosity ($\approx$ 2750 cp) the solids content of gels varied from 150-255 g/L and gel formation time was less in the case of raw mix with carbide sludge (2 hrs) as against the fertilizer and paper sludge (3 hrs). These features show that physical properties (Table-II) of the sludges have a strong influence on the gel parameters. (Table-I).

The infrared spectra of gels Fig.1 (a,b,c) indicate absorptions due to Si-O, N-O, H-O-H, moisture in gel and OH in silicate system.

The DTA/TGA studies indicate an endotherm coupled with loss of uncombined gel moisture at 100-140°C and another endotherm at 380-400°C coupled with dehydroxylation reaction. Beyond 800°C, initiation of phase formation was observed.

The characterisation of gels obtained from these sludges by SEM (Plates 1, 2, 3) reveal the differences in particle size and agglomeration tendencies. The particle size tends to be coarser with gels of paper and fertilizer sludges, while carbide sludge gel shows the finest particle size.

The chemical composition of sinters (Table-III) shows the molar CaO/SiO_2 ratio during these experiments was in the range of 2.38 to 2.58 and the total impurities in the range of 0.6 to 1.8%. In conventional cement the molar CaO/SiO_2 ratio is generally maintained in the range of 2.8 to 3.0.

The lime combinability at 1200°C (Table-IV) was observed to be 98% in the case of paper and fertilizer sludge sinters and in the case of carbide sludge sinter, it was 99%. Generally for conventional cement raw mix at 1200°C this value is around 75-80%. This indicates an enormous improvement in lime combinability by sol-gel process.

The corresponding X-Ray diffraction pattern for sinters at 1200°C show peaks in the range expected for C_3S (Fig.2). The X-ray scans (Fig.3) indicate the predominant presence of monoclinic form in the case of carbide sludge sinter; in paper sludge sinter, the monoclinic form was predominent with minor triclinic, whereas in fertilizer sludge sinter the triclinic for was predominent. The patterns further indicate that the crystallinity of carbide sludge sinter to be the best followed by paper and fertilizer sludge sinters.

The SEM photomicrographs of sinters obtained by using fertilizer, paper and carbide sludge (Plate 4,5, 6) respectively reveal the distinct difference in the morphology, crystallinity and phase composition. The carbide sinters are coarsely crystallined with hexagonal and prismatic platelets of C_3S. Compared to this the fertilizer sinter show less C_3S but well developed rounded to sub-rounded C_2S. The phase composition of paper sinter reveal a mixture of both the silicates with less well developed morphology as compared to the earlier two sinters.

The physical properties of the cement produced from these sinters and tested as per the relevant Indian Standard Test procedure given in Table-IV, indicate excellent early age strength for carbide sludge sinter (1 day 330 kg/cm^2 and 3 day 425 kg/cm^2), followed by paper sludge sinter (1 day 230 kg/cm^2 and 3 days 320 kg/cm^2) and fertilizer sludge sinter (1 day 140 kg/cm^2 and 3 days 270 kg/cm^2). The later age strength development (28 days) is best in fertilizer sinters followed by paper and carbide. The lime combinability as well as the extent of phase formation of sinter discussed earlier is also in agreement with the above observed hydraulic characteristics.

CONCLUSION

Based on the various investigations carried out on the utilisation of by-product lime sludge for manufacture of cement by sol-gel technology, the following conclusions can be drawn.

1) Physico-chemical characteristics of lime sludge influence the process parameters as well as quality of cement produced.

2) The study also indicates that it is possible to manufacture a satisfactory quality cement at as low as 1200°C by sol-gel technique.

3) Sol-gel technology can be successfully adopted for incorporation of by-product wastes such as lime sludge produced by fertilizer, paper and carbide industries, for the manufacture of cement.

REFERENCES

1) D.M.Roy, S.O.Oyefesabi, "Presentation of very reactive Ca_2SiO_4 powder", J.Am.Ceram. Soc., March, 178-180 (1977).

2) D.R.Ulrich, "Sol-gel processing", CHEMTECH, April 242-249, (1988)

3) S.Sakka, "Sol-gel glasses and their future applications" Transaction of the Indian Ceramic Society, Vol. 46 (1) 1-10, (1987)

4) H.Schmidt, "Chemistry of material preparation by the Sol-gel process", J.Non-cryst. Solids, 100, 51-64, (1988)

5) H.G.Sowman, "A New Era in Ceramic Fibres Via Sol-gel Technology", Am.Ceram.Soc.Bull., Vol. 67(12), 1911-1916, (1988)

6) A.K.Chatterjee, et al, Development of Sol-gel technology for cement manufacture, Symposium on Advances in Cementitious Materials, NIST and American Ceramic Society, 26th July 1990, Gaithersburg, MD, USA, pp. 640-660.

Specific Theme I-C

Effect of the Use of Mineralisers, Modifiers and Activators

THERMAL BEHAVIOUR OF MINERALIZED PORTLAND CEMENT RAW MEAL

F Ayed*, R Castanet* and F P Sorrentino**

**Centre de Microcalorimétrie, CNRS Marseille, FRANCE*
***Lafarge Coppée Recherche, Viviers/Rhône, FRANCE*

ABSTRACT

Mineralizers are commonly used in cement industry to accelerate the clinkering reactions, lower the burning zone temperature and to save energy. Because the pyroprocessing uses about 80 % of the total energy requirement, the role of mineralizers and specially calcium fluoride (CaF_2) in clinker mineral formation has received considerable experimental attention.

The impact of the fluorine on the total thermal efficiency can be easily evaluated at industrial scale ; it is due to the lowering of the burning zone temperature which indirectly diminishes the heat loss through the walls.

The distribution of the theoretical heat inside the kiln can be approached by the mean of isothermal high temperature microcalorimeter. This technique, associated with high temperature X ray diffraction and electron microscopy allows, a precise measurement of the enthalpy of reactions as a function of the temperature during the overall process.

The use of calcium fluoride and chloride is shown to accelerate the formation of the belite and to modify the position in the kiln of the exothermal effect during its formation.

RESUME

Les minéralisateurs sont utilisés habituellement dans l'industrie cimentière pour accélérer les réactions de clinkérisation, abaisser la température de la zone de cuisson et économiser l'énergie. Le rôle des minéralisateurs et en particulier la fluorine (CaF_2) a fait l'objet de nombreuses recherches parce que, dans la chaîne de production la cuisson est le procédé le plus gros consommateur d'énergie (80% de l'énergie totale).

L'impact de la fluorine sur l'efficacité totale du processus de cuisson peut facilement être évalué à l'échelle industrielle : il est dû à l'abaissement de la température dans la zone de cuisson, ce qui indirectement diminue la chaleur perdue par les parois.

La répartition de la chaleur théorique à l'intérieur du four peut être mesurée au moyen d'un microcalorimètre haute température. Cette technique, associée à une diffraction X haute température et un microscope électronique permet une mesure précise de l'enthalpie des réactions en fonction de la température pendant la totalité du procédé.

On montre dans cette étude que le chlorure et fluorure de calcium accélérent la formation de la bélite et modifient dans le four, la position du dégagement de chaleur qui lui est associée.

1 - INTRODUCTION

The effects of mineralizers such as calcium halogenides on the clinker formation have been widely studied. We mention here the most recent or significant references (1 to 6).

It is generally admitted that their use presents many advantages. They facilitate the clinker formation by enhancing the quantity of liquid phase, increase the production and reduce the fuel consumption by decreasing the burning temperature. In spite of these advantages, the mineralizers or fluxes are very scarcely used industrially, except for alumina and iron oxides whose presence is unavoidable in the raw material.

The reasons can be found in the economic balance between the cost of the mineralizers and the thermal gain or in others factors occuring at large scale (homogeneity of the addition, risk of volatilization and clogging, mechanical properties of the cement and so on ...). In this paper, we try to answer these questions by an analysis of the thermal distribution in the kiln for a fluorine containing raw meal.

2 - EXPERIMENTAL PROCEDURES

In a first step we have analysed the enthalpy of formation of the main clinker compounds (C_2S and C_3S). Pure silica, calcium carbonate and calcium fluoride (ANALAR grade) are used as starting materials, in the right proportions to obtain di and tricalcium silicate. In a second step,we have used an industrial clinker whose chemical analysis of the raw meal is given in the table 1.

TABLE 1

Chemical composition of the industrial raw meal

SiO2	Al2O3	Fe2O3	CaO	MgO	K2O	LOI	MS	A/F
13,9	3,64	1,62	43,22	0,78	0,25	35,9	2,65	2,24

The quantity of added fluorine (CaF_2) is calculated to obtain, after firing, 1 % of CaF_2 in the sample. This high quantity of mineralizer was chosen in order to enhance the thermal phenomena. The enthalpy of the reaction is measured by the drop technique in a multidetector high temperature calorimeter.

This equipment includes a furnace with carbon resistor and a cell with 56 thermocouples. The temperature of the kiln is fixed and the sample (a few mg), which initially is at room temperature, is dropped into the kiln. The cell measures the heat exchanged by the sample to reach the defined temperature.

Drops of platinum samples are used to standardize the equipment. After this measurement the sample is cooled, removed from the calorimeter and analysed, following the classical techniques (free lime, X ray diffraction, selective dissolution and SEM). Polished sections of the samples are coated with carbon and examined by SEM (backscattered electron mode).

The analyse of the phases were made using a scanning electron microscope Jeol 840 fitted with an energy dispersive X ray detector.

The excitation voltage is 15 KV and the analysis is calculated by the classical ZAF procedure. From the phases analysis and the bulk composition of the clinker, it is possible to calculate for each temperature, the percentage of phases which are formed (7) and to relate it to the measured enthalpy. High temperature X ray diffraction is used to follow continuously the sintering reaction up to 1200°.

3 - RESULTS

Formation of C_2S from 2 $CaCO_3$ and SiO_2 :

- The figure 1 shows the enthalpy of formation of C_2S from a mixture of silica and calcium carbonate without CaF_2 (upper curve) and with CaF_2 (bottom curve).

The first part of the curve a b, corresponds to the enthalpy variation of calcium carbonate and silica.

In the case of the standart sample (no CaF_2), the decarbonation starts at 700°C and goes on until 1100°C (8).

Simultaneously intermediate phases form (C_3S_2, CS) and it is difficult to separate the exothermal effect of the formation from the endothermal effect of the decarbonation.

At 1100°C a small decrease in the curve (after the peak P1) is attributed to C_2S formation. At higher temperature, the slope corresponds mainly to the enthalpy variation of C_2S. At 1450 °C the free lime in the sample is less than 1%

In the case of the raw mix containing fluorine, the opposite effects of decarbonation and C_2S formation, compensate each other.

The formation of C_2S occurs early (after the peak P2) and goes on until 1150°C. The total enthalpy at 1450°C, which corresponds to total :

- formation of C_2S and decarbonation, is the same for both sample, proving that CaF_2 acts on the kinetics of the reaction of C_2S formation and has no action on the final thermal balance.

Formation of C_3S from 3 $CaCO_3$ + SiO_2 :

- The figure 2 shows the enthalpy of formation of C_3S from a mixture of silica and calcium carbonate with and without CaF_2. Until 1000°C, there are nc significative difference between the curves.

At 1000°C, for the reference sample, we see an exothermal effect due to the formation of C_2S (peak P1). When CaF_2 is added, the exothermal peak corresponding to the formation of C_2S occurs early (after the peak P2) and is more important. The two curves end up at the same enthalpy.

Industrial raw meal :

- The figure 3 shows the enthalpy of formation of C_2S from an industrial raw meal with and without CaF_2.Without CaF_2, the decarbonation start at 850°C and we see a large endo-thermic effect which ends at 1100°C (9).

The exothermal effect P1 is attributed to the C_2S formation. At higher temperature, the slope of the line corresponds to the enthalpy of the clinker.

With CaF_2, the decarbonation starts earlier, but the endothermic peak P2 is not as high as for the standard and the exothermal effect corresponding to the C_2S formation occurs earlier.

At 1200°C the large endothermal effect is due to the formation of liquid phase. From, the free lime analysis and the phases analysis by SEM, it is possible to evaluate the percentage of phases formed at each temperature (7).

Table 2 gives these results.

* : means traces.
Yes : means that the percentanges less than 5% and difficult to quantify.

FIGURE 1

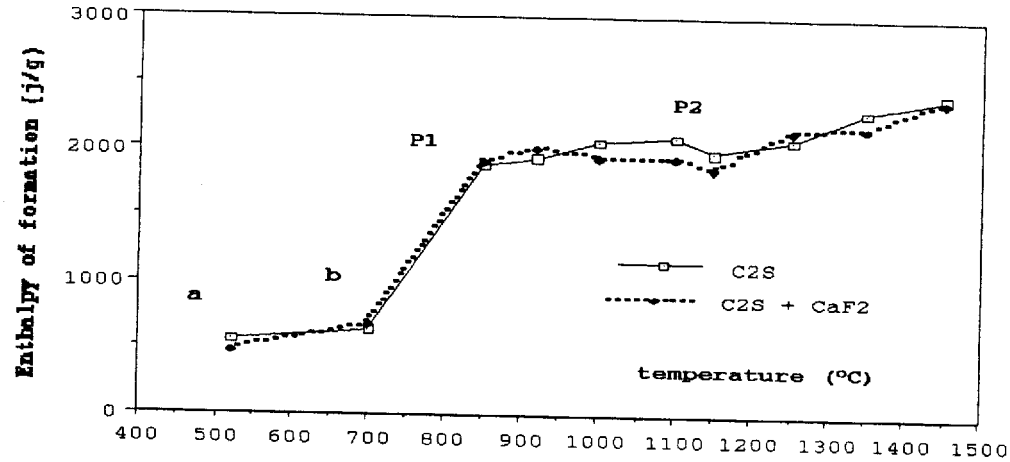

FIGURE 2

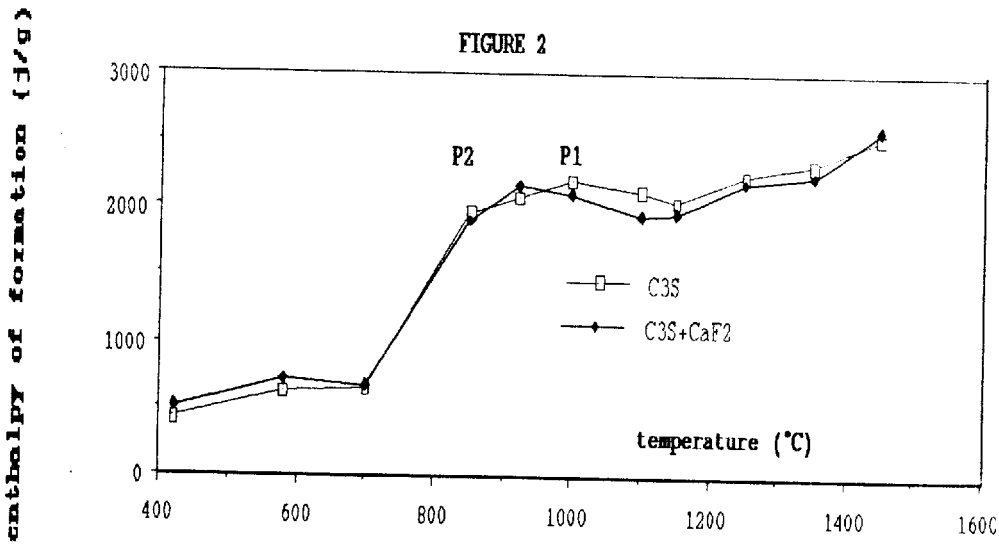

FIGURE 3

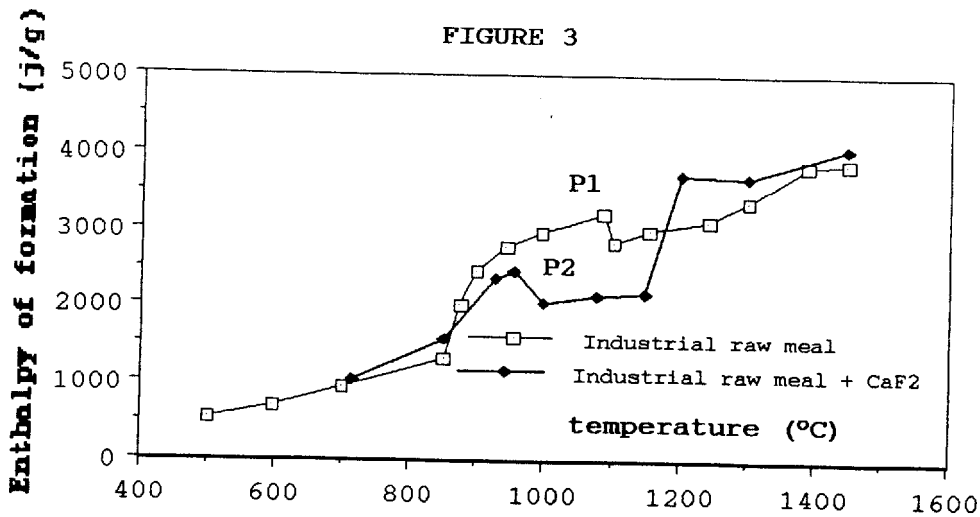

TABLE 2

Burning T° 1000°C	Without CaF2		With CaF2	
	CaO	22,6	CaO	17,9
	C2S	56,3	C2S	61,8
	C3A	7,7	C3A	
	C11A7 CaF2		C11A7 CaF2	8,4
	ferrite	7,4	ferrite	8,8
	MgO	yes	MgO	
	MCAS		MCAS	
	total silicates	49,2	total silicates	59,9

Burning T° 1100°C	Without CaF2		With CaF2	
	CaO	23,4	CaO	11,6
	C2S	55,8	C2S	34,5
	C3A	7,2	C3A	
	C11A7 CaF2		C11A7 CaF2	7,9
	ferrite	7,3	ferrite	8,1
	MgO	yes	MgO	
	MCAS		MCAS	yes
	total silicates	49,5	C3S	33,5
				66,3

Burning T° 1200°C	Without CaF2		With CaF2	
	CaO	18,7	CaO	2,5
	C2S	60	C2S	13,2
	C3A	12,8	C3A	
	C11A7 CaF2		C11A7 CaF2	6,9
	ferrite	6	ferrite	6,4
	MgO	yes	MgO	
	MCAS	yes	MCAS	yes
	C3S	*	C3S	69,7
	total silicates	55,6		78

Burning T° 1300°C	Without CaF2		With CaF2	
	CaO	1	CaO	0,4
	C2S		C2S	2,6
	C3A	10	C3A	
	C11A7 CaF2		C11A7 CaF2	5,4
	ferrite	7	ferrite	7,1
	MgO		MgO	yes
	MCAS	yes	MCAS	yes
	C3S	81,3	C3S	83,6
	total silicates	77,3		88,4

Burning T° 1400°C	Without CaF2		With CaF2	
	CaO	0,9	CaO	0,8
	C2S		C2S	2,4
	C3A	11	C3A	6,9
	C11A7 CaF2		C11A7 CaF2	
	ferrite	9,2	ferrite	10,4
	MgO	yes	MgO	yes
	MCAS		MCAS	yes
	C3S	78,7	C3S	79,3
	total silicates	66,9		75,2

Without CaF_2, the C_3S starts to form at 1250°C and at 1100°C with CaF_2. In this case, $C_{11}A_7$ CaF_2 forms instead of C_3A at temperature up to 1300° and transforms into C_3A at higher temperature.

MgO is found as periclase or as calcium silicate solid solution "54 CaO.16 SiO_2.Al_2 O_3. MgO (10).

Although the quantity of alite in the mineralized sample, is higher than in the standard sample, the belite in this latter case is hardly detectable at T°› 1300° C, due probably to the phase composition.

The quantity of C_3A is higher than the quantity of $C_{11}A_7$ CaF_2 at equal temperature. From 1300°C to 1400°C, the quantity of alite decreases and $C_{11}A_7$ CaF_2 transforms into C_3A.

DISCUSSION :

The table 3 compares the calculated and experimental values of the enthalpy of formation for C_2S and C_3S. The calculated values are based on the previously found data for C_2S and C_3S : ΔH C_2S = -692 j/g and ΔH C_2S = -546 j/g. The experimental values found by drop calorimetry are in good agreement with the calculation.

TABLE 3

	C2S	C3S
Enthalpy	j/g	j/g
Heating from 25° to 850°	1391	1456
decarbonation	1968	2225
heating between 850° and 1100°	344	358
C2S formation	-683	-516
heating C2S from 1100° to 1450°	456	177
transformation into C3S	0	146
heating C3S from 1300 to 1450	0	175
calculated	3476	4021
experimental	3637	3997

The addition of fluoride does not change the theoretical formation of C_2S and C_3S and modifies only slighltly the enthalpy distribution.

Attention must be paid to the early exothermal effect due to the C_2S formation, when the industrial burning process involves a preheater or a precalciner. When the process leads to a burning at the entrance of the kiln or inside the cyclones, the presence of fluorine would lead to an increase of the quantity of liquid phase and a risk of clogging or ring formation.

In figure 4, we attempt to represent the distribution of the clinker formation enthalpy, of the belite percentage, for a raw meal with and without CaF_2, as a fonction of the residence time in a kiln equipped with a preheater. The X axis represents the residence time or the length of the kiln and the Y axis is in arbitrary units.

FIGURE 4

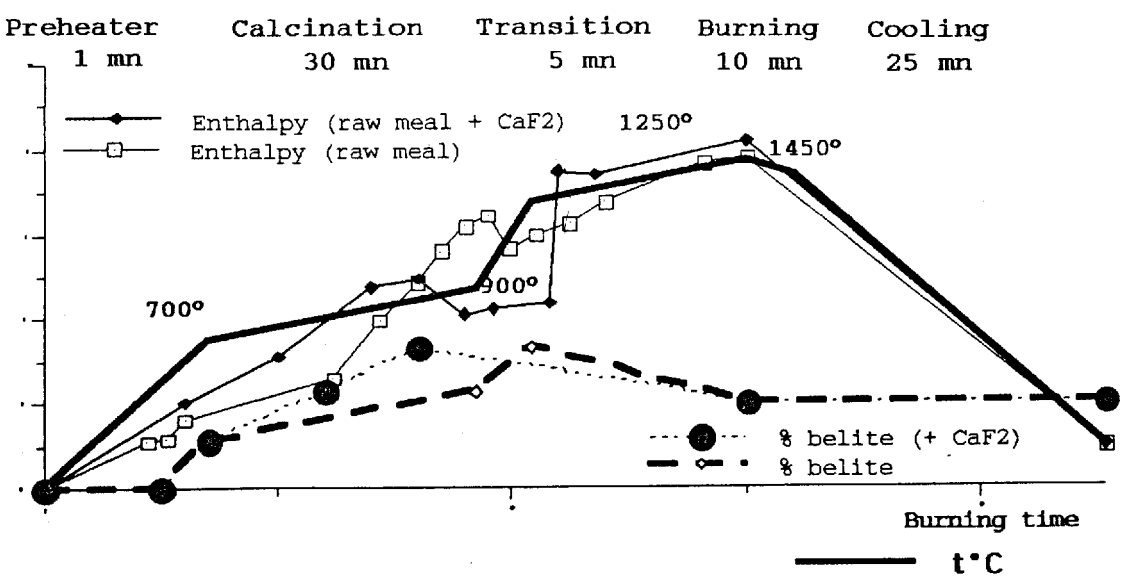

Concerning the effect of fluorine on the industrial raw meal, it is worth noting that the total enthalpy of the clinker formation is not changed, but the distribution is largely modified.

The fact that the change of the temperature of C_2S formation is more important, in the case of the clinker than in pure C_2S, suggests that the fluorine acts mainly by a modification of the liquid phase (in % and quality)

CONCLUSIONS :

In the case of pure C_2S and C_3S, the addition of calcium fluoride to the raw mixture does not change the total enthalpy of formation of these compounds and modifies only slightly its distribution.

In the case of industrial raw meal, the addition of calcium fluoride to the raw meal, does not change the total enthalpy of formation of these compounds but modifies its distribution by accelelating the C_2S formation.

These phenomenum can be explained by an action of the fluorine on the liquid phase occuring earlier.

The risk of clogging or ring formation by using fluorine in processes involving a rapid burning up to 900°C (preheater, precalciner) is not negligible.

REFERENCES :

1. Odler, I.: **"Improving Energy Efficiency in Portland Cement Manufacturing"**, Cement and Concrete Technology by S.N Gosh ABI Books Private Limited, 1991, 175-200.

2. Blanco-Varela M.T, et al.: **"Effect of fluorspar on the formation of clinker phases"**, Cement Concrete Research, 1984, 14, 397-406.

3. Klemm, W.A. et al.: **"Mineralizers and fluxes in the clinkering process"**, Cem. Res.Prog. Am. Ceram. Soc, 1976, 14, 259-291.

4. Goswami, G. et al.: **"Phase formation during sintering of a magnesium and fluorine containing raw mix in a cement rotary kiln"**, Zement-Kalk-Gips, 1990, 5, 253-256.

5. Moir, G.K.: **"Mineralized high alite cement"**, World Cement 1982, 10, 374-382.

6. Surana, M.S. Joshi, S.N.: **"Use of mineralizers and fluxes for improved clinkerisation and conservation of energy"**, Zement-Kalk-Gips, 1990, 1, 43-47.

7. Harrisson, A.M. Taylor, H.F.W.: **"Electron optical analysis of the phases in a portland cement clinker, with some observations on the calculation of quantitative phase composition"**, Cement Concrete Research, 1985, 15, 775-780.

8. Ayed, F. Sorrentino, F. Castanet R.: **"Determination par calorimétrie de dissolution des enthalpies de formation de quelques silicates, aluminates et aluminosilicates de calcium"**, to be published.

9. Ayed, F.: "Contribution à l'étude des phénomènes thermiques lors de la clinkérisation de crus de ciment portland", Ph. D Thesis, 1991, Université de Provence, Marseille (France).

10. Yamaguchi, G. Miyabe H.: **"Precise determination of the C3S cells, interpretation of their X ray diffaction pattern"**, J.Am. Ceram. Soc. 1960, 43, 219-223.

SINTERING MECHANISM OF PORTLAND CEMENT CLINKER WITH ENERGY-SAVING AND EARLY-STRENGTH

Wang Xinrong, Zhu jiaoqun, Xian Yafang and Wang Shanba

Department of Material Engineering, Wuhan University of Technology
Wuhan, Hubei, P R CHINA

SUMMARY

The cement clinker in the paper was formed by sintering at 1250～1350℃ from limestone, clay, gypsum and a calcium fluoride. The sample has the high-strength, early-strength and energy-saving property. High-temperature XRD and EPMA (electron probe microanalysis) were used to study the sintering mechanism of the cement clinker. The clinker contains a great deal of alite, some $C_4A_3\bar{S}$ and a part of high-temperature burned gypsum. The results indicate that the CaF_2 and $CaSO_4$ have obvious mineralization properties during sintering process of Portland cement clinker. Three intermediate phases appeared during sintering process of clinker. At 1100℃ a liquid phase and alite crystal phase appeared. The formation rule of $C_{11}A_7 \cdot CaF_2$ and $C_4A_3\bar{S}$ crystal phases during the sintering process of clinker is analysed in the paper.

摘 要

该水泥熟料是由石灰石、粘土、石膏及萤石经1250～1350℃煅烧而成。它具有早强、高强特性，并可节省大量燃料。本文利用高温X射线衍射，电子探针等分析方法对该熟料烧成过程机理进行了详细研究。该熟料含大量阿利特、一定量的$C_4A_3\bar{S}$和部分高温煅烧石膏。高含量$CaSO_4$和少量CaF_2对熟料烧成起明显矿化剂作用，使熟料烧成中出现三种中间过渡相，并于1100℃左右出现适量液相和析出阿利特晶相。文中还分析了熟料煅烧中$C_{11}A_7 \cdot CaF_2$和$C_4A_3\bar{S}$晶相的形成规律。

1. INTRODUCTION

In order to decrease energy loss during production process of cement, develop economy efficiency and satisfy the needs for various special projects, the cements with the property of energy-saving, early-strength and high-strength have been the subject of a great deal of research. At present, in order to gain the above properties, it is the most efficient method that CaF_2, SO_3, mixed mineralizer is used during sintering process of clinker. Thus, in order to study and produce high-strength and saving-energy cement and control the sintering technique of the clinker with mixed mineralizer, it is important to know the formation process of the clinker mineral phase and the formation rule of the phase with Alumina. G.K.Moir[1] reported that when temperature is higher than 1350℃, with high-sulphur mixed mineralizer ($CaSO_4$ 6%, CaF_2 0.5%) being used, C_3S, C_2S and C_4AF phases exist in the clinker and there is a little $C_4A_3\overline{S}$ phase at 1300℃, but $C_{11}A_7 \cdot CaF_2$ apears only as intermediate phase. Whereas Wang Tiandi [2] gained the cement clinker whose mineral composition contains C_3S, C_2S, C_4AF, $C_4A_3\overline{S}$ and $C_{11}A_7 \cdot CaF_2$ by means of low-temperature sintering with mixed mineralizer CaF_2 and $CaSO_4$. Fong Minfen [3] also studied the formation of the mineral containing Alumina during sintering process of cement clinker with F^- and $\overline{S}$ and the action mechanism of mixed mineralizer, they thought that CaF_2 is a kind of depressant to the formation of C_3A and $C_4A_3\overline{S}$. Xue jungan and Li Xiouyin et al [4] studied the formation rule of the clinker phase containing Alumina with the addition of F^- and $\overline{S}$ and thought that the clinker containing 2.5% SO_3 is advantageous to the formation of $C_4A_3\overline{S}$ at 1250℃ and is advantageous to formation of C_3A at 1300℃.

The new early-strength cement clinker gained by us contains more than 65 % C_3S, 5-8% C_2S and about 5% $C_4A_3\overline{S}$. When the clinker was used in industrial production, its three days' strength sustains 43.0～50.0MPa and twenty eight days' strength is more than 65.0MPa. By means of adding a number of various mixed materials to the clinker, the mixed material cement can be produced, with saving-energy 15-25% than general cement. The composition of the cement clinker is 60～65% CaO, 18-22% SiO_2, 3.0～6.5% Al_2O_3, 0～3.5% Fe_2O_3, 0.6～1.7% CaF_2 and 2.5～8.0% SO_3. in the paper, high-temperature XRD and EPMA were used to study the sintering mechanism of the cement clinker.

2. EXPERIMENT AND MEASUREMENT

2.1 Sample preparation

The clinker used in the paper was prepared from industrial limestone, clay, gypsum and A.R grade CaF_2. Ground industrial raw meal was homogenized and passed the sieves with sieve mesh 0.074mm. The results gained by chemical analysis were shown in table 1.

Table 1. The chemical compositions of industrical raw meal

wt%	SiO_2	Fe_2O_3	Al_2O_3	TiO_2	CaO	MgO	SO_3	L	Σ
limistone	5.02	0.68	1.32	—	51.29	0.62	—	40.61	99.09
clay	59.51	7.04	17.46	0.59	3.25	1.38	—	9.32	98.55
gypsum	7.34	0.61	1.91	—	30.24	0.56	38.58	20.17	99.47

The sample compositions were shown in table 2. The powered sample with suitable amountof water was pressed into 14×24×1.5mm sheetlike sample.

Table 2. Raw meal and clinker compositions of the sample

raw meal compositions				clinker compositions						
limistone	clay	gypsum	CaF_2	CaO	SiO_2	Al_2O_3	Fe_2O_3	MgO	SO_3	CaF_2
76.00	14.51	8.60	0.89	63.65	19.81	5.62	2.41	1.09	5.03	1.35

2.2 Measurement

High-temperature X-ray diffraction measurement was made by D/MAX-RB type rotating target X-ray diffractometer with Japan CN2311B1 type high-temperature device. Measurement condition was as follows: Cuka target, voltage 50 KV, current 150mA, scan speed 10° /min, scan range 2θ =10～60° , heating-up speed 10℃/min and soaking time 20 min under every measured temperature. measurements were made respectially at room temperature, 700℃, 800℃, 900℃, 1000℃, 1100℃and 1200℃.

On the other hand, the raw meals in table 2 with suitable amount of water were pressed into Φ 25×3mm sheetlike samples, then the sample was sintered in high-temperature furnace with 30 min at 1300℃. The heating-up speed was about 10℃/min. The clinker was quenched by-air into room temperature, then was milled into power which was used in general X-ray diffraction. The general X-ray diffraction data were obtained by HZG-FC type X-ray diffractometer, with Coka target, voltage 40kV, current 40mA, scan speed 10° /min.

3. RESULTS AND DISCUSSION

Fig. 1 and fig.2 showed the X-ray diffraction figures of sample. And the X-ray diffration figure of the sample obtained by sintering at 1300℃ and then quenching was shown in fig.3.

From the diffraction figures, it was known that at room temperature (17℃) the main crystal phases of raw meal were $CaCO_3$, $CaSO_4 \cdot 2H_2O$, SiO_2, muscovite and CaF_2. During the process of heating-up to 700℃, the dehydration of dihydration gypsum and the decomposition of clay mineral were finished. The diffraction figureat 700℃ showedthemaincrystalphases in the sample were $CaCO_3$, SiO_2, $CaSO_4$ and CaF_2. At the same time, it was also known that $CaCO_3$had begun to decompose and that the characteristic peaks of CaO appeared at 2.428Å and 1.719Å.

The high-temperature XRD figure at 800℃ showed that a amount of $CaCO_3$ had decomposed, the characteristic peaks of CaO were more outstanding, $CaSO_4$ and SiO_2 were involved in sold phase reaction, therefore all their characteristic peaks decreased. at the moment several new phases appeared in the sample, they were $C_2S \cdot CaCO_3$(3. 017, 2. 718, 2. 680, 2. 636Å) , β -C_2S(2. 888, 2. 784Å) and $3C_2S \cdot 3CaSO_4 \cdot CaF_2$(2.839, 2.804, 2.718, 2.636Å). That was dicalcium silicate and other two intermediate phases had begun to appear at 800℃.

DTA data were obtained using Japan PTC-16A type DTA divice with heating-up spead 10℃/min. From those date it was known that $CaCO_3$ began to decompose at 672℃ , heat absorbing peak' s submit appeared at 792℃ . And decompostition reaction of $CaCO_3$had been finished at 810℃.

The diffraction figure at 900℃ showed that both $CaCO_3$and intermediate phase $C_2S \cdot CaCO_3$had disappeared at the temperature.Then CaO became main crystal phase, on the other hand there were $3C_2S \cdot 3CaSO_4 \cdot CaF_2$, β-C_2S, $CaSO_4$ and SiO_2 phases, and $C_{11}A_7 \cdot CaF_2$ phase (2.674Å) and C_4AF phase (2.658Å) also appeared.

From the diffraction figure at 1000℃ it was known that the characteristic diffraction peaks of CaO phase and SiO_2 phase decreased obviously, which was because CaO and SiO_2 joined further solid phase reaction and formed α'_L-C_2S. From the figure, it was known that the diffraction peaks of $CaSO_4$ and CaF_2 also decreased rapidly, which might be because a part of the two phases joined the above reaction and existed in dicalcium silicatein solid solution, and a part of the two phases formed a little liquid phase appearing at 1000℃.

The diffraction figure at 1100℃ showed CaO phase decreased rapidly, alarge amount of CaO joined reaction process, so was the SiO_2phase.Under the temperature $3C_2S \cdot 3CaSO_4 \cdot CaF_2$ and $C_{11}A_7 \cdot CaF_2$ disappeared at the same timeand suitable amount of liquid phase appeared, while alite phase appeared at the moment.

The diffraction peaks of α'_L-C_2S appeared at 2.761Å, 2.710Å, 2.210Å, 1.981Å and 1.657Å, the diffraction peaks of alite phase appeared at 3.887Å, 2.784Å, 2.784Å, 2.633Å and 1.771Å.

The diffraction figure at 1200℃ showed the main crystal phases of the sample were α'_H-C_2S and alite, at the same time there were also $CaSO_4$ and C_4AF crystal phases.At the moment characteristic diffraction peak of $C_4A_3\bar{S}$ appeared at 3.781Å, which showed that the $C_4A_3\bar{S}$ crystal phase had been formed between 1100℃ and 1200℃.

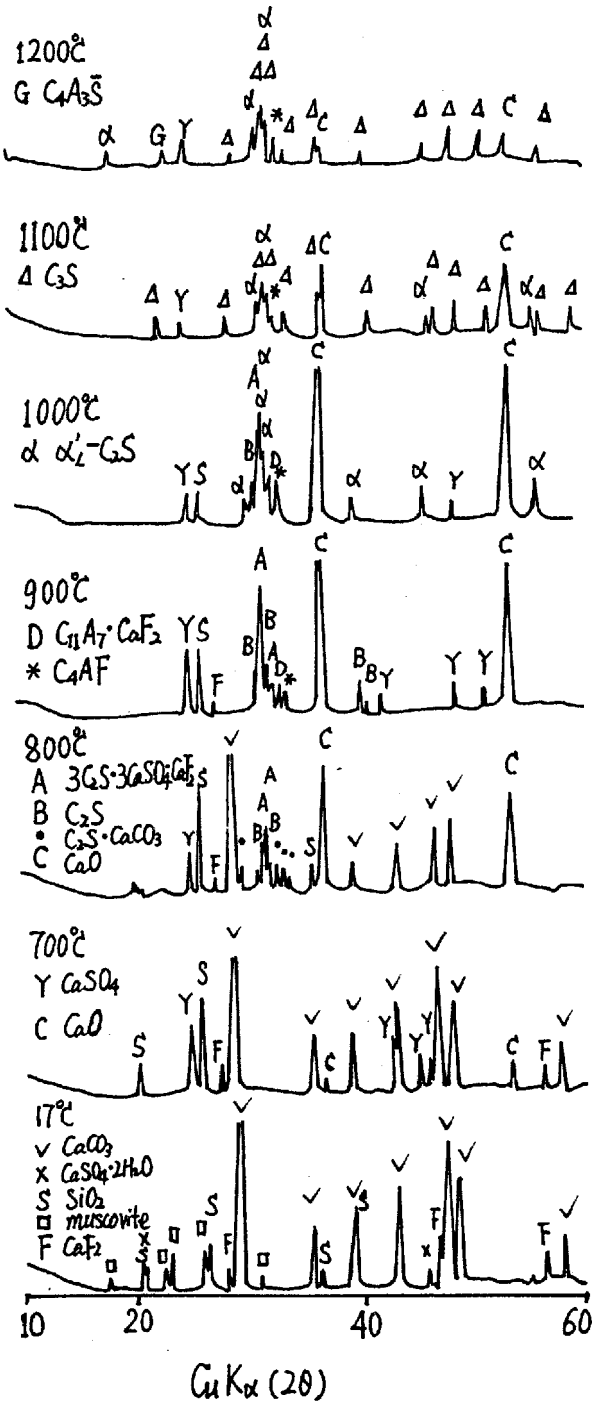

Fig. 1 X-ray diffraction figure of the sample during heating-up process

Fig. 2 was the X-ray diffraction figures of the sample when it was cooled from 1200℃ to 350℃ at the speed of 30℃/min and after it was cooled to room temperature. From the figures it was known that at 350℃ the main crystal phases of the clinker were alite, α'_H-C_2S, C_4AF, $CaSO_4$ and $C_4A_3\bar{S}$(3.759, 2.858Å).But the increasing again of CaO diffraction peak resulted from the decompositon of alite during the process of slowly cooling and

recrystallization of CaO not fully joining reaction. The sample having been heated-up 1200℃ was quenched to room temperature, its main crystal phases were alite, β -C_2S, α -C_2S, C_4AF, $C_4A_3\bar{S}$, $CaSO_4$ andf-CaO.

Fig.3 was the XRD figures of the sample which was socked 30 min at 1300℃ and was quenched to room temperature by air, then was measured by XRD. From above analysis it was known that the sample was domained by alite phase and there were also β -C_2S, C_4AF C_3A, $CaSO_4$ and $C_4A_3\bar{S}$ phase, but f-CaO was so little that it can't be measured out.

The S and F elemental distributions in clinker were measured by JCXA-733 type electron probe X-ray micro-analyzer. The experiment condition was as follows: volatage 20 KV, current 2.0×10^{-8}A.

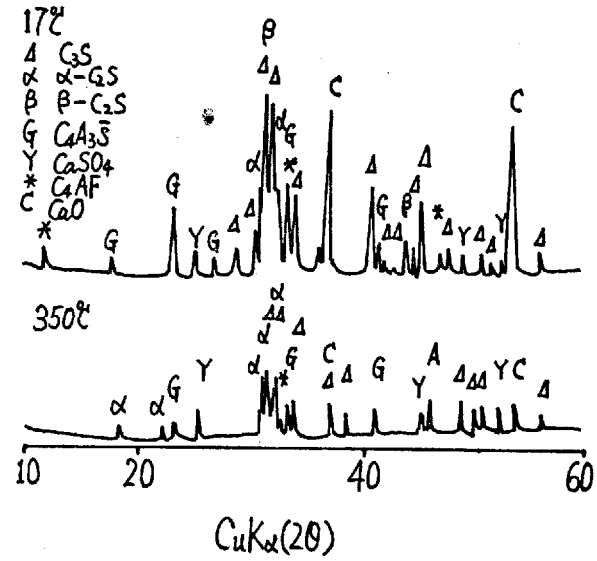

Fig.2 X-ray diffraction figure of the sample during cooling process

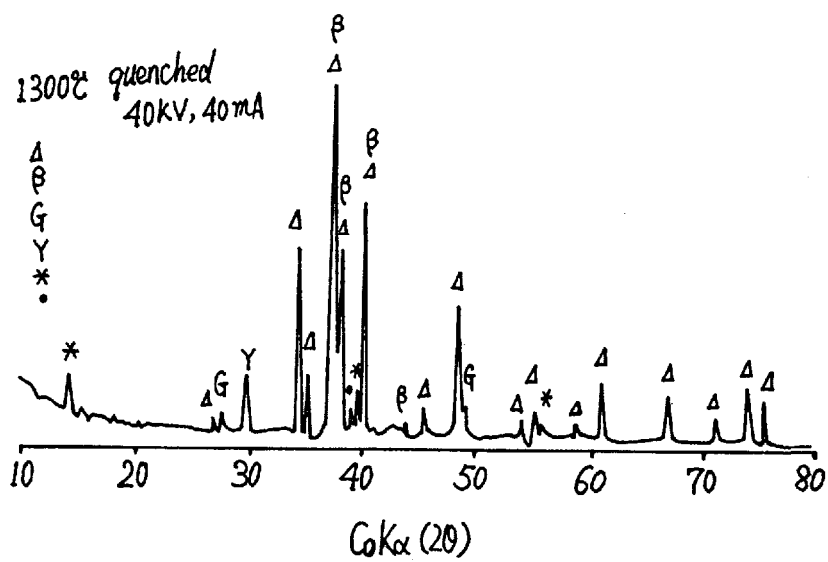

Fig.3 X-ray diffraction figure of the sample sintering at 1300℃ and then quenching

The S and F elemental characteristic X-ray intensity was measured by fixed spot method and the results were compared with those gained by 10S calculating number. The results were shown in table 3.

From table 3 it was known that F elemental concentration ,distribution almost was equal in C_3S, C_2S and intermediate phase. By the mineral content of clinker it was known that in clinker about 70% F element distributed in siliate phases, the other F in intermediate phase. The SO_3 content in cliker was higher, table 3 showed that small amount of S element existed in C_3S in solid

Table 3 F and S elemental characteristic X-ray intensity measured by fixed spot electron probe

	C_3S			C_2S			intermediate phase		
element	1	2	3	1	2	3	1	2	3
F	31	25	32	29	32	31	32	35	38
S	143	126	129	792	796	802	1162	1312	1274

solution, S content was higher in C_2S and it was the highest in intermediate phase. By all the mineral content in clinker it was known that about 30% SO_3 distributed in silcate phase and the other SO_3 in intermediate phase.

From above analysis, it was known that in the sintering process of the Portlant cement clinker with high sulphur mixed mineralizer, because of the mineralization function of CaF_2 and $CaSO_4$, $CaCO_3$ had begun to decompose before 700℃. Intermediate phase $C_2S \cdot CaCO_3$, $3C_2S \cdot 3CaSO_4 \cdot CaF_2$ and $C_{11}A_7 \cdot CaF_2$ existed in 800～1100℃, with temperature heating up they either decomposed or formed liquid phase being advantageous to forming blite and alite phase. Because the high-sulphur mixed mineralizer was used in sample, the liquid phase during the sintering process of clinker early appeared at about 1100℃, which made that alite had formed at 1100℃.

During the sintering process of sample, the formation rule of early-strength minerals $C_{11}A_7 \cdot CaF_2$ and $C_4A_3\overline{S}$ also had outstanding characteristics at about 900℃, high-activated CaF_2 reacted with CaO and Al_2O_3 in sample and formed $C_{11}A_7 \cdot CaF_2$, making C_3A not appear in the sample. With temperature heating up to 1100℃, $C_{11}A_7 \cdot CaF_2$ reacted with CaO, SiO_2, Al_2O_3 and $CaSO_4$ and formed eutectic liquid. With temperature heating up further, a great deal of alite and blite were formed, a large part of F^- ions in liquid phase decreased continously until a certain extent, whether sample being heated-up continously or clinker being cooled, it is not enough to form $C_{11}A_7 \cdot CaF_2$, whereas during the cooling process a part of F^- ions existed in intermediate phase in solid solution, which was testified by EPMA. Thus during the sinkering process and after cooling above 1100℃ the samples didn't contain $C_{11}A_7 \cdot CaF_2$ mineral. From bove analysis, it could be suggested that under the condition of low-temperature reduced under burning, $C_{11}A_7 \cdot CaF_2$ the early-strength and quick-setting mineral was formed in the clinker in which the mixed mineralizer was used.

Under the experiment condition, only when temperature heated-up to 1200℃ $C_4A_3\overline{S}$ mineral phase appeared. The formation of $C_4A_3\overline{S}$ phase didn't result from the solid phase reaction between $CaSO_4$ and C_3A, it was because that during heating-up process the characteristic diffraction peak of C_3A didn't appeared in the X-ray diffraction figure. Whereas C_3A in the clinker produced by sintering at 1300℃ then cooling was formed by liquid phase crystalization during cooling process, it was because liquid phase composition varied with the formation of alite and so on that $C_4A_3\overline{S}$ crystalized out gradually from liquid phase. Because the system wasn't similar to those of the past reports, some point of view in the paper was different from those of the past reports. Fong Xiuji et al [5] studied the formation rule of $C_4A_3\overline{S}$ phase in sulphoaluminate cement and

thought that $C_4A_3\overline{S}$ was formed by high-temperature reaction between CA and $CaSO_4$. I. V. Kravtenko [6] thought that $C_4A_3\overline{S}$ was formed by the reaction of that $C_{11}A_7$, $CaSO_4$ and Al_2O_3. In the paper the formation temperature of $C_4A_3\overline{S}$ phase was accordant with above reports. From above diffration figures it was known that slow-cooling was advantageous to the crystalization of $C_4A_3\overline{S}$ phase from liquid phase, but was disadvantageous to the stability of alite phase, therefore making free CaO add.

Alite phase appeared at 1100℃, but until 1200℃ it became main crystal phase, thus the system clinker must be sintered above 1200℃, but $C_4A_3\overline{S}$ early-strength mineral decomposed above 1350℃. From above analysis, it was known that suitable sintering temperature range of the system clinker was from 1250℃ to 1350℃.

4. CONCLUSION

(1) High-sulphur mixed mineralizer had obvious mineralization during sintering process of Potlant cement clinker, which made liquid phase early appeared at 1100℃ and alite phase crystalized out. The three intermediate phases $C_2S \cdot CaCO_3$, $3C_2S \cdot 3CaSO_4 \cdot CaF_2$ and $C_{11}A_7 \cdot CaF_2$ appeared during the sample sintering process.

(2) High-sulphur and low-alumina clinker was disadvantageous to the end existence of $C_{11}A_7 \cdot CaF_2$ phase, $C_{11}A_7 \cdot CaF_2$ only appeared in intermediate phase and existed in the temperature range from 900℃ to 1100℃. Under the condition of low-temperature reduced under burning, it was known that forming $C_{11}A_7 \cdot CaF_2$ was easy in the cement clinker with mixed mineralizer. In the paper early-strength mineral $C_4A_3\overline{S}$ resulted from the crystalization of liquid phase in clinker above 1200℃.

(3) Electron probe analysis showed that in clinker about 70% F element distributed in silicate phase and the other F in intermediate phase, whereas about 30% SO_3 distributed in silicate phase and the other SO_3 in intermediate phase.

(4) High-temperature X-ray diffraction analysis showed that sintering the cement clinker above 1200℃ was advantageous to forming alite and $C_4A_3\overline{S}$ crystal phases in clinker. The suitable sintering temperature range for clinker was from 1250℃ to 1350℃.

REFERENCE

1. G.K. Moir,: "Mineralised High Alite Cements", World Cement Technology, 1982, 13(10), 374.

2. Wang Tiandi,: "Low-temperature Sintering Mechanism of Fast-hardening Cement Clinker Produced by Gangue and Coal-slag", Collected Papers of Congress on Cement(in China), 1980, 1981, P185.

3. Fong Minfeng,: "The Action Mechanism of Mixed Mineralizer During Producing Process of Cement" Technique data on Producing High-strength Cement by Using Mixed Mineralizer, 1986, 4, P29.

4. Yue Jungan, Li Xiouyin, Tong Xueli, Fan jiajun, Zhang Xiaodong, "The Rule of Formation of Alumina-bearing Phases in Cement Clinker Using F^- and SO_4^{2-} as Combined Additives", Journal of the Chinese Silicate Society, 1985, 13(3), 264.

5. Fong Xiuji, Long Shizong, "The Effection of Phosphorus, Fluorine, Iron and Titanium on the Formation of $C_4A_3\overline{S}$ and the decomposition of $2C_2S \cdot CaSO_4$", Collected Papers of 2nd Congress on Cement (in China), 1988, P339

6. I.V. Kravtenko, V.A. Kharlamov, T.V. Kuznetsova, L.L. Astansky, "Quick Hardening Sulphoaluminate-belite Cement", Cement(USSR), 1979, No.5, P7.

ROLE OF MINERALIZERS IN ALITE FORMATION IN A RICE HUSK ASH - $CaCO_3$ RAW MIX

K C Misra* and P C Borthakur**

**Chemistry Department, J B College*
***Regional Research Laboratory*
Jorhat, INDIA

The influence of three oxide mineralizers, ZnO, CuO and MnO_2 on formation of alite in a raw mix of $CaCO_3$ and RHA (Rice Husk Ash) alone as well as in presence of added C_4AF (Fe_2O_3 + Al_2O_3 + $CaCO_3$) has been investigated. ZnO and MnO_2 in 1-2% dose and CuO in only 0.5% dose can considerably improve alite formation. 1-2% addition of ZnO lowers sintering temperature by 50-100°C. Alite formation is also improved by addition of C_4AF composition to the neat raw meal as well as to those containing ZnO.

DTA suggests that the mineralizing ability of these oxides is not related to their ability to lower the decomposition temperature of $CaCO_3$. A reaction mechanism to explain the role of the mineralizers on formation of C_3S from C_2S is proposed. It is suggested that the reaction is initiated by an attack of the mineralizer on SiO_4 tetrahedron and proceeds through formation of pentacoordinated Si with triangular bipyramidal structure.

Die einfluβ von drei Oxid Mineralisator ZnO, CuO and MnO_2 auf die Formation von Alite in einem grün mischung von $CaCO_3$ and RHA (Reishulse Aschen) alien and auch mit zusatlich C_4AF (Fe_2O_3+Al_2O_3+$CaCO_3$) ist untergesucht. ZnO and MnO_2 in einem Dosis von 1 bis 2% kann verbessern die Alite Formation. Bei einem eingabe von 1 bis 2% ZnO die sintertemperatur ist, in der höhe von 50 bis 100°C niedriger geworden. Die Alite Formation hat auch sich verbessert bei einem eingabe von C_4AF Komposation in einem saubere grün mischung und auch in die mit ZnO.

Die DTA scheines daβ die Mineralisierung fähigkeit der dieses Oxids ist unabhängig von die Fahigkeit der dieses Oxids zum niedrigeren die $CaCO_3$ zersetzung temperatur. Ein Reaktionmechanismus zum erklären die role der Mineralisator auf die C_3S Formation von C_2S ist vorgeschlagen. Es ist schlägt vor da die Reaktion ist eingeführt mit einem angriff von die Mineralisator auf die SiO_4 Tetrahedron and dann weitergeführt durch penta-coordinated Si mit Dreieckig Doppel pyramide Struktur bildung.

*Present address: Chemistry Department, J.B. College, Jorhat-1 (Assam)

INTRODUCTION

Rice Husk Ash (RHA) contains chiefly silica in active form along with trace to small quantities of carbon, Fe_2O_3, Al_2O_3, CaO, MgO, K_2O, P_2O_5 etc[1-3]. The pozzolanic character of RHA was exploited by many workers for development of building materials[4,5]. The present investigators indicated the potentiality of RHA as an argillaceous raw material for preparing high quality portland cement also[6-9]. This investigation is a follow up of the earlier work to look into the high temperature reaction between lime and RHA-Silica for making cement with high alite content.

Raw-meal compositions to achieve very high quantity of alite can be computed in the RHA-$CaCO_3$ system, but the synthesis, is fraught with difficulties due to inadequacy of the liquid phase. High values of Lime-Saturation-Factor (LSF) and Silica-Ratio (SR) also create disadvantages in achieving high alite content[3]. Under these circumstances suitable mineralizers and liquid forming agents are to be incorporated in the raw mix to improve the burnability. The present investigation is carried out using three metal oxide mineralizers viz.CuO, ZnO and MnO_2. Iron-rich melt phases are more efficient in promoting assimilation of lime and formation of C_3S, the order being C_2F>C_4AF>C_6A_2F>C_3A[1-10]. Therefore efforts have also been made to improve alite formation in the system by increasing the quantity of C_4AF through incorporation of additional Fe_2O_3 and Al_2O_3.

MATERIALS AND METHODS

RHA obtained by burning the husk in stack were pulverized to 90μ and mixed up with laboratory grade C_aCO_3 powder to obtain a raw meal having the composition-LOI 38.17, SiO_2 15.86, Al_2O_3 0.225, $CaCO_3$ 44.535, MgO 0.406, K_2O 0.407, Na_2O trace, P_2O_5 0.186, percent by weight. The Lime Saturation Factor (LSF), Silica Ratio (SR) and Alumina Modulas (AM) of the mix corresponds to 99.33, 36.56 and 0.93 respectively. The liquid content of the mix at 1400°C (calculated by Lea and Parker's formula) was 2.28% and the potential phase composition corresponds to C_3S=92.25, C_2S=0.578, C_3A 0.279 and C_4AF=1.103 percent.

Reagent grade ZnO, MnO_2 and CuO (obtained by thermal decomposition of $Cu(NO_3)_2.6H_2O$ was mixed separately and intimately with different portions of raw meal. Calculated quantities of Fe_2O_3, Al_2O_3 and $CaCO_3$ were mixed with different portions of the raw meal. The mixtures as prepared were then placed in a steel mould and pellets were made by applying (approx. 1 ton) pressure. The pellets were heated to the desired sintering temperature in an electrical furnace with fast heating rate and maintained at the temperature for 30 minutes. The products were then allowed to cool (without quenching) inside the furnace. The free lime contents of the samples were determined by glycerol alcohol method. The phase compositions were calculated by applying Nurse's formula[11], designed for clinkers containing P_2O_5.

RESULTS AND DISCUSSION

The variation of alite content in samples doped with different mineralizers at 1350, 1400 and 1450°C temperatures are graphically depicted in Fig.1. The influence of additional

quantity of C_4AF in the compositions is shown in Fig.2.

Fig.1 reveals that the oxides under investigation can enhance the alite quantity to considerable content. With CuO mineralizer, the results follow an erratic trend at all the sintering temperatures. High yield of alite is obtained with 0.5% addition, but the yield falls abruptly with increase of the dose. Odler and Maula[12] earlier reported increase of mineralizing activity of CuO up to 2.5% level of concentration. The difference is probably due to the difference in the method of cooling. CuO probably destabilizers the alite phase and therefore when it is used as mineralizer the sintered products need be cooled rapidly. The alite content increases at a parabolic rate with increase of ZnO dose. A reduction of the burning temperature by 50 to 100°C is observed with 1.0-2.0% addition of ZnO. Tonak[13] also observed a reduction of calcination temperature by about 50°C by the addition of 1-2% ZnO to the raw meal. The present system being liquid deficient, ZnO is acting both as mineralizer and flux leading to higher activity.

MnO_2 seems to act fairly at 1400 and 1450°C. An interesting observation is that with 1.0% MnO_2 a negative effect is seen when the sintering temperature is raised from 1400 to 1450°C. This suggests that MnO_2 lowers the stability of the alite phase. Simple substitution of Mn^{4+} for Si^{4+} and Mn^{2+} for Ca^{2+} and also formation of the compound 2 CaO. MnO_2 which is poorer in lime are assumed to be the reasons of lower alite contents at higher temperature[14]. The rate of increase in alite content with increase in the dose is also not uniform. Thus the mineralising ability of MnO_2 is both temperature and quantity dependent, the optimum dose being 1-2% and temperature 1400°C.

A parabolic rate of increase in alite formation is observed (Fig.2) with addition of C_4AF composition to the neat raw meal. An identical trend with supplemented activity is observed in raw-meal with 2.0% ZnO. Above 70% alite is achieved by the co-action of 2.0% ZnO and 1.0% C_4AF. But addition of C_4AF composition to the raw meals containing 0.5% CuO and 2.0% MnO_2 does not yield any positive result. This is probably due to the destabilising action of the mineralizers on alite phase as mentioned earlier

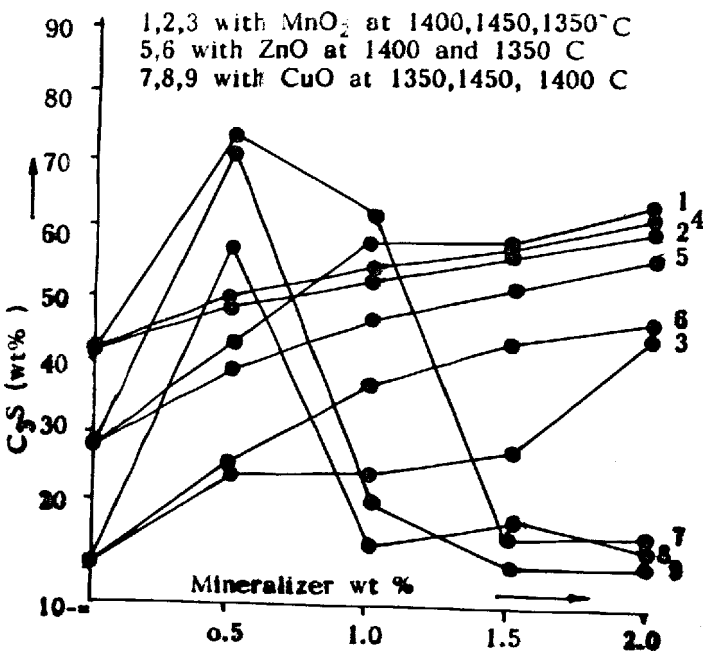

Fig. 1. Variation of C_3S content with mineralizer

Table 1 Samples Description for XRD

Sample/ curve	Mineralizer Composition*	C_3S(% by wt)* 1
1.	2.0% ZnO	77.76
2.	0.5% CuO	64.67
3.	2.0% MnO_2	48.21

*All samples contain 4% C_4AF and burnt at 1400°C, *1 calculated.

The scanning XRD patterns in the 2 θ range 29-34° of three products (compositions in Table 1) as recorded with CuK$_\alpha$ X-radiations (λ =1.54 A°) are shown in Fig. 3.

The diffractograms confirm the presence of alite in the samples[3].

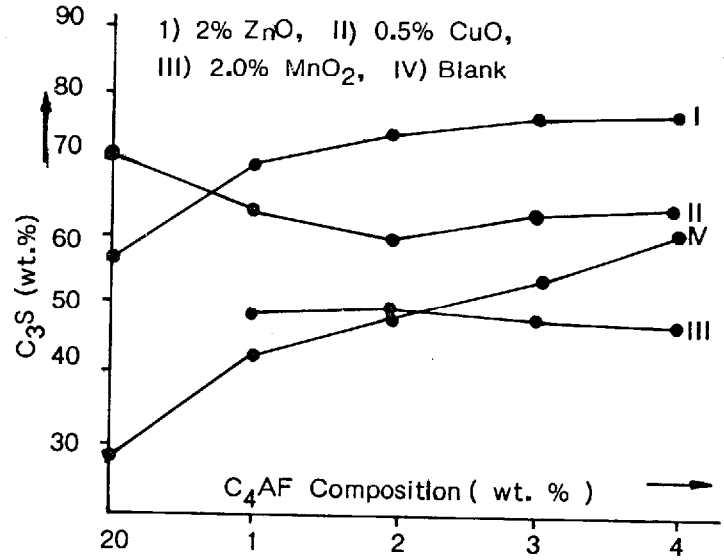

Fig.2. Variation of C_3S content with additional C_4AF at 1400°C

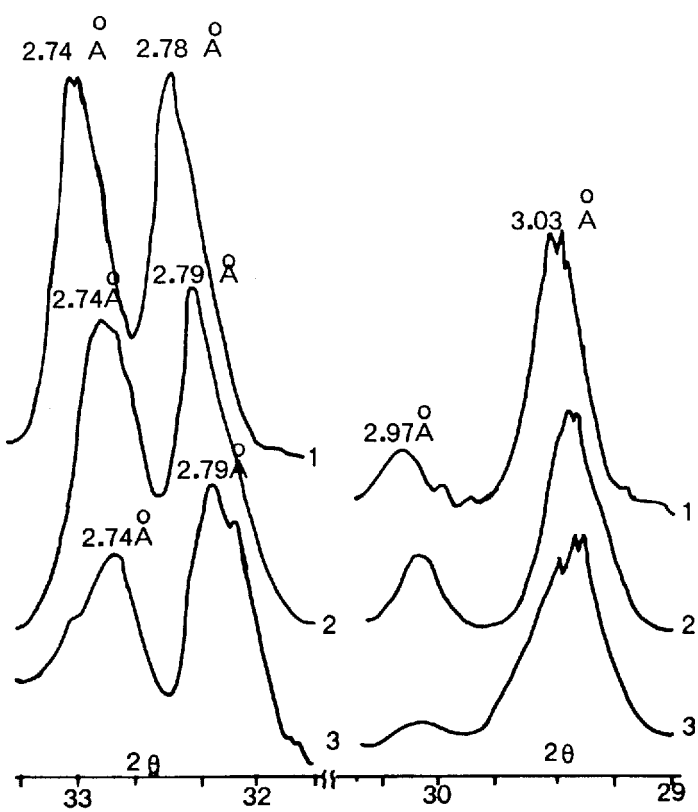

Fig.3. Scanning XRD pattern of products

Influence of the mineralizers on the decomposition characteristics of $CaCO_3$ was investigated with the aid of thermal analysis. The DTA curves (600-1000°C) of raw mix as presented in Fig.4 reveal that the temperature of onset of decarbonation remains fixed at 700°C for all the samples except for the one withMnO_2 (curve IV) where it drops to 675°C. The onset, peak and completion of decarbonation endotherm for **starting** $CaCO_3$ appear at 700, 920 and 950°C respectively (not shown in the Fig). RHA lowers the peak temperature of decarbonation to 860°C (Curve I). A further

insignificant lowering is seen in samples containing ZnO and MnO_2 (curves III, IV) the temperature of completion of decarbonation however remains fixed at 900°C. But in sample withCuO, (curve I) the peak as well as the completion of decarbonation slightly shifts to higher temperature. The mineralizing ability of different oxides is therefore not related to lowering of decomposition temperature of $CaCO_3$. In fact, it is more helpful to alite synthesis if nasent lime can be made available at higher temperature for clinkerisation 15,16.

In the sample containing ZnO+C_4AF (curve II) the decarbonation endotherm remains incomplete and another strong endotherm appears from 891°C due to liquid formation. The finding is in conformity with published literature[17] thatZnO lowers the liquid phase appearance temperature.

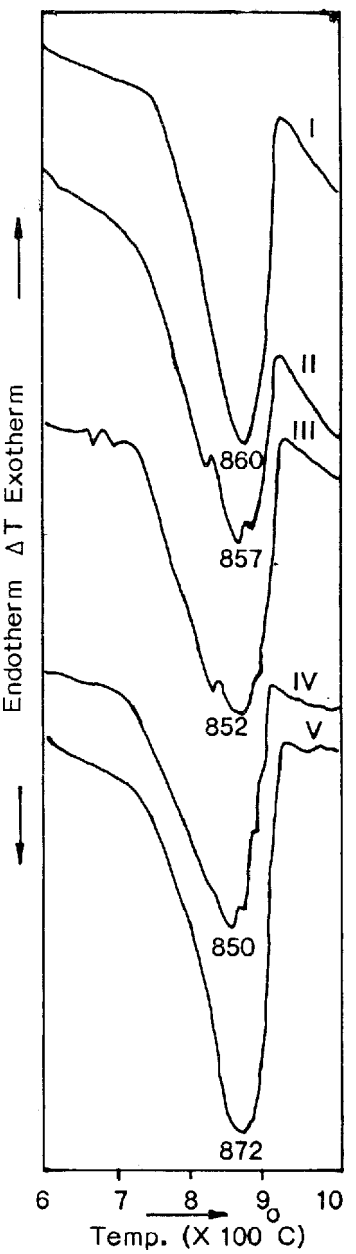

Fig.4. DTA Curves of raw mix

MECHANISM OF MINERALISATION

C_3S exists in dimeric form with the basic unit $Ca_6Si_2O_{10}$ in which deformed SiO_4 tetrahedra are linked together by triplet of Ca^{2+} ion[18-20]. It is obvious that CaO assimilated during formation of C_3S from C_2S goes to convert the -O-Ca-O-linking chain between two Si atoms into $(O\text{-}Ca\text{-})_3$- and builds up CaO octahedra. It is proposed that the process starts with an initial attack on the Si atom (by mineralizer or oxide ion) raising the co-ordination number of Si atom to 5 and converting the structure to triangular bipyramidal. The -O-Ca group trans to the attacking group then leaves with concomitant inversion of the structure to tetrahedral. The active -O-Ca group liberated reacts with free lime to produce columns of CaO octahedra. The scheme of the reaction taking F^- or $O^=$ as mineralizer is shown below:

Sometimes the changes of structure to triangular bipyramidal may not occur; with some deformity the overall tetrahedral structure of the SiO_4 may be retained. On elimination of a -O-Ca-group Cis to the attacking group the structure may become a deformed tetrahedron. Usually the reaction through triangular bipyramidal structure is faster than the other type involving Cis elimination[21]. During the course of reaction the mineralizer group may again be set free by the attack of active -O-Ca-group allowing it to recycle many times. Some mineralizer molecules/ion however may be retained in the silicate structure at

the end of the reaction. Formation of alite with random substitution of oxygen by fluorine can thus be explained.

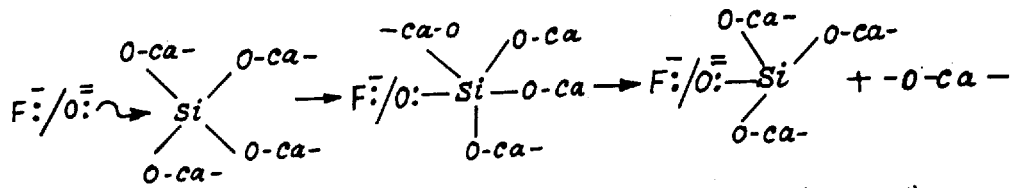

Attack on the SiO_4 tetrahedron may also be initiated by elemental (gaseous oxygen or fluorone mineralizer) generated by high temperature redox reactions. Mobilities in gaseous state being higher than that in ions (compound) an enhanced rate of reaction is expected in such cases.

Any compound or group which can facilitate formation of penta co-ordinated silicon, particularly with triangular bipyramidal structure can therefore act as a good mineralizer. Species like F^-, $O^=$, $SO_4^=$ etc. which act as mineralizer fall under the class of hard bases and so can readily attack Si^{4+}, a hard acid.

ACKNOWLEDGEMENT

One of the authors (KCM) is grateful to Director, RRL, Jorhat for allowing him to work in the laboratory as a guest research worker. The authors are also thankful to Mr. P. Sengupta for his help in translation of the summary.

REFERENCE

1. Borthakur, P.C.; Saikia, P.C. and Dutta, S.N. Indian Ceramics, 23 (2), 25-29 (1980).
2. Jose, J. and Subba Rao, M. Amer Ceramics Soc. Bull. 65(8) 1177-80 (1986).
3. Misra, K.C.: An Investigation on the synthesis of Tricalcium Silicate (Alite) Cement. Ph.D. Thesis (Dibrugarh University) (1990).
4. Rice Husk Ash Cement: Proceeding of a joint workshop on "Production of cement like materials from agro-wastes", Peswar Regional Centre for Transfer of Technology, Bangalore, p. 183 (1979).
5. Boateng, A.A. and Skeete, D.A., Cement and Concr. Res. 20(5) 195-202, (1990).
6. Misra, K.C. and Borthakur P.C. Trans of the Ind. Ceram. Soc. 44 (5), 101-105 (1985).
7. Misra, K.C. and Borthakur, P.C. Proceedings First N.C.B. International Seminar, New Delhi V.3, pp. VII, 40-46 (1987).

8. Borthakur, P.C. and Misra, K.C., Proceedings National Seminar on Disposal and Utilisation of Rice Husk Ash, Organised by National Productivity Council Chandigarh, 1989.

9. Misra, K.C., Bordoloi, D.K. and Borthakur, P.C., A process for making portland cement from rice husk ash, India Patent Appl. 369/DEL/91.

10. Jawed, I., Young J.F., Ghose, A. and Skalany J., Cement & Concr. Res. 14(1) 99-104 (1984).

11. Nurse, R.W., J. Appl. Chem. (London). 2. 708-16 (1952).

12. Odler, I. and Maoula, S. Abdul, Zement Kalk Gips, 33(3) 132-36 (1980).

13. Tonak, Tulini :Cimento Bull : 22, (222), 3-14 (1985).

14. Knoefel, D. Strunge, J. and Bambaur, H.H.: Zement Kalk Gips, 137 (120) 651-55 (1984).

15. Timashev, V.V. and Sazhneva, Z.S.: Tr. Mosk. Technol Inst. i.m. D.I. Mandeleeva, 108, 115-19, (1979).

16. Buchi, R.: World Cem. Technol 12(5), 210-31 (1981).

17. Grach'yan, A.M.: Zubar, G.N. and Kramanovich, G.I.: J. of Appl. Chem of the U.S.S.R.: 46(11), Pt. II, 2731-34 (1973).

18. Fayos. J. and Perez-Mondez, M. Amer. Ceram. Soc. Bull. 65(8): 1991-95 (1986).

19. Perez-Mendez, M.: Howie, R.A. and Glasser, F.P.: Cement and Concr. Res. 14(1), 57-63 (1984).

20. Jaffery, J.W.: "The chemistry of cements", Vol.I, Ed.by H.F.W. Taylor. Academic Press. p. 148 (1964).

21. Bosolo, F. and Pearson, R.G.: "Mechanism of Inorganic Reaction", Wiley Eastern Ltd., (New Delhi, Bangalore), p. 439 (1967).

QUALITY IMPROVEMENT IN CLINKER USING MINERALISERS/ACTIVATORS

A K Parashar, V K Mathur, Shree Gopal and S K Handoo

National Council for Cement and Building Materials
New Delhi, INDIA

SUMMARY

The paper presents case study of two cement plants facing quality and operational problems resulting from poor granulometry, high free lime and inversion of phases besides low output. A combination of mineralisers red mud and gypsum and in the second case MgO bearing materials with blue dust (iron ore waste fines) have been used alongwith the raw mix for improving the clinker quality and simultaneously reducing the energy consumption. The combination of mineralisers TiO_2 and SO_3 being available from waste byproduct red mud in presence of high MgO concentration proved effective in increasing C_3S content by $\sim$ 15 percent besides lowering formation temperature by around 100°C. XRD and optical/ electron microscopic studies reveal increased formation and improved crystal size and distribution in the clinker matrix which resulted in substantially higher compressive strength in the resultant clinkers.

INTRODUCTION

Utilisation of activators/mineralisers available as industrial wastes or inferior materials in the clinkerization process not only reduces the energy consumption and improves clinker quality but also offers a fruitful solution for waste disposal as well as conservation of high grade reserves of limestone. Among various factors for achieving fuel economy in manufacture of portland cement, the role of mineralogical composition of raw materials, fineness of the raw mix and its chemical homogenity are well known and are also practiced to a good extent. A new dimension in this field, which still awaits further detailed investigation and application on industrial scale is the use of mineraliser to induce changes in clinker minerals and its morphology.

Addition of mineralizers or fluxes to raw meal as a possible means of energy conservation in cement manufacture is in principle well established (1). While its practice is fairly extensive in economically profitable situations, the application of mineralizer in this region is still inhibited, not only on grounds of economic viability but presumably also on account of lack of complete perspective of its use. These mineralisers are generally used at a low doses level either individually or in combination with the raw meal.

The reaction effects of mineraliser are multifarious such as, reducing in the decomposition temperature and accelerating the chemical reaction, lowering the temperature of clinker formation, modifying liquid properties, such as viscosity, surface tension etc.

The present paper deals with the use of mineralisers at the plant scale. In first case (I) a combination of mineraliser comprising of red mud - an industrial waste generated from the aluminium industry was added with gypsum to raw meal and in the second case (II) a small dose of dolomitic limestone along with blue dust was used to achieve above desired benefits. The basic objective of conductiong these trials was to make an analytical assessment of the trials with respect to existing quality, optimum dose of additives, process parameters and properties of resulting cement.

PLANT TRIAL

Case I :- Dry process plant of 1200 TPD capacity equipped with double stream Dopol suspension preheater with the following kiln dimension was selected for the investigation : Length = 68 m, $\emptyset$ = 4.2 m, Inclination = 3% and Kiln (r.p.m) = 1-2.

The plant was facing problems in terms of both quality as well as quantity of the product. Production was much below the rated capacity and the quality of the clinker was poor. The chemical characteristics of the existing raw meal, clinker and % phase composition as determined by optical microscopy are presented in Table 1.

The clinker was characterized by high residual free lime and was dusty due to inversion of β-C_2S to γ-C_2S phase. The data provided by the plant revealed that early compressive strength of the resultant cement varied from 16.0-18.0 N/mm^2 (3 days) to 22.0-25.0 N/mm^2 (7 days) at a fineness $\sim$ 3000 cm^2/g (Blaine). The autoclave expansion was more than 1%. Cements were tested as per IS:4031-1968.

In order to simulate almost plant conditions, experiments were initiated on plant raw mixes with activators at laboratory scale.

TABLE 1 : CHEMICAL CHARACTERISTICS OF RAW MEAL AND CLINKER

	LOI	SiO_2	Al_2O_3	Fe_2O_3	CaO	MgO	CaO_f	LSF	SM
				%					
Raw Meal	36.10	12.30	3.15	1.64	43.00	3.20	-	1.09	2.57
Clinker	0.80	23.80	7.00	3.10	60.80	4.20	2.20	0.79	2.36

C_3S=22% C_2S=46% Intersilitial=22% CaO_f= Free lime

Activators fluorogypsum, phosphogypsum and red mud, were added in varying amounts to arrive at optimum mix for the field trial. Amount of F and PO_4^{3-} in fluoro and phosphogypsum were rather low to contribute towards mineralising the reaction. It was therefore aimed to achieve the desired mineralisation from SO_3 being available from gypsum and TiO_2 + Fe_2O_3 combination as available from red mud (2). Burnability investigations were carried out on the series of raw mixes with 6 and 7 percent ash absorption levels so as to provide flexibility in coal quality.

Nodules prepared from mineralised raw mixes ground to 20 percent residue on 90 μ were sintered in laboratory muffle furnace. Subsequent to preliminary burnability investigations bulk clinkers were prepared at their respective sintering temperature (Table 2). The clinkers prepared were subjected to physico-chemical and mineralogical examination. Cements were prepared by adding 5% gypsum (purity 70%).

TABLE 2 : COMPOSITION AND PERFORMANCE OF CLINKER/CEMENT MADE FROM MODIFIED RAW MIXES - LABORATORY STUDY

Sl.No.	Raw mix Composition	Clinker Phases (Percent) (Optical Microscopy)			Physical Characteristics of Cement			
		C_3S	C_2S	Int.	Fineness (cm^2/g)	Compressive Strength N/mm^2 3 d	7d	28 d
Series 1	6% Coal ash							
RMP2 (1400°C)	Raw meal + 2% P	51	34	15	2971	30.3	31.3	43.4
RMP2R3 (1380°C)	Raw meal + 2% P + 3% R	51	22	21	2976	23.2	32.4	42.7
RMR5 (1400°C)	Raw meal + 5% R	50	34	14	2830	22.7	31.5	38.0
Series 2	7% Coal ash							
RMF1 (1400°C)	Raw meal + 1% F	52	29	19	2900	36.8	38.8	46.0
RMF2 (1400°C)	Raw meal + 2% F	46	36	18	3060	28.7	34.6	39.3
RMF3 (1370°C)	Raw meal + 3% F	41	40	19	3100	33.6	38.6	50.3

P - Phosphogypsum F - Fluorogypsum R - Red Mud
CaO_f < 1% at sintering temperatures in series 1 and series 2

The major constituents of fluorogypsum and phosphogypsum are :CaO (30.81%, 31.75%), SO_3 (44.07%, 44.37%), F (0.17%, ND) and P_2O_5 (0.07%, 0.68%) respectively.

The results indicate that activators individually or in combination significantly improved the mineralogy and cementing behaviour (Table 2). Addition of 3 percent fluorogypsum appeared to be the best in terms of strength development, largely due to presence of SO_3 as mineraliser (3,4). Alite content was found to be > 40% in all cases and clinkers showed no sign of inversion on aging.

Taking into account the above findings, economic viability of three activators used and the need for overall improvement, combined activator was used. Raw mix was proportioned as, Limestone: 97.0, Red Mud: 2.0 and Gypsum:1.0 thereby replacing laterite, an expansive raw mix component for the plant by the cheaper material, red mud. During the first phase of the trial with modified raw mix, increase in degree of calcination from existing 36 percent to 43 percent (% LOI in kiln feed at IV stage), rise in kiln shell temperature and erosion of kiln coating was observed.

The rise in shell temperature was due to lack of control on feed rate of coal and kiln feed. It mainly resulted due to excessive heat input than required for clinkerisation reaction coupled with underfeeding of the kiln. Starvation of kiln under intense conditions led to such abnormalities. These were however eliminated when better control on coal and feed rate was exercised. Temperature of clinkerisation was brought down from 1400-1450 to 1360 -1380°C. Improvement in degree of calcination clearly emphasised the need to push more feed to the kiln thus increasing the throughput. Dust generation was reduced from 23 g/Nm^3 to 20.5 g/Nm^3.

In the present case study, incorporation of SO_3 (~0.5%) in combination with TiO_2 in raw meal was found to sufficiently activate the raw mix; improve the reaction kinetics and granulometry since dusty clinker was no more formed. Raw meal clinker linkage showed 7.5 percent ash absorption as compared to about 9% that of the existing clinker. Formation of alite increased from 30 percent to 45 percent along with better development and distribution of phases. XRD analysis of clinker showed absence of γ-C_2S and periclase Fig.1. Mineralising components, though present in small quantities (Table 3), were adequate to modify melt properties, MgO was largely accommodated in clinker phases Fig. 2. As presented in Table 3, cementing behaviour and performance of resulting cement was remarkably improved with addition of activators.

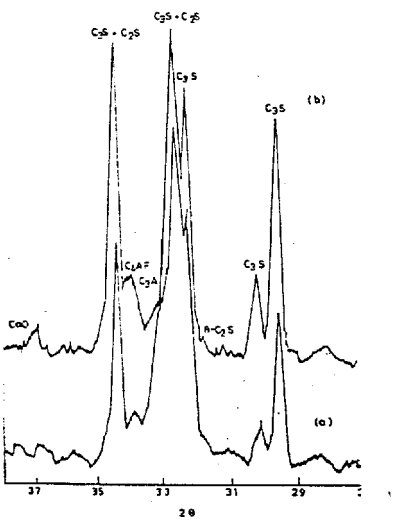

Fig.1: XRD Patterns,
(a) Non-mineralized
(b) Mineralized Clinker

Case II : The second field trial was undertaken at 2200 TPD dry process kiln equipped with precalciner. Of late, the clinker produced was reported to be inconsistant in quality (more free lime) and the plant was facing problems of undesirable buildups in the close vicinity of the burning zone. The average proportions of the raw materials before the trial were limestone 83.0 percent, sweetner 15.0 percent, laterite 2.0 percent. The ultimate aim of the trial was to cut down the consump-

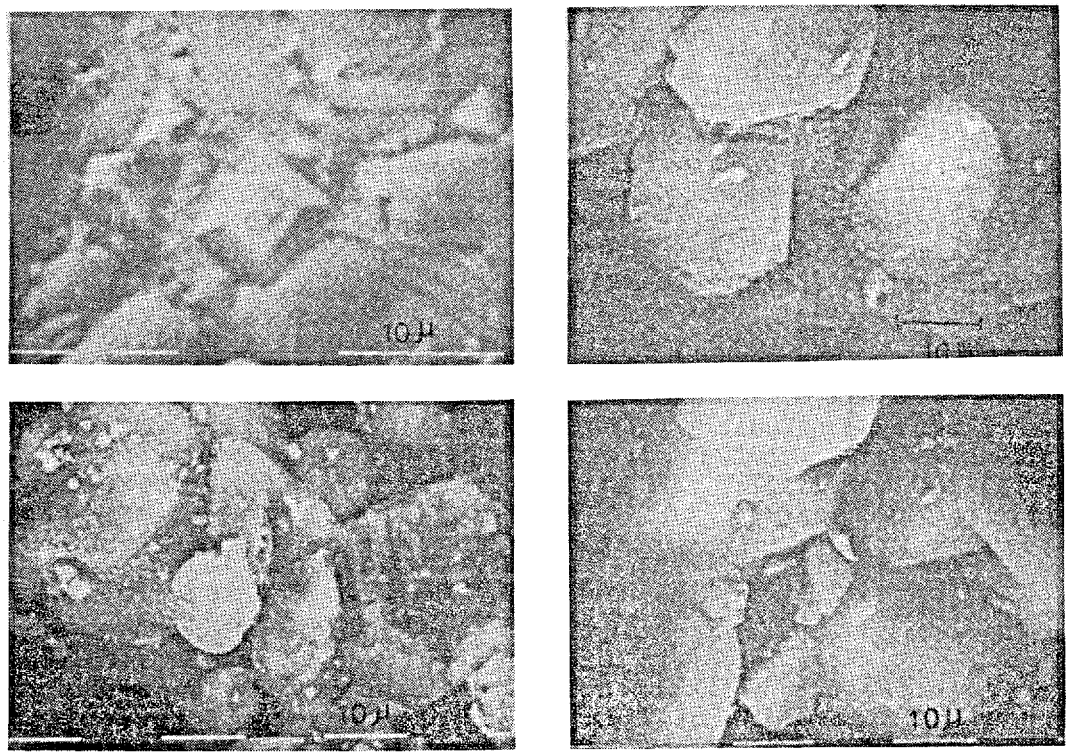

(a) (b)

Fig.2: Scanning Electron Micrographs of Plant Clinkers (a) Without Activator (b) With Activators (Case I)

tion of high grade limestone, which besides being costly factor, was also responsible for high free lime. High free lime, differential burning and quality variation in the feed were causing undesirable coating formation inside the kiln.

Based on above and laboratory investigations/ results and availability of raw materials, the raw mix was modified as per the proportions limestone 88.0, dolomite 3.0, bluedust ($Fe_2O_3 \sim 78\%$) 1.0 sweetner 8.0 percent. Clinker obtained with the above modified raw mix composition was having free lime (< 1 percent) with well developed alite and belite grains. It has also been observed by Han et al (5) that appropriate amount of MgO and Fe_2O_3 lowers the clinkering temperature and also by the addition of MgO, the alite gets converted into small faceted crystals. Mineralogical analysis of clinker from the above raw mixes were performed using XRD analysis, optical and electron microscopy. The diffraction and microscopic analysis show that well developed, crystalline growth with dominance of alite phase (> 50 percent). Very few grains of free lime scattered throughout matrix were noticed (Fig.3).

(a)

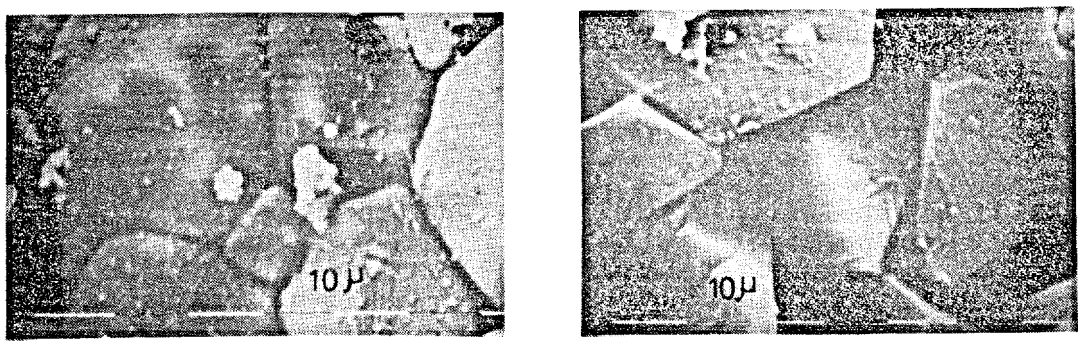

(b)

Fig.3: Scanning Electron Micrographs of Plant Clinkers (a) Without Activator (b) With Activators (Case II)

TABLE 3 : PHYSICO CHEMICAL AND MINERALOGICAL STUDIES OF PLANT RAW MIX, CLINKER AND CEMENT (Case I)

	Chemical Composition (%)								
	LOI	SiO_2	Al_2O_3	Fe_2O_3	CaO	MgO	SO_3	TiO_2	CaO_f
Limestone	37.30	12.06	1.97	1.63	44.75	2.52	-	-	
Red Mud	14.92	8.39	15.48	28.71	14.68	0.92	-	15.0	
Gypsum	20.42	15.57	0.56	0.86	28.66	0.74	31.70	-	
Coal Ash	-	62.51	22.73	6.75	5.05	-	-	-	
Raw Mix	36.90	13.27	2.16	1.72	42.50	2.62	-	-	
Clinker	0.47	23.19	4.71	3.10	61.75	4.37	0.45	0.33	0.89

Proximate Analysis of Coal

Moisture(%)	Ash (%)	Volatile Matter(%)	Fixed Carbon(%)	Calorific Value
2.82	29.70	24.17	43.31	4412 cals/g

Percent Phase Composition of Clinker (OM)

C_3S - 45 C_2S - 26 Interstitial - 24

Performance of Cements

	Fineness (cm^2/g)	Setting Time (min) Intial	Final	Expansion Auto. %	Lechat. mm	Compressive Strength N/mm^2 3d	7d	28d
Before Trial	3208	60	160	>10	6.0	18.0	24.0	36.0
After Trial	3100	100	172	0.60	2.0	26.0	31.0	45.0

The comparative results (Table 4)obtained on the existing and modified raw mix/clinker clearly indicates that reduction in the consumption of high grade material (sweetener) by nearly 50%, utilization of cheaply available low grade raw materials can be achieved besides improvement in the clinker quality.

CONCLUSION

Laboratory and plant applications of activators/modifiers established that technical and economical advantages can be achieved by the proper choice of activators in a given plant and its process conditions. Red mud and the byproduct gypsum have shown the potential and capacity to be used as mineralisers without making any compromise on cost and quality resulting from increased formation, improved crystal size and distribution in the clinker matrix. Optimisation of the materials and process can therefore yield profits with increase in kiln output and improved clinker quality besides conservation of high grade reserves.

ACKNOWLEDGEMENT

The authors have freely drawn upon completed R&D work/status reports of NCB and some of the unpublished work of NCB. This paper is being published with the permission of Director General NCB.

TABLE 4 : PHYSICO CHEMICAL AND MINERALOGICAL STUDIES OF PLANT RAW MIX AND CLINKER/CEMENT (Case II)

Before Trial

	Chemical Composition %						Modulii Values		
	LOI	SiO_2	Al_2O_3	Fe_2O_3	CaO	MgO	LSF	MS	MA
Raw Mix	35.70	11.60	3.70	2.40	43.26	1.77	1.12	1.90	1.54
Clinker	0.33	21.56	6.10	3.49	63.48	2.40	0.91	2.25	1.75
							% Freelime =		1.96

Physical Characteristics of Cement

Fineness (cm^2/g)	Compressive Strength (N/mm^2)			Expansion		% Clinker Phases (OM)			
	3 D	7 D	28 D	% Auto clave	Lechatelier (mm)	C_3S	C_2S	C_3A	C_4AF
2950	18.0	27.0	42.5	0.82	1.5	26	48	21	

After Trial

	Chemical Composition %						Modulii Values		
	LOI	SiO_2	Al_2O_3	Fe_2O_3	CaO	MgO	LSF	MS	MA
Raw Mix	35.70	11.23	3.47	2.54	43.41	2.21	1.17	1.87	1.37
Clinker	0.93	21.15	6.05	3.89	63.54	3.18	0.92	2.13	1.55
							% Freelime		0.83
Limestone	35.69	12.84	2.77	2.13	42.84	1.77			
Blue dust	0.49	8.80	10.15	77.95	0.22	0.16			
Dolomite	46.45	1.38	0.45	0.54	29.72	20.31			
Sweetner	41.54	4.52	0.77	0.51	50.84	0.60			

Physical Characteristics of Cement

Fineness (cm^2/g)	Compressive Strength (N/mm^2)			Expansion		% Clinker Phases (OM)			
	3 D	7 D	28 D	% Auto clave	Lechatelier (mm)	C_3S	C_2S	C_3A	C_4AF
2700	34.0	40.0	45.0	0.28	1.0	51	22	21	

REFERENCE

1 Bucchi, R. (1980) : Influence of the nature and preparation of raw materials on the reactivity of raw mix, Paris 7th ICCC, 1, 259.

2 Maki, I and Hattori, M (1989), 'Influence of minor components on the fine textures of alite in portland clinker', Il Cemento, April, 2, 131.

3 Glasser, F P (1988), 'Influence of minor components in portland cement clinkers' NCB Quest, Nov 2, 1.

4 Oliego-Cuervo, Y B and Glasser, F P (1978), 'Role of sulphates in cement clinkering'. The calcium silico-sulphate phase. Cem and Concr. Res. 8, 455.

5 Han, K S et.al (1989), 'Effect of MgO and SO_3 on the formation of cement clinker'. NCB Quest, May, 2, 1.

FORMATION OF LOW TEMPERATURE PORTLAND CEMENT CLINKER BY USING NON-TRADITIONAL ALUMINOSILICATE ROCK AND MINERALIZER

Sanjaasuren Radnaasediin

Centre for Chemistry and Technology of New Materials
Mongolian State University, Ulaanbaatar, MONGOLIA

SUMMARY

This research deals with the results of physico-chemical intensifications of clinkerization processes and lowering the temperature of formation clinker phases by using non-traditional volcanic rock (alkalic basaltoid) in combination with fluorine-containing mineralizer(CaF_2).

The experiment showed that raw mixes containing basaltoids and CaF_2 make possible production of high alite Portland cement in the temperature range of 1250°-1300°C. Thus, the temperature of clinker phases formation is lowered by 150°-200°C as compared with the traditional technology of Portland cement.

В данной работе рассматриваются результаты исследований по физико-химической интенсификации процесса клинкерообразования и снижению температуры формирования клинкерных фаз путём полной замены глинистого компонента портландцементной сырьевой смеси на нетрадиционную алюмосиликатную вулканическую породу в присутствии фторидного минерализатора.

Установлено, что из базальтоидсодержащей шихты с добавкой фторида кальция можно получить высокоалитовый портландцементный клинкер при температурах 1250-1300°С, т.е. на 150-200°С, ниже по сравнению с традиционной технологией производства портландцемента.

INTRODUCTION

Investigation of the effect of physico-chemical properties of source materials on reactivity of cement raw mix is of paramount practical importance for improving cement quality, saving fuel expenditure and expanding production basis of cement (1,6,7,9). Literary data analysis testifies to that variety of mining species, including volcanic rocks, able to substitute the clay compound in raw mix is likely to increase (6,8).

Efficiency of application of mineralizers in burning clinker is known since long ago. Researchers noted that the use of various mineralizers leads to considerable acceleration of physical and chemical process during solid and liquid phase stage of clinker formation. At present the inclination of use of mineralizers is roused because single and complex mineralizers not only intensify the process of clinker forming phases but also assist to reduce the temperature for the accomplishment of clinker formation process (2-5,7,8).

The present investigation aims at theoretical and experimental substantiation of expediency of using alkaline basaltoids as aluminosilicate raw mix in presence of fluorine mineralizer for synthesis of Portland cement clinker at the temperature lower than in traditional manufacturing process of Portland cement.

Alkaline basaltoids resemble in appearance however the former is distinguished from the latter by their alkaline character of mineral and chemical composition. Basaltoids belong to basic volcanic rocks of alkaline series.

Alkaline basaltoid rocks are widely spread on the territory of Mongolia. Mongolia is rich in fluorspar.

EXPERIMENTAL

Binary and ternary component mixes composed of $CaCO_3$ (or limestone) and basaltoid were investigated, mixes the following ratio (wt%): limestone 76-82%; basaltoid 18-24%; 0,25-2% fluorite (CaF_2) was added. Previously pounded fine starting components are homogenized with acetone in ball mill. They were heated in laboratory silicon carbide furnace. The phase composition (qualitative and quantative) of heated samples was determined by X-ray powder diffraction method. Kinetics of phase formation

was carried out by thermal analysis method on Derivatograph-1500 D. Microstructure of synthesised clinkers, source rocks and hydrated cement samples are studied by petrographic analysis on metalgraphic microscope MIM-7 as well as on scanning electronic microscope J3M-35CF of JEOL company. Chemical composition of clinker phases and distribution of main minor elements by phases were carried out by electronic probe microanalysis on Camebax MBX.

RESULTS AND DISCUSSION

PHASE FORMATION

(A). Figure 1 shows the DTA, DTG and TG curves of binary component mix without CaF_2 of the following ratio and characteristic:

	$CaCO_3$(%)	Basaltoid (%)	$(LSF)_R$	$(M)_S$	$(M)_A$
Raw mix N 1	74,62	25,38	0,93	2,12	1,90
Raw mix N 2	73,92	26,08	0,89	2,12	1,90
Raw mix N 3	70,05	29,95	0,71	2,12	1,90

Analysis of DTA, DTG and TG curves shows that in the investigated raw mixes the process of decarbonization $CaCO_3$ starts at a temperature 630°-650°C and decomposition $CaCO_3$ accomplishes at 970°C. Three exothermic peaks are fixed at 1150°, 1180° and 1235°C in the field of high temperature and endothermic peaks-at 1140°,1160°,1200° and 1235°C.

The peak essence on the DTA peak is identified by X-ray analysis and exothermic peak at 1145°C is linked with the formation of $C_{12}A_7$ and gehlenite by means of interaction between $C_{12}A_{17}$ and SiO_2 and the peak at 1170°C is linked with formation of belite from gehlenite and CaO. Exoeffect at 1235°C is linked with the notable formation of alite phase, though it starts from the formation of 1150°-1200°C with liquid phase. Alite is crystallized in monoclinic form.

In the studied clinkers, belite is in the α-, α'-, and β- crystalline forms. Belite is formed at 900°-950°C solid phase reaction ($CaO+SiO_2$). C_3A is formed by solid and liquid phases; formation of C_4AF starts approximately at 1150°C after melting and with its presence.

In the raw mix N 1 the process of clinker formation is not accomplished at 1400°C and 4 per cent CaO remains free.

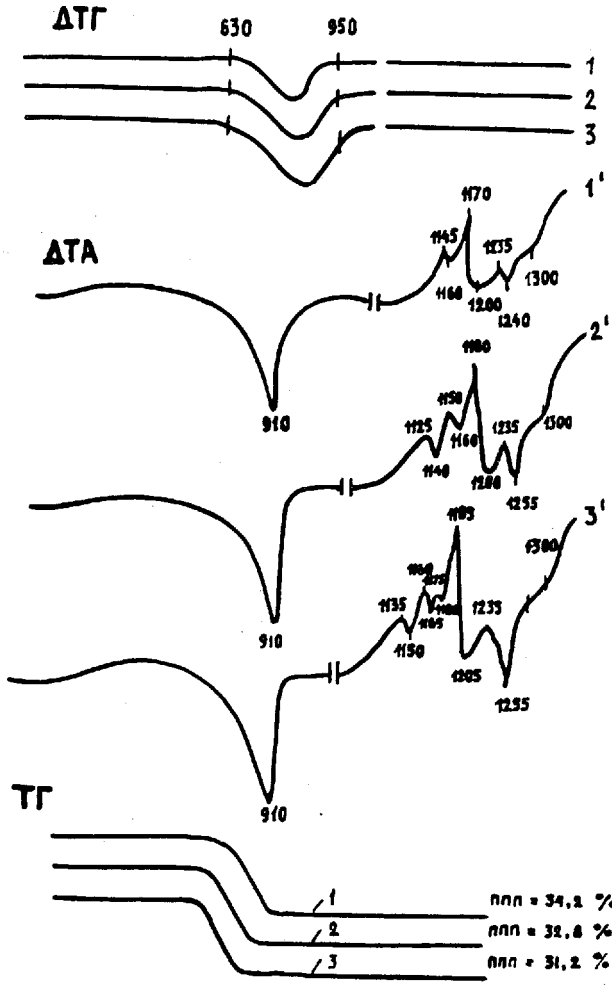

Fig.1 DTA,DTG,TG curves of raw mixes without CaF_2.
1,1'-raw mix N 1
2,2'-raw mix N 2
3,3'-raw mix N 3

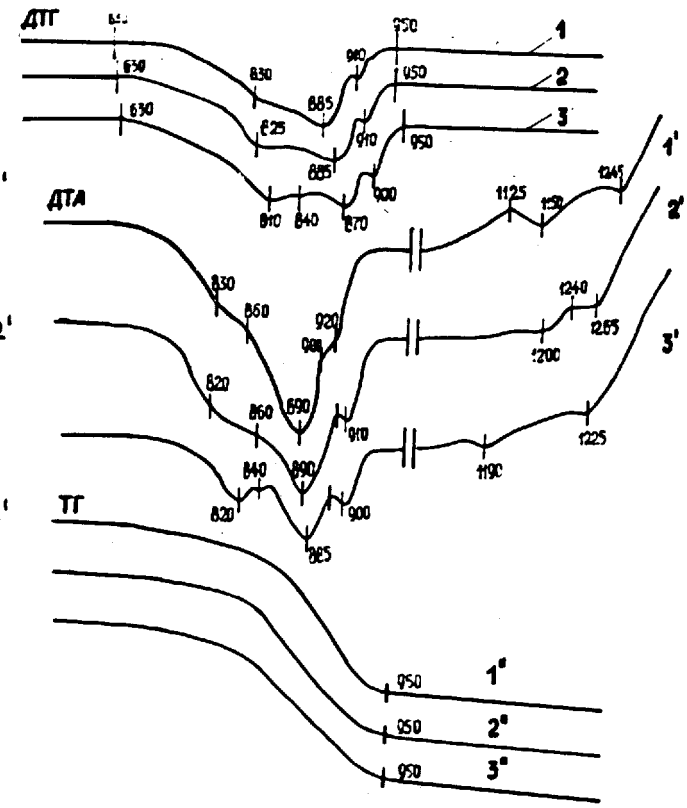

Fig.2 DTA, DTG and TG curves of mix N 1 in presence of CaF_2.
1,1',1"- 0,5wt% CaF_2
2,2',2"- 1,0wt% CaF_2
3,3',3"- 2,0wt% CaF_2

(B). In order to reduce the temperature of clinker formation and to decrease the negative effect of alkalis at the final stage of alite formation, the influence of addition CaF_2 to basaltoid containing raw mixes with $(LSF)_R$=0,93; 0,89 and 0,71. Fig.2 illustrates DTA,DTG and TG curves of raw mix N 1 containing doses of CaF_2 added. In comparison of DTA curves of raw mixes without and with CaF_2, it is obvious, that the kinetics of phase formation process is essentially distinguished. Thermic and X-ray analysis of data showed that decarbonization $CaCO_3$ in the mixes with CaF_2 addition, proceeds within the range of 630°-950°C. However in presence of CaF_2 within the range of given temperatures in the mix "$CaCO_3$+basaltoid"

there take place solid phase reactions leading to the formation of intermidiate unstable compound-carbonate spurrite and to the following decomposition. The spurrite is formed in a short range of temperature (830°-860°C) and decomposes at 900°-920°C.

Presumably fluorine calcium exerts catalitic influence on $CaCO_3$ during decomposition in the range of temperature 730°-920°C, as a result of which, decomposition of $CaCO_3$ takes place with rather less expenditure of heat energy than in the mixes without CaF_2. At rather higher temperature (over 1000°C) CaF_2 plays a new function expressed by that it is affected by chemical reaction of formation of some fluorine containing compounds such as $C_{11}A_7CaF_2$, $2(C_2S)CaF_2$, $C_3A_3CaF_2$, $11CaO*4SiO_2*CaF_2$.

The occurrence of crystalline forms α- and α'-C_2S starting from 800°-900°C with CaF_2 addition is one of the specific features of behaviour of basaltoid containing mixes. In the studied mixes in presence of CaF_2, alite phase starts to be formed approximately at 1100°C which is 150°-170°C lower than in clay containing mixes. Belite phase is formed not through gehlenite, by means of decomposition of spurrite and $11CaO*4SiO_2*CaF_2$.

REACTIVITY OF RAW MIXES

Basaltoid containing binary component mixes have high reactivity by degree of combining of free CaO, and the addition CaF_2 increases the speed of formation of clinker minerals and considerably intensifies solid phase reactions as well as liquid phase process of crystallization of clinker phases. Comparative data of kinetics of combining of free CaO are shown in Fig.3.

In the basaltoid containing binary component mixes (LSF=0,93; 0,89), containing CaF_2 in the proportions of 0,5-1,0wt%, the process of clinker formation accomplishes at 1280°-1300°C.

The study shows the volatility of alkalis grows as burning temperature and quantity of CaF_2 addition increase. The volatility of alkalis in mixes with CaF_2 addition is 50-60%.

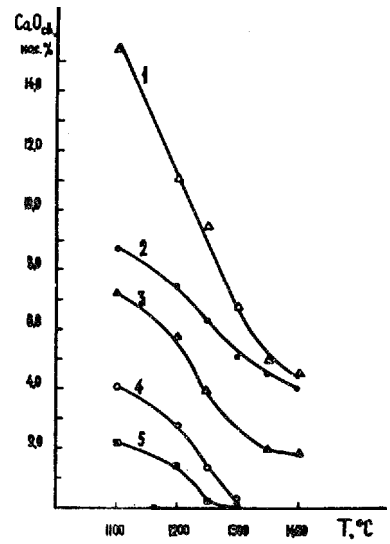

Fig.3. Kinetics of combining of free oxide CaO depending on the burning temperature in the mixes with LSF=0,93=Const.
1-industrial raw mix; 2-$CaCO_3$+basaltoid;
3-$CaCO_3$+basaltoid+Fe_2O_3; 4-$CaCO_3$+basaltoid+CaF_2;
5-$CaCO_3$+basaltoid+Fe_2O_3+CaF_2

CONCLUSION

The physico-chemical basis of low temperature synthesis of Portland cement clinker by using alkaline basaltoids combined with fluorine mineralizer was developed.

Fluorine calcium in the range of temperature 730°-930°C plays the catalyst role in the process of dissociation $CaCO_3$ and causes formation of intermediate compound-carbonate spurrite, while the heat for decarbonization reduces by 20-25%.

ACKNOWLEDGEMENT

The author is indebted to Academician M.M.Shultz, Prof.P.F.Rumyantsev, Prof.A.I.Boikova, Ph.D.Domansky of the institute of Silicate Chemistry (St.Petersbourg), Ph.D.Y.V.Nikiforov of the institute GIPROCEMENT (St.Petersbourg) for their valuable advice and encouragement to carry out this research.

REFERENCES

1.Bucchi,R.:"Influence of the nature and preparation of raw materials on the reactivity of raw mix". 7th Int.Congr.Chem.Cement, Paris,1980,Vol.1, P.1.1/5-1.1/43.

2.Masood,I., Mehrotra,B.P.,Tenri S.P.,Malhotra,S.K.:"Temperature Clinkerization Through use of Mineralizers",J.Sci.Ind.Res.,1985,Vol.44,N 10, 560-566.

3.Johansen,V., Christensen,N.H.:"Rate of Formation of C_3S in the system $CaO-SiO_2-Al_2O_3-Fe_2O_3-MgO$ With addition of CaF_2", Cem.Concr.Res.,1979, Vol.9,1-6.

4.Klemm,W.A., Jawed,I.:"Mineralizers and Fluxes in the Clinkering Process" 7th Int.Congr.Chem.Cement,Paris,1980,Vol.2,p.I.150-I.155.

5.Viswanathan,V.N., Ghosh,S.N.: Mineralizers and Fluxes in Clinkerization. Adv.Cem.Technol., Oxford, 1983,p.177-202.

6.Пащенко,А.А.,Мясникова,Е.А., Мясников,А.А. и др.: Цементы из базальтов, Киев,1983,192р.

7.Лугинина,И.Г., Лугинин,А.Н.: "Влияние фторида кальция на процессы обжига и активность цемента", Цемент,1974, 2,С.15-16.

8.Сычев,М.М.: "К проблеме низкотемпературного клинкеров", ЖПХ, 1987, номер 2,с.355-358.

9.Санжаасүрэн,Р.: "Портланд цементный клинкер низкотемпературного синтеза и его вяжущие свойства", Межвузовский тематич.сборник трудов., 1988, Л.,с.81-84.

EFFECT OF SO_3 ON MINERAL FORMATION AND PROPERTIES OF CLINKERS

Su Dagen*, Chen Weiqing*, Huang Qixiu*, Mai Huo and Zheng Liqiang****

**Department of Inorganic Materials, South China University of Technology, Guanzhou*
***Zhujian Cement Plant, Guangzhou*
P R CHINA

SUMMARY

The effect of SO_3 content on mineral formation and properties of laboratory clinkers and industrially manufactured clinkers with varied clinker moduli were studied at different clinkering temperatures , heating rates , and alkalies , MgO and flourite contents. The results show that SO_3 has either favourable or unfavourable effect on mineral formation of clinkers, especially on the formation of alite . SO_3 shows different dominant effects and has different effects on properies of clinkers under different conditions . The effect mechanism of SO_3 on mineral formation of clinkers has also been studied.Thus, an explanation for the contradictory viewpoints of the effect of SO_3 mineral formation of clinkers has been obtained . It has also been pointed out how to make full use of the mineralization of SO_3 and how to reduce or even eliminate unfavourable effect of SO_3 in practice.

摘要

本文研究了SO_3含量对熟料矿物形成及性能的影响。研究包括实验室熟料及工业生产熟料，研究在不同煅烧温度、不同升温速度、不同的碱、镁、氟含量下SO_3的影响。研究结果表明,SO_3对熟料矿物的形成,特别是alite的形成,同时存在着有利及不利两方面的作用,在不同的条件下所显示的主导作用则有所不同,并对熟料性能产生不同的影响。通过研究SO_3对熟料矿物的作用机理,从而对以往关于SO_3对熟料矿物形成似乎矛盾的观点作出解释。进而指出在实际生产中如何充分发挥SO_3矿化作用及如何减少或消除SO_3的不利影响。

1. INTRODUCTION

Many researchers have reported the effect of SO_3 on the mineral formation and properties of clinkers[1-5], but there are still some contradictory viewpoints on this respect among different researchers . Some authers are emphatic on the favourable effect of SO_3 and cosider $CaSO_4$ as an effective mineralizer which makes the melt appear at lower temperature , decreases the viscosity and surface tension of the melt and increases the mobility of the ions Ca^{2+}, Si_xO^{2-},Al^{3+}, AlO_4^{5-}, Fe^{3+}, and so on [1-2] ; Some other authers have pointed out the particularly favourable composite mineralization of SO_3 in the presence of F^- . In China , the composite mineralizer of SO_3 and F^- has found rather wide application in cement production by shaft kiln and wet process of ratory kiln, and has the effect of increaseing the output, improving quality and saving energy[3-4]. On the other hand ,other authers[5] state that SO_3 high content in clinker is unfavourable to the formation of alite and hence decreases the compressive strength of clinker . They also point out that different SO_3/R_2O mole ratios had different effects on the mineral formation and properties of clinkers in the presence of alkalies . In this paper,the above viewpoints which appear contradictory have been examined and it has been pointed out that SO_3 has either a favourable or unfavourable effect on the mineral formation of clinkers , especially on the formation of alite , depending on the clinker composition and thermal conditions.

Besides , it is very difficult for most cement plants to change their raw materials or fuels in order to decrease the SO_3 content to any great extent in production , whereas it is relatively easy to change the clinker composition including the moduli and minor component of clinker , and the thermal conditions . And hence we search for ways and means to fully exploit the favourable effect of SO_3 while reducing or eliminating its unfavourable effect in practice .

2. EXPERIMENTAL

2.1 Materials

The samples are prepared from C.P. or A.R. reagent $CaCO_3$,Al_2O_3 ,Fe_2O_3, MgO, SiO_2 ,K_2CO_3, Na_2CO_3, CaF_2 and $CaSO_4 \cdot 2H_2O$ which passed 0.080 mm sieve completely.They were fired in a laboratory electric furnace ,under oxidizing atmosphere at different temperatures for 30 minutes and cooled rapidly in air.

2.2 Methods

2.2.1 K_2O and Na_2O are determined by flame photometer.

2.2.2 Soluble alkalies are determined according to ASTM,C-114.

2.2.3 Clinker phase separation is done by salicyclic acid-methanol.

2.2.4 EDAX: Hitachi SEM-X550 with EDX and WDX devices . Voltage:20kV,Callecting time :60 seconds.

2.2.5 The compressive strength of pastes is tested with 20×20×20 mm specimen and w/c ratio :0.30, cured at 20±2℃.

3. RESULTS AND DISCUSSION

3.1 Effect of SO_3 on the minerl formation of clinkers

Table 1 is the free lime (fCaO) content of clinkers burnt at different temperatures with LSF=0.94, IM=1.5,MgO=0.3%,R_2O=0.2% and with different SM and SO_3.

The results show that when MgO and R_2O in the clinker are relatively low the fCaO content increases with the SO_3 content at ordinary burning temperatures (1450℃) , and at lower burning temperature (< 1400℃) , SO_3 can still decrease the f CaO of clinker , especially when the clinker SM is higher , becauce below 1400℃ , the SO_3 in clinker increases the melt amount of clinkers and decreases the melt viscosity,the mineralization of SO_3 shows dominant effect and is beneficial decrease f CaO content of clinker. Besides,the clinkers burnt at 1250℃ and with SO_3 do not crush dust when cooled because the SO_3 in the clinkers stabilizes β -C_2S and restrains it from changing to γ -C_2S. When the equilibrium of melt enters a metastable range , i.e. Ostwald-Miers range. which is characterized by low nucleus forming frequency and high growth rate of the crystals . On the other hand , it is more difficult for the stablized belite to react with CaO to form alite . The optical microscope observation indicates that as the SO_3 content in the clinker increases , the average size of alite increases but the amount of alite decreases . Furthermore , the average size of alite in the clinker with higher SM(2.5) increases less than that with lower SM (2.0).

Table 1 Free lime contents of clinkers of different moduli and burnt at different temperatures

NO	SM	SO_3	f CaO %wt, burning temperature		
			1350℃	1400℃	1450℃
H0	2.5	0	4.85	2.20	0.48
H05	2.5	0.5	3.80	2.00	0.58
H10	2.5	1.0	3.40	1.40	0.76
H20	2.5	2.0	2.90	1.40	1.02
L0	2.0	0	2.20	1.60	0.33
L05	2.0	0.5	1.88	1.40	0.50
L10	2.0	1.0	1.80	1.15	0.82
L20	2.0	2.0	1.76	1.10	0.88

3.2 Effect of SO_3 and Alkalies Contents on Mineral Formation and Properties of Clinker

In preheater and precalciner kilns,the effect of SO_3 and alkalies is often considered together. Figures 1 and 2 show the relationship between K_2O content and the 3-day and 28-day compressive strengths of clinker with SM=2.31-2.33, IM=1.40-1.42 and varied LSF and SO_3 contents.

It can be seen from Fig . 1 and 2 that when K_2O is below 0.8wt%, the 28-day compressive strength of clinker with lower content SO_3 (0.18wt %) is higher than that with higher content SO_3(1.2wt%), and when K_2O is higher the 28-day compressive strength of clinker with lower content SO_3 is lower than that with higher content SO_3,Fig.1 and 2 also show that when the SO_3 content is equal to 0.18% and K_2O is below 0.4 wt %,K_2O hardly affects the compressive strength of clinker. As the K_2O content increases the 28-day compressive strength of clinker decreases noticeably but the 3-day strength changes litte . It is worth pointing out here that the 28-day compressive strength of clinker with higher LSF (0.95) is higher than that with lower LSF (0.91) when K_2O is below 0.8%.

Besides , the SO_3/K_2O mole ratio is of great importance to the clinkering operation of preheater and precalciner kilns.But the effect of alkalies on the mineral formation and properties of clinkers is

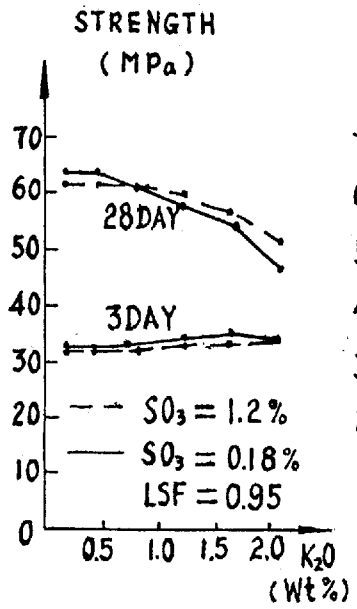

Fig.1 K_2O contents and compressive strength of clinker

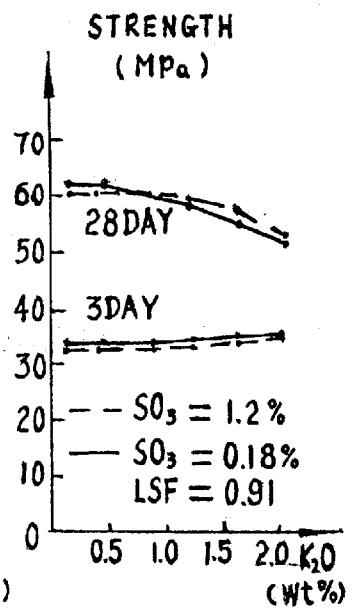

Fig.2 K_2O contents and compressive strength of clinker

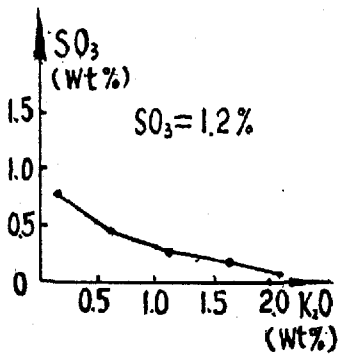

Fig.3 SO_3 content in the silicate phase

greater than that of SO_3. At lower K_2O content (0.4%),SO_3/K_2O mole ratio affects the clinker strength only a litte . The 28-day compressive strength of clinker decreases noticeably with the increase of K_2O content in the clinker.

Fig.3 shows the SO_3 distribution between the silicate phase and the interstitial phase of clinker with varied K_2O contents.The results show that the SO_3 in the silicate phase of clinker gradually decreases with the increase of K_2O content in the clinker.

Table 2 shows that the highest sulphur incorporation levels occur in belite with lower K_2O content (0.5%) and the sulphur in belite gradually decreases with an increase of K_2O content in the clinker.

Moreover,the results of soluble alkalies determination indicated that the soluble alkali contents

Table 2 EDAX measurement

K_2O content in clinker %	the phases	CaO	SiO_2	Al_2O_3	Fe_2O_3	MgO	K_2O	SO_3
0.5	Alite	69.20	26.60	1.85	0.65	0.25	0.34	0.25
	Belite	61.17	33.20	2.08	0.25	0.10	0.10	2.32
	insterstitial phase	49.10	6.05	24.10	17.60	0.45	1.02	1.08
1.1	Alite	69.95	26.90	0.89	0.50	0.24	0.50	0.22
	Belite	62.86	33.50	1.70	0.60	0.15	0.10	1.05
	insterstitial phase	48.80	3.02	25.04	17.30	0.30	1.80	3.78

increase with rise of SO_3 content in the clinker . This agreed with Liu Chongfa [7] . Hence , when the SO_3 content is higher , the amount of SO_3 in belite gradually decreases with the rise of K_2O content , and the unfavourable effect of SO_3 to stabilize belite and hinder alite formation become less too.

3.3 Effect of Heating Rate on Mineral Formation of Clinkers with SO_3

Many researchers have stated that a fast heating rate is favourable to clinkering , which is one of the reasons why precalciner kilns have advantages over long wet rotary klins . In this study all samples were burnt at the same heating rate below 1100 ℃ , but at a faster or slower heating rate between 1100℃ and 1450℃. The heating rate,the average size and amount and distribution of alite determined by optical microscopic is given in Table 3.

It can be seen from Table 3 that at fast heating rate , the average size of alite in the clinker with SO_3 decreases, but its amount increases and its distribution is uniform , and the fCaO content

Table 3 Influence of the heating rate on alite and free lime characteristics

Sample No	Heating rate ℃/min	Average size of alite μm	Alite content %	fCaO content %
H 0.5	35	45	58	0.58
	10	50	56	0.66
H 1.0	35	50	57	0.76
	10	65	54	1.10

also decreases. When the SO_3 content is higher , the favourable effect of fast heating rate is more obvious.

At the Zhujiang cement plant with a SLC kiln of 4000 tpd capacity,the average size of alite decreases and the amount of alite in the clinker increases with higher SO_3 content (1.1%) when the flame is shortened properly and then the temperature and the heating rate increase , so that the 3-day compressive strengths of clinker increases 3 MPa and the 28-day compressive strength becomes more too. The reason is that when the heating rate increases , the crystal size of CaO and belite becomes smaller and they become more reactive , This is favourable for crystallite formation of alite and compensates for the unfavourable effect of low nucleus forming frequency of crystal caused by higher content of SO_3.

3.4 Effect of MgO and F^- on the Burnability of Raw Meal with SO_3

Fig. 4 gives the relationship between MgO and fCaO of the clinker with LSF=0.94 , SM=2.5,IM=1.5, SO_3=1.2 % and K_2O=0.4 % . The results show that adding MgO to the raw meal can decrease the fCaO content of clinker , and the optimum MgO addition is 2.5-3.0 wt % . In addition to reducing the temperature of appearance of melt and viscosity of melt , MgO can also restrain the unfavourable effect of SO_3 on the mineral formation of clinkers. On the other hand ,when MgO content is too high

(>3.0wt%),the more amount of periclase and fCaO occurs.Since the belite phase absorbs larger amount of SO_3, it is unable to absorb the remaining available MgO , which thus precipitate periclase. This is also proved by Arezki Tagnit-Hamou [8].

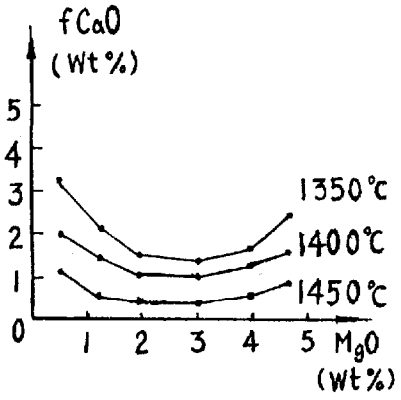

Fig .4 The relationship between MgO and fCaO

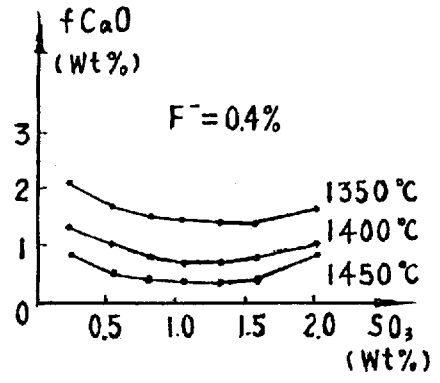

Fig.5 The relationship between F^-/SO_3 and fCaO

F^- and SO_3 composite mineralizer has found rather wide application in the cement manufacture, especially in shaft klin cement plants, where it has been found to be of great benefit .Adding F^- in proper quantity can activate SiO_2,promote decomposition of $CaCO_3$,decrease temperature of appearance of melt and viscosity of melt , and speed up the formation of alite through formation of the transition phase ,Moreover , F^- can restrain the unfavourable effect of SO_3 while strengthening its favourable effect in the clinker .

Fig. 5 shows the influence on fCaO content of clinker with LSF=0.97 , SM=2.0 , IM=1.4 by varied CaF_2, SO_3 contents. It can be seen therefrom that the lowest fCaO content corresponds to the F^-/SO_3 wt ratio range of 0.4-0.5 . It is worth pointing out that when SO_3 content in the clinker is 2.0 wt%,thefCaO of the clinker increases without F^- addition and decreases greatly with F^- addition , and this is also proved by other authors [3].First, F^- forms the transition phase $11CaO \cdot 4SiO_2 \cdot CaF_2$ and then the transition phase decomposes to form C_3S so that the low nucleus forming frequency of crystals caused by higher content of SO_3 may be offseted.In the presence of both F^- and SO_3 , the alite crystal grows more rapidly because of a great decrease in melt viscosity.

4. CONCLUSIONS

4.1 SO_3 has either a favourable effect or unfavourable effect on mineral formation of clinkers, especially alite formation . SO_3 shows different dominant effects and has different effects on properties of clinkers under different conditions . At lower burning temperature (below 1400℃) and

with small amount of MgO , R_2O and F^-,especially for higher SM clinker, SO_3 shows dominant mineralization and is beneficial decrease of clinker fCaO content;at ordinary burning temperature (1450℃) , SO_3 increases the fCaO content of clinkers and has unfavourable effect on mineral formation of clinkers, especially alite formatiomn.

4.2 When K_2O is below 0.8wt% , the 28-day compressive strength of clinker with lower content SO_3 (0.18wt %) is higher than that with higher content SO_3 (1.2wt%) . When K_2O is higher , the 28-day compressive strength of clinker with lower content SO_3 is lower than that with higher content SO_3. The effect of alkalies on the mineral formation and properties of clinkers is greater than that of SO_3.

4.3 Increasing the heating rate is favourable to alite formation in the clinker with a higher content of SO_3 which also increases the amount of alite and is beneficial to increasing the clinker strength , especially the early strength . For the clinker with higher SO_3 content , the favourable effect of increasing the heating rate is particularly notable.

4.4 Adding proper amounts of F^- and MgO to the raw meal can improve the raw meal burnability and restrain the unfavourable effect of SO_3, and mineralization with both F^- and SO_3 can greatly promote mineral formation in clinkers.

REFERENCES

[1] BUDNIKOV, P.P. et AZELITSKAVA, R.D: " A pretreatment of raw materials and its effect on the properties of cement " , Cement- Wapno Gips 1964, 11, 285.

[2] BUDNIKOV, P.P. , KUSNETSOWA, I.P. et SAMELJEW, W.G. :"Eigenschafter von $3CaO \cdot 3Al_2O_3 \cdot CaSO_4$ and sein Zement ", Silikattechnik 1965, 16, 414 (Sonderheft).

[3] Wang Tiandi and Chen Weiqiang :"Effect of the burning temperature on the phase compositions , microstructure and quality of portland cement clinker doped with CaF_2 and/or $CaSO_4$" Proc. of 1985 Beijing Int. Sym . on Cem. and Coner., 1985, Vol.1, 24 .

[4] Li Peiquan , et : " Study of the handening of port land cement from clinker fired at lower temperature " Proc. of 1985 Beijing Int. Sym. on Cem. and Coner.,1985, Vol. 1, 96.

[5] J .Struge , et : " Influence of alkalies suphur on the properties of cement Part I" ZKG 1985,No.3, Part III ZKG 1986, No.7, 1986, No. 8.

[6] Chen Jiagong :"Influence of alkalies of clinker" , Cement No.10/1990.

[7] Liu Chongfa , et al :"Study of the alkalies of portland cement clinker with F^-/SO_3", Cement and House Building Materials. No.5/1989.

[8] Arezki Tagnit-Hamou and Shondeep L Sarkar :"The influence of varuing sulphur content on the microstructure of commercial clinkers and the properties of cement ", World Cement 1990,Vol.21 No.9.

THE INFLUENCE OF SO_3 IN $C_2A_xF_{1-x}$–$C_{11}A_7CaF_2$–C_2S SYSTEM ON FORMATION OF $C_{11}A_7CaF_2$

Yang Yurong, Huang Wenxi, Qian Guangren and Qi Yangyong

Sichuan Institute of Building Materials, Sichuan, P R CHINA

ABSTRACT

The paper reports investigation which have confirmed the relation between burning temperature and formation of minerals, which exists in iron-rich fluoraluminate cement. In order to burn iron-rich fluoraluminate cement at lower temperature , the SO_3 content must be controlled.

摘　　要

本文研究了高铁氟铝酸盐水泥矿物形成与温度的关系，为在低温下烧成该水泥，必须控制 SO_3 含量。

INTRODUCTION

The regular pattern of mineral formation in portland cement where F^- and SO_3 are used as mineralizers has been studied extensively[1-7]. Compound mineralization due to SO_3 and F^- is very obvious[7-13]. The studies indicated that they play an important role in decreasing temperature at which liquid appears and also the viscosity of liquid. Thus alite is formed at a temperature 150-200℃ lower and clinker also is formed at a relatively low temperature of 1300-1350℃. The use of mineralizers could result in an energy saving of 94 -170kcal/kg clinker in semi-dry and wet kiln, and 10-20% in dry kiln. Moreover, by using these compound mineralizeres in portland cement, the strength of cement clinker is raised and the quality of the cement is thus improved. On account of the increased throughput capacity kiln also can be increased by 10-20%. The total economic benefit from all the foregoing is very remarkable. The iron-rich fluoraluminate cement we have studied and developed belongs to the iron-rich phase field of C_6AF_2-$C_{11}A_7CaF_2$-C_2S system. The studies indicate that clinkering temperature reduces by increasing the amount of ferrite phase [14]. In order to lower clinkering temperature and improve the cement properties experiments were performed with SO_3 and F^- added in the raw meal. The regular pattern of mineral formation in the cement with SO_3 added was studied. Addition of SO_3 at low clinkering temperature restricts the formation of $C_{11}A_7CaF_2$ which is regarded as the main mineral of this cement. Therefore, the quantity of SO_3added must be carefully controlled. Formation of cement clinker minerals presents regular variation with burning temperature over the range strided.

1. EXPERIMENTS AND RESULTS

Raw mixture was prepared according to the composition of iron-rich fluroaluminate cement (C_6AF_2=30-60%, $C_{11}A_7CaF_2$=10-40%, C_2S=5-30%). Just the suitable amount of mineralizers was added to the raw mixture prepared with industrial raw materials whose composition is shown as Table 1. The starting materials were ground and mixed in an agate ball mill and compressed into 1.0 mm thick pellets. Burning experiments were carried out in a high-temperature furnace for 45 minutes. The burnt samples were subsequently cooled in air.

Table 1 Chemical composition (%) of raw materials

Material	SiO_2	Fe_2O_3	Al_2O_3	CaO	MgO	LoI
Alumina	3.72	3.91	69.30	1.74	0.33	14.85
Ferrite	7.02	74.95	4.94	4.88	0.70	5.59
Gypsun	2.72	4.59	32.12	32.12	/	SO_3 49.25
Limestone	2.61	0.60	2.17	52.16	/	41.45
Clay	51.50	8.45	15.42	15.92	/	8.50
Fluorite	11.18	0.50	1.40	11.56	0.31	CaF_2 56.13

Industrial gypsum was used as SO_3 source, the quantity to be added was calculated $CaSO_4$ basis. Mineralogy of the clinker samples was determined by XRD. Iron-rich fluoraluminate cement is a kind of lowenergy-consumption cement. Its clinkering temperature is about 1000℃ [14]. Therefore, we firstly experimented on the effect of mineral on cement burning after adding different quantities of SO_3 for a given burning temperature, and thus the effect of SO_3 on minerals formation of cement clinker was studied.

$CaSO_4$ is added to the raw mixture respectively in the quantities of 0, 0.8, 1.0, 1.5, 2.0, 5.0, 9.0 wt% and F^-/SO_3 respectively at the quantity of (except 0 wt% $CaSO_4$) 1.57, 1.26, 0.84, 0.63, 0.25, 0.14. The samples were heated at 1000℃ for 45 minutes and then it subjected to mineral phase analysis by XRD. Results are shown in Fig 1. In addition, a few experiments were conducted in order to study the influence of SO_3on the formation of $C_{11}A_7CaF_2$ at different burning temperatures. On these experiments the raw mixture with 1.5wt% $CaSO_4$ were subjected to burnt respectivly at 950, 1000, 1050, 1100, 1150, 1200, 1250, 1300and 1350℃. The clinkers obtained XRD analysis, and the results are shown in Fig 2.

2. DISCUSSIONS

In order to improve cement clinkering, $CaSO_4$ and CaF_2 together is normally used as a compound mineralizer in portland cement. Compound mineralization is more obvious than of CaF_2 used alone. The

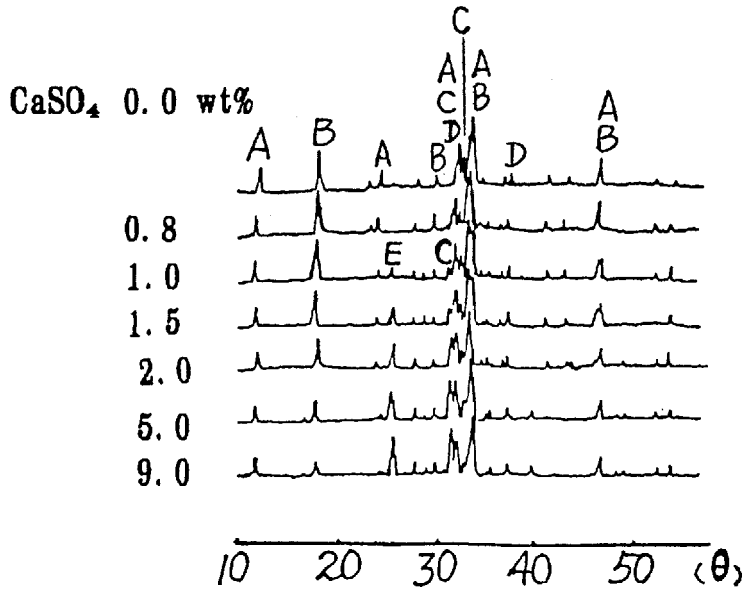

Fig 1 XRD patterns of the samples adding different $CaSO_4$ wt% burnt at 1000℃

A - C_6AF_2
B - $C_{11}A_7CaF_2$
C - β-C_2S
D - CaO
E - $3C_2S3C\bar{S}CaF_2$
F - $C_4A_3\bar{S}$

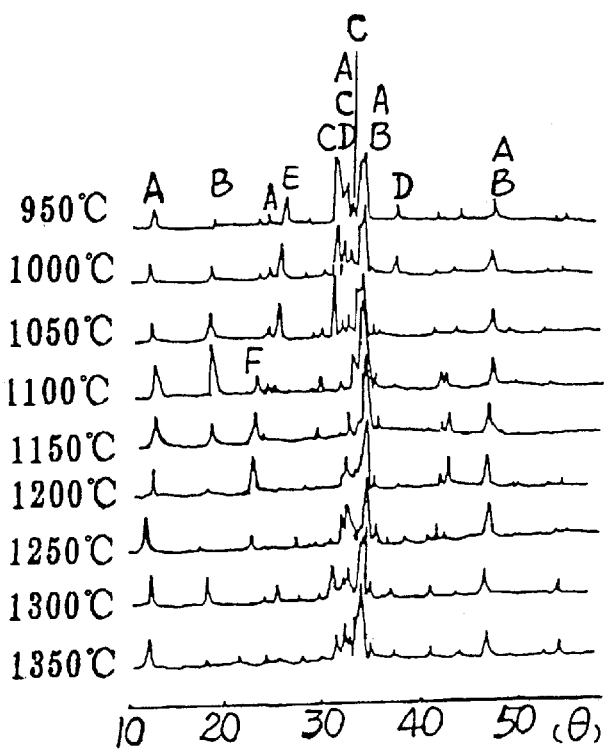

Fig 2 XDR patterns of the samples obtained by burning raw mix adding 1.5 wt% $CaSO_4$ at different temperature

addition of compound mineralizer improve liquid characteristics for clinkering and facilitate C_3S formation. Besides, it also participates in and affects the formation of cement clinker minerals, thus influencing the proerties of the cement. The properties are closely related to the burning temperature, the proportion of the raw mixtures, the F^-/SO_3 ratio of mineralizer, etc.. Normally, 0.8-1.5wt% SO_3 and F^-/SO_3 = 0.2-0.8 are added to raw mixtures, whereupon clinkering temperature drops to 1300-1350℃. When the composition of the cement and the ratio of F^-/SO_3 are in a definite range, $C_4A_3\bar{S}$ and $C_{11}A_7CaF_2$ coexist in the clinker. Both $C_4A_3\bar{S}$ and $C_{11}A_7CaF_2$ possess characteristics of early strength and fast setting. $C_{11}A_7CaF_2$ in clinker sets faster than $C_4A_3\bar{S}$ and it attains highter strength than $C_4A_3\bar{S}$ within an hour. Therefore, when the proportion between the two in the cement is chosen, their characteristics ought to be researched. In order to obtain

cement with higher early strength, but not excessively fast setting, in some published studies about early strength cement, $C_4A_3\bar{S}$ and $C_{11}A_7CaF_2$ were reported to coexist as main clinker minerals. When CaF_2 and $CaSO_4$ are added to such a cement, the effect of decreasing clinkering temperature (energy saving) is considered also. Its clinkering temperature decreases to 1250-1350℃. The iron-rich fluoraluminate cement we have studied can burn at a low temperature of 950-1050℃ even when SO_3 is not added. The composition of cement clinker minerals belongs to the iron-rich field in C_6AF_2-$C_{11}A_7CaF_2$-C_2S system. Because a great quantity of ferrite is present in the cement and other trace elements are added as mineralizer, the hydration rate of $C_{11}A_7CaF_2$ is slowed down. The resulting cement possesses higher early strength and continues to gain strength later. The initial setting time is more than 20 minutes, and final setting time is less than 60 minutes without adding retarder. On this basis, can the clinkering temperature further decrease when SO_3 is added to the raw mix, or can the coexistence of $C_{11}A_7CaF_2$ with $C_4A_3\bar{S}$ improve the cement properties? Up till now, no studies have reported the influence of SO_3 on the formation of $C_{11}A_7CaF_2$ and coexistence of $C_4A_3\bar{S}$ and $C_{11}A_7CaF_2$ in iron-rich field in C_6AF_2-$C_{11}A_7CaF_2$-C_2S system at low clinkering temperature of about 1000℃.

Results in Fig. 1 indicated that, in iron-rich fluoraluminate cement, when the $CaSO_4$ added is less than 1.0wt% the composition of the actual minerals formed are still the very three for (C_6AF_2, $C_{11}A_7CaF_2$, C_2S) which the raw mixtures were designed. Adding SO_3 does not change mineral formation in clinker. Moreover, XRD shows that adding SO_3 does not obviously change f-CaO in clinker (comparing 0.8wt% $CaSO_4$ added with 0 wt% $CaSO_4$), means that its influence on cement clinkering is insignificant. When the quantity of $CaSO_4$ added exceeds 1.0wt% and up to 9.0wt%, the mineral $3C_2S3\bar{C}\bar{S}CaF_2$ is formed.

$3C_2S3\bar{C}\bar{S}CaF_2$ increases with increasing addition of $CaSO_4$, but there are no $C_4A_3\bar{S}$ and f-$CaSO_4$. The $CaSO_4$ added and the CaF_2 in the raw mixture all participate in the formation of $3C_2S3\bar{C}\bar{S}CaF_2$. This reduces the final quantity of $C_{11}A_7CaF_2$ formed. Therefore, Al_2O_3 is an excess because not all of Al_2O_3 is used up in forming the mineral $C_{11}A_7CaF_2$ so that CA forms. Similarly, the final quantity of C_2S reduces with increasing $CaSO_4$. When 9.0wt% $CaSO_4$ is added, XRD data did not indicate any peaks due to C_2S.

Table 2 Compressive strength of clinkers with different contents of SO_3

Sample NO.	SO_3 in clinker (%)	Compressive strength MPa				
		6h	1d	3d	7d	28d
f1	0.20	28.5	47.7	52.8	62.8	78.5
f2	1.15	11.6	19.7	25.3	34.5	38.7
f3	3.05	4.71	15.3	21.7	25.6	26.1
G1	0.14	19.2	35.4	41.3	49.4	64.1
G2	3.51	3.0	18.1	23.4	24.7	29.3

Notes: f1, f2, f3 were obtained by burning in high temperature furnace 2*2*2 cm cement paste
G1, G2 were obtained by industrial test

$3C_2S3\bar{C}\bar{S}CaF_2$, which is a transition phase when compound mineralizer of SO_3 and F^- is used in producing portland cement, has already been studied extensively [6] [18-20]. It is unanimously agreed that this transition phase is present invariably in portland cement by adding SO_3 and F^- at 900-1100 ℃. This agrees basically with our finding mentioned above. When F^-/SO_3 is in the range of 0.101-0.528, this transitional phase forms only at 900-1100℃, which promotes formation of C_2S and plays an important role in low-temperatrure burning of portland cement. But $3C_2S3\bar{C}\bar{S}CaF_2$ can not be retained in the final minerals formed in clinker, because it is a norhydraulic mineral[18]. It is present during the formation process of clinker minerals only as a transitional phase. If $3C_2S3\bar{C}\bar{S}CaF_2$ should exist in clinker, hydraulicity of the cement would be affected seriously. This is confirmed by the data on different SO_3 contents in the clinker of iron-rich fluoraluminate cement with compressive strength of clinker shown in Table 2. Our industrial test is carried out in 3×45 m rotary kiln with shaft preheater. Fig. 3 shows XRD results of clinker (G2) obtained by industrial test (0.2wt% SO_3). As may be seen, the clinker has more $3C_2S3\bar{C}\bar{S}CaF_2$ in the clinker.

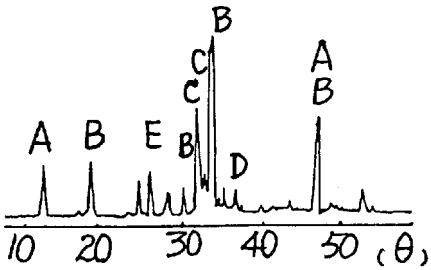

Fig 3 XRD patterns of the clinker (G2) in industrial test
(A, B, C, D, E can be seen about Fig 1, 2)

Moreover, the quantity of $3C_2S3\bar{C}\bar{S}CaF_2$ formed in clinker rises and the compressive strength reduces with increasing addition of SO_3. Thus it can be seen that addition of SO_3 must be strictly controlled in iron-rich fluoraluminate cement at low clinkering temperature , especially the SO_3 content of raw materials. The $CaSO_4$ content in raw mixture prepared must be less than 1.0wt%.

Fig 2 illustrates the regularity of mineral formation in clinker , which is obtained by burning raw mix containing 1.5wt% $CaSO_4$ at different temperatures. The results showed that only $3C_2S3\bar{C}\bar{S}CaF_2$ is present in the sample burnt at 950℃, beside C_6AF_2, C_2S, f-CaO. For 950-1050 ℃, $C_{11}A_7CaF_2$ began to form , and it coexists with $3C_2S3\bar{C}\bar{S}CaF_2$. When the temperature is raised to 1050℃ and above, $3C_2S3\bar{C}\bar{S}CaF_2$ decomposes and disappears. Then $C_4A_3\bar{S}$ began to appear and coexist with $C_{11}A_7CaF_2$. With increase in temperature , the quantity of $C_{11}A_7CaF_2$ formed tends to reduce at 1100-1200℃ . $C_4A_3\bar{S}$ does not reach maximum until 1200 ℃ and then $C_{11}A_7CaF_2$ disappears . After this, $C_4A_3\bar{S}$ begins to decmopose with increasing temperature. At 1300 ℃ $C_4A_3\bar{S}$ decomposes and disappears, then $C_{11}A_7CaF_2$ reappears. As the temperature continues to rise to 1350℃, $C_{11}A_7CaF_2$ decomposes too .

Table 3. Minerals formation process in different varieties of cement

Cement variety	Al/Fe	F^-	F^-/SO_3	Burning temperature℃	Mineral	Reference
Iron-rich cement	2.22-2.94	0.27-0.86	0.05-0.5	1000	$C_4A_3\bar{S}$	[17]
	2.22-2.94	0.27-0.86	0.05-0.5	1100	$C_4A_3\bar{S}$, $C_{11}A_7CaF_2$	[17]
Portland cement			0.101-0.53	950-1100	$3C_2S3\bar{C}\bar{S}CaF_2$	[15]
	2.85	1.0	0.4	1250-1300	$C_4A_3\bar{S}$, $C_{11}A_7CaF_2$	[15]
	2.85	0.5	0.2	1300	$C_4A_3\bar{S}$, $C_{11}A_7CaF_2$	[15]
	2.23	0.5	0.2	1250	$C_4A_3\bar{S}$, $C_{11}A_7CaF_2$	[15]
Our cement	0.92	1.5	0.74	950	$3C_2S3\bar{C}\bar{S}CaF_2$	
	0.92	1.5	0.74	950-1050	$3C_2S3\bar{C}\bar{S}CaF_2$, $C_{11}A_7CaF_2$	
	0.92	1.5	0.74	1050-1200	$C_{11}A_7CaF_2$, $C_4A_3\bar{S}$	
	0.92	1.5	0.74	1200-1300	$C_4A_3\bar{S}$	
	0.92	1.5	0.74	1300	$C_{11}A_7CaF_2$	

The earlier reported studies on mineral formation process in portland cement, with addition of F^- and SO_3, have shown [4, 5, 7, 15] that $3C_2S3\bar{C}\bar{S}CaF_2$ forms at 950-1100℃ and decomposes at 1100℃ and above. $C_{11}A_7CaF_2$ prevents formation of C_3A, as also that of $C_4A_3\bar{S}$. At 1100℃ , $C_{11}A_7CaF_2$ forms first . After that , $C_4A_3\bar{S}$ appears. They can coexist in raw mixture with definite composition . $C_4A_3\bar{S}$ does not decompose until 1300℃, $C_{11}A_7CaF_2$ decomposes at 1350℃. The influence of composition and temperature on regularity of mineral formation has been studied on details [15] . But in iron-rich cement [17] (Al/Fe=2.22-2.94, F^-/SO_3=0.05-0.5) $C_4A_3\bar{S}$ forms first at 1000℃, then $C_{11}A_7CaF_2$ appears. The two phases can coexist . The quantity reaches maximum at 1200℃. Comparison between these studies and our study are shown in Table 3.

There are some similarities in mineral formation processes between iron-rich fluoraluminate cement with SO_3 added and portland cement. But, when 1.5wt% of $CaSO_4$ is added in raw mixture, $C_{11}A_7CaF_2$ forms at first at 1200-1300℃, then the $C_{11}A_7CaF_2$ formed disappears because of the restraining effect of $C_4A_3\bar{S}$. It forms again while the $C_4A_3\bar{S}$ decomposes and disappears with rising temperature. These results have been obtained consequently in our experiments. This is different from that of portland cement or iron-rich cement.

Because of higher CaF_2 contents (F^- more than 1.5wt%) in iron-rich fluoraluminate cement, in which $C_{11}A_7CaF_2$ is regarded as the main clinker mineral, $C_{11}A_7CaF_2$ appears earlier than $C_4A_3\bar{S}$ does. Moreover, Al_2O_3 participates in the formation of $C_4A_3\bar{S}$, which restrains the formation of $C_{11}A_7CaF_2$. $C_{11}A_7CaF_2$ gradually decomposes, and it does not disappear until 1200 ℃, when the $C_4A_3\bar{S}$ contents reach the maximum. With continuously rising temperature, $C_4A_3\bar{S}$ begins to decompose and it does not disappear until 1300℃. Then $C_{11}A_7CaF_2$ forms again. $C_{11}A_7CaF_2$ decomposes and disappears at 1350℃.

3. CONCLUSIONS

3.1. At the clinkering temperature range 950-1050℃ for iron-rich fluoraluminate cement, the $CaSO_4$ contents in raw mixture must be controlled (to be < 1.0wt%). Especially, the SO_3 contents in each raw materaial must be paid due attention. If not, $3C_2S3C\bar{S}CaF_2$ will form, which will reduce the hydraulicity of the cement.

3.2. When $CaSO_4$ is 1.5wt%, in the clinker mineral formation process of iron-rich fluoraluminate cement, $C_{11}A_7CaF_2$ forms first and then $C_4A_3\bar{S}$.

3.3. The formation of $C_4A_3\bar{S}$ restrains that of $C_{11}A_7CaF_2$. When $C_4A_3\bar{S}$reaches the maximum at 1200℃, $C_{11}A_7CaF_2$ dispapears. $C_{11}A_7CaF_2$ does not appear again until the temperature rises to 1300℃ when $C_4A_3\bar{S}$ decomposes and disappears.

REFERENCES

1. R. Bucchi, 7th ICCC, Vol. I, I-1/3 (1980).
2. Feng Peizhi etc., Cement (Chinese), 15, 1985(5).
3. Ne Hua etc., Cement (Chinese), 1985(9).
4. Xu Xianyu etc., 1985 BISCC, Vol. 1, 140, 1985
5. Lu Ping etc., J. Chese. Sil. Soc., 13 (3), 275, 1985
6. Feng Peizhi etc., 1985 BISCC, Vol. 1, 162, 1985
7. Shenwei etc., Technology of Cements, 50, (Academic Press, Beijing), 1986
8. Tong xueli etc., 1985 BISCC, Vol. 1, 120, 1985
9. A. K. Chatterjee, 1985 BISCC, Vol. 1, 174, 1985
10. Li PeiQuian, Journal of China Building Materials Academy, 23, 1981
11. Wang Ansheng, Hunan Building Materials (chinese), 21, 1985(2)
12. Zhong Jingyu, Cement (chinese), 11, 1985(9)
13. Liu Kehui, Zhejiang Cement (chinese), 4, 1985(1)
14. Huang Wenxi etc., 9th ICCC, Indian, 1992
15. Xue Jungan etc., J. Chese. Sil. Soc., 13(3), 264, 1985
16. Liu Baoyuan, j. Chese. Sil. Soc. 12(4), 429, 1984
17. Feng Xinji, J. Chese. Sil. Soc. 12(1), 32, 1984
18. Shi Qixiang, Yunnan Cement (chinese), 1, 1987(4)
19. Zhao Zongyan, Cement (chinese), 33, 1984(7)
20. Zhang Baishou, Jiangxi Building materials, 20, 1988(1)

EFFECT OF SULPHATE ON THE REACTION OF C_3S FORMATION

H M Cheong*, S H Choi*, K S Han and J D Jaung*****

**Department of Inorganic Materials Engineering, Hanyang University, Seoul, KOREA*
***Department of Ceramic Engineering, Inha University, Inchon, KOREA*
****Tong Yang Cement Corp, Seoul, KOREA*

SUMMARY

The effect of sulphate on the reaction of C_3S formation in presence of the clinker liquid phase was studied. The experiments were performed with various sulphate sources, such as $(NH_4)_2SO_4$, $CaSO_4$, and K_2SO_4.

The reaction of C_3S formation was promoted by adding of a small amount of $(NH_4)_2SO_4$ or $CaSO_4$. For its content of more than 3 wt% , however, the formation of C_3S was prevented. When the higher content of $CaSO_4$ or $(NH_4)_2SO_4$ was added, they showed different reaction for preventing of C_3S formation. In case of $CaSO_4$, C_2AS and $C_4A_3\bar{S}$ as intermediate products were formed below 1000°C, and remained upto clinkering temperature. On the other hand, in case of $(NH_4)_2SO_4$, sulphate was enriched at the surface of C_2S grains. The formation of C_3S could be hindered by these two different reactions, respectively.

C_3S grains grew anomalously above 100 μm, when 2 $\sim$ 3 wt% of $(NH_4)_2SO_4$ or $CaSO_4$ was added to the clinker. It might be considered that, below 1400°C, C_3S crystals were precipitated, and the crystals of C_3S were coalesced and/or captured each other with increasing temperature because of their rapid growth rate

K_2SO_4 promoted the reaction of C_3S formation, and it did not prevent that of C_3S formation although an excess of K_2SO_4 was added.

Die Auswirkung des Sulfate auf die Reaktion der C_3S Bildung in der anwesenheit der Klinker flüßieger Phase wurde untersucht. Die Experimente wurde mit verschiedenen Sulfate, d.h., $(NH_4)_2SO_4$, $CaSO_4$, und K_2SO_4 ausgeführt.

Die Reaktion der C_3S Bildung wurde von der Hinzufügung von $(NH_4)_2SO_4$ oder $CaSO_4$ in Kleine Maße gefördert. Jedoch, ist der Sulfatanteil höher als 3 Gew. %, wurde die bildung von C_3S verhindert. Bei dem höheren Gehalt von $CaSO_4$ oder $(NH_4)_2SO_4$ zeigten die verschiedenen Reaktion bei der Verhinderung des C_3S Bildung. In dem Fall von $CaSO_4$, wurden C_2AS und $C_4A_3\bar{S}$ als die zwischenprodukte bei der Temperatur unterhalb 1000°C gebildet und waren die bis Klinkerisierender Temperatur stabil. Gegensätzlich, in dem Fall von $(NH_4)_2SO_4$ wurde das Sulfat an der Oberfläche der C_2S Korngrezen angereichert. Die Bildung von C_3S könnte von diesen zwei verschiedenen Reaktionen, bzw, verhindert werden sein.

C_3S Körnen wächsten sich unregelmäßig übergelegt werden sein, die C_3S Kristalle wurde bei der Temperatur unterhalb 1400°C ausgeschieden und sich wächsten zusammen mit steigenden Temperatur und/oder finden einander wegen deren hohen Wachstumsrate.

K_2SO_4 förderte die Reaktion der C_3S Bildung und nicht behinderte es auch bei der übermäßigen Hinzufügung von K_2SO_4.

INTRODUCTION

Minor components, such as MgO, alkalis, sulphates, and chloride, commonly present in the raw materials of cement, can affect the reactions of the clinker formation. Their effects can be beneficial or harmful. Beneficial effects include acceleration of the clinkering reaction or lowering its temperature. Harmful effects include decrease in alite content, volatilization in the kiln with consequent formation of kiln rings or other deposits.[1,2] Some elements such as SO_3 and P_2O_5 have beneficial effects at low concentrations but harmful ones at higher concentration on the reaction of C_3S formation.[3,4]

Gutt and Smith concluded that, if Al_2O_3 was present and MgO absent, even small proportions of SO_3 could restrict or prevent formation of C_3S.[5] Strange and Knöfel reported that, with increasing the content of SO_3 in the clinkers, the alite content showed considerable decrease, and the belite content correspondingly increase. A higher SO_3 content in the clinker lowered the strength of the cement made from it, and setting time was accelerated.[6] On the other side, Glasser showed that alkali sulphate liquid was virtually immiscible with oxide liquid.[7]

In this study, the effect of various sulphates on the reaction of C_3S formation and the mechanism about the decrease of C_3S content at higher concentration were investigated.

EXPERIMENTAL

Synthesis of γ-C_2S and clinker melt were prepared prior to the addition of sulphates. The composition of the clinker melt was chosen for the invariant point in which C_3S, C_2S, C_3A, and C_4AF were coexisted at 1338℃. Its composition corresponds to 54.8 CaO, 22.7 Al_2O_3, 6.0 SiO_2, and 16.5 Fe_2O_3. As sulphate sources $(NH_4)_2SO_4$, $CaSO_4 \cdot 2H_2O$ and K_2SO_4 of reagent grade were used. $(NH_4)_2SO_4$ was chosen in order to observe single effect of SO_3 because of its decomposition into ammonia and SO_3 below 230℃.

The compositions of raw mixture are shown in Table 1. The desired content of sulphate was varied over a range from 0 to 6.0 wt% as a SO_3 base. When $CaSO_4$ was added, the amount of CaO supplied in $CaSO_4$ was reduced. After mixing, the raw mixes were calcined at 1000℃ for 1 hour, and burned at 1450℃ for 30 minutes. And then the clinkers were cooled in ambient air.

Table 1 Raw Mix Composition (weight percent)

Sample Name	C_2S	CaO	Melt	$(NH_4)_2SO_4$*	$CaSO_4$*	K_2SO_4*
S-0	56.58	18.42	25.00			
S-1	56.01	18.24	24.75	1.0		
S-2	55.45	18.05	24.50	2.0		
S-3	54.88	17.87	24.25	3.0		
S-4	54.32	17.68	24.00	4.0		
S-6	53.19	17.31	23.50	6.0		
C-1	56.01	18.24	24.75		1.0	
C-2	55.45	18.05	24.50		2.0	
C-3	54.88	17.87	24.25		3.0	
C-4	54.32	17.68	24.00		4.0	
C-6	53.19	17.31	23.50		6.0	
K-1	56.01	18.24	24.75			1.0
K-2	55.45	18.05	24.50			2.0
K-4	54.32	17.68	24.00			4.0
K-6	54.19	17.31	23.50			6.0

* : SO_3 base

Raw mixes with 6.0 wt% SO_3 were homogenized, calcined at 1000℃ for 1 hour, and heated upto 1100, 1200, 1300, 1350, 1400, and 1450℃, respectively. As soon as desired temperatures were achieved, the samples were taken out from the furnace, and cooled in ambient air. The intermediate products formed during burning were analyzed.

To investigate reactivity between C_2S and sulphate, raw mixes were prepared by mixing of 25 wt% of clinker melt with C_2S and $CaSO_4$. The molar ratio of C_2S and $CaSO_4$ was 2 : 1. They were calcined, heated and cooled as above procedure.

The content of free CaO and residual SO_3 were analyzed, and XRD, optical microscopy and SEM/EDS were used for analyses of the clinkers.

RESULTS AND DISCUSSION

Table 2 shows the results of XRD and optical microscopy of the clinkers sintered at 1450℃ for 30 minutes with various SO_3 sources and their content. The clinkers free of SO_3 (S-0) produce mostly C_3S which show the equant grains with the size of 10 ~ 20 μm.

When $(NH_4)_2SO_4$ is added, the clinkers with 1 wt% $(NH_4)_2SO_4$ show C_3S crystals of 30 ~ 50 μm. With its addition of 2 wt%, C_3S content decreases, however the grain size increases above 100 μm. Also, when SO_3 is added more than 4 wt%, C_3S crystals do not appear.

$CaSO_4$ also assumes almost similar aspects of $(NH_4)_2SO_4$. The content of C_3S crystals dropps with the increase of $CaSO_4$ addition above 2 wt% . At any rate, its addition of more than 4 wt% eliminates C_3S crystals in clinkers.

K_2SO_4 does not hinder the C_3S formation regardless of its amount. Higher K_2SO_4 in content induces only the formation of crystalline K_2SO_4. C_3S crystals are equant and 10 ~ 20 μm in size.

Table 2 The results of XRD and optical microscopy of the clinkers sintered at 1450℃ for 30 minutes with various SO_3 sources and amount.

Sample No.	Identified phase by XRD	C_3S grain size(μm)
S-0	C_3S(vs) C_2S(vw)	10~20
S-1	C_3S	30~50
S-2	C_3S(s) C_2S(m) CaO(w)	90~150
S-3	C_3S(vw) C_2S(vs) CaO(m)	150~180
S-4	C_2S(vs) CaO(s)	
S-6	C_2S(vs) CaO(s) $CaSO_4$(vw)	
C-1	C_3S	40~60
C-2	C_3S(s) C_2S(m) CaO(w)	90~180
C-3	C_3S(m) C_2S(vs) CaO(m)	160~200
C-4	C_2S(vs) CaO(s)	
C-6	C_2S(vs) CaO(s) $C_4A_3\bar{S}$(w)	$CaSO_4$(vw)
K-1	C_3S	10~20
K-2	C_3S	10~20
K-4	C_3S(vs) K_2SO_4(vw)	10~20
K-6	C_3S(vs) K_2SO_4(w)	10~20

* vs:very strong s:strong m:middle
w:weak vw:very weak

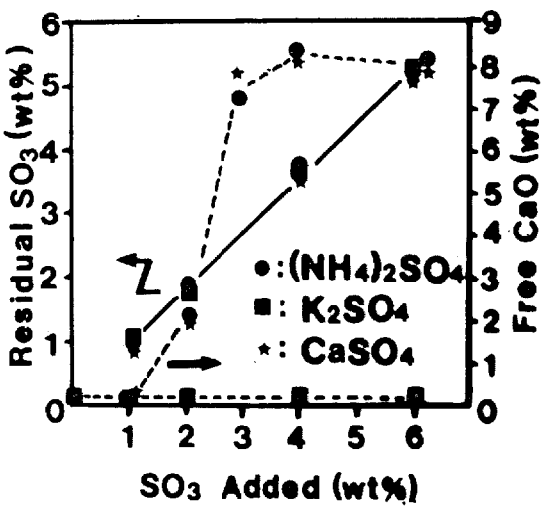

Fig. 1 The value of free CaO and residual sulphate content for the clinkers sintered at 1450℃ for 30 mins. with increasing sulphate contents

Figure 1 is the result of the chemical analyses for the clinkers sintered at 1450℃ for 30 minutes with increasing sulphate contents. The addition of 1 wt% $(NH_4)_2SO_4$ or $CaSO_4$ results in a small amount of free CaO. From 2 wt% of $CaSO_4$ or $(NH_4)_2SO_4$ addition, free CaO content starts to increase. It reaches 8.31 wt% for 4 wt% of the sulphate addition. In contrast, the content of free CaO does not increase for the increase of K_2SO_4 addition. Sulphate in clinkers could reside to the extent of 80 ~ 90 % of added content regardless of sulphate sources.

In the presence of clinker liquid phase, it has been known that C_2S and CaO reacted in the clinker melt to give C_3S.[8] In the reactions of portland cement clinker formation, minor components affect the physical properties of clinker melt, that is, its surface tension and viscosity.

Butt and Timashev reviewed the changes of the physical properties of clinker melt when minor elements were present in a clinker liquid phase.[3] The presence of sulphate in the clinker melt reduces the viscosity and surface tension of the melt. Thus, the dissolution rates of CaO and C_2S are accelerated, so C_3S formation is promoted. Therefore, the mineralizing effect of sulphate may explain why sulphates make the viscosity and the surface tension of the melt dropped.

In order to investigate the hypertrophic growth of C_3S grains, raw mixes with $CaSO_4$ 2 wt% are burned upto 1400, 1450℃, respectively. Produced clinkers are examined under optical microscopy. (Figure 2) As the clinkering temperature is elevated, C_3S crystals grow anomalously, and C_3S grains decrease in number. As shown in Figure 3, the C_3S grains burned at 1450℃ for 30 minutes have a complex surface feature as if they were consolidated and/or captured each other. Maki reported that the crystals of C_3S grew large because of their unstable growth at higher concentration of sulphate.[9]

As the sulphate is added, the dispersibility of particles, only to the reduction of surface tension, becomes higher, and C_3S crystals are precipitated locally. These observations may indicate that,as temperature is elevated,the crystals of C_3S are coalesced and/or captured each other because of their rapid growth rate.

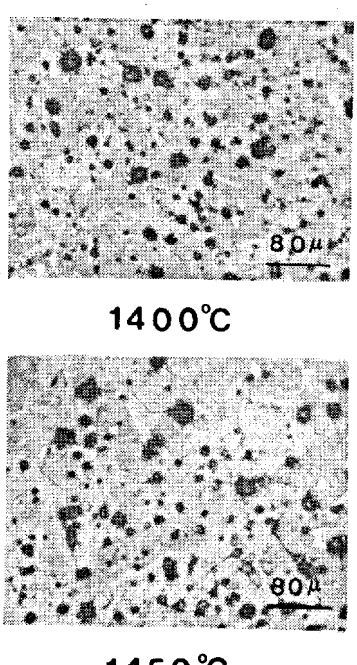

Fig. 2 Micrographs of the clinkers with $CaSO_4$ (2 wt%) heated at each temperatures.

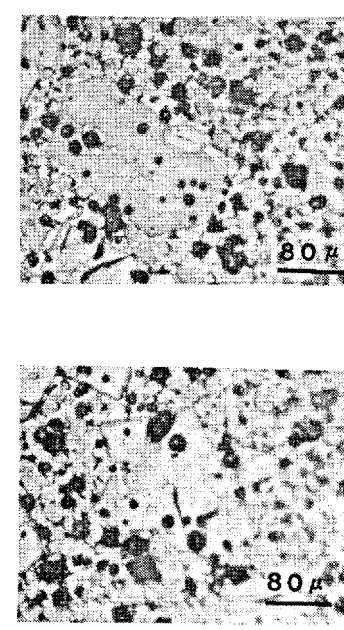

Fig. 3 Micrographs of C_3S grown anomalously (at 1450℃ for 30 min.)

Table 3 shows the intermediate products formed when S-6, C-6, and K-6 are heated at each temperatures. In S-6, a large amount of free CaO resides upto 1450℃. $3CaO \cdot 3Al_2O_3 \cdot CaSO_4$ ($C_4A_3\bar{S}$) is formed and decomposes into $CaSO_4$, $CaSO_4$ remains to 1450℃. In C-6, a large amount of C_4A_3S and $2CaO \cdot Al_2O_3 \cdot SiO_2$ (C_2AS) are formed below 1000℃. $C_4A_3\bar{S}$ remains, but C_2AS is decomposed when sintered at 1450℃ for 30 minutes. Until temperature is elevated to 1450℃, the content of free CaO is smaller to the extent of 1.5 ~ 2 wt% than that of $(NH_4)_2SO_4$. When the samples are soaked during 30 minutes at 1450℃, most of C_2AS decomposes, thus the content of CaO increases suddenly.

On the other hand, K_2SO_4 does not form the intermediate products.

Table 4 shows the intermediate products identified from XRD and C_2S grain size determined from microscopy for investigation of reactivity between C_2S and sulphate. C_2S cystals grow little at 1350 ~ 1400℃, however, they grew to the extent of 30 ~ 50 μm at 1450℃ .

Figure 4 is EDS results of the clinkers burned at 1350℃ and at 1450℃ for 30 minutes. At 1350℃, a large amount of sulphate is enriched at the surface of C_2S. At 1450℃ for 30 minutes, there is no difference in SO_3 content between the surface and the center of C_2S crystals. Thus C_2S crystals don't grow below 1400℃ because of sulphate-rich layer at the surface of C_2S grains. Above 1400℃, they could be developed by the decomposition of sulphate-rich layer at the surface of C_2S grains.

The phenomena that C_3S formation is hindered in presence of excess sulphate could be explained as follows. When $CaSO_4$ or $(NH_4)_2SO_4$ is added, they have the same chemical composition of the starting materials, but they show different appearances. In the case of $CaSO_4$, the intermediate products such as $C_4A_3\bar{S}$ and C_2AS are left over upto clinkering temperature, 1450℃. They catch CaO which would participate C_3S formation. Thus C_3S formation can not occur.

Table 3 The Intermediate Products of S-6, C-6 and K-6 Heated at each Temperatures.

Sample No.	Sintering temp. (℃)	Holding time	Identified phase by XRD	Free CaO content
S-6	1000	1 hr	C_2S(vs) C_2AS(w) CaO(vs)	16.48
	1100	-	C_2S(vs) C_2AS(w) CaO(vs) $C_4A_3\bar{S}$(w)	15.99
	1200	-	C_2S(vs) C_2AS(w) CaO(vs) $C_4A_3\bar{S}$(w)	13.93
	1300	-	C_2S(vs) CaO(s) $C_4A_3\bar{S}$(vw) $CaSO_4$(vw)	11.86
	1350	-	C_2S(vs) CaO(s) $CaSO_4$(w)	10.15
	1400	-	C_2S(vs) CaO(s) $CaSO_4$(w)	9.97
	1450	-	C_2S(vs) CaO(s) $CaSO_4$(w)	8.19
	1450	30 min	C_2S(vs) CaO(s) $CaSO_4$(w)	8.05
C-6	1000	1 hr	$C_4A_3\bar{S}$(vs) C_2AS(vs) C_2S(s) $CaSO_4$(vw) CaO(vw)	1.54
	1100	-	$C_4A_3\bar{S}$(vs) C_2AS(vs) C_2S(s) CaO(vw)	1.37
	1200	-	$C_4A_3\bar{S}$(vs) C_2AS(vs) C_2S(s) CaO(vw)	1.21
	1300	-	$C_4A_3\bar{S}$(vs) C_2AS(vs) C_2S(s) CaO(vw)	1.37
	1350	-	$C_4A_3\bar{S}$(vs) C_2AS(vs) C_2S(s) CaO(vw)	1.33
	1400	-	$C_4A_3\bar{S}$(s) C_2AS(vs) C_2S(s) CaO(vw)	1.46
	1450	-	$C_4A_3\bar{S}$(s) C_2AS(s) C_2S(s) CaO(vw)	1.87
	1450	30 min	C_2S(vs) CaO(s) $CaSO_4$(m) $C_4A_3\bar{S}$(w)	7.73
K-6	1000	1 hr	C_2S(vs) CaO(vs) K_2SO_4(w)	17.43
	1100	-	C_2S(vs) CaO(vs) K_2SO_4(w)	17.31
	1200	-	C_2S(vs) CaO(vs) K_2SO_4(w)	17.37
	1300	-	C_2S(vs) CaO(vs) K_2SO_4(w)	16.99
	1350	-	C_2S(vs) CaO(vs) K_2SO_4(w)	3.35
	1400	-	C_3S	0.63
	1450	-	C_3S(vs) K_2SO_4(w)	0.28
	1450	30 min	C_3S(vs) K_2SO_4(w)	0.22

* vs:very strong s:strong m:middle w:weak vw:very weak

Table 4 The intermediate products by XRD and C_2S grain size by microscopy, for investigation of reactivity between C_2S and sulphate.

Sintering temp(℃)	Soaking time	Identified phase by XRD	C_2S grain size(μm)
1000	1 hr	C_2S(vs) $CaSO_4$(vs)	
1100	-	C_2S(vs) $CaSO_4$(vs)	
1200	-	C_2S(vs) $C_5S_2\overline{S}$(w) $C_4A_3\overline{S}$(w) $CaSO_4$(vw)	
1300	-	C_2S(vs) $CaSO_4$(s) $C_4A_3\overline{S}$(w)	
1350	-	C_2S(vs) $CaSO_4$(m) $C_4A_3\overline{S}$(vw)	10~15
1400	-	C_2S(vs) $CaSO_4$(m) $C_4A_3\overline{S}$(vw)	10~15
1450	-	C_2S(vs) $CaSO_4$(m) $C_4A_3\overline{S}$(vw)	20~25
1450	30 min	C_2S(vs) $CaSO_4$(w) $C_4A_3\overline{S}$(vw)	30~50

* vs:very strong s:strong m:middle w:weak vw:very weak

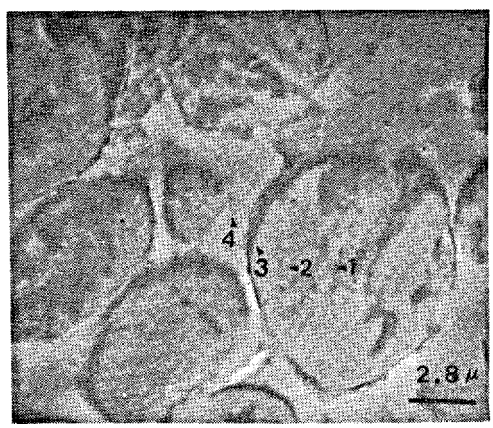

1350 ℃

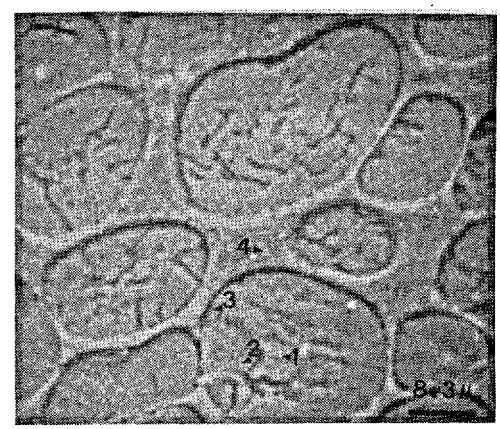

1450℃ 30 minutes

Condition	point No.	CaO	SiO_2	Al_2O_3	Fe_2O_3	SO_3
1350℃	Total	46.66	20.77	10.19	2.67	19.72
	1	54.35	36.27	2.66	1.43	5.29
	2	53.09	37.84	3.07	0.82	5.18
	3	45.84	24.77	5.44	2.68	21.18
	4	30.30	1.47	45.50	Tr	22.73
1450℃ 30 min	Total	57.89	23.26	4.46	3.01	11.39
	1	64.51	30.25	2.08	Tr	3.16
	2	65.15	28.23	1.69	0.97	3.96
	3	65.95	28.30	1.53	0.09	4.13
	4	49.71	4.56	10.07	6.43	29.24

Fig. 4 SEM micrographs and EDS analyses of the clinkers burned at 1350℃ and at 1450℃ for 30 minutes for the investigation of reactivity between C_2S and sulphate

In case of $(NH_4)_2SO_4$, sulphate is enriched at the surface of C_2S grains, so C_2S is prevented from being dissolved into clinker melt.

In contrast, K_2SO_4 does not produce such intermediate products. K_2SO_4 liquid is immiscible with the clinker liquid. Therefore, it could not prevent C_2S and CaO from being dissolved into the clinker melt.

CONCLUSION

1. K_2SO_4 promotes the reaction of C_3S formation, however, it could not prevent that of C_3S formation although an excess of K_2SO_4 (SO_3 base 6 wt%) is added.

2. For the addition of $(NH_4)_2SO_4$ or $CaSO_4$ of 1 wt%, the sulphate could promote the reaction of C_3S formation. For its content of more than 3 wt%, the formation of C_3S is prevented.

3. For the addition of $(NH_4)_2SO_4$ or $CaSO_4$ of 2 wt% and 3 wt%, C_3S grains show the hypertrophic growth above 100 μm. We may consider that below 1350℃, C_3S crystals are precipitated, and the crystals of C_3S are coalesced and/or captured each other with increasing temperature because of their rapid growth rate.

4. When $CaSO_4$ or $(NH_4)_2SO_4$ is added, the chemical composition of the starting materials are the same, but they show different reaction. For $CaSO_4$, C_2AS and $C_4A_3\bar{S}$ are formed below 1000℃. They remain upto clinkering temperature, 1450℃. Thus, these intermediate products catch CaO which would participate the formation of C_3S. In case of $(NH_4)_2SO_4$, sulphate is enriched at the surface of C_2S grains, so this sulphate-rich layer could prevent C_2S from being dissolved into clinker melt.

REFERENCES

1. Taylor,H.F.:"Cement Chemistry".2nd ed.London, Academic press,1990,92p.

2. Bucchi,R.:"Influence of the Nature and Preparation of Raw Materials on the Reactivity of Raw Mix" Seventh International Congress on the Chemistry of Cement,Paris,1980,V1,Sub-Theme I-1.

3. Butt,Y.M. and Timashev,V.V. :"The Mechanism of Clinker Formation Process and Ways of Modification". The Sixth International Congress on the Chemistry of Cement,Moscow,1974,V4,3-64.

4. Han,K.S. and Choi,S.H.:"Effect of MgO and SO_3 on the Formation of Cement Clinker".NCB International Seminar on Cement and Building Materials,2nd,New Delhi,India 1989,V4,IX-54.

5. Gutt,W. and Smith,M.A.:"Studies of Sulphates in Portland Cement Clinker". Cement Technology,1971,2,143.

6. J.Strunge and D.Knöfel, : "Influence of Alkalies and Sulphur on the Properties of Cement; Part-I", Zement Kalk Gips, 1985,38,150. "Part-Ⅱ". ibid,1985,38,441. "Part-Ⅲ". ibid,1986,39,380. "Part-Ⅳ". ibid, 1990, 43,199.

7. Glasser,F.P. and Marr,J.:"Sulphates in Cement Clinkering; Immiscibility between Sulphate and Oxide Melts at 1350℃". Cement Concrete Research,1980,10, 753.

8. Kondo,R. and Choi,S.H.:"Mechanisms and Kinetics of Portland Cement Clinker Formation for a Example of the Solid State Reaction in the Presence of Liquid Phase". Proceedings of The Fifth International Symposium on the Chemistry of Cement,Tokyo,1968,V1,163.

9. Maki,I.,: "Relationship of Processing Parameters to Clinker Properties : Influence of Minor Components".8th International Congress on the Chemistry of Cement,Rio de Janeiro,1986,V1, Sub-Theme I-2 ,34.

EFFECT OF FLUORITE-GYPSUM COMPOSITE MINERALIZER ON THE MICROSTRUCTURE AND PROPERTIES OF PORTLAND CEMENT CLINKER PHASE

Ye Qing*, Kong Jianmin** and Liu Baoyuan**

*Civil Engineering Department, Zhejiang Institute of Technology, P R CHINA
**Cement Research Institute, China Building Materials Academy, P R CHINA

ABSTRACT

XRD, XPS, SEM / EDAX, DTA, high temperature viscometer and chemical analysis have been employed in this study of the crystal chemistry of C_3S or Alite containing $\bar{F}$ and $\bar{S}$ in C_3S (Alite)–CaF_2–$CaSO_4$ system. And the characteristics of liquid phase of portland cement clinker containing $\bar{F}$ and $\bar{S}$ and the microstructure of cement clinker phase containing $\bar{F}$ and $\bar{S}$ are also investigated here. The conclusions are as follows: (i) The replacing form of solid solution and the limits of solubilities of $\bar{F}$ and $\bar{S}$ in C_3S or Alite are obtained. The crystal imperfection and crystalline modification law caused by solid solution are acquaired. Meanwhile, colouring appearance of Alite containing $\bar{F}$ is observed. (ii) Variation law of effect of $\bar{F}$ and $\bar{S}$ on liquid phase performance of portland cement clinker is found. (iii) Effect of $\bar{F}$ and $\bar{S}$ on crystalline appearance and crystal type, and distribution law of $\bar{F}$ and $\bar{S}$ in clinker phase are known.

〔摘　要〕

本文借助 XRD、XPS、SEM / EDAX、DTA、高温粘度计和化学分析等方法，对 C_3S(Alite)—CaF_2—$CaSO_4$ 系统含$\bar{F}$和$\bar{S}$的 C_3S 或 Alite 进行了结晶化学研究以及对含$\bar{F}$和$\bar{S}$的硅酸盐水泥熟料液相性质与含$\bar{F}$和$\bar{S}$的水泥熟料相微观结构进行了研究．得到①$\bar{F}$和$\bar{S}$在 C_3S 或 Alite 中的固溶取代形式和极限固溶量，以及由固溶而引起的晶体缺陷和晶型转变规律，同时观察到含$\bar{F}$的 Alite 的着色现象．②$\bar{F}$和$\bar{S}$对硅酸盐水泥熟料液相性质影响的变化规律．③$\bar{F}$和$\bar{S}$对硅酸盐水泥熟料相结晶形貌和晶型的影响以及$\bar{F}$和$\bar{S}$在熟料相中的分布规律．

1. INTRODUCTION

Al_2O_3 and Fe_2O_3 act as fluxing agents in the $CaO-SiO_2$ system, thus reducing the appearance point of liquid phase to 1338℃ and quickening the reaction of C_3S synthesis. However, the introduction of fluxing agents cannot change the basic law of thermodynamics so that in this system C_3S can only be synthesized or a temperature higher than 1250℃. And the introduction of mineralizer CaF_2 causes the formation of C_3S containing $\bar{F}$ and reliquid phase appearn at 1185℃ (1). Hence, the presence of $\bar{F}$ leads to a variation in the of characteristics of liquid phase in this system, and the solid solution of $\bar{F}$ causes the change of the thermodynamic performance of the C_3S crystal. Meanwhile, it will be definitely be accompanied by a change of its crystal texture and hydraulicity (2,3,4). CaF_2 and $CaSO_4$ act not only as effective mineralizers, but also act as fluxing agents in the production of cement. It is passible to sinter portland cement clinker at a lower temperature, in this way. In this paper, the phase microstructure and performance of portland cement clinker are reported on the basis of application and study on mineralizer.

2. PREPARATION OF SPECIMENS AND TESTING METHODS

i) Preparation of specimens:

(a) Synthesis of clinker monomineral

Pure C_3S is synthesized at 1650℃, crystal type is T_1. Alite is synthesized from the above C_3S by addition of 1% Al_2O_3, 1% Fe_2O_3 and 1% MgO at 1350℃. Specimens of C_3S containing $\bar{F}$ and $\bar{S}$, or Alite is synthesized from the above pure C_3S or Alite to which are added CaF_2 and or $CaSO_4$ at 1350℃. The compounds used are all of analytical by pure grade.

(b) Preparation of specimens for determining the characteristics of liquid phase of clinker.

According to the liquid phase composition at eutectic point (1338℃) of $C_3S-C_2S-C_3A-C_4AF$ quaternary phase system, the proportioning is done by adding alone or both CaF_2 and $CaSO_4$ (external adding).

(c) Low temperature plant clinkers of tained by addition of fluorine–sulphur compound mineralizer. The chemical compositions of such clinkers from there plants are shown in Table 1.

Table 1. Chemical Analysis of Plant Clinkers with Compound Mineralizers

No.	Plant	SiO_2 %	Al_2O_3 %	Fe_2O_3 %	CaO %	F^- %	SO_3 %	CaF_2 %	$CaSO_4$ %	F/SO_3
#1	Wuxian	20.74	6.01	3.93	65.72	1.02	0.74	2.10	1.25	1.38
#2	Jiangshan	18.88	6.15	3.33	64.18	1.19	1.23	2.45	2.09	0.97
#3	Jiangshan	19.15	6.19	3.75	63.34	1.24	1.84	2.55	3.13	0.67

ii) Experimental methods:

(a) Microstructure analysis of clinker monomineral

The specimens were subjected to XRD, QXRD and chemical analysis. Parts were also analysed by XPS, SEM / EDAX, petrographic analysis and high temperature microscope.

(b) Chemical extraction of clinker phase

Silicate phase is obtained from KOH–cane sugar solution extract. Ferroaluminate clinker phase is extracted by using salicylic acid methyl alcohol solution.

(c) Equipment and testing conditions

(aa) X–ray diffraction analyser: D / Max–αA type, (Cu target used) tube electric current of 100mA, tube voltage 40 kv.

(bb) X–ray photoelectron spectroscopy analyzer; KA–ES–300 type.

(cc) Scanning electron microscope ASM–SX type, its energy spectrum is EDAX–9100.

(dd) Rotary viscometer, 1700℃–RV–12 type.

3. RESULTS AND DISCUSSION

(I) Crystal chemistry of C_3S solid solution containing $\overline{F}$ and $\overline{S}$:

a). C_3S ($\overline{F}$) solid solution

(aa). The limits of solubilites of $\overline{F}$ in C_3S:

By detecting and analysing, we obtained the correlation between the amount of CaF_2added and: the free CaF_2 in C_3S (Fig.1); the fCaO in C_3S (Fig.2); variation mine refractive index (Ng) of C_3S ($\overline{F}$) (Fig,3); and C_3S ($\overline{F}$) cell parameter (Fig,4). All the plots showed a formation point 3.4% added CaF_2. The solubility of $\overline{F}$ in C_3S is found to reach the solubility limit when the amount of CaF_2 added is 3.4%. (Limits of solubility of $\overline{F}$ is $1.5 \pm 0.1\%$, that is, the limit of solubility of $\overline{F}$ is 0.18 mol in 1 mol C_3S.)

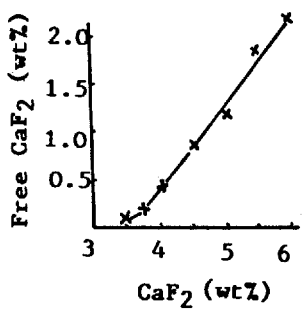

Fig.1 Relationship between the amount of CaF_2 added and free CaF_2 in C_3S

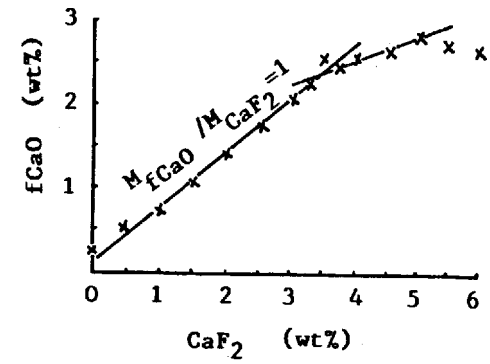

Fig.2 Relationship between the amount of CaF_2 added and fCaO in C_3S

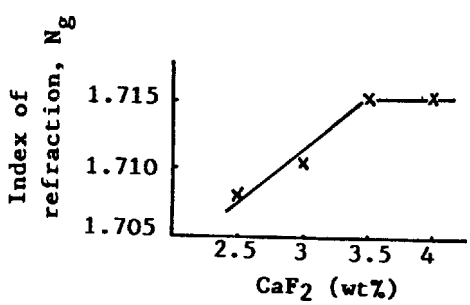

Fig.3 Variation of refractive index with the amount of CaF_2 added for the formation of C_3S–CaF_2 solid solution

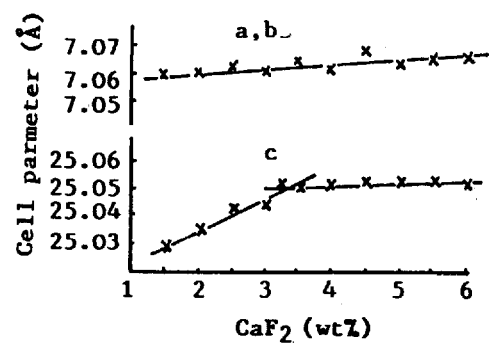

Fig.4 Variation of cell parameters with the amount of CaF_2 added in the formation of C_3S–CaF_2 solid solution

(bb) The solution form of $\bar{F}$ in C_3S:

From XPS analys is the 1S electron energy is 684.8eV for fluorine in C_3S ($\bar{F}$) specimen when the amount of CaF_2added is 3.5%. This is close to the 1S electron energy (684.6 eV) of fluorine in CaF_2, and much different from the 1S energy of fluorine in SiF_4(687.8 eV). The difference of electronic binding energy is enough to indicate that $\bar{F}$ will bond only with Ca^{2+} in C_3S crystal lattice and is impossible to bond with Si^{4+}. Fig.2 also shows that when the amount of CaF_2 added is 0–3.4%, the linear slope of the amount of CaF_2added and fCaO is MfCaO / $MCaF_2$ = 1. Hence, it is definite that two $\bar{F}$ in C_3S takes the place of only one O^{2-}ion which coordinated with Ca^{2+} ion, that no vacancy of Ca^{2+}ion presents. It is namely that the solution reaction of C_3S and CaF_2at 1350℃ is as:

$$O^{2-} \rightarrow 2F^-$$

$$Ca_3O \cdot SiO_4 + xCaF_2 = Ca_3O_{1-x}F_{2x} \cdot SiO_4 + xCaO \quad (0 < x \leqslant 0.09)$$

(cc) Crystal type of C_3S ($\bar{F}$):

By detecting and analysing, it can be seen that with the increase of solubility, the stabilized crystal type of C_3S ($\bar{F}$) will change as T_I(pure C_3S)→ T_{II}(0.5% CaF_2 added) → T_{III}(1.0% CaF_2 added) → M_{II}(1.5% CaF_2 added)→ R (2.0% CaF_2added). $\bar{F}$ acts as stabilizer of high–temperature type of C_3S. And from Fig.4 we can see that with the increasing of solubility of $\bar{F}$, the cell parameter c of C_3S solution increases and a, b direction have no change. Hence, it is confirmed that the solution of $\bar{F}$ is conducted along the c axis of C_3S.

b) C_3S ($\bar{F}$,$\bar{S}$) solid solution

aa) Crystal type of C_3S ($\bar{F}$,$\bar{S}$)

From Fig.5, it is clear that the crystal type of C_3S ($\bar{F}$,$\bar{S}$)depends mainly on the solubility of $\bar{F}$ and relates hardly with solubility of $\bar{S}$. When the amount of CaF_2 added is 1%, $CaSO_4$ is 0%–3%, crystal type of C_3S solid solution is T_{III}. And as the amount of CaF_2 added is 2% and without $CaSO_4$ crystal type is R. When the amount of $CaSO_4$ added is 1%–4%, crystal type is M_{II}. As the amount of $CaSO_4$ added is more than 4%, crystal type is T_{III}. When the addition of CaF_2 is 3%, with the increase of the amount of $CaSO_4$ added, crystal types reduce, and meanwhile superstructure of C_3S solid solution appears.

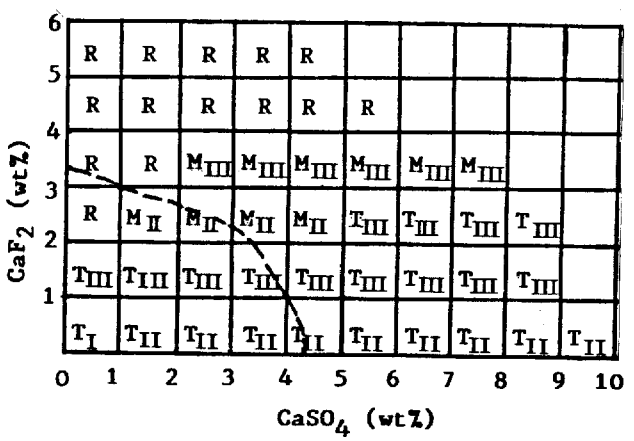

Fig.5 Variation of crystal types containing $\bar{F}$ and $\bar{S}$ in C_3S and limits of solubility of $\bar{F}$ and $\bar{S}$ in C_3S with the amounts of $\bar{F}$ and $\bar{S}$ additives

bb) Solution of $\bar{F}$ and $\bar{S}$ in C_3S

In analysing, when the amount of CaF_2 added is 1%, the limits of solubility of $CaSO_4$ is

4%. (Since traces of liquid phase appear in the specimen at 1350℃). Similarly, when CaF_2 is 2%, $CaSO_4$ is 3.5% and when CaF_2 is 3%, $CaSO_4$ is 1%. Hence, the curve of limits of solution of $\bar{F}$ and $\bar{S}$ in C_3S is obtained. (the imaginary line in Fig.5).

c) Alite containing $\bar{F}$ and $\bar{S}$ or containing both $\bar{F}$ and $\bar{S}$

aa) Crystal types of Alite containing $\bar{F}$ or $\bar{S}$ or both $\bar{F}$and $\bar{S}$

In Fig.6, the variation law of their crystal types is similar to the above C_3S solution in that it depends mainly on the solubility of $\bar{F}$ when 0.5% and 1% CaF_2 is added alone, the crystal type of Alite with $\bar{F}$ [Alite ($\bar{F}$)] is M_{III}; and when the amount of CaF_2 added is equal to or more than 2%, the crystal type is R. When 1% $CaSO_4$ is added alone, the crystal type of Alite with $\bar{S}$ [Alite ($\bar{S}$)] is M_{II}. When the amount of $CaSO_4$ is added equal to or more than 2%, the crystal type reduces to M_I. And when both CaF_2 and $CaSO_4$ are added, for instance, 2% of CaF_2 and $CaSO_4$ within 3%. The limit of the solubility, the crystal types of Alite ($\bar{F}$,$\bar{S}$) are all R. When the limit of solubility is exceeded, symmetrical reducing appears.

bb) Solid solution of $\bar{F}$ and $\bar{S}$ in Alite

When CaF_2 is added alone to Alite, the limit of solubility of $\bar{F}$ is 1.5%; when $CaSO_4$ is added alone, the limit of solubility of $\bar{S}$ is 2.2%. And when they are added together with 1% CaF_2, the limit of solubility of $CaSO_4$ is 3.5%. When CaF_2 is 2%, $CaSO_4$ is 3%, and for 3% CaF_2, $CaSO_4$ is 1%. Then the curve of limits of solubilities of $\bar{F}$ and $\bar{S}$ in Alite is obtained. (The imaginary line in Fig.6).

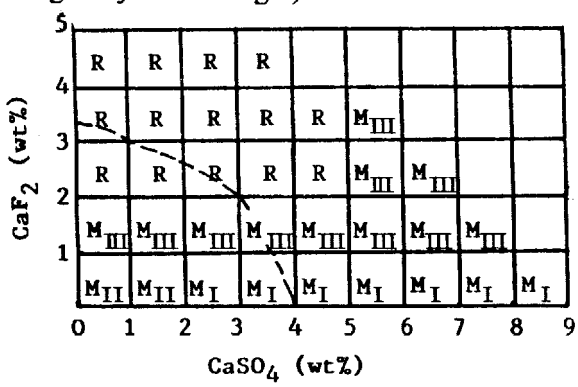

Fig.6 Variation of crystal types and limits of solubility of $\bar{F}$ and $\bar{S}$ in Alite with the amounts of $\bar{F}$ and $\bar{S}$ additives

d) The interrelationship of the solution of $\bar{F}$ and Fe_2O_3 in C_3S

The solid solution of $\bar{F}$ makes Alite coloured in appearance, and its colour changes from greenish–grey (without CaF_2)→ light pink (0.5% CaF_2) → iron red (1% CaF_2)→ dark red (2% CaF_2 added). When $CaSO_4$ is added alone, the colour of Alite will not change. As CaF_2 and $CaSO_4$ are added together, the colour of Alite ($\bar{F}$, $\bar{S}$) is pink. And with increase in the amounts of $CaSO_4$ added, its colour becomes lighter. Hence, the solid solution of $\bar{F}$ influences the solid solution and the coordinating state of Fe^{3+} ion. And the solid solution of $\bar{S}$ weakens the special solution relation between $\bar{F}$ and Fe^{+3}.

Analysing the results listed in Table 2 by SEM / EDAX, we can see that the solibility of Fe_2O_3 in Alite is 0.87%. However, the solubility of Fe_2O_3 reduces with the increase in CaF_2 added in Alite ($\bar{F}$). For instance, in specimen AF3 which has 3% CaF_2 added in Alite, the solubility of Fe_2O_3 is 0.46%.

Table 2. Mutual effect of CaF_2+Fe_2O_3 on their solubilities in C_3S

Sample	Additive amount of C_3S (%)				Crystal type	fCaO %	Color of sample	Fe_2O_3 solubility % (EDAX), in	
	CaF_2	Al_2O_3	Fe_2O_3	MgO				C_3S phase	other phase
Alite	—	1.0	1.0	1.0	M_{II}	0	Greyish green	0.87	—
AF_2	2.0	1.0	1.0	1.0	R	0	Iron oxide red	0.65	—
AF_3	3.0	1.0	1.0	1.0	R	0	Deep iron oxide red	0.46	—
$CFeF_3$	3.0	—	1.0	—	R	0.5	Deep iron oxide red	6.40	2.25

e) Mutual effect of $\overline{F}$ and $\overline{S}$ on their solubilities in C_3S

The solubilities of $\overline{F}$ and $\overline{S}$ in C_3S or Alite have a mutual effect. From the viewpoint of the solutions, $\overline{F}$ affects only the CaO_6^{10-} octahedron, while $\overline{S}$ affects not only the CaO_6^{10-} octahedron, but also the SiO_4^{4-} tetrahedron. According to the law of transformation of crystal types and the tinction phenomenon of Alite ($\overline{F}$), we can find that the solubilities of $\overline{F}$ and $\overline{S}$ in C_3S or Alite interact; and so the limits of their solubilities are inter–dependent.

Because of the interaction and mutual effect of the solubilities of $\overline{F}$ and $\overline{S}$, the appearance of the superstructure of C_3S ($\overline{F}$,$\overline{S}$) shows that the presence of the reducing of tinction phenomenon of Alite ($\overline{F}$) due to the solubility of $\overline{S}$.

(ii) Effect of fluorine and sulphur on the performance of liquid phase of cement clinker

Table 3 shows the results obtained of the effects of $\overline{F}$and $\overline{S}$ on the liquid phase performance of eutectic points of C_3S–C_2S–C_3A–C_4AF system.

Table 3. Viscosity of Liquid Phase of Clinker under Different Temperatures

Specimen number	Mineralizer		Viscosity value, at Pa • S			
	CaF_2 %	$CaSO_4$ %	1340℃	1350℃	1400℃	1450℃
1	0	0	0.115	0.112	0.068	0.040
2	1	0	0.074	0.070	0.049	0.040
3	1	3	0.065	0.064	0.040	0.033

Note: $D = 50s^{-1}$

In Table 3, $\overline{F}$ and $\overline{S}$ cause the viscosity of the system to reduce proving, that these applied elements effectively weaken the association and binding energy of the network structure of the melt. Meanwhile, it is beneficial to the interdiffusion of ions and the reformation of bonds, by virtue of which the chemical reactivity of the substances is increased. Hence, $\overline{F}$ and $\overline{S}$ are characterized by mineralization and one of the reasons there is that they reduce the viscosities of the liquid phase of clinker.

(iii) Effects of Fluorine and Sulphur on the Microstructure of Cement Clinker

a) Effects on crystal morphology of clinker mineral

In the low–temperature clinker to which a compound mineralizer containing fluorine and sulphur had been added , the dissolution of Belite and the conditions of crystallization of Alite vary because of the effect of fluorine and sulphur on the compositions, content, viscosity, and temperature of liquid phase appearance . Fig.7 shows the crystal morphology of Alite in low–temperature clinker.

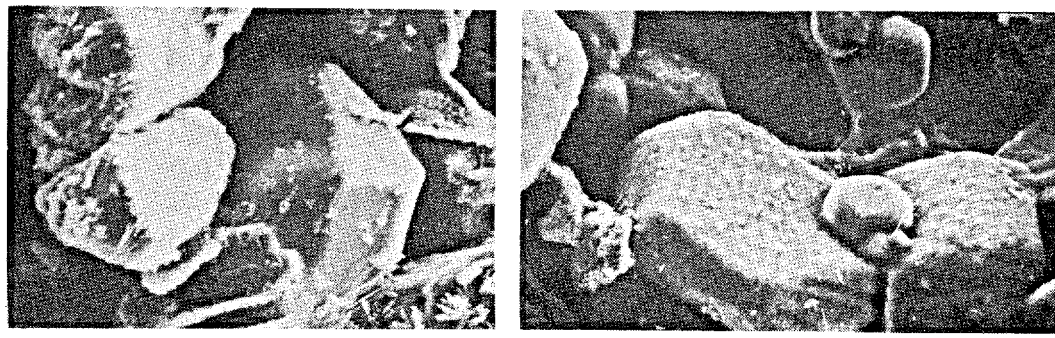

Fig.7 Crystalline morphology of Alite in low–temperature clinker
a. Alite of well–developed grain
b. Alite of directional crystallization and its surface educts

Fig.7a shows the Alite of regular hexagonal 14–hedron at normal sintering temperature (1250–1350℃) and well crystallized. Fig.7b is the regular hexagonal flat Alite obtained at high temperature (> 1350℃), slow cooling and extends alone crystal plane (0001). The ratio of geometrical crystalline axis c / b is 1:4.

b) Effects on crystal types of clinker mineral

From Fig.8a, we can see that in the clinker with 5% $CaSO_4$ mineralizer added in plant raw meal, the Alite is of the monoclinic crystal type, (like any ordinary plant clinker). In the clinker with 3% CaF_2 mineralizer added in plant raw meal, the Alite is trigonal crystal type as shown in Fig.8b. Alite is again trigonal crystal type in the plant clinker to which 5% $CaSO_4$ and 3% CaF_2 had been added as compound mineralizer. (Fig.8c). On other word, the crystal type of Alite in plant clinker obtained by addition of compound mineralizer is similar to that from CaF_2 mineralizer alore added. This proves that mainly $\bar{F}$ affects the crystal type of Alite.

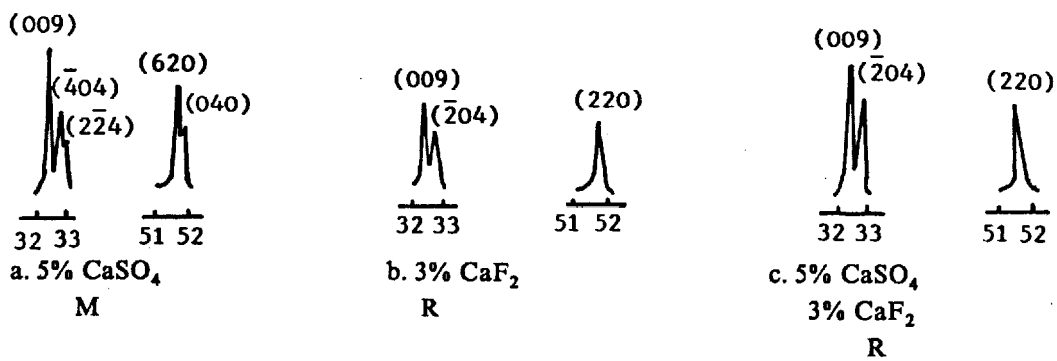

Fig.8 Effects of compound mineralizer on the crystalline forms of Alite

c) Distribution of fluorine and sulphur in low–temperature clinker mineral

In order to study the distribution of fluorine and sulphur in clinker (compositions in Table 1), chemical extraction is used to separate the silicate phase from the ferroaluminate phase. From the results then in Table 4, it can be noticed that the solubility of $\bar{S}$ in silicate phase is within 0.17–1.30%; and the solubility of $\bar{S}$ in ferroaluminate phase is within 0.54–1.32%. Hence, the solubility of $\bar{S}$ in ferroaluminate phase is higher than that in silicate phase. On the other hand the solubility of $\bar{F}$ in silicate is within 0.75–1.60% and in ferroaluminate phase within 0.22–0.31%. This proves that most of the $\bar{F}$ is dissolved in the silicate phase, only a little is dissolved in the ferroaluminate phase or forms $C_{11}A_7 \cdot CaF_2$.

Table 4. Amount and Distribution of $\bar{F}$ and $\bar{S}$ in Clinker Phases

Plant Clinker	Total $\bar{F}$ or $\bar{S}$ in clinker %		$\bar{F}$ or $\bar{S}$ in silicate %		$\bar{F}$ or $\bar{S}$ in ferrite–aluminate %		$\bar{F}$ or $\bar{S}$ in silicate against total $\bar{F}$ or $\bar{S}$ %		$\bar{F}$ or $\bar{S}$ in ferrite–alumiante against total $\bar{F}$ or $\bar{S}$ %	
	$\bar{F}$	$\bar{S}$	$\bar{F}$	$\bar{S}$	$\bar{F}$	$\bar{S}$	$\bar{F}$	$\bar{S}$	$\bar{F}$	$\bar{S}$
1	1.02	0.74	0.75	0.17	0.22	0.54	77.3	23.9	22.7	76.1
2	1.19	1.23	0.85	0.53	0.30	1.28	73.9	29.3	26.1	70.7
3	1.24	1.84	0.89	1.30	0.31	1.32	74.2	49.6	25.8	50.4

4. CONCLUSION

i) C_3S ($\bar{F}$) solid solution

The solution of $\bar{F}$ takes the place of O^{2-} ion in C_3S, which can only coordinate with calcium. High–temperature type of C_3S can be stabilized by $\bar{F}$. The solution of $\bar{F}$ in C_3S is conducted along the c axis. The limit of solubility of $\bar{F}$ is 1.5± 0.1% (1350℃). The molecular formula of C_3S ($\bar{F}$) is $Ca_3O_{1-x}F_{2x} \cdot SiO_4 (0 < x \leq 0.09)$.

ii) C_3S ($\bar{F}$, $\bar{S}$) solid solution

The solution of $\bar{F}$ and $\bar{S}$ in C_3S is mutually is conditioned. The limits of their solubilities are interdependent. The steady crystal type of C_3S ($\bar{F}$, $\bar{S}$)depends mainly on the solution of $\bar{F}$.

iii) Alite ($\bar{F}$)

The colour of Alite is changed from greenish–grey to iron red by $\bar{F}$. The solubility of Fe_2O_3 in C_3S is decreased by $\bar{F}$. High–temperature type of Alite can be stabilized by $\bar{F}$ and the limit of the solubility of $\bar{F}$ in Alite is 1.5%.

iv) Alite ($\bar{S}$)

The solution of $\bar{S}$ hardly changes the symmetry of Alite. The limit of solubility of $\bar{S}$ is 2.2%.

v) Alite ($\bar{F}$, $\bar{S}$)

The solution of $\bar{F}$ and $\bar{S}$ in Alite have a mutual effect. The limits of their solubilities are interdependent. The solution of $\bar{S}$ reduces the colouring of Alite ($\bar{F}$) and the steady crystal type of alite ($\bar{F}$, $\bar{S}$) depends mainly on the solution of $\bar{F}$.

vi) The introduction of CaF_2 and $CaSO_4$ can not change the rheological behaviour of liquid phase of portland cement clinker. However, it can reduce the viscosity of the liquid phase.

vii) The effects of $\overline{F}$ and $\overline{S}$ on the liquid phase of clinker in plant clinkers cause the morphology of Alite crystal to be extended along plane (0001) so as to appear flat. CaF_2 mineralizer significantly influences the crystal type of Alite while $CaSO_4$ has no effect on. Most of $\overline{F}$ is dissolved in the silicate phase in clinker mineral, while most of $\overline{S}$ is in the intermediate phase with a small part of it dissolved in the silicate phase

REFERENCES

1. M. Tanaka and G. Sodoh, Prov. of the Fifth Intern. Symp. on the Chem. of Cement, Tokyo, 1968, Vol.I (1969) 122.

2 . TIMASHEV V.V: "The kineties of clinker formation, the structure and composition of clinker and its phases". Proceedings of the seventh international congress on the chemistry of cement Vol.I Paris 1980.

3. W. Gutt, Proc. of the Fifth Intern. Symp. on the Chem. of Cement, Tokyo, 1968, Vol.I (1968) 101.

4. Ye Qing et al. Journal of China Building Materials Academy, Vol. I (3) 230.

EVALUATION OF AN OPTIMUM PERCENTAGE ADDITION OF FLUORSPAR IN WHITE CEMENT RAW MIX CONTAINING 4% SO_3

H U Shah* and Zafar Iqbal**

**Cement Research & Development Institute, Lahore, PAKISTAN*
***Institute of Chemistry, University of Punjab, Lahore, PAKISTAN*

ABSTRACT

Addition of Fluorspar to a raw mix results in lowering the clinkering temperature of C_3S formation and also increases the speed of formation of silicates. Mixing fluorspar to a raw mix, rich in SO_3 content, certainly helps to produce cement at lower temperature, the cement thus produced shows improved strength properties. Considerable energy savings in terms of temperature reduction, better kiln through-puts, less gypsum requirements and less power consumption can be achieved.

INTRODUCTION

Various studies, on the use of fluxes and mineralizers, for lowering clinkering temperature, increasing the kiln production and energy savings have been carried out in the developed countries. A comprehensive review, on the use of fluxes and mineralizers, in clinkering process has been presented by W.A. Klem and J. Skalny, [1]. Among most of the mineralizers, Flourides have been the most experimented mineralizer. Addition of Fluorspar, to a raw-mix even in small proportion (0.20%) results in lowering the temperature of C_3S formation and increases the speed of silicates formation [2], reduction in clinkering temperature, as high as, 180°C has been reported by the addition of Fluorspar [3]. Mineralization of raw meal with 0.5% F has been found to accelerate the clinkering temperature and rapid formation of C_3S at 1200°C. Addition of minor oxides, MgO and SO_3, particularly at 1300 °C have been claimed to have a further fluxing effect and give slightly higher C_3S content than the composition with only CaF_2 [4]. Doping with compound mineralizers, in the presence of an appropriate amount of SO_3, the cause of decline in hydraulic activity of F-containing alite phase is eliminated [5]. Introduction of 5% SO_3 (introduced as gypsum) into low LSF and high SM raw meal containing 1.6 - 10% MgO, made the clinkerization possible at 1350°C[6].

Addition of large quantities of gypsum(anhydrite) to a rawmix containing limestone and various alumina containing materials results in the production of expansive cement, which comprises C_4A_3S, alite, belite, ferrite, anhydrite and some free lime[7]. Similarly high early strength cement containing C_4A_3S, $C_{11}A_7CaF_2$, βC_2S and C_4AF has been prepared by using $CaSO_4$ and CaF_2 [8]. Utilization of C4A3S replacing C_3S in portland cement system results in saving of energies for burning, since C_4A_3S requires lower temperature for its formation.[9].

The present study is concerned with white cement, synthesized from industrial raw meal containing 4% SO_3 (as anhydrite) in lime-sludge. C_4A_3S, formed due to the presence of higher content of SO_3, has been utilized to replace a portion of C_3S at 1300 °C, that is 300 °C lower than the clinkerization temperature in the kiln. To further enhance the reactivity of raw-mix, different proportions of Fluorspar are added to it. The modifications so induced, both upon the burning behaviour as well as upon the binding properties of the resultant cement, are examined.

EXPERIMENTAL

The materials used were industrial raw-mix and Fluorspar (having 84% purity). The composition of raw-mix determined by chemical analysis is given in Table 1. Varying amounts of Fluorspar (0 to 1% as CaF_2) was added to the industrial white cement raw-mix. The resulting mixtures, after thorough mixing with 36% water were shaped in the form of nodules. After drying in oven at 100 °C, these nodules were burned in a programmable high temperature furnace (1600 °C) from 1300 °C to 1550 °C at a heating rate of 10 °C per minute. Each sample was kept at every fixed temperature for 15 and 30 minutes duration. These clinkers were allowed to cool, first in the furnace to 1280 °C and then rapidly quenched in water. The burning behaviour and the mineralogical composition were followed by chemical analysis of free lime content, XRD (by using Cu Kα source) and DTA/TG. Sufficient quantities of clinker were prepared at 1300 °C with 0.25% F.Spar) to prepare cement designated as cement 1. Physical and mechanical properties of cement 1 were compared with plant cement, designated as cement 2.

RESULTS AND DISCUSSION

1. Burnability Data

As is clear from the residual free lime contents of clinker given in Figures 1 to 5, a good clinkerization degree is obtained even at 1300 °C. Addition of 0.25% fluorspar (as CaF_2) gives 4% free lime combinability temperature as 1300 °C. This is the usual permissible limit of free lime for water quenched clinkers. The enhancement in reactivity of clinkers due to addition of Fluorspar is evident from Figures 1 to 5. The fluorspar

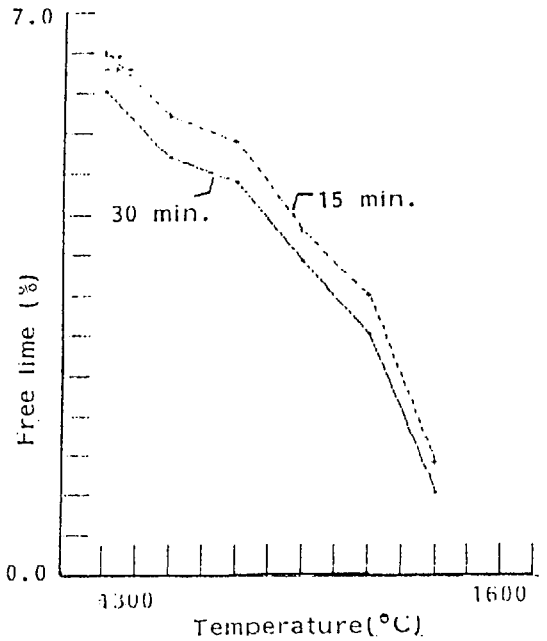

Figure 1 Free lime Vs Temperature without Fluorspar addition for different clinker residence times.

Table 1 Chemical Analysis of raw-mix (%)

lg.loss	34.31
Si02	14.53
A1203	2.60
Fe203	0.25
CaO	40.77
MgO	2.15
SO3	4.38
K20	0.12
Na20	0.09

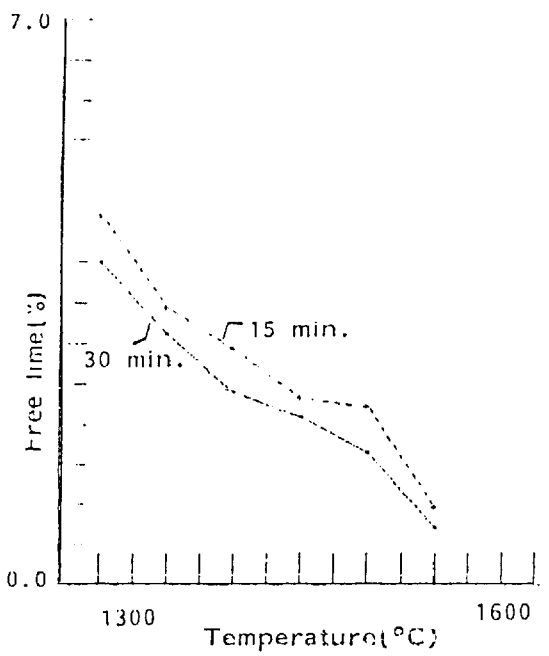

Figure 2 Free lime Vs Temperature with 0.25% Fluorspar addition for different clinker residence times.

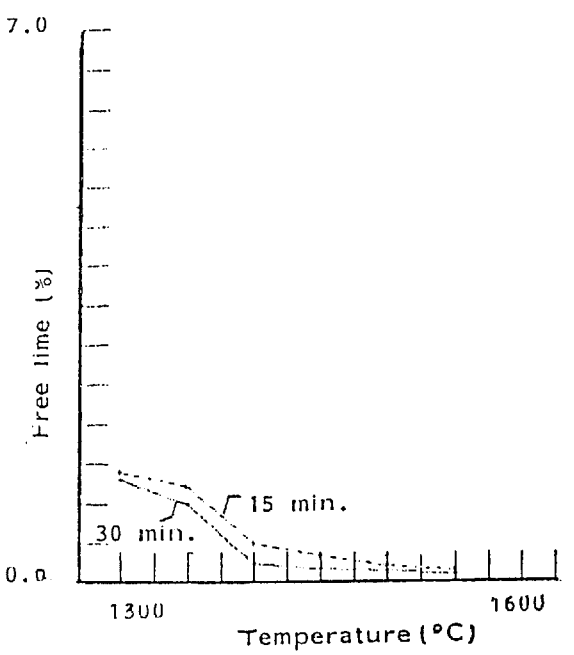

Figure 3 Free lime Vs Temperature with 0.50% Fluorspar addition for different clinker residence times.

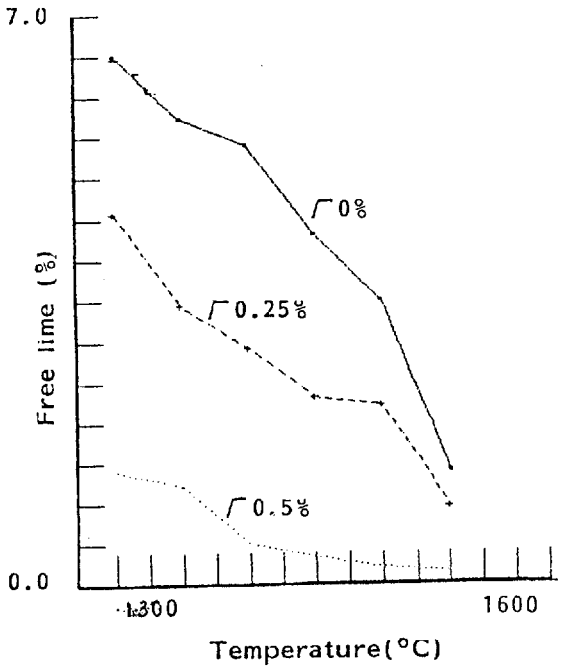

Figure 4 Free lime Vs Temperature different percentages of Fluorspar addition for clinker residence time of 15 min.

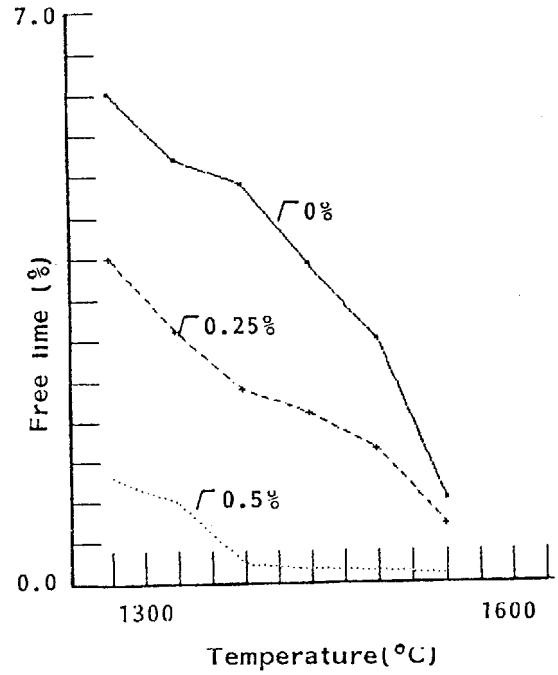

Figure 5 Free lime Vs Temperature with different percentages of Fluorspar addition for clinker residence time of 30 min.

Table 2 Compressive strength of cement 1 and 2

Type	Compressive strength (N/mm^2) 3 days	7 days
Cement 1	9.88	12.77
Cement 2	8.36	9.12

Table 3 Physical Properties of cement 1 and 2

Type	initial set (min.)	Final set (min.)	Expansion (mm)	Fineness (M^2/Kg)	Whiteness
Cement 1	155	205	5.0	420	84.0
Cement 1	160	220	2.0	440	83.3

addition, even in small proportions, lowered the clinkering temperature of C_3S and increased the speed of silicates formation. This is in agreement with the studies of M.T. Blanco et. al. [2], W.A.Klemm et. al [1], V. Johnson et. al. [10] and S. Wei et. al. [5]. The presence of SO_3 in white cement raw-mix depresses the melting point of eutectic mix T_2 for promoting the clinker formation at lower temperature as studied by D. Tong et. al [11].

ii) DTA/TG Studies

From DTA curves, as shown in Figure 6, it can be seen that presence of Fluorspar at all levels reduces further the melt and cement mineral formation temperatures. Due to the presence of SO_3 (as anhydrite) C_3S exotherm is at 1206.7 °C however, with the addition of 0.25% Fluorspar has further reduced to 1150 °C. From temperature 940 °C to onward there are successively other minor exothermic peaks that hint the formation of C_2S, C_4A_3S, $C_{11}A_7CaF_2$, C_3A etc., After 1300 °C decomposition of C_4A_3S starts and corresponding endothermic peaks with TG loss can be observed.

iii) XRD Studies

The presence of minerals C_3S, C_3A, C_4AF and C_4A_3S has been identified in the clinker burned at 1300 °C with and without flux, as shown in Figure 7. The XRD data show a strong peak at 2.16 (d value) this is attributed to the formation of C_4A_3S compound resulted as a consequence of the presence of SO_3 in the raw meal. Above 1350 °C the intensity of this peak starts diminishing due to decomposition of C_4A_3S and intensity of C_3A peak increases. This behaviour is in agreement with the findings of G, Sudoh et. al.[12] and P. Rodrigues [13]. Similarly C_3S peak is found at 1.76 (d value) and βC_2S peak at 1.966 (d value).

iv) Physical and Mechanical Properties of Cements 1 and 2

The physical and mechanical testing of cements 1 and 2 were simultaneously performed with the same set of standard conditions. The compressive strength, setting time, blain specific surface area, Le chatlier expansion together with whiteness of both the cements are given in Table 2. It is evident from the Table 2, that 3 days compressive strength on one inch mortar cube for cement 1 is 18% higher compared to cement 2. The percent increase in compressive strength between 3 and 7 days of cement 2 is 9% whereas, for cement 1 it is 29%. This shows that rate of compressive strength development is much greater for cem. 1 and is attributed to the hydration characteristics of C_4A_3S. At early age, C_4A_3S hydrates more rapidly than C_3A and the rate of this reaction remains relatively high till the depletion of this compound. The combined effect of C_4A_3S and C_3S hydration results in higher strength. The same behaviour has been reported in literature by G. Sudoh et. al [12] and I.F. Xingi et. al. [8].

The cement 1, when ground with gypsum, showed rapid set behaviour, however by adding 3% gypsum (1.26% SO_3) both initial and final set of cement 1 are comparable to setting time of cement 2 as given in Table 3. The expansion observed in case of cement 1 is 5mm, whereas, for cement 2 the expansion is 1.5mm. Whiteness of the cement made with 0.25% Fluorspar is almost the same as cement 2, this show that Fluorspar addition (0.25%) does not effect the whiteness of cement.

CONCLUSION

The present investigations have led us to the following conclusions:

1. Clinker containing alite, belite, tricalcium aluminate and sulpho-aluminate (C_4A_3S) etc., can be prepared from white raw-mix having low iron content and high silica modulus even at 1300 °C in the presence of 4% SO_3 and Fluorspar admixtures.

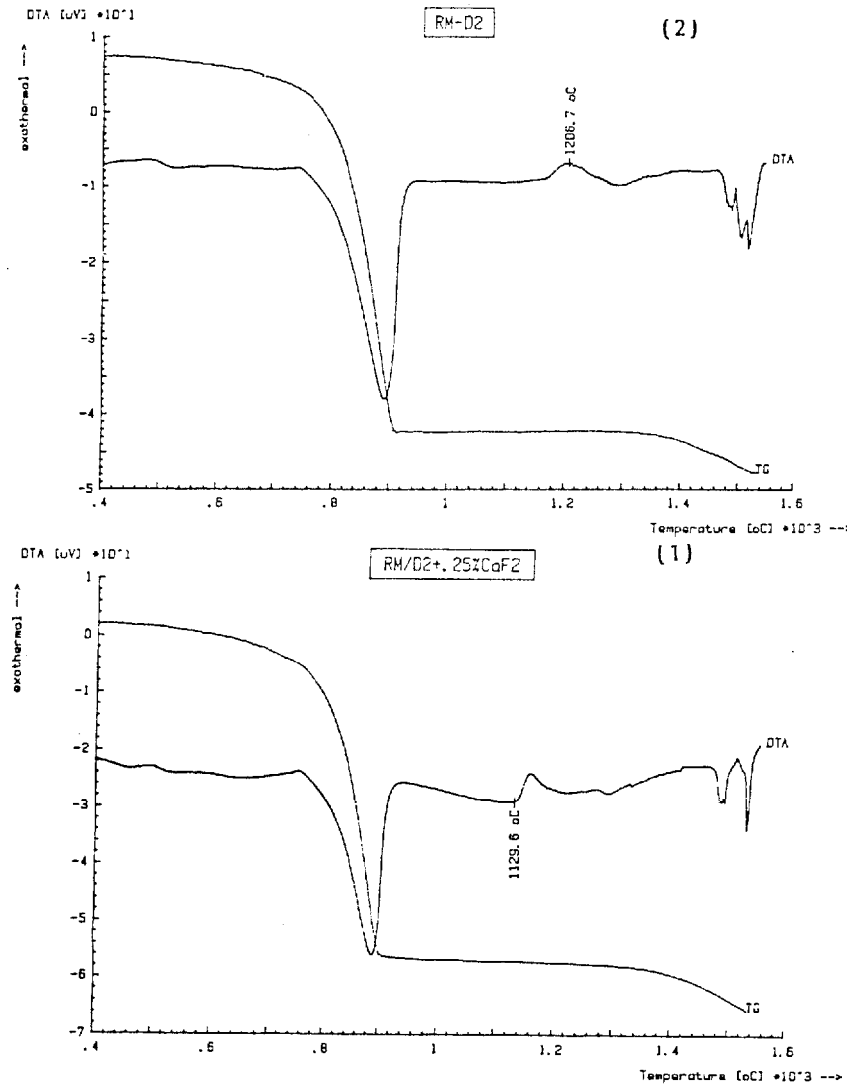

Figure 6 DTA curves for raw mix without (2) and with 0.25% Fluorspar (1) addition.

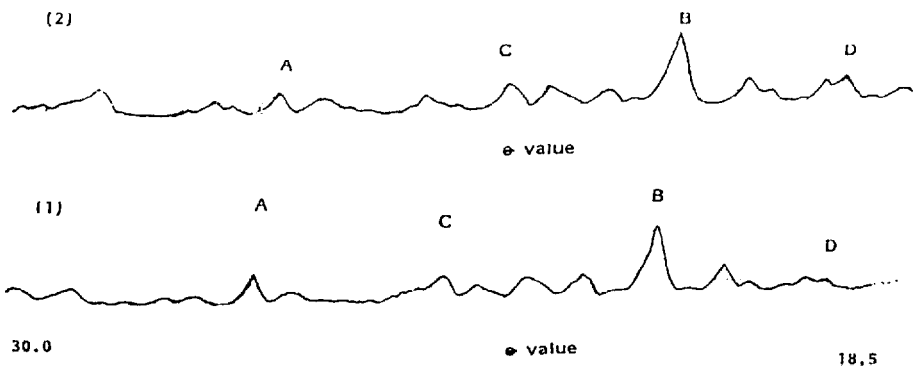

Figure 7 XRD of clinker burned at 1300 °C without (2) and with 0.25% Fluorspar (1) addition.

A = C_3S; B = C_4A_3S; C = β - C_2S; D = Free lime

2. Addition of Fluorspar to a high silica modulus raw-mix containing SO_3 (as anhydrite) increases C_3S content, intensifies the clinkerization process and lowers the burning temperature by nearly 300 °C.

3. Mechanical properties of white cement in the presence of SO_3 and Fluorspar are much better even when the burning temperatures are less.

4. SO_3 emissions from the kiln can be reduced due to the presence of C_4A_3S compound.

5. By utilizing the SO_3 of the raw-mix in clinkering process, gypsum requirements (as a set retarder) can be reduced to half.

REFERENCES

1. W. A. Klemm and J. Skalny, "Mineralizers and Fluxes in the clinkering Process," Cement Research Progress 1976. P. 256-291.

2. M.T. Balanco, A. Palomo. and T.Vazques," Effect of Fluorspar on the formation of clinker phases," Cement and Concrete Research vol. 14 1984. PP 397-406

3. George R. Gouda, "Fluxes Conserve energy in cement manufacture," Rock Products April 1980.

4. W. A. Klemm and I. Jawed, "Burnability of Industrial and Synthetic raw mixes," 7th International Congress on the chemistry of cement vol. II, 1980 PI-150-I-155.

5. S. Wei and F. Mingfen, "A study of effect of CaF^2 on the clinker doped with compound mineralizer," 8th International Congress on the chemistry of cement vol. II, P111-116.

6. I. Teoreance, M. Muntean, M. Bedq and L-Si, "Belitic Portland cements with various contents of Mgo and SO_3," 8th International Congress on chemistry of cement vol. II. P.217-222.

7. S. N. Gosh "Advance in Cement Technology, Pergamon Press, 1983.

8. I. F. Xinji, M.S.Z. Yufeng "Research on early strength cement containing high content of iron," 8th International Congress on Chemistry of Cement, vol. II, P. 286-292.

9. K. Ikeda "7th International Congress on chemistry of cement vol. II P.III -31-36.

10. V. Johansen and N. H. Christensen, "Cement and concrete Research vol 9(1). 1-6 (1979).

11. D-Tong and Z. Tin, "The Role of CaF_2 and $CaSO_4$ in cement clinkering," 8th International Congress on Chemistry of cement, vol. II P-117-121.

12. G. Sudoh et al, "High strength cement in the $CaO-Al_2O_3$ SiO_2SO_3 system and its application," 7th International Congress on Chemistry of cement vol. II.2 V. 152-157.

13. P. Rodrigues "Low Energy clinker formation," 8th International Congress on Chemistry of cement vol. VI, P-49.

INFLUENCE OF $\bar{F}$ ON CRYSTALLINE STRUCTURE OF C_3S

Shanba Wang* and Zhonghui Zhow**

*Wuhan University of Technology, Wuhan, P R CHINA
**Qingdao Cement Plant, Qingdao P R CHINA

SUMMARY

The influence of $\bar{F}$, $\bar{S}$ and $\bar{F}$+$\bar{S}$ on the crystalline structure of C_3S were studied by XRD, IR, Raman spectrometry and chemical analysis. As increasing $\bar{F}$ dissoloved in C_3S, the polymorph was changed to the rohmbic from the triclinic, the numberof spretrum bands of IR and Raman corresponding to [SiO_4] tetrahedron was decreased,the concentrations of SiO_2 in liquid phase in contact with C_3S pastes were decreased and the rate of dissolution of SiO_2 was slowed down, indicating C_3S doped with $\bar{F}$ having denser crystalline structure and higher level symmetry. This is the reason why the hydration of C_3S doped with $\bar{F}$ becomes slow at early age. There is little influence of $\bar{S}$ dissolved in C_3S on the polymorph and crystalline structure of C_3S.

摘　要

用XRD、IR、Raman光谱和化学分析等方法研究了$\bar{F}$、$\bar{S}$和$\bar{F}$+$\bar{S}$对C_3S晶体结构的影响。随着$\bar{F}$的固溶量增加，C_3S由T型向R型转变，晶体各衍射面的d值减小，IR和Raman光谱中属于[SiO_4]四面体的谱带逐渐减少，SiO_2的溶解速度和浆体液相中SiO_2的浓度降低，说明C_3S晶体变致密，对称性提高。这是含F的C_3S早期水化变慢的根本原因。$\bar{S}$的固溶对C_3S的晶型和晶体结构没有什么影响。

INTRODUCTION

Many literatures on the mineralization mechanism and the effect of CaF_2 and $CaSO_4$ on burning portland cement clinker have been published recently, but less on the influence of $\overline{F}$,$\overline{S}$ on the crystalline structure of C_3S. Ye Qing et al (1) reported that the addition of $\overline{F}$ could stablize rohmbic C_3S at room temperature and change triclinic to rohmbic, but $\overline{S}$ change rohmbic C_3S to monoclinic one. Authors (2.3) studied the effect of $\overline{F}$ on the hydration of C_3S and found that the setting time and hydration rate were ratarded at 1 day. For clarifying the reason of lower hydration rate of C_3S doped with $\overline{F}$, the crystalline structure of C_3S doped with $\overline{F}$ and with $\overline{F}$+$\overline{S}$ as well as with $\overline{S}$ were studied by XRD,IR,Raman spectrometry and chemical analysis.

EXPERIMENTS

The samples of C_3S doped with $\overline{F}$ and with $\overline{F}$+$\overline{S}$ as well as with $\overline{S}$ were prepared according to (3). The contents of CaF_2, $CaSO_4$ added and measured as well as fCaO are all listed in Table 1 and 2.

Table 1 Contents of $\overline{F}$ and f-CaO of C_3S Samples doped with $\overline{F}$

Samples	A11	A12	A14	A16
CaF_2 added, %	0.5	1.0	2.0	3.0
$\overline{F}$ measured, %	0.09	0.14	0.39	0.44
f-CaO, %	0.06	0.24	0.42	0.62

Table 2 Contents of $\overline{F}$, $\overline{S}$ and f-CaO of C_3S samples doped with F+S and with $\overline{S}$

Samples	A20	A21	A22	A24	A26
CaF_2 added, %	0	0.5	1.0	2.0	3.0
$\overline{F}$ measured, %	0	0.09	0.16	0.31	0.55
$CaSO_4$ added, %	4.93	4.93	4.93	4.93	4.93
SO_3 measured,%	2.01	1.13	0.96	0.88	1.24
f-CaO, %	1.72	0.69	0.54	0.38	0.23

The peaks of C_3S samples at 2θ =31.5-33.5° and 50.5-52.5° were recorded by XRD and the polymorphes were identified accroding to (1.4). IR and Raman spectra of C_3S samples were carried out by Nicolet 60 XRB IR spectrometer and U 1000 Raman spectrometer respectively. The concentrations of SiO_2 in liquid phase in contact with C_3S pastes(w/c=10) were determined by chemical analysis.

RESULTS

XRD Study

XRD diagrams showed that the polymorphs of C_3S doped with $\overline{F}$ and with $\overline{F}$+$\overline{S}$ were changed to rohmic from triclinic and the symmetry of crystals was changed to higher level from lower level gradually as $\overline{F}$ contents dissolved in C_3S were increased,

but there is not any influence of $\bar{S}$ on the polymorph of C_3S which still remains triclinic (Fig.1 to 2). The results are in agreement with that of Ye Qing et al (1).

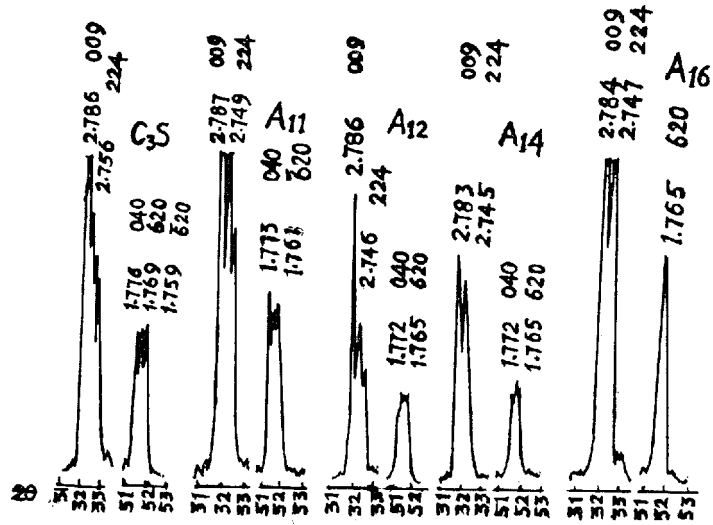

Fig.1 XRD diagrams of C_3S samples doped with $\bar{F}$

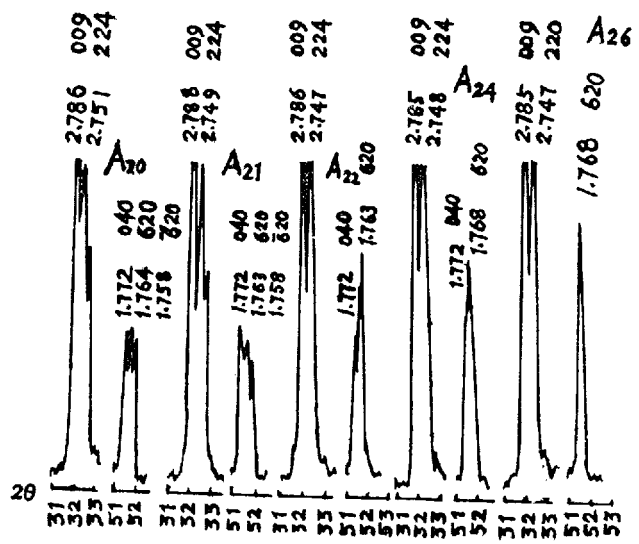

Fig.2 XRD diagrams of C_3S samples doped with $\bar{F}+\bar{S}$

The space d-value of XRD of C_3S doped with $\bar{F}$ and $\bar{F}+\bar{S}$ were decreased slightly (Fig.3), indicating C_3S doped with $\bar{F}$ having a denser crystalline sructure than pure C_3S,which coincided with our previous report of increasing induction period and setting time as well as decreasing hydration rate of C_3S doped with $\bar{F}$ at 1 day (2.3).

IR Study

V.C Farmer (5) pointed out that there were nine degrees of freedom in IR spectrum of isolated $[SiO_4]$ tetrahedron. Because of degeneration there are only four vibration modes:r_1-symmetry stretching vibration, r_2-double bending vibration, r_3-triple stretching vibration and r_4-triple bending vibration. If $[SiO_4]$ tetrahedron

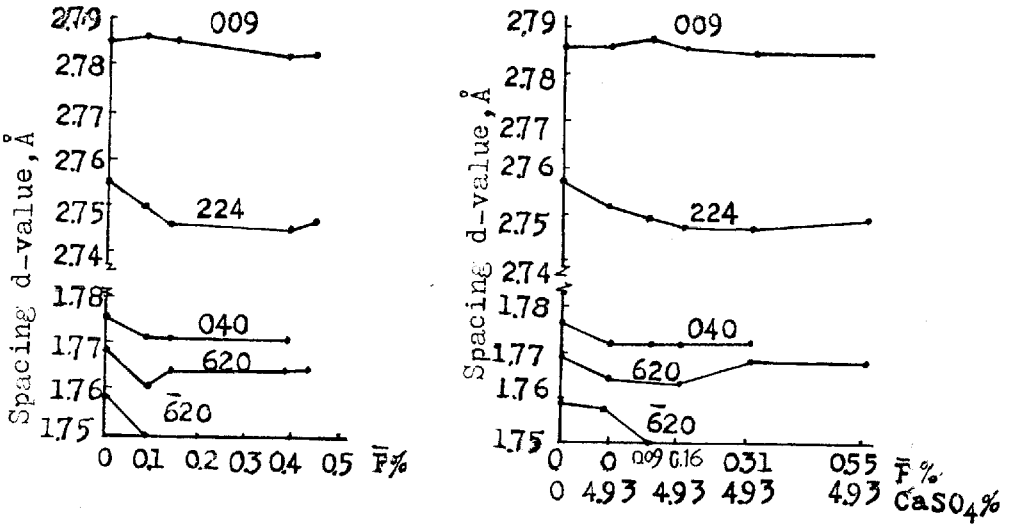

Fig.3 Variation of spacing d-values of C_3S Samples doped with $\bar{F}$ (left) and with $\bar{F}+\bar{S}$ (right)

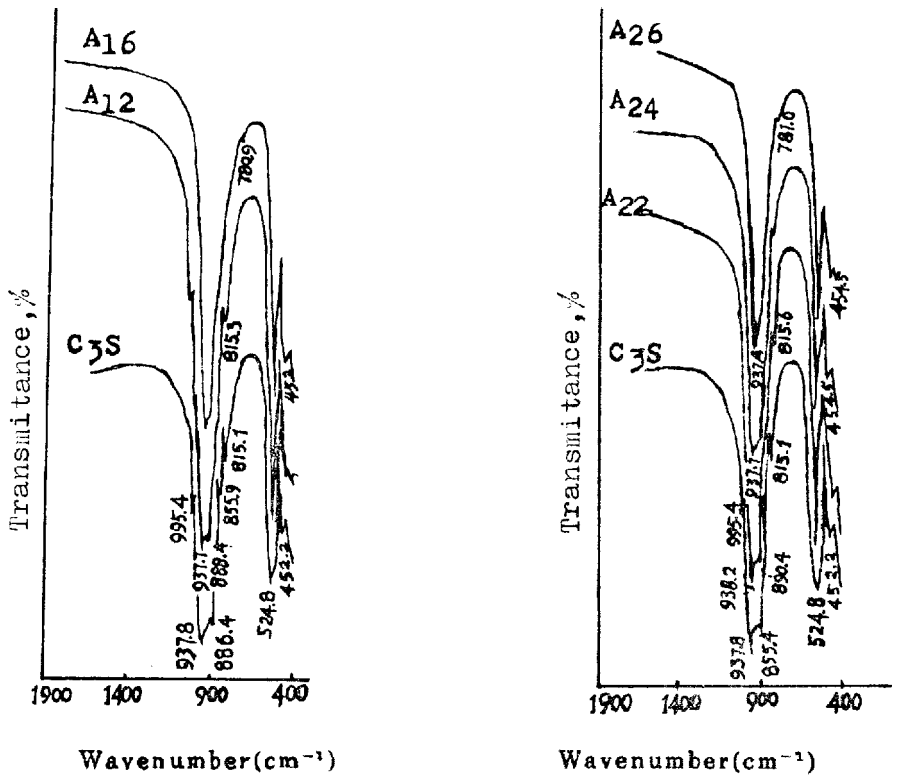

Fig.4 IR spctra of C_3S samples doped with $\bar{F}$ (left) and with $\bar{F}+\bar{S}$ (right)

is well symmetry, there are only r_3 and r_4 vibrations in IR spectrum. For actual silicate minerals, the symmetry of $[SiO_4]$ tetrahedron is disordered because of the effect of cation groups. Therefore only r_1 and r_3 vibration bands occur in IR spectrum. P.Tarte (6) pointed out: r_1=800-900cm^{-1}, r_2=300-350cm^{-1}, r_3=800-1000cm^{-1}, r_4=400-600cm^{-1}. He also considered that the less number of IR spectrum bands, the

higher level symmetry of the crystalline structure. According to M.Handke et al [7], the disappearance of some spectrum bands indicated the improvement of the symmetry of crystalline structure.

Fig.4 (left) shows IR spectra of C_3S samples doped with $\bar{F}$. In Fig.4 (left) r_1 vibtation band splits into two:815cm^{-1} and 856cm^{-1}; r_3, splits into four: 886cm^{-1}, 906cm^{-1}, 938cm^{-1} and 995cm^{-1}. As increasing $\bar{F}$ dissolved in C_3S, the intensities of r_1 bands and all r_3 bands except 937 cm^{-1} are decreased gradually and finally disappeared when the content of $\bar{F}$ dissolved in C_3S is up to 0.44% (A14 sample), which means the enhance of the symmetry of C_3S crystal. The same trends can be found from the spectra of C_3S doped with $\bar{F}$+$\bar{S}$ ($\bar{S}$ added is fixed at a constant) in Fig 4 (right). As $\bar{F}$ content in C_3S is up to 0.55% (A_{24} sample), all bands corresponding to r_3 vibration are engulfed in 937 cm^{-1} bands, again showing increase of the symmetry of C_3S crystal structure. Fig.5 shows nearly the same spectra between pure C_3S and C_3S doped with $\bar{S}$ alone, meaning no change in crystalline structure of C_3S doped with $\bar{S}$ alone. According to M.Handke et al (7),the vibration of Si-O bond depends on the arrangement of O^{2-}. These vibrations depend mainly on the movement of O^{2-}ion, and Si^{4+} is roughly considered to be at rest. The disorder of C_3S crystal lattice does not depend mainly on the superstructure of Si^{4+} but O^{2-}ion. Therefore, the arrangement of O^{2-} around Si^{4+} trends towards regularity as the content of $\bar{F}$ in C_3S is increased.

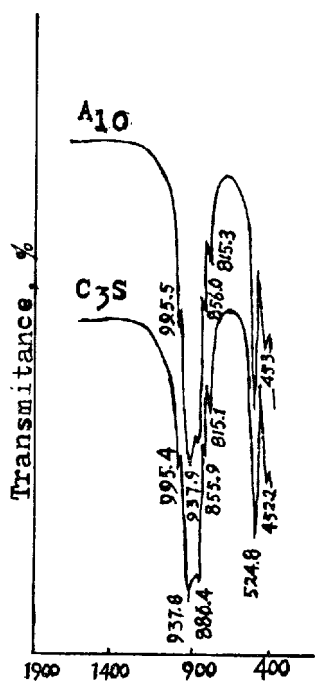

Wavenumber(cm^{-1})

Fig.5 IR spectra of pure C_3S and C_3S sample doped with $\bar{S}$

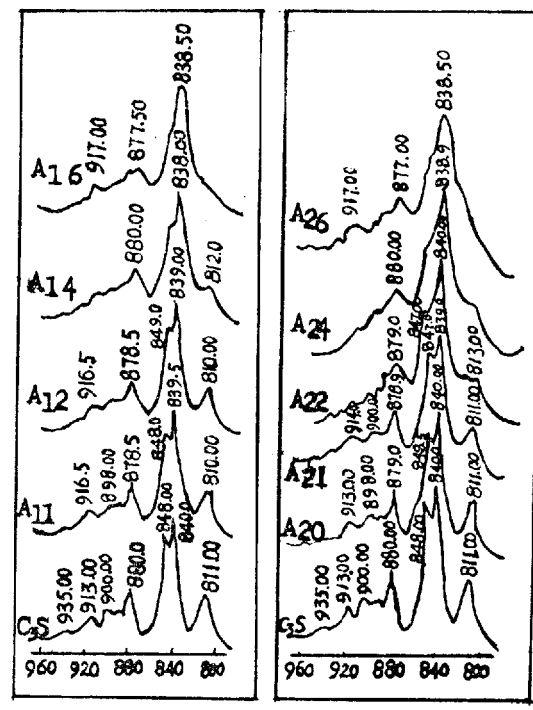

Wavenumber(cm^{-1})

Fig.6 Raman spectra of C_3S samples doped with $\bar{F}$ (left) and doped with $\bar{F}$+$\bar{S}$ (right)

Raman Study

According to the calculation of group theory, isolated [SiO_4] tetrahedron is

possessed of Td symmetry. The symmetry corresponding its various movements is $A_1+E+F_1+3F_2$, in which F_1 and F_2 are corresponding to rotation and pallara movements respectively, and actual vibration is A_1+E+2F_2. Comparing with pure C_3S, only the bands belong to A_1 vibration were changed in C_3S doped with $\bar{F}$, therefore, A_1 vibration is discussed only. Based on the calculation of factor group, there are three bands of A_1 stretching vibration in $[SiO_4]$ tetrahedron,but there are six bands ranged over 800-900 cm^{-1} for pure C_3S, this means that the disorder is occurred in $[SiO_4]$ groups of pure C_3S,and the symmery of $[SiO_4]$ have been changed to C_3V from Td. We can find from Fig.6 that there is not any change in Raman spectra of C_3S doped with $\bar{S}$ alone compared with that of pure C_3S, again indicating little effect of $\bar{S}$ dissolved on the symmetry and crystalline structure of C_3S doped with $\bar{S}$ alone, which is in agreement with the results of XRD and IR.Fig.6 also shows that as increasing $\bar{F}$ dissolved in C_3S whether doped with $\bar{F}$ or $\bar{F}+\bar{S}$, the intensities of 811 cm^{-1} and 900cm^{-1} bands of Raman spectrum were decreased. As the content of $\bar{F}$ dissolved in C_3S up to 0.44%.(for C_3S doped with $\bar{F}$ alone) and 0.55% (for C_3S doped with $\bar{F}+\bar{S}$), both bands of 811 cm^{-1} and 900cm^{-1} are basically disappeared; the intensities of 890cm^{-1} and 848 cm^{-1} bands are also decreasing with increase of $\bar{F}$ in C_3S and finally engulfed in 880cm^{-1} and 840cm^{-1} bands.These results indicate that the degeneracy of Si-O bond vibration in C_3S is increased and the arrangement of O^{2-} coordinated with Si^{4+} trends towards regularity and the symmetry of $[SiO_4]$ tetrahedron is improved with increase of $\bar{F}$ in C_3S.

Study of Chemical Analysis

The improvement of symmetry of $[SiO_4]$ tetrahedron also can be proved from the results of analyzing liquid phase in contact with C_3S doped with $\bar{F}$ and with $\bar{F}+\bar{S}$, showed in Fig.7. The content and rate of SiO_2 solved in liquid phase is decreasing with the increase of $\bar{F}$ dissolved in C_3S whether doped with $\bar{S}$ or not. We had reported previously (3) that as increasing $\bar{F}$ dissolved in C_3S, the heat evolution rate, chemical bound water and the strength at 1 day were decreased and the occurrance of maximum concentrations of Ca^{2+} and OH^- in liquid phase were delayed.The more $\bar{F}$ contents dissolved in C_3S, the more results above. The reason is of improving the symmetry of $[SiO_4]$ terahedron in C_3S crystal by $\bar{F}$ solutioned in C_3S.

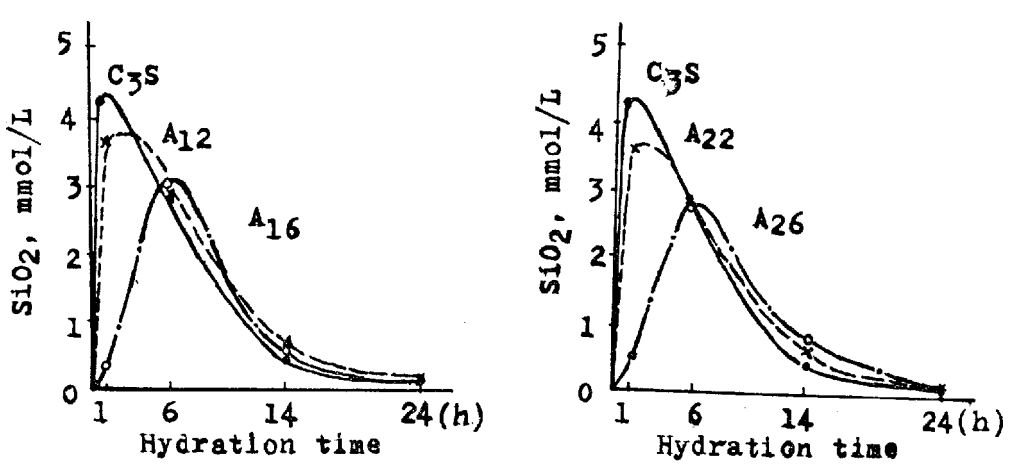

Fig.7 SiO_2 concentrations in the liquid phases in contact with C_3S samples doped with $\bar{F}$ (left) and with $\bar{F}+\bar{S}$ (right)

CONCLUSIONS

Solution of $\bar{F}$ in C_3S improves the symmetry and densification of crystalline structure of C_3S as well as changes the polymorph of C_3S to rhombic from triclinic.

Solution of $\bar{F}$ in C_3S improves the symmetry of $[SiO_4]$ terahedron in C_3S crystal and regularizes the arrangement of O^{2-} coordinated with Si^{4+}.

Solid solution of $\bar{F}$ in C_3S decreases the solubility and concentration of SiO_2 in liquid phase in contact with C_3S paste.

It is the improvement of symmetry and densification of crystal as well as the improvement of symmetry of $[SiO_4]$ in C_3S by solid solution of $\bar{F}$ in C_3S that slows down the hydration rate of C_3S doped with F at early age.

There is little effect of $\bar{S}$ dissolved in C_3S on the polymorph and crystalline structure of C_3S.

REFERENCE

1. Ye Qing, Liu Baoyuan and Xue Jungan: "Crystal Chemistry study of the Solid Solutions of Tricalcium Silicate Containing $\bar{F}$ and $\bar{S}$" Journal of Chinese Ceramic Society, 1989, 17(1), 97-104.

2. Shanba Wang and Wuchang Ding: "Abnormal setting of Portland Cement Doped with CaF_2", Journal of the Chinese Ceramic Society, 1988, 16(4), 304-311.

3. Shanba Wang and Zhonghui Zhow:"Hydration of C_3S Doped CaF_2", Journal of the Chinese Ceramic Society, 1991, 19(4), 318-313.

4. Liu Baoyuan and Xue Jungan:"Effect of CaF_2, $CaSO_4$ Compound Mineralizer on Portland Cement Clinker", Journal of Chinese Ceramic Society, 1984, 12(4), 429-440.

5. V.C.Farmer, "The Infrared Spectra of Minerals" (in chinese), Scientific Publishing House, Beijing, 1982, P227, 49.

6. P.Tarte:"Infrared study of Orthosilicates and Orthogermants", Spectrochimica acta, 1962, Vol.18 467-483.

7. M.Handke, CZ.Paluszkiewicz, and G.Siemiuska:"Spectroscopic Studies of Ca_3SiO_5 Poly-morphism", 7th International Congress on the Chemistry of Cement, Paris, 1980, Vol.1, 21-27.

EFFECT OF FLUORINE-BEARING LIMESTONE ON CLINKER QUALITY

G Goswami, B N Mohapatra and J D Panda

Dalmia Institute of Scientific and Industrial Research
Rajgangpur, INDIA

SUMMARY

The effect of inherent fluorine on clinker mineralogy and cement properties was investigated by incorporating fluorine-bearing limestone in the cement raw-mixes. Clinkers with 0.01 to 0.12% F were produced by sintering the raw-mixes in a pre-calciner kiln and in a laboratory rotary kiln. It is found that with the increase of F content in the clinkers, C3S increases and C3A decreases noticeably. Setting time and early strength of the cement invariably increase with the increase of F. But the strength development from 3-days to 28-days falls when F content reaches 0.12%. It is observed that the effect of inherent fluorine occurring in the form of fluosilicate is more intensive than that of the similar amount of fluorine from external source.

INTRODUCTION

Application of fluorine in cement manufacturing process, both as mineralizer and flux is widely known and a number of studies on its effect on cement properties have been reported. The mean concentration of fluorine in cement raw mix is reported to be only 0.05 % (1) and hence, even the optimum requirement is as low as 0.25 % (2) normally fluorine is added to the normal raw mix in the form of an external source. In our previous investigations (3,4) it was found that cement raw mixes, incorporating the limestone of a particular deposit, having identical chemical and granulometric compostions showed differnces in their burnability, because of the variations in contents of the mineral phlogopite, $K\ Mg_3(Si_3\ AlO_{10})\ (FOH)_2$. Further analyses of a large number of limestone samples from the deposit show that fluorine content ranges from 0.03 to 0.32 % with an averege of about 0.115% and occurs in the form of the mineral phlogopite. In the present investigation, the effect of these fluorine-bearing limestones on the clinker quality and subsequently on cement properties has been examined.

MATERIALS AND PROCEDURES

An industrial and a laboratory prepared raw-mixes incorporating fluorine-bearing limestones from a particular deposit were taken as the base materials. Fluorine contents of the industrial and laboratory raw mixes were 0.11 and 0.04 % respectively (Table-1). Different doses of fluorine were added to the laboratory mix to produce clinkers of variable F contents. The raw mixes were sintered in a laboratory rotary kiln of 2 kg/hour capacity and the clinkers thus produced were taken for comparative study.

Table - 1

Chemical compositions (Wt.%) of the cemnent raw mixes

Components	Raw mixes Industrial	Laboratory
F	0.11	0.04
SiO_2	11.3	12.18
Al_2O_3	2.49	3.01
Fe_2O_3	2.30	2.07
CaO	44.6	44.82
MgO	3.29	1.42
K_2O	0.55	0.54
L O I	35.3	35.85

Mineralogy of the clinkers was examined by X-Ray Diffractometry (XRD), using Ni-filtered Cu-K_α radiation at 40 KV,20 mA. Clinker phases were estimated by Quantitative X-Ray Diffractometry (QXRD). Silicon was used as internal standard and estimations of C_3S,C_2S, C_3A, C_4AF and periclase were made at 2.957, 2.87, 2.70, 2.63 and 2.11 A respectively. Free CaO in the clinker was estimated according to IS:4032 - 1985.

Ordinary Portland Cements (OPC) were prepared incorporating the clinkers produced with identical gypsum content and fineness and then cement properties, including setting time, compressive strength (CCS) and soundness were determined following IS:4031-1988.

RESULTS

Industrial Raw Mix

Chemical compositions of the low and high fluorine-bearing clinkers (designated Clinker-I and Clinker-II respectively) produced from the industrial raw-mix are found to be identical except in their volatile contents (Table-2).Phase analyses, both potential (Bogue) and QXRD values, of the two clinkers are noted in Table-3.

It is found that in general QXRD values for C_3S are higher and those for C_2S and C_3A are lower than the potential phase contents. Although potential phases of the two clinkers are almost identical, QXRD shows that actual phase contents of the two clinkers are quite different. The most distinguishable difference between the two clinker is in their C_3A contents. C_3A in the clinker - I is double that of the clinker - II , which is clearly reflected in the XRD patterns (Cu-K_α) Fig.1. Further, C_3S and C_2S contents in the clinker - II are respectively higher and lower than those in the clinker-I.

Table-2

Volatile contents (Wt.%) of the clinkers produced from the Industrial raw mix.

	Clinker	
Components	I	II
F	0.01	0.12
K_2O	0.26	0.60

TABLE-3

Phase analysis (Wt.%) of the Clinker - I (F=0.01 %) and Clinker - II (F = 0.12 %) produced from the same raw mix.

Clinker	C_3S	C_2S	C_3A	C_4AF	Periclase	Free CaO *
I. (Bogue)	55.9	16.9	8.34	12.17		2.2
(QXRD)	69	12	4	11	1.5	
II. (Bogue)	54.7	18.1	7.7	12.8		1.6
(QXRD)	74	11	2	10	1.5	

* Chemically estimated

Physical properties of the OPC incorporating the clinker - I and II are shown in Table-4. It is found that in identical fineness, the cement containing the clinker - II shows longer setting times, higher 3- and 7-days strength and lower 28- days strength than the cement containing the clinker - I. However, Le-chatelier and Autoclave expansions of both the cements are almost identical.

Laboratory Raw Mix

Fluorine contents retained in the laboratory clinkers produced from the laboratory raw mixes of different doses of fluorine additions were found to be 0.01, 0.04 and 0.09%. The most remarkable effect of F on the mineralization of the clinkers is observed on their C_3S contents (Fig.2). It is found that with the increase of F content, C_3S ($2\theta = 30.2$) content increases and C_2S ($2\theta = 31.1$) content decreases. However, C_3A content does not seem to be much affected.

Physical properties of the OPC containing laboratory clinkers with different amounts of F are shown in Table-5. It is found that with the increase of fluorine content, both setting time and strength in all days increase. But Le-Chatelier and Autoclave expansions remain almost identical.

DISCUSSION

Chemical compositions of clinkers produced from the same industrial raw mix are identical except in their volatile contents, and accordingly their potential clinker phases are also identical (Table-3). However, their actual phase contents as determined by QXRD differ significantly. The clinker - II with higher F is characterized by lower C_3A and higher C_3S contents. In general, clinkers produced from the limestones of the investigated deposit are found to contain higher C_3S and lower C_3A than the respective potential phases and this is caused due to the combined effect of F and MgO (5). In the two examined clinkers, MgO contents are equal and hence any further decrease in C_3A or increase in C_3S can be caused by F only. The clinker - II contains higher K_2O than the clinker - I. But increase in alkali does not change the C_3A content substantialy, particularly when S/R is around 2.4 (6). Thus the difference in mineralogy of the two clinkers is attributed to the F content, which is in accordance with the earlier researches (7-10).

The difference in physical properties of the two cements incorporating clinkers with different F % (Table-4) can be explained by their differences in C_3A and C_3S contents. Higher early strength of the OPC - II is mainly due to its higher C_3S content. After 7- days, the rate of strength development in the OPC - II was lower than that of the OPC - I which might be due to lower amount of C_2S in the clinker - II. Although alkali content is also known to reduce the later strength (8), in the examined cement with 0.60 % K_2O, the effect may not be significant. On the other hand as F is found to have more bearing on the phase assemblage of the clinker, conceivably its effect on the cement properties is more conspicuous.

In the OPC prepared from the clinkers produced from the laboratory raw mix also, cement properties are found to vary with F content (Table- 5). Both setting time and strength are found to increase with the increase of F content. The clinker with 0.09 % F produces 3- days strength much higher than the other two clinkers. This is because of its higher C_3S (Fig.2)-formed due to its higher F content-than that of the other two clinkers. Its strength enhancement over the clinker with 0.01% F is less at 28 days than at 7 days. This shows that with increase of F , its positive effect on 28- days strength decreases. However, the strength of the OPC with 0.09 % F at 28 days is still higher than that produced by the clinker with 0.01% F.

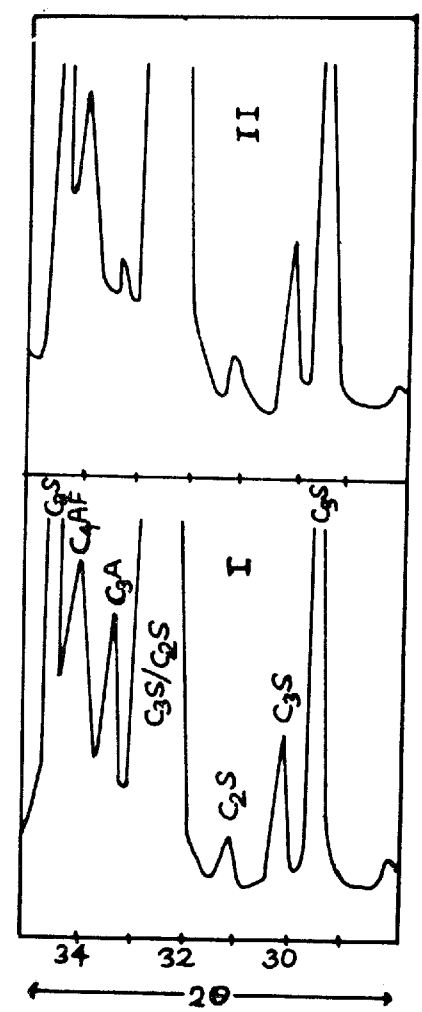

Fig.1 XRD patterns (Cu-K_α) of clinkers produced from the industrial raw mix,
(i) Clinker-I, F = 0.01%,
(ii) Clinker-II, F = 0.12 %

Table-4

Cement properties of the OPC containing clinker I and II produced from the same raw mix.

		OPC I	OPC II
1.	% F in clinker	0.01	0.12
2.	Fineness Sp.Surface (cm^2/ gm)		
	Blaine	2952	2962
3.	Setting time (minutes)		
	Initial	150	175 (117)*
	Final	210	232 (110)
4.	Compressive strength (kg /cm^2)		
	3 days	230	282 (123)
	7 days	305	315 (103)
	28 days	412	354 (86)
5.	Soundness (Expansion)		
5.1	Le-Chatelier (mm)	2.0	2.0
5.2	Autoclave (%)	0.15	0.25

* Figures within parentheses denote values as percentage of the OPC I.

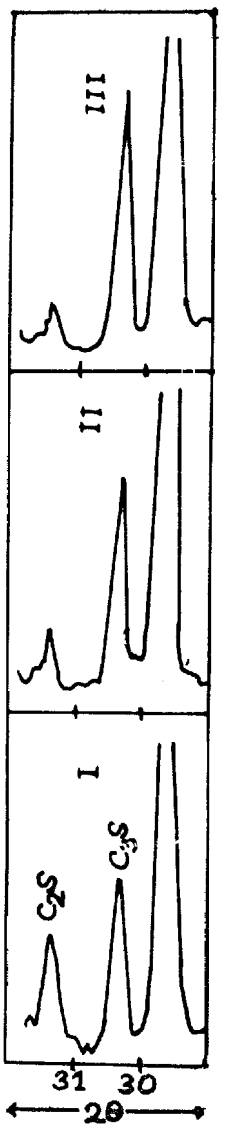

Fig.2 XRD patterns (Cu-K_α) of clinkers produced from laboratory raw mix, (I) F = 0.01 %, (II) F = 0.04 %, (III) F = 0.09 %.

Comparing the properties of the cements produced from the industrial and laboratory raw mixes (Table 4 & 5), it is found that the general trend of change of cement properties is more or less similar in both the cases viz. setting time and early strength increase with the increase of F content with no noticeable effect on autoclave and Le-chatelier expansions. However from the trend of strength developments at 7- and 28-days of the OPC - II (Table-4) and of the OPC, L - III (Table-5), it is conceivable that the effect of F is more pronounced in the former containing inherent F than in the latter with the addition of CaF_2. Although optimum fluorine in clinker is reported to be 0.25 % (2) and application of it even up to 0.33 % with positive effect on 28- days

Table-5

Cement properties of OPC containing clinkers produced from raw mixes with addition of different amounts of F .

	OPC, L-I	OPC, L-II	OPC, L-III
1. % F			
1.1 In the raw mix	0.04 *	0.54	2.04
1.2 Retained in the clinker	0.01	0.04	0.09
2. Cement fineness Sp. surface (cm^2 /gm) Blaine	2963	2905	2952
3. Setting time (minutes)			
Initial	156	172 (110)**	195 (125)
Final	211	227 (108)	260 (123)
4. Compressive strength (kg / cm^2)			
3 days	218	222 (102)	265 (122)
7 days	247	289 (117)	362 (147)
28 days	362	381 (105)	450 (124)
5. Soundness			
5.1 Le-Chatelier expansion (mm)	1	1	1
5.2 Autoclave expansion (%)	0.12	0.12	0.11

* Inherent

** Figures within parentheses denote value as percentage of the L - I.

strength is claimed (12), in the present study, even 0.12 % F from the inherent source is found to affect the 28- days strength. In the investigated limestone, fluorine is present in the form of fluosilicate (4) and the added F to the laboratory raw mix is in the form of CaF_2. It has been reported that fluosilicate proves to be more efficient mineralizer than CaF_2 (7). It is also found that at a temperature 1100 deg. C, emmission of F from the examined limestone, where F occurs in the form of fluosilicate, is much less than that from added CaF_2 and hence at the clinkering temperature, the effect of inherent F naturally becomes more conspicuous than that of the added F .

CONCLUSION

F occurring in the limestone in the form of fluosilicate has got more intensive effect on cement properties, particularly on 28- days strength than the F added to the raw mix. The tolerable limit of the inherently generated F in the clinker is found to be even lower than 0.25 %, which is reported to be optimum F in the normal clinkers (2).

REFERENCES

1. Bucchi.R.: "Influence of the nature and preparation of raw materials on the reactivity of the raw mix", Int. Cong. Chem. of Cement,7th Paris, 1980, Vol. I - 1/3.

2. Moir, G.K.: "Mineralised high alite cement",World Cement 1982, 13 (10) 374-382.

3. Goswami, G., and Panda, J.D.: "Application of microscopy, XRD and DTA in study of cement raw mix burnability", Int. Conf. on Cement Microscopy, 7th Texas, 1985, 81-96.

4. Goswami, G., Mohapatra, B.N. and Panda J.D.: "Effect of fluosilicate on cement raw mix burnability and kiln build-up", Zem-Kalk-Gips,1991, 44(12), 634-37.

5. Goswami, G., Mohapatra, B., and Chatterjee, S.: " Phase formation during sintering of a magnesium and fluorine containing raw mix in a cement rotary kiln",Zem-Kalk-Gips. 1990,43 (5), 253-56.

6. Strunge, J., Knofel, D and Dreizler, I.: "Influence of alkalis and sulphur on the properties of cement, Part IV comprehensive survey", Zem-Kalk-Gips, 1990 ,43 (4) 199-208 .

7. Lea, F.M.: "The chemistry of cement and concrete", 3rd Ed. London Edward Arnold, 1970, 157 P.

8. Odler, I and Abdul-Maula, S.: "Structure and properties of Portland cement clinker doped with CaF ", J. Am. Ceram. Soc.,1980, 63 (11-12), 654-59.

9. Perez. Mendez, M., Trivino Vazquez,F., and Vazquez Moreno, T.: "Effect of fluorine on extracted phases from Portland Cement Clinker", Tonind. Ztg, 1980, 110 (4), 236-42.

10. Wei, S. and Mingfen, F.: "A Study on the effect of CaF on the clinker doped with compound mineralizer", Int. Cong. Chem. of Cement, 8th, Brazil, 1986, Vol.II, 111-16.

11. Page, C.H. and Ghosh, D.: "High strength cement manufacture with mineraliser - A case study", NCB Int. Seminar on Cement and Building Materials, 1st, New Delhi, India, 1987, Vol.3. VI 35-41.

THE EFFECT OF ZnO ON BURNING OF PORTLAND CEMENT CLINKER IN RAPID HEATING-UP BURNING

Xu Guanglang, Huang Wenxi, Lu Zhongyuan and Qian Guangren

Sichuan Institute of Building Materials, Mianyang, Sichuan, P R CHINA

ABSTRACT

The effect of ZnO-doping on the burnability of portland cement clinker has been studied. The burnability of a raw meal has been remarkably improved when a suitable content of ZnO-doping is used in rapid heating-up burning. When 1.5% ZnO is added, the activation energy of clinker formation is reduced. The kinetics of clinker formation is diffusively controlled

本文研究了掺ZnO及快烧条件下波特兰水泥熟料煅烧的易烧性和熟料形成动力学. 结果表明: 少量ZnO 可显著改善生料的易烧性. 掺加ZnO 1.50%, 熟料形成活化能可降低139%. 熟料形成动力学由扩散机制控制.

INTRODUCTION

Cement industry is one of the major energy consuming industries. In cement manufacture, heat consumption comprises 70-80% of the total energy consumption. Therefore, decreasing the sintering temperature of clinker has been attracting increasing attention in the cement circle of various countries.

The use of mineralizers is one of the effective ways to decrease the sintering temperature of clinker. In the 1970s, studies on the mineralizer ZnO were started. D. Knoefel [1], T. Tsuboi [2], I. Odler [3], R. E. Moole [4] et al thought that ZnO was an effective mineralizer and fluxing agent. Adding 1.0% and 3.0% ZnO in raw meal could decrease sintering temperature by 50℃ and 100℃. D. Knoefel, T. Tsuboi and K. Akatsu [5] et al discovered that ZnO was taken up in the interstitial phase preferentially, one half of the ZnO content in clinker entering into the silicate phase (mainly in alite), while the other half entered into the interstitial phase (mainly in ferrite phase). H. Hornain [6] reported that the ratios of mass percentage inthe different phases were Belite : Aluminate: Alite : Aluminoferrile = 1 : 4 : 8 : 17.

Burning with rapid heating-up is a new cement burning technology, which can decrease sintering temperature of clinker by about 150℃ [7]. Meanwhile together with the rapid heating-up burning technology, ZnO adde to the raw meal as mineralizer, can further decrease sintering temperature of clinker. In this paper, the effect of ZnO-doping on the burnablity of portland cement clinker in rapid heating- up burning has been studied. A kinetic model, equation and activation energy for the clinker formation have been developed. Also, the morphology of clinker minerals and the behavior of solid solution of ZnO existing in the mineral phases have been investiged.

BURNABILITY OF CLINKER

Raw meal was prepared from industrial raw materials : KH=0.94, SM=1.74, IM=1.31. The chemical compositions of the raw meal are shown in Table 1. Different amounts of ZnO were added to the raw meal. The raw meal was heated up to 1200℃, 1250℃, 1300℃ and 1320℃at a rate above 800℃/min and burnt for 30 min. The f-CaO content at various conditions are shown in Table 2 and Fig. 1

Table 1 Chemical composition of raw meal

Loss	SiO_2	Fe_2O_3	Al_2O_3	CaO	MgO	Totel
34.56	12.87	3.20	4.19	41.91	0.79	96.08

Table 2 The relation of f-CaO on ZnO-doping and temperature in rapid heating-up burning

t, ℃	ZnO, wt%						
	0	0.50	1.00	1.50	2.00	2.50	3.00
1200	17.79	11.00	9.79	9.33	8.38	7.34	7.19
1250	14.01	3.39	2.41	2.23	2.05	1.84	1.71
1300	3.09	1.54	1.12	0.81	0.63	0.41	0.17
1320	1.61	/	/	/	/	/	/

Table 2 and Fig. 1 show that in rapid heating-up burning, adding 0.50%ZnO can remarkably decrease f- CaO. As the amount of ZnO is added to increase from 0.50% to 3.00%, f-CaO slowly decrease further. The raw meal can be clinkered at 1250℃ (f-CaO <2.00%), when ZnO content equal or more than 2%, while the raw meal without ZnO-doping can be clinkered at 1320℃ only. Thus, it can be seen that ZnO- doping can lower the sintering temperature of clinker by about 70℃ in rapid heating-up burning .

CLINKER FORMATION KLINKERS

1. The kinetic model

The kinetics of clinker formation is very complicated, being influenced by many factors. The possible controlling mechanisms and the corresponding kinetic equations are shown in Table 3 . The equations in Table 3 can be given :

$$fn(\alpha) = Kn(t) \qquad (n = 1, 2 \ldots\ldots 15) \qquad (1)$$

Where α is the reaction ratio
t is the reaction time (min)
Kn is the kinetic constant
Equation (1) can be written as :

$$fn(\alpha) = i + Kn(t) \qquad (n = 1, 2 \ldots\ldots 15) \qquad (2)$$

Where i is intercept

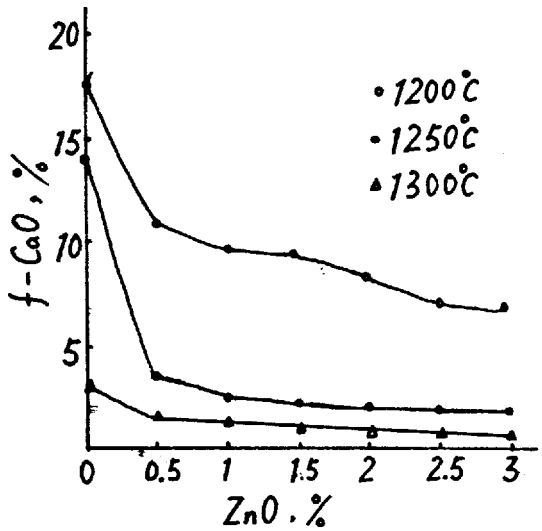

Fig. 1 The relation of f-CaO on factors of ZnO and temperature in rapid heating-up burning

Table 3 Possible controlling mechanisms and kinetic equations of clinker formation[8]

Controlling mechanism	Kinetic equation
Diffusion	$f_1(\alpha) = \alpha^2 = K_1 t$ $f_2(\alpha) = (1-\alpha)\ln(1-\alpha) + \alpha = K_2 t$ $f_3(\alpha) = [1-(1-\alpha)^{1/3}]^2 = K_3 t$ $f_4(\alpha) = 1-2/3\alpha - (1-\alpha)^{2/3} = K_4 t$
Interface chemical reaction	$f_5(\alpha) = -\ln(1-\alpha) = K_5 t$ $f_6(\alpha) = 1-(1-\alpha)^{1/2} = K_6 t$ $f_7(\alpha) = 1-(1-\alpha)^{1/3} = K_7 t$ $f_8(\alpha) = \alpha = K_8 t$
Nucleation and growth of crystal	$f_9(\alpha) = [-\ln(1-\alpha)]^{1/3} = K_9 t$ $f_{10}(\alpha) = [-\ln(1-\alpha)]^{1/4} = K_{10} t$ $f_{11}(\alpha) = [-\ln(1-\alpha)]^{1/2} = K_{11} t$ $f_{12}(\alpha) = [-\ln(1-\alpha)]^{2/3} = K_{12} t$ $f_{13}(\alpha) = [-\ln(1-\alpha)]^{2/5} = K_{13} t$ $f_{14}(\alpha) = f_5(\alpha) = -\ln(1-\alpha) = K_{14} t = K_5 t$ $f_{15}(\alpha) = [-\ln(1-\alpha)]^2 = K_{15} t$

Put the reaction ratios of clinker formation for various time at one particular temperature into the equation (2), make a fit in a computer. If results from fitting show that the coefficient of correlation RF is bigger, the standard variance D_s is smallest, the intercept i is also smallest (for a perfect fitting RF=1, D_s, i=0), it can be considered that the reaction of clinker formation is controlled by that mechanism which the equation represents. From a know ledge of the range of RF, D_s, i, it can be determined as to which kind of mechanism controlls clinker formation reaction and fitted with be right kind of kinetic equation. Meanwhile, the rate constant K of the clinker formation reaction at this temperature is obtained. In the same way, the rate constants at other temperature can be calculated. On the basis of Arrhenius' s formula:

$$K = A\exp(-E/RT) \qquad (3)$$

Where E is the activation energy of reaction (J/mol) R is the molar constant of gas
T is the temperature (K) A is frequrncy factor
K is rate constant
the activation energy of the reaction of clinker formation can be acquired.

2. Experiment and results

Raw meals without ZnO-doping and with 1.5% ZnO-doping were heated rapidly up to 1260-1300℃ and burnt for 3-30 min, the f-CaO content and the loss were measured. The reaction ratios of clinker formation were calculated and the results aree shown in Tables 4 and 5.

Table 4 Reaction ratios α of clinker without ZnO-doping

Temp., ℃	Time, min. 3	5	10	20	30
1260	0.6597	0.7130	0.7388	0.7544	0.7688
1270	0.7007	0.7250	0.7578	0.7672	0.7755
1280	0.7298	0.7428	0.7612	0.7701	0.7804
1290	0.7408	0.7572	0.7806	0.7806	0.7872
1300	0.7514	0.7716	0.7852	0.7967	0.8009

Table 5 Reaction ratios α of clinker with 1.5% ZnO-doping

Temp., ℃	Time, min 3	5	10	20	30
1260	0.8027	0.8587	0.8671	0.8976	0.9071
1270	0.8540	0.8697	0.8880	0.9051	0.9345
1280	0.8632	0.8812	0.9150	0.9174	0.9454
1290	0.8762	0.8975	0.8992	0.9924	0.9571
1300	0.9039	0.9282	0.9398	0.9477	0.9570

Sabstituting the data in Tables 4 and 5 into equation (2), the results from fitting in a computer are shown in Tables 6 and 7.

Table 6 Mechanism and rate constant of formation reaction without ZnO-doping

Temp., ℃	1260	1270	1280	1290	1300
Mechanism and kinetic equation	Diffusion-controlled, Ginsting-Brunshtein of triaxial diffusion $1-2/3\alpha-(1-\alpha)^{2/3}=Kt$ (spherical model)				
RF	0.982	0.981	0.976	0.978	0.979
$D2\times10^{8}$	5.393	6.795	8.303	9.127	9.976
$i\times10^{8}$	1.546	1.742	1.930	2.024	2.116
$K\times10^{4}$	6.731	7.172	7.632	8.121	8.634

The activation energies of clinker formation reaction withaut and with ZnO- doping are obtained by substituting the data in Tables 6 and 7 respectively into equation (3). Table 8

3. Discussion

It is known from Tables 6 and 7 that in rapid heating- up burning, the clinker formation reaction without ZnO-doping and with 1.5% ZnO-doping are all controlled by diffusion, and satisfy the Ginstling-Brunshtein equation (RF>0.97, D_B, i is all in 10^{-8} level), gives the values obstained.

It can be seen from Table 8 that the activation energies of clinker formation reaction without ZnO-doping and with 1.5 % ZnO-doping are respectively 124.09 KJ/mol and 52.12 KJ/mol, the activation energy of the formation of the clinker with 1.5% ZnO-doping decreases by 139% as compared to that without ZnO-doping. It is believed that adding ZnO can accelerate the absorption of f-CaO, and promote the formation of clinker. This

Table 7 Mechanism and rate constant of formation reaction with 1.5% ZnO-doping

Temp., ℃	1260	1270	1280	1290	1300
Mechanism and kinetic equation	Diffusion-controlled, Ginsting-Brunshtein of Triaxial diffusion $1-2/3\alpha-(1-\alpha)2/3=Kt$ (spherical modle)				
RF	0.982	0.980	0.980	0.980	0.980
$D\times10^3$	1.563	2.097	2.357	2.624	3.360
$i\times10^3$	2.637	3.068	3.242	3.366	3.879
$K\times10^3$	1.070	1.099	1.129	1.161	1.191

Table 8 Activation energies of clinker formation reaction withaut and with ZnO-doping

ZnO (%)	0	1.5
E (KJ/mol)	124.09	52.12

is also testified by the studies on burnability. Because the clinker formation reaction is controlled by diffusion, the reaction rate and the activation energy of clinker formation depend on the liquid phase to a great extent. I.Odler[3], D.Knoefel[1] studied the effect of ZnO on liquid phase and clinker burning, and pointed out that adding ZnO decreases the temperature at which liquid phase appears and increases the amount of liquid phase. Owing to the increase in liquid phase, the diffusion rate of the particles in the liquid phase is increased. Therefore, the activation energy of klinker formation reaction decreases and the clinker formation rate is accelerated. Experiments as will as calcutations show that temperature must be raised by 55-76℃, if the reaction rate constant of the clinker without ZnO-doping showed equals that of clinker with 1.5% ZnO-doping. This is entirely in agreement with the results obtained from burnability studies. Therefore, the kinetic model put forward above is reasonable.

RESEARCH ON MORPHOLOGY OF CLINKER MINERALS AND BEHAVIOUR OF SOLID SOLUTIONS CONTAINING ZnO

1. The morphology of clinker minerals

The raw meal with 2% ZnO-doping was heated rapidly up to 1250 ℃ and burnt for 30 min. The morphology of the resulting clinker minerals are shown in Fig.2 as obtained on AMARY-100BSEM. It is seen here from that when

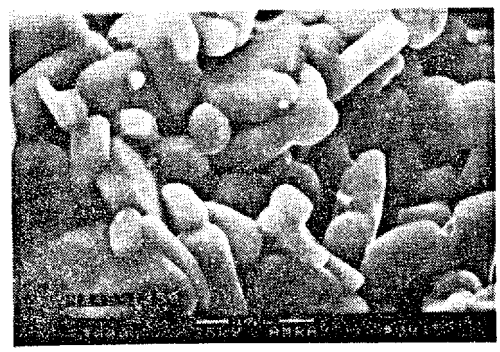

Fig.2 SEM micrograph of clinker with 2.00% ZnO-doping burnt for 30min at 1250℃ in rapid heating-up burning

clinker with ZnO-doping conbined with heating-up burning, majority of alite in the clinker is prismatic, the size of crystal particles relatively smaller (about 10μm), the aspect ratio relatively bigger (L/B=3-4), the interface of minerals distinct, and the distribution of minerals homogeneous. This clinker has a relatively high strength[9]. In normal heating-up burning, the crystal particle size of alite in clinker without

mineralizer is generally 40-55μm or so, while the crystal particle size of alite in Fig. 2 is only about 10 μm. Rapid heating-up burning almost synchronizes the decomposition reaction of limestone and clay, the solid phase reaction of clinker formation and the reaction between the solid and liquid phases[7]. Rapid heating-up burning toghther with ZnO-doping decreases clinkering, the temperature of liquid phase appearance and increases the amount of liquid phase. Thus the crystal particle size of alite decreases and the interface of minerals becomes distinct. Alite with smaller crystal particle size is hydrated easily. Therefore, the clinker has not only superior late strength but also relatively high early strength.

2. The behaviour of solid solution containing ZnO

Raw meals with 1% and 3% ZnO-doping were heated rapidly up to 1300℃ and burnt for 30min. Those with 2% ZnO-doping were heated up to 1200℃, 1250℃ and 1300 ℃ and burnt for 30 min. The solid solubility of ZnO existing in alite, belite and interstitial phase was measured in AMARY-100BSEM with TN-5400 energy spectroscopy. The results are shown in Tables 9 and 10.

Table 9 shows that burning for 30 min at 1300℃ in rapid heating-up burning, the solid solubility of ZnO in all the phases all increases with increase of ZnO-doping. The solid solubility in belite is relatively less, in alite relatively more, in the interstitial phase the highest. The ratio of the solid solubility of ZnO in alite and belite almost does not change (3:1) with increase of ZnO-doping, wherease the solid solubility of ZnO in interstitial phase relatively decreases compared with that in alite and belite with the increase of ZnO-doping.

Table 10 shows that under the condition of rapid heating-up burning, for the same value (2%) of ZnO-doping, the solid solubility of ZnO in alite and belite increases with rise of burning temperature, while that in the interstitial phase decreases. The ratio of solid solubility of ZnO in alite and belite does not change at all (3:1) with rise of burning temperature, but the solid solubility of ZnO in interstitial phase decreases with rise of burning temperature. Thus it can be considered that ZnO is preferentially dissolved by the interstitial phase, while alite and belite form gradually and grow perfectly with rise of temperature, and absorb ZnO from the interstitial phase (liquid phase), with a consequent increase the solid solubility of ZnO in the two phase.

Table 9 Influence of ZnO quantity on the solid solubility of ZnO in clinker at 1300 ℃

ZnO, %		Solid solubility of ZnO, w%	Ratio of solid solubility of ZnO in Alite: Belite: interstitial phase
1.00	Alite	0.43	3:1:19
	Belite	0.14	
	Interstitial phase	2.61	
2.00	Alite	1.04	3:1:13
	Belite	0.36	
	Interstitial phase	4.80	
3.00	Alite	1.78	3:1:12
	Belite	0.55	
	Interstitial phase	6.72	

CONCLUSIONS

1. The burnbility of raw meal can be improved remarkably when a small amount (0.5%) of ZnO is added in rapid heating-up burning. With increase in ZnO-doping, the effect will improve gradually, such as by decrease in the sintering temperature by 70℃ or so.

2. In rapid heating-up burning, the clinker formation reactions without and with 1.5% ZnO- doping are all controlled by diffusion and well satisfy with Ginstling-Brunshtein equation. The activation energy for the clinker formation reaction without and with 1.5% ZnO-doping is respectively 124.59KJ/mol and 52.12KJ/mol.

The activation energy for the clinker formation reaction with 1.5% ZnO-doping decreases by 139% as compared to without ZnO.

3. ZnO is taken up preferentially in interstitial phase in rapid heating-up burning. The solid solubility of ZnO in the various clinker phases changes with the extent of ZnO-doping as will as the burning temperature.

Table 10 Influence of temperature on the solid solubility of ZnO in clinker at 2 % ZnO

Temp., ℃		Solid solubility of ZnO, wt%	Ratio of the solid solubitity of ZnO in Alite: Belite: interstitial phase
1200	Alite	0.63	3: 1: 32
	Belite	0.23	
	Interstitial phase	7.37	
1250	Alite	0.94	3: 1: 17
	Belite	0.31	
	Interstitial phase	5.42	
1300	Alite	1.04	3: 1: 13
	Belite	0.36	
	Interstitial phase	4.80	

REFERENCE

1. Knoefel, D. et al (1978) 'Beeinflussung einiger Eigenschaften des Portlandzementklinker und des Portlandcement durch ZnO und ZnS', Z-K-G 31, 157.
2. Tsuboi, T. et al (1972) 'Die Einflusse von MgO—SO_3 und ZnO auf die Sinterungvon Portlandklinker ', Z-K-G 25, 426
3. Odler, I. et al (1980) 'Einfluss von Mineralisatoren auf das Brennen des Portlandzementklinkers', Z-K- G 33, 132
4. Moore, R. E. (1960) 'Fluorspar boots kiln efficiency', Rock Products 63, H. 12, 108
5. Akatsu, K. et al (1968) 'Some effects of zinc oxide in the raw mix on the portland cement and clinker', Rev. 22nd Gen. Meet. Cem. Assoc. Japan Tokyo p. 40
6. Hornain, H. (1971) 'Sur la repartition des elements de transition et leur influence sur quelques proprietes du clinker et du ciment', Rev Mater. Constr. No 671-672, 203
7. Huang wenxi et al (1985) 'The effect of different burning processes on mechanism of portland cement clinker formation—the formation of tricalcium silicate at low temperature', Pro. of 1985 Beijing Int. Sym. Cement and Concrete P. 226
8. Zhejiang University et al 'The physical chemistry of silicate' the Architecture Industry Publish House of China, 1st impression , 1980
9. Shenwei et al 'Technology of cement', the Architecture Industry Publish House of China, 1st impression, 1986

THE EFFECT OF CALCIUM FLUOROSULPHO-SILICATE ON FORMATION OF CALCIUM SILICATE

Huang Wenxi, Xu Guangliang and Lu Zhongyuan

Sichuan Institute of Building Materials, Mianyang, Sichuan, P R CHINA

ABSTRACT

The study points out that it is the formation of the transition phase $3C_2S \cdot 3CaSO_4 \cdot CaF_2$, and not the liquid phase, which catalyzes the formation of C_3S and C_2S when a suitable CaF_2 and $CaSO_4$ content is present. Furthermore, the effect of CaF_2 and $CaSO_4$, and the transition phase $3C_2S \cdot 3CaSO_4 \cdot CaF_2$ on the formation of portland cement clinker has been studied.

研究指出: CaF_2, $CaSO_4$ 主要是通过形成过渡相 $3C_2S \cdot 3CaSO_4 \cdot CaF_2$, 而不是通过液相促进$C_3S$, C_2S的形成. 还研究了CaF_2, $CaSO_4$和过渡相$3C_2S \cdot 3CaS_4 \cdot CaF_2$ 对波特兰水泥熟料形成的作用.

INTRODUCTION

CaF_2 and $CaSO_4$ are widely used as composite mineralizer. When CaF_2 and $CaSO_4$ are added, portland cement clinker can be sintered at 1200-1350 ℃. Y. M. Butt et al [1] reported that $CaSO_4$ was a kind of effective fluxing agent and mineralizer, and enabled to lower the temperature of liquid phase over 100℃. W. Gutt et al [2] reported that when $CaSO_4$ was added in portland cement, $2C_2S \cdot CaSO_4$ started to form at 950℃ and $2C_2S \cdot CaSO_4$ decomposed to $CaSO_4$ and α'-C_2S at temperatures above 1298 ℃. In CaO-SiO_2-CaF_2 system, W. Gutt et al [3] found that $2C_2S \cdot CaF_2$ formed at 950 ℃ and decomposed to α'-C_2S and CaF_2 at 1040 ℃. S. Akaiwa, C. Gilioli et al [4] [5] reported that $3C_2S \cdot CaF_2$ existed stably from 1100℃ to 1185℃, incongruently melted at 1185 ℃ and decomposed to triclinic C_2S, α'-C_2S and liquid phase. In CaO-C_2S-$CaSO_4$-CaF_2 system [5], only a quaternary compound $3C_2S \cdot 3CaSO_4 \cdot CaF_2$ existed from 1000℃ to 1150℃. The compound coexisted neither C_2S that was not saturated with $CaSO_4$ (1000℃) nor $3C_2S \cdot CaF_2$ (1150℃), $2C_2S \cdot CaF_2$ and $3C_2S \cdot CaF_2$ could form only when F^-/SO_3 (W%) >0.168 in raw meal. Tong Damao et al [6] reported that when CaF_2 and $CaSO_4$ were added in the raw meal of portland cement, the temperature of appearance of liquid phase was lower than before, the fluidity of liquid phase increased, and f-CaO decreased remarkably. It is not through the formation of the transitional phase that the mineralizer promoted the formation of C_2S at lower temperature, but through the fluxing effect. Further studieds [7] have indecated the order of effective fluxing action was: KH>SM>SO_3>IM >CaF_2.

Above all it is not clear whether the action of the in CaF_2, $CaSO_4$ composite mineralizer in promoting the formation of C_2S is caused through the formation of transitional phase or through the fluxing effect, or both. Nor is the mineralization mechanism of CaF_2 and $CaSO_4$ in rapid heating-up burning. For these reasons, we have studied in detail the mineralization mechanism of CaF_2 and $CaSO_4$ on the formation of C_2S and C_3S in normal (20℃/min) and rapid (>800℃/min) heating-up burning from a number of experiments. The optimum CaF_2, $CaSO_4$ content range has been arrived at.

QUATERNARY SYSTEM CaO-SiO_2-CaF_2-$CaSO_4$

1. Experiments and Results

A basic raw mix D (KH=0.96, C_3S=90.67%, C_2S=9.33%) was prepared from chemically pure $CaCO_3$ and SiO_2. Chemically pure CaF_2 and $CaSO_4 \cdot 2H_2O$ were added to it. A_1 and A_2 obtained as follows: A_1: CaF_2 1.50%, $CaSO_4$ 1.50%, F^-/SO_3 0.5 and A_2: CaF_2 0.616%, $CaSO_4$ 3.00%, F^-/SO_3 0.1 in A_2. The mixes A_1, A_2 were heated up to 900 -1400℃ respectively in rapid heating-up rate and normal heating-up rate. The results of XRD are shown in Fig. 1a, b and 2a, b.

2. Discussion

Fig. 1a and b show that in the normal heating-up burning process, when the same content of CaF_2 and $CaSO_4$ is used (CaF_2=0.616-1.50%, SO_3=1.50-3.00%, F^-/SO_3=0.1-0.5), only a transitional phase $3C_2S \cdot 3CaSO_4 \cdot CaF_2$ forms at 1000℃ and disappears at 1200 ℃, C_3S appears at 1100℃, C_3S forms at 1150 ℃ and forms a great deal, when $3C_2S \cdot 3CaSO_4 \cdot CaF_2$ disappears at 1200℃. Above 1200 ℃, C_3S does not increase much.

Fig. 2a and b show that in the rapid heating-up burning process, when the same content of CaF_2 and $CaSO_4$ is used, a transitional phase $3C_2S \cdot 3CaSO_4 \cdot CaF_2$ forms at 950℃ and disappears at 1250℃, in addition, besides little $2C_2S \cdot CaSO_4$ exists in the temperature range of 1020 ℃ to 1050℃ when F^-/SO_3 is relatively smaller (F^-/SO_3=0.1, in the mix A_2). Compared with that in normal heating-up burning, the temperature of formation of $3C_2S \cdot 3CaSO_4 \cdot CaF_2$ decreases and the temperature of disappearence rises respectively by approximately 50℃, C_3S and C_3S form respectively at 1100℃ and 1150℃ after $3C_2S \cdot 3CaSO_4 \cdot CaF_2$ has formed. When $3C_2S \cdot 3CaSO_4 \cdot CaF_2$ disappears at 1250℃, a great amount of C_3S has formed. After 1250℃, the C_3S content does not change basically.

THE MINERALIZATION MECHANISM OF CaF_2 AND $CaSO_4$ ON C_2S AND C_3S

1. Experiment and Results

1.1. Chemically pure $CaCO_3$, SiO_2, CaF_2 and $CaSO_4 \cdot 2H_2O$ were proportioned stoichiometrically to synthesize $3C_2S \cdot 3CaSO_4 \cdot CaF_2$. The mix was burnt for 2 hours at 950℃. That the product obtained was $3C_2S \cdot 3CaSO_4 \cdot CaF_2$, confirmed by XRD and measurement of f-CaO. The synthesized $3C_2S \cdot 3CaSO_4 \cdot CaF_2$ was added to in the basic raw mix D to prepare a series of mixes Dn, as shown in Table 1. The Dn mixes were heated up to 1150 - 1350 ℃ separately in normal heating-up rate and rapid heating-up rate, and burnt for 30 min. The f-CaO contents are shown in Figs. 3a and b.

1.2. The mix D_{30} was heated up to 1100-1350 ℃ separately in normal heating-up rate and rapid heating-up rate, and burnt for 30 min. The results of XRD are shown in Figs. 4a and b. The mix D_{30} was heated up to 1250℃, 1300 ℃ and 1350 ℃, and burnt respectively for 3 min, 5min, 7min, 10min and 30min. The results of XRD are shown in Figs. 5a, b and c.

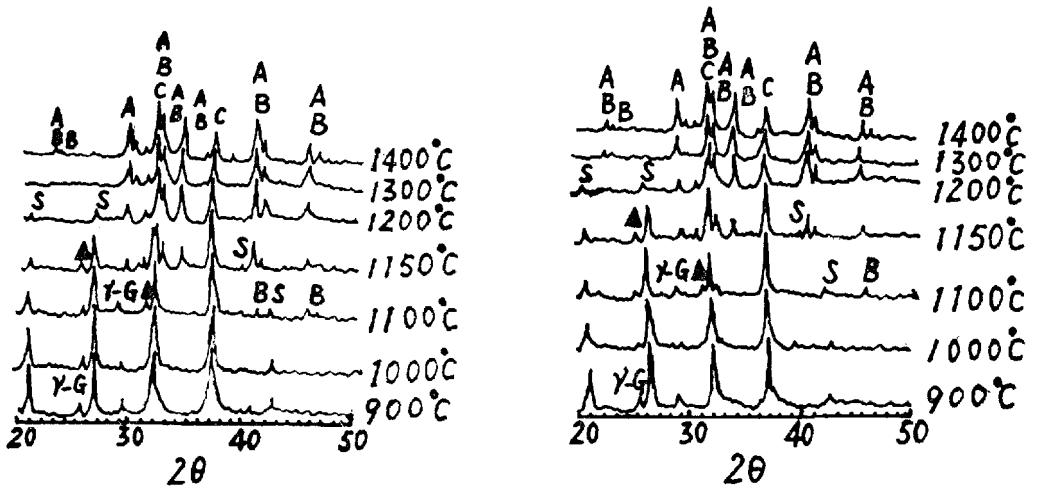

a: mix A_1 b: mix B_1

A: C_3S B: C_2S C: CaO S: SiO_2 γ-G: γ-$CaSO_4$ ▲: $3C_2S \cdot 3CaSO_4 \cdot CaF_2$ ■: $2C_2S \cdot CaSO_4$

Fig. 1. XRD of mixes A_1 and A_2 in normal heating-up burning

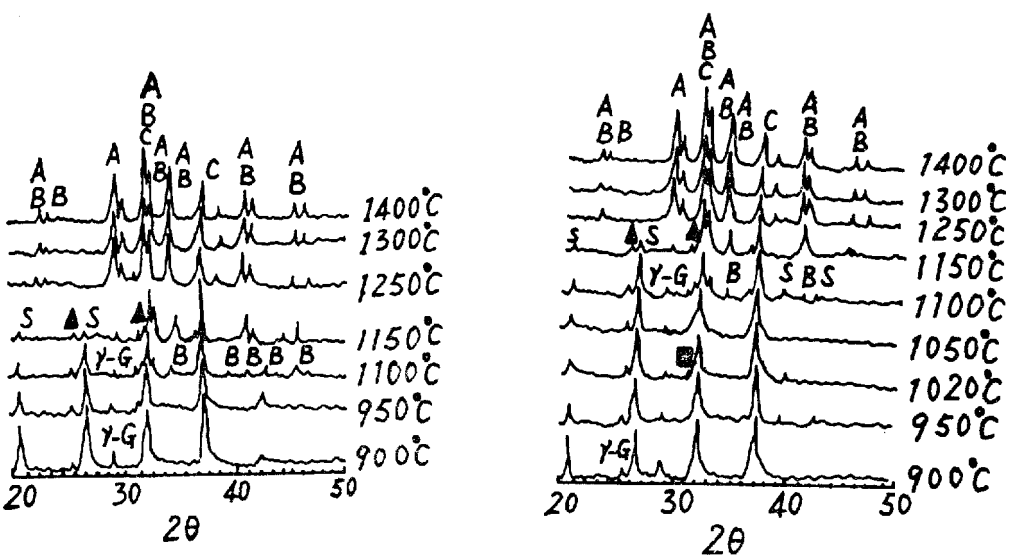

a: mix A_1 b: mix A_2

Fig. 2. XRD of mixes A_1 and A_2 in rapid heating-up burning

Table 1 $3C_2S \cdot 3CaSO_4 \cdot CaF_2$ content in different mixes

Mix No.	D0	D1	D3	D5	D8	D11	D14	D17	D20
3C2S · 3CaSO4 · CaF2 (%)	0	1	3	5	8	11	14	17	20

1, 3. The mixes D_8, D_{11}, D_{14}, D_{17}, D_{20} were heated up to 1200 ℃ in normal heating-up rate and up to 1250℃ in rapid heating-up rate, and burnt for 30 min. The liquid phase content as shown in Table 2 measured with SEM.

2. Discussion

The experiments in the quaternary system $CaO-SiO_2-CaF_2-CaSO_4$ show that except in mix A_1 (F^-/SO_3=0.1) $2C_2S$, $CaSO_4$ appears between from 1020℃ to 1050 ℃ in rapid heating-up burning, when the same content of CaF_2, $CaSO_4$ (CaF_2: 0.616-1.50%, SO_3: 1.50-3.00%, F^-/SO_3: 0.1-0.5) is used. In burning process, only transitional phase $3C_2S \cdot 3CaSO_4 \cdot CaF_2$ appears.

It can be seen from Fig. 4a that in normal heating-up burning, synthesized $3C_2S \cdot 3CaSO_4 \cdot CaF_2$ still disappears at 1200 ℃, C_2S appears at 1100℃ and C_3S appears at 1150 ℃. When $3C_2S \cdot 3CaSO_4 \cdot CaF_2$ disappears at 1200 ℃, a great deal of C_2S and C_3S have formed. Beyond 1200 ℃, C_3S content still increases but not much. The relation between $3C_2S \cdot 3CaSO_4 \cdot CaF_2$ and C_2S, C_3S in Fig. 4a is identical with the results shown in Figs. 1a and b. It can be also seen from Fig. 3a that adding a little $3C_2S \cdot 3CaSO_4 \cdot CaF_2$ can remarkably decrease f-CaO in clinker. This is the case in the temperature range 1150℃ - 1200 ℃. Beyond 1200 ℃ (as shown in Table 2, $3C_2S \cdot 3CaSO_4 \cdot CaF_2$ disappears at 1200 ℃ and liquid phase forms), f-CaO still decreases through not much.

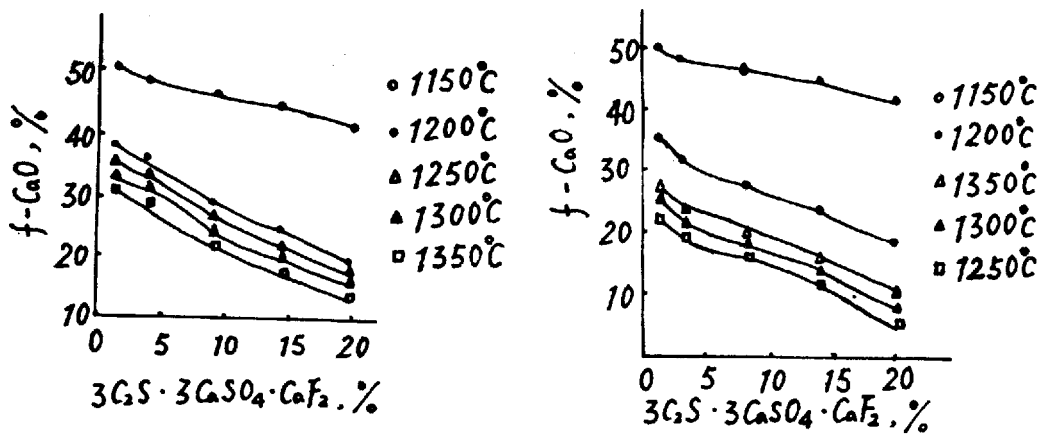

a: normal heating-up burning b: rapid heating-up burning

Fig. 3. Relation of f-CaO content of Dn sample with content of $3C_2S \cdot CaSO_4 \cdot CaF_2$-doping at different burning temperatures for the normal and rapid heating-up modes of burning

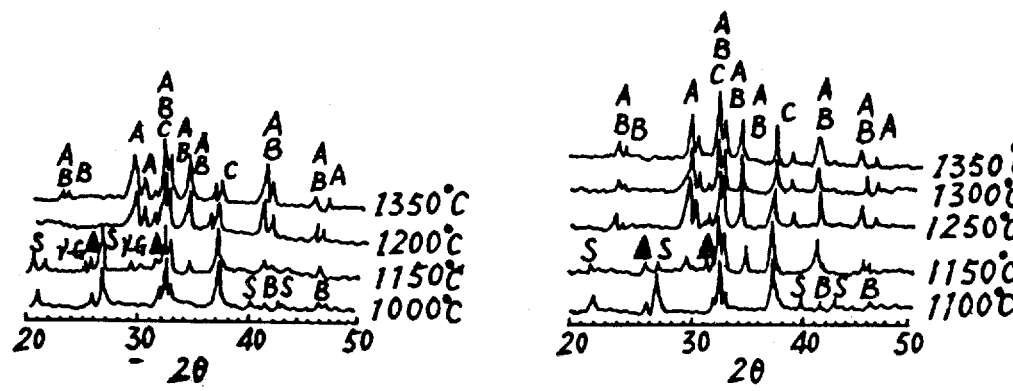

a. normal heating-up burning b. rapid heating-up burning

Fig. 4. XRD of D_{20}

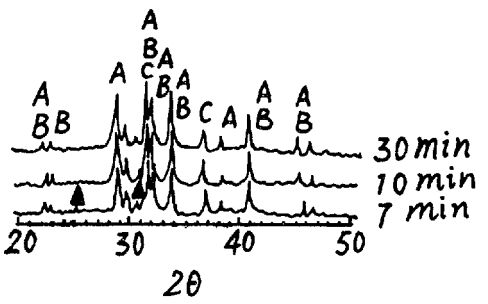

a. at 1250℃

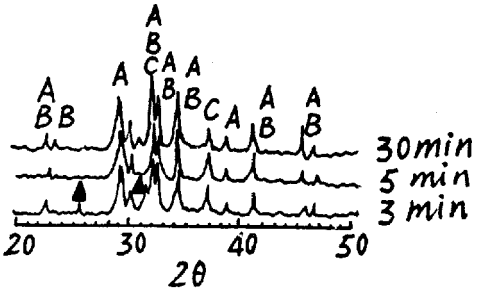

b. at 1300℃

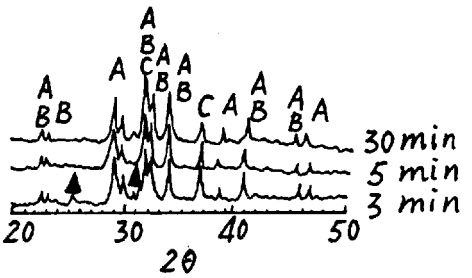

c. at 1350℃

Fig. 5 XRD of D_{20} burnt for various times in rapid heating-up burning

Table 2 Liquid phase content of mixes by different modes

Heating-up mode, temperature and time	Liquid phase content for mix, %				
	D_8	D_{11}	D_{14}	D_{17}	D_{20}
Normal, 1200℃ and 30min	7.1	9.2	10.9	13.3	16.2
Rapid, 1250℃ and 30min	5.1	5.8	6.3	6.7	7.3

The above analysis shows that in normal heating-up burning, after CaF_2 and $CaSO_4$ are added, C_2S and C_3S form mainly when the transition phase $3C_2S \cdot 3CaSO_4 \cdot CaF_2$ exists, while $3C_2S \cdot 3CaSO_4 \cdot CaF_2$ disappears, the C_3S content still increases through not very much. The effect of liquid phase on the formation of C_3S is less important.

It can be seen from Fig. 4b that in rapid heating-up burning, synthesied $3C_2S \cdot 3CaSO_4 \cdot CaF_2$ disappears at 1250 ℃, and C_2S and C_3S appear respectively at 1100 ℃ and 1150 ℃. When $3C_2S \cdot 3CaSO_4 \cdot CaF_2$ disappears at 1250℃, a great deal of C_3S has formed. This is identical with the results shown in Figs. 2a and b. Beyond 1250℃, C_3S does not increase, on the contrary decreases. It can also be seen from Fig. 3b that adding a little $3C_2S \cdot 3CaSO_4 \cdot CaF_2$ can remarkably lower f-CaO content. When temperature rises from 1150 ℃ to 1250 ℃, in the clinker to which synthesized $3C_2S \cdot 3CaSO_4 \cdot CaF_2$ has been added, f- CaO decreases considerably. Whereas it increases beyond 1250℃. This can be explained from Figs. 5a, b and c which shows that while burning for 7min at 1250 ℃, $3C_2 \cdot 3CaSO_4 \cdot CaF_2$ still exists, a great deal of C_2S and C_3S have formed, whereas while burning for 6min at 1300 ℃, 1350 ℃, $3C_2S \cdot 3CaSO_4 \cdot CaF_2$ disappears, C_3S content in clinker almost does not increase. It can be said that C_2S and C_3S form mainly when $3C_2S \cdot 3CaSO_4 \cdot CaF_2$ exists, the liquid phase having little effect on C_3S formation. The time for which $3C_2S \cdot 3CaSO_4 \cdot CaF_2$ exists at 1300 ℃ and 1350 ℃ is shorter than that at 1250 ℃, so the amount of C_3S formed at 1300 ℃, 1350 ℃ is less than that at 1250℃, whereas f- CaO increases the contrary. Table 2 shows that under the same condition, after $3C_2S \cdot 3CaSO_4 \cdot CaF_2$ disappears, the

liquid phase formed in normal heating-up burning is more than that in rapid heating-up burning. Compared with that in rapid heating-up burning, the effect of liquid phase on C_3S formation in normal heating-up burning is greater.

It becomes clear from the foregoing that when the same content of CaF_2 and $CaSO_4$ is used, C_2S and C_3S form mainly when $3C_2S \cdot 3CaSO_4 \cdot CaF_2$ exists no matter whether it is normal heating-up burning or rapid heating-up burning. In the process of burning, $3C_2S \cdot 3CaSO_4 \cdot CaF_2$ forms first from CaF_2, $CaSO_4$ with CaO, SiO_2, then decomposes to form active C_2S. C_3S forms from the active C_2S with CaO immediately. The catalytic effect of CaF_2, $CaSO_4$ on the formation of C_2S, C_3S is mainly through the formation of transitional phase $3C_2S \cdot 3CaSO_4 \cdot CaF_2$. It is secondary that C_3S is formed through liquid phase, that is to say, the effect of liquid phase is less important. The effect of liquid phase in normal heating-up burning is greater than that in rapid heating-up burning.

EFFECT OF CaF_2 AND $CaSO_4$ ON PORTLAND CEMENT CLINKER BURNING

1. Experiment and Results

1.1. The raw meal N (KH=0.94, SM=1.74, IM=1.31) was prepared from industrial raw materials, this chemical composition being: Loss on ignitor 34.58, SiO_2 12.87, Fe_2O_3 3.20, CaO 41.91, MgO 0.79 and Al_2O_3 4.19. Synthesized $3C_2S \cdot 3CaSO_4 \cdot CaF_2$ was added to the extent 10% and 20% to this meal to obtain raw meals NG_{10} and NG_{20}. The raw meals N, NG_{10} and NG_{20} were heated up to 1150-1250℃ separately in normal heating-up and rapid heating-up rate, and burnt for 30min. f-CaO contents in the resulting clinkers are shown Fig. 6.

1.2. Another series of raw meals was prepared by adding different amounts of CaF_2, $CaSO_4$ to the raw meal N, were heated up to 1250 ℃ separately in normal heating-up and rapid heating-up rate and burnt for 30min. f-CaO and $3C_2S \cdot 3CaSO_4 \cdot CaF_2$ contents were measured with XRD and are shown in Table 3. The relation between f-CaO and $3C_2S \cdot 3CaSO_4 \cdot CaF_2$ is shown in Fig. 7.

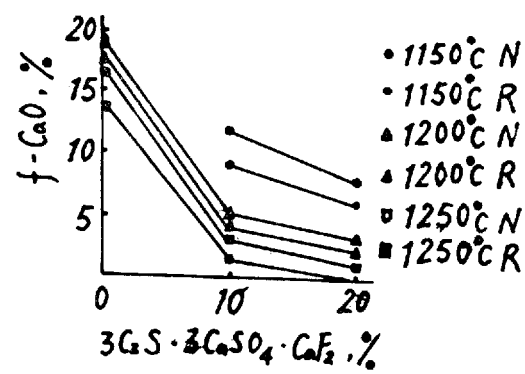

N: in normal heating-up burning R: in rapid heating-up burning

Fig. 6 Relation between f-CaO and synthesized $3C_2S \cdot 3CaSO_4 \cdot CaF_2$

Table 3 Relation between f-CaO and $3C_2S \cdot 3CaSO_4 \cdot CaF_2$ with CaF_2, $CaSO_4$

F^-, %		0.75				0.15	0.45	0.75	1.05
SO_3, %		2.50	2.00	1.50	1.00	1.50			
f-CaO %	Normal	3.61	3.89	4.81	5.66	6.04	5.32	4.81	4.24
	Rapid	1.73	1.98	2.15	2.47	2.81	2.31	2.15	2.06
$3C_2S \cdot 3CaSO_4 \cdot CaF_2$ %	Normal	6.98	5.33	3.41	2.12	1.57	3.02	3.41	4.36
	Rapid	9.23	7.01	4.34	2.83	2.01	3.67	4.34	5.21

2. Discussion

Fig. 6 shows that when synthesized $3C_2S \cdot 3CaSO_4 \cdot CaF_2$ is added to industrial raw meal, f- CaO in the clinker obtained decreases with increase of $3C_2S \cdot 3CaSO_4 \cdot CaF_2$ no matter whether it is the normal heating- up

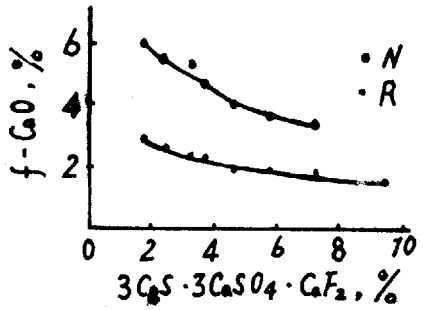

N: in normal heating-up burning R: in rapid heating-up buring

Fig. 7 Relation between f-CaO and content of $3C_2S \cdot 3CaSO_4 \cdot CaF_2$ actually formed

or rapid heating-up mode of burning. It is seen in Fig. 7 that when CaF_2, $CaSO_4$ are added to industrial raw meal, f-CaO in the obtained clinker decreases with the increase in the content of $3C_2S \cdot 3CaSO_4 \cdot CaF_2$ actually formed . It is taken to mean that the mechanism by which CaF2, $CaSO_4$ promotes the formation of portland cement clinker in industrial raw meal is the same as that of CaF_2, $CaSO_4$ in $CaO-SiO_2-CaF_2-CaSO_4$ system in C_2S, C_3S formation, that is to say it is mainly through formationof a transition phase $3C_2S \cdot 3CaSO_4 \cdot CaF_2$ that CaF_2, $CaSO_4$ promotes the formation of clinker.

A suitable content of CaF_2, $CaSO_4$ ought to make help the formation of as much $3C_2S \cdot 3CaSO_4 \cdot CaF_2$ as possible in burning process which is advantageous to the formation of clinker. At the same time , the effect of CaF_2, $CaSO_4$ on the actual operation and cement properties must be paid with attention too . This is the case since a large quantity of $CaSO_4$, C_{aF_2} will make the actual operation difficult, and also have a depreiate effect on cement properties. Therefore, CaF_2, $CaSO_4$content is critical. The optimum CaF_2 , $CaSO_4$ content is respectively 0.75-1.05% F^- and 1.50 - 2.50% SO_3 in portland cement raw meal.

CONCLUSSION

1. In the quaternary system $CaO-SiO_2-CaF_2-CaSO_4$, except $2C_2S \cdot CaSO_4$ exists when $F^-/SO3<0.158$ and in rapid heating-up burning, in the temperature range of 1020-1050℃, only transitional phase $3C_2S \cdot 3CaSO_4 \cdot CaF_2$ appears. In normal and rapid heating-up burning, $3C_2S \cdot 3CaSO_4 \cdot CaF_2$ exists respectively at 1000-1200 ℃ and 950-1250 ℃, C_2S and C_3S start to form respectively at 1100 ℃ and 1150 ℃.

2. When a suitable CaF_2, $CaSO_4$content is used, it is mainly the formation of the transitional phase $3C_2S \cdot 3CaSO_4 \cdot CaF_2$ that causes CaF_2 and $CaSO_4$ to catalyze the formation of C_2S, C_3S. The effect of liquid phase is less important.

3. When CaF_2, $CaSO_4$ is added in industrial raw meals, it is mainly due to the formation of $3C_2S \cdot 3CaSO_4 \cdot CaF_2$ that CaF_2, $CaSO_4$ promotes the formation of clinker. The optimum content of CaF_2, $CaSO_4$ is respectinely 0.75-1.05% F^- and 1.50-2.50% SO_3.

REFERENCES:

1. Butt, Y. M. et al 'The mechanism of clinker formation processes and the modification of its structure', 6th Int. Congr. Chem. Cement. Moscow, 1974

2. Gutt, W. et al 'A new calcium silicosulphate', Nature, 1966, 210, 408

3. Gutt, W. et al 'The system $2CaO \cdot SiO_2-CaF_2$', Trans. Brit. Soc. 1966, 65, 521

4. Akaiwa, S. et al 'Studies on mineralizing effect of CaF_2 and a trinary compound in the system $CaO-SiO_2-CaF_2$', Semento Gijutsu Nempo , 1966, 20, 26

5. Glioli, C. et al 'Studies on clinker calcium silicates bearing CaF_2 and $CaSO_4$', Cem. Concr. Res. 1979, 9, 295

6. Tong Damao et al 'Study on the Effect of Mineralizer' Journal of Wuhan University of Technology , 1986, No. 1, p. 9-18

7. Lin Zongshou et al 'Study on the Meltability of Clinker' Journal of Wuhan University of Technology, 1987, No. 2, p. 169-175

THE EFFECT OF THE COMPOSITE MINERALIZERS OF CaF_2, $CaSO_4$ AND ZnO ON THE FORMATION OF THE PORTLAND CEMENT CLINKER IN A RAPID HEATING-UP BURNING

Lu Zhongyuan*, Huang Wenxi** and Xu Guangliang*

*Sichuan Institute of Building Materials, Sichuan, P R CHINA
**Chengdu Designing & Researching Institute of Industry of Building Materials, Sichuan, P R CHINA

SUMMARY

The authors have combined a rapid heating-up burning (800℃/min) with the composite mineralizers of CaF_2, $CaSO_4$ and ZnO in the burning process of Portland cement clinker. The effect of the composite mineralizers on the burnability, the clinker formation process, the formation kinetics, the microstructure and the physical property of the clinker has been studied. The experiments showed that Portland cement clinker could be formed at about 1050℃.

摘 要

在波特兰水泥熟料的煅烧过程中，作者把快速升温煅烧（800℃/min）和掺CaF_2、$CaSO_2$和ZnO复合矿化剂结合在一起，研究了复合矿化剂对易烧性、熟料形成过程、熟料形成动力学、熟料的微观结构和物理力学性能的影响，实验表明，波特兰水泥熟料可以在大约1050℃形成。

INTRODUCTION

Generally, Portland cement clinker formation occurs at 1450℃ without any mineralizers in the cement raw meal. Such high temperature not only affects the quality and the output of cement,but also results in high energy consumption. one of the methods to lower the formation temperature of clinker is by addition of mineralizers to the raw meal. CaF_2 and $CaSO_4$ are the mineralizers which have been widly used in the cement industry.Asok K.Sarkar, Gilioli.C and W.A.Kleem et al[1,2,3,]had pointed out that addition of CaF_2 to the raw meal would accelerate the formation of C_3S and decrease the temperature of clinker formation by 50℃~200℃. Our research showed [4] , that in rapid heating-up burning technology(rapid burning for short) , due to an extremely rapid temperature rise of the materials, the various processes such as the dehydration of clay, the decarbonation, solid phase reactions,the appearance of liqud-phase,the formation reactions of clinker minerals etc, almost overlap. The whole processes of clinker formation is all along the liquid-solid phase reaction basically, the diffusion rate of particles is enhanced, the reaction activation energy is decreased,the formation of the alite is greatly accelerated.Thus Portland cement can be formed at 1300℃ without any mineralizers added. Results of our study on addition of composite mineralizers of CaF_2, $CaSO_4$ and ZnO to the raw meal followed by rapid burning, indicated that Portland cement clinker formation occurred at 1050℃ (f-CaO<2%).

EXPERIMENTAL

The preparation of cement raw meal pellet: After the raw meal was weighed it was fully mixed on a mixture machine, appropriate quantity of water added and the samples were pressed into tablets of Φ 20×1 mm, and dried at 105±5℃. The clinker samples of the normal heating-up burning (slow burning for short) were also prepared: the raw meal pellets were placed in a high temperature furnace, heated from room temperature. The heating-up rate is controlled at 20℃/min. The clinker sample of rapid burning were prepared as follows: the furnace was kept at the required temperature beforehand and then the raw meal tablets were rapidly introduced into the furnace,the heating-up rate measured reached above 800℃/min.The clinker samples were calcined at a temperature and retention time to be indicated. The samples were taken out and for rapidly cooled and then put into a drying container with silicagel. f-CaO was estimated titration with ethanol-glycerol. Mineral phases and mineral content were determined by X-ray diffraction analysis(XRD for short) . The morphological features were observed by Sweep Electron Microscope (SEM for short).The chemical compositions of clinker minerals were determined by Energy Spectrum Analysis (ESA for short).

RESULTS AND DISSCUSSION

1. The effect of composite minerializers on the burnability of the raw meal.

The raw meal was prepared using industrial raw materials. The chemical compositions of the meal are given in Table 1. The burnability was estimated from the f-CaO contents.Experimental results are shown in Fig 1 and Fig 2. From the results in Fig 2, it is seen that in rapid burning, although the burning temperature of the raw meal without any mineralizers is 200℃ higher than that of the raw meal with composite mineralizers of CaF_2, $CaSO_4$ and ZnO,the f-CaO contents of the former is higher than that of the latter, especially up to the initial 3 minutes of clinker burning .This shows that the burnability of the raw meal with composite mineralizers is better than that of raw meal without mineralizers.Even though the sintering temperature is lower by 200℃ for the former, the cement clinker minerals are formed more easily. The results in Fig.2 indicate that above 800℃ ,the f-CaO contents of rapidly heated samples(curve F) is less than that of the slowly heated samples (curve S) .The portland cement clinker can be formed at about 1050℃ in rapid burning (f-CaO < 2%),but the clinker can be formed at about 1150℃ in slow burning. This shows that when there are suitable composite mineralizers in the raw meal,the burnability of the raw meal can be greatly improved in rapid burning, and the cement clinker is formed easily.This is attributed possibly to the combination of heating and chemical activation. This view has also been expressed by O. Philipp et al[5].

Table 1. The chemical compositions of the raw meal

No.	SiO_2	Al_2O_3	Fe_2O_3	CaO	MgO	SO_3	ZnO	F-	LOSS
1	12.67	3.13	3.38	42.23	1.69		suitable		32.05
2	12.90	3.20	3.67	41.84	1.27		suitable		32.45
3	12.44	3.42	2.73	42.50	1.28		suitable		32.85

2. The effect of the composite mineralizers on the clinker formation in rapid burning

The results of experiment are given in Table 2,3,4,5,Fig.3,4(the raw meals of the samples which were not indicated have the composite mineralizers of CaF_2,$CaSO_4$ and ZnO in Tables and Figures).

Table 2. The minerals formation process of rapid burning sample at 1100℃ with mineralizers

t(min.)	1	2	3	5	10	15	30	45
$CaCO_3$	+	+	-	-	-	-	-	-
CaO	++	+++	++	++	+	+	+	+
C_4AF	+	+	+	+	+	+	+	+
C_2S	+	++	++	++	++	+	+	+
C_3S	-	+	+	++	+++	+++	+++	+++
$C_{11}A_7.CaF_2$	+	+	+	+	+	+	+	-
$C_3S \cdot CaF_2$	-	+	++	+	-	-	-	-

(+++ = a large,++ = middle,+ = a little,- = nil)

Table 3.The minerals formation process of rapid burning sample at 1300℃ without any mineralizers

t(min)	$CaCO_3$	C_3A	β -C_2S	C_4AF	C_3S	CaO(%)
1	+	+	++	+	-	35.02
2	+	+	++	+	++	
3	-	+	++	+	++	
5	-	+	++	+	++	6.80
30	-	+	++	+	+++	3.09
45	-	+	++	+	+++	2.03

*:KH = 0.98 , N = 2.55 , P = 1.25

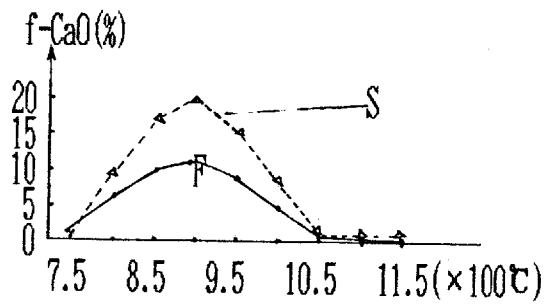

Fig.1.f-CaO content as a function of temp., in the rapid burning(F) and slow burning(S) held for min at various temperatures.

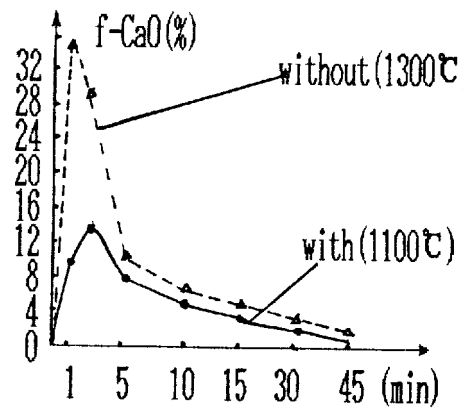

Fig.2. f-CaO contents as a function of the burning time in the raw meal with and without CaF_2, $CaSO_4$ and ZnO

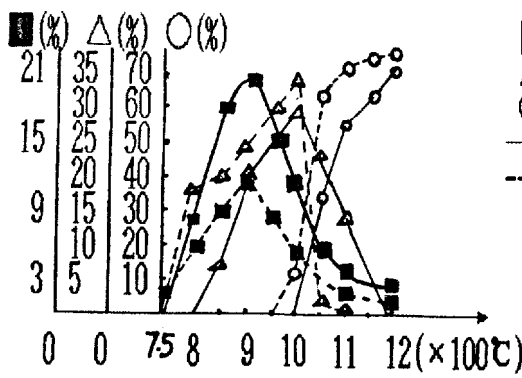

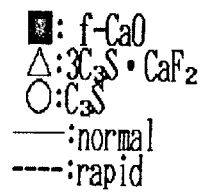

Fig.3.The formation of clinker minerals at various temperature held for 45 min.

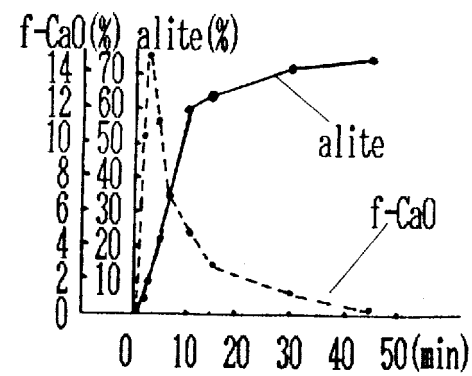

Fig.4 A relation of alite, f-CaO and the time of temp. preservation at 1100℃ in rapid burning

Table 4. Minerals formed during the process of rapid burning to the various temperature for a retention time of 45 minutes

temperature(℃)	750	800	850	900	950	1000	1050	1100	1150	1200	1250	1300
$CaCO_3$	+++	+	-	-	-	-	-	-	-	-	-	-
$2C_2S \cdot CaCO_3$	+	-	-	-	-	-	-	-	-	-	-	-
$3C_2S.3CaSO_4CaF_2$	-	+	+	+	+	+	-	-	-	-	-	-
$3C_3S \cdot CaF_2$	-	+	++	++	++	++	+	-	-	-	-	-
$C_{11}A_7 \cdot CaF_2$	-	-	-	+	+	+	+	+	-	-	-	-
C_4AF	-	-	-	-	+	+	++	++	++	++	++	++
C_2S	-	+	+	+	+	+	++	++	++	++	+	+
C_3S	-	-	-	-	-	+	++	+++	+++	+++	+++	+++
CaO	+	+	++	++	++	++	+	+	-	-	-	-

Table 5. Minerals formed during the process of slow burning to the various temperature for a retention time of 45 minutes

temperature(℃)	750	800	850	900	950	1000	1050	1100	1150	1200	1250	1300
$CaCO_3$	+++	+	-	-	-	-	-	-	-	-	-	-
$2C_2S \cdot CaCO_3$	-	+	-	-	-	-	-	-	-	-	-	-
$3C_2S3CaSO_4CaF_2$	-	-	+	+	+	+	-	-	-	-	-	-
$3C_3S \cdot CaF_2$	-	-	++	++	+++	++	+	-	-	-	-	-
$C_{11}A_7 \cdot CaF_2$	-	-	-	+	+	+	+	+	-	-	-	-
C_4AF	-	-	-	-	+	+	++	++	++	++	++	++
C_2S	-	-	+	+	+	+	++	++	++	++	++	++
C_3S	-	-	-	-	-	-	+	++	+++	+++	+++	+++
CaO	-	+	++	+++	++	++	+	+	+	-	-	-

The results in Tables 2 and 3 show that when the composite mineralizers of CaF_2, $CaSO_4$ and ZnO are added to the raw meals in rapid burning,there is an intermediate transition phase $3C_3S \cdot CaF_2$ formed,$C_{11}A_7 \cdot CaF_2$ replacing C_3A,and the maximum f-CaO content is obviously less than that of the samples without any mineralizers, although the burning temperature is less by 200℃. Comparing Table 2 with Table 5,it can be seen that due to the absence of intermediate transition phase $2C_2S \cdot CaCO_3$ and $3C_2S \cdot 3CaSO_4 \cdot CaF_2$ in the rapid burning, the formation process for the clinker minerals is greatly simplified. In the raw meal with composite mineralizers of CaF_2, $CaSO_4$ and ZnO, within 2 minutes, all kinds of clinker minerals appear in rapid burning. After 10 minutes, all sorts of clinker minerals do not change basically, only the C_3S contents increases, and the $C_{11}A_7 \cdot CaF_2$ and f-CaO contents decrease (Table 2).These results can be got to need over 60 minutes at least in slow burning. This indicates that technology of rapid burning can obviously accelerate the formation of cement clinker minerals,when the burden proportion of raw meal with proper composite mineralizers is suitable.It can be seen in Fig.4 that the alite contents reached 80% and above in rapid burning for 10 minutes. O. Phillipp et al[5] had also observed similar results during the initial stage of burning. The rate of formation of clinker is obviously faster in a high temperature gradient. Gutt and Osborna [6] had reported the formation of $3C_3S \cdot CaF_2$ in $CaO-SiO_2-CaF_2$ system. They considered that this compound was stable between 1110℃~1175℃.It was incongruentaly melting into C_3S,α - C_2S and liquid-phase. Lou Zonghan et al considered $3C_3S \cdot CaF_2$(they considered that its composition was $C_{19}S_7 \cdot CaF_2$)was formed between 1070℃ and 1175℃.Its rate of formation was reached the maximum at 1110℃ and its content also approached a maximum. $3C_3S \cdot CaF_2$ was still unstable within its formation temperature, its reaction of formation and decomposition occurred simultaneously.Formation main occurred below 1110℃, while above 1110℃, its decomposition reaction was main and disapeared at 1170℃.There are the element of C_3S in the $3C_3S \cdot CaF_2$, its decomposition promotes the formation of C_3S. Its function of the promotion is obviously at 1170℃. Our research showed that the steady regions of the $3C_3S \cdot CaF_2$ was between 800℃ and 1000℃ in rapid burning,a great quantity of $3C_3S \cdot CaF_2$ was decomposed at 1050℃.Its decomposition reaction was run out at 1100℃ holding for 45 minutes (Table 4 and Fig.3). The steady region of the $3C_3S \cdot CaF_2$ was between 950℃ and 1050℃ in slow burning, a great quantity of $3C_3S \cdot CaF_2$ was decomposed at 1100℃. Its

decomposition reaction was run out at 1150℃ (Table5) . The steady region of the $3C_3S \cdot CaF_2$ and its decomposition temperature is lower in our research results than that of other researcher , this is the functions of mineralizer ZnO and technology of rapid burning. Comparing Table 2 with Table 4 , it can be seen that there is only a kind of fluoride-based intermediate transition phase $3C_3S \cdot CaF_2$ in Table 2, but there are two kinds of fluoride-based intermediate transition phases $3C_3S \cdot CaF_2$ and $3C_3S \cdot 3CaSO_4 \cdot CaF_2$ in Table 4. This reason is that the clinker minerals in Table 2 are got by a rapid heating-up to 1100℃ holding for different time,but the clinker minerals in Table 4 are got by a rapid heating-up to different temperature holding for 45 minutes. So that the rapid heating-up to 1100℃ in Table 2, it exceed the temperature steady region of $3C_2S \cdot 3CaSO_4 \cdot CaF_2$,so,$3C_2S \cdot 3CaSO_4 \cdot CaF_2$ does not occur.The Fig.4 showed too that the f-CaO contents of rapid burning samples were lower than that of slow burning at 800℃ and over. The formation contents of $3C_3S \cdot CaF_2$ in rapid burning sample were more than 8~20% than that of in slow burning between 800℃ and 1000℃. $C_3S \cdot CaF_2$ contents of rapid burning sample were about 33% at 1000℃,but it was about 26% in slow burning samples. Between 1000℃ and 1050℃, f-CaO content is decreased from 4.5% to about 2%, the content of $3C_3S \cdot CaF_2$ is decomposed from about 33% to 2%, and alite content is increased from about 10% to 58% in rapid burning sample. But in slow bunring sample,f-CaO content is decreased from about 7% to about 4%, $3C_3S \cdot CaF_2$ content is decreased from about 26% to about 20%,alite content increased from zero to about 30%.This indicated that in rapid burning,and CaF_2,$CaSO_4$ and ZnO composite mineralizers added in the raw meal, the portland cement clinker can be formed in lower temperature because of the decomposition of the intermediate transition phase $3C_3S \cdot CaF_2$ promoted the formation of alite. In the normal burning process,C_3S could not be formed at lower than 1200℃ in raw meal without any mineralizers. A little amount of C_3S could be formed at 1300 ℃[1] . While adding the composite mineralizers CaF_2,$CaSO_4$ and ZnO in raw meal, alite can be formed about 10% at 1000℃ and about 58% at 1050℃ in rapid burning.The formation temperature of alite decreased about 300℃. Combining the technology of rapid burning with the composite mineralizers could got such good results, we thought that the reasons were the causes of the following:

The liquid-phase formation temperature of rapid burning sample is 200℃ lower than that of slow burning sample. The technology of rapid burning decreased the liquid-phase viscosity and improved the properties of the liquid-phase [8] and accelerated the alite formation. In rapid burning, $CaCO_3$ could be completely dissociated in preservation temperature for more than 2 minutes at the cement sintering temperature,at the same time a little amount of C_2S and C_3S have been formed (Table 2). The thermodynamic analysis[9] showed that $CaCO_3$ might directly react with SiO_2 or C_2S to form alite. When composite mineralizers CaF_2, $CaSO_4$ and ZnO are added to raw meal, there was an intermediate transition phase $3C_3S \cdot CaF_2$, which was incongruent melting that it transfer to alite at 800~1100℃. This view hasd also been expressed by Gutt [6] . But Gutt considered that the $3C_3S \cdot CaF_2$ transfer to alite at 950~1200℃. The viscosity of the fluoride-bearing liquid-phase formed is lower in low-temperature, which can accelerate the diffusion of particle and promote the formation of alite. ZnO is an efficient mineralizer and flux, which can decrease the burning temperature of the cement clinker, accelerate the f-CaO absorbing reaction [10, 11, 12] , and decrease activation energy of clinker formation. In the process of rapid burning, the various process such as: the decomposition of $CaCO_3$, dehydration of the clay minerals,solid phases react, the appearance of liquid-phase, and the formation of C_3S, C_2S etc approach to overlap, this makes the reaction products (CaO and C_2S etc) under a highly activation state in the formation process of clinker, the whole formating process of the clinker minerals is all along the process of the solid-liquid phase reaction basically, which reduce the reaction activation energy, greatly accelerates the formation of alite.

3. Effect of the composite mineralizers on the microstructure and the minerals of clinker in the rapid burning

No.2 raw meal was sintered rapidly at 1100± 50℃. Samples had been analyzed by XRD, ESA and SEM. The experimental results are given in Table 6 and Fig.5.According to the results of the petrographic analysis and XRD quantitative analysis, when the composite mineralizers of CaF_2, $CaSO_4$ and ZnO are added to raw meal,the main minerals of the Portland cement clinker in low-temperature rapid burning are C_3S 66~74%,β-C_2S 9~16%,C_4AF 12~16%, $C_{11}A_7 \cdot CaF_2$ 4~6%,the alite contents of the clinker are higher than that of general Portland cement clinker, and $C_{11}A_7 \cdot CaF_2$ takes place of C_3A.A large amount of Al_2O_3,Fe_2O_3,ZnO,SO_3 and F^- ions fuse into the alite(Table6) . The crystal of alite well grow crystal size is smaller,the majority of Alite crystal size is less than 10 μ m.A large amount of Fe_2O_3 and a little amount of Al_2O_3,ZnO,SO_3 and F^- ions fuse into the belite, and more SiO_2, ZnO and F^- ions fuse into the C_4AF. The hydration activation and the strength of the cement clinker increased with the increasing content of the solid solution on certainly condition.

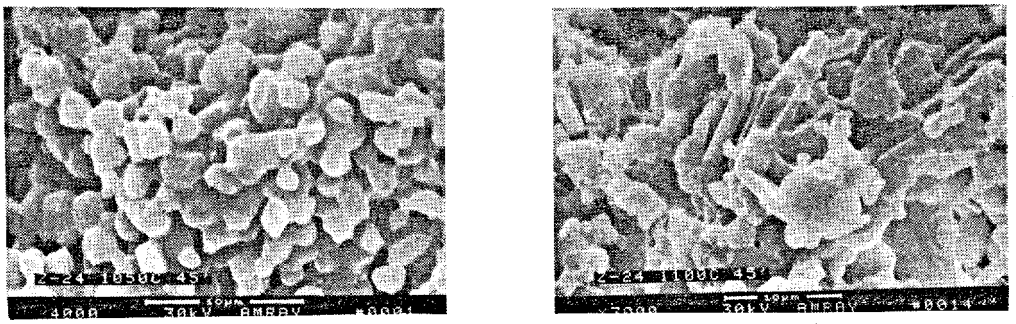

Fig.5. SEM picture of the clinker fromrapid low-temperature burning

Table 6. ESA of various clinker minerals(%)

	CaO	SiO_2	Al_2O_3	Fe_2O_3	ZnO	SO_3	F
Alite	68.92	22.96	3.09	3.27	0.98	0.75	1.15
Belite	61.97	35.28	0.10	1.75	0.41	0.56	
C_4AF	66.36	2.16	9.60	18.16	3.72		1.37

4. The physical properties of Portland cement clinker with the composite mineralizers in rapid low-temperature burning

No-2 and No-3 raw meals were rapidly burning at 1100±50℃. The clinker with 2% gypsum was groud to about 3300 cm^2/g. Then the compressive strength was determined. A contrasting experiment was done using 56.5 MPa (GB 525R) ordinary Portland cement clinker of CHINA JIANGYOU CEMENT PLANT. The results of experiment are given in Table 7.

Table 7. Physical properties of rapid low-temperature burning cement clinker

NO.	setting time(h:min)		compressive strength (MPa)				
	initial	final	1d	3d	7d	28d	90d
1	3:40	6:50	26.3	54.4	81.8	92.9	
2	2:50	4:40	30.5	62.4	71.1	72.5	73.5
3				50.0	61.3	76.3	87.3
4				57.6	63.8	70.8	73.5
5	3:50	8:20		38.6	64.8	70.8	79.8
rdinary cement 56.6MPa				13.9	37.5	57.2	60.0

From Table 7, it is seen that the early age as well as the late age compressive strengths of cement clinker obtained from rapid low-temperature burning are higher than that of the contrasting specimen. Especially one day strength is twice than that of 525#R model ordinary Portland cement. After hydrating for 28 days, the increasing ratio of strength is still larger. This is the reason that the formation

temperature of portland cement clinker in rapid low-temperature burning is lower (about 1100℃) , the crystals size of the clinker minerals with a fine petrographic structure are smaller(Fig. 5),and a lot of impurities fuse into the clinker minerals (Table 6) , the activation of the clinker minerals is higher. According to the general point of view, when there are F^- ions in the cement raw meal, the setting of the cement sintered in low-temperature is very quick. Especially when F^- content is higher,this phenomenon is more common. In Table 7 we can see that when there are much F^- content (over 1%) in raw meal, but the setting time of the clinker sintered at about 1100℃ is regular. This is reason that a large amount of Al_2O_3 fuse into the alite in cement clinker in rapid low-temperature burning (Table 6) , so that greatly decrease Al_2O_3 content which used to form $C_{11}A_7 \cdot CaF_2$, and the setting time can be retarded. The quantitative analysis of XRD showed that $C_{11}A_7 \cdot CaF_2$ content of the clinker is between 4% and 6%, it is less. Especially ZnO etc can decrease the hydration rate of $C_{11}A_7 \cdot CaF_2$[13] , therefore the flash set of cement can not be formed.

CONCLUSIONS

The burnability of the raw meal with the composite mineralizers of CaF_2,$CaSO_4$ and ZnO is better than that of without any mineralizers, though the burning temperature is lower by 200℃, the cement clinker minerals are formed more easily. When there are the composite mineralizers in the cement raw meal, contrasting rapid to slow burning, the experiment results show that a technology of rapid burning can greatly improve the burnability of the raw meal. This is attributed possibly to the combination of heating and chemical activation.

When the composite mineralizers of CaF_2, $CaSO_4$ and ZnO are added to the raw meal,the Portland cement clinker can be formed at about 1050℃.The suitable composition of the main mineral of the Portland cement clinker in rapid low- temperature burning are: C_3S 66~74%, β -C_2S 9~16%, C_4AF 12~16%,and $C_{11}A_7 \cdot CaF_2$ 4~6% (wt.%). The alite content is higher than that of general Portland cement clinker,and $C_{11}A_7 \cdot CaF_2$ replaced C_3A. The strengths of the cement clinker,whether in the early or the late age, are higher.

REFERENCES

1. Asok k.Sarkar 7th Iccc (1980) p141~147(China)
2. Gilioli,c.,Massazza,F.etal Cem.Concr.Res.9,295(1979)
3. Klemm,W.A.and Javed,I.,proc.Mth Intl.Congress Chem.Cem.,Paris(1980) p125~130(China)
4. Huang Wenxi,Wang Xie etal.Proc. 1985 BJ.Intl.Symp.Cem.Concr.Beijing(1985) p226~234
5. Phillipp,O.Proc. 6th Intl.Congress Chem.Cem.,Russian,(1976)(China)
6. Gutt,W.and Osborna,G.J. Trans.Brit.Ceram.Soc.65,521(1966)
7. Tanaka,M.,etal,5th Isscc,Tokyo,I,122(1969)(China)
8. Huang Wenxi, Ye Qiaoming et al 2ND ISCC Beijing, China Vol.1.p203(1989)
9. Huang Wenxi, Lu Zhongyuan Xu Guangliang 9th ICCC,New Delhi,India(1992)
10. Tsubol,T. et al Zement-Kalk-Gips 25,426(1972)
11. Knofel,D.,Zement-Kalk-Gips 31,157(1978)
12. Huang Wenxi,Xu Guangliang, Lu Zhongyuan, 9th ICCC,New Delhi,India(1992)
13. Huang Wenxi, Qian Guangren, et al 9th ICCC, New Delhi,India(1992)

RESEARCH AND APPLICATION OF COMPOSITE MINERALIZER IN ROTARY KILN

LI Peiquan, Liu Changfa, Su Muzhen
Lu Baoshan, LI Guangmin, Ge Wenmin and Chen Yongfan

China Building Materials Academy, Beijing, P R CHINA

SUMMARY

The low temperature burning technology with composite mineralizer has been researched since 1978 and put into operation since 1984. Great benefits have been achieved, mainly as follows: (1) The compressive strength of the clinker is considerably increased. (2) The clinker output is increased by 5～15%. (3) The coal consumption is reduced by 5～15%. (4) The strength of rich alkali clinker and the strength of clinker calcined with high-sulphur low-grade coal are also increased remarkably. (5) The burning operation is easy to control, so the fast speed rotary running rate of kiln is raised. (6) The running period for a rotary kiln is prolonged about 1～1.5 times.

〔摘要〕 1978 年 1 月起，本院开展了复合矿化剂煅烧硅酸盐水泥熟料技术的研究。1984 年 1 月以来，X、T、Q、Z 等水泥厂成功地进行了生产。

本技术主要效果如下:

1.熟料，1 天抗压强度 20MPa 以上，3 天抗压强度 41MPa 以上，28 天抗压强度 63MPa 以上，可以稳定地生产高标号（R）硅酸盐水泥、普通水泥、矿渣水泥、火山灰质水泥、粉煤灰水泥以及快硬水泥、无收缩快硬水泥、道路水泥等等。2.熟料增产 5～15%。3.节煤 5～15%。4.大幅度提高了高碱熟料和高硫劣质煤煅烧的熟料强度。熟料 28 天抗压强度由 53MPa 左右提高到 63MPa 以上。5.煅烧操作方便，控制容易，窑的快转率运转率提高。6.窑皮质量好，有利于窑的长期安全运转。回转窑运转周期提高 1～1.5 倍。

阐述了石膏萤石掺加下，硅酸盐水泥熟料的形成过程和 SO_3，$\overline{F}$在熟料中的分布。介绍了熟料矿物组成和熟料及水泥的物理力学性能。讨论了复合矿化剂技术提高高碱熟料强度的机理。

1. INTORDUCTION

Reducing energy consumption and improving clinker quality are two of the main purposes in the development of cement technology. In order to raise cement output and quality as well as to save energy, great attention has been paid worldwide to low temperature burning with the composite mineralizer.

Quite a lot of theoretical reports about the composite mineralizer have been published [1,2,3] but few about practical application [4,5].

China Building Materials Academy (CBMA) has studied low temperature burning portland cement clinker with the composite mineralizer since Jan.1978. The research project passed administrial appraisal organized by China State Administration Building Materials Industry in Nov. 1982.

The technology has been used in pilot production since Jan. 1984 in X, T, Q and Z cement plants. T cement plant has used the new technique since Sept. 1985. The use of the composite mineralizer in large rotary kilns gives significant social and economic benefits.

2. LABORATORY STUDY

2.1 The formation process of portland cement clinker with the addition of gypsum and fluorite

2.1.1 High temperature XRD— Sample preparation: 5A3 raw meal was prepared from raw materials of J cement plant. The composition of the raw meal is as follows:

The phase trnsformation for 5A3 at high temperature is given in Fig.1.

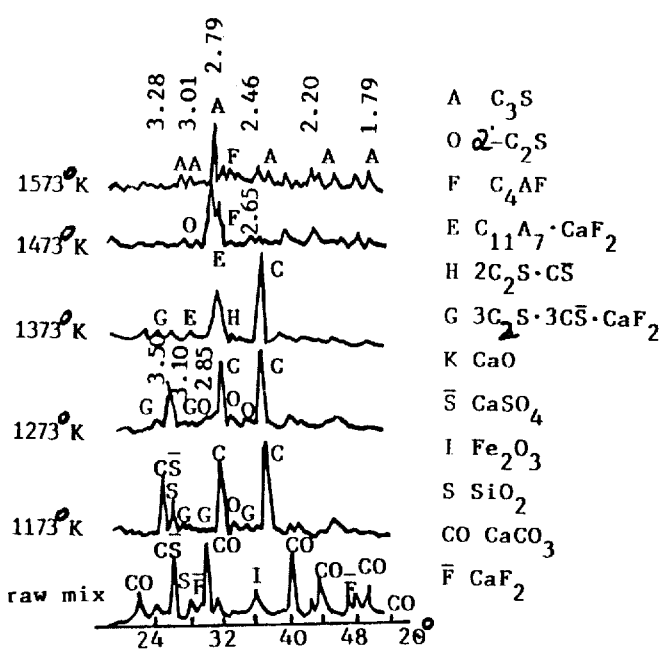

Fig.1 XRD of phase transformation for raw meal 5A3 between 900~1300℃

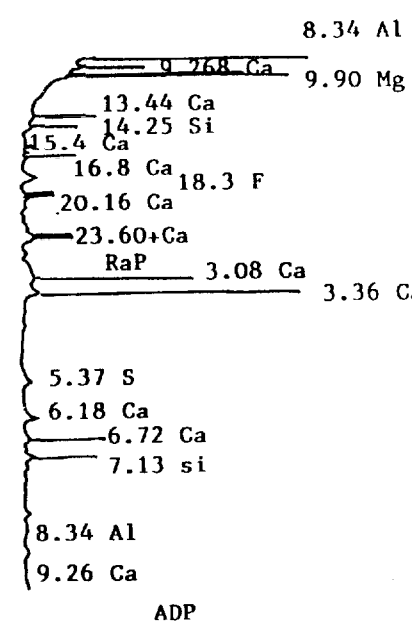

Fig.2 Spectrograms of EPMA for the clinker burned at low temperature.

Loss	SiO_2	Al_2O_3	Fe_2O_3	CaO	MgO	SO_3	$\bar{F}$	K_2O / Na_2O
33.56	13.55	3.66	2.73	43.37	0.33	1.69	1.10	0.47 / 0.07

The result indicates that, with the addition of the composite mineralizer, the low melting point phase $3C_2S \cdot 3C\bar{S} \cdot CaF_2$ appears at 1173 ° K, $2C_2S \cdot C\bar{S}$ occurs at 1323 ° K, and both phases disappear at 1373 ° K. So these two phases are intermediums and play a very improtant role during cement clinkering. The result is in accordance with that by G. Higeto[6].

The introduction of fluorine causes an additional phase $C_{11}A_7 \cdot CaF_2$ to form at 1373 ° K and it begins to decompose at a temperature higher than 1570 ° K. C_2S appears as α'–C_2S at 1173 ° K, which decreases with C_3S formation. C_4AF becomes visibe at 1470 ° K.

2.2 SO_3 and $\bar{F}$distributon in the clinker burned at low temperature

2.2.1 EPMA analysis— EPMA result is shown in Fig.2.

It is known from Fig.2 that, besides Mg, K and Na, SO_3 and $\bar{F}$ also enter the main mineral C_3S of low temperature clinker. The peak for SO_3 is 5.37Å, for $\bar{F}$ 18.0Å. The same elements can also be seen in the minerals C_2S and C_4AF. In other words, for low temperature clinker SO_3 and $\bar{F}$ distribute in silicate phases as well as in interstitial phase, but chiefly in C_3S.

3. PRODUCTION WITH A ROTARY KILN

3.1 Technical and economic benefits for the production

Trial productions have been carried out in large cement plant—X,T,Q(Φ3.5 × 145m wet rotary kiln). Z (Φ4.5 × 50.0m lepol kiln) since Jan.1984.

The main benefits of the technology are as follows:

① The compressive strength of the clinker is greater than 20 MPa for 1 day. 41 Mpa for 3 days, 63 MPa for 28 days. High early strength (R) portland cement, ordinary porland cement, slag portland cement, pozzolana portland cement, fly–ash portland cement and rapid hardening portland cement, non shrinking and rapid hardening cement, portland cement for road etc. can be produced steadily.

② The clinker output is increased by 5～15%

③ The coal consumption is reduced by 5～15%

④ The strength of rich alkali clinker and the strength of clinker calcined with rich sulphur low grade coal are increased remarkably, from about 30 MPa to more than 41 MPa for 3 days, from about 53 MPa to more than 63 MPa for 28 days.

⑤ The operation of low temperature burning is convenient and easy to control. The fast speed rotary running rate of kiln is raised.

⑥ The kiln coating is in good condition and this is favourable to long term safe runing of kiln. The runing period for a rotary kiln is prolonged about 1～1.5 times.

3.2 Clinker

3.2.1 Minerals in the clinkes— The minerals in the clinker burned at low temperature were determined with XRD and the patterns are shown in Fig.3.

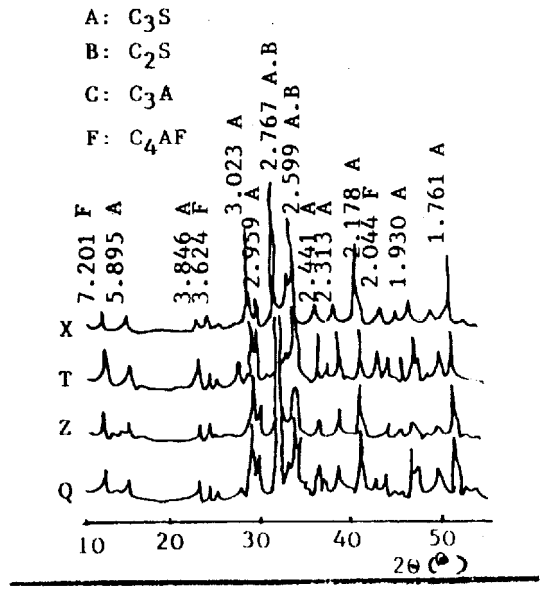

Fig.3 XRD patterns of low temperature burned clinker

Fig.3 shows that the main minerals for low temperature burned clinker are C_3S, C_2S, C_3A and C_4AF.

3.2.2 Physical properties of the clinker— The physical properties for the clinkers burned at low temperature in four plants are listed in Table 1.

Table 1 indicates the compressive strength of low temperature burned clinkers for different ages: above 20 MPa for 1 day, above 41 MPa for 3 days, 63～67.0 MPa for 28 days. Obviously the strength of the clinker is much higher than that of common clinker at 1 day and 3 days.

Table 1 Physical properties for clinkers burned at low temperature

Sample No.	Fineness		Normal consistency %	Soundness	Setting time		Compressive strength MPa days				Bending strength MPa days			
	S m^2/kg	80μm sieve residue %			Initial h:min	Final h:min	1	3	7	28	1	3	7	28
X-1	310.0	5.7	24.00	passed	4:08	5:46		43.0	58.8	65.7		7.0	7.5	8.0
X-2	309.0	8.7	23.75		3:43	6:01		41.4	51.0	64.1		6.7	7.4	8.3
T-1	292.4	4.8	23.50	passed	3:47	4:15		46.5	53.6	63.0		7.3	7.8	8.7
T-2	299.3	3.9	24.25		3:39	4:19		46.7	52.2	62.7		7.1	7.7	8.3
Z-1	292.0	4.4	23.00	passed	4:18	5:38	21.8	45.3	56.9	66.8	4.4	6.8	7.9	8.0
Z-2	295.0	4.8	23.00		3:56	4:31	23.2	45.0	56.6	67.8	4.8	6.6	7.8	8.1
Q-1	299.7	3.2	24.25	passed	3:32	4:26	24.2	44.9	54.0	63.5	5.4	7.1	7.6	8.3
Q-2	301.3	3.4	24.00		3:02	4:02	26.0	46.2	54.0	64.9	6.1	7.1	7.8	8.7

3.3 Cement

Because the clinker burned at low temperature has high strength, especially high early strength, many kinds of high strength grade (R type) cement can be produced steadily, such as portland cement, ordinary portland cement, slag portland cement, fly–ash portland cement, pozzolana portland cement, and rapid–hardening portland cement, non shrinking and rapid–hardening cement, portland cement for road etc.

3.3.1 Portland cement

Table 2 Physical properties of portland cement

Sample No.	SO_3 %	Fineness %	Normal consis–tency %	Sound–ness	Setting time h:min		Compressive strength MPa days			Bending strength MPa days		
					Inital	Final	3	7	28	3	7	28
G0086	2.08	4.6	24.25	passed	3:43	4:33	37.2	50.4	64.4	6.3	7.5	8.5
G0089	2.18	5.0	24.75	passed	2:48	5:01	34.5	47.4	63.2	6.0	7.1	8.4

The physical properties of portland cement are given in Table 2. It can be seen from Table 2 that grade 525 (R) portland cement from low temperature burned clinker actually reaches grade 625 (R) for portland cement of Chinese National Standard.

4. DISCUSSION

Why can this technology increase the strength of rich alkali clinker remarkably?

The reason is that using composite mineralizer can introduce suitable gypsum and fluorite additives to raw meal. When there is a suitable proportion of SO_3 and R_2O, R_2O can form R_2SO_4 instead of detrimental mineral $KC_{22}S_{12}$ etc. So, it is beneficial to late strength. On the other hand, it is predicted that different alkalinity existed in clinker also certainly influences its process of hydration and hardening, and getting different final strength. When the alkali in clinker exists in R_2SO_4, it can transform to liquid phase very quickly in case it meets water because of high solubility of K_2SO_4. Therefore, the alkalinity of liquid phase increases quickly and this impedes diffusion of Ca^{++} in liquid phase. This leads to slow hydration speed of clinker in early hydration period. When the alkali exists in R_2O, it is transformed to liquid phase through minerals hydration, and its speed is slow. The diffusion coefficient of Ca^{++}in liquid phase is weaker, the hydration rate is higher. The differences between two of the hydration speed in early hydration period, are bound to lead to the difference of crystalizing rate, and influence the crystalization and growth of hydration products. As the crystalizing rate of clinker with R_2SO_4 is slow, the structure and crystalization of its hydration products can become perfect. This is also a positive factor to late strength development of clinker.

Regarding the volatility of clinker alkali, generally it is believed that CaF_2 is positive to the volatility of R_2O, and $CaSO_4$ is negative to it. But what is the situation when CaF_2 and $CaSO_4$ coexists? According to our experiments, it is formed that the content of R_2O is unchanged. Obviously, this is also the result of forming R_2SO_4. So, the low temperature burning technique with fluorite and gypsum as a composite additive, in which gypsum will first combine R_2O, in fact, it reduce both

the flying loss of R_2O and the possibility of forming solid solution. At the same time, because of the severe soluble effect of fluorite, it reduces the clinkering temperature, and prevent gypsum from high temperature decomposition. So on the combined effect of both gypsum and fluorite, the mineralizing effect is better developed and the clinker strength is improved. On the other hand, the alite content of the clinker with this technique is usually above 60%, it makes clinker strength enhance greatly, and this is the main factor to improve clinker strength.

5. CONCLUSION

By using the low temperature burning technology with composite mineralizer, following benefits can be achieved:

(1) The compressive strength of the clinker is greater than 20 MPa for 1 day, greater than 41 MPa for 3 days and 63～67 MPa for 28 days. High early strength (R) porltand cement, ordinary portland cement, slag portland cement, pozzolana portland cement, fly-ash portland cement, composite portland cement and rapid-hardening cement, non shrinking and rapid-hardening portland cement, portland cement for road etc. can be manufactured steadily.

(2) The clinker output is increased by 5～15%.

(3) The coal consumption is reduced by 5～15%.

(4) With the addition of the composite mineralizer, $3C_2S \cdot 3C\bar{S} \cdot CaF_2$ appears at 1173 ° K. $2C_2S \cdot C\bar{S}$ forms at 1327 ° K, and these both phases disapplear at 1373 ° K. $C_{11}A_7 \cdot CaF_2$ forms at 1373 ° K, and it begin to decomposes at a temperature higher than 1570 ° K. The clinker alite content with this technique is usually above 60%.

(5) SO_3 and $\bar{F}$ were distributed in silicate phases as well as in interstitial phase, but chiefly in C_3S.

REFERENCES

1. V.N. Viswanathan, S.N. Chosk, "The Mineralizer and Fluxing agent in the Process of Clinker Formation", Cement Technology Progress (in Chinese) pp.113～132.
2. W.A. Kleen, I. Jawed, "The mineralizer and fluxing agent in the calcining process" 7th International Congress on the Chemistry of Cement (in Chinese) pp.125～131.
3. A.K. Sarkar, D.M. Roy and R.M. Smart, "The mineralizer and fluxing agent in the calcined process", 7th International Congress on the Chemistry of Cement (in Chinese) pp.141～147.
4. C.H. Page, D. Ghosk and A.K. Chatterjee, "The influence of mineralzer on the composition and property of industrial clinker", 8th International Congress on the Chemistry of Cement Vol.2 (in Chinese) pp.80～84.
5. Moir, G.K. "World Cement" Vol.10, pp.374～382 (1982)
6. Higeto, G., Sement Gizutsu Nempo, Vol.28, pp.131 (1974)
7. Liu Baoyuan, Li Xiuying, "Journal of the Chinese Silicate Society" Vol.19, No.4 pp.456～465 (1981)
8. Smart, R.M. Roy, D.M., "Cement and Concrete Research" Vol.9, No.2, pp.267～273 (1979)
9. Osokin A., "Proc. of MCTI n.a. D.J. Mendeleer ed" 76, (1973) (in Russian)
10. I.G. Luginina, A.N. Luginin, "Tsement" (2), 15, (1974)
11. S.N. Ghosk, A.K. panl and A. Thakur "T. Mater. Sci." (13) 1603 (1978)
12. Feng Mingfen, Wen Xiuping and She Wei, "A Study of the Effect of Sulphate on Clinker of 1985 Beijing Internatonal Symposium on Cement and Concrete pp.109～119.
13. Gutt. W. et., Swith M.A. (1967) "Studies of the Sub-system $CaO-CaSiO_2-CaSO_4$" "Jrams. Brit Cegam Sec" 66, pp.557.

ACTIVE BELITE CEMENT

Ingo Mielke, Anette Müller and Jochen Stark

Department of Building Materials
University of Architecture and Building, Weimar, GERMANY

SUMMARY

In the active belite cement the belite as the main clinker mineral takes the place of alite. The belite occurs in the α'-modification, which has a high hydraulicity. It is stabilized by incorporated alkalis and by thermal activation.

A further possibility - the chemical activation by the addition of sulfate to the raw meal takes place only in the range of lime standard KSt = 78 - 82, that is the typical range for active belite cement. The 28-day strength of an active belite cement made from a clinker with 5 - 6 % SO_3 is of the same magnitude as that of a belite cement without admixtures. High strength after 3 days is achieved only if α'-C_2S occurs.

ZUSAMMENFASSUNG

Im aktiven Belit-Zement ist der Belit das Hauptmineral anstelle des Alits. Der Belit tritt in der höherhydraulischen α'-Modifikation auf, die als alkalihaltiges C_2S durch thermische Aktivierung stabilisiert wird.

Eine weitere Möglichkeit, die chemische Aktivierung durch SO_3-Dotierung der Rohmehle, wirkt nur im Kalkstandardbereich 78 - 82, das ist der typische Bereich für den aktiven Belit-Zement. Die 28-Tage-Festigkeiten eines aktiven Belit-Zementes aus einem Klinker mit 5-6 % SO_3 liegen in der gleichen Größenordnung wie beim undotierten Belit-Zement. Hohe 3-Tage-Festigkeiten werden nur beim Auftreten von α'-C_2S erreicht.

Active Belite Cement

Research work on the development of an active belite cement (ABC) has been carried out for some years. The aims of this work differ and depend on the economic conditions. The most important aims are:

- the reduction of the energy consumption for the manufacture of cement clinker
- the reduction of the maximum burning temperature, which allows the use of a low grade coal and the reduction of NO_x emission /1,2,3,4,5,6/.

Besides the production of ABC allows the use of limestone or limemarl with a lower $CaCO_3$-content than it necessary for the manufacture of Portland Cement /7,8/.

As early as 1973 a group of reseach workers in Weimar/Germany had the idea to reduce the energy consumption of cement manufacturing by the modification of the phase composition of Portland cement without principally changing the phase composition known from PC-clinker /9/.

In the ABC the belite as the main clinker mineral takes the place of alite. The belite occurs in a modification with a high hydraulicity caused by a thermal or chemical activation. Typical ABC with a lime standard KSt I between 75 and 85 achieves a strength development similar to that of a Portland cement of OPC-type in spite of the low alite content of about 30 % /10,11/.

The thermal activation is realized by quenching of the belite clinker in the temperature range from 1300 to 900 °C with a cooling rate of at least 800 K/min /10,11,12/. The quenching results in the stabilisation of α'-belite by the incorporated alkalis or other foreign oxides up to 5 % /13,14,15,16/. The comparison of the results of the X-ray phase analysis with the strength measurments shows, that the 3-day strength is strongly influenced by the alite content (fig.1). The low 28-day strength of the inactive, slowly cooled belite cements can also be considered as an "alite strength". The increase of the 28-day strength with the cooling rate and the high 28-day strength of ABC is caused by increasing content of α'-belite.

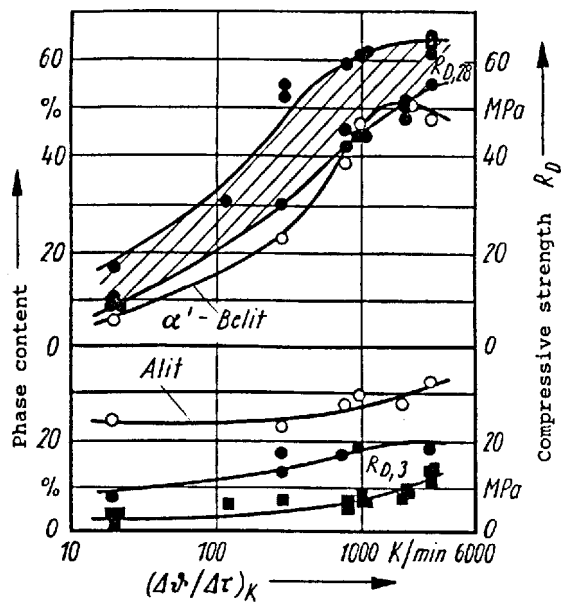

Fig. 1: Compressive strength resp. phase composition versus cooling rate

This result is confirmed by the rate of hydration measured with XRD. The rate of hydration of α'-belite is much higher than of ß-belite and in the same order as that of alite.

The properties of fresh mortars produced from ABC or PC are naerly the same. Small differences appear in the strength development of both cements. Characteristics of ABC are the high strength after 28 days and the lower early strength, as compared with PC. Durability and passivation of steel are ensured by mortars and concretes based on ABC too.

Tests of concrete specimens from ABC produced in a pilot plant with an output of 20 t clinkers/day, were made in connection with the industrial production of prestressed concrete and in connection with the concreting of a road. These tests show a good workability of concrete from ABC. The strength of 20 cm-cube made from site concrete amounts to 17 - 29 N/mm² after 2 days and 38 - 52 N/mm² after 28 days. These concretes do not show any damage after a use of 7 years.

Besides the thermal activation of belite by quenching the chemical activation was investigated too. For that purpose various sulfate materials (anhydrite, flourgypsum and H_2SO_4) were added to the raw meal with the aim of producing a sulfate stabilized belite cement /17,18/. The belites in the clinkers from the raw meals doped with sulfate materials do not contain alkalis as foreign oxides, because these are incorporated in alkalisulfates. In this way the formation and stabilization of α'-belite is prevented even at high cooling rates. The belite occurs only in the ß-modification and contains 3 % SO_3 and 3 % Al_2O_3 as foreign oxides. The formed ß-belite has a higher hydraulic activity than ß-belite without SO_3. For the optimum SO_3-content in clinker of 4...6 % a 28-day strength is achieved, which is higher than that of belite cements without addition at low cooling rates and which is in the same order like undoped belite cements at high cooling rates (fig. 2).

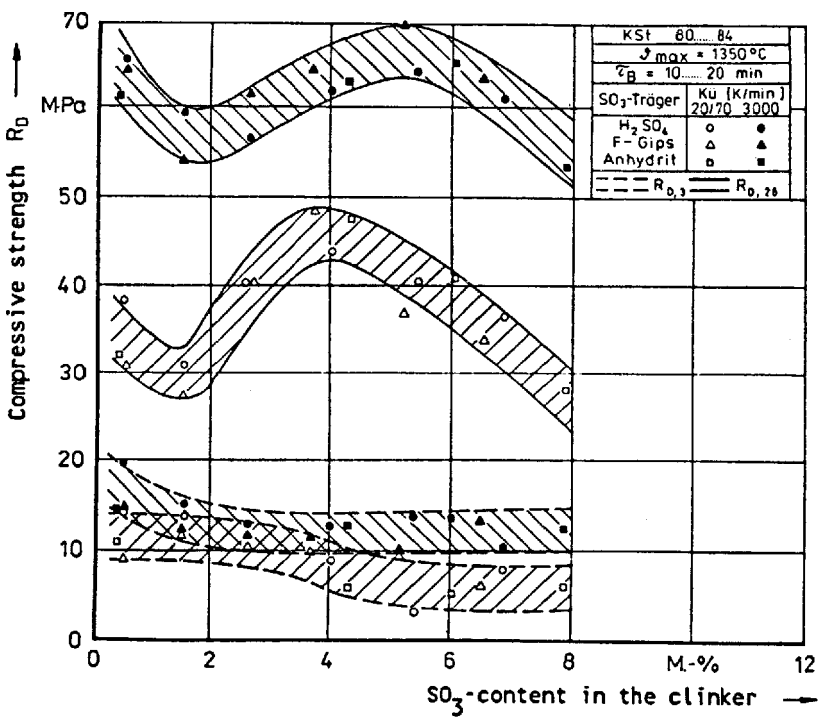

Fig. 2: Compressive strength after 3 and 28 days versus SO_3-content in the clinker for a cooling rate of 20/70 resp. 3000 K/min

The minimum of strenth at about 1,5 % SO_3 in the clinker is caused by two facts:

- The alkalis are connected only with sulfate, no sulfate is incorporated in the belite.
- The alite content is lower than in the belite clinker without SO_3.

Increasing the SO_3-content results in a decrease of alite- content by which the early strength decreases steadily. For SO_3-contents above 6 % the chemical compound $C_4A_3\bar{S}$ appears apart from sulfate containing belite. Because of its potential content in the cement of 10 % at the most this compound has no essential influence on the early strength.

As to the strength there is an optimum range for the lime standard of SO_3 doped belite cement (fig. 3). This range agrees with the optimum lime standard for thermal activated belite cement.

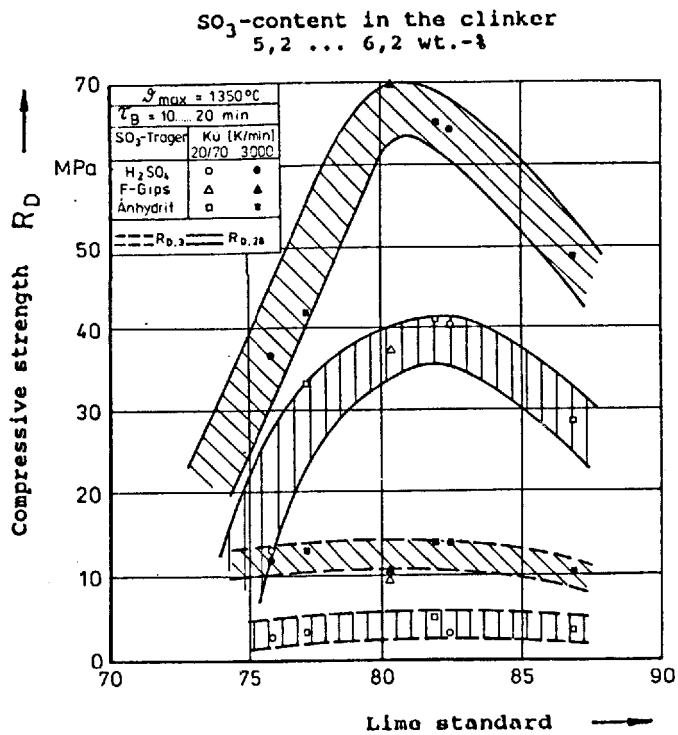

Fig. 3: Compressive strength after 3 and 28 days versus lime standard

ABC based on anhydrite as the CaO-component (sulphuric acid production according to Müller and Kühne) achieved high early strength and very high strength after 28 days in comparison with SO_3 containing ABC from carbonate raw meal /19/. The anhydrite ABC has a very low alkali content of about 0,15 % Na_2O-equ. dependent on the raw materials and a remaining content of 4...6 % SO_3. It contains little alite (< 5 %) and many belite as well as anhydrite and 10 % $C_4A_3\bar{S}$ at the most.

Thus it corresponds to the SO_3 containing ABC with regard to the phase composition and the SO_3-content. In contrast to the ABC doped with SO_3 the belite in the ABC based on anhydrite appears in the α'-modification. It contains about 3 % SO_3 and 3 % Al_2O_3 as foreign oxides and is characteristiced by a high content of excessive stoichiometric CaO. In the anhydrite raw meal α'-C_2S is formed by decomposition of the instatial phase sulfatespurrite $C_5S_2\bar{S}$ /20/. In the SO_3 doped, carbonatic raw meal the

SO_3-content is too low to form $C_5S_2\bar{S}$ even if 10 % $CaSO_4$ is added. Therefore no SO_3 stabilized α'-C_2S can be found in these clinkers (fig. 4).

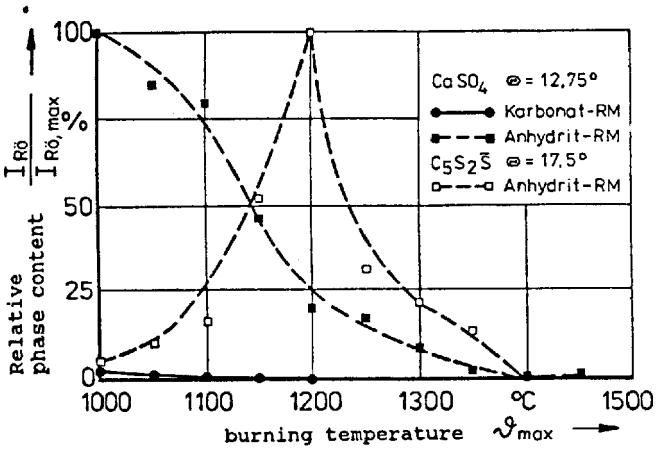

Fig. 4: Relative contents of $CaSO_4$ and $C_5S_2\bar{S}$ versus burning temperature

The sulfoaluminate cement is a further kind of cement often discribed with a high SO_3-content. This cement contains the belite in the α'-modification too, if high cooling rates are realized. The strength of this cement arises from the belite and above all from the $C_4A_3\bar{S}$, by which high early strength is possible at all cooling rates. The 28-day strength is not influenced by the cooling rate too.

In the fig. 5 the strength of sulfoaluminate cement is compared with the strength of the SO_3 doped, carbonate based cement and the anhydrite based cement.

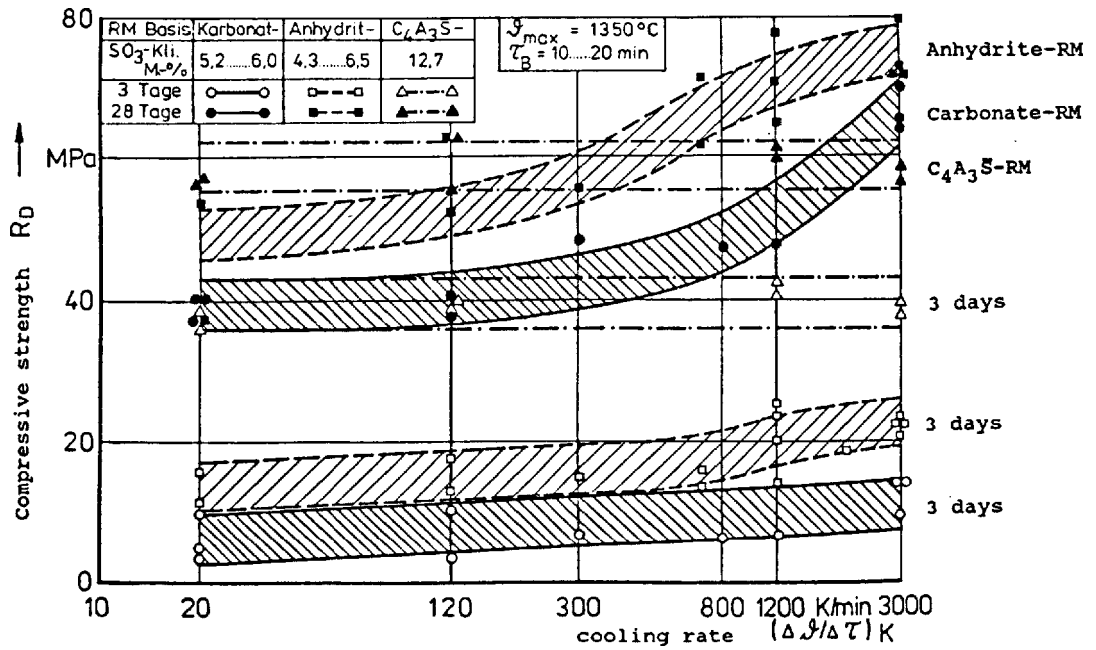

Fig. 5: Compressive strength after 3 and 28 days versus cooling rate for different SO_3 containing belite cements

It shows advantages of the $C_4A_3\bar{S}$-cement with regard to the 3- day strength and advantages of the other cements with regard to the 28-day strength at high cooling rates.

The results of the chemical activation allow the conclusion, that the chemical activation by SO_3 addition cannot replace but only complement thermal activation. The strength of slowly cooled, SO_3 containing belite cements is smaller than the strength of thermal activated belite cements.

Literature

/1/ Mehta, P. K.: Investigations on energy-saving cements. World Cement Technology, London 11 (1980) 4, p. 166-177.

/2/ Sudakas, L. G.; Kraplâ, A. F.; Kougiâ, M. V.; Sokolova, N. A.; Lokšina, E. A.; Evstratova, G. R.: Sostav, teplota obrazovaniâ i gidravličeskaâ aktivnost nizkoosnovnyh klinkerov. Cement, Leningrad 50 (1984) 3, p. 14- 16.

/3/ Sudakas, L. G.; Nikiforov, K. V.; Kougiâ, M. V.; Sokolova, N. A.: Étude des clinkers à basse basicité. 8th ICCC, Rio de Janeiro 1986, Vol.2, p. 322- 326.

/4/ Ludwig, U.; Pöhlmann, R.: Zur Herstellung kalkarmer Portlandzemente. Zement-Kalk-Gips, Wiesbaden 38 (1985) 10, p. 595- 598.

/5/ Ludwig, U.; Pöhlmann, R.: Investigations on the Production of Low Lime Portland Cements. 8th ICCC, Rio de Janeiro 1986, Vol.2, p. 363-371.

/6/ Gies, A.; Knöfel, D.: Influence of alkalies on the composition of beliterich clinkers and the technological properties on the resulting cements. Cem. and Conr. Res., New York 16 (1986) 3, p. 411-422.

/7/ Rangnekar, B. S.; Srinivasan, V. R. G.; Pai, V. N.: An early hardening C_2S phase made by rapid heating technique. 6th ICCC, Moskva 1974, Vol.1, p. 197-200.

/8/ Gosh, S. N.; Mathur, V. K.; Parashar, A. K.: Microstructures and solid solutions of low temperature clinkers. 8th ICCC, Rio de Janeiro 1986, Vol.2, p. 322- 326.

/9/ Schrader, R.; Stark, J.; et al.: Verfahren zur Herstellung von Zement. DD-PS 139 938, 07.09.1973.

/10/ Stark, J.; Müller, A.; Schrader, R.; Rümpler, K.; Dahm, B.; Mielke, I.: Über aktiven Belit-Zement

Teil 1: Silikattechnik, Berlin 30 (1979) 12, p. 357-362; Teil 2: Silikattechnik, Berlin 31 (1980) 2, p. 50-52; Teil 3: Silikattechnik, Berlin 31 (1980) 6, p. 168-171.

/11/ Stark, J.; Müller, A.; Schrader, R.; Rümpler, K.: Existenzbedingungen von hydraulisch aktivem Belit-Zement; Zement-Kalk-Gips, Wiesbaden 34 (1981) 9, p. 476-481.

/12/ Stark, J.; Müller, A.; Seydel, R.; Jost, K.: Conditions of the existence of hydraulically active belite cement, 8th Intern. Congress on the Chemistry of Cement, Rio de Janeiro 1986, Vol. 1.3, p. 306-309.

/13/ Jost, K.; Seydel, R.; v. Lampe, F.; Müller, A.; Stark, J.; Mielke, I.: Phasenbestand und hydraulische Aktivität von Belitklinker, Silikattechnik, Berlin 36 (1985) 12, p. 375-378.

/14/ Müller, A.; Stark, J.; Mielke, I.: Zum Einfluß der Alkalien auf die Festigkeit von aktivem Belit-Zement. 8. ibausil, Weimar 1982, Vortrag Nr. 1.2.7.

/15/ Müller, A.; Stark, J.: Zum Einfluß der Alkalien auf die Festigkeitsentwicklung von aktivem Belit-Zement. Silikattechnik, Berlin 38 (1987) 9, p. 301-305.

/16/ v. Lampe, F.; Altrichter, B.; Müller, A.: Über die Beziehungen zwischen Nebenkomponenten im Belit, Kühlgeschwindigkeit, kristallographischer Modifikation und hydraulischen Eigenschaften. Silikattechnik, Berlin 37 (1986) 7, p.238-243.

/17/ Mielke, I; Stark, J.; Müller, A.: Einsatz von Fluorgips als Mineralisator beim Brennen von aktivem Belit-Zement. 8. ibausil, Weimar 1982, Vortrag Nr. 1.2.6.

/18/ Mielke, I.; Müller, A.; Stark, J.: Mineralphasen im SO_3-haltigen Belitklinker und ihr Einfluß auf die Festigkeit. 9. ibausil, Weimar 1985. In: Wiss. Zeitschr. der Hochsch. für Archit. und Bauwesen, Weimar 31 (1985) 2 B, p. 44-47.

/19/ Müller, A.; Stark, J.; Mielke, I.: Aktiver Belit-Zement auf Anhydritbasis. Silikattechnik, Berlin 35 (1984) 4, p.276-278.

/20/ Stark, J.; Müller, A.; Mielke, I.: Über SO_3-haltigen Belitklinker. Silikattechnik, Berlin 38 (1987) 9, p.301-305.

LITHIUM AS INTENSIFIER IN THE FORMATION OF DICALCIUM SILICATE PHASE

V K Mathur, R S Gupta and S C Ahluwalia

National Council for Cement and Building Materials
New Delhi, INDIA

SUMMARY

Li_2CO_3 dopant lowers the decomposition temperature of $CaCO_3$ and the reaction takes place in two steps. CaO formed at lower temperature reacts with SiO_2 to form β - dicalcium silicate phase (β-C_2S), even at 750°C. The reaction is completed at 1350°C with the formation of β-C_2S alongwith small amounts of γ-C_2S phase by the addition of 1.0 wt. percent dopant. Addition of 5.0 wt. percent dopant brings the final reaction temperature down to 1250°C. The reaction products are β-C_2S and small amount of tricalcium silicate (C_3S) phase. The kinetics of formation of C_2S correspond to first order reaction and the activation energy determined by Ginstling-Brownshtein equation decreases from 180 KJ mol^{-1} in pure system to 130 KJ mol^{-1} with 1.0 wt. percent lithium dopant. There is a general trend towards reduction in Ea up to a concentration of 1.0 percent of Li_2O, after which there is a gradual increase to 145 KJ mol^{-1} at 5.0 percent concentration.

INTRODUCTION

Studies on the kinetics and thermodynamic parameters of the decomposition of pure $CaCO_3$ and the effects of various dopants have been reported earlier (1-5). Some of the workers have reported formation of β-C_2S at the temperature range of 1350 - 1400°C with the help of dopants (3-5). Work has also been done on the thermal dissociation of naturally occurring limestone containing cationic impurities (6-7). A literature survey reveals that systematic study of the 2:1 molar $CaCO_3$: SiO_2 system containing Li_2CO_3 as dopant has received very little attention. Some work with LiCl as mineralizer in the formation of C_2S (8) and of Li_2CO_3 as intensifier (9) in the 3:1 molar $CaCO_3$: SiO_2 mixture has been reported. The present study is on the effect of varying concentrations of Li_2CO_3 on the thermal behaviour of a mixture of $CaCO_3$: SiO_2 (2:1) system.

EXPERIMENTAL

Varying amounts of Li_2CO_3 (calculated as 0.1-5.0 wt. percent Li_2O) were added to a mixture of reagent grade $CaCO_3$ and quartz powder (purity >99.0 percent). The resulting product, after thorough mixing, grinding and passing through a 100 μm sieve were shaped in the form of nodules with small quantity of distilled water. The samples after drying at 100 ± 5 °C for 2 hrs were subjected to quantitative estimation of $CaCO_3$ to ensure complete homogenization. These dried samples were stored for the experimental work.

Thermal, IR and X-ray Diffraction Studies

The measurements were made on Mettler thermal analyser (TA-1), which simultaneously records the DTA, DTG and TG curves. In all cases 60 mg samples were heated at a rate of a 10°C min^{-1} in the platinum crucible of the thermal analyser. The kinetic parameters have been calculated from the decomposition peaks (DTA and DTG).

IR studies were carried out by Perkin Elmer model IR-621 in 1800-400 cm^{-1} region. The samples were prepared in the form of disc of potassium bromide using 2.5 mg sample of dicalcium silicate and 250 mg of KBr and applying a pressure of 700 kg/cm^2.

X-ray diffraction studies were conducted by Phillips model PW 1120 diffractometer with Ni-filtered Cu radiation to identify the phases/products formed at various DTA peaks. The intermediate products formed during heating as shown by DTA peaks have been identified by heating the starting materials ($CaCO_3$ - SiO_2 (2:1) + dopant) to the temperature where the peak ends. The sample is then quenched in liquid nitrogen and stored in air tight containers. The products so formed are then identified by XRD.

RESULTS AND DISCUSSION

Thermal Analysis

The thermal behaviour of the system is given in Fig.1. The thermal curves having Li_2CO_3 (0.1 wt. percent) did not show any peak for the decomposition of Li_2CO_3 due to its amount being very small. With higher percentages of Li_2CO_3, two decomposition peaks were observed. The decomposition of Li_2CO_3 preceded that of $CaCO_3$. As the concentration of the Li_2CO_3 increased to 0.5, 1.0 and 5.0 percent, approximately 2, 6 and 8 percent $CaCO_3$ underwent decomposition in the

first step as determined from TG weight loss curve upto a temperature, where thermal loss completes. This is indicative of the fact that a 5.0 percent concentration of Li_2CO_3 is highly effective in lowering the decomposition of $CaCO_3$. No distinct peak for the decomposition of Li_2CO_3 alone was discerned although an inflexion was observed in the early stages of the peak.

The products formed as discernible by DTA peaks obtained after the decomposition of $CaCO_3$ have also been examined by XRD and infrared spectroscopy.

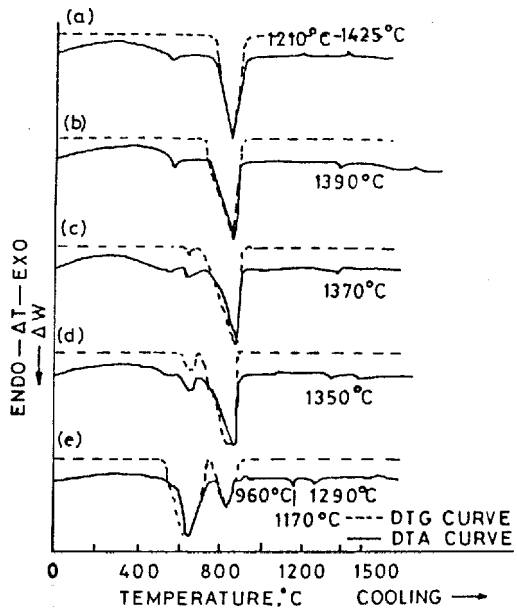

Fig 1: Thermal Curves of (a) $2CaCO_3:SiO_2$ (b) $2CaCO_3:SiO_2$ + 0.1% Li_2CO_3 (c) $2CaCO_3:SiO_2$ + 0.5% Li_2CO_3 (d) $2CaCO_3:SiO_2$ + 1% Li_2CO_3 (e) $2CaCO_3:SiO_2$ + 5% Li_2CO_3

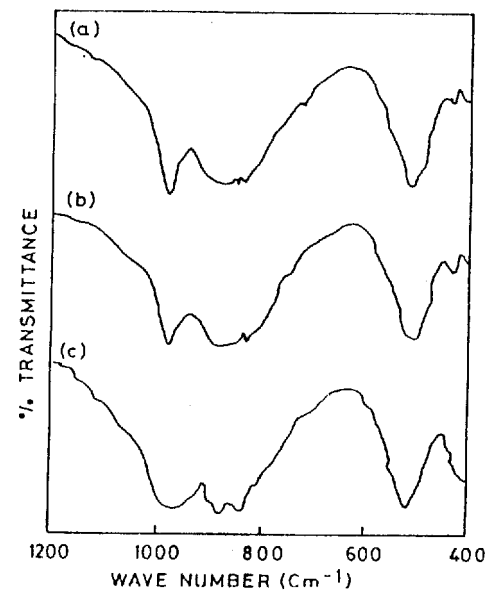

Fig 2: IR Spectra of Li_2CO_3 Doped Dicalcium Silicate Phase (a) 0.1% (b) 1.0% (c) 5.0%

Infrared Studies

The IR spectra of orthosilicates have been studied by Tarte (10). Generally silicates show two main regions of strong absorption, one near 1000 cm^{-1} due to Si-O stretching and the other near 500 cm^{-1} due to Si-O bending, often coupled with other Cation-Oxygen vibrations. The $\nu_1 SiO_4$ frequency is shown by a narrow band of weak or moderate intensity at 800-900 cm^{-1}. The region 800-1000 cm^{-1} broadly corresponds to $\nu_3 SiO_4$ which is complex absorption. The other absorption region 400-500 cm^{-1} corresponds to $\nu_4 SiO_4$. The $\nu_2 SiO_4$ frequency generally occurs around or below 400 cm^{-1}.

The sample $CaCO_3$-SiO_2 (2:1) heated to 1450°C (1h) was used as a reference. Its absorption peaks at 500 and 520 cm^{-1} correspond to β-C_2S phase. It further gave strong absorption bands at 845 and 890 cm^{-1}, which are characteristics of β-C_2S. No absorption bands at 440 and 495 cm^{-1} were observed indicating the absence of γ-C_2S. A strong absorption band at 1000 cm^{-1} further confirms that the product was pure

TABLE 1

Thermal and XRD Studies of $CaCO_3$-SiO_2 (2:1) System in Presence of Li_2CO_3

Concentration of Li_2CO_3 in $CaCO_3$-SiO_2 (2:1) System (% Wt.)	Decomposition of Li_2CO_3 and $CaCO_3$ and other Kinetic Parameters									Final DTA Peak Indicating Formation of Silicate Phase (^oC)	Constituents Formed as Discerned by XRD
	First Peak			Second Peak			A.E.(Ea) from DTG ($KJ\ mol^{-1}$)	Enthalpy (ΔH) ($KJ\ mol^{-1}$)	A.E.(Ea) of Formation ($KJ\ mol^{-1}$)		
	T_i	T_d (^oC)	T_f	T_i	T_d (^oC)	T_f					
0.0	-	-	-	740	850	910	247	160	180	1210	β-C_2S, γ-C_2S, Cristobalite, Free lime (High)
										1425	β-C_2S, γ-C_2S, Free lime (Low)
0.1	-	-	-	710	885	900	207	155	156	1390 (endo)	β-C_2S, γ-C_2S Free lime (0.07%)
0.5	620	650	680	700	880	900	200	135	144	1370 (endo)	β-C_2S, γ-C_2S, Free lime (0.30%)
1.0	620	650	690	690	870	890	187	120	130	1350 (endo)	β-C_2S, γ-C_2S, Free lime (0.43%)
5.0	540	650	740	740	850	890	245	126	145	1290 (endo)	β-C_2S, C_3S, Li_2CaSiO_4, Quartz (0.22%).

β-C_2S. Samples of C_2S having lithium dopants up to 1.0 percent gave an absorption band at 440 cm^{-1} which corresponds to γ-C_2S; the absorption peaks at 500 and 520 cm^{-1} correspond to β-C_2S while a shoulder at 565 cm^{-1} corresponds to γ-C_2S. Lithium doped (5.0 percent) C_2S gave a shoulder at 500 cm^{-1} and 540 cm^{-1} corresponding to β-C_2S. A sharp absorp tion band at 845 cm^{-1} also corresponds to β-C_2S. The band at 815 cm^{-1} can be ascribed to the symmetrical stretching $\upsilon_1 SiO_4$ corresponding to C_3S phase. The IR spectra have been given in Fig.2. The infrared absorption band of C_3S phase tended to overlap C_2S polymorphs and were generally broader as observed by Bensted and Varma (11). A very sharp absorption band at 925 cm^{-1} showed the presence of C_3S phase, which was not shifted due to the presence of Li dopant, indicating that Li^+ substitutes for Ca^{2+} and not for Si^{4+}.

X-ray Diffraction Analysis

The $CaCO_3$-SiO_2 (2:1) system without dopant gave an exotherm at 1425°C and the XRD of the liquid nitrogen quenched sample showed the presence of β-C_2S (d values (A°) 2.80, 2.78, 2.74 and 2.61) γ-C_2S (d (A°) 3.82, 3.01, 2.75 & 2.73) and free lime (d (A°) 2.77, 2.40, 1.70 & 1.45). The pure system, on repeated firing (3-4 times), gave mostly β-C_2S; γ-C_2S has been found to be transformed to β-C_2S.

The Li_2CO_3 doped sample (0.1, 0.5 and 1.0 wt. percent, calculated as oxide) gave endotherms at 1390°C (0.1%), 1370°C (0.5%) and 1350°C (1.0%). Samples quenched from these temperatures showed mixtures of β & γ-C_2S phases along with free lime in the XRD pattern. The 5.0 percent Li_2CO_3 dopant gave four endotherms at 650°C, 850°C, 960°C and 1170°C before giving a final endothermic peak at 1290°C. The sample heated to 1300°C and quenched in liquid nitrogen indicated the presence β-C_2S, C_3S (d (A°) 3.02, 2.76, 2.73), Lithium calcium silicate (d (A°) 2.40, 3.58, 1.99) and quartz (d (A°) 4.27, 3.33, 2.45, 1.81). Free lime, determined chemically, was found to be 0.22 percent. This might be due to substitution of Li^+ for Ca^{2+} and its incorporation in the interstitial sites of C_3S which is quite possible since tetrahedrally-coordinated Li^+ is well established in many compounds (12). The peak at 650°C terminated at 750°C and showed not only the complete decomposition of Li_2CO_3 but also the partial decomposition of $CaCO_3$. Small amounts of β-C_2S and Li_2SiO_3 (d (A°) 4.68, 2.71, 2.34, 1.56) also formed. In the sample quenched at 880°C, Li_2SiO_3 had changed to $Li_2Si_2O_5$ and more β-C_2S was formed, along with γ-C_2S. A small endotherm at 960°C was preceded by a broad weak inflexion which might be due to melting of $Li_2Si_2O_5$ which is also supported by Glasser (13).

The Ginstling-Brownshtein diffusion equation (14) was used to calculate the rate constant K_r and the activation energy (Ea) was calculated by the Arrhenius equation. The activation energy of pure C_2S formation was found to be 180 KJ mol^{-1}, which is in accordance with the activation energy calculated by Meckanzie and Hadipour (15) who determined it to be 165 KJ mol^{-1}, which decreases to 130 KJ mol^{-1} with 1.0 percent dopant through 156 KJ mol^{-1} with 0.1 percent lithium dopant as given in Table 1. The activation energy with 5.0 percent lithium dopant could not be determined due to partial melting.

CONCLUSION

Li_2CO_3 dopant acts as an intensifier and lowers the decomposition temperature of $CaCO_3$. The activation energy (Ea) of $CaCO_3$ decomposition and formation of C_2S is found to be minimum with 1.0 wt. percent of

dopant and then increases slightly with 5.0 wt. percent concentration of Li^+. Li_2CO_3 (5.0 wt. percent) brings down the final reaction temperature to 1290°C with the formation of predominantly β-C_2S and small quantity of C_3S phase and Li_2SiO_3 and $Li_2Si_2O_5$.

ACKNOWLEDGEMENT

The authors are thankful to Dr A K Mullick, Director General, National Council for Cement and Building Materials for providing research facilities. This paper is part of Ph D work of one of the authors (VKM) and is being published with the permission of Director General NCB.

REFERENCES

1 Midgley, H.C.: The polymorphism of calcium orthosilicates. International Symposium on Chem. of Cement, VIth, Moscow, 1974, I, I-I I-2, 63-68.

2 Malik, W.U., Gupta, D.R., Masood, I. and Gupta, R.S. : Kinetic study of thermal decomposition of calcium carbonate in the presence of K_2CO_3 and $BaCO_3$. J Material Science Letters, 1985, 4(5), 532-536.

3 Saraswat, I.P., Mathur, V.K. and Ahluwalia, S.C. : Effect of alkaline earth metal dopants on the thermal decomposition of $CaCO_3$-SiO_2 system Part II. Formation of dicalcium silicate. Thermochimica Acta, 1985, 95, 201-211.

4 Saraswat, I.P., Mathur, V.K. and Ahluwalia, S.C. : Thermal decomposition and phase transformation studies of $CaCO_3$-SiO_2 (2:1) system in presence of sodium and potassium carbonate. Int. Cong. on the Chem. of Cement, 8th, Brazil, 1986, 2, 1.2, 162-166.

5 Tong, Y., Du, Hong and FEI Lun : Hydration process of beta dicalcium silicate followed by MAS and CP/MAS nuclear magnetic resonance. Cement and Concrete Research, 1991, 21, 355-358.

6 Lehmann, H. and Schmidt, H. : Burning behaviour of limestone deposit with a variety of impurities on the phase transformation and decomposition of $CaCO_3$. Toindustrie Ztg, 1961, 85, 83-91.

7 Chattaraj, B.D., Dutta, S.N. and Iyenger, M.S. : Studies on the thermal decomposition of calcium carbonate in the presence of alkali salts (Na_2CO_3, K_2CO_3 and NaCl). J. Thermal Analysis, 1973, 5, 43-49.

8 Packter, A. and Zaidi, S.M.A. : Mineral effect of Li and $CaCl_2$ in the formation of β -C_2S. Silikat., 1976, 27(1), 14-16.

9 Semenov, N. and Zabolotskii, T.V. : Preparation of lithium silicates from Li_2CO_3 mixture. SiO Otd, Akad, Nauk SSSR, 1962, 2, 58-62.

10 Tarte, P. : Infrared study of orthosilicate and orthogermanates. Spectro. Chim. Acta, 1962, 18, 467-483.

11 Bensted, J. and Varma, S.P. : Some applications of infrared and raman spectroscopy in cement chemistry, Part II, Portland cement and its constituents. Cem. Tech., 1974, 5, 378-382.

12 Blanco, M.N., Thomas, H. and Pereire, E. : Alkali metal oxide effect on dicalcium silicate polymorphism. I Rev. Lainoan, Ing. Quim, 1975, 5(2), 125-129.

13 Glasser, F.P. : Crystallization of lithium di-silicate formed from Li_2O-SiO_2. Physics-Chem. Glasses, 1967, 8, 224-226.

14 Qihuang, Feng, Shangren Yu. : A study on the kinetics of the burning of portland cement clinker in different processes. Int. Cong. on the Chem. Cem., 8th, Brazil, 1986, 2, 1.1, 16-20.

15 Mackenzie, K.J.D. and Hadipour, N. : Formation kinetics of portland cement clinker phases II. β-dicalcium silicate and tricalcium silicate. Transactions and J. Brit. Ceram. Soc., 1978, 77(6), 168-172.

EFFECT OF SO_3 AND MgO ON PHASE RELATIONS AND CRYSTAL CHEMICAL STATE OF PHASES IN BELITE-ALUMINOFERRITE CLINKERS

A I Boikova, O I Fomicheva and L V Grishchenko

Institute of Silicate Chemistry, Russian Academy of Science
St Petersburg, RUSSIA

SUMMARY.

The clinkers studied are special binding materials whose properties can change depending on phase relations, chemical composition of the phases and their crystallo-chemical state. Five-component clinkers ($Al_2O_3/Fe_2O_3 \gtrsim 1$) with SO_3 and MgO additions have been synthesized. It has been shown that the influence of SO_3 is closely related to the Al_2O_3/Fe_2O_3 ratio. In high alumina clinkers (Al_2O_3/Fe_2O_3=1.75) sulphur is first consumed for the formation of $C_4A_3\bar{S}$. A high ferrous aluminoferrite phase (C_6AF_2) containing SiO_2 and small amounts of SO_3 and MgO in the solid solution as well as the β- and α'- belites are also formed. The mutual influence of SO_3 and MgO on the stabilisation of α'-belite is antagonistic. In more ferrous clinkers (Al_2O_3/Fe_2O_3<1) belite and calcium aluminoferrite are formed. The latter is less ferrous (C_4AF); it contains a significant amount of SO_3 in the solid solution. Belites and the aluminoferrite phase are characterized by distorted structure and reactive hydration properties.

Исследованные клинкера представляют собой специальные вяжущие, свойства которых могут меняться в зависимости от фазовых соотношений, химического состава фаз и их кристаллохимического состояния. Синтезированы пятикомпонентные клинкера с соотношением $Al_2O_3/Fe_2O_3 \gtrsim 1$ и с добавками SO_3 и MgO. Показано, что роль SO_3 в процессе формирования фаз тесно связана с отношением Al_2O_3/Fe_2O_3. В высокоглиноземистых клинкерах (Al_2O_3/Fe_2O_3=1,75) сера расходуется прежде всего на образование $C_4A_3\bar{S}$. Образуются также высокожелезистая алюмоферритная фаза на основе C_6AF_2, и β- и α'-белит. Совместное влияние SO_3 и MgO на стабилизацию α'-белита противоположно. В более железистых композициях (Al_2O_3/Fe_2O_3 < 1) формируется белит и алюмоферрит кальция. Последний отличается содержанием значительного количества SO_3 в твердом растворе и является менее железистым (C_4AF). Белиты и алюмоферритная фазы клинкеров характеризуются сильно искаженной структурой и активными гидратационными свойствами.

INTRODUCTION

The perspective of developing physico-chemical and technological bases for obtaining high-ferrous clinkers and the efficacy of cements based on them have been reported elsewhere (1). These materials belong to a group of special cements whose relatively lower energy consumption in manufacture results mainly from the low basicity of their main phases - belite and calcium aluminoferrite, and the lower clinkering temperatures. The properties of these materials depend not only on their phase composition and the quantitative phase relations but also their crystallo-chemical states. These are the lattice distortion of the phases due to the influence of impurities, the imperfection of the phases, the change in atomic structure of the phases during phase transformations owing to both the impurities and the thermal schedule of burning, the fine texture of the phases. As shown earlier, the crystal lattices of belite and calcium aluminoferrites undergo the strongest distortions (2). Such imperfectly formed crystals show more active hydration properties.

EXPERIMENTAL

The present paper deals with the study of phase relations in the high-ferrous region of the multicomponent clinker system with SO_3 and MgO, as well as the observation of imperfection of crystal lattices of belite and aluminoferrite phases, and the investigation of hydration properties. Four series of belite aluminoferrite clinkers with a ratio of $Al_2O_3/Fe_2O_3 \geq 1$ were synthesized and studied (Table 1). The table also shows the amounts of SO_3 and MgO added to the five-component (CaO, MgO, Al_2O_3, Fe_2O_3, SiO_2) clinker batches. The burning was carried out at 1350°C which prevented the formation of non-active intermediate compound $2C_2S \cdot \bar{C}S$; the cooling was slow (together with the furnace) and rapid (air-quenching). The phase composition of the clinkers synthesized are given in Table 1. Figures 1 and 2 show the X-ray diagrams of the clinkers studied.

When analyzing the results of phase relations attention is drawn to the following. The influence of SO_3 on phase formation and phase relations greatly depends on the Al_2O_3/Fe_2O_3 ratio. At ratios of $Al_2O_3/Fe_2O_3 \geqslant 1$ (samples 1-10) and with additions of 3.5 and 6 % SO_3, three phases are formed in clinkers: belite in the β- and α'- forms, high-ferrous

Table 1. Chemical and phase composition of clinkers

No	Composition of the initial batch					Addition		Phase composition of clinkers			
								Belite		Alumino-ferrite	$C_4A_3\bar{S}$
	CaO	Al_2O_3	SiO_2	Fe_2O_3	MgO	MgO	SO_3	β	α'		
1	54,0	6,0	25,0	14,0	1,0	–	–	++++	–	++++	–
2						–	3,5	+++	+	+++	++
3		Al_2O_3/Fe_2O_3= 1,75				–	6,0	++	++	++	+++
4						3,0	3,5	+++	+	+++	++
5						6,0	6,0	++++	–	++	+++
6	51,0	18,0	15,0	15,0	1,0	–	–	++++	–	++++	–
7						–	3,5	+++	+	+++	+
8		Al_2O_3/Fe_2O_3= 1,0				–	6,0	++	++	++	++
9						3,0	3,5	+++	+	+++	+
10						6,0	6,0	++++	–	++	++
11*	55,0	14,0	13,0	17,0	1,0	–	–	++++	–	++++	–
12*		Al_2O_3/Fe_2O_3= 0,75				–	6,0	++++	–	++++	–
13*						–	10,0	++++	–	++++	–
14	55,0	14,0	10,0	20,0	1.0	–	–	++++	–	++++	–
15*		Al_2O_3/Fe_2O_3= 0,5				–	6,0	++++	–	++++	–
16*						–	10,0	++++	–	++++	–

* Samples 12,13,15,16 contain some amount of $CaSO_4$

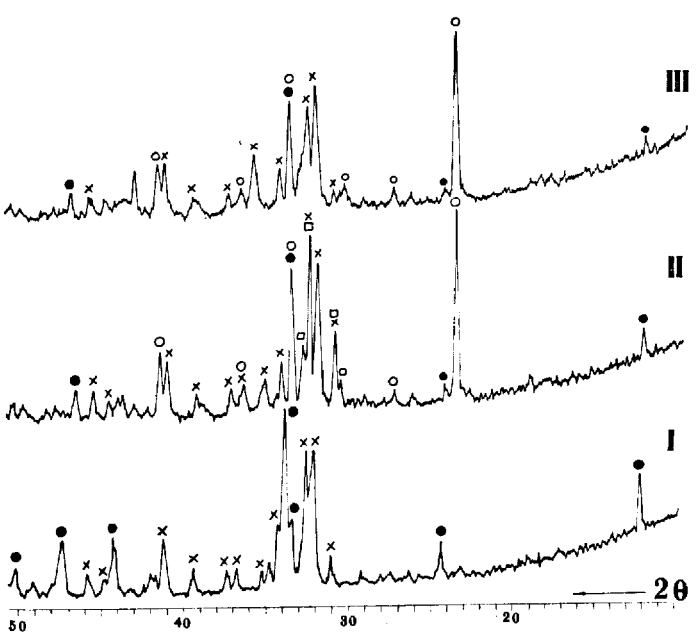

Fig.1. X-ray patterns of clinkers 6 (denoted as I), 8(II), 10(III). x-β-belite; ●-aluminoferrite; o-sulphoaluminate; □-α'-belite.

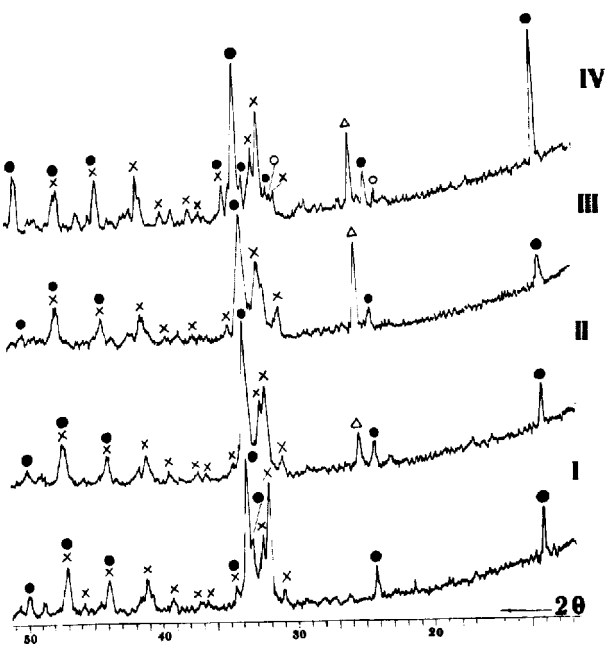

Fig.2. X-ray patterns of clinkers 14 (denoted I),15(II), 16(III), 16—with slow cooling (IY). x-β-belite; ● -aluminoferrite; Δ -$CaSO_4$; o -sulphoaluminate

aluminoferrite based on C_6AF_2 and calcium sulphoaluminate. In spite of the high-aluminate composition of the clinker, aluminoferrite phase with high Fe_2O_3 contetnt is formed. The fact is that SO_3 is first consumed for the formation of $C_4A_3\bar{S}$. With increasing addition of SO_3 the amounts of $C_4A_3\bar{S}$ and α'-belite increase, whereas the amount of the aluminoferrite phase decreases and the aluminoferrite proper becomes more ferrous.

A peculiar behaviour of MgO shows up in the fact that MgO makes it difficult for belite to form α'- modification. Thus by adding 6 % MgO the α'-belite becomes practically absent even in the presence of 6 % SO_3 in the batch. Such a clinker contains 2-3 % periclase. The α'-belite peak (2θ 33°) in the X-ray pattern (Fig.1) of sample II with 6 % SO_3 practically disappears in the X- ray pattern of sample III to which 6 % MgO was added besides SO_3.

In more high-ferrous compositions (Al_2O_3/Fe_2O_3 < 1) two phases are mainly formed: β-belite and a high-ferrous calcium aluminoferrite C_6AF_2. When 6 and 10 % SO_3 are added to the batch, $CaSO_4$ (5-10 %) also appears in the clinker and the other phases contain sulphur as an isomorphous impurity in their lattices. The possible formation of $C_4F_3\bar{S}$ was not confirmed. However by slow cooling a small amount of $C_4A_3\bar{S}$ (3-4 %) appears in these clinkers (Fig.2, curve IY, 2θ=23-24°).

Attention is drawn to the results of electron probe microanalysis. (EPMA) reported in Table 2.Large amounts of sulphur (up to 6-7 %) are present in the lattice of the less ferrous aluminoferrite, namely in the C_4AF-based ones (samples 12,13,15,16). This phase also contains SiO_2 (4-5 %) and MgO (1,5-3,0 %) in solid solution. Sulphur is present in three phases: in $CaSO_4$ proper, as an isomorphous impurity in calcium aluminoferrites, and in the β- and α'-forms of belites.

HYDRATION PROPERTIES

One more crystallo-chemical feature of belite and aluminoferrite phase is also worth mentioning. In the clinkers studied, these phases are products of imperfect crystallization. These phases with strongly distorted lattices are formed in high-ferrous clinkers. Sulphur plays the greatest role in the formation of imperfect crystals. The peaks due to these phases in the X-ray patterns show the diffusion character which is clearly seen when comparing the X-ray patterns for annealed and for

Table 2 Chemical composition of phases according to EPMA

Phase	Sample number	CaO	MgO	Al_2O_3	Fe_2O_3	SiO_2	SO_3
Belite	2	64,5	0,1	0,4	0,6	33,7	0,6
		64,2	0,3	0,5	1,0	32,9	1,0
	3	60,5	0,6	0,8	1,5	32,0	4,1
		60,9	0,7	0,6	1,0	33,7	2,6
	7	64,5	0,1	0,4	0,6	33,7	0,6
		64,6	0,1	0,3	0,7	33,3	1,0
	10	66,7	0,2	0,4	0,7	30,6	1,4
		63,3	0,7	0,6	1,3	32,1	2,0
	12	63,2	0,4	1,0	1,4	29,9	3,1
		61,6	1,6	1,3	1,7	29,9	3,8
	13	63,2	0,6	1,0	1,8	29,7	3,1
		62,4	0,8	1,1	1,4	31,0	3,0
	15	63,2	0,5	1,9	2,0	28,6	3,8
		64,0	0,5	1,8	1,9	29,0	2,8
	16	61,6	0,4	1,1	1,5	31,5	3,9
		61,1	0,5	1,1	1,6	31,3	4,1
Calcium aluminoferrite	2	44,5	0,6	9,0	42,0	3,8	0,1
		44,2	0,7	8,9	41,9	3,9	0,3
	3	43,0	0,7	8,8	43,8	3,3	0,4
		43,1	1,5	8,3	42,8	3,9	0,4
	7	42,7	0,6	10,0	42,4	4,3	0,0
		43,7	0,2	10,7	42,1	3,2	0,1
	10	42,3	0,9	8,1	44,1	4,1	0,6
		43,0	0,7	8,5	44,5	3,1	0,1
	12	47,0	2,6	12,1	28,0	4,9	5,3
		49,2	2,8	12,6	26,3	4,3	4,8
	13	48,6	2,0	11,2	25,9	5,4	6,7
		48,3	2,2	11,0	28,0	4,6	5,6
	15	49,8	1,4	12,2	30,3	4,4	1,8
		46,8	1,1	12,0	31,6	3,5	5,0
	16	48,9	1,5	11,6	31,1	4,5	2,2
		46,7	1,8	11,3	28,6	5,0	6,4
Calcium sulphoaluminate	3	34,3	0,1	49,5	2,5	0,1	13,5
		33,8	0,2	50,0	2,8	0,2	12,9
	7	30,8	0,3	52,9	3,3	0,2	12,4
		33,1	0,1	51,1	3,0	0,3	12,1
	10	31,5	0,1	53,4	3,7	0,2	11,0
		31,6	0,1	52,7	3,0	0,2	12,0

quenched samples of one and the same chemical composition (curves III and IY, Fig.2).

Attention should be drawn to the comparative compressive strengths of these two samples. 28-day strength, namely 30 MPa, of the clinker containing phases (belite and calcium aluminoferrite) with strongly

distorted structures (Fig.2, curves III and IY), is twice as high, namely 14 MPa, as that of the clinker with well-crystallized phases (Table 3, samples 15 and 15').

Table 3. Compressive strength of clinkers.

Al_2O_3/Fe_2O_3 ratio	1,75		1,0	0,75		0,5	
Sample number	3	5	8	12	13	15 rapid cooling	15' slow cooling
28-day strength, MPa	26	25	32	25	32	30	14

The value of compressive strength was obtained as the average sum four measurements. The measurements were made on 1x1x1 cm cubes; w/c= 0.3; the granulometric composition was controlled by sieve N 0071.

The hydration activity of belites, aluminoferrite phases and calcium sulphoaluminates was investigated. The hydration kinetics curves were plotted using the results of X-ray analysis. The experiment was unusual in that the hydration of the indicated phases was studied directly in the clinker. For analysis we chose such maxima in the X-ray pattern for each phase which were overlapped neither by the maxima of the other phases nor by the ones of the hydration products. The w/c ratio was 0.4 for all samples. All ground samples were sieved. The hydration temperature was 20°C. Fig.3 shows the hydration kinetics curves for belites, calcium aluminoferrites and calcium sulphoaluminates occurring in the presence of all the other clinker phases. Analysis of the hydration kinetics curves for belites shows that the distinct character of the process is mainly due to the magnitude of the Al_2O_3/Fe_2O_3 ratio, namely: belites 1,2,3 belong to high-ferrous clinkers. These belites contain a significant amount of SO_3 (3-4 %) in solid solution and possess a strongly distorted structure; belites 4,5,6 belong to less ferrous clinkers and slowly hydrate at the early and later stages.

The curves in Fig.3 show that aluminoferrite phases of high-ferrous clinkers as well as belites are more reactive than the aluminoferrites belonging to clinkers with a higher Al_2O_3/Fe_2O_3 ratio. The low hydration reactivity of the phases in clinker 5 (belite 6, Fig.3a, aluminoferrite 6, Fig.3b) obtained from the same batch as clinker 4 but with slow cooling

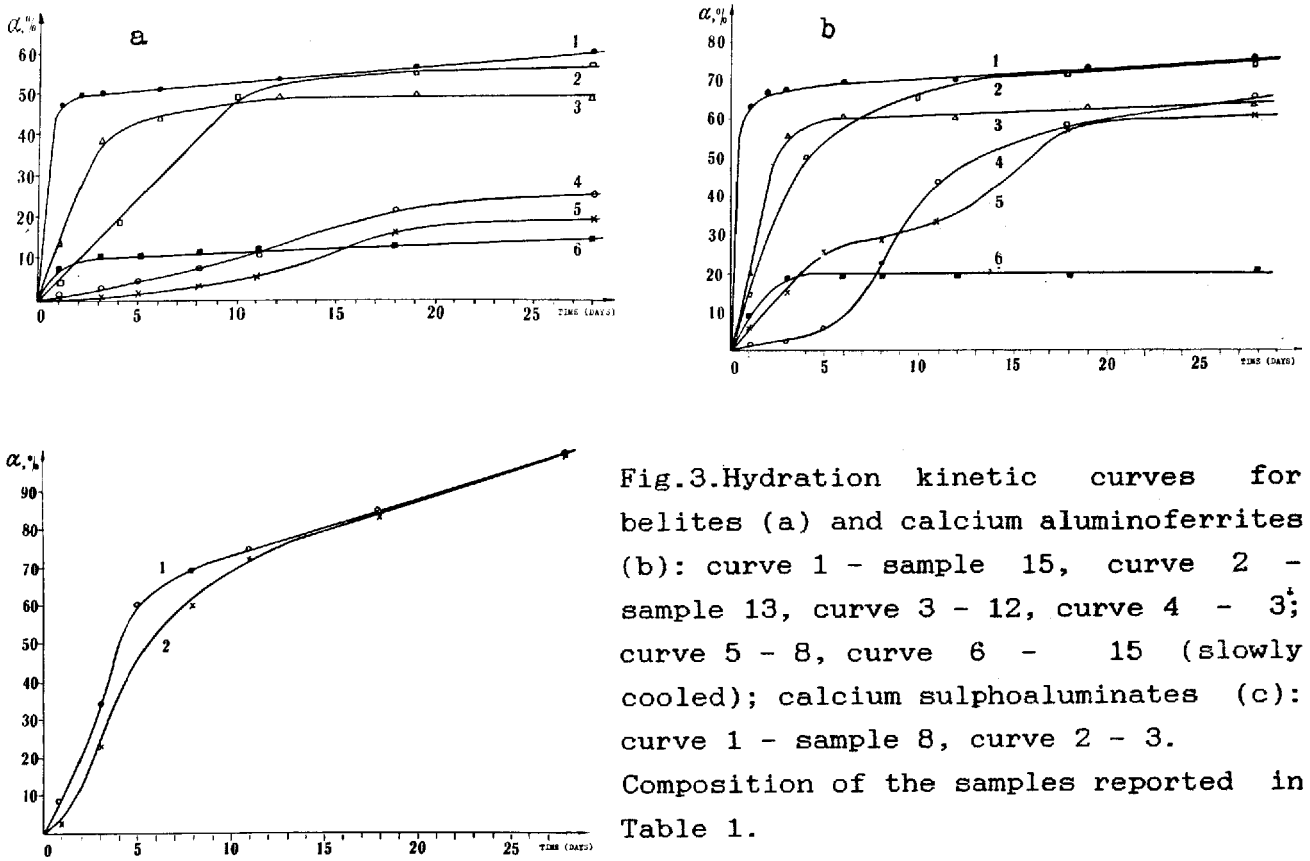

Fig.3.Hydration kinetic curves for belites (a) and calcium aluminoferrites (b): curve 1 - sample 15, curve 2 - sample 13, curve 3 - 12, curve 4 - 3; curve 5 - 8, curve 6 - 15 (slowly cooled); calcium sulphoaluminates (c): curve 1 - sample 8, curve 2 - 3. Composition of the samples reported in Table 1.

can be related to the fact that both the belite and the aluminoferrite in this sample are better crystallized. Besides they contain a much smaller amount of SO_3. As to calcium sulphoaluminates, their hydration process is similar which is confirmed by the kinetics curves. These phases have similar chemical composition and identical X-ray pattern too.

CONCLUSIONS.

It should be noted, that each of the clinkers studied can represent a special binding material with effective properties. The structure of belite and calcium aluminoferrite formed in these clinkers can be strongly distorted. Such phases possess improved hydration properties.

REFERENCES

1. Deng Jun'an, Su Muzhen, Wang Yanmou.: "An investigation into cement $CaO-SiO_2-Al_2O_3-Fe_2O_3-SO_3$ system". 8th ICCC, Brazil, 1986, v.2, 300-305.

2. Boikova, A.I.: "Crystal Chemistry of solid solutions of cement clinker minerals". Tsement, 1982, N 9, 7-10. (in Russian).

ROLE OF MANGANESE ON THE KINETICS OF FORMATION AND HYDRATION OF C_3S PHASE

Ram Prakash*, S C Ahluwalia, N K Katyal** and V K Mathur****

**Minister of State for Electronics, Science & Technology*
Government of Haryana, Chandigarh, INDIA
***National Council for Cement and Building Materials, New Delhi, INDIA*

SUMMARY

Effects of addition of varying concentrations of manganese on the structure and polymorphism of C_3S phase has been investigated. Kinetics of formation of C_3S were obtained by heating a mixture of $CaCO_3$ and SiO_2 in the mole ratio of CaO : SiO_2 (3 : 1) using 0.1, 0.5, 1.0, 2.0 and 5.0 percent MnO_2 by weight. The activation energy (Ea) of formation of C_3S shows a decreasing trend upto 1.0 percent MnO_2 and then rises. Tricalcium silicate shows a polymorphic change from triclinic (T_1) to monoclinic (M_1) with increasing concentration of the dopant, as evidenced from XRD. Electron diffraction of the crushed samples show patterns of several types, of lattice. Microscopic studies revealed that the habit of C_3S crystals changed with the concentration of the dopant. Instead of pseudo hexagonal pure C_3S, typical flower type structures appeared with dopants. Hydration study reveals that the rate of $Ca(OH)_2$ formation is low with doped sample up to 4 h but high in 7 days compared to pure C_3S sample.

INTRODUCTION

Tricalcium silicate exists in six polymorphic modifications i.e. one rhombohedral (R), two monoclinic (M_I M_{II}), three triclinic (T_I, T_{II}, T_{III}). At room temperature C_3S is in triclinic (T_I) form which transforms to monoclinic (M_I, M_{II}) and finally to rhombohedral (R) form on heating upto a temperature of 1100°C (1, 2). These modifications are characterised by having specific symmetries and unit cell dimensions. It has been established experimentally that any of the high temperature forms can be stablised at room temperature by proper selection of dopant, its concentration and thermal treatment. Dopants such as chromium, titanium, manganese, sulphur etc and constituents like Al_2O_3, Fe_2O_3 and MgO present in cement raw mix generally tend to stabilise monoclinic C_3S in the M_i and M_{iii} forms at room temperature (3).

Apart from these effects on the structure of C_3S, the dopants seem to influence the reaction kinetics to a great extent. They influence the formation temperature of silicates, activation energy of various reactions and the rate constants. The polymorphism of C_3S is complicated because of the numerous extremely similar modifications and the very small transformation enthalpies (84-105 KJ/mol).

The work reported here is a part of ongoing study at NCB, which aims at developing the basic understanding of the effect of cationic dopants on the formation kinetics, polymorphism and hydration kinetics of silicate phases.

EXPERIMENTAL

Materials and Sample Preparation

Powdered $CaCO_3$ and quartz (Purity > 99.0 percent) in 3 : 1 molar ratio along with varying concentrations of MnO_2 dopant were separately ground to a fine powder and homogenised in a pot mill. The resulting mixtures, after thorough mixing with distilled water, were shaped into nodules. These nodules were heated to 1500°C for 2 hrs. The pellets were heated repeatedly at the same temperature to ensure completeness of the reaction, which was confirmed each time with estimation of free lime.

Thermal Analysis

Mettler thermal analyser (TA-1) was used to record DTA, DTG and TG curves. The samples (60 mg) were heated to 1500°C at a rate of 10°C/min using α- Al_2O_3 as a reference material. The activation energy (Ea) of $CaCO_3$ decomposition was calculated from DTG curve and were reported earlier (4).

X-ray diffraction studies

The samples were powdered to pass through 45 μm sieve and pressed into a sample holder Rigaku Rad Max B system with wide angle horizontal goniometer and graphite monochromator was used for determining polymorphic transitions in C_3S.

Scanning Electron Microscopy (SEM)

A Philips scanning electron microscope with an energy dispersive X-ray analyser was used for the morphological studies. Fractured specimens of pure and doped C_3S phase were prepared by uniformly blending the sample with resin and giving them a conductive gold coating in vaccum (10^{-5} Torr).

Hydration Studies

The hydration kinetics of pure and doped C_3S have been studied by X ray diffraction. The samples were hydrated taking W/S ratio 0.5 for various ages at room temperature.

RESULTS AND DISCUSSION

X-ray diffraction studies

Tricalcium silicates (C_3S) reportedly exists in various polymorphic modifications in the temperature range from ambient to 1100°C. C_3S with varying percentage of manganese dopant (0.1 - 5.0 wt. percent) shows an appreciable shift in the position of all the lines suggesting modifications of the phase. However the multiplicity and structure of the lines in the region (2θ) = 32-33° and 51-52° remain more or less the same up to 1.0 percent MnO_2. It is observed that structure remains triclinic upto this level. Simple replacement (substitution) of Si^{4+} by Mn^{4+} can therefore be assumed up to 0.1 percent and a solid solution conforming to the following formula could develop $Ca_3(Si_{1-x}\ Mn_x)O_5$ $0 \leqslant x \leqslant 0.003$. Enculescu (5) observed the solubility limit of MnO_2 in tricalcium silicate upto 1.0 %. However, Sakurai (6) has proposed that the only possible substitution is of Si by Mn. It was observed by Knofel (7) that C_3S remains triclinic with lower percentage of MnO_2 dopant (upto 1.0 percent level) and then changes to monoclinic modification with higher concentration of dopant. He proposed a double substitution of Mn^{4+} by Si^{4+} and Mn^{2+} by Ca^{2+} upto 2.2 percent concentration of MnO_2 dopant. However our investigations indicate a mixture of triclinic and monoclinic modification up to 2.0 percent level and a pure monoclinic lattice above that (Fig.1). Kondo and Yoshida (8) have reported that the triclinic modifications are concentration dependent and T_1 transforms to T_{111} as the MnO_2 concentration increases in the range of 0.38 - 3 wt. percent.

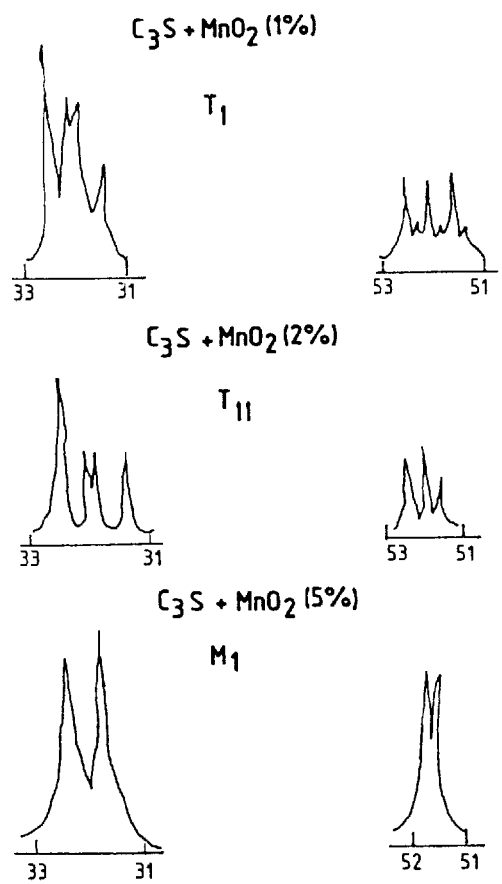

FIG 1 XRD OF MANGANESE DOPED C_3S SAMPLES SHOWING VARIOUS POLYMORPHIC FORMS

The rate constant and activation energies of C_3S formation with and without dopant were calculated as per the method given by Gihuang Feng and Shangren Yu (9) by heating the nodules at a temperature range of 1300-1500°C with 6 levels of 50°C interval for 5, 10, 15, 20, 25, and 30 minutes.

The activation energy (Ea) of C_3S formation as determined by Ginstling-Brounshtein and Arrhenius equation was found to be 600 K J mol^{-1}, quite close to that reported by Meckenzie and Hadipour (10). The activation energy decreased to a minimum at 1.0 percent MnO_2 dopant and then showed an increasing trend (Table 1).

TABLE 1

KINETICS DATA OF $CaCO_3$ DECOMPOSITION AND C_3S FORMATION WITH CONCENTRATION OF DOPANT

Concentration of MnO_2 in $CaCO_3$-SiO_2 (3:1) system	Decomposition of $CaCO_3$		Kinetics of C_3S Formation		
	Peak Td°C	Activation Energy (Ea) KJ/mol	Rate Constant (Kr/10^{-5})	ln Kr	Activation Energy (Ea) KJ/mol
0.0	885	247	9.2	-9.29	600
0.1	870	217	9.3	-9.28	535
0.5	870	200	9.6	-9.25	490
1.0	860	183	10.1	-9.20	480
5.0	860	232	11.5	-9.07	525

SEM Studies

Microstructure investigation of the pure C_3S phase shows that the grains are in the interconnected hexagonal shape and the grain boundary between the crystals can be identified Fig.2(a). The doped phase (MnO_2 0.5 percent) exhibits that the texture consists of loosely connected agglomerates of irregularly shaped grains. As the concentration of dopant increases (1 & 5 percent) the typical flower structure of the sample appears instead of pseudohexagonal shape Fig.2(b,c,d). The crystals are linked together by interstitial phase with Mn^{4+} ions and the crystal size is smaller than in the pure phase. In the case of simple replacement of Si^{4+} by Mn^{4+}, a solid solution conforming to the following formula could develop with lower concentration (7):

$$Ca_3 (Si_{1-x} Mn_x)O_5 \quad 0 \leqslant x \leqslant 0.5$$

Puertas et al (11) have observed the formation of monoclinic tricalcium silicate with Manganese doping and observed two types of formulae in different conditions of kiln atmosphere :

$Ca_3 (Si_{0.954} Mn_{0.036})O_5$ (Oxidizing condition)

$(Ca_{2.903} Mn_{0.097}) (Si_{0.993} Mn_{0.007})O_5$ (Reducing Condition)

In the doped specimens, the stabilizer was detected in grains using non-dispersive X-ray analysis (EDAX) but the distribution of the stabilizer Mn with the grains or in precipitates on crystal boundaries on polymorphic transformation was not determined.

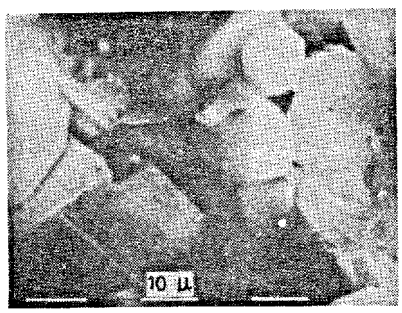

(a) PURE C_3S

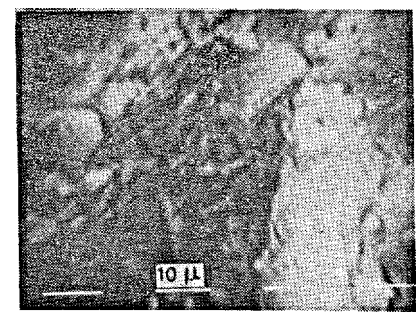

(b) C_3S (0.5% MnO_2)

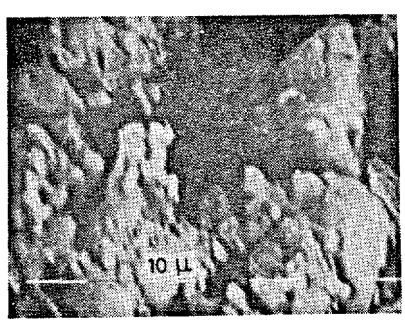

(c) C_3S (1% MnO_2)

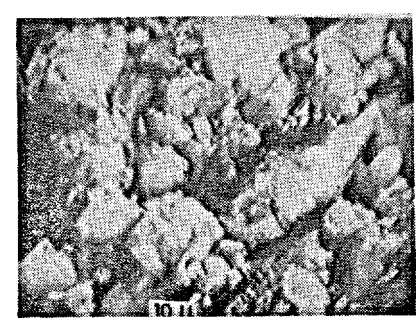

(d) C_3S (5% MnO_2)

FIG 2 SCANNING ELECTRON MICROGRAPHSOF MANGANESE DOPED TRICALCIUM SILICATE PHASE

Kinetics of hydration

The products of hydration of C_3S phase at ambient temperatures are an ill-defined, poorly crystalline calcium silicate hydrate and calcium hydroxide :

$$C_3S + (Y + Z)\ H_2O \longrightarrow C_x\ SH_Y + ZCH$$

X + Z = 3 but X, Y and Z are not necessarily integers. The method used for finding x involves determination of $Ca(OH)_2$ by chemical extraction method.

Calcium silicate hydrate formed by the hydration of C_3S is poorly crystalline, yielding a few broad, weak bands in the X-ray diffraction pattern. This and its uncertain composition have resulted in general use of the notation C-S-H to represent it. Copeland and Kantro (12) reported that the three main X-ray diffraction bands given by C-S-H (peaks at 3.1, 2.8 and 1.8A°) can be indexed as lattice spacings of the mineral tobermorite ($C_5S_6H_5$) and they introduced the term tobermorite gel. Taylor (13) has pointed out that since 3.1A° and 1.8A° spacings are prominent repeat distances within a layer of the portlandite structure the small degree of order in C-S-H may reside in Ca-O parts. $Ca(OH)_2$ is best characterised by the reflection at 4.91A°.

The X-ray diffractograms for 1h, 4h, 1d, 3d, 7d and 28d hydration of pure C_3S and C_3S doped with 0.2, 0.5, 1.0 and 5.0 percent MnO_2 show the appearance of $Ca(OH)_2$ and C-S-H. The results have been analysed using $Ca(OH)_2$ peak at 4.91 A^o and C_3S peak at 3.04A^o. The C_3S and $Ca(OH)_2$ peak intensities have been plotted against duration of hydration for all the samples and are presented in Fig.3.

It is observed that amount of $Ca(OH)_2$ released in all the doped samples is very low up to 4 hrs compared to a pure C_3S sample. In 1 day hydration, the amount of $Ca(OH)_2$ released was found to increase with 1.0 percent MnO_2 dopant and it continuously increases with age of hydration and is nearly complete at 28 days as unhydrated C_3S disappears.

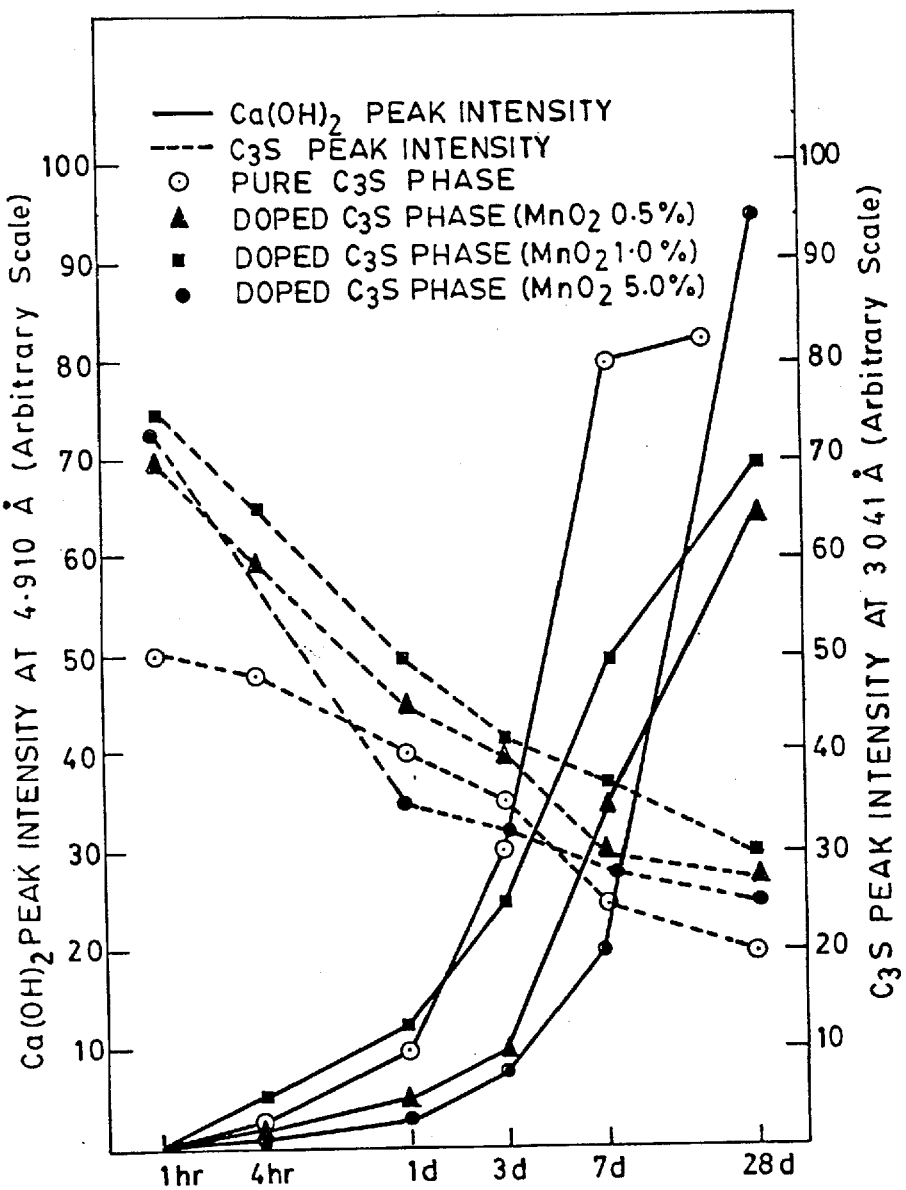

FIG 3 XRD OF PURE AND DOPED HYDRATED C_3S PHASES

CONCLUSION

Manganese dopant lowers the decomposition temperature of $CaCO_3$ and formation of C_3S phase. Activation energy (Ea) of C_3S formation is minimum with 1.0 percent dopant and then increases. MnO_2 up to 2.0 percent level does not alter the basic triclinic structure but higher concentrations lead to the formation of monoclinic C_3S. The hydration study reveals that rate of $Ca(OH)_2$ release is very low in doped samples up to 4h, while it is very high with 1.0 percent dopant between 7 to 28 days relative to hydration of pure C_3S.

ACKNOWLEDGEMENTS

The work described here is a part of research project and PhD programme of one of the authors (N K Katyal) carried out at National Council for Cement and Building Materials. This paper is being published with the permission of Dr A K Mullick, Director General of the Council.

REFERENCES

1. Maki, I. and Kato, K.: "Phase identification of alite in Portland Cement Clinker". Cement Concr. Res., 1982, 12(1), 93-100.

2. Chesley, J.A. and Burnet, G.I.: "A Two Stage reaction sequence for C_3S formation". Cem. and Concr. Res., 1989 19(6), 837-847.

3. Bigare, M., et al : "Polymorphism of Tricalcium Silicate and its solid solutions". J.Am. Ceram. Soc., 1967, 50(11), 609-619.

4. Ahluwalia, S.C. and Mathur, V.K.: "Thermal Studies on the effect of some transition metal oxides on the kinetics of formation and stabilization of β-dicalcium silicate phase". **8th Int. Symp. on Chem. of Cem., Brasil**, 1986, **V1**, 1, 40-45.

5. Enculescu, M.: "Influence of Oxides of Transitional Elements on the Properties of Mineralogical Composition of Cement", **6th Int. Congress on Chemistry of Cement**, Moscow, 1974.

6. Sakurai, T.: "The behaviour of Manganese in Cement Clinker Minerals", Review of the 14 General Meeting Japan Cement Engineering Assoc., Tokyo, 1960, 23-24.

7. Knofel, D., et al: "Incorporation of Manganese in Tricalcium Silicate". Zem kalk Gips, 1984, (12), 651-655.

8. Kondo, R. and Yoshida, K.: "Miscibilities of special elements in tricalcium silicate and alite and the hydration properties of C_3S solid solution". **5th Inter. Symp. on Chem. of Cem., Tokyo**, 1968, (1.1), 262-274.

9. Qihuang Feng, Shangren Yu : "A study on the Kinetics of Burning of Portland Cement Clinker in different Process", **8th Int. Symp. on Chem. of Cem., Basil**, 1986, **V2**, 1.1, 16-20.

10. Mackenzie, K.J.D. and Hadipour, N.: "Formation kinetics of Portland Cement Clinker Phases, II β-dicalcium silicate and tricalcium silicate". J. Brit. Ceram. Soc., 1978, (77), 168-172.

11. Puertas, F., et al: "Influence of the kiln atmosphere on manganese solid solution in Ca_3SiO_5 and Ca_2SiO_4". Cement Concrete Research, 1988, 18(5), 783-788.

12. Copeland, L.E. and Kantro, D.L.: "Hydration of portland cement at ordinary temperature". **Chemistry of Cement**, by H.F.W. Taylor, Academic Press London, 1964.

13. Taylor, H.F.W.: "Calcium Silicate Hydrates". **The Chemistry of Cements**, V1, 1964.

BURNING CEMENT CLINKER FROM THE RAW MEAL USING BARITE AND FLUORSPAR AS A COMBINED ADDITIVE

Xu Xianyu*, Yang Liqun* and Chen Jian**

**Zhejiang University, P R CHINA*
***Zhejiang Clay Minerals Co, Hangzhou, P R CHINA*

By using chemical analysis, EDXA, XRD and minerals phase analysis to study the action and mechanism on Ba^{2+} ion in the process of clinker formation, especially, the relation between the added amount of barite with the strength of cement, and discussing the rule. Some basic researches on the technology of the barite- fluorspar combined additive are made.

Applied the technology to shaft kiln cement factories: 10-15% shaft kiln capacity increase. 2926—3135 KJ/Kg fuel consumption stabilize. 0.5-1.0 T/H cement mill capacity increase.

利用化学分析，EDXA，XRD和矿相分析来研究Ba^{2+}离子在熟料形成过程中的作用和机理，尤其研究了重晶石的添加量与水泥强度的关系，探讨了其规律，对有关重晶石一萤石复合添加剂技术作了基础研究工作。

在立窑水泥厂应用该技术：立窑产量增加10—15%，能耗稳定在2926— 3135KJ/Kg，水泥磨产量提高0.5—1.0T/H。

1. PREFACE

There are most of energy are exhusted in cement production, the way of energy saving is researched in practice and science experiments, one of important ways is, adding various minerlizers in the process of cement burning, to lower the burning temperature.

Many provinces in China are rich in barite resoures, some of that are not exploited due to its poor quality; For the purpose of wide application the natural resource, the paper covers, by means of the methed of activate C_2S, using barite- fluorspar as a composite mineralizer technique in the process of cement clinker formation and the mechanism is investigated. the result is applied in some shaft kiln cement factories, favorourable achievements hava been made.

2. EXPERIMENT AND RESULTS ANALYSIS

(1). Formula and the sample preparing

On the basis of the designed compostion to calculated the formula: adding different amount $BaSO_4$ in raw meals respectively, equal blending, then adding some water in, shaping into the block form, drying at about 110℃, In the end ,put it into highalumina saggar, burning under different temperature.

Table 1: The chemical composition of raw meal(%)

	SiO_2	Al_2O_3	Fe_2O_3	CaO	MgO & Others	Loss	CaF_2	$BaSO_4$
Limestone	0.72	0.17	0.07	55.00	0.45	43.59	/	/
Shale	62.99	15.95	7.33	1.69	6.91	5.13	/	/
Fe powder	17.70	4.78	55.80	5.55	2.50	6.17	/	/
Fluorspar	24.68	0.76	0.29	1.24	0.07	3.27	66.52	/
Barite *	/	/	/	/	/	/	/	99.60

*. For convient research, using the pure chemical reageat ($BaSO_4$) to instead of barite in the experiment.

Table 2: The chemical composition of the designed clinker

	SiO_2	Al_2O_3	Fe_2O_3	CaO	MgO & Others	KH	n	p
96--0	19.60	6.92	4.60	65.76	3.11	0.961	1.70	1.50
93--0	21.12	5.23	4.74	65.47	3.42	0.933	2.12	1.11
90--0	21.54	5.44	5.00	65.18	2.80	0.897	2.08	1.09
87--0	21.98	5.47	5.04	64.02	3.49	0.865	2.08	1.08

(2). INFLUENCES OF BARITE ON THE STRENGTH OF CEMENT CLINKER

Raw meals composition with KH 0.96, 0.93, 0.90, 0.87 is selected respectively, and adding 2% barite, burning at 1350℃ about 30 minutes, cooled abruptly in air.

Then clinkers with 2.5% dihydrate gypsum are grinded up (0.8mm square hole sieve residue 4%). Shaping into 20×20×20mm model to test the pure cement paste strength (W/C=0.30), the result is indicated as Fig. 1

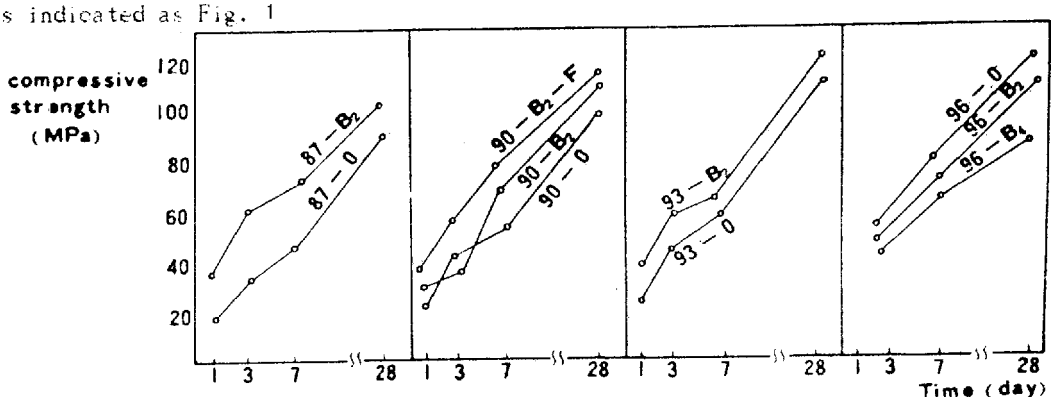

Notes: 90 − 0 : KH=0.90, $BaSO_4$ 0 %; 90 − B_2 : KH=0.90; $BaSO_4$ 2 %
90 − B_2 − F: KH=0.90, $BaSO_4$ 2 %, CaF_2 1 %, on the analogy of this

Fig. 1: The influences of barite on the strength of different composition cement clinkers.

It can be seen from the figure, when KH>0.93, it is obvious that the cement clinker strength decreased after adding 2% barite; as KH<0.93, the strength is increased with barite added especially, more greater amount of increse in strength can be gained in three and seven days; the KH=0.87, the amount of increase in strength is the highest. It comes to the conclusion that the action of barite is relate to the KH. At the same time, batched several groups of raw meal that KH is 0.83, 0.85, 0.90, 0.93, 0.95 respectively, and C_2S% is 30.7%, 27.1%, 23.5%, 18.1%, 12.65%, 9.05% respeatively, the amount of adding barite is changed, according to the same method to study the relation between the amount of barite to the cement clinker strength, and the ratio of BaO and C_2S% when the strength appears the highest. The experiment data showed, the ratio is about 0.027～ 0.083; the conclusion is that C_2S has limited solid — solution of Ba^{2+}.

For further statement the influences of barite on the formation process of clinkers, raw meals of different KH with different amount barite have been used in the study, burning at high temperature about 0.5hr, the fcao in clinkers is measured. (Fig. 2.)

Table 3. The relation of different KH and optimum amount $BaSO_4$

KH	0.83	0.85	0.87	0.90	0.93	0.95
C_2S%	30.7	27.1	23.5	18.1	12.65	9.04
$BaSO_4$%	1.8	1.4	1.2	0.8	0.6	0.3
BaO/C_2S weight ratio	0.039	0.034	0.034	0.029	0.031	0.027

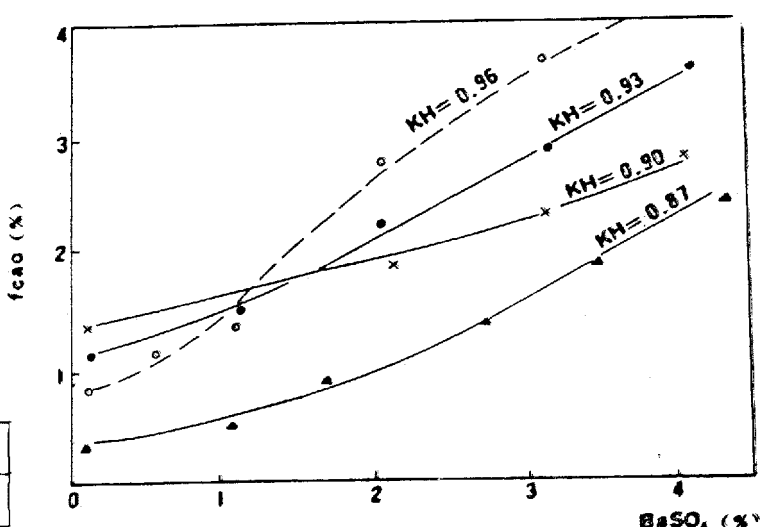

Fig. 2. The relation between Barite% and f_{CaO}

Table 4: Burning 90-0, 90-B_2 raw meals at different temperature, the strength and fcao of their clinkers

		1200℃		1250 ℃		1300 ℃		1350 ℃		# 525
		90-0	90-B_2	90-0	90-B_2	90-0	90-B_2	90-0	90-B_2	cement
Compressing Strength (MPa)	3 days	19.2	19.7	25.6	22.3	21.3	23.0	21.3	28.8	21.9
	7 days	42.7	38.4	50.1	48.6	42.7	57.6	48.3	54.0	44.8
	28days	—	—	60.8	70.7	62.5	74.0	66.5	72.6	63.9
f_{cao} (%)		4.16	4.96	2.26	2.36	1.48	1.53	0.49	0.75	—

This is, with the increase of amount barite, the fcao increases, moreover, x- ray diffraction results of above groups clinker also showed, (Fig. 3.) After adding barite, fcao increased lead to C_3S% decreased, and with increase of KH, more C_3S% is decreased.

For probe into the influence on the clinker burning temperature after adding barite, two raw meal groups (90-0, 90-B_2) are selected in the experiment, burning at 1200℃, 1250 ℃ , 1300℃, 1350℃ respectively about 0.5hr, the fcao in the clinker is measured: Then adding 2.5% dihydrate gypsum in above clinkers, grinding up (controlled the sieve residue is 8%) , shaping into 20×20×20mm model (C/S=1, W/C=0.30), test their strength that compare with #525 cement. (Table 4)

The above is showed, even though fcao increased after adding barite, the 3d, 7d cement strength is higher than that of no barite groups (90-0), and reach to or over #525 cement strength when the burning temperature is at about 1300℃. It is demonstrated, this is an evidence that Ba^{2+} can actrivate C_2S.

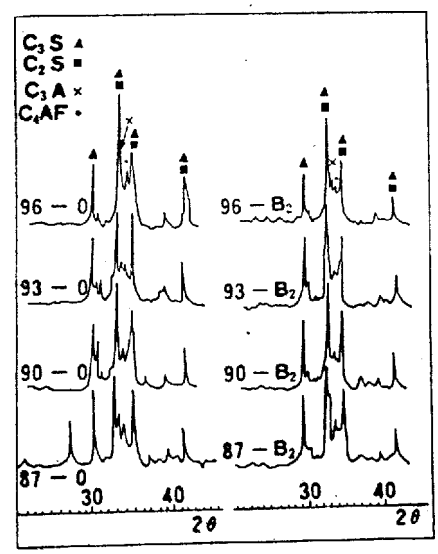

Fig. 3. X-ray diffraction patterns of different KH clinkers

(3). EFFECT OF BARITE AND FLUORSPAR COMBINED ADDITIVE

In order to reduce fcao and increase C_3S% in the clinker, adding 2% $BaSO_4$ and 1% fluorspar in the raw meal (KH=0.90), burning at 1350℃ about 0.5hr, the clinker is obtained. its f_{cao} is shown in Table 5. At the same time, same results are also shown by x--ray diffraction patterns (Fig 4.), C_3S peak in 90-B_2-F clinker is clear higher than that of 90-B_2 and 90-0. It demonstrates that barite and fluorspar combined as a additive, may accelerate adsorbing F_{cao} and increasing C_3S%, so both C_3S and activated C_2S can at the same time act on the strength ofcement clinker. Also can it been seen from x-rays diffraction patterns that a decline in C_3A peak. C_4AF peak rises and $C_{11}A_7$ CaF_2 mineral peak appears after adding fluorspar.

Table 5: The content of f_{CaO} in clinkers

	Amount of barite %	Amount of fluorsper %	F_{CaO}
90-0	0	0	0.84
90-B2	2	0	1.25
90-B_2-F	2	1	0.42

Table 6. Pure cement clinker strength of three clinker groups

		1d	3d	7d	28d
Compressive strength (MPa)	90-0	18.6	42.1	56.5	104.9
	90-B_2	25.1	40.4	64.6	87.7
	90-B_2-F	32.4	55.4	71.9	110.8

Pure cement paste strength of 90--0, 90-B_2, 90--B_2--F groups are tested (Table 6).

It showed that the strength of 90-B_2-F clinker, in different hydration time is higher than that of another two groups, this is consisted with experiment data as before; The important action of barite- fluorspar composite mineralizer is demonstrated in the formation of clinker.

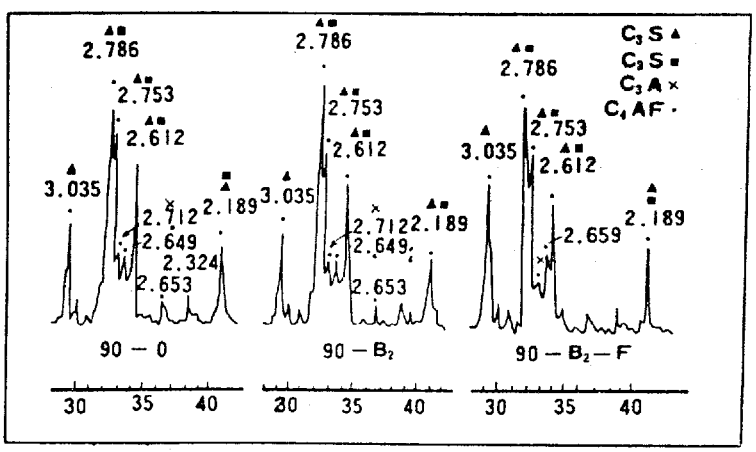

Fig. 4. X-ray diffraction patterns of 90-0, 90-B_2 and 90-B_2-F clinkers

2. DISCUSSION ON THE MECHANISM OF BARITE - FLUORSPAR IN CLINKER FORMATION

The action of barite is related to the C_2S in clinker through above experiments, its also discovered by petrographic analysis (Fig 5.) that C_2S grain morphology is changed obviously, appeared brain-like bar, and the bi-grain bar disappeared; C_3S grains become large and coarse, crystallized completely; Interstitial phase increase obviously. It is suggested that barite has made an important role on the changing of clinker morphology structure.

It is well known that cement clinker is a aggregate body of minerals in the process on the

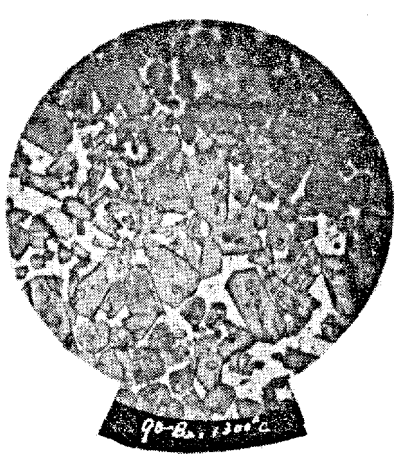

Fig. 5. 90-B_2 petrographic picture

clinker formation, the active mechanism of barite is whether Ba^{2+} selective enters into a mineral or equal distributes on all minerals in clinker. So the 90--B_2 clinker (KH=0.90, with 2% B_aSO_4) is used for the studying, the quantity of Ba^{2+} distribute in minerals are determined by SEM and QXRD (fig 6.) The K_α characteristic spectrum of Ba, Al and Fe (line scanning along AB) showed that Al and Fe are rich in interstitial phase, their content in C_3S and C_2S crystal are less: Ba^{2+} in content C_2S is the highest; in interstitial phase is second, and in C_3S is the least.

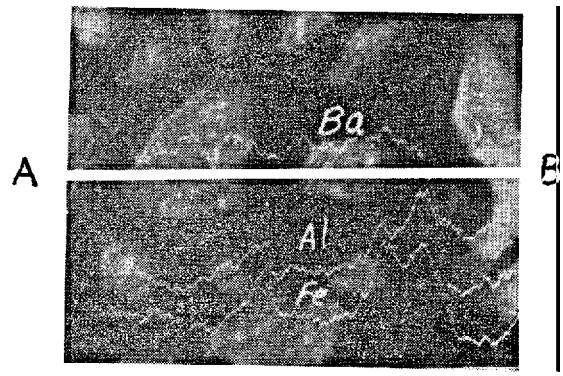

Fig. 6.
The distribution of Ba, Al Fe in clinder minerals

For further interpret the problem, the micro-zone complete energy spectrum analysis of C_3S, C_3S and interstital phase respectively is examined (Fig 7.). results also demonstrate that Ba^{2+} content in C_2S is greater than that of in interstital phase, and in C_3S is less than in interstital phase. It is in agreement with which had reported.

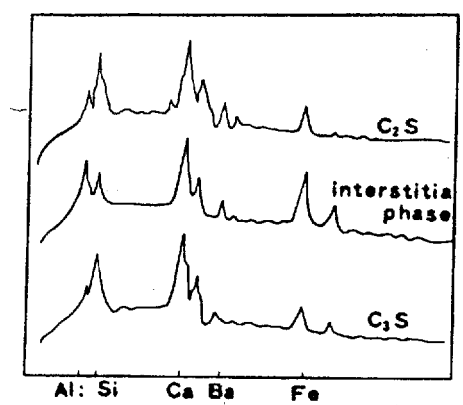

Fig. 7.
The micro-zone complete energy spectrum analysis of C_3S, C_2S and interstitial phase

According to many researchers' studying, 0.2mol Ba^{2+} is displacement of 0.2 mol Ca^{2+} at room temperature that α'-C_2S [$CaO_{1.8} \cdot BaO_{0.2} \cdot Si_1O_2$] can be gained. When 0.8mol Ca^{2+} is replaced by 0.8mol Ba^{2+} the α- C_2S [$CaO_{1.2} \cdot BaO^{0.8} \cdot SiO_2$] is formed: Because of the different variety of C_2S possesses the different structure parameters, α' and α forms are of high coordination number: Ca—O ionic distance increases, Ca — Ca ionic distance shorts, more higher activation can be made. Statement as above, adding moderate barite during cement firing, a definite amount of Ba^{2+} replaced equal amount of Ca^{2+}, C_2S existed in the state of α-or α' form, So C_2S develops more higher strength in the cement hydration and hardenning process.

Otherwise, Ba^{2+} enters partly into interstitial phase, and changes it high temperature viscosity, the growth of C_2S crystal also is promoted. After adding fluorspar, a lot of C_3S and certain amount $C_{11}A_7 \cdot CaF_2$ have formed: Therefore, when using barite- fluorspar as a composite mineralizer in cement burning, the minerals in clinker, C_3S, C_2S, $C_{11}A_7 \cdot CaF_2$ respective develops strength to the full, and make cement with high strength and fast hardenning.

Table 7. The composition of clinkers

	SiO_2	Fe_2O_3	Al_2O_3	CaO	MgO	Fcao	KH	n	p	Loss
1	21.26	4.65	5.42	63.58	3.58	0.15	0.88	2.11	1.17	0.11
2	20.5	4.15	6.30	65.59	1.20	0.16	0.93	1.96	1.52	/
3	20.29	4.25	6.63	66.51	1.79	0.23	0.95	1.86	1.56	/

Table 8. The strength of clinkers

	Setting Time		Bending Strength (MPa)			Compressing Strength (MPa)		
	inital setting time	final setting time	3d	7d	28d	3d	7d	28d
1	3: 47	5: 19	6.9	7.3	8.6	38.8	53.0	69.9
2	4: 55	6: 50	6.7	7.5	9.0	38.0	54.6	76.9
3	3: 50	5: 39	7.5	8.5	8.8	45.2	61.3	75.6

In the end on the basis of the best condition for a synthetical study, three raw meal groups, the KH is 0.88, 0.93 and 0.95 respectively, are made up in our lab, adding moderate barite and fluospar (CaF_2/Al_2O_3=0.20) respectively, burning at 1350℃, grinding the clinkers with gypsum, their strength are measured, results are showed in table 7, table 8. All of these groups cement strength are reach to or over 70MPa, cement clinkers are of high strength and fast hardenning. It full proofs the effect of barite-fluorspar composite minerlizer. The above achievements in scientific research have been applied in several shaft kiln cement factories in China, the synthetical effects of production increasing, energy saving and cement strength promoting are made.

3. CONCLUSIONS

(1). Barite and flourspar have significant effection in the process of cement clinker formation, The action of barite is, Ba^{2+} enters into C_2S by the way of solid-solution, changes C_2S crystal form and makes it in the form of α-or α'-C_2S; High hydraulic activity is obtained. The action of fluorspar is, promoting the formation of C_3S and forming a considerable amount of $C_{11}A_7 \cdot CaF_2$ by means of kinds transitional phases; At the end, the high strength and fast hardenning cement can be made.

(2). The cement clinker's burnability can be promoted, the burning temperature lowered about 100～150℃, 10～15% kiln capacity increase, about 10% coal consumption lower, 2926 ～ 3135KJ/Kg fuel consumption stabilize, and 0.5～1.0 T/H cement mill capacity increase, it has been achieved notable economic benefit in cement prodution.

REFERENCES

1. M. Regourd, M. Bigara, J. Forest, A. Cineier, proc, 5th Int. symp. chemistry of cement 144 —49 (1968).

2. S. SPRUNC, proc, 7th Int. symp. Chemistry of cement 1--2/1- -2/11 (1980)

3. V. V. Timasher, proc. 7th Int. symp. chemistry of cement 1- -3/1 --3 --10 (1980)

4. BORIS. MATKOViC et. al., Am. Cram. SOC. BUH (USA) 60C1]1164—1167 (1981) 60C8] 825- - 829 (1981)

APPLICATION FEASIBILITY OF A CALCINATION CATALYST IN CEMENT MANUFACTURE—A CASE STUDY

S A Khadilkar, P G Lele, C H Page and A K Chatterjee

Research and Consultancy Directorate
The Associated Cement Cos Ltd
Thane, INDIA

SUMMARY

A limestone calcination catalyst based on sodium calcium carbonate developed by an international research institute and of proven performance in lime kilns, was evaluated for use in cement manufacture. The catalyst was characterised for its chemico-mineralogical properties, and its effect in the cement raw mix was studied. This case study presented in this paper illustrates the performance of the catalyst in calcination and in clinkerisation of a cement raw mix at different dosages. The effect of the catalyst on the kinetics of calcination of cement raw mix and its influence on phase assemblage and extent of clinker mineral formation is discussed. The data generated indicates various merits and demerits of its use in cement manufacture.

INTRODUCTION

To enhance productivity and energy conservation in cement manufacture, The Research and Consultancy Directorate of The Associated Cement Cos.Ltd. has carried out comprehensive investigations on feasibility of using various low cost materials in cement manufacture. In this context, the limestone calcination catalyst developed by an international research institute and of proven performance in lime kilns was evaluated for use in cement manufacture. The case-study presented in this paper illustrates the effect of different dosages of the catalyst, on kinetics of calcination and clinker mineral formation and of the various merits and demerits of its use.

CHEMICO-MINERALOGICAL CHARACTERISTICS OF THE CATALYST

Chemical Composition

The full chemical analysis of the calcination catalyst is presented below:

Oxides	SiO_2	Al_2O_3	Fe_2O_3	CaO	MgO	LOI	Na_2O	K_2O	SO_3	Cl	F
%	0.9	0.3	0.07	29.4	1.1	38.9	30.6	0.05	0.01	0.02	0.08

Mineralogy

The X-ray diffraction analysis indicates that the catalyst is composed of the mineral phases Nyererite $[Na_2Ca(CO_3)_2]$ and Tridymite (Fig.1).

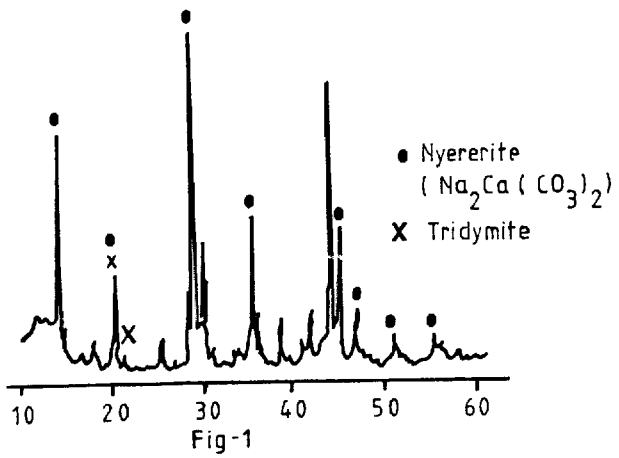

Fig-1
XRD Scan of limestone Calcination Catalyst.

PERFORMANCE EVALUATION

The effect of the calcination catalyst on the kinetics of calcination of cement raw mix and its influence on phase assemblage and extent of clinker mineral formation was studied at three concentration levels, 0.1% (R.Mix-2), 2% (R.Mix-3) and 5% (R.Mix-4) and compared with the cement raw mix without catalyst. (R.Mix-1).

(i) Effect on kinetics of Calcination of Cement Raw Mix

The calcination profile of the four raw mixes was studied by TG/DTA in Mettler Thermal Analyser TA-12 . The results are in Table-1.

TABLE-1 THERMAL ANALYSIS OF RAW MIXES

	Raw Mix-1 without catalyst	Raw Mix-2 1% catalyst	Raw Mix-3 2% catalyst	Raw Mix-4 5% catalyst
1. Onset temp. of calcination °C	575	535	520	510
2. Peak Maxima of calcination °C	835	835	830	825
3. Temp. of completion of calcination °C	860	860	860	860
4. Total Carbonates (%)	75.4	76.6	76.5	76.6
5. Heat of Calcination (Cal/gm)	316.6	314.9	310.9	318.4
6. Percentage Calcination at different ranges of temp.				
600 - 700°C	3.4	4.1	5.0	5.6
700 - 800°C	41.0	39.8	45.8	52.0
800 - 860°C	55.6	56.1	49.2	42.4

Temp °C	Raw Mix - 1				Raw Mix - 2				Raw Mix - 3				Raw Mix-4			
	Free CaO %	Uncombined CaO %	Combined CaO %	Na_2O %	Free CaO %	Uncombined CaO%	Combined CaO %	Na_2O %	Free CaO %	Uncombined CaO %	Combined CaO %	Na_2O %	Free CaO %	Uncombined CaO%	Combined CaO %	Na_2O %
Unfired Raw mix	-	-	-	0.258	-	-	-	0.622	-	-	-	1.00	-	-	-	2.28
700	1.7	95.4	2.9	0.253	1.1	94.8	4.1	0.58	91.2	95.1	3.7	1.00	2.5	93.8	3.7	0.74
800	3.8	54.0	12.2	0.243	33.9	48.9	17.2	0.588	37.5	39.0	23.5	0.982	35.1	30.6	34.3	2.254
900	44.3	53.5	2.4	0.242	48.8	46.8	4.4	0.583	46.2	44.0	9.8	0.99	9.2	35.1	25.7	2.263
1000	70.2	28.9	0.9	0.2298	71.4	22.3	6.3	0.568	61.4	34.3	4.3	0.992	47.2	26.5	26.3	2.247
1100	59.2	28.5	11.8	0.2293	61.8	31.9	6.3	0.547	62.5	21.5	16.0	0.995	41.7	23.5	34.8	2.217
1200	50.5	22.7	26.8	0.2234	51.3	26.7	22.0	0.5233	43.4	23.2	33.4	1.00	28.6	15.7	55.7	2.180
1300	29.8	8.5	61.7	0.2087	23.7	10.6	65.7	0.5194	21.2	10.2	68.6	0.89	25.5	10.4	66.1	1.84
1350	15.2	2.8	82.0	0.2057	16.2	3.0	80.8	0.5177	15.6	3.2	81.2	0.81	19.8	33.2	77.0	1.768
1400	10.0	1.8	87.6	0.2025	12.5	2.8	84.7	0.456	13.2	2.8	84.0	0.76	17.1	2.8	80.1	1.643
1450	8.8	1.2	90.0	0.1999	11.6	2.0	86.4	0.43	12.4	2.2	85.4	0.767	12.0	2.0	88.0	1.465

TABLE - 2 : REACTIVITY / VOLATILITY OF RAW MIXES

The thermal analysis indicates that :

- with the increase in dosage of the catalyst, the onset of calcination is lowered, from a temperature of 575°C for R.Mix-1 (without catalyst) but lowered to 535°C (R.Mix-2), to 520°C (R.Mix-3) and 510°C (R.Mix-4).

- The peak maxima of calcination is decreased by 10°C.

- Although the optimum temperature of calcination is the same, there is an increase in the rate of calcination of raw mix with an increasing catalyst content.

- The heat of calcination (cals/g) shows a decrease with 1% and 2% catalyst; however at 5%, the energy requirement appears to be more which may be due to the higher degree of subsequent solid-solid endothermic reactions occurring at the same temperature range as that of calcination.

Thus, it appears that the presence of the catalyst not only enhances the rate of calcination but also has a catalytic effect on other solid-solid endothermic reactions occurring in clinker phase formation.

(ii) Effect of catalyst on phase assemblage in clinkerisation of raw mix

The influence of different concentrations of the catalyst, on the extent of clinker mineral formation was assessed by techniques standardised in the author's laboratory (Ref. 1,2). The raw mixes (R.Mix-1, 2, 3 & 4) were pelletised and the pellets were fired at temperatures of 700°, 800°, 900°, 1000°, 1100°, 1200°, 1300°, 1350°, 1400° and 1450°C for 20 mins with fresh pellets of the raw mixes taken to each of the above temperatures and retained for 20 minutes. The expansion/shrinkage in diameter of the fired pellets at each temperature was measured and also were analysed for free CaO and total % Na_2O (Table 2) to evaluate the lime consumption and volatility of the raw mixes.

The graphical expansion/shrinkage patterns of the raw mixes in the temperature range of 700°C to 1450°C (Fig.2) are a measure of sinterability and extent of clinker mineral formation in the raw mix. These patterns can be broken up into three conceptual ranges for interpretation: a) 700° - 1100°C, b) 1100° - 1300°C, c) 1300°C -1450°C

a) The pattern upto 1000°C can be interpreted with the help of ternary diagram (fig.3), involving "Uncombined Lime" (lime in carbonate form) "Free Lime" (liberated by decarbonation) and "Combined Lime" (lime in non-carbonate phases like aluminates, ferrites, silicates). The ternary plot is indicative of the progressive liberation and combination of the free lime.

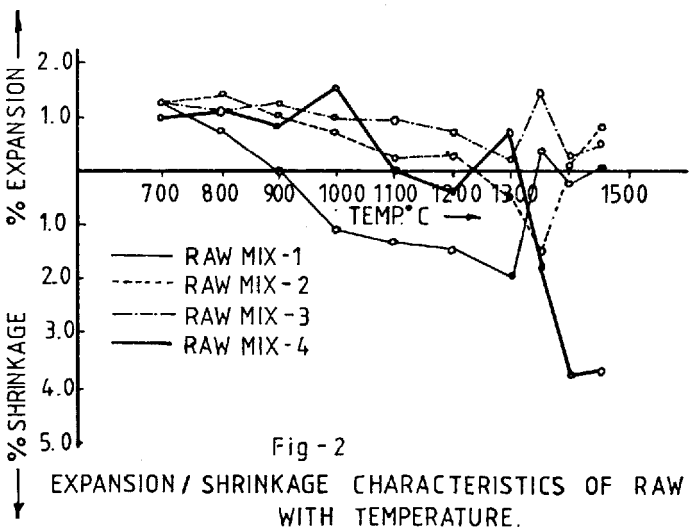

Fig - 2

EXPANSION / SHRINKAGE CHARACTERISTICS OF RAW MIXES WITH TEMPERATURE.

b) In the temperature range of 1100° - 1300°C, the expansion/shrinkage patterns are indicative of the extent of solid - solid reactions in clinkerisation and can be predicted by the plot of expansion/shrinkage and combined lime (Fig.4).

c) From 1300° - 1450°C, the expansion/shrinkage patterns illustrates the nature and temperature of liquid formation and subsequent diffusion reactions resulting in formation of the higher lime silicates.

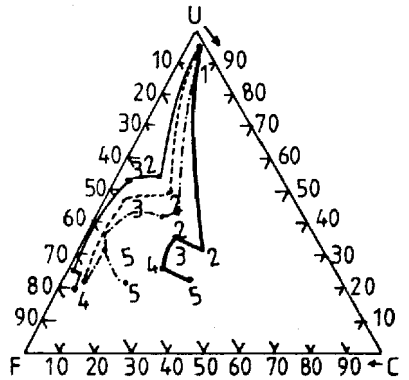

U: UNCOMBINED CaO, F: FREE CaO, C: COMBINED CaO.

1-700°C 2-800°C 3-900°C 4-1000°C 5-1100°C

RAW MIX-1
RAW MIX-2
RAW MIX-3
RAW MIX-4

Fig-3

TERNARY PLOT OF THE RAWMIXES.

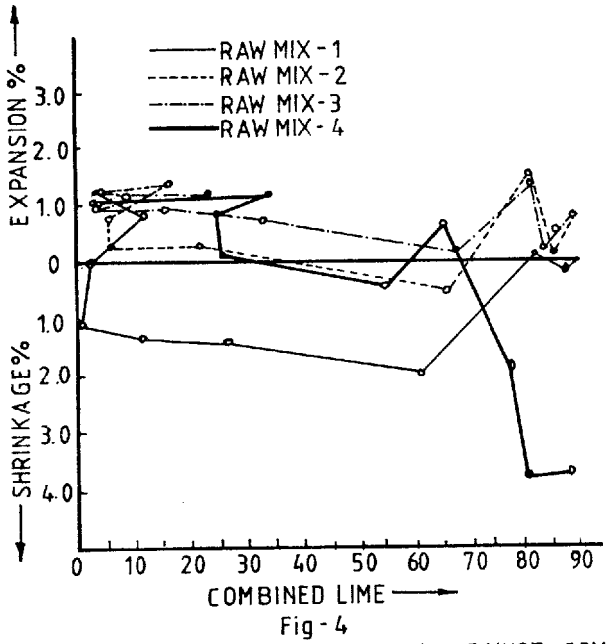

Fig - 4

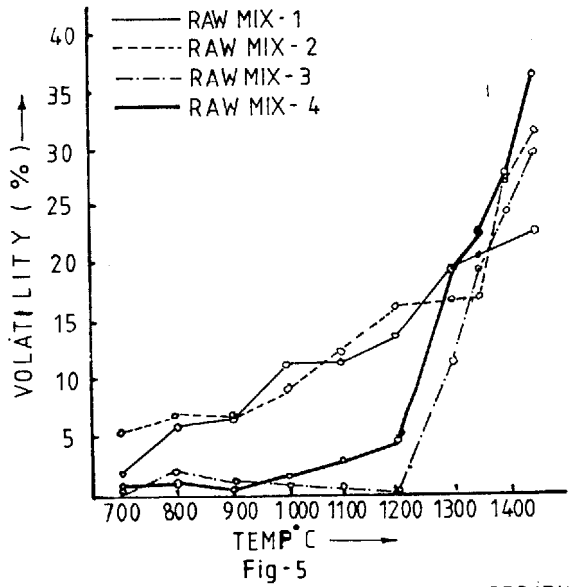

Fig - 5

PLOT OF EXPANSION/SHRINKAGE AGAINST COMBINED LIME. VOLATILITY OF RAW MIXES WITH TEMPERATURE

The volatility of Na_2O with temperature in these raw mixes is presented in Fig.5. (the volatility of Na_2O has been considered on loss free basis at each temperature).

OBSERVATIONS

Based on the data generated, the following observations can be made:

- The ternary plot shows that at higher concentrations of the catalyst (Raw Mixes-3) and 4) the rate of decarbonation is more and the liberated free lime combines to form aluminates and silicate phases.
- The expansion maxima in case of R.Mix-1(without catalyst), R.Mix-2 (with 1% catalyst) and R.Mix-3(with 2% catalyst) are observed when combined lime is 80% while in R.Mix-4(5% catalyst), it is observed when combined lime is 60% (Fig.4) which is indicative of enhanced formation of intermediate phases at the cost of delayed appearance of actual clinker phases (high lime silicates).
- The volatility of the raw mixes with catalyst above 1350° is in the range of 30-36% and the Na_2O contents retained is 1.0-1.46%. This high Na_2O content of the raw mixes, in the temperature range of 1350-1450°C appears to alter the property of liquid formed in the cement clinker, thereby affecting the rate of phase boundary diffusion reactions leading to C_3S formation. This is also supplemented by the XRD analysis of the fired raw mixes at 1450°C (Fig.6), which indicates that with the increase in concentration of the catalyst, the C_3S content gradually decreases.

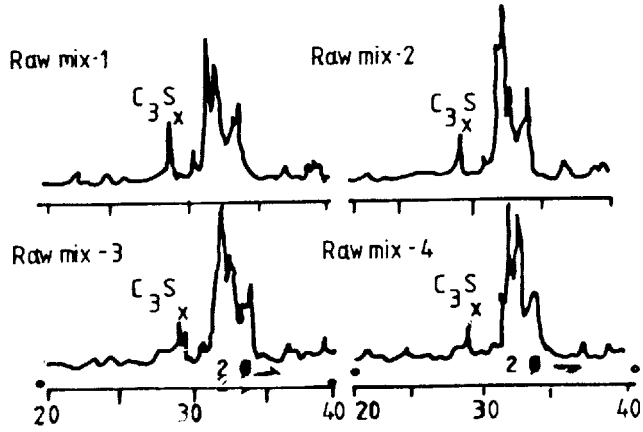

Fig.6 : XRD Scan of Raw Mixes fired at 1450°C

CONCLUSIONS

The calcination catalyst accelerates the rate of calcination of the raw mixes and also enhances the rate of solid-solid endothermic reactions occurring in clinker phase formations upto 1300°C.

The reactivity of the raw mixes with catalyst decreases after the liquidus temperature (above 1350°C) is reached, which can be attributed to the higher Na_2O retained in clinker, presence of which is known to alter the liquid characteristics and thereby decreases the rate of diffusion reactions of C_3S formation. The higher levels of Na_2O contents would also create operational problems in preheater-dry process kiln systems.

The calcination catalyst thus appears to have limitations, for use in cement manufacture unless the catalyst used is recovered from preheater before the material enters the kiln system, whereby its catalytic potential could be completely made use of.

A novel concept for the future is to incorporate the catalyst in a fluidised bed calciner systems, or as a coating on some component of these calciner systems in which case the catalytic potential could be used.

REFERENCES

1. A.K.Chatterjee, C.H.Page and D.Ghosh. "Industrial Experience of using mineralisers for every conservation in clinker formation". Proceedings of Beijing International Symposium on Cement and Concrete, 1985, Vol.I, pp. 174-190.

2. A.K.Chatterjee and C.H.Page. "Industrial applications of mineralisers for improved clinker burning - Illustrative case studies". All India seminar on cement and allied building materials, Jan. 1984 Vol. III, pp. 190-209.

ACTIVATORS FOR ACCELERATED CALCINATION

S Laxmi, A K Ailavadi and M M Ali

National Council for Cement and Building Materials
New Delhi, INDIA

SUMMARY

Calcination consumes substantial thermal energy in the process of cement manufacture. Various chemical additives have been found to enhance the kinetics of reactions. In the present paper effect of waste based additives such as chrome sludge, pyrite cinder, ferrous sulphate, phosphogypsum and some of their combinations has been studied on calcination of cement raw mix. Suitable additives enhanced the rate of calcination by 10-30 percent. Rate of lime assimilation is increased in addition to lowering in clinkerization temperature by 30-60°C. A saving of 65-110 kcal/kg of clinker is observed during calcination in presence of additives. The strength development is also appropriate in these clinkers (40.0 - 47.5 N/mm2 on 28 d basis).

INTRODUCTION

Cement manufacture is a highly energy consuming process which accounts for 40-50 percent of its total production cost. It is therefore obvious that for an industry with such an apetite for energy, the cost and consumption factors of both thermal and electrical energy are very critical. Efforts have been made world over to conserve these energies on micro and macro levels by direct and indirect means. Extensive studies in this direction have led to the modification of process design, installation of heat recovery systems, use of non-conventional fuels,development of alternate technologies for low energy cements and use of chemical additives. Except for the last, all other options need major capital inputs as well as major modifications in the equipments. The use of chemical additives is mainly aimed at reducing thermal energy, therefore gains in electrical power, if any, would only be incidental and an additional benefit.

The chemical additives for lowering energy requirements seem to be one of the approaches wherein triple benefits through : i) reduction in calcination temperature and/or ii) enhancement in rate of calcination, iii) improvement in burnability of raw meal and in turn reduction in clinkerization temperature may be possible. It is also likely that gains in electrical energy, through coarse grinding of raw meal due to enhanced reactivity of calcined product may also be achieved. Various additives for increasing rate of clinkerization of cement raw meal have been reported (1-8). In the present paper it is endeavoured to use certain industrial wastes and chemicals and some of their combinations which would enhance rate of calcination substantially. The studies were conducted on the effect of these additives in varying doses during decarbonation/calcination of limestone as well as cement raw mix at NCB. The present paper reports the effect of the above additives on the rate of calcination, quality of clinker and the cement produced and the energy saving potential of some of the additives in cement manufacture.

EXPERIMENTAL

The raw materials such as cement grade limestone, clay, laterite and industrial raw mixes were used for experimental studies. All the materials were evaluated for their chemical composition, mineralogical characterisation and thermal behaviour using chemical methods, XRD and DTA.

Studies with five different effective additives (I - Calcium sulphate + Ferrous sulphate, II - Phosphogypsum + Pyrite cinder, III - Ferrous sulphate, IV - Chrome sludge, V - Pyrite cinder) in the dosages upto 4 percent by weight of raw meal are presented here. Calcination studies on limestone and raw meals were conducted on samples with a fineness of 10 percent residue on 170 mesh sieve in a muffle furnace at different temperatures between 700 - 900°C with retention times of 5,10, 20, 30 and 60 minutes. The calcined samples were evaluated for loss on ignition, mineralogical characteristics using XRD, DTA for studying rate of calcination, energy of activation and energy consumption during calcination. Raw meals were also evaluated for their burnability. The clinkers prepared on the basis of burnability studies at 1380 °C, were evaluated fpr morphology and mineralogy using SEM and XRD. The cements prepared from these clinkers were studied for strength development characteristics.

RESULTS AND DISCUSSIONS

The data on the effect of potential additives (fig 1) indicate an overall increase in rate of calcination by 10-30 percent during calcination of limestone. Though the enhancement in the rate of calcinabion was observed at all temperatures above 600°C, the effects were more prominent between 700-800°C. Studies conducted with these additives on calcination of raw meals (fig 2) also indicate the same trend.

The extent of enhancement in the rate of calcination was more predominent in the initial stages of decarbonation and the difference from the control decreased as the calcination approached near completion. The rate of calcination was slower beyond 80 percent calcination in all the cases. Considering above, it is clear from Fig 2 that 80 percent of calcination is achieved much faster (15-20 minutes) in raw mixes with additives than in control mixe (60 minutes). Among the various additives the effect of the combination of additives (calcium sulphate and ferrous sulphate) is most predominent indicating its maximum energy saving potential during calcination.

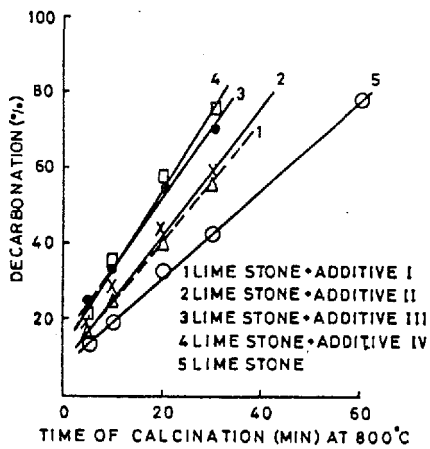

FIG 1 CALCINATION OF LIMESTONE

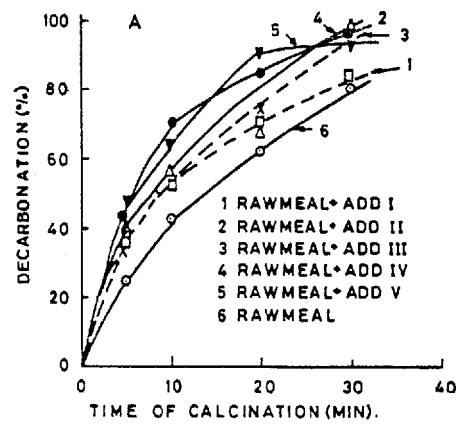

FIG 2 CALCINATION OF RAW MEAL

Mineralogical studies conducted on the calcined raw meal samples (with additives) at 1000 °c indicated the presence of B - C2S and total absence of calcite peak whereas the calcined sample of control mix indicates the presence of calcite, quartz and Ca(OH)2 and absence of B - C2S peak (Fig 3). These findings lead to infer that there is enhancement in the rate of decarbonation and initation of phase forming reactions at lower temperatures due to increased reactivity of mixes in presence of additives.

Studies were also conducted on the effects of various additives on the burnability of raw meals at 1350 °C, 1380 °C and 1400 °c. The burnability data at 1380 °C (Fig 4) showed free lime less than 2 percent in case of raw mixes with additives as compared to control raw meal which showed free lime content of 4.41 percent. The overall results indicated substantial increase in rate of lime assimilation, improved burnability and lowering of clinkerization temperature.

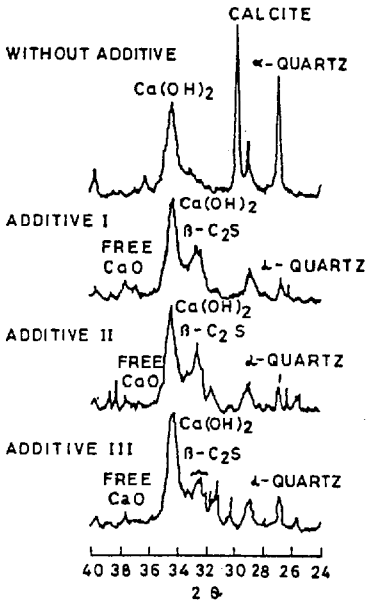

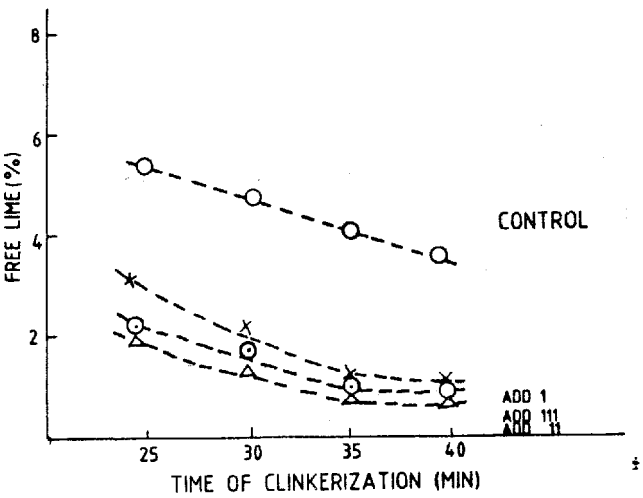

FIG 3 XRD OF CALCINED RAW MEAL (at 1000°C for 30 min)

FIG 4 LIME ASSIMILATION AT 1380°C

XRD studies of clinkers fired at 1350 °C show poor phase development in case of clinkers both with or without additives. However clinker phases were well developed at 1380 °C in case of samples incorpobating additives SEM studies (Plates 1,2) on the above clinkers also indicate better phase development in presence of additives.



PLATES 1&2 - SEM OF OPC CLINKERS WITH ADDITIVES FIRED AT 1380°C (x 1250 & x 2500)

Formation of well developed C2S and C3S phases have been attributed to higher reactivity of raw meals and enhanced rate of reaction. Compressive strength data on the strength development of cements prepared from clinkers with and without additives (tested as per IS-4031-1968) indicate appropriate strength development (Table 1). It is, therefore, clear that incorporation of additives effective in enhancing rate of calcination do not effect adversely strength development of cement.

Table 1

Compressive Strength Of Cement With And Without Additives

S.No.	Sample No.	Fineness (m2/kg)	Compressive Strength (N/mm2) 3d	7d	28d
1.	RM Control	278.0	26.0	38.0	49.5
2.	RM + Add. I	290.0	29.0	38.5	47.5
3.	RM + Add. II	283.0	32.5	40.0	47.0
4.	RM + Add. III	272.0	31.0	39.5	43.0
5.	RM + Add. IV	306.0	21.5	34.5	46.7
6.	RM + Add. V	312.0	31.0	38.5	47.0
7. *	RM-PL Control	275.0	18.3	31.0	41.2
8. *	RM-PL + Add. IV	305.0	24.3	35.5	40.0

* Plant raw meal

ENERGY SAVING POTENTIAL

The energy saving potential of the most effective additives (calcium sulphate + Ferrous sulphate, Phospho gypsum + Pyrite cinder and Ferrous sulphate) has been calculated on the basis of thermoanalytical investigations using DTA/TGA on limestone and raw meal samples containing additives vis a vis control. Incorporation of additives did not result in any appreciable change in temperature of calcination. Similarly activation energies and shape index values were also comparable with control. However on an average net savings of 65-110 Kcal/kg of clinker was observed during calcination based on peak area calculations (Table 2).

Table 2

Energy Consumption and Activation Energies

S.No.	Sample	Activation Energy (Kcal/mole)	Shape Index	Energy Consumption (Kcal/kg)
1.	RM Control	25.77	0.18	237.18
2.	RM + Add. III	25.52	0.17	187.06
3.	RM + Add. II	24.67	0.16	171.58
4.	RM + Add. I	24.04	0.15	151.44

Further a lowering of 30-60 °C in clinkerization temperature has also been observed leading to energy saving to the tune of 15-21 Kcal/kg of clinker. The additives have thus indicated potential benefits for enhancing rate of calcination and lowering clinkerization temperature. The total energy saving potential is of the order of 65-110 Kcal/kg of clinker during pyroprocessing.

CONCLUSION :

The rate of calcination increases in limestone/raw meal appreciably (10-30 percent) in the presence of additives. The choice and the dosage of the additive is however governed by the fineness and mineralogical characteristics of limestone/raw meal. Rate of lime assimilation is increased in the presence of additives leading to decrease in free lime content, formation of C3S at lower temperature, lowering in clinkerization temperature and appropriate phase development. Presence of additives thus improves burnability of raw meals. Calcination process in the presence of additives results in a saving of 65-110 Kcal/kg of clinker. In addition, the clinkerization temp. is lowered by 30-60 °C in the presence of additives. Compressive strength data on the cements from clinkers containing additives have indicated satisfactory performance.

ACKNOWLEDGEMENT

The authors have freely drawn upon completed R&D work of NCB. The paper is being published with the permission of the Director General, National Council for Cement and Building Materials, New Delhi.

REFERENCES

1. Safa, A.I.; Daugherty, K.E.; Mallow, W.A.; Dziuk, J.J. and Funnel, J.B. 'The Potential use of Catalysts in the Cement Industry, Cement, Concrete and Aggregate 1983, p - 21-25.

2. Shearer, J.A., Johnson I and Tuner, C.B. Thermal Decomposition of CaCO3 and formation of - Ca2SiO4. Ceramic society Bulletin, Vol.59, No.5, May 1980, p 521-528.

3. Ghosh, S.N. Paul A.K. and Thakur, K.: Preparation of very Reactive Ca2SiO4 Powder. Journal of Material Science, Vol 13 (7) July 1978, p 1602-1606.

4. Roy, D.M. and Oyefesobi, S.O.; Interaction of NaCl with Limestone during Calcination. Journal of American Ceramic Society, Vol.60, No.314, April 1977, p 178-180.

5. Alimmaryi, S.A. and Tamas F.D.; Burnability of Raw Mix at Rapid calcination conditions, Cem. and Con. Res.10, 1980, p 739-752.

6. Rausbhenefels E, Clinkerability of Cement Raw Meal. ZKG, 29 (2), 1976, p 78-85.

7. Locher, F.W. Low Energy clinker, 8th International Congress on the Chemistry of Cement, Brazil, No.1, 1986, p 57-67.

8. Bhaskar Rao P. Vishwanathan. V.N. Raina S J Arora V.K. and Chatterjee. A.K. Estimation of Heat Requirement for Burning Cement Raw Mixes - a Practical Approach, Cement (Bombay), 11 (4), 1977, p 5-9.

AUTHORS INDEX
(VOLUME II)

A

Abramson, I G – 171,177
Ahluwalia, S C – 56, 146, 406, 420
Ailawadi, A K – 440
Akhmedov, M A – 265
Akhmetov, I S – 74
Akimov, V G – 88
Albats, B S – 10
Alexandrov, A V – 210, 245
Alexandrov, I E – 43
Ali, M M – 440
Andronescu, E – 107
Artykbaev, M T – 265
Asaga, K – 17
Ayed, F – 287

B

Barbanyagre, V D – 196
Bershtein, V L – 261
Bhargava, R – 132
Boikova, A I – 114, 413
Bolwerk, R – 217
Borkar, S A – 278
Borthakur, P C – 301

C

Castanet, R – 287
Chatterjee, A K – 67, 190, 238, 278, 434
Chen Jian – 427
Chen Weiqing – 322
Chen Yongfan – 393
Cheng Jingxiang – 139
Cheong, H M – 335
Choi, S H – 335

D

Daimon, M – 17
Deja Jan – 255
Deng Junan – 94
Dhawan, A K – 118

E

Erofeeva, N T – 62

F

Fadeyeva, N G – 171
Fiodorov, A P – 265
Fomicheva, O I – 114, 413
Fraiman, L S – 232, 245

G

Gandhi, R K – 224
Ge Wenmin – 393
Ghosh, S P – 224
Gore, V K – 67, 238
Goswami, G – 365
Goswami, R K – 56, 177
Grishchenko, L V – 413
Gupta, R S – 406

H

Han, K S – 335
Handoo, S K – 177, 308
Hanehara, S – 3
Hargave, R V – 67
Hirano, Y – 17
Hu Shuguang – 81
Huang Qixiu – 322
Huang Wenxi – 125, 139, 164, 329, 372, 379, 386

I

Ioganson, A K – 232, 245
Iqbal, Z – 351

J

Janecka, L – 23
Jaung, J D – 335
Ji Shang Xing – 36
Jiang Youxing – 125

K

Kanimov, B K – 183
Kapralova, R M – 171
Katyal, N K – 420
Khadilkar, S A – 67, 190, 238, 434
Kong Jianmin – 342
Kougiya, M V – 210, 232
Kouznetsova, T V – 56, 88
Krishnan, N A – 67
Krivoborodov, Yu R – 10
Kurdowski, W – 255

L

Lata Mohan – 118
Laxmi, S – 118, 440
Lele, P G – 190, 238, 434
Lerke, P P – 201, 205
Li Guangmin – 393
Li Peiquan – 393
Liu Baoyuan – 342

Liu Changfa – 393
Liu Xiaoxin – 94
Lu Baoshan – 393
Lu Zhongyuan – 164, 372, 379, 386
Luginina, I G – 114

M

Mai Huo – 322
Mathur, V K – 308, 406, 420
Mielke, I – 399
Miryuk, O A – 74
Misra, K C – 301
Mohan, K – 224
Mohapatra, B N – 365
Mukhamedbaev, A A – 265
Müller, A – 399

N

Nikiforov, Yu V – 177
Nocuñ-Wczelik, W – 250

O

Osokin, A P – 88

P

Page, C H – 67, 190, 238, 278, 434
Pan Yi Zhou – 271
Panda, J D – 365
Panyuskin, V N – 88
Parashar, A K – 308

Q

Qi Yanyong – 329
Qian Guangren – 329, 372
Qin Z G – 153

R

Radnaasediin, S – 315
Raina, K – 132, 146
Rajczyk, K – 250
Ram Prakash – 420
Rumyantsev, P F – 62
Ryazin, V P – 10
Ryzhik, A B – 210, 245

S

Salimov, Z S – 265
Samuel, G – 177
Shah, H U – 351
Shamshurov, V M – 196
Shanba Wang – 29, 294, 358
Sharma, P S – 118
Shirasaka, T – 3
Shkatova, G V – 183
Shree Gopal – 308
Shukla, A K – 101
Shunni Liu – 49
Singh, N B – 101
Singh, S P – 101
Sorrentino, F P – 287
Stark, J – 399
Su Dag[illegible] – 322
Su Muzh[illegible] – 94, 393
Sulimenko, L M – 160

T

Teoreanu, I – 107
Thombare, C H – 278
Timoshenko, T I – 196
Tsurumi, T – 17
Turetski, A M – 43

U

Uchikawa, H – 3

V

Vaisman, A F – 171
Varadarajan, V – 278

W

Wang Xinrong – 294
Wang Yuping – 125
Werynski, B – 23
Wu Zongdao – 94

X

Xia Youming – 139
Xian Yafang – 294
Xu Fengjuan – 36
Xu Guangliang – 164, 372, 379, 386
Xu Xianyu – 427

Y

Yang Liqun – 427
Yang Yurong – 329
Ye Qiaoming – 125
Ye Qing – 342
Yegorov, G B – 43, 183
Yuankui Chen – 29

Z

Zdorov, A I – 261
Zheng Liqiang – 322
Zhonghui Zhow – 358
Zhu Jiaoqun – 294
Zongshou Lin – 49

9th International Congress on the Chemistry of Cement New Delhi, India, 1992

VOLUME III

COMMUNICATION PAPERS — THEME II

NATIONAL COUNCIL FOR CEMENT AND BUILDING MATERIALS
NEW DELHI

9th International Congress on the Chemistry of Cement New Delhi, India, 1992

COMMUNICATION PAPERS

Volume III

ADVANCES IN PORTLAND, BLENDED, SPECIAL AND NEW CEMENTS

Organised by

NATIONAL COUNCIL FOR CEMENT AND BUILDING MATERIALS
NEW DELHI

Co-sponsored by:

Department of Scientific & Industrial Research
Ministry of Science & Technology
Government of India

Cement Manufacturers' Association, India

The India Cements Ltd

J K Cement Works

Madras Cements Ltd

Narmada Cement Co Ltd

Orissa Cement Ltd

This volume is a part of six-volume series of the Congress Papers.
Title of each volume is given below:

I	—	Congress Reports
II	—	Communication Papers - Theme I
III	—	Communication Papers - Theme II
IV	—	Communication Papers - Theme III
V	—	Communication Papers - Theme IV
VI	—	Reports on Special Panel Discussions and Poster Papers

Published by :
National Council for Cement and Building Materials (NCB)
M-10 South Extension Part II New Delhi-110 049 INDIA

No Part of this publication be reproduced without the written permission of the Publishers.

The views expressed in the technical papers printed in this publication are those of authors and not necessarily of the Publishers.

Printed in India by THE OFFSETTERS, New Delhi -110003

PREFACE

Commencing with a one-day meeting in London on 14 January 1918 arranged by the Faraday Society, to discuss "The setting of cements and plasters", which is taken as the first Symposium to deal solely with the chemistry of cement, the subsequent International Symposia and Congresses on the Chemistry of Cement have been held in Stockholm (1938), London (1952), Washington DC (1960), Tokyo (1968), Moscow (1974), Paris (1980) and Rio de Jenairo (1986). At the conclusion of the Rio Congress, it was decided that the next Congress will be held in India. Accordingly, the 9th International Congress on the Chemistry of Cement is being held in New Delhi, India, from 23 to 28 November 1992.

The preparatory and organisational work for this 9th Congress was commenced immediately after the 8th Congress. To start with, all the participants in the previous two Congresses and a large number of individuals and organisations interested in the subject of the Congress were contacted through an extensively worked out and widely distributed Questionnaire. The response was most encouraging. The responses were carefully analysed and the directions which would meet the views of the largest number of participants towards advancing the cement sciences were determined. Based on these findings the first Bulletin was issued in August 1988, providing the necessary preliminary information on the Congress and outlining its scope and essential organisational aspects.

The objectives of the Congress were set to advance the knowledge of chemistry of cements with emphasis on application of this knowledge in both the manufacturing aspects and utilization of cements in practice. Within this broad scope, the thrust was on tracking the scientific progress made in the field since the last Congress, assessing the status of exploitation of the results by the industry and the society, and mapping of the new frontiers of knowledge.

The overall organisation of the Congress was governed by a National Organising Committee which was responsible for all organisational aspects including financial arrangements. Taking into account the suggestions received from various quarters, the International Scientific Committee consisting of 67 experts from 39 countries all over the world was formed which was responsible to finalise : (a) the themes and sub-themes of the Congress, (b) procedures for inviting, receiving and reviewing of papers, (c) selection of authors for general and special reports, and (d) the system for conduct of the proceedings of the sessions and other related scientific and technical matters.

The International Scientific Committee held two meetings in New Delhi in November 1989 and in January 1991. In addition, informal meetings were held with representative groups in Seoul, Tokyo, Paris, Washington DC and Montreal. The International Scientific Committee finalised the Generic and Specific Themes of the Congress. It was decided that for each Generic Theme, there shall be one Principal Review Paper, which shall cover the progress achieved in the area of the Generic Theme between the two Congresses. For each Specific Theme, there shall be one Congress Paper highlighting trends of research and realisation of the results in the industry in the areas related to the Specific Theme. Under each Specific Theme, in addition to the invited Congress Papers, there shall also be Communication Papers. Both the principal review papers as well as the Congress papers were to be presented by the invited experts identified after deliberations of the International Scientific Committee.

Preliminary Abstracts of communication papers were solicited through the Second Bulletin in May 1991. 537 Abstracts were received which were scrutinised by a panel of Indian experts and 513 were short-listed. Authors were requested to send full manuscripts of the paper for detailed review and acceptance for publication and presentation. As many as 412 communication papers from 40 countries were received which were reviewed by a panel of international experts. As a result, 346 communication papers belonging to the four themes of the Congress were finally

accepted for presentation and publication. These were in addition to 21 State-of-the-Art Congress Reports received from invited authors; reports on two Specific themes could not be had because the authors selected expressed their inability at a late stage, making replacement difficult.

In addition to the papers on deliberative thematic sessions, a poster session is being organised on "Advances in Physico-Chemical Evaluation, Characterisation and Quality Control Techniques and Systems" for Clinkers, Particulate Cements, Hydrated Systems and Concrete Systems. The State-of-the-Art Report would be presented by an invited expert and 24 contributions made in the form of posters will be presented during the Congress. In addition, Special Panel Discussions are being organised to survey the newer frontiers of knowledge in the areas of computerisation in cement science and concrete systems; resource economy in cement and concrete making; and cement in hazardous waste management.

The proceedings in six Volumes contain all the above contributions received for the Congress. This **Volume III** contains **Communication Papers on the Generic Theme "Advances in Portland, Blended, Special and New Cements".**

A novel feature of the 9th Congress will be that, in addition to the normal sessions as in the earlier Congresses, there will be three sessions to bring out the technological and techno-ecnomic impact of the scientific advances on the industry. These are intended to provide a better appreciation of the implications of the scientific advances specially on the process control machinery and related industries as well as on operational aspects related especially to energy conservation and environmental improvement. Texts of these Special Lectures will be published in Volume VII of the Proceedings to be brought out after the Congress, along with the texts of Addresses at the Inaugural and Concluding Sessions and List of nearly 550 delegates from 42 countries who are expected to attend the Congress.

I am grateful to the members of the International Scientific Committee for their whole-hearted co-operation, to those who reviewed the Abstracts, and to the International Panel of Reviewers of Manuscripts for providing very useful technical and editorial comments on the communication papers. The co-operation of the authors in accepting and implementing the reviewers' suggestions and revising their manuscripts accordingly is greatly appreciated. Thanks are also due to those authors whose communication papers could not be accepted essentially because the contributions did not fit in with the themes of the Congress and not because of any technical deficiency. We recommend that the authors have those papers published elsewhere.

The unstinted efforts put in by my colleagues in the National Council for Cement and Building Materials in all aspects of organising this Congress, is thankfully acknowledged.

A K Mullick
Chairman
International Scientific Committee
9th International Congress
on the Chemistry of Cement

New Delhi
14 September 1992

GENERIC THEME II

ADVANCES IN PORTLAND BLENDED SPECIAL AND NEW CEMENTS

EXPLANATORY NOTES

The following symbols, which have been universally recognised by cement chemists for formulating more complex compounds, are used interchangeably with the respective oxide formulae throughout this volume:

A	: Al_2O_3	K	: K_2O
C	: CaO	M	: MgO
$\overline{C}$	: CO_2	N	: Na_2O
CH	: $Ca(OH)_2$	P	: P_2O_5
F	: Fe_2O_3	S	: SiO_2
H	: H_2O	$\overline{S}$	: SO_3

Commonly used abbreviations of more general nature are as follows:

DTA	—	Differential Thermal Analysis
EPMA	—	Electron Probe Micro Analysis
IR	—	Infrared
NMR	—	Nuclear Magnetic Resonance
RH	—	Relative Humidity
w/c	—	Water-cement Ratio
XRD	—	X-ray Diffraction.
SEM	—	Scanning Electron Microscope
EDAX	—	Energy Dispersive Analysis of X-rays

CONTENT

Volume III

THEME II A: Advances In Portland and Blended Cements

1. Gypsum-free High Early-strength Cement 3
V V Chistyakov and Ye A Myasnikova

2. The Research on $C_2A_xF_{1-x}$ in Iron-rich Fluoraluminate Cement 9
Huang Wenxi, Yang Yurong, Qian Guangren and Qi Yangyoun

3. Strength Development and Heat of Hydration of Low Heat Cement 16
K Yoshida and H Igarashi

4. Properties of Special Cement Adjusted Particle Size Distribution 23
Kiyohiko Uchida, Yukio Fukubayashi and Suminari Yamashita

5. The Sub-cluster Model of Cement Particle Size Distribution 30
Feng Xiuji and Zhao Fei

6. Production Performances and Utilization of a Special Superplasticized Cement 38
V Alunno Rossetti, F Curcio and L Cussino

7. White Belitic Portland Cements 45
Marcela Muntean, M Dinulescu, Maria Bedö and Florica Paul

8. The Mechanochemical Activation of Belite 51
Luhui Zhong Jinyu, Fan Yueming and Yang Jiazhi

9. Characteristics of Masonry Cement Produced at 975° C in Fluidized Bed Boiler 58
Fu Zicheng, Cui Enshu, Qin Zhigang, Zhong Baiqian and Yang Nanru

10. Ion Exchange Reaction of Granulated Blast Furnace Slag in Acid Solution 65
S Aoki and Y Arai

11. Suitability of Rice Husk Ash Obtained by Fluidized-bed Combustion for Blended Cement 72
N Hara, H Noma, S Honma, S Samrejprasong and S Uparisajkul

12. Reactivity Test for Fine Silicas and Pozzolanic Mineral Additives 79
C Vernet and G Noworyta

13. Activity and Properties of Pozzolan Used in Blended Cements 86
C Urrutia, M Ubilla and M Bobadilla

14. The "Capacity of Exchange" of Pozzolanic Additions: Its Origin and Influence in the Fratini Test 93
Rafael Talero

15. Some Studies on the Activation of Blastfurnace Slag in Cements without Clinker 101
C E S Tango and E Y L Vaidergorin

16. Properties of Very Fine Blastfurnace Slags Manufactured by Jet Mill 108
P J Nieminen and K P K Pylkkänen

17. Chemical Activating of Metallurgical Slag in the Conditions of Granulating 115
V V Vulkov, N A Delchev and N S Nikonova

18. Metallurgical Slags as Blending Materials for Cement Manufacture 121
K M Sharma, R Bhargava, D Yadav and S C Ahluwalia

19. Effect of Structure and Composition on Reactivity of Zeolite-tuff used as Blending Material of Portland Cement 128
Lian Huizhen

20. A Study on the Morphology and Microstructure of Activated Indian Fly ash 135
R N Sharma, S N Ghosh, V K Mathur and A K Solankey

21. Binder Enhanced Refused Derived Fuel Ash: A Study of Hydrolysis. 142
Russell Hill and Kenneth E Daugherty

22. New Technique for Economical Manufacture of Cement Based Binders 149
R Karvinen and P Nieminen

23. Blended Cements Containing Granulated Slags from Ferrochrome Production 154
T V Kuznetsova, V V Mityushin, N S Nikonova and V H Jabirov

24. Study on Effects of Kiln Dust Addition to Portland and Blended Cements 159
S P Ghosh, P Padmanathan and K Mohan

25. Influence of Degree of Hydration of Slag on Slag Cements 166
A F Battagin

26. SO_3 Content of Portland and Blended Cements: Porosity and Behaviour of the Resultant Mortars 173
R Sersale, R Cioffi, G Frigione and F Zenone

27. Limestone Additions to Portland Cement: Uptake, Chemistry and Effects 180
Kevin D Ingram and Kenneth E Daugherty

28. Effect of Pozzolana Additions on Hydration and Performance of Portland Slag Cement 187
K M Sharma, R N Sharma, D Yadav and K C Narang

THEME II B: Developments in New-portland Cements

29. Synthesis and Properties of Low Energy Cements Based on $C_4A_3\bar{S}$ 195
J Beretka, L Santoro, N Sherman and G L Valenti

30. The Crystal Structure of $C_4A_3\bar{S}$ 201
Zhang Peixing, Chen Yimin, Shi Liping, Zhang Guanying, *Huang Wenmei and Wu Jianguo*

31. Sulfate-bearing Solid Solution of Calcium Aluminates and Ferrites 209
Yu R Krivoborodov and S V Samchenko

32. Mechanisms at the Mixed Sulphataluminates Formation in the $CaO-Al_2O_3-(Sr, Ba)\ SO_4$ Systems 216
I Teoreanu, A Puri and M Georgescu

33. Cements Based on Modified Portland and Sulfoaluminate - Belite Clinkers 222
S I Ivashchenko

34. Potentials of Using Dolomitic Limestone in Making Sulphoaluminate - Silicate Cements 227
M M Ali, P S Sharma and R Bhargava

35. Examination of $12CaO.7Al_2O_3$ Phase Doped with Magnesium, ... 233
Iron and Titanium Oxides
Z Konik, A Stock and J Iwanciw

36. Ca_2AlMnO_5: Studies about its Characterization and Hydration 239
F Puertas, M T Blanco, S Martínez and R Dominguez

37. Barium Aluminate Cement — Its Synthesis and Formation Kinetics 245
S J Raina, S Agarwal, M M Ali and S K Agarwal

38. Mechanisms at the Formation of some Unitary Strontium and Bariumsulphataluminats 250
I Teoreanu, M Georgescu, A Puri and A Badanoiu

39. Sulfoferrite Cements 256
A P Osokin, Yu R Krivoborodov and N F Dyukova

40. Kinetics of Aluminoferrite Formation at Different Conditions 262
Chen Yimin, Shi Liping, Su Muzhen and Deng Jun'an

41. Study on Cement in the $C_{11}A_7$. CaF_2-C_2S System 268
Liu Kezhong, Deng Zhongyan, Yuan Mingdong and Tang Jinshu

42. New Energy-saving Cement — Iron-rich Fluoraluminate Cement 277
Huang Wenxi, Qian Guangren, Yang Yurong and Qi Yanyong

43. Hydraulic Binders Based on Condensed Silica Fume and Slaked Lime 284
Harald Justnes

44. High Strength Alkali Steel-Iron Slag Binder 291
Bian Qinghan, Wu Xuequan and Tang Mingshu

45. Comparison of the Microstructure and Performance of Alkali-slag and Portland Cement Pastes 298
Caijun Shi, Robert L Day, Xuequan Wu and Mingshu Tang

46. The Selection of Stimulation Agents for Alkali-slag Cement 305
Chen Zhi Yuan and Liao Xin

47. Alkali Activated Slag Cementitious Material for Drilling Operation 312
W Brylicki, J Malolepszy and S Stryczek

48. The Research of the Reactive Products and Mineral Phase for FKJ Cementitious Material 319
Lu Changgao

49. Investigation of the Possibility of Making Hydraulic Binder by Chemical Activation of Domestic Ash and Mixture of Slag and Domestic Ash 325
N Kostić and B Skenderović

50. Evaluation of Physio-chemical and Hydration Characteristics of Supersulphated Cement 331
K Mohan and S P Ghosh

51. Phosphate-bonded Dental Cements 338
W Jiang and Nanru Yang

52. MgO - Ammonium Polyphosphate Systems 345
Marcela Muntean and Melania Gutul

53. Hardening Processes for Some Refractory Binding Systems Kinetic Considerations and Mechanisms 351
I Teoreanu and N Angelescu

THEME II C: Cementitious Systems Including DSP, CBC etc

54. High-strength Hot-pressed Cement Paste 361
A A Pashchenko, V V Chistyakov and Ye A Myasnikova

55. Contact-condensation Binders Based on Calcium Hydrosilicates 367
Raisa F Runova

56. Mechanical and Microstructural Characterization of MDF Cement-SiC Whisker Composites 373
T H Kim, Y W Park and S H Choi

57. Mechanical Properties of MDF Cement Composites with SiC Powder 380
J H Kim, S H Choi and K S Han

58. Chemistry and Porosity in Modelled MDF Cement Minerals 386
Milan Dràbik, Miloš Krištofik, Ľubica Gáliková and Sadananda Sahu

59. The Increasing Strength Mechanism of the Role of Interfacial Bond in MDF Cement 393
Hu Shuguang

60. Numerical Simulation of MDF Composite Materials 400
R I A Malek and M Uchiyama

61. Chemical Interaction between PVA and Hydrating HAC: Infrared Spectroscopic and Thermoanalytical Investigations 406
S Harsh, Y C Naidu and S N Ghosh

62. Mechanism of Glass-ionomer Cement Hardening 413
E Sakai, K Ono, K Asaga and M Daimon

63. Densifying of Cement Pastes by Chemical Deposition of Silica in the Pores 419
C Atzeni, L Massidda and U Sanna

64. Lithium Salts as Set Accelerators for High Alumina Cement 425
T Matusinović and N Vrbos

65. Solid State Compatibility in the System $CaO-SiO_2-Al_2O_3-CaF_2-CaSO_4$ 431
S Gimènez and M T Blanco

66. Gypsum-free Rapid Hardening and Mixed Portland Cement 438
M A Sanitsky and Ch S Sobol

67. Resource-Saving Coloured Cement-mineral Compositions 444
E P Kholoshin and S V Vavrenyuk

Specific Theme II A

Advances in Portland and Blended Cements

GYPSUM-FREE HIGH EARLY-STRENGTH CEMENT

V V Chistyakov and Ye A Myasnikova

Chair of Cementitious Materials Technology
Kiev Politechnical Institute, Kiev, UKRAINE

SUMMARY

This paper presents results of investigations into kinetics of hydrate and structure formation of gypsum-free cements hardening at a high rate under hydrothermal treatment. Compositions with sulphuric oxides as additives have been developed and studied, they obtain strength at a compression of 38-42 MPa after 4-hour hydrothermal treatment.

РЕФЕРАТ

Приводятся результаты исследований кинетики гидрато- и структурообразования быстротвердеющих безгипсовых цементов в условиях тепловлажностной обработки. Показано, что составы с добавками кислородосодержащих солей серы после 4-х часов пропаривания достигают прочности при сжатии 38-42 МПа.

INTRODUCTION

Lately, there has been a trend towards developing gypsum-free cement compositions (1-3) showing higher physico-mechanical characteristics ascompared to ordinary portland cement. In the light of results of research work reported as yet, gypsum-free cements with potassium bisulphite (4) and sodium sulphate additives were selected. The reason for this choice was that these compositions showed the best compressive strength characteristics in comparison with the other gypsum-free cements containing sulphites or sulphates as additives.

EXPERIMENTAL

Potassium bisulphite and sodium sulphate additives equally intensify the hardening of gypsum-free cements under hydrothermal treatment but produce different effects on water requirements and setting time of the resulting cements (see Table 1). Use of sodium sulphate reduces setting time even compared to a composition based on a clinker without additives. Therefore, compositions with sodium sulphate additive require immediate placement once the mix is prepared. On the other hand, the setting time of a composition with a potassium bisulphite additive conforms to a standard in that its water requirement is 4% lower than that of an ordinary portland cement.

As may be seen in Table 1, blended gypsum-free cements get intensely hardened under hydrothermal treatment in a short-term cycle (4-5 h). The compressive strength immediately after the hydrothermal treatment reaches 38-42 MPa. Compared to this, test specimens based on ordinary portland cement retain a high moisture content after 4-5 h hydrothermal treatment and their compressive strength equals 1.7-3.5 MPa which corresponds to the strength the material acquires by the end of its setting period.

In the present work use was made of the method of disperse system sonic resonance (5), in conjunction with the differential thermal analysis (DTA), infrared spectroscopy (IRS), XRD and variance analysis, to obtain objective data on the kinetics of hydrate and structure formation of the binding agents. Such an approach allows to obtain information not only on the change in elasticity of hardening systems (resonance frequency ω) (5) but monitoring the progress of the dispersion an d compaction processes accompanying the hydration of the binding agents (resonance amplitude A) (6).

Hydrothermal treatment sharply alters the kinetics of structure formation in cement-water dispersion (Fig.1).Analysis of the nature of change in the system dispersion (Fig.1, lower-most curve A-I) is indicative of a multiple rearrangement of its initially formed structuire. Characteristic of the composition based on ordinary portland cement is dilution of the cement paste in 1 and 2.5 h after the start of the hydrothermal treatment. That is caused by rearrangement of the structure as a result of syneresis (the first dilution) and phase transformations of hydrates respecrtively. Elevated values of A for a gypsum-free cement at initial stages of the hydrothermal treatment is indicative of a more intensive dispersion process than the case in ordinary portland cement.

Table 1

Comparative characteristics of cement compositions with gypsum and othersulphite additives

Cycle* of treatment	Additive		Water requirement %	Setting time, h-min		Compressive strength, MPa	
	Type	Amount, mass %		Start	End	Just after treatment	After 28 d of normal hardening
I	Nil	-	31	0-12	0-25	2.0	48
	Gypsum	3	28	2-15	3-20	1.7	43
	Na_2SO_4	1.5	28	0-10	0-15	39.0	55
	$K_2S_2O_5$	1.5	26	1-20	2-20	38.0	61
II	Nil	-	31	0-12	0-25	3.2	50
	Gypsum	3	28	2-15	3-20	3.5	45
	Na_2SO_4	1.5	28	0-10	0-15	42.5	56
	$K_2S_2O_5$	1.5	26	1-20	2-20	40.0	62
III	Nil	-	31	0-12	0-25	23.4	49
	Gypsum	3	28	2-15	3-20	26.7	50.1
	Na_2SO_4	1.5	28	0-10	0-15	44.3	59.1
	$K_2S_2O_5$	1.5	26	1-20	2-20	46.2	60.5

*- Cycles of hydrothermal treatment: preliminary holding + heating to 80°C + isothermal retention at 80°C + cooling off:
I - 0+2+1+1 h; II - 0+2+2+1 h; III - 2+3+5+3 h.

IR spectroscopic data (Fig.2) indicate that there is not only a physical dispersion taking place in this period buit also a breaking of Si-O-Si bonds in the crystal lattice of silicate minerals. This is confirmed by the displacement of the absorption band from 934 cm^{-1} (curve 0) to 920 cm^{-1} (curve ω-I) in the unhydrated cement. Here and further preparation numbers correspond to the point numbers on curve ω-I, Fig.1.

The increased intensity of the bond at 1463 cm^{-1} (fig.2) points to an increased content of slightly crystallized sodium carbonate in the hardening ssystem (this is also supported by the results from XRD). Hence, introduction of potassium bisulphite initiates the process of carbonation of X-ray-amorphous sodium hydroxide when a gypsum-free cement is hardening. Consequently, as a result of a decrease in concentration of sodium hydroxide in the liquid phase the process of clinker mineral hydrolysis will be sufficiently intensified.

Point 3 on the structure formation curves ω-I (Fig.1) corresponds to the moment of setting of gypsum-free composition. The setting mechanism as also the nature of the induction period is the least studied in cement chemistry. According to the experimental data obtained, the set-

ting is preceded by the beginning of compaction of the disperse system (an increase in the value A). As thr cement gets hardened, an increase is noticed in the rate of hydroxylation of dispersion particles. An increase in the intensity of absorption bands in the IR spectrum at 3400 cm^{-1} is indicative of an increase in concentration of the OH^--groups with hydrogen bonds on the surface of the hydrates. These groups are the centers of physical adsorption of water molecules. Thus, one of the causes of hardening is immobilization of the water in the zones which are in immediate contact with hydroxylated particles of dispersion. As this takes place, this immobilized water becomes an element of the structure aand the strength medium.

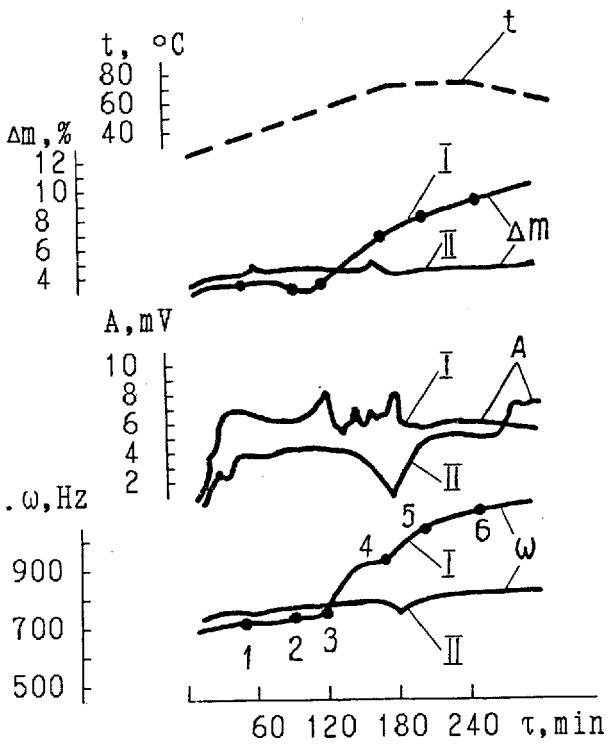

Fig.1. Kinetic curves of cement paste structure formation under hydrothermal treatment: I - Gypsum-free cement with 1.5% $K_2S_2O_5$ additive; II - Portland cement with 3% gypsum; t - temperature of hydrothermal treatment; Δm - a degree of cement hydration -weight loss of test specimen afterheating to 1000°C; A - resonance amplitude; ω - resonance frequency of cement-water paste; figures on curve ω-I correspond to sampling numbers and time

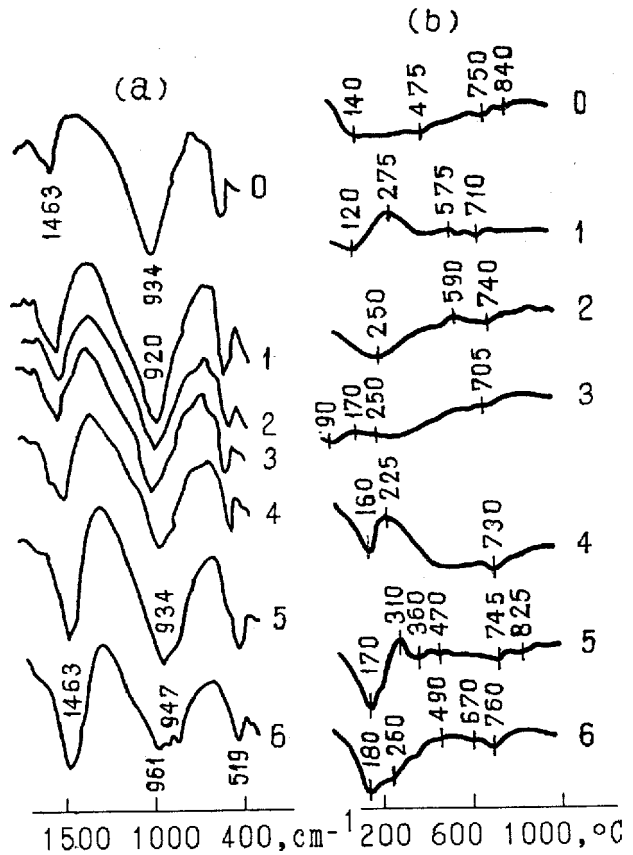

Fig.2. (a) IR-spectra and (b) DTA curves of gypsum-free cement with 1.5% $K_2S_2O_5$ additive getting hardening under hydrothermal treatment. Sampling time 1-6 is the same as in Fig.1, 0 - unhydrated gypsum-free cement

Upon hardening (Fig.1, curve ω-I, point 3) the system elasticity sharply increases, the resonance frequency(the plateau before point 4) is stabilized. Such nature of curve ω-I, is due to the intensive compaction of the system(curve section A-I after point 3(and subsequent recrystallization processes. There are cyclical variations noticed on curve A-I; they point to the break-down processes caused by phase trensformations of primary hydrates. According to the IR spectroscopic data the compaction rate of the new formation does not increase in this period (Fig.2, a).

As the break-down processes are completed, there is a stable increase noticed in the resonance frequency (Fig.1, curve ω-I, interval 4-6) pointing to a system reinforcement. Damping of resonance amplitude variations is an indication of the termination of intensive processes of hydrate recrystallization. The hardening gypsum-free cement is reinforced mainly at interval 4-6. Upon 2.5-h hydrothermal treatment, the degree of hydration of gypsum-free cement is 6.45 % which is twice as high as that of ordinary cement. It should be noted that in this period when the gypsum-free cement is gettiong hardened calcium hydroxide is not registered either in crystalline or in X-ray amorphous form. At interval 4-5, during 45 min, the degree of hydration increases 1.5 times and reaches 9.3 %.

A wave like decrease in values of A at interval 5-6 indicates that the compaction processes predominate over the dispersion ones. It is supported by the absorption band displacement in IR-spectra from 934 to 961 cm^{-1} (Fig.2, a). In the XRD patterns and IR spectra (Fig.2, a), at interval 5-6 crystallization of calcium carbonate is registered, which compound, along with calcium hydrosilicates, becomes one of the structure forming elements of the cement paste.

Thus, the distinctive feature of hydrate formation in the hardening of gypsum-free cement is the intensification of carbonation of amorphous calcium hydroxide. This process accelerates the hydrolysis and dispersion of clinker minerals. As a consequence, calcium carbonate crystallizes in gypsum-free compositions in the period of intensive hardeniong of the cement paste rather than at later hardening stages, as with ordinary portland cement.

Strength tests conducted on the test specimens immediately after the 4-hour hydrothermal treatment demonstrated the following limiting values for compressive strength: ordinary portland cement - 1.7 MPa; with potassium bisulphite additive - 38 MPa and with sodium sulphate - 40 MPa. The gypsum-free cements in question can be produced by the conventional practice, namely, grinding of portland cement clinker with the actice mineral additives.

REFERENCES

1. I.Odler, Ya.Skalny, S.Brunauer: "Properties of the clinker-lignin-sulfonate-carbonate system"/ **Proceedings of VI International Congress on the Chemistry of Cement. M.: Stroyizdat, 1976, V2.** 30-32.

2. **Concretes for Construction under Winter Conditions** / Edited by L.G.Shpynova. Lvov: Vyshcha Shkola, 1985, 80 p.

3. A.Pashchenko, V.Chistyakov:"Gypsum-Free Cements with Non-Perrous Metal Salt Additives"/ Cement. 1986. 10, 11-13.

4. A.Pashchenko, V.Chistyakov, Ye.Myasnikova, P.Sysoyev. Author's certificate No.1622314 (USSR). Binding agent. Published in Bulletin of Inventions. 1991, 3.

5. I.Grankovsky. **Structure Formation in Mineral Binding Systems.** Kiev, Naukova Dumka. 1984, 300 p.

6. A.Pashchenko, I.Grankovsky, V.Chistyakov:"Variation in Dispersion and Condensation Processes in Cement Hydration"/ Journal of Applied Chemistry. 1986, 8, 590-595.

7. V.Timashev, V.Kolbasov. Properties of Cements with Carbonate Additives/ Cement, 1981, 10, 10-12.

THE RESEARCH ON $C_2A_xF_{1-x}$ IN IRON-RICH FLUORALUMINATE CEMENT

Huang Wenxi, Yang Yurong, Qian Guangren and Qi Yangyoun

Sichuan Institute of Building Materials, Sichuan, P R CHINA

ABSTRACT

The paper studies the four kinds of important minerals — C_2F, C_6AF_2, C_4AF, C_6A_2F of ferrite phase $C_2A_xF_{1-x}$ by the methods of rapid burning. The results show that the hydraulic activity of $C_2A_xF_{1-x}$ is initially C_6A_2F > C_4AF > C_6AF_2 > C_2F, lately C_6AF_2 > C_4AF > C_6A_2F > C_2F . The composition of the ferrite phase in clinkers of iron-rich fluoraluminate cement depends on the burning temperature. The ferrite phase in clinkers can exist in the form of C_6AF_2 at lower temperature within 950-1200℃.

摘　　要

本文采用快速升温的方法研究了铁相$C_2A_xF_{1-x}$的四种重要矿物— C_2F, C_6AF_2, C_4AF, C_6A_2F, 结果表明: 早期水化活性依次为 C_6A_2F > C_4AF > C_6AF_2 > C_2F, 后期为C_6AF_2 > C_4AF > C_6A_2F > C_2F. 高铁氯铝酸盐水泥熟料中铁相的组成取决于煅烧温度, 在950-1200℃低温煅烧时该熟料中的铁相以 C_6AF_2 存在.

INTRODUCTION

It is traditionally considered that the hydration activity of the ferrite phase C_4AF is low in portland cement. [1] [2] This view have been understanding. [3] [4] Meanwhile, new varieties of cements which regard calcium ferrite and calcium alumino-ferrite $C_2A_xF_{1-x}$ ($0<X<2/3$) as main mineral compositions are constantly being developed. This paper has studied a series of the ferrite phase solid solutions ($C_2A_xF_{1-x}$) in iron-rich fluoralminate cement which regard $C_2A_xF_{1-x}$, $C_{11}A_7CaF_2$ and β-C_2S as main clinker mineral compositions, using the methods of ordinary burning and rapid burning and the analyses of XRD, IR, rate of hydration heat evolution and Mossbauer Spectrum, and determing setting times and compressive strength. From this, it is obtained that there is much vacancy, cluster and crystal defect in the structure of the ferrite phase with rapid heating-up burning. Thus, hydration activity increases. Hydration development rate for C_6AF_2 in the solid solution $C_2A_xF_{1-x}$ is best. By means of further research for the ferrite phase in iron-rich fluoraluminate cement, it was verified that C_6AF_2 is present in the cement clinker, which is an important guarantee of excellent property of the cement .

1. EXPERIMENTS

A series of solid solutions of the ferrite phases $C_2A_xF_{1-x}$, with increasing solid solubility of Al_2O_3, can be represented as C_2F, C_6AF_2, C_4AF and C_6A_2F. These samples were prepared in the molar ratio. The reagent grades used were of "AR" purity. Industrial raw materials were used and prepared according to the iron-rich fluoraluminate cement clinker, as shown in Table 1, adding 1.0 % mineralizer into the raw mixture. These starting materials mill and pressed into 1. 0mm thick pellets before burning in high temperature furnace. In the method of ordinary burning, the samples were burnt in the hign-temperature furnace raising the temperature at the rate of about 10 ℃/min to burning temperature for pre-determined durations of burning. In the method of rapid beating-up burning (rapid burning), the temperature of the furnace had beforehand risen to the burning temperature before the samples were placed into it Thus, the specimens were exposed directly to the burning temperature (above 800℃/min) for the pre-detemined durations. The samples burnt were cooled in air. The monominerals and the minerals in the cement clinker were examined by means of XRD and Mossbauer spectrum.

Table 1 Chemical compositions (%) of the raw meals

NO.	$C_2A_xF_{1-x}$ in cement	CaO	SiO_2	Al_2O_3	Fe_2O_3	F^-
1#	C_2F	45.08	5.93	20.27	23.50	2.22
2#	C_6AF_2	46.35	5.93	25.65	16.85	2.22
3#	C_4AF	47.05	5.93	28.66	13.14	2.22
4#	C_6A_2F	47.81	5.93	31.92	9.12	2.22

Rates of hydration heat evolution were determined with W/S = 0.8 at temperature of 20℃ by means of a conduction calorimetry. Bound water was determined by the ordinary method of ignition test. Compressive strengths were determined with the mortar of a cement/sand ratio 1:2 by weight and water/cement ratio 0.3-0.35 in case of normal consistency. The clinkers were ground into a fine powder with specific surface area 4500-5000 cm^2/g.

2. RESULTS AND DISCUSSIONS

2.1. The structure characteristic and formation condition of the solid solution $C_2A_xF_{1-x}$

C_2F, C_6AF_2, C_4AF and C_6A_2F on behalf of the solid solution $C_2A_xF_{1-x}$ were separately burnt by rapid burning at 1200-1350℃ for 45 minutes. The free lime content (f-CaO) in samples burnt are listed in Table 2. XRD results of them, that corresponded with f-CaO=0 as shown in the Table 2 are illustrated in Fig. 1. The values of standard characteristic peaks on the XRD charts of four ferrite phases is listed in Table 3 . By means of comparing Fig. 1 with Table 3 , it is seen that four ferrite phases form separately at the temperature, in accordance with f-cao=0 as shown in Table 2, for 45 minutes, i.e, the synthetic temperature of C_2F is 1230℃, C_6AF_2 1250℃, C_4AF 1320℃ and C_6A_2F 1350℃.

C_2F, C_6AF_2, C_4AF and C_6A_2F all belong to the rhombic system. Its characteristic peaks in the XRD were chiefly affected by different Al/Fe ratios, as also by the burning process. These results are shown in Table 4. The regularity in Table 4 shows that the characterisitic peak values (dA) of a series of solid solution decrease correspondingly with increasing Al/Fe, whether by rapid burning or ordinary burning. Meanwhile, dA of the ferrite phase with the same Al/Fe ratio is greater for rapid burning than for ordinary burning. It is quite evident that the progressive change is restricted by the structure change of the ferrite phase.

Mossbauer spectrometry is a method for structure measurement that has been developed during the last twenty years. The structure of solid solution $C_2A_xF_{1-x}$ from its different burning processes can be studied

by means of very profitable Mossbauer parameter in chemical study, isomer shift (IS) and quadrupole (QS). From these, a great deal of information on ferrite phase structure can be obtained. Fig. 2 shows Mossbauer spectra of C_2F and C_6AF_2 in rapid and ordinary burning. Its characteristic can be described as follows: There are considerable amounts of ferromagnetism absorption in C_2F and C_6AF_2 by ordinary burning, which corresponded to two sets of six-line subspectrum of two sublattice in the hyperfine structure. The centre of paramagnetism absorption subsides a little. Besides the ferromagnetism absorption with two sets of six-line subspectrum, in C_2F and C_6AF_2 with rapid burning, paramagnetism absorption increases evidently, especially C_2F.

Table 2 f-cao(%) in the ferrite phases with rapid burning for 45 min.

	C_2F	C_6AF_2	C_4AF	C_6A_2F
1200℃	2.04	2.98	6.09	11.99
1230℃	0	1.65	-	-
1250℃	-	0	-	-
1280℃	-	-	3.68	10.21
1300℃	-	-	2.10	8.07
1320℃	-	-	0	3.04
1350℃	-	-	-	0

Table 3 The stardard peaks value (dA) on XRD charts of four ferrite phases

C_2F	C_6AF_2 *	C_4AF	C_6A_2F
7.36	7.30	7.24	7.17
2.67	2.65	2.63	2.62

Notes: * the data of C_6AF_2 are given according to [1] [10] [11]

Table 4 XRD peak values (dA) of the ferrite phases in different burning

	Ordinary burning				Rapid burning			
	C_2F	C_6AF_2	C_4AF	C_6A_2F	C_2F	C_6AF_2	C_4AF	C_6A_2F
020	7.347	7.280	7.259	7.188	7.369	7.288	7.267	7.225
040	3.681	3.663	3.642	3.623	3.685	3.664	3.651	3.630
200	2.790	2.789	2.780	2.759	2.792	2.789	2.780	2.766
002	2.707	2.684	2.676	2.654	2.709	2.689	2.677	2.659
141	2.673	2.652	2.640	2.628	2.675	2.656	2.641	2.629
161	2.076	2.056	2.048	2.031	2.078	2.060	2.048	2.041
202	1.944	1.934	1.927	1.913	1.944	1.936	1.928	1.915
080	1.842	1.822	1.812	1.806	1.844	1.830	1.813	1.809

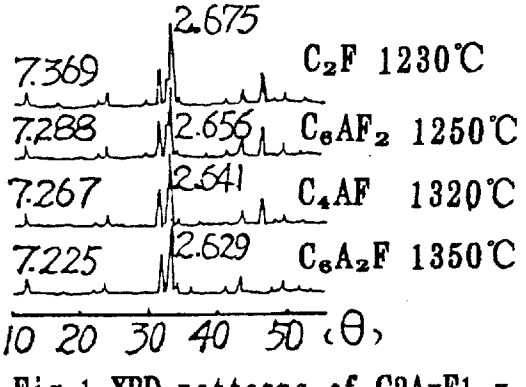

Fig 1 XRD patterns of C2AxF1-x

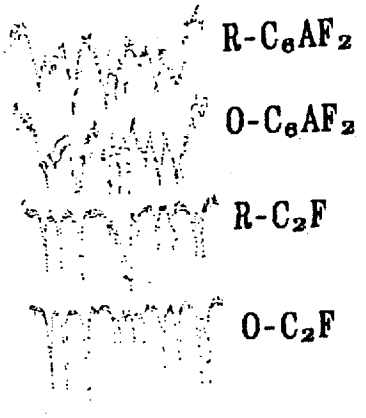

O-ordinary burning
R-rapid burning

Fig 2 Mossbauer patterns of C_{2F} and C_6AF_2

Mossbauer spectra are fitted on a computer by means of least squares method, by which Mossbauer parameteres are obtained and shown in Table 5 and Table 6. The studies had shown [5] [6] [7] that different hyperactive fields exist in the FeO_4 tetrahedra and the FeO_6 octahedra in the ferrite phases, which can be distinguished by means of Mossbauer parameter IS and internal field (Hnf). A set of six-line subspectrum with smaller IS belongs to FeO_4, other one belongs to FeO_6, as shown in Table 5. The doublet with quadrupole is caused by paramagnetism effect (Table 6). FeO_6 and FeO_4 in C_2F structure with ordinary burning account for 50% each. The different amounts of Al^{3+} replace Fe^{3+} in C_2F structure and form C_6AF_2, C_4AF and C_6A_2F in the order of precedence. As shown in Table 5, FeO_6 in C_6AF_2 with ordinary burning is 54.5 %, FeO_4 is 45.5%. It is explained that replacing Fe^{3+} with Al^{3+} occurs prior in the place of tetrahedra and hence FeO_6 and AlO_6 octahedra go up with increasing Al/Fe ratio in $C_2A_xF_{1-x}$ because the ionic radius of Al^{3+} ($r_{Al^{3+}}$= 0.39A) is smaller than Fe^{3+} ($r_{Fe^{3+}}$=0.49A). The tetrahedra layers contract when Al^{3+} replace Fe^{3+}, causing the unit cell to reduce. Meanwhile, the lattice constant (Table 7) in different

ferrite phase structures can also reflect this regularity, which is obtained by means of calculating the values of dA as shown in Table 4.

Table 5 also shows that Fe^{3+} in FeO4 is replaced easier with Al^{3+} by rapid burning, and FeO_6 increase. FeO_6 in C_6AF_2 with rapid burning increases already to 63.7%. For lack of the replaceable effect in C2F, relative distribution of FeO_4 and FeO_6 in the structure can not change with rapid burning. FeO_6 in the ferrite phase with the same Al/Fe ratio increases by rapid burning causing the unit cell volume to reduce. In addition, the covalent bond proportion in the Fe-O bonds and Ca-O bonds in rapid burning weaken (IS increases as shown in Table 5), and interatomic distance and the vacancy increases. Thus, this synthetic result shows that the unit cell volume increases and is related to the increase of lattice constant.

Ordered degree in the structure varies with the burning process, as shown in Table 6. More paramagnetism absorption exists in the structure of the ferrite phase in rapid burning. The study [6] has shown that paramagnetism in $C_2A_xF_{1-x}$ structure depended on superexchange interaction of $Fe^{3+} - O^{2-} - Fe^{3+}$. The superexchange interaction is most strong with $Fe^{3+} - O^{2-} - Fe^{3+}$ angles of 180°, when there is no paramagnetism. Fe^{3+} and Al^{3+} in the ferrite phase structure in rapid burning is not enough time to arrange according to original intrinsic lattice structure, and $Fe^{3+} - O^{2-} - Fe^{3+}$ angles vary at random, and thus easy to form Fe^{3+} and Al^{3+} bunch (cause cluster), causing superexchange interaction to decrease, and then more Fe^{3+} exist in the paramagnetism state. In addition, line width of the sample in rapid burning is obviously greater than ordinary burning. It further explains that two sets of sublattice of FeO_6 and FeO_4 in the ferrite phase structure can again separate into a series of substates with close energy, which contribution stems chiefly from Fe^{3+} cluster. The cluster in rapid burning samples is especially outstanding.

Table 5 Mossbauer parameters of the ferrite phases structure

	$Fe^{3+}_{(Tet)}$					$Fe^{3+}_{(Oct)}$				
	line width (mm/s)	IS	QS	Hnf	area	line width (mm/s)	IS	QS	Hnf	area
R-C_2F	0.173	0.140	0.54	440.2	49.1	0.178	0.330	0.52	512.6	50.9
O-C_2F	0.149	0.139	0.41	439.9	49.7	0.153	0.310	0.51	512.8	50.3
R-C_6AF_2	0.307	0.160	0.79	400.3	36.3	0.317	0.365	0.70	458.3	63.7
O-C_6AF_2	0.223	0.070	0.72	387.8	45.5	0.264	0.351	0.66	443.0	54.5

Notes: R—rapid burning O—ordinary burning

Table 6 The parameters of aramagnetism spectrun

	IS	QS	Area
R-C_2F	0.394	0.64	30.0
O-C_2F	0.317	0.53	3.6
R-C_6AF_2	0.120	1.04	12.2
O-C_6AF_2	0.090	1.03	6.2

Table 7 Lattice constant (dA) of the ferrite phases

	ordinary burning			rapid burning		
	a_0	b_0	c_0	a_0	b_0	c_0
C_2F	5.530	15.050	5.710	5.570	15.170	5.773
C_6AF_2	5.502	14.901	5.709	5.560	15.060	5.750
C_4AF	5.479	14.828	5.677	5.484	14.858	5.685
C_6A_2F	4.428	14.760	5.647	5.460	14.845	5.674

In sum, there is much vacancy and cluster in the structure of ferrite phase with rapid burning, and Fe-O bonds strength weaken. The increased FeO_6 in the structure with increasing Al/Fe ratio gives rise to increased IS and QS, and hence the hydraulic activity of the ferrite phase is affected to a great extent.

2.2 The hydration activity of the solid solution $C_2A_xF_{1-x}$

The hydration behaviour of $C_2A_xF_{1-x}$ solid solution depends on many factors. Many studies on the ferrite phase from ordinary burning have been carried out which have pointed out that [1] [9] hydration rate of the ferrite phase accelerates with increasing Al/Fe ratio. Yet, another says that [8] hydration rate of C_6AF_2 is quicker than any other ferrite phase. Many studies meriting attention have emphasized the effect of sample synthesis conditions on its structure and hydration activity. In this paper, the rate of hydration heat evolution and the degree of hydration of the four ferrite phases from rapid burning were determined. The results in Fig. 3 show that the ferrite phases react with water in the 2 hours, the reaction rate increasing in the order $C_6A_2F > C_4AF > C_6AF_2 > C_2F$, which agree with common view that hydration activity of the ferrite phase rises with increasing Al/Fe ratio. The degree of hydration of the ferrite phases from rapid burning (Fig. 4) represents the hydration rate of each these phases at the hydration age 1d to 28d. At the age of 1d to 3d, their hydration rate increases in the orded $C_4AF > C_6AF_2 > C_6A_2F > C_2F$. At 7d to 28d the hydration rate of C_6AF_2 exceeds not only that of C_6A_2F, but even of C_4AF. From this, the following pattern has been observed:

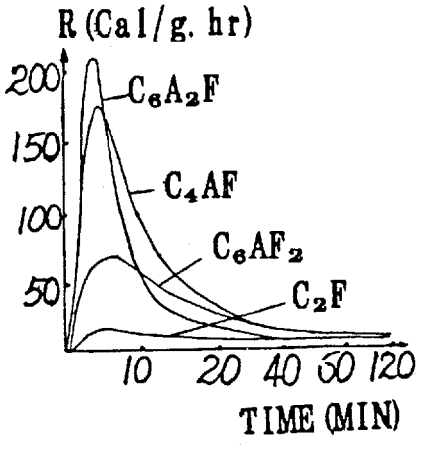

Fig 3 Rate of hydration heat evolution (R) of $C_2A_xF_{1-x}$

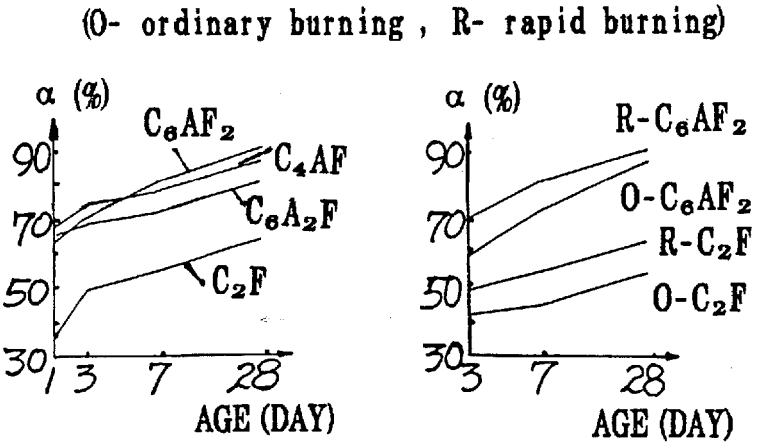

Fig 4 Degree of hydration (α) of $C_2A_xF_{1-x}$

Fig 5 Degree of hydration (α) of C_2F and C_6AF_2

High Al/Fe ratio, except C_2F, is favourable to rise the hydration activity of the ferrite phase in the early period, but low Al/Fe ratio is beneficial to fully develop the hydraulicity in the final period although the hydration rate in the early period is comparatively slow.

The hydration activity of the ferrite phase is closely related with its structure. Fe^{3+} in the ferrite phase is chiefly present in the form of FeO_4 and FeO_6, Fe-O bonds in FeO_6 with high coordination number is weaker than the ones in FeO_4. Mossbauer results show that IS and QS in FeO6 is greater than in FeO_4 increased instability of FeO_6. In hydration process Fe-O bonds in FeO_6 are easy to break, and hence a high Al/Fe ratio is needed to accelerate hydration in the early period. After the hydration has gone on for some time, considerable amounts of hydration products have formed. At this moment, the composition, structure, solubility and micrograph of the hydration products formed play an important role in further development of hydraulicity. In the literature, the hydration products feature of the solid solution C_2F-C_6A_2F [9] were studied. Hydration products of the ferrite phase exist chiefly in cubic $C_3(A,F)H_6$, hexagonal $C_4(A,F)H_{13}$ or $C_4(A,F)H_{19}$ and amorphous hydration product (gel) FH_3 ($Fe(OH)_3$). The ferrite phases with high Al/Fe ratio form more cubic $C_3(A,F)H_6$ and less hexagonal $C_4(A,F)H_{13}$ and gel FH_3. Its hydration in the early period is quick and the hydrates form too fast, which can not be quickly diffused and thus closely concentrate around the grains of still unhydrated ferrite. This is difficult to hydrate further. However, the ferrite phase with low Al/Fe ratio forms more hydrates $C_4(A,F)H_{13}$ and FH_3, the solubilities of which are greater than $C_3(A,F)H_6$ [1]. Although the formation rate of these hydrates is slower in the early period, the hydrates formed in this case do not concentrate around the grains of still-unhydrated ferrite phase, but it is well-dispersed into spaces among the grains of the still-unhydrated ferrite phases. In addition, FH_3 produced in the hydration has a quite important influence on the ferrite phase hydration. When the hydration is complete, the proportion of FH_3 produced is C_6A_2F: C_4AF: C_6AF_2: C_2F = 1: 1.47: 1.89: 2.60 . Obviously, the more the gel products FH_3 , the more favourable it is to full hydration in the final period. The above mentioned factors create favourable conditions for the further hydration of the ferrite phase with low Al/Fe ratio in the final period.

Table 8 Compressive strength (MPa) of C_2F and C_6AF_2

	3d	7d	28d
R-C_6AF_2	18.3	19.4	25.3
O-C_6AF_2	12.2	14.7	24.2
R-C_2F	6.1	8.8	22.0
O-C_2F	0.7	0.9	14.8

Table 9 Results of XRD of No. 2 at different temperature

Temperature	1050℃	1100℃	1150℃	1200℃
XRD peak (dA)	7.296	7.291	7.289	-

Table 8 and Fig. 5 show the results on the hydration rate and compressive strength of the ferrite phases from different burning processes. As mentioned above, more structure vacancy and FeO_6 exist in the ferrite phases structure in rapid burning than ordinary burning, and leads to increased structure instability.

Samples obtained from rapid burning display a higher hydration rate and higher compressive strengths than those obtained from ordinary burning. This difference became more obvious in the early period, and less pronounced in the final period. The hydration rate and strength of C_6AF_2 from the rapid and the ordinary modes of burning approach converge at 28d. This further confirms the preceding views that the hydration rate of the ferrite phase in the early period is controlled by its structure characteristic, wherein further hydration in the final period depends on the composition, structure, crystallization performance and microstructural features of the accumulated hydration products which, together, make up the hydration environment .

2.3 The composition of the ferrite phase in Iron-rich fluoraluminate cement.

Iron-rich fluoraluminate cement is a new type of super high early strength cement that we have studied recently. It consists the of ferrite phase, $C_{11}A_7CaF_2$ and β-C_2S as the main minerals, the ferrite being present in greater content . Therefore, the binding performance and the hydration activity of the ferrite phase are important factors, which affect strength development in the cement. $C_{11}A_7CaF_2$ in the cement ensures higher early strength. The ferrite phase plays a more important role in sustaining the increase to the final strength. In the light of the preceding discussion on the performance of pure ferrite phase mineral, it is seen that, if the ferrite phase exists in C_6AF_2 form in the cement, the aforesaid purpose can still be achieved.

Fig. 6 shows the results of XRD for the samples burnt at 1000℃ , which were obtained by burning four raw meals as show in Table 1. $C_2A_xF_{1-x}$ in them were separately calculated as C_2F, C_6AF_2, C_4AF and C_6A_2F. From this, the effect of different raw samples on mineral formation has been studied. Comparing the XRD in Fig. 1 and Table3 with the result in Fig. 6 , it can be seen that after the raw meals proportioned according to the four ferrite phase components were rapidly burnt for 45 minutes, peak values of ferrite phase in XRD result of its clinker is all close to 7.30 A, 2.65 A that belong to C_6AF_2 ; i, e, the ferrite phase composition in the cement clinkers is all close to C_6AF_2. It shows that the ferrite phase in iron- rich fluoraluminate cement is basicall C_6AF_2 entirely, and is not related to Al/Fe ratio in the ferrite phase.

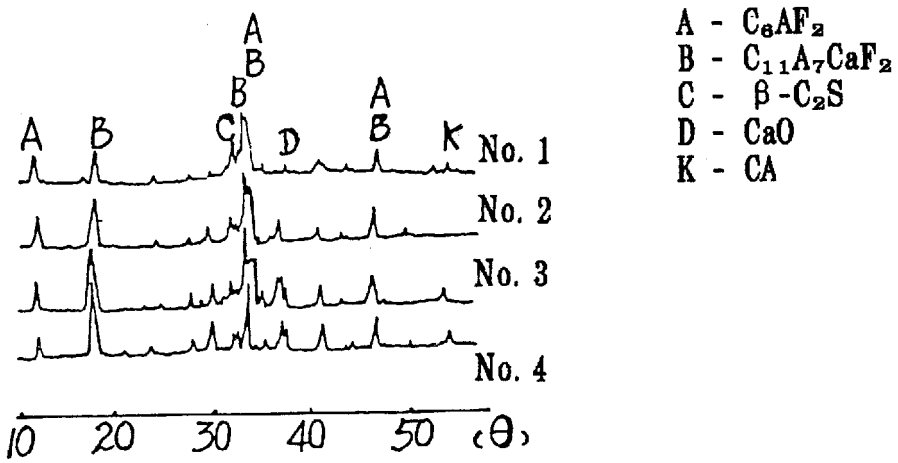

Fig 6 XRD patterns of clinkers at 1000℃

Fig. 6 shows still that because C_6AF_2 is formed practically in every clinker, there is not enough Al_2O_3 to form No. 1 cement clinker minerals as calculated , and thus formation quantity of $C_{11}A_7CaF_2$ reduce and part of CaO exists in the form of free lime. On the contrary, C_6AF_2 is also formed actually in raw meals No. 3 and No. 4 that were proportioned separately according to C_4AF and C_6A_2F, so surplus Al_2O_3 exists after forming the cement clinker minerals, and this in the clinker as CA, and thereby burnability became bad.

Table 9 shows representative peak values on XRD of the cement clinkers that are obtained by burning raw meals No. 2 at different temperatures. The solid solubility of Al_2O_3 in the ferrite phases increases with increasing the burning temperature. The ferrite phase in No. 2 is entirely C_6AF_2 below 1100℃. At 1150℃ the sample has fused and ferrite phase in it has tended to form C_4AF.

To sum up, in iron-rich fluoralminate cement, the final make-up of the ferrite phase formed chiefly depends on the burning temperature, and has little to do with the Al/Fe ratio of the ferrite phase calculated in proportioning the raw meal. The ferrite phases in the cement clinker from low-temperature clinkering are

entirely C_6AF_2. Therefore, in proportioning the cement raw meal, the ferrite phase in it ought to be calculated as C_6AF_2.

Because C_6AF_2 exists in the cement, continued strength development at later ages is better, the cement attaining very high strength at later ages while also having at the higher early strength. The strength at 28d reaches above 625 kg/Cm^2 and do not fall.

3. CONCLUSIONS

3.1 In the structure of the solid solution $C_2A_xF_{1-x}$ from rapid heating-up burning, the FeO_6 octahedra increases, and Fe-O bonds strength weakens, and structure heterogeneity increases. It possesses higher hydration activity.

3.2 The hydration rates of the solid solution of the ferrite phases from rapid burning follow the pattern belows:

Before 1d : $C_6A_2F > C_4AF > C_6AF_2 > C_2F$
1d-3d : $C_4AF > C_6AF_2 > C_6A_2F > C_2F$
7d-28d : $C_6AF_2 > C_4AF > C_6A_2F > C_2F$

Their hydration rate in the early period is controlled by their structure stability, whereto in the final period depends on the composition, structure, solubility and microstructural features of the hydration products. The final strength development of C_6AF_2 is finest.

3.3 The composition of the ferrite phase in iron-rich fluraluminate cement depend on the burning temperature, and has in little to do with the Al/Fe ratio calculated in proportioning the raw meal.

3.4 In iron-rich fluoralminate cement the ferrite phases from low-temperature clinkering are wholly C_6AF_2, which is a guarantee for very high final strength for the cement besides higher early strength.

REFERENCES

1. F·M·Lea , The Chemistry of Cement and Concrete , 102-111 217-314 861 , Third Edition , London, 1973

2. H·F·W·Taylor, Chemistry of Cement , 232 , 1964

3. Feng Xinji , J. of Chinese Silicate Society , Vol.12 (1) , 32 , 1984

4. Zhong Baixi , J. of Chinese Silicate Society , Vol.11 (3), 297, 1983

5. H·J·Whitfield , Aust L.J.Chem. , 20 , 859 , 1967

6. E·F·Bertant , Acta. crystal , 12, 149, 1959

7. D·K·Smith , Acta. crystal , 15 , 148 , 1962

8. M·K·Gharparcy , 5th ICCC , Takyo , Vol.I , 289 , 1969

9. W·Kurdowari , Structure and Performance of Cements , 528 , London , 1983

10. Guo Yong , J. of Chinese Silicate Society , Vol.16 (6) , 481 , 1988

11. Wang Yanmou , J. of Chinese silicate Society , Vol.10 (4) , 1982

STRENGTH DEVELOPMENT AND HEAT OF HYDRATION OF LOW HEAT CEMENT

K Yoshida and H Igarashi

Dept of Cement & Concrete Research, R&D Center
Cement & Light Metal Div , Ube Industries, Ltd
Yamaguchi, JAPAN

SUMMARY

The compressive strength of mortars and heat of hydration of pastes were tested to study the effect of C_2S content of low heat portland cement (LHC), blastfurnace slag content (BFS), pulverized fuel ash content (PFA) and limestone powder addition. The degree of hydration of pastes and the microstructure of mortars were investigated, too.

The development of compressive strength and heat libration of hydration delayed with increasing C_2S content of LHC. The compressive strength at the same heat of hydration increased with increasing C_2S content. The compressive strength before a curing period of 28 days increased by BFS blending, and the maximum sterngth was observed at 60% BFS content. BFS seemed to assist to develop the microstructure of LHC. An increase of compressive strength of the LHC blended with PFA was observed after one year of aging, when a PFA content was 20% and 30%. The compressive strength of the three components cement containing 20% PFA and 0 ~60% BFS increased after 365 days of aging when the content of BFS was less than 20%. The addition of limestone powder (2.5%) to the LHC blended with BFS improved strength during initial curing period.

要約

低熱ポルトランドセメント（ＬＨＣ）のモルタル圧縮強さと水和熱におよぼすC_2Ｓ量、高炉スラグ量（ＢＦＳ）、フライアッシュ量（ＰＦＡ）および石灰石粉添加の影響について検討した。ペーストの水和率とモルタルの微細構造についても検討を行った。

ＬＨＣ中のC_2Ｓ量が増すと強度発現と水和発熱が遅延した。しかし、同じ水和熱での圧縮強さはC_2Ｓ量が増すと増大した。ＬＨＣの材令２８日までの圧縮強さはＢＦＳ混合により増大した。ＢＦＳはＬＨＣの微細構造の発達を促すと思われた。

ＰＦＡを混合したＬＨＣの圧縮強さはＰＦＡ量が２０％と３０％の場合、材令１年で増大した。ＰＦＡを２０％、ＢＦＳを０～６０％混合した３成分系セメントの圧縮強さは、ＢＦＳ量が２０％以下の場合に材令１年で増大した。ＢＦＳを混合したＬＨＣに石灰石粉（２．５％）を添加すると初期材令で圧縮強さと曲げ強さの増大が見られた。

ITRODUCTION

Recently, the development of super low heat cement for mass concrete has been strongly urged to accommodate the construction of large structures and the application of diversified construction methods. Such a cement would have to generate less heat than conventional low heat blended cement, such as that containing blastfurnace slag (BFS) or pulverized fuel ash (PFA) or moderate heat portland cement. Moreover it would exhibit high strength.

Heat generation in low heat blended cement can be greatly reduced by increasing the portion of inorganic admixtures that will be blended with the cement. This, however, may cause problems associated with long-term strength and durability because it would significantly reduce the base cement content. Several methods, therefore, have been proposed to make cement low heat generating. These methods include the use of a base cement known to generate less heat, and controlling the particle size of the base cement or BFS blended (1).

In this study, the authors investigated the effects of the $2CaO \cdot SiO_2 (C_2S)$ content and inorganic admixtures content such as BFS, PFA and limestone powder (limestone) on the strength and heat of hydration of ASTM Type II or IV cement, characterized by the reduced content of $3CaO \cdot SiO_2 (C_3S)$ and $3CaO \cdot Al_2O_3 (C_3A)$. These cement types are known to exhibit good for super low heat properties (2), and have been used in deep-mixing treatments for improving soft clay soil (3). It is an object of this study to clarify the basic properties of these cement types.

EXPERIMENTAL PROCEDURE

Materials

Table 1 shows the Blaine specific surface, chemical composition and mineral composition of low heat portland cement (low heat cement) and moderate heat portland cement (moderate heat cement) with different contents of C_2S, and BFS, PFA and limestone, used for the blended inorganic materials.

Table 1 Blaine specific surface, chemical composition and mineral composition of cement and inorganic admixture

Material		Blaine specific surface (cm^2/g)	Chemical composition (%)										Mineral composition[1] (%)			
			ig. loss	insol.	SiO_2	Al_2O_3	Fe_2O_3	CaO	MgO	SO_3	Na_2O	K_2O	C_3S	C_2S	C_3A	C_4AF
Moderate heat cement		2980	1.0	0.2	22.7	3.9	4.1	64.0	1.0	2.1	0.15	0.43	50	27	3	12
Low heat cement	A	3110	0.4	0.1	25.3	3.6	3.7	62.8	1.1	1.8	0.17	0.44	28	51	3	11
	B	3060	0.8	0.2	26.0	3.4	3.8	61.5	1.2	1.9	0.22	0.29	19	60	3	12
	C	3030	1.1	0.2	26.3	3.3	3.8	60.9	1.1	2.1	0.20	0.31	14	65	2	12
Blastfurnace slag		4360	0.1	—	32.2	13.5	0.4	42.0	6.0	2.2	0.10	0.30	—			
Pulverized Fuel Ash		3360	2.2	83.5	62.4	23.0	3.3	5.2	1.0	0.3	—	—	—			
Limestone		9470	43.6	—	0.17	0.06	0.03	55.5	0.3	—	0.00	0.02	—			

1) Calculated by Bogue equation.

Test Methods

The mortar compressive strength test (Physical Testing Method for Cement - JIS R 5201) and the heat of hydration test (Testing Method for Heat of Hydration of Cement - JIS R 5203) were conducted for each cement sample, excluding the sample containing PFA, which was tested the heat of hydration by the CAJS J-01 method (Testing Method for Heat of Hydration of Fly Ash Cement). The test temperature was set at 20 ℃, for both the compressive strength test and the heat of hydration test. A portion of each

cured sample for the mortar strength was D-dried, after its hydration reactions were halted with acetone, to measure its pore-size distribution by mercury intrusion prosimetry. The paste(w/c=0.4), whose hydration reactions were halted in a similar manner, was analyzed by X-ray diffractometry (with cement added 10% magnesia, serving as the standard material) to determine the X-ray peak area ratio of C_3S and C_3S+C_2S, and by the salicylic acid acetone methanol method(4) to determine the reaction ratio of the BFS.

RESULTS AND DISCUSSION

Effects of C_2S

Fig. 1 and 2 show the effects of the C_2S content on the mortar compressive strength and heat of hydration for portland cement samples with a differrent C_2S content. These results indicate that increasing the C_2S content tends to retard the hydration and the development of strength in similarly aged samples. Verbeck et al. discussed the relationship between the mineral composition and heat of hydration in various types of cement (5). The broken lines in Fig. 2 represent the relationships calculated by applying the coefficients that they proposed. The calculated relationships fairly match these observed during the initial curing period, when the C_2S content is high. These relationships, however, begin to deviate as the C_2S content decreases, which is particularly notable during the initial curing priod.

Fig. 3 presents the effects of the heat of hydration on the mortar compressive strength, showing that the correlation curves shift to the lower heat of the hydration side as the C_2S content increases in the region with a high heat of hydration. This indicates that C_2S is not only lower than C_3S in terms of heat of hydration, but that it is also higher in terms of strength per unit quantity of heat of hydration.

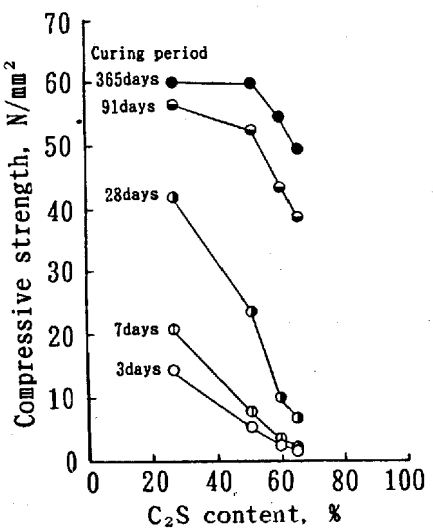

Fig. 1 Relationship between C_2S content and compressive strength

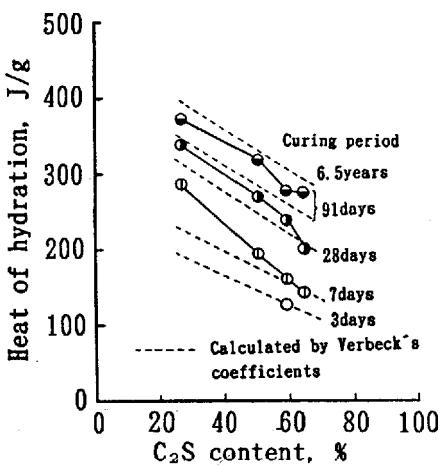

Fig. 2 Relationship between C_2S content and heat of hydration

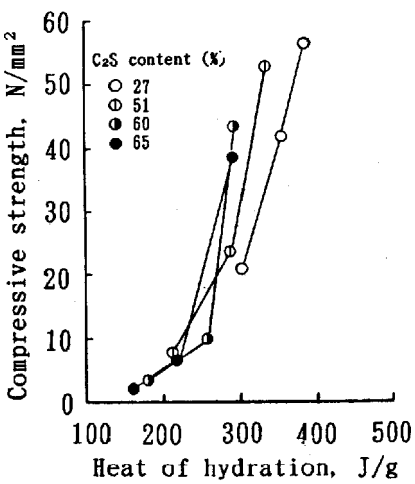

Fig. 3 Relationship between heat of hydration and compressive strength

Effects of BFS

Fig. 4 and 5 show the effects of the BFS content on the mortar compressive strength and heat of hydration for low heat cement(B) with a different BFS content. Mortar strength of samples cured for 28 days or less increases as the BFS content increases, and it attains a maximum at 60% BFS, as shown in Fig. 4. It is known that adding BFS to ordinary portland cement gives the mixture increased strength at longer age, but generally decreases in strength at initial curing period (6). The trends

observed in this study, therefore, are characteristic of low heat cement blended with BFS. Heat of hydration decreases as the BFS content increases, as shown in Fig. 5, which means that adding BFS increases the initial strength without increasing the heat of hydration.

Fig. 6 shows the effects of the heat of hydration on compressive strength, indicating that the correlation for the 100% BFS sample(which contains gypsum) rises sharply with a small increment of heat of hydration. This suggests that BFS leads to a high compressive strength at the same heat of hydration, after the compressive strength increases beyond a certain level.

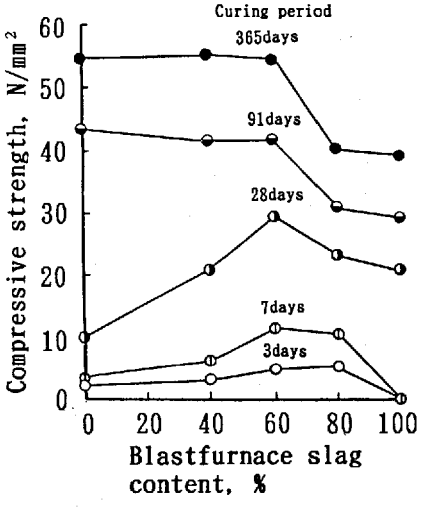

Fig. 4 Relationship between blastfurnace slag content and compressive strength of low heat cement(B) based blended cement

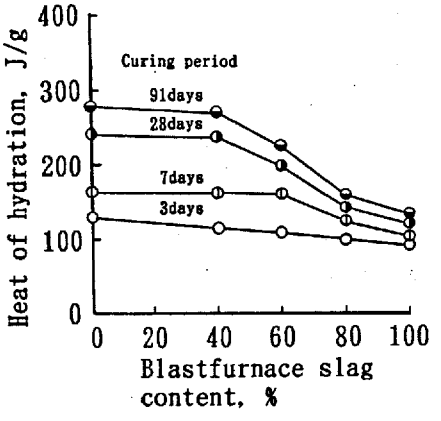

Fig. 5 Relationship between blastfurnace slag content and heat of hydration of low heat cement(B) based blended cement

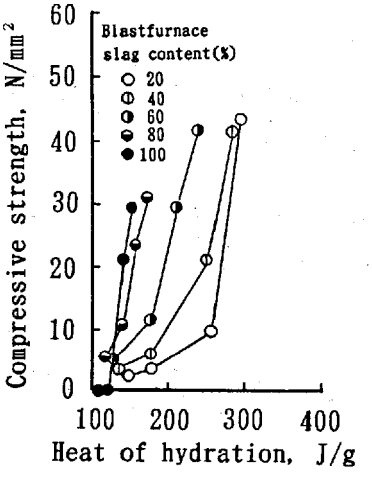

Fig. 6 Relationship between heat of hydration and compressive strength of low heat cement(B) based blendend cement

Fig. 7 shows the effects of the curing period on the reaction ratio of the BFS present in the paste containing 60% BFS. This figure also shows the relative X-ray diffraction intensity (peak area ratio of C_3S and $C_3S + C_2S$ to magnesia). These results indicate that the major reactions of C_3S and C_2S occur at around 3 and 7 to 28 days, respectively, over a curing period of up to 91 days, whereas the reactions of BFS proceed constantly for 91 days. These results, therefore, demonstrate that the reactions of BFS play an important role in this type of cement, even when it is cured for a short period of time.

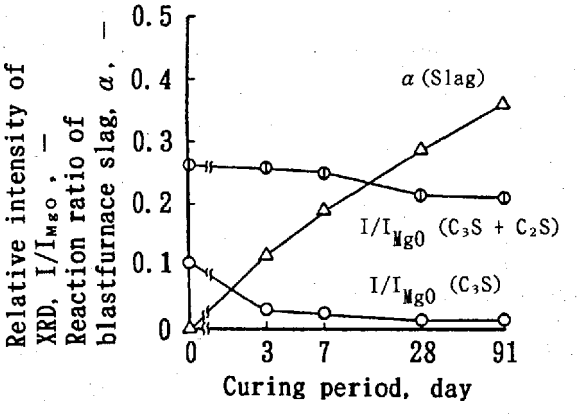

Fig. 7 Reaction ratio of blastfurnace slag and relative intensity of XRD of $C_3S(2\theta=51.7°)$ and $C_2S + C_3S(2\theta=41.3°)$ to $MgO(2\theta=42.9°)$ in low heat cement(B) based blastfurnace slag 60% blended cement

Fig. 8 shows the pore size distributions of the mortar samples, cured for 3 and 91 days, with different BFS contents. Meanwhile, Fig. 9 shows the effects of the total pore volume on compressive strength. Fig. 8 and 9 indicate that the correlation between the total pore volume and the compressive strength is not necessarily negative for all samples cured for 3 days (Fig. 8), but that adding BFS accelerates the decrease in the number of pores of around 10^3nm while increasing the number of pores of around 10 nm (Fig. 9). These results show that the microstructures are well developed in spiteof the low heat of hydration generated.

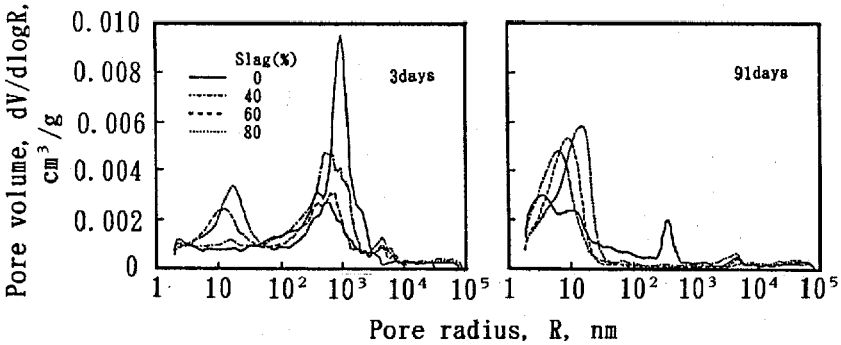

Fig. 8 Pore size distribution of low heat cement(B) based blastfurnace slag cement mortars varing slag content cured for 3 days and 91 days

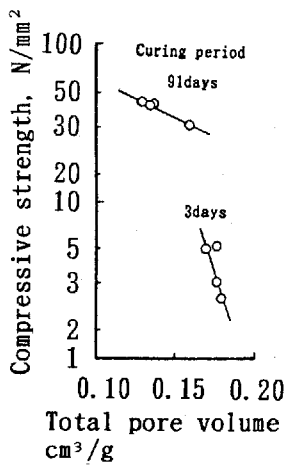

Fig. 9 Relationship between total pore volume and compressive strength of low heat cement(B) based blended cement

Effects of PFA

Fig. 10 and 11 show the effects of the PFA content on the mortar compressive strength and the heat of hydration for low heat cement(B) with a different PFA content. Unlike BFS, PFA increases the compressive strength when its content is 20% to 30% and when the mixture is cured for 365 days, as shown in Fig. 10. This result seems to indicate that, the effects of the pozzolanic reactions on increasing compressive strength are clearly revealed when there is a base cement content of 70% or more. Heat of hydration decreases as the PFA content increases, as shown in Fig. 11. It is particularly noteworthy that it increases with low heat cement content almost proportionally for samples cured for 28 days or less. From this it may be inferred that the hydration of low heat cement is scarcely affected significantly by the presence of PFA in the early hydration period.

Effects of BFS and PFA

Fig. 12 shows the effects of inorganic admixtures content(BFS and 20% of PFA) on mortar compressive strength and the heat of hydration for the low heat cement(B) with different inorganic admixtures content. Also shown for purposes of comparison is the relationship of low heat cement(B) and BFS mixture containing no PFA. Adding PFA to a BFS blended cement generally decreases the compressive strength. Nevertheless, the effects of PFA are diminished when the amount of the inorganic admixtures is 80%. Samples containing PFA and 20% BFS have a higher compressive strength than the samples containing no PFA when these samples are cured for a long period of time. This seem to demonstrate the effects of pozzolanic reaction.

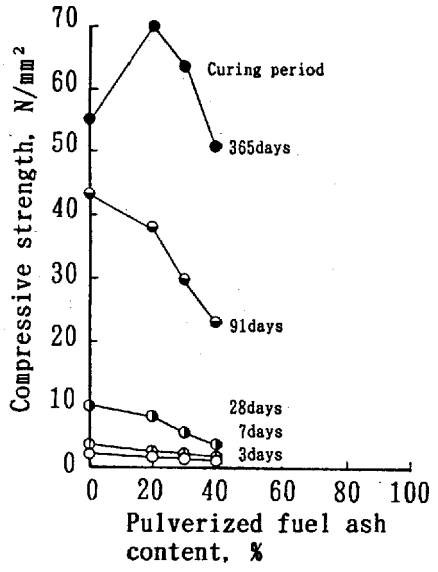

Fig. 10 Relationship between pulverized fuel ash content and compressive strength of low heat cement(B) based blended cement

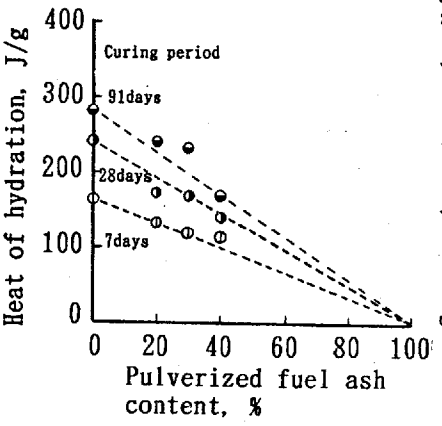

Fig. 11 Relationship between pulverized fuel ash content and heat of hydration of low heat cement(B) based blended cement

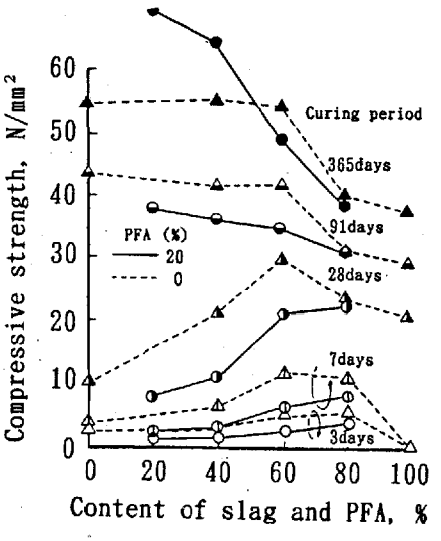

Fig. 12 Relationship between content of inorganic admixture and compressive strength of low heat cement(B) based blended cement

Effects of limestone

Fig. 13 shows the effects of limestone addition on the mortar bending strength ratio and the compressive strength ratio for mixtures of low heat cement(B) and BFS, in which the strength of the blended cement containing 2.5% limestone is compared with the strength of blended cement containing no limestone. As shown, the addition of limestone increases both the bending and compressive strength during the initial curing period. These results match the results obtained by Ohara et al. for BFS blended cement made of 60% ordinary portland cement and 40% BFS (7). Increased strength is considered to result from accelerated hydration during the initial curing period in the presence of limestone, and the formation of calcium carboaluminate hydrates. With mixtures that are cured for a long period, on the other hand, adding limestone decreases the compressive strength ratio of all the samples except those containing 40% BFS, because of the lowered cement content. Nonetheless, no adverse effectscaused by the limestone can be observed regarding the bending strength ratio.

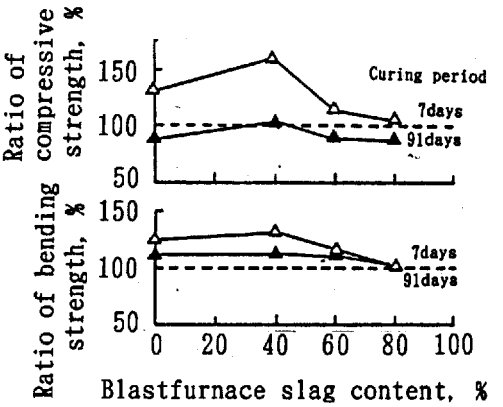

Fig. 13 Mortar bending strength and compressive strength of a mixture of low heat cement and blastfurnace slag, containing 2.5% limestone (relative to the blended cement containing no limestone)

CONCLUSIONS

(1) Increasing the C_2S content retards the development of strength and the generation of heat of hydration in low heat cement. It is, however, notable that the strength per unit quantity of heat of hydration generally increases as the C_2S content increases.

(2) Low heat cement shows improved strength when blended with BFS. The effects of the BFS are particularly noteworthy, when it accounts for 60% of the total amount of the mixture. Moreover, the addition of BFS generally reduces the heat of hydration. The reactions in the BFS continue over 91 days of curing, and play an important role even during the initial curing period. Adding BFS to low heat cement accelerates the decrease in the number of pores measuring around 10^3nm. The improved strength in the presence of the BFS is considered to be the result of well-developed microstructures, in spite of the low liberation of heat.

(3) Adding of PFA to low heat cement, retards the development of strength and the liberation of heat of hydration during a curing period of up to 91 days, but increases the strength of the blended cement when the PFA content is 20% to 30% and the mixture is cured for one year.

(4) The addition of up to 20% PFA to a mixture of low heat cement and BFS improves long-term strength, provided that the BFS content is 20% or less.

(5) The addition of limestone (2.5%) to a mixture of low heat cement and BFS improves both the compressive and bending strength during the initial curing period.

REFERENCES

1) Kanazawa, K., Ninomiya, H., Sogou, S. & Shinkai, C. : "Applicability of Super Low-Heat Cement to Mass Concrete Structures ", Konkurito Kagaku, 1989, 27 (5), 31-37

2) Committee on Cement Research and Development in the Cement Association of Japan, : "Research and Development of Cement for RCD Construction Method" Semento Konkurito, 1990, No.526, 54-63

3) Kobayashi, W. & Okabayashi, S, : "Strength Development of Cement for Deep Mixing Method", Semento Gijutsu Nenpo, 1985, No.39, 490-493

4) Kondo, R & Osawa, E, : "Studies on a method to determine the amount of granuated blast furnace slag and the ratio of hydration of slag in cement ", **Proceeding of 5th International Symposium on the Chemistry of Cement, Tokyo, Japan** 1968, IV, 255-262

5) Verbeck, G. J & Foster, C. W. : "Long-Time Study of Cement Performance in Concrete Chapter 6 - The Heats of Hydration of the Cements ", Proc. Amer. Soc. Test Mater., 1950 50, 1253-1257

6) Ariizumi, A. & Komatsubara, M. : "General Properties of Blastfurnace slag Cement" Semento Gijutsu Nenpo, 1957, No.11, 125-133

7) Ohara, I., Iwabuchi, T., Takegami, H. & Takeuchi, S. : "Effect of Limestone on the Properties of Portland Blastfurnace Slag Cement ", Semento Gijutsu Nenpo, 1987, No.32, 104-107

PROPERTIES OF SPECIAL CEMENT ADJUSTED PARTICLE SIZE DISTRIBUTION

Kiyohiko Uchida, Yukio Fukubayashi and Suminari Yamashita

Central Laboratory, Sumitomo Cement Co Ltd
Chiba, JAPAN

SUMMARY

Particle size distribution of cement substantially influences various properties such as fluidity, strength, and durability during the hydration process, including the texture in the hardened body. Therefore, this paper presents (1)how the components in each particle size group of the ground clinker powder vary according to the kind of clinker and (2) how the properties of cement with same clinker vary according to particle size distribution. Due to the differences in the grindability of minerals composing the clinker, it was found that the chemical composition of the cement varied with each particle size group. In particular, the alminate components of faster hydration, such as $C_{11}A_7 \cdot CaF_2$ and C_3A, were easy to grind and were more contained in the fine particle size group. By substituting the fine particles of the cement with the fine powder which had a low hydration activity, the cement which had a high fluidity and high strength development could be obtained. By adjusting the particle size distribution of cement, it was possible to develop the most suitable special cement such as quick setting cement and cement for centrifugal casting.

要旨

セメントの粒度分布は、セメントの水和性状と硬化体組織を通して、流動性、強度、耐久性等の諸性状に多大な影響を与える。そこで、（１）クリンカー種類によって粉末の粒度群ごとの成分の偏り、（２）同じクリンカーで粒度構成の違うセメントの性状について調べた。セメントを構成する各鉱物の被粉砕性の相違により、粉砕したセメントの各粒度群ごとでその組成は異なっている。特に$C_{11}A_7 \cdot CaF_2$等の水和の速い成分が粉砕され易く、微粉部分に多く含まれる。微粉部分を水和活性の小さい超微粉末に置換することで、流動性が大きく、初期から長期まで強度の大きいセメントが得られる。また、クリンカー粉末の粒度構成を調整することで、瞬結性セメントや遠心成型用セメントといった特殊セメントへの適用が可能である。

INTRODUCTION

Particle size distribution of cement substantially influences various properties of concrete, such as fluidity, strength and durability during hydration process, including the texture of the hardened body[1,2,3,4]. Particle size of cement directly affects the rate of hydration. That is, the smaller is the particle size , the faster is the rate of hydration. However, cement is not a single mineral, but rather consists of several minerals with different compositions. The rate of hydration also differes from the kind of mineral. In addition, the grindability of the cement minerals are generally different from each other. As the mineral composition of cement may become spontaneously unbalanced during the grinding process, it differes from each particle size group[5,6,7].

Therefore, it might be possible to determine the properties of cement by both the particle size distribution and the mineral compositions contained in the particle size groups. This paper presents (1) how the compositions of each particle size group of the ground clinker vary according to the kind of clinker and (2) how the properties of cement with same clinker vary according to a different particle size distribution.

EXPERIMENTS

Two clinkers were used for the experiments, one is ordinary portland cement(OPC) clinker and the other is JET clinker containning 25% calcium-fluoro-aluminate phase ($C_{11}A_7 \cdot CaF_2$). A test ball mill was used to grind JET clinker to a Blaine specific surface area of 5200 (cm^2/g) and OPC clinker to Blaine specific surface area of 5000 (cm^2/g) and 3200 (cm^2/g). The ground clinkers were then classified particle size groups by a centrifugal air classifier. These powders were analyzed chemical compositions by chemical analysis and were measured particle size distribution by a laser diffraction particle size analyzer. In order to produce cement, JET clinker were blended with anhydrite to provide the prescribed ratio (SO_3/Al_2O_3=1.2 : molar ratio) and OPC clinker were blended with gypsum. Then cement adjusted particle size distribution were applied to special cement.

RESULTS AND DISCUSSION

Properties of JET cement with a classified particle size

Table 1 and 2 show chemical and calculated mineral compositions, and Fig.1 shows the particle size distribution found in each particle size group of JET clinker powder. SiO_2 was decreased with the decrease in the particle size of JET clinker powder, while alkali, Al_2O_3 and SO_3 were inversely increased. In the case of JET clinker, it was found that alkali-sulfate was ground most easily, and $C_{11}A_7 \cdot CaF_2$ easily, on the other hand, C_3S was difficult to grind.

It is known that $C_{11}A_7 \cdot CaF_2$ hydrates rapidly and that it adsorps a lot of the chemical admixture. Especially, since $C_{11}A_7 \cdot CaF_2$ in JET clinker powder, after grinding, gathered into the fine particle portion, the hydration of JET cement varied greatly depending on the respective particle size group. Table 3 shows the results of the mortar test of JET cement with a particle size distribution shown in Fig.1.

Table-1 Chemical compositions of JET clinker powder

Clinker	Particle size	Ig.los	Insol	SiO_2	Al_2O_3	Fe_2O_3	CaO	MgO	SO_3	Na_2O	K_2O	Total
JøA	unclassified	0.50	0.24	17.87	14.24	1.65	63.22	0.68	0.37	0.26	0.54	99.57
JøB	under 1 μm	1.95	0.14	14.27	18.30	2.00	57.53	1.40	1.54	0.42	1.76	99.31
JøC	under 5 μm	1.31	0.25	15.07	18.49	1.91	59.50	0.80	0.92	0.32	1.08	99.65
JøD	5 ~ 8 μm	0.86	0.29	16.52	16.43	1.75	61.61	0.69	0.52	0.28	0.69	99.64
JøE	8 ~ 12 μm	0.69	0.17	18.24	14.00	1.55	63.87	0.16	0.37	0.26	0.49	99.80
JøF	12 ~ 18 μm	0.33	0.11	19.30	12.50	1.40	63.85	1.12	0.22	0.25	0.40	99.48
JøG	18 ~ 30 μm	0.18	0.17	19.02	12.34	1.41	64.96	0.61	0.18	0.25	0.37	99.49
JøH	upper 30 μm	0.18	0.42	17.96	13.71	1.89	63.95	0.50	0.25	0.25	0.43	99.54

Table-2 Caluculated mineral compositions of JET clinker powder

Clinker	C_3S (%)	$C_{11}A_7 \cdot CaF_2$ (%)	C_4AF (%)	R_2SO_4 (%)
JøA	66.4	25.6	5.0	1.59
JøB	55.3	33.2	6.1	4.22
JøC	56.6	33.7	5.8	2.73
JøD	62.1	29.8	5.3	1.92
JøD	67.3	25.2	4.3	1.50
JøF	65.1	22.5	4.3	1.31
JøG	72.3	22.1	4.3	1.26
JøH	69.8	24.2	5.8	1.37

R_2SO_4 : Na_2SO_4 + K_2SO_4

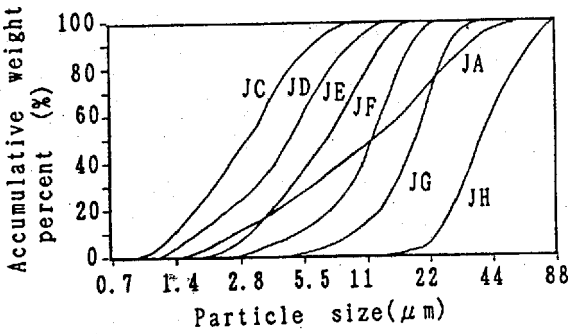

Fig. 1 Particle size distribution of JET clinker powder

Table-3 Results of mortar tests (JET cement)

Cement	Particle size	Handling time (min)	Compressive Strength (MPa)					
			3(h)	6(h)	1(d)	3(d)	7(d)	28(d)
JA	unclaasified	24	15.0	16.7	17.6	25.6	28.3	32.1
JC	under 5 μm	2.5	9.3	14.5	28.3	29.7	32.3	29.6
JE	8 ~ 12 μm	-	-	0.9	17.2	22.8	29.9	37.4
JG	18 ~ 30 μm	420 up	-	1.0	15.0	22.3	35.0	47.8
JI	upper 5 μm	427	-	0.9	17.7	21.8	21.6	43.0
JJ	upper 8 μm	301	-	0.8	17.8	19.6	24.9	38.2
JK	upper 12 μm	341	-	-	17.4	18.6	24.9	38.2
JL	under 12 μm	2.5	21.9	20.3	30.6	32.8	35.4	35.6

It was found that the handling time was reduced when fine particles were excessive. JL of under 12 μm particle size developed maximum strength in the initial period. In spite of same short handling time, JC with finest particle developed lower strength than JL. It was considered that it was difficult to cast JC. The cement removed fine particles (JE to JK) was developed lower strength within 6 hours, but higher strength at 28 days than JA. JG with large particle size developed lower strength at 3 days but higher strength at 7 days than JC. In accordance with time, strength development of cement with large particle size was greater than that of other cements. JC and JL developed very high strength at 1 day but did not develop almost strength afterward. In the case of JET cement, the fine particle (under 5 μm) did not contribute to the strength development on and after 1 day.

Fig. 2 shows rate of heat evolution of the JET cement. The peak of heat evolution of each cement was almost revealed at the same time. The cement which was removed fine particles had small heat of hydration during the initial period, however, the rate of heat evolution increased with time as compared to that of unclassified cement, while the heat of hydration was about the same as that of unclassified cement at 12 hours. This results agreed with that there was little difference in strength development at 1 day.

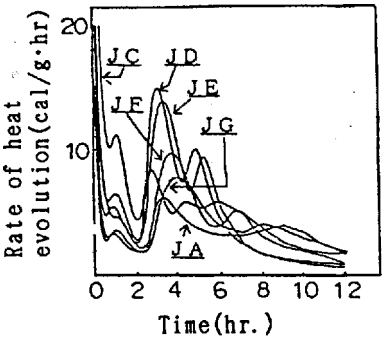

Fig. 2 Rate of heat evolution of JET cement

Properties of OPC with a classified particle size

Table 4 and 5 show chemical and caluculated mineral compositions, and Fig. 3 shows the particle size distribution found in each particle size group of OPC clinker. Similar to the results of the JET clinker, SiO_2 in OPC clinker was decreased with the decrease in the particle

Table-4 Chemical compositions of OPC clinker powder

Clinker	Particle size	Ig. los	Insol	SiO_2	Al_2O_3	Fe_2O_3	CaO	MgO	SO_3	Na_2O	K_2O	Total
PøA	unclassified	0.50	0.08	22.20	5.99	2.87	64.97	1.59	0.73	0.36	0.51	99.78
PøB	under 3 μm	1.92	0.10	20.26	5.92	2.88	62.70	1.58	2.08	0.63	1.59	99.66
PøC	3 ~ 8 μm	0.57	0.07	21.66	6.13	2.98	65.00	1.62	0.76	0.36	0.53	99.72
PøD	8 ~ 15 μm	0.28	0.05	22.37	5.77	2.84	65.60	1.58	0.50	0.29	0.33	99.68
PøE	15 ~ 20 μm	0.22	0.06	22.63	5.81	2.80	65.70	1.58	0.41	0.29	0.27	99.72
PøF	20 ~ 30 μm	0.17	0.07	22.77	5.90	2.76	65.70	1.58	0.38	0.29	0.27	99.97
PøG	30 ~ 45 μm	0.19	0.08	22.84	6.00	2.82	65.40	1.57	0.45	0.30	0.28	99.99
PøH	upper 45 μm	0.12	0.10	22.82	6.40	3.00	64.70	1.60	0.51	0.33	0.33	99.94

Table-5 Mineral compositions of OPC clinker powder

Clinker	C_3S	C_2S	C_3A	C_4AF	R_2SO_4
PøA	49.4	26.4	11.0	8.7	1.77
PøB	52.3	19.7	11.0	8.9	4.38
PøC	52.7	22.7	11.2	9.1	1.80
PøD	53.1	24.3	10.5	8.6	1.27
PøE	51.3	26.3	10.6	8.5	1.16
PøF	50.0	27.7	10.9	8.4	1.16
PøG	47.2	30.0	11.1	8.5	1.21
PøH	41.3	34.4	11.9	9.1	1.37

R_2SO_4: Na_2SO_4 + K_2SO_4

size. On the other hand alkali and SO_3 were increased, but the variations in Al_2O_3 were not clear. As concern as the grindability of minerals in OPC clinker, it was found that alkali-sulfate was ground most easily, and C_3S in OPC clinker was ground more easily than C_2S. Because C_3A and C_4AF gather mainly in the fine and coarse particle portion, such a clear difference of grindability as that observed in C_3S and C_2S could not be recognized in C_3A and C_4AF.

Fig. 4 shows the particle size distribution of cement which was removed fine particles. Table 6 shows results of motar tests. These cement were produced from the

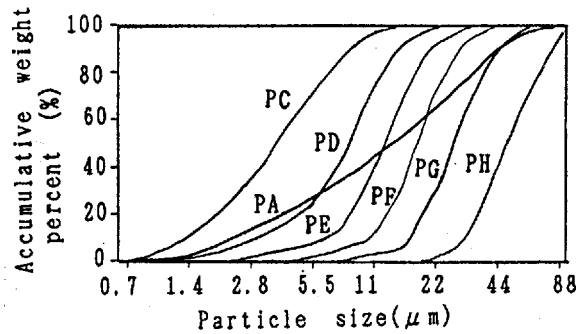

Fig. 3 Particle size distribution of OPC clinker powder

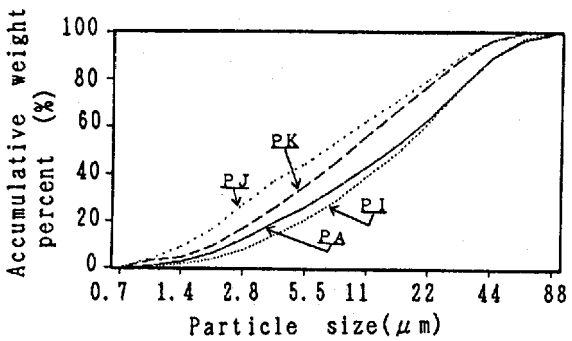

Fig. 4 Particle size distribution of cement which was removed fine particle

Table-6 Results of mortar tests (OPC)

Cement	Particle size	Blaine of cement (cm^2/g)	Flow (-)	Bending Strength / Compressive Strength (MPa) 1 day	3 days	7 days	28days
PA	unclassified	3200	214	3.7/13.6	6.4/25.9	7.1/33.0	8.2/45.5
PC	3 ~ 8 μm	----	114	5.3/35.2	5.0/29.2	5.9/27.6	8.1/41.4
PD	8 ~ 15 μm	----	237	2.9/11.6	6.5/34.7	5.6/40.8	9.1/51.6
PE	15 ~ 20 μm	----	267	2.2/ 8.1	7.4/35.1	8.3/41.3	10.0/49.6
PF	20 ~ 30 μm	----	252	0.0/ 0.0	4.4/19.9	7.1/31.7	8.6/41.2
PG	30 ~ 45 μm	----	141	0.0/ 0.0	2.6/10.1	4.6/20.4	7.0/32.5
PH	upper 45 μm	----	141	0.0/ 0.0	0.0/ 0.0	2.1/ 7.0	2.4/14.1
PI	upper 3 μm	2800	227	- / -	5.3/20.5	6.6/27.7	8.0/42.0
PJ	unclassified	5000	217	- / -	6.0/27.6	7.2/35.5	7.3/47.2
PK	upper 3 μm	3200	261	- / -	6.2/25.7	7.7/36.0	9.6/53.3

OPC clinker that had the particle size distribution shown in Fig. 3 and 4. The relationship was estimated between the strength development and each particle size group in the cement. It was found that the particle size group most closely related with the strength was 0.7 ~ 1.4 μm at 1 day, 1.4 ~ 5.8 μm at 3 days, and 5.8 ~ 22 μm at 7 and 28 days. The particle size group of upper 30 μm contributed to a small extent to the strength development even at 28 days. The cement which was adequately removed fine and corase particles developed higher strength on and after 3 days than the unclassified cement. There was difference in strength development at 3 days beteween PA and PI which was removed fine particles from PA . That was due to the higher content of the 5.8 ~ 22 μm particle size group in PI. PK which was removed fine particle from PJ developed almost same strength at 3 days, but higher strength than PJ on and after 7 days. The strength of PK was the highest at 28 days. In spite of same Blaine surface area as PA, PK developed higher strength than PA. It was considered that PK had fewer particle upper 30 μm than PA and under 3 μm than PJ.

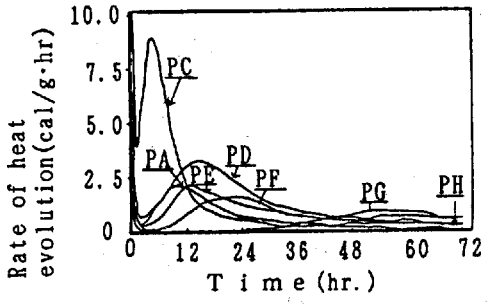

Fig. 5 Rate of heat evoluation of OPC

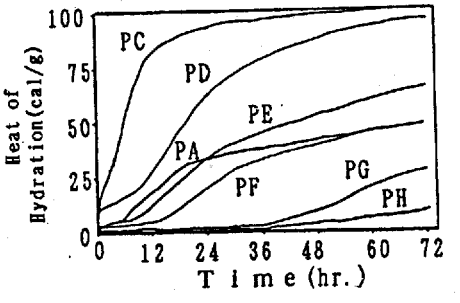

Fig. 6 Heat of hydration of OPC

Fig. 5 and 6 show rate of the heat evolution of hydration of each cement. The heat of hydration of the 15 30 μm particle size group (PE and PF) was low during the initial period, although the heat of hydration at 3 days was approximately the same as that of unclassified cement.

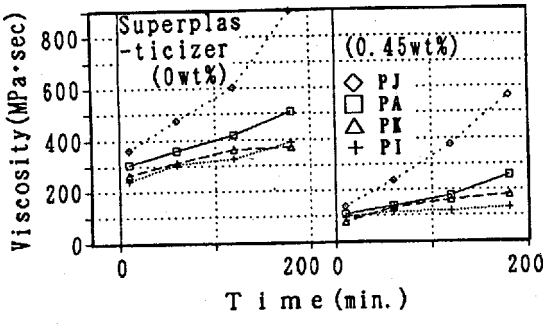

Fig. 7 Change in viscosity of cement paste

Fig. 7 show change in the viscosity of the cement paste. These cement were removed fine particles from OPC clinker. The fine particles (under 3 μm) substantially influenced the viscosity of the cement paste, and the greater the quantity of the fine particles was, the more noticeable the increase of the viscosity of the paste was. It is known that fine particle greatly influenced the flow value. However as the results of mortar test cement for each particle size group shown in table 6, the flow value was decreased in the particle size group of 30 ¯ 45 μm (PG) and upper 45 μm (PH). In spite of same Blaine as PA, the flow value of PK was larger than that of PA. The flow value was reduced both in the case of much fine particles (PC and PJ) and few fine particles (PG and PH).

Table-7 Results of mortar tests (Substitute with fine particles)

Cement		Low active particles	Flow (-)	Bending Strength / Compressive Strength (MPa)			
				3 days	7 days	28days	91days
PA	3200(cm²/g)	nothing	220	5.5/22.8	6.8/31.2	8.1/42.1	8.7/47.9
MA	removed	fly ash 10%	250	5.7/23.1	6.7/33.0	9.0/43.8	10.0/60.8
MB	under 3 μm	slag 10%	252	6.1/25.8	7.2/37.4	8.7/46.1	9.7/55.2
MC	from PA	calcite 10%	249	6.2/29.9	7.9/39.0	9.1/45.3	10.2/55.9

Properties of cement substituted with other particles

It might be possible to produce cement with high fluidity and high strength development by substituting the fine particles of the cement with low active particles[8,9]. The particle size distribution was adjusted by adding 10 % of fine particles of limestone (Blaine 15000 cm^2/g) or fly ash (Blaine 10000 cm^2/g) or slag (Blaine 10000 cm^2/g), respectively, to the OPC clinker which was removed fine particles. As results of mortar test shown in Table 7, both the flow value and strength development of these cement were greater than those of unclassified cement.

APPLICATION OF CEMENT ADJUSTED PARTICLE SIZE

Quick setting cement

Quick setting cement was produced by using fine particles of JET clinker powder. The clinker of quick setteing cement were JøA for S-1 and JøC for S-2, respectively. Table 8 and 9 show mix proportions and test results of the quick setting cement. This cement set within 1 minute and developed the strength of 10 MPa within 10 minutes. It was found that, in spite of less clinker powder, the setting time and strength development of this quick setting cement were superior than commercial one. It might be possible to obtain the cement which offered a better quality by using the fine particles of JET clinker powder.

Table-8 Mix proportions of quick setting cement

Cement	Cl'	Mix proportions (wt.%)				
		Cl'	An	F.A.	Sand	etc.
S-1	JøA	44	11	11	20	14
S-2	JøC	23	7	27	30	13

Cl' :Clinker An:Anhydrite
F.A. :Fly Ash

Table-9 Test results of quick setting cement

Temp. (°C)	Cement	Setting time (sec)	Compressive Strength (MPa)					
			10(m)	1(h)	6(h)	1(d)	7(d)	28(d)
5	S-1	180	5.0	20.9	38.4	44.8	52.3	59.6
	S-2	110	10.3	18.5	26.7	32.2	46.3	62.9
20	S-1	55	13.5	19.4	25.5	46.7	51.6	58.6
	S-2	50	10.9	18.4	23.1	30.4	35.5	54.1

Cement for centrifugal casting

Most of the sludge resulting from centrifugal casting was composed of the fine particles. By removing the fine particles from OPC, the cement was developed which could be applied to centrifugal casting for concrete pile[10]. This cement was produced substituting fine particles

Table-10 Mix proportion of concrete

Slump (cm)	W/C (%)	s/a (%)	Unit weight (kg/m^3)			
			W	C	S	G
8	32.0	40.0	154	480	694	1041

Table-11 Condition of centrifugal casting

	Centrifugal Force (G)	Speed (rpm)	Time (min)
Initial	2	149	2
Medium	10	334	3
Final	30	579	6

Table-12 Curing condition

	Temp. (°C)	Time (hr)
Steam	65	3
Autoclave	180	5

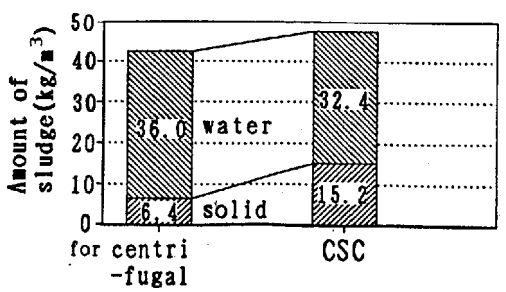

Fig. 8 Amount of water and solids in sludge

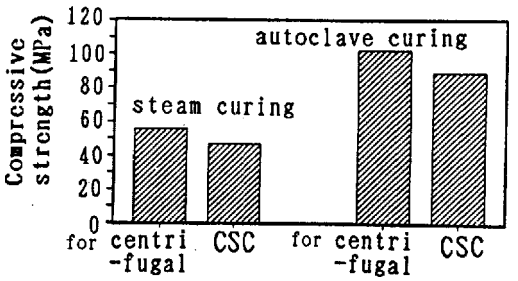

Fig. 9 Compressive strength during both steam curing and autoclave curing

with 25% of silica powder (Blaine 4200 cm^2/g). Tables 10 to 12 show mix proportion of concrete, the condition of centrifugal casting and the curing conditions, respectively. Using the cement for centrifugal casting, the solids in the sludge were reduced by half as compared with commercial silica cement (CSC), as shown in Fig. 8. Because of the large squeezing water during centrifugal casting, the water in the sludge increased. Fig. 9 shows compressive strength during both steam curing and autoclave curing. They were greater by approximately 15 % than that of commercial silica cement because the ratio of water/cement was reduced due to a large squeezing during centrifugal casting. Good results were also obtained in another application for Hume concrete pipe[11].

CONCLUSIONS

(1) Due to the differences in the grindability of cement minerals composing the clinker, the mineral composition of the cement varied with each particle size group of the cement. In particular, the mineral compositions of faster hydration, such as those of $C_{11}A_7 \cdot CaF_2$ were easy to grind and were more contained in the fine particle size group. The grindablity of minerals was different between two clinkers as follows.
JET clinker: Alkali-sulfate > $C_{11}A_7 \cdot CaF_2$ > C_4AF > C_3S
OPC clinker: Alkali-sulfate > C_3A, C_4AF, C_3S > C_2S

(2) The cement produced by classification differed considerably in the properties of initial hydration as compared with the cement which had the same mineral composition, but different particle size distribution.

(3) The fine particles influenced fluidity considerably . The fluidity was reduced when the fine particles were excessive or too few, and an optimum value existed.

(4) By substituting the fine particles of the cement with the low active particles, cement had a high fluidity and high strength development.

(5) By adjusting the particle size distribution of cement, it might be possible to develop the special cement such as quick setting cement and cement for centrifugal casting.

REFERENCES

(1)H. Rittmann, "On the relation between the particle size distribution and the strength of portland cement" (1968), Z.K.G., Vol. 57, No. 9, pp. 390
(2)N. Kataoka, M. Maeno and T. Koga, "Properties of Cement Ground in Roller Mill", (1984), Review of the 38th General Meeting, The Cement Association of Japan, pp. 84
(3)S. Sprung, K. Kuhlman and H. G. Ellerbrock, "Particle size distribution and properties of cement", (1985), Z.K.G., Vol. 74, No. 9, pp. 528
(4)R. A. Helmuth, "Improved cement and energy savings with particle size control", (1981), I.E.E.E. Cem. Ind. Tech. Conf. Vol. 2, pp78
(5)B. Beke and L. Opoczky, "Very fine grinding of cement clinker", (1969), Z.K.G., Vol. 10, No. 12 pp. 541
(6)H. Uchikawa, K. kusaka and N. Kasai, "Effects of Burning Degree of JET Cement Clinker on the Characters of JET Cement", (1973), Review of the 27th General Meeting, The Cement Association of Japan, pp. 49
(7)K. Uchida, Y. Fukubayashi and S. Yamashita, "Particle Size Distribution and Physical Properties of Cement", (1987), Review of the 41st General Meeting, The Cement Association of Japan, pp. 52
(8)B. Beke, "Grinding methods, granutometric composition, and strength development of different cements", (1960), Z.K.G., Vol. 49, No. 9 pp. 419.
(9)K. Uchida, Y. Fukubayashi and S. Yamashita, "Special Cement Using Ultra Finely Pulverized Clinker", (1988), Review of the 42nd General Meeting, The Cement Association of Japan, pp. 62
(10)K. Uchida, S. Yamashita, H. Nukui and K. Kuninishi "Study on the Production of Concrete Pile Using Cement Adjusted Particle Size Distribution", (1992), Extended Abstracts; The 46th Annual Meeting of CAJ.
(11)K. Uchida, S. Yamashita, K. Kuninishi and H. Nukui, "Studies on the Production of Hume Concrete Pipe Using Cement Adjusted Particle Size Distribution", (1992), Extended Abstracts; The 46th Annual Meeting of CAJ.

THE SUB-CLUSTER MODEL OF CEMENT PARTICLE SIZE DISTRIBUTION

Feng Xiuji* and Zhao Fei**

**Wuhan University of Technology, Wuhan, P R CHINA*
***Bengbu Design & Research Institute for Glass Industry*
P R CHINA

ABSTARCT

The general essence of cement grinding process is summarized and the sub- cluster intrinsic equation of cement particle size distribution is derived as the form of $\Phi/(1-\Phi) = K*(1+r_1*w/(1-w)) / (1+r_2*(1-w)/w)$ based on the vague sub-cluster theory.Three sub-cluster parameters with definite physical meaning are obtained and $r_1 * r_2 /K$ is defined as the specific dispersion degree of cement particle size distribution. It is shown that the compressive strengths of cement paste have a good correlation with the specific dispersion degree,and the effect of particle size distribution on mechanical properties of cement can be represented comprehensively by the specific dispersion degree $r_1 * r_2/K$.

摘　　要

本文概括了水泥粉磨过程的一般性本质。依据模糊群子论的基本原理导出了水泥体系粒径分布的群子本征方程$\Phi/(1-\Phi)=K*(1+r_1*w/(1-w))/(1+r_2*(1-w)/w)$,得到了三个具有明确物理意义的群子参数，并将$r_1.r_2/K$定义为粒径分布的比分散度。水泥将体各龄期抗压强对r1.r2/K均有很好的依赖关系，可以用比分散度综合表征粒径分布对水泥性能的影响。

INTRODUCTION

When cement particle size distribution is considered as a structure [1],to further study the component regularity and transforming action in its entirety,the origin and formation of the structure should be investigated so that an internal structure can be found for the experiential external structure and reconstruct the internal structure with a mathematical model.This method is essentially a combination of scientific experiment , mathematical deduction and the structuralism[2].

DERIVATION OF THE SUB-CLUSTER INTRINSIC EQUATION OF CEMENT PARTICLE SIZE DISTRIBUTION

1. Derivation Prerequisite

Many equations have been proposed to describe the particle size distribut of comminuted solids ,and M.E Asim [3] has reviewed these equations in details.It is not difficult from Asim's review to find that there are common places among different investigators when each equation being derived.

(1) A hypothesis was proposed to interpret the mechanisim of crushing breakage based on a physical model.

(2) Probabilistic method or statistical mechanics was used as mathematical tool for deriving the equation.

(3) Equations derived by different authors do not take completely the same form.Different equations are suitable go different situation respectively ,that is to say the applicable range of each equation is cofined to some extent.

Several reasons are responsible for the using restrictivity of the proposed equations.

(1) The proposed physical models do not interpret the mechanisim of crushing breakage precisely due to the complexity of grinding process.

(2) There is no inevitable relationship between the physical hypothesis and mathematical tool,and the mathematical tool is applied to the physical model based on a new hypothetical prerequisite.

(3) Only the crushing action extered on minerals by external forces has been considered, and the resistance of minerals to the crushing of external forces to maintain the structure integrity of minetal crystal lattice was neglected.

Why should the resisting action be taken into consideration? We can make an ideally limit hypothesis that some mineral particles do not have any resisting action on the crushing of external forces, i.e. these minerals particles may coollapse at the first encounter,then it is not difficult to imagine that when this kind of minerals being crushed,they will be broken down to powders with identical size ,it will be meaningless to study the particle size distribution.So the distribution equations derived when the resisting action of minerals being neglected will not be used widely .

Therefore, to derive a widely applicable equation for cement particle size distribution,

several questions should be taken into consideration as follows.

(1)The physical model adopted should reflect the general essence of cement grinding process.

(2)A mathematical method corresponding to the physical model should be used as deriving tool.No mathematical tool should be imposed on the physical prerequisite.

(3)The distribution equation derived should be fitted to experimenntal curves to examine the applicability of the equation .

The authors proposed that the essence of cement grinding process is an inter-competition movement between the crushing action of external forces and the resisting action of minerals, a certain particle size distribution is corresponding to a relative competition balance between the both actions to a certain extent.

2. Derivation process

In above discussion,the general essences of cement grinding process has been abstracted as an inter-competition movement between the crushing action of external forces and the resisting action of minerals.For the sake of convenience and image, these two abstract factors should be specified-be"reduced"or"materialized"as two kind of primary particles,i.e. two kind of partucular principles.A primary particle(Φ_2) being less than a hypothetical diameter (Φ_0)is introduced to represente the crushing action of external forces and another primary particle (Φ_1) being being larger than Φ_0 represent the resisting action of minerals.

It is supposed that sum total of all primary particles in a cement systen be N,the amount of Φ_1 primary particles(principles) in the particle (sub-cluster) of number i be λ_i, the amount of Φ_2 primary particler (principles) in the particle(sub - cluster) of number j is λ_j, the amount of particles in which the amount of Φ_1 principles is λ_i be l_i, the amount of particles in which the amount of Φ_2 principles is λ_j be l_j, the amount of particles containing Φ_1 principles be δ_1 the amount of particles containting Φ_2 principles be δ_2. Then the sub- cluster model of cement particles can be obtained as figure 1.

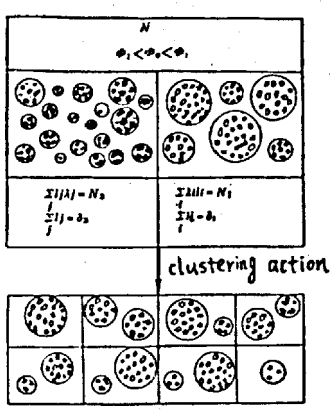

Fig. 1 The sub-cluster model of cement particles

It is also supposed that the probability of Φ_1 principles getting into a certain particle be P_1 and the probability of Φ_2 principles getting into a certain particle be P_2. Then it can be obtained based on the vague sub-cluster theory[4] that

$$\begin{cases} \sum_i \lambda_{1i} l_{1i} + \sum_j \lambda_{2j} l_{2j} - N1 - N2 = 0 \\ \sum_i l_{1i} - \delta_1 = 0, \quad \sum_j l_{2j} - \delta_2 = 0 \end{cases} \tag{1}$$

where N1 is the sum total of Φ_1 principles and N2 of the Φ_2 principles. Meanwhile, the total probability of the system can be written as

$$\Omega = P1^{(\sum_i \lambda_{1i} l_{1i} - \sum_i l_{1i})} * P2^{(\sum_j \lambda_{2j} l_{2j} - \sum_j l_{2j})} * (1-P1)^{\sum_i l_{1i}} * (1-P2)^{\sum_j l_{2j}} * (\sum_i l_{1i})! * (\sum_j l_{2j})! / (\prod_i l_{1i}!) * (\prod_j l_{2j}!) \tag{2}$$

Because any objective cybotactic group will have the most probable distribution form when it is in a relatively steady state under a certain condition, the most probable average cybotactic degrees of Φ_1, Φ_2 principles in each sub-cluster can be obtained by means of Lagrange's method of indeterminatee multipliers as follows.

$$\begin{cases} \overline{\lambda}_1 = 1/(1-P1) \\ \overline{\lambda}_2 = 1/(1-P2) \end{cases} \tag{3}$$

Let's take the following four kinds of cybotactic competition actions into consideration.

(1) The self-clustering action of $\Phi 1 (> \Phi 0)$ principles(determined by the intrinsic character of mineral structure)

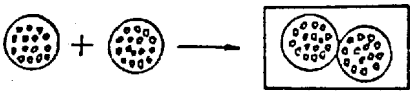

(2) The inter-action between $\Phi_1 (> \Phi_2)$ principles and $\Phi_2 (< \Phi_0)$ principles(i.e.the inter action of resisting-crushing)

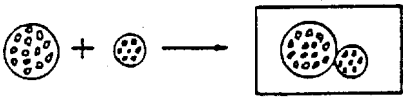

(3) The inter-action between Φ_2 principles and Φ_1 principles(i.e.the inter-action of crushing-resisting)

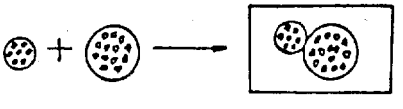

(4) The self-clustering action of Φ_2 principles (determined by the external mechanical energy)

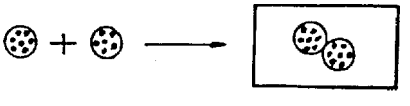

Above-mentioned clustering action is essentially a quasi-chemical reaction process, so following chemical kinetics equations can be founded.

$V11 = K11[N1][N1]$, $V12 = K12[N1][N2]$

$V21 = K21[N2][N1]$, $V22 = K22[N2][N2]$

then

$$P1=V11/(V11+V12)=K11[N1][N1]/(K11[N1][N1]+K12[N1][N2]) \quad (4)$$

$$P2=V22/(V22+V21)=K22[N2][N2]/(K22[N2][N2]+K21[N2][N1]) \quad (5)$$

where both $K12[N1][N2]$ and $K21[N2][N1]$ reflect the inter- action between crushing and resist ing,these two kinds of inter-actions should have the same action velocity,i.e.

$$K12[N1][N2]=K21[N2][N1]$$

Substituting P1,P2 in formula (3) with formula (4) and (5),it can be shown that

$$\begin{cases} \overline{\lambda}_1 = 1/(1-P1)=1+K11[N1]/K12[N2] \\ \overline{\lambda}_2 = 1/(1-P2)=1+K22[N2]/K21[N1] \end{cases}$$

Let r_1 be equal to K11/K12 and r_2 to K22/K21,then

$$\begin{cases} \overline{\lambda}_1 = 1+r_1[N1]/[N2] \\ \overline{\lambda}_2 = 1+r_2[N2]/[N1] \end{cases}$$

In addition

$$w_1=N1/(N1+N2),\ w_2=N2/(N1+N2)=1-w_1$$

where w is the weight fraction or quantity fraction of a principles in sub-clusters.

Under a certain technology condition, weight increase of a particle means the increase of primary particles (principles) in the particle , and the particle size will change correspondingly,i.e. $\overline{\lambda} \propto \Phi$, so

$$\Phi' = \overline{\lambda}_1 K1 = K1\ (1+r_1w_1/(1-w_1))$$

$$\Phi'' = \overline{\lambda}_2 K2 = K2\ (1+r_2(1-w_1)/w_1)$$

Let K be equal to K1/K2,i.e.K=K1/K2,then

$$\Phi'/\Phi'' = K\ (1+r_1w_1/(1-w_1))\ /\ (1+r_2(1-w_1)/w_1) \quad (7)$$

Because the average cybotactic degree of complete sub-clusters is contributed by $\overline{\lambda}_1$ and $\overline{\lambda}_2$,when the minimum cybctactic degree Φmin and the maximum Φmax are known already, the average cybotactic degree can be written as the form of

$$\overline{\Phi} = K1\overline{\lambda}_1\Phi max/(K1\overline{\lambda}_1+K2\overline{\lambda}_2)+K2\overline{\lambda}_2\Phi min/(K1\overline{\lambda}_1+K2\overline{\lambda}_2)$$

$$\text{So } (\overline{\Phi}-\Phi min)/(\Phi max-\overline{\Phi}) = K1\overline{\lambda}_1/K2\overline{\lambda}_2 \quad (8)$$

It is made known from formulas (7) and (8) that

$$(\overline{\Phi}-\Phi min)/(\Phi max-\overline{\Phi}) = K*(1+r_1w/(1-w))\ (1+r_2(1-w)/w) \quad (9)$$

When data of normalized particle size distribytion is adopted, the sub- clustir euqation of cement particle size distribution is obtained as the form of

$$\Phi/(1-\Phi) = k*\ (1+r_1w/(1-w))\ /\ (1+r_2(1-w)/w) \quad (10)$$

where Φ represents a normalized particle size ,w is the weight percent corresponding to the normalized particle size ,K,r_1,r_2,are the related sub- cluster parameters. Because above distribution equation has reflected the essential characteristics of cement grinding process in the most general sense ,the authors define formula (10) as the sub- cluster intrinsic equation of cement particle size distribution.

DISCUSSIONS

1.Physical meaning of the sub-cluster parameters

There are three sub-cluster parameters K,r_1.r_2 in the distribution equation. It is made known from the precondition and process of equation derivation that all these

parameters have definite physical meaning .r_1=K11/ K22, where K11 is determined by the essential character of minerals ,for a given cement,K11 can be considered as a constant.K12 is determined by the resisting action of particles vs external forces.At the initial period of grinding, particle sizes are larger, resisting action is relatively less,so value of r_1 should be larger.At the later period ,particle sizes become smaller,resisting action become strengthening relatively,so r_1 should be smaller .

r_2=K22/K21,where K22 is determined by external mechanical energy,under the condition of continuously stable manufacture k22 can be considered as a constant.It is known from K12[N1][N2]=K21[N2][N1] that the larger(smaller) the K12, the larger(smaller) the K21. Thus at the initial period of grinding ,the value of r_2 is larger ,and at later,r2 is smaller.

Therefore,the smaller the r_1 and r_2 or r_1*r_2 , the better the homogeneity of cement particle size disdtribution.

The physical meaning of K can be known from the following boundary condition. When $r_1 \to 0, r_2 \to 0$,the sub-cluster intrinsic equation will take the form of $K=(\Phi-\Phi min)/(\Phi min-\Phi)$. It is made clear that the larger the value of K,the larger the Φ.So the value of K reflects the total average level of cement particle size distribution.

2. Detemination of the sub-cluster parameters

In order to examin the applicablity of the distribution equation,classified cements are mixed uniformly in different ratio. Particle size distributions of above cements are measured by photo-elextric settlement analysis. The results are given as a form of normalized particle size distribution curves(see fig.2)

In formula (10),let $\Phi/(1-\Phi)=Y, w/(1-w)=X$,then

$Y=K*(1+r_1X)/(1+r_2/X)$

Putting above formula in order,

$$(K-Y)/KX=(r_2Y/KX^2)-r_1 \qquad (11)$$

Formula (11) is essentially a linear equation and the change of K will result in the change of linear relationship.The optimal value of K should enable formula (11) to have the best linear relationship,i. e. the linear correlative coefficient to reach the maximum.So the values of K,r1, r2 can be calculated by linear regression analysis based on the actually measured data (fig.2). The results are given in table 1. The fitness of theoretical equation for actually measured curves is also shown in fig.2.

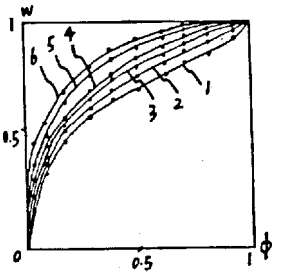

Fig.2 Normalized particle size distribution curves of cements -curves by actual measurement ..points by theoretical calculation

3. Relationship Between Sub-cluster Parameters and Mechanical Properties of Cements.

Many different equations have been proposed for cement particle size distribution,but few have discussed the relationship between distribution parameters and cement properties. The authors have measured the compressive strengths from 1 to 28 days of net paste mini -specimens of cements given in table 1.The results are given in table 2.

Table 1 The sub-cluster parameters of cement with different particle size distributions

No.	K	r_1	r_2	r_1*r_2/K
1	0.585	2.160	6.489	23.360
2	0.265	2.036	2.957	22.719
3	0.165	1.849	1.634	18.310
4	0.125	1.678	1.182	15.867
5	0.073	1.661	0.685	15.586
6	0.063	1.575	0.636	15.410

Table 2 Strength development of cements with different particle size distributions (corresponding to table 1)

NO	Compressive strength (MPa)			
	1d	3d	7d	28d
1	25.5	50.5	63.2	75.5
2	29.9	51.0	66.6	74.5
3	31.4	53.4	67.1	76.0
4	32.3	53.9	72.0	81.3
5	33.3	54.9	76.4	85.3
6	34.3	55.4	81.3	94.6

Curves of sub-cluster parameters vs compressive strengths are drawn in fig.3-fig.6.It is made known from the figures that all the compressive strengths at different hydration ages have a good correlation with r_1*r_2/K,the larger the r_1*r_2/K,the smaller the strength value. Then for a cement with definite chemical composition ,it is possible to forecast its strength development by calculating the sub-cluster parameters.It is known from the physical meaning of sub-cluster parameters that the larger the r_1*r_2,the poorer the homogeneity of partical size distribution,and the value of K reflects the total average level of particle size distribution.So the authors define r_1*r_2/K as the specific dispersion degree of cement particle size distribution.Therefore the effect of particle size distribution on mechanical properties of cement can be represented comprehensively by the specific dispersion degree r_1*r_2/K.

CONCLUSIONS

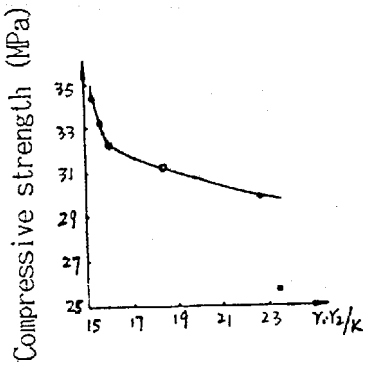

Fig.3 The sub-cluster parameters vs 1d compressive strength

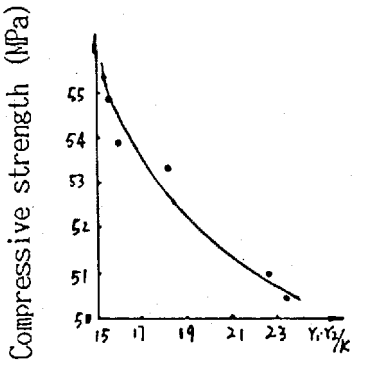

Fig.4 The sub-cluster parameters vs 3d compressive strength

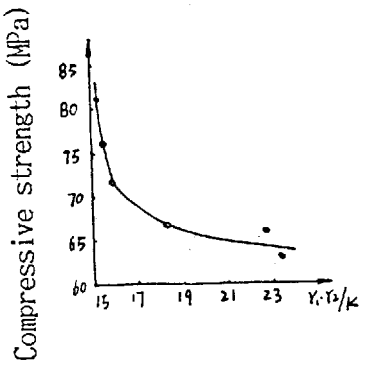

Fig.5 The sub-cluster parameters vs 7d compressive strength

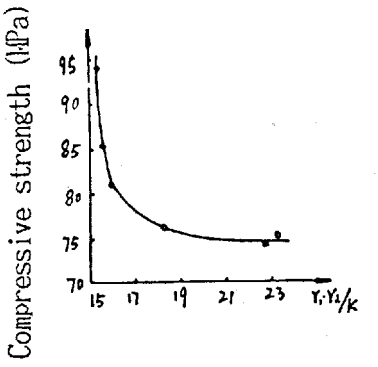

Fig.6 The sub-cluster parameters vs 28d compressive strength

(1) The general essence of the cement of the cement grinding process is summarized as an inter-competition movement between the crushing action of external forces and the resisting action of minerals.The particle size distribution corresponds to the relative competition between the two actions.

(2) The sub-cluster intrinsic equation of cement particle size distribution is derived as the form of $\Phi/(1-\Phi)=K*(1+r_1w/(1-w))/(1+r_2(1-w)/w)$ based on the vague sub-cluster theory. Three sub-cluster parameters with definite physical meaning are obtained and r_1*r_2/K is defined as the specific dispersion degree of cement partical size distribution.

(3) Compressive strengths of cement paste at different hydration periods all have a good correlation with the specific dispersion degree r_1*r_2/K,the effect of particle size distribution on mechanical properties of cement can be represented comprehensively by the specific dispersion degree r_1*r_2/K.

REFERENCES

[1] Zhao Fei,Master academic degree paper of Wuhan Uiversity of Technology(1988).

[2] Jean Piaget,Le Structuralisme,Presses Uiversitaires de france,Paris,1970.

[3] M.E.Asim,Zement-Kalk-Gips,75[6](1986)321.

[4] Jin Riguang,The Vague Sub-cluster Theory,Heilongjiang Press of Science & Technology(in Chinese,1985).

PRODUCTION PERFORMANCES AND UTILISATION OF A SPECIAL SUPERPLASTICIZED CEMENT

V Alunno Rossetti*, F Curcio and L Cussino****

**Università La Sapienza, Facoltà di Ingegneria, Roma, ITALY*
***Unicem spa, Centro Ricerche Guidonia, Roma, ITALY*

SUMMARY

Since the introduction of superplasticizers in concrete technology, two particular problems have been noticed: the first one is the possibility of absorption of the product in the aggregate porosity, the second one is the effect of the addition time on the fluidifying action. In order to overcome these problems a special cement, to which the admixture is added in the cement factory, has been produced at one Italian plant. In this paper the characteristics and the performances of this cement are described.

1. INTRODUCTION

The use of superplasticizing admixtures has greatly changed the concrete practice in many countries, due to the great benefits attainable with their use, in terms of performances, reliability and econonomy.

One problem arising with the use of superplasticizing admixtures is the variability of the effects, as a function of the time of addition to the mix. A second interesting aspect is that the effect of the superplasticizers is believed to be essentially due to adsorption phenomena on the cement particles surface, while the admixture absorbed by the porosity of aggregate particles or adsorbed on it should be ineffective: it could be supposed that a previous adsorption, limited to the cement surface, should minimize the aggregate influence.

In order to reduce the above mentioned variability and to increase the performance of the admixture, the possibility of a direct addition to the cement, instead of the usual addition in the concrete mix, has been studied and a research has been conducted since about 3 years ago. The results obtained in the laboratory were satisfactory and after some experience with a pilot plant, an industrial production at one italian cement plant is now regularly carried on.

In this paper some information is given on the production, performances and applications of this special Super Plasticized Cement (SPC).

2. ADVANTAGES TO FORESEE FROM A SPC

As above outlined, two advantages could be foreseen in using a superplasticized cement.

2.1 Reduced effect of the addition time

The effect of a superplasticizer on the rheological properties of the cementitious mixes, normally depends on the time of addition, in the presence of water.

This effect has been observed both in laboratory tests and in industrial practice, on cement pastes and on concrete. For concrete mixes in industrial practice, Kasami and coworkers (1) for example, found a remarkable increase of slump and slump increment; Collepardi and coworkers (2), examined the effect of an immediate or delayed addition of a sulphonated naphtalene formaldehyde polymer to cement pastes, and found a remarkable effect on their fluidity as measured by means of the minislump test.

To underline the unpredictability of the results, it is worth mentioning that in at least one case the opposite effect (reduced workability for delayed addition) has been claimed (3).

In the industrial practice the addition time can be the very first moment of the contact of the cement with water (as when the admixture is contained in the latter), or it can be quite longer, since the admixture producers, to obtain the best performances of the product, sometimes ask the user to delay the addition to the mix, after that all or the greater part of the required mixing water has been added and the concrete has been thoroughly mixed. In some cases, the admixture is added in the truck mixer at the job site, a long time after the water addition.

The dependence of the effect of the superplasticizer on the time of addition, in some cases can be certainly objectionable: it means indeed that, expecially when a strict control of the timing of concreting operations is not possible, the effect of the superplasticizer is not always and not completely predictable; in turn this can lead to variations of the w/c ratio in attempting to mantain the slump at the prefixed value.

2.2 Effect of the adsorption

The second reason for trying to develop a SPC is the fact, commonly accepted, that the fluidifying effect of the superplasticizers is associated to adsorption phenomena on the surface of the cement particles. It could be supposed that if, due to the production process, the polymer is already adsorbed on the cement surface when the cement comes into contact with water, and if moreover for the same reason the polymer is not or is less adsorbed/absorbed by the aggregates, the fluidifying effect should increase.

It could be objected to this last point, that this is a very simplified way of looking at the phenomenon: many parameters indeed have been taken into account to explain the action of the superplasticizers; among those the most significant could be the amount of adsorption on the individual phases, anhydrous and hydrated. According to Ramachandran (4) for example, the admixture is greatly adsorbed by C3A and C3A-gypsum mixture, leaving only small amounts for the dispersion of the silicate phases. By late addition the admixture is less adsorbed, and more of it is left in solution for dipersing the silicate phases.

Another way of reasoning is that the addition of the admixture to the cement could be seen as a slightly delayed addition in concrete, since its presence as a dispersion of solid particles does not imply immediate appearance in solution and the possibility of immediate action; on the contrary a certain amount of time is required for the solubilization of the product.

3. PRODUCTION OF A SUPERPLASTICIZED CEMENT

On the basis of the preceding considerations a study has been carried out since 1988, in cooperation with an admixture producer, with the task of producing a cement containing the admixture since its production in the cement factory.

The first attempts were based on the addition of a normal sulfonated naphtalene superplasticizer solution to the cement, during the final grinding. The results so obtained, even if encouraging, were not satisfactory, both for the fluidifying effect and for the duration of the effect. Only the availability of a purposely made admixture (again of the sulfonated naphtalene type), gave the possibility of reaching good performances of the product. Also the way of mixing the admixture with the cement has a marked effect on those performances and required the set up of a special stage in the production.

In this way a pilot plant and then a full scale plant for the production of the cement have been set up and today a regular industrial production is carried out.

4. PROPERTIES OF THE SUPERPLASTICIZED CEMENT

4.1 Standard tests

The base cement for the SPC produced so far, is a portland cement (PD) , of the italian type "525" (a rapid hardenig cement, having a crushing strength higher than 52.5 MPa at 28 days). This type was selected since the SPC was meant to have high performances, in view of an initial test utilization in precast and prestressed concrete elements; other types of cement can of course be used.

In table 1 SPC typical characteristics and performances are given, in comparison with those measured on the "parent" portland cement (both according to italian standards). It can be observed that the performances of the two cements are practically the same; if tested on the basis of a constant water/cement ratio this holds for the compressive strength too. On the contrary, when tested on the basis of the same flowability the SPC, requiring about 25 % less water, gives compressive strengths quite higher than the PC.

Cement	PD 525	SPC	
SSB, cm^2/g	4030	3980	
Retained at 40 μm, %	4.4	5.2	
L.O.I. %	0.75	1.6	
Insoluble, %	0.41	0.41	
SO_3	3.30	3.35	
C_3S (clinker)	56.2		
C_2S	19.7		
C_3A	7.7		
C_4AF	9.4		
Paste water dem., %	25.6	20.2	
Initial set, mins	95	300	
Final set, mins	125	395	
		Same w/c	Same consistency
Mortar w/c	0.5	0.5	0.37
Mortar flow, %	118	>200	117
R_{c1}, MPa	26.4	24.2	38.9
R_{c3}, MPa	44.1	44.3	67.0
R_{c7}, MPa	53.3	52.0	81.0
R_{c28}, MPa	64.0	62.9	95.5
R_{f28}, MPa	8.8	7.1	12.4

Tab. 1 - Characteristics of the cements.

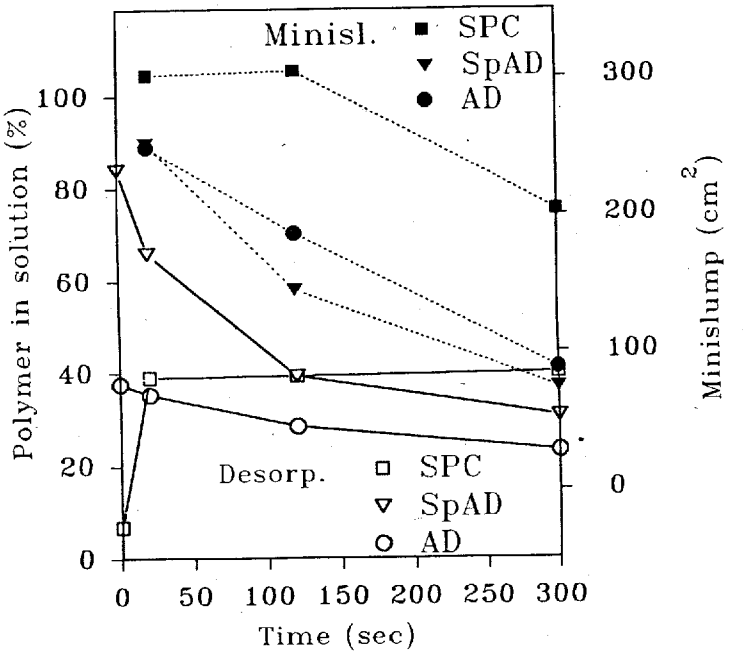

Fig. 1 - Adsorbtion and minislump tests.

4.2 Minislump and absorption tests

In order to obtain some indications on the adsorption phenomena, tests of polymer adsorption and of minislump were performed. For all the tests, the same cement sample was used, and three ways of addition:

- addition of the special admixture (SpAD) to the dry cement in the pilot plant (SPC sample),

- addition of the same admixture (SpAD), but added together with the mixing water (SpAD sample),

- addition with the mixing water of a superplasticizing admixture (AD) having very high performance, commonly used for concrete (AD sample).

As abovesaid, all the admixtures were based on sulfonated naphtalene polimers, and the same quantity was added (1.8 % by weigth of cement).

The minislump (6) tests were performed by energic mixing of the cement with 35% by weight of water (or water + admixture), for periods of time of 20, 120 and 300" and measuring the pat area immediately after the end of the mixing.

In the same samples, part of the mix was used for separating the solution by filtration and measuring the concentration of the polymer, by means of UV absorption spectrometry.

The concentration of the polymer in the solution has been plotted in fig.1 as a percentage of the polymer initially present in the paste; the proportion of polymer adsorbed on the cement can be evaluated by difference. The test for the concentration of the admixture in solution was also performed at "zero time"; this means that water (in the case of SPC) or admixture in water, was passed through the cement, directly over a filtering device.

In fig. 1 results of the adsorption and minislump tests are presented.

The adsorption results indicate that both SpAD and AD are adsorbed until a not very different percentage of the admixture initially present has been dissolved in the contact solution; the SPC cement releases a high proportion of the polymer to the solution, so that at 300" the concentration is the highest, but similar to those already found in the former cases.

The minislump results indicate that the SpAD admixture added to the cement with the mixing water (immediate addition) is equivalent to the AD admixture at 20" and slightly less effective in the same conditions at later times; the SPC, containing the SpAD admixture shows higher fluidity at 20" and is more fluid also at later times.

It can be observed that in a quite short period of stirring, the fluidifying admixture reaches its full effect in all cases; in this period the mean concentration of polymer in solution is quite low for the SPC, having the highest fluidity, because it goes from 7 to 40% of the quantity initially present; on the contrary the concentration of polymer in solution in this period is the highest for SpAD and AD. The fact that the full effect of the polymer is reached for a high concentration of polymer in solution (SpAD and Ad) in one case, and for a low concentration in the other case, could be explained in two ways:

- the polymer in the SPC can really be effective because of the adsorption on the cement particles during the production process,

- addition of the special admixture (SpAD) to the dry cement in the pilot plant (SPC sample),
- addition of the same admixture (SpAD), but added together with the mixing water (SpAD sample),
- addition with the mixing water of a superplasticizing admixture (AD) having very high performance, commonly used for concrete (AD sample).

As abovesaid, all the admixtures were based on sulfonated naphtalene polimers, and the same quantity was added (1.8 % by weigth of cement).

The minislump (6) tests were performed by energic mixing of the cement with 35% by weight of water (or water + admixture), for periods of time of 20, 120 and 300" and measuring the pat area immediately after the end of the mixing.

In the same samples, part of the mix was used for separating the solution by filtration and measuring the concentration of the polymer, by means of UV absorption spectrometry.

The concentration of the polymer in the solution has been plotted in fig.1 as a percentage of the polymer initially present in the paste; the proportion of polymer adsorbed on the cement can be evaluated by difference. The test for the concentration of the admixture in solution was also performed at "zero time"; this means that water (in the case of SPC) or admixture in water, was passed through the cement, directly over a filtering device.

In fig. 1 results of the adsorption and minislump tests are presented.

The adsorption results indicate that both SpAD and AD are adsorbed until a not very different percentage of the admixture initially present has been dissolved in the contact solution; the SPC cement releases a high proportion of the polymer to the solution, so that at 300" the concentration is the highest, but similar to those already found in the former cases.

The minislump results indicate that the SpAD admixture added to the cement with the mixing water (immediate addition) is equivalent to the AD admixture at 20" and slightly less effective in the same conditions at later times; the SPC, containing the SpAD admixture shows higher fluidity at 20" and is more fluid also at later times.

It can be observed that in a quite short period of stirring, the fluidifying admixture reaches its full effect in all cases; in this period the mean concentration of polymer in solution is quite low for the SPC, having the highest fluidity, because it goes from 7 to 40% of the quantity initially present; on the contrary the concentration of polymer in solution in this period is the highest for SpAD and AD. The fact that the full effect of the polymer is reached for a high concentration of polymer in solution (SpAD and Ad) in one case, and for a low concentration in the other case, could be explained in two ways:

- the polymer in the SPC can really be effective because of the adsorption on the cement particles during the production process,

In both the figures, the regression line (continuous) and the 95% confidence interval (dashes) for the regression line have been traced. It can be observed that the interval is about twice for the PD 525 concretes.

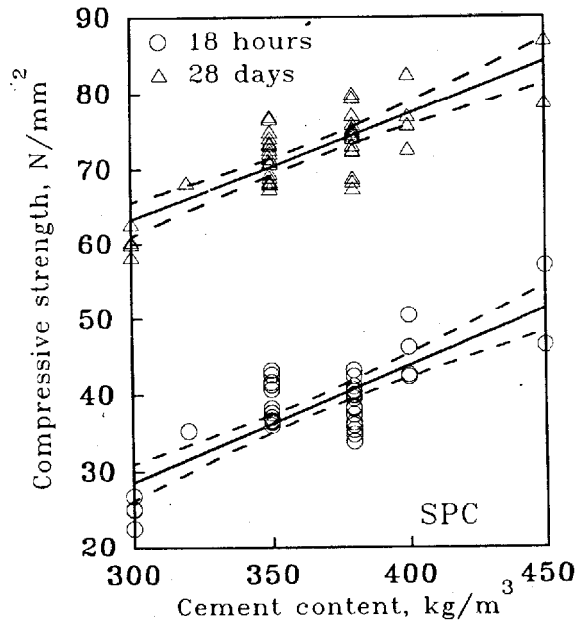

Fig. 2 - SPC strength in concrete.

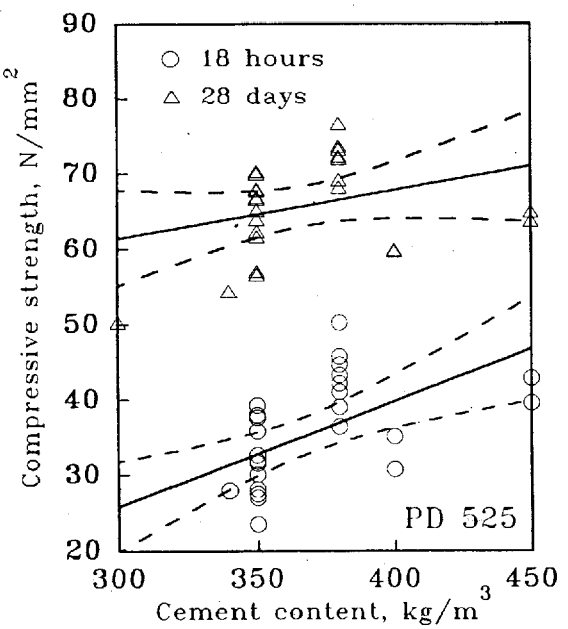

Fig. 3 - PD strength in concrete.

Even if the SPC is already used in precast concrete elements production, homogeneus statistical data are not yet available.

6. CONCLUSION

Industrial production and laboratory testing confirm the advantages of the use of a special cement, containing a superplasticizer added in the cement factory, essentially in reducing the variability of strenght, and in improving the reliability of the concrete.

REFERENCES

1) Kasami H., Ikeda T., Yamane S., in Proceedings of an International Symposium on Superplasticizers in Concrete, Ottawa, Canada (1978)

2) Collepardi M., Corradi M., Baldini G., Pauri M., in VII Int. Congr. on the Chem. of Cement, VI, 20, Paris (1980)

3) Hewlett P.C., in Proceedings of an International Symposium on Superplasticizers in Concrete, Ottawa, Canada (1978)

4) Ramachandran V.S., "Concrete Science", Ed. Heyden / London (1981)

5) Perenchio W.F., Whiting D.A., Kantro D.L., in Proceedings of an International Symposium on Superplasticizers in Concrete, Ottawa, Canada (1978)

6) Alunno Rossetti V., Unpublished data.

WHITE BELITIC PORTLAND CEMENTS

Marcela Muntean*, M Dinulescu*, Maria Bedö and Florica Paul*****

**Politechnic Institute Bucharest*
***Research Design Shareholdings Company for Binding Industry Brasov*
***Construction Institute Bucharest*
ROMANIA

SUMMARY

The paper present the possibility to obtain low firing temperature clinkers from available raw materials, in presence of small sulphate admixtures without lowering the physical-mechanical properties of the resulting cements and simultaneously with good whitnees. Burning ability of the synthesised masses as well as the compositional modification , whitnees and mechanical strengths of the cements were determined.

RESUME

Dans cette oeuvre il s'agit de la possibilité d'obtenir quelques clinkers d'une base température, de matière première usuelle, en présence d'un réduit supplément des sulfates, sans agraver les propriétés physiques et méaniques des ciments résultés et simultanément avec un bon degré de blanc des ces ciments.

INTRODUCTION

The energy-saving fabrication of the white Belitic Portland cement clinkers with satisfactory compressive strengths (above 3o MPa after 28 hardening days) and simultaneously with good whitness from easly available materials, as limestone bentonite and tuff is very interesting for the present binding materials industry /1-7/. Small additions (5%) of $MeSO_4$ (Me = Ca^{2+}, Mg^{2+}, Ba^{2+}) may induce some positive modifications both upon the burning ability, as well as, upon the binding properties of the resulted cements. Concomitently the whitness of the samples with sulphate admixtures is appreciably improved in comparison with that of the reference sample, especially for samples quenched in water or in three ethanol-amine water solutions.

EXPERIMENTAL

A series of laboratory clinkers have been prepared from usual raw materials, characterized by reduced Fe_2O_3 content (Table 1). The raw materials mixtures for clinkers which have lime saturation factors of 8o, 85 and 87, have been finely ground (under 63 μm) and than pelletized (about 1o MPa) and fired in an electric furnace at 1,300° 1,33o° and 1,350° for 3o minutes. Than these clinkers were quenched in various mediums (water and three ethanol amine water solutions, 2% TEA). Clinkers were ground without gypsum to a specific surface area of 350 m^2/kg /8/.

Table 1. Chemical composition of raw materials.

Raw materials	Oxide, %						
	CaO	SiO_2	Al_2O_3	Fe_2O_3	MgO	Me_2O^x	L.I.
Limestone	54.92	0.42	0.28	0.04	0.61	0.45	43.19
Bentonite	11.10	50.09	27.04	0.64	1.41	4.51	10.41
Tuff	4.54	67.98	11.91	0.87	1.06	3.69	9.32

Obs. $Me_2O = Na_2O + K_2O$
SO_3^{2} content is under 0.3 % for each raw materials.

The burning behaviour and the mineralogical composition of the synthesized masses have been followed by chemical, XRD, and SEM analyses. The physical-mechanical properties of the cements have been determined by standard testing methods.

RESULTS.

The free lime content of all samples with sulphate admixtures evidences good clinkerization ability in comparison with that of the reference samples, even for 1,300°C burning temperature (Table 2). The free lime content of the samples is not appreciably influenced by the nature of the quenched mediums. It was observed that, for water quenched samples, their free lime content was greater with 0.05 to 0.15 % in comparison with the samples quenched in the three ethanol amine solution.

For all that, the mineralogical composition of the clinkers with and without sulphate admixtures is influenced by the nature of the quenched medium. As expected, the increase of the synthesis temperature

Table 2. Free lime, %, for TEA water solution quenched samples.

Samples No.	$MeSO_4$ (5%)	Firing temperature, °C/30 minutes. 1,300	1,330	1,350
A	-	1.440	1.115	0.753
A_{Mg}	$MgSO_4$	0.545	0.293	0.036
A_{Ca}	$CaSO_4$	0.790	0.410	0.092
A_{Ba}	$BaSO_4$	0.867	0.499	0.132
B	-	1.790	1.313	0.876
B_{Mg}	$MgSO_4$	1.092	0.635	0.161
B_{Ca}	$CaSO_4$	1.173	0.867	0.582
B_{Ba}	$BaSO_4$	1.250	0.937	0.611
C	-	1.990	1.458	0.953
C_{Mg}	$MgSO_4$	1.330	0.789	0.260
C_{Ca}	$CaSO_4$	1.650	0.999	0.728
C_{Ba}	$BaSO_4$	1.700	1.200	0.759

Obs. A,B,C - reference clinkers with S_K= 80, 85 and 87.

or of the S_K, determine the increase of the content of the well crystallized silicate compounds (C_3S+C_2S). Simultaneously in the clinkers with sulphate admixtures (Fig.1), the XRD data show a maximum line at 3.72 - 3.76 Å attributed to the sulphate aluminate compound ($C_3A_3MeSO_4$) formation /4,7/. Figure 1 show only the mean values of the relative intensity corresponding to the sulphoaluminate compound in water quenched clinkers.

The SEM images show that the iron ions (as Fe^{3+}) distribution in the clinkers is modified both by the cooling medium and the presence of the sulphate admixtures (Fig.2) especially $MgSO_4$. It may be remarked an irregular distribution of the iron ions for water quenched samples in comparison with three ethanol amine water solution quenched samples. Also, the $MgSO_4$ presence determines a lowering of the iron ions of clinkers. The same behaviour

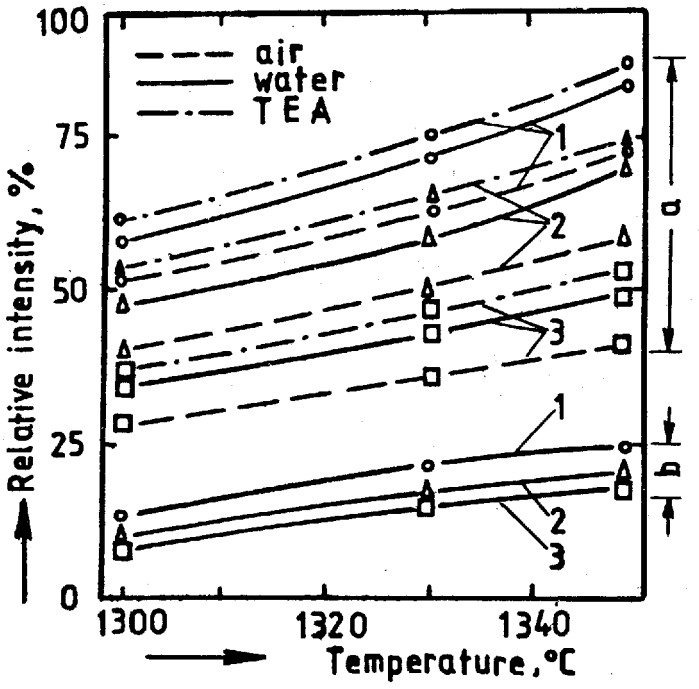

Fig.1 Relative intensity vs. temperature: a)-(C_3S+C_2S); b)-$C_3A_3MeSO_4$, for C, B, A clinkers (1,2,3).

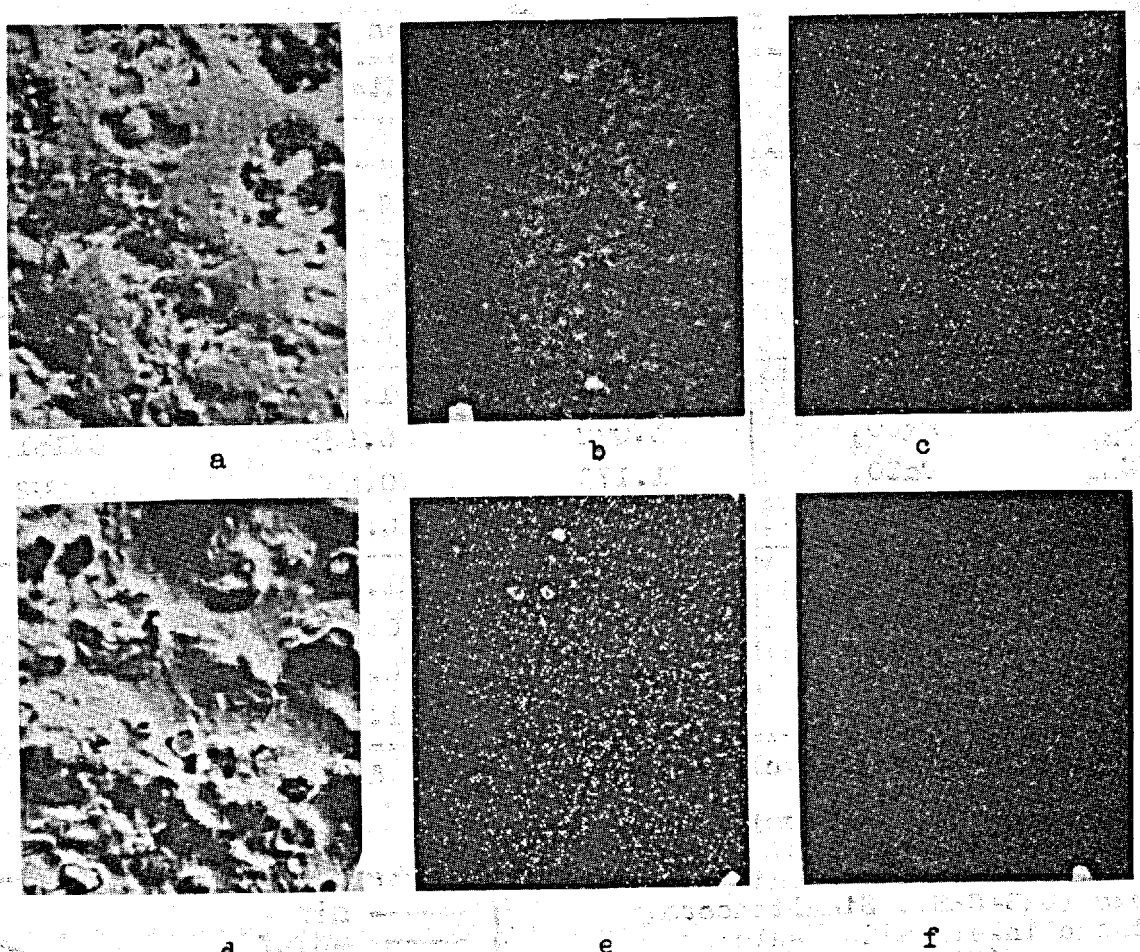

Fig.2 SEM images (5000x) and Fe^{3+} distribution of the B clinker quenched in water (a,b) and in T.E.A solution (d,e); same for B_{Mg} clinker quenched in water (c) and in TEA water solution (f).

are observed in presence of other sulphate admixtures, as calcium sulphate or barium sulphate. As a result, the whitness is better in all samples with sulphate admixtures, especially for TEA water solution quenched samples (Fig.3).

The compressive strengths of the samples quenched in TEA solution, especially for those with 5% sulphate admixture are relatively good and they are very good in presence of 5% of barium sulphate, evan for cements with small S_K (S_K = 80), which was fired at 1,300°C (see Table 3).

For water quenched samples, the compressive mechanical strengths are within 2 to 5 MPa lower than those for TEA water solution quenched samples. Generally, the compressivee strengths of the resulted cements are good, especially for those clinkers which have the lime saturation factors 85 or 87. But one has to take into consideration the nature of the sulphate admixtures and the quenched meidum.

Table 3. Compressive strength at 28 days, MPa.

Samples	Temperature, °C		
	1,300	1,330	1,350
A	18.7	23.4	26.8
A_{Mg}	24.7	29.0	30.3
A_{Ca}	25.0	30.1	31.3
A_{Ba}	28.6	32.0	33.6
B	19.8	25.1	28.2
B_{Mg}	25.5	31.4	33.5
B_{Ca}	27.0	34.2	35.0
B_{Ba}	29.9	36.3	37.2
C	22.7	28.0	30.6
C_{Mg}	28.4	34.4	35.8
C_{Ca}	30.3	36.0	37.9
C_{Ba}	33.1	37.8	39.7

Obs.-specific surface area of the cements = 350 m^2/kg;
-standard samples with binder/sand ratio = 1/3.

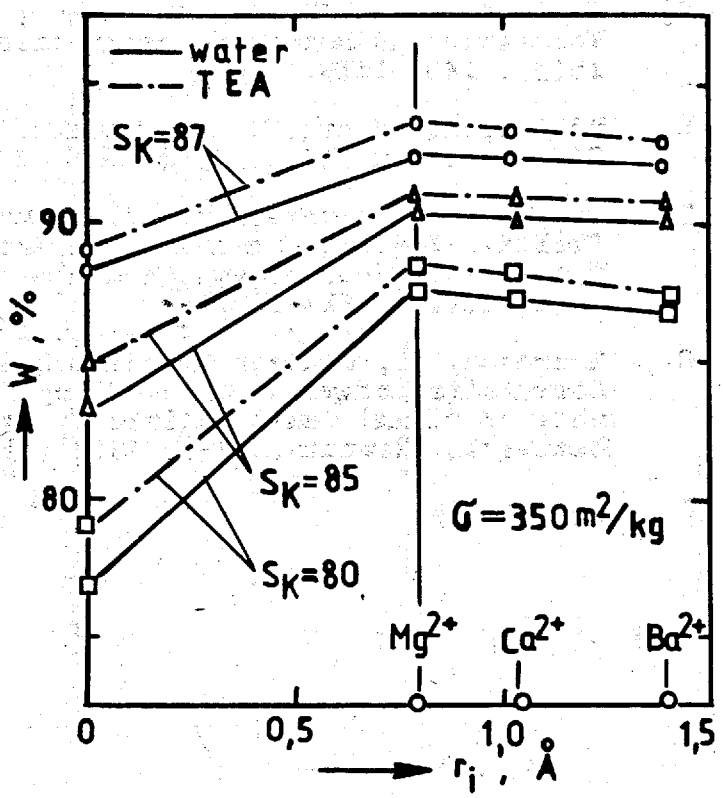

Fig.3 Whitness vs. cation radius of the sulphate admixtures (on ordinate, conventionally W, %, for reference clinkers).

CONCLUSIONS.

White belitic portland cements can be prepared from usual cheap raw materials in presence of the sulphate admixtures. The nature of the sulphates as well as the quenching medium play an important role upon the physical-mechanical properties of cements.

REFERENCES

1. Stark, J., Müller, A and Rümpler, K.; "Existenzbedingungen von hydraulisch aktiven Belit Zement", Z.K.G., 1981, 34(6), 476-482.

2. Mielke, I., Müller, A and Stark, J.:"Despre rolul SO_3 la obținerea cimentului belitic activ", Mat.Construcții, 1985, 13(2), 138.

3. Teoreanu, I., Marcela Muntean; "Expansive sulphate aluminate cements", C.C.R., 1983, 13(5), 711-720.

4. Teoreanu, I., Marcela Muntean and Dragnea, I.:Type 3(CA).M_xSO_4 compounds and compatibility relations in CaO-CaO.Al_2O_3-$M_x(SO_4)_y$ systems", 1986, Il Cemento, 83(1), 39-46.

5. Teoreanu, I and Muntean Marcela ; "Calcium aluminosulphate formation and hardening properties", Rev.Roumaine Chimie, 1974, 15(9), 1483-1489.

6. Muller, A., Stark, J. and Mielke, J.: "Uber aktiven Belit-Zement", Silikatechnik, 1984, 35(4), 276-283.

7. Teoreanu, I., Muntean Marcela., Maria Bedo and Sudrigean, T., "Belitic Portland Cements with various content of MgO and SO_3", The VIII-th Intern.Symp.Chem.Cements, Rio de Janeiro, Brazilia, 1986, 2(1.2), 217-222.

8. Teoreanu, I., Muntean Marcela, Bedo Maria and Sudrigean, T.: Correlation between the cooling medium and the properties of white Portland Cement clinker", Materiale de Construcţii, Bucureşti, Romania, 1989, 19(1), 15-19.

THE MECHANOCHEMICAL ACTIVATION OF BELITE

Luhui Zhong Jinyu, Fan Yueming and Yang Jiazhi

Dept. Inorganic Materials, South China University of Technology
P R CHINA

ABSTRACT

Belite synthesised at 1623K was ground in a vibration mill for 1—70 hours. The variations of mechanochemical properties of the samples, such as particle size distribution; crystal structure; relative lattice strain, surface characteristic and early hydration activity, were studied.

The results show that the grinding would cause the particle size to decrease within 30h, when the grinding is beyond 30h; however, the particle size would be increased. The grinding could also lead the crystal unit cell dimension of belite to change and the crystallinity to descend. With the prolonging of grinding time, both the lattice strain and the early hydration activity were increased greatly. Besides, the technique of inverse gas chromatography (IGC) was used to analyse the surface free energy of the samples. It is concluded that the London—dispersive component and the Polar component increase continuously with grinding, and then decrease when the grinding time is over 30h. The results also indicate that the grinding may greatly raise the compressive strength of belite paste. Therefore, the mechanochemical activation is an efficient method of increasing the hydration activity of belite.

将 1623K 下合成的贝利特置于振动磨内粉磨 1～70 小时，研究了各试样在粉磨过程中所发生的一系列机械力化学性质变化，如试样粒度分布、晶格应变、粉体表面特性及早期水化活性等。结果表明：粉磨作用使贝利特粉体粒度减小，并使贝利特晶胞参数发生变化，同时使贝利特晶体结晶度下降，晶格应变及水化活性增大。随着粉磨时间延长，贝利特粉体表面自由能伦敦色散分量及极性分量不断增大，但当粉磨时间超过 30 小时，贝利特表面自由能反而减小，并使粉体粒度增大。粉磨作用可大大提高贝利特浆体早期强度。因此，机械力化学活化是提高贝利特水化活性的有效方法。

INTRODUCTION

The cements composed mainly of C_2S could be more economical of energy consumption than the ordinary portland cements containing large fraction of C_3S, and it could be superior when used in the form of their hydration products. Since the introduction of an additional mole of CaO (in C_3S Vs C_2S) consumes much energy and yields little inerease in strength, the hydration of C_2S, however, proceeds more slowly than that of C_3S[1]; therefore, how to increase the early hydration activity of belite has been becoming one of the most intreasting projects, and many studies have been made about the synthesis of reactive C_2S previously。 D. M. Roy[2]prepared a kind of reactive βC_2S by spray—drying technique; R. Struillou etc. ,[3] however, synthesised βC_2S by burning the homogeneous mixture of $Ca(NO_3)_2$and SiO_2at 1023K, for $Ca(NO_3)_2$will decompose at this temperture and the reaction between CaO and SiO_2 is very rapid, they found the hydration activity of the βC_2S obtained is much higher than that of βC_2S formed in OPC. An active βC_2S has also been synthesised through a new technique by Yang Nanru, i. e, a mixture of CaO and aerosil with CaO/SiO_2 ratio equalled to 2 was first subjected to hydrothermal treatment at about 373K and then burnt at a temperture not higher than 1123K without adding stabilizer, they found the compressive strength at 14—days hydration was 10 times that of ordinary βC_2S. Meanwhile, it was verified that adding some minor components to the raw mix of C_2S is helpful in increasing the activity of βC_2S. I. Jelenic etc.[5] studied the hydration of B_2O_3 — stabilized α and β modifications of C_2S; then David. L. Kanto etc.[6] investigated the hydration of various βC_2S preparations; and P. Firens etc.[7]researched the nature and concentration effect of stabilizing elements of βC_2S on its hydration rate, they also studied the effect of synthesis temperture and cooling conditions of βC_2S on its hydration rate previously[8]; J. Stark etc. , however, conducted much work about the research of active belite cement[9—11]; other investigators also did many studies on these aspects, but only a few reports about the effect of grinding on the hydration activity of clinker or clinker minerals could be found.[12—13], As we know, the apperent changes of materials in grinding process are the micro-miniaturization and the rise of specific surface area due to the effect of mechanical force. At the same time, the phenomenon of lattice distortion, amorphous state and the increasing of surface free energy of crystal particles may also be produced because of the accumulation of energy, which in turn will lead to changes in physicochemical properties, such as adsorption, wetting, adhesion etc.. These changes in the structure and the physicochemical properties of material arising from the mechanical effect are benificial to heighten the reactivity. With the advancing of grinding technique, more and more highly efficient grinding mills would be manufactured and this would make it much more economical and practical for us to prepare fine materials. Therefore, it is possible to activate belite by the method of mechanochem—isty, and so, in this article, a series of physicochemical changes of belite because of the effect of mechanical force were studied using the theory of mechanochemistry.

EXPERIMENTAL

1. Synthesis of belite

The synthetic mineral belite is prepared with analytical reagents in an electric furnace; the chemical composition of the resulting belite is shown in Table 1.

The mixed raw meal is burnt in the furnace at 1623K for 1 h and then cooled rapidly in air; the content of free lime in the sample is 0. 15% wt.

Table 1 Chemical composition of belite

Composition	CaO	SiO_2	B_2O_3	BaO	P_2O_5
Content% wt.	62. 12	34. 88	0. 5	2. 0	0. 5

2. Grinding conditions

The samples were ground in a vibration mill with Φ15. Φ10, Φ5mm steel balls as grinding media for different times, see Table2, vibration amplitude of the mill is 3mm; vibration frequency is 1500 times/min; the weight ratio of grinding media to sample is 2. 5.

Table 2 Grinding time of samples

Sample	A_1	A_5	A_{10}	A_{20}	A_{30}	A_{40}	A_{70}
Grinding time, h	1	5	10	20	30	40	70

EXPERIMENTAL RESULTS

1. Particle size distribution

All samples were dispersed by ultrasonic

waves before being mearsured and the particle size distributions of sample A_1, A_5, A_{20}, A_{30}, A_{40} were analysed, (see Table 3).

Table3. Particle size distributions of samples

Particle size μm	Cumulative weight%				
	A_1	A_5	A_{20}	A_{30}	A_{40}
0—1	6.1	9.2	13.9	14.7	13.5
1-2	7.9	12.4	18.3	19.5	17.3
2-5	16.9	23.0	34.8	37.2	32.5
5-10	31.8	41.9	57.0	63.4	54.5
10-15	51.5	68.8	86.8	95.3	83.1
15-20	56.2	75.9	90.4	97.5	86.3
20-30	72.1	88.2	98.7	100	90.8
30-40	79.0	90.5	100	100	92.5
40-50	88.8	93.2	100	100	94.4
50-60	94.8	94.6	100	100	93.8
60-80	100	100	100	100	100

Table3 shows that the content of fine particles increases steadily with grinding in the initial 30h; when the grinding time exceeds 30h, however, the particle size increases, the reason is that the samples were first microminiaturized by the outer grinding action in the grinding process, meanwhile, the fine particles can adsorb on each other to form aggregates. In the early stage of grinding, the surface free energy of particles is low because of the low specific surface area, and the opportunity of aggregating between particles by the adsorbing force is smaller, so the particles were microminiaturized constantly with grinding. At the same time, the surface free energy also increases, when the grinding time is too long, the surface free energy will be large enough to cause the fine particles to aggregate together under the effect of surface adsorption, these aggregates were then compressed to form agglomerates under the mechanical pressure. The strength of the agglomerates is high enough and they can not be dispersed by ultrasonic waves, so in Table3, we can find that the partical size increases with grinding when the grinding time is over 30h.

2. Crystal structure

XRD is an effective method to study the crystal structure. The sample A_0 (perfect crystal belite sample) A_1, A_{10}, A_{70} were analysised. (see Fig. 1).

The results show that the crystal forms of belite in sample A_0 are mainly β form, only a little γ-form exists (ds3. 00), and α. α′ form can not be found. Fig. 1 also indicates that the crystal forms of belite do not change after grinding. Meanwhile, it seems that the peaks in XRD patterns divert to high angles, and the distances between crystal faces (d values) decreases constantly with grinding, this indicates that the grinding action will cause the crystal unit cell dimensions of belite to change.

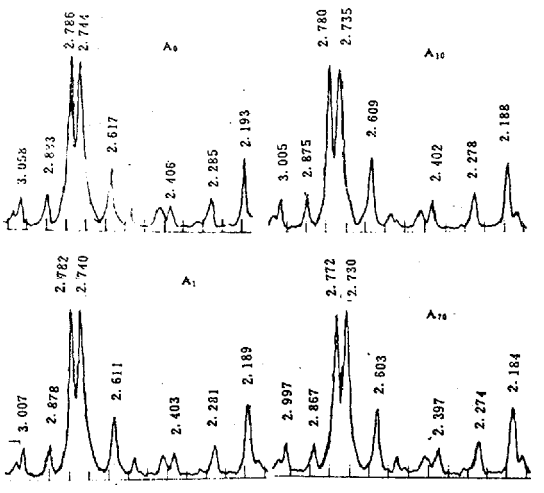

Fig. 1 XRD patterns

The changes of crystal structure will cause the relative scattering intensity and the peaks in XRD patterns to change. The intensity values of all peaks and their half—peak width may reflect the crystallinity and the relative crystal lattice strain of belite. the relation between half—peak width and the lattice distortion may be represented by Halls equation:[14]

$$\frac{\beta\cos\theta}{\gamma} = \frac{1}{D} + \frac{\varepsilon\sin\theta}{\lambda}$$

where B is half—peak width (rad); θ is diffraction angle (°); λ is wave length of X—Ray (A); D is crystallite size (Å); ε is relative lattice strain.

It has been verified that $B\cos\theta/\lambda$ is linearly related to $\varepsilon\sin\theta/\lambda$, so the crystallite size and the relative lattice strain may be semi—quantitatively calculated from the cut distance and the slope respectively. The results are shown in Fig. 2.

Fig2 indicates that with the extending of grinding the relative lattice strain increases rapidly at the initial stage of grinding, then increases slowly and tends to a constant value at last. but the crystallite size of belite decreases continuously.

Using the perfect crystal belite as a standard sample (A_0), then the crystallinity of ground belite may be calculated from the relative scattering intensities of all samples in their XRD patterns[15], see Fig. 3

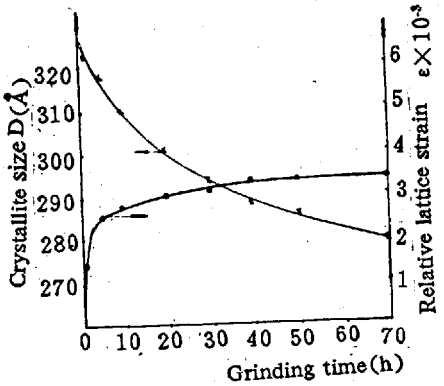

Fig2. Structure distortion of ground belite vs grinding time

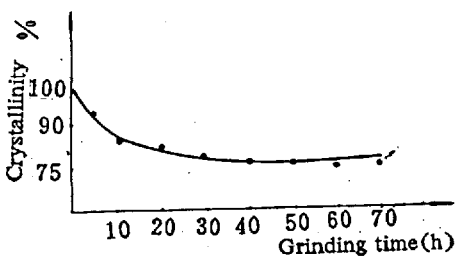

Fig3 Variation of crystallinity of ground belite with grinding.

It can be seen from Fig3 that with the lengthening of grinding, the crystallinity of belite decreases rapidly in the begnning, then decreases slowly, and finally, tends to a constant value. The results of XRD analysis also show that although all characteristic peak intensities weakened after being ground, there exists a large difference in the decreasing amplitude between all peaks. This explains that the grinding effect has selectivity on the crystal faces of belite.

The changes of bonding strength of Si—O bonds and the ionic coordination number of crystal belite may be approximately determined by means of IR, Fig4 is the IR graphs of sample A_1, A_5, A_{20}, A_{40}, A_{70}.

In Fig4, the absorption peaks in the range of 800—1000cm^{-1} are the absorption band (γ_3) of Si—O bonds in $[SiO_4]^{4-}$, and 525cm^{-1} is the absorption band (γ_2) of Si—O bonds. According to J. Schultz etc.,[16], the absorption frequency γ is directly proportional to $K^{0.5}$ (K: Constant of bonding strength), so, when the bonding strength weakens, γ will tend to low wave number; meanwhile, the lower the ionic coordination mumber, the lower the wave number. It can be seen from Fig 4 that there are no changes inpositions and shapes of the peaks in all samples, which indicates that the ionic coordination number and the bonding strength of Si—O bonds will not change during the grinding.

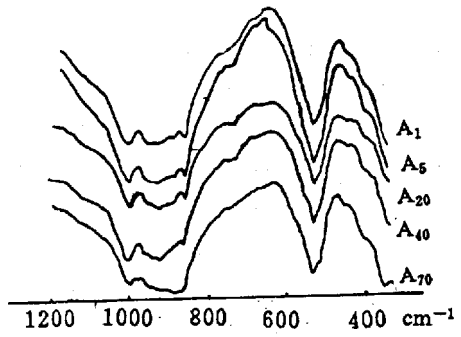

Fig. 4 The IR graphs of sample A_1, A_5, A_{20}, A_{40}, A_{70}.

3. Surface characteristic

In order to study the variations of the surface activity of belite with grinding, the technique of IGC (inverse gas chromatography) was used to study the effect of grinding action on the surface free energy, or the London—dispersion force component and the polar force component.

E. Papirer[17] pointed out that when several kinds of intermolecular interaction occur between the two phases, the free energy of interaction can be given by the sum of London dispersion forces, hydrogen bonds, dipole — dipole interactions, π bonds, donor—acceptor bonds and electrostatic interactions. The dispersion forces are always present, and when one of the phases has its internal interactions limited to dispersion forces (as in saturated hydrocarbons), the surface free energy includes mainly the London—dispersion component (for the other forces are usually negligibly small), for such systems the saturated hydrocarbon (j) may be used as a probe to measure the dispersion force field of the other phase (i) at an interfacial distance dij determined by properties of the hydrocarbon molecules and the dispersion force field of phase i.

Modification of the surface properties of

ground belite is also detectable by IGC. Gray[18] demonstrated a relationship between a chromatographic characteristic (the retention time or the retention volume of a given sulute) and the dispersive component of the surface energy of the chromatographic support. It is a common observation that the specific retention volume (Vg), or the volume (under standard conditions) of carrier gas required to flush the probe through the column containing 1 g of support is linearly related to the number of carbons of n—alkanes injected in the GC. This is also true for belite sample as shown in Fig5.

Further, l_nV_g is connected with the variation in free energy, $\triangle G$, of the system due to adsorption of alkane on the solid surface, If $\triangle G$ of asdorption is equal to $\triangle G$ of desorption, then it is a measure of the surface free energy of the solid. Its volume, however, will depend on the choice of a reference state for the adsorbed molecule of the n—alkanes used as molecular probes for the samples.

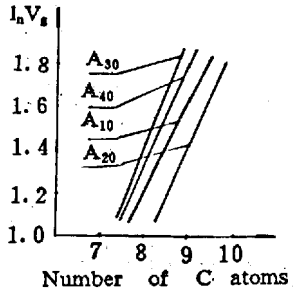

Fig5 Retention volume vs number of C atoms

This choice is necessarily arbitrary. To overcome this theoretical difficulty, Gray proposed determining an increment of $\triangle G$ per CH_2 group, which is simply the slope of the straight line of Fig5. Taking into account Fowkes' [19] assumption which relates the work of adhesion resulting from dispersive reteraction to the mean geometrical value of γ_s^D (the dispersive component of the surface free energy) and γ_L^D (the corresponding value of the alkane or the probe). It is deduced:

$$\frac{\triangle G_{CH_2}}{N.a}=2(\gamma_s^D.\gamma_{CH_2})^{\frac{1}{2}}$$

Where N is the Avogadro number, a is the area of adsorbed CH_2 group or $0.06\times10^{-18}m^2$, γ_{CH_2} is the surface energy of a methylene group which according to Gray is equal to 35mJ. m^{-2} (at 20℃). The γ_s^D of the ground belite samples are collected in Table4, the values, measured at 85℃, are calculated for 20℃, using the relation $d\gamma/dT=-0.056$ mJ. m^{-2}. k^{-1}[20]

Table4 The relation between London—dispersive component and grinding time

Sample		A_{10}	A_{20}	A_{30}	A_{40}
γ_s^D mJ. m^{-1}	at 85℃	22.20	28.08	36.63	29.49
	at20℃	18.56	24.44	32.99	25.85

The conclusions can be obtained from Table 4 that the grinding action is benefical to heighten the London—dispersive component of the belite surface within a suitable grinding time; when the grinding time exceeds 30 h, however, the surface free energy of belite will decrease with grinding. The reason is that many impurities, such as the grinding media wear, could be produced in the grinding process, these impurities would be adsorbed by the grinding surface; meanwhile, the polarization of ions will lead the electric potential field to change and the ions on the surface to distribute again, all these will weaken the surface free energy of belite.

The existance of an energetically homogeneous surface, after treatment, is also apparent when, instead of alkanes, polar molecules are used as molecular probes in the GC experiment. Such molecules will be able to interact with the solid surface through dipole interactions, dipole—induced and dispersive interactions, therefore, it is very diffculut to detect the polar force component, but their interaction intensity may be qualitatively analysed from the retention time of the polar probe molecules.

Fig6 shows the variations of l_nV_g with the logrithm of the vapour pressures of the solutes injected in the column.

The choice of vapour pressure as the varible was made because in a GC experiment the volatility of the probe is obviously important. Fig6 shows that all alkanes fall on a line and the polar molecules fall above another line. This indicates that the polar molecules are retained more strongly than hypothetical alkanes having the same vapour pressure, the reason being that there exists an additional polar interation. With the lengthening of grinding time, the distance between two lines is

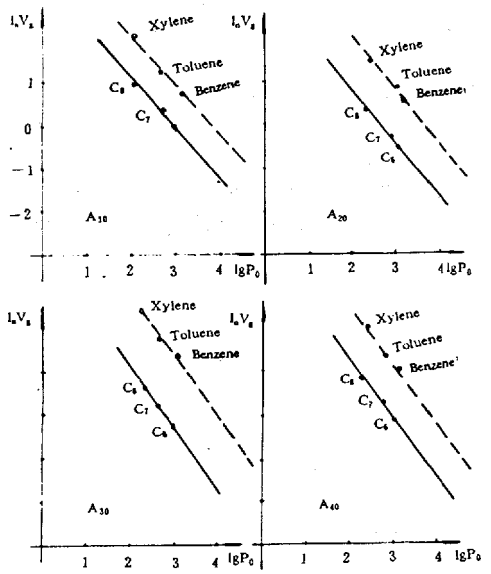

Fig6Retention volume Vs vapour pressure of the solutes

farther, which means that the polar force component of surface free energy is greater. When the grinding time is more than 30 h, howerer, the distance is shortened, which indicates that the polar force component would weaken when the grinding time is too long. As we know, the surface polar interactions of materials come from the polarization and the redistribution of ions on the new surface produced in the grinding process, the longer the grinding time, the more the number of pole—poles on the particle surface and the higher the degree of polarization. This in turn shows stronger polar interactions. But excessive grinding will result in serious destroy which of the surface structure of belite due to the mechanical force. This will result in an amorphous surface structure and make the ions on the surface layer move in a disordered state, so the polar interaction, on the contrary, is weakened.

4. Initial hydration activity.

General evolution of paste electrical conductance during hydration is now well known and hydration rates may be compared by examining the times corresponding to the maximun supersaturations of $Ca(OH)_2$[8], the results are shown in Table5.

Teble5 Times for max. supersaturation(h:m)

Sample	A_1	A_5	A_{10}	A_{20}	A_{30}	A_{40}	A_{70}
t. max	3:25	2:15	1:37	1:05	0:43	0:58	1:22

Table 5 tells us that the maximum supersaturation of $Ca(OH)_2$ occurs earlier when grinding time increases, except for the samples which were ground for over 30 h. This explains that the initial hydration activity of belite would increase rapidly by the grinding within a suitable grinding time; when the grinding time is over 30 h, however, the hydration activity decreased, this change is correctly corresponding to that of the London—dispersive component and the polar force component.

5. Compressive strength of belite paste.

The specimen of cement paste for compressive strength test is 20×20×20mm and the W/C ratio is 0. 28, and the results are shown in Table 6.

Table 6 The compressive strength of samples (MPa)

Hydration age days	A_1	A_5	A_{10}	A_{20}	A_{30}	A_{40}	A_{70}
7	1. 14	3. 68	4. 33	11. 11	14. 30	12. 75	6. 78
14	3. 68	12. 75	18. 87	27. 37	33. 74	26. 33	24. 59
28	12. 01	28. 59	41. 75	42. 57	58. 50	50. 98	42. 89

Table 6 indicates that the grinding action is very helpful for heightening the compressive strength, especially the early compressive strength, of belite paste. The compressive strength at 7—days hydration of sample A_{30} is 14 times that of sample A_1, but excessive grinding is not helpful, because it would cause the particle size to increase and the surface free energy of belite to decrease. It seems that surface free energy is one of the main factors affecting the hydration activity and the compressive strength of belite.

Finally, it indicates that the grinding effect is very helpful for heightening the hydration activity and early compressive strength of belite greatly, but excessive grinding is not helpful. In conclusion, it shows that the treatment with the method of mechanochemical activation of belite is an effective technique to raise its hydration activity and the early compressive strength.

CONCLUSIONS

The following conclusions can be drawn from the experimental results:

1. Grinding for up to 30h would cause the particle size to reduce, but beyond that, the particle size would increase.
2. Grinding could lead the crystal unit cell dimen-

sion of belite to change and the crystallinity to decrease. With prolonging of grinding time, both lattice strain and early hydration activity increased, but the crystal form, ionic coordination number and the bonding strength of Si — O bonds of belite remained unchanged.

3. Grinding would cause the surface characteristics of belite to change. With the lengthening of grinding time, both the London — dispersive component and the polar component of the surface free energy of belite increase continuously, but when the grinding time esceeds 30 h, they will decrease.
4. Grinding may greatly raise the compressive strength of belite paste. Mechanochemical activation is an efficient method of increasing the hydration activity of belite.

ACKNOWLEDGEMENTS

The author gratefully acknowledge Prof. Wei S hiliu for his improving the manucript, and also Zhan Taisheng and Zhang Xiang for their assistance in the experiments.

References

[1] Rangnakar, B. S. ; Srinivasan, V. R. G. and Pai, V. N. ; 5th Int. Congr. Chem. Cem. , Moscow, sept. 1974

[2] Roy, D. M. and Oyefesobi, S. O. ; "Preparation of very reactive Ca_2SiO_4 Powder", J. Amer. Ceram. Soc. , V60, 1977, P178 — 180

[3] Struillou, R. and Arnould , M. ; 7th Int. Congr. Chem. Soc. , V Ⅳ, Partv — 75, paris, 1980

[4] Yang Nanru and Zhong Baigian ; "A study on active β—dicalcium silicate". J. Chinese Ceram. Soc. , V10, 1982, p161—166

[5] Jelenic, I. ; Bezjak, A. and Bujan, M. ; "Hgdration of B_2O_3 — stabilized α′ and β — modifications of dicalcium silicate". C. C. R. , V8, 1978, p173—180

[6] Kanto, D. L. and Weise, C. H. ; "Hydration of various beta—dicalcium silicate preparations". J. Amer. Ceram. Soc. , V62, 1979, p621—626

[7] Fierens, P. and Tirlocq, J. ; " Nature and concentration effect of stabilizing elements of beta—dicalcium silicate on its hydration rate". C. C. R. , V13, 1983, p267—276

[8] Fierens, P. and Tirlocq, J. ; "Effect of synthesis temperture and cooling conditions of beta — dicalcium silicate on its hydration rate". C. C. R. , V13, 1983, p41—48

[9] Stark, J. ; Muller, A. etc ; "Uber aktiven belit — zement". Silikattechnik, V30, 1979, p357—362

[10] Stark, J. ; Rumpler, K. etc ; " Uber aktiven belit — zement ". Silikattechnik, V31, 1980, p50—52

[11] Stark, J, ; Muller, A. etc ; " Uber aktiven belit — zement ". Silikattechnik, V31, 1980, p168—171

[12] Kudrjavceva, N. L. and Chodakov, G. S. ; Silikattechnik, V24, 1973, p63

[13] Schrader, R. and Schumann, H. ; Silikattechnik, V22, 1971, p344

[14] Boldyrew, V. ; Treatise on Mat. Sci. and Tech. V19, 1983, p212

[15] Dhlberg, S. M. and Strickler, D. W. ; "Determination of percent crystallinity of partly devitrified glass by x—ray diffraction", J. Amer. Ceram. Soc. , V45, 1962, p170—171

[16] Schultz, J. , Tsutsumi, K. and Donnet, B. ; " Surface properties of high—energy solids ; Determination of the dispersive component of the surface free energy of mica and its energy of adhension to wate and n—alkanes". J. Colloid and Interface Sci. V59, 1977, p272—276

[17] Papirer, E. ; Schultz, J. and Turchi, C. ; " Surface properties of a calcium carbonate filler treated with stearic acid". Eur. Polymer J. , V20, 1984. p1155—1158

[18] Dorris, G. M. and Gray, D. G. ; J. Colloid and Interface Sci. , V77 1980 p353

[19] Fowkes, F. M. ; " Calculation of work of adhension by pair potential summation. " J. Colloid and Interface Sci. , V28, 1968, p493—505

[20] Wu, S. ; " Interfacial and surface tensions of polymers", J. Macromol. Soc. , VC10, 1974, p1—70

CHARACTERISTICS OF MASONRY CEMENT PRODUCED AT 975 °C IN FLUIDIZED BED BOILER

Fu Zicheng*, Cui Enshu*, Qin Zhigang*, Zhong Baiqian and Yang Nanru****

**Cement Research Institute, China Building Materials Academy, Beijing, P R CHINA*
***Nanjing Institute of Chemical Technology, Nanjing, P R CHINA*

SUMMARY

Crushed marl and low-grade coal were used as raw materials to obtain "blended clinker" at 950–1000℃ in fluidized-bed boiler by addition of small amounts of $CaCl_2$ and CaF_2. The clinker formed at low temperature consisted of C_2S, C_2SCaCl_2, $C_{11}A_7CaCl_2$, $C_{11}A_7CaF_2$, CA, f-CaO, SiO_2, MgO, etc.. It was ground with the appropriate amount of gypsum and slag to produce masonry cement.

The cement hydrates quickly in the early stage. The soundness of the cement conforms to that prescribed in the standard although it contains a high content of free CaO. The development of strength in the later period was satisfactory—the compressive strengths reached 20.6 MPa and 35.6 MPa in 28 days and 180 days respectively.

〔摘要〕 泥灰岩和劣质煤破碎后经少量 $CaCl_2$ 和 CaF_2 处理并作为燃料在 950–1000℃ 的流化床锅炉内煅烧获得"混合熟料"。这种在低温下形成的熟料其组成主要为 C_2S、C_2SCaCl_2、$C_{11}A_7 \cdot CaCl_2$、$C_{11}A_7CaF_2$、CA、f-CaO、SiO_2、MgO 等。用该熟料并掺入适量的石膏和矿渣共同粉磨制得砌筑水泥。

该水泥早期水化快，虽含 f-CaO 相当高但安定性完全合格，其后期强度的发展及其稳定性均令人满意—其 28 天和 180 天抗压强度分别达 20.6MPa 和 35.6MPa。

INTRODUCTION

Fluidized bed boilers (i.e. FBB) are increasingly being used in Chinese industry since they have advantages of using low-grade coal and higher efficiency in heat transfer. But the large amount of cinder from FBB causes pollution and this restricted the popularization of fluidized bed burning technology.

Only small amount of the cinder has been used as blending material of cement so far. The best way, however, to resolve this problem is to transform the cinder into cement clinker in the FBB itself.

It is common knowlege that the sintering temperature of Portland cement clinker is 1450℃ whereas the operating temperature of FBB is 900–950 ℃ at which there is no appearance of liquid phase i.e. no C_3S is formed at this condition. Based on this concept the study tried to make C_2S as much as possible through the solid state reactions at the operating temperature of FBB by addition of the proper amount of calcareous raw materials and small amount of mineralizer.

Two materials, crushed marl and granulated raw meal with coal were respectively used for experiments in both lab and industrial FBB and similar results were obtained from both of the materials. In this paper the results from experiments using marl as main material and the characterics of the cement are reported.

MAIN RAW MATERIALS USED IN EXPERIMENTS

The analysis of raw materials and low-grade coal used in the experiments are shown in Table 1 and Table 2 respectively.

Table 1. Chemical analysis of raw materials

	Loss	SiO_2	Al_2O_3	Fe_2O_3	CaO	MgO	K_2O	Na_2O
Marl-1	36.42	13.92	3.80	1.44	39.96	3.04	0.78	0.05
Marl-2	38.26	10.06	2.85	1.18	43.49	3.10	/	/
Cinder of PX Coal		65.02	27.35	4.47	1.02	1.67		
Cinder of ZX Coal		66.83	28.18	2.58	0.90	1.10		

Table 2. Industrial analysis of low-grade coals

	H_2O %	Ash %	Volatile %	Fixed Carbon %	Heating Value KJ/Kg
PX Coal	1.06	68.09	13.94	17.65	7933
ZX Coal	0.31	51.96	16.86	30.87	14007

RESULTS OF EXPERIMENTS AND DISCUSSION

Preparation of Masonry Cement

The crushed marl (< 7mm) was treated with small amounts of CaF_2 and $CaCl_2$ (using an industrial waste) which adhered to the surfaces of the marl particles, then calcined in a furnace at

950℃ and 1000 ℃ respectively to obtain "clinker" in laboratory.

The industrial test was conducted in a FBB of capacity 20T / hr and equipped with a 3000 KW turbogenerator.

Crushed marl was mixed with low-grade coal and small amounts of mineralizer ($CaCl_2$ and CaF_2) propotionally. Having a heat output of 8047 KJ / kg the mixture was used as fuel for the FBB where the bed temperature was controlled at 950–1000℃ (975℃ on an average) and the fuel was burning well with the result that the output of the boiler reached and even exceeded 20 T / hr.

The so-called "blended clinker" from FBB including calcined marl and cinder of low-grade coal was cooled in an induced draft duct and examined by X-ray diffraction. The main minerals of "blended clinker" were found to be β-C_2S, C_2SCaCl_2, $C_{11}A_7CaX_2$ (X = Cl^- or F^-) and CA as shown in Fig.1. Unreacted components such as SiO_2, MgO and free CaO were also present in it.

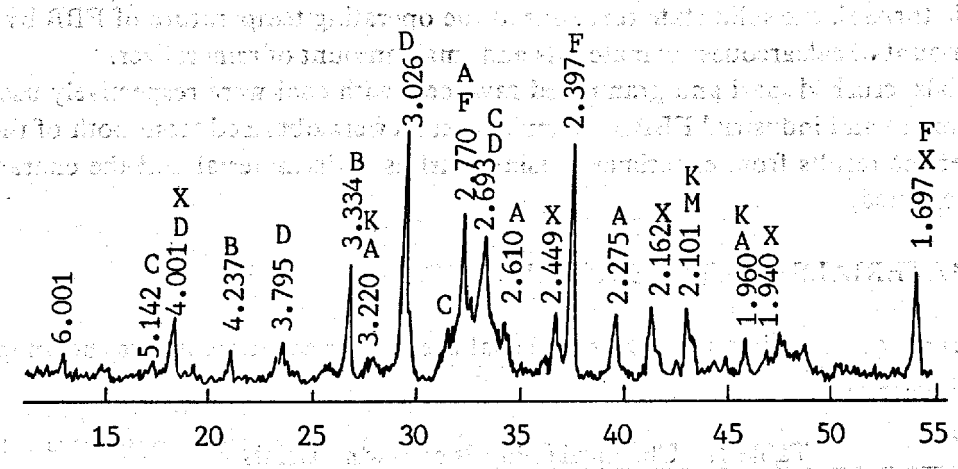

A–C_2S; B–SiO_2; C–C_2SCaCl_2; D–$C_{11}A_7CaCl_2$
M–MgO; X–$C_{11}A_7CaX_2$; F–f–CaO; K–CA

Fig.1 XRD pattern of the clinker–marl calcined at 950–1000℃

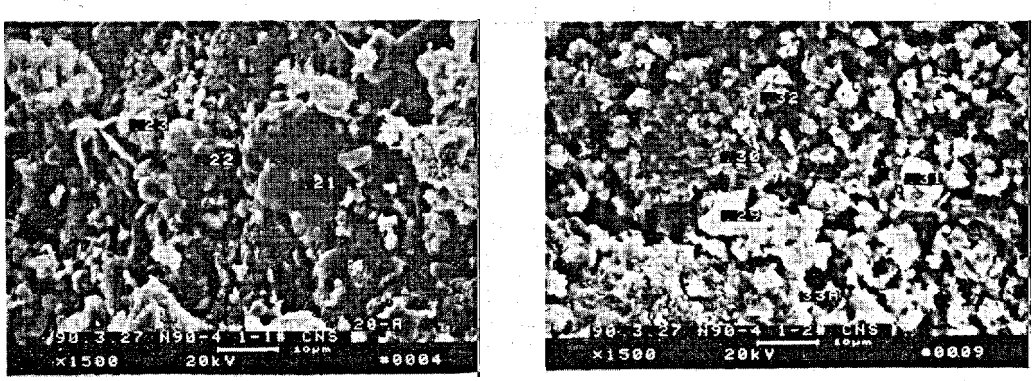

(a) (b)

Fig.2 SEM micrographs of marl caclined at 1000℃
(a) without mineralizer; point 21, 22, 23, f–CaO;samll and round partieles: C_2S
(b) Treated with $CaCl_2$; point 29, 30, 31 32: $C_{11}A_7CaCl_2$;samll particles: C_2SCaCl_2 and C_2S

Fig.2 shows the minerals in the "clinker" when examined by SEM.

The masonry cement in this study was prepared by grinding "blended clinker" with slag and an appropriate amount of gypsum in the proportion "clinker" / slag = 85 / 15. Table 3 shows the chemical composition of these materials.

Table 3. Chemical composition of FBB cinder and masonry cement

	Loss	SiO_2	Al_2O_3	Fe_2O_3	CaO	MgO
FBB cinder (fine)	6.70	37.62	15.35	2.87	32.69	2.91
FBB cinder (coarse)	9.77	37.02	14.36	2.74	31.27	2.63
Masonry Cement	8.58	38.27	13.65	2.76	27.08	3.40

Properties of Masonry Cement

Physical Properties— Table 4 shows the physical properties of the masonry cement made from FBB cinder. These properties are in accordance with the Chinese standard GB3183–82 #175 and close to #225 masonry cement.

Table 4. Physical properties of masonry cement

Sample No.	Fineness* %	Initial Setting Time (hr:min)	Final Setting Time (hr:min)	Normal Consistency %	Soundness	Bending stren. MPa		Comp. stern. MPa	
						7d	28d	7d	28d
9032	4.2	0:56	1:10	36.0	satisf.	2.9	5.7	9.0	24.3
9035	4.7	1:08	2:45	35.0	"	3.1	6.5	10.4	25.7
9038	4.8	0:58	1:50	36.0	"	3.5	6.0	10.1	25.4
9115	9.0	1:30	2:48	36.0	"	2.9	6.4	8.8	20.6

* The residue on 80μm sieve.

Hydration Properties— The heat of hydration was measured by a thermoelectric conduction calorimeter under the condition of w / c = 0.8 and temperature at 20℃. The results can be seen in Fig.3. In order to explain the appearance of of the peaks on the exothermic curve of early hydration, samples hydrated at different ages (10, 50, 90 and 180 min.) were prepared and examined by XRD and DTA. From the results it has been found that the first peak was mainly due to hydration of $C_{11}A_7CaX_2$, CA, a small part of CaO and the formation of ettringite from the reaction between calcium aluminate hydrate and gypsum. The second peak resulted from the hydration of CaO.

The hydration rate was observed by estimating the amount of bound water and $Ca(OH)_2$ which is shown in Table 5.

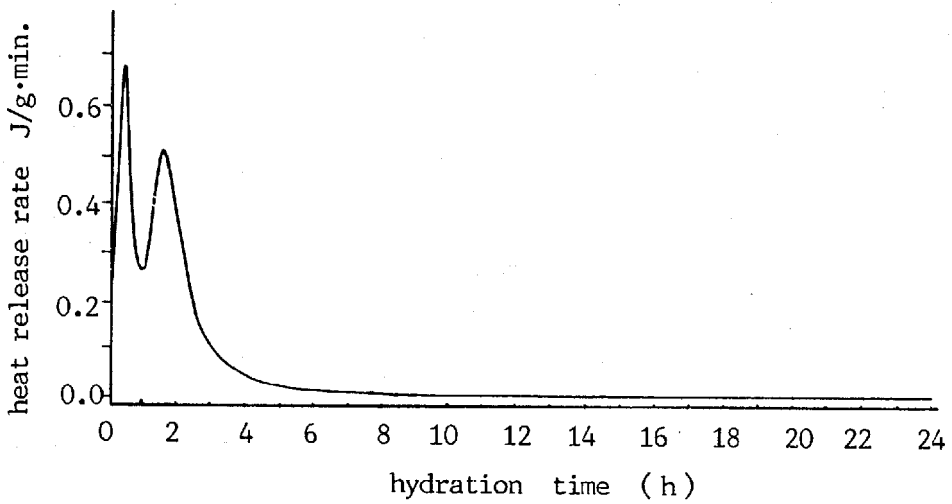

Fig.3 Hydration heat relase of the masonry cement

Table 5. Bound water for samples hydrated at different ages

	2h	6h	1d	3d	7d	15d	28d
% $Ca(OH)_2$	18.29	17.39	16.82	15.66	15.49	13.58	12.84
% Bound H_2O	11.23	13.40	13.95	14.76	/	15.84	16.25

It can be seen from the table that the percentage of bound water increases rapidly in the early stages due to the rapid hydration of $C_{11}A_7CaX_2$ and CA; and the slow increase of bound water content in later stages results from the reaction between $Ca(OH)_2$ and slag to create calcium silicate hydrate. DTA and XRD were employed to determine the hydrates which were found to be ettringite, tetracalcium aluminate hydrate, $Ca(OH)_2$ and calcium silicate hydrate etc. (see Fig.4 and Fig.5).

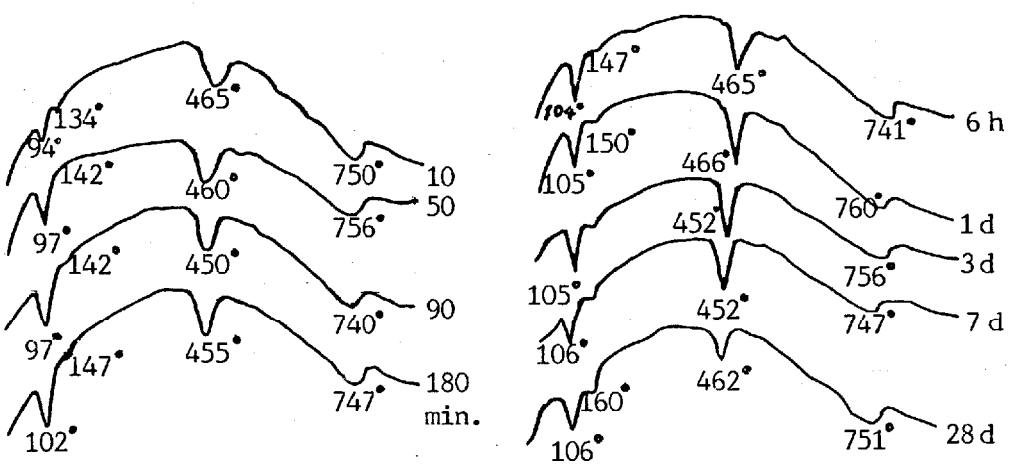

Fig.4 DTA curves of specimens for different hydration ages

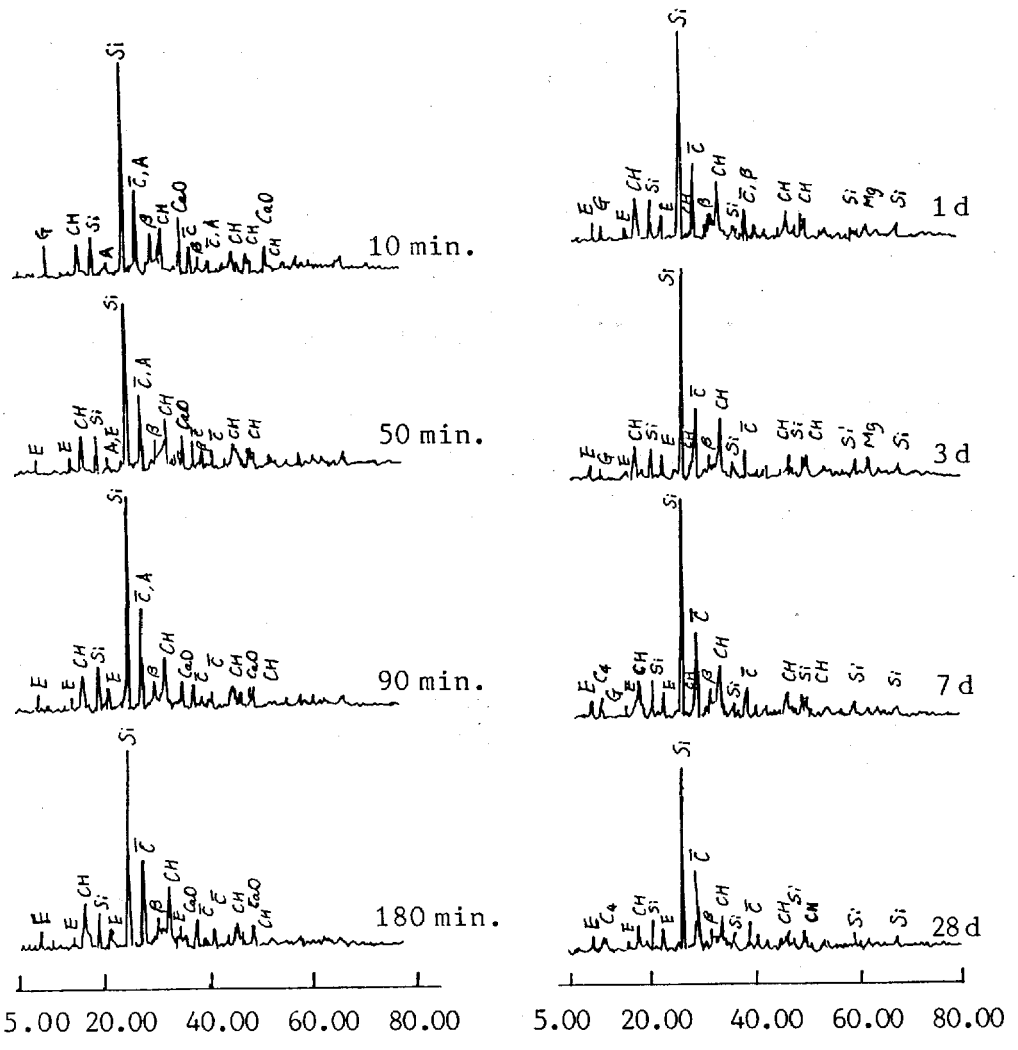

E–$C_3A \cdot 3CaSO_4 \cdot 32H_2O$; G–$CaSO_4 \cdot 2H_2O$; C_4–C_4AHx; CH–$Ca(OH)_2$
A–$Al(OH)_3$; $\bar{C}$–$CaCO_3$; β–β–C_2S; Si–SiO_2; Mg–MgO
Fig.5 XRD patterns of specimens for different hydration ages

Soundness and Long-term Stability—The soundness of the cement produced at 975℃ seems to be doubtful since it contains free CaO as much as 10–12%. So several specimens (w / c = 0.35; 10 × 10 × 40 mm^3) were made and both autoclave expansion and boiling tests were conducted respectively. Results indicated that the expansion percentages ranged from 0.065% to 0.094%, which is much less than 0.5%, the value prescribed by the standard. It stands to reason that the activity of the free CaO formed at low temperature is much better than that formed at high temperature. It hydrates immediately when meeting water and reacts within a short time. For the second reason when milling this cement an appropriate amount of slag was added, which played the role in dilution of free CaO during the early stage and it reacted with $Ca(OH)_2$ to form calcium silicate hydrate which helped in improving the strength of the cement.

Because of the high content of free CaO in the cement, $Al(OH)_3$ from hydration of CA and $C_{11}A_7CaX_2$ are susceptible to form calcium aluminate hydrate. Also the high pH of the cement liquid phase is helpful for the anti-carbonation. No obvious change in the hydration products has

been found in 28 days. The strength of later age increased steadily without falling back and the stability was satisfactory. The compressive strength and the bending strength of the cement reached 35.6 MPa and 7.5 MPa in 180 days respectively.

CONCLUSION

— When calcining marl and low–grade coal at 950–1000℃ in the presence of small amounts of $CaCl_2$ and CaF_2 cement minerals such as β–C_2S, CA, C_2SCaCl_2, $C_{11}A_7CaX_2$ are formed. The compressive strengths of the masonry cement made from the cinder of FBB and slag reached 20–25 MPa (in 28 days).

— In spite of the high content of free CaO in the cement there is no problem of unsoundness because this free CaO formed at low temperature has high activity leading to rapid and complete hydration.

— The late age strength and stability of the cement produced in FBB are satisfactory.

ACKNOWLEDGEMENTS

The authors appreciate the help of their colleagues, Wang Xiangming, Zhang Yuchang, Tong Guishan and Wang Jinyuan in carrying out experimental work. The industrial test was conducted in cooperation with Kang Qifu, Shi Zhenglun from Zhejian University and Cai Jinqiang et al. from Hunan Coal Research Institute.

ION EXCHANGE REACTION OF GRANULATED BLAST FURNACE SLAG IN ACID SOLUTION

S Aoki* and Y Arai**

**Department of Applied Chemistry, Nihon University Junior College*
***Faculty of Science and Engineering, Nihon University*
JAPAN

SUMMARY

It is known that the corrosion of alkali silicate glass in water or in acid solution is caused by the exchange of alkali ion in the glass with the H^+ in water or acid solution. As slag is mainly composed of glass of $CaO-SiO_2-Al_2O_3$ system, it is considered that a similar reaction with glass occurs between slag and water. In that case, the reaction could be expressed as equation (1).

$$Slag-(SiO^-)_2Ca^{2+} + 2(H^+ + OH^-) \rightleftharpoons Slag-(SiOH)_2 + Ca^{2+} + 2OH^- \quad (1)$$

In order to accelerate this reaction, the following two reactions are considered. ① : H^+ (acid) is added to the slag slurry for taking away OH^- as H_2O from the solution. ② : EDTA is added to the slurry for taking away Ca^{2+} as Ca-EDTA.

The present paper mainly deals with method ① in order to accelerate the above reaction.

By adding dilute HCl solution drop by drop into slag slurry, the reaction of equation (1) was remarkably accelerated. Judging from these results, it is assumed that the reaction between slag and water or acid solution, proceeds by ion exchange of Ca^{2+} in slag with the H^+ in water or acid solution. The hydration reaction of slag was examined from the viewpoint of ion exchange of Ca^{2+} in slag with the H^+ in water.

要　　旨

アルカリケイ酸塩ガラスの水または酸溶液による浸食は，ガラス中のアルカリイオンと水または酸溶液中の H^+ とのイオン交換反応により起こるが知られている。スラグは $CaO-SiO_2-Al_2O_3$ 系ガラスであるから，スラグと水との間にも同様な反応が起こると考えられる。その場合，その反応は (1)式で表される。

$$Slag-(SiO^-)_2Ca^{2+} + 2(H^+ + OH^-) \rightleftharpoons Slag-(SiOH)_2 + Ca^{2+} + 2OH^- \quad (1)$$

このイオン交換反応を進行させるには，つぎの二つの方法が考えられる。①スラグスラリーに H^+ (酸) を加え，生成したOH^- を中和し，H_2O とする方法と，②EDTAを加え，Ca^{2+}を Ca-EDTAとしてしまう方法である。ここでは，主に①によるイオン交換反応の進行を検討したもので，スラグスラリーに酸(H^+) を加え，OH^- を中和し，H_2O として除去した場合に，(1) 式のイオン交換反応はどのように進行するか，また，このようにして処理したスラグはどのような性質を持つかを検討した。

INTRODUCTION

For the activation of granulated blast furnace slag (hereinafter referred to as slag), the reaction of slag with acid solution was studied and it was clarified that the basic components, such as CaO and MgO reacted with acid preferably (1). A similar phenomenon is observed in alkali silicate glass and the corrosion of the glass in water or acid solution proceeds by the selective dissolution of alkali ions. It is considered that the solution of alkali ions from alkali silicate glass into water or acid solution is caused by the exchange of alkali ions in the glass with the H^+ ion in water or acid solution. If slag is assumed to be a glass of SiO_2-Al_2O_3-CaO system, the hydration reaction of slag and the reaction of slag with acid solution are supposed to proceed by the ion exchange reaction of the alkaline-earth ions such as Ca^{2+} and Mg^{2+} in the slag with the H^+ ion in the water or the acid solution (2). In this paper it has been examined whether the reaction of slag with acid solution can be made to proceed by ion exchange reaction or not and what kind of properties the ion exchanged slag has.

MATERIALS AND METHODS

Materials

The composition and Blaine values of the granulated blast furnace slags used in this study are shown in Table 1. While slags A and B are normal ones for slag cement, C, D and E were ground specially fine. The differences in composition between the slags are not large.

Table 1 Chemical composition and finess of slags

Slag	CaO	MgO	Al_2O_3 wt%	SiO_2	Fe_2O_3	Blaine cm²/g
A	42.2	6.8	13.4	34.8	0.4	3430
B	42.4	6.8	13.9	34.2	0.3	3980
C	41.7	6.8	13.4	35.0	0.3	6330
D	42.4	6.8	13.4	34.7	0.4	8230
E	41.6	6.9	13.6	35.0	0.4	8690

Ion Exchange Reaction of Slag with H^+ in the Solution

E.L.Shamy studied the alkali removal reaction from alkali silicate glass into water and got the following results (3). When glass comes into contact with water, Na^+ which is modifier in the glass reacts at first with the H^+ in water as indicated in the equation (1)

$$\geqslant SiO^-Na^+ + (H^+ + OH^-) \rightleftharpoons \geqslant SiOH + Na^+ + OH^- \quad (1)$$

(ion exchange reaction of Na^+ in glass with H^+ in water) and Na^+ and OH^- are formed in the water. With the increase of OH^- in the water, it becomes gradually alkaline, and the network structure of silicate in the glass is destroyed by the alkaline water, and the corrosion of the glass proceeds.

If it is assumed that slag is composed of the glass of SiO_2-Al_2O_3-CaO system and Ca^{2+} in slag acts as modifier, it is supposed that slag reacts with water according to the equation (2) and the slurry becomes alkaline when slag is dispersed in water.

$$Slag\text{-}(SiO^-)_2Ca^{2+} + 2(H^+ + OH^-) \rightleftharpoons Slag\text{-}(SiOH)_2 + Ca^{2+} + 2OH^- \quad (2)$$

When the slag is dispersed in water, the pH of the slurry increases fairly high, but the reaction shown in the above equation will stop soon because the degree of dissociation of water is so small as 10^{-7} and the reaction does not proceed any more.

In order to proceed the ion exchange reaction, it is necessary to remove the Ca^{2+} or OH^- out of the system. The following two methods, (a) and (b), were examined for the purpose (4). (a) Neutralize the OH^- formed by adding H^+ and make water. (b) Form EDTA-Ca by adding EDTA.

(a) $2OH^- + 2H^+ \rightarrow 2H_2O$

(b) Ca^{2+} + EDTA → EDTA-Ca + $2H^+$

Since method b has been reported already (4), method a will be principally presented in this paper. We tried to neutralize only the OH^- formed in the slag slurry by adding HCl solution.

Titration Curves of Slag Slurry with HCl Solution

When slag is dispersed and stirred in water, the pH of the slurry increases soon and attains between 10.5 and 11.0 in the equilibrium of equation (2). Then, the slurry is neutralized by adding hydrochloric acid solution using a burette. As a result, the equilibrium of equation (2) moves to the right and the slurry becomes alkaline again soon. So, in order to neutralize it, HCl solution is added again. The slag slurry dispersed in water is apt to become alkaline even after being neutralized, so HCl solution of fixed concentration is added at an appropriate rate into the slag slurry so that the pH of the slurry reaches a stable value. We refer to the plot of the amount of hydrochloric acid solution added against time as the titration curve of slag slurry. In this experiment, 50g slag was dispersed in 500mℓ water and the slurry is stirred at 300 rpm and 2N hydrochloric acid solution was run into the slurry at 50 ℃.

Calculation of degree of ion exchange and some other measurements

The degree of ion exchange between the Ca^{2+} in slag and the H^+ in HCl solution was calculated from the titrated volume of HCl solution and the component of CaO and MgO in slag (referred to as CaO). This was compared with the estimated values of CaO, MgO, Al_2O_3 and SiO_2 in the solution after the titration. CaO and MgO were determined by EDTA method and Al_2O_3 and SiO_2 were determined by an atomic absorption spectroscopy.

The slag treated with HCl solution was separated from the slurry and washed with deionized water. The slag is referred to as acid-treated slag or HCl-treated slag. The acid-treated slag was examined by SEM and analysed chemically. The Ca^{2+} binding capacity of the acid-treated slag was determined from the decrease of Ca^{2+} concentration in the water when 0.5 gram of HCl-treated slag was dispersed in 100 mℓ of 10° DH (hard water, 10mg-CaO/100mℓ-water) for 90 minutes.

Intensity test of slag cements

Slag cement was made by mixing slag, gypsum and slaked lime in the proportion 100/5/1 by weight. Briquettes of size 2.0 x 2.0 x 8.0 cm^3 were made from it with a water cement ratio equal to 0.50. The briquettes were demolded after 24 hours and kept in water at 30℃ till taken out just prior to testing. Compressive and bending strengths of the briquettes were determined at 3, 7 and 28 days using an Amsler hydraulic testing machine.

RESULTS AND DISCUSSION

Titration curve of slag slurry and influence of pH on the curve

Figure 1 shows the titration curves which were obtained by adding 2N HCl solution into the slurry of slag A so as to bring its pH to 7.0, 5.0, 4.0 and 3.0 respectively. Furthermore, the degree of ion exchange calculated from the volume of 2N HCl solution is shown on the Y axis at right.

The shape of all the titration curves is alike. In the initial stages of titration the tendency of the slag slurries to become alkaline is very strong and accordingly the volume of titrated HCl solution increases rapidly. However this tendency becomes weaker with increasing addition of HCl solution and the titration rate of HCl solution becomes slower in order to keep a stable pH. In other words, the rate of ion exchange reaction expressed as equation (2) is fast in the beginning of HCl titration, but the reaction becomes more difficult to

proceed with increasing addition of HCl.

E.L.Shamy concluded that the reaction of alkali removal from alkali silicate glass in acid solution is determined by the rate of transfer of ions through the corrosion layer. It is suggested that the ion exchange reaction of slag in water or acid solution expressed as equation (2) is rate-determined by the transfer of H^+ and Ca^{2+} through the hydrated silicate layer, such as Slag-$(SiOH)_2$ formed by the ion exchange reaction. Therefore, it is supposed that the reaction of slag with acid solution proceeds very fast in the beginning, but slows down later because the hydrated silicate layer formed in the reaction becomes thicker and the movement of H^+ and Ca^{2+} through it gets restricted.

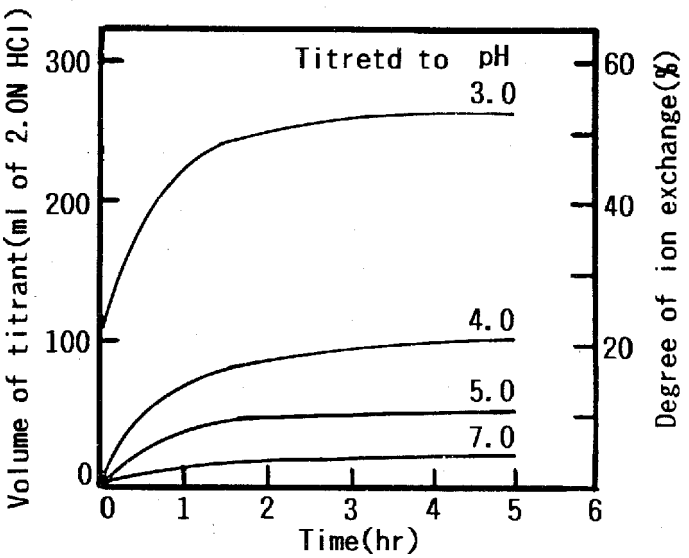

Fig.1 Titration curves of slag A slurries with 2.0N HCl(50g slag/500ml H_2O)

The curve for pH 7.0 is way down in the figure, which means that the rate of the ion exchange reaction expressed as equation (2) is very slow at this pH. However, the lower the pH values of the slurries, the higher the position of the titration curves. At the end of 6 hours reaction the degree of ion exchange of the slags increases progressively from 4 %, through 12% and 18% to 54% for the pH values 7.0, 5.0, 4.0 and 3.0 of the slurries.

Low pH in the slurry means high concentration of H^+ in the slurry. Therefore, when the pH of the slurry is low, the concentration of H^+ on the left side of equation (2) becomes high and the equilibrium shifts to the right side, which signifies the progress of the forward reaction.

Influence of NaCl addition to slurry on the titration curve

Slag D was dispersed in NaCl solutions of various concentrations and then the slurries were titrated with HCl solution so as to bring their pH to 4.0. The titration curves obtained in this series of experiments are shown in Figure 2. The titration curves figure higher with increasing concentration of NaCl in slurries, which means that the ion exchange reaction of Ca^{2+} in slag with H^+ in acid solution is quickened by the presence of Na^+. The degree of ion exchange of the slurries in 6 hours increases from below 40 % in the slurry

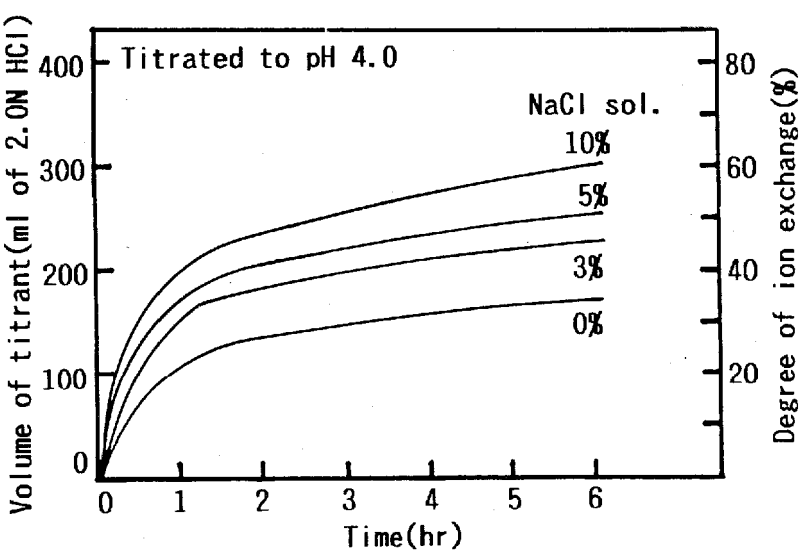

Fig.2 Titraton curves of slag D slurries in the solution of various NaCl concentration with 2.0N HCl(50g slag/500ml solution)

with water to near 70 % in the slurry with 10 % NaCl solution.

In the study of the corrosion of glass containing Na_2O, K_2O and PbO, R.L. Lehman et al. reported that Ca^{2+} moves slowly while Na^+ and K^+ move fast in the corrosion layer (5). Though the mechanism is not clear, it is thought that the movementof Ca^{2+} in the hydrated silicate layer is accelerated in the presence of ions, such as Na^+ and K^+ which are able to move easily in the layer.

Components in the liquid phase of slag slurry by the titration with acid solution

In order to clarify what kinds of slag components and how much of them get dissolved into the liquid phase in the reaction with acid solution, the following experiments were done. The solid and liquid phases were separated by filtration from slurry after the titration with HCl solution. The CaO, MgO, Al_2O_3 and SiO_2 in the liquid phase were analysed. The relationship between the degree of ion exchange and the degree of dissolution of the above components of slag was investigated. Furthermore, the degree of ion exchange and the degree of dissolution of components were calculated from the titrated volume of HCl solution and the analytical values of the components in the liquid phase. The results obtained are shown in Figure 3.

Judging from Figure 3, even though the degree of ion exchange in the slurry increases, which means, increase in the volume of HCl solution added into the slurry, the degree of dissolution of Al_2O_3 and SiO_2 from the slag into liquid phase increases little. On the contrary, the degree of dissolution of CaO and MgO increases with the increase of the degree of ion exchange calculated from the volume of HCl solution added. SiO_2 and Al_2O_3 in alkali silicate glass are network forming components whereas Na_2O, CaO and MgO are modifier components in glass. Therefore, it is assumed that only Ca^{2+} and Mg^{2+} work as modifier components in the slag dissolved in the liquid phase by the ion exchange reaction with H^+ in solution. Consequently, it is considered that Ca^{2+} and Mg^{2+} are dissolved without destruction of the -Si-O-Si-O- network of the slag.

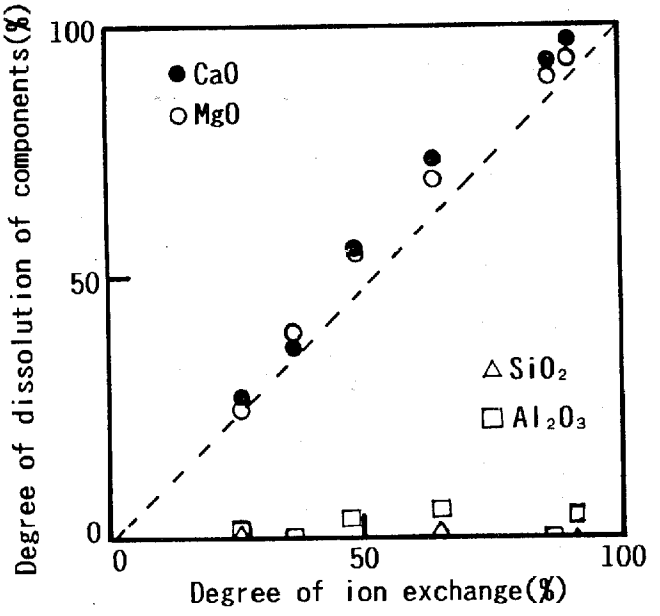

Fig.3 Relation between degree of ion exchange and degree of dissolution of components (50g slag/500ml H_2O)

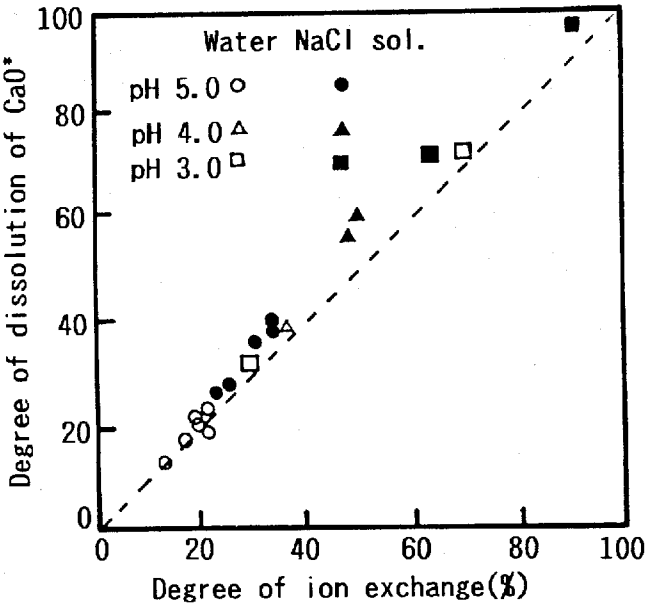

Fig.4 Relation between degree of ion exchange and degree of dissolution of CaO* (CaO*=CaO+MgO)

In order to clarify the ion exchange reaction, the relation between the degree of ion exchange calculated from the titration curves and the degree of dissolution of CaO plus MgO into the liquid phase from the slag with various slurries is shown in Figure 4. The degree of CaO plus MgO dissolution in slag with deionized water coincides precisely with the degree of ion exchange, but with NaCl solution, the degree of dissolution is slightly larger than the degree of ion exchange. From this, it is considered that a part of Ca^{2+} in the slag is replaced by Na^{+} directly.

Relationship between titration curves of slags and their activities

The titration curves of various slags are shown in Figure 5 and their compositions and Blaine values of them are given in Table 1. Though compositions of slags A, B, C, D and E used in this experiment do not differ much, but the differences in their fineness are very large, their Blaine values respectively being 3,430, 3,980, 6,330, 8,230 and 8,690 cm^2/g. As the titration curves are influenced by the fineness of the slag, they figure progressively higher in the figure with the increase in fineness. Which means that the rate of ion exchange reaction of the slag becomes faster, signifying in turn that the activity of the slag becomes higher with increase in fineness of the slag.

In order to know the activity of the slags, the compressive strengths of slag cements made from them were measured. The relationship between the degree of ion exchange after 3 hours at pH 7.0 (refer to Fig.5) and the compressive strenghs of the briquettes of the slag cements at 7 days is shown in Figure 6.

In Figure 6, the strengths increase with the degree of ion exchange of slags. As compressive strength is a measure of the activity of slags, it should be possible to know the activity of a slag

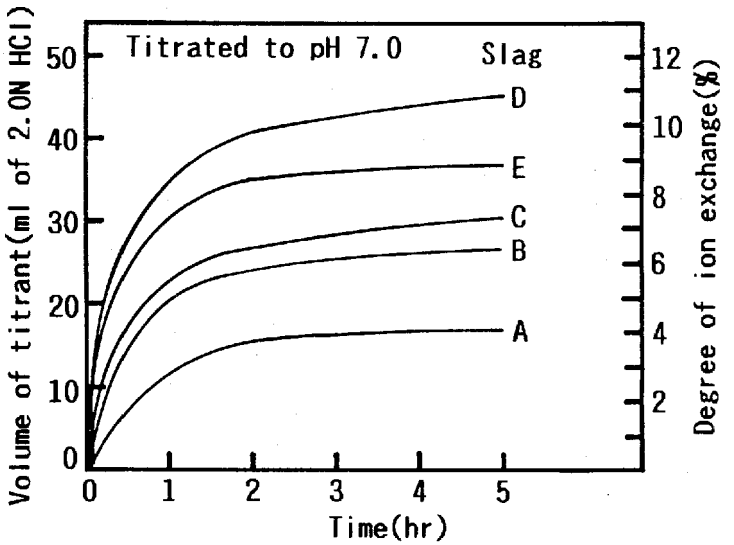

Fig.5 Titretion curves of various slags slurries with 2.0N HCl(50g slag/500ml H_2O) (A:3430cm²/g, B:3980cm²/g, C:6330cm²/g, D:8230cm²/g, E:8690cm²/g)

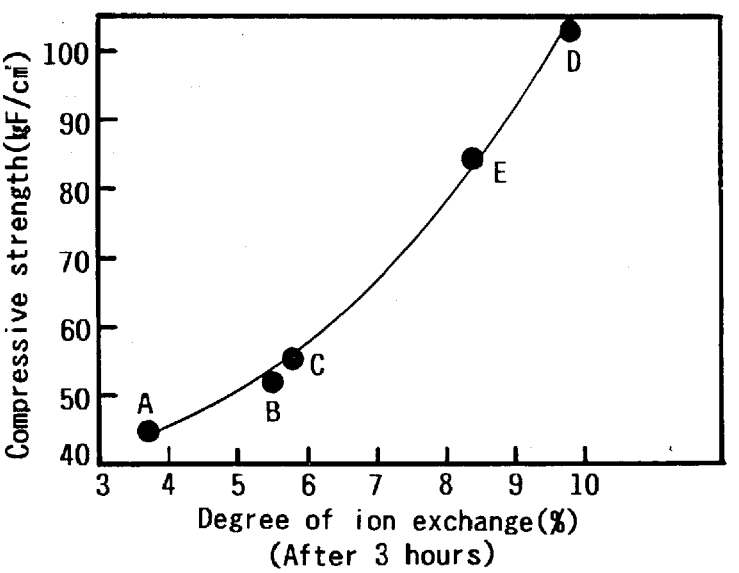

Fig.6 Relation between degree of ion-exchange of various slags after 3 hours and compressive strength of the slag-cement after 7 days (A:slag A, B:slag B, C:slag C, D:slag D, E:slag E)

from its titration curve.

Ca^{2+} catching ability of acid treated slag

Acid treated slag retains the original -Si-O-Si-O- network structure of slag since only the Ca^{2+} in the slag has been exchanged by H^+ in HCl solution. Therefore, it can be presumed that HCl treated slag again takes up Ca^{2+} when dispersed into the Ca^{2+} containing solution. So, the Ca^{2+} uptake ability of acid treated slag was determined.

Figure 7 shows the Ca^{2+} uptake capacity of HCl treated slags after various degrees of ion exchange. The Ca^{2+} uptake capacity is expressed as Ca^{2+} mili ion per gram slag (Ca^{2+} *mion/g* slag) and was determined from the decrease of Ca^{2+} concentration in the water when 0.5 gram of HCl treated slag was stirred in 100*ml* of the hard water (the hardness is 10 DH° (10 mgCaO/100*ml*water)) for 90 minutes.

In Figure 7, the Ca^{2+} uptake capacity of HCl treated slags increases with increase in the degree of ion exchange. This means that HCl treated slag can take Ca^{2+} in again, which incidentally explains the use of HCl treated slag as softener of hard water.

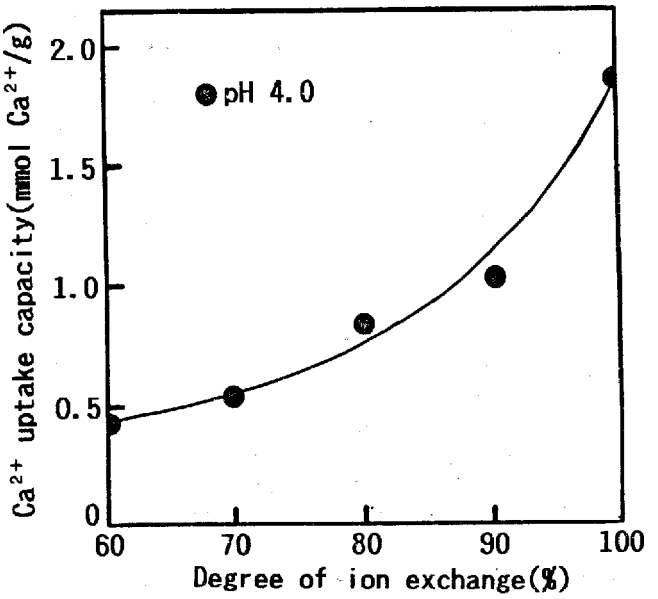

Fig.7 Ca^{2+} uptake capacity of acid trted slag

CONCLUSIONS

The results clarify that the reaction of slag with HCl solution can be promoted by ion exchange reaction of the Ca^{2+} in slag with H^+ in the solution, in which case, Ca^{2+} and Mg^{2+} are dissolved without destruction of the -Si-O-Si-O- network of the slag. The activity of slag can be estimated by the titration curve of slag slurry with HCl solution. The HCl treated slag is expected to find the use as Ca^{2+} catching agent.

REFERENCES

1. Aoki, S., Kiso, M. and Arai, Y.: "Behavior of Granulated Blast Furnace Slag in Hydrochloric Acid Solution", *Gypsum & Lime* , No.191, 24 (1984).
2. Kondo, R.: "Properties and Utilization of Ironmaking and Steelmaking Slags", *J. Iron and Steel Inst. Jap.* , 65, 1794 (1979).
3. Shamy, E.L.: "The rate-determining step in the dealkalisation of silicate glasses", *Phys. Chem. Glasses*, 14, 18 (1973).
4. Aoki, S., Fujisawa, H. and Arai, Y.;"Ion Exchange Reaction of Granulated Blast Furnace Slag in Acid Solution", *Gypsum & Lime* , No.204, 17 (1986).
5. Lehman, R.L., Yoon, S.C., McLaren ,M.G. and Smyth, H.T.: "Mechanism of Modifier Release from Lead-Containing Glasses in Acid Solution", *Amer. Ceram. Soc. Bull.*,57, 802 (1978).

SUITABILITY OF RICE HUSK ASH OBTAINED BY FLUIDIZED-BED COMBUSTION FOR BLENDED CEMENT

N Hara*, H Noma*, S Honma, S Samrejprasong*** and S Uparisajkul*****

Government Industrial Research Institute, Kyushu, JAPAN
***Government Industrial Development Laboratory, Hokkaido, JAPAN*
****Thailand Institute of Scientific and Technological Research, Bangkok, THAILAND*

SUMMARY

It was found out that controlled burning of rice husk by a fluidized-bed burner gives ash comprising amorphous silica with high SiO_2 content and high specific surface area. In addition, the temperature control of fluidized-bed combustion is easily obtainable by controlling the feeding speed of rice husk in case that the air supply is set at the optimum velocity.
Relationship was investigated of its burning conditions with physico-chemical properties of rice husk ash thus obtained. Besides, suitability of this ash as an ingredient for blended cement was compared with those of rice husk ashes obtained by conventional combustion in terms of pozzolanic reactivity with Portland cement or lime at 20°C and 80°C. The results showed that pozzolanic reactivity of the ash obtained by fluidized-bed combustion was excellent and it gave a good compressive strength even in curing at 20°C.

要　約

もみがらを流動床方式で燃焼すると、高シリカ含有率で高比表面積の非晶質シリカより成る灰が得られることを明らかにした。最適な空気供給速度の場合、もみがらの供給速度をコントロールすることによって流動床燃焼温度は容易にコントロール可能である。

その燃焼条件と得られるもみがら灰の物理的・化学的性状の関係を検討した。更に、流動床燃焼で得られるもみがら灰の混合セメント用混合材としての適性を、ポルトランドセメントまたは石灰との養生温度２０℃および８０℃におけるポゾラン反応性として、通常の燃焼法で得られるもみがら灰と比較した。その結果、流動床燃焼で得られるもみがら灰はすぐれたポゾラン反応性を有し、養生温度２０℃でも良好な圧縮強さを示すことがわかった。

INTRODUCTION

Rice husk ash is used as a pozzolanic ingredient with high SiO_2 content for blended cement. Its pozzolanic reactivity is much dependent on its amorphousness and surface area, both of which are well affected by the burning conditions of rice husk (1).
It was found out by the present authors (2) that controlled burning of rice husk by a fluidized-bed burner gives the ash comprising amorphous SiO_2 with high specific surface area. Relationship between the burning condition and properties of the resulting ash was investigated. Furthermore, its suitability as a pozzolanic ingredient for blended cement was compared with those of rice husk ashes obtained by other combustion methods.
Results thus obtained are given and discussed in this paper.

EXPERIMENTAL

1. Fluidized-bed Combustion of Rice Husk

Fig. 1 shows a fluidized-bed burner used for this experiment. The combustion chamber was made of a stainless steel tube with 159 mm in inner diameter and 1000 mm in length. Four litres of silica sand with particle size ranging from 297 μm to 590 μm was used to form a fluidized-bed. Air was supplied through a perforated plate set at the bottom of the

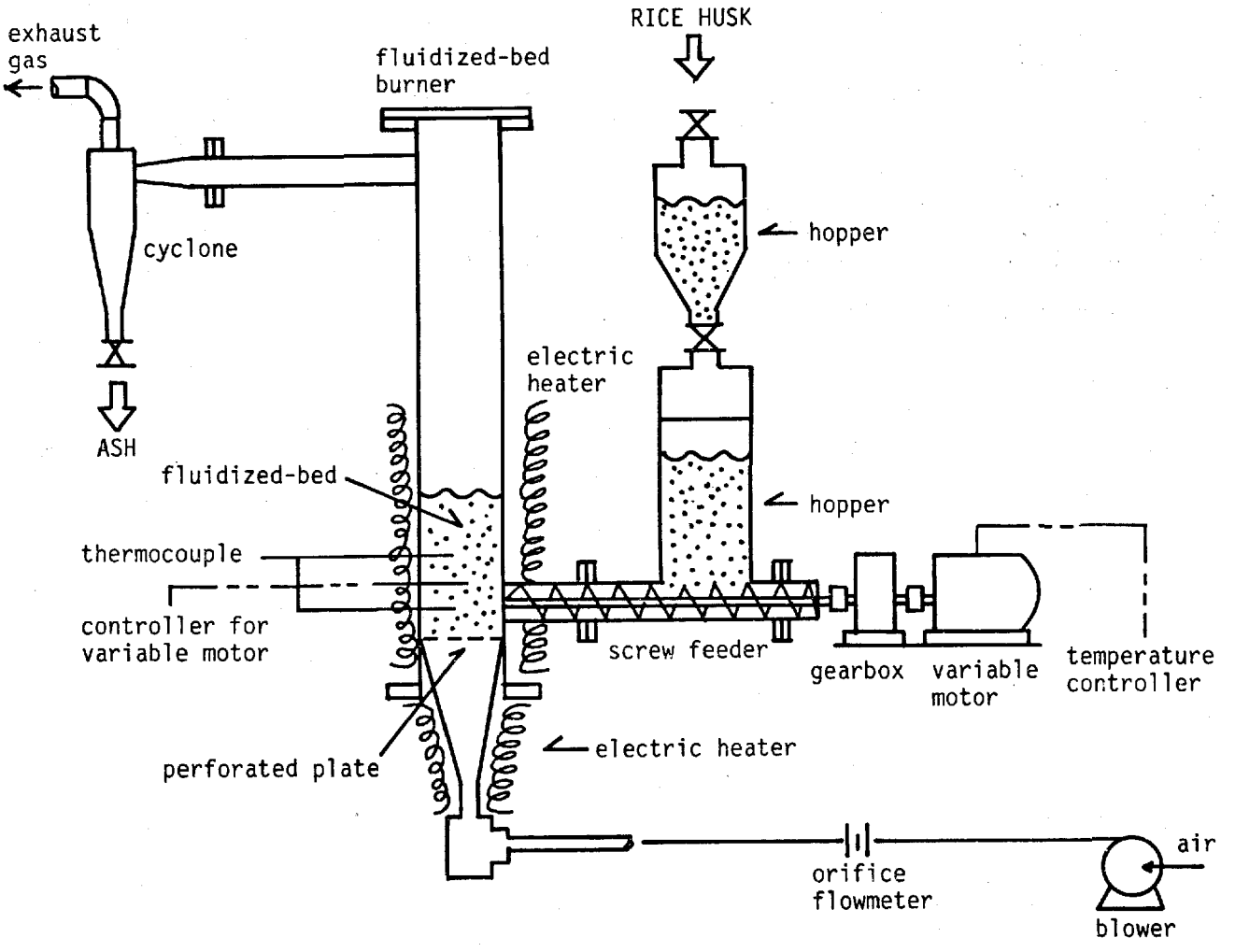

Fig. 1 Fluidized-bed burner for rice husk.

combustion chamber. The fluidized-bed was first preheated by electric heater to 500°C and then feeding of rice husk was started using a screw feeder. Once rice husk was ignited, heating by the electric heater was stopped. The combustion temperature, which was monitored in the fluidized-bed, was controlled only by the feeding speed of rice husk. The air supply was fixed at velocity 15 cm/second. The retention time of ash in the combustion chamber was only a few seconds and the discharged ash was collected through a cyclone collector. The exhaust gas was almost smokeless.
The ash was sampled at combustion temperatures 650, 750, 850, 920 and 1000°C, respectively, and given for scanning electron microscopy (SEM), x-ray powder diffractometry (XRD), surface area determination by N_2 gas adsorption and chemical analysis.
The amorphousness of ash was determined by XRD using its diffraction peak profile (3). Namely, the peak area of broad diffraction attributable to glassy phase of silica ranging from 12° to 35° CuKα2θ was assumed to be proportional to the content of glassy phase by weight, viz. its amorphousness. The amorphousness of the ash obtained by first smouldering for a few minutes on a heating plate and then heating at 600°C for 15 minutes (Sample D in Table 1) was assumed to be 100 % and used as a control, because it showed the highest amorphousness among ashes sampled from various origins.

2. Pozzolanic Reactivity of Rice Husk Ash Blended with Portland Cement

The rice husk ash from fluidized-bed combustion along with two kinds of ashes with different amorphousness, viz. Sample A, B and C in Table 1, were used for this experiment. 1.5 g of each ash, which was ground to less than 30 μm in particle size by an agate pot mill, and 3.5 g of an ordinary Portland cement (OPC)# were well mixed, dispersed in 100 ml of water and kept in a stoppered polyethylene bottle. This mixing ratio corresponds to that of "Class C of Portland pozzolan cement" regulated in the Japanese Industrial Standard (JIS R5212).
These mixtures were cured at 20°C and 80°C for the period from 7 days to 91 days. At required intervals, viz. 7, 14, 28 and 91 days of the reaction time, a portion of each mixture was pipetted, filtered, dried in a vacuum desiccator and given to XRD, differential thermal analysis (DTA) and thermogravimetry (TG). As a control, OPC by itself was hydrated under the same conditions as the above.

3. Hardening Properties of Rice Husk Ash Blended with Lime

Two kinds of rice husk ash, viz. Sample A and C in Table 1, were chosen for this experiment.
Four parts of the ground rice husk ash with particle size less than 30 μm and one part of slaked lime by weight were thoroughly mixed and water was added. The optimum water/solid weight ratio for the mix of the ash from fluidized-bed combustion was 0.6 and for that of the open-field burnt ash was 0.4. This difference in the water/solid ratio was derived from different surface areas of the ashes, viz. 50.8 m^2/g for the former ash and 2.5 m^2/g for the latter. The mixes were press-moulded into a cylindrical compact with 19 mm in diameter and 19 mm high under the moulding pressure of 100 kg/cm^2. The compacts were hardened by curing at 20°C for 3 to 28 days, or by steam curing at 80°C for 1 day.
The hardened compacts were dried in a vacuum desiccator at room temperature and given for measurement of the apparent bulk density and compressive strength. A portion of each hardened compact was finely ground to be given for XRD and DTA-TG.

RESULTS AND DISCUSSION

1. Fluidized-bed Combustion of Rice Husk

The temperature control of fluidized-bed combustion was easily obtainable by controlling

---

Chemical composition (%) : Ig loss 0.6, Insol 0.1, SiO_2 22.2, Al_2O_3 5.6, Fe_2O_3 2.9, CaO 64.4, MgO 1.7, SO_3 1.9, Total 99.4%.
Density 3.16 g/cm^3; Blaine specific surface 3,140 cm^2/g.

the feeding speed of rice husk in case that the air supply was set at the optimum velocity. The fluctuation of combustion temperature was very small during the long run. Chemical compositions and some properties of the ash along with those of ashes obtained from different combustion methods are summarized in Table 1.
The open-field burnt ash was slightly pinkish white-coloured and well crystallized into cristobalite and tridymite. The boiler ash was black-coloured due to residual carbon and partially crystallized into cristobalite. The ash from fluidized-bed combustion was grey-coloured and glassy with high amorphousness.

SEM images of these ashes are shown in Fig. 2.
The ash from fluidized-bed combustion still kept its original texture of rice husk, i.e. porous and brittle, but the boiler ash was well sintered. The open-field burnt ash, which was let stand in a heap of burning rice husk for a few weeks, showed the growth of crystals maybe of cristobalite and/or tridymite. Difference of these textures reflected well their thermal history and had close relations with their specific surface areas.
In fluidized-bed combustion, rice husk charged by a feeder is heated instantaneously up to the temperature of fluidizing sand. The organic matrix of husk may burst to break the texture of husk. Its combustible part is burnt out and the resulting ash is instantaneously quenched by discharging into a cyclone collector. All these processes are completed within a few seconds. These explain the reasons why fluidized-bed combustion tends to produce amorphous silica with high specific surface area.
Specific surface area and ignition loss of the ashes from fluidized-bed combustion obtained at different combustion temperatures are illustrated in Fig. 3. It shows that even in fluidized-bed combustion, the control of combustion temperature is an important factor to control the specific surface area of the resulting ash. Through SEM and XRD study along with these results, it was concluded that 750°C was the optimum combustion temperature to obtain ash with high SiO_2 content, high amorphousness and high specific surface area.

Table 1 Chemical and mineral compositions and specific surface area of RHA.

Sample No.	Ig. loss	SiO_2	Al_2O_3	Fe_2O_3	TiO_2	CaO	MgO	Na_2O	K_2O	P_2O_5	Total
A	3.59	92.46	0.65	0.48	0.03	0.89	0.14	0.30	0.81	0.35	99.70
B	4.24	91.50	0.34	0.19	0.03	0.74	0.54	0.06	1.85	0.49	99.98
C	0.50	97.12	0.14	0.04	tr	0.31	0.35	0.04	1.11	0.37	99.98
D	4.18	91.69	0.14	0.06	0.01	0.58	0.26	0.09	2.54	0.52	100.07

Sample No.	Specific surface area, m^2/g	Amorphousness wt.%	Crystalline phases of silica
A	50.8	85.8	glass
B	11.0	49.9	cristobalite
C	2.5	14.5	cristobalite, tridymite
D	25.6	100.0	glass

Origin of sample :
A. Sapporo, Japan, 1983. From a fluidized-bed burner operated at 750°C.
B. Thailand, 1983. From a RH burner for 3,000 kW electric power generation plant.
C. Malaysia, 1982. Open-field burnt ash.
D. Tosu, Japan, 1981. RH was first let smouldering for a few minutes on a heating plate. The 'charred ash' was further heated at 600°C for 15 minutes.

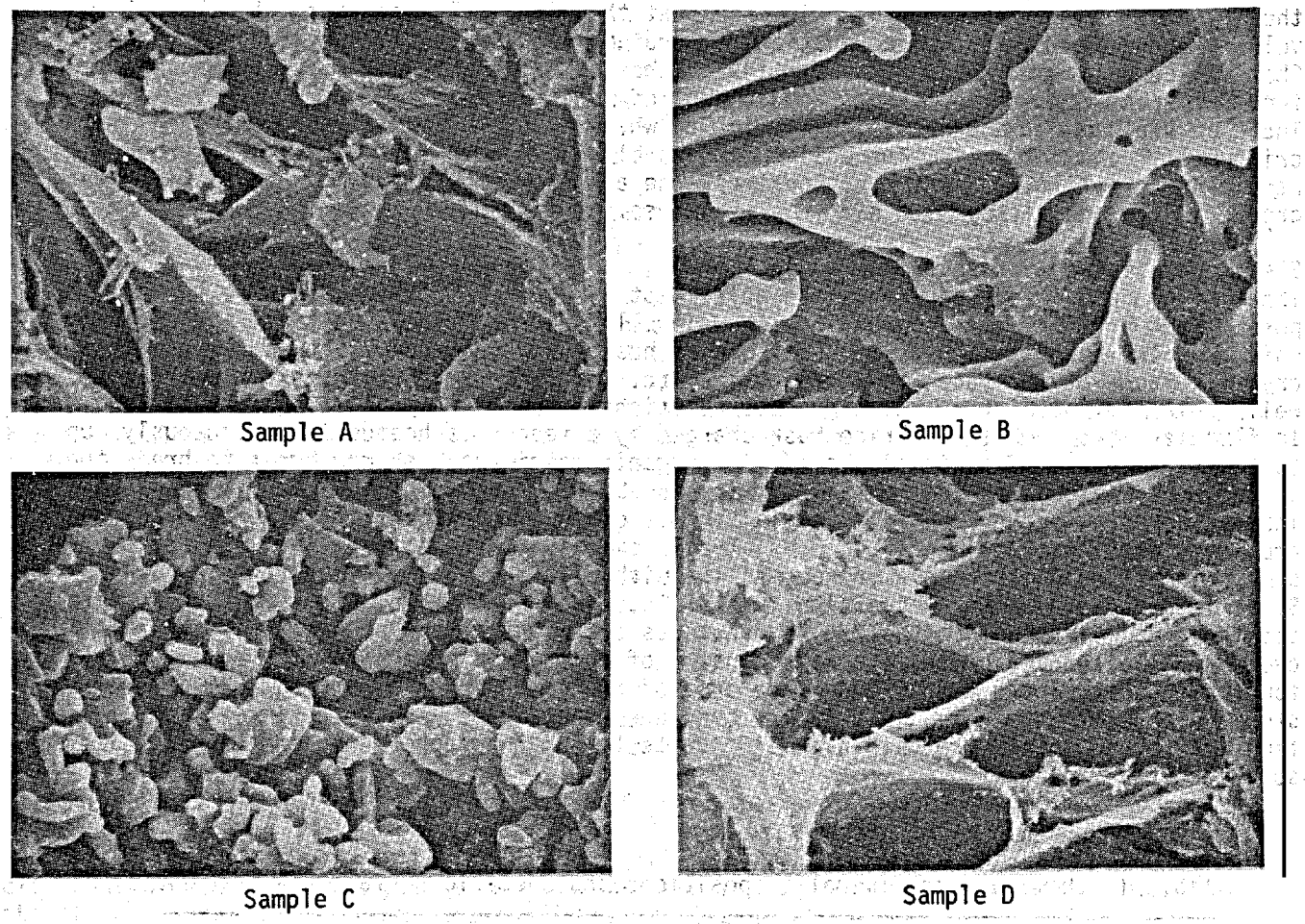

Fig. 2 SEM images of rice husk ashes.
(Refer to Table 1)

2. Pozzolanic Reactivity of Rice Husk Ash Blended with Portland Cement

Pozzolanic reactivity of rice husk ash blended with OPC was discussed based on reaction products determined by XRD and DTA, and uncombined $Ca(OH)_2$ determined by TG from the weight loss due to its dehydration to CaO occurring at temperatures ranging from 450°C to 500°C. The latter results are shown in Fig. 4.
In the reactions at 20°C, OPC gave $Ca(OH)_2$, C-S-H, ettringite and monosulphate. The long term reaction tended to increase the formation of these phases except ettringite. Addition of rice husk ash increased the formation of C-S-H, which was due to the pozzolanic reaction of rice husk ash with $Ca(OH)_2$ liberated by the hydration of OPC. In terms not only of the consumption of uncombined $Ca(OH)_2$ as shown in Fig. 4, but also of the yield of C-S-H estimated by XRD and DTA results, it could be concluded that the amorphous ash from fluidized-bed combustion was more reactive than the others. Besides, addition of rice husk ash decreased the formation of monosulphate. However, that of ettringite was not affected so much as shown in the case of monosulphate.
In the reaction at 80°C, OPC gave $Ca(OH)_2$, C-S-H and a small amount of ettringite and afwillite. Afwillite crystals grew to a size visible even with the naked eye.
When rice husk ash was added, $Ca(OH)_2$ liberated by the hydration of OPC was completely combined with silica in the ash to form C-S-H(I) within the duration of 7 days.
C-S-H(I) was crystallized into 11Å tobermorite with further duration of the reaction.

The crystalline ash gave 11Å tobermorite more easily than the amorphous ones by contraries. Namely, the open-field burnt crystalline ash gave it over 14-day reaction, but the others did over 28 days. The basal spacing of 11Å tobermorite thus formed was in the range from 11.6Å to 11.8Å, which was characteristic of Al-substituted 11Å tobermorite (4). In terms of the formation of 11Å tobermorite at 80°C, rice husk ash seems to have similar or higher reactivity than glassy silica (5) or fumed silica (6).

3. Hardening Properties of Rice Husk Ash Blended with Lime

Apparent bulk densities, compressive strengths and relative strengths of the hardened compacts are summarized in Table 2. It was confirmed from these results that the amorphous ash from fluidized-bed combustion was superior to the crystalline one as an ingredient for pozzolanic cement when it was hardened by curing at room temperature or by steam curing. The amorphous ash consumed all $Ca(OH)_2$ even by curing for 3 days at 20°C, and gave the higher strength than the crystalline one cured at the same temperature for 28 days or at 80°C. Residual $Ca(OH)_2$ detected in the compacts from the crystalline ash cured at 20°C proved its slowness in reaction, which resulted in its low strength under these curing conditions. In addition, the amorphous ash was superior in order to reduce the apparent bulk density of compacts.

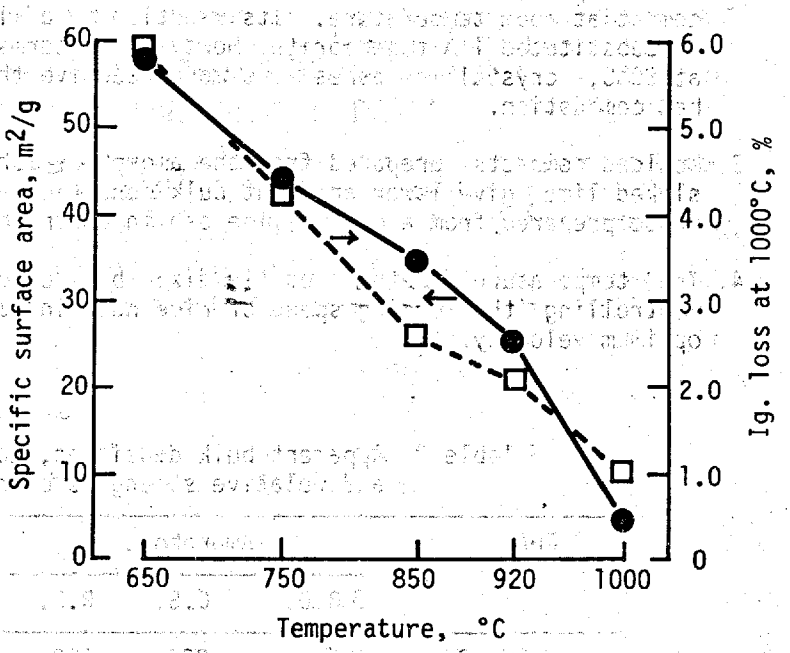

Fig. 3 Specific surface areas and ignition losses of RHAs from fluidized-bed combustion.
Closed circle : Specific surface area
Open circle : Ignition loss at 1000°C

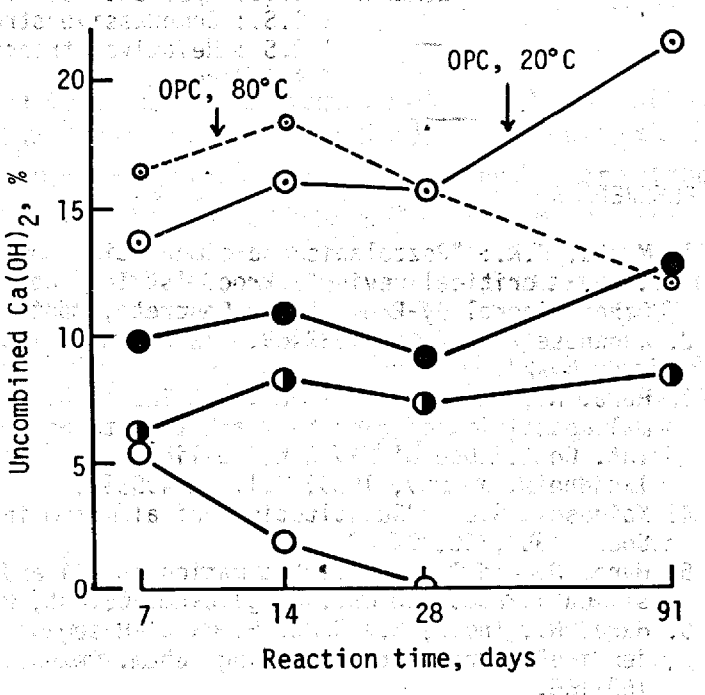

Fig. 4 Uncombined $Ca(OH)_2$ of RHA-OPC mixes reacted at 20°C for 7 - 91 days.
Open circle : Fluidized-bed burnt ash
Half closed circle : Boiler ash
Closed circle : Open-field burnt ash
Circle with dot : OPC (reacted at 20°C & 80°C)

CONCLUSIONS

1. Fluidized-bed combustion of rice husk gives an ash with high SiO_2 content, high amorphousness and high specific surface area, which is suitable to be used as a pozzolanic ingredient for blended cement.

2. The amorphous ash from fluidized-bed combustion has high reactivity with Portland cement at room temperature. Its reaction in a slurry at 80°C gives the formation of Al-substituted 11Å tobermorite. However, in terms of the formation of 11Å tobermorite at 80°C, crystalline ashes are more reactive than the amorphous ash from fluidized-bed combustion.

3. Moulded compacts prepared from the amorphous ash from fluidized-bed combustion and slaked lime give lower apparent bulk densities and higher compressive strengths than those prepared from a crystalline ash in curing both at 20°C and 80°C.

4. The temperature control of fluidized-bed combustion is easily obtainable by controlling the feeding speed of rice husk in case that the air supply is set at the optimum velocity.

Table 2 Apparent bulk densities, compressive strengths and relative strengths of hardened compacts.

RHA	Amorphous			Crystalline		
	B.D.	C.S.	R.S.	B.D.	C.S.	R.S.
20°C, 3d	0.94	224	238	1.22	32	26
20°C, 7d	0.92	118	128	1.23	68	55
	*0.89	167	189	*1.18	73	62
20°C,28d	0.96	206	215	1.17	104	89
80°C, 1d	0.90	158	176	1.18	111	94

Remarks: B.D.: Apparent bulk density, g/cm^3.
C.S.: Compressive strength, kg/cm^2.
R.S.: Relative strength = C.S./B.D, kg/cm^2.
* 2nd run

REFERENCES

1. Mehta, P.K.: "Pozzolanic and cementitious by-products as mineral admixtures for concrete-A critical review". **Proc. 1st Int. Conf. Use of Fly Ash, Silica Fume, Slag and Other Mineral By-Products in Concrete, Montebello, Canada,** 1983, Vol.1, 1-46.
2. Japanese Patent No. 1533469, 12 December 1989. "Fluidized-bed combustion method of rice husk".
3. Hara, N., Yamada, H., Inoue, K., Inoue, N., Tsunematsu, S. and Noma, H.: "Hydrothermal reactivity of rice husk ash and its use for calcium silicate products". **Proc. 3rd Int. Conf. Use of Fly Ash, Silica Fume, Slag and Natural Pozzolans in Concrete, Trondheim, Norway,** 1989, Vol. 1, 499-516.
4. Kalousek, G.L.: "Substitution of aluminum in lattice of tobermorite". J. Am. Ceram. Soc., 1957, **40**, 74-80.
5. Hara, N. and Inoue, N.: "Formation of 10Å and 14Å tobermorite from pozzolanic glassy silica". **Proc. 7th Int. Cong. Chem. Cement, Paris, France,** 1980, Vol. 3, IV-13-18.
6. Hara, N., Inoue, N., Noma, H. and Hasegawa, T.: "Formation and characterization of jennite". **Proc. 8th Int. Cong. Chem. Cement, Rio de Janeiro, Brazil,** 1986, Vol.3, 160-166.

REACTIVITY TEST FOR FINE SILICAS AND POZZOLANIC MINERAL ADDITIVES

C Vernet and G Noworyta

TECHNODES S A
Centre de Recherche Industrielle et Technique du Groupe CIMENTS FRANCAIS,,
FRANCE

ABSTRACT :

We have developed a new reactivity test for fine silica and pozzolanic additives. It is based on the measurement of their reaction kinetics with C_3S. The dormant period duration is measured using electrical conductivity monitoring. At the end of the test, the chemical balance of the filtrate is made, the solid phases are analysed using X–ray diffraction. This allows to evaluate the C_3S reaction rate with pozzolanic additives, in chemical conditions very close to the setting and hardening of cement.
Results for a series of reactive silicas are given, the surfaces of which range from 0.4 to 450 m2/g. The C_3S dormant period is shortened by two mechanisms: (i) portlandite nucleation on ultra–fine particle surface,(ii) dissolution of the silica particles, producing silicate ions, and acting as a "calcium pump". Calcium consumption by reactive silicas increases both the dissolution rates of portlandite, and C_3S. Electron microscopy was carried out for hydrates characterisation, the dissolution of portlandite crystals and the CSH morphology were observed, in agreement with the chemical diagnosis.

1 INTRODUCTION.

The effectiveness of pozzolanic additives depends on their ability for filling pores, and of their chemical reactivity. This one can be evaluated using classical tests, like the CHAPELLE test (1), which measures the potential lime consumption. The experimental procedure (boiling with excess lime) is far from cement hydration conditions. So that it does not reflect the rate at which the cement releases its lime to react with the pozzolana. This is particularly true with reactive pozzolanas and silica fumes.
Another classical test (french standard NF P15 462) consists in reporting on the equilibrium diagram of portlandite the figurative point of the solution in contact of a cement-pozzolana blend. This test is close to the typical hydration conditions, but does not take into account the nature of the hydrates formed by reaction of the lime and pozzolana. Forming calcium aluminates is obviously less favourable than forming CSH, either for rheology or for strength and durability. The aim of this research is to test a series of pozzolanic additives, with large behaviour differences, using a kinetic method. C_3S is used as the lime source, and this enables a progressive and cement-like production of lime . Thus a possible calcium aluminate or sulfoaluminate formation can be easily detected, in the absence of C_3A and C_4AF which could introduce some confusion.

2 - EXPERIMENTAL PROCEDURE.

The kinetic test uses a set of complementary methods: electrical conductivity monitoring (ECM), solid and liquid phases chemical analysis, X-ray diffraction (XRD), thermogravimetry (TG), scanning electron microscopy (SEM), and laser granulometry. We only describe here the unusual procedures.

2.1. Kinetic test using electrical conductivity monitoring.

All the reactions are performed at 25°C. A detailed description of the significance of conductivity variations during cement hydration is given elsewhere (2).
Synthetic C_3S (4000 cm2/g) is blended with finely ground pozzolanic materials. For highly reactive silicas and silica fumes, the blends are composed using the ratio Pozzolana:C_3S = 1:10
For calcined clays and classical pozzolanas, we use the ratio Pozzolana:C_3S = 10:1, and gypsum is added in the ratio gypsum:pozzolana = 1:10
The blends are kept in suspension with a water to solid ratio of 8, allowing a good stirring in each case, even for very fine particles. In these conditions, the pH and concentrations are close to cement conditions. If necessary, for simulation of alkali-rich cements, a K_2SO_4 solution, calculated on the cement composition base, can be used for the test (2). Simultaneous tests can be easily performed with the same stirring speed, (typically 200 rpm) using a magnetic multi-sample stirrer, and a computerized measurement and data acquisition system (conductometric multiplexer). After 72 hours, the suspension is filtered, and the solution and solid phases are analysed using XRD and TG. 10% of finely ground silicium (under 20 microns) are added as an internal standard to the fraction of the solid used for XRD.

2.2. Sample preparation for SEM.

For SEM observation of the microstructure, we use pastes made of the same blends as for conductometric tests. For economy of C_3S, we developed a micro-method. The blends are kept in 1 ml plastic syringes equipped with a micro-filter and a "luer-lock" 3-way valve. The dry blends are pressed to a constant volume, after weighing to obtain a constant porosity (0.5), like in a Blaine cell. The mixing water is introduced after vacuum-exhaustion of the air contained in the cell, by turning the 3-way valve. The samples are kept at 25°C for hydration, and demolded by cutting the end of the syringe and pushing with the piston. Then they are vacuum-dried, cut and carbon-coated for microscopy.

3 - STUDY OF A SERIES OF REACTIVE SILICAS.

We have chosen samples largely differing by their nature, their reactivity, and their particle sizing. Two of them are amorphous hydrated silicas, with a large internal microporosity (ZEOS, TSO).
CABO is an anhydrous pyrohydrolised microsilica. VAW is a silica fume, SILM is a cristobalite

from calcined flint. ATTA is a natural mineral, containing fine attapulgite needles, opal and silica particles. XRD and MAS NMR spectra (not shown here), show large differences of network organisation, and of silanol groups contents for these samples.

3.1. Characterisation.

The particle sizing, and chemical characteristics of these samples are listed below **(table 1)**.

3.2. Kinetic behaviour.

For all the samples, the dormant period duration is shorter than for the standard sample of C_3S **(fig.1)**.

So the accelerating effect of pozzolanas is detectable from the very first hours of hydration.

The conductometric curves show large differences between the lime saturation levels. Two samples rapidly reach the undersaturation domain of portlandite. (ZEOS after 7h, CABO after 32h).

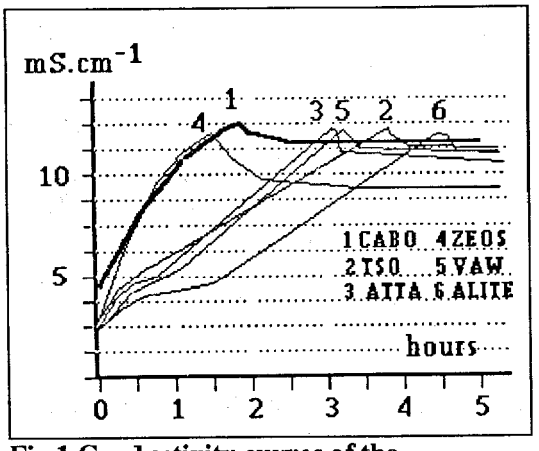

Fig.1 Conductivity curves of the C_3S–silicas blends.

Table 1 Particle sizing and surface.

Sample	CABO	ZEOS	TSO	ATTA	VAW	SILM	ALIT
median diameter (microns)	**0.01**	**8.4**	**11.3**	**12.7**	**8.1**	**1.5**	**11**
% passing at:							
2 microns	**0**	**1.2**	**11.3**	**2.6**	**10.9**	**ND**	**3.1**
1 micron	**0**	**0**	**7.3**	**2.3**	**7.5**	**ND**	**0**
BET (m2/g)	**200**	**250**	**100**	**100**	**10**	**1**	**0.4**

Table 1 (continued) Chemical analysis.

Sample		CABO	ZEOS	TSO	ATTA	VAW	SILM	ALIT
LOI	**%**	**0.0**	**11.0**	**28.2**	**21.4**	**1.3**	**0.97**	**0.6**
SiO_2	**%**	**99.8**	**85.4**	**63.6**	**57.1**	**98.1**	**98.63**	**25.8**
Al_2O_3	**%**	**0.0**	**0.0**	**4.3**	**4.0**	**0.1**	**0.0**	**0.8**
Fe_2O_3	**%**	**0.0**	**0.0**	**1.6**	**2.3**	**0.0**	**0.1**	**0.0**
TiO_2	**%**	**0.0**	**0.0**	**0.2**	**ND**	**0.1**	**0.0**	**0.0**
MgO	**%**	**0.0**	**0.0**	**0.6**	**7.1**	**0.2**	**0.0**	**1.9**
CaO	**%**	**0.0**	**2.5**	**0.0**	**ND**	**0.0**	**0.0**	**0.1**
K_2O	**%**	**0.0**	**0.2**	**0.5**	**0.2**	**0.2**	**0.0**	**0.0**
Na_2O	**%**	**0.2**	**1.3**	**ND**	**0.1**	**ND**	**ND**	**ND**
P_2O_5	**%**	**0.0**	**0.0**	**0.0**	**0.8**	**0.0**	**0.0**	**0.0**

Table 2 – Composition of the solution at the end of the test.

	Ca^{2+} (mM/l)	SiO_2 (μM/l)	Na_2O (mM/l)	K_2O (mM/l)	AL_2O_3 (μM/l)
CABO	19.78	39.84	0.17	0.13	0.72
ZEOS	17.22	59.14	3.13	0.42	0.94
TSO	23.61	40.36	0.13	0.0	1.79
VAW	23.88	33.06	0.18	0.16	0.67
ATTA	24.36	32.54	0.14	0.13	0.49
ALITE (standard)	24.06	71.66	0.14	0.13	0.71

The undersaturation increases with the reactive silica content in the blend. We have verified this on the VAW sample. The C_3S maintains the supersaturation with 10% pozzolana, but with 80% the whole hydration lies in the undersaturation domain. The filtrate analysis at the end of the test gives more details on the ions responsible for the electrical conductivity (table 2). During their dissolution, the samples release a part of their network impurities (for example alkalis for ZEOS and TSO, aluminates for TSO). The silicate concentration is the lowest for the most reactive (therefore soluble) silicas. This is explained by the location of the figurative points in the diagram $CaO–SiO_2–H_2O$: these samples give CSH of lower C/S, that are less soluble. On this diagram, samples ZEOS and CABO fall in the undersaturation domain of portlandite. This confirms the conductometric results.

3.3. Quantitative study of solid phases separated at the end of test.

XRD and TG results enables us to calculate the reactions yields (y_i) of the components (table 3), taking into account the initial composition of the mixes, and the silica content of materials, and based on the reactions [1] and [2] below. The mixes show lower portlandite contents than the standard, but also less residual C_3S (particularly ZEOS and CABO). Here the reaction yield y_2 of portlandite is limited by the availability of silica, which amount is lower than required by the stoechiometry. Portlandite being still present in all the samples, **The reactive silicas have activated the dissolution of C_3S.** This is in agreement with NMR results of HJORTH (3) and BEEDLE (4).

We suggest two possible mechanisms of activation:

– "calcium pump effect", by modification of concentration gradients around the C_3S grains dissolving. The formation of less soluble CSH, and the shift of reactions producing calcium by components consuming calcium can reinforce the diffusionnal mechanism (chemical coupling).

– catalytic effect of large surfaces on the nucleation and growth of portlandite. This effect is clearly visible for TSO and ZEOS samples (**table 3**): for portlandite, the ratio r of the content (TG measurement) to the relative intensity (XRD 2.63 A• line) varies in a 30% range. This kind of variation is classically explained by the enlargement of diffraction lines with the reduction of crystals size, obtained here by increasing the number of nuclei. This is in agreement with the conductometric results, indicating a shortening of the dormant period, when the BET surface of silicas increases (**table 4**).

The differences in reactivity index can be explained by the chemical reactivity of samples (solubility), by their ability to supply inhibitors like aluminium hydroxyde (TSO) to the solution, and by the accessibility of surfaces to OH^- ions, which can be low in the highly microporous samples.

Table 3. **Calculated reaction yields,** based on the following equations:

$$(y_1) * (C_3S + 5.5\ H \dashrightarrow C_{1.5}SH_4 + 1.5\ CH) \quad [1]$$

$$1.5\ (y_1).(y_2) * (CH + S + 4.5\ H \dashrightarrow CSH_{4.5}) \quad [2]$$

	C3S	VAW	SILM	ATTA	TSO	ZEOS	CABO
% H_{tot}	16.97	17.20	17.64	20.50	21.19	23.87	27.18
% H_{CSH}	12.34	12.42	13.58	16.69	17.50	20.85	23.79
% H_{CH}	4.63	11.61	4.05	3.81	3.69	3.02	3.39
I_{C3S}/I_{Si}	0.93	0.82	0.80	0.78	0.75	0.71	0.55
$y_1(C_3S)$	0.47	0.48	0.50	0.53	0.54	0.58	0.69
$y_2(CH)$	0.00	0.04	0.09	0.19	0.22	0.37	0.38
$y_3(S)$	0.00	0.08	0.17	0.71	0.76	0.99	1.04
% C3S	43.94	39.27	37.49	35.34	33.91	29.54	20.19
% CSH	37.03	36.79	39.77	47.75	49.78	57.99	66.11
% CH	19.03	17.10	16.66	15.66	15.17	12.43	13.94
% S	0.00	6.83	6.08	1.25	1.14	0.04	-0.25
I_{CH}/I_{Si}	1.25	1.18	1.09	0.94	0.74	0.63	0.98
r	15.19	14.57	15.23	16.61	20.36	19.61	14.20

Table 4. **Reduction of the C_3S dormant period duration.**

	ZEOS	CABO	TSO	ATTA	VAW	SILM
BET (m_2/g) = s	250	200	100	100	10	1
Reduction of D.Period = d (%)	65.9	57.9	17.6	27.5	26.4	8.06
Reactivity index = d/s	0.26	0.29	0.18	0.27	2.6	8.06

3.4. Morphology of the hydrates.

Portlandite dissolution is clearly visible in the CABO paste **(photo 1)**. The portlandite crystals are large and foliated, whereas they are hardly recognized in the hydrated silicas TSO **(photo 2)**, and ZEOS. In the other samples , portlandite crystals are poorly developed, and partially altered. The CSH morphology depends on the sample reactivity. Appearing with its typical shape of short fibers in the standard C_3S it takes a more honeycomb aspect when the silica consumes more lime. **(photo 3)**.

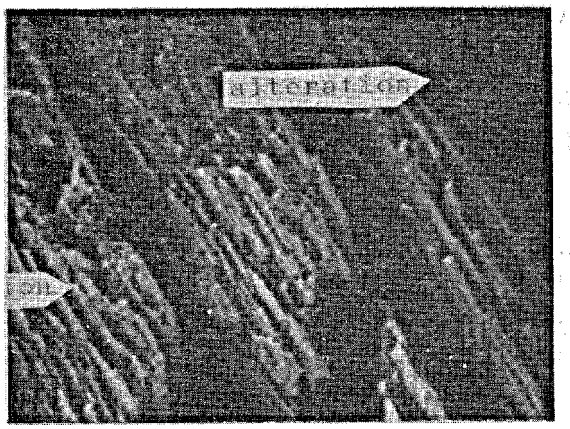

Photo 1. SEM view of CABO paste. Altered portlandite.

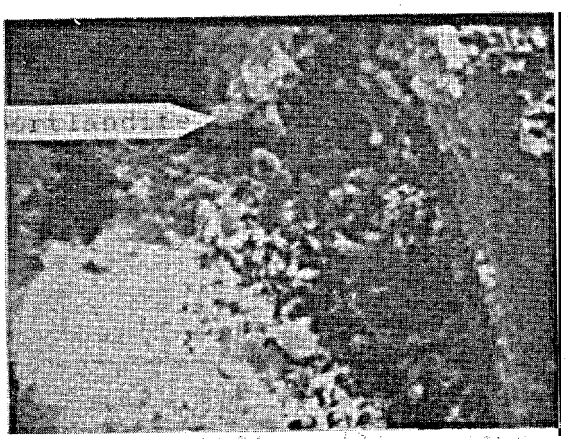

Photo 2. SEM view of TSO paste Poorly crystallized portlandite.



Photo 3 Honeycomb CSH

The agreement between the SEM observations on pastes, and the analysis of solids and solution after filtration, is thus excellent.

4 - OTHER POZZOLANIC MATERIALS.

The above examples cannot be extended to all the pozzolanic materials, because their surfaces and reactivities are of a different order of magnitude. Nevertheless the sensitivity of the test remains adequate, using the blends compositions cited in 2.1.
We have verified the performance of this test in detecting the formation of the sulfoaluminates and other hydrates involved in the hydration of pozzolanas. The modification of the portlandite nucleation is well evidenced in the case of calcined clays and marls. This will be the object of a further paper.

5 - CONCLUSIONS.

The use of synthetic C_3S for studying the reactivity of mineral additives, and a set of complementary methods of investigation, including conductometric test, brings a detailed information on the reactions mechanisms and rates.
Using lime only had not allowed to evaluate the interaction with C_3S and the large kinetic differences observed here.
As for blast-furnace slag and for calcareous fillers, we have shown that pozzolanas react from the very first hours. This result gives a general character to the behaviour of fine additives, taking into account the specific chemical sequence of each type of mineral.
Conductometric measurements allow us to obtain a rapid semi-quantitative view of the reactivity. The risks of aluminates interactions are well detected, and the reaction rates with portlandite and C_3S are easily evaluated. A better quantitative approach, using XRD and TG measurements at the end of the conductometric test, can help to refine the diagnosis.
Last we are lead to redefine the significance of the pozzolanic reactivity: Lime consumption no longer appears to be a pertinent criterion, because it takes into account the formation of aluminate hydrates which are not favourable for rheology, strength and durability. We prefer the reference to the CSH formation by the siliceous part of the pozzolanas. Knowing that CSH of different C/S are not equivalent with respect to their mechanical properties, it appears very useful to survey this ratio.

REFERENCES.

(1) BENOIT O. SIERRA R.
"Détermination de l'activité pouzzolanique par voie chimique." Bull.Labo P et Ch, 26, Juil-Aout 1967, pp D1-D5.

(2) VERNET C.; NOWORYTA G.
"Conductometric test of cement-admixture systems."
9th International Congress on the Chemistry of Cement, New DELHI, 1992. Sub-Theme III-D "Effect of admixtures".

(3) VERNET C. "Low temperature synthesis of belite".
8th International Congress on the Chemistry of Cements, RIO DE JANEIRO, 1986, Theme 1, Vol.2, pp 326-321.

(4) SCHUPPSTULH J. "Investigations dans le système C_3S-C_2S-H_2O."
Thèse Institut des Matériaux non métalliques, Université Technique de Clausthal.(résumée dans Tonin-dustr.Ztg., Dtch, Fev. 1985, Vol.109, pp 77-78.)

ACTIVITY AND PROPERTIES OF POZZOLAN USED IN BLENDED CEMENTS

C Urrutia*, M Ubilla and M Bobadilla***

**Departamento de Ingeniería de Materiales (IDIEM)*
Facultad de Ciencias Físicas y Matemáticas, Universidad de Chile
Santiago, CHILE
***Fca de Cemento Polpaico S A , Santiago, CHILE*

SUMMARY

The aim of this research is to characterize a chilean pozzolan from the chemical and mineral viewpoint and evaluate its effect when it is used as an addition for the cement. The pozzolan is formed essentially of volcanic amorphous glass and a small quantity of quartz and feldspar. The major part of the inert mass is found in the particle size fraction greater than 1.4 mm. A lime and pozzolan mortar made by using the said coarse fraction reaches a less strength than the same ones made with the fine particles (d 0.2 mm) for a similar specific surface.

The addition of pozzolan increases the cement paste water demand from 25% and till a 32% with 50% of pozzolan and produces a delay in the setting from 130 to 190 minutes. The compressive strength decreases with 10% of pozzolan, recovering similar or better strength levels with longer storage. A major content of pozzolan always produces a fall of resistance.

Among other properties, the pozzolan decreases the heat released by the reactions and reduces the expansion of mortar exposed to sulfate solution. However, the mortar made with cement and pozzolan produces a minor resistance when is exposed to a combined medium, sulfate and water solution and dried in a normal environment.

El objetivo del presente trabajo es caracterizar una puzolana chilena de origen volcánico, desde el punto de vista químico y mineral y evaluar su efecto al ser utilizada como adición en el cemento. La puzolana se encuentra conformada mayoritariamente por vidrio volcánico amorfo, algo de cuarzo y feldespato. Las materias inertes se encuentran preferentemente en la fracción gruesa (dp > 1,4 mm), por lo cual esta fracción presenta, a igual grado de molienda una menor reactividad con cal.

La adición de puzolana incrementa el requerimiento de agua de la pasta de cemento, desde un 25% hasta un 32% con 50% de puzolana. El mayor requerimiento de agua, unido a la menor proporción de material activo dc estos cementos, produce un retraso del inicio del fraguado desde 130 hasta 190 min, para los mismos contenidos de puzolana. Con contenidos de hasta 10% de puzolana, la resistencia de compresión cae, especialmente en el corto plazo, recuperándose a edades iguales o superiores a los 28 días. Contenidos mayores producen una caída de resistencia a todas las edades.

Entre otras propiedades, la puzolana disminuye tambien el calor liberado por las reacciones, en una proporción similar al remplazo de puzolana y mejora la resistencia de morteros expuestos a aguas contaminadas con sulfatos. Sin embargo, la menor resistencia de los cementos con puzolana, unida a su mayor permeabilidad en el corto plazo, producen en definitiva una menor durabilidad frente a exposiciones combinadas de aguas saturadas con sales y secado en ambiente normal.

INTRODUCTION

The use of additions is of special interest in our country due to the great potencial we have in this natural resource of volcanic origin. Today, nearly 86% of the total cement volume commercialized in Chile corresponds to cements blended with pozzolan (1). One of the pozzolan that has been in use for over 30 years in the making of cements is the one known as Pudahuel pozzolan whose deposit lies in the surrounding of Santiago. In this research we have considered as our principal aim the contribution to the knowledge of the said volcanic origin pozzolan, so as a way to optimize its use at industrial scale.

The pozzolan was characterized from the chemical and mineral viewpoint. It was shared by sieving in three fractions to analyse the possible enrichment of determinated phases of greater activity in some grading bands. In each one of them the usual test were made for activity measurement. The activity was analysed taking in consideration the pozzolan fineness and comparing three different test methodologies. Finally, cements with different pozzolan content were made and tested to determine the water requirement, setting time, permeability, strength development, heat development and resistance to sulfated water.

EXPERIMENTAL PROCEDURE AND RAW MATERIALS

The pozzolan sample to be analysed was taken directly from the output of the primary crusher and shared by size in three different fractions. These were tested individually (Table 1).

Table 1 Clinker and pozzolan analyses

		Pozzolan	Fraction	(mm)	
	Clinker	Raw	Coarse	Medium	Fine
Component			> 1.4 mm	1.4 - 0.15	< 0.15
Content (%)	--	--	17.0	35.2	47.8
Sp. Gravity	3.12	2.42	2.52	2.41	2.35
CaO (%)	66.7	2.0	4.4	2.9	1.7
SiO_2 (%)	22.8	68.9	60.5	68.7	72.0
Al_2O_3 (%)	4.2	13.4	14.3	14.0	13.0
Fe_2O_3 (%)	3.2	1.9	5.8	1.9	1.3
Na_2O (%)	--	3.4	3.3	3.8	3.1
K_2O (%)	--	3.7	3.2	3.5	4.2
MgO (%)	--	0.6	1.2	0.6	0.4
L. I. (%)	0.3	4.2	3.9	4.3	4.3

In accordance with the X-ray diffraction analyses, the fine fraction essencially contains an amorphous glass material whilst in the coarse ones was concentrated an important quantity of quartz and feldspar.

The activity of the pozzolan and its fractions, grinded in different fineness, was evaluated according to the accelerated test described in ASTM C593 and also curing the specimens at environment temperature. Finally, cement were made with a pozzolan contain rates from 0 to 50% and with a fineness of 3,000 and 4,200 cm2/g. These

cements were prepared by join grinding of clinker, gypsum and pozzolan in a laboratory ball mill. In these cements the effects of pozzolan in the physical characteristic of them were analysed using cement pastes and mortars.

RESULTS AND DISCUSION

Pozzolanic activity

The different pozzolan fractions show, in general, a high water requirement. This high demand can have its explanation in the microstructure type that composes this pozzolan and in the shape of the particles as a result of the grinding.

The pozzolan activity measured in lime mortars shows a strong dependence on the grinding fineness and with the fraction that this represent. This is demonstrated in the accelerated tests as in the mortars cured at environment temperature. The fine fraction essencially composed by a glass phase reaches a compressive strength between 2 and 4 MPa over the coarse fraction grinded to the same fineness. These differences are mantained and even increased in prolongated curing time.

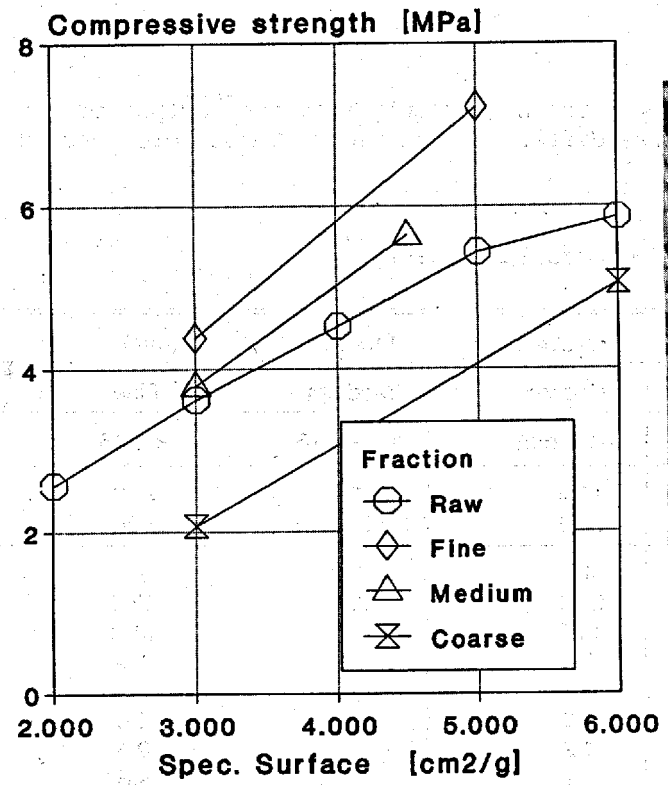

Fig. 1 Pozzolanic activity in mortars lime/pozzolan

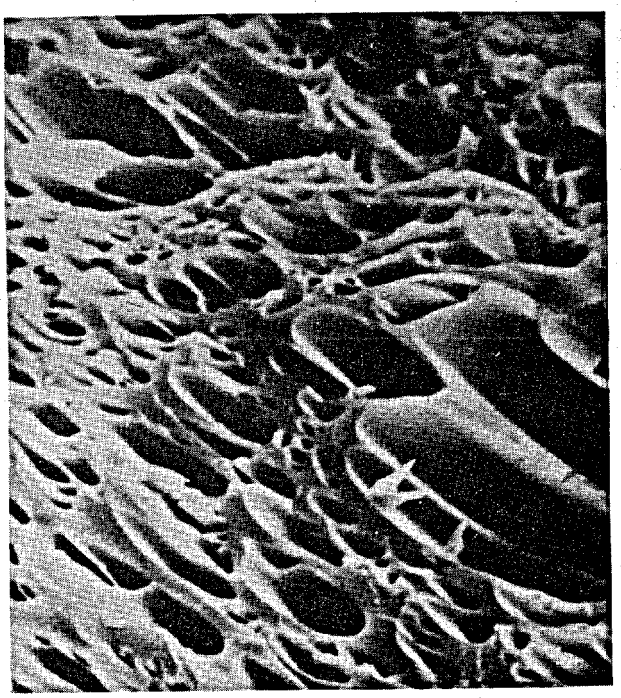

Fig. 2 Pozzolan grain. 1200 times increase

To complement the pozzolanic activity results obtained in the previous blends, additionally a special cement was prepared with Portland cement of 3,000 cm2/g grinded to laboratory scale and with an addition of pozzolan of 30%. In these mortars, depending on the fraction selected and the grinding fineness, it can be reached differences in the mortar compressive strength from 5 to 10 MPa at 28 days, differences that increase with longer curing times.

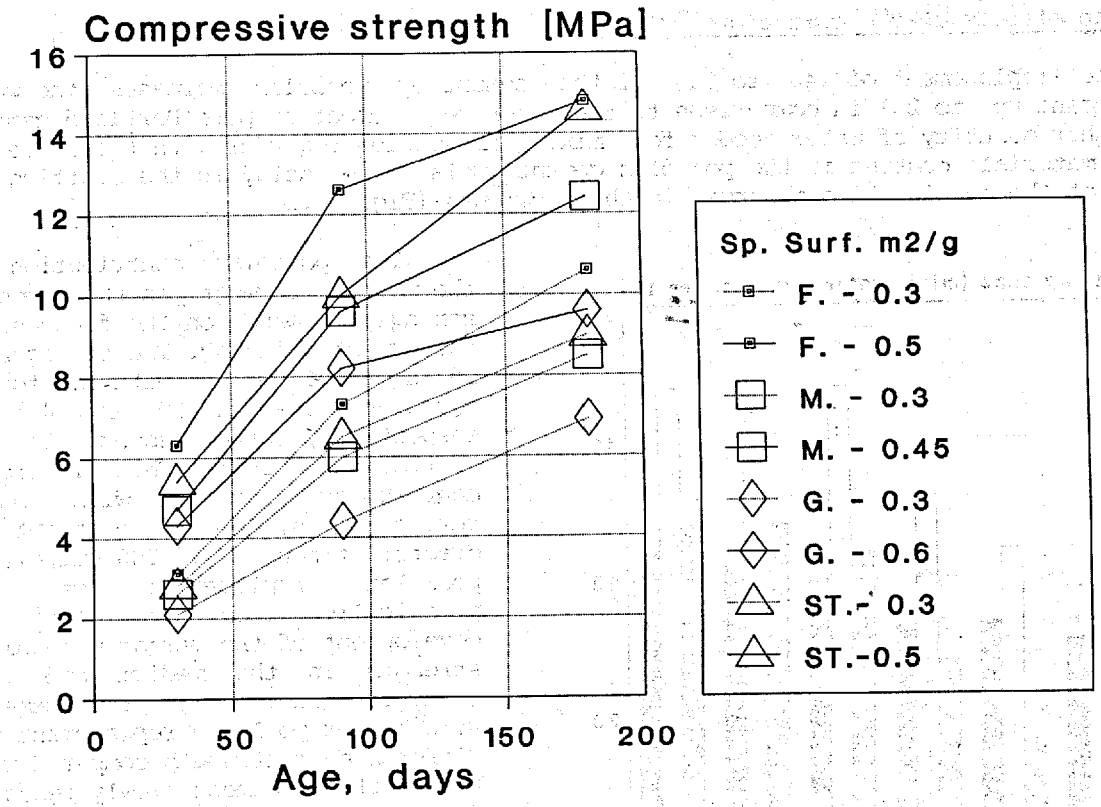

Fig. 3 Pozzolanic activity in mortars. Normal curing. F: fine, ST raw, M: medium and G: coarse fraction.

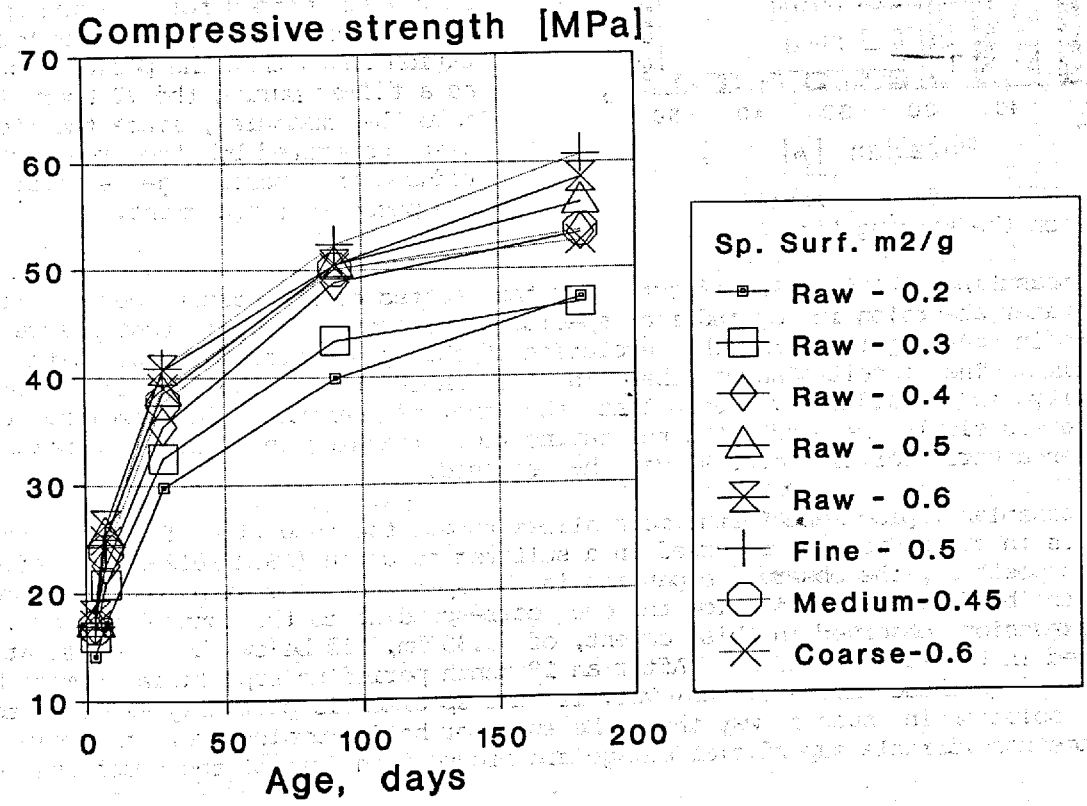

Fig.4 Pozzolan activity in the presence of portland cement.

Pozzolan effects on the cement properties

The replacement of 40 to 50% of the cement by pozzolan increases the water requirement up to 25% in comparison to the water requirement of pure Portland cement. The higher quantity of water needed for mixing the pastes together with the decreased active material content in the pozzolan cement explain the delay in the starting and ending of the setting time observed in these cements (Fig. 5).

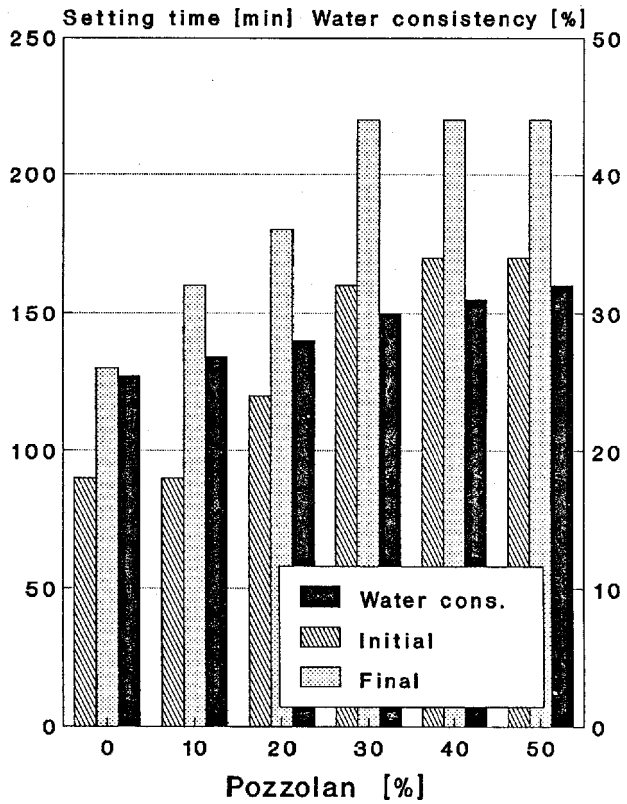

Fig. 5 Effect of the pozzolan on the setting time

The pozzolan contribution to the mortar strength in the cements strongly depends on the fineness of the cement grinding. The strength at 28 days of cement with 10 to 50% pozzolan drops in 10 and 40 MPa respectively with respect to the controling mortar. This difference mantain or increase with longer curing times. However in cements of greater fineness (4,200 cm2/g), a pozzolan replacement of 10% practically does not alter the development of the mortar mechanical strength in the medium and long term. In general, in the cements with higher pozzolan replacement the difference of strength compared with the Portland cement slowly tends to decrease with the curing age.

The investigations made with the Langavant method for measuring the heat generated by the cement hydratation shows that the pozzolan acts, as a filler during the 72 hours that take the measures, since the total heat generated by the reaction is reduced in a percentage similar to the pozzolan replacement.

For measuring the pozzolan effect over the setted cement pastes permeability, test of water absortion in cylindrical specimens were made. This test allows to follow, up in cualitative form, the evolution of the paste microstructure with the curing time. The results shows that in the short term, the Portland cement permeability is considerably less that the one of cement with pozzolan, this difference is slowly reduced with the curing time reaching an equivalent porosity degree when a period of time over 90 days has elapsed.

The pozzolan replacement furthermore allows to get the reduction of the expansion that occurs in cement mortars immersed in a sulfated solution (ASTM 1012-87). After 7 months exposition, the observed expansion in the specimens made with pozzolan cement is found to be from 25 to 50% below the one corresponding to the control mortar. The maximum expansion observed in this cement, of 0.35 mm, is below the specification established in the same standard. After an 18 month period no superficial damage has been observed in these mortars. However, if the specimen is partially exposed to a sulfated solution in such a way that the superior half remains over the solution level, some considerable superficial damage are produced in some of the specimens.

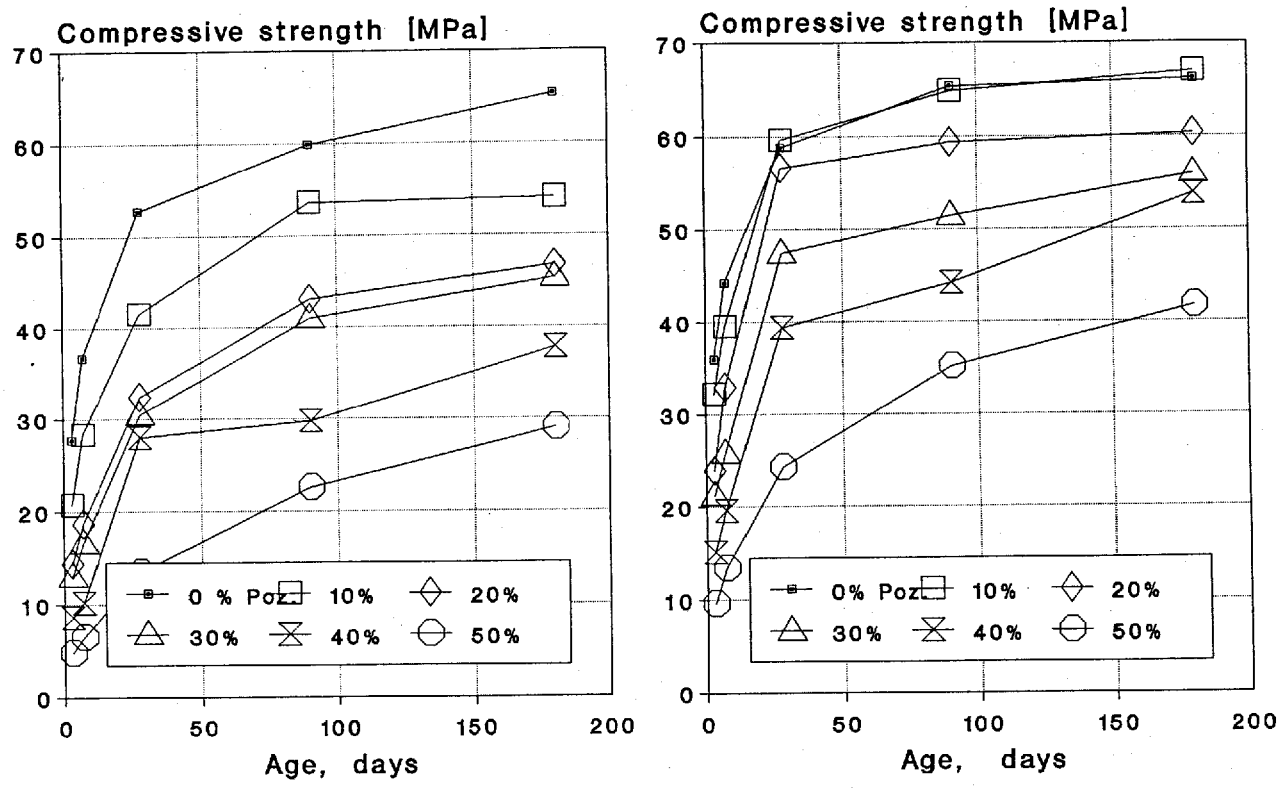

Fig. 6 Effect of pozzolan on the compressive strength of mortars. Cement with 3,000 and 4,200 cm2/g

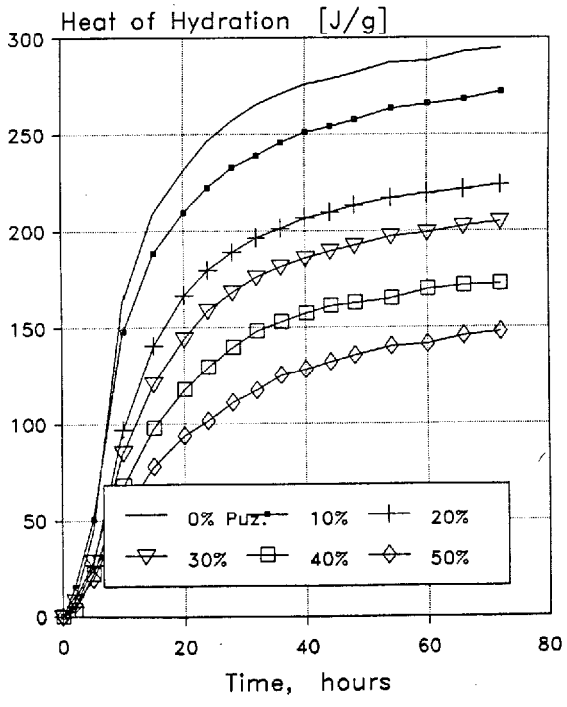

Fig. 7 Effect of pozzolan content on the heat evolution

In a first stage these shows a lost of the superficial grout of fine mortar in the drying section and, after that, in the gradual loosening of the sand grains from the superficial layers. This produces a reduction of the prism section exposed to the air. The observed damage is greater in the cement of less fineness and with a higher pozzolan content. The gradual destruction of the mortar can be explained as a mechanism of crystallization pressure. In this case, in the drying process of the specimen in the zone that remains above the liquid level, a capillary absortion is produced and the sulfated solution slowly climbs up by capillarity through the mortar pores.

In this case, in the drying process of the specimen in the zone that remains above the liquid level, a capillary absortion is produced and the sulfated solution slowly climbs up by capillarity through the mortar pores. In the moment that the solution reaches the drying surface the evaporation of water occurs producing a crystallization of the salt. The pressure generated by the salt crystalls is so strong that destroy the exterior layers of the mortar specimens. The destruction occuring in the specimen will depend then on the permeability of the mortar and on its mechanical strength when the crystallization occurs. In this way it can be concluded that mortars made with cement that have increasing pozzolan contents are more sensible to this kind of attack due to their early permeability and less strength with respect to a mortar made with Portland cement without addition.

CONCLUSIONS

- The impurities of pozzolan are concentrated mainly in the coarse fractions.
- The pozzolan fine fraction have a greater degree of activity than the other fractions.
- The compression strength of a cement blend with a 30% of pozzolan can be increased up to 25% more increasing the pozzolan fineness from 3,000 to 6,000 cm2/g.
- In cements prepared by joint grinding, the lost of strength observed when replacing part of the cement by pozzolan decreases in the cement with greater fineness.
- Pozzolan reduces the heat generated by the cement in the first days in a percentaje similar to that of the replacement.
- Pozzolan addition reduces the expansion of cements exposed to sulfated waters but increase their destruction in front of mixed actions of drying and absortion.

REFERENCES

1. Statistical Bulletin, Cámara Chilena de la Construción, No 218, February - March, 1991.

THE "CAPACITY OF EXCHANGE" OF POZZOLANIC ADDITIONS: ITS ORIGIN AND INFLUENCE IN THE FRATINI TEST

Rafael Talero

Instituto de Ciencias de la Construcción "Eduardo Torroja"
Madrid, SPAIN

SUMMARY

One of the most characteristic properties of the clays is its "CAPACITY OF EXCHANGE". Well, in the present work it has been able to demonstrate that as well as the natural pozzolans like the artificial ones, participate in greater or lesser measure and with greater reason, of that property in function with their contents of Na^+ and or K^- ions.

For that, 100 mixture cements, made up with portland cement "X" and pozzolan "Z", have been tried by means of the Fratini test, determining in its liquid phases correspondingly, their respective contents of Ca^{2+} and OH^-, according to the Specification of Conditions which RC-75 has prescribed (Fratini test).

Nevertheless and furthermore in those most representative, 15, all of them, constituted by the pozzolan "C" or "M" and portland cement P-nº or PY-nº, according to which has been the case, in a veriety of proportions in mass, it has also been determined its corresponding contents of Na^+ and K^+ ions.

The experimental results obtained have demonstrated the previous, that as much has been its CAPACITY OF EXCHANGE in a pozzolan, it is easier to carry out in the same the Fratini test, being able to say by that in a certain way, that iis behaviour in said test results as being more "fictious than fact".

RESUMEN

Una de las propiedades más características de las arcillas es su "CAPACIDAD DE CAMBIO". Pues bien, en el presente trabajo se ha logrado demostrar que tanto las puzolanas naturales como las artificiales, participan en mayor o menor medida y con mayor razón, de esa propiedad en función de su contenido de Na^+ y/o K^+ respectivo.

Para ello, 100 cementos de mezcla-constituidos por cemento portland "X" y puzolana "Z", únicamente- han sido analizados mediante el ensayo de Fratini, habiéndose determinado en su fase líquida correspondiente, sus contenidos de Ca^{2+} y OH^-, respectivos, según prescribe el Pliego de Condiciones RC-75.

No obstante y además en los más representativos, 15, de todos ellos- constituidos por la puzolana C o M y cemento portland P-nº y PY-nº, según ha sido el caso y determinada proporción en masa- se determinó también sus contenidos correspondientes de Na^+ y K^+ en dicha fase líquida.

Los resultados experimentales obtenidos han permitido demostrar lo anterior, así como también que en tanto en cuanto mayor sea dicha CAPACIDAD DE CAMBIO de una puzolana, más facilmente cumplimenta la misma el ensayo de Fratini, pudiéndose decir por ello en un cierto sentido que su comportamiento en dicho ensayo resulta ser "más ficticio que real"..

I.- INTRODUCCION

The term "Exchange Capacity" is used commonly by those researchers of clays and as you know is defined as the total number of available valencies in order to retain changeable cations.

So it effect and according to that, this property of the clays based principally on its "acid nucleous" should be stell more justified for the case of the natural an artificial pozzolans, given its intrinsic pozzolanic activity, represented by its power of fixation of Ca^{2+} in the from of $Ca(OH)_2$, resides fundamentally in the "acid nucleous" of the same, which would have be logically and generally more "acid" than the "acid nucleous" of the same clays since the "acid nucleous" of the pozzolans is constituted by reactive silica, SiO_2^{r-}, and reactive alumina, Al_2O_3, mostly, which are present in the amorphous fraction and vitreous of the natural an artificial pozzolans.

Lastly and before finalizing this introduction, it is worth-while remembering with respect to the power of replacing cationic to equality of the concentration, that follow this order: H^+, Ca^{2+}, Mg^{2+}, K^+, NH_4^+, being the same more directly related to its charge and volume once solvated than with its atomic volumen. To this fact is given the name LIOTROPE SERIES (8).

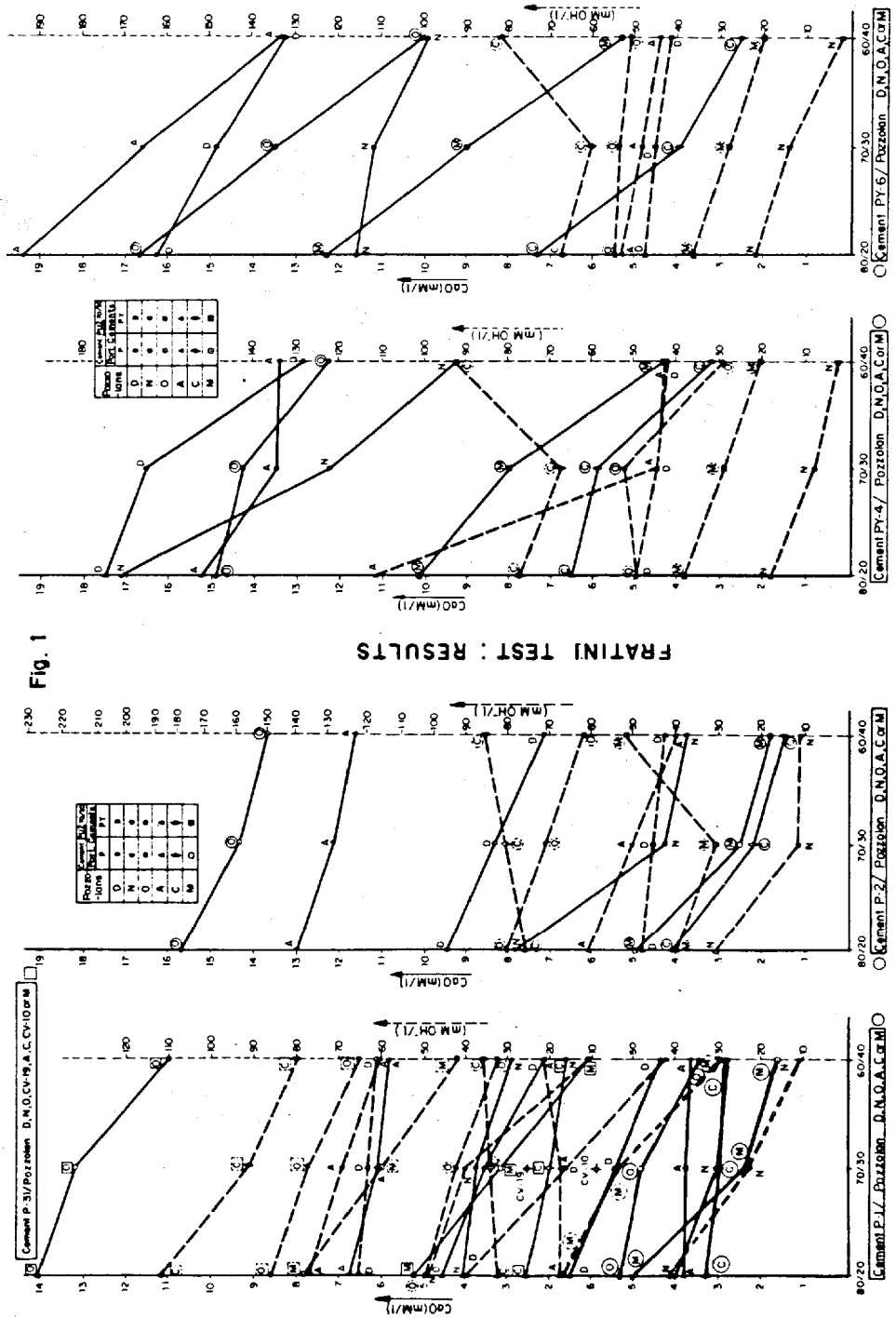

Fig. 1 FRATINI TEST : RESULTS

II.- OBJECTIVE

Try to demonstrate the posibility of the existence of the CAPACITY OF EXCHANGE in the pozzolans, in a similar way in foundiment, as occurs in determined clays.

III.- EXPERIMENTAL PROCEDURE

To demonstrate the possibility of the existance of the CAPACITY OF EXCHANGE in the pozzolans, we prepare 100 mixture cements constituted by portland P-nº and pozzolan "Z" ("Z"=D,N,O,A,C,M, CV-10 and CV-19). Theirs analysis are in Table 1. All were analyzed according to the Fratini test (1). The contents of the Na^+ and K^+ ions were determined by means of atomic absorption.

IV.- EXPERIMENTAL RESULTS OBTAINED

The experimental results obtained are to be found in Fig. 1 and the Tables 2 and 3. The argument and interpretation is carried out concentrating only on those cases nearest to the objective of this work.

For more details see the Doctorate Thesis of R. Talero (1). Among them all its worth while to point out as a matter of interest for those objectives the following:

1.- The pozzolans M and C in this order, in greater or less value, have fixed ions Ca^{2+} in notably superior quantities to the rest of the pozzolans tested and compared with them.

For which on both having M and C contents greater and less respectively, of Na^+ and K^+ and existing direct proportioning between both of them and the contents of Ca^{2+} of its liquid in respect of its Fratini test, it can be basically thought that such alkaline components are the origin and the cause of such an apparently anomalous situation having to base the same on the now known major insolubility of the CaO in the alkaline dissolutions of NaOH or KOH (2). Because such alkaline components of the pozzolan C are much greater than those of the M that scarce in them, would pass to the portlanditic liquid phase of the Fratini test, impeding this way the saturation in portlandite of the same, (1.23 g/l), with which, of origin, the pozzolan C in the Fratini test, will not fix $Ca(OH)_2$ of a satured solution of $Ca(OH)_2$ pure or very close to the saturation of the same, for dealing with portlandite and a part dissolved of the rest of the mineralogical components of the portland cement, but of a dissolution much less than the saturated one; because of the joint presence of the same of the afore mentioned alkalines impeding it, see Tables 2 and 3. From here as can be imagined its quantity of $Ca(OH)_2$ can be situated, set free in said liquid phase beneath that of that other case of the M, that in spite of having potentially more $Ca(OH)_2$ fixed, has left in spite of that more $Ca(OH)_2$ fixed, has left in spite of that more $Ca(OH)_2$ free in the liquid phase given that this last starts of from the saturation in $Ca(OH)_2$ of the same, and that, the C, does not start from it, should of from a dissolution that should be sufficiently below tha saturation (of the now aforementioned joint presence of the same quoted alkalines, Na^+ and K^+).

On the other hand as such as the alkalinity and its influences on its greater or lesser quantity present, in the liquid phase, of the contents of the alkaline components of the corresponding pozzolan, it goes to say as much again as the previous case. As from here that the pozzolan C (the one with the greatest alkaline components, the outcome of the previous reason) which generally heads, the corresponding classifications, due to definitley possessing a greater capacity of cationinc exchange - Na^+ and K^+ by Ca^{2-} in this case- or better perhaps CAPACITY OF EXCHANGE, given the theme which occupies us.

2.- Nevertheless and going into further detail in this CAPACITY OF EXCHANGE of the Pozzolan C, see Table 2, it can be observed what that has happened to the contents of Na^+ and K^+ of the liquid phase of the Fratini test and its evolution in the course of the test in the families of the mixture studied, cements PY-6/C PY-4/C P-31/C P-2/C and P-1/C, respectively, has got to be due mainly to some or all the possible causes of cationic exchanges previously mentioned in the final paragraphs of the indention I-INTRODUCTION which will be according to the LIOTROPE SERIES (8) the Ca^{2+} of each liquid phase (of the portlandite origin freed from hydration of mineralogical components of the fraction of clinker portland respective, in each case) displaces easier to Na^+ than to K^+ of the part of the Pozzolan C of the

corresponding cement paste. From here and the K^+ according to the progress of the exchange process with the Ca^2 at the age of 28 days, should be the contrary of the Na^+, the alkaline cation that is least detected in the liquid phase. And it should be more so the greater the cause or causes that determine the presence of Ca^{2+} in said liquid phase among which are undernamed:

a) the pozzolanic activity of the same pozzolan C,

b) the quantity of cement P or PY within the one same family and or

c) the contents of C_3S, standard of lime and CaO_{comb}, to the equality of mixture, (and the contents of C_3S of the PY-4 is much less than the PY-6 being that 58.19% < 79.43%, occuring logically the opposite with the respective contents of C_3S 19.46% > 2.29%) of said portland matrix cement.

And as for the common factor occurred to the contents of K^+ as much as between the families P-1/C and P-31/C with regard to of the P-2/C, is a futher confirmation that the cause resides in all of the previous three being more evident in all of them thar refers to the low content of C_3S -or high of C_2S- with regard of both portland matrices cements, PY-4 and P-2, in respect of the rest correspondingly PY-6, P-1 and P-31, respectively, compared with those besides the less Specific Surface of the P-2 respect of the P-1 and P-31 principally, and is in the favour of deduced reason. Lastly and if to all that the additional cause is added, that according to the analytical technique of the XRD (1), one of the main components of the pozzolan C us a Zeolite [Na_2Ca_2 (Al, SiO_2- H_2O)], as well as the Phillipsite [K_2Ca_2(Al, Si)$_{16}$ O_{32} 13, $5H_2O$], Graphic 1, in this way it has been too well justified the possibility of the existence of that CAPACITY OF EXCHANGE in the pozzolans, and specially in this case, in the C, as has been demonstrated.

3.- That in the corresponding similar comparative study of the pozzolan O and A, it can be observed as such as although in a lesser measure, but in this case in favour of the O, that on giving greater alkalinity values than the A this confirms its greatest resemblance according to this parameter OH^- with the C, than the A, and cosequently will part more than the A of the causes of the behaviour of the C in this given test.

And furthermore, see Square 1, how the different classifications are obtained to the equality of age and mixture cement of the pozzolans D, O, A, C and M tested in function with the value of alkalinity OH^-, of its respective liquid phase, are nearly all coinciding that it could be obtained from its content of (Na_2O (%) + (0.658 x K_2O (%)). In this way that according to everything previous it is logical that the extreme with the greatest alkaline value should be occupied by the C followed by the O and then the A in this order.

4.- That the pozzolans CV-10 and CV-19 participate in equal measure although in less quantity, of the given reasons for the C and M in the fixation of Ca_{2+} of the liquid phase as like in the alkalinity of the same.

V.- CONCLUSIONS

1st. Generally, to the equality of age the test and mixture cement 60/40, whatever being the accompanying portland matrix common cement, P-nº or PY-nº, correspondingly, the pozzolans which have the least quantity of Ca_{2+} contained its liquid phase respective of the Fratini test, have been the C and the M or M and C, being more abundant the cases corresponding to the order cited in the first place, three, than in the second place, two, and followed later at a relative distance by the N and at a bigger distance by the rest, the A and the O, that in this way to those last two it can be said with fundiment that all the contrary happens to them than to the initial ones aforementioned.

2nd. The pozzolan C has showed at all events an CAPACITY OF EXCHANGE with its liquid phasee which is cause and origin,

- of its apparent major fixation of Ca^{2+} by the same and because of that its "apparent" better behaviour than the rest of the pozzolans with it compared, according to the Fratini test, and
- of the major alkalinity of its corresponding liquid phase.

3rd. The behaviour of the pozzolan C in the Fratini test can be considered then in general, the best of all the pozzolans as tested and compared with it, better including paradoxically than the pozzolan M, which is the one that follows it in said behaviour.

Nevertheless and since said behaviour of the pozzolan C has been on account of its notable CAPACITY OF EXCHANGE, it can be said in a certain way, that its behaviour in said test turns out to be "more fictious than fact".

4th. According to the last two conclusions, of the eight pozzolans studied, generally it can be made- to the equality of the mixture cement-, two groups in function with its pozzolanic activity and because of that, understanding the greater fixation of ions Ca^{2+}, which are the following:

a) as to the of ions Ca^{2+} and the corresponding evolution of alkalinity:

- the group formed by the CV-10, CV-19, N, M and C which corresponding generally a greater fixation of this cation,

- the group formed by the D, O and A or C, and O, to which correspond the exact opposite, and

b) as to the evolution of alkalinity, OH^-:

- the group formed by the rest, headed normally by the pozzolans,

- the group formed by the rest, headed normally by the pozzolans natural canary C, which is the one that has the most Na and K alkaline components.

5th. It can now be said here for notoriety and prominence that the quantities of the necessary liquid phase in order to carry out the volumetric determinations of the Fratini test corresponding to the pozzolans D and N (diatomites) principally, resulted to be notably less than the rest of the tested pozzolans and compared with them and or with whatever traditional pozzolanic cement. (As from here that the results obtained of the same have hed to correspond to the aliquot quantities of the liquid phase, less than the normal).

VI.- DEDUCTION OF INTEREST

In the possible supposition of the fixation, greater or lesser, but simultaneously of Ca^{2+} and OH^- of the liquid phase of the Fratini test of a pozzolanic cement not being proportional between them, but to the contrary, it goes to say greater or much greater fixation of Ca^{2+} than OH^-, which paradoxically would say that "it increases instead of diminishing as it should", a greet possibility exists that in said liquid phase that at the normalized ages of the test a notable quantity of alkalines Na^+ and or K^+ principally, can be found,

- proceeding from the fraction Clinker Portland (perhaps a less probable fact) or

- proceeding from the pozzolan(s) fraction (perhaps a more probable fact), being the cause of that demonstrated CAPACITY OF EXCHANGE of the pozzolan(s) which constitute the pozzolanic cement, which is some surroundings can be a "Pathology" and others can be a "Therapy" for its concrete or mortar correspondent (8).

VII.- GENERAL PRACTICAL ADVICE

Of all the previous it has been deduced that the other distinctive parameters of the by-products of the Fratini test, are in particular RS*, RMC^{2*} and RMF^{3*}, which confirm,

- the degree of suitability of a pozzolan given, to reach a definitive aim, and/or

- the "intention of behaviour" of a pozzolan given in an aggresive or non aggresive determined enviroment, glimpsed or pried firstly by means the Fratini test.

VIII.- BIBLIOGRAPHY

1.- R. Talero: "Contribution to the Analytical Study and Physics-Chemistry of the System: Pozzolanic Cement-Gypsum-Water" (to 22º - 3ºC).- Doctorate Thesis. University Complutense of Madrid, Faculty of Chemical Sciences. Proffesorship of Industrial Chemistry, Nov. 1986, Madrid, and or c/Santa Susana nº 32-4ª.- 28033 Madrid (Spain) and also Book of Conferences (18) Parts 1st and 2nd "The Natural Pozzolans. Fly Ashes and Similars, in the Construction, Cement and Concrete", and Idem "Pathologies and Therapies of the Structures, Concretes and Other Building Materials".

2.- W. Lerch and G. Kalousek: "Simposium on use of pozzolanic materials in mortar and concretes". First Pacific Area National Meeting-ASTM Special Techn. Publ. nº 99, (Oct. 1949). San Francisco, California, USA.

3.- Specifications of General Prescription for the Reception of Cements. RC-75 (decree 1974/1975 of 23rd May, Official State Bulletin num. 206 of 28-8-75)

4.- American Society for Testing Materials. "Standard Methods Samplig and Testing Fly Ash or Natural Pozzolans for use as a MIneral Admixture in Portland Cement Concrete" ASTM C 311-7.

5.- Am4erican Society for testing materials. "Standard Specification for Portland Cement". ASTM C 150-85

6.- Specifications of Conditions for the Reception of Hydraulic Conglomerantes, PCCH-64 Rules and Manuals of the IETCC, CSIC.

7.- American Society for testing Materials. "Standard Specification for Fly Ash and Raw or calcined Natural Pozzolan for Yse as a Mineral Admixture in Portland Cement Concrete". ASTM C 618-85

8.- ASINEL: "Fly Ash and its applications". Graphic Selections (Editions). Paseo de la Dirección, 52. Madrid. Spain.

9.- R. Talero: "Phatologies and preventive Therapies of the concrete: II. The "Capacity of exchange" of the pozzolans Additions (Natural Pozzolans, Fly ashes, activated clays and Similars). Phatology or therapy fior concretes?. Monograph nº 406. Instituto de C.C. Eduardo Torroja, c/Serrano Galvache s/n 28033 Madrid, September 1991.

---

* RS = Resistance to the attack of the sulphate ions or "Sulphatic Resistance"
2* RMC = Comprensive streght
3* RMF = Flexural Strength

NOTE

This research work is a small of the multiples which constitute the Doctorate Thesis of the R. Talero (1). In the next Congresses, Meeting and articles, the rest parts will be published.

TABLE 1

DETERMINATIONS (%)	CHEMICAL DETERMINATIONS — PORTLAND CEMENTS				
	P-1 (3,08)*	P-2 (3,06)	P-31 (3,06)	PY-4 (3,16)	PY-6 (3,21)
LOI	1,60	2,91	3,45	1,64	1,11
I.R.	0,70	1,21	0,86	0,43	0,15
SiO_2	19,18	19,36	18,13	22,10	21,70
Al_2O_3	6,44	6,03	5,30	1,98	1,52
Fe_2O_3	1,75	2,89	3,80	4,46	4,11
CaO	63,94	59,49	61,68	65,59	67,97
MgO	1,48	1,21	1,82	0,83	0,42
Na_2O	0,90	1,23	0,76	0,15	0,43
K_2O	0,52	0,69	0,31	0,05	0,20
SO_3	3,50	4,94	3,86	2,78	2,34
TOTAL	100,01	99,96	99,97	100,01	99,95
$H_2O(105°C)$	0,24	0,93	0,33	0,22	0,22
CaO free	1,90	0,70	0,63	1,20	1,75

DETERMINATIONS (%)	POZZOLANIC ADDITIONS — NATURALS					ARTIFICIALS		
	D (2,59)	N (3,17)	O (3,09)	A (2,41)	C (2,68)	M (2,55)	CV-10 (2,09)	CV-19 (2,43)
LOI	0,23	12,48	0,40	3,92	6,92	0,60	6,92	0,83
I.R.	0,42	0,30	1,10	–	0,43	0,22	0,18	0,12
SiO_2	91,81	64,26	45,12	41,38	54,18	73,53	49,29	45,47
Al_2O_3	1,91	8,42	13,84	19,38	20,10	23,11	29,65	30,09
Fe_2O_3	2,39	4,44	13,82	12,05	3,12	1,19	4,22	16,12
CaO	1,23	11,35	10,48	11,11	2,38	0,63	2,86	4,03
MgO	0,38	–	9,54	10,58	2,04	0,03	1,81	1,12
Na_2O	1,50	–	3,18	1,24	5,64	0,07	0,50	0,20
K_2O	0,12	0,80	2,40	0,44	5,17	0,70	3,60	2,80
SO_3	–	–	0,46	–	–	–	0,94	1,92
TOTAL	99,99	100,05	99,94	100,08	99,98	100,05	99,95	100,78
$H_2O(105°C)$	0,07	3,61	0,55	4,02	4,03	0,16	0,12	0,28
CaO free		CO_2=8,95						

DETERMINATIONS (%)	POTENTIAL CALCULUS BOGUE(%)				
C_3S	51,05	33,47	58,70	58,19	79,43
C_2S	16,48	30,26	7,70	19,46	2,29
C_3A	14,11	11,09	7,62	0,00	0,00
C_4AF+C_2F (2*)	5,33	8,79	11,56	11,75 (2*)	10,19 (2*)
C_4AF+2C_3A (1*)	33,55	30,97	26,80	11,75	10,19
C_4AF+C_3A (1*)	19,44	19,88	19,16	11,75	10,19
Spf.Surf ^{2*}	3192	3015	3248	3233	3287

* Specific Weight (g/cm³)

2* Specific Surface (cm²/g)

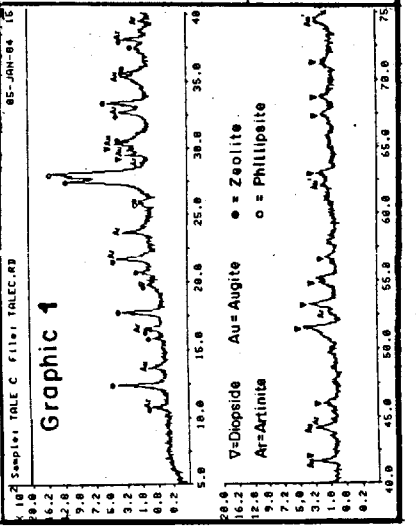

Square 1

Fratini Test

Classification of the Pozzolans D, N, O, A, C and M, thus tested, in function of the contents of :

(A) CaO (mM/l) (B) OH^- (mM/l)

of their liquid phase (from less at great value):

Portland Cements	Mixture Cements Pa and Plz	(A) (B) of their liquid phase (from less at great value):
P-1	10/20	C < A < N < D < M < O
	70/30	M < C < N < A < O < D
	60/40	M < N < C < O < A < D
P-2	80/20	C < M < N < D < A < O
	70/30	C < M < N < D < A < O
	60/40	C < M < N < D < A < O
P-31	80/20	C < N < D < M < O < A
	70/30	C < M < D < N < A < O (<CV-19, <CV-10)
	60/40	C < M < D < N < A < O
PY-4	80/20	C < M < A < O < N < D
	70/30	C < M < O < A < N < D
	60/40	C < M < O < A < N < D
PY-6	80/20	C < N < M < D < A < O
	70/30	C < M < N < O < D < A
	60/40	C < M < N < O < D < A

N = M < A < D < <CV-19 <CV-10 < C

© $CNa_2O(\%) + 0,658 \times K_2O(\%)$ of each pozzolan

TABLE - 2

CONTENTS OF Na^+(Na_2O,%) and K^+(K_2O,%) IN THE LIQUID PHASE OF THE FRATINI TEST, OF THE MIXTURE CEMENTS, PA and PUZ, P-1, P-2, P-31, PY-4 or PY-6/C or M, 80/20, 70/30 and 60/40

NOTE: Na_2O and K_2O g/l		Mixture Cements P or PY/C or M	Mixture Cements PA and PUZ									
			P-1 / C	P-1 / M	P-2/C	P-2/M	P-31/C	P-31/M	PY-4/C	PY-4/M	PY-6/C	PY-6/M
			$Na_2O + K_2O$	$Na_2O + K_2O$	$Na_2O + K_2O$	$Na_2O + K_2O$	$Na_2O + K_2O$	$Na_2O + K_2O$	$Na_2O + K_2O$	$Na_2O + K_2O$	$Na_2O + K_2O$	$Na_2O + K_2O$
AGE (days)	7	80/20	11,6 + 13,2 (24,8)	5,6 + 5,0 (10,6)	11,2 + 10,8 (22,0)	1,2 + 0,8 (2,00)	1,6 + 12,2 (13,8)	1,0 + 1,2 (2,2)	9,8 + 10,0 (19,8)	0,0 + 0,0 (0,0)	9,8 + 9,8 (19,6)	0,2 + 0,6 (0,8)
	28		14,4 + 16,0 (30,4)	6,3 + 14,4 (20,7)	14,2 + 14,8 (29,0)	1,4 + 7,2 (8,6)	15,6 + 20,0 (35,6)	1,6 + 14,6 (16,2)	13,8 + 10,0 (23,8)	0,2 + 2,8 (3,0)	13,8 + 9,8 (23,6)	3,0 + 9,2 (12,2)
	7	70/30	16,0 + 15,4 (31,4)	3,2 + 2,6 (5,8)	11,6 + 11,4 (23,0)	0,8 + 0,4 (1,2)	13,6 + 13,2 (26,8)	3,8 + 3,2 (7,0)	11,2 + 11,0 (22,2)	0,2 + 0,0 (0,2)	11,2 + 12,0 (23,2)	0,3 + 0,8 (1,1)
	28		17,6 + 14,6 (32,2)	4,4 + 12,0 (16,4)	11,0 + 15,8 (26,8)	0,4 + 4,8 (5,2)	14,2 + 13,6 (27,8)	3,8 + 11,6 (15,4)	13,4 + 7,6 (21,0)	0,0 + 2,2 (2,2)	13,8 + 8,2 (22,0)	0,2 + 2,8 (3,0)
	7	60/40	14,8 + 14,8 (29,6)	1,2 + 0,8 (2,0)	10,0 + 10,2 (20,2)	0,4 + 0,2 (0,6)	12,6 + 12,8 (25,4)	2,8 + 2,4 (5,2)	11,2 + 12,2 (23,4)	0,6 + 0,4 (1,0)	11,8 + 12,2 (24,0)	0,6 + 1,0 (1,6)
	28		16,2 + 8,8 (25,0)	2,4 + 7,8 (10,2)	10,4 + 3,0 (13,4)	0,6 + 4,4 (5,0)	14,8 + 10,8 (25,6)	3,0 + 3,2 (12,2)	15,6 + 3,6 (19,2)	0,4 + 3,0 (3,4)	13,4 + 6,8 (20,2)	0,0 + 2,6 (2,6)

TABLE - 3

CONTENTS OF THE Na^+ and K^+* (Na_2O%) IN THE LIQUID PHASE OF THE FRATINI TEST, OF THE MIXTURE CEMENTS, PA and PUZ, P-1, P-2, P-31, PY-4 or PY-6/C or M, 80/20, 70,30 and 60/40

NOTE: Na_2O and K_2O g/l		Mixture Cements P or PY/C or M	Mixture Cements PA and PUZ									
			P-1 / C	P-1 / M	P-2/C	P-2/M	P-31/C	P-31/M	PY-4/C	PY-4/M	PY-6/C	PY-6/M
			$Na_2O + K_2O$*	$Na_2O + K_2O$*	$Na_2O + K_2O$*	$Na_2O + K_2O$*	$Na_2O + K_2O$*	$Na_2O + K_2O$*	$Na_2O + K_2O$*	$Na_2O + K_2O$*	$Na_2O + K_2O$*	$Na_2O + K_2O$*
AGE (days)	7	80/20	11,6 + 8,69 (20,3)	5,6 + 3,29 (8,9)	11,2 + 7,11 (18,3)	1,2 + 0,53 (1,73)	1,6 + 8,03 (19,6)	1,0 + 0,79 (1,79)	9,8 + 6,58 (16,4)	0,0 + 0,00 (0,00)	9,8 + 6,45 (16,2)	0,2 + 0,40 (0,60)
	28		14,4 + 10,5 (24,9)	6,3 + 9,48 (15,8)	14,2 + 9,74 (23,9)	1,4 + 4,74 (6,14)	15,6 + 13,2 (28,7)	1,6 + 9,61 (11,2)	13,8 + 6,58 (20,4)	0,2 + 1,84 (2,04)	13,8 + 6,45 (20,2)	3,0 + 6,05 (9,05)
	7	70/30	16,0 + 10,1 (26,1)	3,2 + 1,71 (4,9)	11,6 + 7,50 (19,1)	0,8 + 0,26 (1,06)	13,6 + 8,69 (22,3)	3,8 + 2,11 (5,91)	11,2 + 7,24 (18,4)	0,2 + 0,00 (0,20)	11,2 + 7,90 (19,1)	0,3 + 0,53 (0,83)
	28		17,6 + 9,61 (27,2)	4,4 + 7,90 (12,3)	11,0 + 10,4 (21,4)	0,4 + 3,16 (3,56)	14,2 + 8,55 (23,1)	3,8 + 7,63 (11,4)	13,4 + 5,00 (18,4)	0,0 + 1,45 (1,45)	13,8 + 5,40 (19,2)	0,2 + 1,84 (2,04)
	7	60/40	14,8 + 9,74 (24,5)	1,2 + 0,53 (1,73)	10,0 + 6,71 (16,7)	0,4 + 0,13 (0,53)	12,6 + 8,42 (21,0)	2,8 + 1,58 (4,40)	11,2 + 8,03 (19,2)	0,8 + 0,26 (0,86)	11,8 + 8,03 (19,8)	0,6 + 0,66 (1,26)
	28		16,2 + 5,79 (22,0)	2,4 + 5,13 (7,53)	10,4 + 1,97 (12,4)	0,6 + 2,90 (3,50)	14,8 + 7,11 (21,9)	3,0 + 6,05 (9,05)	15,6 + 2,37 (18,0)	0,4 + 1,97 (2,37)	13,4 + 4,47 (17,9)	0,0 + 1,71 (1,71)

* K_2O (%) × 0,658 = Na_2O (%)

SOME STUDIES ON THE ACTIVATION OF BLASTFURNACE SLAG IN CEMENTS WITHOUT CLINKER

C E S Tango and E Y L Vaidergorin

I P T - São Paulo, BRAZIL

SUMMARY

The mechanical behaviour of 10 different cements, without clinker, made of activated blastfurnace slag has been investigated. The activation was made with mixtures of gypsum and sodium hydroxide or calcium hydroxide or with only calcium hydroxide. The results from a slag without any activation were used as a reference. An attempt to identify the compounds that were formed and the extent of hydration after 7, 28, 62 and 90 days has been made by means of thermal, X-ray and infrared spectroscopic analysis. The best results were obtained with the gypsum-calcium hydroxide activation, nevertheless the results from the activation with gypsum and soda were also not negligible; the activation with calcium hydroxide alone accelerated the hydration but resulted in lower mechanical strengths. Ettringite, C-S-H and C_4AH_{13} were identified in the hydration products of the gypsum activated slag; in the calcium hydroxide activated slag, only C-S-H and C_4AH_{13} were identified in the hydration products. There were some evidences that the calcium hydroxide had been partially consumed during the hydration process, also due to the formation of calcium carbonate, that was present in all the samples.

QUELQUES ÉTUDES SUR L'ACTIVATION D'UN LAITIER DE HAUT FOURNEAU DANS DES CIMENTS SANS CLINKER

RÉSUMÉ

Le comportement mécanique de micro-eprouvettes de pâtes de 10 differents ciments sans clinker à base de laitier de haut fourneau, activés avec $CaSO_4 . 2H_2O$, NaOH et $Ca(OH)_2$ combinés, ou sans aucune activation, est verifié et confronté au developpement des courbes d'A.T.D. et des spectres Infra-Rouge et de Rayons X. L'activation sulfato-calcique a donné les meilleurs résultats dans les conditions étudiées. Parcontre, l'activation avec soude et gypse n'est pas negligeable; l'activation avec seulement la chaux est importante, mais la quantité de chaux, si d'une coté accelère l'hydratation, d'autre coté affaiblit l'ensemble hydraté. On a trouvé la formation d'ettringite, CSH et C_4AH_{13} avec l'activation sulfato-calcique; les mêmes hydrates avec l'activation sodo-sulfatique; et CSH et C_4AH_{13} avec l'activation calcique; aussi des évidences de que la chaux est partiellement consomée pendent l'hydratation et aussi bien à la cause de la formation de $CaCO_3$, detectable dans tous les échantillons.

INTRODUCTION

The aglomerating properties of blastfurnace slags in the presence of lime are known since 1865, when Germany produced the first hydraulic binder made of these two products[1]. Nowadays blastfurnace slags are mixed in various proportions with cement clinkers for the production of slag cements. In this paper we shall present the results of a study conducted with 10 different kinds of cements without clinker. These cements were made with activated blastfurnace slag which doesn't need the use of high temperature furnaces for its production.

MATERIALS AND METHODS

The activating substances used in this study were hydrated lime ($Ca(OH)_2$), mixtures of gypsum ($CaSO_4.2H_2O$) and sodium hydroxide (NaOH) and mixtures of gypsum and hydrated lime. The slag used was a french one, produced by the "Bouletage"[2] process and ground after being oven dried. The ten mixtures of slag and alkaline activators studies are shown in Table 1. As a reference the tests were also conduted on a slag without activator (cement n. 1).

Table 1 - Mixtures of blastfurnace slag and activators used in this study

Cement N.	Composition of the mixture parts/hundred parts of blastfurnace slag			
	Gypsum	Hydrated lime	Sodium hydroxide	Water(*)
1	-	-	-	23,3
2	5,0	5,0	-	25,4
3	5,0	10,0	-	26,8
4	5,0	15,0	-	30,7
5	5,0	-	1,0	24,2
6	5,0	-	2,0	22,5
7	5,0	-	3,0	21,9
8	-	10,0	-	27,1
9	-	15,0	-	28,7
10	-	20,0	-	30,9

(*) The water was added gradually until the paste released itself from the walls of the mixer.

The mean particle diameters, measured by laser granulometry were the following - slag: $13,8m \times 10^{-6}$; gypsum: $33,1m \times 10^{-6}$; hydrated lime: $3,1m \times 10^{-6}$. Cylinders 20mm in diameter and 40mm in height were molded with all the cements shown in Table 1. These samples were maintained in a water vapour saturated atmosphere, at a temperature of 20°C to 24°C. After 6, 28, 62 and 90 days three samples from each cement were dried in a ventilated oven at 56°C and ruptured by axial compression with a press velocity of 1mm/min. After rupture the samples were ground, dried in an oven, ground again till fineness lower than $100m \times 10^{-6}$ and stored in tight closing vessels. These samples were used for thermal analysis, X-ray and infrared spectroscopy.

RESULTS AND DISCUSSION

Compressive Strength

The results for all the cements are shown in Table 2 and Figs. 1, 2 and 3. The unactivated slag resistance is not to be overlooked but the development was too slow to be considered of practical use. With gypsum-lime activation the fastest grow in the early ages corresponds to lower resistance in higher ages (15,0 parts of lime). A higher amount of lime iniatially increases the strength, acting as a slag resistance development catalizator

but further increases in the amount of lime lower the overall mixture resistance, because the lime itself doesn't contributes very much to the compressive strength.

Table 2 - Compressive strength results

Cement N.	Compressive strength (MPa)			
	7 days	29 days	63 days	91 days
1	9,3	17,6	17,0	20,5
2	25,0	42,8	46,3	47,7
3	29,7	41,9	51,4	55,5
4	32,5	41,0	43,4	47,7
5	16,6	21,5	23,0	26,5
6	23,7	25,5	44,5	44,4
7	28,4	38,4	38,0	37,3
8	21,4	30,6	32,9	32,6
9	21,6	30,1	26,5	30,1
10	18,0	26,0	33,8	33,5

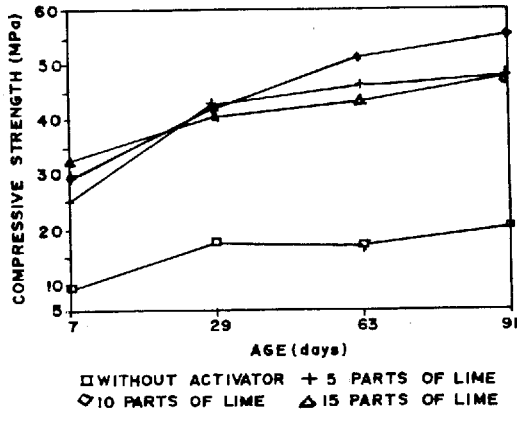

Fig. 1 - Strength development of the gypsum-lime activated slag.

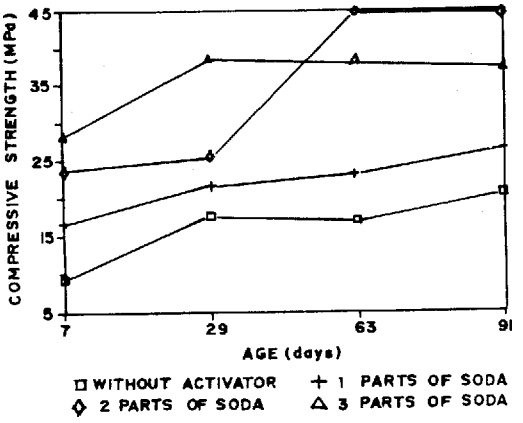

Fig. 2 - Strength development of the gypsum-soda activated slag.

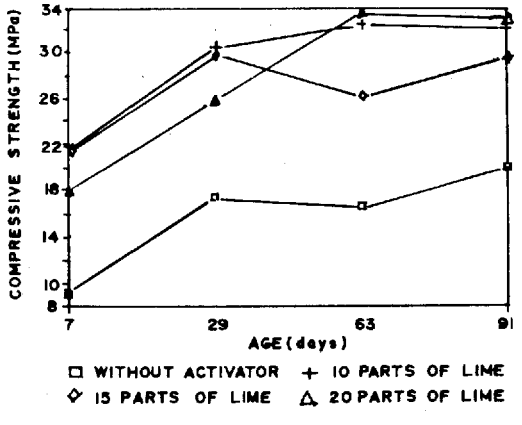

Fig. 3 - Strength development of the lime activated slag.

With gypsum-soda activation, increasing the amount of soda increases the resistance at the early ages but for the higher ages the ideal amount of soda seems to be 2%. The lowest values of compressive strength were obtained with lime as the only activator. At the lower ages the resistance decreased with increasing amounts of lime, but at 63 and 91 days an increase in the resistance with higher amounts of lime was observed. The highest resistance resulted from the gypsum-lime activation. At 7 days the compressive strength of the mixture of 10% lime plus 5% soda was three times that of the unactivated slag and higher than the resistance of the slag alone at 91 days.

Differential Thermal Analysis (DTA)

The DTA curves are shown in Figs. 4 to 7. The peaks at 840°C and 920°C on the slag curve at Fig. 4 represent the slag devitrification, that is, the formation of crystalline compounds (melilite and merwinite). The endothermic peaks observed at the gypsum curve till 190°C represent the transformation of dihydrate in hemihydrate and subsequently into anhydrite. On the lime curve, the endothermic peak at 540°C represents the $Ca(OH)_2$ decomposition.

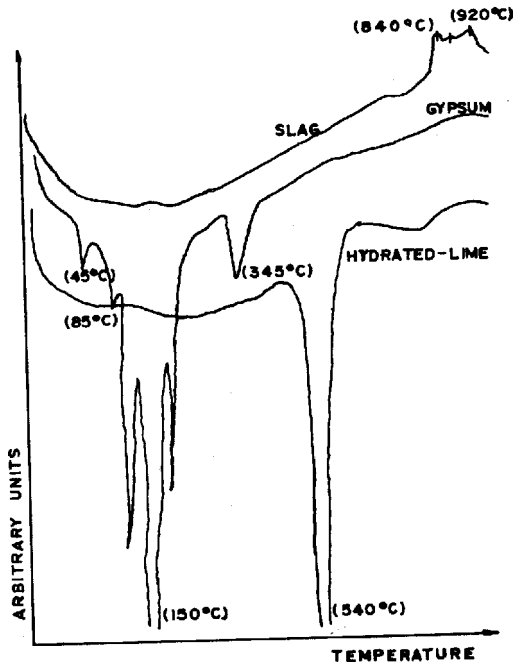

Fig. 4 - DTA curves of the unhydrated slag, of the gypsum and of the hydrated lime.

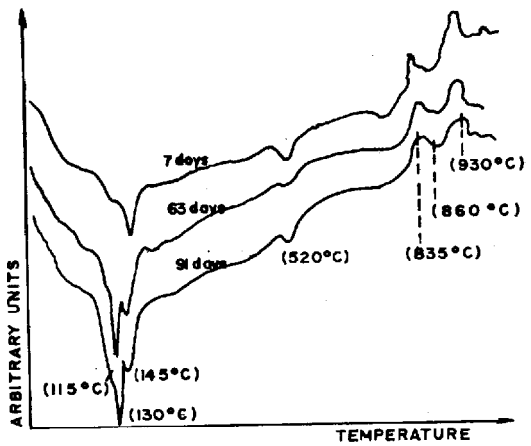

Fig. 5 - DTA curves of the gypsum-lime activated slag (10% lime).

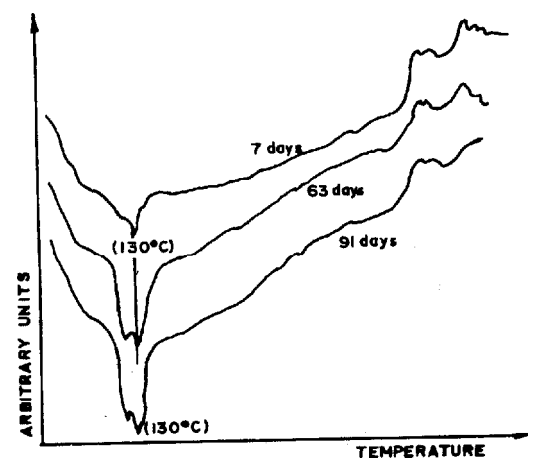

Fig. 6 - DTA curves of gypsum-soda activated slag (2% soda).

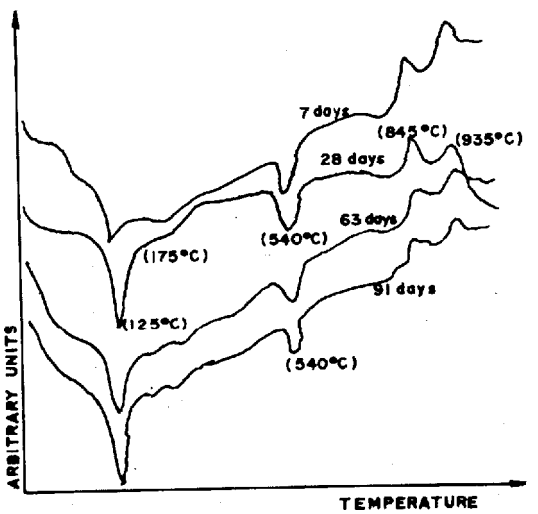

Fig. 7 - DTA curves of the lime activated slag (15% lime).

The unactivated slag DTA curves are similar to that of the unhydrated slag (Fig. 4), but with 91 days of hydration a few differences can be found, a small endothermic peak at 120°C and a lowering of the exothermal devitrification peaks, due probably to the formation of some weak aglomerating hydrates that use up some energy given off by the vitreous fraction.

On the hydrated slag curves, shown in Figs.5, 6 and 7, one can distinguish three main regions:
- the low temperatures region (under 200°C) where we have endothermic peaks due to the hydrated calcium silicates (C-S-H), ettringite and gypsum;
- the central region, about 500°C, where we have the endothermic peaks resulting from the lime decomposition and
- the high temperatures region where the exothermic peaks due to the slag devitrification can be found.

On the gypsum-lime activated slag DTA curves (Fig.5) there are many peaks in the low temperature region due to the formation of C-S-H and ettringite. The lime consumption in the hydration process can be seen from the reduction of the peak at about 500°C with the hydration progress. The peaks at the high temperature region diminish as the peaks due to the hydration products increase.

On the gypsum-soda activated slag DTA curves (Fig. 6) the peaks at about 500°C are absent because there is no lime present in this mixture, but at the age of 91 days a small peak due to the formation of Portlandite ($Ca(OH)_2$) can be found. The endothermic peaks that are present in the low temperatures region are due to the binding hydrates. The sample with the highest amount of soda showed a more simple pattern, with a greater evidency of the ettringite peaks. In any case the exothermic peaks are smaller than the ones observed in the hydrated slag without activator.

The ettringite peak is absent in the low temperature region of the DTA of the slags activated only with lime (Fig. 7). The consumption of lime with the hydration progress is shown by the lower intensities of the peaks about 500°C. The exothermic peaks in the high temperature region almost disappear due to the formation of the cristalline hydrates.

There seems to be a certain relationship between the intensity of the peaks in the low temperature region and the mechanical strength of the different kinds of activated slags, but one must take into account the negative effect on the mechanical strength of an excess of lime.

X-Ray Diffraction

The x-ray diffractograms of the samples hydrated till 63 days can be seen on Figs. 8 to 11. The identification by x-ray diffractometry of C-S-H when not well cristallized is difficult. On the unactivated slag diffractogram (Fig. 8), only the peaks due to merwinite are well defined[3]. The amount of vitreous materials is still large, that can explain the low mechanical resistance.

In the lime-gypsum activated slags diffractograms (Fig. 9) the peaks due to the hydration products ettringite, $CaCO_3$ and C_4AH_{13} can be identified. The intensity of the lime peaks decrease as the hydration progresses, and the peaks due to $CaCO_3$ and C_4AH_{13} increase. The peaks due to ettringite remain quite constant. It seems that the ettringite is formed in the first days of the hydration process.

The same products as with gypsum-lime activation can be identified on the diffractograms of the soda-gypsum activation (Fig. 10) and also the peaks due to merwinite are also still visible. In this case the intensity of the peaks due to ettringite increases with the hydration progress.

On the diffractograms of the lime activated slag (Fig. 11), the following products can be identified: C_4AH_{13}, $3CaO.Al_2O_3.CaCO_3 . 11H_2O$ and $CaCO_3$. The second product is the

first one after carbonation. The peaks due to merwinite and lime are also present. These last ones remain constant during the whole process. Due to the absence of gypsum, ettringite is not formed.

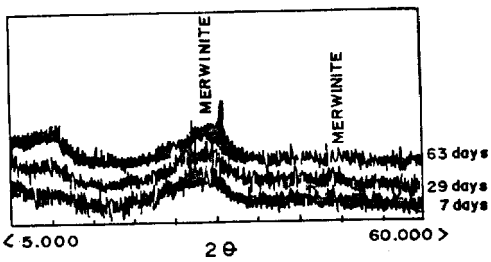

Fig. 8 - X-Ray diffractograms of the unactivated slag.

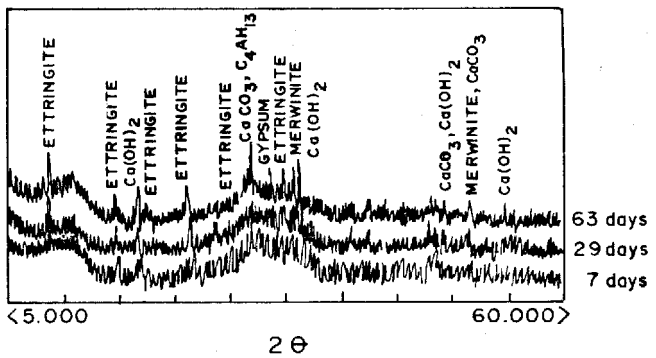

Fig. 9 - X-Ray diffractograms of the gypsum-lime activated slag (10% lime).

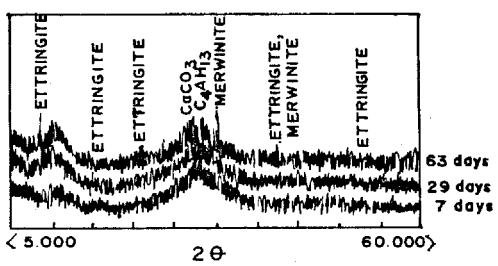

Fig. 10 - X-Ray diffractograms of the soda-gypsum activated slag (2% soda).

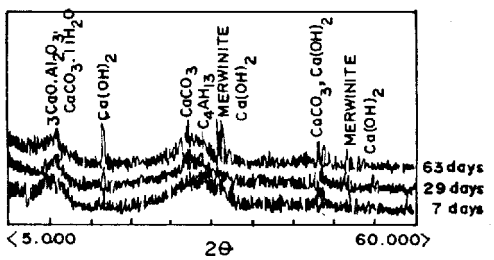

Fig. 11 - X-Ray diffractograms of the lime activated slag (10% lime).

Infrared (IR) Spectroscopy

On Fig. 12 are shown the IR spectrograms of unactivated and activated slags hydrated 63 days. The unactivated slag spectrogram shows only wavebands in the water region ($3480cm^{-1}$) and in the vitreous slag region ($970cm^{-1}$)[4].

The spectrograms of the activated slags are quite similar, only in the lime activated slag spectra there are no wavebands in the ettringite region ($1100cm^{-1}$), due to the gypsum absence. In the lime-gypsum activated slag spectra the waveband at $3644cm^{-1}$ represents the hydroxide. This waveband is absent of the soda-gypsum activated slag spectra indicating that probably all the hydroxide was consumed in the reaction. In these two last spectra the wavebands due to gypsum in the region between $667cm^{-1}$ are $588cm^{-1}$ are missing, probably indicating that most of the gypsum reacted to form ettringite.

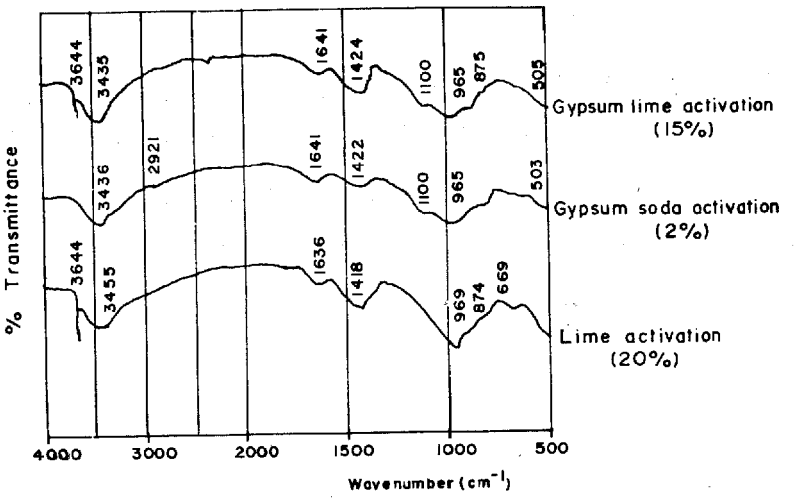

Fig. 12 - Infrared spectrogram of the activated slags after 63 days of hydration.

CONCLUSION

The best activation resulted from the mixture lime-gypsum respectively in the proportions of 10% and 5% of the slag amount. With this mixture the amount of ettringite remained constant after 7 days of hydration, indicating that the amount of gypsum present is sufficiently small to react in the first stages of the reaction, without any risk of further reactions. In this mixture the amount of lime present is still excessive and maybe the addition of a third component to react with the excess of lime, like a pozzolanic material, would result in a better product.

ACKNOWLEDGEMENTS

The work here described was carried out as a part of the agreement between the CNPq-Brazil and CEFI - France, at the Institut National des Sciences Apliquées, INSA in Lyon, Département de Génie Civil, Laboratoire de Matériaux Minéraux, under the supervision of the engineers Jean Péra, Ali Sadr Montazi and with the participation of the engineers Serge Martin - Calle and Sophie Husson.

REFERENCES

1. Lea, F.M.: The chemistry of cement and concrete. 3rd ed. London, Edward Arnold, 1970, 727 p.

2. Alexandre, J. and Sebilescu, J.L.: "Le Laitier de Haut Fourneau", CTPL - Centre Technique et de Promotion des Laitiers, Paris, 1988, 340 p.

3. Cincotto, M. A. and John, V. M.: "Cimento Alternativo à Base de Escória de Alto Forno". Construção - São Paulo, 1990, 43 (2204), 19-22.

4. Dutta, D.K. and Borthakur, P.C.: "Activation of low lime high alumina granulated blastfurnace slag by anhydrite". Cement and Concrete Research, 1990. 20, 711-722.

PROPERTIES OF VERY FINE BLASTFURNACE SLAGS MANUFACTURED BY JET MILL

P J Nieminen and K P K Pylkkänen

Tampere University of Technology, Institute of Engineering Geology
Tampere, FINLAND

SUMMARY

Different types of jet mill pulverized granulated blastfurnace slags from European sources were examined. The slags were characterized according to fineness, surface roughness, water adsorption capacity and chemical composition. The influence of slag properties on the hardening of mortar specimens made of portland cement activated slag was studied. The specific surface area varied between 290-620 m^2/kg (Blaine) and 1000-3000 m^2/kg (gas adsorption). The water adsorption capacity in 7 days varied between 0.2-1.9 %. With the same slag the strength increased with increasing fineness. In some extend the effect of fineness was compensated by using blastfurnace slag of higher alkality.

1 INTRODUCTION

In several countries ground granulated blastfurnace (GGBF) slag is used as a cementitious material in road and concrete construction. To release the hydraulic properties of GGBF slag in order to get needed early strength an activator is usually needed. In addition to the type and amount of activator the properties of GGBF slag itself affect its effectiveness as a hydraulic binder (1).

The cementitious properties of GGBF slag have usually been researched and tried to be classified by determining the fineness, the glass content and the chemical composition of the slag (1), (2). The reactivity of the GGBF slag is often thought to increase with increasing fineness, glass content and C/S -ratio (3), (4).

In the present study the hardening of jet mill pulverized blastfurnace slags from different European sources was examined. In addition to the properties above the slags were characterized according to their specific surface area (SSA) and water adsorption (WA) capacity.

2 EXPERIMENTAL

2.1 Materials

2.1.1 Fineness - The granulated blastfurnace slags originated from Austria, Belgium, England, Finland, France and Germany. The slags were pulverized mainly to three different fineness using jet milling. Slag D1 was ground by ball milling. Particle size distributions measured by laser diffraction method are presented in Figure 1.

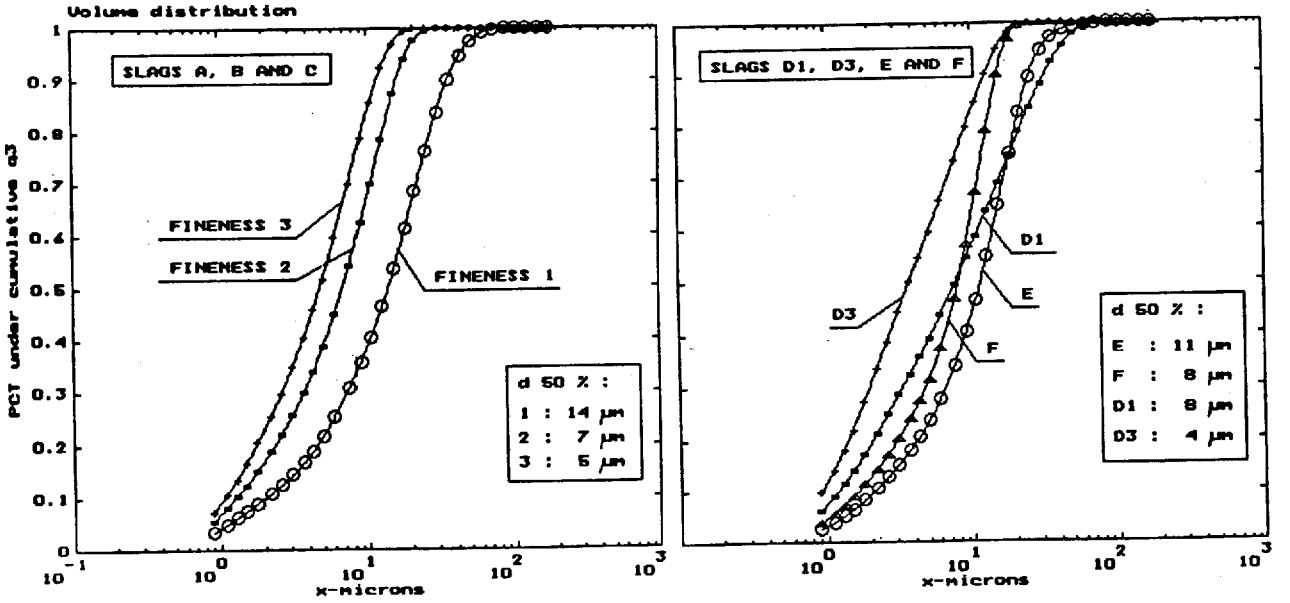

Fig.1 Particle size distributions of used GGBF slags.

Compared to the fineness of Finnish portland cements fineness 1 is coarser than normal hardening cement and fineness 3 about the same as rapid hardening cement.

2.1.2 Specific surface area and water adsorption - The SSA of slags was determined using gas adsorption and permeametry techniques. The applied gas adsorption method was a dynamic single point (p/p_0 = 0.3) method where the carrier gas was helium (70 %) and the adsorbate nitrogen (30 %).

The applied permeametry methods were Blaine and Permaran. Permaran is an apparatus measuring the loss of pressure a compacted sample bed causes to a constant air flow while Blaine -method measures the time needed for a certain pressure increase. The results of the SSA -determinations are presented in Table 1. SSA for slags D1, D3, E and F was determined using only gas adsorption -method. The results are respectively 1100, 1400, 3000 and 1200 m^2/kg.

Table 1. Specific surface areas and water adsorption capacity of GGBF slags.

SLAG	SPECIFIC SURFACE AREA (m^2/kg)			WATER ADSORPTION (%)		
	Gas adsorption	Blaine	Permaran	7 d	28 d	160 d
A1	2100	320	470	1.5	2.3	4.5
2	2500	520	840	1.8	2.9	6.5
3	2700	590	1000	1.9	3.1	7.1
B1	1000	290	430	0.7	1.0	2.2
2	1300	480	750	0.8	1.2	3.0
3	1500	590	920	0.8	1.5	4.2
C1	1500	310	440	1.0	1.4	2.5
2	1600	490	770	1.2	1.7	3.8
3	1700	620	920	1.0	1.6	3.6
OPC	1200	450		5.7	14.4	

The WA -capacity was determined using so called desiccator -method (5). Ovendried samples were placed in dishes into a desiccator with 100 % RH inside. The adsorption of water vapour was followed weighting the samples in 7 days periods up to 160 days. The adsorption capacity was calculated in weight -% of the dry weight of the sample. The results are presented in Table 1. Water adsorption of slags D1, D3, E and F was researched only at the age of 7 and 28 days and the results are respectively 1.0 % and 1.9 % for D1; 0.8 % and 1.2 % for D3; 0.7 % and 0.8 % for E; 0.2 % and 0.4 % for F.

2.1.3 Chemical composition - The chemical composition was examined from slags A, B, C, D and E using x-rayfluorescence -method. The results are presented in Table 2. According to x-raydiffraction analysis slag A is amorphous, slag B consists of merwinitic, slag C of merwinitic and melilitic and slag D of melilitic chrystallization.

Table 2. Chemical composition of used GGBF slags.

SLAG	SiO_2	Al_2O_3	CaO	MgO	S	Na_2O	K_2O
A	37.8	10.6	40.2	8.4	1.2	0.29	0.67
B	34.8	11.6	42.3	8.8	1.0	0.23	0.34
C	36.9	11.3	40.1	8.4	1.0	0.18	0.72
D	36.0	8.5	38.0	11.4	1.8	1.00	1.00
E	38.6	10.1	35.1	10.7	1.0	0.40	1.60

According to the litterature there are several, reactivity indicating, index numbers to be calculated from the amounts of chemical compounds (6), (8). The index numbers differ according to which compounds are considered alkalis and which acids. Some of the indexes are calculated in Table 3.

Table 3. Index numbers measuring the reactivity of used slags.

SLAG	P1	P2	P3	F1	F2	F3
A	1.06	1.28	1.00	1.16	1.56	1.48
B	1.22	1.47	1.10	1.29	1.80	1.70
C	1.08	1.31	1.00	1.17	1.62	1.52
D	1.09	1.38	1.13	1.23	1.60	1.47
E	0.91	1.18	0.94	1.08	1.45	1.34

2.2 Preparation of samples

Specimens of size 4*4*16 cm were used for examining the influence of slag properties on the mortar strength. The specimens were prepared with binder:aggregate -ratio of 1:3 using water:binder -ratio of 0.58. The amount of portland cement activator was 20 weight -% of the total binder. After demolding the specimens were cured in 80 % RH at 20 °C. Some comparative experiments were made with tap water cured specimens. In the most cases the compressive strength of specimens was tested at the age of 1, 7 and 28 days.

3. RESULTS AND DISCUSSION

3.1 Specific surface area and water adsorption

The measurement of SSA and grain size distribution are generally used to determine the fineness of pulverized material. How do this procedures then differentiate the finenesses of studied slags? This is examined in Fig. 2 which presents the relative differences between fineness 2 and 1 and fineness 3 and 1.

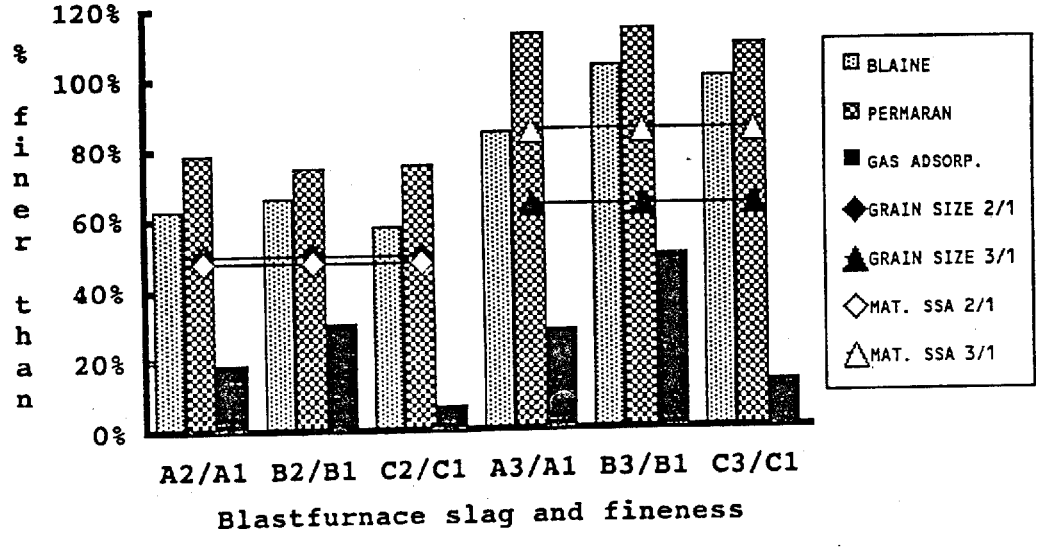

Fig. 2 Relative differences between finenesses determined by different methods.

Compared to the relative differences shown by the medium grain size (d 50 %) or the mathematical SSAs the Blaine and Permaran SSAs seem to show somewhat greater and gas adsorption SSAs smaller difference between finenesses. The last-mentioned is due to the better accuracy of gas adsorption method to measure the inequalities of a separate grain surface rather than the grain size.

The applicability of gas adsorption method to surface texture characterizing appears best when slags with same fineness but of different type are compared. According to Blaine and Permaran SSAs the varying between slagtypes is fairly notable, whereas gas adsorption SSA indicates more variation. The considerably different gas adsorption SSAs of slag A reveals its surface structure more amorphous and microporous compared to slags B and C. This appears also from water adsorption results being biggest for slag A, which may, however, also be due to bigger water affinity of chemical compounds in slag A.

3.2 Compressive strength

The compressive strengths after 80 % RH curing are presented and compared in Fig. 3. There is a notable increase in 7 -day compressive strength changing from fineness 1 to fineness 2 when slags A, B and C are used. Fineness 3 seems to give no further increase. Comparing the fineness 1, slag B is giving approximately 70 % better 7 -day strength than other slags.

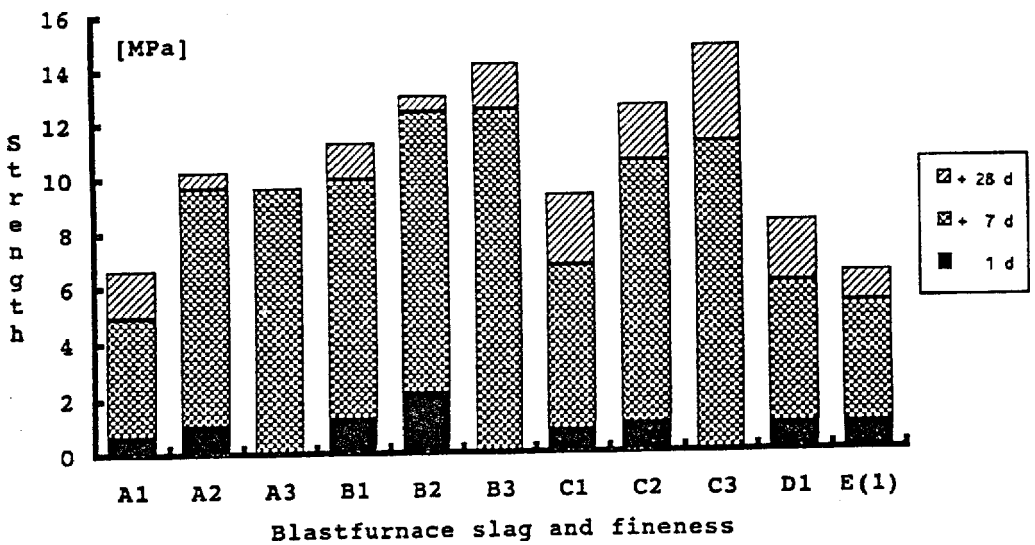

Fig. 3 Compressive strengths of tested mortar specimens after 80 % RH curing.

It is generally known that curing conditions can have a remarkable influence on strength development especially when GGBF slag is used (7). Therefore a couple of experiments were made using water curing. In Figure 4 presented results indicate, that water curing doubles the 28 -day compressive strength compared to 80 % RH curing. There is not great difference between slag types, except slag E giving about 30 % lower strength level at the age of 28 days. Furthermore it is interesting to notice, that using fineness 1 of slag B the same strength level is achieved as with other slags but of much finer grading.

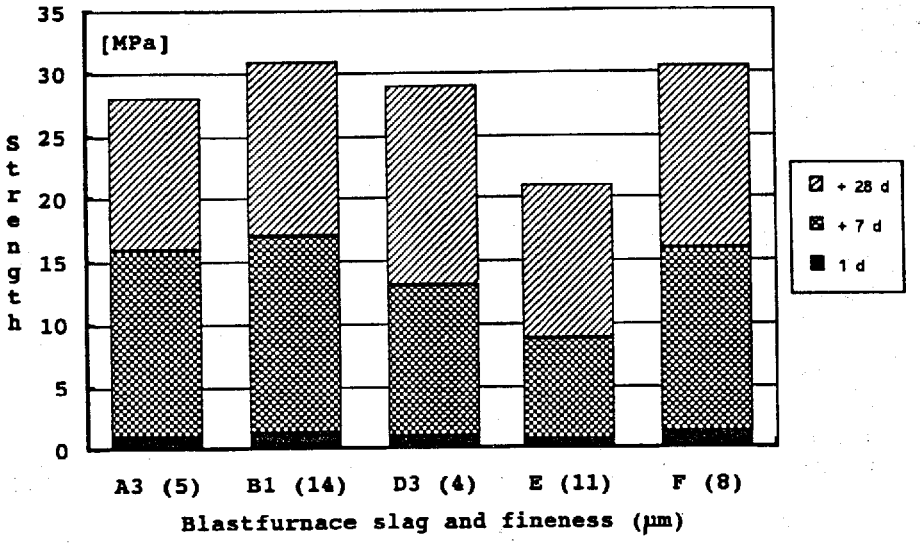

Fig. 4 Compressive strengths of tested mortar specimens after water curing.

The latter result suggests that the chemical composition of the slag may have some influence on the achieved strength level. Examining the calculated index numbers reveals them being in most cases biggest for slag B (containing merwinitic crystallization), which also gives good results in strength tests. For slag E the index numbers are the smallest and so was the strength. Merwinitic GGBF slag has proved active in other researches, too (9).

4 CONCLUSIONS

Ground granulated blastfurnace slags vary not only in chemical composition but in surface structure and water adsorption, too. The roughness of a surface reflects the glass content of the slag. The surface roughness can be evaluated by determining the specific surface area by gas adsorption method. The permeametry techniques measure mainly the fineness and pore size distribution caused by grain size distribution curves of different shapes.

Compared to ordinary portland cements the considerably lower water vapour adsorption capacity of GGBF slags signify better durability in storage conditions.

The presented results suggest that the activity of a ground granulated blastfurnace slag as a hydraulic binder depends mainly on the fineness and the chemical composition of the slag. These properties may to some extent compensate each others effect. The same strength level could be achieved either using coarse slag with higher alkalinity or vice versa.

REFERENCES

1. Lea,F.M.:**The chemistry of cement and concrete.** 3rd ed. London, Edward Arnold,1970,727 p.
2. Sato,K.,Konishi,E.,Fukaya,K.,Koibuchi,K.,Ishikawa,Y.,Iijima,Y.: "Properties of very fine blast furnace slag prepared by classification". **Proceedings 8th International Congress on the**

Chemistry of Cement. Rio de Janeiro 1986. Communications. Theme 3. Vol IV. pp. 239 -244.

3. Smolczyk,H.G.:"Slag structure and identification of slags". **Proceedings 7th International Congress on the Chemistry of Cement. Paris 1980.** Vol I. Principal Reports. Sub-theme III-1. pp. 3 - 17.
4. Daimon,M.:"Mechanism and kinetics of slag cement hydration". **Proceedings 7th International Congress on the Chemistry of Cement. Paris 1980.** Vol I. Principal Reports. Sub-theme III-2. pp. 1 - 8.
5. Kellomäki,A.,Nieminen,P.:"Adsorption of water on the fine fractions of Finnish tills". Helsinki 1986. **Bulletin of The Geological Society of Finland.** Nr 58, Part 2. pp. 13 - 19.
6. DIN 1146-1990:. "Portland-, Eisenportland-, Hochofen- und Trasszement (Portland-, Portland blastfurnace-, blastfurnace slag- and trass cements). March 1990.
7. Kutti,T.: "Alkali activated slag mortar. Mechanical strengths, shrinkage and structure". Chalmers University of Technology. Division of Building Materials. P-90:6.Göteborg, Sweden, March 1990.
8. Demoulian,E.,Gourdin,P.,Howthorn,F.,Vernet,C.:"Influence of slag chemical composition and texture on their hydraulicity". **Proceedings 7th International Congress on the Chemistry of Cement. Paris 1980.** Vol II. pp. III/89-94.
9. Frearson,J.P.H.,Uren,J.M:"Investigations of a ground granulated blast furnace slag containing merwinitic crystallization. **Proceedings 2nd International Conference Use of Fly Ash, Silica Fume, Slag and Natural Pozzolans in Concrete. Madrid 1986.** pp. 1401-1421.

CHEMICAL ACTIVATING OF METALLURGICAL SLAG IN THE CONDITIONS OF GRANULATING

V V Vulkov*, N A Delchev* and N S Nikonova**

**Sofia Technology University, Sofia, BULGARIA*
***D I Mendeleev Institute of Chemical Technology, Moscow, RUSSIA*

SUMMARY

In the presend report are described the results by the researches caried ont in the laboratory of Sofia Technology University and Moscow Technology Institute of Chemistry about the influence of the medium in the process of granulating of the slag melt, The formation of the structure of the slag glass and its hydraulic activity is also investigated. This is a continuation of the developed methol for chemical activation which includes on the granulation of the slag melt in inorganic salts water solutions.

РЕЗЮМЕ

В докладе показаны результаты, проведенных исследовании в Софийском технологическом университете и МХТИ им. Менделеева - Москва полученные при изучении влияния среды гранулирования шлакового расплава на формирование шлакового стекла и его гидровлическую активность. На основе результатов разработан метод химического активирования путем гранулирования шлакового расплава в водных растворах неорганических солей.

INTRODUCTION

Studing the binding properties of the granulated methalurgy slags demands irrefutably the existing connection between activity and physical - chemical specialities in their constitution-chemicalcomposition phase compound and structure. Generaly it is accepted that this connection exits(1, 2,3). Many disputes hare been carried on some ditals: ratio of the glassy to the crystal phase, polymerisation degree of the silicic-oxygen tetraedra, complete replacement of SiO_4^{4-} with AlO_4^{5-}, ratio between complexes with fourfold and sixfold coordination defects as a results of coorision the slassy matrix, the liquid phase separation of the slag glasses (4,5,6,7).This differences however are determened by the initial compound of the slag melt and by the cooling conditions. The exsperiments for increasing the chemical activity of the granulated slag are based on that and come down to two directions: modofication of the slag melt compound, i.e. introduction of ions modificators and changing the conditions of granulating.

Since the end of the sixties, in different coutries has been developed the second direction (8,9,10,11). There are used water solitions of inor - ganic and organic materials (activators) with alcaline or acidic reaction. The effect of the inorganic activators is connected with adsor bation of the alcatine and (or) alcaliearth compounds on the surface and in the granula's pores fixing larger quantities of water molecules, spee ding the processes of interaction between $Si(OH)_4$ and $Ca(OH)_2$ and crystalization of the hydrated formations (8,9,10). It is supposd to be formed active centres of cristalization as a result of chemical interaction of increasing the slag activity, using water solutions of organic substances (11) is pointed out the plastification effect which causes decreasing of the water-cement factor of the activator on the surface of slags' grains and by this way increases the mechanical strength of the slagportland ce ment. These explanations are true and based on the general theories about the processes of hydraulization and hydratacion of the bounding substances.

Having in mind the nature of the glassy state, what granule methalurgy slags are the matter of the process of activation should be researched in the physical-chemically and structural modifications which occured during formation of the slag glass (by the way process of granulation is monequilibrium process by the themodinamics point of view.

EXPERIMENTAL

The matter of the method of activation is the granulating of the slag melt with an initial temperature 1400°C in water solutions of CaO, phospho gyps and $CaCl_2$, which concentration is from 0,1% to 1,0% and expenditure of cooling agent is 4 l/kg slag (12).

The activity of the obtained granulated slags is estimated concerning modification of the mechanikal strenght of compressive of the slag-portland cement, which consists 30% and 50% slag of standart terms of soldification. Finenes of milling (Sn=3200 sm^2/g) and water cement factor (W/C=0,26) were maintained constrant.

Termical analys of the slags is carried out on a derivatograph "Paulik" system, regime: max. temperdture 1000°C; rate of the temperdture increa - sing 10°C/min; sensibility of DTA-sygnal-1/5; sample weight - 1,0 g. Spectral curves of absorption are obtained on a spectrometer "Specord-71 IR"in tablets (KBr), within interval of absorption 2000-400 sm^{-1}. Structure researches, especially polimerizacion degree of silicid-oxygen tetrahedres in the slag glass are carried out using the method of the coplex molibdative kinetic analys (13,14). Activating (E_a) energy and the degree of transformation (α) to overcooling li - gult of the glassy phase we determed by data of DTA usinga package of applicational programms, to be solved straight and reverse tasks of simulative kinetic researches in nonizotermical condi-

tions.

$$\frac{d\alpha}{d\tau} = K(\alpha)^n (1-\alpha) \left| -\ln(1-\alpha)^p \right| \qquad (1)$$

RESULTS AND DISCUSSIONS

The diagram (fig.1) reveals the average modification of the mechanical compressive strenght (in percents) of the slag-portland cement consisting slag granulated in water (nonactivated) and solutions of the already mentioned substrances with different concentration (activated).

Reading the identitive conditions of which were set all cements during the process of hydratation and solidification obtained higher hydraulic activiti (from 8% to 25%) we accept that in is due to only to the increased chemical activity of the slag component. In it's turn this modification is co nected with the change of con ditions of granulating-in solution. Structure modifica-tions on the surface layer of the slags' fractions are possible, as a result of the interaction on the interface boudary surface melt-solution, accelera - ting by the results of the carried out physical-chemi - cally researches. We speci - fied an almost total 993-95% glassing of the melt, based on data of X-ray analys. Carried out electronographic analys proved this con clusion about nonactivated slag and fixes only the presence of micro-crys - talphases in the activated slags. In the chemical activated slags, at heating up, flows degree crystalization within the interval of transformation of slag glass (fig. 2). Primary crystalized phases are - belit (C_2S) and me lilit predominating gelenit component. The transitinal proces kinetic from solid state to overcooled liguid at 700°-740° (fig. 2) is different. The dy namic of it's course expressed by (fig. 3) is higher for activated slags the same for E_a (fig. 4). This is conected with distubanced symetry of the struc ture network ascertained by infra-red spectroskopy by eowering the freguency of vib ration of the bonds Si-0-Si from 1000 sm^{-1} to 930 sm^{-1}. This is a characteristic indication for depolymerization of the silicic-oxygen polihedra. By data of the complex molibdative-kinetic analys, in all slags' struc ture, absented high polymerizational forms with degree $n_i > 25$. There is higher perecentage of oligomeric forms in the activated slags, average 12-13%, compared to 8% in nonactived slag, but the polymerizational degree is lower. The polymerization decreases with the increasing the solution concentration (fig. 6).

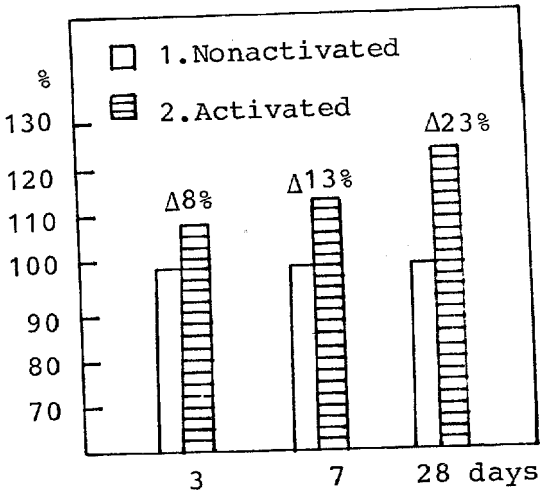

Fig. 1. Changes the slag-portland cement' compressive strenght

The result is a distruction of the silicic-oxygen network or reciprocal process blocking the structure forming in the upper layer under the action the cooling agent particles.

This, it's possible the occurance of nonhomogeneous area with exeess of positive eharges or uncompensated negative charges (acidic -+ or basic-,active centres), of new-phase cristalization. The initial stage of interaction glass-water (solition), as and it's mechanism are simi lar to the explaned in (15) and will be discussed in investigation.

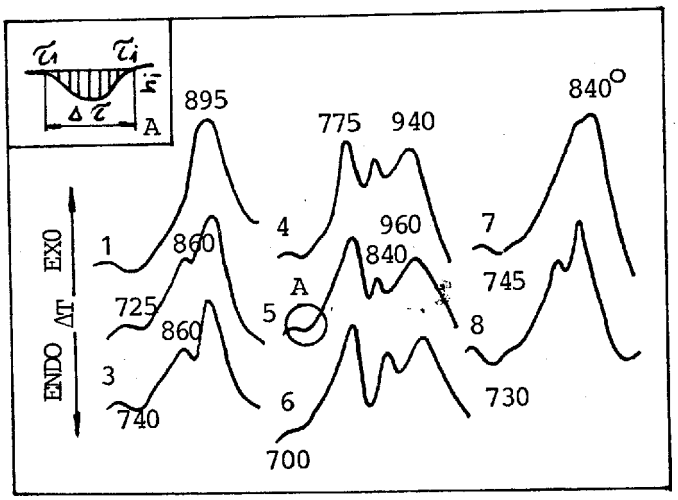

Fig.2. Differential thermal curves of the granulated methalurgy slags 1.Nonactivited. 2.Activited(from 2 to 8)

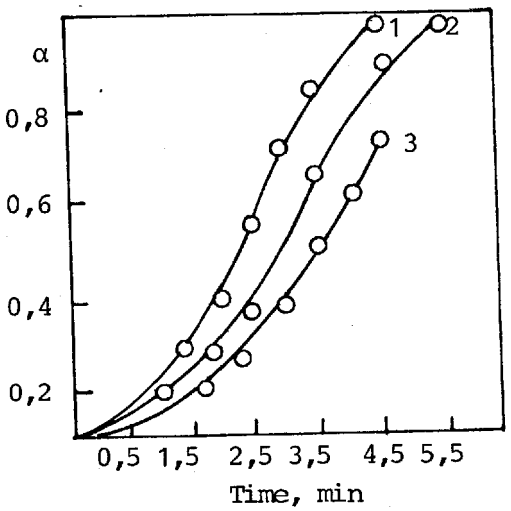

Fig.3. The degree change of transformation of the transition from glass to overcooled liguid of the examined slags

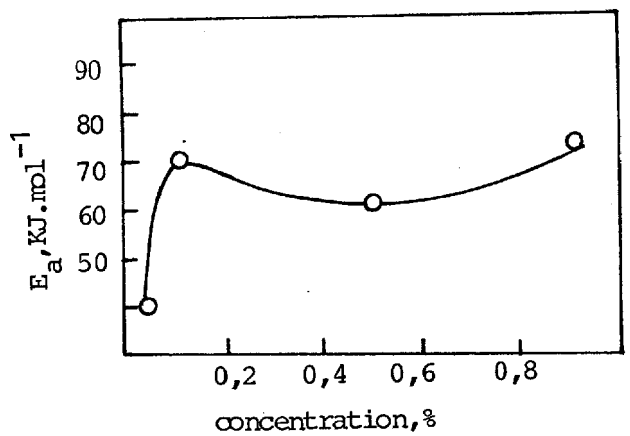

Fig. 4. Change of the E_a of the slag glass by the solution concentration

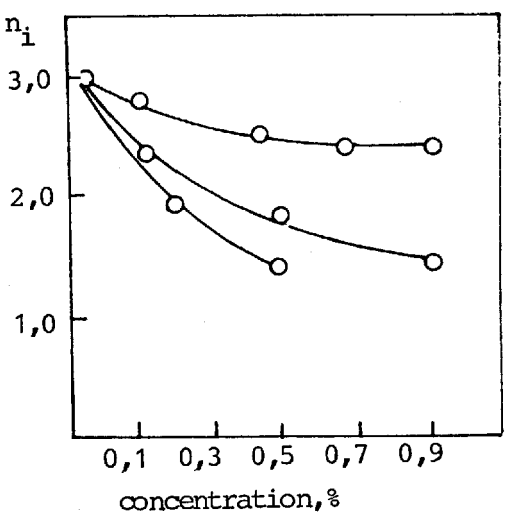

Fig. 5. A change the average polymerizational degree (n_i) of the slag glass by the solution concentration

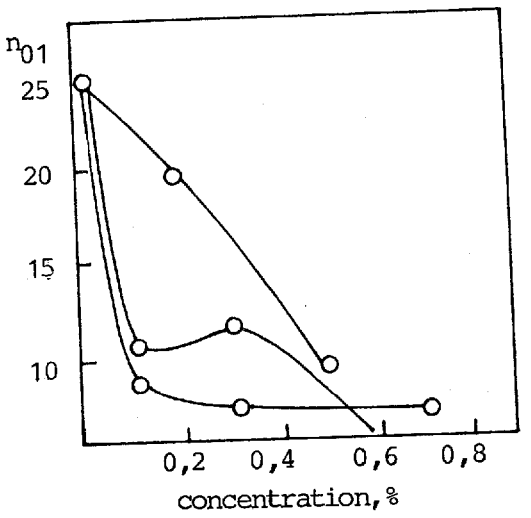

Fig. 6. Polymerization change of oligomeric fruction by the solution concentration

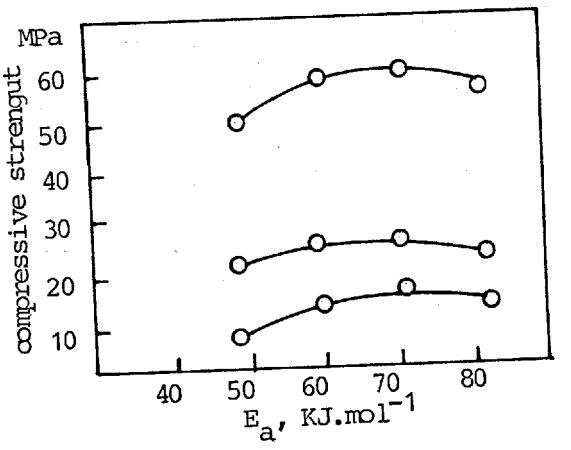

Fig. 7. Hydraulic activity dependency of slag-portland cement by the E_a of the slag component

CONCLUSIONS

The obtained results reveals that the direct connection exists between hydraulic activity and structure of the slag glass, formed in the polymerizational process of the slag melt (fig.7). It's knowledge and studing gives the opportunity to choos the type of the activating agent and regulation the process of activating in order to obtain a product of maximum hydraulic activity.

REFERENCES

1. Voskoboymkov V.G. Dunaev N.Z. Mihalevich A.G.,Svoystva zhidkih domenuih shlakov, Metallourgia, Moskva, 1975.
2. Royak C.M. Pyachev V.A., Shkolnik J.Sh. Structura domenniuh shlakov i ih aktivnost Cement, N 8, 1978.
3. Butt Y.M., Mayer A.A., Isledovanie produktov gibrotermalnoiobrabotki mineralov domennogo shlaka, Sb. Metalurgicheskie shlaki, Moskva, 1962.
4. Kosakavitch P., Rew. metallurgue, N 57, 1966.
5. Myuler R.P., "Priroda", N 8, 1964.
6. Cherou M., Zardinois C., The 5th International Symp. Chemie Cement, Tokyo, 1968, vol. IV, 277-285.
7. Jochanson S.E., Silicatidustrieles, N 3, 1973.
8. Avtorsko svidetelstvo USSR, N 464551, kl. COY B 5/02, 1973.
9. Patent USA, N 3938975, kl COY B 5/50, 1976.
10. Avtorsko svidetelstvo USSR, N 712402, kl. COY B 5/02,1980.
11. Sholnic Y. Sh. Pyachev V.A., Burlakov V.J., Gidravlicheskaya aktivnost domeunih shlakov granulirovanih sulfatno drozhevih brazuki, Izvetie VUZ Stroitelsko i arhitektura, N 7, 1981.
12. Avtorsko svidetelstvo N 12, Bulgaria N 35376, N 35377, 1983 i N 39001, 1984, kl. C 04 B5/02.

13. Ayeer R., Himiya kremnezema , "Mir", Moskva, 1982.

14. Tchekunova E.V., Roe reaktisii polikondeusatsie kremnekislorodiuh anionav v protsesah gidratatsii i degidratatsii silicatov kaltsiya i natrija. Disertatsija na soiskanie nauchnoy stepeni kandidat himicheskih nauk, Moskva, 1988.

15. Shultse H., Izuchenie poverhnostnih sloev buyshhelochennuyh stekol noetodami sektsiomrovaniya u YK-spektroskopii, PUIZIKA i nimiya stekla,2, N 1, 1976.

METALLURGICAL SLAGS AS BLENDING MATERIALS FOR CEMENT MANUFACTURE

K M Sharma, R Bhargava, D Yadav and S C Ahluwalia

National Council for Cement and Building Materials
New Delhi, INDIA

SUMMARY

Granulated blast furnace slag is a potential blending material and is used world over for making blended cements. However, due to inadequate granulation facilities in steel industry and non-availability of these in metallurgical industries, it has to be disposed off in air and is known as air cooled slag having no hydraulic property and as such finds no practical use in cement manufacture. An attempt has been made to utilise these air cooled slags as a blending materials for cement manufacture.Two air cooled slags one from phosphorous industry and the other from steel industry were selected and efforts have been made to activate them chemically by using NaOH and Na_2CO_3, by thermal process and by a combination of these two processes. The resultant slags were used as a blending material for the manufacture of PSC. Performance characteristics of blends prepared with activated and unactivated slags have been reported. SEM and XRD studies of hydrated blends upto 28 days have been presented. Results indicate that a combination of thermal followed by chemical process is most appropriate for the activation of air cooled slags.

INTRODUCTION

The use of granulated blast furnace slag for the manufacture of binary blends of OPC - slag is well established and these blends are now marketed all over the world. In a similar study granulated slag obtained from phosphorous industry has also been utilized for making blended cements (1). Apart from granulated slags huge quantity of air cooled slags having no hydraulic properties is available in India and remains unutilized. The present investigations have been directed towards the utilization of air cooled slags particularly blast furnace and phosphorous furnace slag as a component of slag cement by chemical activation, thermal activation and by combination of the two.Studies have been reported on activation of granulated slags with alkalies and their salts (2,3) and were extended to air cooled slags as well.The blends prepared using OPC, unactivated slags and slags activated by above processes were investigated for performance characteristics. The hydration studies were also carried out using X-ray diffraction and scanning electron microscopic techniques.

EXPERIMENTAL

The raw materials used in the present investigations for making blended cements were ordinary portland cement clinker, air cooled slags from steel and phosphorous industries and gypsum. The elemental analyses of these materials are given in Table 1. These materials were also subjected to mineralogical and morphological studies using X-ray diffraction, optical and scanning electron microscopic techniques. The X-ray diffractograms of air cooled and water quenched (granulated) slags are given in Fig.1 and 2 respectively and scanning electron micrographs are presented in Plates 1 and 2.

OPC-slag blends were prepared by fixing the slag content to 40 percent and overall fineness of slag cement to 400 m^2/kg as per the details given below :

1/ Activation by Chemical Process - Series-I

To study the effect of activation on ground air cooled slags 1 and 2 from steel and phosphorous industry respectively, NaOH and Na_2CO_3 were added in different dosages varying from 1 to 5 percent. The blends so obtained were subjected to the determination of setting time and strength characteristics and the results are given in Table 2.

2/ Activation by Thermal Process - Series-II

Slags 1 and 2 were melted in a laboratory furnace at a temperature varying between 1300 - 1350°C followed by immediate pouring in water to complete the granulation. The granulated slags thus obtained from slag 1 and 2 designated as slag 3 and 4 respectively were dried and ground to a fineness level of 400 m^2/kg. The slag cements were prepared and tested for setting time and strength characteristics (Table 3).

3/ Activation by Thermal Followed by Chemical Process - Series-III

In another series of experiments the slags 3 and 4 obtained above were activated with NaOH and Na_2CO_3 in different dosages and blends

prepared were evaluated for their performance characteristics(Table3).

4/ Effect of Fineness - Series-IV

To see the effect of fineness, blends PSC-3 and PSC-4 were prepared using slag 3 and 4 respectively and ground to different levels of fineness ranging from 250 to 450 m^2/kg. The influence of fineness on compressive strength is given in Fig.3.

Hydration Studies

Blends prepared by air cooled, granulated and granulated slag activated by NaOH were hydrated for 3, 7 and 28 days and the reaction was arrested by acetone and dried under vaccum. The samples were subjected to X-ray diffraction analysis and scanning electron microscopy. Diffractograms and micrographs of selected hydrated samples at 28 days are presented in Fig. 4 and Plate 3 respectively.

RESULTS AND DISCUSSIONS

Results of portland cement clinker (Table 1) indicate the presence of 52.91 percent C_3S and 0.56 percent free lime and considered suitable for the manufacture of blended cements.The X-ray diffraction analysis indicates the presence of 48 percent C_3S and 31 percent C_2S. The optical and scanning electron microscopic studies have shown well developed alite and belite phases (49 and 30 percent) which confirm its suitability for making blended cements.

TABLE 1
ELEMENTAL ANALYSIS OF RAW MATERIALS

Sl. No.	Sample Details	Constituents determined (percent) LOI	SiO_2	Fe_2O_3	Al_2O_3	CaO	MgO	Na_2O	K_2O
1	Clinker*	1.17	22.50	3.68	5.44	65.11	1.25	0.18	0.58
2	Gypsum	18.82	13.58	0.78	0.27	27.93	0.72	0.03	0.07
3	Air cooled BFS	1.12	33.41	0.60 (Feo)	19.01	32.88	9.91	0.14	0.04
4	Air cooled phosphorous furnace slag**	0.38	41.89	0.06 (Feo)	3.27	48.50	1.73	-	-

* CaO_f : 0.56; ** P_2O_5 : 1.08

The elemental analysis (Table 1) of slag samples SL-1 and SL-2 indicates that Al_2O_3 and MgO content of SL-2 is lower as compared to SL-1. However the lime silica ratio of the two slags SL -1 and SL-2 are 1.06 and 1.16 respectively, which are comparable. The X-ray diffraction analysis (Fig.1) has shown the highly crystalline nature of slags. The slag SL-1 contains akermanite, augite and forsterite

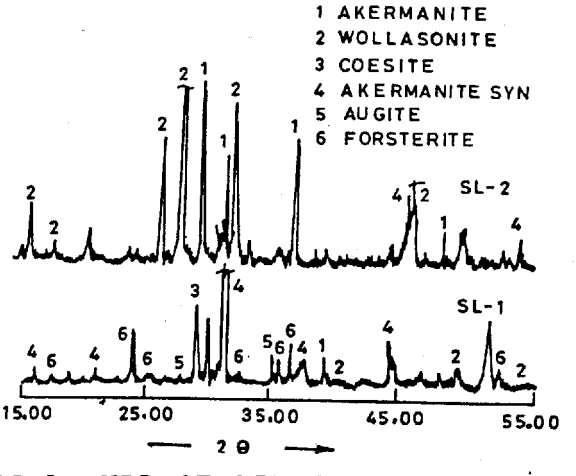

FIG 1. XRD OF AIR COOLED CLINKER

phases whereas SL-2 contains akermanite,pseudo -wollastonite and coesite.

The glass content of SL-1 and SL-2 as determined by optical microscopy was found to be 20 and 18 percent respectively. Chemical composition suggests the suitability of slags whereas the XRD and optical microscopy suggests their non-suitability. XRD of laboratory prepared granulated slags SL-3 and SL-4 (Fig.2) has indicated nearly complete amorphous nature of these slags. The glass content of slags SL-3 and SL-4 was found to be 93 and 92 percent respectively. The scanning electron micrographs of all the four samples are presented in Plates 1 and 2.

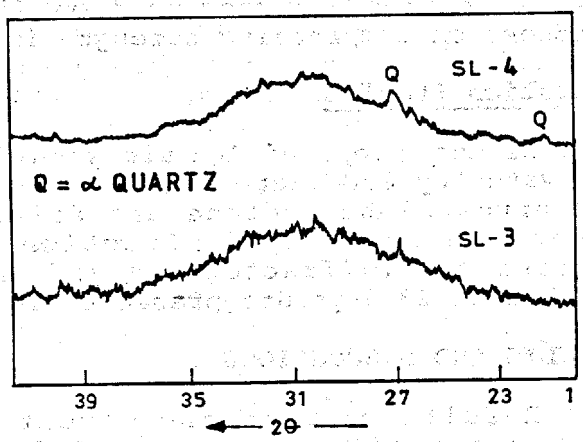

FIG 2 X-RAY DIFFRACTOGRAM OF SLAG SAMPLES

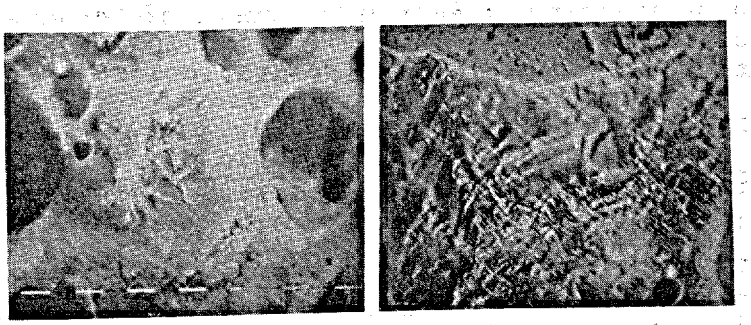

PLATE 1 : SEM's OF SL-1 AND SL-2 —10μ

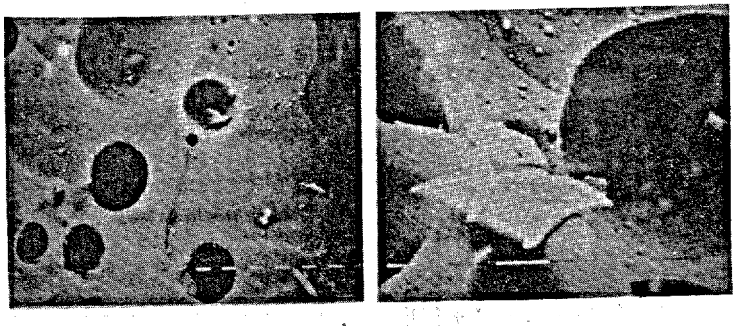

PLATE 2 : SEM's OF SL-3 AND SL-4 — 10μ

Effect of Activators

The slag cements PSC-1 and PSC-2 prepared by the replacement of 40 percent OPC by slags SL-1 and SL-2 show a marked reduction in compressive strength compared to parent OPC. It confirms that the two slags are non-hydraulic. Activation studies indicate a gain in strength by 7 and 10 percent maximum at a level of 5 percent Na_2CO_3 and NaOH respectively(Table 2).

TABLE 2
PERFORMANCE CHARACTERISTICS OF SLAG CEMENTS PREPARED FROM AIR COOLED SLAGS

Sl. No.	Sample No.	Activator (percent by Wt.)		Fineness (m^2/kg)	Setting Time (min) IST	FST	Compressive Strength (N/mm^2) 3d	7d	28d
1	Control OPC	-		315	95	255	26.0	40.2	53.5
2	PSC-1	0			120	280	13.0	20.0	29.1
	PSC-1a	1	NaOH	325	111	260	13.5	20.4	30.6
	PSC-1b	3			105	265	14.8	21.1	31.5
	PSC-1c	5			96	253	15.2	21.6	32.0
	PSC-1d	1			115	265	13.3	20.2	30.0
	PSC-1e	3	Na_2CO_3	325	103	258	14.6	20.9	31.2
	PSC-1f	5			97	255	14.9	21.1	32.1
3	PSC-2	0			113	275	12.1	19.0	28.1
	PSC-2a	1	NaOH	318	110	278	12.5	19.8	29.4
	PSC-2b	3			110	265	13.4	20.6	30.8
	PSC-2c	5			106	260	14.2	21.4	31.5
	PSC-2d	1			114	270	12.1	19.3	28.2
	PSC-2e	3	Na_2CO_3	318	110	265	13.0	20.0	29.1
	PSC-2f	5			98	268	13.9	20.8	30.0

Slag cements PSC-3 and PSC-4 prepared from granulated slags SL-3 and SL-4 indicate an appreciable gain in strength at all the ages and are comparable to parent OPC at 28 days (Table3).

TABLE 3
PERFORMANCE CHARACTERISTICS OF SLAG CEMENTS PREPARED FROM LABORATORY GRANULATED SLAGS

Sl. No.	Sample No.	Activator (percent by Wt.)		Fineness (m^2/kg)	Setting Time (min) IST	FST	Compressive Strength (N/mm^2) 3d	7d	28d
1	Control OPC	-		315	95	255	26.0	40.2	53.5
2	PSC-3	0			110	285	21.8	34.1	51.8
	PSC-3a	1	NaOH	320	103	279	23.0	35.3	52.1
	PSC-3b	3			96	275	24.2	37.2	52.9
	PSC-3c	5			90	265	24.9	38.0	53.0
	PSC-3d	1			105	280	22.1	34.6	51.5
	PSC-3e	3	Na_2CO_3	320	100	272	23.0	35.3	52.0
	PSC-3f	5			96	263	23.6	35.8	52.1
3	PSC-4	0			103	260	19.4	31.2	50.1
	PSC-4a	1	NaOH	316	97	255	20.2	31.9	50.2
	PSC-4b	3			95	254	22.6	33.0	51.6
	PSC-4c	5			93	246	23.2	33.6	51.7
	PSC-4d	1			103	275	20.1	31.4	50.3
	PSC-4e	3	Na_2CO_3	316	95	270	20.9	32.6	50.9
	PSC-4f	5			96	270	21.7	33.1	51.0

A further gain in strength was observed when slag cements PSC-3 and PSC-4 were activated with NaOH and Na_2CO_3. The gain in strength at 3 days was found to be 23.0, 24.2, 24.9 and 20.2, 22.6, 23.2 N/mm^2 at

1, 3 and 5 percent NaOH and 22.1, 23.0, 23.6 and 20.1, 20.9, 21.7 N/mm^2 at 1, 3 and 5 percent Na_2CO_3. From these results it is concluded that NaOH is better activator compared to Na_2CO_3 and 3 percent was considered optimum for activation. The slow activation by Na_2CO_3 could be attributed to the fact that it generates small quantities of lime which on reaction with Na_2CO_3 provides NaOH which eventually carries the activation process.

Effects of Fineness

The studies carried out to see the effect of fineness on compressive strength indicate that the strength increases with increase in fineness and the effect is more pronounced at 3 days. The results are plotted in Fig.3.

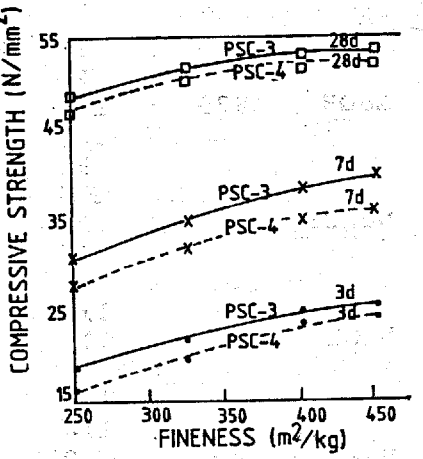

FIG 3: FINENESS VS STRENGTH OF SLAG CEMENTS

Hydration Studies

X-ray diffraction and SEM studies on cement prepared with air cooled slag has indicated the presence of unhydrated phases apart from

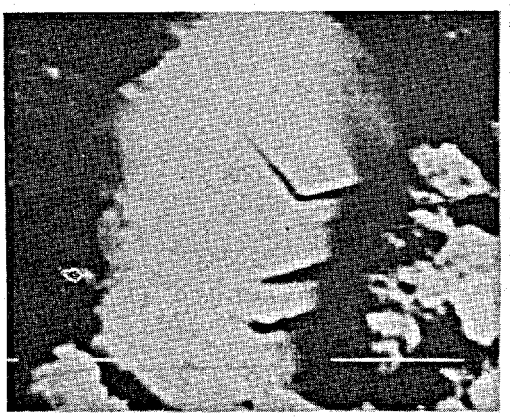

PSC from SL-1

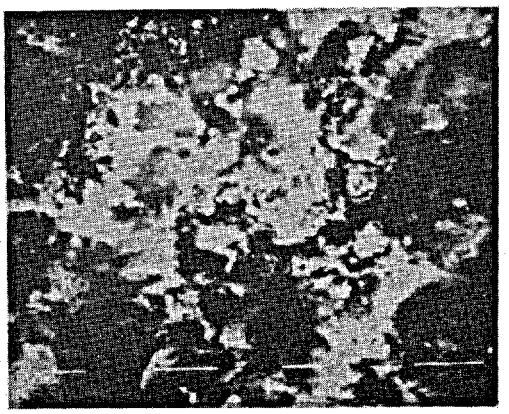

PSC from SL-3

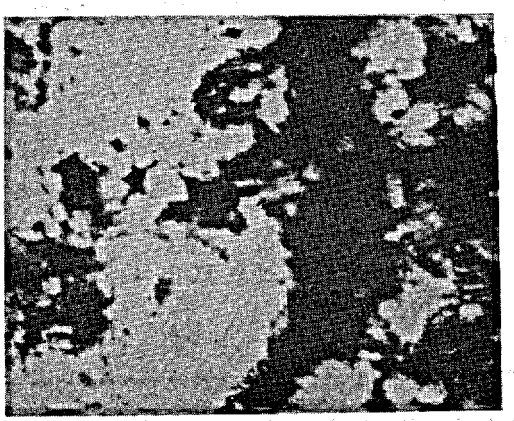

PSC from activated SL-3

PLATE 3 : SEM's OF HYDRATED SAMPLES AT 28 DAYS — 10μ

some hydrated phases of OPC which given small quantities of C-S-H resulting in poor strength. This is further confirmed by the presence of large quantities of $Ca(OH)_2$. In case of cement prepared by granulated slag it has been observed that the amount of $Ca(OH)_2$ decreases with increase in hydration age whereas amount of C-S-H increases. The formation of etterngite has been observed upto 3 days. The rate of hydration further increases at all ages when 3% NaOH is added in above system.

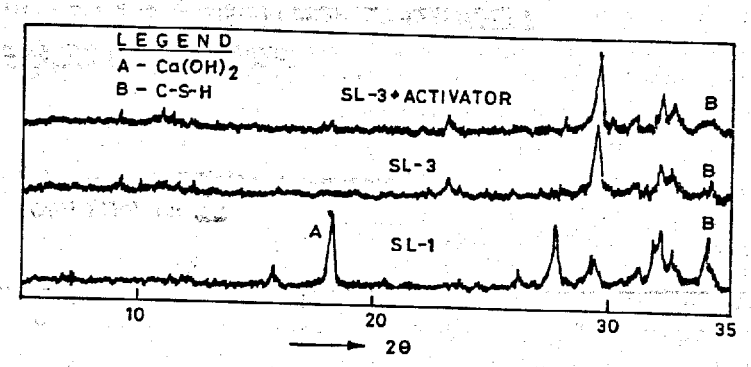

FIG 4 : XRD OF HYDRATED SLAG CEMENTS AT 28 DAYS

CONCLUSIONS

i. Air cooled slags from blast furnace and phosphorous furnace were not found suitable for the manufacture of slag cements.

ii. Activation of these slags was carried out by chemical, thermal and thermal followed by chemical processes. The best results were obtained by slags activated by thermal followed by chemical process.

iii. The compressive strength of slag cements increased with the increase in fineness and the effect was more pronounced at 3 days.

ACKNOWLEDGEMENT

The authors have freely drawn upon completed R&D work/status reports of NCB. This paper is being published with the permission of Director General, National Council for Cement and Building Materials (NCB),New Delhi, India.

REFERENCES

1. NCB :" Technical Suitability of the use of Phosphorous Furnace Slag for the Manufacture of Portland Slag Cement". Project Report, 1989, National Council for Cement and Building Materials, New Delhi, India.

2. NCB :" Development of Indigenous Technology for the Manufacture of Portland High Ash Cements". R&D Report, 1983. National Council for Cement and Building Materials, New Delhi, India.

3. Vionovitch, Dron R : " Effect of Various Activators on Hydration of Granulated Slag". Silica Ind,1976,41,209-12.

EFFECT OF STRUCTURE AND COMPOSITION ON REACTIVITY OF ZEOLITE-TUFF USED AS BLENDING MATERIAL OF PORTLAND CEMENT

Lian Huizhen

Department of Civil Engineering, Tsinghua University
Beijing, P R CHINA

SUMMARY

It is known that zeolite is a kind of crystalline with framing structure, but the pozzolanic reactivity of zeolite-tuff, i.e. zeolitizated tuff, is better than of many uncrystallized volcanic. In order to explain such a unusual behaviour, effect of zeolite content, Si/Al, positive ion and zeolite aqua in cavity of zeolite, fineness, etc. on reactivity of zeolite-tuff are tested. Among of them, the zeolite content and fineness are most sensitive rather than the chemical reactivity. It is confirmed that effect of blending materials should not be only considered according to their chemical reactivity. Compositions take effect on cement by way of their structure. What is the cause of the high reactivity of zeolite-tuff, such a kind of crystalline matter, can be explained.

摘　　要

沸石是一种具有架状结构的结晶，但沸石凝灰岩（即沸石化的凝灰岩）的活性却比非晶质的活性好。为了解释这种不正常的行为，对沸石凝灰岩中的沸石含量、Si/Al比、孔穴中阳离子和沸石水、细度等对沸石凝灰岩活性的影响进行了试验研究。在这些因素中，沸石含量和细度比其化学活性更敏感。这证明混合材料的作用不应只是考虑其化学活性。化学成分通过其结构起作用。沸石凝灰岩这种晶态物质高活性的原因就可以得到解释。

INTRODUCTION

Zeolite is a kind of crystalline with framing aluminosilicate. According to thermodynamics, stability of crystalline is much more than of amorphous. But as early as 1960, some scientists reported that reactivity of zeolite is more capable than that of glass[1][2]. Consequently, products of zeolite-tuff reacted chemically with lime have been studied continually[3][4][5][6]. Interface reaction between zeolite-tuff and cement paste has been investigated, and morphology of products thereof has been described[7][8].

Mokoto Asaka et al treated clinoptilolite tuff by sodium hydrate solution. It is proved that structure of zeolite can not be collapsed until above 2N of NaOH[9]. Lian reported that when concentration of NaOH is 5N, there was no zeolite any longer in tuff, and in solution of 0.1% $Ca(OH)_2$ (this is near the alkality of cement paste), the structure of zeolite is no changed similar to that in 0.5N of NaOH[10]. Owing to such a stable characteristic, zeolite can be used as the sieve sorbent and catalyser.

In order to understand the source of reactivity of zeolite-tuff all-sidedly, effect of varied zeolite content of tuff blended in Portland cement with varied blending amount on strength of cement paste, reactivity of zeolite-tuff, containing varied zeolite, with lime, effect of Si/Al ratio of zeolite and cation in cavity of zeolite on reactivity of zeolite-tuff, etc., are investigated in this paper.

ZEOLITE-TUFF USED FOR EXPERIMENTS

Two types of natural zeolite-tuff

Clinoptilolite-tuff from Nenjiang (in China) and mordenite-tuff from Zhejiang (in China) are used. Amount of ion exchange with NH_4^+ and corresponding zeolite content as well as composition of them are shown in table 1.

TABLE 1
Composition of zeolite-tuff used for experiments

Items			Compositions (%)							
Type of zeolite-tuff	Amount of NH_4^+ exchange (mg/100g)	Zeolite content (%)	SiO_2	Al_2O_3	Fe_2O_3	CaO	MgO	K_2O	Na_2O	LOI
Clinopti-lolite	178.92	84	61.60	14.40	2.20	3.79	1.85	3.13	0.70	12.83
Mordenite	131.57	60	68.96	10.28	1.97	0.92	0.48	0.60	3.40	13.72

Uncrystallization of natural zeolite-tuff

According to the thermostability of the two types of zeolite-tuff, 400°C and 800°C are used for treating above zeolite-tuff for half an hour separately. XRD indicated that structure of zeolite in mentioned tuff has been collapsed and crystallized substantially.

EXPERIMENTS AND ANALYSIS OF RESULTS

Effect of zeolite-tuff with varied zeolite content on strength of cement paste blended with zeolite-tuff by varied amount.

Uncrystallized and original clinoptilolite are mixed in ratio of 0:1, 1:3, 1:1, 3:1, 1:0 to make specimens with varied zeolite content with 84%, 63%, 42%, 25%,and 0%. Those specimens are blended into Portland cement by 5, 10, 15, 20, 30% (by weight of total binder) separately, then to be formed in 2*2*2cm³, W/C is 0.35. The compressive strength are tested after curing for 28 days. Results of tests are shown in fig.1. Every numerical datum is average from 30 groups of specimen.

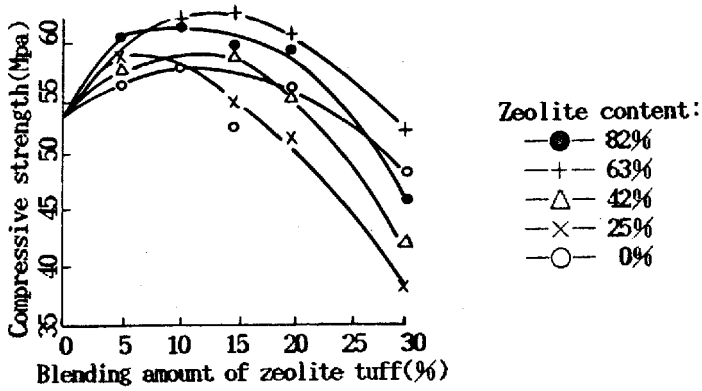

Fig.1 Compressive strength vs. blending amount of zeolite tuff with varied zeolite content at 28th day

It is shown in fig.1 that:

1. When the blending amount of tuff is 5-10% (by weight of the total binder), distinction of strength among specimens in which the zeolite content of tuff is varied seems very little. In fact, owing to "micropowder effect", if some inert material such as quatz sand is ground to be a certain fineness, strength of cement blended with it can also be elevated somewhat[11]. Distinction of strength among those containing varied amount of zeolite is increased with blending amount.

2. There are optimum blending amount of zeolite-tuff to make strength of cement higher for varied zeolite content separately. Alternatively, there are optimum zeolite content to make strength of cement highest for each blending amount of zeolite-tuff.

3. The optimum zeolite content of zeolite-tuff is over 42%, preferably about 63% and the optimum blending amount in that content is 10-20%. All the strength of uncrystalline zeolite-tuff in varied blending amount are lower than that of zeolite-tuff containing zeolite over 42%. When the blending amount is over 30%, strength of cement paste reduce markedly.

As comparison and proofing, the synthetic mordenite sieve sorbent and uncrystallized mordenite tuff are mixed by 0:10, 3:7, 5:5, 7:3, and 10:0 (by weight of total binder) respectively. Results of tested compressive strength are shown in table 2.

TABLE 2

Compressive strength of cement paste blended with 10% of zeolite-tuff containing varied amount of mordenite.

Mordenite to uncrystalline thereof ratio	0:10	3:7	5:5	7:3	10:0
Compressive strength of cement paste (MPa)	66.2	71.7	72.9	69.2	61.9

It is shown from table 2 that varied amount of mordenite tuff has also optimum blending amount; that is, for the same blending amount, there is optimum zeolite content in tuff containing mordenite as blending material of Portland cement.

Chemical reactivity of zeolite-tuff with lime

Specimens as shown in table 2 are mixed with CaO (analytical purity) by ratio of 1:1 (by weight of total binder), and formed with water separately. After curing for 3, 7, 28 days, the soluble SiO_2 and the Al_2O_3 of those paste are examined by cold hydrochloric acid method[12]. Above results of 28th day are shown in fig.2.

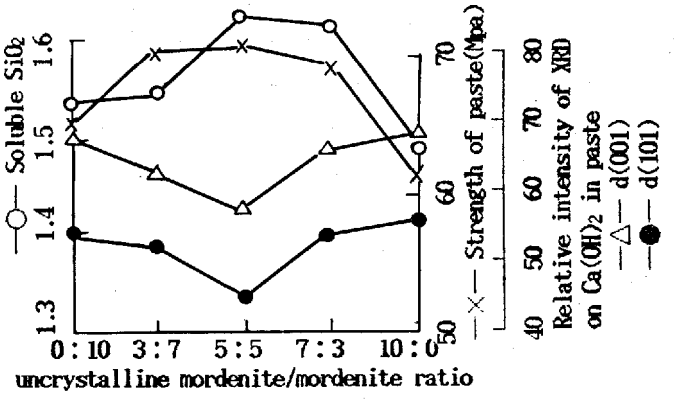

Fig.2 Soluble SiO_2 and Al_2O_3, relative amount of $Ca(OH)_2$ by XRD and strength of specimens comprising lime and zeolite tuff in varied ratio at 28th day

From results of test, it can be seen that:

1. The highest strength of specimen made of zeolite-tuff mixed with CaO can be obtained by suitable zeolite content.

2. The largest amount of soluble SiO_2 occurs in specimens with mentioned ratio of about 5:5.

3. The least relative amount of $Ca(OH)_2$ by XRD in specimens occurs in specimens with mentioned ratio of 5:5 in table 2.

4. Difference strength of specimens containing varied mordenite content is much more than difference of amount of soluble SiO_2 and Al_2O_3 as well as the relative amount of $Ca(OH)_2$. It is considered that the chemical reaction is not the only factor effecting strength of cement paste. Results as above mentioned tally with XRD of zeolite tuff-lime reaction, e.g., in 28-days, the peak values of clinoptilolite in zeolite-tuff are hardly

changed, but of $Ca(OH)_2$ are changed much[13], i.e. the reaction is induced by the amorphous portion of tuff rather than the crystalline zeolite.

Effect of composition on reactivity of zeolite-tuff

1. The cation in cavity of clinoptilolite is changed by ion-exchange, and it results in amount of a kind of cation to be over 50% (by weight of total cation). Mentioned zeolite-tuff which cation have been changed and the original zeolite-tuff are mixed into Portland cement by 10% respectively. Strength of mortar made of those specimens are tested and the results are shown in table 3.

TABLE 3

Change of zeolite water and strength of cement blended with zeolite-tuff by 10%, after ion exchange of zeolite

Type of cation	Compressive strength of cement (MPa)			Zeolite water (%)
	3rd-day	7th-day	28th-day	
Original	15.3	24.9	39.2	
NH_4^+	14.1	24.9	44.2	9.90
Ca^{++}	16.6	27.6	44.3	7.78
Na^+	18.7	28.2	42.0	6.83
K^+	17.2	27.0	39.5	4.32

It is shown from table 3 that the strength of cement paste at 28th day, specially the strength increase rate with ages, is increased with zeolite water. This is due to induction by effect of zeolite water in interface between zeolite-tuff and cement paste[14]. The best effect of cation is Ca^{++}, Na^+, (NH_4^+ does not exist in natural zeolite-tuff).

2. Si/Al ratio and activity ratio of zeolite-tuff after treated by NaOH with varied normality, and strength of cements blended with 10% of above treated zeolite-tuff are tested separately. Results are shown in fig.3.

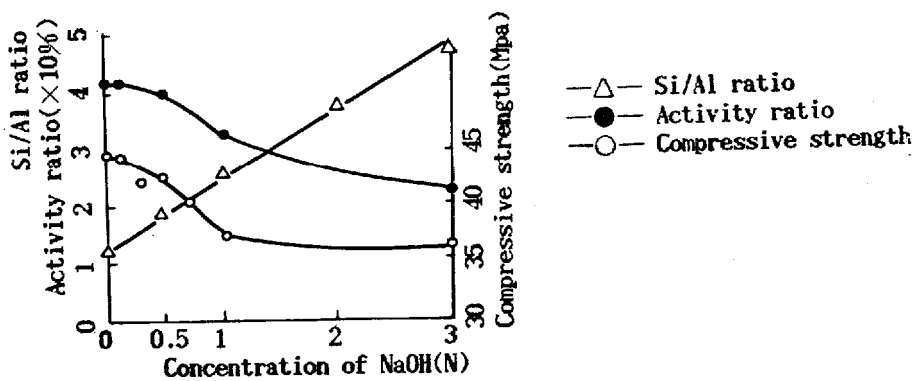

Fig.3 Si/Al and activity ratio of zeolite tuff and strength of corresponding cement vs. normality of NaOH

It is shown that Si/Al of zeolite is decreased with increasing normality of NaOH, and that is identical with change of strength of corresponding cement. But the activity ratio is increased with the normality of NaOH. It is indicated that effect of structure is much more than of the chemical activity. This is different from the case of the other blending materials, strength of which are sensitive to the activity ratio[15].

Effect of fineness of tuff

Zeolite-tuff ground to be 13000, 16000, 19000 cm^2/g of special surface area are mixed into Portland cement by 10, 20, 30%(by weight of total binder) respectively, and W/C is 0.3. Compressive strength of those cement paste at 28th day are shown in fig.4.

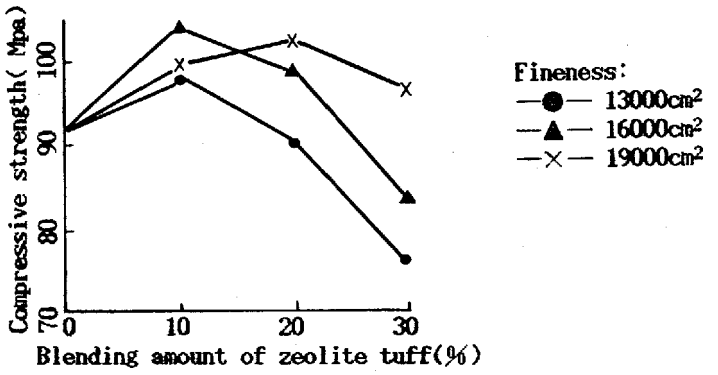

Fig.4 Strength of cement vs. blending amount of zeolite tuff with varied fineness

It is seen that the more amount of zeolite-tuff is blended, the more effect of fineness is. When the blending amount is about 10%, the highest strength occurs by appropriate fineness rather than by the finest. And for the blending amount over 20%, the finely-ground is better. The optimum blending amount is various for varied fineness of zeolite-tuff, and more with fine.

CONCLUSION

1.Reactivity of zeolite-tuff is not due to collapse of crystalline structure substantially, but the reactive portion of amorphous tuff is. And that reactivity of zeolite-tuff is more than of glass is through its special structure-microcrystalline and micro cavity therein as well as zeolite water in cavity.

2. The optimum blending amount which makes the highest strength of cement zeolite-tuff is 5-20% variated with the zeolite content. The optimum zeolite content which makes the optimum blending amount mostly is about 60% or more.

3. The suitable zeolite-tuff for blending material of cement is possessing Ca^{++} or Na^{+} (Ca^{++} is better to avoid harmful effect of Na^{+}) for clinoptilolite-tuff because of change of zeolite water coordinated with the positive ion in cavity.

4. The strength increase rate with special surface area increasing of cement blended with tuff by 30% is more than by 20%, but the optimum, position is varied. When blending amount is less, appropriate fineness is expected rather than the finest, and when blending amount is over 20%, the finer is better.

REFERENCES

[1] Sersale, R. et al: "Pozzolanic activity of zeolites", **Rend. Accad. Sci. Fis. Mat.** (Soc. Maz. sci., Lett. Naples) 27, Ser.4, 1960.

[2] Malquori, G.: "Portland-pozzolanic cement", **4th Int. Sym. on the Chemistry, Washington,** 1960.

[3] Turriziant, R.: "Aspects of the chemistry of pozzolanas", **The Chemistry of Cements,** ed. by H.F.W. Taylor, 1964, p 69-86.

[4] Japanese pattern Bureau open report No. 194526, "Method to produce the hardened calcium silicate".

[5] Drzaj, B. Hocevar, S. and Slokan, M.: "Kinetics and mechanism of reaction in the zeolite tuff-CaO-H_2O systems at increased temperature", **C. and C. R.** 8, 1977.

[6] Guo Jingxong et al: "Study on mechanism of reaction of zeolite in hydration of cement", **Jornal of Chinese Silicate** No. 3, Vol. 8, 1980.

[7] Lian Huizhen: "Morphology of interface between zeolite-tuff and cement paste", **Bond in Concrete** ed. by P. Bartos, Applied Science Publisher, London, 1980, p 34-39.

[8] Lian Huizhen: "Cement paste/zeolite-tuff bond", **Proceedings of 1988 Engineering Foundation conference on advance of Cement Use and Manufacture,** ed by E. Gartner, 1988, P 259-268.

[9] Makoto Asaka et al: "Change in physics chemical properties of clinoptilolite tuff by chemical treatment(III)--Effect of Sodium Hydrate Solution Treatment", **Journal of Society of Rock, Mineral and Deposit,** 75, 257-265, 1980.

[10] See [8].

[11] Yamazaki, H. et al: "Influence of pozzolana and fly ash on concrete", **Concrete Technology,** Nov., 1981 (in Japanese).

[12] Lea, F.M.: "The chemistry of cement and concrete", 3rd ed. Edward Arnold, 1970, p 530.

[13] See [8].

[14] Lian Huizhen, Chen Enyi: "Mechanism of hydration of blended cement I. Strengthening effect of mineral powder on cement used in mortar or concrete", **Proceedings of International concrete conference,** 1990, IRAN.

[15] Lian Huizhen et al: "Evaluation on reactivity of FBC ash and effect factor thereof", **Documents of Appraisal to a special topic 7th Five-Year-Project** (in Chinese), Nov. 1990.

A STUDY ON THE MORPHOLOGY AND MICROSTRUCTURE OF ACTIVATED INDIAN FLY ASH

R N Sharma, S N Ghosh, V K Mathur and A K Solankey

National Council for Cement and Building Materials
New Delhi, INDIA

SUMMARY

Indian fly ashes are, in general, known for low lime-reactivity (LR). The LR value is dependent on the fineness and glass content besides other factors. A recent study on 25 Indian fly ashes showed that the range of glass content (soluble silica) was 8-38 percent and the LR values varied from 9-76 kg/sq cm. Laboratory investigations carried out on the activation of a representative Indian fly ash showed that by thermal or chemical treatment, the LR value of the fly ash could be enhanced by sixty to hundred percent. The chemico-mineralogical and physical characteristics of activated fly ash revealed that the enhancement of reactivity was due to the dissolution of crystalline phases, e.g. quartz, hematite, mullite, etc. In this paper, the effect of chemico-thermal treatment of fly ash on the nature of glass formed is reported. A considerable change in the morphology, texture, microstructure and elemental composition of fly ash paricles was observed by SEM-EDAX analysis. Infrared spectroscopy of the activated fly ash samples showed a lower degree of polymerization with high lime-reactivity.

INTRODUCTION

It is known that the pozzolanic activity of the fly ash arises from the glassy phase; its crystalline constituents, principally α-quartz, mullite, hematite, etc. contribute little, if at all, to pozzolanic activity. The mineralogy and microstructure of fly ash have been studied extensively (1). However, direct analyses has not been mentioned earlier until recently when Uchikawa, et al.(2) reported analyses of the average bulk composition of the glassy phase. Qian et al. (3, 4) have reported additional bulk analyses, as well as the variability in Al_2O_3 content within the particles and microstructure and chemical variation in class F fly ash glass. Shatokhina et al.(5) reported that the amount of cement prepared with mechanically activated fly ash can be decreased by 8-12% compared to that prepared by unactivated fly ash. Ghosh et al. (6) have reported that heat-treatment or by the addition of dopants, the lime-reactivity of an Indian fly ash could be enhanced by sixty to hundred percent.

In this paper, the effect of thermal and thermo chemical treatment of fly ash on the morphology, microstructure and elemental distribution of fly ash by SEM-EDAX analysis is reported. It was also observed that infrared spectroscopy of the activated fly ash samples showed a lower degree of polymerization with high lime-reactivity.

EXPERIMENTAL

Sample Preparation

Mixtures of fly ash with varying concentrations (0.5 to 2%) of soda ash, redmud and iron ore were homogenised and nodulised. The nodules were fired in a muffle furnace at 1300°C for a retention time of 30 minutes and were quenched to ambient air temperature. Nodules made out of fly ash were also subjected to heat-treatment (1300-1500°C) and were quenched similarly.

Scanning Electron Microscopic Studies

These studies were carried out on a Philips Electron Microscope EM-301G with scanning and EDAX attachment (PV-9900). An inbuilt peak identification computer was used for elemental identification and quantitative estimation. X-ray mapping technique was employed to see the elemental distribution in the specimen. The polished surface of the sintered samples were vacuum coated with gold. Specimen used for this study were of the size 5x3x2 mm.

Infrared Spectroscopic Studies

Perkin Elmer I R Spectrophotometer model 621 was used for the present study. Specimen were prepared by adopting potassium bromide (KBr) pellet technique.

Chemical and Physical Characteristics

The chemical composition of fly ash was determined by the complexo-metric (EDTA) method and flame photometry. The lime-reactivity of the experimental and activated fly ashes was evaluated as per IS:1727-1967.

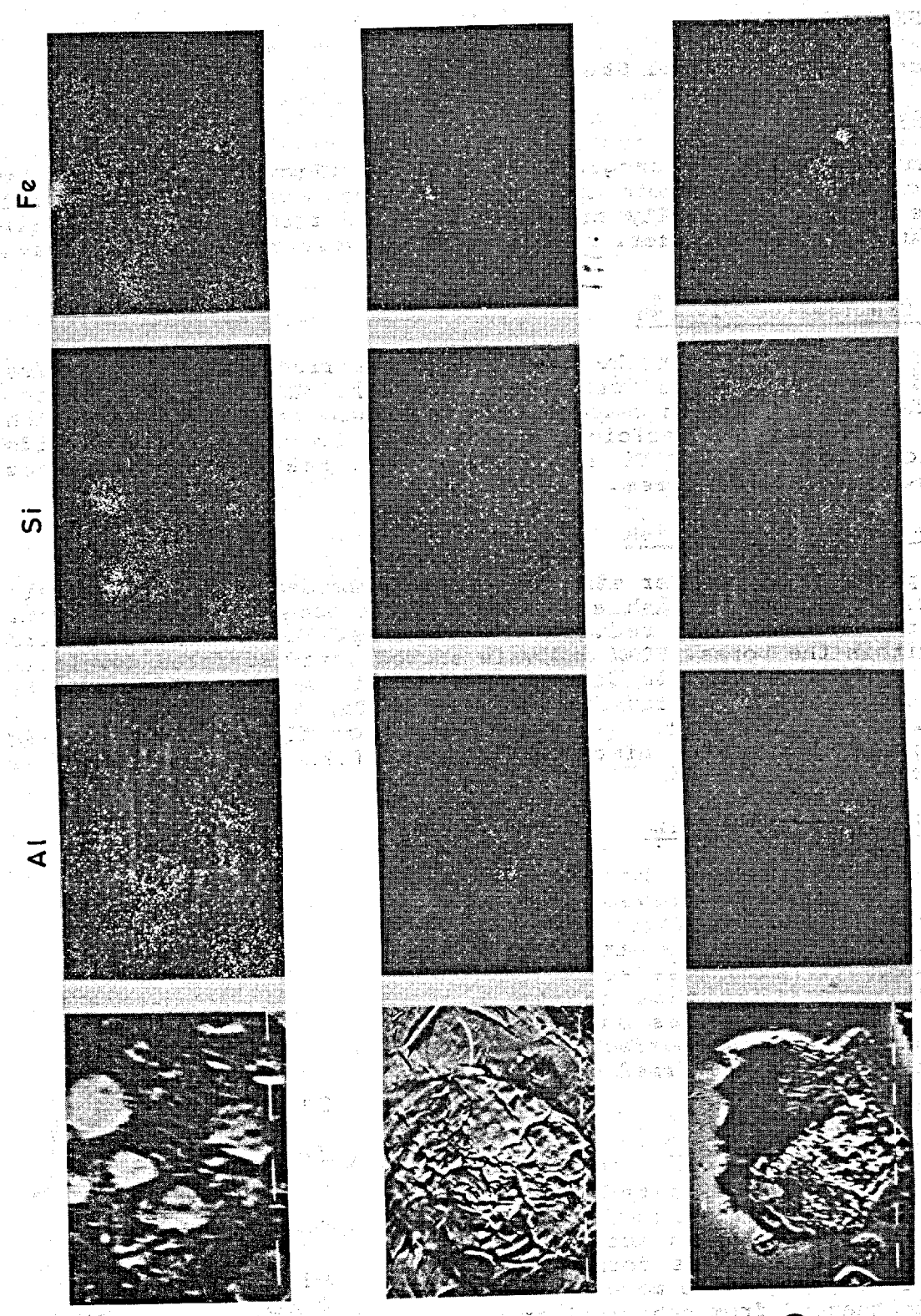

FIG. 1 MICROSTRUCTURE AND ELEMENTAL DISTRIBUTION IN (A) FLYASH SAMPLE, (B) IRON DOPED FLYASH AND (C) THERMALLY TREATED FLYASH

RESULTS AND DISCUSSION

Microstructure/Mineralogical Studies

Fly ash

Scanning electron micrograph of fly ash (Fig.1A) showed it to consists of relatively smooth spheres with some subrounded grains and some oversized particles. Fly ash spheres ranged from as little as one μm to about 10 μm in diameter. Lacy structures were deficient in Al and Si.

Iron Ore Treated Fly ash

Fused mass was found to be abundant. Small fragments of spheroids were found embedded in the fused mass (Fig.1B). EDAX analysis of the zoned surface within the digested spheroids showed that these were rich in Ti, Fe, Ca and Si and deficient in Al and K. Boundaries of spheroids were deficient in Ca and Ti and rich in Fe. Small fragments were observed even inside the pores.

Thermally Treated Fly ash

Few spheroids of smaller size were found embedded in the fused mass on thermally treating fly ash at 1500°C. It is observed that both the size and number of pores reduced drastically. Fused mass was also observed within the pores. EDAX analysis showed zoned surfaces developed within the spheroids rich in iron but deficient in silica compared to that of fused mass. It was found to be rich in Ti, K and Si but poor in Fe and Al. It appears that crystalline silica of fly ash is dissolved into the glassy phase with minor constituents like K and Ti acting as accelerators in the process.

Soda Ash Treated Fly ash

Soda ash destroyed the outer margins of the spheroids leaving them into smaller fragments. These fragments having thin boundaries were rich in Al, Fe and Si. Fused mass seems to be slightly more than that in the original fly ash. Besides mullite crystalline α-quartz was unaffected by soda ash treatment as confirmed by XRD (Fig. 2).

Red Mud Treated Fly ash

When fly ash was treated with redmud the features seen were different than the soda ash activated fly ash. The rate of glass formation was comparatively high. The morphology of spheroids changed from spherical to elliptical form. Mullite was still present. However grains of aluminium-iron-silicate were seen with anhedral crystal outline. Quartz grains were completely digested as shown in Fig. 2.

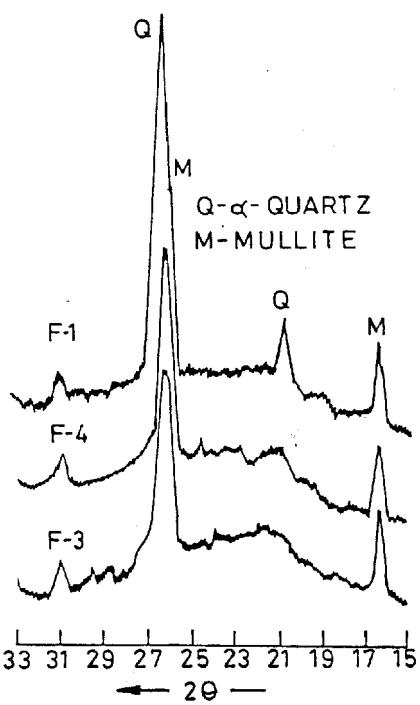

FIG.2: XRD OF CHEMICALLY TREATED FLY ASH

X-ray mapping of original fly ash, iron-doped and thermally treated fly ash samples have been shown in Fig. 1. It is apparent from the maps that the distribution of Al, Si and Fe is more or less similar in original fly ash compared to the treated ones, where the variation of the concentration of these elements, in general, is significant. For example, the concentration of Al in one pocket is high compared to those of the other two elements. This suggests the microinhomogeneity in composition of the treated samples. Lime reactivity of iron-doped/ thermally treated fly ash was found to be higher, however, a correlation between reactivity and microinhomogeneity in elemental distribution is yet to be ascertained.

Infrared Spectroscopic Studies

Infrared spectra of treated and untreated fly ash are presented in Fig.3. Spectra show a number of characteristic bands which are seen to vary with the heat treatment and nature of activators. Activation introduces a number of changes in the spectrum. In all the spectra, a shallow to strong broad band appeared close to 1000-1100 cm^{-1}- ν_a (Si-O-Si or Si-O-Al), is attributed to the asymmetric stretching frequency of the aluminosilicate matrix. Other characteristic shallow broad bands are seen at $\sim$700-800 cm^{-1}- ν_s (Si-O-Si); $\sim$ 450-475 cm^{-1}- δ(O-Si-O); and $\sim$1630-1640 cm^{-1}- δ(H-O-H). In chemically treated fly ash, a few shallow bands were observed at 540, 650, 730 and 790 cm^{-1}. The frequency of the broad absorption band between 1000-1100 cm^{-1} was found to be an indication of the overall degree of polymerisation of the network. This band shifts to lower frequency side in heat treatment as well as in chemically treated samples. Soda ash activation was found to be an exception where it shifts slightly to higher frequency. Broadness and strength of this band increases in treated fly ash. It appears that a lower degree of polymerization is observed with high lime-reactivity.

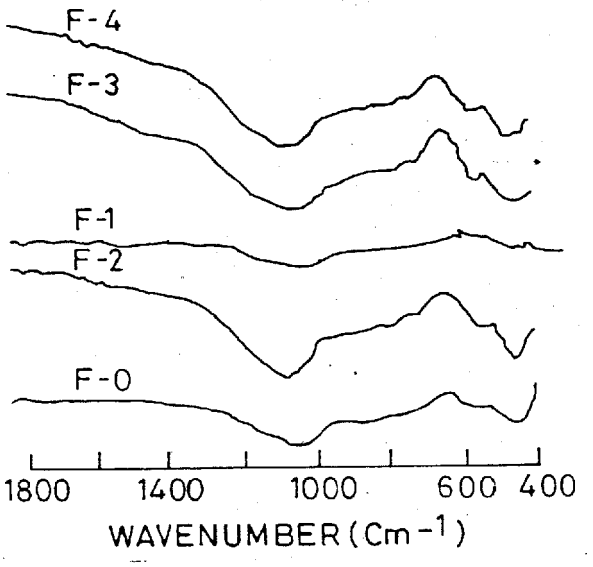

FIG.3: IR SPECTRA OF TREATED AND UNTREATED FLYASH

The chemico-physical properties of fly ash and treated fly ash samples are presented in tables 1 and 2.

TABLE 1

Chemical and Physical Characteristics of Experimental Fly ash

Chemical Analysis (%)		Particle Size	Distribution Percentage
LOI	7.38		
SiO_2	56.30	< 75 μm	76.6
Al_2O_3	24.38	< 40 μm	61.9
Fe_2O_3	4.70	< 20 μm	46.1
CaO	4.26	< 10 μm	13.8
MgO	1.01		
Na_2O	0.16		
K_2O	1.66		
TiO_2	0.20		

TABLE 2

Physical Characteristics of Treated and Untreated Fly ash

Sample No.	Sample	Fineness (sq cm/g)	Specific Gravity	Lime Reactivity (kg/sq cm)
F-0	Experimental Fly ash	4805	2.23	48
F-1	Soda Ash treated	4850	2.35	56
F-2	Thermally treated	5015	2.54	78
F-3	Red Mud treated	4960	2.60	88
F-4	Iron Ore treated	4870	2.76	92

MECHANISM OF GLASS MODIFICATION

In silicate and aluminosilicate systems, structural disorder can be introduced by rapid quenching, network isomorphic substitution and cation modification. Of these, the last two are different aspects of polymerization. Most glasses result from co-melting silica with other oxides, some of which provide elements (Al, Fe, B, P, etc.) capable of replacing Si in the polymeric network of oxygen tetrahedra. Others particularly oxides of alkali and alkaline earth metals (i.e., Na, K, Ca and Mg) induce depolymerization of the polymeric network.

Thus when a lower valency atom (e.g., Al and Fe) is introduced the continuous polymeric nature of the silica network is broken and an excess negative charge must be neutralized by inclusion of a cation (M^+ or 0.5 M^{2+}). Thus, network substitution introduces two forms of disorder

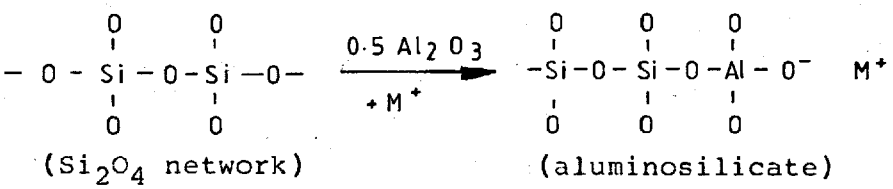

to the already distorted glass structure; a chemical disorder through the random substitution of network atoms and the necessary cations, and a depolymerization of the 3d structure. Modifier elements can further extend the disorder. For example, when soda ash is introduced the resulting glass formed on quenching become increasingly depolymerized relative to the untreated fly ash through reactions such as

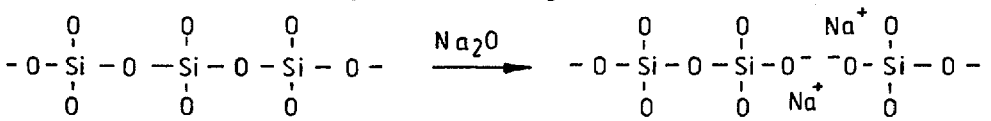

The resulting glass being composed of increasingly smaller silicate (or aluminosilicate) oligomers, with a large number of terminal, negatively charged non-bridging oxygen (NBO) atoms.

CONCLUSIONS

1 Fused mass was found to be most predominant in Iron Ore treated fly ash sample. Fused mass in decreasing order of its abundance was found as follows :

Iron Ore > Red Mud > Heat treated (1500°C) > Soda Ash. The LR values of the treated samples were found in the same order.

2 The distribution of major elements in heated and doped sample appears uneven compared to that in original fly ash sample.

3 IR band in the region 1000-1100 cm^{-1} of the activated fly ash samples shifts down to lower frequency compared to that of the original fly ash.

ACKNOWLEDGEMENT

The investigations presented here are a part of exploratory work carried out in the R&D laboratory of National Council for Cement and Building Materials and the paper is being published with the permission of Director General, NCB.

REFERENCES

1 Sharma, R.C.; Ph.D. Dissertation, submitted to Department of Material Science, IIT Delhi, July 1990.

2 Uchikawa, H., Uchida, S. and Hanehara, S. Effect of character of glass phase in blending components on their reactivity in calcium hydroxide mixture. 8th International Congress on the Chemistry of Cement, Vol. IV (Rio de Janeiro, Brazil, 1986) p 245-250.

3 Qian, J.C. and Glasser, F.P.; Bulk composition of the glassy phase in some commercial PFA's. Mat. Res. Soc. Symp. Proc. Vol. 113 Dec 1-3, 1987, USA, p 39-44.

4 Qian, J.C., Lachowski, E.E. and Glasser, F.P.; Microstructure and chemical variation in class F fly ash glass. Mat. Res. Soc. Symp. Proc. Vol. 113, Dec 1-3, 1987, USA, p 45-53.

5 Shatokhina, L P. et al.: Improvement of the quality of cement with additions of activated fly ash. Tsement 1990(7), p 201.

6 Ghosh, S.N., Sharma, R.N., Mathur, V.K., Sharma, R.C. and Mohan Lata (In Press, IlCemento).

BINDER ENHANCED REFUSED DERIVED FUEL ASH: A STUDY OF HYDROLYSIS

Russell Hill and Kenneth E Daugherty

Department of Chemistry, University of North Texas
Texas, USA

SUMMARY

The explosive production of municipal solid waste in the USA is a dilemma of continuing concern. Disposal alternatives are now being investigated. A method of particular promise has been the production of densified refuse derived fuel dRDF. Municipal solid wastes which have been processed to a composition of 90 % paper, can be extruded into dRDF pellets with a BTU value of close to 8000. This fuel has successively been cofired with coal in spreader-stoker combustion units and cement kilns. A calcium hydroxide binder is often used to produce durable pellets which burn environmentally cleaner than coal.

National production of binder enhanced dRDF could conceivably produce 100 million tons of pellets annually. Ash resulting from combustion would be a substantial by-product.

Avoiding landfilling ash by combining it with cement has already lead to a major research discipline in itself. However, little work has been done concerning the cementitous nature of bdRDF ash.

The present study involves the analysis of a synthetic blend of bdRDF containing lime binder. A number of techniques including XRF, XRD, and FTIR are used to monitor the hydrolysis reactions of cement pastes over a period of time.

INTRODUCTION

Municipal solid waste (MSW) is currently cumulating at a rate of 200 million tons per year. The majority of this waste has traditionally been landfilled. Availability, economics and a growing public concern has forced municipalities and state governments to look for other disposal methods.

One particularly attractive alternative has been to first remove recyclables from MSW and then process the paper residue into densified refuse derived fuel (dRDF) pellets. This fuel can be burned alone or cofired with coal utilizing facilities such as power plants and cement kilns.

The University of North Texas has determined that calcium hydroxide ($Ca(OH)_2$) is an excellent binding agent for dRDF(1). In addition, the binder reduces organic and acid gas emissions as compared to the combustion of coal (2,3).

The major by-product from combustion of binder enhanced dRDF is an ash high in calcium oxide content. Utilization of coal ash in cement has become a major industry, however, comparatively little work has been done with ash from MSW.

Our laboratory has looked at the hydration properties of dRDF ashes with various CaO contents resulting from different amounts of binder. Ashes with little CaO present were amorphous and showed little hydraulic behavior. Ashes high in CaO had crystalline phases and underwent hydrolysis. This paper presents preliminary results on the hydration of ash from dRDF with 16 percent binder.

EXPERIMENTAL

Sample

Densified refuse derived pellets were obtained from Reuter, Inc., Eden Prairie, MN., with a binder content of 8%. The pellets were ground to a fluff material passing a US #5 sieve. Additional reagent grade $Ca(OH)_2$ was added to increase the $Ca(OH)_2$ present to 16% by weight. The mixed material was then ashed in batches at 1000°C for 6 hours in a muffle furnace. The resulting batches were screened and blended. This material was fused for 14 hours in platinum crucibles at 1350°C. The fused product was ground to pass through a 230 mesh sieve and remixed.

Hydration

The ash was placed in a polyethylene bottle and mixed with freshly boiled DI water to give a water/solids of 0.4. The bottle was tightly sealed at ambient temperatures. Samples were periodically removed for analysis. Hydration was stopped by grinding with acetone followed by vacuum filtering on #42 whatman filter paper. The residue was dried for 15 minutes at 100°C and then stored in a desiccator over P_2O_5.

XRF

Samples were ground in an Angstrom Mill and pressed into pellets for approximate analysis at standard conditions. A Model 7200 Applied Research Laboratory X-Ray Fluorescence Analyzer and NBS Fly Ash Standards were used for the analyses.

Free Lime

Analysis of the base ash mixture was obtained using a modified Franke method (5). Analysis of extract was performed using standard conditions on a Perkin Elmer Model 4000 Atomic Absorption Unit.

XRD

Aluminum sample slides were used when sample size permitted. Otherwise glass slides and double stick tape were used. In all cases measures were taken to prevent preferred orientation. A Philips Norelco Model 112045/3 X-Ray Diffractometer utilizing copper K α radiation (30KV 16MA) with a nickel filter and sodium iodide scintillating detector was used at a scan rate of 2° 2θ/min.

FTIR

Samples were packed, according to availability, into a Spectra Tech large or micro sample holder for diffuse reflectance analysis. A Nicolet Model 60SXB FTIR with a D-TGS detector was used to collect 256 scans at $4cm^{-1}$ resolution.

RESULTS AND DISCUSSION

Base Ash (Day 0)

Examination of Table 1 finds the ash differing significantly from typical lignite fly ash composition. Calcium oxide dominates the composition. Alumina silica and magnesium oxide are all present in roughly the same amount. The sulfur content is low because of the inherent low quantity of sulfur found in RDF. The lack of detectable iron is possibly a testimony to the RDF processing's ability to remove ferrous materials for recycling.

TABLE I

*SiO_2	12.70	P_2O_5	0.78	K_2O	0.10
Al_2O_3	11.60	TiO_2	0.40	SO_3	1.07
Fe_2O_3	0	ZnO	0	Cl	0
CaO	63.75	Mn_2O_3	0.01		
MgO	9.32	Na_2O	0.27		

*Data normalized for weight loss

The powder x-ray diffraction pattern (Fig. 1, Day 0) clearly marks the high periclase content but lime peaks are missing. Additional patterns at a slower scan rate of 1° 2θ/min detected a small peak at d=2.40A° indicative of CaO. Analysis for free lime found a lime content of 7.4% ± 0.1%. Thus, the majority of the CaO is presumably combined with the silica/ alumina/ magnesium system. An alite (C3S) phase is identified (based on standard search procedures using JCPDS manuals) as are peaks tentatively considered to be a result of overlap of C3A and Merwinite (C3MS2 or MW).

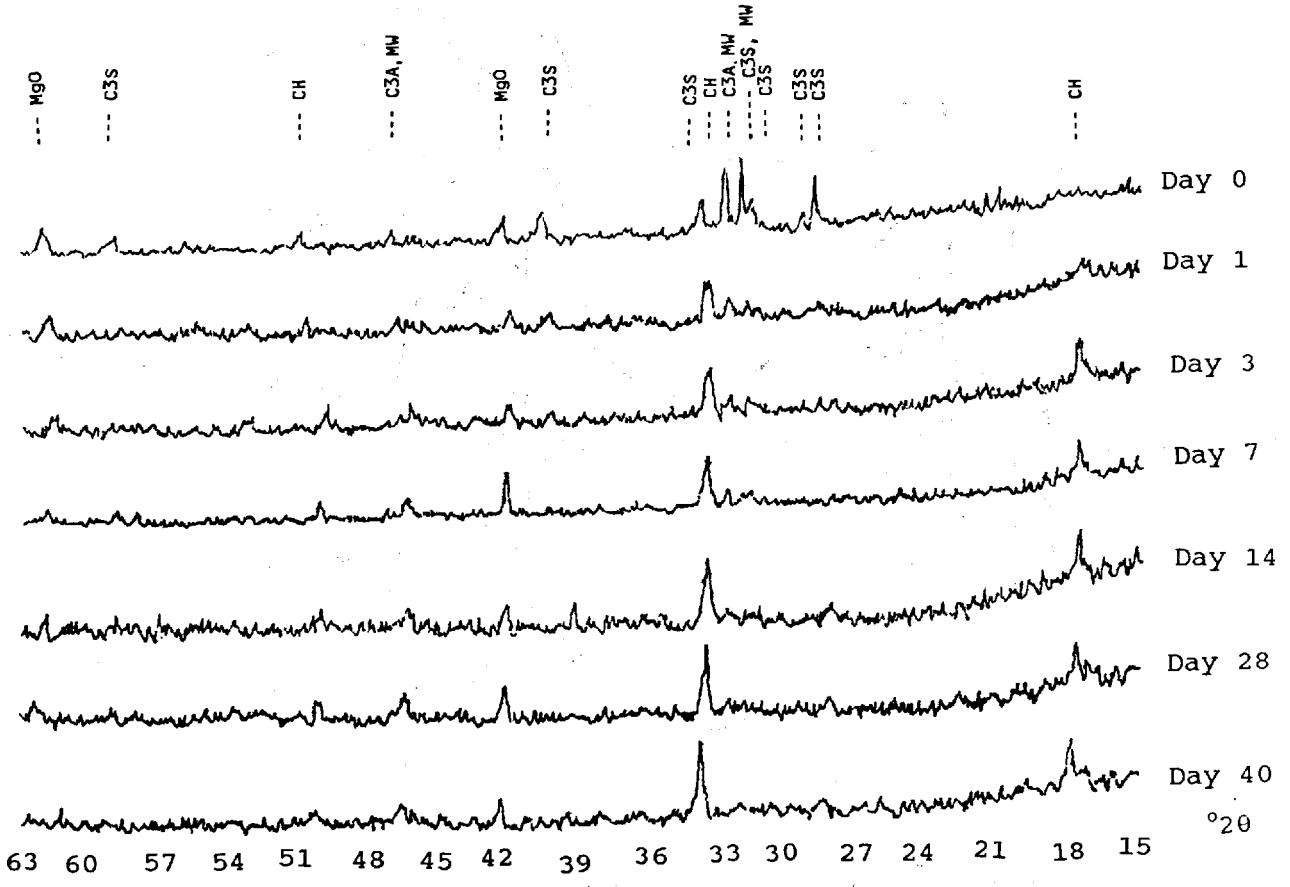

Fig. 1 X-Ray Diffraction Analysis Ash Hydrolysis Products

IR analysis in Fig. 2 (Day 0), display silica characteristic stretch vibrations at 1030cm^{-1} and deformation vibrations at 612 cm^{-1} and 495 cm^{-1}. The similarities between the ash and alite become apparent by referring to Fig. 3. For clarity the two spectra have both had CaO vibrations spectrally subtracted until the peak at 3640cm^{-1} has just disappeared.

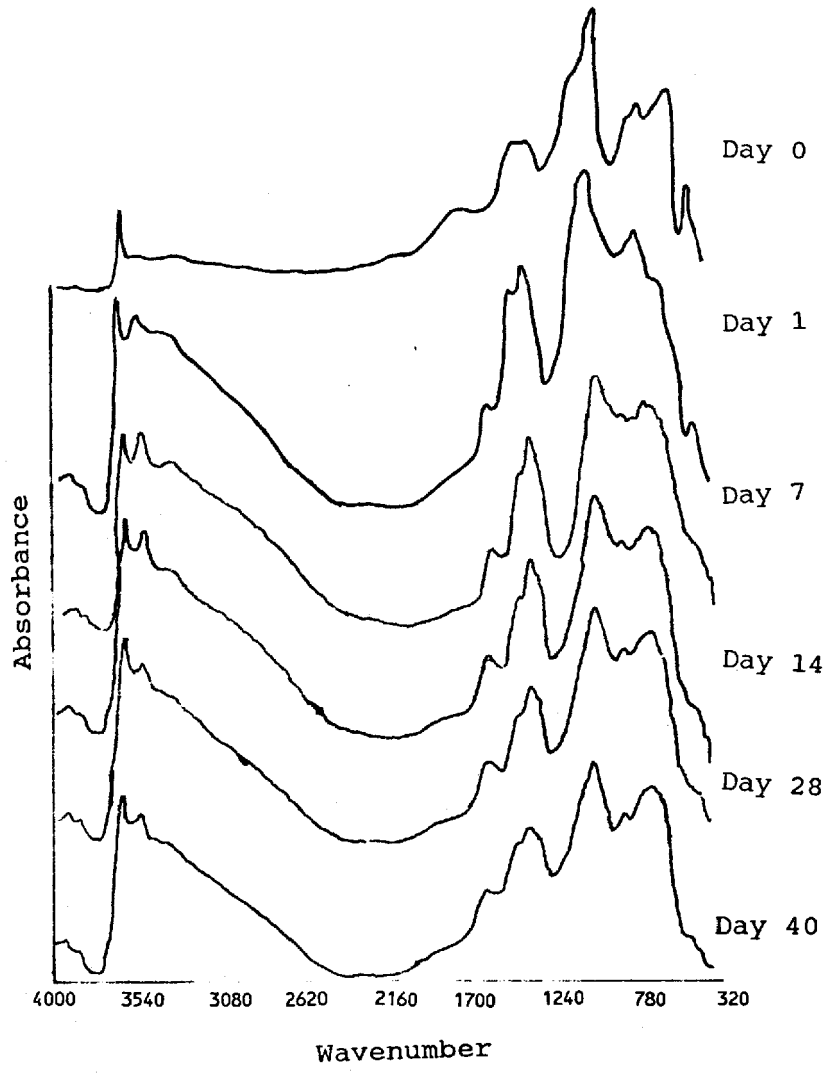

Fig. 2 IR Analysis of Ash Hydrolysis Products

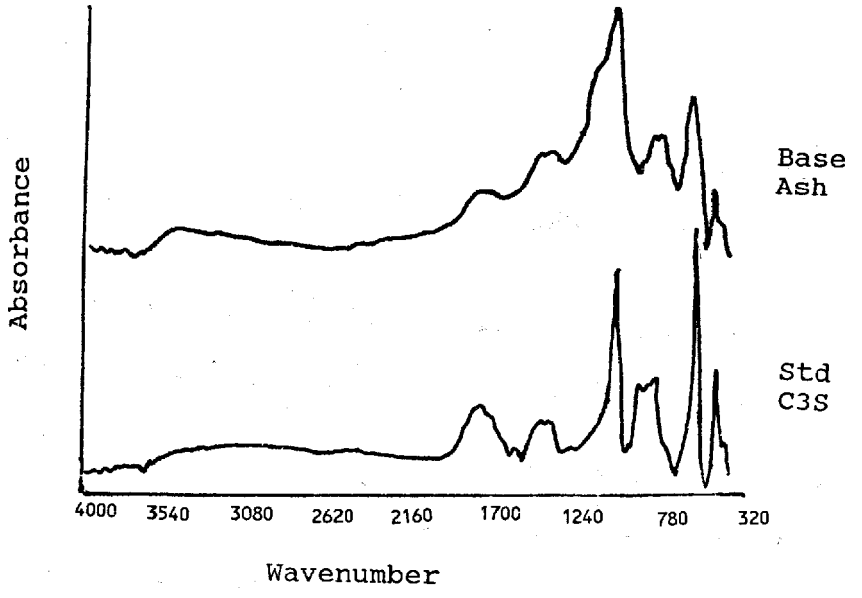

Fig. 3 Comparison of Ash and C3S Std.

Hydration

Figure 1 also allows one to follow the hydration from Day 1 to Day 40. After one day the well defined peaks due to alite and C_3A/Merwinite have largely disappeared. $Ca(OH)_2$ peaks begin to appear due to precipitation. Patterns from Days 14 through 40 possibly indicate the formation of a CSH gel evidenced by diffuse peaks at 50.3° and 28.8°.

Figure 4 displays the same hydration samples after the free lime was extracted. The gradual hydrolysis of alite is much clearer in this series. By day 40 only periclase is evident. The loss of the characteristic gel peaks may be a result of disruption of the open gel structure due to extractions of weakly combined CaO.

The broad expansion of vibration peaks in the 3000° cm^{-1} area and the growth of a peak at 1635 cm^{-1} (Fig. 2) indicate the absorption of loosely bound water as an inner layer within the gel. The loss in intensity of the silica peaks at 612cm^{-1} and 495cm^{-1} as well as the broadening of the silica stretch peak at 1030cm^{-1} marks the hydration of alite. The gradual shift to higher wavenumbers (from 1030 cm^{-1} to 1070 cm^{-1}) of the silica stretch vibration can only be explained by the development of a more rigid structure since water absorption alone would generally lower the peak positions (6).

CONCLUSION

Ash produced from the combustion (1350°C) of dRDF with a high binder ($CaOH)_2$) content (16%) has the potential for forming alite. X-ray, FTIR analysis indicates that the ash binder undergoes hydrolysis to form chains and/or layers of CSH in a nearly amorphous gel system.

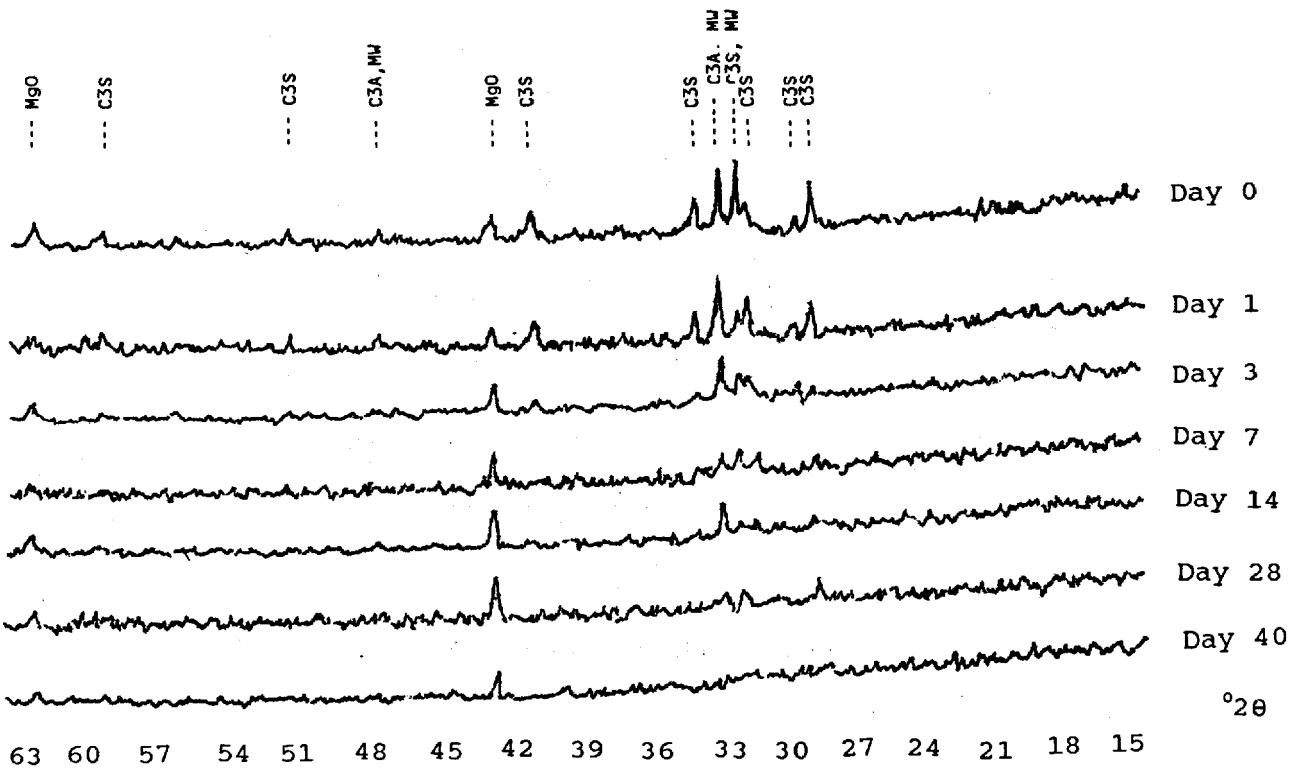

Fig. 4 X-Ray Diffraction Analysis of Ash Hydrolysis Products After Franke Extraction

REFERENCES

1. Daugherty, K.E., et. al.: "An Identification of Potential Binding Agents for Densified Refuse Preparation from Municipal Solid Waste", **Phase 1, Final Report, U.S. Department of Energy ANL1CSV-TM-194,** 1986, 101p.

2. Jen, Jen-Fon: "Analysis of Acid Gas Emissions in the Combustion of the Binder Enhanced d-RDF by Ion Chromatography" **University of North Texas Dissertation**, August, 1988, 186p.

3. Poslusny, M., Moore, P., Daugherty, K.E., et. al.: "Organic Emission Studies of Full-Scale Cofiring of Pelletized RDF/Coal", American Institute of Chemical Engineers Symposium Series, 1988, 84(265), 94-106.

4. Pressler, E.E., Brunauer, S., Kantro, D.L.: "Investigation of the Franke Method of Determining Free Calcium Hydroxide and Free Calcium Oxide", Analytical Chemistry, 1956, 28,96-902.

5. Lehamnn, H., Dutz, H.: "Infrared Spectroscopy Studies on the Hydration of Clinker Minerals and Cements", 4th Inter. Cong. Chem. Cem., Washington, D.C., Paper IV-S6, 1960.

NEW TECHNIQUE FOR ECONOMICAL MANUFACTURE OF CEMENT BASED BINDERS

R Karvinen and P Nieminen

Tampere University of Technology, Tampere, FINLAND

SUMMARY

The mechanism of concrete hardening process is discussed from the point of view, how the size of particles and the amount of different species affect the process. A new technique based on the behaviour of pressurized gas-particle suspension to manufacture fine powders is presented. Experiences in manufacturing cement based and modified binders including grinding of slag, organic additivies and manufacturing of coloured cements are discussed.

INTRODUCTION

Traditionally roller mills, ball mills or tube mills are employed for grinding materials for concrete, namely, cement or blast furnace slag. A large variety of different types of mills is available for the purpose in the market /1/. For manufacturing traditional cements wherein the fineness of the product is not very critical, the above mills fulfil the requirements of users also in respect of energy consumption and cost.

The strength of concrete, its hardening process and the behaviour of mortar are greatly dependent on the size distribution of cement particles. These properties can and are usually altered by using additives. Such modification is needed in the manufacturing of patching and repair mortars /2/. The consumption of those special products is expected to grow rapidly in the near future. The same kinds of problems as encountered with special cements are met with when coloured products are made. For the above purposes the traditional technique is not the best we can imagine.

In this paper the mechanism of concrete hardening process is discussed from the point of view, how the size of particles and the amount of different species in cement affect the process. A new technique to manufacture very fine powders is presented, and some experiences are shown concerning its possibility in manufacturing cement based binders. Also the use of a new technique for manufacture of modified binders in the future is discussed.

THE NEW GRINDING TECHNIQUE

Grinding results on cement based binders to be presented in this paper are obtained with a new type of opposed jet mill, which has been developed by Finnpulva Ltd. in Finland. Called the Pulva FP jet mill, it has been used for grinding many kinds of materials at a pilot plant and in industry in Finland and abroad.

The essential difference between the Pulva FP jet mill and the other mills on the market is generation of a pressurized gas-particle suspension by it using a compressor and a feeder unit. The pressurized suspension flows through acceleration nozzles, imparting to the material particles to be ground a sufficiently high velocity for grinding when the particles from opposed nozzles collide with each other. This is a new principle which substantially reduces mill wear and can be used to produce contamination free products. Finally, an atomized gas-particle suspension flows to a classifier where particles larger than the tolerence limit are separated out. Fig. 1 shows the schematic arrangement of the main components of the mill together with gas and material flows.

The pressurized gas is produced by an oil-free screw compressor in either a single stage or in two stages, depending on the application. The feeder unit consists of a two-valve system, a balancing vessel and a mixing section where the gas-particle suspension is formed. The balancing vessel is needed to lessen fluctuations in material flow caused by the cyclic operation of the valves. Pressurized gas and particles are mixed in the mixing section, where the material to be ground is transported by a screw conveyor from the balancing vessel.

The most important part of the mill is the grinding unit. It consists of nozzles and a grinding chamber. The pressurized gas-particle suspension flows through the nozzles, and the particles are accelerated to a high velocity due to the exchange of momentum between the gas and the particles. In the grinding chamber high-velocity particles injected from the nearly counter-opposed nozzles collide with each other. If the particle velocity is high enough, grinding occurs. Fig. 2 shows the geometry of a converging-diverging nozzle and the nozzle arrangement in a grinding chamber.

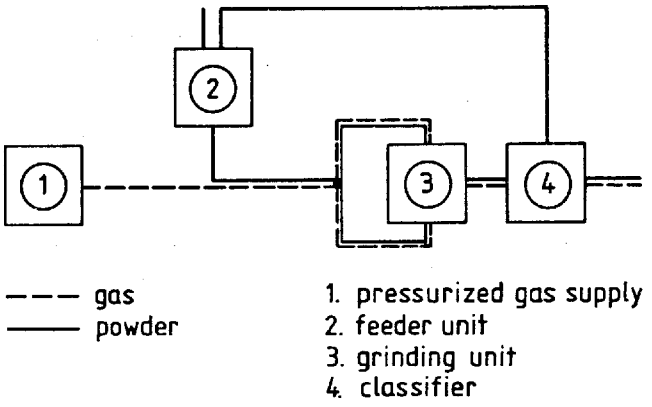

Fig. 1. Schematic diagram of Pulva FP jet mill.

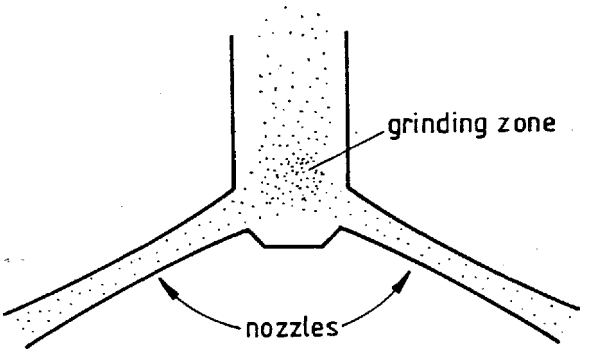

Fig. 2. Geometry and arrangement of acceleration nozzles in the grinding chamber.

After the grinding chamber, the particles are conveyed by the gas flow into a classifier which divides the ground material into coarse and fine fractions. Its operation is based on a highly swirling flow.

The theoretical basis of the two-phase flow governing the phenomena in the Pulva FP jet mill and the relevant details are not discussed in this paper as they are available in the literature /3/.

RESULTS

The Pulva FP jet mill has been used for grinding many materials at a pilot plant in Pirkkala, Finland. There are also several plants of industrial size operating in Finland and abroad. The grinding results of cement based binders presented in this paper are mainly obtained from the pilot plant.

Grinding of slag

Slag is a very difficult material to grind owing to its abrasiveness. An industrial scale factory with the Pulva FP technique is operating at Pyhäsalmi, Finland. An essential feature is that a water content of 6 % in the material is vaporized during the grinding process without any extra drying process. The total energy consumption for grinding, drying and classification is very reasonable, only about 150 kWh/t. The plant's grinding capacity is 2 t/h.

Results of the pilot plant, which gives an idea about the possibility of the Pulva FP jet mill, when very fine powders are needed, are given below. Fig. 3 shows the particle size distribution of the product when wet slag of 5-6 % water content is ground. For that extra fine product d_{50} and d_{98} are 2.99 μm and 9.47 μm, respectively. The total energy consumption including drying and grinding is 450 kWh/t.

The Pulva FP technique also affords the possibility of simultaneous grinding of a wet slag and clinker. In this case the wet slag is ground at the first stage and then the resulting (ground) dry slag is reground with the clinker.

Manufacture of coloured cements

In coloured cements it is essential to have the pigment distributed very uniformly. An other important factor is the pigment particle size, because the amount of pigment will depend on its particle size. Experiments have been conducted in a pilot plant by

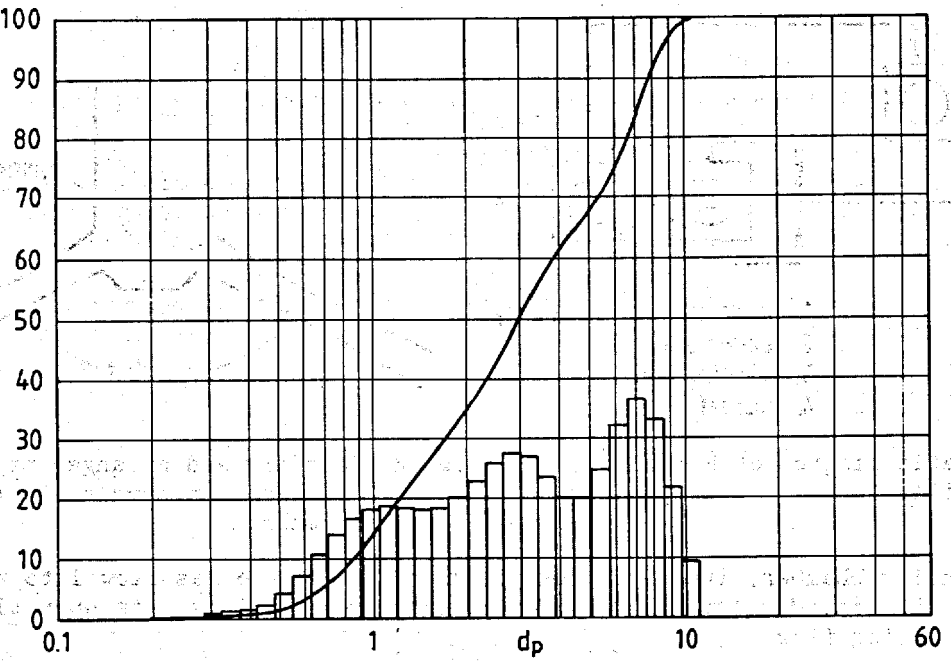

Fig. 3. Fineness of slag product (measured with Silas 850 Alcotel)

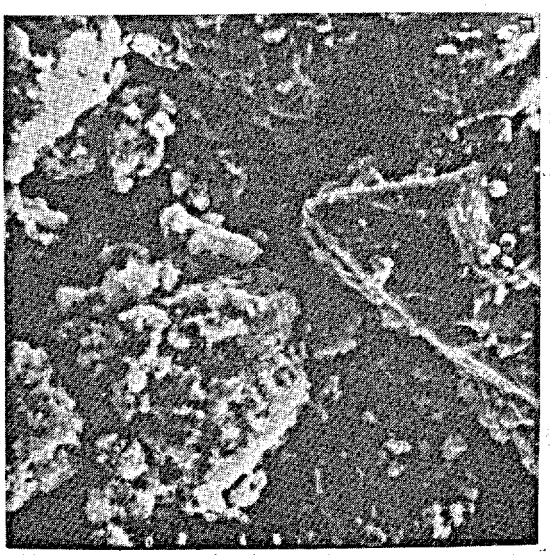

Scanning electroscope picture.

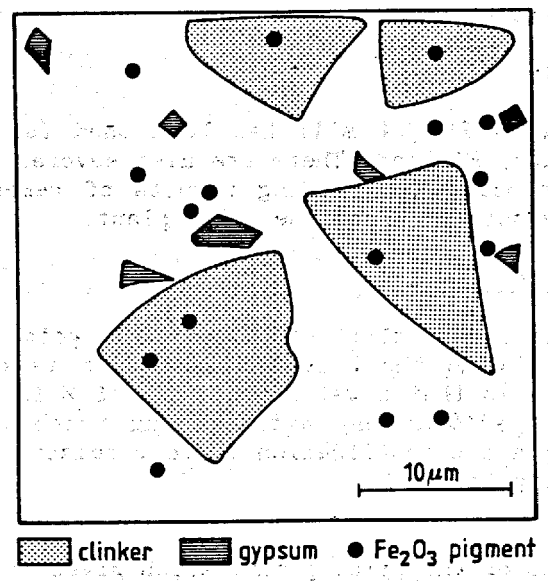

Different materials in scanning picture.

Fig. 4. Microstructure of coloured cement manufactured with jet mill.

simultaneously grinding gypsum and clinker. The results obtained when material consisting of clinker, gypsum and Fe_2O_3 was ground are discussed below.

The feed consisted of 96 % clinker, 2 % gypsum and 2 % Fe_2O_3. The original particle sizes of gypsum and clinker in the feed were same. Fig. 4 shows the results from scanning electroscope on the product obtained. It can be seen that during the grinding process in the Pulva FP jet mill the particle sizes of gypsum and clinker have changed in a different way. The particle size of Fe_2O_3 is also very small, smaller than 1 μm.

It must be observed that small particles of Fe_2O_3 have a great tendency to agglomerate in a dry atmosphere /4/ However, as can be seen from Fig. 4, this phenomenon has been avoided with the use of our mill, because the Fe_2O_3 particles are distributed very uniformly on the surface of clinker particles. This makes for a reduction in the guantity of colour pigment used and uniformes the quality of the binder.

Grinding of organic additives

In dry mortars use is made of different types of organic additives in order to improve the mortar behaviour. The problem is actually, how to make a homogenous suspension of cement, sand and additives.

Experiments were carried out in the pilot plant by grinding a binding agent made of 95 % cement clinker, 4 % redispersible powder and 1 % lignosulfonate. This is a very typical composition in actual practice. The use of organic additive dictates that the temperature be kept low during the grinding process, but this looses no problem with the Pulva FP technique.

In a mortar pin test it was observed that the setting time, when use was made of the binding agent above, was four times longer compared to that if the mixing was made by hand. As a matter of fact the mixing of the additives is a real problem of dry cement based binders. Scanning electron microscope investigation revealed the amount of lignosulfonate to be too large. It covered the cement clinker particle too efficiently. With the grinding technique of this paper, the amount of an expensive additive could be reduced remarkably.

CONCLUSIONS

In this paper some observations concerning a new grinding technique are presented for manufacturing cement based binders. The technique, namely, the Pulva FP jet mill is used already in other branches of industry. With this technique, drying, grinding and mixing of additives can be done simultaneously resulting in very homogenous cement based mortars.

An essential feature of the new technique is that the difficult processes of dosing and mixing of additives can be avoided since these are duly taken care of in the grinding process itself.

The technique also affords the possibility to manufacture a binder from a wet slag sand with d_{50} equal to 7 µm, to which an activator clinker and calcium oxide are added during the grinding process. The total energy consumption including grinding, drying, mixing and classification is very reasonable compared to the other technique in the market.

REFERENCES

1. Haese, U., Powder Processing Machinery and Equipment in Japan. Powder, handling & processing 3 (1991) 105-121.

2. Lea, F.M., The Chemistry of Cement and Concrete 3rd ed. London 1970 Edward Arnold.

3. Karvinen, R., Kauramäki, T. and Nieminen, R., Grinding Principle and Experiences with a New Type of Opposed Jet Mill. Powder, handling & processing 3(1991) 123-128.

4. Büchner, G., Junge, C.-H., Colour fluctuations in the production of coloured concrete. Betonwerk-Fertigteil-Technik Heft 8/82 Banverlag GmbH, Wiesbaden 1982.

BLENDED CEMENTS CONTAINING GRANULATED SLAGS FROM FERROCHROME PRODUCTION

T V Kuznetsova, V V Mityushin, N S Nikonova and V H Jabirov

D I Mendeleev Institute of Chemical Technology
Moscow, RUSSIA

INTRODUCTION

High-basic slags of the low-carbon ferrochrome production, in view of their mineralogical composition, seem to hold good promise for addition to clinker in the process of grinding. But their use in cementing materials' industry is limited by the complexity of granulation, in terms of the dissociation of silicate in the cooling process.

To make these slags effective as an addition to cement, it is necessary to adopt special conditions of granulation. Thus, when the molten slag is cooled slowly, the polymorphous transformation of the $\gamma \rightarrow \beta$ dicalcium silicate takes place simultaneously with crumbling of slags of this kind to dust. On the other hand, when ferrochrome slags are cooled slowly, magnesium oxide crystallizes in large-crystalline configuration (in periclase form), which leads to volumetric changes in the process of hardening slag compositions, making slag-based materials to be of inconsistent behaviour.

When the flame-coloured molten slag is cooled fast enough, the physical stabilization of the dicalcium silicate is to be observed in active α and β forms, while magnesium oxide mostly remains dissolved in the dicalcium silicate, or is a part of the composition of magnesium silicates and picromites.

The aim of this investigation was analysis of the influence of various methods and conditions of granulation on the process of hardening of binding materials, based on portland cement clinker and slags from low-carbone ferrochrome production.

DESCRIPTION OF THE FORMATION OF MATERIALS

The slags analysed in our investigation were of the following chemical composition % wr : SiO_2 24-28; Al_2O_3 4.1-8.3; Cr_2O_3 4-6.2; FeO 0.7-1.5; Fe_2O_3 0.7-1.5; CaO 46.2-55.3 ; MgO 7.0-16.2 .

The flame-coloured molten slag was granulated at 1700-1800 °C , using aerial, aerial-aqueous and aqueous methods at various rates of cooling, regulated by air and water pressure in the granulator.

The methods and conditions of granulation of ferrochrome slag greatly influence the size, porosity and grindbility of the slag granules, physical state of dicalcium silicate crystallites, their polymorphous modification, and, consequently, influence the slag's hydration activity, especially the beginning of hardening.

When the granulation conditions are optimum, dicalcium silicate stabilizes in α and β modifications. While employing the aerial method of granulation, mostly β form of dicalcium silicate has a tendency to stabilize, whereas with the aerial-aqueous method it is the α form. Besides, granulated slags from low-carbon ferrochrome production also contain tricalcium silicate.

Dicalcium silicate in granulated ferrochrome slag has the shape of roundish granules with split edges (size - 10-20 mm), which is connected with the dendrite character of dicalcium silicate crystallites' growth when it is cooled fast.

Granulated ferrochrome slag contains 3-7 % wr of uncombined magnesium oxide, present in the form of periclase. The size of periclase granules considerably depends on the method of granulation. Granules obtained as result of the aerial-aqueous method of granulation are smallest in size.

Magnesium oxide in the granulated slags from low-carbon ferrochrome production is also associated in calcium magnesium silicates : mervinite $3CaO.MgO.2SiO_2$, diopside $CaO.MgO.2SiO_2$, monticellite $CaO.MgO.SiO_2$, $2CaO.MgO.2SiO_2$ and picrochromites.

RESEARCH METHODOLOGY

The cements were prepared by airergrinding granulated slag, portland cement clinker and gypsum in laboratory ball-mill to a fineness of 250-300 m^2/kg. Actual density and periods of hardening were fixed according to the State All-Union Standard 25094-82. Samples were made from the paste of normal density and 1:3 cement mortar. Samples were steamed thoroughly at 60-100°C and kept afterwards for 28 and 90 days under aerial-humid conditions; and in aerial-humid conditions for 7, 28 and 90 days.

HARDENING OF GRANULATED SLAGS FROM LOW-CARBON FERROCHROME PRODUCTION

Normal density of granulated slags ground to a specific surface of 200-300 m^2/kg , correspond to that of portland cement of normal density and a similar specific surface, but the rate of hardening is considerably accelerated. The method of granulation influences the rate of hardening . When the aerial-aqueous method of granulation is used, the rate of hardening is highest of all, whereas slags obtained from aerial or aqueous method of granulation give cements which harden at a slower rate. The rate of hardening also depends considerably on the fineness of grinding of the slags. A slag with a higher specific surfase had a higher hardening rate in almost all experiments. Gypsum, if added to the slag (at 3 to 5 % wr) does not influence the rate of hardening and normal density.

Pure granulated slags possess hydraulic activity, in mixture with gypsum as well as lime. The hydraulic activity of slags was influenced by the methods and conditions of granulation.

After 3 months hardening under normal aerial-humid conditions, the durability of binders, obtained from pure ground does not equal that of the standart portland cement samples. The bending strength of specimens, made from the slag cement, after hardening for 1-3 months under normal aerial- humid conditions or 1-3 months after being steamed thoroughly, is very high. The latter result could be attributed to the peculiarities of the chemical composition of slags, in particular, the presence of oxides of magnesium, chro-

mium and iron in the hardening system. In the process of hydration of the slag's silicate components, this provids the prerequisites for creating elements of asbestos structure, and for self-cladding of stone, based on the ferrochrome slag.

HARDENING OF CEMENTS BASED ON PORTLAND CEMENT CLINKER AND GRANULATED FERROCHROME SLAGS

The normal density and rate of hardening of cements, produced by airergrinding portland cement clinker, slag and gypsum, does not differ much from the respective values of standard portland cement.

Addition of granulated ferrochrome slag to clinker during grinding, whatever the granulating conditions and methods, does not decrease the compressive strength, if the slag content of the cement is up to 18 % wr, and the hardening under normal aerial-humid conditions lasts for 7 and 28 days. After 3 months of hardening slag-cement mixtures containing up to 80 % wr of slags are found to attain the durability of standard cement.

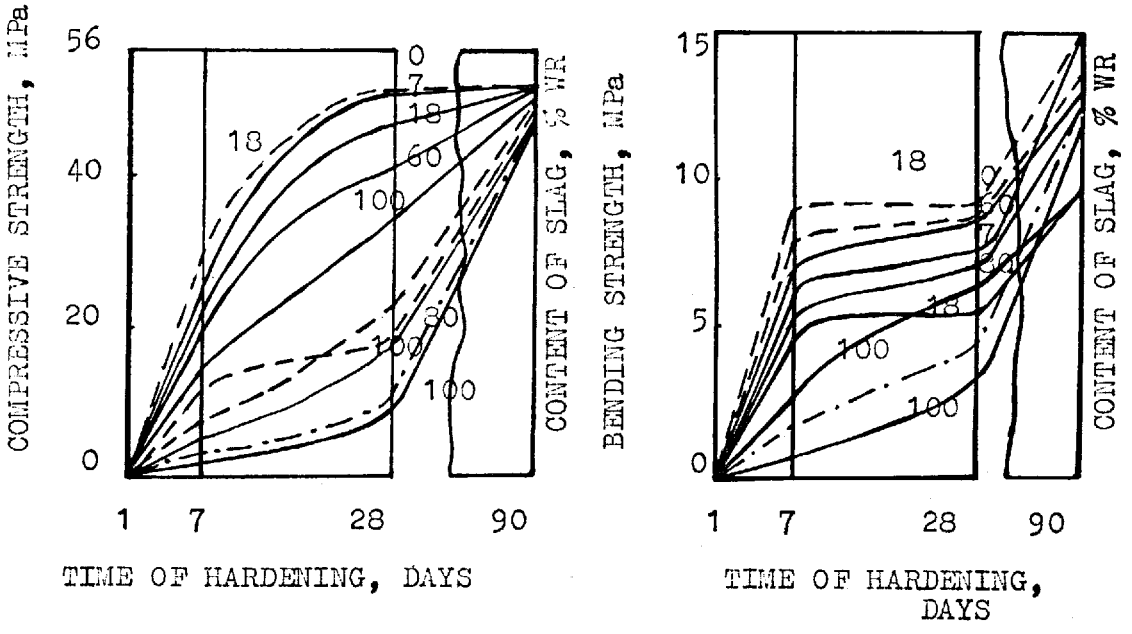

FIG.1 Compressive strength and bending strength of slag cements obtained from granulated ferrochrome slag by aerial (-), aerial-aquatic (--), aquatic (-.-) granulation methods were hardened under normal aerial-humid conditions

If the hardening takes place under conditions of hydrothermal treatment, mixtures containing 18 % wr of slag attain the durability of standard cement samples irrespective of the granulating conditions and methods. After 28 days of thoroughly steaming, mixtures containing 60 % wr (and sometimes - up to 80 % wr) of the slag are found to reach the same level of the durability.

At the end of 3 months hardening under normal aerial-humid conditions, the durability of the slag cements, does not equal the durability of portland cement.

Portland cement containing ferrochrome slag was used in pre-fabricated concrete technology. The cost economics of the cement and technological parameters did not differ from the standard for the plant.

STUDY ON EFFECTS OF KILN DUST ADDITION TO PORTLAND AND BLENDED CEMENTS

S P Ghosh, P Padmanathan and K Mohan

Cement Corporation of India Limited, New Delhi, INDIA

SUMMARY

Effects of adding different quantities of kiln dust upon the physical properties of OPC, PPC and PSC have been studied. Major physical properties of portland and blended cements have been determined with three sets of samples. Test results showed that with increase of gypsum content from 4 to 5% the PPC showed decrease of compressive strength at all ages with 2 to 6% kiln dust addition, whereas in case of PSC the decrease in compressive strength was noticed only after 4% kiln dust addition. In contrast, OPC showed higher compressive strength at all ages with 2-4% kiln dust addition. However, upto 3% kiln dust addition such that gypsum and kiln dust does not exceed 4% in cement, increased the compressive strength at all ages for PPC decreased compressive strength at all ages for PSC and both these trends were observed for OPC. Setting times were found to decrease for both PPC and PSC and increase in case of OPC.

РЕЗЮМЕ

ВЛИЯНИЕ ДОБАВКИ ПЕЧНОЙ ПЫЛИ НА ПОРТЛАНДСКИЙ И СМЕШАННЫЕ ЦЕМЕНТЫ.

Ш.П. ГХОШ, П. ПАДМАНАТХАН И К МОХАН

Изучено влияние добавки разных доль печной пыли на физические свойства портландского, портландско- пуццоланского и шлако-портландского цементов. Сравнение результатов испытания образцов содержащих разные количества пыли и гипса, с соответствующим исходным образцом показало уменьшение прочности на сжатие всех видов цементов, хотя она удовлетворяет требованиям стандарта. С увеличением содержания гипса до 5% ППЦ показал уменьшение прочности на сжатие во всех возрастах с добавкой от 2 до 6% пыли тогда как уменьшение прочности ШПЦ наблюдалось только при добавке 4% и больше пыли. В противовес этому, ОПЦ показал высшие прочности во всех возрастах при добавке от 2 до 4% пыли. Однако, придобавке до 3% пыли, когда количество гипса и пыли совместно не превышало 4% всей массы, прочность ППЦ увеличилась во всех возрастах, но уменьшилась для ШПЦ, а ОПЦ показал обе эти тенденции. Сроки схватывания в этих случаях уменьшились для ППЦ и ШПЦ и увеличились для ОПЦ.

INTRODUCTION

The quantity of kiln dust generated from different kilns in India is estimated to vary from 8 to 15% (1). Though in Indian Cement Plants, dust collection systems are not as efficient as in some other countries (2, 3), in recent years more attention is being given to dust collection.

A number of research work (4-15), has been carried out on the utilization of kiln dust in cement manufacture. Recycling of kiln dust is the most practical proposition provided chemical compositions of the dust permit the remixing. Direct addition of kiln dust during the grinding process of OPC, PPC and PSC is one of the most economic methods of disposal of the waste. However, the quantity of kiln dust which can be added without deterioration of the cement quality depends not only on the quantity of dust but also upon the quantity of the set retarder added in the process.

In the present investigation, the (i) effects of kiln dust addition to OPC (Ordinary Portland Cement), PPC (Portland Pozzolana Cement) and PSC (Portland Slag Cement) on physical properties and also the (ii) effects of gypsum in the presence of kiln dust on the physical properties of OPC, PPC and PSC have been examined.

EXPERIMENTAL

Materials

Three commercial clinker samples, two from wet process kilns and one from dry process SP kiln, kiln dust as well as chemical gypsum samples from respective plants were used in this study along with a fly ash and a granulated blast furnace slag.

Chemical composition of clinkers and kiln dusts are given in Table-1, Clinkers 1 and 2 are from wet process kilns and clinker 3 is from dry process SP kiln, kiln dusts - 1, 2 and 3 are from respective plants.

Table-1 Composition of Clinkers and Kiln dust

Ingredient	Components (wt.%)												
	SiO_2	Al_2O_3	Fe_2O_3	CaO	MgO	SO_3	LOI*	IR**	Free CaO	C_3S	C_2S	C_3A	C_4AF
Clinker-1	22.62	7.02	4.10	61.30	1.70	0.20	1.30	0.46	0.84	21.15	48.89	11.66	12.48
Clinker-2	23.60	6.70	3.80	61.80	1.20	0.36	0.71	0.56	0.53	19.62	52.86	11.32	11.56
Clinker-3	22.36	6.40	4.40	62.16	1.20	1.20	1.64	0.60	0.84	30.36	41.2	9.51	13.39
Kiln dust - 1	22.90	16.04	2.40	32.70	1.00	3.24	21.60	25.93	-	-	-	-	-
kiln dust - 2	23.22	15.46	3.60	32.76	1.00	1.83	22.20	21.04	-	-	-	-	-
Kiln dust - 3	12.54	5.12	1.20	42.56	1.20	0.55	36.46	12.12	-	-	-	-	-

* LOI - Loss on Ignition
** IR - Insoluble Residue

Chemical compositions of chemical gypsum, fly ash and slag are given in Table -2. Chemical gypsums - 1 and 2 are from wet process kilns and chemical gypsum - 3 is from dry process SP kiln.

Table-2 Chemical compositions of gypsum, fly ash and slag.

Ingredient	Constituents (wt.%)							
	SiO_2	Al_2O_3	Fe_2O_3	CaO	MgO	SO_3	LOI	IR
Chem.Gypsum-1	10.46	6.22	0.80	28.56	1.00	37.24	15.70	8.92
Chem.Gypsum-2	6.20	5.80	0.60	29.40	0.80	40.35	15.91	2.29
Chem.Gypsum-3	5.44	4.28	1.00	30.52	0.80	41.16	16.35	5.50
Fly Ash	59.24	31.60	1.60	1.96	0.40	1.26	3.20	88.11
Slag	34.48	26.72	1.10	31.60	4.02	1.09	0.02	1.38

Method

Sample Preparation and Testing - Kiln dusts from respective plants were blended in the laboratory ball mill with different proportions of clinker and gypsum from the same plant. Three sets of samples of OPC, PPC and PSC were prepared: (a) The clinker and kiln dust proportions were varied with fixed gypsum content (4%), (b) Gypsum and kiln dust contents were varied (upto 4% in total) with clinker content remaining fixed (96%), and (c) The clinker and kiln dust contents were varied with higher but fixed content of gypsum (5%).

All compositions were ground to more or less same fineness. PPC and PSC samples were prepared with 15% fly ash and 48% slag respectively.

All the compositions were tested for physical properties as per IS:4031-1988.

RESULTS AND DISCUSSION

Physical test results for different compositions of OPC, PPC and PSC are summarised in Tables 3, 4 and 5.

Ordinary Portland Cement (OPC)

The water requirements of OPC made with and without kiln dust are more or less the same irrespective of the type of clinkers and kiln dusts used. The initial and final setting times of OPC, made with clinkers-1 and 2, kiln dusts-1 and 2 and constant quantity of gypsum (4%) increased marginally with increased addition of kiln dust from 2 to 10%, whereas, with clinker-3 and kiln dust-3, it decreased slightly.

The initial and final setting times of OPC, made with clinkers-1 and 3, kiln dusts-1 and 3 and higher but constant quantity of gypsum (5%) are not affected with increased addition of kiln dust from 2 to 6%, whereas, with clinker-2 and kiln dust-2 these increased.

However, variation in gypsum content with corresponding kiln dust addition such that the both do not exceed 4% in cement shows that the initial and final setting times of OPC made with clinker-1 are not affected with increased addition of

kiln dust from 1 to 3%, whereas, with clinkers 2 and 3 these decreased.

Mohanty, Goswami and Panda (8) found that the initial and final setting times of OPC made with kiln dust decreased marginally with the increased addition of kiln dust from 3 to 8%. However, they observed that the variation in gypsum content with corresponding kiln dust such that the both do not exceed 5% in cement did not affect the setting times of OPC made with increased addition of kiln dust from 1.5 to 2.5%. However, Sastry and Mohan (13) noted that the initial and final setting times of OPC made with kiln dust increased marginally irrespective of the type of clinker used.

Comparison of compressive strength test results with the control specimen in each case show that with constant quantity of gypsum (4% and 5%) increased addition of kiln dust upto 10% affects the compressive strengths at all ages adversely, irrespective of the type of clinker used. This finding is in agreement with the work by Bhatty (12) and Sastry and Mohan (13), but is in conflict with the research work by Mohanty, Goswami and Panda (8), who have reported that with 3-4% of kiln dust, the compressive strengths increased at all ages, whereas with 6-8% of kiln dust the 3 and 28 days compressive strengths were more or less the same as that of the control cement, but 7 days compressive strength is slightly reduced.

However, variation in gypsum content with corresponding kiln dust addition such that the both do not exceed 4% in the cement shows that the 3 days compressive strengths of OPC made with clinkers-1 and 3 did not show significant difference with increased addition of kiln dust from 1 to 3%. However, 7 days compressive strengths of OPC made with clinker - 1 and 3 are not affected. On the contrary, the 28 days compressive strength of OPC made with clinker-1 showed marked improvement and of OPC made with clinker-3 decreased with 1-3% addition of kiln dust. However, the compressive strengths of OPC made with clinker-2 decreased at all ages with 1-3% addition of kiln dust.

With 5% gypsum and addition of 2 to 6% kiln dust, OPC made with clinkers-1 and 2 and kiln dusts-1 and 2 showed higher compressive strengths at all ages as compared to samples having 4% gypsum and there is no change in compressive strength with 6% kiln dust. However, OPC made with clinker-3 and kiln dust-3 and 5% gypsum do not show any change in compressive strength at all ages as compared to samples having 4% gypsum. But increased addition of kiln dust from 2 to 6% adversely affected the compressive strength at all ages.

Portland Pozzolana Cement (PPC)

The water requirements of PPC made with and without kiln dust are more or less the same. The initial and final setting times of PPC, made with clinkers-3, kiln dust-3 and constant quantity of gypsum (4% and 5%) decreased marginally with increased addition of kiln dust from 2-8%. This is in agreement with the results obtained by Sastry and Mohan (13).

Variation in gypsum content with corresponding kiln dust addition such that the both do not exceed 4% in cement shows that the initial and final setting times of PPC decreased with increased addition of kiln dust from 1 to 3%.

Comparison of compressive strengths test results shows that with constant quantity of gypsum (4% and 5%) increased addition of kiln dust from 2 to 8% affects the compressive strengths at all ages adversely. These results are in agreement with the results obtained by Bhatty (12) and Sastry and Mohan (13).

However, variation in gypsum content with corresponding kiln dust addition such that the both do not exceed 4% in cement shows that the compressive strengths at all ages increased with increased addition of kiln dust from 1 to 3%.

Increase of gypsum content from 4 to 6% and addition of 2 to 6% kiln dust to clinker shows a decrease in compressive strength at all ages in comparison to samples having 4% gypsum and 2 to 6% kiln dust.

Portland Slag Cement (PSC)

The water requirements of PSC made with and without kiln dust are more or less the same. The initial and final setting times of PSC, made with clinker-2, kiln dust-2 and constant quantity of gypsum (4% and 5%) increased marginally with increased addition of kiln dust from 2 to 8%. However, these results are in conflict with the results obtained by Mohanty, Goswami and Panda (8), who found that the setting times of the PSC made with 8% kiln dust and control PSC are almost the same.

Variation in gypsum content with corresponding kiln dust addition such that the both do not exceed 4% in cement shows that the initial and final setting times of PSC decreased with increased addition of kiln dust from 1 to 3%.

Comparison of compressive strength test results shows that with constant quantity of gypsum (4%), increased addition of kiln dust from 2 to 8% does not affect the compressive strength at all ages. Increase of gypsum content to 5% and addition of 2 to 6% of kiln dust to clinker shows that the compressive strength at all ages are not affected upto 2% kiln dust addition. However, as the amount of kiln dust increased to 4-6%, compressive strength at all ages decreased. However, variation in gypsum content with corresponding kiln dust addition such that the both do not exceed 4% in cement shows that compressive strengths at all ages decreased with increased addition of kiln dust from 1 to 3%.

ACKNOWLEDGEMENTS

The work described here has been carried out as part of the research programme of the R&D Centre of Cement Corporation of India Limited and this paper is published with the permission of Director(Operations). The authors thank Mr.Ram Chandra for samples preparation and physical testing of samples.

REFERENCES

1. Talcherkar, K.V.: "Report on utilisation of electrostatic precipitators in cement industry". Sub-Committee of panel on cement industry, DGTD, Govt. of India, New Delhi,1972.
2. Talcherkar, K.V.: "The Indian cement industry", Zement-Kalk-Gips,1976,29(7),362.
3. Mishra, J.C., Srivastava, V.K. and Narang, K.C. : "Characterization of kiln dust and exit gases from Indian cement plants". Zement-Kalk-Gips,1978,31(5),230.
4. Davis,T.A. and Hooks, D.B.: "Disposal and utilisation of waste kiln dust from cement industry". U.S.Environmental Protection Agency Report EPA-67012-75-043,1975, 63 p.
5. Peter Max, F. and Erni, H.F.: "Full Production efficiency requires a fresh look at specification", Rock Products, 1978, 81(5),1992.
6. Tettmar, B., Gregory, S. and Khor, I.H.: "Processing of kiln dust", Zement-kalk-Gips, 1978, 31(6), 288.
7. Stearn, E.W.: "What is CKD?", Rock Products,1979,82(6),84.
8. Mohanty, S.K., Goswami, G. and Panda, J.D.: "Utilisation of cement kiln dust in cement manufacture". All India Seminar on cement manufacture,1981. New Delhi, 1981, V3, 537-541.

9. Goswami,G., Mohanty, S.K. and Panda, J.D.: "Hydration study of cement kiln dust blended portland cement by DTA". Seminar on Cement Industry, 6th,Madras, India,1982.
10. Bhatty, M.S.Y. : "Use of cement kiln dust in blended cements". World Cement,1984, 15(4), 126.
11. Bhatty, M.S.Y.: "Use of Cement kiln dust in blended cements - alkali aggreate reaction expansion". World Cement, 1985, 16(10), 386.
12. Bhatty, M.S.Y.: "Kiln dust cement blends evaluated". Rock Products, 1985, 88(10), 47.
13. Sastry, R.R. and Mohan, K.: "Utilisation of kiln dust in the manufacture of OPC and PPC". Cement Industry Annual Review, Bombay, India, 1989, VIII, 87-92.
14. Sharma, G.D.: "Kiln operation vis-a-vis ESP dust-A bold approach at Maihar Cement". NCB International Seminar on Cement and Building Materials, 3rd, New Delhi, India, 1991, V1, I-139-150.
15. El-Sayed, H.A., Gabor, N.A. and Mohran, M.A.: "Reutilization of By-pass kiln dust in cement manufacture". NCB International Seminar on Cement and Building Materials, 3rd , New Delhi, India, 1991, V3, VIII-3-13.

Table-3 : Physical Test Results for OPC

Sl. No.	Composition(Wt.%) CL-1	GYP-1	KD-1	Sp.Sur. (cm^2/gm)	N.C. (%)	Setting time(min) Initial	Final	Le-ch. Expn. (mm)	Compressive strength (kg/cm^2), 3days	7days	28days
01.	96.0	4.0	0.0	2806	24.25	190	245	1.0	330	430	570
02.	94.0	4.0	2.0	2885	24.25	160	215	1.0	320	410	570
03.	92.0	4.0	4.0	2885	24.50	215	280	1.0	280	380	550
04.	90.0	4.0	6.0	2885	24.50	210	275	1.5	270	370	550
05.	88.0	4.0	8.0	2924	24.75	215	285	1.5	240	330	520
06.	86.0	4.0	10.0	2885	24.75	240	310	2.0	220	300	480
07.	96.0	3.0	1.0	2885	24.50	195	250	1.0	330	440	620
08.	96.0	2.0	2.0	2885	24.75	190	245	1.0	310	440	630
09.	96.0	1.0	3.0	2924	25.00	180	245	1.5	300	440	630
10.	95.0	5.0	0.0	3581	23.75	140	185	1.5	350	470	630
11.	93.0	5.0	2.0	2885	23.75	145	185	1.5	320	460	600
12.	91.0	5.0	4.0	2885	24.00	135	180	1.0	300	420	580
13.	89.0	5.0	6.0	3217	24.00	145	185	1.0	260	370	550
	CL-2	GYP-2	KD-2								
14.	96.0	4.0	0.0	2806	27.50	95	135	1.0	280	360	450
15.	94.0	4.0	2.0	2806	27.75	95	145	0.5	270	350	450
16.	92.0	4.0	4.0	2806	27.50	120	170	0.5	280	350	440
17.	90.0	4.0	6.0	2846	27.50	135	180	0.5	270	350	430
18.	88.0	4.0	8.0	2846	27.50	140	190	1.0	270	330	410
19.	86.0	4.0	10.0	2806	27.25	160	200	1.0	260	320	400
20.	96.0	3.0	1.0	2806	27.75	100	150	1.0	250	310	380
21.	96.0	2.0	2.0	2806	28.00	70	90	1.0	220	280	360
22.	96.0	1.0	3.0	2806	28.25	30	55	1.0	210	260	340
23.	95.0	5.0	0.0	2806	27.75	60	95	1.0	320	400	470
24.	93.0	5.0	2.0	2885	28.25	60	95	1.0	320	400	460
25.	91.0	5.0	4.0	2806	28.00	75	120	1.0	290	360	440
26.	89.0	5.0	6.0	2806	28.00	85	125	1.0	270	350	430

Sl. No.	Composition(Wt.%) CL-3	GYP-3	KD-3	Sp.Sur. (cm^2/gm)	N.C. (%)	Setting time(min) Initial	Final	Le-ch. Expn. (mm)	Compressive strength (kg/cm^2) 3days	7days	28days
27.	96.0	4.0	0.0	2846	25.00	230	285	1.0	340	450	600
28.	94.0	4.0	2.0	2846	25.00	230	280	1.0	340	450	570
29.	92.0	4.0	4.0	2885	25.00	225	275	1.0	310	430	550
30.	90.0	4.0	6.0	2846	24.75	215	270	1.5	300	410	540
31.	88.0	4.0	8.0	2885	24.75	220	275	1.5	270	380	540
32.	86.0	4.0	10.0	2885	24.25	205	245	1.5	240	350	510
33.	96.0	3.0	1.0	2846	24.75	185	225	1.0	380	460	600
34.	96.0	2.0	2.0	2846	24.75	155	195	1.0	380	460	570
35.	96.0	1.0	3.0	2846	24.75	145	190	1.0	360	450	550
36.	95.0	5.0	0.0	2846	25.00	230	280	1.0	340	440	600
37.	93.0	5.0	2.0	2846	25.00	225	275	1.0	310	420	600
38.	91.0	5.0	4.0	2846	24.75	220	270	1.0	280	390	550
39.	89.0	5.0	6.0	2885	24.75	225	270	1.0	260	360	550

Table-4 :Physical Test Results for PPC

Sl.	Composition (Wt.%) CL-3	GYP-3	KD-3	Fly Ash	Sp.Sur. (cm^2/gm)	N.C. (%)	Setting time(min) Initial	Final	Le-ch. Expn. (mm)	Compressive strength ($kg./cm^2$) 3days	7days	28days
1.	81.0	4.0	0.0	15.0	3354	26.50	215	255	0.5	310	430	610
2.	79.0	4.0	2.0	15.0	3387	26.50	200	240	0.5	300	420	600
3.	77.0	4.0	4.0	15.0	3387	26.50	200	245	0.5	290	400	600
4.	75.0	4.0	6.0	15.0	3354	26.50	195	245	1.0	270	380	580
5.	73.0	4.0	8.0	15.0	3354	26.25	195	240	1.0	250	350	530
6.	81.0	3.0	1.0	15.0	3387	26.50	175	215	0.5	360	470	630
7.	81.0	2.0	2.0	15.0	3354	26.50	175	215	1.0	350	460	610
8.	81.0	1.0	3.0	15.0	3387	26.50	155	195	1.0	340	440	590
9.	80.0	5.0	0.0	15.0	3354	27.25	250	290	1.0	310	420	600
10.	78.0	5.0	2.0	15.0	3354	27.25	220	260	1.0	280	400	600
11.	76.0	5.0	4.0	15.0	3354	27.25	215	260	1.0	230	350	600
12.	74.0	5.0	6.0	15.0	3354	27.25	215	265	1.0	160	260	520

Table-5 :Physical Test Results for PSC

Sl. No.	Composition (Wt.%) CL-2	GYP-2	KD-2	Slag	Sp.Sur. (cm^2/gm)	N.C. (%)	Settimg time(min) Initial	Final	Le-ch. Expn. (mm)	Compressive strength (kg/cm^2) 3days	7days	28days
01.	48.0	4.0	0.0	48.0	2806	27.25	140	220	0.5	260	340	450
02.	46.0	4.0	2.0	48.0	2806	27.50	145	225	0.5	250	320	440
03.	44.0	4.0	4.0	48.0	2846	27.50	170	240	0.5	250	340	460
04.	42.0	4.0	6.0	48.0	2806	27.50	195	260	1.0	240	330	430
05.	40.0	4.0	8.0	48.0	2846	27.50	205	270	1.0	240	320	420
06.	48.0	3.0	1.0	48.0	2846	28.00	145	210	1.0	250	330	430
07.	48.0	2.0	2.0	48.0	2806	28.25	115	160	0.5	240	330	410
08.	48.0	1.0	3.0	48.0	2846	28.50	80	110	1.0	210	280	380
09.	47.0	5.0	0.0	48.0	2806	27.25	125	190	1.0	290	380	510
10.	45.0	5.0	2.0	48.0	2846	27.50	120	185	1.0	300	380	500
11.	43.0	5.0	4.0	48.0	2806	27.50	175	245	1.0	260	340	450
12.	41.0	5.0	6.0	48.0	2806	27.50	190	275	1.0	240	330	430

INFLUENCE OF DEGREE OF HYDRATION OF SLAG ON SLAG CEMENTS

A F Battagin

Brazilian Association of Portland Cement
São Paulo, BRAZIL

ABSTRACT

A selective dissolution method with EDTA solution was employed to determine the degree of hydration of slags in laboratory-made cements. The principle of this method is based on the fact that clinker phases and their hydrates, and the hydrates formed from the interground slag are largely dissolved whereas the unhydrated slag remains as a residue. Experimental cements with known slag contents were subjected to different curing conditions (temperature and humidity). Correlation of the degree of hydration of slag in the cements to their compressive strength has been attempted.

RESUMEN

El método de disolución selectiva con solución de EDTA fue empleado en el presente trabajo para determinar el grado de hidratación de escorias en muestras de cemento de laboratório.

El principio del metodo se basa en lo hecho que las fases del clinker y sus hidratos y los hidratos desarrolados por la presencia de escoria en el cemento son atacables por la solución de ensayo mientras que los granos todavia anidros de escoria se quedan insolubles.

Cementos experimentales con distintos níveles de contenido de escória fueran ensayados a condiciones distintas de curado (temperatura y humidad). Se intentió averiguar la existencia de correlación entre el grado de hidratación de las escorias y la resistencia mecánica de los cementos con escoria.

1 INTRODUCTION

Towards a better understanding of hydration mechanisms of slags and their influence on the performance of cements and durability of concrete, the results of an investigation on the degree of hydration of the slags in a cement are presented.

The degree of hydration as a mesure of the reaction between cement grains and water is a parameter very difficult to determine. Literature indicates that the degree of hydration is evaluated indirectly based on three different methods. The first one is based on the determination of the amount of chemically combined water. Another consists in determining the heat of hydration due to the exothermic nature of the hydration reactions. The third one is based on comparing the development of compressive strength at different ages to a final value reached after a long hydration period (eg 360 days or more). However these methods are not wholly suitable when applied to cement with additions, such as blast-furnace slag portland cements. This reason is because slags present a different behaviour during hydration compared to the clinker phases.

Accordingly, a different procedure based on the selective dissolution of the phases, capable of mesuring the unreacted slag, was adopted, in the present study.

This study not only tries to evaluate the effect of the curing conditions (temperature and moisture) of mortars on the degree of hydration of slags (not the degree of hydration of the cements proper but also makes an attempt to correlate this parameter to the compressive strength of mortars.

2 EXPERIMENTAL PROCEDURE

2.1 Methods and Materials

The investigations were carried out on laboratory cements prepared with the addition of 35%, 50% and 70% of granulated blast-furnace slag (GBFS) to a high early-strength portland cement (HPC), representative of the industrial production in Brazil. Tables 1 and 2 show the chemical and physical data of the starting materials and Table 3 shows the data for laboratory-made cements.

Table 1 Chemical Physical and Mechanical Data of Starting Materials

COMPOSITION, % in mass	HPC	GBFS
SiO_2	19.46	35.46
Al_2O_3	4.87	12.16
Fe_2O_3	2.81	0.63
CaO	64.09	43.39
MgO	0.48	6.32
SO_3	3.52	-
Na_2O	0.02	0.15
K_2O	0.60	0.50
IR	0.04	-
S	-	-
LOI	3.19	1.10

Physical Data	HPC	GBF
Density, g/cm³	3.11	2.92
Specific surface, $m^2.kg^{-1}$	394	378
Vitrification Degree, %	-	98
Refractive index	-	1.64 to 1.65

POTENTIAL COMPOSITION (BOGUE)	
C_3S	66.2
C_2S	5.8
C_3A	8.2
C_4AF	8.6
$CaSO_4$	6.0

Table 2 Rheological and Mechanical Data for Cement

Parameter		HPC
Initial Setting time, minutes (Vicat Test)		130
Compressive Strength, MPa, at	1 day	19.7
	3 days	35.3
	7 days	41.7
	28 days	50.9

Table 3 Composition and Specific Surface Area for Laboratory-Made Cements

Laboratory Cement	% in mass		Specific Surface ($m^2.kg^{-1}$)
	cement	slag	
1 (control)	100	0	394
2	65	35	388
3	50	50	386
4	30	70	383

The compressive strength was determined according to the Brazilian method (NBR 7215) by using 5 x 10cm cylindrical test specimens in mortars 1 : 3 (cement : sand) cured at 23° ± 2°C, w/c = 0.48.

Dissolution technique was based on a modified **Levelt's** proposition (1) by using a solution containing EDTA, triethanolamine and Na_2HPO_4. Under controlled conditions, this solution can dissolve the unhydrated cement grains and their hydration products, leaving only the unreacted slag grains as undissolved residue.

The undissolved residue was determined in pastes with w/c = 0.48, subjected to the same conditions as mortars whose compressive strengths were determined.

The degree of hydration of slag grains in pastes was calculated from the following equation:

$$Hs = \frac{R_{cement} - R_{paste}}{R_{cement}} \times 100\% \quad (1)$$ where

Hs = degree of hydration of slag in cement paste
R_{cement} = undissolved residue for anhydrous cement
R_{paste} = undissolved residue for the cement paste

2.2 Compressive Strength Results

Table 4 presents the mortar compressive strength results.

Table 4 Mortar Compressive Strength

Age, days	Compressive Strength, MPa			
	Control	Cement 2	Cement 3	Cement 4
3	35.3	26.2	21.0	13.4
7	41.7	36.3	32.6	29.4
14	44.0	45.3	41.1	40.4
21	48.8	47.9	46.8	44.4
28	50.9	51.3	49.6	49.2
91	57.0	59.1	60.9	58.0
180	59.5	61.0	65.6	61.5
360	60.4	64.6	67.9	65.0

From Table 4 we can conclude that at early ages, the higher the cement replacement by slag, the lower the compressive strength. Strength reduction at early ages when compared to the control was expected because slag hydration rate is remarkablebly lower than that of clinker. At later ages (14 to 91 days) both slag and control mortars give almost the same value. At 180 days and beyond the highest values are found for 50% replacement.

2.3 Results of Undissolved Residue as a Measure of Slag Hydration Degree

Table 5 shows the results of selective dissolution of cement pastes and anhydrous cements.

The degree of hydration of slag grains in paste cured at 23° ± 2°C was calculated from equation 1 using the data in Table 5.

Table 5 Undissolved Residues of Cement Pastes

Age days	UNDISSOLVED RESIDUE, %		
	Cement Paste 2	Cement Paste 3	Cement Paste 4
3	29.1	40.2	55.0
7	26.1	36.3	47.6
14	23.5	32.6	45.2
21	23.6	30.6	43.6
28	23.8	29.9	42.8
91	23.4	30.7	42.6
180	18.3	24.4	36.0
360	16.7	21.8	33.7
Anhydrous cement	34.8	48.4	67.6

Table 6 Degree of Hydration of Slag in Pastes Cured at 23° ± 2°C

Age days	DEGREE OF HYDRATION OF SLAG, %			
	Cement 2	Cement 3	Cement 4	Average
3	16.4	16.9	18.6	17.3
7	25.0	25.0	29.6	26.5
14	32.5	32.6	33.1	32.7
21	32.2	36.8	35.5	34.8
28	31.6	38.6	36.7	35.4
91	32.7	36.6	37.0	35.4
180	47.4	49.6	46.7	47.9
360	52.0	54.9	50.1	52.3

Table 6 shows the results so obtained. They show that all the mixtures were able to develop a progressive hydration up to 14 or 21 days. At this age, about 35% of slag grains have already reacted and were converted to hydrated phases. From 28 days to 91 days very little development in hydration was noted, and after 91 days and beyond the hydration rate again increased.

These results accord with those reported by **LUKE and GLASSER** (2). They had shown that 40% of the slag had reacted within the first month but a renewal of slag hydration was noticed to occur only after 6 months as against 3 months in the present study.

At 12 months approximately 50% of slag appears to be unreacted. This fact indicates a very slow hydration of slag as compared to clinker grain. The grain size appears to have a great influence on slag hydration and **Longo** (3) reported that slag particles above 45 μm have a very little effect on the slag hydraulic reactivity.

2.4 Degree of Hydration of Slag in Pastes Cured at 40°C, 60°C and 80°C

The temperature at which a mortar or concrete is cured has a remarkable effect on its mechanical strength. Although high curing temperatures accelerate early strength gain, data in literature report a deleterious effect on later age strength. On the other hand, blast-furnace slag cements are found to respond very well to elevated curing temperature as compared to ordinary portland cement.

In order to investigate the influence of curing temperature on the degree of slag hydration, slag pastes with 50% cement replacement and water to binder ratio of 0.48 were cured at 40°, 60°and 80° ± 2°C up to 28 days. The degree of slag hydration was calculated by the same procedure reported above. In addition, mechanical compressive strengths of mortars subjected to the same conditions were also determined.

Figures 1 and 2 show the results obtained. Figure 1 clearly shows that on raising the curing temperature there is an increase in the degree of hydration of slag. In fact, at 28 days, slag pastes cured at 23°C exhibited a 38% hydration of slag, comparable to the paste cured at 40°C for five days, or to the one cured at 60°C for two days, or even to the one cured at 80°C for first 24 hours.

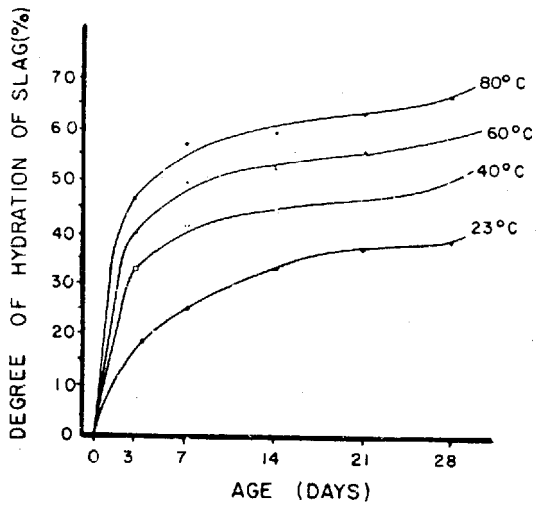

Fig. 1 - Degree of hydration of slag of mortars with 50% replacement in function of curing temperature and age.

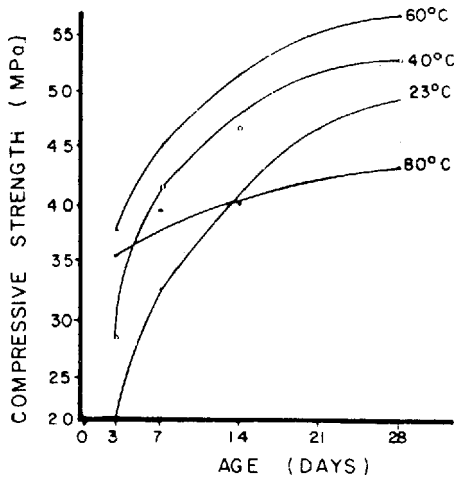

Fig. 2 - Compressive strength of mortar with 50% replacement in function of curing temperature and age.

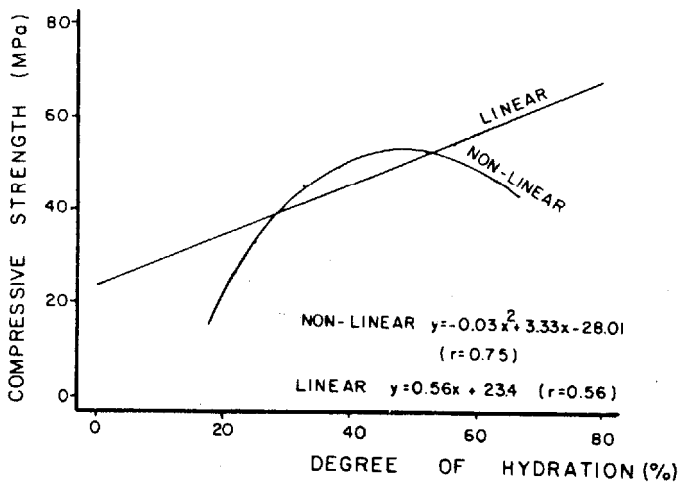

Fig. 3 - Degree of hydration of slag versus compressive strength.

Figure 2 shows the development of compressive strength for slag pastes with age up to 28 days with 50% replacement slag and cured at different temperatures. In general, there is a gain in compressive strength for comparable age with increase in curing temperature up to 60°C.

However, mortar cured at 80°C presented a different behaviour, registering an increase of strength only at early age and a decrease from 14 and up to 28 days (compared to mortar cured at 23°C).

Figure 3 shows the relationship between degree of hydration of slag and compressive strength, not taking into account the age, curing temperature, etc.

By means of a linear regression analysis a correlation coefficient **r** of 0.56 was found. This value suggests a poor linear correlation between degree of hydration of slag and strength. A value of 0.73 is found for **r** if a non-linear regression analysis is carried out. However, correlating mortar strength to degree of hydration of slag in pastes with 35%, 50% and 70% cement replacement and cured at 23°C ± 2°C, a good value of **r** = 0.91 was found.

A similar value (**r** = 0.92) is obtained if a non-linear regression analysis (polynomial) is made.

High **r** values are also found while correlating compressive strength to the degree of hydration of slag in pastes with 50% cement replacement and cured under similar conditions. For 23°, 40°, 60°and 80°C curing temperatures the values of **r** (linear regression analysis) were respectively 0.95, 0.93, 0.97 and 0.99.

The poor correlation between the degree of hydration of slag and mortar strength, without taking into account the curing regime could be explained by **Verbeck and Helmuth's theory** (4). According to them at normal temperatures (23°C in this investigation) the hydration products have enough time to diffuse into cement bulk paste and attains a well defined and uniform distribution. On the other hand, at higher temperatures of curing (40, 60 and 80°C in this investigation), the rate of hydration is so much faster than the rate of diffusion that most of the hydration products remain near the cement grains. As result, the intersticial spaces in the cement paste matrix are not completely filled and voids and pores increases which decrease the later strengths. However, for the same curing regime, the good correlation between the degree of hydration of slag and mortar strength appears to be due to a similar microstructure of the cement paste.

2.5 Degree of Hydration of Slag in Pastes Cured Under Different Moisture Conditions

Concretes with a high content of blast-furnace slag replacing portland cement are known to exhibit a more pronounced effect on strength decrease when cured under prolonged dry condition than concrete with ordinary portland cement.

In order to investigate the relationship of the degree of hydration of slag and the compressive strength of mortars cured inadequately, cement 4 (70% slag content) was chosen. Pastes and mortars were prepared similar to the former procedures mentioned in **2.1.**

Degree of hydration and 28-day compressive strength were determined respectively in pastes and mortars after they were subjected to the following curing regimes:

a) continous moist curing for 28 days at 23° ± 2°C and > 95 percent relative humidity (moisture room);

b) 21 days in moisture room followed by 7 days in a dry room with 23° ± 2° C and 50 ± 4 percent relative humidity;

c) 14 days in moisture room and 14 days in dry room;

d) 7 days in moisture room and 21 days in dry room;

e) 3 days in moisture room and 25 days in dry room and
f) 1 day in moisture room and 27 days in dry room.

Figures 4 and 5 show the results obtained.

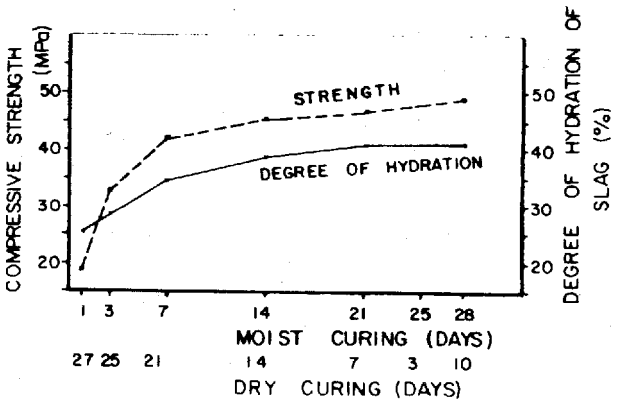

Fig. 4 - Degree of hydration and 28-day compressive strength of mortars with 70% slag subjected to moist and dry curing cycles.

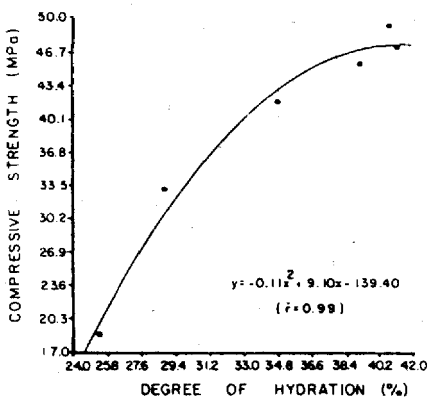

Fig. 5 - Degree of hydration of slag of mortar with 70% slag versus 28 days compressive strength (moist and dry curing cycles).

3 CONCLUSIONS

From the results of tests carried out in this investigation, the following conclusions can be drawn.

- The selective dissolution method proposed by **Levelt** is a valuable tool for estimating the degree of hydration of slag in slag pastes.
- At early ages, the higher the cement replacement by slag, the lower the compressive strength.
- At later ages both slag and control mortars presented almost the same value of strength. At 180 days and beyond the highest values were found for 50% replacement.
- At 14 or 21 days about 35% of slag had already reacted and converted to hydrated phases; a renewal of slag hydration occurred only after 3 months, and at one year 50% of slag appeared to be still unreacted.
- High curing temperatures greatly accelerated the degree of hydration of slag. Although high curing temperatures also accelerated early strength gain, it is not proportional to the increase in the degree of slag hydration at later ages.
- There is poor correlation between the degree of hydration of slag and mortar strength if the curing regime is not taken into account.
- Within the same curing regime, however, a good correlation was obtained. As microstructure is supposed to depend on the curing regime condition, the good correlation, in this case is possibly due to the similar microstructure.

REFERENCES

1. Levelt, F. et alii: "Determination of the slag content of blast-furnace slag cements by means of a solution method". Zement-Kalk-Gips, 1982, Wiesbaden, 35(2) : 97-8.
2. Luke K. & Glasser F.P. - "Selective dissolution of hydrated blast-furnace slag cements". Cement and Concrete Research, 1987, 17(2), 273-82.
3. Longo, A. "Characterization of granulated blast-furnace slag". **Latin American Seminar on the use of blast-furnace slag in Building,** Buenos Ayres, Argentina 1991, 19-26 (in spanish).
4. Verbeck, G.J. et al.: "Structure and physical properties of cement paste." Proceeding of the **Fifth International Symposium on the Chemistry of Cement, Tokyo,** Japan 1968, v3, 1-32.

SO_3 CONTENT OF PORTLAND AND BLENDED CEMENTS: POROSITY AND BEHAVIOUR OF THE RESULTANT MORTARS

R Sersale*, R Cioffi*, G Frigione and F Zenone*****

**Department of Materials and Production Engineering, University of Naples*
***Department of Chemistry, University of Calabria*
****Cementir, Cementerie del Tirreno*
ITALY

SUMMARY

The aim of this work is to search for possible correlations between the alteration in the physical microstructure, due to gypsum addition, and the mechanical behaviour of cement mortars. Experimental investigations on a series of 42 ISO-Rilem mortar samples, differentiated by the type of cement and gypsum content, have pointed out a continuous variation of pore size distribution until a certain amount of SO_3 is reached, beyond which distribution remains unchanged. These experimental results suggest that the mechanical behaviour is significantly affected by the gypsum content of the cement used, owing to the alterations induced in the physical structure of the mortars.

Ce rapport tente d'établir une corrélation raisonnable entre les modifications de la microstructure physique, amenées par l'addition de gypse, et le comportement mécanique des mortiers de ciment. La recherche, accomplie avec une série de 42 échantillons de mortier ISO-RILEM, préparés avec différentes sortes de ciment à teneur variable de gypse, a montrée une variation continue de la distribution de la taille des pores, jusqu'au moment où une certaine teneur de SO_3 est gagnée, au-delà de laquelle la distribution meme reste inchangée. Ces résultant démontrent que le comportement mécanique des mortiers est influencé, d'une façon significative, à la suite des modifications de la structure physique des mortiers, amenées par la teneur de gypse du ciment utilisé.

INTRODUCTION

The influence of gypsum content on the development of mechanical strength is well known (1-3). There is in fact an optimum gypsum content allowing the highest compressive strength value to be reached. Such a content increases with the curing duration, shifting towards lower or higher SO_3 amounts. The phenomenon has been interpreted in different ways: for instance that SO_3 can affect, on the one hand, the reaction rate, particularly at early ages, and on the other, form a tobermoritic gel with different intrinsic strength characteristics. There is indeed little information in literature on the influence of SO_3 on the physical microstructure of cement pastes or mortars.

The aim of this work is to investigate the relationship between SO_3, pore size distribution, total porosity and compressive strength (4-7) of cementitious manufacture.

A prelinimary study on Portland cement had been accomplished by the authors in a previous work (8).

EXPERIMENTAL

Four different Portland cements and two blended cements were prepared. The series of Portland cements were prepared utilizing three different clinkers with C_3A content ranging between 1.6 to 10.7%. The Blaine fineness was equal to 380 m^2/kg. The clinker with the highest C_3A content was ground at two different finenesses (380 and 500 m^2/kg). Phlegraean pozzolana (35%) and blast furnace slag (70%), respectively, were added to the clinker with C_3A intermediate content, in order to obtain two types of blended cements.

The chemical characteristics of the products used are reported in Table 1.

TABLE 1

	C_3S	C_2S	C_3A	C_4AF	Na_2O	K_2O
Clinker N. 1	54.1	24.3	1.6	15.0	0.4	0.3
Clinker N. 2	48.6	24.9	8.4	13.2	0.3	0.9
Clinker N. 3	47.3	26.2	10.7	11.2	0.2	1.0
	SiO_2	Al_2O_3	Fe_2O_3	CaO	Na_2O	K_2O
Phlegraean pozzolana	57.8	19.4	4.1	3.0	3.4	7.6
Blast furnace slag	33.0	12.7	2.6	43.3	0.5	0.4

Increasing amounts of gypsum were added to such blends, in order to obtain seven different cements with a total amount of SO_3 ranging between 1.5 and 4.5%.

In this way a series of 42 different ISO-Rilem mortars were prepared. After a certain age, the hydration was stopped (8) and each mortar subjected to compressive strength tests and mercury intrusion analysis (9) in order to determine the total porosity and pore size distribution, calculated according to Washburn algorithm (10).

RESULTS AND DISCUSSION

Fig. 1 reports the pore size distribution of Portland cement mortars prepared with clinker Nº.1 (Fig. 1a) and clinker Nº.2 (Fig. 1b) as a function of SO_3 content. It can be seen that the SO_3 content does not significantly influence the pore size distribution of the mortars prepared with clinker Nº.1 and cured at 3 and 28 days.

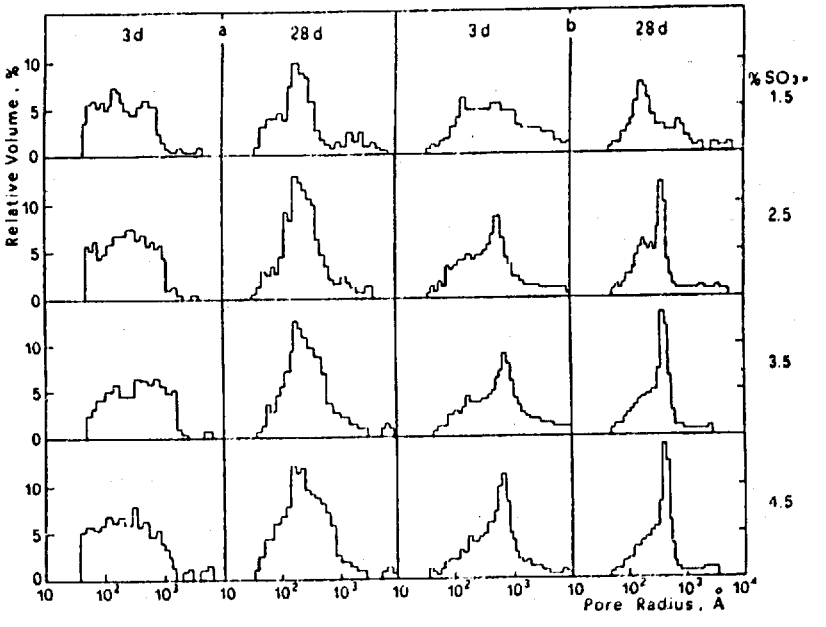

Fig. 1. Pore size distribution of Portland cement mortars prepared with: a) clinker Nº.1 - b) clinker Nº.2, as a function of SO_3 content.

For mortars prepared with clinker Nº.2, we notice however a shifting of the pore size distribution towards the smallest ones. Such variation, at 3 and 28 day curing, is continuous up to a 2.5% SO_3. Afterwards the pore size distribution remains almost constant.

Fig. 2a shows the influence of SO_3 content on pore size distribution of Portland cement mortars prepared with clinker Nº.3 ground to 380 m^2/kg fineness. One can see that at 3 and 28 day curing there is a replacement of the larger pores with smaller ones, according to a linear course up to values of SO_3 content equal to 2.5%. As for clinker Nº.2, the linear course is maintained until the 2.5% SO_3 is reached.

Fig. 2b reports the variations of pore size distribution as a function of SO_3 content for Portland cement mortars prepared with the same clinker Nº.3, but ground to a higher fineness (500 m^2/kg). Pore size distribution at 3 and 28 day curing will not vary up to 2.5% SO_3. For values of SO_3 content over 2.5%, a variation with a linear course up to 4.5% SO_3 is observed. In this case pores ranging from 1000 to 10000 Å disappear giving way to lower sized pores ranging from 100 to 1000 Å.

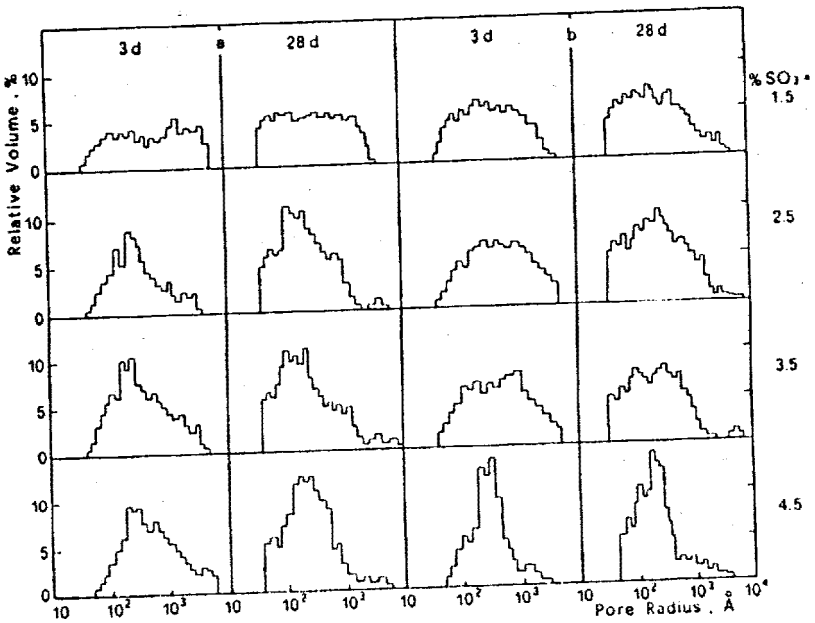

Fig. 2. Pore size distribution of Portland cement mortars prepared with: a) clinker Nº.3 (380 m^2/kg) - b) clinker Nº.3 (500 m^2/kg), as a function of SO_3 content

Pore size distributions for pozzolanic cement mortars are reported in Fig. 3a. In this case a continuous variation up to 4.5% SO_3 is shown. The size of pores for the most part shows values slightly above 100 Å.

Fig. 3b refers to slag cement mortars whose pore size distribution shows the same course as Fig. 3a. In this case, however, the variation achieved after a 28 day curing is much more evident.

All the previous results point out that the pores of slag cement mortars are smaller than those of the other cements previously studied, even when the amount of SO_3 is changed.

Therefore gypsum influences the variations of pore size distribution according to C_3A content. Such variations do not show any kind of correlation with the compressive strength.

As for the values of compressive strength, they may be correlated with total porosity, as shown in figures 4 and 5.

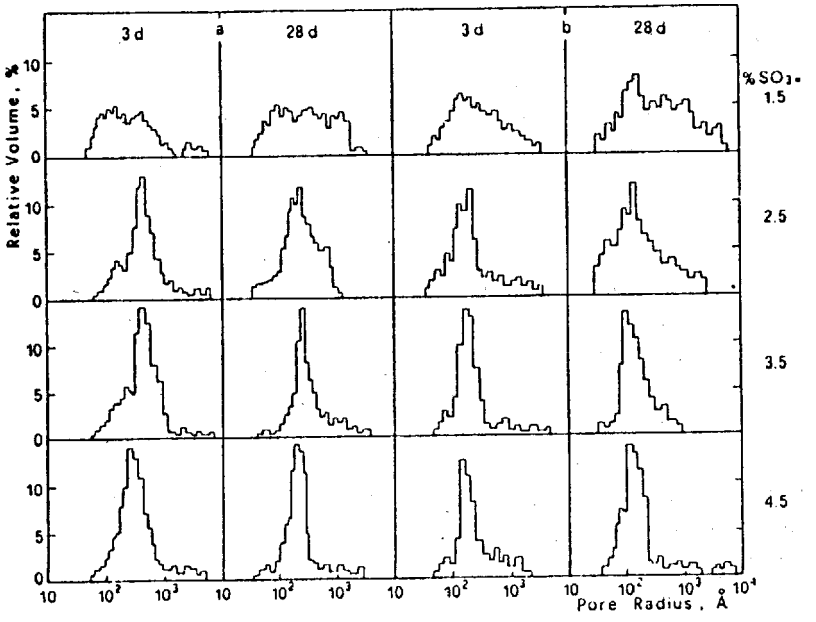

Fig. 3. Pore size distribution of: a) Pozzolanic cement mortars and b) Slag cement mortars, as a function of SO_3 content.

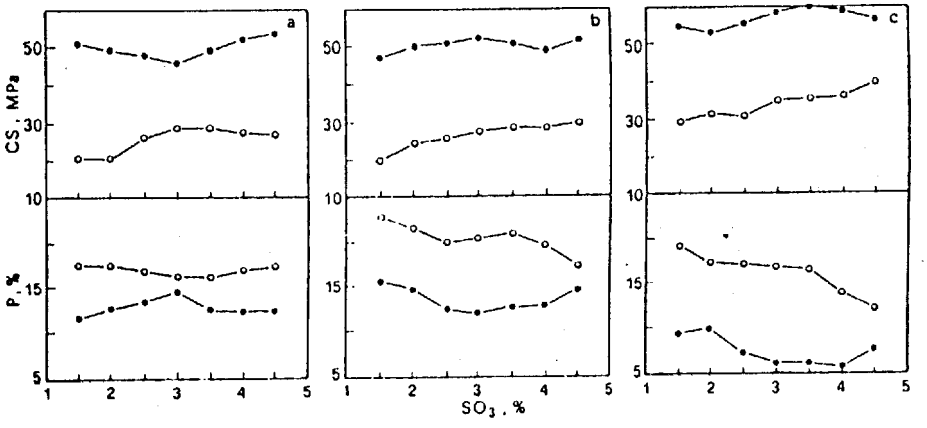

Fig. 4. Compressive strength and total porosity of Portland cement mortars prepared with: a) clinker Nº.1 - b) clinker Nº.3 (380 m^2/kg) - c) clinker Nº.3 (500 m^2/kg), as a function of SO_3 content.

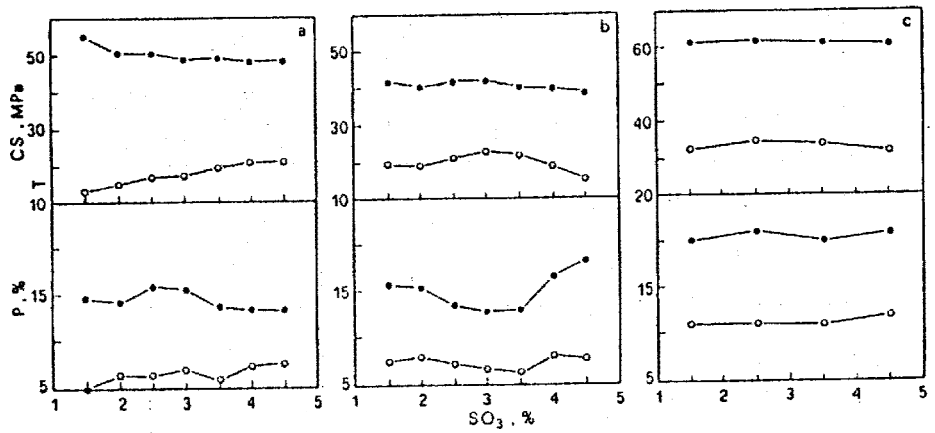

Fig. 5. Compressive strength and total porosity of: a) Slag cement mortars, b) Pozzolanic cement mortars and c) Portland cement mortars prepared with clinker Nº.2, as a function of SO_3 content.

Porosity varies us the SO_3 in such a way that lower values of porosity induce higher values of strength. Therefore, strength variations, due to SO_3 content, largely depend on porosity variations.

It may also be noticed that a variation of fineness because of grinding will only affect the absolute values of total porosity, without influencing the shape of the curves.

CONCLUSIONS

All the results above confirm the influence of SO_3 on mechanical strengths through a variation of total porosity. SO_3 content determines furthermore variations in pore size distribution. Consequently, all the physical properties related to it (such as permeability) also will be influenced.

As for cement mortars prepared with clinkers Nº.2 and Nº.3, when the amount of SO_3 increases, the size of the pores becomes smaller. For low values of SO_3, such shift takes place very quickly up to 2.5% SO_3. For values over 2.5% pore size distribution does not show particular variations.

In mortars prepared with clinker Nº.1, containing small amounts of C_3A, pore size distribution will not vary with SO_3 content.

Variations in fineness do not reasonably influence pore size distribution, which, in the case of blended cements, varies linearly with increase in SO_3 content up to the maximum adopted values.

REFERENCES

1. Frigione, G.: Gypsum in cement. Advances in cement technology, Ed. by Ghosh, S.N.. London, Pergamon Press., 1983, p 485-535.

2. Lerch, W.: "The influence of gypsum on the hydration and properties of Portland cement paste". Proc. Am. Soc. Test. Mat., 1946, 46, 1252-1292.

3. Soroka, I. and Relis, M.: "Effect of added gypsum on compressive strength of Portland cement Clinker". Bull. Am. Cer. Soc., 1983, 62, 695-697.

4. Soroka, I. and Abayneh, M.: "Effect of gypsum on properties and internal structure of PC paste". Cement and Concrete Research, 1986, 16, 495-504.

5. Odler, I. and Abdul-Maula, S.: "Investigation on the relationship between porosity structure and strength of hydrated Portland cement pastes. III: Effect of clinker composition and gypsum addition". Cement and Concrete Research, 1987, 17, 22-30.

6. Odler, I and Roßler, M.: "Investigation on the relationship betweeen porosity, structure and strength of hydrated Portland cement pastes. II: Effect of pore structure and of degree of hydration". Cement and Concrete Research, 1985, 15, 401-410.

7. Atzeni, A., Massidda, L. and Sanna, U.: "Effect of pore distribution on strength of hardened cement pastes". Proc. of the First Int. RILEM Cong. on 'Pore structure and materials properties', Paris, France 1987, Chapman and Hall, 195-202.

8. Sersale, R., Cioffi, R., Frigione, G. and Zenone, F.: "Relationship between gypsum content,porosity and strength in cement. I. Effect of SO_3 on physical microstructure of Portland cement mortars". Cement and Concrete Research, 1991, 21, 120-126.

9. UNI-Unicemento E0704053: "Paste, mortars and concrete - Determination of porosity by mercury intrusion".

10. Washburn, E.W. Proc. Nat. Acad. Sci. USA, 1921, 7, 115-116.

LIMESTONE ADDITIONS TO PORTLAND CEMENT: UPTAKE, CHEMISTRY AND EFFECTS

Kevin D Ingram and Kenneth E Daugherty

Department of Chemistry, University of North Texas
Texas, USA

ABSTRACT

The addition of limestone filler to Portland cement before grinding is an ongoing controversy in Europe and the United States. Does the limestone act as an active participant in the hydration chemistry of Portland cement or is it primarily an inactive diluent? With the addition of calcium carbonate a reaction occurs upon hydration between it and tricalcium aluminate to form calcium carboaluminates. They can control set characteristics in a manner similar to the calcium sulfoaluminates. It appears that cements with higher levels of tricalcium aluminate show either improved characteristics or no decrease in the quality of the cement. In cements with low levels of tricalcium aluminate, deleterious effects on physical properties have been noted. It appears though that if the water/cement ratio, the surface area of the clinker and the particle size of the limestone are controlled, the side effects of limestone addition can be minimized. Also of interest is the uptake of carbonate, especially in a system that contains sulfate. How much carbonate is available for the formation of both the high and low carbonate forms of the carboaluminate and what effect does the formation of carboaluminate have upon the formation of sulfoaluminates?

INTRODUCTION

The new draft European guidelines for concrete (pr ENV 197), set to become effective in 1992 , allow 5% minor additional constituents to be added to ordinary portland cement (OPC). This addition can be limestone, granulated blast furnace slag or fly ash. Because of this, there is an increasing interest in the effects of carbonate additions on the quality of concrete. This interest also extends to the United States where there have been proposals to ASTM to allow a 5% addition of limestone to portland cement.

There is a belief that limestone is an inert addition to OPC. However, some $CaCO_3$ is taken up into the system and reacts with C_3A to form calcium carboaluminates. How much carbonate is available for CCA formation, how does the CO_3^{2-} affect SO_4^{2-} uptake and the ensuing formation of ettringite, and what effect does CCA have upon the quality of the cement are questions that must be answered.

First, in a system containing C_3A and $CaCO_3$, a reaction occurs which forms both a high carbonate form of carboaluminate $C_3A.3CaCO_3.32H_2O$ and a low carbonate form $C_3A.CaCO_3.12H_2O$. These species closely approximate the physical properties of the high sulfate form of calcium sulfoaluminate, $C_3A.3CaSO_4.32H_2O$ (ettringite) and the low sulfate form $C_3A.CaSO_4.12H_2O$ [1].

Mixed ettringite like species containing CO_3^{2-} or OH^- substituting for SO_4^{2-} also have been observed [2]. Ramachandran has reported that in the presence of carbonate, the conversion of ettringite to the monosulfate, which occurs as sulfate levels in the paste decrease, is delayed [3]. It is possible that the incorporation of carbonate into this set controlling species is responsible for this delay in reaction.

Compressive strength is generally increased or not affected in OPC containing up to 5% limestone [4]. In some cements that have lower levels of C_3A, an increase in shrinkage is noticed [5]. This can mean that cements will not meet guidelines for shrinkage in structural concrete. If particle size and surface area of both the clinker and any limestone additions are controlled and the water/cement ratios are regulated, deleterious effects can generally be avoided [6].

In France, where carbonate additions have been allowed for years, reports indicate that limestone cement produces good quality concrete that has a pleasant pigmentation and good physical properties [7,8]. Bertrandy suggests the use of water reducing admixtures to help improve workability in some instances.

EXPERIMENTAL

Powder XRD was conducted on a Phillips model 112045/3 unit with nickel filtered copper K-alpha radiation at 35kV and 15mA.

Infra-red data were obtained upon a Nicolet 60sxb FT-IR utilizing a Spectra-Tech diffuse reflectance attachment and a DTGS detector. CO_3^{2-} uptake was determined by heating samples in a Lindberg furnace and determining the weight loss between 550°C and 850°C.

CO_3 UPTAKE

How much CO_3 is available for reaction with C_3A? Klemm and Adams found about 1.7% maximum (absolute) uptake of a 15% limestone addition was incorporated into a cement system having a 6.4% C_3A content after 129 days [5]. Barker reported 3% uptake in 13% C_3A cement with a 25% limestone addition and 2.5% uptake in a 5% limestone addition to the same clinker after 28 days [9]. There was also a general trend that increasing levels of C_3A elevate carbonate uptake.

Our research with Type ILA cement paste (6.59% C_3A) after 28 days shows a 5.84% uptake in cement containing 3% gypsum and 10% limestone (TABLE I). It appears that carbonate uptake is enhanced in the presence of gypsum, substantiating the fact that sulfate and the resulting sulfoaluminates probably have the largest impact on the cement hydration. Previous work in our lab shows in Type I cements with 12.5% C_3A, up to 3% limestone can be incorporated within 28 days of hydration in a system containing a 5% addition of limestone [10].

TABLE I: % Carbonate Remaining

	5% Limestone	3% Gypsum/ 10% Limestone	25% Limestone
0 day	5.33%	10.63%	25.18%
14 day	4.91	5.56	22.90
28 day	4.64	4.79	21.16
Incorporated Limestone	0.69	5.84	4.02

It is apparent that any CO_3^{2-}/OPC system can incorporate 2-3% CO_3 within 180 days, dependent upon C_3A content. Therefore a 5% inclusion of limestone appears allowable as an active participant in the hydration reaction of OPC. Long term studies are in progress to determine the maximum active percent of $CaCO_3$ versus percent C_3A in OPC.

Work by Bobrowski et al and others [4,11,12], has shown that up to 50% of the gypsum normally added to OPC can be replaced by limestone without any detrimental side effects. The calcium carboaluminates formed act as set control agents in a manner similar to sulfoaluminates. There are also positive effects on

controlling false set that can be brought about by gypsum dehydration.

EFFECTS OF LIMESTONE ADDITIONS

XRD

Low levels of calcium carbonate lead to the formation of the monocarbonate species. Some tricarbonate may also be present [4]. In an OPC system with 5% limestone and no gypsum, a change in the ratio of C-S-H to portlandite is observed (TABLE II). In a 5% gypsum system after 140 days, the ratio of the 2.79 Angstrom line from C-S-H to the 2.63 Angstrom line of portlandite is approximately unity. This is the same as in a hydrated Type ILA clinker sample used as a control without either gypsum or limestone additions. In a 5% limestone system, this ratio approaches 2.5.

TABLE II: C-S-H/ Portlandite
Peak Ratio From XRD (counts)

	5% Limestone	5% Gypsum	Type ILA Clinker
2.79 Angstrom (C-S-H)	130	80	80
2.63 Angstrom (Portlandite)	55	80	90
Ratio 2.79A/2.63A	2.36	1.0	0.89

It has been reported that calcium carbonate accelerates the hydration of C_3S by increasing the hydration zone about the crystal [3,8,9]. The observed increase in intensity of the C-S-H could be attributable to an increase in the rate of formation of C-S-H gel due to the carbonate. However, instead of an actual increase in the C-S-H intensity, the increase in this ratio could be due to a decrease in the crystallinity of the portlandite. This would be brought about by an increased rate of precipitation that the larger number of nucleation sites provided by the calcium carbonate. An early increase in the rate of precipitation might cause some of the portlandite to be amorphous. This also might explain why a limited amount of carbonate is available in the initial hydration since the particles of limestone might be covered by layers of calcium hydroxide.

Infra-Red

Infra-red has been used for years to identify inorganic ions. The first IR analysis of carboaluminates was published in 1960 [13]. Recent advances in FT-IR, sampling techniques and computer

processing have increased the versatility of IR for the analysis of hydrating cement systems [10]. Peaks for carboaluminate hydrates and sulfoaluminate hydrates can be identified (TABLE III). The best peaks are from the OH stretch in hydrated samples. Due to the fact that overlap of the hydration peaks occur, the position and presence of these peaks was determined from the second derivative spectra of the cement systems. Work is underway to utilize both second derivative analysis and various deconvolution methods to refine the analysis of carboaluminates in a cement matrix.

TABLE III: IR Peaks in Type ILA
Cement After 140 Day Hydration

ILA	5% Limestone	5%Gypsum
3640 cm^{-1}	3641 cm^{-1}	3639 cm^{-1}
3547	3566	
		3514
3477		
		3431

Carbonation

One of the more interesting side effects of carbonate additions to portland cement is that atmospheric carbonation damage might be reduced. There are two possible mechanisms for this. The first is that a buffer system is set up so that CO_3^{2-} and CO_2 react in the hydrating cement to produce bicarbonate ion, HCO_3^-. In this scenario 2 moles of CO_2 are required to overcome each mole of incorporated carbonate before attack of the calcium hydroxide proceeds. Another possibility is that the atmospheric CO_2 does attack $Ca(OH)_2$ normally, but the system stays basic longer due to the presence of the calcium carbonate. This would increase the length of time before any metal incased in the cement losses passivity.

Phenolphthalein stains were done on cross-sections of cement with 6.59% C_3A and varying levels of carbonate additions after 140 days of hydration (FIGURE I). One might expect that the system without any limestone filler would develop higher strength and resist the attack of CO_2 better. Low levels of carbonate addition appear to improve the resistance better than does a 25% level of substitution of the cement, possibly due to the increased porosity of high filler cement. In a two year study of weight loss of rebar imbedded in 5% limestone cement, decreased weight loss was observed as when compared to OPC. In the cement with 25% limestone, increased weight loss from the rebar was noted [14].

Figure 1: CO_2 Penetration of 140 Day Hydrated Cement Samples

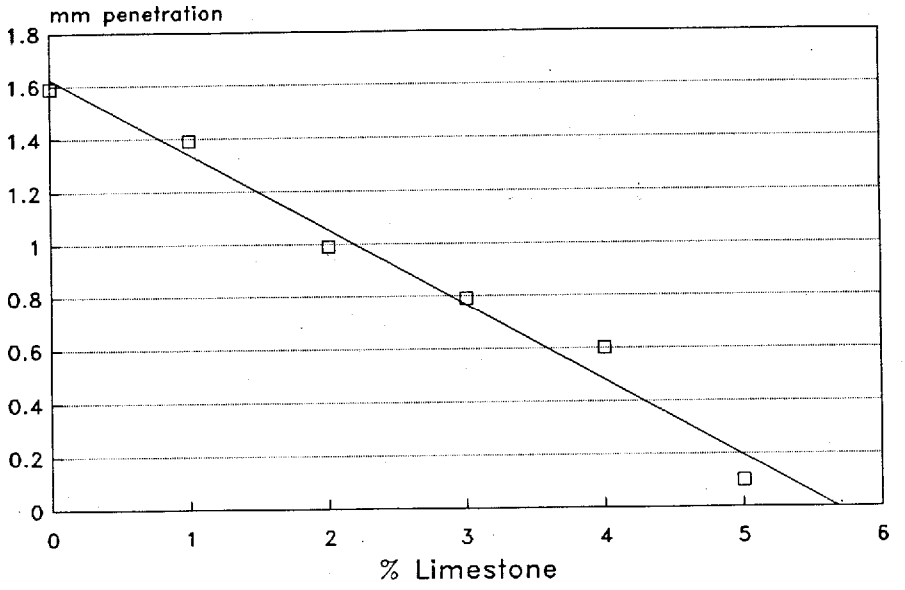

CONCLUSIONS

A beneficial reaction occurs between the C_3A in OPC and the "inert" limestone filler. This reaction leads to the formation of calcium carboaluminates. CCA can exert a positive effect upon the strength of the cement. It also affects the rate of reaction of C_3A and C_3S.

Calcium carbonate is slowly taken up in the system. Approximately 3% is available for reaction after 180 days. In some systems, over 5% limestone may be incorporated after just 28 days.

More long term study is underway to elucidate the effects of calcium carbonate upon strength and to determine the maximum active level of CO_3 in portland cement of varying C_3A contents. Investigations into the effect of calcium carbonate additions to the pH of cements undergoing atmospheric carbonation is also underway.

REFERENCES

1. Lea, F.M. : **The Chemistry of Cement and Concrete,** Chemical Publishing Company, 1971, pp. 202-233.

2. Poellmann, H., H.J. Kuzel and R. Wenda : Cement and Concrete Research, 1990, 20(6), pp. 941-7.

3. Ramachandran, R and Z. Chun-Mei : Durabil. Mater., 4, 1986, pp. 45-66.

4. Bobrowski, G.S. J.L. Wilson and K.E. Daugherty : Rock Products, Feb. 1977, pp. 64-77.

5. Klemm, W.A. and L.D. Adams : in **Carbonate Additions to Cement**, ASTM STP 1064, P. Klieger and R.D. Hooten, Eds., American Society for Testing and Materials, Philadelphia, 1990, pp. 61-72.

6. Ingram, K.D. and K.E.Daugherty : Cement and Concrete Composites, 13(1991) 165-170.

7. Bertrandy, R and P. Poitevin : in **Blended Cements in Construction**, R.N. Swamy, Ed., Elsevier, 1991, pp. 16-31.

8. Regourd, M : in **Proceedings of the 8th Congress on the Chemistry of Cement, Rio de Janeiro, 1986**, vol 1, pp. 119-129.

9. Barker, A.P. and H.P. Cory : in **Blended Cements in Construction**, R.N. Swamy, Ed., Elsevier, 1991, pp. 107- 124.

10. Ingram, K.D., M. Poslusny, K.E. Daugherty, and W. Rowe : in **Carbonate Additions to Cement**, ASTM STP 1064, P.Klieger and R.D. Hooten, Eds., American Society for Testing and Materials, Philadelphia, 1990, pp. 14-23.

11. Negro, A., G. Abbiati and L. Cussino : in **Proceedings of the 8th Congress on the Chemistry of Cement, Rio de Janeiro, 1986**, vol 3, pp. 109-113.

12. Vernet, C. : in **Proceedings of the 8th Congress on the Chemistry of Cement, Rio de Janeiro, 1986**, vol 3, pp. 70-74.

13. Carlson, E.T. and H.A. Berman : Journal of Research of the National Bureau of Standards, 64A, no.4, 1960, pp. 333-341.

14. Livesay, P. : in **Blended Cements in Construction**, R.N.Swamy, Ed., Elsevier, 1991, pp. 1-15.

EFFECT OF POZZOLANA ADDITIONS ON HYDRATION AND PERFORMANCE OF PORTLAND SLAG CEMENT

K M Sharma*, R N Sharma*, D Yadav* and K C Narang**

**National Council for Cement and Building Materials*
***Dalmia Cement (Bharat) Ltd*
New Delhi, INDIA

SUMMARY

The hydration and performance of binary blends of an ordinary portland cement and a blast furnace slag are investigated. Additions of another reactive constituent to the binary blends exert a major influence on the characteristics of the resulting ternary blends. The effect of pozzolana additions on the properties such as setting time, compressive strength and autoclave expansion of blends of portland cement and blast furnace slag has been studied. The ordinary portland cement clinker and blast furnace slag used for the present investigations were obtained from a major cement plant, whereas the pozzolana (flyash) was from a nearby thermal power station. Pozzolana was added (5 to 25 % by weight) to the binary blends and the resulting ternary blends were subjected to hydration and performance studies. The results indicate that addition of pozzolana up to 10 % does not affect the properties of the binary system significantly. It has also been observed that the ternary blends show better sulphate resistance compared to the binary blends.

INTRODUCTION

The ternary blends, known as Pozzolana Metallurgical Cement (PMC), based on portland cement, granulated blastfurnace slag and pozzolana have been investigated in France, Japan, Spain and Germany (1-3). The ternary blends are expected to offer better sulphate and acid resistance as well as a lower heat of hydration. Since the components to be used in our country differ in chemico-physical and mineralogical composition from those obtained elsewhere, the need for the evaluation of ternary systems vis-a-vis binary systems such as slag cement was felt. It was therefore considered essential to study the effect of pozzolana additions to the binary blends of portland cement and blast furnace slag, with a view to reduce the level of portland cement clinker, the costliest component, and also to reduce slag components to conserve grinding energy. The paper highlights the effect of pozzolana additions on hydration and performance characteristics of portland slag cement.

EXPERIMENTAL

Granulated blast furnace slag, portland cement clinker, flyash and mineral gypsum used in the present study were evaluated in terms of chemical and mineralogical characteristics. The results are presented in Table 1.

TABLE 1

Chemical and Mineralogical Composition of Ordinary Portland Cement Clinker, Slag and Flyash

S. No.	Sample Details	Constituent (Percent) LOI	SiO_2	Fe_2O_3	Al_2O_3	CaO	MgO	SO_3	Na_2O	K_2O
1	Clinker	1.74	21.68	2.73	04.33	63.01	5.10	0.27	0.15	0.83
2	Slag	0.81*	32.38	1.32	22.76	30.12	8.72	1.16	0.38	0.95
3	Flyash	8.16	55.65	6.55	25.90	0.51	0.12	Tr.	0.40	0.98

*Gain on Ignition ; Mn_2O_3 Content of Slag : 1.75 %

CLINKER :

C_3S : 58.94, LSF : 0.93,
C_2S : 18.87, SM : 3.07,
C_3A : 6.99, AM : 1.59,
C_4AF : 8.45

SLAG :

Glass Content : 97%
CaO / SiO_2 : 0.93
SiO_2 / Al_2O_3 : 1.42
Gehlenite, Anorthite

FLYASH :

Mullite, α-Quartz, Hematite, Glass Content:30%

Slag cement was prepared by keeping the slag content at 50 percent level. Ternary blends of cement, slag and flyash were prepared by replacing 5, 10, 15, 20 and 25 percent slag component with flyash. Sample details are provided in Table 2.

TABLE 2

Composition of Portland Slag Cement and Ternary Blends

S. No.	Sample No.	Components (Percent by weight) Clinker	Slag	Flyash	Gypsum
1	Control PSC	45	50	00	05
2	PMC - 1	45	45	05	05
3	PMC - 2	45	40	10	05
4	PMC - 3	45	35	15	05
5	PMC - 4	45	30	20	05
6	PMC - 5	45	25	25	05

The performances of all the samples were tested and evaluated according to IS:4031-1988 and the results are presented in Table 3.

TABLE 3

Performance of Slag Cement and Ternary Blends

S. No.	Sample No.	Fineness m^2 / kg	W / C ratio	Compressive Strength (N / mm^2) 1d	3d	7d	28d	90d
1	Control PSC	400	0.37	10.0	40.2	52.3	61.0	66.5
2	PMC - 1	400	0.37	9.0	19.0	33.5	45.6	63.8
3	PMC - 2	400	0.38	8.0	17.8	30.0	44.0	62.0
4	PMC - 3	400	0.38	7.5	16.2	28.8	42.7	60.2
5	PMC - 4	400	0.43	5.8	15.0	21.0	38.0	49.6
6	PMC - 5	400	0.45	3.6	12.5	19.0	29.2	36.8

S. No.	Sample No.	Heat of Hydration (Cal / g) 7d	28d	Setting Time(min) Initial	Final	Autoclave Expansion %	Potential Sulphate Expansion % 14d	28d
1	Control PSC	77.95	85.67	225	300	0.15	0.059	0.065
2	PMC - 1	76.70	82.80	230	305	0.05	0.058	0.065
3	PMC - 2	75.65	82.00	230	303	0.04	0.056	0.060
4	PMC - 3	51.35	82.33	232	306	0.02	0.052	0.050
5	PMC - 4	50.20	79.23	240	310	0.02	0.050	0.048
6	PMC - 5	49.00	75.50	240	312	0.01	0.050	0.048

Portland slag cement and the ternary blends were subjected to hydration studies up to 90 days. Hydrated samples were evaluated by using X - Ray diffraction and scanning electron microscopic techniques. The diffractograms and the electron micrographs of some selected samples are presented in Fig 1 and Plate 1 respectively.

RESULTS AND DISCUSSION

Microscopic characteristics of components

Scanning micrograph of ordinary portland cement clinker shows dominant alite phase having pseudohexagonal shape with a few nodular belite grains in between. Blast furnace slag has continuous glass matrix with reasonably good activity. Flyash, a typical product from Indian coals, shows the presence of finely distributed spherical particles.

Portland slag cement and its performance

Results in Table 3 indicate that the strength, which was 10 N/mm^2 at 1 day, increased to 66.5 N/mm^2 at 90 days. Initial and final setting time were observed to be 225 and 300 minutes respectively. Heat of hydration at 7 and 28 days was found to be 77.95 and 85.67 Cal/g respectively. The autoclave expansion was found to be 0.15 % only. The above results indicate that the slag cement conforms to all the requirements of IS : 455-1976. The very good strength development in the above slag cement despite the presence of low C/S ratio (0.93) and the low lime content (30.12%) of the slag could be attributed to the presence of high C_3S in the clinker.

Effect of Pozzolana Additions

(a) Performance

Indian slag cements are reported to have the poor performances particularly the sulphate resistance, because of the presence of high alumina and low C/S ratio and lime content. The sulphate resistance of these cements could be improved by increasing slag content and overall fineness (4). The results reported by Taneja (5) and Narang (6) on ternary blends using Indian slags have shown contradictory results in terms of strength development. While in general, addition of other hydraulic materials to OPC should reduce the strength (7), Taneja reported improvement. The present study became therefore imperative for a clear understanding of the effect of pozzolana additions to slag cement.

Table 3 shows that a gradual replacement of slag content by flyash i.e. from 5 to 25 % by weight reduces the compressive strength from 10 % to 65 % at 1 day. The reduction, however, diminishes at later ages and in particular at 90 days it is merely 10 % at 15 % replacement level. Strength development in ternary blends upto 15 % replacement level was found to be comparable to slag cement, at later ages. The strength development of the blends at higher replacement levels was found to be very low and did not meet the requirements of slag cement specifications IS : 455-1976. Setting time of the ternary blends are, however, within the specified limits of the slag cement. Heat of hydration measured at 7 and 28 days shows that the heat evolution of the ternary blends is lower. A drastic reduction in autoclave expansion of the ternary blends compared to slag cement was noticed. All the formulations passed the autoclave expansion test as prescribed in IS : 455-1976 with comfortable margin. Sulphate attack studies conducted according to ASTM (C-452-89) have also revealed that the ternary blends show better potential resistance to sulphate compared to slag cement (Table 3) and thereby suggest the suitability of the investigated Indian slags for the manufacture of ternary blends.

(b) Hydration

In the case of slag cement, the initial activation starts as soon as the alkalinity and the presence of $Ca(OH)_2$ in the paste is ensured. The presence of flyash appears to accelerate the contribution of slag owing to the faster uptake of $Ca(OH)_2$ from the solution. Due to the lower amount of C_3S and the larger amount of filler materials, these formulations show lower strengths at early ages. The margin, however, is made up over 28 days owing to the full contribution of slag and the marginal contribution of the flyash.

The hydration products identified at different ages are the same as those of slag cement, i.e. $Ca(OH)_2$, ettringite and solid solution of tri and mono sulphate, C_4AH_{13} and C-S-H. A lower content of $Ca(OH)_2$ as well as a lower C/S molar ratio of the C-S-H are expected in the ternary blend pastes. In addition, the occurrence of the phenomenon of fine power effect can be expected (8). The porosity of gel structure of slag cement hydration can be filled by fine flyash which complements the granulometry

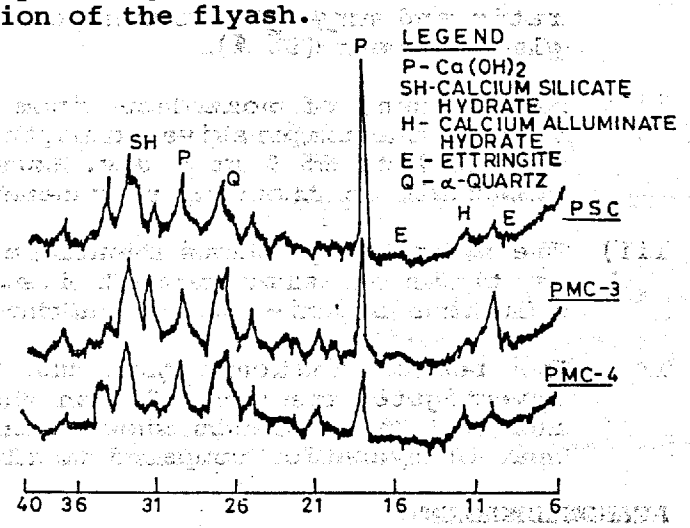

Fig 1 XRD OF 7 DAYS HYDRATED PSC AND TERNARY BLENDS

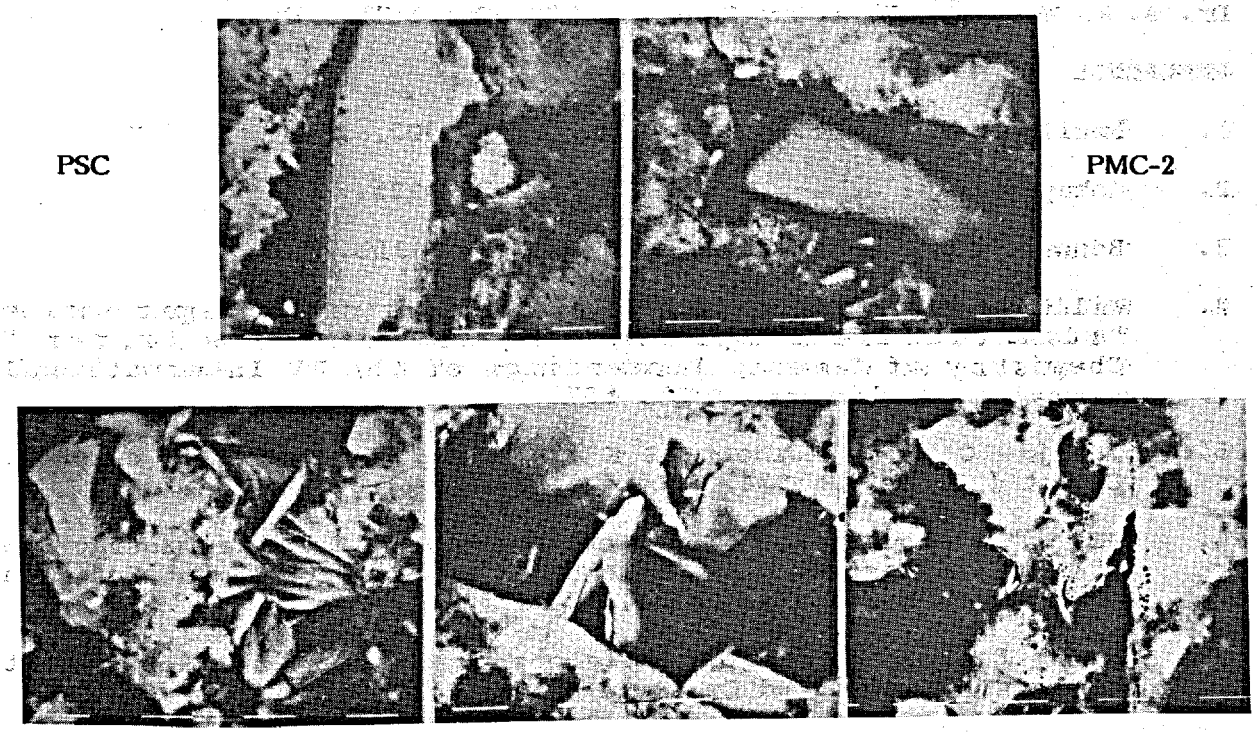

PLATE 1 : SEMs OF HYDRATED SAMPLES AT 90 DAYS

of gel structure and provides more surface area for reaction to proceed. In the prcoess, the flyash uses up lime starting at 14 days and at later ages it also reduces the lime content in the C-S-H structure. Diffractogrames and micrographs of selected samples are presented in Fig. 1 and Plate 1 respectively.

CONCLUSIONS

i) Ternary blends were prepared with Indian slag having a 0.93 C/S ratio and an Al_2O_3 content of 22.76 % and pozzolana with low glass content (30 %).

ii) Replacement of pozzolana from 5 to 25 % by weight with slag lowered the compressive strength of the resulting ternary blends from 10 % to 65 % at 1 day. However, at 90 days, strengths were comparable to those of slag cements.

iii) The hydration products identified at different ages are the same as those of slag cement i.e. $Ca(OH)_2$, ettringite, solid solutions of tri- and monosulphate, C_4AH_{13} and C-S-H.

iv) The results indicate that the Indian slag and flyash samples investigated are suitable for the manufacture of ternary blends and that these blends show better sulphate resistance and lower heat of hydration compared to slag cements.

ACKNOWLEDGEMENT

The authors have freely drawn upon completed R & D work/status reports of NCB. The paper is being published with the permission of Dr. A. K. Mullick, Director General, NCB, New Delhi, India.

REFERENCE

1. Fouilloux P : Rev. Mat. Constr, 1956, 502, 191.

2. Kobayashi K : Japan, Patent 7245, 1972, 925.

3. Beruero M D L : Cem-Hormigon, 1973, 44, 1155.

4. Williams H and Chopra S K : Discussions on the paper entiled "Blastfurnace slags and slag cements by W Kramer " Chemistry of Cement, Proceedings of the IV International symposium, Washington, 1960, 957.

5. Taneja C A and Malhotra S K :" A Sulphate Resisting cement". Cement (India), 1974, VII, (2), 14.

6. CRI : "Development of Indgeneous Technology for the Manufacture of Non Portland High Ash Cement", R & D Report, Cement Research Instiute of India, New Delhi, 1983.

7. Berry E E : " Strength Development of some Blended Cement Mortars", Cement and Concrete Research, 1980, 10 (1), 1.

8. Chopra S K : " Physical properties and Structure of freshly Cementitious Pastes", Symposium on Structure of Portland cement Paste and Concrete, Highway Research Board Special Report 90, Washington (USA), 1966, 9.

Specific Theme II B

Developments in Non-portland Cements

SYNTHESIS AND PROPERTIES OF LOW ENERGY CEMENTS BASED ON $C_4A_3\bar{S}$

J Beretka*, L Santoro, N Sherman* and G L Valenti*****

**CSIRO Division of Building, Construction and Engineering, Victoria, AUSTRALIA*
***Universita di Napoli 'Federico II', Dipartimento di Chimica, Napoli, ITALY*
****Universita della Basilicata, Dipartimento di Ingegneria e Fisica dell' Ambiente, Potenza, ITALY*

SUMMARY

High early strength low energy cements containing $C_4A_3\bar{S}$, β-C_2S or $C_5S_2\bar{S}$ and $C\bar{S}$ were synthesised using, as raw mix components, pure AR-grade materials, commercial materials, and industrial wastes and by-products such as phosphogypsum, fly ash, blast furnace slag and bauxite. The compositions studied were synthetised either separately or together in the $C_4A_3\bar{S}$–β-C_2S–$C\bar{S}$ weight ratio of 1.5:1:1; the latter were referred to as binary and ternary systems. It was found that the impurities present in the industry-derived materials reduced the synthesis temperatures. The addition of fly ash and/or blast furnace slag to the $C_4A_3\bar{S}$-based cements reduced the 1 d compressive strengths but markedly enhanced the 28 d strengths. The ternary system, which contained $C_5S_2\bar{S}$ instead of C_2S, produced cements with very high early and ultimate strength. The compositions examined appear to be stable at room temperature, 100% RH, but strength loss was observed after conditioning for six months to one year at ordinary temperatures and humidities, owing to the carbonation of ettringite.

RIASSUNTO

Cementi a rapido indurimento iniziale, di basso dispendio energetico e contenenti $C_4A_3\bar{S}$, β-C_2S o $C_5S_2\bar{S}$ e $C\bar{S}$ sono stati sintetizzati impiegando, come materie prime, reagenti puri per analisi , materiali commerciali, sottoprodotti e rifiuti industriali quali fosfogesso, ceneri volanti, scoria d'altoforno e residui dell'estrazione della bauxite. Le composizioni studiate sono state sintetizzate sia separatamente che congiuntamente (sistemi binari e ternari) in rapporti ponderali $C_4A_3\bar{S}$–β-C_2S–$C\bar{S}$ di 1.5:1:1. E' stato riscontrato che le impurezze presenti nei sottoprodotti industriali abbassano le temperature di sintesi. L'aggiunta di ceneri volanti e/o scoria d'altoforno ai cementi a base di $C_4A_3\bar{S}$ riduce le resistenze a compressione dopo 1 giorno di stagionatura, ma migliora notevolmente quelle a 28 giorni. Il sistema ternario , avente $C_5S_2\bar{S}$ in luogo di C_2S, dà origine a cementi con elevate resistenze iniziali e finali. Le composizioni esaminate appaiono stabili a temperatura ambiente, 100% U.R. ma, dopo stagionatura da sei mesi ad un anno a temperatura e umidità ambiente, si è osservata una perdita di resistenza meccanica dovuta a fenomeni di carbonatazione dell'ettringite.

INTRODUCTION

In the last few years, much attention has been paid to calcium sulfoaluminate, $C_4A_3\bar{S}$, as a component of cements with high early strengths, and with ultimate strength and dimensional stability similar to that of ordinary Portland cements, OPC (1,2). They are usually referred to as low energy cements (3), supersulfated alumina-belite cements (4), rapid hardening and/or high early strength cements (5), sulfoaluminate cements (6), and non-alitic cements (2). In these cements, the high early strength is due to the rapid formation of ettringite, $C_6A\bar{S}_3H_{32}$, and the later and ultimate strength is attributed to the formation of calcium silicate hydrates.

Cements based on $C_4A_3\bar{S}$ can be produced at temperatures much lower than OPC which require about 1500°C for the synthesis of C_3S. They are relatively friable after firing and require little energy to grind. Furthermore, it is possible to synthesise these cements not only from inexpensive, natural commercial materials such as limestone, gypsum, clay and bauxite, but also from industrial wastes and by-products such as phosphogypsum, fly ash, blast furnace slag and other waste materials containing CaO, Al_2O_3, SiO_2 and SO_3 (2,3,5,7–9). Due to the relatively low firing temperature and ease of grinding as compared with OPC clinker, these cements are also referred to as low energy cements.

Previous work (7,8,10) has shown that replacing pure gypsum with phosphogypsum enables a great reduction in both the temperature and time required for the synthesis of $C_4A_3\bar{S}$, without adversely affecting its hydration properties. In this work, in addition to phosphogypsum, other industrial wastes and by-products such as bauxite fines, blast furnace slag and fly ash were used together with pure AR-grade and commercial materials for the preparation of $C_4A_3\bar{S}$-based cements. Other components of these cements were β-C_2S and $C\bar{S}$.

The different formulations all contained $C_4A_3\bar{S}$, β-C_2S and $C\bar{S}$ in the weight ratio of 1.5:1:1, and can be grouped in three basic systems: the first containing only the three components above, the second including 30% by weight blast furnace slag, and the third including 20% by weight blast furnace slag and 10% by weight fly ash.

$C_4A_3\bar{S}$ was: (a) separately synthesised and mixed with β-C_2S and $C\bar{S}$, each individually synthesised; (b) synthetised together with β-C_2S (binary synthesis) and mixed with $C\bar{S}$ separately synthetised; and (c) synthetised together with both β-C_2S and $C\bar{S}$ (ternary synthesis) in a single firing.

The influence of the synthesis temperature and the nature of raw materials on the physico-mechanical properties of the different compositions was investigated.

EXPERIMENTAL

Raw Materials and Procedures

The principal chemical compositions of the commercial and industry-derived materials used are shown in Table 1. The pure AR materials were not analysed. The planned compositions of the various systems investigated are listed in Table 2, and are identified with the numbers 101, 102 and 103. Large (about 5 kg) mixes were used for each synthesis and XRD was employed to check the phase composition of the fired products. All mixes containing carbonate and hydrated alumina, including bauxite, were fired with a pause of 1–2 h at 850°C, and 1 h at 1000°C, to allow for the escape of CO_2 and H_2O, respectively, from the system.

Table 1. Principal chemical components (%) of raw materials used

Material	CaO	SiO_2	Al_2O_3	Fe_2O_3	MgO	SO_3	P_2O_5	H_2O
Natural gypsum	32.60	3.33	0.35	0.22	0.06	43.40	0.01	20.70
Phosphogypsum	32.60	0.05	0.23	0.02	0.22	44.90	0.47	20.50
Limestone	54.10	1.57	0.38	0.40	0.61	0.05	0.01	42.92*
Clay	1.30	46.80	34.50	1.33	0.12	0.10	n.a.	14.69
Bauxite	0.02	4.70	51.50	15.30	0.04	n.a.	0.04	25.40
Silica	n.a.	99.00	0.37	0.06	n.a.	n.a.	n.a.	0.28
Fly ash	4.80	56.80	25.50	4.20	1.50	0.40	n.a.	0.40
Blast furnace slag	41.10	33.20	14.20	1.57	7.00	2.58	–	0.15

*CO_2

Table 2. Composition (wt%) of systems investigated

	Composition		
	101	102	103
$C_4A_3\bar{S}$	43.0	30.0	30.0
β–C_2S	28.5	20.0	20.0
$C\bar{S}$	28.5	20.0	20.0
Blast furnace slag	–	30.0	20.0
Fly ash	–	–	10.0

Compositions Containing Separately Synthetised Compounds

The $C_4A_3\bar{S}$ was synthetised in a number of ways depending on the raw materials used: (a) from pure AR materials, by calcination at 1350°C for 16 h; (b) from commercial materials, by calcination at 1350°C for 8 h; and (c) from commercial materials with phosphogypsum or with phosphogypsum and bauxite, by calcination at 1170°C for 2 h.

The β-C_2S was synthetised as follows: (a) from pure AR materials, by calcination at 1450°C for 2 x 16 h, with intermittent grinding; (b) from commercial materials, at 1350°C for 16 h; and (c) from commercial materials with 0.5% B_2O_3 β-phase stabiliser, at 1300°C for 7 h.

The $C\bar{S}$ was produced by calcining gypsum (or phosphogypsum) at 850°C for 90 min.

The individually synthetised compounds $C_4A_3\bar{S}$, β-C_2S and $C\bar{S}$ were blended at a weight ratio of 1.5:1:1, sieved to pass a 150 µm screen and used for making mixes of compositions 101, 102 and 103. Firstly, 2 g specimens were mixed with water (w/s = 0.5), placed in a plastic envelop, and hydrated for 1, 3, 7, 14, 28, 56, 90 and 180 d at 23°C, 100% RH. At the end of the hydration period, the specimens were removed, the reaction 'stopped' with acetone, the materials dried with ether, then analysed by XRD and DTA/TGA. Secondly, 25 mm cube specimens and 100 x 12.5 x 12.5 mm bars were cast at a w/s ratio of 0.5, cured at 23°C, 100% RH, and their compressive strength, density and shrinkage/expansion determined by conventional methods.

Compositions Containing Binary and Ternary Synthesised Compounds Using Commercial and Industry-derived Materials

The mixes for the binary and ternary synthesis were prepared from commercial materials (e.g. limestone, bauxite and clay), and industry-derived materials (e.g. phosphogypsum, fly ash and blast furnace slag). The compositions were designed to give fired compounds with the planned weight ratios of 1.5:1 $C_4A_3\bar{S}$–$C_2\bar{S}$; or 1.5:1:1 $C_4A_3\bar{S}$–C_2S–$C\bar{S}$. The mixes containing the binary synthesis products incorporating fly ash, blast furnace slag and clay were identified with the symbols FAC, BSC and CLC, respectively. The ternary synthesis products were identified with the symbols FA^+, BS^+ and CL^+, respectively. The stocks were fired at 1200°C for 8 h and used to make only systems of planned composition 101.

RESULTS AND DISCUSSION

Synthesis of $C_4A_3\bar{S}$

It was found that, depending on the type of raw materials used, different temperature/time regimes were required for full conversion to $C_4A_3\bar{S}$ as follows: (a) with pure AR grade, $CaCO_3$, Al_2O_3 or $Al(OH)_3$ and $CaSO_4.2H_2O$, 1350°C for 16 h; (b) with commercial limestone, alumina and gypsum, 1350°C for 8 h; (c) with commercial limestone, alumina and phosphogypsum, 1170°C for 1–2 h; and (d) with commercial limestone, bauxite and phosphogypsum, 1170°C for 1–2 h.

According to previous findings (7,8), the use of phosphogypsum greatly increases the rate of $C_4A_3\bar{S}$ formation, owing to the presence of mineralisers such as P_2O_5. Furthermore, by incorporating fluxes, such as NaF or CaF_2 (1–2% by weight) into the mixes, the firing temperature could be reduced even further to about 1100°C.

XRD analysis of the fired products revealed that: with (a), pure AR-grade materials, the product was virtually pure $C_4A_3\bar{S}$, with traces of $C_{12}A_7$ and unreacted $C\bar{S}$; with (b), commercial materials, the degree of conversion to $C_4A_3\bar{S}$ was somewhat less than with (a), and the synthetised material contained not only traces of $C_{12}A_7$ but also small quantities of other calcium aluminates, viz. CA, C_3A and traces of $C\bar{S}$; with (c), commercial limestone, alumina and phosphogypsum, traces of $C_{12}A_7$ and CA_2 were detected, but no $C\bar{S}$; and with (d), commercial limestone, bauxite and phosphogypsum, no $C_{12}A_7$ was detected, but the fired material contained traces of CA and CA_2, and significant amounts of gehlenite (C_2AS). The latter compound forms at the expense of $C_4A_3\bar{S}$.

Properties of Systems Containing Separately Synthetised $C_4A_3\bar{S}$, β-C_2S and $C\bar{S}$

DTA/TGA and XRD analysis of the hydrated specimens of compositions 101, 102 and 103 did not reveal any major difference among them in terms of hydration kinetics. Common features of the above systems were as follows: ettringite was the main hydration product and formed to a considerable extent as early as 1 d; calcium silicate hydrate also formed and was detected after 14 d; and relatively large quantities of unreacted β-C_2S were still present at 28 d.

The compressive strengths of all the compositions made of individually fired components are shown in Table 3. As far as the systems of composition 101 are concerned, the results indicate that very good early (1 d) compressive strengths were obtained. The specimens made from pure AR-grade materials had the highest early (1 d) strength, but the ultimate 28 d strength was about the same in all cases.

Table 3. Compressive strength (MPa) for compositions 101, 102 and 103 when components were synthetised separately; cured at 23°C,100% RH, w/s = 0.5

Days at 23°C	Composition		
	101	102	103
Pure AR-grade materials			
1	31.3	16.1	27.6
7	38.5	29.7	45.0
28	37.2	48.5	54.7
Commercial materials			
1	24.4	15.8	15.1
7	33.0	22.1	21.1
28	40.7	40.1	34.2
Commercial materials with bauxite and phosphogypsum			
1	18.2	8.2	7.8
7	34.3	17.9	15.4
28	42.1	41.7	51.4

The densities of the specimens dried to constant weight were of the order of 1720 kg/m^3. The specimens tended to expand slightly from 1–7 d (0.08%), then they shrank a little (0.1% at 28 d, and 0.2% at 90 d), similar to OPC pastes.

As far as the systems of compositions 102 and 103 are concerned, the following observations can be made. In the case of pure AR-grade materials, the addition of blast furnace slag alone (102) has a large negative effect on 1 d strength. However, the 28 d strength of the specimens containing either blast furnace slag (102) or both blast furnace slag and fly ash (103), markedly increases as compared with composition 101.

With the compositions synthetised from commercial materials only, and commercial materials plus bauxite and phosphogypsum, somewhat similar findings were obtained at early ages. However, at 28 d, only composition 102 results were similar to those of composition 101, while in the case of composition 103, compressive strength was lower for commercial materials and higher for commercial materials plus bauxite and phosphogypsum.

The densities of the air-dried specimens, for all the compositions, were of the order of 1550–1650 kg/m^3. All the specimens showed a slight expansion at early ages (1–7 d), thereafter they tended to shrink slightly, similar to OPC pastes.

Properties of Systems Containing Binary and Ternary Synthetised Compounds

The binary synthesis products obtained with fly ash, blast furnace slag and clay were mixed with separately fired $C\bar{S}$ to get the systems FAC, BSC and CLC, respectively, of composition 101. The hydration behaviour of these systems was very similar to that of the systems of composition 101 previously discussed.

The compressive strengths are shown in Table 4. Early (1 d) strengths of 20.4–24.8 MPa were obtained, but the 28 d strength only marginally increased for system FAC, while it more than doubled in 28 or 14 days for systems BSC and CLC, respectively. Similar to the systems synthetised separately, all the specimens showed only slight expansion when kept at 100% RH, and slight shrinkage in drying, giving values similar to that obtainable with OPC pastes.

Table 4. Compressive strength (MPa) for the binary compositions of FAC, BSC and CLC cured at 23°C, 100% RH; w/s = 0.5

Curing days	Composition		
	FAC	BSC	CLC
1	24.8	22.5	20.4
7	36.5	37.3	41.6
28	26.2	50.2	51.4*

* 14 d

The synthesis of the ternary composition, $C_4A_3\bar{S}$–C_2S–$C\bar{S}$, in the weight ratio of 1.5:1:1 (composition 101) was not possible in a single firing at the relatively low temperature of 1200°C with any of the silica sources employed, i.e. fly ash (FA^+), blast furnace slag (BS^+) and clay (CL^+). The fired products did not contain β-C_2S and consisted mainly of $C_4A_3\bar{S}$, a new phase identified as calcium sulfosilicate, $C_5S_2\bar{S}$, and residual $C\bar{S}$. Both β-C_2S and $C\bar{S}$ could probably be obtained at higher temperatures, e.g. 1300°C, by decomposition of $C_5S_2\bar{S}$ (11).

According to the literature (4,5,11), $C_5S_2\bar{S}$ appears to be a slowly hydrating phase. However, very good 1, 7 and 28 d strengths were obtained with these compositions, as shown in Table 5. The values were much higher than those obtained with the compositions of the previous systems, even though a direct comparison is not possible, due to the lower water demand of the ternary systems (w/s ratio of 0.4 instead of 0.5 employed in the experiments). The dimensional stability of systems FA^+, BS^+ and CL^+ was similar to that of the previous ones.

Table 5. Compressive strength (MPa) for the ternary compositions of FA^+, BS^+ and CL^+ cured at 23°C, 100% RH; w/s = 0.4

Curing days	Composition		
	FA^+	BS^+	CL^+
1	49.3	35.4	49.5
7	67.1	51.4	61.7
28	76.2	58.2	69.7

LONG-TERM BEHAVIOUR OF ETTRINGITE-CONTAINING SYSTEMS

It was found that cast specimens, which were left in air at room temperature for six months to one year, showed a considerable loss of strength (35–70%). This is due to the low resistance of ettringite to CO_2 attack. The products of carbonation of ettringite are calcite or aragonite, gypsum and alumina gel.

There is a lack of data in the literature about long-term behaviour of $C_4A_3\bar{S}$-based cements. To the best of the authors' knowledge, only Ref. No. 2 gives compressive strength results at late ages (up to four years) obtained with concretes made of a type of binder similar to those investigated in this paper. No retrogression in strength development was observed at any age within the four-year period examined.

Further experiments are in progress with the purpose of understanding the carbonation mechanism and improving the composition of the $C_4A_3\bar{S}$-based cements, in order to reduce this problem.

CONCLUSIONS

Industrial by-products such as phosphogypsum, fly ash, blast furnace slag and bauxite fines may be conveniently employed for the synthesis of low energy cements based on $C_4A_3\bar{S}$. Compared with pure and natural materials, the industrial by-products allow a reduction of the temperature required for synthesis.

When $C_4A_3\bar{S}$ was mixed with separately synthetised C_2S and $C\bar{S}$ in the weight ratio of 1.5:1:1, hydrated at room temperature, 100% RH, hydraulic binders with good strengths (1 d, 18–31 MPa; 28 d, 37–42 MPa) were obtained. The addition of blast furnace slag, or blast furnace slag and fly ash, reduced the early strengths, but promoted higher ultimate strengths.

With mixes in which the $C_4A_3\bar{S}$ and C_2S were synthetised together (and the $C\bar{S}$ was added separately to the mixes), good early and ultimate strengths were obtained (1 d, 20–25 MPa; 28 d, 26–50 MPa).

The synthesis of $C_4A_3\bar{S}$, C_2S and $C\bar{S}$ in a single firing was not possible at the temperature of 1200°C. The formation of $C_5S_2\bar{S}$ instead of C_2S and $C\bar{S}$ was observed. However, the system containing $C_4A_3\bar{S}$, $C_5S_2\bar{S}$ and residual $C\bar{S}$ developed very good mechanical strength (1 d, 35–49 MPa; 28 d, 58–76 MPa).

The dimensional stability of the pastes was similar to that of OPC pastes, showing very slight expansion at early ages followed by slight shrinkage at later ages.

The cast specimens were stable at room temperature, 100% RH. However, some strength reduction was observed at ordinary temperatures and humidities due to the carbonation of ettringite.

REFERENCES

1. Kurdowski, W., George, C.M. & Sorrentino, F.P.: "Special cements", **Proc. 8th Int. Congr. Chem. Cement**, Rio de Janeiro, 1986, Vol. 1, 292–318.
2. Mudbhatkal, G.A., Parmeswaran, P.S., Heble, A.S., Pat, B.V.B. & Chatterjee, A.K.: "Non-alitic cement from calcium sulfoaluminate clinker: optimisation for high-strength and low-temperature application", **Proc. 8th Int. Congr. Chem. Cement**, Rio de Janeiro, 1986, Vol. 4, 364–370.
3. Mehta, P.K.: "Investigations on energy-saving cements", World Cement Technol., May 1980, 166–177.
4. Ikeda, K.: "Cements along the join $C_4A_3\bar{S}$–C_2S", **Proc. 7th Int. Congr. Chem. Cement**, Paris, 1980, Vol. 2, Theme III, 31–36.
5. Sudoh, G., Ohta, T. & Harada, H.: "High strength cement in the CaO–Al_2O_3–SiO_2–SO_3 system and its application", **Proc. 7th Int. Congr. Chem. Cement**, Paris, 1980, Vol. 3, Theme V, 152–157.
6. Deng Jun-An, Ge Wen-Min, Su Mu-Zhen & Li Xiu-Ying: "Sulfoaluminate cement series", **Proc. 7th Int. Congr. Chem. Cement**, Paris, 1980,Vol. 3, Theme V, 381–386.
7. Santoro, L., Garofano, R. & Valenti, G.L.: "Calcium sulfoaluminate made from phosphogypsum and its hydration properties", **Proc. 8th Int. Congr. Chem. Cement**, Rio de Janeiro, 1986,Vol. IV, 389–394.
8. Valenti, G.L., Santoro, L. & Garofano, R.: "High-temperature synthesis of calcium sulfoaluminate from phosphogypsum", Thermochimica Acta, 1987, **113**, 269–275.
9. Beretka, J. (CSIRO, Australia), Valenti, G.L., Santoro, L. & Cioffi, R. (Universita di Napoli, Italia): "Hydraulic binders and building elements formed from non-traditional materials", International Patent Application No. PCT/AU87/00Y19, 1987.
10. Santoro, L., Garofano, R. & Valenti, G.L.: "Role of phosphogypsum in the hydration of calcium sulfoaluminate", Thermochimica Acta, 1987, **116**, 145–152.
11. Nakamura, T., Sudoh, G. & Akaiwa, S.: "Mineralogical composition of expansive cements rich in SiO_2 and its expansibility", **Proc. 5th Int. Symp. Chem. Cement**, Tokyo, 1968, Pt 4, 351–365.

THE CRYSTAL STRUCTURE OF $C_4A_3\bar{S}$

Zhang Peixing*, Chen Yimin*, Shi Liping*, Zhang Guanying, Huang Wenmei** and Wu Jianguo****

**China Building Materials Academy, Beijing, P R CHINA*
***Shanghai Institute of Building Materials Industry, Shanghai P R CHINA*

ABSTRACT

$3CaO \cdot 3Al_2O_3 \cdot CaSO_4$, ($C_4A_3\bar{S}$), is the main mineral phase in sulphoaluminate cement. In the study an experiment on the mix composition and the burning process of C_4A_3Swere achieved by the orthogonal method and the pure monomineral of C_4A_3Shas been produced. The XRD data of $C_4A_3\bar{S}$were callected by D / max-$\gamma\beta$ type rotational copper target XRA. The indexing for the data was conducted by "TREOR" program of computer and the optimization was made with "9214" refinement program. Finally the revision and the check of the crystal structure of $C_4A_3\bar{S}$were conducted by "POWD12" program.

The results indicated that $C_4A_3\bar{S}$ belong to tetragonal system, and its lattice parameters $a_o = b_o = 13.031$Å and $c_o = 9.163$Å, space group D_{2d}^6–$P\bar{4}C2$, structure formula $Ca_4\,[Al_6O_{12}]\,SO_4$.

〔摘　要〕

$3CaO \cdot 3Al_2O_3 \cdot CaSO_4$, ($C_4A_3\bar{S}$)是硫铝酸盐的主要矿相。本研究是用正交法对$C_4A_3\bar{S}$的配料和烧成工艺进行试验，烧出纯的$C_4A_3\bar{S}$单矿物，在D / max-$\gamma\beta$型铜极转靶X射线衍射仪上进行$C_4A_3S$粉晶衍射累积强度数据收集，经"TREOR"计算程序进行指标化和"9214"精化程序优化处理，最后用"POWD12"程序对$C_4A_3\bar{S}$晶体结构进行修正和验证。

实验结果指出，$C_4A_3\bar{S}$属四方晶系，晶胞参数$a_o = b_o = 13.031$Å，$c_o = 9.163$Å空间群为D_{2d}^6–$P\bar{4}C2$，结构式为$Ca_4\,[Al_6O_{12}]\,SO_4$。

I. INTRODUCTION

$C_4A_3\bar{S}$($3CaO \cdot 3Al_2O_3 \cdot CaSO_4$) is the main mineral phase in sulphoaluminate cement. In 1962, P.E. Halstead and A.E. Moore (1) reported that $C_4A_3\bar{S}$ has a cubic subcrystalline cell ($a_0 = 9{,}195$Å) and a structure of ultramarine sort. In 1972 the revision of structure in subcrystalline cell of $C_4A_3\bar{S}$ with space group of $I\bar{4}3m$ and its atom coordinates were presented by H Sealfeld and W. Depmeier (2). Also, they pointed out that real space group of $C_4A_3\bar{S}$ is $I4_132$, $a_0 = 18.41$Å. In 1988 Feng Xiuji and Liao Guanglin (3) synthesized the monomineral of $C_4A_3\bar{S}$ by the salt–fusing method and determined space group of subcrystalline cell of $C_4A_3\bar{S}$($I\bar{4}3m$, $a = 9.167$Å) and its atom coordinates. They pointed out the space group of real cell of $C_4A_3\bar{S}$($I4_132$) and mineral of $C_4A_3\bar{S}$with four crystal structure type.

II. EXPERIMENT

1. Syntering of monomineral of $C_4A_3\bar{S}$

Measuring the crystal structure of $C_4A_3\bar{S}$ by XRD must use the pure monomineral. It is most difficult to burn pure monomineral of $C_4A_3\bar{S}$ sence the gypsum decomposes to varying degrees and SO_3 volatilizes in the process of sintering. Therefore, it is impossible to burn the pure monomineral of $C_4A_3\bar{S}$ that proportioning is only mode according to molar ratio. By the orthogonal design experiment method we had obtained the pure $C_4A_3\bar{S}$ mineral. A mixture of weight of $C_4A_3\bar{S}$ with chemical pure grade is 44.0564 g $CaCO_3$, 76.6921 g $Al(OH)_3$, 37.0657 g $CaSO_4 \cdot 2H_2O$, and the sintering temperature is 1320 ± 5℃ for 1 hour.

2. XRD of powder crystal $C_4A_3\bar{S}$

The experiment with XRD of powder crystal $C_4A_3\bar{S}$ was obtained on a D / max–γB type of the rotational copper target XRA and repeated three times in all. The results from all the three are basically similiar. 88 diffraction lines were identified and are presented in Figure 1 and Table 1.

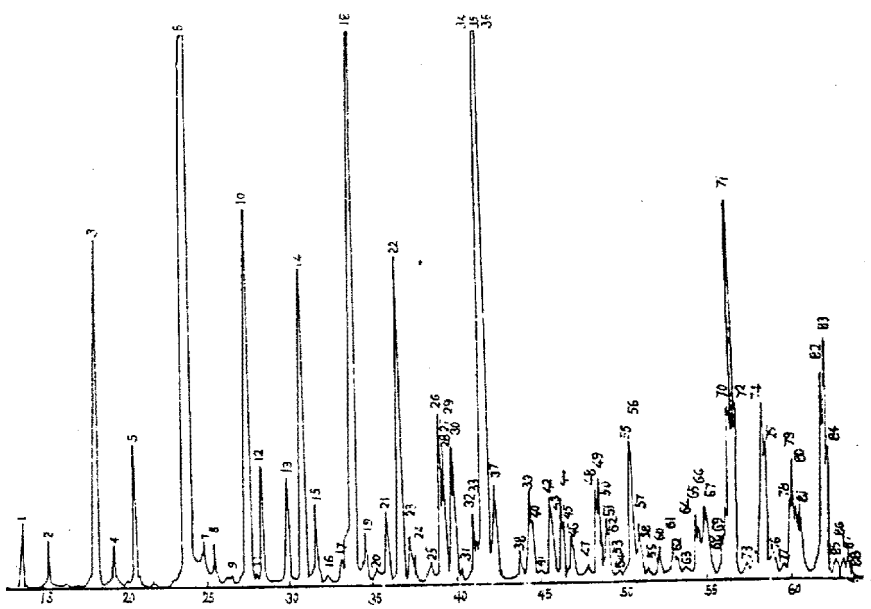

Fig.1 XRD Diagram

Table 1. The XRD data of powder crystal $C_4A_3\bar{S}$

No.	d	I/I_o	HKL	No.	d	I/I_o	HKL
1	6.5056	2	200,111	46	1.9357	1	324
2	5.8242	1	210	47	1.9349	1	324α2
3	4.9187	6	211	48	1.8961	<0.5	523
4	4.6047	1	220,002	49	1.8791	2	622
5	4.3247	2	300,102	50	1.8740	2	404
6	3.7574	100	311,202	51	1.8697	1	404α2
7	3.6001	< 0.5	320,212	52	1.8596	1	700,542
8	3.4984	1	*	53	1.8554	1	414
9	3.3608	< 0.5	321	54	1.8504	<0.5	414α2
10	3.2501	8	400,222	55	1.8378	<0.5	443,334
11	3.2043	<0.5	*	56	1.8058	3	640,711
12	3.1510	2	410,302	57	1.8038	3	533,424
13	2.9879	2	411	58	1.7899	1	720,632
14	2.9118	6	420,331	59	1.7847	1	720α2
15	2.8378	2	322	60	1.7540	<0.5	721,613
16	2.7794	<0.5	421	61	1.7478	1	215
17	2.7058	<0.5	213	62	1.7209	1	504
18	2.6544	34	402	63	1.7162	<0.5	504α2
19	2.6013	1	500,412	64	1.7020	<0.5	225
20	2.5489	<0.5	510,232,223	65	1.6818	1	731,642
21	2.5062	1	431,242	66	1.6744	1	315
22	2.4545	7	511,422,313	67	1.6671	2	650,722
23	2.4201	1	520	68	1.6638	1	524
24	2.4088	<0.5	520α2	69	1.6386	1	633
25	2.3388	<0.5	521,323	70	1.6343	1	325
26	2.3042	4	440	71	1.6285	4	800
27	2.2907	3	004	72	1.6243	8	444
28	2.2840	1	004α2	73	1.6206	3	444α2
29	2.2641	2	502	74	1.5919	<0.5	811
30	2,2598	2	104	75	1.5777	3	713,604
31	2.2351	<0.5	530,411,512	76	1.5740	2	335
32	2.1965	1	413	77	1.5648	<0.5	614
33	2.1914	1	413α2	78	1.5439	<0.5	723
34	2.1712	19	600,531	79	1.5346	1	600,802
35	2.1652	20	333	80	1.5318	2	624
36	2.1613	11	204	81	1.5277	1	006
37	2.1330	2	214	82	1.5240	1	830,812
38	2.0590	1	620,442	83	1.4930	4	751,822,733
39	2.0352	2	540	84	1.4896	4	515
40	2.0219	1	304	85	1.4857	1	206
41	2.0069	<0.5	621,532	86	1.4768	<0.5	216
42	1.9870	1	541	87	1.4643	<0.5	653
43	1.9837	1	433	88	1.4606	<0.5	525
44	1.9601	2	602,513				
45	1.9546	1	513α2				

3. IR spectrum of $C_4A_3\bar{S}$

The IR spectrum of $C_4A_3\bar{S}$ obtained from infrared spectro meter PE–683. The IR spectrum obtained is presented in Fig.2

As Fig.2 shows, the vibration frequency of group of $C_4A_3\bar{S}$ appears at 1250–350 cm^{-1}. At 800–900 cm^{-1} there presents a strong and wide band due to vibration frequency Vas of $[AlO_4]$, and 600–700 cm^{-1} is the band of bending vibration frequency Vs of $[AlO_4]$. The band of 411 cm^{-1} below 500 cm^{-1} is the bending vibration frequency of Al–O–Al in $[AlO_4]$. Meanwhile, due to no absorption band in 700–800 cm^{-1} there presents no octahedron of Al–O in the structure of $C_4A_3\bar{S}$. The vibration frequency at 1193 and 1100 cm^{-1} are dual band due to vibration Vas of neso–$[SO_4]$, and 610 cm^{-1} and 660 cm^{-1} are bending vibration frequency Vs of $[SO_4]$.

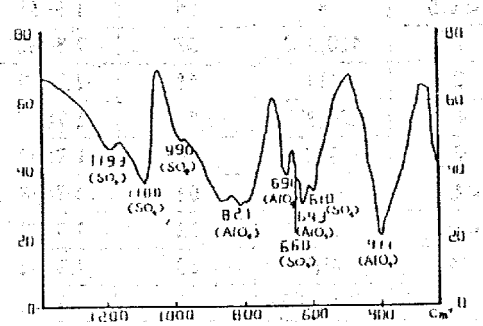

Fig.2 IRS diagram of $C_4A_3\bar{S}$

4. Optical character of monomineral of $C_4A_3\bar{S}$

Micropolarmeter was used to measure optical character of monomineral of $C_4A_3\bar{S}$ under plane polarized light it is colorless and transparent object and has an irregular form mostly. Most of its grains are about 2μ in linear size, and a few of large grains can reach 50μ. Under orthogonal polazed light crystal mineral of $C_4A_3\bar{S}$ appeared 1 grade of grey–yellowy interference colors, inclinedextinction and negative elongation. Under conical rays in the interence figure $C_4A_3\bar{S}$ is uniaxial crystal optically positive. Monomineral of $C_4A_3\bar{S}$measured by the oil immersion method has a refraction index Ne = 1.570 ± 0.002, No = 1.576 ± 0.002 and Ne–No = 0.003. Its crystal system is medium–grade crystal system.

5. Electron–diffraction on monocrystal of $C_4A_3\bar{S}$

Electronmicroscope was used to find out a monocrystal of $C_4A_3\bar{S}$ having complete crystal and 12μ in linear length, shown as photo 1. Fig.3 is the picture of electrondiffraction pattern of moncrystal of $C_4A_3\bar{S}$ that was taken in transmission electronmicroscope H–600. The product of the wave legnth of electronic beam used λ and the distance from the specimen to the photo plate L is 28.8 mmÅ. The spectrum diagram was analyzed and calculated to obtain reciprocal plane lattice of $C_4A_3\bar{S}(a^*c^*)$ as a rectangle and $c_o = 9.14$Å, $a_o = 13.09$Å in the parameter of cell. And, under L≠2n in the reflection index of crystal face (hol) the extiction of system exists, presented as Fig.3. Its Laue spot group is 4 / mm m P–C– that it is of tetragonal system.

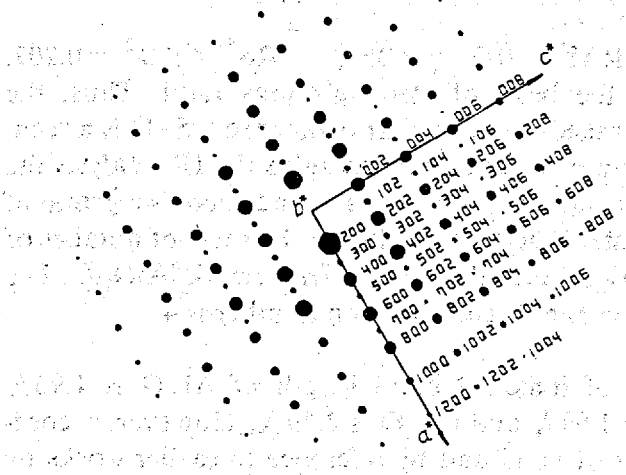

Fig.3 Analytic diagram of electron–diffraction spectrum monocrystal of $C_4A_3\bar{S}$ (b^* // incident electronic beam)

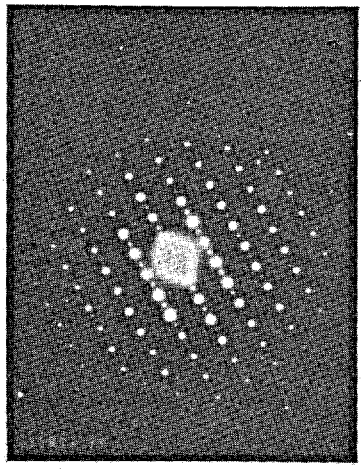

Photo 1. Electro–diffraction pattern of monocrystal $C_4A_3\bar{S}$

III. ANALYSIS OF CRYSTAL STRUCTURE OF $C_4A_3\bar{S}$

1. Indexing for XRD diagram of powder crystal of $C_4A_3\bar{S}$ and determination of parameters of its cell

Indexing for XRD diagram of $C_4A_3\bar{S}$ was conducted on PHNAFACOM–U1550 II computer and by using "TREOR" program. Then, indexing was achieved with the least squares refinement program of "9214".. Finally, $C_4A_3\bar{S}$ was frond to be a tetragonal system with $a_o = b_o = 13.031$ Å, $C_o = 9.163$ Å, $\alpha = \beta = \gamma = 90°$ as the parameters of the crystalline cell.

2. Measurement of space group of mineral $C_4A_3\bar{S}$

Analysis for reflection rule of indexing of diffraction lines indicates that in the diffraction lines of (hol) or (okl) as extinction of system exists when L≠2n. According to the extinction rule the diffraction group of $C_4A_3\bar{S}$ obtained is of number 56, 4/mmm P–C––. There are 3 space groups in it, i.e. D_{4h}^{10}–$P4_2/mcm$, D_{2d}^{6}–$P\bar{4}C2$ and C_{4v}^{3}–$P4_2cm$. When analysis of structure was conducted with the space groups respectively the space groups of $C_4A_3\bar{S}$ obtained should be number 116, D_{2d}^{6}–$P\bar{4}C2$.

3. Calculation of molecular number of $C_4A_3\bar{S}$ in monocrystalline cell

The crystal of $C_4A_3\bar{S}$ measured is $D_o = 2.61$ g/cm^3 in density, the calculated volume of its monocrystalline cell is $V_o = 555.941$ Å^3, and molecular weight of $C_4A_3\bar{S}$ calculated is $M_o = 610.2$ g. According to the formular $Z = \frac{V_o \cdot D_o}{1.66 M_o}$ molecular number of $C_4A_3\bar{S}$ in monocrystalline cell Z had been calculated to be 4. Thus, there are 24 Al, 16 Ca, 4 S and 64 O atoms in the cell.

4.Coordination number and bond length of Al–O, S–O and Ca–O crystal $C_4A_3\bar{S}$

According to pauling's rules $RAl^{3+}/RO^{2-}=0.357$, $RS^{6+}/RO^{2-}=0.207$, $RCa^{2+}/RO^{2-}=0.707$ had been calculated on the basis of Pauling's ions radil. Thus, the coordination polyhedron of Al–O is a regular tetrahedron or regular octahedron, S–O is a regular tetrahedron and Ca–O is a regular octahedron or a cube. According to the IR analysis the Al–O tetrahedron is a regular tetrahedron, its coordination number is 4, and there is a group of tetrahedron Al–O jointed from angles top in crystal $C_4A_3\bar{S}$. And, due to the ratio of number of Al / O which is 1:2 the group of tetrahedron Al–O exists in the form of framework $[AlO_2]^{n-}_{2n}$. The coordination polyhedron S–O is a nesotetrahedron and its coordination number is 4.

According to the theory for closepacking of ions the bond length of Al–O is 1.90Å equaling to the sum of both ionic radius, S–O is 1.69Å and Ca–O is 2.39Å. However, according to the effect of radius ratio and the character of bond and by reference to earlier works by others we propose that the bond length of Al–O is about 1.75Å, that of S–O is about 1.53Å and Ca–O is about 2.39Å.

5.Proposed trial structure of $C_4A_3\bar{S}$ crystal

On the basis of experimental and calculated data, employing of the equivalent spot system and the symmertry elements, and by making reference to earlier works by other we propose a trial structure for $C_4A_3\bar{S}$ crystal. Finally, the trial structure is calculated and revised with "POWD12" simulator of XRD diagram of powder crystal to obtain various atom coordinates in the crystalline structure of $C_4A_3\bar{S}$, given in Table 2, the coordination polyhedron diagram, shown in Figure 4.

Table 2. Various atom coordinates of monocell in crystal of $C_4A_3\bar{S}$

Name and number of atoms	Spot number in equivalent spot system	Starting coordinate of equivalent spot		
		x / a	y / b	z / c
4s	4e	0.249	0.249	0.250
$2Al_I$	2C	0	0	0
$2Al_{II}$	2d	0.500	0.500	0
$2Al_{III}$	4i	0	0.500	0.503
$4Al_{IV}$	4f	0.125	0.125	0.750
$4Al_V$	4f	0.374	0.374	0.750
$4Al_{VI}$	8j	0.124	0.375	0.752
$8Ca_I$	8j	0.256	0	0
$8Ca_{II}$	8j	0.256	0.500	0
$8O_I$	8j	0.133	0.269	0.250
$8O_{II}$	8j	0.297	0.297	0.368
$8O_{III}$	8j	0.073	0.096	0.581
$8O_{IV}$	8j	0.250	0.083	0.720
$8O_V$	8j	0.405	0.074	0.918
$8O_{VI}$	8j	0.427	0.095	0.579
$8O_{VII}$	8j	0.416	0.249	0.780
$8O_{VIII}$	8j	0.426	0.405	0.581

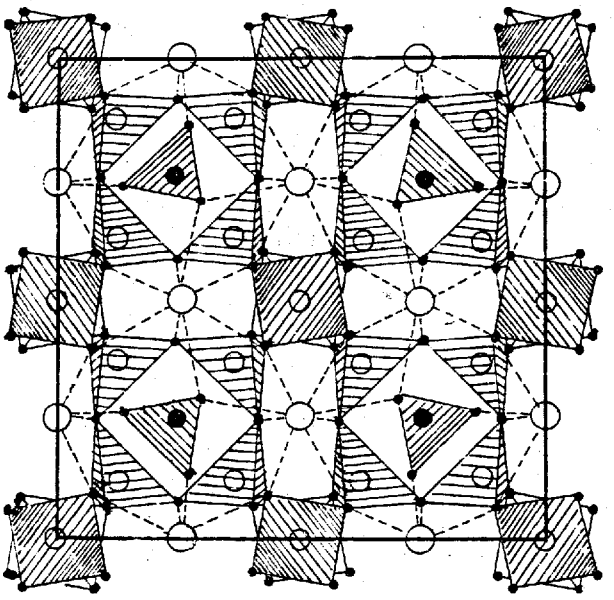

Fig.4 The diagram of coordination polyhedron for crystal
O–CaO; o–Al; ●–S; • –O

It can be seen known from Fig.4 that the crystal structure of $C_4A_3\bar{S}$ is a porous crystal framework which is mainly constructed from groups of Al–O tetrahedron jointed the nodal point. In the framework, there are four square rings jointed from four Al–O tetrahedron by nodal point in every monocells, which froms four square axial hole paths in the direction parallel to axis [001]. In the hole paths the nesotetrahedrons of S–O are respectively distributed at 1 / 4 Co or 3 / 4 Co. And, every square ring is linked by nodes of Al–O tetrahedron to form 8 hexangular axial hole paths parallel to the direction of axis [001]. Ca^{2+} ions are distributed at 0 Co and 1 / 2 Co in the hole paths shown in Fig.5. There are narrow connected seams between hole paths.

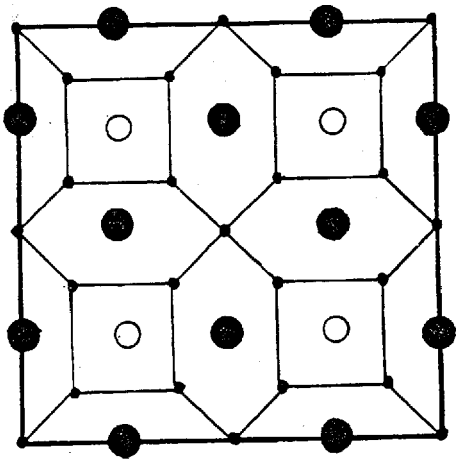

Fig.5 Scheme of crystal structure of $C_4A_3\bar{S}$(Progrection parallel to the direction of axis[001]
●–Ca; • – (AlO_4) ; o– (SO_4)

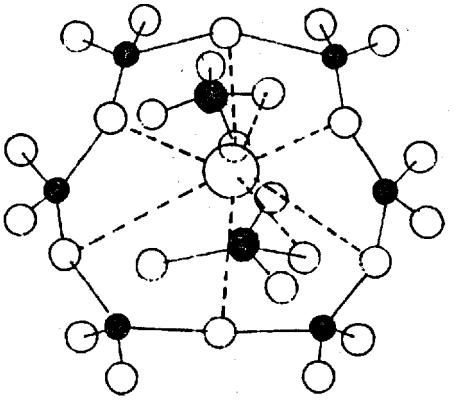

Fig.6 Diagram of coordination structure of Ca–O in crystal structure of $C_4A_3\bar{S}$O–Ca; • –Al; o–0; ●–S

According to Pauling's electrovalence rule the number of positive valence of 16 Ca^{2+} in the monocell just balances with the number of negative valence of $(Al_{24}O_{48})^{24-}$ and $4(SO_4)^{2-}$. Thus, every Ca^{2+} ion has to connect with the tetrahedron of Al–O and S–O in the form of valence bond. As shown in Fig.4, the ion in the form of ionic bond types of cubic ligands being coordination number of 8 are constructed from every Ca^{2+} ion in the form of ionic bond with one oxygen in two tetrahedrons of S–O and one oxygen on the node of every tetrahedron of Al–O in the hexagonal ring, illustrated in Fig.6. However, the layers of its closepacking is |ABCABC| and some distortion appears. It is obvious that the porous structure of $C_4A_3\bar{S}$ and the distorted ligand of Ca–O are more beneficial to its hydration.

IV. CONCLUSION

We had burnt $C_4A_3\bar{S}$ pure mineral containing volatile component by the orthogonal experimental method. Its mix proportion by weight of analylically pure chemical agents was, $CaCO_3$ 44.0564 g; $Al(OH)_3$ 76.6921 g; $CaSO_4 \cdot H_2O$ 37.0657 g; burning temperature was 1320℃ and its isothermal period was 1 hour. More refined XRD data of $C_4A_3\bar{S}$ powder crystal were obtained. Thus we first determined the $C_4A_3\bar{S}$ crystal structure to be tetragonal system. The parameters of its crystal cell are $a_o = b_o = 13.031$ Å, $C_o = 9.163$ Å, $\alpha = \beta = \gamma = 90°$ and $Z = 4$. The space group is D^6_{2d}–$P\bar{4}C2$. Its structural formula is $Ca_4[Al_6O_{12}]SO_4$. Ca–O was determined to be ion type of cubic coordination polynedron being coordination number of 8. Layer of its closepackin is |ABCABC|, but a distortion appears. The mode of crystal structure of $C_4A_3\bar{S}$ has been made. New optical data of $C_4A_3\bar{S}$ crystal was determined to be $Ne = 1.570 \pm 0.002$, $No = 1.567 \pm 0.002$, inclined extiction, negative elongation, uniaxial crystal, optically positive and 1 grade of grey–yellowy interference colors.

REFERENCE

1. P.E. Halstead and A.E. Moore, J. Appl. Chem. 1962, 12(9)413.

2. H. Saalfeld and W. Depmeier, Kristall and Technik, 1972 7(1～3) 229.

3. Feng Xiuji and Liao Guanglin, Journal of Wuhan University of Technology, (China), 1988, (3)1.

SULFATE-BEARING SOLID SOLUTION OF CALCIUM ALUMINATES AND FERRITES

Yu R Krivoborodov and S V Samchenko

NII Cement, Moscow, RUSSIA

SUMMARY

In this paper the results of the investigation sulfocontained solid solution of calcium aluminate and ferrite are described. It is shown that calcium sulfoaluminate can consist of up to 9% of ferrite oxide. In the results of exchange between ions alumina and ferrite calcium sulfoaluminoferrites are obtained. They were synthesized by sintering and melting row mixes. The presence of S-ions in the structure of calcium aluminoferrite leads to the formation of ettringate at the hydration and to have expention of hardening system.

INTRODUCTION

One of the tendency of cement science development occurs due to the nessesity of obtaining binders with special properties which are not available for usual cement. The most detailed investigated and presently widely applicated cements are aluminate and sulfoaluminate ones. Due to a good performance of strengh development and final strength these cements are able to substitude special composite materials, and aplication of these cements provides a high density, crack resistance and low water-permeability.

Calcium sulfoaluminate, beeing the main mineral of sulfoaluminate clinkers, is capable to include in its structure various impurities. It is observed during kilning of raw mixes, having low alumina content. The changes in calcium sulfoaluminate cell by impurities lead to changes of its properties.The formation of ferriferous calcium sulfoaluminate (CSA) becomes possible by the fact that the ionic radii of AL^{3+} and Fe^{3+} are close to each other (0.57 and 0.67 A), so an ion Fe^{3+} may replace Al^{3+} in mineral synthesis with the emegence of solid solutions (1).

EXPERIMENTAL

At present work both an influence of ferrite oxides on structure and properties of calcium sulfoaluminate and its stability under higher temperatures were investigated. To examine the solubility of ferric oxides in CSA, ferric oxide in an amount of 1 to 15% by mass was added to the mineral synthesized earlier. The blends had been held for 20 minutes at a temperature of 1350°C, following which they were analysed.

To investigate solid solutions of CSA and calcium sulfoferrite (CSF), blends were out of minerals synthesized previously, the ratio in all the experiments being from 25 up to 75 mole-%. The blends prepared were treated in the form of pressed briquettes at temperatures of 1050 to 1300°C in steps of 50°C, for 20 minutes each. The cakes obtained were subjected to petrographic and X-ray phase analysis.

Calcium sulfoaluminoferrites were obtained by solid-phase synthesis by the burning of raw mixes intended for the production of calcium aluminoferrites with compositions of C_6AF_2, C_4AF, C_6A_2F, with the addition ofcalcium sulfate and a blend of calcium aluminoferrites having synthesized beforehand with anhydrite, as well as by the crystallization of sulfated aluminoferrite melts (2).

RESULTS AND DISCUSSIONS

To examine the solubility of ferric oxides in CSA, ferric oxide in an amount of 1 up to 15% by mass was added to the mineral having beensynthesized earlier. The blends were held for 20 minutes at a temperature of 1350°C, following which they were analysed. X-ray phase analysis has revealed that the addition of ferric oxides caused a shift in the major diffraction peaks of CSA, this being the more manifest the more Fe_2O_3 added to the mineral (see Table 1). The IR-spectra data show a shift and spreading of the band referring to the various oscillations of the SO_4^{2-} group in the original CSA (absorption bands 1093 and 1180 cm^{-1}) which is due to a change in the coordination environment of that group as a result of the incorporation of ferric oxides whose presence is evidenced by the emergence of absorption bands in the region of 400 to 500 cm^{-1}.

Table 1 X-ray phase analysis of calcium sulfoaluminates modified by ferric oxide

CSA sample description	Position of major diffraction peaks (hkl)		
	422	444	822
No additive	3.750	2.650	2.166
1% Fe_2O_3	3.748	2.644	2.163
3% Fe_2O_3	3.745	2.641	2.161
5% Fe_2O_3	3.740	2.636	2.158
7% Fe_2O_3	3.733	2.636	2.158
9% Fe_2O_3	3.729	2.575	2.138

Such changes in the spectra of CSA samples occur when up to 9% ferric oxides are added; but when the iron content is greater, the formation of an aluminoferrite phase is observable, i.e.the CSA structure can coprise up to 9% ferric oxides, the principal pattern of its crystall lattice remaining unchanged.

The study of the hydration process of modified CSAs through ferric oxide in micropreparations has demonstrated that the oxide available in the CSA structure retards the interaction process of the mineral and water. CSA interacts with water during the first minutes of being mixed with water, whereas the start of the hydration process of modified CSAs is shifted by one hour in proportion to the amounti of ferric oxide

added. By the end of the first day, however, the quantity of ettringite formed levels off, so in the long run this will have no effect on the compaction and expansion process of the hardening system comprising CSAs modified by ferric oxides.

The investigation of powders, consisting of preliminary synthesied minerals (calcium sulfoaluminate, dicalcium ferrite and calcium sulfate), shows, that there is an exchange of aluminate and ferrite oxides between minerals and they are stable under heating up to 1350°C. The following increasing of temperature causes the decomposition of calcium sulfoaluminate and melt appearance, which solves the formed earlier phases. During melt cooling calcium aluminoferrites of varying composition are appeared, which contain sulfur oxide. It has been found that minerals burnt together change their colouring in transmitted light, while the X-ray spectra feature a shift of major diffraction peaks of the minerals as compared with their initial matrices, i.e. an exchange of aluminium and iron ions takes place between the minerals, this becoming the more pronounced as the temperature rises.

The X-ray spectrum microanalysis in samples shows that CSA contains ferric oxide in its composition, and high-basicity CSF carries aluminium oxides (see Table 2), but a broad series of CSA and CSF solid solutions like the aluminoferrite series is not formed. This may be due to the fact that the CSA structure can comprise ferric oxide in a limited amount only, in contrast to high-basicity CSF, which is a solid solution of calcium sulfate in the structure of dicalcium ferrite. As the latter is the initial member of the aluminoferrite series, high-basicity CSF is the "founder" of the series of calcium sulfoaluminoferrites solid solutions.

The mineral composition of cakes from raw mixes meant for the production of aluminoferrite minerals with calcium sulfate is represented by a mixture of such minerals as CSA, CSF and calcium sulfoaluminoferrites.

The results of burning calcium aluminoferrites of compositions C_6AF_2, C_4AF and C_6A_2F together with calcium sulfate testify to the fact that there occurs a fixation of the latter with aluminoferrite minerals, for the X-ray phase analysis does not indicate the formation of other chemical compounds.

Table 2 Composition of calcium sulfoaluminates and sulfoferrites according to X-ray spectrum microanalysis data

Mineral description	Content of oxides, % by mass			
	CaO	Al_2O_3	Fe_2O_3	SO_3
CSA	35.69	47.69	3.12	13.76
CSA	34.26	48.28	5.24	12.20
CSA	36.39	43.15	7.28	13.45
CSF	44.82	3.76	46.09	4.98
CSF	43.58	1.89	48.67	6.01
CSF	42.42	4.41	47.42	5.94

The general aspect of the radiographs of calcium aluminoferrites and sulfoaluminoferrites remains almost unchanged, which is indicative of the fact that the major pattern of the crystalline structure is preserved. In all cases, however, calcium sulfoaluminoferrites differ from calcium aluminoferrites in the intensity of characteristic diffraction peaks and in the shift of interplanar spacings, which is caused by a distortion of the crystal lattice of calcium aluminoferrites by calcium sulfate (see Table 3).

Table 3 Interplanar specings of calcium aluminoferrites and sulfoaluminoferrites

Description of aluminoferrite and sulfoaluminoferrite	Position of peaks (hkl)		
	200	141	202
$6CaO \cdot Al_2O_3 \cdot 2Fe_2O_3$	2.7914	2.6395	1.9285
$6.3CaO \cdot Al_2O_3 \cdot 2Fe_2O_3 \cdot 0.3SO_3$	2.7805	2.6485	1.9318
$4CaO \cdot Al_2O_3 \cdot Fe_2O_3$	2.7830	2.6335	1.9212
$4.4CaO \cdot Al_2O_3 \cdot Fe_2O_3 \cdot 0.4SO_3$	2.7733	2.6401	1.9245
$6CaO \cdot 2Al_2O_3 \cdot Fe_2O_3$	2.7701	2.6230	1.9151
$6.5CaO \cdot 2Al_2O_3 \cdot Fe_2O_3 \cdot 0.5SO_3$	2.7681	2.6395	1.9228

Investigations into the crystallization of calcium sulfoaluminoferrites from the melt show that the composition of crystalls emerging depends on the cooling rate. It has been established

that in the case of a rapid cooling of the melt, the crystalls are enriched in aluminium to a greater extent that is the case solidified melt. In the case of slow cooling, the composition of the crystallizing phase is identical with that of the melt.

The composition of calcium sulfoaluminoferrites produced by the crystallization of melts, as determined by means of X-ray spectrum microanalysis, is presented in Table 4.

Table 4 Composition of calcium sulfoaluminoferrites

Ser. Nos.	Content of oxides, % by mass				Structural formula
	CaO	Al_2O_3	Fe_2O_3	SO_3	
1	30.29	44.74	15.35	10.31	$C_{1.63}A_{0.69}F_{0.31}\bar{S}_{0.21}$
2	34.0.8	26.59	28.35	11.26	$C_{2.08}A_{0.35}F_{0.65}\bar{S}_{0.26}$
3	43.59	16.47	30.18	9.83	$C_{2.92}A_{0.18}F_{0.82}\bar{S}_{0.27}$
4	44.48	16.52	22.16	13.62	$C_{2.30}A_{0.43}F_{0.57}\bar{S}_{0.35}$
5	46.52	17.77	24.26	12.44	$C_{2.21}A_{0.42}F_{0.58}\bar{S}_{0.30}$
6	34.29	45.62	10.23	10.24	$C_{1.23}A_{0.82}F_{0.18}\bar{S}_{0.18}$
7	36.01	47.53	4.41	12.06	$C_{1.85}A_{0.91}F_{0.09}\bar{S}_{0.23}$
8	35.77	46.04	5.73	11.63	$C_{1.85}A_{0.91}F_{0.09}\bar{S}_{0.22}$
9	35.19	47.57	6.63	11.49	$C_{1.72}A_{0.88}F_{0.12}\bar{S}_{0.21}$

The results displayed in Table 4 indicate that in the course of crystallization from melts, there emerge calcium sulfoaluminoferrites which, in the same way as calcium aluminoferrites, have a variable composition and can therefore be described through a general formula of $C_2A_xF_{1-x}\bar{S}_n$, where"x" varies within the limits of 0.1 to 0.8 and "n" ranges from 0.02 to 0.5.

Modifying calcium aluminoferrites by calcium sulfate brings about not only a difference in the of composition hydration products, but also an enhanced hydraulic activity of the solid solutions as compared to that of the source minerals.

By way of comparing the hydraulic activity it is to be noted that the degree of hydration grows with the increase of the A/F ratio in calcium sulfoaluminoferrites, and stands at 67 to 75 % during the first three days.

An analysis of the kinetic curves shows that within three days the minerals interact with water vigorously, but as more hydration time passes, the reactions low down owing to the formation of crystalline hydrates around the non-hydrated grains, and this hinders the access of water to the source minerals. In the hydration of calcium sulfoaluminoferrites ferriferous ettringite is formed the rate of whose formation and stability depend on the composition of the former. In hydrated high-aluminate samples, ettringite is formed during the first hours of interaction with water already (1 to 6 hours), but by 12 hours it recrystallizes into the monosulfate form of calcium hydrosulfoaluminoferrite, which is stable at any time thereafter. In the hardening of this sample, hexagonal calcium hydroaluminoferrites also crystallize during the first hours and at any time thereafter; the formation of cubic crystalline hydrates is observable only by 28 days.

The formation of ferriferous ettringite occurs in the hydration of calcium sulfoaluminoferrire based on C_4AF during the first day of hydration, in the hydration of highly ferriferous sulfoaluminoferrite towards the expiry of three days only, while during the first (1 to 6)hours the monosulfate form of calcium hydrosulfoaluminoferrite is formed.

CONCLUSIONS AND RECOMMENDATIONS

Thus, calcium sulfate, while causing structural alterations in aluminoferrite melts, enters the crystalline phases during their crystallization, and it changes their structure, no new chemical compounds being formed thereby.

In the hydration of calcium sulfoaluminoferrites with gypsum, ettringite is formed right from the moment of their being mixed with water, and it is stable at any later time. This enables these minerals to be used as expansion agents in the creation of self-stressing and expansive cements.

REFERENCES

1. Krivoborodov Yu.R. and Samchenko S.V. :"Phase formation in aluminoferrite systems in presence of calcium sulfate", **Second International Symposium on Cement and Concrete, Beijing**, 1989, 78-81.

2. Samchenko S.V. :"Mineral formation in aluminoferrite systems in the presence of calcium sulfate". Cement, Leningrad, 1989,3,19-20.

MECHANISMS AT THE MIXED SULPHATALUMINATES FORMATION IN THE $CaO-Al_2O_3$-(Sr, Ba) SO_4 SYSTEMS

I Teoreanu, A Puri and M Georgescu

Polytechnical Institute, Bucharest
ROMANIA

SUMMARY

The thermal stability of $SrSO_4$ and $BaSO_4$ suggests the formation of calcium and strontium- . respective calcium and barium sulphataluminates in the $CaO-Al_2O_3$-$(Sr.Ba)SO_4$ systems.The stability conditions as well as the reaction mechanism and the formation of $3(CaO.Al_2O_3).SrSO_4$ and $3(CaO.Al_2O_3).BaSO_4$ compounds. are evidenced. The thermal stability range of mixed sulphataluminates depend on the basicity of $CaCO_3$-Al_2O_3-MSO_4 mixtures. The decompositions of sulphataluminates occur at lower temperatures when the CaO/Al_2O_3 ratio in the starting materials is higher.

ZUSAMMENFASSUNG

Die Temperaturbestandigkeit von $SrSO_4$ und $BaSO_4$ suggeriert die mogliche Bildung von Kalziumstrontium-. bzw. Kalziumbarium Sulfataluminaten in den $CaO-Al_2O_3$-$(Sr.Ba)SO_4$ Systemen. Es werden die Bestandigkeitsbedingungen, sowie auch der Reaktionsmechanismus bei der Bildung von $3(CaO.Al_2O_3).SrSO_4$ und $3(CaO.Al_2O_3).BaSO_4$. festgelegt. Die Temperaturbestandigkeit der Sulfataluminate ist von der Basizitat der Ausgangsmischung $CaCO_3+Al_2O_3+MSO_4$ abhangig. Bei grosseren CaO/Al_2O_3 Werten der Ausgangsmischung findet der Zerfall der Sulfataluminate bei niedrigeren Temperaturen statt.

INTRODUCTION

Conditions of formation, stability, structure and properties of the calcium sulphataluminate - $3(CaO.Al_2O_3).CaSO_4$, its contribution in the hardening of cements which contain it and the development of the mechanical strength, are well known nowadays.

Considering the calcium sulphataluminates behavior and the possibility of using other sulphatic compounds like mineralizers or components of the raw mix to get portland cement clinkers or derivates, to examine other sulphataluminates' formation, their conditions of stability and the corresponding processes' mechanism, produced interest.

In this paper we made some researches in this way, in the $CaO-Al_2O_3-(Sr,Ba)SO_4$ systems. Considering the thermic stability of $SrSO_4$ and $BaSO_4$, the formation of some mixed sulphataluminates- $3(CaO.Al_2O_3).BaSO_4$ and $3(CaO.Al_2O_3).SrSO_4$, respectively appear probable. Thus we are given more information that the investigations already made by ourselves or belonging to others [1-7], especially referring to the formation mechanism of the sulphataluminates mentioned above but also concerning the influence of the initially mixture composition upon the formatting temperatures and their stability.

EXPERIMENTAL, RESULTS AND DISCUSSION.

We used $CaCO_3$, Al_2O_3, $SrSO_4$ and $BaSO_4$ as p.a. reactants. We examined mixtures of $CaCO_3/Al_2O_3/(Sr,Ba)SO_4$ with molar ratio 3:3:1 and 9:3:1. The masses were burned at 600-1450 °C maintaining it for 3 hours at the maximum temperature. The phase composition of the burned samples has been established by X-ray diffraction. In this way we could obtain information about the interaction processes' mechanism and about the temperature when there starts the formation of sulphataluminate compounds, res-pectively their decomposition.

The $CaO-Al_2O_3-SrSO_4$ system

Irrespective of reacting substances' proportion in the initial mixture, until about 800°C, the main chemical process is the dissociation of $CaCO_3$. Some calcium aluminates take from too, CA and $C_{12}A_7$, in the $CaCO_3/Al_2O_3/SrSO_4$ = 3:3:1 mixture, respectively $C_{12}A_7$, in the $CaCO_3/Al_2O_3/SrSO_4$ = 9:3:1 mixture, even from 800°C. The diagrams presented in figs. 1 and 2 shows the formation of $3(CaO.Al_2O_3).SrSO_4$ (3CA.$S\bar{S}$) at the temperatures over 800°C - in the case of the stoichiometric mixture of reacting substances, and, under this temperature in the mixture of reacting substances richer in $CaCO_3$ (ratio $CaCO_3/Al_2O_3$ = 3). The process is accelerated over 1000°C.

The strontium sulphate is consumed until under the limit of X-ray detection, with formation of mixed sulphataluminate, at higher temperatures as compared to those of integral consumption of CaO and Al_2O_3. Thus, it suggest that the formation of 3CA.$S\bar{S}$ is the most probable by the interaction of $SrSO_4$ with calcium aluminates which have been formed before.

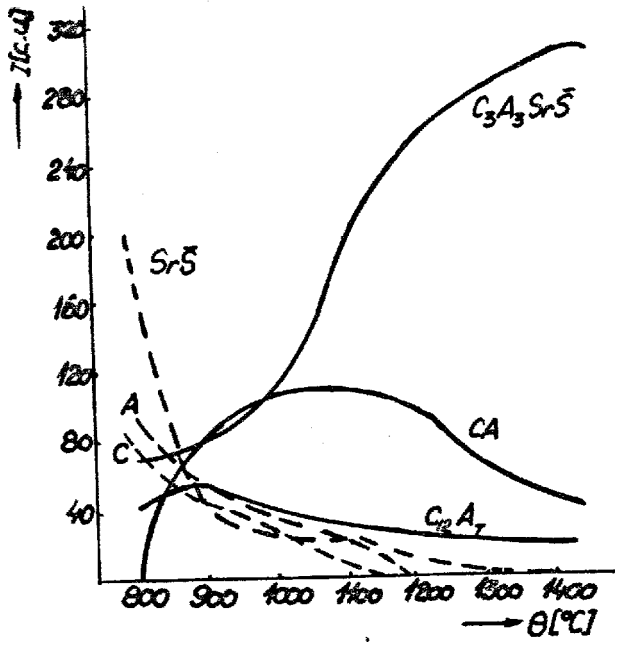

Fig. 1 Evolution of mineralogical composition at the burning of $3CaCO_3+3Al_2O_3+SrSO_4$ mixtures.

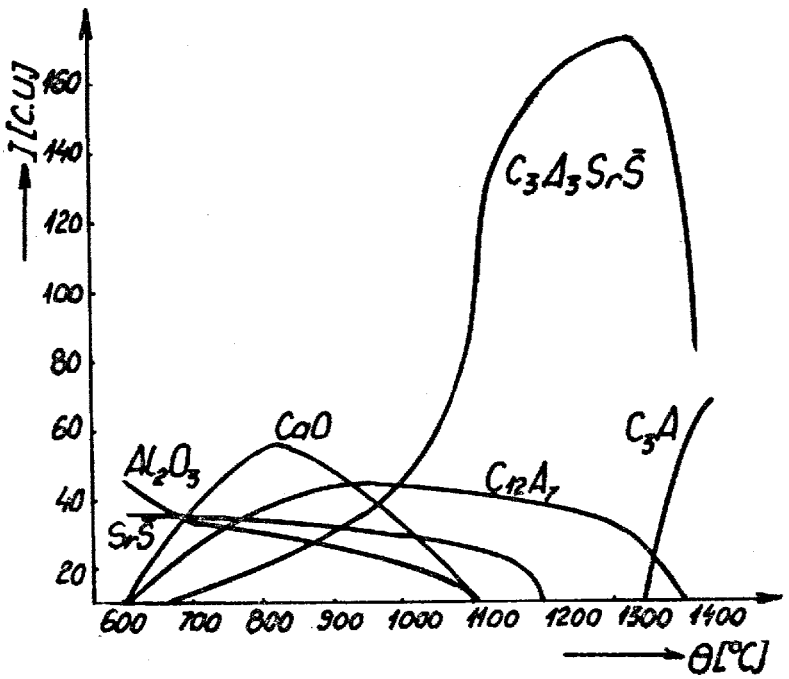

Fig. 2 Evolution of mineralogical composition at the burning of $9CaCO_3+3Al_2O_3+SrSO_4$ mixtures.

We must notice that in the more basical mixtures of reacting substances ($CaCO_3/Al_2O_3$ = 3). $3CA.SrSO_4$ starts to decompose at about 1300°C temperature which is about 100°C lower than the decomposition temperature of stoichiometric mixtures.

At 1300°C, in basic mixture, besides $3CA.S\bar{r}\bar{S}$, is evidenced only $C_{12}A_7$, while over this temperature the existence of tricalciumaluminate has been found, together with $3CA.S\bar{r}\bar{S}$ - this one in a lower proportion, due to it's instability and decomposition.

In the samples burned at temperatures higher than 1100°C, the presence of CaO in not evidenced, although, in the conditions of mixed sulphataluminates' existence, its presence should assert itself: in more basic mixtures which have been investigated, CaO is the only eqilibrum compound with 3CA.SrS, at maximum stability temperature of this one.

The existence of the calcium aluminates can suggest either a partial decomposition of strontium sulphataluminate, with a higher content of strontium sulphate, that the stoichiometric considerate above.

The $CaO-Al_2O_3-BaSO_4$ system

In this system we notice too, the formation of a mixed calcium and barium sulphataluminate. In the stoichiometric mixture of reacting substances corresponding to $3(CaO.Al_2O_3).BaSO_4$ ($3CA.B\bar{S}$), the mechanism of interaction processes is generally similar to these noticed in the

similar mixtures with $SrSO_4$: but we have noticed too the formation of the monobaric aluminate.

The X-ray diffraction patterns evidence the formation of the mixed sulphataluminate, by the interaction of $BaSO_4$ with the calciumaluminates formed before (fig.3). As a result of the formation of $BaO.Al_2O_3$ (BA), the substitution of Ca^{2+} with Ba^{2+} in the aluminous lattice of the mixed sulphataluminate becomes possible, too.

The identification of BA at higher temperatures, especially over the limit of mixed sulphataluminates stability, suggests possible interactions of $BaO(BaSO_4)$ with Al_2O_3, with the formation of this aluminate.

The mixed sulphataluminate is starting with 1000°C, its formation rate grows appreciable over 1100° and its limit of stability is about 1400°C. At the maximum temperature of stability of the $3CA.B\bar{S}$, in conditions of $BaO.Al_2O_3$ and $CaO.Al_2O_3$ (the latter in very small quantities) co-exists with the mixed sulphataluminate.

In the mixture characterized by a $CaCO_3/Al_2O_3/BaSO_4$ ratio 9:3:1, the formation of $3(CA).B\bar{S}$ compound starts from lower temperatures, its limit of stability being inferior to the one which has been noticed at the synthesis of calcium and barium sulphataluminate, from the stoichiometric mixture of reacting substances (fig.4).

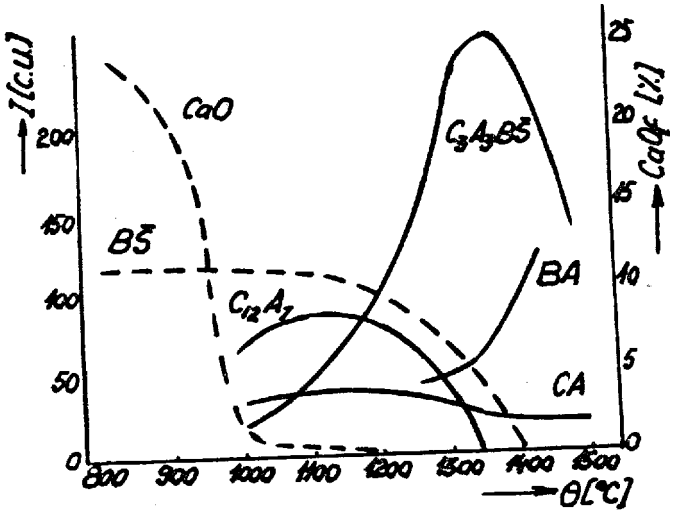

Fig.3 Evolution of mineralogical composition at the burning of $3CaCO_3+3Al_2O_3+BaSO_4$ mixtures.

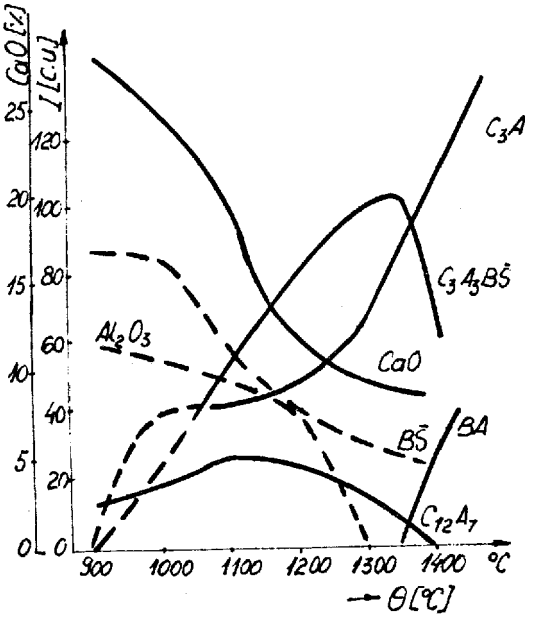

Fig.4 Evolution of mineralogical composition at the burning of mixture: $9CaCO_3+3Al_2O_3+BaSO_4$

In this case too, it is suggested the formation of $3(CA)B\bar{S}$, by the reaction of $BaSO_4$ with calcium aluminate which have been formed before. At the maximum temperature of stability, together with $3(CA).BS$, coexists unreactioned CaO and $BaSO_4$ in important proportions, $3CaO.Al_2O_3$ and small quantities of $C_{12}A_7$. Over this temperature, the quantity of $3(CA).B\bar{S}$ decrease and $C_{12}A_7$ disappears.

The proportion of CaO continues to diminish due to the formation of some important quantities of C_3A, by the saturation in the CaO of CA resulted from the decomposition of $3(CA).B\bar{S}$ and of the rest of $C_{12}A_7$. At 1400°C, the tricalcium aluminate is the main compound: we can notice too, the formation of monobaric aluminate - BA, resulted from the decomposition of sulphataluminate.

Compatibility relations at subsolidus temperatures

The results mentioned above, about the compatibility relations in the $CaO-CaO.Al_2O_3-CaSO_4$ system, and the information obtained in this paper, lead us to the conclusion that in all $CaO-CaO.Al_2O_3-(Ca.Sr.Ba)SO_4$ systems stipulate the same relationships. For subsolidus temperatures the relation corresponding to all the systems mentioned, are shown in fig.5.

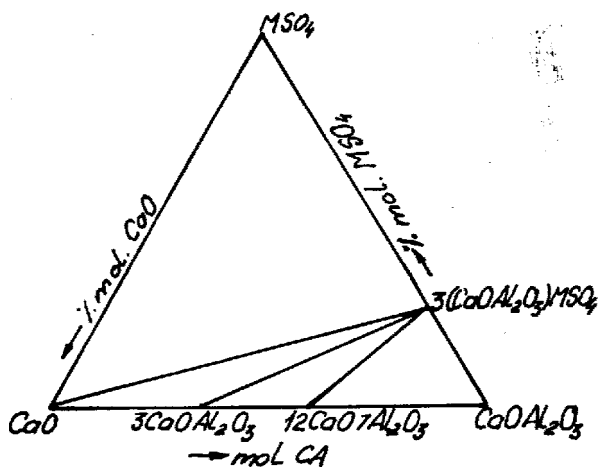

The examination of the diagram in fig. 5 points out that in presence of Sr or Ba sulphate, in raw mixtures for some aluminatebelite clinkers, by stopping the formation of C_3A in favor of $3(CA).Sr\bar{S}$ or $3(CA).B\bar{S}$, a certain quantity avaible.

Fig. 5 Compatibility relations in the $CaO-CaO.Al_2O_3-MSO_4$ systems.

This one, can saturate the silicate $2CaO.SiO_2$ to $3CaO.SiO_3$:

$$3(3CaO.Al_2O_3) + MSO_4 \longrightarrow 3(CaO.Al_2O_3).MSO_4 + 6\ CaO \quad (1)$$

$$6(2CaO.SiO_2) + 6CaO \longrightarrow 6(3CaO.SiO_2) \quad (2)$$

$$3(3CaO.Al_2O_3)+6(2CaO.SiO_2)+MSO_4 \longrightarrow 3(CaO.Al_2O_3).MSO_4+6(3CaO.SiO_2) \quad (3)$$

CONCLUSION

The researches we have made, suggest the formation of mixed sulphataluminates, mainly by the interaction of Sr or Ba sulphate with calcium aluminates, formed before.

The formation temperatures and stability of the investigated mixed sulphataluminates are dependent on initially mix composition ($CaCO_3$. Al_2O_3. $SrSO_4$ or $BaSO_4$): they are lower in the case of more basic mixtures.

The compatibility relations at subsolidus temperatures in the $CaO-CaO.Al_2O_3-SrSO_4$ and $CaO-CaO.Al_2O_3-BaSO_4$ systems. are similar to those indicated above for the $CaO-CaO.Al_2O_3-CaSO_4$ system.

LITERATURE

1. I. Teoreanu. M. Muntean.I. Dragnea - Rev.Roum.Chim. 20. 925. 1975

2. I. Teoreanu. M. Muntean. I. Dragnea - Il Cemento 83.39.1986

3. I. Teoreanu. A. Puri - Rev.Roum.Chim. 34. 357. 1989

4. I. Teoreanu. M. Georgescu - Il Cemento 88.(4).211 1991

5. G. Giglioli. F. Massazza. M. Pozzuoli - Cem.Concr.Res. 1. 621. 1971

6. I. Teoreanu. M. Georgescu. A. Puri. A. Badanoiu - Colocviul Fundamente in Stiinta Silicatilor. vol.III. p.53. Bucuresti 1991.

7. A.S. Muminov a.o. - Izv.Akad.Nauk SSSR Neorg.Mater. 21.(4). 669. 1985.

CEMENTS BASED ON MODIFIED PORTLAND AND SULFOALUMINATE-BELITE CLINKERS

S I Ivashchenko

All-Union Engineering Construction Building Institute, Moscow, RUSSIA

The present work studies the influence of additives on sulfoaluminate-belite and portland clinkers in view of the fact that blended cements based on those find ever greater application industry. It has been established that the presence of modifying additives in the system $CaO-Al_2O_3-SO_3$ intensifies mineral formation reactions and raises the thermal stability of modified $C_4A_3\bar{S}$. It has been demonstrated that additives forming solid solutions with $C_4A_3\bar{S}$ modify the ettringite phase in the hydration process, thereby changing the shape and size of crystals, the resistance to recrystallization, and this exerts a decisive influence on the strength parameters of synthetized sulfated cements. A reciprocal influence of modification has been shown in the production of multicomponent cements based on clinkers of silicate and sulfoaluminate hardening types.

The idea of improving the quality of blended cements through enhancing the properties of the clinkers going into them was put forward earlier by both Soviet and foreign scientists. This mainly concerned enhancing the quality of special cements through boosting the hydration activity of portland cement clinker through modification of its structure by introduction of micro-admixtures. A more promising route to this end would be to improve the properties of not one particular clinker which enters into the composition of blended cements, but to simultaneously improve the properties of several clinker types making up blended cements through the use of inorganic additives to modify portland clinker as well as sulfated, fluorinated and other types of clinkers.

In this work the influence of additives on sulfoaluminatebelite (SAB) and portland clinkers was studied as blended cements based on those are finding ever increasing application in the construction industry. Particular attention was given to modifying sulfated clinkers.

The analysis of information from the literature on modified SAB clinkers and the positive results which have been obtained in modifying raw portland cement mixes made it possible to assume that addition of different modifying agents to raw sulfoaluminatebelite mixes can stabilize the burning process of SAB clinkers, improve their grindability, increase the setting time of the superrapid hardening cements based on those clinkers and improve considerably other building and engineering properties of cements.

Since it is waterless calcium sulfoaluminate that has a decisive influence the properties of SAB clinkers and SAB clinker-based cements, processes which proceed during the synthesis and hydration of $C_4A_3\bar{S}$ in the presence of BaO, SrO, P_2O_5, MgO, CdO, ZnO, Ni_2O_3, CuO, Mn_2O_3, MoO_3, V_2O_5, WO_3, Cr_2O_3, Co_2O_3, TiO_2, SnO_2, PbO, B_2O_3, $CaCl_2$, NH_4F, H_3BO_3, K_2CO_3, Na_2CO_3 were studied. The modifiers were added to the raw mixes in the form of different reagents of AR grade and in the form of different kinds of waste in amounts of 0.5 - 1.0 - 2.0 - 3.0 - 5.0% by mass, to obtain $C_4A_3\bar{S}$.

Cakes burned under optimum burning conditions comprised 90-95% of waterless calcium sulfoaluminate, and the remaining was $C_{12}A_7$ and $CaSO_4$. The presence of modifying agents in the samples only slightly changes the quantitative ratio of minerals formed in the system; however, in this case the size and shape of calcium sulfoaluminate crystals change considerably.

No compounds other than the above mentioned were found in the cakes when additives were used, except for samples containing $CaCl_2$, TiO_2, CaF_2 and MgO. X-ray and petrographic analysis revealed the presence of perovskite, besides $C_4A_3\bar{S}$, $CaSO_4$ and $C_{12}A_7$, in the titan-containing samples. In chlor- and fluorine-containing samples, instead of

$C_{12}A_7$ $C_{11}A_7 \cdot CaCl_2$ and $C_{11}A_7 \cdot CaF_2$ were found, while in MgO-modified samples, free magnesium oxide and magnesian spinel were observed.

X-ray examination of samples did not reveal any additives not entered into the solid solution, while petrographic analysis showed in almost all samples a slight amount of admixtures not entered into the solid solution with calcium sulfoaluminate, their maximum concentration being 5% by mass.

It has been found by petrographic, X-ray and IR-spectrum methods that the additives under study form solid solutions with calcium sulfoaluminate, and this is in line with the data obtained earlier for some additives.

Investigations on the modified samples by IR-spectroscopy have shown that cations of the alkali and alkaline-earth metals replace the Ca^{2+} cations in the calcium sulfoaluminate structure; multivalent cations from the top row of d- and p-elements (Mo^{6+}, W^{6+}, Cr^{6+}, Ti^{4+}, Ni^{3+}, Sn^{4+}) enter into mineral structure fragments containing AlO_6^{9-} - octahedrons and AlO_4^{5-}- and SO_4^{2-}- tetrahedrons; and the ions Zn^{2+}, Cu^{2+}, Co^{3+}, Mn^{3+} in calcium sulfoaluminate enter only into the structure fragments containing complexes AlO_4^{5-} and AlO_6^{9-}. Halogen-containing additives form the modified meionite in the system under study.

The above structural changes have a considerable effect upon the hydration activity of solid solutions of calcium sulfoaluminate, and it has been found that strength properties of samples are, for the most part, directly proportional to the degree of hydration of the modified minerals.

To obtain $C_4A_3\bar{S}$ in additive-containing raw mixes, mineral formation reactions are intensified; in the process $C_4A_3\bar{S}$ is synthesized at a lower (by 50-70°C) temperature and begins to decompose at a higher (by 50-100°C) temperature than in the reference samples, i.e. the range of stable existence of the mineral becomes wider, which can be used for practical purposes. The features of mineral formation reactions in the system C-A-$\bar{S}$ in the presence of additives have been revealed. In particular, it has been found that in raw mixes with a K_2O additive, the synthesis of solid solution of calcium sulfoaluminate is achieved first by direct interaction between Al_2O_3, SO_3 and CaO, bypassing the formation of meionite, and then both reactions of mineral synthesis take place concurrently.

The study on the hydration of monomineral binders obtained has shown that additives forming solid solutions with $C_4A_3\bar{S}$ are also present, after its hydration, in the ettringite causing the change of its shape, size of crystals, resistance to recrystallization, which is decisive for the strength properties of the modified samples. The hydration products

of modified calcium sulfoaluminate as well as of additive-free $C_4A_3\bar{S}$ are $Al(OH)_3$, calcium hydroaluminates and hydrosulfoaluminates have been found.

The improvement of strength properties of the binder based on modified calcium sulfoaluminate is due to the fact that the solid solution resulting from waterless calcium sulfoaluminate exhibits a greater ability to interact with water than "pure" $C_4A_3\bar{S}$. And in the modified system, unlike the reference one, a greater amount of the ettringite is formed, and its crystals are larger and shorter (1:d is from 2:1 to 3:1) which means they are less prone to recrystallization than the additive-free $C_3A \cdot 3C\bar{S} \cdot 31H$.

The reduction in the ultimate compressive strength of the binder based on calcium sulfoaluminate modified by TiO_2, Cr_2O_3, SnO_2, MoO_3, WO_3 is accounted for by the formation of thinner and longer (1:d is from 5:1 to 10:1) crystals of the ettringite and by the occurence in the system of compounds which have no binding properties (perovskite, etc.), and also by the recrystallization of the ettringite into $C_3A \cdot C\bar{S} \cdot 12H$.

These studies have made it possible to identify the additives and fix the optimum concentrations in which they could be added to the raw mixes to obtain $C_4A_3\bar{S}$ which about a significant change in its hydraulic properties, and also has a considerable effect upon the properties of cements based on modified calcium sulfoaluminate. These studies permitted a change-over from laboratory research to pilot and industrial experiments. For industrial experiments, wastes from different industries were used as the modifying agents.

Addition of an optimum amount of waste stabilizes the burning process which can be conducted at a lower (by 50-70°C) temperature than the reference mixes. The modified SAB clinkers had a 10-15% higher grindability than the reference ones.

The addition of modified SAB clinkers to self-stressing cements increases by 1.7-10.2 MPa their strength properties, and by 1.0 MPa the self-stressing of test self-stressing cements, as compared to the self-stressing cements based on reference sulfoaluminate-belite clinker. The increased early strength of the test cements results from a higher hydration activity of the modified calcium sulfoaluminate, calcium alumino-ferromanganates and $C_{11}A_7 \cdot CaF_2$; and the increased ultimate strength of binders is due to a higher activity of dicalcium silicate which has stabilized in its α'-form in the presence of additives. The modified SAB clinkers were added at the stage of grinding to the portland cement, slag cement, self-stressing and oil-well cements. Experiments have shown an improved grindability of cement compounds containing modified SAB clinkers as against the reference sulfoaluminate-belite clinker. Likewise the strength properties of cements with the modified SAB clinker

were 0.5-10.5 MPa higher at any setting time than those of the cements based on the sulfoaluminate-belite clinker without additive. The cements made of modified portland and sulfoaluminate-belite clinkers had their strength and self-stressing increased respectively by 1.0-15.0 MPa and up to 2.4 MPa over the reference cement. This was attributed to the rapid hardening of the structure of cement stone due to an accelerated hydration of the modified minerals of portland and sulfoaluminate-belite clinkers, and also due to the formation at a faster rate and in larger amounts, of the ettringite during the hydration of the modified sulfoaluminate-belite clinker.

Based on the pilot and commercial tests, standards have been drawn up for the production of modified sulfoaluminate-belite clinker and cements based there on, which possess improved building and engineering properties.

POTENTIALS OF USING DOLOMITIC LIMESTONE IN MAKING SULFOALUMINATE - SILICATE CEMENTS

M M Ali, P S Sharma and R Bhargava

National Council for Cement and Building Materials
New Delhi, INDIA

SUMMARY

Presence of MgO as periclase in Ordinary Portland Cement (OPC) beyond certain limits causes unsoundness at later stages of hydration. In non-alitic clinker compositions consisting of $CaO-Al_2O_3-Fe_2O_3-SiO_2-MgO-SO_3$, the mineral phases formed at about 1350^oC are $C_4A_3\bar{S}$, C_2S and C_3MS_2 wherein about 10 percent MgO could be fixed in the form of calcium magnesium silicates by substitutions in C_2S phase. Such cements have shown shrinkage in the range of 0.02 to 0.05 percent under autoclave. However on further increase in MgO, expansions were seen. The cement samples yielded high early strength. The rapid hardening properties were due to generation of ettringite. The formation of clinker using dolomitic limestone at above temperature showed potentials of substantial saving in energy.

INTRODUCTION

The temperature of clinkerization in manufacture of calcium sulphoaluminate and C_2S based cements falls in the range of 1200-1350°C. Such cements are generally called as low energy cements and are characterized by rapid hardening and sulfate-resistant properties (1-3). As the clinker mineral phases are rich in alumina, iron oxide and sulfate, the raw materials required generally are bauxite, laterite, gypsum along with the limestone and clay. The low lime composition (CaO ~ 50%) of clinker indicates the potentials of using low grade limestone.

In the present investigation, it is endeavoured to utilise dolomitic limestone to prepare calcium sulfo-aluminate based clinker in which 8-10% MgO could be fixed in mineral phases with stisfactory performance characteristics.

EXPERIMENTAL

Raw materials such as limestone, dolomite, clay, bauxite, laterite and gypsum were analysed and ground in ball mill to a fineness retaining about 12% residue on 170 mesh. Six raw mix compositions bearing 2 to 12% MgO in clinker were prepared as shown in **Table 1.**

The raw mixes were converted into nodules of 1.5 - 2.0 cm dia in a pan nodulizer and dried in an oven at 150°C. The nodules were fired in an electric furnace at 1350°C for 25, 30 and 35 minutes. The fired nodules were air quenched and stored in dessicator. The clinker samples were evaluated for mineral phases and their morphology using XRD, SEM and OM. The different clinker samples were ground in ball mill. The powder was then blended with 5 % gypsum by weight. The fineness of cement was maintained about 300 M^2/Kg Blaine surface area. The cement samples were evaluated for compressive strength and autoclave expansion as per IS : 4031-1988. The autoclave expansion was determined at a pressure of 300 psi for 3 hours.

RESULTS AND DISCUSSION

The clinker samples obtained in 25 minutes firing at 1350°C were softer and those in 35 minutes were hard burnt. The clinker obtained in 30 minutes were well burnt. The six cement compositions **(Table 1)** differ mainly in MgO, CaO and Al_2O_3 contents. Compositions I to V are rich in MgO and composition VI is lime rich and poor in MgO.

TABLE 1
CHEMICAL COMPOSITIONS OF CEMENT SAMPLES

Component oxides	Compositions					
	I	II	III	IV	V	VI
LOI	1.06	1.21	0.73	0.93	0.80	1.51
SiO_2	13.64	15.11	15.79	15.96	15.67	15.02
Fe_2O_3	6.65	8.33	7.96	7.26	6.60	6.99
Al_2O_3	19.44	22.52	23.02	18.38	18.02	18.12
CaO	41.77	35.72	36.69	38.53	39.28	48.98
MgO	9.24	8.94	8.60	9.43	11.92	2.12
SO_3	6.40	5.47	6.27	7.05	6.12	5.20
Na_2O	0.23	0.25	0.23	0.26	0.21	0.28
K_2O	0.19	0.26	0.21	0.19	0.18	0.22
TiO_2	0.62	0.69	0.72	0.61	0.58	0.55

X -ray diffraction studies (**Fig.1**) have shown presence of mineral phases such as $C_4A_3\bar{S}$, C_2S, C_3MS_2, CSH_2 and C_2AS (**Table 2**). In MgO rich composition calcium magnesium silicate is predominant whereas in composition V, C_2S is predominant and small amount of C_3MS_2 is formed. In a separate study where blends of MgO and pure $C_4A_3\bar{S}$ were fired, the appearance of periclase occured even with one percent MgO inclusion. This indicated that MgO did not affect $C_4A_3\bar{S}$ formation and no change in peak position occurred (d=3.76 A^o). The formation of stable calcium magnesium silicate phase $Ca_3MgSi_2O_8$ in the temperature range of 979 to 1381°C in the system involving CaO -MgO -SiO_2 is well known (4).

TABLE 2

MINERAL PHASES IN CEMENT SAMPLES

Composition	Phases present
I	$C_4A_3\bar{S}$, CSH_2, C_3MS_2, β-C_2S, CS, C_4AF,
II	$C_4A_3\bar{S}$, CSH_2, C_3MS_2, C_2AS, β-C_2S, CS, C_4AF
III	$C_4A_3\bar{S}$, CSH_2, C_3MS_2, C_2AS, β-C_2S, CS, C_4AF
IV	$C_4A_3\bar{S}$, CSH_2, C_3MS_2, β-C_2S, C_4AF
V	$C_4A_3\bar{S}$, CSH_2, C_3MS_2, β-C_2S, C_4AF
VI	$C_4A_3\bar{S}$, CSH_2, C_3MS_2, β-C_2S, C_4AF

Optical microscopic studies of clinker with MgO content of 9.24 % indicated very fine crystals. The clinker is also porous and may be due to high vapour pressure of SO_3 liberated at high temperature. Fracture surface studies, SEM, (**Fig.2**) indicated multifacial cubic crystals of $C_4A_3\bar{S}$. The other granular particles were those of silicate phases. The anhedral grains of C_3MS_2 were comparatively finer and less than 10 micron in size.

The hydration of neat cement showed formation of considerable amount of ettringite, $C_6AS_3H_{32}$ and C_4A_3S in 15 minutes. The hydration of $C_4A_3\bar{S}$ is very fast and in 120 minutes reaction, only small amount of it remained unreacted. The rate of ettringite formation increases with the time due to further reactions and increasing crystallization. Formation of calcium magnesium silicate was seen in all the samples.

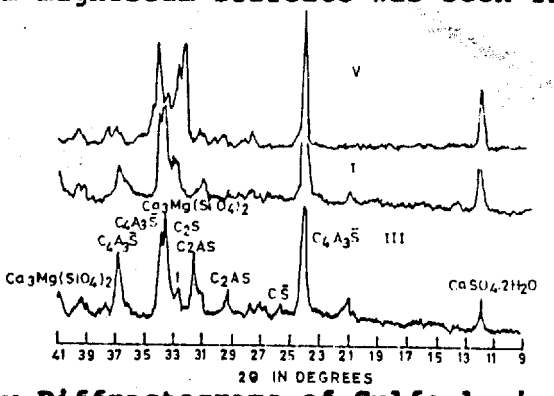

Fig.1 X-Ray Diffractograms of Sulfoaluminate Cements



Fig. 2 SEM of fracture surface of Sulfoaluminate clinker

The optical microscopy of hydrated cement samples (Fig 3) along with the surface showed formation of needle shaped structure in 15 minutes hydration and well developed crystals were seen in 30 minutes. Development of needles and compact structure led to high early strength as shown in Table 3.

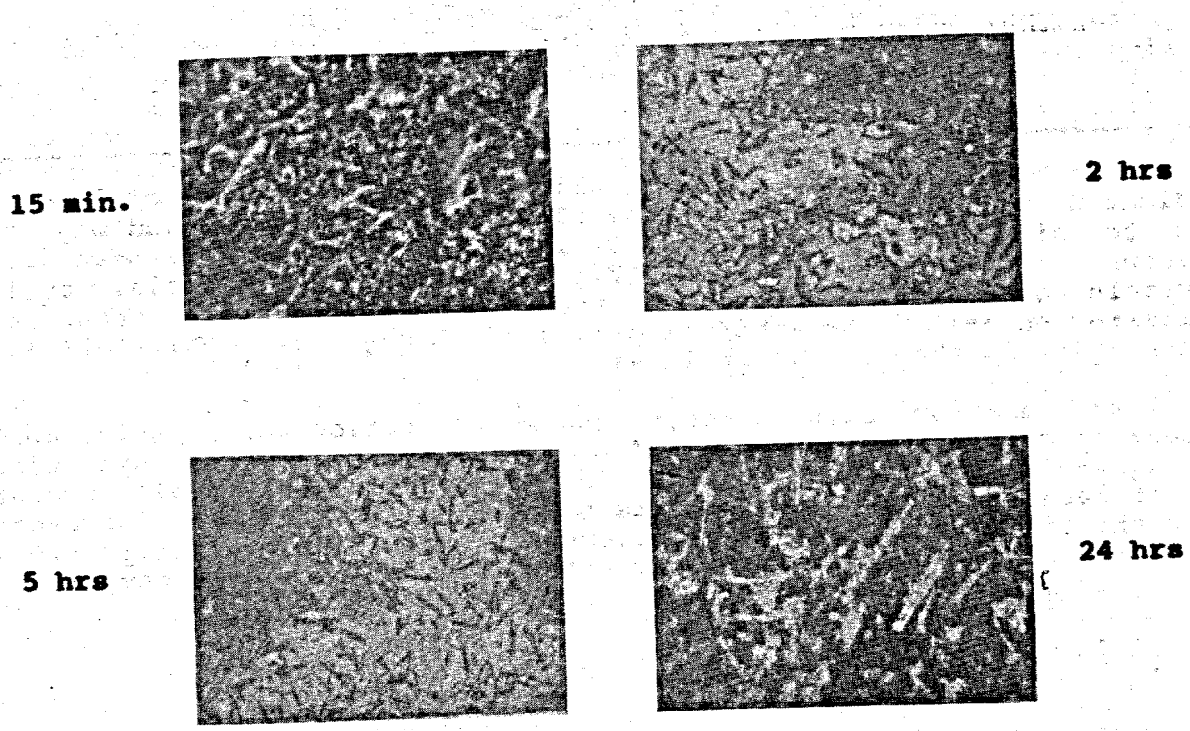

FIG. 3 Micrographs of Hydrated Sulfoaluminate Cement Samples (270x)

TABLE 3

PERFORMANCE CHARACTERISTICS OF CEMENT SAMPLES

Composition	Fineness M^2/Kg	Dimensional change in autoclave (%)	Compressive Strength, N/mm^2			
			1D	3D	7D	28D
I	260	-0.05	37.0	43.5	47.0	49.0
II	250	-0.026	17.0	22.7	24.5	29.0
III	260	-0.036	16.5	21.0	24.0	30.0
IV	240	-0.047	24.5	30.0	34.0	36.0
V	300	0.25	21.5	24.0	30.0	36.0
VI	300	0.40	30.0	41.5	46.0	48.0

Dimensional changes during hydration under autoclave conditions showed shrinkage in the range of 0.02 to 0.05 percent in cement with MgO as high as 10% assimilated as calcium Magnesium silicate. Cement sample (V) with further increase in MgO content i.e. 11.92 % indicated expansion. However the compressive strengths attained at early ages were appreciable for all the samples compared to the minimum values percribed in case of ordinary portland cement. However the rate of strength gain at 1 and 3 days were comparatively higher. The relatively poor strength in composition II and III is due to formation of gehlenite phases in clinker samples and lowering in $C_4A_3\bar{S}$ phase. These cements are suitable for use in sulfate bearing aggressive environment owing to supersaturation with respect to sulfate.

CONCLUSIONS

1 Sulfoaluminate phase bearing clinker prepared at 1350°C have shown substantial assimilation of MgO in the form of stable $Ca_3MgSi_2O_8$ resulting lowering in C_2S.

2 Cement samples with as high as about 10 persent MgO assimilated have shown dimensional stability under conditions of accelerated hydration.

3 The cement samples have higher early strength compared to that of ordinary portland cement.

ACKNOWLEDGEMENT

The authors are thankful to Director General, National Council for Cement and Building Materials, New Delhi, India for giving permission to publish the work done.

REFERENCES

1 Francis Hanayawa:" Technical note on Calcium Sulfoaluminate" **Cement**, 1975, CBI 2:75.

2 Ikada, K.:" Cements along the join $C_4A_3\bar{S}$ - C_2S", **Paris Symposium on Chemistry of Cement**, 1980, Vol.III - 31.

3 Mehta P. K.:" Investigation on Low Energy Cements", **World Cement Technology**, 1980, May, 166-177.

4 Schlandt C. M. and Roy D. M.:" The join Ca_2SiO_4 - $CaMg\ SiO_4$", **J AM Ceram Soc**, 1966, 49 (8), 430 - 432.

EXAMINATION OF $12CaO.7Al_2O_3$ PHASE DOPED WITH MAGNESIUM, IRON AND TITANIUM OXIDES

Z Konik, A Stok and J Iwanciw

Academy of Mining & Metallurgy, Cracow, POLAND

SUMMARY

The phase $12CaO.7Al_2O_3$ is not only a constituent of aluminous and Portland cements, but also a main component of self- disintegrated powder, an intermediate product in alumina and cement technology by J.Grzymek's method.
Pure $12CaO.7Al_2O_3$ as well as material doped with iron, titanium and magnesium oxides added as 0.5;1.0 and 1.5 % wt. was synthesized at 1723K. The samples were cooled in furnace down to 300°C and subsequently in air. A difference in colour was observed in particular group of samples. All the samples were fused; on their surface crystallized polycrystals of 3 to 20 mm length. The most optically perfect polycrystals crystallized from the sample containing 0.5 % wt. Fe_2O_3.
The samples were studied by XRD and by optical and scanning microscopy, and tested by aqueous sodium carbonate solution extraction.
Examination by those techniques shows the influence of MgO, Fe_2O_3 and TiO_2 additions on the quantity of iso- and anisotropic phases of $12CaO.7Al_2O_3$ formed and the size and shape of these crystal phases.
They also revealed considerable differences in the degree of extraction of aluminium oxide from MgO doped $12CaO.7Al_2O_3$ phase in comparison to Fe_2O_3 and TiO_2 doped $12CaO.7Al_2O_3$ phases.

RESUME

La phase $12CaO.7Al_2O_3$ est un constituent important de clinker alumineux et des agglomérés pour la production d'alumine et ciment par la méthode de J.Grzymek.
On a étudie l'influence de Fe_2O_3 , TiO_2 et MgO introduits en 0.5, 1.0, et 1.5 % sur la synthése de $12CaO.7Al_2O_3$ à 1723K. Toutes les échantillons était fonduées et refroidies dans le fourneau jusqu' à la témperature 300°C ,et puis exposées à l'air. Les matériaux avaient été les couleurs differents et les cristaux d'aluminate de dimension entre 3 et 20 mm s'apparaient à leur surfaces. En présence de 0.5 % Fe_2O_3 on a observé les formes parfaitment elevées.
Les aluminates ont éte étudiés par la diffraction aux rayons X, par la microscopie et microscopie à balayage, ainsi que soumis à l'éxtraction par la solution de Na_2CO_3 .
Les résultats montrent que la proportion entre la iso- et anisotrope phase aussi que les dimensions et structure des cristeaux sont influencées par l'addition de MgO, Fe_2O_3 et TiO_2 . Le taux d'éxtraction de Al_2O_3 change en présence de MgO.

INTRODUCTION

Substantial doubts arise when the calcium aluminate phase $12CaO.7Al_2O_3$ is subjected to detailed studies on its structure and properties. There are many controversial data on the structure of this aluminate and its polymorphism. Our own studies on this phase show that the properties of $12CaO.7Al_2O_3$ are strongly influenced by the conditions of synthesis and cooling [1,3,5]. The occurrence of $12CaO.7Al_2O_3$ polymorphs has been also confirmed. It was found that the regular $12CaO.7Al_2O_3$ consists of the two modifications, the optically isotropic and the anisotropic ones [2,4,6].
The results of investigations on $12CaO.7Al_2O_3$ phase doped with magnesium, iron and titanium oxides are presentedin this study.

RESULTS

Pure $12CaO.7Al_2O_3$ phase, obtained from a mixture of weight ratio $CaO:Al_2O_3$ = 0.94, as well as the one doped with iron, magnesium and titanium oxides added as 0.5, 1.0 and 1.5 % wt. were synthesized by heating at 1723K in a superkanthal furnace for 1 hour. Samples were cooled down in the furnace itself up to 300°C and subsequently in air.
A change in colour was observed in one group of samples. Pure $12CaO.7Al_2O_3$ phase and the one doped with magnesium oxide were distinguished by a bright-grey colour, that doped with titanium was beige in clour and that doped with iron was grey-yellow to brown colour.
All the samples were fused whereupon polycrystals of 3 to 20 mm length crystallized on their surfaces.
The most optically perfect polycrystals crystallized in the sample with 0.5 % wt. Fe_2O_3.
The samples were studied by XRD as well as by optical and scanning microscopy, and tested by 12 % aqueous sodium carbonate extraction at temp. 338K. The polycrystal obtained in the sample doped with 0.5 % wt. Fe_2O_3 was observed by optical microscope. The XRD studies were carried out on a Philips diffractometer. The microscopic observations of the 24μm polished sections were carried out in plane polarized light in Reichert MeF-2 microscope and the SEM studies of fractured surfaces in TESLA BS300 scanning electron microscope.
The polycrystals formed on the surfaces of samples doped with 0.5 % magnesium, iron and titanium oxides were cut off the fused materials. Their photographs are shown in Fig.1. The most perfect polycrystals from the sample with 0.5 % Fe_2O_3 are presented in Fig.2.

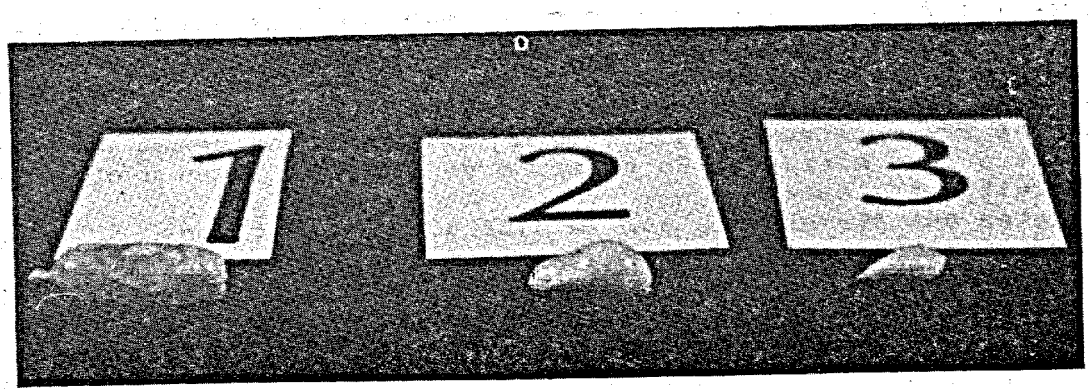

Fig.1. The polycrystal formed on the surfaces of samples doped with 0.5 % magnesium(1), iron(2) and titanium(3) oxides.



Fig.2 The polycrystals formed on the surface of sample doped with 0.5 % Fe_2O_3 .

Observations were carried out on the bottom, middle and upper parts of the polycrystals. It can be seen that the bottom parts as well as all the elongated crystals are composed of a colourless isotropic phase with the xenomorphic inclusions of anisotropic phase exhibiting the skeleton structure (Fig.3 and Fig.4).

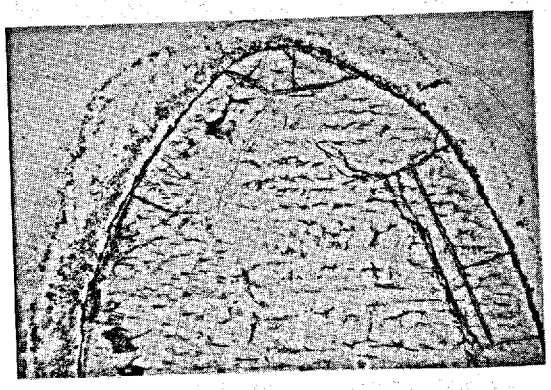

Fig.3 Nicols ||. Magnif. 30x. Polycrystal - the basic colourless mass of isotropic phase - the skeleton phase inclusion are visible.

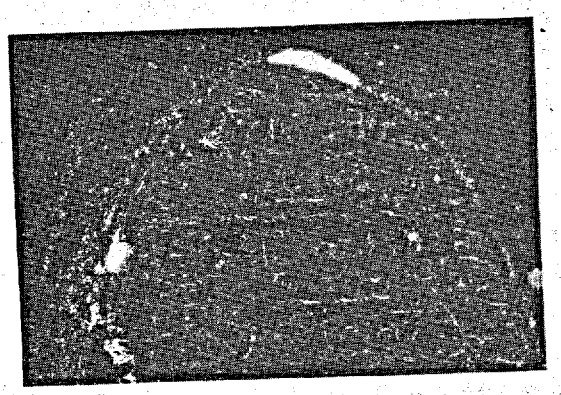

Fig.4 Nicols +. Magnif. 30x.

In all the samples doped with Mg, Fe and Ti oxides, only the regular isotropic optically $12CaO.7Al_2O_3$ phase was detected by XRD. Only slight differences in the peak intensities were found.
As will be evident from the microscopic observations, both modifications of $12CaO.7Al_2O_3$ are present in the samples. The colourless, monolithic crystal matrix is the main part of the samples. The isotropic phase occurring in the samples without additive and in those with magnesium oxide shows monolithic or crystalline microstructure. In the samples with TiO_2 this phase is crystalline and with Fe_2O_3 (1 - 1.5 %) it is monolithic. Samples with 0.5 % Fe_2O_3 exhibit both monolithic and crystalline isotropic modifications. The size and habit of isotropic phase grains is also influenced by the admixtures mentioned above. The anisotropic phase crystallizes as an interstitial phase in the area between the isotropic phase forming the xenomorphic crystals of skeleton structure. Only in the 1.5 % TiO_2 doped sample does the crystalline anisotropic phase coexist with the anisotropic one. The anisotropic phase content in the samples increases with admixture and its distribution becomes more uniform (Fig.5,6,7,8,9,10,11,12,13 & 14).

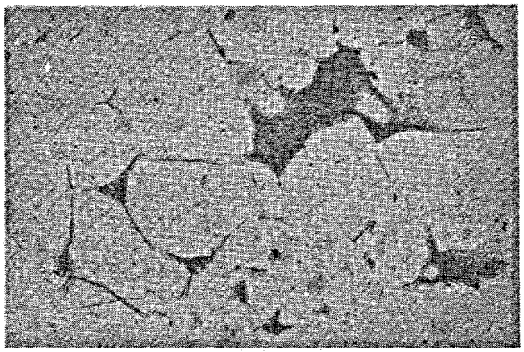

Fig.5 Nicols ||. Magnif. 75x.
$12CaO.7Al_2O_3$ without additive. Isotropic phase grains of basic mass and xenomorphic skeleton crystals of anisotropic phase are visible.

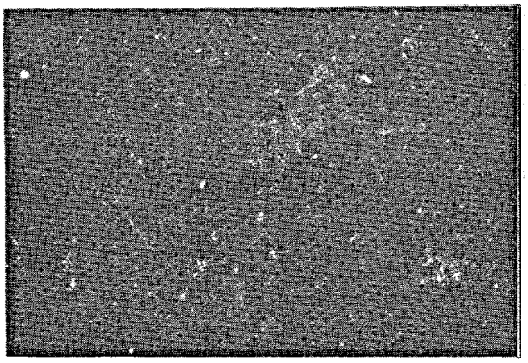

Fig.6 Nicols +. Magnif. 75x.

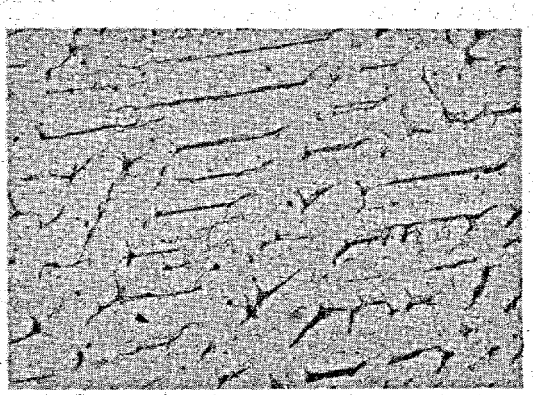

Fig.7 Nicols ||. Magnif. 75x.
$12CaO.7Al_2O_3$ with 1.5 % MgO addition. In colourless isotrpic main phase the xenomorphic skeleton crystals of anisotropic phase are visible.



Fig.8 Nicols +. Magnif. 75x.

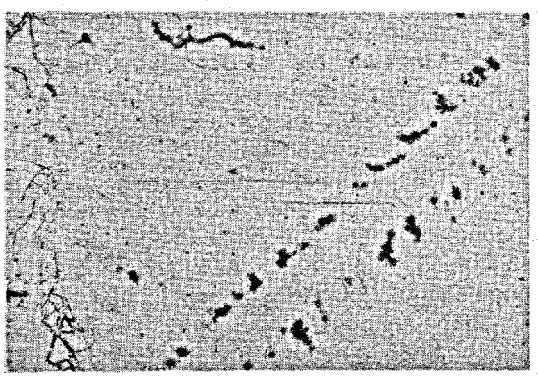

Fig.9 Nicols ||. Magnif. 75x.
$12CaO.7Al_2O_3$ doped with 1.5 % Fe_2O_3. In monolitical colourless isotropic main phase the inclusions of anisotropic skeleton phase ere visible.



Fig.10 Nicols +. Magnif. 75x.

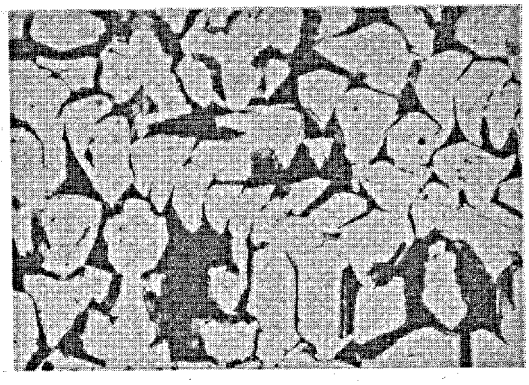

Fig. 11 Nicols ||. Magnif. 75x.
$12CaO.7Al_2O_3$ doped with 0.5 % TiO_2. Visible the basic mass of colourless isotropic crystals and the xenomorphic anisotropic phase.

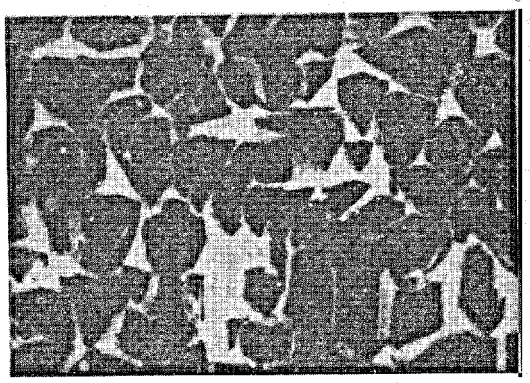

Fig. 12 Nicols +. Magnif. 75x.

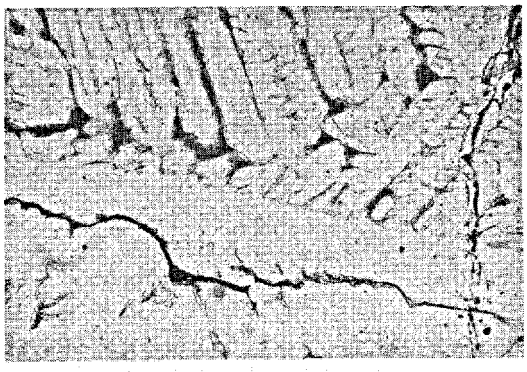

Fig. 13 Nicols ||. Magnif. 75x.
$12CaO.7Al_2O_3$ doped with 0.5 % Fe_2O_3. In the main isotropic phase the anisotropic skeleton phase is also visible.

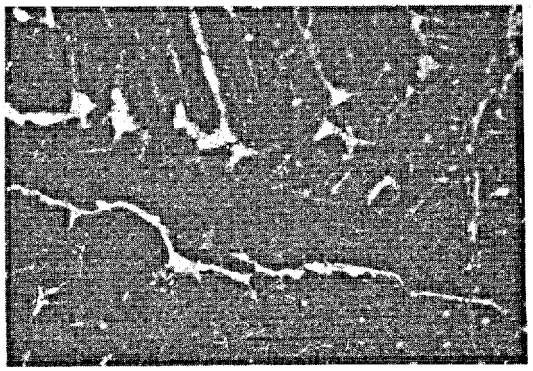

Fig. 14 Nicols +. Magnif. 75x.

Results of the scanning electron microscope observations showed cracks, bulges and cavities on the surface of samples(see Fig. 15, 16).

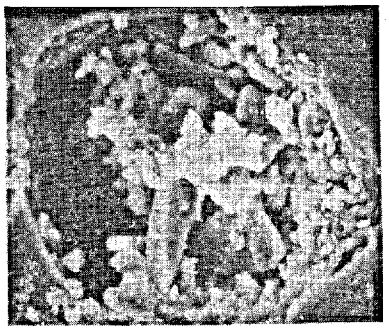

Fig. 15 SEM. $12CaO.7Al_2O_3$ with 0.5 % Fe_2O_3. 2000X.



Fig. 16 SEM. $12CaO.7Al_2O_3$ with 1 % TiO_2. 1000X.

The tests of Al_2O_3 extraction from the $12CaO.7Al_2O_3$ samples show that the MgO admixture brings about a 10 - 20 % extraction decrease when added at 0.5 - 1.5 %. The results of these tests are presented in Fig. 17.

While extracting with 12 % aqueous Na_2CO_3 aluminium is leached out and occurs as an aluminate ion but calcium precipitates as $CaCO_3$. The XRD data indicate that $CaCO_3$ occurs as calcite, vaterite or aragonite, depending on the admixture used in the synthesis. Only in the precipitate after the extraction of aluminate doped with 1 % MgO, are all the above mentioned three phases detected simultaneously. In the other samples $CaCO_3$ occurs as calcite and vaterite. The calcite phase dominates in the precipitates from pure aluminate or aluminate doped with Fe_2O_3. The highest amount of vaterite was detected in the samples containing MgO and TiO_2. In the MgO containing samples unreacted $12CaO.7Al_2O_3$ can be detected.

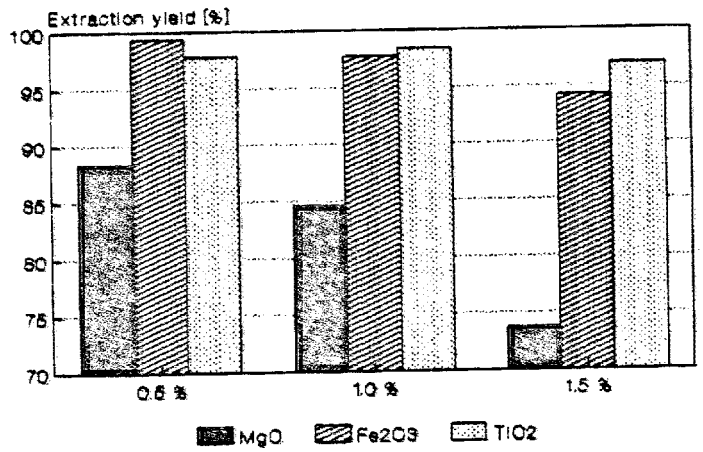

Fig.17. The extraction yield of Al_2O_3 from $12CaO.7Al_2O_3$ phase versus type and percentage of admixture.

CONCLUSIONS

i. The introduction of admixtures of magnesium, iron and titanium oxides into the $12CaO.7Al_2O_3$ phase affects the anisotropic $12CaO.7Al_2O_3$ content as well as the size and habit of isotropic $12CaO.7Al_2O_3$ crystals.
ii. MgO admixtures inhibit alumina extraction from $12CaO.7Al_2O_3$.

REFERENCES

1. J,Grzymek, A.Derdacka-Grzymek, Z.Konik, A.Stok, M.Pyzalski :"Bedutung der Polymorphen Umwandlung des Kalziumaluminats $C_{12}A_7$ als Grundlage des Komplexverfahrens zur Gewinnung von Portlandzement", Eisen und Tonerde. Baustoffindustrie, 1985, 3, 72-74.
2. J,Grzymek, A.Derdacka-Grzymek, Z.Konik, M.Pyzalski, A.Stok, J.Iwanciw: :"The Effect of Synthesis and Cooling Conditions on Phase Properties of the $C_{12}A_7$", 8th International Congress on the Chemistry of Cement, Vol.IV Rio de Janeiro, 1986, 401-406.
3. J,Grzymek, A.Derdacka-Grzymek, Z.Konik, M.Pyzalski, A.Stok, J.Iwanciw: "Some Physicochemical Properties of $12CaO.7Al_2O_3$ Phase in Relation to Al_2O_3 Production from Self-Disintegrating Sinters", Light Metals AIME, 1987, 91-97.
4. Z.Konik, M.Pyzalski, J.Iwanciw, A.Stok :"DTA Studies of $12CaO.7Al_2O_3$ Polymorphism", Journal of Thermal Analysis, 1987, 32, 1727-1729.
5. J.Grzymek, A.Derdacka-Grzymek, Z.Konik, A.Stok, J.Iwanciw :"The New Way of Alumina Lixiviation from Sinters Containing $12CaO.7Al_2O_3$ in J.Grzymek's Method". Light Metals AIME, 1988, 129-134.
6. A.Derdacka-Grzymek, Z.Konik, J.Iwanciw, A.Stok :"Scanning Electron Microscope Observations of Polymorphic Transitions Occuring on $12CaO.7Al_2O_3$ Surface under Electron Beam Action", Journal of Materials Science 1989, 24, 355-358.

Ca_2AlMnO_5: STUDIES ABOUT ITS CHARACTERIZATION AND HYDRATION

F Puertas, M T Blanco, S Martínez and R Domínguez

Instituto de Ciencias de la Construcción "Eduardo Torroja" (C S I C), Madrid, SPAIN

ABSTRACT

A new compound with formula Ca_2AlMnO_5 has been synthesized and characterized. The characterization has been carried out through X-ray Diffraction, IR Spectroscopy and Electron Spin Resonance. It has been established that Ca_2AlMnO_5 has an orthorrombic structure in which manganese in the form of Mn^{3+} is occupying tetrahedral and octahedral positions in the lattice.

The reactivity of Ca_2AlMnO_5 in water has been studied as well. The hydration was done in presence and in absence of gypsum. Both reactions are highly exothermal giving to different products. When gypsum is not present, an hexagonal hydrate and very stable phase containing Mn is formed.The conversion of that hexagonal phase to a more stable cubic form is very slow. In the presence of gypsum, the most important product of hydration is an ettringite-like phase with Mn in its lattice.

RESUMEN

Se ha sintetizado y caracterizado un nuevo compuesto de fórmula Ca_2AlMnO_5. La caracterización se ha realizado a través de Difracción de Rayos X, Espectroscopia IR y Resonancia Magnética Nuclear. Se ha determinado que el Ca_2AlMnO_5 tiene estructura ortorrómbica, en la que el Mn^{3+} ocupa tanto posiciones tetraédricos como octoédricas en la estructura cristalina.

Se ha estudiado, igualmente, la reactividad del Ca_2AlMnO_5 en agua. Ambas reacciones son fuertemente exotérmicas dando lugar a diferentes productos de hidratación. En ausencia de yeso, se forma un hidrato hexagonal muy estable que contiene Mn en su estructura. La conversión de esta fase hexagonal a otra más estable de estructura cúbica es muy lenta. En presencia de yeso, el producto de hidratación más importante es una fase tipo etringita con Mn en su estructura.

INTRODUCTION

Manganese is only occasionally present at levels > 0,5% in cement making raw materials, but may be added, contained within metallurgical slags incorporated into clinkering batches.

The behaviour of manganese in the clinkering process has been studied by many authors (1-4). From these studies it has been implied that in ordinary clinkers, which contain a ferrite phase much of the manganese is incorporated in this phase, rather than silicate and aluminate phases. Puertas and Glasser (5) determined the maximum incorporation limit of Mn in the crystalline structure of Ca_2AlFeO_5, which was close to 6.67% weight. These results are opposed to those obtained by T. Sakurai (6) who noted the existence of a continuous solid solution series in the line Ca_2AlFeO_5-Ca_2AlMnO_5. This author was the first researcher who pointed out the existence of a new compound whose empirical formula was Ca_2AlMnO_5. Sakurai asserted also that this phase (Ca_2AlMnO_5) was isomorphous with the ferrite phase of the clinker of OPC (Ca_2AlFeO_5).

This new compound was also detected when the effect produced by Mn substitution in C_3A (7) was studied. The main conclusion resulted from this work was that in presence of CaO and Al_2O_3, Mn chiefly reacts so as to produce Ca_2AlMnO_5, slightly reducing the contents of C_3A. The non-existence of structural and chemical data about Ca_2AlMnO_5, as well as that its reactive behaviour towards water, are the starting points of this paper which, aims at: i) establishing chemical and structural characterization of the new phase, Ca_2AlMnO_5 and, ii) studying its reactivity to water, in the absence as well as in the presence of gypsum.

EXPERIMENTAL

Ca_2AlMnO_5 was synthesized from reagent-grade materials: Merck reagent $CaCO_3$ and Al_2O_3, and BDH manganese (II) oxalate. The stoichiometric mixture was blended in agate mortar using ethanol as a dispersing medium. The dry sample was heat treated at 1350ºC during 50 hours, applying 4-5 intermediate grinding in order to increase the system homogeneity.

The product obtained was analysed by the following instrumental techniques: X-ray diffraction, IR spectroscopy and Electron Spin Resonance. X-ray d-spacings were determined using silicon internal standard.

The hydration tests were made in the absence and in the presence of gypsum, as follows:

- Hydration in the absence of gypsum: Small portions of the water free samples screened to a particle size < 88 μm, were mixed with a deonized and decarbonated water at a w/c = 0.5. The mixing time was held constant for 3 minutes.

- Hydration in the presence of gypsum: From the hydration reaction of C_4AF with gypsum and water proposed by Fukuhara et at (8), i.e.

$$3C_4AF + 12C\bar{S}H_2 + 10H \longrightarrow 4C_3(A_{0.75}F_{0.25})C\bar{S}H_{31} + 2FH_3$$

Ca_2AlMnO_5/gypsum ratio of 1:4 was established

The homogeneous blends of Ca_2AlMnO_5 and gypsum were mixed with water at a w/c = 0.5.In order to avoid carbonating phenomena in both hydration tests, the pastes were collected and kept in glass tubes which had been previously saturated with N_2.The pastes were extracted and frozen with acetone and ethanol after ageing for 1, 7 and 28 days. These samples were analyzed by XRD, IR spectroscopy, SEM and EDX.

In addition C_2AlMnO_5 hydration in the absence and presence of gypsum was studied by conduction calorimetry, testing the samples in a conduction calorimeter at constant temperature (20ºC) over 24 hours.

RESULTS AND DISCUSSION

a) Chemical and structural characterization of Ca_2AlMnO_5

* X-Ray Diffraction

The record was carried out by means of an angular range of 2θ = 5º to 80º. The d-spacings and relative intensities of the reflections obtained in the test for Ca_2AlMnO_5, along with its respective hkl values corresponding to an orthorombic cell of a primitive type are showed in (9).

Comparing the characteristic diffraction lines of Ca_2AlFeO_5 in the 30-226 file of the JCPDS (10), with those of Ca_2AlMnO_5 proposed in that work, it can be asserted that Ca_2AlMnO_5 is a separate and independent compound from Ca_2AlFeO_5.

The crystallographic analysis applied to Ca_2AlMnO_5 has shown that this compound is isomorph to ferrite phase, Ca_2AlFeO_5, with an orthorhombic structure. The cell parameters of Ca_2AlMnO_5 are:

$$a_o = 5.465 \pm 0.001 \text{ Å}$$
$$b_o = 14.904 \pm 0.002 \text{ Å}$$
$$c_o = 5.244 \pm 0.002 \text{ Å}$$

* **IR Spectroscopy**

The IR spectrum of Ca_2AlMnO_5 (see figure 1) shows bands (320 and 440 cm^{-1}, 725, 770 and 815 cm^{-1}) that, because of their similarity to the Ca_2AlFeO_5 IR spectrum (11), can be considered derived from the vibrations of AlO_6 and AlO_4, respectively.In addition, in Ca_2AlMnO_5 IR spectrum new bands with large intensity located in 375 and 635 cm^{-1} are found. The origin of these absorptions has been clarified by studying IR spectra of the $Ca_2Al_2Fe_{2-x}Mn_xO_{10}$ series (9). These studies showed some changes in the characteristic zone of vibration of AlO_4 and FeO_4 groups (600-800 cm^{-1}) and a new band about 630 cm^{-1} appears when the proportion of Mn replaced in Ca_2AlFeO_5 is raised. Consecuently, we interpret the strong band at 635 cm^{-1} due to Mn-O vibrations of MnO_4 groups. In the 350-450 cm^{-1} zone, an increase of the absorption is produced as the X values, in the mentioned series, are increased. This is noticed in the spectrum by a loss of clearity in the bands due to AlO_6 groups (440 cm^{-1}) originated by the overlapping with a new absorption at 380 cm^{-1}.The very strong band at 375 cm^{-1} in the Ca_2AlMnO_5 spectrum is interpreted as due to Mn-O vibrations of MnO_6 groups in the Ca_2AlMnO_5 structure.

* **Electron Spin Resonance**

By this technique the new compound, Ca_2AlMnO_5 was studied. The spectrum obtained for this phase showed no wide band nor any hyperfine structure which would be an indication of the presence of unpaired electrons either Mn^{2+} (d^5) or Mn_{4+} (d^3). It must be remember that Mn^{3+} (d^4 configuration) has no unpaired electrons and therefore gives no electron spin resonance signals. The results obtained by ESR has showed that Mn in Ca_2AlMnO is the oxidation state +3.

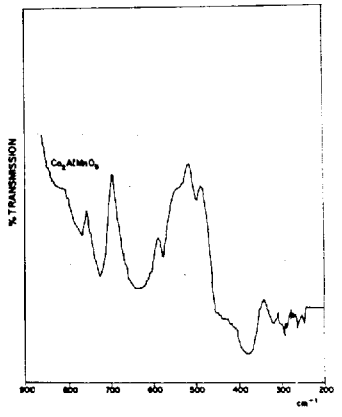

FIGURE 1
IR spectrum of Ca_2AlMnO_5

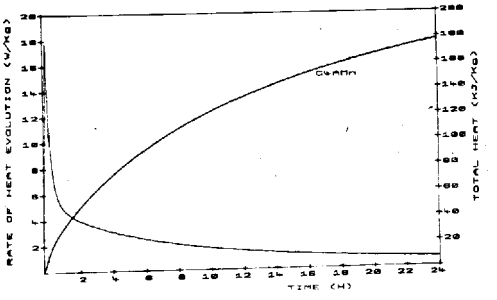

FIGURE 2
Conduction Calorimetric curves
of Ca_2AlMnO_5 hydrated with water

b) Studies about the hydration process of Ca_2AlMnO_5

- Hydration in the absence of gypsum

Figure 2 shows the heat evolution rates and total heat release during the first 24 hours hydration for Ca_2AlMnO_5. This recording has only a single peak corresponding to maximum heat release during the first half hour of hydration. The results obtained, from analysis of the hydrated pastes, by XRD, IR spectroscopy and SEM data, suggest that this heat release peak is due to formation of a hydrate of hexagonal nature.

The results obtained from XRD analysis of C_2AlMnO_5 hydrated pastes show that for one day ageing the hydrates identified are hexagonal, di-calcium, as well as tetracalcium compounds. These hexagonal hydrates remain stable, even after seven days hydration. At 28 days, the major hydration product detected in the sample was a cubic hydrate, although at trace level the presence of hexagonal hydrate still persists.

The IR spectra of the frozen samples (see figure 3) confirm the mineralogical composition as determined by XRD. The IR spectra of the one and seven days pastes are practically identical. The bands located at 3685-90 and 3540-45 cm^{-1}, were assigned by Volant (12) to OH^- group vibrations of a tetracalcium aluminate hydrate (type C_4AH_9). The absorption band at 2990-3000 cm^{-1}, is characteristic of highly hydrated carboaluminates.

Furthermore the bands situated at 780, 600, 530, 420, 305 and 250 cm^{-1} confirm the presence of a hexagonal hydrates. The very strong absorption near 1405 cm^{-1}, is assigned to carbonate-like, probably carboaluminate types.

The IR spectrum of the 28 day sample differs notably from the previous one. A sharp band at 3645 cm^{-1} can be assigned as characteristic of OH^- vibrations in hydrated calcium aluminate of the cubic type. In the 1300-200 cm^{-1} zone, strong bands assignable to cubic hydrates (527, 400 and 375 cm^{-1}) are present. There persist other and much weaker one at 420 and 300 cm^{-1}, attributable to the Al-O and Ca-O vibrations of hexagonal hydrates. SEM and EDX analysis of the pastes reveals that the hexagonal hydrates are present in the form of hexagonal platelets (micrograph nº 1). Point analysis of these platelets proves that these hydrates have Mn, although in considerable lower proportion than in anhydrous Ca_2AlMnO_5. In one day sample, the Al/Mn ratio in these hexagonal hydrates has a mean value of 3.5. In this sample was found, by SEM, amorphous AH_3, but in spite of exhaustive analysis, no manganese oxide or hydroxide was detected.

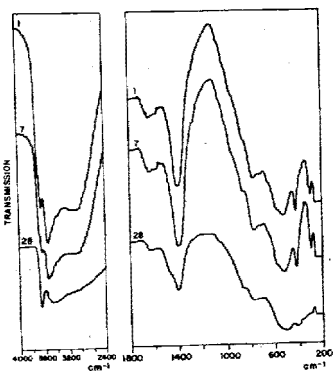

FIGURE 3
IR spectra of hydrated Ca_2AlMn_5 pastes at 1,7 and 28 days

The cubic hydrate at 28 days (micrograph nº 2) shows an Al/Mn ratio in the order of 1.75. This value is remarkably lower than that found hexagonal hydrates (Al/Mn = 3.5), it is assumed that in the cubic hydrates more manganese is incorpored than in the respective hexagonal structure.

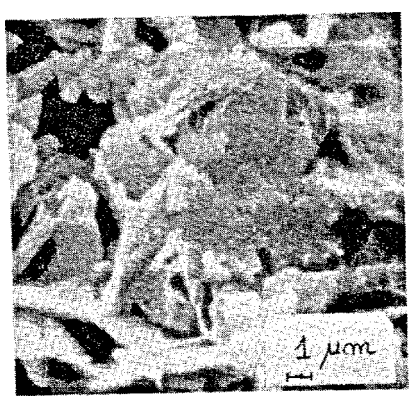

MICROGRAPH 1

Hydrated pastes of Ca_2AlMnO_5 at one day. Hexagonal hydrates



MICROGRAPH 2

Hydrated pastes of Ca_2AlMnO_5 at 28 days. Cubic hydrates

Hydration in the presence of gypsum

Figure 4 shows the heat evolution rate and total heat release in Ca_2AlMnO_5 hydration during the first 24 hours. This calorimetric curve presents a single high intensity signal, associated with heat release in the first half hour of hydration. This signal is attributable, in the light of the results obtained in this research, to the formation of an ettringite like phase.

The retarding effect of gypsum in Ca_2AlMnO_5 hydration is minimal or practically non-existent as can be seen when comparing the calorimetric curves in the absence and presence of gypsum (fig. 2 and 4, respectively). In full agreement with the calorimetric data, XRD analysis, IR spectroscopy and SEM of the hydrated samples at 1, 7 and 28 days, reveal the high ettringite formation rate in Ca_2AlMnO_5 - hydration. In the first 24 hours of hydration, the greater amount of ettringite like phase detected by XRD, is formed; the reaction seems to have exhausted itself by day 7, as the amount of ettringite detected on 28 day is practically identical to the one recorded for the frozen paste after 7 hydration days.

Analysis of the hydrated samples by IR spectroscopy confirms the results described for XRD. Figure 5 shows the IR spectra in the 4000-200 cm^{-1} range, of the hydrated samples of Ca_2AlMnO_5 at 1,7 and 28 days of hydration.

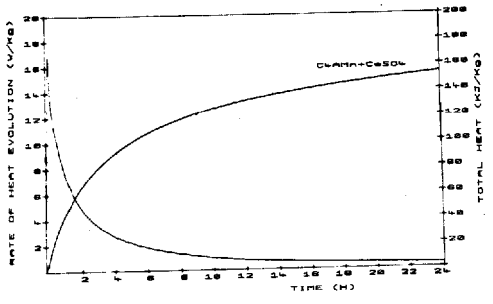

FIGURE 4

Conduction calorimetric curves of Ca_2AlMnO_5 hydrated with water and gypsum

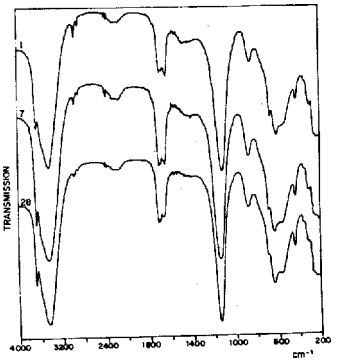

FIGURE 5

IR spectra of pastes in presence of gypsum

The bands which can be used to identify the presence of ettringite in these IR spectra, since there is no overlap with bands attributable basically to gypsum, are positioned at 3635, 3420, 855, 629, 535 and 425 cm^{-1}. These absorptions appear quite clearly in the IR spectrum of the Ca_2AlMnO_5 paste hydrated for one day, its intensity being enhanced at 7 days and showing practically no modification on day 28. Parallel to the increment of intensity of these bands, the sharpness of the gypsum bands are observed to become weaker.

SEM analysis of these pastes shows that the morphology of the ettringite like phases, generated from Ca_2AlMnO_5 hydration, is in the form of longer crystals. The composition of this ettringite phase was determined by EDX. This phase has incorpored Mn in its structure, with a Al/Mn ratio of 3.6.

CONCLUSIONS

The main conclusions drawn from this study can be summarized as follow:

1.- Ca_2AlMnO_5 is a separate and independent compound from Ca_2AlFeO_5. Ca_2AlMnO_5 has an orthorrombic structure in which manganese, in the form of Mn^{3+}, is occupying tetrahedral and octahedral positions in the lattice.

2.- In the absence of gypsum, the hydration reaction of Ca_2AlMnO_5 generates hydrates of the hexagonal type, which contain Mn in their structure. These hydrates have a high degree of stability, and their conversion into cubic hydrates is very slow. In the presence of gypsum, the hydration reaction of Ca_2AlMnO_5 produces an ettringite like phase with Mn incorporated in its structure. Both reactions are highly exothermal.

ACKNOWLEDGEMENT

The authors wish to thank the Dirección General de Investigación Científica y Técnica for the financing of the PB0293 Project without this paper could not have been possible.

REFERENCES

1.- Gutt, W., Osborne, G.J. "The effect of manganese, iron and fluorine on the properties of tricalcium silicate". Transaction of the British Ceramic Society, vol. 68, pp. 129-36 (1969).

2.- Knofel, D., Strunge, J., Bambuer, H.V. "Effect of manganese on the properties of portland cement". Zement-Kalk-Gips. Vol. 12, pp. 651-5 (1984).

3.- Puertas, F., Glasser, F.P., Blanco-Varela, M.T.; Vázquez, T- "Influence of the kiln atmosphere on manganese solid solution in Ca_3SiO_5 and Ca_2SiO_4". Cem. Concr. Res. Vol. 18, pp. 783-88 (1988)

4.- Puertas, F; Blanco-Varela, M.T.; Vázquez, T. "Sustitucion del manganeso en las fases del clinker del cemento portland" Materiales de Construcción, Vol. 39 nº 214 (1989).

5.- Puertas, F.; Glasser, F.P.; "Modification of the ferrite phase in cements by manganese substitution". Advances in Cement Research, Vol. nº 1, pp. 31-34 (1987)

6.- Sakurai, T. "The behaviour of manganese in cement clinker minerals". Review of the 14th General Meeting, Japan Cement Engineering Assoc. Tokyo, pp. 23-24 (1960).

7.- Puertas, F.; Soria, J.; Blanco-Varela, M.T.; Vázquez, T. "Modification on the tricalcium aluminate phase in cements by manganese substitution". Cem. Concr. Res. Vol. 18, pp. 837-842 (1988)

8.- Fukuhara, M.; Goto, S.; Agata, K.; Diamon, M.; Kondo, R. "Mechanism and kinetics of C_4AF hydration with gypsum". Cem. Concr. Res. Vol. 11, pp. 407-414 (1981)

9.- Puertas, F.; Blanco-Varela, M.T.; Domínguez, R. "Characterization of Ca_2AlMnO_5. A comparative study between Ca_2AlMnO_5 and Ca_2AlFeO_5". Cem. Concr. Res. Vol. 20, pp. 429-438 (1990)

10.- JCPDS International Centre for Diffraction Data. Philadelphia. U.S.A.

11.- Tarte, P. "Etude infrarroge du ferrite dicalcium $2CaO.Fe_2O_3$ et des solutions solides $2CaO\ (Al,Fe)_2O_3$". Revue de Chimie Minerale nº 1, pp. 425-438 (1964)

12.- Volant, J. "Etude par spectrométrie infrarrouge d'aluminates de calcium hydrates". Revue des Matériaux de Construction, nº 632, pp. 191-196 ; nº 633-634. pp. 257-272 ; nº 638, pp. 432-450 (1968).

BARIUM ALUMINATE CEMENT — ITS SYNTHESIS AND FORMATION KINETICS

S J Raina*, S Agarwal, M M Ali** and S K Agarwal****

**Excelon Techno Engineers Pvt Ltd*
***National Council for Cement and Building Materials*
New Delhi, INDIA

SUMMARY

Refractory cement based on barium aluminates is a special type of binding material characterised by its extra high resistance to high temperatures and thermal shocks, besides having a higher degree of radiation absorption capacity as compared to calcium aluminate cements. Being soluble in water, it is air hardening type forming a hard mass.

Monobarium aluminate (BaO.Al2O3) is the only phase formed when a mixture of equimolar quantity of AR grade BaCO3 and Al2O3 is sintered at 1450°C in the form of pellets. X-ray diffractogram shows the maximum phase development at this temperature when fired for 3 hours. In the present study on its synthesis, it was found that reaction kinetics favour formation of monobarium aluminate phase at temperatures below 1450°C by using a mineralizer. The activation energy of its formation from pure oxides with mineralizer (MgO 1.5% by weight) is 47.31 Kcal/mole, which is much lower than 68.64 Kcal/mole, the value of activation energy without mineralizer.

* Presently, General Manager, Excelon Techno Engineers Pvt Ltd., New Delhi, India

INTRODUCTION

Barium aluminate cement containing monobarium aluminate (BA) as a dominant phase, is rapid hardening similar to calcium aluminate. However, comparatively higher fusion temperature of barium aluminates leads to significantly improved refractory properties such as refractoriness and higher resistivity to thermal shocks (1-3). Another important characteristic of this cement is its capacity to absorb higher degree of radiation.

The greater reactivity of BA cement towards moisture and tendency to air setting with relatively much lower water content qualifies it for various special refractory applications. It also shows least loss of cold compressive strength during heating to elevated temperatures. It is a best suited material for use in basic refractory concretes.

In the present paper, the formation kinetics of pure monobarium aluminate phase has been studied in presence of a suitable mineralizer in order to reduce the temperature of its formation. The kinetic parameters such as activation energies have also been calculated.

EXPERIMENTATION

Pure BA phase was prepared by repeated firing of equimolar mix of AR grade BaCO3 and Al2O3 at 1450°C in the form of pellets. The formation of pure phase was confirmed by XRD. In order to study kinetics of its formation, the pellets of equimolar mixes were fired at different temperatures varying from 1150° to 1380°C for different retention times. Naber high temperature furnace was used for carrying out the firing.

Mineralogical studies on the partially heated samples were conducted on Rigaku, D/MAX-C, XRD system. The formation of BA was also studied in presence of mineralizers such as CaF2, CaSO4 and MgO in doses of 1% and 1.5% by weight. The relative peak intensity of BA phase corresponding to 2θ = 28.127 was taken as a measure of degree of reaction. The activation energies were calculated by using Arrhenius equation (4,5).

RESULTS AND DISCUSSIONS

Monobarium aluminate was the only phase formed when a equimolar mixture of BaCO3 and Al2O3 was sintered at 1450°C. Maximum phase development was achieved at this temperature when fired for 3 hours. The mineralogical evaluation of the fired samples has shown gradual increase in the intensity of BA phase with increase in temperature and time of reaction. This indicates solid state reaction between corresponding oxides such as BaO and Al2O3. Mineralizers such as CaF2, CaSO4 and MgO when added in 1% by weight of the mix, have shown comparatively higher BA phase formation in presence of MgO at 1350° C. However, an increase in dose of MgO to 1.5% by weight has shown complete stoichiometric formation at 1350°C which was attained without mineralizer only at 1450°C (Fig 1). The effect of mineralizer, CaF2 and CaSO4 was found to be marginal.

B = BaO; A = Al2O3

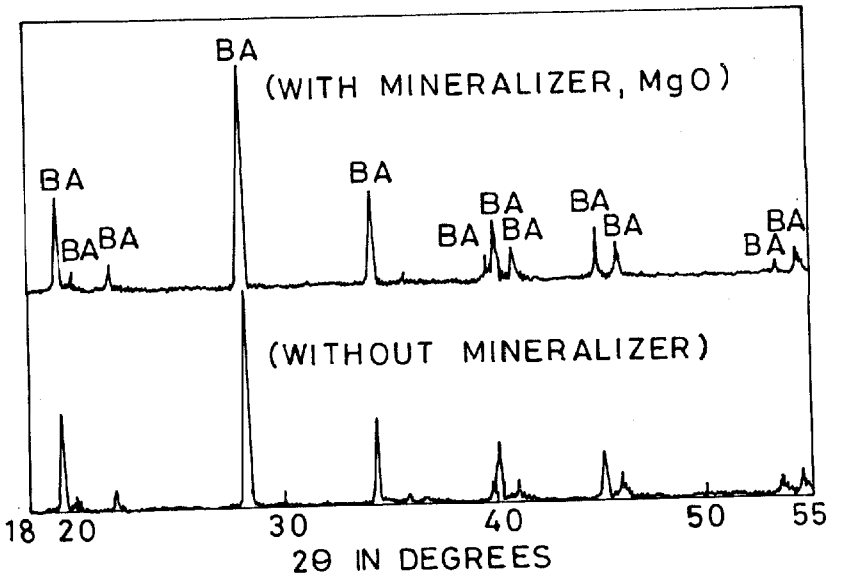

Fig 1 X-ray diffractograms of monobarium aluminate prepared from pure BaO and Al_2O_3

The rate of BA formation was studied by plotting the fraction of BA formed against reaction time at various temperatures. It was found that BA formation obeyed the rate law equation,

$$1 - (1 - x)^{1/3} = Kt$$

where x is fraction of BA formed, t is time and K is the rate constant. The plots of $1 - (1 - x)^{1/3}$ vs t, both with and without mineralizer (fig 2) show straight line relationship, the slope of which gave the value of rate constant, K (Table 1). The temperature dependence of rate constant has been used to calculate the activation energy (Fig 3), which was found to be 68.64 Kcal/mole. However, it was lowered to a value of 47.31 Kcal/mole in presence of minerlaizer (MgO 1.5% by wt.).

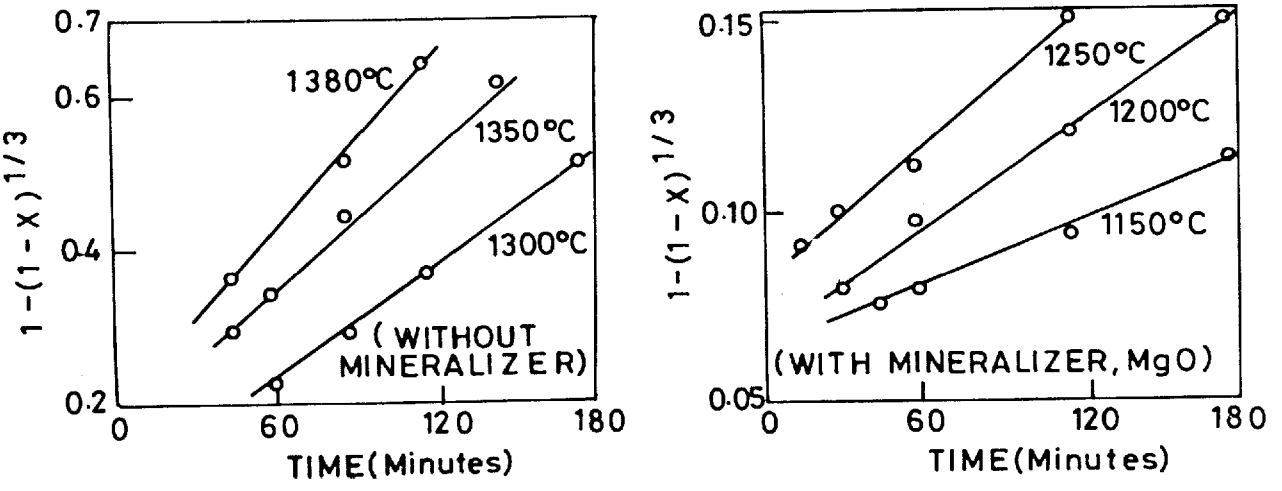

Fig 2 Rate of formation of BaO. Al_2O_3 at different temperatures

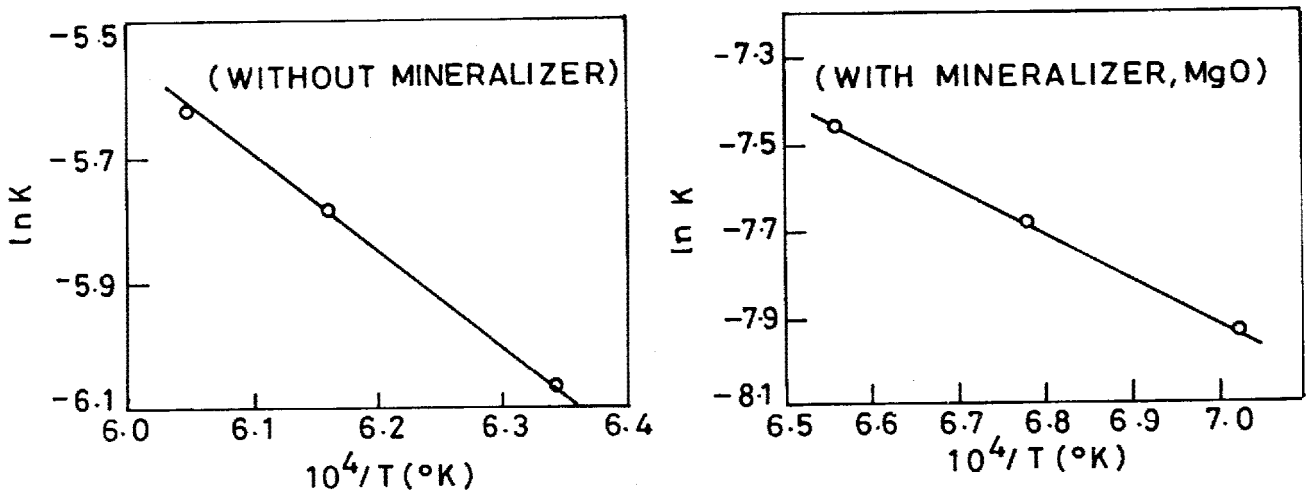

Fig 3 Temperature dependence of reaction rate

Table 1

Values of Activation Thermodynamic Functions

Mixture (mol.ratio)	Temperature (°C)	Rate Constant (K)	Activation Energy (K.cal/mole)
BaCO3+Al2O3	1300	23.3×10^{-4}	
	1350	30.83×10^{-4}	68.64
	1380	36.66×10^{-4}	
BaCO3+Al2O3 +1.5 wt% MgO	1150	35.83×10^{-5}	
	1200	46.00×10^{-5}	47.31
	1250	57.77×10^{-5}	

CONCLUSIONS

i/ The kinetics of formation of monobarium aluminate phase from the equimolar mix of pure BaO and Al2O3, studied in temperature range of 1150°to 1380° C, with and without mineralizers such as CaF2, CaSO4 and MgO, showed MgO to be most effective.

ii/ The addition of MgO, 1.5% by wt. has shown reduction in temperature of formation by 100°C.

iii/ The activation energy for the formation of BA was found to be 68.64 Kcal/mole, which on the addition of mineralizer, MgO, (1.5% by weight), was reduced to 47.31 K.cal/mole.

ACKNOWLEDGEMENT

The authors have freely drawn the information/data from published literature. This paper is being published with the permission of Director General, National Council for Cement and Building Materials, New Delhi, India.

REFERENCES

1. Braniski Al.: "Refractory Barium-Aluminous Cement and Concrete". International Symp. on the Chemistry of Cement, 4th, Washington, 1960, 1075-1091p.

2. Lea F.M.: Chemistry of Cement and Concrete, 3rd. Ed., Edward Arnold, 1970, 542p.

3. Bhaunia D.S., Mitra A. K and Chatterjee M.K.: "Hydraulic Properties of Calcium-Barium Aluminate Cements". Indian Ceramics, 1978, 20, (11), 363-367p.

4. Imlach J.A.: "Non-isothermal Investigation of Reaction Occurring During Clinker Formation". Cement and Concrete, 1976, 6, 747-756p.

5. Ali M.M., Raina S.J., and Singh V.K.: "Kinetics and Diffusion Studies in CA2 Formation". Cement and Concrete Res., 1989, 19 (1),47-52p.

MECHANISMS AT THE FORMATION OF SOME UNITARY STRONTIUM AND BARIUMSULPHATALUMINATS

I Teoreanu, M Georgescu, A Puri and A Badanoiu

Polytechnical Institute, Bucharest, ROMANIA

SUMMARY

By analogy with $3(CaO.Al_2O_3).CaSO_4$ and in correlation with the thermal stability of $SrSO_4$ and $BaSO_4$, the formation of unitary sulphataluminates in the $SrO-Al_2O_3-SrSO_4$, respectively $BaO-Al_2O_4-BaSO_4$ systems, was expected. Researches concerning the processes which occur on burning $MCO_3-Al_2O_3-MSO_4$ mixtures with different behavior of the two investigated systems (with Sr, respectively Ba). A $3(CaO.Al_2O_3)CaSO_4$-like compound is formed only in the mixtures with Strontium. In the system with Barium it is formed a more basic compound $xBaO.Al_2O_3.BaSO_4$ ($x\approx4$)

ZUSAMMENFASSUNG

Analog mit $3(CaO.Al_2O_3).CaSO_4$ und auf Grund der Temperaturbestandigkeit von $SrSO_4$ und $BaSO_4$, ist die Bildung von Sulfataluminaten in Systemen $SrO-Al_2O_3-SrSO_4$, bzw. $BaO-Al_2O_3-BaSO_4$, zu erwarten. Die Untersuchung der Vorgange beim Brennen von $MCO_3-Al_2O_3-MSO_4$ Mischungen verschiedener Basizitat zeigt ein sehr unterschiedliches Verhalten der beiden Systeme (mit Sr, bzw. mit Ba). Eine $3(CaO.Al_2O_3).CaSO_4$-artige Verbindung bildet sich nur im System mit Strontium. In dem System mit Barium entsteht nur eine basischere Verbindung $xBaO.Al_2O_3.BaSO_4$, wobei x ungefahr dem Wert 4 entspricht.

INTRODUCTION

The high thermal stability of the Strontium- and Barium sulphates (the temperature of decomposition is about 1580°C [1]), suggested as possible, the formation of Sr and Ba sulphataluminates in the SrO-Al_2O_3-$SrSO_4$ system, respectively BaO-Al_2O_3-$BaSO_4$ [2-4]. The binary systems Al_2O_3-MO (M=Ca,Sr,Ba) evident the tendency of forming binary compounds of greater basicity, as the alkali-earth metal contained is more electropositive. The most basic calcium aluminate is $3CaO.Al_2O_3$. In the case of SrO-Al_2O_3 system, there appears also a tetrastrontic compound [5], with congruent melting at about 1690°C. For the BaO-Al_2O_3 system.Appendino [6] revealed, at subsolidus temperatures of 900-1400°C, five compounds, more basic than B_3A: B_4A.B_5A.B_7A.B_8A.$B_{10}A$- with incongruity in the solid phase. In the BaO-Al_2O_3 system we notice a wider range of stability for the B_4A and B_8A compounds, as compared to the other Ba aluminates with great basicity mentioned above. Those differences noticed with the MO-Al_2O_3 systems, suggest a possible resemblance between the Sr and Ca sulphataluminate, resemblance which is less probable in the case of Ba sulphataluminate would be expected to be more basic.

In the present paper we have examinated the possibility of the formation of unitary Sr and Ba sulphataluminates, respectively, the mechanisms of the processes involved, as well as the influence of the compositional characteristics of the reactant mixtures upon the formation and thermal stability of the sulphataluminate compounds.

EXPERIMENTAL. RESULTS AND DISCUSSION.

Using $SrCO_3$, $BaCO_3$, Al_2O_3, $SrSO_4$ and $BaSO_4$ p.a., we have obtained mixtures characterized by ratios: $SrCO_3$:Al_2O_3:$SrSO_4$ = 3:3:1, $BaCO_3$:Al_2O_3:$BaSO_4$ = 3:3:1, 3:1:1, and 4.2:1:1, respectively. The choice of this compositions is supported by the above reasons and suggested by the information supplied by [4.6]. The mixtures have been burned at temperatures between 800° and 1450°C, 3-4 hours. Informations regarding the evolution of chemical processes in the investigated mixtures, their mechanism and the nature of compounds which are formed, have been obtained by the X-ray diffraction, thermal analyses and chemical ones (the carbonate content of the burned mixtures)

The $SrCO_3$-Al_2O_3-$SrSO_4$ System

The evolution of the phase composition (fig.1) shows the noticeable intensity of chemical interactions, with the formation of Sr sulphataluminate, even at relatively low temperatures (θ<1000°C) analogous to the Ca one. The Sr sulphataluminate is structurally analogous to the Ca one.

The following reactions are suggested:

$$SrCO_3 (SrO) + Al_2O_3 \longrightarrow SrO.Al_2O_3 + CO_2 \quad (1)$$

$$3(SrO.Al_2O_3) + SrSO_4 \longrightarrow 3(SrO.Al_2O_3).SrSO_4 \quad (2)$$

At lower temperatures, the first reaction may take place at lower speed, in such a way that presence of $SrO.Al_2O_3$ is evidenced at over 1100°C only.

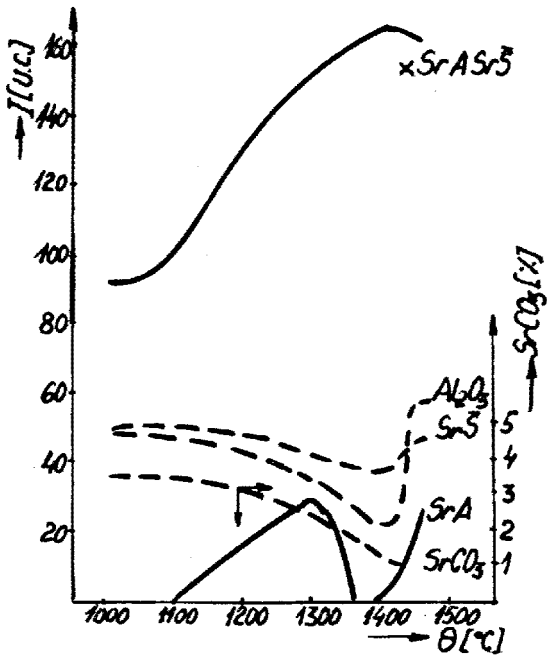

Fig.1 Evolution of mineralogical composition at the burning of $3SrCO_3+3Al_2O_3+SrSO_4$ mixtures.

Between 1100oC and 1300oC we witness a growth in intensity of the diffraction peaks both with the monostrontium aluminate and with Sr sulphataluminate, suggesting a slower rate with reaction no.(2) than with reaction no.(1). This conclusion may also be sustained by the lesser diminishing of the diffraction peaks for $SrSO_4$ than for $SrCO_3$ and Al_2O_3: the description of the sulphataluminate compound can be suggested for this temperature by the $x(SrO.Al_2O_3).SrSO_4$ formula, where $x<3$ (although close to this value).

Between 1300° and 1350°C, the monostrontium aluminate is totally exhausted.

The lesser growth in intensity of the diffraction peaks specific to Sr sulphataluminate may suggest that, within this range of temperature (1300-1350°C) there takes place especially a growth of the ratio $SrO.Al_2O_3/SrSO_4$ ($x \rightarrow 3$) from the sulphataluminate and, to a lesser degree, a growth of its proportion.

The maximum proportion of Sr sulphataluminate is achieved at temperatures of 1350°-1400°C. Over 1400°C, the sulphataluminate compound becomes thermodynamically unstable and decomposes. For the periods of the thermal treatment used, the equilibrium within the system is not achieved, even if a growth in the degree of reactant transformation is apparent with the growth of treatment period from 3 to 4 hours [2].

The $BaCO_3-Al_2O_3-BaSO_4$ System

The research carried out in this system which confirms the hypotheses considerated, reveals the influence exerted by the compound characteristics of the reactant mixtures, upon the formation and thermal stability of the Ba sulphataluminate.

In the case of $3(BaCO_3+Al_2O_3) + BaSO_4$ mixture (corresponding to the hypotetical $3(BaO.Al_2O_3).BaSO_4$), no formation of the sulphataluminate product has been evidenced at any of the burning temperatures (fig.2).

Only $BaO.Al_2O_3$ being formed with the consumption of Al_2O_3 and $BaCO_3$ (BaO), the $BaSO_4$ remaining unchanged in the burned mass. The process is speed up at temperatures over 900°C, being practically finished at about 1100°C.

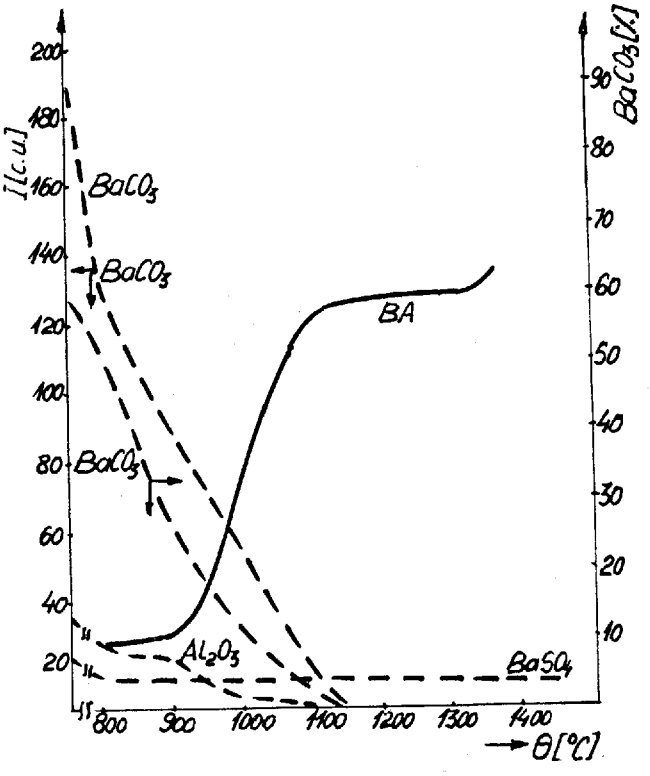

Fig. 2 Evolution of mineralogical composition at the burning of $3BaCO_3+3Al_2O_3+BaSO_4$ mixtures.

With the thermal treatment of the basic mixtures under invesigation: $xBaCO_3+Al_2O_3+BaSO_4$ characterized by $x>3$, the formation of a high basic sulphataluminate compound is noticed (fig.3 and 4), a compound found also in [4], to which the following formula can be associated: $xBaO.Al_2O_3.BaSO_4$. Its structural analogy to the compound mentioned in paper [4] (as resulted from the X-ray diffraction) justifies a value of about 4 for the x coefficient.

The absence of a compound analogous to the Ca sulphataluminate, the only reaction products decelated being $BaO.Al_2O_3$ (BA) and $xBaO.Al_2O_3.BaSO_4$ ($B_xA.BS$), as well as the fact that the $BaO.Al_2O_3$ is formed at temperature lower that the $xBaO.Al_2O_3.BaSO_4$, all this suggested the following succession of chemical processes:

$$BaCO_3(BaO) + Al_2O_3 \longrightarrow BaO.Al_2O_3 + CO_2 \quad (3)$$

$$BaO.Al_2O_3 + (x-1)BaCO_3(BaO) \longrightarrow xBaO.Al_2O_3 + (x-1)CO_2 \quad (4)$$

$$xBaO.Al_2O_3 + BaSO_4 \longrightarrow xBaO.Al_2O_3.BaSO_4 \quad (5)$$

The basic aluminate B_xA is not evidenced by X-ray diffraction.which shows that it is formed by reaction (4) in a rate lower that the one at it is exhausted in the reaction (5). However.the formation of BA is more intense that its' own exhaustion and. consequently. it can be found as a reaction product, besides the $B_xA.BS$.

The Ba sulphataluminate is reported at temperatures of about 1100°C - in case of the more basic mixtures (x=4.2). and at over 1200°C for the mixtures characterized by x=3. It is stable in both situations until about 1400°C.

The growth of the reactant mixtures' basicity causes the acceleration of the forming processes of the Ba sulphataluminate. and a bigger weight of this one in the composition of the reaction products. Fig.3 and 4 suggest at the same time a degree of disorder of the reaction products lattice, bigger in the more basic system.The

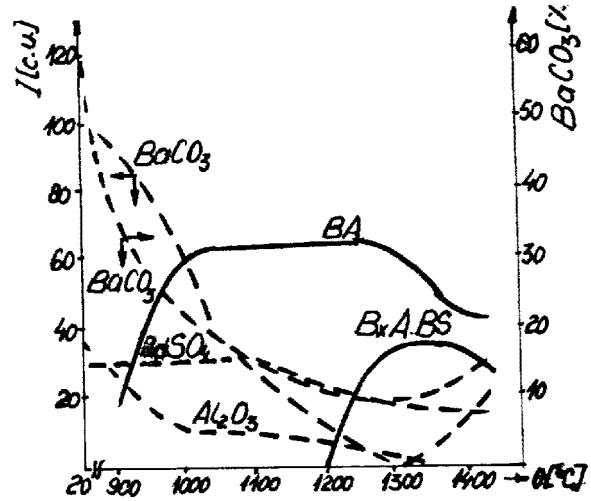

Fig.3 Evolution of mineralogical composition at the burning of $3BaCO_3+Al_2O_3+BaSO_4$ mixtures.

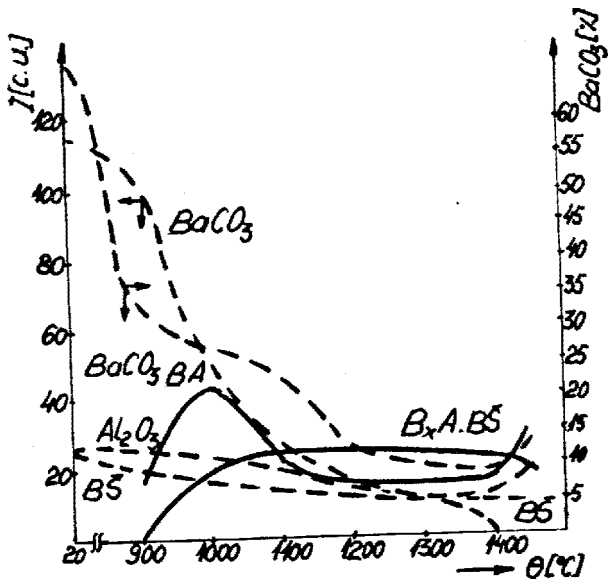

Fig.4 Evolution of mineralogical composition at the burning of $4.2BaCO_3+Al_2O_3+BaSO_4$ mixture.

diminish of the interferences specific to the monobaric aluminate in range of temperature where the intensity of the Ba sulphataluminate interferences stay unchanged, could suggest, like in the case of Sr sulphataluminate the formation of a Ba sulphataluminate first, having a less B_xA/BS ratio, which enriches itself with aluminatic compound.

In the experimental conditions we used, it cannot be relised the entire coversion of the reactants, not at the maximum temperature of stability of the Ba sulphataluminate formed.

The thermal analyses made upon the reactant mixtures, are shown in fig.5.

The endotermal effects at 725-750°C, 850-900°C, respectively at 1150°C can be conferred to the reactants' polymorphic transformations [7].

The effect at the 1150°C, which is specifically to the polymorphic transformation of the $BaSO_4$.can be seen only on the DTA curve of the mixture which correspond to the hipothetical compound 3BA.BS, confirming again that such a compound cannot be formed. The lack of this effect at more basical mixtures, can be considerated a sign for the consumption of the $B_xA.BS$ sulphataluminatic compound.

The dissociation of the $BaCO_3$ is not accompanied by the correspondent endothermal effects on the DTA curves at θ=900°C. These are superposed compensenting themselves, partially or totally, over the exothermal effects of the reaction products' formation.Endothermal effects due to the $BaCO_3$ decompose, are evidenced in the case of the more basic mixtures (fig.5, curve 3, 1230°C). In the same time, exothermal effects corresponding to the formation reaction, appear at higher temperatures only; at such temperatures, vitrification processes are certain (with endothermal melting effects).

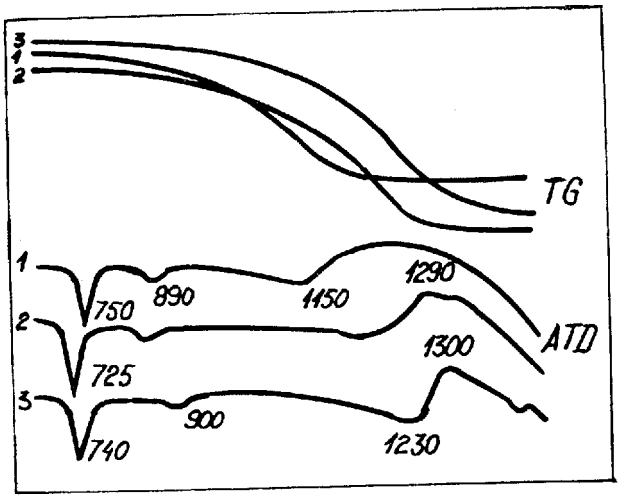

Fig.5 TG and DTA curves of $BaCO_3$:Al_2O_3:$BaSO_4$ mixtures: 1- 3:3:1; 2- 3:1:1; 3- 4.2:1:1.

CONCLUSIONS

The experimental results which have been obtained, evinced important differences in the display of the interaction processes, in the $SrCO_3$-Al_2O_3-$BaSO_4$, and $BaCO_3$-Al_2O_3-$BaSO_4$ respectively:

1-At the thermal treatment of some mixtures corresponding to some sulphataluminates, described by $3(MO.Al_2O_3).MSO_4$ (M=Sr,Ba), the formation of such compound is evinced only in case of the strontium system, having as an intermediate reaction product $SrO.Al_2O_3$. In the Ba system, the only reaction product is $BaO.Al_2O_3$, the reaction between these and $BaSO_4$ taking no place.

2- In the Ba CO_3(BaO)-Al_2O_3-$BaSO_4$ system, it can be noticed the formation of a Ba sulphataluminate, only in the more basical mixtures, this one having the next formula:$xBaO.Al_2O_3.BaSO_4$ (x=4). In this case, the process's mechanism implies the formation of the $BaO.Al_2O_3$ firstly, which saturates itself in BaO, with the result of aluminates which are rich in BaO and able to interact with $BaSO_4$ and to form Ba sulphataluminate.

3- The formation of the Sr sulphataluminate starts with important speed, from temperatures lower than the Ba sulphataluminate's formation, the formation of the latter being more intense in the more basical mixtures. The maximum temperatures of the stability of the two compounds is similar: $\cong 1400^{o}C$.

LITERATURE

1. R.Ripan, I.Ceteanu - Chimia Metalelor,vol I.Bucuresti EDP 1967

2. I.Teoreanu, M.Georgescu, A.Puri, A.Badanoiu - IIIth Nat.Symp. on Fundamentals of Silicates Science, Bucharest 1990, p.53

3. A.S.Muminov a.o - Izv.Akad.Nauk SSSR,Neorg.Mat. 21(4),669,1985

4. V.V.Volkov, H.I.Verbinova, M.M.Sicev - Tement 71(5.)15.1972

5. F. Massazza - Chimica Industria (ialia) 41,108,1959

6. P. Appendino - Annali di Chimica, Roma.61.882.1971

7. *** - Manualul inginerului chimist. Vol I.Bucuresti EDT 1972.

SULFOFERRITE CEMENTS

A P Osokin, Yu R Krivoborodov and N F Dyukova

D I Mendeleev Institute of Chemical Technology
Moscow, RUSSIA

SUMMARY

This paper presents results of investigations of mineral formation processes occured in the system, containing calcium and iron oxides and calcium sulfate. Solid solutions of sulfated calcium ferrites are determined. In the paper there are data showing phase transformations under heating at the range of 1173 up to 1473 K. It is concluded that the formation of sulfated calcium ferrites provides substancial increase of mineral hydraylic activity and change of hydrate product composition.

INTRODUCTION

A new kind of expansive sulfated cement is based on the possibility of an active formation of ferriferous ettringite in the hydration of sulfated calcium ferrites (SCF) (1).The composition of SCF formed in the synthesis is determined by the initial C/F ratio, the $CaSO_4$ content of the system, and depends substantially on the clinkering temperature (2).

RESULTS AND DISCUSSIONS

In the C-F-$C\bar{S}$ system, the interaction of the components starts at 800°C with the formation of the initial CF phase, and is completed at 1100°C. Within the interval of 950 to 1205°C, CF and $CaSO_4$ interact to from calcium monosulfoferrite with a composition of $3CF\cdot C\bar{S}$, which melts incogruently at 1205°C. With a ratio of C/F=2, CF is saturated to become C_2F at 1100 to 1200°C, with subsequent formation of a high-basicity $C_2F\cdot C\bar{S}$ composition which melts at temperatures exceeding 1350°C.

During the formation of solid solutions changes in the positions and intensities of the analytic peaks, and alterations in the characteristics of the unit cell are observed (see Table 1). The IR-spectroscopy data indicated dissolution of the sulfonic-acid group in ferrite matrices thus causing the appearance of absorption bands of asymmetric and symmetric oscillations in the regions 600 and 1110 to 1140 cm^{-1}. During the $3CF\cdot C\bar{S}$ formation, ion introduction into the ferrite structure takes place, causing an increase of the cell parameters, while during the high-basicity phase formation, SO_4 is substituted for FeO_4, which is accompanied by structure compression. The Mossbauer-spectroscopy data corroborate a decrease of the share of tetrahedral iron ions in the $C_2F\cdot C\bar{S}$ structure. The difference in the solid solution types formed on the basis of CF (ion introduction) and C_2F (substitution) respectively results in the fact that the value of calcium sulfate concentration in the hidh-basicity composition is three times higher than that in the low-basicity composition per one mole of calcium ferrite.

The hedration of ferrite phases in the formation of solid solutions is substantially activated, reaching 80% for $C_2F\cdot C\bar{S}$ at an ageof 28 days (see Fig. 1).

Table 1 Structural characteristics of ferrite phases.

Phase composition	Cell parameters, x10, nm			Ca-O bonding energy, kJ/mole	
	a	b	c	total	per atom
CF	9.323	10.740	3.015	3,522.24	1,148.94
$3CF \cdot C\bar{S}$	9.349	10.678	3.023	4,460.73	1,141.31
C_2F	5.579	14.758	5.428	4,555.69	1,092.19
$C_2F \cdot C\bar{S}$	5.355	15.028	5.420	7,380.36	1.084.43

The acceleration of hydration and the presence of calcium sulfate notably change the composition and properties of the monomineral cement stone. At the initial moment of hydration of calcium ferrites, low-basicity hydroferrites are formed, which in one to three days recrystallize into a cubic phase with a composition of C_3FH_6. As a result of recrystallization, the strength of 15.5 MPa attained on C_2F basis after a day of hardening begins diminishing, and by 28 days the specimens have practically no strength. Owing to a low degree of hydration and the recrystallization process in progress, the specimens on CF basis were characterized by a very low strength, and by 28 days they disintegrated. In the hydration process of $C_2F \cdot C\bar{S}$, the hydration products formed are $C_3F \cdot 3C\bar{S} \cdot 31H$ (d= 0.985, 0.747, 0.246 nm), C_4FH_{13} (d= 0.802, 0.395, 0.294

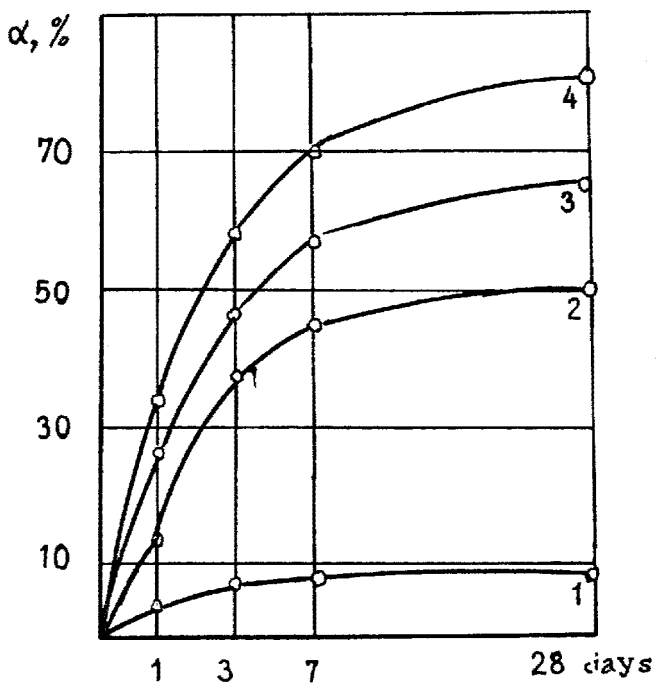

Fig.1 Effect of the hardening duration on the degree of hydration minerals
1 - CF; 2 - $3CF \cdot C\bar{S}$;
3 - C_2F; 4 - $C_2F \cdot C\bar{S}$

nm) and $Fe(OH)_3$; thus the DTA curves display endo effects at 170 to 190°C, 750 to 770°C and an exo effect at 330°C respectively. In the hydration of the low-basicity composition, the monosulfate $C_3F \cdot C\bar{S} \cdot 12H$ is formed in addition to ferriferous ettringite (endo effect at 190 to 220°C and d = 0.890, 0.802, 0.395 nm). For both compositions, no recrystallization of hexagonal hydroferrites into C_3FH_6 is observable, whereas recrystallization of ferriferous ettringite into monosulfate occurs after three days during the hydration of $3CF \cdot C\bar{S}$.

In the combined hydration of SCFs of various compositions with portland cement based on calcium sulfoferrites, analogous phases are formed, with a virtual absence of $Ca(OH)_2$ in the cement stone, which is due to its intensive fixation into ferriferous ettringite. The properties of cement stone depend to a considerable extent on the basicity of the sulfoferrite phase (see Fig.2). In the presence of $C_2F \cdot C\bar{S}$, there occurs a greater expansion and self-stressing of the system at lower stremgth parameters. The low-basicity phase promotes an

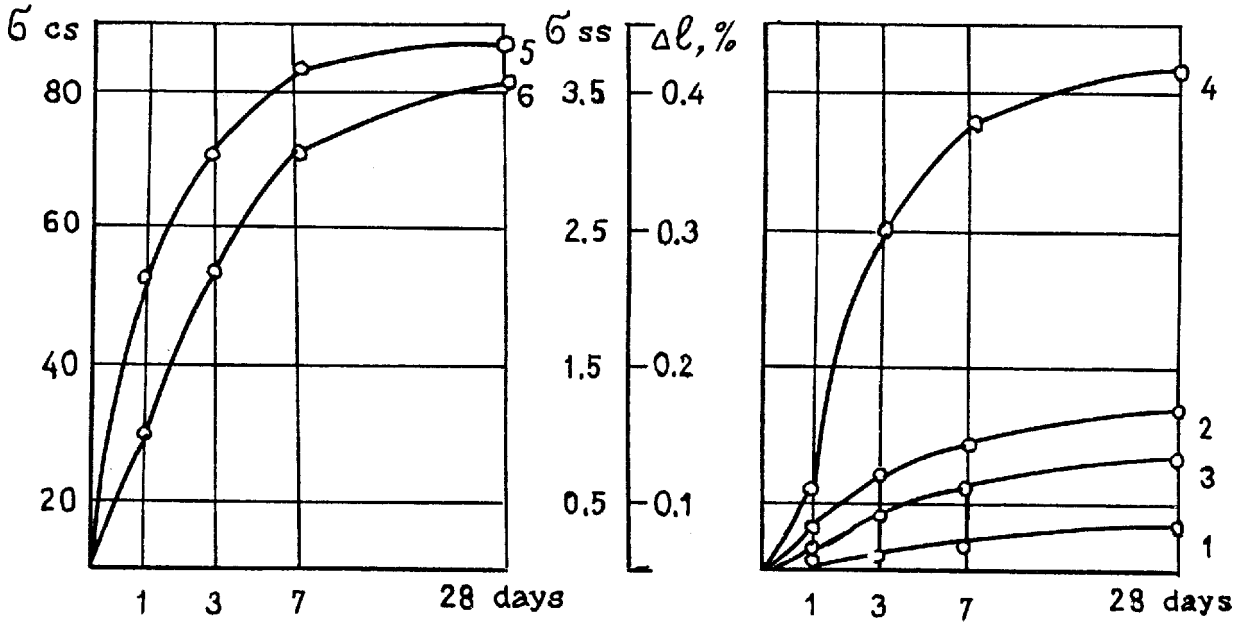

Fig.2 Effect of the hardening duration on the expansion (1,2) self-stressing (3,4) and compressive strength (5,6) of the cement stone based on portland cement carrying 3 $CF \cdot C\bar{S}$ (1,3,5) and $C_2F \cdot C\bar{S}$ (2,4,6)

insignificant expansion of the system (up to 0.15%) and a higher density plus a lower porosity of the cement stone (up to 12 or 14%) following 7 to 28 days of hardening. Sulfoferrite-bearing cements are characterized by a high corrosion resistance as well. Thus, for instance, the resistance factor in sea water in the period 28 to 90 days stood at 0.68 to 0.63 for ordinary portland cement, and when 3 to 8% by mass of $3CF \cdot C\bar{S}$ was added to portland cement, the respective values reached 0.96 to 1.01, rising with the SCF concentration in the cement.

The findings testify that $3CF \cdot CS$ contributes to the production of dense nonshrinking cement stone with an enhanced corrosion resistance, whereas $C_2F \cdot C\bar{S}$ makes it possible to produce expansive cements with a high expansion energy.

During the manufacture of sulfoferrite-bearing clinkers in rotary kilns, the burning temperature varies within the limits of 1200 to 1350°C depending upon the raw mix basicity, and $CaSO_4$ content determines the composition of the sulfoferrite phase (see Table 2).

Table 2 Phase composition of commercial sulfoferrite-bearing clinkers

Cement plant location	Minerals content, % by mass			
	C_2S	$3CF \cdot C\bar{S}$	$C_2F \cdot C\bar{S}$	AF-phase + others
Volsk	35	35	-	30
Voskresensk	35	55	-	10
Mikhailov	30	42	-	28
Sukhoy Log	40	35	-	25
Podolsk	27	9	57	7
Kant	39	21	31	9

In commercial clinkers, the CS content of SCFs may vary between $3CF(0.75 \text{ to } 1.5)C\bar{S}$ and $C_2F(0.8 \text{ to } 1.5)C\bar{S}$, but crystals persist that are similar in composition and stoichiometry.

CONCLUSIONS

Addition 5 to 15% by mass of sulfoferrite clinkers represented in Table 2, when producing portland cement, enables its physical-mechanical

characteristics to be improved, shrinkage to be eliminated, and evenhidly to matre dense watertight concrete with a high corrosion resistance. Besides, with an oriented growth of ferriferous ettringite crystals in cement stone under conditions of magnetic treatment, system self-reinforcement is observable and the bending strength grows five- to ten-fold, which helps cut down cement and steel consumption in the manufacture of reinforced concrete items and structures.

REFERENCES

1. Osokin A.P., Krivoborodov Yu.R.:"Sulfoferriferous cements and their properties" Trudy (Transactions) of the Moscow Institute of Chemical Technology named after D.I.Mendeleyev. Moscow, 1985,137,23-29 (in Russian).

2. Osokin A.P., Akimov V.G.,Krivoborodov Yu.R.:"Investigations of calcium sulfoferrite solid solutions" Trudy (Transactions) of the NIICement Institute. Moscow, 1982,68,81-87 (in Russian).

KINETICS OF ALUMINOFERRITE FORMATION AT DIFFERENT CONDITIONS

Chen Yimin, Shi Liping, Su Muzhen and Deng Jun'an

Cement Research Institute, China Building Materials Academy
Beijing, P R CHINA

SUMMARY

The kinetics of $4CaO \cdot Al_2O_3 \cdot Fe_2O_3$ (C_4AF) formation between 1200℃ and 1350℃ from both mixtures of C_2F+CA+C and C_2F+0.5CA+0.5C_3A and the effect of $C_{11}A_7 \cdot CaF_2$, $C_4A_3\bar{S}$, β–C_2S and β–C_2S+MgO on the kinetics were studied. Between 1200–1300℃, the C_4AF formation is a diffusion controlled process which can be discribed by Ginstling–Brounshtein equation. The kinetics parameters, such as reaction rate constant K and activation energy E, and thermodynamical functions, i.e. activation free $\triangle G$ and entropies $\triangle S$, are given. The diffusion coefficients and diffusion activation energy are calculated by the Fick's second law of diffusion.

The results showed that $C_{11}A_7 \cdot CaF_2$ and $C_4A_3\bar{S}$ will delay the C_4AF formation. $C_{11}A_7 \cdot CaF_2$ makes negative effect in the kinetics and $C_4A_3\bar{S}$ does in thermodynamics. At 1350 ℃, C_4AF will form quickly because of a eutectic. At the presence of β–C_2S and β–C_2S+MgO, an extra eutectic reduces the perfect formation temperature to about 1300℃.

摘 要

本文研究 1200—1350℃ 时由 C_2F+CA+C 和 C_2F+0.5CA+0.5C_3A 形成 C_4AF 的动力学以及 $C_{11}A_7 \cdot CaF_2$、$C_4A_3\bar{S}$、β–C_2S+MgO 对它的影响．在低共熔出现之前（1200—1300℃），反应由扩散控制，可用 Gistling–Brounshtein 方程描述．由此求出了各种条件下反应的活化能、活化自由能和活化熵．还用 Fick 第二定律导出的产物浓度关系式求出了扩散系数和扩散活化能．

结果指出，$C_{11}A_7 \cdot CaF_2$ 和 $C_4A_3\bar{S}$将延缓 C_4AF 形成．其中 $C_{11}A_7 \cdot CaF_2$ 在动力学方面起负作用，$C_4A_3\bar{S}$在热力学方面起负作用．1350℃ 时低共熔液相使 C_4AF 完全形成．β–C_2S 和 β–C_2S+MgO 使低共熔点降低，从而使 C_4AF 形成温度低至 1300℃ 左右．

* The Project Supported by National Natural Science Fundation of China and by Science and Technoloy Development Fundation of Building Materials Field.

INTRODUCTION

The composition of Calcium aluminoferrite in Portland Clinker usually closes to C_4AF. It was belived that it forms by soluting of ferrite to aluminate phase (1), but some authors of present paper suggested (2) that C_2F forms at lower temperature and then aluminate solutes in it gradually. Mackenzie et al (1) published the results of formation kinetics of C_4AF from oxides or C_3A+CF, in which the melting of CF and the eutectic between $CaO+Fe_2O_3$ at about 1240℃ were not considered. In present paper, the solid-state reaction kinetics of C_4AF formation from C_2F+CA+C and C_2F+0.5CA+0.5C_3A is studied and the diffusion coefficient is discussed.

In practical production, CaF_2 and $CaSO_4$ are sometimes added to raw mixtures as mineralizers or flux so $C_{11}A_7 \cdot CaF_2$ and $C_4A_3\bar{S}$ will probably appear during clinkering. Thermodynamic analysis (3) indicated that both of them form more easily than C_4AF. C_2S is always present at fairly low temperature and MgO is one of most common impurities in raw materials. So this paper deals also with the effect of $C_{11}A_7 \cdot CaF_2$, $C_4A_3\bar{S}$, β-C_2S and β-C_2S+MgO on the kinetics of C_4AF formation.

EXPERIMENTAL

Raw materials were A.R. grade reagents $CaCO_3$, Fe_2O_3, Al_2O_3, CaF_2, $CaSO_4 \cdot 2H_2O$, SiO_2 and MgO. The compounds C_2F, CA, C_3A, $C_{11}A_7 \cdot CaF_2$, $C_4A_3\bar{S}$ and β-C_2S were synthesized according to their stoichiometry at suitable conditions. CaO was obtained by heating $CaCO_3$ for 3h at 1100℃. All of them were ground to the size $< 50\mu m$ and average size about $30\mu m$. Samples for kinetic research were prepared according to Table 1. Each of them (3g) was pressed to $\Phi 20 \times 6$ mm and held at 1200℃, 1250℃, 1300℃, 1350℃ for varying time, air quenched and ground to the size $< 50\mu m$ as final specimen.

Table 1. Composition of raw samples

No.	Composition
C40	C_2F+CA+C
C41	C_2F+0.5CA+0.5C_3A
C4F	90%(C_2F+CA+C)+10%$C_{11}A_7 \cdot CaF_2$
C4S	90%(C_2F+CA+C)+10%$C_4A_3\bar{S}$
C4B	90%(C_2F+CA+C)+10%β-C_2S
C4M	85%(C_2F+CA+C)+10%β-C_2S+5%MgO

The reaction extent was determined by quantitive X-ray diffraction using 10% anatase (TiO_2) as internal standard. The determination was performed on Dmax-IIIA X-ray diffractor with Cu target Kα ray, step scanning with each 2θ step 0.002° and present time 0.2 second. Data were collected, stored, and analyzed by computer and the programs for seperating multi-peaks, cutting out the background, and calculating peak areas were employed. The reproducibility of the method was much better than 10%. The peaks used were d=7.25Å for C_4AF, 2.97Å for CA, 4.98Å for both $C_{12}A_7$ and $C_{11}A_7 \cdot CaF_2$, 3.75Å for $C_4A_3\bar{S}$, 2.11Å for MgO and together with 3.15Å for TiO_2.

RESULTS AND KINETICS ANALYSIS

Fig.1 gives the reaction extents as functions of temperature and time and shows, apart from the highest temperature, the best fit with the diffusion-controlled Ginsling-Brounshtein equation: $F(\alpha)=1-2\alpha/3-(1-\alpha)^{2/3}=Kt$, where α is the reaction extent in time t and K is rate constant. Fig.2 to 5 gives part results of other phase determined. According to Arrhenius equation, $K=A\exp(-E/RT)$, the reaction activation energy E and the constant A can be yieled by the linear

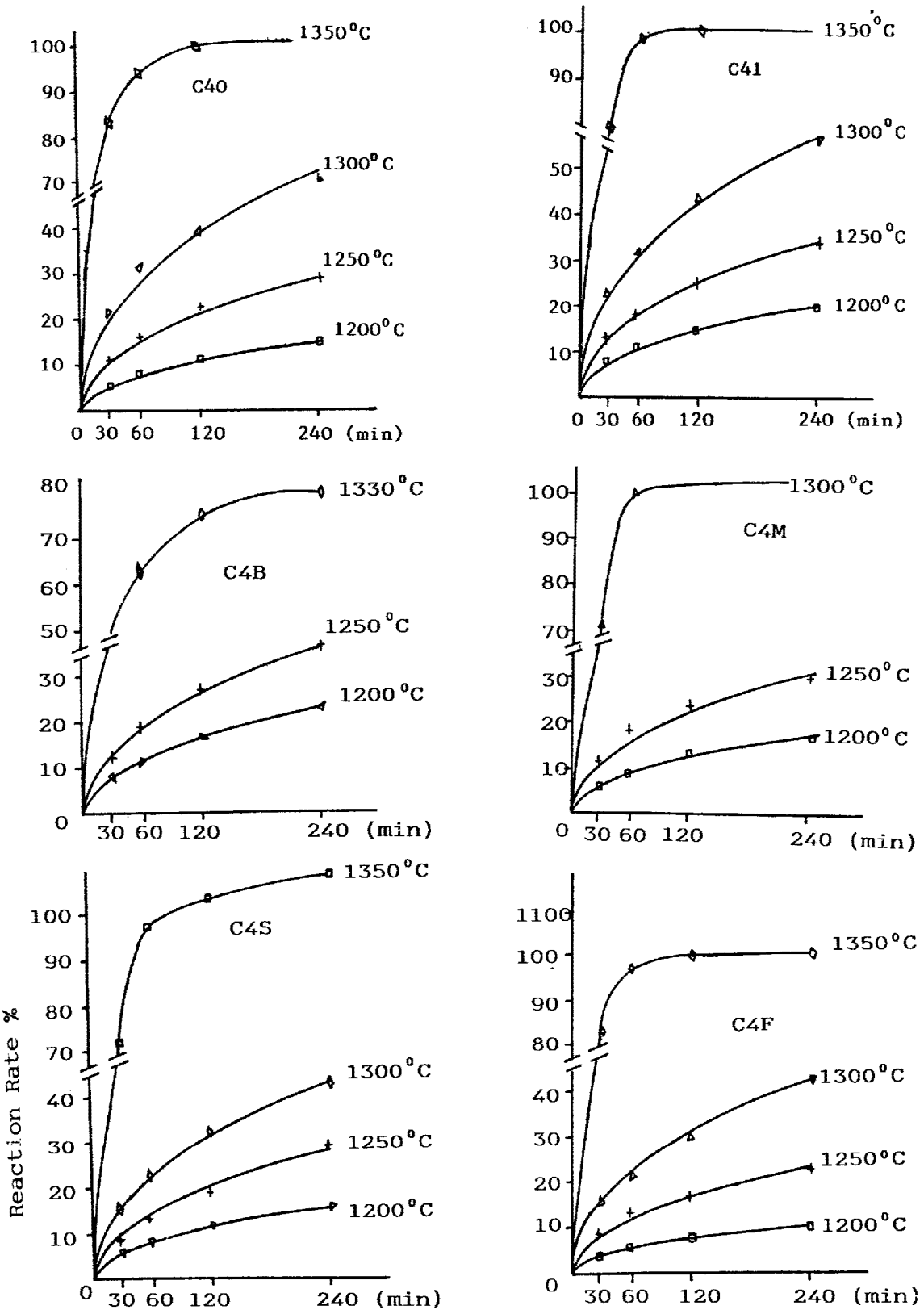

Fig.1 Reaction rate vs temperature and time

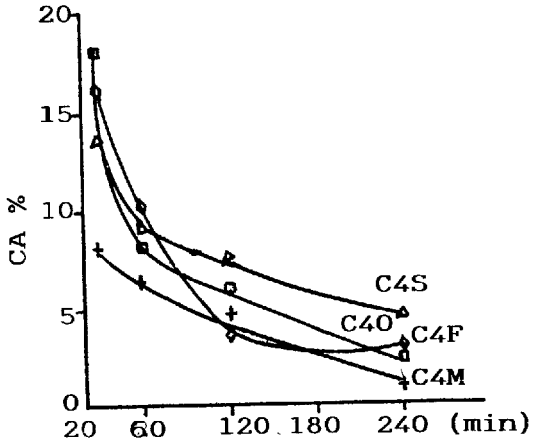

Fig.2 The amount of CA varys with time at 1250°C

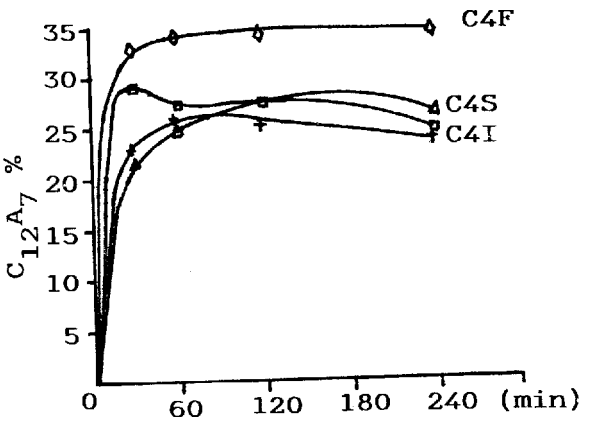

Fig.3 The amount of $C_{11}A_7$(+$C_{11}A_7CaF$) varys with time at 1250 °C

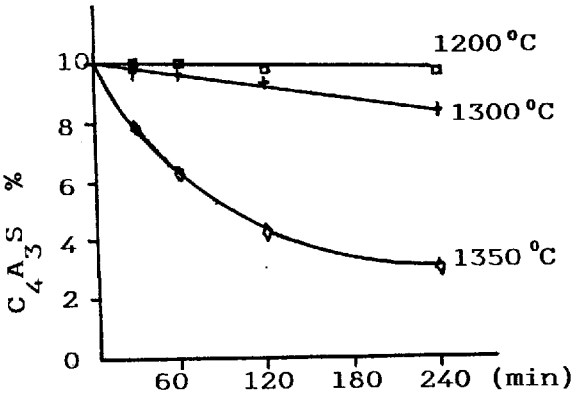

Fig.4 $C_4A_3\bar{S}$ varys with temperature and time in the sample C4S

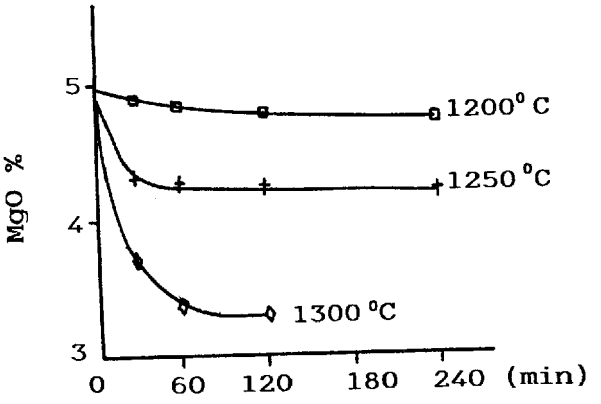

Fig.5 The amount of MgO in the sample C4M

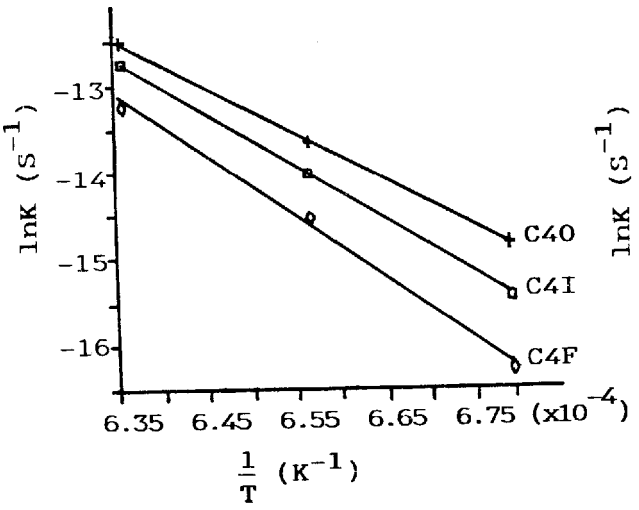

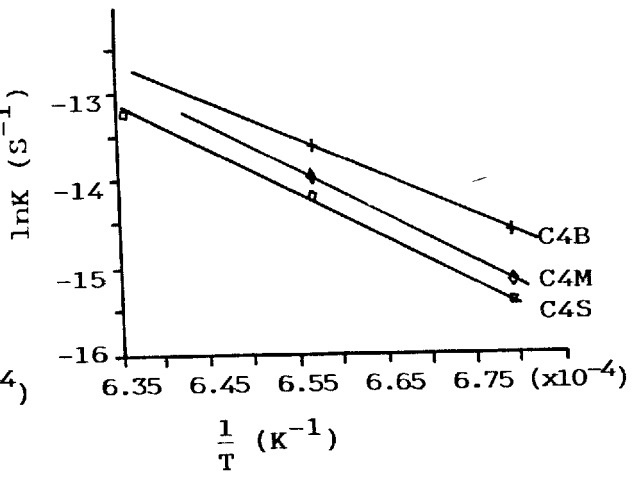

Fig.6 Linear plot lnk vs $\frac{1}{T}$

slopes of lnK vs $-1/T$ (see Fig.6), here T is reaction absolute temperature and R gas constant. Then the activation free energy $\triangle G$ and activation entropy $\triangle S$ are calculated from the equation (1): $\triangle G = RT[\ln(RT/Nh) - \ln k]$ and $\triangle S = (E - \triangle G)/T$, where N Avogardro's number and h plank's constant.

Fick's second law of diffsion for spherical particles states that (4) at time t, the fractional concentration of the product at the distance x from the surface can be represented as $(C-C_0)/(C_s-C_0) = 1-\mathrm{erf}(x/2\sqrt{Dt})$. A computer program has been made to calculate the diffusion coefficients D for each sample at different temperature. Because D depends on diffusion activation energy E_D and temperature T, i.e. $D = B\exp(-E_D/RT)$, (here B is a constant), E_D can be obtained from the linear plot of lnD vs $1/T$. All the calculation results are listed in Table 2.

Table 2. Kinetic parameters, thermodynamic functions and diffusion coefficients

No.	E KJ/mol	A S^{-1}	T ℃	K S^{-1}	$\triangle G$ KJ/mol	$\triangle S$ J/mol.K	D cm^2/S	E_D KJ/mol	B cm^2/S
C40	523.1	$6.593\times^{11}$	1200	1.850×10^{-7}	570	−32.0	0.359×10^{-12}	595.3	4.519×10^{8}
			1250	7.676×10^{-7}	572	−32.1	1.662×10^{-12}		
			1300	27.92×10^{-7}	574	−32.6	7.865×10^{-12}		
C4I	442.9	1.763×10^{9}	1200	3.541×10^{-7}	562	−81.1	0.713×10^{-12}	524.3	2.636×10^{6}
			1250	10.97×10^{-7}	567	−81.8	2.494×10^{-12}		
			1300	35.33×10^{-7}	571	−81.6	10.87×10^{-12}		
C4F	587.8	5.984×10^{13}	1200	0.827×10^{-7}	580	5.21	0.155×10^{-12}	641.2	2.718×10^{10}
			1250	4.501×10^{-7}	579	5.92	0.924×10^{-12}		
			1300	17.43×10^{-7}	580	4.64	4.318×10^{-12}		
C4S	419.3	1.550×10^{8}	1200	2.028×10^{-7}	569	−102	0.395×10^{-12}	466.7	1.436×10^{4}
			1250	6.983×10^{-7}	573	−101	1.496×10^{-12}		
			1300	17.83×10^{-7}	580	−101	4.440×10^{-12}		
C4B	367.8	6.774×10^{6}	1200	4.543×10^{-7}	559	−130	0.933×10^{-12}	412.2	385.0
			1250	12.18×10^{-7}	566	−130	2.817×10^{-12}		
C4M	452.7	2.901×10^{9}	1200	2.572×10^{-7}	566	−77.1	0.507×10^{-12}	493.3	2.063×10^{5}
			1250	8.654×10^{-7}	571	−77.3	1.903×10^{-12}		

DISCUSSION

One of our previous paper (5) indicated that there is an eutectic between aluminate phases at 1360℃ and, when β–C_2S presents, another one at 1322℃ which is reduced to 1291℃ by adding 5% MgO. So the kinetic behaviour at the highest temperature in Fig.1 will not locate in the field of solid–state reaction. At that temperature C_4AF can form quickly through the liquid because of the eutectic. It is certain that the presence of β–C_2S or β–C_2S+MgO accelerates the C_4AF formation at 1300℃ and the results for both of the samples in Table 2 are not correct enough because there are only two temperature points for them.

The values of diffusion activation energy E_D in Table 2 are quite close to E and at the same level to the self–diffusion energy of Al in Al_2O_3 (477KJ/mol) and that of Fe in Fe_2O_3(419KJ/mol) and much larger than that of Ca in CaO (142–168KJ/mol), which means that the process may be controlled by the diffusion of Al or Fe and that the process obeys Fick's second

law of diffusion.

$C_{11}A_7 \cdot CaF_2$ and $C_4A_3\bar{S}$ have negative effects on the C_4AF formation. The former enlarges the activation energy and the later reduce $\triangle S$, so their influence may be in kinekic and thermodynamic, respectively.

Fig.3 shows that at present conditions $C_{12}A_7$ will always appear for all samples as an intermediate. Comparing Fig.2 with Fig.1, it may be seen that $C_{12}A_7$, similar to $C_{11}A_7$ CaF_2, seems playing an negative effect on the process. Maybe its large formula is difficult to diffusion.

CONCLUSION

1. The kinetics of C_4AF formation from both of C_2F+CA+C and C_2F +0.5CA+0.5C_3A between 1200–1300℃ is a diffusion–controlled process, and can be described by Ginstling–Grounshtein equation and obey Fick's second law of diffusion. The reaction activation energy are 523.1 KJ / mol and 442.9 KJ / mol, respectively, and the diffusion activation energy are 595.3 KJ / mol and 524.3 KJ / mol, respectively, close to that of self–diffusion of both Al in Al_2O_3 and Fe in Fe_2O_3.

2. $C_{11}A_7 \cdot CaF_2$ and $C_4A_3\bar{S}$ deduce the C_4AF formation. $C_{11}A_7 \cdot CaF_2$ enlarges its activation energy and C_4A_3S enlarges the $-\triangle S$. Below 1250℃ β–C_2S will somewhat accelerates C_4AF formation and MgO has not shown this effect because of its solution in C_4AF. β–C_2S and β–C_2S+MgO will accelerate C_4AF formation at about 1300℃ by deduce the eutectic temperature.

3. $C_{12}A_7$ is alwalys present as an intermedia phase which might take a similar part as $C_{11}A_7 \cdot CaF_2$ in the C_4AF formation.

REFERENCE

1 K.J.D.Mackenzie and H.Alasti; "Formation Kinetics of Portland Cement Clinker Phases. II. Tetracalcium Aluminoferrite", Trans. J.Brit. Ceram. Soc., Vol. 77, P.162. (1978)

2 Guo Yong, Deng Jun'an, Su Muzhen and Wang Yanmou: "A study on Formation Mechanism of Ferrite Phase in Ferroaluminate Cement",Journal of the Chinese Silicate Society, Vol.16, p.481, (1988).

3 Lu Ping, "Formation of C_4AF, $C_4A_3\bar{S}$, and $C_{11}A_7 \cdot CaF_2$ and Their Hydration in the Early Age", Journal of the Chinese Silicate Society, Vol.13, p.275 (1985).

4 W.D.Kingery, Introduction to Ceramics, John Wiley Sons, Inc., New York, London, Sidney, pp.219–226, (1975)

5 Su Muzhen, Chen Yimin, Shi Liping, Deng Jun'an and Liu Xiaoxing: "Application of Thermal Analysis and Conduction Calorimetry to the Formation and Hydration of Calcium Aluminoferrite", The 5th Conference of Calorimetry and Thermal Analysis, Krocow, Poland, (1991).

STUDY ON CEMENT IN THE $C_{11}A_7 \cdot CaF_2$-C_2S SYSTEM

Liu Kezhong, Deng Zhongyan, Yuan Mingdong and Tang Jinshu

China Building Materials Academy, Beijing, P R CHINA

ABSTRACT

A series of experiments were conducted by means of chemical analysis, petrographic analysis, XRD, TEM, determination of heat of hydration and pore size distribution.

This paper reports in detail the mineral composition of clinker in the $C_{11}A_7 \cdot CaF_2$–C_2S system and the hydration rate and products formed after 5 minutes to 3 months of hydration. This paper also explains why this kind of cement possesses such favourable properties as quick setting and rapid hardening, high "hour" strength and steady development of long term strength.

〔摘　要〕

本文通过水泥材性、熟料岩相鉴定、XRD、TEM、水化热以及孔结构等多方面的试验研究论证了$C_{11}A_7 \cdot CaF_2$–C_2S体系熟料的矿物组成以及该水泥在硬石膏掺与下，从水化5分钟开始到3个月所形成的水化产物和水化速度．同时也阐明了这一体系水泥具有凝结硬化快、小时强度高以及长期强度增长和稳定性好的缘由．

GENERAL

The special cement in the $C_{11}A_7 \cdot CaF_2$–C_2S system possesses the properties of quick setting and rapid hardening, therefore is called "hour cement". The chief mineral compositions of this kind of cement clinker are fluroaluminate ($C_{11}A_7 \cdot CaF_2$) and β–dicalcium silicate (β–C_2S). The fundamental technological properties of the cement are as follows:

Quick setting and rapid hardening, high "hour strength"

Quick setting and rapid hardening and high hour strength are the prominent characteristics of this system cement. At normal temperature (about 20℃), its initial setting time is 1～2min and final setting 2–5 min. without retarding admixture. The setting time can be regulated by adding retarding admixture. The applicable time for concrete construction lasts between 20 to 60 min. The strength of the paste is 30 MPa at 1 hour; > 60 MPa at 6 hours. The concrete strength can reach 20～30 MPa at 3 or 4 hours.

Good low temperature property

This cement not only has high hour strength at normal temperature, but also shows high hour strength at low temperature because of higher heat of hydration.

High long term strength, good stability

The main hydration products of this cement are AFt (ettringite), C–S–H gel and $Al_2O_3 \cdot$ aq. Consequently, strength retrogradation at later age does not exist. The concretes prepared with this cement gain their strength steadily with the increase of their age.

Mini–expansive property

With a suitable amount of slag mixed in this cement, its linear expansion is steady. The linear expansion value of the cement paste specimen cured in water is small, approximately 0.1% at 28 days. The long term linear expansion is steady.

Good corrosion resistance

This system cement has good corrosion resistance property. Its K_1, K_2, K_6 value in 3% Na_2SO_4 solution are all above 1.

The mineral components $C_{11}A_7 \cdot CaF_2$ and $C_4A_3\underline{S}$ (anhydrous calcium sulfoaluminate) which have quick setting and hardening property have been studied closely world over. Regulated–set cement developed in the United States in 1969 was manufactured mainly from calcium fluoroaluminate $C_{11}A_7 \cdot CaF_2$. It is basically a quick hardening cement [1] . Japan introduced this cement and developed it into a super–quick hardening cement comprised mainly of C_3S and $C_{11}A_7 \cdot CaF_2$[2] . Then Germany also imported the American patent and put it into production [3] . A super high early strength cement, W.A. Borge's patent filed in the United States in 1975, was chiefly made of C_2S and $C_4A_3\bar{S}$. The super high early strength cement of $C_4A_3\bar{S}$–C_2S system was also formulated by Japanese [5] .

This paper reports the $C_{11}A_7 \cdot CaF_2$–C_2S system cement developed by our academy in 1973, with main mineral components as $C_{11}A_7 \cdot CaF_2$ and C_2S. According to raw materials and its practical requirements, the content of $C_{11}A_7 \cdot CaF_2$ in clinker may vary between 40–80%. SO_3 / Al_2O_3 ratio in cement should be controlled between 0.5–0.6. This clinker not only has low sintering temperature, but is easily formed and ground as well. The addition of cheap anhydrite and slag lowers the cost of this cement.

This cement has been put into mass production in several cement plants. Its main application areas are emergency repair of airport runway, construction engineering, mine roof bolting projects, watertight engineering, shotcrete construction and casting sand binder, etc. Many years of field application have proved that this cement shows good application results, and are well accepted by customers. Table 1 gives the mineral composition of the clinkers.

Calculated mineral composition of clinkers Table 1

No	Plant add	Calculated mineral composition (%)				Note
		$C_{11}A_7 \cdot CaF_2$	C_2S	C_2F	CT	
1	Lab.	100				Sintered in furnace from chemicals
2	Cement workshop	79.85	10.61	2.03	3.61	
3		51.57	40.36	2.00	2.10	Small rotary kiln
4		33.40	56.88	2.40	1.40	
5	Liulihe	73.40	14.4	2.2	2.6	Rotary kiln
6		71.40	21.5	1.8	2.9	Rotary kiln
7	Suzhou	74.80	16.9	2.7	2.6	Rotary kiln
8	Datong	44.20	38.9	3.3	5.0	Shaft kiln

Table 2 shows the strength of concrete.

Concrete Strength Table 2.

Cement	No.1	Mix proportion cem.:sand:aggr.	w / c	Retarder %	Tem. ℃	Slump cm
$C_{11}A_7 \cdot CaF_2$–C_2S system cement (5# clinker)	1	1:1.8:2.7	0.45	0.50	20	2.1
	2	1:1.47:3.61	0.45	0.50	15	2.5
	3	1:2:3	0.45	0.50	17	

Cement	Compressive strength MPa					/ Applicable time (min)
	3h	4h	6h	1d	28d	
$C_{11}A_7 \cdot CaF_2$–C_2S system cement (5# clinker)	25.3	27.5	30.3	36.5	46.2	30
		20.6	29.1	37.0	58.5	80
		22.6				49.7

Note: No.3 is the construction data of an airport.

TEST AND RESULTS

Test method: prepare the paste according to standard consistency water content, mould specimens in 2 × 2 × 2 cm formed by vibrating at 20℃, then demould and cure them in moist air, place them into water after one day and keep up to the fixed ages. Then specimens were kept in ethanol solution and ground until they pass 0.080 mm sieve. Afterwards put the ground specimens in drier for determination.

Clinker mineral composition

Petrographic analysis shows that its main mineral constituents are $C_{11}A_7 \cdot CaF_2$ and C_2S.

$C_{11}A_7 \cdot CaF_2$:N = 1.609 ± 0.03, round shape, some crystals inter connected.

C_2S: small particle, in small group and not uniform. In addition to the above minerals there is also small amount of white interphase shown in petrographic picture Fig.1.

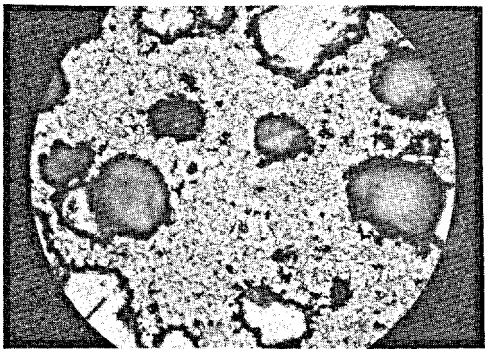

Fig.1 Reflexion (X220)

We can find from the X–ray photograph Fig.2 that $2^{\#}$ clinker containing 79.8% $C_{11}A_7 \cdot CaF_2$ sintered by small–scale rotary kiln and $8^{\#}$ clinker containing 44.21% $C_{11}A_7 \cdot CaF_2$ sintered by shaft kiln exhibit the same X–ray powder pattern as that of $1^{\#}$ clinker of pure $C_{11}A_7 \cdot CaF_2$. Characteristic peaks of $C_{11}A_7 \cdot CaF_2$ appear in $2^{\#}$ and $8^{\#}$ clinker powder pattern (d = 4.9, 3.806, 3.21, 3.0, 2.68, 2.55, 2.445, 2.19, 2.05, 1.94, 1.76), so does the characteristic peak of C_2S (2.77). But the appearance of characteristic peak of f–CaO in $8^{\#}$ clinker is the point that differs from others. (d = 7.399).

The hydrated products from 5 min to 1 hour, 3 hour and up to 3 months are basically ettringite (the characteristic peak is d = 9.8, 2.68, see Fig.3), its amount increases with the reduction of $C_{11}A_7 \cdot CaF_2$ (d = 4.9, 2.68) and anhydrate (d = 2.49, 2.849), no appearance of other hydrated aluminate products, as shown in Fig.3.

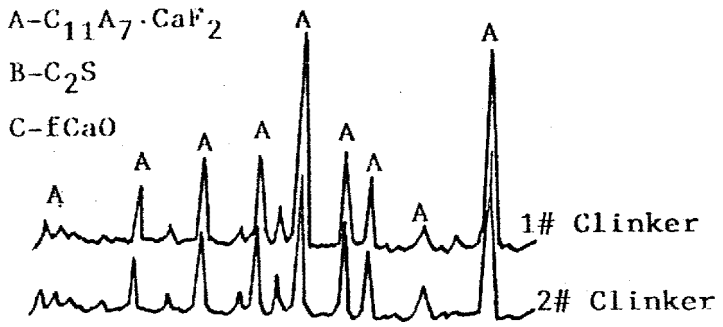

$1^{\#}$: $C_{11}A_7 \cdot CaF_2$, $2^{\#}$: clinker sintered in rotary kiln
Fig.2–1 XRD spectrum of $C_{11}A_7 \cdot CaF_2$–C_2 clinkers

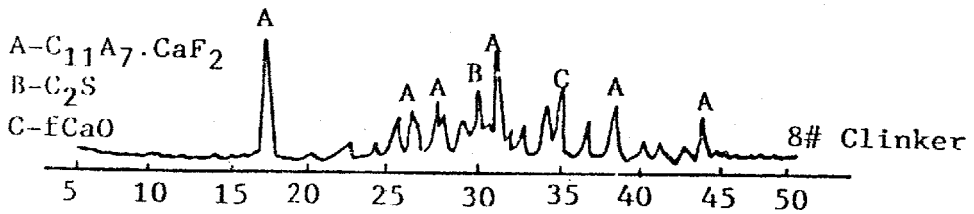

Fig.2–2 XRD spectrum of $8^{\#}$clinker sintered in shaft kiln

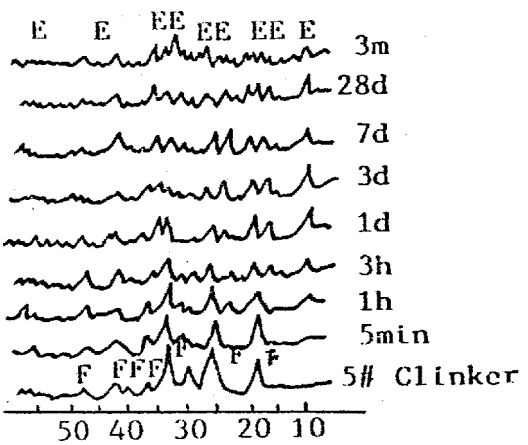

F–$C_{11}A_7 \cdot CaF_2$ E–ettringite
Fig.3. X–ray spectrum of cement pastes at different ages.

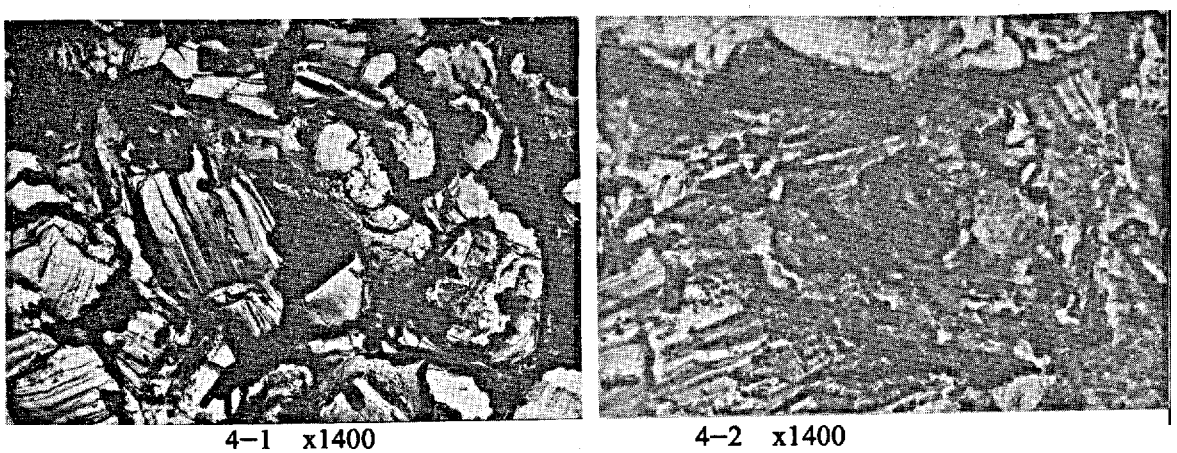

4–1 x1400
Cement paste at 1 hour

4–2 x1400
Cement paste at 6 hour

Fig.4 Electron microscopical photograph of replica

The powder X–ray photographs of large water cement ratio cement paste also confirm that a great amount of AFt appeared with the remarkable reduction of anhydrate and $C_{11}A_7 \cdot CaF_2$ after 5 min. hydration.

The electron microscopic observation (Fig.4) of cement pastes at different ages also shows that a lot of coarse and short rod ettringite crystal are formed, which aspect ratio are 1～1.5, and hydrated aluminium hydroxide spotted on its surface after one hour of hydration. The complete short and coarse etrringite (AFt) is invisible and is coated by foil–like and fibrous CSH gel at 6 hours hydration. Some hydrated aluminium hydroxide is also observed on AFt crystal surface. Dense structure is formed and hydrated products interlock with each other in 7 days.

Heat of hydration

JC139–67 direct approach was adopted to measure the heat of hydration, and comparison was made with the values of 625 and 725# portland cement (see Table 5).

Heat of hydration by comparison test — Table 5

Cement	Heat of hydration cal / g				
	4h	12h	1d	3d	7d
$C_{11}A_7 \cdot CaF_2$–C_2S system cement	59.8	64.3	66.2	69.6	75.2
625# portland cement				49.9	58.0
725# portland cement	8.9	39.7	46.0	59.8	69.1

The heat of hydration of cement depends on the such factors as clinker mineral composition, fineness, hydration rate, etc. This cement releases a great deal of heat in a relatively short period of time since it contains quick hardening ingredient $C_{11}A_7 \cdot CaF_2$ and very fine cement particles, provided the quantity of alkilinity and anhydrate is correctly matched. Compared with 625, 725# portland cement, this cement has both higher hours heat of hydration and total heat of hydration in 7 days.

The pore size distribution lying within the range 25~55000Å (pore radius), measured by mercury intrusion is shown in Fig.5.

The pore peak position of this cement paste at 3 days is at 130Å and that of quick setting and rapid hardening portland cement at 439Å. The total porosity of the former is 0.0674 cm^3/g while the latter is 0.1284 cm^3/g. These results mean that this cement paste has lower porosity and denser structure.

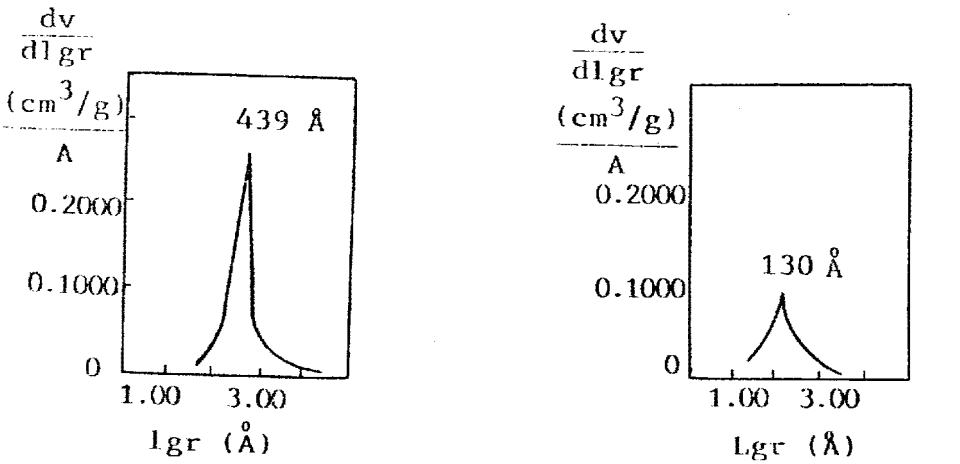

Quick setting and rapid hardening cement $C_{11}A_7.CaF_2$–C_2S system cement

Fig.5. Pore size distribution of hardened cement paste at 3 hours

DISCUSSION

Concerning the factors of clinker mineral compositions, chemical compositions, hydration products, heat of hydration and pore structure, etc, also considering the characteristics of $C_{11}A_7CaF_2$–C_2S system cement, we tried to answer the following two questions:

a. Why the $C_{11}A_7CaF_2$ system cement has the property of quick setting and rapid hardening, and why this cement has high hour strength.

Surely the characteristics of the new type of cement have something to do with the mineral composition of the chinker, the hydration products and their formation rate, quantity, etc.

This cement clinker contains a new mineral $C_{11}A_7 \cdot CaF_2$ which does not exist in ordinary portlant cement, and its content can be controlled in the range 35~80%. The new mineral $C_{11}A_7 \cdot CaF_2$ is responsible for the features of quick setting and rapid hardening as well as high hour strength. Upon contact with water, $C_{11}A_7 \cdot CaF_2$ dissolves and hydrates very quickly, and reacts with the anhydrate, forms a lot of ettringite leading to a very compact network. As seen from the X–ray analysis, a great deal of ettringite has been formed within 5 min. after adding water. This shows a very high hydration rate. Their hydration equations are given as follows.

$$C_2S+2H_2O \rightarrow CSH\ (gel)\ +Ca(OH)_2 \quad (1)$$

$$C_{11}A_7 \cdot CaF_2+CaSO_4+Al_2O_3 \cdot aq+H_2O \rightarrow C_3A \cdot 3CaSO_4 \cdot 32H_2O+CaF_2+Al_2O_3 \cdot aq \quad (2)$$

$$Ca(OH)_2+CaSO_4+Al_2O_3 \cdot aq+H_2O \rightarrow C_3A \cdot 3CaSO_4 \cdot 32H_2O \quad (3)$$

Besides the mineral difference, greater fineness of this cement also contributes to the properties of high hydration rate, accelerated setting and hardening, and quick heat evolution. Most of the heat of hydration has been released at the age of 4 days, accounting for 70% of the total amount as of 7 days. In turn, the heat of hydration promotes the setting and hardening. So this cement can be used in cold weather construction. Moreover, the great amount of expansive ettringite and aluminate hydroxide gel in cement paste combine to form a very compact structure which exihibits not only very quick setting and hardening property and high hour strength, but also good impermeability and corrosion resistance.

b. Long term strength and stability

Long term strength and stability of cement influence concrete durability.

$C_{11}A_7 \cdot CaF_2$–C_2S system cement is different from high alumina cement. Both research and construction practice have proved that the long term strength of retrogradation of high alumina cement is caused by crystalline transformation, which damages the formed structure. For this new cement, we should study and discuss this question from the viewpoint of its hydrated products and the internal microstructure of the cement paste.

As mentioned above, the main products of this cement system are ettringite, CSH and $Al_2O_3 \cdot aq$, $C_{11}A_7 \cdot CaF_2$ reacts with anhydrite, added in the process of grinding, and immediately forms ettringite, instead of forming hydrated calcium aluminate, the problem of crystalline transformation does not exist in this case. Regarding the stabiltity of ettringite, a lot of work has been done and proved its stable at normal temperatures. Our academy made an X–ray powder photograph test on specimens cured in the natural state up to 4 years, and proved the above statement. Other tests carried on self–stressing aluminate cement for stability also reached the same conclusion [7]

The pore structure analysis of the cement paste also supports the argument. The structure of this cement paste is very compact at 3 days, and its porosity is only 0.0674 cm^3 / g. With the increase of hydration age, the cement paste becomes denser and denser for continuous formation of ettringite CSH gel $Al_2O_3 \cdot aq$ and peak position shifts leftward continuously, The porosity of cement paste drops to 0.030 cm^3 / g at the age of 3 months, much denser than ordinary portland cement.

The concrete strength reached 62.7 MPa after curing for 4 years, and strength growth is steady.

CONCLUSIONS

1. Employing suitable limestone, different grade of alumina and small amount of fluorite as raw materials, $C_{11}A_7 \cdot CaF_2$–C_2S system cement can be produced in rotary kiln and shaft kiln at the sintering temperature of 1340～1400℃.

2. The main mineral composition of this system cement are fluoroaluminate and β–dicalcium silicate.

3. This system cement, containing a great deal of quick setting and rapid hardening ingredient $C_{11}A_7 \cdot CaF_2$, hydrates rapidly upon reaction with in water and produces a lot of ettringite, CSH and aluminum hydroxide from 5 min to 3 months.

4. This cement can be used in emergency repair work of airport runway, mine roof bolting, watertight or waterseal projects, shotcrete engineering and casting sand binder.

REFERENCES

1 U.S.Patent No. 3628973, 21, December 1971, "A Process for the Manufacture of Regulated–Set Cement".

2 Hiroshi Uchikawa et al. Ceramics, 1972, 7(4), 249.

3 Rolf Abt.: Beton, 1977, 27(7), 277.

4 U.S.Patent No. 3860433, 14, January 1975.

5 《7th International Congress on Chemistry of Cement》 Vol. 111–31–36, 1980.

6 China Building Blaterials Academy: "The Hydration of Quick Setting and Rapid Hardening Cement".

7 China Building Materials Academy: "The Characteristics and Hydration of Aluminate Self–stressing Cement".

NEW ENERGY-SAVING CEMENT — IRON-RICH FLUORALUMINATE CEMENT

Huang Wenxi*, Qian Guangren, Yang Yurong** and Qi Yanyong****

**Chengdu Designing & Researching Institute of Industry of Building Materials*
***Sichuan Institute of Building Materials*
Sichuan, P R CHINA

ABSTRACT

The mineral compositions of iron-rich fluoraluminate cement are a reasonable compounding of 5 -60% $C_{11}A_7CaF_2$, 20-80% C_8AF_2 and 10-40% C_2S. Because of the modification of mineral compositions and use of the special mineralizers, it reduces the clinkering temperature to 950-1050℃. The cements produced from iron-rich fluoraluminate clinker are characterized by higher hour-strength and better development of strength. At the same time, it has solved the problem —— shortness of setting time of fluoraluminate cement.

高铁氟铝酸盐水泥的矿物组成为 5 -60% $C_{11}A_7CaF_2$, 20-80% C_8AF_2 和 10-40% C_2S, 利用合适的矿物组成匹配和特定的矿化剂可以使水泥熟料的煅烧温度降低至950-1000. 高铁氟铝酸盐水泥具有早强和持续发展的后期强度. 同时, 水泥的凝结时间正常, 解决了传统的氟铝酸盐水泥凝结时间过短的问题.

INTRODUCTION

Rapid development in the fluoraluminate cement has been made at home and abroad, since the man-made $C_{11}A_7CaF_2$ phase was synthesized and added to the clinker of portland cement to make regulated set cement in America . A super-hardening cement mainly composed of C_3S and $C_{11}A_7CaF_2$ phases has been researched successfully in Japan[1]. A fast setting and fast hardening cement made up of C_2S and $C_{11}A_7CaF_2$ phases also has been investigated in China[2]. The phase $C_{11}A_7CaF_2$ is matched with C_3S or C_2S respectively in these kinds of fluoraluminate cements. $C_{11}A_7CaF_2$ is characteristic of fast setting and fast hardening as well as higher initial strength . The excellent cementing of C_3S and C_2S phases plays an important role in the excellent development of late strength . The burning temperature for ordinary fluoraluminate cement is in the range 1250℃ to 1350℃, at least about 150℃ higher than the burning temperature range of 1000℃ to 1100 ℃ for alinite cement . The setting of ordinary fluoraluminate cement is so fast , the initial and final setting times only being only a few minutes , that a regulating of setting time for a practical construction has to depend on expensive retarders. This, in effect, restricts greatly the extensive use of ordinary fluoraluminate cement . A new breakthrough both in energy saving and in properties has been made in the shape of iron-rich fluoraluminate cement not only in our laboratory but also industrial kiln.

EXPERIMENTAL

Raw meal of the cement was prepared from limestone, iron ore, fluorspar and bauxite. Table 1 lists the chemical composition of raw materials. Different kinds of compositions of clinker in the range of mineral composition——$C_{11}A_7CaF_2$ 5-60%, C_6AF_2 20-80% and C_2S 10 -50% are designed . The raw meals are made into pellets with a little water , then they were burnt at 950-1150℃ for 1 hour. The clinkers thus obtained were cooled in air quickly. In 1990 , two industrial tests were done in a special cement factory in Sichuan , China . The clinkers produced were ground to cement with some gypsum. The tests of properties were done according to national standards GB 177-85. GB1346 -77. Cement paste was made at w/c= 0.5 and hydration stopped by methyl alcohol at the desired age of hydration The hydration products were identified by XRD and DTA.

Table 1. Chemical composition of raw materials

Materials	LOI	CaO	SiO_2	Al_2O_3	Fe_2O_3	CaF_2	SO_3
Limestone	41.43	52.16	2.61	2.17	0.60	--	--
Bauxite	14.85	1.74	3.72	69.30	3.91	--	--
Iron ore	5.59	4.88	7.02	4.94	74.95	--	--
Gypsum	--	32.12	2.72	9.40	4.59	--	49.25
Fluorspar	7.39	11.56	11.18	1.40	0.50	56.13	--

RESULTS AND DISCUSSION

1. Mineral Composition of Iron-rich Fluoraluminate cement

The minerals of the clinker of iron- rich fluoraluminate cement clinker belong to the system $CaO-SiO_2-Al_2O_3-Fe_2O_3-CaF_2$. They are $C_{11}A_7CaF_2$, C_2S and C_6AF_2. Obviously, it is quite different from the main minerals of ordinary fluoraluminate cement . As shown in Table 2, the

Table 2. Range of mineral composition for series of fluoraluminate cement

Series of cements	$C_{11}A_7CaF_2$	C_2S	C_3S	Ferrite	Burning temperature	Inventor
Iron-rich fluoraluminate	5- 60	10-40	—	20-80	950-1050 ℃	*
Belite-fluoraluminate	71-72	17-20	—	2-3	1250-1350 ℃	**
Alite-fluoraluminate	20-26	—	50-55	4	1250-1350 ℃	***

Notes: * Sichuan Institute of Building Materials
** China Building Materials Academy
*** Japan (See Reference 1)

ferrite contents of ferrite are 20 to 80 percent higher than those of ordinary fluoraluminate cement Our results show that because of the burning temperature of clinker being 950 to 1050 ℃, no matter what Al/Fe ratios are used as the composition of ferrite phase of clinker , the resulting form of ferrite phase in the clinker is C_6AF_2 . The XRD result of clinker is shown in Fig. 1, corresponding to $C_{11}A_7CaF_2$ (d=4.864, 2.673, 2.179, 1.929), C_6AF_2 (d= 7.287, 3.563, 2.778, 2.673) and C_2S (d=2.778, 2.582, 2.470, 2.169). The burning temperature of iron-rich fluoraluminate cement clinker is related to the matching of minerals. it drops with increase of ferrite phase content, i.e., Fe_2O_3 content, and also enhances with increase of Al_2O_3 content. Table 3 lists the relation between the burning temperature and f- CaO for several samples having different ferrite phase compositions . It is seen from the Table 3 that the clinker of iron -rich fluoraluminate cement can be burnt at 1050℃ without recourse to mineralizers if a suitable mineral composition of clinker is selected. Compounds such as ZnO etc possess directional mineralizing motive by way of accelerating the absorption of CaO. it accelerates the absorption of CaO and can cause the

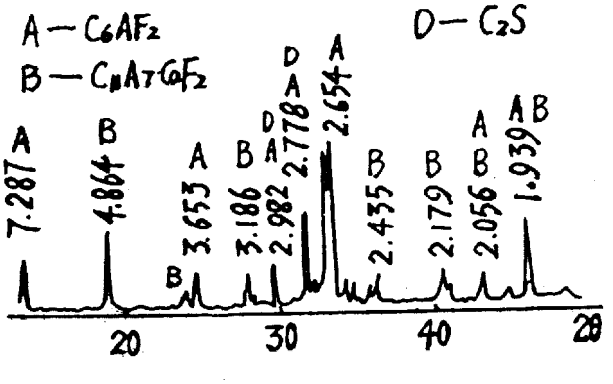

Fig. 1 XRD pattern of clinker

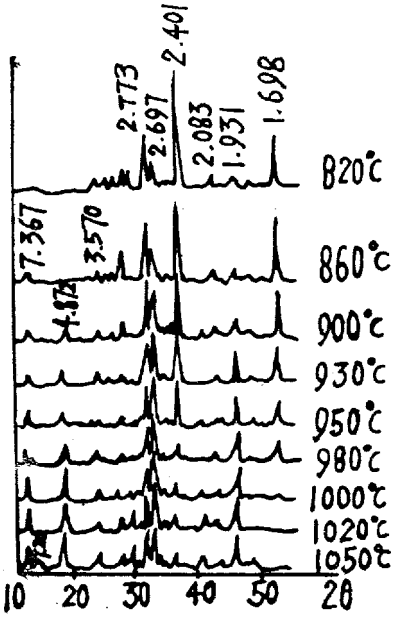

Fig. 2 XRD pattern of clinker formation without mineralizers

Table 3. F-CaO for samples burnt at different temperature

Sample	Content of ferrite (C_6AF_2%)	Without mineralizer		With mineralizer		
		1000℃	1050℃	950℃	990℃	1050℃
F1	20	11.27	3.21	7.17	5.01	1.95
F2	40	7.12	1.74	5.11	3.13	0.97
F3	55	6.40	0	4.50	2.16	0
F4	70	4.74	0	3.77	1.03	0
F5	80	3.92	0	1.91	0	0

burning temperature drop by more than 50℃. Table 3 shows that the clinker of iron-rich fluoraluminate cement can be burnt at less than 1000℃. As is evident from Fig. 2 , the clinker forming process without any mineralizer proceeds as folllows:

$$\text{Bauxite} \rightarrow Al_2O_3+SiO_2 \qquad 530℃$$
$$CaCO_3 \rightarrow CaO+CO_2 \qquad 860℃$$
$$CaO+Fe_2O_3 \rightarrow CaO \cdot Fe_2O_3 \rightarrow 2CaO \cdot Fe_2O_3 \qquad 860℃$$
$$CaO+Al_2O_3 \rightarrow CaO \cdot Al_2O_3 \rightarrow 12CaO \cdot 7Al_2O_3 \qquad 900℃$$
$$2CaO \cdot Fe_2O_3+Al_2O_3 \rightarrow 6CaO \cdot Al_2O_3 \cdot 2Fe_2O_3 \qquad 980℃$$
$$CaO+SiO_2 \rightarrow 2CaO \cdot SiO_2 \qquad 950℃$$
$$12CaO \cdot 7Al_2O_3+CaF_2 \rightarrow 11CaO \cdot 7Al_2O_3 \cdot CaF_2 \qquad 1000℃$$

2. Main Properties of Iron-rich Fluoraluminate Cement

2.1. Strength

The compressive strength of cement paste samples F1, F3 and F5 made in our laboratory and that of cement mortar samples G1 and G2 made in industrial kiln has been determined. The results

Table 4. Strength of paste and mortar samples

Sample	Proportion %		W/C	Blaine surface cm2/g	Setting time		Compressive strength (MPa)				
	Clinker	Gypsum			Initial	Final	6H	1D	3D	7D	28D
F1	100	20	0.39	4540	26′	48′	31.0	65.6	69.3	72.3	86.7
F3	100	10	0.37	4200	38′	1:03	21.6	45.3	53.4	75.2	88.3
F5	100	10	0.31	4050	44′	1:44	10.7	41.3	49.6	59.0	68.2
G1	100	10	0.41	4250	29′	43′	18.6	35.4	41.3	49.5	56.4
G2	100	15	0.41	4550	26′	45′	17.5	36.5	49.6	55.0	63.5

are given in Table 4 . It is obvious that the more the $C_{11}A_7CaF_2$ content, the higher the early strength , i.e., F1>F3> F5 in this series of cement The strength of cement paste for

sample F1 at 6 hours is 31.0 MPa; the corresponding strength of mortar for sample G1 is 19.6 MPa. It is important that the rate of strength development for samples F3 and F5 is higher than for sample F1, which is related to the higher composition of ferrite phase in samples F3 and F5. The compressive strength for samples F1, F3 and F5 at 28 days is respectively 86.7, 88.3 and 68.2 MPa; the compressive strength of cement mortars is also quite high, being respectively 56.4 and 63.5 MPa at 28 days. The iron-rich fluoraluminate cement is a complex system of many phases. Development of cement strength is affected not only by the activity of cement minerals, but also by the composition, morphology and interlinkng of the products produced by the hydration. P. K. Metha [3] and Y. F. Zhu[4] proposed that both ferrite and C_2S phases, resulting from burning at lower temperature and by doping, possess much higher activity of hydration than those of portland cement clinker. The series of our cements are burnt at lower temperature 950 to 1050℃; EDXA analyses for clinker minerals show that there are a lot of minor elements, such as Zn, F, S, Al and Mg, which give the ferrite and C_2S phases much higher activity of hydration. According to the result by I. Jawed[5] the excellent cementing of ferrite phase depends on the medium of hydration; the hydration of ferrite phase in a saturated lime solution and gypsum is retarded strongly. According to our results, the ferrite phase for this series of cements hydrates in the hydration medium of lower concentration with the solution of lime and gypsum. Hence, the ferrite phase can hydrate fully and offer excellent cementing property. The hydration products for F1, at different ages are given in Fig. 3a. The early hydration products for iron-rich fluoraluminate cement are AFt and AH_3 phases within several hours. As the time of the hydration extends, $C_{11}A_7CaF_2$ continues its hydration to form AFt, at the same time, C_6AF_2 begins its hydration to form AFt, C_4AH_{13}, C_2AH_8 and AH_3. At the same time, C_2S hydrates to form C-S-H. The higher the $C_{11}A_7CaF_2$ contents, the higher the quantity of AFt during the early hydration; this makes

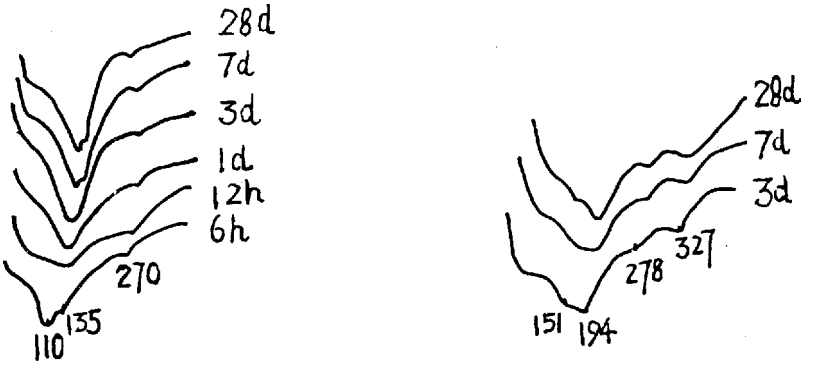

(a) with 20%wt gypsum (b) with 15%wt gypsum

Fig. 3 DTA results of hydration products for sample F1

cement paste with higher hour-strength. C_6AF_2 forms much more gel hydration products FH_3 than does C_4AF during the hydration. Because of the coexistence of a lot of gel hydrates FH_3 with the hydrates AH_3, C-S-H and hexagonal hydro-aluminate, the structure of the hardened cement paste where AFt acts as the main skeleton structure is more and more compact, which assures strength development for this series of cements. The strength of mortar for G1 and G2 with 50% and 40% ferrite phase respectively burnt in the industrial kiln is 56.4, 63.5 MPa at 28 days. For this reason, the mineral composition for this series of cements is an ideal matching.

2.2. Setting Time

A new breakthrough in the properties of iron-rich fluoraluminate cement is that its initial setting time is longer than that of ordinary fluoraluminate cement. As shown in Table 4, although the $C_{11}A_7CaF_2$ content for F1 is more than 40 %wt, the initial setting time is still more than 25 minutes. Beyond doubt, it offers favourable conditions for ordinary constructions, so that not only this kind of cements can be used without any retarder but also they can still have

excellent properties of fast hardening and early strength The reasons why the setting time for iron-rich fluoraluminate cement is favourable are as follows: (1). There exist a lot of minor elements such as ZnO in the structure of $C_{11}A_7CaF_2$. Our work has indicated[6] that the existing of minor elements such as ZnO will change the structure of $C_{11}A_7CaF_2$ and also retard the hydration of $C_{11}A_7CaF_2$ thus restraining the fast setting behaviour of $C_{11}A_7CaF_2$ (2). AFt formed by the interaction between $C_{11}A_7CaF_2$ and gypsum provides a protective layer for the hydration of $C_{11}A_7CaF_2$. The action is much more evident when ZnO and gypsum are used together. (3). The higher the C_6AF_2 content, the longer the setting time of cement (Table .4). This may be related to a lot of FH_3 hydrates formed by the hydration of C_6AF_2

2.3. Effect of Gypsum Content on Strength

The strength of this series of cements is dependent on gypsum contents . Cements produced by the matching of different minerals have the most suitable gypsum contents (Table. 5) The DTA results of hydration products for F1 which contained 15 and 20%wt gypsum respectively are given in Fig. 3 . A comparison of the two reveals that the hydration products which contained 15%wt gypsum are AFm and C_3AH_6, apart from AFt and AH_3 hydrates at 3 days. It shows that although early hydration products are AFt and AH_3, hydrates, such as C_4AH_{13}, C_2AH_8 also will be formed in the absence of gypsum whose products would interact with AFt to form AFm . At the same time hexagonal hydro-aluminate hydrates , such as C_4AH_{13} and C_2AH_8 are easier to change into cubic C_3AH_6;

Table 5. Effect of gypsum addition on strength (2×2×2cm)

Amount added wt%	Compressive strength (MPa)				
	6H	1D	3D	7D	28D
15	29.3	46.7	50.8	50.3	50.7
20	31.0	65.6	69.3	72.3	86.7
25	32.3	59.5	74.0	70.2	89.0

this makes for higher porosity in the hardened cement paste so that the strength goes down or only increases slowly. Hence , a suitable gypsum content must be selected for continued development of strength

CONCLUSIONS

1). The main minerals in iron- rich fluoraluminate cement are $C_{11}A_7CaF_2$, C_6AF_2 and C_2S. Their proportions are matched reasonably ; the series of cements are characteristic of higher early strength and excellent rate of strength development

2). The main hydration products of iron-rich fluoraluminate cement are AFt, AH_3, FH_3, C-S-H, C_4AH_{13}, C_2AH_8 and AFm.

3) The setting time of iron-rich fluoraluminate cement is acceptable. The main reason for the setting time tending to be longer is the effective proportioning of gypsum, ferrite and ZnO in the raw mix.

REFERENCES

1. 内川浩, 松崎安宏 セテミつクス 7(4) 249 (1972)

2. Wang yanmou, Su Muzhen, Cement (in Chinese) (3) 2 (1990)

3. P.K. Metha, World Cement Technology 11 (4) 166 (1980)

4. Feng Xiuji, Zhu Yufeng, Journal of the Chinese Silicate Society 12 (1) 1984

5. I. Jawed, S. Goto and R. Kondo, Cement and Concrete Reserch 16 (6) 441 1976

6. Qian Guangren, Huang Wenxi, Yang Yurong , Qi Yanyong, 9ICCC to be published

HYDRAULIC BINDERS BASED ON CONDENSED SILICA FUME AND SLAKED LIME

Harald Justnes

The Cement and Concrete Research Institute
Foundation for Scientific and Industrial Research
Trondheim, NORWAY

ABSTRACT

The empirical formula of hydraulic binder (CSH-gel) based on condensed silica fume (CSF) and slaked lime (CH) was determined by following the reaction

$a \cdot CH + b \cdot S + c \cdot H = C_aS_bH_{a+d}$

with ^{29}Si MAS (Magic Angle Spinning) NMR (Nuclear Magnetic Resonance) and DTA/TG (Differential Thermal Analysis/Thermogravimetry). The reaction rate of a binder with a predetermined molar C/S-ratio of 1.1 was compared with the reaction rate of pure C_3S at the same water-to-powder ratio (0.70). The reaction between CH and CSF proceeded well at ambient temperature when the mixing water contained alkalies (pH = 13, K/N = 2).

Mortars with binder/sand-ratio 1:3 were made for binders with different C/S-ratios and tested for flexural and compressive strength at 3, 7, 28 and 84 days age. All samples were cured in water at an ambient temperature of 20°C and with an accelerator added to the mix. For mortars with binder with C/S-ratio 1.1, compressive and flexural strength after 28 day curing were 55 and 7 MPa, respectively, tested on RILEM-prisms (40·40·160 mm^3). The rather high strength was obtained in spite of the high water-to-powder ratio (0.70) required for casting.

In addition, the porosity was tested for two samples by capillary suction of water and by MIP (Mercury Intrusion Porosimetry). The porosity was about 10 vol% for both, and with the major part of pore radii between 1 - 10 μm.

INTRODUCTION

This study was undertaken in order to better understand the pozzolanic reaction of condensed silica fume (S = SiO_2) with slaked lime (CH) as the part of investigations concerning pozzolanic activity of S in mixes with both the minerals C_3S (alite) and C_2S (belite) /1/ and with cement /2/. The proposed /2/ mechanism involving the alkalies (N = Na_2O, K = K_2O and H = H_2O) in cement;

$$\begin{array}{lcl} S\ (s) + (N,K)H\ (aq) & \rightarrow & (N,K)SH\ (aq) \\ \uparrow & & + \\ CSH\ (s) + (N,K)H\ (aq) & \leftarrow & CH \end{array} \qquad (1)$$

[(aq) = water-soluble, (s) = solid], lead to the use of partly simulated pore water in this study. The accelerating effect alkalies apparently have on the pozzolanic reaction subsequently initiated the second part of this study; the utilization of slaked lime and condensed silica fume as a hydraulic binder.

Autoclaved mixes of lime and silica are well known as binders, but only a few studies have been made on the reaction between slaked lime and finely divided silica as rice husk ash (95 % S, ≈ 150,000 m^2/kg) at ambient temperature; James and Rao /3/, Cook and Suwanvitaya /4,5/ and Cook /6/.

EXPERIMENTAL

The condensed silica fume (CSF) was a byproduct from a ferrosilicon plant, containing 91.2 % S and with a specific surface of 22,000 m^2/kg. The calcium hydroxide (slaked lime) and calcium oxide (burnt lime) used were of laboratory qualities (Purum). A sample was made of slaked lime (CH) and CSF with C/S = 1.11 (molar ratio) and water/binder = 0.70 (binder is CH calculated as C + CSF) by weight. The water contained 0.1 N alkalies (pH = 13) with K/N = 2. The hydration was stopped after 1, 3, 7, 28 and 84 days of sealed curing by crushing the samples and washing the powder with ethanol. The samples were then dried at 105°C for 1 hour prior to NMR and DTA/TG analyses.

The basic mortar composition (C/S = 1.11) was 1500 g CSF, 1800 g CH and 200 g C with 180 g lignosulphonate as plasticizer. Alkaline water (pH = 13, K/N = 2) was added so that the total w/b = 0.74 (including the water bound chemically in CH). 3500 g dry sand of each of the fractions 0 - 0.5 mm, 0.5 - 2 mm and 2-4 mm was used as aggregate. Flexural strength (3 parallels) was measured on RILEM prisms (40·40·160 mm^3) and compressive strength on their end pieces (6 parallels). The prisms were all cured in wet burlap for 1 day before they were immersed in saturated lime solution. Analogously, mortars with C/S = 2.00, 1.50, 0.90, 0.67, 0.50 and 0.25 were made. The binder aggregate ratio was kept constant, and burnt lime /total lime = 10 % for all mixes.

The solid state ^{29}Si MAS NMR spectra were recorded on a Bruker MSL-200 NMR-spectrometer at 39.76 MHz. This instrument is equipped with a broad banded, double air bearing CP-MAS probe head. Experiments were performed using magic angle spinning (MAS) at 3.1-3.2 kHz, a 5 microsecond pulse width, a 10 second delay between each scan, and approximately 1300 scans for each spectrum. Chemical shift values were calibrated prior to the experiments, using the sodium salt of 3(trimethylsilyl)-1-propane sulfonic acid, DSS.

The DTA/TG experiments were carried out at a NETZSCH 409 STA with a heating rate of 10°C/min and nitrogen as a purge gas. The sample (150 mg) was contained in an alumina

crucible and alumina powder was used as a reference. Weight loss in the range of 100-400°C was assumed to be due to water from the hydration products (excluding CH), while weight losses about 500 and 800°C were interpreted due to the decomposition of CH and CC, respectively.

The samples for MIP were stopped by storing them in ethanol for a few days prior to evacuation. Before the MIP experiments were carried out with the Carlo Erba Porosimeter (Model 1500), the samples were cut into bits with a diameter of ≈ 2-4 mm. This porosimeter records the pore size (radii) distribution of the sample between 58 and 400,000 Å. A contact angle of 117° was used to calculate the pore diameters.

The capillary suction experiments were performed on 2 cm disks (4 parallels), cut from cylinders of ϕ = 10 cm and h = 20 cm, that was predried for two days at 105°C. The principle of the capillary suction method is described in detail by Fagerlund /7/.

RESULTS AND DISCUSSION

Justnes et al have shown earlier /8/ that ^{29}Si MAS NMR may reveal 1) the degree of hydration for the silicon containing cement minerals, 2) the pozzolanic activity of silica fume and 3) the average chain length of the linear poly-silicate anions in the CSH-gel at a given time from a single spectrum. Furthermore, it was demonstrated /1/ that the combination of ^{29}Si MAS NMR data and information obtained from thermo gravimetry (TG) measurements may be used to calculate the stoechiometric factors of the overall hydration reaction of the cement minerals.

The NMR-spectra at 1, 3, 7 and 28 days curing for a slaked lime/silica fume mix with C/S = 1.11 and C_3S /2/ (both with water/binder = 0.70) are shown in Figure 1. The hydration characteristics as obtained from these spectra /1/; degree of hydration for C_3S, conversion degree of CSF and the average length of the polysilicate anions in the CSH-gel in the mixes, are given in Table 1. The detailed interpretation of a ^{29}Si NMR spectrum can be found in /1/, but note that the signal at -70 ppm correspond to C_3S, -110 ppm to CSF and -80 and -88 ppm to the end and middle groups, respectively, in the polysilicate anions in the CSH-gel.

Table 1. Hydration characteristics of a slaked lime/silica fume mix with C/S = 1.11 and C_3S (both with water/binder = 0.70).

Hydration time (days)	C_3S (alite)		C/S = 1.11	
	Hydration degree (%)	Poly-silicate	Conversion (%) of CSF	Poly-silicate
1	22.4	2.50	5.7	3.57
3	37.1	2.65	16.6	3.06
7	48.2	2.89	37.7	3.21
28	67.1	2.66	78.0	3.39
84	87.1	2.84	97.7	4.09

The position of the signals arising from the gel indicates a similar product from both C_3S and CH/CSF. However, the intensity ratios reveal that the average length of polysilicate anions are longer in the CSH-gel originating from the CH/CSF mix than in the gel from alite. The results in Table 1 show that the degree of reaction for CSF is higher than the degree of hydration for alite at 28 and 84 days curing, but much lower at 1 day.

DTA/TG of the lime/CSF mix after 28 days sealed curing gave 18.6 % non-evaporable water and 9.0 % CH of ignited weight (112.2 mg). The balanced reaction is then (relative to dimers in gel);

$$2.37\ CH + 2\ S + 0.84\ H = C_{2.37}S_2H_{3.21} \qquad (2)$$

leading to a (reacted water)/(reacted binder) = 0.23, which is close to the ideal value for alite. The excess mixing water creates capillary pores.

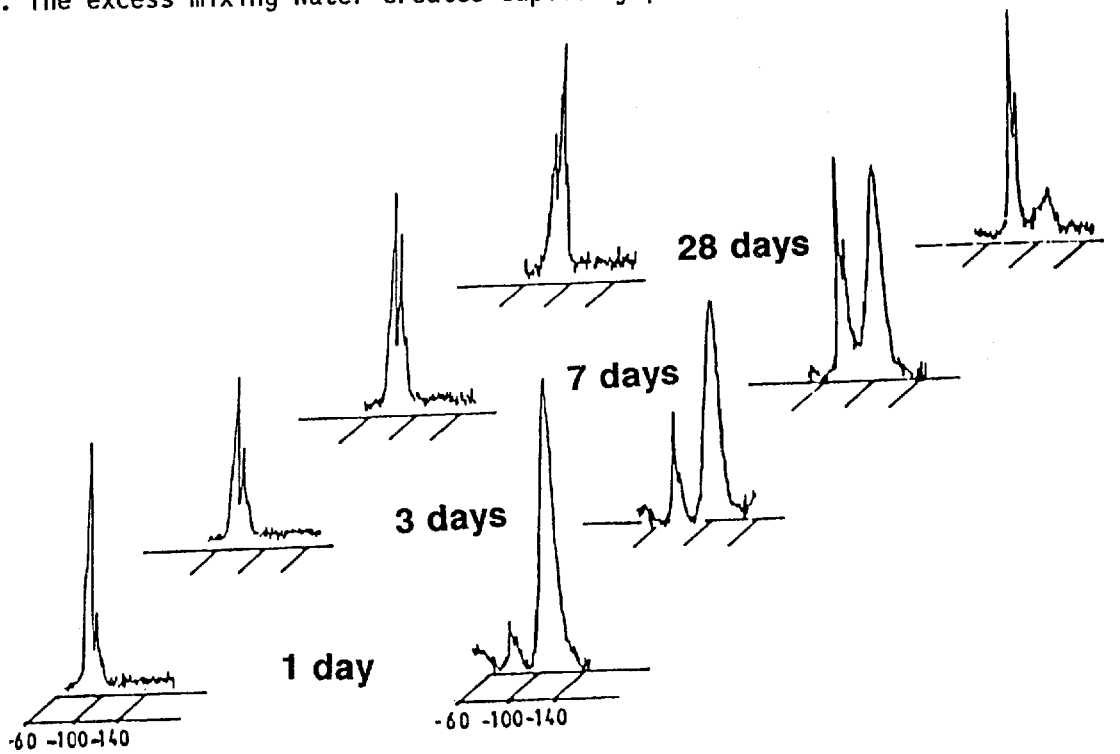

Figure 1: ^{29}Si MAS NMR spectra of C_3S (left) and lime/CSF mix (right) with C/S = 1.11, both with water/binder = 0.70.

The flexural and compressive strength of mortars based on lime/CSF binders with C/S-ratio 2.00, 1.50, 1.11, 0.90, 0.67, 0.50 and 0.25 are listed in Tables 2 and 3, respectively, as a function of curing time. The optimum mechanical properties at 28 days curing seems to be obtained with C/S = 0.50, with 8 MPa flexural and 56 MPa compressive strength. The mix with the lowest C/S-ratio gives the highest early strength in compression.

Mortars with higher early and ultimate strength may be obtained if castable mixes with lower water/binder ratios than 0.70 can be made, since the binder reaction itself only consume water corresponding to a ratio of 0.23 (Eq. 2). The low early strength at ambient curing is probably the most important obstacle for practical use of binders based on slaked lime and finely divided silica.

Table 2. Flexural strength (MPa) of slaked lime/ silica fume mixes as a function of reaction time and C/S-ratio.

C/S-ratio	Hydration time			
	3 days	7 days	28 days	84 days
2.00	3.4±0.6	5.2±0.8	7.0±0.7	-
1.50	3.5±0.3	5.5±0.7	5.9±0.6	-
1.11	3.4±0.1	7.0±0.7	6.9±1.7	7.6±0.8
0.90	3.6±0.2	6.0±1.2	6.3±0.5	-
0.67	5.3±0.2[1]	4.9±0.4	6.4±1.3	-
0.50	3.2±0.7[1]	4.4±0.3	8.1±0.6	-
0.25	4.3±0.3	4.7±0.8	6.0±0.3	-

[1] Strength measured at 4 days instead of 3.

Table 3. Compressive strength (MPa) of slaked lime/ silica fume mixes as a function of reaction time and C/S-ratio.

C/S-ratio	Hydration time			
	3 days	7 days	28 days	84 days
2.00	8.0±0.4	19.9±0.8	45.3±1.8	-
1.50	7.9±0.5	21.7±1.0	47.3±1.9	-
1.11	8.5±0.4	25.9±0.6	54.7±1.4	63.9±2.6
0.90	7.7±0.6	26.5±1.1	52.6±1.8	-
0.67	13.9±0.6[1]	26.9±1.0	56.6±3.2	-
0.50	11.1±0.7[1]	27.9±0.8	56.1±2.2	-
0.25	14.7±0.4	30.2±0.9	42.2±1.4	-

[1] Strength measured at 4 days instead of 3.

Other factors that may need to be varied in order to find optimum hardening conditions is the accelerator type and amount. James and Rao /3/ also state that alkalies have a catalytic effect (Eq. 1) on the reaction between lime and silica in rice husk ash. However, rice husk ash contains by nature about 1 % alkalies.

The pore size distributions from 0.0058 to 40 μm for mortar samples with C/S = 2.00 and 1.50 are depicted in Figure 2. The total porosities were measured to 9.5 and 9.6 %, respectively, while the corresponding densities of the solids were 2.18 and 2.20 g/cm^3. The main part of the porosity seems to be between 10 and 0.1 μm in size.

The water absorption profiles for the same two specimens are plotted in Figure 3. Both samples seem to reach saturation after about 2 hours. The capillary and total porosity (after pressure saturation) accessible for water are 14.5±0.5 and 15.6±0.5 for the sample with C/S = 1.50 and 14.0±0.5 and 15.1±0.5 for the sample with C/S = 2.00.

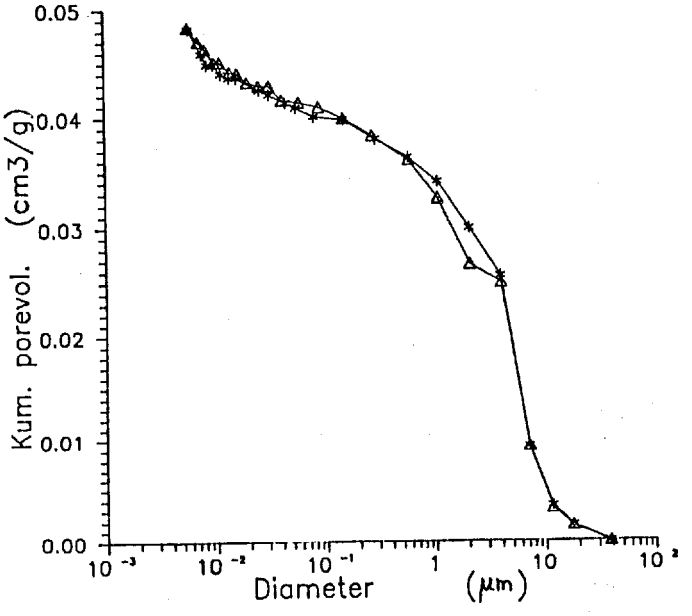

Figure 2: Pore size distribution in mortars with binders of C/S = 1.50 (△) and 2.00 (*).

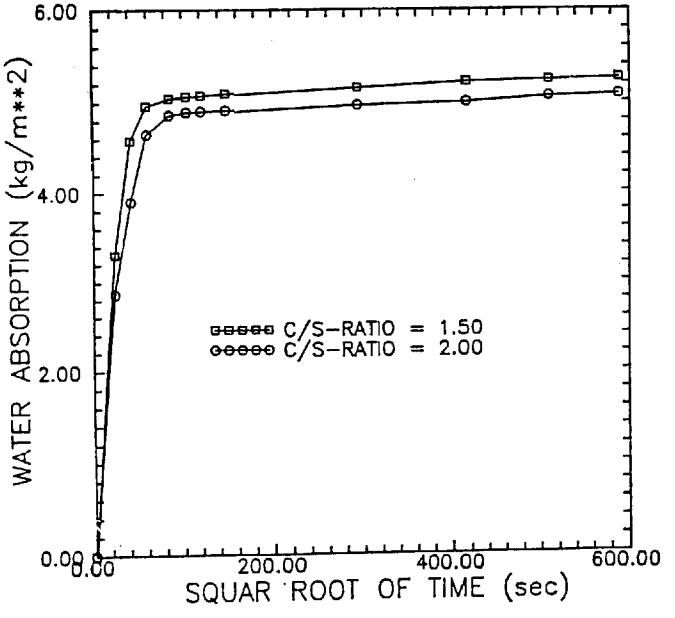

Figure 3: Water absorption during capillary suction for mortars with different binders

CONCLUSION

The CSH-gel formed from the reaction between slaked lime (CH) and condensed silica fume (CSF) accelerated by alkalies has a similar composition as the CSH-gel formed by the hydration of alite. The convertion of CSF is low at the first day of curing, but exceeds that of C_3S at 28 days.

Mortars based on CH/CSF binder exhibits excellent strengths from 7 days on for a wide range of C/S-ratios. However, the early strength is low. The highest early strength seems to be obtained by the lowest C/S-ratio.

Further work should be emphasized on making castable mixes with lowest possible water/binder-ratio, since the reaction itself consumes water corresponding to a water/-binder-ratio of 0.24. The same concept of binder formulation should work on rice husk ash as well, utilizing alkalies as accelerators.

REFERENCES

/1/ Justnes, H., Meland, I., Bjørgum, J.O. and Krane, J.; "A ^{29}Si MAS NMR Study of the Pozzolanic Activity of Condensed Silica Fume and the Hydration of Di- and Tricalcium Silicate." Advances in Cement Research, 1990, 3 (11), 111-116.

/2/ Justnes, H., Sellevold, E.J., Lundevall, G.; "High Strength Concrete Binders. Part A: Reactivity and Composition of Cement Pastes with and without Condensed Silica Fume", **Fourth International Conference on Fly Ash, Silica Fume, Slag and Natural Pozzolans in Concrete, Istanbul, Turkey**, May 3-8, 1992

/3/ James, J. and Rao, M. S.; "Reaction Product of Lime and Silica from Rice Husk Ash", Cement and Concrete Research, 1986, 16, 67-73

/4/ Cook, D. J. and Suwanvitaya, P., **Proc. 1st International Conference of Fly Ash, Silica Fume and other Mineral-by-Products in Concrete, Montebello**, 1983 (ACI SP-79), 2, 831

/5/ Cook, D. J. and Suwanvitaya, P., **Proc. ESCAP/RCTT Third Workshop on Rice-Husk Ash Cement, New Dehli, India**, 1981.

/6/ Cook, D. J., **Proc. 9th Australian Conference on the Mechanics of Structures and Materials, Sydney, Australia**, 1984, 335.

/7/ Fagerlund, G.: "On the Capillarity of Concrete", Nordic Concrete Research, 1982, 1, 6.1.

/8/ Justnes, H., Meland, I., Bjørgum, J.O. and Krane, J.; "Nuclear Magnetic Resonance (NMR) - a Powerful Tool in Cement and Concrete Research." Advances in Cement Research, 1990, 3 (11), 105-110.

HIGH STRENGTH ALKALI STEEL-IRON SLAG BINDER

Bian Qinghan, Wu Xuequan and Tang Mingshu

Dept of Silicate Engineering
Nanjing Institute of Chemical Technology
Nanjing, P R China

ABSTRACT

Steel slag (LDS) from Linz-Donawitz (LD) process partly substituting blastfurnace slag (BFS) to make high strength alkali-slag binder (ASB) has been investigated.

The results show that when less than 20% of LDS was used, the binder strength would be similiar to or even higher than ASB containing no LDS, but beyond 20% the strength would decrease markedly to less than the ASB strength. A binder containing 20% LDS and 80% BFS achieved a compressive strength of 119.4 MPa after 180 days. A 1.5-1.7 modulus of waterglass and a 4-5% alkali dosage are adequate; The presence of CSH(B) as an essential hydrate was confirmed by XRD, DTA and SEM; The pore structure was also studied.

摘　　要

研究了用转炉炼钢过程（即Linz-Donawitz炼钢法）中排出的钢渣（LDS）部分替代高炉矿渣（BFS）制造的高强碱-矿渣水泥（ASB）

结果表明当钢渣用量少于20%时所得碱-钢矿渣水泥的强度接近甚至高于不含钢渣的碱-矿渣水泥（ASB）；如果钢渣用量高于20%，碱-钢矿渣水泥强度将明显低于碱-矿渣水泥含20%钢渣和80%矿渣的碱-钢矿渣水泥180天的抗压强度可达到119.4MPa 适宜的水玻璃模数和碱掺入量分别为1.5-1.7和4.0-5.0%Na_2O 用XRD、DTA和SEM证实了CSH（B）是水泥的主要水化产物 此外，还研究了硬化水泥石的孔结构

INTRODUCTION

Alkali activated blastfurnace slag binder (ASB) has been studied worldwide because of its many advantages, such as high strength both at early and later ages, low heat of hydration, very good durability and energy saving. But in China, mostly blastfurnace slag (BFS, i.e. iron slag) has been used to produce ordinary portland cement and portland-slag cement. As a result, there is no abundant supply of BFS for making ASB. Meanwhile, the sale price of BFS is almost equal to or even higher than that of portland cement clinker in some areas. In the event, substitutes have to be found for BFS to reduce the cost.

Steel slag (LDS) coming out of the steel making process in a LD converter has different compositions at different stages. The average chemical composition of LDS usually lies in the ternary system CaO(MgO)-Al_2O_3 (Fe_2O_3)-SiO_2, and is in close vicinity of the area of BFS and portland cement clinker. In general, it consists of dicalcium silicate, tricalcium silicate, olivine (MS), merwinite (C_3MS_2), dicalcium ferrite, calcium aluminoferrite and RO phase as well as free lime (f-CaO) etc. The amounts of calcium silicates increase with the rise of the alkalinity of LDS (1).

From the theoretical point of view, LDS could reasonably be used to substitute BFS for producing ASB and portland-slag cement.

MATERIALS AND PROCEDURES

1. Materials

Two kinds of BFS (BFS1 and BFS2) and two kinds of LDS (LDS1 and LDS2) were used as raw materials, the alkalinities of BFS1, BFS2, LDS1 and LDS2 were 0.97, 1.12, 2.38 and 4.60, respectively. A waterglass of 3.08-3.30 modulus was used as activator, after adjusting to the required modulus(2).

2. Procedures

The ratio of waterglass was 0.30 for making ASB paste, and 0.44 for mortar. All mortar strengths (aggregate:binder=2.5:1) were tested on the specimens of 4x4x16 cm in size, and paste strengths on 2x2x2 cm specimens. The hydrates and pore structure were also examined on paste.

RESULTS AND DISCUSSIONS

1. Paste Strength

Using LDS2 (Blaine value 412m^2/Kg) and BFS2 (420 m^2/Kg) as raw materials, and 1.7 modulus waterglass as an activator, whose dosage was 3.0% by wt Na_2O on total slag, the compressive strengths of the paste are listed in Table 1.

It can be seen from Table 1 that LDS could partly substitute BFS to make alkali steel-iron slag binder (ASISB), resulting in an increase in compressive strength at all three ages when the amount of LDS less than 20%. LDS might decrease the strength at 28 days when its proportion exceeded 20%, although 3 and 7-day strengths were increased. The paste strengths were obviously reduced as the proportion of LDS was more than 30%.

Table 1 Effect of LDS Proportion on Compressive Strength of Cement Paste

LDS/BFS	compressive strength, MPa, after		
	3 days	7 days	28 days
0/100	4.08	38.38	74.86
10/90	22.14	45.84	81.17
20/80	27.24	44.70	93.22
30/70	26.83	43.43	58.25
100/0	8.02	10.62	17.48

2. Mortar Strength

2.1 Effect of LDS Proportion on Strength-- Using LDS1 (Blaine Value 583 m^2/Kg) and BFS1 (420 m^2/Kg) as raw materials and the same modulus and dosage of waterglass as in the paste experiments, the compressive and flexural strengths determined of the mortar are shown in Table 2. The results are very similar to those of paste in Table 1. It can be concluded that the proportion of LDS in ASISB should not exceed 20% unless high strength is not required and increased use of LDS is desired. An optimum level of LDS might enhance the lime level and cementitious compounds, favouring strength development. For example, when 20% LDS was used, the compressive (and flexural) strengths of ASISB were increased by 13.8% (15.7%), 8.1% (16.3%) and 5.8% (5.9%) at 3, 28 and 180 days, respectively, compared to the control ASB. The strengths decrease with higher amounts of LDS might be explained as due to the increase in free lime and the more capillary pores in the hardened binder due to the rapid setting. In addition, the use of LDS could substantially reduce the cost and benefit the other properties, such as shrinkage, resistances to chemical attacks and abrasion (2).

Table 2 Effect of LDS Proportion on Flexural and Compressive Strength of Mortar

LDS/BFS	flex./comp. strength, MPa, after				
	3 d	7 d	28 d	90 d	180 d
0/100	5.55/43.63	6.81/63.50	7.67/83.02	11.89/105.00	10.47/112.90
10/90	6.43/48.49	7.26/69.87	9.02/92.13	11.53/103.25	10.19/118.00
20/80	6.42/49.64	6.63/67.51	8.92/89.78	9.86/103.30	11.09/119.40
30/70	6.21/49.12	6.80/64.11	8.13/82.10	9.44/89.40	10.13/100.05
100/0	3.27/18.03	3.39/19.46	3.68/23.72	4.60/26.50	5.43/34.28

2.2 Effect of Waterglass Modulus on Strength-- Both 10% and 20% LDS were used and the dosage of waterglass was 5% as Na_2O. The effect of different waterglass moduli on the strength can be seen from Fig.1. From the viewpoint of strength, the most appropriate modulus was 1.5-1.7. The setting time of these ASISB pastes were also determined. It was found that the higher value of modulus would considerably shorten the initial and final setting times.

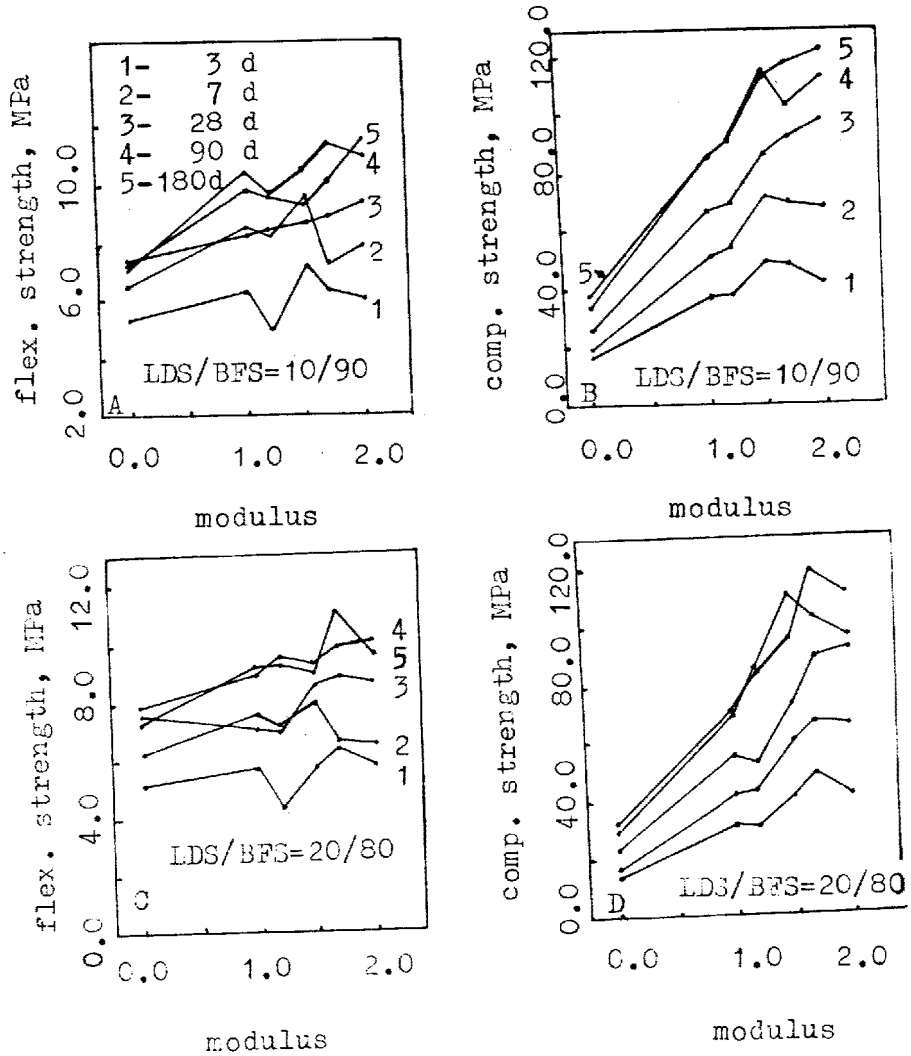

Fig.1 Relations between mortar strength and waterglass moduli. Na_2O 5.0%

2.3 Effect of Alkali Content on Strength-- Both 10% and 20% LDS and waterglass of 1.5 modulus were used. The relationships between mortar strength and waterglass consumption (i.e. the alkali content) are described in Fig. 2. An alkali content ranging from 4.0% to 5.0% as Na_2O might be considered as adequate. Any increase in alkali content could improve the strength only a little and the increase in cost was disproportionable. When 5% alkali was used, the compressive (and flexural) strengths could reach up to 86.43 (8.79) and 72.85 (8.63) MPa at 28 days for ASISB containing 10% and 20% LDS, respectively.

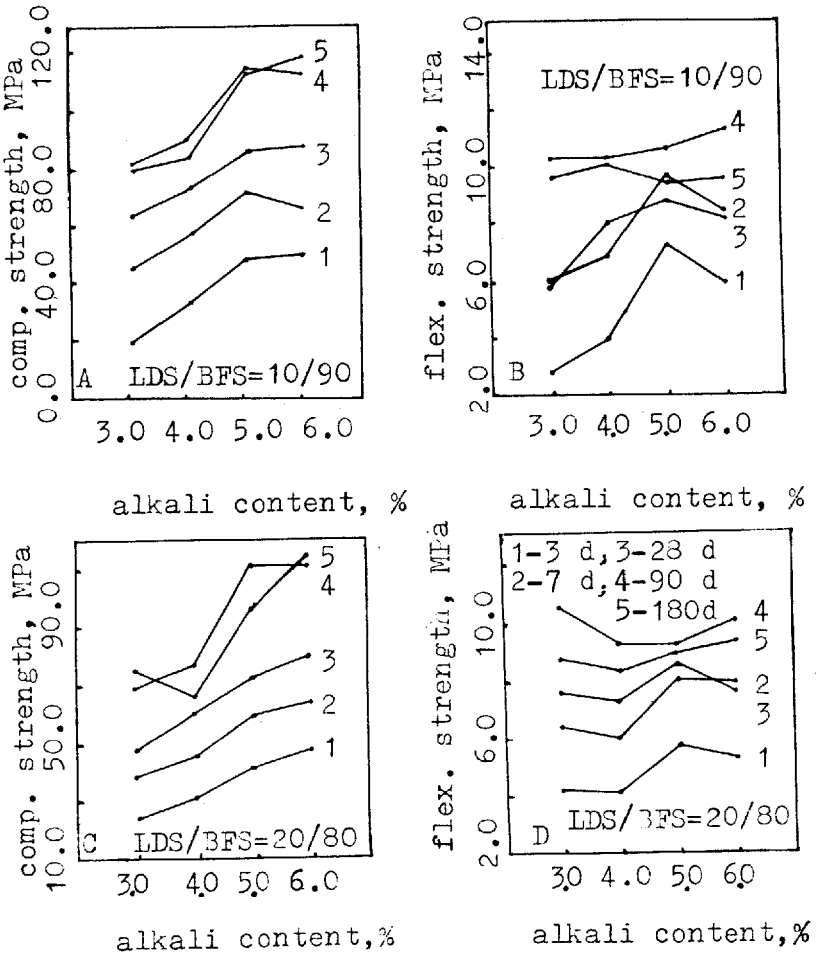

Fig.2 Relationships between mortar strength and alkali content. Modulus of waterglass 1.5

From the above tests, the highest strength ASISB could reach after 180 days was 119.4 MPa for compressive strength and 11.1 MPa for flexural strength. Further, the development of strength within 180 days was positive, i.e. without any decrease in strength.

3. Measurement of Pore Structure

Table 3 shows the results on measurement of pore structure of ASISB paste containing 10% LDS (5.0% Na_2O, waterglass modulus 1.5). It can be deduced that the pore structure varied obviously as the hydration proceeded, the larger pores becoming fewer and the smaller ones becoming more. The total porosity of ASISB paste after 90 days curing was only 4.14%, being very close to that of MDF cement, and there were 21.93% pores of 18.40Å radius. Therefore, ASISB paste exhibits a very densified pore structure, which means high strength and good durability.

4. Study of Hydrates

The hydrates of hardened ASISB paste (10% LDS, waterglass modulus 1.5 and 5.0% Na_2O) at different stages were studied by XRD, and the results

are depicted in Fig.3. The essential hydrate CSH(B) was recognized. These results were also confirmed by DTA and SEM.

Table 3 Pore Structure of Alkali Steel-Iron Slag Binder

	PORE VOLUME DISTRIBUTION									
Hydration Time	<30Å	30–100Å	100–250Å	250–500Å	500–1000Å	>1000Å	MODE	MEAN RADIUS(Å)	MEDIAN RADIUS(Å)	$\frac{\rho(cm^3/g)}{V(\%)}$
3 Days	0.0098	0.089	0.0022	0.0009	0.0013	0.0172	0.0047c.c.at56.14Å	817.9	56.14	$\frac{0.1204}{23.51}$
28 Days	0.0031	0.0036	0.0006	0.0003	0.0007	0.0165	0.0005c.c.at22.35Å	2873	3007	$\frac{0.0249}{4.97}$
90 Days	0.0068	0.0046	0.0008	0.0004	0.0007	0.0073	0.0018c.c.at18.40Å	1352	35.16	$\frac{0.0206}{4.14}$

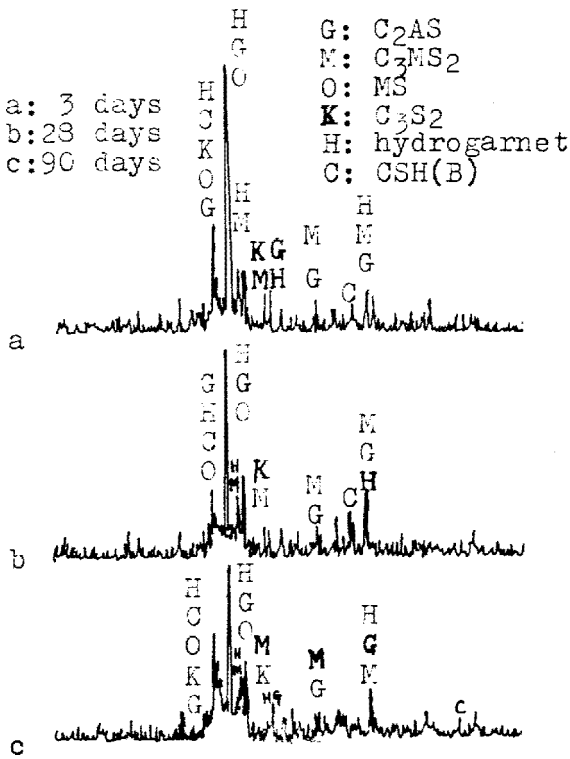

Fig.3 XRD patterns of hardened ASISB paste.

CONCLUSIONS

From the above experimental results, the following conclusions can be drawn:

i) Steel slag (LDS) may partly substitute BFS to make high strength alkali steel-iron slag binder (ASISB). The optimum level of LDS is within 20%, beyond which the strength of ASISB will decrease noticeably.

ii) The adequate modulus and dosage of waterglass for high strength ASISB are between 1.5–1.7 and 4.0–5.0% Na_2O, respectively.

iii) The principal hydrate of hardened ASISB paste is CSH(B).

REFERENCES

1. Tang Mingshu, The Possibility of Producing Cement With Steel Slag Based on the Mineral Composition (in Chinese), 1974.

2. Bian Qinghan, Investigation on Alkali Activated Steel and Iron Slag Binder, M.Sc. Thesis, Nanjing Institute of Chemical Technology (in Chinese), 1988.

COMPARISON OF THE MICROSTRUCTURE AND PERFORMANCE OF ALKALI-SLAG AND PORTLAND CEMENT PASTES

Caijun Shi*, Robert L Day*, Xuequan Wu and Mingshu Tang****

**Department of Civil Engineering, The University of Calgary*
Alberta, CANADA
***Department of Silicate Engineering*
Nanjing Institute of Chemical Technology, Nanjing
P R CHINA

SUMMARY

This paper compares the microstructure and performance of alkali-slag cement (ASC) pastes with those of Portland cement (PC) pastes. CSH(B) with low C/S ratio is the main hydration product in hardened ASC; no crystalline phases such as $Ca(OH)_2$, AFt and AFm exist. At the same time, the ASC pastes, with a high proportion of pores with r<100 Å, show lower porosity than PC pastes. These result in hardened ASC pastes having better mechanical properties and durability than hardened PC pastes.

摘　　要

本文比較了碱一礦渣水泥 （ASC） 漿體和波特蘭水泥 （PC） 漿體的顯微結構與性能。碱一礦渣水泥的主要水化產物爲低碱性的水化硅酸鈣； 没有氫氧化鈣， 鈣礬石和單硫型硫鋁酸鈣那些晶體存在。同時， 碱一礦渣水泥漿體的孔隙率比波特蘭水泥漿體的低，且大多數爲孔徑小于 100 A 的孔。這就使得硬化的碱一礦渣水泥具有比波特蘭水泥漿體更好的力學性能和耐久性。

INTRODUCTION

Modern development of cement and concrete materials is aimed at producing high strength and good durability while maintaining acceptable cost of energy for production. Traditional methods to improve the performance of hardened cement and concrete include (a) changing mineral proportions of clinker, (b) adding chemical or mineral admixtures and (c) polymer impregnation of the pore structure. Much research has confirmed that the potential to obtain high strength from ordinary portland cement is limited by using regular technology.

Alkali-slag cement (ASC), which consists of ground slag with an alkaline activator(s), has advantages of higher strength, denser microstructure, better overall durability, lower production cost and simpler manufacturing technology over portland cement (PC). Russia and some European countries have applied this cement in some practical projects . while many other countries have research in progress [1-6]. The objective of the present paper is to compare the microstructure and performance of hardened ASC pastes with those of PC pastes. Comparisons are based on a large body of research generated by the authors as well as that contained in the literature.

SETTING

Almost all standards require that the initial setting time of cement should not be less than 45 minutes and final set should be less than 12 hours. The setting process of ASC is very different from that of PC; setting of ASC depends upon the reactivity of the slag used as well as the amount and the nature of the alkaline activators used. Table I shows the effect of the modulus and dosage of water glass on the setting of phosphorus slag. The setting time reduces when either the modulus or dosage of water glass increases. The cement will set very quickly if the modulus of waterglass is higher than 1.5. It was also found [7] that the cement will set quite slowly if Na_2CO_3, Na_3PO_4 or NaF is used as an alkaline activator. It seems that the setting of ASC is related to the reaction product of the Ca^{2+} dissolving from the surface of slag grains and the anion or anion groups of activators. The quick set that may result from using waterglass as an activator may thus require use of a set retarder. It has been found that commercial set retarder normally used for PC are, in general, not suitable for ASC-based materials. However, one effective method of controlling ASC setting is to use composite activators.

Table I Effect of the Modulus and Dosage of Waterglass on Setting Times of Alkali-phosphorus Slag Cements [7]

No.	activator[1]	W/S[2]	pH values of solutions	setting time (h:m)	
				initial	final
1	2% M0.5	0.27	13.40	1:02	2:14
2	2% M1.5	0.27	12.98	0:32	1:19
3	2% M2.5	0.27	12.12	0:07	0:12
4	3% M0.5	0.27	13.66	0:47	1:52
5	3% M1.5	0.27	13.11	0:11	0:24
6	3% M2.5	0.27	13.24	0:05	0:07

1 - by weight of Na_2O;
2 - water requirement for normal consistency.

STRENGTH

In addition to the factors which affect the strength development of PC, the nature and the dosage of activators play a crucial role in determining the strength of ASC. Many results confirm that alkaline activators demonstrate selectivity; i.e., the effect that an activator has on strength development may be different for slag of different origins. Matelepszy found that Na_2CO_3 is especially suitable for slags rich in C_2MS , and NaOH is a good activator for slags rich in C_2AS [10]. Smith and Osborne [11], and Bijen and Waltje [12] found NaOH to be the best activator for fly-ash/slag mixtures; waterglass did not show any activation effect on such mixtures. Conversely, Dai and Cheng [13] concluded that waterglass was much better for fly-ash/slag mixtures. Liu [14] developed fly-ash/slag concretes with strengths as high as 76 MPa at 28 days with waterglass as the activator. Fig.1 shows the strength development of alkali-phosphorus slag cement with different activators [15]. The cement with waterglass shows a more rapid strength gain at early age than the cement with Na_2CO_3 activator. Some researchers have also found that the addition of a small quantity of PC is helpful to both the early and the later strength of ASC [1].

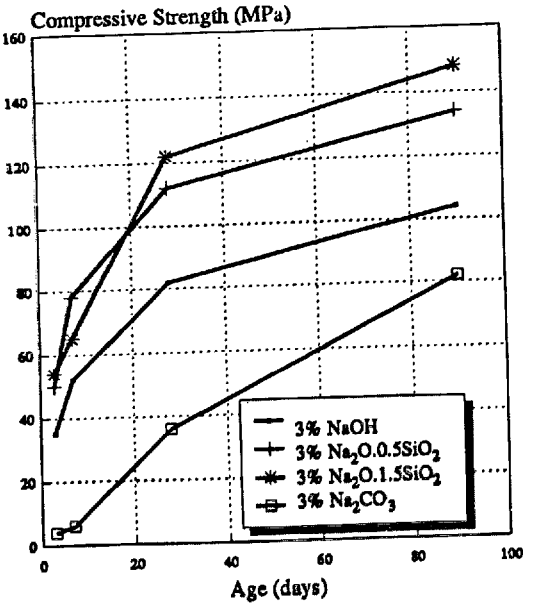

Fig.1 Effect of Different Activators on Strength Development of Alkali-phosphorus Slag Cements [13]

The timing of the addition of the activator also affects the strength of ASC. There are three ways to add the activators: (1) dissolve in mixing water; (2) mix with slag before grinding and (3) mix with slag after

grinding. Usually, method (2) is the most effective because the activators can mix uniformly with slag. Also, some activator(s) may be adsorbed onto the reactive locations on the surface of the slag [1]. Note that some activators may hydrolyse during grinding or storage. In such cases, it is better to use the first method to add the activators.

The characteristics of the slag are also very important. Experimental results indicate that alkali-phosphorus slag cement always shows higher strength than alkali-blast furnace slag cement with all other factors identical, even though phosphorus slag is not as reactive as blast furnace slag if they are used as a mineral admixture to portland cement [8]. This is because blast furnace slag usually contains more Al_2O_3, which is helpful to early strength development but not to later strength gain. Theoretically, the pure SiO_2-CaO system has the highest strength potential [9], the key is how to activate the potential strength of this system.

The strength development of ASC paste is very different from the mortar and concrete if a constant dosage of alkaline activator is used. To maintain equivalent strength, it is better to use constant concentration of solution instead of fixed dosage of activator.

MICROSTRUCTURE

Hydration Products

In hardened ASC paste, C-S-H(B) with a low C/S ratio is the main hydration product; no crystalline $Ca(OH)_2$ and calcium sulphoaluminates C_3AH_6 and C_2ASH_8 have been detected [16]. The appearance of minor crystalline products will depend upon the chemical and mineral composition of the slag used. Several papers have noted the incorporation of alkaline metal ion R^+ into C-S-H or replacement of Ca^{2+} in C-S-H with R^+. The incorporation or replacement varies with the concentration of R^+, reaction age, temperature and the C/S ratio in the system [17,18]. It is widely accepted that the lower the C/S ratio of C-S-H, the more R^+ can be incorporated. Soviet researchers[1] have noted that about 80% of alkalies could be bound by the hydration products at 1 year.

When Na compounds are used as activators, it is very difficult to use XRD to identify the incorporation or replacement. Because the ionic radius of Na^+ (0.95 Å) is similar to that of Ca^{2+} (0.97 Å), the replacement or incorporation of Na^+ thus does not change the structural characteristics of C-S-H and causes little shift of diffraction peaks. When Cs^+ (r=1.69 Å) is used, it was found that the different d-spacing of diffraction peak of C-S-H increases as the dosage of $CsNO_3$ increases (as shown in Table II). SEM/EDS examination also confirmed the presence of R^+ in C-S-H in alkali-slag cement paste. Some people have called the amorphous calcium-alkali aluminosilicate hydrate, "zeolite" [19]. However, it is not appropriate to regard the gel as a zeolite because only the crystalline substance can be called zeolite. It may be more suitable to use C(Na,K)SH gel to represent the main hydration product in hardened alkali-slag cement pastes than to use CSH.

Table II Effect of the Addition of $CsNO_3$ on d-value of Main Peak of Synthetic CSH (80°C, 6 days) [23]

No.	Mixing Proportions	d-values (nm)	d shift (nm)
1	control*	3.3057	0
2	control+0.5%$CsNO_3$	3.3064	0.007
3	control+1.0%$CsNO_3$	3.3082	0.025

* control mix: 1 mol SiO_2+ 1 mol CaO.

Some researchers have noted the presence of silicic acid in ASC pastes [19] despite the fact that the pH value of the pore solution in hardened ASC paste is very similar to that in hardened PC paste. It seems improbable for silicic acid to exist in such a highly alkaline environment. Only amorphous hydration products were identified in hardened ASC pastes cured at room temperature either by XRD or SEM. Tobermorite or xonotlite could be detected in autoclaved ASC pastes with both XRD and SEM [3,6].

Preliminary calculations [21] indicated that the C-S-H(B) formed in ASC pastes has a higher H/C ratio and a lower density than that formed in portland cement pastes, this is in agreement with experimental results [22].

Pore Structure Characteristics

ASC pastes show not only lower porosity, but also a finer pore structure than PC pastes. Table III summarizes the pore size distribution of alkali-blastfurnace slag cement (ABSC), alkali-phosphorus slag cement (APSC) and PC pastes cured at both room temperature and 150 °C. The main pores in ASC pastes are small ones with r<100 Å.

Table III Pore Structure Characteristics of Cement Pastes [6, 23]

paste type	porosity (%)	pore volume (%)		
		18-100 (Å)	100-1000 (Å)	>1000 (Å)
PC[1]	22.3	18.9	69.7	11.4
ABSC[1]	12.7	81.0	15.1	3.9
PC[2]	26.3	14.6	48.7	36.7
ABSC[2]	19.3	96.9	0.4	2.7
APSC[2]	19.7	95.3	4.7	0

1 - cured 28 days at 20°C;
2 - cured 5 days at 150°C.

THERMAL STABILITY

Hydrothermal Conditions

The strength of autoclaved PC at 150°C reaches a maximum value at about 1 day, then drops to only half of the maximum value at 3 days and remains almost constant thereafter (Fig.3). Alkali-blastfurnace slag and alkali-phosphorus slag cements reach a plateau after 1 day. At the same time, alkali-phosphorus slag cement also show higher strength than alkali-blastfurnace slag cement.

Oven-dry Condition

Under oven-dry conditions, ASC pastes also show better performance than PC pastes. Fig.4 gives the strength of the cement pastes oven-dried at 25, 100, 300 and 450°C after these pastes have been cured 28 days in a fog room at 25°C. ABSC pastes show a higher strength than PC pastes over all drying temperatures. Strength of PC paste remains approximate constant. ABSC pastes increase in strength from about 105 MPa at 25°C to about 150 MPa at 300°C, then drop to about 100 MPa at 450°C. Soviet literature [1] state that ABSC pastes have much higher fire resistance than PC pastes. If a small amount of aluminum silicate is added to the alkali-slag cement, the strength of ABSC pastes will be 90-150% of the original strength even after 1000°C oven treatment.

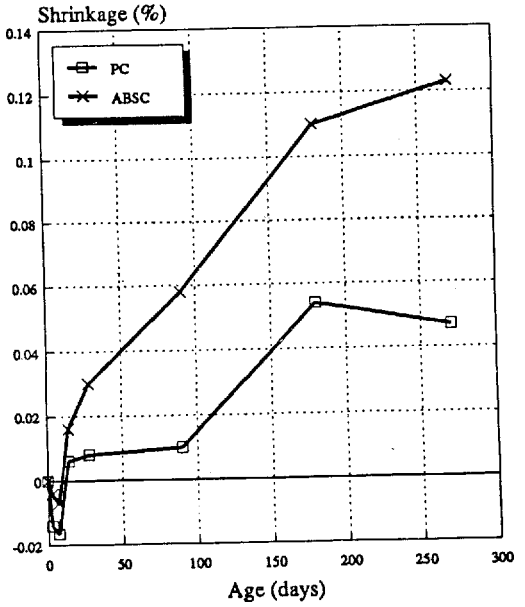

Fig.5 Shrinkage of Cement Pastes in Water at 20°C [25]

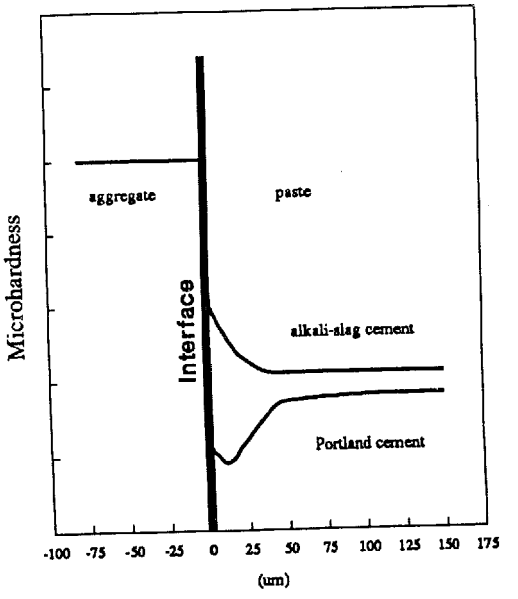

Fig.6 Schematic Illustration of Paste-Aggregate Interface [based on Ref. 1, 26, 27]

SHRINKAGE

Fig.5 shows the shrinkage of ABSC and PC pastes cured in water at 20°C. It can be seen that ASC pastes show larger autogenous shrinkage than PC pastes. This can be explained by the differences in pore structure. ABSC pastes show lower porosity than PC pastes, but the former mainly contains pores with r<100 Å. Time dependent deformation is mainly attributed to fluid and solid movements within the "gel" components of the material. Since ASC pastes have a higher proportion of material in this range, one would expect shrinkage strain to be larger than a material, such as PC pastes, with a coarser microstructure.

INTERFACE BETWEEN CEMENT PASTE AND CONCRETE

The interface between cement paste and aggregate is the weakest zone in the concrete. The main reason is that coarse crystalline substances, such as $Ca(OH)_2$ and AFt are predominant and oriented in the transition zone and weaken the bond between the paste and aggregate. In ASC pastes, no crystalline $Ca(OH)_2$ and sulphoaluminates exist. Also, normally weakening clays or silts on the surface of aggregate can react with the alkaline activator(s) and form cementitious substances [1]. the paste-aggregate interface in ASC concrete is therefore expected to be decidedly different than in PC concrete. Hardness tests indicated that no transition zone appears between ASC paste and aggregate. Fig.6 shows microhardiness across the transition zone of ASC paste and aggregate and PC paste and aggregate. The paste-aggregate interface in ASC concrete should not be the weak link as it is in PC concrete.

Correlation Between Porosity and Strength

Although many relationships between porosity and compressive strength of portland cement pastes have been proposed, most are variations of one of the three types:

$$\sigma=\sigma_o.(1-P)^A \quad \text{.....(1)}$$

$$\sigma=\sigma_o.\exp(-B.P) \quad \text{.....(2)}$$

$$\sigma=D.\ln(\frac{P_o}{P}) \quad \text{.....(3)}$$

where:

σ_o - compressive strength at zero porosity;
P - porosity,
P^o- porosity at zero strength;
σ - compressive strength at porosity P;
A, B, C, D - experimental constants.

All three equations represent a simplification of the system because they consider only total porosity. The pore size distribution, the shape of the pores and the position of pores are also important, but it is both difficult and impractical to include all these parameters. Many experimental results confirm that an acceptable prediction of strength can be obtained by using total porosity. Equation (2) is especially suitable for low porosity systems and equation (3) for high porosity systems. Xu [24] found that both ASC and PC pastes follow the equation (2) within low porosity range:

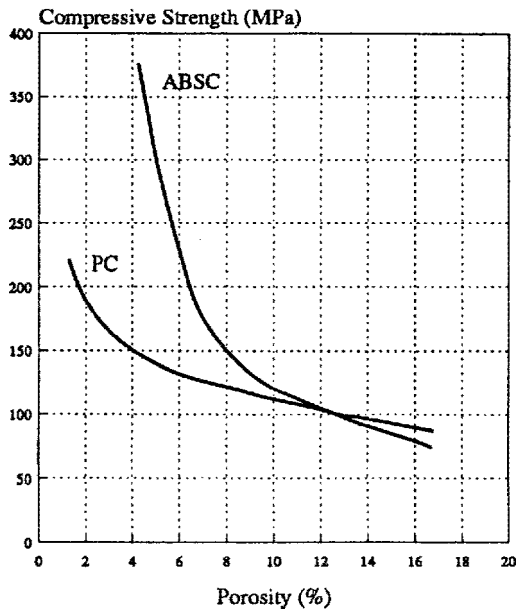

Fig.2 Correlations Between Compressive Strength and Porosity [24]

$$P=11.49\exp(-0.031\sigma) \quad r=0.996 \quad (PC) \ldots\ldots\ldots\ldots (4)$$

$$P=25.26\exp(-0.006\sigma) \quad r=0.941 \quad (ASC) \ldots\ldots\ldots\ldots (5)$$

Below 12% porosity, ABSC paste shows higher strength than PC at the same porosity (as shown in Fig.2). It seems that hardened ASC has higher intrinsic strength than PC pastes.

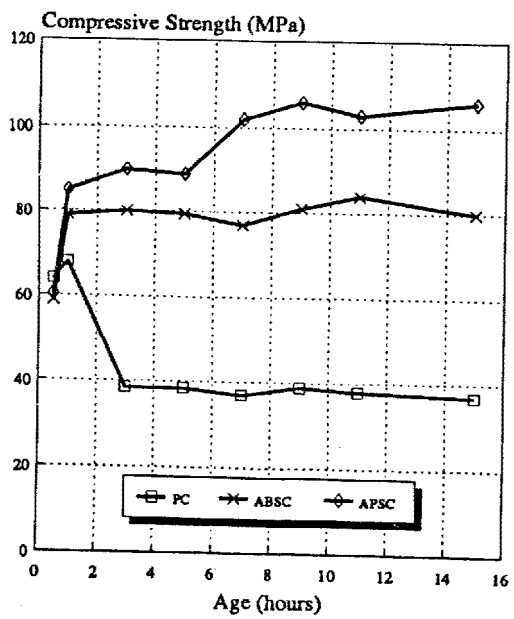

Fig.3 Strength Development of Cement Pastes at 150°C

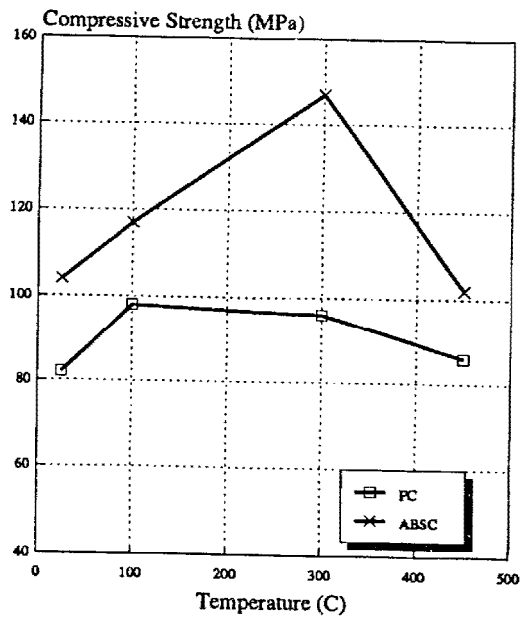

Fig.4 Effect of Oven-dry on Compressive Strength of Cement Pastes [23]

PERMEABILITY, FREEZE-THAW RESISTANCE AND CHEMICAL ATTACK RESISTANCE

Permeability plays a crucial role in determining the durability of cement pastes and concretes. Many researchers have confirmed that permeability primarily depends on capillary pore structure [27,28]. The presence of the transition between PC paste and aggregate results in the much higher permeability of concrete than that of paste. As stated above, ASC pastes show lower porosity than PC pastes and contain mainly pores with r<100°C. At the same time, there is no weak transition zone between paste and aggregate in ASC concrete. ASC pastes and concrete should have superior resistance to water flow and freeze-thaw resistance when compared to PC pastes and concretes.

The expected low permeability of ASC paste and concrete implies high resistance to freeze-thaw attack and attack by aggressive chemicals. An example of this is shown in Table IV [30] where high strength PC pastes appear significantly less resistant to corrosive solution (as measured by a reduction in compressive strength). All solutions have a significant effect on PC paste. Except for ASC2 and ASC3 in 5% $MgSO_4$ solution, the compressive strength of ASC pastes are not significantly affected by the corrosive environment.

Table IV Effect of Various Corrosive Solutions on the Compressive Strength of Cement Pastes[1] [30]

	in water	in 5% Na_2SO_4 solution	in 5% $MgSO_4$ solution	in 5% NaOH solution	in 5% NaCl solution
PC	147.3	106.8	88.8	105.2	95.7
ASC1[2]	155.6	158.2	153.1	151.5	150.6
ASC2[3]	160.8	156.3	112.7	180.6	155.5
ASC3[4]	361.7	371.3	282.7	374.0	352.2

1 - specimens fog-cured 3 days at 80°C and then put in various solutions 28 days at 40°C;
2 - cast with regular technology;
3 - compacted with pressure of 50 MPa;
4 - compacted with a pressure of 500 MPa.

ALKALI-AGGREGATE REACTION

Usually, more than 3% Na_2O is added to slag as an alkaline activator in ASC. There is therefore some concern about alkali-aggregate reaction. The alkalies in ASC can exist in several forms: (1) incorporated into C-S-H; (2) physically adsorbed on the surface of hydration products and (3) free in pore solution. C-S-H with low C/S ratio has a higher uptake of R^+ than C-S-H with high C/S. Thus C-S-H formed in ASC pastes can bind more R^+ than that of formed in PC pastes. About 80% of the R^+ can be bound by hydration products in ASC pastes at 1 year [1]. It can therefore be expected that the free R^+ available for alkali-aggregate reaction is much less than that originally assumed.

It has been found that the rapid autoclave method [31] for evaluating AAR is not suitable for ASC because the AAR reaction occurs before the activation of slags [32]. Also, because ASC contains more alkalies even than high alkali PC, the common mix proportions used to evaluate potential expansion are not suitable for ASC. Mesto measured the expansion of ASC due to AAR by using the mortar bar method [33] and observed a maximum expansion when the opal content was about 5%. In practice, the reactive components in aggregate may be not as reactive as opal. Further studies need to be performed to determine the AAR susceptibility of ASC. Caution should be exercised if reactive aggregates are used with ASC.

SUMMARY

The paper has summarized some important properties of ASC pastes and compared then with those of PC pastes. Some hypotheses about the expected performances of ASC concretes have been made. In particular, the lack of a weak transition zone at the paste-aggregate interface should allow high strength, low permeability and high durability concrete to be manufactured. The main problem for the application of ASC is that alkalies are expensive and in short supply worldwide. Some industrial by-products with high alkali content can be used as the alkaline activators. ASC may have application for special cases, such as the solidification radioactive wastes, in alkaline media, sulphate etc., where cost is not the main factor.

REFERENCES

1. Gluhovsky, V. D.: **Slag-alkali concretes produced from fine-grained aggregates (in Russian).** Vishcha Shkola, Kiev, U.S.S.R., 1981, 223p.
2. Hakkinen, T.: "Durability of alkali-activated slag concrete". Nordic Concrete Research, 1987(6), 81-94.
3. Malolepszy, J. and Petri, M.: "High strength slag-alkaline binders". Proceedings of 8th ICCC, Brazil 1986, V4, 108-111.
4. Douglas, E. and Brandstetr, J.: "A preliminary study on the alkali activation of granulated blast furnace slag". C. C. R., 1990, 20(5), 746-756.
5. Shi, C. and Li, Y.: "Effect of water glass on the activation of phosphorus slag". IL CEMENT, 1989, 86(3), 161-168.
6. Shi, C., Wu, X. and Tang, M.: "Hydration of alkali-slag cements at 150°C". C. C. C. R., 1991, 21(1), 91-100.

7. Shi, C. and Li, Y.: "Investigation on some factors affecting the characteristics of alkali-phosphorus slag cement". C. C. R., 1989, 19(4), 527-533.
8. Shi, C., Tang, X. and Li, Y.: "Studies on the activation of phosphorus slag". Proceedings of the 3rd International Conference on the Use of Fly Ash, Silica Fume, Slag & Natural Pozzolans in Concrete, Norway, June 1989, SP114 (Supplementary Volume), 657-666.
9. Smoiczyk, H. G.: "Structure and identification of slag". Proceedings of 7th ICCC, Paris, 1980, V1, III-I/3-1/17.
10. Malolepszy, J.: "Activation of synthetic melitite slags by alkalies". Proceedings of 8th ICCC, Brazil 1986, V4, 104-107.
11. Smith, M. A. and Osborne, G. J.: "BFS/fly ash cements". World Cement Technology, 1977, 8(4), 223-233.
12. Bijen, J. and Waltje, H.: "Alkali activated slag-fly ash cements". Proceedings of the 3rd International Conference on the Use of Fly Ash, Silica Fume, Slag & Natural Pozzolans in Concrete, Norway, June 1989, SP114, 1565-1578.
13. Dai, L. and Cheng, J.: "An investigation on BFS-fly ash-alkali system". Bulletin of Chinese Silicate Society (in Chinese), 1988, 16(1), 25-32.
14. Liu, C.: "High strength alkali-BFS-fly ash concrete". Proceedings of 2nd Beijing International Symposium on Cements and Concrete, Beijing, 1989, V2, 232-239.
15. Shi, C.: "Activation of Granulated Phosphorus Slag". M. Sc. Thesis, Nanjing Institute of Technology (in Chinese), 1987, 75p.
16. Regourd, M.: "Structure and behaviour of slag portland cement hydrates". Proceedings of the 7th ICCC, Paris, 1980, V1, III-2/11-26.
17. Kalousek, G. L.: "Studies of portions of the quaternary system soda-lime-silica-water at 25°C". Journal of Research of the National Bureau of Standards, 1944, 32, 285-502.
18. Roy, D. M. and Idorn, G. M.: "Hydration, structure, and properties of blast furnace slag cements, mortars and concretes". ACI Journal, 1982, 79(6), 444-456.
19. Talling, B. and Bradstetr, J.: "Present and future of alkali-activated slag concrete". Proceedings of the 3rd International Conference on the Use of Fly Ash, Silica Fume, Slag & Natural Pozzolans in Concrete, Norway, June 1989, SP-114, 1519-1546.
20. Tang, X. and Shi, C.: "Investigations on phosphorus slag binders: Part I - phosphorus binders". Silicate Construction Products (in Chinese), 1988, (1), 28-32.
21. Shi, C., Physical structure of hardened alkali-slag cement (unpublished).
22. Ouyang, S.: "Studies on some characteristics of the CSH system". Ph.D. Thesis, Wuhan University of Technology (in Chinese), 1986, 109p.
23. Shen, X.: "Solidification of radioactive wastes with cements". M. Sc. Thesis, Nanjing Institute of Chemical Technology (in Chinese), 1988, 57p.
24. Xu, Z.: "Relationship between the composition, structure and mechanical properties of low-porosity cementitious materials, and its modification approaches". Ph. D. Thesis, Nanjing Institute of Chemical Technology (in Chinese), 1988.
25. Deng, M.: "MgO expansive cements". M. Sc. Thesis, Nanjing Institute of Chemical Technology (in Chinese), 1989.
26. Bin, Q.: "Investigation of alkali-steel and BFS slag cements". M. Sc. Thesis, Nanjing Institute of Chemical Technology (in Chinese), 1988, 69p.
27. Nyme, B. K. and Illstonm, J. M.: "Capillary pore structure and permeability of hardened cement paste". Proceedings of 7th ICCC, Paris, 1980, V3, VI-181-185.
28. Manmohan, D. and Mehta, P. K.: "Influence of pozzolanic, slag and chemical admixtures on pore size distribution and permeability of hardened cement pastes". Cement, Concrete and Aggregate, 1981, 3(1), 63-67.
29. Chongqing Institute of Architecture and Engineering, Research Report on Alkali-activated Concrete (in Chinese), 1988.
30. Deng, Y., Wu, X. and Tang, M.: "High strength alkali-slag cement". Journal of Nanjing Institute of Chemical Technology, 1989, 11(2), 1-7.
31. Tang, M., Han, S. and Zhen, S.: "A rapid method for identification of alkali reactivity of aggregates". C. C. R., 1989, 13(2), 417-422.
32. Shi, C.: "Alkali-aggregate reaction of alkali-slag cement". Cement and Concrete Products (in Chinese), 1988, (4), 14-16.
33. Mesto, J.: "The alkali reaction of alkali-activated finnish blast furnace slag". Silicates Industriales, Vol.47, No.4-5, pp123-127, 1982.

THE SELECTION OF STIMULATION AGENTS FOR ALKALI-SLAG CEMENT

Chen Zhi Yuan* and Liao Xin**

**Department of Materials Science and Engineering, Tongji University*
***Department of Silicate Engineering, Shangnai Institute of Building Materials*
Shanghai, P R CHINA

SUMMARY

In this paper, we have prove that one of the better ways to improve the properties of alkali–slag cement is the composit method. The results show that the activator has to be a composite agent in which NaOH has the significant role in rasing the strength, Na_2SO_4 affects strengthening at early ages and $NaAlO_2$ at latter ages. And $KA(SO_4)_2 \cdot 12H_2O$ not only has an effect as sulfate in strengthening the early strength, but also as an aluminate in enhancing the latter strength.

RÉSUMÉ

Dans cet' article, nous avons prové que l'un des meilleurs moyens d' améliorer les proporites du ciment–scorie d'alcali est la methode de composite. Les résultats des essais montrent qu' un agent composite est un activateur dans lequel' NaOH joue un rôle significant en augmentations les resistances, Na_2SO_4 affecte surtour sur les resistances initiales, et $NaAlO_2$ sur les resistance a l'agepostérieur. Et $KA(SO_4)_2 \cdot 12H_2O$ non seulement a un effect comme le sulfate en augmentant les resistances initiales, mais aussi comme un aluminate dans d'augmentation de resistances à l'âgepostérieur.

INTRODUCTION

Alkali–slag cement is a kind of cementitious material. Slag is different from other cementitious materials because of its potential reactivity. Besides the physical state and the chemical composition proper of the slag, the activation process determines the cementitious properties of the slag. Activation of slag has to promote the decomposition of slag, as well as formation of the hydration products and of the net–work of hydrates. In this paper, we have proved that one of the better ways to improve the properties of alkali–slag cement is the composite method by which stimulation, assistant stimulation and assistant cementing (i.e.improving the network of hydrates of the paste) take effect together. Thus, it will be useful for the wide use of alkali–slag cements.

EXPERIMENTS

1. Materials:

(1)Slag: Granular blast furnace slag of chemical composition, SiO_2(35.221%), Fe_2O_3(0.75%), Al_2O_3(15.34%), CaO(41.21%), MgO(6.15%) and others(1.33%), and with fineness 3520 cm^2 / g, was used.

(2)Chemical reagents and solutions:

Chemical reagents: NaOH (strong alkali, abb. NH), $KAl(SO_4)_2 12H_2O$ (weak acid, abb. KAS), Na_2SO_4(neutral, abb. NS), and $NaAlO_2$(alkali, abb. NA) were used.

The solutions made with these chemical reagents separately were used as the mixing solution for the alkali–slag cement.

2. Testing Methods

Methods for testing stimulation and assisant stimulation: Using 2 × 2 × 2cm cubic specimen and curing at 20 ± 3℃ under water, the strengths of the specimen with alkali–slag cement with different stimulative agents were measured at 28 days.

RESULTS

We chose NH as an alkaline activator and observed the effects of NS KAS composition as assistant stimulator. Due to the decomposition of KAS in the NH solution as shown in the following equation:

$$2[KAl(SO_4)_2 \cdot 12H_2O]+8NaOH+nH_2O \rightarrow K_2SO_4+3Na_2SO_4+2Na[Al(OH)_4]+(n+12) \cdot H_2O$$

as a sulphate, the effects of K_2SO_4 and Na_2SO_4 are nearly the same. Thus, we combined the NA with NH and studied the effect of assistant activation due to $Na[Al(OH)_4]$. The water content used was determined according to the standard consistency of cement.

1. The effect of NH content

The trend of the relationship (Fig.1) between compressive stength and NH content is just like that of the curve published in reference[1]. But the absolute strengths are different, due to the different slag used. The content of NH which has an effect on compressive strength is in the range 0–8%.

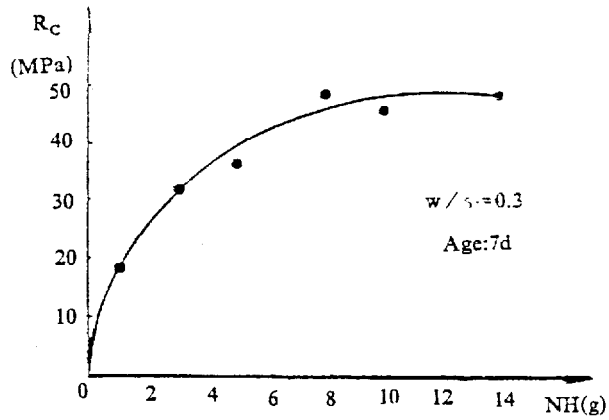

Fig.1 The relationship between compressive strength and NH contents

2. The assistant activaticn of NS and NS+KAS

According to the curve shown above, we combined NH with NS and with NS+KAS in terms of the weight per cent of slag. The results are shown in Table.1.

Table.1. The Compressive strength in different mix proportions

No.	NH %	NS %	KAS %	w / s	Compressive Strength, MPa		
					1 day	3 days	7 days
I	3	/	/	0.3	16.2	30.1	32.1
II	3	1	/	0.3	24.7	34.3	37.5
III	3	2	/	0.3	25.8	37.1	38.9
IV	3	1	1	0.3	29.0	36.8	45.9
V	3	2	1	0.3	25.4	35.1	43.8

From the above data, the assistant activation by sulphate is obvious. In the range we studied, the assistant activation was founed to increase with the contents of NS without KAS. On adding 1% KAS, this increasing trend is apparently not followed but the effect of assisant stimulation is still relatively high.

3. Optimum proportion of composite stimulator

In order to compare the effect of the composite compound on alkali–slag system, three steps were chosen. First, we used the cross experiment design and mean square deviation analysis[2] by compressive strength to obtain the most significient factors in the NH+NS+KAS composite activators. Secondly, the effect of composite activation by NS and KAS was compared with that by NH, and the optimum composite obtained. Lastly, the method of parallel lines [3] was chosen to determine the optimum proportion.

(1)Cross Experimental Design and Mean Square Deviation Analysis— — NH(4%,3%), NS(4 / 3%,1%), KAS(4 / 3%,1%) and Slag (100% with GA,100% without GA) were chosen as four factors of the cross design, and two levels shown in the above brackets were chosen for each factor. Triethanolamine 0.04% on cement weight was

chosen as a grinding agent (GA) for slag. The cross experimental design table of $L_8(2^7)$ was chosen. The results showed that the surface state of slag(with or without grinding agent adsorbed) and the presence of NH were the factors that determined hardening of alkali–slag cement after the slag was actiyated. The NS and KAS affect the strength of alkali–slag in the early age(1–7 d), and NH and NS separately has the non–negligible effect each other on 7–28 d strengths. The best mix proportion of the cross experiment is shown in J4, Table 2.

(2)Comparison and Selection of Composite Form—The mix proportions of the test in Table 2 were investigated to determine the optimizing compounds among NH, NS and KAS.

Table 2 The Compressive Strength with Different Mix Proportions

	NH %	KAS %	NS %	w / s	Compressive Strength, MPa			
					1 day	3 days	7 days	28 days
J1	4	/	/	0.3	17.7	32.7	34.8	43.1
J2	4	1.33	/	0.3	29.7	44.5	46.1	59.8
J3	4	/	1.0	0.3	24.4	38.8	42.7	48.2
J4	4	1.33	1.0	0.3	29.6	42.3	52.7	54.9

From the results shown in Table 2, we chose NH+KAS as the optimizing compound.

(3)The Application of Optimum Seeking Method of Parallel Lines—By this method, the optimizing proportion of the NH+KAS optimizing compound could be obtained. The results are shown in Fig,2 and Table.3.

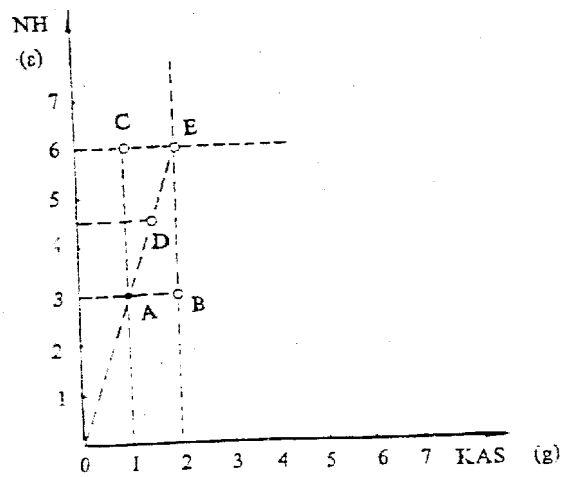

Fig.2 Schematic diagram for parallel line method

In Fig.2 taking testing No.A in Table 3 as a original point, i.e. J2 in Table.2,we chose point B and C. According to the composion of B and C, we prepared the sample and tested it at a particular time. We obtained the compressive strength of testing B and C. The compressive strengths at points B and C are all lower than point A. Thus we took a decision that we need not test the area in the right field of BE and above CE. Then, within the left area, we chose points D and E along the line OA, and obtained the two group strengths of D and E.and found, within the area (NH = 4–6%, KAS = 4 / 3–6 / 3%), the strength increases along the line upward.

Then, we can take R(Z axis), contents of NH (Y axis) and KAS (X axis) as the three dimensional system, and draw Fig.3. On the curved surface, there is a rigid line of high strength. Its projection on XOY plane is a straight line, i.e. Y = 3X. The schematic curve of 7 days age is shown in Fig.3.

Table 3 Strengthes with Different NH / KAS Ratios (by weight)

Testing No.	NH:KAS	Compressive strength, MPa			
		1 days	3 days	7 days	28 days
A	3:1	29.7	44.5	46.1	59.8
B	3:2	24.2	38.1	43.3	45.5
C	6:1	26.5	40.4	45.1	50.0
D	4.5:1.5	38.3	49.2	53.9	65.2
E	6:2	27.5	48.3	54.4	65.7

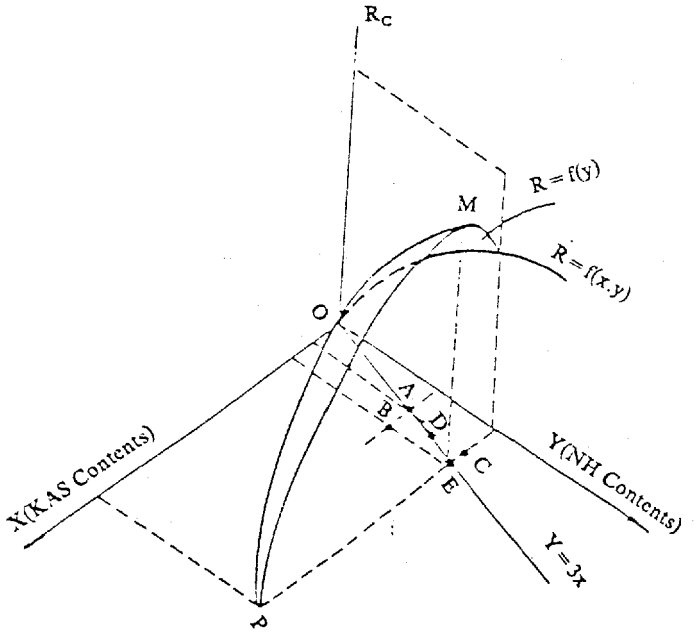

Fig.3 The relationship among KAS, NH and Rc

DISCUSSION

(1)The Assistant Activation Effect of Alkali Sulphate.

The effect of alkali sulphate on the alkali–slag system is to increase the early strength, but its reaction mechanism is yet to be studied.

According to reference[4], a synthetic $C_3AS_3H_{32}$ is formed if the ratio $CaSO_4 / Al_2O_3 > 3$ in the raw materials. If the ratio is within 1–3, the products contain the calcium sulphoaluminate hydrates in two types: high and low sulfur,or solid solution of low sulfur type of calcium sulphoaluminate and tetracalcium aluminate; if $CaSO_4 / Al_2O_3 < 3$, the solid solution of meta stable product and C_4AH_{13} will be formed.

The CaO / Al_2O_3 ratio in slag was about 3. It was suggested that the product of the slag affected by strong alkali is mainly CSH gel. Thus, the CaO / Al_2O_3 ratio decreases due the consumption of a lot of CaO. It cannot form calcium sulphoaluminate hydrate. A.C. Belgel[5] suggested that an incongruent dissolution should take place when

ettringites were in the alkali hydroxide solution. After 24 hours at 25℃, C_2AH_8, C_4AH_{13} and CH would be found in solution. Another reference [6] reported that C_4AH_{13} was present in a product of alkali–slag system. Their data proved the same phenomenon in another point of view.

According to the analyses mentioned above, the early strength mechanism of alkali in the alkali–slag cement is different from that in the portland cement. We consider that, in the alkali–slag system, SO_4^{2-} ions penetrate into the vitreous phase of slag, disturb the stati electric balance of the system, cause the decomposition of slag,thus improving the reactivity of slag. At the same time, the presence of SO_4^{2-} influences the C / S and H / S parameters of CSH phase. It penetrates into CSH and changes the composition and structure of CSH. Being in this process, the alkali sulphate takes the assisant stimulation effect on the early strength.

(2)The Effect of KAS on the Increase of the Strength at Later Age

The optimum conbination,i.e. NH+KAS, raised the strength at all ages. KAS is a sulphate, and appears as a weak acid in the solution. It would decompose to K_2SO_4, Na_2SO_4 and Na〔Al(OH)$_4$〕 in NH solution (pH > 14). Na〔Al(OH)$_4$〕 would be present in the form of AlO_2^- and Na^+. In order to analyses the effect of KAS, we observed the relationship between NH+NA and the strength. The results are shown in Table 4.

Table.4 The Compressive Strengths of Specimen with Different NA Contents

	NH %	NA %	w / s	Compressive strength, MPa			
				1 day	3 days	7 days	28 days
B1	4	0.24	0.3	11.6	29.4	50.2	65.0
B2	4	0.48	0.3	12.4	30.2	47.3	60.7
B3	4	0.72	0.3	9.7	29.0	45.7	54.1

The compositions of J1, J2 and J3 (as shown in Fig.4), were shown in Table.2, and the composition of B1 was converted from that of J2 according to the mol fraction of Al in KAS. In the development of early strength (1–3 days), NS has the early strengthening effect (J3), relative to J1, however, NA inhibits the developement of early strength (B1).And KAS has both the effects of NS and NA(J2). At a later age(3–7 days), the strength of B1 rises rapidly and within 7–28 days the strength increasing rates of B1 and J2 are nearly the same, however that of J1 and J3 rise slowly. Thus, we consider that, in the NH solution, the sulphate and aluminate within the KAS has its own effect on paste strength respectively. KAS can not only develop the early strength, but also improve the strength in the later age by the aluminate. Thus the use of KAS has the practical meaning.

The No.B series show that the raising of NA content on the basis of B1 is without effect for enhancing strength. This phenomenon shows that the hydration products pruducted by reacting with AlO_2^- have to matain a suitable ratio in the paste structure.The change of quantity or properties in the hydration product filling in the paste structure or envelops around the slag grains will lead to different effect on the stimulation hydration and the form of structure. NA was used as a binder in the area of industries and used as an accelerator in the cement concrete construction.NA seems to have the main effect on the paste structure by changing the binding form and thus influencing the hydration and hardening of the alkali–slag system. Finally, the aim of strengthening the system may be achieved.

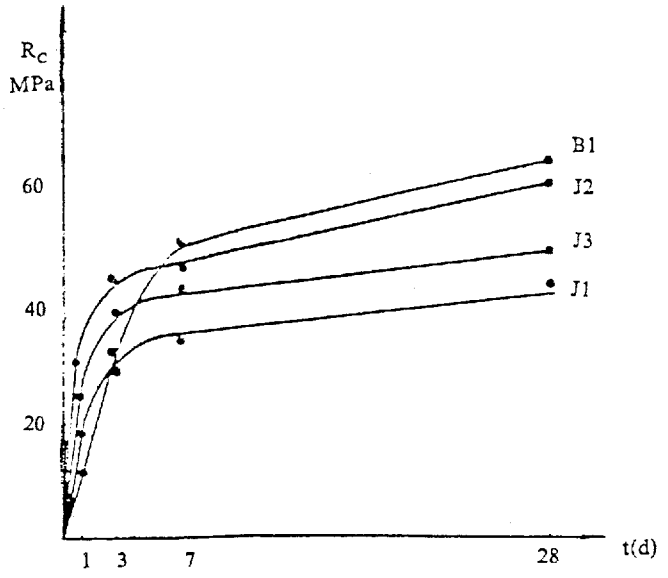

Fig.4 The comparison of Strength development

CONCLUSION

The results show that in the alkali–slag system, the activator has to be a composite agent in which NH has the significant role in rasing the strength, NS affects strengthening at early ages and NA at later ages. And KAS not only has an effect as a sulphate in strengthening the early strength, but also as an aluminate in enhancing the later strength.

REFERENCE

(1)Sersale, R., Aiello, R., Collca, C. and Frigione, G. "Utilisations alternatives des laitiers de haut fourneace", Silic Ind. Vol.41, No.12, 1976, pp.513–519.

(2)Statistics group, Institute of Mathematics, Acadamia Sinica, Common mathematical statistics method, (in Chinese), Science Press, Co. 1973, First edi., Beijing.

(3)Optimum seeking method group, Department of operational research, Institute of Mathematics, Acadamia Sinica, Optimum seeking method, (in Chinese) Science Press, Co. 1975, First edi., Beijing.

(4)He Re Zhang, "Phases study for silicate products made from industrial waste", Beijing Building Materials, 1982.12; 1983.1–3 (in Chinese).

(5)Bepgel A.C. Kopzypalo H.P., Poshyakova, B.A., "Metastable balance of hydrate calcium aluminate in alkali–metal hydroxide", 6th Int. Cong. on the Chemistry of Cement and Concrete, Vol.III (in Russian)

(6)Narang, K.C. and Chopra, S.K., "Studies on Alkaline Activation of BF, Steel and Alloy Slags", Silic. Ind., 1983.9, pp.175–182

ALKALI ACTIVATED SLAG CEMENTITIOUS MATERIAL FOR DRILLING OPERATION

W Brylicki, J Malolepszy and S Stryczek

University of Mining and Metallurgy, Kraków, POLAND

SUMMARY

The investigations on laboratory and technical scale of the alkali activated cementitious materials used in drilling were carried out. The ground granulated blast furnace slag, poorly active was used. The compressive strength, density, setting time and rheological properties of cementitious pastes were determined. The observations of microstructure and microcalorimetric measurements of some samples were also carried out. It was found that the pastes thus obtained could be used in drilling, geotechnics and civil engineering owing to their advantageous properties.

RÉSUMÉ

On a étudié les pâtes contenants le laitier granulé, activé par l'alcalis, utilisés dans les puits profonds. On a déterminé la résistance à la compression, la densité, le temps de prise, les propriétés rhéologiques. On a observé aussi la microstructure des pâtes au microscope à balayage et on a mésuré le dégagement de chaleur pour les échanillons chosies. On a trouvé que les pâtes de laitier activé pourraient être utiliser dans les nombreux constructions grâce à leur comportement favorable.

1. Introduction

It is commonly known that the the setting and hardening of cementitious materials used in drilling (cementing of lining pipes columns, cementing of boreholes, stopping of holes, preventing of drilling fluid escape) takes place under quite different conditions from those obtaining in civil or harbour engineering.
The most important factors influencing the proccess of cement setting and hardening in boreholes are:
- elevated temperature and pressure,
- presence of different active media, such as drilling fluid, aggressive waters, the mineral exploited (petroleum, gas, salt brine).
- a variety of rocks through the depth of the drilled hole (salt beds, anhydrites, gypsum, clays of different structures).

The factors listed above create specific, aggressive media: so the selection of proper materials for cementing must be analysed carefully in each case. The class of cement is firstly chosen depending on the depth of drilling. The conditions obtaining in the borehole determine the type of cement and admixtures for improving the cementing process.

Studies aimed at producing sealing and injection pastes based on activated, ground blast furnace slag as main cementitious material have been carried out at the Academy of Mining and Metallurgy in Cracow, Poland [1, 2].

The phase composition and microstructure of hardened alkali activated slag pastes is strongly influenced by the temperature and duration of curing, besides the type of activator. The following products can be detected in hardened pastes: calcium silicate hydrate CSH I, tobermorite 11A $C_2S_6H_5$, xonotlite C_6S_6H, gyrolite $C_2S_3H_2$, hydrated calcium-sodium silicates as NC_2S_2H, $NC_2S_2H_2$, NC_2S_3H, calcite $CaCO_3$, hydrogarnets $C_xA_yS_2H_n$ with different A/S ratios, sodium zeolites as NAS_2H_3 - sodalite and $NC_2A_5S_{10}H_{12}$ - thomsonite [3]. As it can be easily seen, $Ca(OH)_2$ - portlandite and hydrated aluminates or sulphoaluminates do not occur in slag pastes. This fact is very important, because absence of these phases is responsible for the high corrosion resistance of slag materials. The microstructure and pore size distribution with high fraction of gel pores and low fraction of air and capillary ones gives high tightness and low values of infiltration and permeability coefficients. This is also the reason for the high corrosion resistance [4].

Free Na^+ ions maintain ahigh pH value in the alkali activated slag paste thus improving the interaction with clayey minerals. Another important consequence is the absorption of heavy metals (Zn^{2+}, Pb^{4+}, Cd^{2+}). This fact can be used in ecological engineering (e.g.antifiltration screens) as reported by some authors [5].

2. Experimental

2.1. Raw materials

The following raw materials have been used:
- granulated blast furnace slag from metallurgical plant "Huta im. Sendzimira" in Cracow,
- alkaline activators: sodium hydroxide NaOH, sodium carbonate Na_2CO_3, both of analytical grade.
- ordinary portland cement OPC 35 from "Nowiny" cement work.

The granulated blast furnace slag sample was dried to a constant weight at 105°C and ground in a laboratory ball mill to a specific surface of 3260 cm^2/g as measured by Blaine's method. The chemical composition of the sample so prepared was as follows: L.O.I.- 1.20%, CaO - 42.58%, SiO_2-

38.42%, Al_2O_3 - 7.34%, MgO - 6.66%, Fe_2O_3 - 1.36%, SO_3 - 2.70%, MnO - 0.70%, insoluble residue - 0.24%. The calculated basicity modulus M_z and activity modulus M_a were:

$$M_z = CaO + MgO \,/\, SiO_2 + Al_2O_3 = 1.08$$

and

$$M_a = CaO + MgO + Al_2O_3 \,/\, SiO_2 + MnO = 1.44$$

This slag should be classified as poorly acidic and poorly active. Phase composition studies by XRD and microscopy reveal a dominant vitreous phase content of 83%. The crystalline phases encountered 17% consist mainly of melilites, i.e. solid solutions between gehlenite and akermanite and merwinite. Monticellite, calcite and larnite are present in small amounts.

2.2. Alkali activation of slag pastes and investigation of the products

From the foregonig raw materials injection-sealing pastes were prepared at different water to slag ratios, and different activators and their mixtures. These pastes were subjected to tests following Polish standards [6]. For some pastes the studies of microstructure by SEM and calorimetric measurements were carried out.

2.3. Results

In Table 1 the results of technical parameters determination are presented, particularly those relating to the rheological properties. Using a computer program the following regression equations were presented:

- compressive strength of selected alkali activated slag pastes versus time of setting $R_c = f(t_s)$ (pastes cured at 20°C at RH > 90%) - Table 2,
- initial and final setting as a function of curing temperature $t_i = f(T)$, $t_f = f(T)$ (Table 3)

In Figure 1 the average microstructure of alkali activated slag paste with 5% Na_2CO_3 is shown (28 days hardening in air at RH > 90%). The amorphous product CSH_I (type III following Diamond classification [7]) is clearly visible. In figure 2 the average microstructure of slag paste activated with 5% Na_2CO_3 and autoclaved at 200°C for 4 hours is shown.



Fig.1. SEM 28 for days curing 5500X



Fig.2. SEM for 4h autoclaving at 200°C 3000X

These conditions of curing correspond to those in deep wells, under 2000 m. Apart from the amorphous CSH_I type III, the crystalline plate-like 11.9A tobermorite occurs in this sample.
In Figure 3 the microcalorimetric curves of selected alkali activated slag pastes are presented.

3. Conclusions

The investigations on laboratory and technical scale point to the following advantages from the utilization of alkali activated slag cementitious materials

- possibility of varying some parameters, such as density, setting time, rhelogical properties over a wide range depending on the geological, hydrogeological and technical conditions,
- fulfilment of all requirements by hardened sealing pastes, beside such specially advantegeous properties, as high corrosion resistance [8], low permeability and infiltration coefficients [9] besides controlled shrinkage and expansion [10], unlike pastes made from traditional materials
- low heat of hydration,
- chestness towards drilling fluids and mineralized deposit waters,
- good adhesion to clayey rocks,
- simple method of production of pastes using existing installations.

The sealing and injection mixtures described above are economical and highly efficient when applied in the following works:

a) sealing of lining in boreholes,
b) prevention of drilling fluid escape,
c) sealing and insulation of selected intervals in boreholes,
d) liquidation of eruption during the hole sulphur exploitation,
e) antifiltration barriers and screens realized by grouting,
f) reinforcement of subsoil under industrial and hydraulic structures by grouting [11].

Table 1

Comp. paste BSF+activ. (% by mass of slag)	Water to BSF ratio w/s	Density kg/m³	Conus test AzNII mm	Relative visc. by Ford test s	Plastic visc. Pa·s	App. visc.at shear. rate $1022s^{-1}$	Flow factor	Consistency coef. "k" Pa·s
Slag without activator	0,45	1870	210	24,2	0,35	0,25	-	-
Slag without activator	0,50	1810	230	17,5	0,045	0,06	0,67	0,587
Slag without activator	0,60	1780	250	16,4	0,040	0,043	0,72	0,42
Slag + 3% NaOH	0,50	1830	240 [2]	16,2	0,063	0,07	0,77	0,373
Slag + 5% NaOH	0,50	1840	260	13,8	0,031	0,04	0,76	0,196
Slag + 2% NaOH 3% Na_2CO_3	0,50	1850	220	22,9	0,088	0,10	0,87	0,238

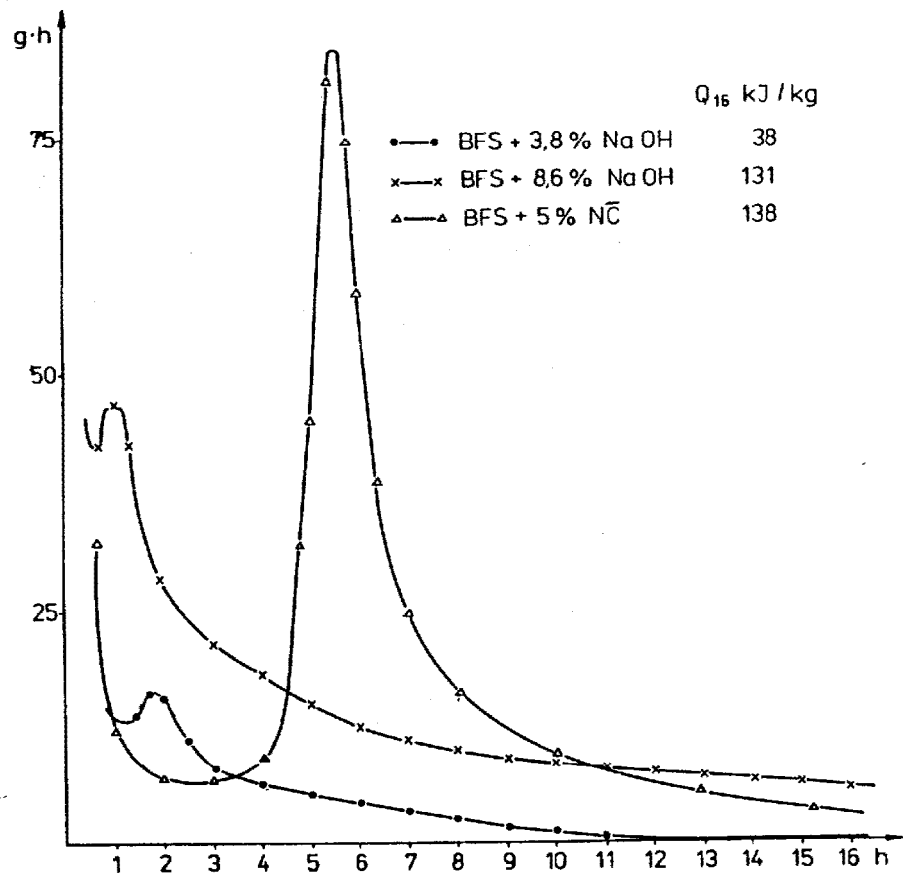

Fig.3 Microcalorimetric curves of some alkali activated slag pastes.

Table 2

Parameters / Independent variable	Compressive strength R , [MPa]					
	Granulated blast furnace slag without admixture w/s=0.5	Granulated blast furnace slag + 2% NaOH w/s=0.5	Granulated blast furnace slag +3% Na_2CO_3 w/s=0.5	Granulated blast furnace slag + 2% NaOH w/s=0.5	Granulated blast furnace slag + 5% OPC +5% Na_2CO_3 w/s = 0.5	Granulated blast furnace slag + 1% NaOH +1% Na_2CO_3 w/s = 0.5
Regression equation	$R = a+bt_v$	$R_c = a+bt_v$	$R_c = a+bt_v$	$R_c = a+bt_s$	$R_c = a+bt_v$	$R_c = a+bt_v$
Coefficient a	0,937	1,067	1,769	1,764	1,754	0,712
Coefficient b	0,256	0,195	0,308	0,275	0,275	0,487
Correlation coefficient	0,929	0,946	0,960	0,971	0,960	0,982
Significance level	0,05	0,05	0,05	0,05	0,05	0,05

Table 3

Parameters / Independent variable	Time of setting [min]					
	Granulated blast furnace slag w/s = 0,5		Granulated blast furnace slag + 5% OPC + 2% NaOH w/s = 0.5		Granulated blast furnace slag + 5% OPC + 2% Na_2CO_3 w/s = 0.5	
	initial	final	initial	final	initial	final
Regression equation	$T_{p1} = \frac{1}{a + bT}$	$T_{p2} = \frac{1}{a + bT}$	$T_{p1} = \frac{1}{a + bT}$	$T_{p2} = \frac{1}{a + bT}$	$T_{p1} = \frac{1}{a + bT}$	$T_{p2} = \frac{1}{a + bT}$
Coefficient a	$-1,689 \cdot 10^{-3}$	$-3,761 \cdot 10^{-3}$	$-4,899 \cdot 10^{-3}$	$-3,854 \cdot 10^{-3}$	$-8,839 \cdot 10^{-3}$	$-6,633 \cdot 10^{-3}$
Coefficient b	$2,929 \cdot 10^{-4}$	$2,341 \cdot 10^{-4}$	$7,377 \cdot 10^{-4}$	$3,460 \cdot 10^{-4}$	$1,040 \cdot 10^{-3}$	$6,446 \cdot 10^{-4}$
Correlation coefficient	0,955	0,997	0,939	0,979	0,989	0,988
Significance level	0,05	0,05	0,05	0,05	0,05	0,05

4. References

1. Polish Patent No.P-285071, 8 May 1990.
2. Polish Patent No.P-284873, 18 April 1990."Spoiwo żużlowo-alkaliczne"
3. Małolepszy J.: Dissertation AGH Kraków, Zeszyty Naukowe Ceramika nr 53, 1989
4. Andreson R., Graham H., Małolepszy J., Deja J.: "Alkali Activated Slag". C.B.I. Research. Stockholm 1988
5. Asano Shunkichi, Toda Fumikazu: 35 th Gen. Meet. Cem. Assoc. Jap. Tech. Sess., Tokyo, 13-15 May 1981, Synopsis. Tokyo, 1981, p.46-47
6. Polish standard PN-85/G-02320. "Drilling cementitious materials for cementing works in borehole"
7. Diamond S.: Proc.Symp."Effects of Fly Ash in Cement and Concrete", Mater.Res.Soc., 1981, p.111-113
8. Machowski M., Małolepszy J. Deja J.: Prace Komisji Górniczo - Geodezyjnej PAN, Górnictwo 1988, 25, s.83-89
9. Brylicki W.,Stryczek S.: "The properties of Alkali - Activated Slags Used in Borehole Cementing Works", Mediterranean Petroleum Conference and Exhibition, Tripoli, Libya, 1992, p.596-604
10. Polish Patent No.P-271470, 21 May 1990. "Spoiwo hydrauliczne"
11. Stryczek S., Brylicki W., Bałasz J., Sztorc S.: "Practical aspects of the utilization of new, alkali activated slag materials as sealing agent in drilling operations", Mediterranean Petroleum Conference and Exihibition, Tripoli, Libya, 1992. p.590-595

THE RESEARCH OF THE REACTIVE PRODUCTS AND MINERAL PHASE FOR FKJ CEMENTITIOUS MATERIAL

Lu Changgao

Suzhou Concrete and Cement Products Research Institute
State Administration of Building Materials Industry, P R CHINA

SUMMARY

In this paper, the study of the reactive mechanism and hydrate products of the fly ash slag—alkali cementitious material (namely FKJ①), Which Na_2SiO_3 is taken as an activator is stressed. By the analyses of the forming process of natural zeolite in natural world, scanning electronic microscope to mineral phase appearance, thermodynamic calculation as well as modern X—ray diffractometer, we consider that, in the FKJ system, the main hydrate products possibly produced are sodium—sillicoaluminate hydrate of analcite type; The secondary products are calcium—silicoaluminate hydrate of scolecite type and sodium—calcium—silicoaluminate hydrate of thomsonite type, meanwhile a small amount of low—alkaline calcium silicate hydrate are also produced.

In the paper, the properties as to good durability, fine carbonation resistance, frost resistance and resistance to chemical attack etc of the FKJ binder are also expounded. Therefore it is possessed of bright prospect in application.

摘　　要

本文着重研究以Na_2SiO_3作为激发剂的粉煤灰渣一碱胶结料(简称FKJ)的反应机理和水化产物。通过分析自然界中天然沸石的形成过程，扫描电镜显微矿相形貌分析，热力学计算及现代X衍射谱线分析，我们认为FKJ系统中可能生成的主要水化产物为方沸石型的水化硅铝酸钠；其次为钙沸石型的水化硅铝酸钙和杆沸石型的水化硅铝酸钠钙；还生成少量的低碱度水化硅酸钙。

论文还阐述了FKJ胶结料有良好的耐久性，即有良好的抗碳化性、抗冻性、耐化学侵蚀性等，故它有广阔的应用前景。

① FKJ refer to the abbreviation of chinese spelling.

1. INTRODUCTION

It's well known that the study and development of blastfunace slag—alkali cementitious material has been carried out in many countries/1/. In recent years, the research in this respect is also undertaken in china/2/. Facing the facts that the fly ash hasn't been sufficiently used and the slag is basically exhausted in home, we pay great attention to the research of FKJ binder which major ingrendient is fly ash. We consider that the reactive mechanism of the FKJ binder differ from that of the blastfurnace slag—alkali binder. In this paper, the main purpose is to reveal the reactive mechanism and hydration products in the FKJ system.

2. ALKALINE MEDIUM IS MAIN CONDITIONS FOR HYDRATION IN FKJ CEMENTITIOUS MATERIAL

FKJ binder is characteristiced by taking alkaline metallic compound as the activator, normally its alkaline reaction is much stronger than that of alkaline earth metallic compound.

The one—valence metallic compounds are various, among which the effect of the Na_2SiO_3 is best according to our test and research, its alkalinity, PH value is **13—14**, in the FKJ system. We consider that the Na_2SiO_3 added in FKJ system not only possess of higher alkaline condition, but also is an important ingredient material to take part in reaction.

3. UNDERSTANDING THE HARDENED MECHANISM OF THE FKJ BINDER FROM ROCK—FORMING MINERAL IN NATURAL WORLD

According to geological information, the great majority of zeolites are formed from reaction between deposited silicoaluminate mineral and water in the pore/3/. the temperature and pressure of some of zeolite in the forming procedure are approximately similar to those in the making of hydraulic cementitious material. For instance analcite and so on are formed by the weathering in the earth's crust, just like water—heat reaction at low temperature.

The formation of zeolite type mineral depends on the chemical constituents and forming conditons for the water—heat mortar in natural world. It is related to the following factors according to analysis.

3.1 In relation to the structural constituents of mother rock

It's indicated by the study that the volcanic glass rock (such as pearlite) is most favourable mother rock for forming zeolite. It is richly possessed of glass structure which main constituents contain SiO_2, Al_2O_3 and some of Na_2O, CaO etc. This factor is similar to the constituent and glass structure for fly ash (amount to **70%**), Blastfurnace slag (amount to **30%**) and activator Na_2SiO_3 in the FKJ binder.

3.2 In relation to the PH value in environment

Sufficient water in pore is fundamental factor that zeolite is hydrated from aluminosilicate, while the PH value in water—solution can be a determine influence on the formation of zeolite. It is very favourable for the fast formation of zeolite when the PH value of water in pore for the volcanic glass rock is as high as **13—14** approximately. The alkality of mix, i.e. PH value approximately equal to **13—14** after the alkaline activator was added into FKJ binder provided necessary condition for fast formation of zeolite type mineral.

3.3 In relation to temperature and pressure

The zeolite is hydrated mineral, therefore it is easily effected by the temperature and pressure. Some of the zeolite is produced under low—temperature and low—pressure. The test indicated that the FKJ binder could be hardened under the conditions of atmospheric temperature and pressure, its conditions about the same.

3.4 In relation to the activity of the basic positive ion and of the silica

The chemical activities of the metallic positive ion, silica oxide and water have influences on the zeolite type crystallized from the solution. The zeolite with high content of metallic positive ion shall have urgely been formed under the condition of high alkalinity. The high or low activity of positive ion have also some influences on the zeolite type formed. This is a more complex problem pending further study.

4. THE HYDRATION CHARACTERISTIC AND POSSIBLE HYDRATION PRODUCTS FOR THE FKJ BINDER

In the FKJ binder system alkali, alkali—earth aluminosilicic acid may be taken as the dispersion system. In the system, the water—sulution of silicic acid carrying negative charge, the metallic ion carrying positive charge, through interaction, cause particls producing coagulation. The more outstanding features are producing strong condensation of the aluminium positive ions in the ash—slag on the silicic gel in the water—glass, forming gel particls. Meanwhile the per gram—molecule of Al_2O_3 can capture 1.0—1.5 gram—molecule of Na_2O, finally to produce sodium silicoaluminate hydrate of four components, i.e.

$$Al_2O_3+4SiO_2+2NaOH+H_2O\rightarrow Na_2O\cdot Al_2O_3\cdot 4SiO_2\cdot 2H_2O. \quad (1)$$

This hydrated products like the analcite in natural world/4/. It forms tetrogon—triakisoctahedron or the gathering of tetrogon—triakisoctahedron with cubic crystal. Its SEM photograph as shown in Fig. 1. It can be seen from the crystal form in the Fig. 1. that there actually is the mineral phase and it can be considered as the main mineral phase in the system.



Figure. 1. The crystal form of SEM(x5000)$Na_2O\cdot Al_2O_3\cdot 4SiO_2\cdot 2H_2O$ mineral phase.

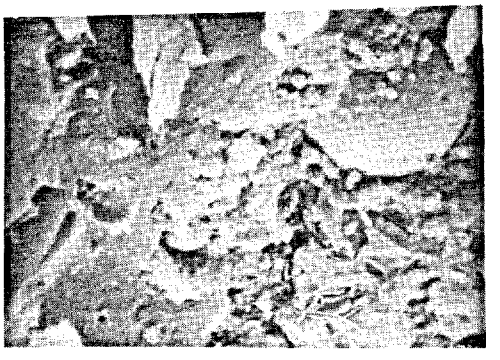

Figure. 2. the crystal form of SEM (x5000) $Na_2O\cdot Al_2O_3\cdot 3SiO_2\cdot 3H_2O$ (left) and 0.5($Na_2O\cdot 4CaO\cdot 5Al_2O_3\cdot 10SiO_2\cdot 12H_2O$) (right) mineral phase.

The active SiO_2 in the ash—slag system or the silicic gel particls in the activator with the active glass Al_2O_3 and $Ca(OH)_2$ have condensated producing gel in the meantime, finally possibly forming calcium silicoaluminate hydrate.

$$Al_2O_3+3SiO_2+Ca(OH)_2+2H_2O\rightarrow CaO\cdot Al_2O_3\cdot 3SiO_2\cdot 3H_2O. \quad (2)$$

Meamwhile, the SiO_2 and Al_2O_3 have made condensation not only with $Ca(OH)_2$, but also with NaOH and producing gel, finally producing sodium—calcium silicoaluminate hydrate possiblly:

$$2.5Al_2O_3+5SiO_2+NaOH+2Ca(OH)_2+3.5H_2O\rightarrow 0.5(Na_2O\cdot 4CaO\cdot 5Al_2O_3\cdot 10SiO_2\cdot 12H_2O). \quad (3)$$

The hydrated products in formula(2)like the scolecite in natural world. Its crystal is usually formed column, bar—radiative collecting body, as shown left section in Fig. 2; The hydrated products of formula(3) like the thomsonite in natural world. Its crystal is usually formed fibre and radiation—ball particls, as shown right section in Fig. 2.

In the ash—slag system, some of minerals having hydraulic activity themselves, such as the $\beta—C_2S$ can be formed hydrated products at atmospheric temperature under catalysis by activator. i.e.

$$2CaO\cdot SiO_2+nH_2O\rightarrow 2CaO\cdot SiO_2\cdot nH_2O(n:1—2). \quad (4)$$

The hydrated products of formula (4) are dicalcium silicate hydrate. Its crystal is usually formed flakeparticl collecting body, as shown in Fig. 3.



Figure. 3. The crystal form of SEM (x5000) $2CaO\cdot SiO_2\cdot nH_2O$ mineral phase.

5. THE THERMODYNAMIC CALCULATION OF HYDRATION FOR THE FKJ BINDER

Based on the above analysis, the possible hydration products formed in FKJ binder system are synthesized into a reactive equation as follows:

$$4.5Al_2O_3+10SiO_2+1.5(Na_2O\cdot 2SiO_2)+5CaO+12.17H_2O\rightarrow Na_2O\cdot Al_2O_3\cdot 4SiO_2\cdot 2H_2O+CaO\cdot Al_2O_3\cdot 3SiO_2\cdot 3H_2O+0.5(Na_2O\cdot 4CaO\cdot 5Al_2O_3\cdot 10SiO_2\cdot 12H_2O)+2CaO\cdot SiO_2\cdot 1.17H_2O. \quad (5)$$

Since the hydration process of inorganic cementitious material is usually reacted between solid and liquid phases and finally the solid products are obtained. Therefore, it may be unnecessary to think about the complicated mechanism of interaction between cementitious materials and water, the hydration process can be analyzed only with the aid of thermodynamic calculation of reactant and hydration products according to the formula: $\triangle Z_T^0=\triangle Ho-\triangle aTlnT-0.5\triangle bt^2-0.5\triangle CT^{-1}+YT$ of coacervate system/6/.

The calculation results show that when temperature t=25℃, i.e. T=298K, the $\triangle Z_{298}^0$ is −253.68 KCal/Mol, When t=100℃, i.e. T=373K, the $\triangle Z_{373}^0$ is−275.37 KCal/Mol, which indicate that the above equation (5) can be carried out, i.e. the equation can be established.

6. THE ANALYSIS OF X—RAY DIFFRACTO—SPECTROGRAM FOR THE FKJ BINDER

In order to expound the reactive mechanism and the produced mineral phase of FKJ cementitious material,

we carried out X—ray examination to the FKJ cementitious material. The recorded curves of diffraction are shown in Fig. 4, the recorded data of diffraction are shown in table 1. By comparing both, it can be seen that mainly produced the crystal phase include: d=5.4006, 3.3505, 3.0395 Å, we considered that it belonged to sodium—silicoaluminate hyarate of analcide type ($Na_2O \cdot Al_2O_3 \cdot 4SiO_2 \cdot 2H_2O$). some of secondary crystal phases also can be found on the spectrogram line in figure. 4, in which d=5.8509, 3.3931, 2.0323 Å, it belongs to calcium—silicoaluminate hydrate of scolecite type; d=2.8033, 2.7032, 2.5494 Å, it belongs to sodium—calcium—silicoaluminate hydrate of thomsonite type; d=4.2620, 3.8615, 2.5001 Å, it belongs to calcium silicate hydrate /3,5/.

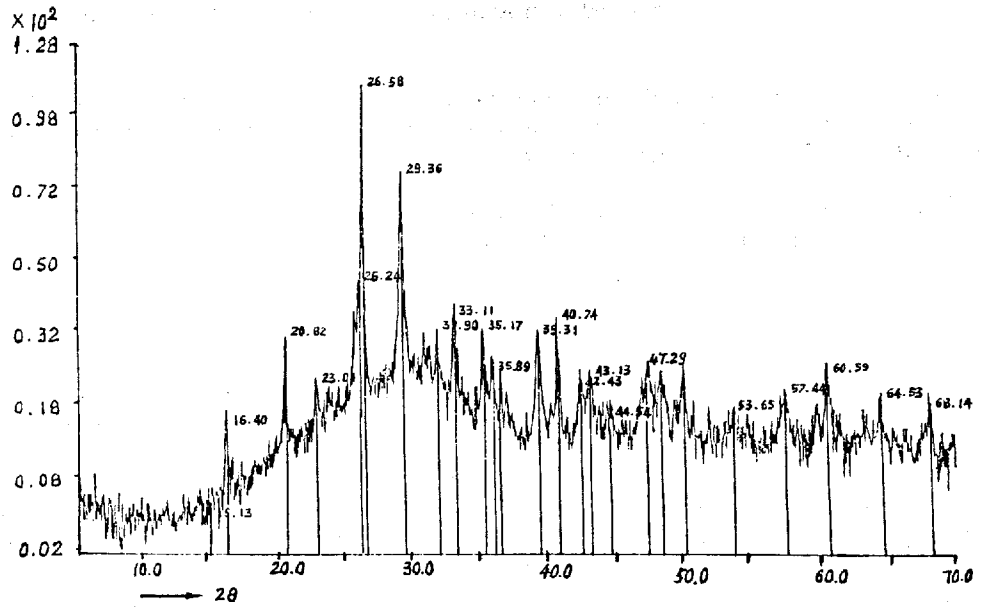

Figure. 4 The X—ray diffracto—spectrogram for FKJ binder specimens

Table. 1 The recorded data of diffraction for FKJ binder specimens

2θ	d(Å)	I/Imax(%)	2θ	d(Å)	I/Imax(%)	2θ	d(Å)	I/Imax(%)
15.1300	5.8509	10.66	29.3600	3.0395	60.14	39.3100	2.2901	19.25
16.4000	5.4006	13.49	31.8975	2.8033	10.66	40.7400	2.2129	16.66
20.8250	4.2620	23.99	33.1125	2.7032	16.66	42.4300	2.1286	10.66
23.0125	3.8615	12.76	35.1725	2.5494	17.50	43.1350	2.0954	10.66
26.2425	3.3931	31.50	35.8900	2.5001	10.66	44.5450	2.0323	10.66
26.5825	3.3505	100.00	36.4650	2.4620	10.66	47.2875	1.9207	11.34

7. THE PRODUCTS AND MINERAL PHASES FOR THE FKJ BINDER AND ITS UNANIMITY OF MACROCHARACTERISTIC

Author consider that the durability and the resistance to chemical attack of silicoaluminate hydrate are better, which are related to the microstruture of its silicon (aluminium) — oxygen tetrahedron. For instance, the sodium — silicoaliminate hydrate of analcite type forms tetrogon — triakisoctahedron crystal, the pore passage in silicon (aluminium) — oxygen crystal lattice mainly consist of hexatomic ring. It forms one — dimensional tube pore passage, pore diameter is about 2.6 Å and unifomly distributed.

Therefore this one mineral phase and micostructure determine a series of fine characteristics.

The FKJ cementitious material is featured with early strength nature, at normal temperature its strength: R_{1d} is above 10MPa, R_{28d} is about 50MPa, the data determined for 1, 3, 5 years have indicated that the strength is slightly increased. Thus, this means mineral phase of produdtion is stable, and has fine resistance to climate.

The FKJ cementitious material has good frost resistance. It can resiste more than 250 cycles of freezing and thawing; It has strong carbonation resistance, its coefficient of carbonation approximated to 1. The experiments have indicated that the FKJ binder has better resisted to erosion by fresh water, corrosion by solphate and attack by sea water.

It is of interest to note that just as natural zeolite mineral, the FKJ binder is possessed of thermal stability and acid resistance. According to our tests, it can be resisted 1200 C high temperature, high concentration of HCl, HNO_3 and aqua regia and 5% concetration of H_2SO_4.

The FKJ binder has good nature of protecting reinforcement. The FKJ samples with reinforcement were respectively placed in atmosphre, sea water and $MgCl_2$ solution (Its concentration is 25°Be') after one year, the reinforcements were not rusty.

8. CONCLUSION

The fly ash slag — alkali cementitious material (namely FKJ) which Na_2SiO_3 is taken as an activator is non — clinker cement. The experimental research shows that their hydrated products are suitably formed under normal temperature and the hydrate products produced are silicoaluminate hydrate of zeolite type.

It is a new cementitious material with early strength, high strength, energy — saving, strong resistance to chemical attack and good durability. It may be widely used in many kinds of construction engineering, in particular suitable to structural concrete for offshore engineering construction, resistance to corrosion engineering. Therefore this material is possessed of certain development prospect and economical significance.

REFERENCES

1. V. D. Glukhovsky etc. Slag — alkaline cement and concrete, in USSR, 1978.

2. Lu Changgao, The preliminary research of the fly — ash slag alkali concrete, 2nd International symposium on cement and concrete, Beijing China, 1989.

3. Zuo Jiexiang, Zeolite, China Building Industry Press, 1980.

4. Beijing University, Optical mineralogy, China geological press, 1979.

5. ASTM, USA, Powder diffraction file, 1963.

6. V. I. Babouchkine etc. Silicate thermodynamics, in USSR, 1972.

INVESTIGATION OF THE POSSIBILITY OF MAKING HYDRAULIC BINDER BY CHEMICAL ACTIVATION OF DOMESTIC ASH AND MIXTURE OF SLAG AND DOMESTIC ASH

N Kostić* and B Skenderović**

**Agricultural Faculty, Belgrade-Zemun*
***Faculty of Civil Engineering, Subotica, YUGOSLAVIA*

SUMMARY

The composition and properties of domestic ash have been examined vis-a-vis fly ash. Domestic ash is what remains after ignition of low quality coal (lignite) and wood mixture in domestic ovens. Experiments were performed to find out the possibility of using ground domestic ash for making hydraulic binder for mortar and concrete.

Domestic ash has better hydraulic activity than fly ash, but has some harmful components (K_2O,Na_2O,free CaO). It can be activated better with $Ca(OH)_2$ than with NaOH. By chemical activation of a mixture of ground slag and domestic ash it is possible to produce a binder of acceptable quality. However, this has a limiting combination in that slag is activated better with NaOH whereas $Ca(OH)_2$ is more convenient for the activation of domestic ash.

INTRODUCTION

Large quantities of ash are produced from the ignition of coal and wood in many cities of Yugoslavia. Large quantities, especially produced in winter, contribute much to pollution of land and ground waters and are a serious problem in pollution control. It would be very good if this kind of ash could be used for production of hydraulic binders for mortars and concretes like flyash is already being used.

For want of sufficient data in literature on the composition and properties of domestci ash, we went by the data on composition and hydraulic activity of different kinds and fractions of domestic ash (reported all was in 2,3,4,5,6). We found that domestic ashes differ in composition depending on the composition and quality of the coal, quantity of the wood used and aslo the burning conditions. Domestic ash contains variable quantities of unburnt coal and other harmful components (Na_2O,K_2O, free CaO, SO_3). It is possible to get rid of most of the unburnt coal and improve the hydraulic activity by using only finer fractions of domestic ash.

With these experiments we wanted to contribute to the efforts to use domestic ash as a raw material for some products. The investigations were confined to the possibility of chemical activation of the hydraulic properties of domestic ash when used alone and in combination with ground slag.

MATERIALS AND METHODS

Domestic ash obtained from the combustion of low-grade coal(lignite) and wood used for heating of houses and flats was used for experiments. Fine fraction (<2mm) of the ash were separated by sieving, which which were then ground to about 5000 cm^2/g and as such used in experiments. Results of chemical analyses of domestic ash, slag and flyash, for control purpose, are given in Table 1.

Table 1 Chemical analysis of slag and ashes

Component	Quantity in %		
	Slag	Domestic ash	Flyash
SiO_2	35,0	35,5	56,8
Al_2O_3	10,1	7,5	20,1
Fe_2O_3	0,83	10,7	6,1
CaO	57,9	15,6	6,9
MgO	4,1	3,0	3,3
Na_2O+K_2O	1,01	7,6	0,43
SO_3	3,01	9,0	3,3
Unburnt coal	-	1,5	1,63
Free CaO	8,3	10,2	2,10
Loss on ignition	-	11,3	3,5

Domestic ash had more CaO and much less SiO_2 then flyash.It had much more alkalies (Na_2O+K_2O), free CaO and SO_3 than flyash which was used as a control.

The mineral composition of the crystalline phases present was obta-

ined by X-ray diffraction analysis and the results are given in Fig.1. In domestic ash the dominant crystalline phases were calcite ($CaCO_3$) and anhydrite ($CaSO_4$), whilst quartz (SiO_2) and calcite ($CaCO_3$) were present in flyash.

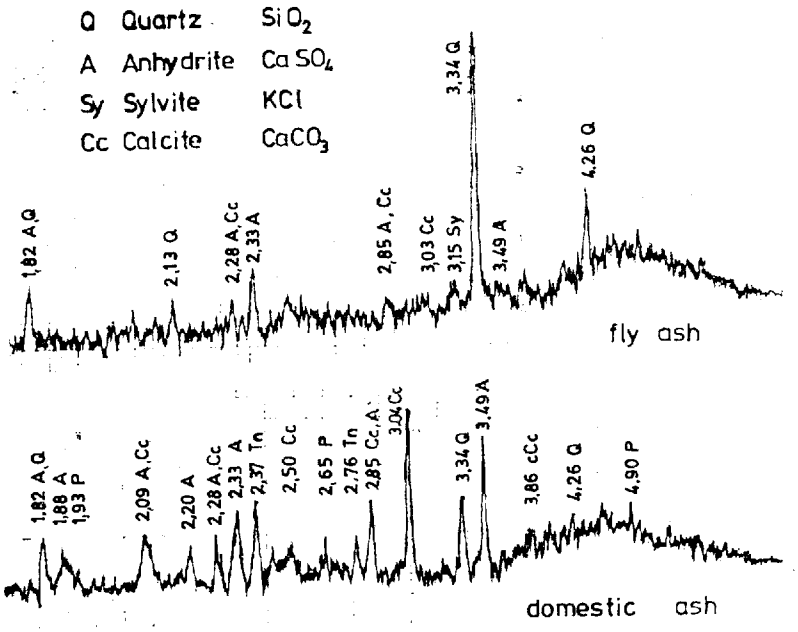

Fig 1 Results of X-ray diffraction analysis of ashes

For testing the hydraulic activity of slag and ashes,some measurements of strangths (7,28 days) and the speed of ultrasonic waves in test prisms (4x4x16 cm) were performed. The test prisms were made of 1:3 mortar in which activated ash, slag or a mixture of slag and domestic ash were used as a binder (in proportion 2:1). The test prisms were cured for 28 days in an atmosphere saturated with steam.

RESULTS AND DISCUSSION

1. Hydraulic properties

Hydraulic properties of ashes and slag can be enhanced by different kinds of chemical activators. In these experiments $Ca(OH)_2$ and NaOH were used for that purpose. The results of measurements of strength and speed of ultrasonic waves transmission through the tested mortars are presented in Table 2. Ashes are activated better by $Ca(OH)_2$, but slag is much better activated with NaOH. It is obvious that domestic ash is much more active and produce more solids (higher speed of ultrasonic waves in mortar) and higher strength of mortar after 28 days of hydratation, than flyash used as control. By reducing the quantity of $Ca(OH)_2$ added,the hydratation improves and the mortar becomes stronger, probably, because domestic ash contains about 10% free, CaO, which in the presence of water gives $Ca(OH)_2$. Activation with NaOH is similar, probably because of the high quantity of alkalies (Na_2O+K_2O) in domestic ash.From the results in Table 2 it is evident that it is possible to produce a good hydraulic binder in mortars with domestic ash with optimum cuantity of $Ca(OH)_2$ as activator. The optimum quantity of activator ($Ca(OH)_2$) depends probably on the

Table 2 Strengths and speed of ultrasonic waves in test mortars after 28 days

	Quantity of activ. in %	Speed of ultra wave in cm/μ sec	Bending strength in MPa	Compressive strength in MPa
Activated with $Ca(OH)_2$				
Flyash	50	0,232	1,88	13,7
Domestic ash	50	0,328	2,71	20,9
Domestic ash	25	0,352	2,99	24,1
Slag	33	-	2,22	23,8
Activated with NaOH				
Flyash	6	0,121	-	0,31
Domestic ash	6	0,324	1,78	10,9
Domestic ash	3	0,323	2,15	16,5
Slag	4	-	2,15	31,2
Slag	6	-	3,46	39,5
Slag	8	-	4,70	44,1

chemical composition of the ash, especially the quantity of free CaO in it. Slag is very effectively activated by NaOH and with addition of proper quantity of activator it can be used as a binder for concrete.

In our experiments we tried to make a hydraulic binder of good quality which could be used for concrete too, by chemical activation of a proper mixture of slag and domestic ash. A 2:1 mixture of ground slag and domestic ash was activated with different quantities of NaOH and mixture of NaOH and $Ca(OH)_2$. Table 3 gives the results of strength measurements of test mortars after 7 and 28 days hydratation, and Fig.2 the results of measurements of ultrasonic wave speed in wet test prisms in the first 28 days of hydratation.

Tabel 3 Strengths of test mortars

Activ.quantity in %		Bending strength in MPa, after:		Compress. strength in MPa, after:	
NaOH	$Ca(OH)_2$	7	28 days	7	28 days
4		0,75	0,90	7,5	8,3
8		2,00	2,11	20,1	20,9
12		3,11	3,18	29,9	30,4
6	2	1,74	1,78	15,2	17,3
4	4	0,91	1,20	7,5	9,4
2	6	0,97	1,03	7,9	8,9

Results are poor while using a mixture of NaOH and $Ca(OH)_2$ as activators, especially when the mixture contained a smaller quantity of NaOH. This could be due to the fact that $Ca(OH)_2$ is poor activator for slag, even as NaOH is not good for ash activation, as we have seen from the results presented in Table 2. The results have improved if the activation was carried out with NaOH alone, but in that case domestic ash hydrates poorly and makes little contribution to strength development. Therefore, it is much better to use only ground slag,activated with appropriate quantity of NaOH, instead of a mixture of slag and domestic ash.

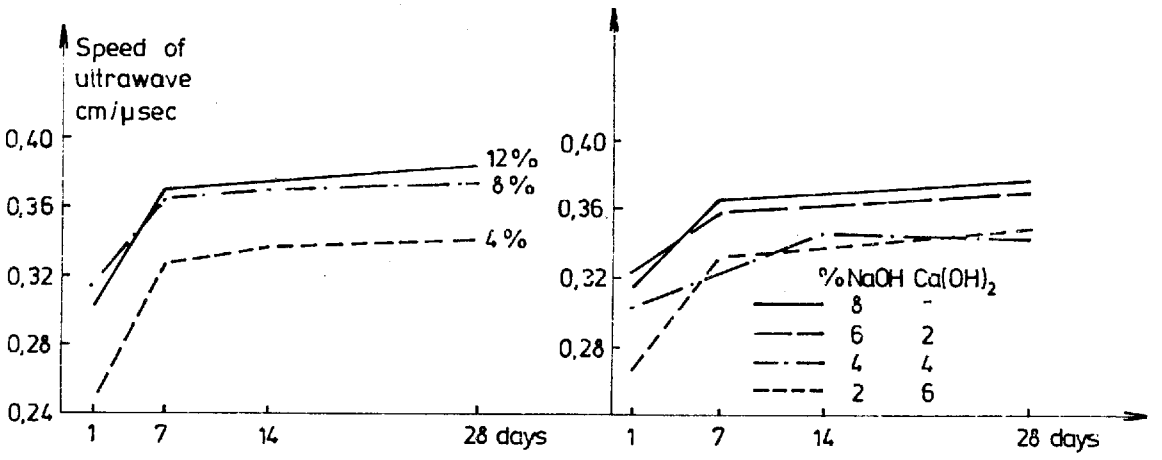

Fig 2 Speeds of ultasonic waves in wet test prisms

From the results presented it can be concluded that it is possible to get a hydraulic binder by activation of mixture of slag and domestic ash by NaOH. But, it is not practical because in such a combination the domestic ash hydrates poorly and makes little contribution to strength development. Hence, it is much better to make binders for mortar by activation of ground domestic ash with proper quantity of $Ca(OH)_2$, and produce binders for concrete by activation of ground slag with NaOH.

CONCLUSIONS

1. Domestic ash, produced by ignition of a mixture of low-grade coal (lignite) and wood in flats and houses, has better hydraulic activity than flyash, but it contains more harmful components.
2. It is possible to produce hydraulic binders by chemical activation of a mixture of ground slag and domestic ash, but results are much better if they are used and activated separately. With ground slag better results are obtained by NaOH activation, whereas domestic ash is activated better with $Ca(OH)_2$.

REFERENCES

1. Junuzović E., Horvat L., Skenderović B.:"Ispitivanje mogućnosti korišćenja šljake različitog porekla kao agregata za malter i beton", Zbornik Građevinskog fakulteta Subotica, 1986, 2, 181.

2. Skenderović B., Lakatoš T.: "Ispitivanje osobina i mogućnosti korišćenja komunalnog pepela za izradu maltera i betona", Simp. o zaštiti životne sredine, Beograd, 1988.

3. Skenderović B., Kostić N.: "Izučavanje hemijskog i faznog sastava komunalnog pepela različitog porekla". Simp. o zaštiti životne sredine, Beograd, 1988.

4. Skenderović B., Lakatoš T.: "Ispitivanje sastava i hidrauličkih osobina komunalnog pepela". Zbornik Građevinskog fakulteta, Subotica, 1990, 6, 105.

5. Skenderović B.: "Uticaj nekih tehnoloških faktora na hidrataciju i osobine maltera u kome je deo cementa zamenjen komunalnim pepelom ", Zobrnik Građevinskog fakulteta, Subotica, 1991, 7, 133.

6. Skenderović B. : "Ispitivanje sastava i hidrauličkih osobina raznih frakcija komunalnog pepela i šljake". II Jugosl. savetovanje o zaštiti životne sredine u procesnoj ind., Dubrovnik, 1991, 214.

EVALUATION OF PHYSIO-CHEMICAL AND HYDRATION CHARACTERISTICS OF SUPERSULPHATED CEMENT

K Mohan and S P Ghosh

Cement Corporation of India Limited, New Delhi, INDIA

SUMMARY

The physical and chemical properties of laboratory prepared supersulphated cement using varying proportions of slag (70 to 85%), anhydrous $CaSO_4$ (10 to 25%) and clinker (2 to 6%) were studied. A total number of 16 blends have been prepared and tested for physical properties, chemical composition and analysed by XRD and DTA. Blends using 70 - 75% slag, 20 - 25% $CaSO_4$ obtained from mineral gypsum and 5% clinker as well as blends using 78 - 81% slag, 13 - 16% $CaSO_4$ obtained from chemical gypsum and 5 - 6% clinker conform to all the requirements of supersulphated cement as per IS:6909-1973. The phases formed in the hydrated products of selected blends as revealed from XRD and DTA results indicate less significant role of ettringite than C-S-H in strength development.

РЕЗЮМЕ

ОЦЕНКА ФИЗИКО-ХИМИЧЕСКИХ И ГИДРАТАЦИОННЫХ СВОЙСТВ СУПЕР-СУЛЬФАТИЗИРОВАННОГО ЦЕМЕНТА

К МОХАН И Ш.П. ГХОШ

Изучены физические и химические свойства супер-сульфатизированного цемента с разными пропорциями шлака (70-85%) обезвоженного $Ca\,SO4$ (10-25%) и цементного клинкера (2-6%). Было приготовлено 16 смесей цемента и каждая смесь испытывалась на физические свойства, химический состав и анализировалась с помощью XRD и DTA. Сравнение результатов испытаний выявило, что смеси, содержащие 70-75% шлака, 20-25% $Ca\,SO4$ из минерального источника и 5% цементного клинкера, а также смеси, содержащие 78-81% шлака, 13-16% $Ca\,SO4$, полученного из химического гипса, и 5-6% цементного клинкера, отвечают всем физическим и химическим требованиям индийского стандарта Is: 6909-1973. Анализ продуктов гидратации некоторых смесей указывает на менее существенную роль эттрингита в наборе прочности таких цементов, чем C-S-H.

INTRODUCTION

Supersulphated Cement (SSC) is a hydraulic cement produced by intergrinding or intimately blending a mixture of a granulated blast furnace slag, calcium sulphate and a small amount of portland cement or clinker or any other source of lime.

Supersulphated cement has a special place because of its low heat of hydration and for its chemical resistance to most of the aggressive conditions generally encountered in the construction industries and to the attack of sulphates in particular (1-3). However, at low and high temperature, this cement is reported to have slow rate of hardening and strength retrogression (3,4).

Earlier investigations (5-7) on supersulphated cement report on the hydration and properties. The present study characterizes the physico-chemical properties of supersulphated cement and their hydrated products at different ages based on different compositions of supersulphated cement.

EXPERIMENTAL

Materials

Two commercial clinker samples - one from dry process SP kiln and another from wet process kiln and one sample of granulated blast furnace slag were used in this study. Anhydrous $CaSO_4$ was prepared in the laboratory by calcining of both mineral and chemical gypsum at 600-650°C for about one hour in the muffle furnace.

Chemical compositions of clinkers and slag are given in Table 1. Clinkers - 1 and 2 are from dry process SP kiln and wet process kiln respectively.

Table 1 Composition of clinkers and slag

Components (Wt.%)	SiO_2	Al_2O_3	Fe_2O_3	CaO	MgO	SO_3	LOI*	IR**	Free CaO	C_3S	C_2S	C_3A	C_4AF
Clinker-1	21.78	7.06	4.70	64.65	0.40	0.16	1.22	0.48	0.87	39.93	32.32	10.76	14.30
Clinker-2	20.54	7.08	3.80	61.90	1.40	0.41	2.70	2.18	0.70	40.00	28.71	12.33	11.56
Slag	36.28	23.80	1.10	32.88	4.17	0.49	0.00	2.38					

Chemical composition of anhydrous $CaSO_4$ are given in Table-2. $CaSO_4$ - 1 and 2 are obtained from calcining of mineral and chemical gypsum respectively.

Table-2 Chemical composition of anhydrous $CaSO_4$

Constituents (wt.%)	SiO_2 + IR**	Al_2O_3	Fe_2O_3	CaO	MgO	SO_3	LOI*
$CaSO_4$ - 1	19.54	1.30	1.50	31.92	0.80	39.27	4.18
$CaSO_4$ - 2	7.64	2.42	0.60	40.14	0.59	45.13	2.24

* LOI - Loss on ignition
** IR - Insoluble Residue

Method

(i) SSC sample preparation - A total number of 16 blends of supersulphated cement (SSC) were prepared in the laboratory by intergrinding varying proportions of slag (70-85%), anhydrous $CaSO_4$ (10-25%) and clinker (2-6%) with the same grinding media charge, duration of grinding and approximately same specific surface, around 4000 cm^2/gm. Out of a total of 16 blends, seven blends of supersulphated cement were prepared from clinker-1 and $CaSO_4$ - 1 and the other blends from clinker-2 and $CaSO_4$ - 2.

(ii) Testing and Analysis - All the blends were tested for specific surface, normal consistency, initial and final setting time, Le Chatelier expansion and compressive strengths at 3, 7 and 28 days as per IS:4031-1988 and also for chemical composition e.g. insoluble residue, MgO and SO_3 as per IS 4032-1988.

One-inch cube specimens of pure paste of selected blends of SSC were prepared with a water : cement ratio of 0.45 and cured for 24 hours in 100% RH atmosphere and then in water for 3, 7 and 28 days. At predetermined time, the hydration was stopped by slicing a portion of the sample and grinding in acetone, and, then drying in a vacuum desiccator. Different fractions of the dried samples were analysed by differential thermal analysis (DTA) and X-ray diffraction (XRD).

RESULTS

(i) Physical and Chemical Tests Results

Physical and chemical test results are summerized below (Fig.1) :-

Sl. No.	Composition (wt.%) Slag	$CaSO_4$	Clinker	Whether conforms to all the requirements of SSC	Comments
1.	70-75	20-25 (from mineral gypsum)	5	Conforms to all the physical and chemical requirements.	-
2.	80-85	10-15 (from mineral gypsum)	5	Does not conform to chemical requirements in respect of SO_3.	Fails primarily because of lower percentage (10-15%) of $CaSO_4$ from mineral gypsum.
3.	78-83	15-17 (from mineral gypsum)	2-5	Does not conform either to physical or chemical requirements.	Fails either because of lower addition of clinker (2%), slag (78%) or $CaSO_4$ (17%)
4.	78-81	13-16 (from chemical gypsum)	5-6	Conforms to all the physical and chemical requirements.	-
5.	72-78	17-23 (from chemical gypsum)	5	Does not conform to physical requirements.	Fails primarily because of lower addition of slag.

(ii) XRD and DTA Results

The phases identified by XRD and DTA in hydrated products of selected SSC blends are prescribed in Table-3. The 3 and 7 days hydration products of SSC blends containing $CaSO_4$ from mineral gypsum show predominance of gypsum, anhydrite and ettringite; the blend containing 70% slag, however, shows nil or insignificant development of ettringite. The 28 days hydration products show predominent development of $CaCO_3$ (due to carbonation during curing), gypsum, silica, anhydrite and ettringite.

The 3 and 7 days hydration products of blends containing $CaSO_4$ from chemical gypsum show predominant development of anhydrite, ettringite and alite. The 28 days hydration products show predominant development of anhydrite, calcium carbonate (due to carbonation during curing) and ettringite.

The hydration products of all the blends are reported to contain major amount of X-ray amorphous compounds which may logically be attributed to the presence of C-S-H. The presence of C-S-H and other forms of hydrosilicates as well as devitrification of slag components are indicated in thermograms by endothermic peaks at 130°-160°C, 710°-755°C and exothermic peaks at 850°-880°C and 980°-1000°C respectively(Fig.2a & 2b).

DISCUSSIONS

The presence of ettringite and C-S-H had been detected (8) on the third day after hydration, the shape and height of ettringite peaks were found to be nearly the same regardless of the time of hydration. Presence of ettringite and C-S-H as main hydration products has also been indicated from XRD and DTA results (5-7) wherein the early strength has been mainly attributed to ettringite formation, but strength development from about 3 days onwards was considered to be due to increasing formation of C-S-H. It has also been noted (5) that ettringite content hardly rises further as from the third to the seventh day, while during the same period, the compressive strength increases substantially indicating that ettringite has small contribution to strength development. In this regard, the inference drawn from results of comprehensive investigations on hydration characteristics and properties of SSC (6) that ettringite formation contributes decisively to the strength development has been contradicted by results of further investigations (9). According to the latter, formation of C-S-H phases starts nearly simultaneously with ettringite formation. The quantity of ettringite nearly remains constant from the fourth or the seventh day latest, while strength increases rapidly upto 28 days. Therefore, in the opinion of Schröder (9), the formation of C-S-H phases is the decisive factor in the strength development of SSC.

The cited physical and chemical tests as well as XRD and DTA results show that ettringite phase formation is less significant in hydrated products of SSC blends containing $CaSO_4$ from mineral gypsum than in the blends with $CaSO_4$ obtained from the chemical gypsum. Also, the 28 days hydration products in both the above cases show insignificant quantity of ettringite, although strength development upto 28 days remained uninterrupted. The test results indicate insignificant role of ettringite in strength development which should be attributed primarily to C-S-H.

Fig.1 - Compatibility fields of different compositions of supersulphated cement for various requirements of specifications.

1. PASSING BOTH PHYSICAL & CHEM. SPECIFICATION.
2. PASSING PHYSICAL SPECIFICN ONLY.
3. PASSING CHEMICAL SPECIFICN ONLY.
4. PASSING NONE OF SPECIFICNS.

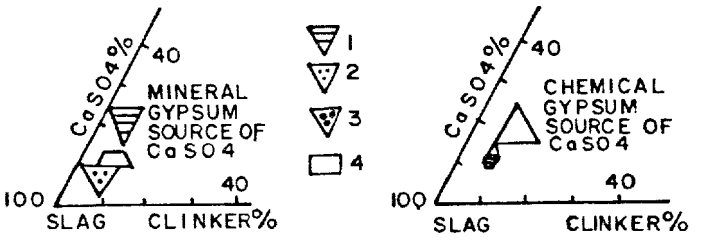

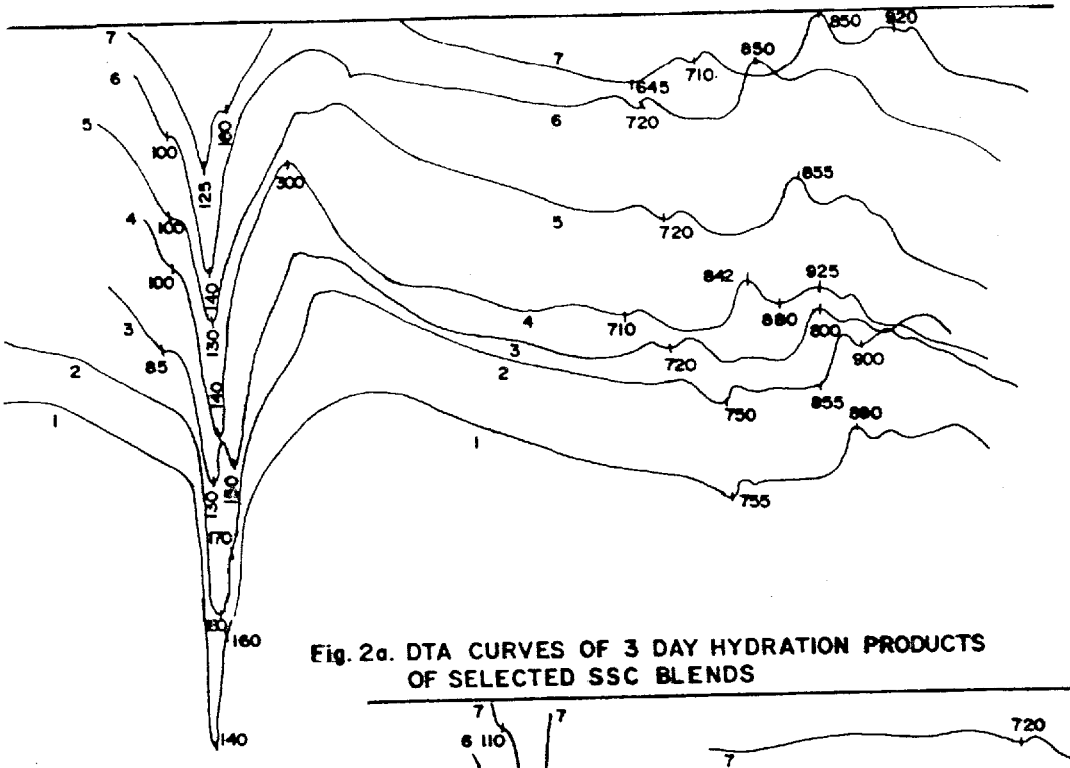

Compositions 1 to 7 in Figs. 2a and 2b are given in Table-3

Fig. 2a. DTA CURVES OF 3 DAY HYDRATION PRODUCTS OF SELECTED SSC BLENDS

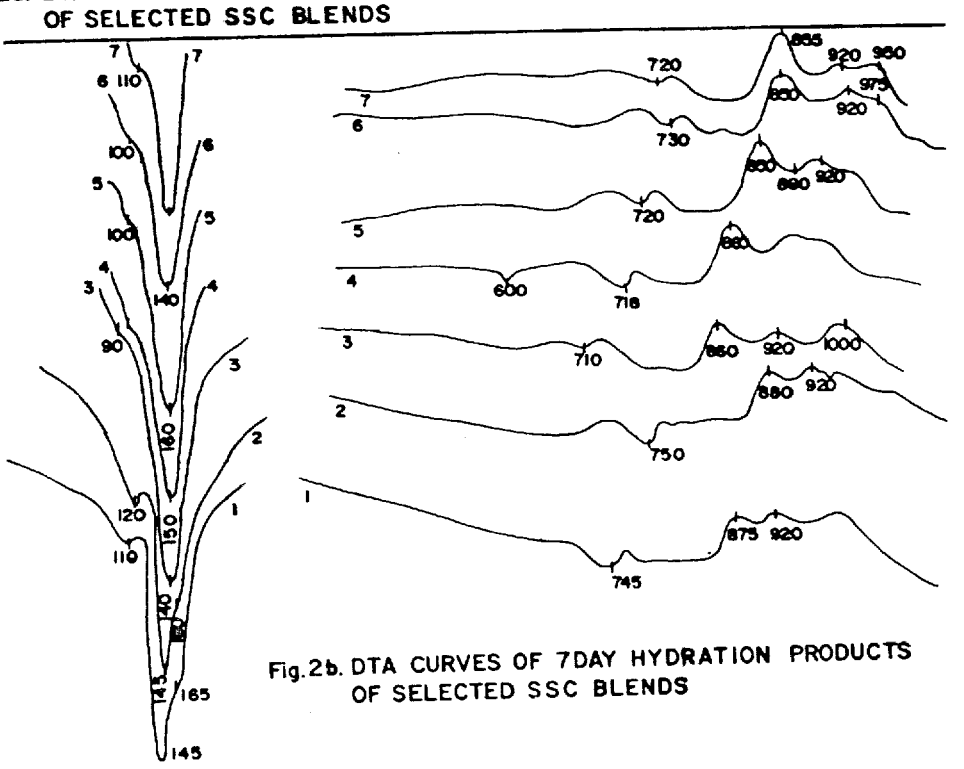

Compositions 1 to 7 in Figs.2a and 2b are given in Table-3.

Fig.2b. DTA CURVES OF 7DAY HYDRATION PRODUCTS OF SELECTED SSC BLENDS

Table-3 Phases identified by XRD and DTA in hydrated products of selected SSC blends.

Sl. No.	Composition (wt.%) Slag	$CaSO_4$-1	Clinker-1	Phases identified at different ages 3 days	7 days	28 days
1.	70	25	5	G,A,S,AL,BL (CL, F, CH)	G,A,AL,BL,S (CL, CH, F)	CC,G,AL,S,A,E, (CL)
2.	78	17	5	G,A,E,S,AL,BL (CH,CL,F)	G,A,E,S,AL,BL (CL)	CC,S,BL,A,G,E, (CL, AL)
3.	85	10	5	G,A,E,S,AL,BL (CL,CH)	A,G,E,AL,BL,S,CL (CH,F)	CC,G,S,BL,A,E,AL (CL)
	Slag	$CaSO_4$-2	Clinker-2			
4.	72	23	5	A,E,AL,BL, (CL,S,F,CH)	A,E,AL,BL (CH,G,CL,F)	CC,A,BL,E, (CL)
5.	78	17	5	A,E,AL,BL,G (S)	A,E,AL,BL,G (S,CH)	A,G,CC,E,BL, (CL)
6.	80	15	5	A,E,AL,BL,CL (S,CH,F,G)	A,E,AL,BL,CL (S,CH,G,F)	A,CC,E,G,AL,BL.
7.	80	14	6	A,E,AL,BL (CH,S,CL)	A,E,AL,Bl (CL,F,G,CH)	CC,A,G,E,BL (CL)

The phases identified by XRD are arranged in order of decreasing frequency. ( ) denotes trace amount. G = gypsum, A = Anhydrite, E = Ettringite, S = SiO_2, AL = Alite, BL = C_2S, CL = C_3A, F = C_4AF, CH = $Ca(OH)_2$, CC = $CaCO_3$. Besides, significant amount of C-S-H is presumed to be present in all cases, although not detectable in diffractograms and thermograms. The thermograms of blends containing $CaSO_4$ obtained from mineral gypsum show after 3 to 7 days hydration prominent endothermic peaks with weight loss at (a) 130°-160°C and (b) 710-750°C and exothermic peaks at (c) 860°-890°C and occassionally at (d) 1000°C. The blends containing $CaSO_4$ obtained from chemical gypsum show, besides above features, a small but distinct endothermic peak accompanied with weight change at around 90°-100°C. This peak is conspicuously absent in both types of blends (with or without mineral gypsum source of $CaSO_4$) containing higher (80-85%) slag and lower gypsum (10-14%) quantity. The exothermic peaks at 860°-900°C and 1000°C presumably indicate devitrification of constituent phases in the slag. In all the cases, the peaks at (a) and (b) are usually more intense for 7 days hydration products than for 3 days hydration.

ACKNOWLEDGEMENTS

The work described here has been carried out as part of the research programme of the R&D Centre of Cement Corporation of India Ltd. and this paper is published with the permission of Director(Operations). The authors thank Mr.Ram Chandra for the samples preparation and physical testing and Mr.U.C.Dumka for chemical analysis of samples.

REFERENCES

1. Kondo, R.: "New types of sulphated slag cement suitable for soil stabilization". Rev.14th Gen.Meeting, Tokyo, 1960, 76-77.
2. Reinsdorf, S.: "Eigenschaften und Verwendung von Sulfathuttenzement (SHZ)". Bauplanung - Bautechnic, 1962, 16, 230-234.
3. Blondiau, L.: "Aptitude de ciment sursulfate a la construction des egouts". Rev.Mat.Constr., 1960, 536, 113-118.
4. Blondiau, L.: "Conversation du ciment sursulfate". Rev.Mat.constr., 1962, 559, 103-114.
5. Smolczyk , H.G.: "Die Hydrationsprodukte hullensandreuher Zemente". Zement-Kalk-Gips, 1965, 18, 238-246.
6. Ludwig, W. and Schwiete, H.E.: "Hydration of supersulphated cement", Tonind Zeitg, 1965, 89, 174-176.
7. Yang, J.C.: "Chemistry of slag-rich cements". Proc. of the Fifth Int.Symp.on the Chemistry of Cement, Tokyo, 1968, V4, 296-309.
8. Kondo, R.and Ohsawa, S.: "Studies on a method to determine the amount of granulated blast furnace slag and the rate of hydration of slag in cements". Proc. of the Fifth Int.Symp. on the Chemistry of Cement, Tokyo, 1968, V4, 255-262.
9. Schröder,F. : "Blast furnace slags and slag cements", Proc. of the Fifth Int.Symp. on the Chemistry of Cement, Tokyo, 1968, V4, 149-207.

PHOSPHATE-BONDED DENTAL CEMENTS

W Jiang and Nanru Yang

Nanjing Chemical Engineering Institute of Technology
Nanjing, Jiangsu, P R CHINA

SUMMARY

A new calcium phosphate cement composed of tetracalcium phosphate and dicalcium phosphate dihydrate was investigated. The results show this cement can set in a short time under certain conditions and develop strength rapidly, forming hydroxyapatite as the final product. Those properties make it suitable for dentistry. The chemistry, kinetics of forming, setting mechanism, mechanical properties, and biocompatibility were discussed.

Ein neuer Calciumphosphate Zement war aus Tetracalciunphosphat und Dicalciumphosphat. Dieser Zement Kann in einer Kurzen Leit setzen und ausserdem schnell Karlt entwickeln, Des Reaktionsproduct ist Hydroxyapatit. Die Eigenschaften dis diesen Systems machen Zement benutzbas zu der Zahnheikunde. Die Chemie, die Reaktionsgeschwindgheit der Bilding, der Mechanismas, des Setzens, die mechanische Eignschaften und die Biovereinbarkeit wertden diskutiert.

INTRODUCTION

In dentistry, cements can be used for cosmetic and temporary filling materials; protective cavity liners; luting agents for crowns, bridges, inlays, and orthodontic appliances; root canal fillings; and pulp capping. Besides in dentistry, cement is also used in bone surgery. Phosphate-bonded cement based on the hardening reaction between a metal oxide or silicate and a concentrated solution of phosphoric acid can be formulated to set within a few minutes and develop strength rapidly. It has found use in a wide variety of dental and medical applications. All dental cements are based on the hardening reaction between a powdered solid and a viscous hydrogen-bonded liquid. These cements themselves fall within Wygant's definition of reaction cement, a term applied to cement other than those which set by hydraulic action. There are three main types of phosphate-bonded dental cement: (1) The dental zinc-phosphate; (2) The dental aluminosilica-phosphate; (3) The dental calcium-phosphate. The self-setting calcium-phosphate dental cement (CPC) which was first reported in 1986 has a good biocompatibility, which makes it potential in many applications. [1] The concept of self-assembling composites are being developed, such composites develop properties as a result of controlling the rates of competing chemical reactions to create composite materials, the initials selection of hydrating anhydrous inorganic phase in the presence of polymerizing macromolecules. [2, 3]

The theoretical basis for reaction illustrated in Fig. 1. Fig. 1 is obtained by plotting the solubility curves for dicalcium phosphate (DCP), CAHPO4, brushite ($2CaHPO_4 \cdot 2H_2O$), tetracalcium phosphate (TetCP), $Ca_4(PO_4)_2O$, and hydroxyapatite (HAp), $Ca_5(PO_4)OH$, which is compositionally similar to native hard tissues, those solubilities plotted as the negative logarithms of the calcium-ion concentrations, pCa, depending on the solution pH. [4] From the perspective of Gibb's phase rule, the plot can be considered as representing a potion of the ternary system: $Ca(OH)_2$-H_3PO_4-H_2O. In a ternary system at constant temperature and pressure, the intersections of the solubility curves for brushite and HAp, for DCP and HAp, and for DCP and TetCP are ternary invariant or singular points, while those for brushite and TetCP, and for DCP and TetCP are metastable; the invariant solutions are supersaturated with respect to HAp. These supersaturations are the basis for the formation of HAp using brushite and TetCP as reactants. Thus, when the solids brushite and TetCP dissolve in an aqueous solution, the system is driven toward metastable invariance, which is continuously disturbed by HAp formation. The objective of this research is using this reaction to develop a new calcium phosphate dental cement.

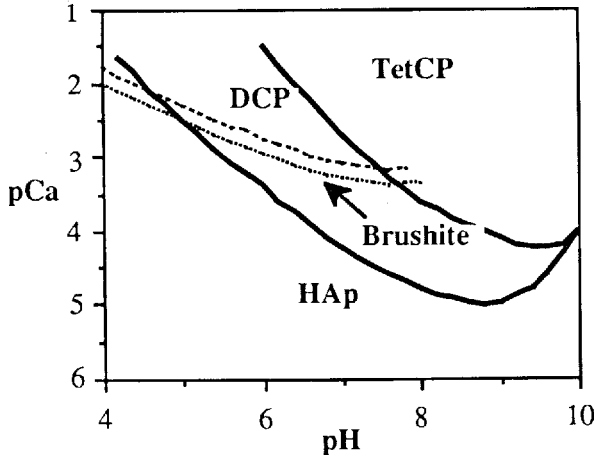

Fig. 1. Solubility curves for DCP, brushite, HAp, and TetCP. Solubility isotherms showing negative log[Ca] and pH of the solutions (after Brown).

EXPERIMENTAL

Powder Preparation

Since tetracalcium phosphate is not commercially available, it was prepared by two ways:

$$2CaHPO_4 \cdot 2H_2O + 2CaCO_3 = Ca_4(PO_4)_2O + 2CO_2 + 5H_2O \quad (1)$$

After weighing, the equimolar mixture starting powders were mixed by ball milling for a half an hour to improve homogeneity. The mixture was hydrothermally treated at 180°C for 2 hours. Then, the powder was put into an alumina crucible. First heated at 950°C for 12 hours and then heated at 1450°C for 4 hours. Powder X-ray results showed that final phase was TetCP.

$$2CaCO_3 + 2CaHPO_4 = Ca_4(PO_4)_2O + 2CO_2 + H_2O \quad (2)$$

In this case, the Phase-pure TetCP was prepared by reaction at 1550°C. Reactants were characterized by X-ray diffraction (XRD) for phase purity. Then tetracalcium phosphate was comminuted in anhydrous ethanol using zirconia grinding media to obtain powders having BET surface areas of 0.95 m^2/g.

Cementing Reaction

The cement system consisted of a powder and a liquid component. The powder contained tetracalcium phosphate and brushite, which were mixed a molar ratio at 1:1. This ratio was selected because it would give a 1.67 Ca/P molar ratio, which is the ratio for apatite, the desired reaction product. Brushite was dry mixed with tetracalcium phosphate in attrition milling to ground to fine particle size. The liquid component was an aqueous solution, containing HPO_4. Additives of apatite powders were used for promoting the reactions and adjusting the setting time. The plastic pastes formed by mixing these two components set rapidly to hard salt-like gels which form in the liquid phase, acting as a binding matrix. The cement-forming reaction is one where hydrogen bridges in the liquid phase are progressively replaced by stronger metal ion bridges, a process which causes the liquid to gel and the gel to harden.

Setting Time

The setting time was measured according to American Dental Association Specification No. 9. Three min. after starting the mix, the specimens placed to the curing box with 90% R.H. and 37°C. A vicat needle (for final set) was smoothly lowered on the surface of cement. The setting time is the time elapsed from the starting of mix to the time when the needle failed to make a perceptible circle on the surface of the specimens. One hour later the specimen was removed from the mold and immersed in distilled water at 37°C. The specimens of age one day to six weeks were tested the compressive and flexural strength.

Calorimetry

The kinetics of the reaction was determined by isothermal conduction calorimetry. In the isothermal method, heat evolved during a reaction is conducted across thermopiles which surround the calorimetic cell. Heat output is therby converted to a voltage output which is recorded against time. In the method used, approximately 3 g of an aqueous phase was innoculated into an equivalent mass of anhydrous reactants that had been placed in a calorimetric cell. This was done inside the body of the calorimeter after both the liquid and solid reactants had achieved thermal equilibrium. The heat evolution attendant to the mixing of the liquid with solids and the subsequent reaction to form hydroxyapatite were measured and recorded. [5] At the termination of the calorimetric experiments, microstructural development was observed, using scanning electron microscopy.

RESULTS AND DISCUSSION

Setting Reaction

Table I lists the results of cement reactions of the tetracalcium phosphate and brushite powder mixture ina molar ratio at 1:1 with various pH aqueous solutions. The BET specific surface area of mixture is 0.94 m^2/g. $Ca(OH)_2$ is used for adjusting basic solutions, and H_3PO_4 is used for acidic solutions. The reactions were conducted at 37°C.

Table I Setting time with various pH aqueous solutions

solution/pH	12.9	10.3	7.0	5.2	2.1
setting time (min)	23.0	134.0	no setting	158.0	25.0

It is obvious that the pH of the solution was very important for setting. For dental cement, a fast setting (less 10 minutes) was needed. In order to reduce setting time, considering biocompatibility, acidic conditions was recommended. 5-20% H_3PO_4 solutions were used, the result shows that 12% was the best. In addition 10% ground hydroxyapatite powder (BET specific surface area of 9.07 m^2/g) was used as filler. The optimum formula shows as Table II. The following tests were basically conducted according to this formula. The setting time of this formula was illustrated in Fig. 2.

Table II Mixing formula

TetCP & brushite (1:1)	12% H_3PO_4	HAp	Setting time
4.5 g	2.5 ml	0.5 g	8.5 min

Kinetics of Forming

Calorimetric experiments were carried at 37°C which is physiological temperature. Fig. 3 shows the calorimaetic curve (the rate of heat evolution obtained). There is an initial period of rapid heat liberation exhibiting as a peak in rate a few minutes after mixing. Initial peaks of this type are primarily associated with wetting, initial dissolution, and establishment of critical degrees of supersaturation. The curve exhibited a main peak at 20 minutes after reaction. Compared to the reaction kinetics at 15 and 25°C temperatures, the magnitude the main peak is greater, the maximum in reaction rate occurs at the shortest time, and the end of measurable heat evolution occurs earliest. [6] It is obvious that setting happens in the acceleratory.

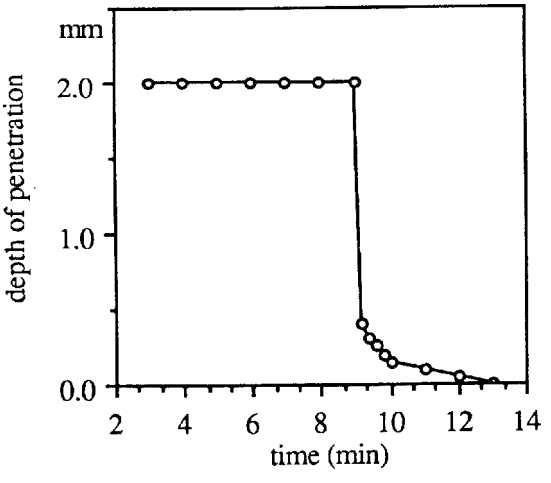

Fig. 2 Depth of penetration against time

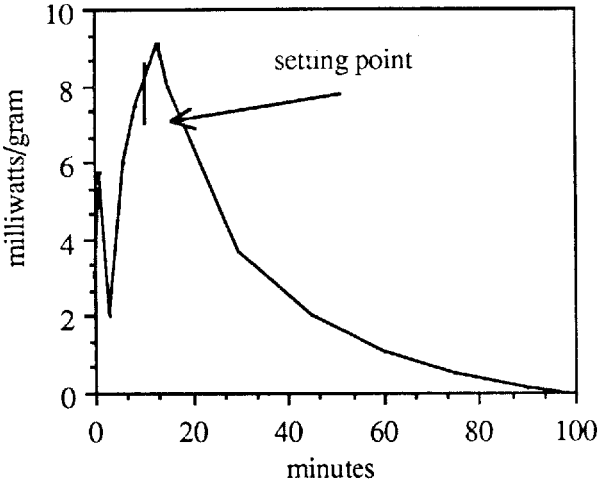

Fig. 3 Calorimetric curve obtained at 37 ° C

The Products of Setting Reaction

X-ray diffraction patterns of the products of setting reaction showed that the tetracalcium phosphate was totally converted to hydroxyapatite illustrated in Fig. 4. The possible reaction of tetracalcium phosphate:

$$CaHPO_4 \cdot 2H_2O + Ca_4(PO_4)_2O = Ca_5(PO_4)_3OH + 2H_2O \quad (3)$$

$$5Ca_4(PO_4)_2O + 2H_3PO_4 = 4Ca_5(PO_4)_3OH + H_2O \quad (4)$$

These dissolution/reprecipition reactions from the setting reaction of calcium phosphate cements. As long as both brushite and TetCP are present in excess and the rates of dissolution of these two salts are greater than that of HAp formation, the solution should continue the conversion of brushite and TetCP to HAp. Thus, the pH of the singular points lies near the physiological pH, and this contributes to the high biocommpatibility of CPC which is essential in biomedical application. For TetCP, the hydrolysis reaction produces $Ca(OH)_2$ as a byproduct (Equation 5). This would increase the pH which also causes the solution to become less supersaturated with respect to HAp.

$$3Ca_4(PO_4)_2O + 3H_2O = 2Ca_5(PO_4)_3OH + 2Ca(OH)_2 \quad (5)$$

TetCP is unique, because it is the only calcium phosphate salt which has a Ca/P ratio higher than that of HAp. Thus it also only can be combined with another salt (other than HAp) to formulate a mixture that has the stoichiometry of HAp.

Mechanical Properties

The mouth is a harsh environment, one ideally suited for destruction. Materials used within it are subject to great forces are continuously exposed to abrasive and corrosive conditions. The average biting force of a person with natural dentition is approximately 170 pounds in the posterior area of the mouth. This works out to represent approximately 28000 psi on a single cusp of a molar tooth. [7] Materials considered for use in restoring chewing surfaces must have sufficient strength to withstand these forces. Two kind samples were tested: a) soft-casting, using flexible spatulas by hand, b) warm-pressing, applying heat and pressure simultaneously. The latter has theoretical meaning. In this experiment, samples were pressed 0.5 to 1 hour under 80-350 MPa at 37-100°C. Because the ratio of the liquid to powder was very important, an eye dropper was used to add the liquid to powder until the powder was wetted to a just paste consistency. After mixing, the sample was put into a 0.5 x 2.5 x 0.25 cm mold.

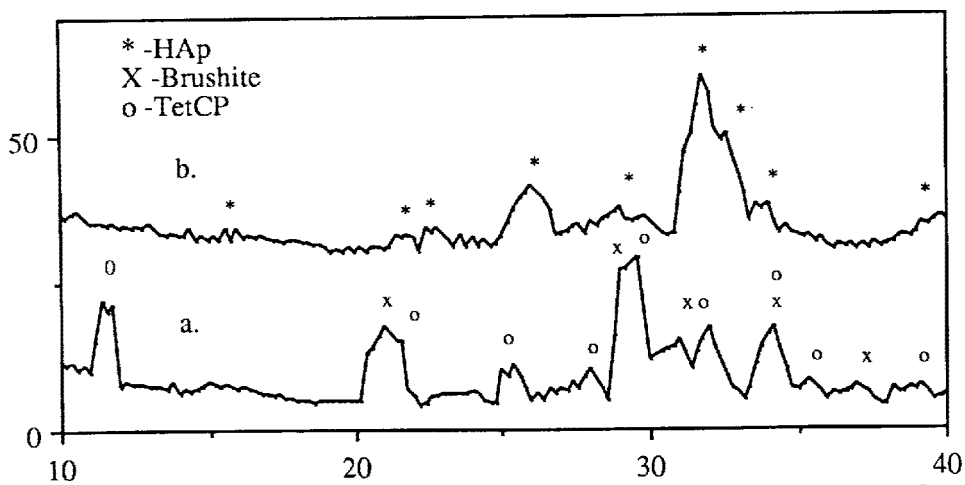

Fig. 4. X-ray diffraction patterns for (a) reactant, (b) after reaction 1 day at 37 ° C

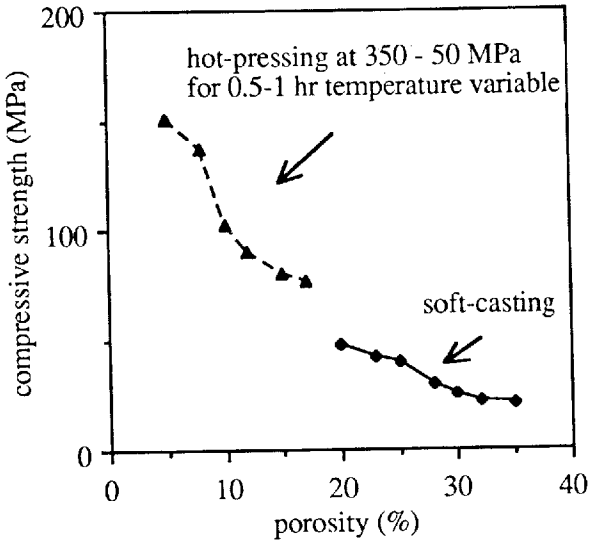

Fig. 5 The relationship between compressive strength (7 day) and porosity of cement paste

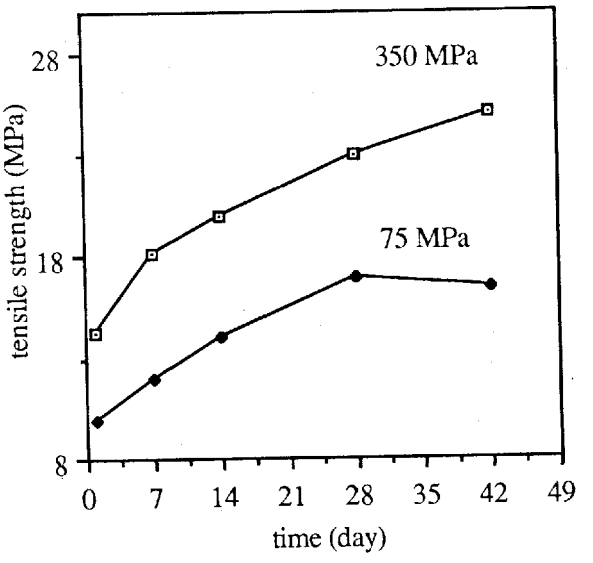

Fig. 6 Tensile strength of warm-pressed samples under 75 and 350 MPa

Factors That Affect Strength

Porosity: Because calcium phosphates are relatively insoluble, the volume occupied by the liquid phase of CPC contains essentially no calcium phosphate materials. As a result, porosity of set specimen is closely related to the solid-to-liquid ratio used. The maximum powder-to-liquid that would still produce a workable paste appears to increase with the particle size of the solids. The strength of cement is strongly dependent on both the total porosity and the maximum pore size in the materials. Dense packing is the essential feature of cementitious materials to reduce both the total porosity and maximum pore size (critical flaws). The packing of particle systems is strongly dependent on the mechanical placing of particles, i.e. the kinematics of the arrangement of particles. Normally, denser packing can be obtained by shear deformation, repeated shear deformation, or balanced vibration. Only by using heavy mechanical compaction was it possible to overcome the locking surface forces and pack the cement as densely as permitted by the particle geometry - typically corresponding to a low solid/liquid ratio - resulting in very high strengths. In Figure 5 the curve shows the relationship between compressive strength and porosity of hardened cement paste in small-scale laboratory experiments under soft-casting and special warm-pressing conditions. Fig. 6 shows the flexural strength of two warm-pressing specimens vs. time.

Particle sizes: Because the calcium phosphates used for this cement are sparingly soluble, it is crucial to control the particle size for proper cement setting and strength of the samples. Firstly, the chemical bonding forces is driving force for setting reaction; secondly, the excess free energy of a high-surface-area calcium phosphate is also sufficient to provide the driving force for setting reaction. According to the classical Gibbs-Kelvin equation, the smaller the particle size, the larger the solubility of powders. In this experiement, the desired particle size of tetracalcium phophate and brushite which is an equimolar mixture was achieved by wet grinding on an attrition mill, and dehydrated ethyl alcohol was used. The specific surface area was test by BET method (Monosorb, Quantachrome Corporation, Syosset, NY). The effect of specific surface area on the compressive strength of specimens at age 28 days which were prepared under warm-pressing at 100 MPa can be seen in Table III.

Table III Effect of Specific Surface Area on Compressive Strength

Specific Surface Area m^2/g	0.5	0.76	0.94	1.32
Compressive Strength (MPa)	31.4	39.7	48.3	51.7

Biocompatibility

To test the compatibility of the dental phosphate-bonded cement, the cements were implanted into the jawbones of Wistar male rats with the age ranged from 15-20 weeks. The implanted samples were used HAP power as a comparative control. After surgical entry to the bone, 1 mm diameter holes were drill in submandibular symphyseal region into which the cement was placed. After the pastes were inserted, the soft tissue was closed with sutures. Rats were sacrificed after 4 and 8 weeks, and the histology was examined. Histomorphometry was carried out on the mass the whole circumference of which were visible in the eyefield of the light microscope with 400 magnification. [8] The interface between bone and cement shows new bone formation.

CONCLUSIONS

The combination of self-setting and high biocompatibility makes the calcium-phosphate cement a potential dental material. Exactly how to get the appropriate mechanical properties is not entirely clear and the subject would probably repay further research.

REFERENCES

1. W.E. Brown and L. Chow, in Cements Research Progress, edited by P.W. Brown (Am. Ceram. Soc., Westerville, Ohio, 1986), pp. 352-79
2. P.W. Brown, in Advances in Cementitious Materials, edited by S. Mindess (Am. Ceram. Soc., Westerville, Ohio, 1991), p. 769
3. L.C. Chow, S. Takagi, P.D. Costantino, and C.D. Friedman in Self-setting Calcium Phosphate Cements, edited by B.E. Scheetz, A.G. Landers, I. Odler, and H. Jennings (Mater. Res. Soc. Proc. 179, Pittsburgh, PA, 1991), pp. 3-24
4. L. Xie, and E.A. Monroe, in Calcium Phosphate Dental Cement, edited by B.E. Scheetz, A.G. Landers, I. Odler, and H. Jennings (Mater. Res. Soc. Proc. 179, Pittsburgh, PA, 1991), pp. 25-40
5. P.W. Brown, and M. Fulmer, J. Am. Ceram. Soc., 74[5] 934-40 (1991)
6. P.W. Brown, N. Hocker, and S. Hoyle, J. Am. Ceram. Soc., 74[8] 1848-54 (1991)
7. H.O. Torres and A. Ehrlich, Modern Dental Assisting, 3rd (W.B. Saunders Company, Philadelphia, PA, 1985), p. 196
8. B.J. Fellows, G. Bauer, H. Gottschalk, H.J. Oel and K. Donath, in Ceramics in Clinical Applications, edited by P. Vincenzini (Elsevier Science Publishers B.V., Amsterdam, Netherlands, 1987), p. 284

MgO — AMMONIUM POLYPHOSPHATE SYSTEMS

Marcela Muntean and Melania Gutul

Polytechnic Institute, Bucharest, ROMANIA

SUMMARY

The binding properties of the MgO - ammonium polyphosphate systems are investigated. Correlation between the nature of the ammonium polyphosphate (especially, the polycondensation degree) and the physical-mechanical properties of the systems, in normal hardening conditions, are also established.

AUSZUG

Es sind die Bindeeigenschaften der MgO - Ammoniumpolyphosphatsystems geforscht Gleichfalls sind die Korrelationen zwischen der Natur des Ammoniumpolyphosphats (besonders das Polykondensation grades), der Hydratationprodukten, der Härte vorgangekinetik, und der Physikalischen-Mechanischengenschaften der Systeme, in normalen Festwerdenbedingungen festgestellt.

INTRODUCTION

A careful investigation of the processes ocurring during the hardening of phosphatic binders has led to the extension of our knowledge regarding acid-oxide type binders. Their hardening may be controlled by the formation of hardly soluble salts which generate hardened space lattice with lower internal tensions /1-3/. The binders made from magnesia - ammonium phosphate (ployphosphate) have a short initial setting time, between 5 and 3o minutes, and final setting time of 2o - 6o minutes /4-9/. In the hardened systems are formed hydrated magnesium phosphate salts as crystalline compounds /3-5/. Mortars and concretes made with magnesia-phosphate cement have a good abrasion resistance and compressive strengths and also, high durability.

EXPERIMENTAL

The magnesia which mainly has MgO, besides small quantities of SiO_2, CaO and Al_2O_3 (under 1.5%) was calcined at 1,3oo°C for one hour and ground to a very high degree of fineness (under 63 μm). The ammonium polyphosphate (APP) with the general formula, $(NH_4)_{n+2}P_nO_{3n+1}$, was prepared by the method described in previous papers, see /1,3,7/. In this case, the polycondensation degree, n, was 1, 10, 20 and 50. The chemical analyses and XRD data show for higher polycondensation degree than 10, belong to long chains with n = 10, 20 or 50, the presence of the tripoly-, tetrapoly- and even pyrophosphate. Sometimes 5% of sodium triphosphate (TPP) was utilised as additive to retard the setting time.

Magnesia-phosphate binders, in which MgO/APP ratio was 2.0, 1.5 and 1.0 were used for tessted with various laboratory-made mortars. Quartz sand of high purity (over 99% SiO_2) and magnesia clinker (burnt at 1,700°C) were used as aggregate for the mortars. The particle size of the aggregate was 300 um maximum. The binder-aggregate ratio of mortars was 30/70. The nature of the hydration compounds, the physico-mechanical properties of the phosphatic systems and the kinetics of the hardening processes were analysed by the usually employed testing methods /3,7,8/.

RESULTS

The kinetics of the hardening processes varies with MgO/APP ratios. The setting time varied, depending on the ammonium polyphosphate nature, i.e. the greater the polycondensation degree, the longer the setting time (see Table 1).

The mechanical strengths of the mixtures with various MgO/APP ratios were good. Especially, they were better for the mixture with MgO/APP ratio 1.5 at higher polycondensation degrees, and for values of the hardening time 100 hours and beyond. The processes which take place at the formation of the hardened structure occur more slowly when the polycondensation degree is higher (n over 20, 50), see Table 2.

In all cases one may observe that, the optimum MgO/APP ratio is 1.5 regardless of the polycondensation degree of the ammonium polyphosphate (see Fig.1). The same fact is also evidenced for samples with

Table 1. Setting time of the phosphatic binders.

Sample No.	Polycondensation degree, n	MgO/APP ratio	Setting time, minutes Initial	Final
1.	1.0	1.0	8.0	17
2.		1.5	6.0 (13)	15 (31.5)
3.		2.0	4.0 (11)	13 (29.3)
4.	10.0	1.0	10.0	19
5.		1.5	8.0 (21)	14 (37)
6.		2.0	5.5 (17)	12
7.	20.0	1.0	17.5	27 (51)
8.		1.5	15.0 (33)	22 (55)
9.		2.0	13.0 (31.3)	20 (48)
10.	50.0	1.0	30.2	60
11.		1.5	21.0 (46)	37.5 (86)
12.		2.0	16.5 (39)	29

Obs. water/binder ratio = 0.45
( ) - the same binder with 5% sodium triphosphate as setting retard additive.

Table.2. Compressive strengths (R_c) of the binders.

Sample No.	MgO/APP ratio	Polycondensation degree (n)	R_c, MPa, at various hardening time (hours) 5	10	100
1.	2.0	1.0	4.6	11.8	14.0
2.		10.0	9.8	16.6	21.4
3.		20.0	10.3	16.2	21.9
4.	1.5	1.0	8.2	13.0	17.7
5.		10.0	13.0	21.2	25.5
6.		20.0	11.9	18.5	26.4
7.		50.0	10.0	14.4	28.3
8.	2.0	1.0	3.1	6.6	11.5
9.		10.0	4.7	9.3	15.1
10.		20.0	5.2	10.7	16.4
11.		50.0	4.3	8.3	17.5

Obs. hardening at room temperature;
water content, 13%.

5% sodium triphosphate used as retarding admixture.

The electron microscope images show a more uniform structure for the phosphatic binder with MgO/APP ratio 1.5 vis-a-vis other phosphatic masses, Fig.2. This fact may explain the better mechanical properties obtained in this system.

The compressive strengths determined on laboratory mortars, under standard conditions, shows that mortars with magnesia clinker as

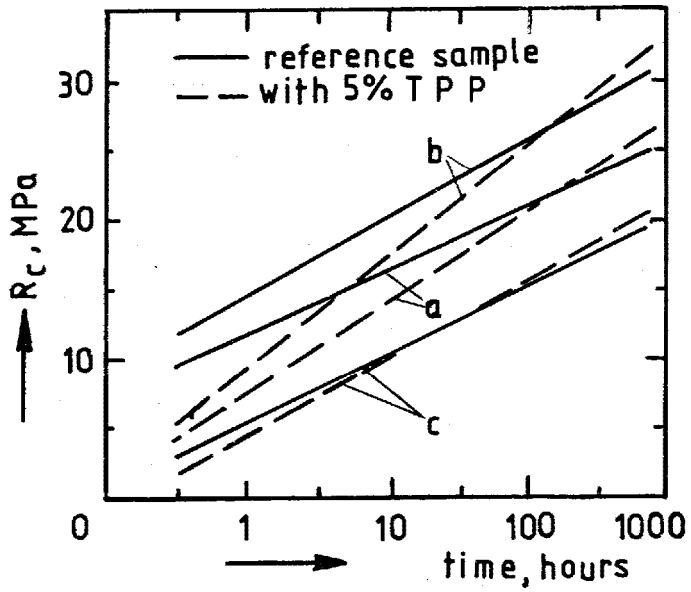

Fig.1. Mechanical strength vs. time for samples with and without TPP, for various MgO/APP ratios (n=10): a) 2; b) 1.5 and c) 1.0

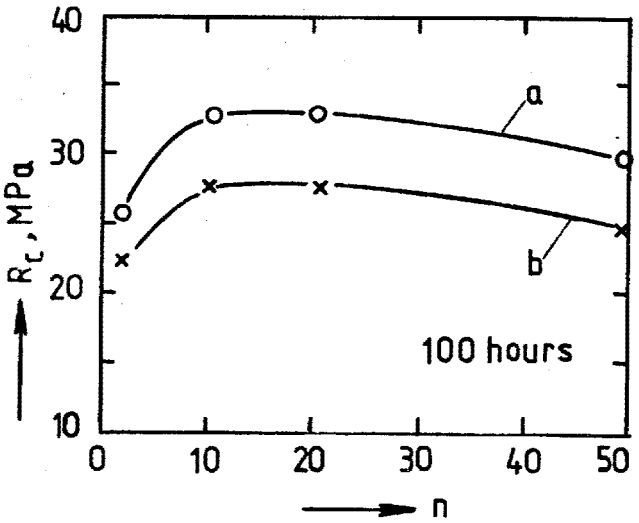

Fig.3. Compressive strength vs. polycondensation degree: a)magnesia mortar; b) silica mortar.

aggregate have a higher mechanical strengths compared to phosphatic binders with silica mortars (Fig.3).

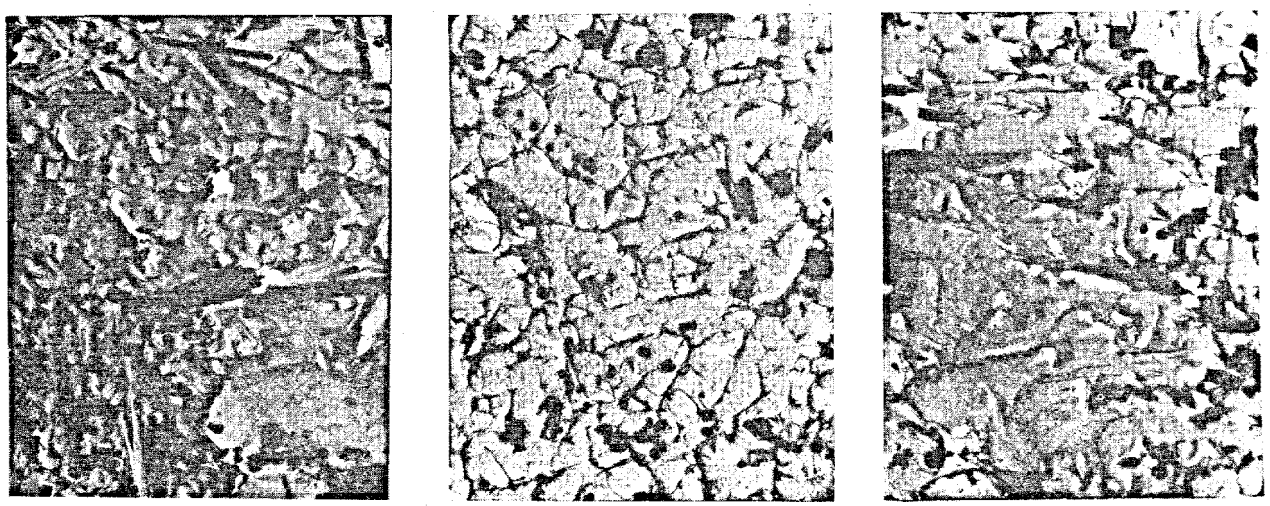

MgO/APP=1 MgO/APP=1.5 MgO/APP=2

Fig.2. EM (5000 x) of the phosphatic binders with various magnesia/APP ratios.

The dependence of compressive strength on polycondensation degree shows a similar trend for both mortars, but with an increase in "n"

the magnesia mortars display higher strengths than silica mortars. The difference lies within 2 to 4.5 MPa. Perhaps, the adherence of the phosphatic binder to the aggregate particles is more tenacious with magnesia mortars.

The XRD data in conjunction with those from DTA show that the nature of the hardened products is similar in all samples, but their proportions, in various MgO - APP systems are different. Frequently, in all phosphatic binders, may be observed unreacted starting materials (especially MgO) together with hydration products as struvite, schertelite, dittmarite (Table 3).

Table 3. Phase distribution in phosphatic binders.

Compounds	n = 10			n = 50		
	MgO/APP					
	1.0	1.5	2.0	1.0	1.5	2.0
MgO	+++	+++	+++	+++	+++	+++
Ammonium polyphosphate	+	-	-	+	-	-
$NH_4MgPO_4.6H_2O$ (struvite)	++	+++	++	++	+++	++
$(NH_4)_2Mg(HPO_4)_2.4H_2O$ (schertelite).	++	+	++	++	+	+
$NH_4MgPO_4.H_2O$ (dittmarite)	++	+	+	++	++	+++
DTA endo-effects: struvite, 94-98°C; schertelite, 110-115°C, dittmarite, 245-250°C.						

In the samples with 5% TPP, $NaNH_4PO_4 4H_2O$ also was identified. The data are in good agreement with the compressive strengths. This may be explained by the greater proportion of struvite in the initial hardening period, responsible for the formation of the hardened structure of the phosphate binders /4,5,7/.

CONCLUSIONS

Binding masses within the MgO - ammonium polyphosphate system may be obtained. They have good mechanical performances for 1.5 MgO/APP ratio, when the polycondensation degree of the ammonium polyphosphate is 10 or 20, even at shorter hardening time. The phosphatic mortars with magnesia clinker as aggregate may be used as refractory masses.

REFERENCES

1. Praizer, A.W., Smith, J.P., Lehr, J.R.;"Characterization of Some Ammonium Polyphosphates", J.Agr.Food Chem., 1965, 13, 316-326.

2. B.El-Jazairi., Concrete., 1982, (12), 67-69.

3. Niculescu Simona.,"Phosphatic binders", MScThesis, Polytech. Inst. Bucharest, 1987.

4. Sugama, T. and Kukacka, L.E.:"Magnesium Monophosphate Cements Derived from Diammonium Phosphate solutions", Cement and Concrete Research, 1983, 13(3),407-511.

5. Sugama, T. and Kukacka, L.E.: "Characteristics of magnesium polyphosphate cements derived from Ammonium Polyphosphate solutions", Cement and Concrete Research, 1983, 13(4), 499-5o8.

6. Adbelrazig, B.E.I., Sharp, J.H. and El-Jazarri, B.: "The chemical composition of mortars made from magnesia phosphate cement" , Cement and Concrete Research, 1988, 18(3), 415-429.

7. Niculescu Simona and Muntean Marcela: "Binding masses within the ammonium polyphosphate MgO system", Materiale de Construcţii, 1988, 18(3), 174-178.

8. Teoreanu, I., Muntean Marcela and Ene Daniela: "The behaviuor towards hardening of the binding mixtures of the oxide-acid systems with TiO_2 and ZrO_2", Materiale de Construcţii, 1989, 19(47, 257.

9. Montague, L.; "Role liant des phosphates condenses dans les composites ceramique-metal", These, Lille - France, 1991.

HARDENING PROCESSES FOR SOME REFRQACTORY BINDING SYSTEMS KINETIC CONSIDERATIONS AND MECHANISMS

I Teoreanu* and N Angelescu**

**Polytechnical Institute of Bucharest*
***Metallurgical Research Institute*
Bucharest, ROMANIA

SUMMARY

Binding systems of interest for low cement content refractory concretes, prepared of high alumina cement and admixtures or high alumina cement and phosphate or chromite bonds carriers are investigated. The influence of the admixtures and of the phosphate or chromite bond carriers is studied related to the nature and formation of the high alumina cement systems hydration and on the cement kinetics interaction with water. Also the paper deals with the peculiarities of the hardening mechanisms in the searched complex binding systems used in refractory concretes.

RÉSUMÉ

On fait l'investigation des systèmes liants d'intérêt pour les bétons réfractaires à bas contenu de ciment, composés de ciment à haut contenu d'aluminium et d'additifs, ou de ciment à haut contenu d'aluminium et des liants porteurs des liaisons phosphatiques ou chromitiques. On y étudie aussi l'influence des additifs et des liants porteurs des liaisons phsphatiques ou chromitiques sur la nature et la formation des phases de hydratation des systèmes à ciment à haut contenu d'aluminium, de même que la cinetique de l'interaction du ciment et de l'eau. Dans le même ouvrage, on examine aussi les particularités des mécanismes de durcissement des systèmes liants complèxes étudies, à utilisation aux bétons réfractaires.

INTRODUCTION

The new generations of low or ultralow cement content refractory concretes have as specific components, together with refractory aggregates, complex binding mixtures, dispersing or superplasticizing additives and ultradispersed mineral powders. Thus the positive consequences of reducing cement content are better used due to the fact that, simultaneously, the cohesion forces of the binding matrix with refractory aggregates are not reduced so the rheological behaviour and hence the concrete workability are greatly improved.

The convergence of effects determined by compositional modifications of the new generations of refractory concretes can be achieved by taking into account the mechanisms of the hardening processes for related binding systems.

Starting from these facts, the present paper deals with investigations of the binding systems made from high alumina cement and additives or of high alumina cement together with phosphatic or chromitic binding systems. This paper studies the influence of the additives and phosphate or chromite bonds carriers on the nature and formation of hydration phases of the systems with high alumina cement as well as on the interaction kinetic of the cement with water. Also the peculiarities of the hardening mechanisms are considered for the complex binding investigated systems to be used in refractory concretes.

EXPERIMENTAL CONDITIONS AND PROCEDURES

A high alumina cement (Alicem 2) with ~ 78.5 % Al_2O_3 and ~ 23.5 % CaO has been used.

The processes involved in hardening - the nature of the new hydrated phases and the cement hydration kinetic, were investigated by means of X - ray diffraction and specific surface measurements BET have also been carried out. The preparated pastes were characterized by a water/cement ratio (w/c) = 0.3 and hydrated under normal temperature conditions.

As additives were used: sodium citrate (CS), Ca-lignosulphonate (LSC), resin melamin-formaldehyde (VIMC11) and resin naphthalene-formaldehyde (VIMC22) - based additive, sodium tripolyphosphate (TFS) and chromic anhydride (CrO_3). The additives have been used in the established proportion (additive/cement ratio = ad/c) considered to be optimal from the point of view of their effect on the corresponding refractory concretes strength - which were prepared, conserved and tested in similar (comparable) conditions. The sodium tripolyphosphate and chromic anhydride were also dosed in higher proportions to highlight binder characteristics, together with the alumina cement.

The mechanical properties of the hardened binding systems have been established by tests carried out on refractory concretes with tabular alumina as aggregate maintaining unaltered all the other preparation and hardening conditions, excepting the binding system composition.

EXPERIMENTAL RESULTS. INTERPRETATIONS

The diffractometric study of the hydration processes in alumina cement either additivated or mixed with phosphatic or chromitic bonds carriers provides both qualitative informations on the nature of the hydrated phases and on the phase composition evolution of the binding systems, quantitative informations on the hydration degree (α) and the process kinetic.

The nature of the hydrated phases

When Alicem 2 cement is hydrated (even up to 7 days) only CAH_{10} (lines 14.2 A; 7.16 A; 3.60A; 2.55 A) and alumina hydroxide (lines 4.85 A; 4.37 A) are to be evident as hydrated phases, although under the same hydration conditions, in pure CA or CA_2 (C = CaO, A = Al_2O_3) pastes respectively, the presence of C_2AH_8 (see /1,2/) is also detected. The absence of the characteristic lines of the calcium hydroaluminate C_2AH_8 could be eventually explained by the significantly reduced speed of the $CAH_{10} \longrightarrow C_2AH_8$ conversion, as well as by the latter presence of the gellic state; the higher radiation background in the diffractograms of the Alicem 2 cement pastes as compared with that of the diffractograms of the monomineral binder pastes can also account as argument for this situation.

The formation of CAH_{10} and of the aluminium hydroxide (see figure 1) through hydration under similar circumstances is reported, similar to the unadditivated Alicem 2 cement, in the case of cement pastes with LSC (ad/c = 0.001), VIMC11 (ad/c = 0.0016, useful substance), VIMC22 (ad/c = 0.0045, useful substance), as well as TFS and CrO_3 used according to a low value of the additive (ad/c = 0.01 for TFS and ad/c = 0.001 for CrO_3). It is noteworthy that for the same hydration period, the intensity of the diffraction characteristic lines for the hydrated products is lower than for nonadditivated cement pastes; this fact, together with a more intense radiation background suggest a more pronounced amorphous character of the hydration products due to their higher dispersion degree (also possible associated with a certain braking effect on the cement hydration process determined by the additives). The additive dispersant effect is clearly highlighted by the measurements of specific surface BET - table 1.

TABLE 1

No samples	Cement samples	ad/c ratio	Specific surface BET, m^2/g
1.	Alumina cement Alicem 2, anhydrous	0	1.197
2.	Alumina cement Alicem 2, three days hydrated	0	2.524
3.	Idem 2 + LSC	0.001	3.094
4.	Idem 2 + CS	0.001	2.571
5.	Idem 2 + VIMC11	0.0016	3.536
6.	Idem 2 + VIMC22	0.0045	5.666
7.	Idem 2 + TFS	0.01	3.438
8.	Idem 2 + TFS	0.25	5.681
9.	Idem 2 + CrO_3	0.001	3.477
10.	Idem 2 + CrO_3	0.4	9.130

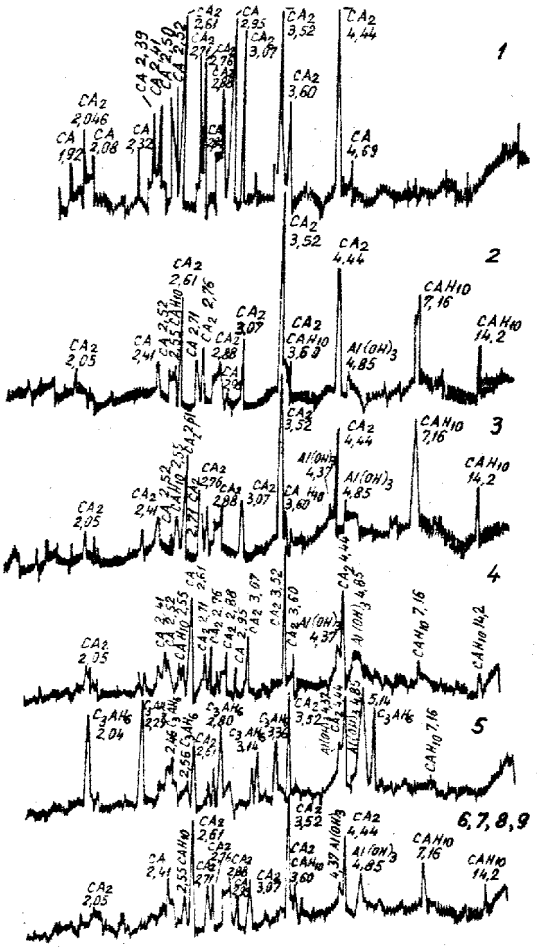

FIG. 1 Diffractograms of the alumina cement Alicem 2,anhydrous and freely hydrated-additivated: 1. anhydrous cement; 2. 3 days hydrated non-additivated cement; 3.7 days hydrated non-additivated cement; 4. LSC additivated cement (ad/c=0.001), 3 days hydrated; 5. CS-additivated cement (ad/c=0.001), 3 days hydrated; 6. VIMC11 additivated cement (ad/c=0.016), 3 days hydrated; 7. VIMC22 additivated cement (ad/c = 0.0045), 3 days hydrated; 8. TFS additivated cement (ad/c=0.01), 3 days hydrated; 9. CrO_3 additivated cement (ad/c=0.001), 3 days hydrated.

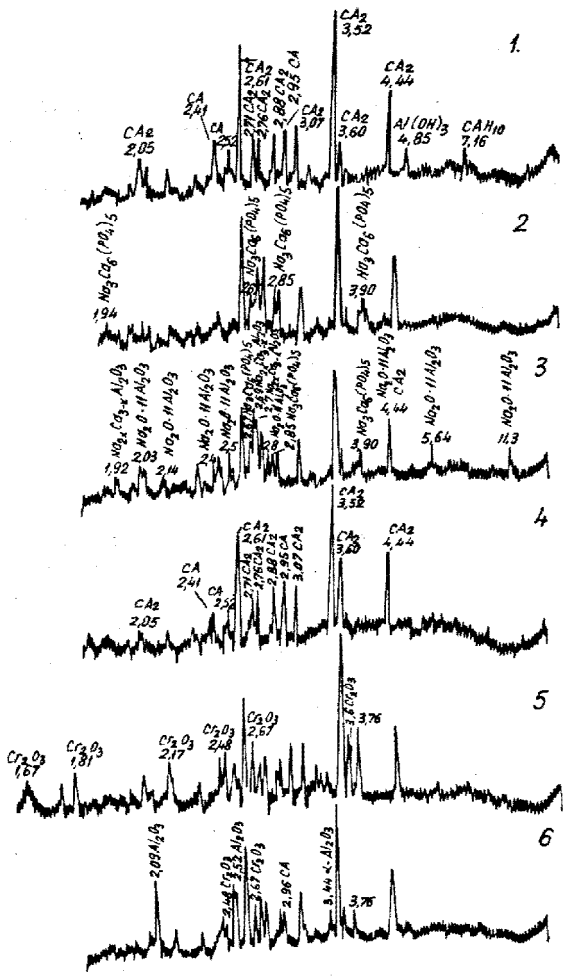

FIG. 2 Diffractograms of the alumina cement Alicem 2, TFS additivated (ad/c=0.25) or CrO_3 additivated (ad/c=0.4), freely hydrated for 3 days and after heat treatment: 1. TFS additivated cement; 2. The same (1) after heat treatment at 1000°C; 3. The same (1) after heat treatment at 1500°C 4. CrO_3 additivated cement; 5. The same (4) after heat treatment at 1000°C 6. The same (4) after heat treatment at 1500°C.

The sodium citrate alumina cement pastes (ad/c = 0.001) have a complete different behaviour. The corresponding diffractogram (figure 1) indicates the formation of a cubic calcium hydroaluminate - C_3AH_6 (lines 5.14 Å; 3.36 Å; 3.14 Å; 2.80 Å; 2.56 Å; 2.46 Å; 2.29 Å; 2.04 Å) due to the conversion of the initially formed hexagonal hydroaluminates. The sodium citrate acts as a promoter of the alumina cement hydration process but also as accelerating agent of the previously mentioned conversion processes. The promotion of the hexagonal hydroaluminates conversion in cubic hydroaluminate with the acceleration of the latter, suggests a possible negative influence on mechanical strength of the hardened binding system, confirmed by the determinations made on refractory concretes.

Alicem 2 cement pastes mixed with significant quantities of natrium - tripolyphosphate (TFS) or CrO_3 (ad/c = 0.25 for TFS and ad/c = 0.4 for CrO_3) have a clearly different behaviour related to the other studied pastes. TFS and CrO_3, for this ratio, exibited their binding capacity as phosphate and chromate bond carriers for the conditions of use of refractory concretes. X - ray diffractograms of the samples (figure 2) clearly show, for normal temperature conditions, both their retarding action on alumina cement hydration and the formation of a great amount of amorphous reaction products; this behaviour is confirmed by the radiation background being more intense that for other samples.

The results of BET specific surface determinations - table 1, confirm the very high degree of dispersion of the corresponding binding systems after 3 days hydration suggested by the X - ray diffraction analysis. The crystalline formations are in lower amounts, than seen in the other examined pastes; the presence of CAH_{10} (7.16 Å) and $Al(OH)_3$ (4.87 Å) were detected. For the samples under high temperature (1000°C and 1500°C) thermal treatment, there were detected, near calcium aluminates from hydroaluminates dehydration, some phosphate and chromate compounds corresponding to the nature of binder as different bonds carrier of the cement (alumina cement Alicem 2) - fig. 2.

The kinetics of the high alumina cement hydration

The kinetics of the alumina cement hydration, of its mineralogic compounds CA and CA_2 with or without additives or phosphate bonds carrier, has been studied through digital X - ray measurements corresponding to the characteristic lines of the calcium aluminates (2.96 Å for CA and 3.52 Å for CA_2) and their degree of transformation for various hydration terms were evaluated.

In order to process the obtained information, a simplified diffusion model was adopted, that the rate of the hydration process is inversely proportioned to the hydration degree. It results:

$$\alpha = k.\sqrt{\lg t} + k_o \qquad (1)$$

were α is the hydration degree, t - the duration of the process, k - rate constant and k_o - integration constant.

Figure 3 shows the data obtained concerning the hydration kinetic of CA and CA_2 from the non-additivated cement Alicem 2 and mixed with TFS as carrier of binding reactions which differ from those

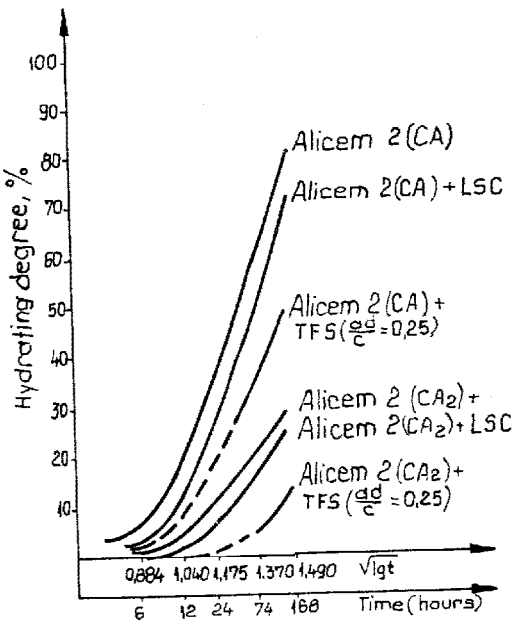

FIG. 3. The kinetics of the hydration process.

that exist in hydraulic binder (relatively high ad/c) - with a strong delaying effect (similar to CrO_3 for ad/c = 0.4) and additivated with LSC - with a moderate delaying effect. For the investigated period two distinct kinetic periods are evident: an induction period followed by a period of rapid hydration (acceleration period), also observed for portland cement clinker and its mineral components /3/. The graphs suggest that the kinetic of the process during acceleration period is controlled by diffusion. Under these circumstances, the hydration process is likely to be a surface process during the induction period, controlled mainly by the nucleation of crystalline hydrates which are thermodynamically stable; this period of time is longer for both CA_2 and retarding additives, especially, when phosphate or chromite carrier bonds together with alumina cement are used.

The mechanisms of hardening for complex binding systems

The mechanical strengths obtained on refractory concrete samples with tabular alumina (with continuous grain size according to the Fuller - Bolomey curve), cured for three days and dried after hardening at 110°C, show the favourable influence of the additives studied with the exception of sodium citrate which has a highly accelerating effect on alumina cement hydration. The sodium tripolyphosphate and the chromium oxide in high proportions - carriers of phosphatic and chromitic bonds respectively, lead under these circumstances, together with the alumina cement, to complex binding systems. At low proportions, TFS and CrO_3, also act favourably due to their strongly dispersing effect; the contribution of their binding bonds is negligible in this case, while their influence on the hydration kinetic is undetermined. Also there is a similar situation for additives LSC, VIMC11 and VIMC22.

From fig. 4 /4/ two domains of the TFS dosage values can be distinguished with positive effects on the development of the resistant hardened structures in the refractory concrete binding matrix; within these domains tripolyphosphate acts as described above, according to different prevailing mechanisms; through the dispersing action on the binding system (I) and through the development of phosphatic bonds (II), respectively. Between these two domains, related to intermediate values of the TFS/cement ratio, when the contribution of the bonds to the system hardening is of low significance, the TFS dispersing action can not compensate its

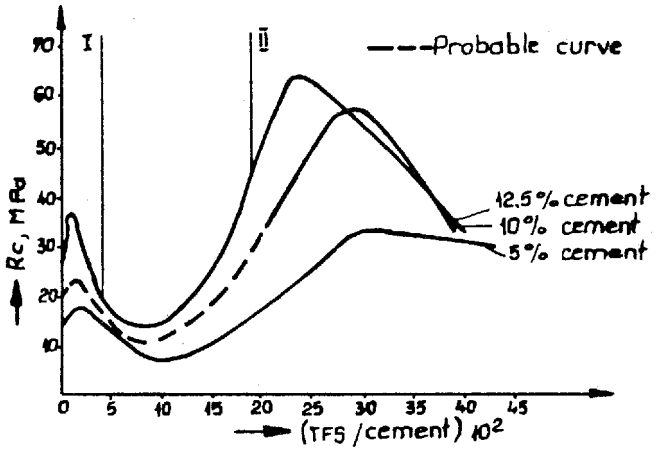

FIG. 4. Compression strength variation, for 3 days freely hardened and 110°C dried refractory concretes, as function of their TFS contents, at different alumina cement dosages: I. domain corresponding to low TFS proportions, with dispersating action; II. domain corresponding to high TFS proportions with prevailing binding (phosphatic) action.

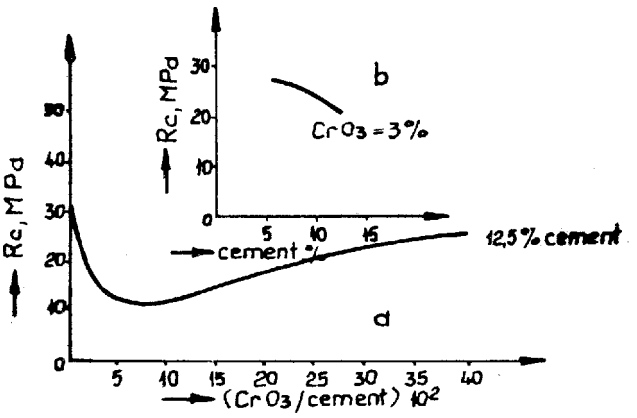

FIG. 5. Compression strength variation, for 3 days freely hardened and 110°C dried refractory concretes, as function of their CrO_3 contents or alumina cement a. compression strength dependence on the CrO_3 contents for 12.5 % alumina cement concretes; b. compression strength dependence on the cement dosage for 3 % CrO_3 concretes.

inhibiting influence on the alumina cement hydration and on the formation of crystallization - polycondensation structures of the new hydrated formations.

Experimental data on the strength of the concretes with alumina cement and chromic anhydride (figure 5 /4/) and information supplied by the BET specific surface determinations (Table 1), corroborated the fact that CrO_3 also contributes to binding, support a hardening mechanism of the main binding system similar to the one previously investigated.

REFERENCES

1. Angelescu, N.: "Concretes with low cement content". Doctorate thesis, Polytechnical Institute Bucharest, 1983.

2. Teoreanu, I., Angelescu, N., Tuclea, D.: Rev. Roumaine Chim. 29 (1), 113, (1984).

3. Teoreanu, I., Muntean, M.: Silicat. Ind. 39 (2), 49, (1974).

4. Teoreanu, I., Angelescu, N.: To be published in Interceram.

Specific Theme II C

Cementitious Systems Including DSP, CBC, etc

HIGH-STRENGTH HOT-PRESSED CEMENT PASTE

A A Pashchenko, V V Chistyakov and Ye A Myasnikova

Chair of Cementitious Materials Technology
Kiev Politechnical Institute, Kiev, UKRAINE

SUMMARY

This paper carries results of investigations into peculiarities of hydrate and structure formation of a cement paste at different temperatures (100-250°C) and forces (25-300 MPa) of pressing. Mechanism of action of various intensifiers of cement hardening has been studied. They provide 5 to 6-fold reduction of pressing force, the specimen strength remaining unchanged. The cement paste showing compressive and bending strength of 380 and 50 MPa respectively has been obtained at a pressing force of 50 MPa and a temperature of 200°C.

РЕФЕРАТ

Исследованы особенности процессов гидрато- и структурообразования цементного камня при различных температурах (t= 100 - 250°C) и давлениях прессования (P = 25 - 300 МПа). Изучен механизм действия различных интенсификаторов твердения цементных составов, позволяющих в 5-6 раз снизить давление прессования без уменьшения прочности образцов. При давлении прессования до 50 МПа и температуре 200°C получен цементный камень с прочностью при сжатии и изгибе, соответственно, 380 и 50 МПа.

INTRODUCTION

Hot pressing allows the production of materials whose density and strength are appreciably superior to the properties of an ordinary paste based on mineral binding agents (1,2). Propagation of this technique in future depends to a large extent on the development of binder compositions capable of hardening at a high rate when a pressure of 20-30 MPa generated by commercial press equipment, is applied. This could be achieved by introduction of efficient additive-intensifiers of hardening into the binding agent during the hot pressing.

EXPERIMENTAL

Test cylinders (o=22.57 mm, S=40 mm^2, height equal to the diameter) were formed in a hot pressing device by two-sided compression. The heating was done by an electric heater mounted around the periphery of the mould. Temperature of the cylinder was monitored by means of a potentiometer thermocouple. The water-cement ratio in all tests was 0.1. The rate of temperature rise was $10^{\circ}C$/min. The total pressing time including heating and isothermal cure for each cycle was the same - 45 min. Thus, as the pressing temperature was increased the isothermal curing time decreased. In the search for compositions capable of hardening actively at low pressures, the effect of pressing ratings (pressure and temperature) on density and strength of the cement paste was studied. Specimens were prepared from a commercial portland cement by applying a pressure of 25, 50, 100, 200 and 300 MPa at 100, 150 and $200^{\circ}C$. After pressing, the test pieces were placed in water to hard for 28 days under normal conditions. The effect of various electrolytes and active mineral additives on the processes of hydrate and structure formation in a hot-pressed cement paste was studied by means of the differential thermal analysis, the X-ray diffraction and IR spectroscopy. The degree of condensation of silicate anions forming calcium hydrosilicates was determined by the molybdate method. The porous structure and the specific surface of the cement paste were studied by the water adsorption-desorption method.

RESULTS AND DISCUSSIONS

As the pressing force increases, the density of the pieces increases, their porosity decreases and hydrates with smaller specific surface are formed (Fig.1). The specific surface of hydrates decreases most intensively when the pressing force increases to 25 MPa. Beyond this value, the cement paste density increases mainly at the expense of porosity reduction; for P 200 MPa this process slows down.

The relation between the relative hardening Rcomp/P of plain cement paste specimens and the pressing force P is shown in Fig.2. It can be seen that firstly there is notable strength gain with increase in P but the effect gradually flattens out later. An increase in the effect of hardening is particularly marked for P 200 MPa, which could imply that the limiting degree of piece compaction has been reached. The data presented allow making a conclusion that there exists an area of effective compaction of the cement paste. This results from the fact that the cement paste contains chemically-bound (hydration) water carried in interlayered and intercrystalline vacancies and physically-bound water adsorbed on the particle surface and filling meso- and macropores.

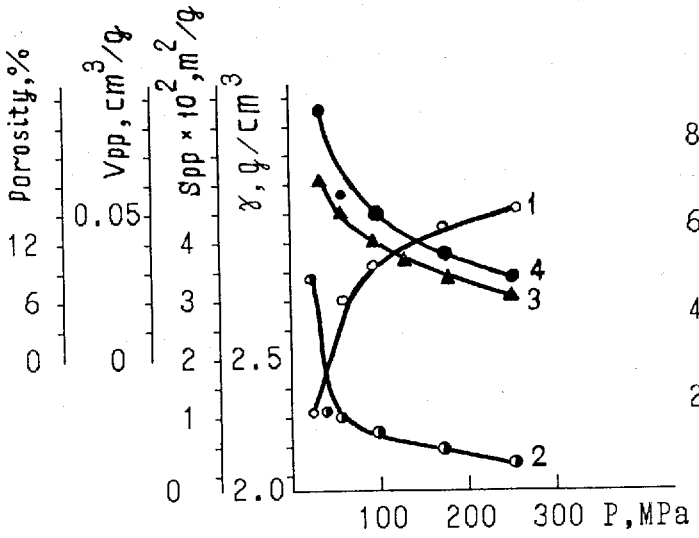

Fig.1. Effect of the pressing force on density, (1); specific surface, S (2); specific V_s(3) and relative porosity of hot-pressed cement paste (4)

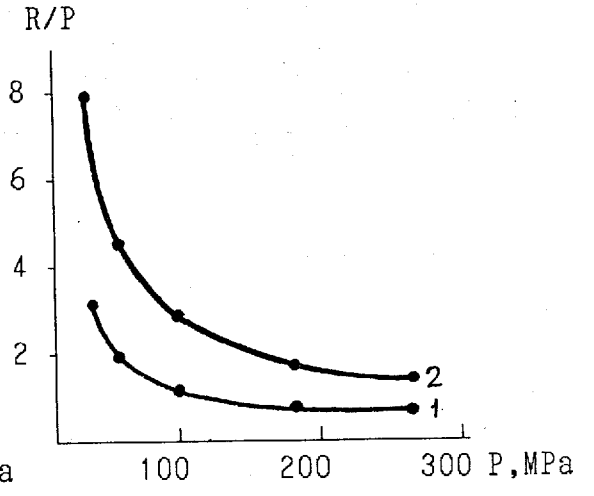

Fig.2. Effect of the pressing force P(t=200°C) on R_{comp}/P ratio:1 - just after pressing;2 - after 28 days of normalhardening

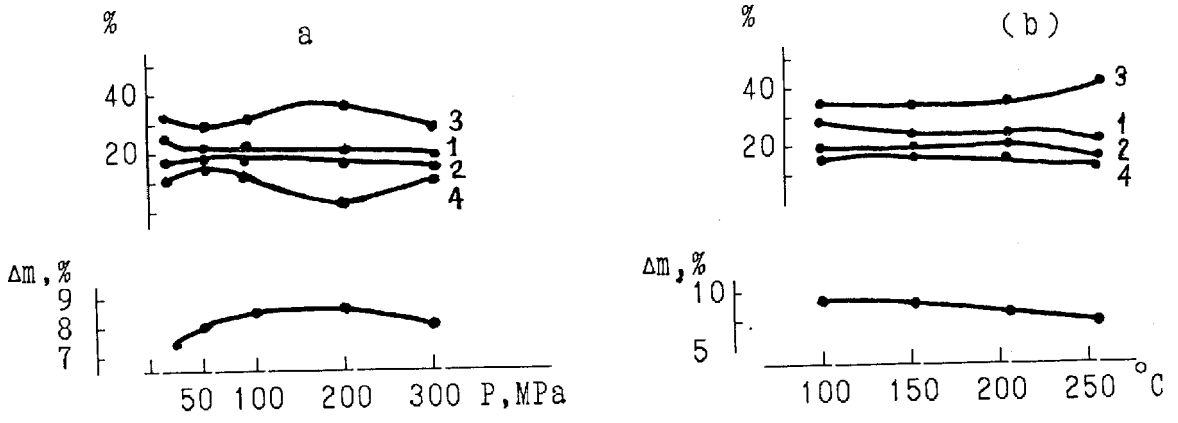

Fig.3. Effect of the pressure (a) and temperature (b) of pressing on the cement hydration degree Δm (a preparation mass loss, %, when heated to 1000°C) and a fraction of bound water, %, at different intervals of characteristic temperatures, °C: 20-290 (1), 290-490 (2), 490-760 (3), 760-1000 (4)

A fraction of the physically-bound water decreases to a greater extent than that of the chemically-bound water as a result of squeezing when the compaction pressure increases. Simultaneously with a total decrease in the content of bound water in the system, the fraction of water which enters into the composition of various hydrates and features different binding energy is redistributed. It can be judged by a change in a loss of the piece mass on heating at appropriate intervals of characteristic temperatures (Fig.3).

Fig.4 presents microphotographs of a cement paste pressed at 25 and 300 MPa wherein morphological differences are clearly defined. For a pressure of 25 MPa applied the new formations represent rounded particles and aggregates, the structure, to some extent, resembling a cement paste produced by vibration. As the pressure is raised, formation of a close-layuered structure can be clearly seen that can point to a topochemical mechanism of hydrate formation (3).



Fig.4. Microphotographs of cement paste structure pressed at 25 MPa (a) and 300 MPa (b), x2000

Compositions containing sodium sulphate and silica waste from ferrosilicon production S = $2 \cdot 10^6$ sm^2/g as additives showed the highest strengths (Table 1). Comparison of strength characteristics between pressed paste specimens without additives (1 and 2) and those with additives (3, 4 and 5) in Table 1 shows that additives help reduce the pressure applied from 300 to 50 MPa without reducing the paste strength. For the same pressing force, additives bring about a maximum of 3-fold increase in strength when tested just after pressing. The salient feature of the new formation composition is the absence of calcium hydroxide in the cement paste. Calcium silicate hydrates are represented mainly by CSH (I) and tobermorite 1.13 nm - $C_5S_6H_5$. The X-ray patterns also show faint lines of okenite - $C_3S_6H_6$ and gyrolite - $C_2S_3H_2$.

In addition, it has been established that sodium sulphate influences the polarizing effects cyclically running in cement water dispersion and controlling initial elementary hydration acts - a process of transfer of a proton by hydrohonium ions and proton reaction with an oxide ion in a crystal lattice of a clinker mineral. Consequently, the retardation effect due to hydrate formation as noted in the induction period for an additive-free composition is less when an additive is introduced. Thus, the amount of new formations increase 3-fold during hot-pressing.

The increase in the strength of the modified compositions has been attributed to the intonsification of hydrate formation processes and formation of calcium silicate hydrates of a higher degree of polymerization when a high pressure is applied at an elevated temperature. The sodium sulphate additive which contributes to an increase in the amount of hydrates also reduced their condensation degree by virtue of the replacement of SiO_4^{4-} with SO_4^{2-} (4). However, the data in table 2 indicate that the condensation processes prevail in the composition with a sodium sulphate additive under conditions of hot pressing.

Table 1

Effect of additives and pressure on cement paste strength

Test piece No	Additive		Pressing force, MPa	Ultimate strength under pressing, MPa	
	Type	Amount mass %		Just after pressing	After 28 d of normal hardening
1.	Nil	-	50	75	208
2.	Nil	-	300	190	384
3.	Na_2SO_4	1.5	50	180	330
4.	Silica fume	10	50	140	285
5.	Silica fume + Na_2SO_4	10+1.5	50	225	375

Table 2

Effect of pressing mode and sodium sulphate additive on the siliceous anion polymerization degree

Pressing mode		Additive	Content of Si_xO_y, %, when x equals				Average polymerization degree	Average basicity
P, MPa	t, °C		1	2	3-8	> 8		
25	20	Nil	79.04	0	0	20.9	19.09	1.75
25	150	Nil	58.1	11.0	0	30.9	66.4	1.90
25	150	1.5% Na_2SO_4	50.7	0	0	49.2	101.9	1.36

CONCLUSIONS AND RECOMMENDATIONS

The experimental data ibtained thus confirm that the hardening effect, under hot pressing, is brought about by formation of a less defective structure of the paste at the cost of both a sufficient reduction in its porosity and formation of new hydrate formations of a higher polymerization degree. Addition of active mineral additives

and electrolytes allows a 5 to 6-fold reduction of the pressure to be applied without reducing the cement paste strength.

Materials of completion made by pressing of such compositions for containers of high-pressure and temperature devices used in the synthesis of superhard materials (diamonds, cubic boron nitrate) have been studied; these have passed production tests too.

The salient features of hot pressed cement paste technique allowed its use for developing the technology for binding, compaction and encapsulation of radioactive wastes of low and medium intensity of radiation.

The studies pursued could be extended to hot pressing of compositions based on mineral substances for manufacture of building blocks, brick, tile. In such cases, use is made of compositions with a lower cement content, which include industrial wastes - slag, ash, moulding sand, silica fume and others.

REFERENCES

1. D.Roy, G.Gouda:"Optimization of Cement Paste Strength"/ **VI International Congress on the Chemistry of Cement. M.:Stroyizdat, 1976,V2,** 310-315.

2. J.Beaudoin, R.Feldman:"High-strength cement pastes - a critical appraisal"/ Cement and Concrete Research. 1985, **15**(1), 105-106.

3. H.Taylor. Chemistry of cement hydration/ **VIII International Congress on the Chemistry of Cement. Rio-de-Janeiro, 1986 - I,** 82-110.

4. N.Nikonova, T.Mashir, M.Smirnova, G.Zheltova. Study of the Structure of Calcium Hydrosilicate Siliceous Anions. Proceedings of MChTI, 1986, **142**, 80-91.

CONTACT-CONDENSATION BINDERS BASED ON CALCIUM HYDROSILICATES

Raisa F Runova

Kiev Civil Engineering Institute, UKRAINE

SUMMARY

This paper presents the results of investigation of the calcium hydrosilicates as independent binders synthesised in the form of dispersed phases of amorphous or unstable crystal structure. Investigations have shown that such substance can be condensed to the water-resistant stone with the strength to 350MPa at the moment of the formation contacts between macroparticles. Based on these binders new composites (metalsilicates and polymersilicates) have been commercially produced.

Эта статья представляет результаты исследований гидросиликатов кальция как самостоятельных вяжущих, синтезтрованных в виде дисперсных фаз аморфной или нестабильной кристаллической структуры. Показано, что такие вещества в момент формирования контактов между макрочастицами конденсируются в водостойкий камень прочностью до 350 МПа. На основе этих вяжущих в промышленности получены металлосиликатные и полимерсиликатные композиционные материалы.

INTRODUCTION

Calcium hydrosilicate phases, which determine the properties of hardening cements have been thoroughly investigated [1,2]. In dispersion state they have been approved for the manufacture of autoclaved materials for heat and thermal insulation [3,4]. In this case, the preferences are tobermorite and xonotlite in the well crystallized phases. The results of our investigations indicate that the synthesised amorphous products based on the system $CaO-SiO_2-H_2O$ possess new properties: during contact, the macroparticles of the compound, in the absence of heat and without chemical changes, condense and form an artificial water-resistant stone. Based on the development from these investigations [5,6,7], such products have been classified as contact-condensation binders (term-applied refers to hydration-condensation), intended for the production of special composite materials.

OBJECTS AND RESEARCH METHODS

Dispersion calcium hydrosilicates were synthesised under hydrothermal conditions conforming to approved methods [1] using chemically pure oxides with a ratio of CaO/SiO_2=0,8 and 1,5, followed by D-drying. Under these conditions, creation of various degrees of arrangement of structure of compound - from the most amorphous phase to dense crystals in a stable structure, is achieved.

The state of the structure of the products obtained was determined with the help of XRD, and also by evaluating the density (pycnometry) of the compound [8]. Practically the same dispersion for the powders was attained during sifting through a sieve: diameter of the particles lies within the limits of 10^{-3} to 10^{-5} cm The surface energy of the powders was determined by calorimetry method.

The characteristic of properties of contact-condensation binders was considered to be the coefficient of water-resistance of the sifted materials - CW which is the relation between the compressive strength of water-saturated samples after 48 h of moulding by pressing to the initial strength achieved just after pressing.

The strength of single contacts, forming the body by mechanism of contact-condensation hardening, was determined by experimental and mathematical analysis described in the work[12]. For this the density and the specific surface of calcium hydrosilicates had been measured. The specimens-cylinders (diameter and height 20mm) had been pressed from these powders and using a model of monodispersion structure a pore volume calculated on mass unit was determined.The body strength at tension(R) was tested and with the help of corresponding nomographs[12] the single contacts(R_1) being formed at specific load (Q_1) have been calculated. Tangent of an angle of line R_1-Q_1 serves as the autocohesion characteristic of the powders (n=tga).

The use of hydrosilicate binders in composite materials in powder form in conjunction with water-dispersion polymers (polyvinylacetate and latex) is suitable for producing thin forming layer systems for protective cover-finishing purposes, and also with metallic powders suitable for the preparation of pressed electric conductors.(The materials were tested by special methods [9,10].)

The nature of the interaction of composite materials was evaluated by DTA, XRD, infra-red spectroscopy and electron microscopy.

BINDER - CONDENSATION PRINCIPLES

Its principles could be analysed based on the experimental results given in Table 1. Amorphous hydrosilicates are formed during the pressing of the stone, which does not

lose strength when immersed in water and possesses a coefficient of water-resistance exceeding 1. Increasing the degree of crystallization in the compounds causes the decrease in peak width as indicated by XRD and the increase in density of the compound to the maximum value, leads to the loss of contact-condensation properties. All this is supported not only by the strength value, but also by the coefficient of water - resistance. This agrees with the earlier results achieved [5] while comparing the properties of silicates of various classes of stable and unstable crystal structures and the conclusions regarding the determining role of the structural state of the compound during its process of condensation to a water-resistant stone [11].

Table 1.

PHYSICAL PROPERTIES OF DISPERSION CALCIUM HYDROSILICATES AND CONDENSED STONE

Hydrosilicate type	Integral width (H), $m \cdot 10^{-3}$ d=0.303-0.305nm (XRD)	Density, $kg/m^3 \cdot 10^3$	Surface energy, kJ·kg	Compr. str. after pressing*, MPa	Coefficient of water - resistance CW
$C_{0.8}SH_2$	255	1.51	102.875	37.5	1.24
	140	1.69	90.456	31.6	1.12
	80	1.85	80.805	28.4	0.75
	75	2.08	33.076	5.3	0
$C_{1.5}SH_2$	230	1.59	81.098	23.8	1.30
	175	1.66	68.284	18.5	1.24
	130	1.71	65.188	13.6	1.07
	47	2.12	27.880	1.8	0

* Samples were pressed with a force of 100 MPa, immersed in water just after moulding.

This phenomenon is associated with free (abundant) surface energy. Material in unstable (amorphous or sub-microcrystal) state possesses the least dense arrangement of atoms and molecules, and hence occupies the maximum volume, that is, it is less dense compared to a similar stable crystal structure. Therefore in the equilibrium of its internal energy, part of it is the kinetic energy at maximum, while surface energy is plentiful at normal conditions. As noted from the experiments (Table 1), its value is inversely related to the density and this energy is discharged during the interaction of the macro-particles of calcium hydrosilicate during contact-condensation hardening.

This fact is supported by the results on the strength of single contacts by the models of the structure of mono-dispersed globules [12]. As may be seen from Fig 1, the best results are obtained when there is no compensation of dipole layers of water. Compounds having minimum density show maximum values of autocohesion constant (n=tga, Fig1) and do not require the application of free water during pressing.

Table 2 illustrates the influence of specific compacting load on the strength and average density of stone. These values are characterised by a straight line relationship up to the attainment of maximum values. A pressing force of 400MPa creates

Table 2

DEPENDANCE OF PROPERTIES OF STONE MADE OF DISPERSION HYDROSILICATE $C_{0.8}SH_2$ UPON PRESSING FORCE

Properties	Pressing Force, MPa								
	10	20	50	100	200	400	800	1600	2000
Compressive strength after pressing, MPa	4	8	19	40	81	125	163	268	356
Average density, kg/m³	790	895	1065	1220	1500	1860	1970	2240	2260

a stone of strength equal to 1/3 of the pressing load. However, these systems condense not only during pressing: it has been demonstrated that water dispersion calcium hydrosilicates layer of 0.1-0.2 mm thickness, applied up on a concrete surface, after drying, forms a water-protective cover, despite the fact that, it is not sufici-ently firm to be utilised as a protective finishing material.

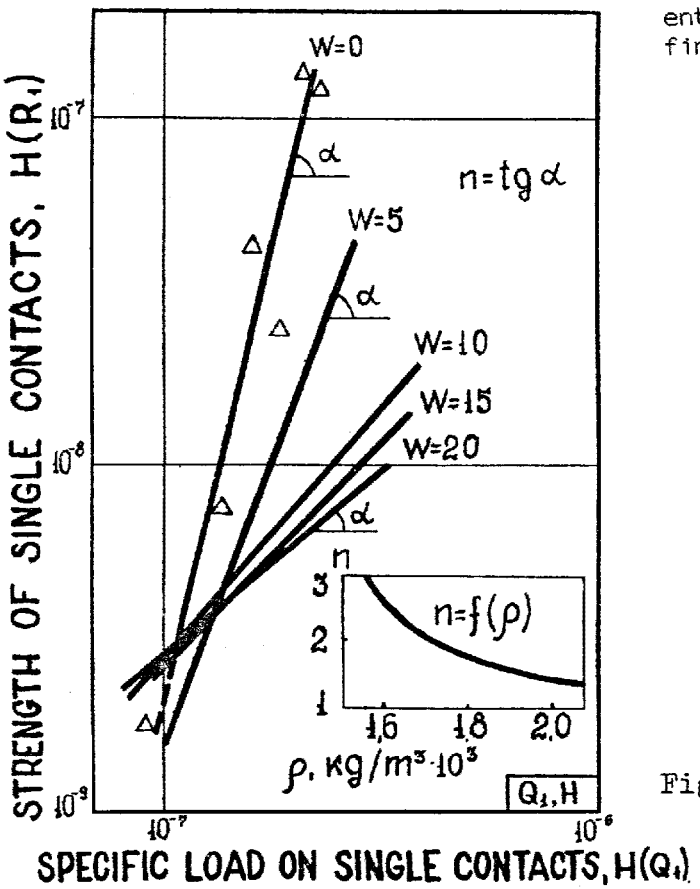

Fig.1.Characteristic of the single contacts of calcium hydrosili cate C/S = 0.8 at 0;5;10;15 and 20% moisture content.

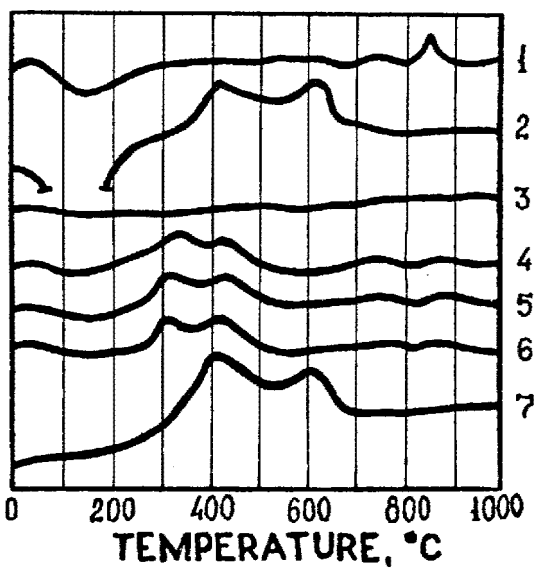

Fig.2.DTA results of calcium hydrosi licate C/S = 0.8(1),polivinyl acetate dispersion/PVAD/(2), wollastonite(3), coatings on hydrosilicate and PVAD base after 48h(4),90days(5) and 360days(6),coating on wolla stonite and PVAD.

Generalising the experimental investigations, hydrosilicate binders may be considered as systems of minerals forming an unstable structure of the following common type CxSyHz. These systems are characterised by a free (kinetic) energy, which is sufficient for creating a mutual attrraction among the macro-particles in addition to the formation of water-resistant bonds between themselves. Such energy might appear not only during the formation of cohesion contacts, but also in the interaction with the particles of another material. This serves as a basis for the effective use of binders in composite materials lacking additive properties.

PECULIARITY OF STRUCTURE FORMATION IN CERTAIN COMPOSITE MATERIALS

During the mixing of hydrosilicate binder with dispersion polyvinylacetate in the ratio of 0.85:0.15 to 0.70:0.30 in parts by mass, compound of viscocity 20-30 seconds are formed. After applying a 0.2 to 2 mm thicklayer of this compound on concrete or brick, it harden within 1 to 1.2 h, thus creating a white or coloured (if a pigment is ed) cover. The impact strength of the layer is 6.3 - 7.4 MPa, adhesion to base 1.6 - 1.8 MPa, coefficient of softening 0.94 - 1.0, frost resistance 35 - 60 cycles and weather resistance 350 - 600 cycles. These properties are characteristic of materials suitable for water-resistant facade paint and testify about the interaction processes in the system, differing from the known anologues, containing water-dispersion polymers [13].

In accordance with DTA the interaction in the system is accompanied with the formation of a complex organic-mineral phase "X", of which it is possible to judge due to the presence of a double exothermal effect with a maximum value at 325 and 420°C , and which is absent in the curves of initial components and compounds with portland cement and wollastonite [Fig 2] The mixing of stripes of absorption for carbon group C=O (1700 cm^{-1}) and group C-O-C (1200 cm^{-1}), characterise the reaction-capabilities of centres of polyvinylacetate molecules, consequently in the stripe region of 1740 cm^{-1} and 1240 cm^{-1} and never noted in similar compounds witn portland cement [13]. It is possible to judge the formation of a donor-concetration ties witn the creation of a complex material. The presence of impoper electron pairs of oxygen atom in the carbonic groups stipulatestheir properties as donor electrons, while calcium hydrosilicate ion acts as an emphasiser to the electron pairs. This is the manner, with which is manifested the peculiarities of the nature of mineral component -the structural state of the loose - dispersion calcium hydrosilicates.

Paints, based on the above system, have been industrially explored and are utilised in facade finishes.

Hydrosilicate binders, when thoroughly mixed with metallic powders to give a homogeneous distribution of particles in volume, give composites upon pressing, by a mechanism of contact-condensation hardening, without recoures to thermal energy.

The structural formation of the composite is based on similar to mechanism condensation processes of compounds with metallic bonding and amorphous silicates with covalent bonding. However, the chemical structure of the system's ingredients is not disturbed, thougth plastic deformation of silicate is likely with an increase in density. Consequently a change in electrical and thermal-physical characteristics of the material is also noted. In the zone between phase interactions becomes the possibility of the proccesses of electron level. Investigations on similar systems with crystallized silicates confirm the effect of active interaction of amorphous silicates with metallic particles. Based on this effect, various special materials have been manufactured for use in electric heating of buildings, and also for the preparation of frictional accessories and others.

CONCLUSION

Amorphous dispersion calcium hydrosilicates, synthesized from oxides or obtained through the hydration of water-free mineral components, possess contact-condensation properties. These materials display a high chemical activity during interaction with water-dispersion polymers with the formation of complicated compounds. They also participate in the physical interaction processes with metallic powders without the formation of new phases. The above mentioned properties are effectively utilised in the preparation of polymer-silicate and metal-silicate composite materials.

ACKNOWLEDGMENTS

This paper generalizes the results of investigations being carried out in Scientific Research Institute of binders and materials named Glukhovsky V D under the supervision of the author. The author appreciates the assistance of her colleagues Kochevych M A, Maksunov S Y and Maistrenko A A, who carried out experimental work.

REFERENCES

1. The chemistry of cements. Ed. by H.F.W. Taylor. London-New York, 1964, 500p.

2. Iluhin, V V :Calcium Hydrosilicate. Synthesis of monocrystals and crystal chemistry. Moscow, Science, 1979.184p.

3. Sasnauskas, K.:"Synthesis of calcium hydrosilicate".KPI:Institution Scientific Works. Chemistry and Chemical Technology,XY, Kaunas, 1973,68-74.

4. Sasnauskas, K.:" Calcium hydrosilicates and their applications".All Soviet Conference, Kaunas, 1990, 5-8.

5. Gluhovsky, V D and Runova, R F:"Properties of Dispersion Products of Hydration of Cement".VI Int..Congr.on the Chemistry.of Cement, .Moscow, 1976, P2, V1.90-93.

6. Glukhovsky, V D, Runova, R F.:" Condensation Properties of Dispersed Products of Portland Cement Hydration and Rehydration". VII Congr.Jnt. de la Chimie des Cements, Paris, 1980, VII,419-422.

7. Glukhovsky, V.D, Krivenko,P V, Runova,R F:" Particularites de Structure le Ciment Durci Contanant des Alcalis".VIII Jnt. Congr. on the Chem. of Cement,Rio de Janeiro, 1986, V VI,614-616.

8. Runova, R F, Kochevih,M A:" Qualitative and Quantitative Characteristics of Contact-Condensation Structural Formations in Dispersion Systems, Represented by Calcium Hydrosilicate". Chemistry and Chemical Technology, 1986, (6),45-49.

9. Karyakina, M I.: Testing of Painting Materials and Covers. Moscow, Chemistry, 1988,272p.

10. Pugachev, Q A.: Technology for the Production of Electric-Conducting Concrete Elements. Novosibirsk, 1988, 198p.

11. Runova,R F.:"Condensation of Dispersion Materials of Unstabie Structure". Cement,1985, (11),15-16.

12. Rebinder, P A, Shukin, E D, Marcholis, L Y.:"About Mechanical Strength of Porous Disperion Bodies. Papers - Academy of Sciences U.S.S.R.1964,V3(154),695-698.

13. Spirin, Y A, Olchincky, A Q, Mchedlov-Petrosyan, O P, Uginchus, D A.:" Interaction of Organic and Mineral Components in Cement Composite Materials". Papers - Academy of Sciences U.S.S.R., 1978, V3(241),654-656.

MECHANICAL AND MICROSTRUCTURAL CHARACTERIZATION OF MDF CEMENT-SiC WHISKER COMPOSITES

T H Kim, Y W Park and S H Choi

Dept of Inorganic Materials Engineering, Hanyang University
Seoul, KOREA

SUMMARY

The addition of SiC whisker enhanced mechanical properties of macro defect-free (MDF) cement, which basically composed of high alumina cement and polyvinyl alcohol/acetate. The contents of the SiC whisker added to MDF cement were in the range of from 2 vol. % to 10 vol. %.

Our study shows that flexural strength and fracture toughness of the composites have been greatly improved, although micropores are produced around the SiC whisker. Such enhanced mechanical properties appear to be related to the suppression of microcrack growth by the SiC whisker, indicating that the SiC whisker having a very high elastic modulus can absorbe energy for crack propagation. The main toughening behavior of the MDF cement composites reinforced with SiC whiskers are related to crack deflection, microcracking, and bridging of cracks.

SiC whisker-zusätze tragten zur Verbesserung der mechanische Eingenschaften des macro defect-free (MDF) Zements, des sich grundsätzlich hoch Tonerdezement und Polyvinylalkohol/Acetat zusammen setzten. Der Gehalt der SiC whisker in den MDF Zement-SiC whisker Verbundwerkstoffen war in dem Bereich von 2 bis 10 vol. %.

Diese Untersuchung zeigt, daß die Biegebruchfestigkeit, und die Bruchzähigkeit der Verbundwerkstoffen erhôht wurden, obwohl die Mikrorißе um die SiC whisker gebildet wurden, Es erschiente, daß solche Erhôhung der mechanische Eigenschaften mit der Unterdrükung des Mikrorißwachstums, die auf den SiC whisker berühte, verbunden ist, d.h., SiC whisker kann, aufgrund ihrer sehr hohe Elastizitätsmodul, die Energie zur Rißausbreitung absorbieren. Haupte Zähesverhalten von MDF Zement-SiC whisker Verbundwerkstoffen wurde von Rißablenkung, Mikrorißbildung, und Rißbrückung gekennzeichnet.

INTRODUCTION

Macro defect-free (MDF) cement has been developed as a high performance cement based material, since it was reported by Birchall *et al.*(1-3). Recently, research and development has been focused on improving mechanical properties of MDF cement composites, especially, fracture toughness by fiber reinforcing (4-7). Alford *et al.*(4) reported that MDF cement with small volume fractions of fibre presented excellent toughness and impact properties. Common fibers for reinforcing cementitious matrix are kevlar fiber, polypropylene fiber, and glass fiber. However, it is not easy to find out a homogeneous mixing method with the fibers.

On the contrary, SiC whisker which is in a form of needle-like single crystal (8) has been popularly used material as a reinforcing phase for ceramics to improve mechanical properties of the materials. SiC whisker is material with a very high elastic modulus (~480GPa) and superior fracture toughness, and excellent chemical stability as well as simple fabrication with ceramics. Since the first reinforcement of SiC whisker to the Al_2O_3 matrix was reported Becher *et al.* (9), SiC whisker reinforcing has been succeeding for the various ceramic matrixes such as Si_3N_4 (10), ZrO_2 (11), mullite (12), cordierite (13).

In this study, flexural strength, fracture toughness and toughening behavior and microstructure of MDF cement composites reinforced by SiC whisker were investigated.

EXPERIMENTAL

A cement used in this study is high alumina cement (Union co. Korea) and its chemical composition is composed of mainly Al_2O_3 (71.92%) and CaO (24.65%) contained several minor components such as SiO_2 (0.56%), TiO_2 (0.02%) and Fe_2O_3 (0.27%). Mineral compositions of the high alumina cement are $CaO \cdot Al_2O_3$ (CA), a small amount of $CaO \cdot 2Al_2O_3$ (CA_2) and αAl_2O_3. Its specific surface area (Blaine value) is 5,410 cm^2/g. Additives are polyvinyl alcohol/acetate (PVA, "Gohsenol KH-17S", Japan) as water soluble polymer, SiC whisker (Tateho, chem. co., Japan) and superplasticizer (sulfonate naphthalene formaldehyde condensate).

Starting materials are listed in Table 1. Ultrasonic dispersion was done with ethyl alcohol as a dispersive agent to dissolve the defects like whisker clusters. PVA, water, and superplasticizer were added 10%, 10%, 3% respectively. These were mixed under conditions of a high shear rate on a twin roll mill and formed to be a sheet. Formed specimens are cured at 5 MPa using warm press (80℃) to remove entrapped air from cementitious matrix. To obtain a full strength and rapid hardening, the specimens after press curing were cured in a dry condition for two days at 80℃.

The evaluation of mechanical properties(flexural strength and fracture toughness) was performed on machined 3mm×4 mm×36mm bars. Flexural strength was determined by the three point bending method with an Instron machine (model 4204, Instron Japan Ind.) under the condition of cross head speed 0.5 mm/min, span length 30 mm. K_{IC}, critical stress intensity factor, was measured by the indentation method using Vickers hardness test and the single edge nothed beam (SENB) method by Instron machine.

Microstructures of SiC whisker reinforced composites and defect factors were observed by SEM/EDS (scanning electron micrograph and energy dispersive spectroscopy).

Table 1 Mixing Proportions of Specimens

(wt. %)

Symbol	HAC	PVA	SiC_w	SP	W/S
G10	100	10	-	3	0.1
S 2	100	10	2	3	0.1
S 3	100	10	3	3	0.1
S 5	100	10	5	3	0.1
S 8	100	10	8	3	0.1
S10	100	10	10	3	o.1

HAC :High alumina cement
PVA :Polyvinly alcohol/acetate
SiC_w : βSiC whisker (vol. %)
SP :Sulfonate naphtalene formaldehyde condensate
W/S :Water/Solid (solid = HAC + SiC_w)

RESULTS AND DISCUSSION

The microstructure of MDF cement composites which did not have SiC whisker is shown in Fig. 1. Region 1 presents interface of particles, which belong to amorphous polymeric phase. Al^{3+} and Ca^{2+} ions partially dissolved from cement grains are detected in this area. 2 and 3 are unhydrated alumina cement grains. Especially, Region 2 is unhydrated $CaO \cdot Al_2O_3$ having a size of more than 10μm and the small particle of Region 3 is αAl_2O_3. Rodger *et al.*(14) reported that water soluble polymer reacts with cations such as Al^{3+} and Ca^{2+} dissolved from cement grains with Infrared spectra measurement. Therefore, these results may indicate that water soluble polymer is not simply acting as an agent for assistant interparticle lubrication. In high alumina cement, the normal hydration reactions are strongly suppressed by polyvinyl alcohol/acetate. The polymer reacts with Al^{3+} and Ca^{2+} ions from the cement to form calcium acetate and a crosslinked product (14).

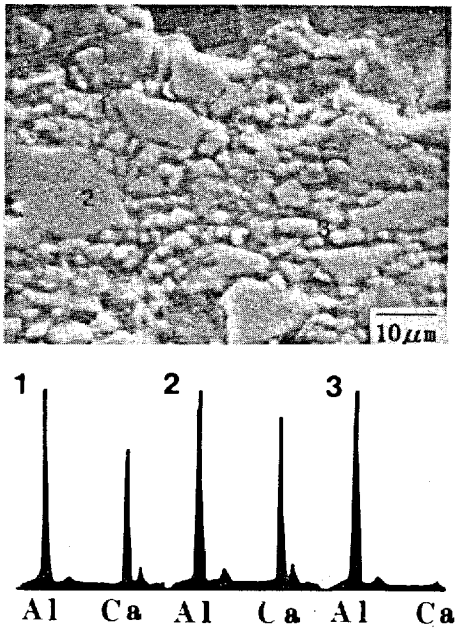

Fig.1 SEM and EDS of macro defect-free cement composites

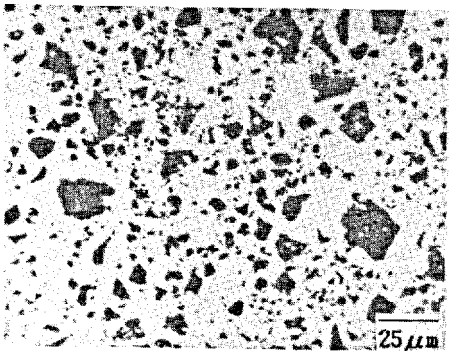

Fig.2 Image analizing of macro defect-free cement composites

Fig. 2 shows the microstructure of polymeric gel matrix and unhydrated particles which are observed by image analyzer. Dark parts are unhydrated particles and white parts are polymeric gel matrix. Kataoka *et al.*(15) reported that the percentage of hydration in MDF cement is about 13%, because the combined water content cementitious matrix is very low as the extent of 6%.

Fig.3 shows the variation of flexural strength of the composites. Mean flexural strength is improved almost 60 % from 150 MPa to 240 MPa. Such enhanced mechanical properties appears to be related to the suppression of microcrack growth by the SiC whisker.

Reinforcing of SiC whiskers in cementitious matrix produces micropores around SiC whiskers. They does not react with polymeric gel matrix as shown in Fig. 4.

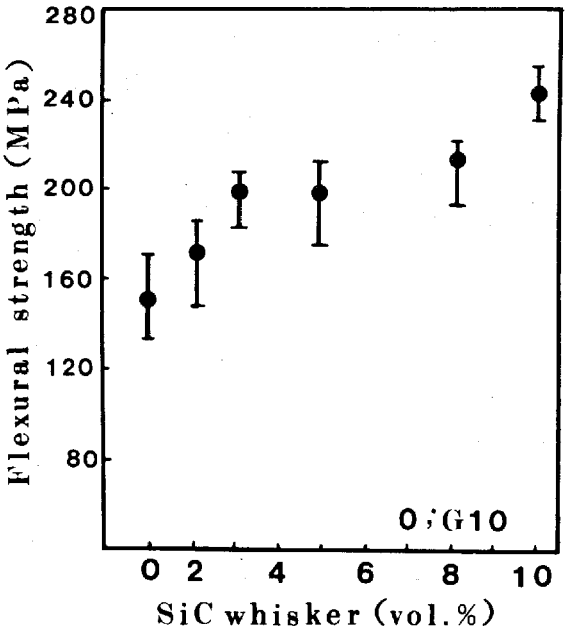

Fig.3 Flexural strength of SiC whisker reinforced MDF cement composites



Fig.4 SiC whiskers in cementitious matrix

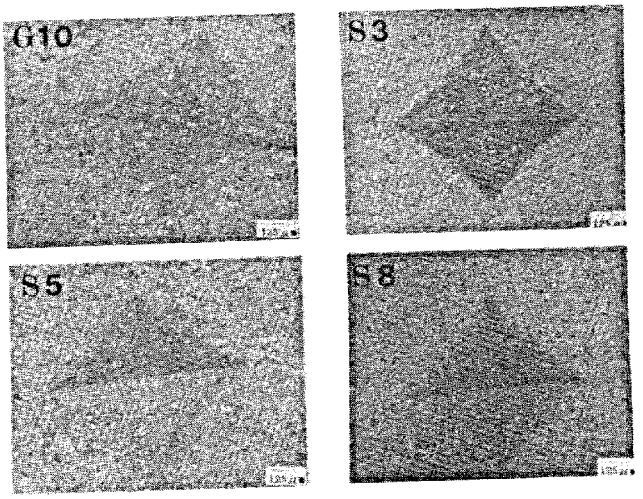

Fig.5 Specimens after indentation loading

Cracks induced by indentation loading are not detected always in cement pastes, because of the heterogeneity between hydration product and unhydrated grain, and the effect of pores in microstructure. Similarly, crack lengths are not equal in MDF cement composites along the indentation direction. Therefore, K_{IC} produced by indentation method does not have a good reliability. Cracks were not observed under 20Kg loading. Cracks were produced with very high loading above 30Kg (Fig. 5). Crack growth were reduced by the addition of SiC whiskers. Especially, crack evolution was not detected in the addition of SiC whiskers above 8 vol. %. By increasing volume fraction of the SiC whisker in the MDF cement composites from 0 to 10 %, K_{IC} value by the SENB method increased from 1.9-2.3 MPa·$m^{1/2}$ to 3.6-4.7 MPa·$m^{1/2}$.

Fig. 6 illustrated that cracks appear to have branching both forward and reverse directions. And these branches are not generally homogeneous in direction. Cracks also develop forking at unhydrated grains. Microcracking at the indenter tips and offsets of the cracks is present along much of the crack length.

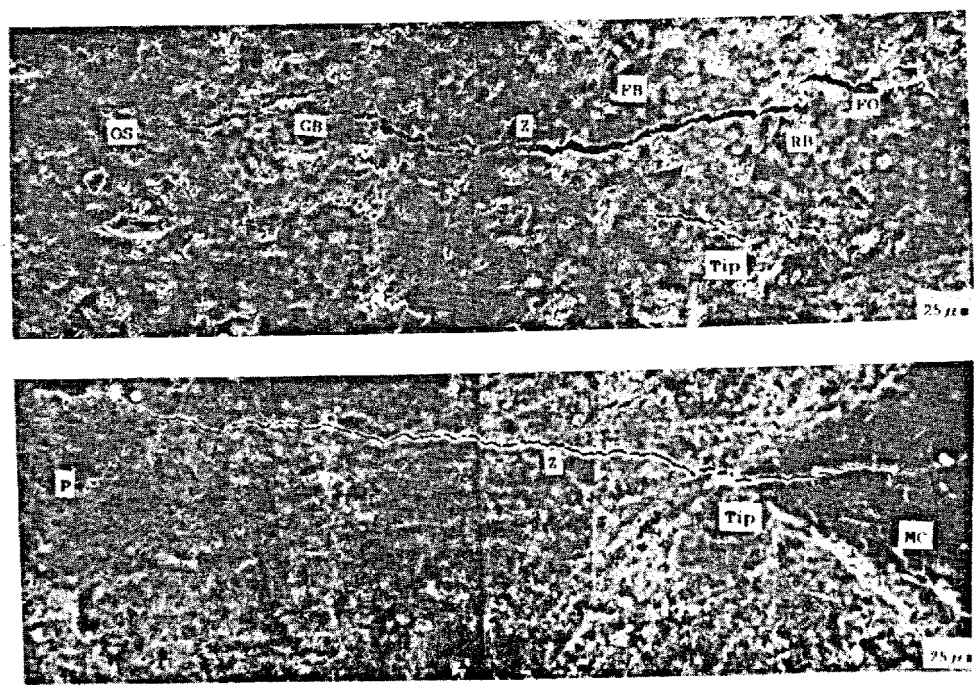

Fig.6 Crack propagation at indent tip (OS:offset, Z:zig-zag, MC:micro crack P:pore, GB:grain bridging, FB:forward branch, RB:reverse branch,)

Struble *et al.*(17) reported that cracks generally appear to pass around unhydrated cement grains, and often branched or forked of their tips, and few microcracks are sometimes observed just ahead of the tips. They also reported that the crack path is often offset with the interjacent material between these offset crack segments forming a bridge across crack.

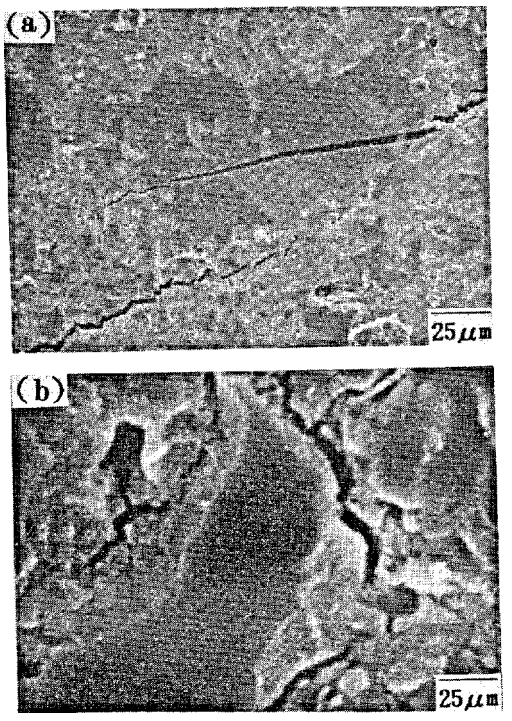

Fig.7 Fracture morphology in MDF cement
(a) transgranular fracture
(b) intergranular fracture

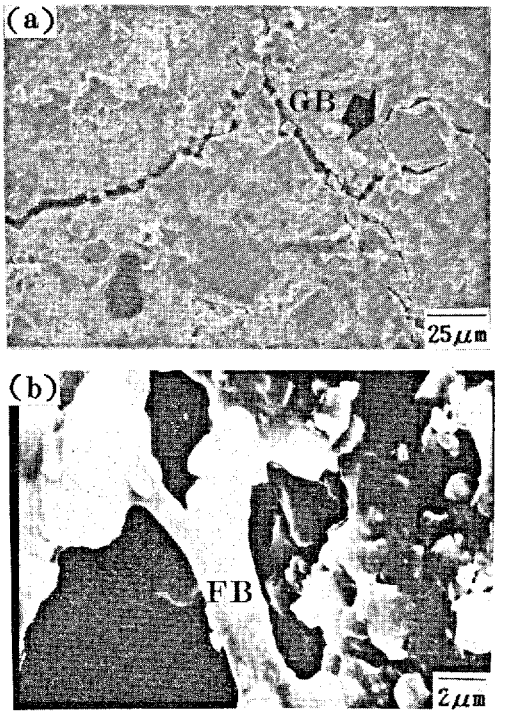

Fig.8 Crack bridging mechanisms in SiC reinforced MDF cement composite
(a) GB:grain bridging
(b) FB:polymer fibril bridging

Fracture morphology is divided into transgranular fracture and intergranular fracture. Fracture behavior of the MDF cement composites generally is of the intergranular type, which is developed through cement grain-polymer interface with a week bonding energy. Brittle and straight morphology of crack propagation are produced through inner cement grains transgranularly (Fig. 7). Popoola *et al.*(18) reported that the fracture of MDF cement can occur at the ceramic-polymer interface, inside the polymeric phase, or transgranularly across ceramic grains.

Fig. 8 illustrates two crack bridging mechanisms in the MDF cement composites which show grain bridging and the polymer fibril bridging.

Fig. 9 shows the crack deflection along whisker/cementitious matrix interfaces. Mai *et al.*(16) reported that it is not possible to locate a fracture process zone a head of the crack tip. Therefore, the toughening mechanisms in the MDF cement composites are predominantly the grain bridging behind advancing crack tips and the polymer fibril bridging across crack faces, indicating a significant role of the polymer in strengthening the composites. Fig.8 is consistent with the theory of Mai *et al.*

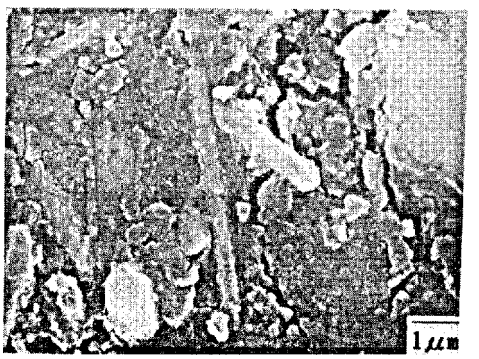

Fig.9 Crack deflection by SiC whisker

CONCLUSION

1. Flexural strength and fracture toughness of MDF cement composites are improved with the addition of SiC whisker. Further improvement in mechanical properties may be due to crack deflection along whisker/cementitious matrix interface.

2. SiC whisker reinforced MDF cement composites consists of unhydrated cement grains, whisker phase, hydrates, polymeric phase and micropores. Fracture process seems to be related to the evolution of microcracks between unhydrates and hydrated gel matrix.

3. Fracture morphology of the composites presents mainly intergranular fracture and parcially transgranular character that are brittle and straight crack propagation.

4. The main toughening mechanisms of SiC whisker reinforced MDF cement composites are characterized by crack deflection, microcracking, and bridging of cracks.

ACKNOWLEDGMENT

The authors gratefully acknowledge the financial assistance of Korea Science & Engineering Foundation.

REFERENCE

1. Birchall, J.D., Howard, A.J. and Kendall, K.: "Flexural Strength and Porosity of Cement", *Nature*, 1981, 289 (29), 388-390.

2. Birchall, J.D., Howard, A.J. and Kendall, K.: European Patent Publication, No. 0021682, 1981, Imperial chemical Industries Ltd.

3. Kendall, K., Howard, A.J. and Birchall, J.D.: "The Relation between Porosity Microstructure and Strength, and Approch to Advanced Cement-Based Materials", Phil. Trans. R. Soc. Lond., 1983, A310, 139-153.

4. Alford, N.McN and Birchall, J.D.: "Fibre Toughening of MDF Cement", *J. Mater. Sci.*, 1985, 20, 37-45.

5. Li, Z.G., Mobasher, B. and Shar, S.P.: "Characterization of Interfacial Properties in Fiber Reinforced Cementitious Composites", *J. Am. Ceram. Soc.*, 1991, 74(9), 2156-2164.

6. Shar, S.P. and Young, J.F.: "Current Research at the NSF Science and Technology Center for Advanced Cement-Based Materials", *Am. Ceram. Soc. Bull.*, 1990, 69(8), 1319-1331.

7. Mobasher, B., Stang, H. and Shar, S.P.: "Microcracking in Fiber Reinforced Concrete", *Cem. Concr. Res.*, 1990, 20, 665-676.

8. Becher, P.F. and Tiegs, T.N.: "Whisker Reinforced Ceramics", Engineered Materials Handbook, Vol.1, Composite, 1987, 941-944.

9. Becher, P.F. and Wei, G.C.: "Toughening Behavior in SiC Whisker Reinfored Alumina", *J. Am. Ceram. Soc.*, 1984, 67(12), C267-C269.

10. Lundberg, R., Kahlman, L., Pompe, R. and Carlsson, R.: "SiC Whisker Reinforced Si_3N_4 Composites", *Am. Ceram. Soc. Bull.*, 1987, 66(2), 330-333.

11. Claussen, N., Weisskopf, K.L. and Ruhle, M.: "Tetragonal Zirconia Reinforced with SiC Whiskers", *J. Am. Ceram. Soc.*, 1986, 69(3), 288-292.

12. Russell, L.M., Johnson, L. F., Hasselman, D.P.H. and Ruh, R.: "Thermal Conductivity of Silicon Carbide Whisker Reinforced Mullite", *J. Am. Ceram. Soc.*, 1987, 70(10), C226-C229.

13. Ashizuka, M., Watanabe, M. and Ikeyama, N.: "Mechanical Properties of SiC Whisker Reinforced Cordierite Composites", *Yogyo-Kyokai-shi*, 1990, 98(4), 408-411.

14. Rodger, S.A., Brooks, S.A., Sinclair, W., Groves, G.W. and Double, D.D.: "High Strength Cement Pastes: Part 2 Reactions During Setting", *J. Mater. Sci.*, 1985, 20, 2853-2860.

15. Kataoka, N. and Igarashi, H.: "Expansion Property of Macrodefect-Free Cement in Water", Proc. of Mat. Res. Soc. Symp., 1988, Part III, S.

16. Mai, Y.W., Barakat, B., Cotterell, B. and Swain, M.: "Mechanisms of Crack Growth Resistance in Macro-Defect-Free Cement Paste", Proc. of Mat. Res. Soc. Symp., 1988, Part II, R.

17. Struble, L.J., Stutzman P.E. and Fuller, Jr. E.R. : "Microstructural Aspects of the Fracture of Hardened Cement Paste", *J. Am. Cerm. Soc.*, 1989, 72(12), 2295-2299.

18. Popoola, O.O., Kriven W.M. and Young, J.F.: "Microstructural and Microchemical Characterization of a Calcium Aluminate Polymer Composite (MDF Cement) ", *J. Am. Ceram. Soc.*,, 1991, 74(8), 1928-1933.

MECHANICAL PROPERTIES OF MDF CEMENT COMPOSITES WITH SiC POWDER

J H Kim*, S H Choi and K S Han*****

**Hanil Cement Co Seoul*
***Hanyang University, Seoul*
****Inha University, Inchon*
KOREA

ABSTRACT

Mechanical properties of MDF cement composites prepared from ordinary Portland cement and SiC powder were investigated. The cement pastes were mixed with 3.0% of hydroxypropyl methyl cellulose and 0.1% of water cement ratio by a twin roll mill, and cured 60 days in a humidity chamber.

The flexural strength of the MDF cement composites with SiC powder was improved due to the following factors: the removal of macropores larger than 100μm, the reduction of capillary pores which may act as the passage of crack propagation, and the increase of Young's modulus by higher content of unhydrated cement. The fracture toughness was enhanced by a crack toughening mechanisms such as grain bridging, polymer fibril bridging and frictional interlocking.

Mechanische Eigenschaften von MDF Zement-SiC Pulver Verbundwerkstoffen, die aus normalem Portland Zement und SiC Pulver hergestellt worden sind, wurden untersucht. Die Zementpasten wurden mit 3.0% Hydroxypropyl-methylcellulose und 0.1% Wasser Zement von Zweirollmühle gemischt und in der feuchter Kammer 60 Tage getrocknet.

Die Biegebruchfestigkeit von MDF Zement-SiC Pulver Verbundwerkstoffen erhöhte, und diese Erhöhung berühte auf den folgenden Faktoren ; die Beseitigung der Makroporen, dessen Durchmesser größer als 100μm ist, die Abnahme der kapillaren Poren, die als den Weg zur Rißausbreitung wirken darf, und die Zunahme der Elastizitätsmodul, die sich aus die größeren Menge von unhydrierendem Zement ergegeben werden. Die Bruchzähigkeit wurden von Rißzähmechanismus, wie Z.B., Kornbrückung Polymerfaserbrückung und Reibungsineinandergriff erhöht.

INTRODUCTION

Recently, MDF(macro-defect-free) hardened cement pastes are produced by adding water soluble polymer, low W/C ratio, and the special process. Their mechanical properties such as flexural strength and toughness have been greatly improved. The strength of these MDF hardened cement pastes can be described by not only the strength-porosity relationship but also the application of fracture mechanisms. Inasmuch as the strength of the hardened cement pastes have the function of the macropores or defects, it may follow Griffith's crack theory.

Therefore, if the Griffith flaw, such as macropores or defects, in the hardened cement pastes can be removed, then the flexural strength of the hardened cement pastes will be increased(1-3). On the other hand, as the Young's modulus of the hardened cement pastes increases, their flexural strength increases remarkably by the rule of mixture(4). Also, if the macro-flaws are removed, the flexural strength of high strength hardened cement pastes may depend on the resistance of crack propagation, K_{IC} value(5).

In this study, in order to improve the flexural strength of the hardened cement pastes, mixing water was reduced to W/C=0.1. Water soluble polymer was added to the pastes to obtain a better dispersion, adhesive and packing effect of particles in the pastes. In addition, the effects of blending material such as fine SiC powder with high Young's modulus on the microstructure and the flexural strength of the hardened cement composites were investigated through the application of the fracture mechanisms.

EXPERIMENTAL

MDF cement composite specimens were prepared from an ordinary Portland cement(Blaine; 3,200 cm^2/g) with water soluble polymer HPMC(hydroxy propyl methyl cellulose) and superplasticizer. Each one was added 3 wt% for content of cement respectively. Four separate samples were similarly prepared by replacing 0, 5, 10 and 15 wt% of fine SiC powder for content of the ordinary Portland cement. After kneaded by a twin roll mill for compact and homogeneous mixing, MDF cment composites were prepared to be in a sheet form by pressing with acryl plate. These specimens were cured for 7, 28 and 60 days in 100% RH at ambient temperature and dried for 7 days in oven at 60^0C. The flexural strength and Young's modulus of the MDF cement composites were determined by three point bending method. Fracture toughness K_{IC} was determined by SENB(single edge notched beam)method with Instron machine(model 4302, Instron Co.). Then, microstructure and crack toughening mechanisms were studied by SEM.

To observe crack growth, 8^0 wedge was inserted into the groove of a double cantilever beam specimen (30x20x2 mm) in holder. The advance of the wedge produces crack turning the screw(Fig.1). The porosity of composites was measured by a mercury intrusion porosimetry.

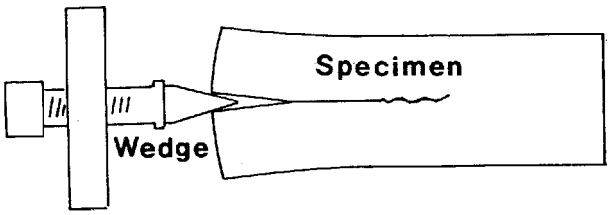

Fig.1 Schematic diagram of double cantilever beam specimen used to observe crack growth.

RESULT AND DISCUSSION

Physical properties measured for MDF cement composites are listed in Table 1. The flexural strength of MDF cement pastes without SiC increased with curing time, as showed in Table 1.

Its values reaches about 96 MPa for the ones cured for 60 days. The flexural strength of a MDF cement composites with SiC powder is 100-105 MPa. The flexural strength of the MDF cement composites increases about

ten times, compared that of ordinary hardened cement pastes.

In Fig.2, macro-pores are completely removed and capillary pores are reduced with the increase of curing time. These phenomena may be partly due to the lubricating effect of HPMC. In addition, the Young's modulus of the MDF cement composites increases remarkably. Young's modulus of hardened cement pastes and MDF cement paste has been described by Hansens' mixture rule(4) and Alford et al.(5). According to the mixture rule, the addition of SiC powder might significantly enhance the Young's modulus of the MDF cement composites.

Table 1. Physical properties of MDF Cement Composites Added with SiC Powder.

Specimen (addition with SiC Powder)	Hydration period	Flexural strength σ(MPa)	Young's modulus Y(GPa)	Fracture toughness K_{IC} (MPam$^{1/2}$)
SiC 0%	7 days	65	45	1.28
	28 days	96	60	
	60 days	96	60	
SiC 5%	7 days	60	48	1.24
	28 days	100	65	
	60 days	105	95	
SiC 10%	7 days	53	50	1.19
	28 days	100	80	
	60 days	100	90	
SiC 15%	7 days	63	50	1.03
	28 days	98	65	
	60 days	98	90	

Therefore, it is assumed that the flexural strength of the MDF cement composite is increased by removing macro-flaws, reducing the capillary pores, and increasing the Young's modulus of the MDF cement composite. On the other hand, Alford et al.(5) reported that when the critical flaw is removed completely, the flexural strength can be achieved only with increasing K_{IC}, resistance against crack propagation. As shown in Table 1, K_{IC} of the MDF cement composite without adding SiC powder was 1.28 MPam$^{1/2}$. This value is about four times higher than ordinary hardened cement pastes which is 0.3 MPam$^{1/2}$. And when SiC powder is added to MDF cement composites, K_{IC} decreases slightly as the content of SiC powder increase.

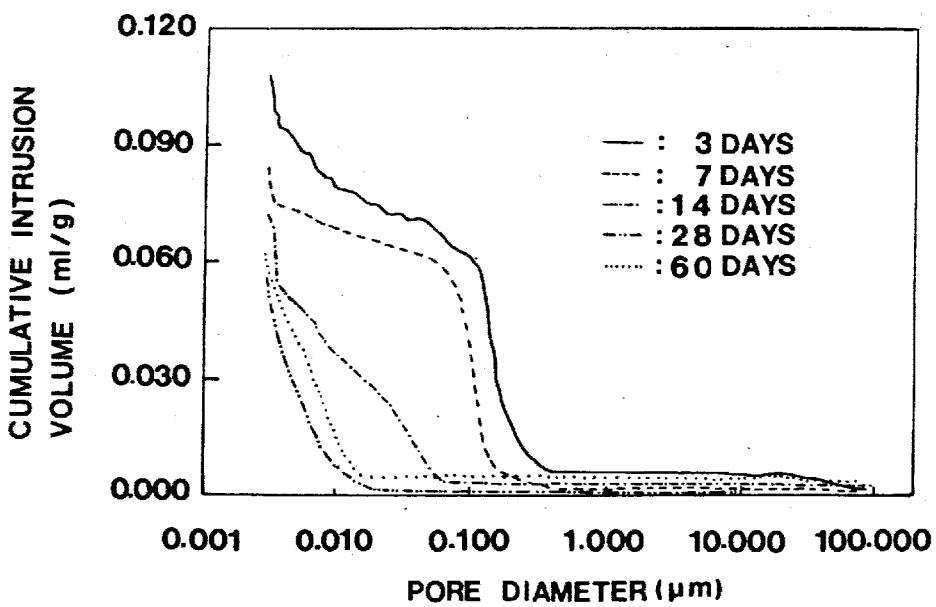

Fig.2 Pore size distribution of 10% SiC powder added to hardened cement paste with various curing time(W/C=0.1).

Struble et al.(6) reported that the crack appears to pass through outer hydration product, inner hydration product, and voids. As shown in Fig.3, when the MDF cment composite was fractured, the crack was propagated with breaking outer CSH gel bonding. Accordingly, K_{IC} value of the MDF cement composite depends on the capillary pores and the bonding force of the CSH gel. Mai et al.(7) reported that when the crack is propagated, crack bridging occurs with various patterns. Generally, grain bridging passes along unhydrated cement grain. The grain bridging would be a principal crack toughening mechanism of the hardened cement paste.

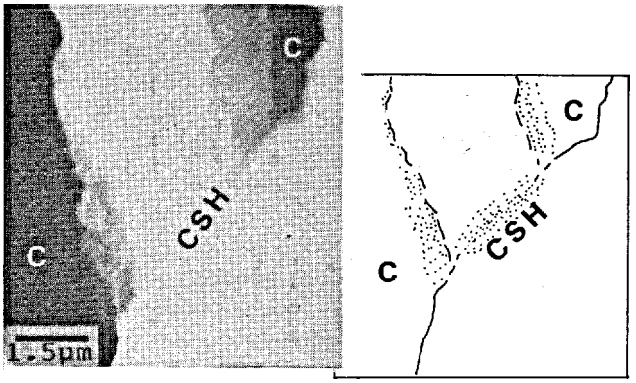

Fig.3 Scanning electron micrographs and schematic illustrations of MDF cement paste, showing examples of C-S-H bonding at crack sites. (W/C= 0.1, cured for 60 days) CSH: C-S-H bonding C: crack

In some of the grain bridging sites, frictional interlocking improves the fracture resistance of hardened cement paste. When the crack is propagated, frictional contact occurred between grains(8). Therefore, the fracture toughness of hardened cement paste can be improved.

And also, a water soluble polymer has considerable adhesiveness on its own, when it is dried. It forms the bond of CSH-polymer-CSH, which produces polymer fibril bridging(9). Fig.4 and Fig.5 illustrate two crack bridging mechanisms, grain bridging and polymer fibril bridging, in MDF cemnt composites.

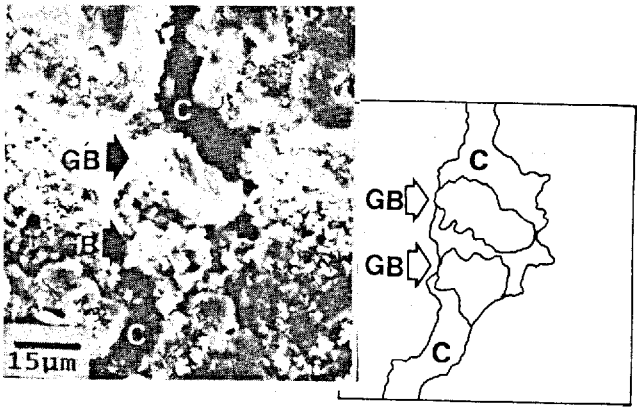

Fig.4 Scanning electron micrographs and schematic illustrations of MDF cement paste, showing examples of grain bridging. (W/C=0.1, cured for 60 days) GB : grain bridging C : crack

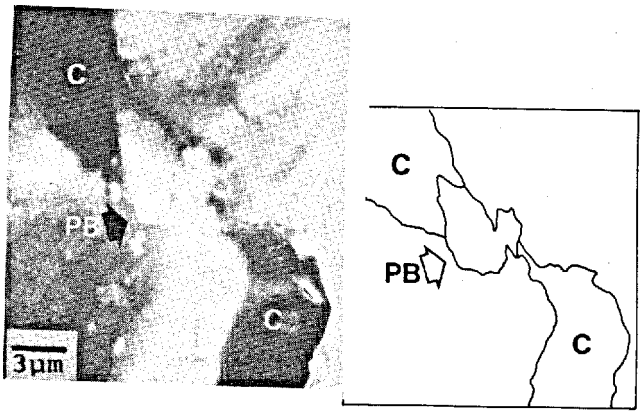

Fig.5 Scanning electron micrographs and schematic illustrations of MDF cement paste, showing examples of polymer fibril bridging. (W/C=0.1, cured for 60 days). PB : polymer fibril bridging C : crack

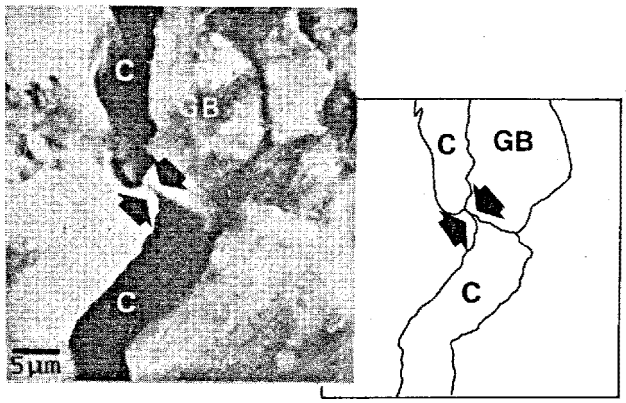

Fig.6 Scanning electron micrographs and schematic illustrations of MDF cement paste, showing examples of frictional interlocking at grain bridging sites.
(W/C=0.1, cured for 60 days)
: Frictional interlocking at grain bridging
C : crack
GB : grain bridging

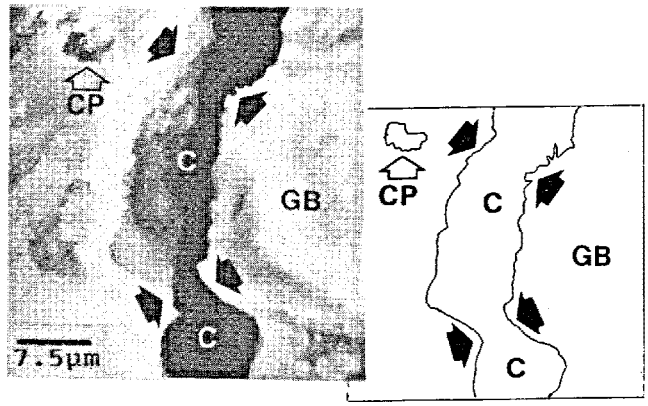

Fig.7 Scanning electron micrographs and schematic illustrations of MDF cement paste, showing examples of frictional interlocking at grain bridging sites.
(W/C=0.1, cured for 60 days)
: Frictional interlocking at grain bridging
C : crack
GB : grain bridging
CP : capillary pore

Fig.6 shows frictional interlocking at grain bridging sites. In Fig.7, the capillary pores present at the normal orientation of crack advance show no effect on the crack propagation. The crack is propagated along the capillary pores which exist at the parallel orientation of an applied stress. Consequently, the high strength mechanism of the MDF cement composite with SiC powder may be related to the removal of macropores. The reduction of capillary pores which may act as the passage of crack propagation, and the increase of Young's modulus with increase of unhydrated cement and the addition of SiC powder.

CONCLUSION

1) The flexural strength and Young's modulus of the MDF cement composites using ordinary Portland cement cured for 60 days without SiC are around 96 MPa and 60 GPa respectively.

2) When SiC powder is added in the MDF cement, the flexural strength is about 100-105 MPa and Young's modulus was about 95 GPa of high value.

3) The flexural strength of the MDF cement composites is improved by removing macropores larger than 100μm, reducing capillary pores and increasing Young's modulus, owing to unhydrated cement grains and SiC powder. In addition to, the fracture toughness is increased by crack toughening mechanism such as grain bridging, polymer fibril bridging and frictional interlocking.

REFERENCES

1. Birchall, J.D., Howard, A.J. & Kendall, K.: "Flexural Strength and Porosity of Cement", Nature, 1981, 289(29), 388-390.

2. Birchall, J.D., Howard, A.J. & Kendall, K.:European Patent Publication, No.0021628, 1981, Imperial Chemical Industries Ltd.

3. Kendall, K., Howard, A.J. & Birchall, J.D.:"The Relation between Porosity, Microstructure and Strength and Approach to Advanced Cement-based Materials", Phil. Trans. R. Soc. Lond., 1983, A310, 139-153.

4. Hansen, T.C.: "Influence of Aggregate and Void on Modulus of Elasticity of Concrete, Cement, Mortar and Cement Paste", J.of Concr. Inst., 1965, No.62-11, 193-215.

5. Alford, N.McN., Groves, G.W. & Double, D.D.:"Physical Properties of High Strength Cement Pastes", Cem. Con. Res., 1982, 12, 349-358.

6. Struble, L.J., Stutzman, P.E. & Fuller.Jr., E.R.:"Microstructural Aspect of the Fracture of Hardened Cement Paste", J. Am. Ceram. Soc., 1989, 72(12), 2295-2299.

7. Mai, Y.W., Barakat, B., Cotterell, B. & Swain, M.:"Mechanism of Crack Growth Resistance in Macro-Defect-Free Cement Paste", MRS, 1988, 13, 187-193.

8. Swanson, P.L., Tairbanks, C.J., Lawn, B.R. & Mai, Y.W.:"Crack-Interface Grain Bridging as a Fracture Resistance Mechanism in Ceramics: I, Experimental Study on Alumina", J. Am. Ceram. Soc., 1987, 70(4), 279-29.

9. Eden, N.B. & Bailey, J.E.:"The Mechanical Properties and Tensile Failure Mechanism of a High Strength Polymer Modified Portland Cement", J. of. Mater. Sci., 1984, 19, 2677-2690.

CHEMISTRY AND POROSITY IN MODELLED MDF CEMENT MINERALS

Milan Drábik, Miloš Krištofík, Ľubica Gáliková and Sadananda Sahu*

Institute of Inorganic Chemistry, Slovak Academy of Sciences
Bratislava, CSFR

SUMMARY

Analysis of X-ray powder diffraction patterns, ^{27}Al MAS NMR spectra and thermal stability of studied models offers evidence of multiatomic chemical bonds $Al(Fe) - O - X$ R (X = H, S, C). Results prove the atomic level of the origin of interactions of clinker phases - Ca_2AlFeO_5 (C_4AF) and $Ca_4(Al_6O_{12})SO_4$ ($C_4A_3\bar{S}$) with carbonous water-soluble polymer - hydroxypropylmethylcellulose (hpmc). Distribution of porosity; dominance of pores $10 < r/nm < < 100$ and total pore volume estimated near by 18 % , are further topical issues in the studied models and are discussed together with the atomic-level changes. Study is in support of the balance of porosity aspects with atomic-level changes in course of synthesis of modelled MDFs.

ZUSAMMENFASSUNG

Rtg. pulver Diffraktometrie, ^{27}Al MAS NMR Spektroskopie und termische Stabilität von studierten Modellen bewiesen mehratomische Bindungen $Al(Fe) - O - X$ R (X = H, S, C). Ergebnisse bestätigten atomisches Niveau der Abstammung der Interaktionen von Klinkerphasen - C_4AF und $C_4A_3\bar{S}$ - mit dem kohlenstoffhaltigen wasserlöslichen Polymer - hydroxypropyl methylcellulose (hpmc). Porositätdistribution, das Übergewicht von Poren $10 < r/nm < 100$ und total Porosität weniger als 18 % , sind weitere Eigenschsften von Modellen und sind im Zusammenhang mit Änderungen im atomischen Niveau disskutiert. Die Arbeit fordert die Gleichwertigkeit der Porositätaspekten und Atomischniveauaspekten während der Synthesen der MDF Modellen.

INTRODUCTION

Macro-Defect-Free materials have been reported from 1981st. These advanced cement-based materials arise utilizing cementitious reactions of proper clinker phase(s) and water-soluble polymer with water added in amounts corresponding to ratios water/solid w/s = 0.2 , under pressure 5 MPa as a route to low-temperature synthesis of ceramic-like materials [1,2]. Introductory studies compare properties of MDFs with hydraulic materials as there is close similarity of the syntheses [1-3] as well with potentialy altered materials (insulators, staticaly exerted metallic parts) [1,2].

Interactions and depth of chemical reactions of inorganic with polymer matrices are discussed as important sources of exceptional properties of MDFs [1,2,4], some aspects of this hypothesis exceed at present experimental results. Aim of this study has been to strengthen experimental physico - chemical knowledge and give an account of the relations of atomic and porosity aspects in course of MDF's syntheses .

EXPERIMENTAL

Study has been carried out on the following simplified model C_4AF + + $C_4A_3\bar{S}$ (mass ratios = 0+1, 1+1, 1+0) + hpmc (0 - 25 mass%) + H (w/s = = 0.2) alternatively without pressure or applying this in initial 30 minutes of syntheses, detailed in table 1.

Table 1: Composition and reaction conditions in course of syntheses

C_4AF	$C_4A_3\bar{S}$	hpmc (%)	H (w/s)	appl.of pressure	duration (hours)	note
1	0	1	0.2	a),b)	1,6,24,7x24	
1	0	5	0.2	a),b)	1,6,24,7x24	a: none
1	0	10	0.2	a),b)	1,6,24,7x24	pressure
1	0	25	0.2	a),b)	1,6,24,7x24	
0	1	1	0.2	a),b)	1,6,24,7x24	b: pressed
0	1	5	0.2	a),b)	1,6,24,7x24	in initial
0	1	10	0.2	a),b)	1,6,24,7x24	30 minutes
0	1	25	0.2	a),b)	1,6,24,7x24	mechanicaly
1	1	1	0.2	a),b)	1,6,24,7x24	
1	1	5	0.2	a),b)	1,6,24,7x24	
1	1	10	0.2	a),b)	1,6,24,7x24	
1	1	25	0.2	a),b)	1,6,24,7x24	

Atomic level changes during syntheses have been followed by X-ray diffractometry, ^{27}Al MAS NMR spectroscopy and thermal analysis of samples taken after 1, 6, 24, 7x24 hours of interactions of components in individual parts of the system. X-ray powder diffraction patterns were measured on the Philips 1540 powder diffractometer using CuKα or FeKα radiation. d-spacings and reagents conversions were identified as described in [5]. Decoupled ^{27}Al MAS NMR spectra of samples taken from system $C_4A_3\bar{S}$ + hpmc + H were measured at 104.2 MHz on Bruker MSL-400 spectrometer with sample spinning rate 4.3 kHz. Actual chemical shifts were compared with standard chemical shifts of ^{27}Al in ettringite, monosulphoaluminate hydrate, hydrogarnet, aluminum hydroxides and in $C_4A_3\bar{S}$ [6-8]. Weight losses (TG) and thermal effects (DTA) have been collected simultaneously using MOM Derivatograph Q 1500 D (table 3).

Distribution of porosity and total pore volume of each sample under study have been estimated on mercury porosimeter Carlo Erba 2000 and compared to published values of MDFs [1-3]. Processing of numerical outputs of individual measurements gave sets of averages of total and relative pore volumes within radii 5 nm to 10000 nm (fig. 2). The connections of porosity distribution, synthesis conditions and atomic-level changes are discussed.

RESULTS AND DISCUSSION

According to qualitative analysis of X-ray powder diffraction patterns late formation (more than 24 hours needed) and significant uniformity of crystalline hydrates occur in systems regardless of reagents ratios at w/s = 0.2. Crystalline hydrates are the members of the monosulphoaluminate-like solid solution -- AFm phase.

Table 2: Unreacted clinker phases, as given by X R D data (d/nm, I_{rel}/I_0), after 7x24 hours

Reagents	Content of hpmc / mass %			
	1	5	10	25
C_4AF + hpmc	0.33	0.46	0.24	0.27
$C_4A_3\bar{S}$ + hpmc	0.31	0.34	0.41	0.42
C_4AF + $C_4A_3\bar{S}$ + hpmc	0.20	0.30	0.21	0.37

Contents of unreacted C_4AF and $C_4A_3\bar{S}$, as extracted from X-ray data after 7x24 hours of interaction (table 2), vary from 0.2 to 0.4, thus conversion proceeds to formation of crystallohydrates. Disharmony between diffractometric conversions and formation of crystallohydrates is the indirect evidence of the primary formation of amorphous hydrates. We have formerly noticed this phenomenon from common distribution of reagents and hydrates (reaction stoichiometry, differential calorimetry) and from ^{27}Al MAS NMR spectra that more precisely account for amorphous phase [9]. Moreover, detailed analysis of ^{27}Al MAS NMR spectra (fig. 1)

gives very important explanation of atomic structure of second coordination sphere of *Al* atoms in studied samples. Comparison of chemical shifts from fig. 1 with standard values of ettringite (8.5 ppm) monosulphoaluminate hydrate (13.5 ppm), hydrogarnet (12.0 ppm), aluminum hydroxides (2 - 6 ppm), $C_4A_3\bar{S}$ (60 - 80 ppm) [6-8] and with the effect of amorphous state on line widths of signals [8,10] results in :

60 - 80 ppm (complex signal) - due to *Al*(4) in $C_4A_3\bar{S}$ [7].

13.2 ppm represents *Al*(6) in AFm phase with second coordination sphere of *Al* consisting of *H* and *S* [7].

10.1 ppm represents *Al*(6) in amorphous phase with second coordination sphere of *Al* consisting of *H*, *S* and *C* : *Al-O-XR* (*X=H,S,C*), where the only source of *S* is clinker phase and the only source of *C* is carboneous polymer.

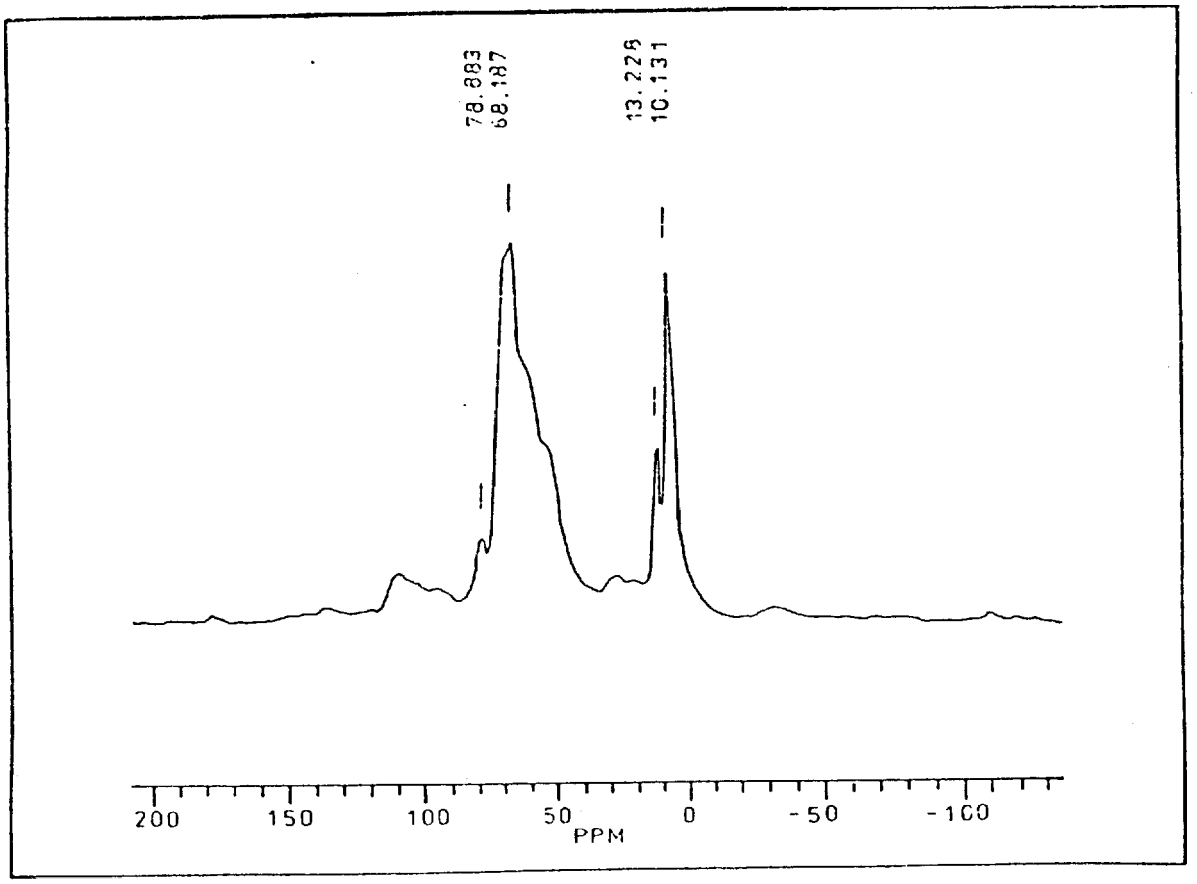

fig. 1 : ^{27}Al MAS NMR spectrum and chemical shifts of $C_4A_3\bar{S}$ + hpmc + H after reaction procedure of MDFs synthesis

Table 3: Results of thermal analysis of reaction products

reagents, conditions	interval(s) TG θ / °C	θ of peaks / °C		
		DTG	DTA endo	DTA exo
$C_4A_3\bar{S}$+C_4AF+H	100-350	190, 280	200, 290	-
+ 5% hpmc	100-220 230-350	280	190	320
w/s=0.2 10% hpmc	100-220 230-350	300	190	320,
t=24hours 25% hpmc	100-250 250-350	300	190	320,335

Table 3 displays weight losses and effects accompanying thermal treatment of samples under study. Within stepwise weight loss first step falls to temperature area typical for dehydration of AFm phase (80 - 220 °C), second step, due to amorphous phase, follows immediatelly (230 -350 °C). Close sequence of the end of second weight loss and the exoeffect on DTA marks the virtue and the border of thermal stability of carbonous part incorporated in amorphous phase. Literature data [11,12] are in support of the discussed relations.

Chemical bonds *Al(Fe)-O-XR* within amorphous phase, occupying due to synthesis conditions and gelation of hpmc [12] originally free space among grains of clinker [13], are reflected in distribution of porosity as well. Fig. 2 presents results of mercury intrusion porosimetry, curves and distributions represent processing of three patterns of samples synthesized without hpmc (marked **a** in fig. 2), 10 patterns of samples synthesized with hpmc (marked **b** in fig. 2) and 10 patterns of samples synthesized with hpmc under pressure (marked **c** in fig. 2). Results visualize effects of hpmc and pressure upon distribution of porosity, in particular :

Reduction of content of pores $100 < r/nm < 1000$ in presence of hpmc (curve **b** and resp. columns in fig. 2).

Minimum amount of pores with $r/nm > 100$ together with dominance (appr. 80%) of pores $10 < r/nm < 100$ (full columns in upper part of fig. 2), medians of pores under the later interval (fig. 2, M_c) and total porosity near by 18 % when pressure applied during synthesis (curve **c** in fig.2).

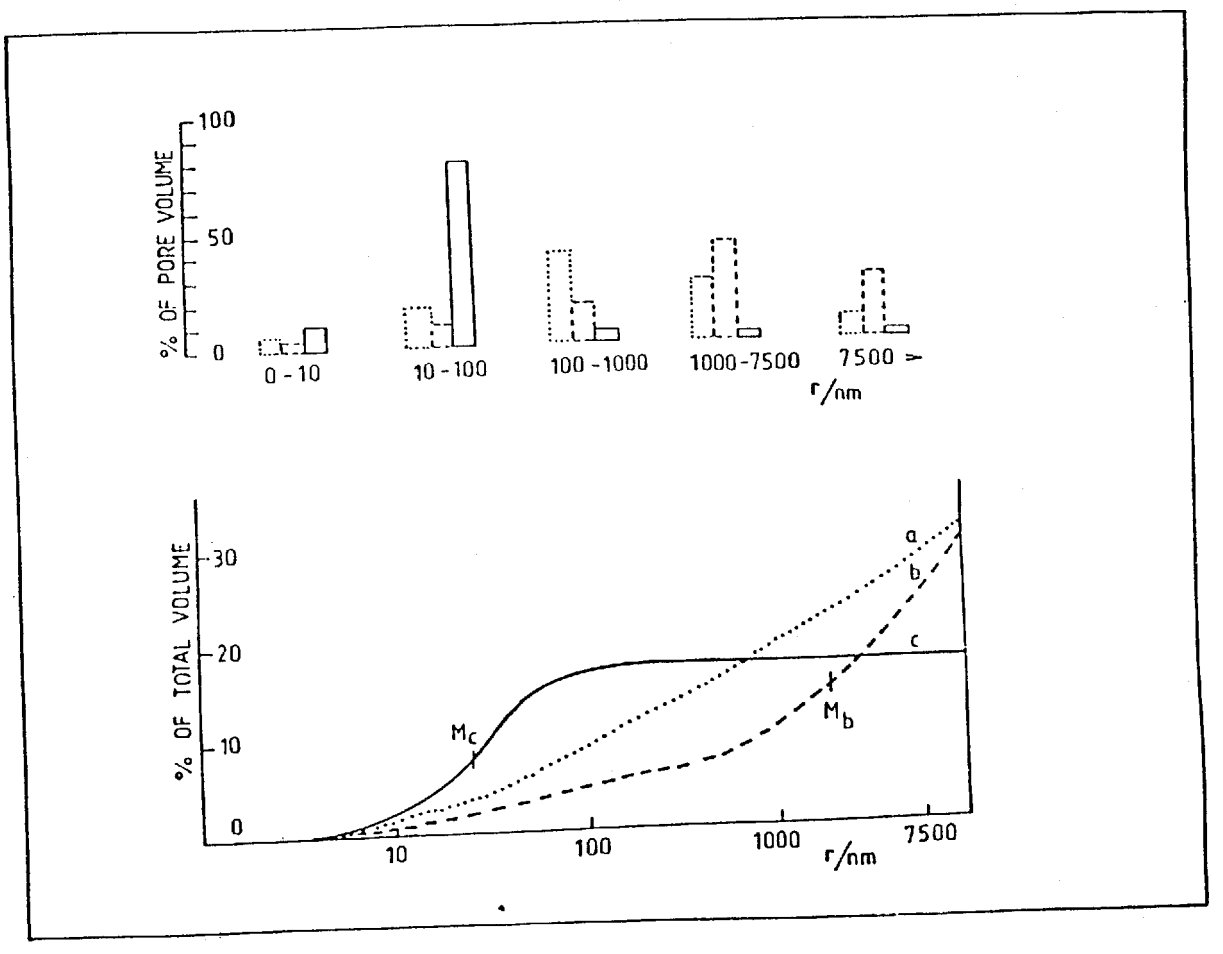

fig. 2 : Porosity distribution of hydration products of $C_4A_3\bar{S}$ + C_4AF (a) with hpmc added (b), pressure applied (c) and corresponding medians of pores (M_b, M_c) ; averages of 25 patterns

CONCLUSION

1. Study of given model :
   i. Displays novel chemical bonds and properties of amorphous reaction product at synthesis conditions relevant to MDF procedure.
   ii. Exhibits influence of synthesis conditions on distribution of porosity; at optimal conditions (pressure applied) interval of dominant pore radii, including medians of pores, is 10 - 100nm.
   iii. Indicates interrelations of local and pore structures and balances the changes of these in course of syntheses.

2. Comparison of external variable, recognized atomic-level changes and porosity values favours the idea of the role of chemistry [1-4, 9, 14] in the course of synthesis of modelled MDFs : Incorporation of carbonous polymer (hpmc) within amorphous reaction product affects both atomic and pore structures. Influence of hpmc on the pore structure is enhanced if pressure is applied during synthesis.

REFERENCES

1. S.R.Tan, A.J.Howard, J.D.Birchall: Phil.Trans.R.Soc.London A322, 479-491 (1987)
2. S.R.Shah, J.F.Young: Ceram.Bulletin 69, 1319-1331 (1990)
3. J.D.Birchall, A.J.Howard, K.Kendall, J.H.Raistrick: Eur.Pat.Specification No.0055035, B1
4. R.N.Edmonds, A.J.Majumdar: J.Mater.Sci. 24, 3813-3818 (1989)
5. M.Drabik, L.Smrcok, L.Stevula, I.Kapralik: Silikaty 31, 299-307 (1987)
6. D.Muller, A.Rettel, W.Gessner, G.Scheller: J.Magn.Reson. 57, 152-155 (1984)
7. M.Drabik, F.Hanic, I.Tkac: Proc.Solid State Chemistry '89, 118-119, Pardubice (1989)
8. R.C.T.Slade, J.C.Southern, I.A.Thompson: J.Mater.Chem. 1, 563-568 (1991)
9. M.Drabik, M.Kristofik, L.Galikova: Proc.Termanal '91, 145-146, Bratislava (1991)
10. G.D.Soraru, F.Baboneau, J.D.Mackenzie: J.Mater.Sci 25, 3886-3893 (1990)
11. A.M.Dunster, J.R.Parsonage: Cem.Concr.Res. 18 758 (1988)
12. Y.Tezuka, K.Imai, M.Oshima, T.Chiba: Polymer Journal 23, 3 189-193 (1991)
13. M.Kristofik, M.Drabik, J.Kozankova: Proc.Progmatech '91, in print
14. M.Drabik, I.Odler: Int.Sci.Fair "World Tech", Vienna 1990

ACKNOWLEDGEMENT Authors are thankful to Dr. I. Tkáč of Institute of Inorganic Chemistry and Dr. O. Žigo of Institute of Construction and Architecture for measurements and inspirative discussions on ^{27}Al MAS NMR (I.T.) and mercury porosimetry (O.Ž.).

* Sadananda Sahu on study leave at

Department of Ceramics, Glass and Cement
Slovak Technical University
812 37 Bratislava, C S F R

THE INCREASING STRENGTH MECHANISM OF THE ROLE OF INTERFACIAL BOND IN MDF CEMENT

Hu Shuguang

Department of Materials Engineering
Wuhan University of Technology, Wuhan, P R CHINA

SUMMARY

The chemical reactions between 12 organic materials and 3 cements have been respectively detected and the micro mechanism of the reaction has been studied by means of FT-IR, XPS technique. The results showed that the significant effects of chemical shift were found in some test specimens and the interactions take place through the active groups of water-soluble polymer and the cations of hydration products. In this paper, the adhesive characters and the actions of beneficial chemical bond on the interface were discussed by using the analysis method of failure. The results indicated, because of the beneficial improvment of bonding behavior on the interface, the force of the interface is often stronger than those of both polymer and cement inner. In this case, the bending strength and properties of the materials can be improved effectively. Therefore, we consider that the role of interfacial bond which improves the structures and bonding behavior between various matrixes is a more important factor to the increasing strength mechanism in MDF cement.

摘　　要

本文运用ＦＴ－ＩＲ和ＸＰＳ技术研究了十二种有机物与三种水泥间的化学反应性，并探讨了反应机制。研究结果表明，在一些反应试样里存在明显的化学反应信息。这种反应主要是通过水溶性聚合物中的活性基团和水化过程中产生的Ca^{2+}、Al^{3+}离子进行的。本文还采用断面分析方法讨论了界面上的粘结特性和有效的键合作用。结果显示，由于界面上粘结性能的改善，使得界面上的粘结强度往往大于相基质的内粘结力。在这种情况下，材料的抗弯曲强度和其他一些物理、化学性能将会有效的提高。作者认为，这种改善了各基质间粘结性能的界面作用是ＭＤＦ水泥材料中一个更重要的增强因素。

INTRODUCTION

MDF (Macro Defect Free) cement materials have high bending strength and some excellent physical and chemical properties. They are expected to have a broad prospect of engineering application [1-2]. As a matter of fact, MDF cement is a new kind of composite materials of polymer cement based. The research work about this kind of material has been developed in recent years, but by now its increasing strength mechanism is still in dispute. The most of viewpoints emphasized the physical action of polymer added in cement. It is suggested that these polymers can improve the pore structure and enhance the toughness. So the bending strength of material can be increased according to Griffith fracture theory [3-5]. On the other hand, some others viewpoints thought that there are certain chemical reactions between polymer and cement, and the reaction plays an important role in the strength and property of the material. As well known, the bending strength of common hardened cement paste is only about 1/10 of its compressive strength. Although the special cold and hot pressed methods can increase cement strength, the experimental results manifested that the ratio of bending/compressive strength is hardly increased whatever methods are used [6,7]. This result seems to reveal that there are different breaking mechanisms for bending and compressive in cement materials.

By obtained research results, it is very clear that physical action of polymer is not enough to explain why the reinforcement effect is not obvious when the porosity is further reduced under the certain extent of porosity, why the strength of composite material is often stronger than the intrinstic strength of matrixes themsleves and why different kinds of polymers have different effects on the strength. We consider the effect of chemical action between the interface is more important and reasonable.

we consider that these polymers used in MDF cement all contain a lot of polar groups which have high activity in water. Meanwhile, as a consequence of the special preparing technique of MDF cement, stirring at a high speed, rolling or extruding, in addition, the high density feature at low water/solid ratio and compacting process, the contact extent between various kinds of particles is strengthened. These make the interface action become a very important factor influencing strength. It is doubtless that this effect is much greater than that in common cement materials. We have verfied this deduction in the investigation of the mico-structure of MDF cement by Positron Annihilation Technique(PAT) [8]. On the other hand, MDF cement is a kind of composite materials according to the feature of composition and structure. Because there are two different property materials in the system, which interact each other to result in the high complex strength. This indicates that there is a certainly complex reinforment action in materials. The complex effect of composite material is realized through the interface of matrix, as we know, when cement materials are damaged, the breakdown mainly takes place in the interface of different hydrate paste. Therefore, it is very important to analyse the interface feaction in MDF cement efficently. In this paper, we investigated the chamical reaction in the interface of MDF cement. Based on the experimental results, the actions of chemical reaction and bonding in the interface were discussed and the increasing strength mechanism of the interface was put forward.

EXPERIMENTAL MATERIALS AND METHODS

Cements used in the experiment were aluminous cement, sulfoaluminate cement and portland cement (commercial products) $CaO.Al_2O_3$ (CA), the main mineral of aluminous

cement, was prepared by chemical reagents (A.R.) in the laboratory. All cements and CA mineral were grinded to Blain specific surface 500m²/kg. The organic materials in the experiment were polyvinyl alcohol(PVA), polyacrylamide(PAM), polyvinyl acetate latex, MC water-reduaing agent, NF water-reducing agent, Sodium carboxy methyl, gelatin, starch, butsdienstyreen rubber, neoprene latex, unsatureted polyesater resin, epoxy resin.

The chemical reaction specimens were prepared by the method as Birchall's [9] , but here water/solid ratio is 0.40. The proportion in weight percent is cement 85%, organic material 15%, The solid organic materials were pretreated by water, mixed and stirred at a high speed, shaped in the special mould by pressure, then demoulded and cured at 50℃ for 3 days. The cured specimens were grinded and dried for 24 hours before tested. The fracture samples were prepared as follows, make up polyacrylamide into homogeneous water-solution, fresh cement paste at water/cement ratio of 0.4 was put into a mirrorlike mould to form a sample ($\phi 30\times 10$mm). One surface of the sample was carved to become a rough surface by a knife fristly, then smeared polymer water-solution on this surface, next the smooth surface of another sample was put on the smeared polymer surface. So a piece of sandwich sample was made. In the experiments, the comparing samples were prepared by using the pure cement paste of water/cement ratio 0.60 to replace polymer water-solution. Curing temperature is 45℃ and age is 28 days. The testing specimens were divided into two groups, one group was dried for 72 hours in a drier before testing and called dry state group, the other group was directly tested after laying 2 hours at room temperature and called as wet state one. All specimens were broken along the designed interface. Instruments and experimental conditions are: IR test, NICOLECT, 60SXB Fourier Transform Infrared Spectrometer, resolution ratio, 0.1^{7-1}cm; sensibility, 0.06cm^{-1}. XPS test, V. G. ESCALAB MKII electron spectrometer, resolution ratio is 0.80 eV; vacuum of work chamber is superior to 1.33 10^{-7}Pa.

RESULTS AND DISCUSSION

Chemical Reaction of Cement and Polymer

The chemical reactions between 12 organic materials and 3 cements have been investigated by FT-IR method.The experimental results discoverd that only PVA and PAM have obviously chemical reaction information with cements. The results are shown in Table 1.

Variations of characteristic absoring band (cm^{-1}) Table 1

polymer	bind	in polymer	in reaction specimens
PVA	ν_{C-OH}	~1100	~1115, intensity weaken
	δ_{OH}	~1123	intensity weaken
	ν_{OH}	3432 (broad-bond)	the peak of free OH appear at 3636
PAM	ν_{C-N}	1025~1045	intensity weaken and tend to disappear
	ν_{C-O}	~1400	peak change into sharp and strong
	ν_{C-O}	~1687	move to ~1665

It can be found from Table 1, that the information of chemical reaction are mainly indicated by those characteristic absorbiong bands which are concerned with hydroxyl(OH) in PVA and amide ($CONH_2$) in PAM. This result revealed that chemical reaction takes place

through those active groups of polymers in specimens, but not all reaction can take place in the polymer with active group. In order to ascertain the micro mechanism of this reaction further, we carried out the XPS study of interface reaction of polyacrylamide and $CaO.Al_2O_3$ system.

The Micro Mechanism of the Chemistry Reaction

The electron binding energies of five elements, C, N, O, Ca, Al, in test specimens prepared by above method were examined by XPS technique.The results are showed in Table 2

The testing results of electron binding energy (eV) Table 2

specimen	C1s	N1s	O1s	Ca2p	Al2p
pure PAM	284.60	399.65	531.95		
hydrate of CA singly			530.40	346.73, 350.14	73.84
hydrate of PAM+Ca	284.60 285.43	399.65 397.60	530.40 531.90	346.73, 350.14 347.70, 350.90	73.84 74.68
chemical shift	+0.53	-2.05	+1.50 -0.05	+0.97	+0.84

The molecular structural formula of PAM is:

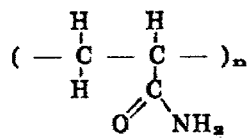

Analyzing the chemical shifts in Table 2, we conclude the variations in reaction are mainly in the C-N bond of amide group. The reasons are, (1) C element appeared a new energy spectrum, binding energy is 285.96 eV, chemical shift is 0.53 eV. This result is deduced to be the breaking of C-N bond. According to theory of XPS analysis, the C1s binding energy increased in reaction means that the place in C-N has been replaced by a higher electronegativity element. This element is only possible to be O in reaction system, and this result predicts the possibility of forming C-O bond. (2) New N1s had a -2.05 eV chemical shift and the result further testified the breaking of C-N bond. As the breaking N element up from C-N bond in amide group, its electron density of nucleus outside enhaces and results in N1s binding energy in inner to decrease. (3) Because O element exists not only in polymer but also in CA hydrate, the further analysis of O structural information is still difficult. Considering from the structure, as result of, if O- C- O group is formed, the outer electrons of C will be redistributed and this C1s binding energy belongs to two oxygens in carboxyl group, which is higher than that in the hydrate and lower than that in the polymer. (4) The chemical shifts of Ca2p, Al2p are 0.97 and 0.84 eV respectively. These are attributed to their link with organic matrixes of higher electronegativity. The information coming from the chemical reaction can be found in both inorganic matrix and polymer here.

As stated above, we conclude the chemical reaction takes place through the breaking of the C-N bond in amide group firstly, then the C is linked with O, next this O is linked

with Ca, Al cations produced during the hydration process, so the beneficial composite structure is formed.

Investigation of Bonding Behavior in Fractured Surface

The amount of adhesive region on the smooth side of the fractured surface was statistically measured by Image Analysis metheod. Table 3 is the results of different interfaces designed under different experimental conditions.

Adhesive amount on fractured surface (%) Table 3

interface	1	2	3	4	5	average value	expriment condition
C-P	21	26	17	25	20	19.8	wet state
	15	17	10	12	8	12.4	dry state
C-C	7	5	8	4	4	5.6	wet state
	4	5	6	4	3	4.4	dry state

note: "C-P" stand for the interface of cement and polymer
"C-C" stand for the interface of cement and cement

Comparing the results in Table 3, we can find that two kinds of interface have obviously different adhesive features. The adhesive areas on C-P interface are much larger than those on C-C interface. This manifests that a good adhesive state has formed between polyacrylamide and aluminous cement during the hydration process. In this case, the bonding force of interface region is stronger than that of hardened paste or polymer inner. So broken surfaces do not always appear in phase interface, some of which are often in polymer inner at wet state condition, and the others are often in hydrate inner at dry condition. As opposed to, the experiment results showed that the broken surface mostly appears in the designed interface for the C-C samples. The results showed that water-solube polyacrylamide can play an important role in improving bond behavior on the interface. Noticing the results came from smooth surface, we consider that it is sure that bonding behavior in practical materials is better. Table 3 also showed that experimental condition had different effect on the bonding results of C-P interface. There was larger amount of adhesion at wet state, which involve both polymer and cement paste, so the exact reason of producing this situation is difficult to be confirmed here. The further examination for this will be carried out below. The effect of dry and wet state on the adhesive result of C-C interface was not found in the experiment.

The micro composition and structure of the smooth region on the fractured surface have been investigated by XPS technique. The results were discussed in three situations. (1) The electron binding energy spectra of pure polymer appeared on the smooth cement surface region. The full lines in Fig.1 are the patterns of C, N, O element binding energy (BE) on the smooth fracture surface, which give the structural information of PAM molecule, C1s=284.60 eV, 285.43 eV; N1s=399.65 eV; O1s=531.95 eV. The dotted lines are the patterns of interface layer with the chemical reaction (Table 2). The structural information of elements on surface is the same as pure polymer instead of the interfacial one which suggests a conclusion that all smooth fractured surface is not actual interface and the breakage takes place in polymer inner. This situation often appears under the wet state condition. According to this result, we can also know it is not accurate to verify the

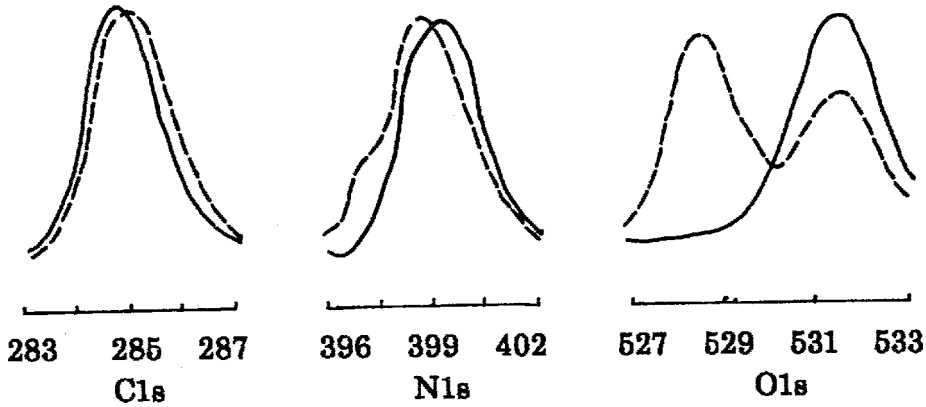

Fig. 1 XPS patterns of C, N, O element binding energy (eV)

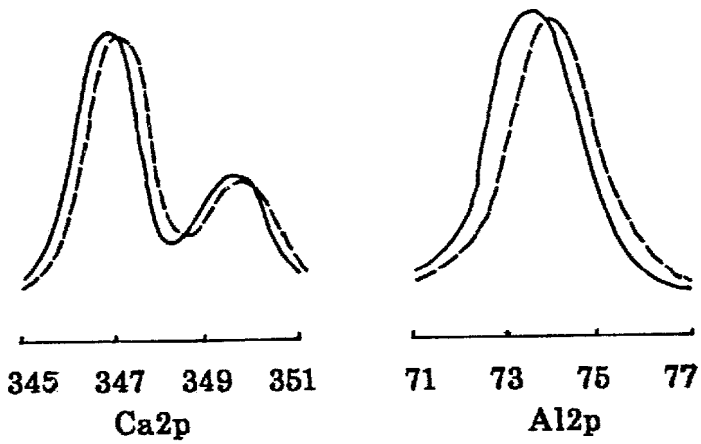

Fig. 2 XPS patterns of Ca, Al element binding energy (eV)

micro surface feature only by the observation of surface image. (2) The fractural surfaces have the real structure information of C, N, O, Ca, Al elements in the interface layer of chemical reaction. The dotted lines in Fig. 2 Ca2p-347.70, 350.96 eV, Al2p-74.68 eV are results, and C1s, N1s, O1s binding energies are the same as those dotted liner in Fig.1. The double peaks of Ca2p in Fig. 2 is the characteric phenomenon (2P1/2, 2P3/2) , but two peaks in O pattern are due to the large difference in chemical state of O. This information showed that some breakage takes place in practical design interface due to weaker bonding force. (3) The fractured surface gave the structural information of pure cement paste inner. The full lines in Fig. 2 show the results, Ca2p 346.71, 350.14 eV, Al2p -73.82 eV. We have two explanations for these results. One is that the fractured surface is in cement inner, which indicated that bonding force between designed interfaces is stronger than that in cement paste inner. The other is that there is no chemical reaction between polymer and cement, and there is some molecular force at most. Because of the weaker adhesive behavior, these places are easily to be broken. Besides materials used, some other factors such as rough surface, gas pore, and so on can all engender this result. In our experiment, two situations may all appear.

According to above results and analyses, we consider that the bonding force between matrixes is often stronger than that in matrix inner, for the composite materials which have chemical reaction between organic-inorganic matrix which can form a beneficial interface layer. In this case, when these composite materials are broken, fractured surfaces are often not in the interface. In our experiment, fractures took place more in polymer side at wet state or in cement side at dry state. That is to say, the interface behavior acquires good improvement. According to the model of breaking analysis of MDF cement [10], it is this improvement of the bonding force in interface that the bending strength and other properties are improved greatly.

CONCLUSIONS

1. Among twelve organic materials, the chemical reaction only take place between water-soluble polymer polyvinyl alcohol or polyacrylamide and cements. The reason is that these polymers provide a lot of active group during the hydration.

2. The micro mechanism of chemical bonding action of polyacrylamide and $CaO.Al_2O_3$ is that, firstly the C-N bond in amide group is broken, next the C links with the O, and then this O links with Ca, Al cations of inorganic matrix.

3. The good bonding state and interface structure are formed between polymer and cement during hydration process, the bonding force in interfaces is often stronger than that in matrixes inner. Therefore, breakdown takes place more often in polymer or in cement inner and does not always in the interface between phases as common cement materials.

4. The improvement of bonding behavior in interface increase greatly the bending strength of materials. This resuls reveals that the weak link between various particles or hydrate phases is the fundamental reason for a low bending strength in cement materials. The experiment results demonstrate that the interface factor play an important role in the promotion strength and properties of MDF cement.

REFERNCES

1. Alford, N. McN. and Birchall, J. D. "The Properties and Potential Applications of Macro -defect Free Cement", Mat. Res. Soc. Proc., Boston, 1984, Vol.42, 265-267
2. Willians, D. F. Mcnamara, F.A. Birchall, J. D. "The Interaction Between MDF Cement and Tissues", J. Mat. Sci., 1984, Vol.19, 637-644
3. Birchall, J. D. Howard, A. J. and Kendall, K. "Flexural Sterngth and Porosity of Cements", Nature, 1981, Vol.289, 388-398
4. Alford,N.NcM."A Theoretical Argument for the Existence of High Strength Cement Pastes", Cem. Concr. Res. 1981, Vol.11,605-610
5. Kendall, K. Howard, A. J. and Birchall, J. D. "The Relation Between Based Materials", 1983, Phil. Trans. R. Soc., London, A310 139-151
6. Roy, D. M. Gouda G. R. and Brobowsky, A. "Very High Strength Cement Paste Prepared by Pressing and other High Pressure Technique", Cem.Concr. Res., 1972, Vol.2 349-366
7. Yudenfreund, M. Oder, I. and Brunaner, S. "Hardened Portland Cement Paste of Low Porosity: I Materials and Experimental Methods", Cem. Concr. Res. 1972, Vol.2 313-330
8. Hu Shuguang and Wang Shiquin, " The Analysis of the interfacial Effect in MDF Cement Materials", J. of Wuhan Univ. of Tech. 1992, Vol.14, No.4 (will be published)
9. Birchall, J. D. Kendall, K. and Howard, A. J. Europen Patent Publication, 1981, No: 0021681
10. Hu Shuguang, "Studies on the Promotion Strength Mechanism of the Role of Interfacial Bond in Polymer Cement Based Composite Materials", (Ph. D. Thesis) 1991, Wuhan University of Technology

NUMERICAL SIMULATION OF MDF COMPOSITE MATERIALS

R I A Malek* and M Uchiyama**

**Materials Research Laboratory, The Pennsylvania State University, USA*
***Tomogami Iron Works, JAPAN*

SUMMARY

The 21st Century Concrete Technology will show considerable shifts in construction methods and equipments. In the area of concrete materials, mix design will likely be more concerned with developments in: new cements for higher early and ultimate strength; mineral admixtures which will lower the water to cement ratio but will still give a dense workable concrete; more effective usage of recycled concrete; curing compounds and sealants that cure, protect, and seal the surface; and development of densified systems containing ultrafine particles and macro-defect-free materials. The major objective will be to produce concrete of improved mechanical properties.

Portland Cement matrices have much lower tensile strength than compressive strength. This is due to the residual large pores and flows after solidification. Various attempts have been taken to improve the mechanical properties of cementitious materials. One of the most recent attempts is the approach of preparing the so-called macro-defect free (MDF) cements, produced originally from high alumina cement and later with ordinary portland cement in combination with a water soluble polymer.

A simulation model for analyzing the mechanical behavior of MDF cement pastes under tensile forces is developed in which the MDF materials are considered to consist of two phases, one is a soft continuous phase made of the polymer gel and the other a hard discontinuous phase made of unhydrated grains. The analysis proceeds by making successive step displacements by inducing increments of force. After each displacement, the total force and total displacement from the initial length are calculated. This process will continue until the maximum strain is reached. After this, re-calculation of the stiffness of the matrix proceeds. Therefore, the present numerical method can follow the stress-strain relationship after the maximum stress. The results of this simulation are presented and compared with experimental results.

* Present adress: Tomogami Iron Works, Japan.

INTRODUCTION

Ordinary Portland Cement matrices are known to have a much lower tensile strength than compressive strength, ascribed to large pores and flows. Various attempts have been undertaken to improve the tensile mechanical properties of cementitious materials. Earlier attempts involved the use of polymer modified cement matrices while others included enhancing the particle packing by blending it with fine particles (DSP*) or using a high pressure[1]. The high pressure densification could be of much benefit when combined with proportioning with fine particles. These materials possess a very high compressive strength but their tensile strength is still low[2]. One of the most recent attempts is the approach of preparing the so-called macro-defect free (MDF) cements produced originally from high alumina cement[3] and later with ordinary portland cement in combination with a water soluble polymer[4]. The MDF materials posses high tensile strength due to the absence of large pores[5-8]. In addition to the pore filling property, the polymer acts as a lubricant to reduce friction and remove air voids during mixing. Furthermore, it reacts with calcium ions produced by cement hydration to develop a polymer-polymer and polymer-cement grains cross-linked network. Alford and Birchall9 showed several applications of products made of MDF cement pastes, ranging from loudspeaker cabinets to armour systems protecting personnel, vehicles and buildings. Recently, the number of studies on the mechanical behavior of MDF related materials is increasing because the potential technical importance of such materials lies in the fact that they possess high tensile strengths combined with high toughness. Recently, Malek[10,11] used high performance fibres to further improve the mechanical properties of the MDF matrices.

Several models have been developed to explain the mechanical behavior of cementitious materials . Higgins and Bailey[12] have improved the tied crack model based on the Dugdale model for OPC pastes. They used the modified Griffith theory to analyze, semi-quantitatively, the observed relationship between flexural strength and notch length. Wittman13 has carried out a numerical analysis on mechanical properties of concrete using the finite element method. He used the circle-idealized aggregate particles to investigate the stress concentration of the interface between the aggregate and the boundary phase. Bazant[14], on the other hand, investigated the microplane model applied to the simulation of tensile mechanical behavior of concrete.

Eden and Bailey [15] developed a model for MDF cement pastes,by using the fiber pull-out mechanism in which the polymer gel acts as an adhesive between two fibrils, buf, Sinclair and Groves[16] rejected it because they didn't find fibrous outgrowth in MDF cement.

PROPOSED MECHANICAL MODEL

In the present model, the MDF materials are considered to consist of two phases, one is a soft continuous phase made of the polymer gel and the other is a hard discontinuous phase made of unhydrated grains. The following two main assumptions are used in the present model: 1) The unhydrated grains are considered as completely stiff particles and thus, their deformation can be ignored. Therefore, the elastic modulus and the maximum strain of the hard phase does not affect neither the soft phase nor the macro-elastic modulus and maximum macro-strain of the material, respectively. The macro-values may, however, be indirectly affected by the size distribution of unhydrated grains. 2) Forces applied to the grain are directed towards one central point in the grain, i.e. no moment nor shear stress occurs around the grain. According to these assumptions, the real microstructure is converted to a pin jointed frame network structure where Hook's low was applied on its members (Figure 1).

* Densified systems containing homogeneously arranged ultrafine particles.

Numerical Analysis

The analysis proceeds by making successive step displacements. by inducing an increment of force around the pin. This will results in a new pin location, which can be generated by solving the linear simultaneous equations. After each displacement, the total

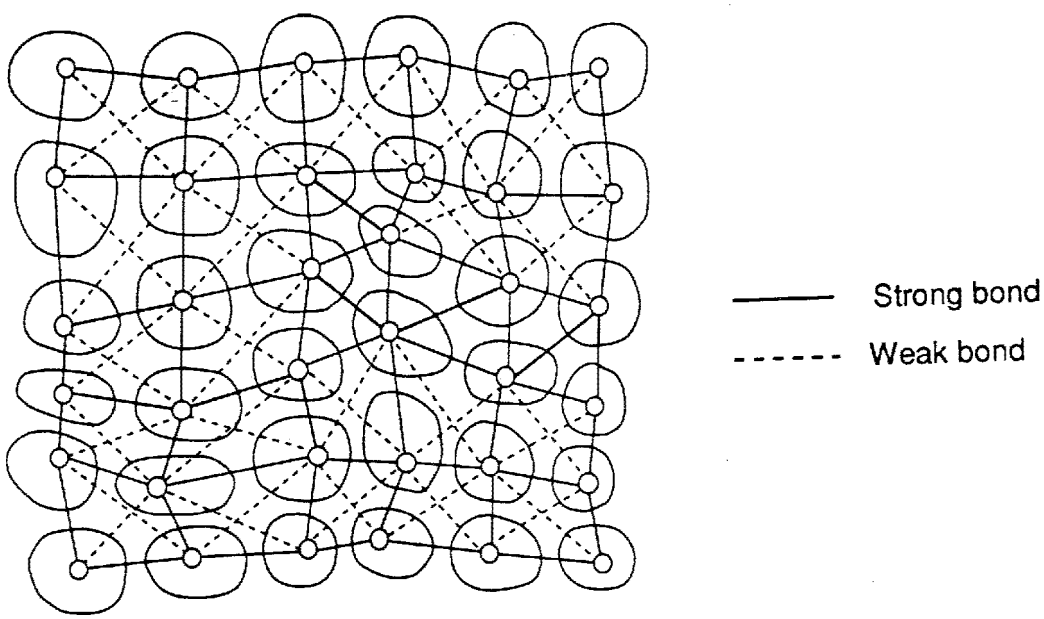

Figure 1. A diagrammatic representation of the mesh

force of each member is calculated by total displacement from the initial length. This process will continue until the maximum strain of the member is reached (i.e. the total force exceeds the maximum strength of the member) and the member is broken. After this re-calculation of the stiffness of the matrix proceeds at zero displacement and then the normal procedure is applied. Therefore, the present numerical method can follow the stress-strain relationship after the maximum stress.

Under uniaxial loading, a two-dimensional frame work can be used in the model without gross errors. The grain location is converted to pin location. The force direction at each member must be determined to be in the actual direction of each displaced member; however, this procedure makes the numerical analysis quite complicated as linear calculations can no longer be applied. In the present numerical analysis, the force direction at each member is determined as the former direction of each displaced member; therefore, linear calculation can be applied. This approximation may be reasonable if the displacement of each member is very small at the force equilibrium. In the present analysis, the small applied step displacement causes a small displacement of each member; therefore, this approximation does not cause gross errors (Fig. 2). Additionally, in the proposed model, the increment of force at each member must be calculated by using the actual elongation of each displaced member; however, this procedure also causes a non-linear calculation. In the present analysis, the elongation of each member is calculated by the inner product of the unit vector of each member and the relative vector of the increment of displacement of each pin. These two approximations are concerned in the procedure of numerical calculation, which can change the complicated calculation into a simple linear calculation. The other approximations are also necessary to

decide the stiffness of each member (micro-stiffness). Each micro-stiffness is dependent on each boundary area, each boundary thickness, and the elastic modulus of the polymer gel.

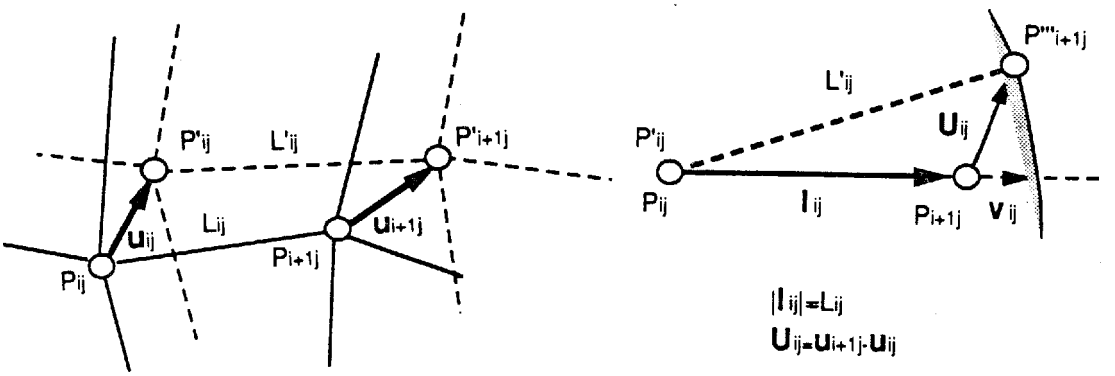

Direction of the elongation of Lij is appoximately equal to the initial direction of Lij. Elongation of Lij is appoximately $|V_{ij}|$: $|V_{ij}| = U_{ij} * I_{ij} / |I_{ij}|$.

Figure 2. Approximation of force direction and elongation used in the present model.

RESULTS OF THE NUMERICAL SIMULATION

Effect of the Particle Size, and Size Distribution

The results show that the elastic modulus will be higher if the particle size is larger since the volume fraction of soft phase is decreased; however, the maximum tensile stress will not be changed if the boundary thickens, and elastic modulus and the maximum strain of the soft phase are fixed.

The effect of the particle size distribution is much more complicated than the effect of the particle size with single distribution because the initial mesh geometry is not simple. The results show that if the particle size distribution is broader, the maximum tensile stress will be lower than that of the material which has the single particle size distribution; however, the elastic modulus of the material will not be always lower. If the geometries of the two initial meshes are not so different, which means that the number of the strong bonds of each mesh is the same, the elastic modulus of the mesh which has the broader particle size distribution will be lower. However, if the number of strong bonds is not the same, the elastic modulus of the mesh which has more strong bonds will be higher.

Generally, a broader particle size distribution will increase the number of strong bonds due to a higher degree of **particle packing**; therefore, a cross-over point may exist in the relationship between the broadness of particle size distribution and the elastic modulus of the material.

Effect of the Boundary Thickness

This result shows that the elastic modulus will be higher if the thickness is smaller; however, the maximum tensile stress will not be changed if the particle size and the mechanical properties of the polymer gel are fixed.

Effect of the Pore Size and Size Distribution

Effect of the Pore Location

The results show that the homogeneous size distribution of the pores increases the maximum tensile stress and elastic modulus of the material. The results show also that if the total pore area projected to the perpendicular section to the loading direction is smaller, the maximum tensile stress and elastic modulus of the material will be higher.

Effect of the Pore Orientation, Geometry, and Size Distribution

The results show that if the pore area projected to the perpendicular section to the direction of loading, which is changed by the pore orientation, is smaller, the maximum tensile stress and elastic modulus of the material will be higher. The proposed model can also analyze the effect of pore size distribution; however, it is practically difficult to do using the small mesh.

Comparison with Experimental Results

Figure 3 shows the analyses of experimental results of FM-1a and FM-1b using the observed particle size distributions. The two specimens were made of two cements of different particle size distributions, polyacrylamide and water. The results of simulations show linear elastic behavior. The experimental results show a good agreement with predicted values up to 0.1% strain. Beyond this the experimental results show non-linear behavior. The deviation of higher strain percentages is due to the fact that the proposed model is established for linear elastic materials, and the mechanical properties of real MDF materials, even dried, are affected by the mechanical properties of the polymer (non-linear behavior).

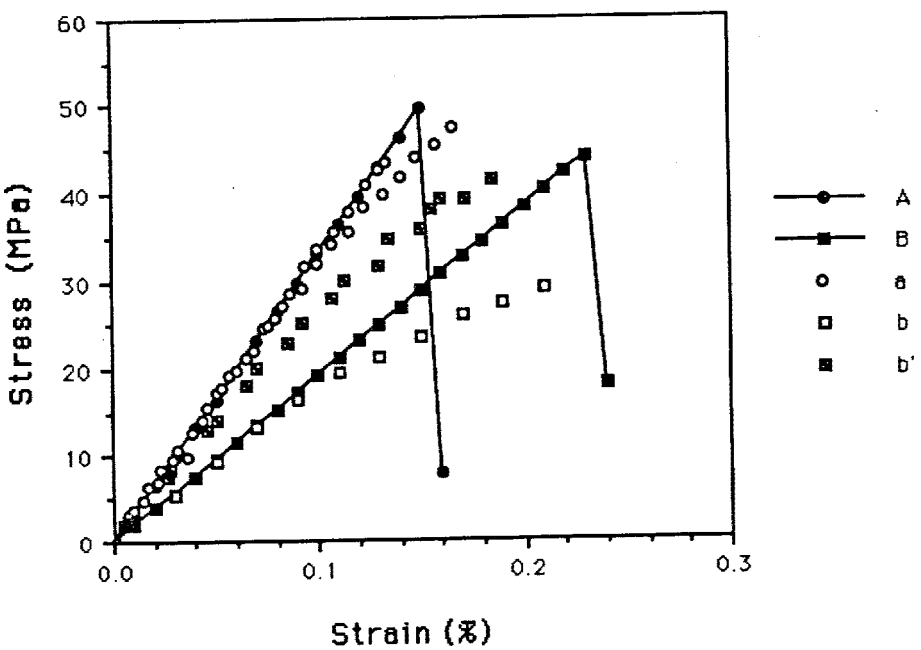

Figure 3. Stress-Strain Relationships Predicted from the Model and Contrasted with the Experimental Results. Letters A and B indicate results of simulation for two specimens FM-1a and FM-1b, respectively. Letters a, b, b' indicate experimental resultsof FM-1a cured for 2 weeks, FM-1b cured for 2 weeks, FM-1b cured for 4 weeks, respectively.

CONCLUSIONS

The proposed simple frame network model can be used to analyze or simulate the tensile mechanical behavior of MDF cementitious materials or composites made of hard inclusions embedded in a soft matrix. The present numerical analysis predicts that particle size distribution and boundary thickness can affect the tensile mechanical behavior of the MDF cement pastes. For example: narrower particle size distribution can give higher strength and elastic modulus, whereas, smaller boundary thickness can give only higher elastic modulus. Also, pore location, pore orientation, and pore geometry can affect the mechanical properties of the MDF cement pastes.

ACKNOWLEDGMENT

Partial financial support of the National Science Foundation is appreciated.

REFERENCES

1. Roy, D.M., and G. R. Gouda. Cement and Concrete Research , **3**, 807-20 (1973).
2. Hjorth, C. Technology in the 1990s: Developments in the Science and Technology of Hydraulic Cements. Ed. Peter Hirsch, et al. London: The Royal Society, 167-73 (1983).
3. Birchall, J. D., A. J. Howard, and K. Kendall. Nature **289**, 388-9 (1981).
4. Rodgers, S.A., *et .al.* Mater. Res. Soc. Symp. Proc. , **42**,.45-52 (1985).
5. Birchall,J. D., Cement and Concrete Research, **16**,31-51 (1986.)
6. Kendall, K., A. J. Howard, and J. D. Birchall. Technology in the 1990s: Developments in the Science and Technology of Hydraulic Cements. Ed. Peter Hirsch, et al. London: The Royal Society, 1983. 139-53.
7. Eden, N. B., and J. E. Bailey. Journal of Materials Science **19**, 150-8 (1984).
8. Alford, N. McN., Cement and Concrete Research, **11**, 605-10 (1981).
9. Alford, N. McN., and J.D. Birchall, Mater. Res. Soc. Symp. Proc. , **42**,. 265-67 (1985).
10. Malek, R.I.A., "Structure/Performance Characteristics of Aramid Fibres Reinforced MDF Cement," 9th Inter. Congr. Chem. Cement (1992).
11. Malek, R.I.A., "Structure/Performance Characteristics of Aramid Fibres Reinforced Cement Matrices," J. of Composite Materials, in press (1992).
12. Higgins, D.D., and J.E. Bailey, J. Mat. Sci., **11**, 1995-2003 (1976).
13. Wittman, F.H., ed. Fracture Toughness & Fracture Energy of Concrete,"Elsevier (1986)..
14. Bazant, Z. P. Fracture Mechanics of Concrete. Ed. George C. Sih, and A. DiTommaso. Dordrecht: Martinus Nijhoff Publishers, 72-85 (1985).
15. Eden, N.B., and J.E. Bailey, J. Mat. Sci., **19**, 2977-90 (1984).
16. Sinclair, W., and G.W. Groves, J. Mat. Sci., **20**, 2946-52 (1985).

CHEMICAL INTERACTION BETWEEN PVA AND HYDRATING HAC: INFRARED SPECTROSCOPIC AND THERMOANALYTICAL INVESTIGATIONS

S Harsh, Y C Naidu and S N Ghosh

National Council for Cement and Building Materials
New Delhi, INDIA

SUMMARY

The nature of chemical interaction between polyvinyl alcohol (PVA) and hydrating high alumina cement (HAC) has been investigated using infrared spectroscopy and DTA/DTG techniques. Infrared spectroscopy results confirmed the formation of metal carboxylates in high alumina cement-polyvinyl alcohol (HAC-PVA) systems, formed by interaction of acetate groups released by polyvinyl alcohol and metal ions released by cement. IR spectroscopy also provided indirect evidence of cross-linking of polymer chains via metal ions. The DTA curves showed that the presence of polyvinyl alcohol suppresses the formation of C_3AH_6 in hydrating high alumina cement systems. A new endothermic peak observed in the DTA curves of HAC-PVA systems at about 250° - 260°C, could possibly be arising from the decomposition of PVA-complexed-gibbsite.

INTRODUCTION

The macro-defect-free (MDF) cement composites developed by Birchall et al (1-3) have very high compressive and flexural strengths (more than 250 MPa and 200 MPa respectively) together with a high modulus of elasticity and relatively high fracture energy. The basic constituents of the system are cement (ordinary portland cement or high alumina cement) and a water soluble polymer such as polyvinyl alcohol, polyacrylamide or hydroxypropyl methyl cellulose. A low water/cement ratio (0.12-0.16) is required to be maintained for achieving high strengths. Thorough mixing of the cement-polymer-water system at such low w/c ratios is achieved by high shear mixing at a roll mill. After roll milling the mix acquires a dough like consistency and can be processed into desired shapes through plastic processing techniques such as calendering, compression moulding etc.

As to the factors responsible for such high flexural and compressive strengths, there is a lack of consensus. Birchall (2) suggested that the removal of relatively large, elongated pores coupled with overall lower porosity is the primary reason for the higher strength of the MDF composites. It was argued (1,3) that the large pores act as flaws and therefore as per Griffith's equation, the reduction in the largest pore size will result in higher flexural strength. Eden et al proposed a model (4) to account for the high flexural strengths of OPC based MDF composites taking into consideration the suggestion (5) that the failure in an OPC paste occurs by the pulling apart of calcium silicate hydrate fibrils. As per this model the flexural strength of MDF cement is considered to be controlled by the shear resistance of the CSH - polymer - CSH fibrilar interface. They further suggested that removal of pores, either large or colloidal is not the principal factor contributing to the high strength. But Sinclair and Groves (6) did not find interlocking fibrous hydrates in OPC as well as HAC based composites as required by Eden's model.

In addition to the microstructural features, the cement- polymer interaction is also expected to play a significant role in determining the strength of MDF composites. The studies by Rodger et al (7) have indicated that strong interactions occur between polymer and cement in both the OPC and HAC based MDF composites. In a recent review of various aspects of cement-polymer interaction for OPC systems, Chandra et al (8) have concluded that the cement polymer interaction is due to ionic bonding between metal ions furnished by cement and anionic groups on polymer chains and results in the cross-linking of the polymer chains. Zhu Hong et al (9) on the basis of their investigations on PC based MDF composites supported the findings of Rodger et al (7) that the physical and chemical interactions between polymer and cement in MDF composites make the polymer chains cross-linked. They further suggested that the largest pore size was not a dominant factor determining the flexural strength of MDF cement and felt that the interactions between polymer and cement gave rise to an "intense composite effect" that made a great contribution to the high flexural strength of MDF cement. However, the mechanism of these interactions and the mode of their contribution towards higher strengths are far from clear.

In this paper we present the results obtained on cement polymer interaction from the infrared spectroscopic and DTA/DTG studies of the high alumina cement-polyvinyl alcohol (HAC-PVA) System.

EXPERIMENTAL

The commercially available high alumina cement (trade name "calandum"), containing 46% Al_2O_3 , 32% CaO, 6% SiO_2 and 5% Fe_2O_3 was used for the preparation of HAC-PVA composite samples. The HAC-PVA mixes at w/c ratio below 0.2 were prepared by mixing the cement with polymer-water gel in a planetary mixer followed by high shear mixing at a roll mill. The dough like material was stripped of the rolls and filled

in 2" cube moulds. The material inside the mould was compacted using a hammer and a rod. After casting, the cubes inside the moulds were kept covered under a damp cloth and were demoulded after 5 hours. The demoulded cubes were cured for 4 days at 50°C and RH 80 and then dried for 1 day at 80°C.

The cured and dried cubes were crushed and ground to a fine powder and subjected to IR and DTA/DTG investigations. For comparative studies two more samples were prepared. One was that of HAC hydrated for 4 days at w/c = 0.3. Another was a mix of HAC and 10% PVA hydrated for four days at w/c = 2.0. The hydration was carried out at ambient temperature (30°-35°C). After 4 days the samples were washed with acetone, dried and ground to a fine powder. The powdered samples were subjected to IR and DTA/DTG investigations.

RESULTS

1/ IR Spectroscopic Studies

IR spectra of HAC-PVA system (samples prepared as KBr pellets) have been reported (7) to show a complete absence of the carbonyl (C=0) band of the acetate group, which appears as a strong band at 1720 cm^{-1} in the spectrum of partially hydrolyzed PVA, and emergence of two new bands at 1570 cm^{-1} and 1415 cm^{-1}. The two new bands were attributed to metal carboxylate absorbances.

The IR spectra of hydrated HAC-PVA systems and that of hydrated HAC only (samples prepared as nujol mull) are given in Figure 1.The 1720 cm^{-1} band of the carbonyl group was not observed in any of the spectra of HAC-PVA system. Further as compared to hydrated HAC only, the spectra of HAC-PVA systems showed a new band at 1560-1570 cm^{-1}, which was one of the bands attributable to a metal carboxylate. These results were in accordance with data reported earlier (7). It was also seen that not

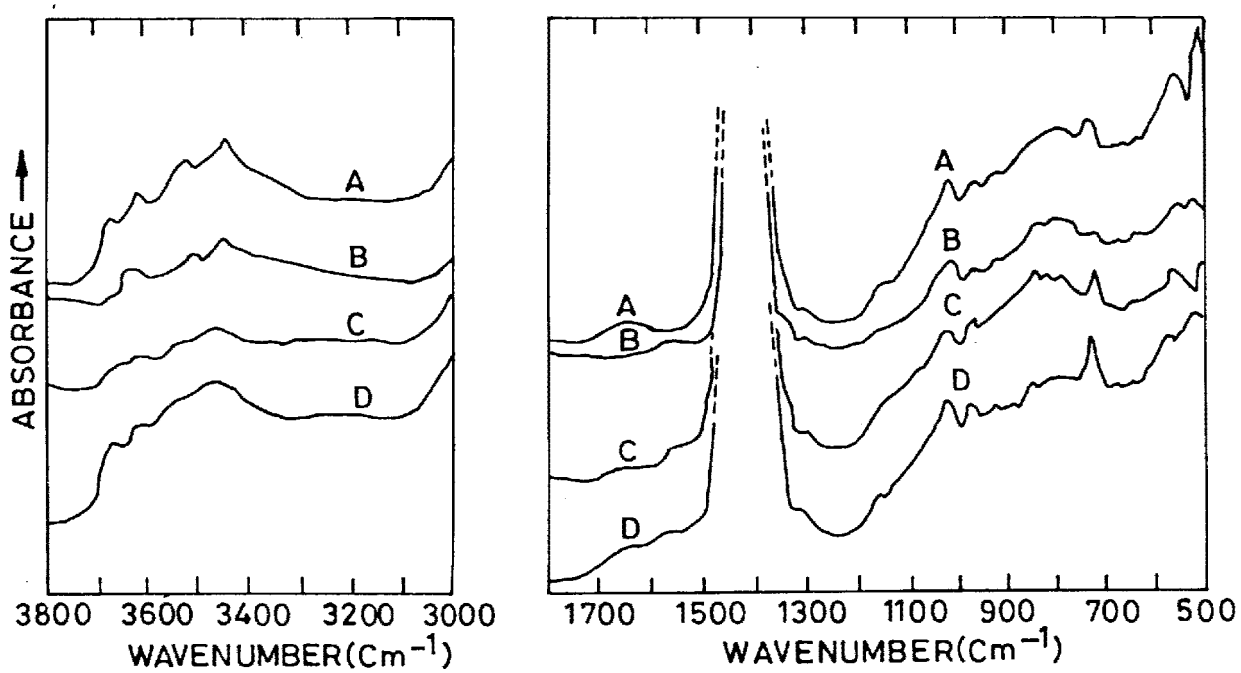

Fig 1 IR spectra of hydrated HAC+PVA systems. **A** - Hydrated HAC (w/c = 0.3); B - Crushed HAC-PVA cube (PVA = 5%, w/c = 0.15); **C** - Crushed HAC-PVA cube (PVA=7%; w/c=0.15); **D**-Hydrated mix of HAC and 10% PVA (w/c=2.0).

Table 1 Infrared Absorption Bands of PVA (7)

Band Position (cm^{-1})	Assignment
1096 m, b	C-O str., OH bend
1245 s	C-O str.,
1370 m	CH bend
1430 m	CH, CH_2, OH bend
1720 s	C=O str.(acetate)
2930 m	CH str.
3360 vs,b	OH str.

s = strong, m = medium, b = broad, v = very, str. = stretch

only the 1720 cm^{-1} band but other bands of PVA as well, such as 1096 cm^{-1} (C-O str., OH bend) band, 1245 cm^{-1} (C-O str.) band and 3360 cm^{-1} (OH str.) band did not appear in the HAC-PVA spectra. We comment specifically on these bands because other IR bands of PVA (Table 1) attributable to CH str. or CH, CH_2 bend fall in the absorption region of nujol and could not be deciphered in the IR spectra presented here.

The vibrational bands observed in the aluminate absorption region (500-1100 cm^{-1}) and the OH absorption region (3400-3700 cm^{-1}) for various calcium aluminates/ calcium aluminate hydrates did not show any appreciable change in going from hydrated HAC to hydrated HAC-PVA systems.

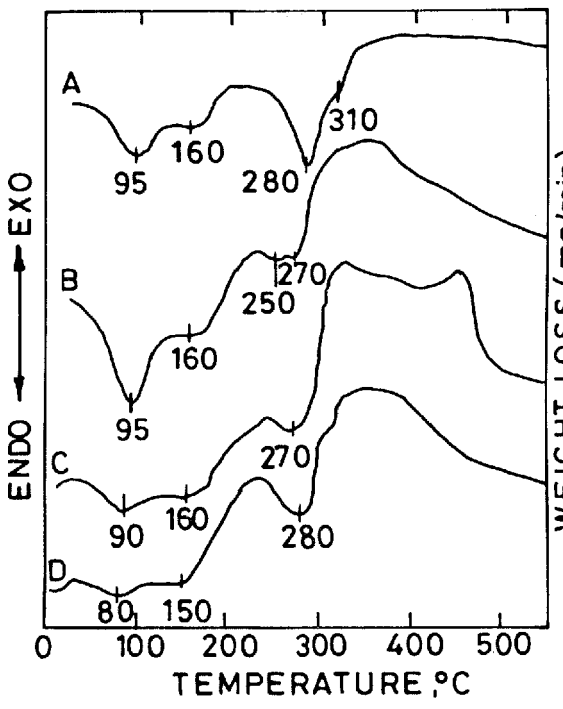

Fig 2 DTA curves of Hydrated HAC+PVA Systems

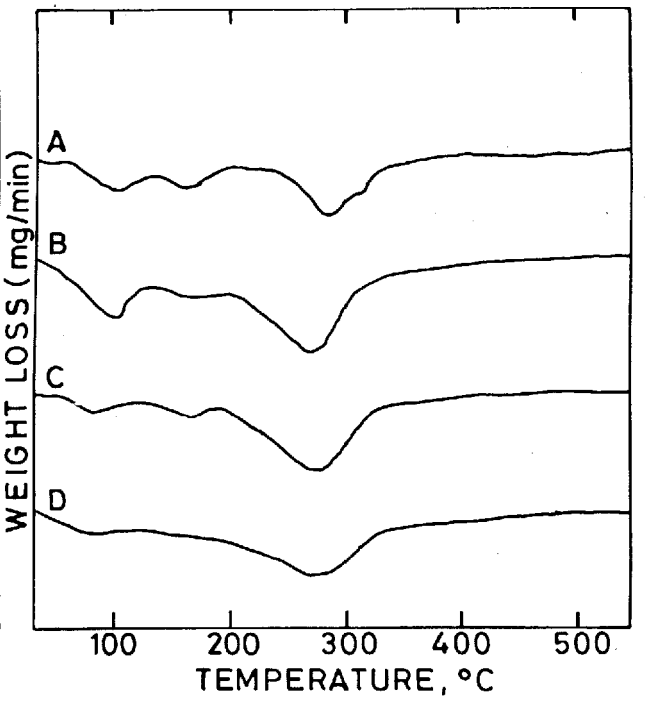

Fig 3 DTG curves of Hydrated HAC+PVA Systems

A- Hydrated HAC (w/c=0.3); **B**- Hydrated mix of HAC+10% PVA (w/c=2.0); **C**-Crushed HAC-PVA cube (PVA=6%, w/c=0.19); **D**-Crushed HAC-PVA cube (PVA=5%, w/c=0.16)

2/ **DTA/DTG Studies**

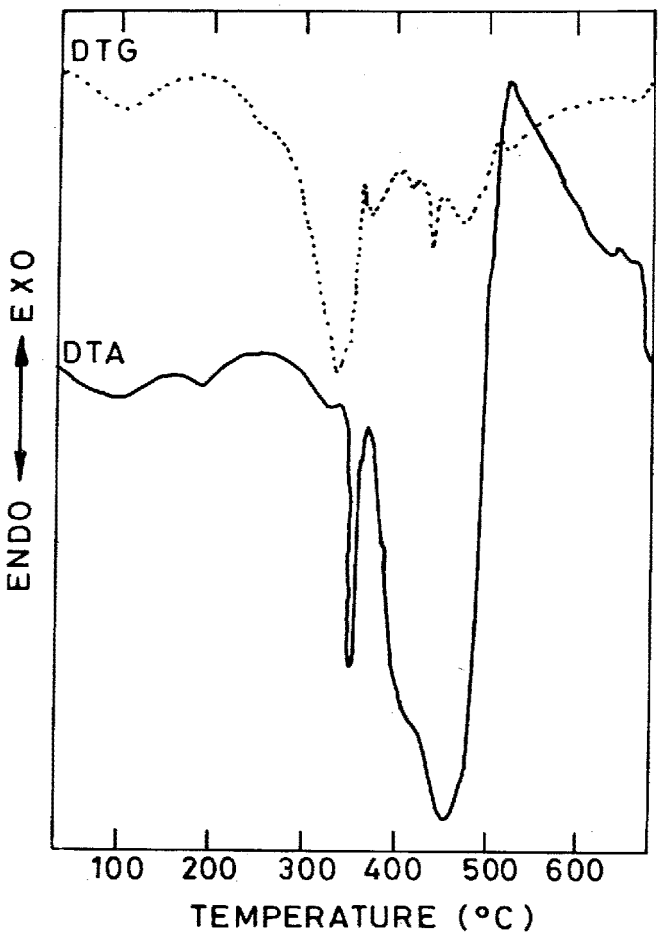

Fig 4 DTA and DTG curves of polyvinyl alcohol

The DTA/DTG data for the hydrated HAC and HAC-PVA systems are given in Figure 2. The DTA curve of hydrated HAC showed endothermic peaks at 95°C, 160°C, 280°C and 310°C (shoulder) corresponding to alumina gel, C_2AH_8, AH_3 and C_3AH_6 respectively. The presence of 4 peaks in the DTG curve (Figure 3) corresponding to weight loss in four stages at about 100°C, 165°C, 280°C and 315°C confirmed the presence of four phases. The DTA curves for the HAC-PVA systems showed some significant differences from the DTA curve for hydrated HAC. The most important differences were observed in the 230°-450°C region where it was observed that (a) The C_3AH_6 peak, observed at 310°C in the case of hydrated HAC, was either absent or greatly diminished in intensity; (b) The relatively narrow peak corresponding to AH_3 at 280°C was replaced by a much broader peak. In one case (curve-B), instead of a single broad peak a broad doublet was observed with individual peaks of the doublet centered at 250°C and 270°C; (c) The 300° -450°C region of the DTA curves for HAC-PVA systems (curves B, C and D) showed presence of exothermic peaks. In the case of curve-C a total of 3 exothermic peaks were observed in this region. A perusal of the DTA curve of polyvinyl alcohol (Figure 4) showed that these exothermic peaks were not attributable to PVA. Further it was seen that none of the peaks observed in the DTA curve of polyvinyl alcohol appear in the DTA curves for HAC-PVA composite system.

DISCUSSION

The infrared spectroscopic and DTA/DTG studies presented in this paper provide evidence of the existence of, and throw some light on the nature of, cement polymer interaction in hydrated HAC-PVA systems. The main observed features of the IR spectra of these systems were (a) The band at 1720 cm^{-1}, corresponding to acetate group of partially hydrolyzed polyvinyl alcohol was not observed; (b) A new peak was observed at 1560-1570 cm^{-1} corresponding to metal carboxylate salts; (c) IR bands of PVA corresponding to C-O str., OH str., and OH bend were not observed; and (d) The IR bands corresponding to calcium aluminate hydrates did not show any appreciable change in going from hydrated HAC to hydrated HAC-PVA systems, except for the changes in the intensity of the peaks reflecting the quantitative changes in the cement phases. As mentioned earlier, the disappearance of absorption band of acetate group and appearance of two new bands corresponding to metal carboxylates has been reported by Rodger et al(7), who also postulated a mechanism for the interaction of polyvinyl alcohol with hydrating HAC systems (Figure 5). As per this mechanism, the partially hydrolyzed PVA is completely hydrolyzed releasing acetate ions in solution, which combine with metal ions present in the system forming carboxylate salts. This would

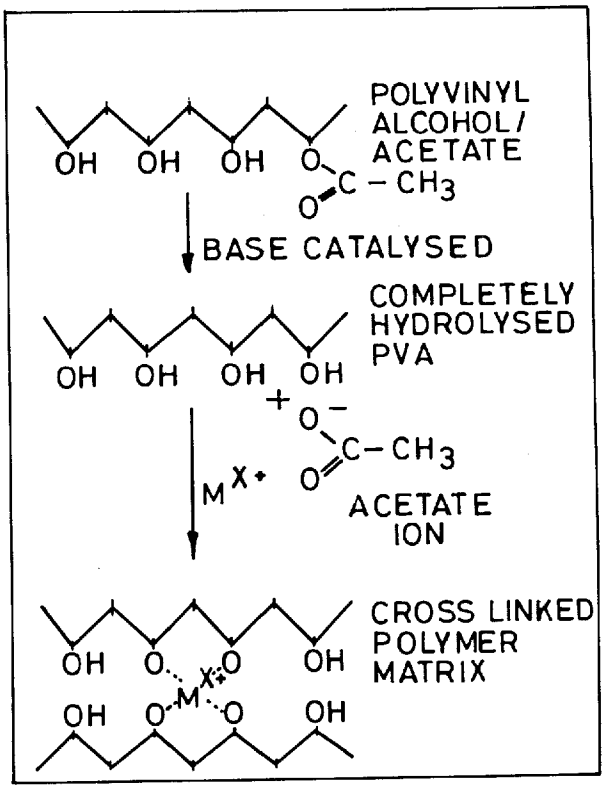

Fig 5 Reaction of PVA with hydrating high alumina cement (7).

account for the disappearance of 1720 cm^{-1} band and also for the new band at 1570 cm^{-1} observed in the IR spectra of HAC-PVA system. (The 1415 cm^{-1} band of metal carboxylates fell in the absorption region of nujol and could not be seen). However, IR spectra did not provide any direct evidence for the next postulated step of the mechanism, i.e.,cross-linking of polymer chains via metal ions. Though, the absence of other IR bands of PVA, i.e., the ones corresponding to the vibrations of C-O and OH groups, can probably be taken as an indirect evidence of cross-linking of PVA chains. Apparently, because of the cross-linking, where the oxygen of the hydroxyl group of PVA is postulated to combine with metal ions from cement, the vibrational modes of PVA such as C-O str., OH str. or OH bend were greatly suppressed and did not appear in the IR spectra of HAC-PVA systems. Lastly, the absence of any significant change in the vibrational bands corresponding to calcium aluminate hydrates indicated that the molecular structure of the various hydrates was not affected by the cement polymer interaction.

The DTA/DTG data presented in this paper has provided new evidence of the interaction of PVA with hydrating HAC and has also shown that the presence of PVA affects the course of hydration of HAC. The DTA curves, clearly showed that the presence of PVA, both at high as well as low water/cement ratios, checked the formation of C_3AH_6 in hydrating HAC systems. The observation relating to the broadening of the 280°C peak both in the DTA as well as in the DTG curves indicated that the PVA probably combined with gibbsite to a much larger extent than with other cement phases present in the system. In one case (Figure 2, curve B) instead of a single broad peak, the DTA curve showed a doublet with peak positions at 250°C and 270°C. This observation suggested that the broadened peaks observed at 270°C and 280°C in the DTA curves C and D (Figure 2) are also not single peaks but a combination of two overlapping peaks. Out of these two peaks, the one appearing at about 270°-280°C could be attributed to AH_3 (gibbsite) decomposition. The new endothermic peak appearing at about 250°-260°C probably arises from the decomposition of PVA-complexed-gibbsite. In a recent study (10) on the interaction between gibbsite and polyacrylamide, the X-ray photoelectron spectra suggested electrostatic complexation of Al in AH_3 with the oxygen of the carbonyl (C=O) group in polyacrylamide. The gibbsite-PVA complex is probably formed through a similar interaction between Al of AH_3 and oxygen of the hydroxyl group. As for the exothermic peaks observed in the DTA curves, the reasons for these were not clear.

CONCLUSION

The studies presented in the paper lead to the following conclusions :

i) The PVA interacts chemically with hydrating HAC both at high as well as low w/c ratios.

ii) The polymer appears to interact with the cement system at two levels : (a) The interaction between the hydroxyl oxygen of PVA and metal ions present in the solution, resulting in the cross linking of polymer chains, (b) The interaction between hydroxyl oxygen of the PVA and metal ions (largely Al) present on the surface of hydrated phases (largely gibbsite), resulting in the bonding of polymer to the surface of hydrated phases.

iii) The acetate groups released by PVA combine with metal ions to form metal carboxylates.

iv) The presence of PVA affects the course of hydration of HAC and suppresses the formation of C_3AH_6.

ACKNOWLEDGEMENT

The work presented here has been carried out as part of the Fundamental and Basic Research programme of the National Council for Cement and Building Materials, New Delhi, India and this paper is being published with the permission of the Director General of the Council.

REFERENCES

1. Birchall J.D., Howard A.J. & Kendall K. : "Flexural strength and porosity of cements". Nature, 1981, **289**, 388-389.
2. Birchall J.D. : "Cement in the context of new materials for an energy-expensive future". Phil. Trans. R.Soc. Lond., 1983, **A 310**, 31-42.
3. Kendall K., Howard A.J. & Birchall J.D. : "The relation between porosity, microstructure and strength, and the approach to advanced cement-based materials". Phil. Trans. R. Soc. Lond., 1983, **A 310**, 139-153.
4. Eden N.B. & Bailey J.E. : "The mechanical properties and tensile failure mechanism of a high strength polymer modified portland cement". J.Mat.Sci, 1984, **19**, 2677-2690.
5. Higgins D.D. & Bailey J.E. :"Fracture measurements on cement paste". J.Mat.Sci.,1976, **11**, 1995-2003.
6. Sinclair W. & Groves G.W. : "High strength cement pastes. Part 1 - Microstructure". J.Mat.Sci., 1985, **20**, 2846-2852.
7. Rodger S.A., Brooks S.A., Sinclair W., Groves G.W. & Double D.D. : "High strength cement pastes. Part 2 - Reactions during setting". J.Mat.Sci., 1985,**20**, 2853-2860.
8. Chandra S. & Flodin P. : "Interactions of polymers and organic admixtures on portland cement hydration", Cem. Conc.Res., 1987, **17**, 875-890.
9. Hong Z., Xuequan W. & Mingshu T.: "The strength increasing mechanism in MDF cement". **International Symposium on Cement and Concrete, 2nd, Beijing, China 1989, V 1**, Topic 2, 352-359.
10. Sugama T., Kukacka L.E., Carciello N. & Hocker, N.J. : "Study of interactions at water-soluble polymer/$Ca(OH)_2$ or gibbsite interfaces by XPS", Cem. Conc. Res., 1989, **19**, 857-867.

MECHANISM OF GLASS-IONOMER CEMENT HARDENING

E Sakai*, K Ono*, K Asaga and M Daimon*****

*Denki Kagaku Kogyo Co Ltd, Special Cement Dept, Tokyo
**Nishi-Tokyo Institute of Technology, Dept of Material Science, Yamanashi
***Tokyo Institute of Technology, Dept of Inorganic Materials, Tokyo
JAPAN

SUMMARY

In this report, mechanism of glass-ionomer cement hardening is discussed by using glass containing florine and acrylic polymer systems. Mean diameters of glass particles used in this experiment were respectively 13 and 4.5 μm. Four types of acrylic polymers with differences in the molecular weight were used. The weight ratios of these polymers related to glass were changed from 1.25 to 2.75. Bending strength of hardened samples was increased by using high molecular weight of acrylic polymer or fine particles of glass. Crystals of hydrated products were not detected when hardened samples were analyzed by using XRD. Large amounts of hydrated products were detected by using DSC and TG/DTA. These hydrated products may be formed by reaction between glass particles and acrylic polymer. The amount of hydrated products increased according to increases of molecular weights of acrylic polymers. By using FT-IR the absorption intensity of -COOH decreased in hardened samples. On the other hand, the absorption intensity of $-COO^-$ increased under same conditions. The bending strength of glass-ionomer cement is increased according to the absorption intensity ratio of $-COO^-/-COOH$. These results may be indicating the bridge formation between metalic ions and acrylic polymers.

Este estudio se trata de los mecanismos de endurecimiento de cemento vidrio-ionomero por uso de un sistema de vidrio contiendo fluor y polimeros acrylicos. Los diametros medios de los tamaños de las particulas de los vidrios son respectivamente 13μm y 4.5μm y los cuatro tipos de polimeros acrílicos tiendo pesos moleculares diferentes. La proporción de los polímeros y vidrios son cambiados de 1.25 para 2.75. La fuerza de ligamento de las muestras son aumentados por uso de los pesos moleculares de polimero acrilico o particulas finas de los vidrios. Las muestras fueram analizadas por método de la difración de los radios-X y los productos de cristales hidratados no son notados. Entretanto, una gran cantidad de produtos hidratados son notados por DSC o TG/DTA. Estos productos hidratados son formados por la reacción de las particulas de vidrios e polímeros acrílicos. La cantidades de productos hidratados son aumentados con aumento de peso molecular de los polímeros acrílicos. Por uso de FT-IR, la absorción de -COOH para polímero acrílico está disminuido en muestras duras. Por otra parte, la absorción de COO^- és aumentado. La fuerza de la ligación de el cemento vidrio-ionomero son aumentados con aumento de la razón de la absorción de $-COO^-/-COOH$. Éstos puedem estar indicando la formación del puente entre ion metalico y polímero acrílico.

INTRODUCTION

MDF(Macro-defect free) cement which is cement-polymer composite proposed by Birchall is well known(1). Many investigators have studies the cement-polymer composite as ultra-high strength cement and chemically bonded ceramics. The hardening mechanism of MDF cement has been ascertained.

Glass-ionomer cement(GIC) that consists of polymer-inorganic materials systems is utilized in dental cement(2). Compressive strength and bending strength of hardened GIC at 50℃ and 1d are 120 - 150MPa and 20 - 30MPa respectively.

Hardening mechanisms of GIC have been investigated by analysis of the liquid phase. It has been reported that the mechanisms of GIC hardening is by the formation of bridges between metal ions and acrylic polymers(3).

The present investigation is essentially an exploration of this mechanism by using differents particle cize of fluorine glass and differents molecular weights of polyacrylic acids. For the purpose of clarifying the formation of bridges and reaction mechanism of GIC, hardened GIC was directly analysized by XRD, thermoanalysis, FT-IR and Wet-SEM/EDX.

EXPERIMENTAL DETAILS

Materials Used

Table 1. Chemical composition of glass.

No	SiO_2	Al_2O_3	CaO	F	P_2O_5	d_{50} (μm)
①	43	33.1	11.4	7.7	0.25	13
②						4.5

The chemical composition of synthesized glasses with fluorine are shown in Table 1. Glasses were synthesized following reference (3). The mean diameter of glass particles used were 13 μm and 4.5 μm. Polyacrylic acids used had molecular weight of 2000, 4000, 20000 and 90000.

The glass/polymer ratios were varied from 1.25 to 2.75. Samples were cured in wet condition for 7d at 50 ℃.

Strength Test

Samples were tested for compressive and bending strength, using a 10X10X80mm beam.

Analysis of Hydrated Products

The hydration products were detected by using XRD and thermoanalysis (DSC and TG/DTA). Morphology of hardened GIC was observed by wet-SEM. Bridge formation between polymers and metal ions was determined by means of FT-IR and Wet-SEM/EDX.

RESULTS AND DISCUSSIONS

Mechanical Properties

Figure 1 shows the influences of molecular weight of polyacryilic acids and the particle size of glass on the mechanical properties of GIC. Figure 2 shows the relation between pore volume and bending strength of hardened GIC. In the strength test method containing molding process ,specimen size, curing

temperature, curing time and so on, more detail investigations are necessary. Therefore, in this report, in order to discuss the tendency of strength development of GIC, relative strength is used. At the same pore volume in samples of hardened GIC, the larger the molecular weight of polyacrylic acids, the greater the bending strength of GIC. Particle size of glass also influences the bending strength. Bending strength of GIC with a small size of glass is larger than that of GIC with a large size of glass.

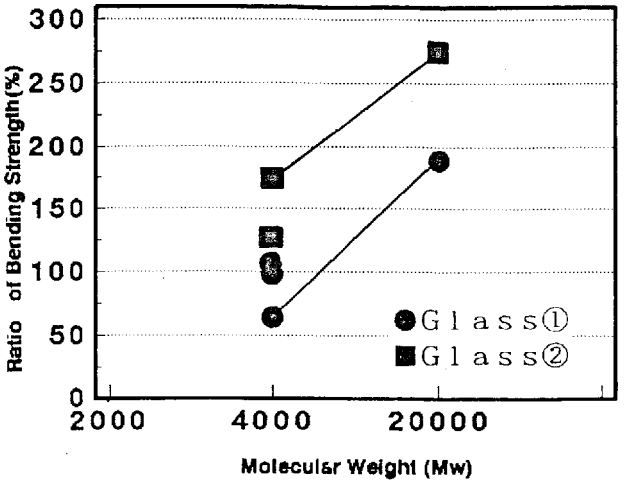

Figure 1. Strength of GIC

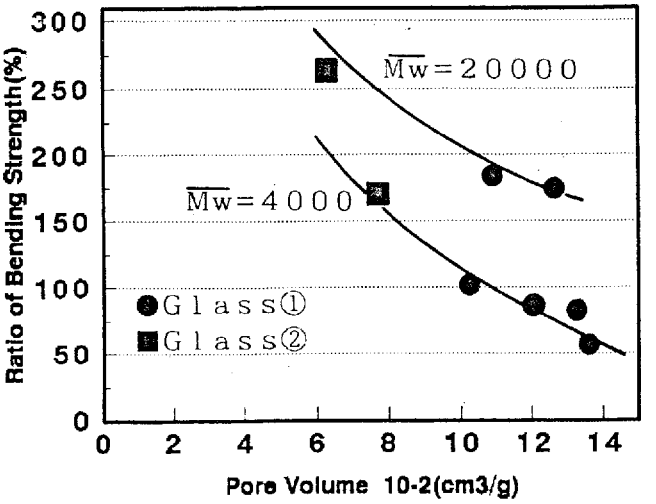

Figure 2. Relation between strength and pore volume

Hydrated Products

Figure 3 and Figure 4 show the DSC curve and TG/DTA curves of hardened GIC. The marked endothermic peak (ΔH_1) and the reduction of weight (TG_1) at 150 ℃ are caused by the decomposition of hydrated products. Crystals of hydrated products are not detected by XRD as shown in Figure 5. Therefore, hydrated products are amorphous phases.

The marked endothermic peak (ΔH_2) and the weight loss of GIC at about 450℃ (TG_2) are caused by the decomposition of polyacrylic acids. These are related to the contents of polyacylic acids.

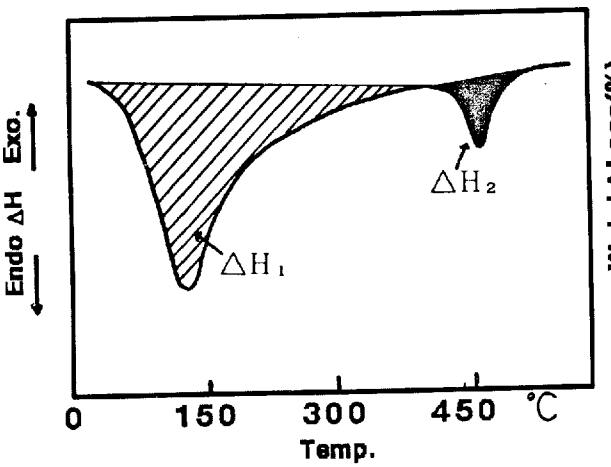

Figure3. DSC curve of hardened GIC

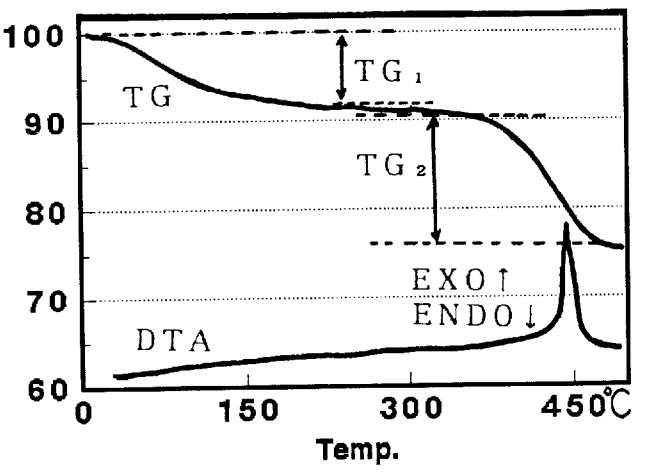

Figure 4. TG and DTA curves of hardened GIC

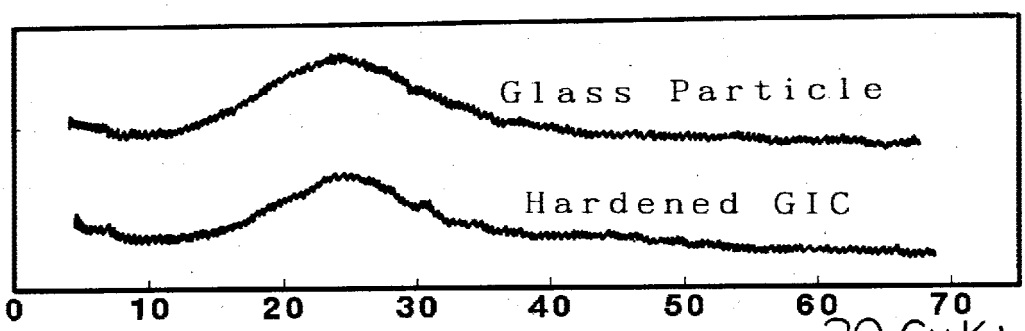

Figure5. XRD patterns of hardened GIC

ΔH_1 and TG_1 are related to the amounts of hydrated products in hardened GIC. Relation between ΔH_1 and the molecular weight of polyacrylic acids is shown in Figure 6. For TG_1 the same results are obtained. ΔH_1 and TG_1 increase with the increase of molecular weight of polyacrylic acids and the decrease in glass/polymer ratio. Therefore, bending strength of GIC is related to the amounts of hydrated products. The bending strength of GIC is increased with the increasing of the amounts of hydrated products. Glass particles were dissolved in polyacrylic acid with low pH. The amounts of hydrated products are associated with the dissolution of glass particles.

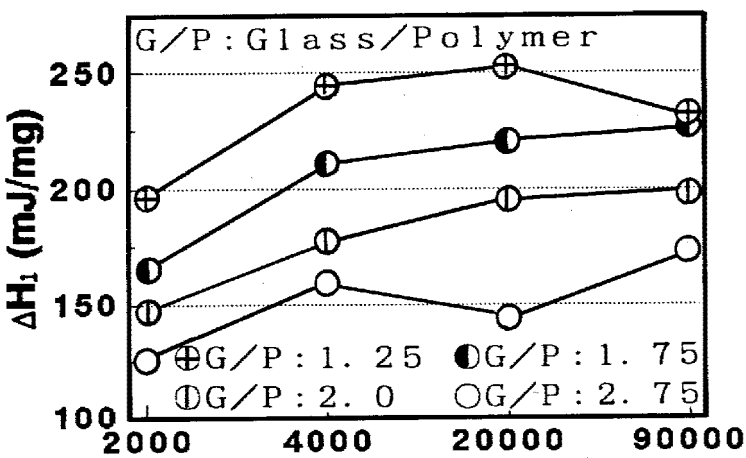

Figure 6. ΔH_1 of hardened GIC

Bridge Formation and Microstructure

Figure 7 shows the FT-IR spectra of hardened GIC and glass particles. In hardened GIC, both peaks of -COOH and $-COO^-$ are observed. Polyacrylic acids contains only the functional group -COOH. Carboxylic ion ($-COO^-$) is produced by the dissociation of -COOH. Carboxylic ion formed the bridge to metal cations from glass particles as follows (4).

$$Me^+ + 2\text{-}COOH \rightarrow -COO^-Me^{2+}{}^-OOC- + 2H^+$$

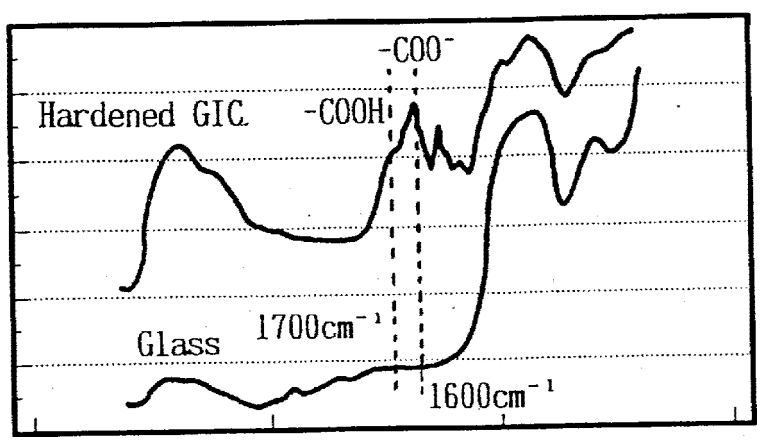

Figure 7. FT-IR spectra of hardened GIC and glass

Figure 8 shows relation between the ratio of $-COO^-/-COOH$ measured by FT- IR and the bending strength of GIC. When same molecular weight of polyacrylic acid is used, the bending strength of GIC is increased with the increase of $-COO^-/-COOH$ ratio. Bridge points between polyacrylic acids and metal ions are increased by the increase of $-COO^-/-COOH$ ratio.

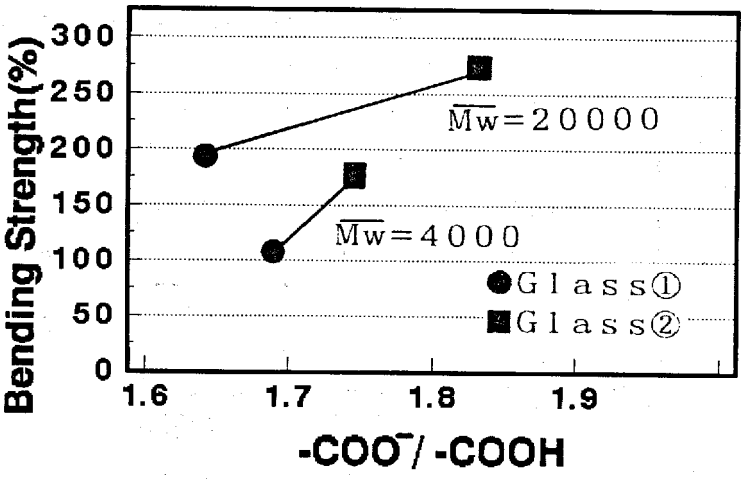

Figure8. Relation between the bending strength of GIC and the ratio of $-COO^-/-COOH$.

Also, the bending strength of GIC with polyacrylic acid having molecular weight of 20000 is larger than that of GIC with polyacrylic acid of molecular weight 4000. Bridge performance of polyacrylic acids is increased by the increase of it'smolecular weight.

Therefore, the strength of GIC is determined by the bridge formation between polyacrylic acids and metal ions, and the amounts of hydrated products containing polyacrylic acids and metal cations.

Microstructure of hardened GIC was observed by Wet-SEM. Unreacted glass particles were surrounded by hydrated products (gel) of reaction between polyacrylic acids and metal ions, dissolved from glass particles as shown in Figure 9.

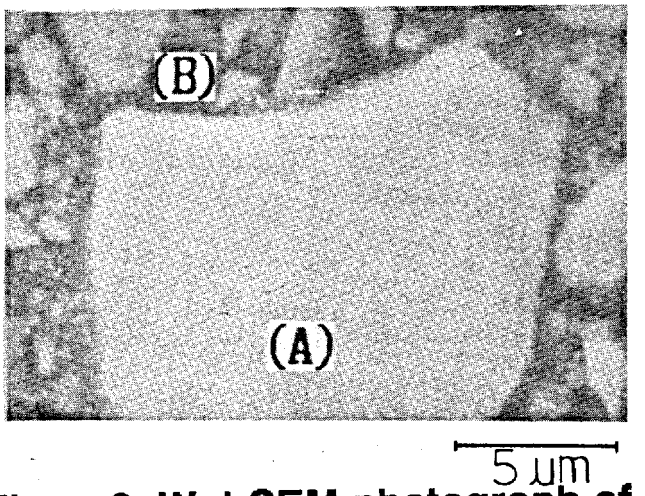

Figure9. Wet-SEM photograph of hardened GIC.

Figure 10 shows the chemical composition of hydrated products and glass particles in hardened GIC measured by Wet-SEM/EDX. The relations among Al/Ca ratio, molecular weight of polyacrylic acids and pH were studied and the results were as follows:

Al and Ca contents are constant in glass particles. When polyacrylic acids with high molecular weight as 90000 is used, the amount of Al in hydrated products is very high compared with glass particles. therefore Ca contents is very low, On the other hand, when polyacrylic acids with low molecular weight are used, Al and Ca contents in hydrated products are increased compared with those of glass particles. These phenomena are related to the pH rather than the molecular weight of polyacrylic acids. pH of polyacrylic acid with molecular weight of 90000 is higher than that of others. By using of polyacrylic acids having low pH(<2), both Ca^{2+} and Al^{3+} ions act as bridge ions, on the other hand, at pH about 3, Ca^{2+} ion mainly act as bridge ion.

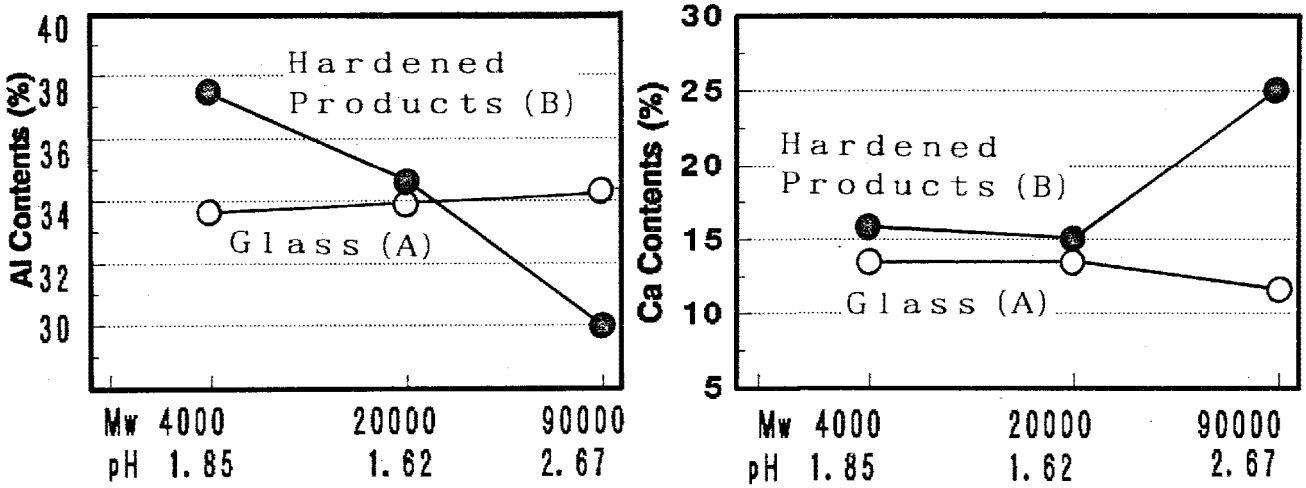

Figure10. Chemical composition of hardened GIC by Wet-SEM/EDX

CONCLUSION

The main conclusions from this investigation are as follows:

(1) Molecular weight of polyacrylic acids and the particle size of glass influence the mechanical propeties of hardened GIC.
(2) Amorphous hydrated products are detected by DSC in hardened GIC. The greater the amounts of hydarted products, the larger becomes the strength of hardened GIC.
(3) In hardened GIC, polyacrylic acids are dissociated as measured by FT-IR. The $-COO^-/-COOH$ ratio is related to the strength of GIC. Bridge between $-COO^-$ of polyacrylic acids and metal ions such as Al^{3+} and Ca^{2+} are formed in hardened GIC.
(4) Mechanical properties of GIC are determined by the amounts of hydrated products formed by bridging of polyacrylic acids and metal ions.

REFERENCES

1. Birchall J.D., Haward A.J. and Kendall K.: "Flexural Strength and Porosity of Cements", Nature, 1981, 289(5796),388 - 389.
2. Wilson A.D. & Kent B.E.: "A New Trablucent Cement for Dentistry" , Brit. Dent. J.,1972,132,133 - 135.
3. McLean J.W. & Wilson A.D.: "Fissure Sealing and Filling with Adhesive Glass-Ionomer Cement", ibid.,1974,136,269 - 276.
4. Chandra S. & Flodin P.: "Interactions of Polymers and Organic Admixtures on Portland Cement Hydration" ,1987,17,875 - 890.

DENSIFYING OF CEMENT PASTES BY CHEMICAL DEPOSITION OF SILICA IN THE PORES

C Atzeni, L Massidda and U Sanna

Dipartimento di Ingegneria Chimica e Materiali
Universitá di Cagliari, Piazza d'Armi, Cagliari
ITALY

SUMMARY

The control of the porosity plays a crucial role in the cement materials technology. Here the possibility is examined to densifying cement pastes prepared with a wide range of water-cement ratios by a impregnating solution of silicic esters. The consequent deposition of silica gel in the pores altered significantly the mechanical and the hygrometric properties.

RÉSUMÉ

Le contrôle de la porosité joue un rôle crucial dans la technologie des matériaux en ciment. Dans ce travail on estime la possibilité rendre plus denses les matériaux en ciment réalisés avec des valeurs différentes du rapport eau/ciment avec l'emploi d'une solution imprégnant d'ester silicique. La déposition de silica gel dans les pores, entraîne des modifications significatives dans les propriétés mécaniques et hygrométriques.

INTRODUCTION

The control of porosity plays a key role in the strive to achieve better quality cement products (enhanced strength and durability), for traditional uses and especially in developing innovative applications (1,2,3,4).

Numerous techniques have been experimented for densifying both the bulk and surface layers: impregnation with monomers (e.g. methylmethacrylate, MMA), which are then polymerized in situ (5,6), the use of reactive fillers such as silica fume and the addition of polymers which allow to work at very low water-cement ratios (7,8), the use of molding techniques such as pressing, rolling and extrusion (3,8).

Nowadays, with the accent on conservation, impregnating solutions of silicic esters have being used for consolidating stone materials, especially the sandstone used for building monuments and scultures. These esters, with the help of a suitable catalyzer, react with the water contained in the pores resulting in elimination of the ethyl and methyl alcohols and deposition of colloidal silica in the pores. The resulting consolidating effect and enhanced durability as regards of weathering and atmospheric pollution are usually considerable (9,10).

Here the possibility is examined of employing the above densifying technique on cement pastes having a variety of water-to-cement ratios and hence porosities.

EXPERIMENTAL

We used a commercial Portland cement (type 425 Italian Standards; ASTM type II) to make up pastes witch water-to-cement ratios (w/c) (by weight) of 0.25, 0.28, 0.31, 0.34, 0.37, 0.40 and 0.43. For the first three with the lowest w/c a naphthalene-sulphonate plasticizing admixture, having a polymer-cement (p/c) ratio of 0.0035 (by weight) was used.

The test specimens (25 mm cubes) were aged for 28 days (7 days under water and 21 days in air). The ones set aside for impregnation were then degassed by keeping them for 5 h at 30°C under 2 10^{-3} mercury pressure. The degassed specimens were then partly submerged in a silicic ester solution (commercial product, 75% ester, specific weight 0.94 g/cm^3) and treated for 15 h (capillary absorption). The specimens were then further aged in a climatic chamber at 25°C and relative humidity of 65% for two months.

Compressive strength tests were then carried out and the capillary absorption of water determined for both the treated and untreated specimens. Porosity was also measured (by forced mercury intrusion up to 200 MPa) and observations made under the scanning electron miscroscope (SEM) to detect alterations in the pore microstructure as a result of treatment with silicic ester.

RESULTS AND DISCUSSION

Table I shows a series of physical influencing parameters in the process of silicic ester solution absorption. As can be clearly seen, the volumic fraction of voids of the pastes is a function of the w/c of the mix. However, under the operating conditions at hand, only some of the voids were reached by the impregnating solution. Changes in (average) specific weight are consequently significant especially at the higher w/c values.

Table I
Physical influencing parameters in the process of silicic ester solution absorption(X_V volume fraction of voids, X_{Vi} volume fraction impregnated, ΔP weight gain in impregnation, ρ_{ut} specific weight untreated samples, ρ_t specific weight treated samples).

w/c	X_V (%)	X_{Vi} (%)	ΔP %	ρ_{ut} (g/cm^3)	ρ_t (g/cm^3)
0.25	11.1	4.0	1.8	2.16	2.16
0.28	13.2	7.3	3.2	2.15	2.16
0.31	15.0	8.3	3.8	2.07	2.08
0.34	18.6	12.9	6.1	2.00	2.01
0.37	26.5	14.2	6.9	1.94	1.96
0.40	30.9	18.4	9.0	1.90	1.95
0.43	36.7	21.6	11.0	1.85	1.89

The process of silica gel formation can be schematized in the following stages:

- evaporation of the solvent;
- formation of silicic acid:
  $Si(O\text{-}Et)_4 + 4\,H_2O \rightarrow 4\,Et\text{-}OH + H_4SiO_4$
- conversion of silicic acid into silica gel:
  $H_4SiO_4 \rightarrow SiO_2 + 2\,H_2O$

Figure 1 shows compressive strength of the treated and untreated specimens versus w/c ratio. As can be seen, the treated material displays superior mechanical properties and in particular strength gain is proportional to the fraction of initial voids (see Figure 2). The greatest improvement in strength was observed for the specimen with w/c of 0.43 while the poorest gain corresponded to w/c 0.25, in keeping with the data on capillary absorption of the ester solution, just a few percent.

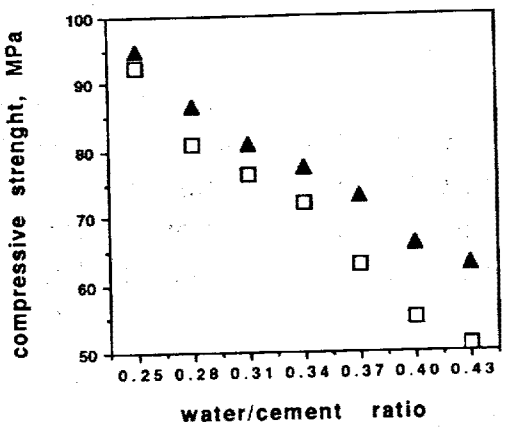

Fig.1 Compressive strength of untreated□and treated specimens ▲.

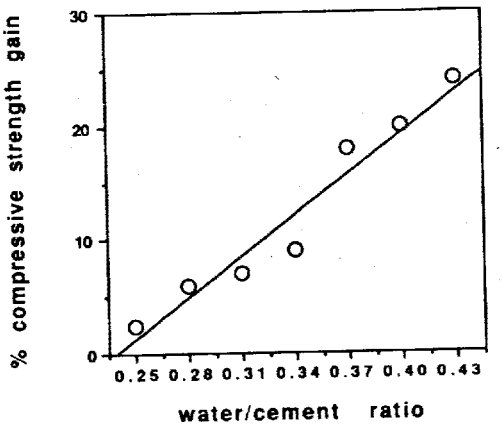

Fig.2 Compressive strength gain percent vs water-cement ratio.

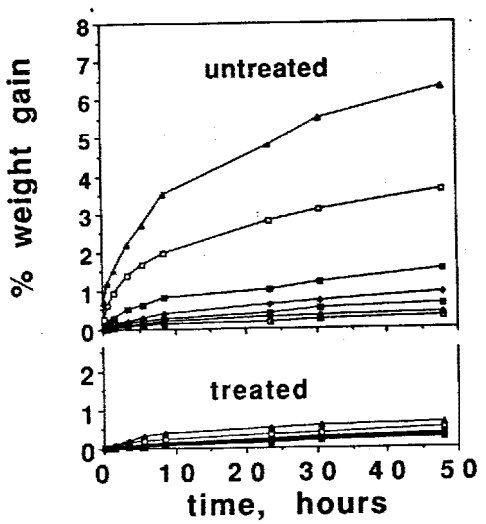

Fig.3 Capillary absorption of water in untreated and treated specimens.

w/c = 0,25 0,28 0,31 0,34 0,37 0,40 0,43

The treatment is especially efficacious in reducing capillary absortion of water, as the data given in Figure 3 show. For instance, after 4O hours the specimen with w/c ratio of 0.43 had absorbed only 14% of the water absorbed by the untreated spccimen, equivalent to the amount absorbed by the systems realized at low w/c (e.g. w/c = 0.31).

The different effect on mechanical properties and on the reduction of capillary absorption of water is associated primarily to the fact that strength depends on both bulk and surface properties while water absorption depends chiefly on surface properties.

Figure 4 shows the porosity of the untreated materials and the impregnated ones after transformation of the ester into silica gel. As can be seen there is a drastic reduction in porosity at w/c = 0.43. However, a marked difference also exists

between the samples taken near to the surface and those extracted from the core of the specimen, a clear indication that impregnation is not uniform and is more efficacious in the uppermost layers. The same considerations hold for all the specimens, bearing in mind that the differences tend to attenuate with decreasing w/c ratio and hence lower permeability of the specimens to the impregnating solution.

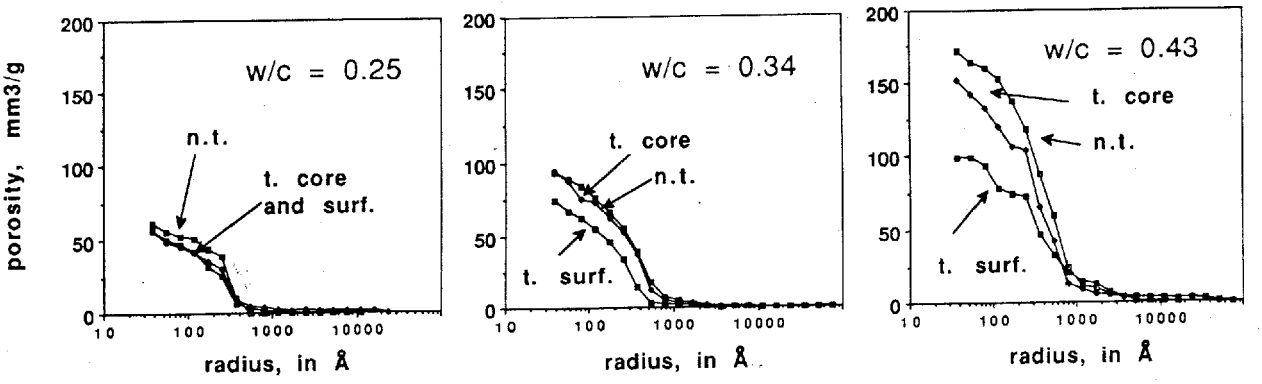

Fig.4 Porosity of the systems prepared at w/c 0.25, 0.34 and 0.43.

The core of the specimen with w/c = 0.43 has the same porosity as the untreated specimen with w/c = 0.34. In turn the core of the latter was observed to have the same total porosity as the untreated specimen having w/c = 0.25.

The above findings were borne out by the SEM observations of the microstructure which revealed considerable differences between the newly formed phases in the surface layers (compact and numerous, Figure 5a) and those in the core of the specimen (filiform and sparse, Figure 5b).

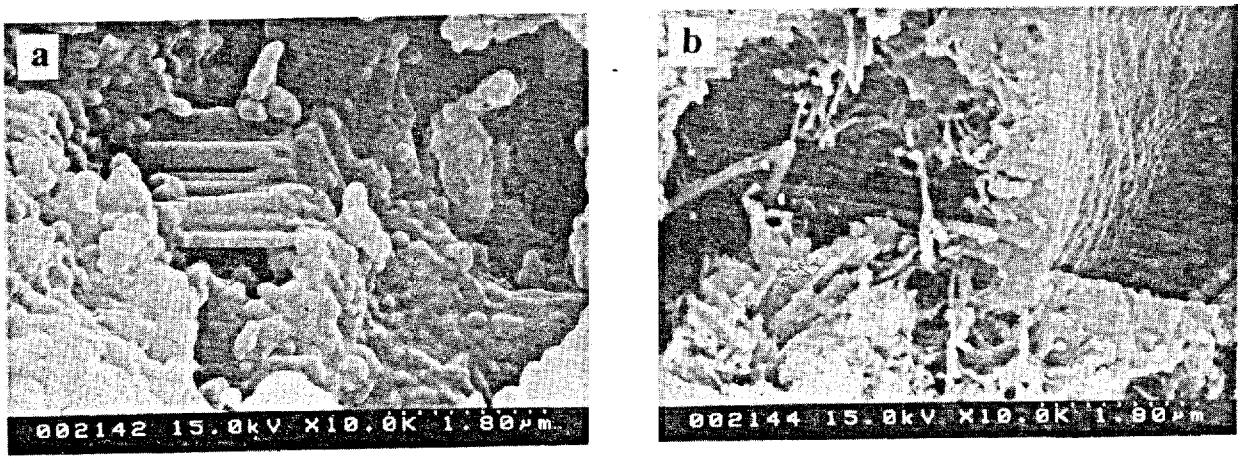

Fig.5 SEM's views of the microstructure after the treatment; a- near surface; b- core.

CONCLUSIONS

The penetration of the silicic ester solution used is dependent upon the material's initial porosity and is negligible for the pastes having lowest w/c ratio (0.25 and 0.28). The difficulties of impregnation are also highlighted by the fact that in the more porous systems (at w/c = 0.43, increase in average weight of over 10%) the amount of newly formed silica was observed to be larger at the surface than at the core of the specimens (a little more than 10 mm apart).

Where the ester was able to penetrate silica gel was deposited in the pores.

This brought about a significant alteration in the microstructure of the material's pores, resulting in superior compressive strength (increase of about 25% in the most favourable case), but above all in a drastic reduction on the ability to absorb water through the capillaries, a factor of major importance for the durability of the cement products.

REFERENCES

1. Sheppard L.M. "Cement renovations improve concrete durability", Ceramic Bulletin, vol.70, n.3, 1991, pp 370-392.
2. Shah S.P., Young J.F. "Current research at the NSF Science and Technology Center for Advanced Cement-Based Materials", Ceramic Bulletin, vol.69, n.8, 1990, pp 1319-1331.
3. Maso J.P. (editor) "**Pore Structure and Construction Materials Properties**", Chapman and Hall, London, 1987.
4. Kendall K., Howard A.J., Birchal J.D. "The relation between porosity, microstructure and strength, and the approach to advanced cement based materials", Phil. Trans. R. Soc. London, A310, 1983, pp 139-153.
5. Dikeou J.T., Kukacka L.E., Backstrom J.E., Steimberg M., "Polymerization makes tougher concrete", American Concrete Institute Journal, october 1969, pp 829-839.
6. Auskern A., Horn W. "Some properties of Polymer-impregnated cements and concretes", Journal of the American Ceramic Society, june 1971, vol.54, n.6, pp 282-285.
7. Metha P.K. "Pozzolanic and cementitious by-products in concrete", Proceedings **Third International Conference on Fly Ash, Silica Fume, Slag and Natural Pozzolans in Concrete**, Trondheim 1987, vol.1, pp 1-43.
8. Double D.D. "Chemically bonded ceramics: taking heat out of making ceramics", Journal of Materials Education, vol.12, 1990, pp 353-381.
9. Littlewood B., Robinson M. "An evaluation of British stone consolidation treatment", Construction Maintenance and Repair, july/august 1990, pp 209-211.

LITHIUM SALTS AS SET ACCELERATORS FOR HIGH ALUMINA CEMENT

T Matusinović and N Vrbos

Department of Chemical Engineering and Technology
University of Zagreb
Zagreb, CROATIA

SUMMARY

The research has been carried out to develop rapid setting and hardening cement materials for repair of concrete. The high alumina cement (HAC) has been used. The effect of alkali metal salts on the setting time has been studied. The influence of concentration of the salts, chemical nature of the anions and the type of the alkali metal cation have all been investigated. The results of the research indicate that lithium salts are very effective accelerators of HAC. By increasing the concentration of the salts, the setting time decreases. The lithium cation has more effect on the setting time than other alkali cations because of its ability to form tetrahedral symmetry while the others will form the octahedral type. The effect of hydroxyl group is greater than the effect of other investigated anions due to the replacement of water molecules by hydroxyl ion in the aluminium environment leading to further centres for oxobridge formation. The measurements of flexural and compressive strength of HAC with lithium nitrate have been made. Lithium nitrate causes decreasing of flexureal and compressive strength of HAC mortars but also causes the strength development at early ages.

ZUSAMMENFASSUNG

Forschungen wurden durchgeführt zwecks Entwicklung von frühhochfesten Zementstoffen schneller Abbindung für Betonreparaturen. Der Tonerdezement wurde benutzt. Es wurde der Einfluss von Alkalimetalsalzen auf die Erstarrungszeit erforscht. Der Einfluss der Salzkonzentration, die chemische Natur der Anionen und der Typ des Alkalimetalkations wurden analysiert. Die Forschungsresultate weisen auf, dass die Lithiumsalze sehr leistungsfähige Akzeleratoren der frühhochfesten Zementstoffe sind. Durch Ernöhung der Salzkonzentration steigt die Erstarrungszeit ab. Das Lithiumkation beeinflusst die Erstarrungszeit mehr als die anderen Alkalikationen, wegen seiner Fähigkeit die Tetrahedrale Symmetrie zu bilden; die anderen Alkalikationen formen octahedrale Typen. Die Wirkung der hydroxylen Gruppe ist grösser als diejenige der anderen erforschten Anionen wegen der Versetzung von Wassermolekülen durch den Hydroxylion in der Aluminium-Umgebung; dies führt zur weiteren Zentren für die Oxobridge-Bildung. Die Messungen der Biegezug- und Druckfestigkeit der frühhochfesten Zementstoffe mit Lithiumnitraten wurden durchgeführt. Das Lithiumnitrat verursacht die Herabsetzung der Biegezug- und Druckfestigkeit des frühhochfesten Mörtels aber auch die Entwicklung von Festigkeit im frühen Alter.

INTRODUCTION

Lithium salts have been reported as set accelerators of HAC pastes, mortars and concretes in patent literature (1-3). S. A. Rodger and D. D. Double studied the effects of lithium salts on HAC by using different physicochemical methods (4). B. R. Currell et al. studied the chemistry of hidration of HAC in the presence of accelerating admixtures (5). Novinson et al. investigated the effect of lithium salts on refractory mortars (6, 7). Although the setting of HAC pastes, mortars and concretes represents a process of fundamental commercial and industrial importance, the chemical processes involved during the hydration are not well understood. The research presented in this paper is an attempt to obtain a better insight into these processes. The practical importance of this research is that the lithium admixtures can be designed for controlled setting reactions.

EXPERIMENTAL

The high alumina cement used was taken from a normal production of "Giulio Revelante", Pula, Croatia. The general analysis of such cement was: CaO, 40.2%, Al_2O_3, 39.0%, Fe_2O_3, 11.7%, FeO, 4.3%, SiO_2, 1.90%. The major clinker phase was monocalcium aluminate with minor phases including $C_{12}A_7$, C_4AF and C_2S. The admixtures used were commercial Analar grade reagents dissolved in demineralized water prior to mixing with HAC. The setting time of HAC in dependence of the pH of lithium salts in mixing water has been measured. The pH of each solution was measured with a standard glass electrode. The electrode was calibrated with buffer solution at 25°C at pH 4 and 9.

The setting time was determined using a modification of the JUS method B.C8.023 (Yugoslav Standard). In our modification the penetration of the needle into hardening paste was measured every 5 seconds due to extremely rapid setting time for lithium salt modified. All experiments used a water/cement (w/c) ratio of 0.24. The salt solution was poured into the bowl and the HAC were added to the solutions. The admixture was mixed together by means of mechanic stirrer for prescribed time intervals. The experiments were repeated three times to obtain reliable standard deviations and statistical means.

For the determination of flexural and compressive strength the specimens (40 x 40 x 160 mm) were prepared acoording to JUS B.C8.022 at w/c ratio of 0.5. The specimens were removed from the mold and kept in a moist room (20°C and 100 percent relative humidity) until the break. Three specimens were tested for each age.

RESULTS

The measurement of the influence of different mass fraction, (w), of lithium nitrate on the setting time of HAC has been done to choose the concentration of the salt which can give setting time convenient for the research. The results of the measurement are shown in Table 1.

The different lithium salts have been tested and the results are shown in the Table 2.

The research of the influence of alkali metal nitrates on the setting time has been made. The results of the research are shown in Table 3.

Table 1 - Lithium nitrate: Comparison of setting times at different mass fractions

Lithium salt	w ($LiNO_3$)/%	Setting time/s
$LiNO_3$	0	16 500
	0.0005	7 330
	0.001	1 650
	0.005	710
	0.01	440
	0.05	F
	0.1	M

F - setting of HAC with lithium nitrate during the mixing time
M - setting of HAC immediately by adding of the lithium nitrate

Table 2 - Lithium salts: Comparison of setting times and pH of 0.01% lithium salts in mixing water

Lithium salt	pH values	Setting time/s
LiOH	12.3	300
Li_2S	11.8	325
Li_2CO_3	11.2	370
$LiBO_2$	10.4	390
Li_2SO_4	6.4	560
$LiNO_3$	5.9	440
LiCl	5.6	360
LiBr	5.4	305

Table 3 - Alkali metal nitrates: Comparison of setting times at 0.01% mass fraction

Alkali metal salt	Setting time/s
$LiNO_3$	440
$NaNO_3$	6 480
KNO_3	7 920
$RbNO_3$	9 360
$CsNO_3$	11 480

The results of the measurement on the compressive and flexural strengths are shown in Table 4.

Table 4 - Compressive and flexural strengths of HAC mortars and HAC mortars made with 0.01% lithium nitrate

Time	Compressive strength/MPa		Flexural strength/MPa	
	HAC	HAC + $LiNO_3$	HAC	HAC + $LiNO_3$
1 hour	x	4.27	x	x
3 hours	x	27.58	x	4.44
1 day	58.70	49.18	8.62	7.32
3 days	67.97	61.87	8.95	7.92
7 days	84.50	70.10	11.10	8.99
28 days	92.60	76.25	11.20	9.65
90 days	96.25	82.08	11.36	10.68

x - test could not be performed because specimens were too soft to be removed from the mold

DISCUSSION

The measurement of the influence of different mass fraction of lithium nitrate on the setting time of HAC has been done. The results of measurement indicate that lithium nitrate accelerates the setting time of HAC even at mass fraction of 5×10^{-4}%. With increasing the fraction of $LiNO_3$, the setting time decreases. With the fraction of 5×10^{-2}% setting occurs during the mixing time, but with the fraction of 0.1% the setting of HAC occurs immediately by adding of $LiNO_3$. The principal hydraulic constituent in HAC clinker is $CaAl_2O_4$ (CA) (8). The hydration process of CA is generally believed to occur through initial dissolution, formation of a metastable gel and subsequent precipitation, principally $CaAl_2O_4 \times 10H_2O$ (CAH_{10}), but also $Ca_2Al_2O_5 \times 8H_2O$ (C_2AH_8). The proportions of CAH_{10} and C_2AH_8 depend on the temperature of hydration. The hydrates CAH_{10} and C_2AH_8 which have hexagonal crystal structures, are metastable with respect to conversion to cubic hydrate C_3AH_6, a process accelerated in warm and moist conditions.

After dissociation of CA, the metastable gel formed will acquire stability by condensation of monocoordinated hydroxyl groups linked to aluminium to form oxobridges between two aluminium centres leading to the crystalline CAH_{10}. Solid-state NMR data indicate that aluminium in CA is entirely 4-coordinated but the principal hydration products of CA, CAH_{10}, C_2AH_8, and C_3AH_6 contain 6-coordinated aluminium. The ^{27}Al NMR work shows that the hydration of HAC proceeds *via* conversion of 4- to 6- fold-coordinated aluminium (9). The oxobridge condensed structure will be affected by alkali metal cations forming coordination linkage with the hydroxyl groups. Of the ions studied, Li^+ should behaviour differently from the other alkali cations due to its ability of forming tetrahedral symmetry with hydroxyl groups, while Na^+, K^+, Rb^+, and Cs^+ will form the octahedral symmetry (10). This is proved by our experimental results (Tables 2 and 3), because lithium ions shows a drastic effect while differences between the other cations are not great and exhibit a definitive trend. The setting time of HAC with the same salts of alkali metal decreases in the following order:

$$Cs > Rb > K > Na \gg Li$$

The sequence follows the trend of crystal radii, hydration numbers and enthalpies of hydration (11). The investigated lithium salts can be classified in two groups, alkaline lithium salts, from lithium hydroxide and very weak acids ($K_A \leqslant 10^{-7}$ mol dm^{-3}) and acid lithium salts derived from strong and very strong acids ($K_A \geqslant 10^{-2}$ mol dm^{-3}) (12). The data could be plotted as setting times vs. pH of the mixing solution. Alkaline lithium salts, (hydroxide, carbonate, sulfide and metaborate) have a linear expression with a negative slope and follow the equation

$$t = 10^{-0.059\ pH + 3.2116}$$

where t is the setting time.

The acids salts (bromide, chloride, nitrate, sulphate) follow a linear plot with a positive slope and seem to obey the equation

$$t = 10^{0.2599\ pH + 1.0935}$$

The effect of hydroxyl group is greater than the effect of the other investigated anions due to the replacement of molecules H_2O by hydroxyl groups in the Al environment leading to a further centre for oxobridge formation. The other investigated anions have a lesser effect while they substitute OH groups in the coordination sphere of Al, which leads to the removal of a hydroxyl group necessary in the process of oxolation. Table 4 shows the results of measurement of compressive and flexural strength for HAC and HAC with 0.01% $LiNO_3$. Lithium salt decreases compressive and flexural strength in comparison with the strength of HAC, but the compressive and flexural strength after 28 days is still high. Along with rapid setting, lithium salt causes the strength development at early ages. Compressive and flexural strength of HAC mortar could be measured only after three hours because specimens were too soft to be removed from the mold but HAC with lithium nitrate showed at the same time a significant strength. This is important for practical use of rapid setting and hardening material.

CONCLUSIONS

We conclude that (1) Lithium salts are very effective accelerators of HAC; (2) with increasing the concentration of the lithium salts the setting time decreases; (3) the pH of the lithium salts in the mixing water is not important; (4) the effect of hydroxyl groups is greater than the effect of other investigated anions, due to the replacement of water molecules by hydroxyl groups in the aluminium enviroment leading to further centres for oxobridge formation; (5) the lithium cation has greater effect on the setting time than other alkali cations because of its ability to form tetrahedral symmetry while other cations will form the octahedral symmetry; (6) the lithium salt caused the strength development at early ages; and (7) proper selection of the lithium salt and the concentration can lead to rapid setting and hardening materials without quality deterioration.

REFERENCES

1. U. S. Patent 3,600,203, A. Altera, assigned to Centro Sperimentale Metallurgico Societa per Axioni, Rome, Italy, Sept. 5, 1969., "Fluidizing Molding Material for Manufacturing Cores and Molds and a Method Therefor".

2. German Patent 648.851, R. Salmoni, Berlin, Germany, Aug. 10, 1937. (in Germ.)., "The Procedure for Reducing the Setting Time of Alumina Cement".

3. U. S. Patent 3,826,665, C. Hovasse and P. Allemand, assigned to Rhone-Progil of Decine, France, March 6, 1972., "Setting and Hardening of Aluminous Cement".

4. Rodger, S. A., and Double, D. D., "The Chemistry of Hydration of High Alumina Cement in the Presence of Accelerating and Retarding Admixtures", Cement and Concrete Research, 1984, 14 (1), 73-82.

5. Curell, B. R., Grzeskowiak, R., Midgley, H. G. and Parsonage, J. R., "The Acceleration and Retardation of Set High Alumina Cement by Additives", Cement and Concrete Research, 1987, 17 (3), 420-432.

6. Novinson T. I. and Crahan J., "Lithium Salts as Set Accelerators for Refractory Concretes: Corelation of Chemical Properties with Setting Times" ACI Materials Journal, 1988, 12 (1), 12-16.

7. Luong T., Mayer H., Eckert H., and Novinson T. I., Journal of the American Ceramic Society, 1989, 72 (11), 2136-2141.

8. Mehta, P. K., Concrete Structure, Properties, and Materials, Prentice-Hall, Inc., Engelwood Cliffs, New Jersey, 1986, p 214-218.

9. Müller, D., Rettel, A., Gessner, W. and Scheler, G., "An Application of Solid-State Magic Angle Spinning ^{27}Al NMR to the Study of Cement Hydration", Journal of Magnetic Resonance, 1984, 57, 152-158.

10. Wells, A. F., Structural Inorganic Chemistry, Oxford Press, London, 1962, 549 p.

11. Cotton, F. A. and Wilkinson, G., Advance Inorganic Chemistry: A Comprehensive Text, Interscience Publishers, New York, 1972, p 189-205.

12. Bailar, J. C., Emeleus, H. J., Nyholm, R. and Trotman-Dickenson, A.F. (Eds), Comprehensive Inorganic Chemistry, Volume 1, Pergamon Press, New York, 1973, p 117-138.

SOLID STATE COMPATIBILITY IN THE SYSTEM $CaO-SiO_2-Al_2O_3-CaF_2-CaSO_4$

S Giménez and M T Blanco

Instituto de Ciencias de la construcción "Eduardo Torroja" (C S I C), Madrid, SPAIN

SUMARY

Phase equilibria in CA-C_2S-$CaSO_4$-CaF_2-CaO system have been studied in order to know the mineralizer effect of CaF_2 and $CaSO_4$ on the raw mix of white cement.

The phase compatibilities in the 5 components system were obtained by adding increasing amounts of CaF_2 to CaO-rich compositions of the system CaO - C_2S-$CaSO_4$-CA (already known through the literature). The experiments have been carried out at 1050°C y 1100°C.

The introduction of an additional component into the quaternary tetrahedra, results in the appearance of the 7 quinary compatibilities at 1050°C and 5 quinary compatibilities at 1100°C.

A consequence of increasing the amounts of CaF_2 to the system, is the appearing of stable phases containing CaF_2 ($C_{11}A_7CaF_2$, fluorellestadite) and the disappearing of C_3A. For those compositions richer in CaO in which $CaSO_4/CaF_2<3$, $Al_2O_3/CaF_2<7$ and $SiO_2/CaSO_4>1$ the formation of alite is produced.

RESUMEN

Las fases en equilibrio en el sistema CA-C_2S-$CaSO_4$-CaF_2-CaO han sido estudiado con el fin de conocer el efecto mineralizador de CaF_2 y $CaSO_4$ en mezclas de crudo de cemento blanco.

Las compatibilidades de fases en el sistema de cinco componentes han sido obtenidas por adición de CaF_2 en cantidades crecientes a composiciones ricas en CaO del sistema CA-C_2S-$CaSO_4$-CaO (conocido por la bibliografía). Los experimentos se realizaron a 1050°C y 1100°C.

La introducción de un componente adicional a tetrahedros de compatibilidad, da lugar a la aparición de 7 compatibilidades quinarias a 1050°C y 5 compatibilidades 1100°C.

Como consecuencia de la introducción de cantidades crecientes de CaF_2 al al sistema se produce la aparición de fases estables conteniendo CaF_2 ($C_{11}A_7CaF_2$ y fluorellestadita) desapareciendo C_3A. Para aquellas composiciones ricas en CaO en las cuales $CaSO_4/CaF_2<3$, $Al_2O_3/CaF_2<7$ y $SiO_2/CaSO_4>1$ se produce la formación de alita a 1050°C.

INTRODUCTION

The saving of energy in the cement industry and, specially the saving of thermal energy during the clinkering process, has mainly been approached in two aspects: the improvement of the technological process and the incorporation of compounds other than those usual, in low proportions, which, without altering the final properties or the product, improve the clinkering condition. Compounds meeting these requirements are named mineralizers and/or fluxes. The mineralizing and fluxing properties inherent in the joint addition of the compounds CaF_2 and $CaSO_4.2H_2O$ have already been described in the literature.

Blanco et al. (1), in studies on the formation of low-energy clinker by using sulfocalcium fly ashes and fluorite as additions to grey raw mix, have found that the molten phase appears at a temperature of 1175°C. The maximum clinkering temperature of this raw mixture is 1350°C, due to the fact that the formation of alite is accelerated by the presence of this molten phase.

Tong and Lin (2) do also conclude that the clinkering temperature of a raw mixture containing CaF_2 and $CaSO_4$ can be reduced down to 1300° - 1350°C. Said authors have determined through a fluidity test that the fluidness of the molten phase containing $CaSO_4$ and CaF_2 approximately doubles the value shown by the quaternary eutectic in the system $CaO - SiO_2 - Al_2O_3 - Fe_2O_3$.

In the process of production of white cement, the incorporation of mineralizing and/or fluxing compounds into the raw mixture is essential to obtain a product showing the right properties at a clinkering temperature close to the clinkering temperature of grey cement clinker.

In addition to CaO, C_2S and C_3S, the phases found in white clinker with added $CaSO_4$ and CaF_2 include fluorellestadite $3C_2S.3CaSO_4.CaF_2$, $3CA.CaSO_4$ and $C_{11}A_7CaF_2$ (2,3). The decrease in the temperature of formation of the molten phase is mainly due to the presence of fluorellestadite.

Galioli et al. (5) have determined the compatibilities in the solid state in the system $CaO - SiO_2 - CaSO_4 - CaF_2$ at 1000°C and 1150°C. In this system, the formation of fluorellestadite ($3C_2S.CaSO_4.CaF_2$) is possible. This phase is compatible with C_2S, $2C_2S.CaSO_4$, CaO, $CaSO_4$ and CaF_2, but not with phases such as $3C_3S.CaF_2$ occurring within the ternary $CaO - SiO_2 - CaF_2$.

In the quaternary system $CaO - SiO_2 - CaSO_4 - CaF_2$, the occurrence of the alite phase has not been established at the temperatures below 1250°C (5,6).

The purpose of the present investigation is to study the quinary compatibilities diagram, in a thermodynamic equilibrium, of the $CaO - SiO_2 - Al_2O_3 - CaF_2 - CaSO_4$ system at temperatures of 1050°C and 1100°C.

EXPERIMENTAL

$CaSO_4.2H_2O$, $CaCO_3$, quartz, CaF_2 and Al_2O_3 have been used in the form of pure reagents (AR) as starting products. C_3A, C_2S, $3CA.CaSO_4$ and $2C_2S.CaSO_4$ were previously synthesized in platinum crucible, starting from the initial reagents, at temperature of 1350°C, 1350°C, 1100°C and 1100°C, respectively, until completion of the reaction. The purity of the phases was checked by XR. CaO and $CaSO_4$ were obtained from the calcination of $CaCO_3$ and $CaSO_4.2H_2O$ at 1000°C and 800°C, respectively.

The study of compatibilities within the quinary system $CaO - SiO_2 - Al_2O_3 - CaF_2 - CaSO_4$ was carried out at 1050°C and 1100°C by addition of CaF_2 at compositions located in the compatibility tetrahedra of the system $CaO - SiO_2 - Al_2O_3 - CaSO_4$ existing in the zone rich in CaO. The tetrahedra chosen are as follows:

1) $CaO - C_3A - 2C_2S.CaSO_4 - CaSO_4$
2) $CaO - C_3A - 2C_2S.CaSO_4 - 3CA.CaSO_4$
3) $CaO - 3CA.CaSO_4 - CaSO_4 - 2C_2S.CaSO_4$

These tetrahedra 1, 2 and 3 were prepared from previously synthesized compounds in proportions of approximately 25% wt. To those homogenized mixtures, CaF_2 was added in proportions of up to 5% wt and were maintained at a controlled temperature during

different periods of time. The phases present were determined by XR and IR methods.

RESULTS AND DISCUSSION

According to the papers of Glasser et al. (4), the compatibility tetrahedra at temperatures comprised between 950°C and 1150°C, in the zone rich in CaO of the CaO - SiO_2 - Al_2O_3 - $CaSO_4$ system are:

1.- CaO - C_3A - $2C_2S.CaSO_4$ - C_2S
2.- CaO - C_3A - $2C_2S.CaSO_4$ - $3CA.CaSO_4$
3.- CaO - $CaSO_4$ - $2C_2S.CaSO_4$ - $3CA.CaSO_4$
4.- C_3A - $3CA.CaSO_4$ - C_2S - $C_{12}A_7$
5.- $3CA.CaSO_4$ - $C_{12}A_7$ - C_2S - CA

The compound $2C_2S.CaSO_4$, present in tetrahedra 1,2 and 3, decompose by effect of temperature into C_2S and $CaSO_4$. The decomposition temperature of $2C_2S.CaSO_4$, indicated by various authors, varies from 1298°C (7) in a closed atmosphere, to 1195°C (8) in the air, to 1200° (9) in the presence of C_3A.

In the quaternary system CaO - SiO_2 - Al_2O_3 - $CaSO_4$, at temperatures above the decomposition temperature of $2C_2S.CaSO_4$, the solid state compatibility tetrahedra which exist are as follows: CaO - C_3A - $3CA.CaSO_4$ - C_2S and CaO - $CaSO_4$ - C_2S - $3CA.CaSO_4$

The addition of CaF_2 to compositions located within the compatibility tetrahedra 1,2 and 3 diminishes the decomposition temperature of $2C_2S.CaSO_4$ down to 1100°C.

Compatibilities within the quinary system CaO-SiO_2-Al_2O_3-CaF_2-$CaSO_4$ at 1050°C

The figure (1) shows the compatibilities found at 1050°C.

The introduction of an additional component into the quaternary tetrahedra of the CaO - SiO_2 - Al_2O_3 - $CaSO_4$ system results in the appearance of the following quinary compatibilities along the range of the compositions studied:

A.- CaO - C_3A - $C_{11}A_7CaF_2$ - $2C_2S.CaSO_4$ - C_2S
B.- CaO - C_3A - $C_{11}A_7CaF_2$ - $2C_2S.CaSO_4$ - $3CA.CaSO_4$
C.- CaO - $C_{11}A_7CaF_2$ - $2C_2S.CaSO_4$ - C_2S - $3C_2S.3CaSO_4.CaF_2$
D.- CaO - $C_{11}A_7CaF_2$ - $2C_2S.CaSO_4$ - $3CA.CaSO_4$ - $3C_2S.3CaSO_4.CaF_2$
E.- CaO - $3CA.CaSO_4$ - $2C_2S.CaSO_4$ - $CaSO_4$ - $3C_2S.3CaSO_4.CaF_2$
F.- CaO - $C_{11}A_7CaF_2$ - $3C_2S.3CaSO_4.CaF_2$ - C_3S_{ss} - C_2S
G.- CaO - $CaSO_4$ - $3CA.CaSO_4$ - CaF_2 - $3C_2S.3CaSO4CaF_2$

Upon addition of CaF_2 to compositions located within the quaternary compatibility tetrahedron 1) CaO - C_3A - $2C_2S.CaSO_4$ - C_2S of CaO - Al_2O_3 - SiO_2 - $CaSO_4$ system, an initial formation of $C_{11}A_7CaF_2$ starts by the reaction of CaF_2 with C_3A according to reaction:

$$7C_3A + CaF_2 \longrightarrow 10CaO + C_{11}A_7CaF_2 \quad (1)$$

resulting in the quinary compatibility volume A.

When the addition of CaF_2 to these compositions is the required to transform the whole C_3A into $C_{11}A_7CaF_2$, the composition is found in compatibility tetrahedron 12. The addition of CaF_2 to compositions of tetrahedron 12 results in the formation of $3C_2S.3CaSO_4.CaF_2$ (fluorellestadite) by reaction of $2C_2S.CaSO_4$ with CaF_2:

$$3(2C_2S.CaSO_4) + CaF_2 \longrightarrow 3C_2S.3CaSO_4.CaF_2 + 3C_2S \quad (2)$$

These compositions are located within the quinary volume C.

In the tetrahedro 21 are located the composition of quinary compatibility volume C which contain the CaF_2 required to react with the whole $2C_2S.CaSO_4$ according to reaction (2). Further addition of CaF_2 to compositions located in this compatibility tetrahedron results in the formation of C_3Sss and the composition will place itself in quinary compatibility volume F.

The addition of CaF_2 to the quaternary compatibility tetrahedron 2) CaO - C_3A - $2C_2S.CaSO_4$ - $3CA.CaSO_4$ results in the formation of $C_{11}A_7CaF_2$ according to reaction (1), and the composition will be located in quinary compatibility volume B. When the amount of CaF_2 for transformation of C_3A is total, the composition is located within compatibility tetrahedron 11.

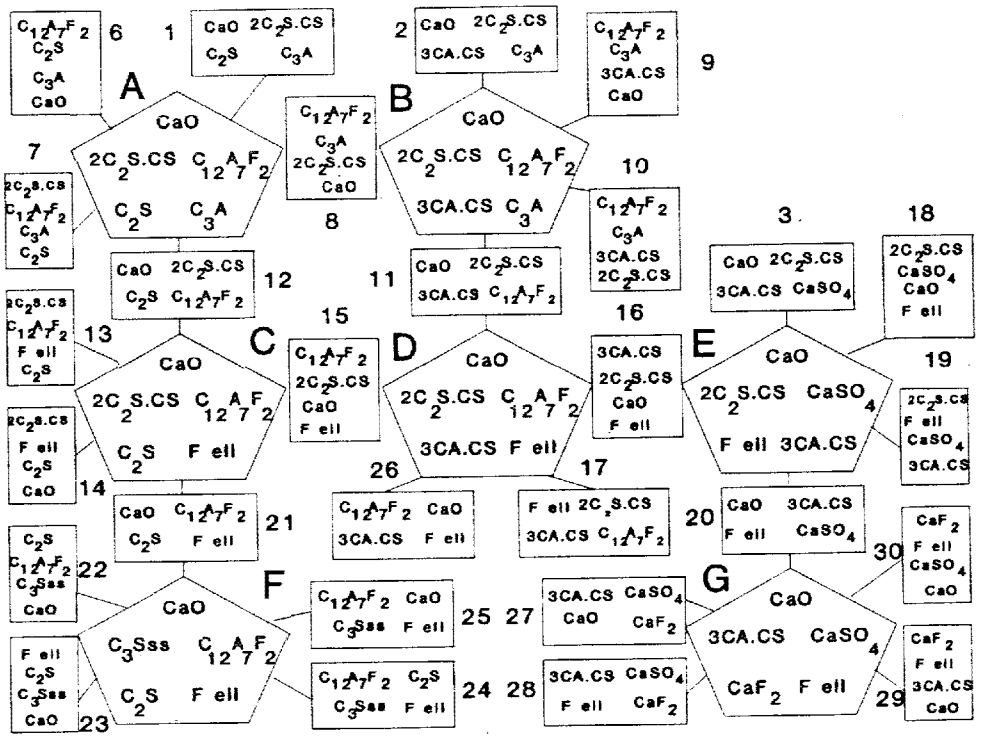

Figure 1.- Solid state quinary compatibilyties al 1050°C in the CaO-SiO2-Al2O3-CaF2-CaSO4 system.

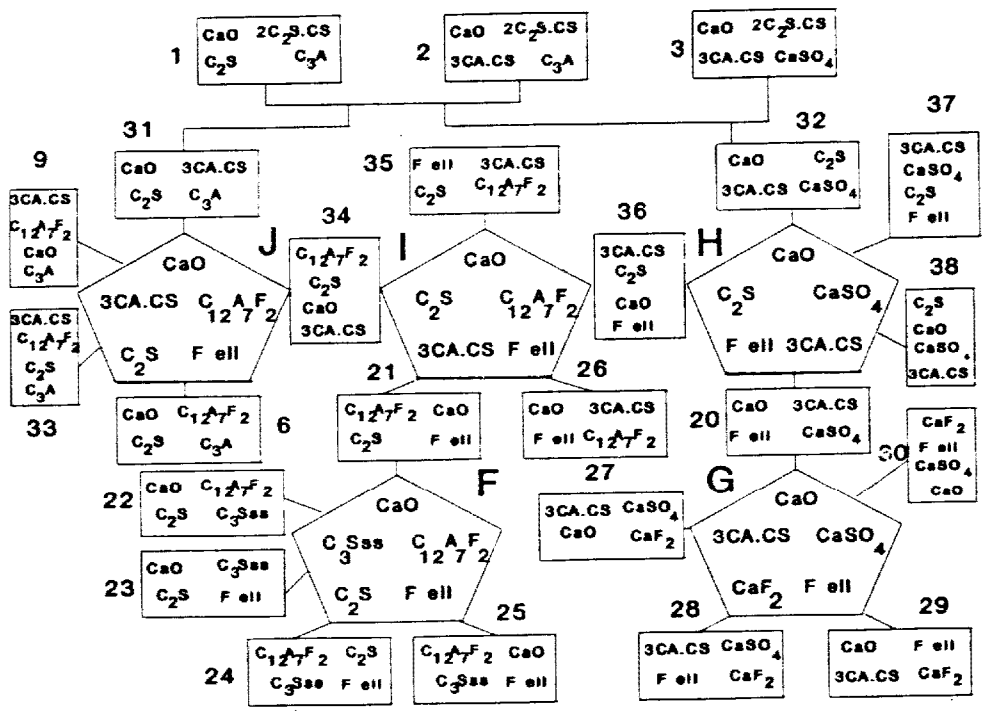

Figure 2.- Solid state quinary compatibilyties al 1100°C in the CaO-SiO2-Al2O3-CaF2-CaSO4 system.

For the compositions proceeding from, compatibility tetrahedron 11, the addition of CaF_2 gives place to the formation of fluorellestadite and $C_{11}A_7CaF_2$, according to the following reaction (reaction 3):

$$36CaO + 21(2C_2S.CaSO_4) + 21(3CA.CaSO_4) + 23CaF_2 \longrightarrow 9(C_{11}A_7CaF_2) + 14Fell$$

These compositions are located in the quinary compatibility volume D.

New increments in the amount of CaF_2 will results in the composition displacing themselves towards compatibility tetrahedra 15 or 26, depending on the proportion of $3CA.CaSO_4$ in the initial composition. The study of the addition of CaF_2 to compositions located in tetrahedron 26 has no interest, since its composition includes no silicate phase.

If the composition is located in tetrahedron 15, a higher proportion of CaF_2 will results in the displacement of the compositions towards quinary compatibility volume C, tetrahedron 14, and quinary compatibility volume F, as remarked before.

On the other hand, adding CaF_2 to the compositions located within the compatibility tetrahedron 3) $CaO - CaSO_4 - 2C_2S.CaSO_4 - 3CA.CaSO_4$; fluorellestadite is formed through reaction

$$3(2C_2S.CaSO_4) + 3CaSO_4 + 2CaF_2 \longrightarrow 2F\ ell \qquad (4)$$

originating the quinary compatibility volume E.

When CaF_2 is added in the amount required to consume the whole initial $2C_2S.CaSO_4$ according to reaction (4), the composition will situate itself in tetrahedron 20. Subsequent additions of CaF_2 will lead into the location of the compositions in quinary compatibility volume G.

In the event that the proportion of $CaSO_4$ in the quinary volume E is not sufficient for the formation of fluorellestadite according to reaction (4), it is possible that the composition shifts according to compatibility tetrahedron 16 and quinary D, as the CaF_2 proportion increases.

Compatibilities in the quinary system $CaO-SiO_2-Al_2O_3-CaF_2-CaSO_4$ at 1100°C

The diagram of compatibilities in the solid state at this temperature is shown in figure 2.

The quinary compatibility volumes identified at 1100°C are:

H.- $CaO - 3CA.CaSO_4 - C_2S - CaSO_4 - 3C_2S.3CaSO_4.CaF_2$

I.- $CaO - 3CA.CaSO_4 - C_2S - 3C_2S.3CaSO_4.CaF_2 - C_{11}A_7CaF_2$

J.- $CaO - 3CA.CaSO_4 - C_{11}A_7CaF_2 - C_3A - C_2S$

F.- $CaO - C_2S - 3C_2S.3CaSO_4.CaF_2 - C_{11}A_7CaF_2 - C_3S$

G.- $CaO - CaSO_4 - 3CA.CaSO_4 - F\ ell - CaF_2$

Starting from the quaternary compatibility tetrahedra of the system $CaO - Al_2O_3 - SiO_2 - CaSO_4$, 1, 2 and 3, the addition of CaF_2 causes the decomposition of $2C_2S.CaSO_4$ into C_2S and $CaSO_4$ at a temperature of 1100°C.

At the same time, phases such as $C_{11}A_7CaF_2$ and F ell do appear producing compatibility volumes H, I and J, since those represented by F and G do not experiment any transformations with temperature, because there is no $2C_2S.CaSO_4$ in their initial composition.

In quaternary compatibility tetrahedra 1 and 2, in those compositions where the ratio $Al_2O_3/CaSO_4>3$, the addition of CaF_2 causes the appearance of $C_{11}A_7CaF_2$ as well as the simultaneous decomposition of $2C_2S.CaSO_4$ according to reaction:

$$2C_2S.CaSO_4 + 10(C_3A) + CaF_2 \longrightarrow C_{11}A_7CaF_2 + 3CA.CaSO_4 + 2(C_2S) + 16CaO \qquad (5)$$

the compositions being located in quinary compatibility volume J. When the reaction of C_3A with CaF_2 is complete, the evolution of the compositions toward another quinary compatibility volume is possible. This only happens in tetrahedron 34. The addition of CaF_2 to compositions located in this tetrahedron results in the appearance of F ell. The reaction is:

$$7(3CA.CaSO_4) + 7C_2S + (16/3)CaF_2 + 4CaO \longrightarrow (7/3)F\ ell + 3C_{11}A_7CaF_2 \qquad (6)$$

These compositions are located in quinary compatibility volume I.

When the amount of CaF_2 is sufficient for reaction (6) being complete, the compositions are located in tetrahedron 21. Additions of CaF_2 to compositions in tetrahedron 21 result in the compositions shifting towards quinary compatibility volume F, with formation of the phases C_3Sss.

As to compositions located in quaternary tetrahedra 1 and 2, with a ratio $Al_2O_3/CaSO_4<3$, and those located in compatibility tetrahedron 3, the reaction produced is the formation of F ell by reaction of CaF_2 with C_2S and $CaSO_4$, simultaneously with the decomposition of $2C_2S.CaSO_4$ (quinary compatibility H).

In the case of compositions located in this quinary volume H, the addition of CaF_2 will results in the displacement of the composition towards tetrahedron 36, if the molar concentration of the total $CaSO_4$ is less than that of C_2S, and towards tetrahedron 20 in the opposite case. The shifting of the compositions upon increasing of the CaF_2 proportion in tetrahedron 36 will be towards quinary volumen I, tetrahedron 21, and quinary compatibility volume F.

The addition of CaF_2 to compositions situated in tetrahedron 20 induces the appearance of the quinary compatibility volume G that, as already mentioned, does no experience any changes with temperature.

In no case has alite been identified at these temperatures, no compositions other than those in quinary volume F.

CONCLUSIONS

The use of mineralizers and fluxes in the cement industry is widely known. It is very difficult to determine the mechanism through which these minor components act, due to the complexity of the phases present. Those minor components are normally encountered in the form of solid solutions, and they often modify the thermodynamic equilibrium phases relation.

In this paper, the solid state compatibilities at 1050°C and 1100°C in the quinary system CaO - Al_2O_3 - SiO_2 - CaF_2 - $CaSO_4$ have been determined in the zone rich in CaO, where the formation of the tricalcium silicate is possible.

The solid state compatibilities show that fluorellestadite and $C_{11}A_7CaF_2$ are the phases which appear upon adding CaF_2 to quaternary compositions CaO - Al_2O_3 - SiO_2 - $CaSO_4$. The quinary compatibility volumes identified are:

A.- CaO - C_3A - $C_{11}A_7CaF_2$ - $2C_2S.CaSO_4$ - C_2S	
B.- CaO - C_3A - $C_{11}A_7CaF_2$ - $2C_2S.CaSO_4$ - $3CA.CaSO_4$	
C.- CaO - $C_{11}A_7CaF_2$ - $2C_2S.CaSO_4$ - C_2S - F ell	1050°C
D.- CaO - $C_{11}A_7CaF_2$ - $2C_2S.CaSO_4$ - $3CA.CaSO_4$ - F ell	
E.- CaO - $3CA.CaSO_4$ - $2C_2S.CaSO_4$ - $CaSO_4$ - F ell	
H.- CaO - $3CA.CaSO_4$ - C_2S - $CaSO_4$ - F ell	
I.- CaO - $3CA.CaSO_4$ - C_2S - F ell - $C_{11}A_7CaF_2$	1100°C
J.- CaO - $3CA.CaSO_4$ - $C_{11}A_7CaF_2$ - C_3A - C_2S	
F.- CaO - $C_{11}A_7CaF_2$ - F ell - C_3S_{ss} - C_2S	1050°C and
G.- CaO - $CaSO_4$ - $3CA.CaSO_4$ - CaF_2 - F ell	1100°C

The initial formation of $C_{11}A_7CaF_2$ is produced by the reaction between C_3A and CaF_2. After the whole C_3A has reacted or into compositions in which it did not previously exist, the addition of CaF_2 results in the appearance of fluorellestadite.

The formation of $2C_2S.CaSO_4$ in this system has been found possible; however, its decomposition temperature is 1100°C, a temperature quite below that indicated in pure state or in the binary systems with C_3A. The solid state decomposition of $2C_2S.CaSO_4$ into $CaSO_4$ and C_2S in compositions in which C_3A is present results in the formation of $3CA.CaSO_4$, a more stable phase with a decomposition temperature of about 1300°C.

At 1050°C, dicalcium silicate is compatible with C_3A, $C_{11}A_7CaF_2$, F ell and CaO. At 1100°C, dicalcium silicate becomes compatible with $3CA.CaSO_4$ and $CaSO_4$ besides $C_{11}A_7CaF_2$ and F ell. The decomposition of $2C_2S.CaSO_4$ does modify the quinary compatibility volumes found at temperatures below 1100°C.

At a temperature of 1050°C, the alite phase has been identified as compatible in solid state in the diagram zone poor in $CaSO_4$ and rich in CaF_2. At that temperature, the alite phase is compatible with $C_{11}A_7CaF_2$, C_2S, CaO and F ell. An increase in the temperature does not change the diagram zone where tricalcium silicate appears.

The formation of alite at temperatures as low as 1050°C is interpreted in the literature as due to the formation of double solid solutions of Al and F (10). In these solid solutions Al replace Si and F atoms to maintain the electron neutrality ($Al^{3+} \longrightarrow Si^{4+}$; $F^- \longrightarrow O^{2-}$). the general formula for these solid solutions is

$Ca_3(Si_{1-x}Al_xO_{5-x}F_x)$, where x can vary from 0 to 0.169. This phase tends to be found in tempered samples, in the rhombohedric polymorphic form of C_3S.

ACKNOWLEDGEMENT

The financial support and encouragement of the M.E.C (project number PB 87-0293) for this work is gratefully acknowledged.

LITERATURE

1.- M.T. Blanco-Varela, T. Vazquez and A. Palomo. Rev. Materiales de construcción No 181 pp.55 (1981).
2.- D. Tong and Z. Lin. 8° Congresso International de quimica do cimento. (1986). Rio de Janeiro (Brazil).
3.- M.T. Blanco-Varela, T. Vazquez and A. Palomo. Cement and Concrete Research, Vol 16 pp. 97-104, 1986.
4.- Y.B. Pliego-Cuervo and F.P. Glasser, Cement and Concrete Research, Vol 9 pp. 51-56, 1979.
5.- C. Gilioli, F. Massazza, M. Pezzuoli. il cemento 2/1972.
6.- S. Giménez, M.T. Blanco, F.P. Glasser, J. Marr. Advanced in cement Research (in press).
7.- W. Gutt, M.A. Smith. Trans. Brit. Ceram. Soc., 66 (11) pp.557-567, 1967.
8.- G.S. Choi and F.P.Glasser. Br. Ceram. Trans. J., Vol.86 pp.13-17, 1987.
9.- F. Hanic, J. Havlica, I. Kapralik, V. Ambruz, L. Galikova, O. Urbanova. Br. Ceram. Trans. J., Vol. 85, pp. 52-57, 1986.
10.- E.G. Shame and F.P. Glasser. Br. Ceram. Trans. J., 86, pp. 13-17, 1987.

GYPSUM-FREE RAPID HARDENING AND MIXED PORTLAND CEMENT

M A Sanitsky and Ch S Sobol

Polytechnical Institute, Lvov, UKRAINE

SUMMARY

This paper presents results of an investigation of early structure-forming processes of portland cement with alkali-bearing compounds additives. The investigation has shown the expediency of using of gypsum-free portland cements in complex with plasticizing-inhibiting components of lignosulphonate type and carbonates, sulphates, alkali metals silicates. Owing to polyfunctional action of said complex chemical additives on the base of gypsum-free portland cements with a fineness of 250 – 400 m^2/kg rapid hardening binders with regulated setting times are produced, they exhibit accelerated strength gain at negative temperatures (up to $-35^{\circ}C$). In addition, the efficiency of mixed binders which contain active mineral additives is substantially increased.

РЕЗЮМЕ

В данной статье представлены результаты исследований процессов раннего структурообразования портландцемента с добавками щелочесодержащих соединений, показавшие целесообразность применения безгипсовых портландцементов в комплексе с пластифицирующе-замедляющими компонентами типа лигносульфонатов и карбонатами, сульфатами, силикатами щелочных металлов. За счет полифункционального действия указанных комплексных химических добавок на основе безгипсовых портландцементов с тонкостью помола 250 – 400 $м^2/кг$ получаются быстротвердеющие вяжущие с регулируемыми сроками схватывания, обладающие ускоренным набором прочности в условиях отрицательных температур (до $-35^{\circ}C$). При этом также существенно повышается эффективность смешанных вяжущих, содержащих активные минеральные добавки.

INTRODUCTION

One of the most radical methods for raising the efficiency of binding system is activation by means of complex chemical additives with polyfunctional effect. It is also possible to make rapid hardening binders based on ordinary portland cement clinkers including binders with accelerated strength gain at frosts as well as mixed multicomponent cements. Plasticizers of technical lignosulphonate type are of considerable practical interest as components of the aforesaid additives. Alkali metal salts are used as a accelerators which improve the rheological properties of a binder due to synergism and promote its hardening rate both at positive and negative temperatures.

Gypsum-free portland cements which represent a finely ground portland cement clinker – set retarder – plasticizer – hardening accelerator – H_2O system are used for enhancing the effectiveness of chemical additives in portland cement compositions. High technical properties as of the rapid hardening and high-strength gypsum-free portland cements developed by S.Brunauer, F.Shkvara, G.S.Royak, L.G.Shpynova et al [1-4] can be attained if the clinker is ground to a fineness of 600-900 m^2/kg. Complex additives having a higher amount of lignosulphonate (i.e. 1.0 – 1.5 mass percent) and lower content of alkali metal carbonate or silicate (0.3 – 1.5 mass percent) are used as a regulator of setting time. When the specific surface is 250 – 400 m^2/kg, however, the binder strength decreases considerably, especially at negative temperatures. Due to the aforesaid effects gypsum-free industrially ground portland cements with complex chemical additives are of practical interest. The said additives incorporate a plasticizing-inhibiting component of a technical lignosulphonate type and alkali metal salts (carbonates, sulphates, etc) which posses regulated setting times and accelerated hardening at both positive and negative temperatures [5].

EXPERIMENTAL

There are, however a number of alkali metal salts, i.e. carbonates, silicates, sulphates, etc, which drastically reduce setting time of portland cement. For this reason, their content is limited to 1 – 2 mass percent. When lignosulphonates in the amounts exceeding 0.3 mass percent are introduced, the kinetics of portland cement hardening considerably slows down.

It has been established that under conditions of high supersaturation of the liquid phase cement paste, at the very beginning of hydration, as a result of exchange reactions of the alkali metal carbonates or silicates and due to the potassium cation tendency to structure-forming with calcium, dihydrate gypsum contained in the portland cement is removed from the early structure-forming processes, as a result of which it is unable to perform its main function as a set retarder of tricalcium aluminate. The crystalline hydrates thus forming, i.e. mirabilite and syngenite, also make for reducing the cement paste thixotropic properties. This makes it necessary to replace gypsum by other retarders when such alkali-bearing additives are introduced.

The processes of early structure-forming in ordinary and gypsum-free portland cements incorporating the said additives are different. As can be seen in Fig.1 the curve at left depicting start of the setting of ordinary portland cement versus the amount of additives indicate a concentration range of K_2CO_3 equal to 1.0 - 2.5 mass percent with non-regulated setting times due to syngenite formation. Gypsum-free portland cement, on the other hand, is free from the above shortcoming (see curves at right) and hence it can be utilized with lower potassium carbonate additives content.

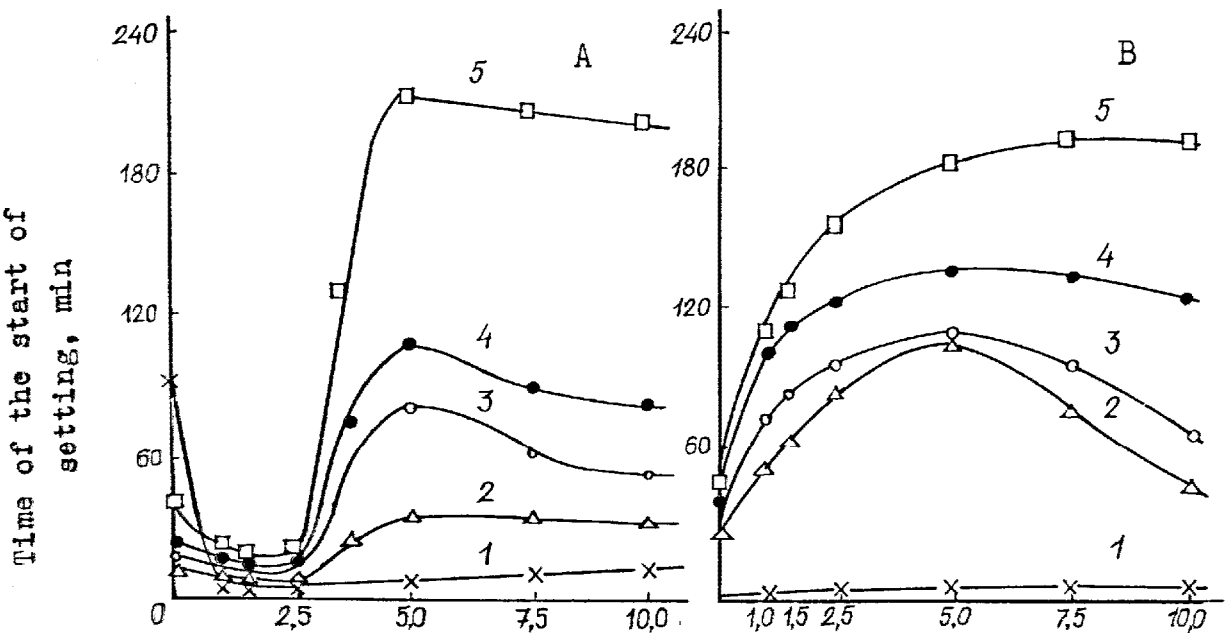

FIG.1 Lignosulphonate* - potassium carbonate additives vs the start of setting of ordinary (A) and gypsum-free (B) portland cements.

(*Lignosulphonate contents 0., 0,3, 0.5, 0.7 and 1 percent cement mass corresponding to curves 1,2,3,4 and 5, respectively)

In the processes of early structure-forming in portland cements incorporating alkali-bearing additives in amounts exceeding 2 mass percent, the liquid phase has a lower concentration of calcium ions as compared to ordinary portland cement. According to X-ray spectral microanalysis data, the alkali metal salt additives are mainly concentrated on the outer hydrates' composition. Therefore, scanning electron microscopy shows formation of more fine crystalline microstructure of the stone, whereas the trimethylsilylation method shows considerable increase in the polymerization rate of silicon-oxygen anions in hydrosilicates. In the process of C_3A hydration with the said additives, crystals of hexagonal AFm-phases are formed which can tightly fit in to each other. So, there is less of cement grains moving apart in the early period of hydration than in the period of ettringite acicular crystals formation. Besides, break-down effects which occur during the transition of the high-sulphate form of calcium hydrosulphoaluminate into the low-sulphate one and which are accompanied by change in crystal habit and density, do not occur with the increase of hardening time. Together, the factors contribute to the forming of a dense, strong but least stressed structure of the cement stone.

DISCUSSION

The mechanism of the setting and hardening processes taking place in gypsum-free portland cement with lignosulphonate and alkali metal salt additives is based on the leading part of a big calcium cation in making structures of new hydrate formations. The structure formation in gypsum-free portland cement binding material can be presented as a complex of successive and parallel processes. The main processes of the early period are: (1) Partial blocking of early C_3S hydration with lignosulphonate molecules, limitation of $Ca^{2+} \rightarrow 2H^+$ protonization and ion exchange; (2) Primary formation of $[Ca_2Al(OH)_6]^+$ peaks which predetermine the AFm-phases formation due to the decrease of Ca^{2+} ion concentration in the cement paste liquid phase; (3) Formation of a protective shell of AFm-phases on C_3A and calcium aluminoferrites surface, followed by their structure stabilization with divalent $[CO_3]^{2-}$, $[SO_4]^{2-}$ anions. The said stabilization reduces adsorption of lignosulphonate molecules from the liquid phase at the early period as well as rejects polarization effects in the cement paste owing to the difference in charge of the silicate and aluminium-bearing hydrating mineral surfaces. As a result of the above processes, cement particles do not agglomerate into coarse clusters even if water require-

ments are reduced, and the cement paste remains plastic. This anti-agglomerating effect manifests itself much better in the case of a complex additive than for its componehts individually.

The directed formation of the cement stone microstructure at the early period of hydration including replacement of the acicular AFm-phases by hexagonal AFm-phases and subsequent stabilization of their structure makes for its compaction and prevents development of break-down effects in the hardened stone which accompany transition of ettringite to a low-sulphate form. As a result, the strength of the stone based on gypsum-free portland cement binding material begins to increase considerably.

The properties of the alkali metal carbonates and sulphates (with plasticizing/inhibiting additives) as highly effective hardening activators manifest full in gypsum-free portland cement in the process of its utilization. The compounds also serve as a setting time regulator for binding material, which makes it possible to obtain quick-hardening and blended portland cements. The properties of these cements can be determined from the type and the amount of plasticizing, inhibiting, alkali-bearing and mineral additives.

Potassium carbonate used as a highly effective hardening accelerator as well as an anti-frost additive (eutectic temperature $-36.5^{\circ}C$) for gypsum-free portland cement allows us to obtain binders with accelerated strength gain at negative temperatures. The expansive stress of these binders is 5 to 10 times lower at early freezing as compared to ordinary portland cement with NaCl, $NaNO_2$, K_2CO_3 additives.

Active mineral additives partially replace clinker in gypsum-free portland cement and interact with alkali compounds thus increasing the rate of alite hydrolysis in the cement stone. In this manner an abundance of hydrosilicates is produced which contributes to the strength due to the formation of more fine crystal structure. It also makes for enhanced durability owing to the fixing of the alkali component of the complex chemical additives.

CONCLUSION

Gysum-free portland cements of industrial fineness (250 - 400 m^2/kg) represent cement system of clinker, active mineral additives and complex chemical additives consisting of plasticizing-inhibiting component of lignosulphonate type and alkali-bearing compounds (carbonates, sulphates,

etc). They allow us to use potential abilities of common portland cements more fully when producing rapid hardening and effective mixed binders. In addition, complex additives, having polyfunctional action, simultaneously regulate setting time of binders and speed up their hardening at negative temperatures (up to $-35^{\circ}C$). Technological control procedures of gypsum-free portland cements binders provide directed action on the processes of their early structure-forming and liquid phase composition. These procedures are determined by choice of the clinker's mineralogical compound, form and amount of chemical and active mineral additives as well as temperature conditions.

REFERENCES

1. ODLER I., SKALNY YA., BRUNAUER S.: "The properties of the clinker - lignosulphate - carbonate system". The 6th International Congress on the chemistry of cement. M., Stroyizdat, 1976. V.2, book 2, 30 - 32.

2. SKVARA F.: "Nove typy bez adrovcovych cementy". Stavivo, 1984, 297-303.

3. ROYK S., PERMINOVA YU., BANDURA V. et al.: "Peculiarities of hydration and hardening processes in the gypsum-free portland cement compositions with low water requirements". Cement, 1981, No.11,6-7.

4. SHPYNOVA L., SANITSKY M., SOBOL CH. et al.: "Peculiarities of cement compositions used at negative temperatures". Cement, 1980, No.9, 11-13.

5. SANITSKY M., SOBOL CH., LOSKUTOV YU., SHEVCHUK G.: "Effective rapid hardening gypsum-free portland cements". Cement, 1989, No.8, 16-17.

RESOURCE-SAVING COLOURED CEMENT-MINERAL COMPOSITIONS

E P Kholoshin and S V Vavrenyuk

Far-Eastern Research Institute for Construction
Vladivostok, RUSSIA

SUMMARY

This paper presents results of investigations concerning the use of high-dispersed cement-mineral compositions as astringent materials in concretes and solutions, as well as in finishing colouring compounds.

The results of investigations showed that the fine-milled mixtures of portland cement and mineral filler modified by chemical additions of supersoftener and organosilicon polymers in the process of grinding improve the physicochemical characteristics of materials on their basis.

АННОТАЦИЯ

В данной работе представлены результаты исследований в направлении использования высокодисперсных цементно-минеральных композиций в качестве вяжущих в бетонах и растворах, а также в отделочных окрасочных составах.

Результаты исследований показали, что тонкомолотые смеси портландцемента и минерального наполнителя, модифицированные химическими добавками суперпластификатора и кремнийорганических полимеров в процессе помола, улучшают физико-механические характеристики материалов на их основе.

INTRODUCTION

Using the industrial waste (ash, tails, rocks, etc.) in the production of the construction materials is a part of the resource-saving technologies and related to the problem of conservation of surroundings.

The most efficient variant of the waste using in cement systems is the joint milling of portland cement and waste by which the mixed astringent materials are produced. The additional milling has for an object to increase the specific surface of cement and filler and, therefore, to raise the chemical activity. It, in turn, allows to control the structurization processes and properties of dispersed structures and, first of all, their physicomechanical characteristics.

Presence of dispersed filler in the portland cement composition leads to improvement of a number of properties of cement stone. A microfiller has significant importance in the creation of the regulated fine-crystalline, fine-capillary structure of cement stone and presents "prepared" substrates at surface of which nuclei of hydrated new formations are arising.

The aim of these investigations is to develop the technology of production and use of cement-mineral compositions (CMC) with prescribed properties due to the joint additional milling of portland cement and filler together with powder polymer admixtures. The investigations include studying the effect of quantity and sort of mineral filler on CMC properties and effect of chemical admixtures on the processes of additional portland cement milling and structurization of cement stone. The area of CMC application as astringent materials in production of footwalk plates, tile, various sorts of concretes and solutions, as well as colouring compounds for finishing of fronts of buildings for various purposes.

EXPERIMENTAL

Investigations have been carried out using high-aluminate cement which has been finished grinding with different mineral fillers (ash-carrying away, waste of porcelain, and brick production, volcanic rocks: pumice, slag, obsidian).

In the process of milling, the powder polymer additions - supersoftener and organosilicon modifier - have been introduced.

Effect of mineral fillers and chemical admixtures on CMC properties have been evaluated through physicomechanical factors and features of cement stone structurization.

RESULTS AND DISCUSSIONS

Mineral fillers used were divided into two groups based on chemical substance determining their activities:

- materials rich in products of roasting of clayish matters (broken porcelain and brick, ash);
- volcanic rocks containing considerable amount of silicates and aluminosilicates in the glassy state (pumice, slag, obsidian).

Investigations have shown that the CMC had the largest strength with ash-filler because the latter was the pozzolanic admixture which is characterized by active binding of calcium hydroxide. The CMC strength with broken brick and porcelain as filler was slightly lower as compared with ash that is explained by presence of considerable content of low-active mullite and cristobalite. It was found that the strength of CMC with the second group fillera do not depend on chemical activity of the latters which is characterized by calcium oxide content relative to the saturation state. The CMC strength in case of volcanic fillers is proportional to the calcium oxide content, the strength decreases correspondingly with the content increase. Investigations showed that the milling fineness is optimum to be 5,000-6,000 cm^2/g.

One of the most important technological stages in CMC development is a modification of dry mixture at its milling stage which provides high quality. Introduction of supersoftener allows to reduce B/T ratio by 20-40 % with simultaneous increase of strength by 40-60 % compared with CMC without admixtures.

Polyphenylsyloxan - organosilicon polymer with phenyl radical C_6H_5- allowing to the most extent to provide the hydrophobicity for dry mixtures, as well as the water-repellent properties for cement stone was used as organosilicon modifier.

Examination of influence of chemical admixtures on the cement grinding processes showed that the polymer complex intensities aprocess of cement powder dispersing and admixtures have additive effect in respect of this process. From viewpoint of the cement stone structurization, it is most advisable to introduce admixtures simultaneously. Thermogravimetric studies confirmed the presence of chemical sorption of organosilicon modifier on the surfaces of portland cement and mineral filler in the course of their grinding.

As a result of additional milling of cement and mineral filler, on the surface of silicate particles, the active centers are forming on which the polymer molecules are chemically inoculated with formation of heterosyloxan structures of SiOMe type. For contact between silicates (cement and filler) and organosilicon modifier, the physical interaction (adsorption) occurs, i.e. polymer intrudes into silicate with creation of bridges simultaneously with chemisorption. Precondition of this interaction is the polymer nature of silicon- oxygen bonds having parameters close to those of the bonds in the crystalline silicate lattice.

An adsorptive polymer layer formed has free ends of hydrocarbon radicals oriented outward and it makes hydrophobic the surface of modified silicates. This property is especially important for CMC having the cement basis because the climatic conditions lead to quick compression and sharp reduction of activity of high-dispersed materials.

On the whole, the technique of mechanosorptive modification of the cement-mineral compositions allows to make the purposeful regulation of activity of mineral materials by introduction of chemical admixtures in the process of their grinding due to successful combination in the proposed method of two conventional kinds of modification - adsorptive and mechanical.

In order to obtain coloured CMC, the pigments are introduced in the course of grinding to be 1-5 % of total dry mass. The introduction of pigments in the course of grinding reduces considerably the expenditure of dyes due to their even distribution over volume. In addition, the water-insoluble pigments introduced in the course of grinding have the property to be wetted when dissolving with water.

If CMC are used as painting compounds, dry milled mix is dissolved with water to the working consistency and applied on the surface by spraying. Painting compounds possess high adhesion to the base and durability.

Using CMC for the production of small products such as footwalk plates, tile etc., as well as various solutions and concretes envisages obtaining the coloured products and materials with high physico-mechanical characteristics.

High physico-mechanical properties of CMC and materials on their basis are due to, first of all, the microstructure of cement stone formed with injection of supersoftener C-3 and organo-silicon modifier complex addition. The addition of C-3 decreases general porousness of cement stone at the expense of cement grout water demand reduction. Organo-silicon modifier, in turn, provides the formation of the fine-porous structure with pore radius r=15-30 um, decreases capillary porousness represented by pores of $r > 200$ A. Cement stone with complex ad mixture has lower integral porousness and higher specific surface than cement-mineral compositions without admixtures.

As to the phase composition of CMC, the above chemical admixtures do not affect the qualitative composition of solid phase. The given type of the admixture complex is characterized by variation of the porous space features. It was found that organo-silicon modifier prevents portlandite ($Ca(OH)_2$) from crystallization into pores and capillaries of cement stone while supersoftener (C-3 type) affects the growth and formation of the stable crystals or calcium hydrosulphoaluminate.

When CMC is used in plastering and painting compounds, the cement content decreases by 50-60 % while the durability of plates increases

due to cement decrease by 30-50 %.

A complex of chemical ad mixtures used is the milling accelerator and in the cement plants it allows to produce the cements of lower marks with a substantial saving of hard-burned brick, especially if mineral powder (ash type) is used.

CONCLUSIONS AND RECOMMENDATIONS

The proposed method of obtaining the cement-mineral compositions, modified in the course of their grinding, allows to purposefully regulate the properties of structurization of cement systems and decrease at the same time the cement expediture.

CMC can be recommended for using as astringent materials in solutions and concretes, as well as durable painting compounds for exterior building finishing.

ACKNOWLEDGEMENTS

This paper is based on the results of planned works of the Far-Eastern Research Institute for Construction, Russian Ministry of Construction.

The authors appreciate the help of their colleagues, V.G. Batrakov and L.P. Crentlikher. The paper is published with the permission of the Institute scientifical and technical council.

REFERENCES

1. Kholoshin, E.P., Vavrenyuk, S.V.: "Modification of Cement-Mineral Compositions by Organo-Silicon polymers", The Collection of Theses of Reports of VII All-Union Conference on Chemistry, Technology of Production and Practical Application of Organo-Silicon Compounds, Moscow, 1990, 364.

2. Kholoshin, E.P., Vavrenyuk, S.V.: "Composite Dry Mixes with Use of Ash". The Collection of Proceedings of XXIII International Conference on Concrete and Reinforced Concrete, Moscow, 1991, 32.

3. "Method of the Dry Finishing Mix Production". Certificate of Authorship No 1471505.

AUTHORS INDEX
(VOLUME III)

A

Agarwal, S — 245
Agarwal, S K — 245
Ahluwalia, S C — 121
Ali, M M — 227, 245
Angelescu, N — 351
Aoki, S — 65
Arai, Y — 65
Asaga, K — 413
Atzeni, C — 419

B

Badanoiu, A — 250
Battagin, A F — 160
Bedo, M — 45
Beretka, J — 195
Bhargava, R — 121, 227
Bian Qinghan — 291
Blanco, M T — 239, 431
Bobadilla, M — 86
Brylicki, W — 312

C

Caijun Shi — 298
Chen Yimin — 201, 262
Chen Zhi Yuan — 305
Chistyakov, V V — 3, 361
Choi, S H — 373, 380
Cioffi, R — 173
Cui Enshu — 58
Curcio, F — 38
Cussino, L — 38

D

Daimon, M — 413
Daugherty, K E — 142, 180
Day, R L — 298
Delchev, N A — 115
Deng Junán — 262
Deng Zhongyan — 268
Dinulescu, M — 45
Dominguez, R — 239
Drabik, M — 386
Dyukova, N F — 256

F

Fan Yueming — 51
Feng Xiuji — 30
Frigione, G — 173
Fu Zicheng — 58
Fukubayashi, Y — 23

G

Galikova, L — 386
Georgescu, M — 216, 250
Ghosh, S N —135, 406
Ghosh, S P — 159, 331
Gimenez, S — 431
Gutul, M — 345

H

Han, K S — 380
Hara, N — 72
Harsh, S — 406
Hill, R — 142
Honma, S — 72
Hu Shuguang — 393
Huang Wenmei — 201
Huang Wenxi — 9, 277

I

Igarashi, H — 16
Ingram, K D — 180
Ivashchenko, S I — 222
Iwanciw, J — 233

J

Jabirov, V H — 154
Jiang, W — 338
Justnes, H — 284

K

Karvinen, R — 149
Kholoshin, E P — 444
Kim, J H — 380
Kim, T H — 373
Konik, Z — 233
Kostic, N — 325
Kristofik, M — 386
Krivoborodov, Yu R — 209, 256
Kouznetsova, T V — 154

L

Lian Huizhen — 128
Liao Xin — 305
Liu Kezhong — 268
Lu Changgao — 319
Luhui Zhong Jinyu — 51

M

Malek, R I A - 400
Malolepszy, J — 312
Martinez, S — 239
Massidda, L — 419
Mathur, V K — 135
Matusinovic, T — 425
Mityushin, V V — 154
Mohan, K — 159, 331
Muntean, M — 45, 345
Myasnikova, Ye A — 3, 361

N

Naidu, Y C — 106
Narang, K C — 187
Nieminen, P — 108, 149
Nikonova, N S — 115, 154
Noma, H — 72
Noworyta, G — 79

O

Ono, K — 413
Osokin, A P — 256

P

Padmanathan, P —159
Park, Y W — 373
Pashchenko, A A — 361
Paul, F — 45
Puertas, F — 239
Puri, A — 250
Pylkkanen, K P K — 108

Q

Qi Yangyoun — 9
Qi Yanyong — 277
Qian Guangren — 9, 277
Qin Zhigang — 58

R

Raina, S J — 245
Rossetti, V A — 38
Runova, R F — 367

S

Sahu, S — 386
Sakai, E — 413
Samchenko, S V — 209
Samrejprasong, S — 72
Sanitsky, M A — 438
Sanna, U — 419
Santoro, L — 195
Sersale, R — 173
Sharma, K M — 121, 187
Sharma, P S — 227
Sharma, R N — 135, 187
Sherman, N — 195
Shi Liping — 201, 262
Skenderovic, B — 325
Sobol, Ch S — 438
Solankey, A K — 135
Stok, A — 233
Stryczek, S — 312
Su Muzhen — 262

T

Talero, R — 93
Tang Jinshu — 268
Tang Mingshu — 291, 298
Tango, C E S — 101
Teoreanu, I — 216, 250, 351

U

Ubilla, M — 86
Uchida, K — 23
Uchiyama, M — 400
Uparisajkul, S — 72
Urrutia, C — 86

V

Vaidergorin, E Y L — 101
Valenti, G L — 195
Vavrenyuk, S V — 444
Vernet, C — 79
Vrbos, N — 425
Vulkov, V V — 115

W

Wu Jianguo — 201
Wu Xuequan — 291, 298

Y

Yadav, D — 121, 187
Yamashita, S — 23
Yang Jiazhi — 51
Yang Nanru — 58, 338
Yang Yurong — 9, 277
Yoshida, K — 16
Yuan Mingdong — 268

Z

Zenone, F — 173
Zhang Guanying — 201
Zhang Peixing — 201
Zhao Fei — 30
Zhong Baiqian — 58

9th International Congress on the Chemistry of Cement New Delhi, India, 1992

VOLUME IV

COMMUNICATION PAPERS — THEME III

NATIONAL COUNCIL FOR CEMENT AND BUILDING MATERIALS
NEW DELHI

9th International Congress on the Chemistry of Cement New Delhi, India, 1992

COMMUNICATION PAPERS

Volume IV

CHEMISTRY OF HYDRATION OF CEMENTS AND CEMENTITIOUS SYSTEMS

Organised by

NATIONAL COUNCIL FOR CEMENT AND BUILDING MATERIALS
NEW DELHI

Co-sponsored by :

Department of Scientific & Industrial Research
Ministry of Science & Technology
Govt. of India

Cement Manufacturers' Association, India

The India Cements Ltd

J K Cement Works

Madras Cements Ltd

Narmada Cement Co Ltd

Orissa Cement Ltd

This volume is a part of six-volume series of the Congress Papers.
Title of each volume is given below :

I—Congress Reports
II—Communication Papers—Theme I
III—Communication Papers—Theme II
IV—Communication Papers—Theme III
V—Communication Papers—Theme IV
VI—Reports on Special Panel Discussions and Poster Papers

Published by :
National Council for Cement and Building Materials (NCB)
M-10 South Extension Part II New Delhi 110 049 INDIA

No Part of this publication be reproduced without the written permission of the Publishers.

The views expressed in the technical papers printed in this publication are those of authors and not necessarily of the Publishers.

Printed in India by Tara Art Press, New Delhi

PREFACE

Commencing with a one-day meeting in London on 14 January 1918 arranged by the Faraday Society, to discuss "The setting of cements and plasters", which is taken as the first Symposium to deal solely with the chemistry of cement, the subsequent International Symposia and Congresses on the Chemistry of Cement have been held in Stockholm (1938), London (1952), Washington DC (1960), Tokyo (1968), Moscow (1974), Paris (1980) and Rio de Jenairo (1986). At the conclusion of the Rio Congress, it was decided that the next Congress will be held in India. Accordingly, the 9th International Congress on the Chemistry of Cement is being held in New Delhi, India, from 23 to 28 November 1992.

The preparatory and organisational work for this 9th Congress was commenced immediately after the 8th Congress. To start with, all the participants in the previous two Congresses and a large number of individuals and organisations interested in the subject of the Congress were contacted through an extensively worked out and widely distributed Questionnaire. The response was most encouraging. The responses were carefully analysed and the directions which would meet the views of the largest number of participants towards advancing the cement sciences were determined. Based on these findings the first Bulletin was issued in August 1988, providing the necessary preliminary information on the Congress and outlining its scope and essential organisational aspects.

The objectives of the Congress were set to advance the knowledge of chemistry of cements with emphasis on application of this knowledge in both the manufacturing aspects and utilization of cements in practice. Within this broad scope, the thrust was on tracking the scientific progress made in the field since the last Congress, assessing the status of exploitation of the results by the industry and the society, and mapping of the new frontiers of knowledge.

The overall organisation of the Congress was governed by a National Organising Committee which was responsible for all organisational aspects including financial arrangements. Taking into account the suggestions received from various quarters, the International Scientific Committee consisting of 67 experts from 39 countries all over the world was formed which was responsible to finalise : (a) the themes and sub-themes of the Congress, (b) procedures for inviting, receiving and reviewing of papers, (c) selection of authors for general and special reports, and (d) the system for conduct of the proceedings of the sessions and other related scientific and technical matters.

The International Scientific Committee held two meetings in New Delhi in November 1989 and in January 1991. In addition, informal meetings were held with representative groups in Seoul, Tokyo, Paris, Washington DC and Montreal. The International Scientific Committee finalised the Generic and Specific Themes of the Congress. It was decided that for each Generic Theme, there shall be one Principal Review Paper, which shall cover the progress achieved in the area of the Generic Theme between the two Congresses. For each Specific Theme, there shall be one Congress Paper highlighting trends of research and realisation of the results in the industry in the areas related to the Specific Theme. Under each Specific Theme, in addition to the invited Congress Papers, there shall also be Communication Papers. Both the principal review papers as well as the Congress papers were to be presented by the invited experts identified after deliberations of the International Scientific Committee.

Preliminary Abstracts of communication papers were solicited through the Second Bulletin in May 1991. 537 Abstracts were received which were scrutinised by a panel of Indian experts and 513 were short-listed. Authors were requested to send full manuscripts of the paper for detailed review and acceptance for publication and presentation. As many as 412 communication papers from 40 countries were received which were reviewed by a panel of international experts. As a result, 346 communication papers belonging to the four themes of the Congress were finally

accepted for presentation and publication. These were in addition to 21 State-of-the-Art Congress Reports received from invited authors; reports on two Specific themes could not be had because the authors selected expressed their inability at a late stage, making replacement difficult.

In addition to the papers on deliberative thematic sessions, a poster session is being organised on "Advances in Physico-Chemical Evaluation, Characterisation and Quality Control Techniques and Systems" for Clinkers, Particulate Cements, Hydrated Systems and Concrete Systems. The State-of-the-Art Report would be presented by an invited expert and 24 contributions made in the form of posters will be presented during the Congress. In addition, Special Panel Discussions are being organised to survey the newer frontiers of knowledge in the areas of computerisation in cement science and concrete systems; resource economy in cement and concrete making; and cement in hazardous waste management.

The proceedings in six Volumes contain all the above contributions received for the Congress. This **Volume IV** contains **Communication Papers on the Generic Theme "Chemistry of Hydration of Cements and Cementitious Systems".**

A novel feature of the 9th Congress will be that, in addition to the normal sessions as in the earlier Congresses, there will be three sessions to bring out the technological and techno-ecnomic impact of the scientific advances on the industry. These are intended to provide a better appreciation of the implications of the scientific advances specially on the process control machinery and related industries as well as on operational aspects related especially to energy conservation and environmental improvement. Texts of these Special Lectures will be published in Volume VII of the Proceedings to be brought out after the Congress, along with the texts of Addresses at the Inaugural and Concluding Sessions and List of nearly 550 delegates from 42 countries who are expected to attend the Congress.

I am grateful to the members of the International Scientific Committee for their whole-hearted co-operation, to those who reviewed the Abstracts, and to the International Panel of Reviewers of Manuscripts for providing very useful technical and editorial comments on the communication papers. The co-operation of the authors in accepting and implementing the reviewers' suggestions and revising their manuscripts accordingly is greatly appreciated. Thanks are also due to those authors whose communication papers could not be accepted essentially because the contributions did not fit in with the themes of the Congress and not because of any technical deficiency. We recommend that the authors have those papers published elsewhere.

The unstinted efforts put in by my colleagues in the National Council for Cement and Building Materials in all aspects of organising this Congress, is thankfully acknowledged.

A K Mullick
Chairman
International Scientific Committee
9th International Congress
on the Chemistry of Cement

New Delhi
14 September 1992

GENERIC THEME III

CHEMISTRY OF HYDRATION OF CEMENTS AND CEMENTITIOUS SYSTEMS

EXPLANATORY NOTES

The following symbols, which have been universally recognised by cement chemists for formulating more complex compounds, are used interchangeably with the respective oxide formulae throughout this volume :

A	:	Al_2O_3	K	:	K_2O
C	:	CaO	M	:	MgO
$\bar{C}$	:	CO_2	N	:	Na_2O
CH	:	$Ca(OH)_2$	P	:	P_2O_5
F	:	Fe_2O_3	S	:	SiO_2
H	:	H_2O	$\bar{S}$	:	SO_3

Commonly used abbreviations of more general nature are as follows :

DTA	—	differential thermal analysis
EPMA	—	electron probe micro analysis
IR	—	infrared
NMR	—	nuclear magnetic resonance
RH	—	relative humidity
w/c	—	water-cement ratio
XRD	—	X-ray diffraction
SEM	—	scanning electron microscope
EDAX	—	energy dispersive analysis of X-rays

CONTENTS

Volume IV

SPECIFIC THEME III-A : Advances in Hydration of Cements at Low, Ambient and Elevated Temperatures

1. Effects of Low Temperature and Freeze-Thaw Cycles on the Stability of Hydration Products 3
   H -M Ludwig and J Stark

2. The Hydration of Class G Oilwell Cement at Low and Ambient Temperatures with Additions of Sodium Aluminate 10
   J S Lota, P L Pratt, K L Scrivener and J Bensted

3. Analysis of the Hydration-Setting Relation : Towards a Comprehensive Approach of the Cement Setting 17
   S P Jiang, J C Mutin and A Nonat

4. The Progress of Portland Cement Hydration : Effect of Clinker Composition 24
   Y Chen and I Odler

5. Determination of Kinetic Parameters in Cement Hydration 31
   R Krstulović and P Krolo

6. Control of the Silicate Hydration Activity with the Knowledge of Charge Transport in Solids taken into Account 38
   L B Svatovskaya, M M Sychev, V Ya Solovyeva, T V Smirnova, N N Shangina, S G Gerke and N I Uman

7. Obtaining High Basicity Clinker and Influence of Complex Additives on its Hydration and Hardening 44
   A Kaminskas and A Mituzas

8. An Investigation into the Hardening of Monostrontium Aluminate 51
   L B Borovkova, T I Borodina, T A Evdokimova, T A Melehina and E P Pakhomov

9. An Investigation into the Hardening of Monobarium Aluminate Cement 57
   L B Borovkova, T I Borodina, T A Melehina and E P Pakhomov

10. Long-term Hardening of Cements with Higher Content of Magnesium Oxide 64
    Yu V Nikiforov and R A Zozulya

11. Hydration of Calciumaluminate and Calciumaluminoferrite Separated from Portland Cement 69
    Anette Müller, Jochen Stark and Silvia Stürmer

12. Hydration of β-C_2S Prepared at 600°C from Hillebrandite : C–S–H with Ca/Si = 1.9 – 2.0 76
    H Ishida, K Sasaki, Y Okada and T Mitsuda

13. Influence of Different Fillers on the Hydration of C_3S 83
    S Husson, B Guilhot and J Pera

14. The Effect of C_3A Polymorphs on Hydration of C_3S 90
G Y Shin and K S Han

15. Hydration Characteristics of Sulphate Solid Solution in the Clinker 97
J S Koo, K S Han, J D Jaung and S H Choi

16. Physical Properties and Early Hydration Reaction of Finely Ground Portland Cements 104
K Yoshida and S Okabayashi

17. The Mechanism of $BaSO_4$ Preventing Calcium Aluminate Hydrates from the Crystalline Transformation 111
Wu Yanrong, Long Shizong and Liao Guanglin

18. The Role of Alkalies in the Hydration of Vitrified Calcium and Magnesium Silicates 118
Jan Malolepszy

19. Hydration Property of Various Cements under Adiabatic Conditions 124
K Kato, Y Fukaya, M Tanaka

20. The Significance of Thermal History for Offshore Grouts 131
A K Crumbie, P L Pratt and H F W Taylor

21. Hydrothermal Stability of Calcium Silicate Hydrates Between 250°C and 400°C 138
N B Milestone, N I Baxter and A R Gainsford

22. Inhibition of Autoclave Reaction of Cement-Quartz Mortars by Prolonged Air Precuring 145
E R Cantrill, M G Stevens and L P Aldridge

23. Thermal Behaviour of Synthesized C–S–H 151
S Ito, T Nishikawa, Y Ito and K Suzuki

24. Thermodynamics and Kinetics in the System $Ca_4(Al_6O_{12})(SO_4) - CaSO_4.2H_2O - H_2O$ up to 75°C 157
Jaromír Havlica and Sadananda Sahu

25. Thermodynamic Approach to Understand the $CaO–Al_2O_3–SO_3$ System 164
J P Bayoux, M Testud and B Espinosa

26. On the Mechanism of Scawtite Formation 170
W Kurdowski and M Pilch

27. Thermokinetics of Cement Hydration under Non-Isothermal Conditions 175
A V Usherov-Marshak and A G Sinyakin

28. Effect of Curing Temperature on the Hydration of Portland Cement Compounds 181
Kiyoshi Asaga, Michio Ishizaki, Shigeru Takahashi, Kazuo Konishi, Takaaki Tsurumi and Masaki Daimon

29. Electrochemical Behaviour of Portland Cement and Gypsum 188
D Menetrier/Sorrentino and F P Sorrentino

30. Relationship Between the Structure and Polycondensation Degree of Silicate Anion of C–S–H Estimated by FT-NMR, GPC and SFC and the Strength of Mortar 195
Hiroshi Uchikawa, Takayoshi Okamura and Minoru Takehiro

31. Observation of the Change of Composition and Surface Structure of Alite Crystal and Estimation of Hydration Reactivity by Etching 202
Hiroshi Uchikawa, Shunsuke Hanehara and Daisuke Sawaki

32. Comparison of Two Methods for Stopping Hydration : Applicaton to the Study of the Initial Dissolution Rate of C_3S 208
C Vernet and G Noworyta

33. A Scaling Approach to the Texture of Hardened Cement Pastes 214
R Maggion, S Bonnamy, P Levitz, D Tinet and H Van Damme

34. Applications of Higher Temperature Conduction Calorimetry to High Alumina Cement Hydration 220
John Bensted, Gary J Audley and Paul N Aukett

35. A Method for Determining the Advancement of the Hydration of C_3S in Diluted Suspensions by Means of Simultaneous Conductimetric and Calorimetric Measurements 227
D Damidot and A Nonat

36. An NMR Investigation of C_3S Hydration in Pastes and in Stirred Diluted Suspensions 234
R Rassem, H Zanni-Théeveneau, C Vernet, D Heidemann, A R Grimmer, P Barret, A Nonat, D Bertrandie and D Damidot

37. X-Ray Microanalysis of Portland Cement Pastes Hydrated at Different Temperatures 241
K O Kjellsen and R J Detwiler

38. A Weighing Method for Cement Hydration 248
P Paulini

SPECIFIC THEME III-B : Structure, Composition and Properties of Cement Hydration Systems

39. Chemistry of Hydration Products Formed in Paste of β-C_2S with $C_{12}A_7$, Aged 16 Years 257
Francisa Hannawayya

40. Intrinsic Bond Properties of Hydrates Formed in the Hydration of Pure Clinker Minerals 265
H Scharf and I Odler

41. Micromineralogical Study of the Influence of Gypsum on the Early Hydration of C_3A Polymorphs 271
Aimin Xu and Shondeep L Sarkar

42. Understanding of the Hydration Mechanisms of $C_4A_3\bar{S}$-Portland Clinker - $CaSO_4$ Mixes 278
L Taczuk, J P Bayoux, F Sorrentino and A Capmas

43. Study on Hydraulic Reactivity and Structural Behaviour of Very Active β-C_2S 285
Yang Nanru, Zhang Hua and Zhong Beiqian

44. Correlation Between the Crystal Structure of Calcium Minerals and their Reactivity with Water 292
M A Sanitsky

45. Structural Changes due to Carbonation in Hardened Cement Pastes 298
I G Richardson, G W Groves, A Brough and C M Dobson

46. Effects of the Carbonation on the Thermal Properties of Tobermorite 304
Seishi Goto and Sadami Ikeda

47. An Investigation on the Optimum Amount of Gypsum Needed for Optimum Strength and for Different Types of Clinker 310
F Milia, Lj Miljkovic, G Papavassiliou, E Chaniotakis and D Frangoulis

48. Hydration and Performance of Cements with Various Amounts and Forms of Added Sulfate 317
F J Tang and S W Tresouthick

49. Structure Formation in the Hardening Stone of Multi Component Cements 324
Z B Entin, Yu R Krivoborodov and V I Shubin

50. State of Formed Mineral Phases and Properties of Binding Systems 331
L G Sudakas

51. Relationship Between Strength and Porosity of Fly Ash Cement Pastes 337
L P Xu and S Y Huang

52. Ettringite from Portland Cement Origin and Ettringite from Pozzolan Origin : Analogies, Differences and Semiquantitative Relations with their Respective Origins : Interrogations 343
R Talero

53. The Composition and Structure of C-S-H Gels in Cement Pastes Containing Blast-Furnace Slags 350
I G Richardson and G W Groves

54. Mechanism and Hydration Kinetics of the Electrothermo-phosphoric Slag as a Component of Mixed Cements 357
N S Nikonova, V V Mityushin, I N Tikhomirova and N M Ketayva

55. Incorporation of SO_4^{2-}, CO_3^{2-} and OH^- in Hydration Products of Tricalciumaluminate 363
H Poellmann

56. Investigations on Pore Structure of Quick Cement 370
D Knöfel and J Wang

57. Fe_2O_3 Solid Solution of Ettringite 377
Yaozhong Xi

58. Effect of ZnO on the Hydration Behaviour of $C_{11}A_7CaF_2$ 384
Qian Guangren, Huang Wenxi, Yang Yurong and Qi Yanyong

59. The Structure and Properties of Hydration of Doped Dicalcium Silicates 391
Yang Shuzhen and Song Hantang

60. Microstructural Studies of Pure and Iron Doped Unhydrated and Hydrated Dicalcium Silicate Phase 397
Ram Prakash, S C Ahluwalia and J M Sharma

61. Influence of Gypsum Morphology on the Structure and Property of Steam Curing Paste Matrix 404
Zongshou Lin and Shunni Liu

62. Investigation on the Hydration of Sr- and Ba- bearing Sulphoaluminate 411
P Yan

63. Investigation on the Structure and Hydration of New Mineral Phase $3SrO.3Al_2O_3.CaSO_4$ 418
Long Shizong, Wu Yanrong and Liao Guanglin

64. Cement-Inorganic Polymer Composites, Microstructure and Strength Development 424
Weiping Ma and Paul W Brown

65. Mechanisms of Limestone Fillers Reactions in the System $\{C_3A–C\underline{S}H_2–CH–C\underline{C}–H\}$: Competition between Calcium Monocarbo- and Monosulfo-Aluminate Hydrates Formation 430
C Vernet and G Noworyta

66. Thermal and Chemical Stability of AFm Phase–Isostructural Group 437
T Nishikawa, K Sato, S Ito and K Suzuki

67. Influence of Anhydrite Particle Size on the Hydration of Sulphoaluminate Belite Cement 443
S Sahu, J Majling and J Havlica

68. Studies of Barium addition on the β-Ca_2SiO_4 Hydration 449
M Gawlicki

69. A Quantitative Study of Paste Microstructures and Hydration Characters of Sulphoaluminate Cement 454
Wang Yanmou, Su Muzhen, Yang Renhe and Lui Baoyuan

70. Early Hydration Characteristics of System $NaNO_2–C_4A_3\bar{S}–CaSO_4·2H_2O$ 461
Yang Huixian and Jin Shuxin

71. Hydration Products of Alkali Activated Slags 468
T Kutti

72. On Hardening Peculiarities of Gypsum-Cement Materials 475
G Y Danko

73. Alkaline Cements 482
P V Krivenko

74. Development of Cementitious Properties in Phosphogypsum-Fly Ash System 489
Manjit Singh and Mridul Garg

SPECIFIC THEME III-C : Structural Models for Hydrated Cement Pastes

75. A Mathematical Model on Rate of Heat Liberation in Early Hydration of Portland Cement and its Application 497
H Okamoto, N Itoh and S Takahashi

76. Prediction of Cement Properties from Description of the Hydration Processes 504
Bjarne Osbaeck

77. Hydration Kinetics and Mechanical Evolution of Concrete During the First Days: Study of the Hardening Mechanism 511
C Vernet

78. Kinetic and Thermodynamic Interpretations of Hydration and Hardening of Portland Cements and their Mineralogical Constituents 518
I Teoreanu, Marcela Muntean and A Volceanov

79. Thermochemical and Kinetic Analysis of Hydration 525
Li Jian—Xi

80. Theory and Practice of Cement Strength Characteristics Prediction 532
A S Koshmai and O P Mchedlov-Petrossyan

81. Sedimentation Method for Analysis of Cement-Ash Composition Properties 536
L P Orentlicher, V G Nikiforova

SPECIFIC THEME III-D : Effect of Admixtures

82. Hydration in Very High Strength Cement Composites 543
A Durekovic

83. Effect Mechanism of Concrete Admixture based on Aromatic Hydrocarbon Sulphonate 550
Chen Yongsu, Wu Zhaoqi and Yu Kuichang

84. Rheological Properties of Cement Mixes Containing Different Organic Dispersant Admixtures 557
J R Baragaño and A Macias

85. Effect of Superplasticizer on the Hydration of Portland Cement 564
N B Singh, Reetika Sarvahi and N P Singh

86. Influence of Superplasticizer on Fluidity of Fresh Cement Paste with Different Clinker Phase Composition 570
E Asakura, H Yoshida and H Nakae

87. The Role of the Nature of Hydration Phases on the Rheological Properties of Cement Dispersions 577
F L Glekel and R Z Kopp

88. Flash-set Behaviour of Oil Well Cement Slurries Containing Lignosulphonates 584
M Michaux and E B Nelson

89. The Influence of Admixtures on the Crystallization of Tobermorite from C–S–H (I) 591
W Kurdowski and T T Nguyen

90. Effect of Cement Characteristics on the Fluidity of Cement Paste Containing an Organic Admixture 597
T Nawa and H Eguchi

91. Effect of Additives on Hydration Workability and Some Other Properties of Portland Cement 604
V K Singh and Barsha Gogoi

92. The Effect of Hydrolyzable Tannic Compounds on Hydration of Cement and its Utilization as a Heat Controlling Agent 612
H Inokawa, K Inada, N Kozakai, A Ohno and K Uchida

93. Application of HPLC in the Characterization of Naphthalene Sulphonate-based Superplasticizers 619
U Costa, M Goisis and G Guerra

94. Conductometric Test for Cement-Admixture Systems 627
C Vernet and G Noworyta

95. Desorption Isotherms of Silica Fume Mortar 634
Elisabeth Atlassi

96. Study on "Farming Silica Fume" Use in Pozzolanic Cements 640
J R Baragaño and V M Villar

97. Hardening of Ordinary and Expansive Cement with Silica Fume Admixture 646
A I Panchenko and L Opoczky

98. Hydration and Strength of Blends CAC–Fume Silica and Stability of Hydrates 651
S Marcdargent, M Testud, J P Bayoux and A Mathieu

99. Study on Hydration Properties of Slag and Silica Fume Blended Cement for Ultra-High Strength Concrete 658
M Shizawa, Y Joe, S Takesue and Y Urakawa

100. Microstructure and Mechanical Properties of Hardened Cement Paste Incorporating Ground Granulated Blast-Furnace Slag 665
T Nishikawa, K Koibuchi, S Ito and M Takatsu

101. The Hydration Behaviour of Metakaolin–$Ca(OH)_2$–Sulphate Binders 671
P S de Silva and F P Glasser

102. Chemical Binding of Water During the Hydration of Portland Cements and Blast-Furnace Slag Cements Blended with Fly Ash 678
Reiner Härdtl

103. 20-Year Study on Hydration of High Magnesia Cement with Fly Ash at Ambient Temperature 684
S S Rehsi and S K Garg

104. Inhibition of Blending Materials on Effect of Excess SO_3 Content in Cement 691
Lian Huizhen and Chen Enyi

105. The Influence of some Fly Ashes and Blast-Furnace Slags on Blended Cement Hydration and Properties 698
W Roszczynialski

106. A Study on Calcium Aluminate Cements Admixtures 705
J P Bayoux, D Sorrentino, J P Falaschi and A Capmas

107. Autogenous Shrinkage Caused by Self Desiccation in Cementitious Material 712
E Tazawa and S Miyazawa

108. The Use of Admixtures in High Alumina Cement Mortar for the Marine Environment 719
N C Baker and P F G Banfill

Specific Theme III-A

Advances in Hydration of Cements at Low, Ambient and Elevated Temperatures

EFFECTS OF LOW TEMPERATURE AND FREEZE-THAW CYCLES ON THE STABILITY OF HYDRATION PRODUCTS

H -M Ludwig and J Stark

University of Architecture and Building, Weimar
GERMANY

SUMMARY

This paper presents results of laboratory investigations to the effects of low temperature and freeze - thaw cycles on the stability of calciumsulfoaluminate- and calciumsulfoaluminatferrathydrates.
The investigations have shown that the influence of negative temperatures affects phase displacements between the AFm - and the AFt - phases.
The quantity of the AFt - phase formed during the low temperature treatments is lager in the case of C_3A - rich cements.

ZUSAMMENFASSUNG

Der vorliegende Beitrag stellt die Ergebnisse von Laboruntersuchungen zur Auswirkung tiefer Temperaturen und von Frost - Tau -Wechseln auf die Stabilität von Calciumsulfoaluminat- und Calciumsulfoaluminat-ferrathydraten dar.
Die Untersuchungen zeigen, daß negative Temperaturen eine Phasen-umwandlung von AFm - zu AFt - Phase hervorrufen. Die Menge an AFt - Phase, die während der Frostbeanspruchung entstand, ist im Falle von C_3A - reichen Zementen größer.

0. Introduction

Influence of cement type and phase composition of Portland cement on resistance to freezing and thawing of concrete has been a subject of discussion for long. Within this set of problems the assesment of the possibility of phase displacements of AFm- and AFt-phases was the intention of the experiments.

1. Materials

Basic cements for the investigations were Portland cement (SRPC 40 A) with a low C_3A content (C_3A = 1.7 %) and a C_3A-rich white cement (C_3A = 10.7 %).
The experiments were carried out with samples of C_3A and $C_2(A,F)$ obtained by salicylic acid extraction from these technical cements.
The results of this extraction are shown the Table 1.
Most of the silicate clinker phases were separated while the aluminate- and ferrite phases were concentrated in the extraction residue. Besides these phases most alkalies and sulphates too were insoluble in the acid solution.
The basic cements and the extracted residue also were studied by XRD (Figures 1 and 2). The materials prepared in thus correspond exactly to the clinker aluminates and ferrites, both in nature and the quantity of incorporated foreign oxides, and in their hydraulic activity.

2. Experimental investigations

The extraction residues were hydrated in saturated lime solution at a solution/residue ratio of 1,0. Hydration of the extraction residue leads to a pore solution similar to that with commercial cements. This is because almost all sulphates and alkalies remain in the residue.
After mixing, the material is placed in small closed bottles until the beginning of the experiments after 90 days' hydration time. Then the water-saturated samples were subjected to following treatments:

- storage at + 20 °C - 30 days
- storage at + 5 °C - 30 days
- storage at - 5 °C - 30 days
- 150 freeze-thaw cycles
  + 20 °C/-20 °C - 30 days

Differential thermalanalysis, thermogravimetry, XRD and scanning electron microscopy were used for examination of the stability of calciumsulfoaluminatehydrates during the frost loading.

Table 1: Results of the salicylic acid extraction

Chemical analysis before and after the extraction:

	SRPC 40 A		PC White	
	basic PC	after extr.	basic PC	after extr.
SiO_2 %	19,8	5,6	22,0	7,5
Al_2O_3 %	4,4	14,9	4,2	19,7
Fe_2O_3 %	5,7	20,4	0,2	0,7
CaO %	65,8	44,4	68,2	44,6
MgO %	1,6	3,1	2,3	9,9
K_2O %	0,70	2,20	0,32	1,41
Na_2O %	0,23	0,51	0,12	0,56
SO_3 %	2,0	7,8	2,2	13,2
CaO_{fr} %	1,9	0,1	0,6	0,1

Main phases before and after the extraction:

SRPC 40 A		PC White	
basic PC	after extr.	basic PC	after extr.
C_3S = 65,6 %	C_4AF = 62,1 %	C_3S = 70,8 %	C_3A = 51,1 %
C_2S = 6,4 %	C_3S = 10,3 %	C_2S = 8,0 %	C_3S = 6,4 %
C_3A = 1,7 %	$CaSO_4$ = 11,4 %	C_3A = 10,7 %	$CaSO_4$ =19,7 %
C_4AF= 17,3 %	MgO = 3,1 %	C_4AF= 0,6 %	MgO = 9,9 %

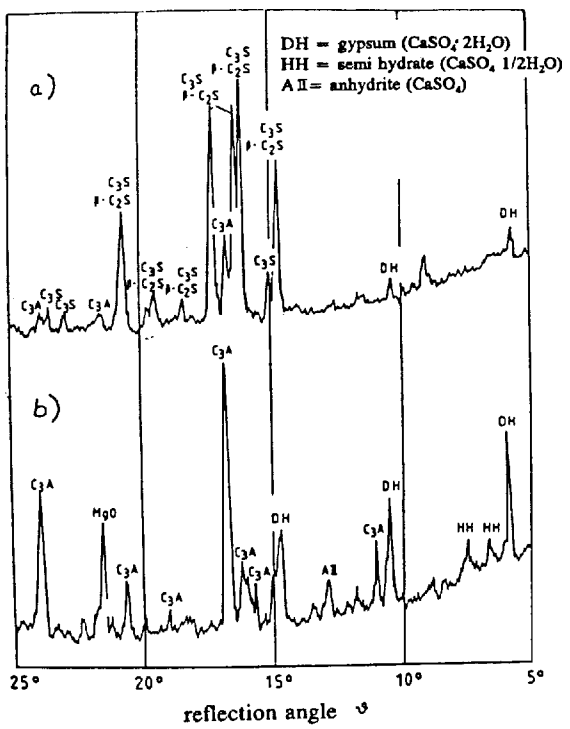

Figure 1: XRD pattern of PCW
a) basic cement
b) extraction residue

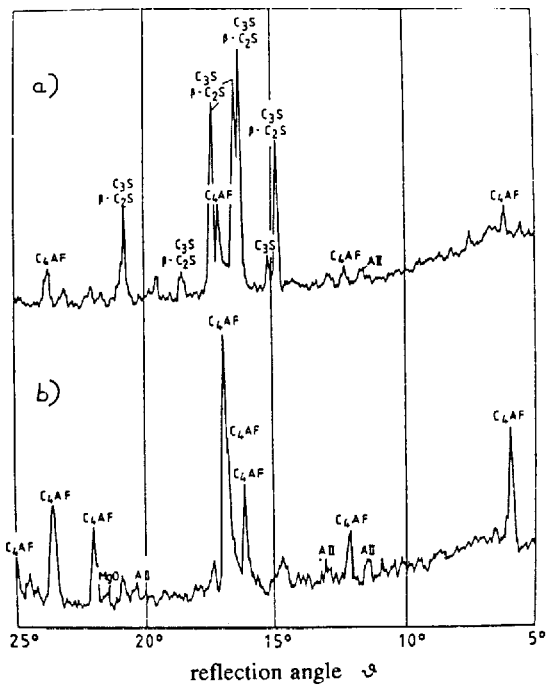

Figure 2: XRD pattern of SRPC
a) basic cement
b) extraction residue

3. Results

DTA/DTG/TG

Results of these investigations are shown in Figures 3 and 4. It is discernible that after a hydration time of 120 days at + 20 °C there is a distinct difference between the hydration products of C_3A-rich residue (PCW) and the residue with a low C_3A-content (SRPC).

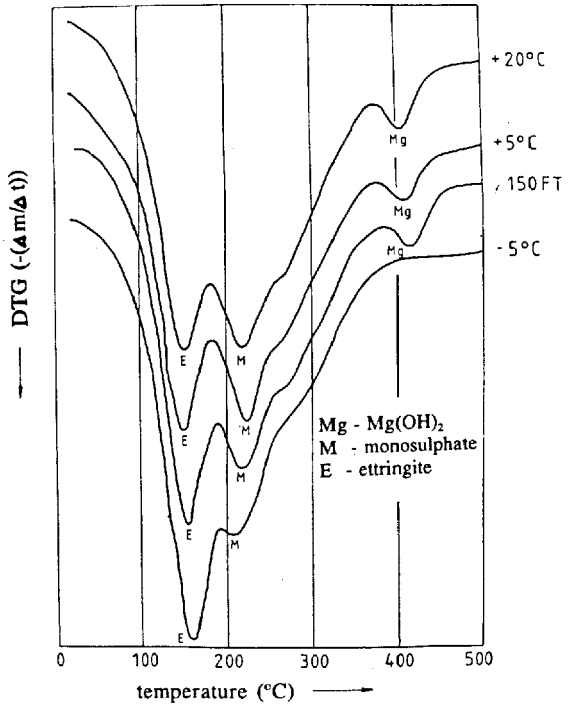

Figure 3: DTG curves of PCW after temperature treatments

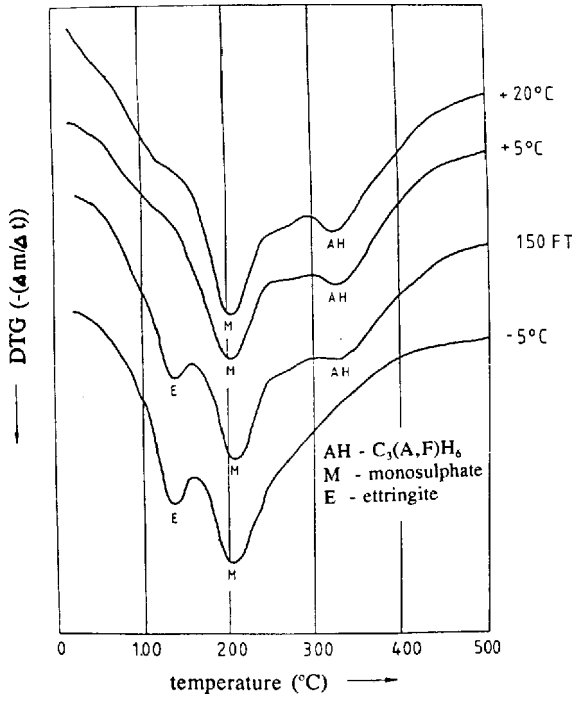

Figure 4: DTG curves of SRPC after temperature treatments

In the case of the PCW both AFm- and AFt-phases were observed. However in C_4AF-rich cement (SRPC) only the AFm-phase appears after this hydration time.

Futhermore, after the temperature treatment a distinct phase displacement from monosulphate or AFm-phase respectively to ettringite or AFt-phase respectively, was observed with decreasing temperature. This dependence was irrespective of the kind of residue.

The quantitative determination of the trisulphate was carried out by means of a calibration curve obtained from mixtures of synthetic ettringite and clinker. Approximate information about the quantity of monosulphate was obtained through thermogravimetry (TG) because in this case no synthetic material was available.

The results are shown in Table 2.

Table 2: Phase content after different treatments

Treatment	SRPC 40 A		PC W	
	AFm	AFt	AFm	AFt
+ 20 °C	61 %	5 %	40 %	33 %
+ 5 °C	57 %	6 %	36 %	37 %
- 5 °C	47 %	14 %	26 %	51 %
150 ft cycles	53 %	17 %	34 %	38 %

The greatest displacement to ettringite was shown at a constantly negative temperature (- 5 °C).

XRD - SEM/ESMA

The investigations by means of XRD and scanning electron microscopy confirmed the results of the thermoanalytical examinations.
The XRD patterns of the samples after the temperature treatments are shown in Figures 5 and 6.
A large quantity of a crystalline solid solution of C_4AH_{13} -monosulphate in addition to the AFm-phase was indicated by the XRD patterns. The AFm phase and the solid solution decreased while the AFt phase increased, with freezing and thawing and at low temperatures.
A quantitative analysis was not possible by XRD since the ettringite of secondary origin showed partially amorphous behaviour.

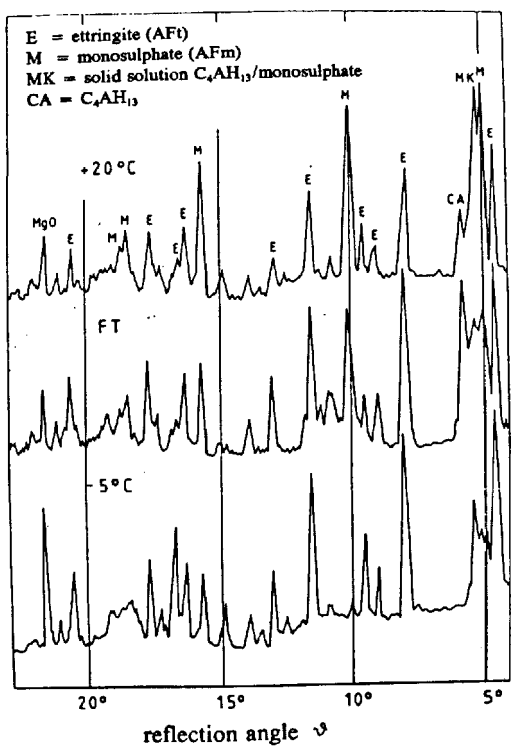

Figure 5: XRD patterns of PCW after temperature treatments

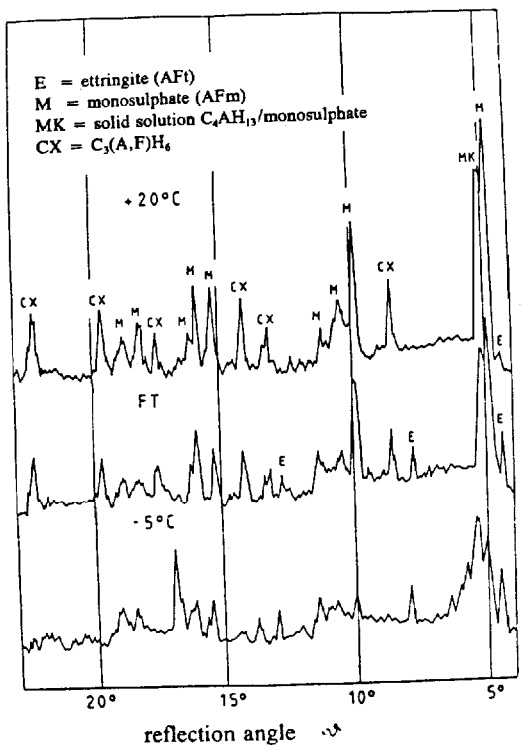

Figure 6: XRD patterns of SRPC after temperature treatments

The increase in the ettringite phase is good to be observed in scanning electron microscopy (Figures 7 to 12). The amount of ettringite needles increased during the freezing and thawing. The AFt formation is similar, regardless of a ferrat or a ferrat-free form.
However, the morphology of ettringite (AFt) which was formed at negative temperatures (- 5 °C) differed considerably from the usual needle - shaped formation.



Figure 7: 120 d-hydrated PCW - storage at +20°C

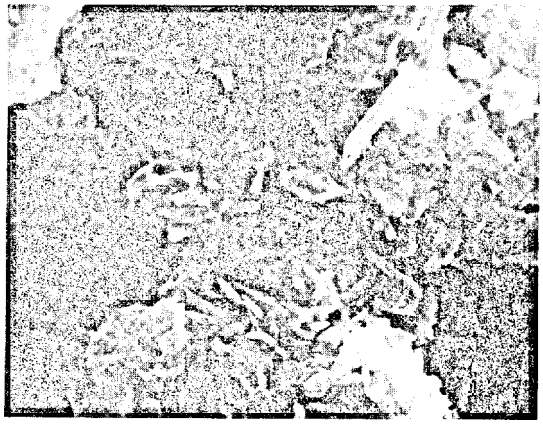

Figure 8: 120 d-hydrated SRPC - storage at +20°C



Figure 9: 120 d-hydrated PCW - 150 ft-cycles / 30 d



Figure 10: 120 d-hydrated SRPC - 150 ft - cycles / 30 d

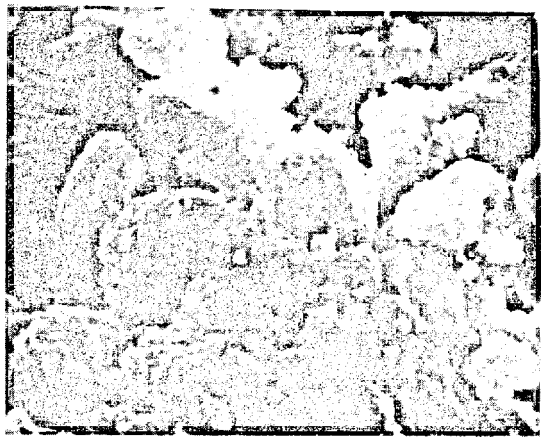

Figure 11: 120 d - hydrated PCW - storage at -5°C / 30 d

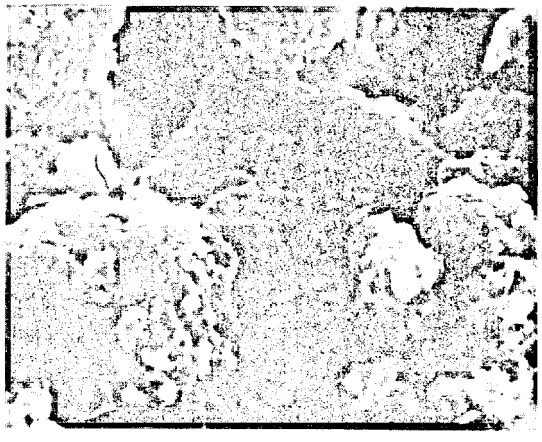

Figure 12: 120 d - hydrated SPRC - storage at -5°C / 30 d

4. Conclusions

The investigations have shown that the influence of negative temperatures affects phase displacements between the AFm- and the AFt-phases. The changes take place independently of the C_3A-content of the basic cements, that means, it is irrespective of whether calciumsulfoaluminate- or calciumsulfoaluminatferrathydrates are present. However, the quantity of the AFt-phase formed during the low temperature treatments is larger in the case of C_3A-rich cements.
Futher investigations are required to answer the question whether the observed phase displacements play a role in frost damages and the degree to which the presence of deicing salts influence these phenomena.

THE HYDRATION OF CLASS G OILWELL CEMENT AT LOW AND AMBIENT TEMPERATURES WITH ADDITIONS OF SODIUM ALUMINATE

J S Lota*, P L Pratt*, K L Scrivener* and J Bensted**

**Imperial College of Science, Technology and Medicine, London, UK*
***BP Plc, Sunbury Research Centre, Middlesex, UK*

ABSTRACT

The microstructure of high sulphate-resistant Class G oilwell cement has been investigated at 20°C and 5°C with additions of sodium aluminate as the accelerating admixture. The progress of hydration was monitored by isothermal conduction calorimetry, thermal analysis, x-ray powder diffractometry, infrared spectroscopy, scanning electron microscopy with backscattered electron imaging and the development of compressive strength. Temperature had a marked influence upon the development of microstructure. Hydration at 5°C showed a significant increase in the formation of ettringite and a decrease in that of C-S-H gel compared with 20°C.

Additions of sodium aluminate produced supplementary peaks on the calorimetry curve. The hydration was accelerated by 0.3 M additions at both 5°C and 20°C, and the greatest increase in the total heat evolved after 1 day was at 5°C. Large additions reduced the amount of calcium hydroxide, increased the coarse porosity and reduced the amount of bound water.

INTRODUCTION

Oilwell cements are used primarily in the oil industry both in exploration and production of oil and gas. Their main purpose is to seal the annular space between the walls of a borehole and the steel casing that lines the well (1). At low temperatures, as found in the North Sea during drilling at or near the surface, the cement hydration reactions are slowed down and admixtures are employed to accelerate these reactions. A better understanding of the effects of temperature and of acceleration upon the development of cement microstructure and properties should lead to improved and more efficient cementing of wells. Class G oilwell cement is essentially a coarsely ground high sulphate-resisting cement, suitable to cover a wide range of well depths and temperatures (2).

EXPERIMENTAL METHODS AND TECHNIQUES

The cement was supplied by Blue Circle Industries with a potential phase composition (Bogue %) of C_3S - 56.6, C_2S - 19.3, C_3A - 1.5 and C_4AF - 15.9. The sodium aluminate ($NaAlO_2$) was supplied by Fosroc Technology, UK. X-ray analysis showed it to be composed of sodium aluminate (95% by weight) with traces of $NaAlO_2.3H_2O$ and $NaAlO_2.2H_2O$. Specimens were prepared using molar concentrations (0, 0.1, 0.3, 0.5 and 1.0 M) of sodium aluminate with distilled water. A water to cement ratio of 0.44 was used throughout (2).

For examination by scanning electron microscopy (SEM), thermogravimetric analysis (TG), infrared (IR) spectroscopy and x-ray powder diffraction (XRD), cylindrical specimens, 11 mm diameter by 35 mm height, were cast after mixing in a Waring blender for 3 minutes and subsequently cured in water baths maintained at either 20°C or 5°C. Prior to casting at 5°C the cement and mix water were chilled at 8°C for 24 hours.

At appropriate curing times the specimens were frozen in a slurry of solid carbon dioxide and methanol and then freeze dried under vacuum. A JEOL 35 CF SEM fitted with a solid state backscattered electron (bse) detector linked to a Kontron image processing system was used to examine the polished surfaces cut from the cylinders after freeze drying.

The heat evolution from freshly prepared samples was measured using an isothermal conduction calorimeter supplied by Wexham Developments Ltd (3).

Compressive strength measurements were obtained by crushing 12.7 mm cubes which had been cured at either 5°C or 20°C for a specified time. Ten cubes were crushed to obtain the compressive strength at each time.

RESULTS

The heat evolution curves of the cement with additions of sodium aluminate at 5°C and 20°C are shown in Figures 1 and 2 respectively. In addition to the peaks produced by the control paste, with increasing addition of sodium aluminate two supplementary peaks appear at both temperatures. These increase in intensity as the dosage is raised. At 5°C, 0.1 M and 0.3 M additions advance the main peak due to C_3S, whereas the 0.5 M and 1.0 M additions retard this peak significantly. At 20°C, only the 1.0 M addition retards the C_3S peak.

The total heat evolved at 1 and 2 days hydration is shown in Table 1. At 5°C it declines as the dosage of sodium aluminate is increased, but after 2 days the total heat output of all the pastes with sodium aluminate is roughly the same. At 20°C all the additions produce an appreciable rise in the total heat at 1 day and the 0.1 M and 0.3 M additions both show an appreciable increase at 2 days.

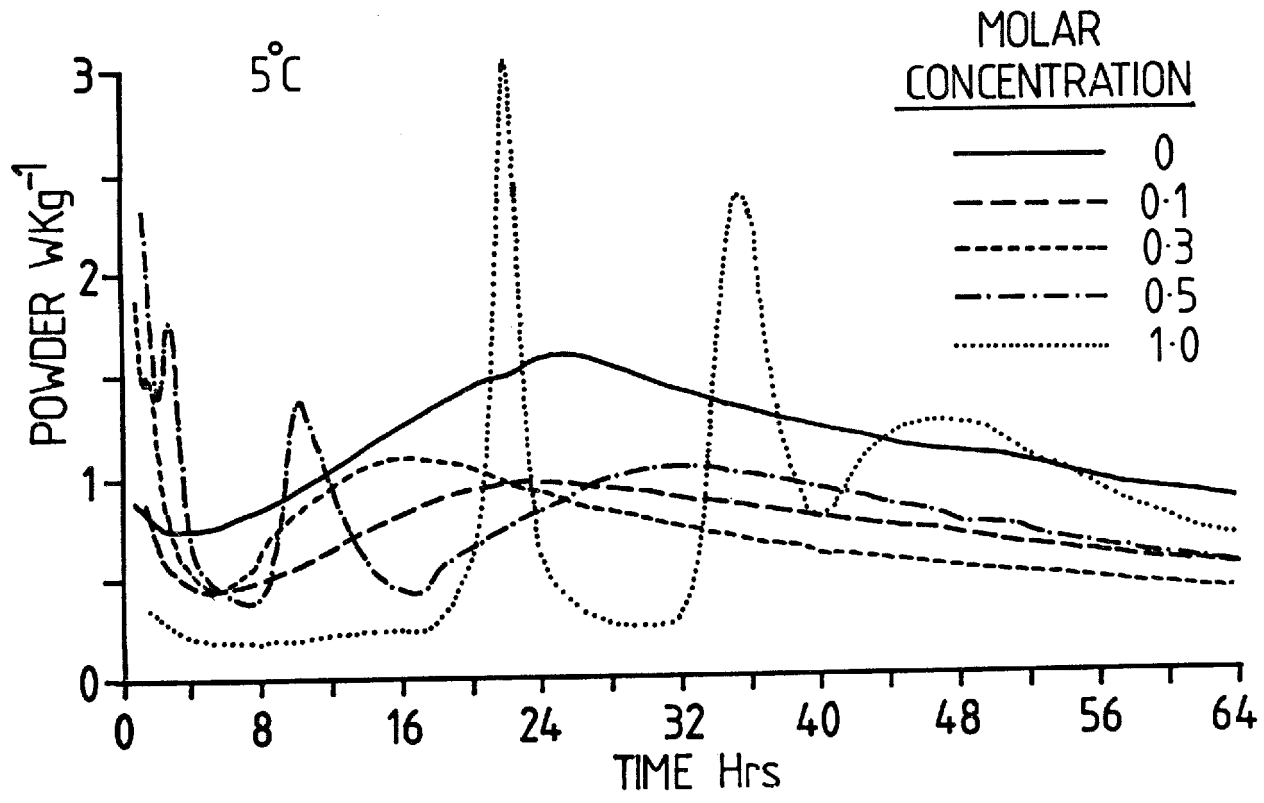

Fig. 1 Heat evolution of Class G oilwell cement hydrated with additions of $NaAlO_2$ at 5°C

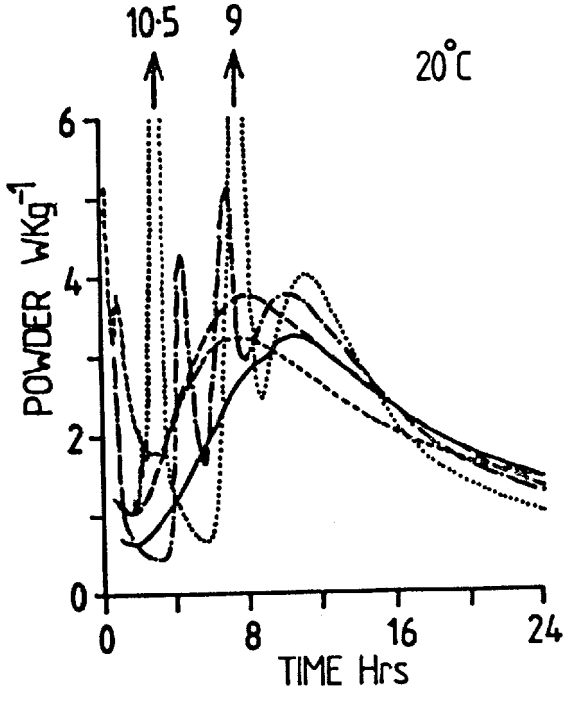

Fig. 2 Heat evolution of Class G oilwell cement hydrated with additions of $NaAlO_2$ at 20°C

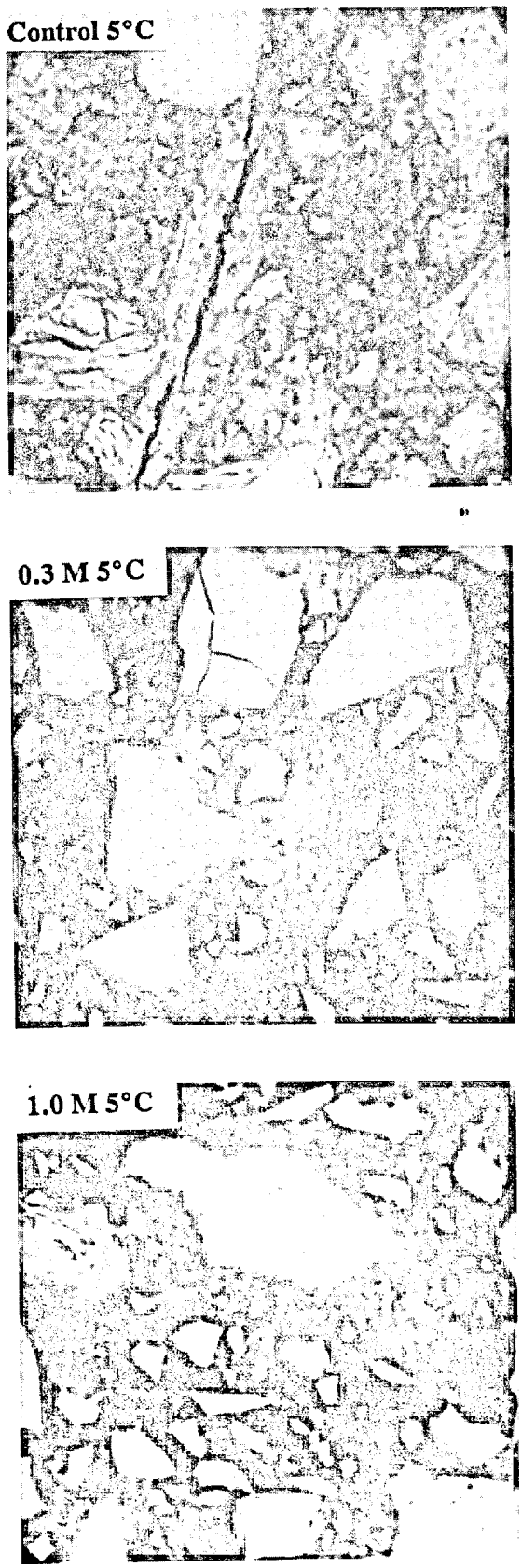

Fig. 3 Bse images of Class G oilwell cement hydrated for 1 day at 5°C

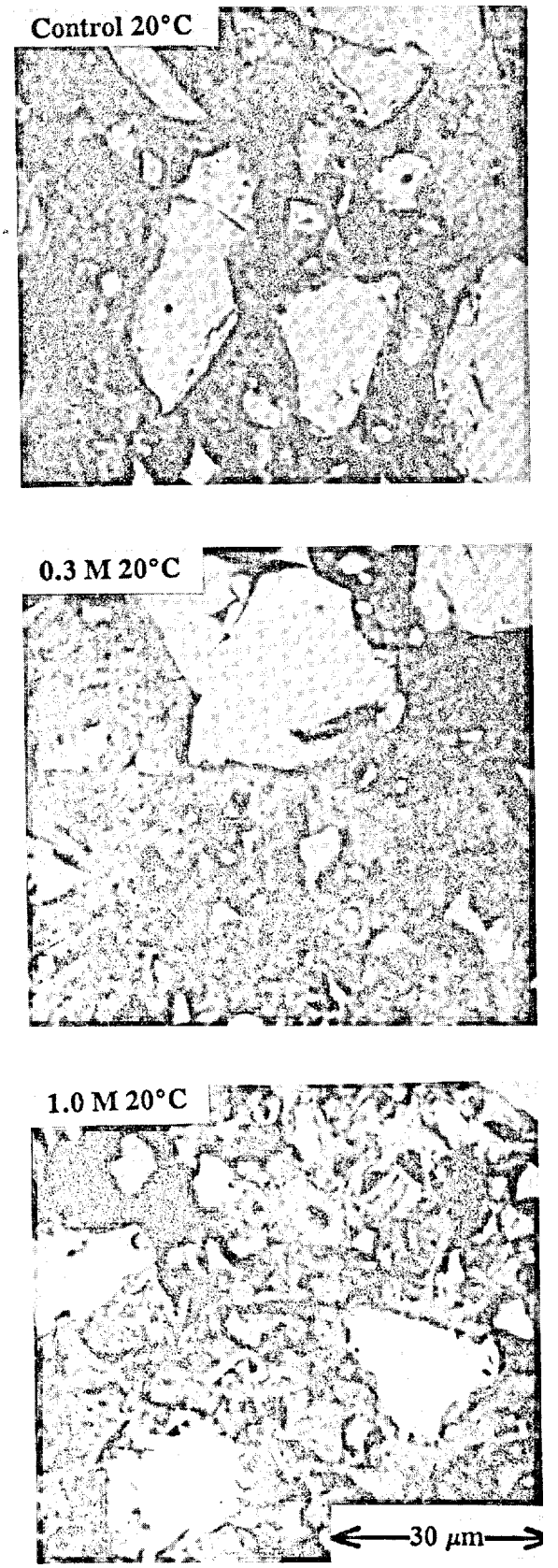

Fig. 4 Bse images of Class G oilwell cement hydrated for 1 day at 20°C

Table 1 Total heat evolved from the Class G oilwell cement with various additions of sodium aluminate (kJ/kg)

Molar addition	5°C		20°C	
	At 1 day	At 2 days	At 1 day	At 2 days
Control	94.4	214.1	173.2	260.6
0.1	59.2	133.8	205.6	288.7
0.3	76.1	136.6	193.0	290.1
0.5	64.8	142.3	194.4	259.2
1.0	42.3	126.8	221.1	271.8

Table 2 Volume % CH

Hydration time	5°C Molar addition of sodium aluminate			20°C Molar addition of sodium aluminate		
	Control	0.3 M	1.0 M	Control	0.3 M	1.0 M
3 hours	1.13	0	0.61	0.70	3.26	3.69
6 hours	1.19	0	1.47	1.18	1.10	0.62
12 hours	2.42	1.67	0.74	3.93	4.02	3.20
1 day	5.30	4.74	0.25	5.43	5.69	2.51
28 days	9.01	12.28	8.34	10.99	10.21	4.24
6 months	not determined			15.43	not determined	
1 year	11.89	not determined		12.02	not determined	

Table 3 Non-evaporable water expressed as % weight loss referred to the ignited cement 1000°C

Hydration time	5°C Molar addition of sodium aluminate			20°C Molar addition of sodium aluminate		
	Control	0.3 M	1.0 M	Control	0.3 M	1.0 M
3 hours	3.27	4.91	6.08	2.35	10.51	11.27
6 hours	4.42	4.98	6.71	3.32	5.81	7.56
12 hours	5.99	7.19	7.54	8.50	9.89	11.06
1 day	7.47	12.58	6.91	8.99	12.17	10.78
28 days	17.05	18.07	17.70	16.87	17.14	11.06
1 year	22.12	not determined		22.95	not determined	

Table 4 Compressive strength development of Class G oilwell cement with 0.1 M addition of sodium aluminate (Nmm^{-2})

Hydration time	5°C		20°C	
	Control (sd)	0.1 M (sd)	Control (sd)	0.1 M (sd)
1 day	0.82 (0.10)	not determined	8.43 (0.43)	10.08 (0.38)
3 days	3.46 (0.25)	7.59 (0.95)	16.25 (1.77)	22.84 (1.77)
7 days	8.59 (0.41)	18.82 (0.45)	21.87 (1.71)	32.21 (2.11)
14 days	14.21 (0.70)	25.47 (0.63)	32.31 (1.48)	33.50 (3.86)
28 days	22.66 (0.65)	28.65 (0.58)	35.18 (2.03)	37.64 (1.27)
3 months	37.58 (2.17)	55.29 (1.63)	45.80 (5.36)	52.90 (0.54)
6 months	51.30 (1.20)	62.43 (2.94)	62.46 (4.02)	72.32 (3.66)
1 year	55.06 (2.86)	73.93 (3.27)	66.02 (4.58)	71.94 (2.77)

sd - standard deviation

Typical bse images of the paste hydrated for 1 day with addition of sodium aluminate at 5°C and 20°C are shown in Figures 3 and 4 respectively. At 5°C the control paste shows a lower degree of hydration than at 20°C. The addition of sodium aluminate does not appear to have increased hydration. At 20°C, the 0.3 M addition shows an accelerated hydration as indicated by a denser C-S-H gel and thicker rims of C-S-H around the anhydrous cores compared to the control. With 1.0 M addition the hydration appears to be accelerated so that the hydration shells around the cement grains have merged with the surrounding C-S-H gel. The latter has a different morphology from that of the control or with the 0.3 M addition to the paste. Furthermore, there is a substantial amount of coarse porosity and the demarcation between the CH and C-S-H gel is not very clear compared to the control paste.

The CH content of the paste measured by TG is shown in Table 2. At 5°C, with 1.0 M additions, the amount of CH that is formed at up to 24 hours is erratic. Beyond 24 hours hydration the 0.3 M addition produces the greatest amount of CH. At 20°C, with 0.3 M and 1.0 M additions there appears to be much more CH at 3 hours than in the control. This increase vanishes by 6 hours and the 0.3 M addition thereafter resembles the control. The 1.0 M addition does not significantly influence the formation of CH after 12 hours hydration and the amount of CH remains low at least up to 28 days.

The measured non-evaporable water (loss on ignition, LOI) content of the paste is shown in Table 3. The LOI shows a pattern similar to the CH content of the paste. At 5°C, 0.3 M additions increase the LOI compared to the control up to 28 days whereas the 1.0 M addition gives erratic behaviour. At 28 days the LOI of all the pastes is of similar magnitude. At 20°C and 3 hours the control has a smaller LOI than at 5°C, while the addition caused a marked increase in LOI. As with the CH content, this increase falls after 6 hours before rising again. With 1.0 M addition the content does not significantly change between 12 hours and 28 days.

The compressive strength development of the paste with 0.1 M addition of sodium aluminate is shown in Table 4. At 20°C, most improvement in strength is found at early ages up to 7 days, whereas at 5°C improvement is found at all ages, being most effective at ages up to 7 days.

DISCUSSION AND CONCLUSIONS

In the control pastes hydration is slower at 5°C than at 20°C for the silicate phases, resulting in the production of smaller amounts of C-S-H gel and CH from 6 hours and onwards. However XRD traces showed that more AFt phase, ettringite, was formed at 5°C than at 20°C especially at early ages (4). At 20 °C the AFt phase was detected only after 28 days. This can be explained by the lowered rate of hydration of the alite phase producing an inadequate covering of C-S-H gel around the hydrating cement grains, thus leaving water and space for the alumina-containing phases to hydrate relatively unhindered. At 20°C the amount of CH after 6 months declines, suggesting that the ferrite phase plays a significant part in the hydration process at later ages, particularly after the hydration of the calcium silicate phases declines. There appears to be an anomaly at the earliest age of 3 hours where more CH is found in the paste at 5°C than at 20°C. This might be due to the increasing solubility of CH in the pore solution at the lower temperature.

With the addition of sodium aluminate two important changes in the hydration mechanism can be seen. From Tables 2 and 3 the amount of CH and the amount of bound water after 3 hours at 20°C are increased by a factor of 5 compared with the control. These amounts decreased substantially by 6 hours and are almost back to normal by 12 hours. The time of this unexpected behaviour at 20°C coincides with the appearance of the 2 new peaks in the heat evolution curves before the main C_3S peak. The erratic CH and LOI content in the pastes with sodium aluminate at early times is accompanied by the formation of calcium aluminate hydrates as shown by XRD (4). This suggests that the addition of sodium aluminate is altering the pore solution chemistry significantly so that the normal sequence of events taking place in the control paste is changed. The

sodium aluminate appears to enhance the hydration of the ferrite phase by removing calcium ions from the pore solution to form calcium aluminate hydrates.

The increased formation of calcium aluminate hydrates, at 5°C and 20°C, particularly with the 1.0 M addition deprives the pore solution of the calcium and hydroxyl ions and of the water required to form them. At 5°C with the 1.0 M addition the heat evolution curve shows that only the first supplementary peak has been passed by 1 day. The total heat evolved is low at 42.3 kJ/kg, very little CH has been formed and very little water has been bound. From the heat evolution curve the hydration of the alite phase begins after 40 hours and the peak extends to 3 days. By this time the strength should have started to develop but it is not surprising that so much porosity remains after 1 day in Figure 3. At 20°C with 1.0 M addition, the hydration shell appears to have become part of the surrounding C-S-H gel and in places no longer acts as a barrier between the pore solution and the unhydrated core, thus exposing a greater surface of the unhydrated cement to the pore solution. This results in erratic hydration causing the paste to set prematurely by increasing the rate of hydration and diminishing rapidly the quantity of free water. IR spectroscopy confirms this by indicating the presence of strong sulphate wavebands up to 28 days hydration which are due to unreacted gypsum (4). From these results it seems reasonable to conclude that 1.0 M additions of sodium aluminate both at 5°C and at 20°C are too much to act as a reliable accelerator in the early stages of hydration. At 20°C the heat evolution curves are dominated by the supplementary peaks and the amount of CH and bound water are lower than for the 0.3 M addition. At 5°C the C_3S peak is retarded from 16 to 48 hours by an increase from 0.3 M to 1.0 M while little or no CH is formed in the first 24 hours as we have seen.

The hydration characteristics of the cement depend upon the temperature of curing and the dosage of the admixture. Overall, the Class G oilwell cement shows a complicated hydration behaviour with the addition of sodium aluminate, suggesting that there is no universal mechanism of acceleration. This draws attention to the need for caution in the application of sodium aluminate in practice.

ACKNOWLEDGEMENTS

The authors are grateful to the Science and Engineering Research Council and to Sunbury Research Centre of BP for the support of J S Lota on a CASE research studentship during the period of this work, and to Blue Circle Industries for supplying the Class G oilwell cement used in this investigation.

REFERENCES

1. Bensted, J.: "Cements with specific applications - Oilwell cements". World Cement, 1987, 18, 72-78.

2. API Specification: 10A-1991: "Specification for well cements". 21st Ed, American Petroleum Institute, Washington DC, 1991.

3. Forrester, J.A.: "A conduction calorimeter for the study of cement hydration". Cement Technology, 1970, 1, 95-99.

4. Lota, J. S.: "The hydration of Class G oilwell cement". PhD thesis, University of London, 1992.

ANALYSIS OF THE HYDRATION-SETTING RELATION : TOWARDS A COMPREHENSIVE APPROACH OF THE CEMENT SETTING

S P Jiang, J C Mutin and A Nonat

Laboratoire de Recherches sur la Réactivité des Solides
Faculté des Sciences Mirande, Université de Bourgogne
FRANCE

SUMMARY

The mechanical evolution and the structure of the cement paste have been analysed in relation with the chemical evolution (electrical conductivity, hydrates formation) of the system. The setting process can be described as following two fundamental steps : the coagulation of cement grains during the first minutes following the mixing, and the rigidification of the coagulated structure which arises simultaneously with the acceleration of hydrates formation.

During the coagulation step, the structure formed is proved to be mechanically reversible. The rigidification of coagulated structure is provided by the hydrates formation in the contact zone. The increase of the paste cohesion at this stage is proportional to the quantity of precipitated hydrates, the structure thus rigidified becoming mechanically irreversible.

Finally, the nature of the forces bringing into play in the coagulation and the rigidification has been discussed. It was suggested that the forces intervening in both phenomena may be the same nature, i.e. hydration forces.

RESUME

L'évolution mécanique et la structure de la pâte du ciment pendant la prise ont été étudiées en tenant compte de l'évolution chimique de la intersticielle et de la formation des hydrates du système. Le processus de la prise peut être décrit par deux étapes fondamentales suivantes : la coagulation des grains de ciment pendant les premières minutes qui suivent le gâchage, et la rigidification de la structure coagulée qui intervient simultanément à l'accélération de la formation des hydrates.

Pendant l'étape de la coagulation, la structure formée est mecaniquement reversible. La rigidification de la structure coagulée est ensuite assurée par la formation des hydrates dans la zone de contact. L'augmentation de la resistance de la pâte pendant cette periode est proportionnelle à la quantité d'hydrates formés, la structure ainsi rigidifiée devenant mecaniquement irreversible.

La nature des forces interparticulaires entrant en jeu dans la coagulation et la rigidification a été également discutée. La discussion suggère que les forces intervénant dans les deux processus pourraient être les mêmes : les forces d'hydratation.

INTRODUCTION

The litterature survey related to the setting of hydraulic binders reveals that very few studies have been taken to establish clearly the susceptible relationship which may exist between the appearance of initial cohesion of the paste during setting and the advancement of hydration of the binder.

People often confuse hydration and setting which are two different aspects of the binder evolution after mixing with water. The name hydration interprets the overall chemical evolution of the cement grains, whereas settting results from the mechanical evolution of the cement paste. Hydration is not setting, indeed, both evolutions may be independently observed. For exemple, the chemical transformation of anhydrous binder into hydrates occurs as soon as it is mixed with water without setting if the suspension is diluted enough and dispersed by stirring in order to prevent contact between particles. Thus the hydrate formation is not a sufficient condition for setting. On the other hand, Sereda (1) obtained, by the compaction of the hydrate powder, a material which has the same mechanical strength as hardened hydrated paste of the same porosity. So hydration, in the meaning of time depending chemical evolution, is not a necessary condition for setting.

The setting is a process of transformation from the initial state, a dispersed suspension, to a final state, a connected and strengthened system of the particles. This transformation in the case of the cement paste, is obtained by a chemical way : cement hydration.

According to the theoritical and experimental studies of Shchukin (2) and Hattori (3), the cement setting seems to result from the following two fundamental steps :
- coagulation establishing contacts between particles, the coagulated structure being mechanically reversible;
- rigidification of coagulated structure by the formation of hydrates in the contact zone, the final structure becoming mechanically irreversible.

This transformation occurs when both the solids and the intersticial solution of the cement paste are subjected to continuous chemical changes from the mixing until the end of setting. However, Shchukin and Hattori's works did not take into account this fundamental feature. One can think that this chemical evolution and especially the change in ionic concentration in solution, particularly at the contact zone between particles, may play an important role in coagulation and strengthening of the coagulated structure. So, the mechanical evolution and the structure of the cement paste must be analysed in relation with the chemical evolution of the system. This amounts to elucitate the susceptible relations between the hydration and the setting (coagulation and rigidification). With this end, an experimental study of the hydration-setting relation has been performed.

EXPERIMENTAL

Materials

In order to avoid problems and artefacts due to multicomponents system, and to minimize chemical entities and reactions, simpler cements like pure alite would be better to use. However, the great quantities required for mechanical measurements often obliged us to use less pure materials. So, we chose a silica-rich portland cement (offered by Ciment Larfarge) refered to as SRPC. The chemical analysis is given in the table 1.

CaO	SiO_2	Al_2O_3	Fe_2O_3	SO_3	MgO	K_2O	Na_2O	C_3S	C_2S	C_3A	C_4AF	CS	free CaO
66.5	24.5	3.0	2.6	2.1	0.8	0.2	0.1	63.7	18.3	3.8	7.0	3.6	1.2

Table1. Chemical and mineralogical analyses of SRPC (%)

Experimental Methods

The advancement of the cement hydration was determined by isothermal microcalorimetric measurements following a procedure described by Damidot (4). The evolution of the interstitial solution was followed by electrical conductivity.

Concerning the evolution of mechanical properties of cement pastes during setting, a cohesimetry method was used. The shear strength (cohesion forces) was measured by applying a couple on a vane immerged in the paste. The measuring range is between 0 and 1200 g/cm².

A particle analyzer CAPA -700 HORIBA was also used to follow particles size evolution in the diluted cement suspension.

RESULTS AND DISCUSSION

The mechanical evolution of the SRPC paste is evaluated by the shear strength, whereas the chemical evolution is represented here by the advancement of cement hydration. The comparison as shown in the figure 1, leads to distinguish the paste mechanical behavior before and during the acceleration of the hydrates formation.

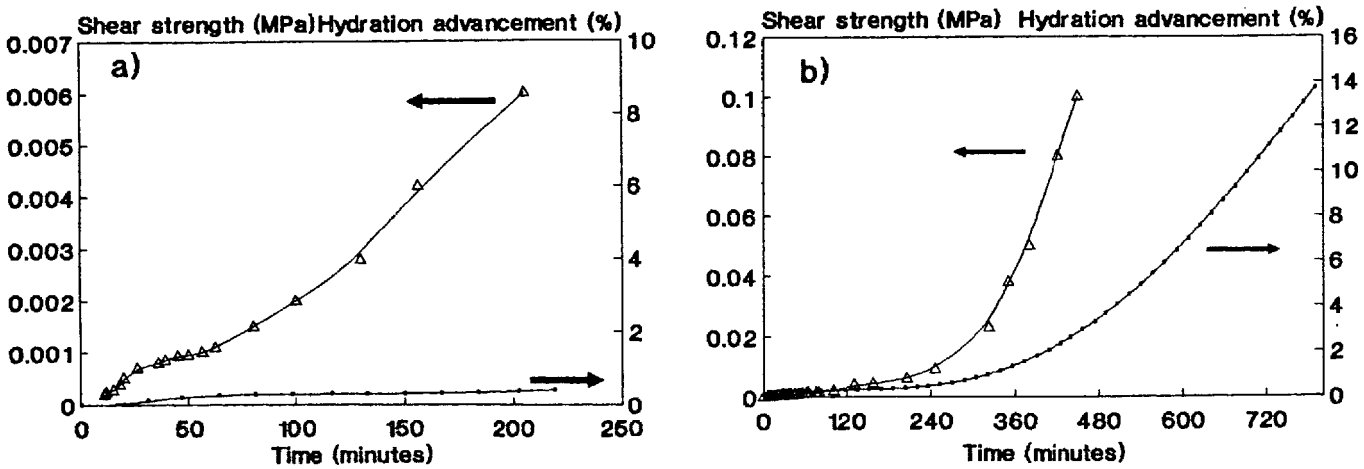

FIG. 1 Evolution of the hydration avancement and the initial strength devolpment versus time in a SRPC paste (W/C=0.4).
a) during first 4 hours hydration b) during first 13 hours hydration

The earliest increase in cohesion appears when there is practically no hydrates formed. This first step in the shear strength evolution can be compared to the viscosity evolution we have measured (5) and that found by Hattori (3). It is attributed to the paste coagulation.

The second increase in cohesion, which is more important, ranges between about 0.01 and 0.1 MPa, it corresponds to the acceleration of hydrates formation. It can be attributed to the paste rigidification. According to the Vicat test, this stage corresponds to the setting of the paste.

The existence of these two steps during the setting can also be exhibited in the figure 2, showing the evolution of the shear strength versus the percentage of transformed anhydrous in hydrates, at the different W/C ratio. From these figures, we

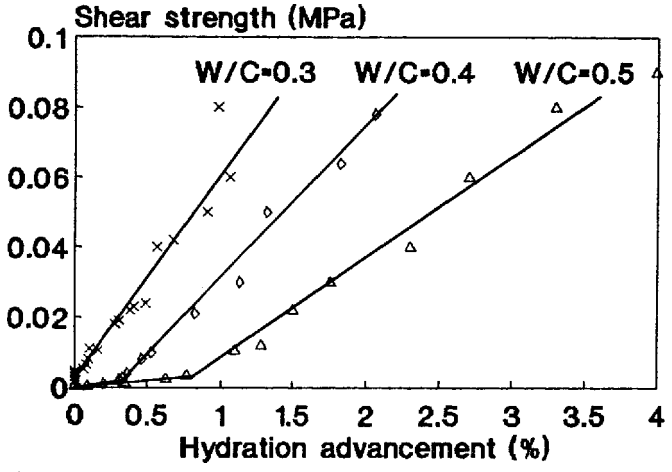

FIG. 2 Evolution of the shear strength versus the hydration avancement for SRPC paste with different W/C ratios.

can see that during the coagulation step, the shear strength is not directly related to the quantity of hydrates formed, whereas during the rigidification step, the paste strength is proportional to the percentage of hydrates formed for a given W/C ratio. So, these curves established more precisely the relation between the hydration and the setting.

The First Increase in Cohesion - Coagulation step

As shown in the figure 2, the formation of coagulation structure in the paste depends very much on W/C ratio. At a small W/C ratio (i.e. W/C = 0.3), it seems even no hydrates needed to forme the initial coagulation structure.

As a stacking of spheroidal particle, for exemple, of C_3S ($\emptyset$ = 10 μm, ρ = 2.8 g/cm^3) in which each ball has 6 linked neighbourings and water fills in the pores, corresponds to a W/C ratio of 0.285. So the initial increase of the paste cohesion expresses a change in the interactions between the stacked particles. These interactions are likely exerted on very close surfaces formed by Ca^{2+}, OH^- and $H_3SiO_4^-$ ions, in an electrolytic solution contained mainly Ca^{2+} and OH^- ions. So, the evolution of the electrical conductivity, which expresses the ionic concentration of the intersticial solution, is of a primary importance in the initial built-up of the coagulation structure. The paste cohesion increases as its electrical conductivity of the intersticial solution increasly evoluted following the mixing with water. In the case of paste mixed with ethylic alcohol (no conductivity evolution) for the same liquid/solid ratio, the paste cohesion was rather small and its evolution was rather constant.

The forces involved in the coagulation process is of mechanically reversible bonds. The figure 3 shows that a remixing of the paste after 1 hour destroyed the structure which is rebuilt afterwards, whereas the hydration advancement remains very small. It becomes irreversible after about 4 hours hydration which corresponds to the acceleration of hydrates formation.

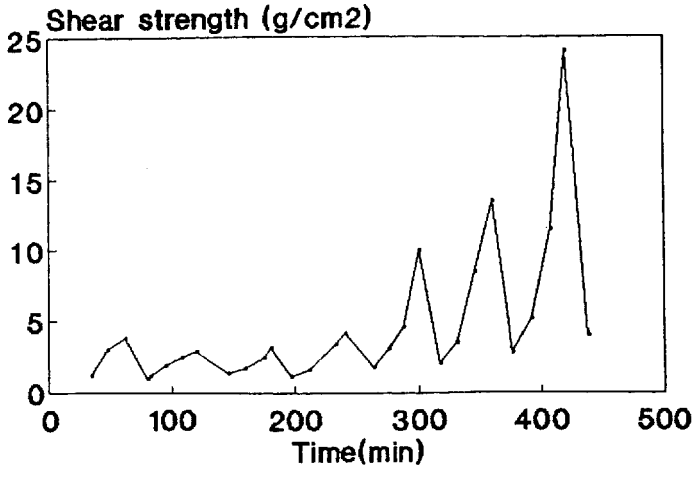

FIG. 3 Effect of successive remixing (5 min each hour) on the shear strength of SRPC paste (W/C=0.35).

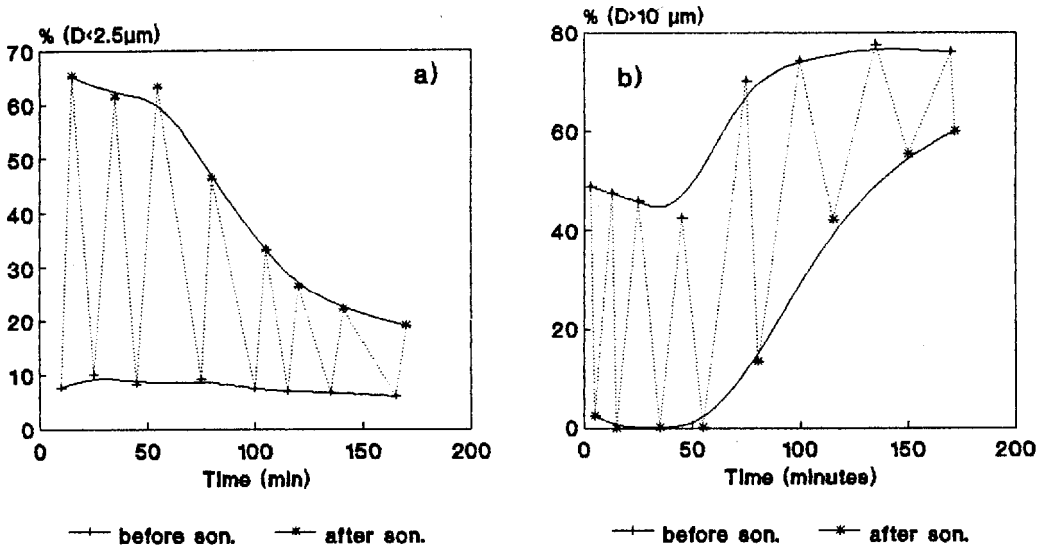

FIG. 4 Evolution of the Particles (the finer (a) and the coarser (b) in a saturated lime solution (W/C=300) subjected periodically to sonification.

However, the close stacking is not essential to obtain the coagulation. The curves of the figure 4 were obtained by granulometric experiments in very diluted suspension (W/C = 300) made in saturated lime water ([CaO] = 22 mmol/l) in order to slow down the formation of hydrates. These curves show the population evolution versus time, of the granulometric classes ranged between 0-2.5 μm and >10 μm before and after 30 seconds of sonification. In such conditions and during the first hour, before sonification, particles are aggregated, they are distributed as 10 % of the the finer particles and 50 % of the coarser ones. the sonification disperses the particles, since the population becomes 60 % of the finer and 0 % of the coarser. 10 minutes after the sonification, the population is the same as before, showing the mechnical reversibility of the interparticular bonds. Then, the coagulation must be due to the same interactions both in paste and in diluted suspension : in paste, the preliminary contact results from the close stacking; in diluted suspension, it results from the chocks between particles caused by stirring, convection flow and brownian motion.

The Second Increase in Cohesion - Rigidification Step

As shown in the figure 2, at the second stage, the paste strength is proportional to the quantity of hydrates formed for a given W/C ratio. For a given percentage of hydrates formed, the smaller the W/C ratio, the more rigid the paste. At this stage, the hydrates are practically uniformally distributed around cement grains, so, the more the number of contact (i.e. the smaller W/C ratio), the greater the part of these hydrates used to make rigid the paste. The strengthening of the paste does occur and the strengthened structure is not easily destroyed unlike the one resulting from coagulation. The result of granulometric experiments in the previously described conditions (figure 4), shows that, during the first hour following the mixing, the sonification disperses particles in the suspension, after then the same treatment makes less and less dispersive : the finer population irreversibly decreases as the coarser one increases, certainly due to particle bridging by hydrates.

But how the hydrates make the paste strengthened? One of the most possible answers to this was proposed by Shchukin (2), who connected the probability of the formation of bridging nuclei between surfaces in contact with various physical and

chemical parameters which have been found to be determinant. However, the proposed model in the case of gypsum nuclei bridging gypsum crystals (or other crystallized phase), seems to be not directly transposable to the strengthening of the cement paste. Indeed, it is difficult to consider C-S-H, the main hydration product, as crystallized phase. The C-S-H are actually poorly crystalline particles precipitated from a supersaturated solution, and their structure is not well established. However experimental evidences show that C-S-H has a layered structure close to tobermorite and jennite (6). Each layer could be regarded as a composite of a main layer and interlayer with a combined thickness of about 1.4 nm . The main layer is a sandwich in which a Ca-O central part is flanked on each side by parallel rows of linear silicate chains. The interlayer consists of H_2O molecules and calcium ions (5).

It is possible to think that C-S-H particles, refered to in the following as nanoparticles, are formed from supersaturated solution according to a classic nucleation process. They could interact with the alite grain surface first and afterwards with each other in the contact zone between cement grains to constitute Shchukin's bridging nuclei. Then, what are the forces involved in these interactions and leading to build up these bridges? The action mode of solvation forces seems to be considered.

As described by Israelachivili (7), at small separation between surfaces, below few molecular diameters, the discrete molecular nature of the solvant cannot be ignored and the short-distance intermolecular pair potential can be quite different from that expected from continuum theories. The solvation forces arise because liquid molecules tend to lie in semi-ordered layer at surface (stratification) and because of the disruption of this ordering during the approach of a second surface.

In many aqueous systems, solvation forces are observed, commonly refered to as hydration forces. They are rather exponentially repulsive, but Israelachivili considered that the short-range hydration forces between smooth rigid surface (e.g. mineral surface) is always oscillatory due to ordered layering of water molecules bound to hydrated surface groups and that the interaction in water is governed by intermolecular effects, i.e. long-range dipole polarization and cooperative H-bonding effects.

This model of particular associations resulting from hydration forces could be applied to the formation of bridging C-S-H. In this case, this kind of interactions would be exerted between the hydrosilicate nanoparticles appearing in the contact zone between cement grains. According to the structure model of C-S-H described above, water and calcium rich interlayers constitute the surface of C-S-H layer; moreover, the environmental medium is a lime supersaturated solution and it can be believed that there is stratification of hydrated calcium ions near these surfaces. The development of hydration forces are favorized by the proximity of the surfaces brought closer by the coagulation process.

According to this mechanism, the nanoparticles stacking in which the interlayer would be constituted by water and calcium ions, forms a true hydrate, in the chemical meaning.

It is the same sort of interactions that lead to hydrates to be fixed on the cement grain surface, which is subjected to a protonation, assuring the strengthening link between them. This interaction mode between superficial ordered layers of hydrated calcium ions could be at the origin of the coagulation as well.

CONCLUSION

In this paper, the initial mechanical evolution and the structure of the cement paste have been studied in relation with the chemical evolution of the system. The cement paste setting process can be described as two fundamental steps : coagulation and rigidification.

The coagulation establishes contacts between cement particles during the first minutes following the mixing. The coagulated structure is proved mechanically reversible. The rigidification of the coagulated structure is provided by formation of hydrates in the contact zone. The increase of paste strength at this stage is proportional to the quantity of precipitated hydrates. The rigidified structure becomes mechanically irreversible.

The nature of the forces bringing into play in the coagulation and rigidification has also been discussed. It suggests that the forces intervening in both phenomena may be the same nature : hydration forces.

REFERENCES

1. Serada P.J., Feldman R.F. and Ramachandran V.S.: "Formation et dévolppement des structures dans les pâtes de ciment durcies", **7th International congress of cement chemistry,** Paris, 1980.

2. Shchukin E.D. and Amelina E.A.: "Contact interactions in dispersed system", **Adv.in Colloïd and interface Sci.**, 1979, 11, 235-287.

3. Hattori K. and Izumi K.: "A rheological expression of coagulation rate theory", **J. Dispersions Sci. Techn.**, 1982, 3(2),129-145.

4. Damidot D.: **"Etude de l'hydratation du silicate tricalcique en suspension diluée par microcalorimétrie isotherme"**, Thesis, Dijon, 1990.

5. Nonat A. and Mutin J.C.: "From hydration to setting", **1st International Workshop on Hydration and setting,** Dijon, France, 3-5 July, 1991.

6. Taylor H.F.W.: "Proposed structure for calcium silicate hydrate gel", **J. Amer. Ceram. Soc.**, 1986, 69(6),464-467.

7. Israelachvilli J.N.: **"Intermolecular and surfaces forces with application to colloidal and biological system"**. Academic Press, London, 1985.

THE PROGRESS OF PORTLAND CEMENT HYDRATION : EFFECT OF CLINKER COMPOSITION

Y Chen and I Odler

Technical University Clausthal
GERMANY

SUMMARY

On a series of portland cement pastes made from cements of different composition the progress of hydration was studied by measuring the amount of nonreacted clinker phases and formed hydration products. It was found that the progress of hydration of the individual clinker phases depended on the overall cement composition as well as water-cement ratio.

ZUSAMMENFASSUNG

An einer Serie von Portlandzementpasten hergestellt aus Zementen unterschiedlicher Zusammensetzung wurde studiert deren Hydratationsfortschritt. Dazu wurde gemessen die Menge der noch nicht reagierten Klinkerphasen und gebildeter Hydratationsprodukte. Es wurde gefunden, daß der Hydratationsfortschritt einzelner Klinkerphasen von der Zusammensetzung des Zementes und dem Wasser-Zement-Wert abhängig war.

INTRODUCTION

Within the present paper we are reporting our data on the hydration kinetics of selected portland cements. The aim of the work was to study the effect of clinker phase composition on the progress of hydration and how the hydration kinetics of the individual phases is affected by the presence of other cement constituents. The investigations were performed on laboratory made cements prepared with a constant sulfate addition and constant fineness and allowed the hydrate at a constant w/c and constant temperature.

EXPERIMENTAL

Four clinkers were synthetized in the laboratory from pure chemicals. Their potential phase composition (Bogue) was as follows:

clinker	C_3S	C_2S	C_3A	C_4AF
A	70	10	10	10
B	60	10	0	30
C	60	10	30	0
D	40	40	10	10

From the clinkers cements were prepared by grinding them with gypsum (SO_3 = 3.0%) to a specific surface area of 300m^2/kg (Blaine).

Pastes made from these cement (w/c = 0.30) were allowed to hydrate at 20 °C for various periods of time; the hydration process was stopped by acetone - ethyl ether extraction. The content of C_3S and C_2S in the pastes was determined by X-ray diffraction on samples preignited to 600 °C (accuracy ± 2.4 g and ± 4.2 g/100 g cem). Also the amount of AFm was determined by this method, however without preignition of the paste (accuracy ± 2.9 g/100 g cem.). To determine C_3A and C_4AF the paste was first extracted with a methanolic maleic acid solution (to remove C_3S, C_2S, CSH and CH). Then the measurement was done again by X-ray-diffraction (accuracy ± 2.0 g/100 g cem.). Gypsum, calcium hydroxide and the AFt phase were determined by DTA (accuracy: ± 0.1 g, ± 0.5 g and ± 0.9 g/100 g cem.). Finally, the combined water was determined as the loss on ignition of the material after acetone-ether extraction. The difference between the total and the sum of phases determined directly was considered to be the CSH phase.

RESULTS

Figure 1 shows the combined water content of the studied pastes after different hydration times. It appears that this value was consistently highest in the hig C_3A cement C whereas it was rather similar in all other cements.

Figures 2 and 3 show the progress of C_3S hydration and the free lime content in the studied pastes. The differences in the progress of C_3S hydration appear generally not too great in different cements. However, an enhanced initial free lime formation in the paste made from cement C suggests an accelerated hydration of C_3S at this stage. The reduced free lime content in the paste made from cement D is due to a reduced C_3S content in the original clinker.

Figure 4 shows the progress of C_3A hydration. The figure includes data for both cements and ground, gypsum free clinkers. Out of the clinkers compared, the C_3A hydration was significantly accelerated in cement C with highest C_3A content. A comparison of data obtained with and without

gypsum revealed a reduced initial C_3A hydration in the former pastes. The progress of C_4AF hydration was not too different from that of C_3A.

From Figure 5 it appears that the amount of the AFt-phase in the studied pastes increased up to a maximum and declined afterwards. This maximum was reached significantly sooner in cement C than in all other cements. The maximum amount of formed AFt was almost identical in all the four cements studied and was obviously controlled by the amount of added gypsum. The rate at which the present AFt was consumed differed in different cements. After 28 days the amount of ettringite in the paste made from cement B was still significant, whereas this phase was absent or present just in very small amounts in pastes prepared from all the three remaining pastes.

From the obtained experimental data it was possible to determine the composition of the pastes studied at any hydration time. Table I shows the composition of the original cement pastes at time zero and after 28 days of hydration (in g per 100 g of original cement). In addition to cement pastes prepared with w/c = 0.30, the Table contains also data for cement A mixed with a higher water-cement ratio i.e. 0.50. It appears, that the hydration of C_3S became increased significantly under these conditions. The Table also includes data for a cement in which a higher amount of gypsum (4.5 rather than 3.0% SO_3) was interground with clinker C. It was found that in this cement the hydration of C_3A was slowed down, yet the amount of AFt present after 28 days was increased. A full interpretation of the hydration progress in cement pastes made from cements A, B, C and D with w/c = 0.30 is shown in Figures 6a-d in which the composition of the paste (in volume fractions) is plotted as function of hydration time.

Tab. I Composition of cement pastes after 0 and 28 days of hydration (in g/100 g original cement)

		nonhydrated material					hydrates				
clinker	hydr. time d	C_3S	C_2S	C_3A	C_4AF	$C\bar{S}H_2$	CH	AFt	AFm	Rest (CSH)	H_2O free
A	0	65	10	9	9	7	-	-	-	-	30
	28	33	10	5	7	0	10	2	0	50	13
	0	65	10	9	9	7	-	-	-	-	50
	28	5	10	4	6	0	22	6	0	80	17
B	0	54	11	0	28	7	-	-	-	-	30
	28	15	11	0	25	0	11	9	0	49	10
C	0	53	12	28	0	7	-	-	-	-	30
	28	21	12	10	0	0	11	0	3	68	5
	0	52	11	27	0	10	-	-	-	-	30
	28	14	11	17	0	0	11	10	1	57	9
D	0	36	41	8	8	7	-	-	-	-	30
	28	18	31	3	6	0	5	3	0	47	17

DISCUSSION AND CONCLUSION

The development of accurately enough analytical methods enabled us to study the progress of cement hydration in a quantitative way. While essen-

cially confirming most previous reports, we were able to show that the kinetics of this process varies in cements of different phase composition and may by affected by the amount of added calcium sulfate and by the water-cement ratio. The obtained findings may be summarized as follows:

The kinetics of C_3S hydration, including the length of the induction period, is little affected by the clinker composition, yet is accelerated with increasing w/c. The observed acceleration due to the presence of larger amounts of C_3A is in line with previous reports (1,2). The kinetics of C_2S hydration is very slow within the first 28 days.

The hydration of C_3A is very fast within the first minutes after mixing with water and slows down subsequently. The amount hydrated in this initial period was found to be even higher in the absence of calcium sulfate. This observation is in line with the assumption, according to which a slow-down of C_3A hydration is one of the ways by which the setting is controlled in the presence of calcium sulfate. Inspide of the very rapid initial hydration, a significant fraction of C_3A remains unhydrated even after 28 days. The hydration of C_4AF progresses distinctly more slowly than that of C_3A. Nevertheless, even here a period of a fast initial hydration may be observed.

The conversion of ettringite (AFt) to monosulfate (AFm) after all free calcium sulfate had been consumed, progresses with a different rate in cements of different composition. Generally, this conversion rate was found reduced in iron-rich cements high in C_4AF. The amount of AFm in mature pastes was found to be rather low, This is possibly due to the fact that a significant fraction of this phase may be closely intermixed with the CSH phase and thus escapes detection.

REFERENCES

1. A. Celani, P. A. Moggi and A. Rio, The effect of tricalcium aluminate on the hydration of tricalcium silicate and portland cement. Proc.5th ICC Tokyo 1968, Vol. II, pp. 387-421.

2. D. Locher and I. Odler. Interaction phenomena in the combined hydration of clinker minerals. Il Cemento 86, 25-36 (1989).

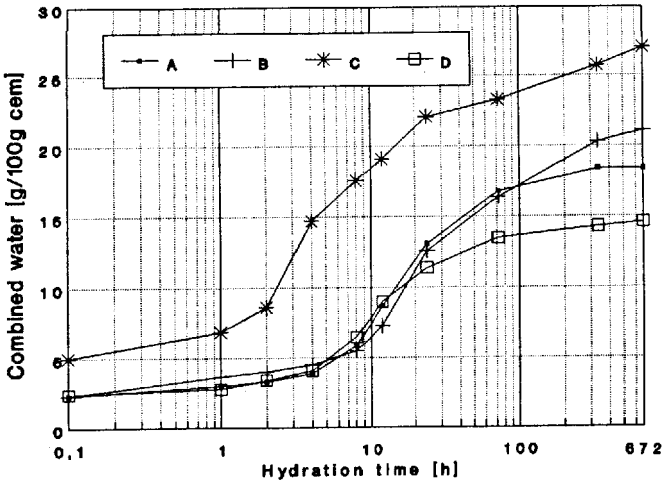

FIG. 1

Combined water content

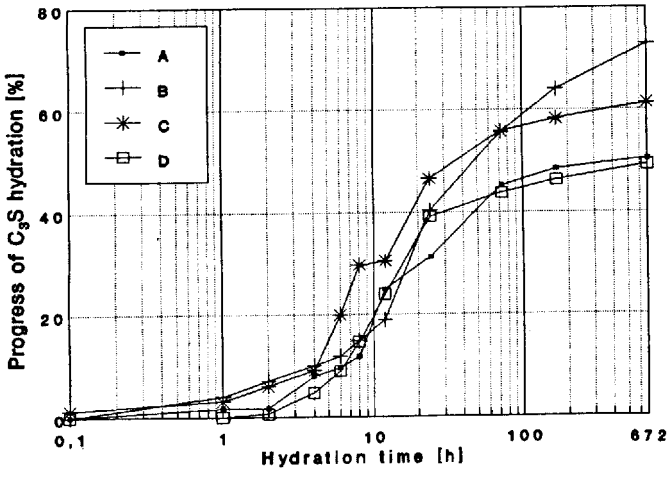

FIG. 2

Progress of C_3S hydration

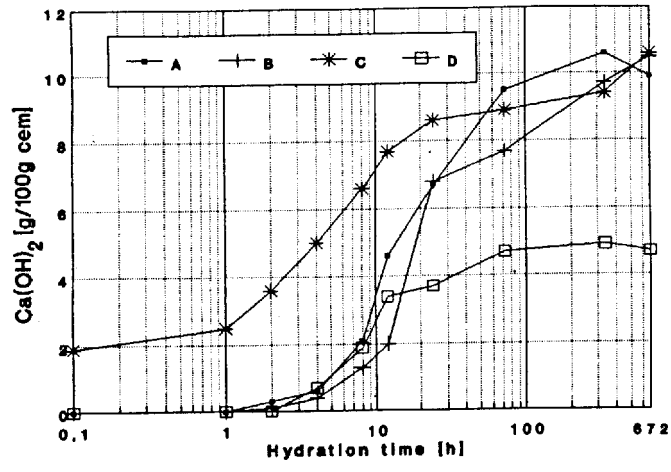

FIG. 3

Free lime ($Ca(OH)_2$) content

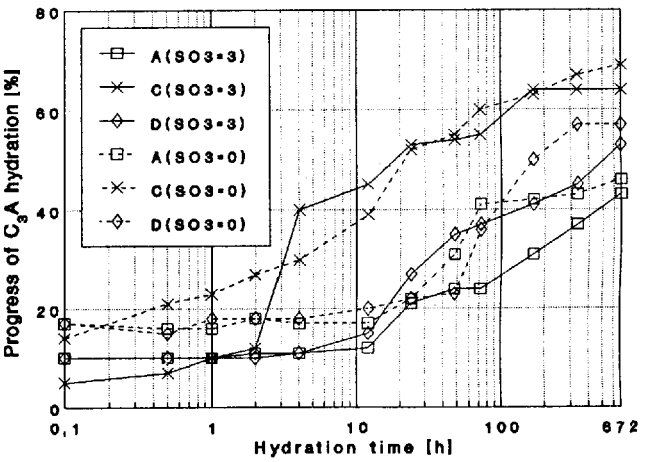

FIG. 4

Progress of C_3A hydration

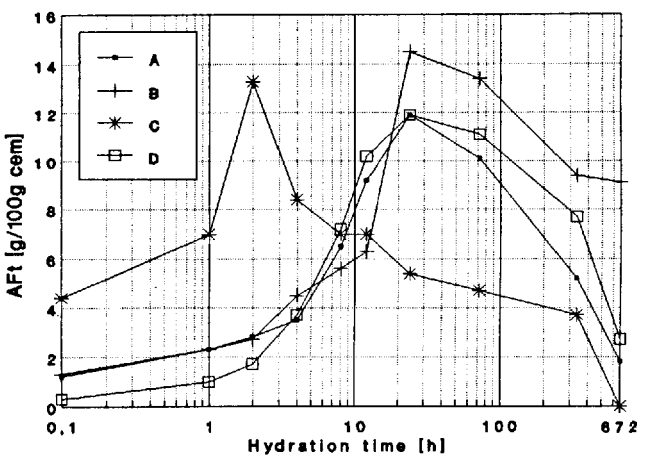

FIG. 5

AFt (ettringite) content

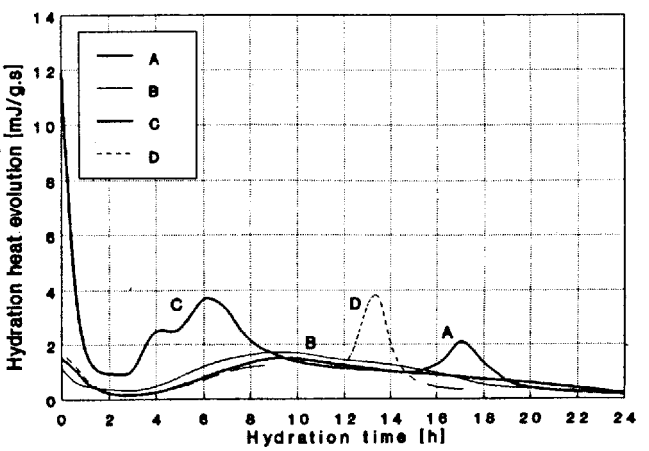

FIG. 7

Hydration heat evolution of pastes made from cements A, B, C and D

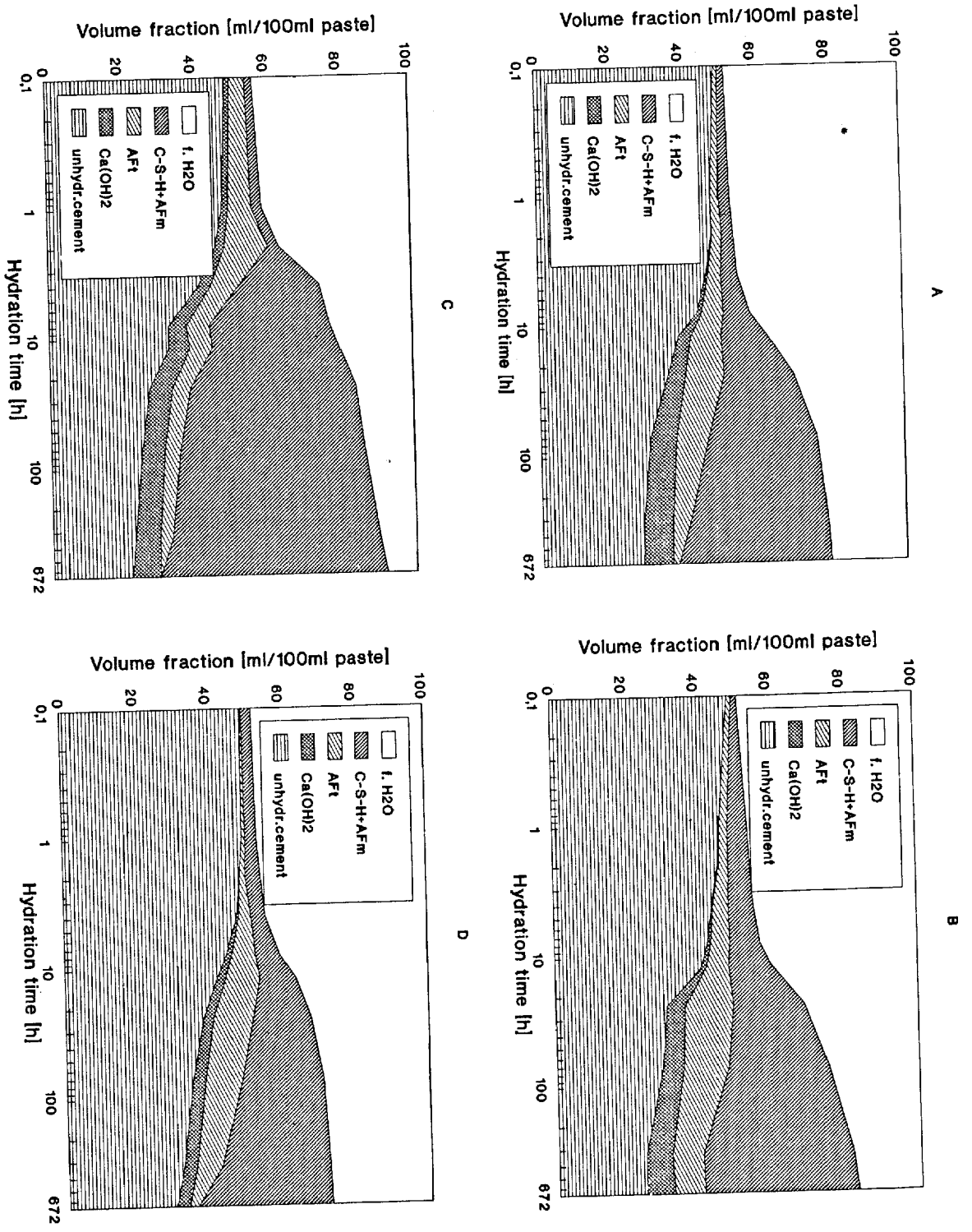

FIG. 6 Composition of cement pastes made from cements A, B, C and D as function of hydration time (in Vol.-%)

DETERMINATION OF KINETIC PARAMETERS IN CEMENT HYDRATION

R Krstulović and P Krolo

Faculty of Technology, Split, CROATIA

The differential microcalorimetric technique was applied in order to study cement hydration. A differential microcalorimeter was used to measure heat evolved during hydration of cement samples; this was a starting parameter in analysis of kinetics of this complex heterogeneous chemical reaction.

Based on the results obtained for heat released and degree of progress of hydration against the duration of hydration, this paper introduces a systematic approach for calculation of the important kinetic parameters in this process.

The induction period, Gibbs free energy of activation, and the equilibrium constant of nuclei formation of new phase during the induction period of cement hydration, were determined by introducing an admixture based on the naphthalenesulphonic acid condensate with formaldehyde into the cement-water system. The Avrami's rate constant and the Arrhenius apparent activation energy were determined as kinetic parameters for the period of accelerated hydration. Mathematical analysis of the hydration kinetics models applied makes it possible to get an insight into the mechanism governing the basic reaction which is characteristic of the hydration process under the given operating conditions.

Zusammenfassung

Für das Studium der Zementhydratation wurde eine differentiele mikrokalorimetrische Messtechnik (DMC) angewandt. Durch die DMC wurde eine quantitative Hydratationswärme von Zementmuster gemessen. Die Hydratationswärme war die Anfangsmessgrösse zur Lösung einiger kinetischen Fragen dieses komplexen heterogenen chemischen Reaktionsablaufs. Auf Grund der Ergebnisse von der freiwerdenden Hydratationswärme und Hydratationsgrad und in der Zeitabhängigkeit wurde eine methodologische Messung und Rechnen der wichtigen kinetischen Parameter in diesem Prozess dargestellt. Die Induktionszeit, Gibbs freie Aktivierungsenergie und Gleichgewichtigskonstante der Formation von der neuen Phase der Nukleation, als sehr wichtige kinetische Parameter in der Induktionszeit der Zementhydratation, werden durch ein Zusatzmittel auf der Basis von Naphtalem-Sullfonsäure mit Formaldehyd im Reaktionsystem vom Zement-Wasser bestimmt. Während der beschleunigten Hydratation, als kinetische Parameter, werden Avramis Geschwindigkeitskonstante und Arrhenius Scheinaktivierungsenergie gerechnet. Auf Grund des Einsatzes der mathematischen Modelle für die Hydratationskinetik kann der Mechanismus eines Hauptreaktionsablaufs, der den Hydratationsprozess unter gestellten Arbeitsbedingungen charakterisiert, kennengelernt werden.

INTRODUCTION

Cement hydration processes, as well as similar physical and chemical processes in ceramic materials, are usually explained by several essential phenomena which occur during the processing of the materials and are closely related to the final product quality and its intended use. The hydration process of cement can be traced by means of the heat evolved during hydration. A knowledge of this phenomenon, and the manner of its progress, provides a better insight into the individual reactions both of the individual constituent phases and the cement as a whole.

In order to study the hydration process and the mechanism governing it, differential microcalorimetry was applied and this proved to be an accurate and simple method. The results thus obtained were used to determine the kinetic parameters. (1, 2)

EXPERIMENTAL

The hydration kinetics of cement was examined by means of a differential microcalorimeter (DMC). Its features make its application possible for precise measurements of cement hydration heat.

The kinetic parameters and the hydration mechanism were determined for a sample of PC-55 type Portland cement in the presence of an admixture. The admixture was a commercial product based on naphthalene-sulphonic acid condensate with formaldehyde (NSF). Table 1 lists the basic properties of the cement and the admixture.

Table 1. Properties of PC-55 cement and the NSF admixture

Chemical composition of cement, mass %

LOI	SiO_2	Al_2O_3	Fe_2O_3	CaO	MgO	SO_3	Insoluble residue
1.38	20.03	5.15	2.68	64.50	2.11	3.12	0.40

Mineral composition of clinker, mass %

C_3S	C_2S	C_3A	C_4AF	CaO_{free}
71.50	22.70	3.02	1.75	1.00

Specific surface according to Blaine ..... 4633 cm^2/g

The NSF admixture is a plasticising and binding retarder, its aqueous solution is dark brown and contains 44.45 % of dry substance; its density is 1.2457 g/cm^3.

Determination of Kinetic Parameters

The hydration process has been divided into three stages. Thus the early stage is viewed as the "induction period", the second stage as the "accelerated hydration period", and the third one as the "retarded hydration period". This study covers the first two stages, i.e. the induction period and the accelerated hydration period.

The induction period is the most important period of hydration, during which the reacting cement-water system prepares for transforming from cement paste into cement stone. It is during this transformation that reactions responsible for later applicative properties of cement take place. (3, 4)

The accelerated hydration period occurs after the induction period, i.e. at the beginning of nucleation of $Ca(OH)_2$ or C-S-H phases, or both simultaneously. Hydration is accelerated in this period, and the degree of hydration (α) shows significant changes. If the basic hydration mechanism is known, and if admixtures are applied which will affect the duration of individual hydration periods, some kinetic parameters can be determined quantitatively. The basic value determined experimentally by the microcalorimetric method is hydration heat Q(t). Its accurate and precise determination makes it possible to obtain kinetic functions such as: change of heat release rate dQ/dt, and change of degree of hydration $\alpha(t)$ with time.

The degree of hydration $\alpha(t)$ is determined by the expression:

$$\alpha(t) = \frac{Q(t)}{Q_f} \qquad (1)$$

where Q(t) is hydration heat at t, and Qf is the final hydration heat. As the hydration of cement occurs at a certain rate, depending on the operating conditions, it is assumed that all hydration heat is released by the end of 72 hours' hydration, which makes it possible to substitute Q_{72} for Qf.

If the value for the degree of hydration is used in mathematical expressions which serve as kinetic models, the mechanism governing hydration reactions in the individual stages of hydration can be established. (4, 5)

Determination of Induction Duration

Induction duration as a measured value provides an insight into the effect the admixture has on cement hydration. This value is determined from the degree of hydration $\alpha(t)$ calculated according to the above expression. The results obtained for duration of induction as a function of the quantity of admixture introduced into the reacting system are shown in Table 2.

Table 2. Change in induction duration t_i with quantity of NSF admixture for PC at 293 K and 298 K at w/c=0.5

NSF	t_i (293 K)	t_i (298 K)
% mass	s	s
0.0	8912.13	8944.38
0.5	15408.29	12839.91
0.8	18399.62	17504.32
1.0	23821.84	18903.20
1.5	29662.27	23921.13

RESULTS AND DISCUSSION

Induction Period

Addition of admixture to cement influences the induction period as per the relation

$$\ln t_i = b\,C + \ln t_i^o \qquad (2)$$

where C is the concentration of admixture introduced. The apparent Gibbs free energy of activation for new phase nuclei formation can be determined from the equation

$$\Delta G_o^{\#} = \left(\ln t_i^o + \ln \frac{k_B\,T}{h}\right) RT \qquad (3)$$

where $\ln t_i^o$ is n$_o$ intercept when the function $\ln t_i = f(C)$ is shown graphically, k_B - the Boltzmann constant, h_o - the Planck constant, R - the gas constant. Results obtained for $\ln t_i^o$ are shown graphically in Figure 1.

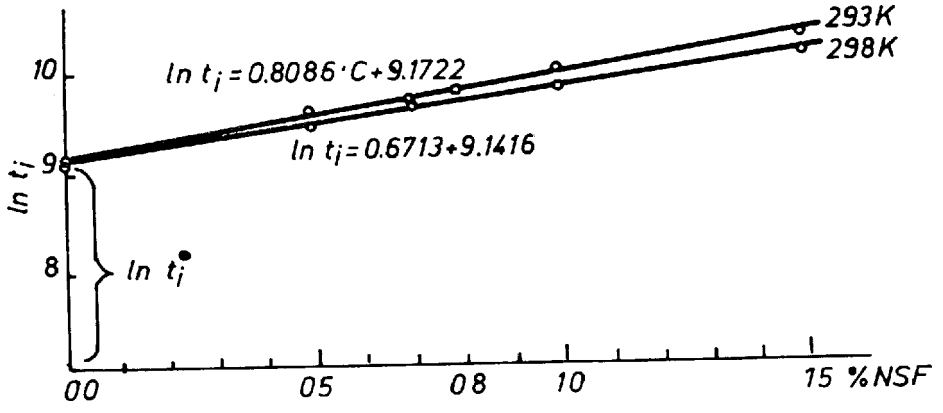

Figure 1. Dependence of $\ln t_i$ upon addition of the NSF admixture to PC-55 cement at 293 and 298 K at w/c = 0.5

The values obtained for $\ln t_i$ are used to determine the value of the apparent Gibbs free energy of activation for new phase nuclei formation.

The admixture, whose activity in the hydration process affects the duration of individual hydration stages, makes it possible to determine the new phase nuclei formation rate constant k. This constant in the induction period is inversely proportional to the duration of this period. The longer the induction duration, the lower the rate constant and the reaction rate. Based on the transition stage theory, the new phase nuclei formation rate constant can be expressed as:

$$k = \frac{k_B\,T}{h} \exp\left(-\frac{\Delta G_o^{\#}}{RT}\right) \qquad (4)$$

while the activated complex formation equilibrium rate K^*, which may be assumed to be a typical transition stage equilibrium constant can be expressed as:

$$K^* = \exp\left(-\frac{\Delta G_o^{\#}}{RT}\right) \qquad (5)$$

Table 3. presents the results obtained for the kinetic parameters in the induction period.

Table 3. The apparent Gibbs free energy of activation ΔG_o, the rate constant k and the equilibrium constant K^* $_o$for new phase nuclei formation for PC-55 with the NSF admixture at 293 and 298 K

T, K	ln t_i^o	$\Delta G_o^{\#}$, kJ/mol	k, s^{-1}	K^*
293	9.1722	94.06	$1.04\ 10^{-10}$	$1.70\ 10^{-17}$
298	9.1416	95.63	$1.07\ 10^{-10}$	$1.73\ 10^{-17}$

Accelerated Hydration Period

The reactions taking place during this period of cement hydration influence the final quality of cement as a binding material. Determination of kinetic parameters, such as the rate constant K_A, the apparent activation energy E_a, and the pre-exponential factor A in the Arrhenius equation is made possible by application of the admixture whose optimal quantity is 0.8% in relation to cement (6, 7). The rising part of the kinetic curve was used to determine the degree of hydration $\alpha(t)$. $\alpha(t)$ shows significant changes in this part of the curve, with linear dependence, and is applied in the kinetic model described by the Avrami's expression

$$\sqrt[3]{-\ln(1-\alpha)} = k_A\, t \qquad (6)$$

The rate constant k_A is determined by establishing the straight line direction coefficient when $\sqrt[3]{-\ln(1-\alpha)}$ is shown as a function of hydration duration.

Based on the results obtained for heat released with time, Figure 2 shows the kinetic curves dQ/dt for different temperatures.

Table 4 presents the results obtained for the constants k_A and ln k_A.

Table 4. Variations in k_A and ln k_A with temperature for PC-55 cement with 0.8% of the NSF admixture added

PC-55 + 0.8 % NSF			w/c = 0.5
T, K	293	298	300
k_A, s^{-1}	$9.4\ 10^{-6}$	$12.1\ 10^{-6}$	$13.8\ 10^{-6}$
ln k_A	-11.57	-11.32	-11.19

The graphical presentation of the Arrhenius equation written in its logarithmic form, Figure 3, is used to determine the value for the apparent activation energy E_a and the pre-exponential factor A.

The activation energy Ea for the cement sample without the admixture amounts to 40.46 kJ/mol. It is 39.73 kJ/mol if the admixture is applied. The pre-exponential factor A is 157.8 s^{-1} for the sample without the admixture, and 112.9 s^{-1} for the sample with it.

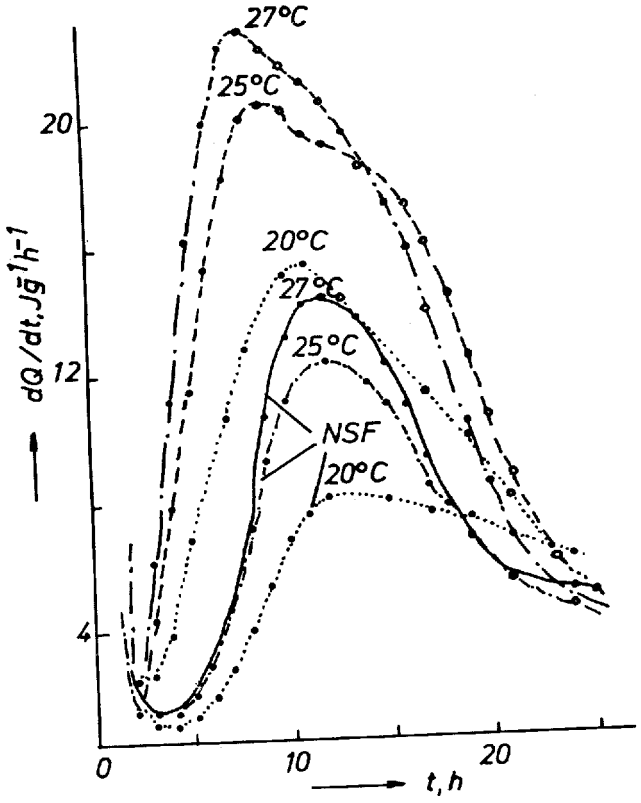

Figure 2. Dependence of dQ/dt = f(t) for PC-55 with and without the NSF admixture

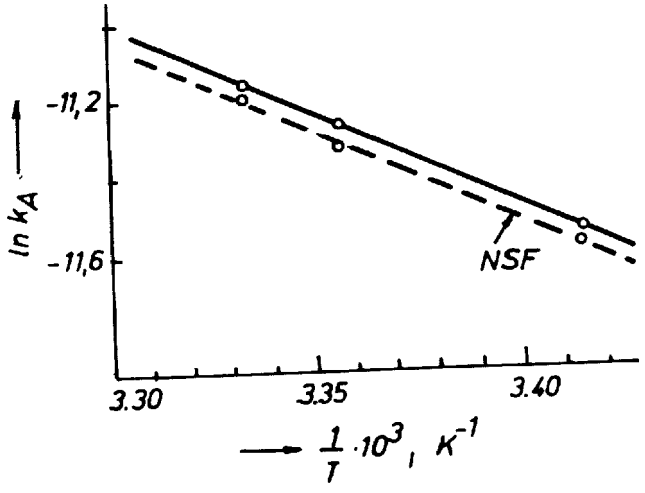

Figure 3. Dependence of ln k_A = f(1/T) for PC-55 with and without the admixture

CONCLUSIONS

Microcalorimetric measurements were used to illustrate a methodological approach for determination of kinetic parameters in the hydration of an industrial Portland cement in the presence of the NSF admixture, a superplasticiser and binding retarder. From the results obtained the following may be concluded:

The role and the influence of the admixture on the mechanism of various processes during the first hours of cement hydration - the quantitative link between the admixture quantity and the values of kinetic parameters (such as $\Delta G_o^{\#}$, K*, k) obtained when mathematical expressions are used as kinetic models confirms that these processes take place during the induction period.

The use of Avrami's equation as the chosen kinetic model satisfies the assumed reaction mechanism (through the rate constant k_A). Validity of the mechanism assumed has been confirmed by Arrhenius' equation.

The apparent activation energy is a specific kinetic parameter indicating the reactive capabilities of cement. Constancy of this value (about 40 kJ/mol) shows that the admixture does not influence the rate of the hydration process (it only modifies some kinetic values) and confirms that the kinetic model was well chosen for the reacting system examined and the conditions under which reactions take place in it.

A change in the value of the pre-exponential factor (A) shows that the presence of the admixture diminishes its value due to adsorption and stabilization of C-S-H phases.

REFERENCES

1. Skalny, J. & Young, J.F.: "Mechanism of Portland cement hydration". International Congress on Chemistry of Cement, 7th, Paris, France 1980, V1, II-1/3 p.

2. Krstulović, R., Krolo, P. & Ferić, T.: "Microcalorimetry in the cement hydration process". Periodica Polytechnica, Chemical Engineering,1989,33(3-4),315 p.

3. Fierens, P., Kabuema, Y., Orszagh, J., Tenoutasse, N. & Tirloco, J. "Reaction mechanism and kinetics of tricalcium silicate hydration in the presence of calcium chloride". International Congress on Chemistry of Cement, 8th, Rio de Janeiro, Brazil 1986, V3, 17 p.

4. Stadelman, C. & Wieker, W.: "Influence of organic compounds on the hydration reaction of tricalciumsilicate", International Congress on Chemistry of Cement, 7th, Paris, France 1980, V4, 199 p.

5. Delmon, B.: "Kinetics of heterogeneous reactions" Moscow, Mir, 1972

6. Krstulović, R., Krolo, P., Žmikić, A. & Ferić, T.:"Determination of the optimal quantity of admixture to cement", Symposium on Cement and Asbestos Cement Technology Development, 14th, Sarajevo, Yugoslavia 1990, Proceedings, 59 p.

7. Krstulović, R., Krolo, P., Žmikić, A., Ferić, T. & Perić, J.: "Comparative examinations of admixtures to cement". International RILEM Symposium on Admixtures for Concrete Improvement of Properties, Barcelona, Spain 1990, Proceedings, 142 p.

CONTROL OF THE SILICATE HYDRATION ACTIVITY WITH THE KNOWLEDGE OF CHARGE TRANSPORT IN SOLIDS TAKEN INTO ACCOUNT

L B Svatovskaya, M M Sychev, V Ya Solovyeva
T V Smirnova, N N Shangina, S G Gerke and N I Uman'

Petersburg Institute of Transport Engineers, Moskovsky
St Petersburg, RUSSIA

ABSTRACT

The work is devoted to investigating the possibilities of controlling the hydration activity of two-calcium β-silicate with the knowledge of the surface character, charge and energy transport in solids and quasi-solids taken into account. Two stages of oxidation processes in β-C_2S paste have been found which reflect cycles of the hydration processes taking place as well as reaction activation by introducing dispersions of substances of a particular character, ions with high degrees of oxidation as well as by temperature decreasing after the critical period of structure formation down to -3 ... -6°C. Proceeding from the knowledge of a specific electronic structure of the surface of the substances to be introduced and water structure, interaction models have been considered.

РЕФЕРАТ

Работа посвящена исследованию возможностей управления гидратационной активностью β-двухкальциевого силиката с учетом представлений о природе поверхности, переносе зарядов и энергии в твердых и квазитвердых телах. Обнаружены две стадии процессов окисления в пасте из β-C_2S, отражающие циклы происходящих гидратационных процессов, а также активирование реакций введением дисперсий веществ определенной природы, ионов в высоких степенях окисления, а также понижением температуры после критического периода образования структуры до -3°... -6° С. Рассмотрены модели взаимодействия, исходя из представлений об особом электронном строении поверхности вводимых веществ и структуры воды.

INTRODUCTION

A conclusion drawn from the discussion of the band structure of the silicate composition, character of active centers and system of hydrogen bonds existing in a binding paste is that it is possible to control the hydraulic activity of a solid, with the following hypothetical mechanisms of influence included.

1.Recombination mechanism

Nonequilibrium charge carriers (electrons), which appear in silicate at a contact with another phase or on illumination with visible light, ultraviolet or X-ray radiation, that is, any radiation with an energy of above 3,5 eV, recombine with holes with the possible formation of quasi-particles such as excitons which in the breakdown release an energy close to the level or band energy. If the heat capacity of silicate is approximately assessed as that following from the Dulong and Petit law, the temperature increase inside the sample taking place due to recombination can reach tens degrees.The practical result of implementing this model is the development of radiactive technologies of cementstone hardening activation, introduction of activating substances capable of interaction with nonequilibrium charge carriers,as the transport of energy and charge carriers through the bond system is used.

Exciton states can initiate polymerisation processes with energy transfer to a chemical bond which breaks and a radical or a pair of radicals is formed. The practical result of applying the model of solid-phase polimerization is both hydration activation based on principles of oxidation catalysis and stone strengthening.

2.Proton-transfer mechanism

Proton and energy transfer through the hydrogen-bond system, possibly with the use of quasi-particles in the form of solitons, enables one to believe that with decreasing temperature due to system entropy lowering and initiation of particular boundary structures from hydrogen bonds, proton and energy transfer processes are activated by the token mechanism, which results in the enhancement of hydrate formation and ston strength. It is not improbable that in appropriate conditions tunneling can also manifest itself.

3.Interaction mechanisms with the peculiarities of the surface electronic structure taken into account

In accordance with [1,2], the following active centers can be single out on the silicate surface, which are distinguished by electronic structure peculiarities - acid electron-acceptor α-centers which can be an electron-pair acceptor and a proton donor;basic α'-centers which can be an electron-pair donor; electron-deficiency (oxidation) h^{+}-centers and electron-donor (reduction) h^{-}-centers. With the peculiarities of the surface structure in conditions of the manifestation of charde and energy transfer taken into account,it is possible to control the hydration activity of silicates, using substances of a particular character or appropriate physical conditions.

EXPERIMENTAL

The investigations were conducted on β-C_2S pastes with substances of different bond character and electronic structure introduced and also with the hydration temperature decreased down to -18°C.

Substances were added to β-C_2S powder in amounts of 3 to 10 mass %, the mixture was tempered with water at the w/S ratio = 0.3 and sample blocks were formed. At particular intervals physicomechanical and physicochemical studies were made by Mossbauer spectroscopy, IR spectroscopy, X-ray phase and derivatization analyses.

RESULTS AND DISSCUSSION

The Table gives the developed models of β-C_2S hydration-activity control and investigation results with the specified substances taken as examples.

Active-center character of the silicate surface	Substance to be introduced or hydration conditions	Possible interaction schemes	Effect of influence: compression strength, %, chemically bound water, %, at the age of, day		
			7	28	60
Electron-deficiency, h^+-centers	Ions with the lowest oxidation degrees $Me^{m+} - ne \rightarrow Me^{(m+n)+}$	Surface passivation due to electron drain and center extiction $h^+ + \bar{e} \rightarrow h^0$ (scheme 1)	$SnCl_2$: 0 / 61	83 / 92	480 / 253
Electron-donor, h^--centers	Ions with high oxidation degrees	Surface-activity enhancement due to the induction of additional active h^{+*}-centers (scheme 2) $h^- - n\bar{e} \rightarrow h^{+*}$	$SnCl_4$: 125 / 188	182 / 203	441 / 263
Acid Lewis centers, $\alpha\square$-centers	Substances A ($\downarrow\uparrow$) having unshared s,p,d-electron pairs	Surface-activity enhancement due to chemical bond weakening in the interaction (scheme 3) $A(\downarrow\uparrow) + \alpha\square \rightarrow A\boxed{\downarrow\uparrow}\alpha$ $H_2O(\downarrow\uparrow) + \alpha\square \rightarrow H_2O\boxed{\downarrow\uparrow}\alpha$	CaF_2: 186 / 179	191 / 206	171 / 205
Basic Lewis centers, $\alpha'(\downarrow\uparrow)$-centers	Substances having vacant s,p,d-orbitals: $Me^{n+}\square$	Surface-activity enhancement due to chemical bond weakening in interactions (scheme 4) $Me^{n+}\square + \alpha'(\downarrow\uparrow) \rightarrow Me^{n+}\boxed{\downarrow\uparrow}\alpha'$ $Me^{n+}\square + H_2O(\downarrow\uparrow) \rightarrow Me^{n+}\boxed{\downarrow\uparrow}OH + H^+$ $H^+\square + \alpha'(\downarrow\uparrow) \rightarrow H^+\boxed{\downarrow\uparrow}\alpha'$	Fe: 130 / 128	147 / 135	165 / 138
			$CaSO_4$: 196 / 167	235 / 219	217 / 179
$\alpha'(\downarrow\uparrow)$-centers	Temperature decrease in the system (cryohydration)	Hydration-activity enhancement due to proton mobility with the token mechanism of proton transport (scheme 5) $H^+\ldots(O\overset{H}{<})_n\ldots O\overset{H}{<} \rightarrow H^+\square$ $H^+\square + \alpha'(\downarrow\uparrow) \rightarrow H^+\boxed{\downarrow\uparrow}\alpha'$	t= -3° to -7°C: Period of critical hydrate structure formation 118 / 132		126 / 129

Note: Strength and chemically bound water of addition-free β-C_2S hardening at t=20°..22°C at the corresponding age are taken as 100%.

The process of Sn(II) oxidation in Sn(IV) in β-C_2S paste and no Sn(IV) reduction were recorded by Mossbauer spectroscopy (Fig.1)

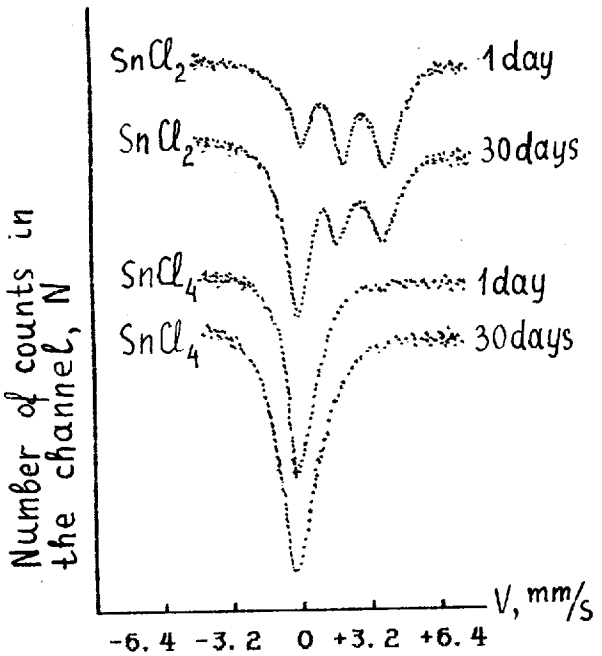

Fig. 1. Mossbauer spectra of $SnCl_2$ and $SnCl_4$ in β-C_2S paste

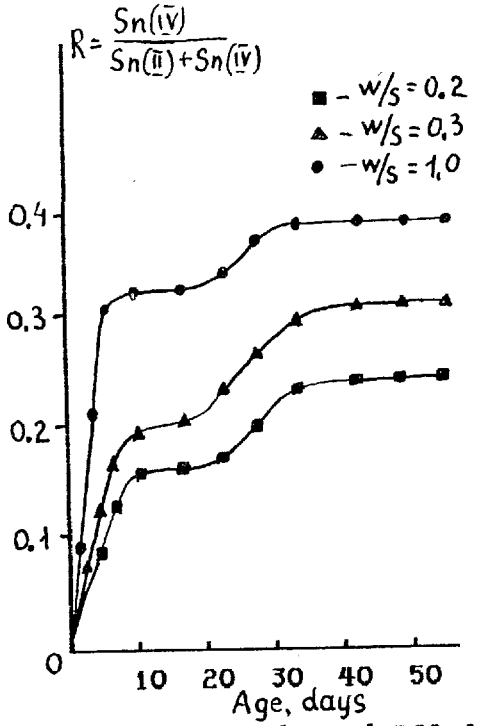

Fig. 2. Kinetic dependence of the Sn(IV) fraction in β-C_2S paste

In this case even on the first day Sn(II) present in the system begins to change to Sn(IY) and by the 30th day the fraction of Sn(IY) increases. It has been established that oxidation of tin (II) occurs in two stages: the 1st stage ends in 7-10 days (depending on the amount of added water), the 2nd one in 23-28 days. In curves showing the kinetic dependence of the four-valent tin fraction two plateaus are observed which correspond to two hydration-process stages characterized by different times of redox reaction running (Fig. 2), that is, hydration processes feature cyclic character. In this case surface reduction reactions can proceed according to scheme 1: $h^+ + e \rightarrow h^\circ$, which results in passivation of the surface at the early age.

Realization of scheme (2) in $-\beta C_2S$ hardening in the presence of substances having elements of high oxidation degrees with the possible induction of h^{++}-centers of the surface suggests the activation role of oxidants in β- C_2S hardening. The experiment has shown that at the age of 2 months the strength of stone samples from β- C_2S with tin increased more than three-fold, since by this age in the system there exists only Sn(IY) either obtained by scheme (1) or initially introduced. The strength enhancement is connected with increase in the amount of chemically bound water and low-basicity hydrosilicates.

Proceeding from the knowledge that in a binding system from the first act of the interaction with water the donor-acceptor system of bonds is realized, one can assume that beneficial for enhancing the surface activity and reactivity of starting solid phases will be compounds with donor properties which contain vacant S, p, d-electron pairs (scheme 3) and compounds with acceptor properties which contain vacant S, p, d-orbitals (scheme 4). The investigations of β- C_2S hardening in the presence of substances featuring different bond character - 3d-row metals: iron, cobalt, nickel and their oxides as well as slightly soluble compounds of ionic bond character with vacant S-orbitals: $CaSO_4$ and CaF_2 showed the following.

According to data of instrumental physicochemical investigations, the introduction of iron, nickel, cobalt increases the hydration activity and strength of the composition, the content of low-basicity calcium hydrosilicates increases therewith.

It has been known that at negative temperatures the boundary water layers and water acquire new properties, including structure-and-mechanical ones, and as a consequence of water cross-linking the mobility of hydrogen ions, active particles of the system, increases (token mechanism) - scheme 5.

It has been found that a specific token mechanism begins to manifest itself in conditions of the existence of particular critical hydrate structures which are formed within 3 to 7 days.

Since the token model of proton transfer being considered includes a system of donor-acceptor bonds and interactions, it can be acted on with substances given in the Table. Fig.3 shows the dependence of the hydration degree for β-C_2S-based compositions on hydration temperature at the age of 28 days. The investigations have shown that the growth of chemically bound water and strength at temperatures from -3° to -7°C is connected with the increase in the content of low-basicity hydrosilicates and the appearance of new hydrate phases.

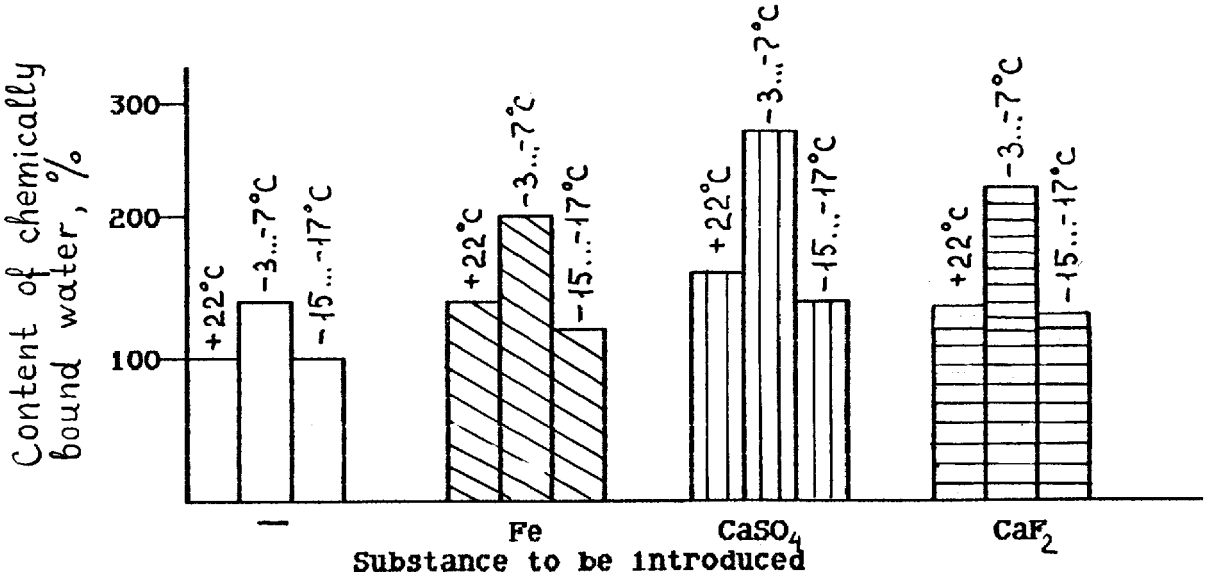

Fig. 3. Dependence of the hydration degree of β-C_2S paste samples on hydration temperature, as substances of different character at the age of 28 days are introduced

CONCLUSIONS AND RECOMMENDATIONS

The knowledge of a specific electronic structure of the surface of silicates and substances to be introduced as well as water and the whole system at decreased temperatures can be used for controlling the hydration activity of β-C_2S-containing products such as belite cements or nepheline slurries. In this case slightly soluble substances introduced in comminution and capable of donor-acceptor interactions at the level of heterogeneous acid-base catalysis such as calcium anhydrite or fluoride, substances containing elements with high oxidation degrees and substances containing elements with partially filled orbi-

tals can activate hydration processes.Temperature lowering down to -3..-7°C after the formation of boundary critical hydrate structures also results in activation of hydration processes and strength enhancement.

REFERENCES

1. Svatovskaya, L.B. and Svchev, M.M.: "Activated hardening of cements" L.,Stroiizdat, 1983.
2. Svchev M.M.,Svatovskaya L.B.,Lukina L.G.,Stepanova I.N.: "Chemical properties of active centers and control of silicate hydration",Proc.of the 8th All-Union Scientific and Technical Meeting on Chemistry and Technology of Cement M.,1991.

OBTAINING HIGH BASICITY CLINKER AND INFLUENCE OF COMPLEX ADDITIVES ON ITS HYDRATION AND HARDENING

A Kaminskas and A Mituzas

Technical University, Vilnius
State Firm "Termolita", Innovations and Science Centre, Vilnius
Republic of LITHUANIAN

This paper presents kinetics of clinker formation which increases lime saturation factor (LSF) up to 0.98-0.99 by introducing in the burning zone dust enriched with carbonate components trapped by electro filters. Mechanism and kinetics of clinker hydration is resumed, when hydration process is simultaneously effected by carbonate and silicate ions.

A higher lime saturation factor (LSF) of clinkers significantly increases strength characteristics of portland cement especially during initial hardening, allows to reduce sharply quantity of alkalies in the cement and saves energy consumption owing to the possibility of obtaining cements with large quantity of hydraulically active additives /up to 5%/ almost without decrease of their initial strength.

However, in practice, production of clinkers even with LSF close to one is accomplished with great deal of technological difficulties and increase of fuel consumption.

In the present paper results of kinetics of the formation and destruction of calcium silicates of high basicity in the course of thermal processing of raw material mixtures are resumed. These raw materials differ in their mineralogical characteristics.

The first group comprises mixtures, constituents of which are large - crystalline and kaoline and marble type components which are not so active. The second group comprises mixtures, whose reactivity is increased by means of mineralisers (mixture 2-1) and magnesite (mixture 2-2), or composite parts of which are natural, almost amorphous marls (mixture 2-3). The third group comprises materials made up by relatively potentially reactive acid oxides and limes of medium - crystal structure and are industrial raw mixes of cement plants.

Granules prepared from the raw materials mixtures were burnt at 600, 750, 850, 950, 1050, 1200, 1350 and 1450°C. In each case retention period was 30 and 60 min. Cakes cooled in the air were ground in the mill and subjected to physico - chemical, XRD and other methods of analysis.

The kinetics of clinker formation was investigated radiographically and by the method of selective solution in 5% H_3BO_3 of calcium orthosilicates (quantity change of soluble SiO_2 and CaO in the solution H_3BO_3 /1/).

Silicates constituted from endless chain (SiO_3^{2-}) and silica oxygen groups which are in glassy state remained untouched.

According to these data, for all the mix batches burnt at different temperatures, contents of $CaCO_3$; free CaO, C_2S and C_3S were calculated; and the quantity of silica soluble in H_3BO_3 was determined (soluble SiO_2).

Data obtained are presented in Figs. 1 and 2. XRD data indicated, that C_3S was present mainly in monoclinic form. However, in the course of isothermal burning trigonal and monoclinic forms are fixed, which is characteristic of real clinkers with large contents of Al^{3+}, Fe^{3+} /4/. This shows, that at burning temperatures <1350°C even with isothermal burning it is impossible to identify a precise connection between crystal form of C_3S and changes in SiO_2 solubility caused by the diverse nature of raw material components.

However, in the alite diffractograms obtained at high temperatures, transition of one form of alite into another can be clearly noticed with temperature and time changes. The order of existence of separate crystal system was: <1350°C - rhombohedral (r); 1350-1400°C monoclinic (m); >1400°C - triclinic (t).

During cooling, monoclinic and triclinic forms of C_3S become stable.

Experimental data obtained testify that:

- Alite formed at high temperatures of isothermal retention undergoes cyclic polymorphous transformation, frequency of which depends on the chemico-minerological characteristics of the raw mix;

- Temperature increase of processing of certain raw materials mixture conditions increase of alite transformation cycles;

- Transformation cycles number growth enlarges reduction probability of alite quantity in cooled clinkers because of fixation of the destroyed alite part in glassy, not active state.

These results formed the basis for the main development of a new method of obtaining portland cement clinkers, essence of which consists in maintaining the temperature of the burnt material in the sintering zone of the rotary kiln at a level which is sufficient for completion of clinker formation reactions and at the same time preventing the polymorphic transformation of alite.

This is achieved by introduction in the burning zone dust enriched with carbonate components (dried or ground limestone) trapped by electro filters.

Introduction of burning process according to the present method allows to bring the LSF of clinkers to 0.98-0.99 while using raw mixes of LSF 0.92-0.93 (Table 1).

Table 1

Data of Chemical Analyses of Lime - Stone Used

No	Title	Chemical composition, %				Modules		
		SiO_2	Al_2O_3	Fe_2O_3	CaO	LSF	p	r
1.	Source raw materials	13,04	3,21	2,90	40,34	0,93	2,1	1,1
2.	Raw materials dust (concentrated)	13,75	3,58	3,10	46,14	1,02	2,06	1,1
3.	Clinker	19,95	4,71	4,44	64,53	0,99	2,2	1,1

Because of the increase in clinker LSF there is a possibility of obtaining cements having a high content of hydraulically active additives. Substitution of part of clinker by these additives allows to significantly reduce energy consumption for cement manufacture.

Study of active additives of this type which simultaneously supply silicate and carbonate ions to the hardening system is especially interesting.

Carbonaceous opoka is an additive of this kind consisting of amorphous SiO_2 and saturated fine - dispersion calcium carbonate.

$CaCO_3$ content in opoka is ~ 45%. Opoka activity is 260 mg CaO/g.

Kinetics and the mechanism of carbonaceous opoka influences on early stage hydration of basic clinker materials C_3S; C_3A and portlandcement were studied at $\pm 30^oC$ for a water - cement ratio w/c=0,3 and at $\pm 80^oC$ for a ratio w/c=0,8.

It can be seen from the thermokinetic curves (Fig.5), that addition of very finely divided carbonaceous opoka increases the rate and completeness of C_3S hydration. However, carbonaceous opoka (fig.6) significantly reduces intensity and completeness of C_3A hydration.

If in the case of hydration of pure C_3A the basic hydration phase is C_3AH_6, in case of opoka addition, calcium hexagonal hydroaluminate with high degree of dispersion and amorphous state dominates. With increase in the duration of C_3A hydration hexagonal crystals of C_2AH_8 (d=2,84; 2,42 etc.) remain stable. A significant quantity of $C_3A.CaCO_3.11H_2O$ (d=7,63) accumulates in a parallel way. Disappearance of endothermic crests at 360-370°C and 540°C, characteristic of C_3AH_6 presence, points out that with the appearance of calcium carboaluminate, C_3A hydration reaction is decelerated to an even greater degree, carbonate ions at hardening temperature, not exceeding 40°C can be a regulator of the setting period of portland cement aluminate part.

Change of hydration kinetics of basic clinker minerals and formation of additional quantity of cementing materials ensure high strength of pozzolana cements.

The test results obtained are presented in Fig.3 and 4, which depict the change in strength data (Curve 1) and linear deformations of mixed cement samples, obtained by inter - grinding of clinker and opoka; and their separate grinding followed by mixing.

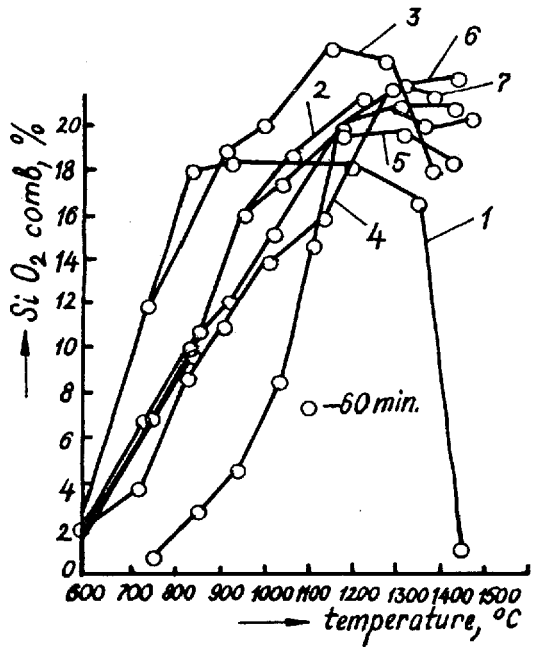

Fig.1

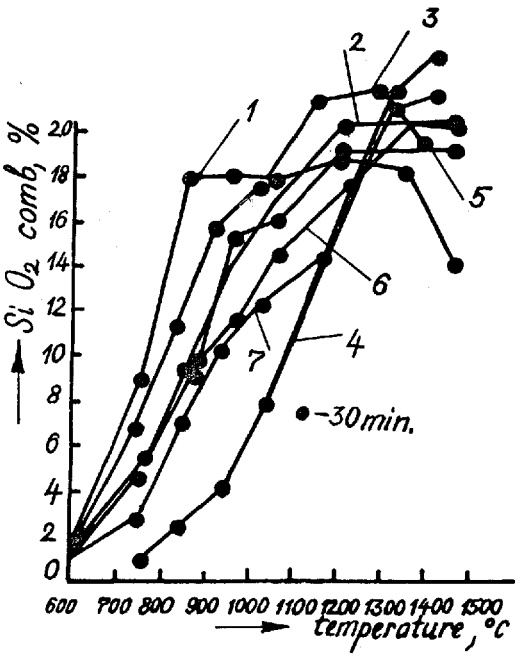

Fig.2

Change of SiO_2 in 5% solution of H_3BO_3 depending on burning temperature: Charge No 2-1 (curve 1); charge 2-2 (curve 2); charge 2-3 (curve 3); charge 1-1 (curve 4); charge 3-1 (curve 5); charge 3-2 (curve 6); charge 1-2 (curve 7).

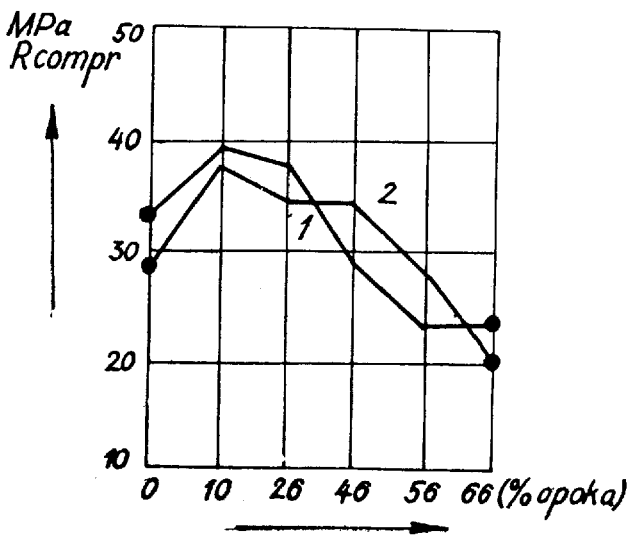

Fig.3. Dependence of samples strength, which hardened 28 days in the water, on quantity of added opoka.

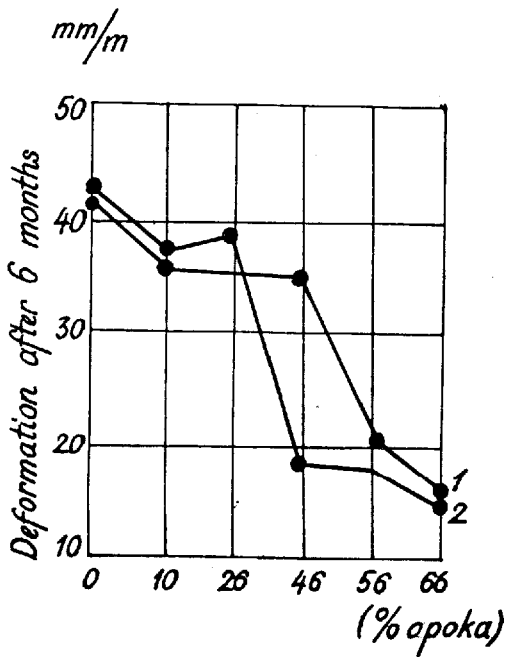

Fig.4. Change of samples linear deformation depending on quantity of added opoka.

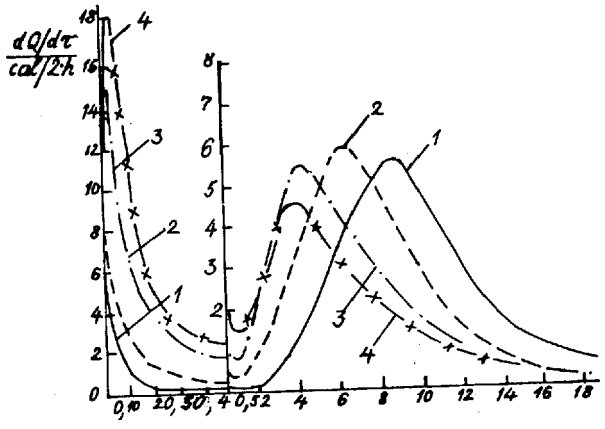

Fig.5.

Thermo kinetic curves of hydration with addition of grinded opoka:t=30°C;W/C=0,5

1 ____ C_3S 100%
2 ____ C_3S 90% + Opoka 10%
3 _ . _ C_3S 70% + Opoka 30%
4 _x_ C_3S 50% + Opoka 50%

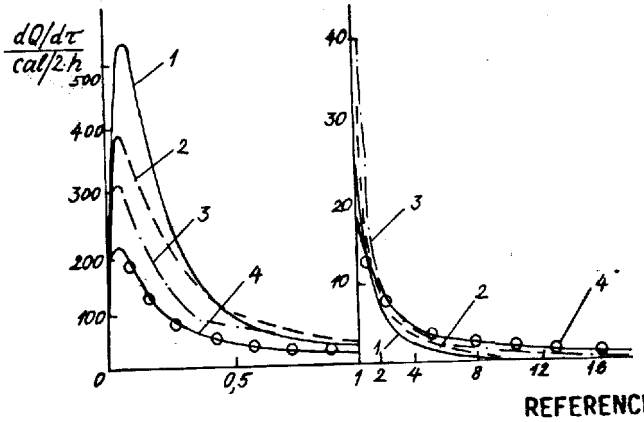

Fig.6.

Thermo kinetic curves of C_3A hydration with opoka addition: t=30°C; W/C=0,5

1 ____ C_3A 100%
2 ____ C_3A 90% + Opoka 10%
3 _ _ C_3A 70% + Opoka 30%
4 _x_ C_3A 50% + Opoka 50%

REFERENCES

1. A.Mituzas "Boron acid in cement chemistry". Cement, 1988. No 5, p.p. 16-17

2. F.M.Li "Chemistry of cement and concrete". Gosstroijizdat, M., 1967, p.p. 130-131.

3. R.I.Bogue "The chemistry of portland cement". Second edition, New York, 1955, p.p. 123-125.

4. A.Ginje, M.Renur "Structure of portland cement minerals". Fifth International Congress on Cement Chemistry. Stroijizdat, M., 1973, p.p. 8-10.

5. J.Mituzas, A.Mituzas "Mecanisme du durcissement de la pate de ciment portland". 7-e Congres International de la chimie des Cements, vol.III. Communication (Sulte). Paris, 1980.

6. A.Kaminskas "Technology of building materials on magnesium raw materials". Vilnius "Mokslas", 1987, p.p. 116-121.

AN INVESTIGATION INTO THE HARDENING OF MONOSTRONTIUM ALUMINATE

L B Borovkova, T I Borodina, T A Evdokimova
T A Melehina and E P Pakhomov

Institute for High Temperatures, Russian Academy of Science, MOSCOW

SUMMARY

Setting characteristics (normal consistency paste of cement,initial and final setting, selfheating) were investigated. Process of curing (increase compressive strength, changes in mass and volume, porosity, degree of hydration, crystalline compositions of hydration products) as a function of the curing time duration (from 0.1 hour to 6 months), amount of the mixing water (H/SA=0.05-1.0), temperature of the environment (20-40°C), Blaine fineness (2500-5200 cm^2/g) and effect of addition of water to the sample during the curing process,were studied.

Comparison of the literature values was carried out.

Maximum strength of air the hardened cement SA (40 MPa after 3 days hardening) was reached by curing with H/SA=0.24, that very close to normal consistency paste of cement (0.27). Obviously, hydrate SAH_{7-10} is formed in the framework and is the cause of strength of the stone SA.

Duration of the hardening by addition to the sample of supplementary water the amount S_3AH_6 increase, but amount of the crystalline AH_3 does not increase. The strenght of the cement stone begins to decrease only after 2-3 months. Obviously, becouse of cement stone has a big porosity (about 20%) a some part of additional volume of the hydration products can be absorb by its structure without considerable damage the last.

АННОТАЦИЯ

Характеристики схватывания (нормальной консистенции теста, начала и конца схватывания, саморазогрева) и твердения (набора прочности на сжатие, изменений объема и массы, пористости, степени гидратации и фазового состава кристаллических продуктов гидратации) были исследованы в зависимости от времени твердения (от 0,1 часа до 6 месяцев), количества воды затворения (H/BA=0,05-1,0), температурных условий (20-40°C), удельной поверхности исходного порошка (2500-5200 $см^2/г$) и количества воды, дополнительно вводимой в образец в процессе твердения.

Выполнено сравнение с имеющимися литературными данными.

Получено, что на воздухе максимальная прочность достигается камнем SA (~40 МПа после 3 дней) при затворении с водоалюминатным отношением 0,24, что несколько меньше нормальной густоты теста (0,27).

Вероятно, гидрат SAH_{7-10} формирует при схватывании структуру камня SA и определяет его прочность.

При поступлении в твердеющий образец дополнительной воды растет количество S_3AH_6; прочность начинает уменьшаться после 2-3 месяцев твердения. Вероятно, формирование на этапе схватывания значительной пористости (20%) позволяет размещать в ней некоторую часть дополнительного объема продуктов продолжения гидратации без разупрочнения структуры камня.

INTRODUCTION

Monostrontium aluminate $SrO.Al_2O_3$(SA) like monobarium aluminate is one of the most highly refractory cements. It has a high potential for use as concrete and ramming masses at 2000 K and more.

SA cement has been studied very extensively in 50-70th years (1-13). However, knowledge on SA hardening characteristics remains insufficient.

In this report the results of the study (14) on the hardening characteristics of SA cement as a function of curing time duration, amount of mixing water, powder fineness and hardening conditions are reported. Compressive strength, mass and volume changes, open porosity, hydration degree and compositions of crystalline hydrates were determined.

Strontium aluminate, produced by solid state sintering at 1820 K, was used as the raw material. X-ray analysis showed that 2-5 % wt. impurities of strontium hexaluminate (SA_6) are present. The Blaine fineness of the powder was 3500 cm^2/g.

EXPERIMENTAL

Water-cement ratio of SA slurry with normal consistency was 0.27, initial and final sets were 20 min and 25 min,respectively. The self-heating of 35 g normal consistency slurry is 5-6 K and after 30-40 min the heating maximum is reached.

A time dependence study of the SA air hardening in 2 hours -6 months period at relative humidity(W) 55±20% and at 21±3°C on samples 14.14.14 mm^3 (Fig.1)was carried out.It showed that after the first day of curing the strength reached 20-35 MPa (Fig.1,a), after a month the strength was 45-55 MPa, and after 6 months it became 50-55 MPa.

The volume shrinkage after 1-3 days of hardening was 2% and after one month 3%. Mass losses (water evaporation) were 5-6% after one day of hardening and 3% after one month. The open porosity of the stone was 20-25%.

Data on the degree of hydration (X(SA)) (Fig.1,b) showed that at the final set of SA normal consistency slurry 20% of the cement mass had hydrated and after one day 55%. Beyond that, over the next 6 months, the hydration degree did not change.

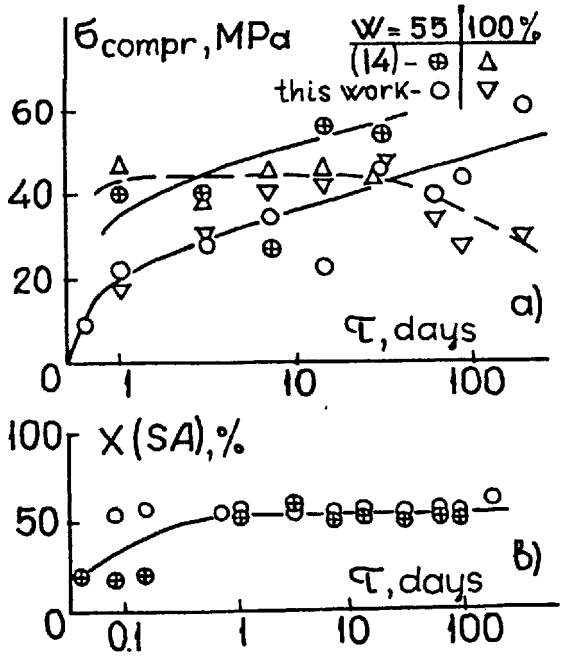

Fig.1 The change of the compressive strength (a) and SA hydration degree (b) as a function of hardening time both for air and at humidity W=100%; H/SA=0.27

X-ray analysis shows the presence of SA, SA and SAH , S AH , AH , SH (sometimes SH) compounds (where A=Al O , S=SrO, H=H O, C=CO). Peak intensities of all crystalline hydration products are not high. The scatter of the values is large.

Investigations on the setting and hardening processes as a function of mixing water content was carried out at water: strontium aluminate (H/SA) mass ratio 0.1 :1.0 (Fig.2). It was found that the setting time increased when the mixing water increased. At H/SA<0.2 setting time is negligible.

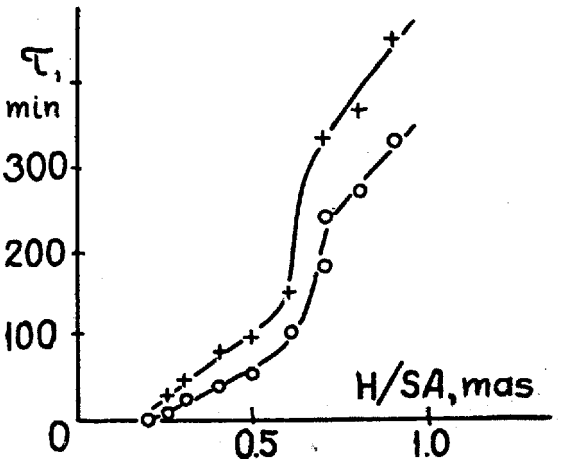

Fig.2 Set times of SA slurry as a function of the mixing water amount (H/SA)

Fig.3 represents the change in compressive strength ( )at 3 and 28 days and 6 months hardening as a function of the mixing water amount. Maximum strength (45-50 MPa) was reached at H/SA=0.24, the late less than the normal consistency slurry (0.27). If mixing water amount is varied, strength of SA stone decreases till 20 MPa at H/SA<0.13 and H/SA> 0.45.It is necessary to note that the scatter of the values is large.

Volume shrinkage and mass losses of patterns are growing with H/SA increasing (Fig.3) from zero at H/SA= 0.1 up to 10-15% at H/SA=0.5.

Hydration degree (X(SA)) and composition of SA hydration products as a function of the mixing water amount for 3 and 28 days and 6 months hardening are represented in Fig.4. With H/SA increasing the hydration degree increases too (Fig.4,a). Complete hydration is observed at H/SA>1.3. The hydration degree is about 40-55% at maximum strength.

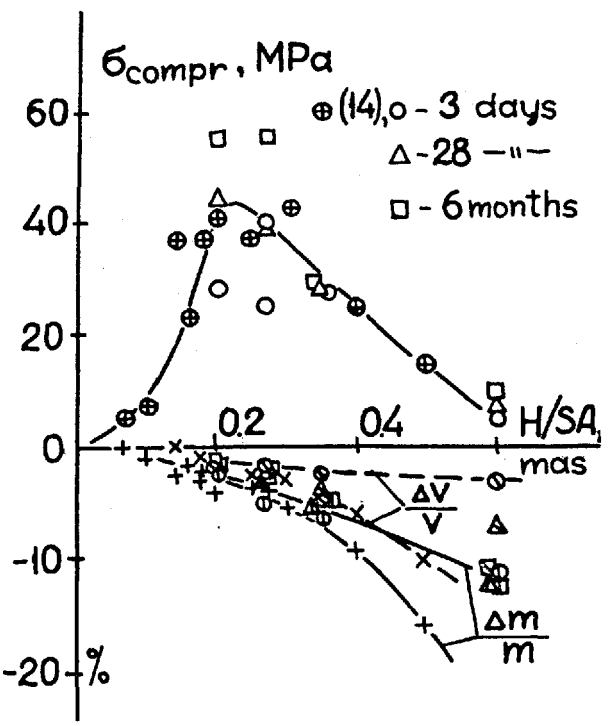

Fig.3 The change of the compressive strength, volume shrinkage mass losses as a function of the mixing water amount after 3 and 28 days and 6 months air hardening

Data on related changes in the composition of hydration products allow to infer that its main mass is X-ray amorphous. Maximum quantity of crystalline SAH forms at the maximum strength (Fig.4,b). When H/SA ratio is rich, S AH quantity is rich too (Fig.4,d). The quantity of S AH begins decreasing after 3-14 days of

hardening. In this time SC' quantity grows (up to I=0.06-0.2). The quantity of crystalline AH_3 is constant and small (Fig.4,c). $I(SH_9)<0.03$.

Data (14) on growth of SA_6 quantity with increase in H/SA were not confirmed.

Influence of temperature on SA air hardening processes was investigated with help of specimens with H/SA=0.3 at 20-40°C over 1-21 days. It was established, that increase in temperature accelereted strength development in the initial stage of hardening. However, after 14 days of hardening, maximum strength is attained at 30°C.

At 30°C, the SA hydration degree is maximum (~55%) and mass losses of samples minimum (4-5%). The shrinkage monotonic growth occurs with temperature increase (up to 10-12% at 40°C). The SC' appearence is marked. At T>30-40°C increase in crystalline AH_3 was not revealed.

When SA powder specific surfase increases, the set is accelerated and the hydration degree and strength also grow, the last taking place more faintly.

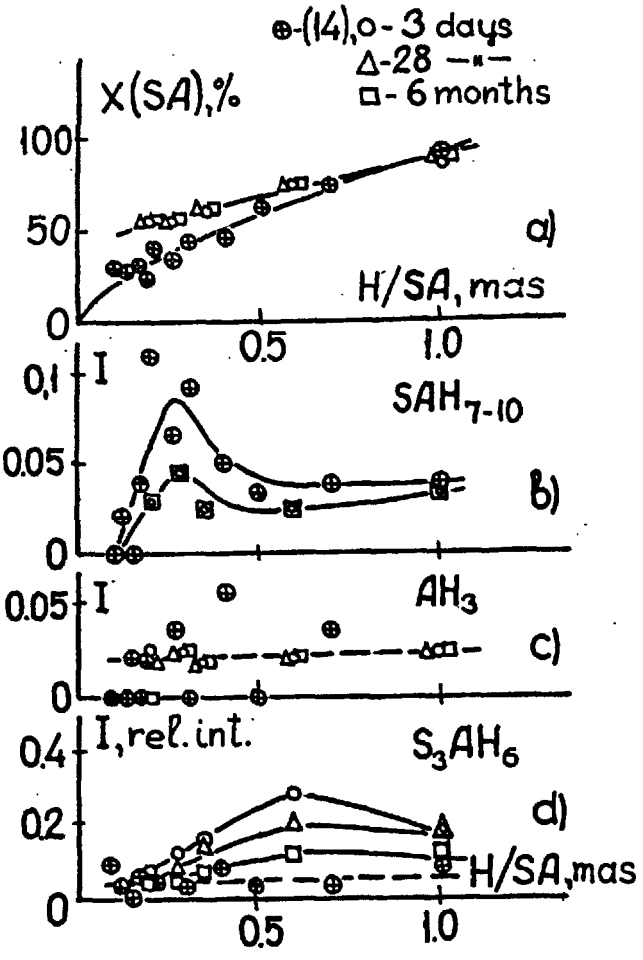

Fig.4 The hydration degree (a) and intensity of main diffraction lines crystalline hydration products compositions as a function at the mixing water amount after 3 and 28 days and 6 months air hardening

At 100% relative humidity (inside desiccator over water) and the hardening during 1-28 days, the strength increase at H/SA=0.27 is similar to hardening in air, at the same time the hydration degree increases up to 80%. After 3 months the strength decreases to 30 MPa and the hydration degree reaches 100%. After 3-4 days of losses change on mass increases (up to 5-10% after 28 days). After start of the hardening, the sample volume decreases to 1% over a period of some days and then slowly increases (up to initial state after 28 days).

Thus SA stone strength, unlike BA, weakly depends on high humidity, i.e. introduction of additional water during the hardening.

Humidity influences on S_3AH_6 amount gradual increase up to I=0.8-1 after 2-3 months (at H/SA=0.3 and 0.7). At the same time the measurable open porosity sharply decreases. As S_3AH_6 quantity begins to decrease [simultaneously the SC' quantity appears and increases (up to I=0.2-0.6)]. At the same time other crystalline hydrates and SA_6 [in contrast to (14)] amounts practically did not change.

We suppose, that during the setting of SA the hydration leads to

SAH_{7-10} formation, which probably provides the stone its strength. Simultaneously, apparently, the main mass of SAH_{7-10} remains X-ray amorphous. When additional water is indroduced during the hardening process, supplementary hydration of SA with S_3AH_6 formation takes place. The loss in strength of SA stone begins when additional quantity of S_3AH_6 crystalline hydrates fill up the pore space in a big way. Probably AH_3 and SH_9 formation takes place during the setting process as a result of SA hydrolysis.

CONCLUSIONS

Monostrontium aluminate is a rapid hardening, high strength (σ_{compr} ≈40-55 MPa), air cured cement, which at the setting stage the stone with porosity 20-25% is forming. The hydration degree is ~45%.

The maximum strength is reached at H/SA=0.24, which is close enough to H/SA=0.27 for the normal consistency slurry. The volume shrinkage is 2%.

The main crystalline hydrate, providing SA stone its strength is probably SAH_{7-10}.

At W=100% the hardening of the SA stone (at H/SA=0.3-0.7) leads to increase in the degree of hydration, and once it reaches 100% (after 1-2 month), the stone strength decreases. At this time additional quantity of S_3AH_6 forms without growth of the crystalline AH_3 quantity.

The optimum SA air hardening temperature is about 30°C.

REFERENCES

1. Carlson, E.T.: "A Study of Some Strontium Aluminates and Calcium-Strontium Aluminate Solid Solutions", J. Res. Nat. Bureau Stand., 1955, 54(6), 329-331; "Some Observations on Hydrated Monocalcium Aluminate and Monostrontium Aluminate", 1957, 59(2), 107-111.

2. Braniski, Al.: "Barium- und Strontium-Zemente", Zement-Kalk-Gips, 1957, N5, 176-184.

3. Braniski, Al.: Rev. Roum. Chim., 1964, N9, 585-599.

4. Braniski, Al.: "Infrarot-Untersuchungen der Hydratation des Mono-Ca-, Sr-, Ba-Aluminats und der silikatischen Ca-, Sr-, Ba-Zemente", Zement-Kalk-Gips, 1965, N4, 164-171.

5. Tarte, P.: Spectrochimica, 1967, 23A, 2127-2143.

6. Braniski, Al.: "Strontiumzemente", Zement-Kalk-Gips, 1967, N3, 96-101.

7. Braniski, Al.: Zement-Kalk-Gips, 1969, N11, 513-516.

8. Мельник, М.Т., Ковалев, Ю.С.: "Высокоогнеупорный алюмоцирконатстронциевый цемент", Вестник ХПИ, техн. неорг. мат., 1972, 70, в.4, 65-67.

9. Ковалев, Ю.С.: "Получение и исследование цементов высшей огнеупорности в системе $SrO-Al_2O_3-ZrO_2$", Автореф. дисс., ХПИ, Харьков, 1976.

10. Мельник, М.Т., Илюха, Н.Г., Шаповалова, Н.Н.: Огнеупорные цементы. Киев, "Вища школа", 1984, 121 с.

11. Надеждина, Т.Н., Побединская, Е.А., Белов, Н.Б.: "Кристаллическая

структура Sr-алюмината $Sr_4Al_4O_2[Al_{10}O_{23}]$", Кристаллография, 1976, 21(4), 826-828.

12. Шутова, В.И., Косоруков, А.А., Овчаренко, Ф.Д.: Взаимодействие окисей стронция и алюминия в гидротермальных условиях", ДАН СССР, 1979, 246(2), 355-357; "Термическое разложение $3SrO.2Al_2O_3.2H_2O$ и $3SrO.Al_2O_3.6H_2O$", Ж. неорг. химии, 1979, 24(1), 153-156.

13. Сиражиддинов, Н.А., Кадырова, З.Р.: Алюминаты и галлаты щелочноземельных металлов. Ташкент, "Фан", 1986, 130 с.

14. Borovkova, L.B., Borodina, T.I., Malenina, T.A., Pekhomov, E.P.: "An Investigation of the Hardening of Monostrontium Aluminate Cement", Prepr. 2 Un. Int. Techn. Conf. on Refractopies., Sept. 23-26, 1991, Aachen, Germany, 430-432.

AN INVESTIGATION INTO THE HARDENING OF MONOBARIUM ALUMINATE CEMENT

L B Borovkova, T I Borodina
T A Melehina and E P Pakhomov

Institute for High Temperatures, Russian Academy of Science, MOSCOW

SUMMARY

Setting characteristics (normal consistency paste of cement, initial and final of setting, selfheating) were investigated. Progress in the curing process (increase compressive strength, changes in mass and volume, porosity, degree of hydration, crystalline compositions of hydration products) as a function of the curing time duration (from 0.1 hour to the 3 months), amount of mixing water (H/BA=0.05-1.0), temperature of the environment (20-40°C), Blaine fineness (1700-4000 cm^2/g) and addition of water to the sample during the curing process were studied.

Comparison of the literature values was carried out.

Maximum strength of the air hardened cement BA after 3 days hardening is ~90 MPa. It was reached by curing in semi-dry consistency with H/BA=0.14 (at normal consistency paste of cement with H/BA=0.21).

Obviously, BAH_7 hydrate is formed and contributes to the strength of the stone BA. At H/BA>0.35 the composition of BA stone is varition from BAH_7 to β-BAH_6.

Detected, that surplus mixing water or introduction of additional water in the hardening stone give an increase amount of the hydration products, that decrease strenght of the hardened BA stone, having a very small porosity (2-5%).

АННОТАЦИЯ

Характеристики схватывания (нормальной консистенции теста, начала и конца схватывания, саморазогрева) и твердения (набора прочности на сжатие, изменений объема и массы, пористости, степени гидратации и фазового состава кристаллических продуктов гидратации) были исследованы в зависимости от времени твердения (от 0,1 часа до 6 месяцев), количества воды затворения (H/BA=0,05-1,0), температурных условий (20-40°C), удельной поверхности исходного порошка (2500-5200 $см^2/г$) и количества воды, дополнительно вводимой в образец в процессе твердения.

Выполнено сравнение с имеющимися литературными данными.

Получено, что на воздухе максимальная прочность ~90 МПа (после 3 дней твердения) достигается камнем BA при затворении в полусухой консистенции с водоалюминатным отношением 0,14 (нормальная консистенция теста H/BA=0,21). Вероятно, гидрат BAH формирует при схватывании плотную структуру камня (П=2-5%) и определяет его прочность. При H/BA>0,35 состав камня изменяется с BAH_7 на β-BAH_6.

Избыток воды затворения или введение в твердеющий камень дополнительного количества воды ведет к росту количества продуктов гидратации и разупрочнению камня BA, имеющего малую пористость.

INTRODUCTION

Monobarium aluminate BaO.Al O (BA) is one of the most highly refractory cements. It has a high potential for use as concrete and ramming masses at 2000 K and more.

BA cement has been studied very extensively in 60-70th years,but then the number of publications decreased. In our opinion knowledge on the hardening characteristics of BA remains insufficient (1-13). The composition and characteristics of BA crystalline hydrates have been investigated (14-16).

In this report the results of the study (17) on the hardening characteristics of BA cement as a function of curing time duration, amount of mixing water, specific surface of powder and hardening conditions are reported. Compressive strength, mass and volume changes, open porosity, degree of hydration and the compositions of crystalline hydrates also have been determined.

Barium aluminate, produced by solid state sintering at 1820 K, was used as the raw material. X-ray analysis showed 5% impurities mainly in the form of tribarium aluminate (B A) and barium hexaaluminate (BA) are present. The Blaine fineness of the powder was 3000 cm /g.

EXPERIMENTAL

Water-cement ratio (H/BA) in the normal consistency paste was 0.21, initial set was 15 min and final set was 25 min. After mixing with water 35 g of slurry BA is selfheating up to 25 C over 15-20 minutes.

A time dependence study of the BA air hardening in 1 to 28 days period at a relative humidity (W) 55+20% and at 21+3 C was carried out. It showed that after first 2 hours curing the strength reached more then 40 MPa, after one day the strength reached 60 MPa and at 28 days the strength was 90 MPa (Fig.1a).

The volume shrinkage after first day of hardening was 3%, then it increased monotonic to 5-6% at 28 days of curing. Mass losses (water evaporation) increased from 1% to 2.5-3% after one and 28 days, respectively. It is important to note that BA set and hardened to a relatively dense stone with 4-5% open porosity .

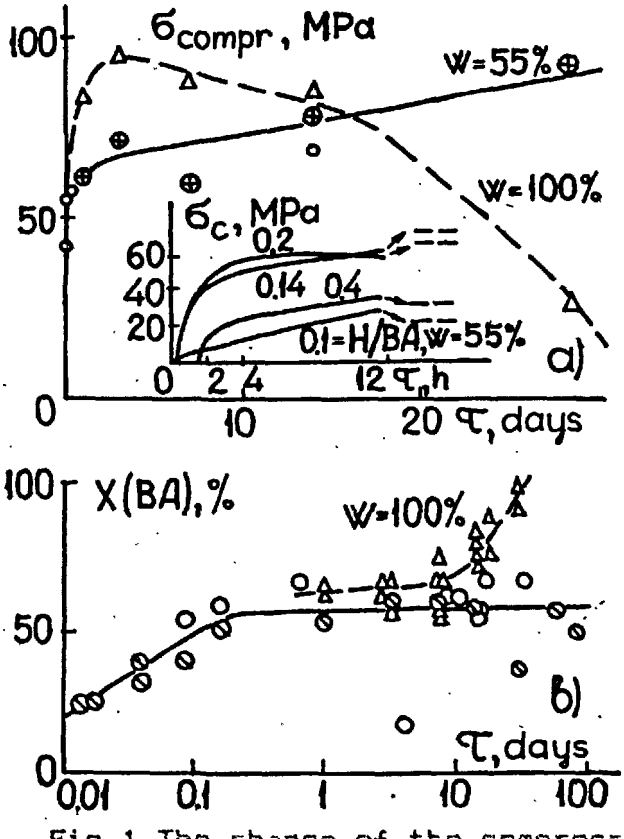

Fig.1 The change of the compressive strength (a), the BA hydration degree (b) as a function of hardening time both for air and at humidity W=100%;H/BA=0.21

Results on degree of hydration X(BA) showed (Fig.1b) that at the final set tne cement was hydrated to the extent of 25-30% whereas after 4 hours the cement was hydrated to the extent of 50-55%. After that the degree of hydration did not change over 1-86 days.

X-ray analysis of sample after hardening showed the presence of different products of BA hydration. It was detected that composition of the hydration products greatly alter on the sample volume. This was probably, due to the inhomogenity of the real water distribution among the cement particles and its selfheating. The main compounds formed are BAH_7(where $A=Al_2O_3$,$B=BaO$, $H=H_2O$, $C'=CO_2$). $BAH_{0.5}$, BAH, α,γ-BAH_2, α,β-BAH_4, BAH_6, AH_3, AH, BH_9 , B_2AH_5 more rarely are found. BC', $(BA)_2C_4H_7$, BH appear at specific conditions.

At the final set the peak intensity of the main crystalline hydrate practically reaches its constant level.

Investigations on the setting and hardening processes as a function of the amount of mixing water were carried out at a mass ratio of water: barium aluminate (H/BA) 0.1:1.0. It was discovered that the period to initial and to final set increases from some minutes to 35 minutes for H/BA=0.1 and to 45 minutes, respectively, for H/BA=0.3. The difference between initial and final set (10 minutes) is practically constant (Fig.2) for this period.

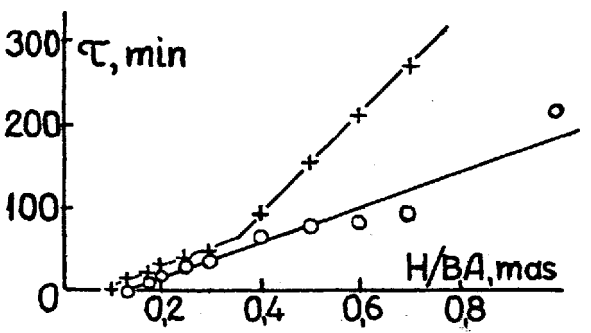

Fig.2 Set times of BA as a function of the mixing water amount (H/BA)

With increasing of amount of mixing water the final setting time grows more faster than the initial setting (up to 270 and 110 min, respectively, at H/BA=0.7). Probably the main crystalline hydrates kind is changed. When the H/BA ratio increases, the critical concentration, which corresponds to the beginning of crystalline hydrate precipitation, occurs more slowly.

Fig.3a represents the change in compressive strength (σ_{compr}) after 3 and 14 days hardening as a function of the quantity of mixing water. The maximum strength ($\sigma_{compr}\approx$80-90 MPa) is reached at H/BA=0.14, i.e. at semi-dry consistency of cement paste. At the normal consistency of cement slurry (H/BA=0.21) the compressive strength is much lower (~70 MPa) and rapidly decreases when the quantity of mixing water is increased (up to 30 MPa at H/BA=0.4).

BA high strength level at H/BA=0.14 is steady at the hardening during the following month. The volume shrinkage up to 14 days hardening increases from 2% at H/BA=0.12 up to 8% at H/BA>0.3. With H/BA increase the losses of sample mass also rise.

The open porosity is small (4%) and constant at $0.13<H/BA<0.45$. The apparent density is maximum at maximum strength.

The degree of hydration and composition of BA hydration products as a function of the amount of mixing water for 1-28 days hardening was obtained by X-ray analyses. The degree of hydration was found to increase with increase in H/BA (Fig.3b). At the maximum strength the degree of hydration is about 40-45%, at normal slurry consistency 55% and at H/BA=0.4 it reaches 75%. Practically complete hydration is observed at H/BA>0.75.

Fig.4 shows that the peak intensity is maximum for all compositions of crystalline hydrate products but at different values of H/BA. At the maximum strength the main crystalline phase was BAH_7. BAH, BH_9, BAH_6 and B_2AH_5 were also observed. Probably the strength decrease at H/BA>0.14 is accompanied by an increase in the degree of hydration of BA, caused by BAH_7 amount decrease and at H/BA>0.35 rapid growth of amounts (in our opinion) new crystalline hydrate β-BAH_6. The X-ray spector similar that of β-BAH_6 was showed in (6). Practically,there is variation in the composition of the BA stone as was noted in (6). It well correlates with

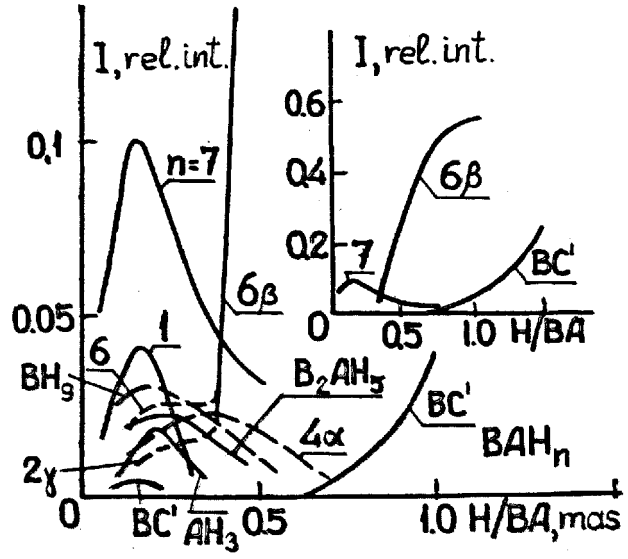

Fig.4 Intensity of main diffraction lines of crystalline hydration products compositions as a function of the mixing water amount after 1-28 days air hardening

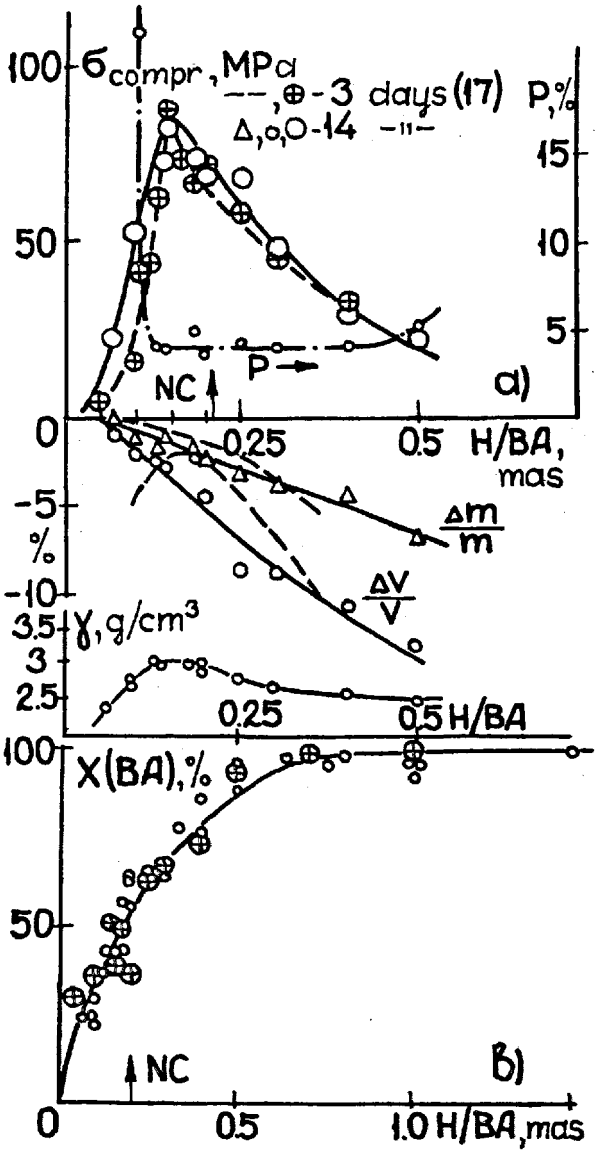

Fig.3 The change of the compressive strength,volume shrinkage, mass losses, open porosity, apparent density (a) and BA hydration degree (b) as a function of the mixing water amount after 3 and 14 days air hardening

the changing of setting time dependence from H/BA (Fig.2) at H/BA>0.35. The obtained results allow to make suppose that finely dispersed BAH_7 is the main crystalline hydrate which contributed to the high strength of BA cement stone.

When hardening in air increase

in the specific surface (from 1700 to 4000 cm^2/g) of BA powder results in: set acceleration; decrease of water amount (from 0.24 to 0.18) for the normal consistency slurry production; increase in the degree of hydration (from 50 to 60%); strength increase (for 28 days $\partial\sigma/\partial\tau$ =0.018 $MPa.g/cm^2$).

Temperature and humidity influence on BA hardening processes. Investigations in this regard were carried out at the H/BA ratio 0.21. It was found that increase in air hardening temperature from 20 to 40°C accelerates strength development. At 30°C it was found that the strength maximum is reached after 7 days hardening. At 40°C the strength begins to decrease after 3 days hardening. At 30°C the degree of hydration is maximum and sample mass losses are minimum. The shrinkage increases at 30 C and beyond.

Investigations on the influence of introducing additional water in hardening samples (H/BA=0.21) were carried out at a relative humidity 100% (in the desiccator over water) over 28 days. The obtained results show (Fig 1a) that during 3-5 days the strength of the samples exceeded that of the over subjected to air hardening at W≈55%; after the following 14 days it becames smaller. At 28 days there is strength decrease up to 20 MPa.

This process is accompanied by essential changes in the volume and mass of samples. After 1-3 days shrinkage changes on an expansion (up to 40% at 28 days), while the mass increases all through (up to 10% at 28 days).

A similar process takes place during water hardening in the core of samples (even as their exterior dissolves in the water).

In this manner, 100% humidity conditions essentially accelerate the strength increase of samples in the first stage of hardening, after a regrogression in strength begins. After 1.5 months the samples totally disintegrate.

X-ray analyses show that at 100% humidity hydration continues to increase for 1.5 months up to completion in BA hydration (Fig.1,b). After 10-14 days the amount of BAH_7, which determines BA cement strength, decreases and the amount of crystalline hydrates β-BAH_6 increases significantly. BC also occurs. The contents of the other BA hardening products remains small and constant. At the beginning, increase in β-BAH_6 amount increases the strength of BA stone, but later tends to destroy it.

CONCLUSIONS

Monobarium aluminate is a rapid hardening,high strength, air cured cement, which upon setting stage forms a dense stone (P<5%).

The cement reaches its maximum strength (σ_{compr}=80-100 MPa) at a semi-dry consistency of the slurry with an H/BA ratio 0.14 during air hardening accompanied by a volume shrinkage ~3%. In this case the degree of hydration is 45-50%.

The main crystalline hydrate, providing BA stone its strength, is finely dispersed BAH_7. Its rapid crystallization during the set leads to the formation of the dense fine crystalline framework. At H/BA>0.35, the main crystalline hydrates become β-BAH_6.

Surplus curing water (H/BA>0.14) and introduction of additional water in the nardening stone result in decrease of the stones strength, despite the crease in the degree of hydration and amount of the hydration products.

The optimum BA hardening temperature is 30°C. At which maximum strength and hydration degree can be reached.

REFERENCES

1. Журавлев, В.Ф.: Химия вяжущих веществ. Л.-М., Гос. н.-т. изд. хим. лит., 1951, 207 с.

2. Braniski, Al.: "Barium- und Strontium-Zemente". Zement-kalk-gips, 1957, N5, 176-184.

3. Braniski, Al.: Rev. Roum. Metall., 1960, 5(1), 165-185.

4. Будников, П.П., Савельев, В.Г.: "Исследование процесса гидратации монобариевого алюмината". Изв. ВУЗов, хим. и хим. техн., 1962, 5, 793-799; Савельев, В.Г.: "Исследование монобариевого алюмината и огнеупорных бетонов на его основе". Автореф. дис., МХТИ им. Д.И.Менделеева, М., 1962.

5. Braniski, Al.: "Infrarot-Untersuchungen der Hydratation des Mono-Ca-, Sr-, Ba-Aluminates und der silikatischen Ca-, Sr-, Ba-Zemente". Zement-Kalk-Gips, 1965, N4, 164-171.

6. Uchikawa, H., Tsukyama, K.: J. Chem. Soc. Japan Industr. chem. Sci., 1966, 69(9), 148-153; Proc. 5 Int. symp. chem. cement, Tokyo, 1968 1-4.

7. Будников, П.П., Куликова, Н.В.: "Получение и свойства силикатов и алюминатов бария". Изв. АН СССР, неорг. матер., 1966, 2(11), 1985-1990

8. Будников, П.П., Куликова, Н.В., Сердюков, В.И.: "Изучение процесса дегидратации алюмината и силиката бария". Ж. прикл. химии, 1967, 90(5), 937-942.

9. Handl, M., Rozanowski, B.: "Widma absorbcyne w podczerwieni produktow reakcji cementu glinowo-barowego z rozna iloscia wody zarobowej" Zement-Kalk-Gips, 1971, N12, 385-387.

10. Мельник, М.Т., Илюха, Н.Г., Бернштейн, В.Л.: "Цемент вищої вогнетривкость в системі $BaO-Al_2O_3-ZrO_2$".Вестник ХПИ, 1972, 70(4), 64-65.

11. Drozdz, M., Wolek, W.: "Le ciment alumineux de barium". Soc. franc. ceram. bull., 1975, 107, 39-52.

12. Мельник, М.Т., Илюха, Н.Г., Шаповалова, Н.Н.: Огнеупорные цементы. 1964, Киев, "Вища школа", 121 с.

13. Сиражиддинов, Н.А., Кадырова, З.Р.: Алюминаты и галлаты щелочноземельных металлов (Ca,Sr,Ba). 1986, Ташкент, изд."Фан", 138 с.

14. Carlson, E.T., Wells, L.S.: "Barium Aluminate Hydrates". J. of Res. Nath. Bureau Stand., 1948, 41(8), 103-109.

15. Thilo, E., Gessner, W.: "Uber Ba-Aluminate und Ba-Aluminathydrate". Z. anorg. allgem. Chem., 1965, 337(5-6), 238-253.

16. Ahmed. A.H.M., D.Glasser L.S.: "Barium Aluminate Hydrates. I.General surrey and preparative methode". J. Appl. Chem. Biotechnol., 1971, 21(4), 103-106; "II. $BaO.Al_2O_3.H_2O$ or 1.1 $BaO.Al_2O_3.H_2O$", 107-108; "III. $BaO.Al_2O_3.2H_2O$ and $BaO.Al_2O_3.0.5H_2O$", 109-112; "Barium Aluminate Hydrates. IV. α-$BaO.Al_2O_3.4H_2O$", 1973, 23, 457-463.

17. Borovkowa, L.B., Borodina, T.I., Melehina, T.A., Pakhomov, E.P.: "An investigation of the hardening of monobarium aluminate cement". Prepr. 2 Un. Int. Techn. Conf. on Refractories, sept. 23-26, 1991. Aachen, Germany, 432-434.

LONG-TERM HARDENING OF CEMENTS WITH HIGHER CONTENT OF MAGNESIUM OXIDE

Yu V Nikiforov and R A Zozulya

Design and Research Institute of Cement Industry "Giprocement"
St Petersburg, RUSSIA

SUMMARY

This paper presents observational data of long-term (over 18-28 years) hardening under normal conditions of cements with magnesium oxide content ranging from 1.8 to 9.5%. Variations in values of dynamic modulus of elasticity of standard specimens (1:3), in strength characteristics and linear expansion of cement stone (1:0) according to MgO content have been studied. A correlation between data obtained and results of the autoclave soundness tests made it possible to draw a conclusion that the normative magnesium oxide content in portland cement clinker can be brought up to 6% without conduction of the autoclave tests.

РЕЗЮМЕ

В докладе приводятся данные многолетних (в течение 18-28 лет) наблюдений за твердением в нормальных условиях цементов с содержанием оксида магния в пределах 1,8-9,5%. Исследовано изменение значений динамического модуля упругости стандартных образцов (1:3), прочностных показателей и линейного расширения цементного камня (1:0) в зависимости от содержания MgO при длительном твердении. Сопоставление полученных данных с результатами автоклавных испытаний на равномерность изменения объема позволило сделать вывод, что нормативное содержание оксида магния в портландцементном клинкере может быть увеличено до 6% без проведения автоклавных испытаний.

INTRODUCTION

The question of a permissible content of magnesium oxide in portland cement clinker is up to now open in spite of numerous investigations in this area. Often the question was raised to what extent methods applied for testing cements with higher MgO concentration are reliable in evaluation of potential unsoundness. In this connection data of long-term hardening of magnesium-bearing cements are of special interest, particularly in comparison with results of the autoclave test at 2.1 MPa which is taken as a standard method in many countries. In the present paper results of 18-28 year observation of cement behaviour on the basis of clinkers with magnesium oxide content from 1.8 to 9.5% are discussed.

EXPERIMENTAL

Cements from clinkers burnt in a pilot plant (in a 7 m long rotary kiln) of natural raw materials were the subjects for investigations. Clinkers of Series I of experiments were characterized by MgO content of 2-7%, by values of lime saturation factor (KH)* 0.90, of alumina modulus 1.6-1.7 and silica modulus 1.9-2.0. Magnesium oxide content in clinkers of Series II varied in the range from 1.8 to 9.5%, value of KH was 0.89, of alumina modulus - 1.2-1.3, silica modulus 2.2-2.3.

For the subsequent grindings clinkers were chosen characterized by a free calcium oxide content below 0.5%. They were ground with addition of gypsum (2.0-2.5% by SO_3) to the specific surface about 300 m^2/kg. The autoclave soundness tests (at 2.1 MPa) were conducted both in pat paste and in prism specimens 0.02x0.02x0.10m of normal consistency paste.

In series I the behaviour of the cement specimens in long-term hardening under the normal conditions was observed with the use of a non-descructive test method by means of determination of values of dynamic modulus of elasticity (DME), this being an indirect characteristic of changes in the hardened cement mortar. The measurements of DME values were taken on standard mortar specimens 0.04x0.04x0.16m at a plant described in (1). For Series II cements direct strength characteristics of standard specimens as well as values of linear expansion of prism specimens (0.02x0.02x0.10m) from normal consistency paste were determined at different hardening ages.

Mortar specimens (1:3) on the basis of cement No.6 (MgO ~ 7.2%) after 18 and 28 years of water hardening were analyzed with the help of XRD and DTA, respectively, for the purpose of determination of periclase and its hydration products. The specimens were preliminary enriched by means of a partial removal of the fine aggregate.

RESULTS AND DISCUSSION

In Table I are given values of the dynamic modulus of elasticity as well as results of the autoclave soundness tests for cements of Series I.

* $$KH = \frac{CaO - 1.65Al_2O_3 - 0.35Fe_2O_3 - f\text{-}CaO}{2.8SiO_2}$$

Table 1. Dynamic Modulus of Elasticity (MPa x 10^2) of Cements after Water Hardening and Results of Autoclave Soundness Tests

Cement No.	MgO content in clinker,%	Tests at 2.1 MPa		Hardening age, years						
		pat paste	linear expansion,%	1/12	1	5	10	15	25	28
1	2.28	B.	0.04	415	444	442	456	453	432	436
2	4.60	H.B.	2.05	408	435	437	448	443	420	417
3	5.52	H.B.	5.1	414	443	434	443	440	433	429
4	6.06	-"-	~11	402	443	441	460	462	451	420
5	6.20	-"-	~12	399	437	432	457	445	438	-
6	7.19	-"-	Failed	399	432	384	324	225	214	228

Note: B - withstood the test; H.B. - did not withstand the test

As can be seen from Table 1, DME values for specimens of cements Nos.1-6 (with MgO content in clinker from 2.28 to 6.20%) after 28 years of hardening varied slightly in spite of a considerable difference in magnesium oxide content. At the same time, the specimens of cement No.6 (MgO = 7.19%) after 15 years of hardening showed a decrease in the DME value by nearly one half in relation to one year hardening, a dense network of fine cracks developed on the specimens. It should be noted that specimens (1:0) of this cement failed the autoclave test.

When comparing data of Table 1 for cements Nos.1-3 it is easily seen that the like DME values for specimens after 28 years of hardening are not adequate to the autoclave test results: the first of them withstood the test while two other cements (with MgO content of 4.60 and 5.52%) did not met the requirements of the standard as to the soundness showing a rather considerable expansion of 2.0 and 5.1%, respectively. This once again confirms the correctness of the point of view expressed earlier in (2,3) that the autoclave cement test method is rather rigid (hydration of free MgO and CaO has an explosive nature) and does not comply with actual operating conditions of concrete (mortar) articles.

The results of series II cements testing (MgO in clinker in the range from 1.76 to 9.51%) are presented in Table 2. The data of Table 2 point to the fact that there is no simple relationship between the value of the linear expansion of the cement stone (1:0) and the strength characteristics of specimens from the cement mortar (1:3). So, the strength of cement No.9 decreased from 45.9 MPa (5 hardening years) to 23.6 and 10.5 MPa at the age of 10 and 18 years, respectively. The values of the linear expansion therewith varied only a fair: from 0.24 to 0.29 and 0.33%, respectively.

Table 2. Strength Characteristics and Linear Deformations of Cements of Long-Term Hardening under Normal Conditions

Cement No.	MgO content in clinker, %	Linear expansion (%) at the age (years)				Ultimate strength (MPa) at: Bending, years				Compression, years			
		1/12	5	10	18	1/12	5	10	18	1/12	5	10	18
7	1.76	0.03	0.10	0.11	0.12	6.8	7.2	6.4	-	53.6	55.5	64.6	-
8	5.20	0.05	0.15	0.18	0.20	6.7	6.5	5.3	4.9	51.9	54.6	60.8	55.9
9	7.65	0.05	0.24	0.29	0.33	6.1	3.7	1.8	1.1	42.7	45.9	23.6	10.5
10	9.51	0.07	0.40	0.47	0.56	6.3	0.9	Failed		45.0	11.5	Failed	

Note: Cements Nos.9 and 10 did not withstand the autoclave test at 2.1 MPa.

The specimens of cement No.10 (9.5 MgO) failed after 10 years of water hardening with linear expansion of the cement stone being only 0.47%. The increase in the MgO content in clinker from 5.20 to 7.65% caused a sharp decrease in the strength of the cement specimens at the age of 10-18 years, i.e. by 2-4 times as against the initial (28-day) strength.

So, the behaviour of the cement stone (1:0) in case of a higher MgO content is not adequate to hardening of the mortar (1:3) and is probably due to the fact that the stresses brought about by periclase hydration are compensated in the first case by a higher strength of the cement stone. Attention should be drawn to the fact that in compliance with the autoclave test results, cements Nos.2-4 are to be considered as sub-standard ones, but 25-28 years of hardening under normal conditions have not revealed any signs of failure of specimens of such cements.

It should be noted that it was not possible by means of the X-ray phase analysis to find the presence of periclase in specimens of mortar after 18 years of water hardening. Presence of $MgCO_3$ and $Mg(OH)_2$ in the hydration products was found by the use of the DTA method in the mortar specimens for cement No.6 after 28-year hardening.

By and large, the data of Tables 1 and 2 point to the fact that the autoclave tests do not always give an impartial assessment of the cement quality as to its soundness. On the other hand, the whole complex of investigations points to the fact that in case of production of portland cement without active mineral additives the amount of MgO in clinker can be brought up to 6% without conduction of the autoclave soundness tests.

CONCLUSIONS AND RECOMMENDATIONS

1. It has been found that for specimens (1:3) prepared of cements

with magnesium oxide content of 2 to 6% which hardened for 28 years the values of the dynamic modulus of elasticity (DME) are similar and they practically did not change as compared with data at the age of 1 year. The specimens of cements with MgO concentration in clinker of 7.2% showed reduction of the DME value by nearly one half even after 15 harden - ing years.

2. It has been established that the linear expansion of specimens of the cement stone (1:0) is not always adequate to behaviour of specimens of mortar (1:3) at the long-term hardening. So, the standard spe - cimens on the basis of cement with MgO content of 9.5% failed by 10 years of hardening while the specimens made of cement paste did not have any defects, with linear expansion making up to 0.47%.

3. The comparison of the long-term cement hardening data with the results of the autoclave tests makes it possible to state that the latter do not always give an impartial assessment of the cement quality as to its soundness. It seems to us that the normative magnesium oxide content in clinker can be brought up to 6% without conduction of the autoclave tests.

ACKNOWLEDGEMENTS

The authors would like to thank Eng. Zh M Orsher for her participation in the investigations.

REFERENCES

1. Porotsky, Ye.M. and Rustchuk, G.M.: "Opredeleniye kachestva tsementa i betona po dinamicheskomu modulyu uprugosti" ("Determination of cement and concrete quality from the dynamic modulus of elasticity"), Tsement, 1950, (1), 13-19.

2. Calleja, J. & Olmo C. del.: "Expansion of cements and methods of its determination". The VI-th International Congress on the Chemistry of Cements, Moscow, 1976, V3, 202-206.

3. Kennerley, R.A., Fletcher, R.A. and Milestone, N.B.: "Effect of Free Lime and Other Factors on the Soundness of Cement". Chemistry Division, Department of Scientific & Industrial Research, Private Bag, Petone, New Zealand, 1981, 2315, p.26.

HYDRATION OF CALCIUMALUMINATE AND CALCIUMALUMINOFERRITE SEPARATED FROM PORTLAND CEMENT

Anette Müller, Jochen Stark and Silvia Stürmer

Department of Building Materials
University of Architecture and Building, Weimar, GERMANY

SUMMARY

This paper presents results of a laboratory investigation in the hydration performance of preparations of C_3A and $C_2(A,F)$ obtained after the extraction of silicates with salicyl acid from technical cements. All method used - XRD, DTA, DCA and SEM - show that $C_2(A,F)$ reacts in the early hydration only somewhat more slowly than C_3A. The investigation have also shown that the initially formed AFT - phase from the $C_2(A,F)$ - rich material has almost the same habit as the ettringite initially form of the C_3A - rich material.

ZUSAMMENFASSUNG

Die Ergebnisse von Hydratationsuntersuchungen an C_3A- und $C_2(A,F)$-Präparaten werden vorgestellt. Die Präparate werden aus technischen Gründen durch Extraktion der Silikate hergestellt. Alle angewandten Untersuchungsmethoden - XRD, DTA, DCA und SEM zeigen, daß $C_2(A,F)$ am Beginn der Hydratation nur etwas langsamer reagiert als C_3A. Außerdem zeigen die Untersuchungen, daß die AFt-Phase, die sich aus $C_2(A,F)$ bildet, in ihrem Habitus dem primär gebildeten Ettringit aus dem C_3A sehr ähnlich ist.

Introduction

The clinker minerals C_3A and $C_2(A,F)$ decisively determine the early hydration of Portland cement. The course of the early hydration influences essential properties of cement such as setting, workability, formation of pore structure, strength development and durability. The hydration products of Calciumaluminates and Calciumaluminoferrites are of special interest in the discussion about durability of cement-bound concrete. The chemical durability of mortars and concrete can be affected by late ettringite formation with and without supply of sulphate from outside. This is especially important, if the concrete is exposed to extreme temperatures e.g. under heat treatment or freezing.

Experimental

For the investigation of the ettringite and AFt-formation it is more appropriate to use the cement minerals C_3A and $C_2(A,F)$ in their original form rather than the synthetically prepared phases. Therefore the hydration was examined with samples of C_3A and $C_2(A,F)$ obtained after separation from technical cements by an organic acid solution. Material prepared in this way correspond to the cement clinker both in nature and quantity of incorporated foreign oxides and in the hydraulic activity.

Basic cements for the investigations were a sulphate-resisting Portland cement (SRPC 40A) with low C_3A-content and a C_3A- rich white cement (WPC). The analytical data and important characteristics of the basic cements are shown in Table 1. The cements were selected both from the point of extreme variation of C_3A - contents and comparable contents of alite and alkalies. The latter aspect must be taken into account, as besides the C_3A - content itself, the interaction with alite and alkalies /1,2/ and the ability of CSH-phases to store calcium sulphate /3/ can play an important role in the late formation of ettringite.

The silicate phases were dissolved from the basic cements with a 15 % salicyl-acid methanol solution. After drying the extracted residue was treated to remove traces of salicyl acid to prevent it from influencing the hydration process of C_3A and $C_2(A,F)$. Table 2 shows the analytical data of the extracted residues from both cements. From these data the phase composition was calculated (Table 3). The analytical data and the phase composition show, that the salicyl-acid methanol solution dissolves the free lime completely and the Calciumsilicates up to 1 - 2 % - related on the original cement. The residue of the extraction contains Calciumaluminate, Calciumaluminoferrites, Calciumsulphate, Alkalies and MgO - all phases which form ettringite or AFt or influence the AFt/ettringite formation by changing the hydration milieu.

TABLE 1: Analytical data, specific weight ρ, surface area A_o, strength β_D and other important data of the basic cements SRPC 40A and WPC

		SRPC 40A	WPC
L.O.I.	(%)	0.65	2.18
CaO	(%)	64.91	66.41
SiO_2	(%)	19.14	21.21
Al_2O_3	(%)	4.25	4.17
Fe_2O_3	(%)	5.64	0.24
SO_3	(%)	2.03	2.36
Na_2O	(%)	0.11	0.13
K_2O	(%)	0.27	0.16
MgO	(%)	1.38	2.60
Σ		98.38	99.46
Free Lime	(%)	1.9	0.6
ρ	(g/cm³)	3.19	3.09
A_o	(cm²/g)	4160	4300
WA *)	(%)	29.5	36.0
β_D 3d	(N/mm²)	26.5	33.9
7d	(N/mm²)	32.7	39.9
28d	(N/mm²)	42.6	58.0
KSt by KÜHL		99	100
SM		1.93	4.81
TM		0.75	17.38
Na_2O aequ.		0.29	0.23
C_3S	(%)	68.6	71.6
C_2S	(%)	3.1	6.8
C_3A	(%)	1.7	10.6
C_4AF	(%)	17.2	0.7
SO_3/Al_2O_3	mol.	0.62	0.72

*) WA= amount of water to reach the standard consistency

TABLE 2: Chemical data of the Residues (L.O.I.-free)

		SRPC 40A	WPC
CaO	(%)	44.5	44.4
SiO_2	(%)	6.1	9.1
Al_2O_3	(%)	16.0	17.5
Fe_2O_3	(%)	20.7	0.71
SO_3	(%)	7.8	11.9
K_2O	(%)	1.43	0.78
Na_2O	(%)	0.35	0.22
MgO	(%)	3.1	9.9

TABLE 3: Phase composition of the residue SRPC 40A

		SRPC 40A
C_4AF	(%)	63.0
C_3A	(%)	7.4
$CaSO_4$	(%)	12.1
C_3S	(%)	7.9
MgO	(%)	3.1
K_2SO	(%)	1.6

The residues were hydrated at a water/cement ratio of 1.0. The residues were either hydrated at 20 °C or subjected to a 6-hour heat treatment with a maximum temperature of 90 °C. Further hydration took place in both cases in small closed bottles at 20 °C. First investigations were carried out with distilled water /4/. However, as in the hydration of cement the mixing water is saturated with $Ca(OH)_2$ after a short time, analogous examinations followed with satured solution of $Ca(OH)_2$. The hydration was stopped at certain ages up to 90 days.

The hydration process was investigated by means of XRD, DTA, difference calorimetric measurements and SEM.

Results

Figure 1 and 2 show the scanning electron micrographs of the hydrated residues from the sulphate-resisting (fig. 1) and the white Portland cement (fig. 2) after a hydration period of 6 hours. The AFt-phase (fig. 1) is initially produced in the hydration of the $C_4(A,F)$-rich residue and ettringite (fig. 2) in the hydration of the C_3A-rich residue. As the micrographs show both crystals are mostly small rods of varying length (1 - 5 µm) with hexagonal cross section. The AFt - phase formed from the $C_4(A,F)$-rich residue has nearly the same habit as the ettringite formed from the C_3A-rich residue.



Fig. 1: Residue of SRPC 40A 6 hours normal hardening; 3000:1



Fig. 2: Residue of WPC 6 hours normal hardening; 3000:1

The course of hydration up to 72 hours was examined by difference calorimetric measurements. Figure 3 shows the rate of heat development of the original cements and the corresponding residues in the first hour of hydration, which is dominated by reactions of C_3A and $C_4(A,F)$. The heat development of the residues is essentially higher than that of basic cements - as was to be expected - but the maxima of heat development of cement and its residue agree in both cases. This shows that the hydration process is not affected by the preceding extraction with salicyl-acid methanol solution. The C_3A-rich residue reaches its maximum somewhat earlier (5 min.) than the $C_4(A,F)$-rich residue, but the hydration heat in the first hour is comparable (SRPC - residue = 206 J/g; WPC - residue = 212 J/g).

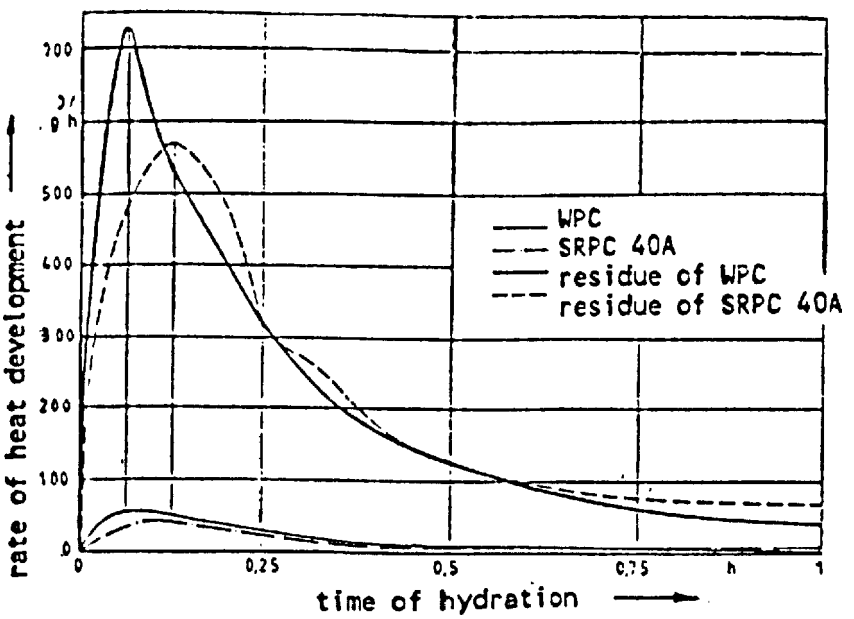

Fig. 3: Rate of heat development in the first hour

Furthermore, the course of hydration up to the complete conversion of C_3A and $C_4(A,F)$ in distilled water and saturated $Ca(OH)_2$-solution was investigated by quantitative XRD. At the beginning of the hydration the C_3A (fig. 4) decreases very quickly. Between 2 and 12 hours there is a 'dormant period'. After 7 days C_3A is not detectable. A dependence of the C_3A- hydration on the hydration medium could not be established.

$C_4(A,F)$ (fig. 5) decreases continuously. A 'dormant period' could not be detected. Contrary to the C_3A-hydration the nature of the medium strongly influences the hydration of $C_4(A,F)$. During the hydration in saturated $Ca(OH)_2$-solution the decrease of $C_4(A,F)$ was decelerated.

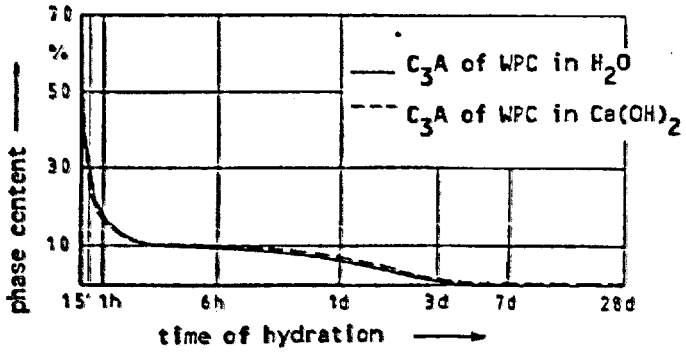

Fig. 4: XRD - decrease of C_3A

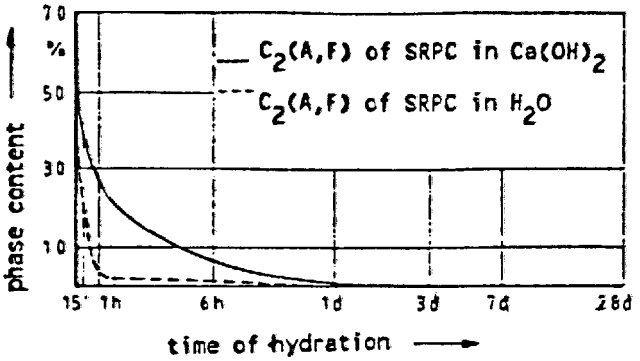

Fig. 5: XRD - decrease of $C_4(A,F)$

The differential thermoanalysis was used for the examination of Calciumaluminate sulphate hydrates which were formed during the hydration process. Figure 6 shows that in the hydration of $C_4(A,F)$-residue the Aft-phase disappears between 1 hour and 3 days. Simultanously the content of AFm-phase - also present after 1 hour - increases. In the case of the C_3A-hydration (fig. 7) ettringite and monosulphate appear after 1 hour and the amount of both rises with increasing hydration time. This phenomenon will be more closely examined in further investigations. After the destabilization of the trisulphate due to heat treatment (max. temperature 90°C) the ettringite of the C_3A-rich material is quickly (1 day) and almost completely reformed. The Aft-phase of the $C_4(A,F)$-residue only occurs again in very small amounts after 28 days . After 90 days the AFt is not detectable.

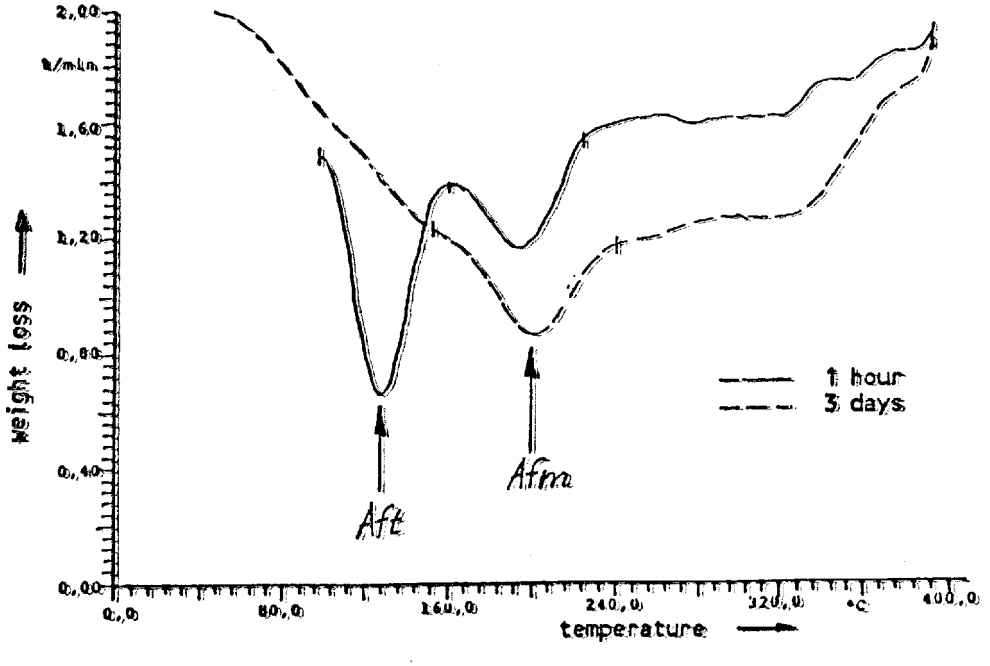

Fig. 6: DTG of the hydrated residue of SRPC 40A

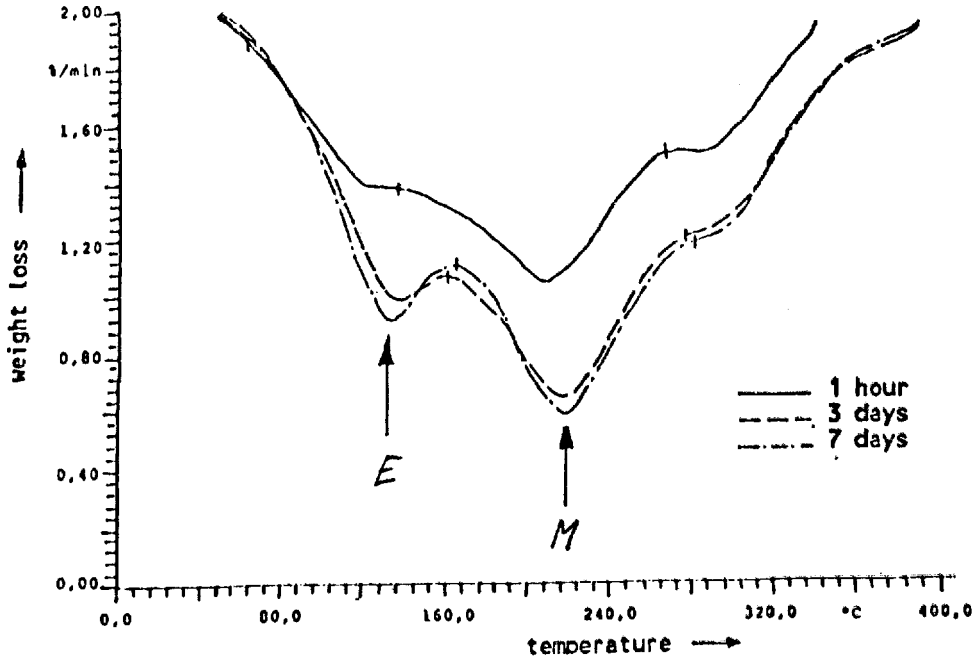

Fig. 7: DTG of the hydrated residue of WPC

Conclusions

The extraction with salicyl-acid methanol solution according to /5/ is a suitable method for prehandling the cement for the investigation of the hydration of C_3A and $C_2(A,F)$ in its original form. Here the two phases hydrate under real conditions of cement hydration with regard to the Calciumsulphate and the incorporated foreign oxides. The absent influence of the portlandite due to the separation of silicates is compensated by using saturated $Ca(OH)_2$-solution as hydration medium.

In the early hydration $C_2(A,F)$ reacts somewhat more slowly than C_3A although the difference is not as large as often described. Also the initially formed AFt-phase from the $C_2(A,F)$-rich residue has almost the same habit as the ettringite initially formed of C_3A-rich residue.

The investigation of the hydration of C_3A and $C_2(A,F)$ separated from cement was to emphasize the importance of the different cement matrix phases for the durability of mortars and concrete.

Literature

/1/ Popovics,S.: Phenomenological approach to the role of C_3A in the hardening of Portland cement pastes, Cem.& Concr.Res. 3, 343-350 (1976)

/2/ Ono,M.;Nagashima,M.;Saito,M.: The stiffening of mortar accompanied with the early hydration of cement, Proc. of the 7th ICCC, Vol. II, 172-175, Paris 1980

/3/ Odler,I.: Interaction between gypsum and the CSH-phase formed in the C_3S-hydratation, Proc. of the 7th ICCC , Vol. II, 492-495, Paris 1980

/4/ Stürmer,S.;Stark,J.;Müller,A.: Hydratation von C_3A und $C_4(A,F)$ - separiert aus sulfatbeständigem und weißem Portlandzement - bei Normalerhärtung und Wärmebehandlung, Wiss. Z. HAB Weimar 35 (1989) 5/6,

/5/ Takashima,S.: Review of the 12th general meeting, Cement Association of Japan, Tokyo 1958, 12-13

HYDRATION OF β-C_2S PREPARED AT 600°C FROM HILLEBRANDITE: C-S-H WITH Ca/Si = 1.9–2.0

H Ishida, K Sasaki, Y Okada and T Mitsuda

Nagoya Institute of Technology, Asahigaoka, Tajimi, JAPAN
INAX Corp, Koie, Tokoname, JAPAN
Onoda Cement Co Ltd, Ousaku, Sakura, JAPAN

ABSTRACT

The hydration at 80°C with w/s=0.5 of β-C_2S prepared from hillebrandite and the decomposition of the hydrates by heating were investigated. The hydration was completed in 24 h and strongly influenced by temperature until the end of the reaction, contrasting with the hydration of normal β-C_2S made by clinkering. The hydrates were C-S-H with or without trace amount of $Ca(OH)_2$, with composition 1.98-2.00$CaO \cdot SiO_2 \cdot 2.5$-$2.6H_2O$ and NMR ratio of Q^1/Q^2=1.0 without Q^0, Q^3 and Q^4, indicating a single chain structure with or without dimer. On heating at 370°C, the X-ray peak at 0.18 nm of C-S-H (0.30, 0.18 nm) disappeared and the NMR Q^0 peak began to appear, due to β-C_2S.

要 旨

ヒレブランダイトより合成したβ－Ｃ２Ｓの80℃における水和反応と、水和生成物の加熱変化を研究した。焼成法によるβ－Ｃ２Ｓと比較した場合、水和反応は24時間で完了し、反応完了時まで温度に著しく依存する。水和生成物 C-S-Hの化学組成は、1.98-2.00 CaO・SiO２・2.5-2.6 Ｈ２Ｏで、Ca(OH)２をほとんど含まない。 固体核磁気共鳴装置による解析の結果、C-S-H はQ^1, Q^2 のみを示し、Q^0, Q^3 、Q^4 を含まない。 Q^1 ／Q^2 の強度比は1.0であり、ダイマーと単鎖のシリケートアニオンの混在が予測できる。 370℃に加熱の結果、C-S-H の特徴的なＸ線回折ピーク（0.30, 0.18nm）のうち、0.18 nm のピークは消失し、ＮＭＲの解析では、β－Ｃ２Ｓの生成によるQ^0 が出現した。

INTRODUCTION

β-C_2S is usually synthesized by high temperature solid phase reaction above 1400°C of CaO and SiO_2 with stabilizing additives. Compared to C_3S, β-C_2S requires less CaO for its preparation and could therefore be considered as an energy-saving material. However, its hydration rate is slower than that of C_3S. Pritts and Daugherty (1) and Shibata et al. (2) have reported that highly reactive β-C_2S can be obtained if no stabilizing agent is used for preparation by high temperature reaction, though it is difficult to make pure β-C_2S. Yang and Zhong (3,4) first made highly reactive β-C_2S using lime and colloidal silica without any stabilizer in hydrothermal suspensions at 100°C followed by heating at 950°C.

We have attempted the synthesis of stable and pure β-C_2S at room temperature without any stabilizer by dehydration below 800°C of calcium silicate hydrates having Ca/Si=2.0. These are α-C_2S hydrate $Ca_2(HSiO_4)(OH)$, hillebrandite $Ca_2(SiO_3)(OH)_2$ and dellaite $Ca_6(Si_2O_7)(SiO_4)(OH)_2$, which give dehydroxylation at 400-450°, 520-540° and 640-700°C respectively. From these, hillebrandite can be purely made by using various forms of silica with lime in hydrothermal suspensions at temperatures of 200-250°C and decomposed easily into β-C_2S on heating at 600°C (5). The β-C_2S is thus obtained as fibrous thin crystal aggregates with a large specific surface area of more than 6 m^2/g, similar to that of hydrothermally formed hillebrandite. This β-C_2S is highly reactive with water and completes hydration in 28 and 14 days with w/C=0.5 and 1.0 at 25°C respectively. The C-S-H has a Ca/Si ratio as high as about 1.95 and contains almost no $Ca(OH)_2$. These characteristics are significantly different from those reported up to now (6,7). In the present work, we have studied the hydration behavior at 80°C of the β-C_2S made from hillebrandite and thermal decomposition behavior of the product.

EXPERIMENTAL

β-C_2S Preparation and its Hydration

Hillebrandite was hydrothermally prepared by using reagent grade CaO and pure quartz (less than 10 um, 99.9% SiO_2) with Ca/Si=2.0 in stirred suspensions at 250°C for 20 h as reported earlier (5). The products used contained trace amounts of xonotlite as an impurity and gave a specific surface area (BET) of 9.7 m^2/g. By heating at 600°C for 1 h, hillebrandite loses hydroxyl groups forming β-C_2S, with the same morphology as the original material (Fig. 1). The β-C_2S thus obtained contains trace amounts of xonotlite, having a BET area of 8.7 m^2/g.

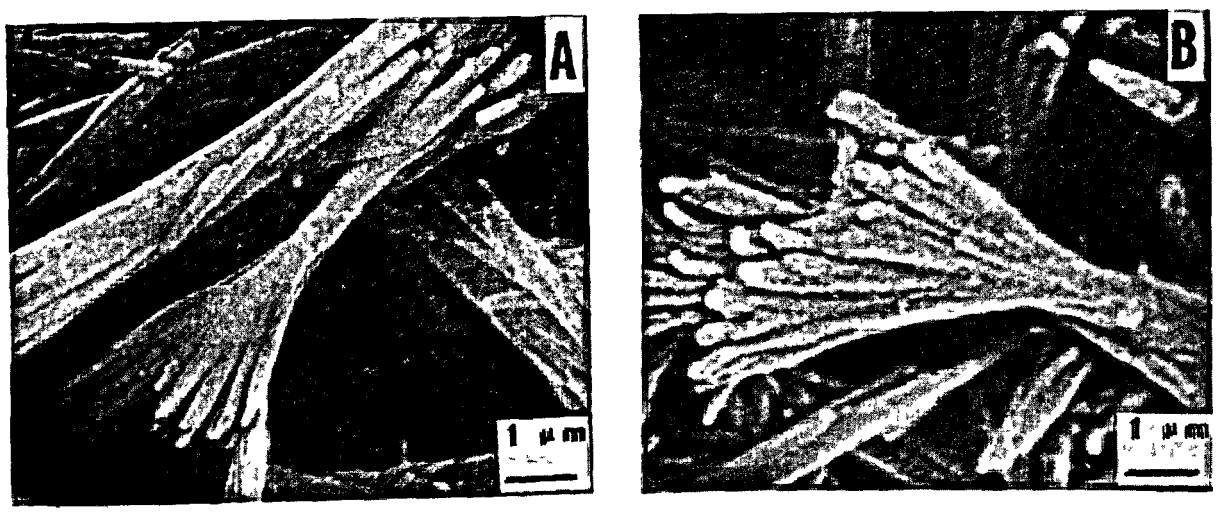

Fig.1 SEM photographs of synthetic hillebrandite (A) and its decomposed β-C_2S (B) at 600°C for 1 h.

The hydration of the β-C_2S was carried out with w/s=0.5 at 80°C. The reaction rate was obtained by a quantitative XRD method. The Ca/Si ratio of the C-S-H was obtained by difference, using determination of $Ca(OH)_2$ by DTA-TGA and by an analytical transmission electron microscopy, ATEM (JEOL-2000FX with NT-5500). These methods were described elsewhere (5,6,7).

Thermal Decomposition of the C-S-H

The C-S-H used for thermal decomposition was of fully reacted β-C_2S cured at 80°C for 24 h. After heating the C-S-H at 200° to 1000°C for 1 h, the decomposition products and variations in the silicate anion structure were determined by XRD and ^{29}Si MAS NMR (JEOL GX-270) respectively. The activation energy of the reaction from C-S-H to β-C_2S was obtained by the heating method.

RESULTS AND DISCUSSION

1. Hydration Behavior

Table 1 shows the results of the β-C_2S hydration cured for 1 h to 28 d. The hydration at 80°C of the β-C_2S was faster than at 25-60°C (6,7), and the hydration was completed in 24 h. In addition, it was strongly dependent on temperature throughout. The results are not in agreement with those given by Brunauer and Kantro using normal β-C_2S made at high temperature with stabilizer (8).

Table 1 Percentages of β-C_2S reacted and chemical compositions of C-S-H in β-C_2S hydrates

Curing time (h)	β-C_2S reacted (%)	Ca/Si of C-S-H		H_2O / SiO_2 molar ratio
		ATEM	TGA-DTA	
1	2	-	-	-
3	21	-	2.00	3.99
6	50	-	2.00	3.09
12	87	-	1.97	2.70
24	100	2.05	1.98	2.50
168	100	1.99	2.00	2.50
672	100	2.03	1.98	2.57

ATEM and TGA-DTA results show the mean values of 30-40 analyses by scanning a 5 um^2 of C-S-H aggregates without $Ca(OH)_2$ and 3-5 measurements respectively.

This is attributed to the fact that the β-C_2S made from hillebrandite has a fibrous form with extremely thin (10-30 nm thick) and elongated laths, resulting in a large surface area. With w/s=0.5, in contrast to the situation with normal β-C_2S, the β-C_2S from hillebrandite is covered with a thin layer of water. Thus the initial reaction occurs directly on the β-C_2S surface to form C-S-H with a Ca/Si ratio of 2.0 without $Ca(OH)_2$ crystallization, and further reaction rapidly proceeds to the interiors of the thin laths without the diffusion control, which is observed in the later stage for normal β-C_2S. This mechanism is supported by the C-S-H morphology, which shows the same lath-like plates as the β-C_2S before hydration.

The Ca/Si ratios of the C-S-H have almost the same values of 2.0 by both ATEM and DTA-TGA methods, without formation of $Ca(OH)_2$ or trace amount of $Ca(OH)_2$, even if formed. This could be due to the different mechanism of hydration between the β-C_2S from hillebrandite and normal β-C_2S with their different surface areas and imperfect crystallinity.

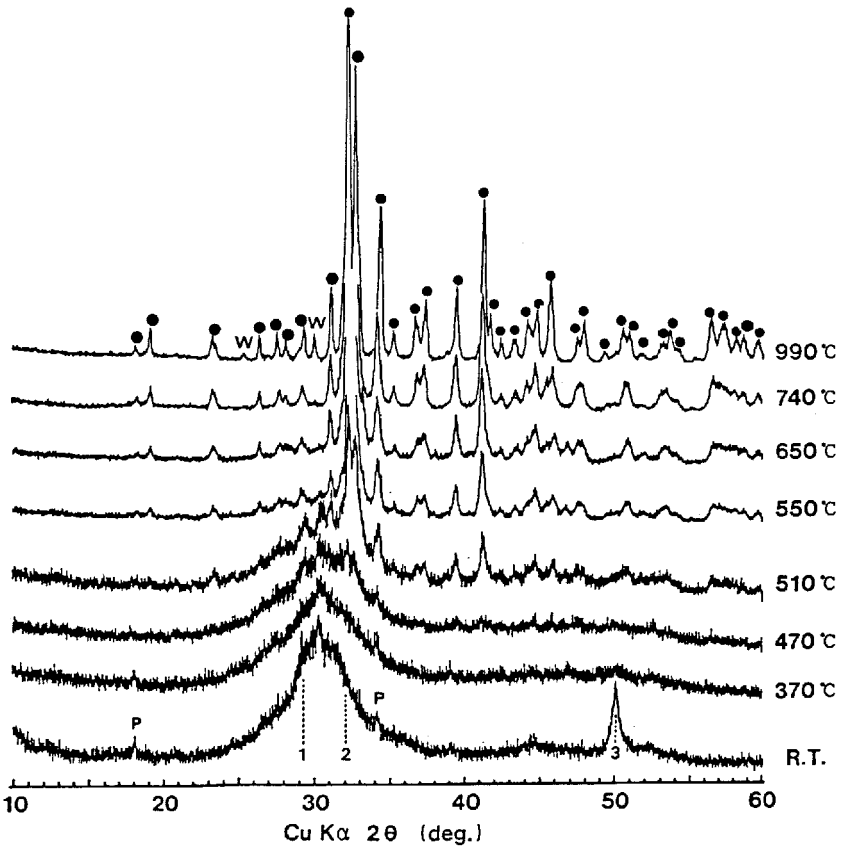

Fig. 2 XRD powder patterns of a fully reacted β-C_2S hydrate, showing C-S-H at 0.304 nm (1), 0.280 (2) and 0.182 (3) with $Ca(OH)_2$ (p). On heating, β-C_2S (●) and wollastonite (w) were formed.

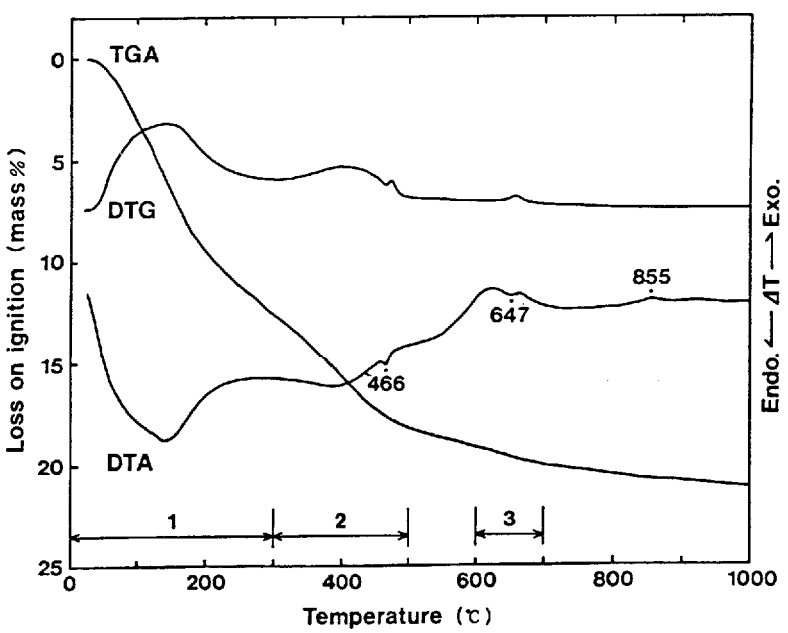

Fig. 3 DTA-TGA curve of a fully reacted β-C_2S hydrate, showing with the differentiation of TGA curve (DTG). Reaction is separated into 3 areas.

2. Thermal Behavior of the C-S-H

X-Ray Diffraction Patterns Fig. 2 shows the XRD powder patterns of a fully reacted β-C_2S hydrate at 80°C for 24 h, and its heated samples at 370° to 900°C. The patterns of the hydrate before heating are similar with those of a fully reacted β-C_2S paste reported by Mohan and Taylor (9), except that the $Ca(OH)_2$ peaks are very weak and the 0.304 - 0.280 nm (2Θ = 29.3-32.1°) shows a symmetrical broad peak. On being heated at 370°C, the 0.304 - 0.280 peak weakened and the 0.182 nm peak (50.1°), contributing to the O - O repeat distance of Ca - O polyhedra in C-S-H, completely disappeared. This evidence shows that the Ca-O polyhedra attached with silicate anions as dimers or chains lose their ordered domains. At 470°C, a small amount of β-C_2S can be observed, indicating that the β-C_2S is directly formed from the C-S-H. With further heating, the dehydrated C-S-H is fully decomposed to β-C_2S at 650°C, indicating higher crystallinity on higher temperature treatment. At 990°C, a little wollastonite was also obtained, probably from decomposition of the xonotlite, which was present as an impurity.

DTA-TGA Curve Fig. 3 shows the DTA-TGA-DTG curve of a fully reacted β-C_2S hydrate at 80°C for 24 h. The weight loss occurs continuously up to 900°C, except for a weak step at 466°C from dehydration of $Ca(OH)_2$ present in traces. The weight loss is divided into three steps; abruptly up to 300°C, gradually at 300-500°C and steadily at 600-700°C. The results are similar to those of a fully reacted C_3S paste reported by Taylor and Turner (10), except that the $Ca(OH)_2$ dehydration-endotherm is very weak, the weak exotherm at 647°C and the weak exotherm occurring at 855°C, due to the crystallization of wollastonite from xonotlite included in the sample.

Silicate Anion Structure

Fig. 4 shows the ^{29}Si MAS NMR results for the fully reacted sample before and after heating same as X-ray analysis. The C-S-H before heating shows strong Q^1 and Q^2 peaks with a Q^1/Q^2 ratio of 1.0, indicating single chain anions with or without dimer. On being heated at 370°C, the dehydrated C-S-H shows a strong and broad Q^0 peak with weakened Q^1 and Q^2 peaks. This evidence shows that the dehydrated C-S-H is an initial or induction stage of β-C_2S formation, accompanying the depolymerization and monomerization. In the specimen heated at 500°C, coexisting of dehydrated C-S-H with β-C_2S according to the XRD pattern, the NMR pattern shows a sharpened Q^0 shoulder with weakened Q^1, indicating an acceleration of monomerization.

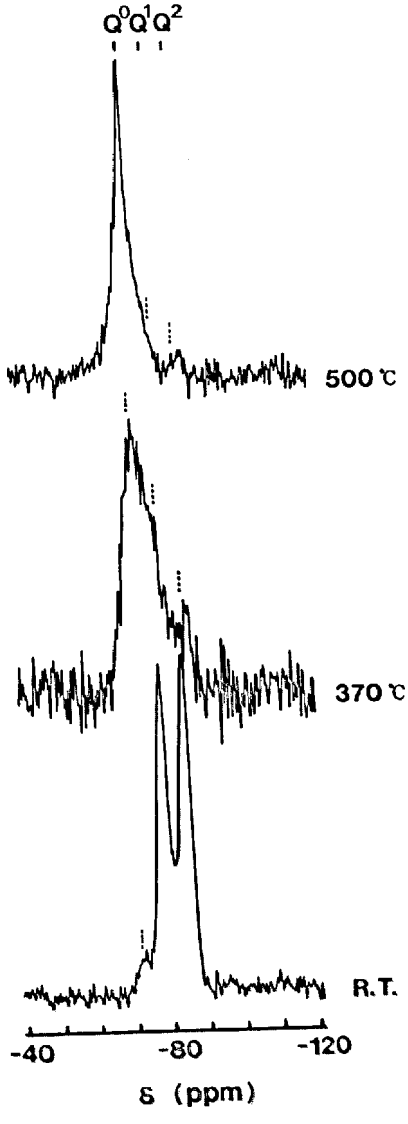

Fig. 4 ^{29}Si MAS NMR spectra of C-S-H in a fully reacted β-C_2S and its heated specimens.

On being heated at 600-700°C, the specimens show a sharp and strong Q^0 by the MAS NMR, while TGA curve continues to show a slight weight loss, indicating a mixture of non-protonated and protonated monomers. This NMR result on heating agreed with those of the fully reacted β-C_2S hydrates formed from hillebrandite at 25° to 60°C (7) and of a mixture of hydro-thermally formed C-S-H and $Ca(OH)_2$ with Ca/Si=2.0 at 100°C (11).

Activation Energy Calucated

The activation energy required for the entire amount of C-S-H to decompose into β-C_2S was 1.45 kJ/mol as shown in Fig. 5.

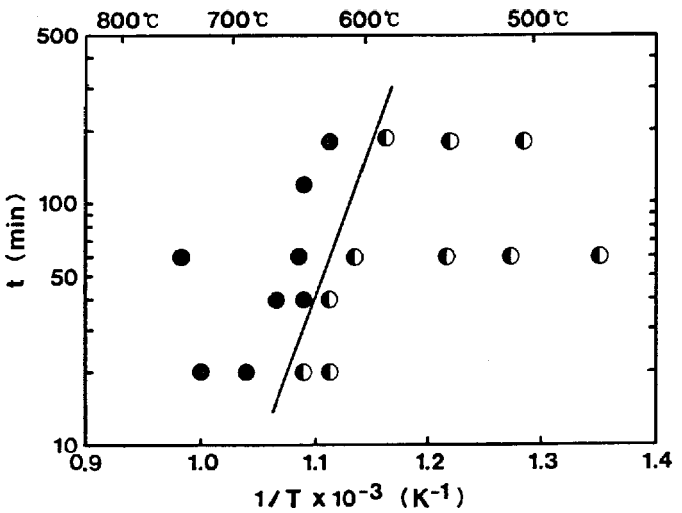

Fig. 5 Dehydration/decomposition of a fully reacted β-C_2S hydrate (C-S-H) to β-C_2S under isothermal conditions, showing β-C_2S (●) and mixture of dehydrated C-S-H and β-C_2S (◑).

ACKNOWLEDGEMENTS

This work forms of a program financed by the Cement Association of Japan, whose support to Mitsuda is gratefully acknowledged. We thank also Emeritus Professor H.F.W. Taylor, University of Aberdeen for critically reviewing the manuscript and for his helpful comments on C-S-H.

REFERENCES

(1) Pritts, I.M. and Daugherty, K.E.: "The Effect of Stabilizing Agents on the Hydration Rate of β-C_2S", Cem. Concr. Res., **6**, 783-795 (1976).

(2) Shibata, S., Kishi, K., Asaga, K., Daimon, M. and Shrestha, P.R.: "Preparation and Hydration of β-C_2S without Stabilizer", Cem. Concr. Res., **14**, 323-328 (1984).

(3) Yang, N. and Zhong, B.: "A Study on Active β-Dicalcium Silicate", J. Chinese Silicate Soc., **10**, 161-166 (1982).

(4) Yang, N., Zhong, B. and Wang, Z.: "An Active β-Dicalcium Silicate Preparation and Hydration", in 8th Intern. Cong. Chem. Cem., Rio de Janeiro, Vol. 3, p. 22-27 (1986).

(5) Ishida, H., Mabuchi, K., Sasaki, K. and Mitsuda, T.: "Low Temperature Synthesis of β-Ca_2SiO_4 from Hillebrandite", J. Am. Ceram. Soc., in press (1992).

(6) Ishida, H., Sasaki, K. and Mitsuda, T.: "Highly Reactive β-Dicalcium Silicate: I, Hydration Behavior at Room Temperature", J. Am. Ceram. Soc., in press (1992).

(7) Ishida, H., Okada, Y. and Mitsuda, T.: "Highly Reactive β-Dicalcium Silicate: II, Hydration Behavior at 25°C Followed by ^{29}Si NMR", J. Am. Ceram. Soc., in press (1992).

(8) Kantro, D.L., Brunauer, S. and Weise, C.H.: "Development of Surface in the Hydration of Calcium Silicates. II, Extension of Investigation to Earlier and Later Stages of Hydration", J. Phys. Chem., **66**, 1804-1809 (1962).

(9) Mohan, K. and Taylor, H.F.W.: "Analytical Electron Microscopy of Cement Pastes; IV, β-Dicalcium Silicate Pastes", J. Am. Ceram. Soc., **64**, 717-719 (1981).

(10) Taylor, H.F.W. and Turner, A.B.: "Reactions of Tricalcium Silicate Paste with Organic Liquids", Cem. Concr. Res., **17**, 613-623 (1987).

(11) Okada, Y., Shibasaki. H., Yang, N. and Mitsuda, T.: " Decomposition of CaO - SiO_2 - H_2O Compounds by Heating: ^{29}Si CPMAS NMR Spectroscopy", Cem. Assoc. Japan, Proc. Cem. Concre., **45**, 64-67, in Japanese (1991).

INFLUENCE OF DIFFERENT FILLERS ON THE HYDRATION OF C_3S

S Husson*, B Guilhot and J Pera

Ecole Nationale Supérieure des Mines de Saint-Etienne
Institut National des Sciences Appliquées de Lyon, FRANCE

The addition of a fine particulate material to a Portland cement can impart an influence on the hydration of the cement with witch is blended or will act just as a simple filler. Such material may be inert or have latent hydraulic properties. This study examines the influence of the three fillers on the hydration of C_3S:

i) zirconia, witch is insoluble in water and only fills up porosity;
ii) limestone filler, whose effect on the hydration of C_3A is well know; its interaction with C_3S has yet to be detailed;
iii) zircon, whose cristalline structure is closely related to the C_3S one; zircon and C_3S also possess a common ion.

Zircon and limestone filler react with C_3S. Limestone filler accelerate C_3S dissolution and modifie the nature of hydrates: carbonated silicates precipitate. Zircon consumes calcium hydroxide and changes the nature of hydrates.

Zircon and limestone filler do not enhance the compactness of the granular stack but their chemical reactivity induces an increase in strength at dosages higher than 20%.

L'ajout de fillers au ciment Portland peut, en plus d'un effet physique de comblement de la porosité, modifier les caractéristiques de l'hydratation du liant. Ceci grâce à un effet pouzzolanique ou non. Cette étude traite de l'influence de trois types de fillers sur l'hydratation du C_3S :

i) une zircone, insoluble dans l'eau, qui n'agit que par le comblement de la porosité ;
ii) un filler calcaire, dont la réactivité avec le C_3A est déjà connue. Sa réactivité avec le C_3S est étudiée ici ;
iii) un zircon, qui possède un ion commun et une structure cristalline voisine du C_3S.

Le zircon et le calcaire réagissent avec le C_3S. Le filler calcaire a un effet accélérateur et modifie la nature des hydrates : un silicate de calcium carbonaté et hydraté précipite. Le zircon réagit avec l'hydroxyde de calcium pour former des nouveaux hydrates.

Contrairement à la zircone, ces fillers n'améliorent pas la compacité de la pâte. Pour des pourcentages supérieurs à 20 % leur action chimique provoque une augmentation des performances mécaniques.

* Actual adress: Weber et Broutin - Servas

INTRODUCTION

Since 1979, fillers have been widely used in Portland Cements with mineral admixtures ("CPJ" cement), in France. They are authorized for additions up to a maximum content of 35%. It was of interest to study their influence on the hydration of Portland Cement.

This paper describes the interaction of three fillers with C_3S zirconia, zircon and limestone filler. Some results on the influence of calcareous filler are available [1] to [3].

EXPERIMENTAL

Materials

- Zirconia (ZrO_2) was chosen because of its insolubility in water. It is an inert filler as it only fills up the porosity.
- Zircon ($ZrSiO_4$) is soluble in basic solutions and its crystalline structure is closely related to the C_3S; it possesses a common ion.
- Limestone ($CaCO_3$) filler is soluble in water; its effect on the hydration of C_3A is well known, although its interaction with C_3S has yet to be ascertained.

The particle size distributions of these fillers are compared with that of C_3S in figure 1.

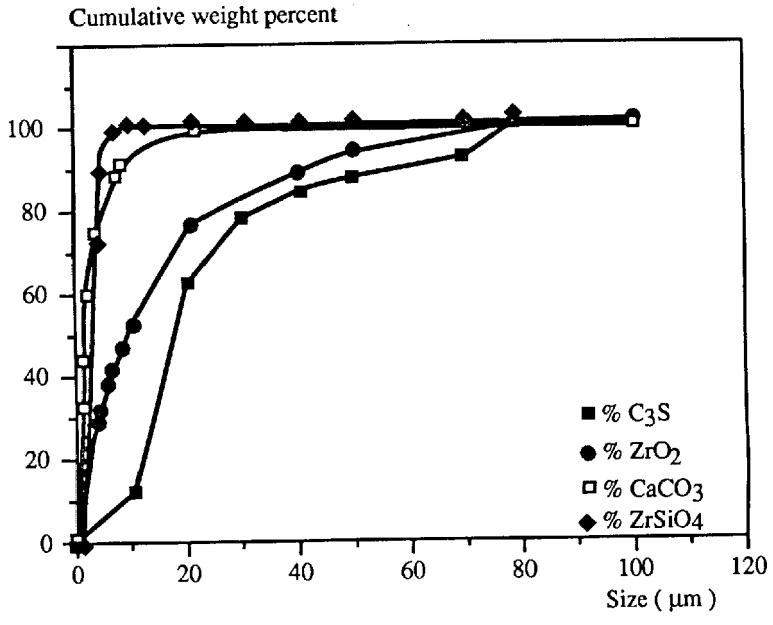

Figure 1 :
Particle size distribution of C_3S and fillers

PHYSICO-CHEMICAL INVESTIGATIONS

The kinetics of hydration of the blended binders was studied by isothermal calorimetry on mixes containing 50% C_3S and 50% fillers. The water to solid ratio was 1.00.

Five mixes with 10 to 50% C_3S substitution by fillers were prepared. All samples were cast at an equivalent consistency in minicylinder moulds (d = 2 cm, h = 4 cm).

The water to solid ratios were respectively:

100% C_3S	:	0.35
C_3S + zirconia	:	0.35 to 0.40
C_3S + zircon	:	0.35 to 0.40
C_3S + limestone	:	0.30 to 0.35

These samples were then cured in lime satured solution at 20°C at different periods for mechanical tests in compression (1, 7, 28 and 60 days). The hydration was stopped by the procedure developed by Bachiorrini and Guilhot [4]. Differential thermal analysis (D.T.A.), Fourier Transform Infra-Red (F.T.I.R.) and X-ray diffraction (X.R.D.) were performed on dried powders selected to be < 100 µm.

RESULTS AND DISCUSSION

Kinetics of hydration

The results of isotherm calorimetry are shown in figure 2.

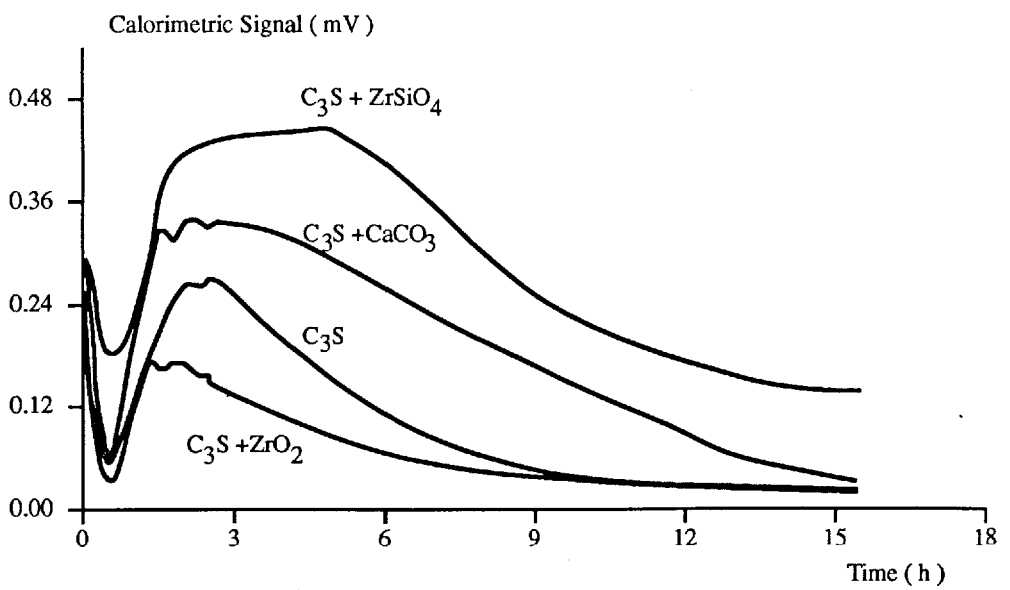

Figure 2 :
Influence of fillers on the kinetics of C_3S hydration

The total mass of the solid sample was 300 mg. The heat released by the hydration of 300 mg C_3S is twice the heat noted for a mix of 150 mg C_3S and 150 mg zirconia. Zirconia does not influence either the kinetics of the reaction or the heat released.

It is quite an inert filler. The heats released for mixes containing limestone filler or zircon are higher than that of plain C_3S; they therefore react with C_3S to develop new hydrates.

Hydrates formed

The hydrates were determined by F.T.I.R. and X.R.D. Zirconia does not modify the nature of hydrates; when limestone was added, the vibration of one SiO_4 group was modified (figure 3). In plain C_3S, the absorption band was present at 450 cm^{-1} while in the blended binder the doublet vibrated at 486 and 462 cm^{-1}.

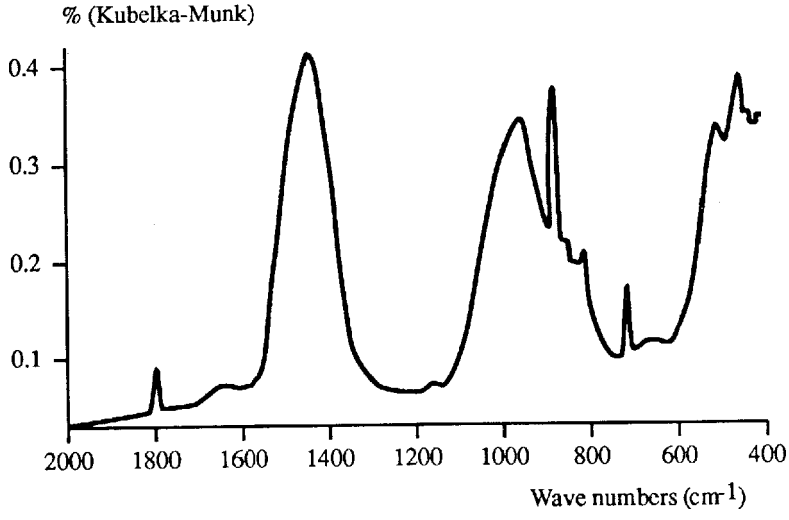

Figure 3 :
F.T.I.R. spectra of 50% C_3S + 50% $CaCO_3$ hydrated mix

A new X-ray peak appeared (2θ = 14.9°: $K_{\alpha Cu}$) and its intensity increased with the carbonate content (figure 4). It could correspond to the formation of carbonated hydrated calcium silicate [1], [5], [6].

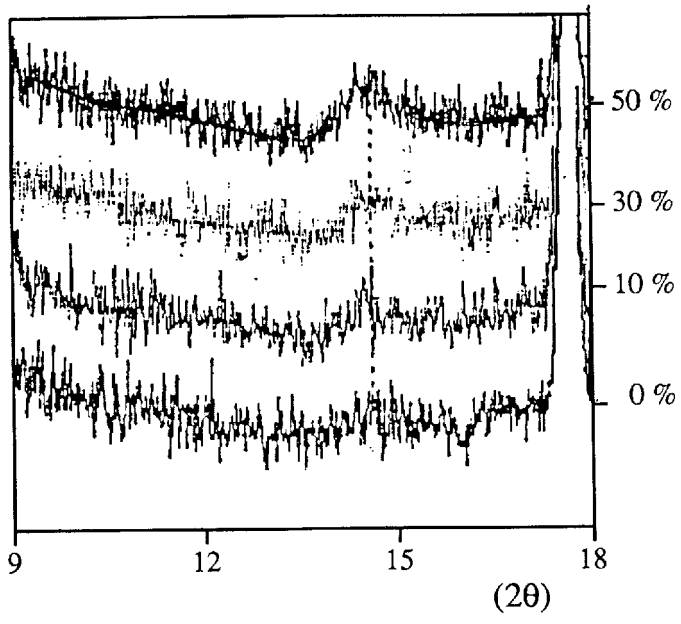

Figure 4 :
XRD spectra for C_3S - $CaCO_3$ hydrated mixes

In the mixes containing zircon, it can be seen that the calcium hydroxide content and the 615 cm^{-1} band intensity decreased with time (figure 5). Zircon exhibits pozzolanic properties.

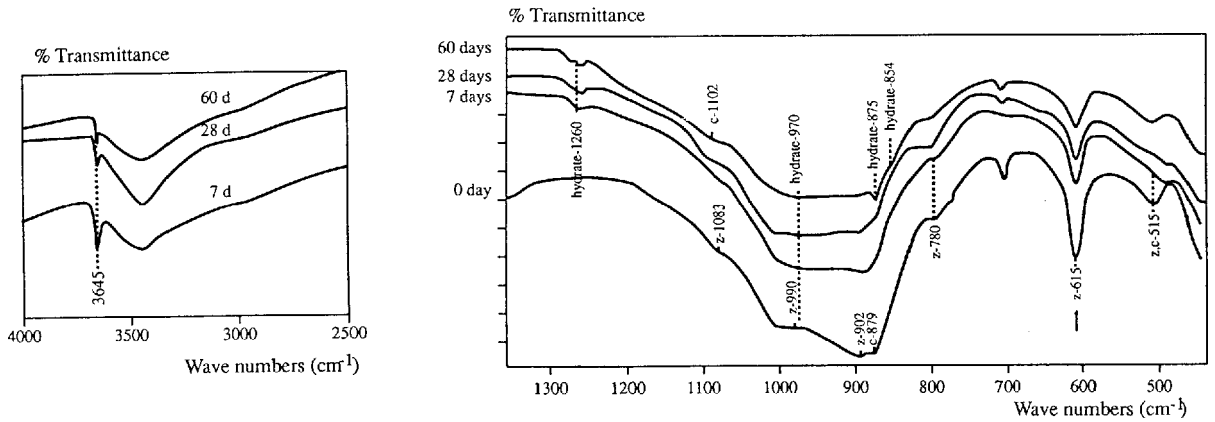

Figure 5 :
F.T.I.R. spectra of C_3S-zircon hydrated mixes

Mechanical strength

The results are reported in figures 6 to 8.

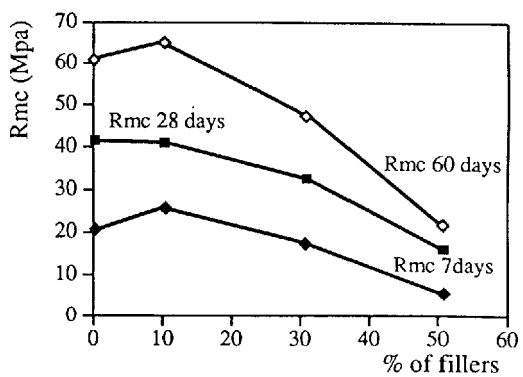

Figure 6 :
Compressive strength of zirconia blended binders

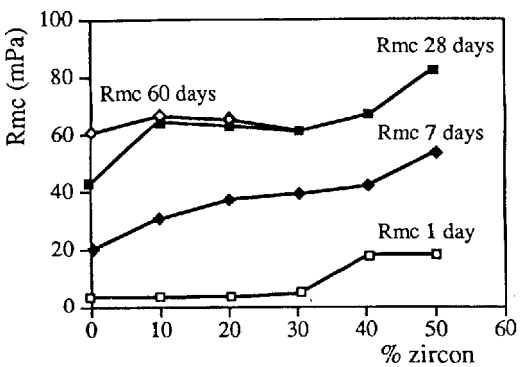

Figure7 :
Compressive strength of zircon blended binders

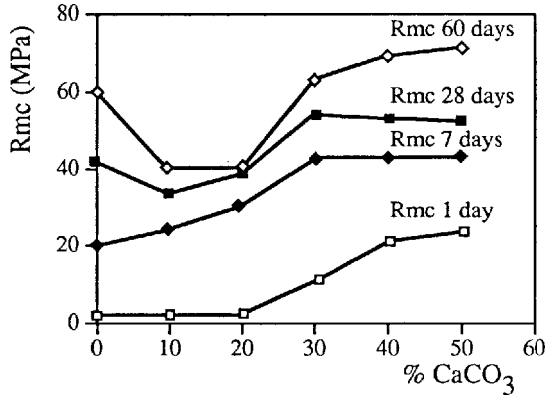

Figure 8 :
Compressive strength of limestone blended binders

With 10% zirconia, the compressive strengh is increased; for higher contents there is a decrease in strengh.

With zircon and calcium carbonate, the best results are obtained for blend contents higher than 20%.

The chemical activity of these fillers can be evaluated using Feret's law:

$$R_c\,(t) = K\,(V_s/V_t)^2$$

where: R (t) is the compressive strengh measured at time t.
V_s is the volume of the solid fraction in the paste.
V_t is the total volume of the paste and K the index of activity.

The K index for mixes containing zircon are higher than the K value for plain C_3S. It proves that this filler shows some pozzolanic activity (figure 9). $CaCO_3$ also reacts with C_3S when the content of $CaCO_3$ is higher than 20%. The zirconia mixes show no chemical activity.

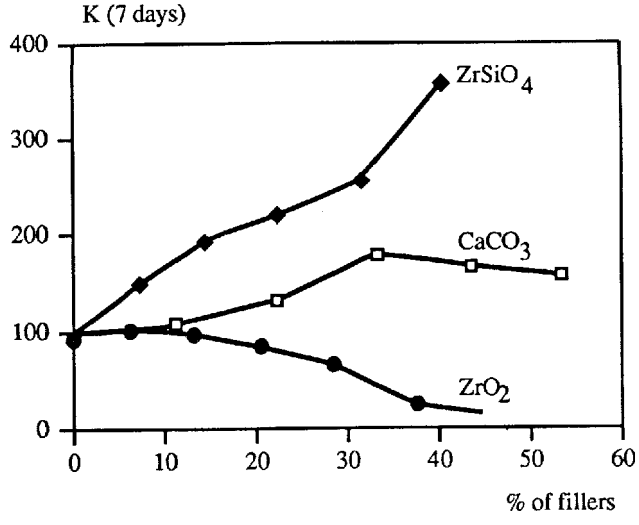

Figure 9 :
Feret's indexes

CONCLUSION

Zircon and limestone fillers react with C_3S. Limestone filler accelerates C_3S dissolution and modifies the nature of hydrates: carbonated silicates precipitate. Zircon consumes calcium hydroxide and changes the nature of hydrates.

Zircon and limestone filler do not enhance the compactness of the granular stock but their chemical reactivity induces an increase in strength at dosages higer then 20%.

REFERENCES

[1] V.S. Ramachandran, Zhang Chun-Mei. Il Cemento, 1986, 83 (3), 129-152

[2] V.S. Ramachandran, Zhang Chun-Mei, Durability Build. Mater., 1986, 4, 45-66

[3] V.S. Ramachandran, 8th Congrès International de la Chimie des Ciments, Rio de Janeiro, 1986, III, 109-119

[4] A. Bachiorrini, B. Guilhot, Cement and Concrete Research, 1982, 12, 559

[5] C. Hemni, Mineral J., 1977, 8, 374

[6] J.J. Pluth, J.V. Smith, Acta Cryst., 1973, B29, 73-88.

THE EFFECT OF C_3A POLYMORPHS ON HYDRATION OF C_3S

G Y Shin* and K S Han**

*Ssangyong Cement Industrial Co, Seoul, KOREA
**Inha University, Inchon, KOREA

SUMMARY

We have studied various effects of different crystalline forms of C_3A including a melt phase of C_3A, on the hydration of C_3S in the system C_3S and C_3A with and without gypsum. Cubic form of C_3A was synthesized by pure C_3A composition, orthorhombic and monoclinic forms were prepared with a C_3A composition of sodium ion substitution. A melt phase of C_3A was formed by rapid quenching of a completely fused C_3A containing a small amount of SiO_2. C_3A polymorphs showed different hydration rates. The hydration of coexistent C_3S was correspondingly influenced by the type of C_3A polymorphs, that is, the lower the hydration rate of C_3A is, the higher the hydration rate of coexistent C_3S is. In the system containing gypsum, a retardation phenomenon as a formation reaction of monosulfate was observed in both sodium substituted C_3A and melt C_3A.

In den Systemen C_3S und C_3A mit oder ohne Gyps wurden die verschiedenen Effekte der unterschiedlichen Kristallformen von C_3A einschließlich einer Schmelzphase von C_3A auf die Hydration von C_3S untersucht. Die kubische Form von C_3A wurde von einer reinen C_3A-Komposition und die orthorhombische und die monoklinische Form wurden von einer mit den Natrium-Ionen substituierten C_3A-Komposition hergestellt. Eine Schmelzphase von C_3A wurde mit schneller Abkühlung von einem voll geschmolzenen C_3A, das eine kleinen Menge von SiO_2 enthält, gebildet. Der C_3A-Polymorphismus zeigte unterschiedlichen Hydrationsraten. Die Hydration von koexistierendem C_3S wurde dem entsprechend vom Typ des C_3A-Polymorphismus beeinflußt. Daß heißt, je niedriger die Hydrationsrate von C_3A ist, desto höher die Hydrationsrate von koexistierendem C_3S ist. Im System, das Gips enthält, war das Verzögerungsphänomen mit einer Bildungsreaktion des Monosulfats in beiden mit Natrium substituierten C_3A und geschmolzenen C_3A festgestellt.

INTRODUCTION

The interaction of tricalcium silicate (C_3S) and tricalcium aluminate (C_3A) is of a great interest to cement chemists because they are two important phases in a cement clinker : the former is responsible for the early strength development, whereas the latter is for the setting behaviour. However, a few limited research has been studied until now, and the effect of C_3A on C_3S hydration has not yet been completely clarified (1-6).

It is well established that most of the alkali in the clinker is contained as a solid solution with C_3A, and the crystalline structure of C_3A changes from cubic to orthorhombic and monoclinic structure depending on the substitution content of sodium. But, little is known about the hydration characteristics of the C_3A polymorphs, especially the effects of the C_3A polymorphs on C_3S during their hydration (7-10). In this study,various effects of the different crystalline forms of C_3A including a melt phase of C_3A, were investigated on the hydration of C_3S in the system C_3S and C_3A with and without gypsum.

EXPERIMENTAL

C_3S was synthesized from a mixture of calcium carbonate, quartz,alumina and magnesium carbonate with a mole ratio of $54CaO \cdot 16SiO_2 \cdot Al_2O_3 \cdot MgO$ by heat treatment at 1450℃ for a few consecutive burning. The final product was checked by XRD and subsequently ground to a fineness of ca 3000 cm^2/g (Blaine). X-ray diffractograms showed that C_3S belonged to a monoclinic phase (11) with a free lime content below 0.3%. Four kinds of C_3A polymorphs were synthesized : cubic phase C_3A(C-C_3A) was prepared by heating a stoichiometric mixture of calcium carbonate and alumina. The Na_2O containing C_3A samples, that is, orthorhombic (O-C_3A) and monoclinic phase C_3A (M-C_3A) were prepared as described by Shin and Glasser (12). The samples were characterized by X-ray diffractograms which were in a good agreement with Regourd and Guinier's data (13). A melt phase of C_3A (G-C_3A) containing a small amount of SiO_2 was prepared by rapid quenching after complete fusion at 1700℃. The sample G-C_3A presumably containing a small amount of glass phase resulted in lowering intensity of X-ray diffraction and increasing free CaO, compared to C-C_3A. The result of chemical composition analysis is given in Table 1, Fig. 1 contains the IR spectra patterns of C_3A polymorphs.

Each sample was prepared by blending of the system 75%C_3S-25%C_3A polymorphs with and without 10% gypsum to the sample as shown in Table 2.

Table 1. Characterization data for C_3A polymorphs.

Item \ Crystalline form		Cubic	Orthorhombic	Monoclinic	Melt
Chemical composition (wt. %)	CaO	62.2	58.0	57.1	60.5
	Al_2O_3	38.0	37.7	37.5	36.9
	Na_2O	-	4.48	5.71	-
	SiO_2	-	-	-	2.9
	Free CaO	0.5	0.8	0.9	2.7
Specific density (g/cm^3)		3.05	3.17	3.18	2.99
Specific surface (cm^2/g)		3010	3010	3005	3010

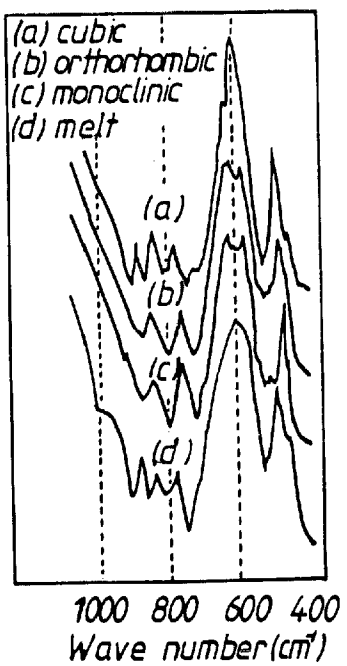

Fig.1. Infra-red spectra of C_3A polymorphs

The multicell conduction calorimeter was used to measure the heat evolution of hydration for the sample with a water to solid ratio of 1.0 at 20 ℃. For the hydration studies, prepared pastes were mixed with distilled water using a constant water to solid ratio of 1.0. They were stored in small sealed polyethylene jars in a curing cabinet at 20±1 ℃. At designed intervals, hydration process was stopped by the addition of acetone and dried in vacuum. The amount of unreacted clinker phases was determined by quantitative X-ray diffraction analysis using samples preignited at 600 ℃. The quality of the phase formed in the hydration process was analysed again by XRD and DT-TGA. The microsturctures of hydrates were observed by SEM. Suspension experiments were conducted for the sample with a water to solid ratio of 50. At the end of reaction periods, the contents were filtrated by G-4 glass filter. The contents of Ca, Al and Na in the filtrate were analysed using an atomic absorption spectrometer.

Table 2. Notation of samples in the system 75%C_3S-25%C_3A polymorphs with and without gypsum.

Sample No.		Used C_3A
Without gypsum	With gypsum	
B C	B C G	cubic
B O	B O G	orthorhombic
B M	B M G	monoclinic
B G	B G G	melt

RESULTS AND DISCUSSION

System C_3S-C_3A polymorphs

The curves of heat liberation (Fig. 2) in the system C_3S-C_3A polymorphs show two distinct exothermic peaks during hydration. The first peak reveals the heat of solution and hydration of each clinker minerals right after the contact with water. The second peak which is related to the interactive hydration of the clinker minerals is discussed.

The second one appears early in the samples BM and BO, compared to the samples BC and BG as shown Fig. 2. Therefore, it can be thought that the hydration of C_3S is affected by C_3A polymorphs. Because the hydration rate of O-C_3A and M-C_3A is slower than that of C-C_3A, the content of released [Ca^{2+}] into solution would decreased. As a result, the heat evolution increase with accelerating the hydration of coexistent C_3S in the samples BO and BM. In the hydration of C_3A, Shin and Glasser (14) reported that [Ca^{2+}] in solution was lower in the Na containing C_3A, compared to the pure C_3A during the same hydration interval. On the contrary the fact that O-C_3A and M-C_3A release lower content of [Ca^{2+}] into solution than C-C_3A, we observe that the concentration of [Ca^{2+}] in the samples BO and BM containing O-C_3A and M-C_3A respectively is higher than that of the sample BC after 6 hours of hydration as shown in Table 3. This observation reveals that the hydration of C_3S in the samples BO and BM is accelerated compared to the sample BC. On the other hand, the concentration of [Ca^{2+}] after 12 hours of hydration in samples BO and BM is extremely lowered, because [Ca^{2+}] in solution is supersaturated earlier and greater $Ca(OH)_2$ precipitate is produced than the sample BC. Early precipitation of $Ca(OH)_2$ is confirmed by DT-TGA analysis as shown in Fig. 3 and this result is consistent with the result of $Ca(OH)_2$ measurement on the paste sample after 12 hours hydration as shown in Table 4. As a result, the samples BO and BM containing Na substituted-C_3A have a higher rate of $Ca(OH)_2$ formation than the sample BC containing pure-C_3A.

The hydration progress of C_3S and C_3A is shown in Fig. 4 and Fig. 5. In the samples BO and BM, the hydration rate of C_3A is low, whereas that of C_3S is high compared to sample BC. Thus, it can be confirmed that the hydration rate of O-C_3A and M-C_3A containing Na_2O is low but that of coexistent C_3S is accelerated. At the same time, in the samples BO and BM, the hydration rate of coexistent C_3S increases in proportion to the content of Na_2O in C_3A. Even though the density of C_3A polymorphs increases according to the Na_2O substitution, no difference is shown between O-C_3A and M-C_3A as shown in Table 1. Accordingly, the difference of hydration rate between O-C_3A and M-C_3A seems to be affected by [Na^+] discharged into solution during the hydration process as shown in Table 3, in addition to the effects of C_3A polymorphs.

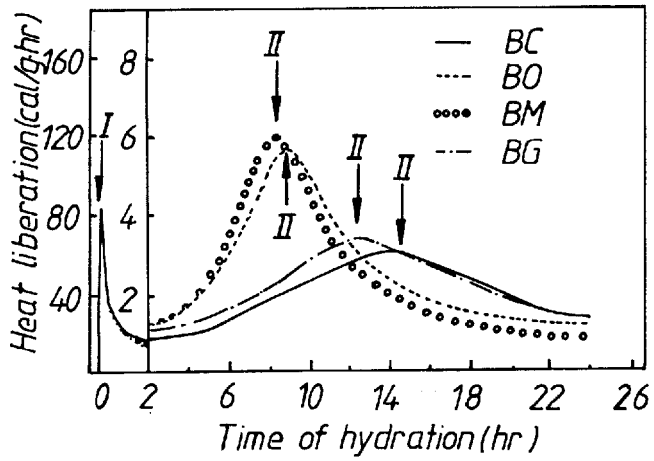

Fig. 2. The cuves of heat liberation in the system C_3S-C_3A polymorphs. (I and II : the apex of 1st and 2nd exothermic peak)

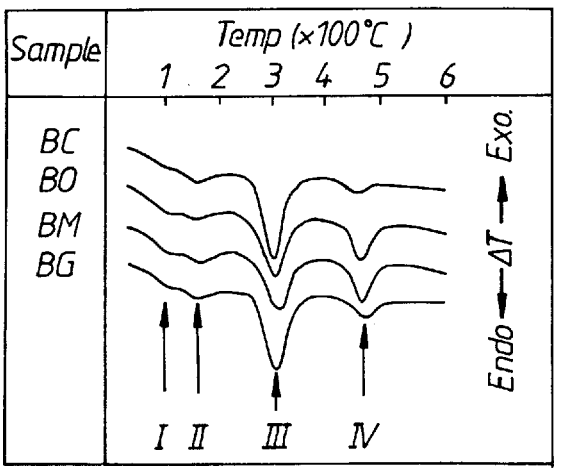

Fig. 3. Thermograms of hydrated products in suspension reaction after 12 hours of hydration. (I=CSH, II=C_2AH_8, III=C_3AH_6, IV=$Ca(OH)_2$)

Table 3. Ions concentration in solution according to the hydration time. (mg/ℓ)

Componet	Sample No.	Hydration time(hr) 1	3	6	12
$[Ca^{2+}]$	B C	933	1014	1071	1193
	B O	1001	1098	1185	970
	B M	1084	1105	1195	973
	B G	958	1023	1073	1161
$[Al^{3+}]$	B C	6.53	4.75	3.88	3.23
	B O	6.85	6.04	3.28	3.25
	B M	8.35	6.58	3.80	3.56
	B G	6.61	5.04	3.52	3.35
$[Na^{1+}]$	B O	144	154	156	198
	B M	172	188	201	237

Table 4. The content of $Ca(OH)_2$ in system C_3S-C_3A polymorphs after 12 hours of hydration.

Sample No.	BC	BO	BM	BG
$Ca(OH)_2$ (%)	5.73	8.94	10.55	6.20

The shape of the second peak of the sample BG containing G-C_3A is similar to that of the sample BC containing C-C_3A, but the heat evolution at the top of the peak is somewhat faster than that of the sample BC. This is because the hydration rate of G-C_3A is somewhat lower than that of C-C_3A due to the existnece of partially glassified C_3A. In other words, Al ion in G-C_3A is acting as a net work former of -Al-O-Al- and the hydration activity is lowered, because of the high bonding energy of Al-O(Oxygen) in G-C_3A compared to C-C_3A(15). Therefore, the hydration of coexistent C_3S is accelerated and the time to reach the second peak is shortened, as stated previously in the samples BO and BM.

This explanation is confirmed by measuring the hydration rate of each sample as shown in Fig. 4 and Fig. 5. The hydration rate of C_3S of the sample BG is higher than that of the sample BC, in spite of the lower hydration rate of C_3A in the same period of hydration. As shown in Table 4, the content of $Ca(OH)_2$ of the sample BC is small compared to the sample BG after 12 hours of hydration. However the shape of the second peak of sample BG is similar to that of the sample BC. This observation indicates that G-C_3A is not completely glassified and maintains cubic phase even in the lower diffraction intensities than that of C-C_3A.

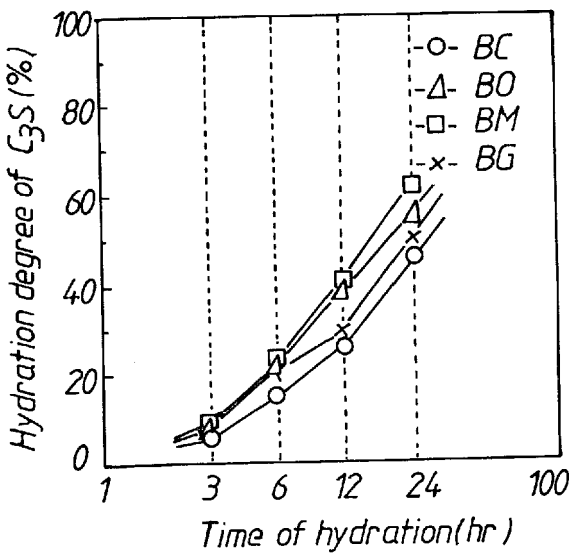

Fig. 4. Progress of C_3S hydration in the system C_3S-C_3A polymorphs.

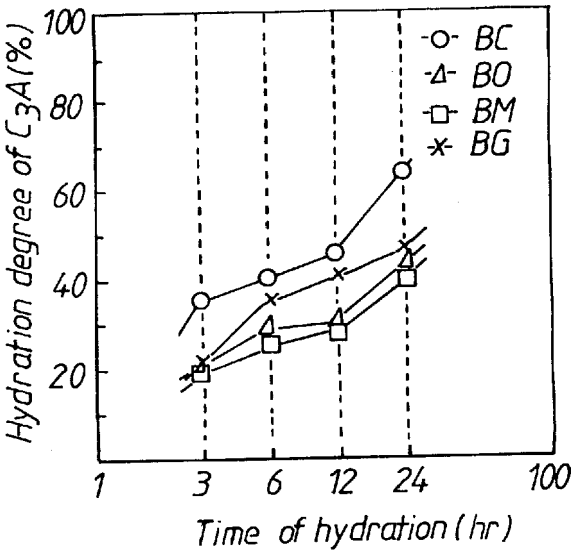

Fig. 5. Progress of C_3A hydration in the system C_3S-C_3A polymorphs.

System C_3S-C_3A Polymorphs-Gypsum

In the presence of gypsum, as shown in Fig. 6, the second peak of samples BOG and BMG appears early compared to the samples BCG and BGG and this trend is same with the case of no gypsum. This is due to the fact that the trend of hydration rate according to the C_3A polymorphs is same as the case of no gypsum as shown in Fig. 7 and Fig. 8, although the hydration rates of C_3A are relatively low, compared to the case of no gypsum. Accordingly, it can be confirmed that the sample showing lower hydration rate of C_3A indicates somewhat a higher hydration rate of C_3S. At the same time, the content of $Ca(OH)_2$ increase as the hydration rate of C_3A decrease as shown in Table 5. Consequently, the interaction between C_3S and C_3A affecting the second peak seems to be similar to the case of no gypsum.

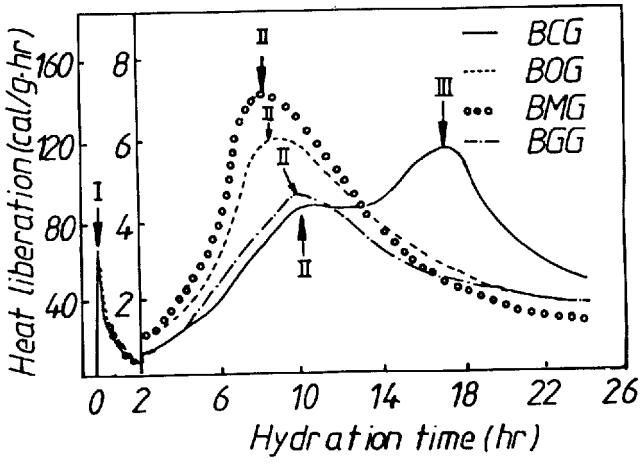

Fig. 6. The curves of heat liberation in the system C_3S-C_3A polymorphs-Gypsum. (I, II and III : the apex of 1st, 2nd and 3rd exothermic peak)

Table 5. The content of $Ca(OH)_2$ in the system C_3S-C_3A polymorphs-Gypsum after 12 hours of hydration.

Sample No.	BCG	BOG	BMG	BGG
$Ca(OH)_2$ (%)	7.37	9.11	10.81	7.81

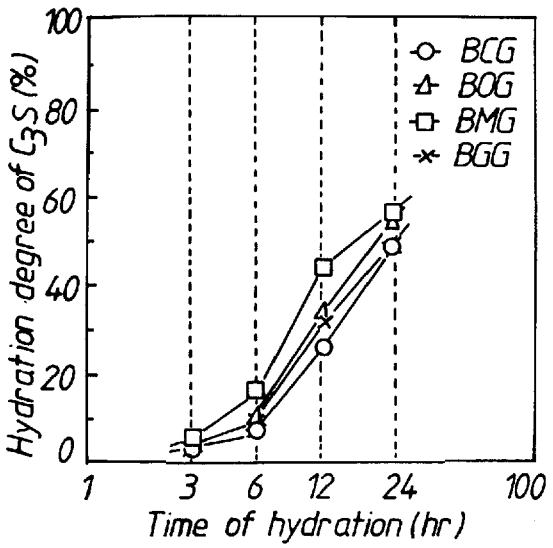

Fig. 7. Progress of C_3S hydration in the system C_3S-C_3A polymorphs -Gypsum.

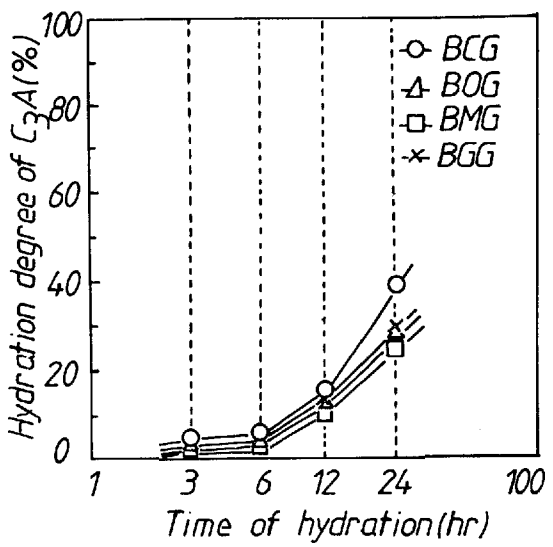

Fig. 8. Progress of C_3A hydration in the system C_3S-C_3A polymorphs -Gypsum.

But the shape of the third peak contribu-ting to the formation of monosulfate changes greatly depending on the types of the C_3A polymorphs. Unlike the other samples, sample BCG reveals the third peak beside the second peak. The time takes 17hr-25min to reach the top of the third peak, and the hydration heat evolution rate at the top is 5.6 cal/g.hr. But from the result of DT-TGA analysis on the hydrated products after 24 hours of hydration as shown in Fig. 9, the peak of monosulfate appears at around 200 ℃ even in the samples BOG and BMG. On the other hand, in the sample BGG containing G-C_3A, the monosulfate peak is not present but significant ettringite peak is observed. Therefore, it is assumed that the formation of monosulfate can be greatly restrained.

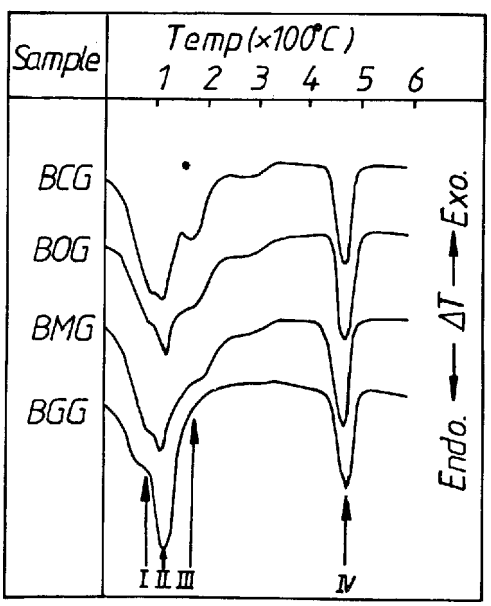

Fig. 9. Themograms of hydrated products in the system C_3S-C_3A polymorphs -Gypsum after 24 hours of hydration. (I=CSH, II=ettringite, III=monosulfate, IV=$Ca(OH)_2$)

SEM-EDS observation shows that the shape of ettringite occurs in different forms according to the added C_3A polymorphs as shown in Fig. 10. The shape of ettringite in the samples BOG and BMG is of a needle type and that of the sample BGG is of a short stick and substrate of foil shape. These variations in the shape of ettringite would have affected the formation of monosulfate. In the samples BOG and BMG, some monosulfate formation occurs by a topochemical reaction because of the retardation of C_3A hydration. But this monosulfate formation is retarded by continuous formation of new ettringite around C_3A particle. In the sample BGG, the the surface of C_3A particle is completely surrounded by the ettringite phase of short stick shape and substrate of foil shape. Such a formation of ettringite disturbs the contact between the unhydrated C_3A and the solution, and the formation of monosulfate is retarded.

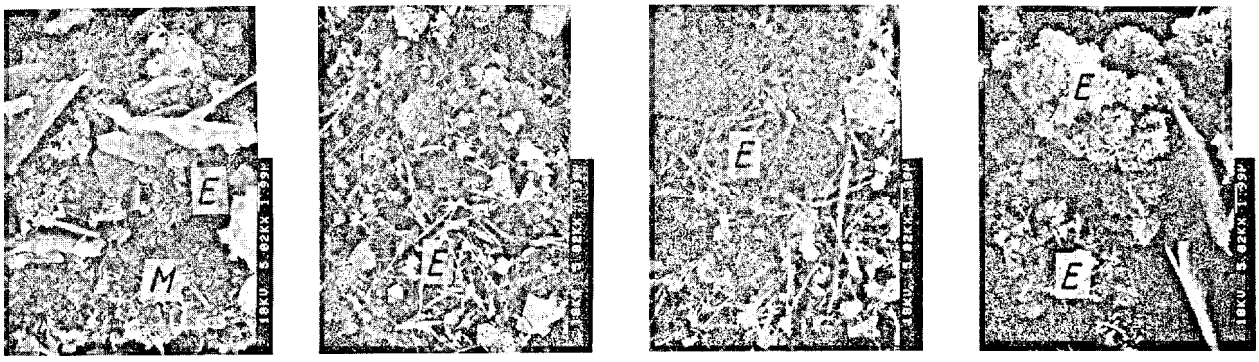

(BCG) (BOG) (BMG) (BGG)

Fig. 10. Morphology of ettringite according to the C_3A polymorphs. (E=ettringite, M=monosulfate)

CONCLUSIONS

When C_3A having different polymorphs is hydrated with C_3S, C_3A polymorphs show different hydration rates and the hydration of coexistent C_3S is affected. Generally the lower the hydration rate of C_3A is, the higher the hydration rate of coexistent C_3S is.

Regardless of the presence of gypsum, the hydration of C_3S is accelerated in the system containing orthorhombic, monoclinic and melt-C_3A, compared to cubic-C_3A. In the system containing Na-substituted C_3A, monosulfate formaiton is retarded by the continuous formation of the new ettringite around the C_3A particle. In the system containing melt C_3A, monosulfate formation is retarded because the surface of melt-C_3A particle is completely surrounded by the ettringite phase of short stick and substrate of foil shape.

REFERENCES

1. De Jong, J.G.M., Stein, H.N. and Stevels, J.M. : 5 th International Congress on the Chemistry of Cement, Tokyo, 1968, VII, 311~320
2. Tenoutasse, N. : Ibid, 1968, VII, 372~378
3. Celani, A., Moggi, P.A. and Rio, A. : Ibid, 1968 VII, 492~503
4. Regourd, M., Hornain, H. and Mortureux, B. : 7 th International Congress on the Chemistry of Cement, Paris, 1980, VIV, 477~482
5. Cottin, B.F. : Ibid, 1980, VIV, 504~508
6. Jones, E.S. and Osbaeck, B. : Ibid, 1980, VIV, 514~519
7. Maki, I., Nishi, M. and Sugimura, T. : Journal of The Ceramic Society of Japan, 1971 V79 (7), 241~245
8. Spierings, G.A.C.M. and Stein, H.N. : Cement and Concrete Research, 1976, V6 (2), 265~272
9. Spierings, G.A.C.M. and Stein, H.N. : Ibid, 1976, V7 (5), 483~492
10. Boikova, A.I, Domansky, A.I. and Paramonova, V.A. : Ibid, 1977, V7 (5), 483~492
11. Taylor, H.F.W. : Academic Press, 1964, VII, 349~409
12. Shin, G.Y. and Glasser, F.P. : Cement and Concrete Research, 1983, V13 (1), 135~140
13. Regourd, M. and Guinier, A. : 6th International Congress on the Chemistry of Cement, Moscow, 1974, Principal paper
14. Shin, G.Y. and Glasser, F.P. : Cement and Concrete Research, 1983, V13 (3), 366~376
15. Tsuyuki, N., Hirota, N., Miyakawa, T. and Kasai, J. : 8th International Congress on the Chemistry of Cement, Brajil, 1986, V6, 400~404

HYDRATION CHARACTERISTICS OF SULPHATE SOLID SOLUTION IN THE CLINKER

J S Koo*, K S Han*, J D Jaung**, and S H Choi***

*Inha University, Inchon, KOREA
**Tong Yang Cement Corp, Seoul, KOREA
***Hanyang University, Seoul, KOREA

ABSTRACT

In synthesized clinker minerals, the effect of sulphate solid solution on the early stage hydration was investigated by microconduction calorimetry, when four different sulphate sources: ammonium sulphate, potassium sulphate, sodium sulphate and calcium sulphate were added to the clinker.

When ammonium sulphate and calcium sulphate were added, the sulphates did not affect clinkering until their contents reached around 1.45%. The sulphates as a solid solution in the clinker accelerated the hydration of alite, however, they did not change the hydration of calcium aluminates.

Particularly, by adding potassium sulphate to the clinker, the sulphate did not affect clinkering, but reduced the hydration of calcium aluminate and enhanced the hydration of alite. In addition, when potassium sulphate was added up to more than 2.0 wt%, the hydration of alite was accelerated by a free potassium sulphate formed separately in the clinker.

Bei synthetischem hergestelltem Klinker, wurde der Effekt von Sulfatmischkristall auf die Hydratcharakterisierung in der Anfangsstufe mit Mikroleitungskalorimeter untersucht. Hier wurde vier verschiedene Sulfate, d.h., Ammoniumsulfat, Kaliumsulfat, Natriumsulfat und Calciumsulfat zu Klinker hinzugefügt.

Bei der Hinzufügung von Ammoniumsulfat und Calciumsulfat wirkten die nicht auf Klinkerisierung bis dessen Gehalte von ca. 1.45% erreicht wurden. Die Sulfate als den Mischkristall in Klinker beschleunigten Hydratation von Alit, jedoch, die haben die Hydratation von Calciumaluminat nicht geändert.

Insbesonders, die Hinzufügung von Kaliumsulfat wirkten nicht auf Klinkerisierung, sondern senkten Hydratation von Calciumaluminat erhöhten Hydratation von Alit. Zusätzlich, wenn Kaliumsulfat mehr als 2.0 Gew. % darauf hinzugefügt wurde, wurde die Hydratation für Alit von freiem Kaliumsulfat, der sich in Klinker getrennt gebildet hat, schnell beschleunigt.

INTRODUCTION

The portland cement clinker takes up sulphate as a solid solution from raw materials and fuel in burning process. It is important to understand how solid solution sulphate affects the initial hydration of cement.

In the reaction of clinker formation, the sulphur compound which is contained in raw materials generally reduces the viscosity and surface tension of melt, so it influences clinkering and changes the physical properties of cement(1-3). The setting time of cement is accelerated by the presence of K_2SO_4. As a result, acicular crystals of syngenite $CaSO_4 \cdot K_2SO_4 \cdot H_2O$ are formed as one of the reaction products(4). In addition, the rate of hydration is affected by lattice defects caused by a minor amount of SO_4^{2-} ions which are believed to enter the crystal lattice as a substitutional replacement for the SiO_4^{4-} during the reaction of clinker formation(5,6).

In this study, the effect of sulphate on the reaction of clinker formation was studied with various sulphate compounds such as $(NH_4)_2SO_4$, $CaSO_4$, K_2SO_4 and Na_2SO_4. The effect of sulphate in the clinker minerals on the early hydration characteristics at the early stage was investigated.

EXPERIMENTAL

Many clinkers having the basic chemical composition(shown in Table 1.) for various sulphate substitutions were prepared by sintering of analytical reagent grade chemicals in a platinum crucible.

Table 1. Composition of the Basic Clinker (wt%)

CaO	SiO_2	Al_2O_3	Fe_2O_3	LSF	SM	IM
68.05	2.55	5.92	3.48	94	2.4	1.7

The clinker was synthesized with the addition of $(NH_4)_2SO_4$, $CaSO_4$, K_2SO_4 and Na_2SO_4 to be 0, 1, 2, 4, 6 wt% as SO_3. The contents of free CaO in the synthesized clinker, the contents of residual SO_3 and solid solution SO_3 were determined by chemical analysis. The content of C_3S phase in the clinker was measured using the point method under a metallurgical microscope. SEM/EDS was in part applied for the component analysis of the minerals and interstitial phase present in the clinker.

The hydration characteristics of the clinker containing various content of SO_3 was investigated by microconduction calorimetry and differential thermal analysis. The clinker samples for hydration were mixed with CO_2-free distilled water at a water/solid ratio of 0.5. Then, they were hydrated at the temperature between 22-24°C for 7 hours, 1, 3, 7 and 28 days.

RESULT AND DISCUSSION

(1) The effect of the different sulphate sources on the clinker formation

Fig.1 shows the result of the chemical analysis for the contents of residual SO_3 and free CaO in the clinker which was sintered at 1450°C for one hour, when the different contents and types of SO_3 were added to the clinker.

It was observed that the content of the residual SO_3 was around 70~80% in the clinker, which seemed to be independent on the kind of sulphate. When the addition of $(NH_4)_2SO_4$ and $CaSO_4$ as the sourse of SO_3 to the

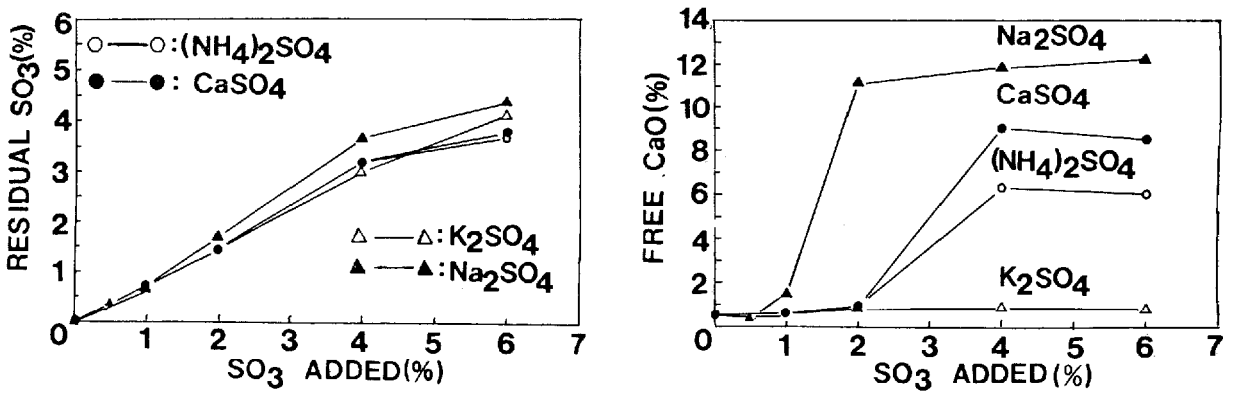

(a) Content of Residual SO_3 (b) Content of Free CaO

Fig.1 Content of residual SO_3 (a) and free CaO (b) in the clinker sintered at 1450°C for 1hr.

clinker were up to 2 wt%, the contents of free lime were less than 1%, whereas when their SO_3 content exceeded 2 wt%, the free lime contents increased and the clinker formation become worse.

By adding a small amount of sulphate, the sulphate in clinker melt acts as a mineralizer and promotes the reaction of the clinker formation by increasing the wetting power of the liquid phase-that is by reducing its surface tension(2,3). In the substitution of SO_3 for C_3S and C_2S phases, $(SiO_4)^{4-}$ group is substituted by $(SO_4)^{2-}$ group or Si^{4+} is substituted by S^{6+}(7). When $(NH_4)_2SO_4$ and $CaSO_4$ are added to the clinker, a critical content of substituted SO_3 is around 1.45%, which dose not affect clinkering.

The reaction of clinker formation is surpressed remarkably by adding only a little amount of Na_2SO_4. However, the contents of free CaO was observed to be less than 1% in the clinker which was burned with the various amounts of K_2SO_4 as a source of SO_3. The addition of K_2SO_4 dose not influence the clinker formation.

It could be considered that K_2SO_4 decreases the viscosity and surface tension of melt and forms an immiscibility with the clinker melt(8,9), and does not restrain the reaction of C_3S formation in the liquid phase.

Fig.2 shows the SEM micrograph and EDS analysis of the clinker added with 4% of K_2SO_4 and sintered at 1450°C for one hour. Pore surface at point 4 shows a greater amount of SO_3 and K_2O than that of C_3S, C_2S and interstitial phase.

After the phase separation occurs as a result of density difference between K_2SO_4(2.8 g/cm^3) and clinker liquid phase(3.02 g/cm^3), K_2SO_4 evaporates through pores during burning. Later, it is condensated or precipitated on the inner surface of the pore with decrease in the temperature.

(2) The effect of the sulphate on the hydration of the clinker

As discussed above, when $(NH_4)_2SO_4$ and $CaSO_4$ were added, the limit of sulphate which did not obstruct the formation of C_3S in the clinker was about 2 wt%. The addition of K_2SO_4 doesn't affect the reaction of clinker formation. When 2 wt% of K_2SO_4 is added to the clinker the sulphate exists in only free K_2SO_4.

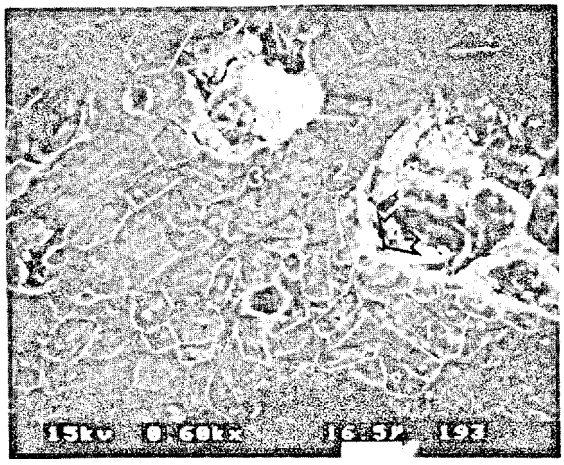

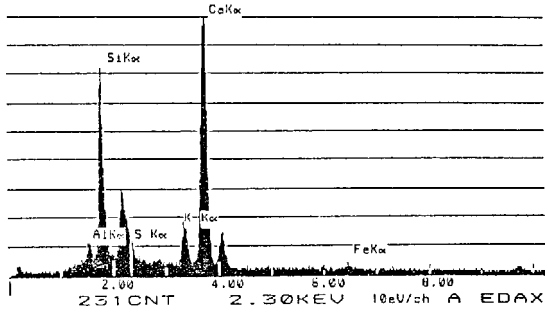

Point 4

Sample No.	Point No.	CaO	SiO_2	Al_2O_3	Fe_2O_3	SO_3	K_2O
K4	Total Area	62.06	21.87	6.64	3.2	3.14	3.40
	1	72.86	25.20	-	-	0.84	1.10
	2	65.17	31.06	-	-	2.38	1.40
	3	57.43	4.55	23.59	12.18	1.26	0.99
	4	52.77	30.60	2.95	0.69	6.48	6.42

Fig.2 SEM micrographs and EDS analysis of the clinkers with 4% of K_2SO_4 sintered at 1450°C for 1hr.

Accordingly, our investigation primarily focussed on free K_2SO_4 on the hydration of clinker, the effect of using the microconduction calorimetry and the differential thermal analysis.

THE EFFECT OF THE SOLID SOLUTION SULPHATE ON THE HYDRATION OF THE CLINKER

The curves of the heat evolution rate with the variation of the solid solution SO_3 are shown in Fig.3.

The first exothermic peak represents the hydration reaction of C_3A. These peaks are not changed by the variation of the amount of SO_3 as a solid solution in the clinker. However, with increasing amount of SO_3 as a solid solution in the clinker, the time to reach the highest point of the 2nd exothermic peak becomes shorter, which corresponds to the hydration reaction of C_3S.

Fig.4 shows the amount of C_3S with a variation of SO_3 for the clinker containing less than 1% of free CaO among the synthesized clinkers added with $(NH_4)_2SO_4$ and $CaSO_4$. The amount of SO_3 as a solid solution in the clinker and C_3S increases as two sulphates are added. Such a large amount of C_3S shortens the hydration time to reach the highest point of 2nd exothermic peak.

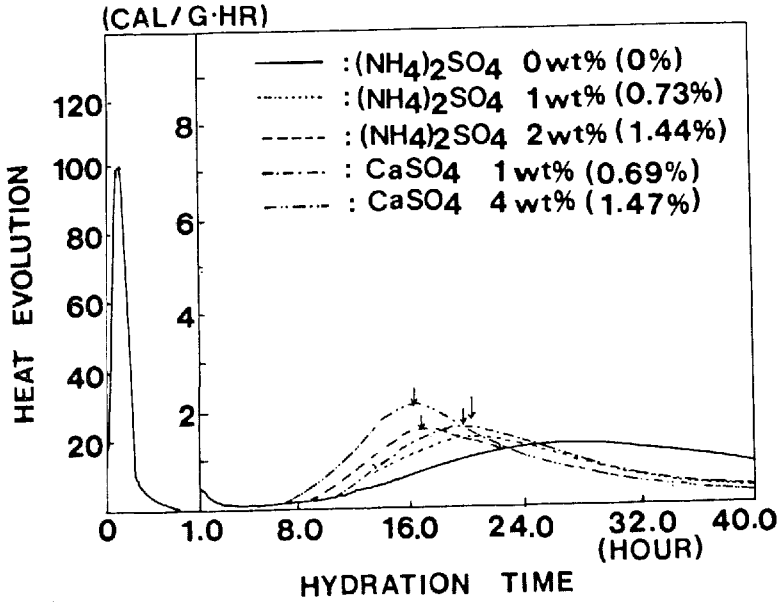

Fig.3 Rate of heat evolution for cement paste with $(NH_4)_2SO_4$ and $CaSO_4$ content. ( ) : Content of solid solution SO_3

On the other hand, it could be also assumed that the solid solution SO_3 in the clinker creates lattice defects, shortens the length of the induction period and enhances the hydration of C_3S(5,6).

THE EFFECT OF THE FREE K_2SO_4 ON THE HYDRATION OF THE CLINKER

Fig.5 shows the result for the effect of free K_2SO_4 remaining the clinker which was synthesized with the addition of K_2SO_4 on the rate of hydration heat evolution of the clinker.

When the clinker was synthesized with the addition of K_2SO_4, the hydration of C_3A is reduced and that of C_3S is rapidly accelerated, as the amount of the sulphate increases. Especially, when K_2SO_4 was added up to more than 2.0 wt%, it can be considered that the hydration of C_3S is remarkably accelerated by the free K_2SO_4 remaining in the clinker(shown in Fig.6) rather than by amount of C_3S product and sulphur trioxide as a solid solution in it.

With respect to the clinker synthesized with the addition of zero and 6 wt% K_2SO_4 respectively, the results of differential thermal analysis on the hydration products is shown in Fig.7 according to the change of the hydration time.

When K_2SO_4 is not added, the endothermic peak appears at around 180°C by the dehydration of C_3AH_X which is the hydration product of C_3A. But when K_2SO_4 is added at 6 wt%, an endothermic peak which is caused by the dehydration of ettringite appears at around 120°C after three days of hydration. At 7 hours hydration, endothermic peaks which are caused by the dehydration of CSH and $Ca(OH)_2$

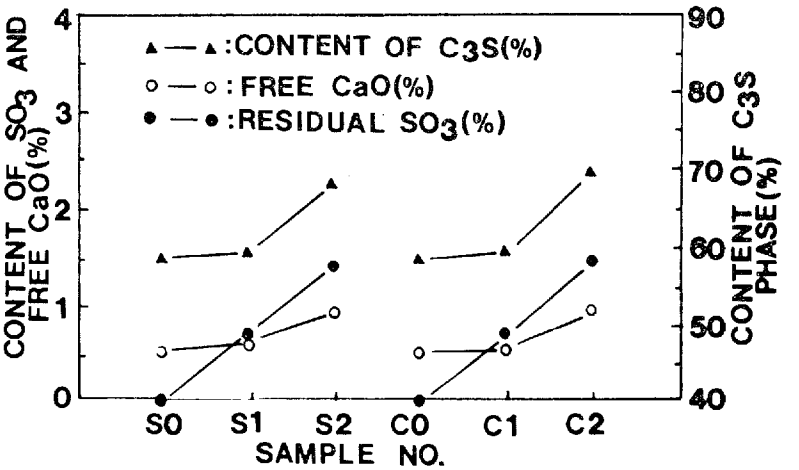

Fig.4 Comparison with contents of free CaO and SO_3 by chemical analysis and contents of C_3S phase for clinkers with $(NH_4)_2SO_4$ and $CaSO_4$ by point method.
S0 : $(NH_4)_2SO_4$ 0 wt% C0 : $CaSO_4$ 0 wt%
S1 : $(NH_4)_2SO_4$ 1 wt% C1 : $CaSO_4$ 1 wt%
S2 : $(NH_4)_2SO_4$ 2 wt% C2 : $CaSO_4$ 2 wt%

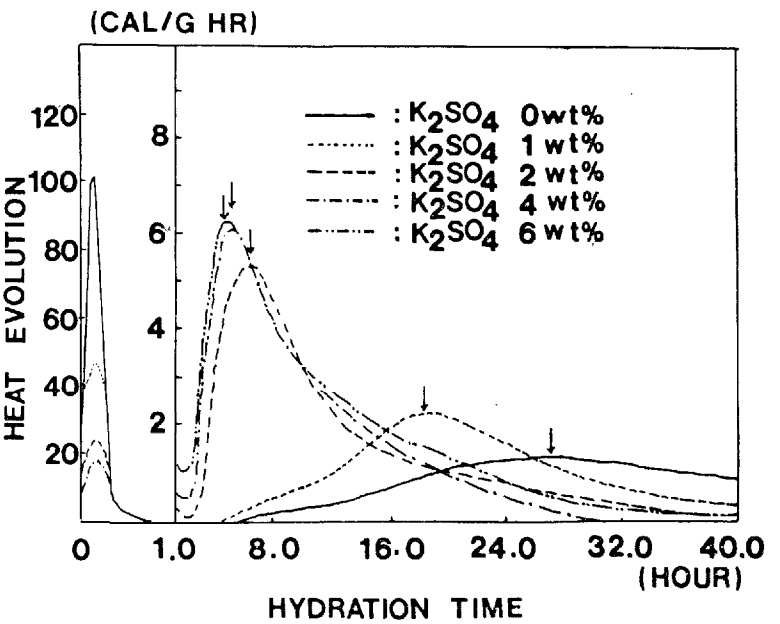

Fig.5 Rate of heat evolution for the clinker added various amount of K_2SO_4.

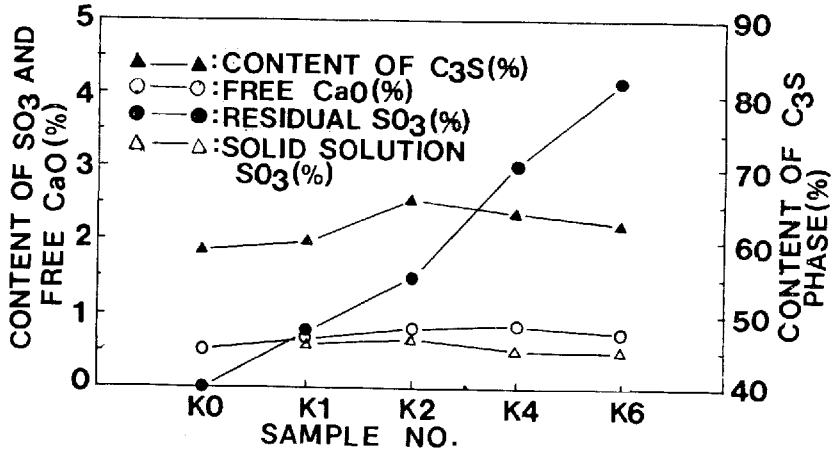

Fig.6 Comparison of free CaO and residual SO_3 of the clinker with various amounts of K_2SO_4, measured by point method. K0 : K_2SO_4 0 wt%, K1 : K_2SO_4 1 wt%, K2 : K_2SO_4 2 wt%, K4 : K_2SO_4 4 wt%, K6 : K_2SO_4 6 wt%

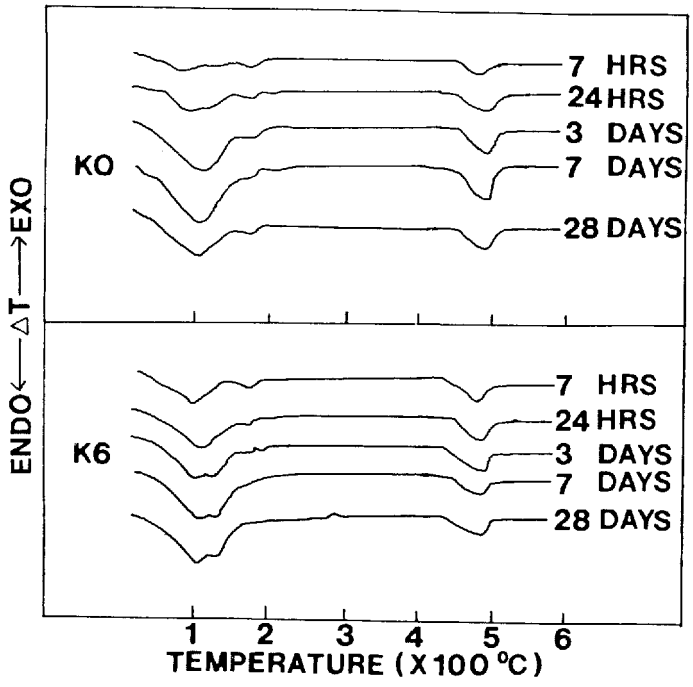

Fig.7 DTA curves for hydration product of the clinker(K0) and (K6) with hydration time. K0 : K_2SO_4 0 wt%, K6 : K_2SO_4 6 wt%

appear at around 100°C and 490°C, respectively.

Since the free K_2SO_4 has higher solubility(136 g/l) than that(2.4 g/l) of gypsum used as a retarder, in the early stage of hydration, the free K_2SO_4 is decomposed into K^+ and SO_4^{2-}, and dissolved SO_4^{2-} can be used to form ettringite(10). So it is considered that the hydration reaction of C_3A is restrained. In addition, the occurrence of 2nd exothermic peak showing the C_3S hydration is accelerated and the induction period is shortened with increasing the concentration of dissolved K^+.(Fig.5)

CONCLUSION

1. By adding less than 2 wt% of $(NH_4)_2SO_4$ and $CaSO_4$ to the clinker, the reaction of clinker formation is enhanced and considerable amount of alite is produced. However, a greater amount of the sulphur trioxide than 2 wt% prevents the clinkering. A critical content of SO_3 is around 1.45%. The sulphate as a solid solution in the clinker accelerates the hydration of alite, however it dose not influence on the hydration of Ca-aluminates.

2. When K_2SO_4 is added to the clinker, the reation of clinker formation is not affected by the amount of sulphate, but the hydration of Ca-aluminate is reduced, although the hydration of alite is promoted. Particularly, by adding up to more than 2.0 wt% of K_2SO_4, the hydration of alite is accelerated rapidly by free potassium sulphate separated in the clinker.

REFERENCES

1) Taylor, H.W.P. : Cement chemistry. London. Academic Press, 1990, p51-56.

2) Butt, Y.M. & Timashev, V.V. : "The mechanism of clinker formation processes and ways of modification" .6th International Congress on the Chemistry of Cement, Moscow, 1974, V4, 3-64.

3) Bucchi,R. : "Influence of the nature and preparation of raw materials on the reactivity of raw mix" . Proceedings of The Seventh International Symposium on the Chemistry of cement, Paris, 1980, V1, 3-43.

4) Odler,I.& Wonnemann,r.: "Effect of alkalies on portland cement hydration - I. Alkali oxides incorporated into the crystalline lattice of clinker minerals" . Cem.Conc.Res., 1983, 13, 477-482.

5) Maycock, J.N. Skalny, J. & Kalyoncu, R.: Crystl defects and hydration - I. Influence of lattice defect. Cem. Conc. Res., 1974, 4, 835-847.

6) Maycock, J.N. & McCarty, M.: "Crystal lattice defects in di-calcium silicate", Cem. Conc. Res., 1973, 3, 701-713.

7) Ghose, A. & Barnes, P.: "Electron microprobe analysis of portland cement clinkers", Cem. Conc. Res., 1979, 9, 747-755.

8) Pliego-Cuervo, Y.B. & Glasser, F.P.: "The role of sulphates in cement clinker reactions-Phase fomation and melting in the system $CaO-Ca_2SiO_4-K_2SO_4$", Cem. Conc. Res., 1977, 7, 477-482.

9) Glasser, F.P. & Marr, J.: "Sulfate in cement clinkering-Immiscibility between sulfate and oxide melts at 1350°C", Cem. Conc. Res., 1980, 10, 753-758

10) Ghosh, S.N.: Advances in cement technology. Oxford, Pergamon Press, 1983, p327-328.

PHYSICAL PROPERTIES AND EARLY HYDRATION REACTION OF FINELY GROUND PORTLAND CEMENTS

K Yoshida and S Okabayashi

Dept of Cement & Concrete Research, R&D Center, Cement & Light Metal Div
Ube Industries Ltd, JAPAN

SUMMARY

In this study, the effect of fine grinding on the physical properties and early hydration reaction of cement is investigated. The cements used are finely ground cements of ASTM Type I－IV, API Class G (oil well cement) and white portland cement, whose mean grain size is about 2 μm. The physical properties of the slurry, paste and mortar prepared from these cements are measured.

Furthermore, the paste prepared from finely ground cement of ASTM Type I is analysed in solid phase and liquid phase, and the early hydration reaction up to 24 hours is considered.

要　約

本報では、セメントの諸物性および初期水和反応におよぼす微粉化の効果について検討した。使用したセメントは、ＡＳＴＭ　ＴｙｐｅⅠ～Ⅳ，ＡＰＩクラスＧ（油井セメント）および白色ポルトランドセメントの高微粉砕品であり、その平均粒子径は約２μｍである。これらのセメントから調製したスラリー，ペーストおよびモルタルの諸物性を試験した。

さらに、ＡＳＴＭ　ＴｙｐｅⅠの微粉セメントのペーストを対象に、液相の分析および固相の解析を行い、２４時間までの初期水和反応について考察を行った。

INTRODUCTION

Cement grinding techniques have recently improved, as a result of the development of new types of pulverizers and classifiers. It has been suggested that grinding cement finely would substantially change its various properties by affecting both physical and chemical properties. Few researchers, however, have discussed the properties of finely ground cement. As a result, characteristics of cements of Blaine's specific surface area exceeding 1,000 m²/kg (1-3) and the details thereof, including details involving the effects of the clinker composition, have largely remained unknown.

In this study, therefore, the authors finely ground various types of cement clinker to a Blaine's specific area of around 1,200 m²/kg in order to investigate the properties of such cement types. The properties investigated included the powder characteristics, penetration into pores, setting/hardening characteristics, heat of hydration, drying shrinkage, neutralization depth, etc. In addition, cement samples with intermittent particle-size distributions were prepared, and medium-size or large cement particles were added to the finely ground particles to investigate the possibility of increasing the strength. Tests results of the above properties suggested that the behaviour of finely ground particles differed significantly from ordinary-sized cement particles in the early hydration reaction. Further, the mechanisms involved in the hydration reactions during the initial stage were also investigated.

EXPERIMENTS

Sample Preparation

In this study, 6 types of cement clinker ordinary (ASTM Type I), moderate-heat of hydration (ASTM Type II), high early-strength (ASTM Type III), low-heat of hydration (ASTM Type IV), oil well (API Class G) and white cement were finely ground in a jet mill to a mean particle size of approximately 2 μm. Gypsum ($CaSO_4 \cdot 2H_2O$) of the same particle size was then added to the above finely ground clinkers to make their SO_3 content 2% to prepare the cement samples. Table 1 shows the fineness and mineral composition of these cement samples. Each sample had a maximum particle size of approximately 6 μm, and its mineral composition remained essentially unchanged before and after grinding.

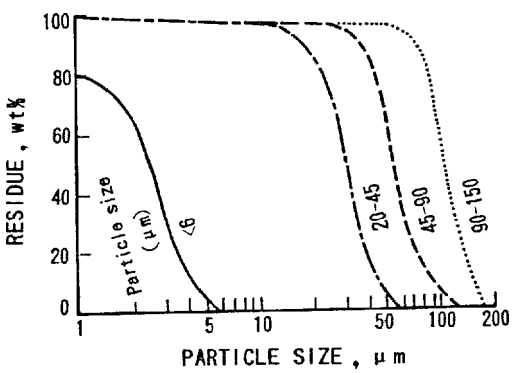

Fig. 1 Particle-size distribution of classified cement clinker

Table 1 Fineness and mineral composition of cement clinker

Cement No.	Cement type	Blaine specific surface (m²/kg)	Mean particle size (μm)	Mineral composition(%)			
				C_3S	C_2S	C_3A	C_4AF
1	ASTM Type I	1336	2.3	56	19	8	11
2	ASTM Type II	1158	2.6	46	32	4	12
3	ASTM Type III	1323	2.1	71	7	8	9
4	ASTM Type IV	1260	2.4	18	62	3	11
5	API Class G(HSR)	1251	2.2	64	16	0	15
6	White cement	1164	2.6	68	19	6	1
7	ASTM Type I	314	15.2	53	22	9	10

To test cement samples with intermittent particle-size distributions, on the other hand, high early-strength cement was ground and classified into four types according to particle size, 6 μm and less, 20 to 45 μm, 45 to 90 μm and 90 to 150 μm. Two or three classified groups were then combined, and a given quantity of gypsum (SO_3 content of cement:2.0%) was added to prepare 23 kinds of cement samples. Figure 1 shows the particle-size distributions of these classified cement samples. Observations showed that they were scarcely different from one another with respect to mineral composition.

Experimental Procedure

The experimental procedure is outlined below:

(1) Penetration into pores: Cement No. 3 was mixed with water at a ratio of 1:4 to prepare slurry. This mixture was then passed through packed sand (mean pore size:250 or 350 μm) and a commercial

glass filter (mean pore size: 4 to 135 μm) to visually observe how the slurry passed through these micropores.

(2) Setting/hardening characteristics: Tests were conducted mostly in compliance with JIS R 5201 specifications. During these tests, sodium citrate was added, as a setting retarder, to the paste or mortar of the finely ground cement. In addition, the mortar strength of the finely ground cement No. 1 (Blaine's specific surface area: 1,260 m^2/kg) was tested at curing temperatures varying from 5 to 65℃. At the same time, the samples had a water/cement ratio which varied from 35 to 65%. To measure the strength of the cement samples with intermittent particle-size distributions, a setting retarder and/or superplasticizer were added. The paste samples for the purpose were prepared with different water/cement ratios, and cured at 20℃.

(3) Heat of hydration: Tests were conducted in compliance with JIS R 5203 specifications. The rates of heat liberation at early stages were measured in some of the tests by using a conduction calorimeter at a water/cement ratio of 100% and a temperature of 20 ℃.

(4) Drying shrinkage and neutralization depth: Tests to determine drying shrinkage were conducted in compliance with the standard procedures of the Cement Society of Japan (CAJS H-11) on mortar samples containing the setting retarder. Phenolphthalein was sprayed onto the cross-sections of samples (age: 98 days) and tested for drying shrinkage.

(5) Early hydration reaction: The following tests were conducted on the cement No. 1 paste sample containing a setting retarder:

i) Ion concentration in the liquid phase: The Ca^{2+}, Na^{+}, K^{+}, Si^{4+}, Al^{3+}, SO_4^{2-}, OH^{-} and citrate ions were quantitatively analyzed.

ii) Unhydrates and hydrates: The X-ray diffraction intensity ratio was determined by the internal standard method (internal standard: containing 10% magnesia, 2θ = 42.9°) for unhydrated alite (2θ = 51.7°), alite +belite (2θ = 41.3°), and calcium hydroxide as a product (2θ = 18.1°).

iii) Degree of hydration: The ignition losses in the paste samples at different ages were determined, and these losses were compared with losses experienced by a one year old sample (ignition base) to determine the degree of hydration.

iv) Pore-size distribution: This was determined for each sample by mercury porosimeter as well as by the nitrogen adsorption method.

v) Microstructure: The microstructures were observed through a scanning electron microscope.

(6) Tapping-packed density: It was measured for cement powders by tapping apparatus. Sample cylinder was 90mm high and 10mm diameter. The cylinder was suffered an unimpeded drop of 5mm. Bumping was continued until one thousand times at a speed of 0.5 times a second.

EXPERIMENTAL RESULTS

Penetration into pores

Table 2 shows the penetration test results. It was difficult for the cement sample to penetrate into pores measuring approximately 120 μm or less, when they were merely dispersed with water. The lower limit of the pore size through which the slurry could pass decreased to approximately 45 μm in the presence of a retarder, and to approximately 20 μm when dispersed with ethanol. In other words, the minimum size of the pores through which the slurry could pass (approximately 20 μm) was roughly 3 times larger than the maximum cement particle size (approximately 6 μm). In any case, it is essential to reduce the size of the largest cement particle and disperse the particles well within the medium in order to improve the penetration of cement into the micropores.

Table 2 Penetration of cement into micropores (Cement No. 3)

Measurement condition		Dispersion Medium		
Method	Mean micro pore size (μm)	Water	Water +retarder	Ethanol
Packed sand	350	◎	◎	◎
	250	◎	◎	◎
Glass filter	135	◎	◎	◎
	110	○	◎	◎
	45	△	△	◎
	8	△	△	○
	4	△	△	△

◎ All passage ○ Partial passage △ Only dispersion medium passage
w/c 400%

Setting

Table 3 shows the setting test results. The setting started at 35 to 48 minutes with cement Nos. 3 and 4, at 88 to 105 minutes with cement Nos. 1, 2 and 5, and at 272 minutes with cement No. 6. However, all cements except No. 4 completely set between 7 to 36 minutes. The addition of a retarder reduced the final setting time of all the cements tested. The accelerated setting was considered to be the result of the greatly reduced

Table 3 Setting time of cement

Cement No.	Retardar (%)	w/c (%)	Setting time (h-min)	
			Initial	Final
1	0.50	41.2	1-32	1-43
2	0.35	40.5	1-22	1-44
3	0.55	41.7	0-35	0-42
4	0.25	39.2	0-48	1-45
5	0.35	39.5	1-45	2-11
6	0.35	42.0	4-32	4-52

quantity of water required to prepare the paste.

Strength

Figure 2 shows the mortar strength of samples cured at 20℃. Cement Nos. 1 and 3 were finely ground to secure rapid-hardening characteristics. They were slightly slower in exhibiting strength than the samples containing no retarder; however, their strength tended to increase faster, once it appeared. Figure 3 shows the mortar strength of samples cured at different temperature levels. Finely ground samples had a higher compressive strength than ordinary cement (cement No. 7) at any curing temperature. However, these samples were slower to manifest their initial strength than commercial super-high-early-strengh cement (jet cement), and their initial strength depended more on the curing temperature. Figure 4 shows the mortar strength for cement No. 1 with different water/cement ratios. Of these, the ones with a water/cement ratio of 35 and 40% were compacted by using a vibrator. It was observed that finely ground cement increased greatly in strength when the water/cement ratio was reduced. The sample with 35% water/cement ratio had a compressive and bending strength which exceeded 100 N/mm^2 and 15 N/mm^2, respectively, when cured for 28 days. Table 4 shows the compressive strength of paste with an intermittent particle-size distribution, in which finely ground particles (6 μm and less), medium-sized particles (20 to 45 μm) and coarse particles (90 to 150 μm) had been mixed in the ratio 20:20:60. The results of the finely ground sample (No. 1) and the sample with a continuous particle-size distribution (63 μm and less) are also shown to provide a basis for comparison. It was possible to reduce the water/cement ratio of the cement sample with an intermittent particle-size distribution, since the paste with 15% water/cement ratio exhibited high strength, exceeding 100 N/mm^2 and 139 N/mm^2, when cured for 3 and 91 days, respectively.

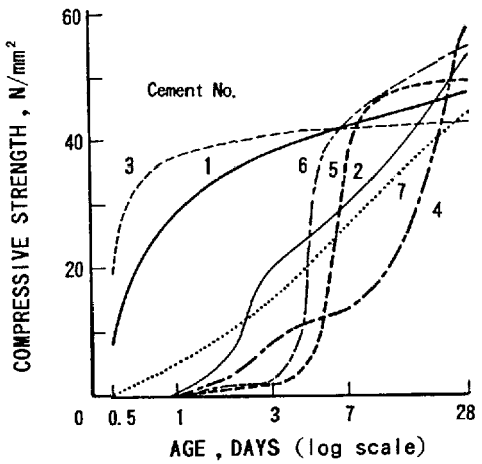

Fig. 2 Compressive strength of mortar (20 ℃)

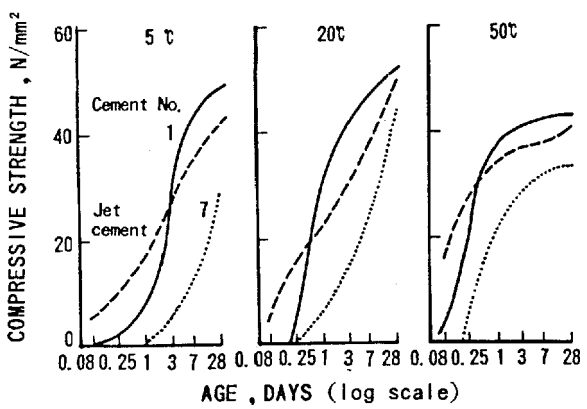

Fig. 3 Compressive strength of mortar cured at various temperatures

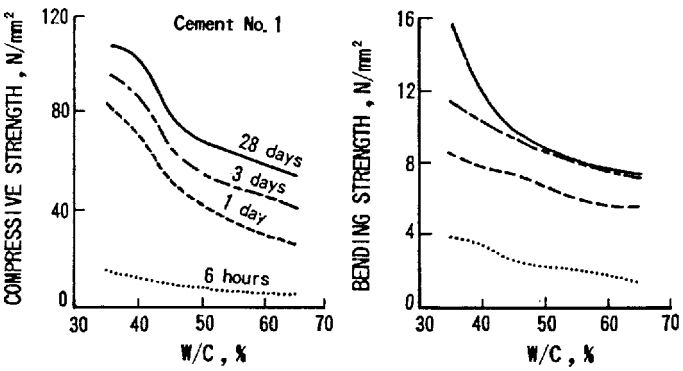

Fig. 4 Relationship between w/c ratio and strength of mortar

Heat of Hydration

Figure 5 shows the rate of heat liberation during early hydration. Each sample tested displayed two exothermic peaks; the first peak corresponding to the initial setting, and the second peak corresponding to the first manifestation of strength. Table 5 shows the heat of hydration of each sample. Cement Nos. 1 and 3 had a fairly high value of 300 J/g or more, when cured for only 1 day, while Nos. 2, 4, 5 and 6

Table 4 Compressive strength of paste

Cement	w/c (%)	Compressive strength (N/mm^2)			
		3 days	7 days	28 days	91 days
Intermittent grading	30	32.2	62.9	97.9	115.5
	25	50.7	83.8	107.7	123.2
<6μm:20-45μm:90-150μm	20	73.6	93.4	122.9	129.3
= 20: 20 : 60	15	100.0	109.1	129.8	139.5
Continuous grading	30	69.6	86.5	114.5	128.6
(<63μm)	25	84.5	100.8	122.2	134.5

Additive: Mighty 150 1.0%

Table 5 Heat of hydration of cement (J/g)

Cement No.	1 day	3 day	28 day
1	308.5	415.3	472.6
2	79.1	278.4	404.0
3	375.9	437.9	489.3
4	41.0	172.9	313.5
5	66.1	144.0	414.8
6	42.3	114.7	415.7
7	—	232.7	394.3

had a low level of 80 J/g, or less, when cured for the same length of time.

Drying shrinkage and neutralization depth

Figure 6 shows the results of drying shrinkage tests on the mortar samples. Cement Nos. 4 and 5 were comparable to cement No. 7 (ordinary cement) in terms of the longitudinal change of mortar, whereas results for cement Nos. 1 and 3 were substantially higher. After the drying shrinkage tests, the neutralization depth of samples cured for 365 days was measured. The neutralization depth was 5 to 6 mm with cement Nos. 4 and 7 (ordinary cement), and 2 to 3.5 mm with other cements. These results indicate that grinding cement finely generally retards neutralization.

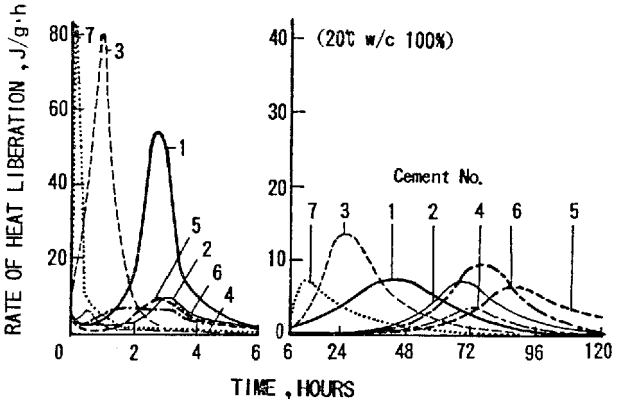

Fig. 5 Calorimetric curves of cement

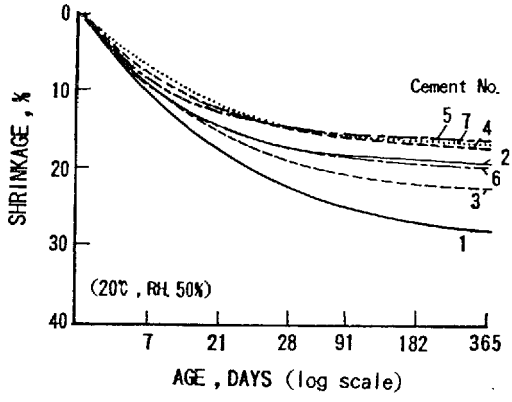

Fig. 6 Drying shrinkage of mortar (w/c 60%)

DISCUSSION

The setting/hardening process of finely ground cement with a setting retarder is discussed based on the analysis of the hydration reaction and the associated structure formation process. Fine grinding of cement greatly increases the amount of water required to pack the pores between the cement particles, and also increases the amount of water required for the hydration reaction during the very early stages (4). A setting retarder, therefore, is inevitably required in order to secure a paste of normal consistency and good workability. Figure 7 shows the amount of retarder required for a mortar flow of 200±5 mm. It is determined by the quantities of C_3A and C_3S present in the cement. Figures 8 through 10 and Photograph 1 show the results regarding the early hydration reactions of the finely ground cement sample (cement No. 1) and the sample to which a setting retarder was added. These results suggest that the following phenomena are involved in the early hydration reactions of finely ground cement:

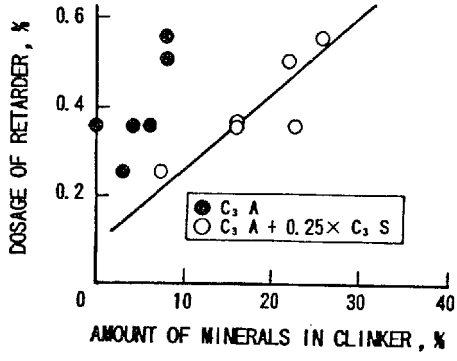

Fig. 7 Amount of retarder required to obtain mortar with a fixed workability

Finely ground cement, which contains no retarder, is hydrated to a notable extent during the kneading process to coat the clinker particles with a solid hydrate film. Gypsum will be consumed faster and precipitate ettringite over the clinker particle surfaces, which will eventually terminate the setting. Though the induction period is somewhat extended (5), the hydration of calcium silicates is reactivated later to initiate hardening. The overall degree of the hydration attainable will be fairly high, given the large specific surface area; however, the hydration speed (as calculated by the hydration depth) will be lower than that of ordinary cement.

A setting retarder, when added to finely ground cement, works to significantly control the hydration reactions that occur immediately after the cement makes contact with water. The citrate ions remaining in the liquid phase of the paste maintain Ca^{2+} and SO_4^{2-} ions at a high concentration (6). The hydration of C_3A starts to occur rapidly as soon as the citrate ions are depleted in the liquid phase, which, however, produces plate-shaped crystals of calcium aluminate hydrate because of

the lowere availability of gypsum. Moreover, the above phenomenon is accompanied by the hydration of alite over the same period, and the resultant C-S-H show the characteristic shapes. Both the initiation and termination of the setting will occur during the period between the disappearance of the citrate ions and the formation of C-S-H. The hydration of calcium silicates is reactivated after the end of the induction period, which lasts for a fairly long time. This reactivation forms Type III C-S-H, thereby initiating strength manifestation. After the hardening reaction has begun, the paste or mortar structures gradually become more dense, partly because of the hydration reaction of belite. However, capillary pores of radius 10 to 50 nm continue to remain, even if the sample is cured for 28 days. Such a phenomenon can be observed with any sample which has been finely ground. Moreover, it is caused by either the pores formed as a result of the agglomeration of finely ground cement particles or the slowly manifesting pore-packing effect of external hydrates.

It has been observed that finely ground cement exhibits a very high strength at a low water/cement ratio. Figure 11 shows the effects of water/cement ratio on the total pore volume of mortar. The mortar has a fairly small pore volume at water/cement ratios of 35 and 40%, both for samples cured for a short time and those cured for a long time. In other words, finely ground cement has good vibration-compaction characteristics, which allows it to develop high strength. Figures 12 and 13 show the results of the tapping-packing tests on powdery cement samples with an intermittent particle-size distribution and the pore-size distributions of the hardened paste samples, respectively. The sample which showed the highest strength under the test conditions was the one which also showed the highest tapping-packed density. Thus, these results confirmed that the packing property of the particles constituting the paste is one of the most important factors in determining the strength of a hardened body. These tests also showed that cement paste with an intermittent particle-size distribution had small capillary pores of radius 10 to 50 nm, unlike the paste of finely ground cement. This finding indicates that this cement paste has a highly densified structure. In order to

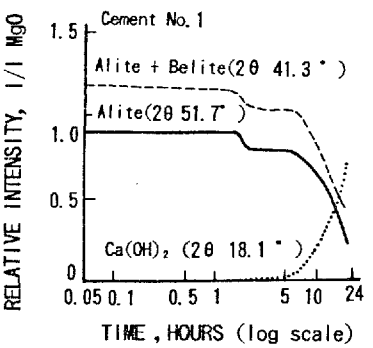

Fig. 9 Intensity ratios of X-ray diffraction of paste (I MgO:2θ 42.9°)

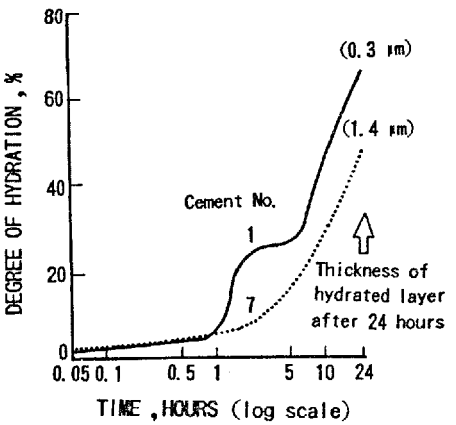

Fig. 10 Changes in the degree of hydration of paste

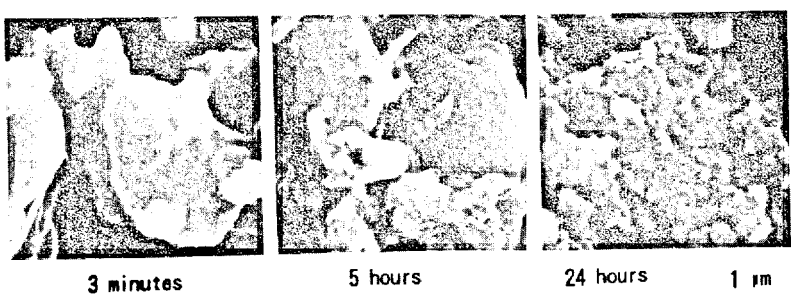

Photo. 1 SEM Phptograhs of paste

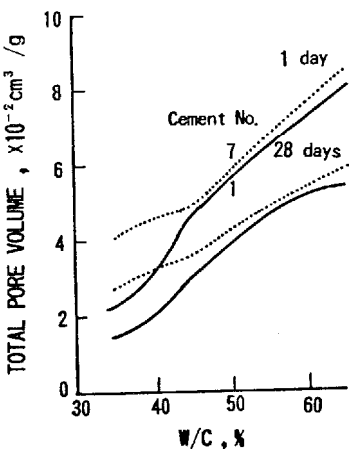

Fig. 11 Relationship between w/c ratio and total pore volume of mortar

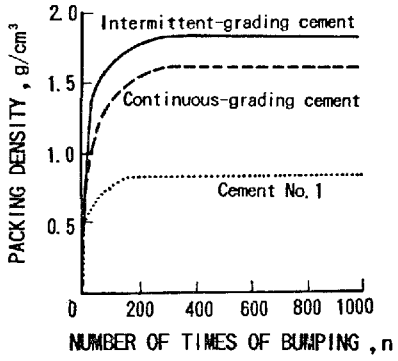

Fig. 12 Changes in the packing density of cement

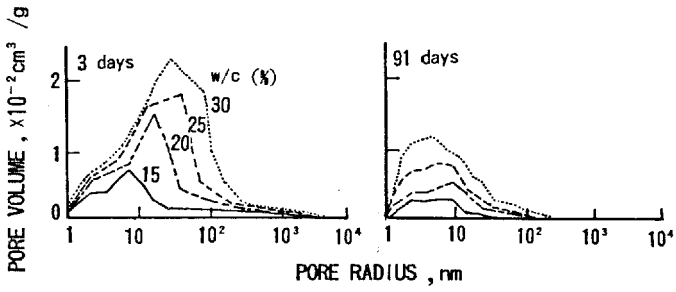

Fig. 13 Pore size distributions of hardened cement paste (Intermittent-grading cement)

investigate the relationship between pore-size distribution and drying shrinkage, the pore-size distribution of mortar samples was measured after they had been precured in water for 6 days. It was found that drying shrinkage tends to increase as the quantity of micropores increases.

CONCLUSIONS

The major conclusions obtained by this study are summarized below:

i) Finely ground cement particles have an improved penetrability into micropores, provided that they are well dispersed.
ii) A retarder is inevitably required to prepare the paste or mortar of finely ground cement, and the amount required depends on the mineral composition of the cement.
iii) Finely ground samples of ASTM Type I and III cements have a mortar compressive strength of 29 N/mm^2 or more at 24 hours, as shown by the JIS R 5201 test.
iv) The mortar compressive strength of finely ground Type I cement is affected by a curing temperature greater than that of super-high-early-strength cement (jet cement). Finely ground Type I cement has a high mortar compressive strength of 100 N/mm^2 or more at low water/cement ratio (35%), when it is compacted by a vibrator and is cured for 3 days.
v) Both heat of hydration and mortar drying shrinkage differ depending on the cement type.
vi) Cement with an intermittent particle-size distribution consisting of finely ground particles (6μm and less), medium-size particles (20 to 45μm) and coarse particles (90 to 150μm), is useful to increase the density and strength of the paste.
vii) Fine grinding of cement notably changes early hydration reactions. It increases the extent of hydration, but decreases the average hydration depth of cement particles.

REFERENCES

1)Beke, B. and Opoczky, L.: "Very fine grinding of cement clinker", Zement-Kalk-Gips, 1969, 5, 541-546.
2)Skavara, F. et.al.: "The effect of cement particle size distribution upon properties of pastes and mortars with low water-to-cement ratio", Cement and Concrete Research, 1981, 11, 247-255.
3)Uchida, K., Fukubayashi, Y. and Yamashita, S.: "Particle Size Distribution and Physical Properties of Cement", Semento Gijutsu Nenpo, 1987, 41, 62-65.
4)Kumar, A. and Roy, D.M.: "Effect of Fineness on Properties of Classified Cements", Cement, Concrete, and Aggregates, 1984, 6, No.1, 47-51.
5)Kondo, R. and Ueda, S.: "Kinetics of Hydration of Cements", **Proceedings of The Fifth International Symposium on the Chemistry of Cement, Tokyo,** 1968, VII, Part II, 203-255.
6)Uchikawa, H. and Uchida, S.: "Influence of Boric Acid on the Hydration of ultra-Rapid Hardening Cement", Semento Gijutsu Nenpo, 1972, 31, 30-33.

THE MECHANISM OF $BaSO_4$ PREVENTING CALCIUM ALUMINATE HYDRATES FROM CRYSTALLINE TRANSFORMATION

Wu Yanrong, Long Shizong and Liao Guanglin

The Department of Material Engineering, Wuhan University of Technology
Wuhan, Hubei, P R CHINA

During a study of the hydration process of $3CaO.3Al_2O_3.BaSO_4$,it was discovered that $BaSo_4$ is able to restrain the CAH_{10}—C_2AH_8—C_3AH_6 crystalline transformation. The hydration products of calcium aluminate contained $CAH_{10}$and C_2AH_8;no $C_3AH_6$was found at a temperature of 30℃ and in the presence of $BaSO_4$. The results of chemical analysis of the solution phase indicate that the restraining effect is attributable to the fact that $BaSO_4$ absorbs Ca^{2+} ions whereby the ratio of Ca/Al in the solution drops,which hinders the formation of higher basicity calcium aluminate hydrates.Therefore the discovery may be used to prevent the long-term strength retrogression of aluminous cement.

摘　　要

作者在研究$3CaO.3Al_2O_3.BaSO_4$水化时，发现$BaSO_4$对水化铝酸钙的晶型转变(CAH_{10}—C_2AH_8—C_3AH_6)有抑制作用.即使在30℃条件下水化,只要有$BaSO_4$ 存在,水化产物仍为(CAH_{10}和C_2AH_8没有C_3AH_6)。通过液相成分分析表明，这种抑制作用是由于$BaSO_4$晶体对液相中Ca^{2+}吸附,使液相中Ca/Al比值降低,不利于高碱水化铝酸钙(C_3AH_6)形成。这一发现有可能利用$BaSO_4$来改善矾土水泥后期强度倒缩问题。

INTRODUCTION

Following the volume of studies on the crystal transformation process of calcium aluminate hydrate,it can be pointed out that organic adm ixtures,such as sulfosalicylic acid, triethanolamine,etc,and inorganic substances, such as dolomite, magnesite, $CaCO_3$ have a restraining effect on calcium aluminate hydrate crystal transformation. The underlying mechanism is that these can react with calcium aluminate hydrate to form calcium magnesium carboaluminate hydrate, ($CaO.MgO.Al_2O_3.CO_2.11H_2O$), and calcium carboaluminate hydrate, $C_3A.CaCO_3.11H_2O$. During a study of the hydration of $3CA.BaSO_4$[1],it was found that $BaSO_4$ can prevent the CAH_{10}—C_2AH_8—C_3AH_6 transformation.Obviously,the restraining action has practical significance to prevent the long-term strength retrogression of aluminous cement.According to the experimental results, $BaSO_4$ did not react with calcium aluminate hydrate to form a new compound. What then could be the reason for this restraining effect of $BaSO_4$? The present study was undetaken towards suggesting a possible mechanism for this.

HYDRATION EXPERIMENTS

1.Analysis of CA hydrate by XRD and DTA

It has been affirmed by many research workers that CA can hydrate at different temperatures as follows:

$$CA+H_2O \longrightarrow CAH_{10} \quad (< 20^{\circ}C)$$

$$CA+H_2O \longrightarrow C_2AH_8+Al_2O_3.aq+C_3AH_6 \text{ (a little)} \quad (>20^{\circ}C)$$

$$CA+H_2O \longrightarrow C_3AH_6+Al_2O_3.aq \quad (> 30^{\circ}C)$$

Two groups of specimens had been designed,one pure CA, the other CA plus $BaSO_4$, at a mole ratio of $CA:BaSO_4$=3:1.They were then allowed to hydrate simultaneously at 30°C for 14,28 days, and at 45°C for 7 days. They hydrates formed were analyzed by XRD and DTA. The results are shown in Fig.1 to 4. The experimental results indicated that,when hydration occurred at 30°C,the hydrates of the barium containing (second) group, at 14,28 days,contained mainly C_2AH_8 (main XRD peaks:10.487,5.223A-) without C_3AH_6, whereas in the hydrates of CA the groups having only CA (first) there was C_3AH_6(5.157,2.299, 2.04A),besides C_2AH_8.The endothermic peak due to C_3AH_6 decomposition was not noticed in the DTA curves of the hy drates of the second group,

but it was obviously noticed in the first group hydrates at 310℃.

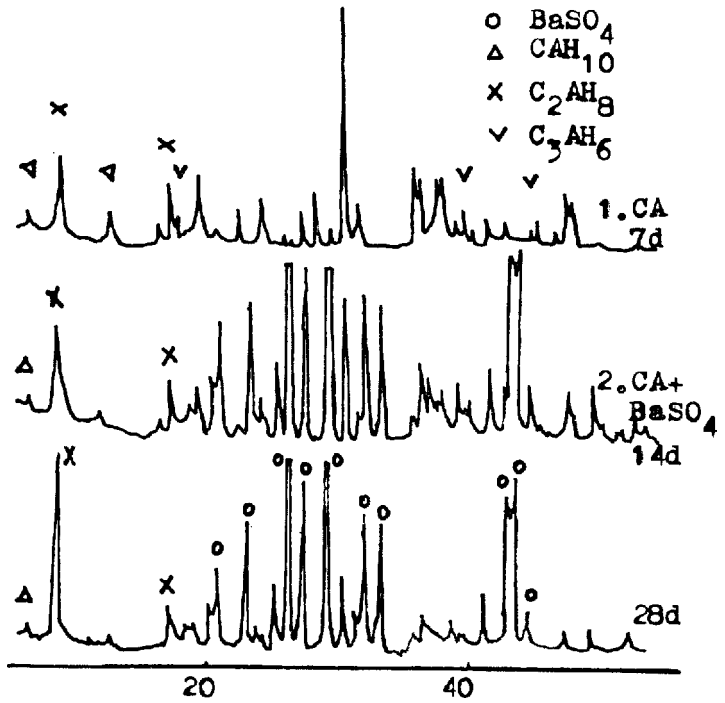

Fig.1 XRD patterns of the hydrates at 30℃

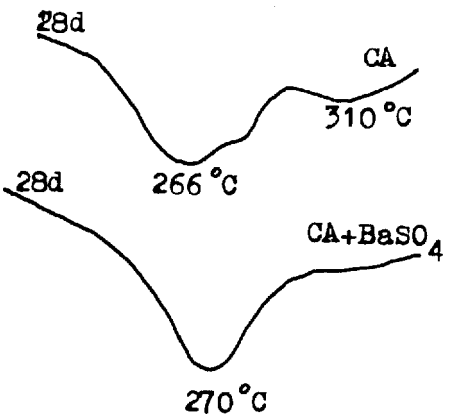

Fig.2 DTA patterns of the hydrates at 30℃

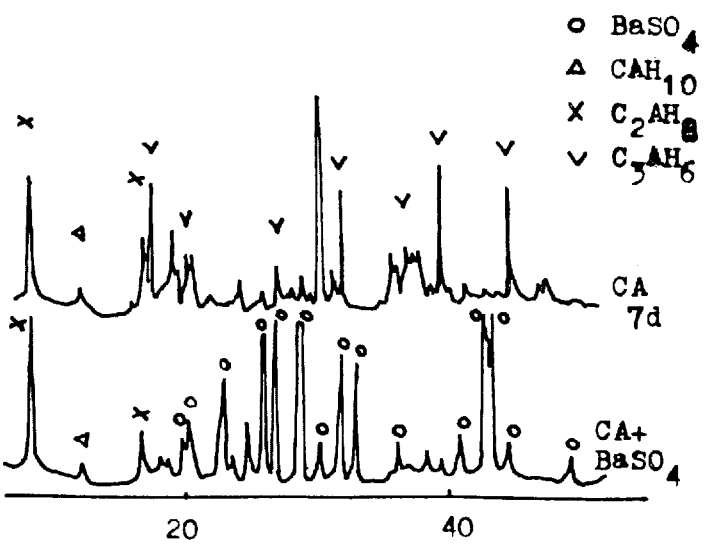

Fig.3 XRD patterns of the hydrates at 45℃

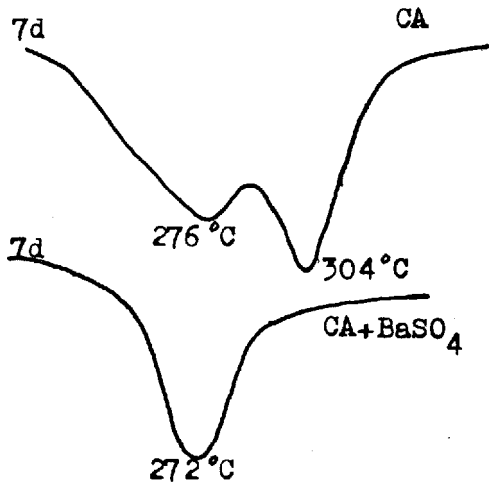

Fig.4 DTA patterns of the hydrates at 45℃

In XRD patterns of hydrated samples at 45℃,the main hydration product for the second group at 7 days was still C_2AH_8(10.468, 5.238), no peaks of C_3AH_6 was found,while the peaks of C_3AH_6(5.138,2.293,2.037A) were obviously found in the XRD patterns of the first group.In DTA patterns,the endothermic peak at 310℃ was not detected in the second group,whereas the endothermic

peak at 304℃ was dominant in the first group.

2. Compressive Strength Test

Compressive Strength test was carried out on 1:2 mortar cubes 2×2×2 cm of size, water/cement ratio 0.41,for the two groups.After demoulding, the cubes were cured in water at 20, 30 and 40℃ respectively,then their compressive strengths were measured at a given age. The results ars shown in Table 1.

Table 1. Compressive Strength of mortars at different ages for different curing temperatures

Binder Group	Specific surface area, cm^2/g	Age days	Compressive strength,kg/cm_2 20℃ cure	30℃ cure	40℃cure
1(CA)	1950	3	512	557	-
		7	554	619	167
		28	550	524	80
2 (CA+$BaSO_4$)	2100	3	451	390	243
		7	553	445	227
		28	599	534	179

From the data in Table 1,it could be seen that,when hydration took place at 20 to 30 ℃ , the strength of group 2 increased steadily,and there was no fall in strength up to 28 days. On the other hands at 20℃ and 7 days age, the strength of group 1 did not increase anymore, but decreased slightly;and at 30℃, the 28-day strength for group 1 regressed remarkably; at 40℃, the strength of both group 1 and 2 were falling,but the regression in group 2 was smaller than in group 1.The foregoing indicated that when CA hydrates at higher than 30℃ and with $BaSO_4$ in the system,the transformation may possibly be restrained, which is beneficial to development of strength of aluminous cement.

ANALYSIS AND DISCUSSION

Experiments here again were based on the two groups of samples used before.Group 1 was 4.74g CA and group 2 was 4.74g CA+2.333g $BaSO_4$. The samples under test were put into volumetric flasks having 100 ml clistilled water.The flask was shaken for 1 minute,then kept in water bath

at 20℃ and 40℃ for varying periods from 1 to 72 hr.At the end of the hydration period , the contents of the flask were filtered.T hen the pH value and molal concentrations of both CaO and Al_2O_3 of the filtrate were determined.The results obtained for 20℃ and 40℃ are shown respectively in Table 2 and Table 3:

Table 2. Results on hydration filtrate from 20℃ for different periods

Binder Group	Hydrate characteristic	1h	4h	8h	12h	16h	20h	40h	72h
	pH	11.62	11.50	11.68	11.73	11.83	11.76	11.83	12.07
1	Mcao	0.0151	0.0164	0.0083	0.0079	0.0071	0.0073	0.0068	0.0065
(CA)	$M_{Al_2O_3}$	0.0127	0.0143	0.0060	0.0056	0.0048	0.0050	0.0036	0.0029
	CaO/Al_2O_3	1.186	1.430	1.370	1.417	1.478	1.464	1.872	2.250
	pH	11.65	11.54	11.71	11.76	11.84	11.80	11.92	12.10
2	Mcao	0.0159	0.0123	0.0079	0.0074	0.0069	0.0070	0.0065	0.0064
(CA+	$M_{Al_2O_3}$	0.0122	0.0121	0.0054	0.0051	0.0047	0.0046	0.0036	0.0029
$BaSO_4$)	CaO/Al_2O_3	1.301	1.019	1.459	1.453	1.457	1. 525	1.807	2.195

Table 3.Results on hydration filtrate from 40℃ for different periods.

Binder Group	Hydrate characteristic	1h	4h	8h	12h	16h	20h	40h	72h
	pH	11.80	11.81	11.89	11.91	12.01	11.91	12.04	12.12
1	Mcao	0.0118	0.0086	0.0076	0.0075	0.0073	0.0074	0.0071	0.0077
(CA)	$M_{Al_2O_3}$	0.0101	0.0061	0.0045	0.0041	0.0038	0.0039	0.0033	0.0031
	CaO/Al_2O_3	1.170	1.410	1.694	1.814	1.935	1.908	2.713	2.509
	pH	11.80	11.85	11.92	11.95	12.05	12.04	12.13	12.19
2	Mcao	0.0016	0.0068	0.0074	0.0073	0.0070	0.0070	0.0068	0.0072
(CA+	$M_{Al_2O_3}$	0.0105	0.0052	0.0044	0.0039	0.0037	0.0036	0.0035	0.0033
$BaSO_4$)	CaO/Al_2O_3	1.108	1.319	1.685	1.828	1.889	1.938	1.969	2.187

The results in Table 2 demonstrate that,when hydration occurred at 20 ℃ , the CaO concentration hydration filtrate of group 2 at any age was lower then that of group 1.

But generally speaking,the difference in the volues of CaO concentration as well as CaO/Al_2O_3 molal ratio between the two groups was small.However,data in Table 3 show that,at 40℃ the CaO concentration for group 2 was much lower than that for group 1 at all ages.It was the same with CaO/Al_2O_3 molal, concentration ratios also, the difference becoming the larger, the longer the hydration period.E.V.Kravchenco[2] considered that increase in the relative CaO content in solution phase was beneficial to stabilize lower basicity calcium aluminate hydrate. From the above experimental results,it was verified that the presence of $BaSO_4$can lower CaO concentration and C/A ratio of solution phase.This could explain the restraining effect of $BaSO_4$ on the crystalline transformation of hydrated calcium aluminate. How could $BaSO_4$ lower the CaO concentration of solution phase? A possible reason for this, according to us ,is that $BaSO_4$ can adsorb Ca^{2+}ion in solution.There is surplus electric charge on the crystal surface of $BaSO_4$, as shown in Fig.5:

Fig.5

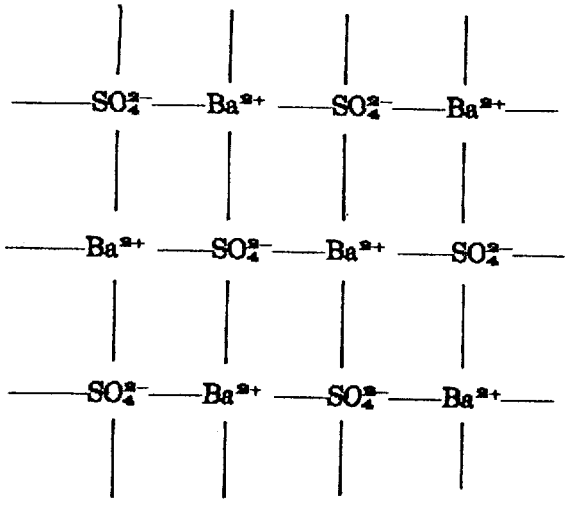

Because of electrostatic attraction,the surplus surface charge can attract ions of the opposite charge.Being slightly disolved in water,CA forms Ca^{2+} ion and AlO_2^-,or $Al(OH)_4^-$ ion . According to adsorption laws,the higher the value of the charge of the adsorbed ion , the smaller the solubility and the dissociation degree of the compound formed from the adsorbed ion and the surface component of the adsorbant,the easier its can be adsorbed. For the reasons described above,$BaSO_4$ adsorbs Ca^{2+} ion first,because the charge of Ca^{2+} ion is higher than that of AlO_2^- ion ,and $CaSO_4$ ($K_{sp}=2.5\times10^{-5}$),formed from Ca^{2+} and SO_4^{2-},has a lower solubility than $Ba(AlO_2)_2$,so AlO_2^- ion is not adsorbed easily. Because the above experiments were conducted with high w/s ratio,the adsorption of Ca^{2+} by $BaSO_4$ may be weak .When the w/c ratio is smaller, the adsorption may be stronger.As adsorption is essentially a physical phenomenon,the ability for adsorption of Ca^{2+} ion by $BaSO_4$ decreases as the temperature increases. Accordingly the restraining action may become weak at higher temperatures(>45℃) or even vanish.

REFERENCS

1. Feng Xiuji,Liao Guang Lin and Long shi Zong. Investigation on the structure and the preformance of 3CA.$SrSO_4$ and 3CA.$BaSO_4$. 1989 Beijing Int.Symp.on cement and concrete.

2. E.V.Kravchenco, 《Aluminons Cement》 ,Moscow (USSR),1961.

THE ROLE OF ALKALIES IN THE HYDRATION OF VITRIFIED CALCIUM AND MAGNESIUM SILICATES

Jan Malolepszy

University of Mining and Metallurgy, Cracow, POLAND

SUMMARY

The influence of Na_2CO_3 and NaOH on the hydration of vitryfied akermanite and diopside at 20-200°C was studied. It was found that ill crystallized CSH phase and carbonate formed as main hydration products at ambient temperature. The crystalline products, such as tobermorite, gyrolite, pectolite and magnesium silicate hydrate appeared as the temperature of hydration increased. α-C_2SH phase was detected in akermanite pastes. The samples activated by Na_2CO_3 exhibited the highest strengths.

RESUME

L'hydratation d'akermanite et diopside à l'état vitreux en présence de Na_2CO_3 et NaOH a été étudié entre 20°C et 200°C. A la témperature ambiante on observe la formation de gel C-S-H et carbonates. Dans les témperatures élevées le tobermorite, girolite, pectolite et hydro-silicate de magnesium cristallisent. α-C_2SH s'apparaît dans les pâtes de verre d'akermanite. Les pâtes activé avec Na_2CO_3 révelent les plus hautes résistances.

1. Introduction

The properties of binding materials obtained from granulated blast furnace slags depend not only on the type of slag, but on the additions introduced in the grinding process and on the method of preparation of mortars and concretes too. OPC clinker, quicklime and gypsum are commonly used additions. As is the usual practice, dry granulated slag is fed into a grinding mill with the activators. The obtained materials are characterized in many cases by a very slow strength development in the initial period of hardening [1-4]. The materials obtained from granulated slags containing considerable amount of alumina may be the exception to the rule. The growing economic crisis in the world induces investigations on the new technologies of binding materials. These technologies should consider low-energy consuming materials in comparison with the commonly produced cements [5-6]. The lowest energy consumption is achieved in the production of binding materials containing no OPC clinker. In the case of activation of granulated slags by small amounts of alkalies (NaOH, Na_2CO_3, water glass) the obtained binding materials are characterized by a very low energy consumption and high early, as well as ultimate strength, freeze-thaw resistance and corrosion resistance [7-14].

Apart from mellitites, the magnesium and calcium silicates, such as akermanite, merwinite, monticellite and diopside can occur in slags. In this work the results of the investigations of akermanite and diopside hydration in alkaline solutions are given. These components have been selected because of their different structure [18]. Akermanite occurs predominantly in the basic slags and diopside in the acid ones. There is no reported data dealing with the hydration of these phases in alkaline solutions though there are some information about the hydration of crystalline or vitrified akermanite and diopside in the presence of $CaSO_4 \cdot 2H_2O$ and $Ca(OH)_2$. In water and in $CaSO_4 \cdot 2H_2O$ or $Ca(OH)_2$ solutions the crystalline or vitrified akermanite hydration takes place to some degree, while the hydration of diopside practically does not occur in normal conditions [14, 19]. However, the hydration of diopside is observed in hydrothermal conditions [1, 14, 15].

In the present work the results of the studies on akermanite and diopside hydration in NaOH and Na_2CO_3 solutions, at temperatures from 20°C to 250°C are shown.

2. Experimental

2.1. Preparation and characteristics of samples

Table 1. Chemical composition of synthetic slags.

Type of slag		Percentage of oxides		
		CaO	MgO	SiO_2
Akermanite	a	41.07	14.86	44.07
	b	41.75	13.90	43.92
Diopside	a	26.20	18.60	55.20
	b	27.80	18.50	53.20

a - theoretical b - real

The slags were prepared from sodium carbonate, alumina, silica gel and magnesium hydroxide of the highest purity, mixed following the calculated chemical composition. The mixtures were fused for 30 min. and quenched with large amounts of water. The chemical composition of synthetic slags is given in Table 1.

The degree of vitrification and phase composition of synthetic slags were determined by means of Reichert microscope. Fractions of glassy and crystalline phases in the tested slags were determined using powder preparation. Glassy phase content in slags exceeded 80%. In synthesized slags the crystalline phase was formed by akermanite and diopside crystals of several microns. X-ray examinations confirmed the results of the microscopic observations.

The synthetic slags were ground in an agate mill to a fineness of 3200 cm^2/g measured according to Blaine method. Sodium carbonate and sodium hydroxide were used as activators. The activation was carried out in two ways. In the first case both activators were used in different amounts. The addition of 5% Na_2CO_3 was applied; it is equivalent to 2.9% Na_2O. The amount of this activator was selected in accordance with the results of our previous investigations [10]. The amount of sodium hydroxide, 3.8%, was equivalent to 2.9% Na_2O.

2.2. Effect of Na_2CO_3 and NaOH on the strength properties of hardened pastes

The powdered slags were mixed with water at a slag/water ratio of 0.5. The pastes were formed into cylinders of 2 cm high and 2 cm in diameter and vibrated for 2 min. The cylinders were steam cured and autoclaved. The conditions of low pressure steam curing were as follows: temperature-80°C, time-6 hrs. The cylinders were autoclaved for a period of 2 hrs at 150, 200 and 250°C. The cylindrical samples were subjected to the compressive strength tests and phase composition examinations. The results of compressive strength tests are given in Tables 2 and 3.

Table 2. Compressive strength of akermanite pastes.

Conditions of curing	Compressive strength [MPa]					
	Type of activator					
	Na_2CO_3			NaOH		
	after treatment	28 days	90 days	after treatment	28 days	90 days
natural curing	-	15.1	17.2	-	9.5	11.5
80°C	21.2	24.1	28.1	13.3	16.5	19.2
150°C	27.2	30.2	33.1	26.2	29.8	32.4
200°C	25.3	29.1	32.8	23.8	28.2	31.3
250°C	23.9	24.2	28.2	21.6	24.1	26.6

Table 3. Compressive strength of diopside pastes.

Conditions of curing	Compressive strength [MPa]					
	Type of activator					
	Na_2CO_3			NaOH		
	after treatment	28 days	90 days	after treatment	28 days	90 days
natural curing	-	10.2	13.1	-	7.4	9.8
80°C	20.5	23.4	27.8	14.3	17.2	20.8
150°C	32.5	41.1	44.3	28.5	38.5	42.1
200°C	37.5	51.3	55.6	31.3	40.7	43.2
250°C	36.5	47.8	51.2	34.2	45.1	47.8

As it can be seen from the data listed above, for the low temperature curing, i.e. 20-80°C the highest compressive strength values can be attributed to the akermanite pastes while in hydrothermal conditions the highest compressive strength values are obtained for the diopside pastes. In both cases the higher compressive strength values are observed for the pastes activated by Na_2CO_3.

2.3. Effect of added activators on the phase composition of hardened pastes

In order to find the reason for the differences in strength properties of slag pastes, the phase composition was studied by means of X-ray diffraction method and scanning electron microscope. The XRD studies of akermanite pastes cured at 20 and 80°C show that the CSH phase (d=3.07; 1.83) and $CaCO_3$ (d=3.03; 2.48; 2.28) are the main hydration products. Some amounts of hydrated sodium and calcium silicates are also detected. For the pastes cured at higher temperatures the intensities of peaks corresponding to the hydration products increase markedly. In the case of vitrified akermanite activated by NaOH the substantial amounts of hydrated sodium silicates such as $Na_2Ca_2[Si_2O_7] \cdot H_2O$ (d=2.86; 2.77; 3.86) and $Na_2Ca[Si_2O_6] \cdot 2H_2O$ (d=2.67; 2.86; 2.06; 3.32; 3.70) are detected. In the presence of Na_2CO_3 the predominant phases are CSH and $CaCO_3$. In the pastes cured above 80°C the αC_2SH phase appears (d=4.22; 3.54; 1.788). The phase composition of hardened diopside pastes differs substantially, particularly when the hydration occurs above 80°C. In the pastes cured above 150°C the CSH I phase, tobermorite, pektolite and gyrolite are present, while the pastes hydrated at 20°C and 80°C show only the CSH and $CaCO_3$. In the vitrified diopside pastes activated by Na_2CO_3 the scawtite phase is formed [d=3.03; 2.89; 1.89]. It should be also noted that some quantity of hydrated magnesium silicate is detected in both akermanite and diopside pastes cured above 80°C. The SEM micrographs are shown in figures 1-3.

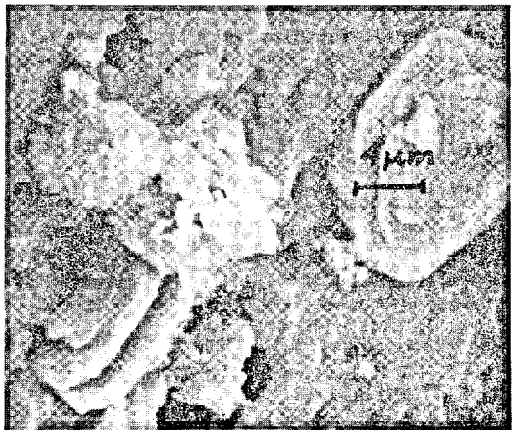

Fig.1. Slag paste of akermanite (Na_2CO_3 as activator) autoclaved cured - 150°C

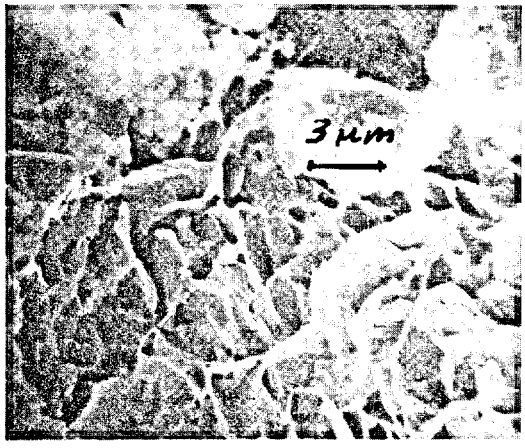

Fig.2. Slag paste of akermanite (Na_2CO_3 as activator) autoclaved cured - 200°C



Fig.3. Slag paste of diopside (Na_2CO_3 as activator) autoclaved cured - 200°C

3. Discussion

The strength results for the akermanite and diopside pastes cured in temperatures 20 and 80°C indicate that the structure of vitrified slags has no effect on the strength characteristics. On the other hand, the type of activator affects significantly the strength properties and highest values are obtained for the pastes

activated by Na_2CO_3. The temperature of curing is another important parameter giving the strength increase. This strength increase results from the higher hydration degree and type of hydration products. The highest strength for the pastes cured above 80°C are observed in the case of diopside slag. The lowering of strength can be explained by the formation of α-C_2SH [Fig. 1] [18].
The strength development in the diopside pastes is strongly influenced by a substantial amount of tobermorite and gyrolite. The CSH phase formed in the pastes shows different morphology. In akermanite pastes a substantial amount of CSH type II according to Diamond classification [18] is present while in [Fig. 2] diopside pastes CSH type IV and I are dominating components [Fig. 3].

4. References

1. P. Budnikow - Granuloranyje domiennyje szlaki i szlakowyje ciemienty. Moskwa 1953
2. F. Schroder - 5th I.C.C.C. - Tokyo 1968 vol. IV pp. 149-179
3. W. Satarin - 6th I.C.C.C. Moskwa 1974 vol III pp. 45-56
4. J. Toreanu, M. Georgescu - 7th I.C.C.C. Paris 1980 vol III pp. 99-104
5. P.K. Mehta - World Cement Technology 1980. 5. p 144-147
6. W. Kurdowski, L. Taczuk - Cement Wapno Gips 1983. 10-11. pp. 271-273
7. W.D. Głuchowski - Gruntosilikati wirobi i konstrukcji Kijew. 1968
8. W.D. Głuchowski - Baustoffindustrie 1974. 3. 9-12
9. W.D. Głuchowski, G.S. Rostowskaja - 7th I.C.C.C. Paris 1980 vol 3/V pp. 164-168
10. J. Małolepszy - 8th Int. Baustoff und Silikatung "Ibausil" Weimar 1982 vol I pp. 158-164
11. J. Małolepszy, A. Derdacka - Cement Wapno-Gips. 1975. 10. pp. 291-295
12. B. Talling, J. Brandstetr - 3rd Int. Conf. Fly Ash, Silica Fume, Slag and Natural Pozzolans in Concrete Trondheim 1979 vol 2 pp. 1519-1545
13. J. Deja, J. Małolepszy - 3rd Int. Conf. Fly Ash, Silica Fume, Slag and Natural Pozzolans in Concrete Trondheim 1979 vol. 2 pp. 1547-1563
14. J. Deja, J. Małolepszy, G. Jaśkiewicz - 2nd Int. Conf. "Durability of Concrete" Montreal. 1991 vol. I pp. 509-525
15. Gorszkow W.S., Aleksandrow S.E. - Kompleksnaja piererabot ka i ispolzowanije mietalurgicieskich szlakow w stroitielstwie. Stroijzdat Moskwa 1985
16. Goworow A.A. - Prociesy gidrotiermalnowo twierdienija szlakowych dispiersji. Naukowaja Dumka Kijew 1976.
17. Kalousek G.L. - Journal Amer. Concr. Inst. 1951. 23. pp. 77-79
18. Diamond S. - 8th I.C.C.C. Rio de Janeiro, 1986 vol 2/2 pp. 1-15
19. Liebau F. - Structural Chemistry of Silicates. Springer-Verlag New York. 1985.

HYDRATION PROPERTY OF VARIOUS CEMENTS UNDER ADIABATIC CONDITIONS

K Kato, Y Fukaya and M Tanaka

Central Research Laboratory, Chichibu Cement Co, Ltd
Tsukimi-cho, Kumagaya-shi, Saitama, JAPAN

SUMMARY

Since the inside of mass concrete is nearly in adiabatic condition, the temperature of the system is elevated due to the heat generation resulting from the hydration reaction of the cement. Under the adiabatic condition, strength development was higher than that cured at 20℃, especially during the early phase of curing. The strengths gradually became similar at 91 days of curing and thereafter. Strength development under adiabatic condition was larger in cements containing much C_2S and also in blended cements containing slag and fly ash. These phenomena were ascribed to the high temperature dependencies of the hydration reaction of these minerals. In case of cements with low water cement ratios cured under the adiabatic condition, those with much C_2S showed larger strength development due to the smoothly advancing hydration as well as the temperature dependency. Under the adiabatic condition, SiO_4^{4-} decreased markedly and polymerization of Si-O-Si was accelerated by the dehydrated condensation. C-S-H products thus tended to form mesh structure which was suggested to be effective for strength development to manifest.

ZUSAMMENFASSUNG

Da ein Volumenelement im Inneren der Betonmasse als adiabat abgegrenzt betrachtet werden kann, braucht zur Ermittlung der Temperatur lediglich die Reaktionswärme berücksichtigt werden, die beim Abbinden des Zements frei wird. Verglichen mit bei konstant 20℃ abgebundenem Beton fiel bei adiabatisch abgebundenem Beton vor allem der anfänglich steile Festigkeitszuwachs auf. Nach Spätestens 91 Tagen jedoch war die Festigkeit in beiden Fällen gleich. Bei adiabatisch abgebundenem Beton korrelierte die Festigkeit mit dem C_2S-Gehalt des Zements, trotz gleichzeitig erhöhtem Schlacke- und Flugasche-Gehalt. Diese kann auf die ausgeprägte Temperaturabhängigkeit der Reaktion dieser Minerale erklärt werden. Bei wasserarmen Zementen zeigten die adiabatisch abgebundenen mit relativ hohem C_2S-Gehalt aufgrund der ausgeglichenen Abbindereaktion und der Temperaturabhängigkeit eine erhöhte Festigkeit. Unter adiabatischen Bedingungen war das SiO_4^{4-} deutlich reduziert und die polymerisation von Si-O-Si war aufgrund der Kondensierung durch Wasserentzug stark beschleunigt. Die C-S-H-Gruppen bildeten eine Gitterstruktur, von welcher wir annehmen, daß sie zur Festigkeit beiträgt.

INTRODUCTION

Since inside of mass concrete is nearly under adiabatic condition, the temperature of the system is elevated by the heat generation accompanying the hydration reaction of cement which in turn is accelerated by the temperature rise. Temperature dependency varies among the minerals and the admixtures composing cements. It is thus considered that their compositions play important roles in the adiabatic temperature rise curve and strength development during the course of hydration. Water cement ratio (w/c ratio) is closely related to the rate of hydration reaction and the heat capacity of cement. The w/c ratio is thus expected to largely affect the adiabatic temperature rise curve. In this study, the adiabatic temperature rise curve as well as the strength development and hydration reaction during the course of temperature rise has been investigated. The correlation of these factors has been discussed.

EXPERIMENTAL

Materials

Portland cements used in the experiments were all industrial products. They were ordinary portland cement (N), moderate heat portland cement (M) and ASTM type Ⅳ cement (L). Their chemical and mineral compositions are shown in Tables 1 and 2, respectively. There were 2 kinds of blended cements used in the experiments. They were MS60 consisting of M blended with 60% of blast furnace slag shown in Table 1 and MF30 consisting of M blended with 30% of fly ash. Two kinds of aggregates were used in the experiments. One had a granulometry of ϕ10 mm - 0.15 mm and was used for mortars with w/c ratios of 30% and 45%. The other had a granulometry of ϕ5 mm - 0.15 mm and was used for mortar with w/c ratio of 60%. The organic admixture used was β-naphthalene sulfonate formaldehyde condensate (NSF).

Table 1 Chemical compositions and specific surface area of cement and admixture

	Composition (%)								Blaine
	CaO	SiO_2	Al_2O_3	Fe_2O_3	MgO	SO_3	Na_2O	K_2O	(cm^2/g)
N	64.1	21.6	5.2	2.9	1.6	2.1	0.29	0.51	3290
M	64.8	23.8	3.7	3.9	1.1	1.9	0.26	0.32	3200
L	64.0	26.6	2.8	2.4	1.0	2.0	0.19	0.45	3250
Slag	44.2	31.9	13.8	0.3	5.2	2.0	0.24	0.40	4430
Flyash	9.0	51.4	24.6	6.2	2.0	0.5	1.85	1.41	3500

Table 2 Mineral composition (%)

Cement	Alite	Belite	C_3Ass	C_4AFss
N	52	23	9	9
M	43	36	3	12
L	33	50	3	7

Measurement of adiabatic temperature rise

Multi-point measurement apparatus for adiabatic temperature rise was used for the measurement(1). Mixing proportion of mortar was 1:5 of cement:aggregate. w/c ratios were selected to be 30%, 45% and 60%. In cement, NSF was added at 0.25% (for that with w/c ratio of 60%) or 0.5% (for those with w/c ratios of 30% and 45%).

Determination of compressive strength

Compressive strength was measured on mortars with mixing properties identical to those used for measurement of adiabatic temperature rise. Mixed mortar was poured into a mold of 40 x 40 x 160 mm in size and cured under sealed condition accurately simulating the adiabatic temperature rise curve. Compressive strength of the mortar was measured at prescribed curing time points. As the control for comparison, compressive strength was measured on mortar cured at a constant temperature of 20℃.

Analysis of hydration products

Mortar used for the analysis of hydration products was that mixed with sintered alumina (ϕ2mm) in place of aggregate. It was cured under the same conditions as employed for the determination of

compressive strength. The hydration reaction was stopped by acetone at the prescribed curing time. It was then analyzed by thermal analysis (TG/DTA, DSC), XRD and analysis of silicate anion by trimethylsilylation(2, 3).

RESULTS AND DISCUSSIONS

Adiabatic temperature rise curve

Adiabatic temperature rise curves of various cements are shown in Figure 1. When the adiabatic temperature rise curves of N, M and L cements with different mineral compositions were approximated by the following formula (1), temperatures of these cements were calculated as follows: N cement; $T=52.0(1-e^{-0.551t})$, M cement; $T=43.2(1-e^{-0.384t})$, L cement; $T=41.0(1-e^{-0.288t})$.

$$T = K\ (1 - e^{-\alpha t}) \qquad (1)$$

where T=temperature, K=final value of temperature rise, α=coefficient and t=time.

In portland cements, K and α values became greater with increase in the ratio of C_3A and C_3S, which had high rate of hydration heat evolution. When compared with M cement, MS60 cement $[T=43.5(1-e^{-0.531t})]$ showed rather low temperature rise until 2 days of curing. The rapid temperature rise was the result of active hydration reaction of slag for 2-3 days. Thereafter, the temperature of MS60 cement remained higher than that of M cement. In proportion to the amount of fly ash, the temperature rise was generally lowered. During a prolonged curing, its temperature approached that of M cement by the active hydration of fly ash [MF30 cement; $T=41.0(1-e^{-0.241t})$. The experiments on w/c ratio provide useful data concerning highly strong concrete with low w/c ratio and large quantities of cement. Heat capacities of mortar used in the experiments were 500.3 cal/℃ for w/c ratio=30%, 519.2 cal/℃ for w/c ratio=45% and 536.6 cal/℃ for w/c ratio=60%. Therefore, for comparable advance in the degree of hydration, the temperature rise became higher as the w/c ratio decreased. However, as shown in Figure 2 indicating the experimental results, the temperature rise was sometimes lower for w/c ratio=30%. This tendency became more marked in cements containing higher C_3A and C_3S as mineral compositions. Among blended cements, this tendency was more marked in cement containing slag than fly ash. Heat evolution for hydration of cement was calculated from the temperature rise and heat capacity. The results are shown in Figure 2. As w/c ratio decreased, the heat evolution of hydration became smaller. The tendency was very marked in N cement.

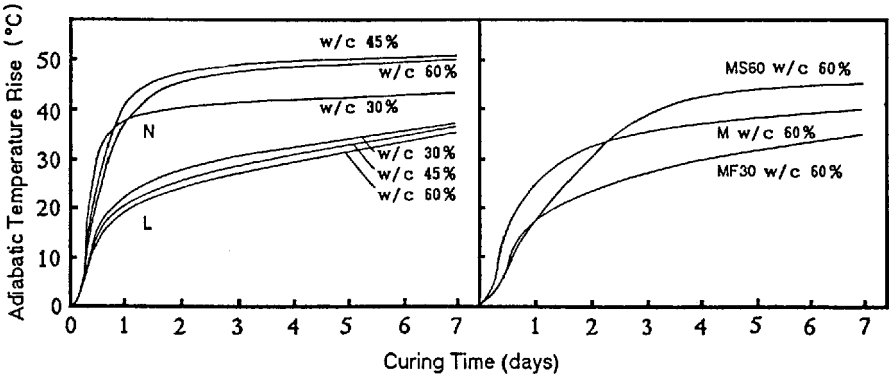

Fig. 1. Adiabatic temperature rise curves

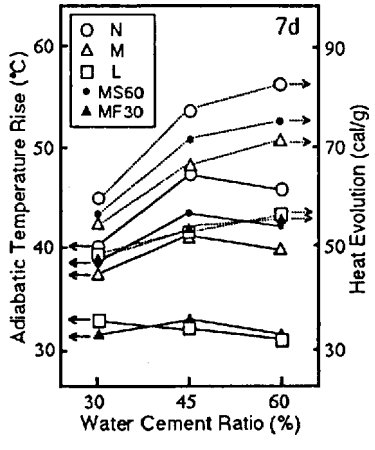

Fig. 2. Influence of w/c ratio on adiabatic temperature rise and heat evolution

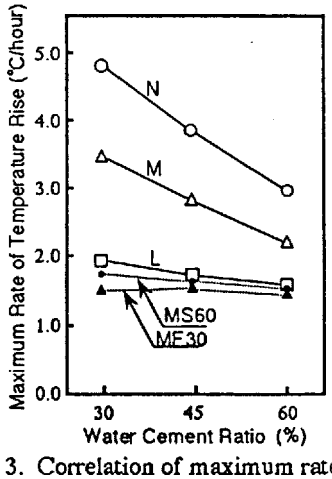

Fig. 3. Correlation of maximum rate of temperature rise to w/c ratio

As shown in Figure 3, the initial rate of temperature rise was higher in cements containing higher of C_3A and C_3S as well as those with low w/c ratio.

Strength development

Strength development during curing of N, M and L cements are shown in Figure 4, both under the adiabatic condition and at 20℃. The compressive strength of mortar at 20℃ for w/c ratio=60% showed the following order due to the difference in the amount of C_3S until 28 days of curing : N > M > L. During the course of adiabatic temperature rise, hydration was accelerated accompanied by temperature rise of the system. While strength of any cement was large, the tendency was very marked in L and M cements, both high C_2S type cements. At 14 days of curing and thereafter, their strengths were higher than that of N cement. This tendency was further accelerated in cements with w/c ratio=30% due to the additive effect of hydration inhibition which occurred in N cement. The strengths of M and L cements reached to the levels of N cement at 7 and 10 days, respectively, of curing. Their strengths remained higher than that of N cement thereafter. On the other hand, the strength of N cement scarcely improved on 7 days of curing and thereafter. This finding suggested a severe depression of hydration reaction. Compressive strengths when cured at 20℃ are plotted in Figure 5 against those cured under the adiabatic condition for the corresponding curing times. The strength development of cement was high during the early phase of hydration under the adiabatic condition than at 20℃. The ratio was higher in the following order with respect to the mineral composition of cement: L> M > N. It was considered to be due to the high temperature dependency of C_2S(4). With respect to the admixtures, both slag and fly ash had high temperature dependencies. Slag was especially revealed to have high strength development under the adiabatic condition. The strength approached to that cured at 20℃ as the curing time prolonged. However, there was no marked inversion until 91 days of curing. In general, it has been reported that strength deteriorated in

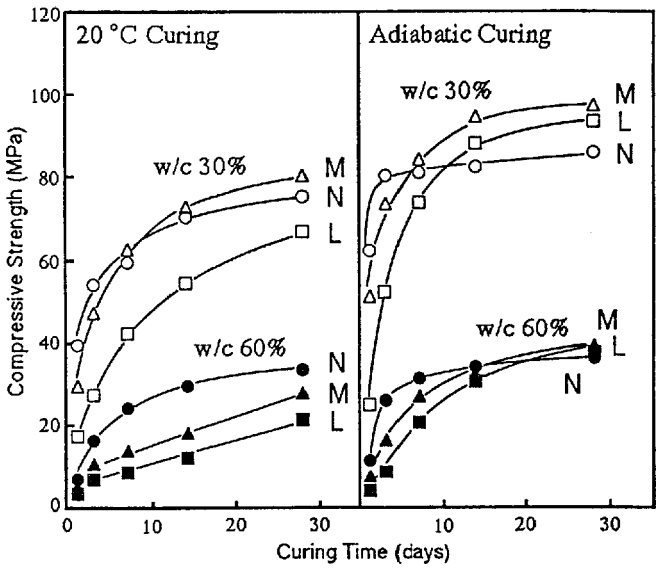

Fig. 4. Strength development

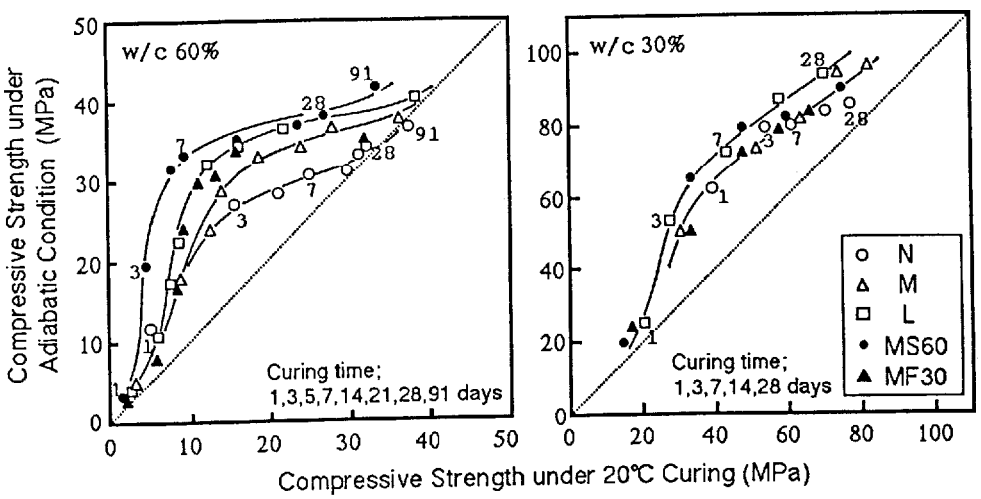

Fig. 5. Comparison of strength between adiabatic curing and 20°C curing

cements subjected to long time curing at high temperature(5). However, our results did not agree with these observations. It could possibly be ascribed to the same initial temperature and gentle temperature rise during the first few hours after mixing.

Hydration reaction during the course of adiabatic temperature rise

Amount of combined water – Changes in the amount of combined water in the hydration products during the course of adiabatic temperature rise are shown in Figure 6. The amount of combined water was high in N and MS60 cements during the early phase of curing within 3 days. This was attributed to the high contents of C_3A and C_3S in cement N resulting in the production of $Ca(OH)_2$, ettringite ($C_6A\bar{S}_3H_{32}$), and monosulfate ($C_4A\bar{S}H_{12}$), all containing much combined water, during the early phase of curing. In cement MS60, large amounts of ettringite and monosulfate were produced during the early phase of curing from the Al^{3+} contained in the slag. Hydration products from the cements were analyzed with DSC and the results are shown in Figure 7. From N and MS60 cements, production of many calcium sulfoaluminate hydrates was identified. M and L cements containing high C_2S showed high peaks at C-S-H. These results were confirmed by XRD analysis. From these results, N and MS60 cements were indicated to consume much liquid phase during the early phase of curing due to the active production of hydration products with large amounts of combined water. In cements with low w/c ratios, the influence was marked to result in strong inhibition of hydration. The retardation in the rate of hydration was considered to affect the adiabatic temperature rise curve and strength development.

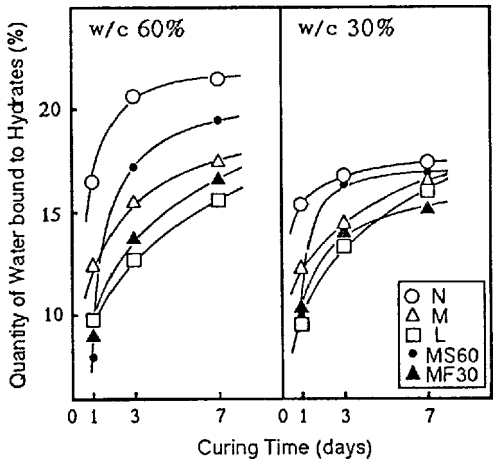

Fig. 6. Correlation of quantity of combined water to curing time

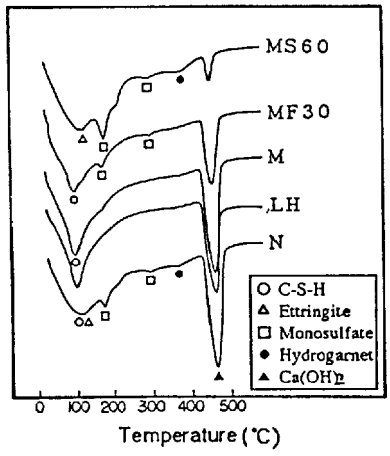

Fig. 7. DSC curves of hydration product after 7 days of curing

Difference in behaviour of silicate anion between curing at 20℃ and under adiabatic conditions – Since C-S-H products were poorly crystallized, they were difficult to be analyzed with XRD. As one of the information concerning C-S-H products, the behaviour of silicate anion was analyzed by trimethylsilylation technique. In Figure 8, gel permeation chromatogram (GPC) of trimethylsilyl derivatives of the hydration products of L cement is shown. Almost all silicate anions in the unhydrated cement were monomers (SiO_4^{4-}). As the hydration progressed, they changed to dimers ($Si_2O_7^{6-}$) and more polymerized polysilicates. Under the adiabatic condition, the decreasing ratio of monomers was high due to the acceleration of hydration with temperature rise. Thus, the amount of polysilicates produced was markedly higher than when cured at 20℃. The average molecular weight of the polysilicate derivatives was 1,700 ($\bar{M}n$) after 28 days of curing at 20℃. Under the adiabatic condition, the value was 2,800 ($\bar{M}n$). The correlation of peak area in GPC of monomer and polysilicate derivatives to compressive strength is shown in Figure 9. There was an inverse relation between the amount of monomer and the compressive strength. The plot of the results lay almost on an identical line for both cured at 20℃ and cured under the adiabatic condition. On the other hand, there was a direct relation between the amount of polysilicates produced and the compressive strength. The plot of the results for curing at 20℃ and under the adiabatic condition were lay on different lines. The

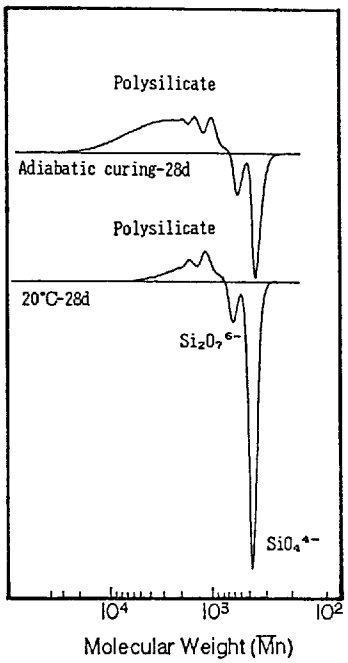

Fig.8. Gel permeation chromatogram of trimethylsilyl derivatives of L cement hydrates

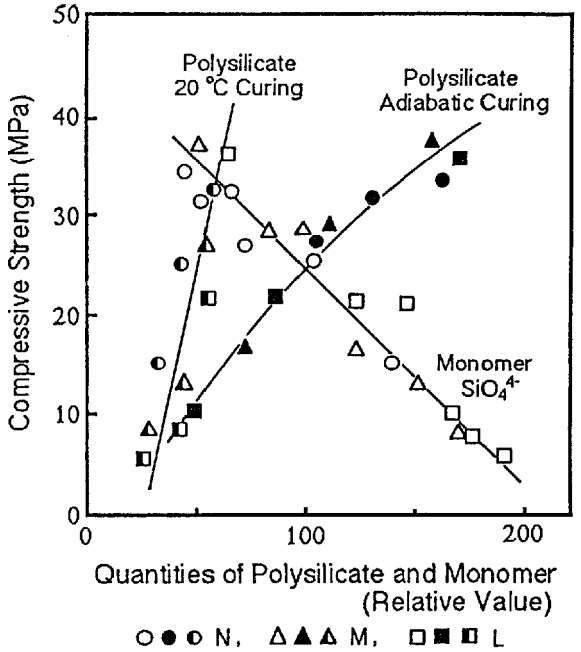

Fig. 9. Relationship between compressive strength and quantities of polysilicate and monomer (SiO_4^{4-})

latter condition showed a large production of polysilicates. From these results, hydration of C_3S and C_2S produced by SiO_4^{4-} was found to be accelerated under the adiabatic condition. With increase in the amount of C-S-H products, the polymerization was accelerated by the condensation of dehydrated silicate anion as shown in formula (2) with the rise in temperature having considerable effect on strength development.

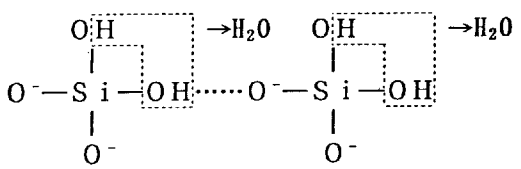

(2)

Correlation of behaviour of silicate anion with w/c ratio – The w/c ratio largely affected the adiabatic temperature rise curves of N and L cements as well as the strength development during the course of adiabatic temperature rise. These effects were discussed with respect to the behaviour of silicate anion. N and L cements were compared with respect to the decrease in SiO_4^{4-} and production of polysilicates. The results are shown in Figure 10. Since N cement contained much C_3A, hydration products containing much water were generated abundantly during the early phase of curing leading to a decrease in free water and thus high concentration of Ca^{2+} ion in the liquid phase. Under such a condition, elution of Ca^{2+} from the surface of C_3S and C_2S was retarded and mutual diffusion of H_2O and Ca^{2+} in the inner hydration products was disturbed. Therefore, invasion of unhydrated C_3S and C_2S inside was inhibited. It was considered that much SiO_4^{4-} that formed C_3S and C_2S remained in such cements and thus the amount of polysilicates did not increase. On the other hand, L cement contained little C_3A and had abundant liquid phase from the early to the late stages of curing. Consumption of SiO_4^{4-} and production of polysilicates advanced smoothly. Based on these properties, marked strength development was indicated by cement with low w/c ratio during the course of adiabatic temperature rise. The degree of polymerization of polysilicates is shown in Figure 11. The average molecular weight of polysilicate TMS derivative products increased as the curing time prolonged. The w/c of cement had only a small influence. There was no large difference between 30% and 60% of w/c ratios. Therefore, decrease in w/c ratio was revealed to influence the rates of hydration of C_3S and C_2S as well as the amount of polysilicates produced. However, it was found that polymerization of Si-O-Si bonds in C-S-H products progressed with temperature and curing time.

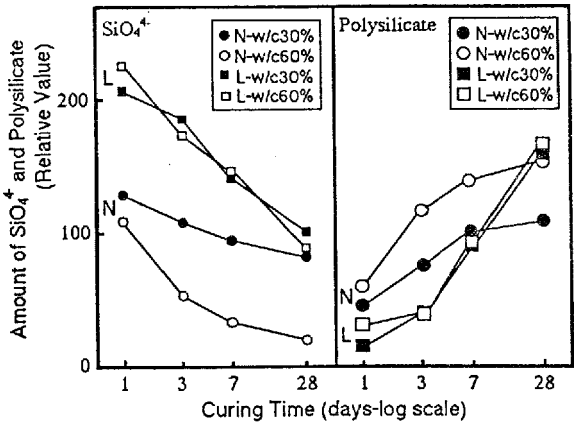

Fig. 10. Influence of w/c ratio on behaviours of SiO_4^{4-} and polysilicate

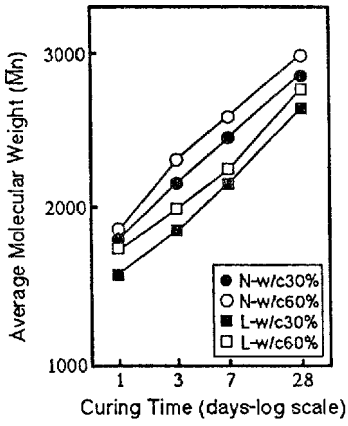

Fig. 11. Correlation of average molecular weight of polysilicate TMS derivatives under adiabatic condition to curing time

CONCLUSIONS

1. Adiabatic temperature rise values were largely influenced by the heat of hydration and mineral composition of cement as well as the admixtures. w/c ratio also significantly influenced the values. As w/c ratio decreased, the heat capacity of the mortar became smaller and the hydration of cement during the early phase of curing was accelerated. However, inhibition of hydration was induced in cements with low w/c ratios. In such cements, the adiabatic temperature rise values showed decreasing tendencies. The tendency was enhanced in portland cements containing much C_3A and in blended cement containing slag.
2. Under the adiabatic condition, strength development was higher than that cured at 20℃, especially during the early phase of curing. The strengths gradually became similar at 91 days of curing and thereafter. Strength development under adiabatic condition was larger in cements containing much C_2S and also in blended cements containing slag and fly ash. These phenomena were ascribed to the high temperature dependencies of the hydration reactions of these minerals. In case of cements with low w/c ratios cured under the adiabatic condition, those with much C_2S showed larger strength development due to the smoothly advancing hydration as well as the temperature dependency.
3. Under the adiabatic condition, SiO_4^{4-} decreased markedly and polymerization of Si-O-Si was accelerated by the dehydrated condensation. C-S-H products thus tended to form mesh structure which was suggested to be effective for strength development to manifest. When the w/c ratio was low, the amount of C-S-H products decreased due to inhibition of the hydration reaction of clinker. However, it was confirmed that the degree of polymerization of polysilicates from C-S-H products was not affected.

REFERENCES

1. K. KATO, S. SAWAKI, Y. FUKAYA, "Effect of gypsum on adiabatic temperature rise of slag cement", CAJ Review of the 43th General Meeting - Technical Session -, 1989, 72p.
2. F. D. TAMAS, A. K. SARKAR, D. M. ROY, "Effect of variables upon the silylation products of hydrated cements", Conf. Hydraulic Cement Pastes, Sheffield, 1976, 55p.
3. H. UCHIKAWA, R. FURUTA, "Hydration of C_3S-Pozzolana paste estimated by trimethylsilylation", Cement and Concrete Research, 1981, 11 , 65p.
4. V. LACH, J. BURES, "The phase composition and microstructure of cement pastes hydrated at elevated temperatures", 6th International Congress on Cement Chemistry, Vol. II, Moscow, 1974, 73p.
5. P. KLIEGER, Proceedings American Concrete Institute, 1957, 54 , 1063p.

THE SIGNIFICANCE OF THERMAL HISTORY FOR OFFSHORE GROUTS

A K Crumbie, P L Pratt and H F W Taylor

Imperial College of Science, Technology and Medicine
London, UK

ABSTRACT

In this paper the development of microstructure has been studied in cement pastes hydrated at constant temperatures from 40°C to 110°C to determine the effect of temperature for periods of time from a few hours to several months. In addition temperature cycles were devised to approximate those developed in large grout bags, with periods of hydration at room temperature after excursions to the high temperature. The microstructure of the pastes was studied by x-ray diffraction, thermogravimetric analysis and backscattered electron imaging of polished sections. The results show that in addition to accelerating hydration, elevated temperature curing affects the composition and type of hydrate phases formed and their distribution in the cement microstructure.

INTRODUCTION

Littlejohn and Hughes (1) have examined the thermal behaviour of grouted support bags for subsea pipelines. The function of these bags is to overcome irregularities in the topography of the seabed and scouring of the seabed under the pipe during service. Their results with OPC grouts showed that in full-size grout bags, 2.1 m^3 in volume, immersed in a tank of seawater at 8°C, a maximum temperature of 110°C was reached 5 hours after filling. This temperature was held for 36 hours in the centre of the grout bag and cooling to 8°C lasted for 12 days. Not surprisingly severe local temperature gradients of up to 2,500°C/m were measured and substantial cracking occurred with marked loss of strength. The purpose of this paper is to examine the development of microstructure in similar cement pastes hydrated at constant temperatures of 80°C and 110°C to compare with that at 25°C. Heat cycles were also applied to approximate to those developed in the full-size grout bags.

EXPERIMENTAL DETAILS

Northfleet OPC provided by Blue Circle Plc was used for this work. The oxide composition and alkali content were typical of the Northfleet product and the x-ray phase analysis, kindly determined by Mr W Gutteridge of the British Cement Association, gave 61% alite, 16% belite, 8% C_3A and 10% C_4AF.

OPC pastes at w/c = 0.4 were cast into small plastic containers. These had loosely fitting caps and were placed inside larger vessels which contained saturated solutions of CH and which were sealed. After an initial hydration time of one hour the samples were cured at temperatures of up to 80°C for times of up to 3 months, and at 110°C for times up to 28 days. The samples probably took about 2 hours to reach their maximum temperatures, a heating rate of over 30°C/hour. After specified times hydration was stopped and the free water subsequently removed by freeze drying. One half of the sample was prepared for microstructural examination in the SEM (scanning electron microscope), using the back scattered electron (bse) imaging on flat polished surfaces. A quantitative analysis of the anhydrous cement and porosity greater than 0.35 μm was made using these bse images in conjunction with a Kontron image processing system. The other half of the sample was used for x-ray diffraction (XRD), thermogravimetric (TG) analysis and differential thermal analysis (DTA). These techniques give information about the phases present in the sample. Fracture surfaces of the dried samples were observed in the secondary electron imaging (SEI) mode of the SEM. This allows the morphology of the cement hydration products to be assessed, though this is liable to have been affected by drying and the regions observed may be representative of weak rather than of typical parts of the material.

Compressive strength data were also obtained for a range of curing temperatures between 25°C and 110°C. All results are means of 8-10 cubes from at least 3 separate casts.

Due to the limited availability of field specimens from large structures, additional experimental work was carried out. OPC pastes were made and cured at 80°C and 110°C for periods of up to 28 days using the techniques described above; after this time they were cured at 25°C in saturated limewater, for times of 7 days, 28 days and 3 months. These specimens were of more direct practical significance and were characterised in the same way as the isothermal samples.

EXPERIMENTAL RESULTS AND DISCUSSION

XRD and DTA

For specimens cured at 25°C the XRD results show the normal behaviour for OPC with the amount of ettringite passing through a maximum at 18 hours and monosulphate beginning to appear after 2 days. Anhydrous C_3A was undetectable after 1 day and C_4AF decreased over the entire 3 months. For curing at 80°C the hydration of both the silicate and the aluminate phases was accelerated while the products of the aluminate

phases were very different from those at 25°C. Ettringite was not detected at any age while monosulphate, which was strong at 3 hours, decreased to below the limits of detection by 2 days. Other AFm phases gave rise to diffuse peaks between 1 and 3 days but the major aluminate product clearly detectable after 18 hours was hydrogarnet. At 110°C neither ettringite nor monosulphate was found; the only aluminate product was hydrogarnet which increased steadily with time.

These results are combined with those for the specimens subjected to an early heat cycle in Table I. This shows that hydrogarnet was present in all the samples examined. In those for which the heat cycle was relatively mild, ettringite or monosulphate, or both, reappeared after varying lengths of time at 25°C. The monosulphate was usually found as $C_4A\bar{S}H_{12}$ (c' = 8.9 Å) but in one case as $C_4A\bar{S}H_{10}$ (c' = 8.2 Å): this difference probably reflects a difference in drying conditions. A number of specimens, mainly those cured at 110°C, gave an unidentified weak peak at 3.86 Å and one specimen gave an unidentified very weak peak at 12.2 Å. The peak at 3.86 Å cannot be attributed to AFt as the other peaks for this phase are not present. Ettringite reappeared after periods of 1-3 months only after treatments not exceeding 24 hours at either 80°C or 110°C. Monosulphate reappeared after treatments of up to 7 days at 80°C. After the 110°C treatments it was found only in one case and was then very weak.

Table I Summary of hydrated aluminate phases from XRD analyses of OPC pastes subjected to early heat cycles at 80°C and 110°C followed by curing at 25°C.

HEAT CYCLE		TIME AT 25°C				HEAT CYCLE		TIME AT 25°C			
Temp	Time	0	7d	28d	3m	Temp	Time	0	7d	28d	3m
80°C	24h	MH	MHX	MEH	MEH	110°C	12h	H	H	HX(E) (M*)	HE
	3d	H	MH	MH	MH		24h	H	H	H(X)	HEX
	7d	H		HM	H(M)		3d	H	HX	HX	H
	14d	H			H		7d	H		HX	HX
							14d	H		HX	HX
							28d	HX			HX

NB: Strongest peak is listed first

H = hydrogarnet M = monosulphate ($CA\bar{S}H_{12}$ 8.9 Å) M* = monosulphate ($CA\bar{S}H_{10}$ 8.2 Å)
E = ettringite X = peak at 3.86 Å ( ) = weak

These results are generally similar to those found by Heinz (2) and Heinz and Ludwig (3,4) and by Wieker and Herr (5) in both cases working on rapid hardening cements (German PZ55) which are higher in SO_3. The absence of both monosulphate and ettringite in samples cured at 110°C, or for greater than 24 hours at 80°C was presumably due to the instability of these phases in the cement paste at these temperatures. AFm phases are thermodynamically unstable with respect to hydrogarnet, although decomposition in cement pastes did not occur in any observed length of time at 25°C. At 80°C or 110°C, the decomposition was clearly more rapid.

The DTA results confirmed the XRD findings, showing no sign of ettringite immediately after curing at 80°C and a notably broader C-S-H endotherm compatible with the incorporation of aluminate and sulphate ions in the gel.

TG Analysis

(i) Non-Evaporable Water From TG - Figure 1 gives losses observed on TG curves between 105°C and 900°C, expressed as percentages of the mass at 900°C. These are used as approximate measures of chemically bound water, though errors arise from the absence of any correction for CO_2 and from other causes. The results confirm the greater degree of hydration at 80°C for all ages up to 3 months and at 110°C for ages up to 28 days, compared with hydration at 25°C.

(ii) Weight Percentage of CH from TG - Figure 2 shows the weight percentages of CH against hydration time for OPC pastes cured at 25°C, 80°C and 110°C. The results are averages from at least 2 separate TG runs, in some cases more. At times up to 28 days more CH is formed at 80°C than at 25°C, but after 3 months, there is no significant difference in CH content with temperature. After 6 hours of hydration at 110°C the rate of formation of CH is much lower than at lower temperatures.

Specimens subjected to the early heat cycle showed a reduction in the amount of CH subsequently formed at ages up to 3 months, compared with isothermal curing at 25°C.

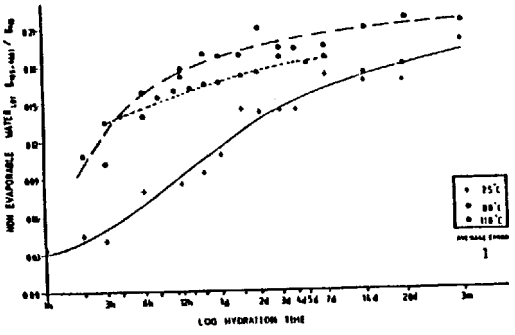

Fig. 1 Non-evaporable water content with time

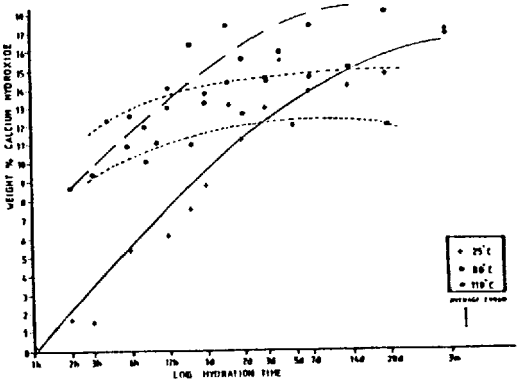

Fig. 2 Weight % CH with time

Microstructure

(i) Bse Imaging with Image Analysis - The volume percentages of anhydrous cement and of porosity > 0.35 μm for pastes cured at 25°C, 80°C and 110°C for times of 1 hour to 3 months were determined using bse imaging. The volume content of anhydrous cement initially, calculated from the w/c ratio (0.4) and cement density (3160 kgm^{-3}) is 44%. On this basis the percentages hydrated were calculated (Figure 3). For the pastes cured at 25°C at times up to about 7 days these are much higher than those typically found using XRD, shown by the idealised curve; they are probably in error due to failure of the image analysis to record the smaller cement grains at the magnification used. Consequently, the results have only comparative significance. They indicate more rapid reaction at 80°C than at 25°C, but do not support earlier conclusions that the ultimate degree of hydration is lower.

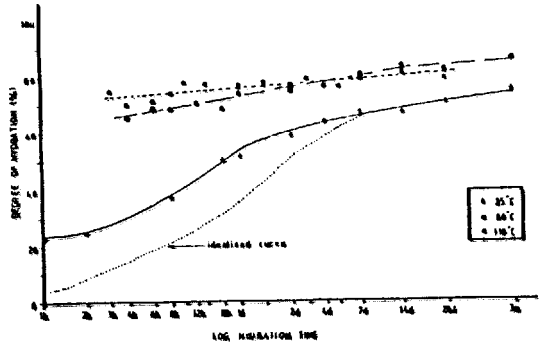

Fig. 3 Degree of hydration with time

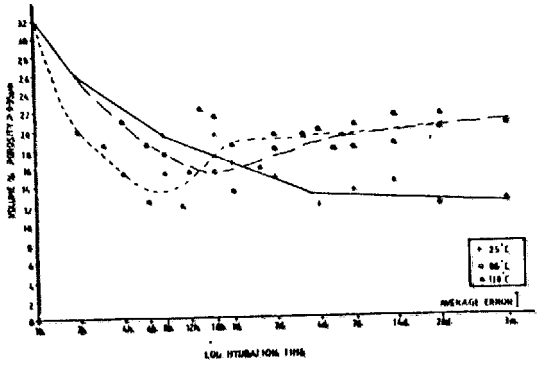

Fig. 4 Porosity > 0.35 μm with time

Figure 4 shows that at 80°C and 110°C the porosity > 0.35 μm in the first 12 hours of curing is significantly lower than that at 25°C. This reflects the higher initial rate of hydration at this temperature. After this decrease the porosity passes through an ill-defined minimum at 8-18 hours, increases by 2 days to more than that at 25°C and shows little further change thereafter up to 3 months. This increased porosity > 0.35 μm for samples cured at 80°C and 110°C occurs despite the higher degree of hydration and is compatible with the conclusion of earlier workers, that an increase in curing temperature results in a coarser pore structure. The initial rapid decrease at 80°C and 110°C is due to hydration products forming in the water-filled space; the subsequent increase is due to the empty shells of the medium-sized cement grains, seen in Figure 5, which are not filled with later hydration products from the larger cement grains.

Accurate discrimination of the CH from bse images of OPC pastes was not possible for the samples cured at 80°C or 110°C. The grey level of the CH was very similar to that of the 'outer' C-S-H gel or 'undesignated' product, Figure 5. The C-S-H peak in the histogram of grey levels is shifted to superimpose upon the CH peak, exposing the porosity peak more clearly. This shift is even greater than that found by Kjellsen et al (6) at 50°C. This suggests that at elevated temperatures the chemical composition or the density of the cement gel differs significantly from that at 25°C.

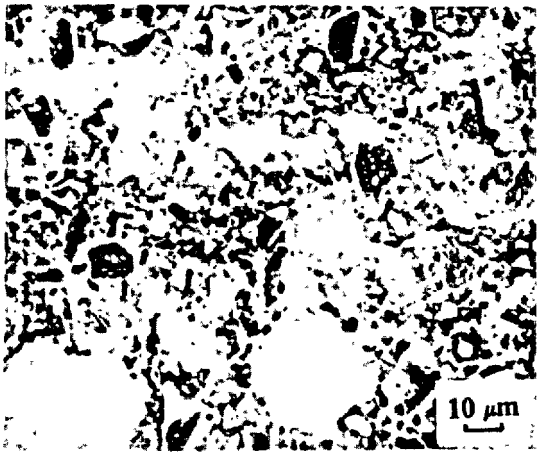

Fig. 5 Bse image of paste cured at 80°C for 4 days

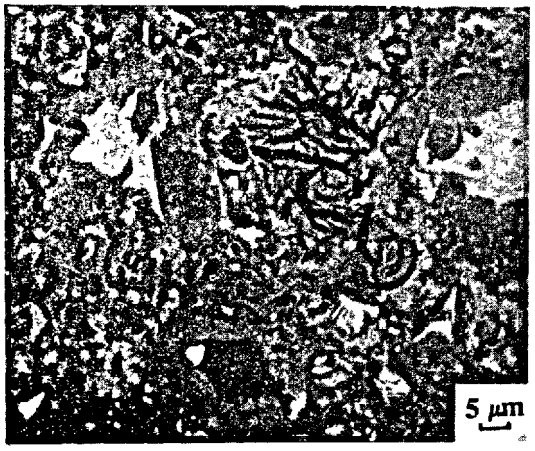

Fig. 6 Bse image of paste cured at 110°C for 12 hours and 25°C for 3 months

(ii) Chemical Composition Of The C-S-H Gel - The chemical composition of the C-S-H gel surrounding the alite and belite grains ('in situ' product) was determined using bse images in conjunction with EDXA; all analyses were the mean of 50 separate measurements from more than one field. The results for pastes cured at 25°C and 80°C for four days indicate that the mean C/S ratio of the 'in-situ' cement gel increases with temperature from 2.1 to 2.4. These preliminary results also indicate that the incorporation of other ions (Al, S, Mg) in the 'in situ' gel decreases slightly with an increase in curing temperature. The higher C/S ratio of the 80°C paste would account for the failure to resolve the CH peak in the histogram of the bse image.

(iii) Effects of Early Cycling - For samples cured for 24 hours at 110°C and then at 25°C for up to three months the amount of coarse porosity was close to that of samples cured at 25°C throughout. The 'in-situ' gel showed a darker grey level which persisted in these specimens, Figure 6, together with a new product often filling many of the once-empty hollow shells of the medium-sized cement particles. This product has a very distinctive dried and shrunken appearance and x-ray microanalysis reveals that it is the ettringite first seen by XRD after 28 days at 25°C following the high temperature cure. Longer times at 110°C resulted in permanent increases in the coarse porosity.

(iv) Phases Visible on Fracture Surfaces - Two new phases in addition to the gel were found on fracture surfaces after curing at 80°C for 8 hours. Tablet-shaped crystals identified as calcium sulphate were either secondary gypsum or anhydrite but neither was found by XRD. Leaf-shaped crystals of low symmetry, Figure 7, appearing to contain Ca, K and S were possibly syngenite, which may have crystallised from the pore solution on drying. After 24 hours at 80°C or 4 hours at 110°C, Figure 8, the leaf-like morphology persisted and minute particles at most 100 μm across appeared amongst the Type II reticular C-S-H gel. These might have been hydrogarnet but they were much too small for EDX analysis. After 8 hours at 110°C most of the anhydrous cement had already reacted and the fracture surfaces were too dense to reveal individual phases.

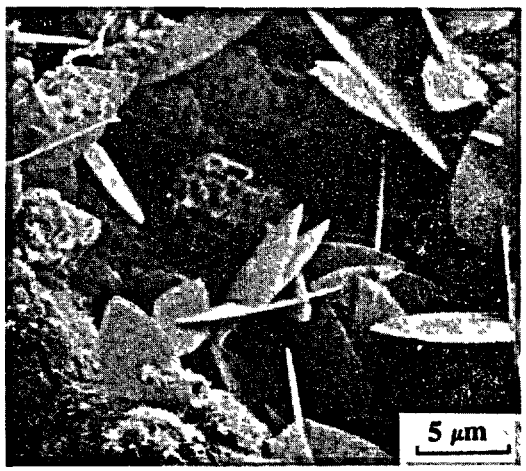

Fig. 7 Paste cured at 80°C for 8 hours

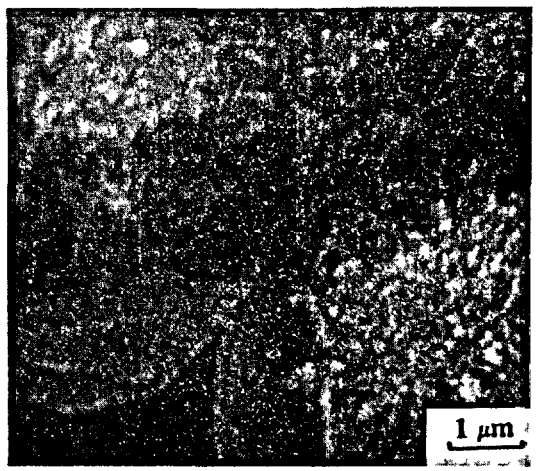

Fig. 8 Paste cured at 110°C for 4 hours

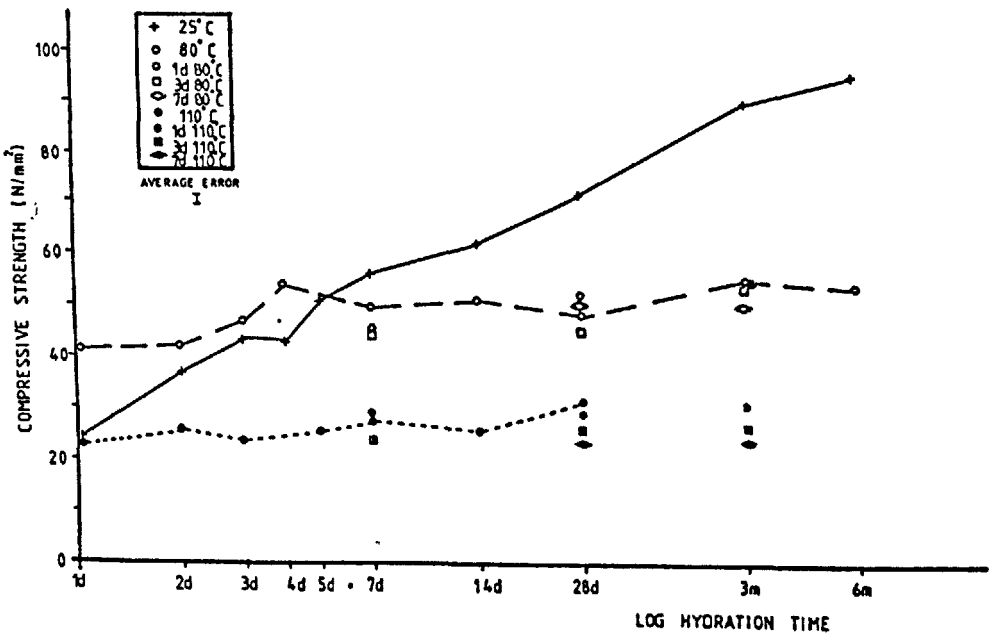

Fig. 9 Compressive strength development

Mechanical Properties

Figure 9 shows the compressive strength development for OPC samples cured at 25°C, 80°C and 110°C for up to 6 months. At 25°C the strength continued to increase up to 6 months as the degree of hydration increased and the amount of coarse porosity fell. At 80°C and 110°C there was very little increase in hydration or decrease in coarse porosity after 1 day and the strength remained low and more or less constant. Pastes cured for 1 day or more at 80°C or 110°C and then held at 25°C under water had strengths similar to those of pastes held at high temperature for the whole period.

CONCLUSIONS

Curing at 80°C and above coarsens the microstructure of OPC pastes, increases the amount of porosity > 350 μm and can reduce the compressive strength permanently.

Curing at 110°C for only 12 hours is sufficient to cause this loss of strength and this is significant for the large grout masses in the pipe-line support bags.

ACKNOWLEDGEMENTS

We are grateful to the Marine Technology Directorate Ltd for financial support for Alison Crumbie, to Blue Circle Plc for the supply of cement and to the British Cement Association and the Geology Department at Imperial College for help with XRD facilities and analyses.

REFERENCES

1. Littlejohn, G.S. and Hughes, D.C.: "Thermal behaviour of grouted supports for pipelines". **Grouts and grouting for construction and repair of offshore structures, a summary report**, Dept of Energy, 1988, OTH 88 289.

2. Heinz, D.: "Deleterious formation of ettringite-like phases in heat treated mortars and concretes", Dissertation, 1986, Technical University of Rhein-Westfalen, Aachen.

3. Heinz, D. and Ludwig, U.: "Mechanism of subsequent ettringite formation in mortars and concretes after heat treatment". **Proc 8th Int Cong Chem Cement, Rio de Janeiro,** 1986, **5**, 189-194.

4. Heinz, D. and Ludwig, U.: "Mechanism of secondary ettringite formation in mortars and concretes subjected to heat treatment". Concr Durability, ACI SP100-105, 1987, 2059-2071.

5. Wieker, W. and Herr, R.: "Some problems concerning the chemistry of Portland cement". Zeit für Chemie, 1989, **29**, 321-327.

6. Kjellsen, K.O., Detwiler, R.T. and Gjørv, O.E.: "Backscattered electron imaging of cement pastes hydrated at different temperatures". Cem Conc Res, 1990, **20**, 308-311.

HYDROTHERMAL STABILITY OF CALCIUM SILICATE HYDRATES BETWEEN 250°C AND 400°C

N B Milestone, N I Baxter and A R Gainsford

DSIR Chemistry, Private Bag, Petone
NEW ZEALAND

ABSTRACT

Pastes of calcium silicate hydrates were prepared from pure C_3S and quartz flour and βC_2S and quartz flour at Ca/Si ratios ranging from 2.0 to 0.5. The samples were initially cured hydrothermally at 150°C for two days before being subjected to exposure up to and above the critical point of water (374°C) for up to eight weeks.

While xonotlite was formed in all samples, it was only the predominant phase when Ca/Si = 1.0 where it remained stable up to 400°C. At higher Ca/Si ratios, a mixture of kilchoanite, killalaite and xonotlite predominated above 300°C with calciochondrodite and $C_6S_2H_3$ forming at or below this temperature. Above the critical point, wollastonite formed as the predominant phase along with some xonotlite. At Ca/Si = 0.5, xonotlite and C_4S_5H formed as the principal phases with C_4S_5H predominating at elevated temperatures. Truscottite only formed from the βC_2S mixtures and was not present above 300°C.

These results have important implications on geothermal grout stability where high Ca/Si ratio grouts can be used to counter corrosion caused by CO_2 rich waters. New fields to be developed have temperatures in excess of 320°C where field exposure details are not available.

ZUSAMMENFASSUNG

Aus reinem C_3S, βC_2S und feinstgemahlenem Quarz wurden Calzium-silicat-hydrat-pasten, mit Ca und Si in den Verhältnissen 0.5 bis 2.0, hergestellt. Die Probenwurden anfangs für zwei Tage bei 150°C hydrothermal gereift bevor sie Bedingungen in der Nähe des kritischen Punktes des Wassers (374°C) ausgesetzt wurden.

Während Xonotlit sich in allen Proben bildete, war es die vorherrschende Phase nur bei Ca/Si = 1.0 und war dann bis 400°C stabil. Mischungen von Kilchoanit, Killalait und Xonotlit herrschten bei höheren Ca/Si Verhältnissen und Temperaturen über 300°C vor. Calziochondrodite und $C_6S_2H_3$ bildeten sich bei oder unter dieser Temperatur. Wollastonit, zusammen mit etwas Xonotlit bildeten sich als die vorherrschende Phase über dem kritischen Punkt des Wassers. Xonotlit und C_4S_5H erschienen als Hauptphasen bei Ca/Si = 0.5, bei höheren Temperaturen herrschte C_4S_5H vor. Truscottit bildete sich nur von den βC_2S Mischungen und wurde bei Temperaturen unter 300°C nicht gefunden.

Diese Beobachtungen lassen wichtige Rückschlüsse auf die Stabilität von geothermalen Betonmischungen zu. Um der Korrosion durch CO_2 reiche Wässer entgegen zu wirken, können Mischungen mit hohen Ca/Si Verhältnissen verwendet werden. Gegenwärtig entwickelte geothermale Felder haben Temperaturen über 320°C, für diese stehen zur Zeit keine Daten zur Verfügung.

INTRODUCTION

In selecting the most suitable cementing system for wells in the Ohaaki Geothermal field, New Zealand, it became apparent that the most durable formulations were those which contained little or no added silica[1,2]. This is in direct contrast to current cementing practise where silica is added to geothermal cements to counter the reduction in strength and the increase in permeability which occur as the temperature is raised[3]. At Ohaaki, high CO_2-content fluids dissolved a readily carbonated binding system based on tobermorite and xonotlite, the preferred binders at high temperatures[4]. There also appears problems in using this system if sulphur compounds are present[2] although the results were not conclusive. Milestone *et al.*[5] concluded that the best compromise for CO_2 durability and strength was addition of less than 15% addition of silica flour when the phases kilchoanite and killalaite were formed at 260°C.

While silicate binders based on the high calcium silica ratio phases have proved more durable under Ohaaki conditions at maximum temperatures of 260°C[1], neighbouring fields have temperatures in excess of 320°C. There have been suggestions of high temperature instability of these phases[6] and certainly they have little strength[3]. This study investigates the formation and stability of a number of calcium silicate hydrate phases formed by addition of silica flour to pure calcium silicates, up to temperatures above the critical point of water (374°C) and considers the implications in geothermal cements.

EXPERIMENTAL

Small 45 x 15 x 15 mm prisms of pure silicate mixtures were prepared from slurries of βC_2S and C_3S plus powdered quartz (silica flour of <200 m^2/kg) mixed in appropriate proportions to give pastes with ratios of Ca:Si from 2.0 to 0.5. The silicates were dry blended with appropriate amounts of silica flour, then moulded with sufficient water to give a firm paste (w/s approximately 0.4) and initially cured in moulds at 60°C in a water bath for three days before being stripped and autoclaved at 150°C (under 0.48 MPa pressure) for two days to fully harden the prisms. This curing regime was used to simulate downhole curing conditions.

Samples were placed in pairs in stainless steel pressure vessels, together with sufficient water to cover the samples at temperature, and heated in tubular furnaces to the required temperature under autogenous pressure. After a given time the vessels were cooled and the samples recovered. A small portion was removed with a wafering saw for X-ray diffraction (XRD). The remainder was replaced in the vessel, distilled water added if necessary, sealed and reheated for a further period of time. The portion removed was dried at 60°C then ground and examined by XRD.

RESULTS

The phases formed on initial curing at 150°C are shown in Table 1. Semiquantitative XRD indicated approximately 25% unhydrated C_3S and 45% unhydrated βC_2S after curing. 11Å tobermorite was found only when the Ca:Si ratio was 1.0 or less for C_3S and 0.5 for βC_2S, αC_2SH being the common phase formed. Excess quartz was present in all samples but only for C_3S at Ca:Si = 2.0 was $Ca(OH)_2$ present. At the lowest Ca:Si ratio some xonotlite was formed with C_3S and truscottite with βC_2S.

Once the temperature was increased, further reactions occurred and only for pastes where Ca:Si = 0.5 did excess quartz remain after 8 weeks curing below the critical point. The various phases formed are detailed in Table 1 for temperature versus time. At one week all C_3S was hydrated at 250°C and higher, while 300°C was needed to hydrate all βC_2S. No evidence was found for gyrolite formation although this phase is commonly reported under hydrothermal conditions when excess silica is present[7].

Ca:Si = 2.0 from C_3S

At 250°C the major phases initially formed were $C_6S_2H_3$ and calciochondrodite with a minor amount of kilchoanite. Some quartz was present at 1 week but it slowly reacted and was not detected after 4 weeks. As the temperature was increased to 300°C, $C_6S_2H_3$ and calciochondrodite continued to be the predominant phases although more xonotlite was formed with time at the expense of kilchoanite. A deposit of calcite formed on the pressure vessel lining indicating loss of calcium from the samples. At 350°C and higher,

xonotlite was the major phase but substantial amounts of killalaite, observed in trace levels at 250°C, were present along with a minor amount of kilchoanite. At 400°C, xonotlite and kilchoanite were the predominant phases with minor amounts of killalaite.

Ca:Si = 1.5

From C_3S, kilchoanite and killalaite were initially formed at 250°C with minor amounts of xonotlite and a trace of $C_6S_2H_3$ but the xonotlite concentration decreased with time. As the temperature was raised to 300°, xonotlite was initially the major phase with smaller amounts of kilchoanite and killalaite but the concentrations of the latter two compounds increased with time. At 350°C xonotlite was the predominant phase after one week but the amounts of kilchoanite and to a lesser extent killalaite increased with time. At 370° xonotlite was the most stable phase with kilchoanite and killalaite remaining as minor phases, the concentration of killalaite decreasing slowly. At 400°C however, wollastonite was formed as the major phase with only small amounts of xonotlite and kilchoanite formed.

This contrasts with the βC_2S pastes where calciochondrodite was initially formed as the major phase at 250°C and only slowly transformed to the kilchoanite/killalaite mixture over 8 weeks. At 300°C xonotlite was formed but the predominant phase remained the kilchoanite/killalaite mixture. This remained the case until 400°C when xonotlite became the predominant phase along with minor amounts of kilchoanite and wollastonite.

Ca:Si = 1.0

For both C_3S and C_2S, xonotlite was the only silicate phase formed below the critical point. No quartz was present until above the critical point, where complete reaction of C_3S with quartz did not occur. While xonotlite was the predominant phase, excess quartz was present along with minor amounts of what is probably poorly crystalline wollastonite.

For βC_2S_2 however, reasonable amounts of wollastonite as well as xonotlite were formed initially at 400°C changing little with time and no free quartz was observed.

Ca:Si = 0.5

From both C_3S and βC_2S the phases formed were xonotlite and the 3.15Å phase, approximately C_4S_5H. Excess quartz was present in all samples. For the βC_2S paste, minor amounts of truscottite were formed initially at lower temperatures but this slowly reacted over 8 weeks.

Precautions were not taken to exclude atmospheric CO_2 while handling samples or filling the pressure vessels. Lost water was 'topped' up with distilled water. Over 8 weeks a layer of calcite formed on the inner surface of the reaction vessels indicating that calcium ions are leached from the samples. This leaching appeared most pronounced in the higher Ca:Si ratio specimens where after 8 weeks a definite skin was observed on the samples which contained a high proportion of xonotlite. Scawtite was not detected in the samples.

DISCUSSION

It is clear that the starting materials have an influence on the phases that are initially formed from hydrothermal treatment ie, after 1 week at test temperature. Truscottite was only formed from βC_2S in the presence of excess silica at low temperatures (150-250°C). It does not prove particularly stable in the presence of excess silica, converting to xonotlite. This is in accordance with work carried out by Luke *et al.*[8] although temperatures recorded in our study were lower than they observed. This indicates that formulations which produce truscottite will not be suitable binding systems for high temperature wells where silica is readily available, such as might be expected in geothermal fluids with high levels of dissolved silica. Gallus *et al.*[9] also noted that problems occurred with truscottite binders in dry steam conditions.

Table 1: Phases formed on hydrothermal treatment

(a) Ca:Si = 2.0 C_3S

		1 wk	2 wk	3 wk	4 wk	8 wk
400°		Xo Kc Ka	Xo Kc Ka	Xo Kc Ka	Xo Kc Ka	Xo Kc Ka
370°		Xo Co Kc Ka	Xo Co Kc Ka	Xo Kc Ka Co	Xo Kc Ka Co	Xo Kc Ka Co(tr)
350°		Xo Kc $C_6S_2H_3$	Xo Kc Ka	Xo Kc Ka	Xo Kc(tr) Ka(tr)	Xo Kc(tr) Ka(tr)
300°		$C_6S_2H_3$ Co Xo	$C_6S_2H_3$ Co Xo	$C_6S_2H_3$ Co Xo	Xo $C_6S_2H_3$ Co	Xo Kc $C_6S_2H_3$(tr)
250°		Co $C_6S_2H_3$ Kc Ka	Co $C_6S_2H_3$ Kc Ka	Co $C_6S_2H_3$ Kc Ka	Co $C_6S_2H_3$ Kc Ka(tr)	Co $C_6S_2H_3$ Kc Ka (tr)
150°	αC_2SH CH qtz					

(b) Ca:Si = 1.5 C_3S

		1 wk	2 wk	3 wk	4 wk	8 wk
400°		Wo Kc Xo	Wo Kc Xo	Wo Kc Xo	Wo Kc Xo	Wo Kc Wo
370°		Xo Ka Kc	Xo Ka Kc	Xo Ka Kc	Xo Ka Kc	Xo Kc Ka
350°		Xo Kc Ka	Kc Xo Ka	Kc Xo Ka	Kc Xo Ka	Kc Ka Xo
300°		Xo Kc Ka	Xo Kc Ka	Xo Kc Ka	Xo Kc Ka	Xo Kc Ka
250°		Kc Ka Xo $C_6S_2H_3$(tr)	Kc Xo Ka $C_6S_2H_3$(tr)	Kc Ka Xo	Kc Ka Xo	Kc Ka Xo
150°	αC_2SH qtz Kc, Ka } tr					

(c) Ca:Si = 1.0 C_3S

		1 wk	2 wk	3 wk	4 wk	8 wk
400°		Xo qtz Wo	Xo qtz Wo	Xo qtz Wo	Xo qtz Wo	Xo qtz Wo
370°		Xo	Xo	Xo	Xo	Xo
350°		Xo	Xo	Xo	Xo	Xo
300°		Xo	Xo	Xo	Xo	Xo
250°		Xo	Xo	Xo	Xo	Xo
150°	Tob qtz					

(d) Ca:Si = 0.5 C_3S

		1 wk	2 wk	3 wk	4 wk	8 wk
400°		C_4S_2H Xo qtz	qtz C_4S_2H Xo	qtz C_4S_2H Xo	qtz C_4S_2H Xo	qtz C_4S_2H Xo
370°		Xo qtz C_4S_2H	Xo qtz C_4S_2H	Xo qtz C_4S_2H	qtz Xo C_4S_2H	qtz Xo C_4S_2H
350°		qtz Xo C_4S_2H	qtz Xo C_4S_2H	Xo qtz C_4S_2H	qtz Xo C_4S_2H	
300°		qtz Xo C_4S_2H	qtz Xo C_4S_2H	qtz Xo C_4S_2H	qtz Xo C_4S_2H	
250°		qtz C_4S_2H Xo	qtz C_4S_2H Xo	qtz C_4S_2H Xo	qtz C_4S_2H Xo	qtz C_4S_2H Xo
150°	Tob qtz Xo					

(e) Ca:Si = 1.5 βC_2S

		1 wk	2 wk	3 wk	4 wk	8 wk
400°		Xo Kc Wo	Xo Kc Wo	Xo Kc Wo	Xo Kc Wo	Xo Kc Wo
370°		Kc Xo Ka	Kc Xo Ka	Kc Xo Ka	Kc Xo Ka(tr) Wo(tr)	Xo Kc Ka(tr) Wo(tr)
350°		Kc Xo Ka	Kc Xo Ka	Kc Xo Ka	Kc Xo Ka	Kc Xo Ka
300°		Kc Xo Co(tr)	Kc Xo Co(tr)	Kc Xo Ka	Kc Xo Ka	Kc Xo Ka
250°		Co Kc Ka Xo(tr)	Co Kc Ka Xo(tr)	Kc Co Ka Xo(tr)	Kc Ka Co Xo(tr)	Kc Xo Co Ka
150°	αC_2SH qtz					

(f) Ca:Si = 1.0 βC_2S

		1 wk	2 wk	3 wk	4 wk	8 wk
400°		Xo	Xo Wo	Xo Wo	Xo Wo	Xo Wo
370°		Xo	Xo	Xo	Xo	Xo
350°		Xo	Xo	Xo	Xo	Xo
300°		Xo	Xo	Xo	Xo	Xo
250°		Xo	Xo	Xo	Xo	Xo
150°	αC_2SH qtz					

Table 1 (Continued)

(g) Ca:Si = 0.5 βC_2S

		1 wk	2 wk	3 wk	4 wk	8 wk
400°		C_4S_5H Xo qtz	C_4S_5H Xo qtz	C_4S_5H Xo qtz	C_4S_5H Xo qtz	C_4S_5H Xo qtz
370°		C_4S_5H Xo qtz	C_4S_5H Xo qtz	C_4S_5H Xo qtz	C_4S_5H Xo qtz	C_4S_5H Xo qtz
350°		Xo C_4S_5H qtz	Xo C_4S_5H qtz	C_4S_5H Xo qtz	C_4S_5H Xo qtz	C_4S_5H Xo qtz
300°		Xo C_4S_5H qtz	Xo C_4S_5H qtz	Xo C_4S_5H qtz	Xo C_4S_5H qtz	C_4S_5H Xo qtz
250°		Xo C_4S_5H qtz Tr(t)	Xo C_4S_5H qtz Tr(t)	Xo C_4S_5H qtz Tr(t)	Xo C_4S_5H qtz Tr(t)	Xo C_4S_5H qtz
150°	To Tr qtz					

Key:
Wo wollastonite
Xo xonotlite
Ka killalaite
Kc kilchoanite
Co calciochondrodite
qtz quartz

Calciochondrodite, $C_5S_2H_3$, and $C_6S_2H_3$ are normally associated with high Ca:Si ratio pastes and temperatures[5] and as expected, are the predominant phases formed initially from C_3S plus silica flour at Ca:Si ≥ 2.0 particularly at low temperatures. $C_6S_2H_3$ would appear to be the initial hydration product of C_3S between 250 and 350°C. It is not formed above 350°C. Calciochondrodite appears to be formed from $C_6S_2H_3$ and is metastable at 370°C. Calciochondrodite is also formed from βC_2S at Ca:Si ≥ 1.5 and could be the initial hydration product of βC_2S at this temperature since Gouda and Roy[10] also found it as the hydration product of βC_2S in their hot pressed pastes at 250°. It was not formed in samples from C_3S at this ratio. At 300°C, however only a trace of calciochondrodite is formed from βC_2S (Ca:Si = 1.5) with the major phases being xonotlite and kilchoanite and a trace of killalaite, more in line with the results of Kalousek and Nelson[11]. At this temperature calicochondrodite slowly reacts to form the lower ratio phases.

Apart from the changes associated with calciochondrodite, changes in phase compositions with time were minor reflecting changes in the initial concentration ratios rather than phase conversions. As the temperature of exposure was raised above 300°C the hydrated species in all mixes became less stable. $C_6S_2H_3$, calciochondrodite and killalaite became metastable with temperature, and xonotlite and kilchoanite predominated. C_4S_5H was only found when excess quartz was present.

For several formulations there were some significant differences between samples exposed at 370°C and those at 400°C, above the critical point of water. Perhaps the most noticeable change is for the Ca:Si = 1.5 sample prepared from C_3S. At 370°C, the phases formed were xonotlite, kilchoanite and metastable killalaite but at 400°C the major phase was wollastonite, βCS, with only minor amounts of xonotlite and kilchoanite formed. The intensities do not change over 8 weeks so that wollastonite must be formed originally from αC_2SH plus quartz rather than from xonotlite. From βC_2S at 370°C, kilchoanite rather than xonotlite was the stable phase with minor amounts of xonotlite and metastable killalaite. But at 400°C, xonotlite was the stable phase along with kilchoanite and a trace only of wollastonite.

Xonotlite has been reported previously as unstable in aqueous systems[8,12,13] although under dry conditions it is stable to over 700°C[14,15]. Xonotlite is stable for several formulations in this study including that from βC_2S at Ca:Si = 1.5 up to 400°C. Heating the reaction vessels usually took up to 3 hours to stabilize at temperature suggesting that xonotlite formation from βC_2S may be slow whereas wollastonite formation from αC_2SH and quartz is relatively rapid. Xonotlite is the predominant phase formed from both βC_2S and C_3S at Ca:Si = 1.0 although at 400°C, both these samples contain some quartz and a trace of wollastonite in equilibria with xonotlite, neither of which was present at 370°C. This suggests that the formula for xonotlite C_6S_6H must allow for a variable concentration, a point made by Kalousek *et al*[14] and that an excess of Ca^{2+} ions are needed to maintain the stability at elevated temperature noted in this study.

The rate of heating of samples and starting materials may be critical in determining which phase is preferentially formed. Mitsuda and Taylor[16] and Mitsuda *et al.*[17] reported that formation of kilchoanite is favoured by rapid heating while xonotlite formation is very dependent on the starting materials. Once formed, both phases appear resistant to transformations to other phases.

It does appear that the only hydrates stable above the critical point are those that are silica rich ie, xonotlite, C_6S_6H and C_4S_5H. While high Ca:Si ratio phases have proved chemically durable at Ohaaki[1,2], their use in higher temperature fields must be considered unsuitable since calciochondrodite, the main although weak binder, and $C_6S_2H_3$ are unstable forming xonotlite and kilchoanite which appear stable in this work.

However, both these have been reported as unstable in aqueous systems, xonotlite by Roy and co-workers[12,13] and kilchoanite by Mitsuda and Fukuo[18]. Wollastonite and C_4S_5H, found in this study have not been considered as potential binding systems and further studies are needed before they can be considered suitable and kilchoanite is not normally considered suitable as a binder[7]. It is clear that further field exposure is needed before a cementing system can be formulated for durability in a geothermal field that is fluid dominated in the region 300-400°C.

CONCLUSIONS

In pastes prepared from calcium silicates and silica flour, only the silica-rich hydrates xonotlite and C_4S_5H, appear stable at temperatures close to the critical point of water. Above the critical point the only stable phases appear to be the anhydrous phases with low Ca:Si ratios, such as wollastonite and kilchoanite although in this study xonotlite and C_4S_5H remained stable for eight weeks.

The phases formed initially depend on the starting materials, and it would seem the rate of heating. Results available are not sufficient to predict which cementing formulation will be stable in geothermal fluids with temperatures close to the critical point of water.

REFERENCES

1 Milestone, N.B., St. John, D.A., Abbot, J.H. and Aldridge, L.P.: "CO_2 Corrosion of Geothermal Cement Grouts", *8th Int. Cong. Chem. Cements.*, Rio de Janeiro, Sept 1986, V 141-144 (1986).

2 Milestone, N.B. and Aldridge, L.P.: "Corrosion of Cement Grouts in Aggressive Geothermal Fluids" *Trans. Geoth. Res. Council*, 14(I), 423-429 (1990).

3 Nelson, E.B.: "Prevention of Strength Retrogression in High Temperature Well Cements", *Proc. SW Pet. Short Course*, Lubbock, Texas (1980).

4 St. John and Abbot, J.H.: "The Microscopic Textures of Geothermal Cement Grouts Exposed to Steam Temperatures of 150°C and 300°C". *Proc 9th Int. Conf. Cement Microscopy.* Reno NV, (1987), 280-300.

5 Milestone, N.B., Sugama, T., Kukacka, L.E. and Carciello, N.: "Carbonation of Geothermal Grouts - Pt. 2: CO_2 Attack at 250°C", *Cement Concr. Res.*, 17 (1), 37-46, 1987.

6 Milestone, N.B.: unpublished results.

7 Nelson, E.B., Eilers, L.H. and Kalousek, G.L.: "Formation and Behaviour of Calcium Silicate Hydrates in a Geothermal Environment", *Cement Concr. Res.*, 11, 371-381 (1981).

8 Luke, K., Taylor, H.F.W. and Kalousek, G.L.: "Some Factors Affecting Formation of Truscottite and Xonotlite at 300-350°C", *Cement Concr. Res.*, 11 (1), 197-203.

9 Gallus, J.P., Pyle, D.E. and Moran, L.K.: "Physical and Chemical Properties of Cement Exposed to Geothermal Dry Steam", SPE Paper 7876 presented at 1979 AIME 4th Symposium. Oilfield and Geothermal Chemistry, Houston, Jan. 1979.

10 Gouda, G.R., and Roy, D.M.: "Characterization of Hot Pressed Cement Pastes", *J. Am. Ceram. Soc.*, 59 (9-10), 412-414 (1976).

11 Kalousek, G.L. and Nelson, E.B.: "Hydrothermal Reactions of Dicalcium Silicate and Silica", *Cement Concr. Res.*, 8, 283-290 (1978).

12 Langton, C.A., White, E.L., Grutzeck, M.W. and Roy, D.M.: "High Temperature Cements with Geothermal Applications", *Proc 7th Int. Congr. Chem. Cement*, Paris 1980, V145 (1980).

13 Buckner, D.A., Roy, D.M. and Roy, R.: "Studies in the System CaO-Al_2O_3-SiO_2-H_2O, II The System $CaSiO_3$-H_2O", *Amer. J. Sci.*, 258, 132 91960).

14 Kalousek, G.L., Mitsuda, T. and Taylor, H.F.W.: "Xonotlite: Cell Parameters, Thermogravimetry and Analytical Electron Microscopy", *Cement Concr. Res.*, 7, 305-312.

15 Dent, L.S. and Taylor, H.F.W.: "The Dehydration of Xonotlite", *Acta Cryst*, 9, 1002 (1956).

16 Mitsuda, T. and Taylor, H.F.W.: "Influence of Heating Rate on the Hydrothermal Formation of Kilchoanite from Lime-Quartz Mixtures", *J. Appl. Chem. Biotechnol.*, 24, 447-451 (1974).

17 Mitsuda, T., Saito, J. and Hattori, E.: "Influence of Starting Materials on the Hydrothermal Formation of Xonotlite at 180°C", *Proc. 1st Symp., Hydrothermal Reactions*, (1982), 823-38.

18 T Mitsuda and K Fukuo, "Synthesis of Kilchoanite", *Min. Jour.*, 6 (1-7), 17-35 (1969).

INHIBITION OF AUTOCLAVE REACTION OF CEMENT-QUARTZ MORTARS BY PROLONGED AIR PRECURING

E R Cantrill*, M G Stevens* and L P Aldridge**

*Department of Materials Science, University of Technology, Sydney, NSW, AUSTRALIA
**Australian Nuclear Science & Technology Organization, NSW, AUSTRALIA

ABSTRACT

Commercial high pressure steam cured (autoclaved) fibre reinforced cement-quartz composite building products were made in Australia during 1957-1985 using asbestos fibres as reinforcement. Since 1982 cellulose has successfully replaced asbestos which has been condemned as a health hazard.

In this study, the hydration of cement/quartz, cement/quartz and proprietary additives was monitored after extended air curing prior to autoclaving at 177°C for eight hours, these conditions being chosen as representing commercial manufacturing conditions. The formation of tobermorite, dicalcium silicate α-hydrate, and portlandite was monitored by DTA instrumentation.

It was found that significant differences in the resulting compositions occurred after saturating with water and reautoclaving for another eight hours, the hydration products underlining the importance of correct precuring.

Preliminary studies are being carried out on the bonding of the cellulose to the cementitious material using theoretical models.

INTRODUCTION

Kalousek & Adams (1951) extended the work of Menzel (1934) on the physical properties of autoclaved cement-quartz mortars of differing ratios and were able to give an interpretation of Menzel's physical results based on the composition of the phases. They showed that the high strengths, obtained with optimum additions of fine quartz, were associated with the formation of 11Å tobermorite/CSH-I, and that the low strengths obtained with lower additions of quartz, were associated with the formation of C_2S α-hydrate.

Their autoclaving temperature was 177°C (350°F) for a curing time of 24 hours and their quartz contents ranged from 0% to 60%. In this report the specimens were autoclaved 8 hours at 177°C for quartz contents of 0 to 80%.

EXPERIMENTAL

The specimens were manufactured using a constant water/(cement* + quartz† + AB‡) ratio of 0.36, AB addition being either 0 or 4%, then exposed to a normal atmosphere containing carbon dioxide at ambient temperatures during overnight curing (16 hours) prior to eight hours autoclaving at 177°C. The intention was to simulate factory conditions of precuring . After sampling for analysis, the remainder of the specimens were immersed in water for two days, then autoclaved for a second eight hours at 177°C ("reautoclaved"), resampled and reanalyzed.

Changes in the reactions were measured from the thermographs by monitoring the peak <u>heights</u> of the four main phases, i.e., portlandite [$Ca(OH)_2$] (endotherm 475-485°C), dicalcium silicate α-hydrate [C_2S α-H] (endotherm 450°C), "CSH-I", and "CSH-II". "CSH-I" and "CSH-II" are tobermorite minerals labelled "CSH-I" if the exotherm appears about 870°C .or "CSH-II" if the exotherms occur about 925°C.

---

* Type I OPC, BCS Cement, Berrima, NSW. SA = 330 m^2/g

† Ground Quartzite, ex Ballarat, Vic. SA = 350 m^2/g

‡ AB is a proprietary argillaceous admixture patented by the Building Boards Division of James Hardie Industries Ltd., Australia.

Various cement/quartz (C/S) ratios were investigated, from 100/00 to 20/80 at 4% intervals.

DTA analyses were conducted on a Rigaku 8008 HT apparatus using a microhead sample holder. Heating rate was 10°C/min. Sample weights varied from 75 to 90mg. Temperatures were measured at the base of the pans. The reference material was a calcined 1:1 mixture of corundum and kaolinite.

RESULTS AND DISCUSSION

The DTA results are similar to those of Kalousek & Adams (1951). With increasing addition of silica (quartz), the portlandite content diminishes while that of C_2S α-H first rises then falls, though both persist as a weak double endotherm up to C/S = 72/28. "CSH-II" rises as a single exotherm up to C/S = 72/28 after which the "CSH-I" exotherm appears beside it. Both species persist up to C/S = 60/40, the "CSH-I" exotherm increasing in relation to the "CSH-II" peak with increasing quartz addition, and with decreasing peak temperatures; in both cases on reautoclaving. After C/S = 60/40, the "CSH-I" exotherm decreases in height as this phase becomes increasingly diluted with unreacted quartz.

Typical thermographs are shown in Fig. 1. The double exotherm 870-900°C in Fig. 1b was observed in portlandite-silica mixtures by Kalousek (1969).

Some unusual minor endotherms were observed at the higher C/S ratios, with peaks at 310, 410, and 530°C. That at 410°C appeared at C/S = 92/08 and disappeared at C/S = 72/28. The first two endotherms persisted at a heating rate of 3°C/min, but the 530°C endotherm did not.

Reautoclaving results in more portlandite being produced for the calcium-rich mixtures [see Fig. 2a]. However as the amount of calcium decreases the proportion of portlandite decreases faster in the reautoclaved samples.

Separate experiments carried out with little curing prior to autoclaving show far greater amounts of portlandite. It appears that prolonged air curing inhibits the formation of

FIG 1: TYPICAL THERMOGRAPHS

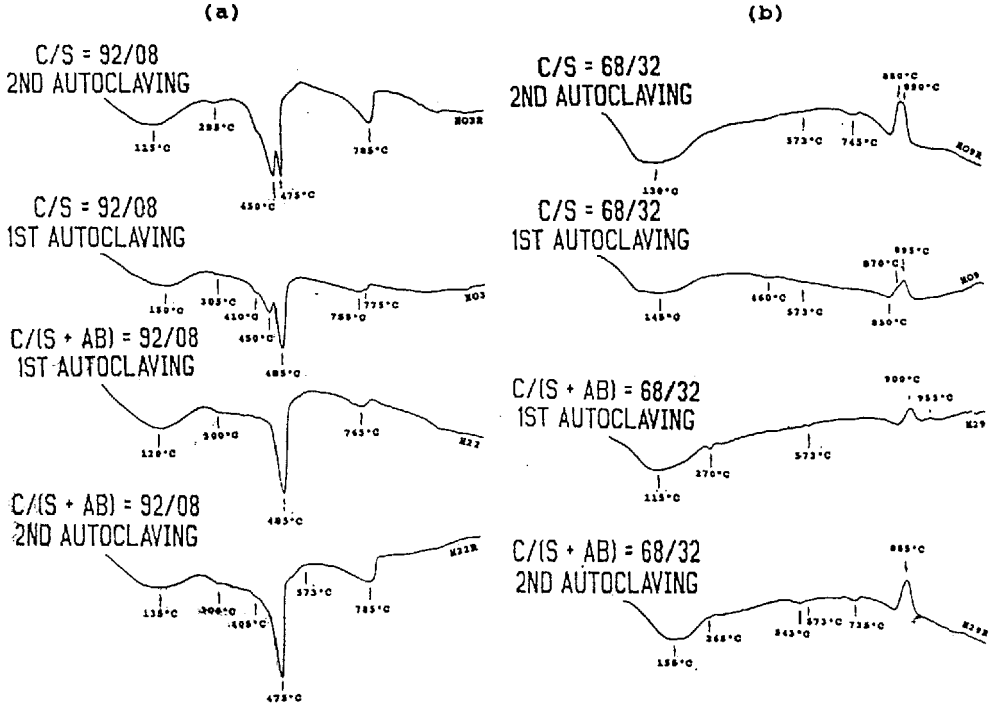

FIG 2: DTA PEAK HEIGHTS vs CEMENT/SILICA RATIO

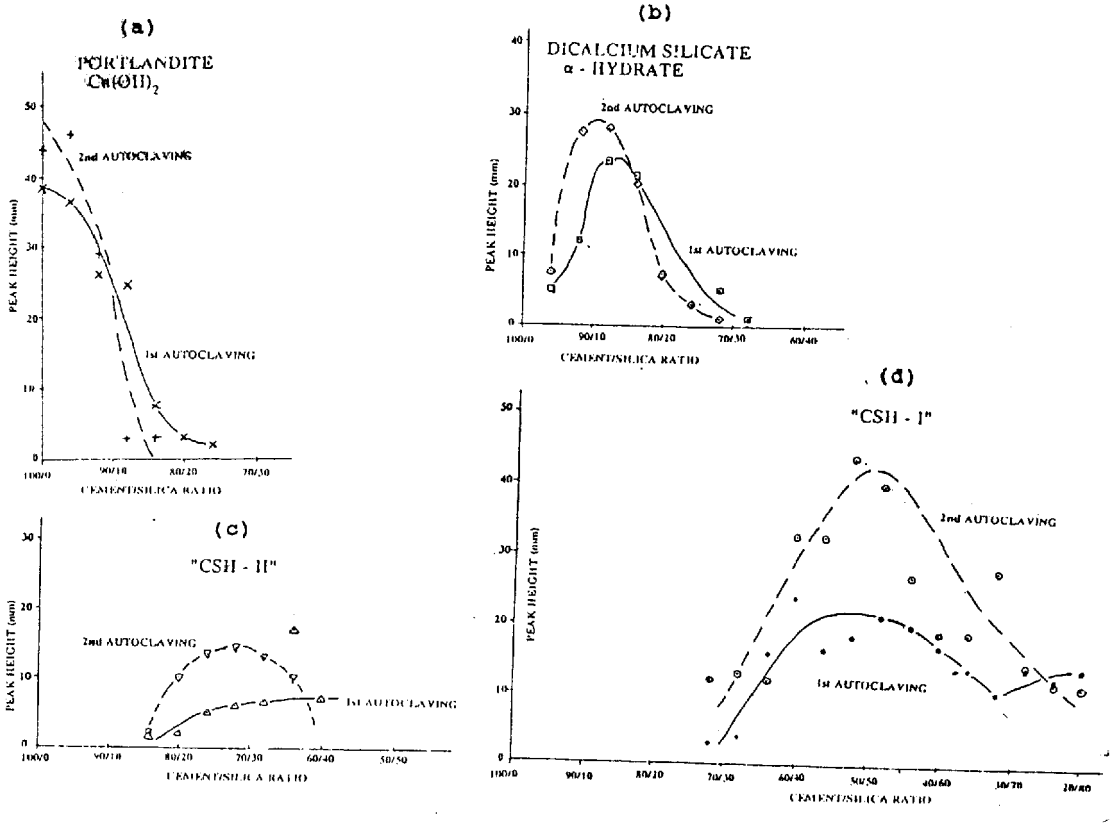

portlandite.

Reautoclaving increases the amounts of C_2S α-H [Fig. 2b] formed and also increases its formation for calcium rich mixtures.

The "CSH-I" and "CSH-II" contents are increased on reautoclaving but the behaviour of "CSH-II" is different.

The "CSH-II" phase [Fig. 2c] is at a maximum co.centration at C/S = 60/40. Reautoclaving causes more of this phase to be produced with a fairly broad and symmetrical rise and fall about the C/S ratio 70/30.

The "CSH-I" [Fig. 2d] has similar maxima about C/S = 50/50 irrespective of autoclaving cycles. The results of the first autoclaving show considerable scatter and the difference between the two autoclaving cycles may be due more to the degree of crystallinity than to the degree of reaction.

From these results it is easy to predict that a second autoclave cycle would give better properties of the cellulose cements. However in practice it is found that a second autoclave cycle breaks down. the cellulose producing a more brittle, inferior product.

In order to understand the bonding of cementitious material to cellulose we have carried out various modelling calculations. All of these have, so far, been carried out using an extended Hückel (1931, 1935) approximation on the bonding between glucose (which represents the cellulose sheets) and portlandite which we have taken to represent cementitious materials. The bonding between the model compounds will be very similar to those taking place between cellulose and the cementitious materials found in autoclaved cement. All of the bonds modelled are, of course, of the hydrogen bonds type. We will report on this work and the work being carried out on the thermal analysis of autoclaved cement/cellulose and cement/asbestos samples in a subsequent paper.

CONCLUSION

From an essentially superficial investigation by DTA, prolonged air curing appears to inhibit the initial autoclave reaction for high C/S ratios due to the limited amount of water available for the initial hydration of the cement. The inhibition of the initial autoclave reaction for C/S ratios >60/40 appears to be in the conversion of "CSH-II" to "CSH-I".

REFERENCES

Hückel E (1931)
Z. Phys. **70** 204

Hückel E (1935)
Int. Conf. Physical Soc. Vol 2 p9

Kalousek G L (1957)
J. Am. Ceram. Soc. **40** 74

Kalousek G L (1969)
Proc. 5th Int. Conf. Chem. Cement, London (1968)
Vol. 3, p523

Kalousek G L; Adams M (1951)
J. Am. Concr. Inst. **48** 77

Menzel C A (1934)
J. Amer. Concr. Inst. **31** 125

THERMAL BEHAVIOUR OF SYNTHESIZED C-S-H

S Ito, T Nishikawa, Y Ito and K Suzuki

Department of Material Science and Engineering, Nagoya Institute of Technology
Gokiso-cho, Showa-ku, Nagoya, JAPAN

SUMMARY

The C-S-H powders with various Ca/Si molar ratios were synthesized by solution method using different mixing techniques. Their characters and thermal behavior were examined by X-ray diffraction, thermal analysis and surface area determination.

Ultrasonic wave mixing was useful for the preparation of C-S-H powder having a uniform composition and a high specific surface area compared with that by stirrer mixing. With increasing Ca/Si ratios, the specific surface area of C-S-H powder and the water mostly discharged up to 300°C decreased. At about 300°C, a discontinuous drop was found by X-ray diffraction on the d-spacing change with temperature, but was not clearly by thermal analysis. From the apparent activation energies for the dehydration of C-S-H, the thermal stability of this water is seemed to be related to the molar ratio of Ca ion and the surface condition of appropriate C-S-H.

For discussing the sintering character, the synthesized C-S-H powders with various Ca/Si ratios were compressed into pellets and then heated at prescribed temperatures up to 800°C. The sintered C-S-H bodies with high ratios were more dense and had a higher hardness than those with lower ratios.

種々のＣａ／Ｓｉ比のＣ－Ｓ－Ｈ粉末を溶液法により混合操作を換えて合成し、その粉末のキャラクターと熱的挙動を調べた。

超音波混合はスターラー攪拌に比べて、組成の均一性と高い比表面積を持つＣ－Ｓ－Ｈ粉末を合成するのに適している。Ｃ－Ｓ－Ｈ中のＣａ／Ｓｉ比が増加すると、粉末の比表面積と３００℃までに放出される水分は減少した。約３００℃で、格子面間隔の急激な変化がみられたが、これに伴う熱変化は認められなかった。Ｃ－Ｓ－Ｈ中の水の熱的安定性は、脱水のみかけの活性化エネルギーからＣａイオンのモル比と表面の状態に関係すると考えられた。

合成Ｃ－Ｓ－Ｈ粉末の焼結性について８００℃まで調べられ、そのＣａ／Ｓｉ比が高いほど、焼結体の密度と硬度が高くなる傾向がみられた。

INTRODUCTION

Calcium silicate hydrate (C-S-H) is a chief cementing and hardening material, exhibits an ill-crystalline state, in the hydrates of portland cement and other lime-silica systems. Numerous studies have been made on its composition, morphology, structure and thermal behavior (1)(2). We already investigated the carbonation and the effects of alkaline-ions on the formation of C-S-H relevance to the hydration of cement, using the synthesized specimens by solution method (3)(4). In this synthesis, the mixing operation plays an important part as well as starting solutions. Ultrasonic wave effects on the chemical reactions and make homogenous products. Concerning the dry shrinkage or the deterioration of cement materials, thermal and chemical stabilities of water in hydrates are important.

In this work, the C-S-H powders with various Ca/Si molar ratios were synthesized by solution method at room temperature, using two different mixing techniques. Chemical analysis, BET, DTA-TG and XRD were carried to characterize the formed C-S-H powder. Some data for thermal stability and physical properties of their compressed bodies are presented.

EXPERIMENTAL

Preparation

The $(C_2H_5O)_4Si$ solution (about 0.444 M) was added into $Ca(OH)_2$ aqueous solution (about 0.01 M), until the solution had prescribed Ca/Si molar ratios. The hydrolysis was processed by ultrasonic wave (39 kHz) or magnetic stirrer mixing (150-200 rpm) under the isolated condition from CO_2. The solution was filtered and the precipitate was dried in a vacuum under 2 mmHg at room temperature. The composition (Ca/Si ratio) of precipitate was calculated from the ionic concentrations in solutions before and after the preparations (3).

The synthesized C-S-H powder was compressed into pellets and then heated at prescribed temperatures up to 800°C for 4 hours. The bulk density and hardness of these sintered bodies were measured.

RESULTS AND DISCUSSION

Formation of C-S-H

By using ultrasonic wave mixing, the gelation time on the C-S-H formation was within 2 hours compared with more than 30 hours by magnetic stirrer mixing. From the chemical analyses for the solutions before and after reaction, the Ca/Si ratios of precipitates were estimated. Products were examined by XRD and DTA-TG methods, and C-S-H was identified as a monolithic phase.

For the preparations at 0.2, 0.8 and 1.5 ratios, the formed C-S-H had those of 0.2, 0.7 and 0.9 respectively. The accuracy of these ratios was

limited with that of chemical analyses and seemed to be ± 0.05.

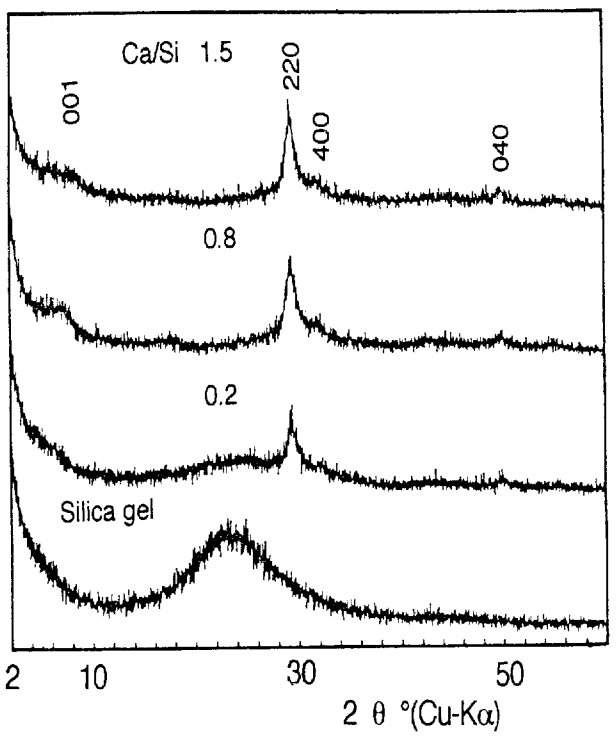

Fig.1. X-ray diffraction patterns of C-S-H and silica gel.

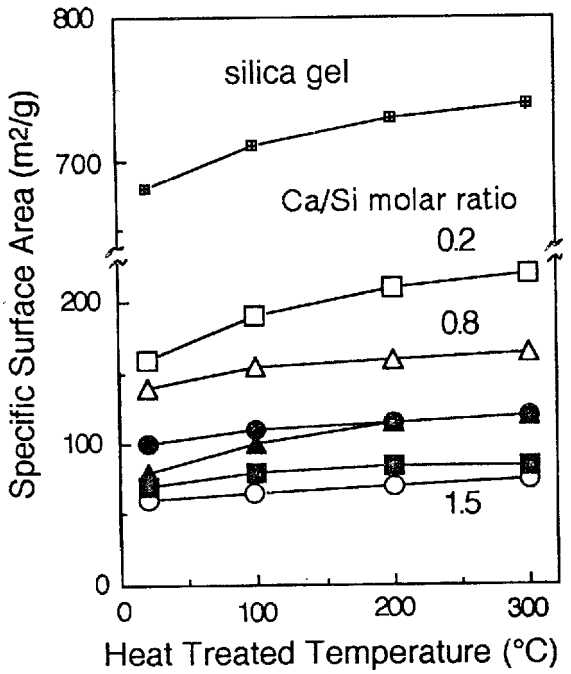

Fig.2. Specific surface area of C-S-H and silica gel.

Fig.1 shows the X-ray diffraction patterns for the C-S-H and silica gel synthesized by ultrasonic wave mixing and dried in a vacuum at room temperature. All C-S-H specimens gave substantially the same patterns as C-S-H (I) reported by various workers (1)(2). However, except for 220 line, 001 as a basal spacing and other lines were very weak, frequently not clearly. For the preparation at 0.2 ratio, an additional broad band of silica gel appeared, but was very weak compared with that made by stirrer mixing.

Specific Surface Area

Fig.2 gives the specific surface area of C-S-H and silica gel powder heat treated at prescribed temperatures in a vacuum. The values for the C-S-H formed at Ca/Si ratio of 0.2 were larger than those at higher ratios, and increased with heating temperature. These values were comparable with data for the hydrothermally formed C-S-H reported by T.Mitsuda et al (2). Silica gel had the surface area over twice as large as every C-S-H. Results from XRD and surface area determination suggest that the C-S-H specimens obtained in this work, even at 0.2 ratio, differ from silica gel in their structure, surface condition and composition.

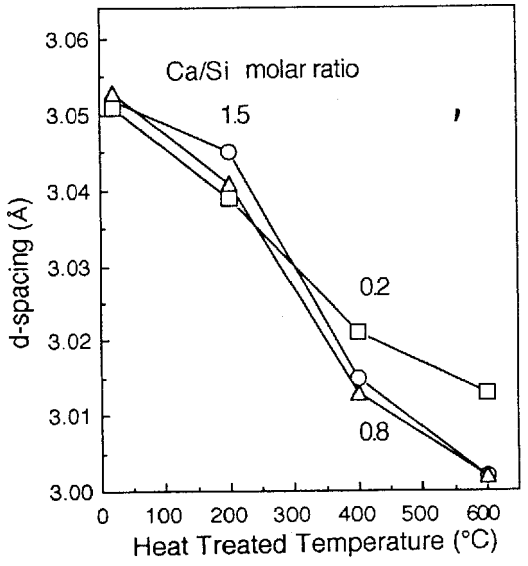

Fig.3. Changes on d-spacing of 220 line with temperature.

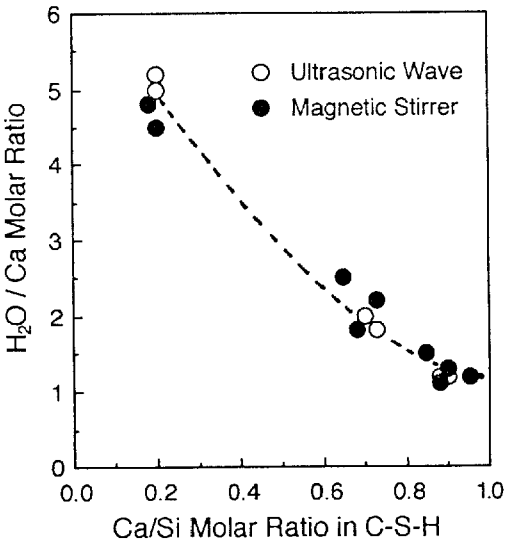

Fig.4. Water content of C-S-H with various Ca/Si ratios.

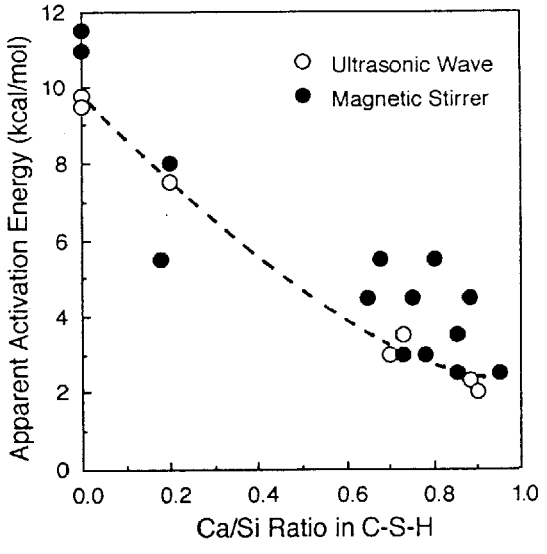

Fig.5. Apparent activation energy for dehydration of C-S-H with various Ca/Si ratios and silica gel.

Water in C-S-H

The water contained in C-S-H changes with preserving conditions as a temperature and a humidity, but about 70% of its amount released rapidly up to 300°C by heating. At this temperature as shown in Fig.3, a discontinuous drop was found on the d-spacing change of 220 line with heat treated temperature by XRD, but was not clearly on the DTA-TG curve. We measured the amount of water discharged up to 300°C by TG method and results are plotted in Fig.4 as H_2O/Ca versus Ca/Si molar ratios determined for the appropriate C-S-H. This ratio decreased from about 5.2 to 1.2 with increasing Ca/Si ratio.

Moreover, the apparent activation energies were calculated from the following equation proposed by H.Monma et al (5);

$$d\ln(\emptyset/T_m^2)/d(1/T_m)=-E/R$$

where $\emptyset$ is a heating rate, Tm is a temperature with the maximum dehydration rate at each heating process measured by DTA-TG and DTG, R is a gas constant and E is an apparent activation energy, and plotted in Fig.5. From these results, the thermal stability of water released below 300°C is seemed to be related to the molar ratio of Ca ion and the surface condition (Fig.2) of appropriate C-S-H.

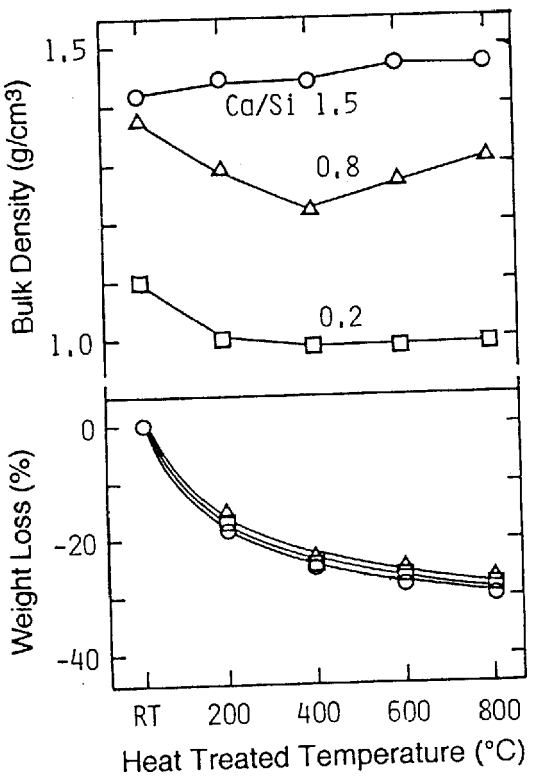

Fig.6. Changes on weight loss and bulk density of compressed C-S-H bodies with heat treated temperature.

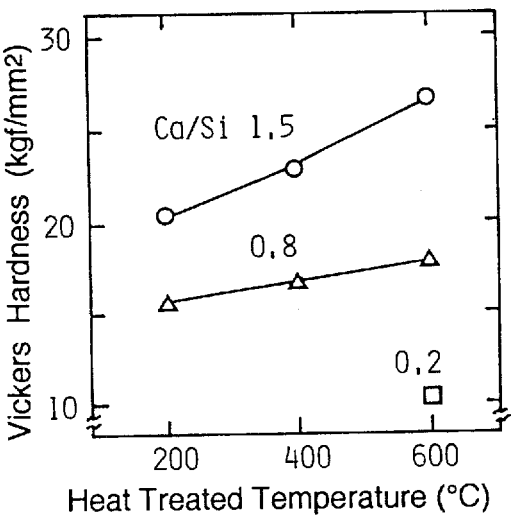

Fig.7. Vickers hardness of sintered C-S-H bodies.

Properties of Sintered Bodies

Fig.6 shows the weight loss and bulk density of compressed C-S-H pellets heated isothermally in atmospheric pressure. The values of weight loss for every C-S-H and at every temperature were the same within an accuracy of this measurement. However, bulk densities at 800°C increased from about 1.0 to 1.5 g/cm³ with increasing Ca/Si ratios. The Vickers hardness number also increased from 10 to 27 at 600°C. These values are comparable with data for graphite and molybdenite respectively (6). These

results indicate that the sintered C-S-H bodies with high Ca/Si ratios are more dense and have a higher hardness than those with lower ratios.

CONCLUSION

(1) Ultrasonic wave mixing shortened the gelation time and was useful for the preparation of C-S-H powder having a uniform composition and a high specific surface area.

(2) For the preparation at Ca/Si ratios of 0.2, 0.8 and 1.5, the composition of formed C-S-H was 0.2, 0.7 and 0.9 ratios respectively.

(3) With decreasing Ca/Si ratios, the surface area and the water of C-S-H, mostly discharged up to 300°C, increased. The apparent activation energy for dehydration of C-S-H increased depending on their H_2O/Ca ratios and surface condition of the appropriate C-S-H.

(4) The sintered C-S-H bodies with high Ca/Si ratios were more dense and had a higher hardness than those with lower ratios.

ACKNOWLEDGMENT

We wish to thank the Toyota Physical and Chemical Research Institute for the support of this work.

REFERENCES

1. Taylor, H.F.W. : **The Chemistry of Cements, vol.1,** Academic Press, 1964, p181-203 and: **Cement Chemistry**, ibid., 1990, p123-166.

2. Mitsuda,T. Kobayakawa,S. & Toraya,H. : "Characterization of Hydrothermally Formed C-S-H", 8th International Congress on the Chemistry of Cement, Riode Janeiro, 1986, Vol III, 173-178.

3. Suzuki,K. Nishikawa,T. & Ito,S.: "Formation and Carbonation of C-S-H in Water", Cement and Concrete Research, 1985, **15**(2), 213-224.

4. Suzuki,K. Nishikawa,T. Ikenaga,H. & Ito,S.: "Effect of NaCl or NaOH on the Formation of C-S-H", Cement and Concrete Research, 1986, **16**(3), 333-340.

5. Monma,H. & Ueno,S.: "Thermogravimetric Analysis of Hydroxyapatite Prepared by the Hydration of Tricalcium Phosphate", Gypsum & Lime, 1979, **159**, 53-58.

6. Weast,R.C. : **Handbook of Chemistry and Physics**, CRC Press Inc. 1986, B p206-207.

THERMODYNAMICS AND KINETICS IN THE SYSTEM $Ca_4(Al_6O_{12})(SO_4)-CaSO_4.2H_2O-H_2O$ UP TO 75°C

Jaromír Havlica* and Sadananda Sahu**

*Institute of Inorganic Chemistry, Slovak Academy of Sciences, Bratislava, CZECHOSLOVAKIA
**Slovak Technical University, Bratislava, CZECHOSLOVAKIA

SUMMARY

Thermodynamics and kinetics of hydration processes of the system $Ca_4(Al_6O_{12})(SO_4)$ - $CaSO_4.2H_2O$ - H_2O in the temperature range 20 to 75 °C were studied by differential calorimetry. Increase in temperature by external heating accelerates all reactions in the initial period. Experiments demonstrate improvement of transport properties in the systems studied and acceleration of the hydration processes. Results enabled estimation of standard enthalpy ΔH° of formation of sulphoaluminate phase $Ca_4(Al_6O_{12})(SO_4)$ in the temperature range studied. The value obtained for standard enthalpy of reaction was used for quantitative evaluation of phase development in the hydrated system.

SUMARIO

Fue estudiada la termodinámica y la cinética del proceso de hidratación del sistema $Ca_4(Al_6O_{12})(SO_4)$ - $CaSO_4.2H_2O$ - H_2O en un rango de temperatura entre 20 y 75 °C, mediante calorimetría diferencial. El aumento de temperatura debido al calentamiento externo acelera todas las reacciones en el período inicial. Los experimentos demostraron el mejoramiento de las propiedades de transporte de los sistemas estudiados, y una aceleración en el proceso de hidratación. Los resultados permitieron la estimación de la entalpa standard ΔH° de formación de la fase de sulfoaminoato $Ca_4(Al_6O_{12})(SO_4)$ en el rango de temperatura estudiado. El valor obtenido de entalpa standard de reacción fue empleada en la evaluación cuantitativa del desarrollo de fase en el sistema hidratado.

INTRODUCTION

Sulphoaluminate phase $Ca_4(Al_6O_{12})(SO_4)$ reacts in the presence of water according to scheme (1) to form ettringite

$$Ca_4(Al_6O_{12})(SO_4) + 8\ CaSO_4 + 6\ CaO + 96\ H_2O \longrightarrow 3\ Ca_6(Al_2O_3)(SO_4)_3.32H_2O \quad (1)$$

which is responsible for the expansive properties of type-K expansive cement. Substitution of tricalcium silicate in portland cement by sulphoaluminate phase and creation of sulphoaluminate belite cement [1] evokes some questions concerning the influence of temperature and initial phase composition on the stability of the hydrated products. Presence of Al^{3+} ions in the sulphoaluminate phase $Ca_4(Al_6O_{12})(SO_4)$ or in calcium sulphoaluminate hydrates : ettringite $Ca_6(Al_2O_3)(SO_4)_3.32H_2O$ and monosulphate $Ca_4(Al_2O_3)(SO_4).12H_2O$ influences the stability of these phases depending on the p*H* value of the system. The p*H* values for ettringite (p*H*<10.7) and monosulphate (p*H*<11.6) to dissappear were established in our work [2]. It was proposed, that the p*H* value determines the behaviour of the hydrating system across the solid-liquid interphase. Attempts at solving this problem by the hypothesis about liquid interlayer near the surface of sulphoaluminate grains is under report [3]. Actual values of p*H* on the surface of the $Ca_4(Al_6O_{12})(SO_4)$, as well as the thermodynamic data of its formation are still not known. On the other hand, the thermodynamic stability of the main products of hydration,

$$Ca_4(Al_6O_{12})(SO_4) + 18H_2O \longrightarrow Ca_4(Al_2O_6)(SO_4).12H_2O + 4Al(OH)_3 \quad (2)$$

$$Ca_4(Al_6O_{12})(SO_4)+2CaSO_4.2H_2O+34H_2O \longrightarrow Ca_6(Al_2O_6)(SO_4)_3.32H_2O+4Al(OH)_3 \quad (3)$$

ettringite and monosulphate was analysed in papers [4-6]. The authors calculated thermodynamic values (ΔH°, ΔS° and ΔG°) from the results of measurements by differential hydrothermal analysis (DHA) which was described in detail earlier [4]. The equilibrium temperature (450 K) determined for the hydrothermal conditions of the reaction,

$$Ca_4(Al_2O_6)(SO_4).12H_2O \longrightarrow Ca_3(Al_2O_6).6H_2O + CaSO_4.0.5H_2O + 6H_2O \quad (4)$$

was used for calculating the values of standard enthalpy ΔH°, standard entropy ΔS° and standard Gibbs energy ΔG° for this reaction (4). The same approach was applied to calculate the thermodynamic data of high sulphate phase ettringite by measurement of the equilibrium temperature of the reaction

$Ca_6(Al_2O_6)(SO_4)_3.32H_2O \rightarrow Ca_4(Al_2O_6)(SO_4).12H_2O + 2\ CaSO_4.1/2H_2O + 19\ H_2O$ (5)

The aim of this work is measurement of the heat of hydration of sulphoaluminate phase and its mixtures with gypsum at various temperatures between 20 and 75 °C and estimation of the thermodynamic data (ΔH°, ΔS° and ΔG°) of formation of sulphoaluminate phase at 298 K.

EXPERIMENTAL

$Ca_4(Al_6O_{12})(SO_4)$ was synthesized by ignition of mixtures of aluminium and calcium nitrates with gypsum by the procedure already reported [7]. The powder thus obtained and containing particles smaller then 63 μm were mixed with gypsum in $Ca_4(Al_6O_{12})(SO_4)$: $CaSO_4.2H_2O$ molar ratios 1 and 2

$$r = \frac{x_{C\bar{S}H_2}}{x_{C_4A_3\bar{S}}} \qquad (6)$$

Where C-CaO, A-Al_2O_3, $\bar{S}$-SO_3, and H-H_2O. The purity of the prepared phases and the composition of the hydrated products were checked by X-ray diffraction analysis. Calorimetric experiments were performed on a differential calorimeter ZIAC [8,9] at 20, 40, 50 and 75 °C keeping water to solid ratio one (w/s=1).

RESULTS AND DISCUSSION

Results of X-ray diffraction phase analysis obtained on products of reactions (1) and (2) given in Table 1 show the presence of monosulphate in systems with lower gypsum content. Hydration of mixtures with $Ca_4(Al_6O_{12})(SO_4)$: $CaSO_4.2H_2O$ ratios equal to or higher than 1 produces ettringite as a stable phase. Increasing the temperature accelerates the hydration process, and the presence of original sulphoaluminate phase was detected only at 20 °C.

As the temperature of the system approaches to 75 °C the dQ/dT value tends to zero. This shows that the system is achieving the equilibrium condition. So we can consider the degree of conversion α at 75 °C is equal to 1. The dependence of ΔC_p was neglected and in converting the ΔH_r° values to the temperature of 298 K, and standard enthalpies of reaction were assessed considering the following relation:

$$\alpha \xrightarrow{\lim} 1 \; Q_{hydr.} = -\Delta H_r^\circ \qquad (7)$$

The values of heat of hydration obtained were used for evaluating the degree of conversion as follows:

$$\alpha = - \frac{Q_{hydr,i}}{\Delta H_{r,i}} \qquad (8)$$

TABLE 1

Hydration products of mixtures in the temperature range 20 and 75 °C and values of heat liberated after 72 h

System	Temp. °C	Phases present in product	Heat liberated after 72 h kJ/mole of $C_4A_3\bar{S}$
$C_4A_3\bar{S}$	20	$C_4A\bar{S}H_{12}$, AH_3, $C_4A_3\bar{S}$	150.8
	40	$C_4A\bar{S}H_{12}$, AH_3	199.0
	50	$C_4A\bar{S}H_{12}$, AH_3	210.2
	75	$C_4A\bar{S}H_{12}$, AH_3	219.7
$C_4A_3\bar{S}$ + $C\bar{S}H_2$	20	$C_4A\bar{S}H_{12}$, AH_3, $C_6A\bar{S}_3H_{32}$, $C_4A_3\bar{S}$, $C\bar{S}H_2$	272.3
	40	$C_4A\bar{S}H_{12}$, AH_3, $C_6A\bar{S}_3H_{32}$	290.1
	50	$C_4A\bar{S}H_{12}$, AH_3, $C_6A\bar{S}_3H_{32}$	310.0
	75	$C_4A\bar{S}H_{12}$, AH_3, $C_6A\bar{S}_3H_{32}$	320.2
$C_4A_3\bar{S}$ + 2 $C\bar{S}H_2$	20	$C_6A\bar{S}_3H_{32}$, AH_3, $C_4A_3\bar{S}$, $C\bar{S}H_2$	326.5
	40	$C_6A\bar{S}_3H_{32}$, AH_3	365.8
	50	$C_6A\bar{S}_3H_{32}$, AH_3	410.3
	75	$C_6A\bar{S}_3H_{32}$, AH_3	420.7

TABLE 2

Values of α at various temperatures and molar ratios of gypsum to sulphoaluminate phase

r	$\Delta H^o_{r,i}$ kJ/mole	20 °C	40 °C	50 °C	75 °C
0	- 219.7	0.68	0.91	0.96	1.00
1	- 320.2	0.85	0.91	0.97	1.00
2	- 420.7	0.78	0.89	0.99	1.00

Results in Table 2 show the proportionality between temperature and the efficiency of hydration. The rate of hydration was highest in system with a molar ratio of gypsum to sulphoaluminate phase, r=1. The values of standard enthalpy of formation of $Ca_4(Al_6O_{12})(SO_4)$ at temperature 75 °C, ΔH_f^o were evaluated for various ratios of gypsum to sulphoaluminate phase. These calculations were performed by using values of standard enthalpy ΔH_f^o of gypsum, water and aluminium hydroxide from the tables reported earlier [10,11] and the results of measurement of standard enthalpy of formation of ettringite and monosulphate from an earlier study [3]. The results obtained are shown in Table 3.

TABLE 3

Values of standard enthalpy ΔH_f^o of formation of $Ca_4(Al_6O_{12})(SO_4)$

r	ΔH_f^o kJ/mole
0	- 8 513.92
1	- 8 506.39
2	- 8 498.14

$\Delta H_f^o = -8506.2 \pm 7.9$ kJ/mole

From the established values of $\Delta H_{r,1}^o$ and the corresponding temperature T_r it follows that

$$\Delta S_{r,1}^o = \frac{\Delta H_{r,1}^o}{T_r} \qquad (9)$$

On assuming that $\Delta C_p = 0$, the entropy balance for reactions yields values in Table 4.

TABLE 4

Calculated values of $\Delta S_{r,1}^o$ and ΔS_f^o

r	$\Delta S_{r,1}^o$ J.mole^{-1}.K^{-1}	$\Delta S_{C_4A_3\bar{S}}$ J.mole^{-1}.K^{-1}
0	631.32	448.55
1	920.10	534.57
2	1208.91	620.60

$\Delta S^o_{C_4A_3\bar{S}} = 534.57 \pm 86.03$ J.mole^{-1}.K^{-1}

The values of ΔS_f^o of sulphoaluminate phase were calculated by using tables [10,11] and results from another study [5]

From the following relation

$$\Delta G^{\circ}_{r,i} = \Delta H^{\circ}_{r,i} + T \times \Delta S^{\circ}_{r,i} \quad (10)$$

the values of standard Gibbs's energy of reactions $\Delta G^{\circ}_{r,i}$ in systems with various r were calculated. By using the following relation

TABLE 5

Calculated values of $\Delta G^{\circ}_{r,i}$ and ΔG°_{f} of $Ca_4(Al_6O_{12})(SO_4)$

r	$\Delta G^{\circ}_{r,i}$ kJ/mole	ΔG°_{f} kJ/mole
0	-407.833	-8078.346
1	-594.390	-8099.055
2	-780.955	-8119.760

$$\Delta G^{\circ}_{r,i} = \sum_{\text{products}}^{i} n_i \Delta G^{\circ}_{f} - \sum_{\text{input}}^{j} n_j \Delta G^{\circ}_{f} \quad (11)$$

the values of standard Gibbs's energy of formation of $Ca_4(Al_6O_{12})(SO_4)$ were obtained (Table 5). The average value of ΔG°_{f} is

$$\Delta G^{\circ}_{C_4A_3\bar{S}} = -8099.053 \pm 41.414 \text{ kJ.mole}^{-1}$$

The results represent gross estimation of thermodynamic values, but on the other hand, these data enable thermodynamic descriptions of reaction involving clinker and hydrated compounds. Considering the fact that standard thermodynamic values of formation are much higher than the values of reaction, the relative error of ΔH°_{f} and ΔG°_{f} is expected to be low.

CONCLUSION

The values of liberated heat of hydration Q were used for estimation of thermodynamic data of sulphoaluminate phase $Ca_4(Al_6O_{12})(SO_4)$ at 298 K.

$\Delta H^{\circ}_{C_4A_3\bar{S}} = -8506.2 \pm 7.9 \text{ kJ.mole}^{-1}$; $\Delta S^{\circ}_{C_4A_3\bar{S}} = 534.6 \pm 86.0 \text{ kJ.mole}^{-1}.\text{K}^{-1}$

$\Delta G^{\circ}_{C_4A_3\bar{S}} = -8009.1 \pm 41.4 \text{ kJ.mole}^{-1}$

REFERENCES

1. Mehta P.K., World Cement Technology 11, 166 (1980).
2. Gabrišová A., Havlica J., Sahu S., Cem.Concr.Res. (in press).
3. Havlica J., Sahu S., Cem. Concr. Res. (in press).
4. Šatava V., Vepřek O., Journ. Amer. Cer. Soc. 58, 357 (1975).
5. Šatava V., Silikáty 30, 1 (1986).
6. Babuschkin V.I., Matvejev G.M., Mchedlov-Petrosyjan O.P.: Thermodynamics of Silicates (in Russian), Strojizdat Moscow 1986.
7. Kaprálik I., Hanic F., Havlica J., Ambrúz V., Br.Ceram.Trans.J. 85, 107 (1986)
8. Oliew G., Wieker W.,Silikattechnik 32, 152 (1981).
9. Oliew G., Wieker W.,Silikattechnik 31, 333 (1980).
10. Barin I., Knacke O.: Thermochemical Properties of Inorganic Substances, Springer Verlag Berlin-Heidelberg-New York 1973
11. Barin I., Knacke O., Kubaschewski O.: Thermochemical Properties of Inorganic Substances, Suplement, Springer Verlag Berlin-Heidelberg -New York 1977.

THERMODYNAMIC APPROACH TO UNDERSTAND THE $CaO-Al_2O_3-SO_3$ SYSTEM

J P Bayoux*, M Testud* and B Espinosa**

**Lafarge Coppée Recherche, Viviers sur Rhône, FRANCE*
***Lafarge Fondu International, Neuilly/Seine, FRANCE*

ABSTRACT

A previous study already published [1] has shown that the Al_2O_3/SO_3 ratio measured in the solution of a dilute suspension containing calcium aluminate cement and calcium sulphate is at the very beginning of the hydration very dependant on the properties of the materials put together particularly those of calcium sulphate. This ratio is a critical parameter in the hydration process that will influence the mechanical properties of calcium aluminate/calcium sulphate mixes.

The thermodynamic study shows that the liquid phase cannot be saturated at the same time with the calcium aluminate and the calcium sulphate. The value for the Al_2O_3/SO_3 ratio greater or smaller than 1 can be explained by an equilibrium at oversaturation towards ettringite and gibbsite. There is an equilibrium between the precipitation of these hydrates which is continously balanced by the dissolution of the anhydrous. The interpretation of the experimental data using thermodynamic equilibrium has led to a much better understanding of the hydration of the calcium aluminate - calcium sulphate mixes.

RESUME

Une étude déjà publiée [1] a montrée que le rapport [Al2O3]/[SO3] mesuré sur une suspension diluée contenant à la fois un aluminate de calcium et un sulfate de calcium est au tout début de l'hydratation très dépendant de la nature des matériaux présents et en particulier du type de sulfate de calcium anhydre ou hydraté. Ce rapport est un paramètre très important qui va orienter la réaction d'hydratation et conditionner les performances mécaniques obtenues en mortier.

L'étude thermodynamique montre que la solution ne peut être à la fois saturée par l'aluminate de calcium et le sulfate de calcium. La valeur du rapport [Al2O3]/[SO3] supérieur ou inférieur à 1 peut être expliquée par un équilibre à sursaturation d'ettringite et gibbiste. Il y a un équilibre entre la précipitation de ces hydrates et la dissolution des phases anhydres. L'interprétation des résultats expérimentaux en utilisant les équilibres thermodynamiques nous a permis d'acquerir une meilleure compréhension de l'hydratation des mélanges aluminates de calcium et sulfate de calcium.

1 - INTRODUCTION

The use of calcium aluminate cements or calcium sulphoaluminate in combination with calcium sulphate and lime to precipitate ettringite during hydration is very often used by of the building industry (screads, sealing products, lining of pipes) or in the mines and tunnels (retaining walls for example). These products for which we can easily regulate the hydration kinetic offer new prospects and a real comfort for those who use them. Hydration kinetics can be monitored as well as length variations which is very helpful in many technical applications, thus implying a good knowledge of the mechanisms.
The purpose of this work is to provide technical background based on thermodynamic calculations helping to understand the fundamental different behaviour of hydrated calcium sulphates on one side and anhydrite on the other when mixed with calcium aluminate cement.

2 - GENERALITIES

In order to understand and give a clearer description of the hydration process of calcium aluminate - calcium sulphate it is very helpful to obtain some information on the thermodynamic equilibrium of the various minerals that one meets in the $CaO - Al_2O_3 - SO$ system.

2.1 - Main hydration reactions

The main reactions in the CaO, SO_3, Al_2O_3 system are :

(1) $3\ CA + 3\ CS\ H_x + (38 - 3\ x)\ H \longrightarrow 3\ C_3A\ 3CS\ H_{32} + 2\ AH_3$
(2) $3\ CA + CSH_x + (18 - x)\ H \longrightarrow C_3A\ CS\ H_{12} + 2\ AH_3$
(3) $6\ CA + C_3A\ 3CS\ H_{32} + 16\ H \longrightarrow 3\ C_3ACS\ H_{12} + 4\ AH_3$

These reactions develop when hydration is complete - for example :

Reaction 1 is the basic reaction which occurs in a mix Calcium Aluminate Cement (C.A.C.)/hemihydrate 60/40 assuming that the C.A.C. contains 60 % CA.

Reaction 2 leading to the formation of calcium monosulphoaluminate corresponds to a mix C.A.C./hemihydrate 87/13 thers containing less calcium sulphate.

Reaction 3 occurs for example in the systems poor in a very soluble calcium sulphate. At the very beginning of the reaction ettringite will precipitate and then when the SO_4 concentration in the solution becomes nil ettringite will transform into calcium monosulphoaluminate releasing more AH_3. All the ettringite is transformed into monosulphoaluminate and if calcium aluminate is still available and when all no sulphate left the typical hydrates of calcium aluminate cements will precipitate.

2.2 - Chemical equilibriums

The chemical equilibria are presented below (fig. 1), are distributed into several groups :

- the first group of equations caracterizes the solubility of anhydrous and hydrates. We have not presented the equation for the calcium aluminate hydrates because we do not need them further in this presentation.
- the second group of equations corresponds to the chemical equilibria in the solution. Most of the time $[CaOH]^+$ and $[HSO_4]^-$ are negligible in neutral solutions but have to be taken into account respectively in basic and acid solutions. We will omit HSO_4^- because of the basicity of our mixes through $[CaOH]^+$ is not to be omitted in the case when lime is added to the system.
- the third group of equation is the total conservation of ions in the solution.
- the fourth group shows the electroneutrality of the solution which is very often the equation that one uses to balance the system. All factors were taken from the litterature [2] and recalculated taking into account the activity coefficient from the Debye Huckel equation.

Fig. 1 - Equilibria equations

Dissolution/precipitation equations

$CaSO_4\ 2\ H_2O \rightleftharpoons Ca^{++} + SO_4^{--} + 2\ H_2O$ $\quad K = 0,234.10^{-4}$

$CaO,\ Al_2O_3 + 4\ H_2O \rightleftharpoons 2\ Al(OH)_4^- + Ca^{++}$ $\quad K = 9,5.10^{-6}$

$Al(OH)_4\ (2\ H_2O)^- \rightleftharpoons Al(OH)_3 + OH^- + 2\ H_2O$ $\quad K = 0,25$ microcrist. / $K = 0,095$ (gibbsite)

$3\ CaO\ Al_2O_3\ CaSO_4,\ 12\ H_2O \rightleftharpoons 4\ Ca^{++} + 2\ Al(OH)_4^- + SO_4^{--} + 4\ OH^- + 6\ H_2O$ $\quad K = 2,9.10^{-30}$

$3\ CaO\ Al_2O_3\ 3\ CaSO_4,\ 32\ H_2O \rightleftharpoons 6\ Ca^{++} + 2\ Al(OH)_4^- + 3\ SO_4^{--} + 4\ OH^- + 26\ H_2O$ $\quad K = 4,9.10^{-44}$

Chemical equilibriums

$H^+ + OH^- \rightleftharpoons H_2O$ $\quad K = 0,681.10^{-14}$

$Ca^{++} + SO_4^{--} \rightleftharpoons CaSO_4$ $\quad K = 10^{2,31}$

$Ca^{++} + 2\ H_2O \rightleftharpoons CaOH^+ + H^+$ $\quad K = 10^{-12,7}$

$H^+ + SO_4^{--} \rightleftharpoons HSO_4^-$ $\quad K = 10^{1,99}$

Conservation

$Ca_{total} = Ca^{++} + CaSO_4 + CaOH^+$

$SO_4 total = SO_4^{--} + HSO_4^- + CaSO_4$

$Al_{total} = Al(OH)_4^-$

$OH_{total} = OH^- + Ca(OH)^+ - H^+ - HSO_4^-$

Electroneutrality

$2\ Ca^{++} + H^+ + CaOH^+ = 2\ SO_4^{--} + Al(OH)_4^- + OH^- + HSO_4^-$

From these equations it is at anytime possible to calculate the sursaturation level of any type of hydrate.
For example, in the case of ettringite oversaturation is defined by a coefficient β which is calculated as follows.

$$\beta = \frac{[Ca^{++}]^6\ [Al(OH)_4^-]^2\ [SO_4^{--}]^3\ [OH^-]^4\ [\gamma_C]^6\ [\gamma_A]^2\ [\gamma_S]^3\ [\gamma_O]^4}{K\ \text{ettringite}}$$

3 - EXPERIMENTAL

3.1 - Raw materials and testing procedure

For the experimental study of the system CaO - Al_2O_3 - SO_3 we decided to use mixes of C.A.C. and calcium sulphates in which.

C.A.C. is commercial Ciment Fondu ® Lafarge
$CaSO_4,\ 2\ H_2O$ is a natural gypsum (purity = 98 %) very finely ground (10 % > 30µm)
$CaSO_4,\ 0,5\ H_2O$ is an hemihydrate containing 75 % calcium sulphate hemihydrate and 25 % anhydrite II
$CaSO_4$ is natural anhydrite. The range of investigation expressed as the ratio C.A.C./sulphate spreads from 100/0 to 70/30 (sulphate is always expressed as % hemihydrate).

For a thorough examination of the hydration mechanisms, dissolution and precipitation, we worked on dilute suspension w/s = 20. This technique enables to extract samples at any time. These samples can then be filtered to separate the solid phase for microscopic or XRD analysis and the liquid for determination of ionic concentration.

3.2 - Hydration of mixes C.A.C./calcium sulphates

The experimental study has shown that calcium sulphates could be classified as

slow or fast sulphates depending on their solubility kinetics. Fast sulphates are hemihydrate and gypsum, anhydrite is the slow one. This difference is discussed in detail in the literature [1]. Typical results are presented below showing the difference between slow and fast sulphates [fig. 2].

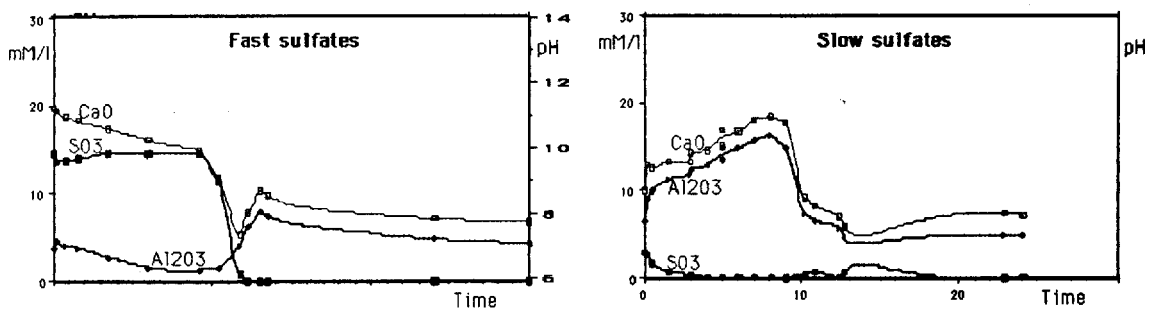

- Fig 2 -
Typical behavour of various calcium sulfates

During the very beginning of hydration there is a drastic difference between fast and slow sulphates. The solution contains mainly SO_3 and CaO whereas on the other side it is Al_2O_3 and CaO. It is this difference that we will explain using the thermodynamic equilibriums. Fig. 2 shows typical behaviours with mixes of 20 % calcium sulphates fast or slow and can be generalized to other mixes as shown on [fig. 3]. In the case of 20 % calcium sulphate additions and up to 90 min. the Al_2O_3/SO_3 ratio ranges from 0,2 to 0,3 in the case of gypsum which goes rapidly into solution and from 2 to 6 in the case of anhydrite which dissolves slower. Replacing gypsum by hemihydrate which dissolves even more quickly leads to a Al_2O_3/SO_3 ratio between 0,11 and 0,04.

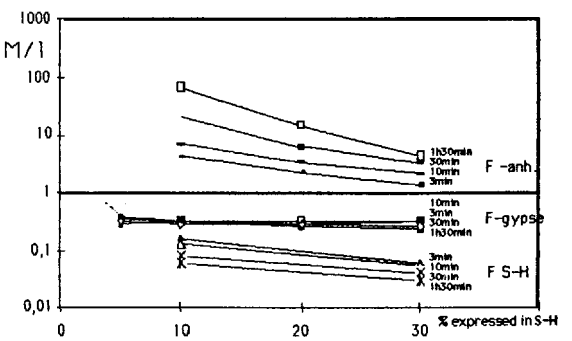

- Fig 3 -
A/S ratios depending on calcium sulfate additions

3.3 - Thermodynamic interpretation

The thermodynamic interpretation consists of finding the right equilibriums in the solution between solid and liquid phases which could explain this difference. Two hypothesis can be made :

3.3.1 - Saturation with calcium aluminate and calcium sulphates - The equilibrium corresponds to a solution saturated at the same time with the calcium aluminate cement and the calcium sulphate.

The results of the calculation are plotted on fig. 4. This figure clearly shows that the assumption of congruent dissolution does not enable to explain the values of the A/S ratio either greater or smaller than one depending on the calcium sulphate.

There must be a precipitation occurring very quickly which would explain these

differences of Al_2O_3/SO_3 ratios. From the theoritical equation and also taking into account the results of E.S.M. examination it is clear that ettringite and gibbsite precipitate.

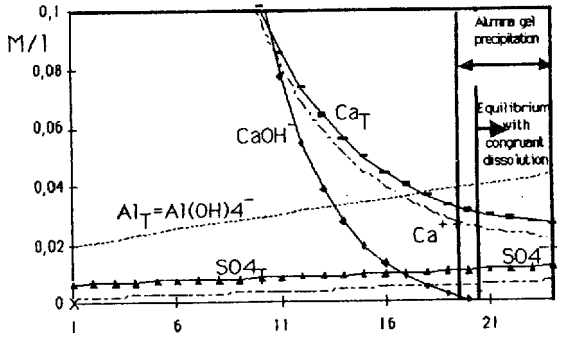

- **Fig 4** -

Theoritical filtrat equilibrium curves at saturation level with CA and CaSO4,2H2O.

3.3.2 - <u>Equilibrium with oversaturation toward ettringite and gibbsite</u> - The equilibrium diagram between $Ca/Al_2O_3/SO_3$ has to be calculated introducing the solubility equations for ettringite and gibbsite. The calculations were done taking into account constant oversaturations toward ettringite or gibbsite. These oversaturation levels, β, correspond to the experimental datas. The calculated theoritical equilibrium diagramm (fig. 5) agrees well with :

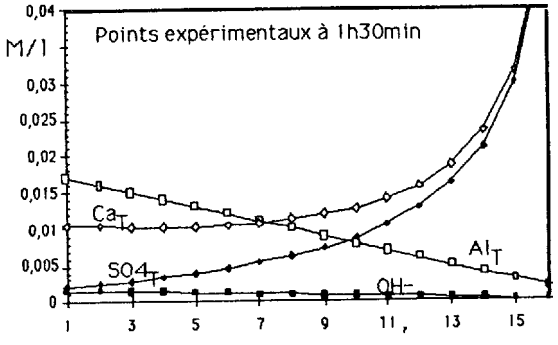

- **Fig 5** -

Equilibrium diagram with oversaturation toward ettringite and gibbsite $k_{ett}=10^{-37}$ and $k_{AH3}=10$

- The values of Al_2O_3/SO_3 greater or smaller than 1 depending on the nature of the calcium sulphate.

- The experimental results which we have pointed on the diagram are for the three different types of sulphates (30 % additions). These sulphates have increasing dissolution kinetic from anhydrite to gypsum to hemihydrate. They fit rather well with the theory. The small differences could be explained by the oversaturation which can slightly vary from one mix to the other.

- The precipitation of ettringite and gibbsite which is associated with the $CaSO_4$/calcium aluminate reaction that we have seen with the E.S.M.

3.3.3 - <u>Mechanism</u> - Once we know the reactions occuring during the initial reaction process a schematical description of the evolution of the system can be proposed. It is a 3 steps process.

As soon as the calcium aluminate cement/calcium sulphate mix is poured in the

water the liquid phase will concentrate in Al_2O_3 and SO_3 ions.

The proportions depend on the respective dissolution kinetic of calcium aluminate and calcium sulphate. The [CaO] corresponds to $[Al_2O_3]$ plus $[SO_3]$ assuming that the dissolution of both calcium aluminate and calcium sulphate is congruent.
Once the solution is oversaturated either in ettringite or gibbsite the hydrate will precipitates. Assuming for example that ettringite precipitate first, this will increase the $[Al_2O_3]$ in the solution and depress $[OH^-]$ and $[Ca^{++}]$ which as a consequence will increase the saturation toward gibbsite till this second hydrate precipitates. Once this occurs the system reaches the theoritical equilibrium decribed by the thermodynamic equations taking into account oversaturation coefficients.

At this third stage the solution precipitates at the same time ettringite and gibbsite. The precipitation is immediately balanced by the dissolution of both anhydrous materials bringing Al_2O_3 and SO_3 ions so as to precipitate ettringite and gibbsite (6 moles [CaO], 3 moles $[SO_3]$, 3 moles $[Al_2O_3]$).

Theoritically $[Al_2O_3]$, $[SO_3]$, [CaO] should remain stable but because of the increasing precipitation kinetic of ettringite the anhydrous materials will not be able to compensate and the system will move. During the course of hydration the oversaturation coefficient varies.

4 - CONCLUSIONS

The ionic concentration of the liquid phase that we have observed during the first step of the hydration of calcium aluminate/calcium sulphate mixes depends on the nature of the calcium sulphate because they don't have the same dissolution kinetic. The $[Al_2O_3]/[SO_3]$ ratio can be greater or smaller than 1. These results have been analysed using thermodynamic equilibriums and a mechanism implying precipitation of ettringite and gibbsite at oversaturation has been proposed. This mechanism fits the experimental datas and leads to a much better understanding of the hydration of calcium aluminate/calcium sulphate mixes.

BIBLIOGRAPHY

[1] Bayoux, J.P., Bonin, A. : "Study of the hydration properties of aluminous cement and calcium sulphate mixes", Proceedings of the International Symposium on Calcium Aluminate Cements, July 1990 LONDON E 8 FN SPON.

[2] Beau, D. : "Action du CO_2 et des agregats calcaires sur les aluminates de calcium hydratés à l'équilibre de solubilité. Influence des ions sulfates". These Universite de Dijon, 1991.

ON THE MECHANISM OF SCAWTITE FORMATION

W Kurdowski and M Pilch

University of Mining and Metallurgy, Cracow
POLAND

SUMMARY

Different mixtures containing Quartz, C-S-H, Tobermorite, Xonotlite and calcium or ammonium carbonate were autoclaved in saturated water vapour. X-ray examination shows that total transformation into Scawtite occurs only in the mixture with Quartz. In C-S-H containing mixtures the simultaneous formation of Tobermorite and Xonotlite diminishes the Scawtite content to 50 %. On the other hand Xonotlite coexists with Calcite in the atmosphere of saturated water vapour at 205°C and 300°C without any detectable quantities of Scawtite formed.

RÉSUMÉ

Les différents mélanges contenants du Quartz, C-S-H, Tobermorite, Xonotlite et le carbonate de calcium ou ammonium ont été autoclavés dans la vapeur d'eau saturée. L'exam en aux rayons X a montré, que la transformation totale en Scawtite a lieu seulement dans le mélange avec du quarz. Dans les mélanges contenants la phase C-S-H la formation simultanée de Tobermorite et de Xonotlite abaisse la teneur en scawtite jusqu'à 50% seulement. D'autre part, Xonotlite coéxiste avec la Calcite dans l'atmosphére de vapeur d'eau saturée à 205°C et 300°C sans quantités detectables de Scawtite formées.

INTRODUCTION

Small quantities of Scawtite are easily formed in cement paste due to influence of CO_2 present in atmosphere and consequently in water. Much greater importance has this phase at high temperature and pressure and in these conditions Scawtite is one of main constituents of the system $CaO-SiO_2-CO_2-H_2O$. In this system Scawtite is the only four-component phase and coexists with Xonotlite, Foshagite, Tobermorite and calcium carbonate. Scawtite is formed in geothermal cements, oil well cements and all building materials which in the production process are thermally treated in CO_2 rich atmosphere. However, there are relatively few informations about its formation (1-4).

In this paper some experimental results are presented with the object to achieve more informations on the conditions of Scawtite formation.

MATERIALS

As a starting materials natural Quartz, amorphous silica (Aerosil Degussa) as well as calcium carbonate, calcium hydroxide and ammonium carbonate as chemically pure reagents were used. Amorphous silica and calcium hydroxide shaken two weeks in CO_2 free water served to obtain C-S-H phase and Xonotlite. Tobermorite was obtained using Quartz and autoclaving with calcium hydroxide at 118°C under saturated water pressure. Xonotlite was obtained from C-S-H phase by autoclaving at 205°C.

METHODS

X-ray was applied and for Scawtite content determination relative intensity of two peaks 0.452 nm and 0.426 nm and as an inner standard Quartz was used. SEM was the second method.

For thermal treatment small autoclave was used and the samples were introduced in the form of a paste in small, open teflon vessels (5).

EXPERIMENTAL RESULTS

The results presented in this point are limited to the mixtures having the C/S molar ratio = 7/6, i. e. corresponding exactly to Scawtite.

Table 1. Phase composition of the samples

Starting mixture	C/S	Temp., °C	Time, h	Phases present *
C + Q + NH_4HCO_3	7/6	205	168	Sc, Q, $C\bar{C}$
C + Q + $CaCO_3$	7/6	205	168	Sc, Q, $C\bar{C}$
		300	48	Sc, Xo
C + S + NH_4HCO_3	7/6	155	168	Sc, To, $C\bar{C}$
		170	72	Sc, Xo, To, $C\bar{C}$
		170	168	Sc, To, Xo, $C\bar{C}$
		190	168	Sc, Xo, To, $C\bar{C}$
		205	168	Sc, Xo, To, $C\bar{C}$
		225	240	Xo, $C\bar{C}$, Sc

* Phases are enumerated in the order of diminishing concentration

As it is seen from table 1 the mixtures of calcium oxide, Quartz and

ammonium carbonate or calcium carbonate after the 168-hour thermal treatment at 205°C are composed of Scawtite with small quantities of Quartz and Calcite. The content of Scawtite in the samples increases quickly to attain 67 %, 85 %, 91 % and 99 % for 6, 12, 24 and 96 hours respectively of thermal treatment at 205°C. A 168-hour autoclaving gave almost pure Scawtite sample.

Mixtures containing amorphous silica have a slightly different composition, namely Tobermorite and in higher temperatures also Xonotlite appears.

When C-S-H phase is used as starting material the content of Scawtite does not exceed about 50% and other coexisting phases are Tobermorite and Calcite (Table 2).

Table 2. Composition of samples

Starting mixture	C/S	Temp., °C	Time, h	Phases present
C-S-H + $CaCO_3$	7/6	205	6	To, Sc, $C\bar{C}$
			16	Sc, To, $C\bar{C}$
			24	Sc, To, $C\bar{C}$
			72	Sc, To, $C\bar{C}$
			96	Sc, To, $C\bar{C}$
			168	Sc, To, $C\bar{C}$, Xo
		225	1	C-S-H, To, $C\bar{C}$
			3	Sc, To, $C\bar{C}$, C-S-H
			6	Sc, To, $C\bar{C}$
			12	Sc, To, $C\bar{C}$
			24	Sc, To, $C\bar{C}$
			72	Sc, To, $C\bar{C}$
			168	Sc, To, $C\bar{C}$

The content of Scawtite increases at the beginning rather quickly to attain 39 % and 49 % for respectively 24 and 96 hours of autoclaving at 205°C. Then no composition changes of the samples are observed, namely the content of Scawtite after thermal treatment during 168 hours is practically unchanged and reaches about 50 %.

In the end, when initial mixtures are composed of Tobermorite, of Xonotlite and $CaCO_3$ after thermal treatment at 205°C and 300°C, the apparently stable phases are Xonotlite and Calcite (table 3).

Table 3. Composition of samples

Starting mixture	C/S	Temp., °C	Time, h	Phases present
To + $C\bar{C}$ + CH	7/6	205	72	To, Xo, $C\bar{C}$
Xo + $C\bar{C}$	7/6	205	72	Xo, $C\bar{C}$
		205	120	Xo, $C\bar{C}$
		225	168	Xo, $C\bar{C}$
		300	48	Xo, $C\bar{C}$

As we can see from the results presented in table 3 Tobermorite is

slowly transformed into Xonotlite, which coexists with Calcite in experimental conditions choosen in our researches.

In all samples which contain Scawtite, independently of its quantity, this phase is formed as very small crystals nondistinguishable under SEM [Fig.1].

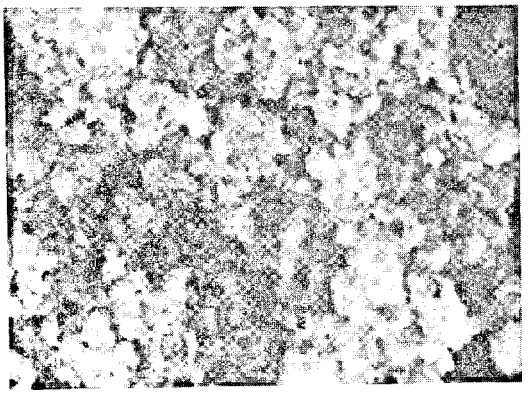

Fig. 1. SEM image of sample composed of Scawtite (10000 x)

The presented results can be explained by assuming that C-S-H phase underwent simultaneous transformation into Tobermorite. It is seen in the phase composition of the sample autoclaved shortly, i. e. only one hour at 225°C. The process can be schematically presented as follows:

$$\text{C-S-H} \longrightarrow \text{Sc}$$
$$\longrightarrow \text{To} \longrightarrow \text{Sc}$$

On the contrary in the mixture of calcium hydroxide, carbonate and Quartz the formation of C-S-H phase and Tobermorite are sluggish and the crystallization of Scawtite prevails. This process can be presented schematically like follows:

$$\text{C} + \text{Q} + \text{C}\bar{\text{C}} + \text{H} \longrightarrow \text{Sc}$$
$$\longrightarrow \text{C-S-H} \longrightarrow \text{Sc}$$
$$\longrightarrow \text{To}$$

Small amounts of C-S-H and/or Tobermorite can not be detected on the X-rays patterns.

CONCLUSIONS

The results of the experiments permit to draw the following conclusions:

a) The best conditions of Scawtite formation exist when Quartz as silica source is used. When amorphous silica is used the quick formation of C-S-H phase gives always large quantities of Tobermorite.

b) Tobermorite does not react with calcium or ammonium carbonate and transforms into Xonotlite.

c) Xonotlite coexists with calcium carbonate without any detectable quantity of Scawtite formed.

REFERENCES

1. Maycock, J.N. and Skalny, J.: Cement Concrete Research, 1974, 4, p. 69

2. Mörtel, H. & Piper, K.: Tonind. Ztg, 1978, 102, p. 513

3. Harker, R.: Mineralogical Magazine, 1965, 34, p. 232

4. Kapralik, J., Stevula, L., Petrovic, I. and Hanic, F.: Cement Concrete Research, 1984, 14, p. 866

5. Kurdowski, W. and Szuba, J.: Cemento, 1987, 84, p. 107.

THERMOKINETICS OF CEMENT HYDRATION UNDER NON-ISOTHERMAL CONDITIONS

A V Usherov-Marshak and A G Sinyakin

Kharkov Civil Engineering Institute, Kharkov
UKRAINE

SUMMARY

Method of calculation of non-isothermal heat evolution under cement hardening at the range from 20 C to 90 C°is offered. Differences in kinetics and completeness of hydration reactions based on thermokinetic characteristics of hardening processes are shown.

Предложен метод расчета неизотермического тепловыделения при твердении цементов в интервале 20 - 80°С. Показаны отличия в кинетике и полноте реакций гидратации по термокинетическим характеристикам процесса твердения.

Thermokinetic analysis data on the rate and completeness of early stages of cement hydration under isothermal and non-isothermal conditions are important for the control of hardening processes/1/. A new approach and a mathematical model for non-isothermal kinetics of heat evolution on the data of differential micro-calorimetry are presented in this report.

Two approaches are adopted in the limits of the kinetics of hydration reactions. Firstly, calculations of constants, discussion of the reaction mechanisms based on the analysis of the non-isothermal experimental relations data, and then adoption , by mathematical means, of non-isothermal relations to the isothermal experimental data/2/.

The results of heat evolution measurements by isothermal and adiabatic means are not identical for real non-isothermal conditions of hardening. The attempts of the non-isothermal dependences by means of graphic analysis were made by Y. Danielson, I. B. Zasedatelev /3/; and by design means by M. Regourd and E. Gotie /4/. However, these methods remain formal and approximate.

In the general case α -parameter of the process depth depends upon temperature and time: $\alpha = \varphi(\tau, T)$. A complete differential of this function is written as follows:

$$d\alpha = (\partial\alpha/\partial\tau)_T d\tau + (\partial\alpha/\partial T)_\tau dT \quad (1)$$

and may be expressed:

$$d\alpha/d\tau = (\partial\alpha/\partial\tau)_T + (\partial\alpha/\partial T)_\tau dT/d\tau \quad (2)$$

where $dQ/d\tau$ - temperature pattern; β

$(\partial\alpha/\partial T)_\tau$ - modification of the degree of transformation with rise in temperature.

It is difficult to determine $(\partial\alpha/\partial T)_\tau$ - under isothermal condition. However this value is presented as the isothermal relation with a "correction multiplier":

$$d\alpha/d\tau = (\partial\alpha/\partial\tau)_T \left| 1 + \beta \frac{(\partial\alpha/\partial T)_\tau}{(\partial\alpha/\partial\tau)_T} \right| \quad (3)$$

Let us find the expression of this multiplier. Usually such analytical relations /2, 5/ are written as follows:

$$(\partial\alpha/\partial\tau)_T = \psi(\alpha, T) \quad (4)$$

The main requirement of the function ψ is a possibility to represent it as a product of two functions. One of them depends upon α, and the other upon T:

$$(\partial\alpha/\partial\tau)_T = f(\alpha)\cdot\varphi(T) \qquad (5)$$

The fulfilment of these requirements permits the description of isothermal data in relation to temperature. But the integration in common appearance:

$$\int_0^{\alpha} d\alpha/f(\alpha) = g(\alpha) = \int_{T_0}^{T}\varphi(T)\,dT \equiv P(T) \qquad (6)$$

is quite complicated especially when determining the appearance of function P /6/. Equation /6/ must contain, for simplification, one parameter and satisfy Arrhenius's law. The value E does not necessarily mean activation energy and is given as a formal parameter:

$$d\alpha/dT = (\partial\alpha/\partial\tau)_T \left| 1 + \frac{\beta\tau E}{RT^2} \right| \qquad (7)$$

Such a simplification permits to suppose that the relation of dynamical velocity of the process to the isothermal one does not depend upon the appearance of the function f /7/. The equation by KEKAM (Kolmogorov, Erofeev, Kozeev, Avraami, Mampel) is used here.

The non-isothermal relation of the transformation velocity in terms of heat emission is repersented by the expression:

$$dQ/d\tau = (\partial Q/\partial\tau)_T \left| 1 + \frac{\beta\tau E}{RT^2} \right| \qquad (8)$$

A series of isothermal thermokinetic curves for different temperatures is the first step. Their number is determined by the exactness desired. It is important to value the interaction between Q and α. In the work /1/ it is shown that a direct proportion $Q(\tau) = Q_{\infty}\alpha(\tau)$ is not well founded, is taken as a simplifying assumption and is checked by phase analysis.

The kinetics of hydration of $3CaO\ SiO_2$ and of cements of different mineral compositions for some temperature regimes has been studied by this method (Fig. 1) The isothermal experiment was carried out in the range 20-80°C, with an interval of 10°C. The water-solid ratio is 0,5.

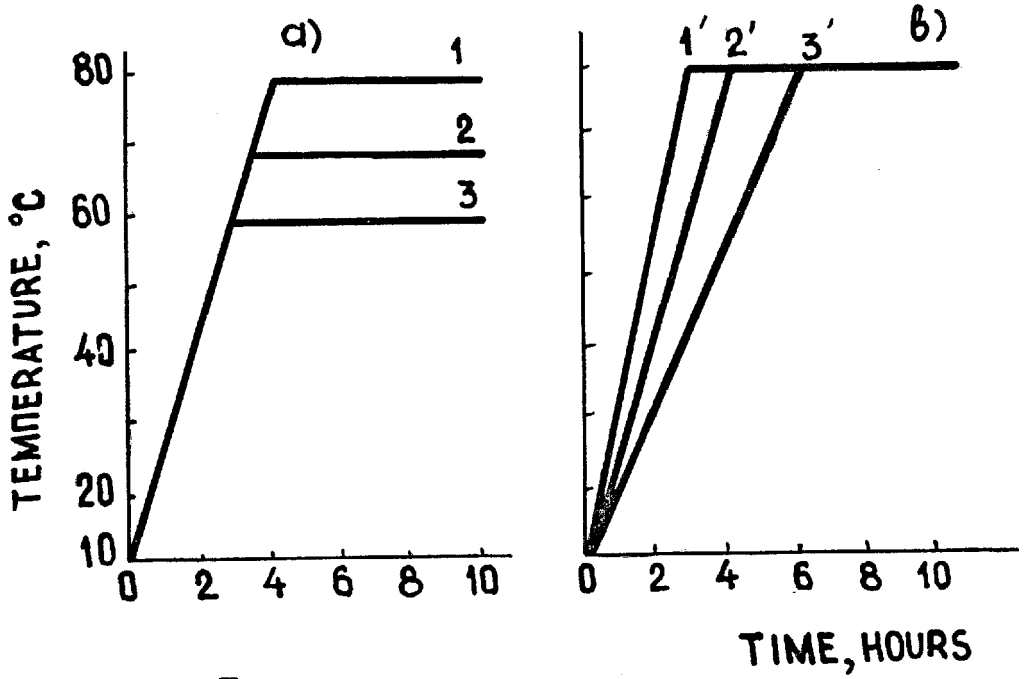

FIG.1 Temperature regimes
а) 1,2,3 - 80,70,60 °C
б) 1',2',3' - velocity of rising temperature - 20,15,10 °C/h

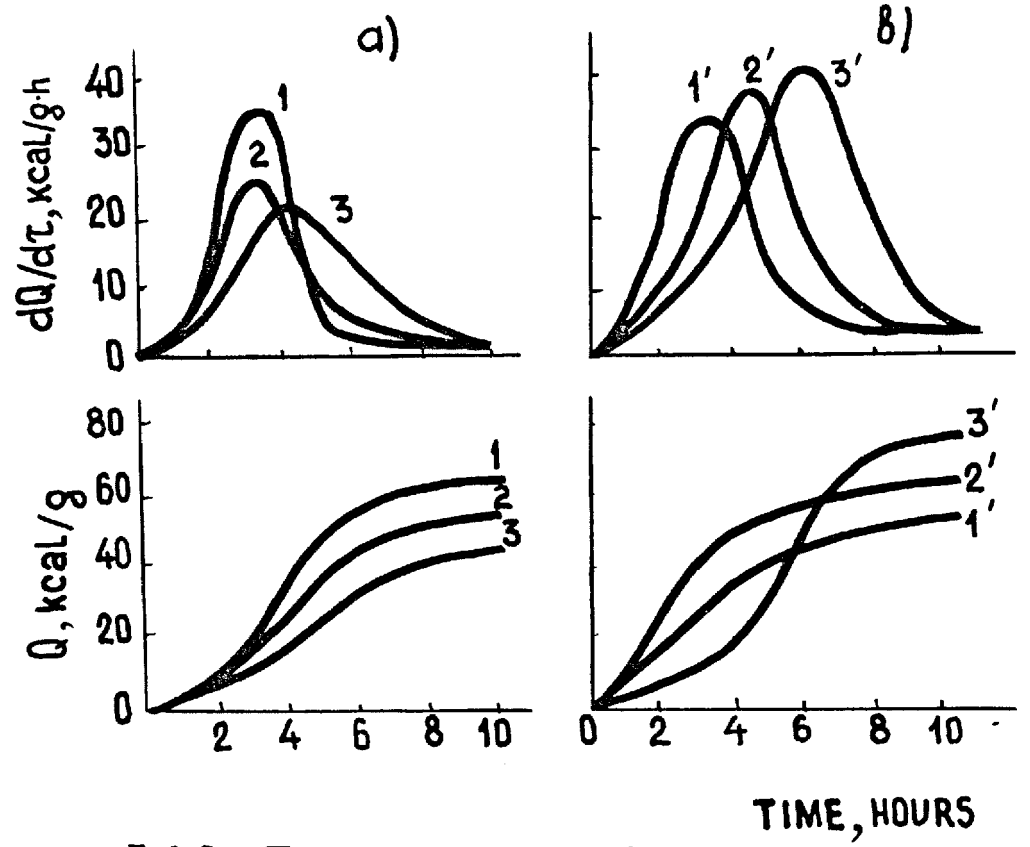

FIG.2 Thermokinetics $3CaO \cdot SiO_2$
а) regimes 1,2,3
б) regimes 1',2',3'

Increasing temperature of isothermal conditioning from 60 to 80 C with a constant rate of heating (Fig. 2a) results in an increase in intensity index and completion of heat evolution. The slowing down of reaction at 80°C is another most visible modification as a result of the rate of temperature rising (Fig. 2b) thus existing a double influence on the thermokinetic characteristics of the hydration of $3CaO \cdot SiO_2$. A smoother rise in temperature- 10°C per hour, furthers the deepening of the hydration processes. Intensive temperature influence retards the process owing to the formation of solid hydrate layers on the mineral grains.

Analysis of thermokinetic hydration under non-isothermal conditions has been carried out with some types of cement . The results of one series of experiments are given in Figure 3a for hydrating Portland cement from the Balakleevsky plant (C_3S - 65,1%, C_2S - 14,6%, C_3A - 5,6%, C_4AF - 13%). Regimes of accelerated hydration are shown in Fig. 1a. In the second case the superplasticizing admixture Surface Active Substance based on modified calcium lignosulphonate was added in the quantity of 0,25% of the cement mass (Fig. 3b).

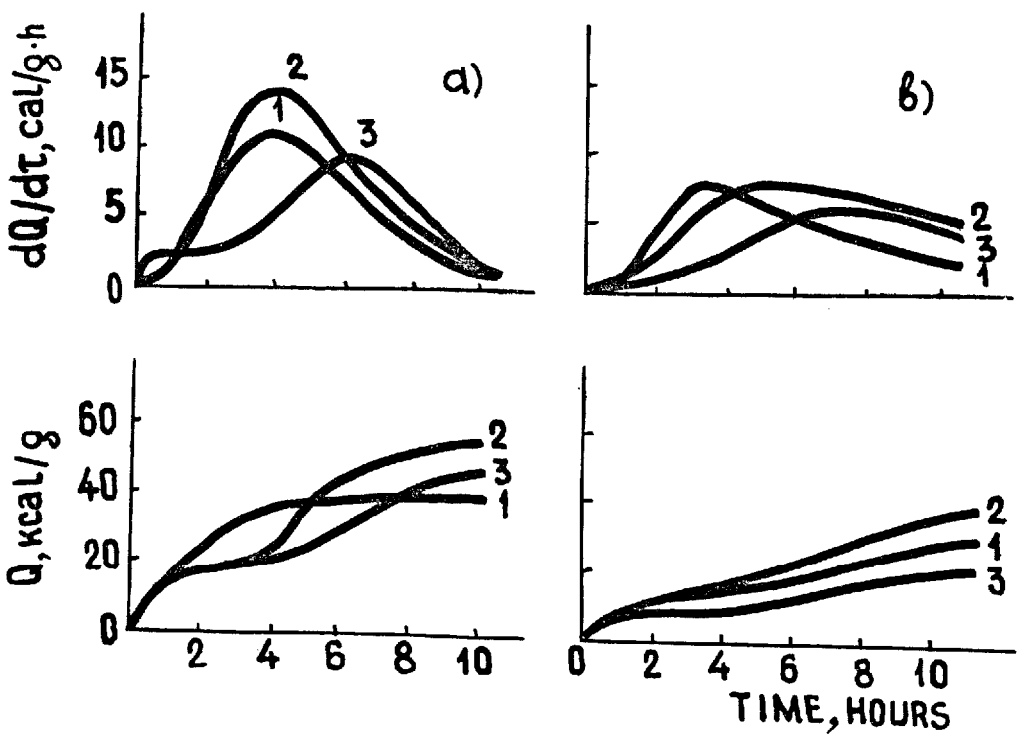

FIG.3 Cement hydration thermokinetics for regimes 1,2,3
a) without admixtures
б) with the presence of superplasticizing

Experimental data showed that raising the temperature above 70°C is of no use from the view point of a complete exploitation of the potential binding characteristics of cement.

When characteristics comes to hydrothermal processing, it is necessary to take into consideration the thermokinetic hydration characteristics of the binder under non-isothermal conditions. The results obtained justify the principle of coherence /8/ of temperature parameters and kinetic hydration characteristics of binders. The model of non-isothermal heat evolution kinetics can be applied for theoretical and practical use when studying different heterogeneous reactions.

REFERENCES

1. Mchedlov-Petrossyan, O. P., Usherov-Marshak, A. V, Urjenko, A. M. :" Heat evolution during binders and concretes hardening", Moscow, Stroiizdat, 1984, 224 P.

2. Braun M, Dolmimor D, Galvey Z. :" Reaction of solids", Moscow, Mir, 1983, 360 P.

3. Zacedatelev, Z. B. & Petrov-Denissov, V. G. :" Heat and mass transmission in concrete", Moscow, Stroiizdat, 1975, 162 P.

4 Regourd , M. & Goutier , E. :" Comportement des ciments soumis au durcissement accéléré", Cim, béton, Plâtres, chauex. 1980, N4, P. 240-249.

5. Barre, P. :" Heterogeneous prosesses kinetics", Moscow, Mir, 1976, 399P.

6. Shestak, V. Y. :" Theory of thermal analysis", Moscow, Mir, 1987, 456P.

7. Ditta, A. & Ryan M. E. :"Thermochimica acta", 1979, 33, 87-92.

8. Mchedlov-Petrossyan , O. P. :" Chemistry of non-organic building materials ", Moscow, Stroiizdat, 1988, 213 P.

EFFECT OF CURING TEMPERATURE ON THE HYDRATION OF PORTLAND CEMENT COMPOUNDS

Kiyoshi Asaga*, Michio Ishizaki**
Shigeru Takahashi***, Kazuo Konishi****
Takaaki Tsurumi***** and Masaki Daimon*****

*The Nishi Tokyo Univ., **Mitsubishi Materials Ltd
***Cement Association of Japan, ****Ube Industries Ltd
*****Tokyo Institute of Technology, JAPAN

SUMMARY

Pastes of portland cement with water cement ratio of 0.3-0.4 were hydrated at 0℃, 20 ℃, 50℃ and 80℃. The hydration percentage of clinker compound was measured by means of quantitative X-ray analysis. And the loss on ignition and amount of $Ca(OH)_2$ were also measured.

The precise hydration ratios of alite, belite, aluminate phase and ferrite phase were obtained by pattern fitting method for X-ray diffraction peaks. The hydration rate of alite at initial stage was faster at high curing temperature almost independent of water cement ratio, and reaction percentage in later stage was not affected by the curing temperature, but by the water cement ratio. The hydration rate of belite was faster at higher curing temperature, not only at initial stage but also after several months. The hydration rate of aluminate phase was very fast at high temperature in initial stage, but was not affected in later stage, and over 90% of aluminate phase reacted within a week regardless of the curing temperature. The hydration ratio of ferrite phase was also affected by the curing temperature at initial stage, but it decreased significantly at any curing temperature after 50% hydration.

C-S-H, $Ca(OH)_2$, Aft and Afm were produced by the hydration of cement at every curing temperature. The amount of $Ca(OH)_2$ was almost proportional to the hydration ratio of alite at low curing temperature. It suggested that the composition of C-S-H did not change remarkable due to the curing time.

1 INTRODUCTION

The hydration rate of portland cement is significantly affected by curing temperature. And there are several of studies for the effects of the curing temperature on the hydration of portland cement[1-3], but the precise analysis of hydration percentage of each compound is very difficult and there are little data on curing at various temperature in spite of the fundamental data of a mass concrete or high strength development concrete[1-3]. Authors discussed on the method of measurement of hydration percentage of each compound by means of quantitative XRD analysis in their previous studies[4-6]. The purpose of this study is to discuss the effect of curing temperature on the hydration rate of each compound and hydration products by measuring the precise hydration percentage of each compound.

2 EXPERIMENTAL

2.1 SAMPLES

Chemical composition and physical test results of the ordinary portland cement used in the experiment are listed in Table 1 and 2. From the calculation of Bogne equation, there is 50% C_3S, 25% C_2S, 8% C_3A and 9% C_4AF in this portland cement.

Cement paste prepared with W/C ratio of 0.30 or 0.40 at 20℃ was sealed in a test tube, and then cured in a incubator at 0, 20, 50 and 80℃ for 3 hours to 91 days respectively. Hydration was stopped by acetone and dried at 110℃ for 24 hours.

2.2 MEASUREMENT AND ANALYSIS OF HYDRATION

Ignition loss of hydrated samples was measured by burning at 1000℃ for 1 hour. Amount of $Ca(OH)_2$ was measured by means of D.S.C. . Hydration ratio of each compound was measured using XRD. For XRD analysis 10% of corundum was added as internal standard, the sample was ground into a fine powder under 5 μm. Measurement was carried out after drying at 200℃ for 24 hours in order to dehydrate the AFm phase. This treatment was necessary to avoid to overlap between the peaks of AFt and belite.

More than three measurements on each sample were carried out to avoid preferred orientation factor of minerals. Hydration ratio was calculated from the integrated intensity of selected peaks by means of pattern fitting calculation program using modified Lorentz function[7].

3 RESULTS AND DISCUSSION

Fig.1 shows the effect of water cement ratio on the reaction ratio and amount of $Ca(OH)_2$ produced in the samples cured at 20℃. The reaction percentage of alite in the both sample cured for 1 day was about 50 %, which was not affected by the water cement ratio. But after 1 day curing, it was affected by the water cement ratio; the hydration rate of alite in the sample with W/C=0.3 decreased with curing time and almost stopped after 28days. On the other hand, it did not so decrease in the W/C=0.4 sample. The reaction percentage of alite at 91 days curing was about 80% and 90% respectively.

In the previous study[4], the hydration percentage of alite in the 5 different samples of commercial ordinary portland cement made by Japanese companies cured at 20℃ in

pastes with W/C=0.35 was about 50% for 1 day curing and 85% for 91 days curing which did not change much among the samples.

The amount of $Ca(OH)_2$ increased with curing time as a same function of hydration of alite.

Figs.2-5 show changes in the hydration ratio of four principal compounds with curing time at various curing temperatures. The standard deviations of reaction percentage of alite was smaller than 2.5% in this study. The hydration rate of alite at initial stage was greatly affected by the curing temperature, the reaction percentage of alite at 1 day curing was about 10% at 0℃, 50% at 20℃, 65% at 50℃ and 75% at 80℃ respectively. Then alite in the samples cured at 0℃ reacted almost proportionally with the log of curing time, but reaction rate of alite cured at high temperature decreased with curing time, and reaction percentage in later stage was not apparently affected by the curing temperature.

The measurement of the reaction ratio of belite was very difficult, the standard deviations of reaction percentage were about 3-9% in this study. The hydration rate of belite was strongly affected by temperature. It was faster at higher curing temperature not only at initial stage but also after several months.

The hydration rate of aluminate phase was very fast at high temperature in the initial stage, but was not affected in later stage, and over 90% of aluminate phase reacted within a week regardless of the curing temperature. The hydration ratio of ferrite phase was also affected by the curing temperature at initial stage, but when the hydration ratio reached about 50%, ferrite phase hardly hydrated thereafter at any curing temperature.

Hydration products were C-S-H, $Ca(OH)_2$, Aft and Afm which did not change due to the curing temperature. Figs.6,7 show changes of the loss on ignition or the amount of $Ca(OH)_2$ produced with curing time. These values increased with curing time in the same manner of the hydration of alite.

Fig.8 shows relation between the amount of $Ca(OH)_2$ and hydration ratio of alite in samples cured at various curing temperatures. In the samples cured at 0℃, the amount of $Ca(OH)_2$ increased proportionally with hydration ratio of alite. In the case of 20℃, the plots appear almost on the same line.
When cured at high temperatures such as 50 and 80℃, the amount of $Ca(OH)_2$ was less than that of 0℃ at first, but slightly more as the hydration proceeded.

The following experimental equation was obtain at 0 and 20℃ curing:

$$Y=1.15X$$

where, Y is the amount of $Ca(OH)_2$ shown as mole, X is the reaction of alite shown as mole.

Litte $Ca(OH)_2$ was produced from the hydration of belite because of the low ratio of hydration at the low curing temperature, and $Ca(OH)_2$ was not produced in the hydration of aluminate and ferrite phase which hydrate according to the following equations:

$$C_3A+3CSH_2+32H \rightarrow C_3A3CSH_{32}\ (AFt), \qquad 2C_3A+C_3A3CSH_{32}+4H \rightarrow 3C_3ACSH_{12}\ (AFm)$$

$Ca(OH)_2$ was produced only from hydration of alite, and C/S ratio of C-S-H did not change remarkably in the curing time. The C/S ratio of C-S-H calculated was 1.85, and the value of C/S of C-S-H produced from curing at high temperature is somewhat larger than 1.85. These C/S values were not so different from the previous data[3].

The increase of the $Ca(OH)_2$ production in the later curing time at high curing temperature may be result of belite hydration.

4 CONCLUSIONS

(1) The hydration rate of alite at initial stage was almost independent of water cement ratio, and reaction percentage in later stage was not affected by the curing temperature, but by the water cement ratio.
(2) The hydration rate of belite was faster at higher curing temperature, not only at initial stage but also after several months.
(3) Over 90% of aluminate phase reacted within a week regardless of the curing temperature.
(4) The hydration rate of ferrite phase decreased significantly at any curing temperature after 50% hydration.
(5) The C/S ratio of C-S-H did not change remarkably due to the curing time at the low curing temperature.

5 REFERENCES

1) Copeland, L.E and Kantro, D.L.: "Hydration of Portland Cement", Proc. 5th Int'l. Sym. Chem. Cements, Tokyo, (1968) Vol.2, PP387-421

2) Young, J.F.: "Hydration of Portland Cement", Instruction Modules in Cement Science (Ed. Roy, D.M.), J. Materials Education (1985), pp1-24

3) Taylor, H.F.W.: "Hydration of Portland Cement", Cement Chemistry, Academic Press, London (1990) pp199-241

4) Ishizaki, M., Asaga, K., Daimon, M. and Takahashi, S.: "Measurement of Reaction Ratio of Each Compound in the Hydration Process of Portland Cement", CAJ Rev., 38-41 (1988)

5) Asaga, K., Ishizaki, M., Tsurumi, T. and Takahashi, S.: "Effect of Firing Condition of Clinker on the Hydration Rate of Each Compound of Portland Cement", CAJ Proc. Cement and Concrete 48-53 (1989)

6) Konishi, K., Asaga, K., Tsurumi, T. and Daimon, M.: "Effect of Heating Rate on the Hydration of Each Compound of Portland Cement", CAJ Proc. Cement and Concrete 68-73 (1990)

7) Ishizaki, M.: "Measurement of Reaction Ratio of Each Compound in the Hydration Process of Portland Cement", Master of Thesis, Tokyo Institute of Technology, (1988)

Table 1 Chemical composition of the portland cement

Ig.Loss	Insol.	SiO_2	Al_2O_3	Fe_2O_3	CaO	MgO	SO_3	Na_2O	K_2O
0.7	0.1	21.8	5.0	2.9	63.9	1.7	2.3	0.26	0.34

Table 2 Pysical properties of the portland cement

Finess	Time setting			Strength			Flow
Blaine specific surface (cm^2/g)	water amount(%)	Initial (hr.min)	Final (hr.min)	Compressive Strength(kgf/cm^2) 3days	7days	28days	(mm)
3382	28.1	2-51	3-52	154	258	408	238

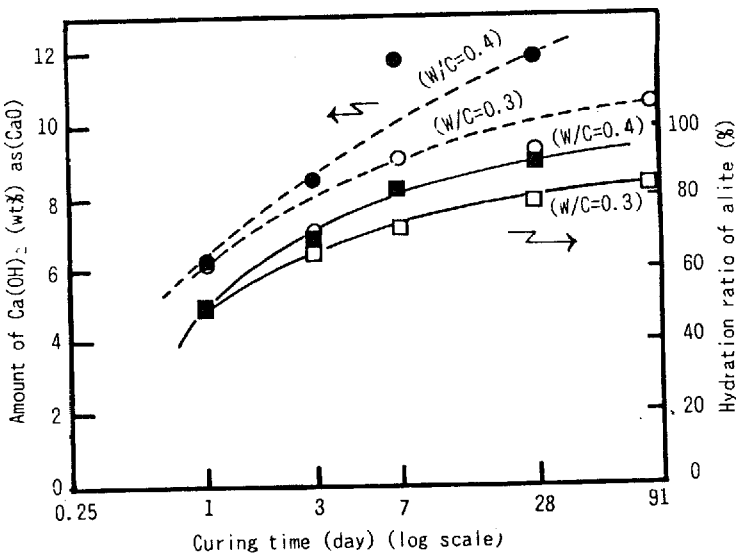

Fig.1 Effect of water cement ratio on the reaction ratio and amount of $Ca(OH)_2$ produced in the samples cured at 20℃

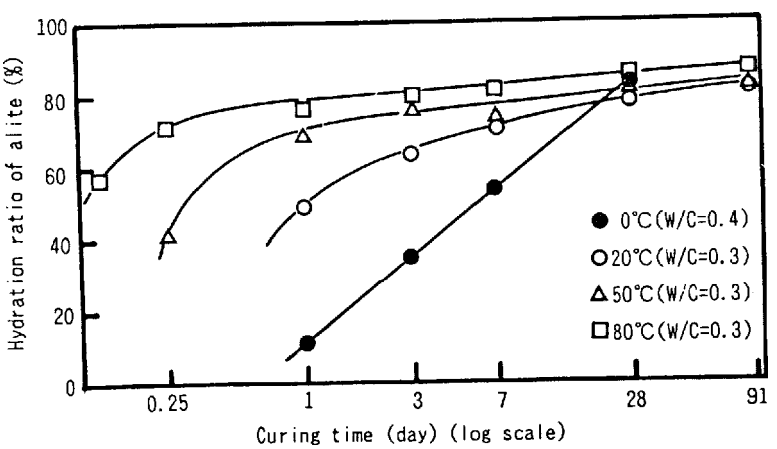

Fig.2 Changes in the hydration ratio of alite with curing time at various curing temperatures

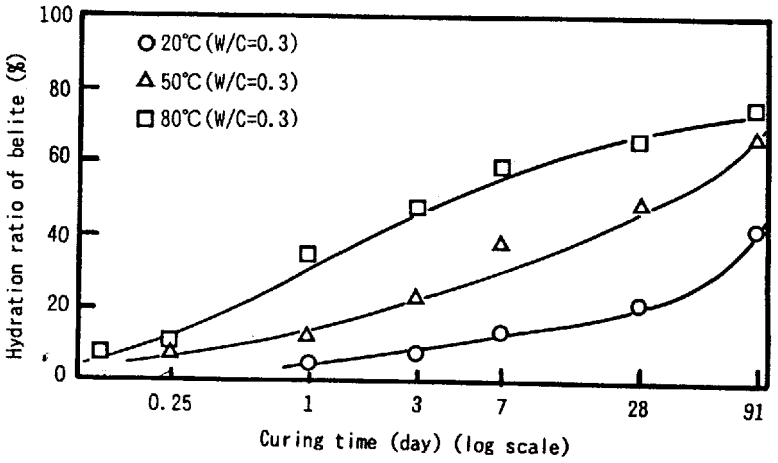

Fig.3 Changes in the hydration ratio of belite with curing time at various curing temperatures

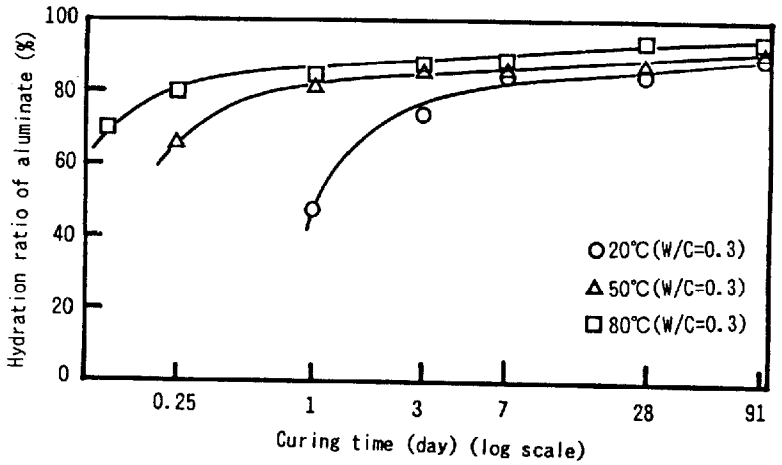

Fig.4 Changes in the hydration ratio of aluminate phase with curing time at various curing temperatures

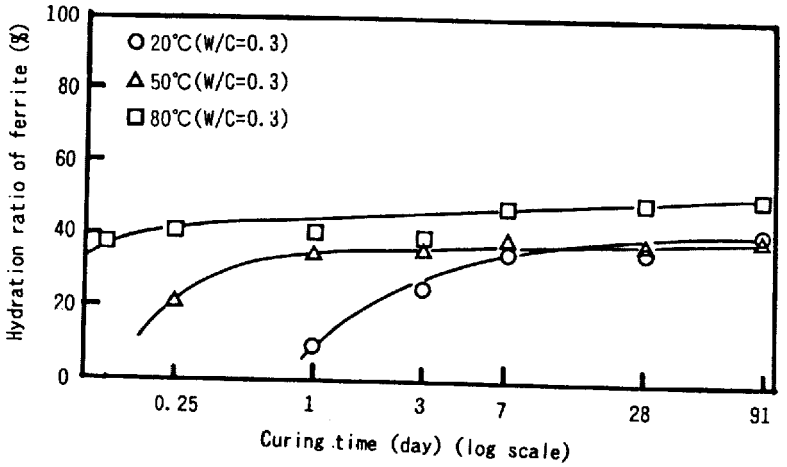

Fig.5 Changes in the hydration ratio of ferrite phase with curing time at various curing temperatures

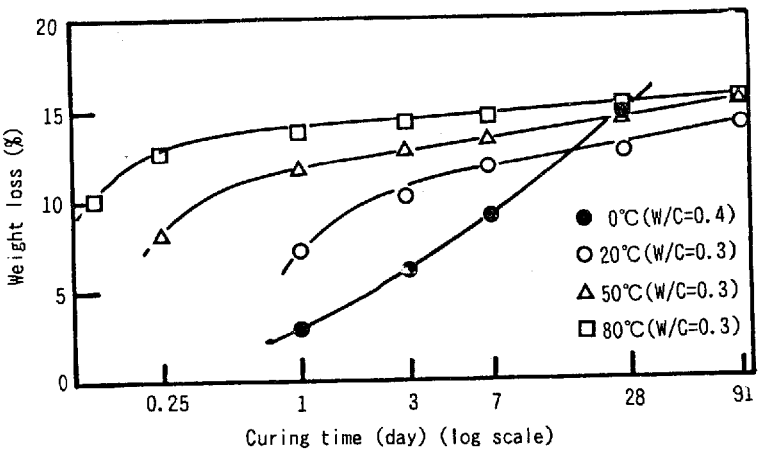

Fig.6 Changes in the loss on ignition with curing time at various curing temperatures

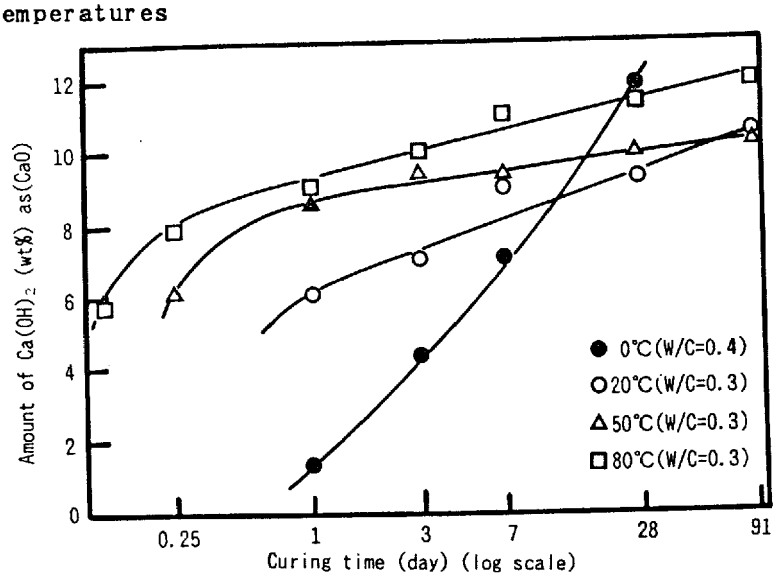

Fig.7 Changes of the amount of $Ca(OH)_2$ produced with curing time at various curing temperatures

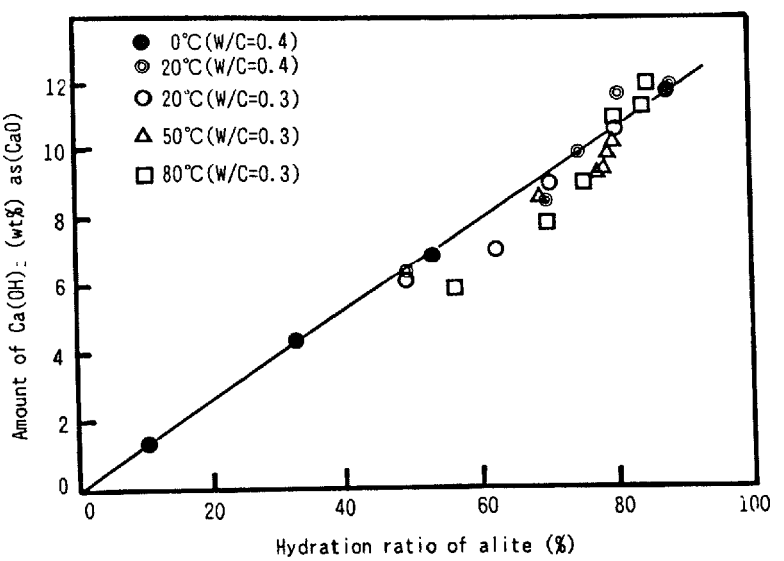

Fig.8 Relation between the amount of $Ca(OH)_2$ and hydration ratio of alite in the samples cured at various temperatures

ELECTROCHEMICAL BEHAVIOUR OF PORTLAND CEMENT AND GYPSUM

D Menetrier/Sorrentino and F P Sorrentino

Lafarge Coppee Recherche, Viviers/Rhône
FRANCE

ABSTRACT

Calcium sulfates are interground with clinker to improve the rheological properties and strengths of cement. The percentage of calcium sulfates, and their quality have been subjected to many experimental studies and attempts at mathematical modelling. Yet, the determination of optimum gypsum content remains empirical. In this study we have tried to understand the mechanism underlying the simultaneous hydration of industrial portland cements, having different C_3A and C_4AF contents, mixed with increasing amounts of gypsum. The use of isothermal microcalorimetry, conductivity, and hydration evolution measurement by the quantity of hydrates produced allow a correct understanding of the phenomena, a possible prediction of the optimum gypsum content and an evaluation of the reactivity of the clinker.

RESUME

Il est bien connu que les sulfates de calcium cobroyés au clinker améliorent la rhéologie et les propriétés mécaniques des ciments. La quantité de sulfate ainsi que sa forme ont fait l'objet de nombreuses recherches et tentatives de modélisation. Malgré cela, la détermination du gypsage optimum reste expérimentale. Dans cette étude, nous avons essayé de comprendre le mécanisme d'interaction entre le gypse et des clinkers industriels de ciment Portland contenant différents pourcentages de C_3A et C_4AF. L'utilisation de techniques telles que microcalorimétrie isotherme, conductivité ou mesure de l'évolution de l'hydratation nous permet de mieux comprendre les phénoménes, de prédire la quantité optimale de gypse et d'évaluer la réactivité des clinkers.

1 - INTRODUCTION

Calcium sulfates are known to improve the rheological behaviour of Portland cement pastes during its initial contact with water, by slowing down the hydration of calcium aluminates.

When the nature and the quantity of the calcium sulfate is adapted to the clinker, the mechanical properties of the cement are also improved. Many results corroborate this phenomenon and we mention here only the most recent or important references (1,2,3,4). Despite these researches and numerous attempts to calculate or to construct a model for the optimum gypsum (5,6), experimental measurement is still the only way to determine its value.

The development of new technologies __ special admixtures, and new grinding processes (high pressure roller press) __ has posed difficulties in controlling the rheological properties and the quality of the cement pastes.

These problems as well as the interaction between admixtures and calcium aluminates, and the increase in water demand (7) due to modification of the particle size distribution by the grinding process are directly connected to the interaction between calcium aluminates and sulfates.

For all these reasons, we have undertaken this study by using an electrochemical approach, involving the measurement of the solution conductivity and ionic concentration during the cohydration of gypsum and cements containing three different C_3A percentages.

2 - EXPERIMENTAL PROCEDURES

Three industrial clinkers of different C_3A and C_4AF contents were chosen. Table 1 shows their chemical and mineralogical composition which is calculated according to the so called" modified Yamaguchi" method reported in other papers (8).

TABLE 1

	N°1	N°2	N°3
CaO	67,15	67,18	65,61
SiO_2	20,88	21,96	22,65
Al_2O_3	6,79	5,11	3,70
Fe_2O_3	2,45	2,61	4,81
MgO	1,24	1,05	0,61
SO_3	0,05	0,90	0,75
Na_2O	0,11	0,11	0,04
K_2O	0,13	0,37	0,80
TiO_2	0,31	0,25	0,19
CO2	0,15	0,20	0,20
P2O5	0,05	0,06	0,26
Mn_2O_3	0,03	0,03	0,06
Free CaO	0,80	0,30	0,55
LSF	95,21	94,84	92,14
SO4(NaK)2	0,09	1,60	1,33
Alite	65,70	72,70	68,60
Belite	12,00	10,50	16,20
Aluminate	14,40	7,80	0,50
Ferrite	7,20	7,80	13,60

The clinkers were interground to about 4000 cm^2/g with different quantities of gypsum, in order to obtain in the cement a total of 1, 2, 3, 4, and 5 % SO_3. The industrial clinkers were ground to the same fineness and used as reference.
The compressive strengths in pure paste (w/c=0,4) were determined on 1x1x10 cm prisms.

The evolution of the hydration was evaluated by the following techniques :

- bound water determination. The hydration is stopped at 24 hours by washing with acetone and ether and the water bound to the hydrates is measured by heating the sample at 1000°C.

- isothermal microcalorimetry. The heat released during the hydration of the cements (w/c=1) is measured up to 24 hours ; special attention is paid to the heat released at 15 minutes and 24 hours.

- conductimetry and ionic measurements. These techniques have already been described in detail (9) and we recall here only their most important features. The hydration is conducted in a special thermoregulated vessel (25°C) under nitrogen in stirred suspension at w/s=20.

A pH and electrical conductivity electrodes and a temperature sensor are installed in the vessel. The numerical values are continuously recorded and processed on a microcomputer.The electrical conductivity which represents the whole of the negatively and positively charged ions in the liquid phase is expressed in milli-Siemens (mS/cm).

At selected times, small volumes of the suspension are taken from the reactor and filtered on millipore filters (0.45µm). The liquid phase is stabilised with HCl, before being quantitatively analysed by Inductively coupled Plasma (ARL 3520).

3 - RESULTS

Table 2 shows the results found by microcalorimetry, heat released at 15 min and 24 hours (columns 3 and 4), the bound water at 24 hours (col. 5) and the strengths (col.6), for different gypsum content (col.2) and approximately the same fineness (col.1).

TABLE 2

Specific surface cm2/g	% SO3	Heat released j/g 15 min	24 hours	Bound water 24 hours	Strengths MPa 24 hours	28 days
			CEMENT N°1			
3750	0	27,5	96,9	13,4		
3905	1	35,0	102,4	10,3	5,5	36
3930	2	11,8	202,1	15,3	11,6	56
4045	3	14,1	154,9	13,0	5,1	60
4090	4	11,4	144,4	14,4	9,6	67
4290	5	8,4	137,8	14,5	8,0	36
			CEMENT N° 2			
3760	0	12,9	143,0	12,4		
3715	1	3,3	92,0	12,8	9,0	55
3875	2	4,5	164,0	13,8	16,3	76
4025	3	12,7	208,0	15,6	21,2	86
4070	4	5,5	182,0	15,5	14,3	71
4240	5	9,3	176,0	16,0	16,2	50
			CEMENT N°3			
3845	0	6,6	61,0	12,9		
3890	1	7,0	116,0	11,4	5,6	50
3940	2	3,4	137,0	14,4	15,4	61
3975	3	8,4	171,0	16,2	12,0	49
4075	4	4,8	158,0	15,7	12,0	47
4180	5	7,2	160,0	15,6		40

Figures 1 to 3 show the evolution of the conductivity versus time. The detail of the curves during the first 10 min is presented within the frame of the figures. In order to clarify the figures, only the most important curves (corresponding to the low % SO_3) are shown.

FIGURE 1

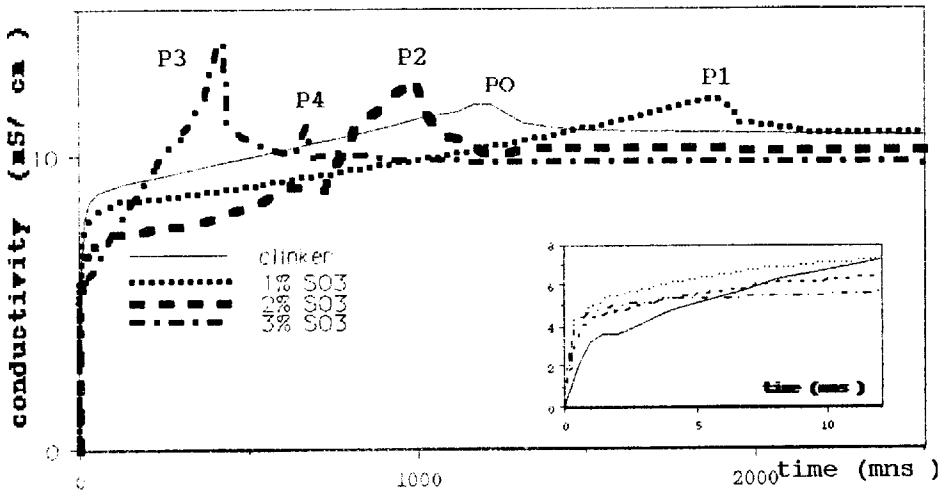

FIGURE 2

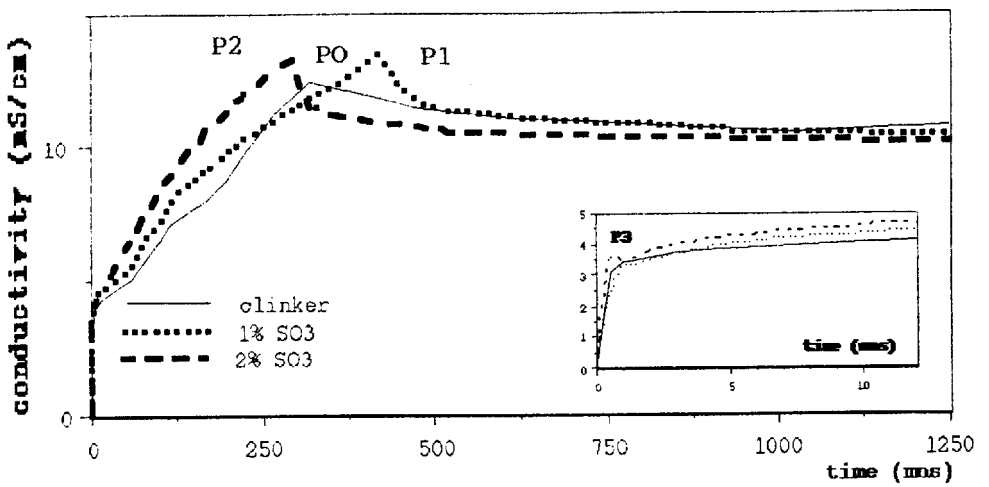

FIGURE 3

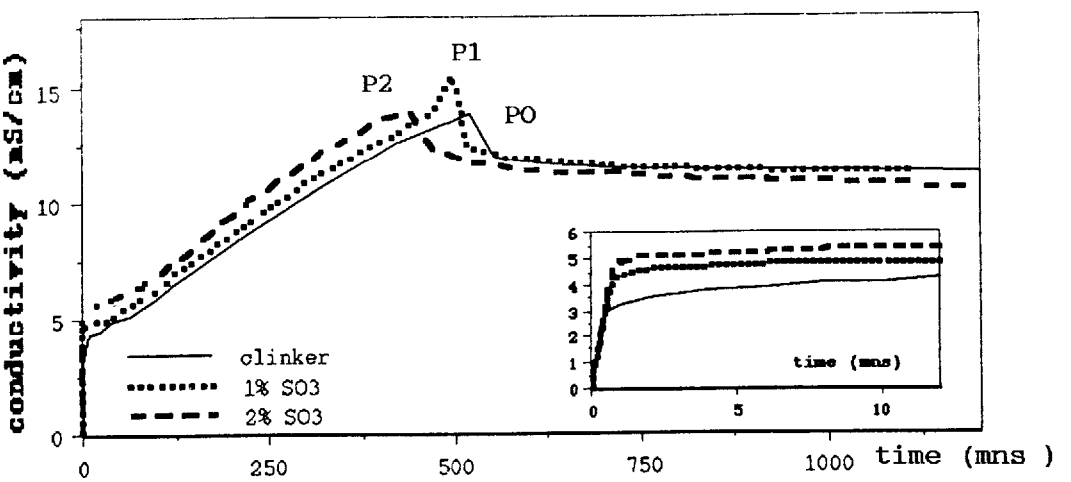

4 - DISCUSSION :

- High C_3A content. The optimum gypsum content, corresponding to the maximum cement strengths is 2% SO_3 at 24 hours and 4% SO_3 at 28 days. The heat released and the bound water at 24 hours presents also a maximum for 2% SO_3. The addition of calcium sulfate increases strongly the conductivity during the initial contact with water, but after 12 mins, the conductivity of the clinker is higher and the addition of 1% SO_3 deletes the occurrence of the large precipitation of the hydrates (represented by the peak P1).

The effect of 2% SO_3 addition is less important during the first few minutes and accelerates the precipitation of the hydrates (P2). The same effect occurs for higher sulfate contents too.
The conductivity curve of the clinker presents a shoulder at 2 mins ; it corresponds to the decrease of the hydration rate due to the precipitation of C_4AH_x. After 3 mins the reaction starts again at a slower rate. We obtain the same type of curve for 1 and 2 % SO_3.

For higher SO_3 contents, the shoulder is replaced by a small peak occurring earlier (30 sec) and corresponding to the precipitation of ettringite. For a sulfate content higher than 3% SO_3, a second peak occurs (P4), attributed to a new formation and precipitation of ettringite.

- Medium C_3A content. The maximum strength results for 3% SO_3 at 24 hours, and remains the same at 28 days. The bound water and the heat released at 24 hours also show a maximum for 3% SO_3. The addition of 1% SO_3 decreases the conductivity during the first few minutes and increases it later : the precipitation of the hydrates (P1) is deleted.

For higher SO_3 contents (2, 3, 4 and 5 %) the conductivity is higher and the precipitation of the hydrates is accelerated (P2) : in this case, a small peak corresponding to the precipitation of ettringite occurs during the first few seconds of hydration.

- Low C_3A, high C_4AF content. The compressive strengths show a maximum for 2% SO_3 at 24 hours and 28 days. Unlike the preceding case, the maximum bound water and heat released at 24 hours corresponds to a higher SO_3 (3%). The addition of 1% SO_3 increases the conductivity during the first few minutes and accelerates the precipitation peak (P1).

The same effect occurs when higher SO_3 contents are added. During the initial hydration, the higher the C_3A content, the higher is the heat released, (27.5 j/g for 14.5% C_3A, 12.9 j/g for 7,8% C_3A and 7,0 j/g with no C_3A). Later, the conductivity of the high C_3A clinker is still high, but there are no differences between medium and low C_3A clinkers. When 2% gypsum (1% SO_3) is inter-ground with the high C_3A clinker, the heat released during the first seconds of hydration is higher than for the clinker itself.

The opposite effect occurs for the medium C_3A clinker and there is no effect when the clinker contains no C_3A. When the addition of SO_3 is 2 %, the heat released at 15 minutes decreases for the high C_3A cement and remains constant for the others.

A comparison of the conductivity curves for the three clinkers was carried out. When the clinker contains high C_3A, the hydration starts rapidly and the conductivity increases, then the hydration rate remains constant and the massive precipitation of the hydrates occurs later.

When the quantity of C_3A is medium to low, the conductivity is lower and the peak occurs earlier (P2, P3). The higher the C_3A content, the later the occurrence of the precipitation peak and the lower the 24-hour compressive strengths.

Figure 4 shows the heat released (hr) at 24 hours as a function of the bound water. The points fit well two straight lines : the upper line corresponds mainly to the low SO_3 content and the bottom line to the high SO_3 content.

FIGURE 4

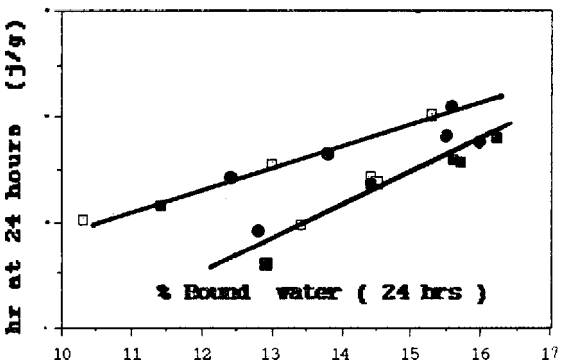

FIGURE 5

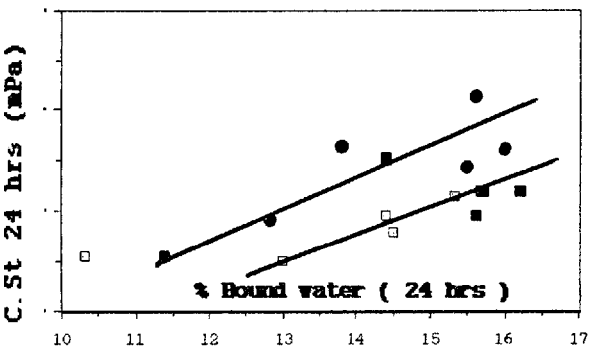

The open squares correspond to the high C_3A content clinker, the black squares to the medium C_3A content, the black circles to the low C_3A content.

The compressive strengths (C.st) are represented as a function of the bound water in figure 5. Like in for the preceding case, the points fit two curves corresponding to the low and high SO_3 content.

These results suggest the existence of different mechanisms of interaction depen- ding on the C_3A content of the clinker and the SO_3 content of the cement. When the C_3A content is high and SO_3 content is low, the ettringite forms and precipitates very fast.

After a few seconds, there are no sulfate or aluminate ions in the solution. The heat released, the bound water, the conductivity, and the strengths increase simultaneously with the SO_3 content.

When both C_3A and SO_3 contents are high, the ettringite also forms and precipitates rapidly but the conductivity still remains high, due to the sulfate and calcium ions coming from the excess of gypsum. The heat released, the bound water, and the strengths decrease but not at the same rate as they increase.

When the C_3A content is medium to low, the first addition of sulfate (1%) reduces the heat released and the conductivity. For higher additions, the heat released, the bound water, the strengths increase simultaneously until a maximum is reached at 3% SO_3. After the maximum, the heat released, the bound water and the strengths decrease together.

When the C_3A content is very low or absent, the increase in conductivity is continuous with the addition of gypsum and we do not observe the deletion of the main peak for low percentage of SO_3 or its acceleration for higher SO_3. We never obtain aluminate or ferric ions into solution, in spite of a precipitation of iron containing ettringite. This implies that the solubility product of this ettringite is attained instantaneously after contact with water.

These results show clearly that the variation of strength as a function of the C_3A and SO_3 contents can be largely explained by the variation of the hydration rate measured in different ways (bound water, electrochemical measurements, heat released). In a previous study of the effect of gypsum on the hydration and strength of C_3S pastes, (10), Bentur explains the maximum strength due to the effect of gypsum on the quantity and the quality of CSH gel. This explanation, found for pure C_3S is not sufficient to explain the simultaneous decreases in hydration rate and compressive strengths and, in the case of cement, the existence of a maximum for these parameters remains to be found.

CONCLUSIONS :

In this study it is shown that :

Electrochemical measurements can be used to follow continuously the hydration phenomena and these agree fairly well with the results found by other techniques, such as microcalorimetry or bound water determination.

Occurrence of a shoulder or peak in the conductivity curve allows a better understanding of the hydration mechanism and could be related to strength development.

Existence of a maximum in the strength curve for an optimum quantity of gypsum is directly related to the evolution rate of the hydration reaction with the SO_3 content. There are at least two mechanisms to account for the increasing and the decreasing part of the curve. The conditions of the predominance of one over the other remains to be explained.

REFERENCES :

1. Ish-Shalom, M. Bentur A.: "Effects of aluminate and sulfate contents on the hydration and strength of portland cement pastes and mortars", Cement and Concrete Research, 1972, 2, 6, 653-662.

2. Odler, I. Wonnermann R.: "Hydration of C3A in Portland cement in the presence of different form of calcium sulfate", **7 International Congress chemistry of cement**, 1980, 4, 510-512.

3. Soroka, I. Relis, M.: "Effect of added gypsum on compressive strength of Portland cement clinker", American Ceramic Society bulletin,1983, 62,(6), 695-703.

4. Kanare, H.M. Gartner, E.: "Optimum sulfate in Portland cement", Cement Research Progress, published by the American Ceramic Society 1984, chapter 13, 213-245.

5. Soroka, I.: "Hydration temperature, gypsum content of cement and compressive strengths of concrete, tentative conclusions", Cement and Concrete Research, 1972, 2, 5, 551-557.

6. Ost, B.: "Optimum sulfate contents of Portland cement", American Ceramic, Society bulletin, 1974, 53, 8, 579-582.

7. Sumner, M.S. Hepher, N.M. Moir, G.K.: "The influence of a narrow cement particle size distribution on cement paste and concrete water demand", Ciments, bétons, platres, chaux, 1989, N° 778, 164-167.

8. Harrisson, A.M. Taylor, H.W.F.: "Electron optical analysis of the phases in a Portland cement clinker, with some observations on the calculation of quantitative phase composition", Cement Concrete Research, 1985, 15, 775-780.

9. Menetrier/Sorrentino, D. et al.: "Electrochemical measurements : tools to characterise the reactivity of hydraulic binders", **Proceedings of the first international workshop on hydration,** 1991, July 3/5 Dijon (France).

10. Bentur, A.: "Effect of gypsum on the hydration and strength of C3S Pastes", Journal of the american ceramic society, 1976, vol 59, 5, 6, 210-213.

RELATIONSHIP BETWEEN THE STRUCTURE AND POLYCONDENSATION DEGREE OF SILICATE ANION OF C-S-H ESTIMATED BY FT-NMR, GPC AND SFC, AND THE STRENGTH OF MORTAR

Hiroshi Uchikawa*, Takayoshi Okamura and Minoru Takehiro****

**Executive Director, Research and Development, Onoda Cement Co Ltd, JAPAN*
***Cement and Concrete Research Laboratory, Onoda Cement Co Ltd, JAPAN*

SUMMARY

The strength of hardened cement paste, mortar and concrete depends on their pore structure and morphology, surface energies and strength of the hydrate, etc. The pore structure including the pore size distribution, the volume and morphology of pores is the main factor controlling the strength. Strength, morphology and surface energy of hydrate itself is an important strength-controlling factor next to the pore structure. Although a lot of research has been focused on the morphology and surface energy of the hydrate and the influence of pore structure on strength, only a little research on the structural factors controlling the strength of hydrate itself has been carried out. This paper deals with the relationship between the polycondensation degree of silicate anion and the strength of mortar, focusing on the polycondensation degree of silicate anion as a structural factor.

Polycondensation degree of silicate anion in C-S-H in a mortar specimen increases with the increase of the curing temperature and age. There are large amounts of silicate anions of heptamer or more and dimer in mortar developing high strength. The higher strengths per unit volume of total pore of autoclaved mortar and silica fume blended white cement mortar cured in water are mainly attributed to the increase in fine pore on which the stress caused by load is poorly concentrated. The higher strength per unit volume of pore of 20 nm or more of white cement mortar cured under a high temperature is attributed to the increase in strength of hydrate itself by the increase of polycondensation degree compensating the decrease in cohesive energy caused by the increase in crystallinity and the formation of different kinds of hydrates.

Résumé

La résistance d'une pâte de ciment, d'un mortier et d'un béton indurés dépend de leur structure poreuse et de la morphologie, des énergies de surface et de la résistance des hydrates, etc... La structure poreuse comprenant la distribution de taille, le volume et la morphologie des pores, constitue le principal facteur contrôlant la résistance. La résistance, la morphologie et l'énergie de surface du seul hydrate sont des facteurs importants du contrôle de la résistance après la structure poreuse. Bien que de nombreux travaux aient été réalisés sur la morphologie et l'énergie de surface de l'hydrate, et sur l'influence de la structure poreuse sur la résistance, il existe peu de recherches sur les facteurs structuraux contrôlant la résistance de l'hydrate. Cette communication présente les relations entre le degré de polycondensation des anions de silicate et la résistance du mortier, en se concentrant sur le degré de polycondensation des anions de silicate en tant que facteur structural.

Le degré de polycondensation des anions de silicate dans le C-S-H d'un spécimen de mortier augmente avec l'accroissement de température de conservation et l'âge. Il existe de grosses quantités d'anions de silicate heptamère ou plus et dimère dans un mortier montrant une haute résistance. Les résistances les plus élevées par unité de volume du total des pores d'un mortier passé à l'augmentation des pores de petites dimensions sur lesquelles la contrainte induite par la charge est faiblement concentrée. La résistance la plus élevée par unité de volume des pores de 20 nm ou plus d'un mortier de ciment blanc conservé à haute température est attribuée à l'augmentation de la résistance de l'hydrate par augmentation du degré de polycondensation qui compense la décroissance d'énergie de cohésion causée par l'augmentation de la cristallisation et la formation de diverses sortes d'hydrates.

1. INTRODUCTION

The strength of hardened cement paste, mortar and concrete depends on their pore structure and morphology, surface energies and strength of the hydrate, etc. The pore structure including the pore size distribution, the volume and morphology of pores is the main factor controlling the strength. Strength, morphology and surface energy of hydrate itself is an important strength-controlling factor next to the pore structure. Although a lot of research (1) (2) (3) has been focused on the morphology and surface energy of the hydrate and the influence of pore structure on strength, only a little research on the structural factors controlling the strength of hydrate itself has been carried out. This paper deals with the relationship between the polycondensation degree of silicate anion and the strength of mortar, focusing on the polycondensation degree of silicate anion as a structural factor.

2. SAMPLE

White cement alone (W) and two types of blended white cement containing 50% of blastfurnace slag (WSL) and 10% of silica fume (WSF) were used for the convenience of the NMR measurement. Ordinary portland cement (OPC) was also used for the other experiment. The fineness and chemical compositions of OPC, white cement, blastfurnace slag and silica fume are shown in **Table 1**.

3. EXPERIMENT

3.1 Compressive strength test of mortar

After the mixing of mortars according to JIS, they were cured for three ways, water curing at 20°C, steam curing and autoclave curing, and submitted to compressive strength test at different specified ages. Steam curing was started 5 hours after the mixing and the mortars heated up to 65°C at the rate of 15°C/min. After maintaining 65°C for 4 hours, they were cooled down in air. Autoclave curing was stated 1 day after the mixing and the mortars heated up to 180°C at the rate of 60°C/min. After maintaining 180°C for 5 hours, they were cooled down in air. Both mortars cured in steam and autoclave were further cured in 20°C water until the specified age. Toyoura standard sand was used as the fine aggregate and no organic admixture was used.

3.2 Determination of pore structure

Part of the samples prepared for the measurement of compressive strength were immersed in acetone at different specified ages to terminate hydration. After drying using the D-drying method, the pore size distributions were determined using a mercury-penetrating porosimeter.

3.3 Determination of composition and structure of C-S-H

(1) EPMA - The point analysis of C-S-H of various types of hardened mortar after 28 days was made using EPMA. The measurements at ten points in the vicinity of unhydrated cement particle were averaged out.

Table 1 Chemical composition of white cement, ordinary portland cement, blastfurnace slag and silica fume (%)

	ig loss	SiO_2	Al_2O_3	Fe_2O_3	CaO	MgO	SO_3	Na_2O	K_2O	Total
White cement	4.7	21.5	4.1	0.2	63.9	1.7	3.1	0.45	0.09	99.7
OPC	1.9	21.1	4.8	2.8	64.6	1.5	2.2	0.26	0.50	99.7
Blastfurnace slag	-	34.1	16.1	0.5	41.7	6.5	0.0	0.20	0.30	99.5
Silica fume	1.0	96.0	0.0	0.4	0.8	-	-	0.21	0.45	98.9

(2) FT-NMR - Hardened mortars dried by the D-drying method were analyzed at a magic angle of 54.7 degrees and a spinning speed of 3 to 4 kHz with a cross-polarization magic-angle spinning nuclear magnetic resonance (CP-MAS-NMR) system of JEOL using a Derlin resin sample cell. ^{1}H-and ^{29}Si-double resonance NMR was used and the mass gated decoupling method was applied to the pulse sequence. A small piece of silicone rubber (-22 ppm from TMS) was used as the internal standard for the calibration of chemical shift and the comparison of peak intensity.

(3) TMS-SFC-GPC - Hardened mortars at 28 days were trimethysilylated according to the Uchikawa et al.'s method (4) using dimethylformamide, hexamethyldisiloxane and trimethychlorosilane. The silicate derivatives produced were kept at 175° C for ten hours to remove the solvents and volatile matter containing monomer, dimer and trimer. Thus prepared samples were analyzed to determine the non-volatile content including polysilicate and the molecular weight distribution of polysilicate derivative was determined by gel permeation chromatography (GPC). The configuration of GPC and the measuring conditions were the same as in the Uchikawa et al.'s method. Part of trimethylsilylated sample was submitted to the separation and analysis of silicate derivatives with a supercritical fluid chromatograph (SFC) of JEOL. A evaporative light scattering detector (ELSD) was used as the detector of SFC and super critical CO_2 was used as the eluent.

4. RESULT AND DISCUSSION

4.1 Relationship in mortar between pore size distribution and compressive strength

The compressive strengths of JIS mortars cured under different conditions are shown in **Fig. 1**. Although the strength of white cement mortar at the early age is slightly higher than that of silica fume blended white cement mortar in the case of water curing at 20°C, the strengths of both mortars are nearly equal to each other after 91 days though the former is lower than the latter after 28 days. The strength of blastfurnace slag blended white cement mortar is the lowest regardless of age among the mortars cured in water. In the steam curing, the strength of white cement mortar is also as high as that of ordinary portland cement mortar and that of blastfurnace slag blended white cement mortar is relatively low. Although the strength of silica fume blended white cement mortar cured in steam is higher than that of white cement mortar during the early age, that of 28 days is nearly equal to that of blastfurnace slag blended white cement mortar. In autoclave curing, the strength of blastfurnace slag blended white cement mortar is higher than that of white cement mortar and that of silica fume blended white cement mortar is relatively low. It is generally known that the effect of silica fume on the improvement of strength at the early age is augmented with the decrease in the W/C ratio. In this experiment, however, it is considered for JIS mortar with a W/C ratio as high as 0.65 containing no organic admixture that the strength of silica fume blended white cement mortar is generally low because the microfiller effect of the dispersed silica fume on the strength is not produced.

The pore size distribution of each type of the hardened cement mortar cured at different conditions are shown in **Fig. 2**. The total pore volume of mortar cured in water at 20° C is low for white cement, blastfurnace slag blended white cement and silica fume blended white cement. The trend is the same as those of mortar cured under condition other than water curing at 20°C.

In water curing at 20°C, the pore volume of 20 nm or more closely relating to the strength (1) (2) is high for blastfurnace slag blended white cement, silica fume blended white cement and white cement at the early age. That of mortar at the later age is high for blastfurnace slag blended white cement, white cement and silica fume blended white cement because silica fume blended white cement mortar is more densified with age.

Although the pore volume of 20 nm or more in mortar cured in steam is high for white cement, ordinary portland cement, blastfurnace slag blended white cement and silica fume blended white cement at the early age, that of blastfurnace slag blended white cement mortar is the lowest after 28 days.

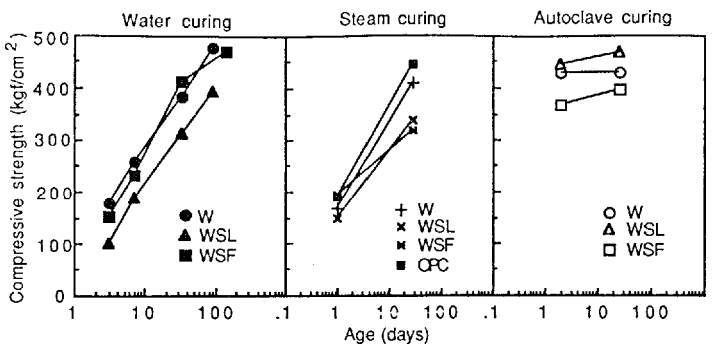

Fig.1 Compressive strength of JIS mortar of each cement cured under various conditions

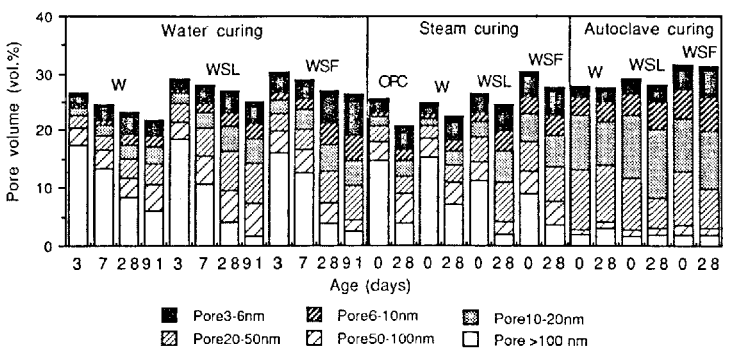

Fig.2 Pore size distribution of hardened JIS mortar prepared from various cements cured under different conditions

The trend of the pore volume of 20 nm or more in autoclaved mortar is similar to that in mortar cured in steam at the later age. Although the pore volume of 20 nm or more is generally related to the strength of mortar, some relationships do not show such a trend. **Fig. 3** illustrates the relationship of the total pore volume and the volume of pore of 20 nm or more with the strength of mortar. Comparing the relationship in mortar cured in water at 20°C between the total pore volume and the compressive strength with that of mortar cured in steam, the strength of mortar per unit volume of pore is high for silica fume blended white cement, blastfurnace slag blended white cement and white cement. The strength per unit volume of pore in autoclaved mortar is higher than those in mortars cured in water at 20°C and in steam. On the other hand, the relationship between the pore volume of 20 nm or more and the strength is approximately expressed by a straight line, especially that in mortar

cured in water at 20°C. The strengths per unit pore volume of 20 nm or more in steam-cured mortars of blastfurnace slag blended white cement, silica fume blended white cement and that in autoclaved mortar of silica fume blended white cement are low. The deviation from the regression line is considered to be attributed to the differences in the strength of the hydrate itself and cohesive energy.

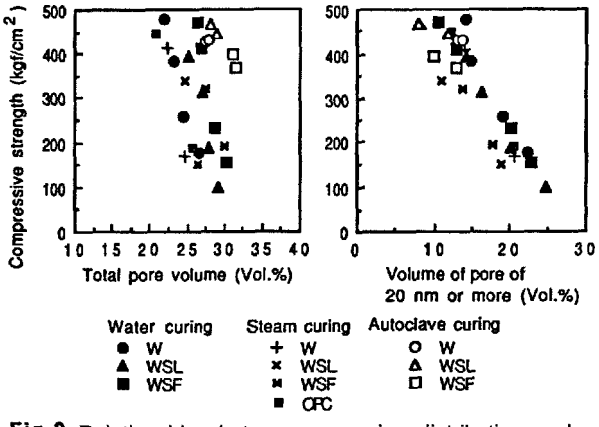

Fig.3 Relationships between pore size distribution and strength of hardened JIS mortar prepared from various cements cured under different conditions

Table 2 Chemical composition of C-S-H in hardened mortar at 28 days measured by EPMA

Cement	Curing condition	SiO_2	Al_2O_3	Fe_2O_3	CaO	MgO	SO_3	Na_2O	K_2O	Total %	C/S molar ratio
W	Water	28 7	2 4	0 2	43.1	2 0	1 4	0.15	0.01	77.9	1.63
		(3.1)	(0 5)	(0.2)	(1.8)	(0.4)	(0.4)	(0.08)	(0.01)	(3 2)	(0.22)
WSL	Water	27.9	4.1	0.2	36.7	1.8	1.4	0.11	0.04	72.3	1.48
		(6.4)	(1.3)	(0 1)	(2.7)	(0.7)	(0.2)	(0.07)	(0 03)	(8 9)	(0.35)
WSF	Water	26 9	2.2	0.2	39.3	1.7	1.3	0.10	0.02	71.7	1.62
		(6 5)	(0.7)	(0.1)	(4.2)	(1 0)	(0.3)	(0.02)	(0 01)	(11 1)	(0.30)
OPC	Steam	29.1	1.8	1.2	42.1	1.0	0 9	0.12	0.10	76 4	1.56
		(1.5)	(0 5)	(0.4)	(3 5)	(0.6)	(0.2)	(0 08)	(0 05)	(2.4)	(0.20)
W	Steam	27.5	2.2	0.1	45.9	1.6	1.5	0.12	0.02	79 0	1.80
		(1.6)	(0 3)	(0.1)	(2.2)	(0.7)	(0 3)	(0.05)	(0.01)	(2.2)	(0.14)
WSL	Steam	22.9	3.6	0.3	33.1	1.2	1.8	0.12	0.08	65.5	1.69
		(3 5)	(1.4)	(0.1)	(5.4)	(0.3)	(1.5)	(0.09)	(0 03)	(6.6)	(0.23)
WSF	Steam	26.8	2.3	0.2	38.3	1.4	1.2	0.08	0.03	70.5	1.56
		(5.2)	(0.6)	(0.2)	(5.3)	(0.9)	(0.4)	(0.07)	(0.03)	(10.3)	(0.25)
W	Autoclave	29.8	1.5	0.1	43.5	1.1	9.3	0.35	0.06	85 7	1.65
		(6.3)	(0.3)	(0.1)	(4.7)	(0.3)	(7.2)	(0.20)	(0 02)	(5.1)	(0.50)
WSL	Autoclave	24.1	3.8	0.1	31.5	0.3	1.1	0 21	0.21	61.4	1.37
		(4 7)	(1.1)	(0 0)	(3 0)	(0 2)	(0.3)	(0.08)	(0.11)	(8.5)	(0.19)
WSF	Autoclave	28.6	2.9	0.1	35.1	1.9	1.4	0.09	0.04	70.0	1.35
		(6 5)	(0 9)	(0 0)	(1.2)	(0.9)	(0 5)	(0.01)	(0 09)	(8 6)	(0.25)

note ; ( ) Standard deviation

4.2 Kind and texture of hydrates

Typical scanning electron micrograph of the fracture surface of each type of hardened mortar after 28 days are shown in **Fig. 4**. From the results of the SEM and XRD, calcium hydroxide, ettringite and monosulfate hydrate are recognized and a lot of type I C-S-H are observed as well as type III C-S-H in mortar cured in water at 20°C. In steam curing, there are the same kinds of hydrates as that in mortar cured in water although type I C-S-H grows slightly larger. In an autoclaved mortar, a lot of hydrogarnets are formed and the peak intensity of XRD caused by (2 2 0) plane of tobermorite increases instead of calcium hydroxide, ettringite and monosulfate hydrate. The network structure of tobermorite similar to that of type II C-S-H is observed frequently in autoclaved mortar of white cement. In an autoclaved mortar of blastfurnace slag blended white cement showing high strength, the tobermorite similar to the morphology of type III C-S-H occupies the majority although the network structure is also observed. On the other hand, it is observed that a lot of foil shaped tobermorites grown from the sphere particles which are considered to be silica fume connect the particles with each other. Such a coarse texture shows that the connecting strength between silica fume particles is relatively weak.

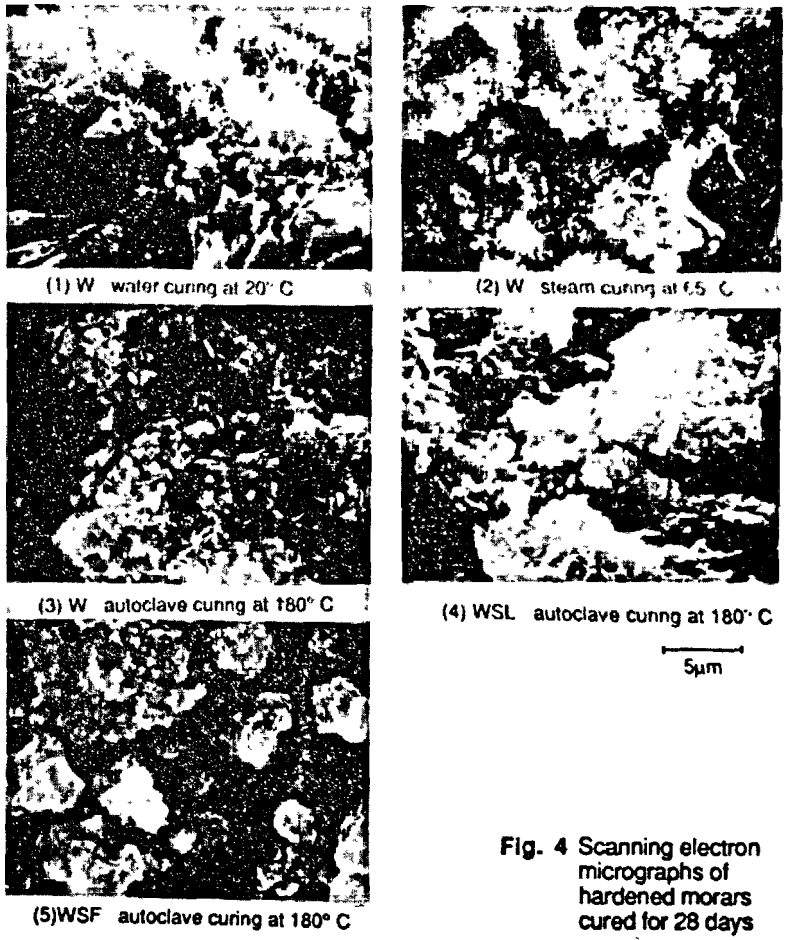

Fig. 4 Scanning electron micrographs of hardened morars cured for 28 days

4.3 Compositions of C-S-H

The composition of C-S-H in each type of hardened mortar after 28 days measured using EPMA are shown in **Table 2.** It is known that C/S molar ratio of C-S-H in hardened blended cement paste varies according to its position precipitated and it decreases with the decrease of distance from unreacted blending component particle (5). In this study, C/S molar ratio of C-S-H in autoclaved mortar decreases to 1.3 to 1.4 by the addition of blastfurnace slag and silica fume though the decrease in it is relatively small in mortars cured in water and in steam because the C-S-H in the vicinity of unhydrated cement particles were analyzed. It is known that the C-S-H of low C/S molar ratio has a large specific surface area and a large cohesive energy (3) (6). In autoclave curing, however, it is considered that the cohesive energy of hydrate decreases regardless of C/S molar ratio due to the change in morphology and texture accompanied with the increase in crystallinity and the formation of tobermorite mentioned earlier.

4.4 Structure of C-S-H

The structures of glass and amorphous phases can be estimated by the powder X-ray diffraction halo patterns (5). The halo patterns for the paste portion in the hardened mortar sample are, however, within 29° and 30° of 2θ (CuKα) in the experiment and almost constant independent of the types of cement and the curing conditions. The structure of C-S-H was, therefore, investigated by the analysis including NMR and TMS.

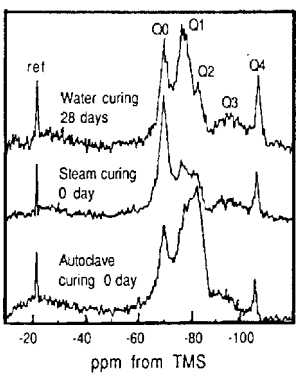

Fig.5 NMR spectra of hardened white cement mortar

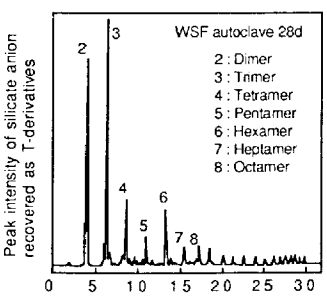

Fig.7 Super critical fluid chromatogram of hardened silica fume blended white cement mortar treated by TMS

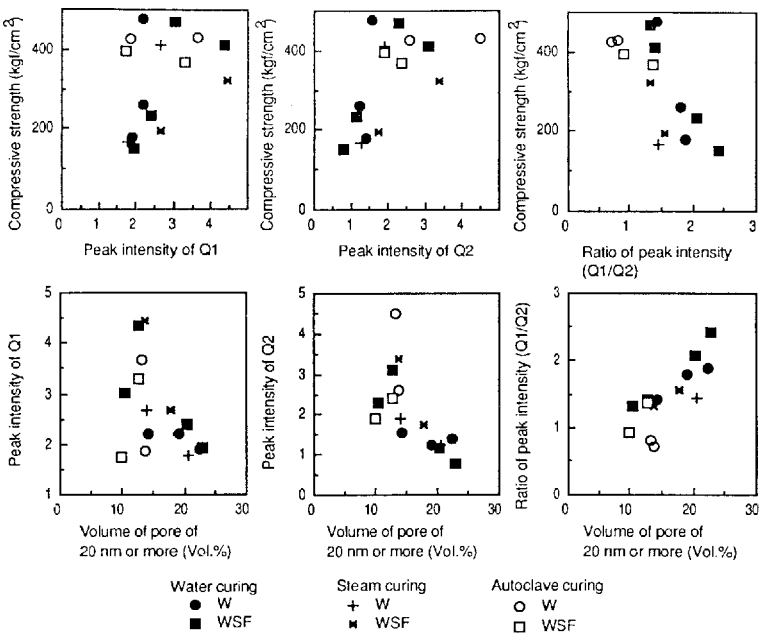

Fig.6 Relationships between compressive strength, pore volume of 20nm or more, NMR peak intensity and peak intensity ratio of hardened mortar

(1) NMR - The results obtained using NMR using hardened white cement mortars cured under different conditions are illustrated in **Fig. 5.** The peak at -22 ppm corresponds to silicone rubber used for reference. According to ^{29}Si-NMR, the structure of silicate anion is divided into five groups, Q_0 (monomer of SiO_4), Q_1(end of chain), Q_2 (middle of chain), Q_3 (ramification point of chain) and Q_4 (three-dimensional structure), depending on the chemical shift. Q_0 and Q_4 in the hardened mortar samples of white cement are derived from unhydrated calcium silicate and fine aggregate of Toyoura standard sand, respectively. Since Q_1, Q_2 and Q_3 are derived from silicate anions in C-S-H, the amount and structure of C-S-H produced can be estimated from the intensity and the intensity ratio of peaks (7) (8). **Fig. 6** illustrates the relationships of the strength and pore volume of 20 nm or more with the peak intensity of Q_1 and Q_2 and with the intensity ratio of Q_1/Q_2. Although there is no direct relationship between the pore size distribution and the polycondensation degree, pore volume of 20 nm or more which is a main controlling factor of the strength is used for the estimation of polycondensation degree to clarify the mechanism of strength development. The peak intensity of Q_0

corresponding to the quantities of unhydrated alite and belite decreases and that of Q_1 and Q_2 corresponding to the quantity of C-S-H produced increase as the hydration proceeds though that of Q_1 decreases at the later age. Since the intensity ratio of Q_1/Q_2 is related to the polycondensation degree of silicate anion in C-S-H, the polycondensation degree increases with the decrease in the intensity ratio of Q_1/Q_2. **Fig. 6** illustrating the relationship between the intensity ratio of Q_1/Q_2 and the pore volume of 20 nm or more reveals that the chain of silicate anion in C-S-H is lengthened with the increase in curing temperature. Compared with the water-cured mortars containing almost the same pore volume of 20 nm or more, their polycondensation degree are in the same level. In steam curing and autoclave curing, however, the polycondensation degree per unit pore volume of 20 nm or more in silica fume blended white cement mortar is lower than that in white cement mortar.

It is inferred from **Figs. 6** and **Fig. 3** that the increase in the strength of mortar per unit volume of total pore by the addition of silica fume is attributed to the increase in fine pore on which the stress caused by load is less concentrated than coarser pore as particularly conspicuously shown in the mortar cured in water at 20°C. The highest strength of autoclaved mortar per unit volume of total pore is also attributed to the same reason as shown in **Fig. 2.** Meanwhile, the low strengths per unit volume of pores of 20 nm or more in silica fume blended white cement mortars cured in steam and in the autoclave are attributed to the low polycondensation degree of silicate anions in C-S-H as well as the cohesive energy lowered by the increase of crystallinity and the formation of different types of hydrate. It is considered that the increase in polycondensation degree accompanied with the increase in strength of hydrate itself compensates the decrease of cohesive energy as shown in steam-cured and autoclaved mortars of white cement developing high strength as almost the same as that of mortar cured in water at 20°C.

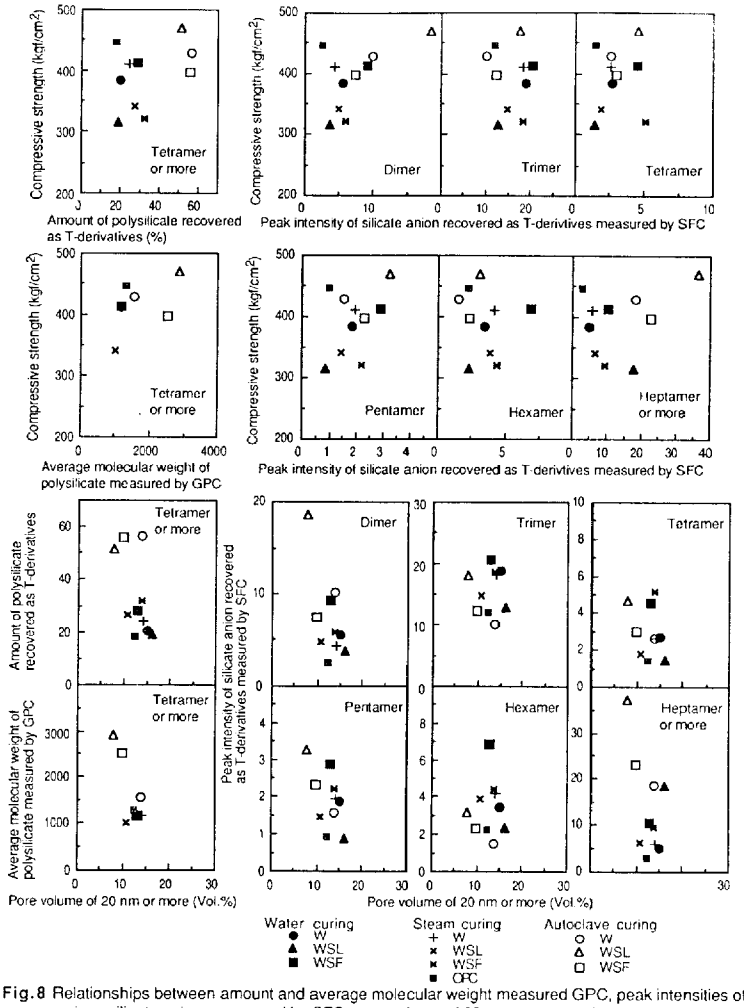

Fig.8 Relationships between amount and average molecular weight measured GPC, peak intensities of various silicate anions measured by SFC, pore volume of 20nm or more and compressive strength

(2) TMS-SFC-GPC - Supercritical fluid chromatogram of hardened white cement mortar after 28 days treated by trimethylsilylation is shown in **Fig. 7.** By the conventional gas chromatography and GPC, it is impossible to separate polymer silicate derivatives clearly. SFC is capable of clear separating and detecting the silicate derivatives of higher polycondensation. SFC using FID as the detector is able to separate polymer silicate derivatives until octamer or so (6). By the use of ELSD as the detector and by the addition of ethanol into eluent as the modifier, the resolution of SFC increases remarkably and the highly polycondensed silicate derivatives can be detected as shown in **Fig. 7.** Monomers, however, can not be detected due to the high temperature setting (90°C) of nebulizer of ELSD.

The relationships of the amount and average molecular weight of polysilicate derivatives measured by GPC and the peak intensities of various silicate derivatives measured by SFC with the strength and pore volume of 20 nm or more in each type of mortar after 28 days are shown in **Fig. 8.** Compared with the mortars containing almost the same pore volume of 20 nm or more, it is recognized that the amounts of silicate anions of heptamer or more and dimer in an autoclaved mortar of white cement are larger than that in autoclaved mortar of silica fume blended white cement. Moreover, the amounts of silicate anions of heptamer or more and dimer in

autoclaved mortar of blastfurnace slag blended cement which develops the highest strength are almost two times as large as that in autoclaved mortar of white cement. This result substantiates the earlier-mentioned mechanism of strength development that the increase in strength of the hydrate itself by the increase in the polycondensation degree of silicate anion in C-S-H compensates for the decrease of cohesive energy caused by the increase in crystallinity and the formation of different kinds of hydrates.

5. CONCLUSION

1) In water curing at 20°C, silica fume blended white cement mortar develops higher strength per unit volume of total pore than the others. Autoclaved mortars develop higher strength per unit volume of total pore than that of water and steam-cured mortars. Although, the strength of mortar is strongly related to the pore volume of 20 nm or more, steam-cured mortars of blastfurnace slag blended white cement and silica fume blended white cement and autoclaved mortar of silica fume blended white cement show a lower strength than the other mortars containing almost the same pore volume of 20 nm or more.
2) In water curing and steam curing, there is no difference in the kinds of hydrates formed and the difference in the C/S molar ratio is relatively small although the well growth of type II C-S-H are observed in mortars cured in steam. In autoclave curing, the addition of blastfurnace slag and silica fume lowers the C/S molar ratio of C-S-H remarkably. The three-dimensional network structure of tobermorite which shows the morphology of type II C-S-H and well grown hydrogarnet are observed.
3) Polycondensation degree of silicate anion in C-S-H increases with the increase in curing temperature and age. In autoclave curing, polycondensation degree varies largely according to the kind of cement used. There are large amounts of silicate anions of heptamer or more and dimer in the autoclaved mortar of blastfurnace slag blended white cement which developed the highest strength. It is considered that the increase in strength of the hydrate itself by the increase in highly polycondensed silicate anions of C-S-H, especially heptamer or more, compensates for the decrease in cohesive energy caused by the increase in crystallinity and the formation of different kinds of hydrates.
4) In the water-cured mortars containing almost the same pore volume of 20 nm or more, polycondensation degrees of silicate anion in C-S-H are in the same level and polycondensation degree of silicate anion in C-S-H is closely related to the strength. In steam and autoclave curing, however, the mortars containing silicate anion of high polycondensation degree develops higher strength per unit pore volume of 20 nm or more. For example, white cement mortar developing higher strength per unit pore volume of 20 nm or more than silica fume blended cement mortar contains larger amounts of highly polycondensed silicate anions, especially heptamer or more and dimer.
5) The higher strengths per unit volume of total pore of autoclaved mortar and silica fume blended white cement mortar cured in water are mainly attributed to the increase in fine pore on which the stress caused by load is poorly concentrated. The lower strength per unit pore volume of 20 nm or more of silica fume blended cement mortar cured under high temperature is attributed both to the low polycondensation degree of silicate anion and low cohesive energy of hydrate caused by the increase in crystallinity and the formation of different kinds of hydrates.

REFERENCES

(1) H.Uchikawa: "Similarities and Discrepancies of Hardened Cement Paste, Mortar and Concrete from the Standpoints of Composition and Structure", Engineering Foundation Conferences Advances in Cement Manufacture and Use at Trout Lodge, Potosi, Missouri, 1988, Vol. 1, p271
(2) H.Uchikawa, S.Hanehara and D.Sawaki: "Effect of Hardened Structure of Blended Cement Mortar and Concrete on their Strength", CAJ Proceedings of Cement & Concrete, 1990, No.44, p330
(3) S.Brunauer, D.L.Kantro and L.E.Copeland: "The Stoichiometry of the Hydration of ß-Dicalcium Silicate and Tricalcium Silicate at Room Temperature", Journal of American Ceramic Society,1958, 80(2), p761
(4) H.Uchikawa and R.Furuta: Cement and Concrete Research, 1981, Vol.11, No.1, p65
(5) H.Uchikawa: "Effect of Blending Components on Hydration and Structure Formation", 8th International Congress on the Chemistry of Cement, 1986, Vol.1, p249-280, Rio de Janeiro.
(6) H.Uchikawa, S.Uchida and T.Okamura: "Role of Fly Ash on the Hydration and Structure formation of Ternary Components Blended Cement Composed of Blastfurnace Slag, Fly ash and Portland Cement", Proceedings Shanghai 1991 Ash Utilization Conference, Vol.2: Ash Use in Cement and Concrete, p65-1.
(7) K.A.Smith, R.J.Kirkpatrick, E.Oldfield and D.M.Henderson: "High-resolution Silicon-29 Nuclear Magnetic Resonance Spectroscopic Study of Rock-forming Silicate", American Mineralogist, 1983, Vol.68, p1206.
(8) N.J.Clayden, C.M.Dobson, G.W.Groves, C.J.Hayes, S.A.Rodger, "Solid State NMR Studies of Cement Hydration", Proc. British Ceramic Society, 1984, (35), p55.

OBSERVATION OF THE CHANGE OF COMPOSITION AND SURFACE STRUCTURE OF ALITE CRYSTAL AND ESTIMATION OF HYDRATION REACTIVITY BY ETCHING

Hiroshi Uchikawa*, Shunsuke Hanehara and Daisuke Sawaki****

**Executive Director, Research and Development, Onoda Cement Co Ltd, JAPAN*
***Central Research Laboratory, Onoda Cement Co Ltd, JAPAN*

SUMMARY

The hydration reactivity of mineral components and the movement of elements during the hydration reaction of cement clinker were studied combining the state-of-the-art surface-structure-determining techniques including atomic force microscopy, in-lens field emission scanning electron microscopy and Auger electron spectroscopy with the etching techniques for optical microscopy. The hydration reactivity is related to the change in color tone by etching the surface of sample. Holes several nm in diameter from which elements are dissolved are developed more on the surface of alite than on that of belite after etching. The rough surface which makes us analogize the existence of network structure is also observed. By etching the surface of alite with water for 30 seconds, the distance between the peak and trough on the surface becomes 11nm and the Ca/Si ratio at the surface decreases to 1.3 because Ca is selectively leached out. The etched depth is proportional to the 1/4th power of the etching time. The Ca/Si ratio at the surface of belite is decreased to 1.6 by the same etching treatment. The etched depth is 2nm in this case. The setting time of cement can be estimated from the change in color tone of clinker alite by etching and this technique can be applied for control of setting time of cement.

Résumé

Les réactivités d'hydratation de composants minéraux et le mouvement des éléments au cours de la réaction d'hydratation dans des scories de ciment a été examinées, en combinant aux techniques de corrosion pour microscopic optique l'état-de-l'art en matière de techniques de détermination de structures de surface, y compris la spectroscopie atomique, la microscopie électronique à balayage à émission de champ intra-objectif, et la spectroscopie électronique selon Auger. La réactivité d'hydratation est rapportée aux changements de couleur induits par corrosion de la surface de l'échantillon. Des trous de plusieurs nm de diamètre dont les éléments ont été dissous, se sont développés après corrosion préférentiellement à la surface de l'alite plutôt que sur celle de la belite. Une surface rugueuse suggérant l'existence d'une structure en réseau est également observée. En corrodant la surface de l'alite avec de l'eau durant trente secondes, la distance entre sommet et fossé à la surface atteignent 11nm et le rapport Ca/Si à la surface décroît à 1.3 parce que le Ca est lessivé de facon sélective. La profondeur de corrodée est proportionnelle au 1/4 de la puissance du temps de corrosion. Le rapport Ca/Si à la surface de la belite décroît à 1.6 avec le même traitement. La profondeur de corrodée est de 2 nm à cette occasion. Le temps de prise du ciment peut être estimé à partir du changement de couleur en corrodant les scories, et cette technique est appliquée au contrôle du temps de prise du ciment.

1. INTRODUCTION

Observation of alite, belite and interstitial phase in clinker with the reflection optical microscope after etching the surface of polished clinker had been developed about a hundred years ago(1), as well as with the transmission optical microscope(2)(3), and is still used for quality control of cement clinker.

In order to clarify the compositional and structural change on the surface of clinker minerals immediately after mixing with water and to establish a simple rapid testing method of setting time using clinker, the authors have investigated the initial hydration of clinker minerals combining the state-of-the-art surface-structure-determining apparatuses including atomic force microscope (AFM), in-lens field emission scanning electron microscope (FESEM) and Auger electron spectroscope (AES) with the etching technique for determining the surface structure and the element distribution in the depth direction in a micro-region.

2. EXPERIMENTAL METHOD

2.1 Sample

Eight ordinary, three high early strength and three moderate heat portland cement clinkers produced in several plants were ground with 2.0% of gypsum as SO_3 by test mill to 3,500 cm^2/g of Blaine specific surface area.

2.2 Etching treatment

A polished surface of clinker was dipped in pure water for 30, 600 and 3,600 seconds or 0.01% aqueous solution of NH_4Cl. Then it was washed with a large amount of ethanol and dried.

2.3 Determination of the surface structure and composition of clinker

The change of surface structure of the clinker minerals before and after etching was observed by in-lens FESEM (JEOL 840) and AFM (Digital scan). The roughness of the surface of alite crystal in the direction of depth was determined by AFM. The distribution of element in the direction of depth from the surface of alite and belite particles was determined by AES (JEOL JAMP-8400).

2.4 Test of setting time

Setting time of cement was measured in the manner described in JIS R 5201.

3. RESULTS AND DISCUSSIONS

3.1 Surface structure and composition of clinker minerals

3.1.1 Change of surface structure of clinker minerals before and after etching - A micrograph of clinker by a reflection optical microscope is shown in **Fig.1**. Alite in the clinker turns brown by the etching treatment and the color becomes darker with the increase of etching time. The color tone of belite remains unchanged by etching. Since the C_3A phase is easily dissolved, the contrast with the color of the C_4AF phase becomes more remarkable. Spherical free CaO particles change in various color tones with the passage of time.

The secondary electron images of the surface of clinker before and after etching with water for 30 seconds observed by in-lens FESEM are shown in **Fig.2**. Since the angle of aperture can be increased by setting the sample in the objective lens of in-lens FESEM, the magnification and resolving power can be augmented as high as of 0.7nm compared with the ordinary FESEM. The particles exists on the surfaces of alite and belite before etching are contaminants. Holes several nm in diameter from which elements are dissolved are developed more on the alite crystal than on the belite crystal after etching. The general structure of them is regarded as a network considering from the roughness of surface. The surface structure of C_4AF phase is not changed so much by etching. Roughness of the surface of alite after etching seems to be caused by dissolution of element from alite and precipitation of hydrate on alite.

The AFM images of the surfaces of alite before and after etching with water for 30 seconds are shown in **Fig. 3**. The smooth surface before etching has a roughness as small as approximately 1 to 2nm and fine scratches at intervals of approximately 50nm regarded as abrasions with grains of abrasive 0.05μm in average

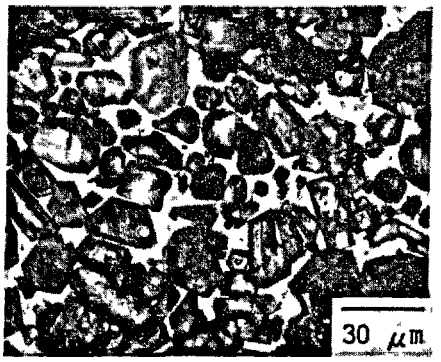

Fig. 1

Reflected light micrograph of clinker etched with 0.01% aqueous solution of NH_4Cl for 30 seconds

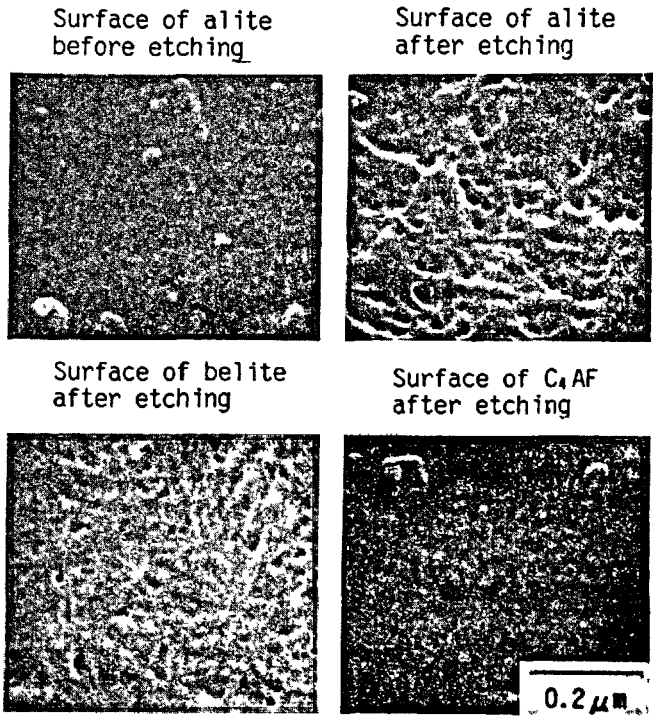

Fig. 2

Secondary electron image of the surface of clinker before and after etching with water by in-lens FESEM

diameter. The roughness of the surface after etching is enlarged by the dissolution of elements and the distance between peaks is approximately 100nm. The roughness of the surface determined by AFM in a high accuracy of 0.1nm in the direction of depth is shown in **Fig. 4**. The distance between the peak and the trough on the surface of alite is 10.3 to 11.5nm. Assuming that the distance corresponds to the size of an alite crystal dissolved, four unit cells with the c-axis 2.5nm long are leached out from the surface in the direction of c-axis. The distance is increased to 18.5 and 39.4nm by increasing the etching time to 600 to 3600 seconds, respectively. The distance is proportional to the 1/4th power of the etching time as shown in **Fig. 5**.

The change in color tone of the polished surface of clinker is attributed to the combination of the interference of beams with different optical path lengths according to the roughness of etched surface and the difference in the passing time of beam through the etched surface phase. The larger the roughness the of surface is, the stronger the interference color becomes.

3.1.2 Change of composition in the direction of depth from the surface of clinker minerals before and after etching - The distribution of element from the etched surface of clinker minerals in the direction of depth can be determined by the ion-sputtering method. Sizes of alite and belite particle are within a range from 10 to 40μm. AES is appropriate for determining the element distribution in the direction of depth from the surface, because the analytical region of surface by AES is 100nm to 1μm in the cross wide direction and ion-sputtering can be applied to AES. The change of composition in the direction of depth from the surface of alite particle according to the etching time is shown in **Fig. 6**. The analytical position is the center of alite. The Ca/Si molar ratio in the surface layer and depths of 3 and 8nm from the alite surface etched for 30 seconds are approximately 1.3, 2.1 and 3.0, respectively. As mentioned above, the position showing the theoretical value of Ca/Si ratio of alite is 8nm deep. The sputtering depth by AES is expressed as that of quartz under the same conditions, therefore it has some possibility to be underestimated. Nevertheless, the depth coincides with the distance between the peak and the trough on the surface of approximately 11nm by AFM. The Ca/Si ratios in the surface layer of belite and at a depth of 3nm from it are 1.6 and 2, respectively. The result indicates that the hydration reactivity of belite is lower than that of alite because Ca ions are dissolved at the beginning of hydration less from a shallower part in belite than in alite.

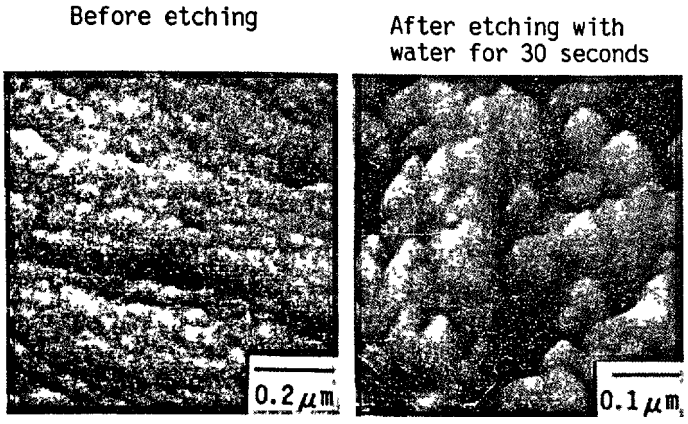

Fig. 3

AFM image of the surface of clinker alite before and after etching with water for 30 seconds

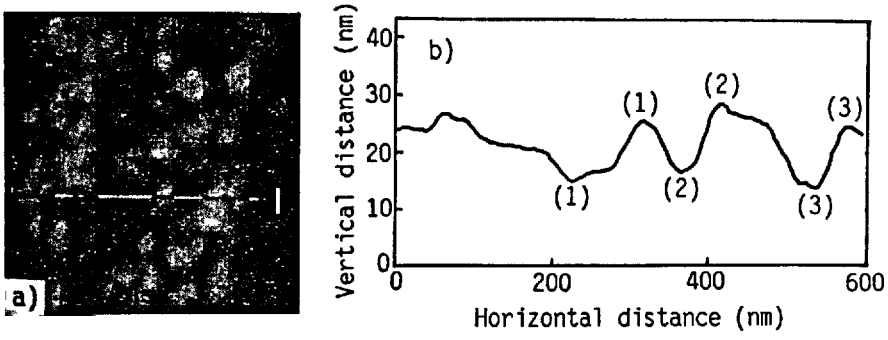

a) AFM image,
b) Surface profile of line I shown in a)

	(1)	(2)	(3)
Horizontal distance [nm]	93.00	57.00	36.00
Vertical distance [nm]	10.34	11.55	10.29
Angle [deg]	6.35	11.45	15.96

Fig. 4

Roughness of the surface of clinker alite etched with water for 30 seconds determined by AFM

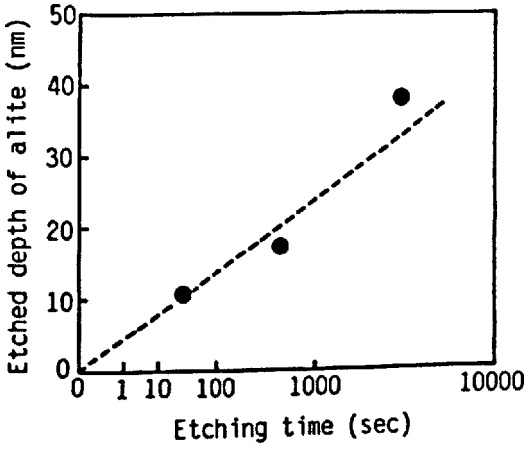

Fig. 5

Relationship between etching time and etched depth of clinker alite

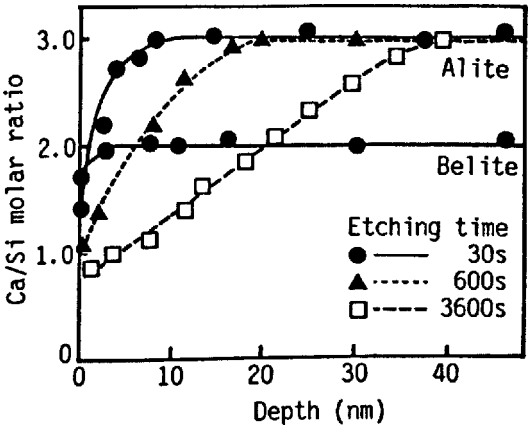

Fig. 6

Change of Ca/Si molar ratio in the direction of depth from the surface of alite particle according to the etching time

In case of alite with zonal structure, the peripheral part coincides with high temperature stable transformation of M_3 akin to trigonal and the inner part coincides with low temperature stable transformation of M_1(4)(5). This result was confirmed by determination of structure and composition of each part by micro-focus x-ray diffractometer and EPMA(6). Since inner part in alite is more easily etched with water than peripheral part, M_1 phase has higher hydration reactivity at initial stage than M_3 phase. Etching depth on alite by water corresponds to Ca ion leached from the surface of alite, and relates to the hydration reactivity of alite. Hydration reactivity at initial stage of cement clinker seems to be estimated by the change of color tone of alite and belite by etching with water.

3.2 Relationship between color tone of alite by etching and setting time of cement

The etching time with pure water, for example 1 hour, is so long that the etched depth of the sample is varied by the effect of ions dissolving from the sample in water and of precipitation of hydrate. If the data of the etching with pure water is required, the data obtained by etching with a solution free from such an effect has to be converted into the data of etching with pure water. It was confirmed by AFM that etching with pure water for 60 minutes corresponds to that with 0.01% aqueous solution of NH_4Cl for 30 seconds.

As alite is the most influential mineral on the properties of cement, standard chart of color tone of alite etched with 0.01% aqueous solution of NH_4Cl was prepared by dipping the same sample after every 3 seconds interval. The pinacoid perpendicular to the c-axis of alite crystal is more slowly etched than the other surface rhomb. Assuming that the area ratio of the pinacoid to the other surface coming out on the polished surface by etching is constant, however, the hydration reactivity of alite may be inferred by the change of color tone after etching. The degree of etching of clinkers was determined by color tone after etching with 0.01% aqueous solution for 30 seconds, compared with standard chart.

The relationship between the degree of etching of alite in clinker and the initial setting time of cement is shown in **Fig. 7**. Classifying the amount of free CaO in clinker into three ranges, that is, less than 0.5%, 0.5-1.0% and more than 1.0%, the degree of etching of clinker closely relates to initial setting time of cement. The more easily clinker is etched, the shorter the initial setting time of cement becomes. For example, the initial setting time varies with a range of 120 and 180 minutes at the same free CaO level. Increase of free CaO of 0.5% in clinker corresponds to shortening of 40 minutes of initial setting time. The same tendency is observed on the final setting time. At the same amount of free CaO and the same degree of etching, estimated initial setting time is shorter in the order of high early strength portland cement, ordinary portland cement and moderate heat portland cement. Thus the setting time of cement can be estimated from the change in color tone of alite in clinker by etching and this technique can be applied for the control of setting time of cement.

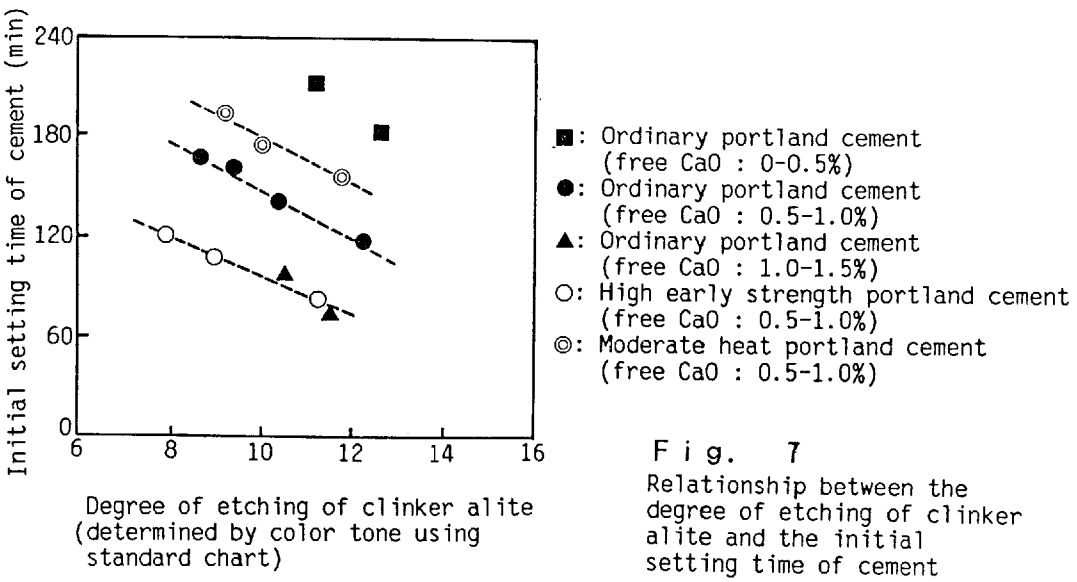

Fig. 7
Relationship between the degree of etching of clinker alite and the initial setting time of cement

4. CONCLUSIONS

The change of surface structure and composition of clinker minerals by etching were investigated using the state-of-the-art surface-structure-determining techniques including AFM, in-lens FESEM and AES. Results obtained are as follows;

1) Holes several nm in diameter from which elements are dissolved are developed more on the alite crystal than on the belite crystal after etching with water. By etching the surface of alite with water for 30 seconds, the distance between the peak and the trough on the surface becomes 11nm. The etched depth is proportional to the 1/4th power of the etching time.

2) The change in color tone of the polished surface of clinker by etching is attributed to the combination of the interference of beams with different optical path lengths according to the roughness of etched surface and the difference in the passing time of beam through the etched surface phase.

3) The Ca/Si molar ratio in the surface layer and depths of 3 and 8nm from the alite surface etched with water for 30 seconds are approximately 1.3, 2.1 and 3.0, respectively. The position showing the theoretical value of Ca/Si ratio of alite is 8nm deep by AES. The depth coincides with the distance between the peak and the trough on the surface of approximately 11nm by AFM.

4) Classifying the amount of free CaO in clinker into three ranges, that is, less than 0.5%, 0.5-1.0% and more than 1.0%, the degree of etching of clinker expressed by interference color closely relates to initial setting time of cement. The setting time of cement can be estimated from the change in color tone of alite in clinker by etching and this technique can be applied for the control of setting time of cement.

REFERENCES

(1) H. Insley, H.F. McMurdie: "Minor Constituents in Portland Cement Clinker", Journal of Research of the National Bureau of Standard, 1938, 20 (2), 173-184.
(2) A.E. Törnebohm: Zement, 1903, 4, p.287
(3) H. Le Chatelier: Experimental Researches on the Constitution of Hydraulic Mortar, McGraw-Hill, New York, 1905.
(4) S. Chromy: "High-Temperature Microscopic Investigation of Tricalcium Silicate and Dicalcium Silicate Phase in Portland Cement Clinker", Journal of American Ceramic Society, 1967, 50 (12), 677-681.
(5) I. Maki, K.Goto: "Factors Influencing the Phase Constitution of Alite in Portland Cement Clinker", CEMENT and CONCRETE RESEARCH, 1982, 12 (3), 301-308.
(6) H. Uchikawa, S. Hanehara, T.Shirasaka: "Relationship between Zonal Structure in Alite and Lamellar Texture in Belite and Their Production Process, Composition and Crystal Structure", 1992, submitted to Supplementary paper for 9th ICCC in New Delhi.

COMPARISON OF TWO METHODS FOR STOPPING HYDRATION : APPLICATION TO THE STUDY OF THE INITIAL DISSOLUTION RATE OF C_3S

C Vernet and G Noworyta

Technodes SA
Centre de Recherche Industrielle et Technique du Groupe, Ciments Francais
FRANCE

ABSTRACT :

We have compared two techniques for stopping hydration: rinsing with ethanol–ether, and cryosublimation after freezing in liquid nitrogen. We have applied both methods to the study of short term hydration of tricalcium silicate. Suspensions with water/silicate = 4, monitored with an electrical conductivity device, were filtered at various times, during the dormant period. Filtrates were kept apart, and the solid fractions rinsed with ethanol–ether. After treatement, the solid parts were remixed with their respective liquid phase, and the hydration rate monitored again. In case of freezing, the same set of suspensions in their bottle were immersed in liquid nitrogen, reheated at 25°C, and then monitored again without filtration. Our results show that the C_3S dissolution rate is modified with both treatments. The effect is more pronounced for freezing, probably because the C_3S grains undergo internal cracking due to ice growth.

Beyond this point, the conductometric analysis has been used to evidence the effect of hydration time upon the C_3S dissolution rate. It is found that during the dormant period, the dissolution rate is a decreasing function of the hydration time, and is limited by diffusion through the hydrates layer. As second diffusional regime, at a higher rate, begins when portlandite precipitates.

RESUME :

Nous avons comparé deux méthodes d'arrêt de l'hydratation: le rinçage à l'éthanol–éther et la cryosublimation après gel dans l'azote liquide. Ces deux méthodes ont été appliquées à l'étude de l'hydratation à court terme du silicate tricalcique. Après application de chaque méthode, les solides ont été remis en suspension dans la phase aqueuse au contact lors de l'arrêt., et l'hydratation a été suivie par conductimétrie, permettant de mesurer la durée de la période dormante.

Nos résultats montrent que la dissolution de C_3S est modifiée par les deux traitements. Cet effet est plus prononcé pour le gel, car les grains de C_3S subissent une microfissuration interne lors de la croissance cristalline de la glace. L'étude des variations de la durée de période dormante des échantillons préhydratés, stoppés et remis en suspension, montrent que la vitesse initiale de dissolution est une fonction décroissante de du temps d'hydratation, et qu'elle est limitée par la diffusion à travers la couche d'hydrates. Un second régime diffusionnel, de vitesse plus grande, commence lors de la précipitation de la portlandite..

1 - INTRODUCTION.

Among the existing methods for stopping hydration, rinsing with organic solvents like acetone-ether or ethanol-ether is the most currently used. This technique implies crushing of the paste before rinsing. Hence, it is of particular interest for the study of suspensions. Cryosublimation, which does not require crushing, can also be used, but it is not rapid enough to follow the rapid initial reactions. In this case, liquid nitrogen freezing of the sample has to be used in order to stop the hydration quickly (1).

We have compared these two methods, and applied them to the study of the early steps of C_3S hydration (dormant period). The first aim of this study was to find the best experimental procedure, knowing the secondary effects of the treatments on the microstructure of the hydrates. The second aim was to study the kinetics of CSH formation during the first hours of hydration.

2 - EXPERIMENTAL.

Two identical series of suspensions with water/C_3S =4 were studied. They were stirred at 25°C at the same speed, and monitored with an electrical conductivity device. Hydration was stopped at different times by both methods, sampling each time two suspensions.

- In the first case, the suspension was filtered under vacuum. The filtrate was kept apart, and the solid residue was rinsed with the solvent and moderately dried by vacuum evaporation. The filtrate and its rinsed solid were then reintroduced in the cell and monitored further.
- In the second case, the suspension in its plastic cell was immersed in liquid nitrogen, allowed to freeze, and then reheated to 25°C, stirred and monitored again.

The samples were finally exposed to the same vapor pressure, to bring the samples in the same standard hygrometric status.

Both methods were applied to different synthetic alites and C_3S samples. The dormant period duration, during the second run, was measured and studied as a function of the time of hydration in the first run. More details on the conductometric techniques and significance of the curves are given elsewhere (2)

Three synthetic alites were tested, the end of the dormant period being easily detectable with the conductivity maximum (the curves of alite N°1 are given at fig.1). The duration of the first run was taken into account, and added to the duration of the dormant period measured during the second run. The intermediate filtration and drying can thus be considered as a simple point on the curves, as if the clock had been stopped during these operations.

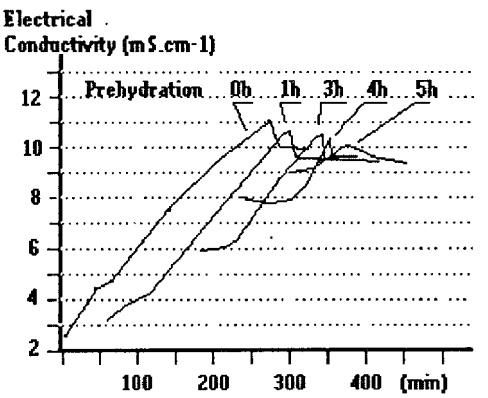

Fig.1 Conductivity curves for alite #1 prehydrated during 0 to 5 hours

When hydration was stopped after the end of the dormant period of the first stirring, a second conductivity maximum, showing a new precipitation of portlandite, occured during the second stirring. In this case, the second dormant period was used for totalisation. The three alites, allowed to hydrate and monitored without further step of treatment, were taken as references for comparison.

3 - RESULTS.

3.1. Rinsing with ethanol-ether.

The total dormant period durations (DPD), are given in table 1, with the calculated differences from the untreated alites. In agreement with a previous work of BARRET and BERTRANDIE (3), an increase of the dormant period duration is found. The variation with respect to the reference increases with the stopping time, that is to say with the progress of reactions of the alite samples during the first step.

Table 1. Dormant period durations with rinsing at time t1.

stopping time t1	ALITE 1 D.P.D	(diff)	ALITE 2 D.P.D	(diff)	ALITE 3 D.P.D.	(diff)
0h15					2h48	(0h26)
0h30			4h25	(- 0h20)		
1h00	5h12	(0h50)			3h03	(0h41)
2h00			5h15	(0h10)	3h36	(1h14)
2h30					4h03	(1h41)
3h00	5h48	(1h26)	5h28	(0h23)	4h43	(2h21)
3h30			5h36	(0h31)	5h12	(2h50)
4h00	5h52	(1h30)			5h28	(3h06)
5h00	6h10	(1h48)			6h37	(4h15)
Reference	4h22	0	5h05	0	2h22	0

A negative difference is found in one case (alite 2 stopped after 30 minutes). This was not observed for other series of C_3S and alites, but the upward trend of the differences was confirmed.

3.2. Freezing with liquid nitrogen.

The conductometric curves are given in fig.2 for alite N°2, and the total dormant period durations in Table 2, for alites 1 and 2. As for rinsing, the difference with regard to the standard increases with the stopping time, here from negative to positive values.

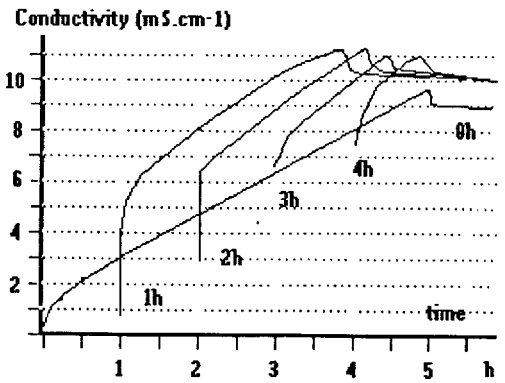

Fig.2 Conductometric curves for alite #2 frozen after 0 to 4h of prehydration

The negative values correspond to an acceleration of the hydration. It is a secondary effect of freezing, when this is applied before the end of the dormant period of the first step. This behaviour was confirmed with other series of C_3S and alites stopped by freezing.

4 – INTERPRETATION.

4.1. Differences of dormant period.

All the differences from the reference dormant periods are plotted on fig.3, as a function of the stopping time t_1. The curves are composed of two parts: the first part, after a short initial increase, shows weak slopes, similar for each alite sample and treatment.

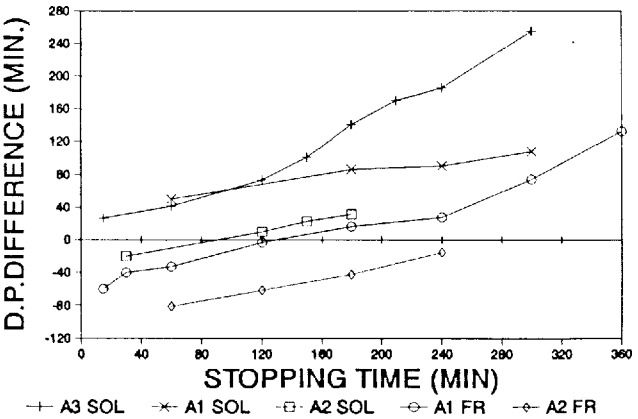

Fig.3 Dormant period difference from reference not prehydrated

Table 2. Dormant period durations with intermediate freezing.

stopping time t_1	ALITE 1 D.P.D	(diff)	ALITE 2 D.P.D.	(diff)
0h15	3h05	(-1h20)		
0h30	3h25	(-1h00)		
1h00	3h32	(-0h53)	3h44	(-1h21)
2h00	4h02	(-0h23)	4h08	(-0h57)
3h00	4h21	(-0h04)	4h23	(-0H42)
4h00	4h33	(0h08)	4h50	(-0h15)
5h00	5h19	(0h19)		
6h00	6h18	(0h18)		
16h00	17h05	(1h05)		
Standard	4h25	0	5h05	0

The second part shows a larger slope, beginning just before the time which corresponds to the reference dormant period.

Plotted as a function of the square root of t_1, the curves seem to be parallel in their first part (fig.4). This is not surprising, since the initial reactions are known to be diffusion-controlled (3). The curves now differing only by a constant, we are questioned about its significance. This constant represents the difference obtained at the very first moments, between the reference and treated alites.

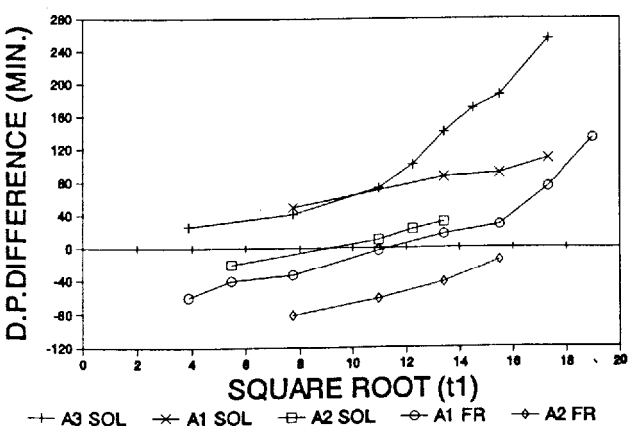

Fig.4 Differences of DPD as a function of $t_1^{1/2}$

- the references are in different states of conservation, more or less aerated with the storage time. The treatment could renew the surface, and lead to an increase in reactivity. In this respect, alites 1 and 3 seem to be in a better state than alite 2, for both treatments.
- the first freezing and ice growth can create some modifications of the alite grains, if they have an internal porosity accessible to water. This could be a good explanation of the negative values of the differences observed in this case, the treated samples becoming more reactive than the references.
This hypothesis was checked by scanning electron microscopy, which confirms the porous structure of the alite samples (photo 1)
- sorption by hydrates or imbibition of organic solvents into the pores of the samples (4) could also be a cause of modification of hydration kinetics and hydrates permeability or structure.

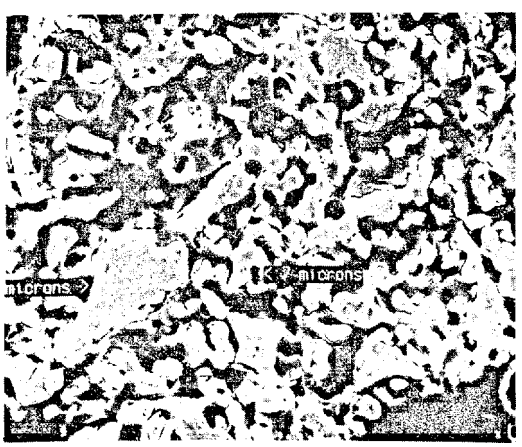

Photo 1 Porosity of alite #1

Table 3. **Correction of the references.**

Alite/treatment	ref.DPD (min)	correction (min)	new ref.DPD (min)
alite 3/solvent	142	- 5 (+/-5)	137
alite 1/solvent	262	- 5 (+/-5)	257
alite 2/solvent	305	-50 (+/-5)	245
alite 1/freezing	265	-103 (+/-5)	162
alite 2/freezing	305	-135 (+/-5)	170

Taking into account these initial differences, the ordinates at time zero were calculated by extrapolation, with a regression method. New reference values were obtained, and are listed below (table3).

The new curves are now superimposed in their first part (fig.5). They appear to be composed of two straight lines, intersecting at a time corresponding to about ten minute before the end of the untreated samples dormant period.

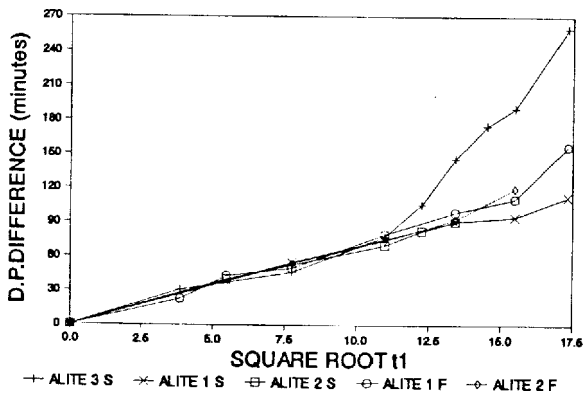

Fig.5 Corrected curves DPD vs $t_1^{1/2}$

The complete corrected curves are plotted on fig.6. A very good fit with a square root law is found, within the experimental errors.

4.2. Effect of treatments upon the dissolution rate of C3S.

Having taken into account the initial perturbations caused by the treatments, it appears that, for a given increase of the square root of the time of stirring in the first step, a proportional increase of the dormant period is obtained in the second stirring step.

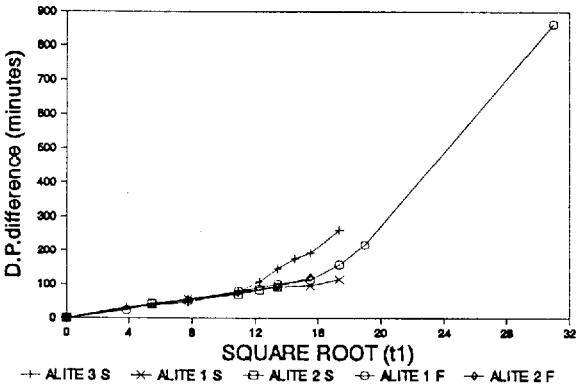

Fig.6 Complete corrected curves.

The existence of such a relation can be related to different causes, but the most evident is the covering of the alite surface by a layer of CSH, the permeability of which is a decreasing function of time (3).
Both treatments are likely to modify the permeability of this layer, by irreversible dehydration and/or sorption of molecules. Applied to a layer, the thickness of which increases with time t_1, the treatments could then induce an additional reduction of the dissolution rate, also function of t_1.

4.3. Effect of treatments upon the portlandite nucleation.

The treatments do not modify the time of portlandite nucleation: Despite the modifications of the CSH layer caused by the treatments, a new dif-

fusional regime takes place when portlandite begins to precipitate. This occurs about ten minutes before the conductivity maximum, when the slope of the curve starts to decrease. This observation is in agreement with the fact that the concentrations detected by conductometry are the resultant of the difference of two ionic fluxes, and that the maximum is dynamical.

In this second regime, the permeability of the layer seems to be governed by the portlandite growth, thus less sensitive to dehydration by solvents or freezing. This is in agreement with NMR results on two samples stopped before and after the end of dormant period, showing no difference concerning the polymerisation of CSH (5).

5 - CONCLUSIONS.

For both treatments, the C_3S dissolution rate increases with the square root of the time of hydration, that is to say with the thickness of the CSH layer. Nevertheless these effects can be modelized, what enables a second use of a sample already partially hydrated. This could be useful in case of working on very small quantities of samples, for example those enriched with rare or expensive isotopes.

The less disturbing treatment is found to be the solvent rinsing one. It could be used to renew the surface of old aerated samples, and this requires additional research.
Freezing leads to an increase of the C_3S reactivity, by fracturation or microcracking of porous samples, and opening new pathways for water. Because it is the only method available to stop the hydration quickly and very early, it can be used with precautions, and requires a reference treated by the same way, after a few second of hydration.

Regarding the hydration mechanisms of C_3S, our results are consistent with a control of the duration of the dormant period by the permeability of the CSH layer, and with the starting of a new period caused by portlandite nucleation and growth.
Portlandite nuclei being formed in the most supersaturated zones, near the interface, it is not surprising to find no effect or a weak effect of seeding experiments with portlandite. This is also in agreement with the dormant period reduction by ultrafine particles, observed elsewhere (6), (7).

Additional work is now required to quantify the reaction rates, and to build a model taking into account the kinetics of portlandite nucleation and growth, and its effects on the CSH permeability.

REFERENCES.

(1) CHANDRA S.; HEDBERG B.; BERNTSSON L.; "Freezing as a method of study of early cement paste hydration."
J.C.C.R., Vol 10, pp 467–469, 1980.

(2) VERNET C.; NOWORYTA G.;
"Conductometric test for cement–admixture systems". 9th International Congress on the Chemistry of Cement, NEW DEHLI, 1992, Theme III, Sub–theme III–D "Effect of admixtures".

(3) BARRET P.; BERTRANDIE D.;
"Experimental study of the barrier effect of calcium hydrosilicate (CSH) leading to a new view on the hydration mechanism of tricalcium silicate." 10th International Symposium on the Reactivity of solids, Dijon, 1984, pp 543–545,

(4) TAYLOR H.F.W.; TURNER A.B.; "Reactions of tricalcium silicate paste with organic liquids."
J.C.C.R., Vol 17, pp 613–623, 1987.

(5) RASSEM R. "Apports de la RMN a l'étude du mécanisme d'hydratation du silicate tricalcique, composant majoritaire du ciment portland."
Thèse Doctorat, 16/05/1990, Université Paris VI.

(6) BEEDLE S.S.; GROVES G.W.; RODGER S.A.; "The effect of fine pozzolanic and other particles on the hydration of C3S." Advances in Cement Research, 1989, 2, N°5, Jan, pp 3–8.

(7) VERNET C.; NOWORYTA G.; "Reactivity test for fine silica and pozzolanic mineral additives. 9th International Congress on the Chemistry of Cement, NEW DEHLI, 1992, Theme II, Sub–theme II–A, "Advances in portland and blended cements."

A SCALING APPROACH TO THE TEXTURE OF HARDENED CEMENT PASTES

R Maggion, S Bonnamy, P Levitz, D Tinet, and H Van Damme

Centre de Recherche sur la Matière Divisée
CNRS - Université d'Orléans
FRANCE

Abstract

An integrated approach involving several nondestructive or mild structural techniques has been developed in order to characterize the textural evolution of hardened cement pastes at all length scales between the size of the elementary colloidal gel particles and the size of the largest void. The starting samples were all prepared with the same w/c ratio (0.4). Their evolution was monitored from one day up to one year. The C_3S/CSH ratio was measured by X-ray diffraction. Mercury intrusion was used as a standard reference method in order to measure the pore size distribution and the pore scaling properties between 1 μm and 10 nm. The specific surface area accessible to water molecules in saturated conditions was measured by proton NMR. Small angle X-ray scattering was used to determine the scaling properties between 45 and 3 nm. A multifractal analysis was performed on digitized transmission electron micrographs. In the later case, a mild stepwise solvent exchange treatment was developed in order to include the water-saturated samples in epoxy resin. The micrographs were obtained on ultra-thin (50 nm) slices.

Most of the specific surface area and porosity evolution (in particular, the disappearance of the capillary porosity peak) was found to occur in the first days of curing, in parallel with the progress of the hydration reaction. However, significant and complex interface morphological changes occur at longer period. The long-term state of this evolution appears to be a surface and pore volume multifractal structure.

Résumé

L'évolution texturale de pâtes de ciment durcies examinée à des échelles comprises entre la taille des particules colloïdales élémentaires et la taille des pores capillaires est étudiée par des méthodes non destructives. Les échantillons de départ sont préparés à un rapport E/C de 0,4. Le temps d'hydratation varie de un jour à plus de un an. Le rapport C_3S/CSH est déterminé par diffraction des rayons X. L'intrusion de mercure est utilisée comme technique de référence pour la détermination la distribution de tailles de pores et des propriétés de loi d'échelle entre 1 μm et 10 nm. La surface spécifique accessible aux molécules d'eau est mesurée par RMN du deutéron dans les conditions de saturation. La diffusion des Rayons X aux petits angles est utilisée pour déterminer les propriétés de loi d'échelle entre 45 et 3 nm. Une analyse multifractale est réalisée sur des images numérisées obtenues par microscopie électronique à transmission. Dans ce dernier cas, un échange de solvants est appliqué sur les échantillons saturés d'eau pour permettre l'inclusion dans une résine époxy. Les micrographies sont obtenues sur des coupes ultra-minces de 50 nm d'épaisseur.

Les résultats indiquent que l'évolution de la surface spécifique et de la porosité intervient dans les premiers jours de l'histoire de la pâte, parallèlement à la progression de la réaction d'hydratation. Cependant, des variations morphologiques complexes se produisent pour des périodes plus longues. A long terme, le résultat de cette évolution est une structure dont la matière et le réseau poreux présentent une organisation multifractale.

1 Introduction

Understanding the physical and mechanical properties of cement pastes requires a thorough knowledge of the matter and void distribution (what we call *microtexture*) at all length scales between the size of the elementary colloidal particles of the hydrated phases and that of the largest voids (microcracks network). *In this paper we shall concentrate on the microtextural characterization of the most important component of cement pastes, CSH gel. Our target is to understand how the capillary porosity of the fresh paste is progressively filled by the hydrated gel as the CSH/C_3S ratio increases, during a curing period extending from 1 day to 1 year.* We examined three microtextural features: the surface area the interface morphology and the pore size distribution. These features are usually studied by methods (BET method applied to nitrogen or water adsorption, scanning electron microscopy, mercury porosimetry) which, though powerful, have the drawback of perturbing the microtexture of the sample either during the sample preparation or during the measurement proper. *It is an integral part of our approach to develop methods which will allow keeping the samples as much as possible in wet, unperturbed conditions.*

2 Sample preparation and hydration rate

All the samples were prepared with a water/C_3S ratio of 0.4. The samples were cast as thin disks of 3 mm thickness and 3 cm diameter. The disks were stored at room temperature in saturated lime slurries during the curing period, in closed polyethylene vessels.

The progress of the hydration reaction, defined as the fraction of anhydrous material converted to hydration products, was monitored by X-ray diffraction, by quantitatively estimating the fraction of unreacted C_3S on the basis of the intensity of its diffraction lines, compared to an internal standard (10% silicon, by weight), as described elsewhere [1].

3 Solid/water interface area

Spin-lattice relaxation time (T_1) measurements of solvent nuclei in dilute or concentrated suspensions of mineral particles have been used as a non-perturbing method for the determination of a solid-liquid interface area. The method is based on the increased relaxation rate of solvent molecules nuclei close to the solid surface (typically within 1 nm from the surface). It has been applied to clay suspensions [2] as well as to fresh or hardened cement pastes ([3], [4]).

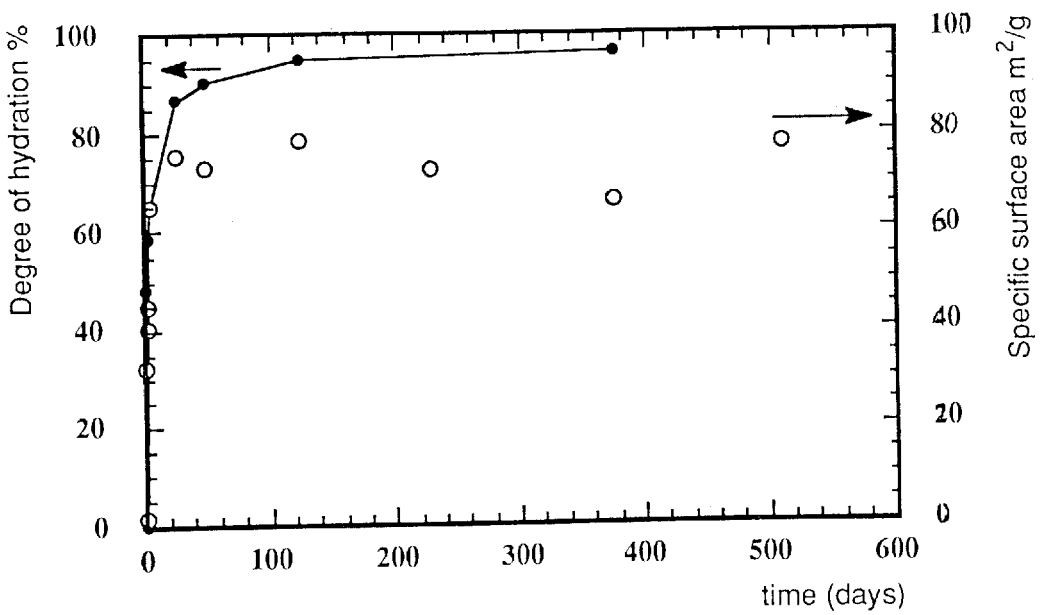

Fig 1: ^2H NMR specific surface area and hydration rate as a function of curing time

An important feature of this method is that, in the case of aggregated particles separated by one or a few layers of solvent molecules (this applies to clay flocs and, most probably, to cement hydrates)) , it does not yield the *total* surface area of the particles but only the *external surface area of the colloidal aggregates*. This stems from the condition of rapid molecular exchange between the interfacial phase and the capillary water or the suspension medium.

In order to determine the evolution of the hydrate particles aggregates surface area with curing time, each sample disk past a given curing time was dried with a paper cloth at room temperature for a few minutes, weighed, and roughly crushed by hand. Several suspensions of the resulting fragments in heavy water were then immediately prepared with increasing solid/heavy water ratios and their deuteron relaxation rate was measured. The interface area was calculated for each sample from the evolution of T_1^{-1} as described elsewhere [2] .

As shown in Figure 1, the evolution of the hydrated products/water interface area is significant and fast in the first 25 days, in step with the progress of the hydration reaction. About 90% of the initial C_3S mass is converted to hydration products after 25 days. The interface area is close to its maximum (~ 0,075 m^2/Kg) for that curing time and tends to decrease slightly afterwards. A preliminary conclusion from this is that *all eventual textural modifications occurring after about 25 days do so essentially at constant hydrate aggregate/water interface area.*

4 Pore size distribution

Although mercury intrusion is a perturbing technique (it involves drying the sample and, at very high intrusion pressure, may even destroy the pore system), it is a standard method for analyzing the pore neck size distribution of porous materials. We analyzed the pore volume distributions after 1, 4, 15, 57 and 375 days curing. The total porosity, defined as the ratio of the total pore volume to the external or apparent volume of the sample, decreases from 0.38 to 0.14 when the hydration reaction progress increases from 0.48 to 0.96 over 375 days. In fact, most of this evolution takes place in the first 50 days, with the rapid disappearance of the capillary porosity peak centered around ~0.7 μm in the first days, followed by a slower decrease to a broader distribution of pores between 0.5 and 0.01 μm.

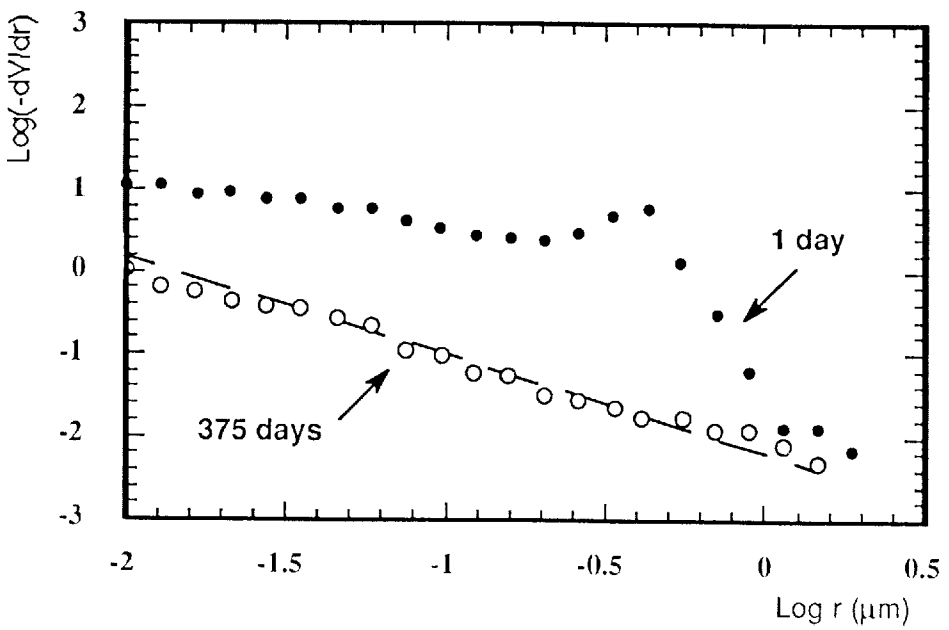

Fig 2: pore diameter (μm) distribution determined by mercury intrusion

Interestingly, the long term evolution of the porosity after 375 days is a broad and smooth distribution which, when examined in logarithmic scales (Figure 2), is clearly suggesting the existence of scaling properties. The slope of this log-log relationship may be interpreted in terms of fractal dimension of the pore walls.

Assuming that a pore volume measurement by mercury intrusion in this material at a given pressure P corresponding to a given pore radius r is equivalent to measuring the pore space *accessible* to balls of dimension r, one can show that [5] :

$$dV_{access}(r)/dr = -(3-D)(D-2).L^{D}.r^{2-D} \qquad (1)$$

This relationship, which predicts a linear Log(dV/dr) *vs* Logr, is only reasonably obeyed in the case of the sample cured for 375 days. It leads to a surface fractal dimension of 3.04

5 Interface morphology

Small-angle X-ray scattering (SAXS) measurements were performed in the q-domain between 0.12 and 2 nm^{-1}. All the measurements were performed in point geometry. The samples were examined in powdered form, after hand crushing of the wet disks.

In the case of mass fractals, the scattered intensity is expected to scale as [6]

$$I(q) \sim q^{-Dm}$$

In the case of surface fractal structures, one would expect

$$I(q) \sim q^{-(6-Ds)}$$

SAXS has already been applied both to cement pastes [7]; and to CSH pastes [8]. A fractal behavior was found in all cases, but the results do not agree quantitatively. However, these discrepancies may be due to differences in materials, preparation or curing conditions. In the case of CSH pastes prepared with water/C_3S= 0.5, a surface fractal behavior is observed with D_S=2.74 [8].

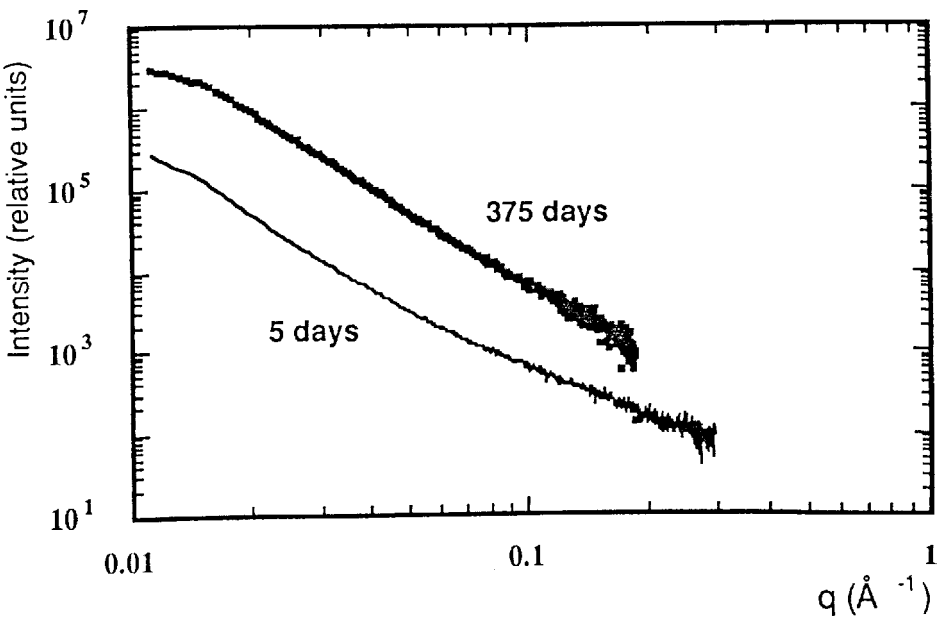

Our Log I(q) *vs* Log q curves (Figure 3) show in general two linear regimes. The first one is observed at small q (long distances), below ~ 0.7 nm^{-1}. The slope is always close to -3 or slightly more negative. This can be interpreted in terms of a surface fractal behaviour with Ds<3. The second regime is observed at large q (smaller distances)) above 0.7 nm^{-1} and is characterized by slopes which range from -1.9 to -2.88. The most straightforward interpretation of this regime is in terms of a mass fractal behaviour with an increasing compact structure with exponents D_m ranging from 1.9 to 2.88.

The scaling exponents exhibit a clear evolution, in parallel with a crossover between the two regimes. At early curing times, the two regimes are clearly distinct, with a crossover around q=0.7 nm^{-1}, which corresponds to a distance close to 10 nm. At longer curing times (one year), the two regimes seem to merge. The two exponents become very close to each other (D_s=2.89 and D_m=2.38) with no clear crossover point. Thus, SAXS suggests that the long term evolution of the CSH paste is close to a compact structure, at least at length scales between 3 and 45 nm.

6 Transmission electron microscopy and multifractal analysis

Figure 4 (a,b,c) shows three typical digitized images of ultrathin slices of samples after curing times of 1, 22 and 400 days, respectively. The inner CSH and the outer CSH are clearly visible on the 22 day sample. A multifractal analysis [9] of the mass, void space and interface on these images shows that these materials are not simple self-similar structures. A qualitative but important observation is that a young paste is a very heterogeneous distribution of compact grains and open voids whereas a mature paste tends towards a homogeneously dispersed space-filling texture.

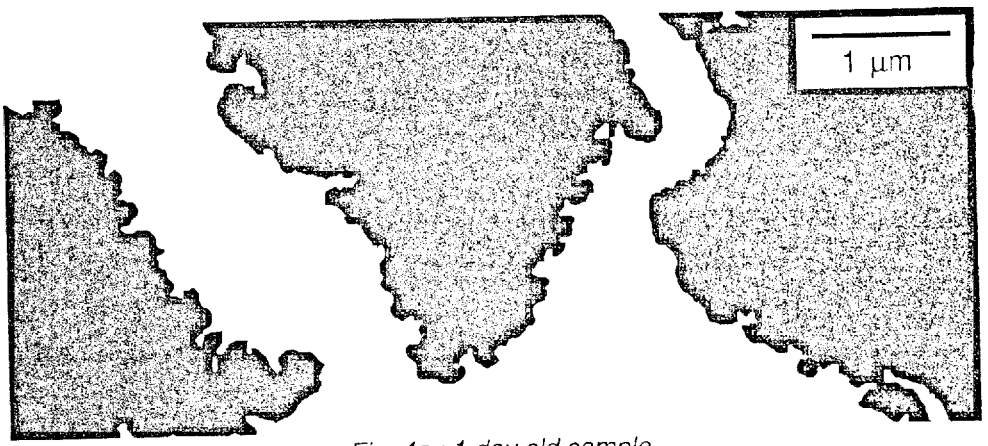

Fig. 4a : 1 day old sample

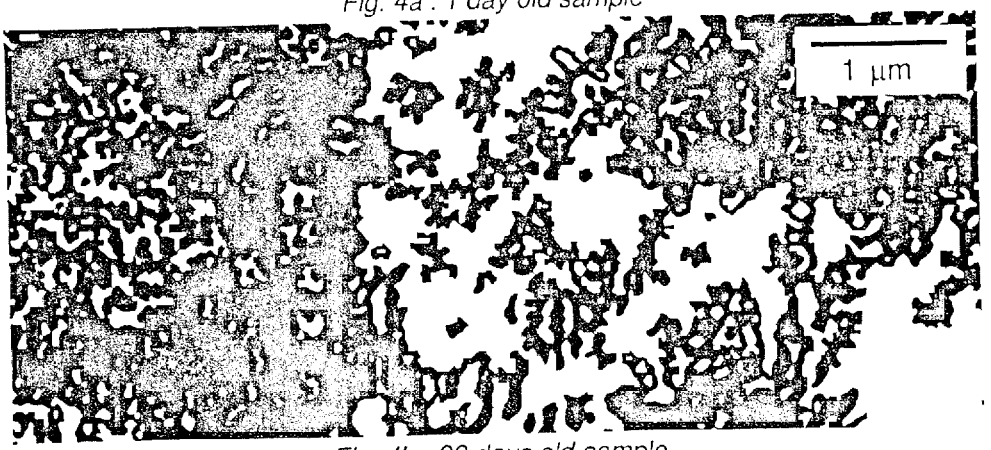

Fig. 4b : 22 days old sample

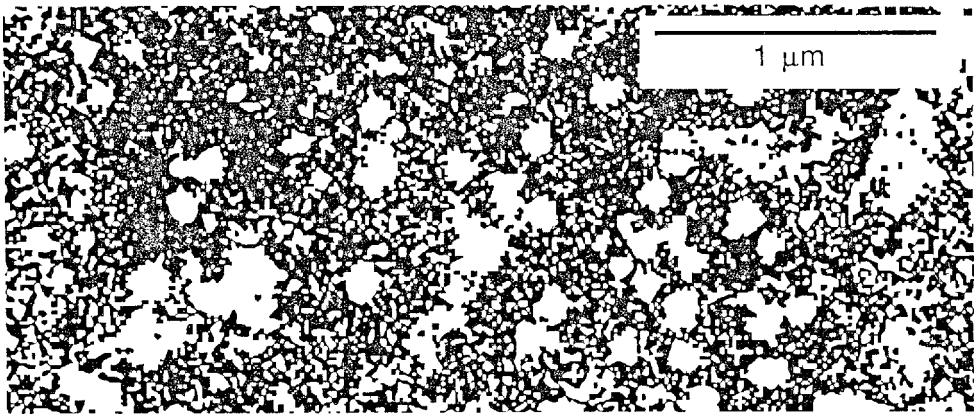

Fig. 4c : 400 days old sample

The main conclusion of this work is undoubtedly that the long term evolution of hardened CSH pastes is a homogeneous fractal structure with a fractal exponent close to 3. Surprisingly, this important *qualitative* change in the paste microtexture occurs long after the initial and fast development of interface area and the filling of the capillary porosity. It is therefore best attributed to textural *rearrangement* processes, occurring at quasi-constant interface area and porosity.

References

[1] Maggion R., Tinet D., Levitz P., Van Damme H. and Faugère A.M., in *Hydration and Setting*, proceedings first Int. Workshop on Hydration and Setting, Dijon 1991, in press

[2] Fripiat J.J., Cases J., François M., Letellier M. and Rouquerol J. (1982), J. Coll. Interf. Sc., **89**, 378-400

[3] Barbic L., Kocuvan I., Blinc R., Lahajnar G., Merljak P. and Zupancic (1982), J. Amer. Ceram. Soc., **65**, 25-31

[4] Letellier M., Van Damme H., Mortureux B. and Regourd M. (1986), Proc. Int. Congress on Cement Chemistry, Rio.

[5] Fripiat J.J. (1989), in *The Fractal Approach to Heterogeneous Chemistry*, (D. Avnir ed.), John Wiley & Sons, Chichester, pp. 331-340

[6] Martin J.E. and Hurd A.J. (1987), J. Appl. Cryst., **20**, 61-78

[7] Winslow D.N. (1985), Cem. Concr. Res., **15**, 817-824

[8] Craievich A.F. (1987), J. Appl. Cryst., **20**, 327-329

[9] Levitz P. (1992), to be published in J. Phys. (Paris)

Acknowledgements : We would like to thank the **A**ssociation **T**echnique de l'**I**ndustrie des **L**iants **H**ydrauliques (**ATILH**) for financial support.

APPLICATIONS OF HIGHER TEMPERATURE CONDUCTION CALORIMETRY TO HIGH ALUMINA CEMENT HYDRATION

John Bensted, Gary J Audley and Paul N Aukett

B P International Ltd, Sunbury Research Centre
Middlesex, UK

SUMMARY

Hydration of high alumina cement (HAC) has been examined in the Setaram C80 heatflux calorimeter at temperatures from 20°C to 180°C. Accurate recording of the initial heat evolution is achieved through an in-situ mixing system. This technique enables hydration phenomena to be studied under both normal and hydrothermal (refractory) conditions. The effects of using different water/cement ratios and employing admixtures are clearly demonstrated. For instance, for the neat HAC at water/cement ratios 0.3 and 0.5, the time at which the major heat peak was observed (which is associated with cement setting), passed through a maximum at 35°C. The hydration reaction was faster at both lower and higher temperatures. This apparent anomaly can be understood in terms of the hydration of CA (the main cementing component) and the problems of nucleation of CAH_{10} at around 35°C. As with Portland cements, calcium lignosulphonates retard the setting of HAC but tend initially to produce greater chemical reactivity. Calcium chloride tends to retard HAC hydration, whereas it accelerates Portland cement hydration at similar concentrations. Much practically useful information on workability, setting and the development of hardening in HAC can be obtained through the application of the higher temperature conduction calorimetry described.

INTRODUCTION

Conduction calorimetry has become a standard laboratory technique for studying the hydration behaviour of cements[1-3], following the development by Calvet[4] of the original Tian calorimeter[5]. Conventional conduction calorimetry has suffered from the following problems:

a) The inability to use it above 95°C meant that hydrothermal cement hydration reactions could not be investigated.

b) It was not possible to record accurately the initial heat peak at the beginning of hydration owing to difficulties experienced in the internal mixing of cements with water.

These problems were overcome with the development of the Setaram C80 heatflux calorimeter. This instrument allows in situ mixing of the cement with water, which enables the first heat peak to be accurately measured. Using the mixing cell, experiments can be carried out up to 180°C, the point at which the vapour pressure of water equals the working pressure of the cell (~1.0 MPa). The technique has been successfully employed in the examination of oilwell cementing formulations over a wide temperature range[6,7]

In the present work the heatflux calorimeter has been applied to the hydration of high alumina cement (HAC). The hydration has been examined under a variety of conditions over the temperature range 20 - 180°C.

The HAC and water were placed in the two respective halves of the mixing cell, separated by a loose fitting lid and a layer of mercury. Mixing was carried out internally within the heatflux calorimeter by means of an automatic reversing mechanism. This permitted the loose fitting lid to fall away and thus allow the cement and water to mix. In this way, it was possible to measure accurately the initial heat peak for the hydration process.

EXPERIMENTAL

Conduction calorimetry was carried out on the Setaram C80 heatflux calorimeter using a Lafarge Ciment Fondu high alumina cement (produced to BS 915:1972[8]) at water/cement ratios of 0.30 or 0.50 within the temperature range 20 - 180°C. In order to ascertain the effect of admixtures, calcium lignosulphonate (CLS) at 0.2% and 0.3% by weight of cement and calcium chloride at 2% by weight of cement were also investigated for their effects upon the hydration process.

The HAC and water were placed in the two respective halves of the mixing cell, separated by a loose fitting lid and a layer of mercury. Mixing was carried out internally within the heatflux calorimeter by means of an automatic reversing mechanism. This permitted the loose fitting lid to fall away and thus allow the cement and water to mix. In this way, it was possible to measure accurately the initial heat peak for the hydration process.

RESULTS

The results of this work are tabulated in Table 1 and illustrated in Figures 1 and 2. Here heat evolution is shown only up to 33 hours, and the curves are to different scales for the heat flow axis so as to aid clarity.

DISCUSSION

In comparison with Portland cement, there is much less heat dissipated at the very beginning of hydration at 20°C[3,6]. A small first heat peak, due primarily to heat of solution and heat of wetting effects arises during the first minutes of hydration. The principal heat peak is the second one. For HAC at 0.30 w/c (sample 1) this second peak occurred at 7.3 hours. The times corresponding to initial and final set (335 and 355 minutes) occurred on the low time side of the second heat peak, a phenomenon similar to that observed with Portland cement, but in this instance due primarily to the onset of significant CAH_{10} formation. Hydration was slow at first and then became rapid, giving a long workability period, in accordance with the slow setting, but rapid-hardening characteristics of HAC. At 0.50 w/c (sample 2), which is above the generally recommended maximum water level of 0.40 for practical usage[9,10], there is much greater heat dissipation during the first few hours and setting is advanced.

Addition of 2% calcium chloride to the HAC at 0.30 w/c (sample 3) effectively retarded the first heat peak. However, it drew out the 'second' heat peak into three peaks, the first of which moved forward to 5.2 hours, but the other two (at 9.6 and 20.6) peaks were effectively retarded in comparison with sample 1 in the absence of calcium chloride. At 0.50 w/c (sample 4) the first heat peak is larger, indicative of greater chemical reactivity, but the second heat peak is retarded and has a pronounced shoulder on the low time side. Clearly 2% calcium chloride, which accelerates Portland cement hydration at 20°C, has a much more complex effect on HAC, tending to retard the setting process and interfering with the smooth hydration of CA to CAH_{10}. Calcium lignosulphonate (CLS) in 0.2% quantities, as with Portland cements, retards the setting and the advent of the second heat peak in sample 5 at 0.30 w/c. For sample 6 compared with sample 2 at 0.50 w/c there is more chemical reactivity at the beginning of hydration, as shown by a greater first heat peak, but further heat is dissipated over a longer time period, which is commensurate with the retardation of setting. Like calcium chloride, CLS interferes with the smooth, effective hydration of CA to CAH_{10}. At 0.3% CLS addition for 0.30 w/c (sample 7) more heat was dissipated in the first 3 hours than for 0.2% addition (sample 5). Repetition with a different CLS (sample 8) produced similar results. For 0.5 w/c (sample 9), in comparison with the corresponding 0.2% CLS addition level (sample 6), there was a greater first heat peak, confirming the greater reactivity produced by CLS at the commencement of hydration, but a similar second heat peak, although this was advanced to 11.9 hours. Yet, the overall effect was retardation of set.

At 35 °C, although the first heat peak was greater than the 20 °C one for HAC hydration at both 0.30 and 0.50 w/c (samples 10 and 11), onset of the second heat peak was comparatively delayed in both instances corresponding to longer setting, despite the higher temperature. This is in line with the observations on the hydration of CA, the major cementing component of HAC, which encounters problems of nucleation in producing CAH_{10} at around ~30 - 35 °C[11]; this would explain the longer setting observed from the delayed second heat peak here. Significant quantities of C_2AH_8 are also formed at this temperature, which, like CAH_{10} contribute towards the setting process.

At 50 °C and 0.30 w/c (sample 12) the hydration rate of the HAC had substantially increased, with setting times and the workability period reduced and the small first heat peak not accurately quantifiable. At 75 °C (sample 13) the small first heat peak had apparently merged into the much larger 'second' heat peak with its maximum at 8.0 minutes. This had a pronounced shoulder on the longer time side indicative of substantial C_3AH_6 formation at this stage of the hydration process. C_3AH_6 is substantially involved in the setting process here.

At 100 °C (sample 14) the shoulder has practically disappeared, since hydration is far less discontinuous by now, and less heat is evolved than at 75 °C, although the peak maximum has decreased to around 7.4 minutes. This trend continued at 140 °C (sample 15), with the peak maximum being brought further forward, the shoulder having disappeared, but the total level of reactivity continuing to fall off. Finally at 180 °C (sample 16), the level of reactivity has only fallen off slightly compared with the situation at 140 °C. At these elevated temperatures the HAC hydration was comparatively less sensitive to temperature changes than at the lower temperatures encountered. This is undoubtedly connected with C_3AH_6 being the dominant hydration product here. Such observations are important in the context of hydrothermal hydration, which has been less well characterised for HAC than for Portland cement[12].

CONCLUSION

Higher temperature conduction calorimetry has been demonstrated to be a valuable tool for studying the hydration behaviour of high alumina cement. The effects of different temperatures, water/cement ratios and admixtures have been clearly pinpointed. Much practically useful data on workability, setting and the development of hardening in HAC can be obtained by employing this technique in laboratory studies.

ACKNOWLEDGEMENT

The authors wish to thank the Lafarge Aluminous Cement Company Ltd of West Thurrock, Essex, UK for supplying the high alumina cement (Ciment Fondu) used in these investigations and BP International Ltd for permission to publish this work.

BIBLIOGRAPHY

1. J A Forrester (1970). A conduction calorimeter for the study of cement hydration. Cement Technology 1 (3), 95 - 99.

2. J Bensted (1980). Early hydration behaviour of sulphate-resisting and white Portland cement. Proceedings of the 7th International Congress on the Chemistry of Cement, Paris, 1980. Volume II: Communications. pp II/1 - 6. Editions Septima, Paris.

3. J Bensted (1987). Some applications of conduction calorimetry to cement hydration. Advances in Cement Research 1 (1), 35 - 44.

4. E Calvet and H Prat (1963). "Recent Progress in Microcalorimetry." Pergamon Press, Oxford.

5. A Tian (1923). Utilisation de la méthode calorimétrique en dynamique chimique: emploi d'un micro-calorimètre à compensation. Bulletin de la Société Chimique de France 33 (4), 427 - 428.

6. J Bensted and P N Aukett (1990). Applications of higher temperature conduction calorimetry to oilwell cementing. World Cement 21 (7), 308 - 320.

7. P N Aukett and J Bensted (1991). Application of heat flow calorimetry to the study of oilwell cements. 5th European Symposium on Thermal Analysis and Calorimetry, 25th - 30th August 1991, Nice. Journal of Thermal Analysis (in press).

8. British Standards Institution (1972). Specification for High Alumina Cement (Metric Units), BS 915:Part 2:1972.

9. H G Midgley (1990). High alumina cement in construction - a future based on experience. "Calcium Aluminate Cements." (Ed R J Mangabhai) Proceedings of the International Symposium held at Queen Mary and Westfield College, University of London, 9th - 11th July 1990, pp 1 - 13. E & FN Spon, London, New York.

10. C M George (1990). Manufacture and performance of aluminous cement: a new perspective. ibid. pp 181 - 207.

11. A Capmas, D Ménétrier-Sorrentino and D Damidot (1990). ibid. pp 65 - 80.

12. G Bell, J Bensted and F P Glasser (1989). Characterisation of hydrothermally-treated calcium silicate and oilwell cement hydration products. Advances in Cement Research 2(6), 61 - 72.

TABLE 1

CONDUCTION CALORIMETRIC DATA

SAMPLE NO	TEMP (°C)	W/C RATIO	ADMIXTURE	1st HEAT PEAK -ΔH (J/g)	1st HEAT PEAK PEAK HEIGHT (mW/g)	2nd & OTHER HEAT PEAKS -ΔH (J/g)	2nd & OTHER HEAT PEAKS PEAK MAX (hours)	2nd & OTHER HEAT PEAKS PEAK HEIGHT (mW/g)
1	20	0.30	-	5.6	3.5	204.5	7.3	20
2	20	0.50	-	4.4	4	312.5	6.6	22
3	20	0.30	2% $CaCl_2$	2.9	1.5	58.2 39.6 97.6	5.2 9.6 20.6	5 3 4.5
4	20	0.50	2% $CaCl_2$	10.2	5	280.9	13.8 sh 14.7	13 14
5	20	0.30	0.2% CLS	3.8	2.5	39.8 161.4	9.1 21.6	2 3.5
6	20	0.50	0.2% CLS	5.1	2.5	306.3	21.5	5
7	20	0.30	0.3% CLS	3.9	2.5	8.3 75.2 74.8	2.8 8.5 25.9	1 2 1.5
8	20	0.30	0.3% CLS*	4.5	2.5	43.3 58.8 78.2	7.7 19.8 30.5	2 1.5 1.5
9	20	0.50	0.3% CLS	6.6	2.5	290.0	11.3	6
10	35	0.30	-	13.7	4	240.5	9.5	22
11	35	0.50	-	32.0	5	310.0	12.4 (minutes)	24
12	50	0.30	-	10.0+	7.5	327.2	77.2	98
13	75	0.30	-	*	*	399.6	8.0 22.0 sh	199 90
14	100	0.30	-	*	*	362.9	7	415
15	140	0.30	-	*	*	339.3	<7	320
16	180	0.30	-	*	*	332.5	<7	375

+ only partially resolvable
* encompassed within main heat peak

sh - shoulder
* different CLS sample

Fig. 1: Conduction Calorimetry Curves For HAC Samples 1 – 9

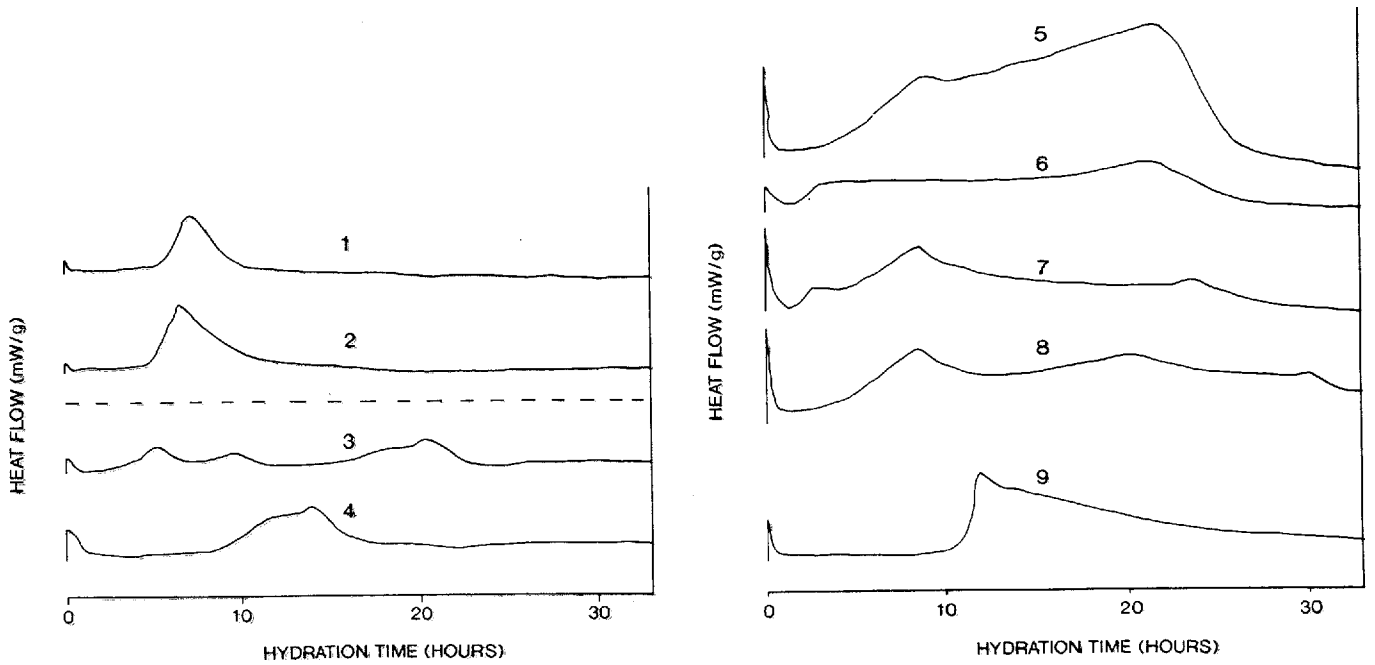

Fig.2: Conduction Calorimetry Curves For HAC Samples 10 – 16

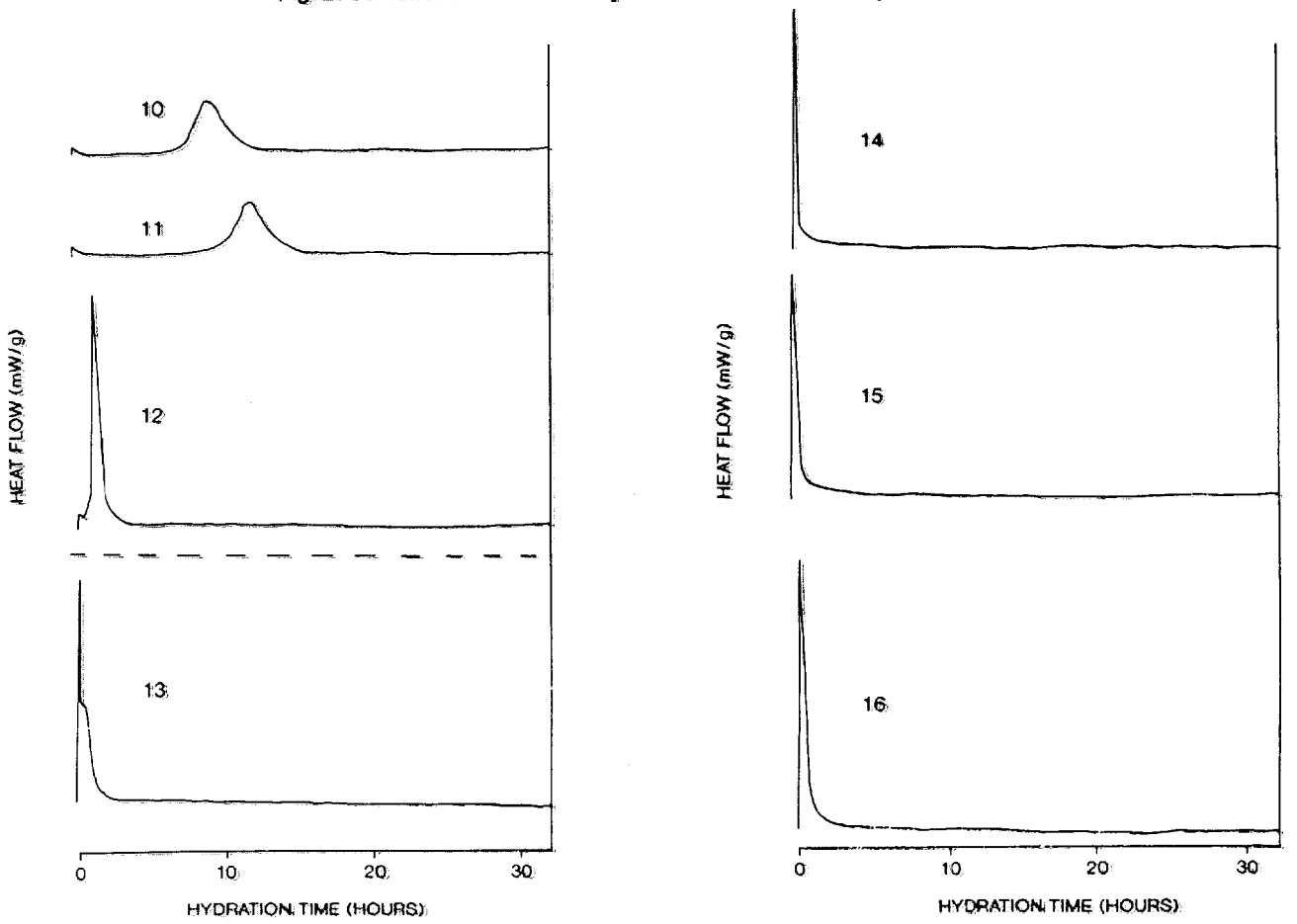

A METHOD FOR DETERMINING THE ADVANCEMENT OF THE HYDRATION OF C_3S IN DILUTED SUSPENSIONS BY MEANS OF SIMULTANEOUS CONDUCTIMETRIC AND CALORIMETRIC MEASUREMENTS

D Damidot and A Nonat

Laboratoire de Recherches sur la Réactivité des Solides
Faculté des Sciences Mirande, Université de Bourgogne
FRANCE

SUMMARY

Hydration of C_3S has often been studied in stirred diluted suspensions by following the evolution versus time of the silicate and calcium concentrations in solution or that of the electric conductivity of the solution. In this way, it is possible to get a quantitative determination of the advancement of the reaction by making hypothesis on the Ca/Si of the precipitated C-S-H only before the precipitation of portlandite.

For getting round this limitation, we developped an isothermal microcalorimetric technique for studying stirred diluted suspensions and allowing to simultaneously measure the heat flow released by the reaction and the electrical conductivity of the solution.

The use of this method in different hydration conditions (e.g. W/C ratio, initial ionic concentrations...), leading to the rate of each reaction involving in the hydration of C_3S, allowed us to distinguish two kinetic steps of precipitation of C-S-H with different diffusion properties.

RESUME

L'hydratation de C_3S a souvent été étudiée en suspension diluée et agitée en suivant l'évolution en fonction du temps de la concentration des ions silicates et calcium en solution ou plus simplement celle de la conductivité électrique de la solution. De cette manière, il n'est possible de déterminer quantitativement l'avancement de la réaction que pendant la période précédant la précipitation de la portlandite et en faisant des hypothèses sur le rapport Ca/Si des C-S-H qui précipitent.

Pour pallier cette limitation nous avons développé une technique de microcalorimétrie isotherme permettant l'étude des suspensions agitées tout en mesurant la conductivité électrique de la solution.

L'utilisation de cette méthode originale dans différentes conditions d'hydratation (W/C, concentration ioniques initiale,..) nous a permis de distinguer, lors de l'hydratation, deux étapes cinétiques de précipitation des C-S-H dont les propriétés par rapport à la diffusion des ions et de l'eau sont différentes.

INTRODUCTION

The most of recent studies on C_3S hydration especially in diluted suspensions (1-3), lead to the conclusion that hydration proceeds by through solution reactions. From precise analysis of the evolution of both calcium and silica concentrations in solution, Barret and Bertrandie (2) showed that hydration process may be divided in five stages during which three different reactions become successively simultaneous; there are :

- R_1, the dissolution of C_3S, with the rate v_1
- R_2, the precipitation of C-S-H, with the rate v_2
- R_3, the precipitation of portlandite, with the rate v_3,

and relations between the three rates have been established. But it is not possible by this way to know the rate of each reaction and then the advancement of hydration, especially after the portlandite precipitation.

On the other hand, the calorimetry offers the advantage to follow continuously the evolution of the system and to give a proportional measure of the reaction rates during the hydration process; it is often used to characterize the evolution of cement hydration in paste. So we try to joint the two methods to study C_3S hydration and we adapted a very sensitive isothermal calorimeter for analysing stirred diluted suspensions.

EXPERIMENTAL PROCEDURE

The experimental device was built up around a TIAN-CALVET isothermal type microcalorimeter. Its high sensitivity (0.3μW) allows to measure the heat evolution rate of very diluted suspensions (some mg of C_3S in 5 cm^3 of water).

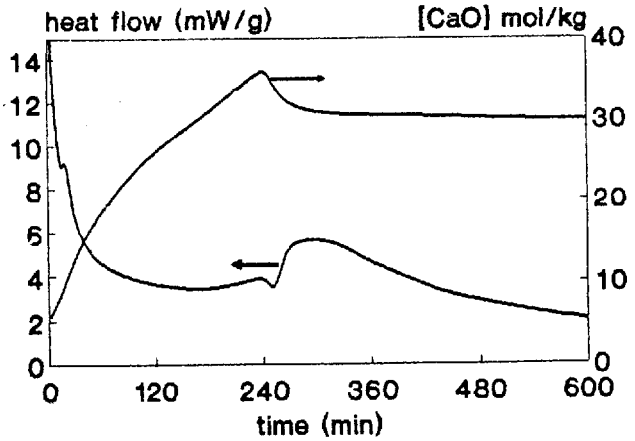

FIG. 1 Typical evolutions of heat flow and conductivity during hydration of C_3S in diluted suspension in water (w/c =18).

When C_3S is hydrated in pure water, lime concentration is proportional to the elecrical conductivity; it may be deduced after calibration. The electrical conductivity of the solution was continuously measured by means of a laboratory-made microelectrode in the calorimetric cell. A full description of the experimental device has been published elsewhere (4). Typical evolutions of both thermal flow and conductivity are presented on figure 1.

C_3S used in this study was supplied by Lafarge Coppée Recherche, it contains less than 0.1% of free lime. The solid was ground, its specific surface, determined by the Blaine's method was 3100 cm^2g^{-1} and its granulometric distribution is centered around 4 μm.

CALCULATION METHOD

Principle of the method

At each time the heat flow $\Phi(t)$ and the electrical conductivity $\Lambda(t)$ of the solution are measured :

$$\Phi(t) = \frac{dQ}{dt} = v_1(t)\,\Delta H_1 + v_2(t)\,\Delta H_2 + v_3(t)\,\Delta H_3 \qquad (1)$$

with v_1 and ΔH_1, the rate and the enthalpy of the C_3S dissolution,
" v_2 " ΔH_2 " precipitation of C-S-H,
" v_3 " ΔH_3 " precipitation of portlandite.

$\Lambda(t)$ is proportional to the lime concentration in solution since the silica concentration is always low and negligible. After calibration or calculation, we obtain $[Ca^{2+}](t)$. At each time, the volume of the solution being constant, $d[Ca^{2+}]/dt$ =

$dnCa^{2+}/dt$, i.e. the variation of the number of mole of Ca^{2+} is equal to the number of calcium ions coming into solution from the C_3S dissolution minus the number of calcium consumed by the C-S-H and CH precipitations, i.e. :

$$dnCa^{2+}/dt = 3v_1(t) - C/S\ v_2(t) - v_3(t) \qquad (2)$$

C/S is the Ca/Si ratio of the precipitated C-S-H. Then, at each time we get a system of two equations with three unknowns :

$$\begin{cases} \dfrac{dQ}{dt} = \Delta H_1\ v_1 + \Delta H_2\ v_2 + \Delta H_3\ v_3 \\ \dfrac{dnCa^{2+}}{dt} = 3\ v_1 - C/S\ v_2 - v_3 \end{cases} \qquad (3)$$

which may be solved only if ΔH_i are known and if relations between v_i are expressed. We have measured and calculated the first, and the second have been established by Barret and Bertrandie (2).

The Relations between v_i

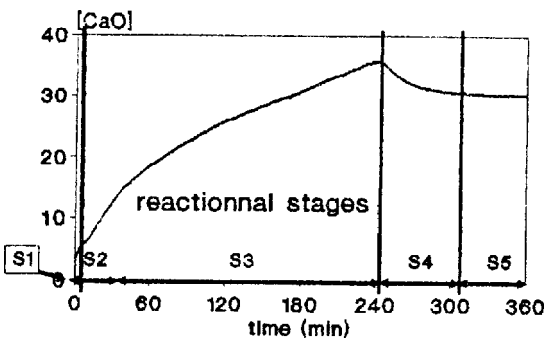

FIG. 2 Schematic representation of the five different stages of C_3S hydration with respect to the lime concentration evolution.

The five stages of the hydration process defined by Barret are located with respect to the evolution of the lime concentration on figure 2.

The first stage - the first stage of the lime concentration evolution corresponds to the congruent dissolution of C_3S producing about 5.5 mmol/kg lime and 1.8 mmol/kg silica. In this stage, only R_1 occurs at the rate v_1.
In the lime-silica-water diagramme, the concentrations in lime and silica reache the supersaturated domain with respect to C-S-H, so C-S-H spontaneously precipitates, that is the second stage.

The second stage - It corresponds to the decrease of the silica concentration untill less than 0.5 mmol/kg due to the precipitation of C-S-H and a plateau in lime concentration which implies a relation between the rate of dissolution of C_3S (v_1) (supplying 3 calcium ions in solution per mole of dissolved C_3S) and the rate of the precipitation of C-S-H (v_2) (consuming 1 calcium ion per mole of precipitated C-S-H). So, there is the following relation between the rates of the simultaneous reactions : $v_2=3v_1$.

The third stage - The lime concentration continuously increases when the silica concentration remains constant. So, the rate of the consuming silica reaction, the precipitation of C-S-H, is equal to the rate of supplying silica reaction, the dissolution of C_3S : $v_1=v_2$.

The fourth stage - When the lime concentration reaches the supersaturation with respect to the portlandite, this one begins to precipitate (R_3), the lime concentration decreases rapidly, i.e. the rate of the precipitation of portlandite (v_3) is greater than the rate of dissolution of C_3S : $v_3>v_1$.

The fifth stage - After the drop in lime concentration, the lime and silica concentrations remain about constant, then the three reactions go on at the same rate $v_1=v_2=v_3$.

Determination of ΔH_1

Enthalpy of dissolution of C_3S, ΔH_1 - ΔH_1 was determined from an experiment in which C_3S was completly dissolved without C-S-H precipitation, that is to say in such a w/c ratio as the lime and silica concentrations are lower than the maximum of supersaturation with respect to C-S-H. Figure 3-a ,shows the heat evolution rate curve during the dissolution of 2 mg of C_3S in 10 ml of water (w/c=5000). From this experiment, the value of ΔH_1 was found to be equal to -132 ± 10 kJ/mol. This value is in a good agreement with that calculated in considering the following equation at pH equal to 11.65 :

$$Ca_3SiO_5 + (4-y)H_2O \rightarrow (3-x)Ca^{2+} + xCaOH^+ + (1-y)H_2SiO_4^{2-} + yH_3SiO_4^- + (5-x-y)OH^-$$

The calculated value is equal to -139 kJ/mol when the enthalpy of formation of each compound according to Petrossian et al (5) and the silicate speciation according to Greenberg (6) are used.

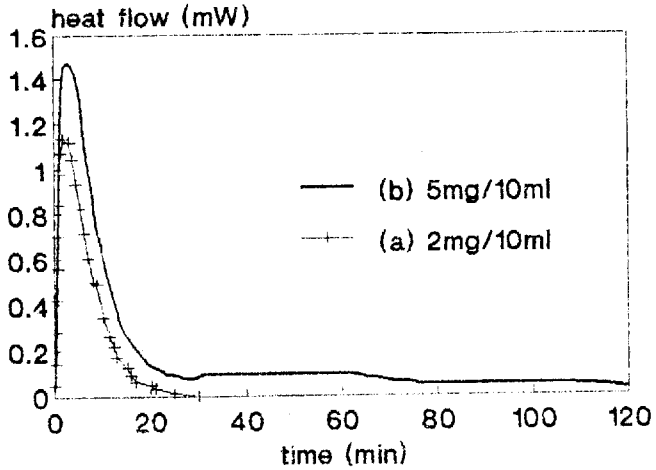

FIG. 3 Heat evolution rate curves versus hydration time from C_3S hydrated at w/c=5000 (a), 2000 (b)

Enthalpy of precipitation of C-S-H, ΔH_2 - Experimental determination of ΔH_2 is more difficult because C-S-H precipitation occurs after or during the dissolution of C_3S. The released heat by the reaction results from the dissolution of C_3S ($x_1\Delta H_1$) and from the precipitation of C-S-H ($x_2\Delta H_2$).

The simplest way consists in dissolving all the C_3S to precipitate C-S-H. Figure 3-b shows the heat evolution rate curve during the hydration of 5 mg of CJS in 10 ml of water (w/c=2000). In such a condition, 84.5% of C_3S is dissolved before reaching the maximum of supersaturation with respect to C-S-H. As soon as this point is reached, C-S-H begins to precipitate from the lime and silica in solution and C_3S continues to dissolve. Considering a C/S ratio equal to 1 in C-S-H, when the solibility equilibrium is reached, $x_2 = 12.10^{-6}$ mol of C-S-H have been precipitated and $x_1=21.10^{-6}$ mol of C_3S have been dissolved. It is then possible to deduce ΔH_2 which is equal to 25±15 kJ/mol. That is an endothermic value which explains the typical shape of the heat evolution rate curve of the figure 3-b.

Enthalpy of precipitation of portlandite, ΔH_3 - The enthalpy value of the portlandite precipitation is well known, ΔH_3 = 16 kJ/mol, it was not been experimentally determined here. Portlandite precipitation produces an endothermic effect too. This enthalpy value is about the same order of magnitude with that of the C-S-H precipitation.

ADVANCEMENT OF THE HYDRATION OF C_3S

At each time, the amount of C_3S consumed by the hydration, $n_1(t)$, is equal to the integration of v_1 between 0 and t, and the percentage of reaction, α, is equal to

$$\alpha(t) = (1/n)\int v_1(t)dt \quad (4)$$

where n is the initial number of mole of C_3S.

Hydration in pure water

The first stage : R_1 is the unique reaction:

$$\Phi = -132\ v_1 \text{ and } dnCa^{2+}/dt = 3v_1,\ v_1(t) = -\Phi(t)/132 \quad (5)$$

The second stage, $v_2 = 3v_1$:

$$\Phi = v_1\Delta H_1 + 3v_1\Delta H_2, \text{ so } v_1 = \Phi/(\Delta H_1 + 3\Delta H_2),\ v_1(t) = -\Phi(t)/57 \quad (6)$$

The third stage, $v_2(t) = v_1(t)$:

$$\Phi = v_1\Delta H_1 + v_2\Delta H_2, \text{ so } v_1(t) = \Phi(t)/(\Delta H_1 + \Delta H_2),\ v_1(t) = -\Phi(t)/107 \quad (7)$$

The fourth stage, $v_3(t) > v_1(t), v_1(t)=v_2(t)$:

$$\begin{cases} \dfrac{dQ}{dt} = -107\, v_1 + \Delta H_3\, v_3 \\ \dfrac{dnCa^{2+}}{dt} = (3 - C/S)\, v_1 - v_3 \end{cases} \quad (8)$$

The fifth stage, the three reactions are going on simultaneously at the same rate :

$$\Phi(t) = v_1\Delta H_1 + v_1\Delta H_2 + v_1\Delta H_3 \text{ and } v_1(t) = -\Phi(t)/91 \quad (9)$$

The evolution of the percentage of the hydration of C_3S by integrating $v_1(t)$ is given on figure 4 with the w/c ratio equal to 13.

A more sophisticated method has been developped considering the change in the C/S ratio in C-S-H according to the well known curve C/S versus lime concentration in solution (7,8). In this case, a fourth reaction, R_4 with the rate $v_4(t)$ and an enthalpy ΔH_4 has to be taken into account. The variation of the enthalpy due to an increase of C/S by the absorption of lime into a tobermorite-like C-S-H has been calculated by Fujii and Kondo (9). They found that the increase of C/S from 0.8 to 2 results in an exothermic effect (-10kJ/mol). The use of this method imposes to solve, for each stage, a system of two equations with two unknowns the coefficients of which are calculated by the algorithm presented on Figure 5. The variation of ΔH_1 and ΔH_2 with the speciation of silicate ions due to the change in pH is taken into account and the evolution of the rate of each reaction is calculated (figure 6). The evolution of the percentage of the hydration of C_3S calculated by this way (figure 4) is not very different from the one obtained with the simpler method. The first method is a good approximation if only the advancement of the reaction is required.

C_3S hydration in saturated lime water

In this condition, the two first stages are practically inexistant (2), so only the equations 7, 8 and 9 have to be considered. The evolution of the percentage of hydration calculated by the two methods is plotted on figure 7 and the evolution of each rate on figure 8.

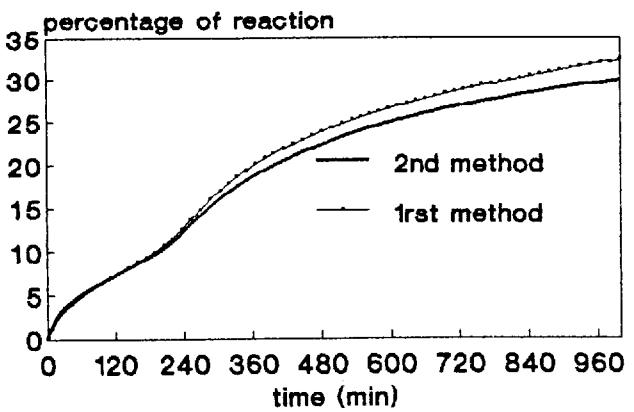

FIG. 4 Percentage of C_3S hydration versus time in water (w/c = 13)

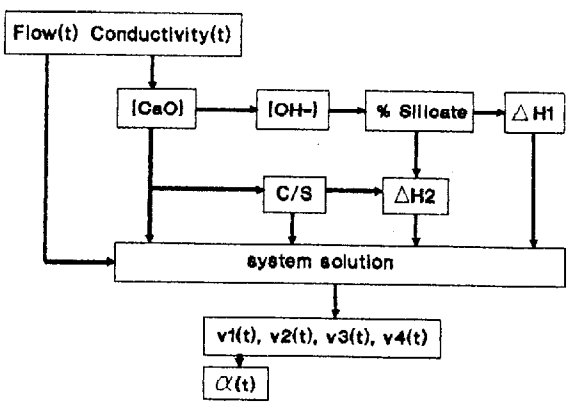

FIG. 5 Solution algotithm

RESULTS AND DISCUSSION

The evolutions of the percentage of hydration versus time obtained under different conditions are plotted on figure 9. C_3S hydration operates in one or two steps according to the initial lime concentration. If the solution is initially saturated with respect to portlandite, the evolution of the hydration shows only one acceleration-deceleration step and looks like the evolution of a cement paste

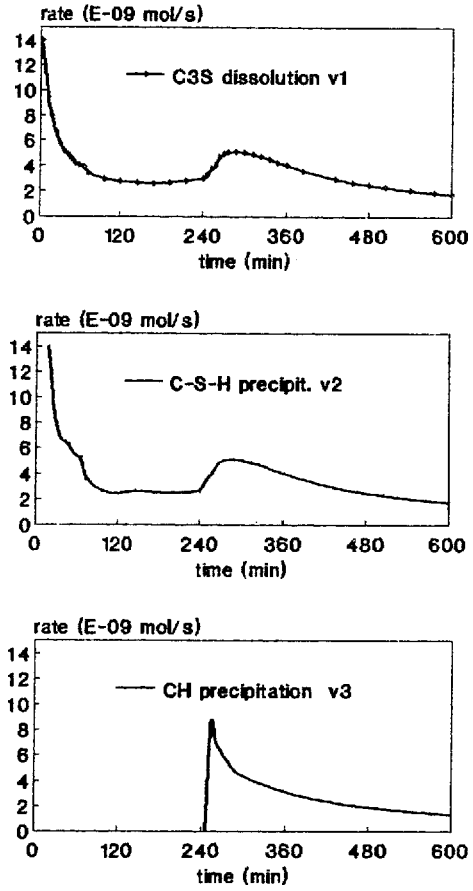

FIG. 6 : Evolution of the rate of each reaction versus time from C_3S hydration in water (w/c=13).

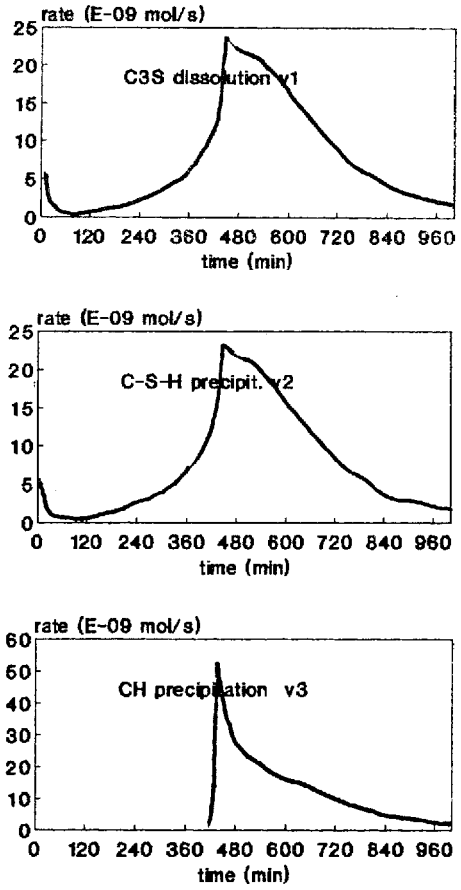

FIG. 8 : Evolution of the rate of each reaction versus time from C_3S hydration in saturated lime solution (w/c=13).

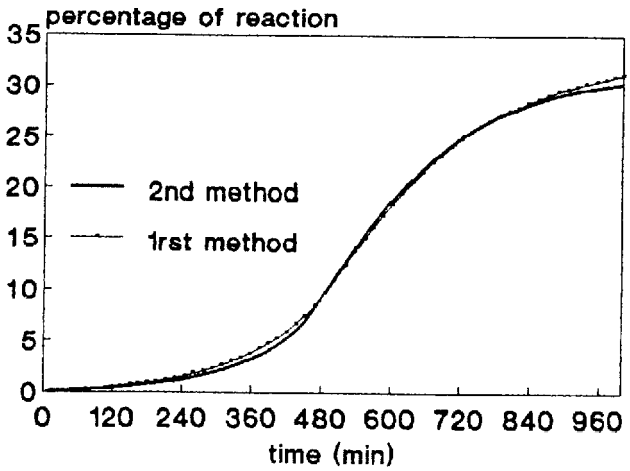

FIG. 7 Percentage of C_3S hydration versus time in saturated lime solution (w/c = 13)

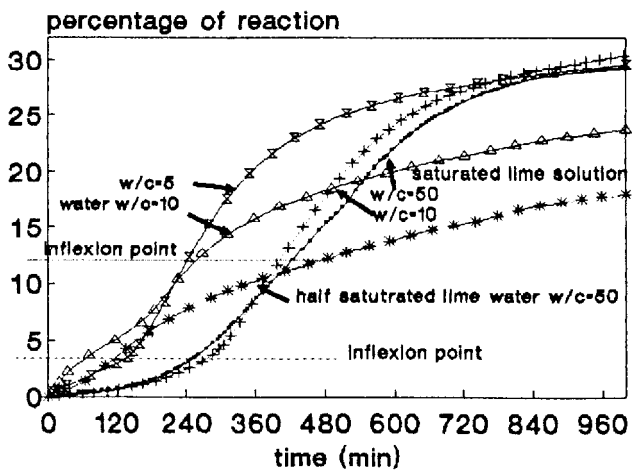

FIG. 9 Evolution of the percentage of reaction from C_3S hydration in different conditions

hydration. If the hydration begins in pure water, the evolution shows two successive acceleration-deceleration steps. The first step occurs as long as the solution remains undersaturated with respect to portlandite. It may be found conditions for which only the first step occurs, for example in an half saturated lime solution with w/c ratio equal to 50. In such a condition, the inflexion point of the evolution curve is located at about 4% of reaction, wheareas it is located at about 13 % of hydration when only the step corresponding to the second one in pure water is observed like in saturated lime water. The inflexion point corresponds to the time from which the reaction becomes limited by a diffusion process of ions and water through the C-S-H layer developed around cement grains. So, it seems that C-S-H precipitated during the first step, i.e. in an undersaturated solution with respect to portlandite, are less permeable than those precipitating in a supersaturated solution with respect to portlandite since the reaction is diffusion-controlled for a thicker layer. According to the C/S versus lime concentration curve, the first step could correspond to the precipitation of a low C/S less permeable C-S-H, and the second one, to the precipitation of a high C/S more permeable C-S-H.

REFERENCES

1. Brown, P.W., Franz, S., Frohnsdorff, G., Taylor, H.F.W.: "Analyses of the aqueous phase during early C_3S hydration", **Cem.Conc. Res.**, 1984, 14, 257-264.

2. Barret, P, Bertrandie, D.: "Fundamental hydration kinetic features of the major cement constituants : Ca_3SiO_5 and β-Ca_2SiO_4", **J.Chim.Phys.**, 1986, 765-775.

3. Gartner, E.M.,Jennings, H.M.: "Thermodynamics of Calcium Silicate Hydrates and their solutions", **J.Amer.Cer.Soc.**, 1987, 70(10), 743-749.

4. Damidot, D., Nonat, A., Barret, P.: "Kinetics of tricalcium silicate hydration in diluted suspensions by microcalorimetric measurements", **J.Amer.Cer.Soc.**, 1990, 73(11), 3319-3322.

5. Babushkin, V.I., Matveyev, G.M., Mchedlov-Petrossian, O.P., **Thermodynamics of silicates**, Berlin, Springer Verlag, 1985.

6. Greenberg, S.A.: "The nature of silicate species in sodium silicate solutions", **J.Am.Chem.Soc.**,1958, 80, 6508-6511.

7. Ménétrier, D.: "**Contribution à l'étude cinétique de la période initiale d'hydratation du silicate tricalcique, composant principal du ciment portland**", Thesis, Université de Bourgogne, 1977.

8. Hannawayya, F.: "Study of the crystallisation properties of tricalcium silicate and dicalcium silicate beta hydrate and the new calcium silicate hydrates CSH III, CSH I and CSH II", 1980, **7th I.C.C.C.**, Paris, 1980.

9. Fujii, K., Kondo, W.: "Estimation of thermochemical data for calcium silicate hydrate (C-S-H)", **J.Amer.Cer.Soc.**, 1983, C220-221.

AN NMR INVESTIGATION OF C_3S HYDRATION IN PASTES AND IN STIRRED DILUTED SUSPENSIONS

R Rassem*, H Zanni-Théveneau*, C Vernet, D Heidemann*****
A R Grimmer*, P Barret****, A Nonat****, D Bertrandie**** and D Damidot******

**Laboratoire de Physique et de Mécanique des Milieux Hétérogénes, FRANCE*
***Technodes, Ciments Francais, FRANCE*
****Institüt für Anorganische Chemie, Berlin, GERMANY*
*****Laboratoire de Recherche sur la Réactivité des Solides, Faculté des Sciences Mirande, FRANCE*

SUMMARY

Tricalcium silicate (C_3S) hydration in pastes and in stirred diluted suspensions has been followed by ^{29}Si and ^{1}H solid state NMR techniques on samples containing ^{29}Si in natural abundance (4.7%) and on totally enriched samples, in order to get informations on the kinetics and on the reactionnal mechanism of the hydrates formation. Two types of systems containing protons were identified: - a Q^0 monomeric species, which appears at the very early times of hydration, during the induction period, and persists after; this species was particularly well revealed by the study of suspensions (^{29}Si in natural abundance) and pastes prepared with enriched C_3S; - a Q^1-Q^2 type calcium silicate hydrate (CSH), which appears during the induction period and grows up continuously. The Q^0 and Q^1-Q^2 species appear before the Ca^{2+} sursaturation of the solutions which leads to portlandite precipitation.

RESUME

L'hydratation du silicate tricalcique (C_3S) en pâte et en suspensions diluées agitées a été suivie grâce à la RMN en phase solide de ^{29}Si et de ^{1}H sur des échantillons contenant ^{29}Si en abondance naturelle (4.7%) et dans des échantillons totallament enrichis afin d'obtenir des informations sur la cinétique et sur les mécanismes réactionnels de la formation des hydrates. Deux types de systèmes protonnés ont été identifiés: - une espèce monomérique Q^0, qui apparaît aux tous premiers instants de l'hydratation, pendant la période dormante, et persiste après; cette espèce a été particulièrement bien révélée par l'étude des suspensions (^{29}Si en abondance naturelle) et des pâtes préparées avec du C_3S enrichi en ^{29}Si; - un silicate de calcium hydraté (CSH) de type Q^1-Q^2, qui apparaît pendant la période dormante et croît après continûment. Les espèces de type Q^0 et Q^1-Q^2 apparaissent avant la sursaturation de la solution en Ca^{2+}, qui conduit à la précipitation de la portlandite.

INTRODUCTION

The ^{29}Si NMR study of tricalcium silicate hydration in pastes (low W/S water/solid weight ratio) was initiated by Lippmaa et al (1); Clayden et al (2) and Rodger et al (3) introduced CP-MAS techniques to follow the growth of hydrated species versus time, especially during the induction period, when the paste remains workable. Our own results obtained in pastes (4) agree with these previous ones.

The present work tries to answer to the following questions: at which time, in the induction period, one can really observe hydrated calcium silicates (CSH) and what is their structure; what is the Q^0 species, previously reported (2,3,4) and how long is it observable in the system; what is the relationship between the end of the induction period, when the Ca^{2+} concentration is maximum and leads to the portlandite precipitation, and the CSH precipitation; finally, are the NMR observations in agreement with some proposed reactionnal mechanism (5).

The phenomena which occur in the very early times of hydration for samples with low W/S ratios are rather complex and take place very quickly. The quantity of hydrates formed after such short hydration times is very small and their characterization is difficult. Indeed ^{29}Si NMR investigations realized on pastes with non enriched C_3S (4) are very long time consuming, especially for very short times of hydration. To enhance the signal sensitivity we enriched the samples with ^{29}Si isotope as Rodger et al have done and shall present results on totally enriched pastes.

On the other hand, one knows that increasing W/S ratio does not change the different hydration stages but slowers the kinetics, which allows a better investigation of the first stage of hydrates formation for low Ca^{2+} concentration. So stirred diluted suspensions were prepared with high W/S ratios.

An attempt of studying C_3S hydration kinetics using ^1H high resolution solid state NMR will be presented also. T_1 measurements give some insight in the different steps of hydration (6) but for a structural point of view they do not allow to distinguish the different types of hydrates.

EXPERIMENTAL

Samples

Paste samples were prepared by mixing anhydrous C_3S with pure water (W/S = 0.5). For proton NMR we used a mixture of H_2O/D_2O water (50%) in order to diminish the dipolar interaction between protons. After the desired hydration times, the reaction was stopped by removing the residual water with aceton-ether.

The ^{29}Si enriched C_3S was synthetized from 99.9% enriched SiO_2.

Diluted suspensions were prepared by mixing C_3S with pure water (W/S = 20 to 2000). Solid samples were obtained by filtration of suspensions at periods corresponding to different hydration stages, then washed and dried by aceton-ether.

NMR experiments

^{29}Si NMR experiments were performed on a Bruker CXP 300 NMR spectrometer, in a 7.03 Tesla field, at a frequency of 59.617 MHz, using the high resolution solid state NMR techniques: Magic Angle Spinning (MAS), proton decoupling and ^1H - ^{29}Si Cross-Polarization (CP). For non enriched samples the mean number of scans varied from 40000, for very poor hydrated samples, to 2000 for samples corresponding to several days of hydration. In the case of ^{29}Si enriched samples only few scans were necessary to observe the signal.

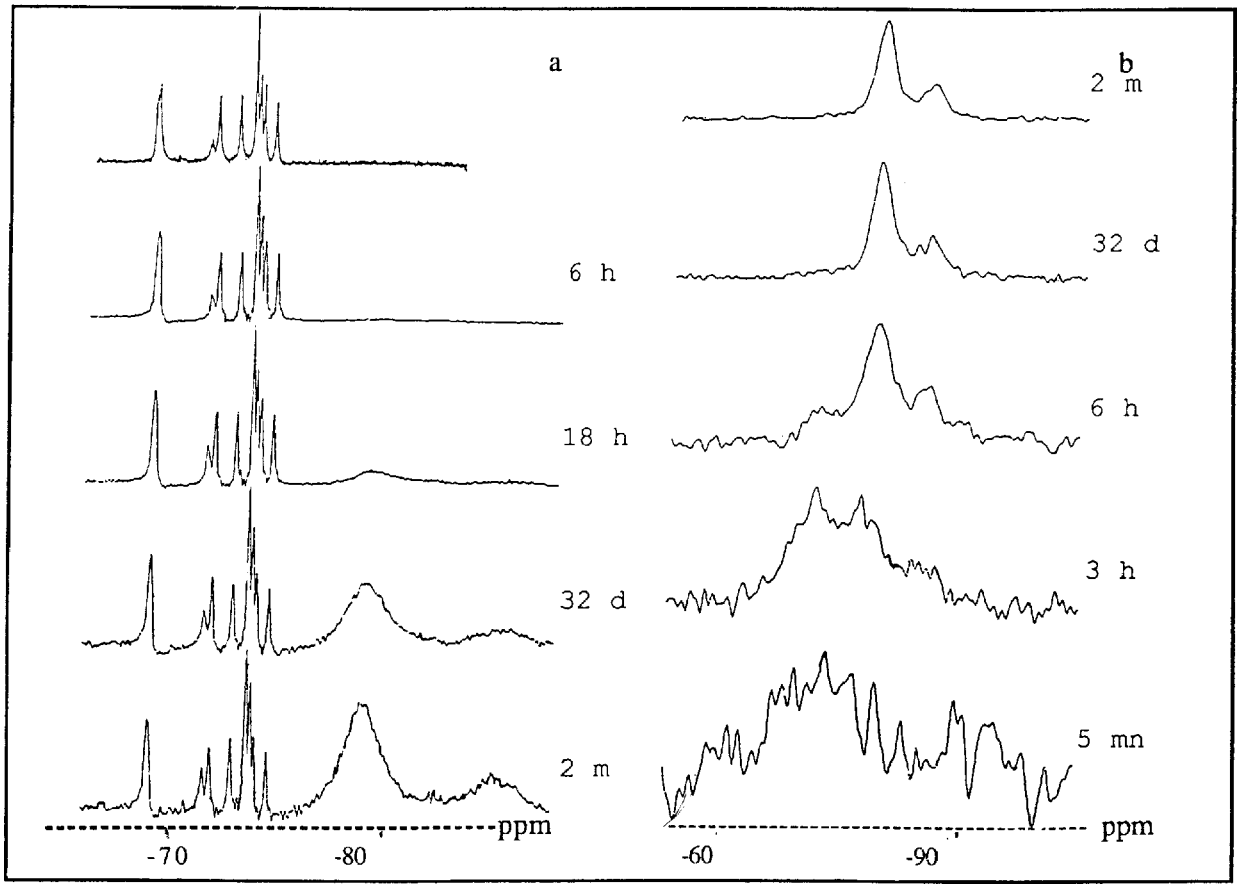

Fig.1. ^{29}Si NMR spectra of hydrated samples of non enriched C_3S. Hydration times are indicated on the spectra. (a) MAS and ^1H decoupling spectra; (b) CP-MAS and ^1H decoupling spectra.

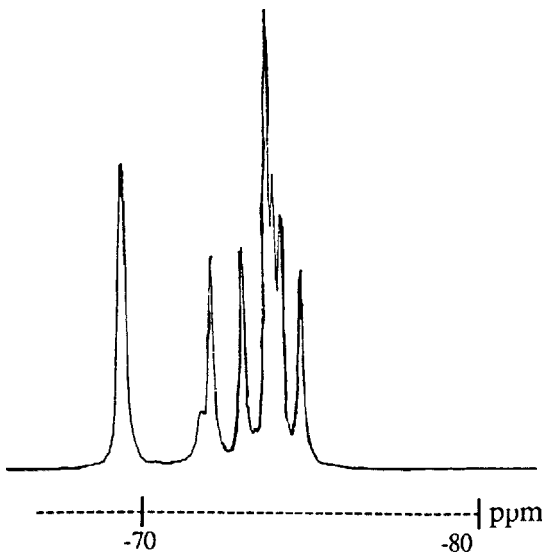

Fig.2. ^{29}Si spectrum of 100% enriched C_3S.

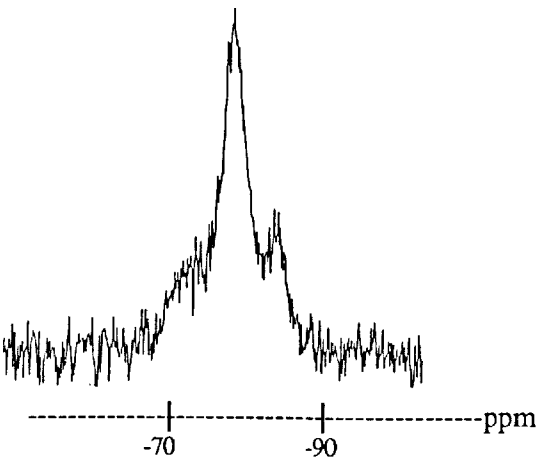

Fig.3. ^{29}Si spectrum of 100% enriched C_3S hydrated 24h.

Q_8M_8 $[Si(CH_3)_3]_8Si_8O_{20}$ was used as a secondary standard, the major peak being at 11.6 ppm relatively to TMS, the tetramethylsilane $Si(CH_3)_4$.

^1H NMR spectra were recorded in a 1.4 Tesla field at 60.58 MHz on a FKS 176/178 spectrometer. The multipulse sequence MREV 8 combined with the MAS technique was used (CRAMPS technique). Between 100 to 1350 FIDs were accumulated with a repetition time of 10s. In all experiments we used liquid hexamethylsiloxan, HMDSO, $(CH_3)_3SiOSi(CH_3)_3$, as an internal standard with a chemical shift close (0.06 ppm) to that of TMS.

RESULTS

^{29}Si NMR spectra of pastes

Non enriched samples - ^{29}Si NMR spectra of samples corresponding to different hydration times are reported on Fig.1.

In Fig.1.a one observes simultaneously the ^{29}Si signal of anhydrous C_3S and hydrated species, CSH. The spectrum of anhydrous species is characteristic of a well crystallized solid and consists of 9 narrow lines lying in the monomeric Q^0 range : - 69.3 to - 74.7 ppm. The CSH spectrum can be detected only after the induction period (6h in the case of the C_3S used in the experiment). It is composed of two broad peaks, characteristic of a non well crystallized system; the first peak, centered at - 79 ppm, corresponds to end-groups Q^1 units and the second one, centered at - 84 ppm, is assigned to chain middle groups Q^2 units.

In CP MAS experiments, only ^{29}Si nuclei in interaction with protons are detected. It revealed to be particularly relevant to study what happens during the induction period, when the quantity of hydrates formed is much smaller than that of anhydrous C_3S. Fig. 1.b shows a broad line centered at - 72 ppm, in the Q^0 range immediatly after the hydration (5 mn). This line is still detected in the middle and at the end of the induction period (3h and 6h).

On the other hand, the Q^1-Q^2 type species appears during the induction period and grows up continuously after.

^{29}Si enriched samples - ^{29}Si spectrum of a totally enriched C_3S sample is presented on Fig. 2. It was obtained with 24 scans only. We present also on Fig. 3. the CP MAS experiment in the case of a sample hydrated 24h. Its acquisition needed 200 scans and shows inambiguously the coexistence of the Q^0 monomeric species with the Q^1-Q^2 one.

^{29}Si NMR spectra of CSH obtained in suspensions

We present on Fig.4.a the variation of CaO concentration versus time for different W/S ratios (0.5 to 50). The curves show the slowing of [CaO] increase in diluted suspensions. On Fig.4.b is reported a typical heat flux curve for W/S = 20 which allows to define different stages in the process. Three samples (quoted 1,2,3 on Fig.4.) were studied corresponding to these different hydration stages. Their spectra are reported on Fig.5.:

- number 1 spectrum consists in a peak located at -72 ppm, characteristic of a Q^0 entity. It is due to a protonated species formed during the first stage of the reaction, which may correspond to the passage of the calcium and silicates ions into the solution, following the reaction:

$$2\ Ca_3SiO_5 + 8\ H_2O \text{ <----> } 6\ Ca^{2+} + 2\ H_3SiO_4^- + 10\ OH^- \qquad (1)$$

- number 2 spectrum shows, in addition to the Q^0 peak, Q^1 and Q^2 peaks, due to the CSH formation following the reaction:

$$\varepsilon\ Ca^{2+} + (2\varepsilon - 1)\ OH^- + H_3SiO_4^- \text{ <----> } Ca_\varepsilon(OH)_{(2\varepsilon - 1)}H_3SiO_4 \qquad (2)$$

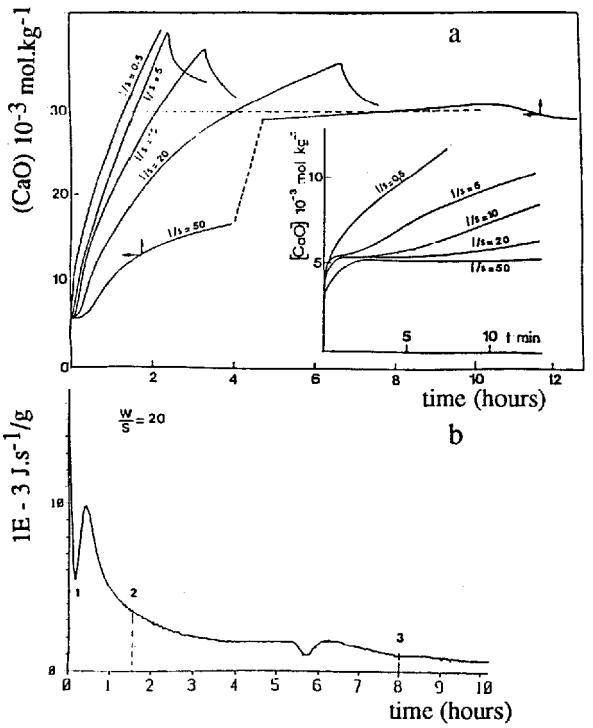

Fig.4.(a) CaO concentration in suspensions versus time;
(b) heat flux curve for W/S = 20.

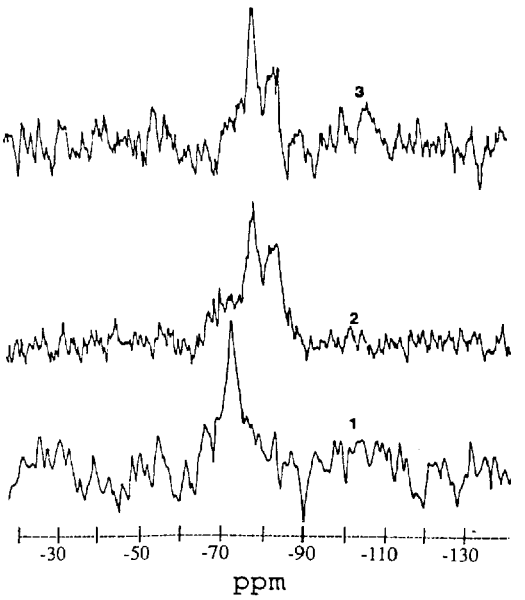

Fig.5. ^{29}Si NMR spectra for CSH obtained from suspensions.

with $0.5 < \varepsilon < 2$
During this stage, reactions (1) and (2) take place simultaneously;
- number 3 spectrum is obtained at a longer hydration time, after precipitation of calcium hydroxyde, portlandite:

$$Ca^{2+} + 2\ OH^- <----> Ca(OH)_2 \qquad (3)$$

It presents the same three peaks, but their intensities are higher, due to the hydration growth.

^{1}H NMR spectra of pastes

The analysis of ^{1}H CRAMPS spectra of CSH obtained in pastes is based on the proton chemical shift variation range determined by Heidemann (7) in a study of well crystallized silicate samples (see Fig.6.). For instance the ^{1}H NMR spectrum of portlandite consists in a line of 5 ppm width and centered at + 1.4 ppm.

We studied samples corresponding to 5mn, 20mn, 1h, 3h and 6h hydration times. They all present rather broad spectra (10 to 17 ppm) in accordance with the amorphous character of the CSH formed in C_3S hydration. They show the existence of SiOH groups, immediatly after the hydration, then the onset of CaOH groups, coexisting with SiOH groups and corresponding to the CSH formation, before the end of the induction period, then the CaOH groups corresponding to portlandite precipitation.

We have reported on Fig.7. and Fig.8. the spectra of samples hydrated 5mn and 3h. The first one presents peaks corresponding to SiOH groups (7.4...13.4 ppm). The maximum of the second one at +2.4 ppm and the shoulders at -1.3 to -3.4 ppm demonstrate that the main amount of protons exists in this sample as CAOH groups.
Beside these CAOH groups, the sample contains even SiOH groups the component lines of which are located at + 15.4 to +6.4 ppm, revealing CSH formation.

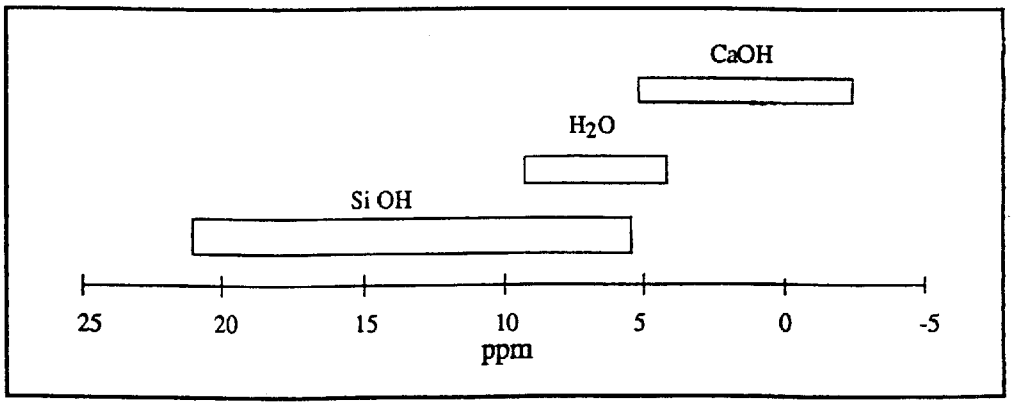

Fig.6. ^{1}H chemical shifts for silicates (7).

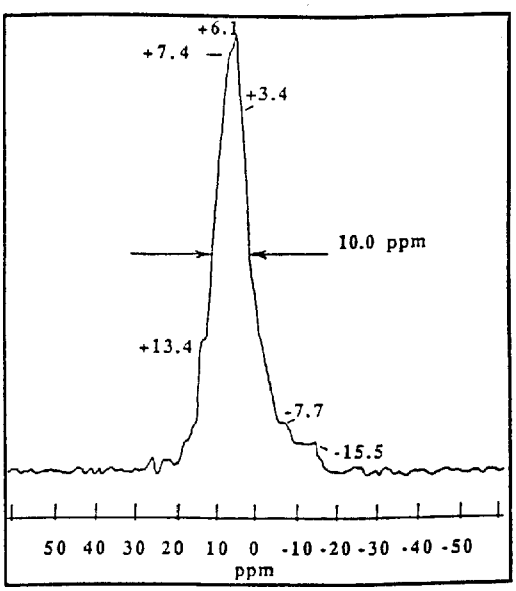

Fig.7. ^{1}H CRAMPS spectra for C_3S hydrated 5mn.

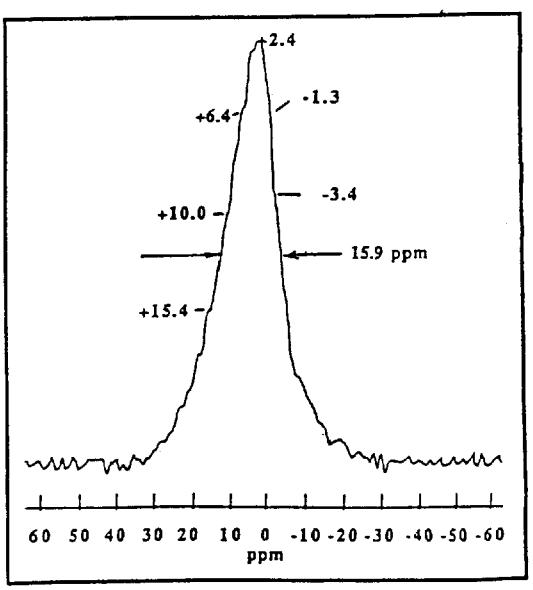

Fig.8. ^{1}H CRAMPS spectra for C_3S hydrated 3h.

CONCLUSION

From this NMR investigation we can conclude that:

- immediatly after hydration a monomeric species arises and persists as long as anhydrous C_3S is present in the system; it may correspond to a hydroxyled species at the C_3S surface.

- formation of Q^1-Q^2 type CSH takes place very early in the induction period, before precipitation of portlandite.

ACKNOWLEDGEMENTS

A part of this work will be published in "First International Workshop on Hydration and Setting" Ed. Chapman and Hall.

REFERENCES

1 Lippmaa, E., Magi, M., Tarmak, M., Wieker, W. and Grimmer, A.R.: "A high resolution ^{29}Si NMR study of the hydration of tricalcium silicate". Cem. Concr. Res., 1982, **12**, 597-602.

2 Clayden, N.J., Dobson, C.M., Hayes, C.J. and Rodger, S.A.: "Hydration of tricalcium silicate followed by solid-state ^{29}Si NMR spectroscopy". J. Chem. Soc., Chem. Commun., 1984, 1396-1397.

3 Rodger, S.A., Groves, G.W., Clayden, N.J. and Dobson, C.M.: "Hydration of tricalcium silicate followed by ^{29}Si NMR with cross-polarization". J. Am. Ceram. Soc., 1988, **71**, 91-96.

4 Rassem, R., Zanni-Théveneau, H., Schneid, I. and Regourd, M.: "^{29}Si high-resolution NMR study of tricalcium silicate hydration". J. Chim. Phys., 1989, **86**, 1253-1264.

5 Barret, P. and Bertrandie, D.: "Fundamental hydration kinetic features of the major cement constituents: tricalcium silicate ($CaSiO_5$) and beta-dicalcium silicate (β-$CaSiO_4$)". J. Chim. Phys., 1986, **83**, 765-775.

6 Letellier, M., Van Damme, H., Mortureux, B. and Regourd, M.: "Mécanismes d'action des fluidifiants étudiés par RMN du proton". **Proceedings of the 8th Intern. Congress on the Chemistry of Cement, Rio de Janeiro, Brasil,** 1986, **2**, 93.

7 Heidemann, D.:"^{29}Si und ^1H Festkörper-NMR-Untersuchungen ankristallinen Hydrosilicaten". Thesis, Berlin, Germany, 1987, 127p.

X-RAY MICROANALYSIS OF PORTLAND CEMENT PASTES HYDRATED AT DIFFERENT TEMPERATURES

K O Kjellsen* and R J Detwiler**

**Swedish Cement and Concrete Research Institute*
Stockholm, SWEDEN
***Department of Civil Engineering, University of Toronto*
Toronto, CANADA

SUMMARY

Concrete cured at elevated temperatures gains strength rapidly at first, but has a reduced ultimate strength. The elevated temperature increases the initial rate of hydration, but allows insufficient time for the hydration products to diffuse into the bulk cement paste. As a result, dense "shells" of hydration products form around the cement grains, hindering further hydration. In previous work involving backscattered electron imaging of pastes hydrated at 50 °C the "shells" appeared as areas of increased signal intensity as compared with the bulk cement paste. They were much less distinct in specimens hydrated at lower temperatures. The question then arose as to whether the difference in intensity was due to differences in chemical composition or in density. Plain portland cement pastes of 0.50 water/cement ratio were mixed, cast, and cured at constant temperatures of 5 and 50 °C. They were hydrated to a degree of hydration of approximately 70% as estimated by the nonevaporable water content and examined using backscattered electron imaging and energy dispersive X-ray analysis. The results show that local differences in signal intensity are due primarily to differences in density rather than composition. Tests reported elsewhere of companion mortar and concrete specimens show the deleterious effect of elevated hydration temperature on both strength and permeability to chloride ions. These results are consistent with the observed distribution of hydration products.

ZUSAMMENFASSUNG

Bei erhöhter temperatur nachbehandelter beton gewinnt zunächst schnell an festigkeit. Seine endfestigkeit ist jedoch gering. Die höhere temperatur bewirkt zwar eine schnellere anfangshydratation, sie lässt den hydratationsprodukten jedoch wenig zeit, in die schüttzementpaste einzudiffundieren. Es bilden sich dadurch um die zementkörner dicke "hüllen" von hydratationsprodukten, die eine weitere hydratation behindern. In vorangegangenen arbeiten, bei denen pasten, die bei 50 °C hydratisiert wurden, mit rückstreuelektronen-bildtechnik fotografiert wurden, erschienen die "hüllen" als flächen mit im vergleich zur schüttzementpaste erhöhter signalintensität. Die hüllen waren bei Exemplaren, die bei niedrigeren temperaturen hydratisiert wurden, weit weniger stark ausgeprägt. Es stellte sich dann die frage, ob der intensitätsunterschied auf unterschiede in der chemischen zusammensetzung oder in der dichte zurückzuführen ist. Pasten aus normalem portlandzement mit einem wasser-zement-verhältnis von 0,50 wurden bei einer konstanten temperatur von 5 und 50 °C gemischt, gegossen und nachbehandelt. Sie wurden auf der grundlage von schätzungen des nicht verdampfbaren wassergehalts auf einen hydratationsgrad von rund 70% hydratisiert und mit rückstreuelektronen-bildtechnik und energiedispersions-röntgenanalyse untersucht. Die ergebnisse zeigen, dass die lokalen unterschiede in der signalintensität in erster linie auf dichteunterschiede und weniger auf zusammensetzungsunterschiede zurückführen sind.

INTRODUCTION

There has been some controversy as to how curing temperature influences the structure of cement paste, mortar, and concrete. In 1968 Verbeck and Helmuth (1) hypothesized that curing at elevated temperatures causes the formation of dense zones of hydration products in the region immediately sorrounding the hydrating cement grains. The low solubility and low diffusibility of the hydration products would prevent them from diffusing to any significant distance from the surface of the hydrating cement grains within the time allowed by rapid hydration. At lower temperatures hydration is slower, allowing more time for the hydration products to diffuse and precipitate away from the dissolving grain surfaces. The distribution of hydration products throughout the paste matrix would thus be more uniform. Verbeck and Helmuth believed different distribution patterns would form early in the hydration process. They found indirect evidence for their hypothesis: however, the techniques available at that time did not enable them to carry out reliable direct studies.

Our results (2, 3, 4) generally support their hypothesis. SEM studies (2, 3) gave strong indications of the existence of dense hydration shells around the hydrating cement grains in specimens hydrated at elevated temperatures and a much more homogeneous distribution of reaction products in the matrix of specimens hydrated at lower temperatures. All specimens were hydrated to a degree of hydration of approximately 70%. However, at approximately 30% hydration no difference in the distribution patterns was observed. Thus our results deviate from the hypothesis in one respect: The formation of the characteristic shells at higher temperatures was not evident in the early hydration process but only at a relatively advanced stage. At the temperatures examined, early hydration was characterized by hollow shell hydration (through-solution). At later stages of hydration the reaction became increasingly controlled by topochemical or local through-solution (intra-shell) mechanisms, with the effect being more pronounced at higher hydration temperature. The higher the temperature, the lower the degree of hydration at which the change in mechanism occured.

The work cited above was based on the examination of polished specimens in the backscattered electron mode. As the incident electron beam in the SEM scans the specimen surface, electrons and X-ray photons with different properties are emitted. The intensity of the backscattered electron signal from a point depends on the average atomic number of the material at that point. The higher the mean atomic number in the interacted region, the more intense the signal. Thus, the intensity depends on both the chemical composition in regard to the atomic number of the elements present and the density of the interacted microvolume. The distinguishable phases are normally unhydrated cement grains, calcium hydroxide, other hydration products, and pores above the size that can be resolved by the microscope at the chosen magnification. We hypothesized that the difference in the backscattered electron images of the mature paste, hydrated at the different temperatures, was due essentially to differences in the density of the other hydration products. In the specimens hydrated at 50 °C hydration products of apparently high density were clearly visible around the hydrating grains, while hydrated phases of low density (i.e. high capillary porosity) appeared in the outer product. In the specimens hydrated at 5 °C there was little difference in density between inner and outer product. Some of the mature specimens examined in the backscattered electron mode were then examined by X-ray microanalysis partly in order to test the previous assumption. This paper reports the result of this investigation.

EXPERIMENTAL

All specimens were made from an ordinary portland cement and distilled water, the properties of which have already been reported (4). The water/cement ratio was 0.5. The curing temperatures ranged from 5 to 50 °C. The mixing temperature was held as close as possible to the intended curing temperature except that the 50 °C specimens were mixed at approximately 35 °C in order to prevent them from stiffening too quickly.

Details of the mixing and curing procedures are as reported earlier (4). The degree of hydration was determined from the amount of nonevaporable water (3).

After curing to approximately 70% hydration the specimens were prepared for backscattered electron imaging. Details of preparation and examination of these specimens are as reported earlier (2, 5). X-ray microanalysis in the form of dot mapping and spot analysis was performed on some of the same specimens used for backscattered electron imaging.

RESULTS AND DISCUSSION

Figure 1 shows a backscattered electron image of a specimen hydrated at 5 °C to about 70% hydration. The hydration products appear to be well distributed throughout the matrix. The inner products can sometimes be distinguished as areas of only slightly higher signal intensity.

Figure 2 shows a backscattered electron image of a specimen hydrated at 50 °C to approximately 70% hydration. Here the signal intensity for the hydration products is much stronger in the inner product than in the outer product.

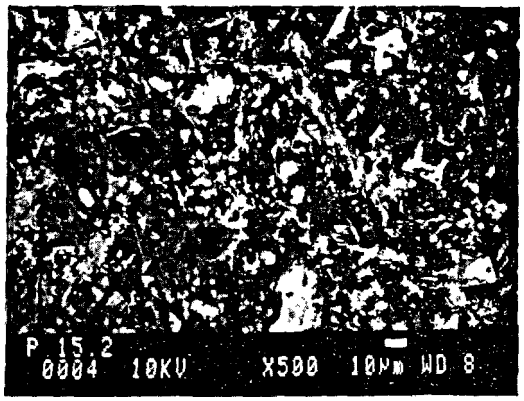

Figure 1: Backscattered electron image of cement paste hydrated at 5 °C to 73% hydration.

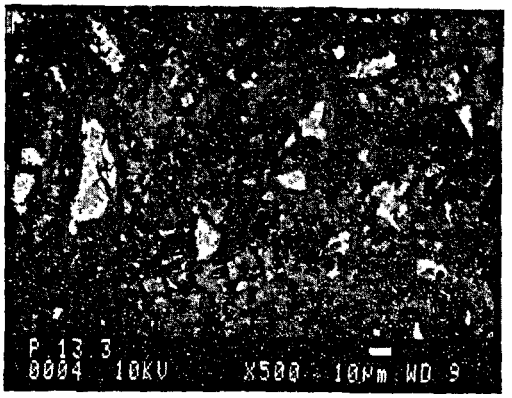

Figure 2: Backscattered electron image of cement paste hydrated at 50 °C to 71% hydration.

Figure 3a shows another backscattered electron image of a field from the specimen hydrated at 5 °C to approximately 70%. Figures 3b to 3f show the elemental X-ray dot maps of the field from Figure 3 A. The unhydrated grain at the right side of the field consists of calcium silicates with only a small area of C_4AF. The CH crystals can be identified from the Ca map (Figure 3b) while the interstitial phases and hydrates are recognized from the Al, Fe, and S images. The lack of systematic difference in the intensity of Ca and Si within the C-S-H indicates that the C-S-H is well distributed throughout the matrix.

Figure 4a depicts a backscattered electron image of a field from the specimen hydrated at 50 °C to about 70%. The resolution of Figures 3a and 4a is poorer than in the previously shown backscattered electron images because the image has undergone the same image processing as the X-ray dot maps. While Figures 1 and 2 were the normal analog CRT (microscope) photographs, the images in conjunction with the X-ray analysis are digitized images of 128 x 128 pixels. Figures 4b to 4f show the elemental X-ray images of the field from Figure 4a. The two unhydrated remnant grains consist almost entirely of calcium silicates. Only very small fractions of interstitial minerals are present. The intensity of both Ca and Si is consistent with the intensity of the hydration product phases of the backscattered electron image. The distribution of the

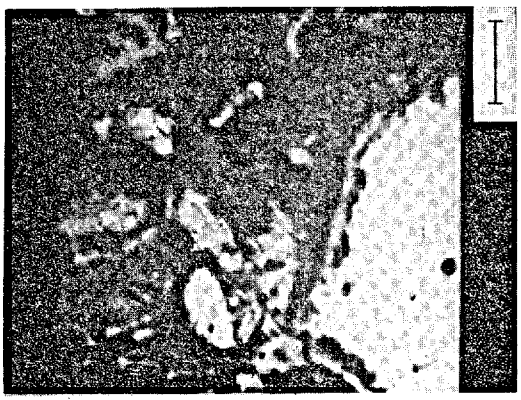

Figure 3a: Backscattered electron image of the paste cured at 5 °C to 73% hydration. The bar denotes 10 um.

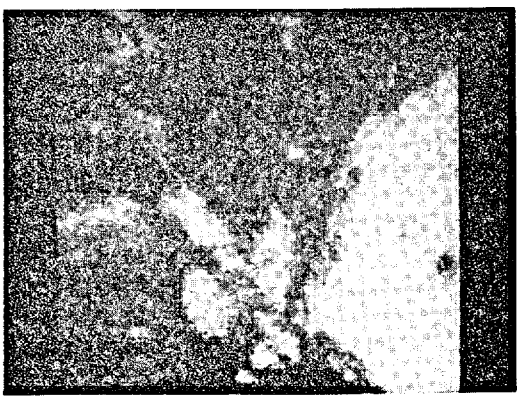

Figure 3b: Ca X-ray image of the field from Fig. 3a.



Figure 3c: Si X-ray image of the field from Fig. 3a.

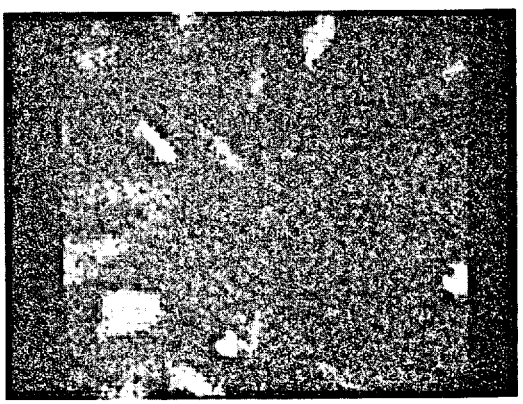

Figure 3d: Al X-ray image of the field from Fig. 3a.

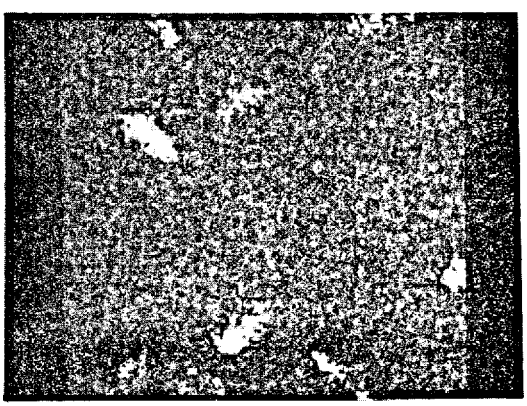

Figure 3e: Fe X-ray image of the field from Fig. 3a.

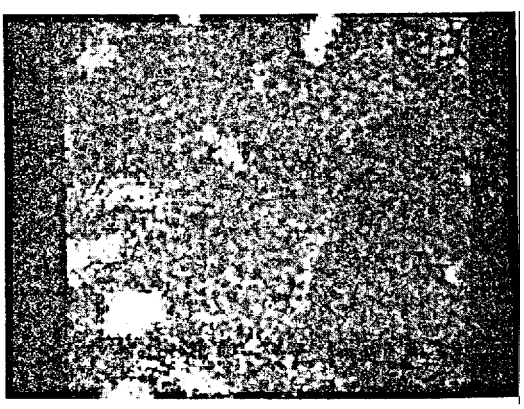

Figure 3f: S X-ray image of the field from Fig. 3a.

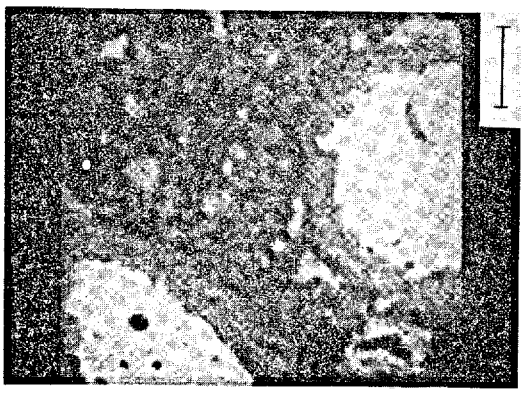

Figure 4a: Backscattered electron image of the paste cured at 50 °C to 71% hydration. The bar denotes 10 um.



Figure 4b: Ca X-ray image of the field from Fig. 4a.

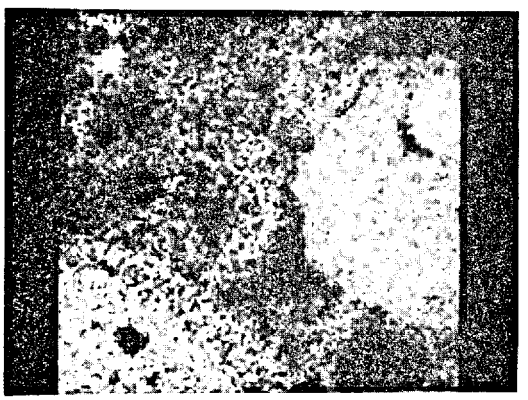

Figure 4c: Si X-ray image of the field from Fig. 4a.

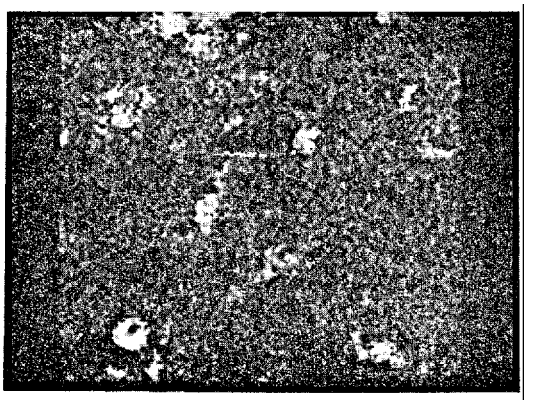

Figure 4d: Al X-ray image of the field from Fig. 4a.

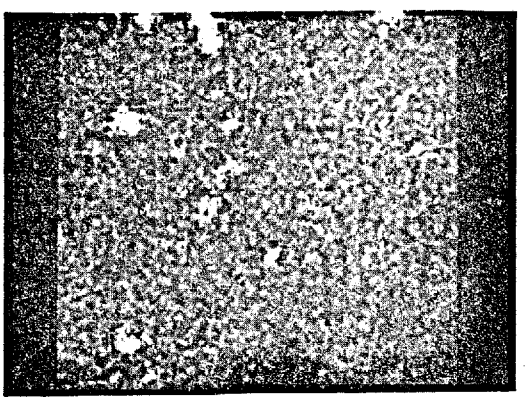

Figure 4e: Fe X-ray image of the field from Fig. 4a.

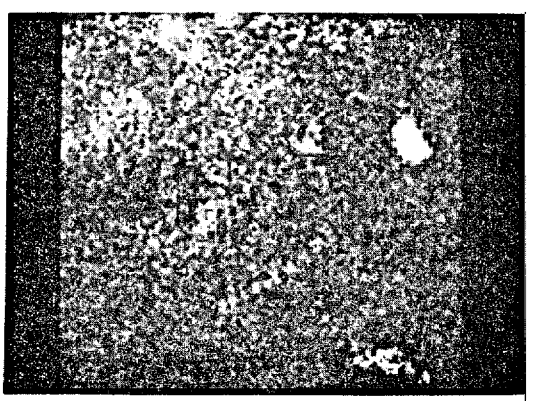

Figure 4f: S X-ray image of the field from Fig. 4a.

other elements appears not to be influenced by hydration temperature. The relatively high atomic number element Fe does not appear to be present in the hydration shells, at least not at detectable concentrations. This is not surprising since the cement grains consist of calcium silicates. However, outside zones of C_4AF an accumulation of Fe within the hydration shells could be expected because of their low diffusivity. According to Taylor and Newbury (6) Fe does not migrate readily in an alkaline environment.As Fe has the highest atomic number compared to the other elements present in cement paste it is conceivable that, if present, it might have influenced the backscattered electron signals of the shells. A series of X-ray spot analyses was performed within the hydration shells and in outer C-S-H phase of the 50 °C specimen. The C/S ratio (weight %) was found to be about 1.9 both within the shells and in the outer C-S-H.

The results obtained from the present X-ray analysis support the assumption made earlier that the differences in intensity of backscattered electron signals from the outer and inner product phases of cement paste hydrated at different temperatures are due mainly to differences in the density of C-S-H. This observation supports the idea that dense shells of reaction products form around the anhydrous grains at higher temperatures, leaving an outer product phase of high porosity. We found (4) indications that the difference in pore volume in the outer product phase was essentially due to an increase in the number of pores in the range of 0.25 to 1.25 microns.

A microstructural feature commonly observed in specimens hydrated at 5 °C are phases of an almost layer-like structure with oriented flat pores. Figure 5 shows two such features. A series of X-ray analyses shows these phases to contain about 24% Al_2O_3, 18% SO_3, and 55% CaO (weight %). This composition largely resembles that of AFm. No indications of these large clusters of AFm were observed at 30% hydration and they are much less developed and more unusual in specimens hydrated at higher temperatures.

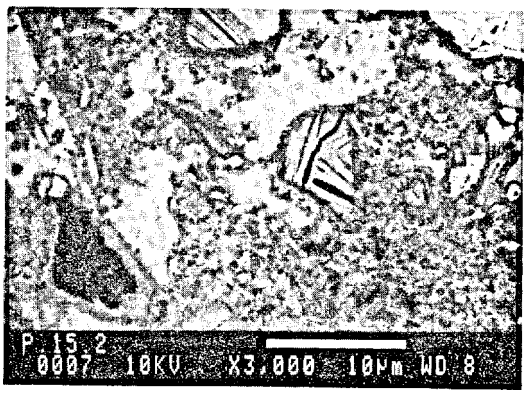

Figure 5: Backscattered electron image of paste hydrated at 5 °C to 73% hydration.

CONCLUSIONS

The X-ray analyses indicate that differences in intensity of the backscattered electron signals from these cement paste specimens are due primarily to differences in density rather than composition. Thus, our earlier interpretation of the backscattered electron images is correct. Cement hydrated at elevated temperatures does form dense"shells" of hydration products surrounding the cement grains, hindering further hydration and leaving the interstitial space relatively porous. Cement hydrated at lower temperatures has a more uniform distribution.

ACKNOWLEDGEMENTS

We would like to express our appreciation for the support provided by the Division of Building Materials at the Norwegian Institute of Technology, where the laboratory work for this paper was performed. We would also like to thank the Royal Norwegian Council for Scientific and Industrial Research (NTNF), Aker Entreprenør A/S, BEA Consult A/S, Scancem Chemical A/S, Rescon A/S, Norcem Betong A/S, Norcem A/S and the Norwegian Ready Mix Concrete Association for their financial support.

The second author gratefully acknowledges the postdoctoral fellowship given by NTNF.

REFERENCES

1. Verbeck, G.J. and Helmuth, R.H. "Structures and Physical Properties of Cement Paste," Proceedings of the 5th International Congress on the Chemistry of Cement, Tokyo, 1968.

2. Kjellsen, K.O.: Detwiler, R.J.: and Gjørv, O.E. "Backscattered Electron Imaging of Cement Pastes Hydrated at Different Temperatures," Cement and Concrete Research, Vol. 20, No. 2, 1990, pp. 308-311.

3. Kjellsen, K.O.: Detwiler, R.J.: and Gjørv, O.E. "Development of Microstructures in Plain Cement Pastes Hydrated at Different Temperatures," Cement and Concrete Research, Vol.21, No. 1, 1991, pp. 179-189.

4. Kjellsen, K.O.: Detwiler, R.J.: and Gjørv, O.E. "Pore Structure of Plain Cement Pastes Hydrated at Different Temperatures," Cement and Concrete Research, Vol 20, No. 6, 1990, pp. 927-933.

5. Kjellsen, K.O.: Detwiler, R.J.: and Gjørv, O.E. "Backscattered Electron Image Analysis of Cement Paste Specimens: Specimen Preparation and Analytical Methods," Cement and Concrete Research, Vol 21, No 2/3, 1991, pp. 388-390.

6. Taylor, H.F.W. and Newbury, D.E. "An Electron Microprobe Study of a Mature Cement Paste," Cement and Concrete Research, Vol. 14, No. 4, 1984, pp. 565-573.

A WEIGHING METHOD FOR CEMENT HYDRATION

P Paulini

Institut für Baustofflehre und Materialprüfung
Universität Innsbruck, AUSTRIA

SUMMARY

Traditionally cement reactions are recorded by calorimetric methods. A simple and accurate kinetic record of hydraulic reactions can be performed with a dipping and weighing method. Changes in sample volume, respectively in their density, are measured continuously during the reaction with a balance. In this contribution the basics of the method will be explained and some examples are given in order to prove the suitability for cement hydration. In the early phase of cement hydration either chemical shrinkage processes or swelling processes can occur. The induction period is defined by a swelling process while the hardening phase is characterized by the appearance of chemical shrinkage. A rough calculation of bond energies leads to values normal for concrete materials.

ZUSAMMENFASSUNG

Zementreaktionen werden traditionell mittels kalorimetrischer Methoden aufgenommen. Eine einfache und genaue kinetische Aufnahme hydraulischer Reaktionen kann auch mittels dem Tauchwägeverfahren durchgeführt werden. Dabei werden die Änderungen des Probenvolumens, respektive deren Dichteänderungen, kontinuierlich während der Reaktion mittels einer Waage gemessen. In diesem Beitrag werden die Grundlagen des Verfahrens erklärt und anhand einiger Beispiele die Anwendbarkeit der Methode auf die Zementhydratation gezeigt. In der Anfangsphase der Zementhydratation können sowohl Schrumpfvorgänge wie auch Quellvorgänge vorliegen. Die Ruheperiode wird durch die Dauer der Quellperiode bestimmt während die Erhärtungsphase durch das Auftreten von Schrumpfvolumen charkterisiert ist. Eine Abschätzung der Bindungsenergie ergibt für Betonmaterialien gängige Werte.

INTRODUCTION

The determination of the kinetic behaviour of cement reactions can be classified into direct and indirect methods. Direct methods like calorimetry or volumetry are carried out continuously during the reaction and their analog output can be transformed to any desired resolution. Direct methods have also a direct relation to energy changes in the reacting sample. Indirect methods require to stop the reaction and need mostly a sample preparation, which leads to discrete measurements. Such methods are quantitative X-ray analysis (QXRA), nuclear magnetic resonance (NMR), differential thermal analysis (DTA), determination of evaporable water and chemical and optical methods. A comparison of some of these methods is given in [1].

ENERGY PRINCIPLES OF CHEMICAL REACTIONS

Energy changes of chemical reactions are described by the 1st and 2nd law of thermodynamic. The inner energy U of a system can be expressed with a heat energy term Q and a volume work W

$$U = Q + W \tag{1}$$

From conservation law of energy it is required that the inner energy of a closed system remains unchanged. This ca be expressed as

$$dU = dQ + dW = 0 \tag{2}$$

Thus we receive for a chemical reaction opposite directed energy terms of the same absolute amount for changes in heat energy and volume work

$$dQ = -dW \tag{3}$$

The direction of the chemical reaction can be determined with the 2nd law of thermodynamic. We divide the entropy S in an inner term dS_i remaining in the system and in a dissipative flux term dS_e released from the system

$$S = S_i + S_e \tag{4}$$

The 2nd law can be written claiming an increase of the inner entropy term dS_i [2]

$$0 \leq dS_i \tag{5}$$

For irreversible chemical reactions it can be shown that energies remaining in the system and dissipative flux energies underlie the following relations [3]

$$T.dS_e < 0 < T.dS_i$$

exothermic reactions	$dQ_R < 0 < dW_{irr}$
endothermic reactions	$dW_{irr} < 0 < dQ_R$

(6)

In an exothermic reaction the heat of reaction dQ_R is an energy loss term, which is released from the system and transferred to the surrounding. Coincidently a positive volume work dW_{irr} is transferred to the system, resulting in a hardening process. An endothermic reaction is characterized by a supply of heat energy to the system with a simultaneous negative volume work (solution process). Hardening processes are therefore exothermic whereas solution processes are of endothermic nature. These relations hold not just for nonequilibrium chemical processes (hydraulic hardening, 2-component resin reactions), they are also valid for equilibrium crystallization like ice formation or stiffening of meltings of metals and polymers.

Chemical reactions can therefore be recorded either by measuring the heat of reaction ΔQ_R or by measuring the volume work ΔW_{irr}. In classical thermodynamics volume work has mostly been neglected because the pressure is regarded as working from outside "on the system". This is valid especially for gas reactions. For liquid and solid reactions the pressure is regarded here as an inner bond pressure p_B working "in the system between particles" !

Figure 1 shows a p-V diagram of a chemical reaction starting at state 0 and ending at state 1. An irreversible process from state 0 to state 1 occurs along the adiabatic path 0 - 2 - 1 and performs a total work according equation (7). We assume that the system allows a reversible process along the path 0-1 with a reversible work according equation (8). This reversible work must also be overcome during the irreversible process and is directed against the total work. The remaining irreversible volume work responsible for material structure changes like hardening can be expressed as difference of these two opposite energies.

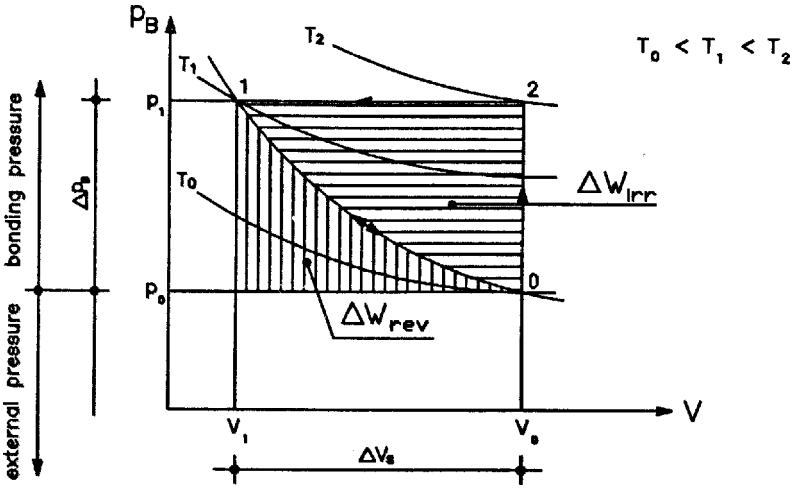

Fig. 1, p - V - Diagram

The total produced volume work ΔW during the irreversible process can be written as

$$\Delta W = -\Delta p_B \cdot \Delta V_s \tag{7}$$

Against this bonding work effects the reversible volume work ΔW_{rev}

$$\Delta W_{rev} = -\int_{V_0}^{V_1} p_B \cdot dV \tag{8}$$

The irreversible bonding work ΔW_{irr} remaining in the system and responsible for material hardening can be stated as

$$\Delta W_{irr} = \Delta W - \Delta W_{rev} \tag{9}$$

We express the bond pressure p_B in terms of volume changes and bulk modulus K

$$dp_B = -K \cdot \frac{dV}{V_0} \tag{10}$$

Under the simplified assumption of a constant bulk modulus K we receive the bond energy produced by a chemical reaction as a true function of the shrinkage volume V_s [4].

$$\Delta W_B = \Delta W_{irr} = \frac{-K}{V_0} \left((\Delta V_s)^2 - \iint d^2V\right) = \frac{-K}{2V_0} \cdot (\Delta V_s)^2 \tag{11}$$

If we express equation (11) in terms of relative volume changes e

$$de = \frac{dV_s}{V_0} \tag{12}$$

we receive the bond energy as

$$\Delta W_B = -\frac{K}{2} \cdot (\Delta e)^2 \cdot V_0 = \sigma_t \cdot V_0 \tag{13}$$

σ_t is the uniform directed bond strength of the material and can be regarded as a uniform tension strength. Thus, the square of the shrinkage volume ΔV_s is a direct unit for the hardening process.

VOLUME CHANGES OF CEMENT PHASE REACTIONS

Portland cement consists of various clinker phases that react with water according to the following symbolic equations:

C_3S : $2.C_3S + 6H \longrightarrow C_3S_2H_3 + 3CH$
C_2S : $2.C_2S + 4H \longrightarrow C_3S_2H_3 + CH$
C_3A : $C_3A + 6H \longrightarrow C_3AH_6$
C_4AF: $C_4AF + 2CH + 10H \longrightarrow C_3AH_6 + C_3FH_6$

All these phase reactions are exothermic processes accompanied by a decrease of volume (chemical shrinkage). Table 1 show for C_3S a comparison of volumes of basic and reaction products. The shrinkage volume V_s as difference between volume of reaction and basic products becomes negative.

C_3S - Reaction	Mol.Wt. g/mol	Density g/cm^3	Mol.Vol. cm^3/mol	
$2.(3CaO . SiO_2)$	456,6460	3,1300	145,8933	
$6\ H_2O$	108,0918	0,9982	108,2867	
Basic Products	564,7378	2,2218	254,1800	$= V_b$
$3CaO.2SiO_2.3H_2O$	342,4538	2,6300	130,2106	
$3.(Ca(OH)_2)$	222,2841	2,2300	99,6790	
Reaction Products	564,7379	2,4566	229,8895	$= V_r$
			-24,2905	$= V_s$

Tab. 1, C_3S - Reaction

Relating the shrinkage volume to the solid mass of the basic product we get for C_3S

$$V_{cs} = \frac{V_s}{M} = \frac{-24.2905}{456.646} = -0.0532 \ cm^3/g$$

Negative shrinkage volumes were found with analogue calculations for all other clinker phase reactions too. The mass related shrinkage volume $V_{cs,u}$ of a full hydrated portland cement can be calculated with the phase constituents according

$$V_{cs,u} = -0{,}0532.[C_3S] - 0{,}0400.[C_2S] - 0{,}1785.[C_3A] - 0{,}1113.[C_4AF] \quad (14)$$

A similar characteristic cement parameter is the volumetric water demand factor F_{wv}. For C_3S it becomes

$$F_{wv} = \frac{V_w}{V_f} = \frac{108{,}2867}{145{,}6933} = 0{,}7422$$

and for portland cement

$$F_{wv,u} = 0{,}7422.[C_3S] + 0{,}6874.[C_2S] + 1{,}2023.[C_3A] + 1{,}3754.[C_4AF] \quad (15)$$

ASTM	C_3S [%]	C_2S [%]	C_3A [%]	C_4AF [%]	Total [%]	$V_{cs,u}$ [cm^3/g]	$F_{wv,u}$
Type I	49	25	12	8	94	-0.0605	0.825
Type II	46	29	6	12	93	-0.0608	0.819
Type III	56	15	12	8	91	-0.0669	0.827
Type IV	30	46	5	13	94	-0.0577	0.812
Type V	43	36	4	12	95	-0.0578	0.808

Tab. 2, Cement Parameters for ASTM - Type Cements

Table 2 shows these cement parameters for ASTM-type cements. In these calculations the remaining mass fraction to 100% was considered with a 30% lower reactivity. Similar values for cement have been reported by other authors too. Using a mean chemical shrinkage volume for cement of 60 cm^3/kg with a mix of 300 kg cement/m^3 and a bulk modulus of 20 GPa we receive with equation (13) a tension strength of 3,24 MPa, well in the range of concrete materials.

The degree of hydration $\alpha(t)$ can be expressed as relation of time dependent shrinkage volume $V_{cs}(t)$ to the ultimate shrinkage volume $V_{cs,u}$

$$\alpha(t) = \frac{V_{cs}(t)}{V_{cs,u}} \tag{16}$$

and can be determined through a continuously weighing of shrinkage volume $V_{cs}(t)$.

WEIGHING METHOD

A simple method to measure volume changes of hydraulic reactions is the use of a dipping and weighing method. This has been applied for cement reactions already in [5,6]. The equipment is very simple and a system plot is shown in Fig. 2. The required components are a self levelling water bath with a thermostat, a digital balance (0,001 g) and a data logger.

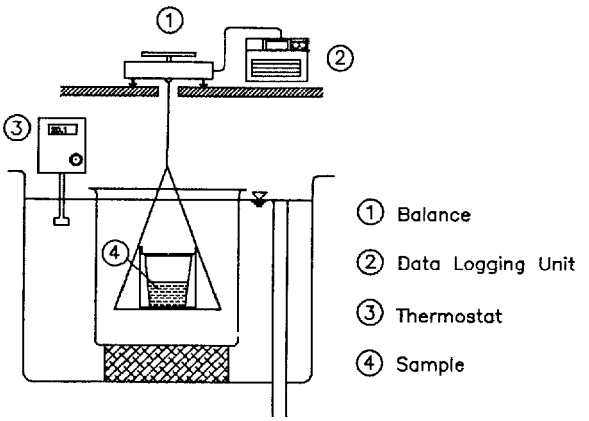

Fig. 2, Immersion Weighing Method

The immersion weighing vessels are divided into a temperature controlled outer water bath and a stabilized inner water bath. The two baths intercommunicate via an aperture of small area or a siphon. The common water level is kept constant. The sample is placed in a plastic case that, in turn, is placed in a vessel to separate it from the inner water bath. An elastic sheet is used to separate the sample from the water bath. The purpose is to avoid density changes by diffusion of dissolved ions to the free water bath. Placing of the sample and covering of the sample holder must be done under water.

The immersion weighing method can be applied to pure cement samples as well as to mortar or concrete samples. Measurements can be taken from the earliest time on, just after placing the sample and calming down of the water level after 1-2 min. The method is suitable for long term runs too, because control procedures like in calorimetry are not necessary. Interpretations of datas from immersion weighing recordings are simple. The shrinkage volume for isothermal storage can be calculated just from mass changes $\Delta G(t)$ and the density of water ρ_w

$$V_s(t) = \frac{G(t) - G_0}{\rho_w} = \frac{\Delta G(t)}{\rho_w} \tag{17}$$

and related to cement mass Z

$$V_{cs}(t) = \frac{\Delta G(t)}{Z \rho_w} \tag{18}$$

In order to get conventional graphs of cement reactions, the original negative shrinkage volume is introduced here with a positive sign. An increase in the reading of an immersion weighing means a volume shrinkage resp. an increase in density.

EXPERIMENTS

The following plots represent typical cement reactions. The plots show V_{cs}- time - diagrams in which positive values mean a volume shrinkage and negative ones a swelling of volume. The reactions were carried out at constant temperatures of 20 °C and with w/c-ratios of 0,40.

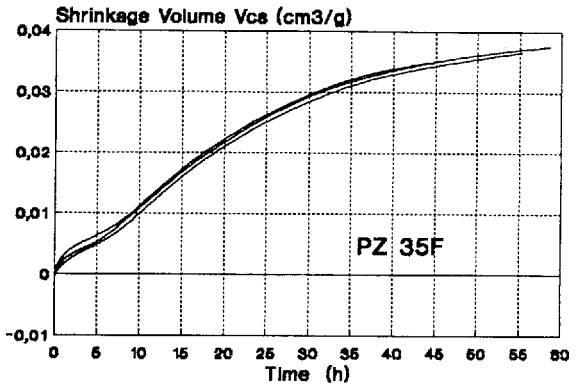

Fig. 3, Repeating Accuracy

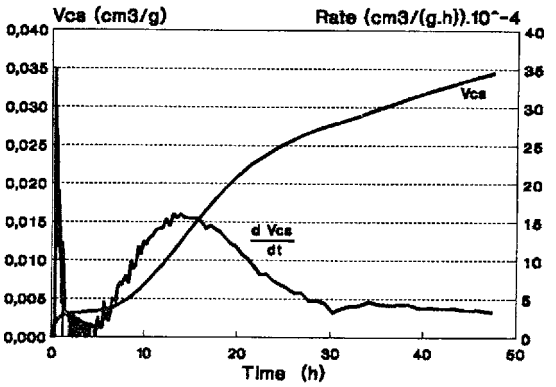

Fig. 4, Normal Cement Reaction

Fig. 3 presents the repeating accuracy of 3 repetitions of a cement reaction. The recordings show a nearly identic behaviour with small variations in the early phase. The reproducibility of the method seems to lie in a sufficient range.

In Fig.4 a reaction of a normal hardening PZ 35F is shown. Differentiation of V_{cs} values against time leads to the reaction rate. These curve has a fluctuating shape because of numerical differentiation. Though, the high early reaction followed by an induction period, and from about 5 hours on the beginning of the acceleration period, can clearly be seen.

Cement reactions recorded with an immersion weighing method differ from each other especially through the type of initial reaction. Fig. 5 shows possible initial cement reactions of different cement types. Distinguishing between the mentioned reaction types leads to the following description:

Type H: high initial reaction, with very fine ground cement types
Type L: low initial reaction, with quicker reacting normal cement types and cements of a medium finesse
Type N: no initial reaction, with normal cement types
Type S: initial swelling reaction (solution-type), change to shrinkage after an induction period, mostly with SRPC and slag modified cement types and with freshly ground cement.

The last mentioned S-type cement reaction explains the hydration mechanism of cement reactions. This can be regarded as sequential reaction of a solution and a crystallization process. In both processes a phase transition is included with well known volume changes during each transition step. As long as the solution process dominates over crystallization, an overall volume swelling results form the process. From the time of supersaturation on, crystallization shrinkage dominates over solution swelling and material hardening begins. The time period of the swelling process can be defined as induction period.

Fig. 6 shows the reaction behaviour of pure C_3A with a Blaine value of 4000 cm^2/g. Relating $V_{cs}(t)$ on the ultimate shrinkage volume of 0.1785 acc. equation (14) we receive the degree of hydration with equation (16).

The influence of concrete admixtures on immersion weighing results of cement reactions has been discussed in [7]. Generally, it can be said that accelerators lead to an immediate shrinkage behaviour while retarders and superpasticizers tend to S-type reactions.

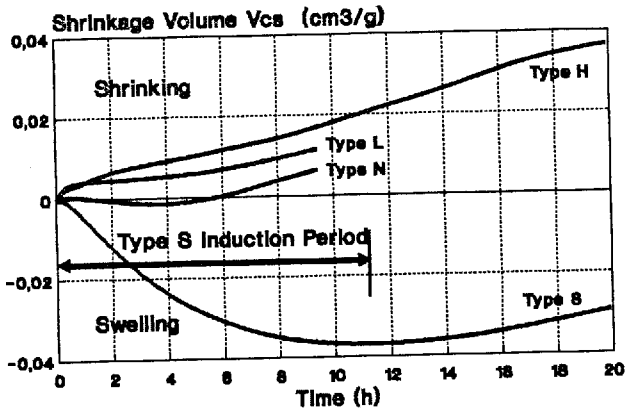

Fig. 5, Initial Reaction Types

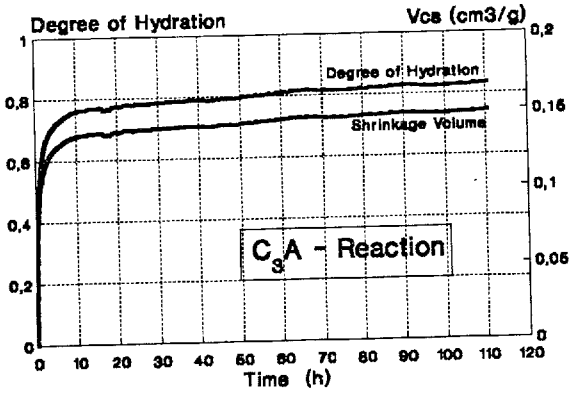

Fig. 6, C_3A - Reaction

CONCLUSION

Immersion weighing of hydraulic reactions represents a simple and accurate method to record kinetic datas of hydraulic processes. The equipment is comparatively cheap so that the method can be used not just in laboratories but also on building sites. The measured reaction curves allow an evaluation of cement types as well as the efficiency of additives or the influence of a temperature treatment. Especially for the early reaction period, the method is more sensitive than calorimetry. The induction period is characterized by the occurrence of a swelling reaction. The acceleration period, during which material strength arises, begins from the time of first occurrence of shrinkage.

REFERENCES

1. Parrot, L.J. et al : "Monitoring Portland Cement Hydration: Comparison of Methods", CCR, Vol.20, pp.919-926, (1990)

2. Glansdorff, P. and Prigogine, I.: "Thermodynamic Theory of Structure, Stability and Fluctuations", Wiley Interscience, London, 1971

3. Paulini, P.: "Kinetik der Zementhydratation und ihr Einfluß auf die Festigkeit von Beton im jungen Alter", Diss., Univ. Innsbruck, 1988

4. Paulini, P.: "Thermodynamics of Hydraulic Hardening", Proc. 1st. Int. Workshop on Setting and Hardening, Jul.1991, Dijon, Chapman and Hall, (in press)

5. Geiker, M. and Knudsen, T.: "Chemical Shrinkage of Portland Cement Pastes", CCR, Vol.12, pp.603-610, (1982)

6. Raffle, J.F.: "Volume Changes during Hydration of Cement Plasters", Proc.Brit.Ceramic Society, 35, pp.295-303, (1984)

7. Paulini, P.: "Reaction Mechanisms of Concrete Admixtures", CCR, Vol.20, pp.910-918, (1990)

Specific Theme III-B

Structure, Composition and Properties of Cement Hydration Systems

CHEMISTRY OF HYDRATION PRODUCTS FORMED IN PASTE OF β-C_2S WITH $C_{12}A_7$, AGED 16 YEARS

Francisa Hannawayya

Hannawayya's Laboratory for Chemical Research and Development
Stockholm, SWEDEN

ABSTRACT

Chemistry of hydration products formed in paste of β-C_2S with $C_{12}A_7$, with and without gypsum at water/solid ratio of 0.5 were studied and examined by: Scanning electron microscopy (SEM) combined with EDAX for samples aged 16 years; and by X-ray diffraction for those of ages 1 day, 7 days, 28 days, 1 year and 16 years. Synthetic anhydrous β-C_2S and $C_{12}A_7$ were prepared by burning process and having of purity 100%. Their chemical composition and densities are presented. Four Series of different alternate compositions of mixtures of β-C_2S with $C_{12}A_7$ were investigated. The main hydration products of the system without gypsum consist of C_2AH_8, CAH_{10}, C_3AH_6 and AH_3. When gypsum is present, the hydration product was initially ettringite ($C_6A\bar{S}_3H_{32}$) of prismatic rod crystals, then after 1 year, monosulphates ($C_4A\bar{S}H_{18}$ and $C_4A\bar{S}H_{12}$) phases are formed. At 16 years aged the hydration products were ettringite and gehlenite hydrate. The author found that Series A and D exhibit high strength within 24 hours and it seems to be a good for applications in the repair of cracked cement-concrete.

SAMMANFATTNING

Kemin beträffande hydratations produkter bildade av β-C_2S med $C_{12}A_7$, med eller utan gips vid vatten/solid förhållande 0.5 undersöktes, och examin med svepelelektronmikroskopi i samband med EDAX endast efter 16 års ålder, och med röntgen diffraktion efter 1 dygn, 7 dygn, 28 dygn, ett år och 16 år. Syntetiska icke hydratiserad β-C_2S och $C_{12}A_7$ var preparationen av brännprocessen hade 100% renhetsgrad. Fyra serier av olika alternative blandning kompositionen av β-C_2S med $C_{12}A_7$ undersöktes. De huvedsakliga produkterna av systemet utan gips består av C_2AH_8, CAH_{10}, C_3AH_6 och AH_3. Då där finns gips, var första produkten ettringite ($C_6A\bar{S}_3H_{32}$) av prismatiska stavkristaller, efter 1 år bildas monosulfater ($C_4A\bar{S}H_{18}$ och $C_4A\bar{S}H_{12}$) faserna. Till sist efter 16 år var produkterna ettringite och gehlenitehydrat. Författaren fann att i serierna A och D utvisa hög hållfasthet inom 24 timmar och det förefaller vara praktiskt tillämpliga vid många reparationer av betongsprickor.

INTRODUCTION

The order of relative importance of the oxides which make up rock forming minerals is, silica, alumina, oxides of iron and lime, etc. It seems desirable to study the system of lime-silica-alumina (or $C_{12}A_7$ + β-C_2S + H_2O). The interest aroused from this study is not only among those engaged in pure science, but also among many in commercial work.

Aluminous cement production had started when the Faraday Society held the first Symposium on the Chemistry of Cements and Plasters in 1918. The knowledge of the material increased rapidly from that time until 1939, as reflected in the paper presented by Sundius /1/ at the Second Symposium held in Sweden 1938.

In the early period of development of high alumina cement. A number of investigations were carried out to determine the most favourable compositions. Bied /2/ believed that the composition should be along the line of C_2S-CA and that the strength decreased as the ratio of C_2S to CA increased. The cementing value of lime-alumina-silica mixes, with and without ferric oxide, of high alumina cement composition was studied by Bates /3/, Endell/4/, Berl and löblein /5/, Solacolu /6/, kühl/7/ and Richter /8/. The high alumina cement zone then falls in the shaded part of the diagram shown in figure 135, Lea /9/, the compounds to be expected in the alumina cement thus being $C_{12}A_7$, CA and C_2S; CA, C_2S and C_2AS; or CA, C_2AS and CA_2 /9/.

Brandenberger /10/ suggests that all the hydrated calcium aluminates may be expressed by the general formulae $mCa(OH)_2 . nAl(OH)_3 . pH_2O$. According to Büssen and Eitel/11/, the composition of the corresponding stable modification must be richer in CaO than Al_2O_3 and they suggest the formulae $12CaO.7Al_2O_3$. A similar result has been reported by Lagerqvist, Wallmark and Westgren /12/ they contend the proportion $9CaO.5Al_2O_3$ to be an alternative possibility. Le Chatelier /13/ was the first investigator to study the hydration reaction of calcium aluminates and their hydrated products. The aluminates, supposed to have the composition CA and C_3A_2, where shaken with one litre of water in portions of 1 and 10 g. An excess of calcium hydroxide was proved in the solution, after some time, and a great portion of aluminum hydroxide and some crystalline calcium aluminate hydrate was formed. Le Chatelier concluded that the setting properties of the anhydrous calcium aluminates should be referred to the suppersaturated solution, which yield hydrated alumina and calcium aluminate hydrates during the setting.

As $C_{12}A_7$ is the essential component of high alumina cement it has been chosen in this investigation together with C_2S. The low silica content is important in high alumina cement in order to obtain hydraulic activity, as it improves both setting time and rapid strength. Therefore, the attention of the present investigation was directed to study the chemistry of hydration products of the system $C_{12}A_7$ + β-C_2S + H_2O in paste form. The purpose was to find out if its hydration products were useful for application of the product in building.

MATERIALS AND METHOD

The initial materials used in this

investigation are:

1- β-dicalium silicate, Hannawayya/14/ synthesized β-C_2S (or $2CaO.SiO_2$), composed of 65.2440% wt. CaO; 33.6675% wt. SiO_2 and 1.0985% wt. Al_2O_3. Table 2 /14/ shows numerous data by X-ray pattern of unhydrated β-C_2S. The data of extreme accurate standard are of great benefit to those who are specialists in cement-concret research.

2- The essential component of high aluminate cement, $C_{12}A_7$ was synthesized by Hannawayya as follows: Calcium carbonate (99% purity) is slightly burnt in a large platinum crucible in a muffle furnace for at least two hours at 1050°C to get CaO, and Al_2O_3 was dried at 1200°C. The materials, reagent weight according to the stoichiometry of $C_{12}A_7$, calcium oxide and aluminum oxide were dry, passed through a No. 48 sieve, and again mixed dry for two hours in bottles on a rotating wheel. The mixture was then heated in open platinum dish in an electric furnace at 1380°C for 24 hours, and cooled rapidly in air. The preparation was ground to pass a No. 200 sieve. The specifications of the compound $C_{12}A_7$ and β-C_2S are given in Table 1.

Table 1.

Compound	Detected by X-ray	Free CaO	Specific surface area cm^2/gm Blaine
$C_{12}A_7$	$C_{12}A_7$, C_3A, (CaO)	0.01%	3900
β-C_2S	β-C_2S (CaO, C_3S)	0.08%	2339

Chemical analyses of the heated sample for CaO and Al_2O_3 are given in Table 2. The results show that the preparations are truly anhydrous. Dry toluene was used for density measurements. This indicates that no reaction occurs between the solid phases and immersion media.

Table 2.

Components of $C_{12}A_7$	mixture weight%	calculated weight %	Density of $C_{12}A_7$
CaO	48.58	48.53	2.68
Al_2O_3	51.50	51.47	
	100.08	100.00	

The system β-C_2S + $C_{12}A_7$ + H_2O, with and without gypsum is studied at water/solid ratio of 0.5. Composition of mixtures used are given in Table 3.

Table 3.

Series	β-C_2S parts vol.	$C_{12}A_7$ parts vol.	$C\bar{S}$ parts vol.	H_2O W/S
A	65	3	-	0.5
B	20	65	-	0.5
C	20	65	15	0.5
D	65	20	15	0.5

Paste specimens with and without gypsum were prepared and stored inside the desiccator containing cold water for the proper period of test, cured at room temperature without being protected from the CO_2 of the air. The hydration system β-C_2S + $C_{12}A_7$ + H_2O paste was examined by X-ray diffraction after 1, 7, 28 days and 16 years. The morphology of the paste aged only 16 years was identified by Scanning Electron Microscopy.

RESULTS, OBSERVATIONS AND DUSCUSSIONS

The relations between the hydration products and the oxide composition in ternary (C-S-H and C-A-H) and quarternary system, $CaO.SiO_2$-$Al_2O_3.H_2O$ (or C-A-S-H) were studied, and recorded photographically by Scanning Electron Microscopy of the paste aged only 16 years. As $C_{12}A_7$ is the essential component of high alumina cement, it was

selected in this investigation with β-C_2S. β-C_2S was chosen for its role in the hydraulic activity. The compound $C_{12}A_7$ has a unit cell larger than that of grossularite and it was thought probable that the open structure of $C_{12}A_7$ /11/ would enable it to incorporate silica into its lattice without any drastic effects. Ditte/15/ assumed that two forms of hydrated alumina are involved, the gelatinous and the crystalline. Hannawayya /16/ by means of X-ray diffraction patterns has shown that the aged gelatinous alumina is crystalline.

The purpose of the present investigations was to explain the connection between the structures of the hydrate and the strength of the paste system, β-C_2S + $C_{12}A_7$ + H_2O. Table 3 shows the compositions.

(i) X-RAY DIFFRACTION DIAGRAMS

(a) 65 parts vol. β-C_2S + 3 parts vol. $C_{12}A_7$ + H_2O, W/S = 0.5.

X-ray diffraction of this series revealed that no new phases had formed after 1 and 7 days. It will be recalled that the products in the mixture are retarded by influencing each other. The only products were unhydrated β-C_2S and $C_{12}A_7$. After 28 days, X-ray diffraction revealed that β-C_2S had decreased to medium strong intensity, while CH and C-S-H had developed. $C_{12}A_7$ had decreased to very weak intensity. After 1 year X-ray diffraction revealed the same hydration products as after 28 days, except that CH had increased to medium strong intensity. After 16 years, X-ray diffraction revealed that the lime, CH, concentration decreases to medium intensity Whereby the silicate hydrates are transformed into lime rich C-S-H. In this medium the strength is good, and this series has useful for practical work. Table 4, Fig. 1.

Table 4. Data of X-ray diffraction of the reaction: X β-C_2S + Y $C_{12}A_7$ + H_2O.

Series β-C_2S + $C_{12}A_7$ + H_2O		1d.	7d.	28d.	1y.	16y.
A	β-C_2S	s	s	ms	m	m
	$C_{12}A_7$	w	w	vw	vw	vvw
	CH	-	-	mw	ms	m
	C-S-H	-	-	bb	bb	bb
Series β-C_2S + $C_{12}A_7$ + H_2O		1d.	7d.	28d.	1y.	16y.
B	β-C_2S	m	m	mw	vw	-
	$C_{12}A_7$	ms	ms	m	m	mw
	CAH_{10}	mw	m	-	-	-
	C_2AH_8	m	mw	-	-	-
	C_3AH_6	-	m	s	ms	m
	C_4AH_{11}	w	w	vw	vw	-
	C_2ASH_8	-	-	m	mw	mw

(b) 20 parts vol. β-C_2S + 65 parts vol. $C_{12}A_7$ + H_2O, W/S = 0.5.

X-ray diffraction of this mixture as in series B revealed that the products after 1 day: a peak of C_2AH_8 of medium intensity and a large amount of unhydrated $C_{12}A_7$. The β-C_2S was of medium intensity. There were peaks of CAH_{10} at 6.2 and 12.4°2θ. Some $C_4A\bar{C}H_{11}$ appeared. After 7 days, C_2AH_8 had decreased rapidly. The peaks of CAH_{10} had increased. Peaks appeared at 17.3°, indicating formation of C_3AH_6. $C_4A\bar{C}H_{11}$ had decreased. Both β-C_2S and $C_{12}A_7$ had decreased. The main hydration products of $C_{12}A_7$ consist of C_2AH_8, CAH_{10}, C_3AH_6 and AH_3. The fist two phases are converted into C_3AH_6 and AH_3 according to the following reactions:

$$3CAH_{10} \longrightarrow C_3AH_6 + 2AH_3 + 18H$$

$$3C_2AH_8 \longrightarrow 2C_3AH_6 + AH_3 + 9H$$

After 28 days, X-ray diffraction revealed that a new gehlenite hydrate (C_2ASH_8) phase appeared with medium peaks of 31.1°, 7.1° and 21.3°. Gehlenite hydrate was formed by reaction of lime, released from β-C_2S during hydration with high alumina component, $C_{12}A_7$. Both β-C_2S and $C_{12}A_7$ had decreased. The C_3AH_6 continued to increase in in-

tensity, reaching a strong peak. There was also some of $C_4A\bar{C}H_{11}$. After 1-year, X-ray diffraction revealed that the unreacted β-C_2S had decreased in intensity. $C_{12}A_7$ had the same intensity as after 28 days. Both C_3AH_6 and gehlenite hydrate (C_2ASH_8) had decreased. Some $C_4A\bar{C}H_{11}$ could be very weakly detected. X-ray diffraction of the paste aged 16 years revealed the same hydration products as after 1 year with decrease of their intensities. The structure is broken up and the strength decreased. See Table 4.

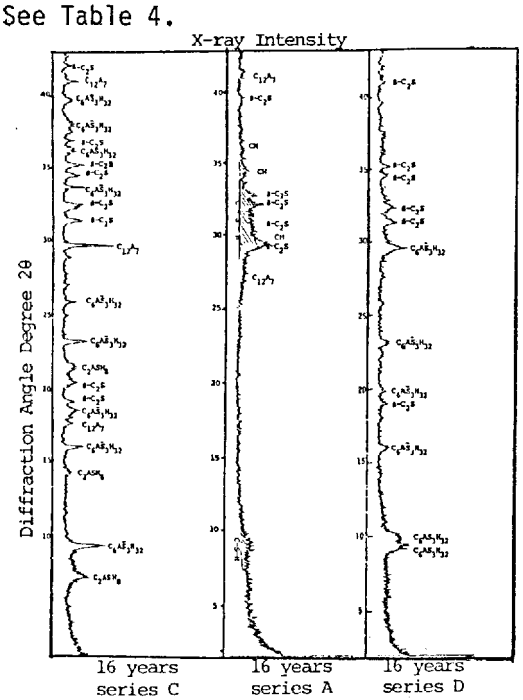

Fig. 1 X-ray diffraction diagrams of the paste 16 years series C, A and D.

(c) 20 parts vol. β-C_2S + 65 parts vol. $C_{12}A_7$ + 15 parts vol. $C\bar{S} + H_2O$.

When gypsum was added, X-ray diffraction after 1, 7 and 28 days revealed that gypsum to some extent retards the hydration rate of the system as in series C. The hydration products of this mixture revealed medium intensity of ettringite after 1 day. Unhydrated $C_{12}A_7$ of strong intensity, and β-C_2S of medium intensity. Gypsum had reached depletion. After 7 Days, ettringite had transfered to monosulphate ($C_4A\bar{S}H_{18}$) with a medium intensity, $C_{12}A_7$ and β-C_2S had decreased. Peaks appeared at 7.1^o, 31.1^o and 21.1^o, indicating formation of gehlenite hydrate (C_2ASH_8). C_3AH_6 could be very weakly detected. After 28 days, peaks appeared at 9.9^o and 19.9^o, indicating formation of $C_4A\bar{S}H_{12}$. The intensity of gehlenite hydrate had decreased. C_3AH_6 had weak intensity. $C_{12}A_7$ had further decreased. The peak of β-C_2S showed a slight decrease. Som $C_4A\bar{C}H_{11}$ was visible. After 1 year, X-ray diffraction revealed that gehlenite hydrate (C_2ASH_8) of medium stromg intensity was the chief hydration product. Monosulphate($C_4A\bar{S}H_{18}$) had increased. $C_4A\bar{S}H_{12}$ had reached medium weak intensity, C_3AH_6 and $C_4A\bar{C}H_{11}$ had the same intensities as after 28 days. $C_{12}A_7$ had decreased to medium weak intensity. After 16 years aged X-ray diffraction revealed a transition stage of monosulphates ($C_4A\bar{S}H_{12}$ and $C_4A\bar{S}H_{18}$) to ettringite, C_2ASH_8 had decreased to weak intensity. β-C_2S and $C_{12}A_7$ had the same intensity as after 1 year. Other products had disappeared. In this series the strength was weak. Table 5 and Fig. 1 show.

(d) 65 parts vol. β-C_2S + 20 parts vol. $C_{12}A_7$ + 15 parts vol. $C\bar{S} + H_2O$.

Continuing with a mixture to which more silicate has been added, i.e series D, X-ray diffraction revealed different hydration products. After 1 day, ettringite had medium strong intensity, Gehlenite hydrate had weak intensity, gypsum had ceased reacting. $C_{12}A_7$ had very weak intensity. Unreacted β-C_2S of strong intensity appeared.

After 7 days gypsum had reached depletion. The gehlenite hydrate increased further. After 28 days, the β-C_2S had decreased and started to release lime (CH) in the solution of amorphous phase (cannot detected by X-ray). After 1 year, a transition stage occurred, in which β-C_2S had decreased to medium intensity, releasing lime. Unreacted $C_{12}A_7$ and gehlenite hydrate were the same as after 28 days. After 16 years aged X-ray diffraction revealed that the main hydration product is ettringite. β-C_2S had decreased, releasing more lime (CH). $C_4A\bar{S}H_{12}$ reacted with more lime and transferred to ettringite. Other hydration products had disappeared. In this medium the strength is good. This series is good for practical application. See Table 5, Fig. 1 and 2.

Table 5. Data of X-ray diffraction of the reaction:

$X\beta\text{-}C_2S + y\bar{C}12A_7 + Z\bar{C}\bar{S} + H_2O$, W/C = 0.5.

Series	β-C_2S + $C_{12}A_7$ + $C\bar{S}$ + H_2O	1d.	7d.	28d.	1y.	16y
C	β-C_2S	m	mw	w	w	w
	$C_{12}A_7$	s	m	mw	mw	mw
	$C_6A\bar{S}_3H_{32}$	m	-	-	-	ms
	$C_4A\bar{S}H_{18}$	-	m	m	ms	-
	$C_4A\bar{S}H_{12}$	-	-	m	mw	-
	C_2ASH_8	-	m	m	ms	w
	C_3AH_6	-	vw	w	w	-
	$C_4A\bar{C}H_{11}$	-	-	w	w	-
Series	β-C_2S + $C_{12}A_7$ + $C\bar{S}$ + H_2O	1d.	7d.	28d.	1y.	16y.
D	β-C_2S	s	s	ms	m	mw
	$C_{12}A_7$	vw	vw	vw	vw	-
	$C_6A\bar{S}H_{32}$	ms	ms	ms	ms	m
	$C_4A\bar{S}H_{12}$	-	-	-	m	-
	C_2ASH_8	w	mw	m	m	-
	$C_4A\bar{C}H_{11}$	-	-	-	vw	-

(ii) SCANNING ELECTRON MICROSCOPY RESULTS

SEM was used to reveal the morphological structure of the various products of hydration. It can be seen how the character of the products of hydration changes with time and environment. EDAX technique is a method of qualitative analysis. The element concentrations shown by X-ray peaks of each compound in the region scanned are not linearly proportional to the peak height over a wide range of concentration. The peak heights are strongly dependent upon the matrix of the compound. Each composite EDAX spectrum was scaled to the same background level.

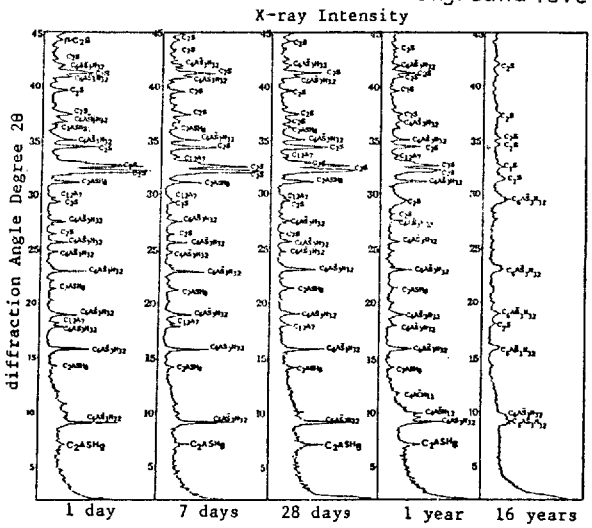

Fig. 2. X-ray diffraction diagrams of Series D.

(a) 65 parts vol. β-C_2S + 3 parts vol. + $C_{12}A_7$ + H_2O, W/S = 0.5.

The silicate in high concentration lime solution gives rise to the lime-rich of C-S-H which grows around the β-C_2S grain like a space lattice consisting of small short rods. In this mixture CH crystallizes as large compact leaf like Portland cement. The strength is good and reaches high values. This series is good for practical application. See Fig. 3

(b) 20 parts vol. β-C_2S + 65 parts vol. $C_{12}A_7$ + H_2O, W/S = 0.5.

The product formed first will be a gel compound. Owing to the large amount of β-C_2S, the CH production is more rapid and its crystallization can be seen after 24 hours of hydration. The larger amount of CH leads to a large number of reaction products. At first C_2AH_8 crystallizes, then C_2AH_n + CH gives rise to C_3AH_6 in the form of round grains with pronounced tendency to form regular crystals. AH_3 and CH can also form CAH_{10} in the form of hexagonal crystals and on the picture there is a mixture of crystals types. The compound is strongly broken up and

the strength decreases. Owing to the high concentration of Al-ions in the solution and the CH released from β-C_2S during hydration, gehlinite hydrate (C_2ASH_8) is formed. See Fig. 4.

(c) 20 parts vol. β-C_2S + 65 parts vol. $C_{12}A_7$ + 15 parts vol. $C\bar{S}$ + H_2O.

The quantity of gypsum is too small to transfer all the $C_{12}A_7$ component to ettringite, so there was a medium strong amount of ettringite. Also gehlenite hydrate (C_2ASH_8) of prismatic crystal habits in hydration product, However, does not give tenacity. Thus the prismatic ettringite crystal in this mixture did not give high tenacity. See Fig. 5.

(d) 65 parts vol. β-C_2S + 20 parts vol. $C_{12}A_7$ + 15 parts vol. $C\bar{S}$ + H_2O.

The β-C_2S gives the solution a certain lime concentration from the beginning in spite of the high reaction velocity of $C_{12}A_7$. This leads to the transformation of aluminate into ettringite ($C_6A\bar{S}H_3H_{32}$) which forms hexagonal rod crystals. Around the β-C_2S grains there are often cracks, where a high lime concentration can build up. There the silicate forms the lime-rich Ca-silicate form with a lot of short staffs which can be seen on the pictures. The C-S-H form is poor in lime, which however increases somwhat when time, whereupon the structure becomes thicker and stronger with good strength. This series is good for practical application. See Fig. 6.

CONCLUSONS

The present study was directed on hydration properties of pastes of β-C_2S + $C_{12}A_7$, with and without gypsum. This study is of interest not only to those engaged in pure science, but also those on the applied wide. X-ray diffraction and SEM revealed that the initial hydration products were the metastable hexagonal hydrate phases, C_2AH_8 and CAH_{10}, which finally were converted to stable phase isometric tricalcium aluminate hexahydrate(C_3AH_6). The β-C_2S did not retard the conversion. When gypsum is present, the hydration products was initially ettringite($C_6A\bar{S}_3H_{32}$) of prismatic rod crystals. Since calcium hydroxide(CH) is a product of the hydrolysis of β-C_2S, the increase of $Ca(OH)_2$ results in the precipitation of monosulphates hydrate ($C_4A\bar{S}H_{18}$ and $C_4A\bar{S}H_{12}$). Finally at 16 years aged, the products were ettringite and gehlenite hydrate. The present author found that Series A and D exhibit high strength within 24 hours and it seems to be agood for application in the repair of cracked cement-concrete.

ACKNOWLEDGEMENT

The author is deeply grateful to Director General Pertil Pettersson and Senior Research Officer Sten Flodin of the Swedish Council for Building Research for help received in supporting part of grant for this research.

REFERENCES

/1/ Sundius, N., Symposium on the Chemistry of Cements, Stockholm, p. 395 (1938).
/2/ Bied, Le Ciment 25, 295 (1920); 26, 135 (1921); 27, 101 (1922).
/3/ Bates, Bur. Stand. Tech. Paper, No. 197 (1921).
/4/ Endell, Zement 8, 319 (1919).
/5/ Ibid. 15, 642 (1926).
/6/ Ibid. 22, 13, 114, 250, 311 (1933).
/7/ Ibid. 20, 261 (1931).
/8/ Ibid. 21, 445 et Seq. (1932).
/9/ Lea, F. M., Third edition, The Chemistry of Cement (1970).

/10/ Brandenberger, Mineral, Pet. 13, 569 (1933).
/11/ Büssen and Eitel, Z. Krist., 95, 175 (1936).
/12/ Lagerqvist and Westgren, Chem. 234, 1, (1937).
/13/ Le Chatelier, (1883), 1056, Diss, Paris (1887).
/14/ Hannawayya, 10th International Conference (ICMA) San Antonio, Texas, U.S.A. (1988).
/15/ Ditte, Compt. Rend. 116, pp.183, 386 509 (1893).
/16/ Hannawayya, F. 8th International conference (ICMA) Orlando, Florida, U.S.A. (1986).

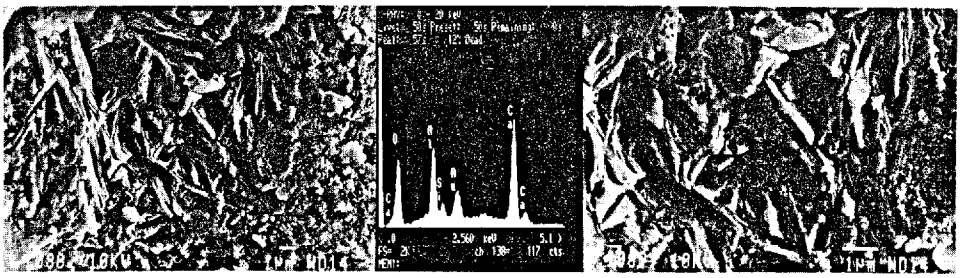

SEM (Fig. 3) Series A.

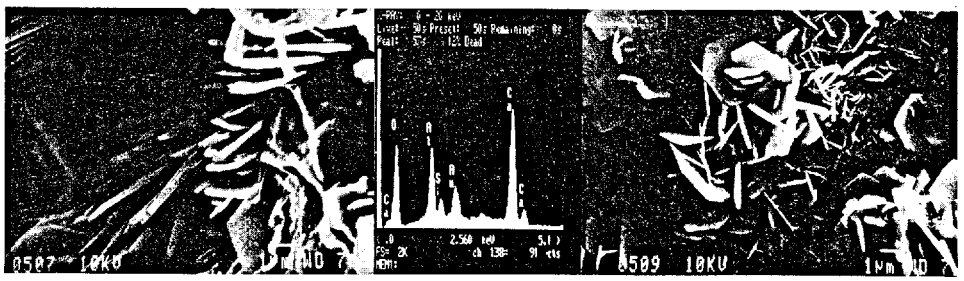

SEM (Fig. 4) Series B.

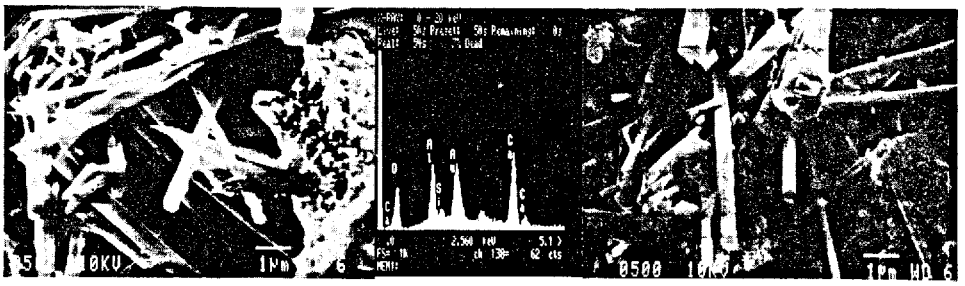

SEM (Fig. 5) Series C.

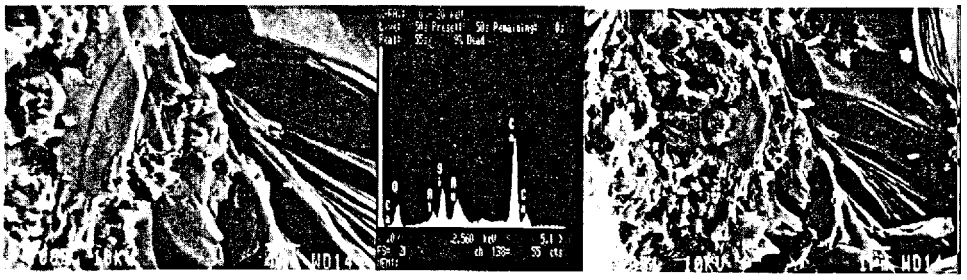

SEM (Fig. 6) Series D.

INTRINSIC BOND PROPERTIES OF HYDRATES FORMED IN THE HYDRATION OF PURE CLINKER MINERALS

H Scharf and I Odler

Technical University Clausthal
GERMANY

SUMMARY

Mature pastes of various clinker minerals i.e. C_3S, C_3A, C_4AF, CA and C_4AF + $C\bar{S}$ consisting of different hydrate phases, i.e. CSH+CH, AFt, AFm, C_3AH_6 and CAH_{10} were mutually compared with respect to their strength properties i.e. compressive and flexural strength, modulus of elasticity and hardeness. Significant differences were found in the bonding characteristics of different hydrate phases when compared both at equal starting water-solid ratios and equal porosities.

ZUSAMMENFASSUNG

Hydratisierte Pasten verschiedener Klinkerminerale, nämlich C_3S, C_3A, C_4AF, CA und C_4AF + $C\bar{S}$, die verschiedene Hydratationsprodukte enthielten (CSH+CH, AFt, AFm, C_3AH_6 und CAH_{10}) wurden gegenseitig verglichen bezüglich ihrer Festigkeitseigenschaften (Druck- und Biegezugfestigkeit, Elastizitätsmodul und Härte). Es wurden gefunden wesentliche Unterschiede in den Bindevermögen verschiedener Hydratphasen beim Vergleich von Pasten, hergestellt mit gleichem Wasser-Feststoff-Verhältnis oder auch solchen, die identische Porositäten auswiesen..

INTRODUCTION

Within our work we studied the intrinsic bond properties of hydration products formed in the hydration of a series of phases common in portland and high alumina cements. In order to eliminate the simultaneous effect of porosity efforts were made to compare pastes of equal porosity. As it is also known that variations of hydration temperature may affect the quality of the hydrates formed, some of the pastes were allowed to hydrate at two different temperatures.

EXPERIMENTAL

Pastes prepared from pure Ca_3SiO_5 (C_3S), $Ca_3Al_2O_6$ (C_3A), $Ca_4Al_2Fe_2O_{10}$ (C_4AF) and $CaAl_2O_4$ (CA) synthetized in our laboratory as well as from C_4AF+CS were studied. Pastes of each starting material were made with several water-solid ratios, all liyng within the range of plastic consistency. Out of these, test specimens 10x10x60 mm^3 were prepared. They were demolded after one day and kept in a saturated lime solution until testing, i.e. 180 days. All samples were prepared and cured at 20 °C, except those of CA where temperatures 5 and 30 °C were employed to obtain two different hydration products. The C_3S pastes were cured also at 90 °C, in addition to 20 °C, to study the effect of curing temperature on strength. To be able to prepare test specimens also from C_3A pastes, their setting had to be retarded by performing the mixing at 5 °C. The pastes were cured at 20 °C subsequently. To produce an AFt phase as product of hydration, blends of C_3A and C_4AF with calcium sulfate were also included in the study. Test speciments made from the former combination expanded and desintegrated in the course of curing, and thus could not be used for strength determination. Specimens made from C_4AF+CS_2 expanded too, but only to a degree at which strength determination was still possible.

Under the described experimental conditions all the pastes included in the study became completely, or nearly completely hydrated by the time of testing. The following strength parameters were determined on the produced test specimens: compressive (σ_C) and flexural (σ_F) strengths, dynamic modulus of elasticity (E, ultrasonic procedure) an hardeness (H, Brinell test). Each value reported represents the average of at least three independent measurements.

In addition to mechanical testing the content of total (w_t) and combined (w_c) water in the samples was also determined. The former parameter was determined as the loss on ignition of a non-treated sample, whereas the latter one as the loss on ignition of a sample that had been extracted with acetone and subsequently with ethyl ether. The porosity of the material was determined as the volume of free water ($w_f = w_t - w_c$) per volume unit of paste. The phase composition of the hydrated samples was determined by X-ray diffraction and DTA.

RESULTS AND DISCUSSION

The strength data found in pastes with different starting water-solid ratio are summarized in Table I. The table also includes the total and combined water values (in grams of water per one gram of original material) and the main products of hydration.

It is apparent that most of the samples picked up distinct amounts of water from the environment in the course of curing. This amount was highest in the samples, yielding ettringite where the hydration was accompanied with a distinct expansion.

The combined water values differed distinctly in pastes prepared from different starting materials but were generally little dependent on the starting water-solid ratio. The highest combined water values were found in pastes yielding AFt and the hydrograrned phases (C_3AH_6) as products of hydration.

The compressive strength, just as the flexural strength, modulus of elasticity and hardeness varied greatly in pastes made from different starting materials and/or hydrated at different temperatures, if compared at equal starting water-solid ratios. By far the highest compressive strengths and moduli of elasticity were found in pastes made from CA hydrated at 5 °C, whereas these values were lowest in pastes made from C_4AF+CS. The flexural strength and hardeness were highest in C_3S pastes hydrated at 90 °C. The lowest flexural strength was obtained in CA pastes hydrated at 30 °C and the lowest hardeness in C_4AF pastes.

In Table II the average ratios between the individual strength parameters for the different binders studied are given. It is apparent that these ratios varied greatly in pastes made from different starting materials and/or hydrated at different temperatures. It may be assumed, that these differences are due mainly to the different morphology of the hydrates formed.

In Figure 1. The compressive strengths found in the individual experimental series are plotted as function of porosity. Similar data for flexural strength, modulus of elasticity and hardeness are shown in figures 2,3 and 4. From the figures it is apparent, that it was impossible to produce all the studied hydrated materials with equal porosities, inspite of similar starting water-solid ratios employed. This was due on one hand to the existing differences in the amount of water taken up from the environment in the course of curing and on the other hand to different amounts of water combined in the course of hydration. Nevertheless, it may be concluded, that even at equal porosities the bonding capacities of different hydrate phases differed. The only exception appears to be the modulus of elasticity whose magnitude seems to be just a function of the overall porosity of the hydrate phase present. A comparison of the Figures 1-4 indicates a lack of a general correlation between the four strength parameters studied. This is due to the fact that the ratio between the parameters studied vary in different hydrated materials.

CONCLUSIONS

The strength properties of hydrates formed from the hydration of different clinker minerals differ if compared both at an equal starting water-solid ratio and equal paste porosity.

Some clinker minerals yield hydrates of different bonding properties if allowed to hydrate at different temperatures. This may be due to differences in the nature of the hydrate phases formed, or to the microstructure of the hydrated material.

The mutual ratio of different strength parameters i.e. compressive and flexural strength, modulus of elasticity and hardeness may vary greatly in different hydration products.

Tab. I Composition and strength properties hydrated clinker mineral pastes

material	w/s	W_{tot} g/gc	W_{comb} g/gc	σ_c MPa	σ_F MPa	E GPa	H MPa	Phases
C_3S	0.35	0.392	0.271	100	4.6	33	221	CSH
20 °C	0.40	0.427	0.286	84	3.3	37	194	+
	0.45	0.470	0.296	69	2.6	23	162	CH
	0.50	0.478	0.296	38	2.3	21	-	
C_3S	0.39	0.379	0.236	89	13.5	32	406	CSH
90 °C	0.43	0.443	0.258	54	10.6	22	270	+
	0.48	0.480	0.266	41	8.2	15	180	CH
C_3A	0.40	0.493	0.326	28	5.8	27	67	C_3AH_6
20 °C	0.44	0.542	0.328	16	3.9	17	63	
	0.48	0.567	0.320	12	3.1	16	44	
C_4AF	0.38	0.441	0.291	26	6.0	21	12	$C_3(A,F)H_6$
20 °C	0.43	0.488	0.307	16	4.6	17	11	
	0.48	0.577	0.317	12	2.9	14	-	
CA	0.25	0.322	0.287	216	12.6	73	155	CAH_{10}
5 °C	0.35	0.451	0.408	207	6.4	61	178	
	0.40	0.516	0.461	192	6.4	55	167	
CA	0.27	0.524	0.479	82	3.7	64	138	C_3AH_6
30 °C	0.30	0.612	0.492	53	2.6	46	130	+
	0.35	0.645	0.495	37	2.5	37	103	AHx
	0.40	0.692	0.492	29	-	27	105	
C_4AF 64.1%	0.36	1.034	0.528	12	4.4	8.7	28	AFt
CS 35.9%	0.38	1.054	0.523	9	5.7	7.4	29	
	0.43	1.040	0.525	10	5.4	6.6	30	
	0.48	1.061	0.535	9	4.9	6.3	28	

W_{tot} total water (in g per 1 g of original substance)
W_{comb} combined water (in g per 1 g of original substance)

Tab. II Mutual ratios of various strength parameters found in hydrated clinker mineral pastes (average values)

Material		σ_F/σ_c	$E/\sigma_c \times 10^3$	H/σ_c
C_3S	20 °C	0.047	0.39	2.29
C_3S	90 °C	0.18	0.37	4.65
C_3A	20 °C	0.24	1.11	3.33
C_4AF	20 °C	0.25	1.01	0.57
CA	5 °C	0.041	0.31	0.82
CA	30 °C	0.054	0.88	2.63
C_4AF+CS	20 °C	0.52	0.73	2.92

σ_F = flexural strength (MPa) E = modulus of elasticity (MPa)
σ_c = compressive strength (MPa) H = hardeness (MPa)

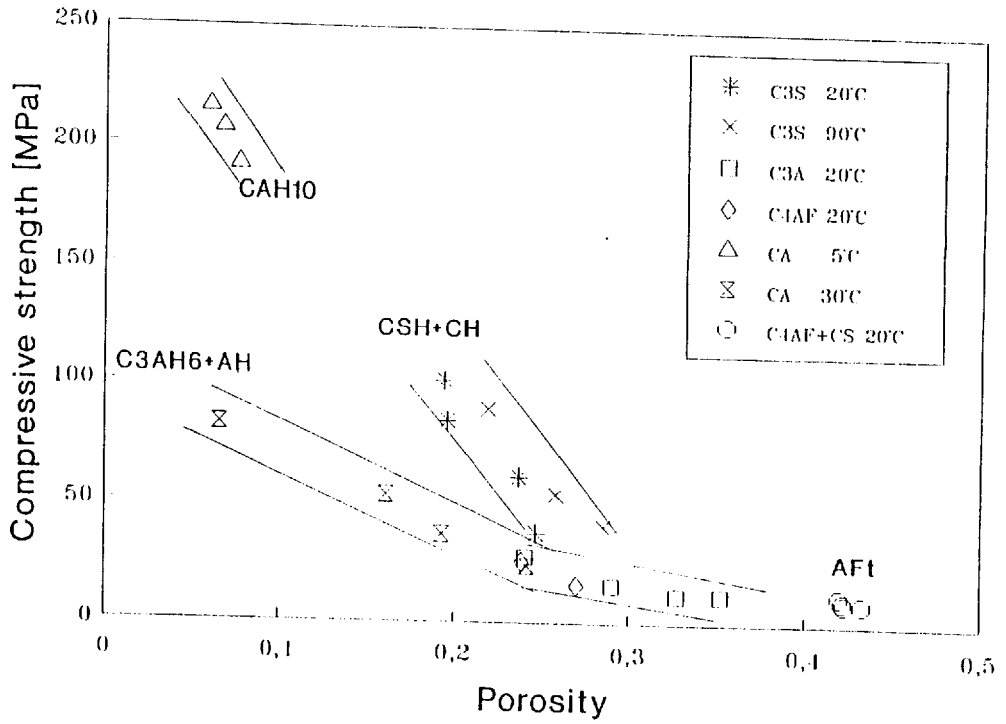

FIG. 1 Compressive strength as function of total porosity

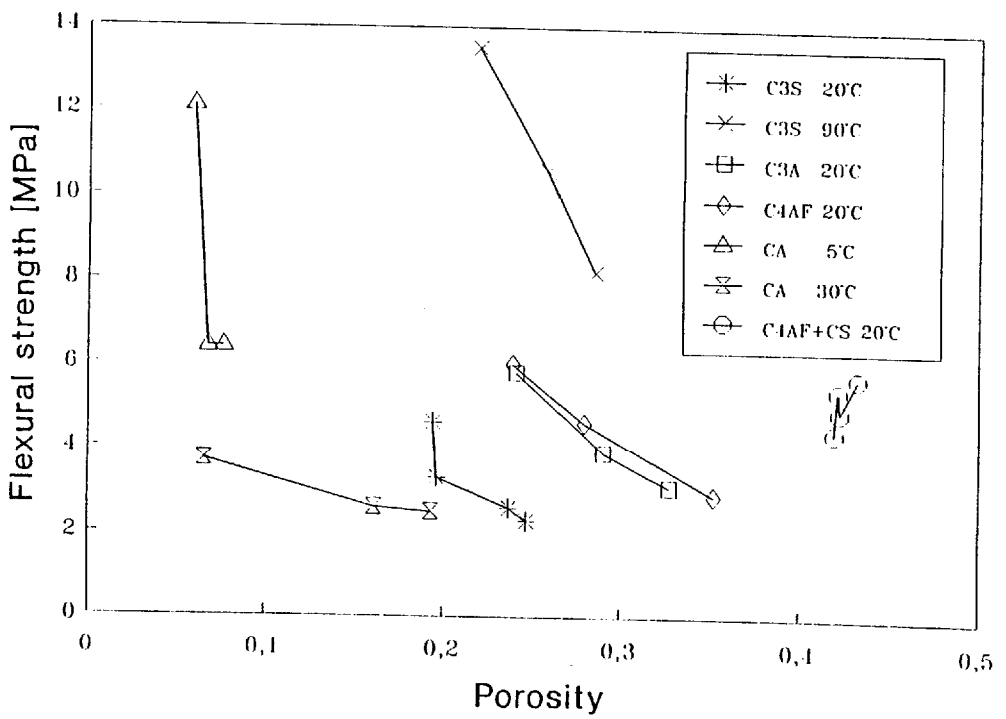

FIG. 2 Flexural strength as function of total porosity

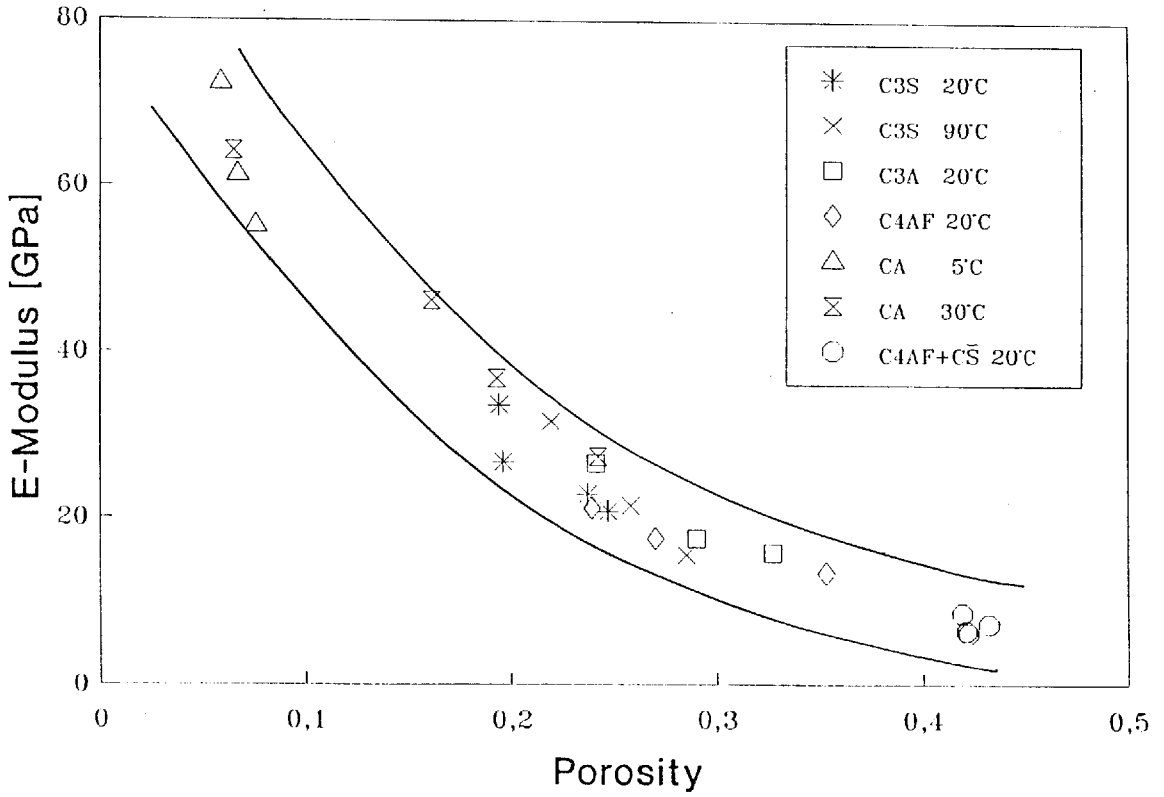

FIG. 3 Modulus of elasticity as function of total porosity

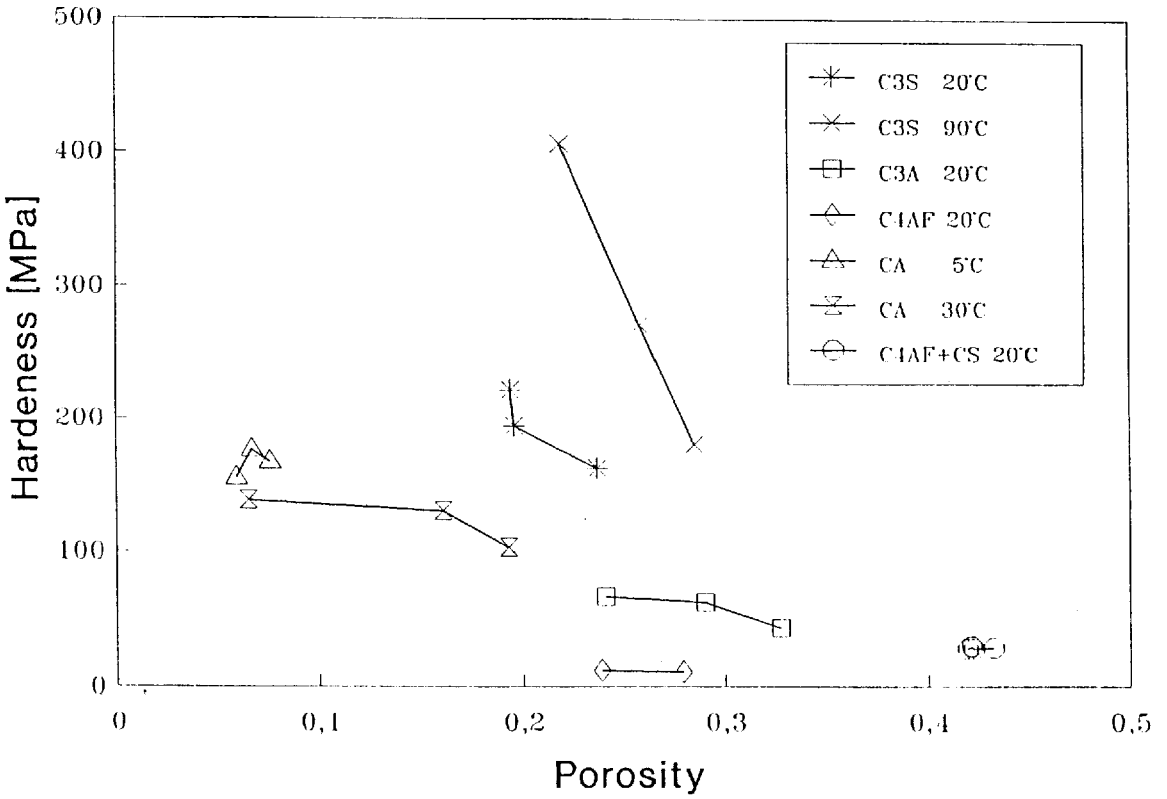

FIG. 4 Hardeness as function of total porosity

MICROMINERALOGICAL STUDY OF THE INFLUENCE OF GYPSUM ON THE EARLY HYDRATION OF C_3A POLYMORPHS

Aimin Xu* and Shondeep L Sarkar**

*Division of Building Materials, Chalmers University of Technology, Göteborg, SWEDEN
**Faculty of Applied Sciences, Université de Sherbrooke, Sherbrooke, Québec, CANADA

ABSTRACT

It is well-established that at least two forms of C_3A (cubic and orthorhombic) occur in cement, offering different reactivities. Since C_3A hydration significantly influences fresh paste rheology and setting time, a detailed micromineralogical investigation of early hydration was carried out. Due to their widespread use, the influence of superplasticizer were also investigated.

Environmental scanning electron microscope (ESEM), the latest development in electron microscopy, enables the examination of wet specimens, allowing real-time comparison of hydration kinetics and distinction between products of orthorhombic and cubic C_3A. Supportive microanalytical techniques used were XRDA, conventional SEM, and DTA/TG.

The results obtained indicate that in saturated gypsum solution, the C_3A_O forms crystalline ettringite faster. Extremely fine fibrous products form very early on the C_3A_C surface, whereas long lath-like crystals begin to grow, often radially, on orthorhombic C_3A. Though the cubic C_3A-gypsum reaction appears to be more vigorous very early, it is associated with the formation of some secondary gypsum on C_3A crystals. In the presence of superplasticizer, a dense membrane begins to cover the surface of C_3A_C crystals. A more open-structured honeycomb formation was observed in the orthorhombic variety. Both forms are accompanied by a distinctly retarded hydration process.

ÉTUDE MICROMINÉRALOGIQUE DE L'INFLUENCE DU GYPSE SUR L'HYDRATATION DES POLYMORPHES C_3A AU JEUNE ÂGE

RÉSUMÉ

Il est bien connu qu'il existe dans le ciment au moins deux formes de C_3A (cubique et orthorhombique) présentant des réactivités différentes. Puisque l'hydratation du C_3A influence de façon significative la rhéologie de la pâte fraîche et le temps de prise, on a effectué une étude microminéralogique détaillée de l'hydratation au jeune âge. On a aussi étudié l'influence des superplastifiants par suite de leur utilisation de plus en plus courante dans le domaine des bétons.

Microscope électronique à balayage environmental (MEBE), la dernière innovation en microscopie électronique, permet l'examen d'échantillons humides. Cette technique offre la possibilité de comparer la cinétique d'hydratation et de différencier les produits du C_3A cubique et orthorhombique. Les techniques microanalytiques de support utilisées furent la DRX, la MEB conventionnelle et la TG/ATD.

Les résultats indiquent que, dans une solution saturée de gypse, le C_3A_O forme de l'ettringite cristalline plus rapidement. Des produits fibreux extrêmement fins se forment très tôt sur la surface du C_3A_C , tandis que de longs cristaux en lattes commencent à croître, souvent de façon radiale, sur le C_3A orthorhombique. Bien que la réaction C_3A cubique / gypse semble être plus active très tôt, elle est accompagnée de la formation de gypse secondaire sur les cristaux de C_3A. En présence de surperplastifiant, une membrane dense commence à recouvrir la surface des cristaux de C_3A cubique. Une structure plus ouverte en nids d'abeilles a été observée dans la variété orthorhombique. Les deux formes sont clairement accompagnées d'un retard d'hydratation.

INTRODUCTION

Although C_3A hydration alone, or in the presence of gypsum, has been researched extensively [1-3], it still continues to generate intense interest among cement scientists and engineers alike. Researchers in the last two decades have conclusively proved the presence of at least two polymorphic forms of C_3A (cubic and orthorhombic) in commercial cements [3, 4]. Since their crystallographic structures are different [5, 6], their hydration behaviour also differs. Secondly, since high dosage of superplasticizers are frequently used in concrete, it has been observed that cement / superplasticizer compatibility differs from one cement to another [7]. This can be related to the polymorphic form of C_3A, besides the C_3A content proper in the cement. C_3A is the first cement component to react when the cement comes in contact with water. Depending upon the C_3A polymorph present, the hydration kinetics will vary, thus influencing on the rheological behaviour of the cement/concrete.

To date, most of the research related to C_3A hydration has been conducted using techniques such as calorimetry [8, 9], XRD analysis [8, 10], DTA [11, 12], ζ-potential measurement [13, 14], infrared-spectroscopy [1], and solution chemistry [15, 16]. None of these can provide adequate information about the morphological development and changes that occur during the very early hydration period, which invariably requires the support of a direct observation technique, such as SEM [8, 9, 17, 18]. However, SEM requires the sample to be dried (by liquid N_2, oven drying, or acetone immersion), which can result in the loss of physically adsorbed water, generate artifacts, such as shrinkage of the colloidal gel, can lead to precipitate formation on solid phases, and most important, it arrests hydration. Most of these can be overcome by using the latest SEM development, called ESEM, which permits cement hydration to be recorded in real-time. ESEM allows retention of moisture in the specimen for at least up to 30 min, sufficient to study the initial hydration of C_3A. Unlike in the standard SEM, the ESEM specimen chamber can be maintained at a relatively low vacuum (5×10^{-3} torr versus 10^{-6} torr), which will not cause violent evaporation. This allows wet specimen imagery at the same high level of resolution as the conventional SEM. It is also equipped with EDX detector for simultaneous elemental analysis.

The authors investigated the very early hydration of both C_3A_C and C_3A_O with gypsum with/without a superplasticizer. Such a comparative study helps to elucidate further the hydration mechanism, establish the difference between C_3A_C and C_3A_O hydration, and predict the rheological behaviour of cement/concrete in the presence of a superplasticizer. For the first time, ESEM was used to study C_3A hydration kinetics. Supportive techniques such as conventional SEM, XRD and DTA examinations on acetone-dried specimens were also used, since it is not always possible to deduce the complete mechanism from a single method. In addition, the C_3A-gypsum mixes were tested for water soluble Ca^{2+}, Na^+, Al^{3+}, and SO_4^{2-} ions at 20°C.

EXPERIMENTAL

Two types of C_3A, cubic and orthorhombic, supplied by CTL, Skokie, Ill., USA, of Blaine fineness 320 m^2/kg and 280 m^2/kg, respectively, were used. The Na_2O content in C_3A_O was 0.12 unit, i.e., the C_3A_O is equivalent to $N_{0.10}C_{2.90}A$ by the dissolution test. The gypsum was of reagent grade purity. The dry mixes of C_3A and gypsum were homogenized by inter-grinding. A locally available commercial sodium naphthalene polycondensate superplasticizer and distilled water was used. Two types of mixes were prepared as follows:

C_3A + gypsum + water (w/s = 0.60; molar ratio of gypsum : C_3A = 3:1, which represents the stoichiometric composition for ettringite formation); and C_3A + gypsum + water with 3% superplasticizer (w/s = 0.60).

RESULTS

DTA/TG The results are shown in Figure 1. Ettringite forms in the pastes hydrated for 10 min, as evidenced by the endothermic peak between 100 and 120°C [11]. The lower decomposition temperature for the C_3A_C + gypsum paste may be due to the unexpected retardation in ettringite formation. At 60 min, the C_3A_O positively forms a higher amount of ettringite. The strong twin endothermic peaks at 146°C/158°C, together with the weak but distinct exothermic peak at 365-375°C are due to unreacted gypsum. The gypsum endotherm is slightly wider (extends to the lower temperature), especially at 10 min for the C_3A_C + gypsum paste. There also exists a very weak endotherm for C_3A_C at 264°C due to the decomposition of calcium aluminate hydrates. The small endotherm at 922°C (not associated with weight loss) for the C_3A_O + gypsum paste is difficult to explain at this stage.

The addition of superplasticizer in the mixing water significantly retards the hydration process and can be related to the weaker endotherm for ettringite and the stronger peaks for gypsum. The gypsum peaks, unexpectedly become stronger at 60 min for the C_3A_C + gypsum paste. For this paste, the weak endotherm at 256-258°C can be compared to that at 264°C for the C_3A + gypsum pastes without superplasticizer. The endotherm at about 700°C is associated with 2.9% and 3.5% weight loss (by the weight of dry paste) for C_3A_C and C_3A_O respectively, which is obviously an effect of the superplasticizer. The weight loss is too high for C_3A_O, since the superplasticizer /(cement+gypsum) ratio is only 0.03. The TG/DTA test for this superplasticizer showed that it is almost completely decomposed at about 500°C accompanied with a strong exothermic effect (which is not seen for the paste samples), some exothermic effects also occur near 800°C, and the total weight loss at 1100°C is only about 60%. The endothermic peak at 908-911°C for C_3A_O paste is comparable to the peak at 922°C for the paste without superplasticizer. The broad endotherm from about 800°C to 1000°C is associated with a large weight loss, 3.1% and 8.9% for C_3A_C at 10 min and 60 min, respectively; and 8.6%

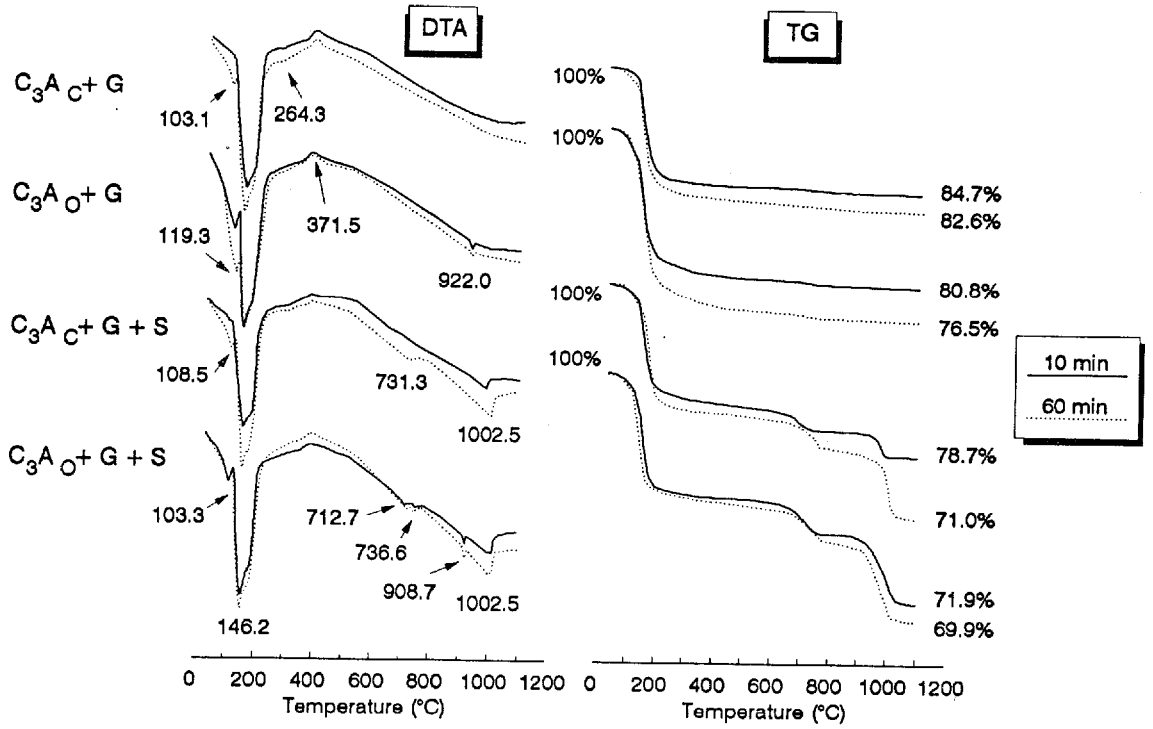

Fig.1. DTA/TG curves of the pastes at 10 and 60 min; G = gypsum and S = superplasticizer.

and 13.4% for C_3A_O.

XRD Figure 2 shows the XRD patterns of the samples hydrated for 10 min. In the presence of gypsum, C_3A_O reacts faster; more ettringite is generated in the paste. For the C_3A + gypsum paste containing superplasticizer, the formation of ettringite is highly suppressed, though C_3AH_6 and C_4AH_{19} still form.

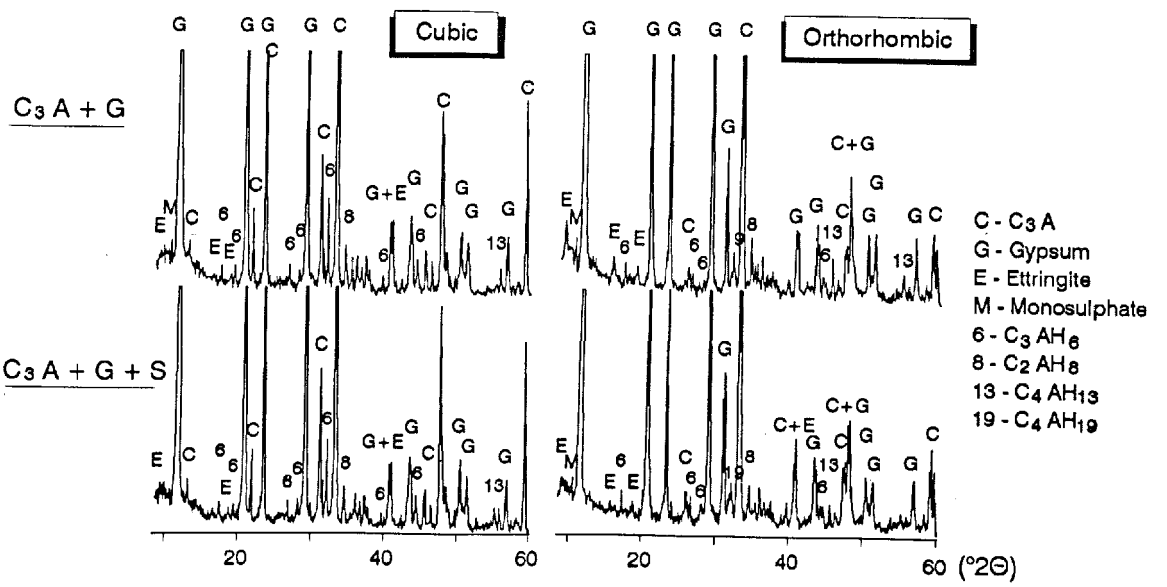

Fig.2. XRD of the hydrated pastes at 10 min.

A semi-quantitative analysis of the main phases, C_3A, ettringite and C_3AH_6, performed by integrating the diffraction intensity of the characteristic peaks, is shown in Figure 3. It can be seen that at 10 min, more C_3A_C reacts compared to C_3A_O, but it is the reverse at 60 min. In the presence of superplasticizer, C_3A_C has a faster reaction rate. However, more ettringite is formed in C_3A_O + gypsum paste, especially in the absence of superplasticizer. The unbalanced amount between the consumption of C_3A and production of ettringite is clearly because of more C_3AH_6 is formed in C_3A_C. This indicates that in DTA results the endothermic effect at 264°C is due to the decomposition of this phase.

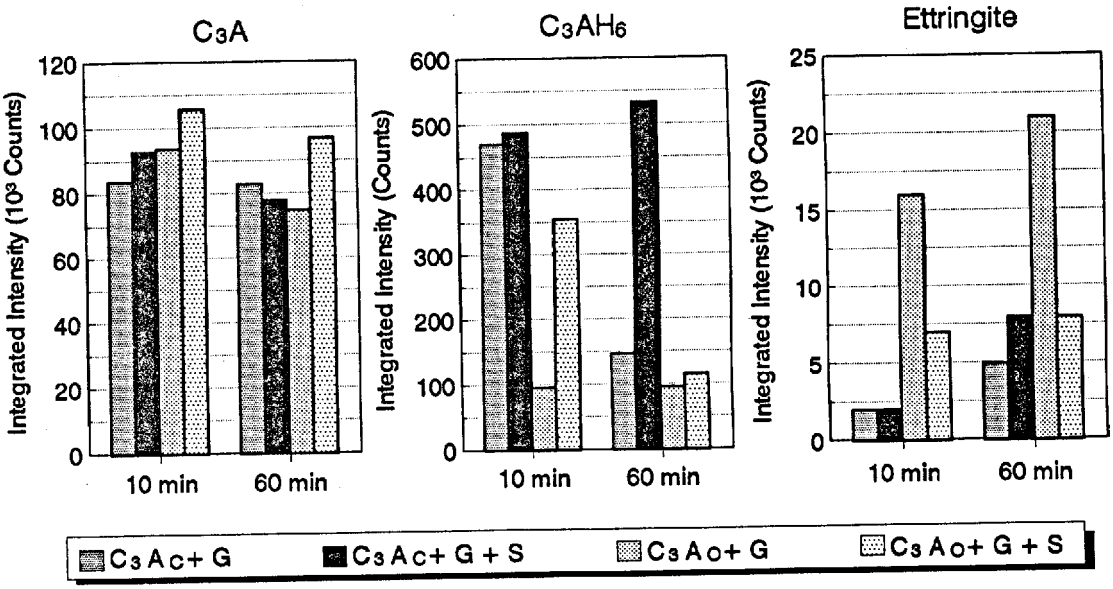

Fig.3. Integrated peaks intensities of C_3A, C_3AH_6, and ettringite.

SEM/EDXA This part of the study represents the combined results of examination of wet samples under the ESEM as well as dried pastes under conventional SEM.

C_3A + gypsum hydrated in water: C_3A_O is covered with thin, remarkably long (10 μm) platy crystals, often with radial distribution (Fig.4), even at 10 min. EDXA shows they contain a small amount of S; the Ca:S:Al ratio is about 3.7:3:1. With progress of hydration, more needle-like crystals appear. Their morphology suggests ettringite (Fig.5), despite a Ca:S:Al ratio of only 2.0:0.5:1. Large gypsum crystals remain undissolved or partly reacted with some short needle-like surfacial rods.

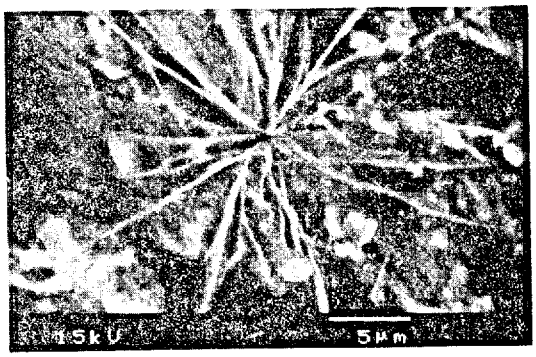

Fig.4. ESEM of hydrated C_3A_O+gypsum at 10 min.

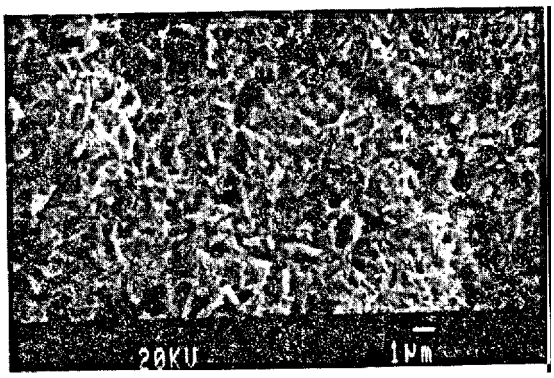

Fig.5. Hydrated C_3A_O + gypsum at 60 min.

C_3A_C , on the other hand, is enveloped by profuse short fibers at 10 min (Fig.6) with Ca:S:Al about 3.2:0.6:1. Although their fibrous appearance suggests ettringite, neither DTA nor XRD shows profuse ettringite phase. These fibrous crystals occasionally appear on the surface of gypsum. Further hydration to 60 min shows little change in the paste's morphological appearance (Fig.7).

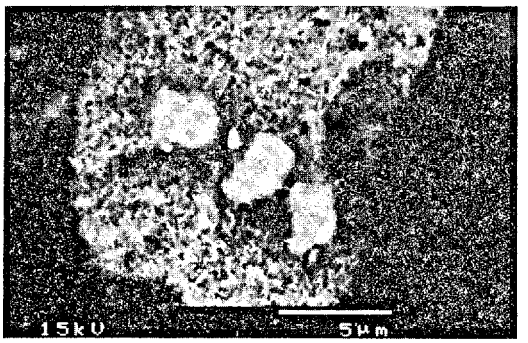

Fig.6. Surface coverage of C_3A_C hydrated in the presence of gypsum hydrated (at 10 min).

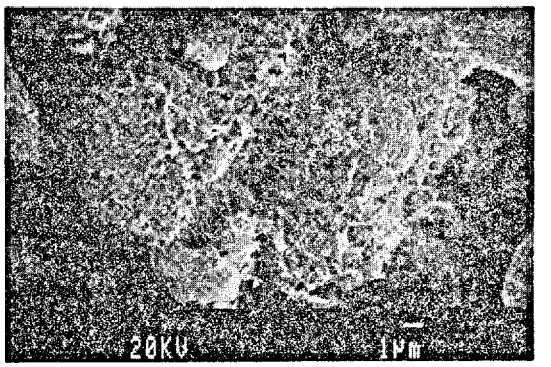

Fig.7. Hydrated C_3A_C + gypsum at 60 min.

C_3A + gypsum hydrated in water containing superplasticizer: At 10 min, the C_3A_O surface is enveloped by a honeycomb structure with a Ca:S:Al ratio of 3.6:2.4:1 (Fig.8). Reticular flakes resembling calcium monosulfo-aluminate hydrate (AFm) appear locally at 60 min (Fig.9).

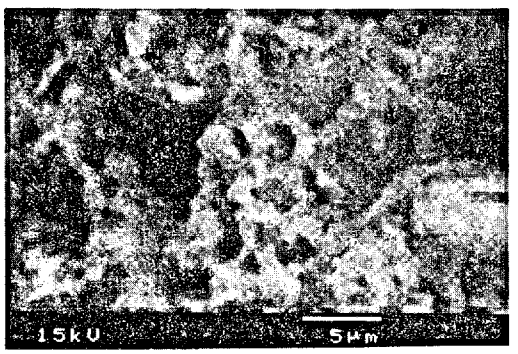

Fig.8. Honeycomb structure in hydrated C_3A_O + gypsum in superplasticizer aq. at 10 min.

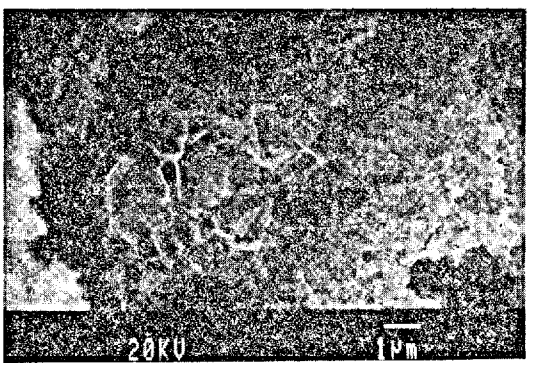

Fig.9. AFm flakes in the same paste at 60 min.

C_3A_C , however, is more drastically affected by the superplasticizer. The surface is rather densely covered with amorphous phases at 10 min (Fig.10). At 60 min, no major surfacial change on C_3A_C is evident, except denser coverage (Fig. 11).

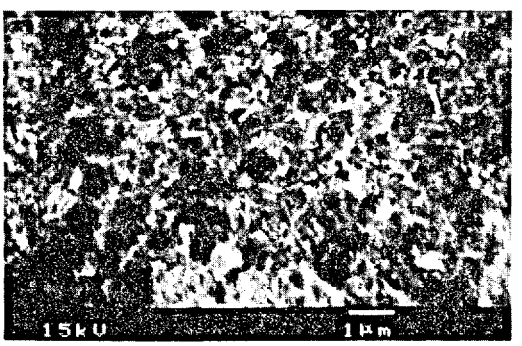

Fig.10. Honeycomb structure in hydrated C_3A_O+gypsum in superplasticizer aq. at 10 min.

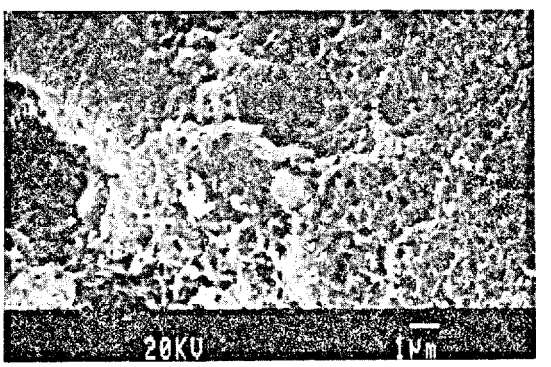

Fig.11. Hydrated C_3A_C + gypsum in superplasticizer aq. at 60 min.

Water Soluble Ions Table 1 shows the change in ionic concentration in C_3A-gypsum-water solutions from 10 to 60 min. Water soluble Ca^{2+} is slightly higher for C_3A_C , while the SO_4^{2-} is higher for C_3A_O, in addition to the distinctly higher Na^+. The table clearly indicates Na^+ release in this dilute solution is completed within the first 30 min. Ca^{2+} and SO_4^{2-}, being nearly balanced, the solution is gypsum saturated. However, the SO_4^{2-} content in the C_3A_O solution is higher due to the presence of Na^+. At 20 min, the C_3A_C solution contains a relatively higher amount of Al^{3+}, though both the absolute values are very low.

Table 3. Solubility Analysis (mmol/l)

Sample	Time (min)	Ca^{2+}	Na^+	Al^{3+}	SO_4^{2-}
C_3A_C	10	14.26	0.23	0.36	12.85
	30	13.84	0.24	0.08	14.18
	60	14.18	0.28	0.09	14.69
C_3A_O	10	14.18	3.46	0.14	14.41
	30	13.68	4.95	0.06	15.21
	60	13.43	4.88	0.06	15.02

1 gram of dry sample per 50 ml distilled water.

DISCUSSION

DTA shows that the main product of the C_3A-gypsum hydration, even as early as 10 min, is ettringite, though at 60 min, the amount produced by the two forms of C_3A is different, it being higher for C_3A_O. This was confirmed by XRD analysis and from SEM observation.

The authors posit that the dense layer that forms promptly on C_3A_C prohibits penetration of ions into the lattice even at very early age. In addition, its greater ability to hydrate results in more hydrates, such as C_2AH_8 and C_4AH_{13}, which cover the grain surface and reduce further ettringite formation. In contrast, thin sheet or flakes growing loosely and radially outward from the surface of C_3A_O gradually transform to large needle-like crystals at a later age, which provides a better condition for the further formation of ettringite. The coating on C_3A is usually explained as ettringite and amorphous $Al(OH)_3$ [13]. This work, however, shows that C_3A_C in the presence of gypsum produces much less ettringite than C_3A_O despite its more apparently vigorous reaction. This may be attributed to amorphous ettringite [19] with some secondary gypsum, though DTA results seems to preclude the existence of the amorphous ettringite phase. DTA data at 60 min indicate that ettringite formed in C_3A_C decomposes at 103°C, compared to 119°C for C_3A_O. However, its amount in C_3A_C is too low to explain the abundance of fibrous phases. On the other hand, the DTA peak for gypsum is broadened to a lower temperature, while the exothermic peak at 371°C remains rather strong and higher than that for C_3A_O. This is a positive indication of secondary gypsum formation. SEM observation of recrystallized gypsum from the solution revealed that this type of gypsum also has a needle-like habit. In the presence of alkali, the gypsum solubility increases [20]. The ionic solubility results in Table 1 also indicate that the chances of secondary gypsum formation are lower for C_3A_O.

Addition of superplasticizer causes rapid formation of a dense layer on C_3A_C and a less dense granular layer on C_3A_O. The eventual formation of ettringite, especially in the C_3A_O is severely retarded, although it still has a higher production rate at 10 min. The superplasticizer was dissolved in the mixing water, possibly putting it in direct contact with C_3A grains. ESEM shows that a layer of newly formed phase rapidly forms on the C_3A grain surface within the first few minutes, suggesting that the superplasticizer is mainly adsorbed by the hydrated compounds, prohibiting further crystallization. Hydrating C_3A_O, which has a higher negative charge on the surface because of more associated OH^- ions acting as potential determining ions [13], develops a stronger hydrogen bond between the superplasticizer and the hydrates formed [21].

In the DTA/TG curves, at temperature higher than about 630°C, endothermic peaks and significant weight loss appear only for the samples with superplasticizer, which can be partly explained due to decomposition of the superplasticizer. Similar effect of lignosulfonate, sucrose, etc was noted by Ramachandran [22] but no explanation was given. Though the weight loss at this temperature is usually considered to be due to the decomposition of $CaCO_3$, this possibility can be ruled out since the XRD patterns do not reveal any phases containing carbonate. Nevertheless, the higher decomposition temperature and the change in thermal effect (compared to that for pure superplasticizer) suggests the interlayer adsorption of the superplasticizer molecules [23] and some chemical reaction with the hydrates.

CONCLUSIONS

This study positively demonstrates that the two polymorphic forms of C_3A hydrate differently. In the presence of gypsum, C_3A_C hydrates react to form ettringite which deposits on the C_3A_C grain thus slowing down the reaction process of this polymorphic form. At the same time, secondary gypsum may also deposit on the C_3A surface. Ettringite forms faster in the C_3A_O system.

Superplasticizer is adsorbed on the surface of C_3A hydrates, reducing the hydration rate. There is a much more compact layer on C_3A_C , and a honeycomb texture on C_3A_O.

The importance of this study lies in understanding why cements containing the same amount of C_3A may exhibit different rheological behaviour. Furthermore, it elucidates the effect of superplasticizer on different polymorphs of C_3A, which can explain the difference in water demand between cements.

REFERENCES

1 Schwiete H.E. & Ludwig U.: "Crystal structures and properties of cement hydration products (hydrated calcium aluminates and ferrites)". **5th Int. Symp. Chem. Cem., Tokyo**, 1968, **V2**, 37-67.

2 Budnikov P.P.: "Role of gypsum in the hardening of hydraulic cements". **4th Int. Symp. Chem. Cem., Washington**, 1960, **V1**, 469-477.

3 Regourd M.: "Structure cristaline et caracteristion de l'aluminate tricalcique - donnees recentes". Presented at International Seminnary on Calcium Aluminates, 14-16, Sep. 1982.

4 Tagnit-Hamou A. & Sarkar S.L.: "The influences of varying sulphur content on the microstructure of commercial clinkers and the properties of cement". **World Cement, Sep.** 1990, 389-393.

5 Moore A.E.: "Polymorphism of C_3A and its solid solutions". **7th Int. Cong. Chem. Cem., Paris**, 1980, **V4**, 417-420.

6 Regourd M.: "Cristallisation et reactivite de l'aluminate tricalcique dans les ciments portland". Il Cemento, 1978, **75**, 323-336.

7 Aïtcin P. C., Sarkar S.L., Ranc & Levy C.: "A high silica modulus cement for high-performance concrete", **Advances in Cementitious Materials**, ed by Mindess S., **Ceramic Transactions, V16**, American Ceramic Society, 1991, 103-122.

8 Breval E.: "C_3A hydration". Cem. Conc. Res., 1976, **V6**, 129-138.

9 Massazza F. & Costa U.: "Effect of superplasticizers on the C_3A hydration". **7th Int. Cong. Chem. Cem., Paris**, 1980, **V4**, 529-534.

10 Sersale R., Sabatelli V. & Valenti G.L.: "Influence of some retarders on the hydration, at early ages, of tricalcium aluminate". **7th Int. Cong. Chem. Cem., Paris**, 1980, **V4**, 546-551.

11 Greene K.T.: "Early hydration reactions of portland cement". **4th Int. Symp. Chem. Cem., Washington**, 1960, **V1**, 359-385.

12 Oyefesobi S.O. & Roy D.M.: "Hydrothermal studies of special types of cement mixed with quartz". Cem. Conc. Res., 1977, **V7**, 165-172.

13 Stein H.N.: "The colioid chemistry of calcium aluminate hydrates". **7th Int. Cong. Chem. Cem., Paris**, 1980, **V4**, 449-454.

14 Roy D.M. & Daimon M.: "Effects of admixtures upon electrokinetic phenomena during hydration of C_3S, C_3A and cement". **7th Int. Cong. Chem. Cem., Paris**, 1980, **V2**, II/242-246.

15 Shin G.Y. & Glasser F.P.: "Chemistry of cement pore fluids. I Suspension reactions of $Ca_3xNa_{2x}Al_2O_6$ solid solutions with and without gypsum additions". Cem. Conc. Res., 1983, **V13**, 366-376.

16 Barret P. & Bertrandie D.: "Hydration de C_3A en présence d'eau de chaux". **7th Int. Cong. Chem. Cem., Paris**, 1980, **V4**, 443-448.

17 Jawed I. & Skalny J., "Surface phenomena during early hydration of tricalcium aluminate". Proc. Int. Sem. Calcium Aluminates, Turin, 1982, pp. 125-129.

18 Kolbasov V.M., Kozyreva N.A. & Dobronravova L.A.: "The peculiarities of initial processes of hydrates forming in C_3A-H_2O systems and the role of its medium in hydrate". **7th Int. Cong. Chem. Cem., Paris**, 1980, **V4**, 455-459.

19 Luke K. & Aïtcin P.C.: "Effect of superplasticizer on ettringite formation". **Advances in Cementitious Materials**, ed by Mindess S., **Ceramic Transactions, V16**, American Ceramic Society, 1991, 147-166.

20 Uchikawa H., Uchida S., Ogawa K. & Hanehara S.: "Influence of $CaSO_4 \cdot 2H_2O$, $CaSO_4 \cdot ½H_2O$ and $CaSO_4$ on the initial hydration of clinker having different burning degree". Cem. Conc. Res., 1984, **V14**, 645-656.

21 Shchukin E.D., Amelina E.A., Andreeva E.P. & Kontorovich S.I.: "Agglutination (bridging) of particles during hydration hardening and the effect of surface active additives". **7th Int. Cong. Chem. Cem., Paris**, 1980, **V2**, II/167-171.

22 Ramachandran V.S.: "Elucidation of the role of chemical admixtures in hydrating cements by DTA technique". **Thermochimica Acta**, 1972, **V3**, 343-366.

23 Dosch W.: "Interlayer adsorption of water and organic compounds on C_4AH_x". N. Jb. f. Mineralogy, 1967, 200-239 (in German).

UNDERSTANDING OF THE HYDRATION MECHANISMS OF $C_4A_3\bar{S}$ - PORTLAND CLINKER - $CaSO_4$ MIXES

L Taczuk*, J P Bayoux*, F Sorrentino* and A Capmas**

**Lafarge Coppée Recherche - Viviers/Rhône*
***LFI International, Neuilly-sur-Seine*
FRANCE

ABSTRACT

Calcium sulpho aluminate cements were developed some years ago and are used today in different applications. One of them is the acceleration of Portland cement by small addition of $C_4A_3\bar{S}$. This paper deals with the understanding of the system C_4A_3S - Portland clinker - and $CaSO_4$ when it hydrates.

The area that we have investigated ranges from 5 % to 20 % $C_4A_3\bar{S}$ and 11 % to 45 % $CaSO_4$ 2 H_2O or 9 % to 35 % $CaSO_4$, the complement material being the Portland clinker. The molar ratio between $C_4A_3\bar{S}$ and the calcium sulphate is chosen to be 8 in order to favour the ettringite formation which is the case most of the time.

Mechanical properties, together with X-Ray diffraction measurements clearly describe the reactions occuring. From these data it is obvious that the nature of the calcium sulphate has a very important effect on the properties. Some recommendations are given concerning the durability of the materials.

RESUME

Les aluminates de calcium ont été développés il y a quelques années et sont utilisés aujourd'hui dans différentes applications dont en particulier l'accelération des ciments Portland par l'ajout de petites quantités de $C_4A_3\bar{S}$. Cette publication traite des mécanismes d'hydratation des mélanges $C_4A_3\bar{S}$. Clinker de Portland et $CaSO_4$.

Les domaines étudiés sont pour $C_4A_3\bar{S}$ de 5% à 20% pour $CaSO_4$ $2H_2O$ de 11% à 45% ou de 9% à 35% CaSO4 pour $CaSO_4$, le complément étant réalisé par le clinker de Portland. Dans les mélanges les rapports molaires entre C4A3S et le sulfate de calcium est de 8 afin de favoriser la formation d'ettringite.

Les propriétés mécaniques complétées par les mesures de diffraction X décrivent clairement les réactions. De ces résultats il apparaît très clairement que la nature du sulfate de calcium est déterminante pour les propriétés mécaniques. Des recommandations sont données pour l'obtention de matériaux durables.

1 - INTRODUCTION

The goal of this study is to determine the influence of various factors on the hydration of the mixes $C_4A_3\overline{S}$ - Portland - $\overline{CS}$. It is well known that during the hydration process ettringite will precipitate according to the following reaction :

$$C_4A_3\overline{S} + 8\ \overline{CS} + 6\ CH \xrightarrow{water} 3\ (C_3A\ 3\ \overline{CS}\ 32\ H_2O)$$

This hydrate is very interesting because it crystallises with a large number of molecules of water, thus bringing low porosity and high mechanical strength.

However the hydration process is not as simple as it seems because the reaction is sometimes diverted from its original track due to the following :

- dissolution blocking effect because of an impervious layer of hydrates.
- lack of available Ca^{++} and SO^{4--} in the solution leading to the precipitation of less rich calcium sulphate phases like $C_3A\overline{CS}$, 12 H_2O (MSH).

Both phenomena have major impact on the structure of the hydrated material. Strength can be much weaker and sometimes dangerous expansion will occur followed by the destruction of the sample.

In the litterature the role of Ca^{2+} ions is mentioned very often [1-5]. When the calcium ion concentration is high it is reported that.

- Very fine high compacity product will precipitate around the anhydrous grains preventing their further dissolution avoiding the completion of the reaction.
- Monosulfoaluminate will precipitate as well as hydrated calcium aluminate along with ettringite.

Without wanting to discard the influence of the lime we think that the nature of the calcium sulphate is also rather important. The various hydrated calcium sulphates have a marked influence on the mechanical properties of mortars [6] because they lead to different precipitation of hydrates [7].
A good knowledge of the mechanisms will lead to a better understanding of the blocking effect.

In this paper we have compared the hydration of $C_4A_3\overline{S}$ when mixed with a typical portland clinker, natural anhydrite or gypsum.

2 - EXPERIMENTAL

2.1 - Raw materials and mixes

In order to describe the phenomena various mixes were prepared with :

- $C_4A_3\overline{S}$: It is a laboratory made calcium sulpho aluminate.
- Portland clinker : We have chosen only one type of clinker containing no calcium sulphate. It is an ordinary clinker (C_3A = 10,5 %, C_3S = 65,6 %, C_2S = 12%, C_4AF = 7,7%, Free lime = 1,1%)
- $CaSO_4$

Two different sources of calcium sulphate were chosen in order to reproduce what can normally be found in Portland cement. We have selected a natural anhydrite of high purity and a gypsum which is used in the Portland factories.

In Table 1 we have presented the mineralogical analysis of the various materials that were used. Portland clinker was chosen instead of cement in order to eliminate the effect of the various phases (gypsum or anhydrite), which are added to the Portland clinker for controlling its set.

Two different systems were investigated :

- with anhydrite where kinetic dissolution is rather slow. [8]
- with gypsum where kinetic dissolution is much faster. [8]

Molar ratios between $C_4A_3\overline{S}$ and $\overline{CS}$ were 1/8 in order to favour ettringite formation. Mixes with 5 % to 20 % $C_4A_3\overline{S}$, associated with $\overline{CS}$, were added to the Portland clinker. The compositions different mix are summarised on Table. 1.

Table.1 Mineral Composition and Physical Characteristics of Used Components (%by wt.)

	C3S	C2S	C3A	C4AF	CaO l	C4A3S	CA	$C\bar{S}$	$C\bar{S}H2$	Dolom.	SiO2	others	Bl. cm2/g
Clinker Portl	65,6	12	10,5	7,7	1,1	-	-	-	-	-	-	3,1	3 800
$C4A3\bar{S}$	-	-	-	-	0,15	90	9	-	-	-	-	0,85	6 000
Gypsum		-	-	-	-	-	-	22	65	10	2	1	2 800
Anhydr.	-	-	-	-	-	-	-	97	2	-	-	1	3 500

2.2 - Tests

2.2.1 - Mechanical properties - Mechanical properties (setting time and mechanical strength) were measured on neat pastes prepared with various W/S ratio. We have made the following assumption for the calculation of the water required to fully hydrate the mix.

Portland releases lime. We consider that only 60 % of the C_3S will quickly react releasing 1,5 mole of lime per mole of CSH formed. C_2S which is less reactive will only contribute at 30 % of its total amount. It will release 0,5 mole lime per mole of CSH formed. [9]

The hydrates which will precipitate depend on the balance between $C_4A_3\bar{S}$ and lime (the molar ratio between $C_4A_3\bar{S}/C\bar{S}$ of 1/8 is always sufficient for ettringite formation, monosulpho should never precipitate). Depending on $C_4A_3\bar{S}$/lime ratios will precipitate either ettringite on its own when lime is sufficient or ettringite + gibbsite when lime is missing.
From these asumptions the calculated W/C ratios ranges from 0,34 to 0,56 [Table 2].

Table. 2 Mineral Compositions and Strength Tests Results of Different Composite Mixes

	Ingredients (%by wt.)				W/C	Setting times		Compressive strength (MPa)					
	$C4A3\bar{S}$	Anhydr	Gyps.	Clink.		init.	final	4h	6h	24h	3d	7d	28d
G5	5	-	11	84	0,34	50	330	0	0	39,7	66,3	79,8	99,3
G10	10	-	22	68	0,41	25	50	0	0	0	1,2	5,2	8,3
G15	15	-	34	51	0,47	15	35	0	0	0	0	0	0
G20	20	-	45	35	0,41	3	8	0	0	14,5	28,7	31,1	45,4
A5	5	9	-	86	0,36	7	18	5,4	9,4	35,1	64	76,8	90,4
A10	10	18	-	72	0,46	6,5	9	7	8	11,9	38,5	51	65
A15	15	27	-	58	0,56	5,5	8	6,4	6,8	14,1	22,7	32,9	47,3
A20	20	35	-	45	0,55	3,5	9	8,1	9,3	17,1	16,3	17,9	20,4

In this table G or A represents gypsum or anhydrite mixes.

The neat pastes were cast at 20°C and kept at the same temperature underwater after 4 hours (anhydrite) or 24 hours (gypsum). The difference in demolding time is a consequence of the set. X-Ray diffraction analysis of the neat paste were performed at different dates in order to follow the reaction process.

2.2.2 - Hydration of diluted suspensions - Diluted suspensions were prepared in a thermostated reactor (W/S = 10) in order to have a better understanding of the dissolution precipitation mechanisms. At various dates, samples were withdrawn from the reactor and the liquid phase was analysed for ionic concentration. Conductivity was measured continuously in the suspension because it gives useful information on dissolution (increase of conductivity) and precipitation (decrease of conductivity).

3 - RESULTS

3.1 - Mechanical properties and hydrates formed

The typical difference between the two series (anhydrite or gypsum) is in the setting time (Table 2). For the mixes with gypsum, setting time is much longer with consequently no early strength. Even with a 20 % $C_4A_3\overline{S}$ addition which reduces the setting time, we have not measured any strength after six hours of hydration. X-Ray analysis of neat paste is presented in Fig. 1. Results are expressed in % of unreacted materials.
These figures show that the more portland clinker present in the mix (or the less $C_4A_3\overline{S}$) the more difficult it is for the $C_4A_3\overline{S}$ to react. It is only with a 20 % addition of $C_4A_3\overline{S}$ and a portland content as little as 35 % that we have a complete reaction of $C_4A_3\overline{S}$.
On the other hand for the case of anhydrite mixes ; setting times are always short and associated with early strength. Fig. 2 shows that $C_4A_3\overline{S}$ reacts much more easily even in the case where the percentage of Portland cement is high.
Anhydrite calcium sulphate is not as quickly soluble as gypsum and tends to favour monosulfo (MSH) precipitation. This is particularly the case for mixes with high clinker percentage. This precipitation of MSH commented in various papers [1,3] is most probably responsible for the non blocking of the reaction.

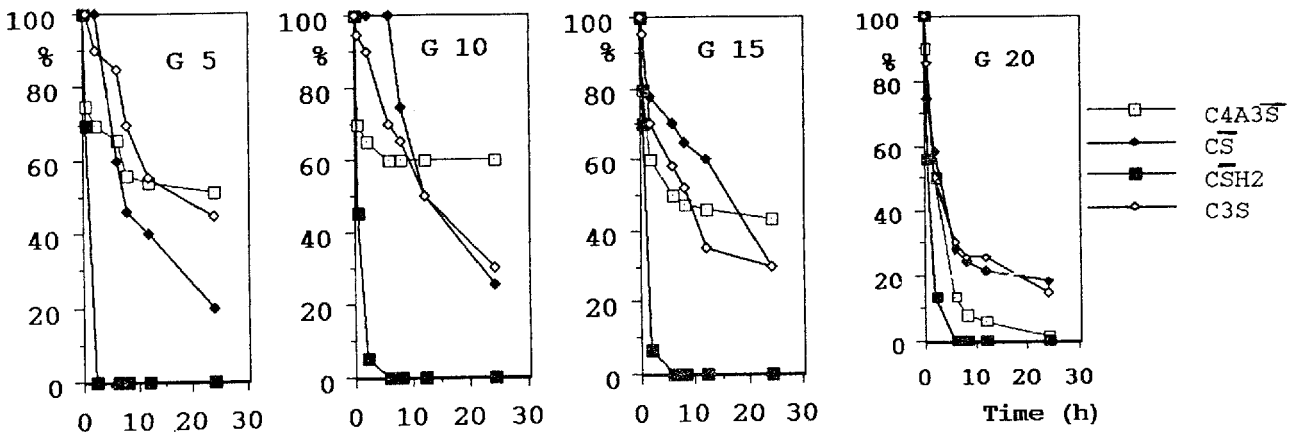

Fig 1. Relative intensities of various phases as a function of hydration time (with gypsum)

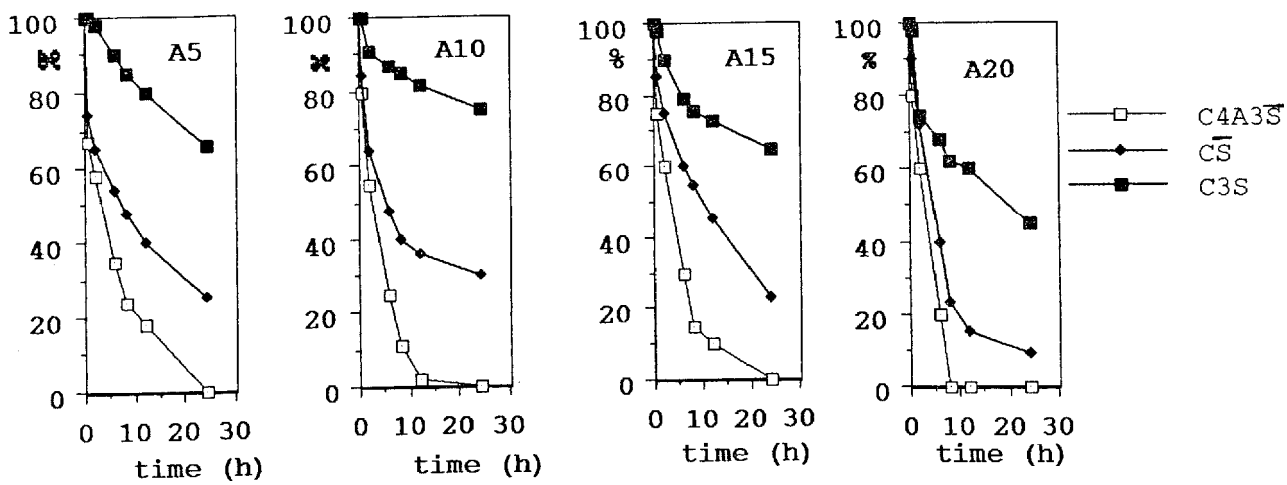

Fig 2. Relative intensities of various phases as a function of hydration time (with anhydr.)

Scanning electron micrographs show that for both series the morphology of hydrates depend greatly on the nature of the calcium sulphate.

Photographs (fig. 3) of A5 and G5 samples after 6 hours hydration show that with gypsum very fine crystals have precipitated. This precipitation is typical of oversaturated solution and leads to the complete covering of all the anhydrous grains.

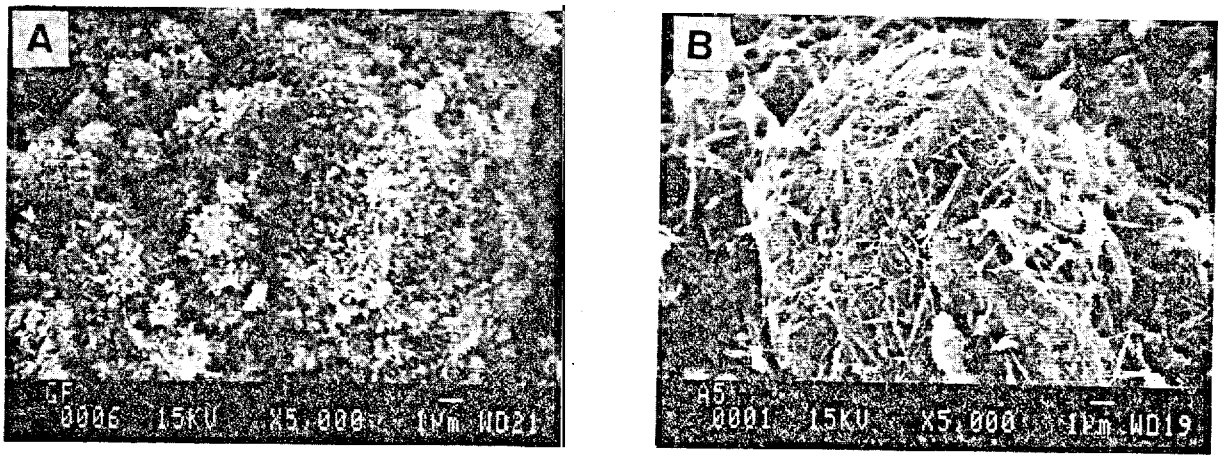

Fig. 3 - Ettringite formed in the $C_4A_3\overline{S}$ - clinker - sulphates pastes hydrated for 6 hr. A) mixture with gypsum B) mixture with anhydrite

With anhydrite, the crystals are much longer and the dissolution of ettringite using glycolethylen revealed the presence of MSH (fig. 4). [10]

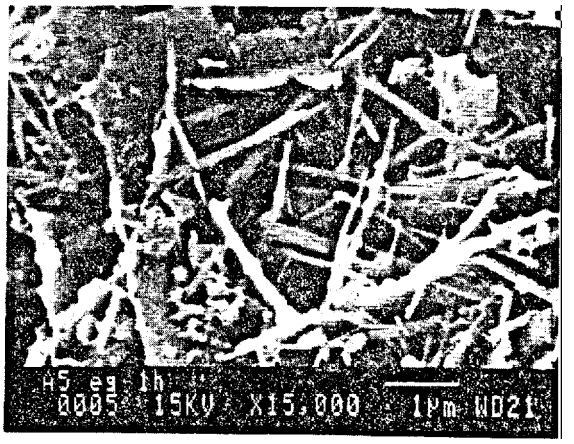

Fig. 4 - Undissolved phase of sample A5 in glycolethylene solution

3.2 - Mechanisms in diluted suspensions

The curves (pH, conductivity, ionic concentrations) presented in Fig. 5 and 6 show the typical difference between anhydrite and gypsum.

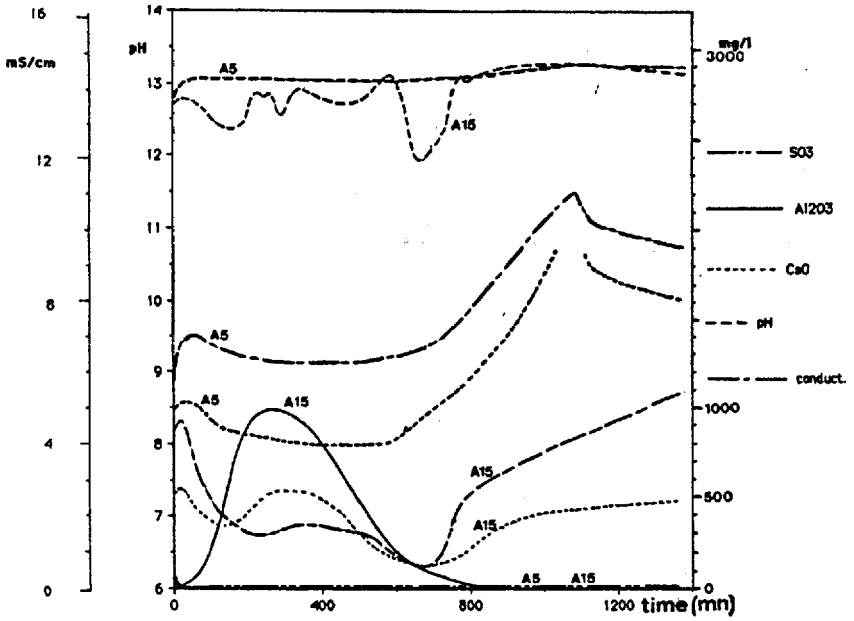

Fig. 5 - The concentration of CaO, Al_2O_3, SO_3 and pH, conductivity as a function of hydration time (with anhydrite)

With gypsum the conductivity curve is very similar to that of Portland cement. The conductivity increases rapidly mainly because of the hydrolysis of C_3S and the dissolution of gypsum ($CaSO_4$ 2 H_2O). Calcium and sulfate concentrations are high from the beginning of the reaction - on the contrary the alumina concentration is very small in the case of anhydrite because hydration proceeds differently. $C_4A_3\overline{S}$ reacts as seen from XRDA and the absence of alumina ion in the solution is probably due to the very fast precipitation of sulphoaluminate hydrates.
These results show that hydration proceeds continuously because of the slow dissolution kinetic of anhydrite.

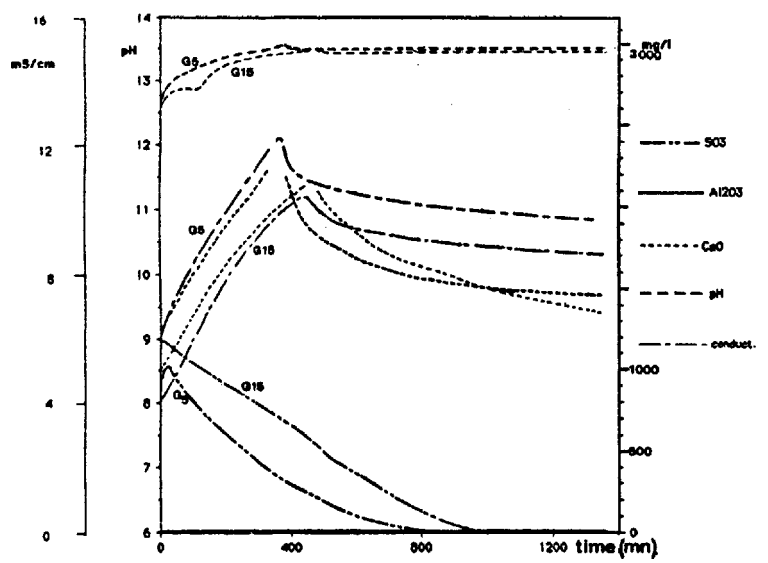

Fig. 6 - The concentration of CaO, Al_2O_3, SO_3 and pH, conductivity as a function of hydration time (with gypsum)

4 - CONCLUSIONS

The results that we have presented show that when mixing $C_4A_3\overline{S}$ - $\overline{CS}$ - to Portland clinker we are able to alter the hydration process simply by changing the reactivity of the sulphates.

Particularly low sulphate ion concentration at the very beginning of the reaction will permit a total hydration of $C_4A_3\overline{S}$, thus preventing fine ettringite crystals from precipitating like a shell on anhydrous grains.
Anhydrite which is slowly soluble favours low [SO_3] ion concentration at the very beginning of the reaction. This is favourable to obtain the complete and quick reaction of $C_4A_3\overline{S}$ ensuring a durable material.

5 - REFERENCES

[1] - Mehta, P.K. : "J. Am. Ceram. Soc.", 1967, v. 50, p. 204.

[2] - Fukuda, N. : "V - JCCC Tokyo 1969", Tokyo 1969, v. IV p. 341,

[3] - Bonin, A., Cariou, B. : "7 - JCCC, Paris 1980", Paris 1980, v. III p. V 159.

[4] - Nakamura, T., Sudoh, G. : "V - JCCC Tokyo 1968", Tokyo 1969, v. IV, p. 351.

[5] - Kurdowski, W., Thiel, A. : "CCR", 1981, v. 11, p. 29.

[6] - Ikeda, K.: "Yogyo Kyokaishi", 1981, v. 89, p. 54.

[7] - Sudoh, G., Ohta, T., Harada, H. : "7 - JCCC Paris 1980", Paris 1980, v. III, p. V - 152.

[8] - Locher, F.W., Richartz, W., Sprung, S. : "Zement-Kalk - Gips Nr 6", 1980, p 271.

[9] - Lea, F.M.: "the chemisty of Cement and Concrete 3 rd ed London Edward Arnold", 1970, 727 p.

[10] - Uchikawa, H. and Suchida, CCR : 1974, Vol 4, pp 821 - 834.

STUDY ON HYDRAULIC REACTIVITY AND STRUCTURAL BEHAVIOUR OF VERY ACTIVE β-C_2S

Yang Nanru, Zhang Hua and Zhong Beiqian

Nanjing Institute of Chemical Technology
Nanjing, Jiangsu, P R CHINA

SUMMARY

The hydraulic reactivity of β-C_2S synthesized under hydrothermal treatment (100℃) followed by heating at 950℃ has been already reported. In order to understand the factors influencing on the reactivity, samples were burned at different temperatures (850℃, 1000℃, 1100℃, 1200℃, 1300℃). For comparison, β-C_2S sintered at 1350℃ without hydrothermal treatment was taken as reference. BET and SEM were used for measuring the specific surface area and particle size, PAT (positron annihilation technique) was used to determine the crystal defects and crystallinity. IR was used to study the behavior of the Si-O and Ca-O bond vibration. The hydration rate of samples were measured by using microconductometer and the content of combined water. From the results, the authors suggested that factors influencing on the hydraulic reactivity of active β-C_2S may be classified into 3 levels, that is, the particle size, defects and its concentration in crystal, attribute of Si-O bond in $[SiO_4]^{4-}$ tetrahedron and coordination number of Ca-ions with oxygen atoms.

摘　　要

作者曾对经水热处理再在950℃下煅烧的β-C_2S的水化活性进行过报导。为了进一步了解影响其水化活性的因素，本文对不同温度下煅烧（850℃，1000℃，1100℃，1200℃，1300℃）的活性β-C_2S进行了研究，并将未经水热处理于1300℃煅烧的β-C_2S作为对比。用BET和SEM测定了试样的比表面积和颗粒大小，用PAT探讨了样品中的晶体缺陷和结晶度，用IR研究了Si-O键和Ca-O键的振动方式，通过水化热和结合水的测量测定了试样的水化速率。由上述结果，作者将影响β-C_2S水化活性的的因素分为3个层次：即颗粒大小；晶体缺陷；$[SiO_4]^{4-}$四面体中Si-O键的性质和钙离子与氧的配位数。

INTRODUCTION

Recently, cement scientists are interested in the activation of hydraulic reactivity of β-C_2S. So many methods have been used for the purpose of increasing the rate of early hydration of it. The authors of present paper, after studying the crystal behavior and hydration process of β-C_2S, believed that the low strength development at early hydration of β-C_2S is not its inherent character, but caused by conditions of formation. A very active β-C_2S has been prepared by heating calcium silicate hydrates at 950℃ without any stabilizer[1-4]. The rapid strength development of this β-C_2S paste took place between 7-28 days instead of after one month in the case of ordinary β-C_2S burned at 1350℃ with or without B_2O_3 as stabilizer. In addition, the structural behavior of active β-C_2S heated at different temperatures was also reported[5-6] For further ascertainment the relationship between hydraulic reactivity and structural behavior of active β-C_2S is presented in the present paper.

EXPERIMENTAL

1. Preparation of samples

Analytical reagent of CaO and aerosol silica were used as starting materials. A mixture of CaO/SiO_2 with mole ratio equal to 2 and W/S equal to 5-10 (by wt.) was treated hydrothermally under 100℃ and 1 atm for several hours, then dried and heated at 850℃, 1000℃, 1100℃, 1200℃ and 1300℃ separately followed by air quench. Samples were marked T-85, T-100, T-110, T-120, T-130 respectively. Another sample marked HA was prepared by heating a CaO/SiO_2 =2 mixture at 1350℃ without stabilizer, used as reference.

2. Experimental methods

(1) Micro calorimeter was used for measuring the heat of hydration; the amount of combined H_2O in specimens after different ages of hydration was measured by C-H analyzer.

(2) The particle size of β-C_2S were measured by scanning electron microscope. The specific surface area was measured by BET N_2 (g) absorption method.

(3) Positron annihilation technique (PAT) was used to determine the crystal defects and crystallinity. In the present paper, the lifetime spectra with more than 10^{*6} counts were recorded at room temperature (25 ± 1℃) by using a fast-slow spectrometer. As a positron source, ^{22}Na from a carrier-free neutral solution of NaCl was deposited on a thin Ni foil; a second identical foil was sealed over the first one and the source so assembled was sandwiched between the specimens under investigation. The time resolution is about 383ps (FWHM) with mean 46.7ps/channel. All spectra were fitted with positronfit extended program.

(4) Infrared spectra of all samples were recorded by using KBr pellets.

RESULTS AND DISCUSSION

1. Hydraulic Reactivity

The amount of combined water after hydration at different stages and heat of hydration were used to evaluate the hydraulic reactivity of β-C_2S. The results are shown in table 1 and fig 1. The amount of combined water increased significantly with the decrease of heating temperature. The reactivity of β-C_2S heated up to 1300℃ (T-130) was much higher than HA. From fig 1. the heat evolution during hydration also indicated clearly the influence of heating temperature on reactivity of β-C_2S.

Samples	1d	3d	7d
T-85	1.60	1.69	3.77
T-100	1.08	2.18	2.62
T-110	1.06	1.77	2.34
T-120	0.97	1.28	1.95
T-130	1.26	1.49	1.57
HA	0.75	0.93	

Table 1. The amount of combined water of samples.

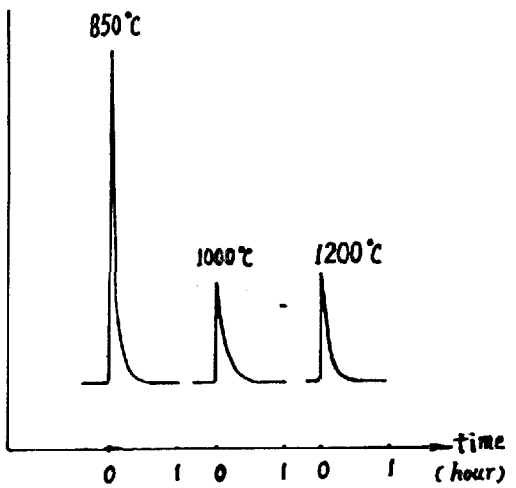

Fig 1. Evolution curve during hydration

2. Particle Size and Crystal Grain Size of β-C_2S.

The particle size of β-C_2S formed at different temperatures are listed in table 2. The specific surface area is also shown in the same table. The grain and particle size evidently increased with increasing temperature. On the contrary, the specific surface area was influenced in an opposite way. Doubtlessly, this must be an important factor affecting the hydraulic reactivity of β-C_2S, which has been reported by the authors.

Samples	Particle Size (μm)	SSA ($m^2 \cdot g^{-1}$)
T-85	0.27	24.60
T-100	0.50	12.43
T-110	0.80	10.62
T-120	1.20	11.14
T-130	1.60	9.07
HA	~ 20	0.78

Table 2. Particle size of samples

3. Results of Positron Annihilation Measurement

The cation cavities with equivalent electrons in solids showed ability to capture positrons. In the present work, PAT was used

to study on the defects in β-C_2S crystals. The results taken from lifetime spectra after free and constraint fitting are shown in table 3.

Samples	τ_1 (ps)	τ_2 (ps)	τ_3 (ps)	I_1 (%)	I_2 (%)	I_3 (%)	$\bar{\tau}$ (ps)	τ_f (ps)
T-85	180±27	337±20	1216±105	39.80±11.71	57.28±11.27	2.92±0.50	302.57	268.83
T-100	210±25	346±38	1174±142	55.22±18.58	42.53±18.05	2.25±0.59	289.53	257.87
T-110	198±19	324±26	1555±436	58.50±14.95	40.95±14.80	0.56±0.18	275.22	236.85
T-120	202±10	349±22	3121±414	71.32±7.74	28.48±7.78	0.20±0.11	249.70	230.02
T-130	202±26	315±26	1684±690	52.66±19.59	46.98±19.47	0.36±0.14	260.42	243.87

Table 3. Positron annihilation character of active β-C_2S (free fitting).

where τ_i --lifetime of positron trapping, i=1, 2, 3; I_i --intensity corresponding to τ_i; Table 3 also gives $\bar{\tau}=\Sigma(\tau_i I_i)$ where $\bar{\tau}$--mean lifetime of positrons, which describes comprehensive (multiple) parameters of positron annihilation character, and $\tau_f = (I_i \tau_i^{-1})^{-1}$, where τ_f --lifetime of free positrons.

Here, in table 3: τ_1 corresponds to short lifetime component which has no relation to any kind of positron state, but does correlate to the character of free electron annihilation; I_1 is corresponding to the free electron density in materials. τ_1 and I_1 increased with incresing heating temperatures of samples.

τ_2 is a long lifetime component. It is possibly contributed by three ways: 1) positrons are trapped on grain surfaces or grain boundaries of β-C_2S crystals, forming an inter-bound state; 2) positrons are trapped in cation cavities; 3) fomation of quasi-positronium. Evidently τ_2 and corresponding I_2 are the most important information characterizing the structural behavior of β-C_2S crystals.

τ_3 is a very long lifetime component, the intensity of which (I_3) is very low, ranging between 0.2~3.5%. Therefore, it is not important for the present case and will not be discussed in the following.

As it has been already reported[5-6] that the formation of quasi-positronium in the above case is impossible, and τ_2 is not mainly contributed by defects caused by thermal fluctuation, but by the positrons trapped on grain boundaries. It can be seen from table 2 that

grain size of all samples of β-C_2S, synthesized at low temperature is much smaller than that of HA. So it might be suggested that the grain boundaries have a more important effect on the value of τ_2. In order to further elucidate we have calculated τ_+ (trapped state lifetime of positron, ps) by equations in reference[7-9], and gave the value ranging from 326.3 to 395.8ps, which is approximate to the measured one, 334ps. The details of calculating procedure has been reported elsewhere[6]. Of course the other factor such as vacancies in crystals is not excluded here, since τ_2 decreases slightly with the increase of temperature if τ_1 is set to be 200ps. On the other hand, I_2 also decreases slightly with the temperature rising if τ_2 is set to be 334ps. This is understandable, for the active β-C_2S is formed from dehydration of calcium silicate hydrates, the later is characterized by poor crystallinity, even in amorphous state with large specific surface area. The active β-C_2S contains large amount of boundaries and vacancies, which is lowered as the heating temperature increases, this is caused by the growth of crystals. The vacancies in crystals are augmented as the temperature rises, which, however, is appreciable only when the temperature is higher than 1300℃ (T-130 gives higher I_2).

4. Infrared Spectra of β-C_2S

The isolated and separated $[SiO_4]^{4-}$ tetrahedron has four vibration modes, but only two of them are infrared active, they are ν_3 --asymmetric stretching vibration, which is triply degenerated at 1050 cm^{-1} and ν_4 --bending vibration, triply degenerated at 625 cm^{-1}. Since $[SiO_4]^{4-}$ tetrahedra are connected with other cations to form crystal lattice, the above vibration modes should be influenced by the surrounding cations. Consequently, the symmetry of $[SiO_4]^{4-}$ tetrahedron decreases and degenerated vibrations split. This did happen in the IR spectra of active β-C_2S. In the case of HA, the absorption bands appear at 906cm^{-1} (very strong), 845cm^{-1}, 868cm^{-1} and 996cm^{-1}, whereas in the spectra of T-850~T-130 samples, there are six vibration bands in the range of 800~1000cm^{-1} instead of four as in the HA spectrum, namely:

848cm^{-1}	medium;
868cm^{-1}	shoulder;
889~894cm^{-1}	very strong;
917~923cm^{-1}	strong;
996cm^{-1}	very strong;
1013cm^{-1}	strong.

Here, not only the triply degenerated vibration ν_3 split almost completely into individuals, but the infrared inactive ν_1 also appears and splits into 848 cm^{-1} and 868cm^{-1} bands. It is reasonable to consider that this is caused by decrease of the symmetry of molecules. As is well known, Ca^{2+} ions in β-C_2S crystals generally possess two kinds of coordination number, some of the Ca^{2+} ions have 7, and others 8. In the case of active β-C_2S, Ca^{2+} ions might be distributed unequivalently in the two lattice sites. Eventually, the $[SiO_4]^{4-}$ tetrahedra become to be in strongly asymmetric state. With the increase of heating temperature, Ca^{2+} ions migrated to the normal lattice sites, and thus caused the change of the intensity of vibration bands. Further study is needed for understanding the above phenomena.

5. Three factors influencing on reactivity of β-C_2S.

There have been many papers reporting the factors influencing on reactivity of cement clinker minerals and cements, such as fineness, crystal defects etc. From above results of our experiments, the factors influencing on reactivity of active β-C_2S may be divided into 3 levels. Each of them has its own character and can be controlled by technological procedures or chemical and physical methods.

The first: Particle size or specific surface area of material--It is well known that fineness of cement clinker significantly influences on hydraulic reactivity of it. Generally we can get very fine powder by a mill grinding. Evidently, it is a mechanical methods and used at the later stage of production. But the fineness usually is limited due to the energy assumption and the equipment used. In cement production, technologists have noticed the effect of crystal morphology and particle size of cement clinker on the hydraulic reactivity. In our sense, the smaller the grain size of β-C_2S, (the more the grain boundaries) the more reactive the β-C_2S will be. Grinding the raw material finer, heating at lower temperature the smaller grain size of mineral could be obtained.

The second: crystal defects in grains--Crystal defects include thermal defects and grain boundaries, the later influences more strongly than the former as indicated by PAT results. The amount of defects increases with diminishing grain size due to more grain boundaries.

The third: Distortion degree of molecules--As is seen from IR spectra, the $[SiO_4]^{4-}$ tetrahedra and thus the molecules of β-C_2S synthesized at low temperature are strongly distorted. This may play the most important role promoting the reactivity of minerals, and might be the inherent cause to increase the early hydration of β-C_2S.

CONCLUSION

1. A very active β-C_2S can be obtained from hydrothermal treatment of a CaO/SiO_2 mixture with mole ratio equal to 2 followed by heating at 850~1300℃. The products are characterized by very fine grain size in the range of 0.27~2.7 μm and ssa. 10~24 $m^2 \cdot g^{-1}$

2. The grain boundaries in β-C_2S particles play a main role in the positron annihilation effect.

3. $[SiO_4]^{4-}$ tetrahedra in β-C_2S crystals are situated in very poor symmetry and Ca^{2+} ions irregularly distributed in the crystal lattice sites.

4. Studying the hydraulic reactivity and structural behavior of β-C_2S the authors believe that the factors influencing hydraulic reactivity of cement clinker mineral might be considered in 3 levels, that is fineness (particle size) or grain size; crystal defects and distortion of molecules. The last one is suggested to be the most important and inherent factor.

ACKNOWLEDGEMENT

The authors would like to express gratefulness to associate professors Wan Yujin and Zhu Yuqun, Southeast University, for kindly offering the chance to run the PAT experiment at their laboratory, and for their helpful discussions.

REFERENCE

1. Yang Nanru and Zhong Baiqian: " A Study on Active β-Dicalcium Silicate ". Journal of the Chinese Silicate Society, 1982, 10[2], 161-166.

2. Yang Nanru, Wang Zhanwen and Zhong Baiqian: " Formation Mechanism of Active β-C_2S ". Journal of the Chinese Silicate Society, 1986, 14[4], 385-391.

3. Zhong Baiqian and Yang Nanru: " Hydration of Active β-Dicalcium Silicate ". Journal of Nanjing Institute of Chemical Technology, 1987, 9[2], 63-72.

4. Yang Nanru, Zhong Baiqian and Wang Zhanwen: " An Active β-Dicalcium Silicate Preparation and Hydration ". 8th International Congress on the Chemistry of Cement, Brasil, 1986, vol. 3, 22-27.

5. Yang Nanru, Zhang Hua: " The Structural Behavior of Active β-C_2S ". Report on the 93rd Annual meeting and Exposition of America Ceramic Society, Ohio, America, 1991.4.28-5.2.

6. Zhang Hua, Yan Nanru, Wan Yuejing, Zhu Yuqun: " Positron Annihilation Study in Very Active β-C_2S ". Journal of the Chinese Silicate Society, to be presented in 1992.

7. W. Brandt: " Positron Dynamics in Solid ", Applied physics, 1974, 5[1], 1-23.

8. Zhou Xianyi, Jiang Huilin, and Wang Shuying: " Positron Annihilation in Large-angle Crystallinic Boundary". Nuclear Technique, 1989, 12[11], 638-641.

9. B. Bergersen, E. Pajanne, P. Kubica, et al: " Positron Diffusion in Metals ". Solid State Communications, 1974, 15, 1377-1380.

CORRELATION BETWEEN THE CRYSTAL STRUCTURE OF CALCIUM MINERALS AND THEIR REACTIVITY WITH WATER

M A Sanitsky

Polytechnical Institute, Lvov, UKRAINE

SUMMARY

In this paper the mechanisms of structural changes in the process of hydration of a number of cement minerals are examined based on the results of crystal chemistry analysis. It has been established that the differences of hydration activity of silicates, aluminates and calcium aluminoferrites are due to the protonizing process peculiarities during interaction between minerals and water, i.e. in calcium silicates the protonization of oxygen ions in the structure proceeds partially and is accompanied by polyfunctional condensation of SiO_4-tetrahedrons in solid phase with $Ca(OH)_2$ leaching, but in calcium aluminates (aluminoferrites) full protonization of all oxygen ions with changing of aluminium's function from anion-forming to one of cation is observed.

РЕЗЮМЕ

В данном сообщении на основании результатов кристаллохимического анализа рассмотрены механизмы структурных изменений при гидратации ряда цементных минералов. Установлены причины различий в гидратационной активности силикатов, алюминатов и алюмоферритов кальция, обусловленные особенностями процесса протонирования при взаимодействии минералов с водой: в силикатах кальция протонирование ионов кислорода в структуре протекает лишь частично и сопровождается поликонденсацией SiO_4-тетраэдров в твердой фазе с выщелачиванием $Ca(OH)_2$, а в алюминатах (алюмоферритах) кальция наблюдается полное протонирование всех ионов кислорода с изменением функции алюминия от анионобразующей до катионной.

INTRODUCTION

Owing to the successes in decoding the crystal structures of the main cement minerals and their hydrate phases, and taking into account the development of silicate crystal chemistry [1-3] and a thorough elucidation of some fundamental chemical notions (Pauling's second rule) [4], it has become possible to interpret in a new way the relation between the structural peculiarities of cement minerals and their reactivity with water, i.ei their hydration (chemical) activity [5].

EXPERIMENTAL

Based on the crystal chemistry analysis of calcium cement minerals, it has been established that they could change their structure in the process of hydration. I n this regard a number of the crystal chemistry factors of cement minerals' activity should be pointed out.

The high hydration activity of alkali earth oxides (CaO, SrO, BaO) can be explained by non-correspondence of the coordination number of their cations to the ion radii ratio V_k/V_a which is charactetistic of octahedrons. This means that their crystal structures have porosity which facilitates oxygen anions protonization in the hydration process. The formation of OH^- groups, i.e. strongly polarized dipoles, necessitates rearrangement of a coordination structure into a laminated one which is less symmetrical. As a result, CaO, SrO and BaO are converted into hydroxides within a short time. This leads to quick setting, too high a rate of heat release and consequently development of break-down effects and formation of s low-strength stone. Similar processes take place in the hydration of a number of cement minerals. They differ only because of differences in their content and structure.

In order to determine the crystal chemistry regularity of the calcium cement minerals' hydration processes, calculations have been made on the local valency balance of the specified decodings C_3S, β- and γ-C_2S, C_3A, C_4AF, C_2F, CA_2, $CaSO_4 \cdot 2H_2O$, $CaSO_4$-II crystal structures. These calculations permit us to point out the structural factors in their hydration activity, i.e. anisotropy of interatomic correlations in coordination polyhedrons and, as a consequence, oxygen anions undersaturated and oversaturated with the cation positive charge. Just undersaturated oxygen anions in the cement minerals' structures can be presented as proton acceptors in the process of hydration which makes further structural changes possible.

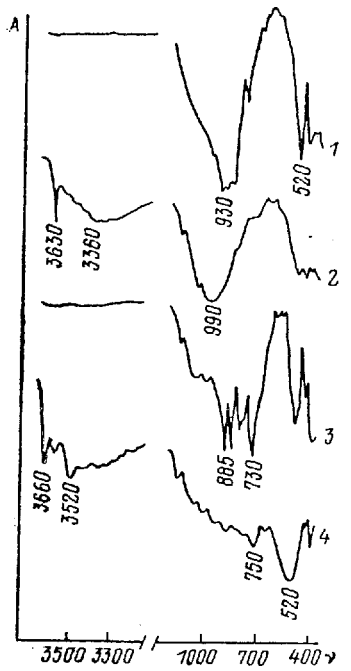

FIG.1 IR absorption spectra of C_3S (1 –nonhydrated, 2 – hydrated for 3 years) and C_3A (3 – nonhydrated, 4 – hydrated for 3 years) minerals. A – absorption, %. ν – wave number, cm^{-1}

According to the degree of hydration activity, clinker minerals can be divided into two groups. The first group represents calcium silicates, the second – C_3A and calcium aluminoferrites. One can study the main patterns of the hydration processes developed in these two groups, taking C_3S and C_3A as examples. C_3A has a higher reactivity with water despite two-fold reduced basicity. Crystal chemistry analysis of the said structures shows why these differences occur.

For C_3A crystal structure, weaker Ca–O links are typical in polyhedrons due to the higher coordination Ca numbers. The anisotropy of chemical links, however, is on the whole higher by 1.7 times (seeTable 1). The total local unbalance of C_3A crystal structure is higher by 3 times than that of C_3S structure. It accounts for higher velocity of the oxygen anions protonizing (see Table 2). A pattern of the processes taking place during C_3S and C_3A hydration is depicted in Fig.1 as revealed by IR spectroscopic analysis. The analysis was carried out with Specord 75 IR spectrophotometer. In C_3S hydration the main absorption band due to stretching vibrations of Si–O bonds is shifted to higher frequency region, i.e. from 930 to 990 cm^{-1} due to the increase of hardening time. For C_3A, the increase of AlO_6–octahedrons bands absorption is observed in the region 700–500 cm^{-1}. AlO_4–tetrahedrons absorption bands intensity being simultaneously decreased in the 900–700 cm^{-1} region. As far as silicates are concerned, it indicates hardwning, i.e. formation of Si–O–Si links. In the case of aluminates, it shows the increase of the aluminium coordination number in hydrate compounds from IY to YI. In the 3700–3300 cm^{-1} region stretching vibration bands of OH^- groups appear as a result of the protonizing process, their intensity in C_3A stone being higher.

Table 1

Characteristic of chemical bonds in C_3S and C_3A structures (z=3)

Poly-hedron	$Ca_9Si_3O_{15}$				$Ca_9Al_6O_{18}$			
	Ratio	CN	Bond force Me – O		Ratio	CN	Bond force Me – O	
			average	Δ			average	Δ
Ca(1)	3	7	0,286	0,125	0,5	6	0,333	0
Ca(2)	3	6	0,333	0,074	0,5	6	0,333	0
Ca(3)	3	6	0,333	0,108	1	6	0,333	0,002
Ca(4)					1	9	0,222	0,107
Ca(5)					3	8	0,250	0,207
Ca(6)					3	8	0,250	0,251
Si(1)	1	4	1,000	0,115				
Si(2)	1	4	1,000	0,037				
Si(3)	1	4	1,000	0,077				
Al(1)					3	4	0,750	0,101
Al(2)					3	4	0,750	0,042

Table 2

Local balance of valencies $\sum v_{ij}$ in C_3S and C_3A structures

Anions	$Ca_9Si_3O_{15}$			$Ca_9Al_6O_{18}$		
	Ratio	$\sum v_{ij}$	Δv_{ij}	Ratio	$\sum v_{ij}$	Δv_{ij}
O (1)	1	2,012	0,012	3	2,215	0,215
O (2)	1	1,940	–0,060	3	2,178	0,178
O (3)	1	2,053	0,053	3	1,893	–0,107
O (4)	1	2,106	0,106	3	1,954	–0,046
O (5)	1	1,965	–0,035	3	1,819	–0,181
O (6)	1	1,855	–0,145	3	1,942	–0,058
O (7)	3	1,992	–0,008			
O (8)	3	2,081	0,081			
O (9)	3	1,956	–0,034			
/Total/	15	30,018	0,780	18	36,003	2,337

DISCUSSION

The pecularities of the protonizing process can be explained by the clinker minerals' structures [5,6] . In C_3S and β–C_2S silicates, common-face links appear between Ca-polyhedrons which cause the structure, acc-

ording to Pauling's rule, to be stressed and unstable. The presence of the fifth part of easily protonized O^{2-} ions not bound with Si^{4+} ion in $C_3S=Ca_3O[SiO_4]$ is the main reason for its increased hydration activity compared to $\beta - C_2S=Ca_2[SiO_4]$. Structural instability is also pecular to calcium aluminates and aluminoferrites. It is entailed by the change of the aluminium (ferrum) coordination number in the process of hydration. Besides, large cavities of 0.3 mm size, caused by $[Al_6O_{18}]^{18-}$ ring groupings availability, are typical of C_3A. This accounts for its structure porosity due to which water molecules penetrate into the lattice, promoting the development of protonization processes. As the link ionicity in AlO_4-tetrahedrons is higher than in SiO_4-tetrahedrons, OH^- groups are formed in the process of hydration of calcium aluminates and aluminoferrites. So the necessity arises to rearrange the structure. Topotactic transitions of aluminium from coordination IY to coordination YI also promote abovementioned. These processes proceed catalytically and so for C_3A, in which all oxygen anions are protonized in the structure, unlike for C_3S, thermal effect is two times higher.

CONCLUSION

There are two processes which determine the hydration mechanism of calcium aluminates and aluminoferrites and their reduced reactivity with water: protonization of all O^{2-} and changing of aluminium's function from anion-forming to one of cation. This leads to a complete destruction of the initial structure of minerals and determine their high hydration activity. In the process of calcium silicates' hardening, a partial protonization of undersaturated oxygen anions takes place. This is accompanied by a rearrangement and complication of the silicon-oxygen motive as well as leaching of calcium ions with subsequent crystallization in pores in the form of portlandite. It follows from this that structural changes entailed by the possibility of protonizing to the inside of the initial crystal are the mobile force belonged to cement minerals' hydration processes and determine their hydration (chemical) activity.

REFERENCES

1. BELOV N.V.:"Essays on structural mineralogy." M.,Nedra, 1976, 344p.
2. ILYUHIN V.V., KUZNETSOV V.A., LOBACHOV A.N., BAKSHUTOV V.S."Calcium hydrosilicates. Synthesis of monocrystals and crystal chemistry". M., Nauka, 1979, 184 p.
3. TAYLOR H.F.W. "Cement Chemistry", Academic Press, 1990, 475 p.

4. PYATENKO YU.A. "On common method of approach to analysis of valency local balance in inorganic structures", Crystallography, 1972, V.17, No.12, pp. 773-779.

5. SANITSKY M.A.: "Some questions on crystal chemistry of cement minerals", Kiev, 1990, 64 p.

6. PASHCHENKO A.A., SANITSKY M.A.: "The mechanisms of structural transformations in the process of hydration of cement minerals". J. of Applied Chemistry, 1990, No 2, 340-343.

STRUCTURAL CHANGES DUE TO CARBONATION IN HARDENED CEMENT PASTES

I G Richardson*, G W Groves*, A Brough and C M Dobson****

**Department of Materials, University of Oxford, Oxford, UK*
***Inorganic Chemistry Laboratory, University of Oxford, Oxford, UK*

SUMMARY

Thin (0.4mm) slices of hardened cement paste have been carbonated for various extents in atmospheres of CO_2 and of air. The slices were sufficiently thin to undergo progressive changes in a relatively uniform manner. Microstructural changes during the course of carbonation were studied by a combination of analytical transmission electron microscopy and solid state ^{29}Si NMR spectroscopy. The C-S-H gel component of the pastes underwent a reduction in Ca:Si ratio accompanied by a polymerization of the silicate chain structure of the gel. The morphology of the C-S-H gel remained in the main unaffected by the changes in composition and structure. The calcium carbonate produced took the form of microcrystals of vaterite or calcite appearing to nucleate initially on fibrils of C-S-H gel in the outer product and ultimately producing dense microcrystalline regions of carbonate in the outer product. Cross-linked silica gel formed only at later stages of carbonation. Calcium hydroxide crystals initially reacted rapidly but the rate of reaction of calcium hydroxide subsequently decreased, which may be attributed to the observed formation of dense layers of microcrystalline calcium carbonate at the surface of the calcium hydroxide crystals.

INTRODUCTION

The topic of the carbonation of concretes has been reviewed by Parrott[1]. The depth of the carbonation reaction increases markedly with increasing water/cement ratio (or decreasing concrete compressive strength) and maximises at an ambient relative humidity of about 60%. In practice, carbonation is usually detected by phenolphthalein indicator sprayed onto a broken surface of the concrete. The fully carbonated zone remains colourless due to its reduced pH. This test however is not effective in revealing partially carbonated cement paste and analysis of the phases present in concrete exposed to carbonation has shown that a partially carbonated zone can extend over a distance comparable to the depth of fully carbonated concrete. Carbonation must therefore be seen as a process which at any given point in the concrete develops with time, leading to progressive changes in the microstructure of the hardened cement paste, and consequent changes in its local properties, such as its permeability. Although all the hydration products present are expected to react with carbon dioxide, the major reactions in cements based on Portland cement are the reaction of C-S-H gel to form ultimately silica gel and calcium carbonate and of CH crystals to form calcium carbonate and water. These reactions can conveniently be studied in the laboratory in pastes of C_3S cement. The stages by which C-S-H reacts, its relative rate of reaction compared to that of CH, and the morphology of the products of the reaction are at present incompletely known. In this paper we report the results of a study of these aspects of carbonation using techniques of analytical transmission electron microscopy (TEM) which is able to resolve the fine details of the partially carbonated microstructure, and ^{29}Si solid state nuclear magnetic resonance, which is able to follow changes in the state of polymerization of the C-S-H gel as it reacts with carbon dioxide.

EXPERIMENTAL PROCEDURE

C_3S was prepared by mixing and pelletizing calcium hydroxide and colloidal silica, followed by firing, crushing and refiring at 1500°C. A white Ordinary Portland Cement was obtained from Aalborg Corporation in Denmark (Bogue composition 65% C_3S, 27% C_2S, 4% C_3A, 1% C_4AF). Silica fume from Elkem Corporation had a silica content of 87.3% with Fe_2O_3, MgO, K_2O and Al_2O_3 as the main impurities. Cement pastes were prepared by hand-mixing with distilled water at the required water:cement ratio. Freshly mixed paste was poured into polyethylene sample vials of 13mm internal diameter which were sealed prior to curing for at least 28 days at room temperature. After demoulding the hardened paste cylinders were cut into discs ~0.4mm thick. Discs were mounted in a chamber for carbonation in which humidity control was obtained by saturated NH_4Cl/KNO_3 solution to hold a relative humidity of 72.6%. The discs were equilibrated in moisture content for at least 24 hours in the chamber before admitting the CO_2-containing atmosphere. The carbonating atmosphere was either pure CO_2 or air with a CO_2 content of approximately 0.05% by volume. Specimens for examination by TEM were prepared from hardened paste discs by grinding to a thickness of approximately 30μm, followed by ion-beam thinning until a hole appeared, the edges of the hole then containing areas thin enough for electron transmission. TEM was carried out in a JEOL 2000FX microscope equipped with a Tracor Northern X-ray analyser. Thermogravimetric analysis of carbonated pastes was carried out in a Stanton Redcroft analyser using a heating rate of 10°C/min.

Specimens for ^{29}Si MAS NMR spectroscopy were ground to a powder. Approximately 150mg of sample was placed into a 7mm diameter ZrO_2 rotor. ^{29}Si spectra were acquired at a resonance frequency of 79.5 MHz on a Bruker MSL 400S spectrometer with magic angle spinning (MAS) at 3-4 kHz, and with high power ^1H decoupling with a field of 60 kHz.

Typically a flip angle of 30° was used with a recycle delay of 10s. Under these conditions relative peak intensities should be within 10% of their true values for resonances with T_1 values up to 30s. Chemical shifts are given downfield of tetramethyl silane at 0ppm.

RESULTS

Thermograviemetric analysis of hardened pastes of C_3S carbonated in pure CO_2 for times ranging from 1h to 4 days showed an initially rapid reaction of CH which became much slower with time and a reaction of C-S-H which while initially slower than that of the CH, decreased less rapidly with time and ultimately overtook the reaction of the CH. This is shown in fig.1, which combines the results of two studies[3,4], one of C_3S pastes of 0.6 water:cement ratio carbonated in CO_2 at times from 1 to 16 hours and the other of C_3S pastes of 0.5 water:cement ratio carbonated in CO_2 at times from 1 day to 4 days, both at a relative humidity of 72.6%.

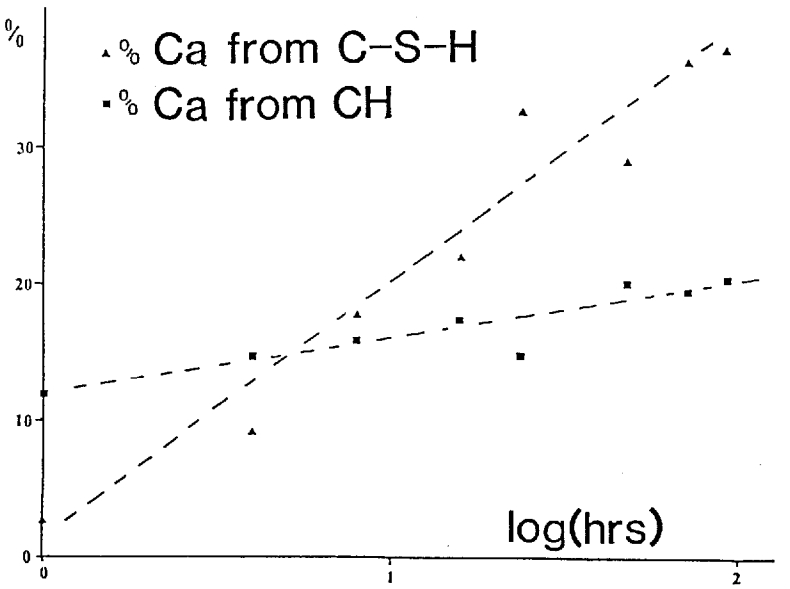

Fig.1 The reactions of CH and CSH during the carbonation of C_3S pastes.

A possible explanation for this effect is that the rate of reaction of CH is initially very rapid at exposed crystal surfaces but that the reaction slows down markedly as access to the surface becomes obstructed by reaction product in the form of calcium carbonate crystals. This explanation is supported by the observation in the TEM of CH crystals embedded in calcium carbonate crystals(3). In the case of C-S-H, the very high surface area would prevent such a process from occurring to the same extent.

The microstructures of C_3S pastes partially carbonated in CO_2 show the following main features.

1. The morphologies of the finely porous relatively homogeneous inner product C-S-H and outer product C-S-H are maintained while the Ca:Si ratio of the C-S-H is reduced by carbonation.

2. At an early stage (after about 4hrs) some regions of gel of very low Ca content form. At the same time, ^{29}Si NMR shows the presence of Q_4 signal indicating the presence of silicate units linked to 4 other silicate units in a three dimensional network.

3. Calcium carbonate appears to nucleate on fibrils of C-S-H in the outer product. Microcrystals of order 100nm size form in pores in the outer product and around C H crystals. The choice of calcite or vaterite crystal structures appears to be finely balanced and both are observed.

4. At a later stage only, very fine (~10nm) poorly crystalline vaterite particles form within regions of inner product gel.

Although quantitative phase analysis for a series of increasing carbonation times has as yet only been performed on C_3S pastes carbonated in pure CO_2, a number of TEM and ^{29}Si NMR observations have been made on the following systems.

a) C_3S/silica fume blended pastes carbonated in CO_2(TEM only)

b) C_3S pastes carbonated in air

c) OPC and OPC/silica fume pastes carbonated in air

A hardened C_3S paste carbonated in air was in most respects microstructurally similar to one carbonated in CO_2. The main difference was that the development of silica gel was delayed in air carbonation relative to the case in CO_2 carbonation(4). Microanalysis showed that at a time of two months a C-S-H gel of Ca:Si ratio approximately 1.0 with little spread in composition was present and NMR spectroscopy showed that C-S-H gel of a higher degree of linear polymerization formed, relative to the case of CO_2 carbonated paste, before any three-dimensionally polymerized silica gel formed. After a further time, however the NMR spectrum showed the start of three-dimensional polymerization as seen in fig.2.

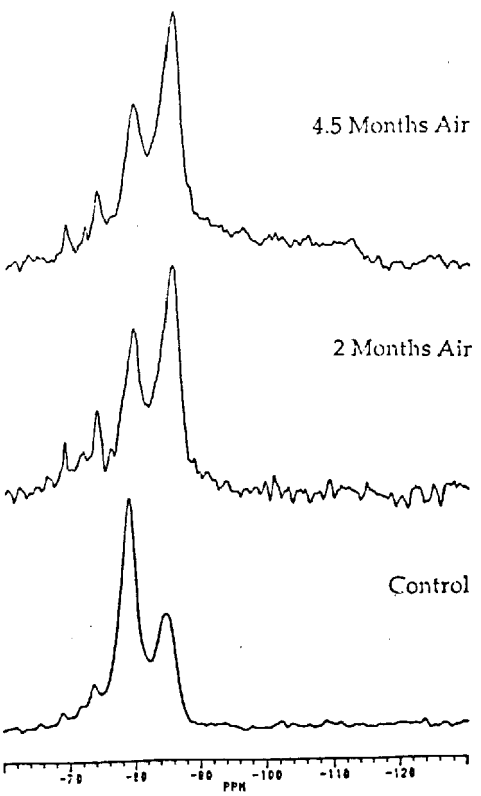

Fig.2 NMR spectra for C_3S paste carbonating in air.

A white OPC paste carbonated in air showed similar features to the C_3S paste although the progress of carbonation appeared to be slower than for a C_3S paste of the same water:cement ratio carbonated at the same relative humidity. Fig.3 shows a characteristic distribution of calcite microcrystals intermingled with fibrillar C-S-H gel in the outer product region of the paste microstructure.

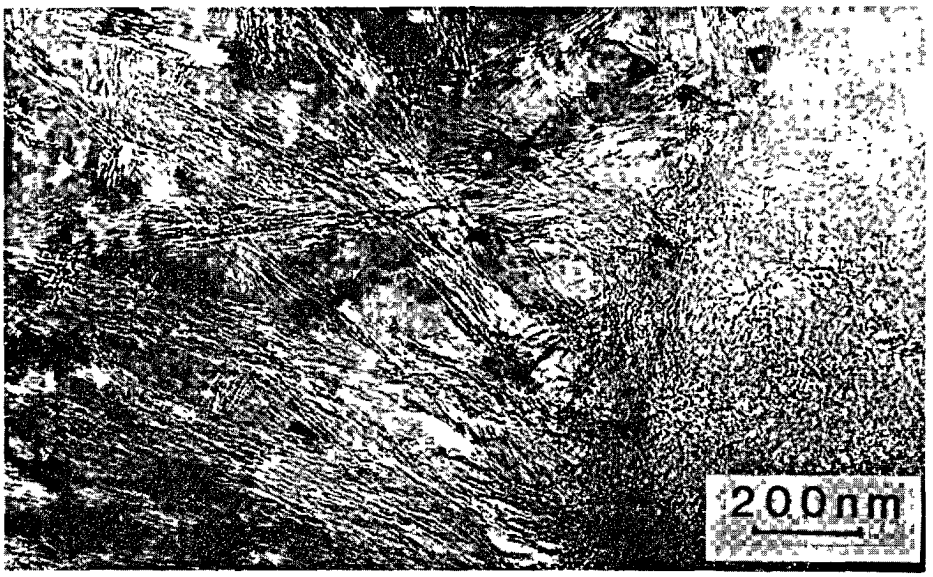

Fig.3 Microstructure of a white OPC paste carbonated in air for 116 days.

In the cases of blends of C_3S and silica fume carbonated in CO_2 or white OPC and silica fume carbonated in air a major difference in the microstructure from the unblended C_3S or OPC pastes lay in the distribution of carbonate. This appeared to be less homogeneous, with local high concentrations of calcite microcrystals in some areas and substantial areas of outer product containing silica fume particle resides which were free of carbonate crystals. A possible explanation for this effect is the absence of coarse porosity within which calcite crystals can readily nucleate in some areas of the outer product of the blended pastes. Such regions of outer product would then behave like inner product C-S-H in unblended pastes in not containing carbonate crystals at least in the early stages of carbonation.

DISCUSSIONS AND CONCLUSIONS

Analysis of the partially carbonated thin discs of hardened C_3S paste indicates that initially CH is the more rapidly reacting phase but that its reaction dramatically slows down so that the reaction of C-S-H becomes dominant. The question arises, to what extent is the carbonation of C_3S pastes a satisfactory model for the carbonation of OPC pastes and what difference does acceleration of the carbonation by increasing the CO_2 content of the atmosphere make to the microstructure? As regards the latter question, the evidence from C_3S pastes is that the use of CO_2 instead of air as the carbonating atmosphere forces the microstructure to depart further from equilibrium by the development of silica gel in some regions at an earlier stage so that a wider spread of gel composition and structure exists in the partially carbonated state than in the case of air carbonation. As regards the former question, the microstructures of partially carbonated pastes of OPC and C_3S carbonated in air appeared similar although the rate of carbonation of the C_3S paste was greater than that of the OPC paste of the same water/cement ratio. Partially carbonated blended pastes of white OPC/silica fume and C_3S/silica fume showed similar features. From this it appears likely that pastes of

C_3S are a good model for pastes of OPC as far as carbonated microstructures are concerned. The advantage of the use of C_3S in laboratory specimens is that it allows a complete analysis of the structure to be more readily obtained.

The progressive development of the carbonated microstructure in thin discs of paste can be considered to indicate the variation in microstructure with depth in a bulk specimen carbonate in air where the degree of carbonation below a fully carbonated zone decreases with depth. At the greatest depths showing signs of carbonation it can be expected that the surfaces of CH crystals will have reacted and carbonate microcrystals will have nucleated at their surfaces and on C-S-H fibrils in solution-filled voids within the outer product. At lesser depths C-S-H gel will have been converted without change of morphology into a more highly polymerized gel of lower Ca:Si ratio, while regions between C-S-H fibrils in the outer product become increasingly filled with carbonate microcrystals. The net loss of calcium from inner product regions arising from the fact that they do not contain large enough pores to allow the nucleation of carbonate crystals at this stage will lead to shrinkage unless this is restrained, in which case porosity may develop in the inner product. The filling of outer product porosity containing pore solution with carbonate microcrystals will lead to a reduction in permeability and in rates of diffusion through the paste. As the carbonation front is approached regions of silica gel containing a small concentration of calcium will appear and possibly very small vaterite crystallites may appear within the inner product, although it is uncertain as yet whether these form during un-accelerated carbonation.

In the carbonation of concretes in service macro-heterogeneity of the cement paste microstructure can be expected to lead to fluctuations in the degree of carbonation and hence in the microstructure from point to point at a given depth below the surface. A further factor present in service and not readily reproduced in the laboratory is the fluctuation in ambient humidity and temperature. It appears to be remarkably difficult to achieve complete carbonation of thin discs held under constant conditions in the laboratory even under the highly accelerating environment of pure CO_2 and it is possible that complete reaction is more readily obtained under fluctuating conditions.

REFERENCES

1. Parrott, L.J.: "A review of carbonation in reinforced concrete", Building Research Establishment, Garston, Watford WD2 7JR, U.K. 1987.

2. Parrott, L.J. & Killoh, D.C.: "Carbonation in a 36 year old in-situ concrete". Cem. Conc. Res. 1989, **19**, 649-56.

3. Groves, G.W., Rodway D.I. & Richardson I.G.: "The carbonation of hardened cement pastes". Adv. in Cem. Res. 1990, **3**, 117-125.

4. Groves, G.W., Brough,A., Richardson I.G. & Dobson, C.M.: "Progressive changes in the structure of hardened C_3S cement pastes due to carbonation". J. Amer. Ceram. Soc. 1991, **74**, 2891-96.

ACKNOWLEDGEMENT

The support of the Science and Engineering Research Council under grant GR/F44557 is acknowledged.

EFFECTS OF THE CARBONATION ON THE THERMAL PROPERTIES OF TOBERMORITE

Seishi Goto and Sadami Ikeda

Faculty of Engineering, Yamaguchi University
Ube, Yamaguchi, JAPAN

ABSTRACT : 11A Tobermorite was synthesized and used for carbonation experiments. There were two types of 11A tobermorite. One showed X-ray diffraction peaks at 7.7°, 28.9°, 29.9° (CuKα) while the other showed the peaks at 8.1°, 28.9°, and 29.4°. They were exposed to an atmosphere of 5%CO_2-N_2gas at 25℃ at 100% and 75% RH. The carbonation products were vaterite at the early stage and calcite in the later stage. When tobermorite was heated to 900℃, wollastonite was produced, but when carbonated tobermorite was heated, the products were pseudo-wollastonite and wollastonite. The amounts of wollastonite and pseudo-wollastonite seemed to depend on the degree of carbonation.

РЕЗЮМЕ: Для исследования карбонизации были синтезированы две модификации 11A тоберморита. Одна с характерными на рентгенограмме пиками при 7,7°, 28,9°, 29,9° (CuK) и другая с пиками при 8,1°, 28,9° и 29,4°. Полученные модификации выдерживались в среде 5%CO_2-95%N_2 газа при температуре 25°C и влажности 100% и 75%. Продуктом карбонизации на ранней стадии является ватерит, а на поздней стадии - кальцит. В результате нагрева тоберморита до 900°C образуется волластонит. Однако, продуктами нагрева карбонизованного тоберморита являются псевдоволластонит и волластонит, соотношение между которыми, очевидно, зависит от степени карбонизации.

1. INTRODUCTION

Carbonation of tobermorite is a fundamental and important problemin the durability of concrete. Many kinetic studies on the carbonation of concrete have been carried out. However, in most cases, the extent of carbonation was measured as the thickness of the neutralized layer by means of phenolphthalein and also from the changes in porosity or poresize distribution(1). The thickness is affected by the condition of thesample, such as wet or dry. Sometimes, a rewetted sample shows a lesser thickness than a dry one(2). This does not mean decarbonation by rewetting. It only means that the alkalinity is diffused towards outside by rewetting. Thus, measurement of the thickness of the neutralized layer doesnot accurately indicate the extent of carbonation.

Ariizumi et al.(3) reported on the measurement of extent of carbonation by using radio isotope of $^{14}CO_2$, but made no precisely mention of the quantitative observation. Nevertheless, it is one way to measure the carbonation directly and quantitatively, but $^{14}CO_2$ is hard to deal with T.Fukushima and F.Tomosawa(4) measured the distribution of $Ca(OH)_2$ and $CaCO_3$ and succeeded in a way, but there is no information about the carbonation of CSH. In a previous report, the authors mentioned about the rateof absorption of CO_2 gas in hardened cement pastes(5).

This study was aimed at obtaining some quantitative information of carbonation of tobermorite. To this end, tobermorite was synthesized and carbonated with 5%CO_2-N_2 gas at 23℃ at 100% or 75% RH, and studied by means of XRD and DTA.

2. EXPERIMENTAL

2.1 Synthesis of Tobermorite

Tobermorites were synthesized hydrothermally at 156℃ to 200℃ with various C/S ratios, 0.6~1.5, and with water or 1N KOH solution. The reagents of $Ca(OH)_2$, SiO_2 and Al_2O_3 were all of special grade.

The compositions of mixtures and hydrothermal condition of samples prepared for carbonation experiments are shown in Table 1. These samples were washed with KOH in deionized water and subsequently subjected to XRD and DTA analysis.

Table 1 The Hydrothermal Condition of Sample Preparation

Sample No.	Temp.(℃)	Time(days)	Composition
1	156	3	C/S = 0.60
2	156	3	C/S = 1.00
3	180	2	C/S = 0.83
4	200	1	C/S = 0.60
5	200	1	C/S = 0.83
6	200	1	C/S = 0.83

2.2 Carbonation

A few grams of sample was ground and put on a plate and the plate set in a chamber in which the humidity-regulated 5%CO_2-N_2 gas was passed at room temperature of about 23℃.

2.3 Observation of Carbonation

The carbonated samples were examined by XRD and DTA. XRD of the samples subjected to DTA analysis were also taken. The XRD used was Geiger Flex 2027 (Rigaku Co.Ltd) and target was CuKα. About 10 mg of sample was used for DTA. The rate of temperature rise was 10℃/min.

3. RESULTS AND DISCUSSION

3.1 Synthesized Tobermorite

XRD patterns and DTA curves of synthesized tobermorites are shown in Fig.1. XRD patterns show well crystallized tobermorite, though there are also some minor components of SiO_2, $Ca(OH)_2$ and/or α-C_2SH. There are two types of tobermorite. One (hereafter named type A), whose sample number was 4, 5 and 6 in Table 1, has peaks at 7.7°, 28.9°, and 29.9°. The other (type B), whose sample number was 1, 2 and 3 in Table 1, has peaks at 8.1°, 28.9°, and 29.4°. In type A, peaks of (400) and (008) were separated. Previously, we mentioned that the separation of these peaksis influenced by the concentration of K^+ ion(6). Samples in this study were all synthesized with KOH solution, but type A samples were prepared at relatively high temperatures.

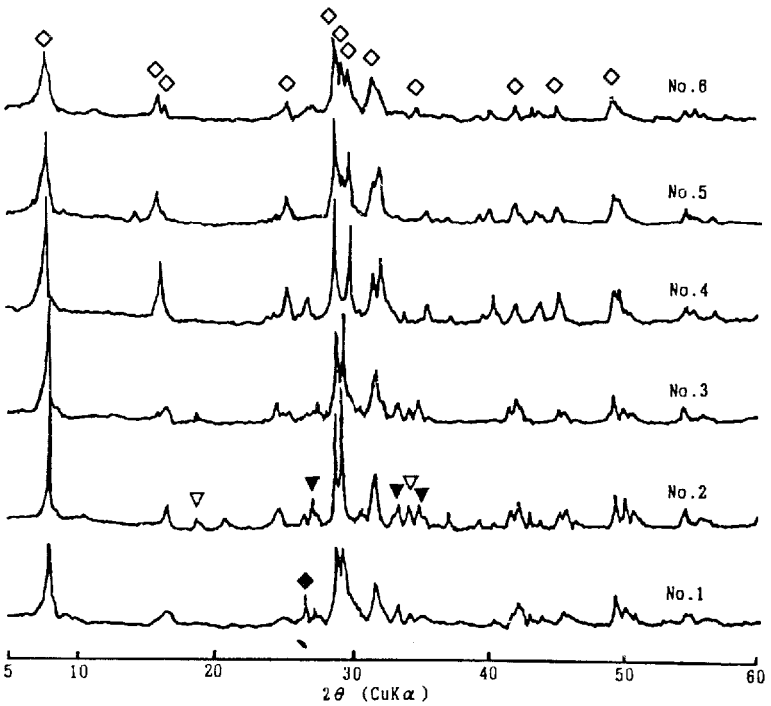

Fig.1 X-ray Powder Diffraction Pattern of Synthesized Tobermorite.
◇ : Tobermorite, ◆ : Quartz, ▽ : $Ca(OH)_2$, ▼ : α-C_2SH

In the DTA curves shown in Fig.2, an endothermic peak due to dehydration of tobermorite is observed around 180℃ while an exothermic peak due to formation of wollastonite is observed around 800℃. In the type B samples, another endothermic peak is observed just before the exothermic peak.

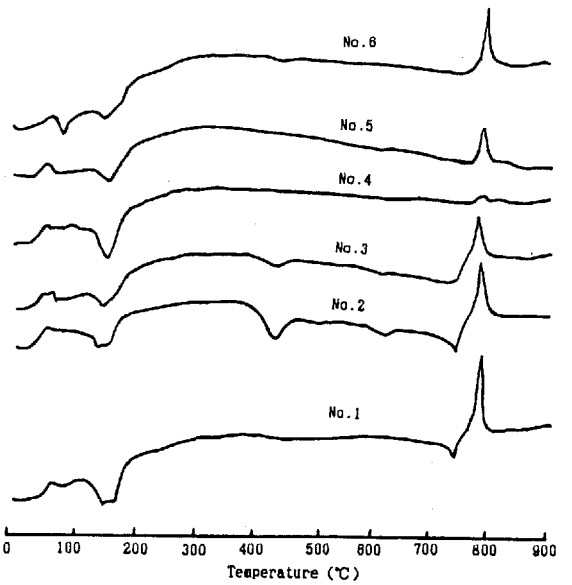

Fig.2 DTA curves of Synthesized Tobermorite.

3.2 Carbonation reaction

The XRD patterns of the carbonated sample (No.5) are shown in Fig.3. It suggested that the rate of carbonationi very high at 100% RH. In 2 to 4 days, the tobermorite peak mostly disappeared and the vaterite peak appeared, at early stage. Calcite formed at a later stage. At 75% RH, the rate of carbonation was relatively low and tobermorite persisted for morethan 16 days. The results of all other samples are not shown. However, they were more or less the same, but some aditional effects due to the crystallinity of tobermorite were also obtained.

Regarding the effects of humidity on the carbonation of concrete, it has been observed that the rate of carbonation increases with decreasing humidity; below the humidity of the 70%, the rate decreases with decreasing humidity. Results obtained here are, however, at higher humidity, and the rate of carbonation is faster. Humidity was found to play a very important role in th e carbonation of concrete. Especially important is how the pore is filled with aqueous solution(5). Since we used powder-like samples for carbonation, the effects of humidity on the rate of carbonation might appear somewhat different from that of concrete.

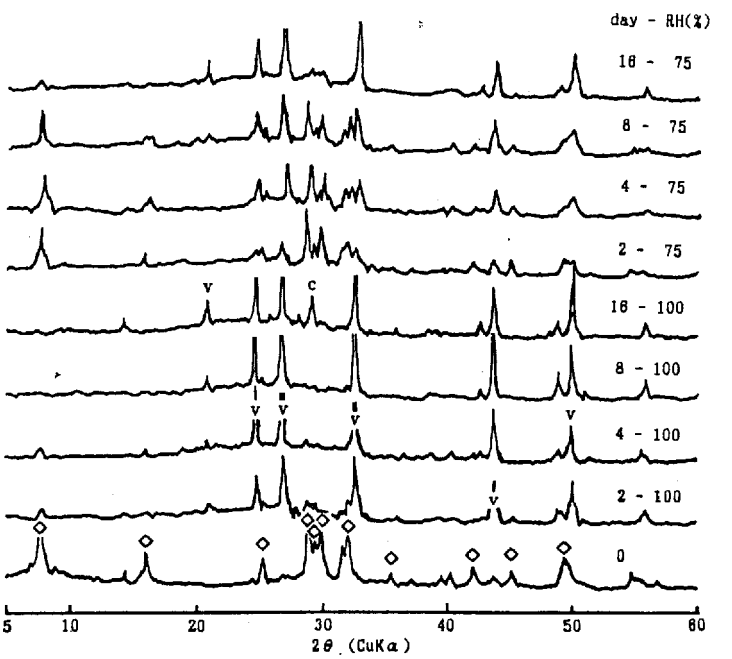

Fig.3 X-ray Powder Diffraction Pattern of Carbonated Sample No.5.
◇ : Tobermorite, V : Vaterite, C : Calcite

The DTA curves of carbonated samples (No.6) are shown in Fig.4. After carbonation, a broad endothermic peak appeared at about 500℃ (450~600℃) and a relatively sharp one at 600~650℃. The former peak was attributed to the formation of vaterite and the latter to the formation of calcite. The endothermic peak arising due to the decarbonation of vaterite was influenced by humidity. Samples carbonated at lower RH showed relatively smaller and sharper decarbonation peaks. An exothermic peak due to wollastonite was found to decrease with carbonation.

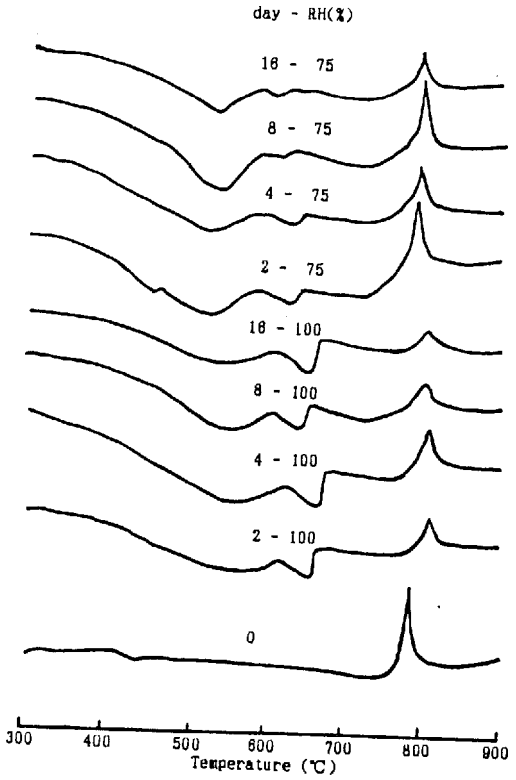

Fig.4 DTA Curves of Carbonated Sample No.6.

3.3 Effect of carbonation on formation of wollastonite

The XRD patterns of carbonated samples after heating up to 900℃ are shown in Fig.5. They showed wollastonite and/or pseudo-wollastonite. Uncarbonated sample showed only the wollastonite peak. With increase in carbonation time, the pseudo-wollastonite peak was found to increase in intensity. In the sample carbonated at 100% RH, even at 2 days carbonation, the pseudo-wollastonite peaks are very strong while the wollastonite peak decreased with increase in carbonation time.

When a mixture of silica and lime is heated above 900℃, pseudo-wollastonite is usually obtained. In the carbonated tobermorite, silica geland $CaCO_3$ are present just as in a mixture of silica and lime. Thus, pseudo-wollastonite is produced by heating the carbonated sample. The structural arrangement of Ca and Si atoms in uncarbonated tobermorite are simillar to that in meta-kaolin, and thus, wollastonite is obtained on heating the sample.

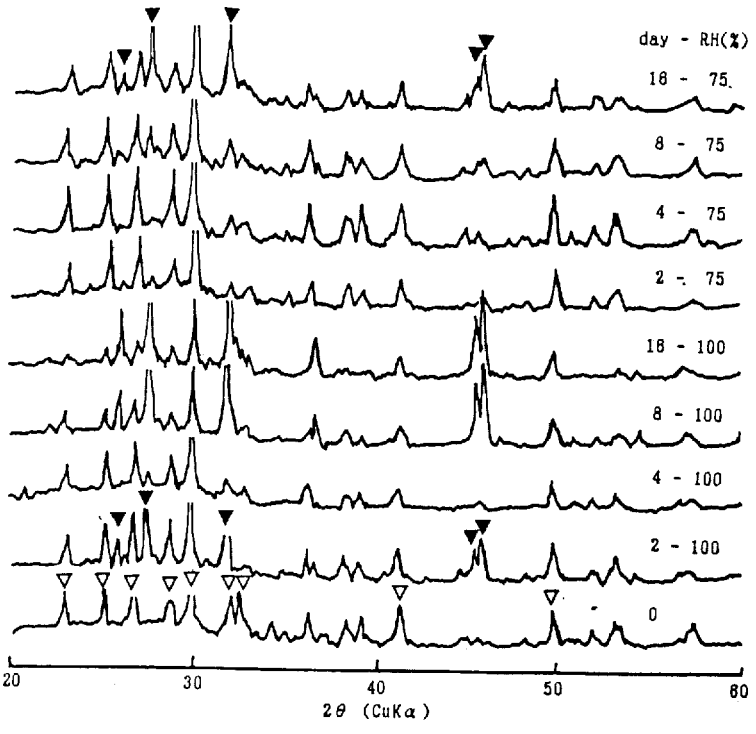

Fig.5 X-ray powder Pattern of Carbonated sample No.3 after DTA Measurement. ▽ : Wollastonite, ▼ : Psuedo-Wollastonite

Techniques have not yet

been worked out to a quantitative analysis of wollastonite and pseudo-wollastonite. But a combination of this wollastonite/psuedo-wollastonite analysis and quantitative XRD analysis of $Ca(OH)_2$ and $CaCO_3$ will be considered to arrive at a better understanding of the mechanisms and kinetics of the carbonation of concrete.

4. CONCLUSIONS

Carbonation of tobermorite was performed using synthesized 11A tobermorites. Two types of 11A tobermorites was obtained as indicated XRD and DTA. They were exposed to an atmosphere of 5%CO_2-N_2 gas at 23℃ at 100% and 75% RH. The results obtained are as follows.

i) The carbonation products were vaterite and silica gel at early stage and calcite at later stage.

ii) The rate of carbonation was faster at higher humidity.

iii) Wollastonite was obtained by heating uncarbonated tobermorite and pseudo-wollastonite by heating the carbonated one. Their amounts seemed to depend on the degree of carbonation.

Acknowledgment: We thank for the financial suport of 1989's Research Fund of Japanes Cement Association.

REFERENCES

1) R.Kondo, M.Daimon and T.Akiba, Proc.5th Int'l Symp.Chem.Cem., Tokyo 1968, Vol.III 402-409 (1968)

2) H.Ohga, T.Saeki and S.Nagataki, Semento Gijutu Nenpo, 43 564-569 (1989)

3) S.Ariizumi, N.Kondo and M.makita, Semento Gijutsu Nenpo, 14 513-519 (1960)

4) T.Fukushima And F.Tomosawa, Semento Gijutu Nenpo, 43 570-575 (1989)

5) H.Shima, K.Asaga, M.Daimon and S.Goto, Semento Gijutu Nenpo, 43 552-557 (1989)

6) K.Asaga, M.Daimon, S.Goto and R.Kondo, Proc.7th Int'l Cong. Chem.Cem., Paris, Vol. III VII-40 - VII-45 (1980)

AN INVESTIGATION ON THE OPTIMUM AMOUNT OF GYPSUM NEEDED FOR OPTIMUM STRENGTH AND FOR DIFFERENT TYPES OF CLINKER

F Milia*, Lj Miljkovic, G Papavassiliou***
E Chaniotakis* and D Frangoulis*****

**Institute of Materials Science, NCSR Demokritos, Attikis, GREECE*
***On leave from University of Nic, YUGOSLAVIA*
****Titan Cement Industry, Kamari, Attikis, GREECE*

ABSTRACT

In order to investigate the influence of the different SO_3 on the hydration properties of cement paste, two different kind of cement samples were produced: i) laboratory-samples with an almost constant total SO_3 content, ii) industrial samples produced from the same clinker but with a different amount of gypsum. These samples were examined by using ^1H NMR, atomic absorption, XRF, and strength measurement techniques. The NMR results are in agreement with the gypsum behaviour obtained by other techniques. In addition it is observed that the SO_3 contained in clinker is retarding the hydration process of the cement paste.

Pour étudier l' influence des differents SO_3 sur les propriétés d' hydratation de la pate du ciment, nous avons produit deux differents echantillons: i) echantillons de laboratoire aven un contenu total en SO_3 presque constant. ii) echantillions industrielles produit du même clinker mais avec un different contenu de platre. Ces echantillons ont été étudié avec les techniques ^1H RMN, absorption atomic, FRX et mesures de resistance en flexion et en pression. Les resultats de RMN sont en concordance avec le comportement du platre obtenu par d' autres techniques. Il est aussi observé que le SO_3 contenu dans le clinker retarde le process d' hydratation de la pate du ciment.

I. INTRODUCTION

The final amount of sulphates in a cementeceous product originates from three different sources: (i) The raw material, (ii) the fuel, and (iii) the natural gypsum which is added at the end.

There is a lot of work done, referring on the influence of gypsum on the hydration properties of cement, see for instance refs.[1, 2]. It is well established by now that gypsum percentage is related to the setting time and strength development, via its influence on the hydration rate, whereas an optimum amount of gypsum maximises strength and minimises drying shrinkage. However as far as we know, only a little work has been done, regarding the influence of parameters like the sulphate content of the raw materials, on the hydration properties of cement. In order to investigate this problem we decided to apply a combination of conventional methods (setting time and strength measurements, Atomic Absorption (A.A.), XRF) and novel methods (proton NMR). Our aim is to get a deeper understanding and clarify the factors which play a decisive role in the behaviour of the final product.

II. EXPERIMENTAL WORK

1) Sample preparation.

White clinker samples, originating from different raw materials and thus containing different amounts of SO_3, were produced in the laboratory (from now on referred as samples "a"). These samples were ground together with different percentages of natural gypsum in order to get samples with almost the same SO_3 content. In addition, industrial samples of white cement were produced (from now on referred as samples "b"), from the same clinker but with a different amount of gypsum.

2) NMR measurements.

The hydration process and hardening of both sample groups, "a" and "b" was investigated by of proton NMR spectroscopy.

Proton NMR spectroscopy gives valuable information on the behaviour of protons in different chemical and physical environment. Different kind of proton groups have different values of the proton spin-lattice T_1 and spin-spin T_2 relaxation times. It is already published by us and other groups [3-6] that different kind of proton groups have been identified during the solidification of the cement paste. We may thus, conclude that NMR techniques allow a continuous and simultaneous monitoring of the above mentioned proton groups. In addition, it is established by now[5] that the rate of spin-lattice relaxation $1/T_1$ of the exchangeable water (mainly water in micropores) is related to the flexural and compressive strengths.

3) Chemical and crystallographic analysis.

Chemical and crystallographic analysis were performed by using A.A. and XRF techniques.

4) Setting time and strength measurements.

Finally, setting time and strength measurements were performed and compared with the NMR results.

III. RESULTS AND DISCUSSION

1) NMR results.

Fig. 1 shows a set of curves of spin-lattice relaxation time vs. hydration time for samples "a".

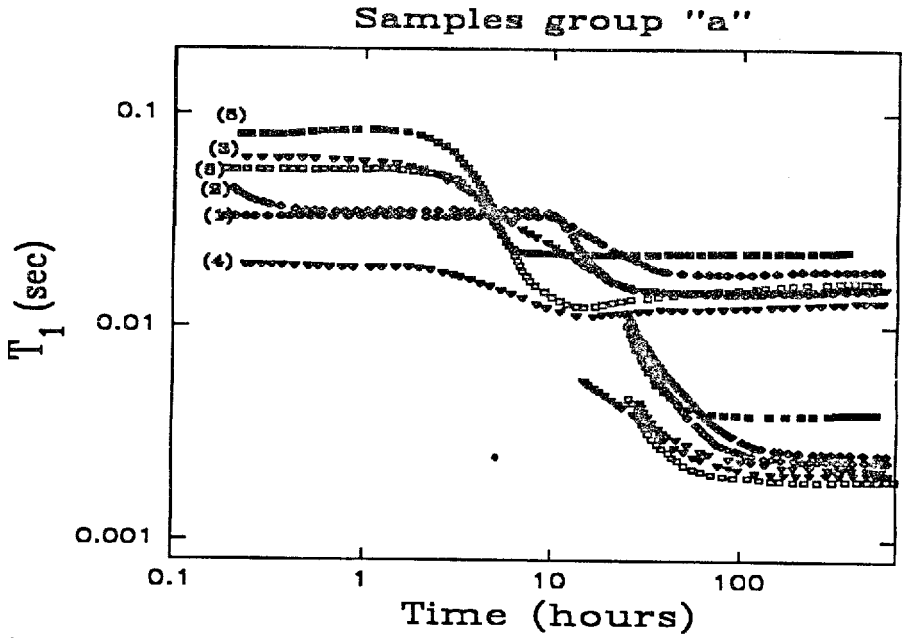

Fig. 1: Proton NMR spin-lattice relaxation time T_1 as a function of the hydration time for the group "a" of samples. (Gypsum Percentage: (1) 2.7%, (2) 3.5%, (3) 4.4%, (4) 4.6%, (5) 5.3%, (6) 5.5%).

As we can see, different cements although with the same final amount of SO_3, exhibit interesting differences in their behaviour of the hydration and hardening processes. Due to the industrial importance of these first results, and in order to clarify and isolate the factors which play a decisive role and affect the properties of the final product, a second group of samples (samples "b") was produced as referred above. NMR measurements were repeated for this second group of samples (fig. 2).

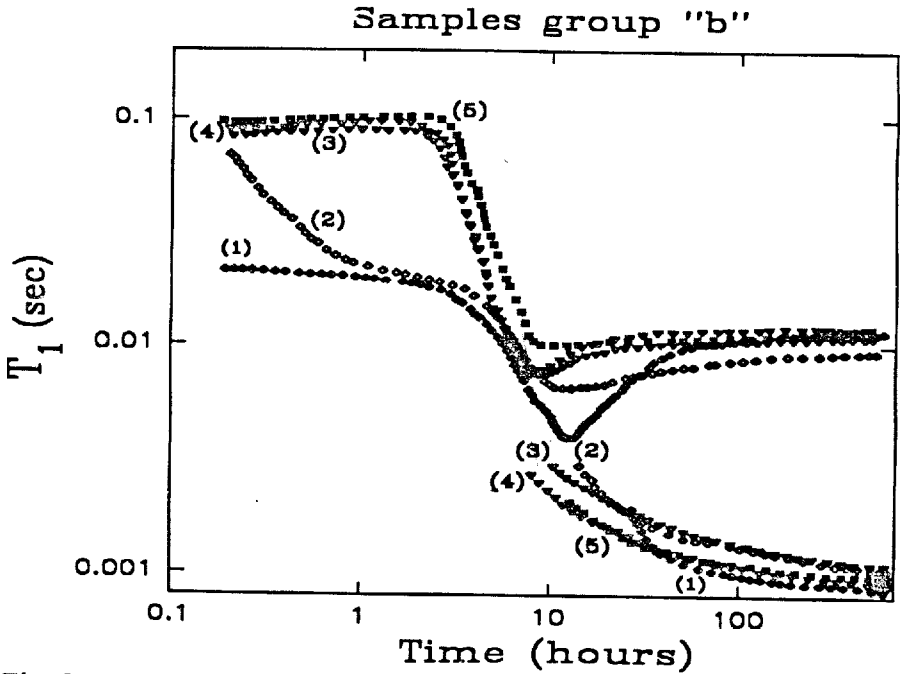

Fig. 2: Proton NMR spin-lattice relaxation time T_1 as a function of the hydration time for the group "b" of samples. (Gypsum Percentage: (1) 0%, (2) 2.7%, (3) 3.5%, (4) 4.6%, (5) 5.5%).

2) Physical results

In order to relate the NMR measurements to the hydration properties of cement, the strength and setting time of samples "b" (Table I, Table II) were measured according to the EN 196 standard procedure.

TABLE I: Strength measurements of Samples Group "b" (Nt/mm^2)

% GYPSUM	1 DAY	2 DAYS	7 DAYS	28 DAYS
0.0	14.8	26.5	40.4	53.4
2.7	15.2	23.7	36.3	48.8
3.5	17.8	26.2	40.4	52.8
4.6	21.6	30.0	43.5	54.4
5.5	20.7	29.0	43.1	54.3

TABLE II: Setting Time measurements of Samples Group "b"

% GYPSUM	W/C	INITIAL (min)	FINAL (min)
0.0	0.4	80	115
2.7	0.4	70	85
3.5	0.4	155	225
4.6	0.4	170	230
5.5	0.4	190	250

3) Chemical results

Finally, in order to interpret the T_1 relaxation time vs. hydration time, the samples "a" were analysed chemically with A.A. (Table III), whereas the clinker of the samples group "b" was analysed with the help of XRF (Table IV).

TABLE III: Atomic Absorption Chemical Analysis of Samples Group "a"

	No 1	No 2	No 3	No 4	No 5	No 6
Gypsum*	2.7%	3.5%	4.4%	4.6%	5.3%	5.5%
SiO2	21.68	20.32	21.60	19.64	21.82	21.44
Al2O3	5.81	7.18	6.20	6.57	6.30	6.43
Fe2O3	0.27	0.19	0.24	0.27	0.25	0.29
CaO	65.34	65.58	65.72	65.56	64.63	65.07
MgO	0.82	0.71	0.69	0.89	0.86	0.89
SO3	2.94	2.94	2.74	2.67	2.56	2.65
K2O	0.56	0.44	0.24	0.21	0.10	0.13
Na2O	0.04	0.08	0.04	0.07	0.05	0.05
Free CaO	1.09	1.43	1.63	3.34	2.52	1.59
C3S	48.99	49.83	46.94	51.90	37.04	44.31
C2S	25.19	20.67	26.51	17.16	34.62	28.04
C3A	14.94	18.71	16.02	16.95	16.27	16.55
C4AF	0.82	0.58	0.73	0.82	0.76	0.88

* (Gypsum percentage is included in total SO_3 which is shown in row 8)

TABLE IV: XRF Chemical Analysis of the Clinker from Samples Group "b"

SiO2	Al2O3	Fe2O3	CaO	MgO	K2O	SO3
23.16	5.96	0.23	68.28	1.17	0.18	0.82
Free CaO	C3S	C2S	C3A	C4AF	--	--
0.50	61.58	19.94	15.40	0.70	--	--

IV. DISCUSSION.

In order to understand and clarify the results of the samples of group "a", we proceed our discussion with the explanation of the results of the samples of group "b", where the only changing parameter is the gypsum percentage.

The time evolution of T_1 of the clinker (gypsum % = 0.0) belonging to group "b" is shown in fig. 3. The corresponding curves for the whole group "b" are shown in fig. 2. In all cases, we observe that T_1 is almost constant during the early hydration time (the initial rapid hydration of the first few minutes is impossible to follow), rapidly decreases during the period when the compressive and flexural strength starts to increase, and finally splits into two components. These two components (T_{1s}~1.5 μsec, T_{1l}~10 μsec) are associated with water in pores [5, 7].

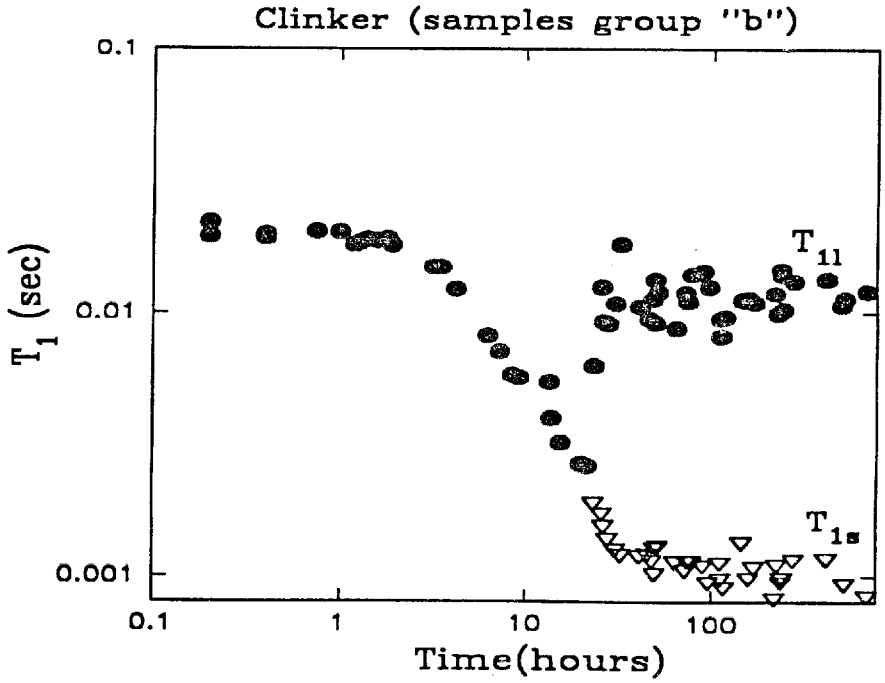

Fig. 3: White Cement Clinker from group "b".

G. Best et. al.[7] recently reported, that water protons in cement pores could be separated into three different groups according to spin-lattice relaxation times: T_{1a} = 1.8 μsec (corresponding to micropores with a percentage = 22%), T_{1b} = 9.5 μsec (corresponding to medium-size pores with a percentage = 42%), and T_{1c} = 50μsec (corresponding to macropores with a percentage = 36%). The above is explained by a trimodal pore size distribution. In contrast to other methods (mercury porosimetry, nitrogen adsorption, SANS, e.t.c), NMR has exactly the ability to measure continuously macropores with a diameter >1μm in wet samples, which are correlated to the flexural-strength weakness of cement [8]. Within a given pore there is a fast exchange between water molecules in the bulk and on the surface of the pore [5], so that,

$$T_1^{-1} = n(T_{1surf})^{-1} + (1-n)(T_{1bulk})^{-1} \quad (1)$$

T_{1bulk} belongs to the free water and T_{1surf} to the water bonded on the pore surface. Since $T_{1bulk} >> T_{1surf}$ we conclude that

$$T_1^{-1} = n(T_{1surf})^{-1} \quad \sim r^{-1} \qquad (2)$$

where n is the percentage of surface water molecules which is proportional to the surface to volume ratio S/V of the pore, and r is the average radius of the pore. In the advanced stages of cement hydration we have an almost continuous T_1 distribution which reflects the pore-size distribution. In reality, at late stages of hydration the porous structure of the cement seems to be a fractal object [5, 9].

We approximated the T_1 distribution with two components for the following reasons:

i) Water in micropores <100 nm corresponding to gel porosity[7] has, due to fast exchange [5], the same T_1 as the gel which means that there should be a strong short T_1 component corresponding to both gel and gel-micropores. ii) The "long" component which corresponds to large voids was omitted due to a low signal-to-noise ratio.

In contrast to ref. [8] where all three components (T_{1a}, T_{1b}, T_{1c}) were constant as a function of hydration time, we observe that in our case the shorter component, attributed to micropores, decreases almost steadily. This should be explained by the existence of an effective T_1 corresponding, according to relation 2, to a steady shift of the pore-size distribution to smaller values. Indeed, this is in agreement with ref. [7] where mainly the macropore and micropore percentages change drastically (decreases, increases respectively). Since strength development is related to the pore-size distribution, the T_1 measurements offer a powerful tool in estimating strength non destructively. We observe that:,

1) The setting time (Table II) corresponds to the initial period, where T_1 remains almost constant and the cement paste maintains it's workability. Cement samples with an increasing gypsum percentage have a longer initial T_1 plateau which corresponds to a longer final setting time. The strange T_1 behaviour of the sample with gypsum percentage 2.7% is accompanied with a reduction of the setting time and could be attributed to false setting. The observed small discrepancies should be attributed to the high sensitivity of the NMR method, which is able to follow details impossible to follow with the conventional setting time measurements.

2) The initial T_1 values seem to be proportional to the gypsum concentration. Since clinker was the same for all the samples, this behaviour could be attributed to the different amounts of created enttringite that prevents the fast hydration of C_3A.

3) Lower T_{1s} values correspond to higher strength development. Indeed, from Table I we observe that clinker's strength in early times is by far lower than the corresponding strength of samples with gypsum percentages between 4-5%. However, these strength values become after 28 days comparable. This is in agreement with the T_{1s} measurements (Fig. 2), where the T_{1s} values of the clinker are, between 10 and 30 hours, sufficiently higher (lower strength) than the T_{1s} values of the samples with gypsum concentration between 4-5%. Similarly with the strength measurements, these T_{1s} values become comparable at the later stages of the hydration. In addition, samples with a gypsum percentage lower than 4% have higher T_{1s} values (lower strength) which is in good agreement with Table I.

Taking the above into consideration we return in Fig. 1 which shows T_1 vs. hydration time results for samples "a". Here we observe remarkable differences in the T_1 behaviour, in comparison to the "b" group of samples, which can be summarised as follows:

1) The initial T_1 values are not increasing with increasing gypsum percentage, as in samples "b".

2) The setting time, estimated from the T_1 curves, as a function of the gypsum percentage does not behave similar to the "b" samples, but seems to be mainly influenced by the SO_3 content of the clinker (Fig. 4).

3) All samples of the "a" group exhibit considerably higher T_{1s} values - and thus lower strength - as compared to the "b" samples. One reason might be that the pore size distribution is, according to relation (2), shifted to larger pore-sizes. This could be assigned to the lower C_3S content of samples "a" in comparison to samples "b", as shown by the Atomic Absorption and XRF results of Tables III and IV.

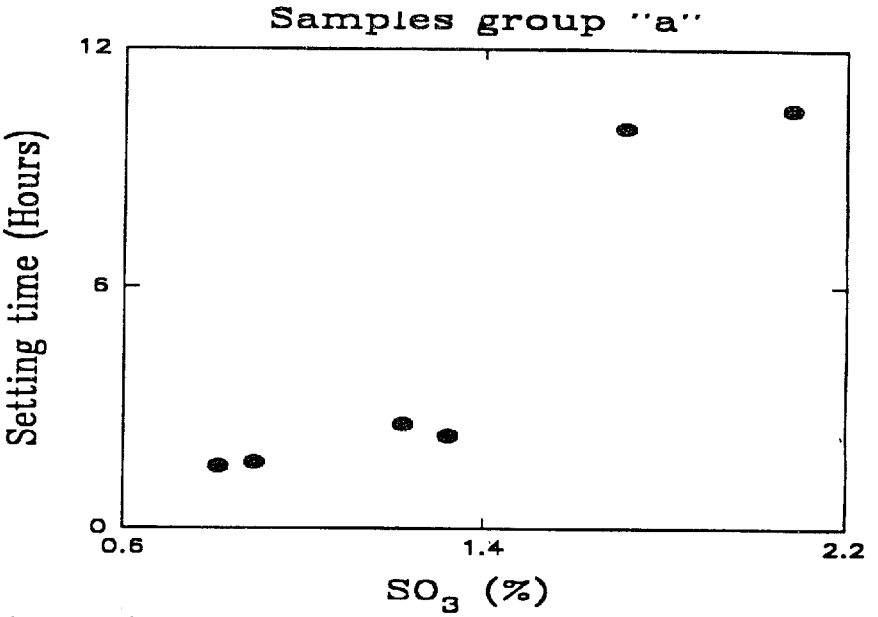

Fig. 4: Setting time as a function of the clinker SO_3 percentage. The total SO_3 content is, for all the samples, almost the same (see Table III).

ACKNOWLEDGEMENTS

This work was supported by a NATO-SFS Grant.

REFERENCES

1. W. Lerch, "The Influence of Gypsum on the Hydration and Properties of Portland Cement Pastes", Proceed. Am. Soc. Test. Mater. 1946, **46**, 1252 .

2. I. Jelenic, A. Panovic, R. Halle, and T. Gacesa, "Effect of Gypsum on the Hydration and Strength Development of Commercial Portland Cements Containing Alkali Sulphates", Cem. Concr. Res., 1977, **7**, 239 .

3. D. D. Lasic, M. M. Pintar, and R. Blinc, "Are Proton NMR Observations Supportive of the Osmotic Model of Cement Hydration?", Philos. Magaz. Lett., 1988, **58**, 227.

4. L. J. Schreiner, J. Mactavish, L. Miljkovic, M. M. Pintar, R. Blinc, G. Lahajnar, D. Lasic, and L. W. Reeves, "NMR Lineshape Spin-Lattice Relaxation Correlation Study of Portland Cement Hydration", J. Am. Ceram. Soc., 1985, **68**, 10.

5. L. Barbic, I. Kocuvan, R. Blinc, G. Lahajnar, P. Merljak, and I. Zupancic, "The Determination of Surface Development in Cement Pastes by Nuclear Magnetic Resonance", J. Am. Ceram. soc., 1982, **65**, 25.; R. Blinc, J. Dolincek, G. Lahajnar, A. Sepe, I. Zupancic, S. Zumer, F. Milia, and M. M. Pintar, "Spin-Lattice Relaxation of Water in Cement Gels", Z. Naturforsch., 1988, **43a**, 1026.

6. F. Milia and Y. Bakopoulos, "Surface Induced Spin-Lattice Relaxation of Water in Tricalcium Silicate Gels", Z. Naturforch., 1991, **46a**, 697.

7. G. Best, A. Cross, H. Peemoeller, M. M. Pintar, "Distribution of Pore Sizes in Hydrating Cement by Modelling of the Proton NMR Relaxation", to be published.

8. J. P. Birchall, A. J. Howard and K. Kindall, "Flexural Strength and Porosity of Cements", Nature, 1981, **289**, 388.

9. A. J. Allen and P. Schofield in "Scaling Phenomena in Disordered Systems", eds. R. Pynn and A. Skjaltorp, NATO ASI. 1985. **B133**. 189. Plenum Press. New York.

HYDRATION AND PERFORMANCE OF CEMENTS WITH VARIOUS AMOUNTS AND FORMS OF ADDED SULFATE

F J Tang and S W Tresouthick

Construction Technology Laboratories, Inc
Skokie, Illinois, USA

SUMMARY

Low- and high-alkali cements containing various levels of sulfate were prepared in the laboratory from a Type I clinker by intergrinding with an appropriate sulfate source that included gypsum, calcium langbeinite, and aphthitalite. The cements were hydrated at 23°C, and the amount of aluminate consumed up to 24 hours of hydration was determined using a quantitative X-ray diffraction method. Strength and expansive properties of mortars prepared with these cements were also determined using ASTM standard test methods. It was found that the rate of aluminate consumption during the first hour of cement hydration was about the same for all the cement intergrinds. At 24 hours, however, aluminate hydration in high-alkali cements was roughly twice that found in low-alkali cements. To counteract this effect, higher amounts of gypsum were required. Better control of the aluminate hydration up to 24 hours generally resulted in higher 28-day strengths. High-alkali cements showed tolerance for higher gypsum additions without exhibiting excessive expansion. No single optimum SO_3 level for strength development was evident in this present study; instead, the data seem to suggest that it can vary depending on curing time.

SINOPSIS

Se prepararon en el laboratorio con un clinker Tipo I, cementos poco y altamente alcalinos, conteniendo diferentes cantidades de sulfato, intermoliendos con sulfatos apropiados que incluyeron cal, langbeinite y aphthitalite de calcio. Los cementos se hidrataron a 23 grados centígrados y se determinó la cantidad de hidratación consumida a las 24 horas por el método de difracción cuantitativa de rayos X. Asimismo, se determinó la resistencia y las propiedades expansivas de morteros preparados con estos cementos usando los métodos de prueba estandard de ASTM. Se encontró que el cambio en el consumo de aluminato durante la primera hora de hidratación del cemento fué aproximadamente el mismo en todos los cementos intermolidos. Sin embargo, a las 24 horas, la hidratación del aluminato en los cementos altamente alcalínos fué de aproximadamente el doble que en los cementos poco alcalinos. Para contrarestar este efecto, se requirió de mayores cantidades de cal. Un mejor control de la hidratación del aluminato a las 24 horas, se obtuvo generalment con resistencias mayores a los 28 días. Los cementos altamente alcalinos mostraron mayor tolerancia a la adición de cal no exhibiendo expansión excesiva. El nivel óptimo de SO_3 para el desarrollo de resistencia no fué evidente en el presente estudio; de hecho, los resultados parecen sugerir que este varía dependiendo del tiempo de curado.

INTRODUCTION

One major observation reported in our earlier paper [1] on the influence of sulfate source on hydration and properties of cement paste in cement interblends was the vast difference in cement behavior between intergrinding and blending gypsum. The interground cement not only gave overall better paste properties, but also showed lower aluminate hydration rate up to 24 hours, similar to the observation of Osbaeck and Jons [2]. This present study was undertaken to resolve inconsistencies in some test results obtained from different methods of cement preparation and help provide a truer picture of commercial cement hydration.

EXPERIMENTAL

Cement Preparation

Cements were made by intergrinding mixtures of low alkali, low sulfate Type I plant clinker (Table 1) and sulfate-containing compound in a heated steel ball mill. Mill temperatures were similar to those found in commercial finish mills.

Table 1: High C_3A Clinker Analysis (Mass %)

Oxide Analysis		Potential Compound Composition*	
SiO_2	21.38		
Al_2O_3	6.12	C_3S	59.9
Fe_2O_3	2.44	C_2S	17.6
CaO	67.25	C_3A	12.1
SO_3	0.02	C_4AF	7.4
MgO	1.14		
K_2O	0.22	Free CaO = 0.7% (Determined by modified Franke method)	
Na_2O	0.12		
TiO_2	0.26		
P_2O_5	0.11	Residue after salicylic acid-methanol extraction = 19.10%	

*Standard "Bogue" formulae (as in ASTM C 150)

Two sets of cements were produced: low alkali cements made with only added gypsum, and those containing either calcium langbeinite ($2CaSO_4 \cdot K_2SO_4$) or aphthitalite [$K_3Na(SO_4)_2$] which will be referred to as "high alkali cements." For each set of cements, several levels of sulfate were added in the form of gypsum to cover a wide range of compositions (Table 2). The cements were ground to cement fineness of approximately 3800 cm^2/g (Blaine), typical of most U.S. Type I cements. Sieve analysis performed on two low alkali cements containing 3% and 5% SO_3 showed them to have very similar amounts retained on the 325 mesh and 10 micron sieves.

Hydration of Cements

Cements were hydrated and the rates of C_3A and C_4AF hydration determined as already reported [1]. Testing was expanded to include conduction calorimetry study at 23°C in a Wexham calorimeter for cement pastes hydrated at a w/c = 0.50.

Physical Testing

Cements were tested for mortar flow and compressive strength at fixed w/c ratio by ASTM C 109, and mortar bar expansion by ASTM C 1038.

TEST RESULTS AND DISCUSSION

Rate of Aluminate Hydration

The amounts of C_3A and C_4AF consumed during hydration up to 24 hours are given in Table 3. The low hydration rates shown in the table during the first hour of hydration clearly indicate the

Table 2: Cement Intergrind Composition

Cement Code	Sulfate Source Used	Mill Temp. (°C)	Cement Total SO_3 %	Total Alkalies as Na_2O
IG-1	Gypsum	100	2.0	0.3
IG-2	Gypsum	45	3.0	0.3
IG-2A	Gypsum	100	3.0	0.3
IG-2B	Gypsum	110	3.0	0.3
IG-3	Gypsum	100	4.0	0.3
IG-4	Gypsum	100	5.0	0.3
IG-5	Calcium Langbeinite	100	3.0	1.0
IG-5A	Calcium Langbeinite	110	3.0	1.0
IG-6	Calcium Langbeinite/ Gypsum	100	4.0	1.0
IG-7	Calcium Langbeinite/ Gypsum	100	5.0	1.0
IG-8	Calcium Langbeinite/ Gypsum	100	6.0	1.0
IG-9	Gypsum/Aphthitalite	100	3.0	1.1
IG-10	Gypsum/Aphthitalite	100	4.0	1.1
IG-11	Gypsum/Aphthitalite	100	5.0	1.1
IG-12	Gypsum/Aphthitalite	100	6.0	1.1

effectiveness of intergrinding in controlling early aluminate hydration reaction. These rates are substantially lower than those reported in our previous paper[1] on similar cements made by interblending separately finely ground clinker and sulfate compounds. Rates obtained at 24 hours are similar to those reported by Osbaeck and Jons [2]. One explanation for the aluminate control effectiveness of interground sulfate may be better physical distribution providing a more rapid supply of Ca^{2+} and SO_4^{2-} to the hydrating aluminate surfaces.

Cements IG-2 and IG-2B show the effect of milling temperature on aluminate hydration rates. The latter cement contained almost three times as much hemihydrate as measured by DTA. There is very little difference between the hydration rate of the two cements, suggesting that gypsum is as effective as hemihydrate provided it is interground.

Table 3: Percentages of C_3A and C_4AF Consumed during Hydration

Hydration Time	2-Min.		5-Min.		12-Min.		30-Min.		60-Min.		24-Hours	
Cement Paste	C_3A	C_4AF	C_3A	C_4AF	C_3A	C_4AF	C_3A	C_4AF	C_3A	C_4AF	C_3A	C_4AF
IG-2	3	0	3	0	3	0	4	0	4	0	20	3
IG-2B	4	3	5	6	6	4	6	4	6	6	13	13
IG-5A	2	0	2	0	3	0	3	0	3	0	51	23
IG-9	2	0	4	1	4	0	4	0	5	0	36	16
IG-1	-	-	-	-	-	-	-	-	-	-	48	19
IG-3	-	-	-	-	-	-	-	-	-	-	14	0
IG-4	-	-	-	-	-	-	-	-	-	-	10	0
IG-6	-	-	-	-	-	-	-	-	-	-	22	9
IG-7	-	-	-	-	-	-	-	-	-	-	18	15
IG-8	-	-	-	-	-	-	-	-	-	-	14	13
IG-10	-	-	-	-	-	-	-	-	-	-	28	27
IG-11	-	-	-	-	-	-	-	-	-	-	19	22
IG-12	-	-	-	-	-	-	-	-	-	-	15	6

Note: Typical standard deviations are 1% for C_3A and 3% for C_4AF

Rates of aluminate hydration in both high alkali cements (IG-5A, IG-9) are virtually the same as their low alkali cement counterparts (IG-2, IG-2B) during the first hour of hydration. This is true even with the cement made with just added calcium langbeinite. At 24 hours, however, the hydrated amounts of both C_3A and C_4AF are about twice as much for the high alkali cements as those found in low alkali cements. For high alkali cements to obtain aluminate hydration rates at 24 hours comparable to low alkali cements, higher gypsum addition was needed, as in IG-7, IG-8, IG-11, and IG-12 cements.

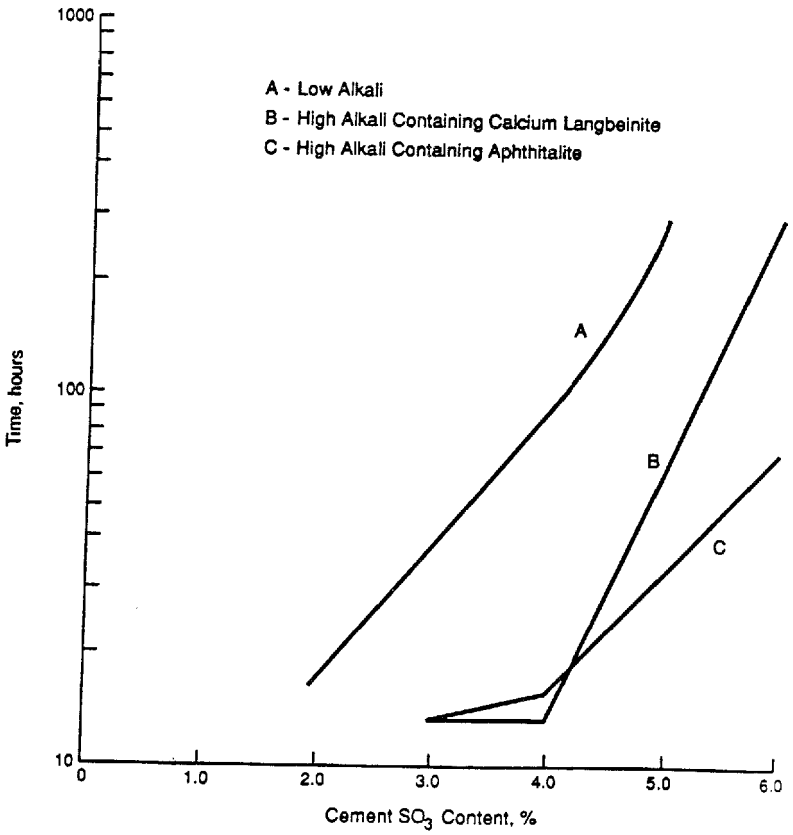

Figure 1: Cement SO_3 Content vs Time of C_3A Renewed Hydration

Conduction Calorimetry Data

Results of calorimetry runs at 23°C of all cements hydrated at w/c = 0.50 are shown in Table 4.

Each cement gave a typical heat of hydration curve consisting of heat peaks associated with the C_3S acceleratory hydration reaction, and C_3A renewed hydration reaction.

The data clearly indicate the profound effect of cement sulfate content on the hydration of C_3A. An almost linear plot obtained on a semi-log scale of sulfate content versus C_3A renewed hydration, shown in Figure 1, illustrates this effect. Unlike the low alkali cements whose plot consists only of a single sloped line, the high alkali cements gave a plot that contained a flat portion extending up to the 4 percent SO_3 level. This extra sulfate seems needed to overcome the accelerating effect of alkalies on C_3A hydration.

Table 4: Conduction Calorimetry Data

Paste Mixed at W/C = 0.50, 23°C

Cement Code	Sulfate Source	Cement SO3 Level, %	Peak Location (Hours)	
			C_3S Peak	C_3A Peak
IG-1	Gypsum	2.0	8.9	16.1
IG-2A	Gypsum	3.0	9.7	41.1
IG-3	Gypsum	4.0	9.7	88.9
IG-4	Gypsum	5.0	9.7	308.9
IG-5	Cal. Langbeinite	3.0	6.7	12.8
IG-6	Cal. Langbeinite/Gypsum	4.0	8.1	12.9
IG-7	Cal. Langbeinite/Gypsum	5.0	7.8	65.0
IG-8	Cal., Langbeinite/Gypsum	6.0	7.8	280.0
IG-9	Gypsum/Aphthitalite	3.0	7.8	12.8
IG-10	Gypsum/Aphthitalite	4.0	7.8	15.6
IG-11	Gypsum/Aphthitalite	5.0	7.8	37.0
IG-12	Gypsum/Aphthitalite	6.0	7.8	63.0

C_3S heat peak location for cements containing about 3% SO_3 level and higher was virtually unchanged, occurring at about 10 hours for low alkali cements and roughly two hours sooner for the high alkali cements. The latter may explain the often reported short setting times and early strength development of high alkali cements.

Table 5: Amount of C_3A Hydrated at Approximate Time of C_3A Renewed Hydration

Cement Paste Code	Cement SO_3 Level, %	Time of C_3A Renewed Hydration	Percent C_3A Hydrated
IG-1	2.0	17 Hours	44
IG-2B	3.0	42 Hours	63
IG-3	4.0	89 Hours	70
IG-4	5.0	309 Hours	78

Quantitative analysis by XRD was conducted on samples of paste prepared from low-alkali cements (IG-1, IG-2A, IG-3, and IG-4) at the moment of C_3A renewed hydration. Results are presented in Table 5. The data show that C_3A continues to hydrate at an appreciable rate despite the presence of large amounts of gypsum in the cement. In cement paste having the highest gypsum addition (IG-4), the disappearance of gypsum was noted approximately 10 days prior to the occurrence of the third heat peak (C_3A renewed hydration). At the emergence of the third heat peak, neither AFt nor AFm phase was detected in any of the four cement pastes; instead a broad line at 8.8 - 8.0 Å normally associated with the C_4AH_{19} - $C_4A\bar{S}H_{12}$ solid-solution series[3] was observed. Its presence, particularly in Cement IG-4 paste, is interesting since there is enough gypsum in the cement to form $C_4A\bar{S}H_{12}$ from the estimated amount of C_3A. This suggests that sulfate is also being used up in reactions other than just hydration of C_3A and C_4AF: incorporation into the calcium silicate hydrate may be one of them [4,5].

Mortar Flow and Strength

ASTM C 109 mortar test results are given in Table 6. For low-alkali cements, the flow decreased as cement sulfate level increased. This reduction appears to be directly related to the increasing hemihydrate content of the cement resulting from dehydration of gypsum during grinding. The strength results seem to indicate at least two optimum sulfate levels: one sulfate level for early ages and another one for 28 days. Lower sulfate levels tend to promote higher 1-day strength while higher sulfate levels seem to favor 28-day strength.

Table 6: ASTM C 109 Mortar Test

Cement Code	Sulfate Source	Cement SO_3 Level, %		Compressive Strength, psi			
			Flow	1d	3d	7d	28d
IG-1	Gypsum	2.0	110	1650	3670	5160	7000
IG-2A	Gypsum	3.0	109	1370	3920	5840	6610
IG-3	Gypsum	4.0	103	1300	3490	5810	7450
IG-4	Gypsum	5.0	93	1210	2580	3670	7340
IG-5	Calcium Langbeinite	3.0	108	2720	4070	4680	5500
IG-6	Cal. Lang./Gypsum	4.0	110	2560	4260	4910	5590
IG-7	Cal. Lang./Gypsum	5.0	95	1720	3900	4980	5880
IG-8	Cal. Lang./Gypsum	6.0	101	1730	2890	3850	5970
IG-9	Aphthitalite/Gypsum	3.0	102	2630	3960	4450	5220
IG-10	Aphthitalite/Gypsum	4.0	103	2140	4240	4890	5490
IG-11	Aphthitalite/Gypsum	5.0	103	1480	2800	4350	6160
IG-12	Aphthitalite/Gypsum	6.0	104	1470	2410	3140	5610

The high alkali cements containing calcium langbeinite gave very similar flow to their low-alkali cement counterparts confirming calcium langbeinite's effectiveness as a set-control agent. It is also notable that in spite of its large amounts (5.5%) in the IG-5 cement, flow was not adversely affected as might be expected due to rapid syngenite and gypsum crystallization. XRD qualitative analysis of paste made from the same

cement showed a slow conversion of calcium langbeinite to syngenite and gypsum which may help explain its relatively high flow. Calcium langbeinite was detected in the paste as late as 60 minutes.

Consistent with the calorimetry data, the positive effect of alkalies on early strength is demonstrated in the very high one-day strengths of cements containing either calcium langbeinite or aphthitalite. At 28 days, however, the mortar strengths of high alkali cements were always lower compared with that of low-alkali cements. Additional sulfate, added as gypsum, caused some reduction of early strength, but it had a definite improvement at 28 days. These are consistent with earlier observations of Lerch [6] and also later by Osbaeck and Jons [2].

Correlation with Rate of Hydration of Aluminate

Mortar strength at 28 days and the amount of C_3A hydrated at 24 hours were plotted for all cements (See Figure 2). The plot clearly shows an inverse correlation between 28-day mortar strength and amount of

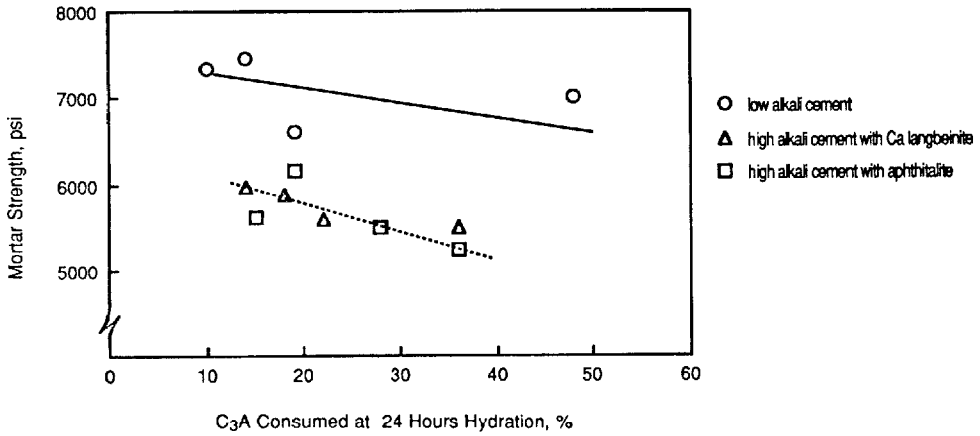

Figure 2: 28-day Mortar Strength vs C_3A Hydration

C_3A hydrated at 24 hours. Low and high alkali cements lie on distinctly different lines. The plot for low alkali cements was always found above that of the high alkali cements, indicating their higher strengths at 28 days.

Mortar Bar Expansion

Results of the mortar bar expansion test in accordance with ASTM C 1038 are given in Table 7. The table also includes additional measurements obtained at 28 days. The results clearly show that expansion is directly related to the sulfate content of the cement, and the maximum safe limit appeared to be influenced by the alkalies in the cement. For low-alkali cements, 4% SO_3 level seemed to be the limit; for high alkali

Table 7: Mortar Bar Expansion (ASTM C 1038)

Cement Code	Cement SO_3 Level, %	% Linear Expansion	
		14 Days	28 Days
IG-1	2.0	0.006	0.003
IG-2A	3.0	0.002	0.001
IG-3	4.0	0.015	0.013
IG-4	5.0	(0.042)	(0.038)
IG-5	3.0	0.007	0.005
IG-6	4.0	0.005	0.004
IG-7	5.0	0.020	0.017
IG-8	6.0	(0.073)	(0.071)
IG-9	3.0	0.005	0.007
IG-10	4.0	0.004	0.004
IG-11	5.0	(0.025)	(0.024)
IG-12	6.0	(0.109)	(0.113)

Note: Bracketed values denote expansion exceeding the ASTM C 150 limit.

cements, slightly more SO_3 was tolerated. The reason for this apparent tolerance for higher sulfate in high-alkali cement may be related to the accelerated hydration of C_3A resulting in faster consumption of sulfate and thus also hastening the conversion process from AFt to aluminate solid solution series. The additional expansion measurements taken at 28 days generally showed slightly lower values than those at 14 days prescribed by the test. This means most of the aluminate expansive reaction probably had already been completed by 14 days.

CONCLUSIONS

Aluminate hydration rates in interground cements during the first 24 hours of cement hydration are roughly two times lower than those found in cement interblends(1). By intergrinding gypsum, all cements have virtually the same initial rate of aluminate hydration up to 1 hour regardless of alkali content. However, at 24 hours, the high alkali cements have rates approximately twice as much as their low alkali cement counterparts. To obtain comparable hydration rates, high alkali cements need higher amounts of gypsum addition. The low alkali cements have better strength performance at 28 days than high alkali cements, but 1-day strengths are much higher for the latter cements. High alkali cements seem to be able to tolerate more sulfate without causing excessive expansion, and this higher sulfate addition also improves their 28-day strengths. The data obtained in this study are generally consistent with our conceptual model of a stronger cement paste structure resulting from hydration of C_3S with minimal interference from C_3A hydration achieved by intergrinding the sulfate source with the clinker.

REFERENCES

1. Tang, F.J. and Gartner, E.M. Influence of Sulfate Source on Portland Cement Hydration. Advances in Cement Research. Vol. 1, No. 2, April, 1988.

2. Osbaeck, B. and Jons, E.S. The Influence of the Content and Distribution of Alkalies on the Hydration Properties of Portland Cement. Proceedings of the Seventh International Congress on the Chemistry of Cement, Paris, 1980. Paris, Edition Septima, 1980. Vol. II pp. 135-40.

3. Roberts, M.H. Calcium Aluminate Hydrates and Related Basic Salt Solid Solutions. Proceedings of the Fifth International Congress on the Chemistry of Cement, Tokyo, 1968 Part II, Vol. II pp. 104-117.

4. Copeland, L.E., Bodor, E., Chang, T.N., and Weise, C.H. Reactions of Tobermorite Gel with Aluminates, Ferrites, and Sulfates. J. Res. Dev. Lab., Portland Cement Association 9 (1), 1967, pp. 61-74, PCA Res. Bull. 211.

5. Kalousek, G. L. Analyzing SO_3-Bearing Phases in Hydrating Cements. Materials Research and Standards, June, 1965, pp. 292-304.

6. Lerch, W. The Influence of Gypsum on the Hydration and Properties of Portland Cement Pastes. Proceedings ASTM 46. pp. 1252-1291, 1946.

ACKNOWLEDGMENTS

The research reported in this paper was conducted at Construction Technology Laboratories, Inc., with the sponsorship of the Portland Cement Association (PCA Index No. 90-9) under CTL Project H40007. The contents of this paper reflect the views of the authors, who are responsible for the facts and accuracy of the data presented. The contents do not necessarily reflect the views of the Portland Cement Association.

STRUCTURE FORMATION IN THE HARDENING STONE OF MULTI COMPONENT CEMENTS

Z B Entin, Yu R Krivoborodov and V I Shubin

NIICement, Moscow, RUSSIA

SUMMARY

The paper present a study of hydration processes occured in finely ground multicomponent cements (FGMCC). The composition of a liquid phase is determined at the age of 10 min. up to 28 days after mixing. CaO concentrations in a liquid phase reaches maximum within 1-24 hours after mixing, thereafter it rapidly decreases. Firstly alkali oxides content drops, but by the age of 28 days it increases again. At all ages of hardening pH of a liquid phase remains at the level of 12.8-13.2, and the basicity of phase is mainly provided by K and Na hydroxides.Preferable concentration of Ca, Na and K ions near surfaces of quarts and ash particles provides unhomogenity of liquid phase pH in microvolumes and, thus, leads the differences in hydration rate of clinker minerals at various areas of hardening cement paste.

INTRODUCTION

Research in recent years has shown that finely ground multicomponent cement (FGMCC) constiture one of the efficient linders. There contain a large amount of active mineral additives or fillers (1,2,3).

The higher specific sugjace of FGMCCs is of particular importance, since the mechanical activation of the grain surface of both clinker and additive during comminution is the principal cause of their imporoved compressive strength and plastifiability.

The transition zone (TZ) between the cement stone and the additive particles plays a special role in determining the structure of FGMCC stone and its strength. The TZ could be thought of as a material layer up to 5 or 7 m thick immediately contacting the additive surface. Considering that the number of additive particles in FGMCCs is comparable to the number of clinker grains, TZs account for 15 to 20% of the total volume of cement stone, including the volume of the clinker and additive particles that have failed to react.

RESULTS AND DISCUSSIONS

Hydration of an additive, even an active one such as blastfurnace slag, is possible only when there is hemisorption, on its surface, of alkali or calcium ions diffusing through the layer of new formations.

Table 1 contains data on the composition of FGCCs aim slag-ash ($N^{O}1$) and slag-sand ($N^{O}2$) and the following components: clinker 45%, slag 10%, fly ash or quartz sand 40%, gypsum 5%. The liquid phase was expressed from the cement paste samples according to a technique a lready reported (4).

As easarly as after one hour hydration, the pH value reached 13.0 in both cement and contins ied to be maintained at that level despite a substantial decrease of the calcium oxide content of the pore solution. At this time, the pH value is susrained mainly by alkali oxides. Considerable fluctuations in the SiO_2 content of the liquid phase are observed, its content being generally antibate to that of CaO.

In slag-sand cement, the SiO_2 content of the liquid phase is higher

and the Al_2O_3 content is lower than the respective values for slag-ash cement.

The sixeable increase in SiO_2 and Al_2O_3 contents of the liquid phase at 28 days hydration accomprenced by a sigficant drop in the centration of CaO, indicates that the processes occurring in the TZ resulting in the hydration of the additive grains continue in this case as well, ions from the alkali oxide becoming the main during factor.

Table 1 Changes in liquid phase composition hydration FGMCC.

Cement specimen	Hydration time	pH	Chemical composition, mg/l					
			SiO_2	Al_2O_3	Fe_2O_3	CaO	SO_3	R_2O ($Na_2O+0.65K_2O$)
N°1	10 min	12.75	8.64	0.35	0.28	842	4,442	9,004
	1 hour	13.00	8.24	0.51	2.20	902	4,034	4,831
	1 day	13.20	5.06	0.40	0.35	466	377	3,385
	28 days	13.20	23.26	13.03	1.08	140	14	4,956
N°2	10 min	12.70	6.14	0.66	0.32	535	4,236	8,050
	1 hour	12.80	47.55	1.57	3.53	449	4,207	4,783
	1 day	13.15	8.00	0.89	0.40	611	109	3,071
	28 days	13.00	117.40	2.80	0.16	124	14	6,019

The growth and compaction of the surface layer due to new formations prevents alkali oxides from penetrating to the yer unreached surface of the additive, thus retarding the hydration process. Hence the internal portion of the additive grain may altogether unhydrated, and from the so-called Yung's microconcrete.

Of particula interest in this respect are data on the chemical composition of the contact zone behocen the cement matriz and the additive. To determine the nature of interaction of quartz, ash and slag grains with the cement matrix during FGMCC hydration the X-ray spectrum microanalysis (XSMA) of the TZ was carried out. By observing the fracture surface of specimens in a scanning electron microscope, areas containing additive particles were selected the XSMA method was used to indentify the material composition at each point along the line passing

through the cement stone and the centre of the additive grain at intervals of 2 to 4 μm (see Fig.1).

The XSMA results of an area for composition 2 FGMCC stone hardened for 28 days indicated a substantial inhomodeneity of TZ. The ratio of CaO to the total of aluminium, ferric, magnesium, sulphur and alkali metal oxides in the area of the cement matrix averages 6.11. In the TZ at the boundary with quartz it rises to 8.53. This is due to the fact that quartz particles play the role of a substratum in portlandite crystallization. On the quartz surface bordering upon portlandite, there are also deposited calcium hydrosulfoaluminates in colloidal form. In this area, a higher concentration of aliminiun and sulphur oxides is observed which causes the ratio of CaO to other oxides to decrease to 4.46. The crystallization of aluminate phases near the surface of quartz grains brings about a change in the ratio of the phases in the areas of the cement matrix enriched with portlandite, but not contiguous to quartz. In these zones, the aluminium oxide content is lower than in the other areas by a factor of 2 to 5.

An essential feature of the area of cement stone adjoining portlandite is that it also contains a ligh concentration of alkalis and ferric oxide in the form of $Fe(OH)_3$.

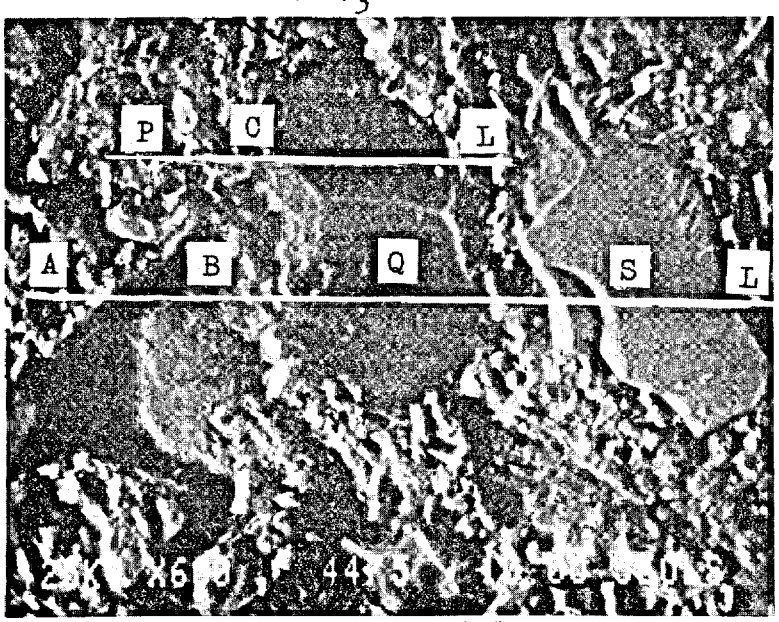

Fig.1 Diagram of an area of hardened FGMCC:
A - Cement matrix area; B - TZ of quartz and cement stone; Q - Quartz grain; S - Slag grain; C - Contact zone of quartz and portlandite field; P - Portlandite field; L - Line along which the XSMA was carried out.

In the TZ of the cement stone and slag particle, no selective crystallization of portlandite occurred.

The concentration of basic oxides corresponds to their content in the cement stone mass, but a greater concentration of alkalis is noted.Alkaki ions migrate towards the active surface of slag particles,whereas quartz particles interact in the first place with calcium ions and portlandite crystals, with which they are in immediate contact.It is here that the formation of low-basity calcium hydrosilicates occurs,thus strenthening the TZ.

The difference in the composition of varios FGMCC TZ areas containing fly ash is even more noteable. The CaO content drops rapidly in the direction from the cement stone towards the ash particle surface.At the same time, the SiO_2 content of the TZ is higher than that on the particle surface proper, and reaches 42 to 43 %. The Al_2O_3 content increases as well. The ash particle surface is depleted of SiO_2 and Al_2O_3, whereas it is enriched in Fe_2O_3. Thus, the TZ accomodates a shell consisting of primary low-basicity calcium hydrosilicate and hydroaluminate.

An enhanced concentration of alkali oxides observable in individual areas of the TZ deserves particular attention. This could be explained by a local build-up of osmotic pressure in TZ microvolumes and the resulting water inflow, a swelling and destraction of the contact layer, which eventually speeding up the hydratation of the additive particles. At the same time, no build-up of osmotic pressure takes place in the cement stone macrovolumes since such microinhomogeneities are distributed with statistical uniformity in the stone volume, in close cicinity of one another.

As a result, instead of osmotic transfer there as an inhibition of migrates of both water and alkali hydroxides, which manifests by an increase in the R_2O content of the liquid phase at the age of 28-days as shown in Table 1. This probably explains the greater resistanse to alkali silica reaches in concreates made of blended cements when a reactive aggregate is foreseen.

Based on the data obtained, an attempt was made to assess the phase composition of the cement stone in the TZ. The following assumptions

were made for the purpose: (i) The sulphur oxide present is fixed into a low-basicity form of hydrosulfoaluminate C_4ASH_{12}; (ii) Aluminium oxide remaining after the formation of C_4ASH_{12} forms hexogonal C_4AH_{13}; (iii) Calcium oxide remaining after the formation of aluminate phases forms hydrosilicates of the CSH or C_2SH type; (iiii)With a CSH basicity of less than 0.8, the formation of a silica gel is possible, in which case the CSH basicity was assumed to be 1.0, and (v) Ferric oxide initially separated in the form if hydroxide $Fe(OH)_3$.

Table 2 shows data on the TZ phase composition for samples of fly-ash cements aged 7 and 28 days respectively.

Table 2. Phase composition of TZ in 7 and 28-day hydrated cements.

	7 days										28 days						
	TZ areas																
Phases	1	2	3	4	5	6	7	8	9	10	1	2	3	4	5	6	7
C_4ASH_{12}	11	8	5	7	9	24	10	7	10	5	6	12	7	6	7	8	11
$C_4AH_{(12-19)}$	42	31	25	32	25	38	46	40	37	58	14	30	37	52	21	24	34
CSH	38	-	-	-	-	5	37	-	30	12	44	30	40	7	36	54	-
C/S	0.72	-	-	-	-	1	1.15	-	1	1	1.5	1	0.9	1.2	1.29		-
Silica gel	-	39	43	34	43	17	-	33	11	10	-	17	-	19	-	-	35
$Al(OH)_3$	-	16	22	6	18	-	-	13	-	-	-	-	-	-	-	-	12
$Fe(OH)_3$	6	3	3	15	2	7	3	3	3	9	14	3	9	5	7	5	4

As is clear from the table, typical of the 7-day age is the presence of low-basicity CSH and silica gel near the ash particles. It is only at the point of contact with crystals that a silicate hydrate with a basicity of of 1.3 to 1.5, and 2,o are observed at the portlandite boundary. But CSH with a basicity of 0.9 to 1.0 remains predominant, and areas represented by hydrogel SiO_2 are preserved as well.

CONCLUSIONS

Hence, the TZ composition in FGMCCs with diverse fillers is, to a great extent, determined by the types and reacting ability of additives.

Hence, this has to be taken into account when forecasting the strength characteristics of such binders.

REFERENCES

1. Kuznetsova T.V., Makashev S.D., Entin Z.B.: "Cements with mineral admictures: State of the aft and prospects". 8th International Congress on the Chemistry of Cement, Rio de Janeiro, Brazil 1986, V1, p 207-210.

2. Shubin V.I., Entin Z.B., Lebedev A.O. : "Problems of the efficient comminution of cements". "Tzement",1988, No. 9 (in Russian).

3. Entin Z.B., Shubin V.I., Nefydova L.S., Rudneva G.A., Fominykh N.S., Lebedev A.O. : "Finely ground multicomponent cements".Transations of NIICement, Proceedings of the 15th All-Union Conference "Fundamentals of enhancing production efficiency and cement quality", Moscow, the USSR, 1990, (in Russian).

4. Dankova M. : "The method of pore water expressing of hardened cementitious materials". Silikaty (Inorganic Matirials), 1988, V.32, No. 3, p 257-264 (in Czech).

STATE OF FORMED MINERAL PHASES AND PROPERTIES OF BINDING SYSTEMS

L G Sudakas

Design and Research Institute of Cement Industry "Giprocement"
St Petersburg, RUSSIA

SUMMARY

In studying the phosphate binding systems it has been established that variations in amorphous/crystalline hardening products ratios from completely amorphous to completely crystalline phases make it possible to change strength characteristics and to find optimal parameters with an increase in strength of 30-50%. On the example of the hydration binding systems it has been shown that variations in the phase formation dynamics in hardening can provide a means of strength raising. The strength of systems with drastic changes in the morphology of new formations in the process of hardening (as with the non-modified systems on the basis of alinite cements) can be considerably improved (by 20-30%) through introduction of additives making the microstructure variations with time smoother.

РЕЗЮМЕ

Установлено, на примере фосфатных вяжущих систем, что изменение соотношения количества аморфных и кристаллических продуктов твердения в пределах от полностью аморфных до полностью кристаллических позволяет изменять прочностные характеристики и находить оптимальные параметры с повышением прочности на 30-50%. Показано, на примере гидратационных вяжущих систем, что средством повышения прочности может являться также изменение динамики фазообразования при твердении. Прочность систем с резкими изменениями в процессе твердения, морфологии новообразований (как у немодифицированных систем на основе алинитовых цементов) может быть существенно на 20-30%, повышена за счёт введения добавок, делающих изменение микроструктуры во времени более плавным.

INTRODUCTION

Various methods of modification of the phase state of the hardening products were used as a means of improving properties of binding systems of different chemical nature in the physicochemical laboratory of the Institute of Giprocement when solving concrete engineering problems. One of the most decisive factors of the phase state is the degree of the crystallochemical order. It is well known that hardening products occurring in traditional binding systems vary from a completely crystalline (e.g. in gypsum materials) to a rather amorphous phase, for example in portland cements.

Since the advent of the "microconcrete" theory of V N Young (1) the concept of combination of crystalline and amorphous structures in the cement stone is used. It is thought to be the best version from the point of view of its strength. One finds suggestions on artificial introduction of crystalline additives such as SiO_2, other foreign crystalline seeds and reinforcing components (2,3) into the hardening compositions. Through modification of the hardening conditions it is possible to vary the degree of the crystallochemical order of the products formed, thus creating the required ratios between the crystalline and amorphous formations. The extreme expression of this idea is "self-reinforcement" after V V Timashev, where the objective was to attain a specified (needle) habitus in a part of the products formed (3).

EXPERIMENTAL

Our studies of relations between ordered and disordered forms of new compounds as a factor of the strength concerned the phosphate binding systems, that are relatively simple in their hardening mechanism. Such systems harden due to the direct acid-base interaction and in this respect can be considered as model ones. These types of hardening compositions (Table 1) have advantages over a purely crystalline or purely amorphous ones.

Table 1. State of phases formed and strength of phosphate binding systems

System	Composition of the main crystalline product	Presence (+) or absence (-) of amorphous new formations	Compressive strength level, MPa
$MgO + H_3PO_4$ *	$MgHPO_4 \cdot 3H_2O$	-	60.0-70.0
$MgFe_2O_4 + H_3PO_4$	$MgHPO_4 \cdot 3H_2O$	+	up to 120.0
$ZnO + H_3PO_4$	Zinc phosphates	-	up to 60.0
$ZnFe_2O_4 + H_3PO_4$	Zinc phosphates	+	up to 200.0
$CuO + H_3PO_4$	$Cu(PO_4) \cdot 3H_2O$	-	up to 80.0
$CuFe_2O_4 + H_3PO_4$	Copper phosphates	+	up to 180.0
$Al(OH)_3 + H_3PO_4$	-	+	up to 50.0

* - a 50%-acid was used in all cases

The quantitative assessment of influence of the crystalline-to--amorphous hardening products ratio was performed for magnesium phosphate ($MgO + H_3PO_4$ + quartz filler) and iron phosphate (iron cinders + + H_3PO_4 + quartz filler) self-hardening molding sands (Fig.1). Variable ratios between the crystalline and amorphous forms of new compounds were achieved with the help of different (concentration and neutralization) methods of mixing agent modification (4). It is seen from Fig.1 that by changing this ratio it is possible to vary the strength of associated systems over a wide range. Optimum ratios between the crystalline and amorphous compounds can be found for each binding system.

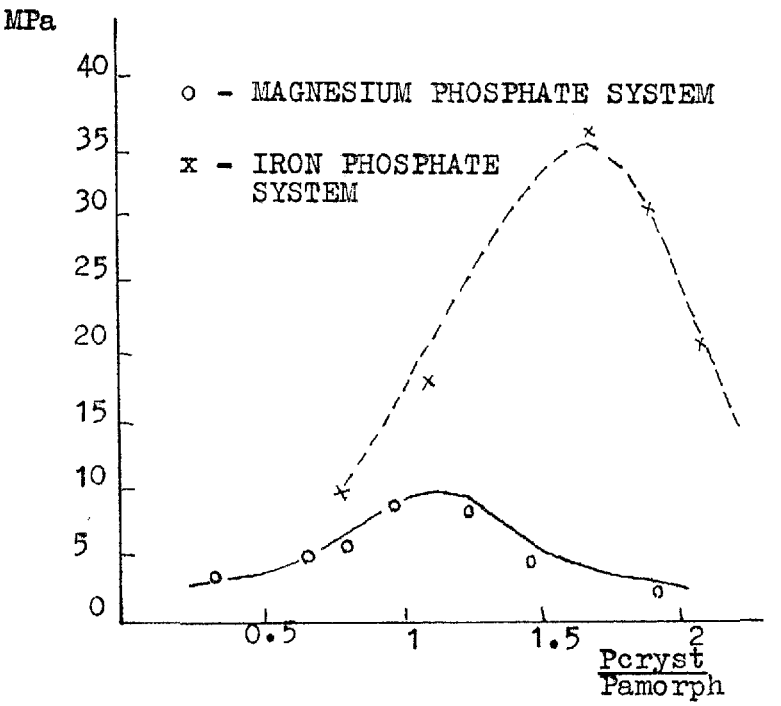

FIG.1 Influence of the crystalline-to--amorphous new compounds ratio on the strength of magnesium phosphate and iron phosphate systems

Through variation of these ratios it is also possible to alter substantially important practical characteristics of hardening systems such as linear and volume deformations. It is well known (5,6) that the positive deformations under hardening can have their origin in the crystallization pressure as one of the main factors. At the same time the amorphous structures possess the ability to relax the strain decreasing the absolute effect. Fig.2 shows the linear deformations for the magnesium phosphate systems as a function of the crystalline-to-amorphous hardening products ratio.

Microstructure of hardening systems is also an integral reflection of the hardening product phase state. Study of hardening of hydraulic cements (alinite and low-lime) obtained by energy-saving technologies shows that control of this factor can contribute to tackling the main problem of these cement types, i.e. to maintain high strength. Alteration of the hardening dynamics was used as a microstructure control means in these cases.

Shown in Fig.3 are photomicrograms illustrating changes in microstructure of a hardening system in alinite cement. In the variant of plain cement (without additives) (Fig.3a) even in the first day occurs mass formation of new morphologically independent phases filling the whole space which we do not observe in the event of the modified (in our case by citric acid compounds) system. In the second case (Fig.3b)

the initial formation of independent phases is suppressed, and the basic structure motives are maintained. Absence of drastic structural changes in the alinite systems hardening results in a higher final strength. In the case referred to, the 28-day strength was 35-37 MPa for the variant without additives and 45 MPa for the modified one. Similar behaviour was observed for other clinker types too (7), when smooth changes in the hardening system microstructure have all advantages over a non-uniform process. Through modification of the system on this principle it has been possible for us to increase the activity of the low-lime cement (KH (LSF) = 0.82; n (silica modulus) = 2.6; p (alumina modulus) = 1.2) from 38-41 MPa to 48-50 MPa.

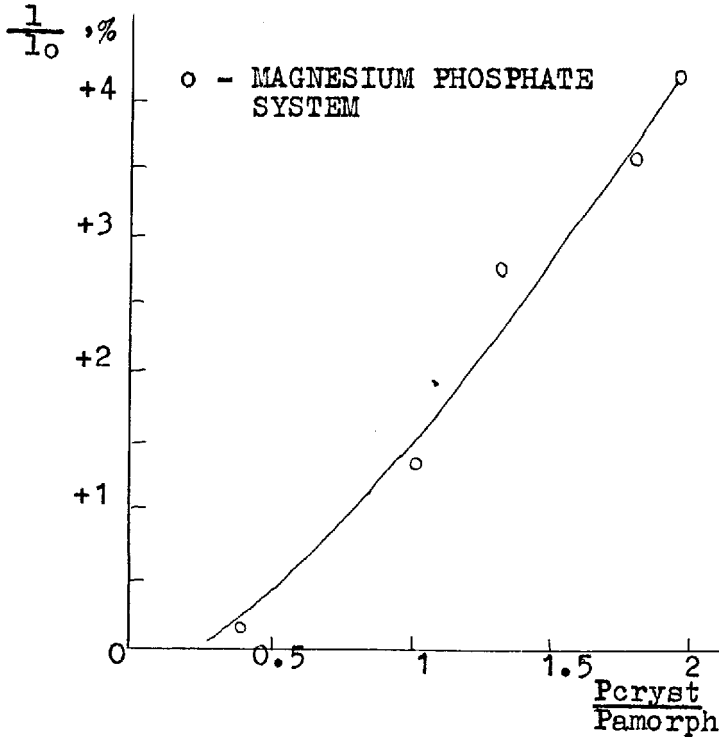

FIG.2 Influence of ratios between crystalline and amorphous new compounds on deformations under hardening of magnesium phosphate binding systems

CONCLUSIONS AND RECOMMENDATIONS

The phase state of the binding system hardening products can be used in practice as an object of the effective control of their properties. Thus both static and dynamic approaches are useful. In the first case the aim of the system modification is to achieve particular crystallochemical and morphological characteristics of new formations in the materials hardened. At the dynamic approach attention is drawn to the nature of variations in the microstructure of the hardening objects with time.

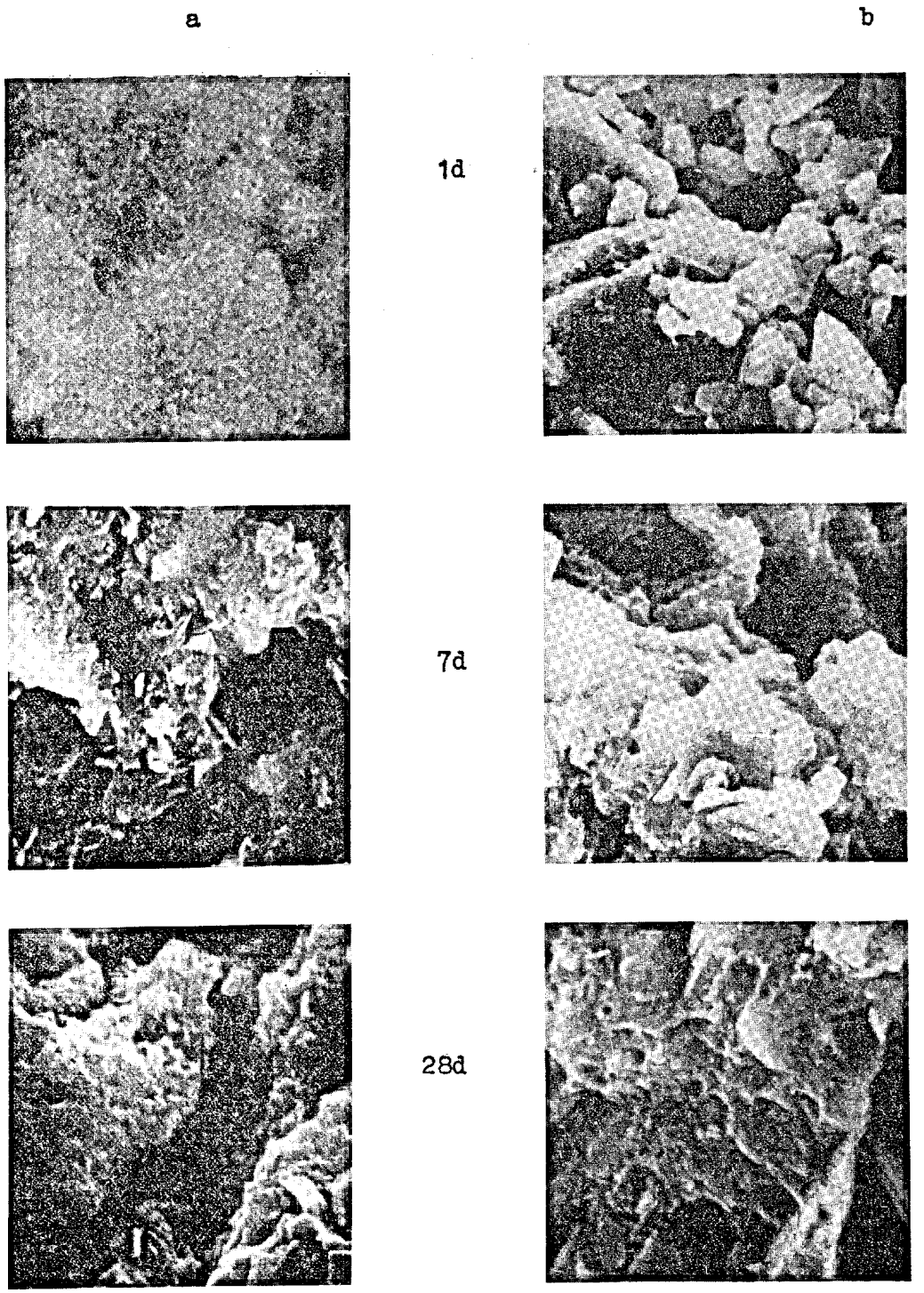

FIG.3 Microstructure of hardening alinite cement:
a - non-modified system; b - modified system

Application of these principles can result in a 20-50% increase in the systems strength, as well as in a drastic change in the deformations under hardening. We have used the static approach with a particular success in the systems with a low content of the binding component - phosphate self-hardening molding sands, and the dynamic approach - for raising the alinite and low-lime cement strength.

ACKNOWLEDGEMENTS

The author would like to record his thanks to L I Turkina, A F Kraplya, A S Tsvang for their assistance in carrying out our works in this direction.

REFERENCES

1. Young, V.N.: "Mikrobeton" ("Microconcrete"), Tsement, 1934, (7), 6-17.

2. Sereda, P.Ya., Feldman, R.F. and Ramachandran, V.: "Obrazovaniye i razvitiye struktury v tverdeyushchikh tsementnykh pastakh". ("Formation and development of structure in hardening cement pastes"). VII-th International Congress on the Chemistry of Cement, Paris, France, 1980, 334-336.

3. Timashev, V.V.:"Sintez i gidratatsiya vyazhushchikh materialov" ("Synthesis and hydration of binding materials"). Moscow, Nauka, 1986, 362p.

4. Sudakas, L.G.: O regulirovanii svoistv fosfatnykh vyazhushchikh sistem (On control of properties of phosphate binding system). Khimiya i tekhnologiya silikatnykh i tugoplavkikh nemetallicheskikh materialov. Leningrad, Nauka, 1989, p 286-297.

5. Kalousek, G.L. and Benton, E.I.: "Mechanism of sea water attack on cement pastes". Journal of the American Concrete Institute, 1970, 67(2), 187-192.

6. Kravchenko, I.V., Kuznetsova, T.V., Vlasova, M.T. & Yudovich, B.E.: Khimiya i tekhnologiya spetsialnykh tsementov (The chemistry and technology of special cements). Moscow, Stroiizdat, 1979, 208p.

7. Kraplya, A.F.: "Vliyaniye gipsa na formirovaniye prochnosti tsementnogo kamnja" ("Influence of gypsum on formation of cement stone strength"). Tsement, 1991,(3-4), 22-26.

RELATIONSHIP BETWEEN STRENGTH AND POROSITY OF FLY ASH CEMENT PASTES

L P Xu and S Y Huang

Shanghai Institute of Building Materials
Shanghai, P R CHINA

SUMMARY

In the present study, porosity and pore size distribution were measured and strength versus porosity relationships were plotted for both fly ash cement and pure portland cement pastes. Strength versus porosity relationship has been found to be different between fly ash cement and pure portland cement pastes. Based on the test results and previous work by Huang Shi-Yuan, a mechanism for the change in strength characteristics and durability of fly ash cement is proposed.

文 摘

本文测定了纯硅酸盐水泥和粉煤灰水泥浆体的孔隙率和孔分布，探讨了强度与孔隙率间的关系。结果发现这两种水泥浆体的强度与孔隙率间的关系是有区别的。根据试验结果和黄士元以前的结果，提出了针对粉煤灰水泥浆体强度和耐久性变化的机理。

INTRODUCTION

As is well known the early strength of fly ash cement is rather low, but its strength at later ages may be as high as, or even may exceed the strength of ordinary portland cement of the same water-cement ratio. This is usually explained by the very low pozzolantic reaction rate of fly ash. However, unlike the hydration reaction of cement clinker, the degree of pozzolanic reaction of fly ash with $Ca(OH)_2$ released by cement hydration, is rather low. It has been reported that the reaction degree of fly ash with $Ca(OH)_2$ is about 2-20% at 7-180 days (1) and that with cement is 8.1% at 7 days and 35.0% at 90 days (2), and thus the decrease in porosity due to the pozzolanic reaction is not so obvious as to cause such a large increase in strength.

In this paper, the relationship between the strength and the porosity and pore structure of fly ash cement pastes are discussed. A comparison with those of ordinary portland cement has also been carried out. A mechanism of strength change of fly ash cement is proposed.

EXPERIMENTAL MATERIALS AND METHODS

Ordinary portland cement and ground fly ash were used in the tests. The fly ash cement consisted of 70% portland cement and 30% ground fly ash. Comparison between fly ash cement pastes and portland cement pastes were always made for the same water-cement ratio. Porosities of pastes were measured by helium pycnometric method and pore size distributions by mercury porosimetry.

TEST RESULTS

Porosities and pore size distributions of fly ash cement and ordinary cement pastes

Tests for comparison of porosities and pore size distributions of fly ash cement and ordinary portland cement pastes were conducted under identical conditions. The results are shown in Fig 1 and Fig 2 respectively.

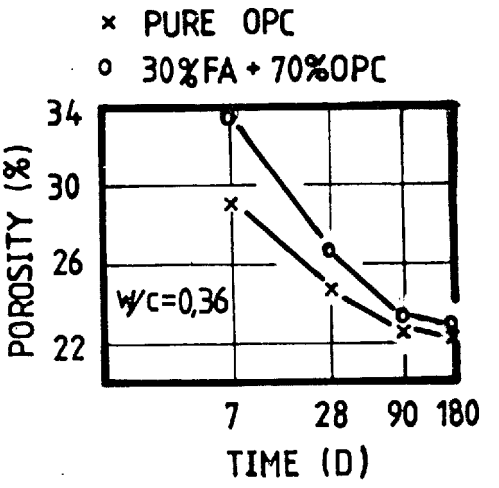

FIG.1 Change in porosity with time in OPC and fly ash cement pastes

From Fig 1 it can be seen that at early ages the porosity of fly ash cement paste is much higher than that of ordinary portland cement paste due to the lesser amount of hydrates formed from the fly ash cement paste. This is because the proportion of portland cement is less in fly ash cement paste, very few pozzolanic reaction products are formed, and only at later ages does the porosity of the fly ash cement paste approach that of portland cement paste, and even then it is still larger than the later.

Pore size distribution results (Fig2) also show that at 28days both the porosity and the pore size of the fly ash cement

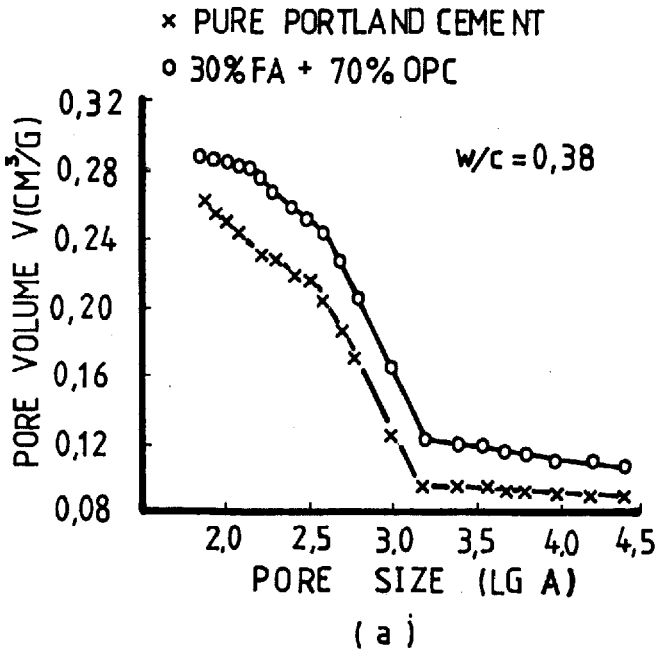

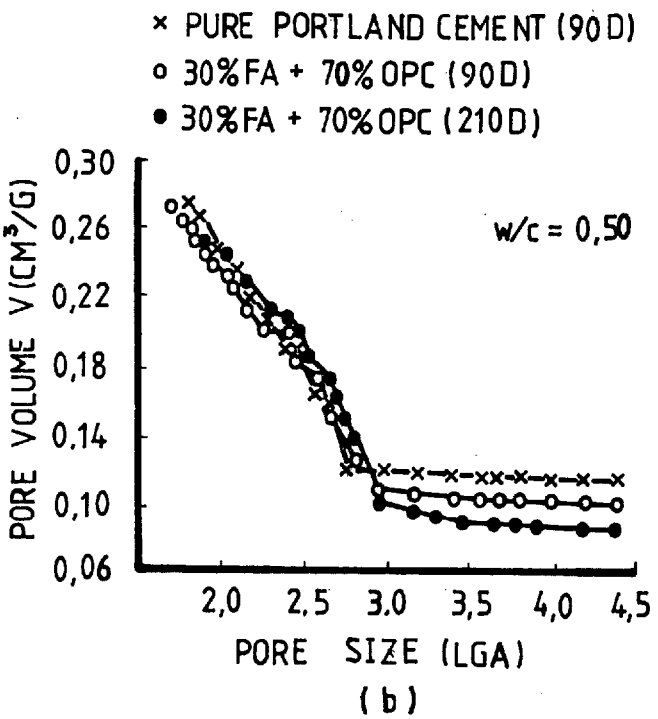

FIG. 2 Comparative pore size distribution of fly ash cement and OPC pastes
(a) 28 DAY (b) 90 DAY and 210 DAY

paste are considerably greater than those of the odinary paste. However,at later ages pores larger than 1000A in the fly ash cement paste are much less than those in the ordinary portland cement paste.

Strength versus porosity for fly ash cement vis-a-vis ordinary cement paste

Correlation of porosity with strength has usually led to semi-emprical equations of the following types:

$$R = R_o (1-P)^A \quad \text{——(1)}$$
$$R = R_o \exp(-BP) \quad \text{——(2)}$$

where R_o is the strength at zero porosity, called instrinsic strength here, P is the porosity and R is the strength at porosity P, A and B are constants.

Test results at different water-cement ratios and different curing ages were plotted in Fig 3 using equation (2). The R_o value obtained by extrapolation and the B value by calculation for both fly ash cement and portland cement pastes are shown in Table 1.

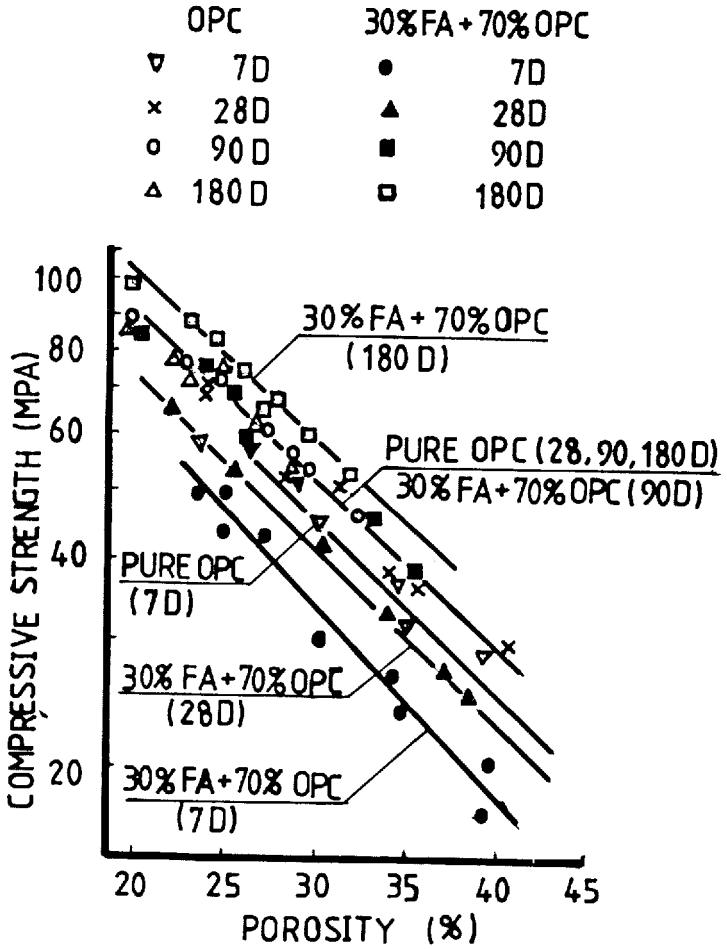

FIG. 3 Strength-porosity relationship of cement and fly ash cement pastes

Table 1. R_c and B values for fly ash cement and pure cement pastes

R_c and B value	Type of cement	curing ages 7d	28d	90d	180d
R_c (MPa)	OPC	266	275	275	275
	FAC	233	240	276	346
B	OPC	5.71	5.48	5.48	5.48
	FAC	6.37	5.83	5.48	5.96

From Fig 3 it is found that all the points from the test results nearly lie upon one straight line for pure portland cement pastes cured beyond 28 day, which means that pure cement paste may be considered to have its own intrinsic strength value R_c. However, it is altogether different with fly ash cement paste at that the strength-porosity relationships for different curing ages differ from each other and follow different line. The intrinsic strength values for fly ash cement pastes increase with the curing age and those at later ages may even exceed that of pure cement paste.

DISCUSSION

The strength character of fly ash cement, namely rather low at early ages but high at later ages, may not be very convincingly explanied by the change in porosity caused by cement hydration and pozzolanic reaction alone. The structure factors also should be considered.Huang Shi-Yuan(3) in his previous work observed the microstructure of fly ash cement paste by SEM and pointed out that a gap zone could be easily observed between the fly ash grains and the hydrates around them in the early age pastes, which had also been reported by K.Takemoto (4), and that the bond between the fly ash grains and the hydrates was the weakest zone. So much so, when a load is applied, solid phase of fly ash grains could not completely perform its bearing capacity together with the hydrates. However, The gap is gradually filled with the hydrates formed by the pozzolanic reaction of fly ash, the bond gradually strengthens so that at later ages the fly ash grains together with hydrates can bear load completely.

Therefore, from the materials' structure view points, strengthening of the bond between fly ash grains and the hydrates around them, decrease in the $Ca(OH)_2$ content in pastes and refinement of the pore structure of pastes with curing time may be the reasons behind the strength characteristics and durability performance of fly ash cement.

CONCLUSIONS

i). At earlier ages the porosity of fly ash cement paste is much higher than that of pure cement paste, and only at later ages does porosity of the fly ash cement paste approach that of pure cement patse.

ii). The relationship between strength and porosity for pure cement pastes nearly conforms to a straight line in the Fc-P plot regardless of the curing age (>28days), but that for fly ash cement patses at different ages differs from each other.

iii). The state of bond between fly ash grains and the hydrates around them is one of the important structural factors affecting the strength charateristics of fly ash cement.

REFERENCES

[1] Huang Shi-Yuan, Cheng Ji-Ping, The evalution of pozzolanic reactivity of ashes, 8th. I.C.C.C. Vol 4, pp.41-45.

[2] Li Shi-qun, D.M.roy, A.Kumar, Quantitative determination of pozzolanas in hydration systems of cement or $Ca(OH)_2$ with fly ash of silica fume, C.C.R., Vol 15, pp.1079-1086.

[3] Huang Shi-Yuan, Hydration of fly ash cement and microstructure of fly sah cement pastes, CBI Research, 1981, No2.

[4] K.Takemoto, Hydration of pozzolanic cement, 7th ICCC SUB-THEME 4.

ETTRINGITE FROM PORTLAND CEMENT ORIGIN AND ETTRINGITE FROM POZZOLAN* ORIGIN: ANALOGIES, DIFFERENCES AND SEMIQUANTITATIVE RELATIONS WITH THEIR RESPECTIVE ORIGINS: INTERROGATIONS

R Talero

Instituto de Ciencias de la Construcción "Eduardo Torroja"
Consejo Superior de Investigaciones Científicas - Serrano Galvache S/n
Madrid, SPAIN

SUMMARY

The ettringite is formed on many occasiones when a concrete of cement is attacked by sulphatic waters.

In this work a semiquantitative analysis and study was made by XRD and SEM of the ettringite (2θ = 9.08º) in the solid phase of the Fratini test, using the cements P-1 (14.11% C_3A) P-31 (7.6% C_3A) and PY-6 (0.00% C_3A), five pozzolans, D, O, A, C or M and five mixture cements PUZ 70/30, PY-6/D, O, A, C or M, respectively, mixed with gypsum (natural stone), $CaSO_4.2H_2O$, in proportions to give 7.0% or 21.0% SO_3. Identical analysis and study was made of the correspondent mixtures of each pozzolan plus $Ca(OH)_2$ and gypsum.

The experimental results obtained demonstrated:

1st.- Ettringite formed from pozzolan origin may be similar and with less size than the ettringite formed from the C_3A origin in portland cement, according to the XRD and SEM techniques.

2nd.- The rate of formation of ettringite from pozzolan must be notably greater than the rate of formation of ettringite from portland cement.

3rd.- The topo-chemical mechanism of the ettringite formation will have be carried out, in its case, with previous solution in water of ALL the necessary reactive materials, included the "reactive" alumine, Al_2O_3, or better perhaps, "aluminate anion" (tetra-or pena-coordinated alumine (2)).

Interrogations: See them, at the end of this paper.
*.- Naturals, Fly Ashes, Activated Clays and Similars.

RESUMEN

La ettringita se forma en muchas ocasiones cuando un hormigón de cemento portland es atacado por aguas sulfatadas.

En el presente trabajo se ha realizado un análisis y estudio semicuantitativo de la ettringita por DRX (2θ = 9.08º) y ME en la fase sólida del ensayo de Fratini de tres cementos portland P-1 (14.11% C_3A), P-31 (7.62% C_3A) y PY-6 (0.00% C_3A), cinco puzolanas, D,O,A,C y M y cinco cementos de mezcla PUZ 70/30, respectivamente, mezclados con yeso, $CaSO_4.2H_2O$, en proporciones tales que la mezcla-conglomerante selenitosa tuviera 7.0% y 21.0% de SO_3, respectivamente, así como también a las correspondientes mezclas selenitosas de cada puzolana con $Ca(OH)_2$ R.A.

Los resultados experimentales obtenidos nos han demostrado:

1º.- La posibilidad real de formación de la ettringita de origen puzolana, la cual según las técnicas analíticas de DRX y ME ha resultado ser similar aunque de menor tamaño, que la ettringita de origen C_3A del cemento portland.

2º.- La velocidad de formación de la ettringita de origen puzolana ha de ser notablemente superior a la velocidad de formación de la ettringita de origen C_3A del cemento portland.

3º.- El mecanismo topo-químico de formación de la ettringita, deberá llevarse a cabo en su caso, con disolución previa en agua de todos los materiales reactivos necesarios, incluida la alúmina "reactiva", Al_2O_3, o mejor quizás, "anion aluminato", o "alúmina tetra-o penta-coordinada.

Interrogaciones: Véanse al final de este trabajo. *Naturales, Cenizas Volantes, Arcillas Activadas y Similares)

I.- INTRODUCTION

The attack on portland cements by the sulphates, involves formation of expansive ettringite from C_3A. Regarding pozzolanic cements and pozzolans, a substantial bibliography exits.

The question remains as to whether portland cements with pozzolan form or do not form, ettringite when they are attacked by sulphate ions, or do these cements resist attack otherwise.

It may be concluded that:

1st.- One of causes of the non formation of ettringite, is the low concentration of $Ca(OH)_2$ in the liquid phase due to the reaction with the pozzolan. The first part of the theory of Lafuma is in harmony with this hypothesis.

2nd.- Another cause may be the formation of products of reaction in form of tobermorite CSH gel, from the pozzolan.

3rd.- A third cause may be the high surface area of the pozzolans that plugs the pores of the paste, impeding accesss of the aggresive solutions.

II.- OBJECTIVES

1st.- To confirm or disprove the formation of ettringite of portland origin and pozzolan origin.

2nd.- Establishment of differences between the ettringite of such differents origins

3rd.- Establishment of relations between the quantitity ettringite formed and or some chemical parameters of its reagent originary.

III.- EXPERIMENTAL PROCEDURE

The Fratini test was done using two non sulphate-resisting portland cements P-1 (14.11% C_3A) and P-31 (6.62% C_3A), a portland cement PY-6 (0.00% C_3A) of high sulphate-resistance, and five pozzolanic cements PUZ 70/30, which were preapred mixing in such proportions, the portland cement PY-6 and the pozzolans D, O, A, C and M, to those five appropiately mixed with $Ca(OH)_2$ see Table 1 and with the amounts of gypsum, $CaSO_4.2H_2O$, expresed to give 7% and 21% of SO_3 (see Table 2). Once prepared and adequately mixed such plaster-bearing mixture (20 g) contained 100 ml distilled water, mixed and stored at 40ºC.

Following the ages of 1, 7, 14, 21, 28, 60, 90, 275 and 730 days, each sample of the solid phase of each one of the plaster-bearing mixtures was sampled.

Each sample subjected to XRD in a nitrogen atmosphere. The analysis was carried out choosing selected ettringite peaks such as $2\theta = 9.08º$ and $2\theta = 15.788º$. Other similar samples were analyzed adequately by SEM.

IV.- EXPERIMENTAL RESULTS OBTAINED

The graphic representation of the experimental results was semilogarithmic. All the experimental results in the Figures 1 a), b), c), d), e) and f), in the Graphic 1 and the Photos 1 a) and b) and 2 a) and b).

1st.- The case of 7.0% SO_3 or 21% SO_3, the pozzolans studied, except for the D give a more rapid ettringite formation, generally 7 to 14 days, and in the case of pozzolan M, in much greater quantity.

2nd.- Generally the intensity of peak of the ettringite of pozzolan origin M only or/in a pozzolanic cement PUZ, PY-6/M 70/30, has resulted as being notably superior, in both cases of 7.0% SO_3, and of the 21.0% SO_3, than the corresponding of whichever of the portland cements equally tested P-1 or P-31 only.

This does not coincide absolutely with what could be hoped for of the theoretical steiquimetric calculations carried out to the effect of their respective dosifications, Table 2, since according to the same, the quantity of ettringite that should be formed in each case has to be:

As from here, and given the great existing disparity between the real and the theoretical the only explanation possible of such notable differences is that the activity of the $Al_2O_3^{r-}$ in spite of its notable minority in the presence of that of the C_3A*, in whichever on the corresponding cases compared, must be of such a magnitude, that it forms ALLthe ettringite of which it is able MUCH MORE RAPIDLY than that of the C_3A of portland cement. Because of that it can be said with fundament that such a notable reactivity of the $Al_2O_3^{r-}$ could be found in the physical-chemical state IDEAL for this process, while that of the C_3A would be found in the oppsite, that is to say, in the NON IDEAL or at least, less ideal form of the same and results, up to the point that the same, on the line of the obtained results, self-restraining and limiting the formation of all the ettringite than by steichiometry it would be able to form.

For which and despite the paradoxical, the mentioned fact demonstrated that at equality of age the test and especially the initial ones, the ettringite formed from $Al_2O_3^{r-}$ of the pozzolans, is greater than ettringite formed from C_3A of the portland cement, making it able to say for whatever cause that the rate of formation, of the ettringite formed from $Al_2O_3^{r-}$ of the pozzolans should be notably superior to the rate of formation of the ettringite formed from C_3A of the Portland Cement.

* Quantity of reacting, C_3A and "reactive" Al_2O_3, see Tables 1 and 2, divided by its respective molecular weights:

- Molecules $Al_2O_3^{r-}$ of the pozzolan M only with $Ca(OH)_2$R.A.
  and 7.0% SO_3 ..... 4.9×10^{-4}
  or 21.0% SO_3 ..... 3.2×10^{-4}
- Molecules $Al_2O_3^{r-}$of the pozzoland M in pozzolanic cement PY-6/M 70/30
  with 7.0% SO_3 ..... 5.4×10^{-4}
  or 21.0% SO_3 ..... 3.5×10^{-4}
- Mole cules C_3A of the portland cement P-1
  with 7.0% SO_3 ..... 95.8×10^{-4}
  or 21.0% SO_3 ..... 61.3×10^{-4}
- Molecules C_3A of the portland cement P-31
  with 7.0% SO_3 ..... 52.2×10^{-4}
  or 21.0% SO_3 ..... 33.4×10^{-4}
- Molecules C_3A of the portland cement PY-6
  with 7.0% SO_3 ..... 6.6×10^{-4}
  or 21.0% SO_3 ..... 4.2×10^{-4}

V.- GENERAL CONCLUSIONS

1st.- The quantity of ettringite, formed depending on its intensity of peak, $2\theta = 9.08º$, of portland cement, origin keeps, as was to be expected, a narrow relationhip with the content of C_3A the same, of greater or lesser value in this order, or gthe portland cements P-1, P-31 and PY-6, thus tested, are totally coinciding with that which has been obtained in function with its respective content of C_3A.

2nd.- ALL the chosen and tested pozzolans in this work have fixed sulphate ions in order to form ettringite, not being able to say, that because of that the same "are susceptible to the harmful attack of the same" and so have to provoke ALL of them forcibly because of said attack against aggresive bad consequences to the civil works that with which they are carried out well mixed with hydrated lime or with portland cement.

3rd.- The first maximum of formation of ettringite (and generally the greatest in all of them) of pozzolan origin, usually surpasses in almost all cases except some occasions that of the pozzolan A, in at least 7 days, to the maximum correspondent of the formation of ettringite from portland cement origin (its C_3A), in spite of that by stechiometry the contrary should have occured; on the other hand the greatest part of the total ettringite to form by them in the case of 7.0% of SO_3, whether mixed separately with hydrated lime or mixed separately with the portland cement PY-6, is origineed during the first 21-28 days of the test.

4th.- The rate of formation of the ettringite formed from $Al_2O_3^{r-}$ of the pozzolan, should be notably superior to the rate of formation of the ettringite formed from C_3A of the portland cement.

Therefore,

- The ettringite formed from $Al_2O_3^{r-}$ of the pozzolan can be denomitated with fundament "ETTRINGITE OF RAPID FORMATION", symbolizing it as "Ett-rf",

- The ettringite formed from C_3A of the portland cement can be denominated with fundament "ETTRINGITE OF SLOW FORMATION", symbolizing it as "Ett-lf", a and

- The ettringite so named previously in its case, can be denominated "TOTAL ETTRINGITE" the which could be different, in absolute value, from one age to another of the test, and could be symbolized by "Ett-T"; and could be at once all of them,

  . "Primary" = "1st" or "early", by corresponding with the first maximum formed by the same, and in all cases, in the initial ages of the test, or

  . "Secondary" = "2nd" or "slow", by corresponding with the latter maximum, formed by the same, in all cases, in the intermediate and/or final stages of the test damage.

5th.- The quantity of ettringite formed (depending on its intensity of peak (2= = 9.08º) of pozzolan origin alone or along with the portland cement PY-6, MAINTAINS a direct relationship with the contents of Al_2O_3 (%) and/or the modules Al_2O_3 (%), or A/F, of the same, since the classification that would be obtained, of lesser or greater value in this order, are practically coincidents, specially those of the fundamental age of the test of 1, 7, 14, 21, 28 and 730 days, see Square 1.

Nevertheless and since said sttringite has to come from the $Al_2O_3^{r-}$ chiefly from the pozzolan, the classification which should be obtained from such pozzolans in function with its respective content of $Al_2O_3^{r-}$ of lessr or greater value in this order, would have to be the 4th of the latter Square 1.

Such 4th classification of the latter Square 1, can not be verified because of a simple analytical method, rapid and reliable, in order to determinate the EXACT CEMENT OF $Al_2O_3^{r-}$ "reactive" SiO_2, or SiO_2^{r-} and "reactive" $Fe_2O_3^{r-}$, (especially the first, whose case occupies us) of a pozzolan not actually existing (not being that parhaps of technological interest, since the final behaviour of the cement of the corresponding mixture is going to depend greatly whatsmore on the portland cement which accompanies it in each case). On the other hand, such 4th classification of the later Square 1, does not necessarily implicate.

- that both contents, of total Al_2O_3 (%) and Al_2O_3 (%) of each pozzolan have to be obligatory and forcibly equal, and less although perhaps than in the a artificial pozzolans, Fly Ash type Similar ones, than in the natural ones, and

- that the content of $Al_2O_3^{r-}$ (%) of each pozzolan has to be always in direct function with its corresponding total content of Al_2O_3 (%).

6th.- The pozzolanic activity of a given pozzolan-greater or lesser fixation but simultaneous of Ca^{2+} and OH^- of the liquid phase in agreement for substituting pozzolan the portland cement matrix - according to the Fratini test, in the form of pozzolanic cement mainting a certain relationship with its degree iof greater or lesser sensitivity, to the attack of sulphate ions and as such with the quantity of ettringite of pozzolan origin(s) which it is made up of (3).

7th.- According to that which has been previously shown, the intensity of peaks of the att-rf formed by each one of the pozzolan of those tested in the first ages of the test of 28 days, could be an indication semiquantitative and comparatively approximate enough to the most probable content of $Al_2O_3^{r-}$ (%) of each one of them with reagard to the rest, of which, the purport of the experimental results obtained would supply a similar classification of the 4th of the Square 1.

8th.- Of the individual and comparative study carried out among the pozzolan M, C and D, it has been observed like C and D, qualitatively, they have their $Al_2O_3^{r-}$ reather similar to that of M, although in less quantity, especially D, which has to have it scarcely.

9th.- Generally all the gypsipherous conglomerate mixtures with the 21.0% of SO_3 have potentiolanny originated during the test a greater quantity of ettringite than their correspondent of the 7.0% SO_3; the cause with could be said to be with fundament that those

have been found nearer to its stechiometric than these. It has been deduced from that, the real possibility of that of the 21.0% of SO_3, could be perhaps more appropiate for its use in an accelerated method of the test.

10th.- The topo-chemical mechanism of the etrringite formation must be carried out, in tis case, with previous solutions in water on ALL the necessary reactive materials, included the "reactive" alumine, $Al_2O_3^{r-}$, or better perhaps, "aluminate anion" (=tetra and/or penta-cordinated alumine (2)).

VI.- INTERROGATIONS

According to 2nd, 3rd, 4th, 5th and 6th the conclusions, it is work asking with fundament that on both of them ettringite, the ett-rf and ett-lf in quantity, rate of formation and distinctive origins-one of the $Al_2O_3^{r-}$ of pozzolan and the other of the C_3A of a portland cement-and on implicity reaching a competitive process of fixation of SO_3 (in form of gypsum) and different disruptions by unisonous formation of ettringite of different origin and ethiology more or less expansives, in the same appropiate plaster-bearing, it is valid to ask oneself:

How oculd their expansive efects be...?

Finally, in what would they express themselves...?

a) In an ADDITION, SINERGISM, ANTAGONISM or INVERSION of the EXPANSIVE ACTION of both?, and such

b) How would the portland cements with POZZOLAN(S), only until a 40% of mass, and specially those of the matrix portland cement of high sulphate resistance behave in face of an attack of the sulphate ions?.

c) How long does it take a concrete with pozzolan(s)-natural and/or artificial- damage when is attacked by sulphate waters?... More or less time that its corresponding cement portland concrete?.

d) In affirmative case (in short time) would it be possible to prevent that aggresive sulpatic attack at those concretes with pozzolans/artificial and/or naturals), manufacturing the pozzolanic cement and placing its concrete forms?

THE ANSWERS DEMOSTRATIONS AND VERY BAD OR VERY GOOD CONSEQUENCES, in the next national or international Conference or Congress.

NOTE

This research work is only a little of the multiples which constitute the Doctorate Thesis of the R. Talero (1). In the next Congresses, Meeting and articles, the remaining parts will be pusblished.

VII.- BIBLIOGRAPHY

1.- R. Talero: "Contribution to the Analytical Study and Physics-Chemistry of the System: Pozzolanic Cements - Gypsum - Water (to 20º ±3ºC)". Doctorate Thesis Complutense University of Madrid Faculty of Chemical Sciences. Nov. 86; Instituto de Ciencias de la Construcción "Eduardo Torroja", c/Serrano Galvache s/n, 28033 Madrid (Spain).

2.- J.S. Moya and S. Aza: "Aluminum - 27 and Silicon - 27 Magic-Angle Spinning Nuclear Magnetic Resonance Study of Kaolinite-Mullite Transformation". J. Amer. Ceram. Soc. 71 (19) C 418- C 421 (1988).

3.- R. Talero: "The Capacity of Exchange of Pozzolanic Additions: Its Origin and Influence in the Fratini Test". 9th International Congress on the Chemistry of Cement, New Delhi, India, 23-28 November 1992.

a) Ettringite formed from C_3A of the portland cements P-1, P-31 and PY-6, respectively, see Tables 1 and 2 and to calculate:

Reaction: $C_3A + 3(CaSO_4 2H_2O) + nH_2O \qquad 3CAO.Al_2O_3.3CaSO_4.31H_2O$

18.35 g of portland cement P-1 (14.11% C_3A) + 1,65 g Gypsum + nH_2O 7.26 g ettringit.
11.74 g " " " P-1 (14.11% C_3A) + 8.26 g Gypsum + nH_2O 7.58 g "
18.51 g " " " P-31 (7.62% C_3A) + 1.49 g Gypsum + nH_2O 6.46 g "
11.81 g " " " P-31 (7.62% C_3A) + 8.16 g Gypsum + nH_2O 4.13 g "
17.86 g " " " PY-6 (1.0% C_3A) + 2.14 g Gypsum + nH_2O 0.82 g "
11.43 g " " " PY-6 (1.0% C_3A) + 8.57 g Gypsum + nH_2O 0.52 g "

b) Ettringite formed from $Al_2O_3{}^{r-}$

- of the pozzolan M + $Ca(OH)_2$ + Gypsum + H_2O, and
- of the pozzolan M (30%) + portland cement PY-6 (70%) + Gypsum + H_2O

see Tables 1 and 2 to calculate, also taking into account these previous considerations:

1st.- A pure metakaolin normally has around 2.08% of $Al_2O_3{}^{r-}$

2nd.- Pozzolan M employed in this work contains at least 50.35% metakaolin (rest quarz).

3rd.- The quantity of pozzolan M employed in preparing the Gypsum - bearing Fratini of the 7.0% SO_3 or 21.0% SO_3 with the mixture, cement PY-6/M 70/30 plus plaster, has been respectively 17.57 x 0.3 = 5.271 g and 11.24 x 0.3 = 3.372 g.

Reaction: $Al_2O_3{}^{r-} + 3CaO + 3(CaSO_4.2H_2O) + nH_2O \longrightarrow C_3A.3CaSO_4.31H_2O$

17.57 g of cement PY-6/M 70/30 + 2.43 g Gypsum + nH_2O ⟶ 1.23 g ettringite
11.24 g of " PY-6/M 70/30 + 8.76 g Gypsum + nH_2O ⟶ 0.79 g ettringite
4.78 g of pozz. M + 3.01 g Gypsum + nH_2O ⟶ 0.61 g ettringite
3.09 g of " M + 7.88 g Gypsum + nH_2O ⟶ 0.39 g "

TABLE-1

DETERMINATIONS (%)	CEMENTS P-1 (3,08)*	P-31 (3,06)	PY-6 (3,21)	POZZOLANS D (2,59)	O (3,08)	A (2,41)	C (2,68)	M (2,55)
LOI	1,60	3,45	1,11	0,23	0,40	3,92	6,92	0,80
I.R	0,70	0,86	0,15	0,42	1,10	-	0,43	0,22
SiO_2	19,18	18,13	21,70	91,81	45,12	41,38	54,18	73,53
Al_2O_3	6,44	5,30	1,52	1,91	13,84	19,36	20,10	23,11
Fe_2O_3	1,75	3,80	4,11	2,39	13,82	12,05	3,12	1,19
CaO	63,94	61,68	67,97	1,23	10,48	11,11	2,38	0,63
MgO	1,48	1,82	0,42	0,38	9,54	10,58	2,04	0,03
Na_2O	0,90	0,76	0,43	1,50	3,18	1,24	5,64	0,07
K_2O	0,52	0,31	0,20	0,12	2,40	0,44	5,17	0,70
SO_3	3,50	3,86	2,34	-	0,46	-	-	-
TOTAL	100,01	99,97	99,95	99,99	99,94	100,08	99,98	100,05
H_2O (105°C)	0,24	0,33	0,22	0,07	0,55	4,02	4,03	0,16
CaO Free	1,90	0,63	1,75					

DETERMINATIONS (%)	POTENTIAL CALCULUS BOGUE (%)		
C_3S	51,05	58,70	79,43
C_2S	16,48	7,70	2,29
C_3A	14,11	7,62	0,00
C_4AF+2C_3A	5,33	11,56	10,19
C_4AF+C_3A	33,55	26,80	10,19
C_4AF	19,44	19,18	10,19
Spf. Surf.	3192	3248	3287

*.- Spf. Weight (g/cm³)
2 .- Spf. Surface (cm²/g)

CHEMICAL ANALYSIS OF THE GYPSUM

DETERMINATIONS (%)		MINERALOGICAL COMPOSITION (%)	
H_2O (40°C a 217°C)	20,13	$CaSO_4.2H_2O$	95,58
CO_2 (217°C a 1000°C)	0,75	$CaSO_4.\frac{1}{2}H_2O$	y/o
R.I.	0,26	$CaSO_4$	2,47
SiO_2	0,04	$CaCO_3$	0,75
SO_3	45,87	$MgCO_3$	0,81
CaO	32,54		
MgO	0,36		
Na_2O	0,02		
K_2O	0,01	TOTAL	99,61
TOTAL	99,98	H_2O a 40°C	0,41

GRAPHIC 1

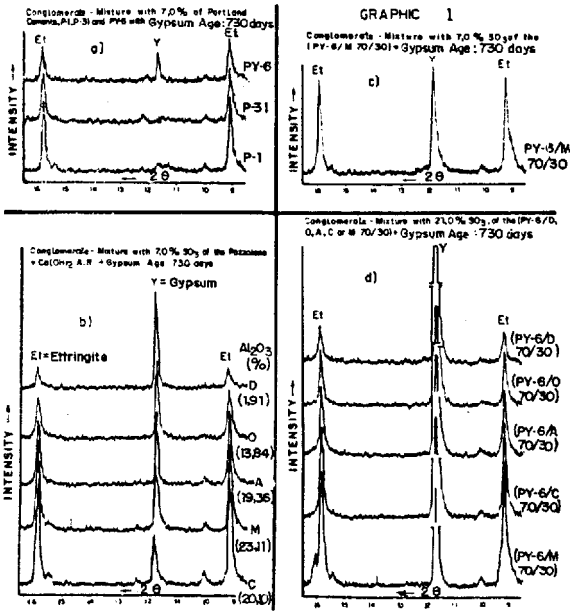

FIG. 1

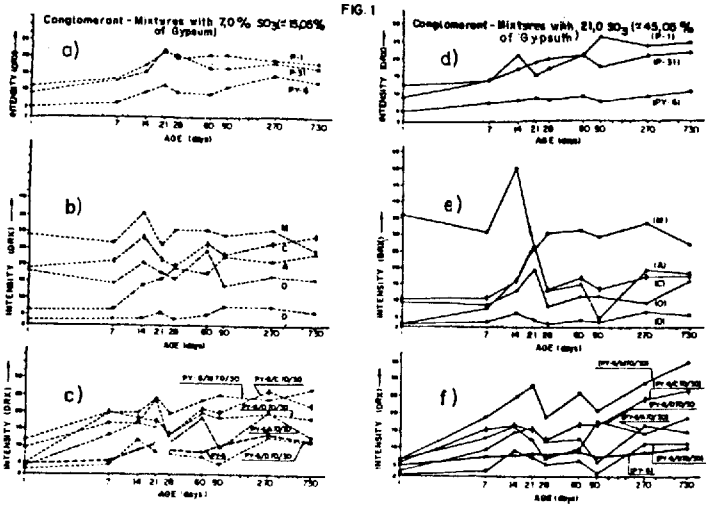

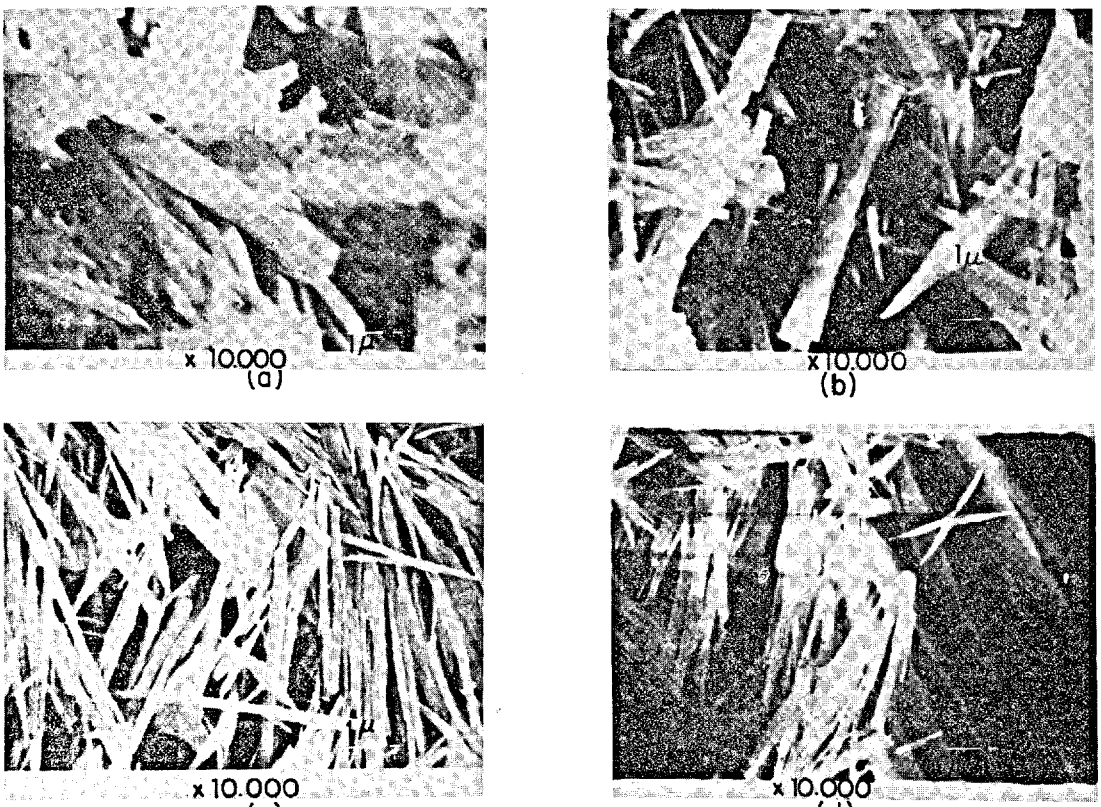

Phot. 1.- Different photomicrographs of the: (a) y (b) are Ettringites from portland cement origin (from its C_3A)or "Ett-lf"; (c) y (d)are Ettringites from pozzolanic addition origin (from its $Al_2O_3^{r-}$)or "Ett-rf". Ages: (a) and (e), 7 days; (b) and (d), 5 years. Shows as the Ett-lf has greater size than Ett-rf because its formation is much more slow and quite at the contrary, the Ett-rf.

Table 2

Materials	CEMENTS																POZZOLANS	
	PORTLAND						POZZOLANICS 70/30										D,O,A,CÓM	
	P-I		P-31		PY-6		PY-6/D		PY-6/O		PY-6/A		PY-6/C		PY-6/M		4,78 g	3,09 g
	% SO_3 of the conglomerant-mixture , cement + gypsum																	
	7,0%	21,0%	7,0%	21,0%	7,0%	21,0%	7,0%	21,0%	7,0%	21,0%	7,0%	21,0%	7,0%	21,0%	7,0%	21,0%	7,0%	21,0%
Cement (g)							PY-6-0	(PY-6-D)	PY-6-0	(PY-6+O)	PY-6+A	(PY-6+A)	PY-6+C	(PY-6+C)	PY-6+M	(PY-6+M)		
							12,32+5,28	7,88+3,38	12,33+5,29	7,89+3,38	12,34+5,29	7,90+3,38	12,32+5,28	7,88+3,38	12,30+5,27	7,87+3,37		
	18,35	11,74	16,51	11,84	17,86	11,43	17,60	11,26	17,62	11,27	17,63	11,28	17,60	11,26	17,57	11,24	---	---
	1,65	8,26	1,49	8,16	2,14	8,57	2,40	8,74	2,38	8,73	2,37	8,72	2,40	8,74	2,43	8,76	3,01	9,03
$Ca(OH)_2$ A-R(g)																	12,21	7,88

Square 1

Parameter	Classification	Classification of the tested Pozzolans D,O, A,C and M inf(≠parameters)	Fundamental Ages of the Test
real < [ettringita] <	1ª	D < O ≶ A < C < M	1,7,14,21,28 y 730 days
real < A/F <	2ª	D < O < A < C < M	
real < Al_2O_3(%) <	3ª	D < O < A < C < M	
theoretical < $Al_2O_3^{r-}$(%) <	4ª	D < O ≶ A < C < M	

THE COMPOSITION AND STRUCTURE OF C-S-H GELS IN CEMENT PASTES CONTAINING BLAST-FURNACE SLAGS

I G Richardson and G W Groves

Department of Materials, University of Oxford, Parks Road
Oxford, UK

SUMMARY

The microstructures of ground granulated blast-furnace slag (GGBFS)/OPC blends (slag fraction 0→1) and activated blast-furnace slag cements have been examined using electron microprobe analysis (EMPA) and analytical transmission electron microscopy (ATEM). Both slag and alite (or belite) inner product C-S-H most often have a fine homogeneous morphology but slag inner product is characterised as having a high content of Mg and Al. Mg,Al-rich precipitates often form in this region with an accompanying coarsening of the I.P. C-S-H morphology. It is shown that the slag inner product can be envisaged as a mixture of a single-phase C-S-H, with a composition equivalent to that of the O.P. C-S-H and a Mg,Al-hydroxide, similar to the naturally occurring mineral hydrotalcite. In the GGBFS/OPC blends, the mean Ca:Si ratio of the single-phase C-S-H steadily decreases with increasing slag fraction towards the value of the anyhdrous slag. As the Ca:Si ratio of the C-S-H decreases the Al:Ca ratio increases. Compositional variations are shown to occur on a region to region, and occasionally sample to sample, basis, but these follow the linear relationship between mean Al:Ca and Si:Ca ratios. These results are discussed in terms of a model for the structure and composition of C-S-H gels.

INTRODUCTION

Although much is known of the hydration chemistry of cements incorporating ground, granulated blast furnace slag (GGBFS)[1] there is relatively little knowledge of the microstructure of hardened pastes at the level of resolution which can be achieved by transmission electron microscopy with associated high resolution microanalysis (TEM). This paper presents the results of this technique together with electron microprobe analysis applied to hardened pastes of GGBFS/OPC blends.

In such blends, C-S-H gels with a range of compositions are found. In particular a relationship between the Al:Ca and Si:Ca ratios has been found and this relationship is discussed in terms of a structural model of C-S-H gel.

EXPERIMENTAL

The cements were prepared from single batches of an OPC (Blue Circle, Northfleet) and a GGBFS (Cemsave, Frodingham Cement Co.). The oxide compositions of these cements are shown in table 1. Pastes were prepared by mixing the required amounts of solids with de-ionized water at a water:solids ratio of 0.4. The resulting paste was placed in a plastic tube which was then sealed in a plastic bag. Curing took place in a water bath, generally set at 20°C. The preparation of specimens for TEM and EMPA followed standard techniques as described in detail elsewhere[2].

Table I Oxide compositions supplied with the Blue Circle NORTHFLEET OPC and Frodingham Cement Co. CEMSAVE GGBFS

	OPC	GGBFS
Na_2O	0.19	0.64
MgO	1.33	7.74
Al_2O_3	6.19	11.00
SiO_2	20.00	37.20
SO_3*	2.65	3.68
K_2O	0.86	0.55
CaO	65.90	41.70
TiO_2	0.30	0.68
Mn_2O_3 **	0.60	0.73
Fe_2O_3**	3.03	0.38

* Most sulphur in GGBFS is present in its lowest oxidation state.
** Mn and Fe are present in the glassy slag in lower oxidation states. Some colloidal and free iron are likely to be present in the GGBFS.

RESULTS AND DISCUSSION

The microstructure of a hardened paste can be broadly divided into outer product (O.P.) formed in the originally water-filled spaces and inner product (I.P.) formed within the original boundaries of the anhydrous grains. C-S-H gel is a major phase in both O.P. and I.P. In O.P. its morphology changes with the proportion of GGBFS in the GGBFS/OPC blend. As

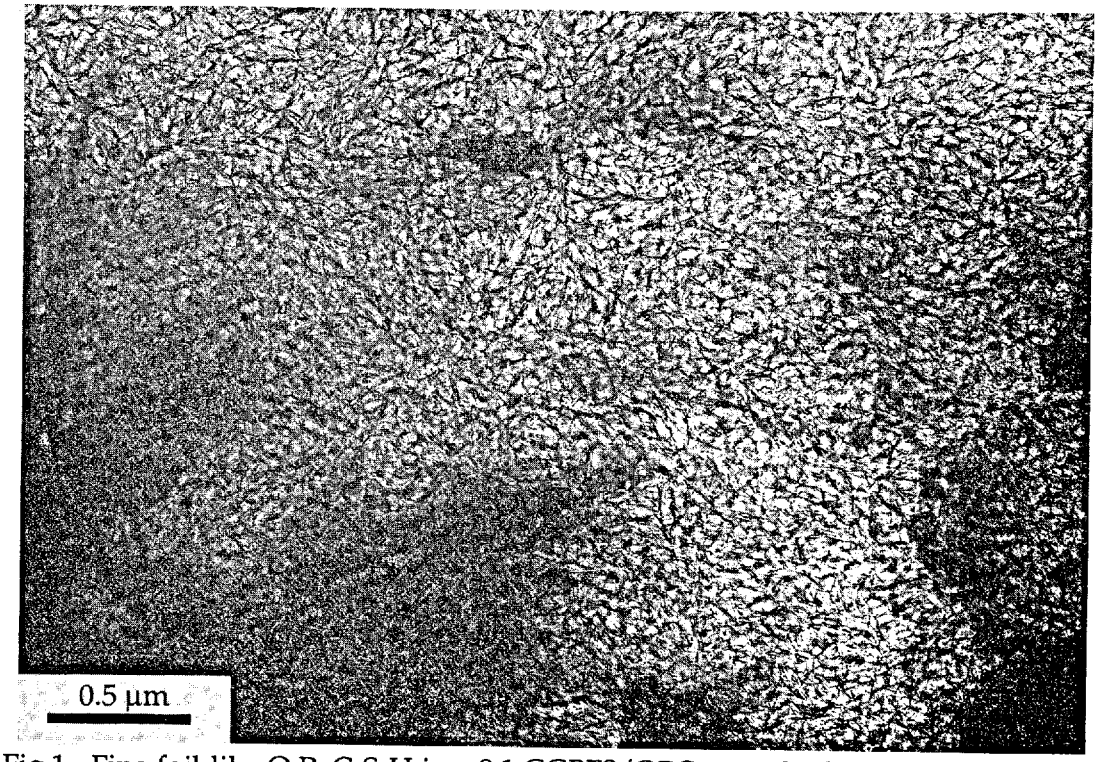

Fig.1 Fine foil-like O.P. C-S-H in a 9:1 GGBFS/OPC paste hydrated for 14 months.

the fraction of GGBFS increases, a fine foil-like morphology gradually replaces a more linear fibrillar morphology. The foil-like morphology, an example of which is shown in fig.1, appears to be more effective in filling space without leaving large pores which may help to account for the beneficial effects of slag in reducing rates of diffusion through the paste[3]. Inner product C-S-H may be derived from alite or belite grains in the OPC fraction or from slag grains. In the former case the C-S-H appears morphologically identical to that occurring in OPC pastes. In large grains the C-S-H generally has a homogeneous texture with very fine-scale porosity; small grains often display C-S-H of relatively coarse texture. The main point of distinction of slag grain inner product, which also most commonly has a fine homogeneous texture, is its high content of Mg and Al, and the presence of laths or platelets which are particularly rich in Mg and Al. Sometimes these take the form of well-developed platelets which may be oriented normal to the boundary of the grain, and which appear to occupy the major part of the I.P., as reported previously [4,5] but in other regions, even in 3 year-old pastes, the plates or in this case possibly laths, are randomly oriented and less well-developed and a high proportion of C-S-H is present in the I.P. An example of such a region in a 3-month old paste is shown in fig.2. Various stages of development in this Mg,Al-rich precipitate can be seen simultaneously within the same specimen.

The Ca:Si ratios of C-S-H gels in O.P., I.P. derived from alite and I.P. derived from slag grains do not differ significantly from one another, nor is there any significant change in Ca:Si ratio with the curing time of the paste. These statements apply to average values. There is considerable local variation in gel composition within any one specimen, so that localized data sets, even if these are large, cannot be taken to establish composition averages and trends. All the C-S-H gels show a similar trend of reducing Ca:Si ratio with increasing proportion of GGBFS in the blend. The trend is shown graphically for O.P. C-S-H in fig.3 - the trend for I.P. C-S-H is closely similar. The earlier result of Harrison et al[6] that the Ca:Si ratio of a C-S-H in a 40% slag blend was only marginally lower than that of a C-S-H in an OPC paste can be considered not typical of the general trend.

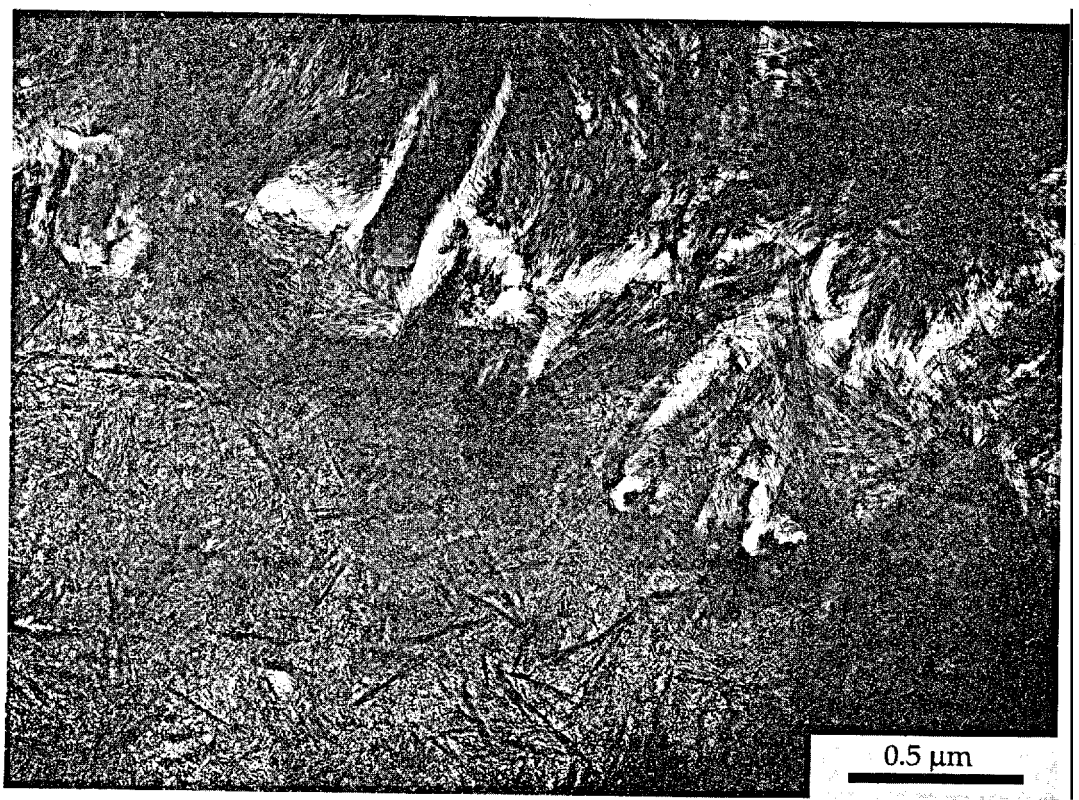

Fig.2 Mg,Al-rich particles (laths or platelets) randomly distributed in slag I.P. (lower left). Upper right shows O.P. with fibrillar C-S-H, AFm plates and relicts of AFt. Paste is a 50% GGBFS/OPC blend hydrated for 3 months.

Although the I.P. C-S-H from slag grains does not differ significantly in Ca:Si ratio from C-S-H in other locations, the overall composition of slag I.P. is distinctive in having a high Mg and Al content. Mg in particular forms an excellent chemical marker for slag I.P. in EMPA, since as reported previously[6], Mg does not migrate from the volume originally occupied by the slag grain and becomes relatively more concentrated as the grain reacts to form the inner product. EMPA analysis is of course unable to resolve even the more well-defined of the Mg,Al-rich precipitates which develop within the slag I.P. Even with TEM microanalysis, although it was often apparent that the analysed volume of slag I.P. contained precipitate, it was not possible to analyse with any certainty C-S-H completely free of precipitation, as can be envisaged from an examination of fig.2. The results of microanalysis by both techniques can therefore be expected to show Mg:Ca and Al:Ca ratios resulting from some level of combination of precipitate and C-S-H in the analysed volume. An example of both EMPA and TEM results is shown in fig.4, for a 3:1 GGBFS/OPC blend. All the data falls quite well on a single trend line which can be described by the equation

$$Al:Ca = a + b\,(Mg:Ca)$$

where a represents the Al:Ca ratio of single-phase C-S-H gel and b the Al:Mg ratio of the Mg,Al-rich precipitate phase. Following this type of analysis for 9 blend compositions in the full range from 0% GGBFS to 100% GGBFS showed that the Al:Ca ratio in the single phase C-S-H component of the slag I.P. (alite/belite I.P. for 0% GGBFS) increased steadily from 0.042 at 0% GGBFS to 0.185 at 100% GGBFS. The Al:Mg ratio of the precipitate remained relatively constant over the bulk of the composition range with an average value of 0.42 although the end members, 0% and 100% GGBFS had anomalously low and high values, respectively. Outer product C-S-H, for which the same difficulty of a finely inter-mixed second phase did

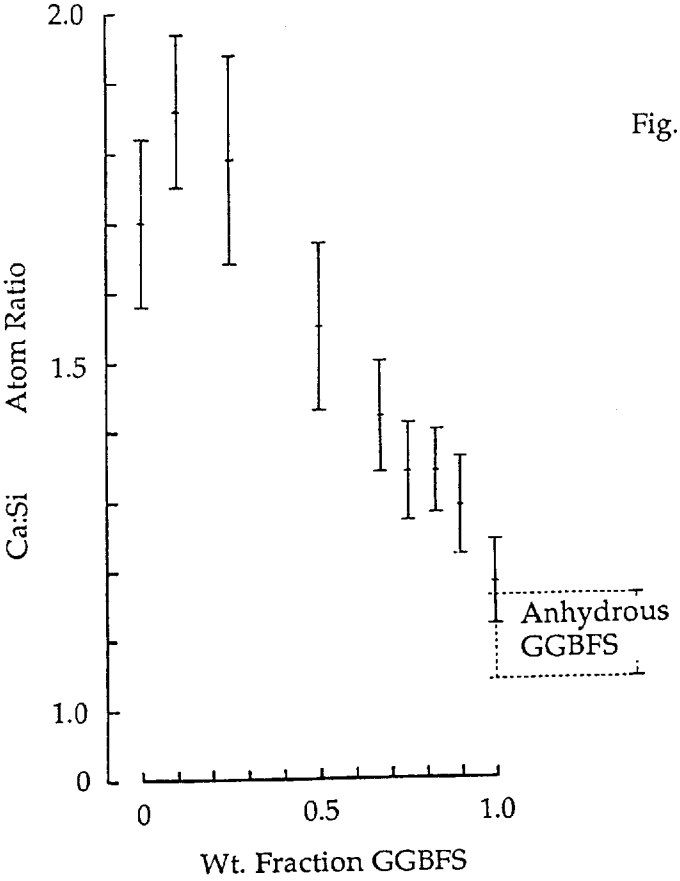

Fig.3 Variation of Ca:Si ratio of O.P. C-S-H with proportion of GGBFS in the blend.

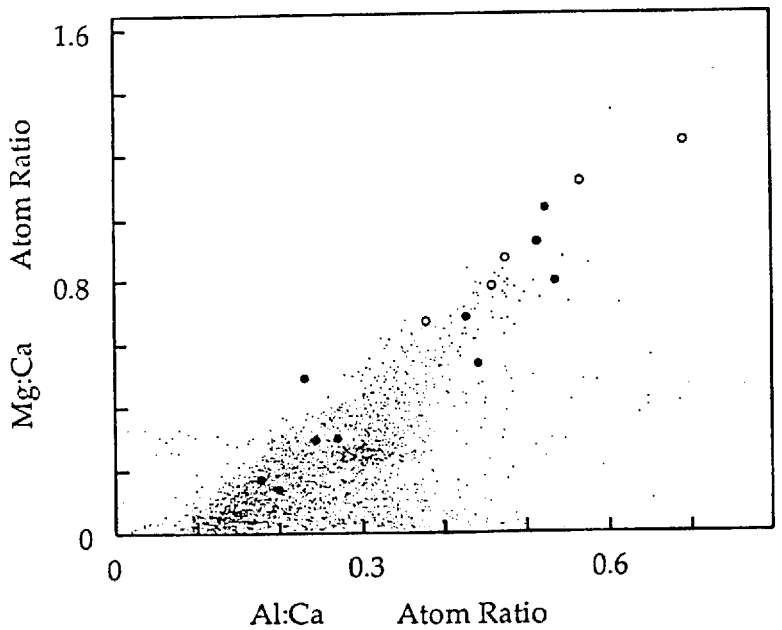

Fig.4 Mg:Ca against Al:Ca atom ratio plot for an area in a 3:1 GGBFS/OPC paste analysed by EMPA (fine points) and TEM analysis of inner product (filled circles) and inner product seen to contain precipitates in the analysed volume (open circles).

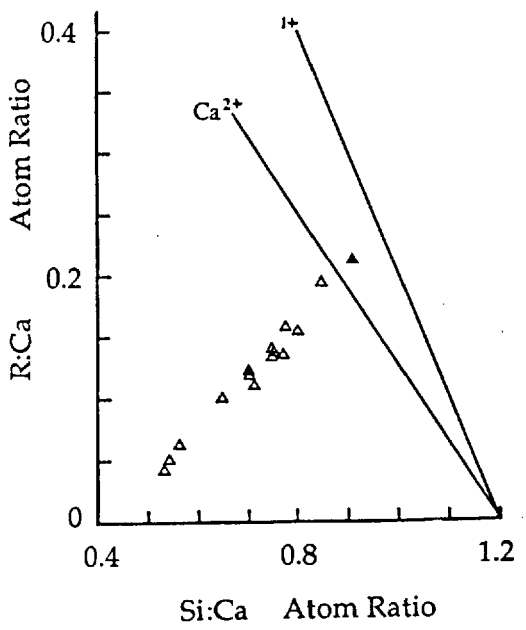

Fig.5 Mean R:Ca against Si:Ca atom ratio plot for O.P. C-S-H in GGBFS/OPC hardened cement pastes.

not arise, showed a similar trend in Al:Ca ratio, varying from 0.052 to 0.194 over the 0% to 100% GGBFS range. It is thus clear that inner product can be viewed as a single-phase C-S-H which is compositionally equivalent to O.P. C-S-H, intermixed over a range of scales with varying amounts of a Mg,Al-rich phase. The amount of trivalent ion, Al or Fe which can be incorporated in the structure of C-S-H gel increases as the Si:Ca ratio of the C-S-H increases. Fig.5 shows that the relationship is approximately linear and can be represented by the equation

$$Si:Ca = 0.44 + 2.25\ (R:Ca)$$

where R is mainly Al with the addition of minor amounts of Fe. It is worth considering the implications of this result in terms of a structural model for C–S–H gel. Taylor[7] has considered that C-S-H gel in hardened OPC pastes may be made up of a combination of tobermorite-like units and jennite-like units in which a large number of the "bridging" silicate tetrahedra in the dreierketten chain structure are omitted. The tobermorite-like dimer units, T_2 and jennite-like dimer units J_2 have no bridging tetrahedra. Polymerized units of chain length 3n-1 (where n=1,2,3 etc.), T_{3n-1} and J_{3n-1}, are built up by uniting shorter chains with bridging tetrahedra. Taylor[7] considered that C-S-H gel incorporating Al could be accounted for by a mixture of T_2 units with J_{3n-1} units and AFm-like layers incorporating the Al but mixed so intimately and on such a fine scale as to be indistinguishable as a separate phase. However in this case a higher proportion of AFm-like layers, incorporating more Al, would bring a higher Ca:Si ratio for the gel, contrary to the trend shown in fig.5. The trend observed can be accounted for by considering a series of C-S-H phases with a range of Si:Ca ratios in which in each phase a similar fraction of Si atoms is replaced by Al or Fe. This implies a structural limitation to the substitution of Si atoms by Al or Fe; it will be assumed that this limitation corresponds to Al or Fe substituting for Si only in "bridging" sites. The substitution of R (Al or Fe) for Si can be incorporated in a general model which retains the dreierketten theme but which unlike Taylor's model allows some variation in the number of Si-OH groups in the chain

$$Ca_XH_{(6n-2X)}(Si_{1-a}R_a^{[4]})_{(3n-1)}O_{(9n-2)}\cdot\underset{c}{\overset{c+}{I}}a_{(3n-1)}\cdot zCa(OH)_2\cdot mH_2O$$

Within this general model, Taylor's tobermorite-like unit is given by X=2.5n, z=0 and the jennite-like unit by X=2.5n z=2n. I represents an interlayer charge-compensating cation which may be an alkali metal or Ca. In the general model the average chain length is given by the average value of 3n-1 and is not necessarily an integer. As the chain length increases, so do the number of bridging sites which can be substituted and the Si:Ca ratio of the gel. The experimental points in fig.5 therefore represent compositions of gels of chain length increasing with Si:Ca ratio from a value at the lowest Si:Ca ratio only slightly greater than that of the dimer which, as it contains no bridging tetrahedra, contains no Si which can be substituted by Al or Fe. Analysis shows that as the average chain length increases above that of the dimer, the inclusion of bridging tetrahedra rapidly increases the maximum possible R:Ca ratio until a chain length of about 5(n =2) is reached, after which the increase in R:Ca with increasing chain length becomes much more gradual. The lines drawn in fig.5 represent the R:Ca versus Si:Ca relationships for infinite chain length, for the cases of charge compensation by Ca and alkali metal cations respectively. The solid triangle in fig.5 is an experimental point for a pure GGBFS cement activated by KOH, in which charge compensation of Al substitution for Si by K ions might be expected to occur. The general model is disucssed in greater detail in reference 8.

SUMMARY AND CONCLUSIONS

Hardened GGBFS/OPC cement pastes contain C-S-H gel which varies in morphology and composition with the blend composition. The Ca:Si ratio of the gel decreases approximately linearly with the weight fraction of GGBFS, and the Al:Ca ratio increases approximately linearly with the Si:Ca ratio of the gel. The latter trend can be accounted for in terms of a general model of the C-S-H structure based on dreierketten chains in which Al substitutes for Si in the bridging tetrahedra.

ACKNOWLEDGEMENT

Thanks are due to SERC for financial support (IGR) and to C.R.Wilding for the supply of material and helpful discussions.

REFERENCES

1. Taylor, H.F.W. :p.276 "Cement Chemistry", Academic Press, London 1990.

2. Richardson, I.G.: "The Microstructure and Composition of Hardened Cement Pastes", D.Phil Thesis, University of Oxford, Oxford U.K. 1991.

3. Page, C.L., Short, N.R. & El Tarras, A.: "Diffusion of chloride ions in hardened cement pastes", Cem. Conc. Res. **11**, 395 (1981).

4. Feng, Q.L., Lachowski, E.E. & Glasser, F.P.: "Densification and migration of ions in blast furnace slag-Portland cement pastes", Mat. Res. Soc. Symp. Proc. **137**, 419 (1989).

5. Feng Q.L. & Glasser, F.P.: "Microstructure, mass transport and densification of slag cement pastes", Mat. Res. Soc. Symp. Proc. **178**, 57 (1990).

6. Harrisson, A.M., Winter, N.B. & Taylor, H.F.W. : "Microstructure and microchemistry of slag cement pastes"., Mat. Res. Soc. Symp. Proc. **86**, 199 (1987).

7. Taylor, H.F.W.: "Proposed structure for calcium silicate hydrate gel", J. Amer. Ceram. Soc. **69**, 464 (1986).

8. Richardson, I.G. & Groves, G.W.: "The incorporation of minor and trace elements into calcium silicate hydrate (C-S-H) gel in hardened cement pastes", to be published in Cem. Conc. Res. (1992).

MECHANISM AND HYDRATION KINETICS OF ELECTROTHERMO-PHOSPHORIC SLAG AS A COMPONENT OF MIXED CEMENTS

N S Nikonova, V V Mityushin, I N Tikhomirova and N M Ketayva

Chair of Cement, Moscow Chemico Technological Institute
Moscow, RUSSIA

Utilization of electrometallurgical slags in mixed cements is an interesting proposition from born economic and environmental view points.

The object of our investigation was to study the setting process of compositions containing granulated electrothermophosphoric slag and self-spilled slag from low-carbon ferrochrome production.

Binder compositions, uncorporating up to 90 % wr of electrothermo-phosphoric slag and up to 10 % wr of self-spilled slag, were sealed with water and sodium sulphate solution (concentration 1.02 g/cm^3) and subjected to hydrothermal treatment at 90°C.

Formation of silicate anion structures in hydration products was studied by the kinetic molybdate complex method.

Granulated electrothermo-phosphoric slag mainly consist of glass. The crystalline phase consists of anorthite, melilite and hydroxyapathite.

Self-spilled slag contains up to 70 % wr γ -C_2S, besides periclase and picrochromites.

The results of determination of mass-molecular distribution of silicate anions (Table 1) show that the electrothermo-phosphoric slag consists of a large number of phases, which have anions with a degree of polymerization about 275. These anions belong to the glass component of slag. This is also due to the oligomeric anions.

Table 1

Fractions of anions	Electrothermo--phosphoric slag		Self-spilled slag	
	n_i	q_i	n_i	q_i
Monomeric	1	20.26	1	9.66
Dimeric	2	28.61	2	54.54
Oligomeric	9.68	7.81	3.31	15.68
Polymeric	275.78	43.32	56.77	20.12
The mean mass degree of polymerization	120.35		13.76	

n_i - mean degree of polymerization of fraction (i) of anions;
q_i - mass part of anions (%) of fraction (i) in mass-molecular distribution.

The self-spilled slag mainly consists of phases (γ - C_2S with admixture of β-C_2S) with monomeric silicate anions. However, mass-molecular distribution indicated up to 35 % of polymeric anions (which relate to the glass of slag).

The glass component of slag react more intensely with water during the isothermal treatment of the electrothermo-phosphoric slag. This manifests by a lowering of the polymerization degree of the high molecular fraction of anions and a decrease of its part in mass-molecular distribution from 51 % to 9 % after 3 hours of isothermal treatment (Table 2).

Table 2

Fractions of anions	Treatment, hours									
	1		3		5		7		9	
	n_i	q_i	n_i	q_i	n_i	q_i	n_i	q_i	n_i	q_i
Monomeric	1	39.1	1	78.8	1	72.9	1	58.9	1	71.3
Dimeric	2	4.5	2	5.7	2	0	2	6.3	2	0
Oligomeric	9.7	4.7	14.3	5.9	24.0	15.4	18.0	6.4	27.6	7.4
Polymeric	42.1	51.7	66.0	9.6	59.0	11.7	40.0	28.4	45.7	21.3

At the same time, there is formation of additional monomeric anions, which belong to the hydroxyapathite - $Ca_5(PO_4)_3OH$ (as shown by X-ray and thermal methods).

After 5 hours of isothermal treatment, the liquid phase loses calcium ions whereupon the hydroxyapathite becomes unstable and partially dissolves. This is confirmed by a decrease of the monomeric anions in the mass-molecular distribution, which can not be explaned by hydration of the crystalline phase of slag with the monomeric structure of anions, because this component of slag is more inert than glass. At the same time, the amount of new formation increases. This new formation has 20-60 tetrahedra united to each other in the structure of the anion. On the other hand, the type of thermogram and X-ray diffractogram changes, namely, area of the peak, which corresponds to the exothermic reaction of the crystallization of glass (930-960°C) decreases. These changes characterize unregulated structure of the glass. It means that the glass further dissolves. Consequently, the appearance of the supplementary amount of phase with oligomeric anions could be attributed to a new phase, which is a weakly crystalline hydrosilicate (Say CSH gel).

After 7 hours, processes of polycondensation of silicate anions occurs, bringing regularity of structure to the weakly crystalline hydrosilicates of calcium. The corresponding X-ray diffractogram indicates a peak at 1.83 Å, which is attributed to CSH gel or the weakly crystalline phase CSH(1).

After 9 hours of the isothermal treatment, the rate of these processes increases and the mean degree of polymerization sharply rises. Thereupon, condensation of CSH gel occurs and, consequently, CSH(1) phase with a higher degree of crystallization than earlier forms. X-ray diffractogram indicates three distinct peaks for this phase.

A few remarks are worth making on the kinetics of the mean mass degree of polymerization (N_{middle} - integral quantity) as also strength development of the material with time (Fig.1). The value of N_{middle} changes from 120 to 8-10 after 3 hours of the isothermal treatment. The maximum value corresponds to the degree of polymerization of the initial slag, whole the minimum value corresponds to the maximum retention of hydroxyapathite in the hardened products and intense dissolution of glass.

The relatively gently sloping section of the acceleration curve (Fig.2) corresponds to the accretion of the reaction products of CSH gel, whereas the steep section corresponds to the weakly crystalline phase CSH(1). After 9 hours, a slumpis observed in the strength of stone formed on the CSH gel and hydroxyapathite base. Consequently, the gel structure reforms and this transformed to phase CSH(1). However, after prolonged treatment, this slump must be made good by the growth in the new formation and by improvement in the morphology and conditions of accretion of the new formation.

Addition 10 % wr of self-spilled slag does not change the sequence of phase formation but speeds up these processes.

Hydroxyapathite, which formed first in this system, reaches its maximum in 1 hour of isothermal treatment, as shown by the mass-molecular distribution. It corresponds to the maximum retention of monomeric anions (69 %) in mass-molecular distribution. Absence of polymeric anions reflects the complete decomposition of the high-polymeric glass component of the slag, however, low-base hydrosilicates with high-polymeric anions too are absent yet. Phases with oligomeric anions with up to 8 tetrahedrons largely constitute (about 26 %) the mass-molecular distribution. These phase belong to CSH gel which still forms after 1 hours and the oligomeric fragment of the slag's glass component.

After 3 hours of the isothermal treatment, the fundamental process, which is taking place in the hardened system, is polycondensation of silicate anions, which results in the strengthening and consolidation of the gel structure. This gel then turns into CSH(1). After 3 hours, the peak 1.83 Å already appears on the X-ray diffractigram.

After 5 hours, the amount of active glass component of slag considerably decreases (exothermic effect of crystallization of the glass is absent on the thermogram). Processes of polycondensation proceed in the direction of raising part and mean degree of polymerization of the polymeric and the oligomeric fraction of anions. Consequently, the weakly crystalline phase CSH(1) builds up intensely in the hardened products. The mean degree of polymerization and the degree of crystallization of calcium hydrosilicates increase (demonstrated by the X-ray method).

Table 3

Fractions of anions	Treatment, hours							
	1		3		5		9	
	n_i	q_i	n_i	q_i	n_i	q_i	n_i	q_i
Monomeric	1	69.3	1	52.1	1	41.4	1	43.6
Dimeric	2	0	2	0	2	0	2	0
Oligomeric	8.5	25.8	12.2	6.2	14.5	7.38	39.6	13.9
			32.4	6.5	28.2	34.7	55.5	21.2
			35.1	22.0				
Polymeric	0	0	112.1	13.2	420.9	16.52	149.7	21.3

After 9 hours, the phase formation processes tend to slow down, indicating that the balance between the solid and the liquid phases of stone will be reached soon. In the mass-molecular distribution, the rate of fall in the amount of monomeric anions slows down, but its amount rather increases in absolute terms (from 41.4 % in 7 hours to 43.6 % in 9 hours). This leads to a lowering of the mean mass degree of polymerization (Fig.2). It should be mentioned here that every deflection in the kinetic curve of this quantity represents a change of phase composition or structure of the hydration products. Appearance of supplementary monomeric anions in the mass-molecular distribution (decrease of hydroxyapathite in the solid phase composition) is signalled by the appearance of a new compound which has anion presented by one tetrahedron. By X-ray and thermal methods this new formation has been identified as phase A. It is phosphosilicate of calcium and sodium whose composition de-

pends on the liquid phase composition. At the moment of its crystallization and change, an exothermic effect appears on the thermogram within wide limits 660-690°C, which, in effect, characterizes phase A. Appearance of this fairly high-base phase is conditioned by the increase in the ratio Me/SiO_2 (where Me: Ca^{2+} Na^{+}) present in the liquid phase of the hardening stone. The increase relative to the preceding period of phase formation occurs owing to the intensive withdrawal of silica, in turn, caused by the fall of low-base hydrosilicates CSH(1) in the solid phase. On the other hand, the amount of phosphorus, which easily enters in the CSH(1) structure, is limited, so phosphate anions accumulate in the liquid phase. Consequently, conditions of formation of relatively high-base phosphosilicate compound are created. Furthermore, enough silica is present in the liquid phase at this moment compared to that when mass crystallization of hydroxyapathite took place. Accordingly, the new phase is just hydroxyapathite and not pure phosphate. Phase A forms due to fairly low concentration of $Ca(OH)_2$ in liquid phase and the high binding degree of lime.

Introduction 10 % wr of self-spilled ferrochrome slag does not greatly alter the order of phase formation processes during initial hardening, but it does speed them up. After 7-9 hours of the isothermal treatment, phase A (phosphosilicate) appears together with the phases which were obtained during the hardening of electrothermo-phosphoric slag. Consequently, addition of the self-spilled ferrochrome slag activates the hardening and helps the reaction proceed to completion.

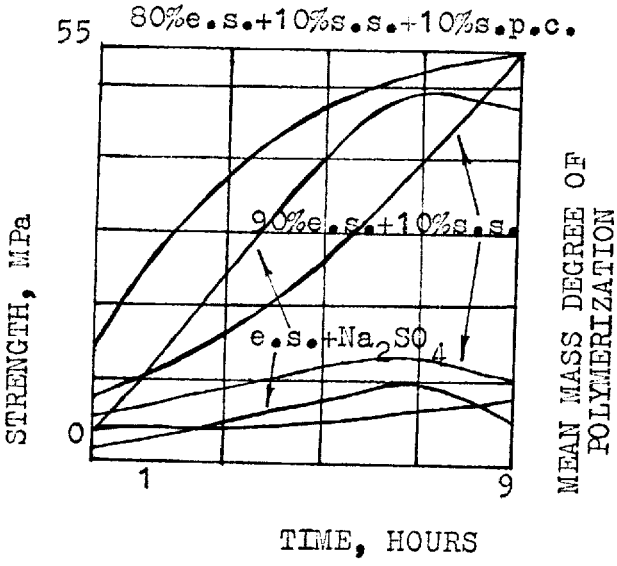

Fig.1

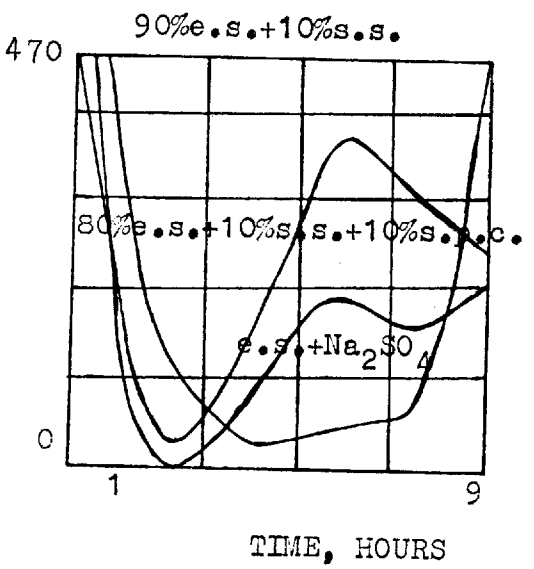

Fig.2

INCORPORATION OF SO_4^{2-}, CO_3^{2-} AND OH^- IN HYDRATION PRODUCTS OF TRICALCIUMALUMINATE

H Poellmann

Mineralogical Institute of University Erlangen-Nuremberg
Erlangen, GERMANY

SUMMARY

The addition of sulfate-containing salts to cements is necessary for the control of setting and hardening. Different hydration products are crystallizing in the course of hydration. It has been shown recently, that the common ions carbonate and hydroxide can influence the type of crystallizing hydrates and their formation. Nevertheless these salts can occur as well in the cycle of deterioration of concrete.
Two different families of hydrates are occuring :
1. Ettringites
2. Lamellar calcium aluminum hydroxi salts
In this investigation ternary solid solutions containing sulfate, carbonate and hydroxide were synthesized and characterized.
In the course of hydration phase compositions are changing. The influence of temperature, water content and additional carbonate is discussed. The X-ray patterns of different hydration stages were studied. Transformation reactions of ettringites and lamellar salts can be caused by sulfate deficiency or carbonate reactions. The following ternary solid solutions could be established :
1. Ettringites :

$$C_3A \cdot (x)CaCO_3 \cdot (y)Ca(OH)_2 \cdot (z)CaSO_4 \cdot nH_2O$$
$$0 < x < 2$$
$$0 < y < 1.5(3)$$
$$0 < z < 3$$

2. Lamellar calcium aluminum hydroxi salts

$$C_3A \cdot (x)CaCO_3 \cdot (y)Ca(OH)_2 \cdot (z)CaSO_4 \cdot nH_2O$$
$$0.33 < x < 0.66$$
$$0.17 < y < 0.50$$
$$0 < z < 0.17$$

Ettringites can form complex solid solution series whereas lamellar calcium aluminum hydroxi salts have only limited ternary solid solutions mainly close to the composition of semi-carbonate. Nevertheless binary solid solutions can occur to an increased extent.

INTRODUCTION

Tricalciumaluminate and $CaSO_4 \cdot aq$ are among the constituents of ordinary Portland cements. In the course of hydration different hydration products are formed. It can be distinguished between two main groups of hydration products - 1. Ettringites 2. Lamellar calcium aluminum hydroxi salts.

It was shown recently, that the common ions OH^- and CO_3^{2-}, which are present all time, can influence the hydration behaviour and the course of hydration. In these cases new hydrates and complex solid solutions are formed. In this investigation mainly the different ternary solid solution will be described and variations in the chemical behaviour will be discussed. At the present stage of knowledge at first ettringite is crystallizing untill all sulphate ions are consumed. Then in a second heat evolution which takes place the conversion of ettringite into lamellar calcium sulphoaluminatehydrate or scaling off effects occur. These reactions are influenced drastically under the presence of carbonate or hydroxide anions. In recent studies it was shown that the ettringite formed in the early stages of hydration does not convert into calcium monosulphoaluminate but in the presence of OH^- and CO_3^{2-} instead semicarbonate and monocarbonate are crystallizing. Solid solutions are occuring(3,4,5,6). (7) have shown that at the very early stages the primarily formed ettringite undergoes a chemical change from the low sulphate form(solid solution) to a higher sulphate-containing ettringite caused by the availability of SO_4^{2-} at the beginning of these reactions.

These facts can influence the stochiometric calculations of sulphate because it can be replaced by carbonate- and hydroxide- ions. An increased quantity of sulphate-containing phases can be formed. The new crystallizing different solid solutions will be discussed and the varying compositions in the various courses of hydration will be described.

EXPERIMENTAL

The composition and hydration reactions of new compounds were studied by pastes made from tricalciumaluminate, gypsum, lime and calcite at different concentrations. Tricalciumaluminate was synthesized in a laboratory furnace from reagent grade Al_2O_3 and $CaCO_3$.

The hydration products were filtrated in a glove.box to avoid influence of additional CO_2 from air. The samples were tested by X-Ray analysis, infrared spectroscopy, thermal analysis, chemical analysis and optical and electron microscopy. The course of hydration was studied by calorimetric methods. X-Ray powder diffraction data were collected from moist (100 % rel. humidity) and dried (35 % rel. humidity) samples using Si (a_o=5.4308Å) as internal standard. All lattice parameters were refined by least squares methods. Thermal and chemical analysis were made from samples dried to constant weight at 35 % relative humidity. Sulphate was measured by nephelometric methods.

RESULTS

I. Solid solution of ettringites

Ternary solid solution of sulphate-, carbonate and hydroxide- ettringite has been described by (3,5). As given by many authors often there is a sulfate deficiency in the ettringite structure(1,2). Detailed reactions on early hydration reactions is given by (2,9,10,11,12). The sulfate de-

ficiency was explained by complex ternary solid solutions (7).

In the course of ettringite-crystallization the chemical composition varies due to the availability of sulfate. At the very early beginning of ettringite crystallization really sulfate-poor ettringites are formed. With increasing reaction time and better available sulphate ion more sulphate-enriched ettringites are precipitating. The compositions of ettringites can be determined by X-Ray methods. On the variation of a_o the ternary solid solutions can be estimated. For a less sensitive measurement the (100)-reflection of ettringite can be taken into account. This gives sometimes practical hints if only this reflection can be registered. The course of lattice parameter a_o of ternary solid solutions of ettringites is shown in (Fig. 1).

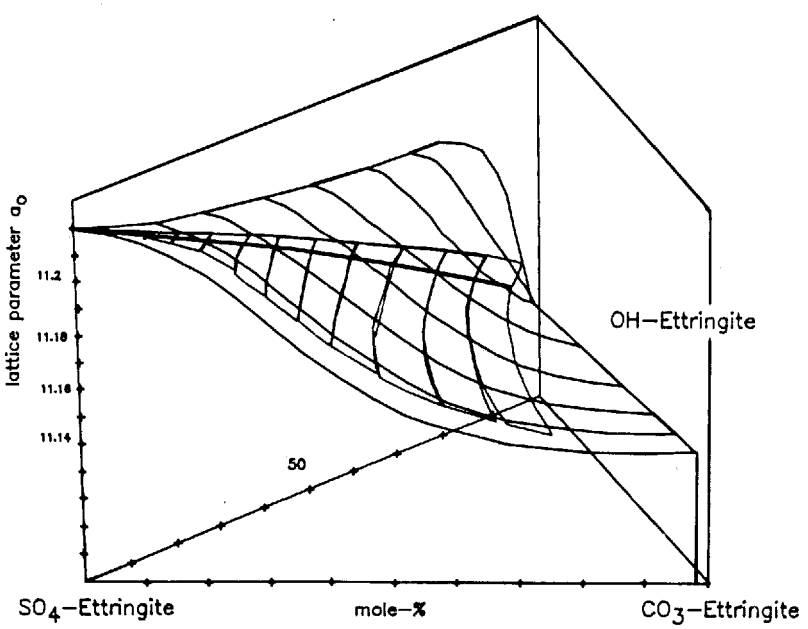

FIG.1 Variation of lattice parameter a_o of ettringites in the ternary system SO_4-ettringite - CO_3-ettringite - OH-ettringite

Due to the availability of sulphate, carbonate and hydroxide a wide range of solid solutions occur. With increased content of sulfate in ettringite the stability increases enormously. The pure sulphate-ettringite is the most stable phase of the complete solid solution series. Only in the carbonate rich part of the system there occurs a miscibility gap.

If no carbonate ions are present and the whole sulphate is consumed a transformation to monosulfate occurs. Ettringite remains stable when carbonate is present. The new hydrates which are formed are semicarbonate and moncarbonate. Ternary solid solutions of lamellar calcium aluminum hydroxi salts, which are closely related in composition to semicarbonate, can crystallize as well.

II. Solid-solution of lamellar calcium aluminum hydroxi salts

At the moment no tedailed information on solid solutions of lamellar calcium aluminum hydroxi salts containing sulfate, hydroxide and carbonate simultaneously is available. In the follwing fig. 2 the phase relations in the ternary system of lamellar phases are shown schematically. Some ternary solid solution to a limited extent occurs in the case of semicarbonate within the phase diagram. Two new ternary phases could be detected in this system.

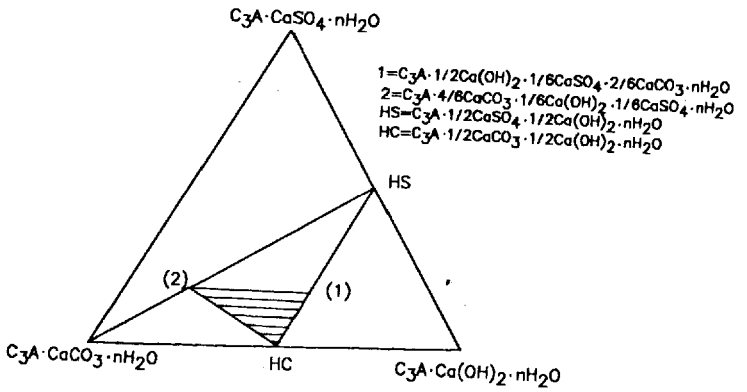

FIG 2. Ternary system of lamellar calcium aluminum hydroxi salts containing OH^-, CO_3^{2-} and SO_4^{2-}

The area of ternary solid solution is marked by lines in the system between HC, 1 and 2. Within some pseudobinary systems the two new ternary compounds could be detected. Their composition can be given by :

1. $C_3A \cdot 1/6CaSO_4 \cdot 1/2Ca(OH)_2 \cdot 2/6CaCO_3 \cdot nH_2O$
2. $C_3A \cdot 1/6CaSO_4 \cdot 1/6Ca(OH)_2 \cdot 4/6CaCO_3 \cdot nH_2O$

The X-Ray powder patterns of these phases are closely related to the one of semicarbonate - therefore it is difficult to distinguish between these phases solely by simple X-Ray measurements. With the aid of a more sophisticated equipment it is possible to establish the solid solutions and their limitations.

The following important results were obtained by measurements with high resolution diffractometry :

1. Ternary solid solutions with semicarbonate occur.
2. Two intermediate ternary compounds are formed in the system.
3. No solid solution between monocarbonate and monosulfate occurs, instead ettringite is precipitating.
4. In the presence of sulfate-ions no semicarbonate is crystallizing but

instead ternary solid solutions are formed.
5. By precise X-Ray measurments it is possible to distingiush between the ternary compounds.

SUMMARY AND DISCUSSION

In the follwing fig. 3 all the compositions with ettringite- and monosulfate-structure, containing sulfate, carbonate and hydroxide are shown. In both structure types ternary solid solutions are formed.

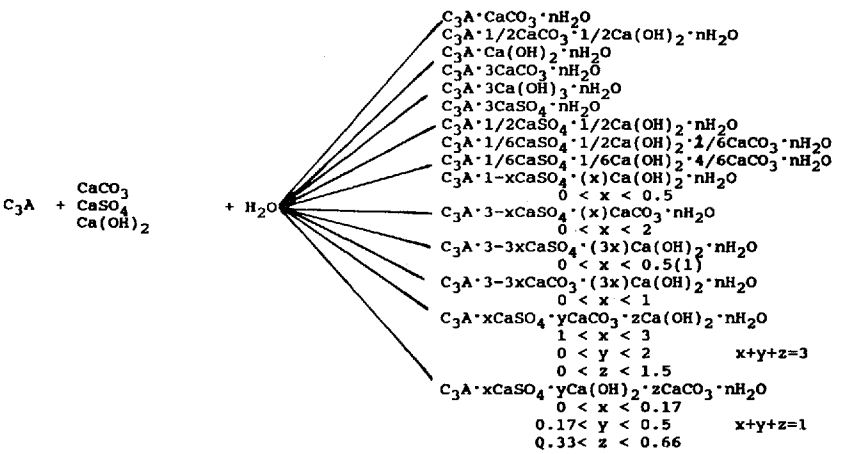

FIG. 3 Phases and solid solutions containing sulfate, carbonate and hydroxide

It is worthwhile to mention, that these ions can influence very strongly the hydration behaviour, the ccurse of hydration and the types of hydrates which are formed. The new ternary hydrates can only be identified by precise X-Ray measurements using least squares techniques. In most cases in technical products these phases must occur because of similar conditions and compositions. The content of different anions can vary in wide ranges. In the course of hydration and due to the availability of anions the compositions of all hydrates can be charged and conversion reactions may occur.

ACKNOWLEDGEMENT

Thanks are due to Deutsche Forschungsgemeinschaft for financial help and Dowell-Schlumberger(St. Etienne/Cambridge) for providing new equipment

REFERENCES

1. Brown,P.W., Libermann,C.O. & Frohnsdorff,G.:"Early hydration of tricalcium aluminate in solutions containing calcium sulfate", J.Am.Ceram Soc., 1984, 67, 793-799.

2. Collepardi,M., baldini,G. & Pauri,M.:"Tricalciumaluminate hydration in the presence of lime, gypsum or sodium sulphate", Cem.Concr.Res., 1978 8, 571-580.

3. Kuzel,H.-J. & Pöllmann;H.:"Hydration of C_3A in the presence of $Ca(OH)_2$ $CaSO_4 \cdot 2H_2O$ and $CaCO_3$",Cem.Concr.res., 1991, 5, 885-895

4. Kuzel,H.-J. & Meyer,H.:"Effect of CO_2 on the hydration of pastes", Proc. 1st. Symp. Hydr. of Cements, 1991, Dijon

5. Pöllmann,H., Kuzel,H.-J. & Wenda,R.:"Compounds with ettringite structure", 1989, N.Jb.Min.Abh. 160, 135-158

6. Pöllmann,H. :"Solving X-ray powder pattern prcblems dealing with layer structures in the field of calcium aluminum hydroxi salts" - Proc. EPDIC 1, 1991

7. Muhamad,M.N., Barnes,P., Fentiman,C.H., Hauserman,D., Poellmann,H. & Rashid,S.:"A time resclved synchrotron energy dispersive diffraction study of the dynamic aspects of the sysnthesis of ettringite during mine packing", Cem.Concr.Res., (1992), in press

8. Schwiete,H.E., Ludwig,U. & Jäger,P.:"Investigation in the system $3CaO \cdot Al_2O_3$ - $CaSO_4$ - CaO - H_2O", Highway res.Board, Special Report 90, 1966 353-367

9. Stein,H.N.:"Some characteristics of the hydration of $3CaO \cdot Al_2O_3$ - $CaSO_4$ - CaO - H_2O", Sil.Ind., 1963, 28, 141-145

10. Taylor,H.F.W.:Cement Chemistry. Academic Press, 1991, 141-145

11. Vernet,C.:"Sequence and kinetics of hydration reactions of C_3A with gypsum, lime and calcareous fillers", Prcc.VIII.Int.Con.Chem.Cem. Rio de Janeiro, 1986, Vol.III, 70-74

APPENDIX

X-ray data of ternary lamellar phases

1. $C_3A \cdot 1/6CaSO_4 \cdot 1/2Ca(OH)_2 \cdot 2/6CaCO_3 \cdot nH_2O$
2. $C_3A \cdot 1/6CaSO_4 \cdot 1/6Ca(OH)_2 \cdot 4/6CaCO_3 \cdot nH_2O$

The X-ray data of $C_3A \cdot 1/2Ca(OH)_2 \cdot 1/2CaCO_3 \cdot nH_2O$ which are relatively similar are not included, because these data can be obtained from the JCPDS-cards.

1. X-Ray data of $C_3A \cdot 1/6CaSO_4 \cdot 1/2Ca(OH)_2 \cdot 2/6CaCO_3 \cdot nH_2O$

d	I/I_o	h k l	d	I/I_o	h k l
8.26	100	0 0 6	2.231	10	2 0 10
4.13	80	0 0 12	2.220	20	1 0 20
3.89	30	1 0 8	2.065	15	0 0 24
3.519	5	1 0 10	2.054	20	1 0 22
2.885	60	1 1 0	1.992	20	1 1 18
2.753	25	0 0 18	1.945	10	2 0 16
2.722	10	1 1 6	1.759	10	2 0 20
2.633	10	1 0 16	1.666	10	3 0 0
2.556	30	1 1 9	1.652	10	0 0 30
2.449	20	2 0 4	1.633	5	3 0 6
2.365	25	1 1 12	1.545	5	3 0 12
2.318	15	2 0 8			

2. X-Ray data of $C_3A \cdot 1/6CaSO_4 \cdot 1/6Ca(OH)_2 \cdot 4/6CaCO_3 \cdot nH_2O$

d	I/I_o	h k l	d	I/I_o	h k l
8.20	100	0 0 6	2.206	30	1 0 20
4.10	80	0 0 12	2.166	5	1 1 15
3.88	30	1 0 8	2.050	15	0 0 24
3.506	5	1 0 10	2.043	20	1 0 22
2.884	40	1 1 0	1.985	10	1 1 18
2.732	20	0 0 18	1.940	10	2 0 16
2.722	10	1 1 6	1.753	10	2 0 20
2.620	10	1 0 16	1.666	10	3 0 0
2.553	15	1 1 9	1.641	10	0 0 30
2.449	35	0 2 4	1.632	5	3 0 6
2.36	25	1 1 12	1.609	5	2 1 16
2.315	10	2 0 8	1.543	5	3 0 12
2.228	10	2 0 10			

INVESTIGATIONS ON PORE STRUCTURE OF QUICK CEMENT

D Knöfel and J Wang

Laboratory for Chemistry of Construction Materials, University of Siegen
Siegen, GERMANY

SUMMARY

The pore structure of three different types of quick cement pastes in the system C-S-A-F-SO_3-CaF_2 was inverstigated at varied hydration periods (2h up to 1 year), temperatures (5°C and 20°C) and storage conditions (in water; in open air and in a CO_2-cabinet with 1 vol.-% CO_2 at 20°C and 65% relative humidity). The hydration behaviour, the carbonation process, the influence of temperatures and the relation between the pore structure and the technological properties of quick cement pastes are discussed.

The results have shown, that the low temperature retards the hydration of alit and only influences the porosity of early hydrated cement pastes, as well. The carbonation causes an increase of the total porosity of cement paste (especially an increase of the capillary pore content). The carbonation effects a deterioation of the chemical and mechanical properties of the quick cements.

ZUSAMMENFASSUNG

Die Porenstruktur des Zementmörtels aus drei Schnellzementen im System C-S-A-F-SO_3-CaF_2 wurden nach Hydratationszeiten zwischen 2 Stunden und 1 Jahr bei Lagerung in Wasser, in Luft und in 1 Vol.-% CO_2 bei Temperatur von 5°C und 20°C untersucht.

Es zeigte sich, daß die frühere Hydratation des Alits durch die niedrigere Tempertaur verzögert wird. Die Carbonatisierung verursacht eine deutliche Zunahme der Gesamtporosität (insbesondere eine Zunahme des Kapillarporenvolumens). Durch die Carbonatisierung werden die technologischen Eigenschften der Schnellzementen beeinträchtigt.

INTRODUCTION

Cement paste is a product of the chemical reactions of cement with water. Most of the added water is consumed in hydration reactions, while the excess water, if it evaporates, leaves an equal volume of pores whose amount and size distribution characterize each cement paste. The pore, with sizes varying from 0.03 µm to about 10 µm constitute the so-called capillary porosity. This, along with the gel porosity (radius smaller than 0.03 µm) and air pores (radius larger than 10 µm) (1) influences essentially the engineering properties and durability of cement mortars.

Kjellsen et al (2) found that the curing temperatur plays an important role in determination of the pore structure of hydrated cement pastes. A high curing temperature increased the volume of the large pores. The air pollution with aggressive gases (3) and the carbonation of the hydrated cement pastes (4-8) could impair the microstructure of the cement mortars and result in an increased porosity.

In the system C-A-S-F-CaF_2 Uchikawa and Tsukiyama (9) reported an investigation of the pore structure of Jet Cement pastes hydrated at 20°C. They found that the high degree of hydration of Jet Cement at earlier ages resulted in a small pore size and a low porosity because of a larger formation of ettringite in cement pastes.

This paper describes an investigation of the pore structure of quick cement mortars at different curing temperatures (5°C and 20°C) and under different storage conditions (in water, in open air and in 1 vol.-% CO_2).

EXPERIMENTAL PROCEDURE

Three different types of quick cement pastes from the system C-S-A-F-SO_3-CaF_2 (10) were prepared. The characteristics of the different types of quick cement are given in table 1 and 2.

No.	SiO_2	Al_2O_3	Fe_2O_3	CaO	MgO	Na_2O	SO_3	F^-	TiO_2	LOI
A	16.6	11.9	1.12	56.0	1.85	1.09	7.84	1.29	0.07	2.03
B	14.2	19.0	1.25	48.7	2.57	0.86	7.12	0.96	1.17	4.05
C	12.2	21.1	1.00	44.9	1.67	1.11	12.8	0.49	0.69	4.17

Table 1: Chemical composition of quick cements (wt.-%)

The quick cement mortars were prepared with different water cement ratios (A=0.5, B and C=0.57) in 15 x 15 x 60 mm molds, and were demolded after 24h. The mortar prisms were stored in curing tanks at temperatures of 20°C and 5°C until performance of test. The hydration of the cement mortars was stopped with acetone. The prisms were crushed to a size of 2 to 4 mm and measured after a drring period of at least 7 days at 70°C.

No.	C_3S	$C_{11}A_7 \cdot CaF_2$	$C_4A_3\bar{S}$	C_2S	C_4AF	W/C	β_{2h}	β_{28d}
A	70	25	-	-	5	0.50	11.5	53.2
B	-	60	-	30	10	0.57	15.4	48.6
C	-	5	60	30	5	0.57	7.2	48.3

* : Specific surface of quick cements was 5000 ± 200 cm^2/g (according to Blaine).
** : Water cement ratios A=0.5, B and C=0.57.
*** : β_{2h} and β_{28d} are compressive strengths of cement mortars after 2h and 28d.

Table 2: Mineralogical composition and compressive strength (N/mm^2) of quick cements after 2h and 28d.

The carbonation behaviour of quick cements was tested on mortar prisms. After a previous water storage of 27 days , a set of prisms was stored in open air, another in a carbonation cabinet with 1 vol.-% CO_2 (20±2°C, 65±5% rel. humidity). The reference samples (H_2O-series) were stored in water at 20°C during the whole period of the experiment.

The pore size distribution of the cement mortars were obtained by using the mercury intrusion method. The porosimeter (AUTOPORE II 9220, Micromeritics) was capable of detecting pore size of radii 0.001 µm to 300 µm.The compressive strength of quick cement mortars in accordance to DIN 1164 part 7 were determined by measurements of 15 x 15 x 60 mm molds.

RESULTS AND DISCUSSION

There are three different types of pores (air pores, capillary and gel pores) in hydrated cement mortars. Most of the air pores are ball-shaped, their amount and size distribution are unchanged with increasing hydration. Therefore the air pores are not discussed in this paper.The porosity of capillary and gel pores of cement mortars at 20°C and 5°C are listed in table 3.

The measurements of the porosity of cement mortar A at 5°C after 2h and 6h is impossible because of the strong retard of hydration of alite-rich cements at low curing temperatur. According to the reference (11) the reason can be that the " dormant " period of the hydration of alite, because of the low curing temperature, was increased.

Table 3 shows that the pore volume of capillary pores of cement A at 20°C decreases with additional hydration from 8.4% (after 1d) to 3.5% (after 28d) and at 5°C from 11.6% to 5.1%. In contrast the pore volume of gel pores increase at 20°C from 5.5% (after 1d) to 6.3% (after 28d) and at 5°C from 3.2% to 7.6%. The rapid increasing of the gel porosity at longer storage at 5°C can be attributed to the greater hydration and better formation of the calciumsilicathydrate of alite.These results are largely corresponding to those of Walz and Bonzel (12) who reported a favourable formation of the longer fibroid calciumsilicathydrate at the low curing temperature than 20°C.

mortar	porosity	2h	6h	1d	7d	28d
A	cap. p.	15.2	12.2	8.4	6.7	3.5
A	gel p.	3.7	4.9	5.5	5.7	6.3
B	cap. p.	14.6	13.0	11.1	6.4	4.1
B	gel p.	3.7	4.4	5.9	8.8	9.4
C	cap. p.	17.5	16.9	15.0	12.8	10.6
C	gel p.	3.0	2.6	3.8	4.8	5.9
a	cap. p.	0	0	11.6	8.7	5.1
a	gel p.	0	0	3.2	4.9	7.6
b	cap. p.	14.5	13.3	11.7	8.0	6.2
b	gel p.	3.8	3.5	4.0	7.2	8.9
c	cap. p.	15.4	15.6	15.4	12.0	11.1
c	gel p.	3.5	2.9	2.8	5.4	6.0

* : cap. p. = capillary porosity (%), gel p. = gel porosity (%)

Table 3: Porosity (%) of capillary pores and gel pores of quick cement mortars at 20°C (A,B,C) and 5°C (a,b,c).

The capillary pore volume of cement mortars at 5°C, is with the help of these longer calciumsilacathydrate fibre reduced quicker than at a temperature of 20°C. At the same time the pore volume of the gel pores increase. This pore structure development of cement mortars plays a very important role for the strength development. This is the reason why the cement mortars at longer storage and at a temperature of 5°C have a higher strength development than the mortars which were stored at 20°C.

The difference in porosity of the cement mortars B and C between different curing temperatures are smaller because of the high degree of hydration at earlier ages is dependent on the mineralogical composition of $C_{11}A_7 \cdot CaF_2$ and $C_4A_3\bar{s}$.

Figure 1 shows the capillary and gel porosity of the cement mortar B at different storage conditions (in water, in open air and in CO_2-enriched air). The 1 vol.-% CO_2-concentration in CO_2-cabinet is about 30 times higher than the CO_2-concentration in natural atmosphere. The storage period of 28d and 180d in the CO_2-cabinet corresponds to a storage of about 3 and 18 years in natural atmosphere.

As expected the capillary porosity decreases with increasing hydration from 5.1% (after 28d in water) to 4.2% (after 180d in water) and the gel porosity raises from 8.4% to 9.5%. In comparison with the pore development in water the capillary and gel porosity shows with increasing " unfavourable " storage (in water - in open air - in CO_2-enriched air) a reversed tendency. The capillary porosity of the carbonated cement mortars increases up to 10.5% (after 180d in CO_2-enriched air). This is about two times higher than the reference sample (4.2%, after 180d in water). The gel porosity decreases at the same time up to 5.3% (after 180d in CO_2-enriched air) which is lower than the reference sample (9.5%, after 180d in water). The reason therefore is that the intruded CO_2-molecules react with the hydratedproducts in the pores and causes the decomposition of the hydrates which promotes an increase of the capillary pores. This makes the CO_2-difussion easy and further decomposes the hydrates quite easy.

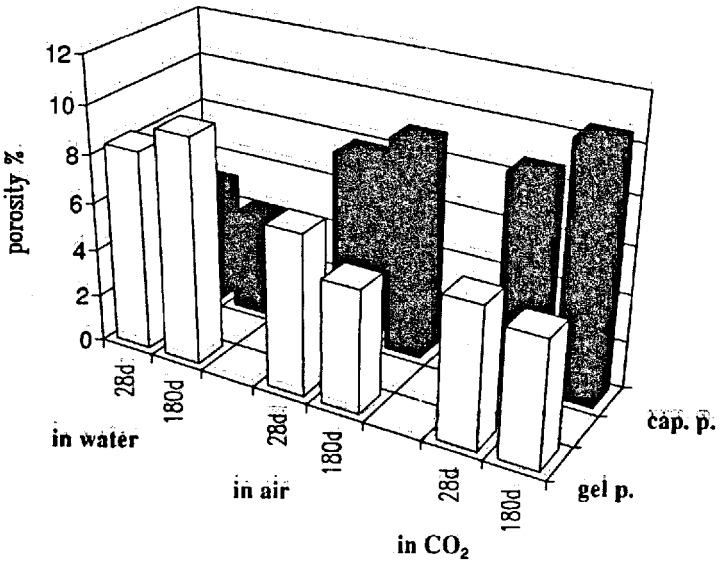

Fig. 1: Porosity of capillary pores and gel pores of cement mortar B after 28 and 180 days´ storage in water, air and in 1 vol.-% CO_2

The strength development of the porous cement mortars are clearly decreased with the additional carbonation of the hydrates. Table 4 shows that the compressive strength of the quick cements B and C decreases from 78.2 N/mm^2 and 72.7 N/mm^2 (reference sample, after 180d in water) down to 47.2 N/mm^2 and 27.9 N/mm^2 (totaly carbonated, after 180d in CO_2-enriched air).

Contrary to the results obtained from cement mortars B and C these results show a favourable compressive development of the quick cement A after carbonation. The compressive strength increases from 79.4 N/mm^2 (reference sample, after 180d in water) up to 85.9 N/mm^2 (after 180d in CO_2-enriched air). These results can be attributed to the considerable formation of $Ca(OH)_2$ in cement pastes of cement A which causes a higher amount of $CaCO_3$ in the cement mortars.

mortar	time	in water	in air	in CO_2
A	28d	9.0/54.0	9.4/67.0	9.7/71.8
A	180d	8.5/67.5	7.7/60.9	14.6/89.4
A	1a	9.9/79.4	7.1/57.8	14.7/85.9
B	28d	7.0/52.8	9.1/68.8	8.3/64.0
B	180d	7.1/65.0	8.1/58.7	7.6/53.1
B	1a	8.1/78.2	8.0/56.3	6.9/47.2
C	28d	6.6/48.7	7.3/62.6	6.0/46.3
C	180d	7.0/60.4	7.0/54.4	5.2/33.3
C	1a	7.8/72.7	6.3/46.1	4.7/27.9

Tabele 4: Strength development of cement mortars in water, air and 1 vol.-% CO_2 (bending strength / compressive strength, N/mm^2)

CONCLUSION

The low curing temperatur (5°C) could mostly retard the hydration of the alite-rich cement from the system C_3S-$C_{11}A_7{\cdot}CaF_2$-$C_2(A,F)$ at earlier ages, but it has no negative effect on the hydration of cements from the $C_{11}A_7{\cdot}CaF_2$-C_2S-$C_2(A,F)$- and $C_4A_3\bar{s}$-C_2S-$C_2(A,F)$-system.

The cement mortars which were stored at 5°C in comparison with the cement mortars stored at 20°C show a higher strength development at longer periods of hydratation because of a better cristallization of hydrated products at low curing temperature in cement pastes.

The effect of carbonation of the porosity or microstructure of mortars is quite significant. With additional carbonation the porosity of capillary pores increases and at the same time the porosity of gel pores decreases. This means that the carbonation causes an increase of the large pore volume. These results suggest that the carbonation could reduce the durability of quick cement mortars.

The influences of carbonation on the strength development of quick cement are dependent on the mineralogical composition of the cement clinker. The alite-rich cements from the C_3S-$C_{11}A_7{\cdot}CaF_2$-$C_2(A,F)$-system have a better capability of resistance to carbonation than the cements from $C_{11}A_7{\cdot}CaF_2$-C_2S-$C_2(A,F)$- and $C_4A_3\bar{s}$-C_2S-$C_2(A,F)$-system because of a large formation of hydroxyde and C-S-H-gel with higher alkalinity in hydrated cement pastes.

REFERENCES

1. Romberg, H.: "Zementsteinporen und Betoneigenschaften". Beton-Information, 1978, 5, 50-55

2. Kjellsen, K. O., Detwiler, R. J. and Gjorv, O. E.: "Pore structure of plain cement pastes hydrated at different temperatures". Cement and Concrete Research, 1990, 20, 927-933

3. Scholl, E. and Knöfel, D.: "On the effect of SO_2 and CO_2 on cement paste". Cement and Concrete Research, 1991, 21, 127-136

4. Goodbrake, C. J., Young, J. F. and Berger, R. L.: "Reaction of hydraulic calcium silicates with carbon dioxyde and water". J. Am. Ceram. Soc., 1979, 62, 488-491

5. Sauman, Z.: "Carbonization of porous concrete and its main binding components". Cement and Concrete Research, 1971, 1, 645-662

6. Suzuki, K., Nishikawa, T. and Ito, S.: "Formation and carbonation of C-S-H in water". Cement and Concrete Research, 1985, 15, 213-224

7. Saumen, Z. and Lach, V.: "Long-term carbonization of the phases $3CaO{\cdot}Al_2O_3{\cdot}6H_2O$ and $3CaO{\cdot}Al_2O_3{\cdot}SiO_2{\cdot}4H_2O$". Cement and Concrete Research, 1972, 2, 435-446

8. Maycock, J. N. and Skalny, J.: "Carbonation of hydrated calcium silicates". Cement and Concrete Research, 1974, 4, 69-76

9. Uchikawa, H. and Tsukiyama, K.: "The hydration of jet cement at 20°C". Cement and Concrete Research, 1973, 3, 263-277

10. Knöfel, D. and Wang, J.: "Untersuchungen zum Schnellzement im System CaO-SiO_2-Al_2O_3-Fe_2O_3-SO_3-CaF_2". Tonind.-Ztg., 1992 (in print).

11. Ghosh, S. N.: Advances in cement technology, Pergamon Press Ltd., Oxford England, 1983, p. 334

12. Walz, K. and Bonzel, J.: "Festigkeitsentwicklung verschiedener Zemente bei niederer Temperatur". Beton 1961, 11, 35-48

Fe_2O_3 SOLID SOLUTION OF ETTRINGITE

Yaozhong XI

Research Institute of Cement, China Building Materials Academy
P R CHINA

ABSTRACT

Ettringite solid solutions with 0–100% mole substitution of Fe_2O_3 for Al_2O_3 were synthesized. Their XRD, DTA and TGA analyses were carried out. The results show that (i) the cell parameters and thermal properties change continuously with increasing replacement of Fe_2O_3 in the ettringite lattice, and $\{Ca_3Al_{(1-x)}Fe_x(OH)_6 \cdot 12H_2O\}_2 (SO_4) \cdot 2H_2O$ $(0<x<1)$ is a complete solid solution without a miscibity gap, (ii) a cell grows with more incorporation of Fe_2O_3 in ettringite, and the cell parameter c_o of ferrite ettringite is about 0.1 Å bigger than that of aluminate ettringite and (iii) the coordination water in ferrite etrringite loses more easily at a temperature 6℃ lower than that in aluminate ettringite.

〔摘要〕

根据教科书和辞典资料，Fe_2O_3 在三硫型水化硫铝酸钙中固溶极限为 75%（克分子）。本研究合成 Fe_2O_3 的克分子百分含量从 0—100%的各种固溶体混晶，精确地测定了它们的晶胞参数，并做了失重和差热分析。结果证明，Fe_2O_3 在三硫型水化硫铝酸钙中为完全的连续固溶，随 Fe_2O_3 量增加晶胞参数 a_o 基本不变，c_o 增加，全铁端员差热曲线主吸热谷较全铝端员降低约 6℃。

1. INTRODUCTION

Ettringite, a complex solid solution and having studied by several cement researchers, is one of the most important hydrates for both ordinary cements and special cements. The setting, strength, expansion and durability of concrete are closely related to the formation and stability of ettringite. The composite mineralizer (gypsum plus fluoride), for example, is used extensively for shaft kiln cement burning in China. The cement produced by such technology has better early strength, impermeability, bond strength as well as smaller shrinkage [1]. More ettringite formed during early hydration is partially resposible for the above improvements.

The composition of ettringite, formed in cement and concrete and designated as AFt phase, is quite different from that of pure phase $[Ca_3Al(OH)_6 \cdot 12H_2O]_2(SO_4)_3 \cdot 2H_2O$, depending on impurities in cement. The dissolution of impurity elements changes the properties of ettringite. Al^{3+} in the columns of ettringite can be replaced by Ti^{3+}, Cr^{3+}, Mn^{3+} and Fe^{3+} [2], not by B_2O_3 and the first transision series V^{3+}, Co^{3+} [3]; CaO in the columns can be substituted by SrO, not by BaO [4]; SO_4^{2-} in the channels may be substituted by CrO^{2-} [5], CO_3^{2-}, OH^-[6], SO_3^{2-}, Cl^-, NO_3^-, ClO_3^-, $C_6H_5COO^-$ [7] and so on. Si^{4+} substitutes not only Al^{3+}, but also SO_4^{2-}.

It is reported that Fe_2O_3 solid solution in trisulfoaluinate hydrates is limited, the maximum molecular ratio of Fe_2O_3 to Al_2O_3 is 3, and the formula is $C_3(F_{0.75}A_{0.25})(C\bar{S})_3 \cdot H_x$[7]. The conclusion was based on the synthesis by G. Malquori and V. Cirilli [8]. They added mixed solutions of ferric sulphate and aluminium sulphate to limewater and synthesized Fe_2O_3 solid solutions with Fe_2O_3 mole percentage below 75%.

In order to gain a clear idea of whether Fe_2O_3 solid solution in ettringite is limited or not, and the effect of Fe_2O_3 dissolution in ettringite on cell parameters and thermal stability, 160 syntheses were made, Fe_2O_3 solid solutions containing mole percentage 0–100% of Fe_2O_3 were prepared, and their crystal data and thermal stability were measured.

2. EXPERIMENTAL

Analar reagents $CaCO_3$, $Al_2(SO_4)_3 \cdot 18H_2O$, $Fe_2(SO_4)_3 \cdot XH_2O$ were used, and CaO was obtained by decarbonation of $CaCO_3$ at 1000℃ for 3.5 hours in a muffle furnace. Various solid solutions of ettringite with different amount of Fe_2O_3 were prepared at 25℃ by mixing mixed solutions of $Al_2(SO_4)_3$ and $Fe_2(SO_4)_3$ (different ratio) with equal volume of excessively–saturated limewater in polyvinyl bottles shaken for 30 hours and stored for 20 days. The precipitates were filtered out rapidly using a suction bottle, washed by absolute alcohol, and dried at pressure 160 mm Hg to constant weight in a vacuum desiccator normally for 6 days with silica gel and soda–lime in the bottom. Attention was paid to avoiding contamination from atomspheric carbon dioxide during the synthesis. The solid solutions synthesized were checked with the optical microscope to be homogeneous crystals. No impurity phase was detected by XRD and DTA.

Cell parameters were measured using a Rigaku D / MAX–rA difractometer with Cu $K\alpha_1$ radiation, $\lambda = 1.5405$ Å, accelerating votage 40 KV, current 200 mA. The measure had three steps: (i) the cell parameters and powder data for the two end members (aluminate ettringite and ferrite ettringite) are determined accurately.[9], and the powder data have been accepted by the International Centre for Diffraction Data as JCPDS standard to replace the original data; (ii) relatively strong lines (100), (110), (112), (212), (304), (312) and (224) (Fig.1) were selected from diffraction

lines of the end menbers, and the 2θ changes of the above lines were determined by step scan (step width 0.02 °) and Si internal standard method; and (iii) the cell parameters of ettringite solid solutions with different Fe_2O_3 were calculated with the modified 9214 microcomputer program and corrected using accurate cell parameters of the two end menbers. The standard deviation of calculation of cell parameters is ± 0.04Å.

The results show that for measuring angle 2θ the internal standard method is better than the step scan. The latter is affected by votage, specimen density after pressing, surface flatness of specimens, the position of the specimen holder etc.

TGA was performed using SHIMATZU DT–2A thermal analyzer heating 200 mg sample in the air at a rate 100℃ / min., and DTA using Dupont 1090 thermal analyzer heating 15 mg sample in the air at 10℃ / min.

3. RESULT AND DISCUSSION

3.1 XRD patterns for aluminate ferrite ettringite solid solutions

Fig.1 gives the XRD patterns for solid solutions of ferrite mole substitution percentage for aluminate 0%, 30%, 60%, 90%, 100%. Roughly speaking, these solid solutions have the same patterns, and they are isomorphs. However, with Fe_2O_3 mole substitution rate increasing, some diffraction peaks appear or go up, and some disappear or go down, e.g. the line d=4.69 (104) on pattern of Fe 0% and Fe 30% disappears quickly, line d=4.744 (201) neaby appears gradually (see pattern Fe 100%). D–value and indexes of diffraction lines appearing on all the patterns are marked on the pattan of Fe 0% for the use in determination of cell parameters of Al–Fe ettringite.

3.2 Variation of cell parameters

Variation of cell parameters for Fe–Al ettringite is shown in Table 1 and Fig.2, which indicates that a_o keeps constant or slightly decreases with Fe_2O_3 content increasing (this is not definite, because 0.02 Å difference of a_o between aluminate ettringite and ferrite ettringite is within the error scope 0.04Å), and that c_o increases with Fe_2O_3 content in solid solutions from 21.40 Å of Al–ettringite to 21.50 Å of Fe–ettringite having the difference 0.1 Å.

According to Shannon and Prewitt [10], the ion radius of six–coordinated Al^{3+} is 0.535 Å, that of six–corrdinated Fe^{3+} 0.645 Å, and their difference 0.11 Å, approximately equal to the c_o difference between ferrite ettringite and aluminate ettringite. This shows that the crystal data determined are reliable and the substitution of larger Fe^{3+} for Al^{3+} makes the columns $[Ca_3(Al,Fe)(OH)_6 \cdot 12H_2O]^{3+}$ longer. The curves of a_o and c_o in Fig.2 are continuous, proving that the solid solution series of $C_3A \cdot 3CaSO_4 \cdot xH_2O$ and $C_3F \cdot 3CaSO_4 \cdot xH_2O$ is a continuous one of substitution type or complete isomorphic one, not a limited one described in current literature [7,8]. The c_o curve can be used to estimate Fe_2O_3 content for the binary Fe_2O_3–Al_2O_3 ettringite solid solutions.

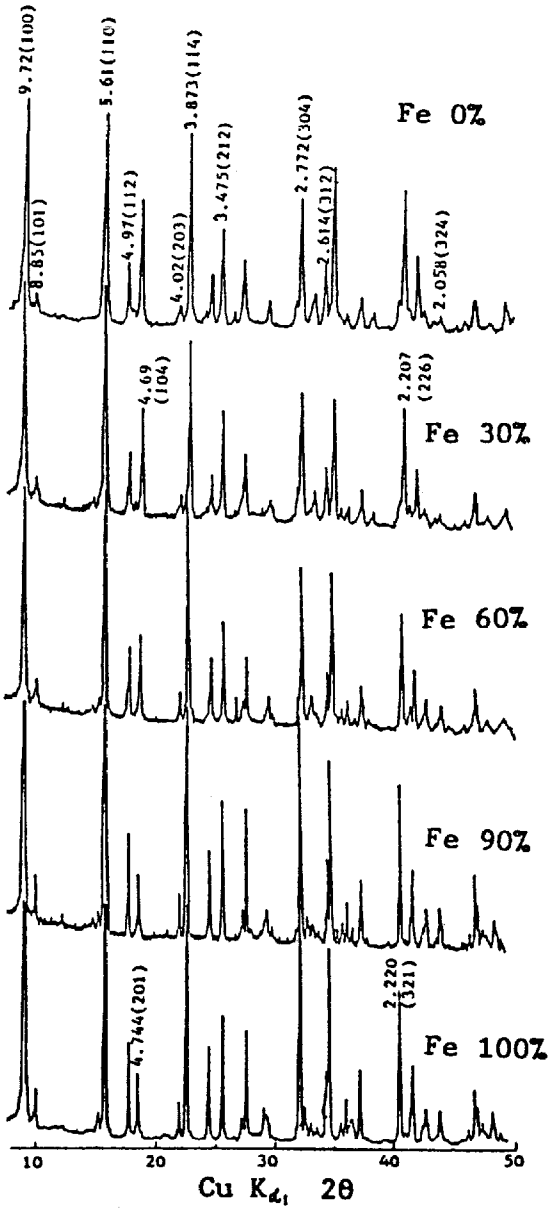

Fig.1 XRD patterns for solid solutions with different Fe_2O_3

Table 1 Cell-parameters for Al_2O_3-Fe_2O_3-solid solutions of ettringite

$\frac{F}{F+A}$ mole ratio	0	15	19	44	60	71	73	74	75	87	90	100
a_o	11.223	11.223	11.231	11.216	11.212	11.202	11.206	11.212	11.202	11.203	11.202	11.201
c_o	21.400	21.413	21.414	21.431	21.452	21.462	21.474	21.467	21.475	21.480	21.488	21.500

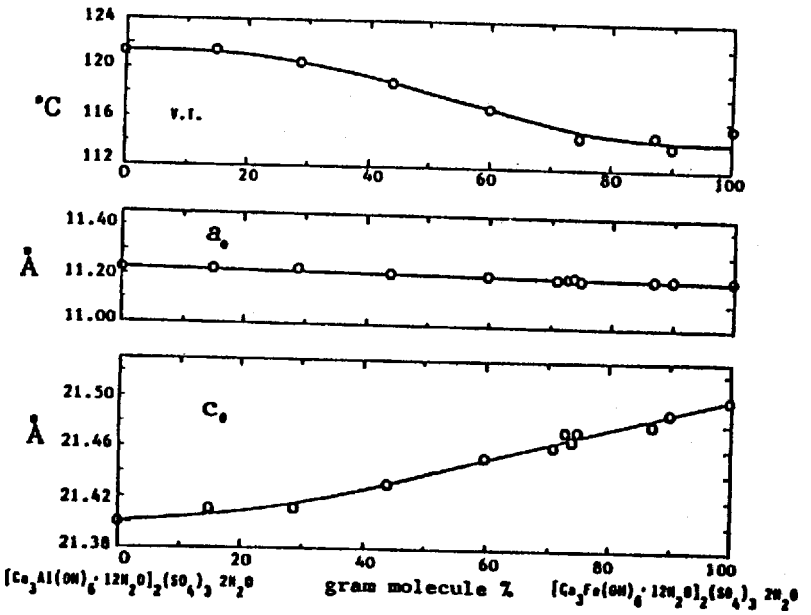

Fig.2 Variation of cell parameters and main endothermal valley temperatures with ferrite content in trisulfoaluminate–ferrite hydrate solid solutions: upper, main endothermal valley temperature of DTA; middle, a_o; lower, c_o

3.3 Thermal analysis

The TGA and DTA curves for Fe_2O_3–Al_2O_3 solid solutions are shown in Fig.3 and 4, from which the water loss up to 800℃ and the temperature of main endothermal valleys are obtained and listed in Table 2. The number of water molecules in the ettringite molecule were culculated from the water loss.

Table 2 Water loss at 800℃ and main endothermal valley temperature for trisulfoaluminate–ferrite solid solutions

$\frac{F}{F+A}$ (%)	0	15	29	44	60	75	87	90	100
800℃ water loss (%)	43.75	–	43.6	–	42.0	41.3	41.7	–	–
H_2O moleoules in an ettringite	30.8	–	30.7	–	29.5	29.1	29.3	–	–
main endothermal valley temperature(℃)	121.3	121.4	120.4	118.9	116.9	114.6	114.8	114.0	115.6

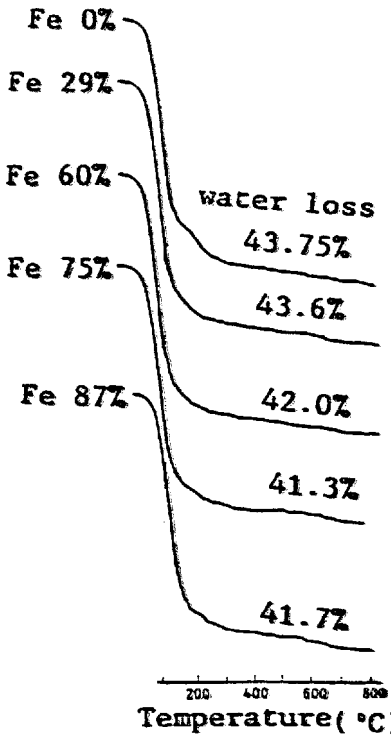

Fig.3 TGA curves of the Fe_2O_3–Al_2O_3 ettringite, samle weight 100 mg, heating rate 100℃ / min

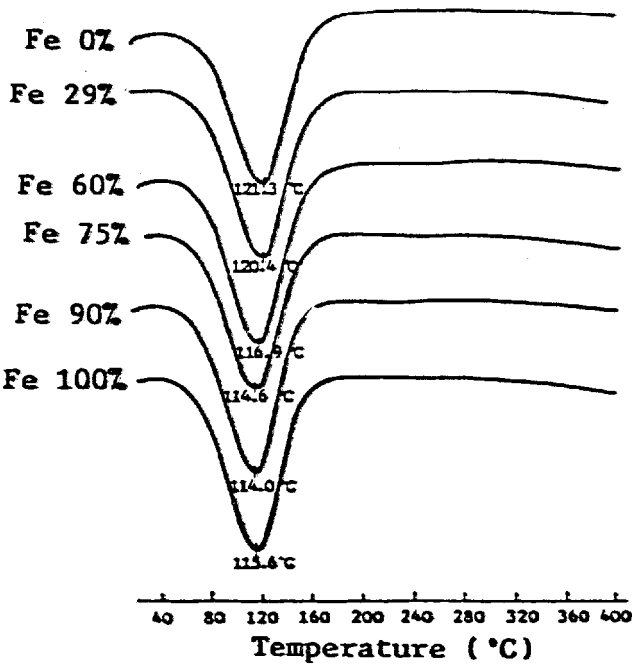

Fig.4 DTA curves of the Fe_2O_3–Al_2O_3 ettringite, sample weight 15 mg, heating rate 10℃ / min.

Fig.3 shows that the Fe_2O_3–Al_2O_3 solid solutions lose water beginning at 30℃ and most rapidly at 70℃. There is a small water–loss step at about 200℃ besides the main water–loss step on the TGA curve of all–aluminate ettringite (Fe 0%), and the other solid solutions with Fe_2O_3 have only one water–loss step. With Fe_2O_3 increasing, the steps move towards the low temperature side and the dehydation temperature lowers. The water loss at 800℃ can be considered as the sum of structure water and crystallization water (free water, abosprbed water and capillary water was removed in a 160 mm Hg pressure vacuum desiccator). It is seen from Table 2 that every molecule of aluminate ettringite has 31 H_2O, and that the molecule of the solid solution with 75% Fe_2O_3 has 29 H_2O, indicating that the ettringite with higher Fe_2O_3 loses the coordination water more easily.

The DTA curve for ettringite has a large endothermal valley at 100–160 ℃ and a small one at 260–300℃. The former is due to the loss of coordination water, and latter is due to the loss of structure water in $[Al(OH)_6]^{3-}$ [7]. The second small endothermal valley sometimes can not be distinguished especially when Al_2O_3 in ettringite is partially or completely replaced by Fe_2O_3. The curves in Fig.4 have one large endothermal valley, the temperature of which lowers from 121℃ of the all–aluminate end member to 115℃ of the all–ferrite end member by about 6℃, consistent with the result of Midgley and Rosaman [11]: endothermal valley for the all–aluminate end menber at 110℃, that for the all–ferrite end menber at 103℃. The valley temperature comes down more markedly for solid solutions with Fe_2O_3 25%–75%. The larger Fe^{3+} substitution for Al^{3+} causes ettringite cells to expand along the c axis, the binding force towards H_2O is weakened, and thus dehydration temperature comes down.

The third endothermal valley on the DTA curve of trisulfoaluminate hydrate reported early may belong to an other phase.

4. CONCLUSIONS

4.1 The solid solutions between $[Ca_3Al(OH)_6 \cdot 12H_2O]_2 \cdot 2H_2O$ and $[Ca_3Fe(OH)_6 \cdot 12H_2O]_2(SO_4)_3 \cdot 2H_2O$ form in any proportion, and their cell parameters and thermal properties change continuosuly. The solid solution series is continuous or entirely isomorphic.

4.2 Fe^{3+} substitution for Al^{3+} in ettringite leads to the maximum increase by 0.1 Å for c_o (the difference between end menbers) and no marked change for a_o, namely, the substitution makes the columns longer, and the distance a_o between columns almost constant.

4.3 The dissolution of Fe^{3+} in ettringite causes the main endothermal valley to move towards lower temperature, maximally by 6℃, showing that the stability of Fe_2O_3 ettringite to be a bit poor.

REFERENCES

1. Zhong Jingyu, Wen Ziyun, Wu Huiying and Yang Jiazhi, Proceedings of 1985 Beijing International Symposium on Cement and Concrete, China Building Industry Press, 1986, Vol.1, 68–91.

2. Bensted, J. and Prakash Varma, S., Cement Technology, 1971, 2(3), 100.

3. Bensted, J. and Prakash Varma, S., Cement Technology, 1971, 2(3), 73–76.

4. Bensted, J. and Prakash Varma, S., Cement Technology, 1972, 3(5), 185–187.

5. Bensted, J. Parkash Varman, S., Silicates Industries, 1972, 37(12), 315–318.

6. Poellmann, H., Kuzel, H.–J. and Wenda, R., Cem. Concr. Res., 1990, 20(6), 941–947.

7. Lea, F.M., The Chemistry of Cement and Concrete, Third Edition, Edward Arnold Ltd. 1970, pp.221, 229, 334.

8. Malquori, G. and Cirilli, V., Proceedings of the Third International Symposium on Chemistry of Cement, London, 1952, 321–328.

9. Xi Yaozhong, Guisuanyan Xuebao (J. Chin. Silicate Soc.), 1988, 16(3), 557–564.

10. Liebau, F., Structural Chemistry of Silicates, Springer Verlag, 1985, 308.

11. Midgley, H.G. and Rosaman, D., Chemstry of Cement, Proceedings of the Foruth International Symposium, Vol.1, National Bureau of Standard, Monograph 43, 1960, 260.

EFFECT OF ZnO ON THE HYDRATION BEHAVIOUR OF $C_{11}A_7CaF_2$

Qian Guangren, Huang Wenxi, Yang Yurong and Qi Yanyong

Sichuan Institute of Building Materials, Mianyang, Sichuan
P R CHINA

ABSTRACT

The effect of ZnO-doping on the hydration and setting of $C_{11}A_7CaF_2$ was investigated. The results showed that on the one hand ZnO-doped $C_{11}A_7CaF_2$ can retard the hydration of $C_{11}A_7CaF_2$ remarkably and alter the behavior of the hydration products, which reduces the heat of hydration, results in prolonging of the induction period and setting time, prevents C_3AH_6 from forming hydration product. Beside, the results are correlated with the crystal structure of ZnO-doped $C_{11}A_7CaF_2$. On the other hand, the compounding of ZnO and gypsum will retard the hydration of $C_{11}A_7CaF_2$ more strongly.

本文研究了ZnO对氟铝酸钙的水化和凝结的影响. 结果表明: ZnO可以显著延缓氟铝酸钙的水化, 改变水化产物的性质, 如降低水化热, 诱导期和凝结时间延长, 阻止C_3AH_6的形成. ZnO和石膏的复合将使延缓效果更为明显 . 同时, 上述结果和氟铝酸钙的晶体结构存在密切联系.

INTRODUCTION

It is well known that $C_{11}A_7CaF_2$ has the characteristic properties of fast setting and fast hardening. The behavior of fluoraluminate cement is controlled by the hydration and hardening of $C_{11}A_7CaF_2$ to a considerable extent. Extensive studies on $C_{11}A_7CaF_2$ have been carried out by H. Uchikawa[1]. S.B.Wang[2] proposed that a small amount of $Ca(OH)_2$ or $CaSO_4$ does not retard $C_{11}A_7CaF_2$ hydration . It is only when 220%wt gypsum is added that the initial setting time is to be more than 45 minutes. Therefore , the key to altering the behavior of fast setting lies in modifying the structure and hydration process of $C_{11}A_7CaF_2$. The retarding effect of ZnO on C_3S and C_3A has been generally confirmed[3, 4, 5]. The main purpose of this work is to study the possibilities of changing the behavior of fast setting of $C_{11}A_7CaF_2$ througth solid solution formation of $C_{11}A_7CaF_2$ when containing a small percentage of ZnO.

EXPERIMENTAL

$C_{11}A_7CaF_2$ was prepared by heating a homogeneous mixture of analytical grade $CaCO_3$, Al_2O_3 and CaF_2 in a laboratory furnace for 4 hours at 1350℃. The synthesized samples were cooled slowly. The mixture of raw materials containing various amounts of ZnO are shown in Table 1. XRD data

Table 1. ZnO contents of samples

Samples	F0	F05	F15
ZnO %	0	0.5	1.5

indicated that the synthesized $C_{11}A_7CaF_2$ is a pure compound. Infrared spectroscopy has been used for structural analysis. The mixtures containing various proportion of synthesized $C_{11}A_7CaF_2$, analytical grade $CaSO_4 2H_2O$ and $Ca(OH)_2$ were ground to a Blaine fineness about 8000 cm^2/g. The samples in suspension (w/c=10) were stirred for a predetermined time and filtered liquid was used for liquid analysis. DTA, TG, and XRD were simultaneously used for identifying the hydration products of remaining in suspension after stopping the reaction by grinding the samples in methyl alcohol A conduction calorimeter was used to measure the rate of heat evolution during the hydration.

RESULTS AND DISCUSSION

1. Hydration characteristics of $C_{11}A_7CaF_2$ and ZnO-doped $C_{11}A_7CaF_2$

1.1 Hydration with pure water

There is a great difference in the hydration rate between $C_{11}A_7CaF_2$ and ZnO-doped $C_{11}A_7CaF_2$ in the presence of pure water. Fig.1a shows the result obtained from liquid analysis. When sample F0, which is pure $C_{11}A_7CaF_2$, is contacted with water the peak concentration for Al_2O_3 is obtained at about 10 minutes, then begins to drop. In the liquid phase for the sample F15 containing 1.5%wt ZnO , the same is achived in 45 minutes. It is only in 5 hours that Al_2O_3 concentration for both F0 and F15 tends to approximately approach each other. S.B.Wang[2] has proposed that there is a relation between the time that Al_2O_3 concentration in liquid phase reaches a maximum and initial setting time. Hence, it can be seen from Fig.1a that the initial setting time for sample F15 containing ZnO-doped $C_{11}A_7CaF_2$ is much longer than for sample F0 which is pure $C_{11}A_7CaF_2$. By comparing the heat evolution curves Fig.2a, there are distinct differences in the rate of heat evolution for different samples. For the sample F0, the first peak is not only a very sharp (220J/g.h) on appearing immediately after contacting with water, but also followed by a second peak when the first peak ends . The induction period of hydration for sample F0 can not be seen in the heat evolution curve. When ZnO is added to the structure of $C_{11}A_7CaF_2$, it reduces remarkably the initial

rate of heat evolution of ZnO-doped $C_{11}A_7CaF_2$. The initial rate of heat evolution for sample F15 doped 1.5%wt ZnO is 25J/h.g, equal to one-ninth that of pure $C_{11}A_7CaF_2$. At the same time, the time when the second peak occurs is postponed with increase in ZnO content, the delay corresponding to

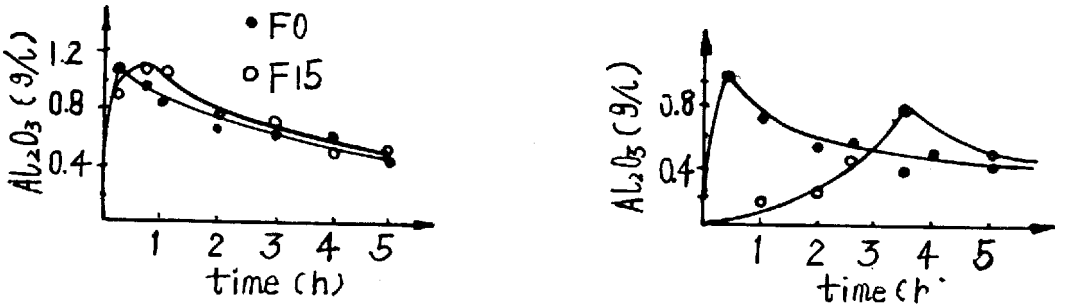

(a). With pure water (b). With CH and 10%wt $C\bar{S}H2$

Fig. 1 Liquid analysis results for hydrated samples with pure water as well as the solution of CH and $C\bar{S}H_2$

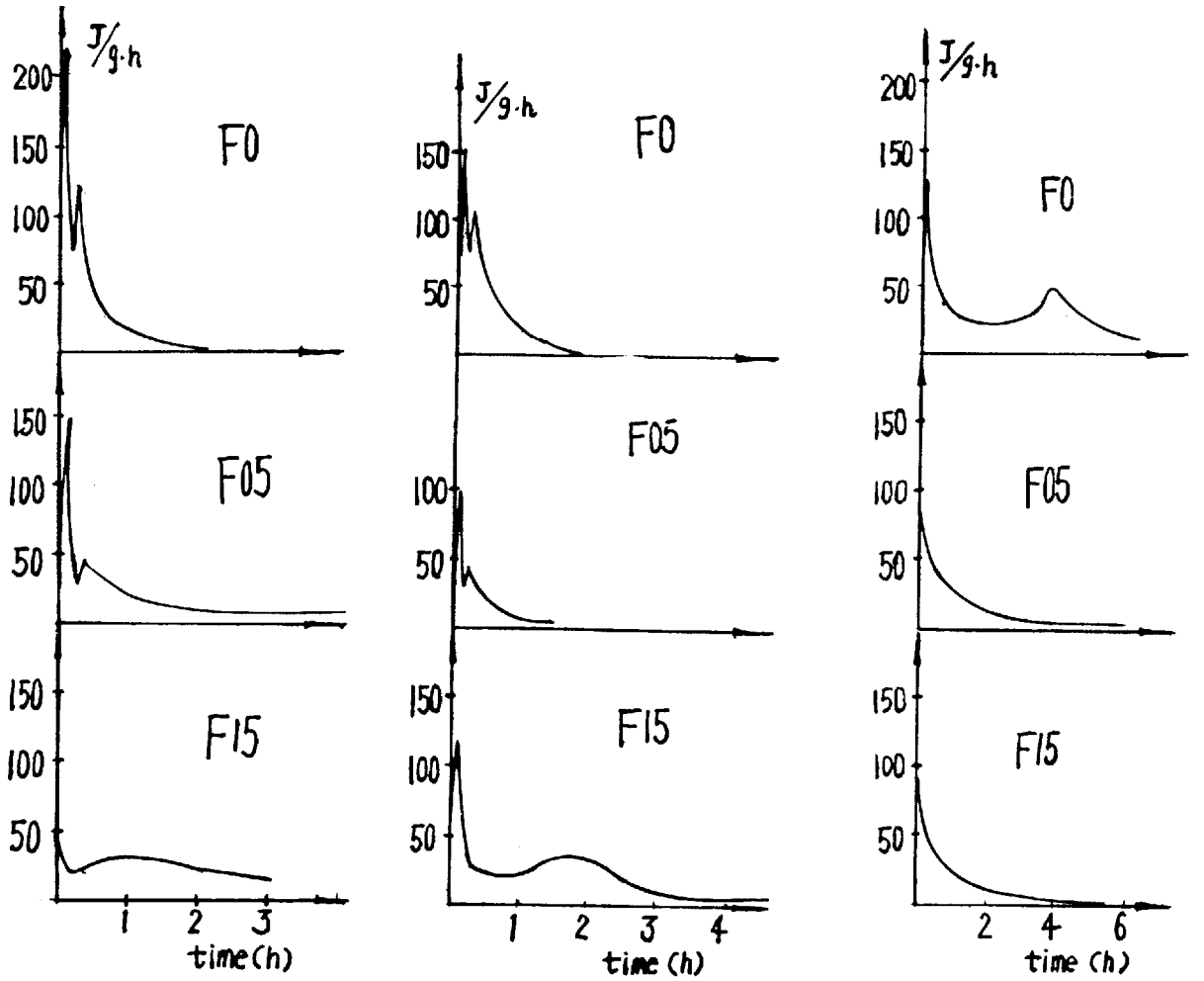

(a). With pure water (b) With CH and 10%wt $C\bar{S}H_2$ (c) With CH and 20%wt $C\bar{S}H_2$

Fig. 2 Rate of heat evolution for samples with pure water as well as the solution of CH and $C\bar{S}H_2$

the prolongation of the induction period. Thus, the induction period of ZnO -doped $C_{11}A_7CaF_2$ becomes clear. It is generally considered that the heat evolution curve of portland cement correlates with the time of initial and final setting. Table 2 shows the results of setting time of samples in pure water. Obviously, ZnO is possessed of effect of making the setting of $C_{11}A_7CaF_2$ retarded.

1.2 Hydration with $Ca(OH)_2$+$CaSO_4 2H_2O$ solution

The effect of gypsum on the hydration of $C_{11}A_7CaF_2$ in saturated solution of $Ca(OH)_2$ is quite complicated. The variation in the Al_2O_3 concentration produced by $C_{11}A_7CaF_2$ in suspension solution of saturated $Ca(OH)_2$ and 10%wt $CaSO_4 2H_2O$ is shown in Fig. 1b. The hydration characteristics of sample F0 in a solution of saturated $Ca(OH)_2$ and 10%wt $CaSO_4 2H_2O$ is

Table 2. Setting time in pure water for samples

Samples	F0	F05	F15
Initial, min	0	12	23
Final, min	14	25	41

much similar to that as in pure water, hydrating rapidly and the Al_2O_3 concentration reaching a maximum in about 10 minutes. However, for the sample F15 doped with 1.5%wt ZnO, the time in which Al_2O_3 concentration reaches a maximum is extended from 45 minutes in pure water to three and a half hours. Because $CaSO_4 2H_2O$ is added to the system ZnO-$C_{11}A_7CaF_2$-$Ca(OH)_2$-$CaSO_4 2H_2O$, it further retards the hydration of ZnO -doped $C_{11}A_7CaF_2$. Studies on the rate of heat evolution of hydration of samples in the solution of $Ca(OH)_2$ and $CaSO_4 2H_2O$ Fig. 2b indicated that the induction period for sample F0 when hydrated in saturated $Ca(OH)_2$ and 10%wt $CaSO_4 2H_2O$ is still too indistinct to be observed. With $CaSO_4 2H_2O$ concentration raised to 20%wt Fig. 2c, the induction period for sample F0 is extended remarkably. Also, the induction period for samples doped with ZnO is found to increase with increase of ZnO content in the presence of solution of $Ca(OH)_2$ and $CaSO_4 2H_2O$. This trend becomes more and more clear when $CaSO_4 2H_2O$ content is increased. Table 3 shows the setting time of $C_{11}A_7CaF_2$ when hydrated in a solution of $Ca(OH)_2$ and $CaSO_4 2H_2O$. According to Table 3, the setting time for sample F0 is still much shorter, only 3 minutes. But the initial setting time for sample F15 is extended to 49 minutes. The above results indicate that the fast setting behavior of $C_{11}A_7CaF_2$ can not be changed when a little $CaSO_4 2H_2O$ is added. Effective compounding of ZnO, $CaSO_4 2H_2O$ and $Ca(OH)_2$ can cause the fast setting of $C_{11}A_7CaF_2$ to be retarded remarkably. It is considered to be connected with both the structure of ZnO-doped $C_{11}A_7CaF_2$ and the behavior of the hydration products.

2. Structure characteristics of $C_{11}A_7CaF_2$ and ZnO-doped $C_{11}A_7CaF_2$

Table 3. Setting time for samples with CH and $C\bar{S}H_2$

Condition		F0	F05	F15
CH+10%$C\bar{S}H2$	Initial, min	3	22	49
	Final, min	24	34	73
CH+20%$C\bar{S}H2$	Initial, min	134	180	180
	Final, min	156	*	*
Note: * stands for no setting within 5 hours				

The crystal structure of pure $C_{11}A_7CaF_2$ is investigated by IR. All the results are not all the same like what Shen Mao[6] proposed. On the basis of Schroed and Iyer's[7] results, it may be concluded from Fig. 3 that there exist two kinds of coordinated groups, i.e., coexistence of AlO_4 tetrahedra and AlO_6 octahedra in the structure of pure $C_{11}A_7CaF_2$. Both the coexistent forms and the structural hole with distortion of the coordinated groups make pure $C_{11}A_7CaF_2$ with much higher hydration activity.

Table 4. Synoptic results of hydration Products for $C_{11}A_7CaF_2$ with pure water

sample	time	hydration products		
		C_2AH_8	C_3AH_6	AH_3
F0	0.5	s	s	s
	1	s	s	s
	5	s	s	s
F05	0.5	s	s	s
	1	s	s	s
	5	w	s	s
F15	0.5	w	0	w
	1	s	0	s
	5	s	0	s
Note : w=weak, s=strong				

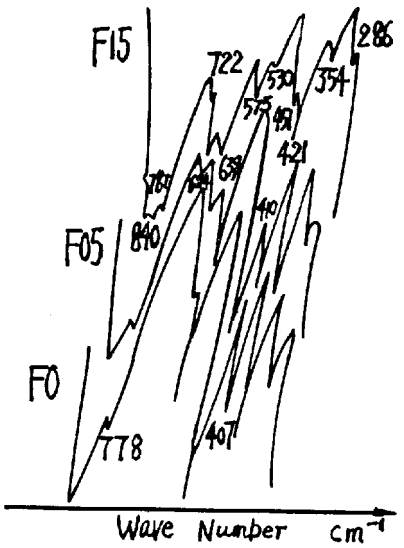

Fig.3 IR spectra for samples

The effect of ZnO on the structure of $C_{11}A_7CaF_2$ has three fold possibilities as follows: (1) structural hole size of pure $C_{11}A_7CaF_2$ may be changed to be smaller, the thermodynamic stability may be raised, when ZnO is incorporated into the structure of pure $C_{11}A_7CaF_2$ forming solid solution of ZnO-doped $C_{11}A_7CaF_2$. (2) The Al-O bond strength of AlO_4 and AlO_6 in the structure of $C_{11}A_7CaF_2$ is enhanced. As ZnO content is increased, it is observed from Fig. 3 that the characteristic frequencies of isolated AlO_4 and AlO_6 groups are shifted respectively to higher number, for example, $407cm^{-1}\rightarrow410cm^{-1}\rightarrow421cm^{-1}$ for isolated group AlO_4 and $778cm^{-1}\rightarrow780cm^{-1}\rightarrow787cm^{-1}$ for isolated AlO_6 group. The characteristic strength of vibration is also decreased correspondingly. The results show that the strength of Al-O bond in the structure of $C_{11}A_7CaF_2$ is enhanced with increase in ZnO content. (3) With the characteristic strength of vibration for the isolated AlO_4 and AlO_6 groups weakened gradually, the new frequencies of vibration for ZnO-doped $C_{11}A_7CaF_2$, ex., $635cm^{-1}$ for sample F05 and $639cm^{-1}$ as well as $722cm^{-1}$ for sample F15, are present in the IR spectra as ZnO content is increased, which is not the case for sample F0. In view of Schroed's results, these new frequencies correspond to the forming of condensed AlO_4 and AlO_6 groups. It may be concluded that both condensed AlO_4 and AlO_6 are gradually substituted for isolated AlO_4 and AlO_6, which substitution is in favour of increase of stability in the structure of ZnO-doped $C_{11}A_7CaF_2$. It is important that, consistent with the hydration behavior of ZnO-doped $C_{11}A_7CaF_2$, the rates of both heat evolution and hydration for ZnO-doped $C_{11}A_7CaF_2$ fall due to the modification of the structure, as a result the fast setting behavior of $C_{11}A_7CaF_2$ also is basically changed.

3. Characteristics of hydration products for $C_{11}A_7CaF_2$ and ZnO-doped $C_{11}A_7CaF_2$

3.1 Hydration with Pure Water

The hydration products for samples as a function of time are determined by DTA and XRD. The

results are summed up in Table 4. For sample F0 , the peaks at 82, 157, 220, 275 and 330 ℃ are observed at hydrating 30 minutes , which are assigned to the hydrates C_2AH_8 (157℃), C_4AH_{13} (220℃), AH_3 (80, 275℃) and C_3AH_6 (330℃) by Feldman [8]; For the sample F05, although the hydration rate is slower than for pure $C_{11}A_7CaF_2$, the products are just the same as for pure $C_{11}A_7CaF_2$. For the sample F15, the hydration products are altogether different from both samples F0 and F05 . There exist hydrates C_2AH_8, C_4AH_{13} and AH_3 but not C_3AH_6 within several hours of hydation . The results confirm the fact that formation of hydrate C_3AH_6 will be avoided as long as there exist suitable ZnO contents in the structure of $C_{11}A_7CaF_2$. Kalousek et al[9] proposed that the peak at 330 ℃ is equal to loss of 4.5 crystalline water for C_2AH_8 hydrate, i.e., $C_2AH_8 \rightarrow C_2AH_{1.5}+4.5H_2O$. Based on the equation , a changing tendency of hydrate C_2AH_8 as a function of time is calculated by rates of weightlessness at the peak 330℃ from DTA-TG curves. At the same time , formation of hydrate C_2AH_8 as a function of time can be plotted by rates of weightlessness at the peak 157℃ from DTA-TG curves. As is shown in Fig. 4 , C_2AH_8 hydrate decreases corresponding to the increase of C_3AH_6

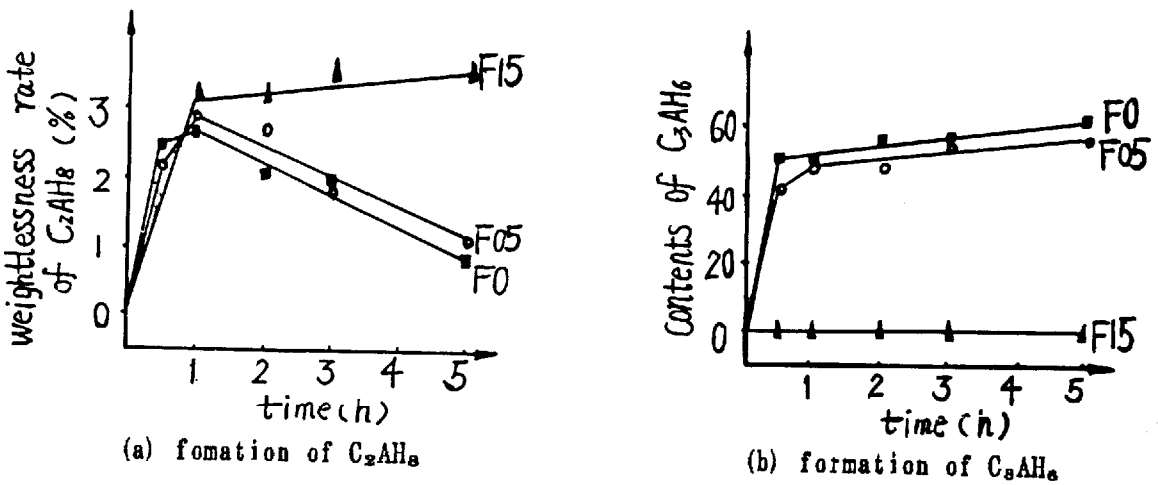

(a) fomation of C_2AH_8 (b) formation of C_3AH_6

Fig. 4 formation of hydrates C_2AH_8 and C_3AH_6 vs time

Table 5. Synoptic results of hydration products for $C_{11}A_7CaF_2$ with CH and $C\bar{S}H2$

Sample	Time (h)	Hydration products				
		AFt	AFm	C_2AH_8	C_3AH_6	AH_3
F0	0.5	w	0	s	w	w
	1	0	s	s	s	s
	5	0	s	w	s	s
F05	0.5	w	0	0	0	w
	1	w	w	w	0	w
	5	s	w	w	w	s
F15	0.5	w	0	w	0	w
	1	s	0	w	0	w
	5	s	w	s	0	s
Note : w=weak, s=strong						

hydrate. It is ascribed to the transformation from C_2AH_8 to C_3AH_6, which promotes hydration and fast setting of $C_{11}A_7CaF_2$.

3.2. Hydration with $Ca(OH)_2+CaSO_4 2H_2O$ solution

The hydration products in the presence of saturated $Ca(OH)_2$ and 10%wt $CaSO_4 2H_2O$ are shown in Table 5. It is evident that for sample F0, a large number of C_2AH_8 hydrates are formed beside a few of AFt hydrates at half an hour ; at the same time, the cubic hydrate C_3AH_6 can be observed which increases with time ; the AFt peak disappears and AFm forms in an hour. In comparision with the results obtained in pure water , the hydration for pure $C_{11}A_7CaF_2$ in the presence of $Ca(OH)_2$ and $CaSO_4 2H_2O$ is almost the same as the former . Upon contacting with water , the Al_2O_3 concentration reaches a maximum in no time; at the very moment, the SO_4^{2-} concentration in the system is very few. The results confirm the views proposed by Locher[10] that the much higher rate of hydration for pure $C_{11}A_7CaF_2$ does not keep its dynamic balance with the SO_4^{2-} concentration from the dissolution of gypsum in the system .Hence, a part of both $C_{11}A_7CaF_2$ and SO_4^{2-} react to give AFt; but remaining $C_{11}A_7CaF_2$ hydrates as the same as in pure water to form hydrates C_2AH_8, C_4AH_{13}, AH_3 and C_3AH_6 because of the absence of gypsum, which react with the AFt formed into AFm hydrate. The initial rate of hydration is lowered with addition of ZnO to the structure of $C_{11}A_7CaF_2$. It is easy for ZnO-doped $C_{11}A_7CaF_2$ to reach a dynamic balance with the SO_4^{2-} concentration from the gypsum dissolved in the liquid phase, resulting in formation of AFt hydrate which increases with the time of hydration.

CONCLUSIONS

(1) It is confirmed that not only the rate of hydration for $C_{11}A_7CaF_2$ is retarded but the fast setting behavior also is changed when suitable ZnO contents are added to the structure of $C_{11}A_7CaF_2$. The fast setting of pure $C_{11}A_7CaF_2$ can not be changed just by a small amount of gypsum. The effect of set retarding is most remarkable when the compounding effect of ZnO and gypsum is used.

(2) The hydration products formed by pure $C_{11}A_7CaF_2$ and ZnO-doped $C_{11}A_7CaF_2$ are different . The forming of C_3AH_6 hydrate can be avoided when enough ZnO is added to the structure of $C_{11}A_7CaF_2$.

REFERENCES

1. H. Uchikawa, Cem. Concr. Res. 3, 263, (1973)
2. Wang Shanba, J. Soc. Sili. 16 (4) 304 (1988)
3. I. Boikova, Tsment , 5, 3 (1978)
4. M. Handke et al , 8ICCC , Paris, 2, 21 (1986)
5. I. Odler , J. Am. Ceram. 3, 13 (1980)
6. Shen Mao, "新ひいセメントヒコンクリト" pp167 , (translated in Chinese)
7. R. A. Schroder J. Inorg. Chem. 28 , 1155 (1966)
8. R. Feldman , J. Am. Cerm. Soc. 49 (5) 268 (1966)
9. G. L. Kalousek, C. W. Davis, W. E. Schmewtz J. Amer. Concr. Inst. 45, 693 (1949)
10. F. M. Locher, Z-K-G 33 (6) 271 (1973)

THE STRUCTURE AND PROPERTIES OF HYDRATION OF DOPED DICALCIUM SILICATES

Yang Shuzhen and Song Hantang

Wuhan University of Technology
P R CHINA

SUMMARY

In this paper, several dicalcium silicates (β -C_2S) obtained by impurities have been studied. A study of the structure and properties of these doped dicalcium silicates revealed that the doping with MgO or $BaSO_4$ enhanced their activity and rate of hydration, K_2O had a similar effect rough less pronounced.

The lattice distortion and crystal size in β - dicalcium silicates were measured by X-ray powder diffraction technique, the bindiing energies of $2P^3$ for Ca and 2P for Si were obtained by X-ray photoelectric spectrum, the vibrations of the chemical bonds in silicate anion $[SiO_4]^{4-}$ were examined by FT-IR and Laser Raman spectra and the heat evolution during hydration reaction for β - dicalcium silicates were determined by microcalorimetry. From the results of XRD, XPS, FT- IR, Raman and micro-DSC, the relationship between the microstructure and properties of doped dicalcium silicates and the mechanism of activation due to impurities were discussed. It pointed out that the essential factors causing the enhancement of activity and acceleration of hydration reaction are the lattice distortion, crystal size, intercrystalline imperfections, the crystallochemical environment change and chemical shifts of the electron binding energies of Ca and Si atoms in doped β - dicalcium silicates.

摘　要

本文通过研究掺杂 β -C_2S的结构和性能，揭示了掺杂MgO和$BaSO_4$增强 β -C_2S的活性和加速水化反应速度，掺杂K_2O增强作用不甚明显。

用XRD测定了晶格畸变与晶粒大小，XPS测定了Ca和Si原子的电子结合能，FT－IR和Laser Raman 测定了结构基团的振动谱和micro-DSC测定了早期水化速率，并讨论了微观结构和性能之间的关系以及掺杂活化的 机理。指出晶格畸变、晶粒细化、界面缺陷、Ca和Si原子周围化学环境改变与电子结合能位移是掺杂 β -C_2S活性增 加和水化加速的根本原因。

INTRODUCTION

β-C_2S is one of the main minerals of cement. It is characterized by low formation temperature and high long term strength, But its slow rate of the hydration reaction and low early strength limits its content in cement clinker. Hence accelerating its hydration reaction and enhancing its early strength are an important problem in the chemistry of cement.

Recently belite cement clinker containing active β-C_2S has been one of the frontier areas in cement research. Changing the compositions of the raw material to form salt aluminum oxide sulfate and salt aluminum oxide fluoride (1) (2) or changing the burning and cooling conditions of the clinker (3), or doping with other ions to activate (4) may enhance the activity of belite cement clinker and increase the amount of β-C_2S in cement clinker so that not only the burning temperature of the clinker can be reduced, but also the early strength enhanced.

Doping is one of the methods of activating β-C_2S. This paper tries to discuss the nature of impurity activating β-C_2S by determining the structure and properties of β-C_2S doped with MgO, K_2O and $BaSO_4$.

SYNTHESIS OF DOPED β-DICALCIUM SILICATES

The mixtures of $CaCO_3$ and SiO_2 in the ratio 2:1 by weight, 3%MgO, 2%K_2O, 2%$BaSO_4$ were added separately and homogenized in agate mortar and then pressed into pellets with a liquid press. Clinkers were obtained from these pellets by burning them in platinum vessels at 1400℃ for 4 hours in a silicon-molybdenum electric furnace. No free-CaO was detectable in these clinkers when determined chemically with pheno-nitrobenzene by microscopy. XRD results indicated the products to be β-dicalcium silicates belonging to the monoclinic system. Their space group was $P2_1/n$.

MICROSTRUCTURE OF DOPED β-DICALCIUM SILICATES

1. Crystal lattice distortion and crystalline grains size.

The crystal lattice distortion and crystal size were evaluated by X-ray diffraction. The diffraction lines are sharp for the large and perfect crystallites and they are widened when the lattice is distorted or the crystal grains are fine. Their width changes with the magnitude of distortion and the fine grains.

The diffractograms of the specimens were obtained on Rigaku D-MAX/ⅢA diffractometer. The test conditions : 40kv/30mA, CuKα 2θ, 1° −1° −0. 3mm−carbon monochromator −0. 8mm−detector, preset-time counting (PT=40sec.), step width 0.02° . The pure and large grains of β-C_2S were considered as standard specimen. The averages of several diffraction lines of doped dicalcium silicates measured were computed on difference-mean square of the diffraction figuration and listed in Table 1.

Table 1 The Magnitude of Lattice Distortion and Crystalline Grains Size of Doped β-C_2S

Measurement Date / Specimens	Lattice Distortion (arc)	Crystalline Grains Size (Å)
1# (the pure)	standard	standard
2# (with 3% MgO)	0.003684	210
3# (with 2% K_2O)	0.002161	558
4# (with 2% $BaSO_4$)	0.003726	207

Data in Table 1 showed that the crystal lattice of β-dicalcium silicates is distorted and their crystallites were grown down. The magnitude of lattice distortion increased in the order 2% $BaSO_4$ > 3%MgO > 2% K_2O while the crystal sizes decreased in the same order.

2. The electronic binding energies of doped β-dicalcium silicates.

The binding energies of doped β- dicalcium silicates were determined by XPS on VG ESCALAB MKII multifunction electron spectrometer. Their data and chemical shifts are listed in Table 2.

Table 2 The Binding Energies of XPS (ev)

Determined Date / Specimens	Ca2P3		Si2P	
	Binding Energy	Chemical Shift	Binding Energy	Chemical Shift
1# (the Pure)	346.85	/	101.55	/
2# (with 3%MgO)	346.90	+0.05	101.60	+0.05
3# (with 3% K_2O)	346.60	−0.15	102.25	+0.70
4# (with 2% $BaSO_4$)	347.20	+0.35	101.75	+0.20

The date in Table 2 illustrate that the binding energies of Ca 2P3 and Si 2P changed and chemical shifts were produced.

The electron binding energies of the electron shells in an atom are under the influence of the electron charge distribution in the outermost shell of the atomic nucleus. The electronic arrangement in the outermost shell of the atomic nucleus determines the chemical charateristics of the atom. In other words, the atomic size, electrovalence and electronegativity are the factors of determining electron binding energies. The crystal distortion and fine grains are related to the characteristics above of the doping atom. The data of the ionic radius and electronegativity as related to this paper are listed in Table 3 .

Table 3 Relative Ionic Radii and Electronegativities

Element	Ca^{2+}	Si^{4+}	O^{2-}	K^{+}	Mg^{2+}	S^{6+}	Ba^{2+}
Ionic Radius (Å)	0.99	0.42	1.32	1.33	0.66	0.30	1.34
Electronegativity	1.0	1.8	3.5	0.8	1.2	2.5	0.9

As shown above , in MgO doping , Mg^{2+} radius being much less than that of Ca^{2+}, Mg^{2+} are filled in the interionic gaps in β-C_2S. Since the electronegativity of Mg^{2+} is more than that of Ca^{2+} , in order to maintain electrical neutrality, the chemical environment of Ca and Si atoms changed, which resulted in the crystal lattice distortion and the electron binding energies shifts.

By doping with K_2O, Ca^{2+} ions were replaced by K^+, The ionic radius of K^+ is higher than that of Ca^{2+}. This brought about ion deformation and lattice distortion. Also, as the charge of K^+ is not equivalent to the charge of Ca^{2+}, oxygen vacancies were produced after replacing each other. The electronegativity of Ca^{2+} being different from that of K^+ and the ions polarization changing , These brought about the shift in electron binding energies .

By doping with $BaSO_4$, Ca^{2+} were replaced by Ba^{2+} and $[SiO_4]^{4-}$ were replaced by $[SO_4]^{2-}$, not only their radii are different , but also the chemical polarity force of Ba^{2+} is less than that of Ca^{2+} and $[SO_4]^{2-}$ more than $[SiO_4]^{4-}$. These resulted in bonds of Si-O and Ca-O to change and the electron binding energies to shift. Moreover , all impurity ions collect in the crystal grain boundaries easily. They resist grains growing up and make boundary imperfections and fine grains (4).

3. The vibration spectra of silicate anion in doped β-dicalcium silicates.

IR spectra of the samples in the form of a KBr pellet were recorded on a Nicolet 60 SXB Fourier Transform Spectrometer and Raman spectra were obtained on a JOBIN YVON U-1000 Laser Raman Spectrometer with the conventional technique usually applied for powder samples.

Fig.1 and 2 show the FT-IR and Raman spectra of doped β-dicalcium silicates. Table 4 lists the FI-IR and Laser Raman spectra date of β-C_2S. These date are in accordance with earlies reports (5).

Comparing the vibration spectra of doped β-dicalcium silicates with that of pure β-C_2S, it was obsevered that the vibrations of silicate anion $[SiO_4]^{4-}$ were retained. This showed that the basic structure of doped β-C_2S did not change, but a fine change in the absorption bands was obsevered.

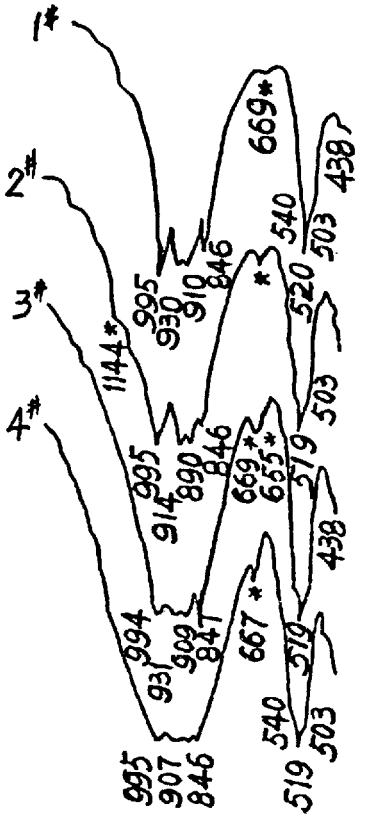

Fig. 1 FT-IR spectra of Doped β-dicalcium silicates

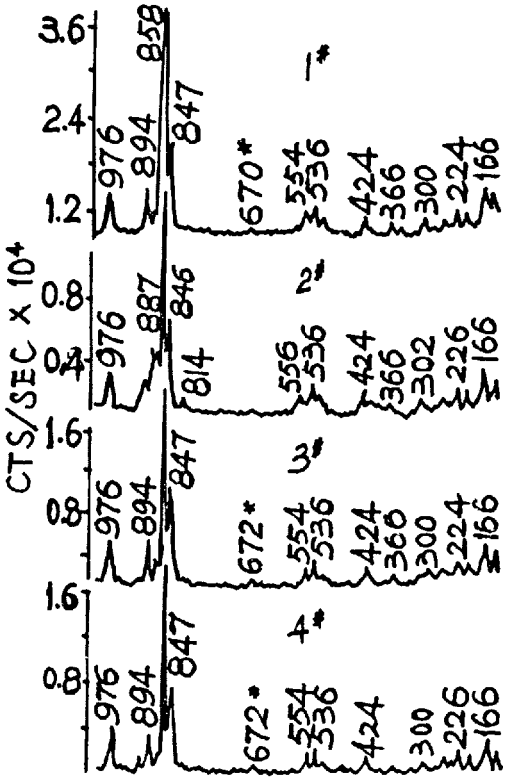

Fig. 2 Laser Raman Spectra of Doped β-dicalcium Silicates

*——the bands for marking * were the Si-O-Si vibrations produced because of little glasses in the samples.

In the MgO doped sample , the band at 950 cm^{-1} widened and its intensity decreased. On the other hand, the bands at 930 and 910 cm^{-1} shifted at 16～20 cm^{-1} and the intensity of the band at 846 cm^{-1} decreased in FI-IR spectra. The bands for the range 849～876 cm^{-1} were changed obviously, the intensity countings of all bands were decreased over half as many as that of pure β-C_2S in Raman spectra. These showed that the silicate anion $[SiO_4]^{4-}$ was distorted and there was crystal disorder.

By doping with K_2O, the band due to Si-O stretching and O-Si-O bending vibrations did not change much basically, but these bands were widened, their intensity decreased and resolution were reduced in FT-IR spectra. The intensity countings for Raman spectra bands were reduced over one half. These showed that the disorder of the crystal was increased after K^+ replaced Ca^{2+} in β - C_2S.

By doping with $BaSO_4$, not only the bands of $[SiO_4]^{4-}$ were widened considerably, but also the intensity of the bands at 995 cm^{-1} and 846 cm^{-1} decreased and the band at 930 cm^{-1} disappeared in FT-IR spectra. The relative intensity of the band at 894 cm^{-1} was decreased and other bands were reduced over one half in Raman spectra. These showed that crystal disorder intensifies and subcrystalline grains increase in number.

Table 4 FI-IR and Laser Raman Data of β-C_2S

Spectra	Si-O stretching Vibration	O-Si-O Bending Vibration	Ca-O, Si-O Mixed and Lattice Vibration
FT-IR (cm^{-1})	995 930 910 846	540 520 503 438	
Raman (cm^{-1})	976 914 894 876 858 847 824	554 536 516 424	366 346 300 256 224 202 166 146

HYDRATION CHARACTERISTICS OF DOPED β-DICALCIUM SILICATES

Group β-dicalcium silicates were powdered for 4 hours in agate ball grinding mill, and their early stage hydration reaction and heat evolution were determined by means of SETARAN C-80 microcalorimeter at 30℃ test temperature. Sample weight was 206.10 mg, and water to powder ratio 10:1. The data on heat of hydration are listed in Table 5. Fig.3 shows the hydration heat evolution curves.

Doping β-C_2S with MgO enhanced hydration reaction but less obviously before 5 hours. However after 5 hours and up to 24 hours the total heat evolution increased. The acceleration of hydation bore an obvious relation to MgO doping which caused lattice distortion and fine grains.

Doping β-C_2S with K_2O slowed down hydration reaction before 6 hours but increased thereafter. The acceleration effect was less pronounced in all; The total heat evolution increased but less obviously.

Doping β-C_2S with $BaSO_4$ visibly enhanced the hydration heat evolution during the first 12 hours. The total heat evolution was increased and the hydration reaction was accelerated visibly. These had a direct relation to doping with $BaSO_4$ when caused maximum shift in the electron binding energies, lattice as well as silicate anion $[SiO_4]^{4-}$ distortions and the minimum crystal grain.

Table 5 Heat of Hydration of Doped β-C_2S

Heat of Hydration (J/g) Specimens / Time (h)	1# (the pure)	2# (with 3%MgO)	3# (with 2%K_2O)	4# (with 2%$BaSO_4$)
0.5	2.219	2.512	2.345	2.847
1	3.894	4.354	4.187	5.401
2	8.165	9.253	8.332	11.263
3	14.529	15.618	14.696	18.590
16	149.602	185.191	155.338	177.864
24	158.604	206.587	172.504	186.405

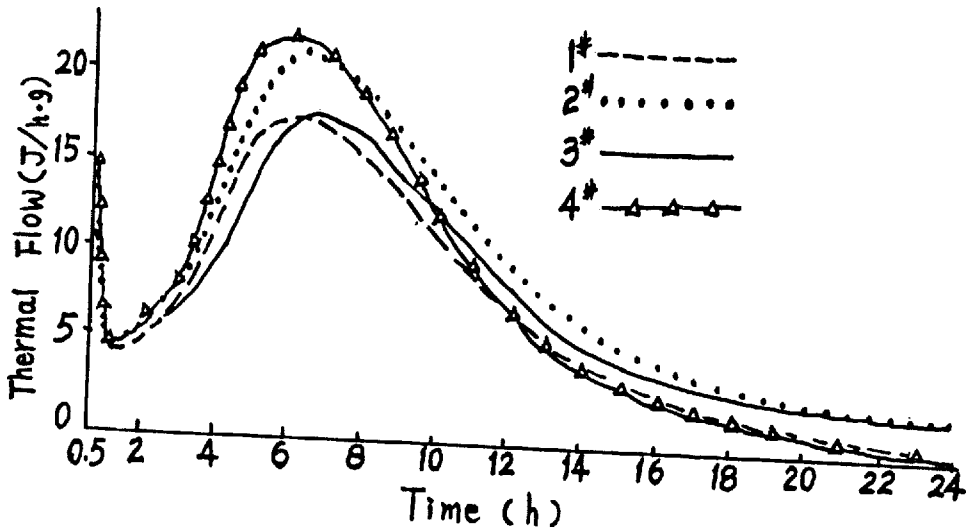

Fig. 3 The Hydration Heat Evolution Curves of Doped β-C_2S

To sum up, upon of doping β-C_2S the crystallchemical environments for both Ca and Si atoms were changed. The crystal lattice was distorted and the crystal structure disorder increased. This made access of H_2O into internal-structure of doped β-dicalcium silicates easier. The crystal grains were fine, intercrystalline imperfections and interface energies were increased. These caused doped β-dicalcium silicates to react with water easily. This is why the hydration reaction of doped β-dicalcium silieates was accelerated.

REFERENCES

1. G.SUDOH, T.OHTA, H.HARADA, 7econgres Intern. de chimie du Ciment, Paris 1980.
2. G. V. KuRolev, Proc. Vth Int. Cong. Chem. Cem. Vol I 298, Tokyo 1968.
3. Yang Nanru, Zhong Baigian, Wang Zhanwen et al., J. of the Chinese Silicate Soc., 10, (2) , 161 (1982); 14, (4), 285 (1985); 8th Int. Cong. on the Chemistry of cement, Vol. 3,22 (1986) Brazili;J. of Nanjing Inst. of Chem. Tech. 9, (2), 63 (1987).
4. Feng Xiuji. Long Shizhong, Wang Lan ,Wang Yanguo et al. Proc. of 1985 Beijing Int. Sym. on Cem. and Conc, Vol. 1, 54(1985); J. of the chinese Silicate Society, 13, (4), 424 (1985); 16, (6) , 552(1988); 16,(2) 104(1988); 15,(6), 489(1987); CCR 17, (4), 532,(1987).
5. MIROSLAW HANDKE, Appl. Spectrose. Vol 40.No 6,873 1986.

MICROSTRUCTURAL STUDIES OF PURE AND IRON DOPED UNHYDRATED AND HYDRATED DICALCIUM SILICATE PHASE

Ram Prakash*, S C Ahluwalia and J M Sharma****

*Minister of State for Science and Technology & Electronics, Govt of Haryana, INDIA
**National Council for Cement and Building Materials, New Delhi, INDIA

SUMMARY

Microstructural features and grain size distribution of pure and iron doped dicalcium silicate pastes were studied upto 180 days using electron and optical microscopy. The development of morphological features have been compared and related with the degree of hydration obtained from thermal studies. There are two interesting features that are observed in the mature paste. The first is the occurence of "pockets" of partially hydrated C_2S grains covered with well known acicular C-S-H. The second feature are areas which resemble irregularly fractured calcium hydroxide crystals. Long term hydration shows the existence of crumpled foils and interlocking fibres of calcium silicate hydrates and $Ca(OH)_2$ of various degree of crystallinity. No clear relationship has emerged from the studies regarding the rate of hydration from the kinetic studies and the strength development.

INTRODUTION

β-dicalcium silicate is an important component of ordinary portland cement and is generally present in Indian Cements in an amount almost equal to C_3S phase. The hydration of C_3S phase is faster and dominates the behaviour of ordinary portland cement particularly during the early days. Young and Tong (1). have reported the microstructural development of hydrated β-C_2S paste at various ages using SEM.

Kinetics of hydration of β-C_2S phase have been reported from thermal and allied studies (2-4). Some work has also been reported by Williamson on the scanning electron microscopy of hydrated β-C_2S upto 1 year and microstructural features have been compared with hydrated C_3S (5). However,no systematic study has been reported on the effect of iron on the hydration behaviour of the C_2S phase.

This paper deals with the microstructural features and grain size distribution of pure and iron doped hydrated C_2S phase upto 180 days. Compressive strength of these pastes for some selected samples were taken. An attempt has also been made to relate the microstructural features with the strength development in mortars using pure and iron doped C_2S phase.

EXPERIMENTAL

i) **Prepration of Dicalcium Silicate :** Calcium carbonate and quartz (>99.0 % pure) in the mole ratio of $2CaO:SiO_2$ (2:1)were mixed,homogenized and pelletized and repeatedly fired at 1450°C till virtually no free lime(CaO f) was left. Formation of dicalcium silicate was determined by XRD.

ii) **Preparation of Doped Dicalcium Silicate :** 0.5, 0.7, and 1 % of Fe_2O_3 by weight was mixed and, homogenized with dicalcium silicate phase and fired at 1400°C with a retention period of 30 minutes and air cooled to ambient temperature. The pellets were ground to a fineness of 4000 cm^2/g.

iii) **Hydration of C_2S Phase :** Pure dicalcium silicate and iron doped dicalcium silicate phase of fineness 4000 cm^2/g (Blaine) were mixed with distilled water (w/s = 2.0) sealed and kept in an incubator at 40° C for different ages (3 to 180 days). The hydration of the paste was arrested by treating with anhydrous acetone and dried under vaccum for 2 hours. The dried samples were ground to pass through 100 μm sieve and stored in sealed vials.

iv) **Casting of Pure and 0.7 % Fe_2O_3 Doped C_2S :** Pure dicalcium silicate and 0.7 % Fe_2O_3 doped dicalcium silicate were cast in 1:3 C_2S to graded standard sand using w/s ratio of 0.5. The samples were kept at 40°C and more than 90% relative humidity for 24 hours, demouled and kept under distilled water at 40° C until required for testing. The samples were used for strength determination and the fractured cubes were used for optical microscopic study.

v) **X-Ray Diffraction Study :** The samples were ground to pass 45 μm sieve and pressed into a sample holder.Rigaku Rad Max B system with wide angle horizontal goniometer and graphite monochromator was used for establishing the mineral composition.

vi) **Thermal Study:** The dried samples were subjected to thermal studies by Netz thermal analyser upto 1050°C using Al_2O_3 (already heated to 1500°C) as a standard and keeping heating rate at 10°C / min.

vii) **Optical Microscopic Study :** The microstructure of the samples were investigated on polished sections etched with hydrofluoric acid by means of incident light microscopy using Zeiss Optical Microscope.

viii) **SEM :** Philips model S(T)EM 301 G was used for the microscopic studies . The samples for SEM were prepared by uniformly blending the powdered sample with a resin and giving them a conductive coating in vaccum of the order of 10^{-5} torr.

RESULTS AND DISCUSSION :

Hydrated samples of pure and iron doped C_2S at 3, 7, 14, 28, 60, 90 and 180 days were evaluated for the weight loss at temperature 400-550°C, assuming that the major loss in weight is due to the decomposition of $Ca(OH)_2$ formed. In case of pure C_2S, the amount of $Ca(OH)_2$ increases upto the age of 60 days and then declines. Similar observations were made in hydrated C_2S doped with 0.5% Fe_2O_3. In case of hydrated C_2S doped with 0.7 Fe_2O_3, the loss increases upto 90 days and then declines while in 1.0% Fe_2O_3, the loss increases from 3 to 180 days in hydrated samples continuously (Table-1). The results indicate that the reactivity decreases in the order :

Pure C_2S > 0.5 % Fe_2O_3 C_2S > 0.7 % Fe_2O_3 C_2S > 1.0 % Fe_2O_3 C_2S.

Table 1 indicates that the degree of hydration is increasing with age in pure and iron doped C_2S eventhough the fixation of $Ca(OH)_2$ starts at 60 days or later on.

TABLE 1
Percentage Loss in weight between temperature 400-550°C due to the decomposition of $Ca(OH)_2$ by thermal technique TG

S.No.	Sample	3d	7d	14d	28d	60d	90d	180d
1.	Pure C_2S	1.10	2.30	3.10	3.25	4.50	3.05	2.39
2.	0.5% Fe_2O_3	0.55	2.04	2.59	3.14	2.96	2.36	1.99
3.	0.7% Fe_2O_3	0.18	1.47	1.85	2.58	2.76	2.77	2.17
4.	1.0% Fe_2O_3	0.16	0.56	0.94	1.89	1.99	2.08	2.54

Compressive Strength : The compressive strength of pure and 0.7%Fe_2O_3 doped C2S were determined and the values (table-2) indicate that the pure C_2S phase gave higher early age strength and was over taken by iron doped C_2S at 7days indicating that the presence of iron slows down the hydration particularly at younger age. However, the data is insufficient to come to any conclusion.

TABLE 2
Compressive Strength of Pure and 0.7 % Fe_2O_3 doped C_2S in Kg/cm^2

Sample	3d	7d	28d
Pure C_2S	3.4	40.0	200.0
0.7% Fe_2O_3 C_2S	2.8	52.0	430.0

Optical Microscopy : Crystalline calcium hydroxide (CH) formed during the hydration of pure and doped C_2S can be easily followed from the optical microscopy. The CH phase is randomly distributed throughout the paste during the early stages of hydration (Plate 1). At later ages of hydration, the $Ca(OH)_2$ grows and intersect one another (Plate 2).

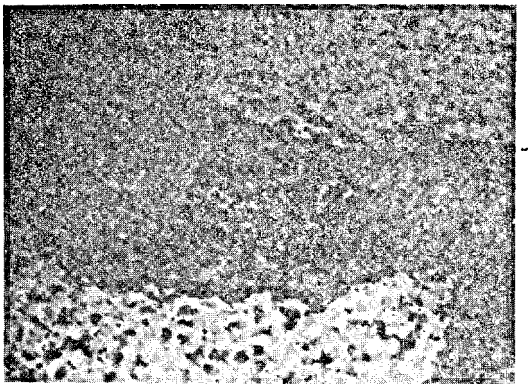

PLATE 1

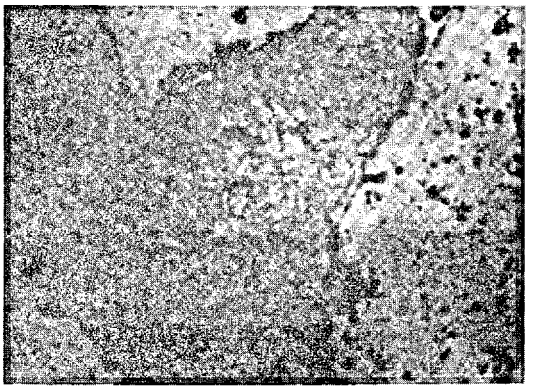

PLATE 2

SEM Observations : The microstructure feature of pure and iron doped C_2S appears to be different because of the formation of different crystal sizes of pure and iron doped C_2S system.

(a) Microstructure of Pure and Iron Doped Dicalcium Silicate:

In pure dicalcium silicate phase (Plate 3 a), the crystal sizes are of the order of 11-19 um having elongated and distorted shapes. 0.5, 0.7, 1.0 percent by weight of Fe_2O_3 doped C_2S were examined for their morphology. The grain size distribution is given in Table (3). Size of doped dicalcium silicate decreases as the concentration of Fe_2O_3 dopant inceases. Addition of Fe_2O_3 not only reduces the crystal size of C_2S but also the shape of the crystal whereas pure C_2S has elongated crystals, the 0.5 % Fe_2O_3 containing C_2S has elongated as well as rectangular shapes (Plate 4 a). The average size of the crystals are smaller than the pure C_2S . Addition of 0.7% Fe_2O_3 to C_2S shows the presence of rounded shapes of the crystals and further decrease in size (Plate 5 a). C_2S doped with 1 % Fe_2O_3 has rounded as well as distorted rounded shapes (Plate 6 a).

TABLE 3
Grain Size Distribution of Pure and Iron Doped C_2S.

C_2S Concentration of Fe_2O_3 Wt %	Grain Size um
0.0	11 - 19
0.5	6 - 19
0.7	5 - 15
1.0	5 - 13

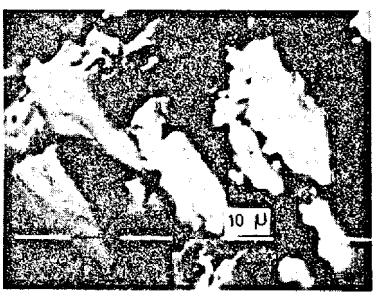

(a)

0d



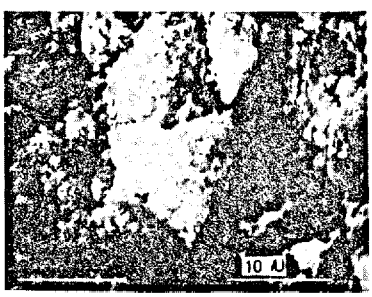

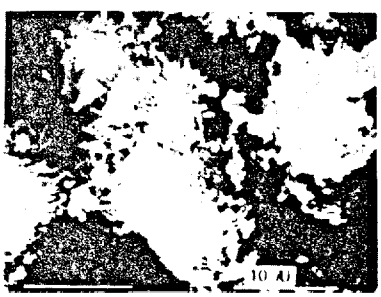

(b) 3d (c) 7d (d) 28d

PLATE 3 (a to g) SEMs OF UNHYDRATED AND HYDRATED C_2S

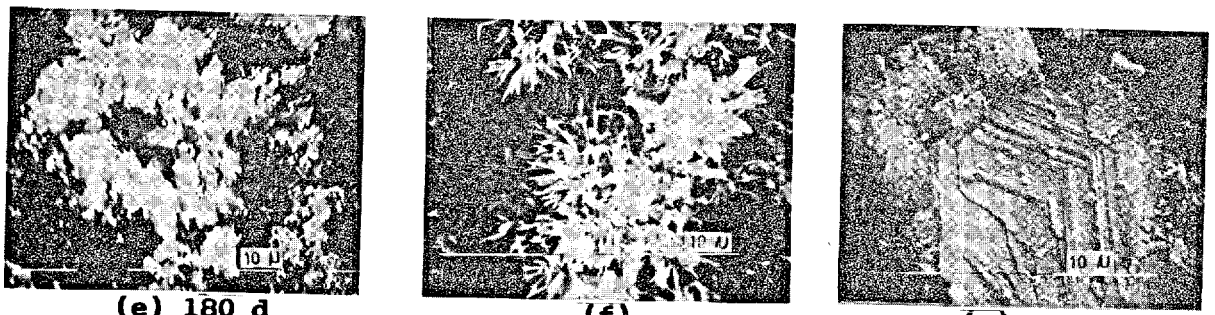

(e) 180 d (f) (g)

(b) **Microstructure of Pure Hydrated Dicalcium Silicate:**

Evidence of hydration products is seen with outermost C-S-H growing but does not shows a definite acicular morphology (Plate 3 b & c). At 28 days (Plate3 d) C-S-H is well developed and continued development of the paste microstructure was observed and the structure becomes more dense. After 180 days of hydration (Plate 3 e) clear distinction of hydrated C_2S from unhydrated core can be made. The hydrated C_2S can be seen as the well developed aciculae C-S-H. Two other features have been observed in the mature paste (Plate 3 f & g). The first is the occurence of pockets of partially hydrated C_2S grains covered with acicular C-S-H and the second feature are areas which resemble irregularly fractured $Ca(OH)_2$ crystals. Long term hydration shows the existence of crumpled foils and interlocking fibres of calcium silicate hydrates and $Ca(OH)_2$ of various degree of crystallinity. Also in the younger paste(7 days) the fractured calcium hydroxide crystals are not very large but increases with age as has also been reported earlier (6).

(c) **Microstructure of Iron Doped Hydrated Dicalcium Silicate:**

The hydrated doped C_2S (0.5% Fe_2O_3) shows hydration has progressed at 7 days but no well defined structure is seen (plate 4 b). At 28 days (plate 4 c). The hydration products showed the linkage of the C-S-H gel very well but still seen some voids and small amount of calcium hydroxide can also be seen on the surface of the crystal. At 180 days (plate 4 d) ,the voids which were seen up to 28 days were filled with gel structure of C-S-H (1) and strong bonding appears.

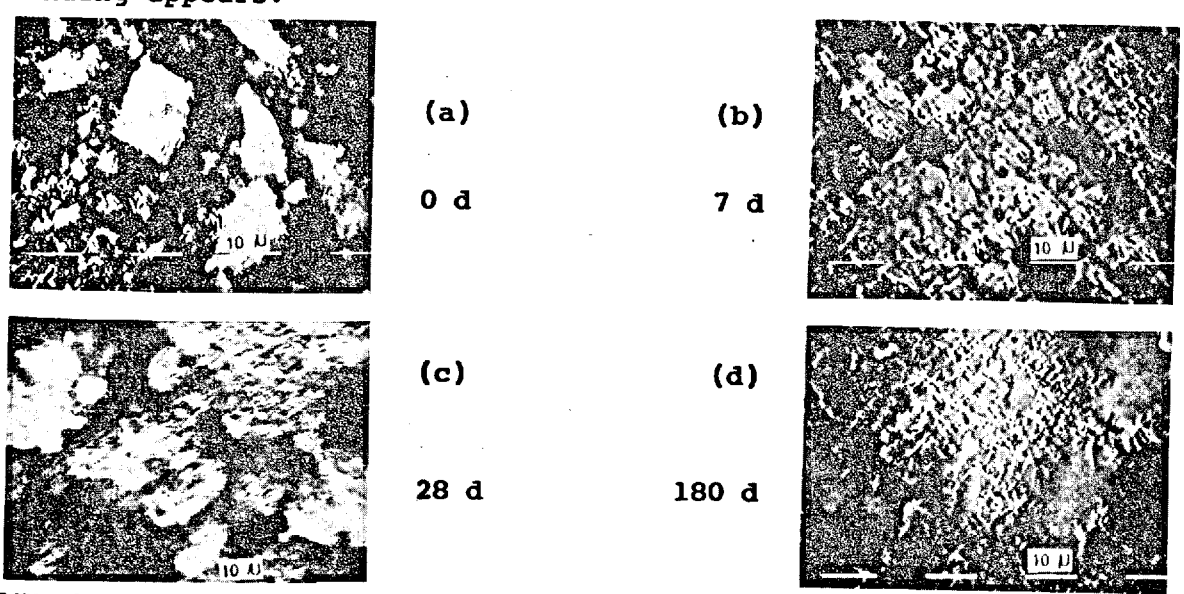

(a) (b)

0 d 7 d

(c) (d)

28 d 180 d

PLATE 4 SEMs OF UNHYDRATED AND HYDRATED C_2S DOPED WITH 0.5 % Fe_2O_3

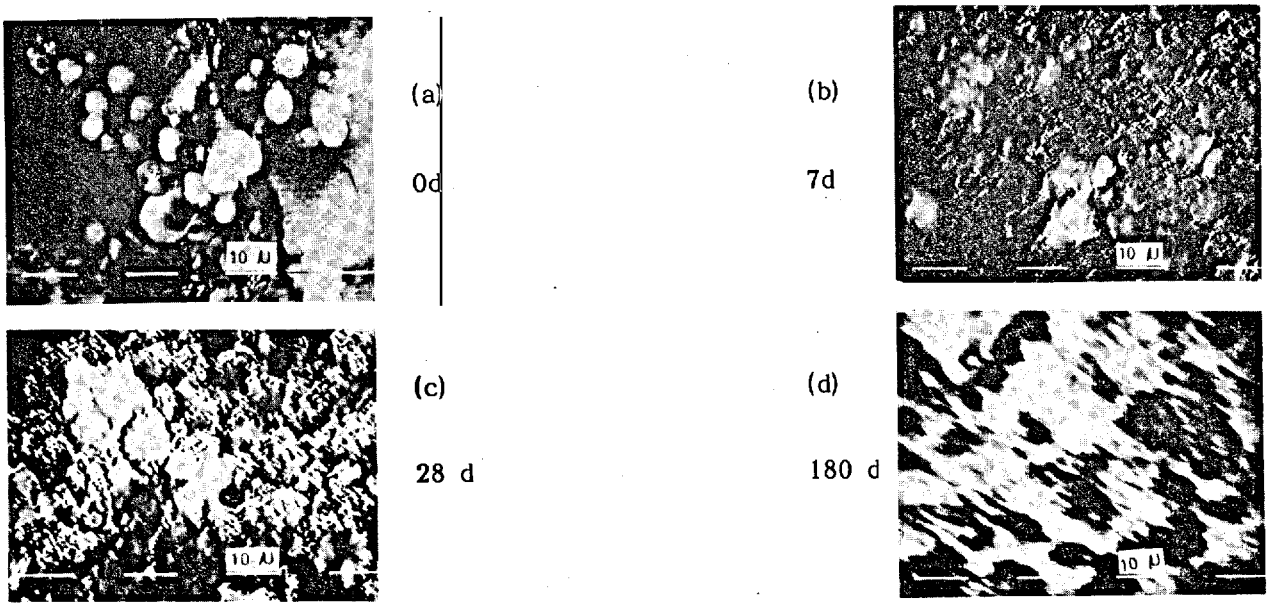

PLATE 5 SEMs OF UNHYDRATED AND HYDRATED C_2S DOPED WITH 0.7 % Fe_2O_3

At 7 days (Plate 5 b) the hydration products of 0.7% Fe_2O_3 C_2S are very poorly developed but at 28 days (plate 5 c) of hydration, the hydration products are not acicular in nature and CSH gel is seen in the gaps. The hydration starts at the surface of the crystals as can be clearly seen . At 180 days of hydration (plate 5 d) , no clear well developed aciculae of C-S-H is seen and uneven distributed iron dopant is seen .

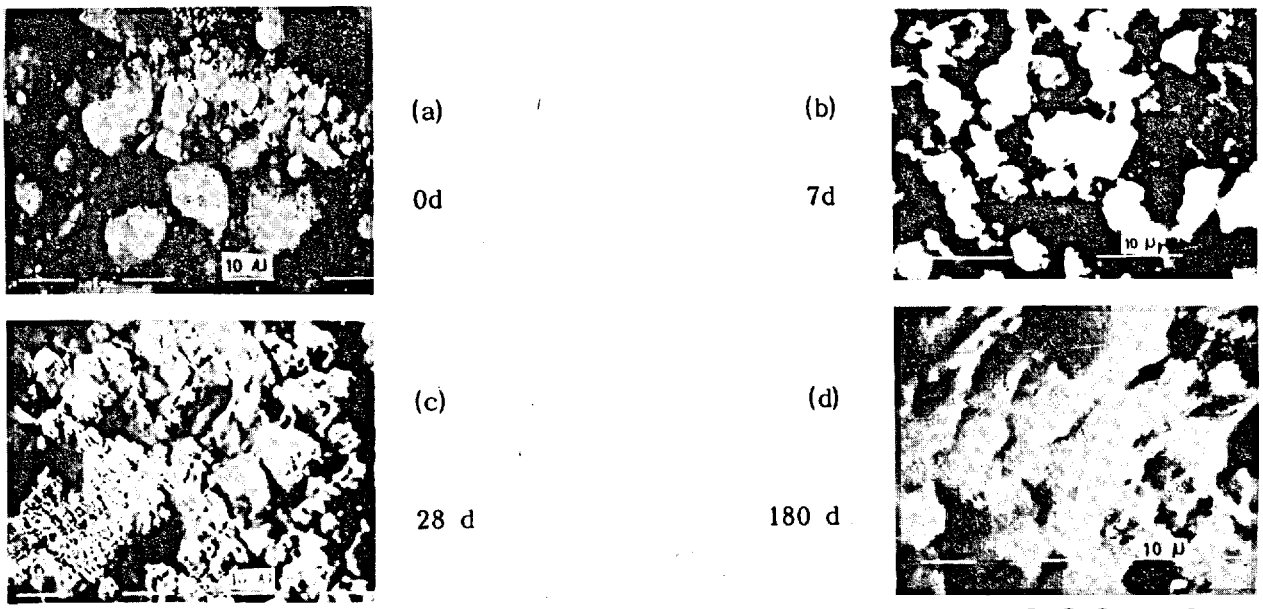

PLATE 6 SEMs OF UNHYDRATED AND HYDRATED C_2S DOPED WITH 1.0 % Fe_2O_3

No hydration is seen upto 7 days of hydration for 1% Fe_2O_3 doped C_2S (Plate 6 b) and at 28 days (plate 6 c) poor hydration is observed but at 180 days of hydration (plate 6 d) appreciable hydration has occured but no C-S-H gel in acicular form is observed. Hydration looks minimum in this case.

Hence SEM studies indicate that the degree of hydration increases with age which has already been confirmed by thermal study as well.

CONCLUSION

1. Doping of C_2S phase with Fe_2O_3 not only reduces the grain size of C_2S but also the shape of the crystal and effect increases with increase in amount of dopant.

2. Presence of Fe_2O_3 adversely affects the rate of hydration of C_2S phase at early age.

3. Compressive strength of doped C_2S phase is lower at early age but surpassed that of pure C_2S phase at 7 days , which may be due to altered mineralogical features and reduced grain size of C_2S doped with Fe_2O_3.

4. No clear corelation between the kinetic studies and compressive strength could be established.

ACKNOWLEDGEMENT

The work carried out here is a part of research project and Ph D programme of one of the author (JMS) at National Council for Cement and Building Materials. This paper is being published with the permission of Dr A K Mullick, Director General of the Council.

REFEREMCES :

1. Young J F and Tong H S: "Microstrusture and strength development of beta - dicalcium silicate paste with and without admixtures" Cement and Concrete research, 1977, 7, 627 - 636.

2. Shibata S, et al.: "Preparation and hydration of β-C_2S without stabilizer", Cem. Concr. Res., 1984, 14, 323.

3. Asaga K, et. al :" Effect of thermal history and addition on the hydration of β-Ca_2SiO_4",Proceeding of the 8th International Symposium on Chemistry of Cement, 1986.

4. Yimin Chen, Liping Shi :" The method for quantitatively studying β-C_2S Hydration," Journal of China Building Academy, 1991, 3(2), 11 and 1991, 3(2), 1991.

5. Williamson R B : " Solidification of Portland Cement," Rpt. No.UC-SESM-70-23, Univ. California, Berkeley, CA. (Dec. 1970, 109; Progr. Mater. Sci., 1972, 15(3), 189-286.

6. Kawada N and Nemoto A : Zem.-Kalk-Gips, 19(2) 65-71 (1967).

INFLUENCE OF GYPSUM MORPHOLOGY ON THE STRUCTURE AND PROPERTY OF STEAM CURING PASTE MATRIX

Zongshou Lin and Shunni Liu

Dept of Materials Engg, Wuhan University of Technology
Wuhan, Hubei, P R CHINA

SUMMARY

The influence of gypsum morphology on the microstructure and property of paste matrix is studied by means of extruded porefluides from cement paste, chemical analysis, ion emission spectrometry, SEM, DSC and mercury pressure porosimetry etc. Results show that SO_4^{2-} ion concentration is always higher in paste added with anhydrite than that with gypsum, but OH^- concentration varies with curing condition. The coarse ettringite crystals uniformly form in the solution far from the solid grains and the size of C-S-H gel also tends to reduce when anhydrite is used. The higher SO_4^{2-} concentration and lower OH^- concentration is helpful to form uniform compact structure and raise the strength of paste matrix.

INTRODUCTION:

Usually, the strength of protland cement by steam curing is 10-15% lower than that by room temperature curing. But in a certain condition, above conclusion can be changed. Reference (1) report that when anhydrite is used to replace gypsum in cement and the content of anhydrite is relatively increased, the use of curing condition for example at 55-75°C with steam curing for 4-6 hours will largely raise the early strength and the long term strength. Above results show that in steam curing condition, the change of the morphology and the content of gypsum has a very important effect on the strength of portland cement. Therefore it is very valuable to study the mechanism of kinds of gypsum on strength of cement.

EXPERIMENT AND RESULT:

1. The ingredient of raw materials

The chemical composition of raw materials is listed in Tab. 1

The ingredient of cement is shown in Tab. 2

Tab.1 Chemical composition of raw materials

raw meal	loss	SiO_2	Al_2O_3	Fe_2O_3	CaO	MgO	SO_3	Total
clinker	1.70	20.64	5.64	4.58	65.48	1.34	0.30	99.95
anhydrite	4.86	5.34	1.41	0.67	37.78	2.59	46.03	98.68
gypsum	20.39	1.42	0.90	0.33	32.28	0.38	44.02	99.72

Tab.2 the ingredient of cement (%)

sample	clinker	anhydrite	gypsum	water - reducing agent	S. A.
A10	90	10		0.7	3900
G 5	95		5	0.7	3860
G10	90		10	0.7	3930

2. The method and result of experiment

2.1 The experiment of strength

4x4x16cm test specimen is used. W/C=0.33, C/S=1:2.5. After the test specimens are formed, firstly they are placed into curing room (20°C) for 5 hours, secondly the temperature of curing room is raised at the rate of 15°C/min to 65°C and the specimens are cured at 65°C for 4 hours, then are cooled to 20°C and are placed into water to cure for a different day. the results are listed in Tab. 3.

Tab.3 the results of strength test

specimen	tensile strength (MPa)				compression strength (MPa)			
	1d	3d	7d	28d	1d	3d	7d	28d
A10	8.7	9.4	10.0	10.3	61.7	76.0	76.1	86.4
G 5	7.8	8.3	8.4	8.7	53.1	58.0	61.7	65.7
G10	7.5	7.9	8.2	8.6	48.8	52.9	56.7	66.3

2.2 The experiment of fluid[8],[9]

The cement paste with W/C=0.56 is mixed for 5 minutes, then sealed into the Igitite packet to cure. After being cured at 20°C for 5 hours, part of the sample is placed into another curing room with steam of 65°C to cure for 4 hours then placed into water to cure for the experiment.

About 300g sample is packed in a piece of nylon cloth and pressed with a filter press to a specific pressure intensity value (220MPa) The constant-pressure time depends on the curing time of sample.

The fluid gained from the filter press is immedientlly filtered and the OH^- concentration of part of the filter-fluid is titrated by the chlorhydric acid standard solution with indicator methyl red. 5% HCl solution is added to another part of filter fluid to neutralize the OH^- ion and the concentration of Al, Ca and S is measured by means of ion emission spectrometry. The Ions concentration of samples A10 and G10 is shown in Tab. 4.

2.3 The deterimination of hydrate

250g cement with W/C=0.24 is formed (2x2x2cm test model is used) and cured at 20°C for 5 hours, at 65°C for 4 hours then placed into water for a specific time. The specimens are pounded and stopped hydration by absolute ethyl alcohol and the shape of hydrate in specimens is observed by means of SEM.

Part of above specimens is dried for 48 hours in the decarburizing atmosphere and -740mmHg vacume. The pore distribution of the specimen is measured by means of mercury pressure.

Another part of specimen is ground in absolute ethyl alcohol, then filtered and washed by absolute ethyl alcohol and acetone respectively for three times. The residue is ground in agate mill for 4.5 hours with grinding aid benzene and dried with cool wind. The content of chemical binding water and ettringite of specimens are respectively measured by means of TG and the chemical fractionation and the results are shown in Tab. 5 and Tab. 6. the content of $Ca(OH)_2$ of samples A10 and G10 cured for 3 days is measured by

means of DSC and the result is listed below; A10 : 8.84%, G10 : 7.61%. The total porosity ratio is A10 : 58.1mm³/g, G10 : 63.1mm³/g. The most probable aperture is A10 : 125A°, G10 : 150A°.

Tab.4 the ion concentration of fluid in paste matrix pore

curing time	ion concentration (m mol/l)							
	(OH^-)		(SO_4^{2-})		(Al^{3+})		(Ca^{2+})	
	A10	G10	A10	G10	A10	G10	A10	G10
1h	80.8	78.9	34.7	30.4	0.6	1.6	29.0	28.0
3h	73.2	76.5	40.0	32.5	1.0	1.3	28.3	28.5
5h	75.9	75.2	42.0	33.8	0.9	0.7	28.0	28.3
13h	83.8	87.9	70.8	58.6	2.7	2.4	16.5	16.9
1d	84.4	92.3	73.1	61.2	3.6	2.9	14.8	15.3
3d	129.7	135.5	47.2	41.9			1.9	2.4
7d	133.8	178.3	45.8	29.5			1.6	2.1

Tab.5 the chemical binding water content (%)

curing time	5h	13h	1d	3d	7d	28d
A 10	0.85	9.83	10.08	11.06	11.48	12.46
G 10	0.65	8.32	9.42	10.22	10.40	10.92

Tab.6 the content of ettringite (%)

curing time	1d	3d	7d
A10	5.23	7.08	7.04
G10	4.20	6.29	6.04

DISSCUSSION:

In the curing condition (65°Cx4hours), the gypsum morphology has a very obvious effect on the cement strength. The 1 day compression strength of cement with anhydrite is 12.9MPa higher than that with the same amount of gypsum and 28 days strength is also 20.1MPa higher.

A lot of study on the dissolving content of different morphologic gypsum in a greater W/C condition is done. But Tai Liangku and others[4] pay a specific attention to the change of the dissolving content of gypsum with W/C and the result is shown in Fig. 1.

In strength test, W/C of A10 and G10 is 0.33 and the gypsum/water is 0.30. From the results Fig.1, it can be seen that the dissolving-content of gypsum ($CaSO_4$g/l) in A10 is larger than that in G10, that is to say, the hydration solution of cement with anhydrite has higher Ca^{2+} or SO_4^{2-} ion concentration.

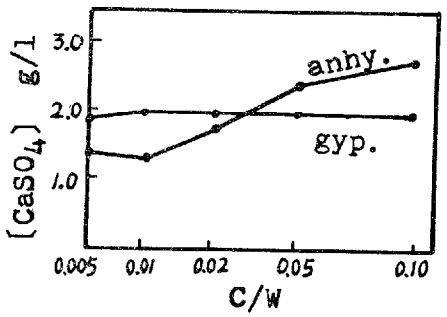

Fig.1 the effect of C/W on the dissolving content of gypsum (time; 5 minutes)

As cement hydrates, a great deal of Ca^{2+} and OH^- ion is given, at the same time, gypsum also releases a lot of Ca^{2+} and SO_4^{2-} ion, therefore the concentration of $Ca(OH)_2$ will speedily saturate and the crystal of $Ca(OH)_2$ quickly educes. The chemical equilibrium relations can be expressed as (time; 5 minutes) follows;

$$CaSO_4\ (solid) \rightleftharpoons Ca^{2+} + SO_4^{2-} \quad (1)$$

$$Ca(OH)_2\ (solid) \rightleftharpoons Ca^{2+} + 2OH^- \quad (2)$$

Above equilibrium relations show that after $Ca(OH)_2$ crystal educes the rise of Ca^{2+} ion concentration in solution will cause the fall of OH^- ion concentration. Because anhydrite has higher $CaSO_4$ dissolving content than gypsum, the hydration solution of cement with anhydrite will have higher concentration of SO_4^{2-} and Ca^{2+} ion, which can cause the concentration of OH^- of solution to fall relatively. In steam curing condition, $Ca(OH)_2$ crystal can educe quickly, therefore the equilibrium can move speedily towards the fall of OH^- ion concentration. It can be confirmed by the experiment results of Tab.4. The concentration of SO_4^{2-} ion in fluid of A10 with anhydrite is always higher than G10 with gypsum. But before steam curing the concentration of OH^- ion of A10 is proximate with that of G10, after steam curing the OH^- ion concentration of A10 is always lower than that of G10 and the concentration difference is the greater and greater with the curing time.

From above results it can be known that the main cause affecting the hydration and strength of cement with different morphologic gypsum is the $CaSO_4$ dissolving content in the steam curing condition. The fluid of cement with anhydrite has higher SO_4^{2-} ion concentration but lower OH^- ion concentration, or the lower alkalinity in the steam curing condition.

Reference (5) reports that the PH value corresponding to the formation of ettringite of portland cement is about 12.5-12.9 and this ettringite crystalizes by the spot chemical reaction. This kind of ettringite causes the change of volume and doesn't raise the strength of paste matrix. But at the initial stage of hydration at which the concentration of $Ca(OH)_2$ is not saturated and the PH value of solution is about 11.5-11.8, ettringite can crystalize speedily from solution and the crystal is helpful to the rise of strength. From reference (5) it can be seen that ettringite tends to crystallize from solution when the alkalinity of solution is relatively lower.

Therefore ettringite of sample A10 with a lower alkalinity in the steam curing condition will tend to crystallize from solution. The results of SEM can also confirm this one. The SEM results show that the ettringite crystal of A10 cured for 1 day is different from that of G10. The former has coarse and uniformly distributive ettringite crystal and the greater part of ettringite forms in the pore space far from the solid grains. The latter has slim and non-uniformly distributive ettringite crystal and a lot of cavity in the structure is observed. More interesting, The size of C-S-H gel in paste matrix of A10 cured for 28 days is 2-4 times smaller than that of G10.

The pore distribution measurement resluts show that the porsoity ratio and the most probable aperture in paste matrix of A10 cured for 3 days tends to fall and the paste matrix structure tends to compact. The content of chemical binding water and ettringite of A10 is always larger than that of G10.

CONCLUSION:

1. The SO_4^{2-} ion concentration in the pore fluid or solution of paste matrix added with anhydrite is always higher than that with gypsum. The OH^- ion concentration of paste with anhydrite is almost proximate to that with gypsum before steam curing, but after steam curing the former has always lower OH^- ion concentration than the latter and the concentration difference is the greater and greater with the curing time.
2. In the steam curing condition, anhydrite is helpful to the uniform distribution of hydrate, the change of size and structure of C-S-H gel and ettringite crystal and the fall of the porosity ratio and the most probable aperature in the paste matrix.
3. The main factors affecting the microstructure of paste matrix are the SO_4^{2-} and OH^- ion concentration. The higher SO_4^{2-} ion concentration and lower OH^- ion concentration is helpful to form the uniform compact structure and to raise the strength of paste matrix cured with the steam of 65°C.

REFERENCE:

1. Zongshou Lin & Shunni Liu "the theory of choose hydration of obtaining high strength cement and Its application" Joural of Wuhan University of Technology, Vol. 12, No. 4, 1990
2. P. Longute, L. Burglen and A. Zelwer, "Rew. mater. constru." P. 676, Vol. 35 (1973)
3. Xun Jungan, Xu Wenxia and Ye Mingxun "Study on the liquid separated from the pore of cem. paste" Jour. of the Chinese silic. soci. Vol. 11, No.3, 1983

4. Tai Liangku and others "Dissc. on mechanism of anhydrite used as the set-controlling admix. of cem." study report of RIBM, 1984

5. Xun Jungan & Wu Zhongwei "The application of expansion and self-stress cement" Published by the Chinese building industry, P. 435, 1985

INVESTIGATION ON THE HYDRATION OF Sr- AND Ba-BEARING SULPHOALUMINATE

P Yan

Institute of Nonmetallic Materials, Technical University Clausthal
Clausthal-Zellerfeld, GERMANY

SUMMARY

The hydration of two new types of calcium sulphoaluminate ($3CaO3Al_2O_3SrSO_4$ and $3CaO3Al_2O_3BaSO_4$) has been studied with XRD, SEM and isothermal calorimetry. The results show that both minerals are rapidly hardening, and exhibit better hydraulic properties than their homologue $3CaO3Al_2O_3CaSO_4$. They hydrate moderately in the initial period and faster later on. Ultimate strength is reached in 7 days. The hydration process and the quality of formed hydrates of $3CaO3Al_2O_3SrSO_4$ and $3CaO3Al_2O_3BaSO_4$ are not analogous to those of $3CaO3Al_2O_3CaSO_4$. $3CaO3Al_2O_3SrSO_4$ produces trisulphate phase similar to ettringite, C_2AH_8 and $SrSO_4$. Only C_2AH_8 but not C_3AH_6 is formed and C_2AH_8 does not convert into C_3AH_6 even if hydration takes place at over 40°C. $3CaO3Al_2O_3BaSO_4$ produces $BaSO_4$ and C_2AH_8. When it hydrates at over 40°C C_2AH_8 formed in the initial stage is transformed into C_3AH_6.

Die Hydration zweier neuartiger Sulphoaluminate ($3CaO3Al_2O_3SrSO_4$ und $3CaO3Al_2O_3BaSO_4$) sind mit XRD, REM und Kalorimetrie untersucht worden. Die Ergebnisse ergaben, daß die beiden Mineralien schnell erhärten und bessere hydraulische Eigenschaften als ihre Homologie $3CaO3Al_2O_3CaSO_4$ haben. Sie hydratisieren gemäßigt im Anfangsstadium, aber schneller später. Die Endfestigkeit wird in 7 Tage erreicht. Der Hydratations-verlauf und die Qualitäten der gebildeten Hydrate von $3CaO3Al_2O_3SrSO_4$ und $3CaO3Al_2O_3BaSO_4$ sind nicht analog zu $3CaO3Al_2O_3CaSO_4$. $3CaO3Al_2O_3SrSO_4$ bildet eine Trisulfatphase ähnlich dem Ettringit, daneben C_2AH_8 und $SrSO_4$. Anstelle von C_3AH_6 bildet sich C_2AH_8, das sich nicht in C_3AH_6 umwandelt, auch wenn die Hydration bei Temperatur über 40°C stattfindet. $3CaO3Al_2O_3BaSO_4$ stellt $BaSO_4$ und C_2AH_8 her. Das am Anfang gebildet C_2AH_8 wird zu C_3AH_6 umgeformt, wenn die Hydration bei über 40°C stattfindet.

INTRODUCTION

It is known for long time that strontium and barium silicates and aluminates have cementing properties similar to those of calcium silicates and aluminates. Cements can be obtained in which lime is replaced by strontium or barium[1-3]. $3CaO3Al_2O_3CaSO_4$ (abbr. $C_3A_3CaSO_4$) is a good cementing mineral. It may be expected that its homologue, $3CaO3Al_2O_3SrSO_4$ (abbr. $C_3A_3SrSO_4$) and $3CaO3Al_2O_3BaSO_4$ (abbr. $C_3A_3BaSO_4$) have cementing properties, too. Feng Xiuji et. al.[4] have developed a Ba-bearing sulphoaluminate cement. This cement can be burned at a lower temperature, has high strength and hardens very rapidly. It can be applied as a high early-strength cement or a radiation shielding cement.

But now about the hydration of both $C_3A_3BaSO_4$ and $C_3A_3SrSO_4$ is known very little. Because of the unsolubility of $BaSO_4$ and a limited solubility of $SrSO_4$ in water, the hydration process and properties of the hydrates of both minerals are possibly very different from their homologue $C_3A_3CaSO_4$.

In the present work three kinds of Ca sulphoaluminates i.e. $C_3A_3CaSO_4$, $C_3A_3SrSO_4$ and $C_3A_3BaSO_4$ were synthesized and mutually compared. The mechanical strength of pastes was measured. The hydration process and hydrates of $C_3A_3SrSO_4$ and $C_3A_3BaSO_4$ were investigated with X-ray diffraction (XRD), scanning electron microscopy (SEM) and isothermal calorimetry.

EXPERIMENT

Three different sulphoaluminates were synthesized. Mixtures of $CaCO_3$, Al_2O_3 and $CaSO_4.2H_2O$ or $SrSO_4$ or $BaSO_4$ with stoichiometrical molar ratios of $C_3A_3CaSO_4$, $C_3A_3SrSO_4$ or $C_3A_3BaSO_4$ were homogenized and compacted. Then they were put into a platinum crucible and burnt at 1300°C for 4 hours for $C_3A_3CaSO_4$, 6 hours for $C_3A_3SrSO_4$ or 10 hours for $C_3A_3BaSO_4$. By X-ray diffraction it was verified that the products were these minerals. The synthesized minerals were ground to a specific surface 5800 cm^2/g ($C_3A_3CaSO_4$), 5100 cm^2/g ($C_3A_3SrSO_4$) and 4500 cm^2/g ($C_3A_3BaSO_4$). Bar specimens 15*15*60 mm^3 were prepared and cured in moist air at room temperature for one day before demolding. The specimens were then cured in water either at 20°C or at 40°C. The mechanical strength of the specimens was measured at the present age. The sample residua after strength determination were washed right after testing with acetone and then with ethylether to stop the hydration. The phase composition and morphologie of the hydrates at different ages were investigated using XRD and SEM. The hydration progress was also observed using isothermal calorimetry (hydration temperature 20°C and w/s=0.7).

RESULTS AND DISCUSSIONS

On the basis of results of mechanical strength measurement(Table 1), it was shown that both $C_3A_3SrSO_4$ and $C_3A_3BaSO_4$ have better cementitious properties than $C_3A_3CaSO_4$. Their ultimate strengthes are obteined within seven days and may decline moderately afterwards.

Table 1. Mechanical Strength of Pastes(MPa)

Samples	Hydr. Tem. (°C)	w/c	3-day		7-day		28-day	
			flex.	compr.	flex.	compr.	flex.	compr.
$C_3A_3CaSO_4$	20	.45	7.2	41.1	6.4	45.4	9.8	44.4
$C_3A_3CaSO_4$	40	.45	9.4	49.1	9.8	44.4	11.3	41.1
$C_3A_3SrSO_4$	20	.45	12.3	94.1	12.1	118.3	12.2	98.0
$C_3A_3SrSO_4$	40	.45	13.9	90.0	14.9	99.0	7.1	78.5
$C_3A_3BaSO_4$	20	.35	10.9	81.4	10.8	95.4	5.3	94.6
$C_3A_3BaSO_4$	40	.35	13.7	82.5	11.8	83.0	7.7	51.3

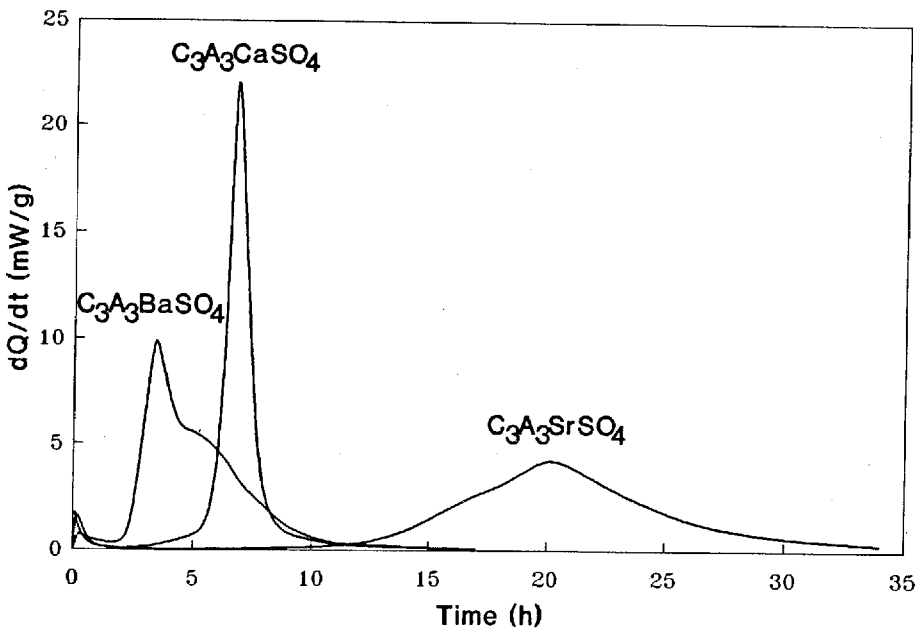

Fig. 1
The hydraulic calorimetric curves of sulphoaluminates

The hydration heat evolution curves for three sulphoaluminates (Fig.1) showed that their hydration process is different from that of calcium silicates or aluminates. There is only a small exothermal peak on the curve in the initial stage of hydration, which indicates their low infiltration heat. The hydration reaction goes into an induction period within one hour after hydration begins. The hydration reaction accelerates again in a few hours and a great exothermal peak appears on the curve. This indicates that clinker minerals begin to hydrate in a significant degree. The total heat of hydration of $C_3A_3CaSO_4$ (92 J/g) is smaller than those of $C_3A_3SrSO_4$ (146 J/g) and $C_3A_3BaSO_4$ (121 J/g), but is released in short time. The second exothermal peaks of $C_3A_3SrSO_4$ and $C_3A_3BaSO_4$ are more extended than that of $C_3A_3CaSO_4$. So the hydration reaction of both minerals takes place moderatly and they have better workability than $C_3A_3CaSO_4$.

The hydration process and the qualities of the formed hydrates were investigated using XRD and SEM (Fig. 2-4). $C_3A_3SrSO_4$ hydrated at 20°C yields first a trisulfate phase similar to that of ettringite. The composition of this trisulfate phase would be $C_3A3(Ca,Sr)SO_4 \cdot xH_2O$. Because the solubility of $SrSO_4$ (=0.014 g/100mL hot water) is lower than that of

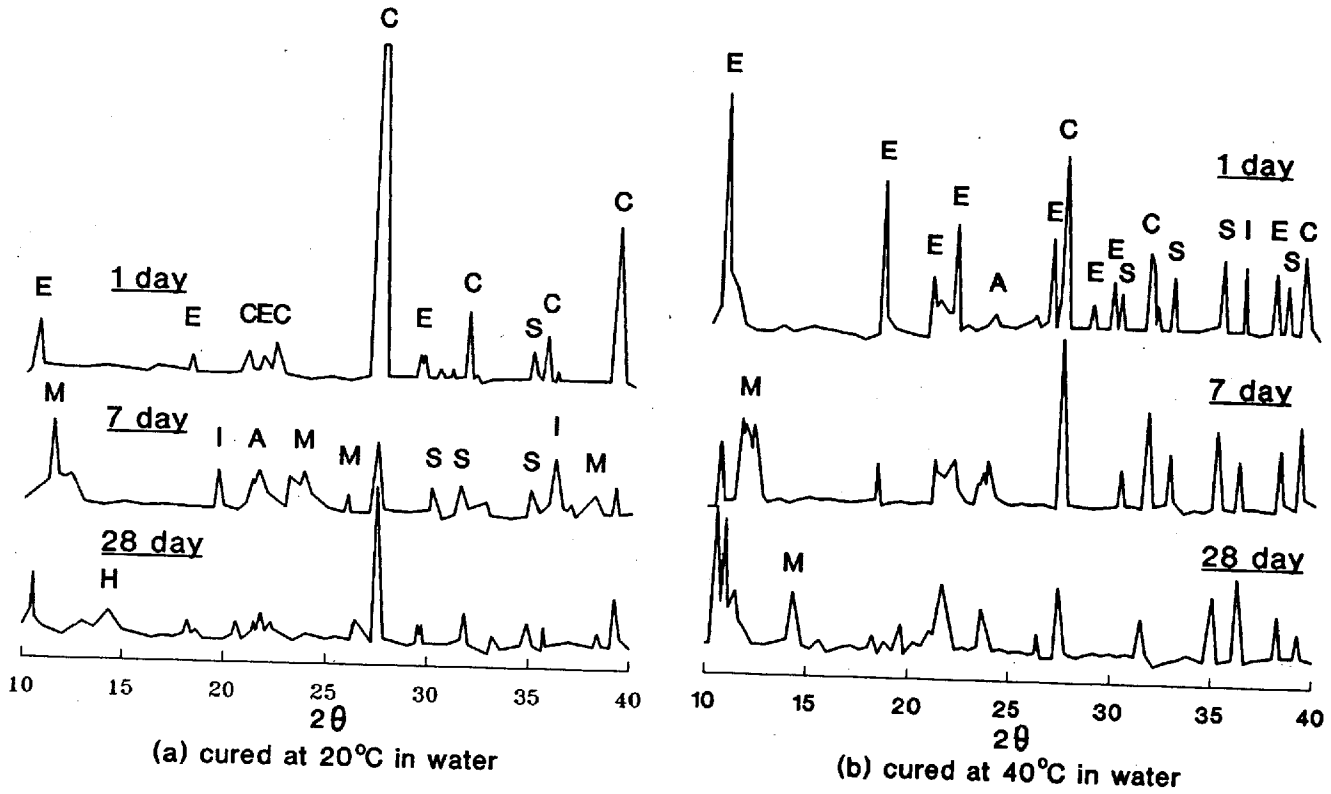

Fig. 2 XRD patterns of $C_3A_3SrSO_4$ paste
A: $Al(OH)_3$, C: $C_3A_3SrSO_4$, E: Trisulfate,
M: Monosulfate, H: CAH_{10}, I: C_2AH_8, S: $SrSO_4$

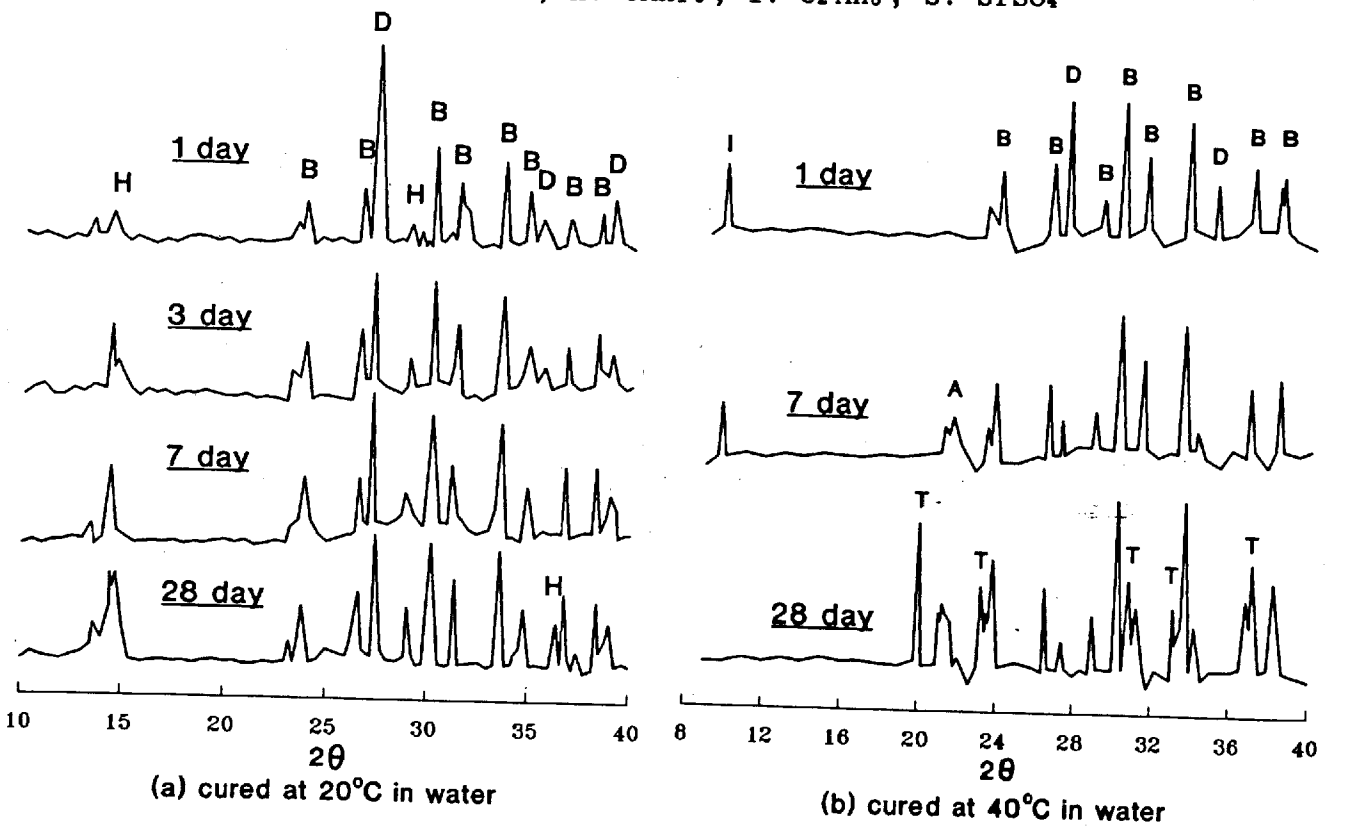

Fig. 3 XRD patterns of $C_3A_3BaSO_4$ paste
A: $Al(OH)_3$, B: $BaSO_4$, D: $C_3A_3BaSO_4$, H: CAH_{10}, I: C_2AH_8, T: C_3AH_6

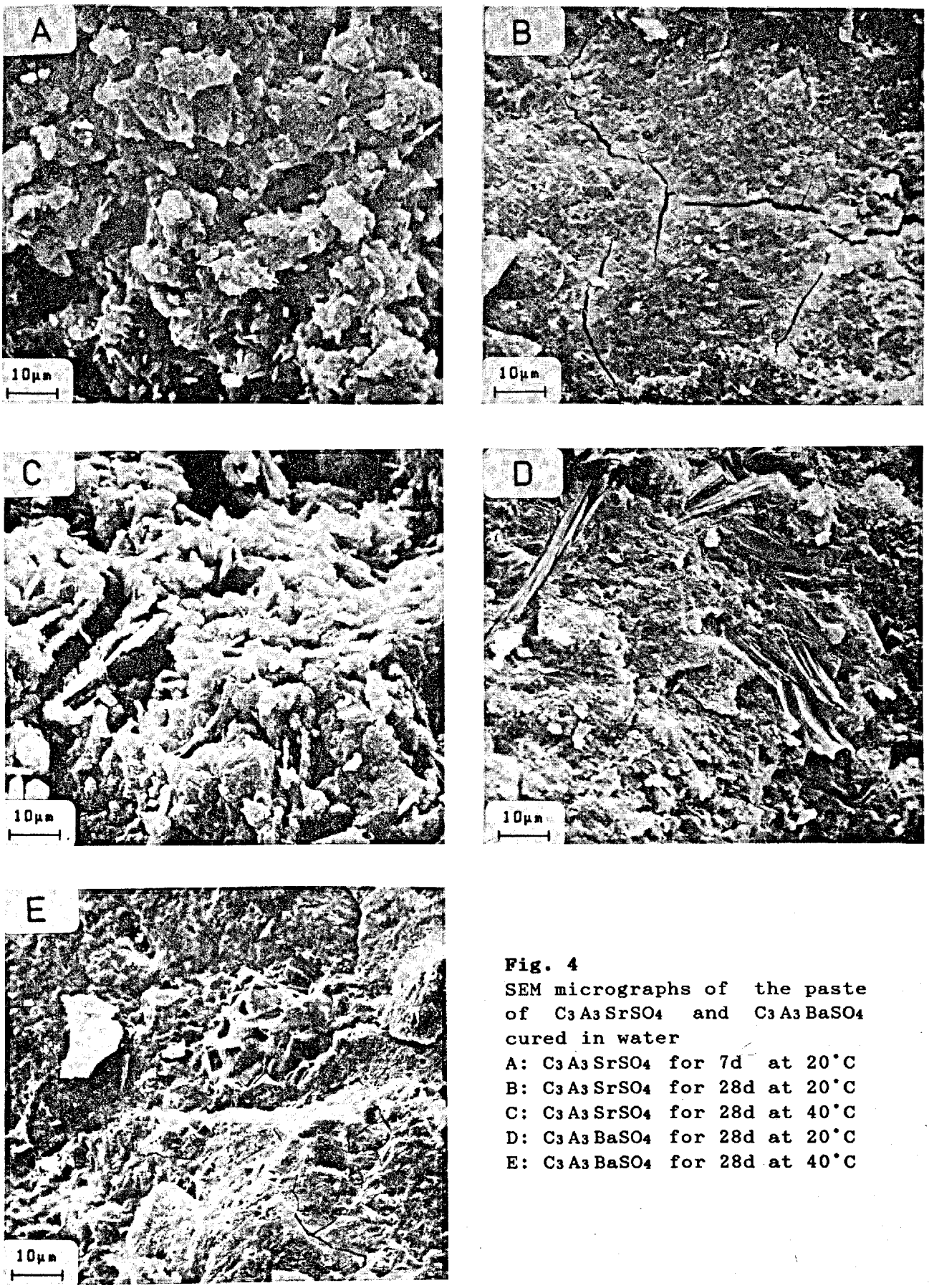

Fig. 4
SEM micrographs of the paste of $C_3A_3SrSO_4$ and $C_3A_3BaSO_4$ cured in water
A: $C_3A_3SrSO_4$ for 7d at 20°C
B: $C_3A_3SrSO_4$ for 28d at 20°C
C: $C_3A_3SrSO_4$ for 28d at 40°C
D: $C_3A_3BaSO_4$ for 28d at 20°C
E: $C_3A_3BaSO_4$ for 28d at 40°C

$CaSO_4$ (=0.162 g/100mL hot water), the saturation of $SrSO_4$ in solution is reached faster and then precipitation takes place rapidly. The trisulfate changes into monosulfate due to the dificiency in sulfate, and C_2AH_8 is formed simultaneously. Monosulfate and C_2AH_8 are plate-like crystals and interlace each other to form a compact crystalline network. $Al(OH)_3$ deposits in the network. A dense paste structure is formed (Fig. 4A) and a high strength is obtained. After most $C_3A_3SrSO_4$ has reacted with water the precipitated $SrSO_4$ reacts again with monosulfate which has formed in paste to yield trisulfate and CAH_{10} is formed simultaneously. During transformation of monosulfate into trisulfate, there is a change of the volume. Because of this volume change takes place in a hardened paste, the paste structure becomes damaged. In the SEM photo of the sample whose hydration continued for 28 days (Fig. 4B), some cracks appear in a dense paste structure. This damage of paste structure explains the decrease of strength at later ages. $C_3A_3SrSO_4$ hydrating at 40°C goes through the same process. The hydration process progresses more rapidly because of a higher hydration temperature (Fig. 2 and 4C). The network structure that can not be formed and transforms fully is not so dense as which hydrated at 20°C. So the mechanical strength of the paste hydrated at 40°C is lower than that hydrated at 20°C. According to general believe on the hydration of aluminates[5], Ca aluminates hydrated over 35°C yield cubic crystal of C_3AH_6 and this results in low strength. However, $C_3A_3SrSO_4$ hydrated at 40°C never produces C_3AH_6, but instend, first C_2AH_8 and then CAH_{10}. This ensures that the paste strength would not be greatly reduced during the later period of hydration.

As to the hydraulic process of $C_3A_3BaSO_4$, $BaSO_4$ precipitation took place as soon as Ba^{2+} and SO_4^{2-} entered the liquid phase because of the unsolubility of $BaSO_4$ (=0.000336 g/100mL hot water). Consequently, there is not possibility for the formation of hydrated sulphoaluminates and $Ba(OH)_2$. $C_3A_3BaSO_4$ can form only $BaSO_4$ and hydrated aluminates. It was observed by XRD studies (Fig. 3) that a large amounts of $BaSO_4$ became precipitated within the first day of hydration. As $BaSO_4$ crystallizes C_2AH_8, then CAH_{10} are formed. Hydrated aluminates yield large plate crystals whereas $BaSO_4$ precipitates in form of microcrystals that fill the space between hydrated aluminate crystals. They together produce compact paste structure that enables the paste to have a very high strength both in the initial and later periods of hydration(Fig. 4D). The hydration rate of $C_3A_3BaSO_4$ at 40°C is faster than that at 20 °C. A high degree of $C_3A_3BaSO_4$ hydration was already found after one day and its hydration was almost completed within three days. C_2AH_8 and $BaSO_4$ crystals can form together a firm network which leads to high strength of the paste in early stage. But the paste strength may be reduced in later stage as cracks are formed(Fig. 4E) due to the volume change accompanying the conversion of C_2AH_8 to C_3AH_6 and $Al(OH)_3$.

CONCLUSIONS

Both $C_3A_3SrSO_4$ and $C_3A_3BaSO_4$ exhibit better cementitious properties than $C_3A_3CaSO_4$. Their ultimate strength is reached within seven days. The

strength may decline in the later stage due to phase transformation and crack formation.

At room temperature $C_3A_3SrSO_4$ yields initially a trisulfate phase similar to that of ettringite, as well as C_2AH_8 and $SrSO_4$. The trisulfate transforms gradually to monosulfate. However, trisulfate is formed again in the final stage of hydration. The volume changes accompanying this phase transformation lead to some decrease of the mechanical strength at later stages. C_2AH_8 plate crystals instead of C_3AH_6 cubic crystal are observed when $C_3A_3SrSO_4$ hydrates at 40°C, therefore the strength remains high.

$C_3A_3BaSO_4$ yields $BaSO_4$, and plate crystals of C_2AH_8 and CAH_{10} that form a firm network. A high paste strength is achieved fast. The hydrates of $C_3A_3BaSO_4$ at 40°C in initial period are C_2AH_8 and $BaSO_4$, whereas C_3AH_6 is formed from C_2AH_8 in the later period. That causes a small decline of the longtime strength.

ACKNOWLEDGEMENT

The author wishes to thank Prof. Dr.-Ing. I. Odler for critically reading the manuscript and for many helpful suggestions and comments.

References

1. Braniski, A.: "Barium- und Strontium-Zemente", Zement-Kalk-Gips, 1957, 10(5), 176-184.
2. Braniski, A.: "Ähnlichkeiten und Verschiedenheiten der Calcium-, Strontium- und Bariumzemente", Zement-Kalk-Gips, 1961, 14(1), 17-26.
3. Braniski, A.: "Strontiumzemente", Zement-Kalk-Gips, 1967, 20(3), 96-101.
4. Feng, X. Liao, G. and Li, Z.: "The study of new type of Ba-bearing sulphoaluminate cement", Symposium of the 4th Conference of Chinese Silicate Society on Cement and Concrete, 1988, Tianjin (to be published).
5. Lea,F.M.: **The Chemistry of Cement and Concrete**, 3rd Edition, Londen, Edward Arnold, 1970, p 507-520.

INVESTIGATION ON THE STRUCTURE AND HYDRATION OF NEW MINERAL PHASE $3SrO.3Al_2O_3.CaSO_4$

Long Shizong, Wu Yanrong and Liao Guanglin

Department of Material Engineering, Wuhan University of Technology
Wuhan, Hubei, P R CHINA

ABSTRACT

With Sr^{2+} ions replacing three Ca^{2+} ions of calcium oxide of calcium sulphoaluminate ($3CaO.3Al_2O_3.CaSO_4$).New mineral $3SrO.3Al_2O_3.CaSO_4$ is synthesized at 1623K in the paper. Characteristic peaks of x-ray diffraction of $3SrO.3Al_2O_3.CaSO_4$ are as follows:3.777_{100}, 2.18_{80}, 2.671_{81}. The kind of new mineral belong to the isometric system.Its cell parameter(a) is 9.25212 ± 0.00057A.The refraction index of $3SrO.3Al_2O_3.CaSO_4$(n) is equal to 1.5494.Besides,the hydration activity of the new mineral is the same as that of $3CaO.3Al_2O_3.CaSO_4$, and its ability of radiation protection is very good. The hydration products of $3SrO.3Al_2O_3.CaSO_4$ are $3SrO.Al_2O_3.3CaSO_4.XH_2O$ (XRD Peaks:9.927; 5.734),similar to ettringite: $SrO.Al_2O_3.10H_2O$ (XRD Peaks:14.43.7.213)and aluminum hydroxide gel.

摘　　要

以Sr^{2+}离子取代 $3CaO.3Al_2O_3.CaSO_4$($C_4A_3\overline{S}$)前面三个Ca^{2+}离子,在1623K制得 $3SrO.3Al_2O_3.CaSO_4$新矿物。它的XRD峰为3.777_{100},2.181_{80},2.671_{81};属立方晶系,a=9.25212±0.00057A;折射率n=1.5494.这个新矿物与$C_4A_3\overline{S}$一样水化活性高,与水化合迅速形成类似钙矾石的针状晶体,其组成可能是$3SrO.Al_2O_3.3CaSO_4.XH_2O$(XRD峰9.927,5.734),水化产物还有 $SrO.Al_2O_3.10H_2O$(XRD峰14.43,7.213)和氧化铝凝胶,这个新矿物有可能用作防辐射材料。

INTRODUCTION

The mineral, calcium sulfoaluminate $3CaO.3Al_2O_3.CaSO_4$,is well known by all of us. It has high hydration activity and a new series of cement products was formed with it as a main mineral.With $BaSO_4$ and $SrSO_4$ replacing $CaSO_4$ of $3CaO.3Al_2O_3.CaSO_4$,the author[1] has prepared two kinds of new mineral: $3CaO.3Al_2O_3.BaSO_4$ and $3CaO.3Al_2O_3.SrSO_4$, and has studied their structures and hydration performances.The literature stated that the mineral $3SrO.3Al_2O_3.SrSO_4$ could be prepared with Sr^{2+} ion replacing the four Ca^{2+} ions of $3CaO.3Al_2O_3.CaSO_4$. But if with Sr^{2+} ions only replacing the front three Ca^{2+} ions of $3CaO.3Al_2O_3.CaSO_4$, could a new mineral be formed? And if it could be formed how about its performance? The paper aims at dealing with these problems preliminanily.

SAMPLE PREPARATION

Analytically pure $Al_2O_3.Sr(NO_3)_2$ and $CaSO_4.2H_2O$ were ground and homoge neously mixed with the molar ratio of $Sr(NO_3)_2:Al_2O_3:CaSO_4.2H_2O$ =3:3:1. After the mixture was pressed a circle cake of ψ 2.5×0.5cm was made.And then the cake was put into a platinum crucible and burned in a furnace at 1473K for 2 hours.Then the temperature continued to rise to 1623K and after the cake was burned for 4 hours at the temperature, it was fet ched out. After rapid cooling in the air, it was ground and a white powder crystal was prepared.

XRD AND REFRACTIVE INDEX OF THE NEW MINERAL PHASE

Analysis of the powder sample prepared was performed with XRD. Testing Conditions:Cuk,

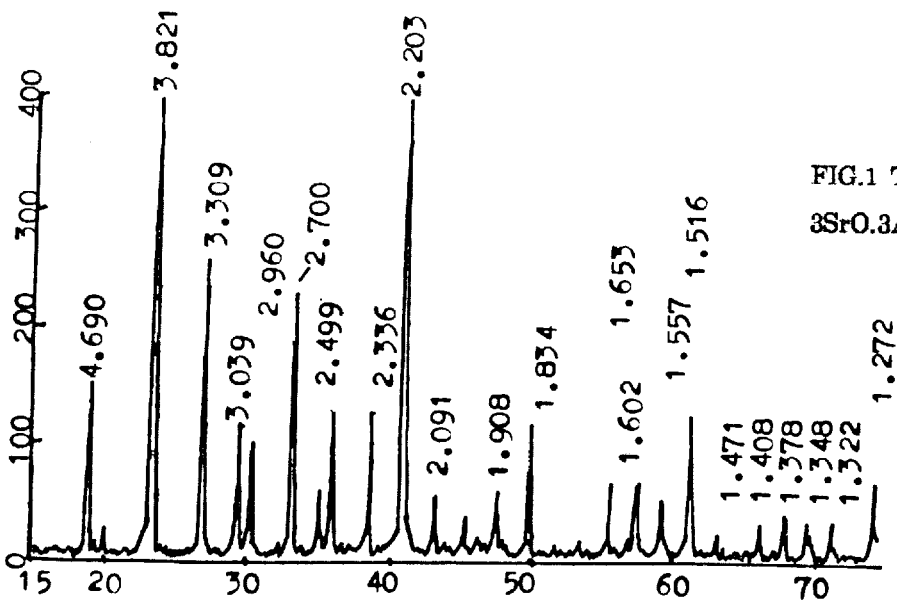

FIG.1 The XRD Pattern of $3SrO.3Al_2O_3.CaSO_4$

Voltage of tube :40KV Electric current :30mA Fig.1 shows the XRD pattern of $3SrO.3Al_2O_3CaSO_4$. After being processed by the computer the diffraction data of mineral were gain shown in Table 1.

Table 1.

No.	hkl	I/I_o	d(A)	No.	hkl	I/I_o	d(A)
1	200	4	4.626	11	431	10	1.814
2	211	100	3.777	12	521	2	1.689
3	220	30	3.271	13	440	7	1.636
4	310	11	2.926	14	600	5	1.542
5	222	31	2.671	15	611	13	1.501
6	321	13	2.473	16	622	4	1.395
7	400	12	2.313	17	631	6	1.364
8	330	50	2.181	18	444	5	1.335
9	332	4	1.973	19	550	4	1.308
10	422	7	1.889	20	721	6	1.259

The new mineral $3SrO.3Al_2O_3.CaSO_4$ belongs to the cubic. Its cell parametres are as follows:$a=9.25212\pm0.00057A$, $\alpha=\beta=\gamma=90^\circ$. The refractive indexn, which was measured by immersion method,is 1.5494.

INVESTIGATION ON THE HYDRATION OF THE NEW MINERAL

1.Hydration Condition

Firstly,the powder sample was homogeneously mixed with water with a ratio of w/c= 0.32. Secindly,the sample was sealed inside a small plastic bottle.Finally,the bottle was put into the water-bath under 20℃temperature in order to hydrate at a constant temperature.

2.Analysis of the hydrates with XRD

The samples which had hydrated after lday, 3 days and 21 days were fet ched out and ground into powder respectively.The Analysis of them with X RD was done.The XRD Patterns of the hydrates were shown in Fig.2.

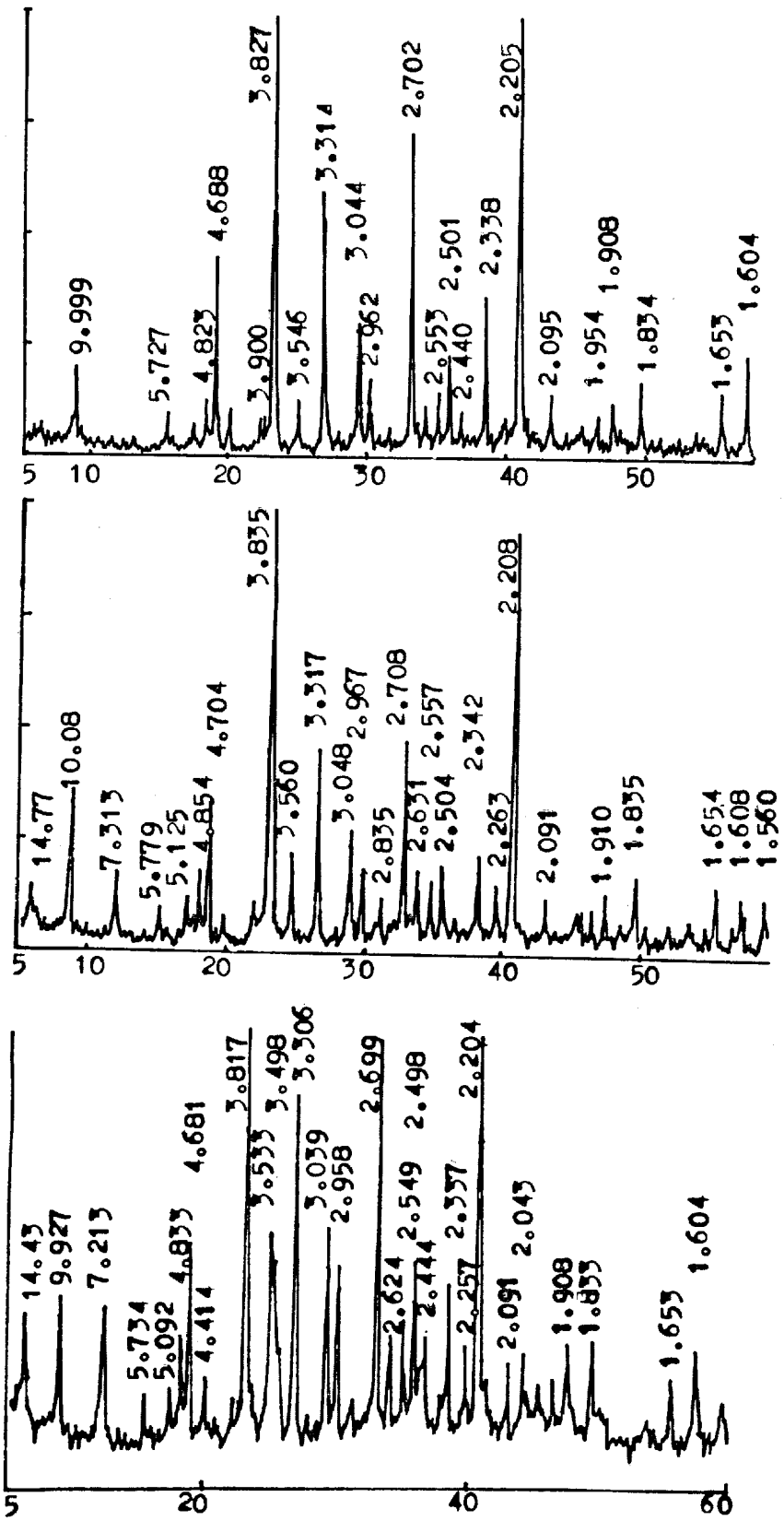

Fig.2.The XRD Patterns of the Hydrates of $3SrO.3Al_2O_3.CaSO_4$

From the XRD of hydrates after 1 day,we can see that there appeared the peaks of XRD 9.999, 5.727,2.828 and 3.980,which were corresponding to those of ettringite $3CaO.Al_2O_3.3CaSO_4.32H_2O$, but the values were greater than those of ettringite.This is because the radius of Sr^{2+} ion is bigger than that of Ca^{2+} ion. As to the XRD of the hydrates after 3 days,the peaks which were similar to ettringite intensified and there appeared such new peaks as 14. 768,7.313 and 3.56,which were corresponding to those of $CaO.Al_2O_3.10H_2O$ and the values were slightly bigger than those of CAH_{10}.And as to the XRD of the hydrates after 21 days,the peaks above which were corresponding to those of ettringite and CAH_{10} continued to intensify,but no new diffraction peak was found. From the results of our experiments, we inferred that the hydrates of $3SrO.3Al_2O_3.CaSO_4$ may be $3SrO.Al_2O_3.3CaSO_4.xH_2O$and $SrO.Al_2O_3.yH_2O$.

3.Analysis of the hydrates by Scanning Electron Microscope

From the SEM photographs.we can see the needle crystal which is similar to ettringite, aluminum oxide gel and sheet crystal.

4.DTA of the Hydrates

Fig.3 shows the DTA pattern of the hydrates after 21 days. In the pattern, there are two

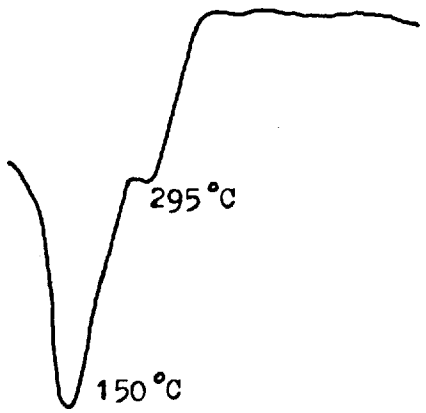

Fig.3 The DTA Pattern of the hydrates after 21 days.

endothermic valleys. One which is at 295℃is corresponding to the endothermic decomposition of $Al_2O_3.aq$.The other which is at 150℃ is corresponding to the endothermic decomposition of the crystal which is similar to ettringite crystal. From the above results of hydration, we can conclude preliminarrily:The hydrates of $3SrO.3Al_2O_3.CaSO_4$ at 20℃ may be $3SrO.Al_2O_3.3CaSO_4.xH_2O$, $SrO.Al_2O_3.yH_2O$ and aluminum oxide gel. The hydration reaction equation may be written as follows:

$$3SrO.3Al_2O_3.CaSO_4+H_2O\rightarrow 3SrO.Al_2O_3.3CaSO_4.xH_2O+SrO.Al_2O_3.yH_2O+Al_2O_3.aq$$

But the exact structures and performances of the two new hydrates are needed to be studied further.

REFERENCS

1. Feng Xiuji,Lao Guaglin and Long Shizong,Investigation on the structure and the preformance of 3CA.$SrSO_4$ and 3CA.$BaSO_4$.1989 Beijing Int.symp.on cement and concrate.

CEMENT-INORGANIC POLYMER COMPOSITES, MICROSTRUCTURE AND STRENGTH DEVELOPMENT

Weiping Ma and Paul W Brown

Materials Research Laboratory
The Pennsylvania State University, USA

ABSTRACT

The purpose of this study was to build on the general concepts from MDF cement technology by identifying inorganic polymers to replace organic polymers as the admixture. A method has been developed for processing this novel material. The flexural strength is greatly improved by reinforcing high alumina cement (HAC) with sodium phosphate-based inorganic polymers, such as $(NaPO_3)_n$ and $(NaPO_3)_n{\cdot}Na_2O$. The heat evolved during the first 48 hours of hydration has been studied for both modified and pure samples by isothermal calorimetry. It was found that phosphate-based inorganic polymers strongly accelerate the hydration reactions. X-ray diffractometry was used to characterize the hydrates and SEM was used to analyze microstructure. Experimental results indicate that phosphate-based inorganic polymers cause the formation of an amorphous cementitious phase which was responsible for the development of strength during the cement hydration.

INTRODUCTION

New cementitious materials developed in recent years have strengths that are much greater than those of conventional hydraulic cements. Many exhibit properties closer to those of ceramics than to those of concrete. The different routes to generating strong cementitious materials include warm pressing, chemical modification, high-shear mixing with polymer additions, and the incorporation of fibrous and particulate second phases [1]. Very early reports indicate that different investigators have tried to use of secondary constituents in concrete to get high strength materials. The available literature of interest dates back to the beginning of this century [2]. However, a class of high strength cement pastes called macrodefect free cements (MDF cements), originally developed by Birchall et al. [3,4] has generated a high level of interest recently [5,6,7]. The purpose of our project is to build on the general concepts from MDF cement technology by identifying cement-inorganic polymer composites instead of organic polymer as the admixture [8]. It is the specific goal to apply the fundamental basis of MDF cement technology for the development of an entirely new class of cement-based materials. Cementitious materials modified by phosphate-based inorganic polymers show high strength and durability, thus, this material offers the potential for use in a range of applications.

A wide range of materials have been studied by various investigators to develop phosphate-bonded materials. The reactions have resulted in the formation of materials which have been used in diverse applications, such as alumina refractories [9] and bioceramics [10]. For example, sodium hexametaphosphate forms rubberlike polymers and yields high strength mortars with fireclay aggregates. These materials are used in high alumina refractories, and are particularly useful for bonding basic aggregates [9]. The PO_4 group provides a basic building block that results in a series of compounds that are analogous to silicate compounds formed on the basis of SiO_4 build block [11]. Thus, sodium phosphate polymer $NaPO_3$ may be represented by the following (where n varies from 6 to 21):

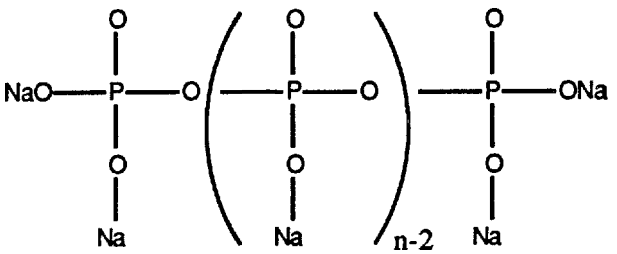

A method has been developed for processing novel HAC-sodium phosphate composites. The flexural strength is greatly improved by reinforcing high alumina cement with sodium phosphate-based inorganic polymers. The mechanisms influencing the mechanical properties of this material are investigated. The results obtained provide the information of the microstructure of cement-inorganic composites and how it affects the mechanical properties of this material. The results of isothermal calorimetry shows that the phosphates strongly accelerate the hydration reactions of HAC.

EXPERIMENTAL

1. Materials

High alumina cement, also known as calcium aluminate cement, used in this study is Secar 71 cement, which obtained from Lafarge, Inc. A typical analysis of the cement showed 71.3 wt% Al_2O_3, 26.8 wt% CaO, 0.68 wt% SiO_2, 0.46 wt% MgO, 0.37 wt% Na_2O, 0.09 wt% Fe_2O_3, 0.04 wt% SO_3 and 0.02 wt% K_2O. BET surface area was found to be 0.96 m^2/g, and density 3.0 g/cm^3. The particle size distribution range is about 0.9 ~ 45.0 μm. X-ray powder diffraction indicated that it consists of CA, CA_2 and $C_{12}A_7$. The percentage of SiO_2 contained in silica fume was 95.32 wt%. Sodium Hexametaphosphate $(NaPO_3)_n$ and Sodium Metaphosphate $(NaPO_3)_n{\cdot}Na_2O$ were employed as the admixtures. X-ray powder diffraction shows that both $(NaPO_3)_n$ and $(NaPO_3)_n{\cdot}Na_2O$ are amorphous.

Mixing is based on the general concept from MDF technology, and high shear mixing was employed instead of standard mixing to improve the homogeneity. Thus, lower water to cement ratios can be used. To prepare the cement pastes, cement and phosphate were mixed with deionized water in the high-shear mixer cell and mixed in speed of 60 rpm for 3 minutes. All samples mixed at room temperature. Compaction was used in an attempt to

decrease the porosity and in increase the density of the hardened paste. The cement pastes were then sealed in plastic bags for about 12 hours at room temperature. The samples were then cured at room humidity, at 100% r.h. or were directly immersed in water.

2. Measurements

Calorimetric studies were performed to test reactivities of the materials by determining the rates of heat evolution during the reactions. Each reactant was allowed to equilibriate separately at 25°C for about half an hour prior to mixing. The heat of hydration of the samples were recorded for 48 hours.

The phase identification were explored using X-ray diffraction analyses which were performed on a Scintag Automated X-ray diffractometer interfaced with a microVAX computer. The scan rate used was 2°2θ per minute. Preparation of hardened samples consisted of grinding the sample in a mortar and pestle, and mounting a portion on a glass slide. All diffraction patterns were obtained at room temperature.

Microstructure of samples were observed using an International Scientific Instruments ISI-DS 130 dual stage Scanning Electron Microscope (SEM). Samples were prepared by carefully cutting the pellets with a razor blade. A small, relatively flat surface piece was then formed a contact between the specimen and the holder with silver paint. The sample was then sputtered with gold to provide a path for charge built up on the surface.

Three point bend load determinations were made using an Instron testing machine at a loading rate of 0.01 cm/minute. The results given are typically the average values of six specimens.

RESULTS AND DISCUSSION

The heat evolved during hydration was studied for both modified and pure cement by isothermal calorimetry during the first 48 hours of hydration. Figure 1 compares the rates of heat evolved during the first 48 hours of hydration for pure cement and two sodium phosphate modified samples. It shows that both of sodium phosphate-modified samples have much faster hydration rates. The samples with sodium phosphate exhibited hydration reactions almost immediately upon mixing, and the peaks occurred within the first three hours. However, the pure cement occurred after about 18 hours. Because only one peak was observed during the first 48 hours of hydration for all samples, it probably corresponds with hydration of CA. The total heats evolved are shown in Figure 2. It shows that cumulative heat for samples modified by sodium phosphate is lower than pure cement. It can be concluded from these data that adding a phosphate-based inorganic polymer strongly accelerates the hydration reaction.

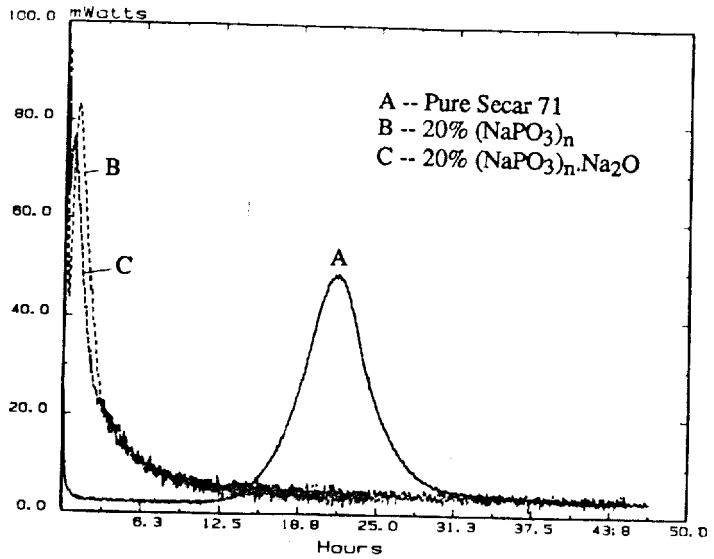

Figure 1. Comparison of the rate of heat evolved during the first 48 hours of hydration for pure cement and modified samples.

Figure 3 shows four x-ray diffraction pattens; pure HAC and samples modified with 10 Wt.%, 20 Wt.% and 30 Wt.% $(NaPO_3)_n$ additions, respectively. All samples were cured in air for one day at room temperature. It shows that the difference in the x-ray diffraction pattens is minimal, denoting that products formed by phosphate-based inorganic polymer and HAC are amorphous. A conclusion can be made as that a new crystalline reaction product does not seem to form at the room temperature in these mixtures. Further studies are underway to reaction mechanism in this system [12].

Table 1 shows the results of the measurements of the flexural strengths for pure HAC and modified samples using two phosphate-based inorganic polymers. All samples were hydrated at a water/solid ratio of 0.182, and a phosphate/cement ratio of 0.1. It can be seen that the phosphate modified cements have higher strengths than pure one. As shown in the table, strengths increased very rapidly with age for about 3 to 7 days for both pure HAC and modified cements. After 7 days, the strengths began to decrease until 28 days of hydration. The values slowly increased again after 28 days of hydration until ten months. The differences between pure HAC and the modified cement are significant. The reason for lower strength between one month and three months is that the hydration of HAC results in the conversion of hydration products CAH_{10} and C_2AH_8, which are chemically unstable at normal and higher temperature, to cubic C_3AH_6 and alumina gel. This change results in an increase in porosity and in strength loss [12,13]. Table 1 also shows the results of 10% silica fume replaced the same amount of HAC. The strength is very high at early ages as shown, but decreases from 48 MPa to 24 MPa between one and three days. However, it is found that the modified cements still have much higher strengths than pure cement.

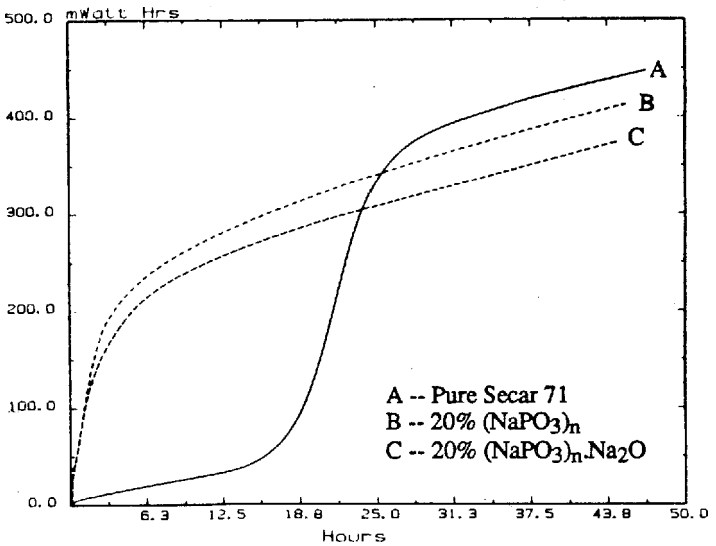

Figure 2. Total heat evolved for pure cement and modified samples.

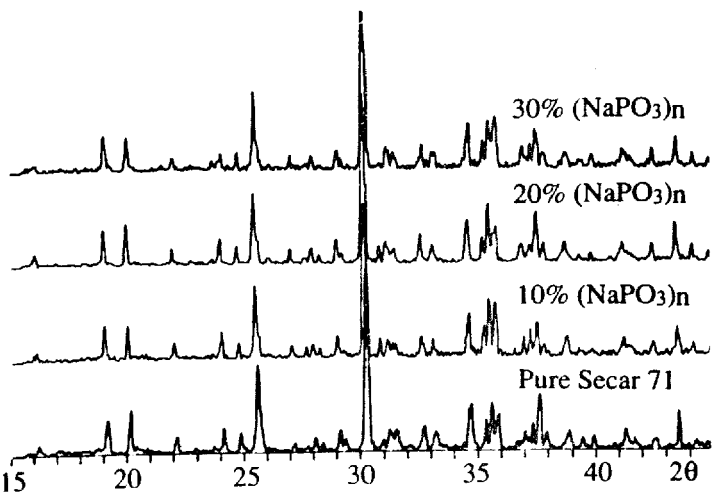

Figure 3. XRD of pure cement and three modified samples containing three addition levels of $(NaPO)_n$ and cured in air for one day at room temperature.

X-ray diffraction results are not entirely consistent with the analysis of the microstructure of the hardened pastes using the scanning electron microscope (SEM). While x-ray diffraction do not indicate the growth of new crystalline phases in these mixture, the micrographs indicate that there is some degree of order in the newly developed phases. The microstructure of the fractured surface of a $(NaPO_3)_n \cdot Na_2O$ modified sample as seen in Figure 4 (a) shows hexagonal crystal embedded in a matrix. Although large pores were removed during sample processing, small pores (~5 μm diameter) can still be seen. The $(NaPO_3)_n$ modified sample (b) shows columnar-like phases in the binding matrix.

Table 1 Flexural strength for HAC and modified samples

No.	Materials	Amount (g)	Flexural Strength (MPa) 1D	3D	7D	14D	28D	90D	300D
03	Secar 71	80	7.3	9.4	13.7	12.3	11.0	11.9	12.1
	DI Water	16							
	Secar 71	80							
01	$(NaPO_3)_n.Na_2O$	8	20.1	34.5	33.8	24.5	27.3	~	34.5
	DI Water	16							
	Secar 71	80							
23	$(NaPO_3)_n$	8	33.7	39.3	33.7	32.5	18.3	20.7	27.3
	DI Water	16							
	Secar 71	70							
27	$(NaPO_3)_n$	7	48.1	24.3	32.3	24.3	~	24.8	28.1
	Silica fume	7							
	DI Water	21							

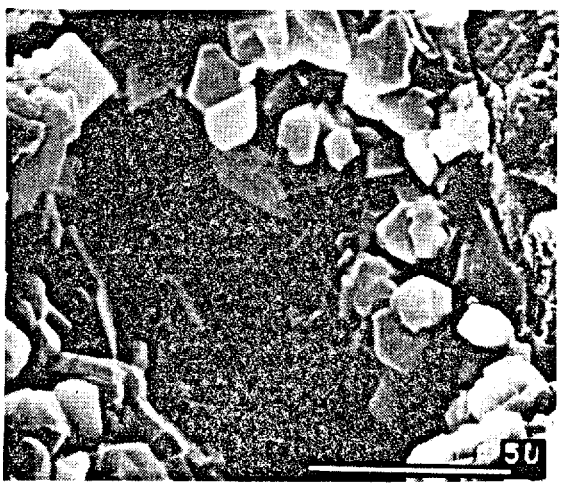

(a)

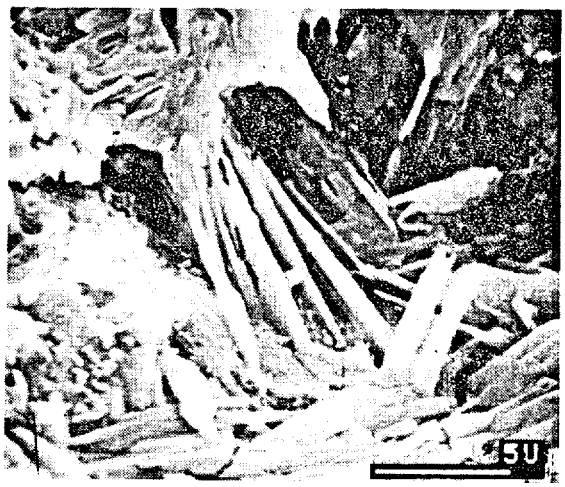

(b)

Figure 4. SEM images of $(NaPO_3)_n$ and $(NaPO_3)_n \cdot Na_2O$ modified samples.

CONCLUSIONS

(1) High alumina cement modified by phosphate-based inorganic polymers exhibit much faster hydration rates. However, hydration evolves less total heat than for pure HAC.

(2) The phosphate-containing products formed in this system are x-ray amorphous. However SEM shows phases exhibiting distinct morphologies.

(3) The strength is greatly improved by the addition of sodium phosphates.

ACKNOWLEDGEMENT

The authors gratefully acknowledge the support of the Air Force Office of Scientific Research, Aerospace Science Directorate.

REFERENCES

1. D. M. Roy, "New Strong Cement Materials: Chemically Bonded Ceramics," Science 235 (1987) pp. 651-658.
2. S. Chandra, and P. Flodin, "Interactions of Polymers and Organic Admixtures on Portland Cement Hydration," Cem. Concr. Res., 17 (1987) pp. 875-890.
3. J. D. Birchall, A. J. Howard, and K. Kendall, "Flexural Strength and Porosity of Cements," Nature 289 (1981) pp. 388-389.
4. J. D. Birchall, "Cement in the Context of New Materials for an Energy-Expensive Future" Technology in the 1990s: Developments in the Science and Technology of Hydraulic Cement, Ed. P. Hirsch et al., (1983) pp. 31-51.
5. W. Sinclair and G. W. Groves, "High Strength Cement Pastes Part 1 Microstructures," J. Mater. Sci. 20 (1985) pp. 2853-60.
6. J. F. Young, "Macro-Defect-Free Cement: A Review," Specialty Cements with Advanced Properties, Ed. B. Scheetz, et al., Mat. Res. Soc. Symp. Proc. Vol. 179. (1991) pp. 101-21.
7. C. S. Poon and G. W. Groves, "The Microstructure of Macro-Defect-Free Cement with Different Polymer Contents and the Effect on Water Stability," J. Mater. Sci. 23 (1988) pp. 657-70.
8. W. Ma, and P. W. Brown, "Mechanical Behaviour and Microstructural Development in Phosphate modified High Alumina Cement," Submitted to Cem. Concr. Res.
9. J. E. Cassidy, "Phosphate Bonding Then and Now," Ceram. Bull. 56 (1977) pp. 640-643.
10. P. W. Brown, and M. Fulmer, "Kinetics of Hydroxyapatite Formation at Low Temperature," J. Am. Ceram. Soc. 74 (1991) pp. 934-40.
11. D. M. Roy, "Recent Advanced in Phosphate Chemically Bonded Ceramics," MRS Int'l. Mtg. on Adv. Mats. Vol. 13 (1989) pp. 213-227 .
12. W. Ma and P. W. Brown, "Investigation of Hydration in the HAC-Phosphate System," (in preparation).
13. R. N. Edmonds and A. J. Majumdar, "The Hydration of Secar 71 Aluminous Cement at Different Temperatures," Cem. Concr. Res., 19 (1989) pp. 289-94.
14. R. N. Edmonds and A. J. Majumdar, "The Hydration of Monocalcium Aluminate at Different Temperatures," Cem. Concr. Res., 18 (1988) pp. 311-20.

MECHANISMS OF LIMESTONE FILLERS REACTIONS IN THE SYSTEM {C_3A–$C\underline{S}H_2$–CH–$C\underline{C}$–H} :

COMPETITION BETWEEN CALCIUM MONOCARBO- AND MONOSULFO-ALUMINATE HYDRATES FORMATION

C Vernet and Noworyta

Technodes SA
Centre de Recherche Industrielle et Technique, du Groupe Ciments Francais, FRANCE

ABSTRACT

In the system { C_3A–$C\underline{S}H_2$–CH–$C\underline{C}$–H }, carbonate ions released by limestone dissolution compete with sulfate ions released by gypsum, to react with aluminate ions coming from C_3A. In presence of monocarboaluminate, the conditions of existence of monosulfo–aluminate in the system are not well established. We have revisited the problem using experimental conditions allowing the monosulfoaluminate formation. The hydration kinetics was monitored and the solids and liquid phases analyzed.

It is found that in the quaternary system, monosulfo– and monocarboaluminates can coexist at equilibrium with portlandite and calcium aluminate hydrate, for an adequate initial composition. Nevertheless, the evolution of the system remains far from equilibrium, as long as C_3A is still present, and this allows the formation of metastable phases. A review of the available data in the literature, including our results, is shown in a diagramatic form, explaining the reaction pathways followed by the different mixes which have been studied. The above apparent discrepancies are then eliminated and the data included in a general view.

A practical consequence relative to the chemical stability of the fillerized cements exposed to carbonation or sulfate attack, can be derived from this study. Knowing that the stability of carboaluminate is better than that of monosulfoaluminate and aluminate hydrate, the durability of fillerized cements should be improved in adjusting the gypsum amount, so as to favourize carboaluminate formation.

N.B. For word-processing reasons, the bars on the top of symbols for SO_3 and CO_2 have been replaced by underlines.

1 - INTRODUCTION

Among the cement mineral additives, limestone fillers are now used in a general way in France, where their use was developed during the 80's. Beyond their filling role, they are known to show various chemical activities, which are difficult to characterise with classical methods, including calorimetry. Reactivity tests in acid media **(1)** are too far from the actual hydration conditions. Dissolution is then operated by a protonation mechanism of carbonate ions, since in basic media it proceeds by shifting the solubility equilibrium of calcium carbonate, with formation of less soluble compounds for example, calcium carboaluminate, in presence of calcium aluminates. During cement hydration, carbonate ions coming from limestone fillers, and sulfate ions from gypsum, compete to react with aluminate ions from C_3A. In this matter, the data found in the literature do not seem to be in total agreement **(2 to 5),(7)(8)**, particularly concerning the monosulfoaluminate formation. In a previous paper **(5)**, we had studied a range of compositions favourizing the carboaluminate formation, which is the general case in cements.
Supposing that the apparent discrepancies of the available data had arisen from the different experimental conditions and molar ratios which had been used, we have further revisited the system {C_3A-$C\underline{S}H_2$-CH-$C\underline{C}$-H} in the conditions of monosulfoaluminate formation.

2 - EXPERIMENTAL.

2.1. Methods

The reagents were synthetic C_3A, doped with 0.25% Na2O, and analytical grade calcite, gypsum and portlandite, finely ground (about 4000cm2/g). The experiments were performed at 25°C, using a water to solid ratio of 16. The dry blends were introduced and kept in suspension during 6 days in a kinetic reactor allowing multiparameters measurements. The parameters monitored were the electrical conductivity, the thermal flow (heat release rate), and the pH of the suspension. The ionic concentrations of sodium, potassium, sulfate and calcium were measured using an online SKALAR analyzer. Samples of the suspension were kept on the base of the variations of the monitored parameters. The filtrates were analyzed using the classical spectrometric methods. The results were used to calibrate the online analysis. The solids were rinsed with ethanolether, moderatly dried, and analysed using thermogravimetry and X-ray diffraction, the latter using silicium as an internal standard. X-ray peaks were identified using ref **(9),(10),(11)**.

2.2. Domain of compositions

All the mixes contained an excess of portlandite, with the aim of maintaining the lime saturation, whatever the reactions can be.
Three runs were performed in a first set, using the proportions of reagents listed in **table** 1.

Table 1 Mixes for kinetic study.

RUN	MOLE FRACTIONS		
	$C\underline{C}$	$C\underline{S}$	C_3A
# 1	0.528	0.061	0.411
# 2	0.514	0.104	0.381
# 3	0.492	0.142	0.365

Table 2 Conductometric tests.

RUN	MOLE FRACTIONS		
	$C\underline{C}$	$C\underline{S}$	C_3A
# 4	0.00	0.13	0.87
# 5	0.11	0.12	0.78
# 5	0.18	0.11	0.71
# 6	0.36	0.08	0.56
# 7	0.53	0.06	0.41
# 8	0.69	0.04	0.27
# 9	0.82	0.02	0.16

This domain of compositions corresponds to C_3A-rich cements in which a part of gypsum is partially replaced by calcium carbonate. A second series of tests were performed, using only the conductometry, on mixes with a large variation of the $C\underline{C}/C_3A$ ratio (table 2) Other conductometric tests were also performed on fillerized cements.

3 - RESULTS.

3.1. Kinetic measurements

A typical series of evolution curves **(run # 3)** is shown at fig.1. The following abreviations are used for simplification of the diagram:
C = electrical conductivity.
dQ/dt = heat flux.
$C\underline{S}$ = gypsum
$C\underline{C}$ = calcium carbonate.
CH = portlandite
TSA = Ettringite.
MSA = Mono-sulfoaluminate hydrate.
MCA = Mono-carbo-aluminate hydrate.
HCA = Hemi-carboaluminate hydrate.
HSA = Hemi-sulfoaluminate hydrate.
C4 = C_4AH_{13} solid solution.

In this run, the gypsum proportion seems to be sufficient to control the C_3A initial reactions. Ettringite and a small amount of MCA are formed first. This corresponds to a splitting of the initial heat flux peak. After the gypsum depletion, **(mark 1)**, the ettringite dissolves and forms MSA and MCA :

$TSA + C\underline{C} + 3C_3A + 25H \rightarrow MCA + 3MSA$

A part of the portlandite is used by the C_3A to form HSA and C_4AH_{13} :

$C_3A + CH + 12\,H \dashrightarrow C4$

$C_3A + CH + MSA + 10\,H \dashrightarrow 2\,HSA$

This is a typical out of equilibrium situation, maintained by the dissolution of C_3A. These reactions are slowed down by the layer of hydrates, until the depletion of ettringite **(mark 2)**. Then the HSA and C_4AH_{13} react with carbonate ions, and HCA appears. MSA, MCA and the calcium concentration increases.

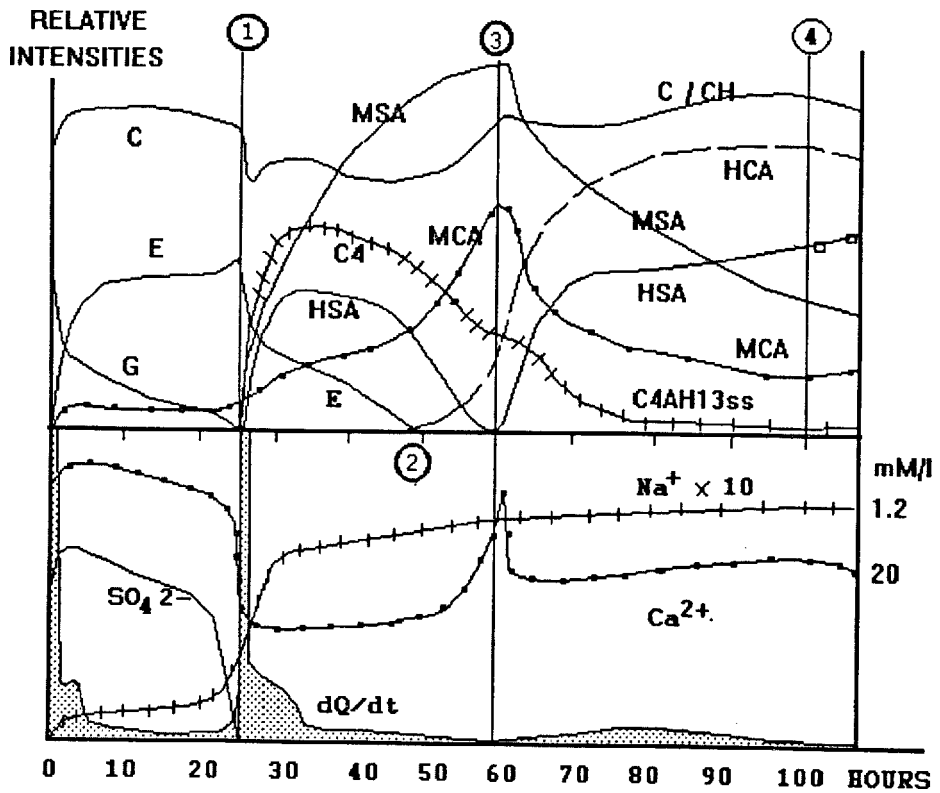

fig.1 kinetic diagram for run # 3.

2 HSA --> 2 MSA + CH
2 HSA + C$\underline{C}$ --> MSA + HCA + CH
2 C_4AH_{13} + C$\underline{C}$ --> 2 HCA + CH.
C_4AH_{13} + C$\underline{C}$ --> MCA + CH

A conductivity maximum, and a minimum heat flux are observed, at the C_3A depletion **(mark 3)**.
Then MSA and MCA react rapidly with C_4AH_{13} to form HCA and HSA.

MSA + C4 --> 2 HSA
MCA + C4 --> 2 HCA

The MSA is depleted after 100h **(mark 4)**, and then the hydrates begin to react more slowly, tending to reach the equilibrium. Finally, a solid solution HSA + HCA is obtained after 6 days. The theoritical composition (TSA + MCA + excess C$\underline{C}$) could take a very long time to be reached. The proportion of gypsum was lower for run #1 than for run #3. Run #1 depicts an immediate depletion of the ettringite. Afterwards the sequence is similar to the #3 one. The C_3A is depleted at about 30h, in #3, v.s. 60h in #1. The MSA is also rapidly depleted. Run #2 is an intermediate case, and behaves as expected.

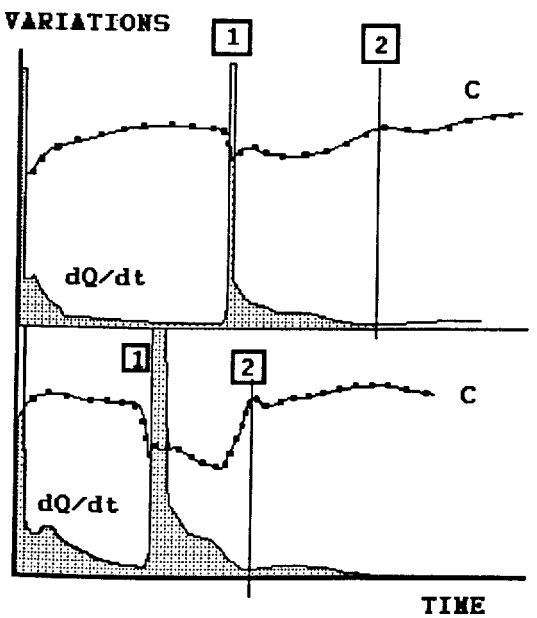

fig.2
Comparison between runs # 1 (upper) and # 2

The conductometric cuves depict the differences in reaction rate between runs #1 and #2 (fig.2). In the latter, the conductivity drop is greater at the gypsum depletion time **(mark 1)**. This drop is due to the calcium and sulfate concentration drop, minus the increase related to the release of alkalis by the C_3A dissolution. It is lower in run #1 than in #2, because a lower gypsum content produces less ettringite, which reacts afterwards with less C_3A.

The conductivity increase after the ettringite depletion **(mark 2)** is larger than in #1. In the latter the C_3A produced more C_4AH_{13} and HSA, because of the lower amount of ettringite, giving less MSA. This is confirmed by a greater heat flux peak in #2 at this moment.
The detailed analysis of the kinetic sequence now allow to interpret the conductometric curves in this system. In the second series of tests, the variation of the calcite content, for a constant amount of gypsum, leads to shifts of the events described above (fig.3).

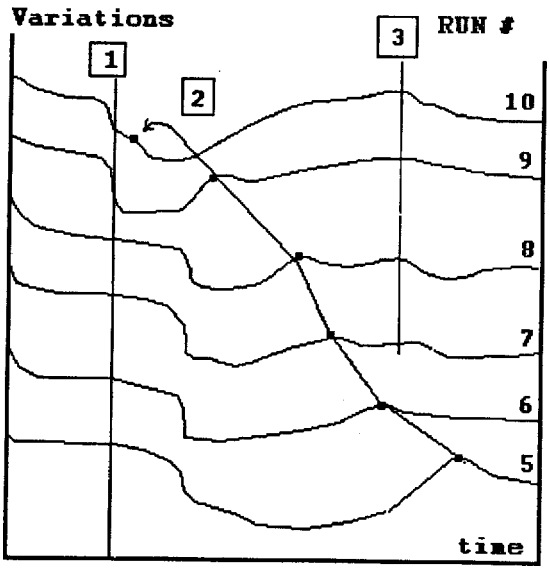

fig.3 **Conductometric curves for runs #5 to #10.**

- The gypsum depletion **(mark 1)** occurs at the same time in runs #5 trough 8, but 4 h sooner in run #9 and #10. In the latter, a large part of the C_3A has reacted in the first hours with calcium carbonate, and the carboaluminate has lowered the "braking" action of the sulfate, probably by a decrease of the permeability of the hydrates layer.
- The larger the amount of calcite, the sooner the C_3A depletion **(mark 2)** occurs. On the contrary, the monosulfate depletion **(mark 3)**,do not seem to be shifted as much.

The same effects are observed for cement suspensions, taken in the same conditions.

4 - DISCUSSION.

4.1. Representation of the reaction pathways. Comparison of the data in the literature (fig.4).

To represent the reaction pathways in the quaternary diagram { $C\underline{S}H_2$ - $C\underline{C}$ - C_4AAH_{13} - CH }, we have used a triangular section of the tetrahedron, obtained for a constant value of the portlandite mole fraction (0.5 is the minimum to form C_4AH_{13} with C_3A). The triangle { $C\underline{S}H_2$ - $C\underline{C}$ - C_4AH_{13} } is composed of 6 zones corresponding to the phases which can coexist, by set of three. The available data (calculated mole fractions), are plotted on this diagram at <u>fig.4.</u>

The observed final phases rarely agree with the location of the equilibrium points, except for hydrates obtained by precipitation from solutions, or equilibrated during several months (point 11 from ref.7). Monosulfate formation have been observed for the points located in the triangle {MCA-MSA-C_4AH_{13}}, and in a transient way, for other points located in the triangle {TSA-MCA-$C\underline{C}$}.
It seems that using C_3A or cement for experimentation leads to metastable intermediate products. The theoritical domain of MSA stabilization is composed of triangles **C**,($C\underline{C}$ depletion), **D**,($C\underline{C}$ and TSA depletion), and **E**,($C\underline{C}$, TSA and MCA depletion). The points # 8, 9 and 10 represent the above kinetic study (runs 1, 2 and 3). The point # 10, for example, lies within the {MCA - TSA - $C\underline{C}$} triangle. Then these 3 phases are expected to coexist at equilibrium. The results of fig.1 have shown that the mix in run #1 uses a particular pathway to reach the equilibrium state, and that equilibrum was long to be reached.

4.2 <u>Kinetic appoach</u>

On a kinetic point of view, the formation of intermediate phases is obvious. The most insoluble phase form first. But the solubility of the hydrates depends on the concentrations, and can change when ions are used up **(12) to (14)**. A less soluble phase can form if the latter more soluble one has been depleted by a chemical reaction. This occurs when anhydrous phases like C_3A or cement can lead the system far from equilibrium.

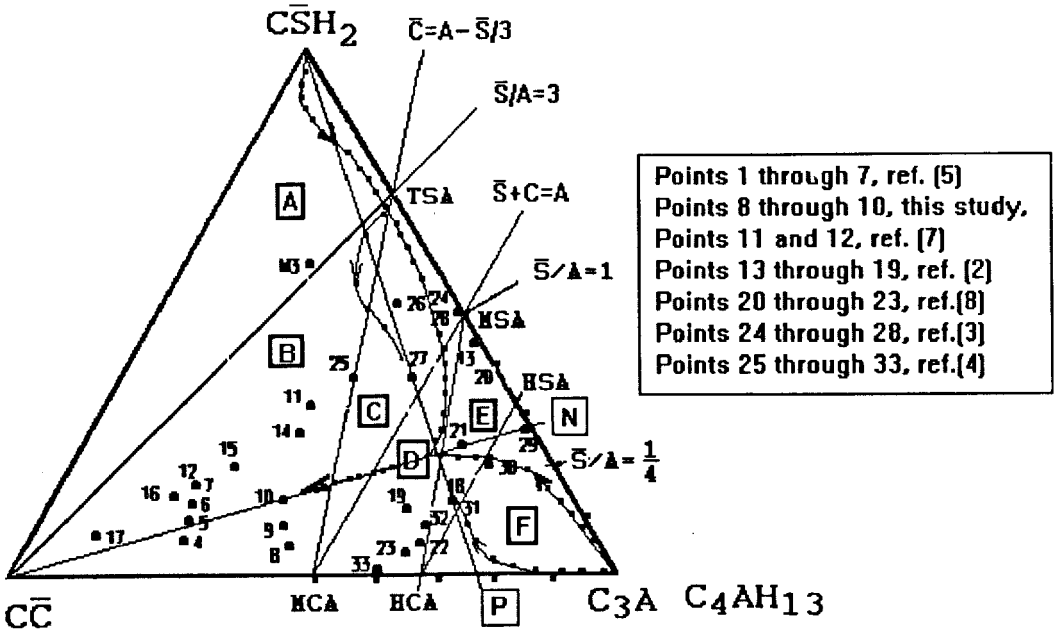

<u>fig.4</u> **Plot of the experimental data in the C_3A-$C\underline{C}$-$C\underline{S}H_2$ diagram**

Depending on their reactivity, they can act as "magnetic attractors" and track the points in their way in the diagram, until they have been depleted.
Thus in run #1, the figurative point passed trough the A, B, C, D, and E triangles, until depletion of the C_3A. MCA and MSA appear when TSA begin to dissolve, for lack of sulfate ions. HCA appears when TSA is depleted, the figurative point being then in the MCA–MSA–HCA triangle.

There is still a behaviour to be explained in the run #3, that is the formation of C_4AH_{13}. For this, we propose to consider the concentration gradients around the C_3A grains (**fig.5**). Taking into account the interaction between diffusion and precipitation, it is possible to describe the formation of the hydrates in a set of domains close to equilibrium. The hydrates precipitate at a finite distance from the C_3A interface, depending on their precipitation rate constant, and on the diffusion coefficients of the constitutive ions (**15**).

Experimental data confirm this model in the calcite transition zone (**16**) (**17**), and around the C_3A grains (**18**). **Thus the hydrates layers are ordered from the interface**, and are close to the hydrates belonging to the same triangle of the equilibrium diagram.

Depending on the initial composition, the thickness and the sequence of the hydrate layers will be different.

For example, the stabilization of TSA by an increase of gypsum will suppress the MSA and HSA. In the same view, C_4AH_{13} and HCA will be expected in close contact with C_3A, separated from TSA by a MCA layer.
This explains why the number of phases is greater than expected for equilibrium, and all the unexpected results in the literature. The reaction pathway can be represented in the equilibrium diagram, by splitting the hydrates in two goups, both giving intermediate pathways (**fig.4**).

The first group is composed of the hydrates close to C_3A, and the second is composed of the external hydrates, formed at the junction of diffusion gradients of aluminate ions and outer ions like sulfate and carbonate. In the case of run #1,(**fig.4**), both pathways tend to join on the line CC–mark N, which represents the composition of the hydrates when TSA and C_3A have been depleted. The remaining hydrates coexist with the remaining CC, which was in excess, and they tend to reach the overall composition.

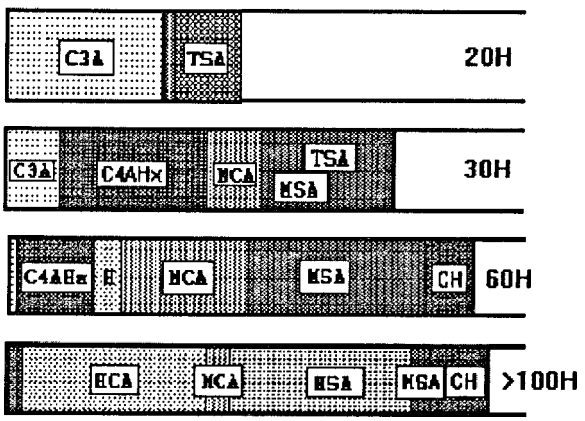

Fig.5 Order of precipitation layers v.s. time and distance from C_3A.

We have also represented the pathways for **point #27**, the behaviour of which was unexpected, because of the absence of MSA formation. The paths tend to reach point #27 and to join the $C\underline{S}H_2$ mark P line. But in the first stage, they pass by the triangles corresponding to the observed behaviour (**3**), and we can understand that MSA will begin to appear after the depletion of CC. This may take a very long time if C_3A is depleted first, taking into account the low reactivity of the hydrates.

5 - CONCLUSIONS.

The consideration of the concentration gradients around the C_3A grains, and the use of a representation of the pathways followed by the hydrates enable the comprehension of the different behaviours of limestone fillerized cements. It seems that monosulfate–aluminate hydrate can form at equilibrium when the kinetic conditions are gathered.
Among the practical consequences of this work, we shall point out the performance of the conductometric technique to evaluate the reactivity of limestone fillers. This can be performed in chemical conditions very close to the cement ones.

We can also use the equilibrium diagram to foresee the behaviour of fillers. Given the better stability of carbonated hydrates versus CO_2 attack, the use of limestone fillers is a way of improving durability. The resistance to sulfate has been reported to be better than the standards, using limestone fillers **(19),** but this cannot be the case into the triangle MSA-MCA-C_3A. Precautions have thus to be taken in the formulations of cements, and proportions will play an important role. Given the higher solubility of the C_4AH_{13} and parent solid solutions, it seems preferable to avoid the triangle MCA-MSA-C_3A, and to aim the triangle TSA-C$\underline{C}$-MCA, in its central part.

References.

(1) LONGUET P."Réactivité des fillers calcaires." Ciments Platres et Chaux, 1982, 742, 3/83

(2) RAMACHANDRAN V.S. "Cement with calcium carbonate addition."
8th ICCC, RIO, 1986, pp 178-182.

(3) KUZEL H.J.; MEYER H.W. "Effect of CO2 on the hydration of pastes." 1rst Workshop on cement hydration, DIJON, 1991. (13 pages).

(4) NEGRO A. ABBIATI G. CUSSINO L.
"Calcium carbonate substitute for gypsum as a set regulator." Il Cemento, 4/1986, pp 537-544.

(5) VERNET C. "Sequence and kinetics of hydration reactions of C3A with gypsum, lime and calcareous fillers." 8th.ICCC, RIO, Vol.3, pp 70-74.

(6) ZHANG F. ZHOU Z. LOU Z. "solubility product and stability of ettringite."
7th ICCC, PARIS, 1980. II-88 II-93.

(7) MANABE T. "Studies on calcium monocarboaluminate hydrate." CAJ Rev, 1961, pp 48-55.

(8) BENSTED J. "Further hydration investigations involving portland cement and the substitution of limestone for gypsum." World Cem, Dec.1983, pp 383-392.

(9) POLLMANN H. "solid solutions of complex calcium aluminate hydrates containing Cl^-, OH^-, and CO_3^{2-} anions". 8th.ICCC, RIO, 1986, 2.1, pp 300-306.

(10) KAPRALIK I. HANIC F. "Phase relations in the subsystem $C_4A_3\underline{S}$- $C\underline{S}H_2$-CH-H_2O of the system CaO-Al_2O_3-C$\underline{S}$-H_2O referred to hydration of sulphoaluminate cement." JCCR, Vol.19, pp 89-102, 1989.

(11) FISCHER R. "Reinvestigation of the system $C_4A.nH_2O$-$C_4A.CO_2.nH_2O$."
JCCR, Vol.12, pp517-526, 1980.

(12) BARRET P. BERTRANDIE D. BEAU D. "Calcium hydrocarboaluminate, carbonate, alumina gel and hydrated aluminates solubility diagram calculated in equilibrium with CO_{2g} and with Na^+ ions." JCCR, Vol.13, 1983, pp 789-800.

(13) SOUSTELLE M. et coll. "Stabilité thermodynamique des phases dans le systeme CaO-Al_2O_3-CO_2-H_2O." JCCR, 1985, Vol.15, pp 421-430.

(14) SATAVA V. "Determining the standard enthalpy of formation, Gibbs' energy of formation and absolute entropy of 3CaO.Al2O3.CaCO3.11H2O." Silikaty, 31, 117-120. 1987.

(15) VERNET C."Evolution de la microstructure des hydrates. Aspects théoriques." 8th ICCC, RIO, 1986, Vol.6, pp 358-360.

(16) NEGRO A. BACCHIORINI A. CUSSINO L.
"Interazione carbonato di calcio-alluminati. "Seminario Internationale Torino,Alluminati di calcio, 1982, pp 219-229.

(17) OLLIVIER J.P.Thesis, Toulouse, 1975.

(18) BAUSSANT J.B. VERNET C. DEFOSSE C. "Growth of ettringite in diffusion controlled conditions. Influence of additives on the crystal morphology." 12th. ICCM, , 1989, New-Orleans, pp 186-197.

(19) SOROKA I. "Effect of calcareous fillers on sulfate resistance of portland cement."
Ceram.Bull.,Vol.55, N°6, 1976, pp 594-595.

THERMAL AND CHEMICAL STABILITY OF AFm PHASE-ISOSTRUCTURAL GROUP

T Nishikawa*, K Sato**, S Ito* and K Suzuki*

*Nagoya Institute of Technology, Gokiso-cho, Showa-ku, Nagoya, JAPAN
**NKK Co, Ltd, Marunouchi, Chiyoda-ku, Tokyo, JAPAN

SUMMARY

In this paper, some isostructural compounds of AFm phase were synthesized by the use of chemical reagents in the liquid-liquid or solid-liquid systems. The resulting solid phases were characterized by XRD, DTA and SEM. Firstly, the basal spacing of the synthesized compounds, which represented the hydrated anion species in the interlayer region, were measured after drying. Though their values might also depend most on the amount of interlayer water.

Secondly, thermal stability of these compounds was measured by DTA-TG. Two stages of weight loss were observed in each compound. One was attributed to the dehydration of the interlayer water and the other to the dehydration of the hydroxide ion. These dehydration temperatures varied with the interlayer anion species.

Thirdly, the chemical stability of the compounds was evaluated by measuring the concentration of the ionic species and the solid phase, after immersion in distilled water. The AFm phase easily decomposed to the AFt phase, gypsum and alumina gel. The compound containing NO_3^- ion partially exchanged to that containing hydroxide ion. Other compounds, containing CO_3^{2-} or Cl^- ion in the interlayer region did not. For the latter two compounds, solubility product Ksp and the standard Gibbs free energy of formation could be calculated. The thermodynamical stability of the AFm phase-isostructural group 's discussed.

要旨

本論文では、液相－液相または液相－固相系の純薬合成によりＡＦｍ相の類似化合物を合成した。得られた固相はＸＲＤ，ＤＴＡ，ＳＥＭで評価した。最初に、合成化合物の層間隔を乾燥後測定した。この値は層間域の水和した陰イオン種に対応したが、層間水量にもかなり依存すると考えられる。

第二に、これら化合物の熱安定性をＤＴＡ－ＴＧで測定した。各々の化合物で２段階の重量減少が認められた。一つは層間水の脱水によるもので、他の一つは水酸基イオンの脱水によるものである。これらの脱水温度は層間の陰イオン種により変化した。

第三に、蒸留水中に浸積した後、イオン種の濃度と固相を調べることにより、化合物の化学安定性を評価した。ＡＦｍ相は容易にＡＦｔ相、２水石膏、アルミナゲルに分解した。硝酸イオンを含む化合物は、部分的に水酸基イオンを含む化合物に変化した。また、層間域に炭酸イオン、塩素イオンを含む化合物は変化しなかった。後の２つの化合物について溶解度積と標準生成自由エネルギーが求められ、ＡＦｍ相類似化合物の熱力学的な安定性について考察した。

1. INTRODUCTION

Calcium monosulpho-aluminate hydrate, $3CaO \cdot Al_2O_3 \cdot CaSO_4 \cdot 12H_2O$, is usually recognized as the AFm phase in the long-term hydration process. Recently, the use of blast-furnace slag instead of portland cement brings the high alumina content in cement and easily produces the AFm phase besides the AFt phase. Although the AFm phase is a metastable phase thermodynamically compared to the AFt phase, or is noticed in the concrete after long term.

AFm phase also has a layer structure and shows the exchangeable property in the interlayer region[1]. Actually, under a given condition, several isostructural compounds of the AFm phase were observed in concrete. For example, Freidel's salt, in which chloride ion exists instead of sulphate ion, is observed in the concrete penetrated or corroded by sea water. While, in the concrete after carbonation, another compound, in which the carbonate ion changes place with sulphate ion, is found. Effect of these compounds on concrete strength or durability has not been revealed completely.

However, these exchangeable properties in the interlayer region can be used as indicator of the host-guest reaction. Therefore, definite synthesized methods of monolithic compound has been expected, for example, while using blast furnace slag.

In this paper, the synthesis of some isostructural compounds of AFm phase by using chemical reagents in the liquid-liquid or solid-liquid systems has been discussed. The resulting solid phases were characterized by XRD, DTA and SEM. Finally, their thermal and chemical stability are discussed.

2. EXPERIMENTAL

Preparation of the starting materials

The following chemical reagents were added to distilled water up to a given concentration and filtered. The solutions used in this experiment were $Ca(OH)_2$ (0.02 mol/l), $Ca(NO_3)_2$ (0.4 mol/l) and $CaCl_2$ (0.5 mol/l) aqueous solution.

Ettringite ($3CaO.Al_2O_3.3CaSO_4.32H_2O$) was synthesized by mixing a calcium hydroxide aqueous solution and aluminium sulfate solution and allowing the mixture to react under a CO_2-free condition. The synthesis method in detail has been mentioned elsewhere[2].

Calcium aluminate ($CaO.Al_2O_3$) was synthesized using $CaCO_3$ and Al_2O_3, which was mixed in the Ca/Al molar ratio of 1.0 and sintered at 1500 ℃ for 3 hrs.

Recommended synthesis method

1)$3CaO \cdot Al_2O_3 \cdot CaSO_4 \cdot 12H_2O$ (AFm-S): Synthesized ettringite was added to distilled and CO_2-free water. Water/solid weight ratio was kept at 125 ~ 150. This suspension was boiled for 4 hrs with magnetic stirring and then filtered[3]. At different water/solid ratio or temperature, initial ettringite , alumina gel or gypsum was co-existed.

2)$3CaO \cdot Al_2O_3 \cdot Ca(NO_3)_2 \cdot 10H_2O$ (AFm-N): $Ca(OH)_2$ and $Ca(NO_3)_2$ aqueous solutions were mixed and added to CA powder to maintain the stoichiometric composition. This suspension was stirred at room temperature for 24 hrs. Other solution or powder combinations brought to form alumina gel and aluminium hydroxide.

3)$3CaO \cdot Al_2O_3 \cdot CaCl_2 \cdot 10H_2O$ (AFm-Ch): $Ca(OH)_2$ and $CaCl_2$ aqueous solutions were mixed and CA powder added to maintain the stoichiometric composition. This suspension stirred at room temperature for 24 hrs. Using the different kind of solution or adding the impertinent amount of CA powder brought to form alumina gel and aluminium hydroxide.

4)$3CaO \cdot Al_2O_3 \cdot CaCO_3 \cdot 11H_2O$ (AFm-Ca): $CaCO_3$ and CA were added to $Ca(OH)_2$ aqueous solution and then stirred ultrasonically at 45 ℃ for 4 hrs. The precipitate obtained

contained a small amount of calcite ($CaCO_3$). At other experimental conditions, several kinds of calcium aluminate hydrates were mainly formed.

Characterization of synthesized AFm phase-isostructural compound

The precipitates were dried in 10^{-2}mmHg vacuum for 24 hrs., and identified with XRD for their basal spacing, SEM for the morphology and EDAX for the chemical composition. Thermal stability was determined by DTA-TG. Chemical stability was evaluated by immersion of these compounds in distilled water followed by measurement of the dissolved ionic concentration.

3. RESULTS AND DISCUSSION

Identification of compound

The precipitates were investigated by XRD. In the XRD patterns of the precipitates, AFm phase-isostructural compound alone was observed except in AFm-Ca, in which calcite co-existed. Accordingly, the basal spacings were calculated from these 001 reflections and listed in Table 1. These values after drying were lower than those observed at normal conditions. The difference of basal spacing was caused not only by the size of the interlayer anion but also the amount of interlayer water, the latter was obtained from thermal test.

Table 1 Basal spacing of AFm-isostructural compound

Sample	Basal spacing (Å)
AFm-S	8.93
AFm-N	8.66
AFm-Ch	7.85
AFm-Ca	7.56

The results of chemical analysis as measured by EDAX are shown in Table 2. For all the compounds, the observed values relatively coincided with the calculated values. In the interlayer region of AFm-S and AFm-Ch, the interlayer ions existed closely. The Ca/Al molar ratio must be equal to 2.0 , but a slight deviation was observed.

Table 2 Chemical analysis measured by EDAX

Sample	Ca(wt%)		Al(wt%)		S(wt%)		Cl(wt%)		Calculated
	OBS.	CAL.	OBS.	CAL.	OBS.	CAL.	OBS.	CAL.	Ca/Al mole ratio
AFm-S	52.3	57.1	27.8	28.6	19.9	14.3			2.16
AFm-N	64.2	60.0	35.8	40.0					2.16
AFm-Ch	45.2	50.0	30.4	25.5			24.4	25.5	1.69
AFm-Ca	59.4	66.7	40.6	33.3					1.80

Fig 1 shows the morphology of each compound. Hexagonal plates were observed in all the compounds. The size of plates for AFm-S was 20 μ m in diameter and 1 μ m in thickness. The sizes of other compounds were approximately 10 μ m in diameter and less than 1 μ m in thickness. The plates for AFm-Ca almost aggregated to become radial.

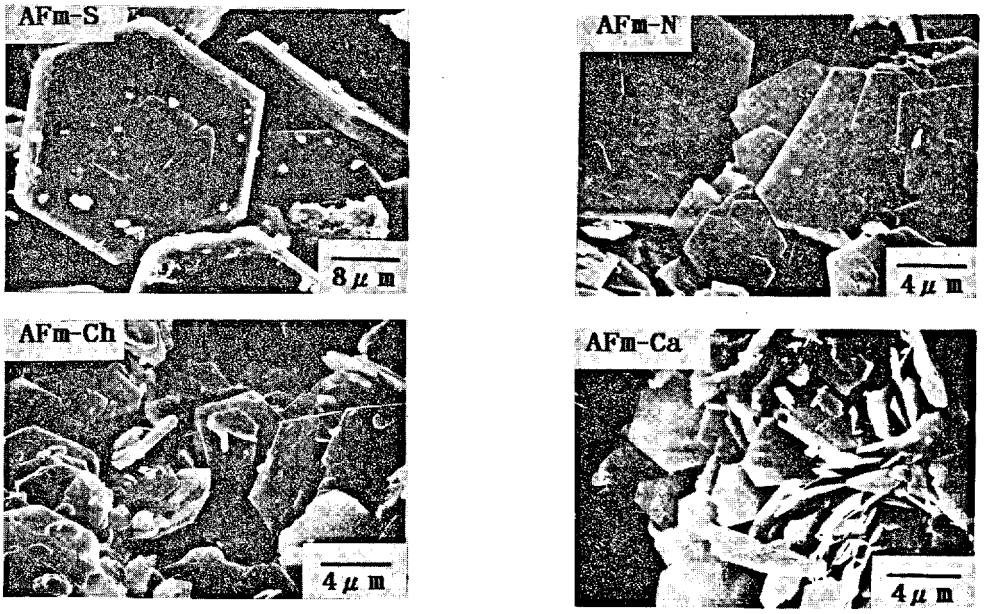

Fig.1 SEM micrographs of AFm compounds

Thermal and chemical stability

Fig.2 shows the DTA-TG results of each compound. Weight loss accompanied with an exothermic peak was roughly divided two stages. One was attributed to the dehydration of the interlayer water and the other to the dehydration of the hydroxide ion in the interlayer region. The dehydration temperature varied with the interlayer anion specimen. The amount of hydrated water was noted down at each plateau step of TG curves. Above that temperature, weight loss and DTA peak may be due to the volatilization of other ion specimens, that is the decarbonation for AFm-Ca at approximately 700 ℃.

Table 3 shows the concentrations of ionic specimens and solid phase after immersion in distilled water. The AFm-Ca and AFm-Ch did not change, but others decomposed or changed to other stable compounds. Gibbs free energy of formation for the former compounds could be calculated[4]. The thermodynamic equations for the two compounds could be written as follows, supposing that they have the same amount of water.

$$4Ca^{2+}(aq.)+2AlO_2^-(aq.)+CO_3^{2-}(aq.)+4OH^-(aq.)+9H_2O(liq.) = 3CaO.Al_2O_3.CaCO_3.12H_2O(AFm\text{-}Ca)$$

$$4Ca^{2+}(aq.)+2AlO_2^-(aq.)+2Cl^-(aq.)+4OH^-(aq.)+10H_2O(liq.) = 3CaO.Al_2O_3.CaCl_2.12H_2O(AFm\text{-}Ch)$$

For AFm-Ca,

$$\Delta G^\circ_{AFm\text{-}Ca} = 4\Delta G^\circ_{Ca^{2+}} + 2\Delta G^\circ_{AlO_2^-} + \Delta G^\circ_{CO_3^{2-}} + 4\Delta G^\circ_{OH^-} + 9\Delta G^\circ_{H_2O} + RT\ln\{[Ca^{2+}]^4[AlO_2^-]^2[CO_3^{2-}][OH^-]^4\}$$

Here, the ΔG°'s with subscript of the solid phase or ionic species are the standard Gibbs free energy of formation. The activity of the solid phase and the activity coefficients of the ionic species were assumed to be unity. The concentration of carbonate ion could not be measured , and so this was obtained from the charge valency

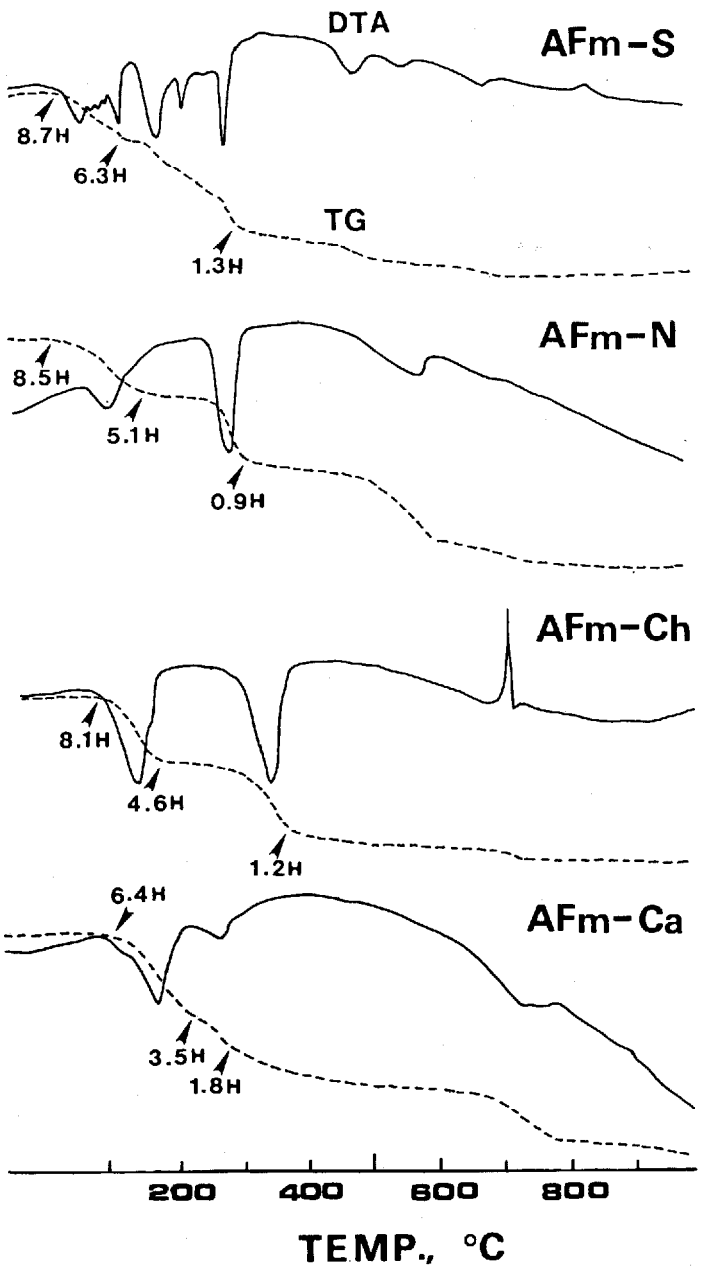

Fig.2 DTA-TG curves of AFm compounds

Table 3 Concentration of ionic specimens and resultant precipitate

Sample	$[Ca^{2+}]$	$[AlO_2^-]$	$[X^{2-}, Y^-]$	$[OH^-]$	Resultant precipitate
		mmol/l			
AFm-S	2.29	1.94	SO_4^{2-} tr.	5.10	AFt, Gypsum Calcite, Bayerite
AFm-N	5.85	2.84	NO_3^- 2.84	5.01	AFm-N, C_4AH_{13}
AFm-Ch	5.02	2.45	Cl^- 4.26	3.16	AFm-Ch
AFm-Ca	2.54	2.17	CO_3^{2-} -	2.00	AFm-Ca

equation in liquid phase. The $\triangle G^\circ$ of each ionic species was taken from the thermodynamic table[5]. The Ksp(AFm-Ca), corresponded to the value of blanket in above equation, was 2.8×10^{-30}. The $\triangle G^\circ$ (AFm-Ca) was -1805.8 kcal/mol. The Ksp(AFm-Ch) was 6.9×10^{-30} and $\triangle G^\circ$ (AFm-Ch) was -1741.8 kcal/mol. These values were lower than that for AFm-S, which was -1859.14 kcal/mol. Actually, the amount of water molecule for AFm-Ca or AFm-Ch was smaller than that of AFm-S. Thus $\triangle G^\circ$ was smaller compared to that of AFm-S. These calculated results suggested that the most stable compound in this group was AFm-S, but it changed easily with the amount of water.

4. CONCLUSIONS

(1) Calcium monosulpho-aluminate hydrate phase-isostructural compound
{ $3CaO \cdot Al_2O_3 \cdot Ca(X,Y_2) \cdot 12H_2O$: SO_4^{2-},CO_3^{2-} as X and NO_3^-,Cl^- as Y } could be synthesized as monolithic phase.
(2)Basal spacing of synthesised compounds depended mostly on the amount of interlayer water.
(3)Two stages of weight loss in TG curve were observed for each compound. One was attributed to the dehydration of the interlayer water and the other to the dehydration of hydroxide ion. The dehydration temperature varied with interlayer anion species.
(4)The compound containing NO_3^- ion partially exchanged to that of containing hydroxide ion. Other compounds, containing CO_3^{2-} or Cl^- ion in interlayer region did not. For the latter two compounds, solubility product Ksp and standard Gibbs free energy of formation could be calculated.

REFERENCES

1) K. Murakami et al., Gypusum and Lime, **114**,202(1971).
2) T. Nishikawa et al., Cement and Concrete Res., **22**,6(1992).
3) H.Y. Ghorab et al., ibid., **15**,93(1985).
4) K.Suzuki et al., ibid., **15**,213(1985).
5) V.I.Babushkin et al., "Thermodynamics of Silicate" Springer-Verlag(1985)

INFLUENCE OF ANHYDRITE PARTICLE SIZE ON THE HYDRATION OF SULPHOALUMINATE BELITE CEMENT

S Sahu*, J Majling* and J Havlica**

*Department of Ceramics, Glass and Cement, Slovak Technical University
Bratislava, CZECHOSLOVAKIA
**Institute of Inorganic Chemistry, Slovak Academy of Sciences
Bratislava, CZECHOSLOVAKIA

SUMMARY

Sulphoaluminate belite cement clinker with the main phases C_2S, $C_4A_3\bar{S}$ and C_4AF was synthesised from limestone, fly ash, phosphogypsum and a small amount of corrective bauxite at 1200 ^{0}C. The influence of particle sizes (specific surface) of a constant amount of added anhydrite during hydration process of this cement was investigated.Results show that the rate of formation of ettringite is proportional to the specific surface of anhydrite. An optimum fraction of particle size helps in gaining the high initial compressive strength. The particle size of anhydrite plays an important role in the mechanism of ettringite formation and influencing the properties of the hydrated cement paste.

SUMARIO

El clinquer de Sulfoaminoato de Belita, con las fases principales C_2S, $C_4A_3\bar{S}$ y C_4AF, fue sintetisado a partir de cal, hollhn, yeso, y una pequeña cantidad de bauxita como corrector, a 1200 ^{0}C. Fue investigada la influencia del tamaño de las partheulas (superficie espechfica) de una cantidad constante de anhidrido añadido durante el proceso de hidratación de este cemento. Los resultados muestran que la velocidad de formación de etringuita es proporcional a la superficie espechfica de anhidrido. Una fracción con tamaños de partheulas óptimos, ayuda en la obtención de una alta resistencia inicial a la compresión. El tamaño de las partheulas de anhidrido juega un rol importante en el mecanismo de formación de etringuita, y en las propiedades de la pasta de cemento hidratada.

INTRODUCTION

Gypsum is used as a set retarder in Portland cement. Gypsum reacts with C_3A of Portland cement in the presence of water to form ettringite on the surface of original aluminate grains leading to the retardation of the reaction and in this way controls the setting behaviour of Portland cement (1).

Grinding of clinker and gypsum together in industrial mill shows that the finer fraction is dominated by gypsum : in fact 90 % gypsum has granule sizes below 40 μm (2). This is due to the fact that grindability of clinker and gypsum is being inversely proportional (3). The granulometry of cement as well as the grinding condition affects the role of gypsum (4).

Ettringite the main initial hydrated product is responsible for the setting and hardening properties of the Sulphoaluminate belite cement (5) as well as the expansive character of expansive cements. In the case of sulphoaluminate belite cement, the sulphoaluminate phase $C_4A_3\overline{S}$ reacts with $C\overline{S}$ in the presence of water to form ettringite according to the following scheme

$$C_4A_3\overline{S} + 8\,C\overline{S} + 6C + 96\,H \rightarrow 3C_6A\overline{S}_3H_{32}$$

The mechanism and kinetics of ettringite formation which influences the microstructure development also determines the strength development and other properties of this cement. In work (6) the influence of different kinds of calcium sulphates have been studied and it has been shown that the solubility of calcium sulphate changes the mechanism of ettringite formation. The solubility of anhydrite is directly proportional to the specific surface of the anhydrite (2). In work (7) the influence of pH on the stability of different hydrated products in the system $CaO\text{-}Al_2O_3\text{-}SO_3\text{-}H_2O$ has been studied and shown that at pH > 10.7 ettringite is the stable phase and at pH > 11.2 monosulphate is the stable phase. On the basis of these findings a hypothetical model has been developed to explain the role of liquid interlayer in the mechanism of ettringite and monosulphate formation (8).

In this work it has been studied how in real situation the particle size/ specific surface of the added anhydrite influences on the hydration of sulphoaluminate belite cement.

EXPERIMENTAL

The sulphoaluminate belite cement was prepared from limestone, fly ash, bauxite and phosphogypsum. For the present study an optimized clinker of the work (5) has been considered. The chemical composition and the phase composition according to modified Bouge's calculation are given in Table 1.

Table 1. Chemical composition and calculated phase composition of the sulphoaluminate belite cement (SAB).

Oxides	Wt.%	Phases	Wt.%
CaO	53.94	C_2S	52.94
SiO_2	18.47	$C_4A_3\overline{S}$	15.7
Al_2O_3	15.41	C_4AF	17.64
Fe_2O_3	5.88	$C\overline{S}$	5.8
SO_3	6.56		
Fineness	296.5 $m^{-2} \cdot kg^{-1}$		

The presence of the listed phases were identified by X-ray diffraction method. Pure chemical grade gypsum was sintered at 1200 ^{0}C for one hour, was ground and sieved to different particle sizes. 15 Wt.% of anhydrite of different particle sizes were mixed with the ground Sulphoaluminate belite cement to prepare the following mixtures, Table 2. Before conducting the hydration study the mixtures were thoroughly homogenized.

For compressive strength measurement test pieces of cement paste of the size 1×1×3 cm. were prepared. After 24 hours of hydration in the humid chamber they were demolded and further left in the humid chamber for hydration. Samples after 24 hours of hydration were taken for mercury intrusion porosimetry (MIP). The heat evolution characteristics were studied by a differential calorimetry ZIAC (9,10).

Table 2. Description of the mixtures

Sample no	85 Wt. %	15 Wt. % CS and particle sizes(μm)	Specific surface of $C\bar{S}$ kg m^{-2}
P1	SAB+	(70-100)	87.9
P2	SAB+	(45-70)	112.5
P3	SAB+	(36-45)	124.4
P4	SAB+	(5-36)	167.7
P5	SAB+	(5-20)	302.0

RESULTS AND DISCUSSION

The kinetics of hydration process of sulphoaluminte belite cement with various fineness of anhydrite has been shown by the trends in heat evolution from calorimetric study Fig.1. It is evident that the increase of specific surface of anhydrite which directly influences the total specific surface accelerates the ettringite formation in first period of hydration and lowering of the second peak. In the case of P5 where the finest fraction of anhydrite is present there is almost no effect on the second peak.

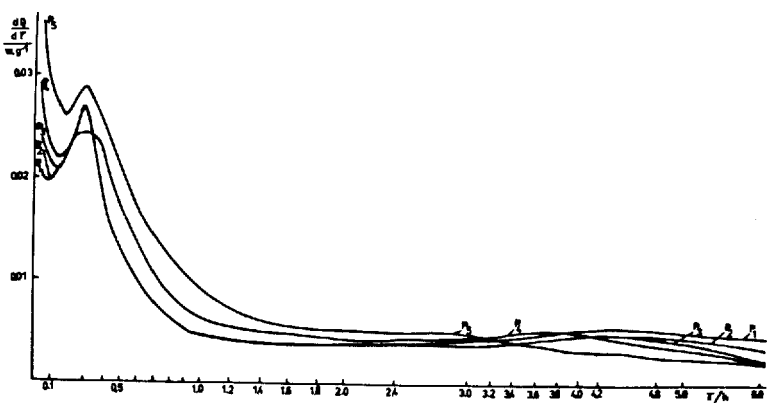

Fig. 1. Trends in heat evolution of Sulphoaluminate belite cement in the presence of different particle sizes of anhydrites

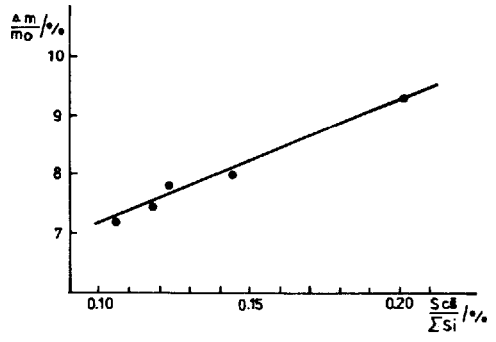

Fig. 2 Dependence of mass loss due to ettringite on the surface ratio r($C\bar{S}$)

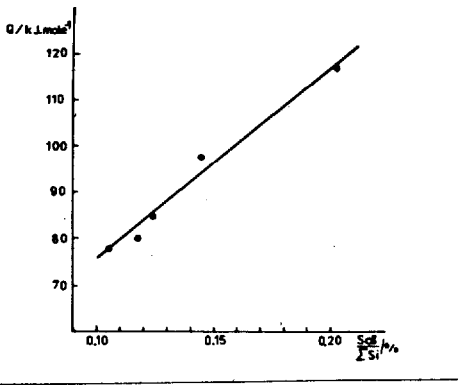

Fig. 3 Dependence of liberated heat in first period on the surface ratio r($C\bar{S}$)

Similar effect was observed in our yet unpublished work (11) where the influence of particle size of the individual minerals in the modelled system C_2S-$C_4A_3\bar{S}$-$C\bar{S}$ was studied. It was observed that when finest fraction of $C\bar{S}$ and coarse fractions of C_2S and $C_4A_3\bar{S}$ are present in the system the initial hydrated product is gypsum instead of ettringite. But in the present studied systems no such gypsum formation was observed. So it can be predicted that the heat evolution in the first period is partly contributed due to the conversion of anhydrite to gypsum. The second peak is most probably due to the second step of ettringite formation.

By analysing the specific surface of individual minerals, which are calculated from the content of individual phases in the original cement and considering all the minerals having the same grindability and contributing equally to the total surface it can be seen that the contribution of surface of anhydrite to the total surface is proportionally highest in the case of P5 Table 3. Where r in table 3 s the relative specific surface of individual phases represented by the following relation.

$$r = \frac{S_i}{\sum S_i}$$

S_i - Specific surface of phase i

Table 3 Contribution of individual phases to the total specific surface

Mixture no	Specific Surface total $m^2\,kg^{-1}$	r %			
		C_2S	$C_4A_3\bar{S}$	C_4AF	$C\bar{S}$
P1	265.2	50.30	22.36	16.77	10.57
P2	268.9	49.29	22.05	16.54	11.72
P3	270.6	49.62	21.91	16.43	12.37
P4	277.1	48.14	21.39	16.05	14.42
P5	297.3	44.88	19.94	14.96	20.22

Considering the amount of ions in the liquid phase in the starting system is proportional to the surface of $C\bar{S}$. As the solubility of anhydrite is proportional to the specific surface (2), it is expected that higher content of sulphate ions in the system and lowering the pH value in the liquid phase. Change in the specific surface of anhydrite most probably influences both the rate of ettringite formation and the dissolution of silicate phase. These conditions retard the formation of silicate hydrates and on the other hand prefer the formation of ettringite which can be observed from the TG results Table 4 and Fig. 2 The dependence Q (heat evolved) in the first period (first peak) on the r ($C\bar{S}$) is shown in Fig. 3. It shows that with increase in r($C\bar{S}$) value the heat evolved in the first period increases.

Table 4. Weight loss from TG measurement

Sample no	Total Wt. loss	Wt. loss due to ettringite
P1	15.2	7.2
P2	15.7	7.4
P3	15.3	7.8
P4	15.3	8.0
P5	17.6	9.3

Porosity measurement by mercury intrusion porosimetry shows that there is no large variation in the pore size distribution of the samples. But the change in total porosity and specific surface indicate that when relatively finer fraction as well coarser fraction of anhydrite is present the total porosity is lower and specific surface is relatively higher Table 5.

Table 5. Total surface and Specific surfaces from MIP

Sample no	Total Porosity	Specific surface $m^2.g^{-1}$
P1	18.84	18.44
P2	21.46	15.86
P3	21.01	15.13
P4	22.32	14.01
P5	19.49	16.29

This is most probably due to the relatively faster formation of ettringite and negatively influenced by fast drop of water in the system and hindering the rate of dissolution of silicate phase. Compressive strength measurement after one day (Table 6) shows contrary results when coarser (P1) as well as finer fraction of anhydrite (P5) is present, the values are relatively lower. It is not very much clear why in the presence of finer fraction of anhydrite the strength is lower. Comparing the differences in strength $\Delta\sigma_{7\text{-}1}$ (7 days - 1 day) it is evident that the values are almost the same but $\Delta\sigma_{28\text{-}7}$ for samples P4 and P5 is higher. This rise in strength is most probably contributed by hydration of silicate phase, which was hindered by the fast formation of ettringite and causing significant drop of water content in the system.

Table 6. Compressive strengths in MPa

Sample no	1 day	7 days	$\Delta\sigma_{7-1}$	28 days	$\Delta\sigma_{28-7}$
P1	29.0	53.0	24.0	55.0	2.0
P2	35.0	58.0	23.0	59.0	1.0
P3	33.0	56.0	23.0	62.0	6.0
P4	31.0	43.0	23.0	60.0	17.0
P5	29.0	52.0	23.0	70.0	18.0

CONCLUSIONS

From the present study it can be concluded that the solubility of anhydrite plays a vital role in the rate of formation as well as in the mechanism of ettringite formation, which influences the microstructure development and other properties of the hardened body. Some more study is required to analyse the influences in detail to develop a high strength sulphoaluminate belite cement as well as proper expansive cement.

REFERENCES

1. J. Bensed: Progresses in Cement Chemistry (ed. S. N. Ghosh), Pregmon press, 1984, 308.

2. J. P. Bombled, 7 th. ICCC, Paris, Communication, III, VI-164, 1980.

3. G. Frigione and R. Di Lena: Cemento 72 (1) 13, 1975.

4. I.P Meric, 7 th. ICCC, Paris, principal report I, I-4/I, 1980.

5. P.K. Mehta: " investigations on energy saving cements" World cement Technology, 11, 166, 1980.

6. S. Sahu, J, Havlica, V. Tomkova, J. Majling: Influence of different kinds of calcium sulphates on the hydration of sulphoaluminate belite cement, Thermochemica Acta 174, 45, 1991.

7. A.Gabrisova, J. Havlica, S. Sahu: "Stability of Sulphoaluminate hydrates in water solution with various pH values", Cem. Concr. Res. 21, 1023, 1991.

8. J. Havlica, S. Sahu: "Mechanism of Ettringite and Momonosulphate formation" Cem. Concr. Res. (in press).

9. G. Oliew, W. Wieker, Silikattechnik, 32, 152 (1982).

10. G. Oliew, W. Wieker, Silikattechnik, 31, 333 (1981).

11. S.Sahu et al. Influence of particle size of the individual minerals in the system C_2S-$C_4A_3\overline{S}$-$C\overline{S}$-H_2O(Unpublished work).

STUDIES OF BARIUM ADDITION ON THE β-Ca_2SiO_4 HYDRATION

M Gawlicki

University of Mining and Metallurgy, Cracow
POLAND

SUMMARY

The hydration in the water suspensions of β-Ca_2SiO_4, Ba_2SiO_4, β-$Ca_{1.98}Ba_{0.02}SiO_4$, and β-$Ca_{1.94}Ba_{0.06}SiO_4$ was studied. It was found that the presence of barium ions in the structure of β-dicalcium silicate brings about the increase of hydration rate. The BaO/CaO molar ratio in the suspensions of two phases doped with barium is much higher than in the initial, anhydrous samples. It may be caused by the fact that Ba^{2+} ions are not incorporated easily into the structure of CSH phase.

RÉSUMÉ

On a étudié l'hydratation de β-Ca_2SiO_4, Ba_2SiO_4 et de solutions solides β-$Ca_{1.98}Ba_{0.02}SiO_4$ et β-$Ca_{1.94}Ba_{0.06}SiO_4$ à la suspension aquense. On a établi qu'à la présence de Ba^{2+} ions dans la structure de β-silicate bicalcique la vitesse de l'hydratation augmentait. Le rapport BaO/CaO dans la phase liquide de solution solides hydratées est plus élevé qu'à la phase initiale ayant l'hydratation. Cet effet pourrait être la consequence d'un fait que Ba^{2+} ions ne prennent pas une part dans la formation de CSH.

INTRODUCTION

As it is commonly known, the rate of β-Ca_2SiO_4 hydration is strongly influenced by the type and amount of foreign ions introduced to the calcium orthosilicate structure. According to many authors the β-Ca_2SiO_4 stabilizers replacing Si^{4+} cations in the $[SiO_4]^{4-}$ tetrahedron reduce the rate of hydration. This assumption results from the studies of Pritts and Daugherty [1]. These authors synthesized the β-orthosilicate phase using many stabilizers entering the structure on the positions both Si^{4+} and Ca^{2+} or interstitially and found that the hydration process was hindered. The highest rate of hydration was observed for dicalcium silicate β-polymorph prepared without any stabilizer. The studies of strength development for cements produced with barium addition, as well as the studies of clinker minerals doped with barium [2] suggest that barium introduced to the Ca_2SiO_4 structure can accelerate the hydration process.

EXPERIMENTAL

The initial materials used in the investigations were β-Ca_2SiO_4 stabilized by thermal treatment i.e. by repeating heating and cooling [3] and barium doped orthosilicates of the following composition:

$Ca_{1.98}Ba_{0.02}SiO_4$ - i.e. 99% by mole Ca_2SiO_4 + 1% by mole Ba_2SiO_4,
$Ca_{1.94}Ba_{0.06}SiO_4$ - i.e. 97% by mole Ca_2SiO_4 + 3% by mole Ba_2SiO_4.

The samples doped with barium were subjected to the same thermal treatment as the initial "pure" calcium orthosilicate. The XRD studies showed that the γ-Ca_2SiO_4 content did not exceed 3%. The sample $Ca_{1.94}Ba_{0.06}SiO_4$ contained, apart from the β phase, some amount of α'-Ca_2SiO_4, not exceeding 5%. The Ba_2SiO_4 synthesis was also carried out. All the samples were ground to the specific surface of 3400 cm^2/g, as measured by Blaine method. The hydration was carried out in pastes prepared at solid to liquid ratio - l/s = 0.5, 0.6 and 0.7 or in the suspensions at l/s = 50, 100 and 200, respectively. The suspensions were continuously mixed in sealed polyethylene containers at room temperature. The time of hydration was in the range from 1 hour to 28 days. The XRD studies of hydrated solid samples showed that the Ba addition caused the acceleration of the β-Ca_2SiO_4 hydration at every l/s ratio, particularly within the first 3 days. At later ages the differences between the hydration degree for particular samples reduced and practically disappeared after 28 days.

The studies of hydrated suspensions were practically limited to the chemical analysis of calcium and barium ions concentration in the liquid phase being in equilibrium with the hydrating material. The analysis was carried out by ASA method and by complexometric titration. The selected results are shown in tables 1-4. The concentrations of calcium and barium cations are expressed as CaO and BaO contents. The total CaO and BaO concentration in liquid phase was calculated following the procedure given below:

$$C_{MeO}=C_{CaO}+0.336*C_{BaO};$$

where:
C_{MeO} - total CaO and BaO concentration calculated as CaO,
C_{CaO} - CaO concentration,
C_{BaO} - BaO concentration.

The percentage of CaO, BaO and MeO leached out from solid (P) was calculated as follows:

$$P = \frac{\text{content of CaO,BaO or MeO in liquid phase}}{\text{content of CaO,BaO or MeO in unhydrous phase}} * 100\%;$$

In all the series the "degree of leaching" for MeO was related to the l/s ratio. The CaO and BaO contents in the solution increased with l/s ratio. The differences reduced with time of hydration. This relation is presented in tables 1 and 2. In the other tables only the results obtained at l/s = 100 are shown.

Table 1. Liquid phase analysis of β-Ca_2SiO_4 samples hydrated in the suspensions at different l/s ratio.

Time of hydration	CaO concentration in the liquid [mg/dm^3]			Percentage of CaO leached out from the solid		
	liquid to solid ratio - l/s					
	50	100	200	50	100	200
1h	410	266	152	3.15	4.08	4.67
3h	507	319	205	3.89	4.59	6.30
6h	547	391	265	4.41	6.01	8.14
12h	664	428	296	5.10	6.57	9.09
24h	729	462	314	5.60	7.10	10.05
3d	844	646	360	6.48	8.73	11.49
7d	952	749	394	7.31	11.51	12.10
14d	1168	895	451	8.97	13.75	13.86
28d	1430	1225	614	10.98	18.80	18.80

Table 2. Liquid phase analysis of Ba_2SiO_4 samples hydrated in the suspensions at different l/s ratio.

Time of hydration	BaO concentration in the liquid [mg/dm^3]			Percentage of BaO leached out from the solid		
	liquid to solid ratio - l/s					
	50	100	200	50	100	200
30min	6302	3654	2000	37.70	43.71	47.91
1h	6431	3795	2060	38.53	45.40	49.28
3h	6840	3947	2080	40.91	47.21	49.72
6h	7219	4160	2095	43.22	49.78	50.08
12h	7715	4181	2090	46.09	50.00	50.02
24h	8365	4203	2095	50.10	50.15	50.08
3d	8358	4187	2100	50.00	50.03	50.20
7d	8360	4182	2090	50.05	50.01	50.02
14d	8365	4182	2088	50.10	50.01	50.00

Table 3. Liquid phase analysis of β-$Ca_{1.98}Ba_{0.02}SiO_4$ samples hydrated in the suspensions at l/s ratio = 100.

Time of hydration	CaO+BaO concentration in the liquid [mg/dm^3]			Percentage of CaO and BaO leached out from the solid		
	CaO	BaO	MeO	CaO	BaO	MeO
1h	270	13	275	4.23	7.39	4.27
3h	330	14	335	5.18	7.95	5.20
6h	409	18	416	6.42	10.22	6.43
12h	449	24	458	7.04	13.64	7.47
24h	471	28	481	7.39	15.91	7.47
3d	659	36	672	10.34	20.45	10.44
7d	757	56	777	11.88	31.82	12.07
14d	932	78	963	14.62	44.32	14.96
28d	1200	84	1231	18.83	47.72	19.12

Table 4. Liquid phase analysis of β-$Ca_{1.94}Ba_{0.06}SiO_4$ samples hydrated in the suspensions at l/s ratio = 100.

Time of hydration	CaO+BaO concentration in the liquid [mg/dm^3]			Percentage of CaO and BaO leached out from the solid		
	CaO	BaO	MeO	CaO	BaO	MeO
1h	258	53	287	4.22	10.23	4.56
3h	304	69	329	4.93	13.32	5.22
6h	392	78	416	6.42	10.22	6.43
12h	428	87	450	7.00	16.80	7.14
24h	452	134	501	7.40	25.87	7.95
3d	633	157	690	10.36	30.31	10.95
7d	712	187	780	11.65	36.10	12.38
14d	889	211	966	14.55	40.73	15.33
28d	1144	236	1230	18.72	45.56	19.52

DISCUSSION

The slow reaction of the dicalcium silicate with water involves serious difficulties in the evaluation of its degree of hydration by QXRD, particularly at early stages, i.e. within first 24 hours. On the other side the amount of calcium hydroxide forming during this reaction cannot be taken as a measure of the reaction progress. The determination of $Ca(OH)_2$ can be, however, useful in comparative studies of many factors ifluencing the hydration process.

The results thus obtained indicate that barium incorporated to the structure of β-Ca_2SiO_4 accelerates the hydration process both in pastes and in the suspensions of calcium orthosilicate with water. In both samples doped with barium the CaO content in the liquid phase was higher

than in the "pure" Ca_2SiO_4 sample. The total BaO and CaO concentration were much higher. It should be underlined simultaneously that the highest concentrations were observed for the β-$Ca_{1.98}Ba_{0.02}SiO_4$ sample. The rate of hydration for these samples was the highest. The lower CaO concentrations in the β-$Ca_{1.94}Ba_{0.06}SiO_4$ suspensions are probably the consequence of different phase composition of the unhydrous samples and higher Ba^{2+} concentration in the liquid phase.

As it results from the data given in tables 3 and 4, the barium ions are transferred to the solution more easily than the calcium ions.The percentage of leaching BaO from the $Ca_{1.98}Ba_{0.02}SiO_4$ and $Ca_{1.94}Ba_{0.06}SiO_4$ structures after 14 days hydration is higher than 40% and after 28 days-45%, respectively, while the percentage of CaO leaching is 14.6% and 18.8%, respectively. The percentage of BaO leaching in these samples approaches the maximal value (50%) for Ba_2SiO_4 hydration in the suspension (table 2). This value is in a good accordance with the data of Hanna, Cook and Kantro [4]; the Ba_2SiO_4 hydration products are barium hydrosilicate with BaO/SiO_2 ratio = 1 and barium hydroxide. Much higher BaO to CaO molar ratio in the solution than in the anhydrous sample suggests that the barium ions do not incorporate easily into the CSH phase structure.

REFERENCES

1. Pritts, I.M. and Daugherty, K.E.: "The effect of stabilizing agents on the hydration rate of β-Ca_2SiO_4",Cement and Concrete Research, 1976, 6, 783-796.

2. Kurdowski, W.: "Influence of barium on the Portland Cement Clinkier prperties", Prace Komisji Ceramicznej PAN, Ceramika, 1972, 18, 32-38. (pol).

3. Gawlicki, M. and Nocuń-Wczelik, W.: "Influence of thermal treatment on transition $\beta \rightarrow \gamma$-C_2S", 7-th International Congress on the Chemistry of Cement, Paris, 1980 vol.II, I-161 - I-165.

4. Hanna, K. M., Cook, R. L. and Kantro, D. L.: "Hydration of dibarium silicate", Journal of Applied Chemistry, 1970, 20, 334-340.

A QUANTITATIVE STUDY OF PASTE MICROSTRUCTURES AND HYDRATION CHARACTERS OF SULPHOALUMINATE CEMENT

Wang Yanmou*, Su Muzhen**, Yang Renhe** and Lui Baoyuan**

*State Administration for Building Materials Industry
**China Building Materials Academy, Guanzhuang, Beijing
P R CHINA

SUMMARY

The hydration characteristics of sulphoaluminate cement and paste microstructures were investigated by quantitative analysis of various phases (including: crystals, gels and pores). The effects of contents of various phases on expansion and strength are discussed.

〔摘　要〕

本文通过硫铝酸盐水泥石的相（晶体，胶体和孔）定量分析，研究了硫铝酸盐水泥的水化特性，结构形成过程．这里讨论了硫铝酸盐水泥的膨胀机理以及孔、胶体含量、晶体含量对该水泥石强度的综合影响。

INTRODUCTION

Industrial sulphoaluminate cement (SAC) clinker, which is composed mainly of two minerals: $C_4A_3\bar{S}$ and C_2S, is blended with different amount of gypsum to form approximately two varieties of cement: the first one is high early strength cement with amount of gypsum below 20%, and the other is expansive cement with gypsum above 20%. In China, the capability of producing sulphoaluminate cement (SAC) is about 500,000 ton per year. Also its usage is readily increasing.

In the past, some authors [1,2,3] investigated hydration characteristics, paste microstructure and mechanism of expansion are high early strength of SAC. However, most of their results were qualitive and not systematized because of the limitation of research methods or measuring techniques. Cement paste is considered as a complex system composed of several phases, each of which has a certain microstructure. For example, the system of SAC paste consists of hydrated phases (AFt crystal and gel), unhydrated phases ($C_4A_3\bar{S}$, C_2S, $C\bar{S}H_2$ and a little amorphous substances) and pores (gas phase). Determination of the contents of phases in the system and investigation of their variations make it possible to study the influence of each phase on the system and the combined effects of several phases on the mechanical behavior of the system. A modified method of QXDA, TGA and methyl displacement pycnometry were used for measuring the main phases composition of SAC pastes quantitatively.

EXPERIMENTAL

1. Materials

Sulphoaluminate cement clinker for this experiment was produced by Shijiazhuang Building Materials Plant, Hebei Province, China. Natural gypsum was from Hebei, China. Their chemical compositions was shown in table 1. Clinker and gypsum were ground saparately to obtain the required fineness. Different types of SAC were obtained by blending gypsum into clinker at the rates of 0, 5%, 15%, 25%, 35% and 45% by weight of cement, and then each of them was homogenized in a mixer, marking SA–0,SA–5,SA–15,SA–25,SA–35 and SA–45 respectively.

Table 1. Chemical compositions

	I.L.	SiO_2	Al_2O_3	Fe_2O_3	CaO	MgO	SO_3
SAC Clinker	1.84	9.78	29.49	1.58	42.81	2.49	10.02
Gypsum	22.98	0.53	0.35	0.11	32.05	2.43	41.11

2. Sample preparation

Cement is mixed with water at water to cement ratio of 0.3 and then cast into moulds of 2 × 2 × 2 cm and 1 × 1 × 6 cm with the aid of vibration. The pastes are demoulded after being stored a fog room for a day, then placed under water for curing up to the ages required.

3. Methods of Quantitative Analysis of phases in SAC paste

3–1 Measurement of porosity

Methyl displacement pycnometry is used.

3–2 Measurement of crystal content

A modified QXDA method [4] is adopted. It is more accurate than conventional methods for quantitative phase analysis and particularly efficient for those whoes "pure" phases with high crystallinity that are impossible, difficult to obtain, or prepare. Weight percentages of AFt, $C_4A_3\bar{S}$, $C\bar{S}H_2$and C_2S are determined by this method.

3–3 Measurement of gel content

Gels in SAC pastes are mostly produced by the hydration of $C_4A_3\bar{S}$ and $C\bar{S}H_2$ in addition to a little amount of C–S–H gel and other gel. In order to simplify the problem, only the contribution to gels due to the hydration of $C_4A_3\bar{S}$ and $C\bar{S}H_2$ is considered here. The gel content of this part can be calculated based on the quantitative results of crystals in cement and in cement paste as well as water content in cement paste (determined by TGA). see reference [4]

EXPERIMENTAL RESULTS

1. Characters of Expansion and Strength

With the increase of gypsum content added into cement, SAC can be divided into two types: high early strength cement and expansive cement, as shown in Fig.1 and shows that compared to 0% gypsum, all others show lower fc. As when gypsum content in cement is below 20%, cement pastes exhibit no expansion or low expansion but very high early strength and when gypsum in cement is above 20%, cement pastes exhibit obvious expansion. Although early strength reduces a considerably, 28 days strength still remains high is shown in Fig.2.

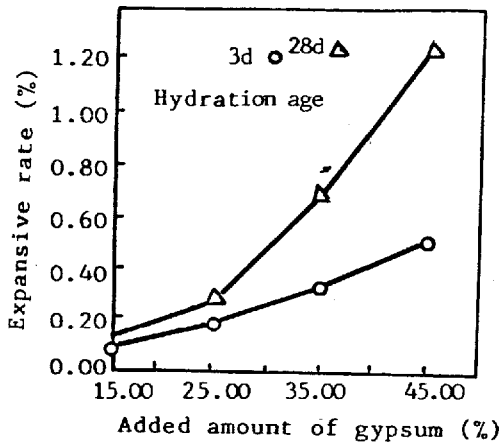

Fig.1 Expantion of sulfoaluminate cement paste

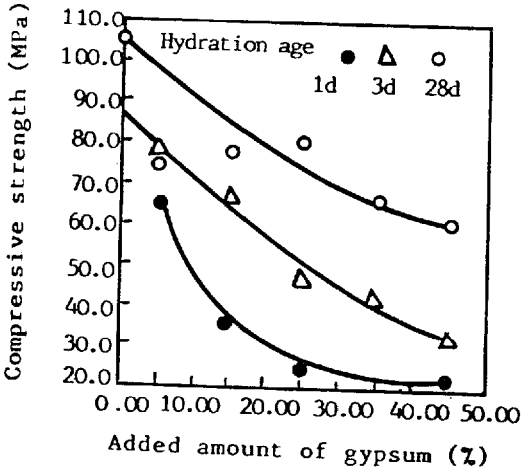

Fig.2 Compressive strength of sulfoaluminate cement pastes

2.Hydration Characteristics of SAC

Mineral composition of SAC determined by QXDA is shown in table 2. Hydration of SAC is very closely related to the proportion of gypsum in it. Hydration degree of $C_4A_3\bar{S}$ in SAC pastes is illustrated in Fig.3. Hydration degree is defined here as the ratio of the phase content in cement paste to that in cement after climinating the influence of water in cement paste. $C_4A_3\bar{S}$ in pure cement clinker hydrates slowly at 1 day. Hydration of $C_4A_3\bar{S}$ accelerates remarkably as soon as gypsum is blended into the cement clinker. Hydration degree of $C_4A_3\bar{S}$ at 3 days and 28 days increases linearly with amount of gypsum. increacing gypsum content in SAC will accelerate hydration of $C_4A_3\bar{S}$ during the middle and late period. At the gypsum content of 45%, $C_4A_3\bar{S}$

hausted by 28 days through hydration . The data on hydration degree at 1 day are around a horizontal line which indicates a limit (about 68%), of hydration degree. It can be seen from Fig.4 that residual gypsum in SAC pasts hydrated for 28 days does not appear until the amount of gypsum added into SAC exceed 15%, the hydration degree of α–C_2S in cement pastes at hydration of 28 days is shown in Fig.5. Only as residual gypsum appears in SAC pastes, α–C_2S starts to hydrate remarkably and its hydration degree rises with residual gypsum content.

Table 2. Phase composition of SAC determined by XRD

Sample	$C_4A_3\bar{S}$	α-C_2S	β–C_2S	$C\bar{S}H_2$
SA–0	58.4	10.6	0.6	
SA–5	56.84	17.83		4.83
SA–15	50.84	14.87		11.16
SA–25	48.8	14.5		22.1
SA–35	36.12	11.56		20.47
SA–45	33.33	10.34	4.5	35.94

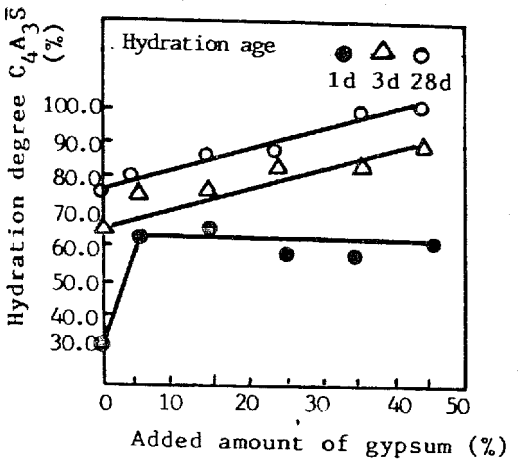

Fig.3 Hydration degree of $C_4A_3\bar{S}$

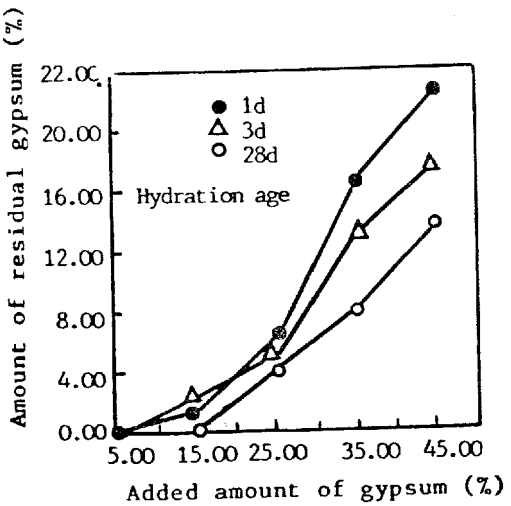

Fig.4 Residual gypsum in cement pastes

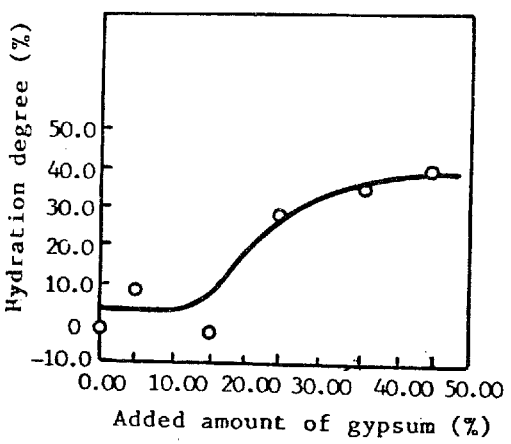

Fig.5 Hydration degree of α–C_2S cured for 28 d

3. Formation of Sulphoaluminate Cement Hydrates

Variations of AFt and gel in SAC pastes with addition of gypsum are given in Fig.6 and Fig.7 respectively. During the early period of hydration (1 day) hydrates in the paste of SAC clinker are less than those in other pastes because of low hydration speed of $C_4A_3\bar{S}$. Later a large amount of hydrates are produced with the acceleration of hydration. Most of the hydrates are gel in addition to a little amount of AFt crystal due to lack of $CaSO_4$ in the clinker paste. However, if a small amount of gypsum is added SAC clinker, SAC pastes are satuated in $CaSO_4$ during the early period and AFt crystal rapidly reaches about 15~20%. Then growth of AFt crystal slows down with exhaustion of $CaSO_4$ such as is the situation at 3 days and 28 days (Fig.6). When the percentage of

gypsum in SAC is more than or equal to 25%, SAC pastes always keep the saturation of $CaSO_4$ due to existence of residual gypsum during the whole period of 28 days. Therefore, there is a distinct growth of AFt at every age of hydration as seen in Fig.6. Hydration reaction proceeds in a state of imbalance and particles of reacting substances with different size are unevenly distributed in cement paste. Only gypsum is in excess so that the environment around $C_4A_3\bar{S}$ particles is saluated in $CaSO_4$ parts of the cement paste. So, both hydration degree of $C_4A_3\bar{S}$ and growth of AFt rise with residual gypsum content. In SAC pastes with residual gypsum, excessive Al^{3+}, SO^{2-} ions easily react with Ca^{++} ions in C_2S to readily form AFt crystals so as to promote hydration of C_2S. Gel content in SAC pastes reduces with the increase of gypsum added to SAC increase.

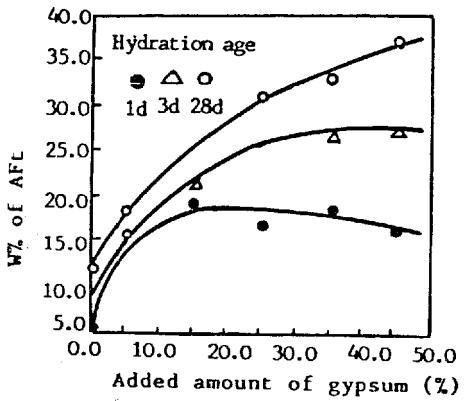

Fig.6 Variation of AFt with adding of gypsum

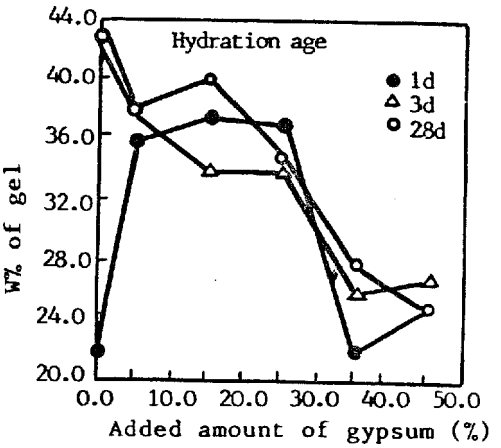

Fig.7 Relation between gel contents and adding amount of gypsum.

4. Pore Structures of Sulphoaluminate Cement Pastes

The growth rules and characteristics of hydrates control the formation of pore structure in SAC pastes. The variation of porosities as a function of the amount of gypsum added to SAC are shown in Fig.8. Gels produced by hydration of SAC make the hardened cement paste into a dense structure. For example, hardened cement paste of SAC clinker has higher percentage of gel and low porosity. The sample at 28 days hydration corresponds to a porosity, at only 13.1%. Porosity increases with the decrease of gel content and occurrence of expansion in SAC pastes.

DISCUSSION

1. Relationship between Phase Composition and Expansion of Sulphoaluminate Cement Pastes

According to the experimental results above, expansion of SAC pastes is directly relevant to the growth of AFt crystal if structure strength and density of cement pastes are enough. Although SAC is a low alkali cement (PH = 9.5~ 10.5), its hydration reaction can retain sufficient growth of AFt crystals to make the cement SAC expand provided this system is satuated in $CaSO_4$. So, the appearance of residual gypsum in cement pastes is a mark of expansion. It can be seen from Fig.1, Fig.4 and Fig.6 that the occurrence of obvious expansion, appearance of residual gypsum and remarkable growth of AFt after a day all correspond to addition of gypsum above 20%, which accounts for the intrinsic connection between them. Relationship between the rates of expansion and quantity of AFt growth of SAC pastes in cement pastes cured for a day is illustrated in Fig.9. Under certain condition of water to cement ratio, growth of AFt crystal can be controlled by changing amount of gypsum in SAC so as to gain the expansion required. Our experiments result show that SAC with

45% gypsum has a good performance as self stressing cement. Its expansion may selfstressing in about 28 days because $C_4A_3\bar{S}$ is nearly exhausted by this period.

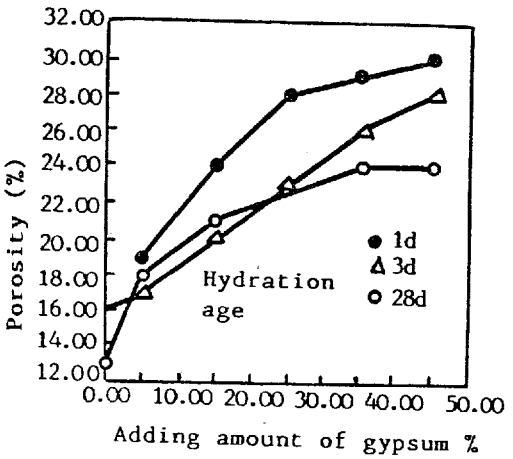

Fig.8 Relation between porosity and adding amount of gypsum

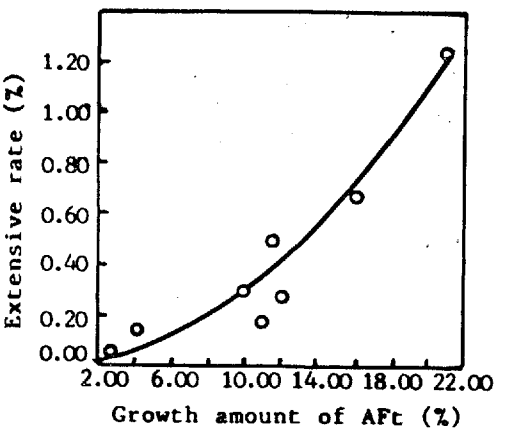

Fig.9 Relation between expansion rate and growth amount of AFt

However, $C_4A_3\bar{S}$ content in industrial SAC clinkers vary from 40% to 70% and $C\bar{S}H_2$ contents in various raw gypsum minerals are different as well. So, it is necessary to perform quantitative phase analysis of industrial SAC clinkers and raw gypsum in order to obtain the optimum gypsum content added to SAC.

2. Relationship between Strength and Phase Composition of SAC Pastes

High early strength SAC may easily achieve the strength above 60 MPa during the period of 1–3 days. The reasons are as follows:

2–1 SAC has a high speed of hydration so that there are plenty of hydrates formed during the early period of hydration.

2–2 AFt crystals in SAC pastes exceed 15% in a day. Although these AFt crystals can not cause expansion of the system as there exists a large amount of pore in the cement paste during the early period of hydration, they can pack hydrates around them tightly so as to densify the structure of the cement paste.

2–3 There is high proportion of gel in the hydrates of high early strength SAC. When SAC is mixed with water, $C_4A_3\bar{S}$ and $C\bar{S}H_2$ begin to dissolve. Al^{+++}, SO^{--} and Ca^{++} from $C_4A_3\bar{S}$ and $C\bar{S}H_2$ may more faster in the solution to form gel which seems easier to precipitate in large pores farther from cement particles. In addition, the gel itself has a dense structure.

Consequently, at water to cement ratio of 0.3, high early strength SAC pastes hydrated for 1–3days are as dense as portland cement pastes hydrated for 28 days (Porosity = 20%).

Low porosity is a structure characteristic of SAC paste main. Strength logarithm of cement paste is related to porosity as shown in Fig.10, when porosities are in the rangs above 20%, relation between strength logarithm and porosity is linear, but in the range below 20%, the curve deviates down from the straight line. It amy be considered that crystals and unhydrated amorphous substances as micro aggregates in cement paste diverge into gels. Effect of gel content (or

microaggregate content) on strength logarithm can be illustrated in Fig.11. Under the condition of same porosities, the higher gel contents, the lower strength of SAC pastes. And the lower porosities are the strength falls steeply. These results explain that the intrinsic strength of gel in SAC pastes is lower than that of other solid phases, though they have a strong action of densifying cement paste. SAC clinker pastes have the high proportion of gels so as to cause deviation of the strength logarithmic curve down from the straight line. The effect of solid phases on strength seem to be important to the SAC pastes with low porosity.

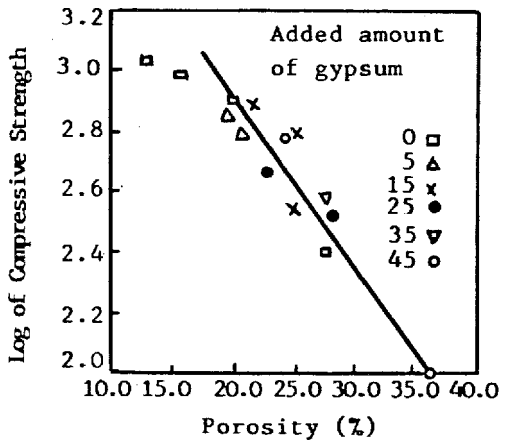

Fig.10 Relation between compressive strength and porosite

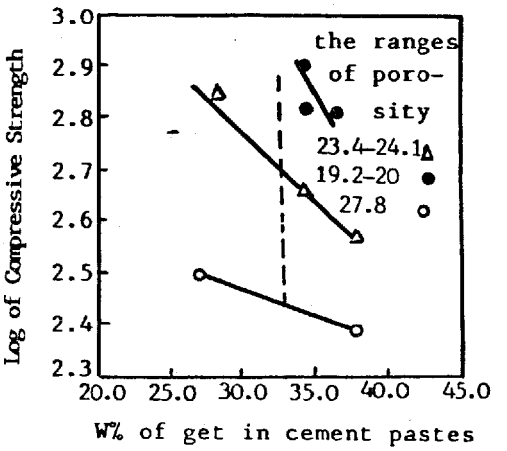

Fig.11 Effect of gel on compressive strength

CONCLUSIONS

1. Gypsum accelerates hydration of $C_4A_3\bar{S}$ and C_2S of in SAC.

2. Remarkable growth of AFt crystals during the middle and late period of hydration cause expansion of SAC paste. Appearance of residual gypsum in SAC paste is prerequisite condition for large growth of AFt and expansion.

3. That dense structure of cement paste can be obtained during the early period of hydration is the chief reason for high early strength of SAC.

4. Gels in SAC paste have lower intrinsic strength than other solid phases but have a strong action of densifying structure of the cement paste.

REFERENCES

1 Xue Jungan, Wu Zhongwei "Expansive and Self-stressing Cement and Their Application", Building Industry Publishing House, 1982.
2 Deng Junan, Ge Wenmin, Su Muzhen, Li Xiuying "7th Internation Congress on the Chemistry of Cement Proceeding", Vol.IV, Paris.
3 "Journal of The Chinese Ceramics Society", Vol.6, No.3, 1978.
4 Yang Renhe "China Building Materials Academy", (Internal data).

EARLY HYDRATION CHARACTERISTICS OF SYSTEM $NaNO_2$–$C_4A_3\bar{S}$–$CaSO_4 \cdot 2H_2O$

Yang Huixian and Jin Shuxin

Wuhan University of Technology, Wuhan, P R CHINA

SUMMARY

The effects of $NaNO_2$ on the hydration processes are studied mainly with C80 microcalorimeter. Thermodynamical parameters in some stages of hydration reaction in the presence of $NaNO_2$ are calculated and the hydration products are investigated as well with electronmicroscope, electron probe and x—ray microanalyser. The mechanism of the effects of $NaNO_2$ on the reaction is discussed.

摘　　要

本文采用 C80 微量热仪研究了 $NaNO_2$ 在水化过程中的作用，计算了在 $NaNO_2$ 存在的条件下水化反应的动力学参数。同时采用电子显微镜和电子探针以及 X 射线观察和研究了水化产物，讨论了 $NaNO_2$ 对反应的作用机理。

1. INTRODUCTION

$NaNO_2$ is a chemical antifreezing additive, crrosion inhibitor, and plasticizer for fresh concrete in China. Since the later 1970s $NaNO_2$ has been used as a chemical additive in winter construction of sulphoaluminate cement. It is effective for lowering freezing point of the liquid phase in the fresh concrete of sulphoaluminate cement, mean while $NaNO_2$ can promote greatly the hydration and hardening process of sulphoaluminate cement[1].

In this paper, the hydration reaction thermodynamical characteristics of $C_4A_3\bar{S}$, including reaction rate constant K and reaction stage coefficient N are studied in the presence of $NaNO_2$. Its hydration products are investigated as well with SEM and EPXMA.

2. THE THERMOGRAM OF HYDRATION REACTION AND ITS ANALYSIS

2. 1 Hydration Reaction of $C_4A_3\bar{S}$

The burden of sulphoaluminate cament is mainly calcium sulphoaluminate(it is abbreviated to $C_4A_3\bar{S}$) made strictly according to the chemical composition. The pure mineral, prepared by calcination in high temperature and tested for specification, is used for the experiment. The X—ray diffraction spectrum is shown in Fig 1. The peaks 3. 743 Å, 2. 647 Å, 2. 163 Å, 1. 622 Å are the standard characteristic peaks of $C_4A_3\bar{S}$.

The admixed water was added into $C_4A_3\bar{S}$, which was mixed with gypsum according to molar ratio 1 : 2, and therefore the $C_4A_3\bar{S}$—$CaSO_4 \cdot 2H_2O$ — $2H_2O$ three—component system was formed. The hydration thermogram of $C_4A_3\bar{S}$ is given in Fig 2. As shown in Fig 2 there are some characteristics in the hydration reaction, which are stated below.

2. 1. 1 At the beginning of hydration, a instantaneous thermal effect occurs and continues for approximately 10 minutes. The analysis indicated that the rate of heat evolution ($R = dQ/dt$) increases steady at high speed for 1 minute after the hydration begins and a decrease follows. Then the rate of heat evolution R reaches the first maximum (6mw) at the 4th minute. Later, R decreases rapidly to the second maximum (R=5mw) at the 10th minute. Afterwards the rate of heat evolution R increases rapidly, since a main flow of hydration heat of $C_4A_3\bar{S}$ arrives.

2. 1. 2 AT the 10th minute after the beginning of hydration, when the instantaneous early thermal effect does not finish, the hydration reaction starts entering into a new tide. Then the rate of heat evolution of $C_4A_3\bar{S}$ (R) reaches the third maximum of the hydration curve, R = 21mw. Later, the hydration reaction is restrained gradually, and the rate of hydration decreases.

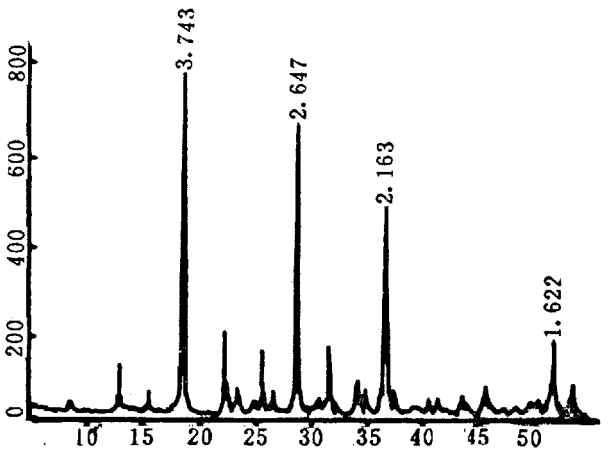

Fig. 1 the result of X—ray diffraction of $C_4A_3S\bar{S}$

About the reason for restraining hydration reaction, we could consider that hydration products

precipitate on the surface of clinker particles and form a boundary layer. Hence, hydration rate begins to decrease.

According to the tangential method of the heat evolution curve, the hydration reaction enters into a new stage of lower rate of hydration R=3mw at the 140th minute after beginning of hydration reaction. For this case, it's considered that the reaction is in the diffusion control stage. The hydration heat evolution curve is divided into three hydration stages (see Figure 2) with reference to the definition method in the C_3S hydration kinetics:

Stage AB: Accelaration period (the 10th to 50th minute);
Stage BC: Decelaration period (the 50th to 140th minute);
StageCD: Diffusion period (after the 140th minute).

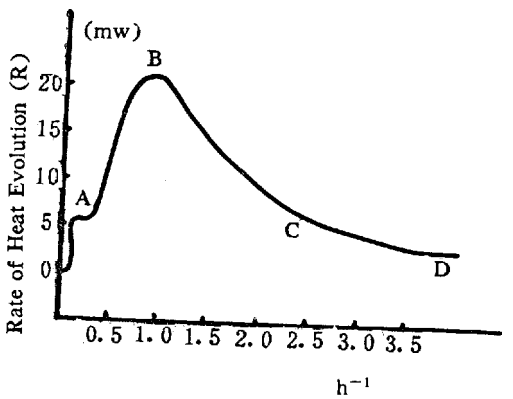

Fig. 2 Heat evolution curve (1)

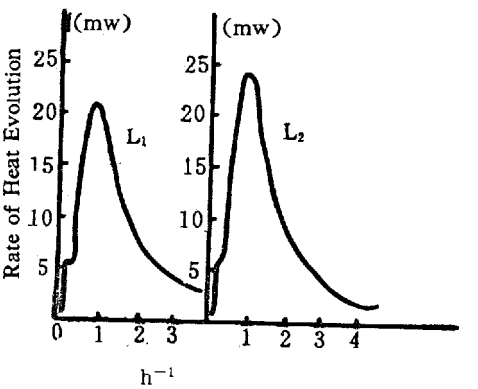

Fig. 3 Heat evolution curves (2)

2. 2 The Effect of $NaNO_2$ on The $C_4A_3\bar{S}$ Hydration

There are two curves L_1 and L_2 in the fig 3, L_1 is a plain curve, there is no $NaNO_2$ in the plain sample; L_2 is the target curve. There is $NaNO_2$ of 2% the weight of $C_4A_3\bar{S}$ in the target sample. The thermal characteristics values in the hydration process are given in table 1.

Table 1 The characteristic parameters of thermaldynamic curves

samples	height of peaks H (mw)	moment of peak top T (min)	integral hydration heat (J/g)			
			2 h	3 h	4 h	16 h
L_1	21	50	405.8	493.0	500.2	732.3
L_2	24	46	454.0	537.0	583.3	768.2

As shown in Fig 1 and table 1, the characteristic values in the rate curve of heat evolution in hydration reaction increase apparently after adding $NaNO_2$. For example, the height of the peak rises 24mw from 21mw, the moment of the peak moves to 46th from 50th minute, the peak width ($\Delta T=T_2-T_1$) shifts to 123rd from 128th minute. The hydration heat of the sample at every time is more than the plain sample without any additive. The result indicates that $NaNO_2$ greatly promotes the hydration reaction of $C_4A_3\bar{S}$.

3. THERMAL KINETIC CHARACTERISTICS OF $C_4A_3\bar{S}$ HYDRATION REACTION

3. 1 Analysis Method

The thermal kinetic characteristics are described with a kinetic formula of the cement hydration[2]:

$$[1-(1-\alpha)^{1/3}]^N=Kt \qquad (1)$$

where K is the reaction rate constant; N is the reaction stage coefficient; α is the degree of hydration at time t. With the equation (1), the lines, having different slopes, are given in the curves of $\ln[1-(1-\alpha)^{1/3}]$ versus ln t, so we can recongnize the characteristics of hydration mechanism and get the values of K and N. In order to find the solutions of the rate constants (values K and N) of the hydration reaction, first of all, we can get the final hydration heat(P_∞) and half decay period(τ) for the hydration rate reaching 50% with Knudsen equation (2)[3]:

$$1/P=1/P_\infty+\tau/[P_\infty(t-to)] \qquad (2)$$

where to is the beginning time of the acceleration period and P is the hydration heat at time t.

3. 2 Thermal Kinetic Analysis

3. 2. 1 The final hydration heat (P_∞) and hydration reaction Half—decay period(t)—With Knudsen equation, the experimental results were processed. The relationship between 1/P and $1/(t-to)$ is given in figs. 4 and 5. We can make a regressive processing for the data in fig 4 and get equation (3):

$$P=3.33\cdot10^{-3}/(t-to)+7.66\cdot10^{-4} \qquad (3)$$

the relative coefficient r=0. 990

By the same processing of the data in Fig 5 we get the equation:

$$1/P=2.87\cdot10^{-3}/(t-to)+8.13\cdot10^{-4} \qquad (4)$$

the relative coefficient r=0. 993

The thremal kinetic parameters of samples L_1 and L_2 are got from equations (3) and (4):

L_1: $P_\infty=1.31$(KJ/g), t=4. 3(h);

L_2: $P_\infty'=1.23$(KJ/g), t=3. 5(h).

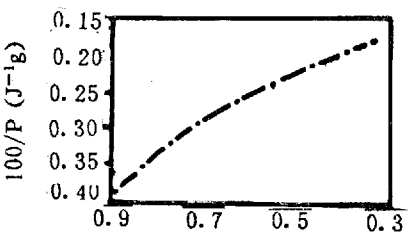

Fig. 4 Kinetic curve (1)

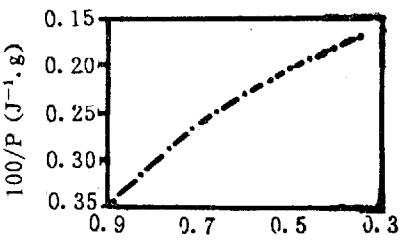

Fig. 5 Kinetic curve (2)

3. 2. 2 Values K and N of acceleration, deceleration and steady—state period. —From the hydration heat at different time P_t and P_∞ relative hydration degree α is given. Processing data by $\ln[1-(1-\alpha)^{1/3}]$

and ln(t—to) we have figures 6 and 7. The (a), (b), (c), (d) , (e) and (f) in Fig 6 and Fig 7 are the hydration degree curves of accelaration, decelaration, and steady—state periods respectively.

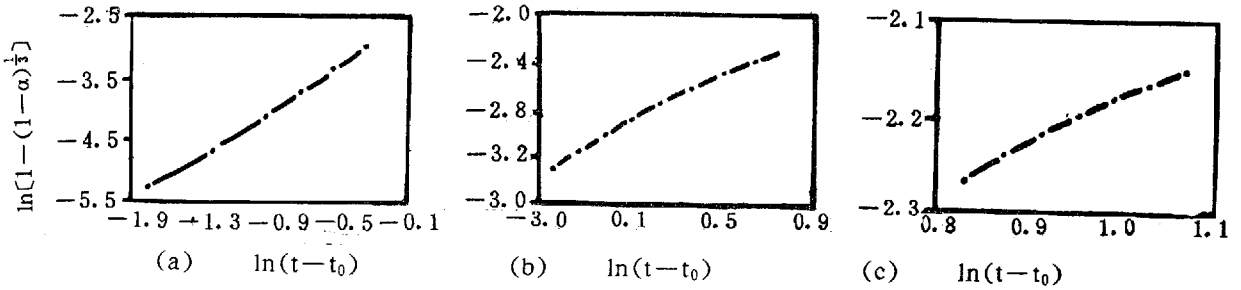

Fig. 6 The hydration degree curves of sample L_1

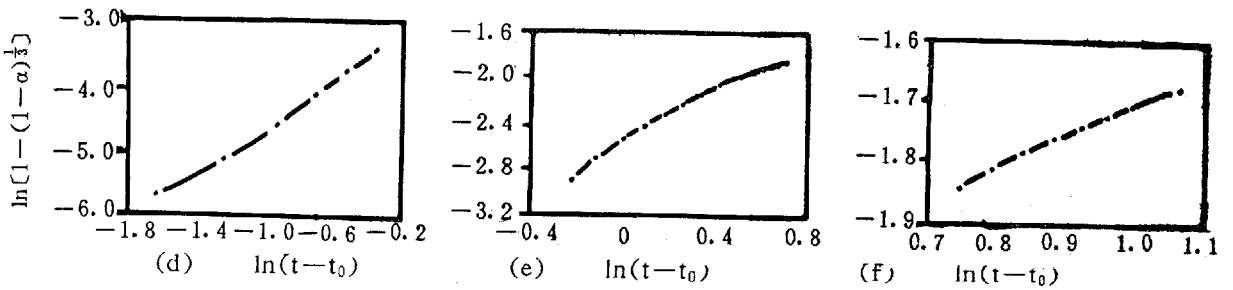

Fig 7 The hydration degree curves of sample L_2

By equation (3), $N = 1/b$, $K = e^{an}$, so we can calculate the values K and N in different hydration stages. The results and the hydration reaction charactreistics of Portland cement at 45℃ are given in table 2. From the experimental analysis and the results of data processing we could know: a)after adding $NaNO_2$, the final hydration heat is changed from 1.13(kJ/g) to 1.23(kJ/g); and the chemical reaction half—decay period is shortened from 4.3h to 3.5h. b) In the acceleration period, the hydration reaction rate constant increases from 0.11 h^{-1} to 0.17h^{-1} after adding $NaNO_2$. As a resistant coefficient of hydration reaction, the value N decreases from 0.69 to 0.66. c)In the decelaration period the constant of hydration reaction rate increses from 0.06 to 0.09 and the value N decreases from 0.95 to 0.92. d)In the decay period, the constant of hydration reaction rate increases from 0.005 to 0.01 and the value N decreases from 1.96 to 1.89.

Table 2 The kinetic parameters in every stages

samples	accelaration		decelaration		steady—state	
	K(1/h)	N	K(1/h)	N	K(1/h)	N
L_1	0.11	0.69	0.06	0.95	0.005	1.96
L_2	0.17	0.66	0.09	0.92	0.01	1.89
Portland cement	0.06	—	0.13	—	0.004	—

As showm in Fig 7, there is a good linear function relationship between $\ln[1-(1-\alpha)^{1/3}]$ and ln(t—

t_0). Let: $\ln[1-(1-\alpha)^{1/3}]=a+b\ln(t-t_0)$, then we can get a, b, r of every period, see table 3.

Table 3 The linear parameters in every periods

samples	parameters	accelaration	decelaration	steady—state
L_1	a	−3.2	−3.03	−2.69
	b	1.44	1.05	0.51
	r	0.987	0.991	0.997
L_2	a	−2.73	−2.57	−2.24
	b	1.52	1.09	0.53
	r	0.991	0.991	0.997

4. SEM AND EPXMA ANALYSIS FOR HYDRATION PRODUCTS

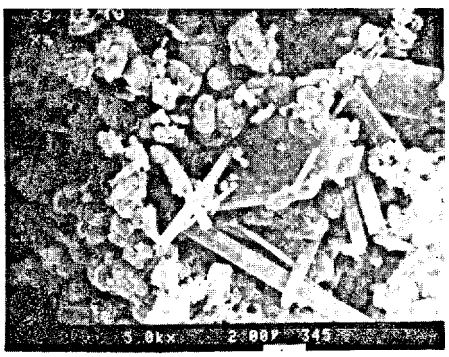

Fig. 8 sample L_2



Fig. 9 sample L_1

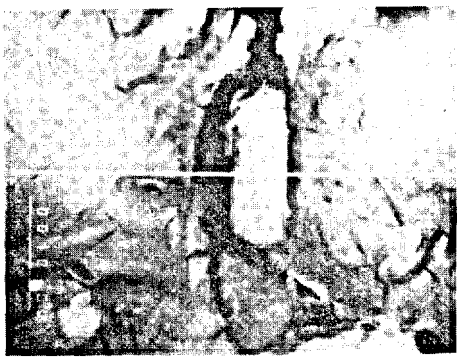

Fig. 10 EPXMA (1)

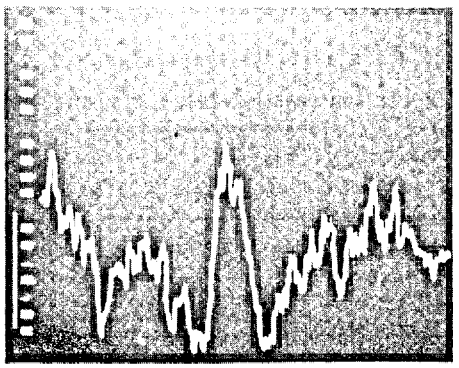

Fig. 11 EPXMA (2)

In order to understand the function of $NaNO_2$, the L_2 were analyzed by SEM 7 (Japanese model SX—40) and EPXMA (Japanese model JCXA—733) after thermal experiment and surface polishing. The results are given in Fig 8. As shown in the figure, there are a lot of ettrengite crystal in hydration products. We can

find a bundle of lathy ettrengite crystals which grow very well. The end of this well crystallized ettrengite is out of products which are $Al(OH)_3$ gels and non—hydration clinker particles. Fig. 9 is of plain sample L_1. Besides $Al(OH)_3$ gels and clinker particles, there are ettrengite crystals, which are in the minority and grow very badly. SEM investigation for sample L_1 presents that we can not find the field of view like sample L_2. The results of electron probe analysis for sample L_2 are given in Figs. 10 and 11. Fig. 10 is the micromorphology of sample L_2. The white lathy product is identified as a ettiengite in the center of Fig. 11. Around the ettrengite is $Al(OH)_3$ gel, the white horizontal line is a basic line of the probe scanning. Fig. 11 is a distributive curve of nitrogen at the same field of view fig. 10, the main peak in which corresponds to the ettrengite crystal in the center of Fig. 10.

It is clearly shown in Fig. 11 and that the nitrogen element concentrates in the ettringite crystals of the center of the field of view . Recently, studies clearly show[5] that hydration calcium sulphoaluminate is one of a isomophic products of the group of hydration calcium aluminate. The SO_4^{2-} in its structural fomula can be replaced by some ions, for example, Fe^{3+}, Si^{4+}, Al^{3+}, and some anions, OH^-, CO_3^{2-}, SiO_3^{2-}. Whether the NO_2^- can go into a ettringite crystal is not dealt with in any references. Fig 11 shows that nitrogen is contained in the ettringite crystal and can enter the ettringite crystal in the form of NO_2^-. The NO_2^- replaced some SO_4^{2-} in the ettringite crystal and therefore formed a new kind of solution solid.

5. CONCLUSION

5. 1 The thermal kinetic characteristics of $C_4A_3\bar{S}$ in hydration process are studied. The thermal kinetic parameters (the rate constant of hydration reaction K and chemical reaction stage coefficient N) and calculated in this paper.

5. 2 The study on the hydration process of $C_4A_3\bar{S}$ shows that there is a instantaneous early thermal effect at the beginning of reaction and contimues for ablut 10 minutes, followed by a tide period of reaction, resulting in the formation of the main peak of hydration reaction until the main peak ends at the 140th minute and enter the lower hydration rate period. Therefore, we divide the hydration process of $C_4A_3\bar{S}$ into primary, acceleration, deceleration and decay period.

5. 3 A little of $NaNO_2$ can apparently change the hydration kinetic characteristics of $C_4A_3\bar{S}$, increase the hydration reaction rate constant K and decrease the chemical reaction stage coefficient N.

5. 4 The reason why $NaNO_2$ changes the hydration thermal kinetic characteristics is considered as that NO_2^- enters into the ettringite crystal and replaces some SO_4^{2-} and forms a new kind of solution solid.

6. REFERENCE

1. Yang Hui—Xian, Tian Ran—Jing, Influence of $NaNO_2$ on Hydration Processes of Sulphoaluminate Cement, in China, Feb. 1986;
2. P. Barmes, Structure and Performance of Cements, p262, Applied Science Publishers, 1983;
3. T. Knudsen, 7th International Congress on the Chenistry of Cement, Paris, Vol. 2, P170—175, 1980;
4. Wu Xue—Quan, Kinetic Study on Hydration of Blast Furnace Slag Cement, in China, Oct. 1988;
5. V. S. Ramachandran, Concrete Admixtures Handbook, Noyes Publications, p8—9, 1984.

HYDRATION PRODUCTS OF ALKALI ACTIVATED SLAG

T Kutti

AB Färdig Betong, Central Laboratory, Göteborg
SWEDEN

SUMMARY

This paper deals with the hydration products of NaOH-activated blast furnace slag formed at normal curing conditions. On the basis of results obtained by means of scanning electron microscopy and literature data, it is suggested that hydrated alkali activated slag consists of two main phases. One of them is CSH-gel. The other one is a gel rich in silica which governs the shrinkage properties, the permeability and the tensile strength of alkali activated slag paste, mortar and concrete.

ZUSAMMENFASSUNG

Dieser Artikel handelt sich um die Hydratationprodukte der Hochofenschlacke bei Erregung mit Natronlauge. Beruhend auf eigenen mikroskopischen Untersuchungen und auf Literaturdaten wird vorgeschlagen, dass die Reaktionprodukte bei alkalischer Erregung der Hochofenschlacke entstehen hauptsächlich durch zwei Phasen. Die eine Pfase ist CSH-gel. Die andere Phase ist ein kieselsäurereiches Gel, das Schwinden, Permeabilität und Zugfestigkeit des Alkalischlackenmörtels und des Alkalischlackenbetons bestimmt.

INTRODUCTION

The first major investigation regarding the use of alkali activated slag as a binder was published in 1940 by Purdon /1/. The early work of Purdon aimed at showing how blast-furnace slag, by means of free caustic soda dissolved in the mixing water, could be converted into a rapid hardening cement with a high early strength and high later age strength. The concept of Purdon has later been tested in numerous research works. The results are uniform. The compressive strength of the cement is substantial. However, the flexural strength diminishes on drying /2, 3, 4/.

In several research works /4, 5, 6/ it has been reported that mortar and concrete of alkali activated slag are afflicted with microcracks. The presence of microcracks decreases the flexural strength and makes the material more permeable for gases and water. Byfors et al. /4/ showed a good correlation between the frequency of cracks and the flexural strength of the specimens, whereas the compressive strength did not correlate with the number of cracks. Häkkinen /5/ found strong cracking even in moist cured samples and concluded that the formation of cracks is not exclusively a result of drying. Vesikari /6/ suggested that the original formation of the cracks must take place during the hydration process caused by early shrinkage.

Kutti /7/ measured moisture-dependent length changes and found great discrepancies in deformation properties between NaOH-activated slag mortar and control mortar with ordinary Portland cement and blast-furnace cement: (i) during water curing at the early stage of hardening, the alkali activated slag specimens demonstrated a significant contraction, while the other specimens showed swelling, (ii) drying shrinkage was substantial, (iii) drying shrinkage per unit water loss was considerable at normal humidity as well as at higher levels of humidity, and (iv) the portion of irreversible shrinkage due to the first drying was larger than for the control samples of mortar. He concluded that the hydration products of alkali activated slag contain an unstable gel phase, which is responsible for the unique shrinkage properties as well as for the microcracks, the decrease in flexural strength on drying and the low resistance of gas and water penetration.

The hydration mechanism(s) of alkali activated slag and the hydration products being disengaged in the slag-alkali activation system are not very well understood. Different theories regarding the hydration mechanism have been proposed. However, it is generally considered that CSH-phases are always formed, and that the C/S ratio of these phases is lower than within CSH of Portland cement /8, 9/. The formation of other phases and compounds than CSH is dependent on the type and amount of activator used, the structure and the composition of the slag, and the thermal conditions under which the hardening process takes place /10, 11/. Research carried out by using scanning electron microscopy (SEM) has shown that gel phases are the predominant phases at an early stage of hydration; prolonged periods of hardening or hydrothermal treatment cause an increase in the amount of crystalline phases /11/.

In the present work, the hydration products of NaOH-activated slag, formed at normal curing conditions, are discussed. On the basis of SEM investigations and literature data, an outline of a model on the cementitious components of the cement is proposed, which would explain some of the properties and features of mortar and concrete with alkali activated slag.

EXPERIMENTAL

Pastes of NaOH-activated slag (AS) were examined after two hours and two months of hydration by means of SEM. The aim of the studies was not to identify the compounds, but to obtain an idea of their states in different stages of hydration. For the studies, ground granulated blast-furnace slag of Swedish origin was used. Swedish slag is of low basicity, has a rather low alumina content, and is usually finely ground. A typical composition of the slag is given in TABLE I.

TABLE I. Physical properties and chemical composition of ground, granulated, Swedish blast-furnace slag.

True density (kg/m^3)	Blaine (m^2/kg)	Glass content (%)	Oxides (%)				
			CaO	SiO_2	$Al2O_3$	MgO	FeO
2950	500	95	40.3	37.1	9.6	10.5	0.4

The preparation of the pastes for the SEM investigations was made as follows:

a) AS paste examined two hours after mixing was prepared directly on the specimen holders. Small quantities of slag were stirred with a thin stick into drops of 8% NaOH-solution. Two hours later the samples were put into liquid nitrogen at -195°C and then immediately placed in the scanning electron microscope.

   Portland cement (PC) paste, made of ordinary Portland cement (Blaine specific surface area 390 m^2/kg) and distilled water, was prepared in an identical manner and used as control sample.

b) AS paste examined after two months of hydration was prepared according to conventional SEM technique. Samples were cut from a hardened AS paste prism (40x40x160mm). The prism was cast in a steel mould, stripped 1 day after casting, initially cured in water for 6 days and then stored in a climate room at +20°C, RH=55%. The slag used and the strength of the activator added were the same as in a). The water/binder-ratio was 0.29.

RESULTS

Figure 1 shows a SEM-micrograph of hydrated AS paste after two hours of hydration. In the same figure, AS paste (Figure 1a) is compared with PC paste (Figure 1b). The photos show hydration products precipitated on the surfaces of the slag grains as well as on the surfaces of the Portland cement grains. The slag grains are completely covered by these products. The components are globular and voluminous, forming a continuous structure. In the case of the Portland cement grains, the precipitation is not so uniform over the surfaces, and appears to be prevalent on certain specific faces. The particles seem to be smaller and stratified, forming a more open structure. The micrographs indicate that the hydration of AS starts early, and that the process appears to proceed

in a more uncontrollable manner than in PC.

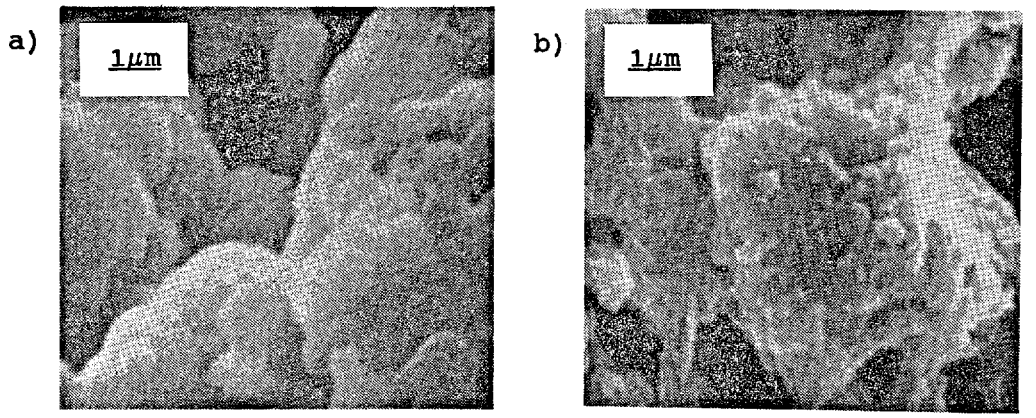

Figure 1. SEM micrographs of pastes after 2 hours of hydration. Magnification x10.000.
a) NaOH-activated slag. b) ordinary Portland cement.

Figure 2 shows hydration products of AS paste after two months of hydration. From these photos two different phases can be distinguished. One phase is globular and voluminous, forming a continuous mass similar to that in Figure 1a. Cracks are visible in this mass. The other phase is also continuous, but its character is irregular and porous, and has certain similarities to the CSH-phase of hydrated Portland cement. The main difference between the photos in Figures 1a and 2a is the additional CSH-like phase, magnified in Figure 2b.

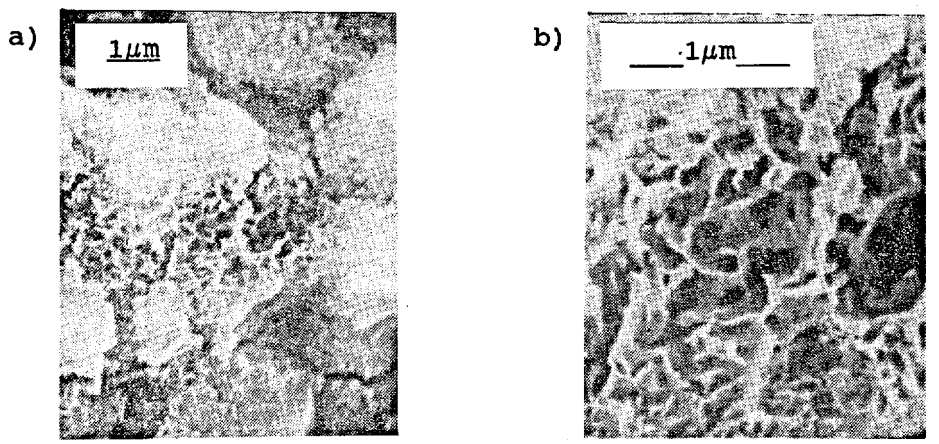

Figure 2. SEM-micrographs of NaOH-activated slag paste after 2 months of hydration.
a) Magnification x10.000. b) Magnification x30.000.

DISCUSSION

From the SEM investigations, two main phases in hydrated AS were discerned. One of them was developed in a later stage of hydration and has been identified as CSH-gel /12/. The other one was formed during the very early stage of hydration and has (up to this stage) not been identified.

According to Glukhovsky et al. /10/, the initial phases formed in alkali activated slag are rich in silica-hydrosilicates and silica acid. The silica acid can be polymerized into silica gel. In alkaline solution, the initial stage of polymerization occurs within only a few minutes /13/. Silica gel is microamorphous and may be described as a coherent, rigid three-dimensional network made of contiguous particles of colloidal silica. A silica gel freshly prepared is unstable and begins to shrink, expelling water from the mass /14/. During this synerisis process, free liquid enmeshed in the gel is spontaneously expelled. Synerisis comes to an end when the water content of the gel is still high, about 90%. On further drying, the structure of the gel continues to shrink and a number of the particle-to-particle bonds throughout the structure gradually break. The shrinkage is essentially irreversible /13/.

The deformation properties of silica gel agree with those reported for AS mortar /5, 6, 7/. It is therefore not improbable that the gel formed during the early stage of hydration is a type of silica gel.

Based on the SEM investigations and the considerations mentioned above, an outline of a model on the cementitious components of AS paste is hereby proposed. It is suggested that AS paste consists of two main hydration products. One of them is a type of CSH-gel, which has certain similarities to that of hydrated Portland cement or hydrated blast-furnace cement; it is most likely that the C/S ratio of the phase is rather low /8, 9/. The other one is a gel rich in silica with properties similar to those of silica gel, herein called AS-gel. A general outline of the type of bonds in AS paste in two different stages of hydration and under two different moisture conditions is illustrated in Figure 3.

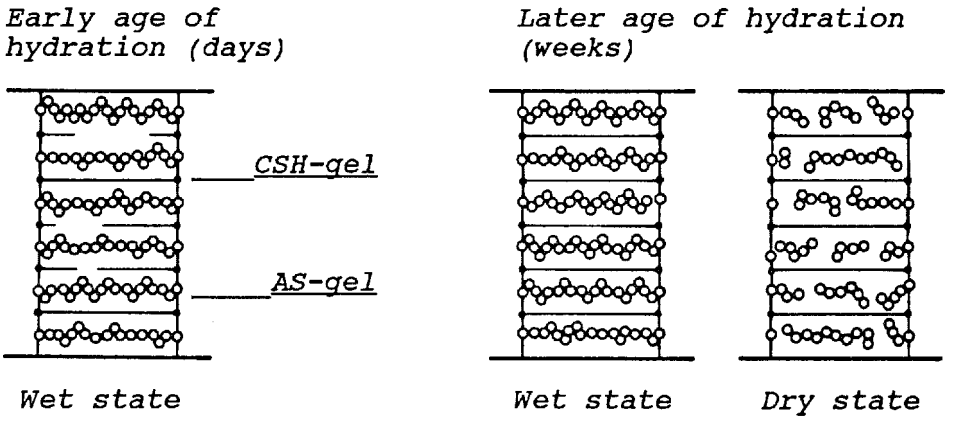

Figure 3. Model on bonds in AS paste in wet and dry states at two different ages.

The formation and properties of the CSH-gel are presumably similar to those of the CSH-phase formed in Portland cement. This implies that the component grows continuously in the course of time, and that the gel is quite stable with respect to drying. Drying shrinkage is restricted, and the compound contributes both to the compressive and the tensile strength of the paste, irrespective of the moisture state in the material.

The formation, structure and properties of the AS-gel are quite different. The gel is formed principally during the very early stage of hydration. The compound is voluminous, continuous, and contains a surplus

of water /14, 15/. The water in the gel is not firmly combined, and is easily emitted. On drying, the gel shrinks substantially, causing cracking within the gel. It is presumed that the gel contributes both to the compressive and tensile strengths of the paste in wet state, while in dry state principally to that of compression. In wet state the tensile strength is considerable.

The AS-gel determines the shrinkage properties, permeability, and tensile strength of the AS paste. During drying, a number of breaks in the particle-to-particle bonds throughout the AS-gel structure occur, thereby forming cracks in the paste. The appearance of the crack pattern in mortar and concrete is due to the cement/aggregate ratio of the mix /5/. At high ratios the cracks become long and continuous, which greatly affects the flexural strength of the specimen.

The outline of the model proposed here is applicable to AS cured at normal temperatures and not to AS treated at higher temperatures. It is known that, as a certain structure of silica gel has been formed, it can be modified further in wet state by heat treatment or autoclaving. The treatments enlarge the pore size and reduce the surface area by a process of dissolution and redisposition of silica. The coarsened gel structure results in decreased shrinkage during drying /13/. This favourable effect of heat treatment on shrinkage of AS has been established earlier /16/, and gives further credibility to the model.

REFERENCES

/1/ Purdon, A.O.: "The action of alkalis on blast-furnace slag". Journal of the Society of Chemical Industry, Vol 59, 1940.

/2/ Kutti, T., Malinowski, R. and Srebnik, M.: "Investigation of mechanical properties and structure of alkali activated blast-furnace slag mortars". Silicates Industriels, 1982-6.

/3/ Kutti, T. and Malinowski, R.: "Influence of the curing conditions on the flexural strength of alkali activated blast-furnace slag mortar". Nordic Concrete Research, No 1, 1982.

/4/ Byfors, K., Klingstedt, G., Lehtonen, V., Pyy, H. and Rombén, L.: "Durability of concrete made with alkali activated slag". **Third CANMET/ACI International Conference on Fly Ash, Silica Fume, Slag and Natural Puzzolans in Concrete,** Trondheim, 1989, SP 114-70, Vol 2.

/5/ Häkkinen, T., Pyy, H. and Koskinen, P.: "Microstructural and permeability properties of alkali activated slag concrete". Research reports 486, Technical Research Center of Finland, Espoo, 1986.

/6/ Vesikari, E.: "Frost resistance of F-concrete". Research reports 474, Technical Research Center of Finland, Espoo, 1987.

/7/ Kutti, T.: "Alkali activated slag mortar". P-90:6, Division of Building Materials, Chalmers University of Technology, Göteborg, Sweden.

/8/ Regourd, M.: "Structure and behaviour of slag Portland cement hydrates". **7th International Congress on the Chemistry of Cement,** Paris, 1980, Vol I, Principal reports, Subtheme III-2.

/9/ Gluchovsky, V.D.: "Alkalischlackenbeton". Baustoffindustrie, Heft 3, Juni 1974.

/10/ Gluchovsky, V., Zaitsev, Y. and Pakhomov, V.: "Slag alkaline cements and concretes". Silicates Industriels, 1983-10.

/11/ Malolepszy, J.: "Activation of synthetic melilite slags by alkalies". **8th International Congress on the Chemistry of Cement**, Rio de Janeiro, 1986, Vol IV.

/12/ Kurdowski, W., Academy of Mining and Metallurgy, Krakow, Poland, (personal communication).

/13/ Iler, R.K.: **The Chemistry of Silica**. John Wiley & Sons, 1979.

/14/ Lea, F.M.: **The chemistry of cement and concrete**. Third edition, Edward Arnold Publishers Ltd, London, 1970.

/15/ Lieber, W.: "Neue Schnellmethode zur Ermittlung hydraulischer Eigenschaften von Hüttensanden". Zement-Kalk-Gips, Heft 3, 1966.

/16/ Andersson, R., Gram, H-E., Malolepszy, J. and Deja, J.: "Alkali Activated Slag". Swedish Cement and Concrete Research Institute, CBI research fo 1-88, 1988.

ON HARDENING PECULIARITIES OF GYPSUM-CEMENT MATERIALS

G Y Danko

Byelorussian State Polytechnic Academy
Minsk, Republic of BELARUS

SUMMARY

This report is devoted to the results of investigations on the hydration processes of mixed gypsum-cement binders containing 70-95 % of gypsum and their influence on the kinetics of material structure formation. Research data on the hydration and hardening kinetics of gypsum and cement based composition at high quasi-static pressures from 10 to 250 MPa are cited.

Artificial stone materials based on gypsum binders and portland cements set quickly and capable of hydraulic hardening . However, in 1 to 3 months and sometimes after 1 to 3 years, deformations may appear under humid conditions, resulting in destruction of products or structures. This is related to the formation of a tri-sulfate variety of calcium hydrosulfoaluminate (ettringite) from high-base calcium aluminates contained in portland cements, and calcium sulfate. The ettringite solid phase in the system undergoes a 2.84 times increase compared with the absolute volume of the initial solid phases (C_3A + $CaSO_4 \cdot 0.5\ H_2O$).

The forms and conditions of ettringite formation have already been studies [1]. It is known that , to avoid the formation of ettringite, the content of high-base calcium aluminates (C_3AH_6 and C_4AH_{13}) in portland cement can be decreased or they can be converted into low-base calcium aluminate (C_2AN_8).

The aim of this study was to investigate the regularities of hydration processes in mixed gypsum binders which are the basis of materials obtained by filter compaction and to study their role in the structure formation of artificial stones [2]. This, in turn required investigation of the hydration rate and its impact on the artificial stone structure-forming kinetics, including physico-mechanical properties, within a wide range of pressures (from 10 to 250 MPa).

Such a study is of great practical importance, as it may help in determining the zones of stable properties in products throughout their service life.

For artificial stones manufactured using conventional techniques (casting, vibrocompaction, etc.), hydration degree is the main factor of structure formation, whereas for compacted artificial stones, specific compaction pressure is the main factor [2].

In the course of the present investigation the hydration degree of gypsum binders, samples of which were manufactured using filter compaction technique, was determined by measuring the amount of chemically bound water through calcination and, at the same time, by the results of X-ray diffraction and differential thermal analyses. The residual water-to-solids ratio was calculated from the formula:

$$(W/S)_{res} = \frac{M_n - K}{K} \qquad (1)$$

where M_n is the freshly formed sample weight, g

$$K = \frac{M_c}{1 + (W/S)_{in}} \qquad (2)$$

Mc is the mixture weight,
(W/S)in is the mixture initial water-to-solids ratio.

The investigation of the impact of specific compaction pressure on the hydration degree of monomineral gypsum binder and gypsum-cement-pozzolana (GCP) binder (70, 20, 10) showed (Fig.1) that the rate and degree of hydration decrease with increase in specific compaction pressure.

The hydration degree is influenced by, in addition to compaction pressure, a limiting factor such as a sharp drop in water content due to lower residual water content (W/S)res and high water losses due to evaporation, especially after 1 to 3 days. For instance, if the compaction pressure is increased from 10 MPa to 250 MPa the stone density increases by 28 per cent while the residual water content becomes 4 times lower for the

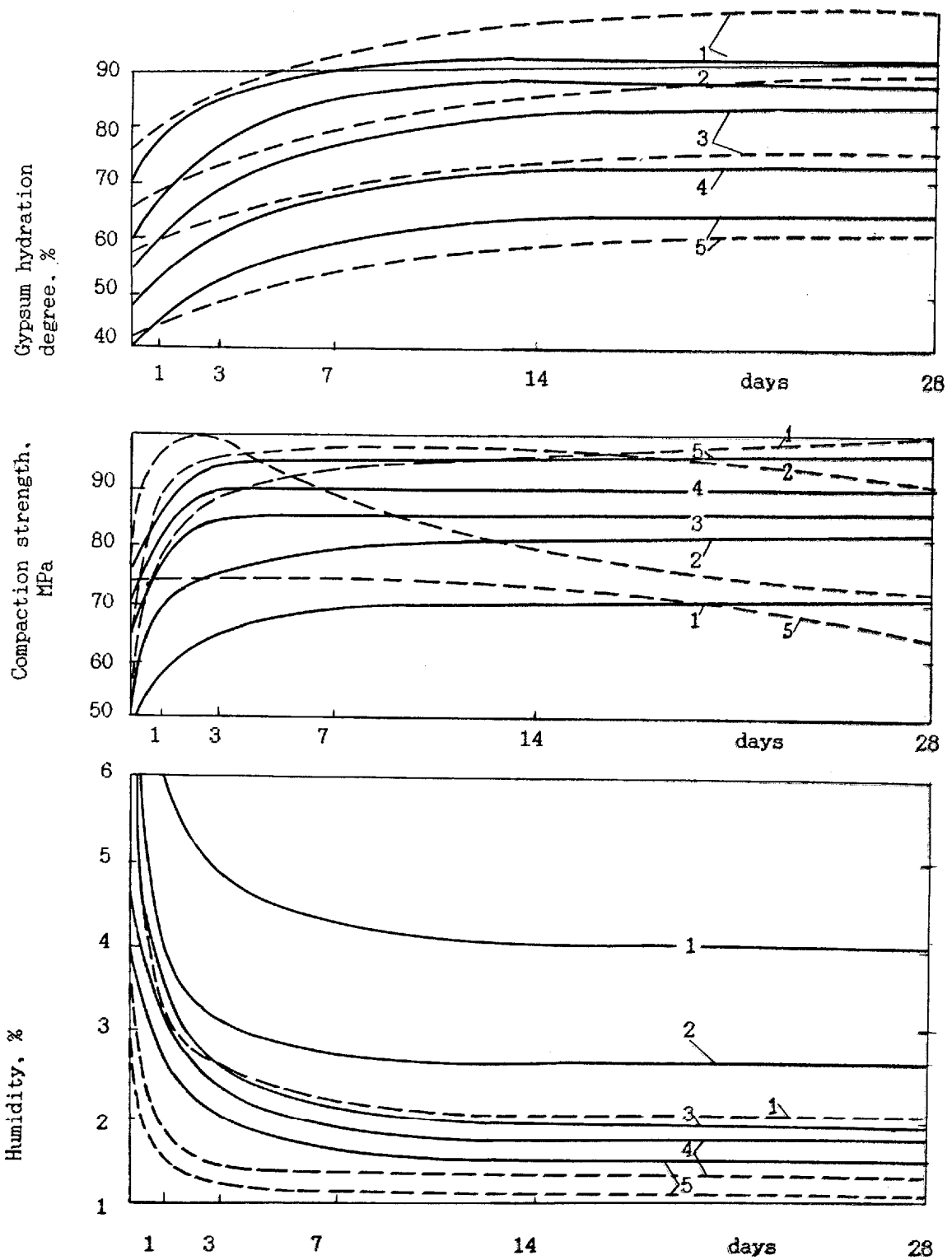

Fig.1. Changes of gypsum hydration degree - a), strength - b), humidity - c), of artificial stone made from - - gypsum and ——— GCP binder with time, depending on compaction pressure: 1 - 10 MPa, 2 - 50 MPa, 3 - 100 MPa, 4 - 150 MPa, 5 - 250 MPa.

gypsum-cement-pozzolana and 5 times lower for the gypsum binder. The water evaporation rate in the stone has the same ratio. In 28 days the water content in the gypsum-cement-pozzolana binder of artificial stone was 2 times higher than that in the gypsum binder while the hydration degree of calcium sulfate hemi-hydrate of the GCP was lower throughout the pressure range. This can be attributed to the modifying role of portland cement and pozzolana addition.

The analysis of changes in the strength properties of the compacted artificial stones showed that the strength of the samples within the first day primarily depends on the specific compaction pressure irrespective of the hydration degree provided it is not lower than 40 per cent. Within the subsequent 1 to 3 months when hydration reaches 100 per cent the strength properties depend on the hydration degree at the initial period (before the sample compaction), the density and possibilities for future hydration and may differ by 2 or more times.

Under dry air storage conditions, the strength of artificial stones based on GCP binder manufactured at 100, 150 and 250 MPa compaction pressure stabilized within 3 days due to lack of moisture. At 10 and 50 MPa compaction pressure , the strength continued to increase slowly. In the samples based on gypsum binder the strength kinetics basically depends on the pressure applied; at 10 MPa the strength increased for 28 days and more; at 50 MPa it stabilized within 3 days; at 100 MPa the strength started to drop after 3 days.

Unlike the dry storage conditions, the strength of artificial stone samples obtained by filter compaction and stored over water progressively increased within the first month , while during the subsequent 12 months it was determined by the above factors ($P_{spec.}$, ρ, $\alpha_{in.}$). For instance, for gypsum samples at 10 MPa compaction pressure the strength reached its maximum within 6 to 7 months and stabilized further on; at 20 MPa compaction pressure the strength increased 18 months and reached the values for samples obtained at 50 MPa compaction pressure, which became maximal after 6 to 9 months; the strength of samples obtained at 100 MPa and 200 MPa reached its maximum within 2 and 1 months, respectively, which amounted 75 per cent of the strength of samples obtained at 20 MPa, and subsequently dropped by 20, 30 per cent.

The GCP-based samples of artificial stones reached their maximum strength at 50 and 100 MPa compaction pressure in 12 and 4 months, respectively, with subsequent stabilization; at 150 and 200 MPa their maximum strength falls within 1 to 2 months and is lower than at 50 and 100 MPa, and subsequently drops as in gypsum-based samples.

The compaction pressure for each mixture based on mineral binders has specific optimal and extreme values. This is attributed to possible internal stresses and destructive phenomena occurring with further hydration of the mineral binders under extreme conditions.

Volzhensky A.V. and Chistov Y.D. [1] showed that the service life of such artificial stones depends on the ratio of volume concentration of the non-hydrated binder, porosity (P) and strength (R) of the stone.

Our experimental data prove that filter compaction of gypsum binders makes it possible to obtain durable materials with lower porosity as compared to dry compaction, by pre-hydration in the process of mixing gypsum mixtures and by controlling the compaction rate, which means that material structure with pre-set properties (R, ρ, P) may be formed. The optimum combination of the above parameters may improve the strength properties by 50 to 70 per cent with their subsequent stabilization and durability through con-

tinued hydration of binders, which results in self-compaction and self-stressing of the artificial stone structure. For gypsum-based materials (including GCP-based) obtained by filter compaction technique, with the initial strength reached at 50 MPa compaction pressure and with at least 12 per cent porosity, an increment of up to 50 per cent on strength and durability may be reached.

The same approach to increasing the durability is valid for ettringite formation in gypsum-cement mixtures as well, e.g. if the volume of hydration products in mineral binders, including ettringite, does not exceed the actual porosity of the material and its strength provides for compensation of its internal stresses, the material will be durable under humid conditions as well.

To avoid the formation of expansive ettringite, such techniques are available as exclusion from portland cement of high-base calcium aluminates although this one is hard to implement due to deficit of this raw material. Among other means to this end are: creation of conditions in the setting gypsum-cement-water system which hamper the stability of high-base calcium hydrosulfoaluminates by introducing acidic mineral additions and reducing the concentration of free calcium oxide; and decomposition of ettringite by introducing magnesium sulfate or solutions of alkaline carbonates, or by thermal treatment.

The author of the present paper studied the technique of reducing the calcium oxide concentration through its absorption by organic substances. As is known, oils readily damage concrete, destroying hydrosilicates in the chemical reaction with calcium hydroxide which results in the appearance of water-insoluble decomposition products expanding in volume. At the same time exact doses of oil, for example, silicon-organic liquids, or fatty acids, may extend the durability of cement-containing mixtures and improve their water resistivity. For insyance, it was proved that, to obtain durable gypsum-cement material based on portland cement containing 63 per cent CaO and Al_2O_3, a mineral addition of 0.33 g/g activity tripoli is necessary at 42 per cent on cement weight, or of silicon-organic liquid at 0.35 per cent.

In the course of experiments the presence of free calcium oxide and ettringite was also checked by chemical methods as per GOST 25094-82 "Active mineral additives, test methods" and using the X-ray diffraction analysis for the integral intensity of analytical diffraction peaks of calcium hydroxide.

Table 1contains data on free calcium oxide contents in artificial stone samples of different compositions and their compressive strength for the same ages. The artificial stone samples were manufactured from the same grades of binders by casting and filter compaction techniques.

Analysis of the data obtained showed that free calcium oxide content was lower for cast samples of artificial stone than for the filter compacted ones for any reasonable period in the experiment. This shows a higher rate of chemical interaction of the components in cast samples.

In the filter compacted samples of gypsum-cement artificial stone, whose molding mixtures were mechanically activated, the free calcium oxide content was considerably higher than in the unactivated ones, or in the mixtures based on pozzolana portland cement (PPC) and slag portland cement (SPC). At the same time, their strength was higher than that of gypsum-cement samples after mechanical activation of the molding mixture. This can be attributed to the presence of pozzolana additive in PPC and SPC, which absorbs free calcium oxide at a higher rate with mechanical activation, but at the same

Table 1.
Free calcium oxide content in artificial stones manufactured by different techniques

Composition,%	Manufacturing technique	Age at test	CaO content in solution, g/l, after 7 days	Compressive strength, MPa
Gypsum hemihydrate - 90 Portland cement - 10	Cast	1 day	0.30	3.2
		7 days	0.24	5.9
		6 months	0.06	8.4
	Filter compaction	1 day	0.36	25
		7 days	0.28	32
		6 months	0.10	53
	Activation, filter compaction	1 day	0.46	28
		7 days	0.34	36
		6 months	0.30	56
Gypsum hemihydrate - 80 Portland cement - 20	Cast	1 day	0.27	3.2
		7 days	0.16	5.7
		6 months	0.04	9.7
	Filter compaction	1 day	0.27	17
		7 days	0.25	33
		6 months	0.09	50
	Activation, filter compaction	1 day	0.35	18
		7 days	0.25	34
		6 months	0.12	44
Gypsum hemihydrate - 90 Portland cement - 10 SOL - 0.5	Cast	1 day	0.08	2.6
		7 days	0.06	3.7
		6 months	0.03	9.1
	Filter compaction	1 day	0.36	25
		7 days	0.28	32
		6 months	0.10	53

time decreases the strength through higher specific surface of the soft substance. Mineral additions in SPC are less active than in PPC, and compacted samples had lower strength.

In the artificial stone samples of all compositions manufactured by filter compaction technique, listed in the Table 1, absorption of free calcium oxide was considerably slower than in the cast samples. This can be explained by the lower hydration rate of the former. The strength development rate during the first day was higher in filter compacted samples than in cast samples but subsequently decreased. A high rate of free calcium absorption within the first day was observed in compositions containing silicon organic liquid (SOL). The SOL activity reaches 27 g/g in calcium oxide absorption while the activity of tripoli is 0.3 g/g.

X-ray diffraction analysis confirms the chemical analysis data. The compositions studied with the same content of components provide a safe ettringite content in the samples while the hydration degree of the binder and the C_3S in the samples ensures their durability.

Higher compaction pressures do not step up ettringite formation in GPC compositions. For instance, at 50 MPa and higher specific compaction pressures, the diffractograms show

the ettringite lines with d=9.8, 5.5, 3.9 Å which are not much higher than the background and at any rate not higher than those of the samples compacted at 10 MPa. At the same time, the samples compacted at higher pressures (≥50 MPa) reveal small peaks with d=9.5, 7.91, 6.4, 2.85 Å which seem to belong to the hydrate ($2CaO_8 \cdot 3SiO_2 \cdot 2H_2O$). Gypsum-sand compositions show lines with d=3.54 Å which may be taken to indicate the presence of α-hydrate of 2-calcium silicate ($2CaO \cdot SiO_2 \cdot H_2O$).

This fact proves that high pressure act similar to thermal processing on the hydration of minerals and facilitate the formation of very strong minerals with the interaction of sand and gypsum.

The study on hardening of gypsum-cement binders, some of the data on which are given in the present paper, shows that the hydration processes in mixed gypsum binders after filter compaction are determined by a number of factors as follows:

1. Higher compaction pressure decreases the hydration degree due to lower hydration rate and residual water content, as well as higher evaporation rate of the residual moisture within the first day.

2. The strength of artificial stone within the first 3 days is determined by the specific compaction pressure and later it depends on the hydration degree of the molded samples, the residual water content and porosity.

3. The content of lime-absorbing additives (both inorganic and organic) in the composition should be equivalent to that of cement (C_3S and Al_2O_3) and their chemical interaction.

4. Silicon-organic liquids have an ability to absorb quickly free calcium oxides, especially within the first setting day and are a highly effective stabilizing additive in gypsum-cement compositions.

5. Mechanical activation by molding of gypsum-cement mixtures accelerates the hydration process and steps up the strength of artificial stone with less pozzolana additions.

6. High compaction pressures (over 100 MPa) facilitate the appearance of calcium silicate hydrates in gypsum-sand compositions on silicon base and intensify their formation in gypsum-cement mixtures.

The above relation make it possible to create gypsum-cement compositions for manufacturing strong (50 to 90 MPa) water-resistant and durable products for use as finishing materials.

REFERENCES

1. Volzhensky, A.V.: Mineral binders. Moscow, Stroyizdat, 1986, 464p. (in Russian)

2. Lyashkevich, I., Danko, G. & Raptunovich, G.: Structure and properties of pressed gypsum and gypsum-cement materials. Cement and Concrete Research. USA, 1990, 20, 357-368.

ALKALINE CEMENTS

P V Krivenko

Civil Engineering Institute, Kiev
UKRAINE

SUMMARY

This paper presents results of studies on regularities of directed formation of hydration products in a system: Me_2O-MeO-Me_2O_3-SiO_2-H_2O within the ratio range MeO:SiO_2=0-3 and Me_2O_3:Me_2O=0-21, which enable to establish the main factors affecting the intensity and completion rate of the structure formation processes at all stages. The relashionship between the strength, deformative properties, fire- and corrosion resistance and hydration product phase composition of a cement body have been established and hardening conditions for reaching the target phase composition have been investigated. The data obtained were taken as the basis for development of a wide range of alkaline cements with predicted properties. The examples on synthesis of highly efficient slag-alkaline and fly ash-alkaline binders, alkaline portland, slag-portland and pozzolana portland cements and their properties are presented. Durability problems of the cement body and concretes are discussed and substantiated.

В статье представлены результаты изучения закономерностей направленного формирования продуктов твердения в системе Me_2O-MeO-Me_2O_3-SiO_2-H_2O в диапазоне соотношений MeO:SiO_2=0-3 и Me_2O_3:Me_2O=0-21, которые позволили установить основные факторы, обуславливающие интенсивность и степень завершенности процессов структурообразования на всех стадиях. Установлена взаимосвязь между прочностью, деформативностью, жаро- и коррозионной стойкостью и фазовым составом продуктов твердения цементного камня, а также определены условия формирования заданного фазового состава. Полученные данные явились основанием для разработки целого ряда щелочных цементов с прогнозируемыми свойствами. Приведены примеры синтеза высокоэффективных шлакощелочных и золощелочных вяжущих, щелочных портланд- и шлакопортландцементов, щелочного пуццоланового портландцемента и их свойства. Обсуждены проблемы долговечности цементного камня и бетонов и обоснована повышенная долговечность разработанных цементов.

INTRODUCTION

Change in traditional views on regularities of revealing the binding properties by mineral substances became possible owing to establishing in 1957 by V.D.Glukhovsky (1,2) the fact that alkali metal (Li, Na, K, Rb, Cs) compounds, which, owing to their high solubility, had earlier been excluded from the traditional cements, possessed binding properties. That was made by comparing and revealing the analogy between processes of structure formation of artificial stone based on cement and processes of formation and chemical weathering of silicate rocks.

The conclusions drawn were taken as the basis for creation of alkaline cements, which were themselves a combination of alkalies and aluminosilicates of natural and waste product origin. Interaction of these constituents results in the creation of a cement body with formation, upon hydration, of alkaline and mixed alkaline-alkali-earth hydroaluminosilicates analogous to natural minerals and formations, namely: hydronepheline, analcime, natrolite, sodium-calcium hydrosilicates and other zeolite-like products.

Differing from hitherto known attempts to activate the traditional systems by means of alkali metal compound additives, which served only as activators and hence were introduced in small quantities (3,4), in alkaline cements the alkaline compounds were considered to be not only activators but as self-dependent structure-forming new formations governing the formation of alkali-containing zeolite-like phases. That's why their content was increased. A break from the traditional views on the role of alkalies in improving the hydraulic binding properties by mineral substances caused the fundamental changes in traditional cement systems based on high-basic minerals (5-12).

RAW MATERIALS

Resulting from the higher chemical activity of alkaline compounds as compared to alkali-earth ones, the raw materials base for these cements varies within wide range: from clays and "burnt" rocks to artificial glasses and high-basic clinker minerals. In overall, the alkaline binder can be represented by the system: Me_2O-MeO-Me_2O_3-SiO_2-H_2O.

Naturally the properties of the cements to be synthesized will depend to a large extent on the chemical, mineralogical and phase compositions of the dispersed (solid) phase and the dispersion (liquid) phase of this system. The regularities of the influence of the chemico-mineralogical composition of dispersed phase within the ratio range MeO:SiO_2= 0÷3 and Me_2O_3:Me_2O=0÷21, represented by C_3S, β-C_2S, C_3S_2, CS, C_3A, $C_{12}A_7$, CA, CA_2, C_3MS_2, C_2MS_2, CMS, $C_{4.5}AS_{2.5}$, C_2AS, C_3AS_3, CAS_2, $C_2A_{0.75}M_{0.25}S_{1.25}$, $C_2A_{0.5}M_{0.5}S_{1.5}$, $C_2A_{0.25}M_{0.75}S_{1.75}$, basic blast-furnace slag, neutral blast-furnace slag, acid blast-furnace slag, nickel slag, lea d slag, copper slag, its structural peculiarities, kind of alkali component anion (OH^-, CO_3^{2-} · SiO_3^{2-}, SO_4^{2-}) and hardening conditions /T=293±5K ÷ 373±5K/ on the intensity of formation and hydration product phase composition had been investigated in the work presented in this paper.

PROCESSES OF HYDRATION AND HARDENING

Studying the structure formation processes in the above mentioned systems enabled to represent this process as a complex of consecutively and simultaneously flowing changes, the foremost of which are (after Rebinder P.A.): destruction of the initial dispersed phase to size of certain units of un-stable structure; their contact interaction with formation of dispersion coagulation thixotropic units; creation on their base of condensation-crystallization structure of hydrated new formations.

Destruction of the dispersed phase of alkaline cement, in contrast to that of portland cement, has its own peculiarities caused by the lower ionicity of the initial minerals as compared to that of portland cement ones, and the presence of alkaline compound in the dispersion medium. As a result of this the processes of dispersion ar ecaused by the break, firstly, of covalent bonds Si-O-Si, Me^{3+}-O-Me^{3+}, Si-O-Me^{3+} and not by protonization of the ion ones as it takes place in high-basic systems with C/S>1.5. It becomes possible in the presence of alkaline cation, which at the stage of destruction-coagulation structure formation acts as destruction catalyst by the scheme:

$$\equiv Si\text{-}O\text{-}Si\equiv + OH^- \rightleftarrows [\equiv \overset{OH}{\underset{|}{Si}}\text{-}O\text{-}Si\equiv]^- \rightleftarrows \equiv Si\text{-}OH^- + \equiv Si\text{-}O^-$$

and at the following stage prevents the reverse reaction of formation of siloxane bond at the expense of formation of bonds of Si-O^--Na^+ type. Further the alkaline silicates being formed can enter into cation-exchange reactions with alkali-earth ions Me^{2+} present in the cement solid phase by the scheme:

$$\equiv Si\text{-}O\text{-}Na^+ + OH^- \rightleftarrows \equiv Si\text{-}O\text{-}Na\text{-}OH$$

$$\equiv Si\text{-}O\text{-}Na\text{-}OH + Me^{2+} \rightarrow \equiv Si\text{-}O\text{-}Me\text{-}OH + Na^+$$

This is confirmed by the wave-like character of the change in Na_2O concentration in the solution of hardening cement /Figure 1 /. The anion constituent of alkaline component affects essentially the structure formation processes. The anions being introduced in the dispersion medium as soluble silicates and aluminates (SiO_3^{2-}, AlO_2^-), analogous to the primary destruction products of aluminosiliconoxygen frame of dispersed phase serve as their additional reserve and are the most efficient. The anions: CO_3^{2-}, SO_4^{2-}, OH^-, SiF_6^{2-}, Cl^- change the solution properties and take part in the formation of complexes promoting the introduction of the reaction products into the solid phase.

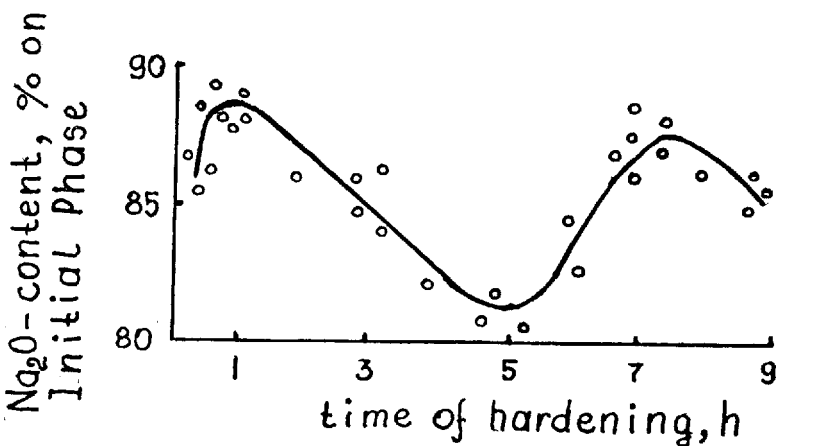

Fig. 1 Change in Na_2O-content in liquid Phase of the Hardening Binder Based on Glass $C_{4.5}A\,S_{2.5}$ and NaOH

Further, by accumulation of the reaction products, firstly there occurs a formation of dispersion - coagulation structures with subsequent development of condensation structures. The progress of this process is accompanied by a decrease of the free alkali content in a cement body as a result of its bonding into new formations of alkaline - alkali-earth composition. Thus, if at the initial stages of interaction the alkaline cation acted as catalyst of destruction, at the subsequent ones it took part equally actively with Ca^{2+} and Mg^{2+} in the formation of a new phase composition.

It was established that the intensity of the above processes depends upon the dispersed phase basicity and its structural peculiarities, the amphoteric oxide (Me_2O_3) content and the nature of the alkaline component.

With increase of dispersed phase basicity, the development of structure formation processes is intensified. However quick hydration under high - alkaline medium conditions results in the release of a large quantity of tobermorite gel in the early period. This creates conditions unfavourable for crystal growth and leads to the formation of an imperfect structure. With decrease of dispersed phase basicity, the new

formation basicity decreases, which positively affects the strength and stability of the cement body in time; however the intensity of the structure formation processes at this becomes slower.

The Me_2O/Me_2O_3 ratio essentially affects phase composition formation.With increase of Me_2O_3 content in a system, there is an increase also in the quantity of slowly crystallizing alkaline or alkaline-alkali-earth hydroaluminosilicates, which govern the development of strength at the later stages of structure formation processes in the hydration products.
In the systems containing ferrous oxides (for example, Na_2O-CaO-MgO-Al_2O_3-FeO-Fe_2O_3-SiO_2-H_2O), presence in the dispersion medium of alkaline catalyst influences the change of coordination form of the latter at the expense of going from the inactive form ($Fe^{2+(IV)}$) into the active one ($Fe^{3+(VI)}$), in which it shows the amphoteric properties.

HYDRATION PRODUCTS

The constant presence of a high-alkaline medium creates the conditions, first of all, for primary formation of low-basic compounds and, secondly, governs the crystallization of alkaline and alkaline-alkali-earth compounds, analogous to natural minerals (Table 1). The first ones are represented mainly by low-basic hydrosilicates and hydrogarnets and appear, as a rule, at the initial stages of structure formation processes. The second ones, as a result of their slower crystallization, are formed at the later stages.

Being formed preferentially in the pore space, they fill it and promote the creation of strong crystallization contacts with the primary phases causing the formation of a more dense and homogenous structure. New formation composition depends upon the initial composition of the alkalies.For example, the thermodynamic calculations fulfilled for the system with $M_b > 1$ (slag + NaOH) /13 /, testify to the fact that at hardening of such composition jismondine and calcium zeolite had been formed side by side with low-basic calcium hydrosilicates. On the other hand, in the system with $M_b \leq 1$ (slag + NaOH) the alkaline hydroaluminosilicate of jismondine type had been formed preferentially.

The most characteristic feature of the phase composition of an alkaline cement body is absence in it of $Ca(OH)_2$, high-basic hydrosilicates, hydroaluminosilicates and hydroferrites, which in many cases, deteriorate the properties of ordinary portland cement.

PHYSICO-MECHANICAL PROPERTIES

Taking the established peculiarities of the structure formation processes and the relationship between cement body properties and new formation phase composition as well as the conditions of its formation as the basis, we developed a wide range of alkaline cements, namely: the slag-alkaline binders, fly ash-alkaline binders, alkaline portland- and alkaline slag-portland cements, alkaline portland cements based on feldspar rocks, alkaline portland cements based on zeolites, alkaline aluminate cements, etc. (14). By their properties these were much superior to traditional portland and high alumina cements, and depending on their composition, could reach the following characteristics:
- lower (by 2-3 times) values of heat of hydration and shrinkage compared to portland cement;
- increased density and water impermeability, predominance of gel pores;
- higher compressive strength (2-3 times that of traditional cements), reaching 120-150 MPa;
- ability to quickly gain strength while hardening under normal conditions compressive (strength at 1 - day age at T = 293±2K is 30-50 MPa) and ability not to interrupt the processes of hydration and hardening up to T = 243K;

- higher frost resistance (more than 1000 cycles) compared to traditional cements, resistance to salts in solutions of mineral salts, alkalies, acids, organic media; heat-resistance (up to 1873K) and fire-resistance (more than 100 cycles), resistance to combined action of heat and aggressive media, especially to molten metals.

Table 1 Solubility of New Formations of the Slag-Alkaline and Portland Cement Stone

Mineral	Stoichiometric formula	Solubility, kg/m³
	Slag-alkaline binder	
CSH(B)	$5CaO\ 6SiO_2\ nH_2O$	0.050
Xonotlite	$6CaO\ 6SiO_2\ H_2O$	0.035
Riversidite	$5CaO\ 6SiO_2\ 3H_2O$	0.050
Plombierite	$5CaO\ 6SiO_2\ 10.5H_2O$	0.050
Gyrolite	$2CaO\ 3SiO_2\ 2,5H_2O$	0.051
Calcite	$CaCO_3$	0.014
Hydrogarnet	$3CaO\ Al_2O_3\ 1,5SiO_2\ 3H_2O$	0.020
Sodium-calcium hydrosilicate	$(Na,Ca)SiO_4\ nH_2O$	0.050
Thomsonite	$(Na,Ca)Al_2O_3\ Si_2O_5\ 6H_2O$	0.050
Hydronepheline	$Na_2O\ Al_2O_3\ 2SiO_2\ 2H_2O$	0.020
Natrolite	$Na_2O\ Al_2O_3\ 3SiO_2\ 2H_2O$	0.020
Analcime	$Na_2O\ Al_2O_3\ 4SiO_2\ 2H_2O$	0.020
	Clinker binder	
Calcium hydroxide	$Ca(OH)_2$	1.300
C_2SH_2	$2CaO\ SiO_2\ nH_2O$	1.400
CSH(B)	$5CaO\ 6SiO_2\ nH_2O$	0.050
4-Calcium hydroaluminate	$4CaO\ Al_2O_3\ 13H_2O$	1.080
3-Calcium hydroaluminate	$3CaO\ Al_2O_3\ 6H_2O$	0.560
Calcium hydro-sulphoaluminate	$3CaO\ Al_2O_3\ 3CaSO_4\ 31H_2O$	high

BEHAVIOUR IN CONCRETES

Use of alkaline cement makes for flexibility in the requirements on aggregate quality and increases the efficiency of the concretes produced. The strength characteristics of heavy- and light-weight concretes are being improved through use of this cement. Further, special pre-treatment of coarse and fine aggregates is not necessary as up to 5% of clayish and 20% of dustish particles in them is permitted. Besides, active interaction of the alkaline medium of a cement body with aggregate surface occurs with formation, over the width of cement - aggregate contact zone, of the compounds representing by themselves zeolite-like new formations. Investigations on the distribution of microhardness over the contact zone width of alkaline concretes based on different aggregates showed that a shell strengthening the aggregate had been formed over it as a result of the processes. This, in effect, makes it possibile to produce highly efficient concretes using low-grade aggregates and alkali - aggregate reaction (AAR) is not observed in them.

Corrosion of alkaline cement in case of using the different wood aggregates was not observed too. Hence it is possibile to produce light-weight concretes and materials under steam treatment, obviating long-term and expensive pre-treatment processes of these aggregates, and the moulded articles can be cured at normal temperatures.

Persistence of an alkaline medium of the hardening cement for a long time guarantees safety of reinforcement steel in an alkaline concrete and its high frost resistance. Investigations have shown that the passive state of the reinforcement in concrete is caused by formation over the metal surface of a protective oxide film, liable to remain unaffected in an alkaline medium for a long time.

DURABILITY PROBLEMS

Observations on ancient constructions in Italy, Greece, Cyprus and Egypt, repaired by modern concrete, snow that the parent concrete in them which had been exposed to the influence of running water and sea wind for two thousand years had not been destroyed, while the modern portland cement concrete used in their repair essentially destroyed after 10 years(15).

Analysis of the ancient concrete structures shows that the presence, in their raw material mix composition, of sodium and potassium carbonates led to the formation of weakly crystalline calcite as well as weakly crystallized phases of zeolite type: $Na_2O(K_2O)Al_2O_3$ (2-4)SiO_2 $2H_2O$.

Similarity of the compositional structure of alkaline cements with the ancient ones results in similarity of cement body new formation phase compositions. Besides, the alkaline cement body has some peculiarities distinguishing it from the less durable Portland cement one(16). It explains the superior properties in service of alkaline concretes, for example slag-alkaline, observed over more than 30 years.

CONCLUSION

From the characteristic peculiarities of alkaline cement structure and the similarity of its compositional structure with that of ancient cement it could be concluded that they are superior in durability to all binders or cements in use at present.

REFERENCES

1. Glukhovsky, V.D., Pashkov, I.A., Yavorsky, G.A.: "A New Building Material." Bull. of Tech. Inform. Glavkievgorstroya, Kiev, USSR, 1957.

2. Glukhovsky, V.D.: The Soil Silicates. Kiev, USSR, Gosstroiizdat Publish., 1959.

3. Jilin, A.I.: The Soluble Glass: Its Properties, Production and Use. Sverdlovsk, USSR, GONTI-NKTM Publish., 1939.

4. Purdon, A.O.: "The Action of Alkalies on Blast-Furnace Slag." J.Soc.Chem.Ind., V59, 1940, 191-202.

5. U.S.Patent No 3,689,294, 1 September 1972, "The Portland Cement Compositions and Method of Producing."

6. U.S.Patent No 3,960,582, 8 June 1976, "Low Porosity Cement and Process for Producing Same."

7. U.S.Patent No 4,405,372, 1 June 1976, "Gypsum-Free Cement Compositions."

8. Forss, B.: "F-Cement Low Porosity Slag Cement for the Precasting Industry." International Conference on Slag and Blended Cement, Birminghem, USA, 1982.

9. Skvara, J., Kolar, K. & Novotny, I.: "The Cement for Use at Low Temperature." 7 International Congress on the Chemistry of Cement, Paris, France, 1980, V3, 57-61.

10. Royak, S.M., Galperina, T.Ja. and others.: "Gypsum-Free Slag-Portland Cement an Effective Binder for Concrete." Tsement, 1984, V11, 18-20.

11. Shpynova, L.G., Ostrovsky, O.L., Sanitsky, M.A. and others: Concretes for Winter Concreting. Lvov, USSR, Vischa Schkola Publish., 1985.

12. Paschenko, A.A., Sanitsky, M.A., Shevtchuk, G.Ja.: "The Peculiarities of the Portland Cement Compositions with Alkali Metal Salt Additives." Tsement, 1990,V7, 17-19.

13. Raksha, V.A.: "Investigation of Influence of Slag Chemical Composition on Properties of Slag-Alkaline Binders and Concretes." Author's Abstract for Cand. Degree, Kiev, USSR, 1975.

14. Glukhovsky, V.D.: "The Alkaline Binding Systems." Tsement, 1990,V6, 3-7.

15. Davidovits, I.: "Ancient and Modern Concretes: What is the Real Difference?" Concrete International, 1987, V9, 12.

16. Krivenko, P.V. "Physico-Chemical Basis of Slag-Alkaline Stone Durability." Tsement, 1990, V11, 2-5.

DEVELOPMENT OF CEMENTITIOUS PROPERTIES IN PHOSPHOGYPSUM-FLY ASH SYSTEM

Manjit Singh and Mridul Garg

Central Building Research Institute, Roorkee, INDIA

SUMMARY

An investigation was carried out to study the hydraulic behaviour of a system composed of calcined phosphogypsum, fly ash and portland cement at 27° to $60^{o}C$. Data show that with increase in temperature from 27° to $60^{o}C$, the strength is increased. The enhancement in strength with increase in temperature is attributed to the pozzolanic action of fly ash blended with the calcined phosphogypsum. A mix proportion of binder containing 40:40:20::calcined phosphogypsum:fly ash:portland cement parts by weight developed maximum strength (31.0 MPa) when cured at $50^{o}C$ for 28 days. The new system/hydraulic binder can be used in the manufacture of prefabricated components such as boards, tiles and building blocks.

INTRODUCTION

Large quantities of phosphogypsum (4.0 million tonnes) and fly ash (35.0 million tonnes) are produced as by-products of phosphoric acid manufacture and thermal power plant respectively. These materials pose serious problems of disposal and health hazards. Phosphogypsum contains impurities of phosphates, fluorides, organic matter, alkalies and free moisture which prevents its direct use as building material (1). Several beneficiation techniques ranging from washing, thermal and chemical treatments of phosphogypsum have been developed in the laboratory (2). Fly ash is used to little extent (1.0 million tonnes) in blended cements, concrete, clay fly ash/lime-fly ash bricks etc. (3). Hydraulic binders based on calcined gypsum, fly ash or granulated blast furnace slag have been investigated earlier (4,5).

To increase the use of phosphogypsum and fly ash as building material, a system containing calcined gypsum (hemihydrate), fly ash and portland cement has been formulated at 27° to 60°C. The new system/binder was evaluated for its strength development upto a period of 28 days through differential thermal analysis (DTA), X-ray diffraction (XRD) and scanning electron microscopy (SEM).

EXPERIMENTAL

Raw Materials

The raw materials of chemical compositions:calcined phosphogypsum - CaO 38.00%, SiO_2 1.10%, R_2O_3 (Al_2O_3 + Fe_2O_3) 0.04%, MgO trace, K_2O + Na_2O 0.09%, SO_3 52.10%, P_2O_5 1.41%, F 0.50%, H_2O 6.10%, Fly ash - CaO 2.60%, SiO_2 70.60%, R_2O_3 24.40%, MgO 0.73% and H_2O 0.20% and portland cement - CaO 62.50%, SiO_2 24.76%, R_2O_3 7.50%, MgO 3.0% and H_2O 0.46% were used to formulate the system. The impurities of phosphogypsum were made inactive by the addition of lime to the calcined material. Table 1 shows composition of system investigated.

Table 1 - Compositions (wt.%) of the System Investigated

Composition	Calcined Phosphogypsum	Flyash	Portland Cement	Retarder
A	30	50	20	0.10
B	40	40	20	0.10
C	35	45	20	0.10
D	50	35	15	0.10

Hydraulic binder /system was produced by blending the dried fly ash, portland cement and retarder with the ground calcined phosphogypsum (passing 150 micron IS sieve). DTA (Stanton Redcroft, U.K.), XRD (Philips, Holland) and SEM (Model 501 Philips, Holland) were used to identify the hydraulic products in the system.

The compressive strength of system was determined on 2.5cm cubes cast at normal consistency and cured at 27° to 60°C in 100% RH for a period of 1 to 28 days as per IS:4031-1968, specification for methods of physical testing of hydraulic cements.

RESULTS AND DISCUSSION

Hydration of System

DTA

Fig. 1(a) shows results of DTA for composition 'B' at 27°C. With increase in curing period upto 28 days, the intensities of gypsum and lime endotherms reduced, whereas ettringite endotherm increased. Small depression at 760° to 780°C indicates tobermorite (CSH). The intensity of endotherms at 140°C - 150°C and 760° - 780°C increased while that at 440°C reduced with the increase in curing temperature from 40°C to 60°C, indicating thereby enhanced formation of ettringite and tobermorite and reduction of lime (after 3 days) respectively. Fig.1(b) shows DTA of the hydraulic binder cured at 50°C. The tobermorite endotherms detected at all curing temperatures (27°, 40°, 50° and 60°C) is formed as a result of

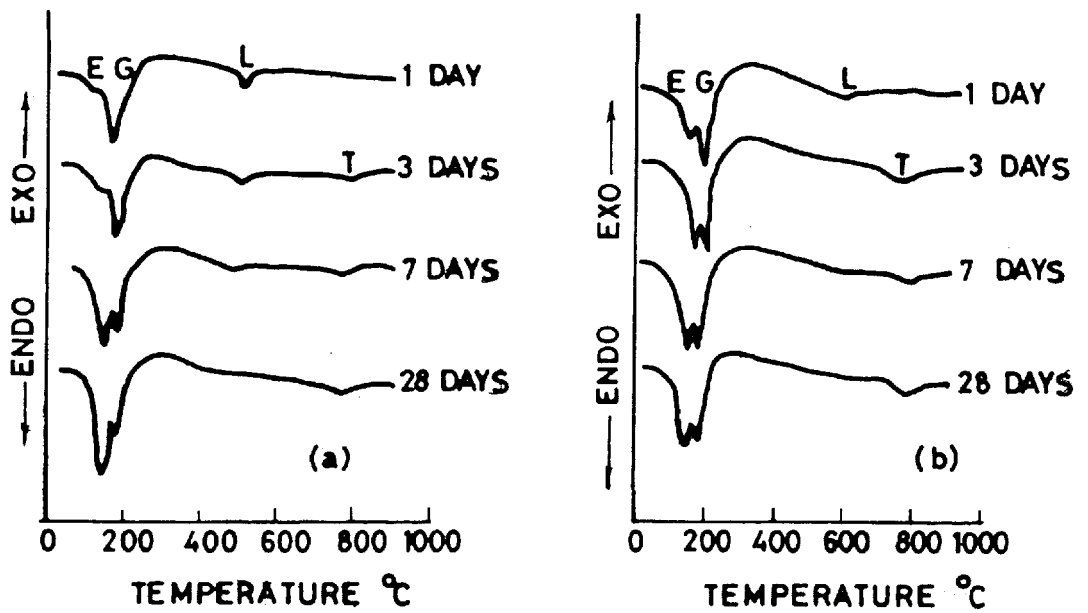

FIG. 1. Differential Thermograms of binder 'B' cured at(a) 27°C and (b) 50°C (E=Ettringite, G= Gypsum, L = Lime and T= Tobermorite)

hydration of both the portland cement and the pozzolanic reaction involving reaction of SiO_2 and Al_2O_3 of fly ash with $Ca(OH)_2$. The decrease in the formation of ettringite at 50° and 60°C shows that lime released by the hydration of portland cement is converted into tobermorite. Thermograms of other compositions (A,C and D) were found similar to thermograms of composition 'B'.

XRD

XRD of hydraulic binder 'B' hydrated at 50°C for a period of 1,3,7 and 28 days is shown in Fig.2. Reflections for ettringite (5.9405, 4.7476, 3.4554, 3.0394,

2.7526, 2.3926, 2.2739, 2.0832, 1.8974, 1.8574, 1.8050, 1.6625, 1.5788 and 1.3640°A) and tobermorite (3.7824, 3.359, 3.1517, 3.0054, 2.8030, 2.2118, 2.0386 and 1.6221°A)are formed at 27°, 40°, 50° and 60°C. The intensity of these reflections

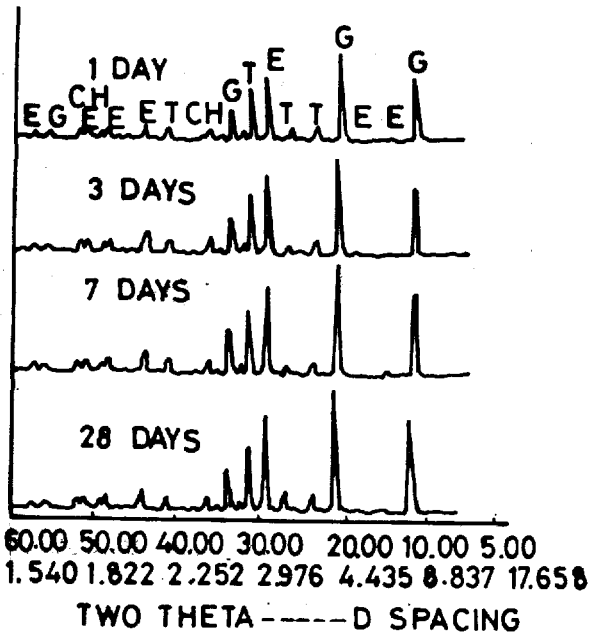

FIG.2. X-ray diffractogram of binder B hydrated at 50°c (G= Gypsum, E= Ettringite, T= Tobermorite CH= Calcium hydroxide)

were increased with increase in temperature and curing period indicating enhanced formation of ettringite and tobermorite. Disappearance of reflections at 2.447 and 1.796°A at 50°C confirms increased formation of tobermorite.

SEM

At 1 day hydration of binder, agglomerated needles of ettringite interspersed with fly ash spheres were formed. Between 3 and 7 days, ettringite needles and

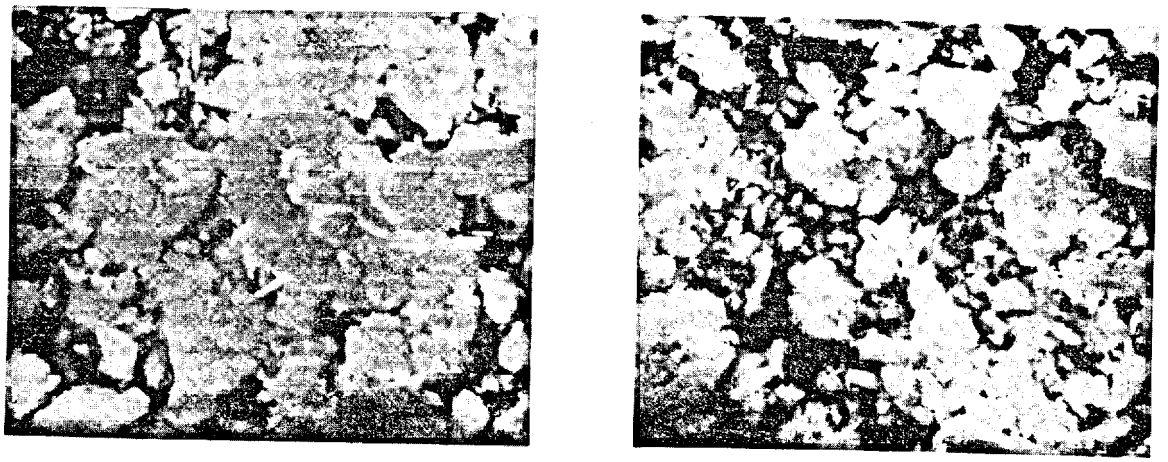

(a) x 1250 (b) x 1250

FIG. 3. SEM of binder 'B' hydrated for (a) 7 days and (b) 28 days at 50°C

hydrated plates of tobermorite developed. At 28 days of hydration, dense structures containing ettringite, tobermorite and fly ash spheres were detected. These results corroborate the findings reported by He Jun Yuan et al (6). SEM of system 'B' hydrated at 50°C for 7 and 28 days are shown in Fig.3(a) and (b).

Strength Development

It was found that with the increase in temperature of hydration from 27° to 60°C and the curing period from 1 to 28 days, the strength of all the systems i.e. A.B,C and D increased (Fig.4). However, at 50°C (c) and 60°C (d) the maximum

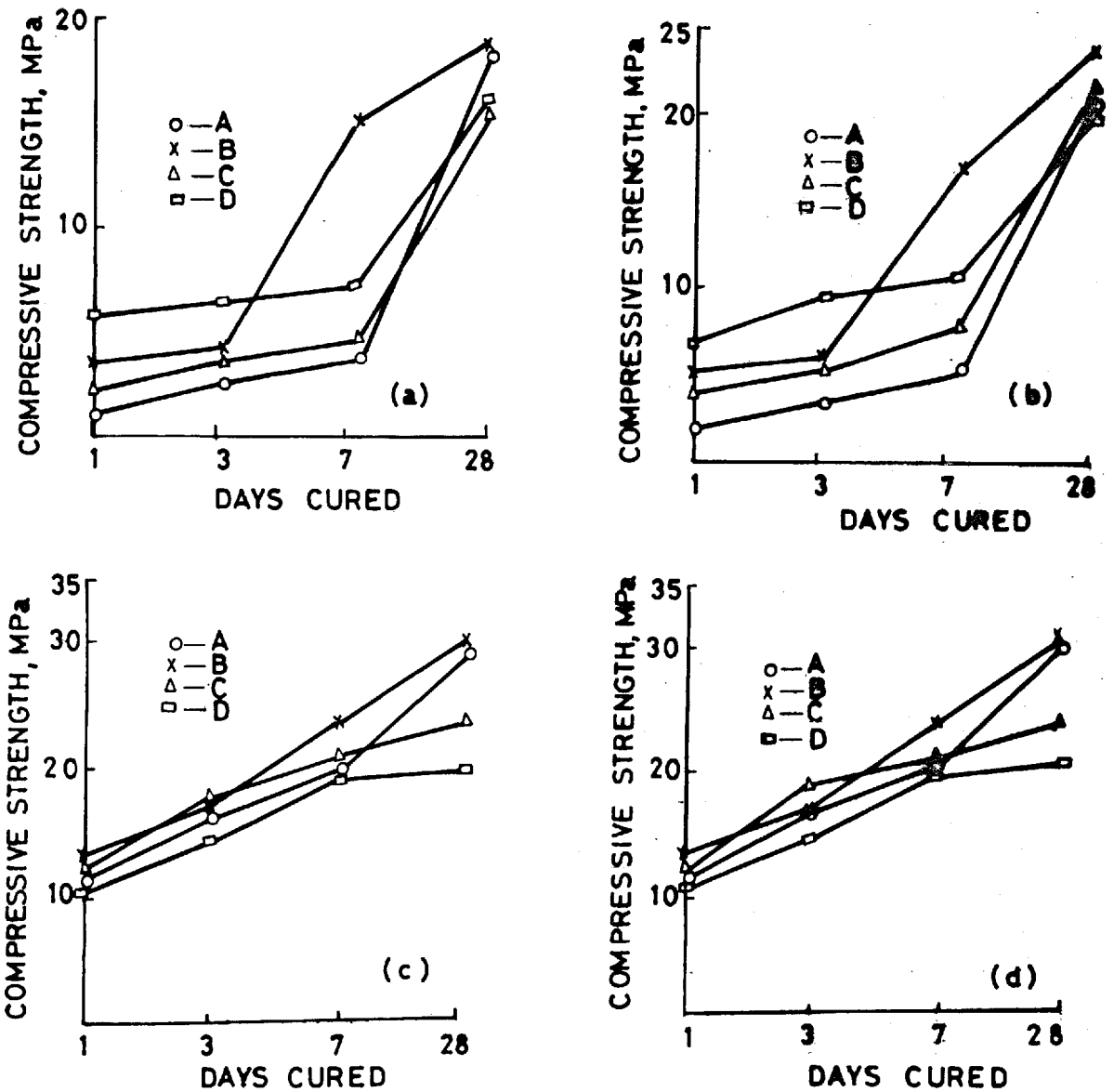

FIG. 4. Relationship between compressive strength and curing period at (a) 27°c (b) 40°c (c) 50°c and (d) 60°c

strength development was noted than obtained at 27°(a) and 40°C (b). The level of strength development at 50° and 60°C was more or less similar. The system 'B' gave maximum attainment of strength than the other compositions due to enhanced formation of ettringite and tobermorite compounds in the former than latter. The early age strength (1 to 3 days) is attributed to the hydration of hemihydrate plaster and portland cement whereas latter age (7 to 28 days) strength development is due to ettringite and tobermorite. The ultimate high strength obtained at 28 days at 50° and 60°C may be ascribed to the reduction in ettringite and increase in tobermorite formation.

CONCLUSIONS

1. The study demonstrates that lime in phosphogypsum-fly ash-portland cement system reacts with SO_4^{2-} and SiO_2 to form ettringite and additional tobermorite.

2. Enhancement in strength development of system at 27° to 60°C is due to increase in the pozzolanic reaction. Maximum strength is attained at 50°C.

3. The hydraulic binder composed of above system may be eminently used as building material in prefabricated components.

ACKNOWLEDGEMENT

The work reported in this paper forms a normal research programme at the Central Building Research Institute, Roorkee (India) and is published with the kind permission of the Director.

REFERENCES

1. Taneja, C.A & Singh, Manjit:Evaluation of phosphogypsum for different building materials, Chemical Age of India, 1977, 20, 108-111.

2. Singh, Manjit : Utilisation of phosphogypsum for building materials, **Building Research Note No. 9,** Central Building Res. Instt.Publication, Roorkee, India, March 1988.

3. Rehsi, S.S. : Fly ash utilisation - Its potential and prospects, **National Workshop on Utilisation of Fly Ash,** Central Building Research Institute, Roorkee, India.1988, A31-A34.

4. Singh, Manjit, Garg, Mridul & Rehsi, S.S. : Water resistant gypsum binder from waste phosphogypsum, **International Congress CIB'89 - Quality for Building Users throughout the World, Paris (France),** 1989, Theme II, 2, 339-352.

5. Santoro, L., Aletta, I and Volenti, G.L. : Hydration of mixtures containing fly ash, lime and phosphogypsum, Thermo-Chemica Acta, 1986, 78, 71-80.

6. He Jun-Yuan, Barry, E. Scheetz & Roy M. Della. : Hydration of flyash portland cements, Cement and Concrete Research 1984, 14, 505-512.

Specific Theme III-C

Structural Models for Hydrated Cement Pastes

A MATHEMATICAL MODEL ON RATE OF HEAT LIBERATION IN EARLY HYDRATION OF PORTLAND CEMENT AND ITS APPLICATION

H Okamoto*, N Itoh* and S Takahashi**

*Maizuru College of Technology, Shiraya, Maizuru, Kyoto, JAPAN
**R&D Laboratory, The Cement Association of Japan, Toshima, Kita-ku, Tokyo, JAPAN

SUMMARY

Early hydration properties of cement are generally represented by the rate of heat liberation. They are very important properties to make clear reaction mechanism of cement, the development of strength and thermal stress of concrete. A mathematical model on the heat liberation curve has not been fully studied yet because it shows very complicated curve.

The present study has been carried out for the purpose of curve fitting by a mathematical model on rate of heat liberation in early hydration of portland cement. We propose the model combining hyperbolic function with logarithm. Furthermore we consider the application of it to estimation of shoulder, strength properties and heat quantity of hydration by specification.

セメントの初期水和特性は、一般に水和発熱速度によって表される。それらは、セメントの反応機構、コンクリートの強度発現や熱応力を明らかにするためには、極めて重要な性質である。発熱曲線に関する数理モデルは、それが非常に複雑な曲線となるため、まだ十分な研究がなされていない。

本研究は、ポルトランドセメントの初期水和発熱速度について、数理モデルによる曲線あてはめの目的で行われたものである。数理モデルとして双曲線に対数を組み合わせたモデルを提案した。また、この応用としてShoulder の評価法、規格試験によって得られる強度特性および発熱量を検討したものである。

1. Introduction

The knowledge on early hydration properties of cement has become very important to understand behavior of fresh concrete and early age concrete.
Early hydration properties of cement are generally represented by the rate of heat liberation. It is considered that the characteristic is highly relied upon with the development of a conduction calorimeter which can be measured with a high accuracy in recent years.

Time-history of the rate of heat liberation indicates very complicated curve which forms several peaks[1]. Study on modelling the heat liberation curve has not been fully carried out up to now[2].

The present study has been carried out for the purpose of curve fitting by a mathematical model on rate of heat liberation in early hydration of cement and of its application, selecting cement of four types the object of investigation. For this we propose the model combining hyperbolic function with logarithm.
The following items are investigated for the present study:
(1) To examine agreement between measurement obtained from heat liberation test and calculation by proposed model.
(2) To evaluate shoulder quantitatively.
(3) To investigate relationship between strength and accumulated calorific value.
(4) To compare with heat quantity of hydration by JIS specification.

2. Mathematical Model on Rate of Heat Liberation

Generally, time-history curve of the rate of heat liberation in early hydration for portland cement is shown in Fig.1. Hydration process is divided into five stages as follows; the first stage is initial rapid reaction period, the second stage is induction period and it stops temporarily, the third stage is rate-increasing period, the fourth stage is deceleratory period so -called 'shoulder and the fifth stage is final period of slow reaction. In this curve, there are three peaks inwhich the first peak appears within about ten minutes, the second peak appears in about 8 hours and the third peak appears about 13 hours, after contact with water. The third peak approaches the second peak, and becomes relatively small but occasionally does not appears.. Accordingly, neglecting the third peak the first and the second peaks are considered as the object of the present study.

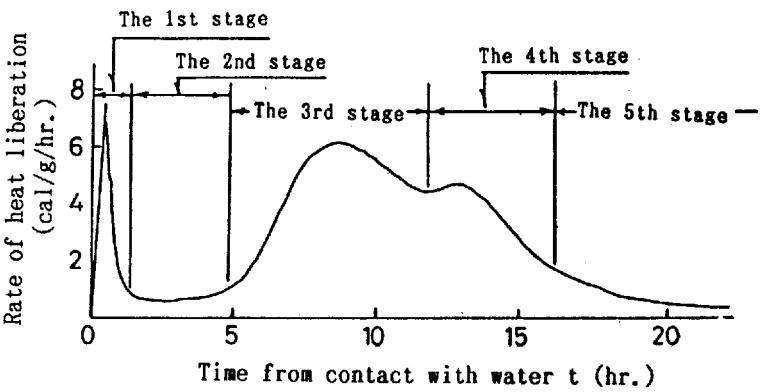

Fig.1 Schematic curve of rate of heat liberation

Modelling on behavior investigates by two methods inwhich one applies rational formula by general law of nature or the other experimental formula fitting the experimental results faithfully. The present study depends on the method of the latter.
A typical relationship between the rate of heat liberation and the elapsed time from contact with water is shown in Fig.2, plotting semilog graph paper.

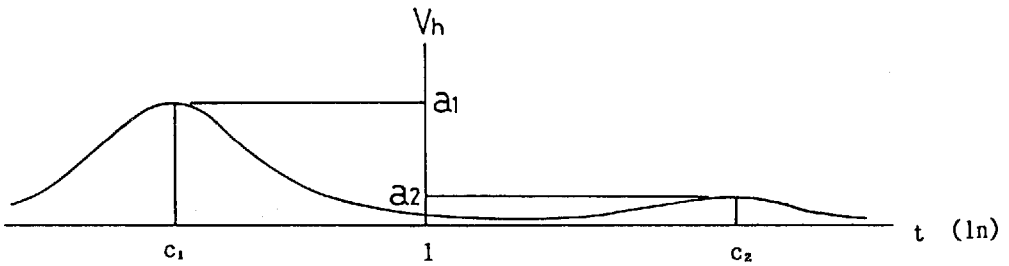

Time from contact with water t (hr.)

Fig.2 A typical curve of rate of heat liberation

As a result of many considerations, we introduce a mathematical model on the heat liberation curve in early hydration of cement as follows. It is the following equation combined hyperbolic function with logarithm.

$$V_h = a_1 \cdot \mathrm{sech}\{b_1 \cdot \ln(\frac{t}{c_1})\} + a_2 \cdot \mathrm{sech}\{b_2 \cdot \ln(\frac{t}{c_2})\} \quad \cdots\cdots\cdots\cdots\cdots\cdots (1)$$

where, V_h: the rate of heat liberation(cal/g/hr.), t: the elapsed time from contact with water(hr.), a_1: the maximum value of rate of heat liberation in the first peak(cal/g/hr.), b_1: the degree of curvature in the first peak, c_1: the arriving time of the first peak value(hr.), a_2: the maximum value of rate of heat liberation in the second peak(cal/g/hr.), b_2: the degree of curvature in the second peak, and c_2: the arriving time of the first peak value(hr.). In this case, $t>0$, $V_h>0$; $a>0$, $b>0$, and $c>0$. Six parameters in this model represent symbolical characteristics of a curve. Six parameters applying the data obtained by conduction calorimeter to Eq.(1) were calculated by means of the method of non-linear least squares.

3. Experimental Method

Rate and amount of heat liberation were automatically measured by conduction micro calorimeter of twin-type within 48 hours. Cement was used four types which are ordinary portland cement, high-early-strength portland cement, moderate heat portland cement and blast-furnace slag cement. These chemical composition and physical properties are shown in Table 1. Tests were carried out on cement paste with water-cement ratio of 50% under curing temperature of 10℃, 20℃, 30℃ and 40℃.

Table 1 Chemical composition and physical properties of cement

Type of cement	Chemical composition (%)										Physical properties	
	ig.loss	insol.	SiO_2	Al_2O_3	Fe_2O_3	CaO	MgO	SO_3	Na_2O	K_2O	S.G.*	Bl.**
Ordinary	1.1	0.3	21.4	5.1	2.9	64.3	1.6	2.1	0.33	0.60	3.15	3330
High-early	0.9	0.0	20.5	4.8	2.7	65.4	1.6	2.7	0.21	0.24	3.14	4340
Moderate	0.7	0.1	23.1	3.7	3.9	63.4	1.6	2.0	0.08	0.48	3.20	3400
Blast-furnace	0.6	0.1	27.3	10.3	1.5	52.3	4.0	1.9	0.27	0.52	3.01	3970

* Specific gravity

**Blaine specific surface(㎠/g)

4. Results of Fitting of Proposal Model and Discussions

Experimental results of the rate of heat liberation and calculated results of time -history obtained by Eq.(1) are shown in Fig.3, on ordinary portland cement, under curing temperature of 20℃, 30℃ and 40℃. Raising curing temperature, the peak becomes higher and its arrival time becomes faster.

Compared with cement of three types of ordinary portland cement, high-early-strength portland cement, and moderate heat portland cement, under curing temperature of 30℃, they are shown in Fig.4. They show therefore that calculated results much agree with experimental results. But as a result the difference between measured values and calculated values was observed in the start of the first peak, because a apparatus used for this study possessed a large time constant. Other results also showed a same tendency as above.

Six parameters and accuracy of Eq.(1) to experimental results are indicated in Table 2. In this study, accuracy is calculated by Eq.(2),

$$S=\sqrt{\frac{1}{n-p}(Vmi-Vci)^2} \quad \cdots\cdots\cdots\cdots\cdots\cdots\cdots\cdots\cdots\cdots(2)$$

where, S: square root of unbiased variance(cal/g/hr.), n: number of the data, p:number of parameter, Vmi: experimental value, and Vci: estimated value.

Curvature in the second peak of curve is given by the following formula,

$$K_2=a_2\cdot(b_2/c_2)^2 \quad \cdots\cdots\cdots\cdots\cdots\cdots\cdots\cdots\cdots\cdots(3)$$

where, K_2: curvature of the second peak of curve.

These calculated results are also indicated in Table 2.

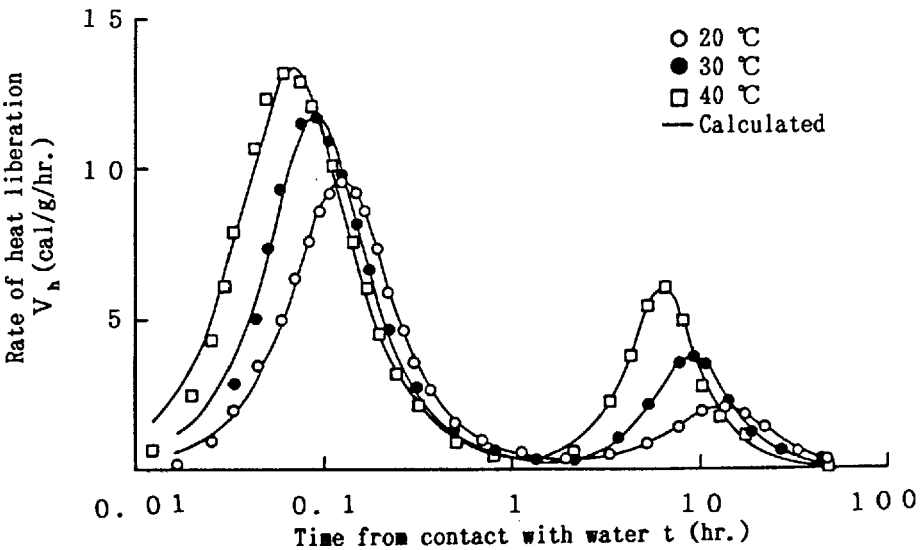

Fig.3 Heat liberation curves of ordinary portland cement

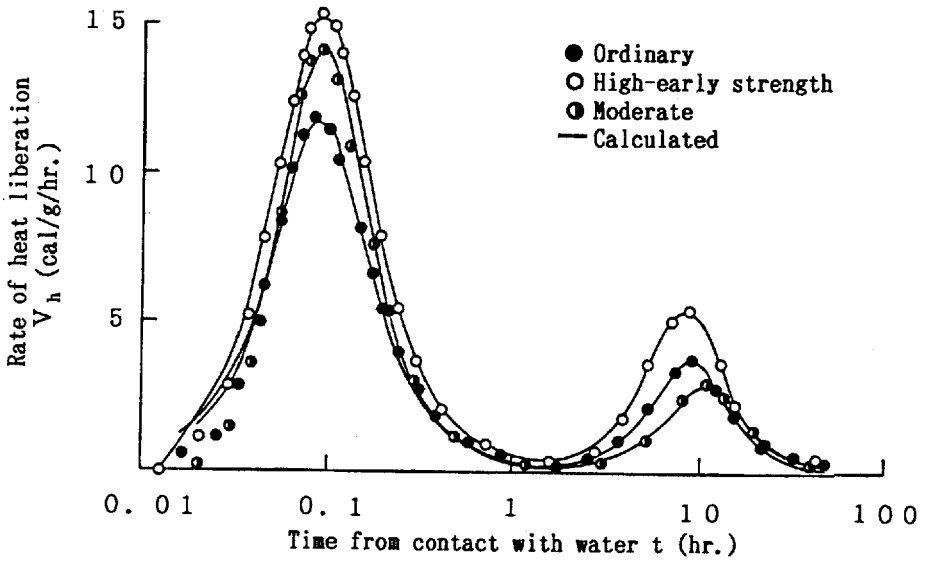

Fig.4 Heat liberation curves of various cement under temperature of 30℃

Parameters a_1, a_2 and b_2 increased, and c_1 and c_2 decreased, with the rise of curing temparature, but parameter b_1 failed to show a certain tendency. S which represents standard deviation ranges from 0.093 to 0.391 cal/g/hr.

Curvature which represents the peak intensity increased with the rise of curing temparature as shown Fig.5.

Consequently, it is recognized that the model proposed in this study fits the heat liberation curve of portland cement well.

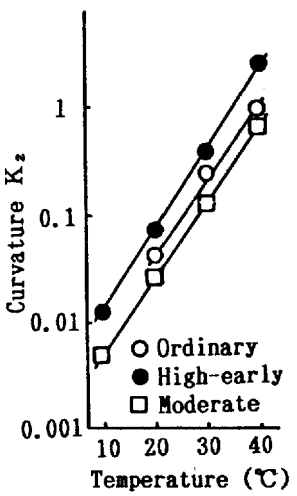

Fig.5 Curvature of the second peak

Table 2 Calculated results by proposed model

Type of cement	Curing temp.	a_1	b_1	c_1	a_2	b_2	c_2	K_2	S
Ordinary	20	9.59	1.75	0.125	2.09	1.90	13.0	4.45×10^{-2}	0.093
	30	11.8	1.80	0.090	3.77	2.33	8.97	0.254	0.230
	40	13.4	1.63	0.069	6.02	2.59	6.36	1.00	0.350
High-early	10	5.24	1.65	0.276	1.62	1.87	21.1	1.26×10^{-2}	0.250
	20	10.1	1.85	0.151	3.10	2.01	13.1	7.31×10^{-2}	0.164
	30	15.4	1.77	0.093	5.59	2.30	8.60	0.398	0.202
	40	23.9	1.69	0.067	10.4	2.58	5.18	2.58	0.391
Moderate	10	5.30	1.98	0.278	0.87	1.66	21.9	4.99×10^{-3}	0.133
	20	10.3	2.12	0.145	1.68	1.89	14.7	2.77×10^{-2}	0.135
	30	14.1	1.93	0.095	2.99	2.26	10.8	0.131	0.246
	40	14.0	1.82	0.074	5.04	3.00	8.24	0.668	0.357

5. Evaluation of Shoulder on Blast-furnace Slag Cement

It is necessary to evaluate quantitatively the shoulder which associates with the conversion of AFt phase into AFm phase.
Therefore, we propose the following method. Primarily, the above calculation by Eq. (1) is carried out except the data at the interval of shoulder. Next, we obtain the area estimated by using the value subtracted the calculated value from the measured value, at the interval, as shown in Fig. 6. Then calorific power of shoulder can be evaluated by the subtracted area.
The heat liberation curves of blast-furnace slag cement are shown in Fig. 7.
Parameters and calorific power of shoulder by the subtracted area are indicated in Table 3. As curing temperature increased, calorific power of shoulder increased.

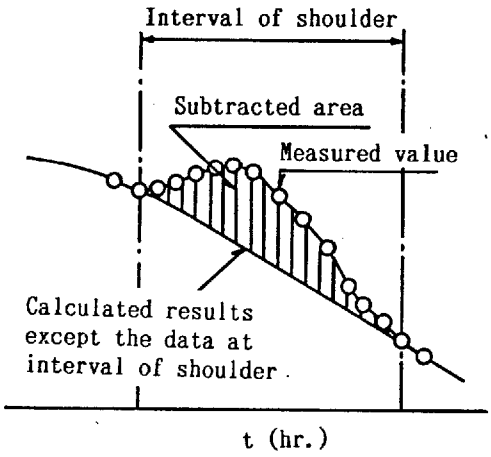

Fig. 6 Evaluation of shoulder

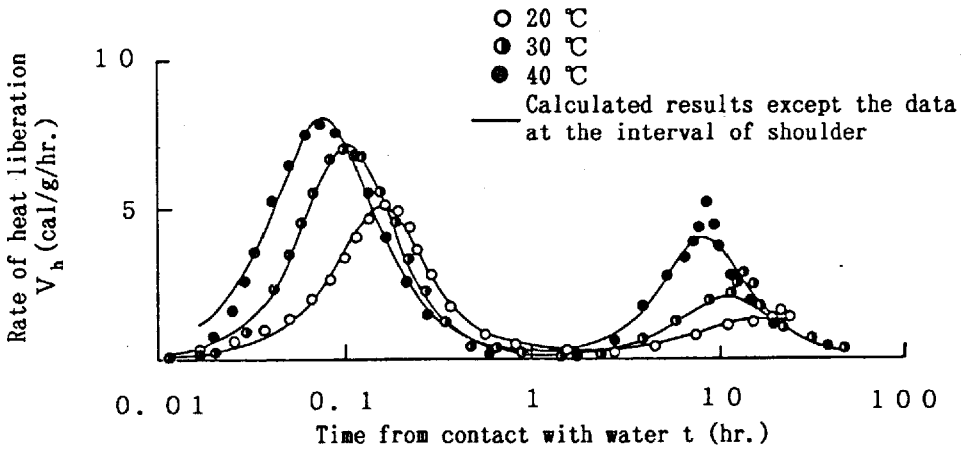

Fig. 7 Heat liberation curves of blast-furnance slag cement

Table 3 Parameters and calorific power of shoulder on blast-furnace slag cement

Curing temp.	Parameters								Calorific power of shoulder(cal/g)
	a_1	b_1	c_1	a_2	b_2	c_2	K_2	S	
20	5.07	1.93	0.160	1.31	1.33	19.2	6.74×10^{-3}	0.129	0.664
30	7.19	1.91	0.104	2.12	1.88	11.2	5.94×10^{-2}	0.140	2.35
40	8.07	1.76	0.079	4.03	2.16	8.31	0.274	0.243	2.82

6. Strength and Accumulated Calorific Value

As a engineering application of this modelling, it investigates relationship between the accumulated calorific value obtained by calculation and the compressive strength by JIS specification at early age. This relationship is shown in Fig.8, at the age of 3 days and 7 days. In consequence, it obtained a good linearity.

7. Comparison with Heat of Hydration by Dissolution Heat Method

As compared with heat quantity of hydration by dissolution heat method of JIS specification and the accumulated calorific value obtained by this model, it is indicated in Fig.9, at 7 days, under curing temperature of 20 ℃. Theoretically, both are equal. It gives approximately straight line, and approaches the isopleth.

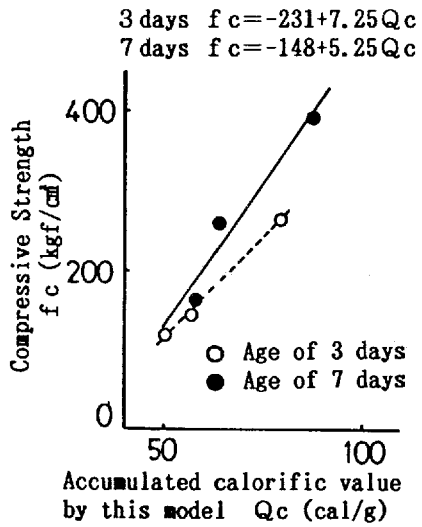

Fig.8 Relationship between strength and accumulated calorific value

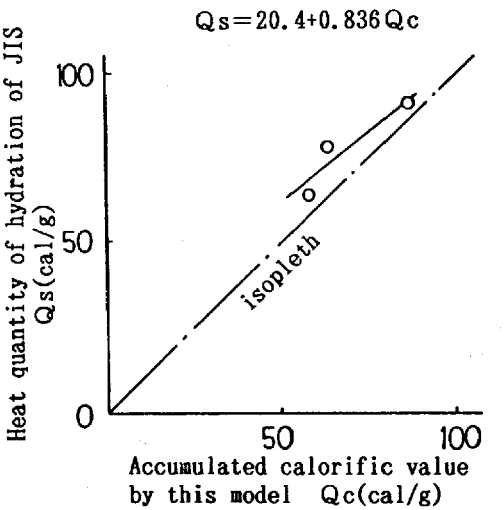

Fig.9 Comparison of heat quantity of liberation

8. Conclusions

Conclusions obtained from the present study are as follows:

(1) On the heat liberation curve in early hydration, the proposed model agrees with experimental results on portland cement of three types, except for the difference in the start of the first peak.
(2) Six parameters in this model represent symbolical characteristics of a curve.
(3) Calorific power of shoulder can be evaluated by applying this model.
(4) Relationship between accumulated calorific value and strength at early age is in proportion.
(5) As compared with heat quantity of hydration by dissolution heat method of JIS specification and the accumulated calorific value obtained by this model, its relationship is shown by linearity.

References

[1] Taylor, H.F.W.: Cement Chemistry, Academic Press, pp.226-242, 1990
[2] Pommersheim, J. and Clifton, J.R.: Mathematical Models of Cement Hydration, Cements Reseach Progress, pp.281-307, 1979

PREDICTION OF CEMENT PROPERTIES FROM DESCRIPTION OF THE HYDRATION PROCESSES

Bjarne Osbaeck

F L SMIDTH & CO A/S, Technical Division
Copenhagen, DENMARK

SUMMARY

Several of the properties important to the user of Portland cement and other hydraulic cements are direct results of the hydration reactions taking place between the components of the cement and water. From a stoichiometric description of the hydration reactions coupled with calculations of the volumetric and thermodynamic changes associated with them it seems possible to obtain good estimates of the physical changes occurring as a result of the hydration reactions including binding of water, formation of specific hydrates, changes in porosity and heat development. From the calculation of porosity it is possible to obtain estimates of porosity-related properties such as strength and durability.

A model based on the principles outlined above is presented and examples are given on its applicability as a tool for prediction of cement properties from cement characteristics and for evaluation of experimental results.

RÉSUMÉ

Plusieurs des propriétés qui présentent de l'importance pour l'utilisateur du ciment de portland et d'autres ciments hydrauliques résultent directement des réactions d'hydratation ayant lieu entre les composants du ciment et l'eau. A partir d'une description stoechiométrique des réactions d'hydratation reliés aux calculs des changements volumétriques et thermodynamiques associés à ces réactions, il semble possible d'obtenir de bonnes estimations des changements physiques sous forme de résultat des réactions d'hydratation comprenant la fixation d l'eau, la création d'hydrates spécifiques, des changements dans la porosité et dans l'évolution thermique. Il est possible, à partir de calculs, d'obtenir des estimations des propriétés reliées à la porosité telles que résistance et durabilité.

Un modèle basé sur les principes précisés ci-dessus est présenté et des exemples sont donnés sur son applicabilité comme moyen pour la prédiction des propriétés de ciment à partir des caractéristiques du ciment et pour l'évaluation des résultats expérimentaux.

INTRODUCTION

As long as portland cement has been used as a binder in construction materials there has been a need for being able to predict the development of engineering properties like strength and heat development as a function of important influencing factors. Curing time, temperature and initial porosity of the cement-paste (water-cement ratio) have been identified as important factors for more than a hundred years and empirical models for quantification of their influence have been proposed in large numbers through the years.

In the 1940's Powers and Brownyard proposed models for the cement paste system on a physical basis and brought cement and thereby concrete research a large step forward (1). Their models were based on calculations of volumetric changes in the hydrating cement paste and their correlation to the engineering properties like strength and permeability. Their models were based on a generalized description of portland cement. The influence of the compound composition of portland cement was dealt with by giving empirical (statistical) equations for the constants in the main models to describe the effect of the cement composition.

A more direct approach to describing the influence of the compound composition on porosity and strength of portland cement was used by Joens and Osbaeck in 1982 (2) and by Parrott in 1985 (3) but based on the same principle as the models by Powers and Brownyard. The modeling was based on an individual treatment of the reactions of the compounds of portland cement. By merging the individual contributions the total changes in the cementitious system can be calculated.

A more strict and comprehensive model build on the same ideas as in our work in 1982 is the topic of the present paper. The treatment is based on general stoichiometric, volumetric and thermodynamic calculations on chemical reactions and can thus be applied to any cementitious system of interest. The basic ideas and some examples of use are outlined in the following.

DESCRIPTION OF THE MODEL

Basic principles

Portland cement clinker consists of a mixture of minerals which are able to react with water under the formation of new solid phases, hydrates. The hydration reactions all have the following physical consequences: An increase in the volume of solids, a decrease in total volume of the system and a development of heat.

By calculating the phase changes in the system as the hydration proceeds and using the basic physical data available on the relevant phases one can obtain an estimate of the total physical changes occuring in the system during hydration. Properties of technical importance that can be calculated include the change in total volume ("chemical shrinkage"), porosity and the development of heat. From the porosity it is possible to obtain estimates of strength. Also the porosity and the description of the hydrate composition can give a basis for considerations regarding durability of the material. The principles of the model are shown in Fig. 1.

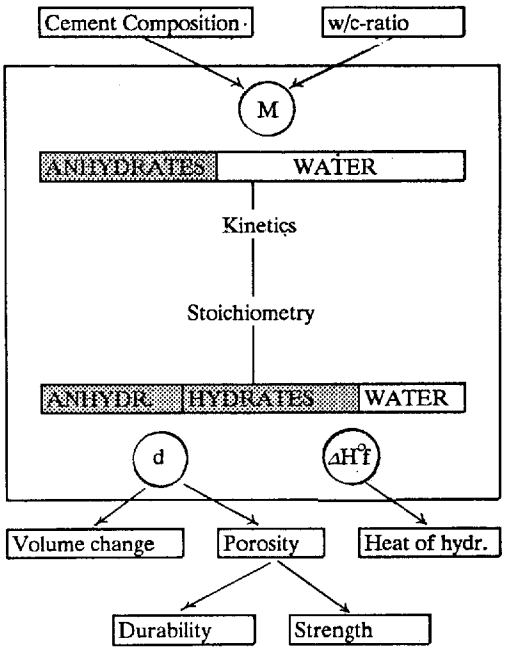

Fig.1 Basic principles of the stoichiometric model for calculating physical changes in cement paste as a function of cement composition, w/c-ratio and degree of hydration.

To be able to calculate the properties mentioned above one has to define the initial system and to calculate the composition of the system at specific ages (maturity levels) during the hydration. This requires the formulation of a set of reactions to descripe the hydration of the basic minerals and kinetic data to define how long the reactions have proceeded. From a phase compositional description of the system and a set of basic data including molar weight density and enthalphy of formation for the phases involved a volumetric and energetic description of the system at any maturity level as well as the changes occured compared to the initial system can be calculated.

Thus, the basic model includes a description of the phase changes in the system, a set of kinetic data (or equations) to define the maturity level of the system, and a data-base of compound specific data to be used for the calculation of the physical changes. Other factors of practical importance like temperature, moisture, and other cement factors than the major compound composition can be incorporated into the model by describing their influence on the kinetics or the product composition.

Description of the initial system

A description of the initial system includes a description of the cement and information about the amount of water added. The description of the cement in the basic form of the model is fairly simple and includes the following compounds

C_3S, C_2S, C_3A, C_4AF, C (free) and $C\bar{S}H_2$

An example of a set of input data is given in Table 1.

Table 1. Input data. (Example)

Compound	Amount (g)
C3S	55
C2S	20
C3A	8
C4AF	11
C	1
$C\bar{S}H2$	5
Cement (Σ=)	100
Water	50

This description can of course be extended to meet specific requirements such as the inclusion of mineral admixtures such as slag, fly ash and pozzolanas as part of the cementitious system. Fineness of the cement and some chemical factors (e.g. alkalies) are important factors for the development of cement properties but their influence can be built into the model through the kinetic description.

Reactions. Stoichiometry

As a first approximation to a description of the multiple reactions occurring during hydration of portland cement a reaction sequence as shown in Fig. 2 has been chosen.

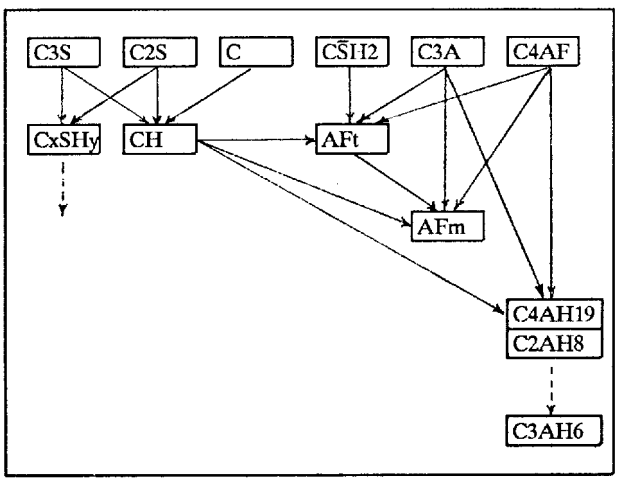

Fig.2 The hydrate formation sequence built into the model

The two calcium silicates (C_3S and C_2S) form a mixture of C-S-H-gel and calcium hydroxide (CH). C-S-H-gel is not a well defined compound and its composition, especially with regard to water content, is variable and depends on environmental conditions and age. Consequently, the model is prepared for variable entries of the stoichiometrical ratios of C/S and H/S. At present a tentative composition of $C_{1.6}SH_4$ is used. Obviously, since the C-S-H-gel is the major part of the hydrate mass of portland cement compositions its treatment by the model is very important. During the testing of the model special attention to this component must be given. A very likely necessary step will be to let the composition and density of this component change with maturity and possibly other factors to obtain a closer estimate of reality.

The C_3A phase will react with gypsum ($C\bar{S}H_2$) to form ettringite ($C_3A \cdot 3C\bar{S} \cdot 32$ H) (abbr. to AFt) as long as gypsum is present in the system. When gypsum is depleted further reaction of C_3A will result in formation of monosulphate ($C_3A \cdot C\bar{S} \cdot 12$ H) (abbr. to AFm) at the expense of ettringite. When the ettringite is used up further hydration of C_3A will result in formation of a mixture of C_4AH_{19} and C_2AH_8 or just C_4AH_{19} if CH is present. This will normally be the case in a portland cement system. The possibility of letting these latter hydrates age to form the stable cubic hydrate C_3AH_6 is an obvious step for the future development of the model.

The ferrite phase (C_4AF or $C_2(A,F)$) is assumed to undergo the same reactions as C_3A with the one exception, that formation of AFt, AFm and $C_4(A,F)H_{19}$ implies the presence of CH to compensate for the lime deficiency of $C_2(A,F)$. Consequently the CH amount will decrease as $C_2(A,F)$ reacts.

Data on individual compounds

To be able to carry out the necessary calculations the following basic data must be available for each of the compounds involved in the description: The molar weight, the density and the heat of formation. The set of data used at present is presented in Table 2.

Table 2. Data for the individual compounds. Molar weight (M), density (d), and standard enthalpy of formation (ΔH_f°).

Compound	M (g/mole)	d (g/cm3)	$-\Delta H_f^\circ$ (kcal/mole)
C3S	228.33	3.20	688.10
C2S	172.25	3.28	538.00
C3A	270.20	3.03	861.00
C4AF	485.98	3.77	1440.00
C	56.08	3.32	151.90
$C\bar{S}H2$	172.18	2.32	483.06
H	18.02	1.00	68.32
C1.6SH4	221.88	2.00	754.00
CH	74.10	2.24	235.80
AFt	1255.15	1.76	4193.00
AFm	622.54	1.95	2100.00
C4AH19	668.58	1.80	2409.00
C2AH8	358.25	1.97	1291.00

The density data has mainly been taken from Appendix I in Ref.(4). Where ranges in densities are given an average value is adopted. For C_2S the value for the β-modification is used. For C-S-H the value 2.0 g/cm³ has tentatively been adopted.

The hydrates of the C_3A and the ferrite phase $C_2(A,F)$ are assumed to be the same and the characteristic figures used for these hydrates are chosen corresponding to the pure Al_2O_3-forms. Since the calculation of the hydrate amounts is performed on a molar basis this implies, that the (A,F)-hydrates have the same molar volume irrespective of the A/F-ratio. This is considered to be a fair approximation.

Obtaining thermodynamic data for anhydrates and especially hydrates relevant to the portland cement system requires a great deal of research. For some compounds several but differing values can be found, while for others values are hard to find, or missing. The values are to be used for calculation of heats of reaction. These will usually come out as small differences between large figures. The precision of the basic data is therefore critical. At the present stage the values recorded in the National Bureau of Standards Circular No. 500 (5) have been adopted for most of the anhydrates, gypsum, calcium hydroxide and water. The values for AFt and AFm have been calculated from heat of reaction data measured by Berman & Newman (6) and the values for C_4AH_{19}, C_2AH_8 and $C_{1.6}SH_4$ from contributions from structural elements. The values have been found to give characteristic heats of hydration close to experimental values reported in the literature.

The ferrite phase creates a problem also in this respect as probably no thermodynamic data on mixed A-F-hydrates has been established. Since in the model $C_2(A,F)$ is assumed to form the same hydrates as C_3A (though with the consumption of CH) a simple use of a standard heat of formation figure for the anhydrate together with the values for the pure Al_2O_3-hydrates does not give reliable results. Consequently, a correction of the value for $C_2(A,F)$ has been made to give reaction values for this compound of the same order of magnitude as reported in the literature.

Kinetics

At present the kinetics are dealt with simply by incorporation of an interchangeable database stating degrees of hydration at different ages for the five anhydrates that are used in the model. The values can be results of actual measurements on a given cement or be estimates based on results from the literature. The set of kinetic data used in the examples of this paper and representing typical average values for cements at standard fineness (around 300 m²/kg (Blaine)) are given in Table 3.

Table 3. Degree of hydration (%) at different ages for the individual compounds. (Example)

Compound	Time (Days at 20°C)				
	1	3	7	28	Ult.
C3S	45	60	75	85	100
C2S	5	10	20	30	100
C3A	25	50	75	85	100
C4AF	10	25	35	45	100
C	100	100	100	100	100

An obvious step for future developments would be to incorporate mathematical expressions for calculation of degree of hydration as a function of time and factors influencing the kinetics. These could be input variables as stated above or factors derived by the model itself. An example of the latter is the change in kinetics that occurs when gypsum is depleted from the system.

Model output

From a definition of the initial composition of the cementitious system including added water and the kinetic state of the system the model calculates the actual composition of the cement paste and a series of derived physical properties of scientific and engineering interest.

The first part of the output concerns the composition of the paste specified by residual anhydrates, formed hydrates, residual water (H) and new pores formed by the chemical shrinkage (P_s). The calculated results based on the input data of Table 1 and 2 and the database in Table 3 is shown in Table 4. Of special interest is the description of the aluminate hydrates which reflects the phase changes between AFt, AFm and C_4AH_{19}.

Table 4. Composition of the cement paste (vol. %) at different ages. (Example)

Compound	Time (Days at 20°C)					
	0	1	3	7	28	Ult.
C3S	21.1	11.6	8.5	5.3	3.2	0.0
C2S	7.5	7.1	6.8	6.0	5.3	0.0
C3A	3.3	2.4	1.6	0.8	0.5	0.0
C4AF	3.6	3.2	2.7	2.3	2.0	0.0
C	0.4	0.0	0.0	0.0	0.0	0.0
$C\bar{S}H2$	2.7	0.0	0.0	0.0	0.0	0.0
C1.6SH4		15.6	21.3	27.8	32.7	48.7
CH		6.8	8.7	10.4	11.5	12.6
AFt		7.5	1.3	0.0	0.0	0.0
AFm		1.3	9.7	11.4	11.4	11.4
C4AH19		0.0	0.0	4.1	7.5	20.9
C2AH8		0.0	0.0	0.0	0.0	0.0
H	61.5	42.0	36.6	27.5	20.6	-2.8
Pa	0.0	2.4	2.9	4.3	5.4	9.1

The second part of the output concerns integral or general data for the cement paste as a whole (Table 5). The volumetric changes are here expressed in cm³/100 g of cement. Also the important volumetric factors like total porosity (residual free water + pores formed by chemical shrinkage) and the gel-space-ratio as introduced by Powers and Brownyard are calculated. The following calculation formulas have been used.

$$P = (V(o)-V_s(t))/V(o)=(H(t)+P_s(t))/Vo$$
$$X = V_{hydrat.s}(t)/(V(o)-V_{anhydrates}(t))$$

The output data includes the hydration-derived properties which are usually measured when studying cement such as bound water, heat of hydration and strength. The strength calculation is based on gel-space-ratio. Models based on this parameter were found to give the best estimates of strength as a function of e.g. w/c-ratio and maturity (degree of hydration). The strength values in the table are based on the model:

$$S = S_o \cdot X^N \qquad (S_o = 100,\ N = 2)$$

The constant can be varied to match the output of different strength measuring methods. By adopting the constant, $S_o = 100$ values close to ISO-mortar-strength values are obtained.

Table 5. Physical consequences on the paste of the hydration processes.(Example)

Property		Unit	Time (Days at 20°C)					
			0	1	3	7	28	Ult.
Total volume	(V)	cm3/100g	81.3	79.4	78.9	77.8	76.9	73.9
Chem. shrinkage	(Pa)	cm3/100g	0.0	-1.9	-2.4	-3.5	-4.4	-7.4
Solid volume	(Vs)	cm3/100g	31.3	45.2	49.2	55.4	60.1	76.2
Increase in solid vol.		cm3/100g	0.0	13.9	17.9	24.1	28.8	44.9
Porosity	(P)	%	61.5	44.4	39.5	31.8	26.0	6.3
Gel-space ratio	(X)		0	0.413	0.509	0.628	0.708	0.937
Degree of hydration		%	0	31.4	45.0	59.1	68.9	100
Bound water		g/100g	0	15.9	20.2	27.6	33.2	52.2
Heat of hydration		cal/g	0	43.1	59.6	78.4	91.0	126.3
Strength (arbitrary)	(S)	MPa	0	17.1	25.9	39.4	50.1	87.8

EXAMPLES OF USES OF THE MODEL

Porosity reduction and strength as a function of water-cement-ratio and degree of hydration

Most investigators agree that there is a strong relationship between the reduction in porosity as the hydration processes proceed and the development in strength and reduction in permeability of cement paste. The present model can give a quantitative estimate of porosity as a function of degree of hydration at different initial water-cement ratios. Tendency curves calculated with an average value of the specific increase in solid volume of 0.40 cm³/g are shown in Fig. 3.

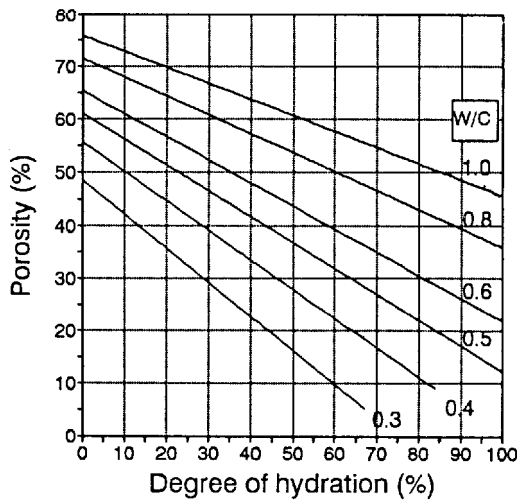

Fig.3 Porosity as a function of degree of hydration and water-cement ratio. (Calculated tendency curves)

Coupled with correlation between porosity and permeability the model can work as a tool to predict the necessary degree of hydration at a chosen w/c-ratio or the necessary w/c-ratio at a specified degree of hydration to bring the permeability below a certain limit. Additionally, coupled with a strength/porosity model a prediction of the strength level as a function of these two parameters can be estimated (Fig. 4).

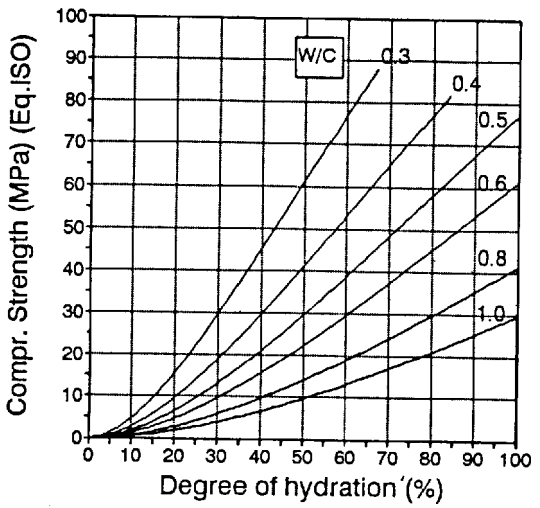

Fig.4 Strength as a function of degree of hydration and water-cement ratio. (Calculated tendency curves)

Volumetric contribution from the C_3A-phase

The influence of the C_3A-phase on the engineering properties of portland cement paste is one of the controversial issues of cement chemistry. An old experiment by Lerch with pure C_3A has been used for decades as evidence for the opinion that C_3A does not contribute to the strength development of portland cement. However a vast of amount of evidence during the previous years has shown that an increasing amount of C_3A in portland cement contributes positively to the strength development of portland cement paste. But the contribution of C_3A is difficult to describe due to the fact that its hydration reaction is strongly dependant on the amount of gypsum present. Gypsum influences the kinetics as well as the composition of the hydrates. The present model is prepared for distinguishing between the different forms of hydrates formed as a function of the gypsum content as well as the physical consequences of these differences. Fig. 5 shows the development of solid phase volume as a function of the degree of hydration of C_3A in two cases with differing amounts of gypsum.

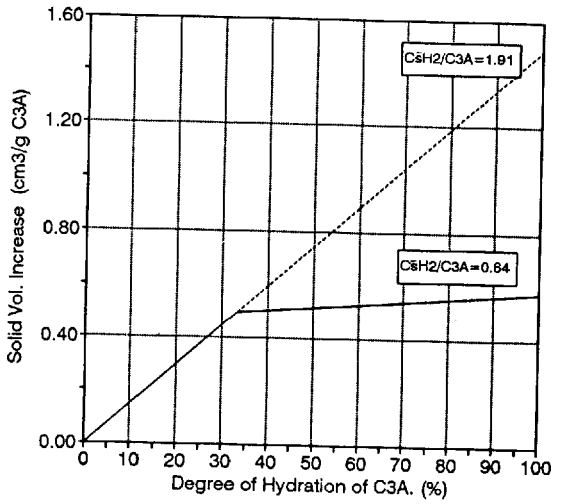

Fig.5 Solid volume increase due to C3A hydrating with different amounts of gypsum.

The examples clearly indicate that by keeping the gypsum/C_3A at an adequate level, a continuous strong increase in solid volume is avoided. This continuous increase in solid volume would probably be beneficial to the strength development due to the porosity reducing effect but could also create problems due to expansive forces associated with the formation of ettringite.

Strength as function of cement composition

The ability of the presented model to predict the influence on compressive strength of the C_3S- and the C_3A-content is illustrated by the examples in Table 6. The calculated increases in strength at different ages with an increase in C_3S- or C_3A-content correspond well to values obtained by many investigators by simple statistical analyses.

Table 6. Effect of C3S- and C3A-content on cement strengths.

Composition	A	B	B-A	C	D	D-C
C3S	50	60	+10	50	50	
C2S	25	15	-10	25	25	
C3A	8	8		3	13	+10
C4AF	12	12		17	7	-10
C	1	1		1	1	
$C\bar{S}H2$	4	4		4	4	
Cement (Σ=)	100	100		100	100	
Water	50	50		50	50	
Strength (*)						
1d	14.4	17.3	2.9	14.0	14.7	0.7
3d	23.8	27.9	4.1	21.9	25.9	4.0
7d	38.4	43.2	4.8	34.8	42.1	7.3
28d	49.5	54.3	4.8	45.7	53.3	7.6

(*) : Compressive strength (MPa) (ISO-mortar level)

Heat of hydration estimated from cement composition

Heat of hydration values at different ages have been calculated for cement compositions representing average values for the ASTM type I, II, IV and V compositions used in the classical work on heat of hydration by Verbeck and Foster (7). The resulting values are plotted together with the experimental values of Verbeck and Foster in Fig. 6.

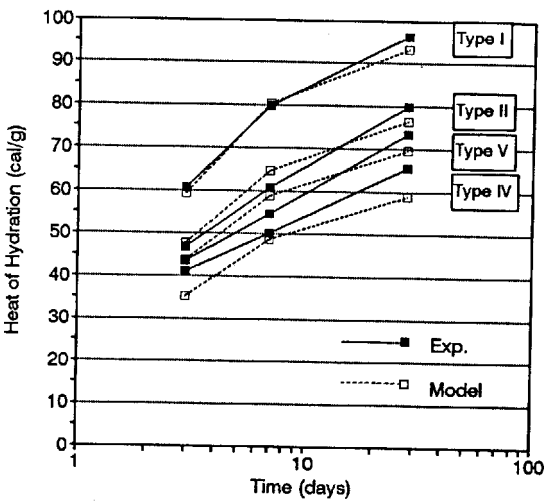

Fig.6 Heat of hydration for different types of cements. (ASTM classification).

Taking into consideration that a fixed set of kinetic data (that in Table 3) has been used for all cements the estimates of the model seem surprisingly good. By adjusting the kinetic values, the model estimates could easily come closer to the experimental values. In fact, one of the interesting possibilities with the model is its use for estimations of individual degree of hydration data from the more easily obtainable derived physical consequences like heat of hydration.

CONCLUSION

A model based on a fairly simply stoichiometric description of the hydration processes coupled with volumetric and thermo-chemical calculations seems to be able to give realistic predictions of several chemical and physical properties associated with cement paste during the hydration of portland cement. The model can be a useful tool for educational purposes, for cross-checking of experimental results, basic data and theories, and for predictive work in practice. It can be elaborated and refined by working with it and testing it against experimental values, and extended in accordance with existing possibilities and needs.

ACKNOWLEDGEMENT

The work presented in this paper was made as a contribution to the United States Strategic Highway Research Program (SHRP) project C-201 "Concrete Microstructure".

REFERENCES

1. Powers,T.C. and Brownyard,T.L.:"Studies of Physical Properties of Hardened Portland Cement Paste". PCA Bull. 22, 1948.

2. Joens,E.S and Osbaeck,B.:"The Effect of Cement Composition on Strength Described by a Strength-Porosity Model". Cem.Concr.Res.,1982,12,167-168.

3. Parrott,L.J.:"Modelling the Development of Microstructure". Proc.of Eng.Found.Conf., Henniker,1985,43-73.

4. Taylor,H.F.W (Ed):"The Chemistry of Cements". Vol. 2, Acad.Press, 1964.

5. Rossini,F.D et al.:"Selected Values of Chemical Thermodynamic Properties". Circular of the National Bureau of Standards 500. Washington, 1952.

6. Berman,H.A. and Newman,E.S.:"Heat of Formation of Calcium Trisulfoaluminate at 25°C". Proc. of the Fourth Int. Symp. on the Chem. of Cement. Washington, 1960,I,247-257.

7. Verbeck,G.J. and Foster,C.W.:"The Heats of Hydration of the Cements" Proc. of Am.Soc. Test. Mat.,1950,50,1235-1262.

HYDRATION KINETICS AND MECHANICAL EVOLUTION OF CONCRETE DURING THE FIRST DAYS: STUDY OF THE HARDENING MECHANISM

C Vernet

Technodes SA
Centre de recherche Industrielle et Technique du Groupe, Ciments Francais
FRANCE

ABSTRACT.

In order to study the relations between the physico-chemical and the mechanical behaviour of concrete, we have used the conductometric, calorimetric and ultrasonic methods together. A series of mortars calculated on the base of concrete formulations have been studied. During the very first days of hydration, the compressive strength is not proportional to the overall reaction yield of cement. This can be explained by the occurrence of micro-stresses, located around large crystals in course of growing. These stresses tend to reduce the mechanical yield of hydration reactions. They originate from the crystallisation pressure, the LE CHATELIER (or chemical) contraction, and from self-dessication in low-permeability concretes, of low water /cement ratio.

A better strength can thus be obtained by reducing the size of the crystals. This is the case in high performance concretes, into which ultra-fine particles has a catalytic effect on portlandite nucleation. Admixtures can also modify microstructure. It is found that the mechanical yield of the hydrates is enhanced by the best superplasticizers.

1 - INTRODUCTION.

The modelisation of concrete strength during the first days is of economical interest. So far, the actual previsional techniques uses a calorimetric calibration of concrete, and temperature measurements on the formworks and within the pieces (1). This calibration requires the determination of an activation coefficient. When ARRHENIUS' law is used, this assumes that the hydration reactions can be considered as a single chemical reaction. This approximation is generally valid, for standard mortars without admixtures (2). But the increasing complexity of concrete formulations has led us to reconsider this question, in the case of high performance concrete.

We had previously studied hydration kinetics of concentrated cement suspensions, using multiparameter measurements. This work has allowed a better understanding of the chemical sequence (3). Afterwards we applied this technique to the study of cement-admixture couples (4). On this base, it is now possible to deal with more complex problems, and to enlarge our study to the mechanical evolution.

2 - EXPERIMENTAL.

2.1. Methods.

The following parameters have been monitored systematically:

- the electrical conductivity. In the case of mortars, it depends also on the actual water/solid ratio, and allows to monitor the water uptake (4).
- the thermal flux, measured by isothermal calorimetry, giving after integration the hydration heat. The chemical contraction is related to the latter, and the linearity has been verified by experimentation (5) (6).
- the ultra-sound attenuation, measured with a relay-probe which allows to monitor the transition from plastic to solid state (7).
- the ultra-sound velocity, which is related to the dynamical elasticity modulus.

In addition, the compressive strengths were measured every hour, by averaging the results of at last 6 cylinders.

2.2. Mixes composition.

For practical reasons, the measurements were made on the finer part of concretes (i.e. less than 5mm). The strength of these mortars extracted from the concrete formulation correlate well with those of concrete during the first days, as so far as the strength is not yet limited by the presence of the aggregates and their transition zone. A first set of formulas was derived from high slump concretes, with 28 days strength about 60 MPa, for building prestressed triangulated beams (**table 1**).

The working conditions required to maintain the slump at a high level during 3 hours, and a setting time lower than 10 hours.

Table 1 : first set of concretes.

portland cement (70%C3S, 8%C3A, 4000cm2/g)	425 Kg/m3
silica fume	40 Kg/m3
sand 0-5 mm	750 Kg/m3
water/(cement+f.s)	0.49
gravel 6-10mm (concrete case)	1050 Kg/m3

Table 2 : admixtures formulations (binder=cement+silica fume)

code	composition (by weight of cement)	Water/binder
S.A.	no admixture	0.49
MLRET	melamine 2% + retarder 0.5%	0.33
PNSRET	polynaphtalene-sulfonate 2% + Retarder 0.5%	0.33
F201	retarded superplasticizer 2%	0.33
F202	retarded superplasticizer 2%	0.33

Table 3. Second set of mortars. Proportions of concrete formula

concrete code	T	U
Portland cement (C3S:70%; C3A:8%; 4000cm2/g)	400	415
silica fume	0	35
Sand	675	755
water/(cement+FS)	0.35	0.35
accelerator without chlorides.(% of binder)	3	0
melamine.(% of binder)	3.6	2.5

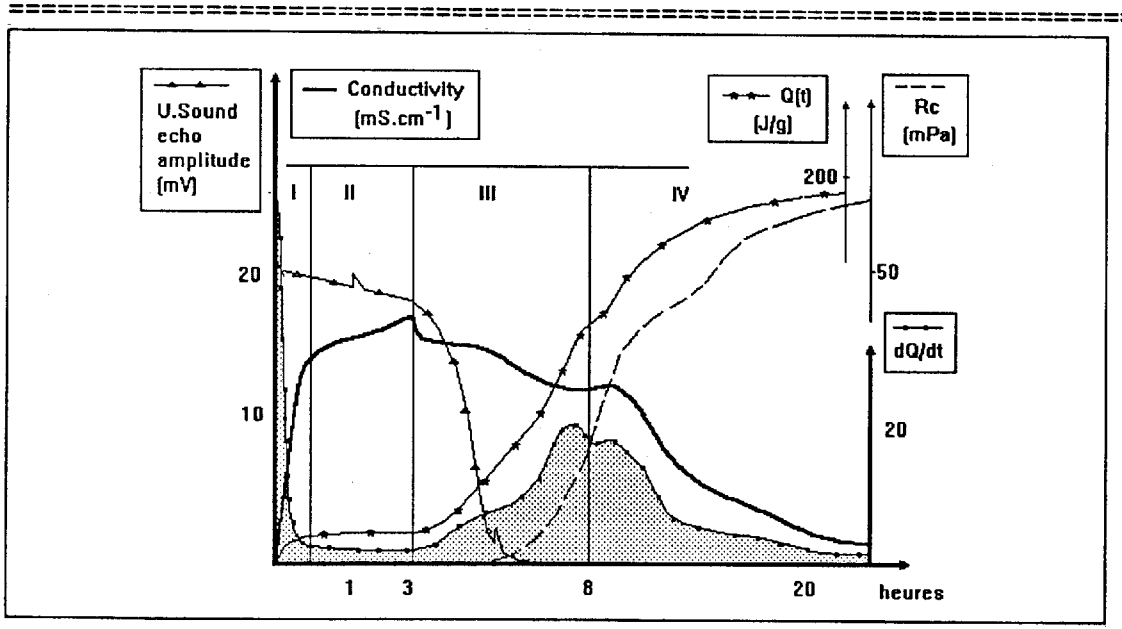

Fig.1 Mortar of concrete T. Hydration kinetics and mechanical evolution.

On the base of table 1, five concretes were made, taking five combinations of admixtures. The latter ones contained mixes of superplasticizers and a retarder (**table2**). A second set of concretes was formulated for high initial performances (**table 3**)

3 - RESULTS.

3.1. Kinetic behaviour of the concrete mortars.

fig. 1 and **fig.2** show the diagrams obtained for mortars T and U:

The conductivity and heat curves display typical singular points, clearly deciphering 4 main periods in the hydration sequence.

- During the initial stage, (I), the conductivity and heat rate increase rapidly, due to the high dissolution rate of cement. A little drop of the ultrasonic echo amplitude, due to ettringite and CSH formation is noticed.
- The dormant period, (II), is characterizzed by low heat rate and slow increase in conductivity, progressive lime supersaturation, and slow variation of sound amplitude.
- The setting or accelerating period (III) begins with the precipitation of portlandite, which acts as a trigger to activate the reactions. It is characterised by a conductivity maximum and an increase in heat rate. The electrical conductivity decreases, due to the water uptake. The sound echo amplitude decreases more rapidly, until the interconnexion of the whole grains is complete, corresponding to the end of setting. Then the heat flux increases faster.

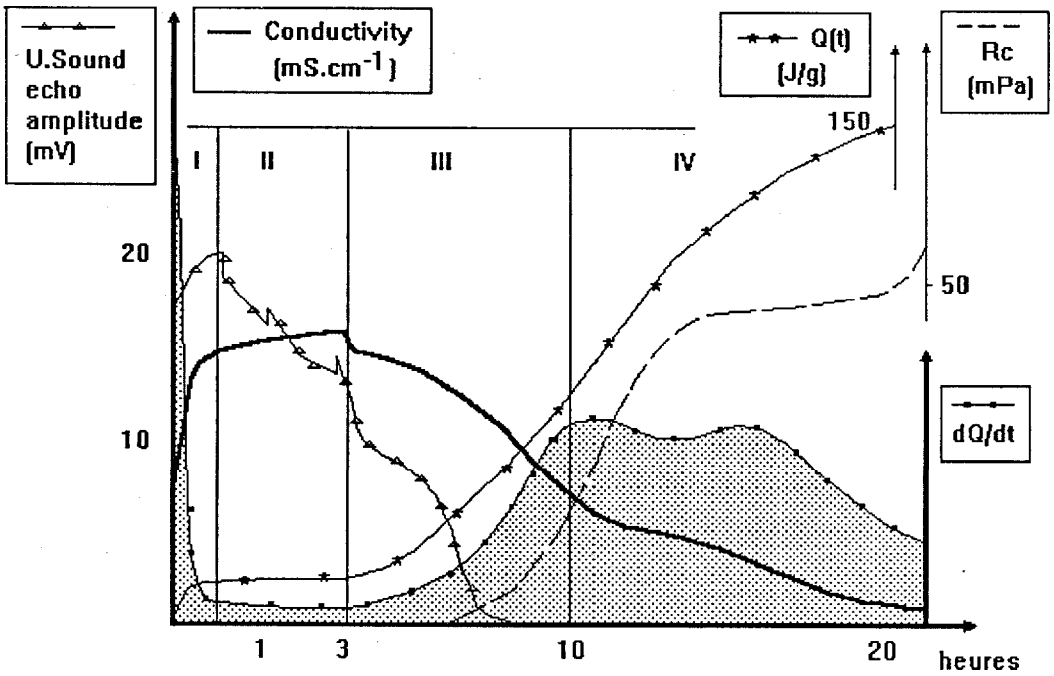

Fig.2 Mortar of concrete U. Hydration kinetics and mechanical evolution

The hydration reactions begin to fill the pores, and the strength becomes measurable, and increases rapidly.

- Then comes the hardening period (IV), from the gypsum depletion on. The alkalis from the C_3A's network are released into the solution, during the fast formation of monosulfoaluminate from ettringite and excess C_3A. This leads to an increase in conductivity or a variation of the slope. Because of its high enthalpy, the C_3A dissolution often gives a thermal peak superimposed on the "silicates" peak. In fact, when gypsum is in adequate proportions, its depletion is synchronized with the main silicates reaction (3) (optimum coupling). After the renewed C_3A hydration, a plateau or a slow down of the strength increase are generally observed, followed by a new increase.

The effect of the acccelerator in the T formula **(fig.1)** can be observed, and compared to the U behaviour **(fig.2)**. The dormant period is shorter in the former (1 h resp. 3h). The maximum setting acceleration takes place earlier for T than for U (about 7h, resp. 10h), and so the sulfates depletion (8h, resp. 15h), showing a strong interaction between the accelerator and the C_3A.

The superplasticizer effect can also be observed. When its amount is increased from 2.5% **(fig.1)** to 3.6% by weihgt of cement **(fig.2)**, the ultrasound echo remains higher during the dormant period, showing a better maintain of the fluidity.

The more striking experimental result obtained here is the existence of significant differences between the hydration heat and strength curves shapes. This also applies to the five mortars of the first set.

3.2. Mechanical yield of hydration.

For a detailed analysis of the mechanical evolution, we are lead to research a ratio giving the strength obtained for a given reaction yield, and we define the "**mechanical yield of hydration**":

$$r(t) = K(t)/Q(t) \qquad [I]$$

where, **Q(t)** is the hydration heat,

and **K(t)** is the strength evolution, normed using FERET's formula:

$$R(t) = K(t).\ c^2/(c+e+v)^2,$$

where R(t) is the strength, and c, e, v, resp., the volumes of binder, water, and entrained air.

The [I] formula then enables to compare rigorously the performances of the mortars, in function of time or of the hydration yield A(t). The latter can be obtained using:

$$Q(t) = A(t)*Q_f$$

where Q_f is the heat for complete hydration.

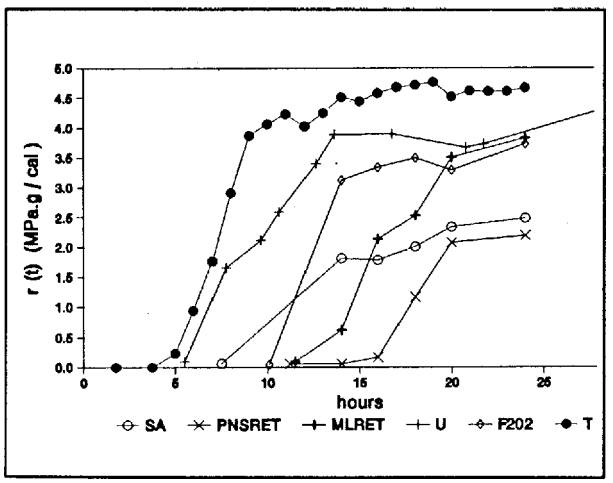

fig.3 Mechanical yield of hydration r(t), as a function of hydration time.

3.3. Results.

3.3.1. The evolution of r(t) versus time, compared for the two sets of mortars, is illustrated in **fig.3.**

The general shape of the curves indicate a non-uniform mechanical evolution kinetics: first the mechanical yield remains lower than measurable. Then it increases sharply during a few hours. The curves show afterwards a plateau or a slope change. Finally the mechanical yield continues to increase slowly. (The variations depicted here are significant, the incertainty on the strength values being of the order of magnitude of the size of the symbols on the graph.)

The nature and amount of admixture modify the time during which the yield remains null, the rate of the initial increase, the intermediate events, and the final value:
- some admixtures (T, U, F202) display a rapid increase and a high value bettweeen 10 and 24h. The MLRET formulation shows a smaller increase initially, but tends to match the last curves after 24h.
- the PNSRET and SA (without admixture) mortars show a lower yield.

- 3.3.2. Evolution of r(t) as a function of the hydration yield A(t)

The more striking result of this set of measurements is depicted by the points along the abcissa axis: with a number of admixtures, the mechanical yield remains close to zero, since the hydration yield is already significant **(fig.4)**.
For example, A(t)=0.22 for PNSRET at zero strength.

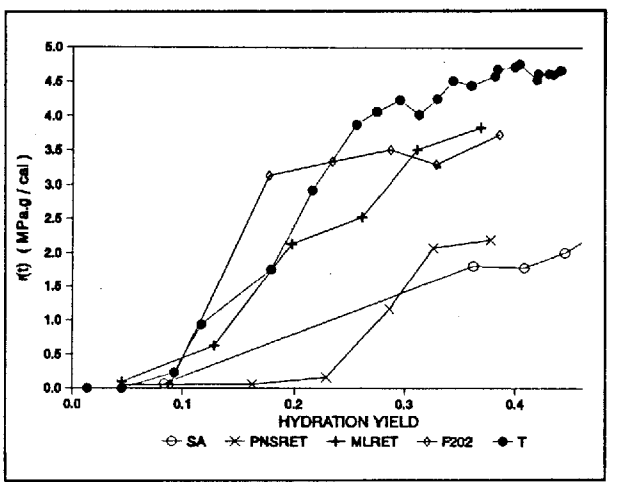

fig.4
Mechanical yiels of hydration r(t), as a function of hydration yield.

To obtain the same mechanical yield, (say 2 MPa.g/cal), the necessary hydration yields are:

0.15 (F202),
0.18 (T and MLRET),
0.32 (PNSRET), and
0.45 (SA=without admixture).

4 - ANALYSIS OF THE HYDRATION MECHANICAL YIELD FACTORS.

4.1 Factors of the mechanical yield

In agreement with the ideas of LE CHATELIER **(8)** and FREYSSINET **(9)**, confirmed by POWERS **(10)**, the hydration yield, represented by the heat release, lead to a mechanical evolution depending on the hydrates nature (adhesion), of their

arrangement around the grains (contact surface) and into the capillary pores. But Powers had observed that the strength is lower for C_3A-rich cements, than expected from the "gel/space ratio" model. To explain this deviation, we suggest to classify the phenomenons at a microscopic scale in two opposite groups.

(i) Phenomenons accounting for an increase of the hydration mechanical yield.

The "stick" formation is mainly concerned, namely hydrates like the CSH. Their amorphous structure enables the formation of a large number of "sticking points". The quantity of stick and its rate of formation are related to the chemical events.

(ii) Phenomenons accounting for a a decrease of the hydration mechanical yield.

In the absence of external agression of concrete, these are mainly related to the creation of micro-stresses:

- The chemical shrinkage or LE CHATELIER contraction, caused by a decrease of the molar volumes, attached to the hydration reactions. The "stick" production thus leads to autogenous stresses of thermodynamical origin.
- The self-dessication, wich increases for low permeability and water reduced concretes. It is caused by the uptake of the CSH water to make new internal hydrate, if free water is lacking.
- The structural expansion by crystals growth. The crystals can act as microjacks, and create an extra-porosity, pushing aside the walls in contact. This applies to portlandite and ettringite crystals, used for this purpose in expansive cements.
- The thermal volume variation, the importance of which is evident.

4.2 Structural consequences.

At the microscopic scale, strains are expected at each interface between CSH and rigid particles, like portlandite crystals and sand grains. Part of the hydrates will fill the microcracks generated when the local elastic limit is exceeded (auto-healing).

At the macroscopic scale, to some extent, contraction may exceed expansion in non-expansive cements. Shrinkage is the instantaneous resultant of these factors. A linear relationship between strength and chemical yield thus cannot be obtained before all the above mechanisms have reached a steady state.

4.3. Back to the results.

fig. 1 and 2, indicate that during the setting period, the healing rate is high enough to balance the expansion stresses. This can be related to the small size of crystals, with respect to the available space for their growth at this moment. On the contrary, the crystals expansion seems to be higher during the hardening period, since the crystals size are bigger and the pores become filled-up. This could explain the plateau of mechanical yield at this moment.

4.4. Role played by admixtures.

The tendency of admixtures to reduce the size and the crystallinity of ettringite **(10)** and portlandite is well established. The reduction of the structural expansion, and a subsequent enhancement of the hydration mechanical yield is then expected. Our results also seem to be indicative of a modification of the mechanical yield of the hydrates themselves, in the LE CHATELIER's view of adhesion.

- A first type of admixture seems to delay or accelerate the strength evolution simply by shifting the chemical events. In this case, the same hydration mechanical yield is expected to be found for the same chemical yield. (see the comparison of SA and PNSRET in fig.3 and 4).

- A second type of admixtures, not only shifts the chemical events (retarded F202 and MLRET, accelerated T and U), but also modify the mechanical yield, for the same chemical yield.

This leads us to assume an effect of these admixtures on the adhesivity of hydrates, by a modification of either the nature of their adhesion bonds, or their surface of contact.

5 - CONCLUSIONS.

5.1. Practical consequences about strength prevision.

The use of an overall activation energy for cements has to be validated in presence of admixtures, when they reduce the coupling between aluminates and silicates reactions. In this case, two activation energies had to be calculated. But this

implies the determination of both the reaction enthalpies and reaction rates of the components, that can be tedious. An alternative method is the calculation of an overall activation energy in each step of the chemical sequence. This parameter can be measured on mortars extracted from the actual concrete formula, including admixtures, and using a set of isothermal monitorings.

5.2. Consequences for high performance concrete optimisation.

The concept of hydration mechanical yield leads to the following suggestions:
- a first approach is to reduce the autogenous internal stresses, i.e. researching a lower hydration yield of cement for a given strength. This is limited by the possibilities of water-reduction. A second limit is due to self-dessication, which tends to increase when the cement/water ratio is over the stoichiometric value
- a second approach is to reduce the internal stresses by an improved distribution at the microscopical scale. This role can be played by fine particles and admixtures enabling the reduction of the crystals size.
- a third way could be the enhancement of the adhesion of hydrates, by increasing the amount of the most effective ones (CSH), and/or their chemical linkage.

REFERENCES.

(1) IDORN M. POULSON E. ANDERSEN B.; THAULOW N.; "Contemporary concrete technology urgently needed for modern constructions."
ASCE, NEW YORK, May 1981, 81-131.

(2) REGOURD M.; GAUTHIER E.; "Comportement des ciments soumis au durcissement accéléré."
Ciments, Bétons, Plâtres et Chaux, N°725, 4/1980, pp 240-249.

(3) VERNET C. "Conduction calorimetry and hydration kinetics - A thermodynamical and analytical approach of the interactive behaviour of cements."
8th International Congress on the Chemistry of Cement, 1986, RIO DE JANEIRO, Theme 2, Vol 3, pp 64-69.

(4) VERNET C.; NOWORYTA G.; "Conductometric test for cement-admixture systems."
9th. International Congress on the Chemistry of Cement, NEW DEHLI, 1992, Theme III, sub-theme II-D.

(5) BUIL M. These de doctorat, L.C.P.C., 1979.

(6) PARROT L.J.; GEIKER M.; GUTTERIDGE W.A.; KILLOH D. "Monitoring portland cement hydration : comparison of methods."
J.C.C.R., Vol 24, pp 919-926, 1990.

(7) BOCQUET M.; MOREAU M.; PELLETIER J.L.; Sonde ultrasonique à relais.ENSAM, Paris. Brevet français déposé en 1983, étendu à la CEEE et aux pays d'Amérique du nord en 1984.

(8) LE CHATELIER Henri; "Recherches expérimentales sur la constitution des mortiers hydrauliques." Paris, 1904, DUNOD ed., pp 88-96.

(9) FREYSSINET E. in "Science et Industrie", Jan 1933, p 3
and also in "Accélération de la prise et du durcissement des liants hydrauliques par la chaleur.", Commentaires faisant suite à l'exposé présenté par J.BROCARD le 15/06/1948 à l'ITBTP.
Annales de l'ITPTP, Dec.1948, N°54, pp 20-23.

(10) POWERS T.C.; BROWNYARD T.L.;
J. Am. Concrete Inst., 18, pp 101-249 (1946)

(11) BAUSSANT J.B. Thèse de doctorat, UFR des Sciences et Techniques de l'Université de Franche-Comté, 1990, N°156.

KINETIC AND THERMODYNAMIC INTERPRETATIONS OF HYDRATION AND HARDENING OF PORTLAND CEMENTS AND THEIR MINERALOGICAL CONSTITUENTS

I Teoreanu, Marcela Muntean and A Volceanov

Polytechnic Institute Bucharest, ROMANIA

SUMMARY

Reaction free enthalpy is used as measure of water reaction intensity of mineralogic constituents of clinker and respectively, Portland cements. In this way it is outlined the dependence of hydration degree of the minerals within clinker and cements on reaction free enthalpy for several periods. For normal Portland cements and for their basic constituents the mechanical strengths are also depending on reaction free enthalpy. The alteration of the above mentioned dependences versus time has provided information about the influence of binder nature upon intrinsic mechanical properties of the hardened system. Kinetic models were suggested for hydration process lime-development of mechanical strengths for the studied systems, during their hardening properties.

RESUME

L'enthalpie libre de reaction est utilisée comme mesure de l'intensité d'interaction avec l'eau des constituants mineralogiques du clinker et respectivement des ciments portland. On met en evidence, ainsi, la dependence de la grandeur l'enthalpie liber de reaction au degré d'hydratation des minéraux de clinker et des ciments pour différents délais d'hydratation. Pour les ciments portland et aussi pour leurs constituants, les resistences mécaniques sont aussi dependantes d'enthalpie libre de reaction. La modification pendant le temps des dependences mentionnées a fourni des informations concernant l'influence de la nature du liant pour les proprietes mécaniques intensèques du système endurci. On a été suggérés les modeles cinétiques du proces d'hydratation et aussi pour le developpment pendant le temp aux resistences mecaniques des systèmes analysés pendant l'endurcissement.

INTRODUCTION.

The magnitude and development of mechanical strengths of mineral binders, during hardening, depend essentially on their nature and reactivity, reflected by the rate of their reaction with water, the rate of formation and the nature of the hardening structures. For binders from the same family - particularly Portland silicate binders - with main hardening structures of the silicate type, the final role for mechanical strengths evolution, their values of different periods of hardening and for comparable conditions of production, hardening and testing, is defined by the reactivity of the binder. A measure of reactivity is the free enthalpy value for the reaction with water, considered order standard conditions ($\Delta^r G^o_1$).

The present work deals with the examination of several relations such as degree of hydration - hydration free enthalpy, mechanical strengths - hydration free enthalpy, for different periods, for both monomineral binders and mixtures of Portland cement minerals, respectively Portland cement clinkers. Also, kinetic models are suggested, for the cases studied, in order to describe the evolution of hydration degree. Statistical analyses have been developed to investigate these relations.

EXPERIMENTAL PROCEDURE AND CALCULATIONS.

Monominerals of Portland cement were obtained by solid state reactions: C_3S, β-C_2S, C_4AF, C_3A. These minerals as well as their mechanical mixtures, respectively Portland clinkers were studied in terms of their hydration degree and mechanical strengths (Kuhl microsamples) for different periods of hydration - hardening. Table 1 shows the minerals, compositions and standard values of hydration free enthalpy corresponding to the investigated binders. Comparison of the determined hydration degree (α) and mechanical strengths (R_c) versus hydration standard free enthalpy has been achieved using the calculation methodology proposed by Egorov et al. [1] and used by them to outline and interpret the correlation $R_c = f(\Delta^r G^o_1)$. According of reaction standard free enthalpy have been performed using relation:

$$\Delta^r G^o_1 = \Delta^r G^o_{C_3S} + \Delta^r G^o_{C_2S} + \Delta^r G^o_{C_3A} + \Delta^r G^o_{C_4AF} \qquad (1)$$

where, $\Delta^r G^o_{C_3S}$, $\Delta^r G^o_{C_2S}$, $\Delta^r G^o_{C_3A}$, $\Delta^r G^o_{C_4AF}$ denote standard free enthalpy for hydration reactions of C_3S, C_2S, C_3A and C_4AF (where, C=CaO, S=SiO_2, A=Al_2O_3, F=Fe_2O_3); these values have been established based on information from [2], using the equations (see [1]):

$$\Delta^r G^o_{C_3S} = -0.0725\ (\%\ C_3S)\ ;\ \Delta^r G^o_{C_2S} = -0.0100\ (\%\ C_2S)\ ; \qquad (2)$$

$$\Delta^r G^o_{C_3A} = -0.1543\ (\%\ C_3A)\ ;\ \Delta^r G^o_{C_4AF} = -0.0878\ (\%\ C_4AF)\ \text{kcal/100 g}$$

Data on degree of hydration were worked out according to the diffusion model proposed by Turriziani and coworkers [3] :

$$\alpha \sim \sqrt{\lg t} \qquad (3)$$

On the processing and interpretation of data, use has been made even of the data from literature as follows: [1] - for mechanical strengths and [4,5] - for degree of hydration of Portland cement minerals for long periods of time (including the results previously obtained by some of autors [6]).

Table 1

No.	Indicator	Composition	$\Delta^f G_1^o$ kcal/100 g	No.	Indicator	Composition	$\Delta^f G_1^o$ kcal/100 g
1.	C_3S	Tricalcium silicate	7.25	8.	AC_2	50% C_3S + 10% β-C_2S 30% C_3A + 10% C_4AF	8.50
2.	C_2S	β-dicalcium silicate	1.00	9.	AC_3	65% C_3S + 15% β-C_2S 10% C_3A + 10% C_4AF	7.28
3.	C_4AF	Tetracalcium ferro-aluminate	8.78	10.	AC_4	15% C_3S + 50% β-C_2S 25% C_3A + 10% C_4AF	6.32
4.	C_3A	Tricalcium aluminate	15.43	11.	AC_5	40% C_3S + 40% β-C_2S 10% C_3A + 10% C_4AF	5.72
5.	AS_1	80% β-C_2S + 20% C_3S	2.25	12.	CA	clinker with a potential mineralogical composition similar to AC_3 mixture	7.28
6.	AS_2	60% β-C_2S + 40% C_3S	3.50	13.	CB	item with AC_5	5.72
7.	AC_1	55% C_3A + 35% C_3S + 5% β-C_2S + 5% C_4AF	11.51				

RESULTS AND DISCUSSION.

The interaction process with water, in paste, of Portland cement minerals as well as their mixtures (including clinkers) exhibits an accelerating period followed by a slow one (called "induction period"), the latter being longer when binder activity - indicated by its hydration standard free enthalpy ($\Delta^r G_1^o$) - is more reduced. The kinetics of the process, for the accelerating period is conveniently described by a diffusion model [3] (previously reported by the authors [6]). The transformation rates of C_3S and C_4AF remain, during this period, at quasisimilar values provided that the induction period of the latter is somewhat longer and its degree of hydration is, at the beginning of the accelerating period, somewhat more reduced. Obviously different behaviours and in opposite directions are exhibited C_3A and β-C_2S. As expected, mixtures of calcium silicates richer in β-C_2S (AS_1 and AS_2 compositions) show an intermediate behaviour, but closer β-C_2S as the content of this component is larger (Fig.1.a.). At the same time, it is to be noted that a mixture of 50% C_3S, 30% C_3A with only 10% β-C_2S and 10% C_4AF, respectively, showed a hydration degree, in time, closer to C_3S although there is a larger amount of C_3A (Fig.1.b).

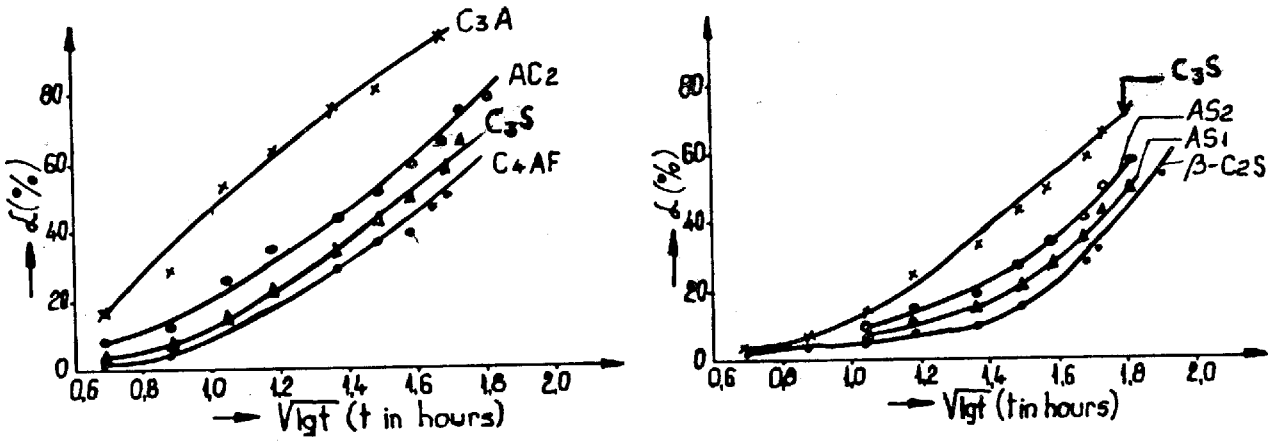

Fig.1. Hydration degree vs.time for mineralogical constituents of Portland cement and for the corresponding polymineral mixtures

Similar findings as in the case of hydration kinetics were obtained for the kinetics of mechanical strength development on hardening of the individual mineralogical components of Portland clinkers, and their mixtures or clinkers (Fig.2.); the latter taking into account the simultaneous effects of both reaction intensity and the development spatial structures of on specific mechanical characteristics, themselfs, in turn, dependent on hydration-hydrolysis process rates and the nature of the hydrated formations.

Figure 2 shows that for long hardening periods of time, the silicate structures formed tend to achieve higher strengths than the base aluminate structures and tend to even superior strengths when they proceed from β-C_2S hydration than from C_3S hydration (considered for long periods of hardening), may be to the higher polycondensation degree of the hardened structures, for the same hydration degree. In other therms, for the same hydration degree, the base aluminate structures have lower mechanical strengths than the silicate ones and the latter have higher strengths when result his from β-C_2S interaction with water than from C_3S hydration, see Figure 3 (the upper limits of a for β-C_2S and C_4AF were under 60%).

For binding systems with preponderant silicate minerals, when the amount of C_3A and C_4AF do not exceed 30%, the hydrosilicates (whatever their origin - see [1]) are essential for the mechanical strengths "design" of the hardened binding systems. On this basis for these types of binders a unique relation $R_c = f(\alpha)$ is suggested and which is statistically acceptable. A one such relation shown in Figure 4; it is linear for values between 5 and 75 % for the hydration degree.

Basing on previous data on hydration kinetics, one can justify not only the correlation of induction period with $r_{G_1}^{0}$ but with the hydration degree too, at least for mixtures with preponderant silicates content and for certain periods of hydration.

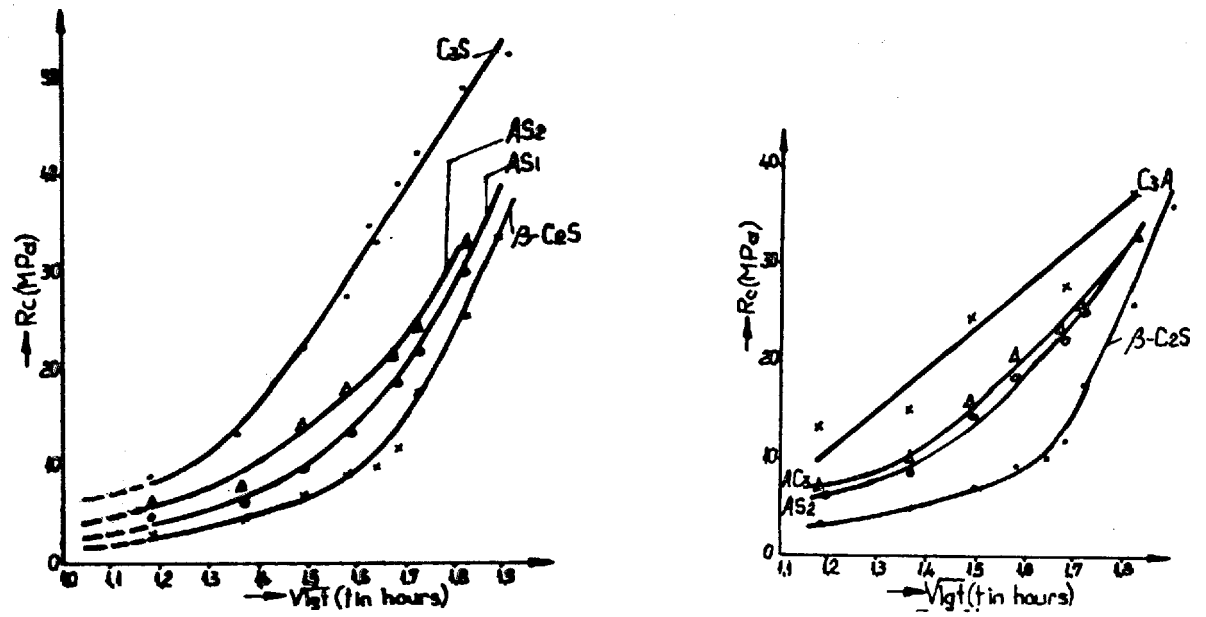

Fig.2. Time dependence of the mechanical strengths developed by the mineralogical constituents of Portland cement and of polymineral compositions respectively

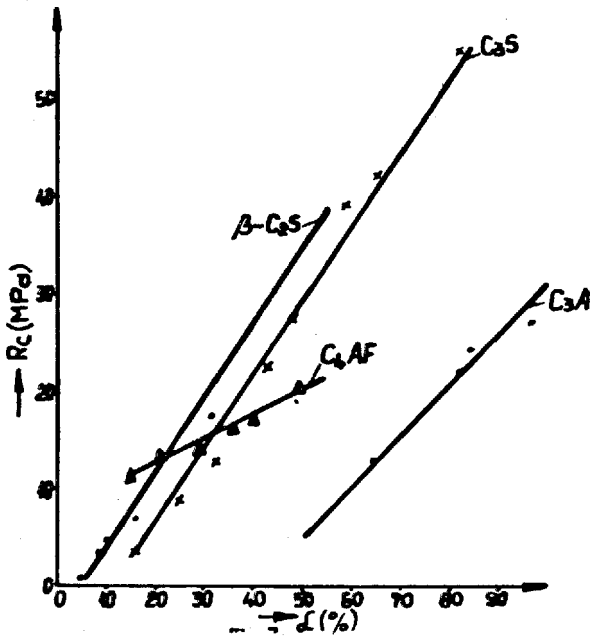

Fig.3. Mechanical strength vs. hydration degree for mineralogical Portland cement constituents.

Although the kinetics of hydration processes can be described by similar diffusion models for the greatest part of their development, the difference in the nature of mineral components suggests that specific mechanisms will depend on this nature. This assumption can explain why C_4AF having a value for Δ^rG^o greater than of C_3S (Table 1) exhibits for the hydration degree lower values for periods of the process (t > 28 days). As a result, if one tries to correlate the values of hydration degree (α) with Δ^rG^o, the data obtained for C_4AF do not show the same dependence as in the case of the other binders; this finding is to be somewhat valid for C_3A, too. Silicate minerals, like mixtures of minerals and clinkers with of majority content of silicates, have values for Δ^rG^o between 1 kcal/100 g for β-C_2S and 8 kcal/100 g for aluminosilicate mixtures (clinkers).

For these binders, which have the standard hydration free enthalpy in 1 - 8 kcal/100 g range, linear correlation between α and Δ^rG^o (see Fig.5) has been established for both short hydration periods (3 hours) and long periods (up to 90 days).

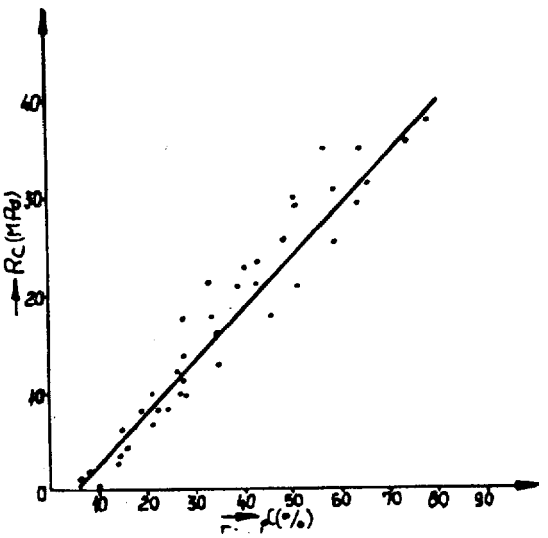

Fig.4. Mechanical strength vs. hidration as degree at silicate binder hardening

The increase in slope of the variation lines, with increases in hydration time , corresponds to the transition from the induction to the accelerating period of the hydration process; for periods over 3 days the slope does not change anymore. High aluminates content mixtures show for periods under 7 days , values for the hydration degree larger than given by the linear correlation $\alpha = f(\Delta^r G_1^o)$ for $1 \leq -\Delta^r G_1^o \leq 8$.

This behaviour can be explained by the rapid hydration of the C_3A so that it is hydrated more than 80 % after 7 days. For longer hydration periods, the unhydrated mixture becomes relatively poorer in aluminates and rich in silicates than the initial mixture, so that it becomes similar to the binders characterized by $\Delta^r G_1^o$ values between 1 - 8 kcal/100 g ; the relation $\alpha = f(\Delta^r G_1^o)$ is linear over the entirer $\Delta^r G_1^o$ domain as it is shown in Fig.5. The differences of behaviour as for higher C_3A content compositions are so much the more accentuated as the process duration is shorter, that is when contribution of C_3A hydration is more important.

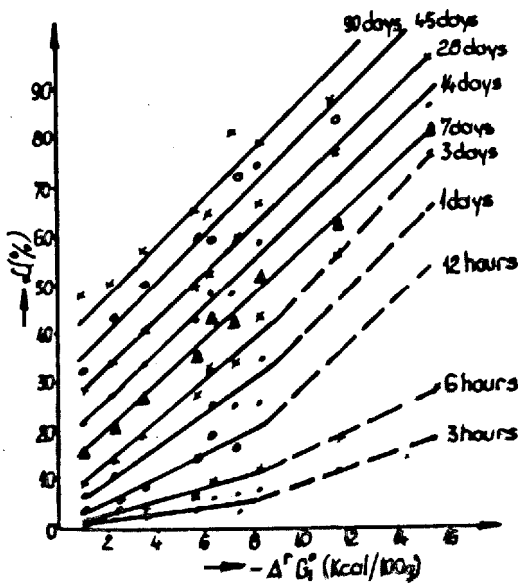

Fig.5. Hidration degree vs. standard free enthalpy

The linear dependence of hydration degree with binders reactivity, for $-\Delta^r G_1^o$ between 1 and 8 kcal/100 g can be extrapolated for the mechanical strengths developed by the binders during hardening.

Silicate compositions show that, up to certain hardening periods, the mechanical strengths developed increased with $\Delta^r G_1^o$ (see Egorov et.al.[1]), demonstrates in fact the present work for a much larger compositional spectrum and consequently for larger limits of hydration standard free enthalpy, i.e. $1 \leq -\Delta^r G_1^o \leq 8$ kcal/100 g (fig.6); above the upper limit of standard free enthalpy the mechanical strengths of binding compositions, preponderant of aluminate type, do not increase anymore for periods up to 14 days or

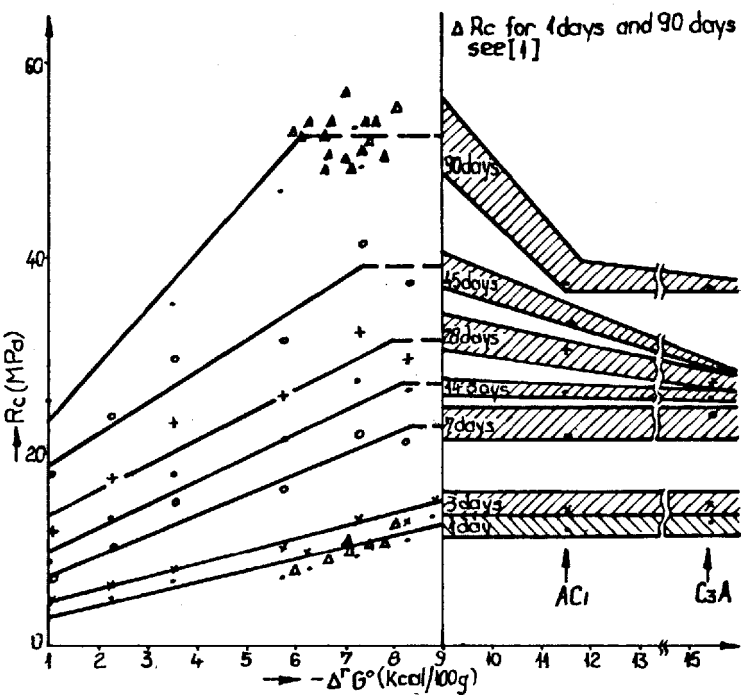

Fig.6. Compressive strengths vs. standard free enthalpy for different hardening periods.

tend to decrease for larger periods of time. For the range $1 \leqslant -\Delta^r G_1^o \leqslant 8$ kcal/100 g a linear dependence between R_c and $\Delta^r G_1^o$ is established, corresponding to a hardening period of 1...28 (45) days (Fig.6). Statistical analysis of the data shows very good correlation coefficients. The results are in good agreement with those reported and interpreted in [1].

For a 90 days hardening, a such dependence is no longer evident, at least for more active binders characterized by a 6 to 8 kcal/100 g standard free enthalpy ($-\Delta^r G_1^o$). The development of the mechanical strengths of the binders, particularly for the most active of them is considered to be determined to a great extent by the structural phenomena, i.e. development of crystallization - polycondensation structures and not by the interaction with water, whose intensity in real terms is measured through the standard free enthalpy ($\Delta^r G_1^o$).

REFERENCES

1. G.B.Egorov et al., Tsement, 86 (8), 10 (1987).
2. V.I.Babushkin, G.M.Matveev, O.P.Mchedlov-Petrosian., Thermodynamics of silicates., Heidelberg Springer Verlag., (1985).
3. R.Turriziani, A.Rio, M.Collepardi., Ind.Ital.Cem., 35 (10), 635 (1965).
4. Iu.M.Butt, L.N.Rashcovich., Tverdenie viajushcih pri povishenih temperaturah., Gostroizd., Moskva (1965).
5. D.L.Kantro, S.Brunauer, C.H.Weise., J.Phys.Chem.,66, 1804 (1962).
6. I.Teoreanu, Marcela Muntean., Silicat.Ind., 39 (2), 49 (1974).

THERMOCHEMICAL AND KINETIC ANALYSIS OF HYDRATION

LI Jian—XI

Wuhan University of Technology
Wuhan, P R CHINA

SUMMARY

In this paper, hydration of C_3S is reviewed and investigated in terms of kinetics and thermochemistry. A simpler procedure for kinetic evaluation is developed and results of the study on the effect of psd and shape of cement particles on the rate constants are presented. Kinetic studies confirm that the rate--determining process is mainly boundary reaction for hydration of alite in cement but diffusion plays a important role in hydration of pure C_3S. The rate constants obtained run from 0.02-0.05 $\mu m.h^{-1}$.

摘　　要

本文从动力学及热化学的角度对C_3S的水化进行了研究，并对C_3S水化机理进行了讨论，提出了一种较为简单的动力学计算方法。其中同时考虑了多颗粒及颗粒形状对动力学的影响。并给出了一种动力学计算中颗粒形状校正的方法，动力学的研究表明，对于阿里特而言，水化早期速率的控制主要是界面反应，对纯C_3S，扩散反应起较大作用。反应速率常数约在0.02--0.05 $\mu m.h^{-1}$范围内。

INTRODUCTION

The mechanism and kinetics of hydration of cement phases have been extensively investigated. Twokinds of theories on C_3S hydration, namely the "protective layer" and the "nucleation and growth", were suggested by most investigators. The effects of psd on the hydration and the kinetics of C_3S, and cement, have been increasing emphasizeed, [1], [2] and some procedure for the kinetic calculation for C_3S have been derived too. A. Bezjak et. al[1] had developed a procedure to evaluate the rate constants for those hydration processes where the overall advance of the reaction is determined by different rate laws in polysize specimens. However, in order to obtain procedures for evaluation of actual rate constants, the effects of psd as well as the shape of powder are of equal importance. Inthis paper, some aspects of C_3S hydration bave been reviewed and analyzed from the kinetics and thermochemistry. A new mechanism of C_3S hydration is discussed. Based on this, a kinetic procedure is developed, in which the effects of both psd and shape of particles are considered.

THEORETICL PART

Spherical model

All investigators believe that the hydration process of C_3S or alite is composed.of a series of conversion of C_3S hydrates, i. e.

$$CSH(\text{I}) \longrightarrow CSH(\text{II}) \longrightarrow CSH(\text{III}) \qquad (1)$$

which manifest many complex phenomena. Fox example, CSH(I) is believed to relate to induction period whereas its conversion to CSH(II) falls under the acceleratory period, which corresponds to the se cond peak in the dQ/dt vs t curve. In terms of "protective layer" mechanism, the "induction period" is caused by the lower permeability of CSH(I). A.Bezjak et.al [1] developed an expression including both resistances due to interaction and diffusion processes:

$$\frac{d\alpha}{dt}\left(\frac{1}{Ki}+\frac{Z}{D_{yz}}+\frac{\delta}{D_y}\right)-\frac{m_o}{P_t}=M\cdot\psi\cdot C_{ty} \qquad (2)$$

where m_o denotes the original mass of C_3S; Pt, the surface area of unhydrated residue at time t; Z, the depth of hydration; K_i, the rate constant of surface interaction, as shown in Fig.1,(a). If

$$K_{\text{I}}=\frac{\rho}{M\cdot\psi\cdot C_{ty}}\left(\frac{1}{K_i}+\frac{\delta}{D_y}\right)$$

and $$K_{\text{II}}=\frac{\rho}{2M\cdot\psi\cdot C_{ty}},$$

$$dt=\frac{d\alpha(K_{\text{I}}+2K_{\text{II}})\,m_o}{Pt\cdot\rho} \qquad (3)$$

where ρ is the intensity of C_3S, K_{I} and K_{II} are function of D_y, D_{yz} and C_{ty} and they will change when the hydrate phase transition occurs. A set of K_{I} and K_{II} will characterize the feature of hydration controlled by interaction and diffusion (or I/D) mechanism in a certain period, so that the "protective layer" theory can be briefly represented by:

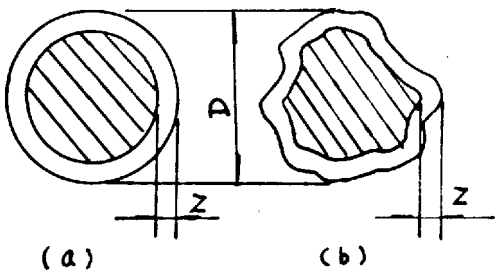

FIG.1 Comparison of spherical particle with a non-spherical one of the same diameter D,

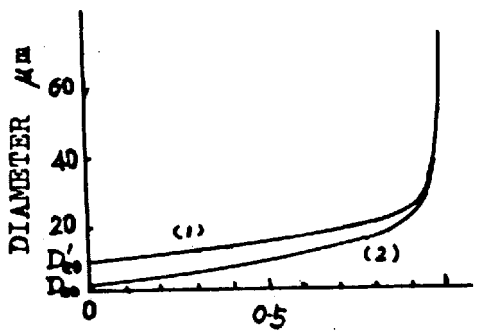

FIG.2 De-a interdependence.(1) -Spherical model, (2)-Nonspherical model.

$$(K_I, K_{II}) \rightarrow (K'_I, K'_{II}) \rightarrow (K''_I, K''_{II}) \quad (4)$$

For spherical model:

$$P_t = 3 m_0(1-\alpha)/\rho . R^{2/3} \quad (5)$$

and $$Z = R[1-(1-\alpha)^{1/3}] \quad (6)$$

by insertion into to Eq. 3 and integrating it when $t_0 \neq 0$ $Z_0 \neq 0$, we get:

$$t - t_0 = K_I(Z-Z_0) + K_{II}(Z^2 - Z^2_0) \quad (7)$$

or $$(t-t_0)/(Z-Z_0) = K_I + K_{II}(Z+Z_0) \quad (8)$$

If we plot $(t-t_0)/(Z-Z_0)$ vs $(Z+Z_0)$, a straight line will be obtained, of which K_I is the intercept and K_{II}, the slope. If $K_I = 0$, the rate--determining process is diffusion and $K_D = 1/K_{II}$. If $K_{II} = 0$, the rate--determining process is boundary reaction and $K_i = 1/K_I$. If $t_0 = 0$, $Z_0 = 0$. We can also get:

$$t_0 = K_I Z + K_{II} Z^2 \quad (9)$$

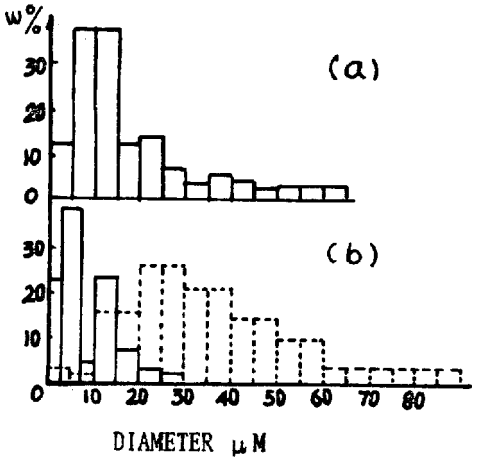

FIG. 3 Diagram of psd (Huaxin Cement). (a) Original cement H; (b) Separated sample H
———, the fine part H_1,
·····, the coarse part H_2

Ploting t/Z vs Z, K_I and K_{II} can also be evaluated in the same way mentioned above. t/Z reflects the hydration rate. When t/Z increases it indicates a decrease of hydration rate, and when it decreases, an increase.

For a polysize system, as seen from the Eq 10, Z is a variable, independent of R, so that if t, K_I and K_{II} are fixed, Z of particles of various sizes will hold constant. It will be found convenient for kinetics of a polysize system to introdrue "equivelent degree radius" Re. A spherical particle with an original radius Re has a hydration degree α_e equal to the mean α of the system at time t. According to this definition and the independence of Z from R we get:

$$Re = \frac{Z}{1-(1-\alpha)^{1/3}} \quad (10)$$

$$\alpha = \sum wi . \alpha_i = \sum wi[1-(1-Z/Ri)^3] \quad (11)$$

If psd is known, the relationships between α, Re (or De) and Z can be derived. For example, a relationship of De-α with psd of the sample H determined by us is given in curve (1) of Fig. 2 and Fig. 3. If a practical α (corresponding to α) is known, De and Z can be got from the and De- α curve and using Eq. 9 or Eq. 10, K_I and K_{II} can be obtained. If K_I and k_{II} are known in advance, α is predicatable.

Non-spherical model

For a C_3S particle of any shape with a specified original diameter D which can be defined in many ways, e. g. the maximum diameter, Stockes diameter, etc, if its specific surface of the unhydrated residue at time t is St, the α-z relationship can be:

$$d\alpha = \rho P_t \, dz/m_0 \quad (12)$$

and $$P_t = (1-\alpha) m_0 S_t \quad (13)$$

so that $$d\alpha = \rho(1-\alpha)S_t \cdot dZ \quad (14)$$

If S'_t denotes the specific surface of the unhydrated residue of the corresponding spherical particle with an original diameter D which is equal to the specified D of the non-spherical

Table 1 Mean Sphericity ϕ

	Blaine (cm^2/g)		
	Ho	H1	H2
S'o	2179.4	5843.3	1137.0
So	5076.94	17037.4	1415.17
ϕ	0.4293	0.3430	0.8034

particle, seen in Fig.1,(b), sphericity ϕ_t can be denoted S'_t/S'_1 .Thus we get:

$$S_t=S'_t/\phi_t=3/\phi_t\ (R-Z) \tag{15}$$

$$\frac{d\alpha}{dz}=3(1-\alpha)/\phi_t(R-Z) \tag{16}$$

In general ϕ_t varies with reaction time, but by assuming that the shape of the particle is retained through the hydration as is also ϕ_t, a constant ϕ, shown in Fig.1, Eq.9 can be integrated whereupon we arrive at :

$$(1-\alpha)^{\phi}=(1-\frac{Z}{R})^3 \tag{17}$$

This is a basic equation for the non-spherical model. When $\phi=1$, it reverts to the spherical model. It can be proved that the agreement of Eq. 17 with the values practically determined is very good. In a polysize system Eq.10 becomes:

$$(1-\alpha)^{\phi_i}=(1-\frac{Z}{Ri})^3 \tag{18}$$

where ϕ_i is the sphericity of particles with specified original diameter D_i. The mean degree α is :

$$\alpha=\sum wi.\ \alpha_i=\sum Wi\,[1-(1-\frac{Z}{Ri})^{\phi i/3}] \tag{19}$$

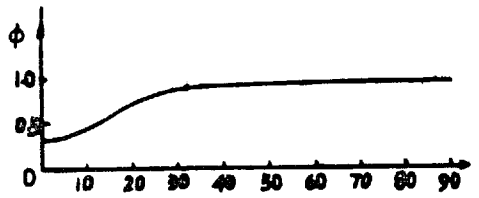

DIAMETER μM

FIG.4 Relationship beween ϕ and D

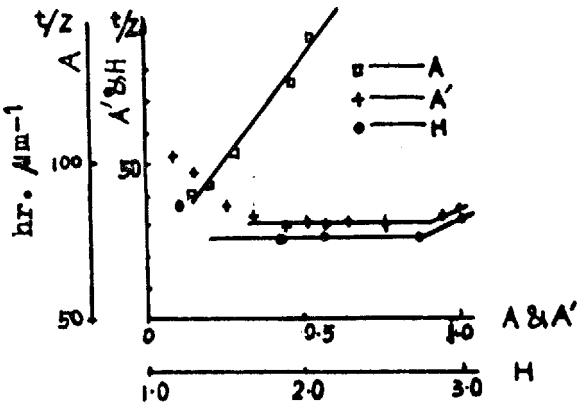

HYDRATION DEPTH μM

FIG.5 Kinetic curve

where $\alpha_i=1$, if $Ri<Z$. The definition of De in spherical model holds here, so the De-α in non-spherical system can also be evaluated by Eq.10, and Eq.19 in the same way as above from the spheric model. The curve(2) in Fig .1 is a morphology corrected De-α curve with the same psd as curve(1) .There are a great difference between the two curves but the shape of them are very similar so that we can obtain the curve (2) in a simplified way in which the curve (1) is parallelly shifted down to the point where Deo is $6/S_o.\rho$. In this way the determination of ϕi can be left out. S_o is the experimentally determined specific surface of the system, and D'_{eo} , D_{eo} are equivelent degree diameters of the spherical and the non-spherical models when $\alpha=0$. When substituting Eq.12 into Eq.3 and integrating it, we get also Eq.8 (or Eq.9. if $t_0=0$, $Z_0=0$). This means that all the calculating processes for kinetics in spherical model hold in a non-spherical model also.

EXPERIMENTAL PROCEDURE

A large number of kinetic data of α-t on C_3S or alite in cement and the psd have been reported by many anthors[1]. A cement sample H from Huaxing plant in China was used in our studies.The phase composition of the clinker was calculated after chemical analysis. C_3S 65.40, C_3S 8.09, C_3A 7.34, C_4AF 10. 64 and f cao 1.01.This cement contains 5% gypsum and 10% furnace slay, which were ground in a circuit mill system in the plant. The determination of psd was carried out in Micron Photo Sizer SKC-2000. The cement was size graded into two grades in a particularly made cyclone in order to determine ϕ_i shown in Table 1 and Fig.3 and 4. The sample was paste-hydrated at w/c=0.4 at 20℃ . After various ages randing from 4 hours to 10 days the specimens were ground, washed with aecohol (water free), dried in vacuum and examined by x-ray diffraction.

According to Eq.10,18 and 19,as well as psd and ϕ_i determined, the De-α curve is obtained, seen curve(2) in Fig.1, and the values of Z and t/Z of various ages can also be evaluated, shown in Table 2. Plotting t/Z vs Z, a straight line is obtained after 10 hours (Z=0.257mm) as shown in Fig 5,

$K_I = 26.23$ and $K_{II} = 0$. The control step is mainly the boundary reaction with a rate constant of $K_i = 0.0381$($\mu m.h^{-1}$). After four days a conversion happens. As compared with the data α-t and psd from A. Bezjak et all [1], similar patterns are obtained and shown in Fig .5 and 6. The hydration rates of the pure C_3S of samples A and C are controlled by I/D process but those of sample A', C' and alite in cement are controlled by boundary reaction only. The sample C' in Fig 7 showing a horizontal line during 14-32hr, undergoes a conversion at about 32 hours. If $t_0 = 32hr$, $Z_0 = 0.8939 \mu m$, plotting $(t-t_0)/(Z-Z_0)$ vs $Z+Z_0$, another horizontal line is obtained seen in Fig.6, which indicates that the reactivity is decreased after t=32hr, and the conversion occurring during the progress of C_3S hydration would not necessarily be one from boundary reaction to diffustion - controlled process. The results are shown in Table 3.

DISCUSSION

A typic curve of t/Z vs Z, has a conversion point (tc, Zc). In the period of t< tc, the hydration rate increases with time, therefore the hydration process is not controlled by I/D, until tc. A possible explaination is that the process is controlled by the "nucleation and growth" mechanism (or K_N). Fig.8. shows the α-t curves derived from the K_N mechanism. The rate-determining step is I/D after tc, so we get:

$$t - tc = K_I(Z - Zc) + K_{II}(Z^2 - Zc^2)$$

which means that the curve of t vs Z does not pass through the origin. For the sample H in the period 10hr~4 day, $K_{II} = 0$ so we have:

$$t = K_I Z + (tc - K_I Zc) \qquad (20)$$

But we obtain a straigt line pass through the origin when plotting t vs Z, seen in Fig.9. The other samples have also the similar features, which suggests a possible hydration model shown in Fig. 10. The two curves $\alpha(K_I, K_{II})$ intersect at t_c, but are not tangential to each other. For overcoming these difficulties, it will be very useful to assume; a) C_3S can be considered as a solid solutiln of C_2S and Cao . A local hydration occurs on C_3S Surface particularly at Ca-O-Ca bondings, after initial dissolution and wetting processes; b) The CSH (I) is made of monomeric silicate and $C/S = 2.0$-2.5 [3], [4]. The configuration is "C_3S-like" [3] i.e. some Ca^{2+} ions in C_3S are replaced by H^+ ions (happening largely at the Ca-O-Ca bondings) and the other ions will remain almost unchanged. The deduction are that the IR spectra of SiO_4^{4-} tetrahedra and x-ray diffraction property and many other properties of CSH(I) are very similar to those of C_3S. So a normal measuring instrument may not be sufficiently sensitive to the change from C_3S to CSH (I); c)The conversion from CSH(I) to CSH(II) is controlled by nucleation and growth mechanism and happens simultaneously in various sized particles owing to the same physicochemical conditions. And so does the CSH(II)to CSH (III) conversion; d) C_3S liberates heat in two steps in the progress of hydration:

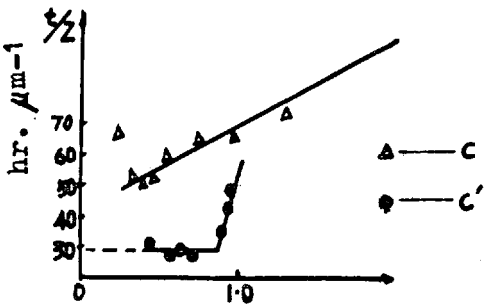

HYDRATION DEPTH μM
FIG.6 Kinetic curve.

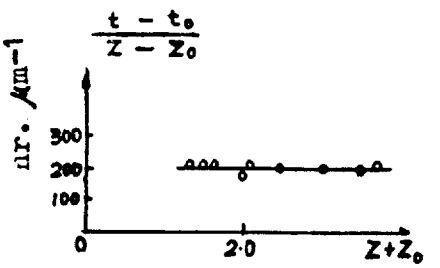

HYDRATION DEPTH μM
FIG.7 Kinetic curve

$$C_3S + nH_2O \xrightarrow{\Delta H_1} CSH(I) + Ca^{2+} + 2H^-_{aq} \xrightarrow{\Delta H_2} CSH(II) + mCH \qquad (21)$$

According to the assumptions, we can see that there are two kinds of hydration rates; a) the formation rate of CSH(I), denoted by dZ/dt or $d\alpha(K_I, K_{II})$ machanism; b)the conversion rate of CSH(I) →CSH (II), denoted by dX/dt, which is detemined by nucleation and growth mechanism, or (K_N) , seen in Fig.11. dZ/dt is the actual hydration rate and dX/dt deals with the hydration rate practically detected by normal measuring meters e.g. the x-ray diffraction meter. At the first stage

of hydration (the induction period) dZ/dt > dX/dt, and Z>X. However dx/dt will increase as hydration progresses and then it will increase as hydration progresses and then it will exceed dZ/dt, so that X tends to approch Z, seen (a) and (b) in Fig.11. At time t_c when Z=X+△, △ only a very thin CSH(I) layer perhaps may remain in the whole hydration, dX/dt is limited by dZ/dt and the two rates become one after tc. In the whole process dZ/dt is controlled by (K_I, K_{II})

In terms of thermochemistry, acording to the assumptions, it is clear that during the induction period the heat evolution is mainly due to the formation of CSH(I) and $Ca^{2+}_{aq}+2OH^-_{aq}$. But in the acceleratory period when dX/dt is large enough, the heat evolution results from the following tow reactions:

$$Ca^{2+} + 2OH_{aq} + CSH(I) \xrightarrow{\triangle H_2} CSH(II) + CH \quad (22)$$

$$C_3S + nH_2O \xrightarrow{\triangle H} CSH(II) + mCH \quad (23)$$

The CSH(I) in Eq.22 is referred to that formed in the induction period. As can be seem from the asumptions, CSH(I) can be regarded as C_2S gel situated in the configuration of C_3S, thus the reaction heat $\triangle H_1$ and $\triangle H_2$ can be approximately evaluated. If the specific surface of CSH(I), or C_2S gel, is in the range 200-400 m^2/g[5] and the surface energy of C_2S is about 0.25 cal/m^2 [6], the forming heat of CSH(I) is about 534.52—534.13 kcal/mol and $\triangle H_1$ can be estimated in the range of -4.342～-12.955 kcal/mol, thus $\triangle H_2$=-12.955～-21.508 kcal/mol. (△H is -25.85 kcal/mol[6]). A heat evolution curve dQ/dt--t of pure C_3S was constructed from meaeurements made in a conduction calorimeter. Seen in Fig.13, Q1, Q2 and Q3 are cumulative heats evolved per gram C_3S in the initial(t_1), induction(t_2), and acceleratory(t_3) periods, and α_1, α_2 and α_3 the hydration degree respectively, υ (the mean dα/dt value during 0-t_3), which can be approximately regarded as a constant in the early period of hydration for I/D process, is then:

$$\upsilon = \frac{Q_3}{\triangle H_1 t_1 + \triangle H_2 (t_2 - t_1)} \quad (24)$$

$$= 0.02159 \sim 0.0229 g/gC3S.hr$$

where Q_3, t_2 and t_3 practically determined are -30.80cal/gC_3S, 2.19hr and 13hr. The corresponding rate constant Ki is about 0.02537-0.02694 $\mu m.hr^{-1}$ which agrees with the experimentally determined values of pure C_2S hydration before.

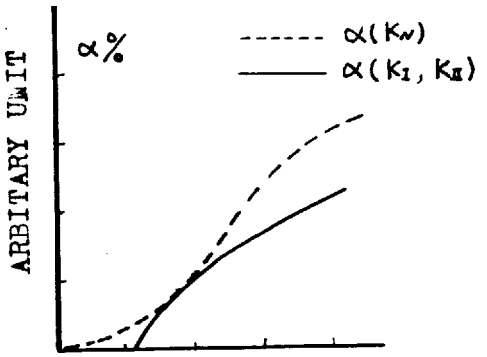

FIG.8 $K_N \rightarrow (K_1, K_{II})$ conversion model

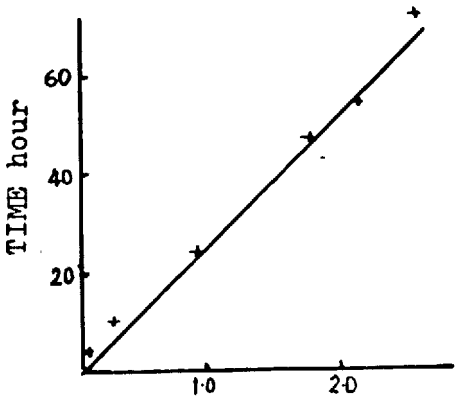

FIG.9 Relationship of t and Z

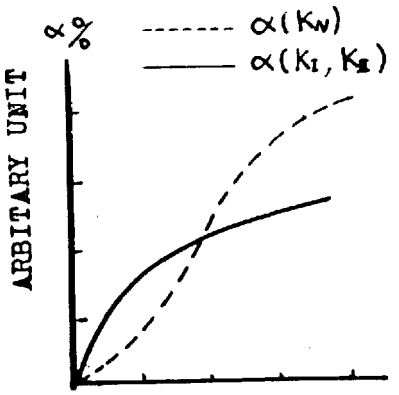

FIG.10 $K_N \rightarrow (K_1, K_{II})$ conversion model

CONCLUSION

i) At early hydration, the resistance due to diffusion is very small for alite in cement except pure C_3S. The rate constants will change with the progress of hydration just as shown by many

investigators, but it appears much later than we expected, e.g. in our observation, 4 days are needed after C_3S contacting with water for the change to take place.

ii) The rate constants evaluated by us are much smaller than those of others, which is an inevitable results of the morphological correction carried out by us .

iii) ϕ_i increases with decrease of particle size D_i or with increase of specific surface. This could be the cause since larger particles must be preferentally ground in a tube mill and these should higher sphericities.

iv) If we accept that C_3S liberates heat in two steps in the progress of hydration, it is possible that the peak II in $dQ/dt \sim t$ curve is caused by the reaction expressed in Eq. 22, and 23, i.e. the acceleratory period may not necessarily exist. In the whole processes the controlling step is I/D with a only set of K_I and K_{II} until CSH(III) or a marked concentration change in the solution occurs. And the change of rate constants does not always mean increase of the resistance due to diffusion.

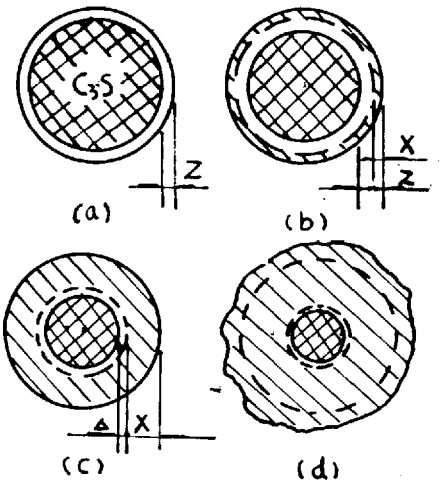

FIG. 11 Hydration model. a) At early hydration. CSH(I) is formed according to (K'_I, K'_{II}) mechanicm. b) CSH(I)→CSH(II) conversion begins, c) dZ/dt and dx/dt is unified at time tc, d) At the later period, CSH(III) appears.

Table 2 Degree of Alite Hydration and Kinetic evaluation

time(h)	a	De	z	t/z
0	0.0338	3.75	0.021	187.2
10	0.2686	5.2	0.257	38.84
24	0.5412	8.0	0.915	26.23
48	0.7189	10.8	1.863	25.77
56	0.7491	11.5	2.12	26.37
72	0.8040	13.0	2.724	26.43
96	0.8268	13.6	3.010	31.90
144	0.8647	15.3	3.72	38.68
240	0.8842	16.8	4.305	55.74

Table 3 Rate Constants for Alite Hydration

Values of Rate Constant for Alite hydration	H	A	A'	C-2	C-2'
Ki(μmh^{-})	0.3081	0.025	0.033	0.0238	0.0351 0.005*
KD (μmh)	0	0.0039	0	0.0357	0

* t<32hr; Ki=0.0351 t>32hr; Ki=0.005

REFERENCES

1、 S.N.Ghosh: Advances in Cement Techmology. Pergamon Press, 1983, translated in Chinese by Yang Nangru, 262P.

2、 A.Bezjak & 1. Jelenic " On the Determination of Rate Constants for hydration Processes in Cement Pastes" Cement and Concerte Reserch, 1980, P10--553.

3、 P. Barret "Hydration Mechanism of Calcium Silicate (C_3S, C_2S) Cement Compounds, Through the General Concepts of the Reactivity of Solids" 8th International Congress on the chemistry of cement, Brasil. 1986 Vol.III 86P.

4、 N. J.Clayden and C. M. Dobson "The Application of Solid State Nunclear magnetic Resonance Spectroscopy Technipues to the Study of the Hydration of Tricalcium Silicates" 8th International Congress on the Chemistry of Cement, Brasil, 1986, Vol.III 51P.

5、 keiichi Murakami and Hirobumi Tanaka "Contribution of calcium Thilsrlphate to the Acceleration of the Hydration of Portland Cement and comparison with Other Soluble Inorganic Salts" Proceedings of The Fifth International Symposium on the Chemistry of Cement, Tokyo, 1968, Vol. II. PARTII P422--430.

6、 В.Н.Бабушкин Г.М.Матвеев, О.П.Мчедлов--Петросян; Thermodynamics of Silicates, translated into Chinese by Pu xinchan, published by the Building Industry Publishing House of China, 1983, 195--252P.

THEORY AND PRACTICE OF CEMENT STRENGTH CHARACTERISTICS PREDICTION

A S Koshmal and O P Mchedlov-Petrossyan

NPKO Yuzhgiprocement, Kharkov
UKRAINE

SUMMARY

This paper presents results of solving the problem of express predictions of cement stone strength characteristics.The prediction method is based on the analysis of change nature of distributed resistive and capacitance parameters of system "cement-water".Prediction of strength characteristics is being carried out during three hours at absolute discrepancy from the results of standard physical-and-mechanical tests not more than ± 1.96 MPa,and relative discrepancy being not more than 4.5 %.

АННОТАЦИЯ

В докладе представлены результаты решения задачи экспрессного прогнозирования прочностных характеристик цементного камня.Метод прогнозирования основан на анализе характера изменения распределенных резистивно - емкостных параметров системы цемент-вода.Прогноз прочностных характеристик осуществляется в течение трех часов при абсолютном расхождении с результатами стандартных физико-механических испытаний,не более - I,96 МПа, и относительном расхождении,не более 4,5 процентов.

INTRODUCTION

Important problem of express prediction of strength characteristics of cement stone is usually tried to be solved on the base of studying the nature of change of one or two parameters of cement-water hardening system.For this purpose there are used such parameters as specific electric conductivity, pH level, dielectric permeability, heat release velocity, velocity of ultrasound wave distribution and reflection , contraction and surface strain.From the experience we know that this method doesn't go for express prediction of strength characteristics adequate to physical-and-mechanical tests of cement stone.

The hardening paste represents an unbalanced heterogenous dynamic cement-water system, development laws of which are determined by hydration and structure-forming processes.From the physical point of view the cement paste is a microinhomogeneous capillary-porous body. Its structural-and-mechanical parameters are functions of coordinates and they have statistical values. Macroscopically such systems are regarded as homogeneous ones because the probability of finding anywhere a solid phase particle or a pore with preset characteristics doesn't depend on coordinates. Such factors as chemical composition and morphology of hydrate compounds, surfaces of initial binder particles and their hydration products, relative quantity of capillaries and pores, ion composition and liquid phase concentration, forms of water molecules bond with solid phases, and unbound water quantity as well as deviation cement-water system from the equilibrium state are changed during hardening process.

The general property of dynamic systems is that side by side with regular dynamics, i.e. natural evolution of the phase space, there arises stochastic dynamics as a result of specific local unstability in separate phase volumes of the space.The distinctive property of the cement paste as a dynamic system is that equal in quantity system characteristics (in particular,that of strength) can be formed by means of different combination and interaction of regular and stochastic dynamics mechanisms at set time interval. For different cement-water systems the identical values of any physico-chemical parameters to be measured can correspond to the same or different system states with the same probability with which different values of these parameters can correspond to the same state. Hence no one physico-chemical parameter can be used itself for effective prediction of cement-water system state. Thus,the solution of cement quality prediction problem according to the "indirect characteristic - strength index" principle has no necessary and sufficient generality. We have worked out the method of strength indicies express prediction at set-theoretical level in the terms of mathematical logic and distributed electro-chemical values.

THEORY

The cement paste as a dynamic system can be described by a mathematical model M in the form of ordered set:

$$M = \langle \Theta, A, B, H \rangle , \qquad (1)$$

where: Θ - time moments set of system evolution; A - set of states; B - set of all possible processes; H - set of system characteristics.

In a general case the dynamic system phase volume is a function of time. Therefore system evolution time is included in its coordinates. As a result, the interaction of regular and stochastic dynamics mechanisms forms the $a \in A$ system state at $\tau \in \theta$ preset time moment. In this case even weak stochastic processes can lead to the significant deviation from the linear dependence between $b \in B$ and $h \in H$ elements of M ordered set, what means the system nonintegrability [1].

In general case between elements $a \in A$, $h \in H$ and $\tau \in \theta$ there is no one-to-one correspondence. If it is impossible to establish such correspondence, let us determine conditions of providing for equivalence relation between $a \in A$ and $h \in H$. If this relation takes place, some value of $\tau_i \in \theta$ has single-valued functional dependences: $f(R_i) = f(a_i, \tau_i)$; $f(R_i) = f(b_i, \tau_i)$ and consequently $f(R_n) = f(a_n, \tau_n)$, where R is strength characteristic; i, n are correspondingly indicies of arbitrary and final values of cement-water system parameters. Then equivalence relation will also be established between $f(R_i) = f(a_i, \tau_i)$ and $f(R_n) = f(a_n, \tau_n)$. This means a principal possibility for prediction of R_n strength characteristic. From the theory of sets it follows that functional dependences indicated are single-valued and simultaneous ones if a, h, τ parameters are identical directly or inversely in dimensionality [1]. Thus the equivalence relation required is provided for when the $a \in A$ parameter has time dimensionality and its a^{-1} inversion (i.e. frequency) is the dimensionality of $h \in H$ parameter.

We have shown that there arise electrochemical phenomena in hardening cement-water systems. These phenomena are caused by disbalanced double electric layers (DEL) on solid and liquid phases boundaries and commensurability of DEL thickness with distance between solid phases with different surface charges [2]. Cement-water system electrochemical description is based on the known Graham's model for DEL in a modification that ignors specific ion adsorption:

$$\sigma = -\sigma_2 = \varepsilon E, \qquad (2)$$

where σ - surface density of solid phase electrostatic charge; σ_2 - surface density of the charge of DEL diffusion region; ε - liquid phase dielectric permeability; E - electrostatic field intensity in DEL diffusion region. The expression 2 is easily transformed into $\sigma = \varepsilon i / \lambda$ and then into $\sigma / i = \varepsilon / \lambda = t$, where i - current density of charges (ions) exchange during interphase interaction in the DEL field; λ - specific electric conductivity of cement-water system; t - some parameter having time dimensionality and describing system state at a preset time moment (τ_i) of its evolution. Thus the $t \in A$ parameter and its $t^{-1} \in H$ inversion provide for equivalence relation between elements of M ordered sets. This allows prediction of cement stone strength characteristics.

In heterogeneous interpretation electrochemical parameters of cement-water system are functions of coordinates and one can say only about some average statistical values of quantities to be measured. This means, in particular, that $\varepsilon / \lambda = t$ parameters are not concentrated, but are distributed over all phase space. Consequently practical determination of the t value as a function of distributed parameters is possible. On this basis we have developed a principally new method for express prediction of cement stone strength characteristics.

CONCLUSIONS AND RECOMMENDATIONS

This method uses high-frequency relaxation oscillator, the circuit of its positive feedback including a special metering cell - a solion. In this cell the cement paste to be investigated fulfils a function of variable electric resistance (of R distributed resistive layer) and that of one of capacitor plates (of C distributed capacitance) simultaneously. The geometric constant of the cell is to correspond to the following condition: $\varepsilon/\mathcal{L} = t = RC$. Oscillation frequency is determined by $1/2\pi RC$ relation. The change of t parameter during cement hardening process is determined by output voltage change, the voltage being proportional to electric oscillations frequency change.

The practical use of the method developed allows to carry out the cement strength characteristics prediction with reliability of $\alpha \geqslant 95$ % in three hours after mixing a binder to be investigated with water, the absolute discrepancy from results of direct physical-and-mechanical tests according to GOST 310.1.76 - GOST 310.3.76, GOST 310.4.81 being not more than $\pm$ 1.96 MPa and the relative discrepancy being not more than 4.5 %. In the same way one can predict strength decrease with indication of its causes, analyse a realization level of clinker potentialities, control setting time, pseudo-setting, structure and density homogeneity of cement stone, predict its corrosion resistance in any agressive media, control preset type cement production process.

ACKNOWLEDGEMENTS

This paper is based on the results of a number of investigations on electrochemistry of cement-water system, carried out in the physical-and-chemical laboratory of Yuzhgiprocement. The paper is published with the permission of General director of the institute.

REFERENCES

1. Дмитриев А.К и Мальцев П.А. Основы теории построения и контроля сложных систем. Л.: Энергоатомиздат, 1988, 192 с.

2. Kochmai A.S., Mtchedlow-Petrossian O.P.: "Phenomenes electrochimiques intervenant aux premiers stades d'hydration et de formation gresso International de Quimica do Cimento, Rio de Janeiro, finep, 1986, v.3, p.290-294.

SEDIMENTATION METHOD FOR ANALYSIS OF CEMENT-ASH COMPOSITION PROPERTIES

L P Orentlicher and V G Nikiforova

Building Materials Department
Moscow Civil Engineering Institute, Moscow
RUSSIA

SUMMARY

Attention is given to the possibility of sedimentary research method of cement-ash compositions, which are related to the processes of structural formation. It is stated that cement, ash and cement-ash suspensions have not two, but three periods of sedimentation. Technological recommendations are made on kinetics of the sedimentation process and control of constructive structure forming composition.

INTRODUCTION

Determining water-retaining power of cement-ash compositions by means of sedimentation method in concentrated slurries one can get a certain quantity of free, separated water. But information on the character of the structures obtained, causes underlying their formation, "freedom degree" of retained water etc, is quite necessary to estimate the technical characteristics of cement-ash composition. These characteristics cannot be obtained while determining the total quantity of water retained in cement-ash composition. To analyse them one must examine bleeding mechanism, its successive phases, as well as their differences in bleeding speed.

EXPERIMENTAL

The experiments were carried on portland cement "400" and on ash of a thermal power station of dry sampling.

The chemical compositions of cement and ash are presented in Table 1.

Chemical cement-ash composition

Table 1

Type of material	Oxide content,%								
	SiO_2	Al_2O_3	Fe_2O_3	CaO	MgO	K_2O+ Na_2O	TiO_2	SO_3	loss on ignition
portland-cement	21.2	6.0	4.3	66.0	1.1	0.8	-	0.4	-
ash	64.0	28.6	3.5	1.7	0.2	0.9	1.7	0.4	up to 5

To investigate bleeding kinetics the slurry was prepared in the following way: a sample of solid material (cement+ash) was mixed for 30 sec, then a predetermined proportion of water was added, the slurry obtained was mixed for 4 min and then carefully transferred into a graduated cylinder. Water-to-solid phase ratio was equal to 1.0 and 1.2. In a definite interval of sediment upper boundary sedimentation, that was determined taking into account experiment errors, the time between the beginning and end of the experiment was registered.

Then graphs were constructed. The ratio of relative bleeding ΔH to the initial volume of slurry H_0 was plotted versus the sedimentation time (min) and speed of sedimentation (cm/min).

The cement-ash composition compounds tested are presented in Table 2, and the sedimentation kinetics curves are shown in Fig.1.

Table 2

Cement-ash composition compounds

Compound №	Proportion,%	
	Cement	Ash
1	100	-
2	80	20
3	60	40
4	50	50
5	40	60
6	20	80
7	-	100

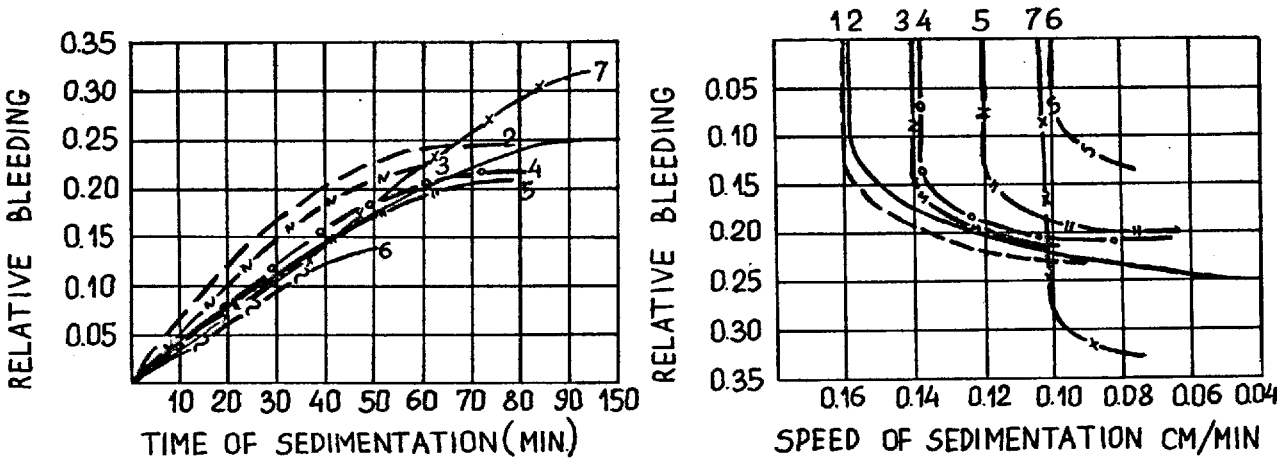

FIG.1 Kinetics of cement-ash mixture sedimentation when W/S.P.= 1,2
See table 1 for compound number

E.M. Porotsky (1) pointed out that sedimentation curves consisted of two parts: rectilinear and curvilinear.

RESULTS AND DISCUSSIONS

The authors suggest that sedimentation curves should be divided not into two, but into three periods, namely,of constant speed,transition and constant relative bleeding. Bleeding curves allow to determine the constant speed period continuity, complete bleeding time and other characteristics.

Analysing the relation of relative bleeding on sedimentation speed, one can note that 20-80% ash introduction decreases the initial speed of sedimentation from 0.16 to 0.10 cm/min for 1.2W/SP and from 0.14 to 0.06 cm/min for 1.0W/SP. At the same time, at 1.2 W/SP constant speed period and constant bleeding period are prolonged by 1.4 times, but transition period is shortened by 4 times.

When W/SP = 1.0 due to ash admixture in cement, sedimentation process changes as described above, except for the third period, which is shortened by 2 times as compared to that for pure cement slurry.

Comparing cement and ash sedimentation curves one can note their prime difference. Cement slurry has a short first, a durable second and a short third period. Ash slurry, on the other hand, has a durable first and two subsequent short periods. These deductions are proved for W/SP = 1.2 as well as when W/SP = 1.0.

Hence to get the densest sediment possible it is necessary either to increase sedimentation speed, e.g. decreasing medium toughness, or to prolong the constant speed period without changing it by means of early coagulation prevention before the sediment begins to set.

Constancy of bleeding speed indicates that new products resulting from reactions in the first period do not greatly affect the surface contours of solid phase particles. It is quite possible that the structure of the hydration product stratum percolated by water during bleeding, that is,the stratum formed first, is rather porous (2).Solid phase particles are yet separate. T. Powers (3) explained the fact in the following way: grains covered with gel are divided by a thin water stratum of several angstrom units thickness. The whole mass forms one floc and the flocculent structure is a homogeneous collection of particles in itself.

The first, namely, the constant speed period is governed by Stokes law because there is no contact between the solid phase particles. The free fall of particles takes place by gravity in dispersive medium. There is no interrelation between particles and slurry fixation depends only on hydrodynamic factors.

The second transition period is a period of flocculation and the beginning of sediment structure formation. The period was not singled out before. The floc is characterized by slower solid phase settlement due to particle collision and liquid backward flow action from vessel bottom. Both Stokes law and frictional flow law, as well as Kozeni-Karmann's permeability theory govern flocculation period.

During the third, constant bleeding period sediment formation processes come to an end. Cement and cement-ash slurry sediment setting begins.

So, the sediment is formed during the third period, whereas there was only floc during the second period. The later it appears and the sooner it settles, the higher the formed sediment density. If the floc exists for a long time a porous sediment with less strong contacts is formed due to coagulation.

Optimal compound 3 (c:a=60:40%), established from earlier experiments, differs slightly in sedimentation kinetics from neat cement (compound 1). Initial speed of cement sedimentation is 0.16 cm/min when W/SP = 1.2; for the optimal compound it is 0.14 cm/min. Cement slurry transition period comes to an end when the relative bleeding is 0.23 and the sedimentation speed is 0.08 cm/min. The corresponding values for optimal compound are 0.19 and 0.12 cm/min. Cement slurry third period is completed when the relative bleeding is 0.25 and sedimentation speed is 0.04 cm/min; for the optimal compound when $\Delta H/H_0$ =0.21 and sedimentation speed is 0.09 cm/min.

CONCLUSIONS AND RECOMMENDATIONS

Decrease in the sedimentation speed of cement as well as cement-ash composition takes place due to coagulation process setting in whereas in the case of ash it is due to their complete settlement and actual completion of sedimentation. Cement-containing composition sedimentation speed differs from that of neat cement coagulation.

It is most essential from an industrial engineer's viewpoint that the former be many times greater than the latter, because the slurry would then be denser. If setting stops bleeding process to its actual physical completeness, then there can appear a stratum of completed "sedimentation zone" at the bottom but W/SP is of initial value above(2). Thus there won't be homogeneity of solid phase in finite sediment, the sediment won't be homogeneous.

According to the existing concentrated slurry theory, sedimentation is carried on sooner provided coagulation takes place, but porous, voluminous sediment results from it (4).

REFERENCES

1. Пороцкий Е.М. Исследование водоудерживающей способности цемента - Труды /Гипроцемента ВНИИ Цементов, 1948, вып. X - 59с.

2. Powers T."Physical Properties of Cement Slurry and Stone". In: The Fourth International Congress on Cement Chemistry.M.1964, p.p. 402-438.

3. Powers T. "Physical Structure of Portland Cement Slurry".In: Cement Chemistry /Edited by H.F.U. Taylor M.; 1969 - p. 501.

4. Фролов Ю.Г. Курс коллоидной химии М.; Химия, 1982 - 400 с.

Specific Theme III-D

Effect of Admixtures

HYDRATION IN VERY HIGH STRENGTH CEMENT COMPOSITES

A Durekovic

Civil Engineering Institute of Croatia
Zagreb, CROATIA

ABSTRACT

Hydration was investigated at normal temperature in cement composites of water to solid ratio of 0.28. Samples with and without superplasticizer admixture were prepared using ordinary portland cement (OPC) in which 0-5-10 and 15 per cent of weight was replaced by condensed silica fume (CSF).The observation period was from 4 hours up to 50 days.

Hydration degrees of alite and tricalcium aluminate determined by QXDA,formation of free calcium hydroxide detected by applying of DTA/TGA,Si-anion polymerization parameters obtained by molybdate method as well as the results of L.o.i and insoluble residue support the conclusion that hydration in cement composites was suppressed when low w/s-ratio was used. The setting behavior of fresh mixes and the effect of superplasticizer on the reaction of individual components extended the interpretation.

The 28 day compressive strength results which were registered up to 108 MPa confirmed research that very high strength cement composites were under investigation.

ZUSAMMENFASSUNG

Die Merkmaele der Hydratation die in der Zementkomposite mit einem Wasser/Feststoff-Wert vom 0,28 und bei der Raumtemperatur stattfindet wurden erforscht. Ein reiner Portlandzement (PZ von ASTM Type I) und ein Siliziumstaub (CSF) aus der FeSi-Produktion verwendete man fuer die Vorbereitung der Proben. Dabei tauschte man die bestimmte PZ-Anteile mit dem gleichen Gewicht des CSF (0-5-10 und 15 Gew. %) aus. Die Probereihe mit und ohne Zugabe einen Betonverfuessiger (von Melamin-basis) wurde vorbereitet.Die Hydratation studierte man in der Zeitspanne von 4 Stunden bis zu den 50 Tagen.

Das Hydratationsgrad des Alits und des Trikalziumaluminats wurde mittels QXDA determiniert und das befreite Kalziumhydroxyd stellte man mittels DTA/TGA fest. Die Polymerisationsvorgaenge der Si-Anionen wurden mit der Molybdatmethode verfolgt.Die L.o.i-Werte,der Anteile des Unloesliches wie auch die Abbindezeiten der zementierenden Mischungen wurden auch gemessen.

Alle Forshungsergebnisse deuten darauf hin, dass unter den benutzten Testbedingungen und beim gewaelten W/S-Wert, die Hydratationsprozesse erschwert und verlangsamt wurden.

Die Druckfestigkeit der Probekoerper (Alter:28 Tage), die bis zu 108 MPa gemessen war, bestaetigte dass der Zementkomposite der hohe Festigkeit untersucht worden waren.

INTRODUCTION

Very high strength (VHS) cement composites are characterised,apart from their extraordinary strength, also by a low water to solid ratio.A very frequently used w/s-ratio lies between 0.20 (below which are values typical for so-called DSP materials, see for example Ref./1/) and the value about 0.30. VHS cement composites often incorporate non-hydraulic or hydraulic fine cement supplementary materials. One of them is condensed silica fume (CSF).

The CSF-containing VHS cement composites have already been an object of investigation /2-7/ but some of the conclusion for partial objects, as in the case of CSF-reactivity /4,5,7/ are quite divergent. This paper presents the investigation results of hydration in the VHS cement composites prepared from OPC-CSF blends.

EXPERIMENTAL

Research was carried out using an ordinary portland cement (OPC), condensed silica fume (CSF) from ferrosilicon alloy production, a superplasticizer of melamine-formaldehide type (solution with 20 % of dry substances) and distilled water. The OPC had a density of 3.12 g/cm^3, a Blaine value of 2710 cm^2/g. CSF (SiO_2 content of 86.92 % and bulk density of 0.20 kg/dm^3) was from the same stock as described in Ref./8/. The basic parameter fixed in all pastes tested was a water to solid ratio of 0.28.

At room temperature four pastes were made in series without superplasticizer using OPC and by replacing the OPC weight with following weight part of CSF: 0% (paste sign PC), 5% (paste sign 5P), 10% (paste sign 10P) and 15% (paste sign 15P). In the superplasticized series of four pastes,which contained an equivalent amount of CSF (paste with "s"-index:PC^s,5P^s,10P^s and 15P^s), the dosage of liquid superplasticizer was always 4% per weight of OPC+CSF. The materials were weighed and mixed for 3 minutes in "Toni-Technik" cement mixer. Immediatelly after setting they were immersed in water for further hydration at 20^{0}C. Hydration was stopped after 4 hours,10 hours,and 1, 3, 7, 28 and 50 days by grinding the paste under acetone and drying in vacuum.

In addition, 4x4x16 cm size samples of the same 8 mixes described were made and tested for compressive strength. Those 8 mixes were also prepared for determination of setting time.

Chemical analysis of the investigated pastes were carried out according to Yugoslav standard JUS B.C8.020 (and BS 4550:Part II).

Quantitative X-ray diffraction analysis (QXDA) was made according to the fundamental principals described in Ref./9,10/, using Cu(K_α) radiation and Philips 1130 diffractometer. The hydration degree of tricalcium aluminate was determined from the intensity of 440 diffraction maxima, while the intensity of alite diffracton maximas I_β(620,040) itself served for determination of the degree of alite hydration. Suprapur, fine pulverized calcium fluoride was used as the internal standard.

DTA/TGA was employed to detect variations in the free lime content of hydrated pastes. The amount of calcium hydroxide was determined by measuring abrupt weight loss in temperature range of 510-600^{0}C.

Polymerization of Si-anions was tested by molybdate method using a procedure based on the works published in Ref./11,12/ and which is fully described in Ref./13/.

RESULTS AND DISCUSSION

Before presenting the results it should be pointed out that the danger of significant warming of setting cement composites which could be caused by development of hydration heat had to be minimized. This was done by demolding samples and transfering them to curing water immediately after the pastes had set. The 28 day hardened mixes have shown the following compressive strengths: PC=78.9; 5P=95.5; 10P=99.0; 15P=90.0; PC^s=81.5;

$5P^s$=97.5; $10P^s$=108.0 and $15P^s$=93.5 MPa. The results corroborate that the mixes prepared for investigation were composites of very high compressive strength.

The reactivity of the tricalcium aluminate and the alite at different time of reaction are presented in Figure 1 and Figure 2. From the beginning of C_3A-hydration (Fig.1) in the mix without superplasticizer (HRWR) and with the lowest dosage of CSF (sign 5P) it was found that there was a slightly higher degree in C_3A-hydration in comparison to the other mixes. This could be speculative explained due to the adsorption of Ca- and sulfate-ions on the CSF surface similar to the mechanism as suggested for the process at much higher w/s-ratio /14,15/. As hydration progresses the interparticular space, which was initially small because of the low w/s-ratio used, will be filled up with originated hydration products. The mobility of small amount of available water in tested composites came to be reduced and the growth of hydration products restricted.

The most significant retardation of C_3A hydration in the tested samples by action of the superplasticizer was found in the pure OPC paste. The reason for this lies in the fact that presence of CSF in the OPC-CSF blends changes the particle size distribution and thus, at the same time, enlarges the specific surface /16/ which consequently causes an increase in superplasticizer demand /16/. Certainly, all this happens in hydrating OPC-CSF composites where in the pore solution the Ca-ions are present and strong "anchoring joint effect" /17/ on the CSF particles may exists.Later in hydration,as Fig.1 shows, the conversion of C_3A in all superplasticized mixes was supported. Undoubtedly this was a consequence of the improved dispersity of the solid particles by the action of HRWR during mixing with water by preparing the pastes. Because the dosage of the HRWR was kept constant in all superplasticized mixes the highest C_3A hydration degree after 28 days was found in the pure PC mix (sign PC^s), which in anhydrous state had the lowest specific surface and therefore the realised particles dispersity was most efficient.

During hydration of the alite in the tested composites (Fig.2) the differences between the mixes regarding the CSF content and effect of superplasticizer,were more distinctly shown in comparison with the results of C_3A given above, but there are similarities in the problems. The results could be considered in two interwals:the early stage and the later period of alite hydration. Conditionally it could be said that the change from the early stage to the later period of hydration varied from 1 up to the 7 days (depending on the CSF content increase in the mixes and HRWR presence). A small amount of CSF (5%,sign 5P), probably acting as nucleating sites of hydrates and causing also a decrease of the Ca-ions concentration /15,18/, improved in the mix without HRWR the alite hydration during the early period of reaction. By continuing hydration and especially with a higher dosage of CSF,the densifying of composites structure and the resulting problems in mobility and availability of water as well as the lack of space for the new originated products, which are all factors relevant for mineral conversion process /19/, lead to the suppression of alite hydration. The presence of HRWR in the tested composites (samples marked with "s"-index) also caused retardation of alite in the early stage of hydration, but the improved dispersion of solid particles by mixing with water enables a higher degree of alite conversion later in hydration.

A low water dosage in relation to the amount of solids (OPC+CSF) and the presence of superplasticizer also reflect on the results of the loss on ignition (Loi), which are shown in Figure 3, and the formation of calcium hydroxide (Figure 4) during hydration.
The results obtained after 28 days in testing the composites agree with the results of lower riched level in hydration of C_3A and alite discussed up to now.

The results of free CaO shown in Figure 4 are calculated from DTA/TGA curves which method seems to be the most convenient for investigation of

hydration in VHS cement composites because there is evidence that especially at low w/s-ratio the calcium hydroxide released is poorly crystalline or even partly amorphous /20,21/. All the results shown in Figure 4 are absolute values lower than those which were found in OPC and OPC-CSF composites of higher w/s-ratios as reported in several papers /8,13,22/. Between 3 and 7 days,depending of the present CSF-amount, a change occured in the balance of the lime released vs. lime consumed by the pozzolanic reaction and this point of time was the peak of the CaO_{free} curves.

Parallel with the consuming of the free lime another indication of the pozzolanic reaction in hydrating and CSF-containing cement composites are the changes of insoluble residues which are given in Table 1. The results for pure PC paste are practically constant around 0.5%. At the beginning of hydration in the OPC-CSF blends the insoluble residues are logically very close to the value of the CSF-amount added to each mix. Table 1 reproduces also the consequence of HRWR-double layer formation on CSF particles during the early stage of hydration and the advantage of the improved particle dispersity by the action of the superplasticizer for the CSF conversion by pozzolanic reaction later in hydration.

The extent of pozzolanic reaction could also be estimated using the parameters from molybdate method. Evaluation of molybdate complexing curves was already descrieb in earlier papers /13,23/. One of those parameter is the part of SiO_2 contained in the residual-polymeric fraction (Res-Poly) of silica anions which decreases with the progressing of cement paste hydration. The pozzolanic reaction also influences some changes in the size dispersion of Si-anions /8,13,24/. According to the SiO_2 parts in residual-polymeric fraction of Si-anions, given in Table 2, and the SiO_2 parts in Res-Poly fraction of anhydrous mixes the estimated parts of CSF involved in the pozzolanic reaction after 50 days were as follows: 5P=67%, $5P^S$=78%, 10P=52%, $10P^S$=61%, 15P=35% and $15P^S$=45%.
Obviously, a significant portions of CSF were not completely converted by pozzolanic reaction. Therefore is it very likely that the remaining unreacted solid particles in the cement composites of very high strength, or at low w/s-ratio, may act as the internal filler as mentioned by S.Diamond /25/ in the case of DSP composites. And also, it does not disproved the opinion mentioned by Brunauer et al./26/ that the pastes prepared with a w/s-ratio below a certain value are unable to reach complete hydration.

Finally, the setting time results of cement pastes investigated are presented in Figure 5. The results show the usual behavior of fresh cement mixes by the action of a superplasticizer and by the presence of CSF but with one exception. Atypical prolongation of the final time of setting in CSF-containing blends without HRWR admixture is the overall manifestation of the slowing in the formation of hydration products which are responsible for setting behavior. This confirms also other aspects of hydration suppression discussed before in the paper.

CONCLUSION

Hydration processes in VHS cement composites of w/s=0.28, i.e. the reaction of clinker minerals (C_3A/alite) and the conversion of CSF by pozzolanic reaction were suppressed during the observation period (from 4 hrs up to 50 days) when compared to hydration in cement composites of higher water to solid ratios. The hydration reduction is more strongly exhibited by increasing the CSF content in the blends.

The amount of released calcium hydroxide in hydrating OPC-CSF blends of w/s=0.28 has had a tendency to be fully consumed by pozzolanic reaction.The balance between the CH released by hydration and the CH consumed by the pozzolanic reaction was very obviously determined by the amount of water available for reaction in the mixes.

Hydration in VHS cement composites is also essentialy influenced by the

presence of a superplasticizer. The presence of HRWR,when considerd for the end results, was of an advantage for this hydration process.

ACKNOWLEDGEMENT
This investigation was financial supported by Ministry of Science, Technology and Informatics of Republic Croatia, under GN 2-15-008.

REFERENCES

1. Bache,H.H.",Densified cement/ultra fine particle based materials",presented at 2nd Int.Conf.on superplasticizer in concrete,Ottawa,Canada,1981. 1-33.
2. "Very high strength cement-based materials",MRS Symp.Proc.,Vol 42, Pittsburgh,USA,Ed.J.F.Young,1985.
3. Mino,I.,et al.,Proc.8th ICCC,Rio de Janeiro,Brasil,Th.2-Vol 3(1986)167.
4. Aitcin,P.C.,et al.,MRS Symp.Proc.,Vol 85,Pittsburgh,USA,Eds.L.J.Struble, P.W.Brown (1987) 261.
5. Sarkar,S.L.,Aitcin,P.C.,Cem.Concr.Res.,Vol 17 (1987) 591.
6. Carles-Gibergues,A.,et al.,ACI SP-114,Vol 2 (1989) 1101.
7. Đureković,A.,Tkalčić-Ciboci,B.,Cem.Concr.Res.,Vol 21 (1991) 1015.
8. Đureković,A.,Popović,K.,Cem.Concr.Res.,Vol 17 (1987) 108.
9. Euw,v.M.,Silicate Ind.,Vol 23 (1958) 643 (in French).
10. Jelenić,I.,et al.,Cem.Concr.Res.,Vol 8 (1978) 173.
11. Thilo,E.,et al.,Z.anorg.allgem.Chem.,340 (1965) 261 (in German).
12. Frydrich,R.,Chem.Berichte,Vol 97 (1964) 151 (in German).
13. Đureković,A.,Cem.Concr.Res.,Vol 18 (1988) 532.
14. Uchikawa,H.,Uchida,S.,Proc.7th ICCC,Paris,France,Vol III (1980) IV-24.
15. Grutzeck,M.W.,et al.,ACI SP-79,Vol 2 (1983) 643.
16. Đureković,A.,Popović,K.,Proc.5 RILEM Int.Symp.-Admixture for Concr., Barcelona,Spain,1990,Publ.Chapman and Hall,London,GB (1990) 1.
17. Buil,M.,et al.,ACI SP-91,Vol 2 (1986) 959.
18. Ogawa,K.,et al.,Cem.Concr.Res.,Vol 10 (1980) 683.
19. Taylor,H.F.W.,et al.,Mat.et Construct.(Paris)Vol 17,No102 (1984) 457.
20. Groves,G.W.,Cem.Concr.Res.,Vol 11 (1981) 713.
21. Ramachandran,V.S.,Cem.Concr.Res.,Vol 9 (1979) 677.
22. "Condensed silica fume in concrete"-FIP State of Art Report,Publ.Thomas Telford,London,GB,1988.
23. Đureković,A.,Popović,K.,Advan.Cem.Res.,Vol 1,No 3 (1988) 138.
24. Uchikawa,H.,et al.,Proc. 8th ICCC,Rio de Janeiro,Brasil,Theme 3-Vol IV (1986) 245.
25. Diamond,S.,MRS Symp.Proc.,Vol 42,Pittsburgh,USA (1985) 233.
26. Brunauer,S.,et al.,Cem.Concr.Res.,Vol 3 (1973) 129.

TABLE 1: Changes of insoluble residue (%)during hydration in VHS cement composites of w/s=0.28 (mixes with HRWR are with "s"index).

Paste CSF(%)	PC 0	5P 5	10P 10	15P 15	PC^s 0	$5P^s$ 5	$10P^s$ 10	$15P^s$ 15
Hydration (h)(days)								
4	0.60	4.10	8.16	11.95	0.50	4.46	9.93	14.27
1	0.55	3.56	5.87	11.08	0.55	4.08	8.36	11.48
3	0.60	3.07	5.91	8.86	0.52	3.29	6.50	10.13
7	0.61	2.80	5.42	7.70	0.60	3.07	5.10	8.20
50	0.52	1.16	2.32	4.42	0.60	0.85	1.52	3.56

TABLE 2: Proportion (%) of SiO_2 in residual-polymeric fraction of Si-anion during hydration in VHS cement composites of w/s=0.28 (mixes with HRWR are with "s"-index).

Paste	PC	5P	10P	15P	PC^s	$5P^s$	$10P^s$	$15P^s$
CSF (%)	0	5	10	15	0	5	10	15
Hydration (h)(days)								
4	0.0	17.5	29.2	40.1	0.0	17.7	28.8	41.8
7	0.2	12.4	23.0	30.5	0.0	12.2	22.4	31.0
50	0.3	6.0	15.3	20.5	0.3	4.0	12.5	17.4

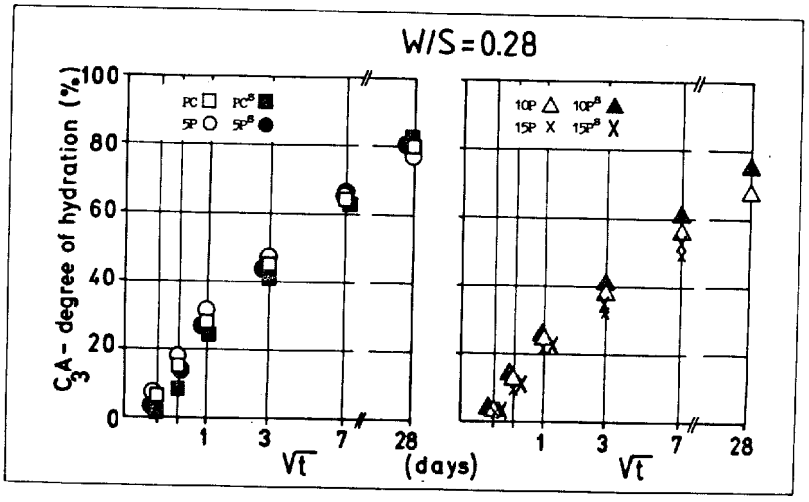

FIGURE 1:

Degree of hydration of C_3A in VHS cement composites of w/s=0.28 in a function of time (superplasticized mixes are with "s"-index).

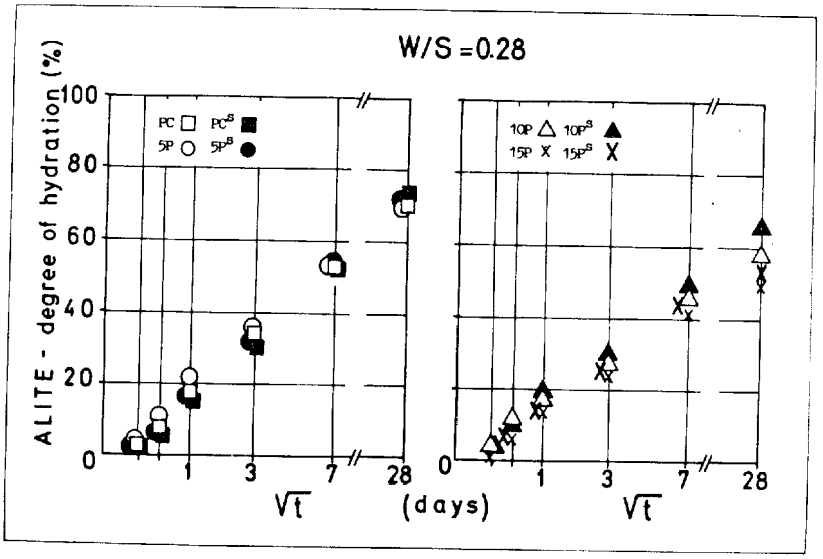

FIGURE 2:

Degree of hydration of alite in VHS cement composites of w/s=0.28 in a function of time (superplasticized mixes are with "s"-index).

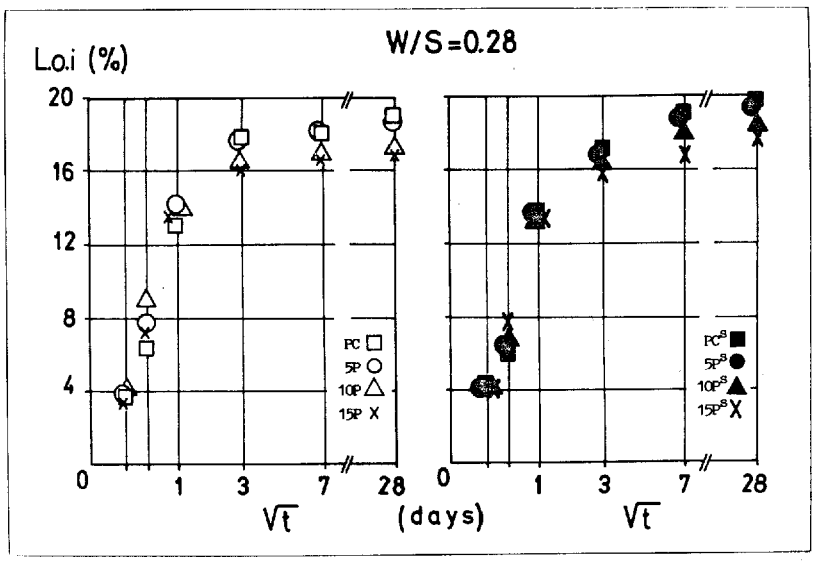

FIGURE 3:

Loss on ignition (Loi) results of VHS cement composites of w/s=0.28 in a function of time (superplasticized mixes are with "s"-index)

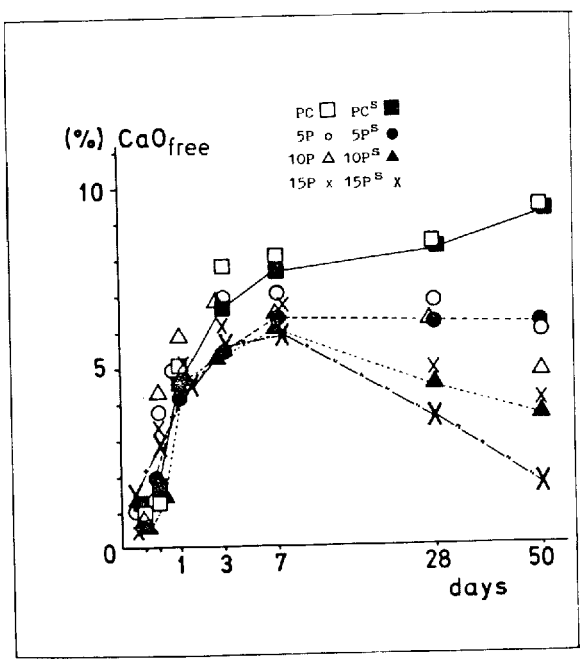

FIGURE 4:

Free lime content (expressed as CaO) in VHS cement composites of w/s=0.28 in a function of time (superplasticized mixes are with "s"-index).

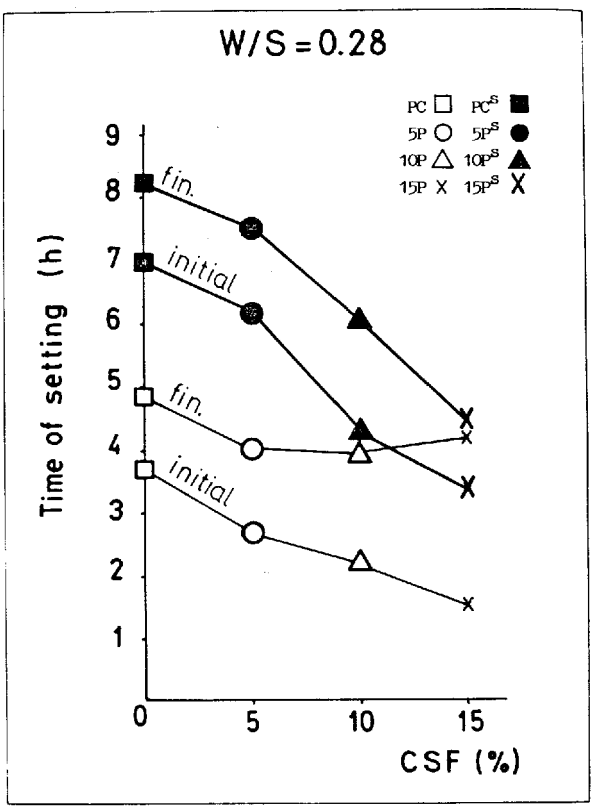

FIGURE 5

The setting times of VHS cement composites of w/s=0.28 (superplasticized mixes are with "s"-index).

EFFECT MECHANISM OF CONCRETE ADMIXTURE BASED ON AROMATIC HYDROCARBON SULPHONATE

Chen Yongsu, Wu Zhaoqi and Yu Kuichang

Cement Research Institute, China Building Materials Academy
Beijing, P R CHINA

ABSTRACT

The effect of Type N aromatic hydrocarbon sulphonate superplasticizer is studied on the surface properties, rheological behaviour, rate of hydration and hydration products. The mechanism of enhancement of flowability of fresh concrete and compressive strength, flexural strength, impermeability, resistance to freezing and thawing, and drying shrinkage of hardened concrete are elaborated.

〔摘　要〕

本文研究 N 型芳香族磺酸盐超塑化剂对水泥浆体流变性，水泥表面性能，水化速率及水泥产物的影响，改善新拌混凝土流变性的机理，以及提高硬化混凝土抗压强度、抗折强度、抗渗性、抗冻融性以及干缩性的效果。

INTRODUCTION

China started to study superplasticizer in 1974. Five products have been put into market since, with an annual production of 15,000 tons [1]. Recently a new product known as Type N aromatic hydrocarbon sulphonate superplasticizer was developed by adopting a by–product from coking plant as a raw material and used in practice.

TEST RESULTS AND DISCUSSION

Test materials

Admixture: Type N aromatic hydrocarbon sulphonate superplasticizer (abbreviated as Type N admixture below).

Cement: Silicate cement having the following chemical composition.

Table 1. Chemical composition of the cement (%)

SiO_2	Al_2O_3	Fe_2O_3	CaO	MgO	R_2O
20.98	6.02	5.75	65.75	0.62	0.24

The effect of Type N admixture on the rheological behaviour of fresh cement paste

1. Isothermal adsorption

Type 751G spectrophotometer was adopted. The test results are shown in Fig.1. It is indicated that the adsorbed quantity increases and reaches a saturation value gradually as the concentration of the solution increases.

2. Zeta–potential

It is shown from Fig.2 that as the concentration of solution increases the absolute value of zeta–potential of cement particle in suspension rises rapidly, and then tends to a stable value gradually (–29 mv), while the zeta potential of cement particle without admixture addition is only –5 mv.

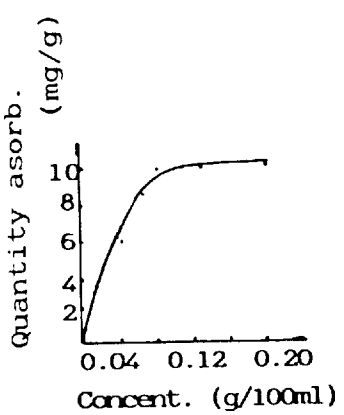

Fig.1 Isothermal adsorption curve

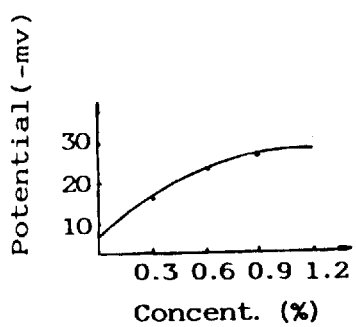

Fig.2 Zeta–potential curve

3. Rheological behaviour of cement paste

Type Fan 35A viscometer was used for determining the rheological properties of cement pastes with different water–cement ratio and content of Type N admixture. The results are shown in Fig.3 and 4. The yield stress of cement paste (Sy) with Type N admixture is much lower than that of control at the same water–cement ratio. Even if the water–cement ratio is reduced by 15% the cement paste with addition of Type N admixture still has lower yield stress. The reduction of yield stress with the increase of Type N admixture content shows the capability of the admixture to improve the flowability of cement paste.

Type N admixture, at a range of dosage, enhances plastic viscosity, (η_p) which makes the cement–water system more stable, and less bleeding for concrete occurs.

The increase of flow behaviour index n′ [2] and reduction of fluid consistency index k′ also indicate the improvement of rheological properties of cement pastes by adding Type N admixture.

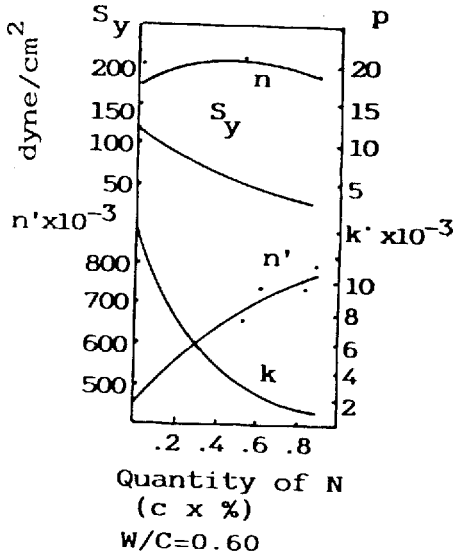

Fig.3 Rheology at the same W / C

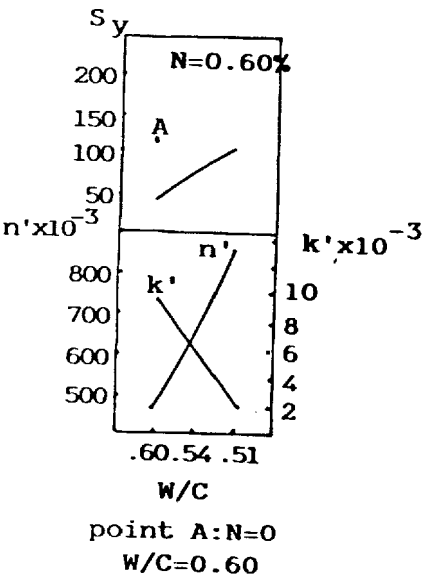

Fig.4 Rheology at different W / C

The effect of Type N admixture on cement hydration

1. Effect on heat evolution rate of hydration at early stage

The heat evolution rate of cement hydration within 24 hours was determined by conduction micro–calorimeter. The results are shown in Fig.5. Comparing with the control sample, the sample with Type N admixture has a lower hydration rate in 8.5 hours, and shows a significant heat evolution peak in 15 hours, and evolves about the same amount of heat in 24 hours.

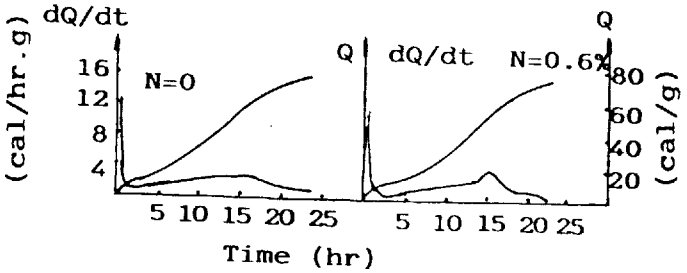

Fig.5 Heat evolution rate

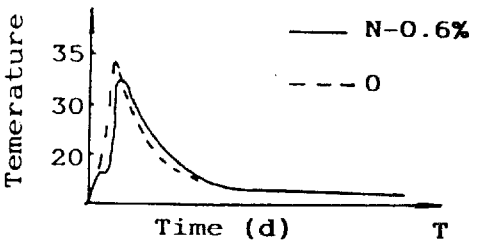

Fig.6 Temperature rising curve

2. The effect on heat of hydration

In Fig.6 the heat evolution peak is delayed for 3 hours, and the highest temperature obtained is lowered by 2.3℃ for sample with Type N admixture. The total heat evolved in one day however, is about the same for both samples with and without the admixture.

The above results show that Type N admixture slightly retards early hydration of cement, but does not affect the rate of hydration after the appearance of heat evolution peak. It seems that the influence of Type N admixture is not to accelerate the rate of hydration, but to affect hydration products and micro–structure.

The effect of Type N admixture on hydration products

Fig.7 is the X–ray diffraction patterns determined by Type D_{max}–IIIA diffractometer. There is no new hydration product found in the patterns of the sample with Type N admixture. But the charactristic peak of calcium hydroxide in this sample appears at 24 hours, delayed for 16 hours. The above results are also verified by data obtained from thermal analysis and scanning electron microscopy. (Fig.8, 9 and 10).

Study with SEM and EPMA shows that there is some change in morphology and degree of crystallization. More ettringite crystallines were detected in samples with Type N admixture, while $Ca(OH)_2$ was better crystallized in samples without the admixture.

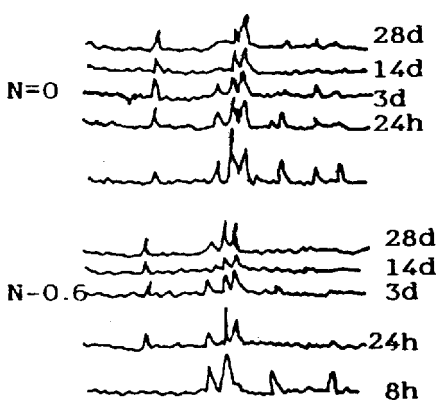

Fig.7 X–ray diffraction patterns

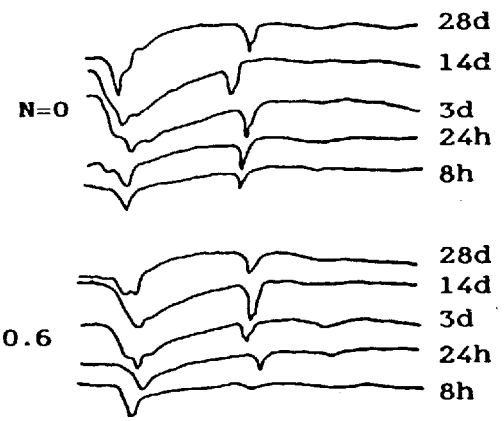

Fig.8 Thermal analysis curves

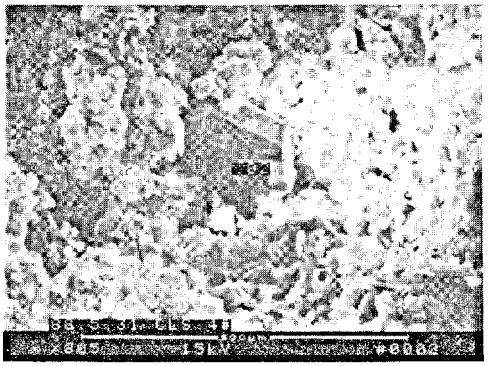

Fig.9 SEM photo of control sample

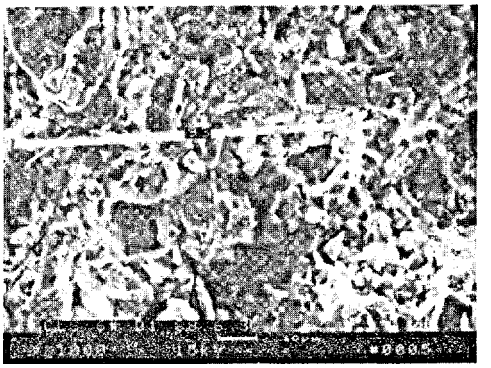

Fig.10 SEM photo of sample with N

The effect of Type N admixture on pore structure of hardened cement paste

1. Pore size distribution of hardened cement paste

Type SERIFS 200 mercury porosimeter is applied to measure pore size distribution of the samples taken from concrete cured for 3, 7 and 28 days.

Table 2. Effect of Type N admixture on pore size distribution

Type N (%)	W / C	Sl (cm)	Ac (%)	Tv. ($\times 10^{-6}$ ml / g)			Ms. (Å)		
				3d	7d	28d	3d	7d	28d
0	0.61	5.7	1.3	134	107	84	1500	1000	600
0.6	0.51	6.3	2.6	107	105	71	1000	500	150

Tv.: Total volume; Ms.: Most probable pore size; Sl: slump; Ac: Air content

Table 2 indicates that the total pore volumes are virtually the same for both samples with and without Type N admixture, but that the size of the most probable pore is smaller for the sample with the admixture than that for the sample without it at the same age, though for both samples the size of the most probable pores become smaller as the hydration proceeds.

2. Characteristics of the bubbles in the hardened concrete

Table 3 shows the influence of Type N admixture on the spacing factor, the mean surface area and the size distribution of the bubbles in hardened concrete. It can be seen that the spacing factor of the concrete with the admixture (411μ) is smaller and the fraction of small pores is greater than those of the concrete without it (624μ). It is shown from the above results that Type N admixture improves the characteristics of the pores and enhances the strength and durability of the concrete [3].

Table 3. Effect of Type N admixture on characteristics of the bubbles

Type N (%)	Sf (μ)	(Asa (mm²/mm²)	Pore size distribution (%)								
			Pore size (μ)								
			< 100	100 ∫ 300	300 ∫ 500	500 ∫ 1000	1000 ∫ 2000	2000 ∫ 3000	3000 ∫ 4000	4000 ∫ 5000	>5000
0	624	7.34	14.4	25.6	15.6	22.2	12.3	4.4	2.2	2.2	1.1
0.6	411	7.81	17.2	42.6	10.5	14.4	9.1	3.8	1.4	1.0	0

* Sf: space factor ** Asa: Average surface area of pores.

The effect of Type N admixture on physical and engineering properties of the concrete

The test results are shown in Table 4 and 5, and Figs 11 and 12.

Table 4. Effect of Type N admixture on concrete properties (1)

Type N (%)	W / C	Sl. (cm)	Compressive strength (MPa)					Flex. str. (MPa)		Elastic modulus (MPa)
			1d	3d	7d	28d	90d	7d	28d	
0	0.68	5.8	4.72	12.8	20.4	30.4	38.1	3.08	3.91	29800
0.6	0.59	5.2	8.31	21.5	32.6	42.5	49.7	3.51	4.27	30900

* Concrete proportion: 1:2.34:3.60; Cement: silicate cement.

Table 5. Effect of Type N admixture on concrete properties (2)

Type N (%)	W / C	Sl. (cm)	Bd. (kg / m³)	Ac (%)	Ip.	Freezing and thawing			Loss of strength (%)
						Cy.	Comp. strength (MPa)		
							Normal curing	Freezing and thawing	
0	0.68	6.0	2355	1.0	–	100	40.7	37.5	7.9
0.6	0.61	5.6	2315	1.6	S12	200	45.9	44.4	3.1

Bd.: bulk density; Ip.: impermeability; Cy.: cycles
Concrete proportion: 1:2.34:3.60; Cement: slag cement

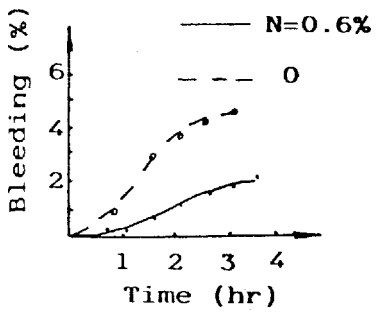

Fig.11 Curves of bleeding vs. time

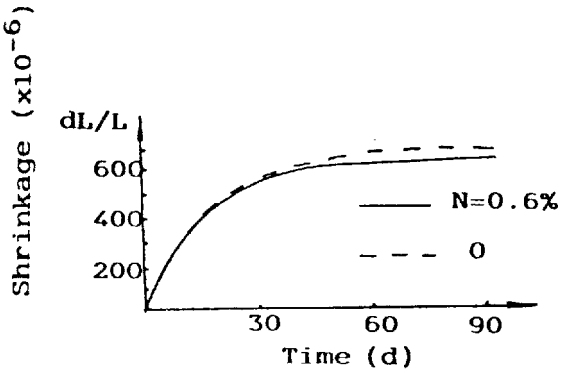

Fig.12 Drying shrinkage curve

Effect of Type N admixutre

The following mechanism is proposed by studying the above test results.

As a surfactant added into fresh cement paste Type N admixture is first adsorbed on cement particles, achieving a high negative zeta–potential, which improves the rheological behaviour and workability of the cement paste [4].

After the adsorption of Type N admixture on the cement, water molecules become difficulty to lodge from the cement particles because of the static electrical repulsion and space–hindering effect, so that the hydration process is retarded, slowly developing a homogeneous early structure of hydration products, which is beneficial to the strength of hardened concrete.

Besides, the addition of Type N admixture improves the pore structure of the concrete by reducing large pore volume and spacing factor, which makes contribution to the durability and strength of the hardened concrete.

REFERENCES

1. Wu, Z.W.: "Concrete in China–Paste, Present and Future", Proceedings of The Second Beijing International Symposium on Cement and Concrete, Beijing, China, 1989, V.1, 16–24.

2. Smith, D.K.: Cementing, Millet the Printer, Inc., Dallas, Tex., USA, 1976, 104–107.

3. Mindess, S. and Young, J.F.: "Concrete, Prentice–Hall, Inc., Englewood Cliffs, New Jersey, USA, 1981, 170–172.

4. Massazza, F. and Costa, U.: "Rheological Problems Related to the Use of Cement", Il Cemento, 1982 (4), 217–219.

RHEOLOGICAL PROPERTIES OF CEMENT MIXES CONTAINING DIFFERENT ORGANIC DISPERSANT ADMIXTURES

J R Baragaño* and A Macías**

**CIDE-ASLAND, SA, Villaluenga de la Sagra, Toledo, SPAIN*
***Building Sciences Institute Eduardo Torroja, Madrid, SPAIN*

ABSTRACT

The effect of lignosulfonate, sulfonated naphthalene and melamine- formaline condensates upon the rheological properties of cement pastes made with three types of cement has been investigated.The studied cements were: low tricalcium aluminate (C_3A = 2.5%), high alkali (Na_2O equivalent = 0.95%) and high fineness Portland Cement (S.A, Blaine = 5002 cm^2/gr).

Plastic viscosity and yield stress of pastes with different concentrations of admixtures through coaxial cylinder viscometer measurements were determined. The combined effect of sodium gluconate and sulfonated naphthalene - and melamine - formaline on the slump retention was examined by measuring the thickening time with a consistometer. Results on compressive and flexural strengths and initial and final setting times are also discussed for the three types of organic dispersants admixtures.

Results show that the efficiency of superplasticizers admixtures depends on the type, of cement, the C_3A /calcium sulphate ratio being the decisive factor. Superplasticizers formulation based on naphthalen sulfonated promote a more fluidifying effect and less slump loss than sulphonated melamine formulations. The presence of sodium gluconate extends retention of improved workability and increases compressive strengths at least in a 20 per cent. With simultaneous addition of lignosulphonate the first effect is even more significant.

RESUMEN

En el presente trabajo se analiza el efecto de la adición de lignosulfonato, resina de naftalen sulfonato y resina de melamina sulfonada en las propiedades reológicas de pastas de cemento. Los cementos estudiados fueron: cemento bajo en aluminato tricálcico (C_3A = 2,5%), cemento con alto contenido en álcalis (Na_2O equivalente = 0,95%) y cemento Portland de finura elevada (S.E. Blaine = 5002 cm^2/gr).

Se midieron la viscosidad plástica y el umbral de cizallamiento de pastas con distinta concentración de aditivos empleando un viscosímetro de cilindros coaxiales. También se examinó el efecto de la adición conjunta de gluconato sódico y resina de naftalen sulfonato - y melamina - en la retención del aumento de trabajabilidad registrando el tiempo de espesamiento con un consistómetro. Por último, se presentan resultados de resistencias a tracción y compresión y de tiempos de inicio y final de fraguado para los tres tipos de aditivos orgánicos dispersantes considerados.

Los resultados muestran que la eficiencia de los aditivos superplastificantes es función del tipo de cemento, siendo la relación C_3A/ sulfato cálcico el factor determinante. Las formulaciones de aditivos superplastificantes basadas en resina de naftalen sulfonato conducen a un mayor efecto fluidificante y a una menor pérdida de trabajabilidad que las formulaciones basadas en resina de melamina. La presencia de gluconato sódico mejora la retención del aumento de fluidez y aumenta las resistencias a compresión en, al menos, un 20%. Con la adición simultánea de lignosulfonato el primer efecto es aún más notable.

COMPOSITION (wt%)	CEMENT A	B	C
SiO_2	21.8	20.3	20.2
Al_2O_3	3.5	4.5	4.7
Fe_2O_3	4.0	2.8	2.5
CaO	64.9	63.5	64.8
MgO	0.96	2.3	1.1
SO_3	2.3	2.7	3.2
K_2O	0.48	1.1	0.85
Na_2O	0.07	0.23	0.09
TiO_2	0.23	0.27	0.26
P_2O_5	0.10	0.15	0.08
L.O.I	1.4	1.8	2.0
FREE CaO	0.90	0.90	1.5
INSOL	0.57	0.60	0.67
C_3S	59.0	59.6	59.8
C_2S	18.1	14.1	12.9
C_3A	2.5	7.2	8.2
C_4AF	12.2	8.5	7.6
SPECIFIC WEIGHT	3.15	3.12	3.12
SURFACE AREA (BLAINE)	3503	4261	5002

TABLE I

Chemical analysis and physical properties of the cements used

INTRODUCTION

Wherever cement slurries or concrete grouts are pumped, their rheological properties are of interest. Also, nowadays, a great deal of attention has been devoted to the problem of developing high-strength chemically stable cements. In order to adjust a slurry at a given water to cement (w/c) ratio for pumpability or to get a high-strength concrete, dispersants, called superplasticizers, are added (1).

The two superplasticizers more frequently used in concrete are sulfonated naphthalene formaldehyde condensate(SNF) and sulfonated melamine formaldehyde condensate (SMF). Both substances are capable of greatly increasing fluidity of concrete, but the slump loss due to the progress of hydration reaction and physical agglomeration, is a draw-back for many practical purposes.

In the present study the effect of lignosulfonated, sulfonated naphthalene and melamine - formaline condensates upon the rheologic properties of cement pastes made with three types of cement have been investigated. The modifications due to the addition of lignosulfonate to the SNF and SMF and the retard in slump loss by addition of a salt of carboxylic acid (sodium gluconate, G) is also studied.

EXPERIMENTAL

Materials

Table I shows the chemical composition and the physical properties of the three cements studied: A, low tricalcium aluminate (C_3A = 2.5%); B, high alkali (Na_2O equivalent = 0.95%) and C, high fineness Portland cement (S.A. Blaine = 5002 cm^2/gr).

The composition of the different mixes tested and of the admixtures used are shown in Table II. In this table the numbers and symbols utilized in figures are also indicated.

SYMBOL	N	COMPOSITION OF MIXES
▽		CEMENT
+	1	CEMENT + SMF
*	2	CEMENT + SNF
□	3	CEMENT + 70% SMF + 30% L
x	4	CEMENT + 70% SNF + 30% L
◊	5	CEMENT + 97% SMF + 3 % G
△	6	CEMENT + 97% SNF + 3 % G
⧗	7	CEMENT + 67.9% SMF + 29.1% L + 3% G
○	8	CEMENT + 67.9% SNF + 29.1% L + 3% G

TABLE II

Composition and Identification of the mixes tested

Techniques

Viscosity- Cement pastes of constant w/c ratio with and without admixtures were prepared. The w/c ratio was chosen for each cement for obtaining similar rheological parameters in all cements in order to maintain the same experimentals conditions: A, w/c = 0.34; B, w/c = 0.44 and C, w/c = 0.34.The organic admixtures in form of a powder were added to the mixed water and stirred in an electrical mixer for 1 minute until complete dissolution. After that, the cement was put in the mixer and mixed with the solution at low-speed for another minute, then allowed to digest for 2 minutes and finally mixed again at high-speed for 1 minute.

Rheological flow curves were obtained by using a coaxial cylinder type viscometer (CERILH). The shear rate was first increased up to the maximum of 100 rpm at a rate of increase of rpm/minute and then decreased at the same rate.

Thickening Time Test- The cement pastes with and without admixtures were prepared with the same characteristics and in the same way that

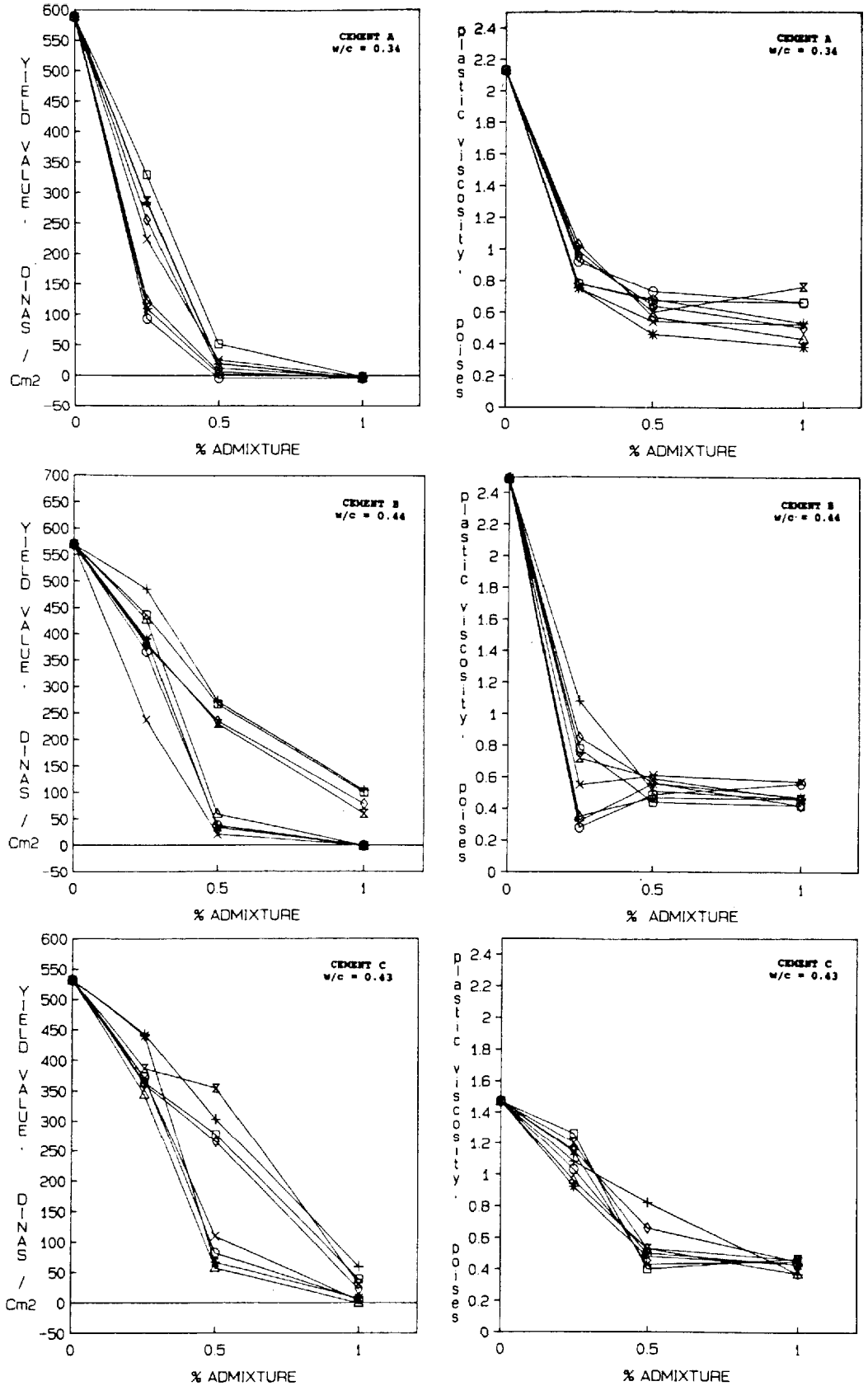

FIG. 1

Yield value and Plastic Viscosity for the cement pastes tested (see identification on Table II)

cement pastes for viscosity measurements. The determination of thickening time, that is, the period of time at which a given cement slurry remains in a fluid state under given conditions was done with a Halliburton Pressurized Consistometer at room temperature and pressure. Experiment was completed when consistency reached 100 Bearden units (equivalents to 10 V).

Determination of setting time- The initial and final setting times were determined in the presence or absence of the admixtures with the Vicat needle. The w/c of the pastes was that at the standard consistency.

Compressive and flexural strength measurements- Blank mortar specimens with w/c ratio equal to 0.5 and c/s ratio of 1:3 were made for the three cements studied. The slump was determined according to ASTM C 230. This slump of the mortar specimens without admixtures fixed the w/c ratio of the mortar specimens with the admixtures. Prisms of 4 x 4 x 16 cm were made for determining the compressive and flexural strength at 1, 7 and 28 days.

RESULTS

In figure 1 the values of yield value (left part) and plastic viscosity (right part) are shown. They are calculated from the rheological flow curves assuming that cement pastes behaved according to the Bingham Model. In this figure it can be seen that all the admixtures tested independently of the concentration produce a decrease in the yield value for the three cements. This effect is sharper for SNF admixtures than for SMF compositions. The addition of L to SMF or SNF generates a little increase of the yield value; on the contrary, the addition of G makes this yield value to diminish. In general the simultaneous addition of both G and L to SNF and SMF produces the lowest yield values.

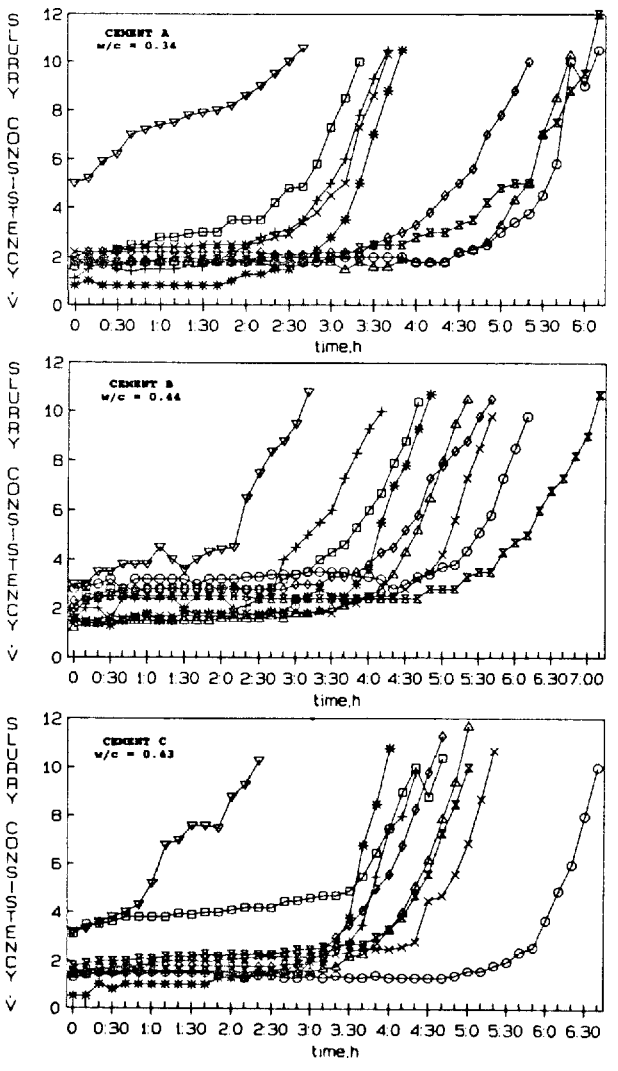

FIG. 2

Slurry consistency of the cement pastes tested (see Table II for identification of curves)

By comparing the three cements tested it can be seen that cement A plus 1% of admixture generates pastes with yield values close to zero for both SNF and SMF; cement B plus the same admixture percentage only generates yield values near zero for the SNF formulations as in SMF compositions yield values above 50 dynes/cm2 are produce. Finally, cement C plus 1% of SMF formulations produces pastes with yield values below 50 and near zero with SNF formulations. As a general rule it can be said that the admixtures have a more significant effect in cement A than on cements B and C (w/c ratio of cement A is 23% < w/c ratio of cements B and C). Cement B is the one needing the highest dosage of admixture for producing the same plasticizer effect.

The results of viscosity may be considered less interesting as the usual and important practical question is whether concrete will flow under the minimum applied stress rather than how fast it will flow. In any case the general tendency observed by which all the admixtures tested whatever the cement is, make the viscosity to decrease until a minimum; after that, viscosity is maintained or even it can increase again. The highest viscosity has been measured in cement A (it agrees with its lowest fineness); the lowest one in cement C, the cement with the highest fineness (S.A. Blaine = 5002).

Figure 2 shows the evolution with time of the consistency of cement A pastes without and with 0.5 wt of cement admixture as well as the evolution of cement B and C pastes without and with 1% wt of cement admixture. These admixture percentages were chosen because of the viscosity results. In the figure it can be observed that the addition of G to SNF or SMF makes the time at which the paste has a flowly consistency considerably longer. Also this

CEMENT + ADMIXTURE	W/C	SLUMP	ARf (%) 1d	7d	28d	ARc (%) 1d	7d	28d
A	0,5	89	-	-	-	-	-	-
A + 0.5% SMF	0.456	95	61.5	23.7	15.7	51.8	35.9	21.4
A + 0.5% SNF	0.422	94	61.5	22	11.4	75.4	37.6	20.4
A+0.5% (70%SMF+30%L)	0.433	94	26.9	5.1	-7.1	25.4	11.6	-6.4
A+0.5% (70%SNF+30%L)	0.411	91	38.4	6.7	-7.1	40.5	15.1	-2.3
A+0.5% (97%SMF+3%G)	0.433	88	53.8	23.7	17.1	62.2	53.8	28.3
A+0.5% (97%SNF+3%G)	0.411	92	50	20.3	15.7	60.3	49.2	23.9
A+0.5% (67.9%SMF+29,1%L+3%G)	0.411	90	11.5	8.4	-1.4	9.4	20.2	2.9
A+0.5% (67.9%SNF +29.1%L+3%G)	0.400	90	15.3	1.7	-4.2	16	20.8	3.1
B	0.5	83	-	-	-	-	-	-
B+1% SMF	0.433	85	20.8	18.4	-1.2	36	10.8	8.9
B+1% SNF	0.400	82	35.4	13.1	4.9	55.4	13.9	13.5
B+1% (70%SMF+30%L)	0.400	88	20.8	1.31	-3.7	34.4	3.8	-1.2
B+1% (70%SNF+30%L)	0.378	84	37.5	5.2	-3.7	33.6	4.02	-2.9
B+1% (97%SMF+3%G)	0.411	88	41.6	15.7	12.3	46.1	24.3	21.9
B+1% (97%SNF+3%G)	0.389	87	31.2	3.9	-1.2	40.9	16.9	13.7
B+1%(67.9%SMF+29.1%L+3%G)	0.389	87	16.6	-6.5	-6.1	2.8	4.2	-4.5
B+1%(67.9%SNF+29.1%L+3%G)	0.367	78	20.8	11.8	-2.4	20.2	13.5	0.7
C	0.5	87	-	-	-	-	-	-
C+1% SMF	0.422	87	-10.9	7.3	10.2	42.5	15.7	12.7
C+1% SNF	0.389	87	27.2	8.5	7.9	55.1	20.6	18.3
C+1%(70%SMF+30%L)	0.400	93	-10.9	-13.4	-17.0	19.01	-6.6	-5.7
C+1%(70%SNF+30%L)	0.378	83	18.2	2.4	-1.1	39.1	12.5	8.1
C+1%(97%SMF+3%G)	0.411	88	12.7	14.6	6.8	49.4	25.5	22.2
C+1%(97%SNF+3%G)	0.389	91	20	6.1	0	48.2	19.8	17.4
C+1%(67.9%SMF+29.1%L+3%G)	0.400	88	5.4	-9.7	-13.6	23.9	2.5	-2.8
C+1%(67.9%SNF+29.1%L+3%G)	0.378	83	16.3	2.4	0	38.0	10.6	6.2

TABLE III

Increments of flexural and Compressive strengths of mortars tested

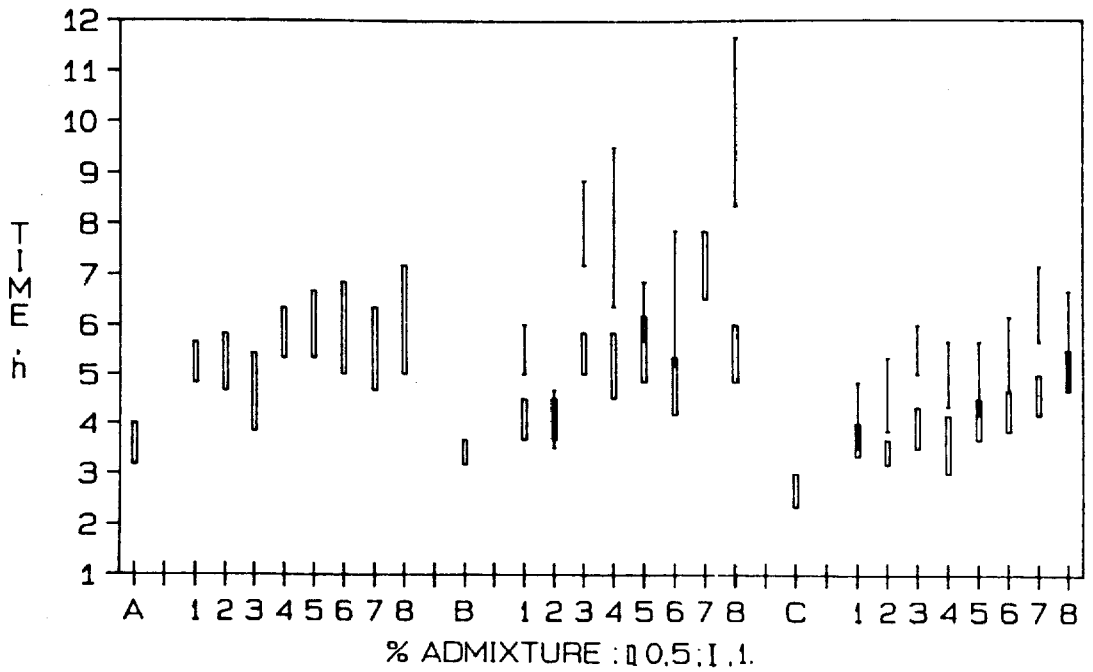

FIG. 3

Initial and final setting times for the cement pastes tested (A, B and C) (see Table II for identification of composition of mixes: numbers 1 to 8)

figure shows that the simultaneous addition of G an L has a synergetic effect of making those times longer even in the cases in which L has little or no effect. It appears that, in general, SNF provokes lower loss of slump.

Initial and final setting times for the three cement pastes with and without admixtures are shown in figure 3. From the results it has been deduced that all the admixtures tested make the initial and final setting to be delayed and make duration of setting to be longer. Longest setting has been measured for SNF and SMF admixtures with G+L addition.

Finally, in Table III the increments of flexural and compressive strengths are shown. These measurements were done at constant slump fitting the w/c ratio. The highest increments of strengths were obtained for cement A with 0.5 % of SNF or SMF while the lowest ones were found in cement B with 1 % SMF or SNF. SNF produces higher resistances although it also produces a reduction in w/c ratio compared with SMF;then it is possible that for the same w/c ratio SMF increases the strengths. The addition of L to SNF or SMF admixtures has a negative effect in strength development which could be balanced by the simultaneous addition of G which increases resistances especially after long periods of time. From the strength results it appears that the efficiency of admixtures is superior in cement A, cement B being less suitable to be used with superplasticizers.

DISCUSSION

The time of retention of improved workability when superplasticizers are added is critical for those uses in which a long time transport or manipulation of concrete is required and it depends on the kind of admixture and of the cement type (2).The mechanism of action of superplasticizers is quite complex but there exists the general agrement for which the fluidifying action is associated which the adsorption of the macromolecules of the polymer onto the cement grains delaying the hydration rate.At the beginning of hydration of cement, tricalcium aluminate and calcium sulphates are virtually the only substances taking part in the hydration reactions (3). The initial hydration takes place at the cements particles surfaces and its extend depends chiefly on the reactivity and on the amount of C_3A , on the proportion of calcium sulphates, on the surface area, on the particle size distribution of the cement and on the temperature of the cement paste.

The progress of hydratation reactions can destroy the adsorption layer of admixtures and so to eliminate its fluidifying effect. According to C_3A content of the cements (see Table I) cement A should be the cement with the slowest hydration rate, the longest set period (see Fig. 3), the lessest water demandant and the slowest process of thickening (see Fig. 2). Effectively, these expectations were in good agreement with the results. Consequently the effect of admixtures on cement A was optimum, that is, the amount needed

for reaching a certain fluidifying effect was minimum. On the contrary, cement C with the highest C_3A content (8.2 % wt) must be the cement in which admixtures behaved worst. But we also have to consider other factors such as fineness and C_3A /$CaSO_4$ ratio. This last variable has an enormous importance being its value of 1.38, 4.86 and 3.45 for cement A, B and C respectively. According to that, cement A is again the better cement to be utilized which admixtures and cement B is now the worst, which is in good agreement with the present results. Also this cement is the one with the highest alkali content and some authors have suggested that high alkali contents in OPC may interact with water reducers and destroy its plasticizing ability (4).

The retention of improved workability depends on the admixture and the type of cement. Mixes containing melamine resin superplasticizers loss slump before than those containing naphthalene resins which is in good agreement with results of others researchers.

Mixing superplasticizers and retarders is one way of ameliorating the problem of loss of workability which has been proposed (5). The delay in initial and final setting times caused by gluconate has the effect of improving the retention of workability. This effect is promoted when lignosulphonate is present. Gluconate has also a possitive effect in the development of resistances. Comparing times of retention of consistency (Fig. 2) and setting times (Fig. 3) we can deduce a direct relation between them.

CONCLUSIONS

- The efficiency of superplasticizers admixtures dependes on the C_3A /$CaSO_4$ ratio of the cement. Increasing this ratio leads to decreasing the fluidifying effect of the admixture.

- Superplasticizer formulations based on SNF generates more fluent and less slump loss cement pastes than formulations based on SMF.

- The association of L with SNF or SMF has not a pernicious effect, amelioring in general the rheological properties of cement slurries but lowering the increment of resistances.

- The simultaneous addition of G and SNF or SMF extends the period of time of retention of improved workability and increases resistances. In presence of L the first effect is even sharper.

ACKNOWLEDGEMENT

The authors wish to thank the "Dirección General de Investigación Científica y Técnica" for financial support through his "ayudas al intercambio de personal investigador entre industrias y organismos públicos de investigación".

REFERENCES

(1) Ramachandran, V.S., American Concrete Inst. Special publication nº 68, (1981), pp. 393-407.

(2) Baufill, P.F.G., Magazine of Concrete Research, 32 (110),(1980), pp. 17-27.

(3) Locher, F.W., Richartz, W. and S. Sprung. Zement-kalk-Gips 29 (1976), N 10, pp. 435-442.

(4) Ramachandram, V.S., Feldman, R.F. and Beaudoin, J.J., Concrete Science, Treatise on Current Research, London: Heyden & Son Ltd., (1981).

(5) Edmeades, R.M. and Hewlett, P.C. Proceedings of Admixtures Congress, Lancaster, (1980) pp.49-72

EFFECT OF SUPERPLASTICIZER ON THE HYDRATION OF PORTLAND CEMENT

N B Singh, Reetika Sarvahl and N P Singh

Department of Chemistry, University of Gorakhpur
Gorakhpur, INDIA

SUMMARY

Owing to its importance the mechanism of action of superplasticizer namely Lico-superplast (LSP) on the hydration of ordinary portland cement (OPC), has been studied by using various techniques. The LSP increased the setting time and reduced the water requirement. The extent of hydration up to 3 days is found to be nearly the same in the presence and absence of LSP, however, beyond 3 days of hydration the value is higher in the presence of LSP. The electrical conductivity of the cement suspensions in water increased with hydration time and the amount of cement disperesed. In presence of LSP the conductivity is much higher but remained practically constant with time. Further the concentration of Na^+ and K^+ ions in the liquid phase extracted from the hydrating cement increased with time and the values were higher in presence of LSP. Free lime value also increased with time but always lower in the presence of LSP. Compressive strength values also increased with time and LSP. Spectroscopic studies have revealed that LSP is adsorbed over anhydrous surface of cement and some chemical interaction also occurs with $Ca(OH)_2$. The overall mechanism of hydration has been discussed.

INTRODUCTION

Superplasticizers also known as high range water reducing admixtures or super water reducers are generally used in the construction industry as concrete admixtures[1-5]. They reduce water content by a much as 20 to 33%. Apart from this the other advantages are the improvement in concrete workability, slump, setting time, development of early strength etc. These admixtures increase the early strength development and are useful in constructing and resurfacing pavement. The introduction of these superplasticizers has opened up new possibilities for the use of concrete in construction, particularly, for resurfacing bridge decks and constructing other highway facilities. Superplasticizers are four catagories:

(1) Sulphonated-melamine-formaldehyde condensate.
(2) Sulphonate naphthalene-formaldehyde condensates.
(3) Modified lignosulphonates, and
(4) Other superplasticizers such as sulphonic acid esters or carbohydrate esters etc.

The effect of each superplasticizer will be different on the concrete mixes. However, the variation will also depend on, water-cement ratio, cement content, concentration of superplasticizer, the stage when it is added to the concrete, temperature etc. It is bserved that in the presence of superplasticizers, hydration and hence the rate of uptake of free water slows down in the early stages of hydration. Two theories have been proposed to explain the mechamism of hydration in presence of superplasticizers. In one theory, it is claimed that the higher liquidity of superplasticized cement pastes is due to the larger amount of free water present during the early hydration stages. Perhaps the superplasticizer from some coating around the cement argain and/or the reaction products. In the other theory it is assumed that superplasticizers are adsorbed over anhydrous and the hydrated product surfaces.

A large number of studies have been made to understand the above proposed mechanisms, but so far it has not been possible to establish the actual mechanism of action of superplasticizers during the hydration of cement. The propose of this article is to evaluated the effect of Lico-superplast on the hydration of cement.

EXPERIMENTAL

Materials : Portland cement of Blain surface area 4300 cm^2/g having the following mineralogical composition was used for hydration studies.

C_3S	C_2S	C_3A	C_4AF
68.2%	10.1%	9.5%	10.1%

Lico-superplast obtained from NCB, Ballabhgarh was used as a superplasticizer and is abbreviated as LSP.

Methods : Setting time (w/s = 0.23) in presence of different amounts of LSP was determined with the help of a vicat apparatus and water reduction was also determined with the help of the same apparatus, but the needle was replaced by a plunger. Non-evaporable water contents (w/s = 1.0) of the hydrated samples hydrated at different intervals of time were determined by heating a known amount of the sample at 1000°C. Free lime determinations (w/s = 1.0) were determined by modified Franke method. Compressive strengths (w/s = 0.25) of cubes (8x8x8 cm^3) were determined

with the help of an AIMIL compression testing machine. The cubes were cured in water.

Electrical conductivities of the suspensions of portland cement in water as well as in LSP solutions were measured with the help of Chemita Digital conductivity meter using a conductivity cell. The suspensions were strirred continuously magnetically.

Adsorption studies of LSP over anhydrous and hydrated cements were made with the help of Bausch & Lomb spectronic-2000 - spectrophotometer. Spectra of different concentrations of LSP in water were recorded in the wavelength range of 200-350 nm. λ_{max} was obtained at around 228 nm. From the optical density at λ_{max}, a calibration curve was plotted. Anhydrous and hydrated cement (24 h) were shaken with water and LSP solution (0.001%) for different intervals of time and the optical density of the filterates were determined at λ = 228 nm and from the calibration curve, the amount of LSP adsorbed was determined.

RESULTS AND DISCUSSION

The variation of setting times in the presence and absence of LSP is given in table 1. From the table it is clear that both the initial and the final setting times increase with LSP concentration indicating that LSP retards the hydration.

Table 1

Setting time

S.No.	Conc. of LSP (%)	Initial setting time (min)	final setting time (min)
1	0.0	57	150
2	0.2	74	218
3	0.4	82	238
4	0.5	88	242
5	0.6	108	252
6	0.8	122	262
7	1.0	145	290

Percent water reduction increases as the concentration of LSP increases and the water reduction is around 23% in presence of 2% LSP.

The variation of non-evaporable water content with hydration time (upto 90 days) in the presence and absence of 1.0 wt % of LSP is given in Fig. 1. Upto 3 days, the extent of hydration is lower in the presence of LSP but after 15 days the hydration increases. Thus during early hours LSP modifies the setting behaviour giving an impression that it acts as a retarder or there is no effect, whereas at longer period of hydration it acts as an accelerator.

The variation of free lime with hydration time in the presence and absence of 1.0 wt % LSP is given in Fig. 2. The free lime is higher in the presence of LSP and the value is highest at 28 days of hydration. It appears that either the extent of hydration is lower in the presence of LSP or LSP reacts with $Ca(OH)_2$, decreasing its concentration. Qualitative tests have indicated that LSP dissolves $Ca(OH)_2$. The decrease in free

lime concentration after 28 days, may be due to the fact that at longer period of hydrations, the crystallinity of CH is much decreased and the total amount could not be detected.

The variation of electrical conductivities with hydration time for different amounts of Portlandcement dispersed in 100 ml water are given in Fig. 3. As the amount of cement is increased, the conductivities are increased with time. This is due to increased concentration of ions in the solutions. The electrical conductivity values increased with the amount of cement but remained practically constant

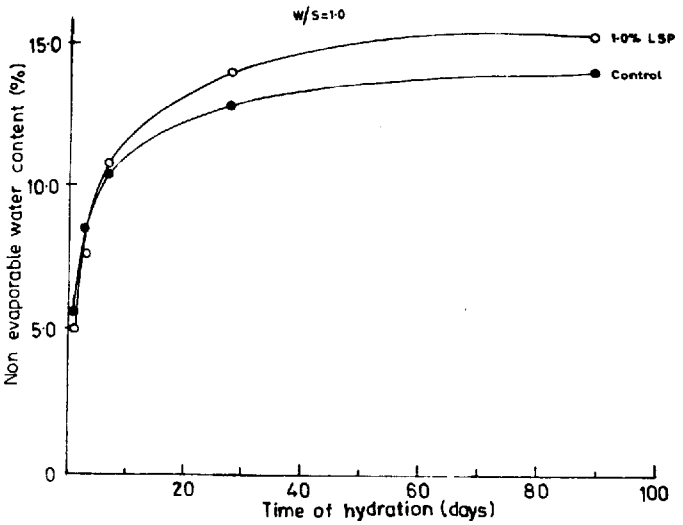

Fig. 1 Variation of Non-evaporable water content with Hydration time.

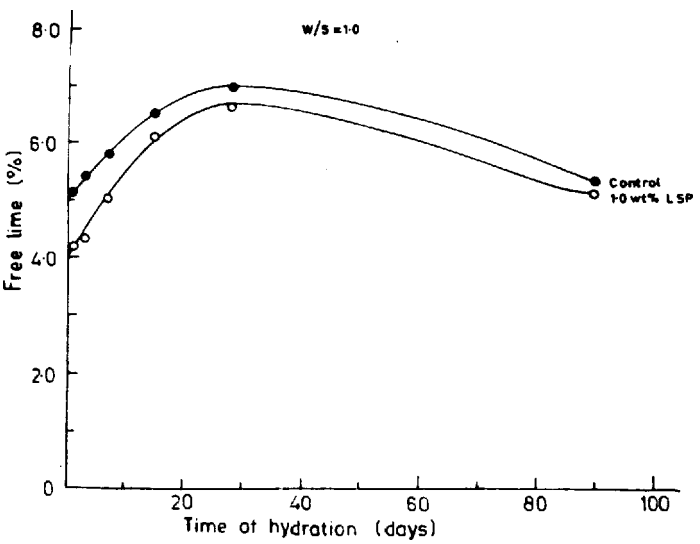

Fig. 2 Variation of Free Lime with Hydration time.

with hydration time in presence of 1.0 wt % LSP. It appears that in the initial stages more ions enter into the solution as the amount of cement is increased but at same time LSP is probably adsorbed over the anhydrous as well as hydrated cement blocking further dissolution of ions into the solution. Probably this situation persisted during the time of experiment i.e. 7 hours.

The values of Na^+, K^+ and Ca^{++} ion concentrations in solutions were found to be higher in presence of LSP and increased with time. This is only because of the interaction of LSP with cement, as a result of which solubility of different ions is increased. The Na^+ ion concentration is found to be maximum because LSP also contains Na^+ ions. It is difficult to conclude anything from this result.

Spectroscopic studies have shown that around 35% LSP is adsorbed over cement surfaces within 5 minutes and after that it is practically constant. Colour change and a broad peak in the absorption curve shows that there is some chemical interaction between LSP and CH.

The variation of compressive strength with hydration time is given in Fig. 4. The value increased with time and concentration of LSP. At 90 days of hydration the strength is increased by 25% and 42.5% in the presence of 1.0 and 2.0 wt % LSP respectively.

The overall results indicate that during plastic state or early stage of cement hydration, LSP is adsorbed over cement surfaces and as a result the extent of hydration is decreased. However, after the plastic state, the LSP modifies the structure and increased the cementing properties either by chemical interaction or decreasing the pore size.

Mor and Mehta[7] have already shown that in presence of superplasticizers pore sizes are decreased and as a result the compressive strengths are increased.

The basic unit of LSP is a naphthalene formaldehyde condensate and contains large number of polar groups. These molecules either enter inter-

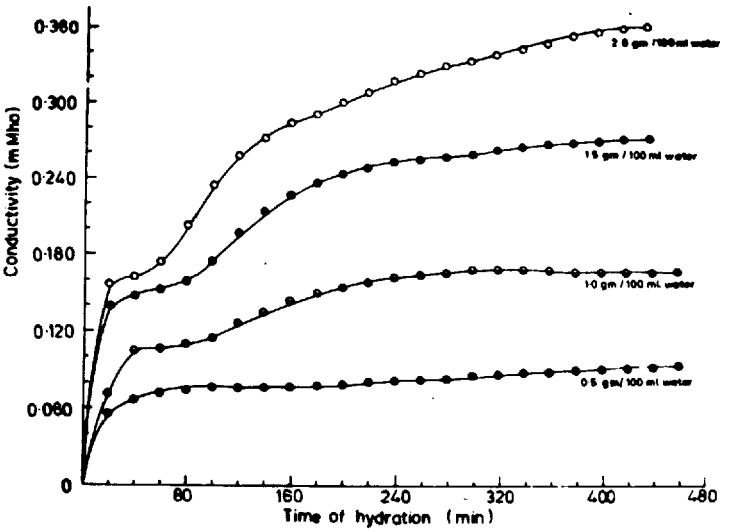

Fig. 3 Effect of Different Amount of cement on the electrical conductivity of the suspensions.

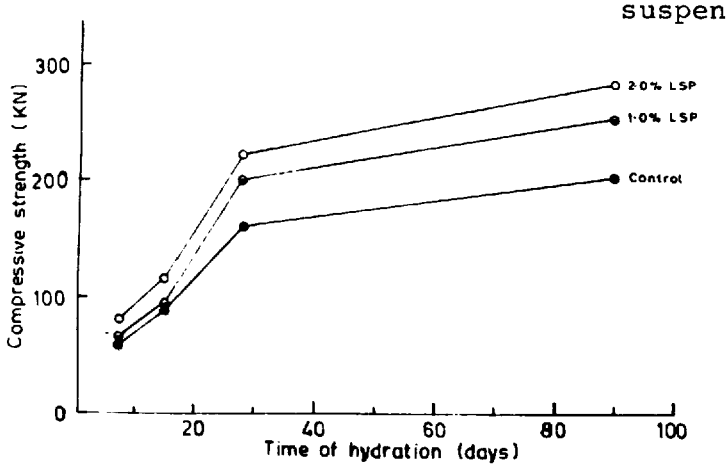

Fig. 4 Variation of Compressive Strength with hydration time.

layer sites of hydration products or absorbed over cement surfaces and the hydration products grow despite the sorbed LSP . It appears that in presence of LSP, the growth of hydration products are poor during plastic state and hence the hydration is retareded. But once the growth of hydration product starts it accelerates with time and in the later stage of hydration, LSP acts as accelerator.

From the above discussion it may be concluded that LSP either enters the interlayer sites of the hydration products or weakly adsorbed and after the plastic state, lowers the port size. This decrease in pore size may be due to LSP as well as increased hydration products. As a result of this the later stage of hydration is accelerated and the compressive strength is increased. The overall mechanism of hydration is given in Fig. 5.

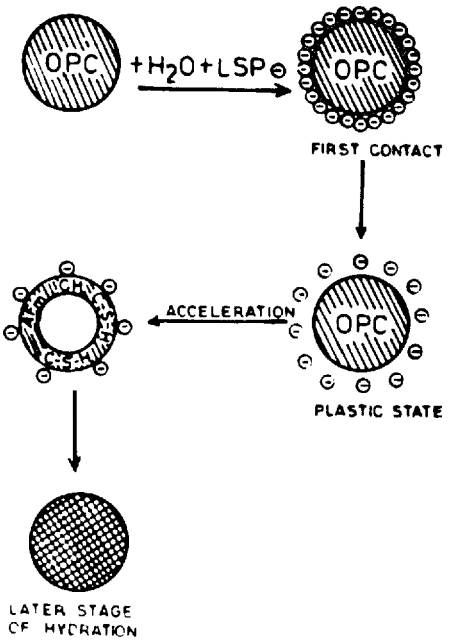

Fig. 5 Mechanism of hydration of cement in presence of LSP.

ACKNOWLEDGEMENTS

The authors are thankful to Prof. S. Giri, Head chemistry department, Gorakhpur University, for providing necessary laboratory facilities. One of us (R.S.) is thankful to CSIR for financial support.

REFERENCES

1 Ghosh R.S. & Malhotra V.M. "Use of Superplasticizers as water reducers", Cement, Concrete and aggregate, 1979, 1(2), 56 (Winto)

2 Lee D.Y. & Yang J.J.F. and Klaiher F.W. : American Society for Testing and Materials 1985, 19

3 Jerath S. and Yamane L.C. : Ibid, 1987, 12

4 Lahallih S.M. Absi, Halabi M. and Ali A.M. : Cem. Concr. Res., 1988, 18, 513

5 Yilmaz V.T. and Glasser F.P. : Adv. Cem. Res., 1989, 2(7), 111

6 Miljkovic L. Mac, Torish J.C., Jain Jin Pinter M.M., Blinc R. and Lahajnar G. : Cem. Concr. Res., 1986, 16, 864

7 Mor A. and Mehta P.K. : Cem. Concr. Res., 1984, 14, 754

8 Ramachandran V.S. : Cem. Concr. Res., 1972, 2, 179

9 Kondo R., Daimon M. and Sakai E. : Cemento, 1978, 75, 225

INFLUENCE OF SUPERPLASTICIZER ON FLUIDITY OF FRESH CEMENT PASTE WITH DIFFERENT CLINKER PHASE COMPOSITION

E Asakura, H Yoshida and H Nakae

Cement Research Institute, Mitsubishi Materials Corporation
JAPAN

SUMMARY

To clarify the influence on the fluidity of fresh cement paste by phase composition of Portland cement clinker, six experimental cements were prepared using natural raw materials. In the preparation, C_3S/C_2S or C_3A/C_4AF in each of these cements was changed, with the content of interstitial phase or silicate phase kept constant. Fluidity, zeta potential, adsorption of naphthalene sulfonate formaldehyde type superplasticizer (hereinafter abbreviated as NSF) and the amount of hydration product in fresh cement paste were measured respectively. The obtained results are as follows.

The apparent viscosity of NSF-added fresh cement paste and the amount of apparent saturated NSF adsorption increased respectively with incremental C_3S/C_2S or C_3A/C_4AF after 10 minutes of hydration. On the other hand, the absolute zeta potential of NSF-added cement reduced with incremental C_3S/C_2S or C_3A/C_4AF.

The apparent viscosity of fresh cement paste rose with time elapse. Especially this viscosity rise was remarkable in the cement of low C_3S/C_2S or low C_3A/C_4AF. It is presumed that this viscosity rise resulted from sedimentation of cement paste.

RESUMÉ

De manière à clarifier l'influence de la composition de phase du clinker de ciment Portland sur la fluidité d'une pâte de ciment frais, six ciments expérimentaux ont été préparés en utilisant des matières brutes. Dans ces ciments, C_3S/C_2S ou C_3A/C_4AF ont été modifiés, alors que le contenu de la phase interstitielle ou de la phase au silicate a été maintenu constant. La fluidité, le potentiel zêta, l'adsorption du superplastifiant de type à naphtaline sulfonée formaldéhyde (NSF) et la quantité du produit d'hydratation de la pâte de ciment frais ont été mesurés. Les résultats obtenus sont les suivants.

La viscosité apparente de la pâte de ciment frais avec NSF et la quantité de l'adsorption NSF saturée apparente augmente avec C_3S/C_2S ou C_3A/C_4AF à 10 min. d'hydratation. La valeur absolue du potentiel zêta du ciment avec NSF diminue avec l'augmentation de C_3S/C_2S ou C_3A/C_4AF.

La viscosité apparente de la pâte de ciment frais augmente avec le laps de temps. Plus particulièrement, une augmentation dans la valeur est rem rquable pour le ciment avec un faible C_3S/C_2S ou C_3A/C_4AF. Ce qui incite à contribuer à la sédimentation de la pâte de ciment.

INTRODUCTION

In recent years, superplasticizer has been used to improve the fluidity of fresh concrete and to produce high-strength concrete. A number of studies have ever been deployed to clarify the influence of superplasticizer on fluidity of concrete(1), the hydration of cement (2-6), its adsorption property against cement(5-8). However, many of these studies used cement clinker minerals from pure reagents(2-4, 6-9). There are only a few studies which were made using clinkers synthesized from natural materials with respect to the rheological properties(9).

The purpose of this study is to clarify the influence on the fluidity of cement paste by clinker phase composition which is determined from Bogue's equation. Furthermore, the amount of superplasticizer adsorption into cement particles, the fluidity, the amount of hydration product and the zeta potential were respectively measured using experimental cements of different C_3S/C_2S or C_3A/C_4AF.

CEMENT PREPARATION

Clinkers were prepared using natural raw materials. Raw meals were first calcined for 1.5 hours at 1000 °C and then burned at 1450 °C in an electric furnace until the amount of free lime reduced below 1.0%. By this treatment, two series of clinker were prepared; S-series of different C_3S/C_2S in silicate phase and I-series of different C_3A/C_4AF in interstitial phase. Table 1 shows the mineral composition determined from Bogue's equation. Each clinker was ground to $3200\pm100 cm^2/g$ in Blaine specific surface area with gypsum equivalent to 2.0% as SO_3.

Table 1 Characters of cement used

Sample	Mineral composition* C_3S	C_2S	C_3A	C_4AF (%)	Free CaO (%)	Na_2Oeq (%)	Inter-** stitial phase (%)	Blaine (cm^2/g)	BET (m^2/g)	n*** value	Average*** particle size (μm)
S-1	43	34	9	10	0.19	0.65	18.3	3230	0.79	0.99	15.4
S-2	54	23	10	10	0.27	0.64	18.3	3270	0.80	0.99	15.4
S-3	67	10	9	10	0.81	0.31	18.8	3230	0.78	0.99	15.7
I-1	54	24	3	16	0.20	0.48	18.4	3190	0.81	0.98	15.3
I-2	54	23	8	11	0.52	0.44	18.3	3230	0.78	0.99	15.5
I-3	55	23	14	5	0.46	0.28	17.7	3280	0.80	0.99	15.9

NOTE; * : Calculated by Bogue's equation
** : Residues after salicylic acid methanol treatment.
*** : Measured with laser-diffraction particle size distribution analyzer and calculated from Rosin-Ramler equation using 1 to 48 μm residues

EXPERIMENTAL

Adsorption amount of NSF

Superplasticizer-- β-naphthalene sulfonate formaldehyde high condensate (NSF: KAO MIGHTY 150) was added to water at the rate of 0 to 1.6% against specific cement weight. Subsequently each cement was mixed with water at water-cement ratio (W/C) of 0.5 for 2 minutes. After 10 minutes of hydration, the liquid phase was centrifugally separated from the pastes. Then, NSF concentration in the liquid phase was measured by a total organic carbon analyzer (Shimadzu TOC-5000). Furthermore, the adsorption amount was determined from the difference between residual NSF content in the liquid phase and the quantity of initially added NSF.

Flow curve

Paste flow curves were obtained from the measured results by a coaxial rotational viscometer with double cylinder (Mettler Contraves 115 with MS-DIN125). The cement pastes were prepared as prescribed above. Fig. 1 shows the procedure for measuring the flow curve at a regular interval which is roughly

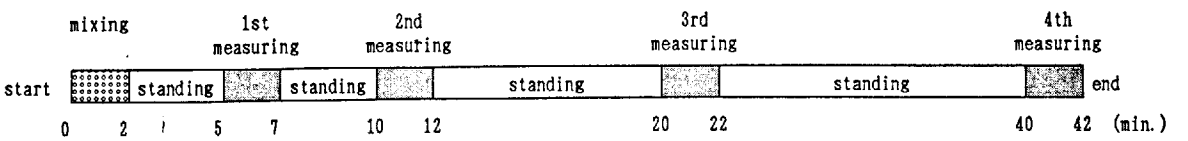

Fig. 1 Measuring procedure of flow curve

equivalent to the procedure used in slump loss measuring test of fresh concrete. In measuring shear stress, the shear rate was continuously accelerated from $0s^{-1}$ to $1000s^{-1}$ per minute and subsequently decelerated to $0s^{-1}$ in one minute. Then, the apparent viscosity of each paste was measured at shear rate of $200s^{-1}$.

Zeta potential

Zeta potential of cement particles in the above liquid phase was measured using an electrophoresis type zeta meter (Pen Kem System 3000). Small quantity of cement particles was sampled from the above cement paste and then added and dispersed into the liquid phase by a ultrasonic vibrator.

Hydration products

Each cement was hydrated on W/C=0.5 and 0.0～1.6% NSF. After given times, the sample was dispersed in acetone and subsequently hydration was discontinued. Then, the hydrated samples were dried in the air of 12% in relative humidity. Hydration products from the samples were identified with XRD and TG-DSC. Subsequently the amount of ettringite in each sample was analysed by an ethylene glycol-methanol extraction method(10).

Sedimentation volume of paste

Each cement paste (W/C=0.5 NSF:0.0～1.6%) was dispersed in a measuring cylinder. After 40 minutes of hydration, the sedimentation volume thereof was determined as a volume against weight of paste sedimented on the cylinder bottom.

RESULT

Adsorption amount of NSF

Fig. 2 shows the apparent adsorption isotherm curves of NSF on cement. These curves were similar to Langmuir's type of isotherm. The apparent adsorption amount of saturated NSF became high with increase of C_3S/C_2S or C_3A/C_4AF. As for cement containing 3% of C_3A, the apparent adsorption amount of saturated NSF was very small. On the other hand, the apparent adsorption amount of same NSF in cement containing 8% or more of C_3A was nearly constant.

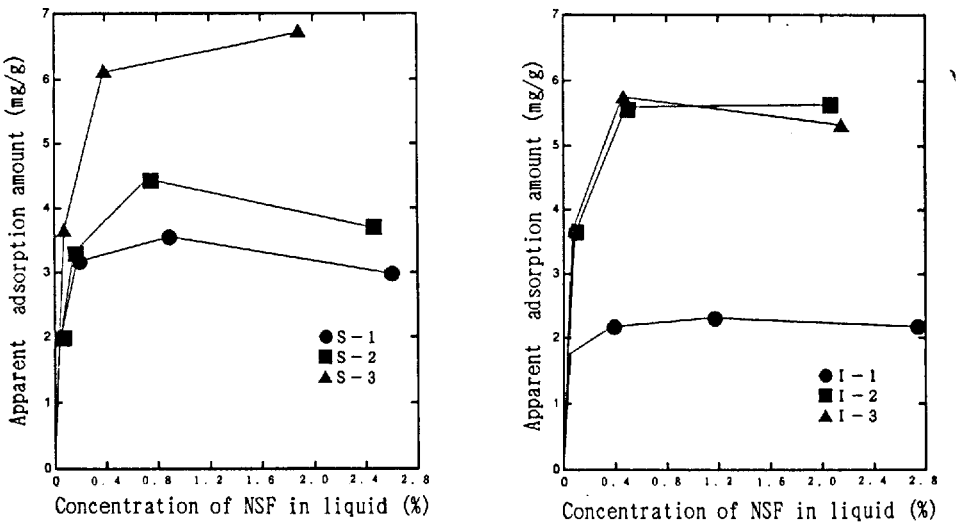

Fig. 2 Apparent adsorption isotherm of NSF on cement

Flow curve

Figs. 3～8 show the flow curves of the pastes. Regarding cement pastes containing no NSF, the apparent viscosity of each paste after 10 minutes of hydration rose with decremental C_3S/C_2S or incremental C_3A/C_4AF (Fig. 3). Particularly the influence on the viscosity by the latter was greater than that by the former. The apparent viscosities of same cement pastes showed almost no ageing change (Figs. 3, 4).

For NSF addition, the paste after 10 minutes of hydration showed a behavior approximate to Newtonian's flow. The apparent viscosity of each paste continued to lower with incremental NSF until the NSF reached the saturated adsorption. When cement particles were saturated with NSF, the apparent viscosity of cement paste remained unchanged even after further addition of NSF. Furthermore, apparent viscosity difference was almost not found among cements of different clinker mineral composition (Figs. 5～8). In the case of NSF addition up to 0.4% max, the apparent viscosity of pastes rose with incremental

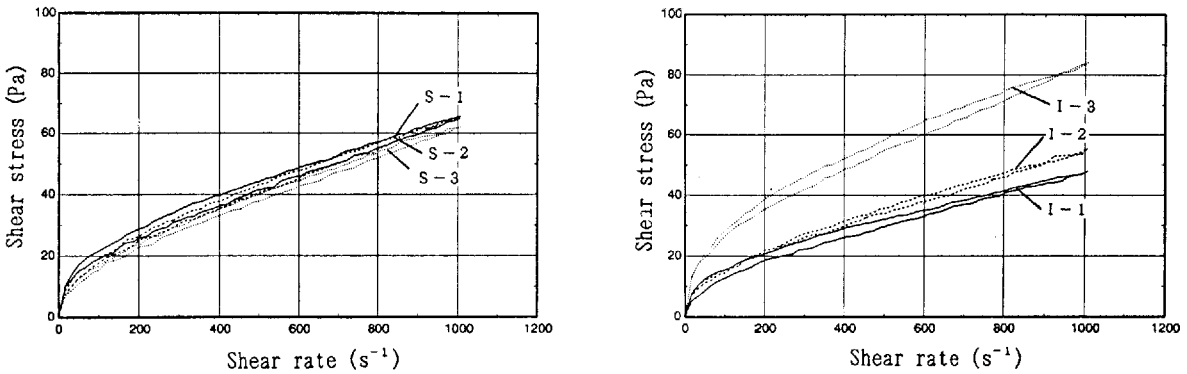

Fig. 3 Flow curves of NSF non-added cement pastes (after 10 minutes of hydration)

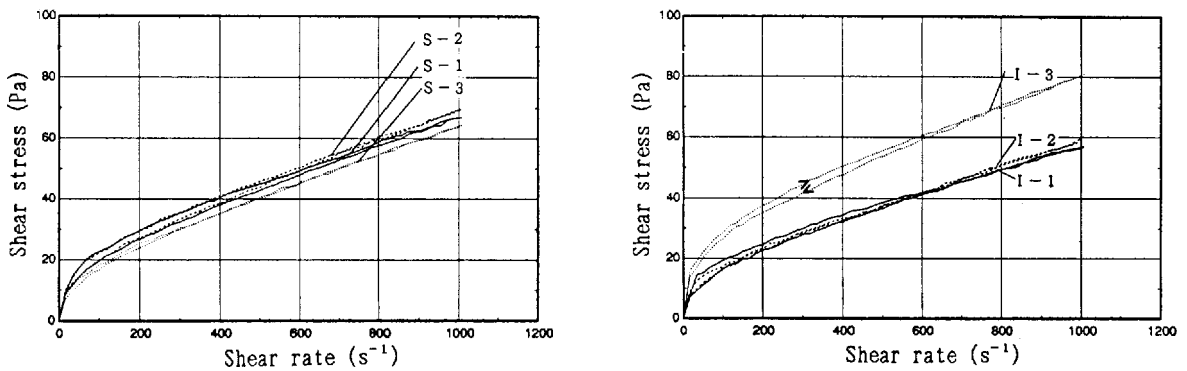

Fig. 4 Flow curves of NSF non-added cement pastes (after 40 minutes of hydration)

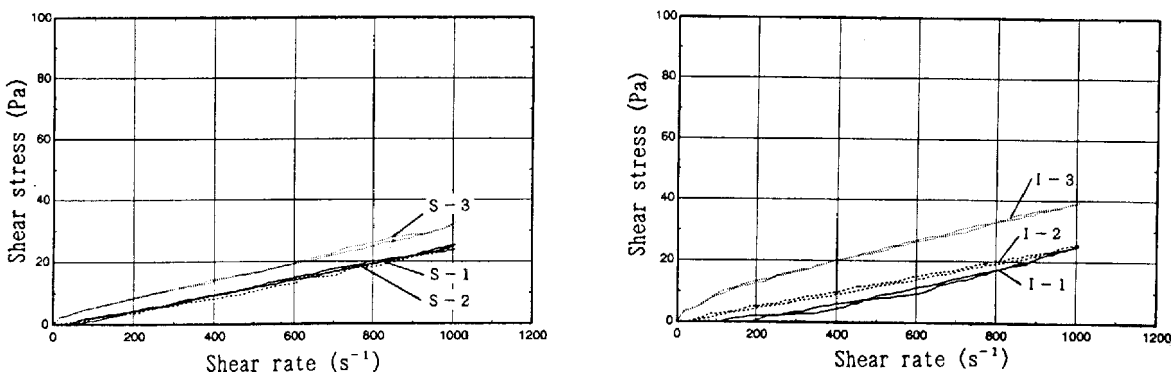

Fig. 5 Flow curves of NSF 0.4%-added cement pastes (after 10 minutes of hydration)

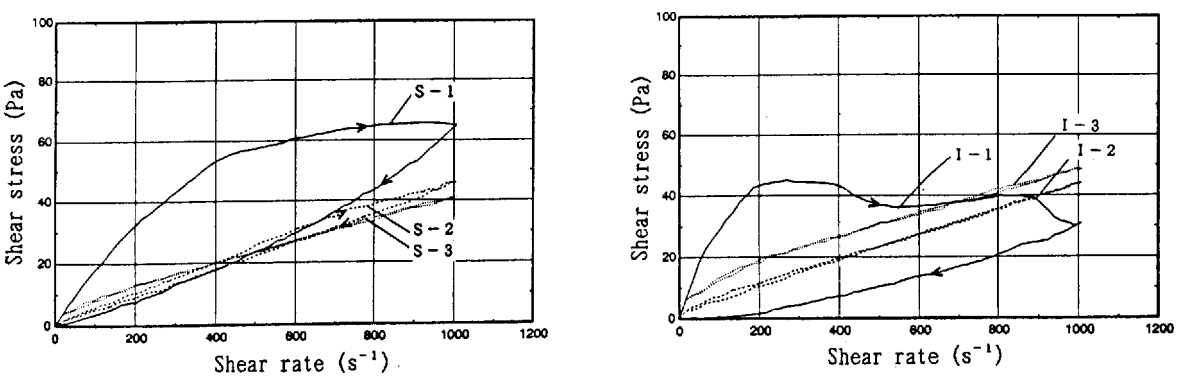

Fig. 6 Flow curves of NSF 0.4%-added cement pastes (after 40 minutes of hydration)

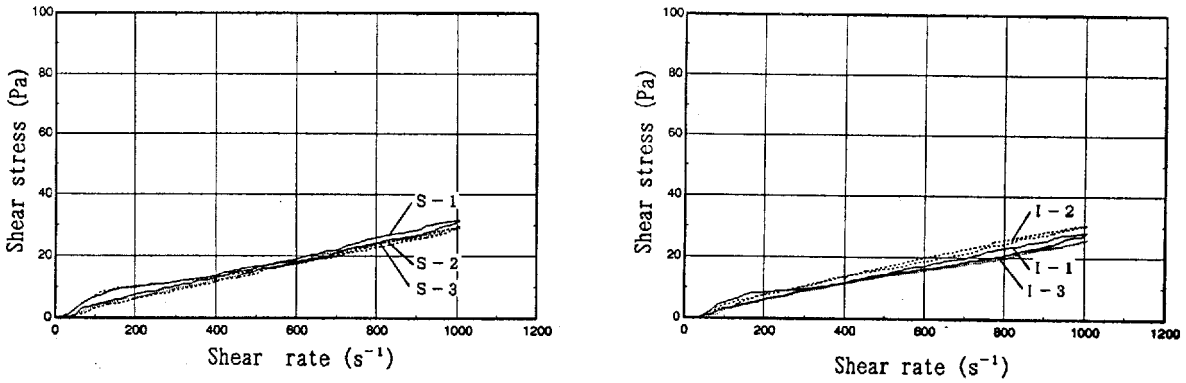

Fig. 7 Flow curves of NSF 0.8%-added cement pastes (after 10 minutes of hydration)

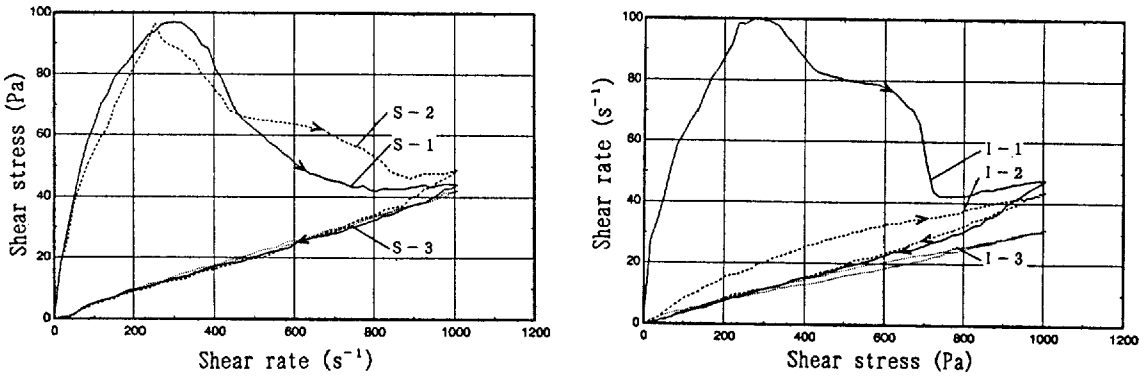

Fig. 8 Flow curves of NSF 0.8%-added cement pastes (after 40 minutes of hydration)

C_3S/C_2S or C_3A/C_4AF (Figs. 5~8). The apparent viscosity after 40 minutes of hydration was higher than that after 10 minutes, caused by incremental addition of NSF.

Zeta potential

Table 2 shows the zeta potential of cement. As shown, the zeta potential of cement containing no NSF was 0mV to +7mV, having increased with decremental C_3S/C_2S or C_3A/C_4AF.

As for cements containing NSF, the absolute zeta potential of each cement continued to increase with incremental NSF until cement particles were saturated with NSF. This absolute zeta potential also increased with decremental C_3S/C_2S or C_3A/C_4AF, when NSF was added up to 0.4% max. As shown, the absolute zeta potential after 40 minutes of hydration was lower than that after 10 minutes. It reduced remarkablly particularly in cement samples which are not saturated with NSF.

Table 2 Zeta-potential of cement (mV)

Sample	10 minutes of hydration				40 minutes of hydration		
	NSF non-added	NSF added			NSF added		
		0.2%	0.4%	0.8%	0.2%	0.4%	0.8%
S-1	+0.1	-32.1	-33.6	-34.8	-26.6	-33.1	-34.0
S-2	+1.1	-33.1	-30.7	-33.0	-31.0	-32.4	-37.4
S-3	+6.5	-19.4	-20.7	-27.7	- 3.1	-15.1	-31.9
I-1	+5.6	-30.1	-31.9	-33.5	-31.5	-33.4	-34.2
I-2	+3.7	-28.0	-27.0	-31.1	-30.7	-28.6	-34.9
I-3	+0.5	-10.9	-16.2	-25.1	- 1.9	- 4.1	-29.0

Hydration products

As regards hydration products in hydrated samples, whether NSF added or not added thereto, only ettringite was identified by XRD and TG-DSC. Fig. 9 shows the amount of ettringite in hydrated samples.

The amount of ettringite didn't depend on variation of C_3S/C_2S, but the amount of ettringite increased with incremental C_3A/C_4AF. Any of cement samples containing NSF showed the increase of the

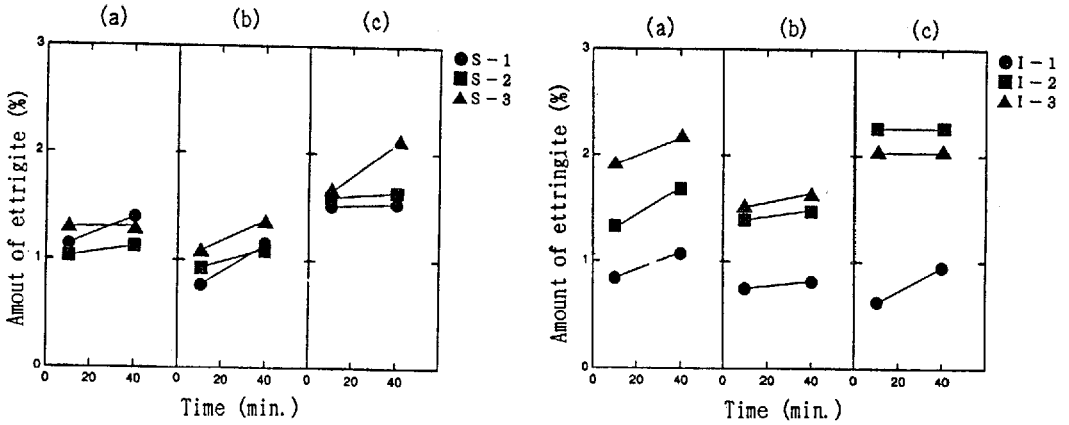

(a) Plaine (b) 0.4% NSF (c) 0.8% NSF

Fig. 9 Time tendency of the amount of the ettringite in cement

amount of ettringite depending on incremental C_3S/C_2S. Further, the amount of ettringite was very small in cement containing 3% of C_3A, while those in cement containing 8% or more of C_3A were nearly constant.

Sedimentation volume of paste

Fig. 10 shows the relationship between the sedimentation volume and apparent viscosity of NSF-added cement paste after 40 minutes of hydration. As shown, this relationship was good.

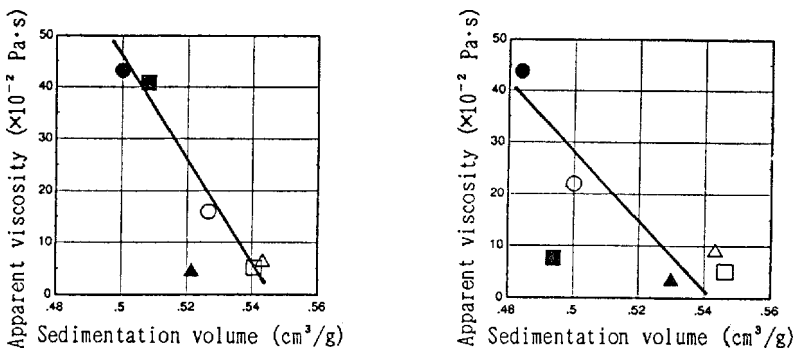

Fig. 10 Relation between sedimentation volume and apparent viscosity of cement paste with different content of NSF

DISCUSSION

Fluidity of NSF non-added cement paste

The apparent viscosity of NSF non-added cement paste rose with decremental C_3S/C_2S or incremental C_3A/C_4AF. This tendency of viscosity rise relates to the amount of ettringite. In other words, probably this tendency reveals that ettringite gives inverse affect to the rheological property of NSF non-added cement pastes(11, 12).

Fluidity of NSF-added cement paste

The absolute zeta potential of NSF-added cement paste increased and the apparent viscosity thereof after 10 minutes of hydration lowered reversely. Such a phenomenon can be explained as follows; NSF adsorbed in cement paste acts to raise the absolute zeta potential and, as a result, increasing inter-particle repulsive force stabilizes particle dispersion.

Cement containing high ratio of C_3S/C_2S or C_3A/C_4AF adsorbed a large amount of NSF. When addition of NSF is small, the absolute zeta potential reduces and the apparent viscosity of paste increases reversely. Addition of NSF at less than saturated NSF adsorption amount makes the absolute zeta potential smaller and also the apparent viscosity of paste higher, because of insufficiency in NSF adsorption into cement particles. When NSF is further added to a paste in which NSF was adsorbed, therefore, the absolute zeta

potential of the paste increases slightly, while the apparent viscosity thereof remains almost unchanged.

These pastes show similar apparent viscosity in spite of different mineral composition. From the result of NSF adsorption into I series of cement, the amount of NSF adsorption into C_3A is considered to be larger than that into C_4AF. This differs from the adsorption character in pure clinker mineral synthesized from reagents.

The apparent viscosity of pastes after 40 minutes of hydration was higher than that after 10 minutes. The viscosity rise is remarkable particularly in pastes containing low ratio of C_3S/C_2S or C_3A/C_4AF. Judging from hydration product and sedimentation volume in and of paste, such a phenomenon is considered to result not from hydration product but from sedimentation of cement particles. The dispersed cement particles are easy to slip from each other and, as a result, facilitate production of cement paste of low sedimentation volume. This acts to raise the apparent viscosity of pastes after 40 minutes of hydration.

On the other hand, the pastes of high apparent viscosity after 10 minutes of hydration showed slight rise of the apparent visosity after 40 minutes. Considering the lowered absolute zeta potential, it is presumed to be caused not by sedimentation but by secondary aggregation of cement particles(13).

CONCLUSION

1. The apparent viscosity of NSF non-added cement paste rises with decremental C_3S/C_2S or incremental C_3A/C_4AF in cement. Cement paste of high apparent viscosity is considered to closely relate to the amount of ettringite which is more formed in such a cement paste.
2. The apparent viscosity of NSF-added cement paste, after 10 minutes of hydration, rises with incremental C_3S/C_2S or C_3A/C_4AF in cement. In the addition of small NSF, the absolute zeta potential of cement with high saturation adsorbability is low because NSF is only adsorbed in a part of the particles surface. This low absolute zeta potential is presumed to cause the apparent viscosity to rise during the initial hydration of cement.
3. The apparent viscosity of NSF-added cement paste rises with time elapse. Particularly the viscosity rise is remarkable in cement paste of low C_3S/C_2S or C_3A/C_4AF. Such remarkable rise is condidered to be caused by sedimentation of cement particles.

References

1. Daimon, M. and Roy, D. M. : "Rheological properties of cement mixes: I. Methods, preliminary experiments, and adsorption studies", Cement and Concrete Research, 1978, 8(6), 753-764, (ENG.)
2. Collepardi, M., Corradi, M., Baldini, G. and Pauri, M. : "Hydration of C_3A in the presence of lignosulfonate-carbonate system or sulfonated naphthalene polymer", 7th International Congress on the Chemistry of Cement, 1980, VI, 524-528, (ENG.)
3. Massazza, F. and Costa, U. : "Effect of superplasticizers on the C_3A hydration", 7th International Congress on the Chemistry of Cement, 1980, VI, 529-534, (ENG.)
4. Ramachandran, V. S. : "Adsorption and hydration behavior of tricalcium aluminate-water and tricalcium aluminate-gypsum-water systems in the presence of superplasticizers", ACI Journal, 1983, 80(25), 235-241, (ENG.)
5. Sakai, E., Yamanaka, S., Daimon, M. and Kondo, R. : "Influence of sodium aromatic sulfonates on the hydration of cement", Nippon Kagakukaishi, 1977(2), 208-213, (JPN.)
6. Suzue, S., Okada, E. and Hattori, K. : "Adsorption of superplasticizer on cement", CAJ Review, 1981, 35, 108-110, (Eng.)
7. Costa, U. and Massazza, F., : "Adsorption of superplasticizers on β-C_2S-changes in zeta potential of particles and the rheology of pastes", Il Cemento, 1984, 81(3), 127-140, (ENG.)
8. Nawa, T. and Eguchi, H. : "Effect of sulfate on adsorption behavior of superplasticizer", CAJ Proceedings of Cement & Concrete, 1989, 43, 90-95, (JPN.)
9. Inokawa, H., Takahashi, K. and Uchida, K. : "Relationship between the rheological property of cement pastes and hydration of cement in the presence of water reducer", CAJ Review, 1984, 38, 64-67, (ENG.)
10. Uchikawa, H. and Uchida, S. : "The analysis of ettringite in hardened cement paste", Cement and Concrete Research, 1974, 4(5), 821-834, (ENG.)
11. Chiocchio, G., Mangialardi, T. and Paolini, A. E. : "Effects of addition time of superplasticizers on workability of Portland cement pastes with different mineralogical composition", Il Cemento, 1986, 83(2), 69-80, (ENG.)
12. Kucharska, L. : "Effect of products of the hydration of C_3A on rheology of clinker and cement pastes.", "Rheology of fresh cement and concrete", ed. by BANFILL, P. F. G., Chapsman & Hall, London, 1991, 47-54, (ENG.)
13. Uchida, S., Okamura, T., Takehiro, M. and Uchikawa, H. : "Influence of characters of cement on fluidity of fresh cement paste and mortar with organic additives", CAJ Proceedings of Cement & Concrete, 1990, 44, 86-91, (JPN)

THE ROLE OF THE NATURE OF HYDRATION PHASES ON THE RHEOLOGICAL PROPERTIES OF CEMENT DISPERSIONS

F L Glekel and R Z Kopp

Institute of Chemistry, Uzbek Academy of Sciences
Tashkent, UZBEKISTAN

SUMMARY

The paper presents results of investigations of parameters affecting rheologic properties of binder-water-admixture system for all the main clinker components (C_3S,C_2S,C_3A, C_4AF in combination with $CaSO_4 2H_2O$ and without it). Calcium lignosulfonate and polimeric electrolyte based on salicylic acid,wich differ in composition and action mechanism (in first one surface activity is predominant, while for the second one - chemical activity) were used as admixtures. It is shown that the main factors were the specific surface of the new formations which should correspond to relief interphase surface of solid phase particles, their affinity for this surface and between each other. Such new formations can, like products of cement hydration, be modified by the admixture at the stage of colloid dispersity degree (I), so result gelir-like products of reaction between chemically active admixtures and cement suspension liqu id phase (II).

Приводятся результаты изучения параметров,влияющих на реологические свойства системы вяжущее-вода-добавка для всех основных компонентов клинкера (C_3S,C_2S,C_3A,C_4AF в сочетании с гипсом и без него).В качестве добавок взяты лигносульфонат кальция и полиэлектролит на основе салициловой кислоты, различающиеся составом и механизмом действия (для первого он определяется преобладанием поверхностной,для второго-химической активности). Показано,что наиболее значимыми факторами оказались дисперсность новообразований и их сродство к поверхности частиц твердой фазы, рельеф которой они должны сгладить, и между собой. Такими новообразованиями могут быть как модифицированные добавкой на стадии коллоидной степени дисперсности продукты гидратации вяжущего (I), так и гелеобразные продукты реакции химически активных добавок с жидкой фазой цементной суспензии (II).

INTRODUCTION

The practice of using admixtures-plasticizers,which allow to control the rheological parameters of concrete mixes,shows that when using preparations of identical composition with different cements, the results are often not reproducible. It is generally accepted that this owes to difference in the mineral composition of the cements. But the data on admixture plasticizing effect on Portland cement clinker components is limited and concerns mainly tricalcium aluminate (C_3A).

Systematic investigations on the influence of admixtures calcium lignosulfonate and polymeric electrolyte based on salicylic acid which differ in composition and mode of action, were carried out on the main clinker components (C_3S,C_2S, C_3A and C_4AF) in combination with gyps and without it.

EXPERIMENTAL

The admixtures were introduced in the form of aqueous solutions together with the mixing water. The changes in the processes of structure formation at early stages (5 min) induced by the admixtures introduced were characterized by a complex study of the liquid and solid phase composition, specific surface and plastic strength (P_m); rheological properties were evaluated from the change in consistency of freshly prepared grout (spread,S).

Influence of the composition and structure of low- and highmolecular SAS on the formation and properties of surface hydrate layers (films was studied using the special methodology in limited concentrated systems, the abundance of free water being absent. The additive in the form of aqueous solution was added with minimum of water in the mineral dispersion C_3A, C_3S and C_4AF; after a minute's mixing the sample was placed inside a vacuum device,where the free water was extracted. The powder treated in this manner was hydrated in the steam phase.

RESULTS AND DISCUSSIONS

A very high increase in specific surface of the water-modified samples (from 2 to 13 m^2/g for C_3S and from 1,8 to 30-35 m^2/g for C_3A and C_4AF) at relatively small degree of hydration shows a very high specific surface of the initial hydrates formed.

The isotherm of water evaporation, sorption-desorption analysis on modified aluminates and silicates of calcium show differences in the influence of additives of different nature on the kinetics and the degree

of hydration as well as on the specific surface of the hydrates.

Besides, the higher the polymer chemical activity for binding Ca^{2+}, the lower the hard phase dispersion at modifying, that speaking about its product of interaction with Ca^{2+} in the formation of screening layers.

In the absence of admixtures, for monomineral systems there is a distinct inverse relationship between the hydration activity of the initial phase the crystalchemical peculiarities and the specific surface of hydrates, on the one hand, and the mix consistency at the initial stage of structure formation, on the other. The minerals are respectively arranged in the following order:

$$CaSO_4 \cdot 2H_2O > C_2S > C_3S > C_4AF > C_3A$$

Indeed, the aluminate phases rapidly react with water with formation of well crystallized calcium hydroaluminate tending to formation of phase contacts, and thus resulting in rapid loss of water suspension fluidity. In silicate suspensions, the initial products of hydration are calcium hydrosilicates localized on the surface of the ititial grains and do not have a noticeable tendency to structure formation and therefore fluidity is substantially higher.

In principle, admixtures-plasticizers liquefy dispersions of all minerals;however all other conditions (identical concentration,method of introduction, liquid-to-solid ratio, temperature) remaining the same, the effectiveness of plasticizing action varies relative to different minerals:

For the Lignosulfonate	For the Polyelectrolyte
$C_4AF > C_3S > C_2S > C_3A$	$C_4AF > C_2S > C_3S > C_3A$

It is seen that introduction of either admixture has the highest effect for calcium aluminferrite while it has the least effect for tricalcium aluminate. The main difference in the nature of hydration products of the two mineral is connected with the fact that C_4AF form substantial amount of products of colloid degree of dispersity along with well crystallized calcium hydroaluminate. Therefore it is suggested that the inincreased effect of plasticizers on C_4AF favours better hydrolysis of this mineral and specific surface of new formations (1,2), as a consequence of the formation and localization of such products in the zone of particle contacts.

To find out the main factors due to which poly -mineral systems with admixtures acquire the ability to plasticizing, regression coefficients were determined by the experiment designed in accordance with multifactor composition plan of the second order. The matrix of planning

of full factor experiment was constructed with allowance for five independent variables: x_1-x_5 – C_3A, C_4AF, C_3S, C_2S, $CaSO_4 \cdot 2H_2O$ respectively. Dependent variables: Y_1– S without admixtures, Y_2– with lignosulfonate, Y_3– with VRP-1, Y_4 and Y_5 – ΔS respectively for LSK and VRP-1. Regression analysis is carried out by SM-4 computer using standart programs.

$$Y_1 = 50{,}7 - 0{,}385x_1 - 0{,}257x_2 - 0{,}050x_3$$

$$Y_2 = 69{,}8 - 1{,}560x_1 + 0{,}705x_2 + 0{,}231x_5 + 0{,}151x_4$$

$$Y_3 = 74{,}9 - 1{,}111x_1 + 0{,}080x_2 - 0{,}445x_3 + 0{,}180x_5$$

$$Y_4 = 13{,}0 + 0{,}915x_2 - 1{,}310x_1 + 0{,}314x_4$$

$$Y_5 = 20{,}2 + 0{,}490x_2 - 0{,}562x_1 - 0{,}320x_3$$

It is seen that in polymineral systems in water suspensions without admixtures, the presence of C_3A is the most negative factor, the second negative factor being C_4AF (table 1).

When the admixtures are introduced, the negative effect of C_3A increases while in the presence of calcium aluminoferrite it becomes one of the main positive factors.

Gypsum in this case becomes important – in all compositions containing aluminate phases, especially in the presence of C_3S. With as well as without plasticizers, introduction of gypsum leads to increase in concrete fluidity (spread) by 10–15%. This indicates that fine disperse products of gypsum interact with aluminate phases, forming calcium hydrosulfoaluminate under conditions of high oversaturation and it is this rather than gypsum itself that has a plasticizing effect. In this connection the role of calcium silicates governing lime oversaturation in a liquid phase of mineral suspension is shown. It appeared to vary with the type of plasticizer introduced into the composition: in the presence of LS the most significant additional factor increasing admixture effect is C_2S, while in the presence of VRP-1 C_3S becomes more important but as a negative factor. This is in good agreement with the peculiarities of the action of the admixtures considered. In contrast to CSA LS, which does not lime and stabilized hydrates at the stage of their formation and growth, VRP-1 immediately reacts with $Ca(OH)_2$ with the formation of poorly soluble products of colloid degree of dispersity (VRP-Ca), which form hydrate-polymeric layer on the surface of silicate thereby inhibiting their hydration.

As a result, formation of calcium hydrosulfoaluminate in the initial stage, which is higher the higher the VRP-1 dose, takes place at lo-

Table 1 - Influence of composition of the mixes on the efficiency of the action of plasticizers (w/c=0,50;filler-highly-disperse sand)

Composition of mix,%					Spread, mm			Δ S, % to water mix	
C_3A	C_4AF	C_3S	C_2S	$CaSO_4$	Without admix	With 0,3% LST	With 0,3% VRP-1	LST	VRP-1
10	10	50	20	10	44	61	53	39	20
–	10	50	20	10	47	80	64	49	36
10	–	50	20	10	44	62	49	41	11
–	–	50	20	10	45	70	57	55	27
10	10	–	20	10	41	72	65	76	59
–	10	–	20	10	40	91	71	127	78
10	–	–	20	10	46	77	60	67	30
–	–	–	20	10	55	85	68	54	22
10	10	50	–	10	43	64	58	49	35
–	10	50	–	10	45	77	60	71	33
10	–	50	–	10	50	69	60	38	20
–	–	50	–	10	50	75	61	50	22
10	10	–	–	10	40	41	72	2	80
–	10	–	–	10	50	62	76	24	52
–	–	–	–	10	62	74	71	19	14
10	10	50	20	–	41	41	41	0	0
–	10	50	20	–	45	80	64	78	42
10	–	50	20	–	45	70	60	55	33
–	–	50	20	–	50	69	64	38	28
10	10	–	20	–	44	44	40	0	0
–	10	–	20	–	52	97	72	86	38
10	–	–	20	–	52	66	61	27	17
–	–	–	20	–	56	71	75	27	34
10	10	50	–	–	43	41	41	0	0
–	10	50	–	–	42	75	62	78	48
10	–	50	–	–	44	46	69	4	58
–	–	50	–	–	53	71	64	34	21
10	10	–	–	–	46	46	70	0	52
–	10	–	–	–	45	85	85	89	89
10	–	–	–	–	42	45	40	2	0

wer oversaturation,i.e.under the same conditions as in C_3A-$CaSO_4$-H_2O system what governs the loss of suspension fluidity by the reasons similar to those for C_3A-H_2O composition where calcium hydroaluminate is a structure forming element.

Hence, the role of binder composition in plasticizing effect varies with the nature of the admixture which determines the peculiarities of its action mechanism.

The type and properties of a binder determine the optimum dose and the mechanism of action of an admixture. It was established that admixtures with predominantly chemical activity (electrolytes, polymeric electrolytes) have the highest effect on the binders, cohereis the products of hydration at early stages are localized in volume (expanding compositions, gypsum pozzolana cement binders). The most effective regulators for the binders cohereis the products of hydration are localized on the surface of cement particles (Portland cement and mixed binders based thereon) are surface-active agents. At this there is no onevalue dependence of the plasticizing action of the admixture on the design mineral composition of Portland cement. Difference in structure and localization on the cement particle surface of particular clinker minerals could be one of the factors influencing the initial stages of hydration the mineral composition itself is connected with the conditions of clinker production.

The above data, in combination with those on investigations of the physico-chemical processes taking place at the initial stages of structure formation and determining the rheological behaviour of the considered mono- and polymineral compositions in the presence of admixtures (3) point to the following. In all the cases, regardless of the nature of the dispersion phase and the plasticizer, the necessary condition for plasticisation is the presence in the system of small quantities of new formations of colloid degree of dispersity which participate in formation of "smooth" surface of contacting particles. For the monomineral systems studied, the source of such products is calcium aluminoferrite.

CONCLUSION

As a result of investigations on the effect of fine aggregate (sand) on the structure formation processes of cement suspension in a concrete mix, it was established that the plasticizing effect of admixtures depends on the sand grain composition, the geometry and the surface properties of its particles. For a given granulometric composition,

the maximum effect is achieved for a sand with smooth surface while using admixtures whose action mechanism is connected with hydrate stabilization at the stage of nucleus formation.

REFERENCES

1. Glekei F.L.,Kopp R.Z.,Akhmedov K.S. Regulation of hydration structure formation by surface active agents.Tashkent: Fan,1986,223p.

2. Ibraimov A.Yu. The study of initial stages of hydration in ultimate concentrated systems binder-water at the presence of admixtures: Thesis abstract. Tashkent, 1981.

3. Glekel F.L.,Kopp R.Z., Musaeva N.A. ets. "The role of mineral binder nature in the effect of plasticizing admixtures". J.Appl.Chem., M-L.,1989,[illegible]5,1026-1028.

FLASH-SET BEHAVIOUR OF OIL WELL CEMENT SLURRIES CONTAINING LIGNOSULPHONATES

M Michaux and E B Nelson

Etudes et Fabrication Dowell Schlumberger
FRANCE

SUMMARY

In oil well cementing, lignosulphonates are commonly used to extend the setting time of Portland cement slurries. In some cases premature stiffening or "gelation" of the slurry occurs when unrefined lignosulphonate retarders are used. In an effort to explain this phenomenon, the hydration behaviour of low-C_3A Portland cement slurries, C_3A-gypsum-lime systems and C_4AF-gypsum-lime systems, containing refined or unrefined lignosulphonates, was studied. The results showed that unrefined lignosulphonates destabilize the hydration process of C_4AF-gypsum-lime mixtures, causing a flash set. Similar behaviour was also detected in low-C_3A Portland cement slurries. The problem can be prevented by two methods - use of refined lignosulphonates, or delayed addition of unrefined lignosulphonates. It was thought that ferrite phase does not hydrate similarly to C_3A; the role played by the possible formation of a protective layer of amorphous iron hydroxide onto C_4AF grains is discussed.

RESUME

Les lignosulfonates sont couramment utilisés lors de la cimentation des puits pétroliers pour augmenter le temps de prise des coulis de ciment Portland. Dans certains cas, un épaississement prématuré du coulis se produit lorsque des lignosulfonates non raffinés sont employés. Dans le but d'expliquer ce phénomène, le comportement au cours de l'hydratation de coulis de ciment à faible teneur en C_3A, de systèmes C_3A-gypse-chaux et C_4AF-gypse-chaux, a été étudié. Les résultats ont montré que le lignosulfonate non raffiné déstabilise le processus d'hydratation des mélanges C_4AF-gypse-chaux, ce qui provoque une prise éclair. Un comportement analogue a également été mis en évidence dans les coulis de ciment à faible teneur en C_3A. Cet inconvénient peut être évité par deux méthodes: soit en utilisant des lignosulfonates raffinés, soit en ajoutant, après quelques minutes, les lignosulfonates non raffinés au coulis de ciment. L'hypothèse a été suggérée que l'hydratation de la phase ferritique s'effectue différemment de celle du C_3A; le rôle joué par la formation éventuelle d'une couche protectrice d'hydroxyde de fer amorphe sur les grains de C_4AF est discuté.

INTRODUCTION

Oil well cementing consists of filling the annulus between casing and formation with a cement slurry in order to maintain the casing and above all to achieve good zonal isolation. The cement slurry is pumped down inside the casing to be cemented, exits the bottom, and displaces drilling mud while moving up the annulus. To properly achieve this placement, cement slurries must be designed with dispersants and retarders to obtain good rheological properties and long enough setting times at temperatures which can sometimes exceed 200°C.[1] The most commonly used retarders for well cements are the sodium and calcium salts of lignosulphonic acids. These polymers, derived from wood pulp, are usually unrefined and contain various amounts of saccharide compounds. Analyses have shown that the main impurities are pentoses (xylose and arabinose), hexoses (galactose, mannose and rhamnose) and corresponding aldonic acids (especially xylonic acid).[2,3] The saccharide compounds content can be as high as 10% of the crude lignosulphonate. In most commercial lignosulphonates, xylose is the principal impurity.

Refined lignosulphonates (RL) can be used without any problem over a wide temperature range. By contrast, premature detrimental stiffening of the slurry often occurs when unrefined lignosulphonates (UL) are used at temperatures above 50-60°C. This problem is illustrated in Figure 1, which shows the effect of UL upon the rheological properties of an API Class G cement slurry (i.e., HSR cement; $C_3A<3\%$)[1] conditioned for 20 minutes at 85°C. A steady increase in the plastic viscosity and yield value was observed with UL concentration. Interestingly, Figure 1 also shows that if the addition of UL to the slurry is delayed for several minutes, the problem is resolved. If a RL is added instead, no adverse rheological effects were noted and the additive acted as an efficient dispersant (Figure 2). This dispersing effect was reinforced when the addition of RL was delayed. These results led us to suspect that the rheological behaviour of a cement slurry is largely a function of the evolution of hydration products during the first few minutes after slurry mixing.

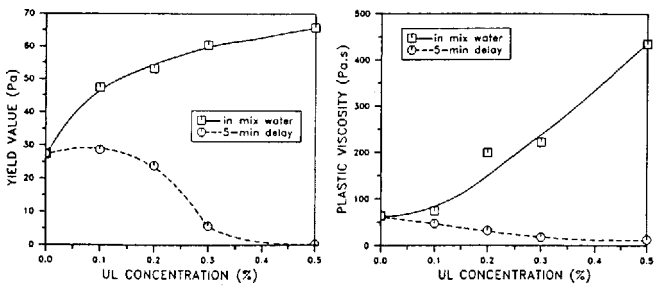

FIGURE 1: YIELD VALUE & PLASTIC VISCOSITY vs UL CONCENTRATION
(UL in mix water or 5-minute delayed addition)
CLASS G CEMENT - W/C = 0.44 - T = 85 deg.C

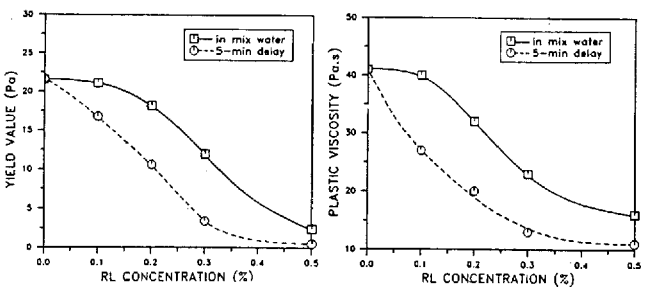

FIGURE 2: YIELD VALUE & PLASTIC VISCOSITY vs RL CONCENTRATION
(RL in mix water or 5-minute delayed addition)
CLASS G CEMENT - W/C = 0.44 - T = 85 deg.C

It is known that the aluminate phases (C_3A and C_4AF, or more precisely $C_2A_nF_{(1-n)}$ with $0<n<0.7$) in Portland cement are the most reactive at short hydration times, and have the greatest influence on slurry rheology. The mechanisms of hydration of these phases are still not completely understood, and several theories have been described in the literature.[4-11] Nevertheless, it would seem that the formation of a more or less protective layer of ettringite on surfaces may somehow be involved. Studies on pure aluminate phases have shown that lignosulphonates can accelerate the formation of ettringite.[12,13] This should result in an excessive rate of early stiffening in cement slurries. Actually, some rheological anomalies in Portland cement slurries containing lignosulphonates, which are mainly used as water-reducing additives in construction industry, have been reported.[14-17] It is usually suggested that these anomalies take place because lignosulphonates slow down the dissolution rate of calcium sulphates, making "undersulphated" a cement normally well sulphated when mixed neat.[15-17] Cements containing large quantities of natural anhydrite instead of gypsum and hemihydrate were shown to be more sensitive to the presence of lignosulphonates.[17]

The present study was undertaken in an effort to explain how unrefined lignosulphonates can destabilize low-C_3A Portland cements which are commonly used in oil well cementing.

RESULTS AND DISCUSSION

A preliminary series of experiments was performed to determine the effects of UL, RL and xylose on the hydration of pure C_3A (cubic form, Blaine fineness: 3200 cm^2/g) and C_4AF (Blaine fineness: 3400 cm^2/g).

Gypsum of reagent grade was added to the phases in the relative amounts observed in most OPC (25% by weight of C_3A; 10% to 25% by weight of C_4AF). 5% calcium hydroxide (containing about 10% calcite as impurity) was also added to obtain a pH similar to that found in cement slurries. The progress of hydration was followed using heat-flow conduction calorimetry (using a SETARAM C80 calorimeter).

The effect of RL upon the hydration of C_3A at 30°C is shown in Figure 3. The concentration by weight of C_3A was varied from 0% to 2%, and a regular progression of "setting time" (heat maximum on the thermogram) with concentration was observed. The rate of conversion from ettringite to monosulphate was probably reduced as well, because the heat-flow peak was widened and its intensity was lowered. An analogous series of thermograms was recorded with UL, at concentrations up to 1% (Figure 4). The same direct relationship between the length of the induction period and concentration was observed; however, UL was shown to be a more efficient retarder than RL. The ability of UL to retard C_3A was severely curtailed by a relatively small increase in temperature, as shown in Figure 5, where the curing temperature was 50°C, but the trend in retardation was the same.

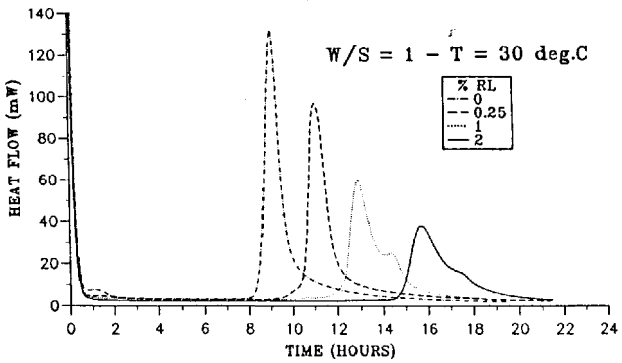

FIGURE 3: EFFECT OF RL ON HYDRATION OF C3A - 25% GYPSUM - 5% LIME SYSTEM.

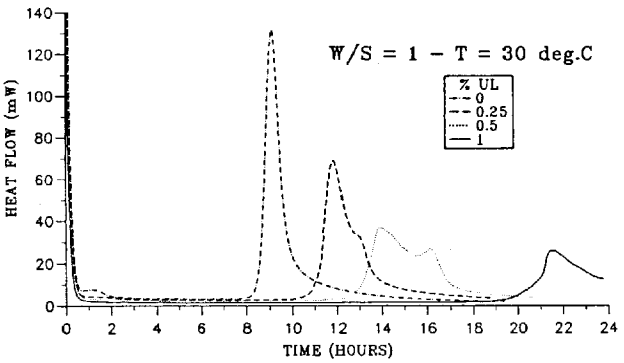

FIGURE 4: EFFECT OF UL ON HYDRATION OF C3A - 25% GYPSUM - 5% LIME SYSTEM.

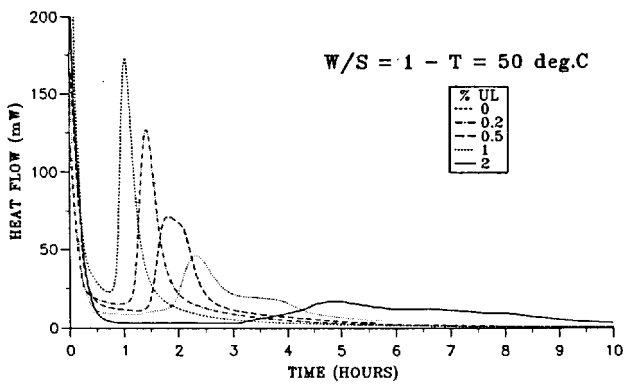

FIGURE 5: EFFECT OF UL ON HYDRATION OF C3A - 25% GYPSUM - 5% LIME SYSTEM.

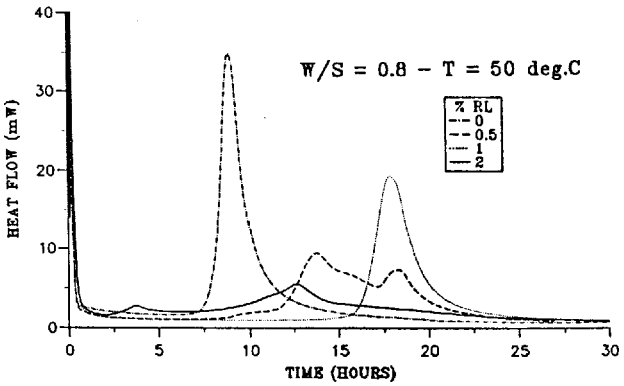

FIGURE 6: EFFECT OF RL ON HYDRATION OF C4AF - 10% GYPSUM - 5% LIME SYSTEM.

As the reactivity of C_4AF is much reduced compared to C_3A, studies were made at 50°C. Much different results were obtained when the retarders were added to this phase. From 0% to 2% RL the shape of the thermograms was completely modified (Figure 6). The intensity of the heat-evolution peaks was significantly reduced and the peak practically disappeared when 2% RL was present. At low concentrations (<1%) RL retarded the formation of ettringite and its conversion to monosulphate, but at 2% it had a neutral or perhaps slightly accelerating effect on the rate of ettringite formation, and a significant retarding effect on its conversion. UL had a completely different effect upon the hydration of C_4AF. Whatever its concentration, the rate of ettringite formation was dramatically accelerated (Figure 7). The induction period was no longer visible with 1% UL, and a flash set was observed in the presence of 2% UL. This led us to suspect that the principal impurity in UL, xylose, might be responsible. Indeed, as shown in Figure 8, only 0.5% xylose was required to induce a flash set.

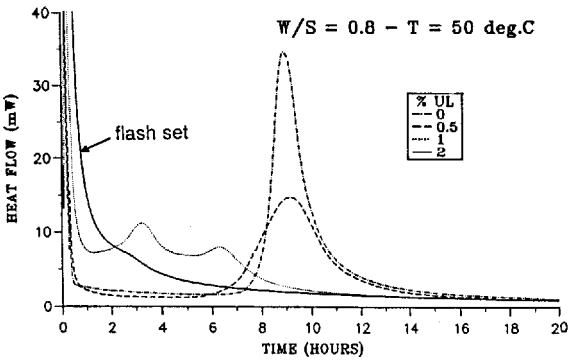

FIGURE 7: EFFECT OF UL ON HYDRATION OF C4AF - 10% GYPSUM - 5% LIME SYSTEM.

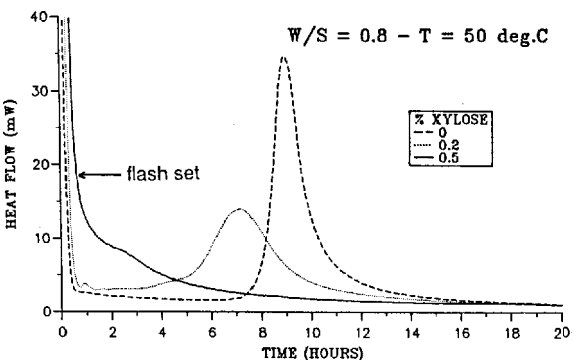

FIGURE 8: EFFECT OF XYLOSE ON HYDRATION OF C4AF - 10% GYPSUM - 5% LIME SYSTEM.

To confirm the information supplied by the thermograms, the evolution of the gypsum (G), ettringite (E) and lime (L) concentrations in the C_4AF pastes was followed by thermogravimetric analysis. The results are presented in Table 1. The system without retarder showed a normal progressive decrease of the gypsum concentration leading to an increase of the ettringite concentration. The reaction was fast at early times and then slowed down. Similar behaviour was noted when 1% RL was present in the system, except that the initial formation of ettringite was delayed. The addition of 1% UL resulted, after a 15-minute induction period, in a very fast consumption of gypsum and conversion of ettringite to monosulphate which could be detected by X-ray diffraction. It can also be noted that, in the three systems, about 1.5% lime disappeared during early hydration. This amount being largely in excess of that necessary to saturate the solution (about 0.1% is required), it can be assumed that a part of lime was involved in the formation of first hydrates. After this fast consumption, lime concentration remained almost constant despite the continuous formation of ettringite. This led us to think that other hydrates have been formed at early ages. At the end of the induction period, the UL-containing system showed a gradual consumption of lime which corresponds to the instability of ettringite and the formation of monosulphate and calcium aluminate hydrates.

To investigate the effects of UL and xylose further, we increased the initial gypsum concentration to 25%. As shown in Table 2, the same acceleration of gypsum consumption was observed; however, the gypsum concentration levelled off and allowed the formation of ettringite to continue for several hours. Again, the initial formation of ettringite was delayed in the presence of UL, whereas this effect was not seen with xylose. In the case of xylose an initial rapid formation of ettringite occurred after which further formation appeared to be blocked. It can also be noted that lime concentration was lower in systems containing UL or xylose.

At this point one might speculate that a simple addition of gypsum to a UL-containing cement slurry would solve the viscosification problem; unfortunately, this is not the case. Notice that the amount of ettringite in the UL and xylose systems is substantially higher than that for the additive-free system. It is known that high concentrations of ettringite viscosify a cement slurry.

The next step in our investigation was to measure the consumption of gypsum in real cements when the above additives are present. The slurries were conditioned in an atmospheric consistometer (EG + G Chandler Engineering Model 1250) at 85°C, at which temperature the gelation problem becomes more apparent. After various times, samples were taken and the hydration was stopped by drying with acetone and ether. Table 3 shows the consumption of gypsum when 0.3% (by weight of cement) UL was added to a Class G cement in which

Table 1: Effect of RL and UL on Hydration of C_4AF - 10% Gypsum - 5% Lime System. W/S = 0.8 - T = 50°C

Time	Neat			1% RL			1% UL		
(min)	% G	% E	% L	% G	% E	% L	% G	% E	% L
0	8.6	0	3.8	8.6	0	3.8	8.6	0	3.8
15	6.6	4.6	2.3	8.4	0.5	2.5	8.1	0.6	2.0
30	6.4	4.9	2.4	5.5	4.4	2.1	6.2	0.4	1.7
60	5.7	5.7	2.4	4.6	7.2	2.0	0	0	0.8
120	5.0	8.0	2.3	3.3	7.6	2.1	0	0	0.9
240	3.3	11.3	2.2	2.6	10.9	1.9	0	0	0.4
360	1.1	14.7	2.1	1.4	14.2	1.6	0	0	0.4
480	0	18.6	1.7	0.8	16.1	1.7	0	0	0.2

Table 2: Effect of UL and Xylose on Hydration of C_4AF - 25% Gypsum - 5% Lime System. W/S = 0.8 - T = 50°C

Time	Neat			1% UL			0.5% Xylose		
(min)	% G	% E	% L	% G	% E	% L	% G	% E	% L
0	19.2	0	3.3	19.2	0	3.3	19.2	0	3.3
15	16.9	5.6	2.0	19.0	0.5	2.6	8.9	14.4	1.3
30	17.2	5.5	2.1	10.1	14.3	1.5	6.5	21.0	1.0
60	14.8	6.9	2.1	8.5	18.3	1.4	6.8	23.6	0.7
120	13.5	10.0	2.2	7.0	22.0	1.4	5.3	26.5	0.9
240	11.8	13.9	2.0	4.9	25.2	1.1	6.0	23.0	0.7
360	10.2	17.2	1.7	3.3	27.8	0.9	3.0	32.9	0.9
480	8.8	20.5	1.5	1.6	29.3	0.7	4.6	28.5	0.9

virtually all calcium sulphate is present as gypsum (3.91%). Compared to the neat slurry, the consumption of gypsum was accelerated but did not go to completion within 420 minutes; however, a viscosification of the slurry was observed. This situation is roughly analogous to that shown in Table 2 where the amount of gypsum is sufficient to prevent a flash set. In Table 4 the behaviour of another Class G cement is shown. Notice that the total calcium sulphate content was less (2.22%), and that most of it (1.84%) was present as hemihydrate (no anhydrite could be detected). The neat slurry demonstrated good control of gypsum consumption; therefore, the cement was not undersulphated (i.e., no flash setting was observed). It can also be noted that hemihydrate very quickly rehydrated into secondary gypsum. Similar control was observed when 0.3% RL was used (accompanied by a slow rehydration of hemihydrate) and when 0.3% UL was added to the slurry 10 minutes after mixing, and in both cases the slurry was very well dispersed. However, complete eradication of gypsum occurred within 5 minutes when 0.3% UL was added normally (i.e., in mix water) or when 0.15% xylose was present, and a severe gelation problem was observed. This situation could be compared with that shown in Table 1 where the amount of gypsum is not sufficient to prevent a flash set.

The results described above have established three principal points - (1) the C_4AF-gypsum-lime system is dramatically accelerated by UL; (2) the effects of UL on the hydration of C_4AF are observable in low-C_3A Portland cement systems; (3) the products of hydration during the mixing stage are critical to the performance of the slurry.

It is generally recognized that hydration products of the C_3A and C_4AF are similar, except for the partial substitution of aluminium by iron in hydrates and possible formation of amorphous iron hydroxide from C_4AF.[9,13] It can be assumed that iron hydroxide may play a major role in the retardation mechanism of the ferrite phase. At this point in our study, we speculated that the RL and UL might affect the fate of iron hydroxide in different ways.

The effects of the lignosulphonates on the formation of iron hydroxide (FH_3) were studied by preparing high-pH solutions of the retarders, adding a known amount of iron chloride, and measuring by ICP spectrometry the amount of iron remaining in solution after stirring for 1 hour. The amount of precipitated iron was deduced from the amount of iron remaining in solution. A comparison between UL and RL is shown in Figure 9. As the concentration of UL increased, the amount of precipitated FH_3 decreased. At 0.8 g/L UL, which corresponds to a concentration much lower than those found in the liquid phase of cement slurries containing 0.3% UL, the precipitation of FH_3 was completely prevented. Analysis of the solution by UV spectophotometry at 280 nm showed that the iron was complexed. A later experiment showed that xylose also prevents the precipitation of FH_3. RL, however, has no effect upon the precipitation of FH_3 at concentrations up to at least 4.0 g/L, corresponding approximately to those usually found in cement slurries containing 0.3% RL.

In the scope of additional tests, it was shown that UL was not capable of destabilizing FH_3 already formed. This might explain why flash set did not occur when UL was added to the cement slurry a few minutes after mixing.

It is known that hydration of aluminate phases is retarded in the presence of lime.[6,7,11] However, it can be seen in Figures 10 and 11 that this retarding effect was much less pronounced on C_3A-gypsum system than on C_4AF-gypsum system for which a flash set occurred in the absence of lime. It is believed that these differences are not explained solely on the basis of the temperature difference 30°C to 50°C. Considering these results with

Table 3: Effect of UL on Hydration of a Class G Cement (1). W/C = 0.44 - T = 85°C

Time	% Gypsum	
(min)	Neat	0.3% UL*
10	3.57	3.17
20	3.63	3.12
30	3.72	2.91
40	3.57	2.86
60	3.57	2.79
100	3.52	2.71
120	3.10	2.57
180	Set.	2.50
300	-	2.50
420	-	2.43

* UL in mix water.

Table 4: Effect of RL, UL and Xylose on Hydration of a Class G Cement (2). W/C = 0.44 - T = 85°C

Time	% Gypsum				
(min)	Neat	0.3% RL	0.3% UL*	0.3% UL**	0.15% Xyl.
5	1.84	0.65	0	1.95	0
10	1.75	0.94	0	1.84	0
15	1.71	1.13	0	1.75	0
20	1.65	1.11	0	1.69	0
30	1.48	1.23	0	1.81	0
60	1.27	1.36	0	1.86	0
90	1.10	1.38	0	1.72	0
120	0.80	1.36	0	1.50	0

* UL in mix water.
** UL added to the slurry 10 minutes after mixing.

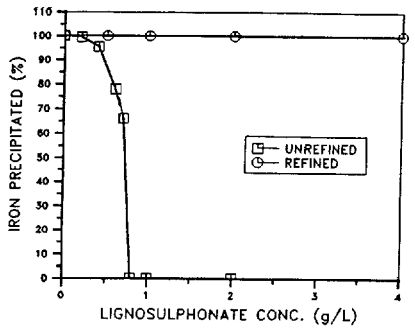

FIGURE 9: INFLUENCE OF LIGNOSULPHONATES ON PRECIPITATION OF IRON HYDROXIDE.

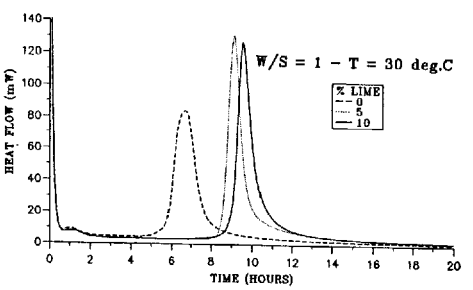

FIGURE 10: EFFECT OF LIME ON HYDRATION OF C3A - 25% GYPSUM SYSTEM.

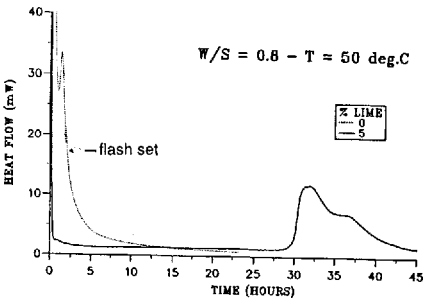

FIGURE 11: EFFECT OF LIME ON HYDRATION OF C4AF - 25% GYPSUM SYSTEM.

those reported in Tables 1 and 2, it is suggested that lime is involved in the formation of first hydrates from C_4AF, perhaps to form a protective layer of amorphous FH_3. With regard to previous results, it can be assumed that the formation of this layer is prevented or perhaps just delayed in the presence of some impurities, such as xylose, contained in UL.

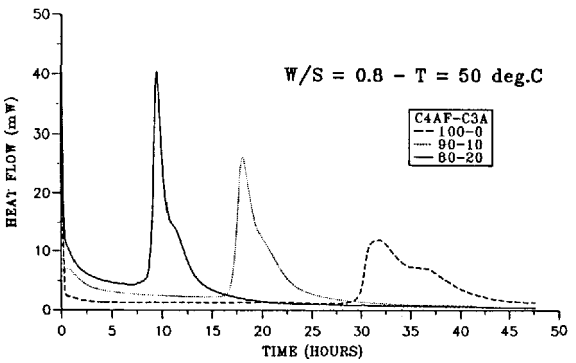

FIGURE 12: HYDRATION OF C4AF-C3A MIXTURES WITH 25% GYPSUM AND 5% LIME.

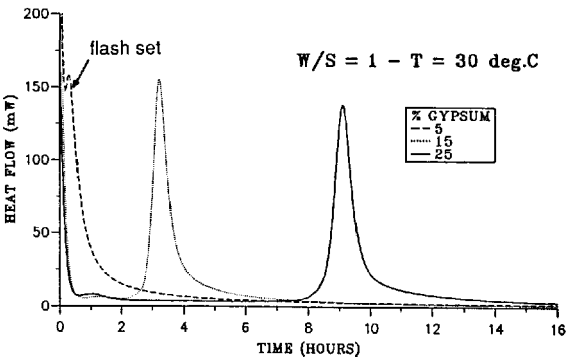

FIGURE 13: EFFECT OF GYPSUM ON HYDRATION OF C3A - 5% LIME SYSTEM.

Most oil well cements have a C_3A content less than 3%. Because this phase is much more reactive than the ferrite phase, low amounts of C_3A will compete with C_4AF in consuming gypsum, resulting in significant acceleration of C_4AF-gypsum-lime systems (Figure 12). Therefore, although C_3A is not accelerated by UL, it can indirectly contribute to destabilize UL-containing cement slurries. In addition, it can be seen in Figure 13 that the length of the induction period of the C_3A-lime system was not at all proportional to the gypsum concentration. Consequently, oil well cements must contain the appropriate amount of calcium sulphate in order to properly perform over a wide temperature range and in the presence of some additives having detrimental side effects such as UL.

CONCLUSIONS

The results of this study have challenged the conventional wisdom concerning the importance of ferrite phase in Portland cement systems. We have shown that C_4AF does not always mimic the behaviour of C_3A, and its response to additives can greatly affect the performance of cement slurries. Unrefined lignosulphonates, which contain residual sugars such as xylose, apparently cause rheological difficulties by preventing the proper control of C_4AF hydration. The fact that delayed addition of unrefined lignosulphonates restores proper control shows that the initial hydration products are critical, and there is a short period just after mixing during which the interstitial phase of cement can be completely destabilized.

Our results also suggest that, unlike C_3A, the proper formation of ettringite is not the only prerequisite to control C_4AF hydration. A protective layer of amorphous iron hydroxide on C_4AF surfaces may be an additional requirement during the first few minutes after mixing. It must however be pointed out that this assumption does not exclude the possible participation of alumina gel and/or C_4AH_n in controlling C_3A and C_4AF hydration, as sometimes proposed in the literature.

Our hypothesis is based on the fact that the presence of lime was shown to be essential to prevent a flash

set in C_4AF-gypsum system at 50°C, and was involved in the formation of first hydration products. By contrast, lime had only a slight retarding effect on C_3A-gypsum system at 30°C. In addition, it was demonstrated that unrefined lignosulphonates, contrary to refined lignosulphonates, prevented the formation of iron hydroxide by forming a complex with iron.

The extent of viscosification in cement slurries containing unrefined lignosulphonates will depend, among other factors probably, upon the amount of calcium sulphates. A more or less important viscosification will occur if, after the accelerated reaction between C_4AF and gypsum, calcium sulphates are still present to control the hydration of interstitial phase. A premature flash set will take place if they are no longer available after this initial reaction. It is likely that the dissolution rate of various forms of calcium sulphates present in the cement is a critical parameter as well.

ACKNOWLEDGEMENTS

The authors would like to thank the management of Dowell Schlumberger for permission to publish this paper.

REFERENCES

1. Nelson, E.B.: **Well cementing.** Amsterdam, Elsevier, 1990.
2. Mouton, Y.: "De l'influence des sucres présents dans les lignosulfonates sur la prise des mortiers et bétons". Bulletin Liaison Laboratoire Ponts et Chaussées, 1972, **58**, 117-134.
3. Milestone, N.B.: "The effect of lignosulphonate fractions on the hydration of tricalcium aluminate". Cement Concrete Research, 1976, **6**, 89-102.
4. Jawed, I., Goto, S., Kondo, R.: "Hydration of tetracalcium aluminoferrite in presence of lime and sulfates". Cement Concrete Research, 1976, **6**, 441-454.
5. Skalny, J., Tadros, M.E.: "Retardation of tricalcium aluminate hydration by sulfates". **Journal American** Ceramic Society, 1977, **60**, 174-175.
6. Collepardi, M., Baldini, G., Pauri, M., Corradi, M.: "Tricalcium aluminate hydration in the presence of lime, gypsum or sodium sulfate". Cement Concrete Research, 1978, **8**, 571-580.
7. Collepardi, M., Monosi, S., Moriconi, G., Corradi, M.: "Tetracalcium alumino-ferrite hydration in the presence of lime and gypsum". Cement Concrete Research, 1979, **9**, 431-437.
8. Chatterji, S.: "Mechanisms of retardation of C_3A: a critical evaluation". **International Congress on the Chemistry of Cement, 7th, Paris, France** 1980, **V4**, 465-470.
9. Fukuhara, M., Goto, S., Asaga, K., Daimon, M., Kondo, R.: "Mechanisms and kinetics of C_4AF hydration with gypsum". Cement Concrete Research, 1981, **11**, 407-414.
10. Plowman, C., Cabrera, J.G.: "Mechanism and kinetics of C_3A and C_4AF, extracted from cement". Cement Concrete Research, 1984, **14**, 238-248.
11. Tsuyuki, N., Hirota, N., Miyakawa, T., Kasai, J.: "The physical properties and the hydration mechanism of C_3A in the presence of $CaSO_4.2H_2O$ and $Ca(OH)_2$". **International Congress on the Chemistry of Cement, 8th, Rio de Janeiro, Brazil** 1986, **V6**, 400-404.
12. Collepardi, M., Monosi, S., Moriconi, G., Pauri, M.: "Influence of gluconate, lignosulphonate, glucose on the C_3A hydration in the presence of gypsum with or without lime". Cement Concrete Res., 1984, **14**, 105-112.
13. Collepardi, M, Monosi, S., Moriconi, G, Pauri, M.: "Influence of gluconate, lignosulphonate, and glucose admixtures on the hydration of tetracalcium aluminoferrite in the presence of gypsum with or without calcium hydroxide". Journal American Ceramic Society, 1985, **68(5)**, 126-128.
14. Hersey, A.T.: "Slump loss caused by admixtures". ACI Journal, 1975, **72(10)**, 526-527.
15. Coulon, C.: "Anomalies rhéologiques apportées par des plastifiants à base de lignosulfonate". Silicates Industriels, 1979, **10**, 235-239.
16. Ranc, R.: "Intéractions entre les réducteurs d'eau-plastifiants et les ciments". Ciments, Bétons, Plâtres, Chaux, 1990, **782**, 19-21.
17. Dodson, V.H., Hayden, T.D.: "Another look at the portland cement/chemical admixture incompatibility problem". Cement, Concrete, and Aggregates, CCAGDP, 1989, **11(1)**, 52-56.

THE INFLUENCE OF ADMIXTURES ON THE CRYSTALLIZATION OF TOBERMORITE FROM C-S-H (I)

W Kurdowski and T T Nguyen

University of Mining and Metallurgy
Cracow, POLAND

SUMMARY

The influence of calcium, aluminium, sodium and chromium chloride and sulphates on the process of Tobermorite crystallization from C–S–H phase under thermal treatment in saturated water vapour was examined. All sulphates except chromium were accelerators, however only calcium chloride was a strong accelerator and all others were retarders. Thus, the influence of both components of salt added i. e. of cation and anion is visible.

INTRODUCTION

The transformation of C–S–H into Tobermorite as a result of thermal treatment of building materials is of great importance. As it is well known the properties of building materials are among others dependent on their mineralogical composition. Taylor (1) and Dyczek (2) have demonstrated the importance of the content of Tobermorite and/or C–S–H phase. Tobermorite is a crystalline product of the transformation of a gel C–S–H phase thus the process increases the content of crystalline phases and changes the microstructure as well as the porosity of the material.

In spite of the importance of the transformation of C–S–H phase into Tobermorite there are few researches concerning the influence of admixtures on the course of this process (3–5). The aluminates ions and alkalies accelerate the transformation (3,4) and on the contrary chromium hamper this process (5). The influence of sulphates ions was also under examination (6).

This paper presents the results of the examination of the influence of some chlorides and sulphates on the crystallization of Tobermorite from C–S–H– phase.

MATERIALS AND METHODS

As a starting material the C–S–H phase was used with the C/S molar ratio equal to 1. The C–S–H phase was obtained by mixing the silica gel (Aerosil Degussa) with calcium hydroxide in water suspension during two weeks. The disappearance of calcium hydroxide was controlled by X–ray and thermal analysis [Figs. 1 and 2]. After two weeks C–S–H samples were washed with acetone and then with ether and dried at 40°C.

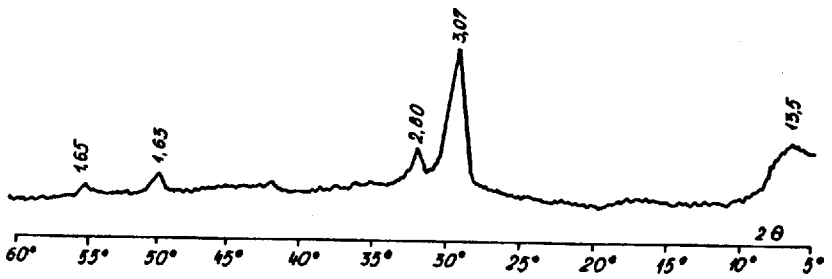

Figure 1. X–ray pattern of C–S–H

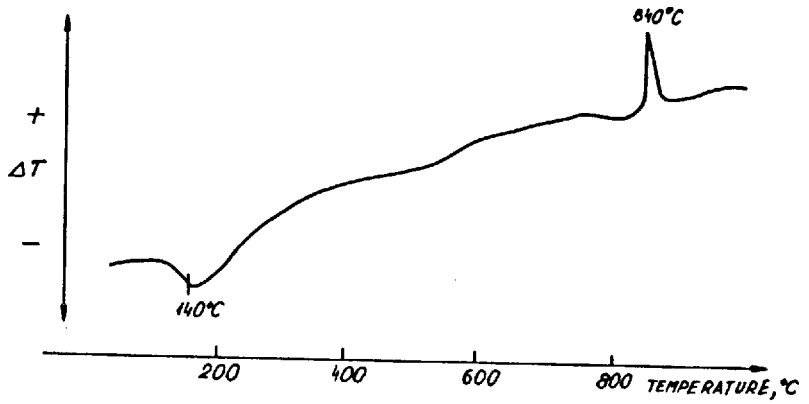

Figure 2. DTA of C–S–H

As the admixtures the following salts were added:

sulphates	chlorides
$CaSO_4 \cdot 1/2H_2O$	$CaCl_2 \cdot 6H_2O$
$Al_2(SO_4)_3 \cdot 18H_2O$	$AlCl_3 \cdot 6H_2O$
$Cr_2(SO_4)_3 \cdot 6H_2O$	$CrCl_3 \cdot 6H_2O$
$Na_2SO_4 \cdot 10H_2O$	NaCl

The quantities of additions were 1, 3 and 5 % on ignition free basis.
All reagents were chemically pure.



Figure 3. SEM image of Tobermorite

To have the standard Tobermorite 1.13 nm the sample was prepared using Quartz and calcium hydroxide and autoclaved at 118°C during four weeks. SEM image is shown in Fig. 3. X–ray pattern contained all peaks of 1.13 nm Tobermorite.

The process of transformation of C–S–H into Tobermorite was observed by SEM and the quantitative X–ray analysis was applied. For this purpose the surface of two peaks: (002) 1.13 nm and (650) 0.167 nm was measured.

All samples were autoclaved in a small chamber, which was introduced to laboratory dryer. The chamber was previously filled with water in a such quantity to have saturated water vapour. The samples were introduced in form of paste in a small, open teflon vessel. This procedure was described in our previous paper (7).

For autoclaving the isothermic condition was choosen and the temperatures of thermal treatment were: 110°,120°, 130°, 140° and 150°C.

EXPERIMENTAL RESULTS

All the sulphates accelerate the transformation of C–S–H phase into Tobermorite. As an example the influence of gypsum is presented in Fig. 4. There is an optimum content of gypsum which lies

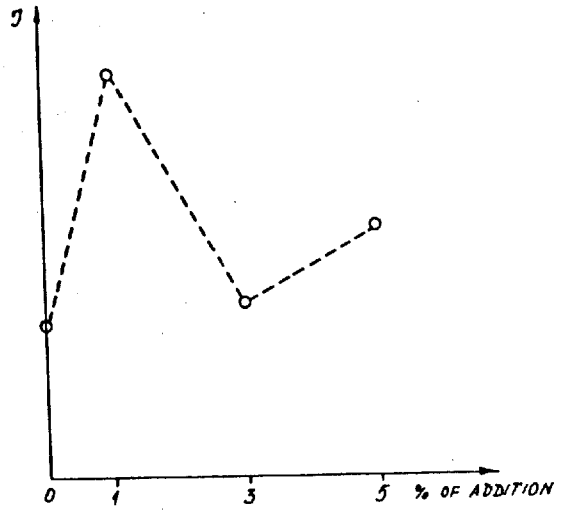

Figure 4. The intensity of Tobermorite peaks in relation to addition of $CaSO_4.1/2H_2O$, thermal treatment at 150°C during 48 h

around 1%. For higher addition, namely 3 and 5 % the acceleration of the process is lower and additionally a small amount of anhydrite can be detected.

The alumina sulphate accelerates in a similar manner the crystallization of Tobermorite but the influence is greater and is increasing with increased amount of addition. The alumina has a distinct influence on the crystals' habit and „band" forms can be be observed [Fig. 5].



Figure 5. The SEM image of Tobermorite formed in the sample containing 5 % of aluminium sulphate, 150°C, 120h

Among the sulphates the only exception is chromium sulphate which totally masks the crystallization of Tobermorite. Even after 120 hours of thermal treatment at 150°C no Tobermorite crystals can be

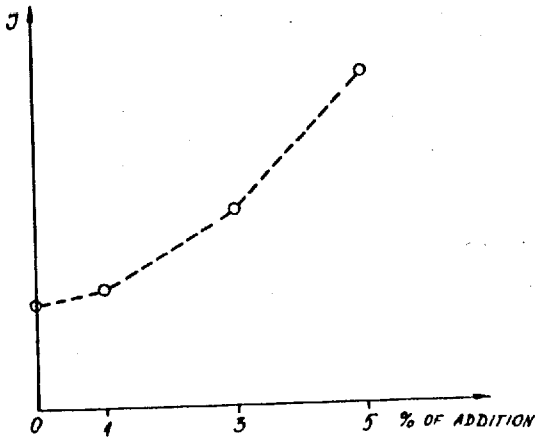

Figure 6. Intensity of Tobermorite peaks in relation to the quantity of calcium chloride added, 150°C, 48 hours

detected under SEM. However in case of 1% of addition very small amounts of these crystals are observed.

Calcium chloride is the most intensive accelerator of crystallization of Tobermorite. In case of this admixture the first plates of Tobermorite can be observed in the sample autoclaved 2 hours at 150°C. The influence is increasing proportionally to the amount added (Fig. 6). The Tobermorite crystals can also be detected by SEM in the samples autoclaved at 110°C during 48 hours.

The unexpected results gave aluminium chloride. This salt was a retarder of Tobermorite formation and its influence was proportional to the quantity added. For 1% of addition the crystals of Tobermorite was visible under SEM, but already for 3 % of $AlCl_3$ the presence of Tobermorite was not dedected neither by X–ray nor by SEM.

NaCl has rather no effect on the transformation of C–S–H phase into Tobermorite. A very limited retardation effect can be noted for the highest addition, i. e. for 5 %.

In the end chromium chloride is a very strong retarder. Even for 1 % of addition after 120 h of thermal treatment at 150°C the process is far from completion while in the sample without chromium the transformation is fully accomplished [Fig. 7].

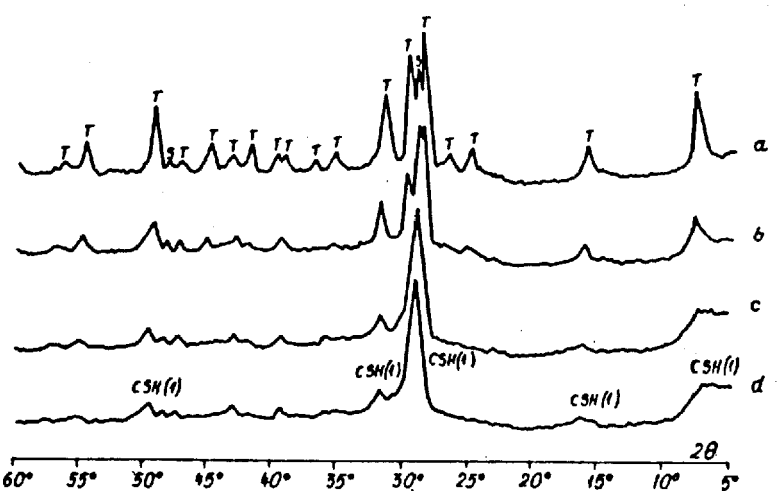

Figure 7. X–ray pattern of the samples with chromium chloride addition autoclaved at 150°C during 120 h: a) 0 %, b) 1 %, c) 3 %, d) 5 % of CrCl

Table 1. Minimum time of the thermal treatment at 150°C for Tobermorite to be detected under SEM

Admixture	content %	time of treatment h
$CaCl_2.6H_2O$	1	6
	5	2
$CaSO_4.1/2H_2O$	1	8
$Al_2(SO_4)_3.18H_2O$	1	8
	5	8
$AlCl_3.6H_2O$	1	24
	5	–*
$Cr_2(SO_4)_3.6H_2O$	1	48
	5	–*
$CrCl_3.6H_2O$	5	–*
NaCl	1	12
none		10

*time of treatment 120 hours

The results are summarized in Table 1 in which the minimum time of autoclaving needed for detection of Tobermorite crystals under SEM is presented.

CONCLUSIONS

From the obtained results the following conclusions can be drawn:

a) the strongest accelerator is calcium chloride,

b) the influence of added salt depends simultaneously on the cation and on the anion. For example $CaCl_2$ is an accelerator but $AlCl_3$ is retarder, but $Al_2(SO_4)_3$ is accelerator,

c) only chromium salts are always strong retarders independently if they are added as chlorides or sulphates,

d) the understanding of the mechanism in question needs further researches.

REFERENCES

1. Crennan, J.M., Dyczek, J. and Taylor, H.F.W.: Cem. Concr. Res., 1972, 2, 277–289.
2. Dyczek, J.: Ceramics (in Polish), 42, Educational Fasciles of Univ. of Min. and Metallurgy, Kraków, 1979.
3. Chan, C.F. and Mitsuda, T.: Cem. Concr. Res. 1978, 8, 135–138.
4. Sakiyama, M. and Mitsuda, T.: Cem. Concr. Res., 1977, 7, 681–686.
5. Tashiro, T. and Kawaguchi, K:. **6th ICCC**, Moscow 1974, vol. II/I, 227–232.
6. Sauman, Z. and Valtr, Z., ibid., page 227–232
7. Kurdowski, W. and Szuba, J.: Cemento, 1987, 84, 107–116.

EFFECT OF CEMENT CHARACTERISTICS ON THE FLUIDITY OF CEMENT PASTE CONTAINING AN ORGANIC ADMIXTURE

T Nawa and H Eguchi

Central Research Laboratory, Chichibu Cement Co, Ltd
Kumagaya-shi, Saitama, JAPAN

SUMMARY

The effect of cement characteristics on the fluidity of cement paste containing an organic admixture has been investigated using a rotational viscometer. The mechanism of the effect of cement characteristics on the fluidity was also investigated from the viewpoint of the hydration of cement, adsorption of the admixture and the zeta potential of the cement particles. The fluidity of a cement paste containing a superplasticizer depends on the fine fraction smaller than 10μm, the type of gypsum, and alkali sulfates in the cement. The hydration and adsorption studies showed that the effect of cement characteristics on the fluidity of cement paste had a slight correlation to hydrate deposition, but was rather closely related to adsorption of the admixture, especially that on C_3S. On the other hand, the zeta potential study showed that the cement paste was a system composed of heterogeneous particles having different surface potentials. The interpretation of the results from the fluidity study and the mechanism of action of an organic admixture are discussed in terms of cement particle heteroflocculation.

概要

セメントのキャラクターが有機質混和剤を添加したセメントペーストの流動性に及ぼす影響について回転粘度計を用いて検討し、さらにその影響のメカニズムについてもセメントの水和性状、混和剤の吸着性状およびセメント粒子のゼータ電位から検討を加えた。その結果、高性能減水剤を添加したセメントペーストの流動性はセメント中の10μm以下の微粒分、せっこう形態および硫酸アルカリによって変化するのを見い出した。また、セメントの水和性状および混和剤の吸着性状の検討結果より、セメントペーストの流動性に及ぼすセメントのキャラクターの影響は水和物の析出よりも混和剤の吸着、特にC_3Sへの吸着と密接に関係していることが分かった。一方、ゼータ電位の測定結果からはセメントペーストは表面電位の異なるヘテロ粒子から成る系であることが分かった。これらの結果に基づきセメントペーストの流動性に及ぼすキャラクターの影響および有機質混和剤の作用機構についてセメント粒子のヘテロ凝集から考察した。

INTRODUCTION

The rapid development of organic admixtures such as superplasticizer and their various applications to concrete has brought about improvement in the quality of cementitious mixtures including fluidity, strength and durability. Therefore, the study of the effect of organic admixtures has been more important in order to control the quality of ready mixed concrete and to identify its physical properties.

Although the effects of an admixture upon the fluidity of cementitious mixtures have long been studied, there are still many unidentified points concerning the mechanism of their action. It is, however, generally agreed that the action and effectiveness of the admixture are affected by the various characterisrics of cement. Whiting (1) reported that the alkali content as well as the fineness and the C_3A content of cement affects the required dosage of superplasticizer. Hattori et al.(2) and Basile et al.(3) pointed out that the effects of superplasticizer were affected by the amount and the type of gypsum. It is well known that alkali reacts preferentially with sulfur in raw materials and generally forms alkali sulfate in the clinker. Therefore, the fineness and sulfates such as alkali sulfate and gypsum are closely related to the mechanism of action of the superplasticizer.

In this study, the effects of fineness and sulfates on the fluidity of cement paste containing superplasticizer were investigated. In addition, the mechanism of action of the superplasticizer is discussed with respect to the hydration of cement, the adsorption on cement and the zeta potential of cement particles.

EXPERIMENTAL

Materials

Table 1 shows the chemical composition of the clinkers used in the study. In order to clarify the effect of fineness on the fluidity of cement paste, 11 types of cement were prepared by grinding the mixture of two clinkers, C1 and C2, and gypsum using different grinding procedures. Dihydrate and hemihydrate were added to achieve 2% of the total SO_3 content. The Blaine fineness and particle size distribution of the cements are shown in Table 2.

On the other hand, for examining the effect of sulfates on the fluidity of cement paste the cement was prepared using two clinkers, HR and LR. Clinkers HR and LR contained different amounts of alkali sulfate corresponding to 0.47% and 0.22%, respectively, of soluble alkali (converted to Na_2O). Each clinker was separately ground to a Blaine fineness of 3,000cm^2/g and then blended with dihydrate(D), hemihydrate(H) or anhydrite(A) to achieve 2.1% of total SO_3 content. Thus, six different cements were prepared and hereafter referred to as HR-D, HR-H, HR-A, LR-D, LR-H and LR-A, which indicate the combination of clinker and gypsum. C_3A, C_4AF and C_3S were prepared by calcining a stoichiometric mixture of $CaCO_3$, Al_2O_3, Fe_2O_3 and SiO_2. Their Blaine finenesses are 3,600±100cm^2/g. The organic admixture used in this study was a commercial superplasticizer (NSF) which mainly consisted of highly condensed sodium naphthalene sulfonate formaldehyde. It was a 42% aqueous solution with a density of 1,200 kg/m^3.

Measurement and Methods

The fluidity of the cement paste was determined by the apparent viscosity using a rotational viscometer. The apparent viscosity (η) is calculated from the shear stress (τ) at a 300 rpm shear rate (γ) using the following equation:

$$\eta = \tau / \gamma \qquad (1)$$

The amounts of adsorbed NSF were calculated by differences in concentration of an admixture in the liquid phase before and after adsorption. The concentration of NSF in the liquid phase was determined by UV absorption at 270-293 nm.

Table 1 Chemical composition of clinker

Sample	ig.loss	insol.	SiO_2	Al_2O_3	Fe_2O_3	CaO	MgO	SO_3	Na_2O	K_2O
C1	0.4	0.0	22.2	5.2	3.4	65.1	1.9	0.5	0.34	0.49
C2	0.7	0.1	22.3	5.1	3.0	64.8	2.1	0.6	0.24	0.46
LR	0.4	0.1	22.7	5.1	3.2	66.7	1.0	0.2	0.22	0.77
HR	0.5	0.1	21.9	5.2	3.3	65.6	1.5	0.5	0.55	0.83

The hydration of cement was stopped by dispersing it in acetone. The amount of ettringite in the hydrate sample was determined by the TG-DSC method. The heat evolution of cement as a function of time was determined using an isothermal conduction calorimeter.

The zeta potential was measured using an electrophoretic technique. Suspensions with a 0.2g sample in a 60mℓ solution of NSF were used at room temperature.

RESULTS

Rheological Study of Cement Paste

Figure 1 shows the apparent viscosity of cement pastes prepared using cements with different Blaine finenesses. The paste was allowed to hydrate for 15 minutes. There is an apparent viscosity increase with an increase in Blaine fineness when the variation of Blaine fineness of cement was large. On the other hand, there was not a very clear correlation detected when the fineness variation was small.

Hattori(4) pointed out that the action of the superplasticizer became significant when the particle size was smaller than 10 μm. Fig.2 shows the correlation between the fine fraction amount ($\leqq 11\mu$m) and the viscosity of the cement paste. A fairly good correlation between viscosity and particle fineness can be seen. It was also indicated that the correlation was affected by the kind of clinker and/or gypsum.

Fig.3 shows the correlation between the apparent viscosity of the cement paste and the added amount of NSF. The paste was prepared from cements with different amounts of alkali sulfate and different types of gypsum with hydration allowed for 15 minutes. For cement prepared with

Table 2 Fineness and particle size distribution

No.	kind of clinker	kind of gypsum	Blaine (cm^2/g)	Residue(%) 11μm	31μm	62μm
1	C1	Dihydrate	2970	36.7	72.4	94.8
2			3180	38.4	74.8	96.1
3			3570	42.1	79.0	97.8
4			4320	51.5	87.0	100.0
5		Hemi-	2930	36.3	69.4	93.8
6		hydrate	3110	40.9	74.2	95.8
7	C2	Dihydrate	4250	55.0	89.4	100.0
8			4310	50.4	88.0	100.0
9			4360	45.5	84.5	98.6
10			4460	52.6	88.2	99.1
11			4520	57.8	87.8	96.9

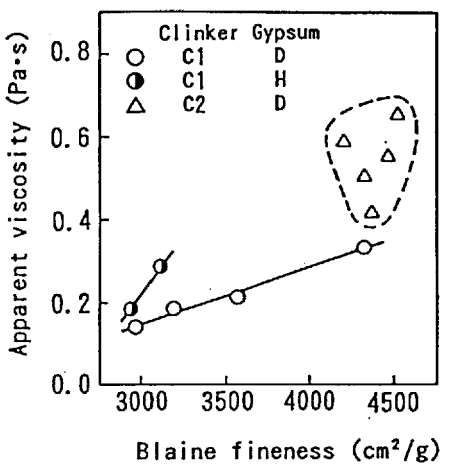

Fig.1. Relation of Blaine fineness to apparent viscosity of cement paste (W/C=0.3, NSF Cx1.4wt%)

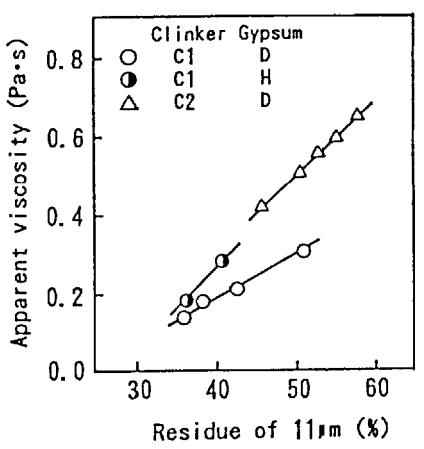

Fig.2. Relationship between fine fraction of cement particles and apparent viscosity of cement paste (W/C=0.3,NSF Cx1.4wt%)

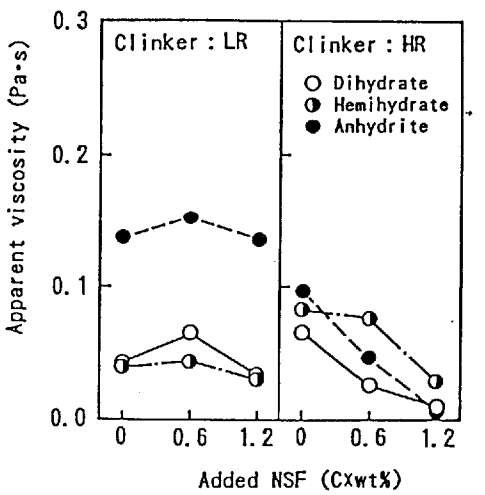

Fig.3. Effect of sulfate on apparent viscosity of cement paste (W/C=0.5, hydration time of 15min.)

clinker HR containing a large amount of alkali sulfate, the viscosity of the paste significantly decreased with an increase in the amount of added NSF. This decreasing tendency was affected by the type of gypsum added, i.e. the decrease in viscosity is enhanced by the low rate of gypsum dissolution. On the other hand, for a cement prepared with clinker LR containing a small amount of alkali sulfate, the addition of less than 1.2wt% NSF only slightly affected the viscosity irrespective of the kind of gypsum.

These results indicated that the fine fraction, the type of gypsum and alkali sulfate in cement influenced the rheological behavior of cement paste containing a superplasticizer.

Hydration

It was observed, for almost all cements, that the apparent viscosity was increased linearly in proportion to the formed ettringite, which was the hydrate product from C_3A and C_4AF with gypsum. In Fig.4, the correlation between apparent viscosity and the amount of ettringite produced with up to 75 minutes hydration is shown. It was found that the correlation between them was different depending on the amount of alkali sulfate in the clinker. These results suggested that the effect of cement character on the viscosity of the cement paste cannot be explained only by the friction between particles due to the deposition of hydrates.

Adsorption of NSF on cements

Fig.5 shows the influence of fineness on the amount of adsorbed NSF onto cement particles. The amount of adsorption increased with increasing fineness, and the saturated adsorption (at 1.4wt% dosage of NSF) increased at a rate of about 0.1mg/100cm^2.

The sulfates in cement showed a more significant influence on the adsorption of NSF than the fineness. Fig.6 shows the adsorption isotherms for cement with different alkali sulfate contents. For cements prepared with clinker HR containing a large amount of alkali sulfate, saturated adsorption amounts were about 3-5mg/g irrespective of the type of gypsum.

On the other hand, for cements prepared with clinker LR containing a small amount of alkali sulfate, saturated adsorption amounts were considerably higher than those for cements prepared with clinker HR. Their saturated adsorptions were about 7-15mg/g and varied depending on the type of gypsum.

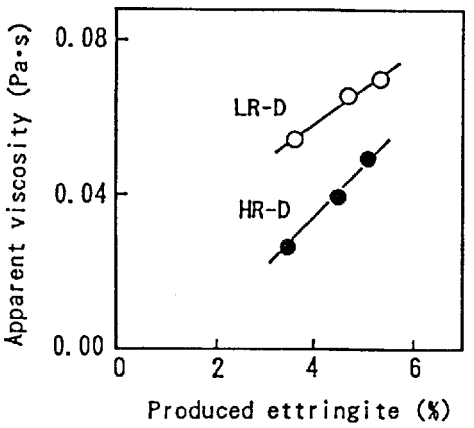

Fig.4. Relation of amount of ettringite produced to apparent viscosity of cement paste(W/C=0.5, NSF Cx0.6wt%)

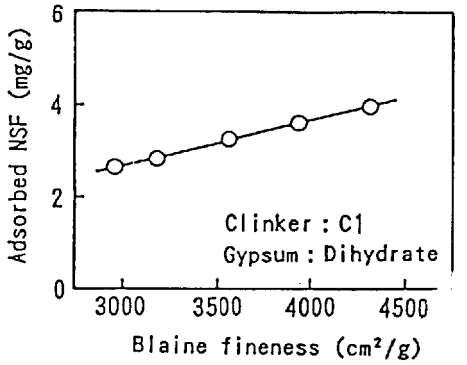

Fig.5. Effect of Blaine fineness on amount of adsorbed NSF on cement (W/C=0.3, NSF Cx1.4wt%, 5min.)

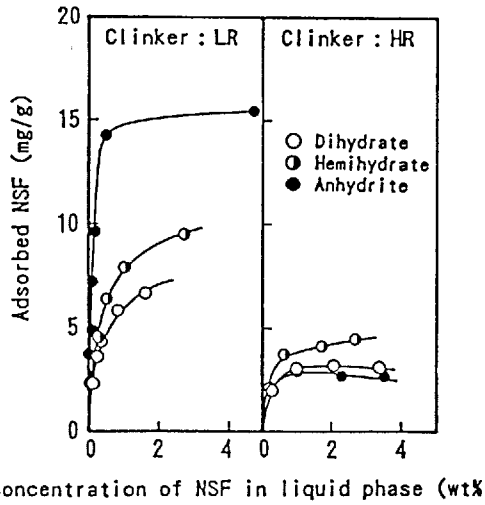

Fig.6. Effect of sulfate in cement on amount of adsorbed NSF on cement (W/C=0.3, NSF Cx1.4wt% ,10min.)

Effect of Alkali Sulfate and Gypsum on Adsorption onto Clinker Minerals

Fig.7 shows the adsorption isotherms of NSF on synthesized C_3A, C_4AF and C_3S. The saturated adsorptions of C_3A and C_4AF were very high, about 300mg/g, while that of C_3S was only 2mg/g. Hemihydrate and alkali sulfate inhibited the adsorption of NSF onto C_3A and C_4AF, but had slightly increased that on C_3S. These results suggested that the increased adsorption amount of NSF onto cement prepared with clinker LR containing a small amount of alkali sulfate (see Fig.6) was explained by the insufficient inhibition of its adsorption on C_3A and C_4AF by alkali sulfate.

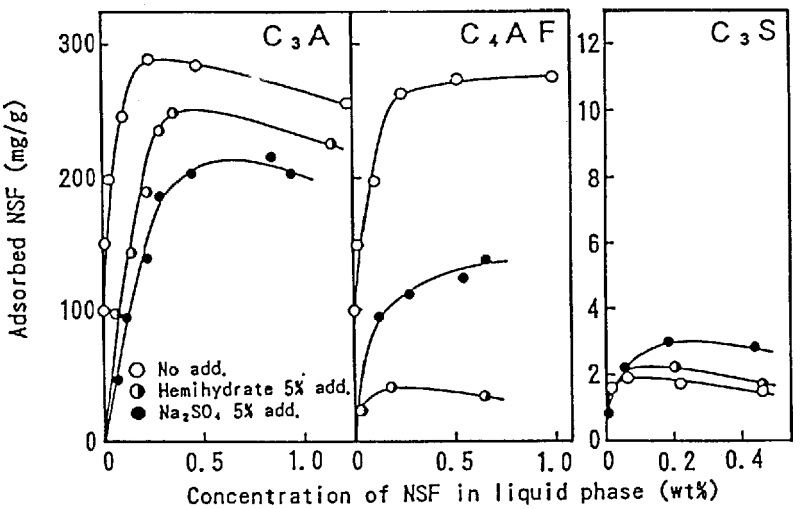

Fig.7. NSF adsorption isotherms onto C_3A, C_4AF and C_3S (W/S=5.0, 10min.)

The rate of adsorption of NSF on C_3A, C_4AF and C_3S is shown in Fig.8. The rate of adsorption had the following order: $C_3A > C_4AF >> C_3S$. The evidence coincides with the result obtained by Ramachandran(5). Accordingly, with mixing water added, the superplasticizer molecules were first adsorbed onto C_3A and C_4AF, and then the remaining ones onto C_3S. An intriguing question is: how does the amount of adsorption on C_3S change when the sulfates inhibit the adsorption on C_3A and C_4AF ?

It is well known that the hydration of C_3S in cement is retarded by adsorption of an admixture on its surface (6). Thus, the adsorption amount onto C_3S can be approximated from the degree of hydration retardation of C_3S in cement. Fig.9 shows the second peak position (t_1) of the heat evolution curve derived from the hydration of C_3S. With the amount of added NSF being the same, the hydration of C_3S was further retarded in cement prepared with clinker HR containing a larger amount of alkali sulfate. Similar effects were also observed for gypsum. It is concluded that dissolved SO_4^{2-} ion originating from gypsum and alkali sulfate inhibited the adsorption of NSF onto C_3A and C_4AF, and enhanced that on C_3S.

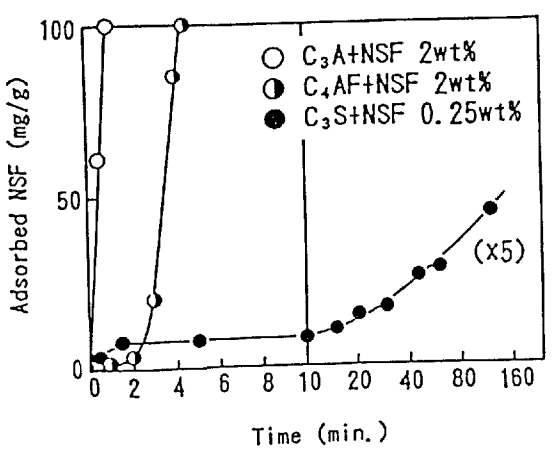

Fig.8. Adsorption rate of NSF on C_3A, C_4AF and C_3S (W/S=5.0)

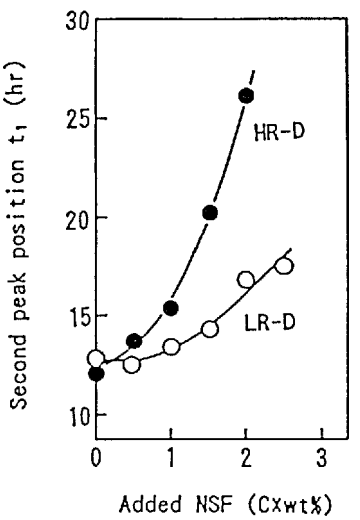

Fig.9. Effect of NSF on hydration of C_3S in cement (W/C=0.5)

Zeta Potential

In the absence of the admixture, the zeta potential value of C_3S was -9 mV and that of C_3A was 23 mV. In saturated $CaSO_4$ solution, the zeta potential values of C_3S and C_3A were reduced to -12 mV and 0 mV, respectively.

Figure 10 shows the zeta potential values of C_3A and C_3S in the presence of an admixture. They were both negative values and their absolute values increased as the concentration of NSF increased. The absolute zeta potential value of C_3S was smaller than that of C_3A. Thus cement paste is a system consisting of particles having different signs and/or zeta potential values.

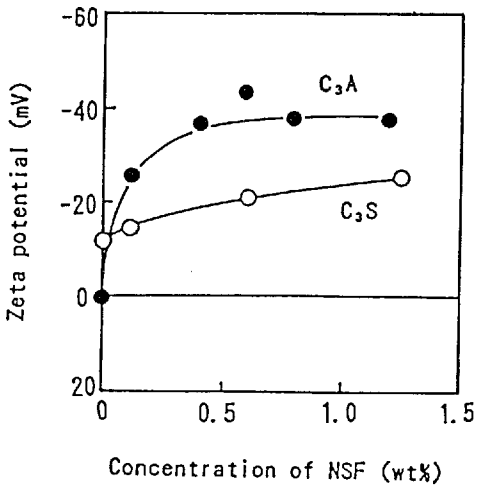

Fig.10. Zeta potential of C_3A and C_3S in saturated $CaSO_4$ solution as a function of NSF concentration

DISCUSSION

This rheological study showed that alkali sulfate improved the fluidity of cement paste. It has also been found that alkali sulfate increased the adsorption of C_3S. It is generally agreed that the action of superplasticizers is primarily due to their being adsorbed onto cement particles and exerting an electrostatic repulsion among them resulting in their dispersion. Several attempts have been made to explain the action of an admixture in terms of DLVO theories(7-9). The model previously chosen was based on a simple interaction between two particles both having the same potential. Such a model, however, is unreasonable for cement paste which consists of particles having different values and/or potential signs. Under such conditions, flocculation has to be investigated from the viewpoint of heteroflocculation. With heteroflocculation, the electrostatic interaction potential (V_A) and van der Waals attraction potential (V_R) between two spherical particles of surface potential ϕ_1 and ϕ_2, respectively, are given by the following equations (10,11).

$$V_R = \frac{\varepsilon a_1 a_2 (\phi_1^2+\phi_2^2)}{4(a_1+a_2)} \left[\frac{2\phi_1\phi_2}{\phi_1^2+\phi_2^2} \ell n \frac{1+\exp(-\kappa H_0)}{1-\exp(-\kappa H_0)} + \ell n\{1-\exp(-2\kappa H_0)\} \right] \quad (2)$$

$$V_A = - Aa_1a_2 / 6(a_1+a_2)H_0 \quad (3)$$

where ε is the dielectric constant of the dispersion medium, κ is the Debye-Hüchel recipocal length, a_1 and a_2 are the radii of respective particles, H_0 is the distance between the surface, and A is the Hamaker constant.

The flocculation/dispersion of particles is determined by the extent of the potential energy barrier (Vmax) on the total potential energy (Vt), namely, the sum of V_R and V_A.

Fig.11 shows the Vt curves between particles with different zeta potential values at an ionic strength of 0.35 mol/ℓ. The Hamaker constant of cement is $A=2\times10^{-21}$J based on the results of Hattori(6). In the absence of an admixture, the signs of the zeta potential for C_3A and C_3S are different,thus providing attraction between the particles (curve 'a' in Fig.11) resulting in rapid flocculation. In the presence of gypsum, however, the zeta potential of C_3A is reduced to zero, thus reducing the electrostatic attraction to relieve flocculation (curve 'b' in Fig.11). This can easily explain the fact that gypsum inhibits the flash set and/or quick set of cement.

On the other hand, in the presence of a superplasticizer, there is a repulsion between cement particles because the signs of the zeta potential for both C_3A and C_3S are the same. In such cases, the potential energy barrier (Vmax) is governed by the zeta potential with a smaller absolute value (curves 'c','d' and 'e' in Fig.11). From the results shown in Fig.10, the zeta potential of C_3S governed the flocculation of particles in a system containing an admixture. As previously mentioned, moreover, the zeta potential of C_3S significantly changed by the adsorption of the superplasticizer on C_3S.

Based on these results, the differences in fluidity of cement paste due to alkali sulfate and/or gypsum can be explained by the following mechanisms: alkali sulfate and gypsum inhibit the adsorption of NSF onto C_3A and C_4AF. This results in an increase in superplasticizer molecules adsorbed onto C_3S. The stable dispersing condition of cement particles is then maintained, resulting in a decrease in viscosity of the cement paste.

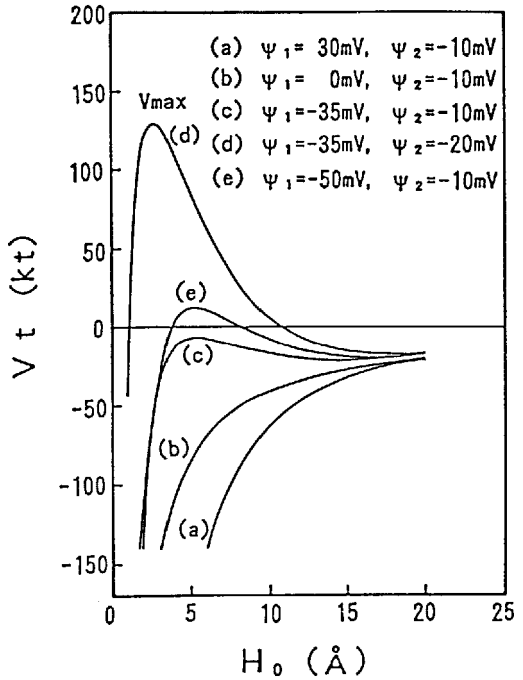

Fig.11. Calculated total potential energy(Vt) between particles ($a_1=a_2=1\mu m$, T=20℃)

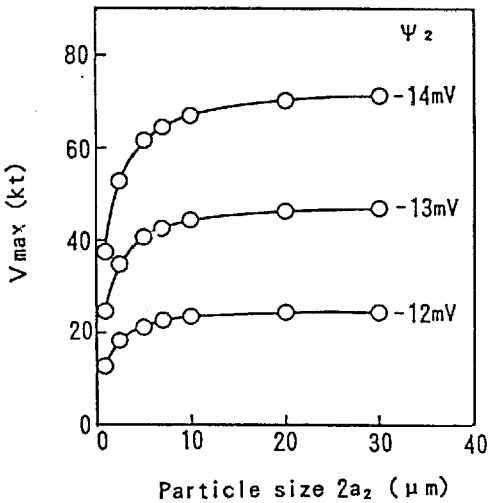

Fig.12. Change in potential energy barrier (Vmax) with particle size ($a_1=1\mu m$, $\phi_1=-35mV$, T=20℃)

The change in adsorption amount of the admixture due to fineness of the cement was not larger than that due to sulfates. Another explanation is thus required for the effect of fineness on fluidity. From equations (2) and (3), it is found that the heteroflocculation is influenced only not by the zeta potential but also by particle size. Fig.12 shows the effect of particle size on the potential energy barrier (Vmax). Vmax showed a marked decreasing tendency as the particle size become small, especially 10μm or less. It is thus explained why the viscosity of cement paste increased as the fine fraction (≦10μm) of cement increased.

In conclusion, the effects of superplasticizer is ascribed to its adsorption onto cement particles that leads to changes in the zeta potential of C_3A and C_3S to the same sign. Electrostatic repulsion among particles then leads to their dispersion. Dispersion of cement particles in this case was explained from the viewpoint of heteroflocculation which depended on the zeta potential of C_3S with a small absolute value as well as on particle size.

REFERENCES

1. Whiting, D., FHWA report,1981,169p
2. Hattori,K.,Okada,E.& Mizunuma,T.,CAJ Review of 38th General Meeting,Tokyo,1984,112-115
3. Basile,F., Biagini,S. & Ferrari,G., Cem.Concr.Res.,1987,17(5),715-722
4. Hattori,K., Concrete Journal(Japan),1976,14(3),12-19
5. Ramachandran,V.S., Il Cemento,1986,83(1),13-38
6. Kondo,R.,Daimon,M. & Sakai,E., Il Cemento,1978,7(3),225-229
7. Hattori,K., J. Soc. Materials Sci.(Japan),1980,29(318),240-246
8. Daimon,M. & Roy,D.M., Cem.Concr.Res.,1979,9(1),103-110
9. Muhua,T. & Roy,D.M., Cem.Concr.Res.,1987,17(6),983-994
10. Hogg,R.,Healy,T.W. & Fuerstenau,D.W., Trans.Faraday Soc.,1966,62,1638-1651
11. Hamaker,H.C., Physica,1937,4,1058-1072

EFFECT OF ADDITIVES ON HYDRATION WORKABILITY AND SOME OTHER PROPERTIES OF PORTLAND CEMENT

V K Singh and Barsha Gogoi

Department of Ceramic Engineering, Institute of Technology
Banaras Hindu University, Varanasi, INDIA

SUMMARY

The effect of some organic and inorganic additives on the properties of ordinary Portland cement has been studied by mixing 0.5 to 3.0 percent tartaric acid, tannic acid, dextrine, sodium bicarbonate and ammonium chloride by weight of cement. 1:3 Cement-sand mortar was utilised for determining flow properties and water retention value was determined by subjecting the mix to a suction of 50 mm of mercury. The setting time, percent flow and water retention values were found to vary with the quantity of additive. Workability increased with increase in water content of the mix. Dextrine and ammonium chloride were effective in improving both workability and water retention values. Tartaric acid produced a very high water retention value and dextrine a highly workable cement mortar.

INTRODUCTION

Consistency is used to indicate the wetness [1,2] of a mix and it must not be necessarily assumed that the more wet a mix, the easier it is to place. If the mix is too wet, segregation will occur and it may be difficult to place it and obtain a good surface finish. The mixing and placing of mixes of coarse and fines [3] play an important role in determining the quality of the product. Satisfactory mixing [4], so as to produce a uniform dispersion of the fines throughout the mix, coating of all the particles of aggregate-coarse and fines, is too obvious a necessity to need mention. The ease with which a mix can be placed depends on the workability [5] of the mix, i.e. the ease with which the material flows and at the same time remains coherent and resists segregation. All the work done or the energy expended in compacting a concrete mix is not usefully employed. The applied energy is the sum total of the work lost and the work performed usefully; the work performed usefully can be subdivided into that performed in overcoming the internal friction of the concrete itself and that required to overcome the surface friction between the concrete and the mould and the reinforcement. The portion of the work which is solely dependent on the characteristics of the mix is that used in overcoming the internal friction of the concrete which is termed 'useful internal work'.

Cement requires about 1/4 of its weight of water to become completely hydrated. It has been found that the strength of concrete continues to increase with reduction of water cement ratio to 0.20 or even less. On the other hand, if water is in excess which does not enter into chemical combination with the cement it forms water voids, or may subsequently dry out leaving air voids.

The factor affecting workability is the quantity of water in the mix. Since the water to cement ratio is fixed by the strength required, the only way of increasing the quantity of water in the mix is to increase the quantity of cement also in the mix [6]. For constant grading and workability, the quantity of free water (excluding that absorbed by the aggregate) required in the mix is constant and independent of the quantity of cement. Though this cannot be accepted as an invariable rule, it does open the possibility of fixing the quantity of water per meter^3 of mix to give it optimum workability. A very finely ground cement requires more water to produce the same workability which a coarsely ground cement will produce with less.

The danger of segregation of constituents must be considered because the wetter the mix, the larger the aggregate size or the coarser the grading [4], greater is the risk of segregation. The tendency for segregation can be prevented by cohesiveness of the mix and this depends on the specific surface of the aggregate and cement put toghether, and increases with these. It is necessary to increase the proportion of fines and increase the cohesiveness to prevent segregation: (i) when the mix is lean; (ii) when the mix is very wet; (iii) when handling conditions are likely to promote segregation, as when it is jolted during transport, dropped into the mould from a height or discharged down chutes; (iv) when the mould or reinforcement contains much small details and sharp corners; and finally (v) when it is pumped.

Water Retention - The water retaining properties of many cements [7], specially masonry cements, help to increase their adhesion to bricks or other building units by not allowing their water to be absorbed into the pores of the building units. In the case of oil well cement, the property desired is that the cement slurry should not lose its mixing water into the surrounding soil when placed in position. Water retaining properties can be imparted to cement by certain additives. The trouble with additives, if present in quantities sufficient to produce the desired effect, is that they may decrease the strength of the cement to unacceptable level. The effect of additives [8-14] on the setting, workability. water retention, water proofing properties of cement, etc, have been reported by several investigators. Organic molecules function as accelerators or retarders by reacting with cement constituents and form amorphous constituents in the

---

In the text, C = CaO. A = Al_2O_3. S = SiO_2 thus C_2S = $2CaO.SiO_2$, C_3A = $3CaO.Al_2O_3$.

mix. Some acids and hydroxy arboxylic acids [8] which have labile protons react with basic hydrated cement compounds present in Portland cement paste to form salts and consequently decrease the set time. The need to delay set time further is sometimes essential in tropical countries where a slow set rate might be advantageous. In the present investigation workability and water retention values of cement - sand mortar have been studied by mixing different quantities of two organic retarders, namely, tartaric acid and dextrine, and two inorganic additives namely sodium bicarbonate and ammonium chloride, besides tannic acid (organic) which accelerate the setting slightly.

EXPERIMENTAL

Workability experiments have been carried out by taking cement mortars having different cement-sand ratios with and without additives. Sand used was ordinary river sand, the particle size of which is given in Fig. 1. Reagent grade tartaric acid, tannic acid, dextrine, sodium bicarbonate and ammonium chloride in quantities 0.5-3.0 percent were weighed and mixed intimately with cement in dry condition in a small pot mill. This was mixed with sand in the ratio of 1:3 and varying amounts of water added. The cement used was ordinary Portland cement (OPC) of composition given in Table I. Its initial setting time was 35 minutes and consistency 31% water.

Table I Composition of Cement

Constituents	Percent
SiO_2	17.45
Fe_2O_3	6.60
Al_2O_3	7.00
CaO	59.81
MgO	2.76
Insoluble residue	2.30
Loss on ignition	2.10
SO_3	1.78

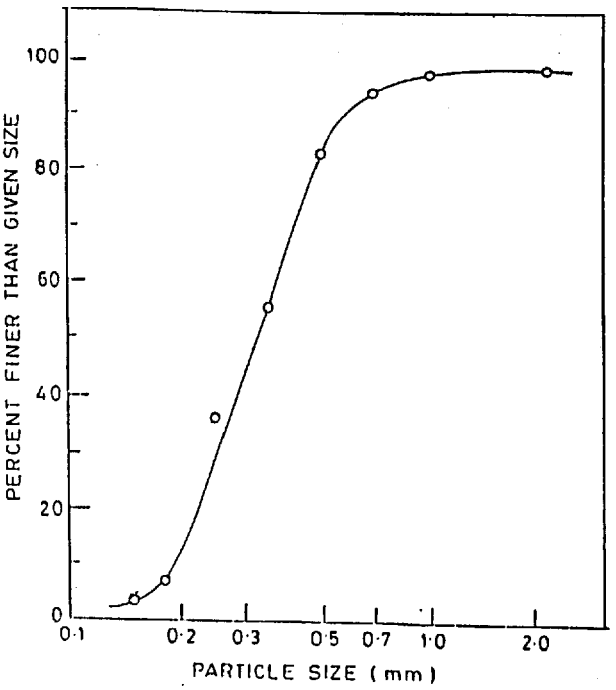

Fig. 1 Cumulative analysis of sand

Determination of Workability - Workability of the mortars with different percentages of additives and water contents were determined by using a flow table [7] having a cam designed to drop the table by 12.5 mm (bump). Spread diameter of the mortar was measured after giving 15 bumps in 15 seconds and flow was calculated by the formula given below:

$$\% \text{ flow} = \frac{\text{spread diameter - initial diameter}}{\text{Initial diameter}} \times 100 \qquad (1)$$

Determination of Water Retaining Capacity - From the workability curves between percent flow versus water/solid ratio (percent water added) for different mixes, the water required to give a flow of 110 percent was determined. Water retention values were determined as per IS:4031 by maintaining a vacuum of 50 mm as measured on a mercury manometer. Mortar was mixed to such consistency as ould give a fl w of 110±5 per ent. Immediately after making the flow test, the mortar was remixed and a performed dish filled up to its rim, after putting a wet filter paper at the bottom of the dish. After maintaining the suction for 60 seconds, the mortar was remixed and filled in the flow. mould and tested for its workability. Water retention value was calculated as follows:

$$\text{Water retention value} = \frac{A}{B} \times 100 \qquad (2)$$

where A = flow after suction, and
B = flow immediately after mixing (before suction).

Setting time with additives was determined using a standard Vicant apparatus. Experiments were performed at 27°C for various tests as per IS:4031.

RESULTS AND DISCUSSION

The presence of materials other than the hydration products greatly affect the workability and water retention values of cement mortars. The flow is determined by: the frictional resistance between its layers, the viscosity of the cement paste, the separation between the particles which in turn, depends on the amount of cement paste, and the grading of aggregates. The effect of the proportion of coarse and fines has been studied by taking cement-sand mortars of different proportions (Fig. 2). Mixes from 1:1 to 1:4 proportions showed increase in the percent flow which was proportional to the quantity of water added. 1:4.5 and 1:5 cement-sand mixes gave yield value at 19.5% water after which the flow again became proportional to the quantity of water added.

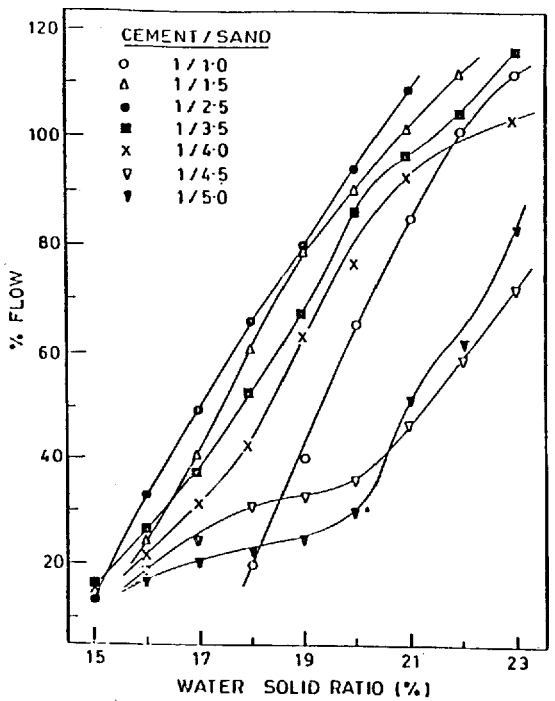

Fig. 2 Workability of different mixes of cement and sand.

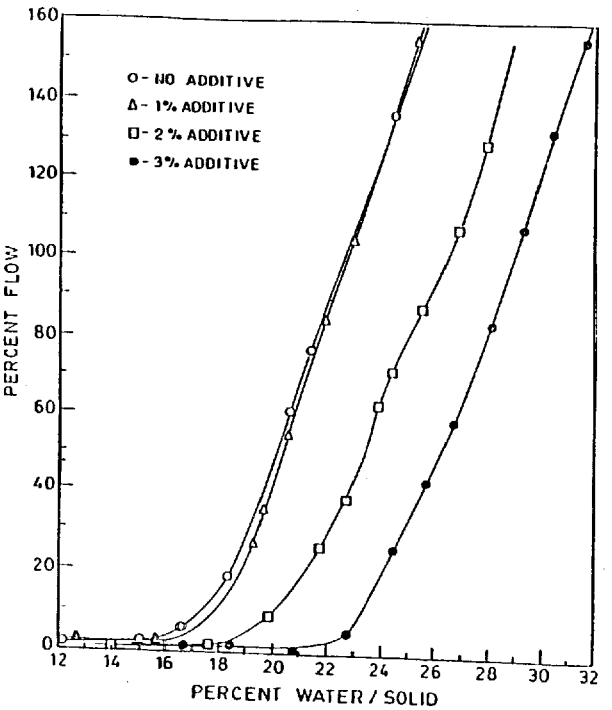

Fig. 3 Effect of tartaric acid on the workability of cement mortar

1:3 Cement-sand mortar requires about 16% water by weight (water/solid ratio about 0.16) of the mix to produce an initial flow which could be measured by flow table. Addition of 1.0% tartaric acid (Fig. 3) required a little more water than even 1:3 cement-sand mortar to give the initial flow. Further increases in tartaric acid content of the mix demanded more water to produce the initial flow. All the curves were almost parallel to that obtained without any addition. 1:3 Cement sand mortar gave a water retention value (as measured by equation '2' of 45%, while with just 1.0% addition of tartaric acid, the water retention value increased to 95%. Change in tartaric acid content from 1.0 to 3:0% in the mix did not alter much the water retention value of the cement mortar.

When the amount of dextrine added was increased from 1.0% to 2.0%, the position of

the curve in the flow vs percent water added shifted towards higher workability values. Addition of 3.0% of dextrine demanded a little more water to produce the initial flow and the position of the curve shifted towards lower workability values up to a flow of 50%, but beyond that it shifted towards higher workability values. Up to 87.0% flow, the values were close to that of 1.0% dextrine addition but thereafter they increased further and gave 160% flow with only 21.6% water (Fig. 4). Dextrine remains interpersed in the mix and affects both workability and water retention values. When the amount was increased from 1.0 to 3.0% the water retention values increased from 57.4 to 75.5%.

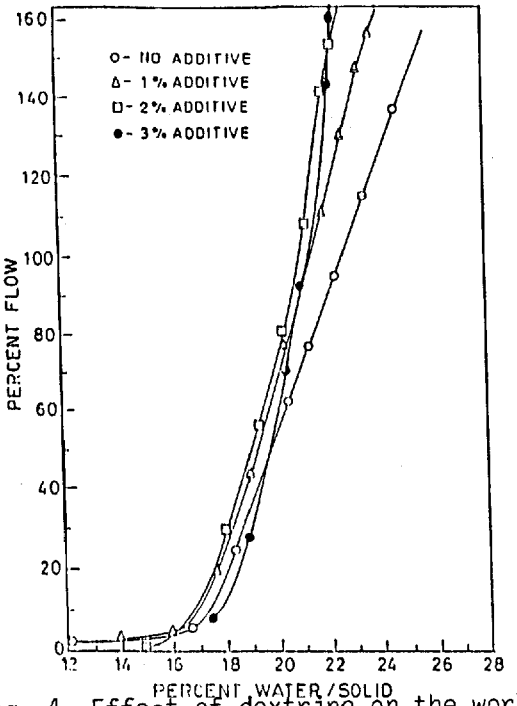

Fig. 4 Effect of dextrine on the workability of cement mortar

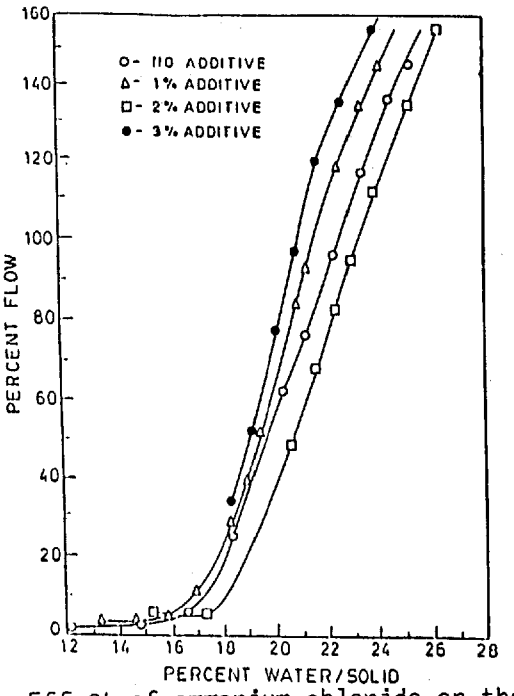

Fig. 5 Effect of ammonium chloride on the workability of cement mortar

Fig. 5 shows that, on addition of 1.0% ammonium chloride, the position of the curve in the flow vs percent water added shifted towards higher workability values as compared to 1:3 cement-sand mortar. On addition of 2.0% NH_4Cl, the position of the curve shifted towards lower workability values. A 3.0% addition gave the highest workability. It has been shown that set regulating salts form complex [14] salts analogous to the calcium aluminate sulphate hydrates. Calcium chloride acts as retarder when present in low concentrations but accelerates setting at higher concentrations [13]. This may be due to the higher solubility of calcium aluminate chloride at higher concentrations. NH_4Cl reacts with cement in a similar way. and increase or decrease in the concentration of NH_4Cl did not affect the workability values proportionately. Water retention values were 67.8, 67.25 and 66.8% with 1, 2 and 3 percent addition of NH_4Cl respectively (Fig. 7).

Sodium carbonate, bicarbonate and silicate react with calcium hydroxide to form alkali which may cause the precipitation of aluminium hydroxide. This process can improve the water retention values of cement mortar. At higher concentrations, aluminium hydroxide starts dissolving and it is difficult to correlate the workability values with the amount of addition. Fig. 6 shows that the addition of 1.0% sodium bicarbonate lowered the workability values, but at 2.0% the position of the curve shifted towards higher workability values. Further increase lowered the workability values again. However, water retention values increased from 56.5% to 60.7% when the additive was increased from 1.0 to 3.0% (Fig. 7).

Fig. 8 shows the workability curves for cement mortar with 0.5 to 3.0% tannic acid. Workability increased with increase in percent tannic acid and water content. Water retention values calculated with the help of formula '2' are given in Table II. It can be

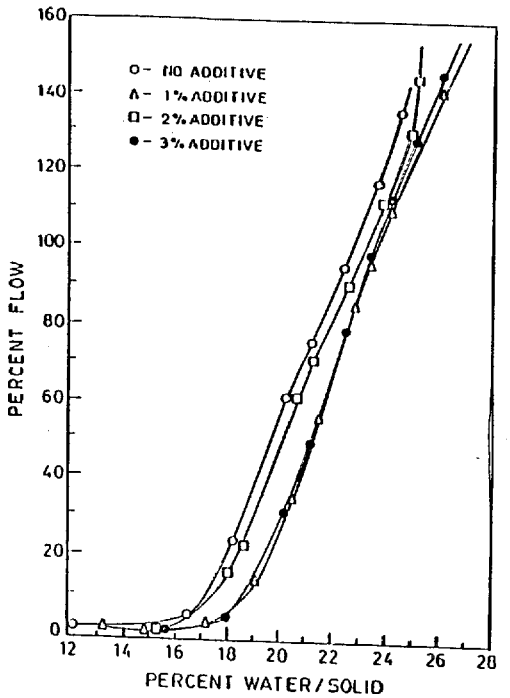

Fig. 6 Effect of sodium bicarbonate on the workability of cement mortar

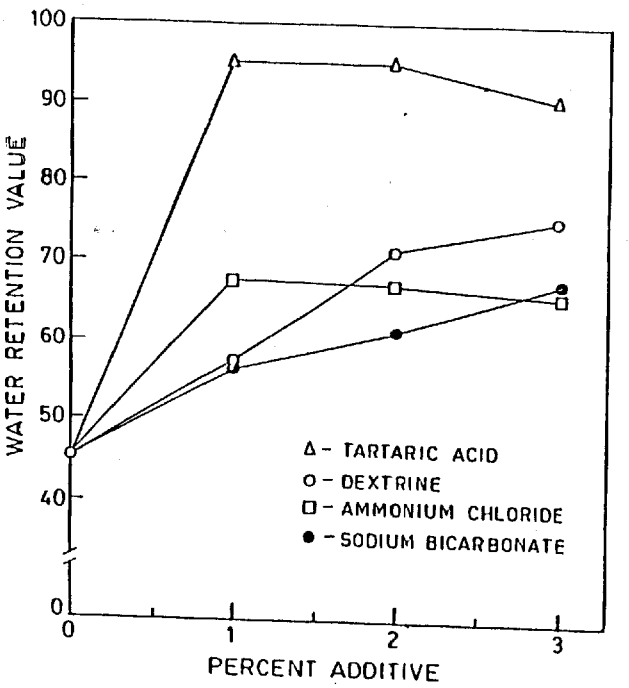

Fig. 7 Effect of retarders on water retentivity of cement mortar

Table II Water retention value of cement mortar with different percentage of tannic acid

Tanni %	Water %	% Flow (B)	% flow after suction(A)	Water retent value (A/B)
0.5	20.0	110.5	55.6	50.3
1 0	19.8	112.0	50.5	45.1
1.5	19.6	112.5	45.6	40.5
2.0	19.4	108.0	38.0	35.2
3.0	18.8	109.0	34.9	32.0

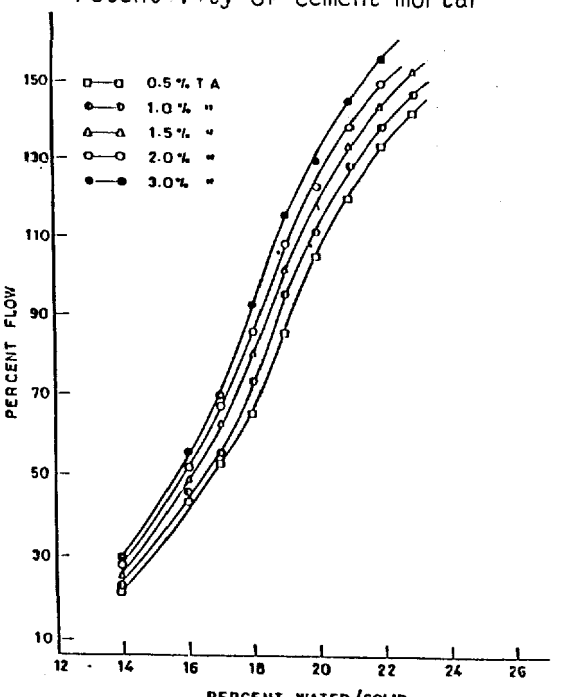

Fig. 8 Effect of tannic acid on the workability of cement-sand mortar

seen that 0.5% tannic acid in the mix gave 50.3% water retention value and 1.0% gave a value equal to that for cement without any addition. Increase in tannic acid from 1.5 to 3.0% decreased the value from 40.5 t 32.0%. Also, tannic acid when mixed with cement acts as accelerator. Table III shows the initial and final set times of cement with 0.5-2.0% tannic acid. The initial set time decreased from 30 to 20 minutes and the final set from 180 to 101 minutes. Table III also shows the compressive strength of mixes with 0.5 to 2.0% tannic acid determined as per IS:4031 on 1:3 cement-sand mortar after curing at 27°C for 28 days in more than 90% relative humidity. A little lowering in the strength was observed and the values obtained were comparable with the strength of cement without any addition.

Organic acids [8] have a distinct behaviour towards the setting of cement due to the presence of functional groups [11], its nature, chain length, etc. The mechanism of set

retardation has been reported [9]. Set retardation may be primarily due to retarding of the hydration of $3CaO.SiO_2$ through adsorption of organic admixtures on to $Ca(OH)_2$ nuclei. Adsorption on to the initial hydration products of $3CaO.Al_2O_3$ can also retard further hydration [14]. The hydration process may be affected also due to the chemical interaction between C_3A, C_3S, C_2S etc. and the organic materials [12] to yield amorphous materials, chelates or organic acid salts of Ca^{2+} or Al^{3+} which are interpersed in the crystalline mass. Inorganic additives dissolve during the first few minutes of the action of water on cement. The reaction of sodium bicarbonate with calcium hydroxide would precipitate $CaCO_3$ according to the equation:

$$NaHCO_3 + Ca(OH)_2 \rightarrow CaCO_3 + NaOH + H_2O \quad (3)$$

The resulting hydroxide would then act as if it was added as such and the result would be acceleration of hydration and set. Ammonium chloride accelerates set because of heat liberation. Different values of setting time with 1.0% additives are given in Table IV.

Table III Setting time and strength of cement with different quantities of tannic acid

Tannic acid %	Initial setting time, min	Final setting time, min	Compressive strength, kg/cm² 28 days
0.0	35	280	215
0.5	30	180	202
1.0	25	125	198
2.0	20	102	180

Acidic additives react with $Ca(OH)_2$ and $Al(OH)_3$ to form Ca^{2+} and Al^{3+} salts and water is liberated which may be helpful in increasing the workability of the mix [$Ca(OH)_2 + 2H^+ \rightarrow Ca^{2+} + 2H_2O$]. When tannic acid ($H_6TA$) reacts with the hydrated phases, calcium and aluminium tannates are formed which remain distributed in the cement mix and affect setting, workability and water retention values of cement.

$$Ca(OH)_2 + H_6TA \rightarrow Ca(H_4TA) + 2H_2O \quad (4)$$

$$Al(OH)_3 + H_6TA \rightarrow Al(H_3TA) + 3H_2O \quad (5)$$

Table IV Effect of additives on the setting time of cement

Additive	Additive %	Initial setting time, min	Final setting time, min
Sodium bicarbonate	1.0	20	145
Ammonium chloride	1.0	26	135
Tartaric acid	1.0	97	305
Dextrine	1.0	370	-

Similar behaviour is expected with other additives, the resulting variation in set time and other properties depending on the activity of the functional group (Table II-IV). Addition of 1.0% sodium bicarbonate and ammonium chloride gave compressive strength values of 175 and 165 kg/cm² respectively whereas it was about 100 kg/cm² with 1.0% tartaric acid and dextrine, which might increase with the age of sample.

Some additives improve more than one property. Workability aids sometimes also act as air entraining agents which are materials that trap air inside cement mortar. Hydrophili groups, such as COO^-, NH_3^+ act sometimes as air entraining agents [13]. Contamination with CO_3^{2-} or its deliberate addition to cement can cause the formation of scawtite [$Ca_7(Si_8O_{18})2H_2O$] and $C_3A\ CaCO_3.12H_2O$. Some ternary phases including 11 Å tobermorite, can also accommodate small amounts (1.0%) of CO_3^{2-} inside their structure [15]. Sodium bicarbonate addition to ordinary Portland cement mortar increases the water retention values but flow properties are not affected appreciably. A feature of agents to which much attention has been devoted recently is their ability to reduce the water requirement by increasing the water retention values. The effect of organic substances and their effect in altering setting time and improving the workability is most marked in cement mortar and concretes. The organic matter may or may not be harmful depending on its nature. The danger is that the cement, under bad curing conditions, may be prevented from hydration and setting, and develop only a very low strength.

CONCLUSIONS

Workability in the mortars studied was affected by the proportion of coarse and fines as also the type and the quantity of additive. It increased with increase in the water content of the mix. Organic materials are more effective in improving workability. Tartaric acid produced a very high water retention value and dextrine a highly workable cement mortar.

REFERENCES

1. Orchard. D.F.: Concrete Technology, Vol. 1, London, Applied Science, 1973, 157 p.

2. Dewar, J.D.: Relation Between Various Workability Control Tests for Ready Mixed Concrete", Cement and Concrete Association, London, 1964, p. 15.

3. BS: 812-1960: "Sampling and Testing of Mineral Aggregates, Sands and Fillers", British Standard Institution, London, 1960.

4. Cusens, A.R.: "The measurement of workability of dry concrete mixtures", Mag. Concr. Res., 1956, 8 (22), 23.

5. Singh, V.K. & Khare, V.K.: "Studies on the workability of cement-lime-sand mortars". Trans. Ind. Ceram. Soc., 1978, 37 (1), 28.

6. Bogue, R.H.: The Chemistry of Portland Cement, New York, Reinhold, 1955, 567 p.

7. IS: 4031-1968: "Indian Standard Methods of Physical Test for Hydraulic Cement", Bureau of Indian Standard, New Delhi, India, 1968.

8. Diamond, S.: "Interaction between cement minerals and hydroxy-carboxylic acid retarders", J. Am. Ceram. Soc., 1973, 56 (6), 323.

9. Young, J.E.: "Review of the mechanism of set retardation in Portland cement paste containing organic admixture". Cem. Concr. Res., 1972, 2, 415.

10. Rakhimbae, S.M. & Bash, S.M.: "Effect of rganic substances on the hardening time of Portland cement", Z. Prikl. Khim. (Leningrad), 1968, 41, 2618.

11. Mueller, L.: "Effect of amino compounds on the setting and hardening of Portland cement", Zem.-Kalk-Gips., 1974, 27, 69.

12. Singh, V.K., Narang, K.K. and Ali, M.M.: "Effect of sulphanilic acid on Portland cement", Trans. Ind. Ceram. Soc., 1979, 38 (3), 85.

13. Lea, F.M.: The Chemistry of Cement and Concrete. 3rd Ed. London, Edward Arnold, 1970, 301 p.

14. Glasser, F.P. & Taylor, H.F.W.: The Chemistry of Cements, Vol. 2, ed. by H.F.W. Taylor, London, Academi Press, 1964, 323 p.

THE EFFECT OF HYDROLYZABLE TANNIC COMPOUNDS ON HYDRATION OF CEMENT AND ITS UTILIZATION AS A HEAT CONTROLLING AGENT

H Inokawa, K Inada, N Kozakai, A Ohno and K Uchida

Central Laboratory, Sumitomo Cement Co Ltd
JAPAN

SUMMARY

In order to develop a heat controlling agent in mass concrete, effects of hydrolyzable tannic compounds (tannic acid) on hydration of cement were studied. Tannic acid are hydrolyzed gradually to generate stronger retarding compounds like gallic acid in alkaline solution. The rate of this reaction depends on temperature; the higher temperature is, the more retarding compounds are formed. So in the hydration processes, tannic acid shows a different behavior from other retarders like lignosulfonate, gluconic acid sodium salt and so on. It was found that tannic acid has a significant effect on the temperature-dependence of retardation and can control the adiabatic temperature rise of mass concrete.

マスコンクリート用の水和発熱抑制剤を開発するために、加水分解性タンニン化合物（タンニン酸）がセメントの水和に与える影響を調べた。タンニン酸はアルカリ溶液中で加水分解し、没食子酸のような強いセメントの水和遅延性物質を徐々に生成する。この反応速度は温度に依存し、温度が高ければ高いほど、より多くの遅延性物質を生成する。よって、タンニン酸はセメントの水和反応に他の遅延剤（リグニンスルホン酸塩、グルコン酸塩他）と異なる影響を与える。

すなわち、タンニン酸は水和遅延の温度依存性が大きく、マスコンクリートの断熱温度上昇を制御することができる。

INTRODUCTION

The mechanism by which hydrolyzable tannic compounds (tannic acid) retards the hydration of cement is not well understood.[1] Tannic acid is a compound in which gallic acid is present in the form of an ester,[2] and hydrolyzes readily under alkaline conditions to generate gallic acid and glucose, which are known for their strong retardation effects on the hydration of cement. Tannic acid is, therefore, expected to exhibit different effects on cement hydration than those of the substances known as ordinary retarders, i.e. lignosulfonate and sodium gluconate.

In this research, the effects of tannic acid on the rate of heat of hydration of cement were studied at different temperatures. These effects were then compared to the effects of lignosulfonate and sodium gluconate on the same processes of cement hydration. The relationship between setting time and the rate of adiabatic temperature rise confirms that the retardation effect of tannic acid on cement hydration differs from those of lignosulfonate and sodium gluconate. The effect is utilized to develop a heat controllig agent with tannic acid as a main ingredient.

EXPERIMENTAL

The cement used was normal portland cement. The reagents used were as follows: high-purity tannic acid (Ta-P, purity: 90%, gallic acid: less than 0.1%), industrial grade tannic acid (Ta-I, purity: 68%, containing 5% of gallic acid), reagent grade sodium gluconate (Gl), commercial AE water reducing agent (LS, lignosulfonate base), commercial AE water reducing agent (SG, oxycarboxylate base) and reagent grade gallic acid (Ga).

High performance liquid chromatography (h.p.l.c.) was utilized,[3] using a normal phase column (NUCLEOSIL 50-5; 4.0mm×250mm, supplied by GL Sciences Inc.), where an absorption at 280 nm was measured using a UV detector under the following conditions. The solvent used was n-hexane/methanol/THF/formic acid (55/61/11/1) containing oxalic acid 450 mg/l, at a flow rate of 1.5 ml/min. The samples for h.p.l.c. were prepared by the following procedure: 20 ml of 10% NaOH were added to a mixture of 10 g of dried Ta-I and 100 ml of distilled water, and the mixture was stirred at 20°C or 30°C for a given time. 1 g of each mixture was added to 0.5 ml of 10 wt% H_2SO_4 and 100 ml of methanol. The mixture was filtered by a 45 μm filter, and 5 μl of the mixture was injected.

A conduction calorimeter and testing apparatus for measuring adiabatic temperature rise, supplied by Tokyo Riko, were used. The amount of cement sample was 4 g (W/C: 50%) for the former, and the mix proportion of mortar was cement (1200 g), sand (6000 g) and water (800 g), sealed in a container, for the latter. The apparatus for DTA used was Seiko's TG-DTA30, where approximately 60 mg of accurately measured, D-dried cement paste was heated at 20°C/min.

RESULTS AND DISCUSSIONS

1. Temperature dependences of effects of tannic acid or other organic substance on the hydration of cement

Fig.1 to 5 show the effects of Ta-P, LS and Gl on hydration of cement at different temperatures by conduction calorimeter.[4] Peak time of cement hydration is defined as the time at which the rate of cement hydration is maximum. The following phenomena are observed:

(1) Effects of tannic acid on cement hydration are as follows. The higher the temperature of cement hydration, the greater the retardation effect of tannic acid on cement hydration and the lower the rate of heat of hydration of cement (Fig.2).

(2) Effects of LS and Gl on cement hydration are as follows. The higher the temperature of cement hydration, the higher the rate of heat of hydration of cement (Fig.3 and Fig.4).
(3) As the amounts of Gl increases, the peak time of cement hydration increases, but the max. rate of heat of cement hydration is constant.
(4) The main product of hydrolysis of Ta-P is Gallic acid (Ga), and its retardation effects are much greater than the effects of Ta-P itself (Fig.5).

These results indicate that the effects of tannic acid on cement hydration are much different from those of the other compounds tested, in particular with respect to dependence on temperature.

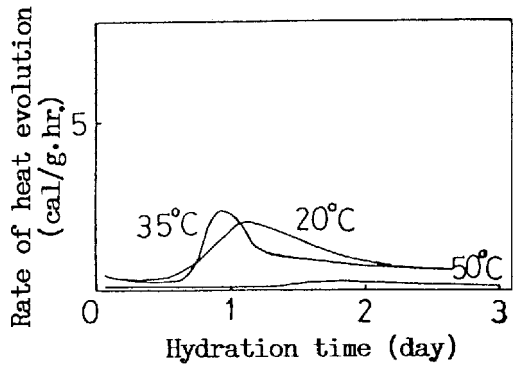

Fig.2 Heat of hydration evolution of cement in the presence of Ta-P (0.5%)

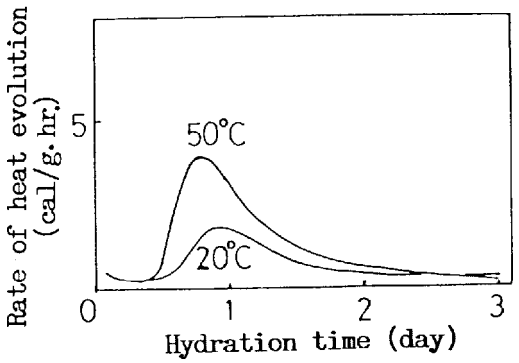

Fig.4 Heat of hydration evolution of cement in the presence of LS (0.5%)

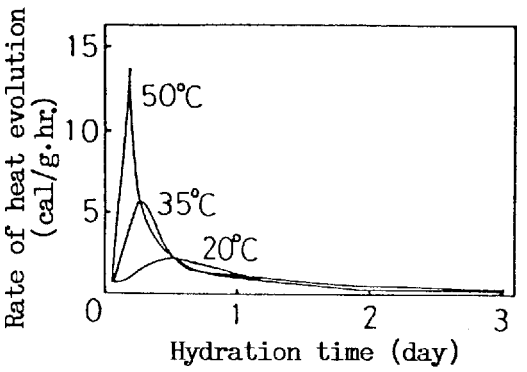

Fig.1 Heat of hydration evolution of cement in the absence of organic chemical admixtures

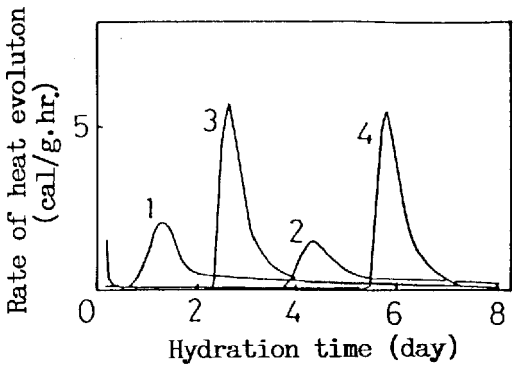

Fig.3 Heat of hydration evolution of cement in the presence of Gl
1: 20°C 0.15% 3: 50°C 0.15%
2: 20°C 0.25% 4: 50°C 0.25%

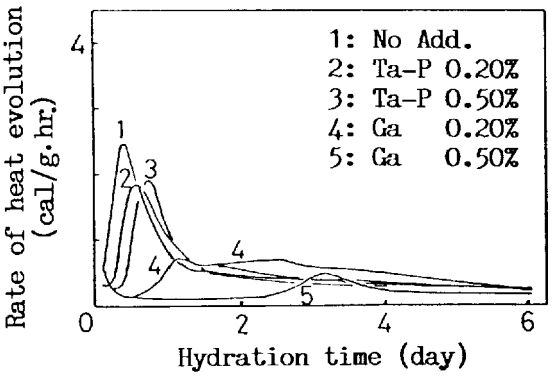

Fig.5 Effects of Ta-P and gallic acid on heat of cement hydration at 20°C.

2. Hydrolysis of tannic acid under an alkaline condition

Tannic acid is a compound in which galloyl groups are bonded to glucose through the ester bond (poly galloyl glucose), and is considered to be hydrolyzed under an alkaline condition. Alkaline hydrolysis of industrial grade (Ta-I) was analyzed by normal phase h.p.l.c..[3),5)] Fig.6 shows the hydrolysis of Ta-I in the presence of NaOH; the amount of Ga increases with time. Particularly noted is a sharp increase in amount of Ga at 0 to 24 hr at 30°C. The side reactions, such as decarboxylation of Ga into pyrogallol, were also detected (retention time of Ga: 3.6 min, pyrogallol: 3.3 min). As the number of galloyl groups linked to glucose increased, retention time also increased.

When Ta-I is hydrolyzed in alkaline at 20°C, Ga is formed slowly by hydrolysis reaction, it seems that Ga is transformed into pyrogallol. At 30°C, on the other hand, Ta-I hydrolyzed quickly to generate Ga and lower moleculer tannin compounds, and the amount of Ga increased steeply at a retention time in the range of 0 to 24 hr.

In a theoretical cement water system, Ta-I undergoes alkaline hydrolysis reactions, and is transformed successively from a condition of many galloyl groups linked to glucose and then to gallic acid and fewer galloyl groups linked to tannic compounds. Retardation of hydration is greatly affected by the presence of low molecular weight phenolic hydroxide groups.[6)]

The polyphenols, such as Ga and pyrogallol as decomposition products, have more phenolic hydroxide groups than tannic acid and exhibit larger retardation effects than Ta-I, and it is considered that the retardation of hydration will change with time in a cement-water system in the presence of Ta-I, this phenomenon was applied to make an agent to control the heat of hydration of cement.

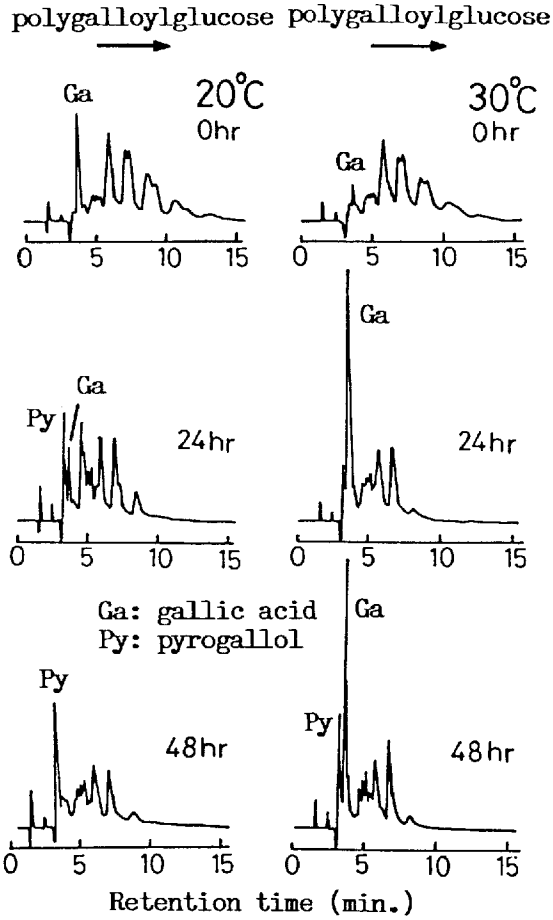

Fig.6 Hydrolysis of Ta-I in the presence of NaOH at 20°C and 30°C

3. Influence of Gl addition on the retardation effect of Ta-I on cement hydration

Here, starting time of the temperature rise is defined as the time at which the temperature starts to increase rapidly in a test of adiabatic temperature rise, and the maximum rate of temperature rise is defined as the maximum rate at which the temperature rises. Increasing the amount of Gl, while keeping the amount of Ta-I constant, increases the starting time of the temperature rise and, at the same time, greatly decreases the rate of temperature rise from 1/2 to 1/3 (Fig.7). Increasing the Ta-I quantity, on the other hand, has only a minor effect on the starting time of the cement hydration, and decreases the rate of temperature rise greatly to around 2°C/day (Fig.8 and Fig.9).[7)] An agent (TF) to control heat evolution resulting from hydration of cement has been developed in response to these results.

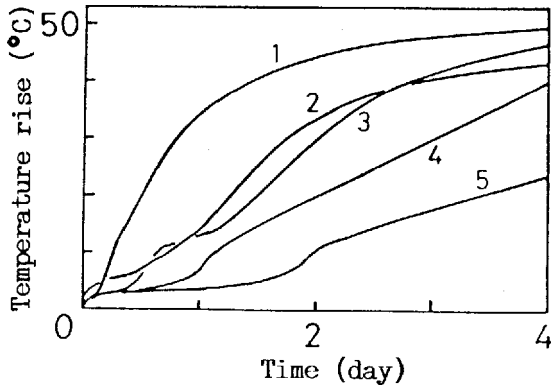

Fig.7 Influence of Gl in the presence of Ta-I (mixing temperature, 20°C)

1: LS 0.25%
2: Ta-I 0.25%+Gl 0.10%
3: Ta-I 0.25%+Gl 0.15%
4: Ta-I 0.25%+Gl 0.20%
5: Ta-I 0.25%+Gl 0.25%

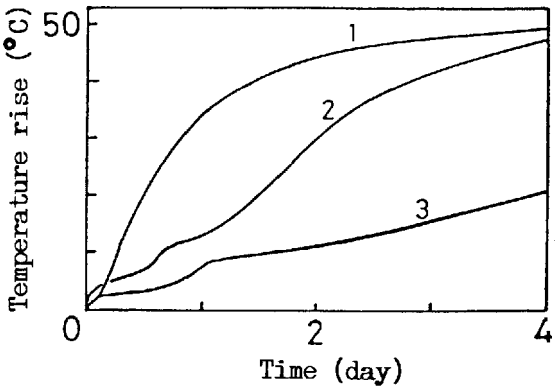

Fig.8 Influence of Ta-I dosage on temperature rise of mortar (mixing temperature, 20°C)

1: LS 0.25%
2: Ta-I 0.25%+Gl 0.15%
3: Ta-I 0.35%+Gl 0.15%

4. Differences in the rates of adiabatic temperature rise between TF and LS or Gl

Fig.10 shows the temperature increase curves at mixing temperature levels of 20 and 30°C. LS causes rapid heat evolution as the mixing temperature is increased from 20°C to 30°C. Gl shows a similar behavior in the rate of temperature rise, with the rate of the maximum temperature rise being essentially unchanged, though the

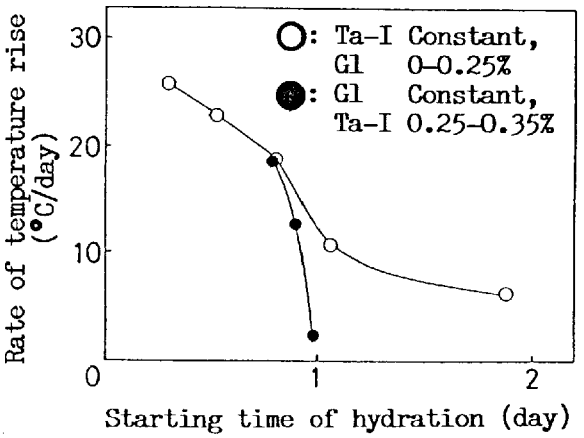

Fig.9 Relationship between the rate of temperature rise and starting time of hydration

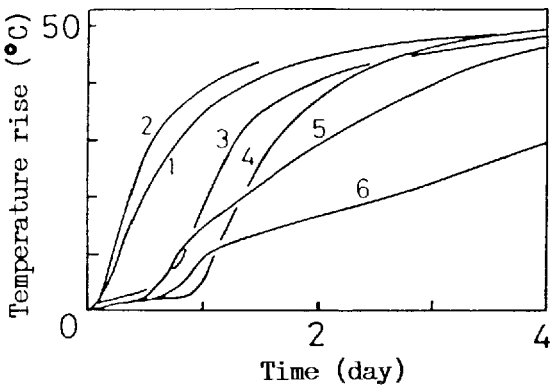

Fig.10 Influence of heat controlling agent on temperture rise of mortar (20°C, 30°C)

1: LS 0.25%, 20°C 4: Gl 0.25%, 30°C
2: LS 0.25%, 30°C 5: TF 0.40%, 20°C
3: Gl 0.25%, 20°C 6: TF 0.40%, 30°C

starting time of the temperature rise is a little retarded. By contrast, TF is capable of reducing the rate of temperature rise, and the starting time of cement hydration is slightly retarded. Of special note is the fact that the rate of maximum temperature rise is further reduced as the mixing temperature is increased from 20 to 30 °C. In other words, it has been demonstrated that the hydration of cement can be controlled by utilizing the temperature-dependence of the hydrolysis of tannic acid and the hydration-retarding nature of its hydrolysis products.

5. Cement hydrates formed during the adiabatic curing process

Paste specimens having the same cement compositions were placed in the atmosphere of the adiabatic temperature rise tests. They were withdrawn from the test system periodically to stop hydration by D-dry, and were analyzed for their DTA behavior. The results are given in Fig.11. LS was rapidly hydrated to form hydrates and, at the same time, was observed to form $Ca(OH)_2$ rapidly. Gl, though retarding hydration during the initial stage, caused rapid formation of $Ca(OH)_2$ as soon as the hydration started. TF is characterized by a hydration process that occurs gradually. TF caused a gradual formation of hydrates in parallel with a gradual increase in $Ca(OH)_2$ formation as the cement hydrated.

6. Application of the heat controlling agent in mass concrete

Next, the example of applying a TF agent for controlling the heat of hydration of cement in concrete is described.[8] A 1×1×10 m, concrete block was laid, and its temperature at the center was monitored. Each of the four sides was insulated with expanded polystyrene to a thickness of 20 cm to achieve a model of 1-m thick slab laid on an existing 1×1×10 m concrete block (Fig.12).

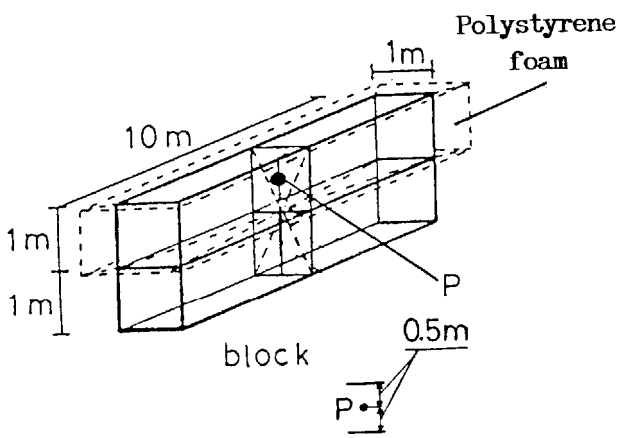

●: Temperature meas. point

Fig.12 Size of concrete block

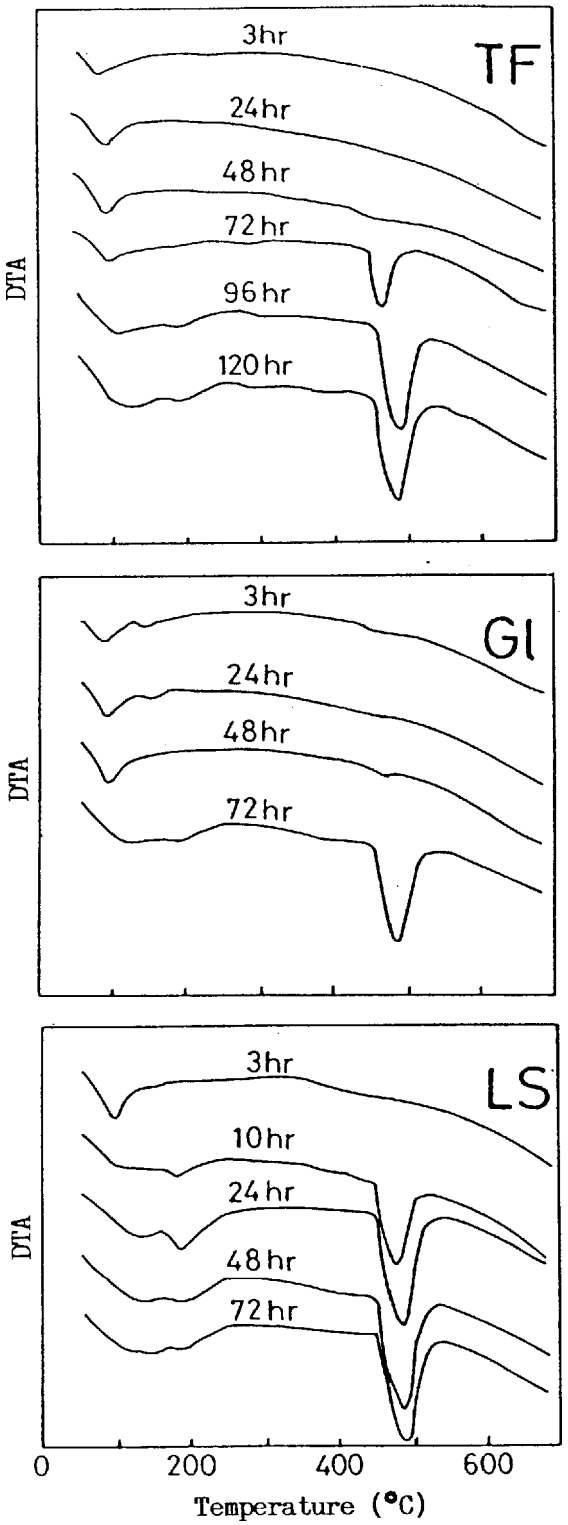

Fig.11 Results of DTA of the hardened cement paste

The temperature of the concrete slab to which an AE water reducer was added increased sharply, as shown in Fig.13, because it was laid in the hot atmosphere of summer (28.4°C, concrete temperature at placing). The temperature of the slab containing the TF, however increased only moderately. The highest temperature of the center of the concrete for this model of slab was 5°C lower, due to the release of heat from the upper and lower faces. Its core strength was higher as a result. The use of a heat controlling agent appears to reduce thermal stress of mass concrete.

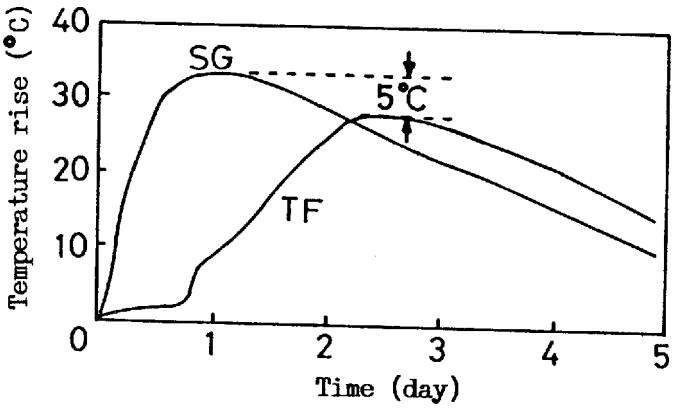

Fig.13 Temperature rise at the center of concrete block

CONCLUSIONS

(1) Tannic acid has a significant effect on the temperature-dependence of retardation. Its retardation effect is greater at higher temperatures.
(2) Tannic acid is hydrolyzed under an alkaline condition to form gallic acid and low molecular weight hydrolyzable tannic compounds. The hydrolysis is accelerated by increases in temperature.
(3) Tannic acid can control the rate of temperature rise of concrete, and can therefore control the adiabatic temperature rise of mass concrete.

REFERENCES

1. Singh,V.K., Narang,K.K. and Mandal,U.K.: "Effects of Tannic Acid on Cement",Indian Ceram., 1979, 12(11), 289-294.

2. Roux,D.G., Ferreira,D. and Botha,J.: "Structural Considerations in Predicting the Utilization of Tannin", J.Agric.Food Chem., 1980, 28, 216-222.

3. Nishizawa,M. and Yamazaki,T.: "Tannins and Related Compounds Part 9", J.Chem.Soc. PERKIN TRANS, 1983, 1, 961-965.

4. Inokawa,H., Inada,K. and Uchida,K.: "Influence of Organic Chemical Admixtures on Temperature Rise of Concrete", CAJ PROCEEDINGS OF CEMENT & CONCRETE, 1987, 41, 86-89.

5. Hemingway,R.W. and Hillis,W.E.: "Behavior of Ellagitannins, Gallic Acid, and Ellagic Acid Under Alkaline Conditions", Tappi, 1971, 54(6), 933-936.

6. Banfill,P.F.G. and Saunders,D.C.: "The Relationship between the Sorption of Organic Compounds on Cement and the Retardation of Hydration", Cement Concrete Res., 1986, 16(3), 399-410.

7. Inokawa,H., Inada,K. and Uchida,K.: "Influence of Heat of Hydration Reducing Agent on Concrete", CAJ PROCEEDINGS OF CEMENT & CONCRETE, 1988, 42, 156-159.

8. Inada,K., Kozakai,N., Inokawa,H. and Uchida,K.: "Effect of Heat Controlling Agent in Mass Concrete", CAJ PROCEEDINGS OF CEMENT & CONCRETE, 1990, 44, 198-203.

APPLICATION OF HPLC IN THE CHARACTERIZATION OF NAPHTHALENE SULPHONATE-BASED SUPERPLASTICIZERS

U Costa, M Goisis and G Guerra

Italcementi SpA, Bergamo, ITALY

SUMMARY

Eight commercial samples of sulphonated naphthalene formaldehyde condensates (SNF) have been analysed via High Performance Liquid Cromatography (HPLC) and up to 20 different molecular weight fractions have been identified. The tested SNF differed mainly in the amount of residual monomer present.

Composition of condensates with respect to the distribution of polymer fractions have been correlated with results of concrete workability and strength tests as well as with conduction calorimetric measurements of rate of cement hydration.

The various condensates tested shown differences involving both plasticizing efficiency and retarding effect on cement hydration but not as regards mechanical strengths from 24 hrs onwards.

INTRODUCTION

The use of superplasticizers in concrete technology is increasing owing to the substantial advantages they offer in terms of both concrete quality and economy of casting operations. This can largely justify the large number of papers published so far on the influence exerted by these admixture on the properties of both fresh and hardened concrete. But, relatively fewer a studies have been devoted to investigate the mechanism of action of superplasticizers and particularly of the two mostly widespread families, namely naphthalene-formaldehyde and melamine-formaldehyde sulphonated condensates. In these studies it was suggested that the plasticizing action is caused by the modification of the zeta potential as well as by the steric hindrance resulting from the adsorption of admixture molecules on the hydrated cement particles [1] [2] [3].

In more recent years, adsorption has been the object of more comprehensive investigations focussed on the influence of the molecular weights of condensates.
As regards sodium sulphonated naphthalene formaldehyde condensate (polymer), Collepardi [4] reported that only a minimum amount of sodium salt of 2-naphthalene sulphonic acid (monomer) is adsorbed on the particles, and that as a result, workability of cement is only negligibly affected. Conversely, polymer adsorption is more substantial and is shown to affect paste workability remarkably.

An increase in adsorption associated with the increasing degree of polymerization was also observed [5]. Moreover, no further significant increase in the polymer adsorption was detected beyond a certain molecular weight [6]. Gel Permeation Chromatography (GPC) was used to demonstrate that the effectiveness of sulphonated naphthalene formaldehyde condensate (SNF) depends on the content in both monomer and low molecular weight fractions [7].

Roy [8] developed a GPC method to determine the distribution of molecular weights of laboratory-synthetized SNF. Using two different types of gels, good agreement between the average molecular weights was found. Also melamine-based condensates have recently been investigated by means of Size Exclusion Chromatography (SEC) which enabled obtaining reproducible measurements of molecular weight distribution in these polymers before and after adsorption [9].

For the purpose of further contributing to the study of the mechanism of action of superplasticizers, a series of commercial SNFs was characterised by HPLC. Analyses were conducted before and after the adsorption of polymers on the cement paste. Data thus obtained were subsequently compared with the results of concrete workability and strength tests as well as with calorimetric measurements of the rate of cement hydration.

EXPERIMENTAL

Materials

Eight commercial samples of sodium sulphonated naphthalene condensate were examined. Samples were industrial products of different origin. Sample No. 1 to 5 were in the form of dry powders whereas the remaining three were aqueous solutions. Table 1 shows the chemical analysis of the samples as well as the percent contents of active matter calculated by subtracting sodium sulphate from the dry matter content.
Tests on concrete were carried out on a Ptl cement class 42.5 whose composition is given in Table 2. The river aggregate employed had a maximum particle size of 20 mm.

The composition of concrete is shown in Table 3.

TABLE 1: Chemical properties of naphthalene sulphonates (SNF)

Elementary Analysis

SAMPLE / DETERMINATION	1	2	3	4	5	6	7	8
Cl- %	0.02	<0.01	0.02	0.02	0.26	<0.01	0.20	1.13
NO3- %	<0.01	<0.01	tr.	tr.	<0.01	<0.01	<0.01	tr.
SO4-- %	10.05	1.10	6.75	1.15	5.00	0.54	1.15	0.73
K %	0.03	0.01	0.09	0.03	0.03	0.02	0.04	0.03
Na %	11.52	8.65	10.70	9.22	10.90	3.64	3.84	4.11
Ca %	0.15	1.19	0.04	0.04	0.04	0.64	<0.01	0.03

Composition

SAMPLE / DETERMINATION	1	2	3	4	5	6	7	8
Dry matter %	100	100	100	100	100	40.26	39.35	40.93
Sodium sulf.%	14.86	1.63	9.98	1.70	7.39	0.80	1.70	1.08
SNF* %	85.14	98.37	90.02	98.30	92.61	39.46	37.65	39.85

* Calculated by subtracting sodium sulphate from dry matter content

After dissolution in approximately 1/3 of mixing water, the SNF was added to the cement and aggregate which had previously been mixed together with the remaining 2/3 of water. Admixture dosages reported are in any case expressed as dry active matter % by weight of cement.

Investigation Techniques

High Performance Liquid Chromatography - HPLC analysis was carried out using ion-pair chromatography as suggested by T.G. Miller [10]. The apparatus and testing conditions adopted are summarised in Table 4.

TABLE 2: Composition of cement

L.O.I. %	4.59
SiO2	21.33
Al2O3	4.28
Fe2O3	1.69
CaO	60.86
MgO	3.31
SO3	2.54
Na2O	0.14
K2O	0.77
SrO	0.15
Mn2O3	0.11
P2O5	0.07
TiO2	0.23
Specific gravity, g/cm3	3.12
Specific surface, cm²/g	3800
Compr.Strength on ISO mortar, N/mm²	
at 2 days	21
at 7 days	36
at 28 days	53

TABLE 3: Composition of concrete

Water	kg/m3	: 175
Cement	kg/m3	: 350
Aggregate	kg/m3	: 1.880
Admixture*	kg/m3	: 1.225

* expressed as active matter

Adsorption Measurements - Adsorption of the different admixtures on cement was determined by measuring their concentration in the starting solution as well as in the solution filtered from the paste after 5-min hydration. The amount of active matter added was 1% by weight of cement. After agitation for 3 minutes, the mix was allowed to rest for 2 minutes. The contact solution was subsequently filtered on a 0.7 µm glass fiber filter. UV spectrophotometric measurements were conducted at a wavelength

of 293±1 nm.

TABLE 4: Instrumentation and operating conditions in HPLC

HPLC SYSTEM	Perkin Elmer Analyst System equipped with - LC 260 4-solvent pump, LC 235 diode-array detector, ISS 200 autosampler
COLUMN	Perkin Elmer Pecosphere C18, 3.3 cm and 0.46 cm I.D.
SOLVENTS	A) 0.01 M of tetrabutylammonium hydroxide (TBAH) and 1% (v/v) of glacial acetic acid in ultrapure deionized water B) 0.01 M of TBAH and 1% (v/v) of glacial acetic acid in acetonitrile
SOLVENT PROGRAMME	Gradient from 40% of B to 100% of B in 10 min; 100% of B for 2 min; gradient from 100% of B to 40% of B in 5 min; 40% of B for 5 min. Flow rate: 1ml/min
INJECTION VOLUME	15 µl of aqueous solution. Starting 2% solutions (2 g of SNF in 100 mL of H2O) and relevant contact solutions were diluted 20 times for injection purposes
UV DETECTION	wavelength = 280 nm ; bandwidth = 15 nm

Complementary Tests - Composition and adsorption data of admixtures were correlated to conduction calorimetry measurements in order to assess the influence of the various products on the initial hydration rate of cement. For this purpose, conduction calorimeters of the types described in [11] were utilised. The plasticizing effect was evaluated on concrete mixes by flow measurements [12]. Workability was determined soon after mixing and also after 30 and 60 minutes in order to assess its decrease with time.
Furthemore, mechanical strengths on 10-cm side concrete cubes were tested at 1, 2, 7 and 28 days.

RESULTS

Adsorption

Figure 1 shows the amounts of polymer adsorbed and expressed as % by weight of cement. It can be observed that adsorption was similar for all the various naphthalene sulphonates. Percentages of adsorption were found to range between 0.33 and 0.35% by weight of cement.

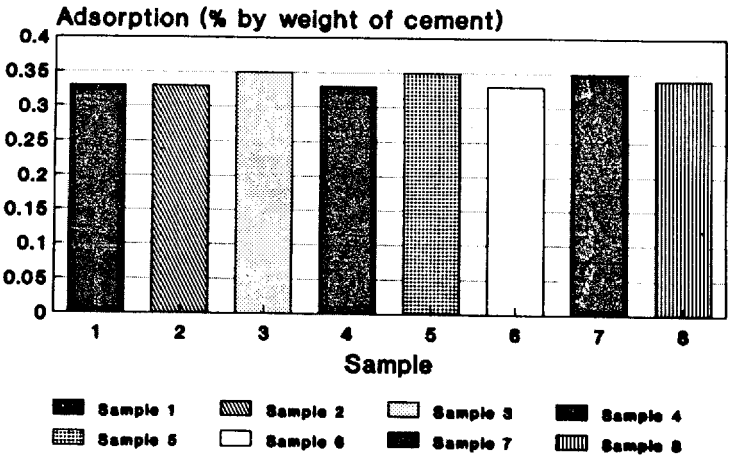

FIG. 1: % adsorption of SNF on cement after 5 minutes'hydration. Dosage: 1% by weight of cement

Liquid Chromatography

Chromatograms from the various samples were found to be qualitatively similar to those given in Figure 2.

Chromatograms are characterized by 20 peaks with retention times ranging between 1.2 and 8 minutes as well as by a wide, unresolved band extending between 8 and 11 minutes. An outstanding chromatogram is that of sample No 7 in which an intensification of the peaks regarding fraction with retention times ranging between 7 and 8 minutes is observed (Figure 3).
The occurrence of two small elution bands at a retention time shorter than one minute was ascribed to the presence of some impurities.

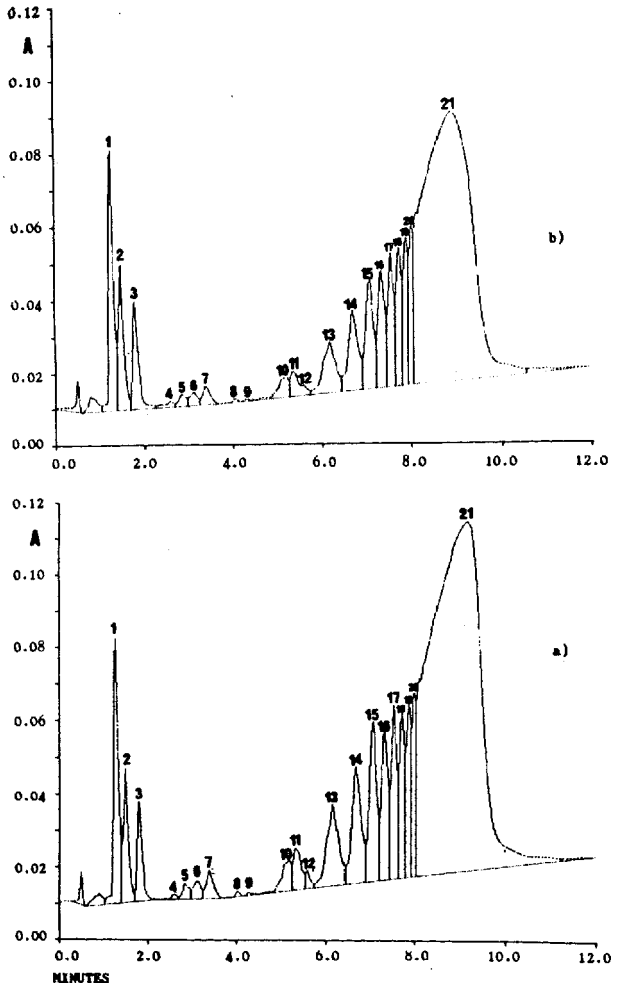

FIG. 2: HPLC chromatograms of SNF No 1
a) before adsorption b) after adsorption

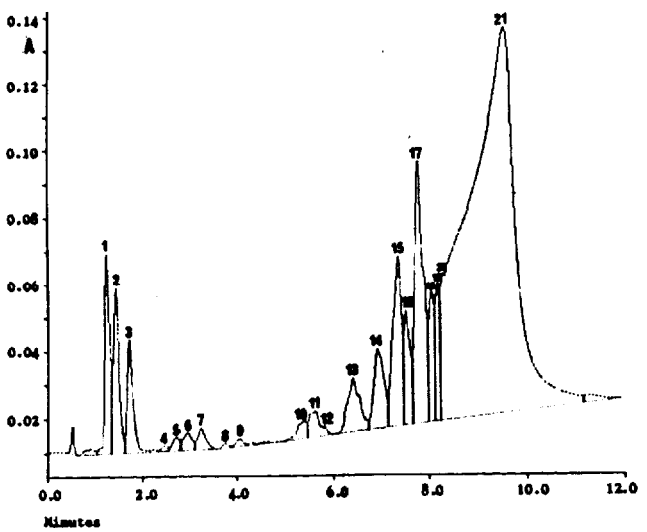

FIG. 3: Chromatogram of sample No 7

The first peak at 1.2 minutes has a retention time which coincides with that of the monomer. All subsequent peaks were in turn attributed to the occurrence of condensate fractions with increasing molecular weights. Using the UV diode-array detector, the UV spectrum of each eluted fraction was determined. Figure 4 exemplifies a typical UV spectrum relevant to fractions No 1, 13 and 21 of sample No 1. As can be noted, the monomer has its maximum absorbance (A) at 270-275 nm whereas subsequent oligomers are located at increasing wavelengths which reach as far as 295 nm in fraction 21. Hence, the areas subtended to the various peaks in the chromatogram strongly depend on the wavelength selected for the UV detector and not only on the concentration of the specific fractions.

It was possible to obtain a quantitative determination of the monomer concentrations in the products investigated from the relevant reference standard (Eastman, 2-naphthalenesulphonic acid sodium salt). The data reported in Table 5 show a very low absorption. The difference between each peak area in the chromatograms of the SNFs solutions after and before adsorption was referred to the peak area of the samples before absorption. It was thus possible to get a relative evaluation of the extent of adsorption on cement for the various eluted fractions.

Figure 5 shows the % area variations for each of the peaks. It can be observed that the first two oligomers are not adsorbed at all. The maximum adsorption occurs in those fractions which correspond to the intermediate peaks (No. 4-12). The % variation of total areas subtended to all peaks gives values ranging between 21% and 27%.

These values referred to the weight of cement become 0.21 and 0.27% respectively and therefore are lower if compared with those obtained from UV adsorption measurements i.e. 0.33%-0.35%.

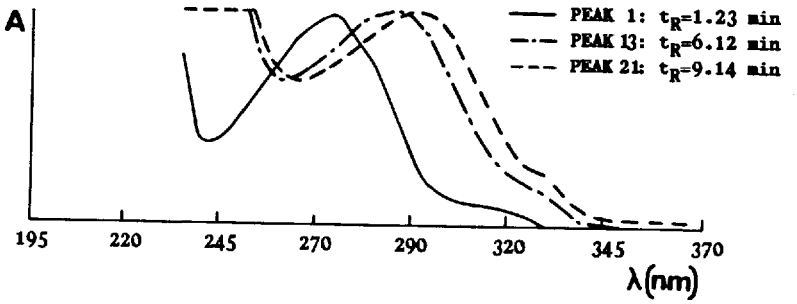

FIG. 4: UV spectrum of fractions 1, 13 and 21 of sample No 1

Rate of hydration

The heat evolution curves of cement pastes having a w/c ratio of 0.40 and with added with 0.5% and 1% of superplasticizer were recorded up to 72 hours of hydration. Curves are noticed have the same common profile as well as two peaks, one situated at about 1 minute of hydration and the second between 9 and 16 hrs. The first peak, attributed mainly to the rapid hydration of alumina phases, is little influenced by admixtures. The second one associated with the hydration of alite shows differences in both position and intensity according to the type and dosage of admixture employed. A synthesis of the effect exerted by the different SNFs on the intensity and position of the second peak can be observed in Figure 6. Here the points relevant to pastes to which different admixtures were added are located on the left-hand side and are shifted downward with respect to the points representing plain pastes. This fact denotes an overall retarding effect exerted by SNFs on alite hydration. The extent of such an effect is minimum for sample No 1 and maximum for sample No 8 whereas it is shown to increase with increasing admixture dosages.

TABLE 5: Monomer content in different SNFs

SAMPLE	BEFORE ADSORPTION (wt. %)*	AFTER ADSORPTION (wt. %)
1	4.90	4.70
2	5.02	4.74
3	5.65	5.22
4	3.37	3.08
5	2.55	2.35
6	4.16	3.84
7	3.78	3.37
8	3.06	2.86

* referred to the active matter

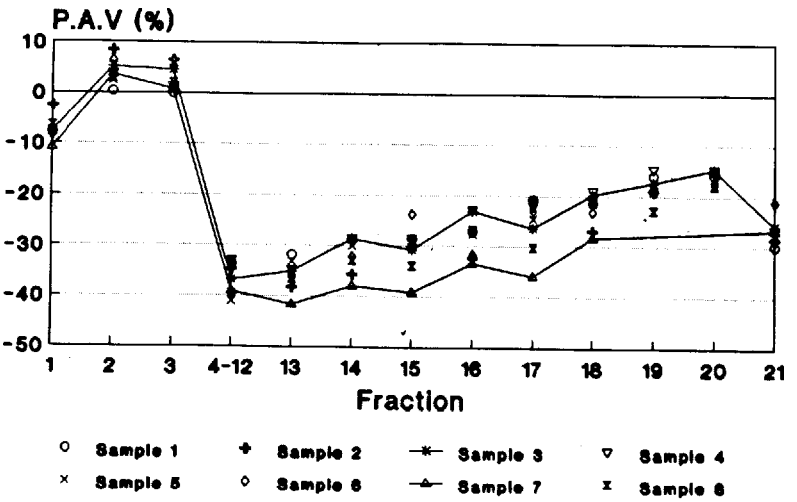

FIG. 5: Peak area variation in %(P.A.V.) of condensate fractions

Concrete Properties

Workability values obtained from concretes to which 0.35% of SNF was added, are summarised in Figure 7. The plasticizing effect exerted by most part of the products

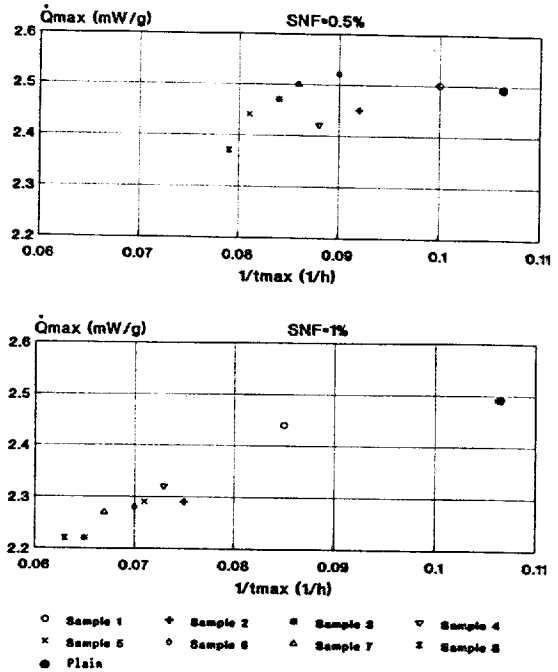

FIG. 6: Maximum heat evolved ($\dot{Q}$.max) corresponding to the 2nd peak of the conduction calorimetry curve as a function of the inverse peak time (1/tmax)

is very similar. Only samples No. 3, 5 and 7 give some lower results. Loss of workability with time follows almost parallel trends so that workability differences recorded soon after mixing as well as at 1 hour are roughly equivalent. Compressive strengths of the concretes are given in Figure 8. Values at 24 hrs and at longer curing ages indicate slight differences between the tested products, likely due to the variability of the determination.

CONCLUSIONS

- HPLC enabled to identify up to 20 different molecular weight fractions present in sodium sulphonated naphthalene formaldehyde condensates.

- Fractionation of the polymers was qualitatively, though not quantitatively, similar for examined SNFs which differed however in the amount of residual monomer.
- Chromatographic analysis conducted after adsorption tests on paste confirmed the occurrence of a limited adsorption of the monomer and of the first two oligomers. Adsorption attains its maximum in fractions with intermediate retention times.

- The various SNFs tested highlighted differences involving both plasticizing efficacy and retarding effect on alite hydration but not as regards mechanical strengths from an age of 24 hrs onwards.
- Modifications in the composition of polymers with respect to the distribution of oligomer fractions having retention times which ranged

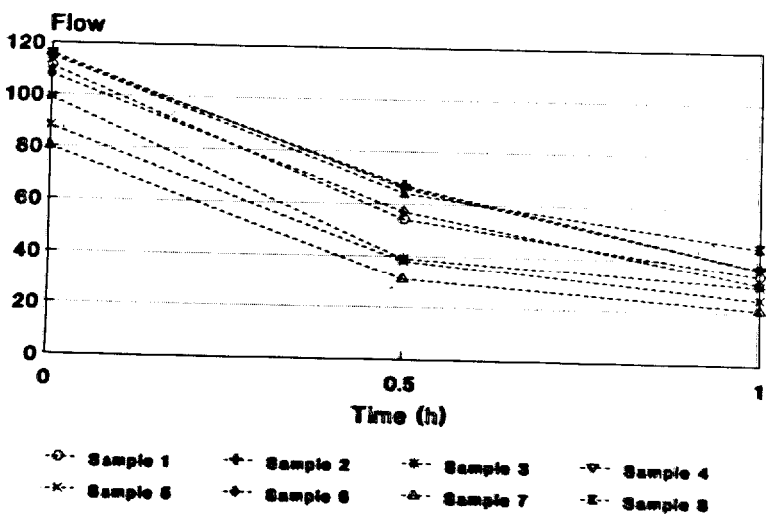

FIG. 7: Workability of concretes as a function of time. SNF dosage = 0.35 by weight pf cement

between 7 and 8 minutes appeared to exert an appreciable influence on both plasticizing and retarding effects.

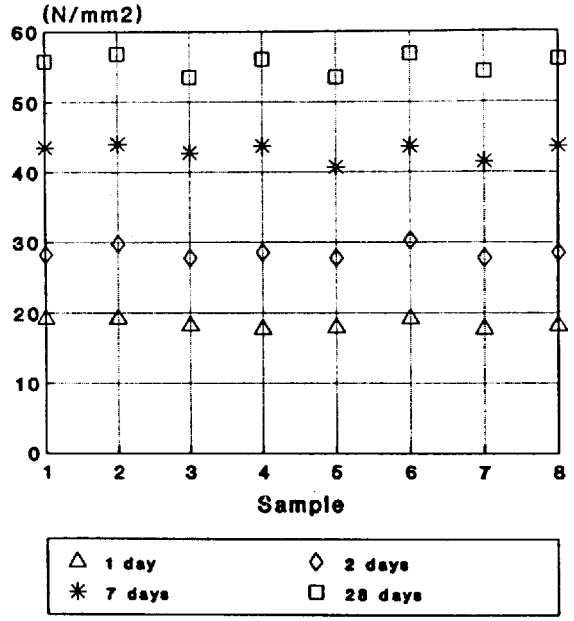

FIG. 8: Compressive strength of concretes added with 0.35% of SNF

REFERENCES

[1] F. MASSAZZA, U. COSTA, A. BARRILA', Developments in the Use of Superplasticizers, ACI SP-68, 1981, V.M. Malhotra Ed., 499-512

[2] U. COSTA, F. MASSAZZA, A. BARRILA', Il Cemento 1982, (4), 323-36

[3] P.J. ANDERSEN, D.M. ROY, J.M. GAIDIS, Cem. Concr. Res. 1987, 17 (5), 805-13

[4] M. COLLEPARDI, M. CORRADI, G. BALDINI, M. PAURI, 7th Int. Congr. on the Chemistry of Cements (Paris, 30 June-5 July 1980), VI-20-5

[5] M. COLLEPARDI, M. CORRADI, M. VALENTE, Developments in the Use of Superplasticizers, ACI SP-68, 1981, V. M. Malhotra Ed., 485-98

[6] P. BASILE, S. BIAGINI, G. FERRARI, M. COLLEPARDI, 8th Int. Congr. on the Chemistry of Cement (Rio de Janeiro, September 22-27, 1986), vol. VI, 264-8

[7] F. BASILE, S. BIAGINI, G. FERRARI, M. COLLEPARDI, 8th Int. Congr. on the Chemistry of Cement (Rio de Janeiro, September 22-27, 1986), vol. VI, 260-3

[8] D.M. ROY, G. VARADI, F.D. TAMSS, G. PALYI, B. BARTHA, Cem. Concr. Res. 1984, 14 (3), 439-42

[9] J.C. CUNNINGHAM, B.L. DURY, T. GREGORY, Cem. Concr. Res. 1989, 19 (6), 919-28

[10] T.G. MILLER, J. of Chromatography 1985, 347 (2), 249-56

[11] F.MASSAZZA, M.T. FRANCARDI, U. COSTA, Cembureau - Manifestations Thermiques de l'Hydratation au Cours de la Prise du Ciment (Paris, april 1969), 1-154

[12] UNI 8020/Nov. 1979, "Determination of consistency of freshly mixed concrete using a flowtable"

CONDUCTOMETRIC TEST FOR CEMENT-ADMIXTURE SYSTEMS

C Vernet and G Noworyta

Technodes SA
Centre de Recherche Industrielle et Technique du Groupe Ciments Francais
FRANCE

ABSTRACT :

Monitoring the electrical conductivity during cement hydration allows an accurate measurement of the dormant period duration of C_3S with standardised experimental conditions: the conductivity maximum is always well defined. The time of gypsum depletion can also be measured using this method, as C_3A contains a sufficient amount of alkalis: a second maximum or a slope inflexion can be observed. This technique thus allows to detect and quantify the chemical secondary effects of admixtures. More than 1000 tests were made on cement–admixture systems, varying the nature of cements, and the nature and the amount of the admixtures. Our results have yielded general rules on the secondary retarding effects:
– Different kinds of cement or different cements of the same class show distinct behaviours when used with the same admixture, depending on the proportions and reactivity of their components.
– For a given cement, different admixtures show secondary effects of variable intensity.
– For each system, there is a critical amount of admixture above which an exponential variation of the retarding effect is observed.
As a consequence, each system requires the assessment of the secondary effect variations with respect to the concentration of admixture, in order to obtain its "characteristic curve".

RESUME :

La mesure en continu de la conductivité électrique durant l'hydratation des ciments permet de déterminer avec précision la durée de la période dormante de C_3S, dans des conditions expérimentales standardisées: le maximum de conductivité correspondant est toujours bien défini. Le temps d'épuisement du gypse peut aussi être mesuré par cette méthode, lorsque le C_3A contient une teneur suffisante en alcalins: un second maximum ou un changement de pente peut alors être observé. Nous avons développé un appareillage spécifique et testé un grand nombre de couples ciment–adjuvant, en faisant varier la nature du ciment, la nature et la proportion d'adjuvant. Les résultats de plus de 1000 tests permettent de tirer des règles générales concernant les effets secondaires retardateurs des adjuvants:
– Différentes sortes de ciments ou différents ciments de la même classe montrent des comportements différents quand en présence d'un même adjuvant, selon la réactivité et les proportions de leurs constituants.
– Pour un ciment donné, différents adjuvants montrent des effets secondaires d'intensité variable.
– Pour chaque couple, il existe une teneur critique en adjuvant, au delà de laquelle l'effet retardateur prend une allure exponentielle.
Pour caractériser les interactions ciment–adjuvant, il faut donc dans chaque cas tracer la courbe caractéristique donnant les variations des effets secondaires en fonction de la teneur en adjuvant.

1 - INTRODUCTION.

The "cement-admixture system" concept has a field recording origin, particular combinations of cements and admixtures having shown unexpected behaviours in concrete. Research on the working mechanisms of admixtures have shown chemical interactions with certain C_3A-rich cements. The control of C_3A by sulphates is affected by lignosulfonates- or polynaphtalenesulfonates-based admixtures (1) (2).
The retarding effect of superplasticizers and water-reducers also varies with the type of cement, but the phenomena are not yet completely understood. Field-recording shows that these variations cannnot be simply counterbalanced by the use of accelerators.
Because of the complexity of the interactions involved, it is not yet possible to predict all the secondary effects of admixtures. With the increasing complexity of the formulations used to day, rapid optimisation tests are required in two complementary domains:
- Rheological tests, pertinent with respect to the concrete behaviour.
- Chemical tests, allowing to evaluate the specific effects of an admixture on the cements components.
We intend here to describe a test of the second type. It is based on the conductometric monitoring, during 24 to 72 hours, of cement pastes, mortars, or stirred suspensions with water to solid ratio (W/S) of 4. We have studied the effects produced on portlandite nucleation and gypsum depletion, at different temperatures, and with various amounts of admixtures.

2 - EXPERIMENTAL.

2.1. Apparatus.

An original measuring device, that we have called "Conductometric multiplexer", allows the simultaneous monitoring of 10 suspensions or pastes, and the input of values into a computer.
For suspensions measurements, we have developed closed cells, stirred at the same speed by the same magnetic stirrer. Attention was paid to solid-liquid diffusion problems, in order to ensure the best repeatability. In order to prevent the abrasion of reacting grains by the magnetic stirring, the bar was suspended to an axis held by the cover. The electrodes are square section rings made of 316L stainless steel, machined to follow the internal surface of the cells. For routine measurements, the cells are kept into a temperature regulated box, adjustable between 10 and 50°C. Outside this range, special cells with a double wall were developed.

2.2. Optimisation of experimental procedure.

The first type of admixtures acts by mean of their concentration, namely the accelerators like calcium chloride, nitrate, or formate. In this case the amount of admixture is calculated on the solution base, and not on the cement base. A second type acts by adsorption on solids or reaction with surfaces. The amounts are then calculated on the cement base, that is the classical method.
Rigorously, we have to apply these principles to the electrolytes present in the cement itself, such as alkali sulphates. This is possible when the clinker analysis is available: then we can use a solution containing 80% of the potential content of the clinker, taking into account the reaction yields generally obtained. Another method always applicable but time consuming, is to filter a cement paste with the adequate W/S, and use the filtrate in place of the mixing water.

3 - SCIENTIFICAL BASE OF THE TEST.

3.1. Variations of the electrical conductivity during cement hydration.

The monitoring of the electrical conductivity, and of the thermal flux, combined with the analysis of solution and solids during the hydration, have given detailed information about the sequence and mechanisms of reaction (3) (4) (5). Thanks to this research, it is now possible to interpret the conductometric curves easily.

Fig.1 shows the chemical evolution diagram of a concentrated suspension of cement (W/S = 4), and the corresponding variations of conductivity. The measurements have been conducted on the same sample, with a multi-sensors apparatus (6). This diagram is in good agreement with date from the literature.

-<u>During the mixing period (I),</u>
- As shown by the initial thermal peak, the dissolution rate of clinker components and gypsum is high. The ions passing into solution increase instantaneously the conductivity.
- After a few minutes, depending on the W/S, the solution becomes supersaturated with respect to ettringite and CSH. Precipitation of CSH begins. This slows down hydration, by covering particles with hydrates. So the thermal flux dQ/dt rapidly decreases.

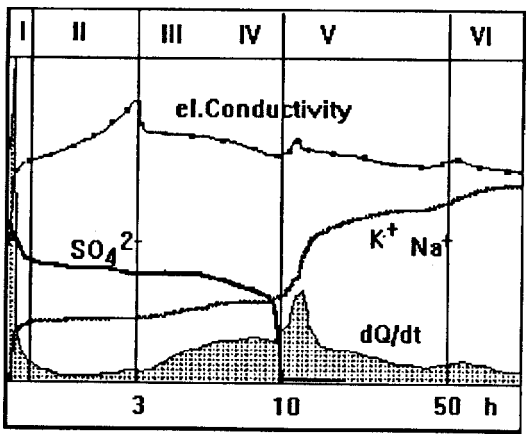

<u>FIG.1</u> Hydration kinetics of a Portland cement.

-<u>During the dormant period (II)</u>
The reactions continue slowly, forming ettringite and CSH. The solution becomes richer in calcium, because only half of the calcium of C_3S is used to make CSH. The other part goes into the solution (in Ca^{2+} and OH^- ions form). Because of the slow nucleation mechanism of portlandite, the solution becomes supersaturated with respect to this hydrate, what causes the increase in conductivity.
-In the presence of hemi-hydrate $CaSO_4,1/2H_2O$, the solution can become supersaturated with respect to gypsum, the precipitation of which can lead to a little decrease, or a plateau of conductivity (false setting can then occur).
- From a critical level of supersaturation, the portlandite begins its precipitation, that give a sudden decrease of conductivity, after reaching a maximum. <u>We shall define this moment as the end of the dormant period,</u> the duration of which characterises the ability of C_3S to bring the solution at its maximum supersaturation level. The higher is the initial water content, the higher is the time required to reach this maximum. The dormant period is thus longer for suspensions than for mortars (**fig.2**).

- <u>During the acceleration, or setting period (III)</u>
Reactions are accelerated due to portlandite precipitation, the total dissolved ions being now consumed by precipitation. This period begins with an increase of the thermal flux, and.a slow decrease of the conductivity. This decrease is larger for pastes than for suspensions, given the increase of the water uptake (**fig.2**).

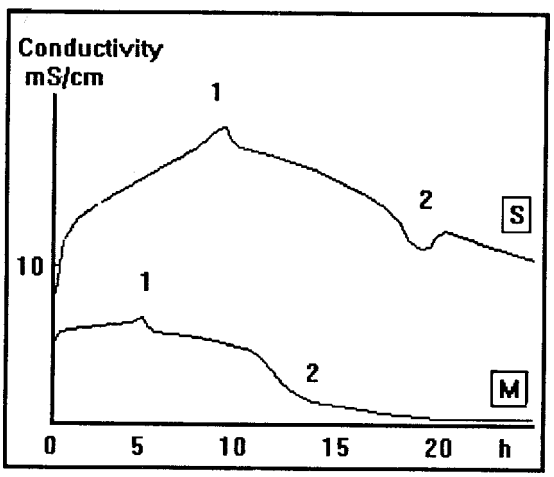

<u>Fig.2</u> Comparison between the conductometric curves of a suspension (W/S=4) and a mortar of the same cement (W/S=0.5).
S=suspension. M=mortar.
Mark 1: end of the dormant period.
Mark 2: gypsum depletion.

- <u>During the hardening period (IV),</u>
- The depletion of gypsum generally occurs. Hydration is disturbed by this sudden event. In the absence of sulfate ions, ettringite begins to dissolve to give new hydrates (monosulfoaluminate), by reaction with the excess C_3A.The rapid uptake of C_3A gives a thermal peak and speeds up the reactions of C_3S (**8**). When the C_3A network contains alkalis, these are released into the solution, and a conductivity peak or a slope variation is observed. <u>We thus have a simple way to detect and measure the time of sulfate depletion.</u> This occurs generally earlier in pastes than in suspensions (**fig.2**), but the time evolved between the end of the dormant period and the sulfate depletion remains in the same order of magnitude.

We can see here an effect of the interaction mechanism between C_3S and C_3A reactions, more efficient in pastes because of the closeness of the grains (8). The increase of strength is maximum during this period.

– During the slowing down period (V)

The increase of the hydrates layer thickness prevents water from reaching the interface, and the reactions are slowed down. The thermal flux decreases. The conductivity of suspensions increases slowly in the case of alkali-rich cements, and decreases slowly in the other cases. The conductivity of mortars and pastes decreases rapidly and reaches a low level, because of water uptake and because of the filling of capillary pores. (fig.2) At longer times, when ettringite is depleted, monosulfoaluminate then reacts with the C_3A in excess, to give hydrated calcium aluminate and parent solid solutions. (IV)

3.2. Interpretation of the conductometric Signal.

The electrical conductivity is the resultant of four main terms:

– the first one is relative to the solution concentrations, which vary with the difference of the dissolution and precipitation ionic fluxes.

– The second term is related to the mobility of the ions and to the dielectric constant of the solution. The latter can be considered as a constant in diluted solutions, but not into the capillary pores of cement, where water molecules interact with the surfaces. This effect can be neglected if we measure the conductance at a low frequency (typically 1 to 10 kHz).

– The third term is related to the variations of the W/S ratio during hydration. Neglecting the microstructural effects, the conductivity of a paste is proportional to the volume fraction of liquid.

– The fourth term is related to the geometric pathway of the electric current which may vary in a material where the pores are in course of filling.

Despite the presence of these different causes of variation, the practical aspects of conductivity measurements, their sensitivity and accuracy, have accounted for our choice. Given the different working possibilities (7), we have to choose the most pertinent experimental conditions with respect to the aims of the test, namely the evaluation of the chemical secondary effects of admixtures. Thus we are lead to work on suspensions, for which the other causes of variations of conductivity can be neglected. Given the W/S ratio, we can standardize the experimental conditions, and have a rigorous comparison of the cement–admixture systems.

4 – APPLICATIONS. SECONDARY EFFECTS OF SUPERPLASTICIZERS AND WATER-REDUCERS.

4.1. Control of C_3A reactions by sulphates, in presence of admixtures.

Examples of results obtained on C_3A blended with portlandite and calcium sulphates are given below.

– Series of blends with the same C_3A content and 3 fractions of the same gypsum, sieved to obtain different sizes (fig.3).

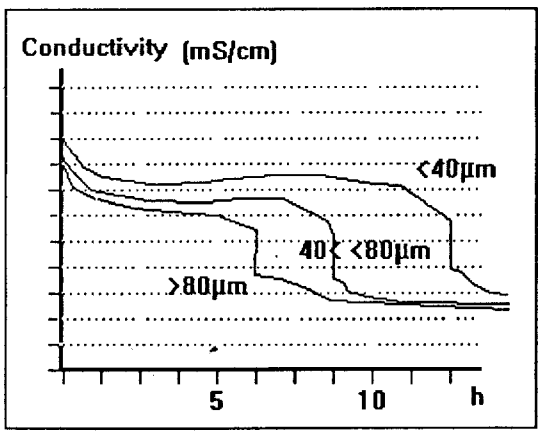

Fig.3 C_3A + gypsum with different fineness.

The gypsum depletion time is easily evidenced by the conductivity drop due to the decrease of the calcium sulfate concentration. The results seem to be opposite to the common sense: the finest gypsum is the last to be depleted. The interpretation of this behaviour requires to consider the concentration gradients around the C_3A grains during mixing: The finer is the gypsum, the more rapid is its initial dissolution, and the larger is the sulfate flux towards the C_3A interface. Thus the ettringite is more rapidly formed, and the C_3A dissolution is slowed down immediatly.

Table 1. **Depletion times of calcium sulphates for the same C_3A (hours).**

	Anhydrite	gypsum	hemi-hydrate
Without admixture	**2h**	**4h**	**6.5h**
With admixture (PNS)	**2h**	**6h**	**15.0h**

The more powerful is the initial "braking action", the longer the depletion of sulfates lasts.

- Series with the same C_3A and different kinds of calcium sulfate.

The last explanation is confirmed by this series of tests. A more reactive sulfate like hemi-hydrate is consumed later than gypsum. A less reactive one, like anhydrite, is depleted earlier, because it is a less powerful "brake" for C_3A than gypsum. This effect is enhanced in presence of polynaphtalenesulfonates **(table 1)**.

From this table, we can infer a modification of the "braking power" of sulphates, probably by a competitive adsorption of sulphates and sulfonates on the active dissolution sites of C_3A. A poor control of the C_3A reactions can lead to rheological secondary effects: we observe then a stiffening of concrete, which is a kind of attenuated flash set. So in C_3A-rich or reactive cements, hemihydrate can be a better controlling agent than gypsum, in presence of plasticizers. It can also be more beneficial to add a part of the admixture after mixing, to give the sulphates enough time to control the C_3A reactions.

4.2. Retarding effects of water-reducers.

Gluconate-based water-reducers slow down the C_3S reactions during the dormant period, and delay the gypsum depletion. Fig.4 shows the relative dormant period durations (namely the ratios to dormant period of the cements without admixture) and relative depletion times of about 20 cement-admixture couples, of various natures and compositions.

The dormant period duration increases rapidly when the amount of admixture increases. As sugars, gluconate probably poisons the hydrates nucleation. An excess of admixture can then lead to a loss of initial strength, and problems during the removal of the formworks. The retarding effect varies with the type and fineness of cement: preliminary tests can help avoiding these incidents.

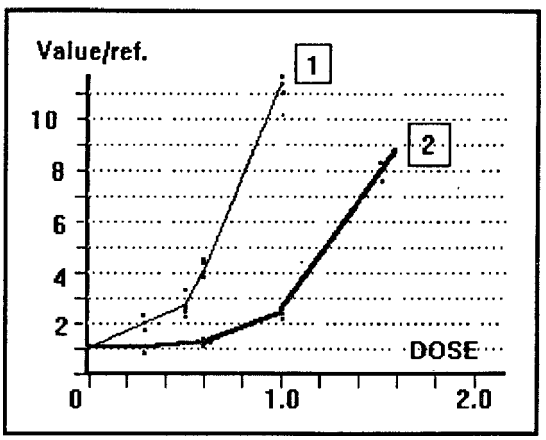

Fig.4 Gluconate based water-reducers.
1 Dormant period duration/REF
2 Gypsum depletion time/REF

4.3. Secondary effects of superplasticizers.

- 4.3.1. Dormant period.

Polynaphtalene-sulfonate (PNS) based plasticizers show a less retarding effect on C_3S than gluconates. Their behaviour yet varies widely, depending on the cement used. The dormant period is generally linearily related to the admixture amount, when it is below about 1%. Over this value, the variation becomes exponential (fig.5), particularly with low C_3A or low surface cements, which are easier to plasticize.

We conclude that in C_3A-rich or in finely ground cements, a large part of the admixture is consumed by the initial reactions, thus the remaining admixture is no longer sufficient to poison the portlandite nucleation. For the same reasons, this kind of cements is difficult to maintain in a fluid state during a long time, in the absence of a retarder.

- 4.3.2. Gypsum depletion.

As seen in 4.1., the affinity of PNS for aluminates leads to disturb the initial control of C_3A by sulphates. The duration of sulphates depletion tends to increase in the case of weak control, and to decrease in the case of strong control. Nevertheless we have to take into account the C_3A-C_3S interaction in pastes and mortars. The largest part of sulphates is consumed during the setting period, after the dormant period. This is well confirmed by conductometric measurements, performed on a great number of samples.

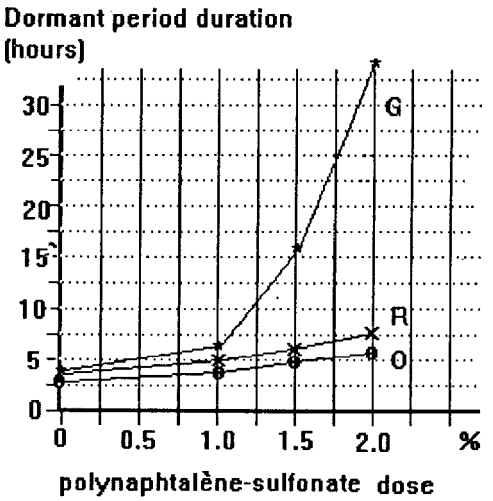

Fig.5 Secondary effects of PNS-based superplasticizers on portlandite nucleation.
G : low C_3A cement.
R, O, high C_3A cements.

The general trend is the conservation of the time evolved between the end of the dormant period and the depletion of suphfates, independently of the dormant period duration. In many cases also, the remaining admixture content is probably too low to affect the reactions rates during this period.

4.4. Effects of retarders with temperature.

Conductometric measurements can be useful to evaluate the retarders. Non-linear effects are also observed in this case (fig.6).
The variation of the dormant period duration versus the amount of retarder, (here a phosphate-based one), is shown at 3 temperatures.

The curves are similar below 1%, with an increase of the slope over 0.5% Over 1%, the curves at 20 and 30°C become different, with a linear increase at 20°C, and a decrease at 30°C.

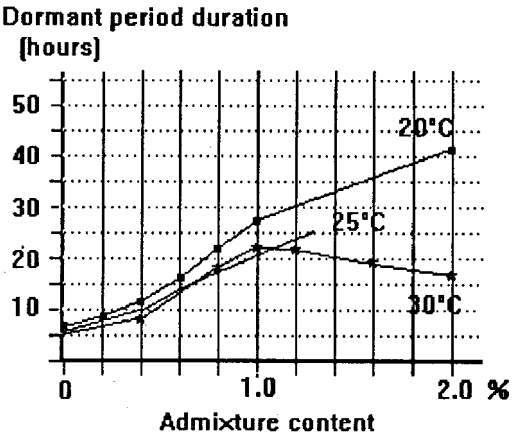

Fig.6 Effect of a retarder on the dormant period duration, at 3 temperatures.

The interpretation of this behaviour can be related to the nucleation kinetics of portlandite: a temperature increase favours nucleation, because the portlandite solubility decreases with temperature. At 30°C, at the 1% dose, the thermal activation begins to compensate the inhibition of the nucleation by the retarder, and the trend is reversed.

5 - CONCLUSIONS.

Here we only have discussed some applications of the conductometric measurements, which can be used for many other studies. In the cement-admixtures optimisation domain, the conductometric mutiplexer technique allows to monitor a large number of systems, and to build progressively a data base.
The general idea derived from this study is the the cement-admixture "coupling" concept. Already used in mechanics and electronics, this expression have been applied to chemical reactions in the field of irreversible thermodynamics. This notion, intuitively understood by field operators, finds a theoretical and experimental base in the mechanisms of interaction between molecules and hydrates.

It appears particularly that:
- with a given cement, different molecules behave in different ways, leading to secondary effects of different intensities.
- with a given admixture, different cements behave in different ways, according to their fineness, content and reactivity of components.
- in many cases, there is a critical level of admixture dose, over which the secondary effects vary in a non-linear trend.

The "cement-admixture coupling" has thus evident and practical consequences. Each system requires to be tested and optimised in the lab. In this respect, the conductometric multiplexer can be a useful tool, particularly to optimise formulations using a mix of different admixtures, because the effects are not additive. The interactions between admixtures and cements can be characterized by the curves of variation of dormant period and gypsum depletion durations, as a function of the admixture content. These curves enable a rigorous comparison of the chemical behaviour of each system. After determining the composition domain meeting the requirements, a limited number of verifications of the rheological behaviour on convenience concretes then becomes sufficient, resulting in a large economy of means.

REFERENCES.

(1) AITCIN P.C.; BAALBAKI M. "La compatibilité ciment portland-adjuvant, une histoire qui se répète" In "Les superplastifiants". Recueil des conférences présentées à l'Université de Sherbrooke.1990 pp 41-48.

(2) MANABE T.; KAWADA N. "Abnormal setting of cement paste owing to calcium lignosulfonates." Semento Konkurito, N°162, pp 24-27.

(3) BARRET P. "Les mécanismes d'hydratation et de durcissement des ciments."
Conférence prononcée à l'Hotel de la Société d'encouragement pour l'Industrie Nationale. 30 Nov. 1978.

(4) MENETRIER D. Thèse de doctorat, Université de Dijon, Juin 1977.

(5) VERNET C.; DEMOULIAN E.; GOURDIN P.;HAWTHORN F. "Cinétique de l'hydratation des ciments portland."
7ème Congrès International de la Chimie du Ciment, Paris, 1980.
Vol.II, pp II-267 à II-272. (SEPTIMA Ed. Paris).

(6) VERNET C. "Etude de la cinétique des réactions d'hydratation des ciments industriels. Méthodologie et applications."
Thèse CNAM, 28 Oct.1982, PARIS.

(7) VERNET C. "Kinetics of mortars hydration and mechanical evolution during the first days. Study of the hardening mechanism."
9th International Congress on the Chemistry of Cement. New Dehli, 1992, Sub-theme III-C "Structural models for hydrated cement paste."

(8) VERNET C. "Conduction calorimetry and hydration kinetics - A thermodynamical and analytical approach of the interactive behaviour of cements."
8th International Congress on the Chemistry of Cement. Rio De Janeiro, 1986, theme 2, Vol.3, pp 64-69.

DESORPTION ISOTHERMS OF SILICA FUME MORTAR

Elisabeth Atlassi

Division of Building Materials
Chalmers University of Technology
Gothenburg, SWEDEN

SUMMARY

It has been shown previously that condensed silica fume (CSF) changes the form of the water vapour isotherm of the first desorption of mortar. The pore structure or at least the pore openings become more refined. The purpose of the present study is to find out if these alterations are sensitive to drying. Preliminary results concerning the second desorption isotherms of mortar with a CSF-to-cement ratio varying between 0 and 25% and a water to cement ratio varying from 0.3 to 0.6 are presented and compared to the first desorption isotherm.

The results show that the pore structure refinement obtained with CSF is preserved after drying to about 40% relative humidity but the prominent 'shoulder' in the capillary region of the first desorption isotherm vanishes or diminishes. The irreversible structural changes in the capillary region are in the same order of magnitude in a mortar with 10% CSF as in one without.

RESUMEE

Il a eté montré auparavant que l'utilisation de la fumée de silice condensée change la forme de l'isotherme de la vapeur de l'eau de la première désorption. Les pores ou au moins les ouvertures des pores deviennent plus étroites. L'objet de cet étude est de déterminer si ces altérations sont sensibles à la dessiccation. Ici sont presentés des résultats préliminaires de la deuxième désorption de mortier où 0 à 25% de silice a eté ajouté. Le rapport eau-ciment varie entre 0.30 et 0.60. Les isothermes de la deuxième désorption sont comparée à celles de la première.

Les résultats indiquent que l'affinement de la structure poreuse est conservée aprés une dessiccation jusqu'à environ 40% de humiditée relative, Mais "l'épaule" dans la région capillaire de l'isotherme de la première désorption diminue ou disparait. Les changements structurelles irréversibles dans les capillaires sont à peu près les mêmes dans le mortier avec 10% de fumée de silice que dans celui sans silice.

INTRODUCTION

The position of the water vapour isotherm from the first desiccation of concrete is shifted when condensed silica fume (CSF) is incorporated in the mix [1-4]. This indicates that the pore structure or at least the size of the continuous pores becomes more refined, which has also been proved by other methods, such as mercury intrusion tests [5]. The CSF-mortar contains more evaporable water per weight of cement than a CSF-free one above 11 % ambient relative humidity. In a mix with w/c=0.50 and with up to 15 % CSF added, the total pore volume is somewhat higher. There is also a 'shoulder' on the isotherm of CSF-mortar between about 75 and 95 % relative humidity which becomes more prominent the more CSF that is incorporated in the mix [4].

However during desiccation the concrete or mortar is subjected to strong stresses from the surface tension of the water meniscuses which cause structural changes in the paste phase. Thus the desorption isotherm from a second desiccation will not look like the one from the first, especially in a mix with a lot of larger capillary pores [6].

How then does a CSF-concrete react to desiccation? Is it more stable or more sensitive to drying than ordinary Portland cement concrete?

In order to answer these questions, second desorption isotherms were included in an extensive investigation of the water vapour isotherms and the pore structure of silica fume mortar being carried out at present at Chalmers University. It also includes isotherms from the first desorption, absorption and scanning experiments. Preliminary results from the first desorption have recently been published [4]. The compositional parameters in the study are the original water to cement ratio (0.30 to 0.60) and the amount of silica fume added (0 to 25% calculated on cement weight). Since silica fume is always used together with a superplasticizer, the type of superplasticizer also varied. Two different cements were used.

Since the method requires long measuring periods [4,7] the investigation was carried out on well-cured specimens in order to eliminate the influence of additional hydration as much as possible during the test. On the basis of pore structure development data [5] a minimum period of 90 days water curing was chosen.

In this paper some preliminary results from the second desorption will be presented and compared with the first desorption isotherms.

EXPERIMENTAL DETAILS

Materials

The experimental details, such as raw materials, mix compositions, specimen preparation and method have previously been described in detail [4]. Thus only the essentials will be given here together with some supplementary information.

Two types of cements were used; a Swedish standard Portland cement (OPC) with a specific surface area (Blaine) of about 380 m^2/kg and a low heat, sulphate resistant (LHSR) cement with a specific surface area around 330 m^2/kg from Sweden. The condensed silica fume of Norwegian origin contained 86-89% SiO_2. It had a specific surface area of 15 000 - 20 000 m^2/kg (Blaine). The aggregate was quartz sand 0.25 - 2 mm. Two kinds of superplasticizers were also used; a naphthalene based powder from Japan, called Mighty 100, and a melamine based 33% solution. The mix water added was always corrected for the water content of the solution.

The mix proportions of the 8 mixes used for the analysis in this study are given in Table 1.

Table 1: Composition of Mortar Mixes.

Mix	w/c by weight	CSF/C by weight	Aggr./C by weight	Cement type	Superplast. SP/C=0.4%
N510	0.50	0.10	2.88	OPC	Napht.
N500	0.50	0	3.00	OPC	Napht.
N310	0.30	0.10	1.35	OPC	Napht.
N610	0.60	0.10	3.65	OPC	Napht.
N525	0.50	0.25	2.70	OPC	Napht.
L510	0.50	0.10	2.88	LHSR	Napht.
M510	0.50	0.10	2.88	OPC	Mel.
I510	0.50	0.10	2.88	OPC	None

Method

The isotherms were determined by the desiccator method. Each point on the isotherm was obtained independently by allowing separate saturated specimens to dry in selected relative humidities (RH:s) until they reached equilibrium weight. The humidity inside the desiccators was controlled by saturated salt solutions, giving 11.3%, 42.3%, 75.5% and 94.6% RH. Sodium lime pellets were used to avoid carbonation of the specimens.

The specimens, 2 to 4 mm thick discs, were wet sawed from 40*40 mm water cured prisms. The first and second isotherm were not obtained on the same specimens. The specimens used to obtain the first desorption isotherm had been water stored for a minimum of 90 days. The four RH:s were started on different occasions from the age of 90 days upto 180 days.

The specimens used to obtain the second desorption isotherm were all water stored for 90 days and then in 42.3 % ambient RH for 290 days. After that they were remoistened in three stages; first to 86% RH, then 96.5% RH, and finally the specimens were resaturated by capillary suction. The desiccation in the four RH:s were also in this case started at different times.

RESULTS AND DISCUSSION

Estimation of Evaporable Water

Bringing such thin specimens to weight equilibrium takes a long time, especially with the denser mixes, and in this case it has not been possible to terminate the experiments yet. Therefore the amount of evaporable water in the specimens still undergoing dessication can only be estimated. Since the traditional relationships between degree of hydration, amount of nonevaporable and total pore volume are not valid in CSF-pastes [4], a procedure which renders knowledge of the degree of hydration unnecessary has been applied (described in [4]). It is based on the following suppositions:

* The amount of nonevaporable water and the pore volume remain constant throughout the drying experiment.
* The material proportions of the specimens are the same as in the original mixes.

* The mean value of the loss on ignition of two samples from each mix could be used as ignited specimen weight.
* No carbonation takes place.

(In future all specimens will be analysed by thermogravimetry and the uncertainties of this estimation will be eliminated.)

The We/C used for the desorption isotherms is based on the minimum weight recorded during approximately 300 days of drying. For some of the most dense mixes the absolute minimum value has not yet been reached in some relative humidities.

Each point is based on the results from at least two specimens, which to some extent eliminates the non-systematic error due to inhomogeneities in the specimen. The standard deviation is 0.43 %-units which leads to the fact that more than 95% of the values of the individual specimens are within ± 0.8%-units from the presented mean values. There may however be a systematic error caused by continuing water uptake in the air pores, which varies with the duration of storage in water.

First and Second Desorption Isotherms

Figure 1 shows that the first isotherm is displaced upwards to the left and there is a prominent shoulder between 75 and 90 % RH when CSF is used. The larger the addition of CSF the greater the displacement upwards and the smaller the pore sizes that are affected. This indicates that the pore structure seems to become more refined. At RH above 40%, where meniscuses are formed, it may however be caused by a narrowing of the pore openings without a change in the actual pore sizes.

When the mortars desiccate a second time the shape of the isotherms changes. The general refinement of the pore structure, i.e. the displacement of the isotherm upwards remains but the shoulder more or less vanishes from the isotherms of CSF-mortars. This indicates that some of the hydration products are relocated to new sites when they are subjected to the strong surface tensions that occur during drying and eventually a more even pore size distribution is obtained. The irreversible structural changes in the capillary region are in the same order of magnitude in a mortar with 10% CSF added as in one without. Thus the changes must take place in the hydration products of the cement and not in the products from the pozzolanic reaction. If the CSF-addition is as high as 25% there is still a 'shoulder' left after the second desiccation. Then the cement will not release enough calcium hydroxide (even if it is fully hydrated) to ensure the pozzolanic reaction with the CSF. The remaining shoulder could be due to the fact that unreacted very small CSF grains are left and act as a filler in the capillary cavities and obstruct the redistribution of the hydration products. The CSF grains may also react to other components of the cement, such as the alkalies, and form another type of hygroscopic gel.

As expected We/C is lower at RH:s between 30% and 85%. However the values at 11% and 94% are higher for the second desiccation than the first. It is possible that hydration and/or carbonation during the experiment gives an apparently higher value for the second desiccation. In that case the whole second isotherm should be displaced slightly downwards. But it may also indicate that the structural changes during the first drying include formation of new chemical bonds. The thermogravimetrical analysis will give a clearer picture of the underlying reasons.

In Figure 2 the desorption isotherms for CSF-mortars with two different w/c ratios but the same CSF/C ratio are shown. Besides the same observations as above it is evident that the irreversible structural changes become greater with a higher w/c ratio, in the same manner as in ordinary Portland cement mortar [6].

Using different types of superplasticizers (SP) or none at all had almost no effect on the first desorption isotherms [4] nor has it on the second desorption isotherms (Figure 3). The small variations recorded are within the measuring error.

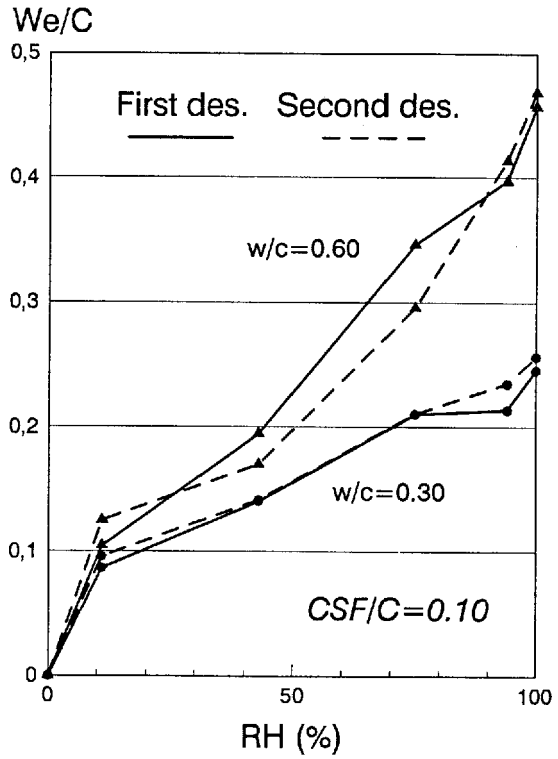

Figure 1: Desorption isotherms for mortar with different amounts of silica fume.

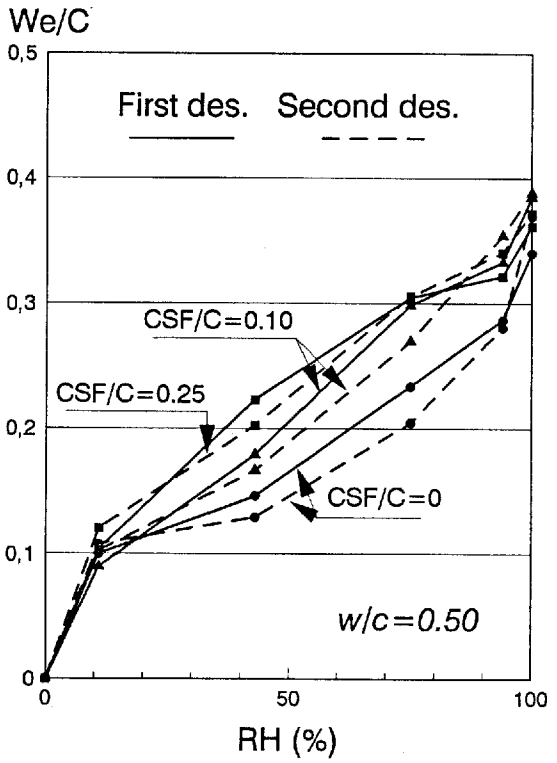

Figure 2: Desorption isotherms for silica fume mortar with different w/c-ratios.

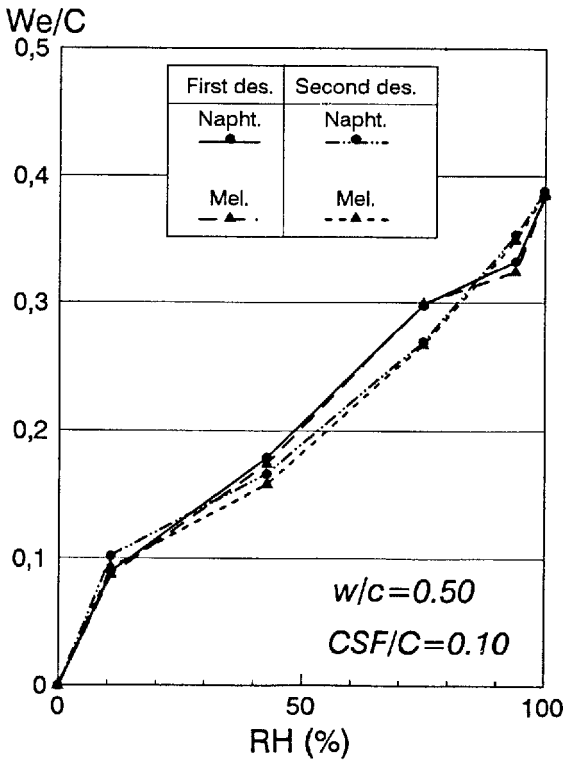

Figure 3: Desorption isotherms for silica fume mortar with different superplasticizers.

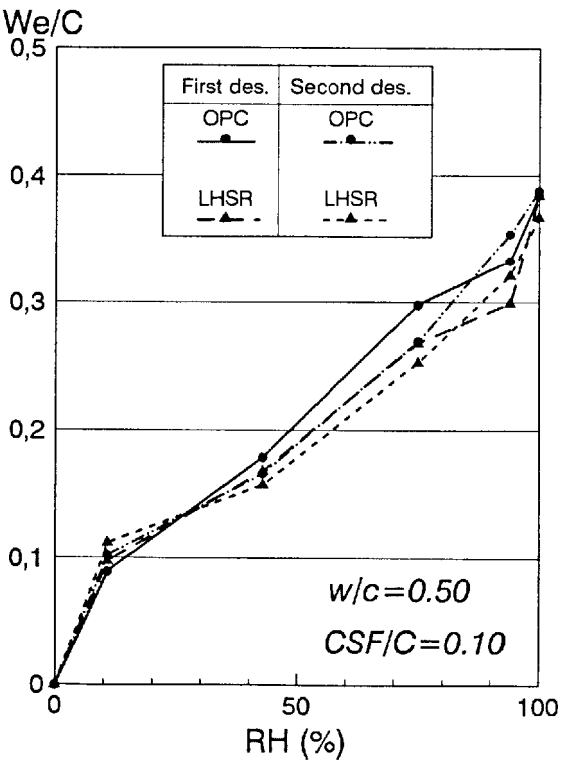

Figure 4: Desorption isotherms for silica fume mortar with different cements.

The low heat sulphate resistent cement (LHSR) mortar which without CSF has a coarser pore structure and a more even sloping first desorption isotherm than the OPC mortar [8]. When 10% silica is added the pore structure of the LHSR-mortar seems to be slightly less sensitive to drying than the finer one obtained with the other cement as can be seen in Figure 4.

CONCLUSIONS

Based on the preliminary results from water stored mortar specimens the following conclusions may be drawn:

* The general refinement of the pore structure that is obtained when silica fume is used is preserved after drying to 42.3% RH but the prominent 'shoulder' of the first desorption isotherm disappears or diminishes.

* Since the structural changes are of the same magnitude with and without silica fume they must take place in the hydration products of the cement and not in the products from the pozzolanic reaction.

* As in plain OPC concrete the structural changes become greater the higher the w/c ratio.

* The type of superplasticizer did not affect the changes between the first and the second desorption to any degree that was detectable in this preliminary analysis.

REFERENCES

1) Sellevold E.J., Bager D.H., Klitgard Jensen E. and Knudsen T., **Silica fume - cement pastes: Hydration and pore structure**, Condensed Silica Fume in Concrete, The Norwegian Institute of Technology, Trondheim, Report BML 82:610, 1987, p. 20-47.

2) Nilsson L.-O., "Desorption isotherms for silica-fume/cement mortars", report IF-8431, Elkem A/S, Kristiansand Norway, 1984.

3) Atlassi E., Nilsson L.-O. and Xu A., "Moisture sorption properties of concrete with admixtures and industrial by-products - implications for durability", **2:nd International Seminar on Durability of Concrete**, Gothenburg 1989, Publ. D9:1989, pp. 9-17, Swedish Council for Building Reasearch, ed.: Berntsson, Chandra and Nilsson.

4) Atlassi E, "Some moisture sorption properties of silica fume mortar", **4:th International symposium on Fly Ash, Slag, silica Fume and Natural Pozzolans in Concrete**, Istanbul, Turkey , 1992.

5) Feldman R.F. and Huang Cheng-yi, "Properties of portland cement-silica fume pastes: I. Porosity and surface properties", Cement and Concrete Research, Vol. 15, 1985, p. 764-774.

6) Helmuth R A and Turk D H, "The reversible and irreversible drying shrinkage of hardened portland cement paste", Journal of The PCA Research and Development Laboratories, May 1967.

7) Atlassi E., "High strength concrete - The influence of mix proportions on some mechanical and physical properties", **Concrete for the Nineties**, Leura, Australia, 1990.

8) Atlassi E., "Influence of cement type on the desorption isotherms of mortar", Nordic Concrete Research 10, 1991, p. 25-36.

STUDY ON "FARMING SILICA FUME" USE IN POZZOLANIC CEMENTS

J R Baragaño and V M Villar

CIDE/ASLAND, SA, Villaluenga de la Sagra Toledo
SPAIN

ABSTRACT

Since industrial silica fume is not readily available in Spain, the possibilities have been studied of using calcinated rice husk ash as an alternative.

The possibilities of calcination, related problems, the characteristics of the ash obtained and the cement properties thereof were studied at a cement plant in Spain, in order to ascertain the industrial benefit of the ash.

A comparison was made with bibliography on Asiatic ashes, Norwegian industrial silica fume and the product obtained at an optimum burning temperature.

By adding 25% of "farming silica fume", a 10% gain is obtained on the 28 day compressive strength compared with the same cement without addition, but the rheological properties are not very accurate.

Other vitrous components, such as fly ash, copper slag or even chemical water-reducing agents must be added to the developed product in order to improve its workability.

The use of 5% "farming silica fume" and 20% copper slag yields cements with very good, improved pozzolanic properties, adequate rheology and mechanical strength.

The latter blended cement has a better performance than those containing 25% of either copper slag or silica fume.

RESUMEN

En España no existe humo de sílice, de ahí que para su uso se utilice el procedente de los paises nórdicos, el cual se suministra en sacos o big-bag, a precios elevados.

Por este motivo se ha estudiado la posibilidad de encontrar una alternativa a través de la calcinación de cáscaras de arroz.

En una fábrica de cemento del Sur de España se ha estudiado la problemática de su calcinación, las características de las cenizas obtenidas y su comportamiento en cementos con el fin de lograr un doble valor a las mismas, es decir, aprovechar su potencia calorífica en un secadero y utilizar las cenizas como un producto de elevada reactividad puzolánica.

La adición de un 25% de este "humo de sílice agrícola" da lugar a un aumento de resistencias, a 28 días del 10%, cuando se ensaya en mortero normalizado, pero sus propiedades reológicas no son apropiadas.

Para mejorar dicho comportamiento reológico es necesario mezclarlo con otros componentes vítreos como cenizas volantes, escoria de cobre e, incluso, con aditivos químicos reductores de agua.

La mezcla de 5% de este "humo de sílice agrícola", con 20% de escoria de cobre, produce cementos con alto valor puzolánico que tienen una adecuada reología, con mejores resistencias mecánicas que las conseguidas con 25% de escoria de cobre o 25% de humo de sílice.

1. INTRODUCTION

Since silica fume is not produced in large quantities in Spain, it is imported from northern Europe. Its marketing, normally containing additions of super-plasticisers, doubles the already high cost of the product. For this reason, the use of "farming silica fume", rice husk ash (RHA), has been studied as a feasible alternative for obtaining good-quality pozzolanic cements. The subject is more widely-known in several Asian countries and there are many publications available on the matter. (1-9).

The problems involved in the use of RHA include, among others, the low apparent density of the rice husk and the ash obtained from burning it, as well as the difficulty of achieving the most suitable quality for the proposed aim. The principal advantage lies in its ability to react with the lime and its high pozzolanity, yielding products with high chemical and mechanical strengths.

Taking advantage of the fact that a cement plant in the south of Spain uses rice husk as a dryer fuel, the different possibilities of burning it, its properties, the characteristics of the ash produced and the cements obtained with such ash have been studied.

The practical aim of this study is to combine the benefit of the calories generated in rice husk combustion with the use of the ash produced for manufacturing pozzolanic cements.

2. RICE HUSK, PROPERTIES AND CALCINATION

A sample of the rice husk used in the afore-mentioned cement plant in an average month has been studied, determining its characteristics in an air-dried sample.

The results obtained are as follows:

Water content in air:	3.8%
Residual water content:	4.1%
Total water content:	7.9%
Apparent density:	96.3 g/l
Real density:	1.91 g/cm^3
Higher caloric power:	3640 cal/g
Lower caloric power:	3350 cal/g

The higher caloric power is determined according to the ASTM standard D-3286 and the lower caloric power is deduced in respect of the water content formed and collected in the combustion of the calorimetric bomb.

The thermal differential analysis (TDA), made with NETZSCH STA-429 equipment, reveals an exothermic reaction at 280ºC and two endothermic peaks at 510 and 550ºC, with stable burning at approximately 700ºC.

The industrial combustion is performed in a specially designed auxiliary furnace, at 750ºC.

The ash produced in an oxidizing atmosphere is then stored in aireated conditions.

3. RICE HUSK ASH, PREPARATION AND TESTING

3.1 RHA Preparation

In the tests carried out on a semi-industrial scale, the Portland cement and the additions were ground separately. The RHA granulometric curve according to the Coulter instrument reveals the following significant parameters:

45 micron rejects:	26.0%
3-30 micron fraction:	44.0%
Average diameter:	31.0 microns

The central part of the curve has the steepest slope; 50% of the particles are between 30 and 79 microns, with a very small quantity of fines and coarse particles.

3.2 RHA Chemical Analysis

Table 1 summarises the RHA chemical analysis compared with the oscillations taken from the bibliography on 14 samples of Asian RHA and a sample of silica fume imported in Spain.

Table 1

Chemical analysis of RHA and silica fume

%	RHA SPAIN	RHA ASIA	SILICA FUME
SiO_2	86.5	88.7 - 93.2	88.1
Al_2O_3	0.77	0.0 - 0.41	1.1
Fe_2O_3	0.59	0.20 - 0.46	2.3
SO_3	0.22	0.0 - 0.81	0.10
CaO	4.4	0.41 - 1.7	**0.51**
MgO	0.34	0.29 - 0.84	1.6
Na_2O	0.15	0.08 - 1.1	0.73
K_2O	2.7	1.8 - 6.4	1.5
P_2O_5	0.57	0.0 - 0.44	0.06
LOI	2.5	3.0	4.0

Although the calcination of Spanish RHA is more efficient than the others shown in Table 1 (minimum LOI), the SiO_2 content is lower and the CaO content is higher, which makes it potentially less pozzolanic than the Asian RHA and silica fume. However, the insoluble residue, according to UNE 80-224, is 4.9%, for which reason practically 80% of the SiO_2 is soluble and therefore reactive.

4. RICE HUSK ASH BLENDED CEMENTS

The industrial cements (see Table 2) have been measured out carefully, controlling the mixtures by means of analytical methods. Copper slag, which appears in the industrial blended cements, has been used in Spain for about 15 years (10). Admixtures were used, when necessary, in the corresponding laboratoy cement tests.

The most interesting results obtained are indicated below.

4.1 Fineness

Although with regard to industrial Portland cement, the progressive addition of RHA scarcely modifies the granulometric reject, the specific Blaine surface increases considerably. The addition of copper slag, which is difficult to grind, gives rise to the greatest reject and reduces the specific surface in the cements that contain it. The difference between the real specific weight of the pure Portland cement (3.1 g/cm^3) and RHA (1.9 g/cm^3) causes certain problems when determining the specific surface.

4.2 Setting time

The water content for normal consistency increases exponentially with the percentage of RHA up to abnormal values (41%) and decreases when copper slag is present.

The initial and final Vicat setting times increase according to the percentage of mixing water required for normal consistency and the RHA content.

Although the setting time is somewhat lengthened by adding admixtures to the cement with 25% RHA (see Table 2), it has little effect on the quantity of water required in order to achieve a correct consistency in the paste, which continues to be a handicap for the good performance of this cement.

TABLE 2

BLENDED CEMENTS WITH RHA

BLENDED CEMENT : REFERENCES	1	2	3	4	5	6	7	8
MIX PROPORTIONS:								
I-55 Industrial Cement, (%)	100	95	85	75	75	75	75	75
Rice Husk Ash, (%)		5	15	25	25	25		5
Cu Slag, (%)							25	20
Lignosulphonate, (%)					0,80			
Melment F-10, (%)						1,0		
PHYSICAL PROPERTIES:								
Fineness, > 63 µm, (%)	0,80	0,86	0,94	1,1	1,1	1,1	2,6	2,2
Blaine Surface, (m^2/kg)	486	510	585	633	633	633	473	559
Pozzolanic Index: 8 days	-	-	+	+			-	-
15 days	-	-	+	+			-	+
28 days	-	+	+	+			+	+
H_2O normal consistency (%)	30,5	32,0	36,5	41,0	36,2	37,5	23,5	26,0
Setting Time: I (min)	115	122	136	155	190	180	155	140
F (min)	140	154	179	220	245	210	190	190
Rheology: Yield Value, (dy/cm^2)	628	675	>900	>900	220	414	128	252
Viscosity, (poises)	12,9	13,6	> 25	> 25	3,1	21,4	1,6	3,2
Compressive Strength:								
1 day , (N/mm^2)	24,5	24,5	25,0	17,6	8,2	20,3	11,6	14,0
	(100)	(100)	(102)	(72)	(34)	(83)	(47)	(57)
3 days, (N/mm^2)	40,4	40,8	41,2	29,6	15,4	34,6	23,8	27,5
	(100)	(101)	(102)	(73)	(38)	(86)	(59)	(68)
7 days, (N/mm^2)	52,5	55,1	55,7	39,4	28,1	46,7	34,0	37,4
	(100)	(105)	(106)	(75)	(54)	(89)	(65)	(71)
28 days, (N/mm^2)	64,4	69,6	78,6	54,1	43,7	63,8	44,1	52,8
	(100)	(108)	(122)	(84)	(68)	(99)	(69)	(82)
90 days, (N/mm^2)	69,7	82,1	102,2	65,5	52,0	80,4	58,2	68,1
	(100)	(118)	(147)	(94)	(75)	(115)	(84)	(98)

4.3 Rheology

In order to confirm the above observations, the viscosity of the 8 cements indicated in Table 2 was tested in a coaxial-cylinder viscometer. The water/cement ratio in the pastes was 0.50. The results obtained, yield value and viscosity, provide information on the rheological nature of each cement and its predictable performance in the workability of the corresponding mortars and concretes.

Increasing RHA additions give rising values of the rheological constants, which are already high in pure Portland cement. The pastes with 15 and 20% RHA are difficult to work, hence it is impossible to use them in the manufacture of industrial cement.

Copper slag, both at 25% (see example 7 in Table 2) and at 20% plus 5% RHA (see example 8), produces very fluid and workable pastes, thereby explaining the good performance of the mortars obtained with the corresponding cements.

These results are only obtained in the cements containing 25% of RHA with the addition of lignosulphonate, since in the case of Melment F-10, the aforesaid values are still very high, especially the viscosity, thereby confirming the difficulties brought about by the high ash content.

On the other hand, copper slag, with a completely vitreous nature, not only affects the amount of water required to make the paste (23.5% compared to 30.5% in pure cement), but its plasticity is also extraordinarily good.

4.4 Pozzolanic Index

After testing the pozzolanic index according to the standard UNE 80-280 in all the cements, the good pozzolanic quality of the RHA and copper slag additions was confirmed in the cements that contain them. The Fratini Index is positive in the cements containing 15% and 25% of RHA over a period of 8 days. When the cement contains 5% of RHA (see cement no. 2, Table 2), its pozzolanic characteristics are revealed after 28 days. With 25% of copper slag (see cement no. 7), the Fratini Index is positive at 28 days, while the mixture of 5% RHA and 20% copper slag produces cements with a positive pozzolanicity reading after 15 days.

There is a mutual effect, found in tests, between RHA and copper slag, improving their common pozzolanic characteristics.

4.5 Compressive strength

The mortars were prepared according to European standards (EH-196) and tested at 1, 3, 7, 28 and 90 days. In Table 2, below the corresponding values expressed in N/mm^2, the ratio with pure Portland cement (value 100) is shown.

The compressive strength of cements with 5 and 15% RHA additions, obtained in standardised mortars, increased after the first age. At 28 days, the compressive strength had improved by 8 and 22%, respectively. At 90 days it had increased by 18 and 47% in each case. When 25% RHA was added, the mortars were very dry and the predictable strengths could not be developed due to the reduction in the workability detected as the RHA percentage was increased, as indicated above.

The use of admixtures in standardised mortars (see examples 5 and 6, Table 2) is, in the case of cement with 25% RHA added, not a real solution, since the strengths only improve with Melment F-10. Lignosulphonate, added at 0.8% in weight, produced poor results at all ages.

In other words, neither of the two water-reducing agents has a beneficial effect on the overall rheology/strengths, nor provides the necessary solution for obtaining high quality cements.

Copper slag, added at 25% (see example 7 in Table 2), compared with the same percentage of RHA (cement no. 4), provides very workable mortars with strengths that improve gradually over time, although at short ages they are somewhat low. When in the last example 5% of copper slag was replaced with RHA, increased strengths were obtained at all ages. At 90 days, it gives the same results as pure cement, with a very much improved workability.

5. CONCLUSIONS

The calcination at 750ºC of Spanish rice husk produces a residue formed mainly of highly-reactive amorphous silica, which should subsequently be ground in order to facilitate its combination with lime.

Since the lower caloric power of the rice husk is 3350 Kcak/kg, it could be interesting to use it first as a fuel and then use its ashes in the manufacturing process of cements with additions.

The pozzolanity of RHA (Fratini Index) is extremely high, since at 8 days the test is positive with 15% added to the Portland cement.

Comparing its chemical analysis with Asian RHA (taken from the bibliography) and with silica fume (imported in Spain from northern Europe), it has slightly lower values of SiO_2 and a higher content of Al_2O_3, Fe_2O_3 and CaO, with approximately 80% of SiO_2 soluble and reactive.

When manufacturing blended cements with this RHA, the water content for normal consistency increases exponentially with the percentage of RHA added. With 15% of RHA the mortars have a very poor workability, but the strength is 22% and 47% higher than pure Portland cement at 28 and 90 days, respectively.

When the RHA is increased to 25%, the rheological constants become so difficult that it is impossible to obtain a blended cement with an acceptable workability.

Although by adding water-reducing agents the workability of the mortar is improved, the strengths obtained are lower than those attained with 15% RHA.

On the contrary, cement containing 25% copper slag, which offers very good rheological characteristics, gives relatively low strengths. A partial substitution of 5% of such component with RHA improves not only the pozzolanicity, but also the strengths at all ages, achieving at 90 days the same strength as that of pure cement.

In order wods, excellent pozzolanic-type cements can be obtained with maximum values of RHA of 10% and vitreous slags up to a total of 20-25%, producing very workable mortars with high chemical and mechanical strengths.

REFERENCES

1.- Hara, N.: "Hydrothermal reactivity of rice husk ash and its use for calcium silicate products". Third Camet/ACI, SP 114-23, 499-507 (1989)

2. Hwang, C.L. and Wu, D.S.: "Properties of cement paste containing rice husk ash". Third Canmet/ACI, SP 114-35 733-762 (1989)

3.- Joseph, S. and Baweja, D.: "Preliminary investigations on a Vortex furnace and gasifier for the continous of heat and amorphous rice husk ash". NBCT Techical Record 523, Edited by David J. Cook, November 1987.

4.- Khalaf, Al and Yousig, H.A.: "Use of rice husk ash in concrete". Inst. J. Cem. Compos. Lightweight Concr, 6 (4) pp. 241-248 (1984) and Cem. Abstr. 102. 171592 (1985)

5.- Khan, M.H., Mohan, K and Taylor, H.F.W.: "Pastes of tricalcium silicate with rice husk ash". Cem. Concr. Res., 15 (1), pp. 89-92 (1985)

6.- Mehta, P.K.: "Properties of blended cements made from rice husk ash". J. Amer. Concr. Inst. 74 (9), 440-442 (1977).

7.- Patent: Britain 2, 106, 087 (1983)

8.- Patent: British UK Appli. 2,050,341 (1981)

9.- Uchikawa, Uchida, S. and Hanehara, S.: "Relationship between structure and composition of amorphous phase and hydraulic reactivities in blending components, such as slag, fly ash, rice husk ash and silica fume". Cem. Assoc. Japan 39th. Gen. Meeting, pp. 36-43 (1985)

10.- Baragaño, J.R. and Rey, P.: "The study of a non traditional pozzolan: copper slag". Proc. of 7th Int. Congr. on the Chemistry of Cement. París 1980.

HARDENING OF ORDINARY AND EXPANSIVE CEMENT WITH SILICA FUME ADMIXTURE

A I Panchenko* and L Opoczky**

*Rostov-on-Don Civil Engineering University, RISI, Rostov-on-Don, RUSSIA
**SZIKKTI, Budapest, HUNGARY

SUMMARY

Investigation results of hardening kinetics of ordinary and expansive cement with silica fume admixture are presented in this paper. Based on research results of X-ray diffraction, thermal analysis (DTA, DTG), kinetics of deformations as well as some mechanical preperties a mechanism of hardening of two types cement was studied. An efficiency of silica fume admixture to the cement, mortar and concrete is shown for the increase of srength and frost resistance, lowering of the permeability and improvement of pore structure. Some aspects of structure formation and synthesis of the strength of cement stone, mortar and concrete containing silica fume are discussed.

РЕЗЮМЕ

В статье представлены результаты исследований кинетики твердения обычного и расширяющегося цементов с добавкой микрокремнезема. Основываясь на результатах рентгено-фазового и дифференциально-термического анализов, кинетики деформаций и некоторых физико-механических свойствах, изучен механизм действия добавки микрокремнезема на твердение цементов двух указаных видов. Показана эффективность использования микрокремнезема в качестве добавки к цементному камню, раствору и бетону для повышения прочности и морозостойкости, снижения проницаемости и улучшения поровой структуры. Обсуждаются некоторые аспекты структурообразования и синтеза прочности цементного камня, раствора и бетона.

INTRODUCTION

Silica fume (SF) is a by-product of the smelting process in the production of ferrosilicon. At present the use of SF as a new high-grade pozzolanic admixture in cement and concrete is attracting increasing attention.

Precise data on the annual output of SF in the world are not available but judging by various sources of information it approaches to one million tons.

The main purpose of this investigation was to study the complex process of hydration and hardening, structure formation and properties of cement stone and concrete with silica fume addition (SFA) and the mechanism of SFA effect. Nowadays the mechanism of action of SFA in producing strength is explained, on the one hand, by CSH gel formation having C/S ratio lower than during cement hydration without SFA (1). On the other hand, SFA effect is connected to a filler effect securng more perfect structure formation of cement stone (2).

It is suggested that increase in bond strength is one of the main reasons for the substantial improvement in strength and some other properties of concrete with SFA. The expansion of cement stone as well as the physical and mechanical properties of mortars and concretes depend not only on the activity of expansive cement but on the technological factors effecting the lime concentration in the mixing water (3,4,5). Since SF has high hydraulic activity, its use is one of the effective methods for lowring lime concentration and regulation of expasion and some other properties.

EXPERIMENTAL

The following binder materials were used in the present investigation: portland cement from the Russia and Hungary, expansive cement, alumina cement, natural gypsum, silica fume from the Russia and Hungary, as well as superplastisizer "S-3". Silica fume from the Russia and Hungary were of approximately the same and quite high hydraulic activity (about 430 mg CaO/g) and grinding fineness about 20...21 m^2/g (according to BET method).

Deformation of the samples during freezing were registered by dilatometer in the ranges $+20^{o}C...-50^{o}C$ and $+20^{o}C...-150^{o}C$. The porous structure of cement stone was studied by high-pressure mercury porosimetry. To study the hydration process, X-ray diffractometry and thermal analysis (DTA, DTG) were applied.

Physico-mechenical properties of the concrete, mortar and cement stone were evaluated in accordance with Russia Standard requirements. Bond strength of cement stone with hardened concrete was defined in accodance with Hungarian EMISz 264 method.

RESULTS AND DISCUSSION

It is known that SFA inplace of cement in 1:1 ratio by mass improves the strength of hardened concrete. Provided all other compound parameters, mix workability, mixing conditions mode remain the same, it can be taken that concrete strength will depend on two factors. Firtly, increase in the strength of concrete can be due to strengthening of cement stone which means that concrete strength gain must be affected by cement paste volume concentration in concrete volume and will increase when cement paste volume concentration increases. Secondly, compressive strength of hardened concrete as a multicomponent material mostly depends upon bond forces of thecement stone with the fine and coars aggregates. In this case increase in volume concentration of cement paste above an optimal amount necessary to "glue" together inert aggregates must not lead to increase in the compressive strength of concrete.

Test results of compressive and bending strength (Table 1) show that 10% SFA improves the strength than 1.5 times. The same amount of SFA to the cement paste does not practically change its strength. As expected strength of the cement-sand mortar with 10% SFA is

also improved, thouth less than for concrete, being about 26%.

Table 1 Compressive and bending strength

	Compressive strength, MPa			Bending strength, MPa		
	Cem.stone	Mortar	Concrete	Cem.stone	Mortar	Concrete
Without SFA	64.4	37.2	41.1	16.0	9.8	8.6
10% SFA	66.0	47.1	63.0	16.3	10.9	12.0

Fig.1 illustrates that when raising cement stone volume content in concrete volume unit, SFA introduction decreases strength gain. That proves the assumption stated above that strength increase of concrete with SFA is not due to cement stone strengthening, but to improved bond forces between cement stone and aggregate.

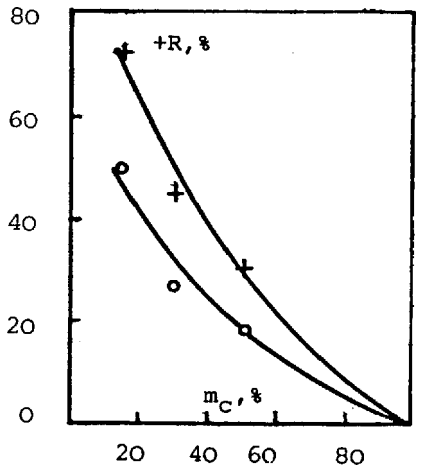

Fig.1 Increase of concrete strength with various amount of cement: o - after 28 days; + - after 28 days, drying and water saturation.

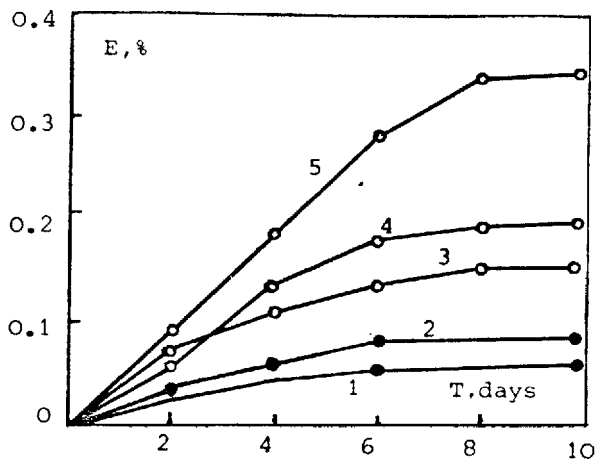

Fig.2 Kinetics of concrete deformation (hardening in water): 1 - PC100%; 2 - PC90%+SF10%; 3 - EC90%+SF10%; 4 - EC95%+SF5%; 5 - EC100%.

Test results of concrete with an expansive cement (EC) show that SFA has similar influence on the compressive strength (R_c) of concrete with portland cement (given in Table 2) However, in case of bending strength (R_f) its influence is different. A 10% SFA to normal concrete increases R_c/R_f ratio from 6.6 to 7.6 indicating a lag in the gain rate of R_f compared to R_c. In EC concrete this ratio does not practically change and the absolute value of R_f is more than 1.4 times higher than in normal concrete with 10% SFA.

Results obtained on bond strength with old concrete deserve special attention. A 10% SFA was dose to PC as well as an EC based on the PC. PC cement stone had a bond strength with old concrete equal to 4.4 MPa. After 10% SFA R_b increased up to 5.6 MPa, i.e. by 27%. SFA when effected together with expansive addition (EC+SF), increased bond strength to 8.9 MPa, a twofold increase over PC. Such size able effect may be explained, on the one hand, by the presence of SF and, on the other hand, owing to the increased amount of ettringite formation in the interfacial zone that provides its strengthening (8).

Table 2 Strength of the PC and EC concretes with SFA

Strength	Binders used				
	PC100%	PC90%+SF10%	EC100%	EC95%+SF5%	EC90%+SF10%
R_c, MPa	37.0	56.1	41.0	58.8	63.0
R_f, MPa	5.6	7.4	7.1	8.9	10.5

Use of EC together with SF allows to control the volume of concrete expansion (Fig.2) and hence influence its structure formation. As was illustrated above (5), by so decreasing the volume of expansion of EC concrete without changing the amount of formed ettringite, one can substantially raise the waterproofness and frost resistance of concrete. As seen from Fig.2, a mere 5% SFA decreases expansion of EC concrete by 1.7 times and 10% SFA does so more than twice. Simultaneosly, a refined porous structure is being formed in cement stone.

It is seen from Fig.3 that 10% sfa into PC stone does not substantially altber its overal porosity, though considerably influences the pore size distribution by decreasing the average size of the prevailing pore volume. Special attention should be drawn to the fact that in expansive cement stone with SFA micropores of 0.007...0.02 μm size predominate and micropore volume (more than 0.1 μm size) is 5 times less than in PC. Such pore size distrebution allows to suppose substantial improvement in frost resistance. This supposition is proved by low temperature dilatometric tests the data of which are presented in Fig.4.

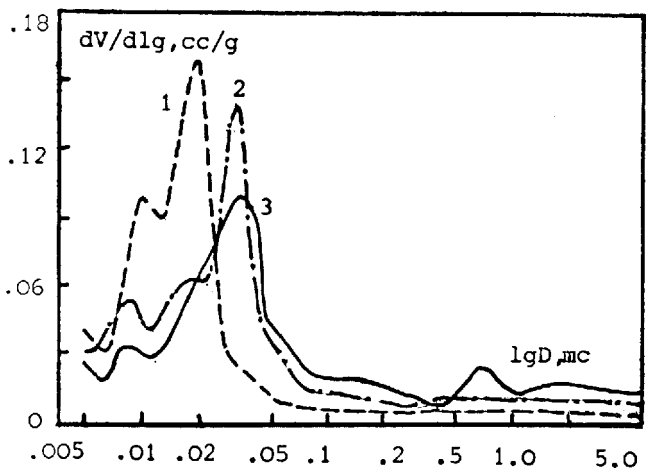

Fig.3 Pore structure of the cement stone:
1 - EC90%+SFA10%; 2 - PC90%+SFA10%; 3 - PC100%.

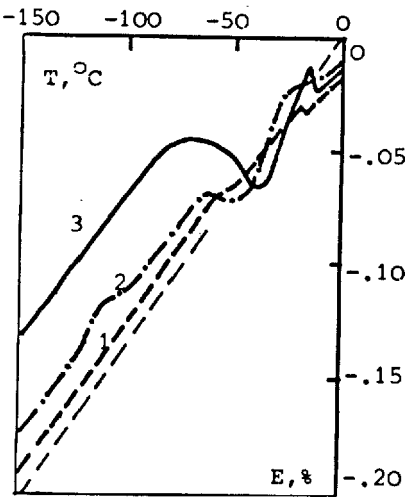

Fig.4 Dilatometric curves:
1,2,3 - look at Fig.3.

Investigation on the hydration of sulfoaluminate expansive cement with SFA is of certain interest since no data on are available in literature. Investigations have been conducted by X-ray diffraction and thermal analyses of cement stone from PC+SFA, PC+AC+G+SFA and AC+G+SFA (sulfoaluminate composition SAS)

Fig.5 illusrates that along with known phases formed as a result of portland cement hydration, the X-ray diffractograms of PC+SAS and SAS show one rather intense peak at .285 nm as well as two peaks with less intensity at .171 and .166 nm. Appearance of these peaks can be explained by the formation of a phase belonging to hydrogarnet group the formula of

which may be written down as $3CaO \cdot Al_2O_3 \cdot xSiO_2 \cdot (6-2x)H_2O$.

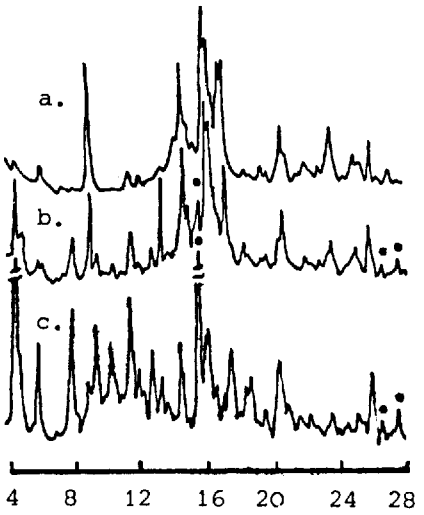

Fig.5 X-ray diffractograms of cement stone: a - PC+SFA; b - PC+EA+SF; c - EA+SF.

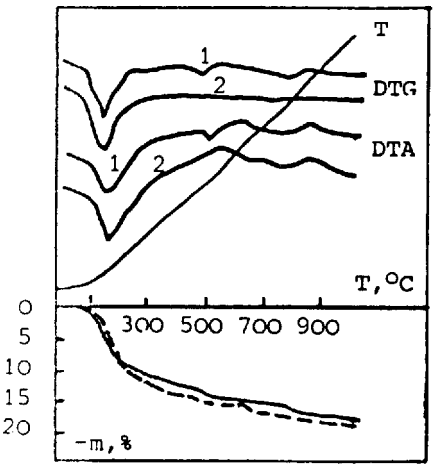

Fig.6 Thermograms of cement stone: 1 - PC+SF; 2 - EC+SF.

Formation of hydrogarnets at normal temperature is possible in this case due to the amorphous state of SF particles and their high chemical activity. The DTA curve (Fig.6) shows an endothermic peak at 783 K (510 °C) attributed to CH decomposition. However in the DTA of PC+SAS this peak completely absent. This absence of lime has been suggested to be due to its consumption in the formation of hydrogarnets.

REFERENCES

1. Sellevold E.J. and Radjy F.F. Condensed silica fume in concrete: water demand and strength development, SP-79 ACI, 1983, 677-694.

2. Condensed silica fume in cncrete. FIP State of art report. London, 1988, 37.

3. Mehta P.K. Cement and concrete research, 1973 Vol.3

4. Kuznetsova T.V. High-alumina and sulfoalumina cements. Moskow, 1986, 203.

5. Panchenko A.I. Control of expansion and structure formation of expansive cement. Cement and concrete research, 1990, 602-609, Vol.20.

6. Gjorv O.E. et al. Effect of condensed silica fume on steel-concrete bond. Trondheim, 1986, Report BML 86.201.

7. Monteiro P.J.M., Gjorv O.E., Mehta P.K. Effect of condesed silica fume on the steel-cement paste transition zone. Cement and concrete research, 1989, 114-123, Vol.19.

8. Monteiro P.J.M., Mehta P.K. The transition zone between aggregate and type K expansive cement. Cement and concrete research, 1986, 111-114, Vol.16.

9. Huang Cheng-yi and Feldman R.F. Hydration reactions in portland cement-silica fume blends. Cement and concrete research, 1985, 585-592, Vol.15.

HYDRATION AND STRENGTH OF BLENDS CAC-FUME SILICA AND STABILITY OF HYDRATES

S Marcdargent*, M Testud*, J P Bayoux* and A Mathieu**

*Lafarge Coppée Recherche, Viviers/Rhône, FRANCE
**LFI International Neuilly, Neuilly-sur-Seine, FRANCE

ABSTRACT·

Hydration products of CAC-fume silica blends in fine mortars at high Water/CAC ratio are studied under various hardening temperatures along with their stability under subsequent thermal treatment. Structural characteristics, compressive strength and bound water, as well as X-Ray mineralogical estimation of hydrates shows that the reactive Silica of the fume, in the presence of admixture Tripolyphosphate (otherwise useful for the rheology of fume blends), stabilizes hexagonal hydrate formed at 20°C against thermal conversion, and co-hydrates with CAC at 38°C into C2ASH8. The elementary chemical and mineralogical effects of fume silica upon strength has been clearly differenciated from its particle size effect upon performance by using a high W/CAC ratio, despite the fume and TPP presence, in opposition to the good practice for Calcium Aluminate Cements.

RESUME

On a étudié les produits d'hydratation des mélanges CAC-fumée de Silice en mortier, sous diverses conditions de température, et leur stabilité sous traitement thermique ultérieur. Les caractéristiques structurelles telles que l'eau liée et la résistance à la compression, ainsi que l'estimation semi-quantitative des hydrates par Diffraction X ont montré que la fumée de silice en présence de l'adjuvant Tripolyphosphate (nécessaire par ailleurs pour la rhéologie des mélanges), stabilise l'hydrate hexagonal formé à 20°C vis à vis de la conversion thermique, et entre en combinaison d'hydrate à 38°C pour former C2ASH8. L'effet élémentaire chimique et minéralogique de la fumée de silice sur la résistance mécanique a pu être clairement distinguée de son effet granulométrique sur les performances en utilisant un rapport Eau / CAC élevé, malgré la présence de fumée de silice et de Tripolyphosphate, en dérogation aux bonnes pratiques d'emploi des ciments alumineux.

1 - INTRODUCTION, OBJECTIVES

Calcium Aluminate Cements (CAC) and particularly "ciments alumineux fondus" [1] provide high early mechanical strengths when cured at low temperature. However, the so-called conversion phenomenon, which converts hexagonal hydrates (namely CAH10) into cubic hydrate (C3AH6), with a subsequent loss of compactness and of mechanical strength, makes it necessary to use a small amount of gauging water related to cement content. The good practice [2] and various publications [3] [4] point out this rule which enables CAC to fulfil the necessary requirements. Nevertheless, it is of general interest either to make easier mix-designs at low gauging water (use of fume silica), or to avoid conversion.

The hydration of CAC in the presence of fume silica has already been described [5], and such blends are well-known in Low- and Ultra-Low-Cement-Castables [6]. In the refractory field, the above mentioned drawbacks are not pertinent. In other fields, these blends have not yet been much developped.

Experimental work has shown that low water, high compacity mortars can be achieved by combining CAC with some fume silica and defloculating agent such as Sodium Tripolyphosphate (TPP). The high compacity and mechanical strength provided at low temperature remain unaltered after a severe heat treatment at 50°C or 70°C, and a large proportion of unconverted hexagonal hydrates subsists.

The objective of this study is to observe and quantify the chemical effect of active Silica, provided by fume silica (independently of its water-reduction effect which increases performance) upon the hydration, conversion and mechanical strength of CAC mortars.

2 - EXPERIMENTAL CONDITIONS

It was decided to study fine mortars, (not pure pastes) in order to have several free parameters and to test materials reflecting better the real ones. The mix design, involving siliceous sand up to 0.2 mm, is based on the following principles

1/ Fume silica : (f)/CAC ratio varies from 0 to 30/70

2/ Water/Cement ratio : W / CAC is constant = 0.6. This ratio is, on purpose, very high and is aimed at making complete hydration into hexagonal hydrates possible. Of course, it is out of the proper range according to good practice and standards, and one must not be surprised of the poor performances obtained, particularly after heat treatment. On the other hand, the chemical effects of silica fume upon conversion are better shown this way.

3/ Gauging water is used at a constant proportion of dry mortar : 20%. Except for the second-order effect of fume silica and sand specific volume difference, this constant ratio ensures a similar solid volume fraction for fresh mortars, hence a similar initial compactness for comparing mechanical strengths.

4/ From the above two conditions it appears that the ratio CAC / Mortar is constant = 1/3. So, the mortar equalling the total of CAC + Sand + fume silica, the total Sand + fume is constant for a given amount of CAC. The various amounts of fume are brought in addition to CAC and in substitution to sand.

5/ The large range of fume silica, together with the constant water amount, would result in a large range of consistency incompatible with a good placing of mortar. The problem has been solved by using two different fine sands, the finest requiring more water to be gauged. So, increasing fume silica (which decreases mortar water demand) has been accompanied by increasing the proportion of the finest sand (which increases mortar water demand).

6/ The theoritical 0.6 W/CAC ratio experiments have been complemented by some experiments at W/CAC ratio = 0.3, which are consistent with the good practice for CAC.

The CAC used is Ciment Fondu Lafarge™, chemical composition Al2O3:39.3%, CaO:37.4%, SiO2: 4.0%, Fe2O3: 13.9%, FeO : 2.9% for the major oxides.

Siliceous sands are S1, ranging to 100µm and S31, ranging from 40 to 200µm. Fume Silica is a commercial product from VAW, 96% SiO2 and 6.8 m^2/g Blaine

Sodium Tripolyphosphate is used at 0.5% of (CAC + fume): dose "a". Some experiments are made with either 0 or 3 x 0.5% (dose 3a).

Mix design of mortars, by weight

Binder 100		Water	Mortar (w/mortar=0.2)			TPP %
CAC	fume	w/cac=0.60	mortar	siliceous sands		/binder
100	0	60.0	300	100	100	0.5
95	5	57.0	285	95	90	0.5
92	8	55.2	276	92	82	0.5
86	14	51.6	258	86	72	0.5
80	20	48.0	240	80	60	0.5
70	30	42.0	210	70	40	0.5
W/CAC=0.3						
100	0	30.0	150	50	-	0.5
86	14	25.8	129	29	-	0.5

After water addition to the dry constituents, a 3 min mechanical gauging is applied in an AFNOR standard mixer. Placing in 2x2x10 cm steel moulds is made on a vibrating table. The moulded mortar is kept 1 day in a humid chamber, then the demoulded samples are kept under water in closed boxes. According to hardening schedules, the boxes are stored at 20°C or 50°C.

During setting and early hydration, the temperature of mortars increased for a few hours by no more than 6°C for W/CAC = 0.6 compositions and 9°C for W/CAC = 0.3. This almost isothermal hardening, necessary to get hexagonal hydrates, was achieved due to the small size of samples and steel moulds.
Hardening schedules : a/20°C permanent. b/20°C up to 24 hours + 50°C up to 7 days. c/20°C up to 28 days + 50°C for 7 or 28 d. d/ 38°C permanent.
The measurements and observations are - compressive strength and bound water.
- X-Ray diffraction : 2 Theta values for Cu radiation;height in mm :7.0° C2ASH8 hydrated gehlenite; 12.3° CAH10 hexagonal hydrate; 17.3° C3AH6 cubic hydrate.

3 - TYPICAL FEATURES OF COMPRESSIVE STRENGTH

Fig. 1 shows compressive strength of mortars made of respectively CAC and CAC + fume (86+14) and TPP, hardened at 20°C or heat treated ("converted") at 50°C (for 7 days after 1 or 28 days at 20°C, or for 28 days after 28 days at 20°C).

High strength (40 MPa) is obtained for both mortars at 24 hours, which is typical for CAC; then a steady increase of strength develops up to 65 MPa if temperature is 20°C. Through treatment at 50°C for 7 days, pure CAC mortar strength drops dramatically down to 17 MPa according to conversion phenomenon, which is fully damaging at the high Water/CAC ratio used.CAC + fume and TPP mortar, on the contrary, is strengthened by a 7 days 50°C treatment, the same way as at 20°C, after 1 or 28 days of 20°C hardening. This is the new property which gives CAC-fume mixtures their interest. By a 28 days (long) 50°C treatment, however, a significant decrease of strength is observed, down to 30 MPa, which indicates that strength stabilization provided by fume does not last for ever. The stability depends on completion of hardening at 20°C and on duration of heat treatment : Another measurement made after 4 months at 20°C + 3 months at 50°C gave 46 MPa, which is better in spite of a longer time of 50°C treatment. The series of fume/CAC ratios, from 0 to 30/70 shows the effect of fume content upon conversion resistance of mortars (with TPP). **Fig. 2** shows the "residual" strength after a 50°C treatment following a 20°C hardening : 1day + 7 days, 28 days + 7 days, 28 days + 28 days. For 7 day treatments, residual strength increases steadily with fume/CAC ratio up to 20/80, then decreases slightly. If 50°C treatment is as long as 28 days, a plateau is observed between ratios 8/92 and 14/86 (even a decrease), making 14/86 ratio mortar unstable. Mortar with ratio 20/80 appears stable even after a long 28 days 50°C treatment.

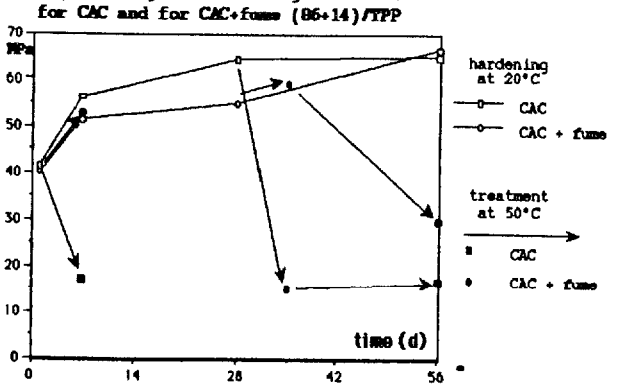

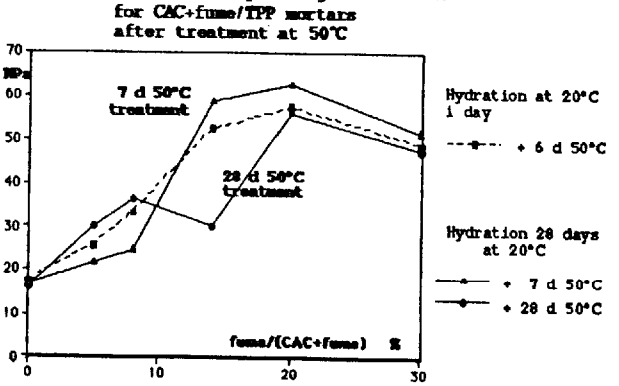

4 - INFLUENCE OF TRIPOLYPHOSPHATE

Addition of fume silica to mortars involves the use of a defloculating agent, the most common among them being Tripolyphosphate (TPP). Besides its rheologigal effect which is neglected in this study, TPP exhibits a chemical effect upon setting time, as well as on hydration and conversion which appears on compressive strength and bound water. Performance of mortars either with zero fume or 14/86 fume/CAC ratio, with various doses of TPP (normal dose "a" = 0.5 /(CAC + fume), zero TPP, and 3xa dose) are shown on Fig. 3, 4, 5, 6 and 7.

Fig. 3 Setting time vs % fume for CAC+fume mortars with various TPP amounts

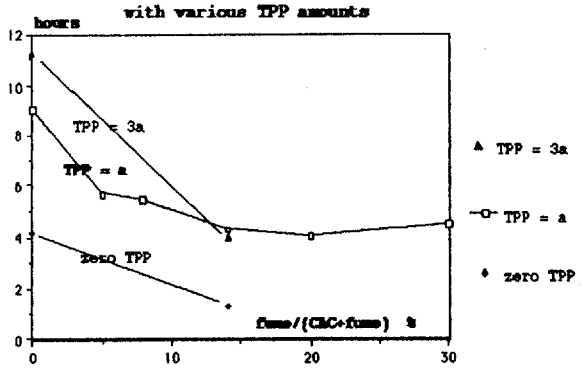

Fig. 4 24 h. comp. strength vs % fume for CAC+fume mortars with various TPP amounts

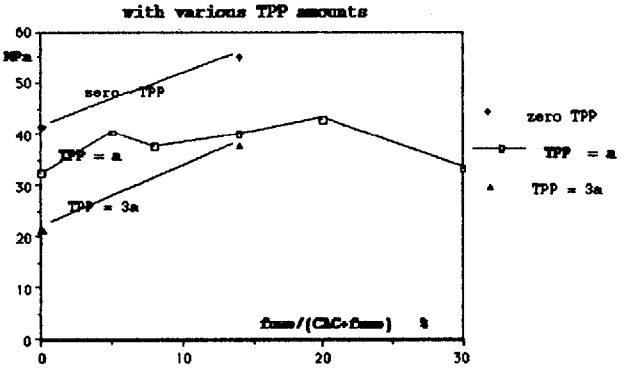

Fig.5 28 d comp. strength vs % fume and residual after 50°C treatment CAC+fume mortars, various TPP amount

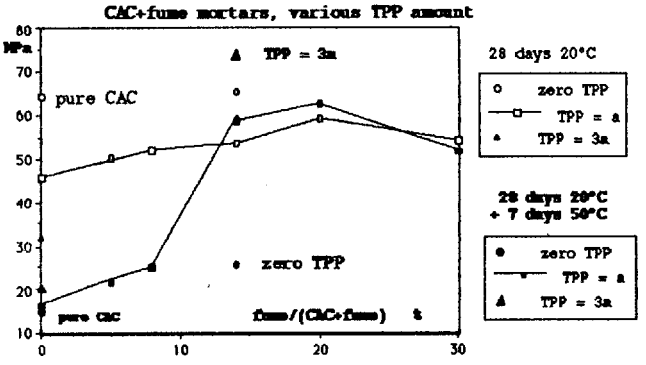

Fig. 6 28 d bound water vs % fume and residual after 50°C treatment CAC+fume mortars, various TPP amount

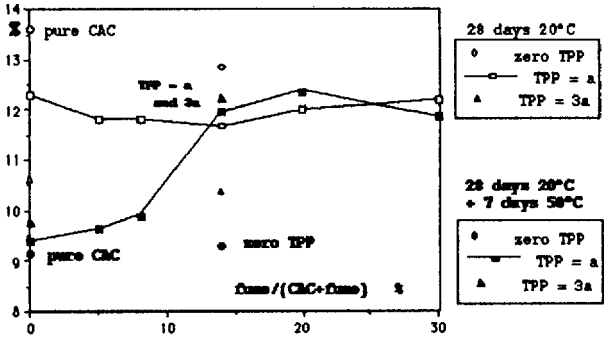

Setting time (**Fig. 3**) is shortened if the proportion of fume increases, whatever the amount of TPP; for instance at zero TPP, pure CAC sets at 4 hours but setting time is only 1.5 hour with 14/86 fume/CAC. If TPP increases to the normal dose "a", these setting times are respectively 9 and 4 hours. So the retarding effect of TPP balances exactly the accelerating effect of fume for a 14/86 fume/CAC ratio and normal dose of TPP. Compressive strength at 24 hours is directly related with setting time as it is shown on **Fig. 4**.

Compressive strength and bound water at 28 days and after a subsequent 7 days 50°C treatment are shown respectively on **Fig. 5 and 6**. They are perfectly in accordance with each other. It appears that addition of fume above 10% stabilizes performances of CAC, provided that TPP is present (see point zero TPP at 14 % fume). Another set of results shows that the loss of stability under long (28 days) 50°C treatment exhibited by the 14 % fume mortar (TPP dose a) disappears if TPP is three times this dose. **Fig. 7** gives the compressive strength vs time at 20°C and after heat treatment for 14/86 fume/CAC ratio mortars, containing zero, a, or 3xa dose of TPP. From the point of view of bound water and strength, it is clear that fume silica stabilizes the performances of CAC, independently of its water-reduction effect, provided that TPP is present. A significant result is found for a fume/CAC ratio above 14/86. At the boundary (14/86), a better stability is reached by increasing the TPP dose.

5 - HARDENING AT 38°C

Mortars have been placed in moulds for 24 hours in a 38°C wet atmosphere immediately after gauging, then demoulded and kept under water at 38°C. After 56 days, a test of thermal stability has been made for 28 days at 50°C.

Fig. 8 shows compressive strength vs time, compared with the 20°C hardening for a CAC+fume (86+14) /TPP mortar. Compressive strength grows linearly from 1 to 28 days and reaches the same level than at 20°C (losing only the high early strength at 1 and 7 days). After 56 days hydration at 38°C, a subsequent treatment at 50°C for 28 days does not alter the performance. Pure CAC at 38°C in comparison reaches at 24 hours the low typical strength of converted mortars,
and remains at this level afterwards (Let us recall that the high W/CAC = 0.6 ratio used is designed to show the thermal stability of hydrates but is incorrect for a normal use of CAC).

Fig. 9 shows the effect of % fume on the compressive strength of CAC+fume+TPP mortars. A steady improvement occurs between zero and 14 % fume/(CAC+fume), in the same fashion as the effect of fume on the stability of mortars hydrated at 20°C and then treated at 50°C. High levels of strength are reached, similar to 20°C unconverted mortars.

In case of zero TPP, strength for 0 and 14 % fume are given. The beneficial effect of 14 % fume is strongly reduced but strenth is nevertheless higher than for converted mortars.

Results for 38°C hydrated mortars tested at 56 days for stability, for 28 days at 50°C, do not differ from untreated mortars and have not been drawn on Fig. 10. Whatever the fume content, with TPP, mortars hydrated at 38°C are thermally stable in compressive strength.

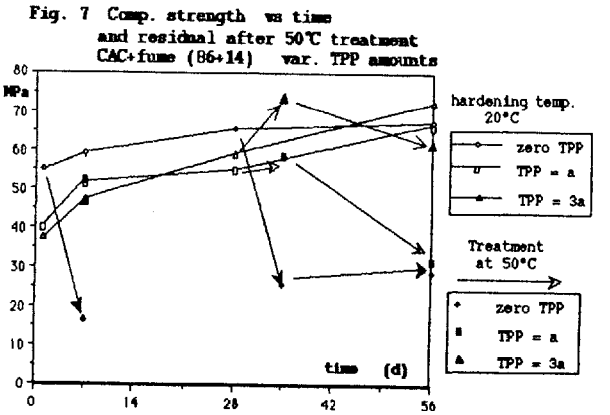

6 - MORTARS GAUGED AT W/CAC RATIO = 0.3

In order to recall that the correct practice for CAC mortars is to use a W/CAC ratio less than 0.4 and to show the performances obtained with fume silica, some results are given in that case for 0 and 14 % fume/(CAC+fume)-TPP mortars.

Fig. 10 and 11 represent compressive strengths vs time for mortars gauged at W/CAC = 0.3. Apart from the higher strength resulting from the lower W/CAC ratio, and a better behaviour under 50°C treatment at 24 hours, The CAC without fume behave the same way as for W/CAC=0.6; however, strength developped at 38°C are a little better than after 50°C treatment. With 14 % fume, the results are very good, 50°C treatments increasing the strength level, and 38°C treatment yielding a level of strength almost as high as at 20°C.

7 - MINERALOGICAL X-RAY EXAMINATION

The choice for mortars, and not pure pastes, explained earlier, is not very favourable for a fine examination of mineralogic phases by X-ray diffraction.

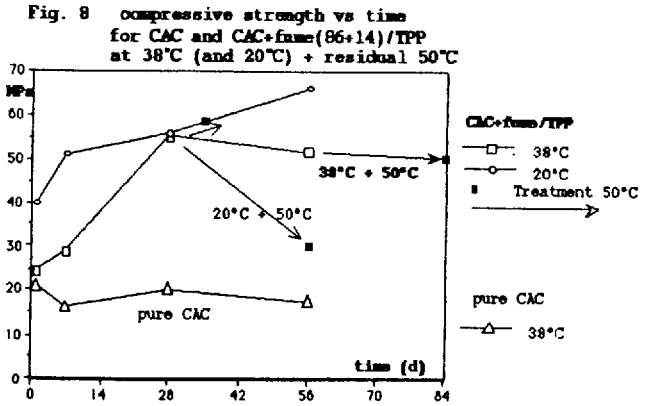

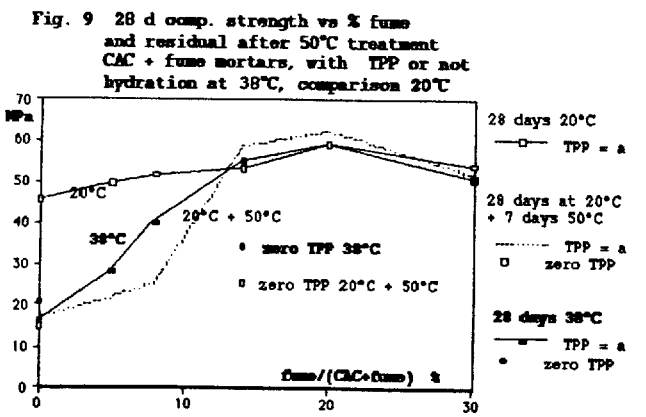

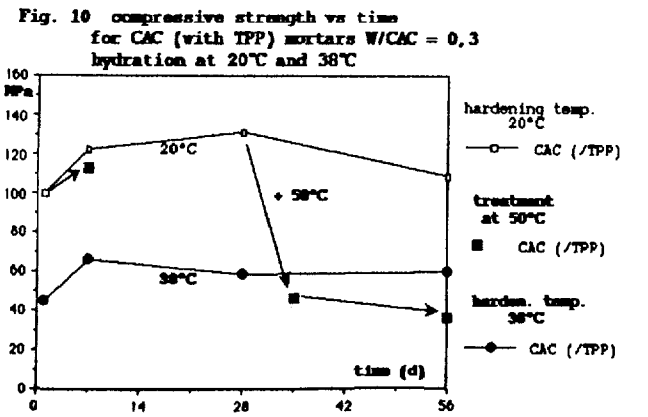

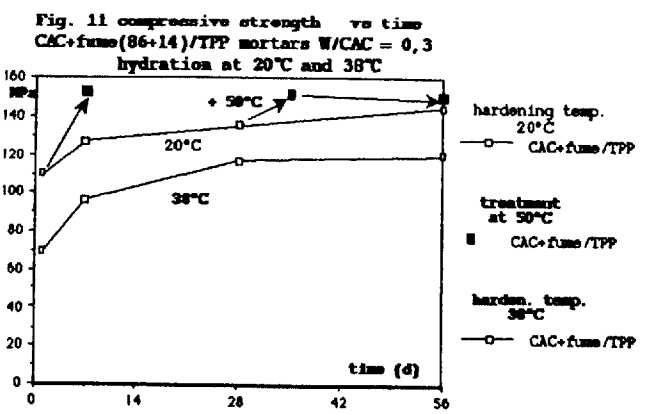

Fig. 12 CAH10 at 28 d 20°C vs % fume and residual after 7 d 50°C treatment
CAC + fume mortars, with TPP or not

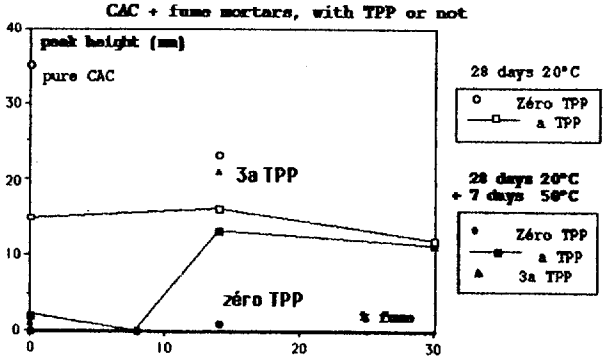

Fig. 13 CAH10 at 56 d 20°C vs % fume and residual after 50°C treatment
CAC + fume mortars, with TPP or not

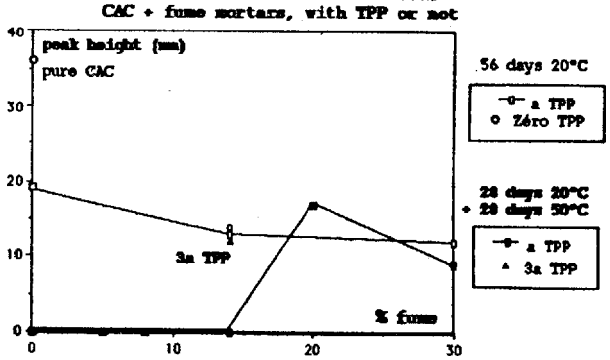

However, the principal hydrated constituents can be observed and the variation of their amounts can be estimated by the height of their diffraction peaks.

The height of peaks above base line is given in mm on the chart. Numerical values must not be examined too accurately, but used as an indication on the nature of the phenomena. Only mortars at W/CAC ratio = 0.6 are presented.

Hexagonal CAH10 and cubic C3AH6 hydrates **Fig. 12 and 13**

These figures show the relation between % fume and CAH10, respectively at 28 and 56 days at 20°C or after a 50°C treatment. It appears that the constant level reached at 20°C by mortars containing dose "a" of TPP drops to zero after 50°C treatment if fume is less than 14%. At this amount, it remains stable through a 7 days treatment but drops to zero after 28 days at 50°C. Besides, at 14% fume, a mortar without TPP loses CAH10 even after 7 days 50°C whereas a mortar with dose 3xa TPP keeps CAH10 unchanged even after 28 days 50°C. This result is in agreement with the variations of strength, high strength being associated with CAH10, as well as with bound water variations. It is also related to the variations of the C3AH6 peak height as shown on **Fig. 14 and 15.**

Fig. 14 C3AH6 vs % fume formed at 20°C for 28 days then by 7 d 50°C treatment
CAC + fume mortars, with TPP or not

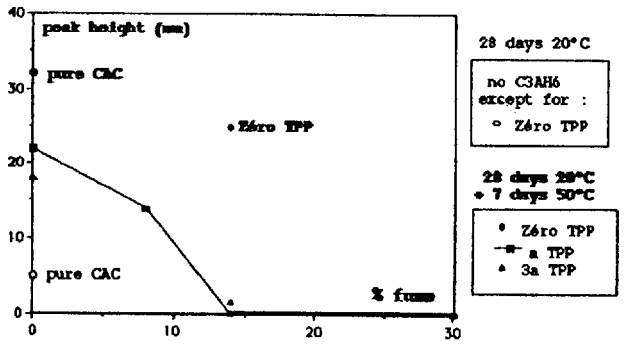

Fig. 15 C3AH6 vs % fume formed at 20°C for 56 days then by 28d 50°C treatment
CAC + fume mortars, with TPP or not

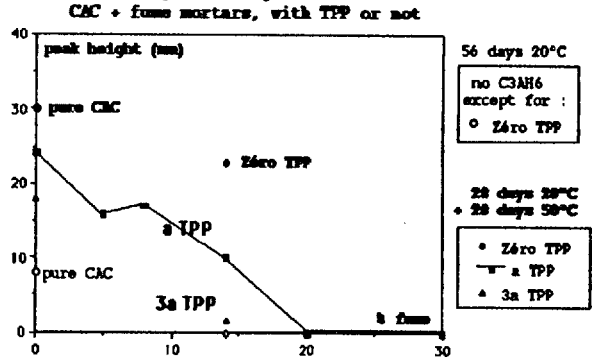

C2ASH8 hydrate **Fig. 16**

At 20°C, little C2ASH8 is formed, if large amount of fume is present, increasing with % fume. The effect of TPP is not clear, due to inaccuracy in the measurement of small peaks. By treatment at 50°C, C2ASH8 always appears, increasing if fume increases from zero to 14 %, stable above.

Fig. 16 C2ASH8 vs % fume formed at 20°C and after 50°C treatment
CAC + fume mortars, dose "a" TPP

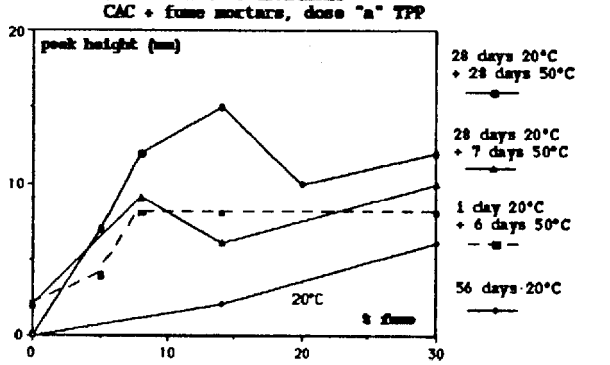

Hydration at 38°C **Fig. 17 and 18**

At 38°C, no hexagonal CAH10 hydrate is present. Pure CAC gives only cubic C3AH6 between 1 and 7 days, then is stable. C2ASH8 is not formed.

For CAC+fume and TPP mortars, the level of C3AH6 reached at 7 days decreases if the % fume and TPP dose increase. On the other hand, C2ASH8 is formed and increases with time up to 28 days. It increases

Fig. 17 C3AH6 formed at 38°C vs time various % fume and TPP

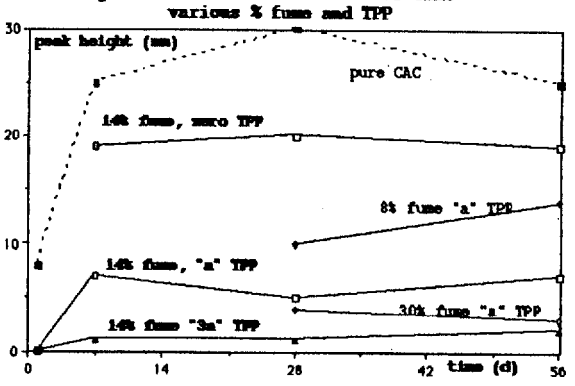

Fig. 18 C2ASH8 formed at 38°C vs time various % fume and TPP

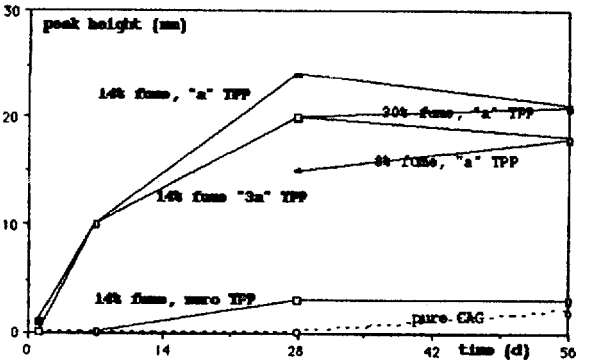

also with % fume up to 14%, then it is stable. If TPP is not present, C2ASH8 is not formed. These results are in agreement with kinetics of strength growth, 38°C hardening giving CAC+fume/TPP mortars a steady strength growth during 56 days whereas pure CAC rapidly reaches the low level of "converted" material.

- **DISCUSSION OF THE EFFECT OF FUME**

Fume silica must be associated with Sodium Tripolyphosphate, not only to be defloculated and provide better compactness resulting from optimised granulometry, but also to play a beneficial part towards hydrates.

The first effect, on 20°C hydrated CAC mortars, is to stabilize hexagonal hydrate CAH10 against thermal conversion to cubic hydrate. This effect increases with the % fume; it is achieved above 14% fume/(CAC+fume) at 0.5%TPP/(CAC+fume) and can be improved at lower fume contents if %TPP is higher. During heat treatment, some C2ASH8 is formed if fume and TPP are present and contributes to maintain better compressive strength even if some conversion occurs.

The second effect is to orient 38°C hydration towards C2ASH8 instead of C3AH6, the more so as the % fume increases and provided TPP is present. The formation of this hydrate takes place for a long period of time and the resulting strength grows steadily to reach at 56 days a level as high as for 20°C CAH10 hydrated mortars. Once again TPP must be present.

CONCLUSION

This study originates from the fact that blends of CAC and fume silica with TPP admixture provide a means of reducing gauging water through a better granulometry of mortars and concretes. This now classical effect can be profitable to fulfil the low Water/CAC ratio required for the good practice of CAC, but has been put apart In this study, this property has been avoided in order to show more clearly the other effects of fume silica upon mechanical strength through hydration and conversion behavior. Mortars gauged with a high W/C ratio, containing more than 14% fume and 0.5% TPP hydrated at 20°C exibit the well-known early and 28 days high strength of CAC, even after a severe 50°C treatment, because of a CAH10 hydrate stabilisation brought about by fume + TPP. Such compositions cured at 38°C hydrate to C2ASH8 and reach at 28 days the same strength as at 20°C.

BIBLIOGRAPHY

[1] British Standard BS915 Part 2,1972; French Standard. : "Norme AFNOR NF P 15 315", 1991.

[2] French descriptive Standard. : "Fascicule de Documentation P 15 316" 1991.

[3] George, C.M. : Structure and Performance of Cements. P. Barnes Applied Science Publisher 1983 p 2-9.

[4] George, C.M. : La bonne et la mauvaise utilisation des bétons de ciment alumineux.Journées Ciments Alumineux, Collège des architectes et techniciens, Barcelone, Avril 1991 Bate S.C.C. : L'expérience en Grande Bretagne, les causes, les suites. Ibid, Avril 91.

[5] Bentsen, S. Seltveit, A. Sandberg, B. : Effect of microsilica on conversion of HAC Proc. Internat. Symposium Calcium Aluminate Cements, London, July 1991 p 294-319.

[6] Bayoux, J.P. George, C.M. Letourneux, J.P. : Theory and practice of fume silica/aluminous cement interactions. Part I UNITECR Los Angeles 1989, Part II A.C.C. Dallas 1990, Part III A.C.C. Cincinati 1991.

STUDY ON HYDRATION PROPERTIES OF SLAG AND SILICA FUME BLENDED CEMENT FOR ULTRA-HIGH STRENGTH CONCRETE

M Shizawa*, Y Joe*, S Takesue** and Y Urakawa***

*Cement Division, Tokuyama Soda Co, Ltd
**Cement and Concrete Research Center, Tokuyama Soda Co, Ltd
***Slag Department, Kobe Steel Co, Ltd
JAPAN

SUMMARY

This report presents the results of studies concerned with blended cement for ultra-high strength concrete. The blended cements were consisted of portland cement, ground granurated blast furnace slag and silica fume. The effect of fineness of portland cement, fineness of slag and mixing proportions of blended cements on the properties of paste, mortar and concrete in very low water cement ratio was investigeted.

The results obtained are summerized as follows;

1. Workability of fresh mortar and concrete of blended cement became worse with the increase in the fineness of portland cement and/or pulverized slag.
2. Workability of fresh mortar and concrete of blended cement was improved by substituting portland cement with suitable amount of pulverized slag and/or silica fume.
3. Heat of hydration of blended cement became larger with the increase in the fineness of portland cement and/or pulverized slag.
4. Heat of hydration of blended cement was enlarged by substituting portland cement with suitable amount of pulverized slag and/or silica fume.
5. At the early ages, by means of increasing the fineness of portland cement and pulverized slag, strength development was improved. However, after 7 days, there was no relationship between strength and fineness of these materials.
6. At the later ages, strength development was improved by substituting portland cement with 10 to 30% silica fume.
7. Slag blended cement, the specific surface area of pulverized slag was about 800 m^2/kg, was superior in improvement of the strength development at the later ages.

要　約

この報告書は超高強度コンクリート用の混合セメントに関する研究の結果を報告するものである。この混合セメントはポルトランドセメント、スラグ粉末およびシリカフュームからなる。これらの混合セメント中のポルトランドセメント、スラグの粉末度および混合比率がペースト、モルタルおよびコンクリートの物性におよぼす影響について調査を行った。

以下にその結果について示す。

1．混合セメント中のポルトランドセメントおよび／もしくはスラグ粉末の粉末度が増加するに連れてフレッシュモルタルおよびコンクリートのワーカビリチーは低下した。
2．適量のスラグ粉末および／もしくはシリカフュームを混合することによりフレッシュモルタルおよびコンクリートのワーカビリチーは改善された。
3．混合セメント中のポルトランドセメントおよび／もしくはスラグ粉末の粉末度が増加するに連れて水和熱は大きくなった。
4．適量のスラグ粉末および／もしくはシリカフュームを混合することにより水和熱は大きくなった。
5．初期材令においてポルトランドセメントやスラグ粉末の粉末度が増加するに連れて強度発現性は改善された。しかしながら、材令７日以降となると粉末度と強度との間に関係が認められなくなった。
6．１０～３０%のシリカフュームを混合することにより長期強度発現性は改善された。
7．ほぼ800 m^2/kg の比表面積を有するスラグ粉末を混合したセメントの長期強度発現性は改善された。

1 INTRODUCTION

In recent years, high strength concrete is increasingly used for construction of tall reinforced concrete buildings and long span bridges. And the demand for strength level becomes higher and higher. Already ultra-high strength concrete above 100 MPa can be obtained by using both silica fume and superplasticizer. Generally, in order to get high strength concrete, decreasing of water cement ratio (W/C) of concrete is the most effective method. But, workability of fresh concrete becomes worse with the decreasing of W/C. By the development of superplasticizer, the desirable W/C to keep workability has been decreased. However, in order to get stronger concrete more than 120 MPa, cement must be changed. Mixing of cementitious ingredients to portland cement is one of effective method to reduce W/C. In addition, to achieve high strength concrete, higher cement contents are used and, consequently, this may lead to higher hydration temperature which could have deleterious effect.

The objective of this study is to develop the blended cement for ultra-high strength concrete having enough workability and low heat evolution. We investigated the effects of fineness of portland cement and fineness of blast furnace slag and mix proportions of portland cement, blast furnace slag and silica fume on the properties of low W/C paste, mortar and concrete. Finally, some results obtained from following experiments are presented.

2 EXPERIMENTAL

2.1 Raw Materials

Ordinary portland cement (N-OPC) was used for the base cement. It belonged to JIS Classification. Fine ordinary portland cement (H-OPC) which was got by pulverizing of N-OPC by vibration mill was used, too.

Ground granurated blastfanace slags (GBS) were used for a kind of supplementary cementitious material. Blaine specific surface area (BSA) of these slags were varied from about 400 to 1200 ㎡/kg

For another kind of supplementary cementitious material, compacted silica fume (SF) was used.

In order to adjust the amount of SO_3 of blends =2.0%, ground desulfo-gypsum (GYP) was added.

Chemical composition and some physical properties of these materials are listed in Table 1 and 2, respectively.

Superplasticizer (SP) was a sulfonated naphthalen formaldehyde condensate high-range AE type water reducer.

2.2 Paste and Mortar Tests

The blends for paste and mortar tests were prepared by mixing of above mentioned raw materials. Mixing proportions of these blends are listed in Table 3.

2.2.1 Paste Tests

Heat of hydration of these blends were measured according to the method of CAJS J-01 (dissolution method). And, rate of heat liberation of some blends were measured by conduction calorimeter.

Table 1 Chemical Composition of Starting Materials

Materials (%)	Ordinary Portland Cement (OPC)	Blast Furnace Slag (GBS)	Silica Fume (SF)	Desulfo Gypsum (GYP)
SiO_2	21.6	34.1	93.0	
Al_2O_3	5.0	14.5	0.6	
TiO_2	0.4	1.3		
Fe_2O_3	2.8		1.1	
MgO	1.6	5.4	0.3	
CaO	63.6	43.0	0.3	31.8
Na_2O	0.24	0.19		
K_2O	0.50	0.37		
SO_3	2.0	S-0.8		44.5

Table 2 Blaine Specific Surface Area (BSA) and Specific Gravity (SG) of Starting Materials

Materials	BSA(㎡/kg)	SG(-)
N-OPC	335	3.16
H-OPC	644	3.16
GBS41	414	2.92
GBS81	805	2.92
GBS116	1163	2.92
SF	21000	2.26
GYP	700	2.30

Water blends ratio (W/C) of these paste was 40%.

2.2.2 Mortar Tests

Flow value of fresh mortar and mortar compressive strength were measured according to the method of JIS R 5201 (4x4x16cm prizm). And, air content of fresh mortar was measured according to the method of ASTM C 185. Mix design of every mortar was blends(binder):sand:water = 1:2:0.3 and SP was added 2.0% of binder. Used sand was the mixture of SOMA-standard sand and TOYOURA-standard sand. Its proportion was SOMA:TOYOURA = 3:2. Prizm specimens were cured in water at 20 ℃.

2.3 Concrete Tests

Following the paste and mortar tests, certain compositions of blends were selected for concrete tests. Mixing proportions of blends are listed in Table 4. Test items were slump, slump flow (measurement of spread width of fresh concrete for slump-test), air content and compressive strength. These measurements were carried out according to JIS-method. These concrete tests carried out in the condition of W/C=30% and 25%. In the case of W/C=30%, the amount of SP was fixed. And in the case of W/C=25%, the amount of SP was decided according to the value of slump of fresh concrete (22 cm). Cylindrical specimens of concrete of 10cm in diameter were cured in water at 20 ℃. Furthermore, measurement of pore size distribution of concrete specimens by mercury intrusion porosimeter and measurement of the amount of $Ca(OH)_2$ of concrete specimens by X-ray diffractometer were carried out.

3 RESULTS AND DISCUSSION

The results of paste and mortar tests are shown in Table 5 and the results of concrete tests are shown in Table 6.

3.1 Paste and Mortar Tests

Table 3. Mixing Poportion of Blends for Paste and Mortar Tests (%)

No.	N-OPC	H-OPC	GBS41	GBS81	GBS116	SF
1	100					
2		100				
3	50				40	10
4		50			40	10
5	50		40			10
6	50			40		10
3	50				40	10
1	100					
7	80				20	
8	60				40	
9	40				60	
10	20				80	
11	95					5
12	75				20	5
13	55				40	5
14	35				60	5
15	90					10
16	70				20	10
3	50				40	10
17	30				60	10
18	80					20
19	60				20	20
20	40				40	20
21	20				60	20
22	70					30
23	50				20	30
24	30				40	30

Table 4. Mixing Poportion of Blends for Concrete Tests (%)

No.	N-OPC	H-OPC	GBS41	GBS81	GBS116	SF
1	100					
2	60		40			
3	60			40		
4	60				40	
5	90					10
6		100				
7		60		40		
8		90				10
9	100					
10	80			20		
11	60			40		
12	40			60		
13	80		20			
10	80			20		
14	80				20	
15	60		40			
11	60			40		
16	60				40	
9	100					
17	90					10
18	85					15
19	80					20
20	80			10		10
21	60			30		10
22	60			20		20

3.1.1 Effect of Fineness of OPC

Heat of Hydration- Heat of hydration of H-OPC paste was about 15% larger than N-OPC during all curing ages. Heat liberation curves of N-OPC and H-OPC are shown in Fig. 1. The second peak of hydration of H-OPC appeared at shorter age and its hight became higher than N-OPC.

Heat of hydration of H-OPC base blends (ternary blends) was larger than N-OPC base blends. The increase in heat of hydration of these cements per BSA 10m²/kg of OPC was about 0.4cal/g.

Workability and Air Content- Flow value of H-OPC fresh mortar was smaller than N-OPC. And, air content of H-OPC fresh mortar was larger than N-OPC. The ralationship between fineness of OPC and flow value, air content of mortar of blends was similar to pure OPC.

Mortar Compressive strength- At the early ages, mortar compressive strength of H-OPC was higher than N-OPC. However, after 7 days, compressive strength of N-OPC became higher than H-OPC. Mortar compressive strength of H-OPC base blends was higher than N-OPC base blends during all curing ages. But, at later age, the strength difference between N-OPC base blends and H-OPC base blends became smaller in compliance with the curing time.

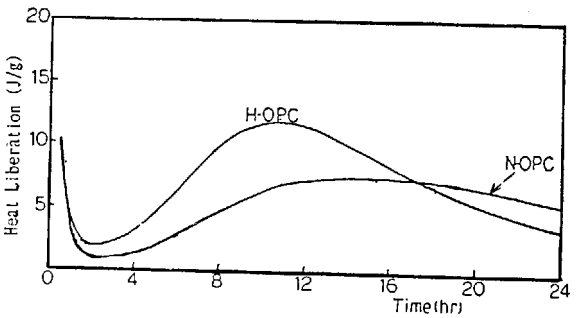

Fig. 1 Heat Liberation of OPC

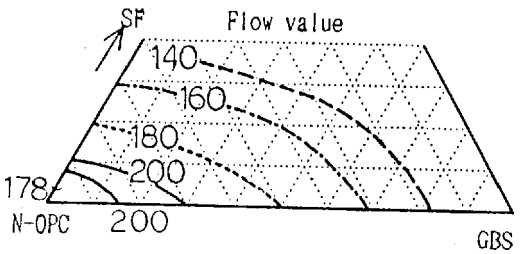

Fig. 2 Mortar Flow Value of Ternary Blends

Table 5 Paste and Mortar test Results of blends

No.	Flow Value (mm)	Air cont -ent (%)	Compressive Strength (MPa) 1D	7D	28D	Heat of Hydration (cal/g) 7D	28D
1	178	3.5	29.2	73.8	81.6	73.6	85.4
2	153	4.1	41.0	64.9	69.3	86.8	97.3
3	174	3.9	22.2	58.9	74.8	72.0	78.9
4	145	5.2	29.6	64.8	79.9	78.0	84.0
5	217	2.7	9.3	46.1	71.6	61.3	74.1
6	196	2.4	16.9	59.5	81.9	72.1	76.0
3	174	3.9	22.2	58.9	74.8	72.0	78.9
1	178	3.5	29.2	73.8	81.6	73.6	85.4
7	211	7.8	19.6	55.0	72.0	86.6	97.0
8	190	4.2	15.5	60.0	83.5	80.2	93.3
9	173	3.1	14.6	52.5	76.7	66.2	74.6
10	143	2.3	19.8	39.9	53.8	44.0	51.2
11	201	4.1	26.1	68.3	88.7	74.5	88.8
12	198	3.8	21.8	59.7	77.0	78.9	91.7
13	182	3.4	20.7	61.7	84.8	76.0	86.0
14	166	3.3	20.7	52.4	70.8	58.0	66.0
15	195	3.8	27.4	69.9	97.4	77.2	96.3
16	186	2.7	24.6	61.9	83.8	77.9	91.7
3	174	3.9	22.2	58.9	74.8	72.0	78.9
17	155	3.8	23.8	47.5	64.8	50.1	57.9
18	172	2.1	26.8	66.7	101.5	73.0	96.0
19	167	3.7	24.8	59.4	80.9	70.7	84.0
20	161	4.2	24.7	52.6	72.8	63.0	70.5
21	132	3.6	26.0	42.2	53.4	44.2	50.4
22	155	3.8	24.0	59.3	95.1	62.9	90.0
23	149	4.1	23.4	58.1	82.6	64.0	78.6
24	137	4.1	20.4	50.8	73.1	55.3	63.2

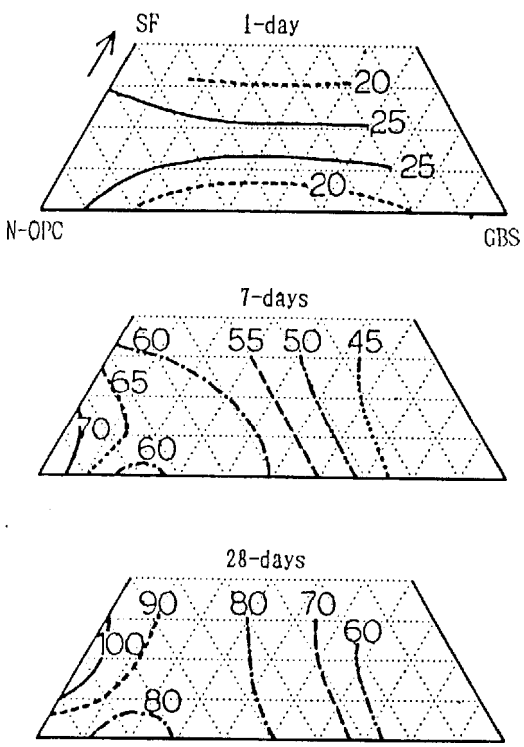

Fig. 3 Mortar Compressive Strength of Ternary Blends

Heat of hydration per compressive strength (Q/S) of H-OPC was higher than N-OPC. Because the heat of hydration of H-OPC was larger than N-OPC, in spite of decreasing of strength development ratio of H-OPC compared with N-OPC at later ages. It is not considered that pulverizing of OPC is an effective method to get ultra-high strength concrete.

3.1.2 Effect of Fineness of GBS

Heat of Hydration- By means of increasing the fineness of GBS, heat of hydration of ternary blends were increased during all curing ages.
Workability- By means of increasing the fineness of GBS, flow value of fresh mortar was decreased.
Mortar Compressive Strength- At the early age, by means of increasing the fineness of GBS, mortar compressive strength of ternary blends were increased. However, ratio of strength development of ternary blends containing GBS116 was decreased at later ages. Ternary blends containing GBS81 was superior in the strength development during all curing ages.

3.1.3 Effect of Mixing proportion

The contour line of mortar flow and mortar compressive strength of ternary blends are shown in Fig. 2 and Fig. 3, respectively.

Heat of Hydration- During all curing ages, Heat of hydration of GBS blends containing 0 to 50% GBS116 were larger than N-OPC. And heat of hydration of SF blends containing 5 to 10% SF was larger than N-OPC.

Heat liberation curves of blends are shown in Fig. 5. By means of increasing the content of SF the second peak of ternary blends were lowerd. But, the patterns of heat liberation curves were not change so much. On the other hand, by means of increasing the content of GBS, the second peaks of ternary blends were shifted from 13 to 18 hours.
Workability- Mortar flow value of GBS blends which containing less than 50% GBS116 were larger than N-OPC. And mortar flow value of SF blends containing less than 15% SF were larger than N-OPC.

Table 6 Mix Desiges of Ultra-high Strength Concrete and Concrete Test Results of Blends

No.	W/c	Bind-er	Water	Aggregete (kg)		SP	Slump	Slump Flow	Air	Compressive Strength (MPa)			
	(%)	(kg)	(kg)	Fine	Coarse	(%)	(mm)	(mm)	(%)	3D	7D	28D	91D
1	30	550	165	691	1013	1.65	180	266	2.6	51.4	69.1	82.1	88.3
2	30	550	165	675	1013	1.65	249	666	2.7	33.3	55.6	79.9	88.4
3	30	550	165	675	1013	1.65	230	561	2.8	41.1	65.7	89.6	96.0
4	30	550	165	675	1013	1.65	127	219	2.8	36.8	53.8	65.1	73.7
5	30	550	165	672	1013	1.65	195	298	2.4	47.0	65.1	86.5	98.2
6	30	550	165	691	1013	3.50	189	323	3.9	53.8	64.7	76.1	81.4
7	30	550	165	675	1013	3.50	248	675	3.5	30.4	58.6	80.6	87.6
8	30	550	165	672	1013	3.50	210	387	3.8	49.1	62.1	76.0	92.9
9	25	660	165	603	1010	2.40	218	361	2.4	56.2	76.3	92.6	98.0
10	25	660	165	593	1010	1.55	222	504	1.9	57.2	77.5	99.0	103.6
11	25	660	165	584	1010	1.40	229	496	1.7	50.7	77.3	99.9	107.8
12	25	660	165	574	1010	1.30	222	419	2.0	44.9	69.1	95.3	104.6
13	25	660	165	593	1010	1.55	226	547	2.1	50.1	71.9	86.2	96.6
10	25	660	165	593	1010	1.55	222	504	1.9	57.2	77.5	99.0	103.6
14	25	660	165	593	1010	1.65	225	453	2.5	54.4	67.5	74.3	88.1
15	25	660	165	584	1010	1.20	229	520	1.7	40.6	65.2	86.9	90.9
11	25	660	165	584	1010	1.40	229	496	1.7	50.7	77.3	99.9	107.8
16	25	660	165	584	1010	2.20	220	414	2.6	45.9	68.5	82.3	85.9
9	25	660	165	603	1010	2.40	218	361	2.4	56.2	76.3	92.6	98.0
17	25	660	165	579	1010	1.85	217	354	2.4	56.4	76.1	101.1	109.9
18	25	660	165	567	1010	1.75	213	324	2.4	53.1	75.1	102.8	108.8
19	25	660	165	556	1010	2.10	213	309	2.4	51.0	74.3	103.2	112.9
20	25	660	165	551	1010	1.90	219	416	1.7	54.1	79.9	105.2	113.4
21	25	660	165	565	1010	1.80	225	409	1.7	50.7	76.6	101.4	119.1
22	25	660	165	546	1010	2.20	217	377	1.7	46.8	74.0	102.1	121.5

too. The maximum flow value was obtained for the 20% GBS116 blends.

Mortar Compressive Strength- At the early ages up to 7 days, mortar compressive strength of N-OPC was larger than any other ternary blends. After 7 days, mortar strength of GBS blends contaning 40% GBS116 took maximum value in the binary GBS116 blends. At 28 days, mortar strength of SF blends containing 20% SF was the highest.

Fresh mortar of GBS blends containing about 20% GBS116 entraped large amount of air. This phenomenon showed that the mixing proportion and packing properties of pulverized materials carried out important role for flow charactaristics of slurry.

3.2 Concrete Tests

3.2.1 Effect of Fineness of OPC

Workability- In the case of W/C=30%, in order to take same slump level, H-OPC and H-OPC base blends needed more than two times of amount of SP compared with N-OPC and N-OPC base blends. This showed that H-OPC is not easier to flow than N-OPC.

Concrete Compressive Strength- At the early ages up to 3 days, concrete compressive strength of H-OPC was similer to N-OPC. After 7 days, compressive strength of N-OPC became higher than H-OPC. However, compressive strength of N-OPC base blends were higher than H-OPC base blends during all curing ages.

3.2.2 Effect of Fineness of GBS

Workability- By means of increasing the fineness of GBS, value of slump and slump flow of fresh concrete became worse. But, difference between workability of GBS81 blends and GBS116 blends were not so much .

Concrete Compressive Strength- During all curing ages, concrete strength of GBS81 blends were surpass GBS41 and GBS116. Strength development of GBS81 blends concrete at later ages were superior to OPC. And there was the maximum point in the range from 20 to 40%. On the other hand, the blends containing GBS41 and GBS116 were not larger than N-OPC. Super pulverized GBS did not contribute to concrete strength.

3.2.3 Effect of Mixing Proportions of Blends

Workability- Slump flow of GBS blends containing 20 % GBS took the maximum value. The excess addition of GBS (more than 20%), Workability of GBS blends became worse. Even though, in the case of 60% GBS blends, workability of that was larger than OPC.

In W/C=25%, slump flow of fresh concrete of SF blends were decreased by substituting N-OPC with over 10% SF. But, by Additing of GBS, SF blends could take very larger slump flow value than N-OPC.

Concrete Compressive Strength- After 28 days, concrete strength of GBS blends containing 20 to 60% GBS81 became larger than N-OPC. During all curing age, that of GBS81 20% blends was larger than N-OPC. Even though, after 28 days, strength of GBS blends containing GBS41 and GBS116 did not become larger than N-OPC. Until 28 days, concrete strength development of SF blends containing 10% SF were similar to OPC. After 28 days, strength of SF blends were about 10% larger than OPC. Concrete strength of SF blends containing 10 to 20% SF were not depend on the content of SF at later ages.

At the early ages up to 3 days, concrete strength of ternary blends (N-OPC,GBS81 and SF) were lower than N-OPC. But after 7 days, became higher. Especially,the ternary blends containing about 40 % cementitious ingredients, became about 20% larger than OPC at 91 days.

3.2.4 $Ca(OH)_2$ and Pore Volume in the Hardnened Concrete

Relative amount of $Ca(OH)_2$ and pore volume of mortar part of hardened concrete are shown Table 5.

Generally, it is well known that pore volume becomes smaller, with the increasing in the strength of concrete. In this experiment, pore volume of each specimenes became smaller with the increasing of curing time and strength. However, different kind of blends consisted by various cementitious materials introduced different decreasing pattern of pore volume. At 28 days, pore volume of GBS blends containing 40% GBS81 were small compared with others. At 7 days, pore volume of H-OPC was relative small, but at 28 days, it did not decrease so much. Strength development of H-OPC showed same charactaristics for pore volume reduction.

The amount of $Ca(OH)_2$ in W/C=25% concrete was smaller than W/C=30%. Similally, that of H-OPC

Table 8 Amount of $Ca(OH)_2$ and Pore Volume in Concrete Specimens

Concrete Specimen Number	Amount of $Ca(OH)_2$ 28D	Pore Volume (cc/g) 7D	28D
1	**********	0.0326	0.0189
2	**	0.0318	0.0188
3	**	0.0245	0.0156
4	trace	0.0275	0.0146
5	********	0.0327	0.0177
6	**	0.0215	0.0177
7	trace	0.0289	0.0143
8	*	0.0261	0.0155
9	*********		
15	*		
11	*		
16	trace		
19	****		
22	trace		

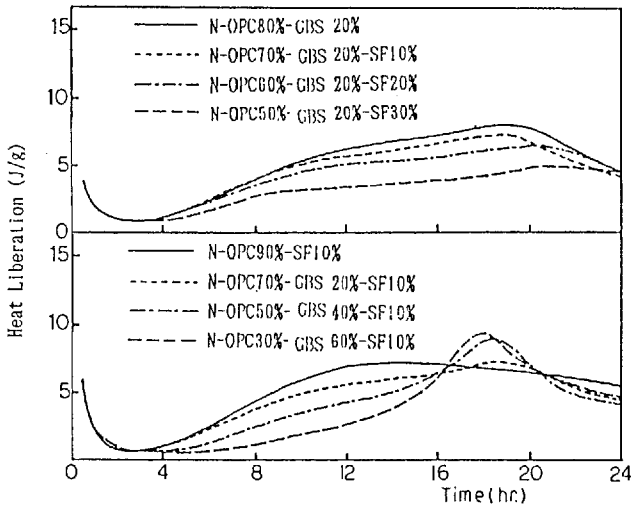

Fig. 4 Heat Liberation of Ternary Blends

base blends was smaller than N-OPC.

These phenomena are concerning to the difference between the hydration structure of N-OPC and that of H-OPC and N-OPC at the early ages. Rapid reaction of hydration makes high CaO/SiO_2 hydrate (C-S-H) and this hydrate inhibits proceedig of hydration.

The amount of $Ca(OH)_2$ of GBS blend became smaller than N-OPC. In the case of GBS116, the amount of $Ca(OH)_2$ was hardly existed. Because GBS consumed $Ca(OH)_2$ which was produced by hydration of portland cement.

4 CONCLUSIONS

From the results presented in this paper, the following conclusions can be drawn.

(1) Workability of fresh mortar and conctrete of blends became worse with the increase in the fineness of base OPC and/or GBS.
(2) Workability of fresh mortar and concrete of blends was improved by substituting OPC with suitable amount of GBS and/or SF.
(3) Heat of hydration of blends increased with the increase in the fineness of base OPC and/or GBS.
(4) Heat of hydration of blends was enlarged by substituting OPC with suitable amount of GBS and/or SF.
(5) At the very early ages, the strength development of mortar and concrete was improved by increase the fineness of base OPC and GBS. However, after 7 days, there was no relationship between strength development and fineness of these materials.
(6) At the later ages, the strength development of mortar and concrete was improved by substituting OPC with 10 to 30% SF.
(7) GBS blends, BSA of GBS was about 800m^2/kg, is superior in improvement of the strength development of mortar and concrete at later ages.

Consequently, GBS 40% blends, BSA of the GBS is about 800 m^2/kg, is superior in using for ultra-higth strength concrete, judging by workability, heat of hydration, amount of $Ca(OH)_2$, pore volume and strength.

REFERENCES

1. KOKUBU, K.: "Finely ground powder of blastfurnace slag",Concrete Journalof JAPAN, Vol.26, No.4 April 1988, 25-31.
2. YONEKURA, A.:"Silica Fume", Concrete Journal of JAPAN, Vol.26, No.4, April 1988 19-24.
3. YOSHIDA and S. OKABAYASHI, "Properties of Finely-ground Cements"; CAJ Proceedings of Cement & Concrete , No.43, 1989, 54-59

MICROSTRUCTURE AND MECHANICAL PROPERTIES OF HARDENED CEMENT PASTE INCORPORATING GROUND GRANULATED BLAST-FURNACE SLAG

T Nishikawa*, K Koibuchi**, S Ito* and M Takatsu*

*Nagoya Institute of Technology, Gokiso-cho, Showa-Ku, Nagoya, JAPAN
**Dai-ichi Cement Co, Ltd, Asano-cho, Kawasaki-ku, Kawasaki, JAPAN

ABSTRACT

In this paper, the hardened cement paste(HCP) were prepared with containing fine blast-furnace slag as ordinary portland cement replacement. The microstructure and mechanical properties of HCP after curing in moist air or in water at 25 ℃ for 1, 3 months, were investigated and discussed.

The larger combined water, smaller void amount and small amount of calcium hydrate were measured on the HCP containing slag. Carbonation progressed slowly compared with that for the slag-free HCP. These quantitative analysis of hydrates indicated the formation of characteristic C-S-H having low Ca/Si molar ratio and high water content.

The replacement of slag brought the compressive development, though did not the bending strength development at least in early stage of hydration. The fracture toughness and the fatigue parameter n in the crack propagation rate equation, was lower than those for the slag-free HCP.

The composition and amount of hydrate must be related to the durability or strength of concrete. The fracture surface in HCP containing slag suggested that crack propagated preferentially through the C-S-H and calcium hydroxide. Corresponded to microstructure and mechanical properties of HCP, the bending strength and fracture toughness accompanied with instantaneous fracture was probably dependent on the component and mechanical properties of hydrates. While, the fatigue behavior was mainly dependent on the property of C-S-H, in which the crack propagated easily or not.

要旨

本論文では、普通ポルトランドセメントを微粉砕高炉スラグに一部置換したセメント硬化体を作成し、２５℃の湿空中および水中で１または３カ月養生した後、微細組織と機械的特性を検討した。スラグ含有の硬化体では、結合水が多く、空隙量、水酸化カルシウム量が少ない。また炭酸化は、スラグを含まない硬化体に比べ緩やかに進む。水和物の定量結果より、Ｃａ／Ｓｉモル比が低く、含水量の多い特徴的なＣ－Ｓ－Ｈの生成が予想される。

水和初期段階におけるスラグの置換は、圧縮強度の増加をもたらすが、曲げ強度の増加はあまり認められない。破壊靭性値および亀裂進展速度式中の疲労パラメータｎは、スラグを含まない硬化体に比べ低い値を示した。水和物の組成および生成量がコンクリートの耐久性や強度に関連すると考えられる。スラグ置換された硬化体の破壊面観察より、亀裂は主にＣ－Ｓ－Ｈや水酸化カルシウムを横切って進展していた。こうした微細組織と機械的特性を対比することにより、瞬時破壊を伴う曲げ強度や破壊靭性値は、水和物の構成成分やそれらの機械的特性に依存すると考えられる。一方、疲労挙動は、亀裂進展の容易さにかかわりなく、Ｃ－Ｓ－Ｈの特性に依存する。

1. INTRODUCTION

The durability of cementious systems has been investigated based on the mechanical properties of concrete. In these studies, the type of cement, mix proportion of concrete and cured environment were mainly studied to reveal the direct effects upon the durability of concrete. The chemical and physical changes of hydrates in cement paste part were also important, but were not discussed except the pore structure.

While, ground granulated blast-furnace slag is commonly used as the blended portland cement, due to the improvement of log-term strength and resistance to chemical attack. In our previous paper, the relation between microstructure of hydrate and strength of concrete containing blast furnace slag was discussed, concerning with the amount and composition of hydrate.

In this paper, the hardened cement paste(HCP) were prepared in laboratory with containing fine blast-furnace slag as ordinary portland cement replacement. The microstructure and mechanical properties of HCP after curing in moist air or in water at 25 ℃ for 1, 3 months, were investigated and discussed. Especially, the fatigue properties of HCP under static or cyclic load condition was also investigated. This mechanical properties fairly reflected the different microstructure.

2. EXPERIMENTAL

Sample preparation and characterization

The chemical compositions of used ordinary portland cement, ground blast furnace slag (Blaine specific surface area; 8490cm^2/g, average particle size; 3.4 μ m in diameter) and anhydrite were listed in Table 1. The cement pastes were prepared with water/solid ratio, 0.30 in slag HCP containing slag as cement replacement of 40 wt% (PCS or PCSW series in this experiment) or 0.28 in slag-free HCP (PC series), respectively. These pastes contained calcium lignosulfate of 1 wt%/solid as water reducer and anhydrite of 5 wt%/slag only for slag HCP as activator. These pastes were cast in 2 x 2 x 10 cm and cured in moist air or water at 25 ℃ for 1 to 3 months.

Table 1 Chemical composition of raw material

Material	Chemical composition (wt%)								
	SiO_2	Al_2O_3	Fe_2O_3	CaO	MgO	SO_3	S	Na_2O	K_2O
cement	21.5	5.4	3.1	63.0	2.7	2.1	0.0	0.40	0.40
slag	34.5	13.5	0.5	41.9	6.8	0.0	0.9	0.17	0.29
anhydrite	0.0	0.0	0.1	40.5	0.0	56.5	0.0	0.00	0.00

The amount and composition of hydrates were identified by XRD and estimated by TG-DTA and EDAX as described elsewhere [1]. The observation of microstructure was performed by SEM and the porosity was measured by immersion into kerosene. The bending strength and compressive strength of each HCP were measured and fracture toughness was by SENB (Single Edge Notched Beam) method.

Fatigue behavior of HCP

Cyclic fatigue test was conducted on a high frequency cycling instrument of a piezo stack type. Cyclic and static fatigue tests were performed in tension under maximum

applied stress (σ_{max}), which was 70 to 100% of mean bending strength, to measure the time to failure (t_f). This instrument provided a sinusoidal cyclic frequency of approximately 100 Hz with a stress ratio ($R=\sigma_{min}/\sigma_{max}$) of 1.0, 0.7 or 0.1 and one-side oscillation[2].

3. RESULTS AND DISCUSSION

Characterization of HCP

In any HCP, calcium hydroxide, calcium carbonate and unreacted alite were observed by XRD, but the last compound was not detected quantitatively. Table 2 showed the amount of former two compounds, the Ca/Si mole ratio in C-S-H and void volume of each HCP. The mechanical properties of HCP were also listed. For example, PCSW 1 was the HCP containing slag of 40 wt% , which was cured in water for 1 month. The larger combined water, smaller void amount and small amount of calcium hydrate were measured for the slag HCP. Carbonation for slag HCP progressed slowly compared with that for the slag-free HCP. The amount of combined water was corresponded to Ca/Si mole ratio in C-S-H, that was, C-S-H having low Ca/Si molar ratio exhibited the high water content.

Table 2 Amount of compound and mechanical properties of HCP

HCP	Amount of compound (wt %)			Ca/Si mole ratio in	Void volume	Compressive strength	Bending strength	Fracture toughness
	$Ca(OH)_2$	$CaCO_3$	H_2O*	C-S-H	(%)	(MPa)	(MPa)	(MPa·$m^{0.5}$)
PC1	1.9	0.8	8.4	1.8	6.2	72.5(Sd. 7.9)	4.2(Sd. 0.7)	-
PCS1	0.4	0.6	10.6	1.5	6.3	92.1(6.6)	3.7(0.8)	-
PCSW1	0.9	0.7	14.5	1.5	0.1	80.4(12.3)	13.1(2.9)	-
PC3	9.0	5.8	9.1	2.1	16.2	80.5(6.6)	11.4(2.0)	0.30
PCS3	2.7	3.1	11.7	1.6	14.9	92.3(9.6)	3.1(0.7)	0.15
PCSW3	3.1	2.8	15.4	1.5	0.2	100.9(12.5)	7.6(1.5)	0.15

* The amount of H_2O corresponded to the weight loss below 450℃

The microstructure of each HCP after bending test was shown in Fig.1. In slag-HCP, the unreacted slag fairly remained. The crack in any HCP propagated through the C-S-H and calcium hydroxide[3], rather than around or through unreacted slag or cement particles.

The bending and compressive strength of each HCP were shown in Table 2 and Fig.2. The higher compressive strength were observed for any slag-HCP compared with those for slag-free HCP. However, the bending strength for slag-HCP did not increase with curing time[4]. Furthermore, the fracture toughness for slag-HCP was 0.15 $MPam^{0.5}$, which was lower than those for slag-free HCP[5]. These weakness in tension suggested that crack easily propagated in C-S-H or CH. As the amount of CH in slag HCP was smaller than that in slag-free HCP, crack propagation rate was mainly contributed by the properties of formed C-S-H, which was related to the low Ca/Si mole ratio for slag HCP.

Fatigue properties of HCP

In order to express the fatigue behavior quantitatively, the data were normalized using the following equation derived from the crack propagation rate equation on the subcritical crack growth, $V=A(K_I/K_{IC})^n$ where V is crack growth rate, K_I is stress intensity factor and K_{IC} is its critical value[2]. A, n are constants known as fatigue

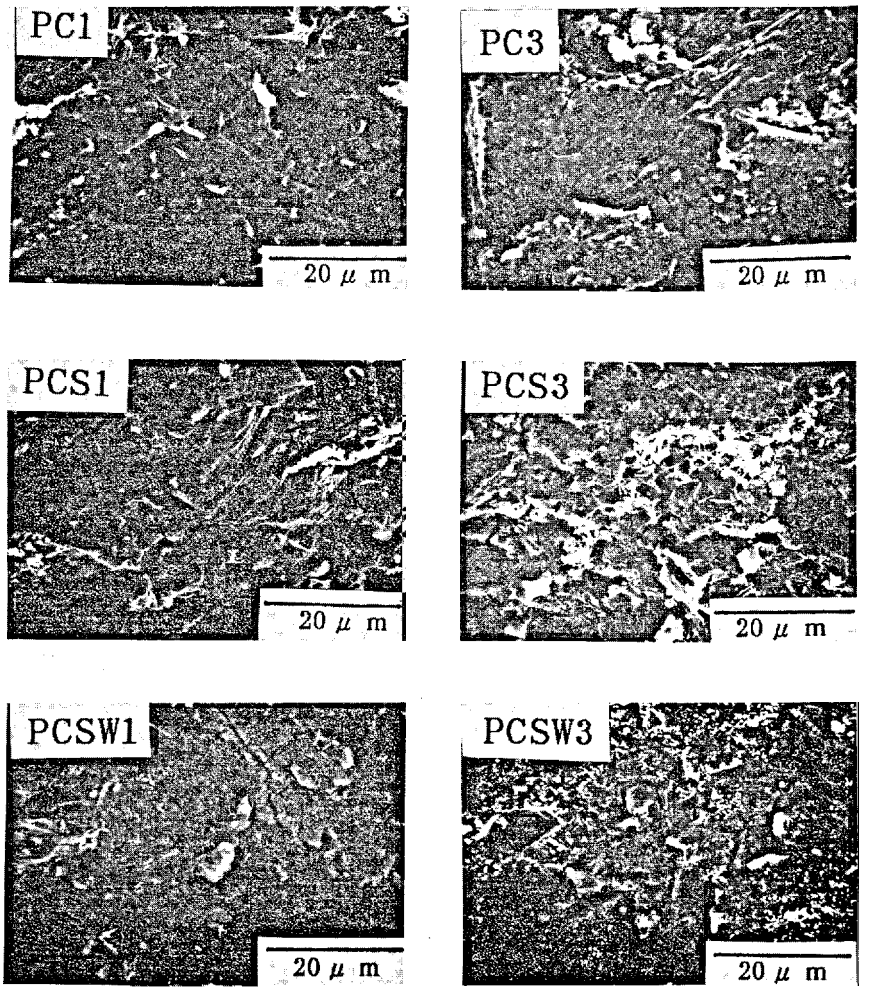

Fig.1 Micrographs of fracture surface in HCP

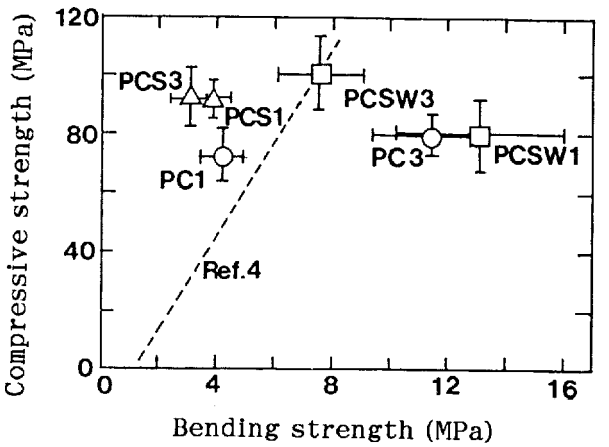

Fig.2 Compressive and bending streth of HCP

parameters of the material at a given load condition.

$$\log(\sigma_{max}/S_f)=[-1/(n+1)]\log(t_f \cdot g^{-1}) - \log[(n+1)/\sigma_{max}]^{1/(n+1)} \quad (1)$$

where σ_{max} is maximum applied stress , S_f is the bending strength, t_f is time to failure, and g^{-1} is the term relative to the applied stress wave-form.

The other fatigue parameter ΔA was calculated from the constant value A,

$$\log \Delta A=\log\{t_f\}_S-\log\{t_f \cdot g^{-1}\}_C + \log[(n_s-2)/(n_c-2)]+(n_s-n_c)\log(\sigma_{max}/S_f) \quad (2)$$

where n_s or n_c is the n value at static or cyclic fatigue test, respectively.

The fatigue results normalized by above equation were shown in Fig. 3. Static fatigue test results were indicated by the solid line and the range of standard deviation by the dashed line, as obtained by the least square method. The acceleration to the short life side under cyclic test became clear with stress ratio, but their tendency were different in each case.

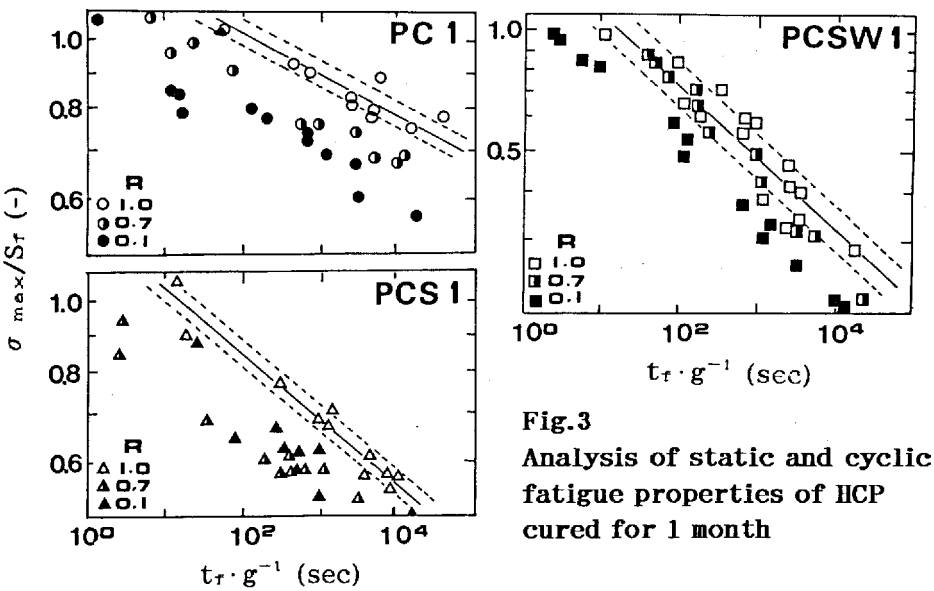

Fig.3
Analysis of static and cyclic fatigue properties of HCP cured for 1 month

The fatigue behavior also could be discussed using fatigue parameters. The material having large n value was hard to fracture at applied stress under its bending strength. The small n value suggested the fracture depended on applied stress. The change of n values of HCP with stress ratio was shown in Fig.4. The n values for any HCP were constant with stress ratio, but n values for PC1 were larger and suggested the tough material. This fatigue behavior corresponded to larger fracture toughness. The change of log Δ A with stress ratio was also shown in Fig.4. Its positive value means the

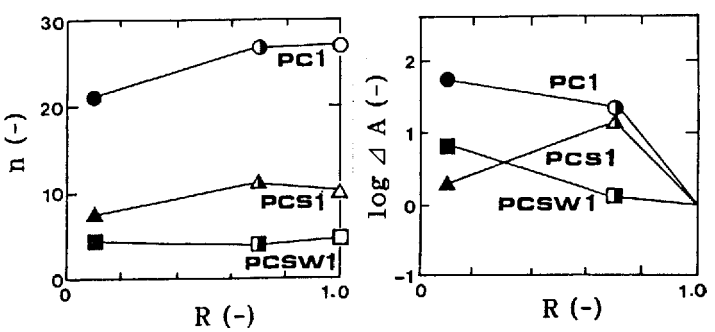

Fig.4 Relations between stress ratio R and fatigue parameter n (left) and log Δ A (right)

acceleration to the short life side. The PC1 was affected significantly by stress ratio under cyclic fatigue, but for the specimen PCSW1 did not. Two kinds of fatigue mechanism must be discussed for HCP, similar to other ceramics. One is the crack propagation mode due to mechanical cyclic stress at crack tips and the other is fractography at the fracture surface behind the crack tips. For any HCP, the crack deflection always occurred. Therefore, the larger deflection might occur in HCP having the tight bonded C-S-H, which formed in PC1. Then, these deflections might brought the complicated crack path to accelerate toward the short life side under cyclic fatigue.

4. CONCLUSIONS

Microstructure and mechanical properties of hardened cement paste incorporating ground granulated blast-furnace slag were investigated and the following conclusions were obtained.

(1) The larger combined water, smaller void fraction and small amount of calcium hydrate were measured on the HCP containing slag. Carbonation progressed slowly compared with that for the slag-free HCP.

(2) The replacement of slag increased the compressive strength of HCP, though not the bending strength, at least in early stage of hydration. The fracture toughness and the fatigue parameter n in the crack propagation rate equation, was lower than those for the slag-free HCP.

(3) The fracture surface in HCP containing slag suggested that crack propagated preferentially through the C-S-H and calcium hydroxide.

(4) The bending strength and fracture toughness accompanied with instantaneous fracture was probably dependent on the component and mechanical properties of hydrates. While, the fatigue behavior was mainly dependent on the property of C-S-H.

REFERENCES

1) T.Nishikawa et al., CAJ Proc. of Cement & Concrete **44**,98(1990)
2) M.Takatsu et al., J.Ceram.Soc. Japan, **98**,1343(1990)
3) I.Jawed et al., Cement & Concrete Res., **17**,433(1987)
4) J.J.Beaudoin et al., ibid., **15**,105(1985)
5) J.J.Beaudoin, Il Cemento, **4**,195(1985)

THE HYDRATION BEHAVIOUR OF METAKAOLIN - $Ca(OH)_2$ - SULPHATE BINDERS

P S de Silva and F P Glasser

Department of Chemistry, University of Aberdeen
Aberdeen, Scotland, UK

Summary -

Metakaolin ($Al_2Si_2O_7$) is a pozzolanic material obtained by heating kaolin in the temperature range 450-800°C. Metakaolin is used in blended cements but it can also be considered for use in OPC free binders. In the present study, the use of metakaolin as a pozzolanic material was investigated. The hydration behaviour of metakaolin/$Ca(OH)_2$ system was studied with and without sulphates. Early hydration was studied by calorimetry. The development of solid hydrates, pore fluid chemistry and the microstructural development of these systems up to 180 days cure are discussed in relation to compressive strength development.

Sulphate additions are favourable for strength properties. The presence of mica impurity in kaolinite is found to have a major effect on the pore fluid composition. During calcination, the alkali content of muscovite mica is activated and is readily and rapidly released during subsequent reaction with gypsum and calcium hydroxide. This influences the formation of hydrates, as shown by microstructural studies. In general, the hydration behaviour of metakaolin/calcium hydroxide system shows pronounced similarities to OPC hydration, especially in terms of heat evolution and set characteristics.

Résumé

Métakaolin ($Al_2SiO_2O_7$) est un matériaux ayant des propriétès pozzolaniques qui est obtenu en cuissant du kaolin entre 450 et 800°C. Métakaolin est utilisé dans les 'blended' cements et peut aussi être envisagé dans le ciment Portland sans liants. Dans le travail rapporté ici, l'utilisation du métakaolin en tant que matériaux pozzolanique a été étudiceé. L'hydratation du système métakaolin/$Ca(OH)_2$ a été étudiée seule ou en présence de sulphates. Le début de l'hydratation a été suivie par calorimetrie. L'évolution des hydrates formés, de la composition de la solution et de la microstructure, a été suivie en relation avec la résistance durant les 180 premiers jours de l'hydratation.

L'ajout de sulphates est bénéfique pour la résistance. La présence d'impuretés de mica dans la kaolinite à une influence marquée sur la composition de la solution. Pendant la calcination, les alkalins contenus dans la muscovite sont activés et ainsi assent plus rapidement en solution. Ceci influence la formation des hydrates comme le démontre l'étude de la microstructure. En général, l'hydratation du système métakaolin/$Ca(OH)_2$ présente beaucoup de similarités avec l'hydratation du ciment Portland spécialement en ce qui concerne la chaleur dégagée et les caractéristiques de la prise.

INTRODUCTION

'Metakaolin' (MK) is a nearly-anhydrous solid obtained by heating kaolin in the temperature range 450-800°C. Metakaolin shows pozzolanic properties and is known to be a useful blending agent for cement. It can also be considered for use in cement-free binders, especially in tropical or sub-tropical countries where kaolin is widely available.

Metakaolin reacts with $Ca(OH)_2$ and water at 20°C to yield a number of hydration products: C-S-H, C_4AH_{13}, C_2ASH_8 and C_3AH_6 (1,2). Addition of gypsum gives initial rapid formation of ettringite, which is subsequently converted to monosulphate (3,4).

Mechanical properties of $MK/Ca(OH)_2$ binders have been reported by Murat (5). Palomo and Glasser (6) reported the effects of NaOH activation in obtaining chemically-bonded, cementitious materials from metakaolin. At or near ambient temperature cures gave a gel binder with good strengths.

In the present investigation the hydration behaviour of the $MK/Ca(OH)_2$ system has been studied in the presence of different secondary activators: NaOH, Na_2SO_4 and ß-anhydrite ($CaSO_4$) with and without NaOH. The extent and kinetics of various competing reactions at early stages of hydration were investigated by calorimetry. The evolution of the chemical environment of both solid and liquid phases during hydration and the microstructures up to 180 days cure are discussed and related to compressive strength.

MATERIALS AND EXPERIMENTAL

Metakaolin was obtained by heating kaolin (Table 1) at 730°C for six hours; Na_2SO_4 (AnalaR), NaOH (AnalaR) and $Ca(OH)_2$ (GPR) were obtained from BDH, Poole, England and ß-anhydrite obtained from ICI. The mix formulations prepared in this study are given in Table 2. Calorimetric data were obtained at 40°C, using a JAF conduction calorimeter, from mixes with a w/s ratio of 0.8.

Cylinders of 4.2 cm diameter and 8.2 cm height, were prepared according to the above mix formulations and cured in a humidity chamber at 40°C and 98% relative humidity. After the strength measurements, the samples were treated with acetone and ether to stop hydration and carbonation and dried at 50°C in a nitrogen atmosphere. The hydrates present in the pastes were subsequently identified by XRD and DTA techniques.

Table (1)
Analysis of Kaolin

Oxide	wt. %
SiO_2	55.23
Al_2O_3	41.23
TiO_2	0.04
Fe_2O_3	0.83
MnO	0.01
SO_3	0.04
MgO	0.34
CaO	0.09
Na_2O	0.02
K_2O	2.02
P_2O_5	0.15

L.O.I. = 13.0%

A separate set of 4.2 x 8.2cm cylinders was prepared and cured at identical conditions to study the chemistry of the aqueous phase of mixtures. Al, Si, K, Na, Ca and sulphate present in the pore fluid extractions were analysed: procedures are given in (7).

The microstructure and morphology of the hydrated pastes were determined by transmission and scanning electron microscopy using a JEOL 2000EX Temscan.

Table (2)
Mix Formulations

3:1 Metakaolin : $Ca(OH)_2$ compositions

Mix No.	MK/CH (mass ratio)	W/S (mass ratio)	Aqueous
a	1	0.8	H_2O
b	1	0.8	0.5M NaOH

3:2 Metakaolin : $Ca(OH)_2$ - sulphate compositions

Mix No.	MK/CH (mass ratio)	Source of sulphate	SO_3/Al_2O_3 molar ratio)	W/S (mass ratio)	Aqueous
c	1	ß-anhydrite	0.1	0.8	H_2O
d	1	ß-anhydrite	0.1	0.8	0.5M NaOH
e	1	Na_2SO_4	0.1	0.8	H_2O

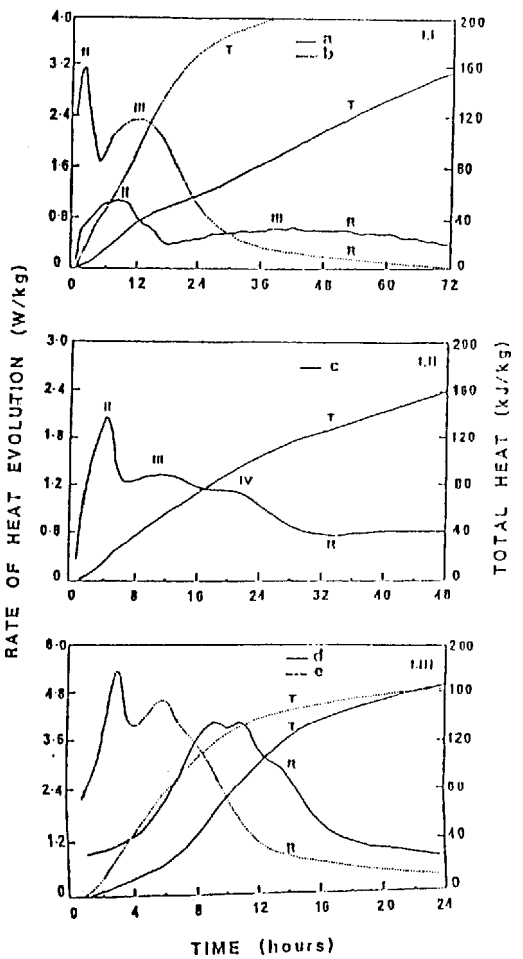

Fig. 1 Rate of heat evolution (R) (left scale) and total heat output (T) right hand scale) of mix formulations (Table 2).

RESULTS

Since $Ca(OH)_2$ was always added, the text will generally note only the secondary activator(s) which were used in conjunction with $Ca(OH)_2$.

Calorimetry

The patterns of rate of heat evolution and total heat evolution are shown in Figure 1. Apart from the rapid heat evolution which occurs immediately after initial mixing of the paste, termed exotherm I, the rate of heat evolution patterns of the systems without sulphates (a,b) consists of two main exotherms, designated II and III (Fig. 1.i). In the presence of sulphates (Fig. 1.ii and 1.iii), in addition to exotherm I, three other peaks are present, viz. II, III and IV. A detailed study of these exotherms in relation to the microstructural development and their effects on thermochemistry are reported in (4). When sulphate is absent the two exotherms, preceded by exotherm I, were due to the formation of hydrates, mainly C_4AH_{13} and C-S-H. In the presence of sulphates, after exotherm I, changes in the rate of heat evolution pattern were due to three major reactions; (i) formation of ettringite, (ii) formation of C_4AH_{13} and C-S-H and (iii) transformation of ettringite to monosulphate. It has been shown by theoretical calculations of heat evolutions that processes (i) and (ii) are exothermic while (iii) is endothermic. Thus the appearance

of peaks III and IV were due to the occurrence of an endotherm superimposed on the broad exotherm from C-S-H formation.

Development of hydrates during middle and late period of hydration

Development of hydrates, as identified by XRD and DTA, is given in Table 3. In systems without sulphate. the hydrates present at 3 days are C_4AH_{13}, C-S-H and C_2ASH_8. Hydrogarnet appears in both systems after 3 days of hydration. As the hydration progresses, gehlenite hydrate and C_4AH_{13} disappear. This sequence is most rapid in the system activated with NaOH.

In systems with sulphates, after 24 hrs hydration, the solids present are monosulphate, C-S-H and C_4AH_{13}. Monosulphate also disappears after some time with the appearance of hydrogarnet. Sulphate is probably partly sorbed in C-S-H and partly retained in solid solution in "C_4AH_{13}". Gehlenite hydrate also appears. The C_4AH_{13} phase is either absent or present only in traces in the sulphate-activated systems, especially after longer cure durations. Some sulphate was present in the pore solution. The initial development of ettringite and its subsequent phase transformations are clearer in system (c) than in alkali/sulphate activated systems such as (d). In all systems, most of the $Ca(OH)_2$ had reacted by 10 days.

Compressive Strength Development

Compressive strength development of the samples are given in Fig. 2. All activators tend to improve early strengths of the MK/$Ca(OH)_2$ system. The effect of NaOH on the strength is significant at early stages, but less or insignificant at later stages. However, continuous strength gain occurs for at least 180 days.

Beta-anhydrite makes a considerable contribution to the strength, although strength of this system remains nearly constant between 28 and 90 days after which it again rises. The effect of beta-anhydrite/NaOH system shows higher late strengths than the system activated by NaOH only.

Scanning Electron Microscopy

As revealed by SEM, NaOH in the absence of sulphates creates a featureless, massive structure at early stage of hydration, with essentially no visible porosity. This explains the high early strengths (Fig. 2). However, at later stages in this system the matrix becomes inhomogeneous and crystalline (Fig. 3.i and 3.ii). The increasing crystallinity of hydrates may be responsible for the lessened or insignificant effect of NaOH on the strength at late stages. In the presence of sulphates, NaOH gave an amorphous structure even at late stages.

The morphology of the hydrates were also strongly influenced by the nature of the activators used. Na_2SO_4 gave well crystallized C_2ASH_8 as hexagonal platelets, whereas in system(a), the same phase had a less regular, more rounded plate-like appearance. A

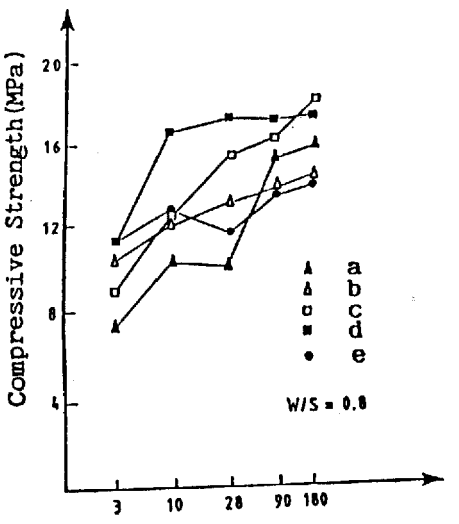

Fig. 2 Compressive strength development for compositions in Table 2.

Table (3)
Hydrates identified by XRD and DTA

Curing time	a	b	c	d	e
24hr	CH,C_4, C-S-H	CH,C_2,C_4, C-S-H	AF_m,C_4,CH, C-S-H	AF_m,C_4, CH,C-S-H	AF_m,C_4, CH,C-S-H
28 days	C_2,C_4, C_3,C-S-H	C_2,C_3,C_4, C-S-H	C_3(tr),C_2,C_4, C-S-H	C_3,C_2,C_4, C-S-H	C_3,C_2,C_4, C-S-H
90 days	C_2,C_4, C_3,C-S-H	C_4 tr),C3, C-S-H	C_3,C_4(tr),C_2, C-S-H	C_3,C_2, C-S-H	C_3,C_2, C-S-H
180 days	C_2,C_4(tr), C-S-H	C_3,C-S-H	C_2,C_3,C-S-H	C_3,C_2, C-S-H	C_3,C_2 C-S-H

a,b,c,d,e - Mixtures as described in Table (2).
CH-$Ca(OH)_2$, C_4-C_4AH_{13}, C_3-C_3AH_6. C_2-C_2ASH_8, AF_t-ettringite, AF_m-monosulphate.

detailed correlation of porosity and microstructure with strength is reported in (7).

Pore Fluid Analysis

An important observation on the pore solution data is the presence of potassium (Fig. 4). The K^+ content of the pore fluid is surprisingly high, given that no potassium was added. Since the kaolin used in these experiments contained 2.02% K_2O, mainly in the form of muscovite, it is supposed that heating activates muscovite and felspar. In contact with Ca at high pH, thermally activated minerals undergo ion exchange and/or reaction. Systems supposedly formulated without an alkali activator,(a and c) actually contain significant K^+ which contributes substantially to the observed alkalinity, hence the pH is in the range 12.6 - 12.8; OH^- and K^+ approximately charge balance each other. The pore solution K^+ content increases at early stages (3-10 days), but subsequently decreases with time. As disclosed by AEM, some of the potassium is absorbed by C-S-H; the composition of C-S-H of systems (a) at 28 days is $C_{1-1.3}SA_{0.17}K_{.015-.03}$. Other aspects of pore solution chemistry are described in (7).



3i

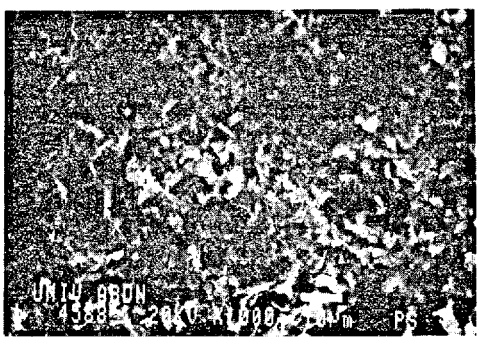

3ii

Fig. 3 SEM of fracture surfaces of NaOH activated system (b) at 3 days (3.i) and 90 days (3.ii).

DISCUSSION

The present study reveals more information about the hydration behaviour of metakaolin, which shows many similarities to that of Portland cement. According to calorimetric

studies, both systems are characterised by rather large heat evolutions during the first 24 hours; 180kJ/kg for an OPC, and comparable values for metakaolin systems. Portland cement liberates heat in bursts, each correlating with particular mineralogical changes. Metakaolin systems behave similarly.

As with Portland cement a continuous strength gain occurs with time, even after 28 days. There is a nearly linear relationship between compressive strength and log [cure time]. Formulation affects the slope of the curve, but not the general relationship between cure time and strength. For the best combination - beta-anhydrite and CH activator - 20 MPa is obtained at 6 months, with no indication of a limit having been reached. Mechanical properties of MK systems mostly depend on the space filling properties of the hydrates, as with OPC. Space filling is not a simple or straightforward process and is affected by phase transformations occurring during hydration as well as changes to the crystallinity and morphology of hydrates.

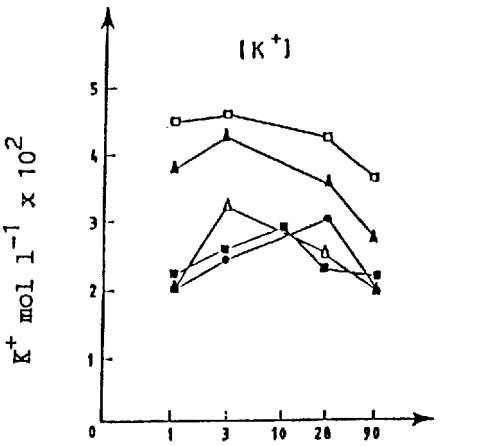

Fig. 4. Pore solution K^+ concentration (symbols as indicated in Fig. 2).

The main phase transformation process occuring in the absence of sulphates is the formation of dense hydrogarnet - most probably containing silicon - from less-dense C_2ASH_8 and C_4AH_{13}, which are metastable. This transformation occurs most rapidly in formulations with NaOH. Mass balance calculations show that the above transformation is associated with a decrease in solid volume. This would lead to an increase in porosity and degradation of the microstructure, which results in limiting paste strengths. This is one of the reasons for the observed effect of NaOH on the strength properties at late stages. In sulphate-containing systems, hydrogarnet is also formed as a transformation product where it is mainly associated with disappearance of monosulphate. This formation of hydrogarnet subsequent to set is reminiscent of the well documented process of conversion in high alumina cements (HAC). As with HAC, strength continues to improve once the conversion reactions are completed.

The information regarding the effect of mica-like impurities on the hydration is important. When muscovite is present as an impurity, it is apparently activated by heating, and its dissolution or ion exchange increases the pH of the pore fluid, hence increases the ratio of $CaOH^+/Ca^{2+}$. This, in turn, enhances the solubility of aluminium and silicon species. The gross inequalities in solubilities of three main constituents are somewhat reduced with the result that gehlenite hydrate and C-A-S-H gel are able to develop. At later stages, C-A-S-H acts as one of the hosts for released potassium. Therefore, the release of K from activated mica changes the overall chemistry, hence the hydrate balance. Thus, in obtaining metakaolin from kaolinite, it is important to choose a temperature which also activates any alkali-containing impurities.

CONCLUSIONS

The hydration behaviour of metakaolin cement systems show pronounced similarities to OPC hydration, especially in terms of heat evolution and set characteristics. NaOH, $CaSO_4$ and the combination of these two are effective activators for $MK/Ca(OH)_2$ reactions. Strength is mainly associated with the space filling

properties of the hydrates. An important phase transformation may occur during hydration; formation of relatively dense hydrogarnet from less-dense, hexagonal hydrates. Formation of hydrogarnets temporarily affects strength gain properties, but with the completion of the conversion reactions, strength gain resumes.

Muscovite in the raw material is activated during calcination and releases potassium, with subsequent enhancement of metakaolin reactivity, most notably with $Ca(OH)_2$ and $CaSO_4$. Therefore, in the calcination of kaolinite, the conditions that favour the activation of muscovite merit further investigation. Pozzolanic mixes made without Portland cement probably have sufficient strength for a range of applications.

REFERENCES

1. Ambroise, J., Murat, M. and Pera, J.: "Investigations on Synthetic Binders Obtained by Middle-Temperature Thermal Dissociation of Clay Minerals". Silicate Industriels, 1986, 7-8, 99-107.
2. Taylor, H.F.W. Chemistry of Cements Vol. 2, London, Academic Press, 1964.
3. Turriziain, R. and Schippa, G.: 1954, Ric. Sci. 24 2645.
4. De Silva, P.S. and Glasser, F.P.: "Hydration of Cements Based on Metakaolin: Thermochemistry". Adv. Cem. Res. 1990, 3 167-177.
5. Murat, M.: "Hydration Reaction and Hardening of Calcined Clays and Related Minerals: I Preliminary Investigation on Metakaolinite". Cem. Conc. Res. 1983 13 259-266.
6. Palomo, A. and Glasser, F.P.: "Chemically-Bonded Cementitious Material Based on Metakaolin". British Ceramic Transactions and Journal, 1991 (submitted).
7. De Silva, P.S. and Glasser, F.P.: "Pozzolanic Activation of Metakaolin". Adv. Cem. Res. 1991, (in press).

CHEMICAL BINDING OF WATER DURING THE HYDRATION OF PORTLAND CEMENTS AND BLAST-FURNACE SLAG CEMENTS BLENDED WITH FLY ASH

Reiner Härdtl

Institute for Building Research, Aachen University of Technology
Aachen, GERMANY

SUMMARY

The hydration mechanisms of portland cement clinker are influenced by the latent-hydraulic and pozzolanic reaction of granulated blast furnace slag and fly ash, materials used in blended cements or as concrete additive, respectively. As a result of teir use the structure of the hydration products and other related properties of hardened cement paste can change significantly. The scope of this paper is the investigation of the effect of fly ash on the amount of chemically bound water in combination with portland and blast furnace slag cements.

In the early stage of reaction the hydration of portland and blast furnace slag cement is accelerated by the use of fly ash which results in a higher amount of bound water after 1 and 2 days. At higher ages the amount of bound water is not increased essentially by the pozzolanic reaction of the fly ash. The dominant part of water bound in the CSH-phases produced by pozzolanic reaction is transformed from the reaction partner $Ca(OH)_2$. As a result there is only a small increase in the volume of the hydration products scarcely reducing the total porosity of the cement paste. The pore size distribution, however, is changed distinctly.

ZUSAMMENFASSUNG

Durch ihre latent-hydraulische bzw. puzzolanische Reaktionsfähigkeit beeinflussen Zementzumahlstoffe oder Betonzusatzstoffe wie Hüttensand und Steinkohlenflugasche die Hydratationsmechanismen des Portlandzementklinkers. Dies kann zu einer deutlichen Änderung der Struktur der Reaktionsprodukte und daraus resultierender anderer Eigenschaften führen. Ziel dieses Beitrages ist es, die Wirkung von Flugasche in Kombination mit Portland- und Hochofenzementen auf die Hydrationsmechanismen anhand der chemischen Wasserbindung zu untersuchen.

In der Frühphase der Reaktion wird die Hydratation von Portland- und Hochofenzement durch die Verwendung von Flugasche beschleunigt, was zu eine höherer Wasserbindung nach 1 und 2 Tagen bewirkt. Durch die puzzolanische Reaktion der Flugasche in höherem Alter wird der Gehalt an chemisch gebundenem Wasser nicht wesentlich erhöht. Der größte Anteil des durch die puzzolanische Reaktion in den CSH-Phasen eingebundenen Wassers wird aus dem Reaktionspartner $Ca(OH)_2$ umgesetzt. Dies hat nur eine geringe Volumenzunahme der Reaktionsprodukte zur Folge, wodurch die Gesamtporosität des Zementsteins kaum reduziert wird. Die Porengrößenverteilung wird dagegen deutlich verändert.

INTRODUCTION

The amount of water chemically bound in hardened cement paste during hydration is a parameter to determine the degree of reaction between cement and water. Taking into account the water-cement ratio, the quantity of gel produced by hydration and the reduction of porosity can be calculated, values from which mechanical properties, pore structure or the resistance against various attacks can be estimated /1/.

In the last years the quantity of additives like granulated blast-furnace slag and fly ash used as components of blended cements or directly added to concrete in the mixer is increasing. The latent-hydraulic or pozzolanic reactivity of these materials influence the hydration characteristics of cement. As a result the structure of the hydrated phases and other properties of the hardened cement paste change. In this paper the effect of fly ash on the chemical binding of water in combination with different portland cements and slag cements is studied.

EXPERIMENTIAL

Eight different cements complying with the German cement standard DIN 1164 were used. Three portland cements (C1 to C3) from different cement plants, one portland filler cement (C4, 18% limestone filler) and four cements containing blast-furnace slag (C5 to C8) were selected. In the case of cements C5, C6 and C8, which originate from the same cement plant, the slag content varied between 26, 50 and 77 wt.%. With 49 wt.% of slag cement C7 has approximately the same slag content as C6, but was produced using a different clinker and a different slag. The main properties of the cements are summerized in Table 1.

Table 1: Properties of cements

Cement	Type of cement	slag content wt.%	specific surface cm^2/g	2d-strength N/mm^2	28d-strength N/mm^2
C1	Portland cement	-	2690	17.8	49.9
C2	Portland cement	-	3380	28.5	45.6
C3	Portland cement	-	3870	24.7	55.8
C4	Portland-filler cement	18[1)]	4650	20.9	50.5
C5	Portland-slag cement	26	3490	21.0	48.7
C6	Blast-furnace slag cement	50	3700	16.2	48.8
C7	Blast-furnace slag cement	49	3530	13.4	45.1
C8	Blast-furnace slag cement	77	3900	9.8	49.7

1) Limestone filler

A low-calcium fly ash equivalent to ASTM-Class F fly ashes from a dry-bottom furnace was used. The fly ash had a specific surface of 3790 cm^2/g, and 16.5 wt.% residue on 40 μm sieve. The glass content was about 80 wt.% and the loss on ignition was 1.7 wt.%.

Mortars were produced from mixes with 450 g cement or cement+fly ash and 1350 g standard sand (0.08 to 2 mm) in accordance with DIN 1164. The ratio of fly ash to cement (f/c) was 0, 0.25 and 0.50. The ratio water to binder w/(c+f) = 0.60 was held constant for all mixes. The mortars were demoulded after 24 hours and stored under water (20 °C) until testing.

For chemical analysis pieces of arround 50 g were broken from the mortars, dried at 105 °C and ground to a fineness < 63 μm. The amount of chemically bound water was determined by Karl-Fischer titration. This method gave very good correlations to results determined by thermogravimetry (TG). The amount of free $Ca(OH)_2$ in cement paste was analysed by extraction with Franke method. With extraction not only CaO in free $Ca(OH)_2$ is determined, but also CaO-components of other hydration products are extracted /2,3/. By reducing the measured values by a factor of 0.85, a good correlation was found with results obtained by TG for all mixes. Pore size distribution was determined by mercury intrusion porosimetry in the range of 100 μm to 1,8 nm.

RESULTS AND DISCUSSION

Early stage of hydration

Figure 1 shows the amount of bound water per unit of cement at an age of 2 days. Portland cements C2 and C3, and portland-filler cement C4 have the highest amount of bound water. Portland cement C1 has a slower initial reactivity, therefore the degree of hydration is lower at this age. With increasing slag content the amount of bound water decreases. This is attributed to the slow latent-hydraulic reaction of the slag which has to be activated by the reaction of portland cement.

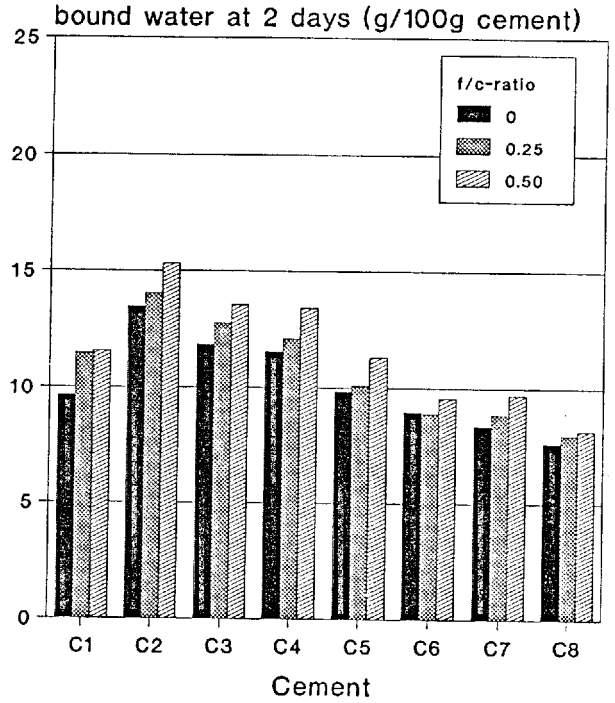

Figure 1:
Bound water at 2 days

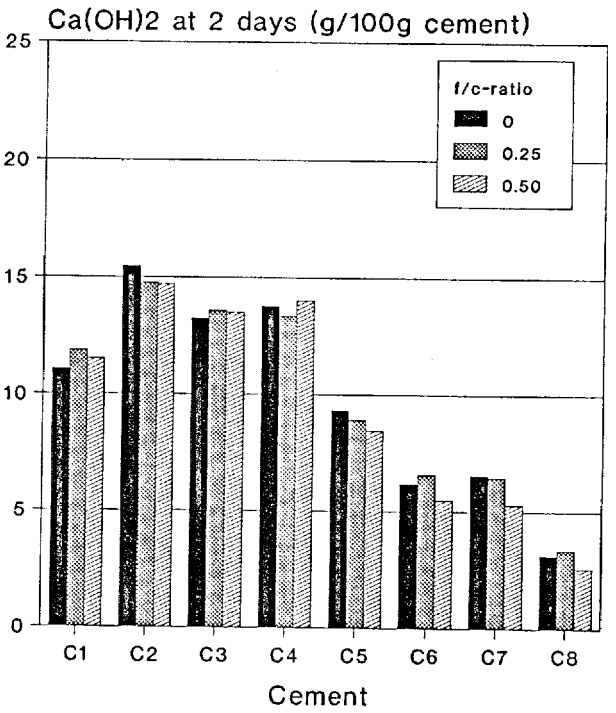

Figure 2:
Ca(OH)2-content at 2 days

If fly ash is used, the amount of water bound in the hydration products related to the cement content increases with increasing fly ash content. Assuming that pozzolanic reaction of fly ash has not started at that age /4/, it indicates an acceleration in the hydration of the cement components. This enhancement is explained by several researchers, e.g. /4,5,6/ due to the presence of fine filler particles acting as nucleation sites onto which additional hydrates can form. In tendency, this effect is remarkable for all cements irrespectively of their slag content.

In contrast to bound water, the amount of $Ca(OH)_2$ liberated by cement hydration at 2 days is not changed significantly by fly ash within the possible scatter of test results (Figure 2). Independent of the fly ash content, the measured values of the fly ash mixes are in some cases larger, in the other cases they are lower than the mortars without additive. After 1 day of hydration the $Ca(OH)_2$-content of the mixes with f/c = 0.25 is generally lower for all cements than the mixes without fly ash.

These test results imply, that the higher amount of water combined by accelerated reaction of cement is not bound in $Ca(OH)_2$, but in other hydrated phases. In early hydration age of portland cement mainly the clinker minerals C_3S and C_3A are reacting. An enhanced C_3S-hydration of cement would increase the binding of water as well as the liberation of $Ca(OH)_2$ provided of an unchanged composition of the produced calcium silicate hydrates. On the other side, the hydration of C_3A (and also of C_4AF) consume $Ca(OH)_2$ for their reaction to produce calcium aluminate hydrates. Taking these mechanisms in consideration, a parallel enhancement of both reactions can be concluded by the use of fly ash. As result, the amount of bound water

is increased whereas the content of $Ca(OH)_2$ remains unchanged. This result is valid for all investigated cements independent of their slag content. Whether there is any change in the reaction of the slag cannot be answered at the moment.

Influence of pozzolanic reaction

The start of the pozzolanic reaction of fly ash can be estimated by the reduction of the $Ca(OH)_2$ content in the cement paste. Figure 3 compares the development of $Ca(OH)_2$ of mortars without (f/c =0) and with fly ash (f/c = 0.25) for cements with different slag contents (C2,C5,C6,C8). With increasing slag content the amount of free lime decreases because the latent hydraulic reaction liberates no or only small amounts of $Ca(OH)_2$. The slag in cement C6 (50 wt.% slag) consumes some $Ca(OH)_2$ for their reaction (see Fig.3).

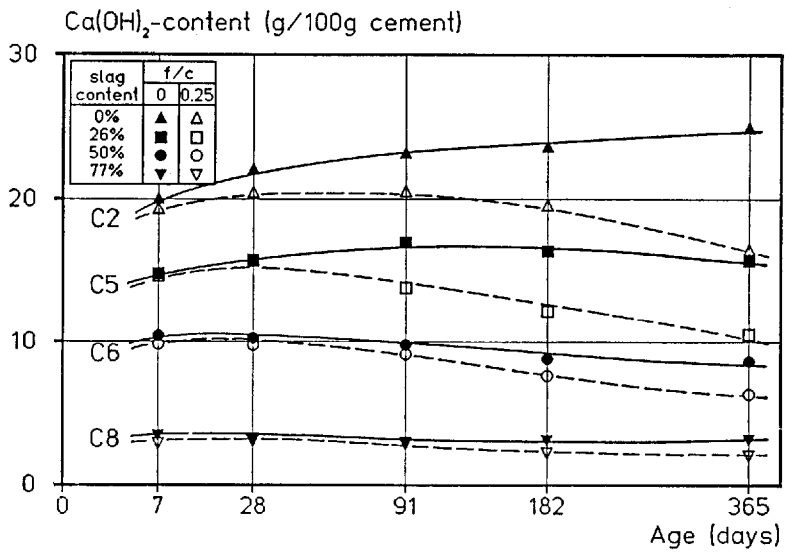

Figure 3: Development of $Ca(OH)_2$ content

With increasing hydration time the $Ca(OH)_2$ content is reduced by fly ash. For portland cement this consumption has the highest value indicating a high degree of pozzolanic reaction which has started at an age of arround 7 days. With increasing slag content the reduction of $Ca(OH)_2$ decreases. For cements containing 26 and 50 wt.% slag the pozzolanic reaction starts after a hydration time of 28 days. In the mortar containing cement C8 with 77 wt.% slag the alkalinity of pore solution is reduced in a proportion that only a small amount of fly ash is dissolved and accessible for pozzolanic reaction /7/. Therefore the consumption of $Ca(OH)_2$ is only low.

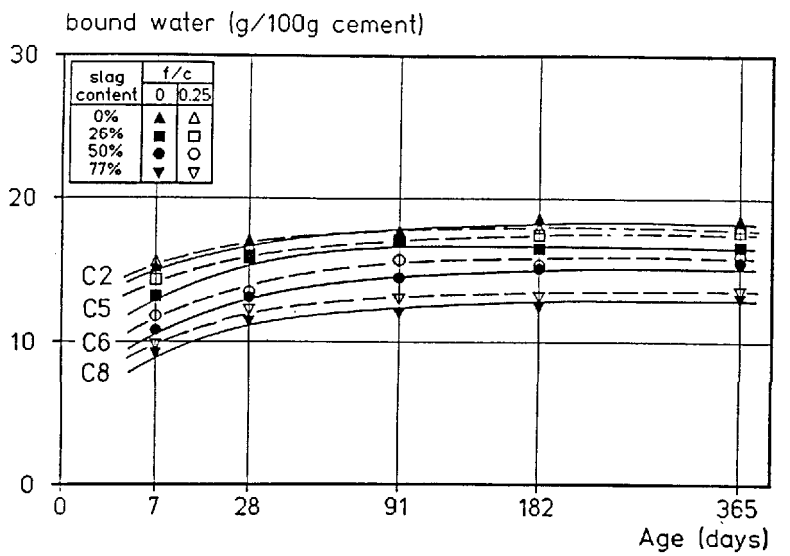

Figure 4: Development of bound water

The development of the amount of bound water shows an increase with time for all mixes (Figure 4). In the mortars there is less water combined in the hydration products with increasing slag content mainly resulted by a smaller $Ca(OH)_2$ content. Therefore the amount of water bound in the CSH-phases is nearly equal for all cements (Figure 5). CSH-phases in this context simplified means all hydration products in their various compositions except $Ca(OH)_2$. Only cement C7 shows higher values probably indicating a higher reactivity of the slag.

The curves of the amount of bound water of the fly ash containing mixes show the same development as the mortars without additive. In tendency the values of the fly ash mixes are slightly higher compared to the corresponding reference mixes. The difference nearly corresponds to the increased amount of bound water resulted by the determined enhancement of cement reaction in the early stage of hydration. This means that no significant quantity of additional water is bound in the phases produced during the pozzolanic reaction of fly ash. The water combined in $Ca(OH)_2$, liberated during cement hydration, is transformed to new CSH-phases formed by the pozzolanic reaction of the glassy fly ash components and $Ca(OH)_2$. The time the pozzolanic reaction starts and the degree of this reaction, both factors depending on the slag content of cement, have no influence on the total amount of bound water.

In contrast to that, the amount of water combined in CSH must be increased by pozzolanic reaction of the fly ash. This is confirmed by the results at an age of 365 days shown in Figure 5. Especially for cements C1 to C4, where the pozzolanic reaction has already reached a high degree, there is a distinct increase of water bound in CSH with increasing f/c-ratio. This effect is deminished with increasing slag content of the cement. For cement C8 containing 77 wt.% slag, where only low pozzolanic reaction was determined, the slight increase of water bound in CSH is mainly dependent on the enhancement of cement hydration in the early stage of hydration.

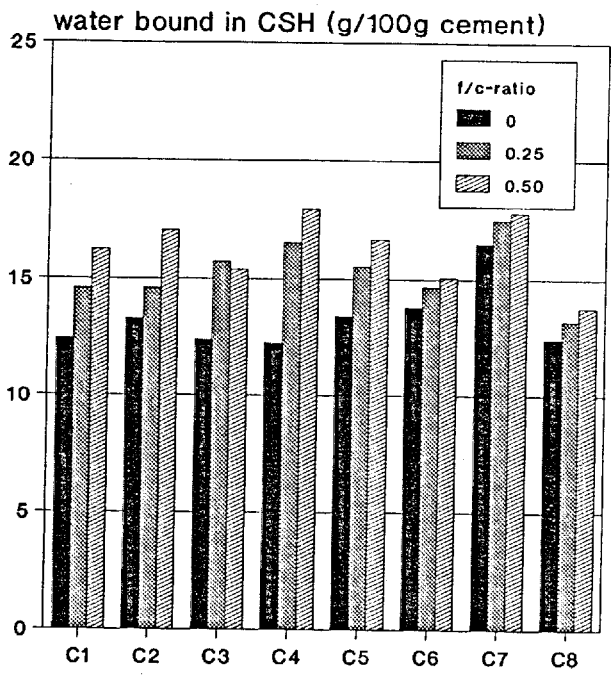

Figure 5:
Water bound in CSH-phases at 365 days

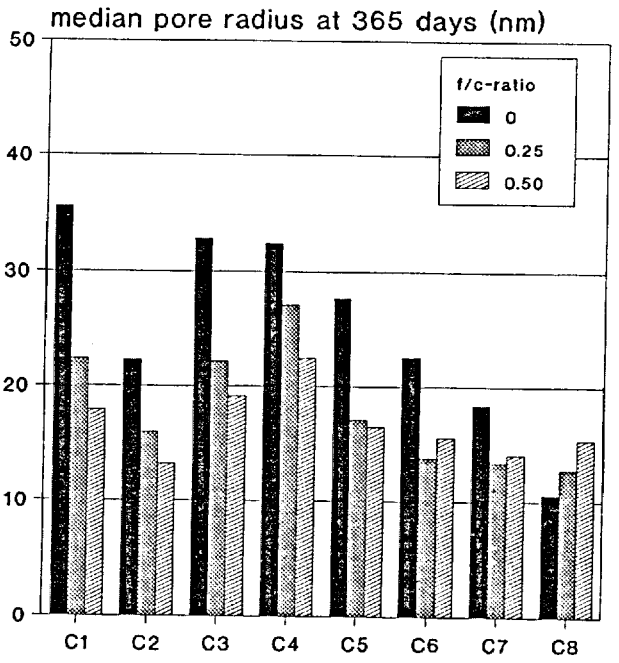

Figure 6:
Median pore radius at 365 days

Change in pore structure

By the chemical binding of water during cement hydration phases are formed with a higher specific volume compared to the unreacted cement particles. Therefore the total porosity of cement paste is generally reduced with increasing degree of hydration. Because no additional water is bound during pozzolanic reaction, no significant change in total porosity is caused by the reaction of fly ash /8/.

On the other hand, the pore size distribution is shifted to finer pores with increasing fly ash content. This effect is shown in Figure 6 where the median pore radius is used to characterize the measured pore size distributions. During pozzolanic reaction the amount of coarse cristallin $Ca(OH)_2$ is reduced and transformed to CSH-gel building very fine gel pores whereas the quantity of capillary pores decreases. Only in cement C8 which has already a very dense pore structure due to the latent-hydraulic reaction of the large content of slag and where no significant pozzolanic reaction of fly ash was determined, fly ash cannot lead to a further densification.

CONCLUSIONS

The use of fly ash accelarates the hydration of cement in the early stage of hydration acting as a nucleation site onto which additional hydrates could form. This enhancement is subjected to the C_3S-reaction as well as to the hydration of C_3A resulting in a larger amount of bound water whereas the $Ca(OH)_2$-content remains nearly unchanged. This behaviour is valid for portland cement, portland filler cement and blast furnace-slag cement irrespective of their slag content.

During the pozzolanic reaction of the fly ash there is no significant amount of additional water chemically bound in the hydrated phases. The water combined in $Ca(OH)_2$, liberated during cement hydration, is transformed to new CSH-phases formed by the pozzolanic reaction of the glassy fly ash components and $Ca(OH)_2$. The degree of pozzolanic reaction and the slag content of cement have no significant influence on this behavior.

ACKNOWLEDGEMENT

The investigations for this publication were supported by the VGB -Technische Vereinigung der Großkraftwerksbetreiber e.V., Essen-.

REFERENCES

/1/ Powers, T.C.: The nonevaporable water content of hardened portland-cement paste - Its significance for concrete research and its methods of determination. ASTM-Bulletin No.158, 1949, pp. 68-76

/2/ Ramachandran, V.S.: Differential thermal method of estimating calcium hydroxide in calcium silicate and cement paste. Cem. Concr. Res., Vol.9, No.6, 1979, pp. 677-684

/3/ Shebl, F.A.; Helmy, F.M.; Ludwig, U.: Investigations relating to the determination of calcium hydroxide by the Franke method. TIZ-International, Vol.107, 1983, No.7, pp. 476-479, No.9, pp. 646-648

/4/ Sybertz, F.; Wiens, U.: Effect of fly ash fineness on hydration characteristics and strength development. Int. Conf. on Blended Cements in Construction, Sheffield 1991, (Swamy, R.N. (Ed.))

/5/ Dalziel, J.A.; Gutteridge, W.A.: The influence of pulverized-fuel ash upon the hydration characteristics and certain physical properties of a portland cement paste. Cement and Concrete Association, Technical Report No.560, 1986

/6/ Larbi, J.A.; Bijen, J.M.J.M.: Effects of water-cement ratio, quantity and fineness of sand on the evolution of lime in set portland cement systems. Cem.Concr.Res., Vol.20, No.5, 1990, pp. 783-794

/7/ Fraay, A.L.A.; Bijen, J.M.J.M.; de Haan, Y.M.: The reaction of fly ash in concrete - A critical examination. Cem.Concr.Res., Vol.19, No. 2, 1989, pp. 235-246

/8/ Härdtl, R.: Effect of the combination of slag cements and fly ash on the pore structure of cement mortars. 4. Int. Conf on the Use of Fly Ash, Silica Fume, Slag and Natural Pozzolans in Concrete, Istanbul, 1992 (to be published)

20-YEAR STUDY ON HYDRATION OF HIGH MAGNESIA CEMENT WITH FLY ASH AT AMBIENT TEMPERATURE

S S Rehsi and S K Garg

Central Building Research Institute
Roorkee, INDIA

SYNOPSIS

The paper presents data on compressive strength, tensile strength, volume expansion and hydration products in high magnesia cement (MgO content 10%) blended with 30% fly ash, by weight hydrated for 20 years in water at an ambient temperature of 27 $\pm 2^{o}$C. The data show that the fly ash imparts soundness i.e. volume stability in high magnesia cement. The characterisation of the X-ray diffractogramss and differential thermal analysis of the hydrated high magnesia cement, with and without fly ash, confirms the formation of CSH, ettringite, $Mg(OH)_2$, $Ca(OH)_2$ and $CaCO_3$. In addition, the presence of unhydrated MgO, quartz and mullite in high magnesia cement with fly ash and unhydrated MgO in high magnesia cement without fly ash, is also indicated. The scanning electron micrographs are given to show the microstructure of the hydration products.

INTRODUCTION

Investigations were undertaken in the late sixties to develop technology for utilising high magnesian limestone in cement manufacture (1). Some of the findings, which have already been reported (2-4), showed that incorporation of reactive siliceous materials such as fly ash, 'Surkhi' (powdered calcined clay pozzolana etc.) in high-magnesia cement (MgO content upto 15%) imparts the desired soundness i.e. volume stability as determined by the standard autoclave test (5). Subsequently, a long-term study was undertaken to determine whether the incorporation of fly ash is also effective in stabilising high-magnesia cement on hydration at ambient temperature of 27 $\pm 2^{o}$ C. The results obtained at different periods of hydration show that the fly ash is effective in stabilising high-magnesia cement having 10% MgO (6-9). This observation is confirmed by the data obtained at 20 years of hydration and reported here.

MATERIALS USED

1. High Magnesia Cement : The high magnesia cement was obtained by grinding high magnesia cement clinker produced in a pilot plant rotary kiln using raw meal consisting of high magnesian limestone and clay, with 4% gypsum by weight to a specific surface (Blaine) of 3423 cm^2/g. The chemical composition of the clinker was : CaO 61.68%, SiO_2 21.45%, Al_2O_3 4.41%, Fe_2O_3 2.46%, MgO 10.0% and free CaO 2.45%.

2. Fly Ash : The chemical composition of the fly ash used was : SiO_2 59.17%, Al_2O_3 25.59%, Fe_2O_3 7.13%, CaO 2.74%, MgO 1.28%, SO_3 0.28% and loss on ignition 3.15%. Its lime reactivity test strength determined according to IS:1727-1960 (10) was 59.8 kg/cm^2.

3. Water : Normal tap water was used.

TEST PROCEDURES

1. Test specimens consisting of rectangular bars 2.5cmx2.5cmx25cm (effective gauge length), 7.07 cm cubes (face area 50 cm^2) and 8-shaped briquettes having 2.5x2.5cm section at the centre, for measuring wetting expansion, compressive strength and tensile strength respectively, were cast following the method specified in IS:1727-1960 and IS:269-1958 (11). The mortar mix used for casting the test specimens consisted of 1 part of high magnesia cement with and without 30% fly ash and 3 parts of single-sized standard Ennore sand (passing 800 micron and retained on 600 micron IS: sieves) by weight.

   The specimens for the study of hydration products by differential thermal analysis (DTA), X-ray diffraction and scanning electron microscopy were 2.5x2.5cm in section and 12.5cm long. These were cast using neat high magnesia cement paste, with and without 30% fly ash, by weight at standard consistency. Demoulding after 24 hrs of moist curing, all the test specimens were kept in water maintained at 27 ± 2°C and were taken out at the time of testing

2. The DTA was carried out by raising the temperature of the furnace at a uniform rate of 10°C per minute. The specimen block was of the pattern of Grimshaw et al (12). The differential thermocouple made of chromel and alumel wires were connected to a sensitive galvanometer.

3. X-ray differactograms of the hydrated high magnesia cement with and without fly ash, were taken by a Philips X-ray Diffractometer (Model No. 1730) using Nickel filtered CuK_{α} radiation.

4. Scanning electron micrographs of the hydrated high magnesia cement with and without fly ash, were taken by a scanning electron microscope (SEM 501, Philips, Holland).

RESULTS AND DISCUSSION

Development of Strength

Data on the development of compressive strength and tensile strength in high magnesia cement (HMC) with and without 30% fly ash by weight, obtained at 3,7,28,90,180 and 365 days and 2,3,4,5,6,7,12,14,15 and 20 years of storage in water at 27 ± 2°C is shown in Fig.1. It shows that the compressive strength as well as the tensile strength of high magnesia cement without fly ash observed after 90 days and continued to fall thereafter. As compared to this, the compressive strength and the tensile strength of high magnesia cement containing 30% flyash by weight continued to rise appreciably during the first two years and crossed over the corresponding strength in high magnesia cement with-out fly ash within 230 days and 100 days, respectively. The upward development of strength in high magnesia cement containing fly ash during the first 2 or 3 years and its remaining more or less constant thereafter indicates a strong stabilising influence of fly ash.

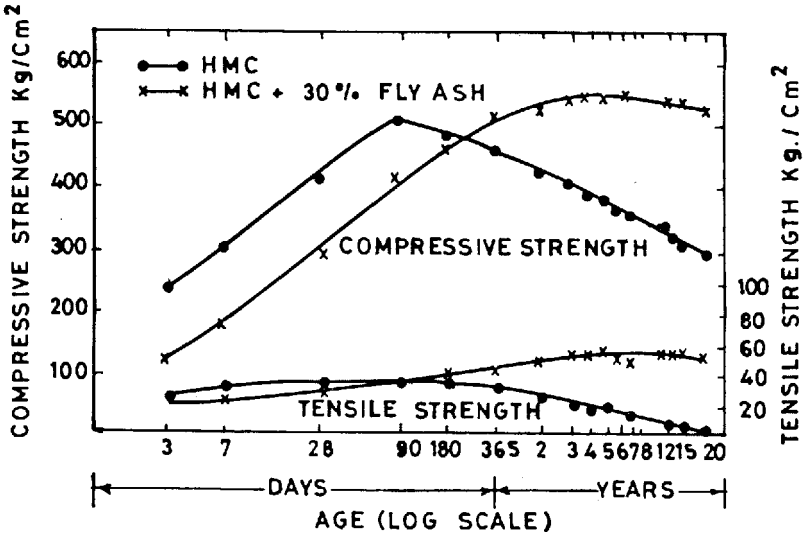

Fig. 1. Development of compressive strength in high magnesia cement with and without fly ash on continuous storage in water at 27 ±2°c for 20 years

Wetting Expansion

Further evidence of the efficacy of fly ash in stabilising high magnesia cement is provided by the data on wetting expansion, determined in terms of percentage increase in length of 2.5x2.5x25cm bars measured by a length comparator (10), over a period of 20 years and shown in Fig.2.

It can be seen that in sharp contrast to high magnesia cement without fly ash which showed an expansion of 1.833 % after 14 years (5110 days) of storage in water at 27 ± 2°C, the expansion in high magnesia cement containing 30% fly ash, by weight, at 20 years (7300 days) of storage in water at 27±2°C was only 0.263%.

The bars made with high magnesia cement (HMC) showed bending due to excessive expansion during continuous storage in water at 27±2°C. At 15 years (5475 days), these bars could not be fitted in the length comparator for taking measurements.

Hydration Products

DTA thermograms of high magnesia cement with and without 30% fly ash, by weight, hydrated by continuous storage in water at 27±2°C for different periods upto 20 years are shown in Fig.3 and Fig.4 respectively. The first endothermic peak in all these thermograms is at 115-140°C.

It can be seen that all the thermograms of high magnesia cement hydrated for different periods are identical. Similarly, all the thermograms of high magnesia cement containing fly ash hydrated for different periods are identical except for the one at 28 days hydration. In this thermogram, there is an additional endothermic peak at 510°C.

The identification of endothermic peaks at 115-140°C, 400-410°C, 510-530°C, 770-780°C and 880-900°C in Fig.3 shows the presence of free water/CSH/ettringite, $Mg(OH)_2$, $Ca(OH)_2$, $CaCO_3$ and CSH respectively in high magnesia cement at all ages of hydration upto 20 years. The endothermic peaks at 115-140°C, 400-410°C, 770-780°C, 800-870°C and endothermic peak at 550°C in Fig.4 also show the presence of these minerals together with unburnt carbon, in high magnesia cement containing fly ash at all ages of hydration except at 28 days which shows an additional endothermic peak of $Ca(OH)_2$ at 510°C.

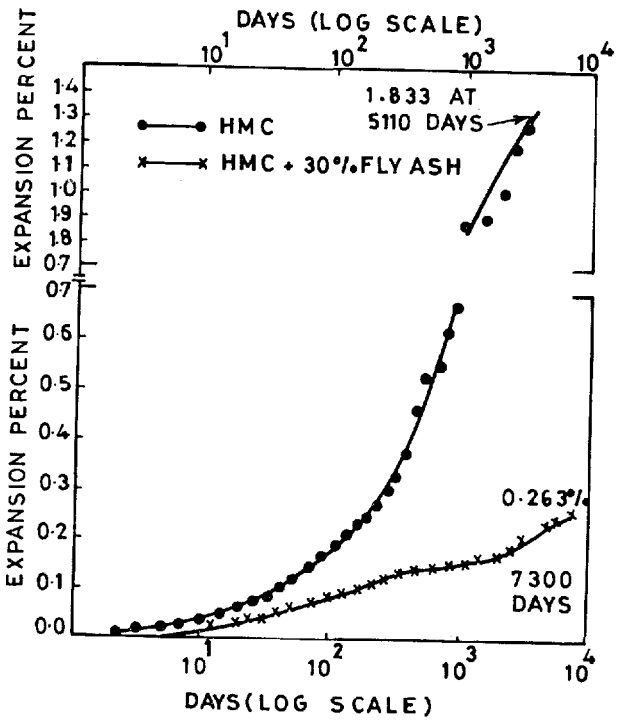

Fig. 2. Wetting expansion of high magnesia cement with and without fly ash on continuous storage in water at 27 ± 2 °c for 20 years.

X-ray diffractograms of high magnesia cement with and without fly ash hydrated for 20 years are shown in Fig.5. Their characterisation confirms the formation of CSH, ettringite, $Mg(OH)_2$ and $CaCO_3$. In addition, the presence of unhydrated MgO, quartz and mullite in high magnesia cement with fly ash and unhydrated MgO in high magnesia cement without fly ash is also indicated.

Figs. 6 & 7 show scanning electron micrographs of the hydration products in high magnesia cement, with and without fly ash, hydrated for 20 years.

CONCLUSIONS

The following conclusions can be drawn from the 20 years data on development of strength and wetting expansion reported here.

1. High magnesia cement containing 10% MgO can be effectively rendered sound i.e. volume stable, under normal hydration conditions of temperature and pressure, by the addition of 30% fly ash, by weight.

2. Hydrated high magnesia cement with and without fly ash, contains CSH, ettringite, $Mg(OH)_2$, $Ca(OH)_2$ and $CaCO_3$ as hydration products. In addition, the presence of unhydrated MgO, quartz and mullite in high magnesia cement with fly ash and unhydrated MgO in high magnesia cement without fly ash is also indicated.

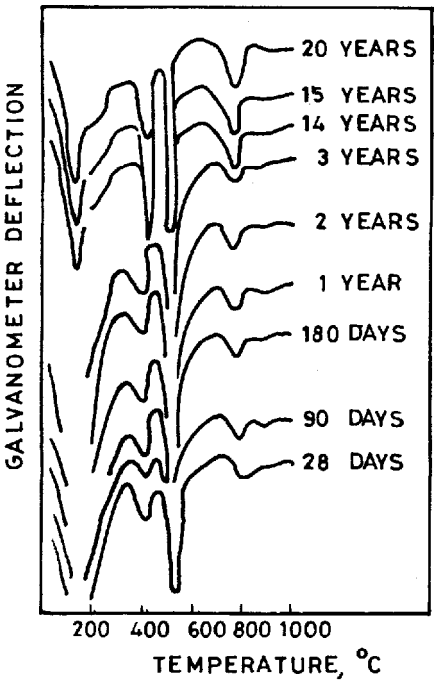

Fig.3. DTA Thermograms of high magnesia cement hydrated for different period upto 20 years in water at 27± 2 °c

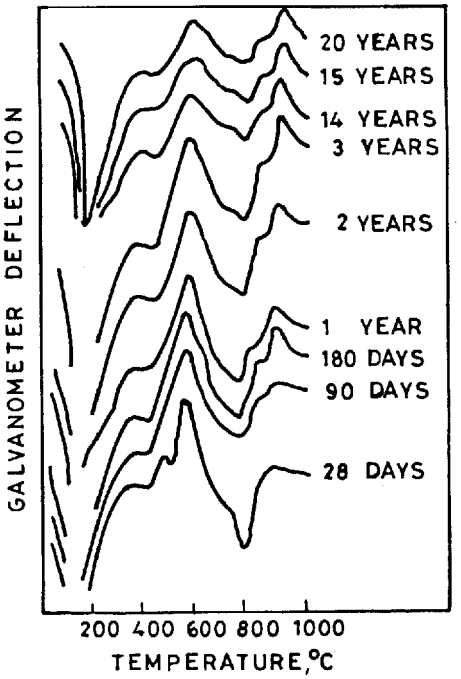

Fig.4. DTA thermograms of high magnesia cement containing 30% fly ash, by weight hydrated for different periods upto 20 years in water at 27 ± 2 °c

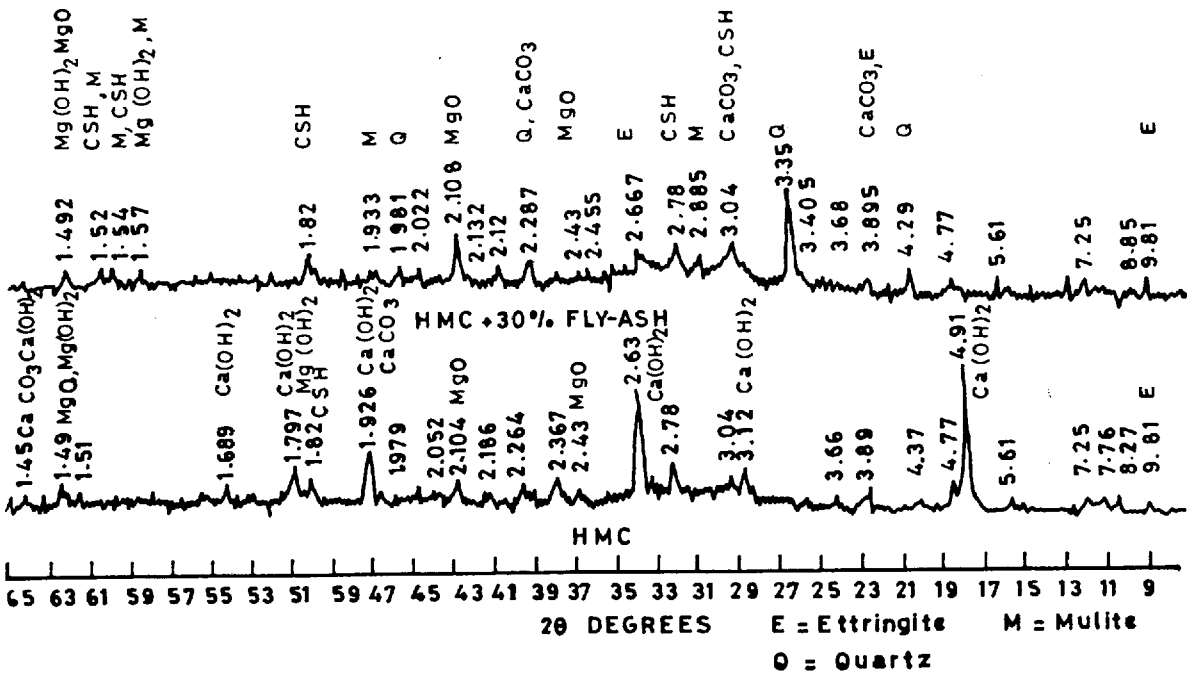

Fig. 5. X-ray diffractograms of high magnesia cement with and without fly ash hydrated for 20 years in water at 27 ± 2 °c

(a) 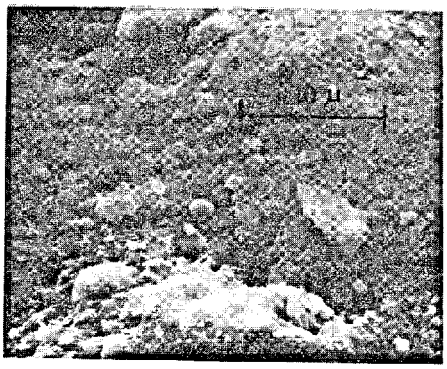

(b) 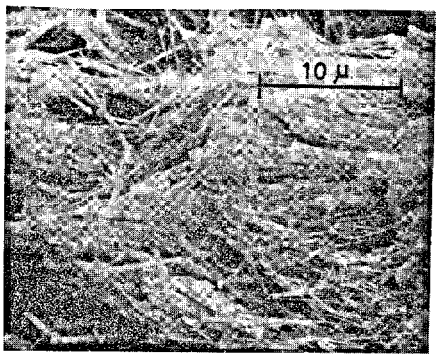

Fig. 6 Scanning electron micrographs showing (a) a general view and (b) needle-like crystals in high magnesia cement hydrated for 20 years in water at $27\pm2^{o}C$.

(a) 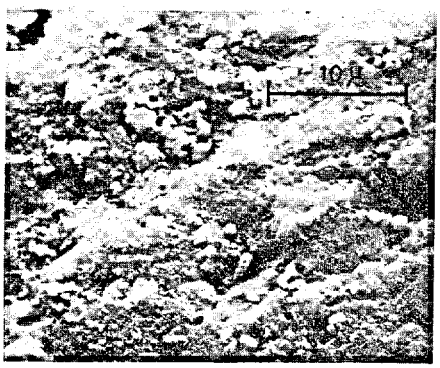

(b) 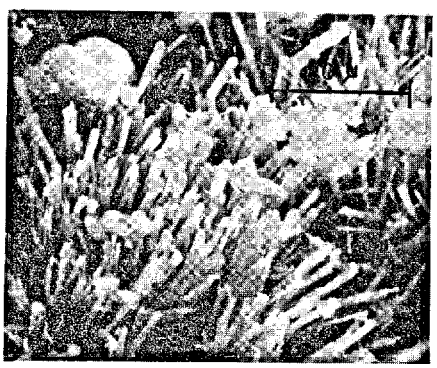

Fig.7 Scanning electron micrographs showing (a) a general view and (b) needle-like crystals in high magnesia cement with 30 percent fly ash, by weight, hydrated for 20 years in water at $27\pm2^{o}C$.

3. The data provide a good basis for the cement industry in countries having vast reserves of high magnesian limestone, to undertake production of sound high magnesia cement utilising fly ash. As shown in an earlier study (3) any other reactive siliceous material such as 'Surkhi' in place of fly ash, would be equally effective in stabilising high magnesia cement.

ACKNOWLEDGEMENT

The study reported here formed a part of the normal research programme at Central Building Research Institute, Roorkee (U.P.), India, and is presented by the permission of Director.

REFERENCES

1. Rehsi, S.S., Physico-chemical studies on the utilisation of high magnesian limestone for making Portland cement, Ph.D.Thesis, Punjab University, Chandigarh, India, May 1968.

2. Rehsi, S.S. & Majumdar, A.J., High magnesia Portland cements : Studies on cements prepared with reagent grade chemicals, Magazine of Concrete Research, 1969, 21 (67), 67-68.

3. Rehsi, S.S. and Majumdar, A.J., High magnesia Portland cement : Study of Cement prepared with commercial raw materials, Indian Concrete Journal, 1969, 43(6) 221-226.

4. Majumdar, A.J. & Rehsi, S.S., Mechanism of stabilisation of high magnesia Portland cements by reactive silica under autoclave conditions, Magazine of Concrete Research, 1969, 21(68) 141-150.

5. Indian Standards Institution, IS:4031-1968, Method of physical tests for hydraulic cement (Second reprint), New Delhi, 1976, 16-21.

6. Rehsi, S.S. and Garg, S.K., Room temperature stabilisation of high magnesia cement with fly ash, Zement-Kalk-Gips, 1975, 28(2), 84-87.

7. Rehsi, S.S., Magnesium Oxide in Portland cement, Advances in Cement Technology, Edited by S.N.Ghosh, Pergamon Press Ltd., Oxford, U.K.,. 1983, 467-493.

8. Rehsi, S.S. and Garg, S.K., Long-term study on stability of high magnesia cement containing fly ash, Durability of Building Materials, 1985, 2, 265-273.

9. Rehsi, S.S and Garg, S.K., 15-year study of high magnesia cement with fly ash at ambient temperature, Proc. First NCB International Seminar 'Pragmatic Strategies for Productivity and Modernisation', New Delhi, 1987, 4, X48-X57.

10. Indian Standards Institution, IS:1727-1960 Methods of test for pozzolanic materials, New Delhi, 1968, 22-28.

11. Indian Standards Institution, IS:269-1976, Specification for ordinary and low heat Portland cement (3rd revision), New Delhi, October, 1976.

12. Grimshaw, R.W., Heaton, E. and Roberts, A.L., Constitutions of refractory clays : Introduction and thermal analysis methods, Trans. Brit. Ceram. Soc., 1945, 44, 69-92.

INHIBITION OF BLENDING MATERIALS ON EFFECT OF EXCESS SO_3 CONTENT IN CEMENT

Lian Huizhen and Chen Enyi

Department of Civil Engineering, Tsinghua University
Beijing, P R CHINA

SUMMARY

It is known that excess SO_3 will make strength of cement reducing and unfavourable expanding. But it is shown by experiments that such harmful effect of SO_3 can be inhibited by suitable blending material. When the added blending material is more than a certain proportion, strength decreases gently, and owing to adding the blending material by suitable proportion, there is possibility of increasing SO_3 content in cement to be 4-5% without unfavourable expansion, i.e. when cement is blended by suitable proportion, the strength can not be reduced by excess SO_3. Furthermore, it would be better to use anhydrite instead of gypsum as a supplier of SO_3.

摘　要

水泥中超量的SO_3会造成水泥强度下降和有害的体积膨胀。但实验表明，合适的混合材料可以抑制SO_3这种有害的作用；当混合材料掺入超过一定量时，可使水泥强度下降减缓，而由于加入适量的混合材料，就有可能使水泥中SO_3含量增加到4～5%而不致产生有害的体积膨胀；在水泥中加入合适掺量的混合材料，可避免因水泥中SO_3过量而降低强度。试验还证明，用硬石膏替代二水石膏以提供SO_3时上述抑制作用更为明显。

INTRODUCTION

There are stipulations in specifications of most countries to limit the amount of SO_3 in cement, as excessive amounts of SO_3 may cause setting time fast by contrast, and induce harmful expansion and strength reducing[1]. In case of utilization on industrial solid waste containing SO_3 to be blending material of cement, to allow the excessive amounts of SO_3 would make good sense. Moreover, that is favourable to utilizing various kind of waste gypsum. I. Odler reported that fineness of cement and the form of SO_3 existing are important factors to effect the resultant expansion and strength of cement besides phase composition of clinker itself. Thus it may exist the possibility to increase the amount of added calcium sulphate if other relevant factors are opitimized[2]. C. Ouyang et al considered that substitution of a portion of Portland cement with fly ash is an effective means to inhibit the internal sulphate attack[3]. Observation by E. Irassar shows that PFA mortars presented a decreasing expansion rate within the time and it was zero at 90 days. And in Portland cement mortar, expansion rate was approximately constant until 180 days, even 360 days[4]. This is due to the "dilution effect" called by Mehta[5], i.e. effect of relative decrease of C_3A in cement.

Above mentioned results are attractive for industrial practice. Within this paper, influence of different blending materials and different form of calcium sulphate on effect of the amount of SO_3 in cement are explored further.

MATERIALS USED

Natural zeolite-tuff containing clinoptilolite from Nenjiang of China, fly ash from Beijing and FBC ash from Hubei of China are used as blending materials of Portland cement. Gypsum and anhydrite (from gypsum burned at 500°C for two hours) are used as set regulator of cement. Composition of above materials are shown is table 1.

TABLE 1
Chemical compositions of blending materials used

Materials	SiO_2 (%)	Al_2O_3 (%)	Fe_2O_3 (%)	CaO (%)	MgO (%)	K_2O (%)	Na_2O (%)	SO_3 (%)	LOI (%)	Activity ratio (%)
FBC ash	69.17	16.26	8.14	1.22	1.00	1.31	0.16	2.62	1.22	20.0
Clinoptilo-lite tuff	61.60	14.40	2.20	3.79	1.85	3.13	0.10	0	12.83	26.9
Fly ash	51.62	17.49	11.33	1.39	0.83	2.40	0.08	0	12.88	11.9
Gypsum	4.27	1.87	0.45	32.47	1.82	--	--	33.08	27.73	--
Anhydrite	9.75	2.00	0.80	36.39	0.93	--	--	42.76	6.72	--

ABOUT THE SETTING TIME

By experiments, it is known as follow[6]: for Portland cement, the minimum amount of SO_3 is about 1.3% (to make the initial setting time to be about one hour), but if the FBC ash containing II-$CaSO_4$ (an anhydrite similar to above mentioned burned gypsum) is mixed with clinker by 3:7, the minimum amount of SO_3 in form of II-$CaSO_4$ is about 2%. Along with the blended amount increasing, the minimum amount of SO_3 in form of II-$CaSO_4$ is increased over a certain degree (e.g. 3%), the setting time would delay with the amount of blending materials increasing, i.e. the blending materials could exercise a

moderating influence on effect of setting time of cement. Therefore, the setting time concerned is considered satisfactory to be employed in this paper, and only strength and expansion are being discussed.

TESTS AND RESULTS

Effect of FBC ash

Anhydrite is used for control the amount of SO_3 in cement blended with FBC ash by varied amount. Compressive strength of specimens are shown in fig.1 (cured under standard condition).

In fig.1 it is shown that when FBC ash is blended, the strength reducing with amount of SO_3 increasing is gently. More FBC ash is blended, more effect is marked.

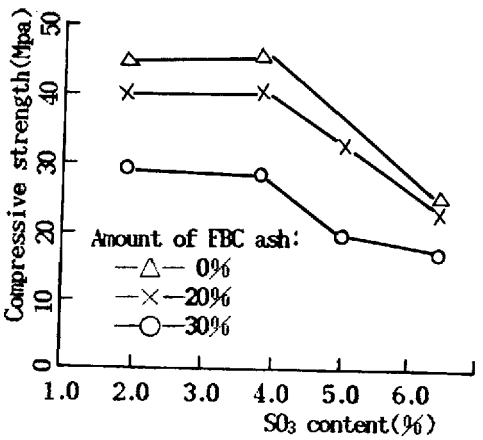

Fig.1 Change of Compressive strength with the amount of SO_3 as blending FBC ash by varied blending amount

Fig.2 shows the change of the linear expansion of cement paste vs. the blending amount of FBC as SO_3 is varied to 2.6%, 3.8%, 4.7%.

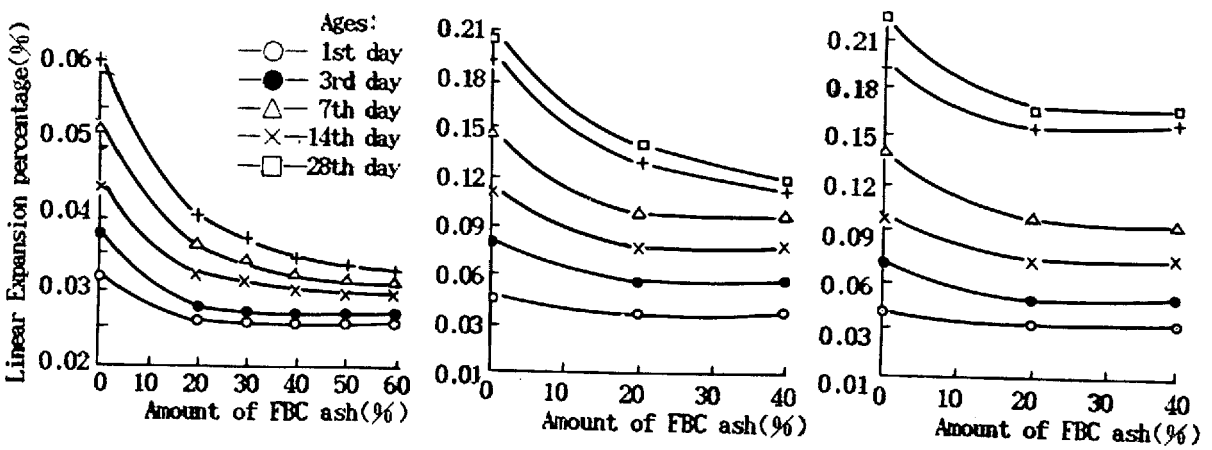

Fig.2 The linear expansion of cement paste vs. the blending amount of FBC ash as SO3 is varied

From fig.2, it is shown that the linear expansion have been inhibited markedly so long as FBC ash is blended over 20% (by weight of total binder), and hardly effected by the further increase of blending amount of FBC ash. This inhibited effect is enhanced with ages. More the amount of SO_3 exists, more evident above mentioned situation is. In other hand, see fig.3, as SO_3 is below 4%, the linear expansion increases quickly with the amount of SO_3 and the increase rate elevates with age. But when SO_3 is over 4%, expansion at varied ages hardly increases with the amount of SO_3.

Effect of SO_3 in different form

Anhydrite and gypsum are used in Portland cement by varied dosages separately, Compressive strength of mortar with above specimens are shown in fig.4.

It is shown from fig.4 that either earlier or later, strength of mortars with anhydrite are higher than with gypsum, and the optimum of SO_3 in form of anhydrite is higher than in form of gypsum, i.e. if anhydrite is used, SO_3 content in cement can be increase to exceed the limit. The linear expansion of mortar with anhydrite is less than with gypsum, and the longer the age runs the large the difference of expansion is.

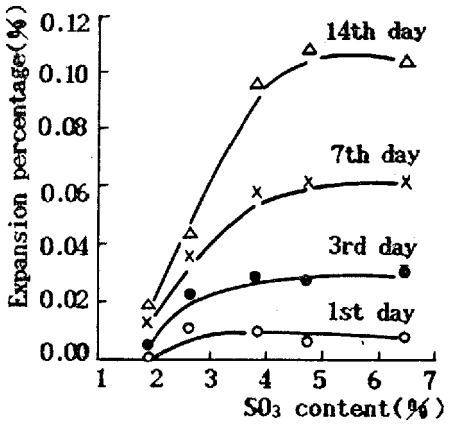

Fig.3 Linear expansion vs. SO_3 content in case of blending FBC ash by 40% at expected ages

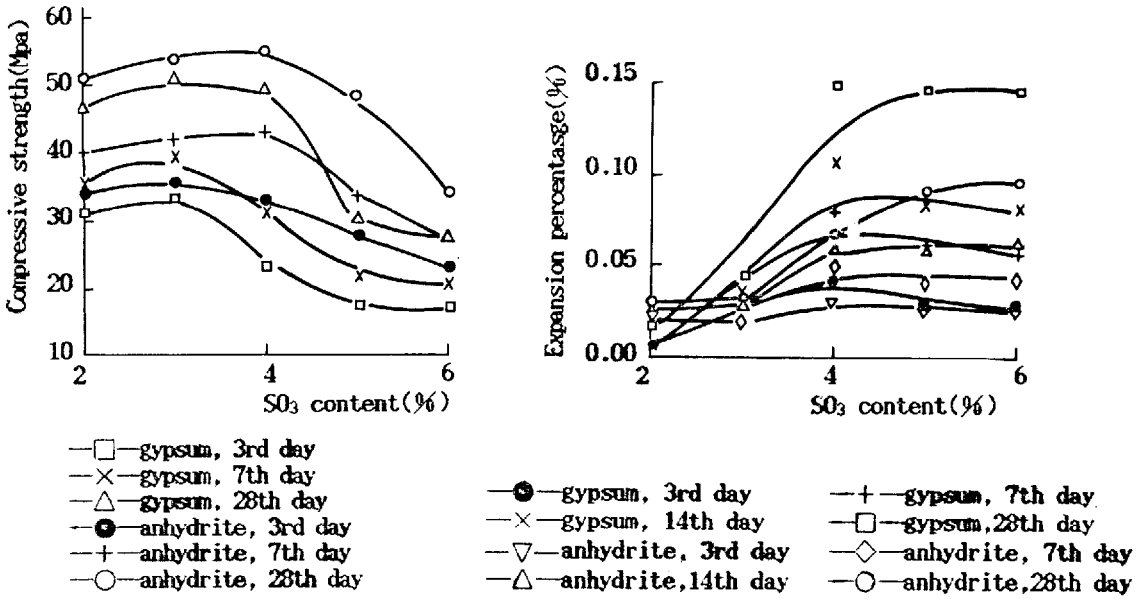

Fig.4 Compressive strength and expansion of Portland cement mortar vs. amount of SO_3 in different form

Comparison of influence of different blending materials on effect of SO_3 in varied form and amount in respect of strength

As shown in fig.5, using anhydrite and blending zeolite-tuff and fly ash separately, the earlier strength of both are lower than that of the plain, but in case of zeolite-tuff, slopes of the strength decrease with the amount of SO_3 increasing is very gently. The more zeolite-tuff is blended, the less strength decreases. In case of fly ash, when SO_3 is over a certain value, strength does not decrease with increasing SO_3 any more, and the more fly ash is blended, the little that value is. This law is similar at the latter age, but strength of cements blended with zeolite-tuff are higher than that without blending, and the change of strength with increasing SO_3 is not visible any longer.

When gypsum is used instead of anhydrite in above specimens the law is similar to using anhydrite (see fig.6).

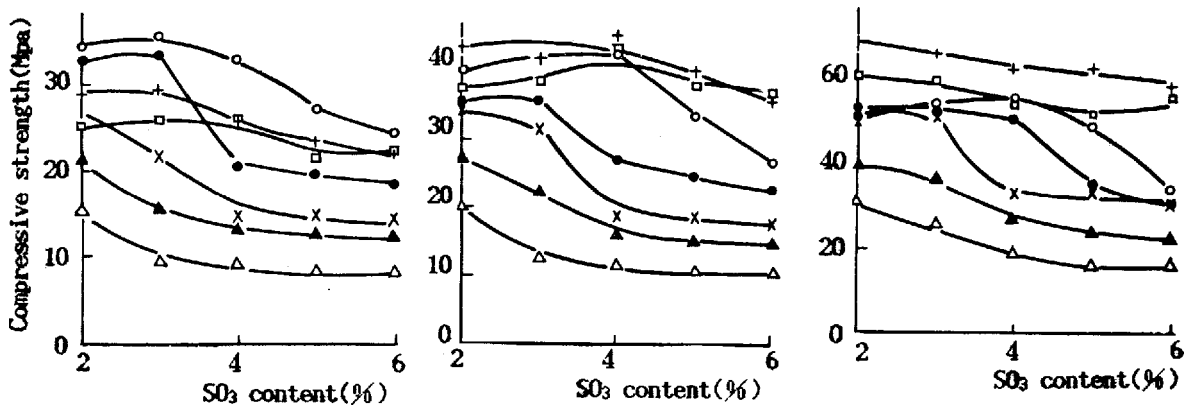

Fig.5 Compressive strength of cement blended with zeolite tuff and fly ash separately vs. amount of SO_3 supplied by anhydrite at expected ages

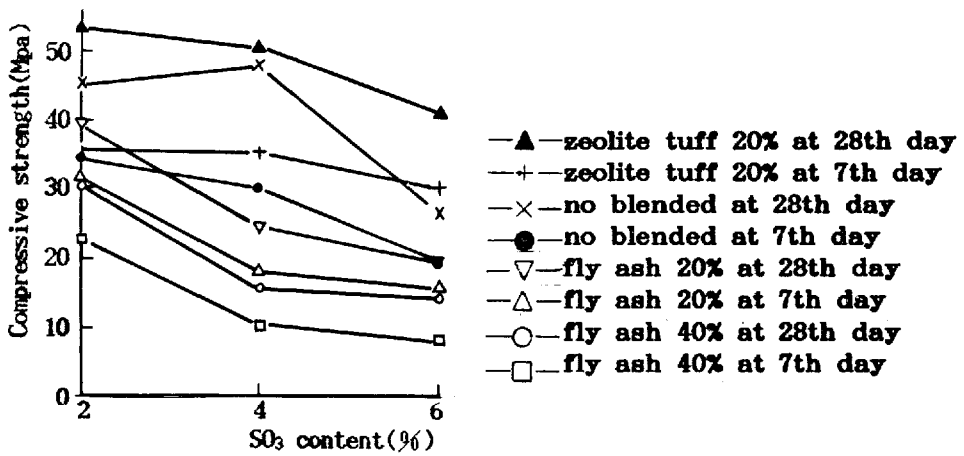

Fig.6 Compressive strength vs. SO_3 content supplied by gypsum

Comparison of influence of different blending materials on effect of SO_3 in varied form and amount in respect of linear expansion

Fig.7 is the relationship between expansion percentage of cement mortar blended with fly ash at 28th day and the blending amount as SO_3 is varied.

It is shown in fig.7 that the expansive percentage of mortar blended with fly ash is less than of that without blending material, and nothing to do with the blending amount so long as fly ash is blended to be over 20%.

When zeolite-tuff is blended, the inhibition effect is different from of fly ash somewhat (see fig.8). It is shown that at the earlier stage, expansion increases slightly with blending amount, and it is in reverse at the later age, the more amount of SO_3, later this reverse. But the expansion rate with age decreases with the amount of zeolite-tuff increasing. When the amount of zeolite tuff increases to be 30%, the expansion does not increase any more, even decrease for SO_3 being 6%.

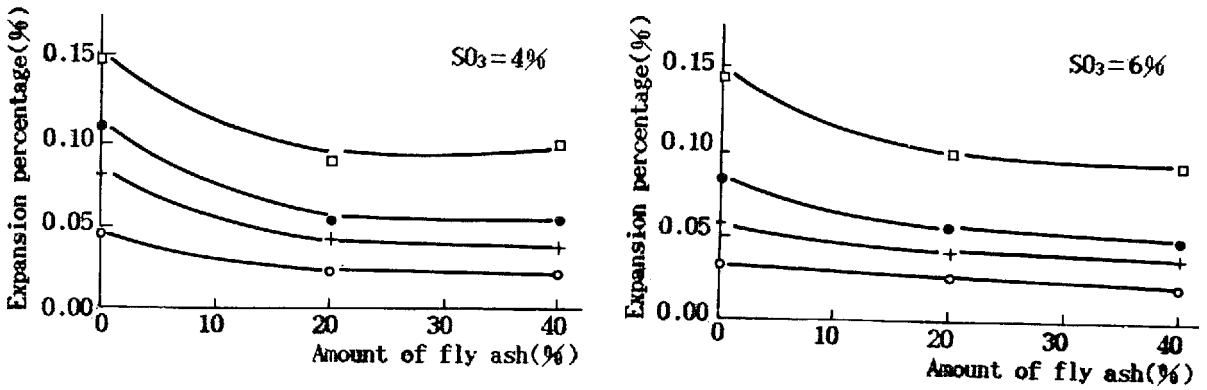

--at 3rd day, --at 7th day, --at 14th day, at 28th day

Fig.7 Linear expansion percentage of mortar vs. blending amount of fly ash at expected ages in case of varied amount of SO_3 supplied by anhydrite

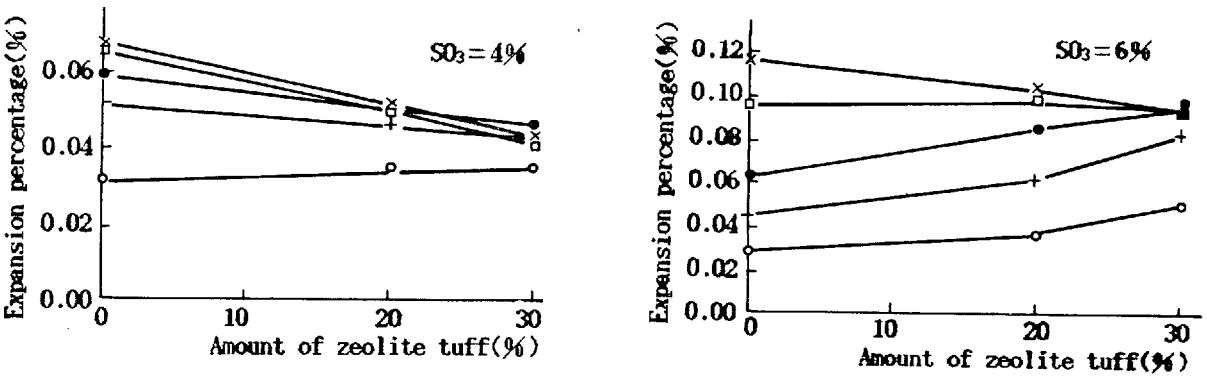

○—at 3rd day, +—at 7th day, □—at 14th day, ×—at 28th day

Fig.8 Linear expansion percentage of mortar vs. blending amount of zeolite tuff at expected ages in case of varied amount of SO_3 supplied by anhydrite

DISCUSSION

1. The decrease of strength and unfavourable expansion of cement products as excess SO_3 content in cement can be exhibited by blending materials, but there are different effects when different blending material are used. So that the "dilution effect" of C_3A can not be satisfactory for explaining the exhibition effect of blending materials as above mentioned on effect of excess SO_3 content.

2. To compare with Portland cement without any blended, even though the amount of SO_3 is added to be 6%, in case of blending zeolite tuff or FBC ash, strength decrease of cement is less, and expansion percentage is more less.

3. The exhibition on effect of SO_3 is deal with the activity of blending materials. Zeolite tuff and FBC with activity ratio more than 20% are much better than fly ash with activity ratio about 10%. Mechanism of that will be discussed in other papers.

4. It can be considered that when a blending material with high activity is used in Portland cement, it is possible to exceed the SO_3 content to be at least 4-5%. It would be favourable for untilizing the industrial solid wastes containing SO_3.

REFERENCES

[1] Information and standard institute, National Building Materials Academy of China, **Revisal on Cement Standard**, Construction Industrial Publishing House of China, Nov. 1977, (in Chinese).

[2] Odler, I.: "The possibility of increasing SO_3 content in cement", **Proceeding of 1988 EFC on Advances of Cement Use and Manufacture.**

[3] Ouyang, C. et al: "Internal and Extra Sources of Sulphate Ions in Portland Cement Mortar, Two Types of Chemical Attack", **Cement and Concrete Research** 18(5), 1988, p 699-709.

[4] Irassar, E.F.: "A Discussion of the paper "Internal and Extra Sources of Sulphate Ions in Portland Cement Mortar", by C. Ouyang, A. Nanni and W. F. Chang", **Cement and Concrete Research** 19, 1989, p 662-664.

[5] Mehta, P. K.: "Effect of Fly Ash Composition on Sulphate Resistance of Cement", **ACI Journal** 83 Nov. 1986, P 994-1000.

[6] Lian Huizhen et al: "Influence SO_3 fixed in FBC ash on the setting time of cement paste", **Proceeding of Results of the 7th-Five-Years Science and Technology Project** (in Chinese), 1991.

THE INFLUENCE OF SOME FLY ASHES AND BLAST-FURNACE SLAGS ON BLENDED CEMENT HYDRATION AND PROPERTIES

W Roszczynialski

University of Mining and Metallurgy
Kraków, POLAND

SUMMARY

The fly ashes from the bituminous coal burning and the granulated blast-furnace slags of low basility were used as blended cement components. The reference ordinary portland cement (95 % OPC clinker + 5 % gypsum) and blended cements with the fly ash or blast-furnace slag added as 45 % cement replacement were subjected to the extensive studies. The investigations of the hydration process using calorimetry, porosimetry, DTA and TG were carried out together with the standard examinations. The results put the light on the effect of admixtures on the hydration and properties of hydrated cement pastes. The long-term studies of the corrosion resistance against the sulphate attack were also carried out. At it results from the 15 years observations the fly ash containing cements show very high corrosion resistance, better than the blast-furnace slag cements. It should be mentioned also that strength development of fly ash cements is lower as compared with the slag cement.

RÉSUMÉ

On a étudié les ciments composés contenants jusqu`au 45% des cendres volantes ou des laitiers à faible teneur en CaO. L`hydratation de ces ciments a été examinées par la calorimetrie, la porosimetrie, l`ATD et TG, ainsi que par les méthodes standarisées pour les mortiers. Les examinations à long terme (15 ans) ont montré la résistance éxcellente à la corrosion au milieu de sulfates pour les mortiers contenantes les ciments pouzzolanique.

INTRODUCTION

The activity of fly ashes and blast furnace slags does not determine, in an equivocal way, their applicability as cement admixtures [1,2]. The best evaluation can be achieved by direct investigations of blended cements with the admixtures mentioned above [2,3]. Unfortunately, some results are obtained after many months or years exposure or curing; it relates particularly to the studies of the corrosion resistance. The physical and chemical studies of cement hydration by use of different methods allow to predict the behavior of some materials.

In the presented work the relations between the course of the hydration process and practical properties of blended cements with fly ash and blast furnace slag are shown. The pure OPC is used as a reference material.

EXPERIMENTAL

1. Materials

The investigations were carried out for cements of the following compositions:

cement A: 52% OPC clinker + 3% gypsum + 45% PFA
cement B: 52% OPC clinker + 3% gypsum + 45% BFS
cement C: 95% OPC clinker + 5% gypsum

The chemical composition of particular components of blended cements is presented in table 1.

Table 1. Chemical composition of OPC clinker, PFA, BFS and gypsum

Oxide	Percentage in particular components			
	OPC clinker	PFA	BFS	gypsum
SiO_2	21.66	48.80	38.66	8.38
Al_2O_3	5.03	25.42	8.08	1.53
Fe_2O_3	2.84	8.70	2.51	1.67
CaO	67.56	3.74	44.24	30.32
MgO	1.52	6.36	3.31	0.92
SO_3	0.35	0.43	1.96	36.77
L.O.I.	0.10	5.60	0.72	20.01
free CaO	0.83	-	-	-
act. SiO_2	-	19.13	-	-
act. Al_2O_3	-	6.53	-	-

2. Influence of fly ashes and blast-furnace slag on cement hydration

The studies of cement hydration were carried out by means of calorimetry, mercury porosimetry, DTA and TG.

2.1. Calorimetric studies

The results of calorimetric studies are shown in figure 1.

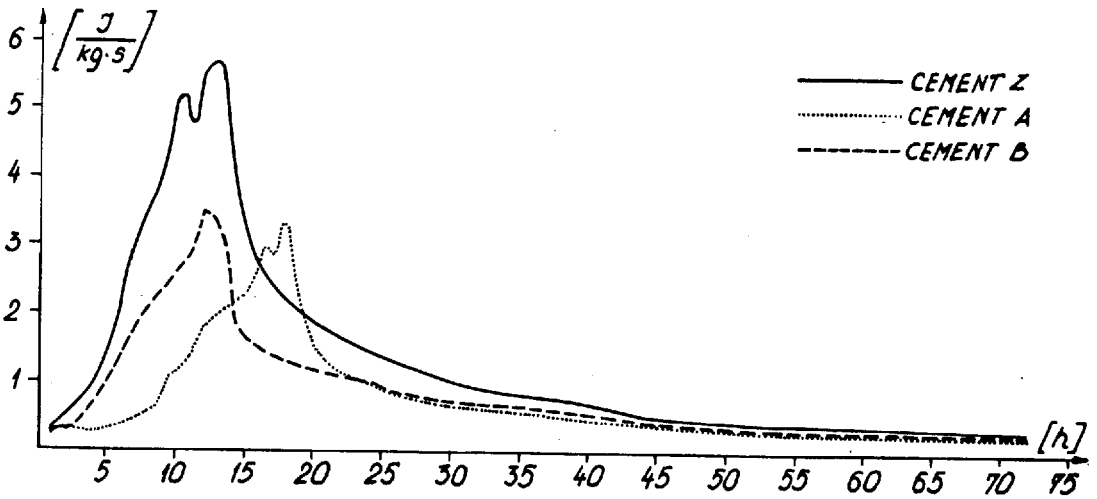

Figure 1. Microcalorimetric curves of cements.

The addition of fly ash reduces the heat evolved during the first three days hydration more than in the case of blast furnace slag addition. This is the consequence of the very slow pozzolanic reaction of fly ash and relatively higher rate of slag hydration. The decceleration of heat evolution process, illustrated as a shift of maximal heat evolution peak position, results from the presence of 3 % unburned coal content in fly ash. The hydrofobic grains of coal disturb the wetting of material and, as a consequence, hinder the hydration of clinker minerals.

2.2. Porosity measurements

The pastes cured in standard conditions for 1, 3, 7, 28, 90 days as well as 1 and 3 years were studied by mercury porosimetry and subjected to the compressive strength tests. The compressive strength versus porosity is plotted in figure 2.

For the particular porosity values the slag containing paste shows higher compressive strength than the paste without admixture. The paste with fly ash exhibits the compressive strength decrease at the same porosity as compared to the paste without admixture. It results from the advantageous microstucture of hydrated slag cement paste [4].

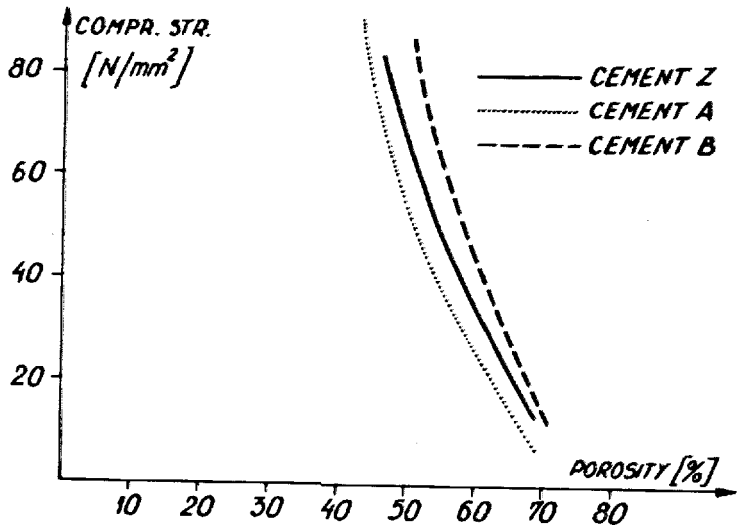

Figure 2. Relation between the compressive strength and porosity.

2.3. DTA and TG studies

In the DTA and TG investigations the calcium hydroxide content in the hydrated pastes was determined. The results are presented in figure 3.

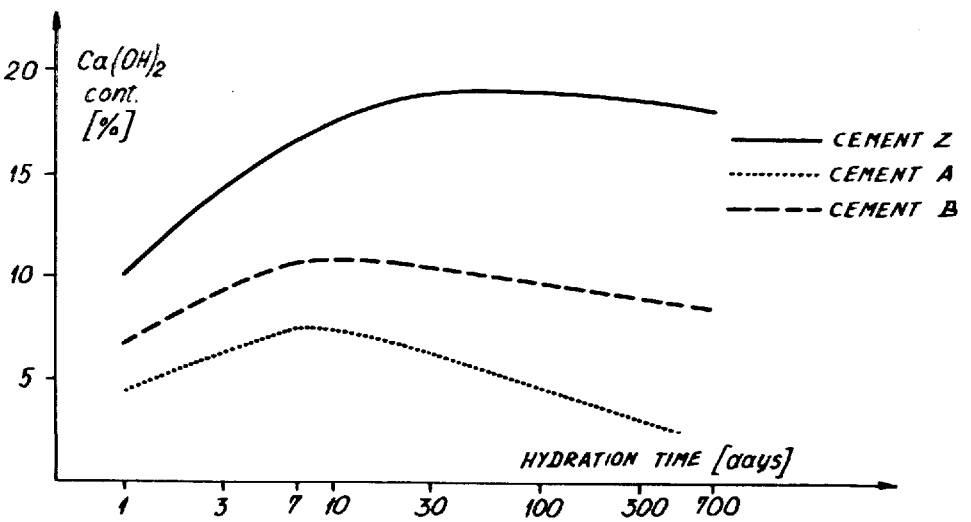

Figure 3. $Ca(OH)_2$ content in the pastes as a function of time of hydration.

Owing to the pozzolanic reactions of fly ash with the hydrating paste the continous consumption of $Ca(OH)_2$ takes place. The calcium hydroxide content decrease in the slag cement results mainly from the partial OPC clinker replacement by slag.

3. Influence of fly ash and blast-furnace slag on the properties of cement

The most important properties of pozzolanic and metallurgical cements are: strength development and corrosion resistance, particularly on the attack of sulphates.

3.1. Strength of mortars

The results of the compressive strength tests are presented in figure 4.

It can be seen that the pozzolanic cement, at early stages of hardening, shows lower strength development than the slag cement and this difference is the greatest after 1 month. At later ages this relation changes. After 300 days hydration the strength of pozzolanic cement is higher than that of slag cement and after 500 days the R_c value for pozzolanic cement is even higher than the R_c for reference OPC (at this age the compressive strength of OPC does not change practically).

Such a differencies reflect the kinetics of slag hydration in metallurgical cement and the pozzolanic reaction kinetics occuring in the fly ash cement.

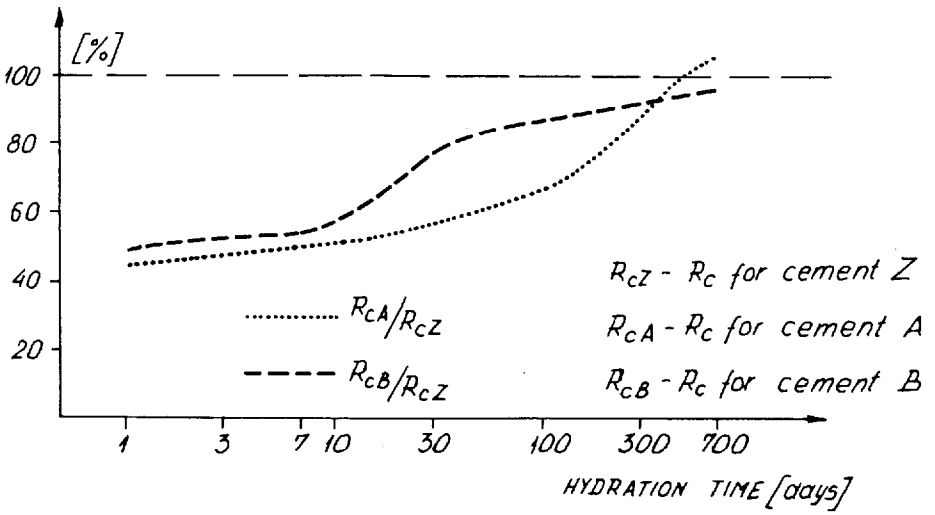

Figure 4. Influence of fly ash and blast furnace slag addition on the compressive strength of mortars.

3.2. Resistance to the attack of sulphates

The results of 15 years observation of the corrosion re- sistance in sulphate containing media are shown in figure 5.

Both the admixtures used in blended cements preparation increase the corrosion resistance. However, after 3 years storage in agressive medium (2% $MgSO_4$) it is evident that the fly ash addition gives better corrosion resistance than the slag addition. After 12 years storage in sulphate solution the slag cement bars exhibit cracks and significant volume increase. During the 15 years observation the fly ash containing mortars have not revealed any symptoms of destruction or deformation.

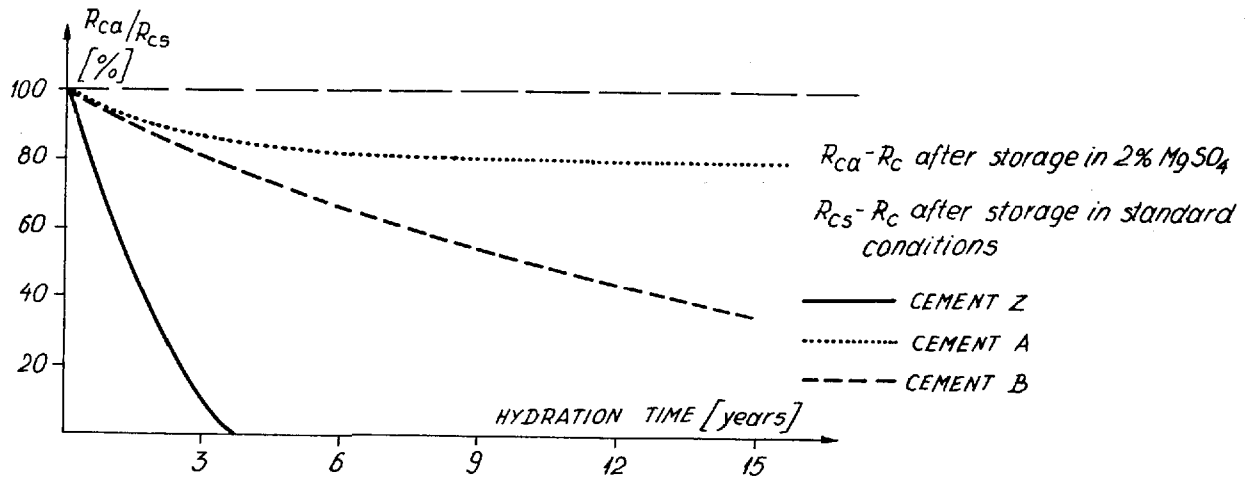

Figure 5. Influence of fly ash and blast furnace slag on the corrosion resistance

DISCUSSION

The studies of pozzolanic cement (45% fly ash by mass of cement) and metallurgical cement (45% blast furnace slag by mass of cement) strength development and corrosion resistance have been carried out for many years giving the results which could be predicted on the basis of the hydration investigations.

The rate of heat evolution is related to the strength development of cement [5]. The lowest heat evolution rate within first 3 days and strength development within first 300 days were observed for pozzolanic cement samples. After longer period of hardening the strength of pozzolanic cement becomes higher than the strength of metallurgical or ordinary portland cement without any admixture. It results from the active behavior of pozzolanic additive at later ages [6,7] involving the modification of microstructure. The porosity measurements show the lowest total porosity as well as the bettter pore structure of pozzolanic cement pastes after a long hardening (1 year, 3 years etc.).

The DTA and TG studies confirm the efficiency of fly ash as a calcium hydroxide binding agent. The high corrosion resistance is a consequence of decreasing calcium hydroxide content. The resistance to the attack of sulphates is also caused by the presence of the hydrated calcium silicates of low Ca to Si ratio showing high durability in corrosive media.

REFERENCES

1. Mehta,P.K.: "Supplementary Cementing Materials for Concrete". chapter 1 "Natural Pozzolans". ed. V.M. Malhotra. Ottawa, 1987, p.3-33.

2. Roszczynialski,W. & Gustaw,K.: "Activity of fly ashes used as a pozzolanic admixture to cement". International Congress on the Chemistry of Cement, 8th, Rio de Janeiro 1986, Vol.IV, p.257-262.

3. Berry,E.E. & Malhotra,V.M.: "Supplementary Cementing Materials for Concrete", chapter 2 "Fly Ash in Concrete". ed. V.M. Malhotra. Ottawa, 1987, p.37-167.

4. Małolepszy J: "The hydration and the Properties of Alkali Activated Slag Cementation Materials" (pol.), Zesz.Nauk. AGH, Nr 1297, Cracow, Poland. 1989, 126 p.

5. Luhr,H.P. & Efes,Y.: "Influence of the Granulometry of Fly-Ash with Low Ignition Losses on the Strength Development of Concrete". (rus.), International Congress on the Chemistry of Cement, 6th, Moscow 1974, Vol.III, p.103-108.

6. Manmohan,D. & Mehta P.: "Influence of pozzolanic, slag and chemical admixtures on pore size distribution and permeability of hardened cement pastes". Cement Concr. and Aggreg., 1981, Nr 1, p.63-67.

7. Samanta,C. & Chaterjee M.K.:"Sulphate Resistance of Portland-Pozzolanic Cements in Relation to Strength". Cem. and Concr. Res., 1982, Nr 6, p.726-734.

A STUDY ON CALCIUM ALUMINATE CEMENTS ADMIXTURES

J P Bayoux*, D Sorrentino*, J P Falaschi and A Capmas**

*Lafarge Coppée Recherche, Viviers/Rhône, FRANCE
**Lafarge Fondu International, Neuilly-sur-Seine, FRANCE

SUMMARY

Calcium Aluminate Cements are widely used in all kind of mixes in association with other mineral compounds and additives. They are also used in refractory products such as the castables with low or ultra low cement contents. These concretes are very dense products and require a large set of additives to make these products flow better and set at a given time.Very often all these formulated products are prepared empirically, the success depending greatly on the experience. The purpose of this work is try to understand the mechanisms in order to optimize the use of the actual additives and develop new ones, simpler and more efficient.

In order to overcome this challenge, an extensive research programm has been launched in which the effect of additives on cement properties, when used individually, will be systematically studied.

Gradually, we will move to more complex systems using 2 or 3 additives together.
To start with, we have decided to focus on trisodium citrate (CT) which is a basic additive used to fluidify aluminous cement pastes [1,2]. This additive is said to give the level of fluidity ; other additives added to it will contribute to a stability of this level and accelerators will determine the setting time.
To fully describe the effect of trisodium citrate, a wide selection of tests has been used, ranging from hydration of diluted suspensions, to rheological and mechanical properties associated to mineralogical analysis.

RESUME

Les aluminates de calcium sont de plus en plus utilisés au sein de produits formulés contenant d'autres minéraux et des adjuvants. C'est en particulier le cas dans les produits réfractaires LCC et ULCC qui sont très denses et qui demandent pour leur mise en place et le réglage de leur prise l'emploi d'un jeu complexe d'additifs. Le plus souvent ces produits sont formulés de façcn empirique les formules obtenues dépendant de l'expérience du formulateur. L'objectif de ce travail est d'essayer de comprendre les mécanismes d'action de ces adjuvants afin de mieux les utiliser et d'en développer de nouveaux plus simples et plus efficaces.

Un programme de recherche ambitieux a été lancé. Dans ce programme différents additifs seront étudiés d'abord individuellement puis en association. Nous avons commencé par le citrate trisodique (CT) qui est un additif de base utilisé pour fluidifier les pates de ciment [1, 2].

Afin de décrire précisemment l'action du citrate trisodique de nombreux essais ont été réalisés depuis l'étude de suspensions diluées jusqu'aux propriétés rhéologiques et mécaniques associées aux analyses minéralogiques.

1 - INTRODUCTION

1.1 - Materials

In order to take into account the influence of the reactivity of the cement, we have prepared, by sintering, two laboratory clinkers which were then ground to 4000 Blaine. The chemical and mineralogical analysis are shown in table 1.

Table 1 - Chemisty (%) and Mineralogy of cements (impulse/sec)

Cement	Insol	SiO_2%	Al_2O_3	CaO	MgO	K_2O	Na_2O	TiO_2	P.F	TOTAL
R	2.60	0.19	70.88	28.42	0.11	0	0.21	0.04	0.45	100.22
S	12.00	0.30	72.11	26.95	0.18	0.03	0.30	0.12	0.20	100.26

Cement	C12A7	CA	CA2	Aα
R	100	2643	1363	107
S	-	3129	765	476

The two laboratory cements are very different. One is reactive (R) the other is slow reacting (S). Cement R contains $C_{12}A_7$ estimated around 3% ; from the chemical analysis : CA $\tilde{-}$ 46% CA2 $\tilde{-}$ 46,5%. Cement S contains no $C_{12}A_7$; from the chemical analysis : CA $\tilde{-}$ 56% CA2 $\tilde{-}$ 29%.
The trisodium citrate (CT) is an industrial grade product which was used in the solid form in every test.

1.2 - Tests and analytical methods

1.2.1 - Mechanical tests - The rheological properties were measured using the shock table technique. For this flow test, the ASTM table was used and the mortars were prepared according to the EN 196-1 European Standard. The proportions and mixing procedure are detailed in this standard [3]

- Setting, mechanical strengths.

EN 196-1 Standard mortars were also used to determine the setting time while neat pastes were chosen to determine their mechanical strength and identify the nature of the hydrates forming at different dates, depending on the amount of additive added to the cement.

1.2.2 - Diluted suspensions - This test was used as a complement to the rheological and mechanical charateristics. The reactions occuring in a stirred suspension of water / solid ratio = 5, placed in a temperature controlled water bath at 20°C, are followed by measuring continuously the electrical conductivity K, the pH and temperature T.
Conductivity is a very interesting parameter to follow dissolution and precipitation reactions because both are associated with variations of ionic concentrations in the liquid phase. [4].
From these suspensions, samples can be taken at various dates and both solid and liquid phases can be separated by filtration. The liquid phase is used for the determination of the ionic concentrations using plasma emission spectrometry (I.C.P) whereas the solid phase is, after aceton/ether quenching, characterized by X Ray Diffraction and when necessary, by scanning electron microscopy.

2 - RESULTS

2.1 - Rheological behaviour

The flow properties vary, depending on the amount of additive and time, as already observed [5].

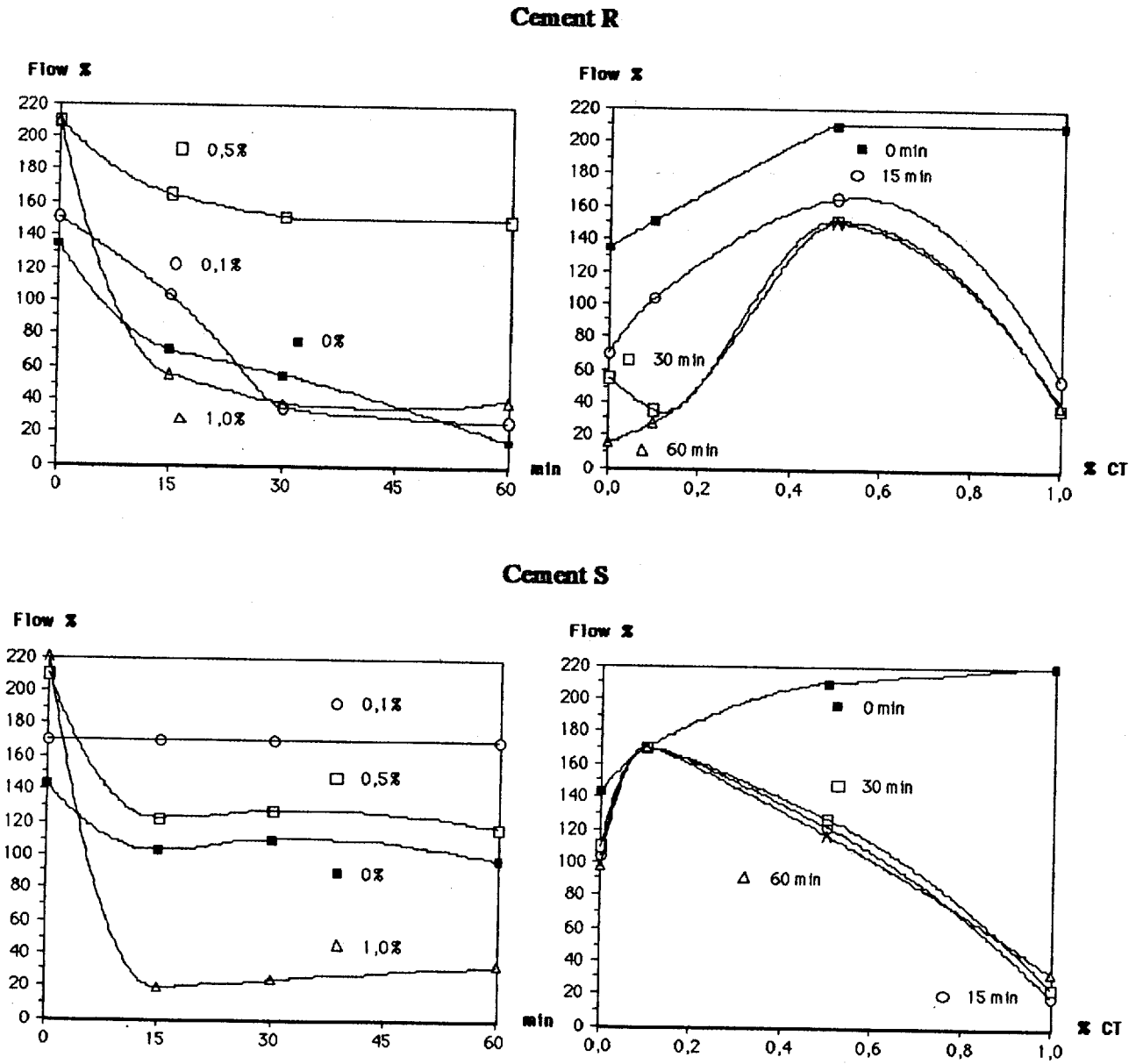

Fig. 1 - Flow Properties of AFNOR MORTARS with trisodium citrate

Results presented on Fig 1 show that CT has with both cements a similar behaviour: increasing the amount of additive first improves the flow and then decreases it dramatically when too large amounts are added. The optimum is not the same with both cements and depends on its reactivity : the more reactive the cement, the more additive is required.

A stable rheology is easier to achieve with the least reactive cement and fortunately the best initial flow leads to the more stable rheology.

2.2 - Setting time and strength

Additions of trisodium citrate delay the set of the cement [2, 3, 6]. For both cements a 0.5% addition of CT leads to a set occurring later than 10 hours. This has a direct influence on the mechanical properties. As already described, we have measured the mechanical properties on neat pastes [Fig.2].

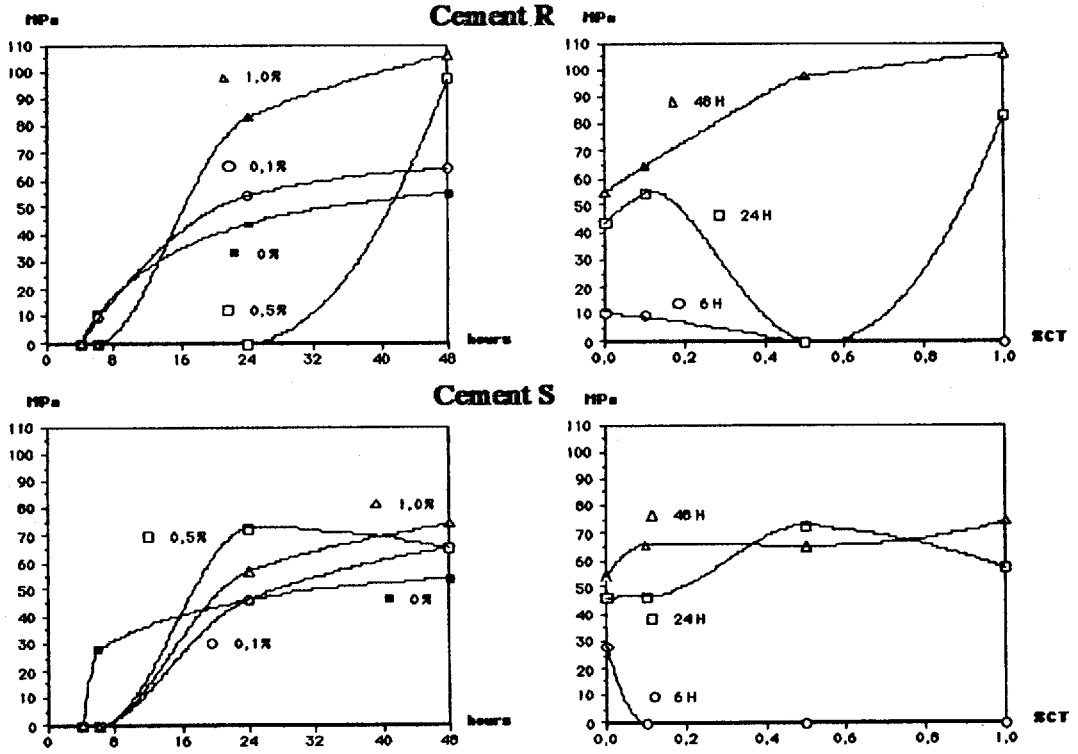

Fig. 2 - Neat Paste Mechanical Strength (W / S = 0,35)

As seen with the mortars but the results are not presented here, small addition of trisodium citrate reduces the early mechanical strength.
The 24 hours strengths are very peculiar with the Secar R : an addition of 0.5% trisodium citrate delays the hydration process to such an extent that no strength can be measured. This has not been clearly explained but is confirmed by the mineralogical analysis and loss on ignition measurements presented in Fig 3.

The mineralogical analysis clearly shows that addition of CT modifies the nature of the hydrates formed.
With both cements S and R CAH_{10} tends to form very quickly leading to a rapid increase of the loss on ignition. Another calcium aluminate hydrate, C_2AH_8 also forms and it is with the slow cement that it forms quicker. AH_3 also precipitates in massive quantities. When adding increasing amounts of trisodium citrate the hydrates differ. In the case of cement S, C_2AH_8 no longer forms quickly and CAH_{10} is slightly delated. Larger additions lead to a larger formation of CAH_{10} after 6 hours.

C_3AH_6 and AH_3 do not show the same variations when comparing both cements : C_3AH_6 forms spontaneously in both neat pastes without additive. When adding large amounts it no longer forms in the case of cement S whereas it is still present and even forming earlier with cement R.
AH3 is very peculiar. In the case of cement S decreasing amounts are formed when increasing the CT%. Cement R behaves differently. On its own it precipitates less AH_3 but increasing quantities form with a maximum which moves towards shorter times when larger CT increments are added. AH3 seems to form at the expense of CAH_{10} : CAH_{10} clearly increases when AH_3 decreases along with C_3AH_6.

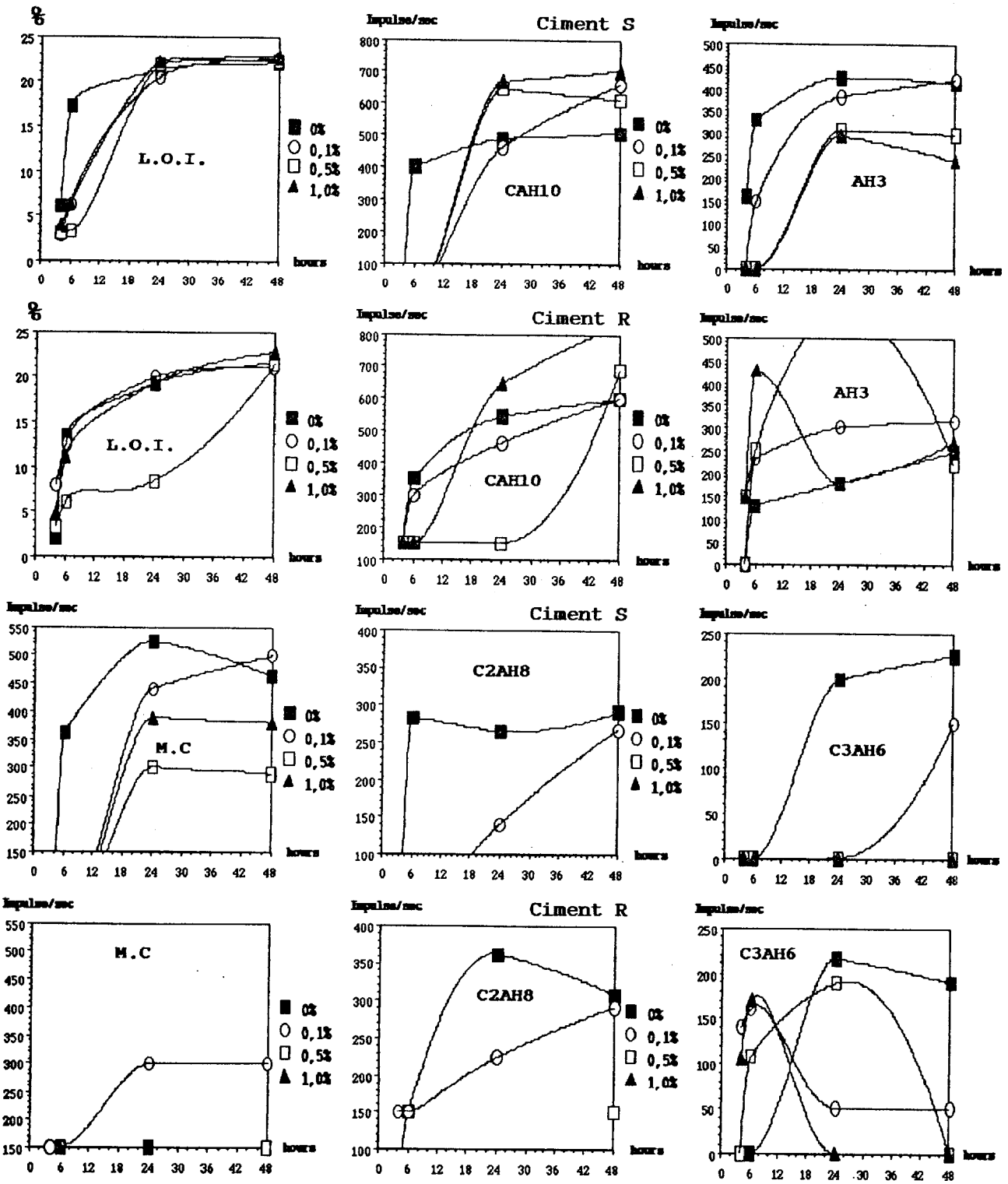

Fig . 3 - Mineralogical Analysis

3 - ELECTROCHEMICAL STUDIES

- Pure cements

Cements R and S were at first investigated on their own, qualitatively (chemical reactor) and quantitatively (liquid and solid phase analysis). The 3 typical curves obtained with the chemical reactor on cement R appear on Fig 4.They allow to understand quickly but accurately the main steps of hydration : dissolution, hydrates nucleation, massive precipitation.

The companion K curve for cement S is comparatively drawn on the same figure. They are broadly the same, but differences can be easily detected, which are indeed related to the mineralogical and crystal size compositions of both cements. These curves are characteristics of the hydraulic reactivity of the cements, and start to be used on an industrial basis. The ionic concentrations cannot be discussed in detail, whereas the loss on ignition curve is given, which represents the overall hydration degree.

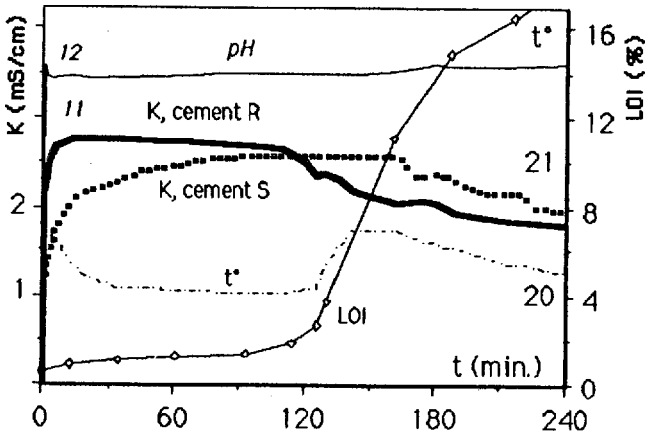

Fig. 4 - Typical K, pH and t° curves for cement R.

- Cements with admixtures

The influence of CT has been mostly studied on cement R. For the qualitative electrochemical part of the study, 7 dose rates of CT have been tried : 0.05, 0.1, 0.2, 0.3, 0.5, 0.8, and 1%, while 2 dosages 0.1 and 0.8% have been selected to realize the quantitative liquid phase determinations.

Figure 5 shows the most typical conductivity curves obtained ; the other ones would be intermediate between the others. A limited study has been done with two levels of CT, with cement S. (0.1 and 0,5%)

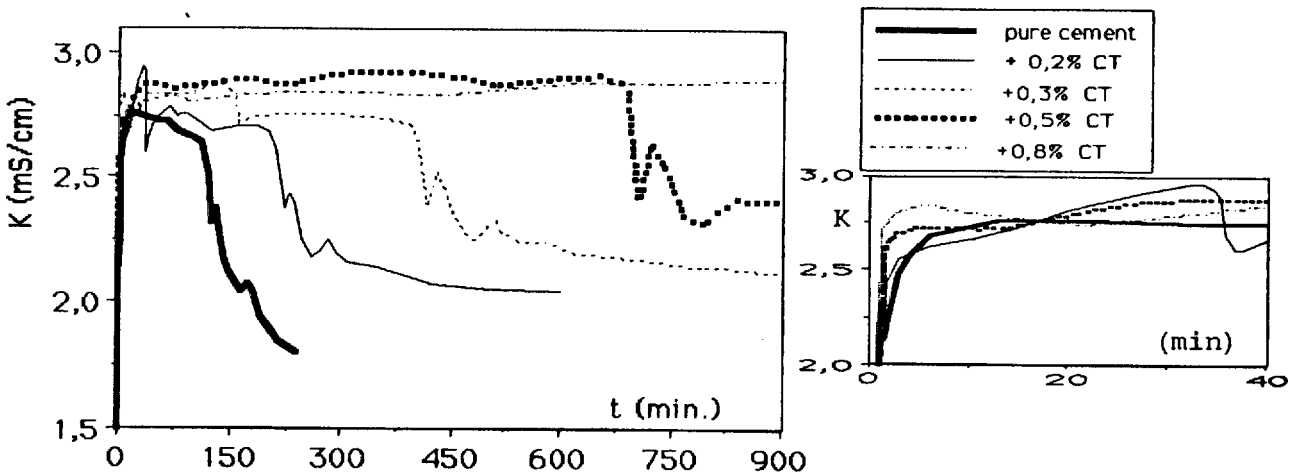

Fig. 5 - Effects of CT additions on the chemical characteristics of cement R

4 - DISCUSSION

Two main properties of the CT admixture will be discussed : the setting time and the fluidizing effect.

- Setting time in this study and, contrary to what Lankard and Hackman observed with 1% CT [1], continously increases with increasing admixture dosages.

We however point out that the relationship is not linear. Setting time drastically increasing with higher % CT. This delayed set fits well with the extended period of the conductivity plateau [Fig.5].This one, although not fully coinciding with the set time is however closely related to it ; therefore, the explanation of the lengthening of the K plateau will help understanding the increased setting time. Several data are important to be considered ; some of them, which we have not been able to include in the paper, will be integrated for discussion :

- the highest ionic concentrations [Ca^{2+}, $Al(OH)_4^-$] vary as a function of CT%, but the variation trend is opposite ; it is somewhat depressed for the lime : 22 to 15m Mol/l for 0.8% CT, while it is enhanced for alumina : 20 to 24 m Mol/l, for 0,8% CT. This results in a large modification of the C/A molar ratio : 1.1 for pure cement to 0.7 for 0.8% CT, which in its turn, has a drastic implication on the nature of the hydrates formed. Even if considering the displacement of the hydrates solubility curves in the CaO. Al_2O_3 - H_2O diagram due to the Na^+ supply from the additive, it is however clear that the kinetic path described by the liquid phase will be placed in the AH_3, CAH_{10}, area and no more in the C_2AH_8 one. This is exactly what show the XRD spectra of the suspensions and neat pastes samples. The observation by S.E.M of samples taken during the conductivity plateau was really instructive : a gelatinous layer, alumina rich-if not pure alumina - was covering the grains, as we already observed on CA grains hydrated at 27° - 30° C [4]. In this respect we agree with Rodger and Double paper [7].

- Fluidizing effect is strongly related with the phenomena occurring at a very early age, and particulary with the dissolution process. It is observed that, the concentration values of both main ions diminish as a function of increasing additive %, due to an overall slowing down of the dissolution rate. However these ions are not equally depressed, alumina being at that time much more lowered than lime, which results in very high C/A molar ratios (above 5 for 0.8% CT). From this, it is obvious that lime rich hydrates, such as C_2AH_8, C_3AH_6 or even monocarboaluminate may initially be formed, what has been observed with the neat paste studies.

5 - CONCLUSIONS

This paper illustrates the modifications of characteristic properties (set time, rheology, strength), with increasing dose rates of the trisodium citrate.The drastic setting time increase is explained based on chemical and morphological observations, the fluidizing effect is well related to an overall slowing down of the dissolution process.
The opposite behaviour of the main ions Ca^{2+} and $Al(OH)_4^-$, at very early stages (high C/A ratios explaining C_3AH_6 formation) and during the nucleation period (low C/A) well explains why lime rich hydrates can be initially produced, while alumina rich hydrates are formed during the main hydration course.This successful methodology, will be now applied to a series of single or combined admixtures.

REFERENCES

[1] Lankard, D.R. and Hackman, L.E. : "Use of admixtures in refractory concretes", 1983, Bull. Amer., Ceram. Soc., 62, 1019-1025.

[2] Sharp, J.H et al. : "The effect of admixtures on the hydration of refractory calcium aluminate cements", London 1990, 127-141, in : Calcium Aluminate Cements, Proc. 1rst Int. Symp. (ed. R. J.Mangabhai).

[3] EN 196-11987 F. European Standard. methods for cements testing ; strength determination.

[4] Capmas, A., Ménétrier - Sorrentino, D. and Damidot, D.: "Effect of temperature on setting time of calcium aluminate cements" , pp 65-80, in ref 2.

[5] Mathieu, A. : "Admixtures for calcium aluminate cements in refractory concretes; Lafarge Fondu International", 1988, Internal Report.

[6] Letourneux, J.P. : "Adjuvants des Ciments Alumineux, Etude bibliographique", 1985, Lafarge Coppée Recherche, Internal Report.

[7] Rodger, S.A. and Double, D.D.: "The chemistry of high alumina cement in the presence of accelerating and retarding admixtures", 1984, Cement Concrete Research, 14, pp73-82.

AUTOGENOUS SHRINKAGE CAUSED BY SELF DESICCATION IN CEMENTITIOUS MATERIAL

E Tazawa and S Miyazawa

Faculty of Engineering, Hiroshima University
Kagamiyama Higashi-hiroshima, JAPAN

SUMMARY

Influences of water-cement ratio, types of cement and admixture on autogenous shrinkage of cement paste were experimentally investigated. It could be seen from the experiments that the magnitude of autogenous shrinkage of cement paste increased with decrease in water-cement ratio. Especially, when water-cement ratio was decreased to 0.17 by addition of superplasticizer and condensed silica fume, more than 4000×10^{-6} of linear shrinkage was observed without evapolation. Observed values of autogenous shrinkage varied with specimen size: the larger the specimen size, the smaller the autogenous shrinkage. For mortar and concrete, large amount of autogenous shrinkage was observe on specimen with low water-cement ratio. Autogenous shrinkage decreased with increase in the volume concentration of aggregate.

要　旨

セメントペーストの自己収縮(Autogenous shrinkage)に及ぼす水セメント比、セメントの種類、混和材料の種類の影響について実験的に検討した。セメントペーストの自己収縮は水セメント比が小さくなる程大きくなり、特に、高性能減水剤およびシリカヒュームを用いて水結合材比を0.17まで下げた場合、4000×10^{-6}以上の自己収縮が計測された。自己収縮には寸法効果が認められ、供試体寸法が大きくなる程小さくなった。モルタルおよびコンクリートについても、水セメント比が小さい場合は大きな自己収縮が認められた。モルタルおよびコンクリートの自己収縮は、骨材の体積濃度の増加と共に減少した。

INTRODUCTION

The combined volume of cement and water decreases with hydration, which results in the formation of intrinsic voids in hardened cement paste. Then the moisture in capillary pores decreases even without evaporation, which phenomenon is called self desiccation (1,2). Shrinkage of concrete due to self desiccation is known as autogenous shrinkage. Since its magnitude is of the order of 100×10^{-6} for ordinary concrete (3), it has been ignored for practical purposes. But it has recently become possible to make concrete with very low water-cement ratio using superplasticizers and condensed silica fume. And it has been reported that self desiccation is relatively large in concrete with low water-cement ratio (4,5). In our laboratory, autogenous shrinkage of cement pastes was measured over a wide range of water-cement ratio and its mechanism was explained in relation to the moisture movement inside a specimen (6,7,8). In this study, the influence of specimen size, type of cement, admixture and volume concentration of aggregate on autogenous shrinkage has been experimentally studied.

EXPERIMENTAL PROCEDURES

Materials and Mix Proportion

Ten types of commercial cement available in Japan were used. Test results for the chemical components and physical properties of these cements are shown in Table 1. Three types of pozzolans (condensed silica fume, fly ash and meta-kaolin) were used as admixtures (Table 2). Five types of superplasticizers were used, as shown in Table 3. In order to reduce autogenous shrinkage of cement paste, two types of drying shrinkage reducing agent and three types of expansive admixtures (Table 4) were used. Coarse aggregate was crushed rhyolite (maximum size : 20mm) and fine aggregate was decomposed granite or crushed rhyolite. Mix proportion of concrete is shown in Table 5.

Table 1 Physical properties and chemical composition of cements

	Specific gravity	Blaine fineness (cm^2/g)	Ig.loss (%)	Insol (%)	SiO_2 (%)	Al_2O_3 (%)	Fe_2O_3 (%)	CaO (%)	MgO (%)	SO_3 (%)	Na_2O (%)	K_2O (%)	TiO_2 (%)	P_2O_5 (%)	MnO (%)	S (%)	Cl (%)	Total (%)
N	3.13	3520	1.7	0.5	21.4	5.3	3.1	63.4	1.0	2.0	0.39	0.43	0.26	0.08	0.19	–	0.003	99.8
M	3.18	2990	1.1	0.2	23.6	3.3	4.0	64.0	0.8	1.7	0.30	0.32	0.16	0.06	0.09	–	0.000	99.6
H	3.13	4250	1.0	0.2	20.4	5.1	2.8	65.4	0.9	2.9	0.33	0.40	0.24	0.10	0.28	–	0.001	100.0
S	3.17	3390	1.3	0.3	21.7	3.6	4.5	63.9	1.0	2.3	0.27	0.37	0.20	0.09	0.26	–	0.002	99.8
G	3.01	3500	1.4	20.5	17.8	4.3	3.4	48.5	1.1	1.6	0.24	0.34	0.19	0.06	0.22	–	0.002	99.7
O	3.17	3120	1.3	0.3	22.0	3.6	4.6	64.0	0.9	2.2	0.26	0.38	0.20	0.09	0.27	–	0.001	100.1
A	3.01	4420	0.5	–	5.9	49.7	4.6	35.1	0.6	–	0.06	0.18	2.50	0.08	0.02	–	0.003	99.2
W	3.03	3700	2.9	0.4	21.6	4.5	0.2	66.1	0.6	2.5	0.07	0.48	0.06	0.04	0.00	–	0.001	99.5
F	2.94	3160	2.2	11.2	19.6	5.4	2.8	54.2	1.0	2.2	0.36	0.42	0.26	0.08	0.17	–	0.003	99.9
B	3.03	3510	1.7	2.4	24.8	8.6	2.2	54.4	2.6	1.4	0.29	0.39	0.38	0.06	0.46	0.23	0.006	99.9

N : Ordinary portland cement. M : Moderate heat portland cement. H : High-early strength portland cement. S : Sulfate resisting portland cement.
G : Geothermal cement. O : Oil well cement. A : Alumina cement. W : White cement. F : Fly ash cemnt (B-type). B : Brast-furnace slag cement (B-type)

Table 2 Chemical composition of pozzolans

	ig. loss	SiO_2	Al_2O_3	Fe_2O_3	CaO	MgO	Na_2O	K_2O	TiO_2	P_2O_5	C	Total
Silica Fume SF	1.3	96.5	–	–	0.12	–	0.14	0.64	–	0.17	–	98.9
Fly ash FA	1.0	63.1	20.7	4.19	6.93	1.37	0.35	0.85	–	–	0.85	99.2
Meta-kaolin MK	0.7	52.0	44.6	0.5	0.03	0.04	0.2	0.1	1.9	–	–	100.1

Table 3 Main component of superplasticizers

	Main components
SP1	β-naphthalen sulfonate formaldehyde high condensates
SP2	Polyalkylallyl sulfonates and reactive macromolecule
SP3	Naphthalen sulfonate condensate and lignin sulfonate derivative
SP4	Polycarboxylic asid ether compound
SP5	Aromatic aminosulfonate macromolecule

Table 4 Drying shrinkage reducing agents and expansive admixtures

	Main components		Main components
D1	Alchol alkylene oxide	E1	$3CaO \cdot Al_2O_3 \cdot CaSO_4$
D2	Glycol ether	E2	CaO
		E3	CaO

Table 5 Mix proportion of concretes

w/c	Unit content (kg/m³)					ad. (%/C)
	W	C	SF	S	G	
0.20	160	720	80	443	1075	0.75*1
0.30	195	649	0	586	993	0.40*2
	190	570	63	586	993	0.40*2
0.50	180	360	0	799	1056	0.14*3

*1 Aromatic aminosulfonate macromolecule (SP5)
*2 β-naphthalen sulfonate formaldehyde high condensates (SP1)
*3 Lignin sulfonic acid

In Figures 3 to 12, mix proportions are symbolically presented as (type of cement)(water-cement ratio %)-(replacement ratio of admixture %)-(dosage of chemical admixture %).

Measurement

Autogenous shrinkage until 24 hours age - Autogenous shrinkage of cement paste was measured for 24 hours after casting, where cement paste was cast into a foamed styrol mold and the original length was measured at the time of initial set (Fig.1). Moisture evapolation was not permitted by vinyl sheet and wet cloth covering the surface of specimen immediately after casting. For each condition, two specimens were prepared.

Autogenous shrinkage for a long period - Cement paste was cast into a steel mold and it was covered with vinyl sheet and wet cloth immediately after finishing its surface. And it was stored at 20°C and 90±5% R.H. for 24 hours. After demolding at the age of one day, the specimens were sealed on all the surfaces with aluminium tape (0.05 mm in thickness) and butyl rubber tape in order to prevent both permeation and evaporation, and were stored in the room at 20°C. Three sizes of specimen were used; 2x2x16cm, 4x4x16cm and 10x10x40cm beams (Fig.2). Length change of specimen was measured with dial gauge(1/1000mm). Some of the specimens were immersed in water (20°C) at the age of 24 hours without being sealed. And length change in water curing was measured for a long period. For each condition, three or two specimens were prepared.

TEST RESULTS AND DISCUSSIONS

Influence of Mix Proportion on Autogenous Shrinkage of Cement Paste

Autogenous shrinkage of cement paste which was measured from the time of initial set was shown in Fig.3. It can be seen that autogenous shrinkage is generated after the time of final set. Autogenous shrinkage increased with decreasing water-cement ratio (w/c). In case of w/c=0.23, addition of condensed silica fume

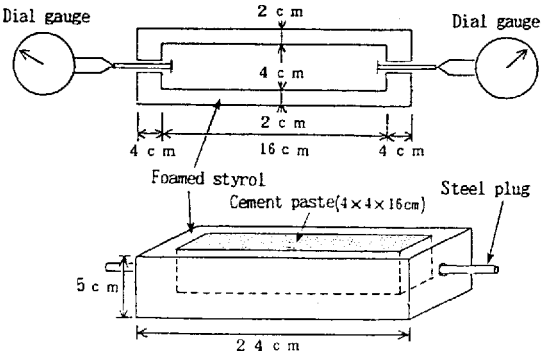

Fig.1 Measurement of autogenous shrinkage until the age of 24 hours

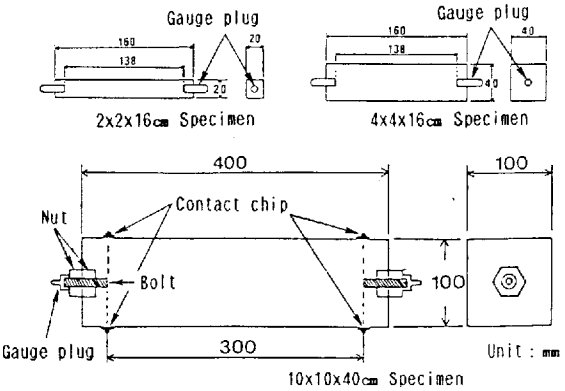

Fig.2 Measurement of autogenous shrinkage after the age of 24 hours

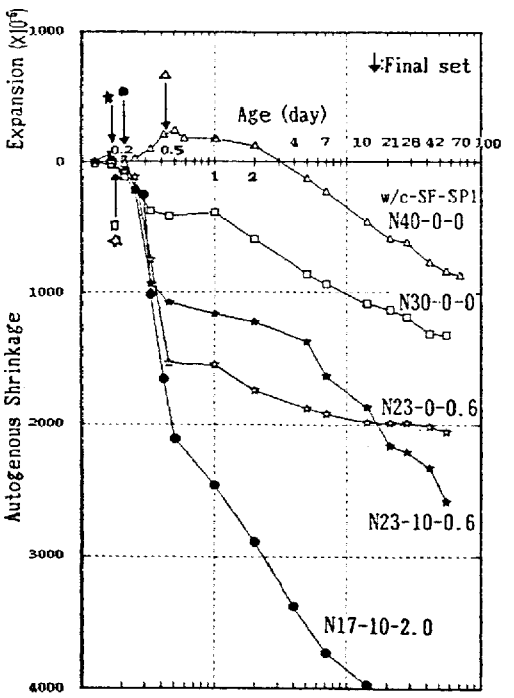

Fig.3 Autogenous shrinkage of cement paste (4x4x16cm)

increased the autogenous shrinkage. Especially, when water-cement ratio was decreased to 0.17 by addition of superplasticizer and condensed silica fume, more than 4000×10^{-6} linear strain was observed.

Influence of Specimen Size

Autogenous shrinkage of cement paste, which was made from high-early strength portland cement, was measured on specimens of different sizes. The original length was measured at 24 hours after casting. Autogenous shrinkage of cement paste increased with decrease in specimen size for any mix proportion, as shown in Fig.4. This size effect is thought to be related to the moisture movement inside a specimen, which is described as follows.

Absolute volume reduction due to hydration will give rise to intrinsic voids in the space that had been occupied by unhydrated cement and water. Since free water will keep continuity by the attracting force among molecules, it will move into the inner part of the specimen, compensating the absolute volume reduction (7,8). If the movement of water results in its continuous distribution, the pressure difference corresponding to the size of the meniscus is transmitted between solid phases and a large amount of autogenous shrinkage will be observed. On the other hand, if the permeating velocity of water is less than the rate of absolute volume reduction, water is discontinuously distributed in the cross section and the pressure difference is not transmitted between solid phases, therefore autogenous shrinkage will not be so large.

Self Desiccation in Water Curing

Length change was measured for unsealed specimens which were stored in water after demolding. With w/c=0.17, a large shrinkage was observed despite increase in the weight of the specimen with permeation of curing water (Fig.5). With w/c=0.30, shrinkage was observed for 10x10x40cm specimen, while swelling was observed for smaller size specimens(Fig.6). These phenomena can be explained by the fact that interstitial void increasing with progressive hydration is filled with water only on the surface portion of the specimen with low water-cement ratio or large size, since the rate of absorption of water from outside is less than the rate of void formation.

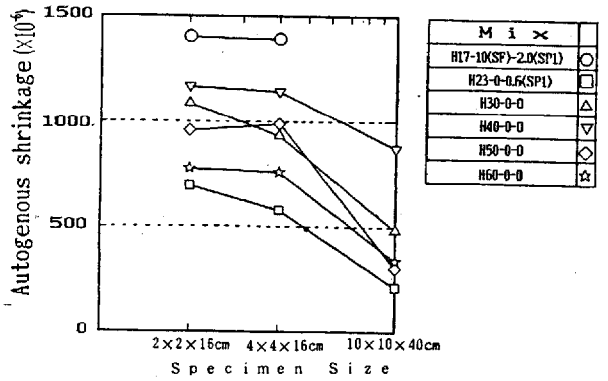

Fig.4 Influence of specimen size on autogenous shrinkage (The original length was measured at 24 hours after casting)

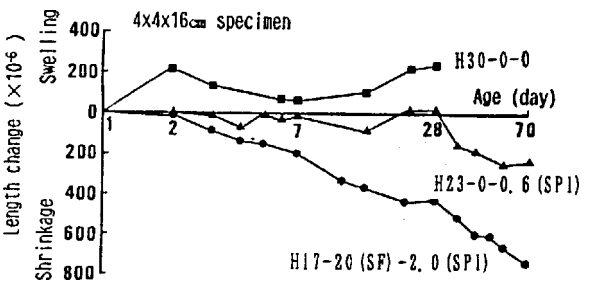

Fig.5 Length change of cement paste in water

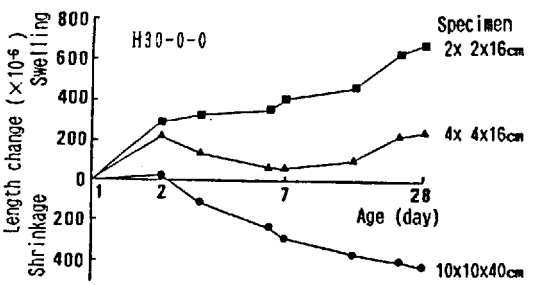

Fig.6 Length change of cement paste in water

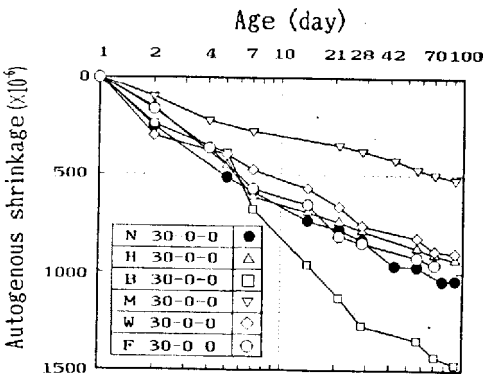

Fig.7 Influence of cement on autogenous shrinkage of cement paste (4x4x16cm)

Influence of Type of Cement and Admixture

Influence of materials (type of cement, pozzolan, superplasticizer, drying shrinkage reducing agent and expansive admixture) on the magnitude of autogenous shrinkage was experimentally investigated. Linear shrinkage was measured for 4x4x16cm beams, where the original length was measured at 24 hours after casting.

Cement - Influence of type of cement was studied for cement paste with w/c=0.30. A great deal of autogenous shrinkage was observed regardless of the type of cement and equilibrium was not established even after 90 days of sealed curing (Fig.7 and 8). Autogenous shrinkage of blast-furnace cement paste was larger, while that of moderate heat portland cement paste and sulfate resisting cement paste was less, compared to ordinary portland cement paste.

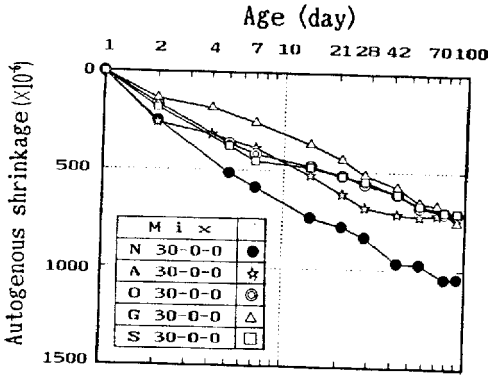

Fig.8 Influence of cement on autogenous shrinkage of cement paste (4x4x16cm)

Pozzolan - Influence of addition of pozzolan on autogenous shrinkage was studied for ordinary portland cement paste with w/c=0.40. Ten percent of cement was replaced with pozzolans, such as fly ash, condensed silica fume and meta-kaolin. Addition of these pozzolans decreased autogenous shrinkage of cement paste (Fig.9). With w/c=0.23, however, addition of condensed silica fume increased autogenous shrinkage (Fig.3). This is because that the water content required for continuous distribution is decreased by micro filler effect of condensed silica fume.

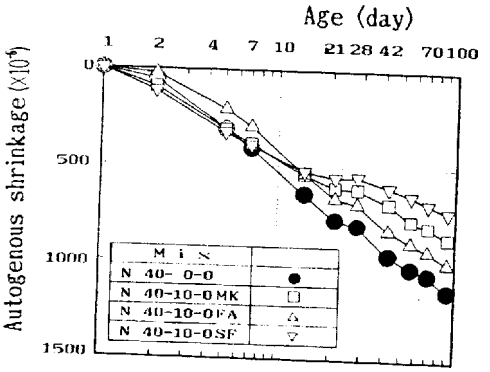

Fig.9 Effect of pozzolan on autogenous shrinkage of cement paste (4x4x16cm)

Superplasticizer - Influence of superplasticizer was studied for ordinary portland cement paste with w/c=0.30. The dosage of superplasticizer was so fixed that fluidities of the fresh cement pastes were the same for the different types of superplasticizers. Autogenous shrinkage slightly decreased with dosage of superplasticizer, as shown in Fig.10.

Shrinkage reducing admixture - Drying shrinkage reducing agents, such as alkylene oxide type and glycol ether type, which are commercially available in Japan, were used in order to reduce autogenous shrinkage. Ordinary portland cement was used, and water-cement ratio was 0.30. The dosage of the agents was 2% of the cement weight. It can be seen from Fig.11 that autogenous shrinkage of cement paste can be effectively decreased especially by the dosage of alkylene oxide type agent, which reduces the surface tension of water by half.

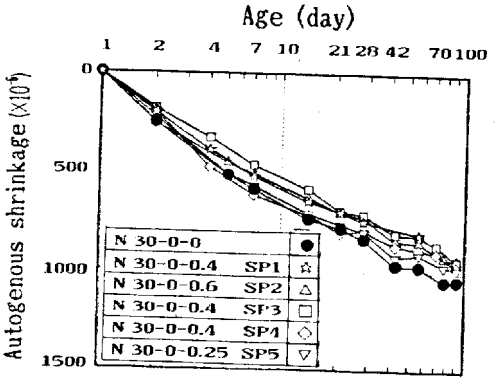

Fig.10 Effect of superplasticizer on autogenous shrinkage of cement paste (4x4x16cm)

Expansive admixture- Effect of expansive admixture was studied for ordinary portland cement paste with w/c=0.30. Ten percent of cement was replaced by expansive admixtures, such as calcium sulfo-aluminate type or CaO type. It can be seen from Fig.11 that expansive admixtures can be effectively used to reduce autogenous shrinkage of cement paste. Expansive admixture E3

(CaO type) is the most effective for reducing autogenous shrinkage of cement paste.

Autogenous Shrinkage of Mortar and Concrete

Autogenous shrinkage of mortar specimen, where volume concentration of aggregate (crushed rhyolite) was changed as 0, 0.1, 0.3, and 0.5, are shown in Fig.12. Pickett (9) and Hobbs (10) theoretically estimated drying shrinkage of concrete as a function of aggregate concentration. Theoretical values calculated by their methods are presented by dotted lines in this figure, where there is little difference between the values obtained by the two methods. In these calculations, the observed values of the modulus of elasticity and Poisson's ratio of cement paste and aggregate were used. Autogenous shrinkage decreases with increase in the volume concentration of aggregate. The experimental results are almost the same as the calculated ones for 4x4x16cm mortar specimen.

Autogenous shrinkage of concrete specimens measured on 10x10x40 cm beams, where crushed rhyolite (maximum size : 20 mm) and pit sand (decomposed granite) were used, is shown in Fig.13. Large amount of autogenous shrinkage was observed on concrete with low water-cement ratio, and it was increased by addition of condensed silica fume.

CONCLUSIONS

(1) Autogenous shrinkage of cement paste increased with decreasing water-cement ratio. When water-cement ratio was decreased to 0.17 by superplasticizer and condensed silica fume, more than 4000×10^{-6} linear strain was observed on 4x4x16 cm beam specimen.

(2) Autogenous shrinkage of cement paste with low water-cement ratio was increased by addition of condensed silica fume.

(3) Autogenous shrinkage of cement paste is increased with decrease in specimen size.

(4) Type of cement had great influence on the magnitude of autogenous shrinkage of cement paste. Autogenous shrinkage of blast-furnace slag cement paste was much larger than that of ordinary portland cement paste.

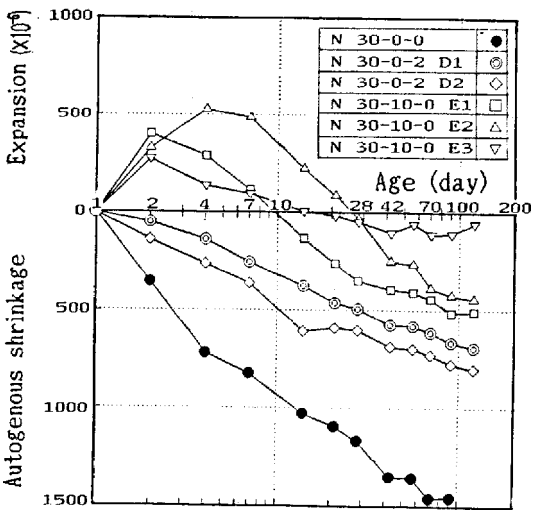

Fig.11 Effect of drying shrinkage reducing agent and expansive admixture on autogenous shrinkage of cement paste (4x4x16cm)

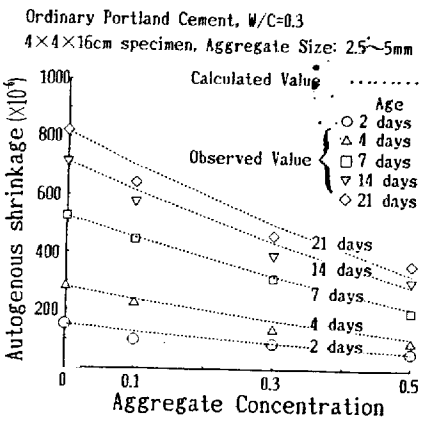

Fig.12 Influence of aggregate concentration on autogenous shrinkage of mortar (4x4x16cm)

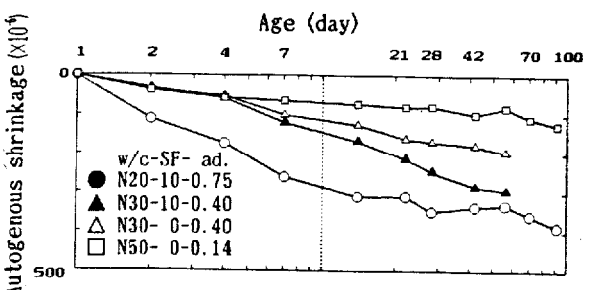

Fig.13 Autogenous shrinkage of concrete (10x10x40cm)

(5) Autogenous shrinkage could be effectively decreased by addition of drying shrinkage reducing agent or expansive admixture which were well selected.

(6) Addition of aggregate decreased autogenous shrinkage of mortar. This effect was estimated by the customary composite models.

(7) Large amount of autogenous shrinkage was observed on concrete with low water-cement ratio containing condensed silica fume.

REFERENCES

1. Powers,T.C. & Brownyard,T.L. : "Study of the Physical Properties of Hardened Portland Cement Paste, Part 9. General Summary of Findings on the Properties of Hardened Portland Cement Paste". Bulletin No.22, Portland Cement Association,1948

2. Copeland,L.E. & Bragg,R.H. : "Self-Desiccation in Portland-Cement Paste". Bulletin No.52, Portland Cement Association,1955,1-11

3. Davis,H.E. : "Autogenous Volume Change of Concrete". Proc. of ASTM,40,1940,1103-1110

4. Paillere,A.M.,Buil,M. & Serrano,J.J. : "Effect of Fiber Addition on the Autogenous Shrinkage of Silica Fume Concrete". ACI Material Journal,Vol.86,No.2,1989, 139-144

5. Mcgrath,P. : "Self-desiccation of Portland Cement and Silica Fume Modified Mortar". Ceramic Transactions, Advanced in Cementitious Materials,Vol.16,The American Ceramic Society,1990,489-500

6. Tazawa,E., Miyazawa,S. & Shigekawa, K. : "Macroscopic Shrinkage of Hardening Cement Paste due to Hydration". CAJ Proceedings of Cement & Concrete,No.45,1991,122-127(in Japanese)

7. Tazawa,E. & Miyazawa,S. : "Autogenous Shrinkage of Cement Paste with Condensed Silica Fume". Fourth CANMET-ACI International Conference on Fly Ash, Silica Fume, Slag and Natural Pozzolans in Concrete, Istanbul, Turkey, 1992 (to be published)

8. Tazawa,E., Miyazawa,S. & Sato, T. : "Autogenous Shrinkage of Cement Paste". Extended Abstracts, The 46th Annual Meeting of CAJ,No.46,1992 (in Japanese, to be published)

9. Pickett,G. : "Effect of Aggregate on Shrinkage of Concrete and Hypothesis Concerning Shrinkage". Journal of ACI,1956,581-590,

10. Hobbs,D.W., "The Dependence of the Bulk Modulus, Young's Modulus, Creep, Shrinkage and Thermal Expansion of Concrete upon Aggregate Volume Concentration". Materials and Structures/Research and Testing,Vol.4,No.20,1971,107-114

THE USE OF ADMIXTURES IN HIGH ALUMINA CEMENT MORTAR FOR THE MARINE ENVIRONMENT

N C Baker and P F G Banfill

School of Architecture and Building Engineering
Liverpool University, UK

SUMMARY

High Alumina Cement (HAC) mortars, made at 5°, 20° and 40°C, were mixed using seawater, de-ionised water and reconstituted seawater. The admixtures used were: an accelerator, a superplasticiser, anti-washout, air-entrainment, water-proofer and an ethylene-vinyl acetate (EVA) polymer latex dispersion. Results on strength and hydrate development, permeability and chloride ion migration, and short term durability against freeze/thaw and wet/dry cycling in seawater are presented. The accelerator gave good early strengths but poor resistance to freeze/thaw. The superplasticiser gave poor resistance to freeze/thaw. Air entrainer, waterproofer, polymer latex and anti washout admixture all inhibited conversion to some extent but the latex gave poor strength and durability. Air entrainer and waterproofer gave good freeze/thaw protection even for fully converted samples. The anti-washout admixture gave poor flexural strength at one year.

SOMMAIRE

On a fabriqué les mortiers du ciment alumineux à 5, 20 et 40°C avec l'eau de mer, l'eau pur et l'eau salée artificielle, et avec quelques adjuvants. Ici on présente des résultats du durcissement, de la conversion cristalline, du perméabilité, de la diffusion des chlorures et du durabilité contre le gélation/degélation et contre le mouillage/séchage.

INTRODUCTION

HAC is known to have superior qualities in resisting attack by seawater and many other hostile chemical environments. HAC is widely recommended as being more durable than ordinary portland cement in seawater (1,2). Conversion does continue but is usually very slow (as little as 15% in 34 years) except in the tidal zone or in warm waters. HAC made with w/c < 0.4 has been found to be particularly resistant. Some authors have suggested that HAC mixed with seawater was more likely to lead to problems, due to formation of chloroaluminates, (3) and some that it might even be better (1). Halse and Pratt (4), for instance, found that although there was early retardation with seawater and HAC, the later microstructure was very similar to that with fresh waters.

A research programme was set up to investigate the durability of HAC mortars, mixed with sea and fresh waters and with various common types of admixtures. The aim was to provide information on the effectiveness of a range of admixtures which would be useful to those designing mixes for marine applications such as repair work. Information on the effects on fresh properties has already been reported (5); this paper reports results on hardened properties.

EXPERIMENTAL PROGRAMME

Materials

HAC (Ciment Fondu) from a single batch supplied by Lafarge Aluminous Cement Co Ltd was used throughout with a standard graded sand. Three different mixing waters were used: de-ionised water (di), Irish Sea water, settled but not filtered (sw), and reconstituted seawater (corrosion test mixture - BDH Chemicals (rsw)), see Table 1. Each mix was made with one of the above waters alone and also containing additional sea salts in an amount intended to simulate the use of unwashed sea-won sand (di + ss, sw + ss and rsw + ss). The amount of corrosion test mixture needed to achieve this was 6.6g total solids per kg of sand in the mortar. In every case the total water/cement ratio was 0.4 and the sand/cement ratio was 1.5. The admixtures used were chosen to represent a range of types such as might be used in marine work, whether for bulk work or for repairs. The admixtures and their dosage rates were:

lithium citrate accelerator at 0.025% by weight of cement (Accel)
superplasticiser (FEB SP3) at 0.6% by weight of cement (SP)
anti-washout (Conplast UW) at 1% by weight of cement (AWO)
air-entrainer (Cormix AE1) at 45ml/50kg of cement (AEA)
water-proofer (Palace "Intrapruf") at 1:30 in the mixing water (WP)
EVA dispersion polymer (Vinamul 3281) at 5% solids by weight of cement (EVA).

In each case the proportions used were the maximum recommended by the manufacturer. Including the nil admixture this programme resulted in a factorial design of 126 mixes (7 admixtures x 3 waters x 3 temperatures x 2 aggregate salts content).

Table 1. Composition of sea waters (ppm by weight of each species)

Species	Cl^-	Na^+	$SO_4^=$	Mg^{2+}	Ca^{2+}	K^+	$CO_3^=$	Br^-
Sea Water (sw, Irish Sea)	19000	10500	2650	1350	400	380	160	65
Reconstituted (rsw)	16200	9960	1830	570	440	-	-	-

Mixing and test methods

The materials, except for admixtures, for each mix were brought to the temperature (5, 20, 40°C) at which they would eventually be cured. Each batch of about 5kg was dry mixed, in a Kenwood Chef domestic mixer, at 120 rev/min for 1 minute, then 1 minute of hand mixing with the mixing water plus admixture, followed by 1 minute at 250 rev/min.

The following test methods were used:

Early strength - The ultrasonic pulse velocity (UPV) by the PUNDIT instrument, hardness by Schmidt

rebound hammer and crushing strength of 75mm cubes were measured at 7 and 28 days.
Hydrate composition and conversion - Finely ground samples from crushed cubes were tested by Derivative Thermogravimetry using a Stanton Redcroft TG750 instrument.
Water permeability - The Figg procedure (6) was carried out on a cylindrical specimen 40mm diameter by 120mm long using a 10 mm hole drilled in one end.
Chloride ion migration - This was observed in a multi-sample system set up to allow chloride ions to migrate from a reservoir containing rsw through 3mm thick discs cut from 40mm diameter specimens into a chamber containing di water. The changing chloride ion concentration in the latter was monitored by repeated tests with an ion selective electrode and the diffusion coefficient calculated from the slope of the line of concentration against time.
Durability - A laboratory programme of wet/dry and freeze/thaw cycling was carried out in di water, sw and rsw. After 7 days curing in the temperature controlled tanks, each specimen (prisms 160 x 40 x 40mm) received 120 cycles spread over a 12 month period during which it stood in water to depths of alternately 25 or 100 mm (wet/dry) or in water to a constant 100mm depth but alternately frozen at -5°C and thawed at +20°C. UPV, Schmidt hardness, weight loss and length change were recorded at intervals over the year's exposure, together with visual assessment. At the end of the year each specimen was tested for flexural strength. In addition a long term exposure trial has been established in a west coast marine site, but this will form the subject of a future paper.

RESULTS

A large amount of data has been accumulated and space permits only selected significant features to be presented here. Analysis of Variance was carried out to assess the significance of the factors in the factorial design and only those factors found to be significant are described. In this context significant means that there is a less than 1% probability that the effect mentioned is due to chance.

Early strength

Admixture, temperature and the interactions between them had a statistically significant effect on compressive strength, UPV and Schmidt hardness at 7 and 28 days. Additionally water had a significant effect on compressive strength only. Fig. 1 shows the pattern of 28 day cube strengths. Strengths at 20°C were nearly always higher than those at 5°C with 40°C being lowest of all. The same pattern was seen for the UPV and Schmidt hardness.

Hydrate composition

Admixture, temperature and the interaction between them were the only significant effects on the degree of conversion. There was no difference between the results after 7 and 28 days curing. Fig. 2 shows the results averaged over all six mixing waters.

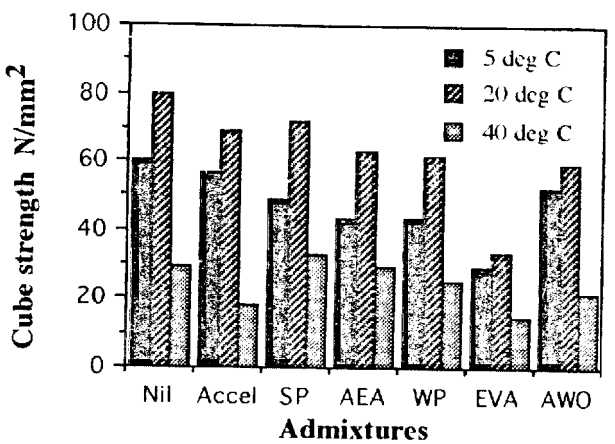

Fig. 1. Effect of admixtures on 28 day cube strength (averages over all waters).

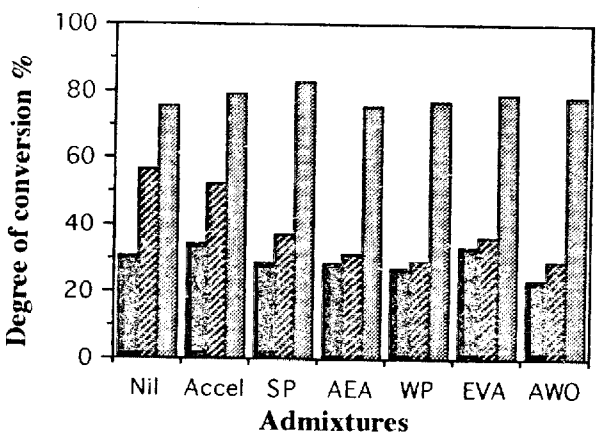

Fig. 2. Effect of admixtures on the degree of conversion at 28 days (averages over all waters)

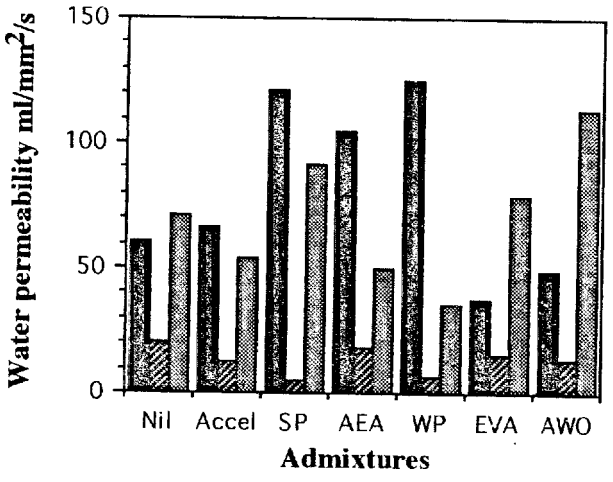

Fig. 3 Effect of admixtures on water permeability (averages over all waters).

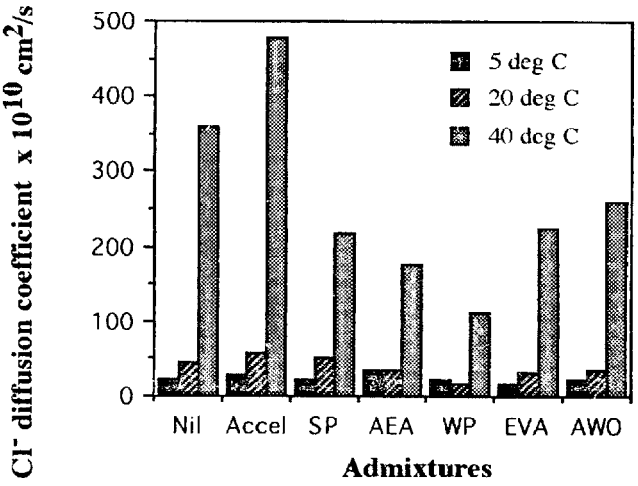

Fig. 4 Effect of admixtures on chloride diffusion (averages over all waters).

Water permeability

Temperature was the only significant effect on water permeability. Fig. 3 shows the results averaged over all six mixing waters.

Chloride migration

Admixture, temperature and the interaction between them were the only significant effects on chloride ion migration. Fig. 4 shows the chloride diffusion coefficient averaged over all six mixing waters.

Short term durability testing

Flexural strength after one year - Four way Analysis of Variance shows that the effects of the various factors on flexural strength are complex. Temperature, admixture, water and exposure regime were significant at the 1% level, as were every two- and three- factor interaction except mixing water/ exposure regime and admixture/ mixing water/ exposure regime. Table 2 shows the effect of freeze/thaw and wet/dry cycling on the flexural strength after one year.

Weight and length changes - All specimens gained in weight during the wet/dry cycling and only those containing accelerator lost weight through spalling under freeze/thaw cycling in sw and rsw. Experimental difficulties resulted in too much missing data to allow Analysis of Variance to be done on length change. Mortars containing superplasticiser, waterproofer, EVA and anti washout admixture made at 5°C tended to contract, while the remainder expanded.

DISCUSSION

Table 3 summarises the findings relating to the effects of admixtures, mixing temperatures and environment. The effects of the admixture types varied according to the test under consideration, but generally the EVA polymer dispersion performed poorly across a wide range of parameters. Air entraining agent, waterproofer, EVA and anti washout all offered some protection against conversion and also against spalling in freeze/thaw, but this is not reflected in an improved strength at a later age when compared with the

Table 2 Flexural strength (N/mm^2) of prisms after 1 year of freeze/thaw exposure.

Mix water	Temp °C	Admixture Nil	Accel	SP	AEA	WP	EVA	AWO
		Exposed to DI water						
DI	5	5.7	4.2	5.5	4.4	4.2	6.1	6.1
	20	7.9	9.8	7.7	7.9	8.1	7.8	8.2
	40	7.8	5.7	5.7	7.6	5.0	4.3	5.0
SW+SS	5	4.1	4.8	3.9	4.1	4.2	6.2	7.0
	20	6.1	7.7	6.2	5.5	7.5	8.7	6.0
	40	6.4	5.3	8.7	8.2	6.4	6.5	4.3
		Exposed to seawater (SW)						
DI	5	7.0	8.7	7.5	4.9	4.2	7.2	8.0
	20	7.5	10.5	6.7	6.2	6.4	7.3	8.0
	40	6.9	6.4	5.5	7.5	7.3	4.3	5.5
SW+SS	5	7.6	7.2	4.3	4.8	5.3	4.6	7.7
	20	5.7	4.2	6.0	5.3	5.7	5.9	4.8
	40	8.1	5.8	8.5	8.6	8.7	6.0	5.5
		Exposed to reconstituted seawater (RSW)						
DI	5	6.1	6.9	5.9	4.8	4.4	6.8	7.3
	20	7.8	9.5	6.4	6.3	7.1	7.5	8.6
	40	7.3	7.2	6.2	7.3	7.0	4.4	4.3
SW+SS	5	4.1	4.3	4.8	4.0	4.8	5.3	5.1
	20	5.6	7.6	6.3	5.4	5.5	7.0	6.1
	40	8.2	4.3	8.4	7.8	8.3	6.9	5.1

nil, accelerator and superplasticiser. Although the strength of the mixes was not as good as for the nil admixture, anti washout admixture gave very good protection against spalling in freeze/thaw and was some use in preventing washout. The superplasticiser did not give the dramatic increase in workability that would be expected in portland cement mixes, but seemed to offer other benefits: good cube and flexural strengths with some increase in flow but a similar setting time to the control. The accelerator also gave good results despite high conversion levels. It should be noted that only in the cases of the accelerator and superplasticiser had previous research considered the suitability or otherwise of the admixture for use with HAC and in most cases only anecdotal evidence was available.

As expected, temperature of mixing and curing is very important in both the early and long term performance of HAC. HAC exposed to 40°C is highly converted and other results such as strength are highly dependent on the level of conversion and the effects of other variables are largely swamped by the effect of conversion. Somewhat more surprisingly the 5°C samples, with their very low early conversion levels, did not perform correspondingly well in all tests. They performed badly in the laboratory durability trials, with spalling, poor flexural strength and high water permeability. Further work will be needed to investigate this unexpected behaviour, but later, unexplained, conversion may have played a part.

Mixing water type rarely produced significant effects but there is some evidence that a slight reduction in strength occurs with salt waters. It was slight and might not be a problem if fresh water was not readily obtainable, providing the potential problem of reinforcement corrosion is addressed.

The freeze/thaw cycling clearly had a more deleterious effect on the samples than the wet/dry cycling, but there seemed to be less of an effect due to the type of water in which the samples were stood. Salt waters appeared to lead to more spalling within the freeze/thaw groups but not in the wet/dry tests.

CONCLUSIONS

This comprehensive study has shown that the effects of admixtures are so complex that potential users of high alumina cement in the marine environment must carry out trials on any admixture which is being considered for use. Such trials must take place in the actual conditions which the material will face in practice.

Table 3 Summary of influences on test results

Test parameter	Admixture types: Nil	Accelerator	SP	AEA	WP	EVA	AWO
Chloride diffusion	-	v.high at 20°C	-	low at 5 and 40°C	low at 40°C	-	-
Conversion	high at 20°C	high at 20°C	-	inhibited	inhibited	inhibited	inhibited
Cube strength	high	high	high	medium	medium	low	medium
UPV 28days	high	high	medium	medium	medium	low	medium
Hardness	hard	hard	hard	medium	medium	soft	medium
Flexural strength 1 year	-	good	good	-	-	-	poor
Weight change	loss in freeze/ thaw in SW and RSW	loss in freeze/ thaw in SW and RSW	loss in freeze/ thaw in RSW	-	-	-	-
Visual	-	20°C mixes spalled in freeze/thaw	20°C mixes spalled in freeze/thaw	40°C mixes v.good in freeze/thaw	40°C mixes v.good in freeze/thaw	-	5°C mixes v.good in freeze/thaw

Test parameter	Mixing temperature: 5°C	20°C	40°C
Chloride diffusion	low	medium	high
Water permeability	high	medium/low	high
Conversion	low	medium	high: dominates all effects
Cube strength	medium	usually highest	lowest
UPV	medium	high	low
Hardness	medium	hardest	softest
Flexural strength after 1 year	generally low in freeze/thaw but often high in wet/dry	usually best in freeze/thaw but poor with added salt	usually poor when DI used but good with added salt
UPV over 1 year	usually highest and still rising, especially for nil and accelerator	slightly rising trend	started lowest but rose steeply apart from nil which was falling at 1 year
Length change	contracted	expanded by variable amounts	expanded by variable amounts
Visual	most except AWO were etched in freeze/thaw	some early spalling in freeze/ thaw with accel and SP	some spalling in both freeze/ thaw and wet/dry

Test parameter	Environment: DI	Freeze/thaw in: SW	RSW	DI	Wet/dry in: SW	RSW
Flexural strength	---------- rarely exceeded 8 N/mm^2 ----------			----- good results for 20°C mixes: many >8N/mm^2 -------		
Weight change	-	loss	loss	gain	-	most gain
Visual	beige/brown below water line	grey, spalling	grey, spalling below water line	beige/brown	grey	grey

REFERENCES

1. Gjorv, O.E. "Long term durability of concrete in seawater". **J. Amer. Concr. Inst.,**, 1971, 68, p60-67.
2. George, C.M. "Industrial aluminous cements" in **Structure and Performance of Cements** (ed. P. Barnes), Applied Science Publishers, 1983, p415-470.
3. Neville, A.M. and Wainwright P.J., **High Alumina Cement Concrete,** Construction Press, London, 1975.
4. Halse,Y. and Pratt, P.L. "The development of microstructure of high alumina cement" in **8th International Conference on Chemistry of Cement,** 1986, Communications theme 3, vol IV, p317-321.
5. Baker, N.C. and Banfill, P.F.G. "Properties of fresh mortars made with HAC and admixtures for the marine environment" in **Calcium Aluminate Cements,** (R.J. Mangabhai ed.) Spon, London, 1990 p142-151.
6. Figg, J.W. "Methods of measuring the air and water permeability of concrete". **Mag. Concr. Res.,** 1973, 25, (85), p213-9.

ACKNOWLEDGEMENTS

We are grateful to the Science and Engineering Research Council and Lafarge Aluminous Cement Co. for financial support under the CASE award scheme.

AUTHORS INDEX
(VOLUME IV)

A

Ahluwalia, S C – 397
Aimin Xu – 271
Aldridge, L P – 145
Asaga, K – 181
Asakura, E – 570
Atlassi, E – 634
Audley, G J – 220
Aukett, P N – 220

B

Baker, N C – 719
Banfill, P F G – 719
Baragano, J R – 557, 640
Barret, P – 234
Baxter, N I – 138
Bayoux, J P – 164, 278, 651, 705
Bensted, J – 10, 220
Bertrandie, D – 234
Bonnamy, S – 214
Borodina, T I – 51, 57
Borovkova, L B – 51, 57
Brough, A – 298
Brown, P W – 424

C

Cantrill, E R – 145
Capmas, A – 278, 705
Chaniotakis, E – 310
Chen Enyi – 691
Chen, Y – 24
Chen Yongsu – 550
Choi, S H – 97
Costa, U – 619
Crumbie, A K – 131

D

Daimon, M – 181
Damidot, D – 227, 234
Danko, G Y – 475
de Silva, P S – 671
Detwiler, R J – 241
Dobson, C M – 298
Durekovic, A – 543

E

Eguchi, H – 597
Entin, Z B – 324
Espinosa, B – 164
Evdokimova, T A – 51

F

Falaschi, J P – 705
Frangoulis, D – 310
Fukaya, Y – 124

G

Gainsford, A R – 138
Garg, M – 489
Garg, S K – 684
Gawlicki, M – 449
Gerke, S G – 38
Glasser, F P – 671
Glekel, F L – 577
Gogoi, B – 604
Goisis, M – 619
Goto, S – 304
Grimmer, A R – 234
Groves, G W – 298, 350
Guerra, G – 619
Guilhot, B – 83

H

Han, K S – 90, 97
Hanehara, S – 202
Hannawayya, F – 257
Härdtl, R – 678
Havlica, J – 157, 443
Heidemmann, D – 234
Huang, S Y – 337
Huang Wenxi – 384
Husson, S – 83

I

Ikeda, S – 304
Inada, K – 612
Inokawa, H – 612
Ishida, H – 76
Ishizaki, M – 181
Ito, S – 151, 437, 665
Ito, Y – 151
Itoh, N – 497

J

Jaung, J D – 97
Jiang, S P – 17
Jin Shuxin – 461
Joe, Y – 658

K

Kaminskas, A – 44
Kato, K – 124
Ketayya, N M – 357

Kjellsen, K O – 241
Knöfel, D – 370
Koibuchi, K – 665
Konishi, K – 181
Koo, J S – 97
Kopp, R Z – 577
Koshmai, A S – 532
Kozakai, N – 612
Krivenko, P V – 482
Krivoborodov, Yu R – 324
Krolo, P – 31
Krstulovic, R – 31
Kurdowski, W – 170, 591
Kutti, T – 468

L

Lerke, S G – 38
Levitz, P – 214
Li, J -X – 525
Lian Huizhen – 691
Liao Guanglin – 111, 418
Long Shizong – 111, 418
Lota, J S – 10
Ludwig, H -M – 3
Lui Baoyuan – 454

M

Macias, A – 557
Maggion, R – 214
Majling, J – 443
Malolepszy, J – 118
Manjit Singh – 489
Marcdargent, S – 651
Marzena Pilch – 170
Mathieu, A – 651
Melehina, T A – 51, 57
Michaux, M – 584
Milestone, N B – 138
Milia, F – 310
Miljkovic, Lj – 310
Mitsuda, T – 76
Mituzas, A – 44
Mityushin, V V – 357
Miyazawa, S – 712
Müller, A – 69
Muntean, M – 518
Mutin, J C – 17

N

Nakae, H – 570
Nawa, T – 597
Nelson, E B – 584
Nguyen, T T – 591
Nikiforov, Yu V – 64
Nikiforova, V G – 536
Nikonova, N S – 357
Nishikawa, T – 151, 437, 665
Nonat, A – 17, 227, 234
Noworyta, G – 208, 430, 627

O

Odler, I – 24, 265
Ohno, A – 612
Okabayashi, S – 104
Okada, Y – 76
Okamoto, H – 497
Okamura, T – 195
Opoczky, L – 646
Orentlicher, L P – 536
Osbaeck, B – 504

P

Pakhomov, E P – 51, 57
Panchenko, A I – 646
Papavassiliou, G – 310
Paulini, P – 248
Pera, J – 83
Petrossyan, O P M – 532
Pilch, M – 170
Poellmann, H – 363
Pratt, P L – 10, 131

Q

Qi Yanyong – 384
Qian Guangren – 384

R

Rachel J Detwiler – 241
Ram Prakash – 397
Rassem, R – 234
Reetika Sarvahi – 564
Rehsi, S S – 684
Richardson, I G – 298, 350
Roszczynialski, W – 698

S

Sahu, S – 157, 443
Sanitsky, M A – 292
Sarkar, S L – 271
Sasaki, K – 76
Sato, K – 437
Sawaki, D – 202
Scharf, H – 265
Scrivener, K L – 10
Shangina, N N – 38
Sharma, J M – 397
Shin, G Y – 90
Shizawa, M – 658
Shubin, V I – 324
Shunni Liu – 404
Song Hantang – 391
Singh, N B – 564
Singh, N P – 564
Singh, V K – 604
Sinyakin, A G – 175
Smirnova, T V – 38
Solovyeva, V Ya – 38
Sorrentino, D M – 188, 705
Sorrentino, F P – 188, 278
Stark, J – 3, 69

Stevens, M G – 145
Sturmer, S – 69
Su Muzhen – 454
Sucakas, L G – 331
Suzuki, K – 151, 437
Svatovskaya, L B – 38
Sychev, M M – 38

T

Taczuk, L – 278
Takahashi, S – 181, 497
Takatsu, M – 665
Takehiro, M – 195
Takesue, S – 658
Talero, R – 343
Tanaka, M – 124
Tang, F J – 317
Taylor, H F W – 131
Tazawa, E – 712
Teoreanu, I – 518
Testud, M – 164, 651
Tikhomirova, I N – 357
Tinet, D – 214
Tresouthick, S W – 317
Tsurumi, T – 181

U

Uchida, K – 612
Uchikawa, H – 195, 202
Uman, N I – 38
Urakawa, Y – 658
Usherov-Marshak, A V – 175

V

Van Damme, H – 214
Vernet, C – 208, 234, 430, 511, 627
Villar, V M – 640
Volceanov, A – 518

W

Wang, J – 370
Wang Yanmou – 454
Weiping Ma – 424
Wu Yanrong – 111, 418
Wu Zhaoqi – 550

X

Xu, L -P – 337

Y

Yan, P – 411
Yang, H -X – 461
Yang Nanru – 285
Yang Renhe – 454
Yang Shuzhen – 391
Yang Yurong – 384
Yaozhong Xi – 377
Yoshida, H – 570
Yoshida, K – 104
Yu Kuichang – 550

Z

Zanni-Theveneau, H – 234
Zhang Hua – 285
Zhong Beiqian – 285
Zongshou Lin – 404
Zozulya, R A – 64

9th International Congress on the Chemistry of Cement New Delhi, India, 1992

VOLUME V

COMMUNICATION PAPERS — THEME IV

NATIONAL COUNCIL FOR CEMENT AND BUILDING MATERIALS
NEW DELHI

9th International Congress on the Chemistry of Cement New Delhi, India, 1992

COMMUNICATION PAPERS

Volume V

PERFORMANCE AND DURABILITY OF CONCRETE AND CEMENT SYSTEMS

Organised by

NATIONAL COUNCIL FOR CEMENT AND BUILDING MATERIALS
NEW DELHI

Co-sponsored by:

Department of Scientific & Industrial Research
Ministry of Science & Technology
Government of India

Cement Manufacturers' Association, India

The India Cements Ltd

J K Cement Works

Madras Cements Ltd

Narmada Cement Co Ltd

Orissa Cement Ltd

This volume is a part of six-volume series of the Congress Papers.
Title of each volume is given below:

I	—	Congress Reports
II	—	Communication Papers - Theme I
III	—	Communication Papers - Theme II
IV	—	Communication Papers - Theme III
V	—	Communication Papers - Theme IV
VI	—	Reports on Special Panel Discussions and Poster Papers

Published by :
National Council for Cement and Building Materials (NCB)
M-10 South Extension Part II New Delhi-110 049 INDIA

No Part of this publication be reproduced without the written permission of the Publishers.

The views expressed in the technical papers printed in this publication are those of authors and not necessarily of the Publishers.

Printed in India by THE OFFSETTERS, New Delhi

PREFACE

Commencing with a one-day meeting in London on 14 January 1918 arranged by the Faraday Society, to discuss "The setting of cements and plasters", which is taken as the first Symposium to deal solely with the chemistry of cement, the subsequent International Symposia and Congresses on the Chemistry of Cement have been held in Stockholm (1938), London (1952), Washington DC (1960), Tokyo (1968), Moscow (1974), Paris (1980) and Rio de Jenairo (1986). At the conclusion of the Rio Congress, it was decided that the next Congress will be held in India. Accordingly, the 9th International Congress on the Chemistry of Cement is being held in New Delhi, India, from 23 to 28 November 1992.

The preparatory and organisational work for this 9th Congress was commenced immediately after the 8th Congress. To start with, all the participants in the previous two Congresses and a large number of individuals and organisations interested in the subject of the Congress were contacted through an extensively worked out and widely distributed Questionnaire. The response was most encouraging. The responses were carefully analysed and the directions which would meet the views of the largest number of participants towards advancing the cement sciences were determined. Based on these findings the first Bulletin was issued in August 1988, providing the necessary preliminary information on the Congress and outlining its scope and essential organisational aspects.

The objectives of the Congress were set to advance the knowledge of chemistry of cements with emphasis on application of this knowledge in both the manufacturing aspects and utilization of cements in practice. Within this broad scope, the thrust was on tracking the scientific progress made in the field since the last Congress, assessing the status of exploitation of the results by the industry and the society, and mapping of the new frontiers of knowledge.

The overall organisation of the Congress was governed by a National Organising Committee which was responsible for all organisational aspects including financial arrangements. Taking into account the suggestions received from various quarters, the International Scientific Committee consisting of 67 experts from 39 countries all over the world was formed which was responsible to finalise : (a) the themes and sub-themes of the Congress, (b) procedures for inviting, receiving and reviewing of papers, (c) selection of authors for general and special reports, and (d) the system for conduct of the proceedings of the sessions and other related scientific and technical matters.

The International Scientific Committee held two meetings in New Delhi in November 1989 and in January 1991. In addition, informal meetings were held with representative groups in Seoul, Tokyo, Paris, Washington DC and Montreal. The International Scientific Committee finalised the Generic and Specific Themes of the Congress. It was decided that for each Generic Theme, there shall be one Principal Review Paper, which shall cover the progress achieved in the area of the Generic Theme between the two Congresses. For each Specific Theme, there shall be one Congress Paper highlighting trends of research and realisation of the results in the industry in the areas related to the Specific Theme. Under each Specific Theme, in addition to the invited Congress Papers, there shall also be Communication Papers. Both the principal review papers as well as the Congress papers were to be presented by the invited experts identified after deliberations of the International Scientific Committee.

Preliminary Abstracts of communication papers were solicited through the Second Bulletin in May 1991. 537 Abstracts were received which were scrutinised by a panel of Indian experts and 513 were short-listed. Authors were requested to send full manuscripts of the paper for detailed review and acceptance for publication and presentation. As many as 412 communication papers from 40 countries were received which were reviewed by a panel of international experts. As a result, 346 communication papers belonging to the four themes of the Congress were finally

accepted for presentation and publication. These were in addition to 21 State-of-the-Art Congress Reports received from invited authors; reports on two Specific themes could not be had because the authors selected expressed their inability at a late stage, making replacement difficult.

In addition to the papers on deliberative thematic sessions, a poster session is being organised on "Advances in Physico-Chemical Evaluation, Characterisation and Quality Control Techniques and Systems" for Clinkers, Particulate Cements, Hydrated Systems and Concrete Systems. The State-of-the-Art Report would be presented by an invited expert and 24 contributions made in the form of posters will be presented during the Congress. In addition, Special Panel Discussions are being organised to survey the newer frontiers of knowledge in the areas of computerisation in cement science and concrete systems; resource economy in cement and concrete making; and cement in hazardous waste management.

The proceedings in six Volumes contain all the above contributions received for the Congress. This **Volume V** contains **Communication Papers on the Generic Theme "Performance and Durability of Concrete and Cement Systems".**

A novel feature of the 9th Congress will be that, in addition to the normal sessions as in the earlier Congresses, there will be three sessions to bring out the technological and techno-ecnomic impact of the scientific advances on the industry. These are intended to provide a better appreciation of the implications of the scientific advances specially on the process control machinery and related industries as well as on operational aspects related especially to energy conservation and environmental improvement. Texts of these Special Lectures will be published in Volume VII of the Proceedings to be brought out after the Congress, along with the texts of Addresses at the Inaugural and Concluding Sessions and List of nearly 550 delegates from 42 countries who are expected to attend the Congress.

I am grateful to the members of the International Scientific Committee for their whole-hearted co-operation, to those who reviewed the Abstracts, and to the International Panel of Reviewers of Manuscripts for providing very useful technical and editorial comments on the communication papers. The co-operation of the authors in accepting and implementing the reviewers' suggestions and revising their manuscripts accordingly is greatly appreciated. Thanks are also due to those authors whose communication papers could not be accepted essentially because the contributions did not fit in with the themes of the Congress and not because of any technical deficiency. We recommend that the authors have those papers published elsewhere.

The unstinted efforts put in by my colleagues in the National Council for Cement and Building Materials in all aspects of organising this Congress, is thankfully acknowledged.

A K Mullick
Chairman
International Scientific Committee
9th International Congress
on the Chemistry of Cement

New Delhi
14 September 1992

GENERIC THEME IV

PERFORMANCE AND DURABILITY OF CONCRETE AND CEMENT SYSTEMS

EXPLANATORY NOTES

The following symbols, which have been universally recognised by cement chemists for formulating more complex compounds, are used interchangeably with the respective oxide formulae throughout this volume:

A	:	Al_2O_3	K	:	K_2O
C	:	CaO	M	:	MgO
$\bar{C}$	:	CO_2	N	:	Na_2O
CH	:	$Ca(OH)_2$	P	:	P_2O_5
F	:	Fe_2O_3	S	:	SiO_2
H	:	H_2O	$\bar{S}$	:	SO_3

Commonly used abbreviations of more general nature are as follows:

DTA	—	Differential Thermal Analysis
EPMA	—	Electron Probe Micro Analysis
IR	—	Infrared
NMR	—	Nuclear Magnetic Resonance
RH	—	Relative Humidity
w/c	—	Water-cement Ratio
XRD	—	X-ray Diffraction.
SEM	—	Scanning Electron Microscope
EDAX	—	Energy Dispersive Analysis of X-rays

CONTENTS

Volume V

SPECIFIC THEME IV-A: Physico-chemical Aspects of Early History of Concrete on its Durability

1. The Effect of Cement C_3S Level on Concrete Properties 3
   S Kelham and G K Moir

2. Influence of Cement Composition on Concrete Mix Properties 9
   L A Fedner, V S Shestoperov and J E Vasiliev

3. Influence of the Components of Portland Cement on the Rheological Behaviour of Fresh Concrete 14
   Masaru Honda, Tatsuo Ikabata and Norio Yokota

4. Calcium Suiphate Optimization in Low Water/Cement Ratio Concretes for Rheological Purposes 21
   A Tagnit-Hamou, M Baalbaki and P C Aitcin

5. Durability of Mortars and Concretes with Varying Lime Standards 26
   C Fuhr, A Müller and D Knöfel

6. Activated Belite-Rich Cements - Ready for Practical Use? Investigations of Pore Fluids and Durability 32
   C Fuhr and D Knöfel

7. Influence of Constituents on the Surface Absorption Characteristics of Concrete 39
   W J McCarter and H Ezirim

8. Consideration about the Durability of Mortars with Granulated Blast-Furnace Slag as Fine Aggregate 46
   A F Battagin and L Scandiuzzi

9. Durability Aspects of Cements with High Limestone Filler Content 53
   Y Tezuka, D Gomes Jr, J M Martins and J G Djanikian

10. Influence of Gypsum Content in Portland Cements on Sulphate Resistance 60
    G Frigione and F Zenone

11. Influence of Cement Characteristics on the Protective Value of the Concrete Cover 67
    R Torrent and J Gebauer

12. Optimization of Portland Cement According to Frost Resistance Factors 74
    G I Gorchakov and A B Andreyeva

13. Effect of Diatomaceous Earth on Blended - Cement Properties 78
    C Urrutia, E Gomez and A Rojas

14. The Influence of Limestone Additions on Rheological Properties and Water Retention Value of Portland Cement Slurries 84
    Claudio Sbrighi Neto and Vicente C Campitelli

15. The Influence of the type of Cement on the Properties and Microstructure of High-Performance Concrete 89
    Shondeep L Sarkar and Moussa Baalbaki

16. Effects of the Initial Structure of the Cement Paste in Fresh Concrete on the First Developments of Strength. Influence of Superplasticizers 95
C Legrand and E Wirquin

17. The Effect of Curing Conditions on Chloride Diffusivity in Silica Fume High Strength Concrete 100
Tang Luping and Lars-Olof Nilsson

18. Permeability and Diffusion of Gases in Concrete 107
U Costa, M Facoetti and F Massazza

19. Evaluation of Compatible-superplasticizer for the Production of High-strength Concrete 115
M Rollet, C Levy and R Cavailles

20. Influence of Cement on Thermal Cracking of Concrete at Early Ages 122
R Springenschmid and R Breitenbücher

21. Retarded Expansion for Cooling Shrinkage Compensation in Mass Concrete 129
Wang Yuqing and Lou Zonghan

22. Durability of Concrete with Different Cements and Aggregates Under Sustained Load 136
Wojciech G Piasta

23. Effect of Particle Packing and Mix Design on Chloride Permeability of Concrete 143
R I A Malek

24. Determination of Consistency of Cement Paste - A Fresh Look 150
S G Shashiprakash, T S Nagaraj and B K Raghu Prasad

25. The Development of Standards for Cements 157
P J Jackson and J M Lawton

SPECIFIC THEME IV-B: Cement-aggregate Compatibility and Structure Property Relationship Including Modelling

26. Influence of Intermilling Silica Fume and Rhyolite in Icelandic Cement on Alkali Silica Reaction 167
Gudmundur Gudmundsson and Jon S Möller

27. The Alkali-Silicate Reaction in some Brazilian Dams 174
V A Zampieri, Y Kihara and L Scandiuzzi

28. Correlation of Concrete Strength with Cement Activity and Physico-mechanical Characteristics of Coarse Aggregate 181
I A Sulkowsky and A G Milrud

29. Microstructure of Interfacial Zones Between Hardened Sulfoaluminate Cement Paste and Aggregate 184
Wang Yanmou, Li Shaozheng, Lu Yonghua and Su Muzhen

30. Relationships Between Mechanical Properties of Mortars and the Hydraulic Radius of their Pores 191
S P Jiang, Ch Detriche and J Grandet

31. Correlation Between Fly Ash Effects on Permeability and Sulfate Resistance of Concrete 196
Parviz Soroushian and Abdulrahman Alhozaimy

32. Modelling and Verifying Portland Cement Concrete Strength - Time Relationship up to 50 Years Ages 203
C E S Tango

33. Relationship of Concrete Strength Development with Age 210
I A Sulkovsky and A G Milrud

34. A Mathematical Model for Blended Cement 213
G Tognon and S Cangiano

35. Mathematical Modelling of the Kinetics of Binder Hardening and its Application to Production Control of Concrete 220
K H Schlüssler

36. Models for the Development of Strength and Porosity with Time in Cements with and without Carbonate Additions — A Qualitative Durability Evaluation 226
C E S Tango, M C Florindo and V C Campitelli

37. The Diffusion Equation of Cl^- Ion Through Cement Mortar 233
X L Wu, L P Xu, Q B Yang and S Y Huang

38. Modelling of Lime Mortar Carbonation 239
K Van Balen and D Van Gemert

39. Modelling the Rheological Behaviour of Fresh Concrete 247
R I A Malek

40. Dependence of the Flow Characteristics of Concrete on the Density of Cement Stone 253
I A Sulkowsky and A G Milrud

41. Physical Determination of Corrosion of Concrete due to Evaporation of Pore Liquid 256
I P Vyrodov and V M Lekarev

42. Kinetics of Impregnation of Reinforced Concrete with Inhibitors and Other Special Solutions 262
I P Vyrodov and V M Lekarev

SPECIFIC THEME IV-C: Physico-chemical, Biological and Thermal Degradation Including Environmental Effects

43. Relation between the Degree of Hydration of Slag Cement and the Frost Resistance of the Respective Mortar 269
H-M Ludwig and J Stark

44. Concrete Durability Enhancement by Internal Timed Release of Antifreeze or Anticorrosion Chemicals for Increased Resistance to Freeze/Thaw and Corrosion 276
Carolyn M Dry

45. Mechanisms of Deicer Scaling of Concrete 282
Q B Yang, X L Wu and S Y Huang

46. Evaluation of Various Concrete Deicers 289
P P Hudec, C MacInnis and F Achampong

47. Influence of the Type of Cement on the Corrosion Behaviour of Steel in Concrete 296
P Schießl and M Raupach

48. Corrosion Susceptibility of Galvanized and Mild Steel Reinforcement in Blended Cement Concretes 302
Kalyan Dass, S S Rehsi, Tilak Raj, P C Gupta and K B Jain

49. Corrosion Characteristics of Steel in Blast Furnace Slag-Portland Cement Blends 309
H T Cao, D E Macphee, L Bucea and V Sirivivatnanon

50. Sulphate Attack on Concrete: Prediction of the AFt Stability from Phase Equilibria 316
D Damidot and F P Glasser

51. Effect of Sea Water on Calcium Monosulfate Hydrate Containing Amino Acid 322
Naomitsu Tsuyuki, Satoshi Suzuki and Junichi Kasai

52. The Behaviour of a Low Energy Cement and Two Blended Cements in Na_2SO_4 and Sea Water Media 329
M T Blanco, S Garcia, S Gimenez, A Palomo, F Puertas and T Vazquez

53. Mechanism of Deterioration of Gypsum-cement Binder Materials 335
C Ostrowski

54. Cement Type Influence on Properties and Durability of Mortars Prepared with Water and Sea Water in Sea Agression Conditions 342
Bogomil D Daraktchiev

55. Investigation into Delayed Ettringite Formation in Concrete 348
J Stark, K Bollmann and K Seyfarth

56. The Resistance of PFA Concrete to Acid Groundwaters 355
J D Matthews

57. Studies on the Carbonation of Hydrated Cement and Its Effect on Microstructure and Strength 363
H Matsusato, K Ogawa, M Funato and T Sato

58. Carbonation of Portlandite Single Crystals and Portlandite in Cement Paste 370
J R Johnstone and F P Glasser

59. Effects of Some Additives on Dynamics of Carbonation of Concrete 377
B Skenderovic

60. Effects of Air-Pollution on Chemism and Dynamics of Concrete Carbonation 383
B Skenderovic and G Lomic

61. Effect of the Carbonation Process on the Concrete Deterioration by $CaCl_2$ Aggression 389
M Collepardi and S Monosi

62. Aggressivity of Phenol Homologues Solutions and Caused Corrosion of Cement Composites 396
V Živica

63. Corrosion of Hardened Cement Pastes by Formic Acid Solutions 402
A Bajza

64. Electrochemical Degradation of Cementitious Materials 409
A Gerdes and F H Wittmann

65. An Impact of Thermal-treated Argillaceous Ochre on Properties of Decorative Cement 416
N A Sirajiddinov, Kh L Usmanov and D K Adylov

66. Durability of Concrete on High-Aluminate Portland Cement at Action of the Sign-variable Temperatures 420
Vas I Kolomiets, B I Popov and Val I Kolomiets

67. Equipment to Measure Thermal Expansion of Cementitious Materials 427
R I A Malek

68. Pore Structure and Transport Parameters of Concretes Containing Blended Cements 431
P Distler, J Kropp and H K Hilsdorf

69. Durability Evaluation of Plain and Blended Cements in Aggressive Media 438
O S Baghabra Al-Amoudi, Rasheeduzzafar, Mohammed Maslehuddin and Sahel N Abduljauwad

70. Performance and Durability of Cement Concrete Using Portland Pozzolana Cement 445
S C Maiti and N K Jain

71. Some Characteristics of a Fifty Year Concrete 452
M A Cincotto and V M John

SPECIFIC THEME IV-D: Special Concrete and Cement Composites

72. Constitution of Mortars and Pull-out of Steel Fibres 461
B Marchese and G Marchese

73. Interface and Internal Compatibility in a Copper Fibre Cement Compact Composite 468
P Kittl, G Diaz and V Martinez

74. High-strength and Durable Composites with Non-metalic Reinforcement 474
V V Glukhovskiy, N Z Mikhailishina and V P Serbin

75. Composites: Cement and Glass Fibre 479
V P Serbin, V V Glukhovskiy and R V Serbina

76. FRC Reinforced with Short Polypropylene Fibres Fracture Process 485
J R L Dyczek, M A Petri

77. Strengthening & Toughening Mechanisms in Carbon Fiber Reinforced Cements 492
N Banthia, J Sheng and M Pigeon

78. Structure/Performance Characteristics of Aramid Fibres Reinforced MDF Cement 499
R I A Malek and M N Salama

79. Physical, Chemical and Mechanical Characterization of Geopolymers 505
A Palomo, A Macias, M T Blanco and F Puertas

80. Strength Properties of Epoxy-modified Mortars without Hardener 512
Y Ohama, K Demura and T Endo

81. Several Aspects Concerning Modification of Cement Compositions by Polymer Agents 517
L J Lavrega

82. Effects of Addition of Different Quantities of Polymer Dispersions on Hydration of Portland Cement and Characteristics of Mortar 525
B Skenderovic

83. The Applications of Polymer Concrete Based on Methylmethacrylate for the Machine Tool Industry 531
Peter J Koblischek

84. Influence of Some Water Soluble Polymers on the Mechanical Properties of Cement Polymer Composites 538
Kamala Gopinathan and D V Ramana Rao

85. Increasing Water-Resistance of Phosphogypsum by Polymer Admixtures 544
M V Chumak and O S Popova

86. Improving Ductility of Concrete by Incorporating Natural Rubber Latex 550
B Kameswara Rao, K T Sundara Raja Iyengar and T S Nagaraj

87. Experimental Investigation of Fracture Properties of Ordinary Concrete and Polymer Cement Concrete 557
Wang Xinyou, Chen Gaixin and Wu Keru

88. The Composition, Properties and Application of Compound Expansive Agent 564
Wang Yanshen, Jiang Yunan, Zhang Gueiqing and Ma Kueihong

89. Properties of UEA Shrinkage-compensating Concrete and Its Application in Engineering for Asian Games 571
You Baokun, Wu Wanchun, Yu Faming, Han Lilin and Chen Fuyin

90. Effectiveness of Expansive Additives in Avoiding Early Age Thermal Cracking 578
L Ebensperger and R Springenschmid

91. FaL-G: The Lucid Concrete Media 585
P Veerabhadra Rao, N Kalidas and N Bhanumathidas

92. Strengthening Effect of Dehydrated Phases of Calcium Silicate Hydrate on Cement Concrete 589
Feng Naiqian and Ji Xihuang

93. Preparation of Novel Porous Materials from Fly Ash, Gypsum and Portlandite by means of Steam Curing-utilization of Limestone Slime and Measurement of Physical Properties of Fired Bodies 596
K Ikeda and C Tashiro

94. Improved Formulations with High Early Strength and Regulated Set 602
M M Ali, S K Handoo, N K Jain and S C Ahluwalia

95. Durability of High Strength Calcium Sulphate Free Cement 608
I P Yanev and M Z Radenkova-Yaneva

96. Volume Stability of High Magnesia Cements 614
K M Sharma, R Bhargava, S C Ahluwalia and K C Narang

97. Study of High-strength Blended Ferro-aluminate Cement Mortar and Concrete 621
Wang Yanmou, Zhang Liang, Su Muzhen and Deng Junan

98. The Hydrate Character and Durability of Gangue Cement 628
Xu Bin

99. Durability of Cement Materials Modified with Melted Sulphur 635
D A Ugincius, K I Mokritsky and L I Degteriova

100. Development of Durability-improving Admixtures for Concrete 641
Y Ohama, K Demura, K Tachibana, T Endo and Y Sato

101. Structure Formation of Cementless Concrete made with Slag Sand and High-Calcium Ash from Thermal Power Plants 647
S I Pavlenko and A B Oreshkin

102. Activated Mixed Binders and Concretes Based Upon Them 653
L A Kuznetsova, V M Dymsky, G A Korableva and T N Kobystcha

103. Use of Circulating Sand Activators in Separate Mixing Technology of Concrete 658
B V Gusev, A G Milrud, A E Lutin, I A Sulkowsky and B B Akhmedov

104. Advances in use of Sea Water for Preparing of Concrete Mixtures for Reinforced Concrete by Means of a Special Water Treatment 661
B D Darakchiev and L V Pantofchieva

105. New Technique to Examine Homogeneity of Particle Dispersion in Slag/Cement Blend and its Effect on Concrete Durability 668
R I A Malek

Specific Theme IV A

Physico-chemical Aspects of Early History of Concrete on its Durability

THE EFFECT OF CEMENT C_3S LEVEL ON CONCRETE PROPERTIES

S Kelham and G K Moir

Blue Circle Industries PLC, Technical Centre, Greenhithe, Kent, UK

SUMMARY

Five specially prepared cements, differing only in their relative proportions of C_3S and C_2S, have been subjected to a wide range of tests. With continuous water curing the early strengths were strongly correlated with the C_3S content but at 28 days and later the strengths and properties such as rate of carbonation were very similar. However, with exposure to a drying atmosphere after 24 hours moist curing, the higher C_3S cements performed much better than the low C_3S cements.

Although the high C_3S cements generally performed as well as or better than the low C_3S cements, they did give higher peak temperatures in simulated large pours.

The high C_3S cements were also more effective in activating the hydration of ground granulated blastfurnace slag and gave higher strengths in blends containing 70% ggbs even after 1 year of water curing.

RESUME

Cinq ciments spécialement préparés, dont diffèrent seulement les proportions relatives de C_3S et de C_2S, ont été soumis à toute une gamme d'essais. Avec la cure continue en eau, il y avait une corrélation marquée entre la résistance initiale et la teneur en C_3S mais à 28 jours et plus tard, la résistance et les propriétés telles que le taux de carbonatation étaient très semblables. Toutefois, avec l'exposition à une atmosphère de séchage après une cure humide de 24 heures, les ciments à une teneur plus élevée en C_3S étaient beaucoup plus performants que ceux à une teneur basse en C_3S.

Bien que les ciments à une teneur élevee en C_3S se comportaient aussi bien que ou mieux que ceux à une teneur basse en C_3S, ils ont donné des températures de pointe plus élevées lors du coulage simulé de grands volumes.

Les ciments à une teneur plus élevée en C_3S étaient également plus efficaces à activer l'hydratation du laitier de haut fourneau granulé et broyé et ont donné de plus hautes résistances dans des mélanges contenant 70 % de laitier de haut fourneau granulé et broyé même après un an de cure en eau.

INTRODUCTION

Changes in cement properties over recent decades have resulted in the strengths of standard concrete mixes increasing by approximately 50% [1]. This implies that concretes designed to meet a specified strength requirement will now have lower cement contents and higher water/cement ratios than was previously the case.

It has been argued that improvements in cement strengths may thus have led to the production of less durable concretes. The most notable change in the physical and chemical properties of cements identified in [1] was an increase in C_3S content. This historical link has resulted in the association of increasing cement C_3S contents with decreasing concrete durability.

The effect of cement C_3S content on concrete properties has been studied by Ben-Bassat, Nixon and Hardcastle [2], who used three production cements with widely differing C_3S contents. They concluded that with good curing the differences were insignificant, but with poor curing the faster hydration of the high C_3S cement produced more durable concrete. However, the cements used differed in other important respects, eg C_3A, SO_3 and alkali metal contents, which would be expected to influence cement hydration and concrete properties.

MATERIALS AND TEST METHODS

Cements were prepared from five clinkers produced in a batch rotary kiln with target C_3S contents of 25%, 35%, 45%, 55% and 65%. Except for corresponding reductions in C_2S content from 50% to 10% (total silicates ≈ 75%) the contents of other phases were maintained as constant as possible with C_3A 8-9%, C_4AF 10-12% and Eq Na_2O 0.6%. The physical and chemical properties are summarised in Table 1. Blends containing 50% and 70% of a ground granulated blastfurnace slag (ggbs) commercially available in the UK were prepared using all the cements except that with a target C_3S content of 25%.

Table 1. Physical and chemical properties of cements

Target C_3S	Bogue analysis (%)				Eq Na_2O	SO_3	SSA	+45 µm
(%)	C_3S	C_2S	C_3A	C_4AF	(%)	(%)	m^2/kg	(%)
25	24	50	9	12	0.59	2.8	354	18.8
35	34	42	9	11	0.57	2.6	352	12.5
45	42	34	8	11	0.54	2.9	351	13.2
55	54	23	8	11	0.66	2.9	355	12.7
65	68	9	8	10	0.64	2.8	347	9.1

Most tests were carried out on a concrete mix of type C1, BS 4550 : Part 3.4 (1:2.5:3.5, 0.6 w/c) using aggregates to BS 4550 : Parts 4, 5 (crushed rock and graded sand), referred to as Mix C. The same materials were also used to produce 0.5 w/c concretes (Mix E). Concrete was generally cured for 24 hours at 20°C before demoulding. One set of mix C concretes was prepared and cured at 5°C.

Compressive strengths of 100 mm. concrete cubes were determined at ages up to 1 year. After demoulding cubes were stored either in water at 20°C or in air at 20°C, 50% rh. Air stored cubes were immersed in water for 24 hours before testing. The mixes prepared at 5°C were cured in water at 5°C to an age of 28 days and then in water at 20°C.

Porosity and carbonation measurements were carried out at 1 year on cast cylinders, 150 mm diameter, 50 mm height, which were exposed to air at 20°C, 50% rh after either 24 hours or 28 days of curing. The capillary porosity was measured using a published method [3] and the cylinders then split and the depth of carbonation measured by applying a solution of phenolphthalein to the fracture surfaces.

A controlled thermal leakage semi-adiabatic calorimeter was used to measure temperature rises in simulated 3m pours.

EXPERIMENTAL RESULTS

Strength results

The compressive strength results for the mix C (0.6 w/c) concretes containing the five cements with water curing are shown in Fig 1. Up to seven days the strengths increase with increasing C_3S content. At 28 days C_3S level in the range 35% to 65% had little influence on strength. At later ages the highest strengths were given by the 35% and 45% C_3S cements. Very similar results were obtained for mix E (0.5 w/c) concretes and EN 196 Pt 1 mortars (0.5 w/c). The air cured cubes showed no increases in strength after 28 days and the later strengths were approximately equal to the 7 day water cured strengths. All the 0.6 w/c concrete strength results are given in Table 2.

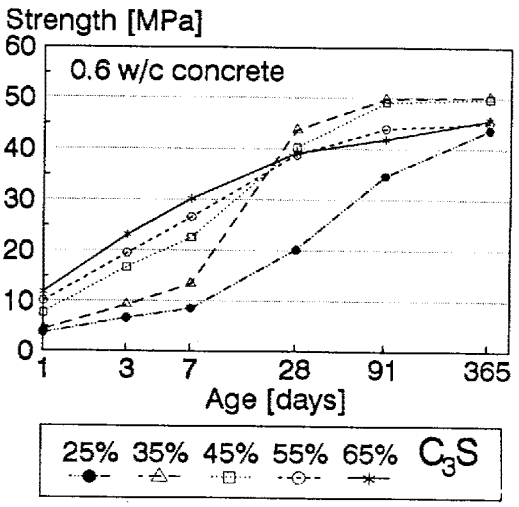

Fig 1 0.6 w/c concrete strength development.

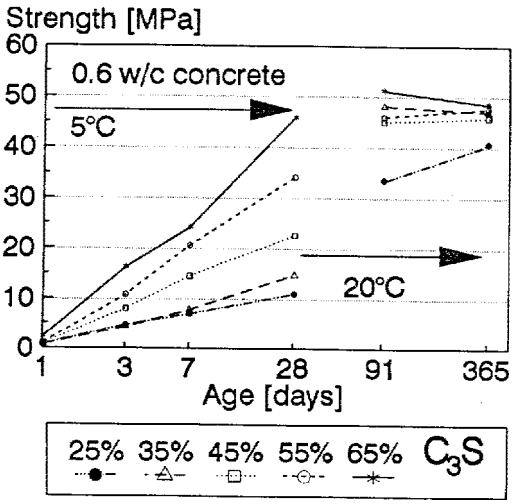

Fig 2 0.6 w/c concrete strength development at 5°C.

Table 2 0.6 w/c concrete strength results [MPa]

Blend/cure	C_3S	Age [days]					
	[%]	1	3	7	28	91	365
Water cured	25	3.8	6.7	8.6	20.2	34.7	43.7
	35	4.5	9.3	13.4	43.7	49.7	50.1
	45	7.7	16.7	22.6	40.3	49.1	49.7
	55	10.1	19.5	26.6	38.8	44.0	45.1
	65	11.8	23.1	30.2	39.2	41.9	45.7
Air cured	25	-	-	8.8	13.7	14.5	14.8
	35	-	-	12.7	17.6	19.1	18.5
	45	-	-	20.7	26.8	26.4	23.6
	55	-	-	24.0	30.2	32.3	28.4
	65	-	-	27.1	31.2	32.9	31.4
Water cured 5°C for 28 days then 20°C	25	0.6	4.7	6.9	10.9	33.5	40.7
	35	0.7	4.3	7.7	14.6	48.1	46.9
	45	0.9	7.9	14.4	22.5	45.6	45.8
	55	1.0	10.7	20.5	34.0	45.9	47.6
	65	2.2	16.2	24.1	45.9	51.2	48.6
50% ggbs water cured	35	1.6	4.4	8.9	25.4	48.8	57.6
	45	2.6	7.0	12.6	30.8	48.9	55.6
	55	3.3	8.5	14.9	33.3	47.4	56.8
	65	5.0	11.5	16.6	34.2	46.8	54.5
70% ggbs water cured	35	0.6	2.5	6.0	15.1	24.4	29.3
	45	1.2	4.8	11.4	26.0	35.0	44.9
	55	1.5	5.3	11.4	27.5	38.3	47.8
	65	2.2	6.6	12.0	28.9	41.0	51.9

The strengths of the mixes prepared and cured at 5°C are shown in Fig 2. Up to 7 days all the strengths are lower than those obtained at 20°C, with the lower C_3S cements affected more than the high C_3S cements. After 28 days at 5°C the 65% C_3S gives a higher strength than at 20°C. The 35% and 45% C_3S cements do not show the rapid increase in strength between 7 and 28 days observed with 20°C curing. Subsequent storage at 20°C produced strengths similar to those obtained with continuous 20°C curing.

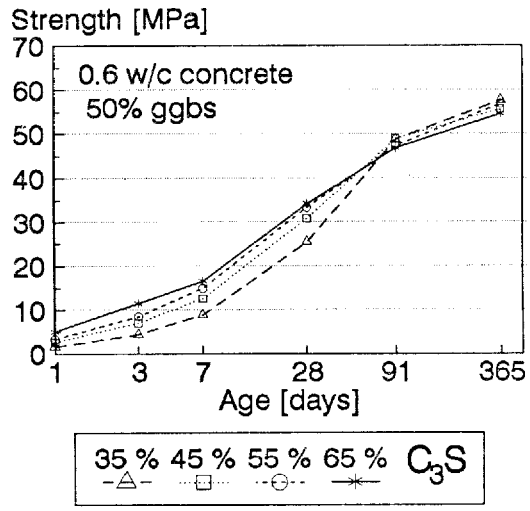

Fig 3 0.6 w/c concrete strength development for 50% ggbs blends.

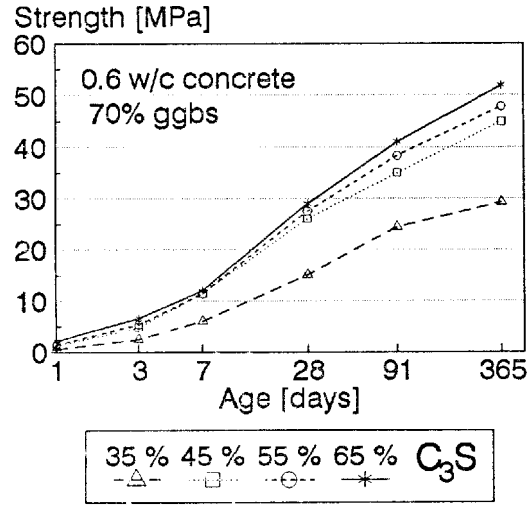

Fig 4 0.6 w/c concrete strength development for 70% ggbs blends.

The strengths of the 50% and 70% ggbs blends are plotted in Figs 3 and 4. Note that no blends were prepared from the 25% C_3S cement and that all the relevant OPC strengths were approximately the same at 28 days and later.

The 50% ggbs blends all give the same strengths at 91 and 365 days, but up to 28 days the strengths increase with increasing cement C_3S content. The strengths of the 70% ggbs blends remain dependent on cement C_3S content up to 365 days, with the 35% C_3S cement giving particularly low values. At 91 days all the 50% ggbs blends give strengths approximately equal to the OPC strength but only the 65% C_3S cement 70% blend gives the same strength as the OPC. The 35% C_3S cement 70% blend gives only half the equivalent OPC 91 day strength.

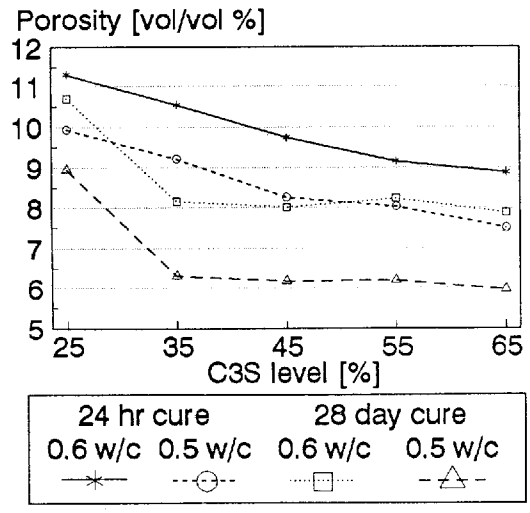

Fig 5 Capillary porosity of 0.6 w/c concrete conditioned at 20°C, 50% rh.

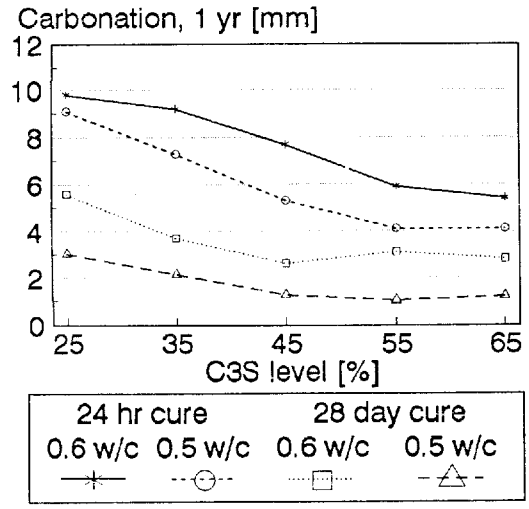

Fig 6 Depth of carbonation of 0.6 w/c concrete after 1 yr at 20°C, 50% rh.

Porosity and carbonation results

The capillary porosity and depth of carbonation were measured after 1 year of exposure at 20°C, 50% rh. The results are presented in Figs 5 and 6. The porosity and carbonation results have similar dependencies on C_3S content, w/c ratio and curing. With 24 hour curing the quality of the concrete increases steadily with increasing cement C_3S content while with 28 day curing the results are independent of C_3S content except at very low values. This agrees well with the strength results.

Large pour simulation results

The peak temperatures and the times at which they occurred for simulated 3m pours are given in Table 3. The peak temperatures increase with increasing cement C_3S content.

Table 3 - Large pour simulation data

Cement C_3S content [%]	Peak temperature [°C]	Time of peak [hours]
25	43.2	65
35	49.3	110
45	53.6	90
55	57.3	70
65	57.2	70

DISCUSSION

The OPC results generally support the findings in [2] that in well cured concrete of a given cement content the C_3S content of the cement has little influence on the concrete properties but in poorly cured concrete the quality of the concrete increases as the cement C_3S content increases. If the 25% C_3S cement is excluded the results are consistent with a simple model in which the rapid C_3S hydration and the slower C_2S hydration proceed independently and the total degree of hydration at any time determines the concrete properties. The C_2S appears to hydrate more slowly in the 25% C_3S cement than in the others. This may be due to a reduction in the activation of C_2S hydration by C_3S hydration [4].

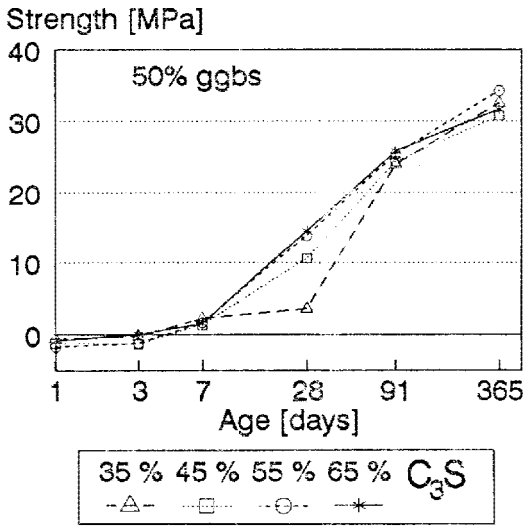

Fig 7 Contribution of ggbs to strength in 50% ggbs blends.

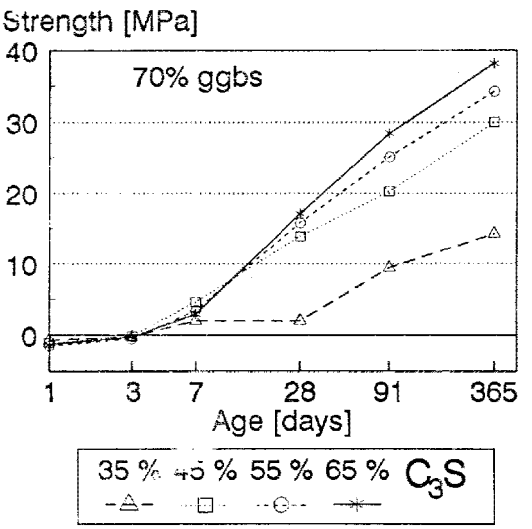

Fig 8 Contribution of ggbs to strength in 70% ggbs blends.

By subtracting the relevant proportion of the OPC strengths from the ggbs blend strengths the contribution of ggbs hydration to the blend strengths can be estimated. Results of such calculations are shown in Figs 7 and 8. The 50% ggbs results suggest that ggbs hydration is delayed in blends with low C_3S cements, leading to different levels of hydration at 28 days, but subsequent hydration rates are unaffected, leading

to ggbs contributions at later times independent of cement C_3S content. However, the 70% blend results show a large dependence of ggbs contribution to strength on cement C_3S content at ages up to 1 year. Without data at later ages it is not clear whether this is due to a reduction in the rate of hydration, as in the 50% blends, or a limit on the extent of possible hydration, perhaps related to the lime/ggbs ratio in the blend.

CONCLUSIONS

Within the range giving acceptable cement properties (35-65%), an increase in cement C_3S level leads to:-

Higher early strengths.

Almost unchanged 28 day strengths when tested under standard laboratory conditions.

No change in the potential durability of well cured concrete.

Improved potential durability of poorly cured concretes.

Increased peak temperatures in large pours.

More rapid strength growth when combined with ggbs.

REFERENCES

[1] Concrete Society. "Changes in the properties of ordinary Portland cement and their effects on concrete." Concrete Society technical report No 29, Concrete Society, London, 1987.

[2] Ben-Bassat M., Nixon P. J., Hardcastle J.: "The effect of differences in the composition of Portland cement on the properties of hardened concrete." Magazine of Concrete Research, June 1990, 42, No 151, 59-66.

[3] Kelham S.: "A water absorption test for concrete." Magazine of Concrete Research 1988, 40, No 143, 106-110.

[4] Odler I. and Schuppstuhl J.: "Combined hydration of tricalcium silicate and ß-dicalcium silicate." Cement and Concrete Research, 1982, 12, No 1, 13-20.

INFLUENCE OF CEMENT COMPOSITION ON CONCRETE MIX PROPERTIES

L A Fedner, V S Shestoperov and J E Vasiliev

Moscow Automowile and Highway Institute, Moscow, RUSSIA

SUMMARY

This paper prasents resalts of a laboratory investigation in the influence of morphological, chemical and mineralogical composition of cement on principal structural and technological properties of cements and cement mixes.

For several years cement properties cataloguing was carried out at Moscow Automobile and Hihgway Institute. Influence of morphological,chemical and mineralogical composition of cement on principal structural and technological properties of cement and cement mixes such as water-demand, plastisizing capacity,deformation ability (shrinkage and creep), strength and freezing resistance has been studied.The programme of cement testing involved investigation of two types of concrete mix.

Type 1 mix with setting cone= 2-3 cm was used to study plastisizing capacity by adding technical lignosulphonate (0.2% from cement mass).Water-demand, influence of steamig on strength , deformation ability and freezing resistance have also been investigated.Thermal moist curing was carried out in the range 2+3+6+4, t=80°C.

Type 2 mix was used to study the mix ability to preserve mobility with time. Besides influence of different hardening conditions (dry air and moist air conditions) on concrete strength has been considered.

Shrinkage and "basic" linear creep for the concrete with cement content between 320 kg/m^3 and 400 kg/m^3 and water consumption between 180 kg/m^3 and 205 kg/m^3 were determined.

TABLE 1.

Clinker miniralogical composition.

Type of clinker		Cement index mark	Content of minerals			
alite	alluminate		C_3S	C_2S	C_3A	C_4AF
C_3S<60%	C_3A=5-8%	Ks, Kr; V; Nl, Nk, Nv; Yl,Yn; Po, Pr.	56-59	12-19	6-8	12-15
	C_3A>8%	M ; Y	58-59	16-17	9	12
	C_3A<5%	CHm ; O	62	15-17	4	14-17
C_3S>60%	C_3A=5-8%	Vs; Al; Br,Bq; Z; Bk, Bs, Bg, Bo.	60-68	10-20	5-7	11-14
	C_3A>8%	Sp	61	13	10	12

The cubic strength of concrete in most of the test was: at 7 days - about 30 MPa, at 28 days= 40 MPa.Prolonged loading of the drying-proof prisim samples was carried out at the age of 7 days (the loading was 20 - 30 % of the prism compression strenght). Shrinkage observation started at the age of 2 - 3 days. Long-term deformation development was observed no less than a year. From Table 1 which presents mineralogical composition of clinkers you can see that these are mostly average alluminates containing between 5% and 8% of C_3A. Only three clinkers can be regarded as high alluminates (9-10% C_3A) and two of then low alluminates(4% C_3A). As for the content of another cement mineral C_3S the investigation presents 7 overage alites (up to 60% C_3S) and 10 high alites (over 60% C_3S). Besides normal Portland cement M400, 500, 550 and 600 4 kinds of alinite cements made with application of low-temperature synthesis technology were tested. As to the morphological composition the study also deals with practically al kinds of multy-purpose cements widely used in

the Russia such as pure clinker-cements (PC),cements with mineral additions (PC Ma), fast-hardening (FHC) and platisized cements (PC pl) (see Table 2).

To manufacture the concrete mix river quartz sand with medium sized particles (fineness modulus=2) and road metal made from dense limestone with 5-20 mm fraction were used. The data of Table 2 which gives general results relating to the influence of the above-mentioned factors on the concrete strength make it possible to draw the following conclusions:

TABLE 2.

Concrete strength

Cement index mark	Influence of dry storing: R_{28} dry storing condition / R_{28} normal storing condition			
	without TMC	with TMC	with LST	with TMC and LST
600 & 550	0,70	0,99	0,80	1,01
500	0,80	1,01	0,78	1,04
400	0,83	1,03	0,84	1,01
400 LTS	0,87	1,01	0,85	0,98

Cement index mark	Influence of TMC: R_{28} with TMC / R_{28} without TMC		Influence of LST: R_{28} with LST / R_{28} without LST	
	without LST	with LST	without TMC	with TMC
600 & 550	0,96	1,00	1,04	1,07
500	0,99	0,83	1,16	0,97
400	0,98	0,89	1,05	0,98
400 LTS	1,05	1,06	1,04	1,04

1. Maximum strength loss while dry hardening was observedwith the concretes based on highly durable cements,and the concretes based on alinite cements had the minimum strength loss. As for the steamed concrete the influenceof dry storing on strength is practically si-

milar for the 4 groups of cement.

2. Plasitisized concretes based on highly durable cements also showed considerable strength loss while dry hardening as compared to the cement M 400.

TABLE 3.

Cement index mark	Concrete creep: Creep rate $C_{365} \times 10^{-5}$, MPa^{-1} without TMC	Concrete creep: Creep rate $C_{365} \times 10^{-5}$, MPa^{-1} with TMC	Concrete creep: Effect of thermal moist curring (TMC) C_{365} with TMC / C_{365} without TMC
600 & 550	4,7	4,3	0,91
500	5,7	6,0	1,05
400	4,7	6,0	1,26
400 LTS	12,6	9,2	0,73

Cement index mark	Shrinkage of concrete: Shrinkage E, mm/m without TMC	with TMC	Effect of TMC: E with TMC / E without TMC, without LST	Effect of TMC: E with TMC / E without TMC, with LST	Effect of LST: E with LST / E without LST, without TMC	Effect of LST: E with LST / E without LST, with TMC
600 & 550	0,38	0,30	0,78	0,85	0,93	1,05
500	0,40	0,34	0,86	0,85	1,07	1,02
400	0,42	0,36	0,86	0,90	1,06	1,12
400 LTS	0,64	0,46	0,85	0,79	1,02	0,95

3. After stearming all kinds of concretes except those containing for low temperature synthesized cements showed stength reduction on the 28-th day the most cosiderable drop being observed with plastisized concretes.

4. Itroduction of lignosulphanate (LST) additive with simaltaneous reduction of water consumption and preservation of permanent mix mobility resulted in increased concrete strength without thermal moist curing (TMC). It also increased the strength of the steamed cocrete containing M 600, M 550 and low temperature synthesized cement.But it almost didn't change the strength of the concretes based on M550, M400 cements with thermal moist curing.

The data of Table 3 concerning concrete deformation ability eanble us to draw the following conclusions:

1. The rate of creep of the Portland cement concrete ranges widely. For the concretes without moist curing the creep rate of C_{365} ranged from 2MPa to $10x10^{-5}$ MPa^{-1} and for the streamed concretes from 3 to $12x10^{-5}$ MPa^{-1} . The LST cements have higher absolute values (twice as high) and wider creep range (from 7 to $24x10^{-5}$ MPa^{-1}). Concrete shrinkage rangeed from 0,23 to 0,56 mm/m for the concretes without moist curing it to 0,2 - 0,45 mm/m for the steamed concretes contining Portland cements. Maximum values of shrinkage for LTS cement concretes ranged between 0,54 and 0,82 mm/m and between 0,35 - 0,60 mm/m respectively.

2. Effect of steaming on prolonged concrete deformation is very complicated. It depends on mineralogical and material composition of cement, namely on additives presence.

For example, the concretes containing pure clinkered cements showed creep reduction by 10% on the average after thermal moist curing and the deformation of cemens with active mineral additives practically didn't change. For fast hardening cements the creep has considerably increased (by 50 %).The creep of the steamed concrete based on plasticized cement has considerably increased as well. As to the steming effect it should be noted that approximately half of the samples based on ordinary Portland cements showed increased creep,a quarter of them had reduced deformation and for the rest creep rate did not change after moist curing. As far as shrinkage is concerned we can say that it usually decreases after steaming (by 15 - 20 % on the average).

3. Influence of active mineral additives on concrete creep and shrinkage which was evaluated by comparing the deformation of pure clinker cements and cements with mineral additives from one plant comes to the following. Introdaction of trenel and pozzolanic additives slightly influenced deformation of the concrete without thermal-moist curing (by ± 10 %). It increased creep and reduced shrinkage after steaming. At the same time slag introduction didn't affect the concrete shrinkage after thermal moist curing despite higher water and cement consumption.

Water retaining capacity was studied while, cataloguing cements. It was shown that the liquid phase distribution in cement systems is determined by water-retaining capacity and is connected with the chemical and physical processes taking place in the material.

The significance of chemical and mineralogical cement composition was pointed out too. It was established that lower coagulating water retaining capacity and increased water yelding by various techniques improves structural and technological properties of cement systems only if the yielded water is removed from the material texture.

Otherwise, the uniformity of the material will be worse, it will desintegrate and show anaesotropic properties.

INFLUENCE OF THE COMPONENTS OF PORTLAND CEMENT ON THE RHEOLOGICAL BEHAVIOUR OF FRESH CONCRETE

Masaru Honda, Tatsuo Ikabata and Norio Yokota

Central Laboratory, Sumitomo Cement Co. Ltd., Chiba, JAPAN

SUMMARY

The concrete-slump test is the most generally and widely used test to determine the rheological properties of fresh concrete. In previous examinations of the rheological behaviour of fresh concrete and cement paste, the formation of ettringite affected the concrete slump, and the water-soluble alkali and OH^- concentrations in hydration solution had little effect on the rheological properties of cement paste. Cement samples of differing amounts of alkali or free lime in clinkers were produced in order to adjust the water-soluble alkali or OH^- concentrations. The influence of the components of these cements on the slump of fresh concrete were examined. As a result, the content of orthorhombic C_3A in cement is the primary determining factor of the rheological properties of concrete. When the amount of orthorhombic C_3A increased, the heat generation increased and the concrete slump decreased. On the other hand, when the amount of free lime increased, the concrete slump decreased slightly.

要　旨

スランプ試験は，コンクリートの流動性の評価方法として，最も一般的で，広く用いられている試験方法である．コンクリート及びセメントペーストの流動性に及ぼすセメントの水和性状について調査したところ，コンクリートのスランプに対しては，接水直後のエトリンガイト生成量の影響が見られ，セメントペーストの流動性に対しては，水溶性アルカリ及びOH^-量の影響がわずかに見られた．

そこで，水溶性アルカリ量と関連の大きいクリンカー中のアルカリ量あるいはOH^-量と関連の大きいフリーライム量を段階的に変化させたセメントを製造し，これらのセメントの諸特性が，コンクリートのスランプに及ぼす影響について検討した．

コンクリートのスランプに最も大きな影響を及ぼす因子は，セメント中の斜方晶C_3Aの量であり，斜方晶C_3Aが増加すると，接水直後の水和発熱が増加し，スランプの低下が見られるようになる．また，セメント中のフリーライムもコンクリートのスランプに影響を及ぼし，フリーライムが増加するとスランプがわずかではあるが低下する．

INTRODUCTION

The ability to control the workability and hardness of concrete by altering the component materials is one of the desirable features of modern concrete production. The rheological behaviour of fresh concrete has a close relationship to its workability and has a significant effect on the durability of hardened concrete. The rheological behaviour of fresh concrete is an important factor in high-flowability concrete and in low-water content/high-strength concrete which has been developed recently. It is common to find, during trial tests, that concretes of the same mix proportion but of differing cement brands and types vary in their flowability.

It is believed that particle size and distribution of cement, as well as hydration reactivity of C_3A solid solutions affect the rheological behaviour of the fresh concrete.[1)2)3)] In addition, it has been reported that the effect of the water/cement ratio or the interaction with water reducing agents might be more important than these mentioned factors.[4)5)]

In a previous, unreported study, the formation of ettringite in the cement pastes of high-slump cements and low-slump cements were measured at 3 minutes and 6 minutes after being mixed with water by using a Differential Scanning Calorimeter. In the high-slump cement paste (Fig.1), there was no noticeable increase in ettringite between the two test times. However, in the low-slump paste, the ettringite measured at 6 minutes was 2 to 4 times greater than that in the first 3 minutes, and total formation of ettringite was greater than in the high-slump cement.

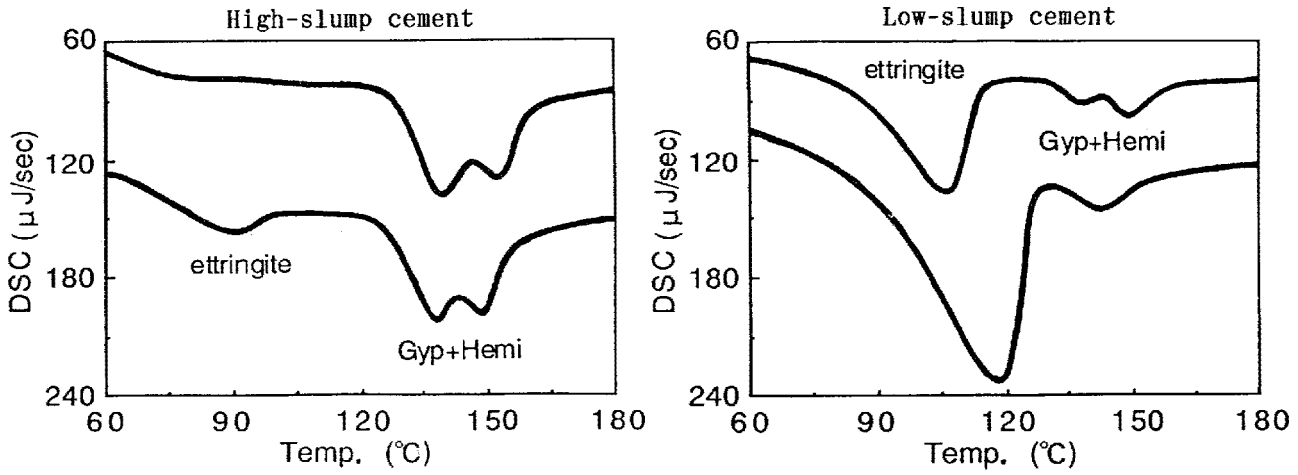

Fig.1 The formation of ettringite in the cement paste of high-slump cement and low-slump cement

Another unreported investigation into the effects of Portland Cement on the rheological properties of commercial cement(included 50 different samples) showed that the water-soluble alkali, OH^- concentration in solution and particle-size distribution of cement all have little effect on the rheological properties of cement paste. There was a slight positive correlation between the water-soluble alkali and the flowability of cement paste and a slight negative correlation between the OH^- concentration and flowability. There was also a slight negative correlation between flowability and the particle-size distribution in the fine portion of cement. However, a later study of this last factor showed a greater negative correlation[6)7)] than was achieved in the first test.

The concrete-slump test is the most generally and widely used test to determine the rheological properties of fresh concrete, and therefore, the influence of the various components of Portland Cement on the concrete slump were investigated in this paper.

EXPERIMENT 1

Preparation of cement

Accordingly, an intensive investigation was conducted into the effects that the concentration of water-soluble alkali and OH^- have on hydration in cement paste immediately after being mixed with water. Clinkers of differing amounts of alkali or free lime were produced in order to adjust the water-soluble alkali or OH^- concentrations. Two types of NSP kilns in two factories were used for preparation of the clinkers. The prepared clinkers were ground to cement with a specific surface area of 3,200 to 3,400 cm^2/g. Twenty-five samples of cement varying respectively in their alkali content and twenty-five samples varying respectively in their free-lime content were prepared.

The particle-size distribution of cement is limited by the grinding equipment. The grinding equipment at the two factories could not be altered for the various size parameters within the required time limits of this study. As a result, that part of the study having to do with particle size-distribution was abandoned.

Measurement of concrete slump, content of alkali and free lime

The alkali content of the twenty-five different samples of cement was analyzed by JIS method and the free-lime content of twenty-five free-lime samples was analyzed by the glycerine ethanol extraction method. The concrete samples were mixed in the proportions listed in Table 1 using a forced-mixing type mixer. After mixing the concrete samples, the slump of each concrete was measured.

Table 1 Mix proportion of concrete

Max.size of coarse aggregete (cm)	Water-cement ratio W/C (%)	Sand-aggregate ratio S/(S+G)(%)	Unite content (kg/m^3)				
			Water W	Cement C	Fine aggregate S	Coarse aggregate G	Chemical * admixture
25	55.0	39.9	155	282	746	1122	C×0.35

* Lignosulfonate

Experimental results

Fig.2 shows the relationship between the concrete slump and the alkali content

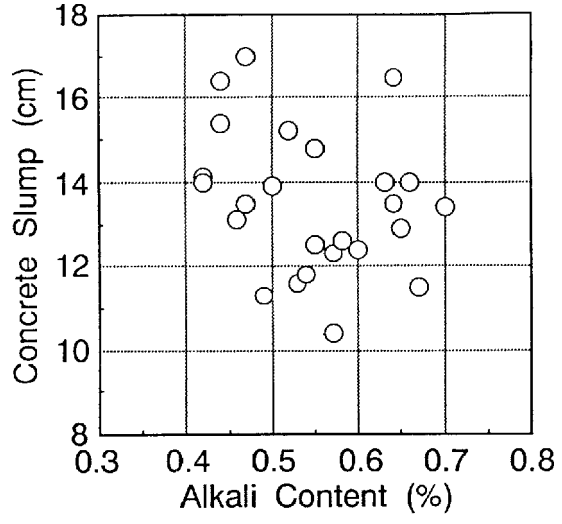

Fig.2 The relationship between the concrete-slump and alkali content

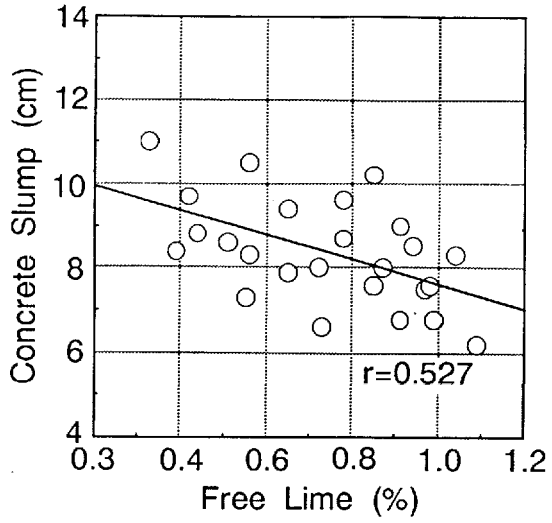

Fig.3 The relationship between the concrete-slump and free-lime content

(in Na_2O equivalents) of the twenty-five samples varied by alkali content. There was no noticeable correlation between the concrete slump and the alkali content, found in the range of 10cm to 18cm in concrete slump and 0.4% to 0.7% in alkali content.

Fig.3 shows a slight negative correlation between the concrete slump and the free-lime content found, in the range of 6cm to 11cm in concrete slump and 0.4% to 1.1% of free-lime content. The values of concrete slump in the free-lime sample were somewhat lower than those in the alkali content group.

After the slump test was performed on all of the samples, ten samples from both alkali and free-lime groups were separated from the other samples and were use for series A and F in EXPERIMENT 2.

EXPERIMENT 2

The water-soluble alkali and OH^- concentrations in hydration solution of series A and F cements were analyzed, and the heat generation of hydration using a Conduction Calorimeter were measured. The content of the C_3A solid solutions and alkali-sulfate phases were determined by a combined method of salicylic acid-methanol selective dissolution and X-ray diffraction. The methods applied to these measurements are as follows.

Measurement of water soluble alkali and OH^-

5.0g of cement sample were placed into a flask containing 50mL of water and stirred with a magnetic stirrer for 3 minutes at room temperature. The resultant solution was filtered through a dry filter paper using a weak vacuum. A 10mL aliquot of filtrate was transferred to a 100mL beaker and OH^- in solution is titrated with 0.05mol/L hydrochloric acid using phenolphthalein indicator. A second 10mL aliquot of filtrate was transferred to a 100 mL volumetric flask add 2mL of calcium solution(56,000 mg/L) was added to the solution. This was diluted to 100mL and the Na_2O and K_2O contents were determined by atomic absorption spectrometry.

Determining of C_3A solid solutions and alkali sulfate phases

The clinkers corresponding to series A and F cements were finely ground by an agate ball mill. 2.0g of clinker powder were weighed and poured into salicylic acid methanol solution and stirred with a magnetic stirrer for 30 minutes at 20 ℃ to dissolve calcium silicate. The C_3A solid solutions and alkali-sulfate phases in residue material were measured by X-ray diffraction.

Measurement of particle-size distribution

The particle-size distributions of series A and F cements were measured by using a laser diffraction particle size analyzer in a dispersion solvent.

Measurement of heat generation of hydration

The heat generation of hydration was measured immediately after being mixed with water by using the Conduction Calorimeter at a water/cement ratio of 0.5 and a constant temperature of 20 ℃.

Experimental results

Table 2 gives measurement results of each test. The series A and F cements have similar particle-size distributions, in the range of 3,200 to 3,400 cm^2/g blaine specific surface area, 1.05 to 1.11 in n value and 0.051 to 0.062 in k value which were obtained from the Rosin-Rammler equation. Therefore, the series A and F cements are examined together in a later part of this paper.

Table 2 Mesurement results of each test

Sample	Slump (cm)	Water soluble		X-ray diffraction peak height (cm)				Heat generation peak height (cm)
		eq.Na_2O (wt%)	OH^- (mmol/L)	Cubic C_3A	Ortho. C_3A	$K_3Na(SO_4)_2$	K_2SO_4	
Series A	10.4	0.310	0.189	21.0	14.4	15.2	14.8	11.5
	12.5	0.234	0.155	15.1	9.9	10.4	15.5	11.4
	12.4	0.336	0.374	25.3	9.0	14.3	6.7	9.8
	13.4	0.364	0.339	25.4	11.3	12.3	11.2	11.4
	14.9	0.302	0.224	8.9	8.6	5.4	10.3	9.5
	15.5	0.343	0.199	11.2	5.1	3.1	8.1	10.2
	16.4	0.335	0.190	15.1	4.0	5.5	10.4	8.9
	17.1	0.290	0.197	14.7	4.9	8.2	10.0	9.3
	11.7	0.425	0.308	5.8	14.1	1.3	26.3	10.8
	15.5	0.434	0.304	17.7	8.0	11.8	14.9	11.2
Series F	11.0	0.308	0.157	6.5	17.9	0.1	16.4	11.6
	9.7	0.292	0.195	5.3	25.9	0.4	20.3	14.2
	8.3	0.230	0.234	9.7	22.5	3.7	14.6	13.0
	8.7	0.279	0.279	7.2	19.0	1.3	9.9	13.1
	7.6	0.270	0.342	5.1	24.5	0.2	20.3	12.8
	8.6	0.231	0.190	7.9	22.0	3.1	15.4	14.2
	6.3	0.244	0.377	8.3	26.0	3.3	11.9	14.1
	8.1	0.298	0.290	5.3	22.8	1.3	14.6	13.0
	7.6	0.267	0.294	10.5	21.3	3.0	12.3	13.4
	6.8	0.265	0.305	6.2	18.7	0.1	16.1	13.0

Fig.4 shows the relationship between the water-soluble alkali concentration and the concrete slump. The weak negative correlation between the concrete slump and the water-soluble alkali was found.

Fig.5 shows the relationship between the contents of orthorhombic C_3A and the concrete slump. There was a significant correlation between the concrete slump and the peak height of orthorhombic C_3A in the X-ray diffraction pattern.

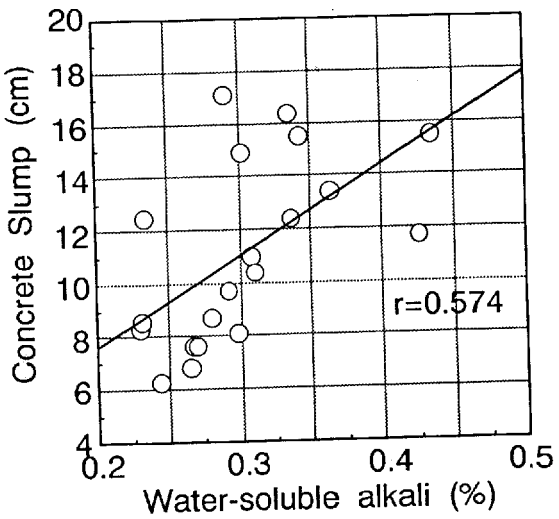

Fig.4 The relationship between the concrete slump and water-soluble alkali

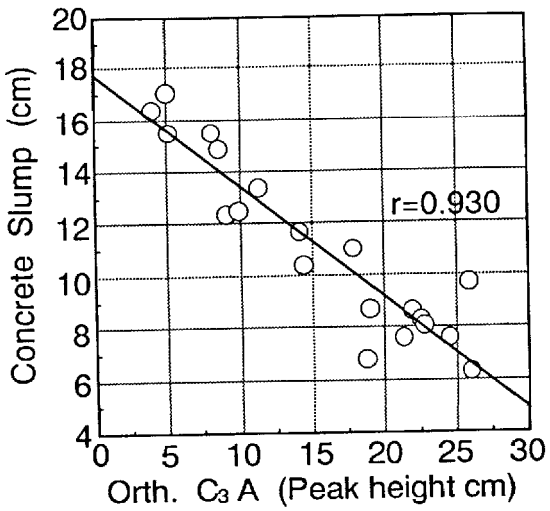

Fig.5 The relationship between the concrete slump and orthorhombic C_3A

As seen in Fig.6, the concrete slump was also strongly related to the first peak height of the heat-generation curve.

Fig.7 shows the relationship between the concentration of OH^- in solution and the concrete slump. In the series F cements, the concrete slump tends to decrease with an increase of OH^- concentration. However, in the series A cements, there is no noticeable correlation between the concentration of OH^- and the concrete slump.

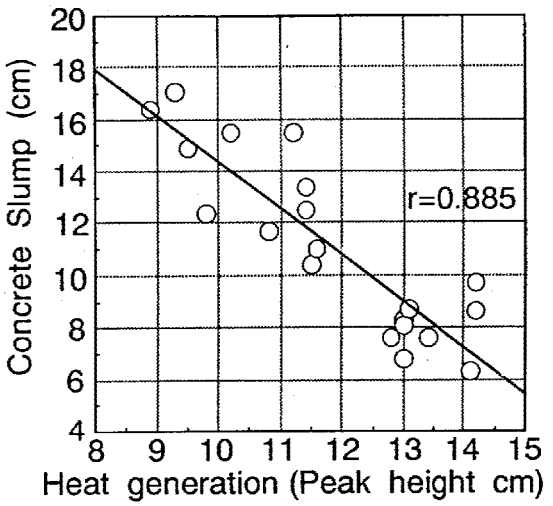

Fig.6 The relationship between the concrete slump and heat generation

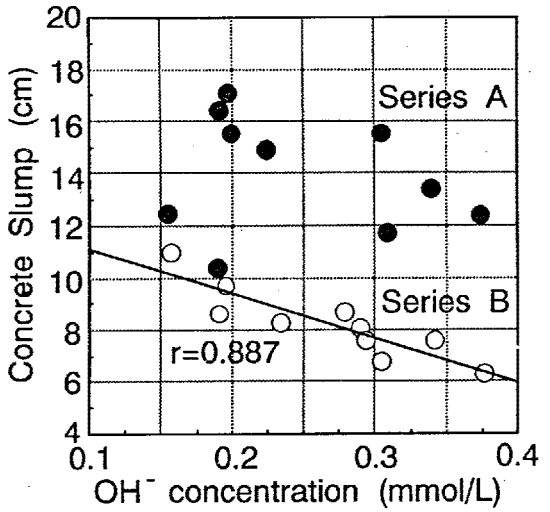

Fig.7 The relationship between the concrete slump and OH^- concentration

DISCUSSION

The hydrate of C_3A solid solutions combine with large amounts of mixing water in the first few minutes after being mixed with water and this reduces the rheologically required portion of the water. The free lime also consumes some mixing water.

It was recognized that the reactivity of the cubic C_3A is higher than that of orthorhombic C_3A.[1] However, when the calcium hydroxide and calcium sulfate coexist in the hydration solution, the reactivity of orthorhombic C_3A became much higher than that of cubic C_3A.[3)7)] The orthorhombic C_3A forms ettringite more than the cubic C_3A, and this reaction generate more heat in the first few minutes after being mixed.

Moreover, it was reported that the alkali sulfate in cement reacted with water-reducing agents, and affected the rheological behaviour of the cement paste.[8] However, the relationship between the water-soluble alkali and concrete slump shown in Fig.3 compares with that between the orthorhombic C_3A and concrete slump. It is clear that the effect of the orthorhombic C_3A on the concrete slump is grater than that of the water-soluble alkali which closely relates to the content of alkali sulfate.

The free lime also combines with the mixing water in the first few minutes after being mixed, but the combined water with free lime is less than that of the orthorhombic C_3A. Thus, the content of orthorhombic C_3A in cement is the primary determining factor on the rheological properties of concrete, while the content of free lime seems to play a smaller indirect role.

In order to confirm the results of this investigation, the clinkers which contained less orthorhombic C_3A were produced using the high-sulfur fuels and low-alkali content raw mixes, by the same kiln which prepared the series F clinkers. The concrete slump of the cements obtained from these clinkers were tested. As a result, it was confirmed that the concrete slump of these cements was improved by 6cm to 10 cm and was

nearly the same value as those in the series A cements by decreasing the orthorhombic C_3A. Fig.8 shows the photographs of the tests for slump, the left one is before the improvement and the right one is after the improvement.

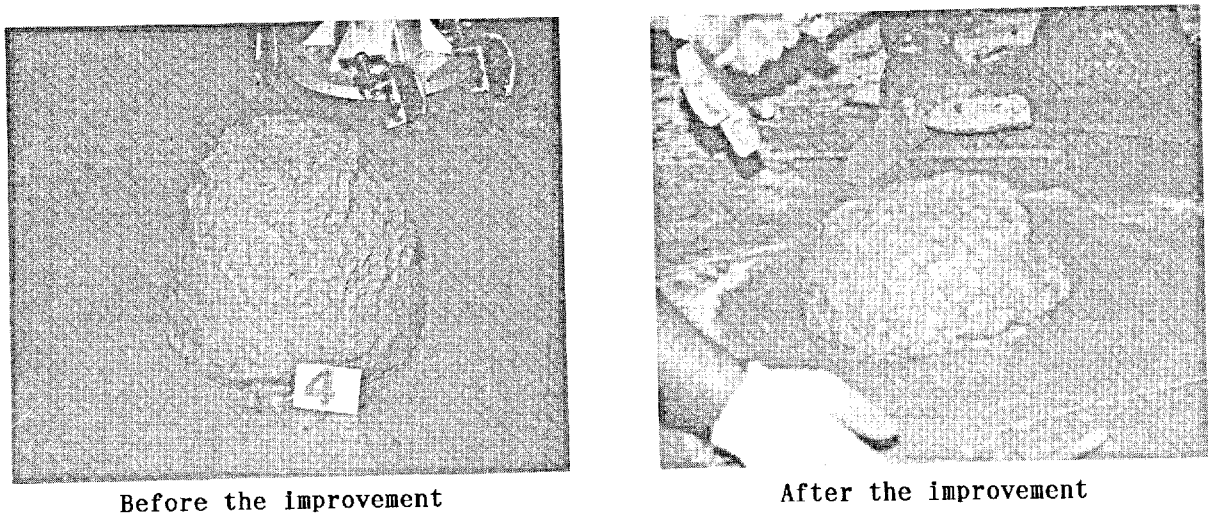

Before the improvement

After the improvement

Fig.8 The photographs of the test for slump

CONCLUSIONS

The cement which contains less orthorhombic C_3A has high flowability of cement paste and high concrete slump.

The free lime contained in cement also affects the concrete slump, but it's effect isn't greater than that of orthorhombic C_3A.

REFERENCES

1. P.Barnes "Structure and Performance of Cement" London,Applied Science Publishers,1983 p.267
2. R.A.Helmuth "Structure and performance of fresh Cement paste";Proc.7th Int. Cong.Chem. Cement,Paris,V1-0/16-0/30
3. S.Sprung "Influence of the composition of clinker and cement on the rheological behaviour of fresh concrete";Proc.8th Int.Cong.Chem.Cement,Rio,1984,vol.6,p279-283
4. I.Odler,T.Becker and B.Weiss "Rheological Properties of Cement Pastes";IL Cemento vol.3,p303-310,1978
5. J.Gebauer and Schramli "Variations in Water Requirement of Industrially produced Portland Cement";Ceramic Bulletin,vol.53,No.2,1974,G161-168
6. T.Ikabata,H.Yoshida,K.Uchida and M.Honda "Low Heat Cement and Particle Size Distribution";Review of 43th General Meeting of Cement Assoc.Japan,1989,p104-109
7. K.Sigeru,M.Suzuki,T.Ikabata and M.Honda " Effect of alkali sulfate in clinker on the hydration and properties of Portland Cement";Proc.Annul Meeting Cer.Assoc.of Japan 1985,p717-718
8. T.Nawa and H.Eguchi "Effect of Alkali sulfate on Rheological Behaviour of Cement Paste";Review of 42th General Meeting of Cement Assoc.Japan,1988,p52-55

CALCIUM SULPHATE OPTIMIZATION IN LOW WATER/CEMENT RATIO CONCRETES FOR RHEOLOGICAL PURPOSES

A Tagnit-Hamou, M Baalbaki and P C Aitcin

Faculté des sciences appliquées, Université de Sherbrooke, Sherbrooke (Québec), CANADA

SUMMARY

The gypsum content of portland cement is now optimized to meet the acceptance requirements of national standards. Such standard tests are performed on standard pastes or mortars having a water-to-cement of approximately 0.50. Pure water is always used for these tests, never any admixtures. The critical factors usually influencing the optimum gypsum content are: initial setting time, early compressive strength, and 28-d compressive strength. However, from field and laboratory experience, it has been found that the optimum amount of gypsum is not always optimum from a rheological point of view for superplasticized grouts, mortars and concretes of low water-to-cement ratios.

The rheological behaviour of different cements having different calcium sulphate contents will be presented and discussed. It will be shown in particular that, when the sulphate content of a particular cement is optimized to meet the best the present acceptance requirements, it can behave like an undersulphated or oversulphated cement from a rheological point of view when mixed in the presence of a superplasticizer, due to a strong interaction between the cement, its sulphates, and the superplasticizer. In one case it was found that a 0.5 percent change in the optimum dosage of calcium sulphate improved drastically the rheological behaviour of that particular portland cement.The two calcium sulphate optimization processes were never found to be irremediably conflicting, but in some cases, a compromise between the two optimum values can be beneficial for the field user.

These results tend to prove that a tighter control of the amount of calcium sulphate and of grinding conditions will have to be implemented in cement plants that want to serve a market in which the use of water reducers and superplasticizer will increase with the years.

RESUME

Actuellement la quantité de gypse dans le ciment Portland est établie en fonction des normes nationales d'acceptation des ciments Portlands. Les essais normalisés sont effectués sur des pâtes ou des mortiers normalisés ayant un rapport eau ciment de l'ordre de 0,50. L'eau utilisée lors de ces essais est une eau pure à laquelle on n'ajoute jamais d'adjuvant. En général, les facteurs qui influencent la quantité optimale de gypse sont: le début de prise, la résistance initiale et surtout la résistance à 28 jours. Malheureusement, à partir de mauvaises expériences de chantier et de laboratoire il apparaît que la quantité optimale de gypse n'est pas toujours optimale du point de vue rhéologique pour les coulis, les mortiers et les bétons superplastifiés ayant un faible rapport eau ciment.

Le comportement rhéologique de différents ciments ayant différentes quantités de sulfate de calcium sera présenté et discuté dans cet article. Nous montrons particulièrement que lorsque la quantité optimale de sulfate de calcium est ajoutée à un ciment en tenant compte des normes actuelles ce dernier peut se comporter du point de vue rhéologique comme un ciment sous-sulfaté ou sur-sulfaté suite à une interaction entre le ciment, le sulfate de calcium et le superplastifiant. Dans un cas particulier nous avons trouvé qu'une addition de 0,5% de gypse a un ciment déjà gypsé en fonction des normes d'acceptation actuelle améliorait significativement sa rhéologie. L'optimisation de l'ajout de gypse selon les normes actuelles et selon le comportement rhéologique du ciment ne sont pas irrémédiablement opposées et un compromis entre ces deux valeurs optimales peut être bénéfique pour les utilisateurs de ce ciment.

Ces résultats tendent à prouver qu'il faudra exercer à l'avenir un meilleur contrôle de la quantité de sulfate de calcium que l'on ajoute et des conditions de broyage dans les cimenteries qui desservent un marché où l'utilisation de réducteurs d'eau et de superplastifiants augmentera dans les années à venir.

INTRODUCTION

The role played by gypsum in controlling the setting time and hardening rate of portland cement has been well-established and the mechanisms involved understood. Using calcium sulphate to control C_3A hydration through the formation of ettringite has been thoroughly documented [1-3]. In fact, the gypsum content of portland cement is regularly tested during the production process to ensure optimum values for conformity to standards. The acceptance requirements for portland cement in most countries are based on the performance of a standard cement paste or a standard mortar, made with standard sand and tap water, at a water-to-cement ratio of about 0.50.

ADDING CALCIUM SULPHATE

Cement producers know that both the quantity and the dissolution rate of the sulphate added to clinker are important. Indeed, depending on its form, calcium sulphate dissolves at different rates: hemihydrate ($CaSO_4 \cdot 2H_2O$) liberates sulphate ions must faster than gypsum, which, in turns, does so much more readily than anhydrite. The alkali sulphates from the clinker (K_2SO_4, Na_2SO_4 or $(K,N)_2SO_4$) dissolve faster than any based on calcium [2].

Generally speaking, gypsum is added to portland cement clinker as a source of sulphate ions. But in order to increase the dissolution rate, the processing of the clinker with the added gypsum must yield some soluble hemihydrate. If the temperature during grinding isn't adequately controlled, however, excessive hemihydrate formation can render the cement liable to false set. Too low a temperature results in a lack of hemihydrate, which can cause flash set.

Despite the production problems outlined here, the current acceptance tests for portland cement perform satisfactorily for concretes having compressive strengths of 20 to 40 MPa.

THE EVOLUTION OF COMPRESSIVE STRENGTH

Over the last two decades, compressive strengths for concrete have increased well beyond 40 MPa, to the point that designers not uncommonly specify compressive strengths of 100 MPa and even greater [4]. Attaining these limits depends on lowering the water-to-cement ratio far below 0.40 with superplasticizers. In fact, a 10 to 15 L/m^3 addition of superplasticizer can yield flowing field concretes (slump greater than 200 mm) with water-to-cement ratios as low as 0.22 for compressive strengths over 100 MPa. Using a superplasticizer can reduce the mixing-water requirement by 40 to 50 L/m^3 compared to normal-strength concrete. In doing so, it brings the cement particles in such close proximity that the hydrates can bridge the gaps between them rapidly, developing very strong bonds. On the other hand, it creates rheological problems.

When using the portland cements now marketed to make very low *w/c* (very high-strength) concretes maintaining slump long enough for easy placement is more of a problem than attaining the desired strength. In addition, not all cements conforming to the standards react in the same way for this application. Some are quite compatible with superplasticizers, others show poor rheology [5]. One must wonder therefore why cements that behave identically when used to make standard paste or mortar at $w/c = 0.50$ react so radically different in the 0.20 to 0.40 range with superplasticizer.

Occurances of this lack of compatibility are likely to increase in frequency since the very low water-to-cement ratios of today's HSCs are the result of less mixing water and more cement. Accordingly, there is less water to accept sulphates, with a concomittant increase in cement particles. This means, in relative terms, that there are more C_3A sites hydrating, but less sulphate going into solution by lack of water. It follows, therefore, that the sulphates must dissolve very rapidly for good C_3A control when superplasticizers are used, otherwise the sulphonate end of the superplasticizer molecules will bond to the C_3A, resulting in rapid slump loss.

CASE STUDIES

The rheological behavior of various cements was investigated using a test that measures the flow time through a Marsh cone of slurries mixed in a high-shear mixer. Measurements were taken 5 and 60 min after mixing. Before testing the slurries, their optimum superplasticizer dosage was determined for a given *w/c* ratio. Optimum here was the point at which an increase in superplasticizer did not affect slurry rheology under the test conditions.

Table 1 gives the chemical and Bogue compositions of the tested cements, all of which conformed to ASTM standards.

Table 1 Chemical and Bogue compositions of the tested cements

Sample	1	2	3	4	5	6	7	8	9	10
SiO_2	21.06	21.05	20.90	20.30	20.78	20.58	20.46	20.29	20.62	21.6
Al_2O_3	4.07	4.01	4.14	5.63	5.68	5.71	5.71	5.68	5.66	4.5
Fe_2O_3	3.21	3.09	3.19	2.56	2.45	2.45	2.43	2.44	2.46	5.6
CaO	62.39	62.64	62.48	62.44	63.27	63.05	62.20	62.89	62.77	60.8
MgO	2.50	2.17	2.23	2.80	2.89	2.87	2.84	2.92	2.91	2.8
SO_3	3.31	3.28	3.30	3.13	2.46	2.88	3.22	2.83	2.53	2.5
K_2O	0.94	0.88	0.97	1.16	1.17	1.17	1.14	1.20	1.21	0.53
Na_2O	0.22	0.22	0.19	0.15	0.13	0.14	0.13	0.20	0.14	0.30
CaO_F*	0.39	0.36	0.30	—	—	—	—	—	—	—
LOI	3.09	2.73	2.93	0.99	0.32	0.39	0.73	0.46	0.55	0.57
C_3S	52.6	54.3	53.7	49.4	50.9	50.1	46.6	52.0	50	38
C_2S	20.7	19.4	19.4	20.9	21.2	21.2	23.5	18.9	21.4	33
C_3A	5.3	5.4	5.6	10.6	10.9	11	11	10.9	10.8	2.4
C_4AF	9.8	9.4	9.8	7.8	7.5	7.5	7.4	7.4	7.5	17.1

* CaO_F : Free lime

Example 1: Rheologically well-balanced cement

Cements 1, 2, and 3 were mixed with the *w/c* ratio maintained at 0.35 with 0.6% superplasticizer. The flow times at 5 and 60 min (see Table 2) were nearly identical for the three samples due to well-balanced reactive phases (C_3A and C_3S), fineness, and sulphate content.

Table 2 Flow time through the Marsh cone

	Flow time (s)	
Sample	After mixing for 5 min	After mixing for 60 min
1	69	83
2	67	85
3	65	84

Example 2: Influence of the degree of sulfphurization on rheology

As demonstrated by Samples 4, 5, 6, 7, 8, and 9, some cements exhibit very different rheology despite quite similar chemical compositions and fineness. These slurries had a *w/c* ratio of 0.45 with 0.6% superplasticizer.

Table 3 Flow time through the Marsh cone

Sample	Blaine fineness (m^2/kg)	Flow time (s)		
		After mixing for 5 min	After mixing for 60 min	SD* (%)
4	377	53	63	71
5	372	53	63	69
6	383	54	61	103
7	386	59	77	71
8	371	55	99	68
9	353	59	139	66

* SD : Clinker sulphurization degree = $\frac{SO_3 \cdot 100}{1.292\ NaO_2 + 0.85\ K_2O}$

Table 3 shows the difference in sulphurization degree (SD) of these cements, with the data indicating an inverse relationship between SD and flow time. To illustrate, the flow time after 60 min of mixing ranged from 61 s for SD = 103 (Cement 6) to 139 min for SD = 66 (Cement 9). These findings indicate that alkali sulphates from the clinker affect cement-paste rheology.

Example 3: Undersulfated Cement

In Québec, a special modified ASTM Type II cement is used at a high *w/c* (0.60) for dam construction. However, rheological problems develop at *w/c* = 0.40 when sulphonate-based water-reducing admixture or superplasticizers are used. From the chemical analysis of Cement 10 given in Table 1, it can be seen that this cement has a SO_3 content of 2.5%, significantly below the 3% specified by ASTM C 150.

As indicated in Table 4, 1.5% superplasticizer was needed to recover slurry fluidity at *w/c* = 0.40.

Table 4 Flow time through the Marsh cone

W/C	Flow time (s)		
	Superplasticizer (%)	After mixing for 5 min	After mixing for 60 min
0.60	0	42	55
0.50	0	NF*	NF
0.40	1	68	NF
0.40	1.5	55	85
0.40	2	54	77

* NF : No flow

To verify if the cement was actually undersulphated, various amounts of calcium hemihydrate ($CaSO_4 \cdot 1/2H_2O$) were added to the mixing water, maintaining the *w/c* at 0.40 and a superplasticizer content of 1%. Figure 1 reveals that increasing the hemihydrate content to up to 1 percent improves slurry fluidity with 1% superplasticizer at *w/c* = 0.40 to the point that it equals the 5 and 60 min flow times of slurry with 1.5% superplasticizer but no additional hemihydrate.

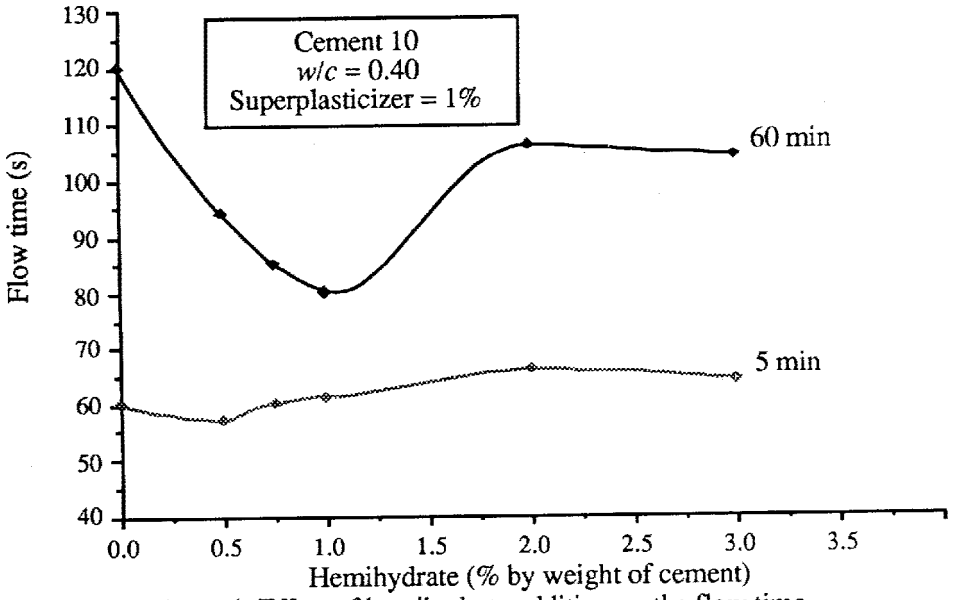

Figure 1 Effect of hemihydrate addition on the flow time

CONCLUSIONS

Up to now, the calcium sulphate content of portland cement has been adjusted to comply with national standards primarily on the basis of rheological and strength behavior of standard pastes and mortars made with tap water at a water-to-cement ratio of about 0.50. This practice has provided satisfactory results for the most commonly used concretes at *w/c*> 0.40 and having a compressive strength of 20 to 40 MPa.

Superplasticized high strength concretes, however, are characterized by a much lower *w/c* in the 0.22 to 0.40 range with compressive strengths of 50 to 100 MPa. In such concretes, the solubility rate of the calcium sulphate present in the cement becomes a critical factor in controlling rheological behavior, since they contain less water to accept the sulphate ions, but more C_3A that must be controlled.

The recent trend towards HSC adds a new factor in cement production control, which should really offer no real difficulties if the importance of calcium sulphate content and rate of solubility receive the attention they deserve. It should be noted that there are existing cements that exhibit complete compatibility with superplasticizers. Nevertheless, cements produced without regard to cement superplasticizer compatibility at low *w/c* could be at a disadvantage in the near future in the growing HSC market.

ACKNOWLEDGEMENTS

The authors express their gratitude to the Nature Sciences and Engineering Research Council and the Network of Centres of Excellence on High-performance Concrete for their financial support of this research.

REFERENCES

1. Taylor, H.F.W.: **Cement Chemistry**, Academic Press Inc.,San Diego, 1990, 475 p.

2. Frigione, G.: **Gypsum in cement.** Advances in Cement Technology, edited by S.N. Ghosh. New Delhi, Cement Research Institut of India, 1983, p. 485-536.

3. Bensted, J.: **Hydration of Portland cement.** Advances in Cement Technology, edited by S.N. Ghosh. New Delhi, Cement Research Institute of India, 1983, p. 307-348.

4. Aïtcin, P.C.: **From gigapascals to nanometres.** Advances in Cement Manufacture and Use, edited by E. Gartner. New York, Engineering Foundation, 1983, p. 150-130.

5. Ranc, R.: "Interactions entre les réducteurs d'eau plastifiants et les ciments". Ciments, Bétons, Plâtres, Chaux, Janvier 1990, 782 (1/90), 3 p.

DURABILITY OF MORTARS AND CONCRETES WITH VARYING LIME STANDARDS

C Fuhr*, A Müller and D Knöfel***

**Lab. for Chem. of Construction Materials, University of Siegen, Siegen, GERMANY*
***University of Architecture and Building, Weimar, GERMANY*

SUMMARY

To assess the effects of lime content on the durability of mortars and concretes, cements with graded lime standards 69-97 were investigated. Priorities were set up on the strength- and porosity development and the carbonation behaviour. Moreover investigations on elastic modulus, behaviour in an SO_2 - enriched atmosphere and the freeze-thaw-cycling resistance were carried out. The max. hydration time of the samples presented in this paper is 180 days. Investigations will be continued up to a hydration time of two years.

Up to now investigations of ABC with lime standard 80 have shown that there are no differences in carbonation after 4 years between concretes made from PC and ABC cement. This was found out by analysing drill cores which were taken from a road partly built of ABC and PC concrete. Investigations of specimen stored in 1 vol.-% CO_2 show that there is no higher carbonation depth of ABC than PC mortar after a simulated 60 years storage in normal atmosphere. One reason for this positive result can be seen in the lower porosity of the ABC mortars.

ZUSAMMENFASSUNG

Um die Auswirkungen des Kalkgehaltes auf die Dauerhaftigkeit von Mörteln und Betonen festzustellen, wurden Untersuchungen an Zementen mit abgestuftem Kalkstandard von 69-97 durchgeführt. Ein Schwerpunkt der Untersuchungen liegt auf der Festigkeits- und Porositätsentwicklung sowie dem Carbonatisierungsverhalten. Daneben wird das dyn. E-Modul, das Verhalten in SO_2 -angereicherter Atmosphäre sowie der Frost-Tauwechsel Widerstand untersucht. Das max. Alter der Proben in den hier vorgestellten Untersuchungen beträgt 180 Tage. Die Untersuchungen werden bis zu einem Hydratationsalter von zwei Jahren fortgesetzt.

Bisherige Untersuchungen an ABZ mit KSt II 80 haben gezeigt, daß z.B. die Carbonatisierungstiefe 4 Jahre alter Betone aus ABZ sich nicht von der von Betonen aus PZ unterscheidet. Diese Ergebnisse wurden durch Analyse von Bohrkernen erhalten, die aus einer Straße aus ABZ und PZ entnommen wurden. Untersuchungen an ABZ und PZ Mörteln, die in 1 Vol.-% CO_2 gelagert wurden zeigen im Hinblick auf ihre Carbonatisierungstiefe bei einer simulierten Lagerungsdauer von 60 Jahren in natürlicher Atmosphäre, keine Unterschiede in der Carbonatisierungstiefe. Ein Grund für diese positiven Ergebnisse ist die geringere Porosität der ABZ-Mörtel.

INTRODUCTION

The manufacturing conditions of activated belite-rich cements (ABC) are well known. Quick clinker cooling and the incorporation of the alkali oxides into belite are especially important (1,2). This effects the stabilisation of the high temperature modifications α- and α'- C_2S, which causes higher hydraulic activity. ABC has a lime standard of about 80. Its alite content of about 30% garantees a sufficient early strength; its ß- belite content of about 50% causes a high strength after longer periods. The properties of fresh mortar and the strength development of ABC were already tested on cements made in the laboratory and such made in a pilot plant (3). With regard to the durability of belite-rich cements there are contradictory statements (4,5).

The following report shows the results of investigations on the durability of cement pastes, mortars and concretes of laboratory cements with varying lime standards.

TEST PROGRAM

The experiments based on 5 cements made from natural raw materials by burning in an electrical furnace and grinding in a ball mill. The lime standard (LS III) varied from 69 to 97. Cement 1 contains no alite. Aluminates and ferrites have less CaO than usual. Cements 2, 4 and especially cement 3 are typical belite cements whereas cement 5 is a typical portland cement. Details are given in fig.1.

Cement pastes with a w/c-ratio of 0.35 and mortars with a w/c-ratio of 0.50 were prepared in accordance to DIN 1164 in 4·4·16 cm^3 molds. The concrete prisms were produced by the use of gravel with the grading line AB 8. The aggregate/cement-ratio was 4.34, the w/c-ratio 0.55. The prepared specimen were used for investigations of the degree of hydration, porosity, strength development and carbonation.

The porosity of cement pastes and mortars was measured by mercury intrusion porosimetry. After a hydration period of 7, 28, 90, 135 and 180 days a plate was cut from the prisms and crushed in small pieces of 2-4 mm. The hydration was stopped with acetone followed by a drying period of at least 14 days at 70°C.

The carbonation behaviour was tested on mortar and concrete prisms. After a previous water storage of 28 days for the mortars and 7 days for the concretes the specimen were stored in air until the 72nd day. The storage continues either in open air, protected from rain, or in a carbonation cabinet with 1 vol.-% CO_2 and a climate of 23°C and 65% rel. humidity. The prisms were stored in 1 vol.-% CO_2 for 63 and 108 days and for longer periods. They are compared with prims stored in the open having the same age of hydration, i.e. 135 and 180 days. The carbonation depth was determined by spraying the freshly cracked prisms with ethanol.- phenolphthalein solution.

RESULTS

Strength development

The strength development of the five investigated cements is effected by the lime standard in a typical way (fig.2). After 7 days the mortar made from cement 1 achieves a compressive strength of only 5.7 N/mm^2. At the same time the mortar made of cement 5 shows a compressive strength of 49.0 N/mm^2. During further hydration the rate of hydration of cement 1 increases up to 90 days while the hydration rate of cement 5 decreases. After 180 days there is only a little difference in compressive strength between cement 1 with 52.9 N/mm^2 and cement 5 with 60.2 N/mm^2.

Fig.1: Test program

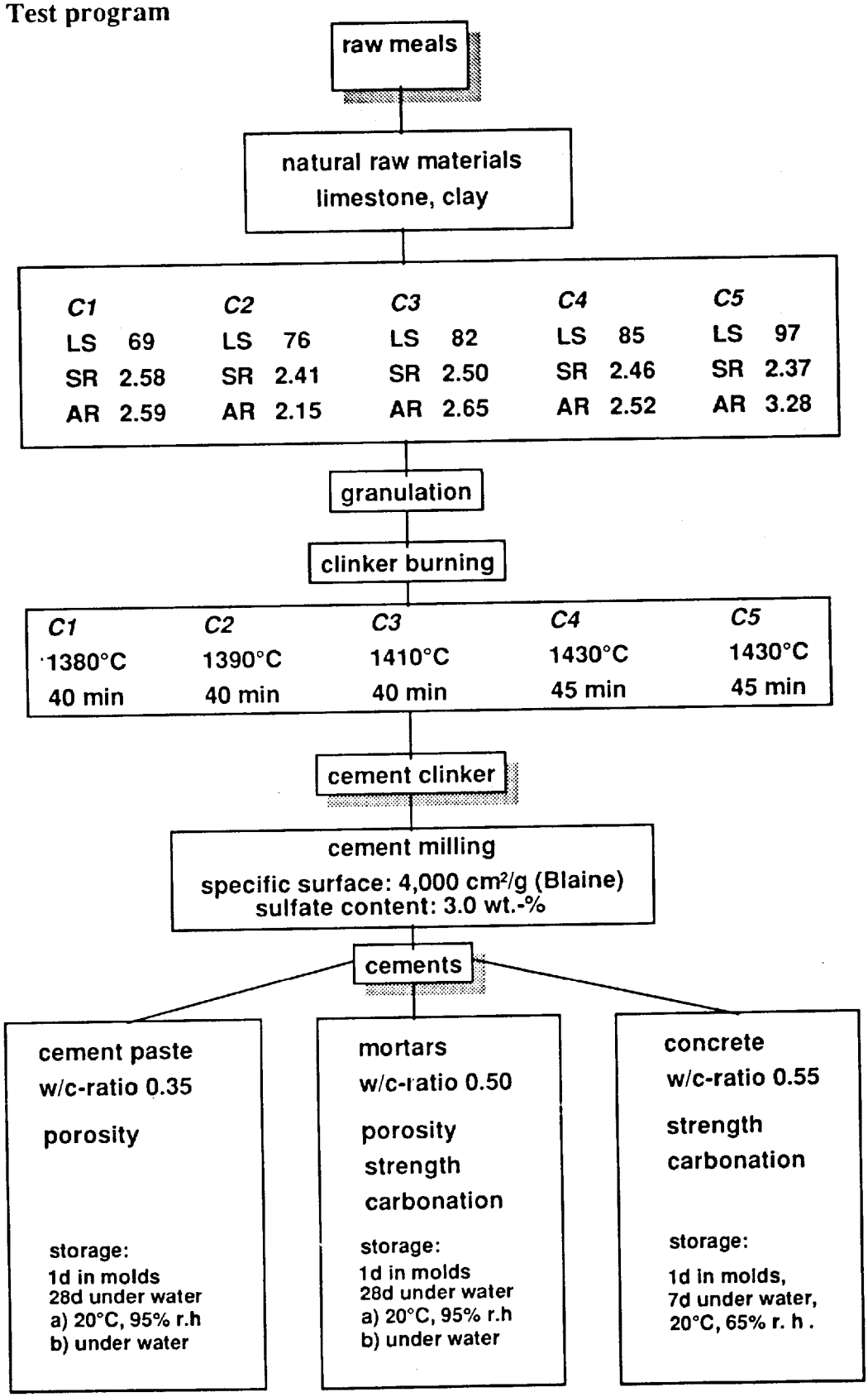

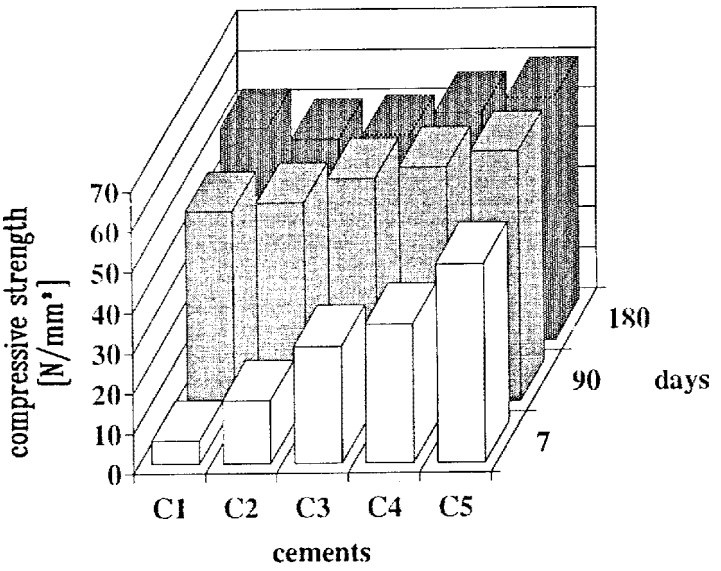

Fig. 2: Compressive strength of the cement mortars after 7, 90 and 180 days' of hydration

Concrete prisms achieve the following amounts of compressive strength after 180 days:

cement 1	β_D = 20.3 N/mm²
cement 2	β_D = 47.0 N/mm²
cement 3	β_D = 54.7 N/mm²
cement 4	β_D = 59.2 N/mm²
cement 5	β_D = 58.6 N/mm²

These results show two facts more clearly than those obtained from the mortars:

-The strength behaviour of cement 1 is rather different to that of the other cements.

-Concretes made from the belite-rich cements 2-4 nearly have the same strength as concrete from portland cement 5.

The strength investigations were completed by measurements of the periodic velocity of ultrasonic pulse. The dynamic modulus of elasticity calculated from this data amounts:

cement 1	E = 27,900 N/mm²
cement 2	E = 36,000 N/mm²
cement 3	E = 38,700 N/mm²
cement 4	E = 40,700 N/mm²
cement 5	E = 40,800 N/mm²

The gradation of the modulus of elasticity of the concretes goes rather confirm with their gradation of compressive strength.

Porosity

The capillary pore system of mortars and concretes is of decisive importance for the durability. Fig.3 shows the capillary porosity of the mortars from all five cements after various times. After 7 days the capil-

lary porosity decreases with an increasing lime standard. After 90 and 180 days there is a similar dependence, but the differences between the cements become smaller. The belite cements 2, 3 and 4 nearly have the same capillary porosity after 180 days; it amounts to 2.50%. The portland cement 5 has a little higher porosity of about 3.11%, in comparison with the belite cements it is 24% higher. The highest porosity was measured for cement 1 with 4.20%. Considering the influence of hydration time on the capillary porosity cement 1 shows the most significant decrease of porosity between the 7th and 90th day. For longer hydration periods the capillary porosity decreases only a little bit.

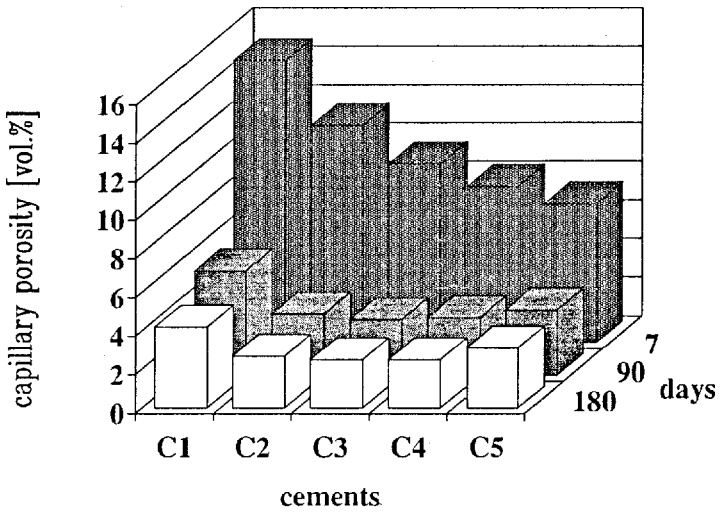

Fig. 3: Capillary porosity of the cement mortars after 7, 90 and 180 days' of hydration

Carbonation

sample	depth of carbonation [mm]			
	mortar		concrete	
	107d/63d	152d/108d	107d/63d	152d/108d
C1	2,4 / 4,4	3,0 / 5,5	2,2 / >20	1,9 / >20
C2	1,3 / 2,5	1,5 / 2,4	2,4 / 7,0	1,5 / 8,4
C3	1,1 / 1,9	<1,0 / 2,2	1,8 / 4,1	1,5 / 4,1
C4	<1,0 / 1,7	1,3 / 2,0	1,5 / 4,2	1,2 / 5,6
C5	<1,0 / 1,7	1,2 / 2,7	1,3 / 4,1	1,1 / 4,0

Table 1: Carbonation depth of the cement mortars after 107 and 152 days' storage in air or 63 and 108 days' storage in 1 vol.-% CO_2.

The higher carbonation depth of those prisms stored in the CO_2-cabinet result from the CO_2-concentration which is 30 times higher than in natural atmosphere. The 63 and 108 days' storage in 1 vol.-% CO_2 corresponds to a storage of 5 and 9 years in natural atmosphere.

As expected sample c1 with LS 69 shows the highest carbonation depth. By storage in the open sample C2 and C3-C5 have a similar carbonation depth. Storage at higher CO_2-concentration shows a clear difference between C2 and C3-C5 after 63 days. This is a result of the lower hydration progress of cement 2. Cements 3 and 4 have the lowest carbonation depth during the whole period of investigation. Cement 5 which is, with LS 97, corresponding to a commercial portland cement shows a similar carbonation depth.

In accordance with the results obtained from the mortars, the concrete from cement 1 shows the highest depth of carbonation after a hydration time of 135 and 180 days. Concretes from cements 3 - 5 have a very similar carbonation depth while concrete 2 shows a little bit higher carbonation. These results can be attributed to the slower hydration of cement 1 and 2 and the lower amount of portlandite formed during hydration in comparison with the other cements. This is also a reason for the accelerated corrosion of these specimen stored in higher CO_2-concentration. In the simulation tests concretes made from belite-rich cements 3 and 4 show the same good results as concrete from portland cement 5.

CONCLUSION

The aim of the presented investigations was to show that not only cements of portland type, but as well belite-rich cements have a sufficient durability. The results led to the conclusion, that mortars and concretes prepared from cements with lime standard 80 show similar properties as cements with lime standard 90 and higher. The compressive strength of mortars and concretes made from belite-rich cements are equivalent to those of portland cements after longer periods. Only the cement with the low lime standard of 69 shows a more unfavourable strength.

The capillary porosity which strongly influences the durability only shows a continuous increase with decreasing lime standard at early periods of hydration. After hydration times of 135 and 180 days the mortars made from the belite cements have the lowest capillary porosity, followed by the portland cement with a little higher porosity and the cement with a lime standard of 69 with a clearly higher porosity.

The carbonation behaviour essentially follows the dependence between capillary porosity and lime standard. Mortars and concretes prepared from belite cements show the same carbonation depth like the portland cement after open air curing as well as after storage in atmosphere with raised CO_2-concentration. This effect shows that the influence of the lower $Ca(OH)_2$-content, formed during the hydration of belite cements is smaller than the influence of porosity on the carbonation behaviour. Investigations on the $Ca(OH)_2$ - content of cement pastes confirm this.

ACKNOWLEDGEMENT

We wish to express our acknowledgement to Ministerium für Wissenschaft und Forschung des Landes Nordrhein Westfalen, Düsseldorf, for the financial assistance extended to this research project.

REFERENCES

1. Stark, J. et.al.: "Manufacture of active belite cement with regards to the reduction of energy consumption". Il Cemento, 1987, 84, 239-250.
2. Gies, A. and Knöfel, D.: "Influence of alkalies on the composition of belite-rich clinkers and the technological properties of the resulting cement". Cement and Concrete Research, 1986, 3(16), 411-422.
3. Müller, A. et al: "Zum Stand der Entwicklung eines aktiven Belit-Zementes". Zement-Kalk-Gips, 1985, 6(38), 303-304.
4. Knöfel, D. and Fuhr, C.: "Durability of activated belite-rich cement mortars". Ceramic Transactions, 1991, 16, 715-727.
5. Kelham, S. and Moir,G.K.: "Influence of cement C_3S level on concrete durability".**5th Int. Conference on Durability of Building Materials and Components , Brighton, England** 1990, 465-470.

ACTIVATED BELITE-RICH CEMENTS - READY FOR PRACTICAL USE? INVESTIGATIONS OF PORE FLUIDS AND DURABILITY

C Fuhr and D Knöfel

Laboratory for Chemistry of Construction Materials, University of Siegen, Siegen, GERMANY

SUMMARY

Belite-rich cements were subjected to comparative tests with commercially available portland cements (PZ 35F, PZ 35L NW/HS) and a blastfurnace slag cement (BSC) over a period of one year. The investigations covered the development of strength, the carbonation and porosity behaviour as well as the alkali content of the pore solution. The last mentioned aspect is of interest in particular with regard to a possible alkali silica reaction of belite-rich cements treated with alkali. In addition, a carbonating period of approximately thirty years was simulated.

The problem of low early strengths arising with belite-rich cements was substantially improved by chemical and physical activation. As for their carbonating behaviour, the activated belite-rich cements are comparable with the analysed BSC and PC cements, with their total porosity being lower. The investigations have shown that the alkali content of the pore solution of activated belite-rich cements is only insignificantly higher than those of portland and blastfurnace slag cements.

ZUSAMMENFASSUNG

Belitreiche Zemente wurden im Vergleich zu handelsüblichen Portlandzementen (PZ 35F, PZ 35L NW/HS) und einem HOZ über einen Zeitraum von einem Jahr getestet. Die durchgeführten Untersuchungen beschäftigen sich mit der Festigkeitsentwicklung, dem Carbonatisierungs- und Porositätsverhalten sowie dem Alkaligehalt in der Porenlösung. Letzteres ist besonders in Bezug auf eine mögliche Alkali-Kieselsäure Reaktion der mit Alkalien dotierten belitreichen Zemente von Interesse. Desweiteren wurde eine Carbonatisierungsdauer von ca. 30 Jahren simuliert.

Die bei belitreichen Zementen auftretende Problematik der geringen Frühfestigkeiten konnte durch chemische und physikalische Aktivierung deutlich verbessert werden. Beim Carbonatisierungsverhalten sind die aktivierten belitreichen Zemente durchaus mit den untersuchten PZ und HOZ vergleichbar, die Gesamtporositäten sind geringer. Wie die Untersuchungen zeigen, ist der Alkligehalt der Porenlösung der aktivierten belitreichen Zemente nur geringfügig höher als der von PZ und HOZ.

INTRODUCTION

The preparation conditions as well as the strength development of various belite-rich cements have been investigated by several authors (1,2,3). With regard to the durability of belite-rich cements in comparison with commercial portland cements the porosity and carbonation behaviour are also of interest. Results of investigations concerning this problems, conducted by the authors, are already available (4,5). Another question which should be investigated is how the higher alkali content of the activated belite-rich cements caused by chemical activation affects to the alkali content of the pore solution. There are two possibilities: either the alkali contents of the pore fluid is substantially higher than that of portland cements or the integration of the alkalis in the hydrate phases of belite and aluminate is intensified.

The alkali content of the pore solution is of practical interest with regard to a possible alkali-silica reaction using alkali reactive aggregate for concrete production. It has to be considered, that the alkali-silica reaction is primarily an attack of hydroxide ions on the silica aggregate and not a direct consequence of the presence of alkalis in pore the fluid. Diamond (6), for example, mentioned that the content of hydroxide ions is considerably influenced by the alkali content.

This paper presents the results of investigations of pore fluids and some remarks concerning the durability of belite-rich cements and reference cements.

ANALYSIS OF THE CEMENTS

Preparation of the cements

All investigations were accomplished on 7 cements. Three of them were prepared using two industrielly produced portland cement clinkers (PC, PCN), and PC-clinker plus blastfurnace slag (BSC). The natural raw materials for the other four cements (BL, BAL, BT, BAT) were limestone, clay and quartz. The raw mixture was burnt in an electrical furnace for half an hour at 1350°C. The cements BAL and BAT were chemically and physically activated belite-rich cements. Chemical activation was achieved by adding pure sodium carbonate (BAL) to the raw mixture or by using clay with a high K_2O content as a raw meal component. Physical activation was achieved by quick clinker cooling, the cooling gradient being 1,000 K/min. BL and BT are non activated belite-rich cements. The PC cement was prepared using a PZ 35F clinker, the PCN using a PZ 35L NW/HS and the BSC using 50 wt.-% PC-clinker and 50 wt.-% blastfurnace slag.

All cements were ground down to a specific surface of 4,000 cm^2/g (according to Blaine) in a laboratory ball mill, with anhydrite and hemihydrate being added as sulfate base (at a ratio 1:1). The total cement sulfate content was 3.2 wt.-% SO_3.

Characterization of the cements

The chemical composition was quantitatively determined by AAS, with the clinker phases being qualitatively by analysed x-ray diffractometry. The chemical analysis was accomplished as per the instruction of Paus and Langmyhr (7). The ignition loss was determined at 1,000+/-50°C. The results in detail are given in table 1.

Cement	BL	BAL	BT	BAT	PC	PCN	BSC
wt.-%							
K_2O	0.296	0.323	0.342	1.327	0.892	0.668	0.681
Na_2O	0.065	0.929	0.050	0.294	0.115	0.020	0.167
CaO	62.535	61.742	64.116	60.557	64.354	63.141	53.628
Al_2O_3	6.045	5.869	4.887	4.452	5.006	3.784	6.970
Fe_2O_3	2.741	2.731	2.550	2.507	2.531	6.135	1.663
MgO	0.517	0.522	0.650	0.632	1.011	0.856	3.974
SiO_2	23.315	22.460	23.101	22.460	19.679	20.962	26.096
SO_3	2.910	3.220	3.090	3.210	3.270	3.460	3.100
LOI	0.600	0.850	0.600	1.350	1.400	0.950	0.200
Σ	99.024	98.646	99.386	95.809	98.258	99.976	96.479

Table 1: Results of the chemical analysis of the cements

The high content of Na_2O for BAL and K_2O for BAT respectively are obvious. The relatively high K_2O content of the PC and PCN can probably be explained by raw meal components containing a high amount of potassium. The higher SiO_2 content of the BL, BAL, BT and BAT cements as compared to the PC and PCN cements reflects itself in a lower C_3S content as well as higher β- and α-C_2S contents, which can be seen from the valuation of the phase composition (table 2). These are so-called belite-rich cements.

Clinkerphases	BL	BAL	BT	BAT	PC	PCN	BSC
α - C_2S	-	+	-	++	-	-	-
β - C_2S	+++	+++	+++	+	++	++	++
C_3S	++	++	++	++	+++	+++	+++
C_3A	+	++	+	+	+	+-	+
C_4AF	++	+	+	+	+	++	+
sulfatebase							
$C\bar{S}$	+	+	+	+	+	+	+
$C\bar{S}H_{0.5}$	+	+	+	+	+	+	+

(+++ a lot, ++ medium, + few, +- possible, - not found)

Table 2: Valuation of the phase composition

Only the BAL and BAT cements contain α-C_2S, because this phase is stabilized by a higher alkali content. As a cement with high sulfate resistance PCN has a low C_3A and a high C_4AF content. Aluminate could not be proved by x-ray diffractometry. Valuation of the phase composition by x-ray diffractometry was also used for comparative measurement to find out the changes and destruction of clinker- and hydrate phases caused by expression of the pore fluids.

INVESTIGATIONS OF THE PORE FLUIDS AND THE EXPRESSED SAMPLES

Expression of Pore Fluid

Cement pastes with a w/c-ratio of 0.42 were prepared in accordance with DIN 1164. The cement pastes were filled into 250 ml PE bottles and rotated for 24h to avoid sedimentation. The bottles were stored at 23°C and 65% rel. humidity until performance of the test. The pore fluid was expressed after a hydration period of 12h, 48h, 7d, 28d and 90d. The apparatus used for expression of pore solution was designed after a similar device reported by Gunkel (8). It employed a max. operating pressure of 530 N/mm² applied to a specimen of hardened cement paste weighing roughly 260 g.

Analysis of Pore Fluid

The pore solutions were investigated with regard to pH, the K^+-, Na^+-, Ca^{2+}- and Al^{3+}-ion concentration using atomic absorption spectroscopy. The SO_4^{2-}-contration was determined by ion chromatography. The measurement of pH was carried out by a glass elctrode, which in a highly alkaline medium can involve measuring inaccuracies, despite the use of saturated calcium hydroxide solution (pH 12.64 at 20°C) as a standard solution. The pore solutions of all cements are highly alkaline, the pH varying between 13.3 and 14. These values cannot be explained by the presence of pure calcium hydroxide solution. The pore fluid is rather a concentrated solution of alkali hydroxides.

The analyses showed that after 28 days there is only a slight change in concentration of the different cations. The increase of the potassium and sodium concentrations during hydration can be explained by the progressive solution of sodium and potassium cations and the simultaneous reduction of the pore fluid quantity. The equivalent percent Na_2O was calculated to assess the effective total alkali content.

Besides the portland cements prepared in our laboratory we used a commercial portland cement PC 35F , with an equivalent percent Na_2O of 3.2 wt.-% for comparison. The development of the equivalent percent Na_2O during hydration is shown in fig. 1.

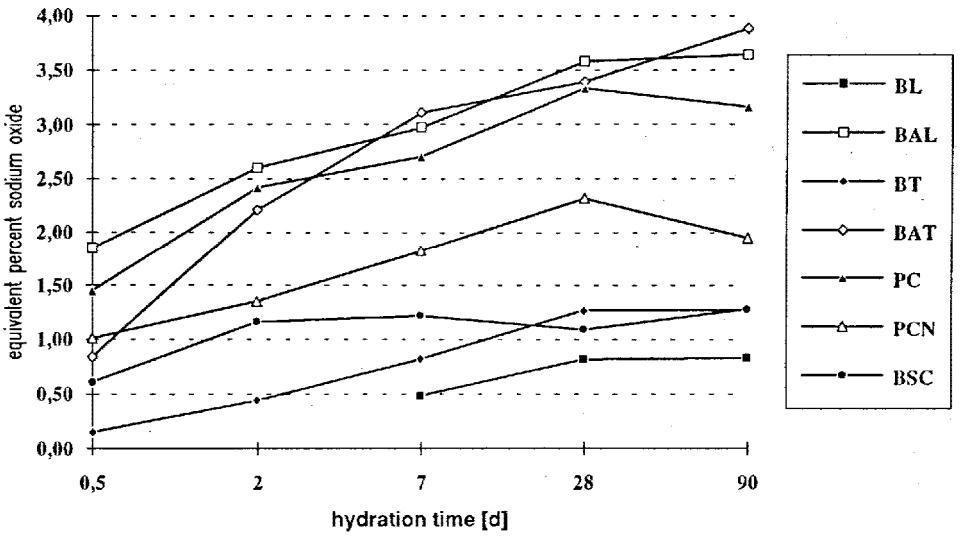

Fig. 1: Development of the equivalent percent Na_2O during hydration.

After 90d the equivalent percent Na_2O is 3.3 for PC, 3.6 for BAL and 3.9 for BAT. As compared to the other four cements, for example BSC with 1.2 and PCN with 2.3 equivalent percent Na_2O, the differences between the three cements mentioned above are not so great. The higher alkali content of the BAL and BAT cements is only partly found in the pore fluid. The other part is integrated in the clinker phases belite and aluminate and their hydration phases.

The quick decrease of the Ca^{2+} concentration of 100-400 ppm after 12h to 1-12 ppm after 7 days can be attributed to ettringite formation, which can also be followed by the concentration development of aluminum. As part of the fast reactive phase C_3A, at first Al^{3+} is dissolved and then integrated in the hydration products. The activated belite-rich cements BAL and BAT show this decrease, which points to integration a little bit earlier than the non activated belite-rich cements BL and BT. This points to a higher rate of hydration. The reason for the "alumina maximum" in the pore solutions of the BAL and BAT can be seen in the formation of orthorhombic C_3A, which is favoured by the high sodium and potassium content of these cements. Cubic C_3A which appears for example in ordinary portland cements dissolves more slowly than orthorhombic C_3A.

The development of the sulfate concentration also points to the formation of ettringite at the beginning of hydration. The main part of sulfate is integrated in ettringite and/or monosulfate after 7 days. Sulfate concentration increases as hydration proceeds as a consequence of the reduction of pore fluid while the amount of sulfate ions in the residual solution remains constant. This becomes obvious when the sulfate concentration of the pore solution is related to the total amount of water determined by ignition loss. The details are given in (9).

X-ray Diffraction Analysis of the Expressed Specimen

The expressed specimen were qualitatively analysed by x-ray diffractometry at different rates of hydration. After max. 90 days of hydration non hydrated clinker phases and hydration products could be proved. This suggests that the clinker phases and hydration products were at least not completely destroyed. The presence of hydration products after expression suggests that only pore solution was expressed and the bound water remained in the specimen.

INVESTIGATION OF DURABILITY

Compressive Strength

The compressive strengths of the activated belite-rich cements BAL and BAT are, depending on the w/c-ratio and storage conditions, after a hydration period of 90 or 180 days comparable to those of an ordinary PZ 35F and a PZ 35L NW/HS. Strengths of the BSC are already reached after 7 or 28 days. Details of strength data and assertions concerning porosity and carbonation development are given in (9).

Porosity

In order to determine the total porosity and the differential pore size distribution, the specimens of mortars and hardened cement pastes were investigated using mercury intrusion porosimetry. As found out in some earlier investigations by the authors, the total porosity of the activated belite-rich cement BAL in comparison to the portland cement PC, depending on w/c-ratio and storage conditions, is lower or equal. Compared to all other cements, the BAL has the lowest total porosity.

Carbonation Behaviour

The carbonation depth was determined by spraying freshly cracked mortar prisms with ethanol. phenolphthalein solution.

To test the long term carbonation behaviour of about 60 years in natural atmosphere, the specimen were stored at a concentration of 1 vol.-% and a climate of 20°C and 65% rel. humidity for 2 years. The reference samples were stored in open air, protected from rain.

The low total porosity of the activated belite-rich cements implies a carbonation depth that is comparable to that of portland cement. This may partly compensate the low calcium hydroxide content of the belite- rich cements. The carbonation resistance of the belite-rich cements increases with longer periods of hydration. After simulated 60 years, no sample of the belite-rich cements had a carbonation depth over 2.5 cm (mortar prisms measuring 5·5·25 cm), while one sample of the PCN (w/c=0.58) was totally carbonated. The activated belite-rich cements generally showed a lower carbonation progress than PCN and BSC.

CONCLUSION

The investigations show positive results for the activated belite-rich cements. The compressive strengths of BAL and BAT cements at early ages show an increase in comparison to the non activated belite-rich cements and are comparable to the compressive strengths of PCN and BSC cements. The carbonation behaviour of activated belite-rich cements, which is comparable to that of a portland cement, is partly due to the lower total porosity of activated belite-rich cements.

As the investigations have demonstrated, a higher alkali content of cement clinker does not result in a higher alkali content of the pore fluid. The alkali concentration of the pore solution of activated belite-rich cements, with regard to a possible alkali silica reaction, is not more critical than that of commercial portland cements. The investigations have clarified further important points for assessing the employment of belite-rich cements in practice. At present tests are being made to determine the diffusion behaviour of chloride ions together with other environmental simulation tests.

Investigations of concretes are unfortunately impossible at the present time, because the belite clinkers can only be prepared in small amounts in our laboratory (9). The next step will be the testing of the production of belite cements in a small industrial facility.

ACKNOWLEDGEMENTS

The research program was supported by the Deutsche Forschungsgemeinschaft, Bonn. We appreciate the assistance of Dipl.-Ing. A. Fiedrich and Mrs. M. Sauer for practical work, and Dipl.-Min. R. Jäger for discussion.

REFERENCES

1. Gies, A. and Knöfel, D.: "Influence of Alkalies on the Composition of Belite-rich Cement Clinkers and the Technological Properties of the Resulting Cements". Cement and Concrete Research, 1986, 16, 411-422.

2. Knöfel, D. and Gies, A.: "Einflüsse erhöhter Mangan- und Alkaligehalte auf die Zusammensetzung belitreicher Zementklinker und die Zementeigenschaften". Silikattechnik 1988, 39, 119-120.

3. Müller, A. and Stark, J.: "Zum Eifluß der Alkalien auf die Festigkeitsentwicklung von aktivem Belit zement". Silikattechnik, 1987, 9 (38), 301-305.

4. Knöfel, D and Fuhr, C.: "Durability of Activated Belite-rich Cement Mortars".Ceramic Transactions, 1991, 16, 715-727.

5. Fuhr, C. and Knöfel, D.: "Dauerhaftigkeit von aktivierten belitreichen Zementmörteln". TIZ, 1992 (in print).

6. Diamond, S.: " A Review of Alkali Silica Reaction and the Expansion Merchanism. Part 1: Alkalies in Cements and in Concrete Pore Solution". Cement and Concrete Research 1975, 5, 329-346.

7. Langmyhr, F.J. and Paus, P.E.: "The Analysis of Inorganic Materials by Atomic Absorption Spectrophotometry and the Hydrofluoric Acid Decomposition Technique, Part IV". Anal. Chim. Acta 1969, 44, 445-446.

8. Gunkel, P.: "Die Zusammensetzung der flüssigen Phase erstarrender und erhärteter Zemente". Beton-Information 1983, 1, 3-8.

9. Fuhr, C.: Dissertation, University of Siegen, 1992 (in preparation).

INFLUENCE OF CONSTITUENTS ON THE SURFACE ABSORPTION CHARACTERISTICS OF CONCRETE

W J McCarter and H Ezirim

Department of Civil and Offshore Engineering, Heriot-Watt University, Edinburgh, Scotland, UK

SUMMARY

It is now recognised that the surface properties of concrete play a major role in the durability of reinforced concrete The ability of concrete to imbibe and transmit water by capillarity is taken as a starting point for assessing these surface characteristics . In this paper , the influence of mix constituents on the water absorption characteristics of concrete is investigated . These mixes have water-cement ratios, cement-contents and strengths typical of those used for *extreme* exposure conditions . These characeristics are quantified in terms of both depth of penetration of the water front and the cumulative volume gain per unit cross-sectional area . Typical data are presented . It is shown that the sorptivity characteristics of concrete are not a simple function of constituent proportions or strength . Data are also presented on chloride concentration profiles on samples subjected to cyclic wetting and drying , and diffusion . The tests show that chloride concentrations within the cover region can increase rapidly under a cyclic regime.

RESUME

Il est maintenant reconnu que les caractéristiques du béton au voisinage de sa surface libre joue un rôle majeur sur la durabilite du béton armé . De plus l'évaluation des propriétés de surface nécessite de prendre en compte en tout premier lieu la capacité du béton à absorber et à transmettre l'eau par capillarité . Dans cet article , l'influence de la composition du béton sur les caractéristiques d'absorption d'eau est étudié . Les mélanges testés ont , des rapports eau sur ciment , des dosages en ciment et des résistances comparables à ceux retenus pour les cas d'exposition *extreme* du matériau . Les caractéristiques d'absorption sont quantifiées à la fois par la profondeur de pénétration du front d'eau et par la quantité d'eau traversant une section unitaire . Des exemples typiques sont présentés . Il est montré que les caractéristiques d'absorption du béton ne sont pas une simple fonction des proportions des constituants ou des résistances . Des informations sur les profils des concentrations en chlorure sont données dans deux cas d'une part dans des échantillons soumis à des cycles successifs d'humidification et de séchage (progression capillaire) et d'autre part dans des échantillons saturés d'eau au contact d'une solution du chlorure (progression par diffusion) . Les tests montrent que les concentration en chlorure dans la zone de recouvrement des armatures augmentent rapidement lors du régime cyclique .

INTRODUCTION

Concrete , which was once thought to be a maintenance-free, durable material, has, over the last 25 years , shown this not to be the case . One of the most serious and widespread causes of concrete deterioration is the ingress of deleterious ionic species , in particular the ingress of chlorides. Chlorides come from many sources : salt-water or salt-laden air affects marine and coastal structures ; calcium chloride may have been added to the mix as an accelerator (although current standards now ban its use in reinforced and prestressed concrete) ; in the Middle East , brackish water is sometimes used to mix (and cure) the concrete . In the United States and Europe , extensive use of de-icing salt for winter maintenance is a cause of serious problems . Leaking bridge joints and decks , and spray from passing traffic , exacerbate the problem.

The long term performance of concrete structures is controlled , in the main , by the permeation characteristics of the cover region and terms such as absorption , permeability and diffusion have been used in this respect . The process of deterioration in concrete is largely as a result of errant water . The extent of , not only corrosion but also freeze-thaw damage , sulphate attack and alkali silica reaction all depend on the availability of moisture . It is generally agreed , that it would be a useful step forward to find a single property which reflects the ability of concrete to absorb and transmit water. To this end , the sorptivity (1) of concrete is taken as a starting point . Ideally , one would wish concrete to have zero sorptivity as a serviceability criterion.

BACKGROUND

Since the surface region of above-ground concrete structures will be subjected to drying action of wind and sun , it will , therefore , have a non-uniform water-content . The degree of saturation will vary from virtually zero at the dry exposed surface increasing (although not in a linear fashion) to a fully saturated state within the bulk concrete . The problem of water movement into the surface region thus becomes one of unsaturated flow and will , necessarily , involve capillary suction forces . The theory of unsaturated flow has been applied to porous building materials (1 , 2) and the term *sorptivity* used to characterise the uptake of water by these materials . The sorptivity , S , is defined in the relationship,

$$i = S\sqrt{t}. \qquad \ldots(1)$$

where i is the cumulative volume gain per unit cross-sectional area of inflow surface , t is the elapsed time and S is the sorptivity Invariably , data display an intercept value on the t = 0 axis . Sorptivity and permeability must not be confused ; permeability relates to the movement of water through a saturated material under a pressure differential , sorptivity is concerned with the movement of water into a partially saturated material under capillary suction forces . It is the latter definition which concerns this paper .

A number of studies have reported sorptivity values for concrete ; however , no direct comparisons can be made as curing methods ; test surface ; temperature at which the sample was conditioned and time interval over which the sorptivity was determined are quite different . For example , sorptivity values have been obtained for concretes made with ordinary Portland cement (OPC), (3) with 1:2:4 and 1:3:6 mix proportions , by weight , and water-cement ratios varying between 0.4 and 1.0 . The samples were wet cured for 10 days and then conditioned at 40°C prior to testing . Values were obtained over the initial hour and were in the range 0.73-2.4 $mm/h^{1/2}$. For concrete initially cured under hessian for five days and then allowed to dry naturally in a laboratory (4) for 2 months before being tested , gave values of 0.69 - 1.43 $mm/h^{1/2}$ when tested over the initial 20 minutes absorption (1:2.18:3.96 mix proportions with water-cement ratios 0.55 and 0.70) . Data have also been reported (5) for concrete samples (1:2.5:3.5 mix proportions with water-cement ratios 0.56 - 0.59) made with Portland cement with partial replacement with pulverised fuel ash (pfa) and ground granulated blast-furnace slag (ggbs) . The samples , in this

instance , were wet cured for 28 days and then conditioned at 105°C . Sorptivity values were in the range 7.6 - 28.4mm/h$^{1/2}$. Conditioning at elevated temperatures , however , can cause undesirable effects such as micro-cracking or alteration to the pore structure . Furthermore , as capillary suction forces are related to the degree of saturation of the concrete , drying samples to virtually zero saturation will result in large suction forces . All these factors combined will result in sorptivity values which are unrealistic and artificially high .

Sorptivity , as defined above , is useful in quantifying the volume of water absorbed ; it does not , however , give any indication on the depth of penetration of the water front during an absorption cycle . Ho et al (6 , 7, 8) have presented data on the depth of penetration of water into concrete samples. It was found that the depth of penetration of water into concrete was given by the relationship,

$$d = S' \sqrt{t} \qquad \ldots(2)$$

where d in the depth of penetration of the water-front from the suction surface and S' is a sorptivity coefficient based on the *depth* of penetration . Once again , data display a small intercept value on the t = 0 axis. Typical (24-hour) values for S' lie in the range 2.0 - 18.0 mm/h$^{1/2}$ depending on the curing regime. The 28 day strengths (F_{28}) of the concrete were in the range 28 - 42MPa . For plain OPC concrete mixes with varying mix proportions and cement-contents (9) , gave sorptivity (S') values in the range 2.19 - 4.74 mm/h$^{1/2}$ when tested over a similar time scale (F_{28} values : 36 - 59MPa) .

EXPERIMENTAL

An experimental programme was undertaken to obtain sorptivity data for a range of concrete mixes whose strengths were in the range 40-70MPa with constituents and proportions typical of those encountered in practice . Samples were tested over a 25-hour absorption period. Tests were also conducted on the influence of cyclic wetting and drying on chloride ion concentration profiles within concrete . These tests form part of a long term programme on chloride movement into concrete and only preliminary results are presented .

Mix Proportions

The mixes used are detailed in Table 1 below . Samples were cast from single batches of concrete as either 150mm cubes (for sorptivity tests) or 300x150mm cylinders (for cyclic and diffusion tests). All samples were demoulded after 24 hours .

On demoulding , five faces of the cubes were sealed with a latex based paint with the top (cast) surface remaining unsealed. This ensured 1-dimensional movement of moisture . The samples were placed under polythene for a further 7 days after which time they were left in a laboratory atmosphere (23°C,55%RH) until testing , which was a period of approximately five months. The method of curing employed is detailed in national codes (10) . Natural drying of the sample thus negated problems that could be encountered during elevated temperature drying . Testing after this time also ensured that the beneficial effect of pfa and slag , resulting in densification of the paste matrix , would be complete .

The sides of the cylinders were sealed and placed under polythene for 7 days . After this time,they were cut in half with a water cooled diamond saw parallel to the ends of the sample . The cut surface was wiped dry and the samples left in a laboratory atmosphere for approximately five months before testing. In order to eliminate the influence of a casting gradient which could exist through the sample , the cut surface was exposed to a 5.0 molar sodium chloride solution . The cut surface could thus be regarded as having had 7 days continuous moist curing before cutting.

Measurements

Sorptivity (Mixes 1 - 8) - Samples were placed in trays (suction surface downwards) and filled with water to approximately 10mm above the suction surface (ie cast) . After 25-hours the samples were split and the water front determined by dusting the fractured surface with a water sensitive dye (duramine green) . This also provided a permanent record of the position and shape of the water-front . Over the 25 - hour period the cumulative volume gain of the samples was monitored by means of a micro-computer controlled weight-gain measuring system with measurements being taken every 15 minutes over the test period .

Cyclic and Diffusion (Mix 9) - The samples were placed in trays as above , but the water was replaced by 5.0 molar sodium chloride solution . A cycle comprised 2 days continuous absorption followed by 12 days drying in a laboratory atmosphere . This regime was evaluated from the local rainfall data which indicated that approximately two days in fourteen days had a significant amount of rainfall . Samples for diffusion tests were initially saturated with water and then placed in the solution until required for chloride analysis . Drillings on the samples were taken after 3 and 6 cycles (ie.6 and 12 weeks) using a 20mm drill bit at depths 0- 10 ; 10-20 ; 20-30 ; 30-40mm . Chloride ion concentration was determined using a spectrophotometric technique employing a Technicon Auto Analyser . The chloride levels are expressed as percentage weight of cement.

Mix	1	2	3	4	5	6	7	8	9
Coarse	Granite	Gravel	Gravel	Granite	L/stone	Crushed Gravel	Gravel	L/stone	Crushed Gravel
Fines	Natural	Natural	Natural	Granite	L/stone	Natural	Natural	L/stone	Natural
OPC	421	-	-	418	245	160	332	-	400
SRPC	-	263	255	-	-	-	-	400	-
PFA	-	-	109	-	-	-	-	-	-
GGBS	-	263	-	-	244	160	-	-	-
MS	-	-	-	36	-	-	28	-	-
20mm	891	-	738	725	701	792	837	717	736
10mm	445	825	370	363	350	400	419	358	368
Sand	505	762	600	512	565	560	538	554	736
water	160	200	160	200	215	160	180	200	160
w/c	0.38	0.38	0.44	0.44	0.44	0.5	0.50	0.50	0.4
Plast.	-	1.3	0.40	1.36	-	1.20	-	-	-
AEA	-	-	-	0.45	-	0.28	-	0.35	-
F_{28} (MPa)	66	58	37	51	61	37	55	42	53

Table 1. Summary of mixes studied

(Note:L/stone=limestone;MS=micro-silica;Plast.=plasticiser; AEA=air-entraining agent;constituents are in kg/m^3)

RESULTS AND DISCUSSION

Sorptivity results , based on cumulative volume gain (S) and depth of penetration (S') , are presented in Table 2 for mixes 1 - 8 and based on the data obtained over the initial 25-hours . Typical i vs. $\sqrt{t}$ curves are displayed in Fig.1 . The effective surface porosities of the concretes have also been evaluated and are obtained from the ratio i/d (at 25 hours) , expressed as a percentage . Results for 3 and 6 cycles of wetting and drying and 6 and 12 weeks diffusion , are presented in Fig.2.

The experimental data obtained from the data logging system confirmed , in most cases , that the cumulative volume gain of the sample could by approximated by the square-root time relationship as given in equation (1) (see Fig.1) . A small downward curvature in this curve is evident , however , in

mixes 6 and 8 . In most cases , there was a small positive intercept with the time=0 axis (i< 0.2mm) The results from the test programme are lower than those obtained by other workers (see above however , this discrepency can be attributed to several factors:

MIX	1	2	3	4	5	6	7	8
S (mm/h$^{1/2}$)	0.16	0.55	0.49	0.38	0.39	0.58	0.43	0.61
S' (mm/h$^{1/2}$)	3.53	5.13	5.05	4.18	3.76	4.70	4.79	4.43
Effective Surface Porosity (%)	8.3	9.1	9.2	8.3	11.3	12.5	8.7	10.0

Table 2. Summary of results for 25-hour sorptivity tests

(1) the samples in the current test programme were not conditioned at an elevated temperature , bu brought into equilibrium in a laboratory atmosphere . Furthermore , the samples were cured unde polythene and not in a submerged state .

(2) S was obtained from the slope of the i vs.$\sqrt{t}$ curve and based on the results obtained over the 24 hour test period . Published results have been determined over time scales ranging from a few minutes to several hours .

(3) low water-cement ratios are employed and are more typical of those used for *extreme* conditions.

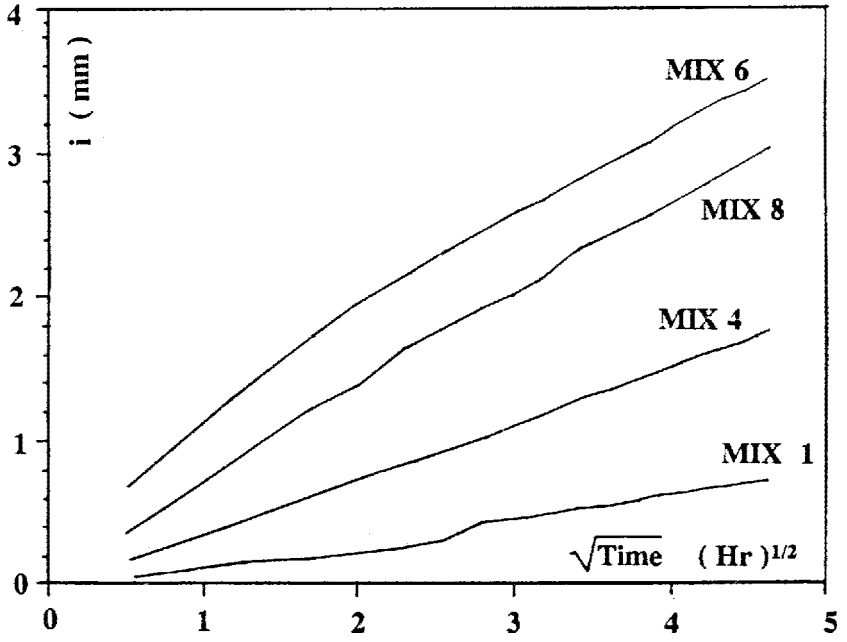

Fig.1 Typical i vs $\sqrt{t}$ curves for a selection of mixes

The lowest sorptivity values (S=0.16 and S'=3.53 mm/h$^{1/2}$) were obtained from a plain OPC mix (mix 1) with no admixtures or replacement material . This mix should be compared to mix 2 which has the same water-cementitious material ratio and sorptivity values of , respectively , 0.55 and 5.13 mm/h$^{1/2}$. Since the samples were approximately five months old , the influence of the slag in densifying the pore structure would be expected to be complete . The increase in these values , which is contrary to what would be anticipated , could be attributable to a combination of factors :

(a) as capillary suction forces are inversely proportional to the pores radius and occur in the evacuated capillary cavities ; a fine pore network , although reducing permeability as defined above , would result in increased capillary suction forces . This would draw water into the concrete at an increased rate .

(b) the slag mix uses a 10mm maximum size aggregate . This will result in a less circuituous capillary pore network around the aggregate than if a 20mm aggregate had been used .

(c) the curing regime , although complying with current specifications , is not an effective method for slag cement and could have resulted in a more porous surface region .

Considering mixes 3 , 4 , and 5 , all with a water-cementitious material ratio of 0.44 , increasing the cementitious material content results in a general reduction in the sorptivity coefficients . Of this group , mix 5 (slag replacement) has the highest effective porosity . Considering (c) above , could show that the curing method employed was not adequate and has obviously had an influence on the hydration characteristics of this mix , resulting in a more porous concrete than would be expected .

Mixes 6 and 8 , both have a high sorptivity coefficient , S , and effective surface porosity . Not only do these mixes have a high water-cementitious material ratio but they also contain an air entraining agent.

Examination of the split surfaces revealed that , during the initial 24-hours , the water moved into the concrete as a well-defined wet front , although this horizon was uneven in nature and not parallel to the suction surface .The water tended to take a tortuous path around the coarse aggregate and the mean depth of penetration was recorded for each sample . The sorptivity coefficients , S' , for the mixes tested were within the range 3.53 - 5.13 mm/$h^{1/2}$. This is in the lower end of the range of previously published data and is , perhaps not surprising as the strength of the mixes in Table 1 are higher . What is of interest is the narrow range of values , considering the large variations in mix proportions and constituents . In the 25 hour test period , the water front had advanced , typically , from 16 mm (mix 1) to 27 mm (mix 2)

Chloride Profiles

The influence of cyclic wetting and drying on chloride concentration is displayed in Fig.2 . Under the cyclic regime , chloride solution will , in part , move into the concrete under capillary suction forces ; this will be a much faster process than that of diffusion . Fig.2 reveals that the increase in chloride ion concentration under cyclic wetting and drying is greater over the surface 15mm than the same concrete subjected to a diffusion test where the *driving force* is concentration gradient . At greater depths , the difference between the two regimes is not as significant . Based on the data in Fig.2 , a diffusion coefficient of this mix was calculated as 3.41×10^{-8} cm^2/sec.

CONCLUDING COMMENTS

Work has been presented on the water absorption characteristics of a range of concrete mixes , together with data on chloride concentration profiles within concrete under both cyclic and diffusion regimes . Many of the mixes in Table 1 would satisfy the durability requirements outlined in codes of practice , for example , BS8110:Part 1:1985 (10) recommends a cement content greater than 350kg/m^3 and a water-cement ratio not greater than 0.5 for concrete exposed to *extreme* conditions) . Considering the range of mix constituents and strengths , the sorptivity coefficients , S' , are limited to the range 3.53- 5.13mm/$h^{1/2}$, whereas S coefficients varied from 0.16 to 0.61 mm/$h^{1/2}$. Prolonged cyclic wetting and drying of concrete shows that chloride levels can build-up within concrete in a relatively short period of time. It is apparant that the first wetting (absorption) cycle after a prolonged dry period will move water and chlorides rapidly through the cover region of concrete .

Many factors influence the absorption characteristics of concrete ; water-cement ratio , cement content, curing regime , even aggregate size and distribution will have an influence on sorptivity characteristics. It becomes apparant that no single material property will adequately characterise the near surface absorption properties of concrete . Any durability model for concrete must , in part , be based on readily available material characteristics obtained from *in-situ* performance tests on concrete structures . This must form part of a routine monitoring strategy to obtain a database for any particular structure ;

only then can realistic predictions be made as to likely deterioration rates for a particular exposure condition or compliance with the specified design life .

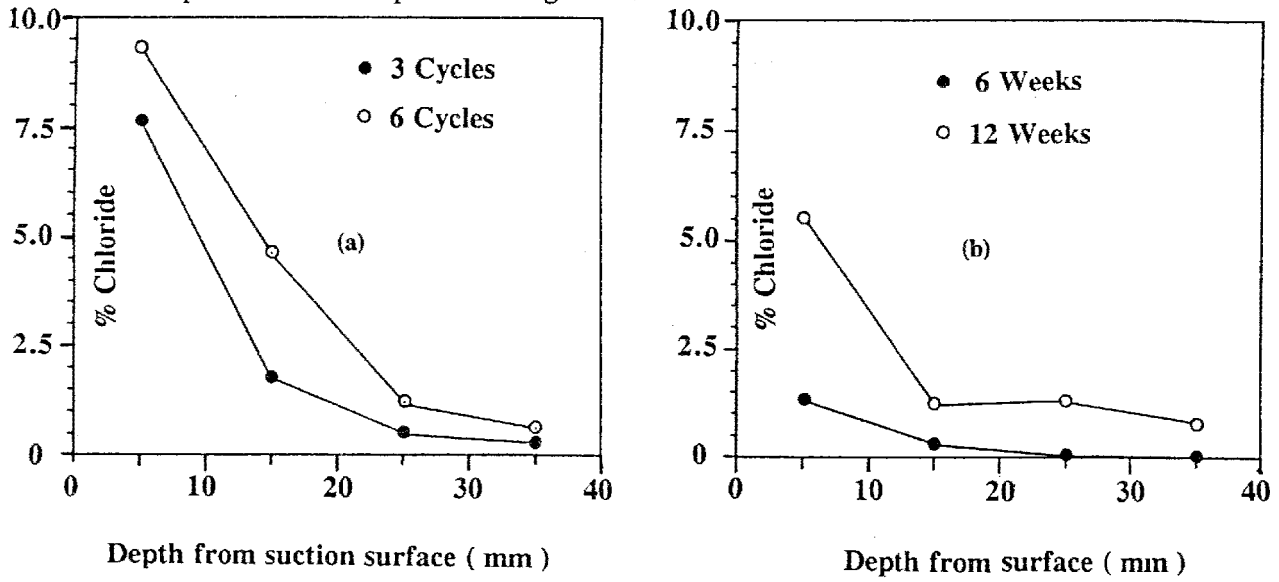

Fig.2 Chloride profiles for concrete (Mix 9) under (a) cyclic and (b) diffusion regimes

REFERENCES

1. HALL,C. 'Water movement in porous building materials - I. Unsaturated flow theory and its application' , **Building and Environment** , Vol.12. , 1977 , pp 117-125

2. IDEM 'Water movement in porous building materials - IX.The water absorption and sorptivity of concrete' , **Ibid** , Vol.22 , 1987 , pp77-82

3. IDEM 'Water sorptivity of mortars and concretes:a review', **Magazine of Concrete Research** , Vol.41 , No.147 , 1989 , pp 51-61.

4. BASHEER,P.A.M.,MONTGOMERY,F.R.,LONG,A.E. and BATAYNEH M. 'Durability of surface treated concrete',Proc.Int.Conf. on Protection of Concrete , Dundee , Sept. , 1990 , pp211 - 221 .(Edited by R.K.Dhir and J.W.Green)

5. KELHAM,S. 'A water absorption test for concrete' , **Magazine of Concrete Research** , Vol.40 , No.143 , 1988 , pp106-110.

6. HO,D.W.S. and LEWIS,R.K. 'Concrete quality as measured by sorptivity', **Trans of the Instn. of Engrs.** , Aust. , Vol.CE26 , No.4 , 1984 , pp 306-313.

7. IDEM 'The water sorptivity of concretes : the influence of constituents under continuous curing', **Durability of Building Materials** , No.4 , 1987 , pp 241-252.

8. HO,D.W.S.,CUI,Q.Y. and RITCHIE,D.J. 'The influence of humidity and curing time on the quality of concrete', **Cem. and Conc. Res.** , Vol.19 , No.3 , 1989 , pp 457-464.

9. McCARTER,W.J.,EZIRIM,H. AND EMERSON,M 'Absorption of water and chloride into concrete',**Magazine of Concrete Research** , Vol. 44 , No. 158 , 1992 , pp 31-37

10. BRITISH STANDARDS INSTITUTION 'Structural use of concrete' , **BS8110 , Part 1** , Section 6 , 1985

CONSIDERATION ABOUT THE DURABILITY OF MORTARS WITH GRANULATED BLAST-FURNACE SLAG AS FINE AGGREGATE

A F Battagin and L Scandiuzzi

Brazilian Association of Portland Cement, São Paulo, BRAZIL

ABSTRACT

Due to their latent hydraulic properties, granulated blast-furnace slags (gbfs), by-products of iron manufacture, have been used extensively in the Brazilian cement industry since the beginning of the 50's. Their use not only can help to conserve energy in cement manufacture but also promotes special properties to portland cement.

This paper deals with the study of an alternative utilization of gbfs as fine aggregate in concrete, taking into account that it is impossible for Brazilian cement industry to consume nowadays, the total slag produced by steel plants.

Results of comparative studies by means of scanning electron microscopy (SEM) and durability tests in mortars containing gbfs, natural sands and pyrex glass as fine aggregate are shown.

RESUMEN

Debido a sus propiedades hidraulicas intrínsecas, las escorias granuladas, subproducto de la fabricación del hierro en los altos hornos están siendo utilizadas en la industria brasileña del cemento desde la decada de 50. El uso de escória, siderúrgica no solamiente determina la disminución del consumo energético de fabricación del cemento mas tambien tienen capacidad de influyr directamente en la durabilidad del cemento y otras propiedades.

Este trabajo ofrece resultados que demostran la viabilidad técnica de un uso alternativo de la escoria siderúrgica, que consiste en su utilización como árido fino en hormigones dada la imposibilidad de su utilización total por parte de la industria como aditivo en el cemento.

Se destacam los aspectos de la durabilidad de argamasas que contienen escória siderurgica como árido fino comparativamente a otros áridos como arenas naturales y de machaqueo, y vidrio pyrex.

1 INTRODUCTION

Due to their latent hydraulic properties gbfs have been used after their drying and grinding in the manufacture of blast-furnace slag cement (up to 70%) or portland cement with additions (up to 35%) all over the world. In fact, gbfs not only helps to conserve energy in cement manufacture but also improves cement properties like the resistance to sulfate attack, the alkali-aggregate reaction prevention, the decrease of the heat of cement hydration etc.

Table 1 shows the utilization of gbfs in Brazil and one can deduce that in 1986 about 2/3 of total slag production was destinated to the cement industry.

Table 1 - Brazilian Utilization of gbfs in 1986[1]

USES	Percentage of utilization
Recycled material	1.2
Cement manufacture	64.7
Road making	9.0
Stock pile	12.9
Other	12.2
Total	100

Although in many countries the use of gbfs as aggregate to replace natural sand is well established, in Brazil at present, gbfs have found application as fine aggregate only in the civil work at steel plants. This fact is due mainly to:

- the use of gbfs as an hydraulic binder is more advantageous;
- there is no divulgation of utilization of gbfs as fine aggregate;
- the behaviour of slag as aggregate concerning the durability of concrete is not yet totally clarified.

However, the increase of gbfs stocks with the generation of about 5,000,000 ton of slag per year, nowadays, and more and more scarceness of natural sands in the biggest cities and urban centers, estimulated the development of an investigation about the use of gbfs as fine aggregate[2].

Although the mentioned research has included the study of physical, mechanical and rheologycal properties of mortar with gbfs as fine aggregate, this paper deals only with the durability of these mortars.

2 EXPERIMENTAL

2.1 Materials

A typical gbfs and two cement types, respectively, an ordinary portland cement (OPC) with high alkali content and another blast-furnace slag portland cement (BPC), representatives of Brazilian production were chosen.

Table 2 - Material Characterization

Composition and Properties	OPC	BPC	Slag
Specific surface Blaine ($m^2.kg^{-1}$)	343	336	-
Compressive Strength (MPa)			-
3-days	25.4	17.2	-
7-days	31.8	25.4	-
28-days	39.5	37.8	-
Setting time (Vicat Test)			
Initial set (h:min)	4:00	4:25	-
Final set	n.d.	5:35	-

Table 2 - (Contin.)

Composition and Properties)	OPC	BPC	Slag
SiO_2 (%)	20.63	27.12	35.94
Al_2O_3 (%)	5.31	8.82	14.35
Fe_2O_3 (%)	3.14	2.51	0.85
CaO (%)	62.16	51.76	40.22
MgO (%)	1.16	3.69	6.62
SO_3 (%)	2.74	2.32	0.04
Na_2O (%)	0.28	0.19	0.11
K_2O (%)	0.98	0.69	1.00
LOI (%)	3.11	2.40	n.d.
IR (%)	0.93	0.83	n.d.
Degree of vitrification (%)	-	-	99%
Slag content (%)	0	43	100

Table 3 - Slag Grain Size Distribution

Size fraction (mm)			% in mass
	> 4.8		0
4.8	-	2.4	6
2.4	-	1.2	41
1.2	-	0.6	33
0.6	-	0.3	14
0.3	-	0.15	4
	< 0.15		

2.2 Test Procedures

In order to investigate the slag reactivity two series of tests were carried out. In the first serie autoclave was used to accelerate cement hydration according to ASTM C 151/83[3] - **Autoclave Expansion of Portland Cement** - with mortars replacing original pastes. Another serie of tests comprised the development of tests according to ASTM C 227[4] - **Potential Alkali Reactivity of Cement-Aggregate Combination (Mortar Bar Method)**. All mortar test specimens were monitorated by SEM to find out any correlation with their microstructure.

Simultaneously, in order to accumulate comparative data, other kinds of fine aggregates were tested like natural sands (**IPT sand**, the Brazilian standard sand; **Jundu sand**, a natural siliceous sand consisting of rounded particles of α - quartz with about 98% of SiO_2), Cantareira sand, an artificial sand consisting of a crushed granitic rock and pyrex glass.

Table 4 shows the composition of mortars used to evaluate the different aggregate reactivity and behaviour.

Table 4 - Composition of Mortar

Mortar nº	Aggregate	Cement	Composition (in grams)		
			cement	aggregate	water (*)
1	pyrex glass	BPC	300.0	675.0	197.3
2	slag	BPC	300.0	675.0	184.6
3	Cantareira sand (crushed granite)	BPC	300.0	675.0	158.3
4	Jundu sand	BPC	300.0	675.0	121.0
5	IPT sand	BPC	300.0	675,0	140.0
6	pyrex glass	OPC	300.0	675.0	175.0
7	slag	OPC	300.0	675.0	189.9
8	Cantareira sand	OPC	300.0	675.0	160.0
9	Jundu sand	OPC	300.0	675.0	126.0
10	IPT sand	OPC	300.0	675.0	143.0

(*) water required for a flow of 112.5 ± 7.5% according to ASTM C-109[5].

2.3 Results and Discussion

Tables 5 to 7 show the results obtained.

Table 5 - Autoclave Test Results

Mortar nº	Aggregate	Cement	Expansion (%)
1	pyrex glass	BPC	0.00
2	slag	BPC	0.00
4	Jundu sand	BPC	0.02
6	pyrex glass	OPC	0.00
7	slag	OPC	0.01
9	Jundu sand	OPC	0.06

Table 6 - Potential Alkali Reactivity ASTM C 227 Test Results (BPC)

Days	Expansion (%)				
	Pyrex Glass	Slag	Crushed Granite	Jundu Sand	IPT Sand
14	0.01	0.00	0.00	0.00	0.00
56	0.01	0.01	0.01	0.00	0.01
90	0.02	0.01	0.01	0.00	0.00
180	0.03	0.01	0.02	0.01	0.01
270	0.03	0.01	0.01	0.01	0.01
360	0.03	0.01	0.01	0.01	0.02

Table 7 - Potential Alkali Reactivity ASTM C 227 Test Results (OPC)

Mortar nº	Expansion (%)				
	Pyrex Glass	Slag	Crushed Granite	Jundu Sand	IPT Sand
14	0.34	0.01	0.00	0.00	0.00
56	0.73	0.01	0.01	0.01	0.01
90	0.79	0.01	0.01	0.01	0.01
180	0.86	0.01	0.01	0.01	0.01
270	0.86	0.02	0.02	0.01	0.01
360	0.86	0.02	0.02	0.01	0.01

Table 5 shows that the accelerating of mortar hydration rate by autoclave did not result in unsoundness of slag mortar, that is, slag activation by $Ca(OH)_2$ originated from silicate hydration is not liable to an expansive phenomenon.

Tables 6 and 7 show that slag mortar bars of ASTM C 227 test made for both BPC and OPC (high alkali) did not result in remarkable expansion after one year.

On the other hand, pyrex mortar with OPC resulted in 0.86% expansion in length at 360 days. In addition, experimental results show that pyrex mortar with BPC did not exhibit expansion due to the fact that BPC is a well-known inhibitor of expansion due to the alkali-aggregate reaction (AAR). In this case, it was supposed that there is an incorporation of the whole solube alkalis into C-S-H structure, i.e., there is no available alkaline ions to react with the aggregate.

2.4 Mortar Microstructure Evaluation by SEM

The aim of this serie of tests was to contribute to the study of both mortar volume changes and paste-aggregate bond.

After preparation, all samples revelead to be very similar under SEM showing a well-compacted and bad crystallized texture. On the other hand, pores are filled generally by a crystalline or a gel material, sometimes with a well defined morphology.

Since mortar 6 has shown the highest expansion. It was taken as reference for the study of the microstructure. In fact, in mortar 6, pyrex glass used as aggregate exhibits a reaction rim (figure 1) with a massive development of gel. Massive gel presents cracks (figure 2), but cracking pattern appeared to be occasioned by sample preparation due to the shrinkage phenomenon during sample drying. Figure 3 shows a pore filled by a massive gel, with a textured surface (botryoidal material).

BAKKER[6] has studied the mechanism of the AAR and has proposed a model to explain the concrete deterioration. According to this author, reactive silica from aggregates reacts with alkali hydroxides from pore solution and originates an expansive hydrated alkaline silicate gel. According to CHATTERJI[7] and co-workers the penetration of alkaline and hydroxyl ions from the pore solution through the surface of reactive aggregate causes a progressive destruction of its structure.

Simultaneously, silica is partially liberated and may migrate both outside or inside aggregate. Expansion occurs only when penetration of both alkaline and hydroxyl ions are larger than outside migration of silica.

Botryoidal gel formed in the interface of pyrex glass appear to be the expansive alkaline gel reported by BAKKER[6] although its chemical nature have not been studied by EDS (energy dispersive spectrometry). However its morphology is very different from that described by DAVIES and OBERHOLSTER[8] as typical products of AAR found in old dams. In this case, time and the porous structure (presence of voids, pores and cracks) could be responsible for a better crystalline development with the formation of crystalline products as lamellar, needles, rose-like crystals etc.

Volume stability of mortar 1 can be explained by the use of BPC reported by many authors as an inhibitor of expansion due to AAR. In this case C/S ratio of C-S-H of BPC (1.7 to 1.4) is lower than C/S ratio of C-S-H of OPC (2.0 to 1.7) and consequently BPC has a better ability to incorporate alkalis in C-S-H. On the other hand, pastes of BPC has little free $Ca(OH)_2$ and according to CHATTERJI[7] this fact promotes the silica migration from pyrex glass. Consequently, the reaction rim of pyrex glass is supposed to have formed a non expansive hydrated calcium silicate gel.

Slag mortar 7 (Figure 4) presents an hydrated layer around the coarse slag grain with massive gel formation. As mortar not presented expansion DAVIES and OBERHOLSTER's model could be proposed in this case. Since slag are rich in CaO, calcium ions could be the inhibitor according to the former autors' theory, with gel presenting in its composition both alkalis and calcium. In this case reaction between slag aggregate and cement paste would originate a massive non expansive gel C-S-H type with alkalis incorporation.

Autoclaved mortars 2 and 7 are similar to non autoclaved mortars and just present a larger reaction rim, accelerated by the highest temperature and pressure conditions, with both gel and crystal formation (Figures 5 to 7). Slag aggregates rich in Al_2O_3 SiO_2 and CaO are hydraulically active and form a transitional zone which increases the bond instead of causing expansive stress. Consequently tensile strength is increased as obtained in a former study[2] dealing with the evaluation of mechanical and rheologycal properties of mortars with slag as fine aggregate.

3 FINAL REMARKS

Former studies[2] about mechanical and rheologycal implications of the use of slag as fine aggregate are now completed with the tests of durability carried out in the same slag mortars. Results of tests suggest from the point-of-view of durability the viability of the use of slag replacing natural sands as fine aggregate.

Therefore one can conclude that slag aggregate hydration is a non expansive phenomenon that leads to an increasing of both the tensile strength and the bond in the interface paste-aggregate.

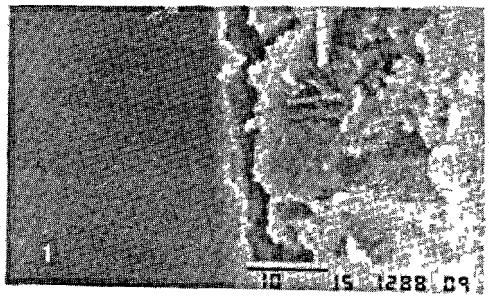

Fig.1 - Mortar 6 with 0.86% expansion after ASTM C-227 test (one year) showing a reaction rim in pyrex glass.

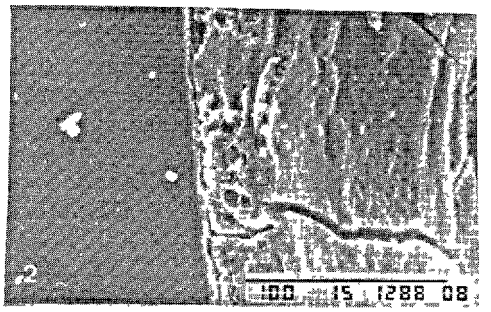

Fig. 2 - Development of massive gel in mortar 6.

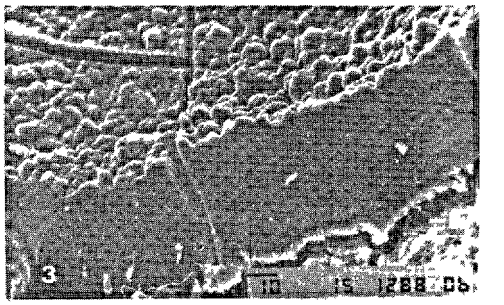

Fig. 3 - Detail of a pore of mortar 6 with massive gel development and textured surface with botryoidal material.

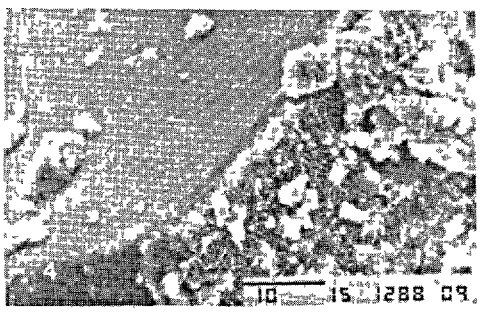

Fig. 4 - Slag aggregate of mortar 7 with a darker reaction rim. Mortar did not present expansion.

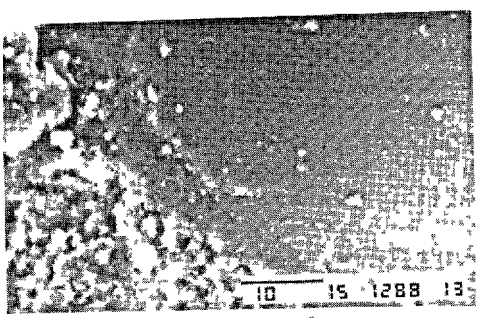

Fig. 5 - Progressive reaction rim in slag grain of mortar 2 after autoclave test.

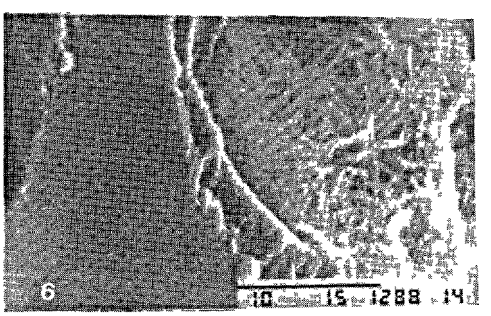

Fig. 6 - Needle-like material formed in a pore of mortar 2 after autoclave test.

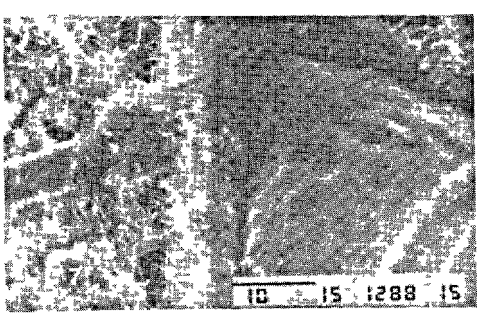

Fig. 7 - A reaction rim of about 5µm in a slag grain of mortar 2 after autoclave test. Mortar did not present expansion and bond was improved.

RFFERFNCES

1. Chehebe, J.R. et alii: "Generation and destination of slag in Brazilian Siderurgical Industry". In: BRAZILIAN INSTITUTE OF SIDERURGY. **Seminar on Siderurgical Industrial Wastes, Rio de Janeiro, Brazil, 9-10, june, 1987**, p. B.1-B.37 (in portuguese).

2. Scandiuzzi, L & Battagin, A.F.: "Utilization of granulated blast-furnace slag as fine aggregate". São Paulo, Brazilian Portland Cement Association, 1989. (Technical Study nº 95) (in portuguese).

3. ASTM C-151-84: "Autoclave expansion of portland cement". Annual Book of ASTM Standards, American Society for Testing and Materials, Philadelphia, 1986. v.04.01.

4. ASTM C-227-87: "Potential alkali reactivity of cement-aggregate combinations (mortar-bar method)". Annual Book of ASTM Standards, American Society for Testing and Materials, Philadelphia, 1988. v.04.03.

5. ASTM C-109-86: "Compressive strength of hydraulic cement mortars (using 2-in. or 50-mm cube specimens)". Annual Book of ASTM Standards, American Society for Testing and Materials, Philadelphia, 1986. v.04.01.

6. Bakker, R.F.M.: "About the cause of the resistance of blast-furnace cement to the alkali-silica reaction". In: **International Conference on Alkali-Aggregate Reaction in Concrete, 5th, Cape Town, South Africa, 1981.** p. 252/29-1-7.

7. Chatterji, S. et alii.: "Studies of alkali-silica reaction, part 6: Practical implications of a proposed reaction mechanism". Cement and Concrete Research, 1988, 18(3), 363-368.

8. Davies, G. & Oberholster, R.E.: "The alkali-silica reaction products, a mineralogical and an electron microscopic study". In: Bayles, J. **International Conference on Cement Microscopic, 8th, Orlando, 1986.** p.303-326.

DURABILITY ASPECTS OF CEMENTS WITH HIGH LIMESTONE FILLER CONTENT

Y Tezuka*, D Gomes Jr, J M Martins** and J G Djanikian****

Brazilian Portland Cement Association, São Paulo, BRAZIL
***Serrana Cement Group, São Paulo, BRAZIL*

SUMMARY

Studies of fillerized cements from clinkers with high C_3A content have shown an accelerated hydration reaction and the formation of carboaluminate.

Our paper started with clinker of low C_3A content and 36 cements were prepared in laboratory with 5, 10, 15, 25 and 35 percent calcite and dolomite limestone, by weight, to evaluate their durability performance.

Pastes and mortars were tested by diffusibility of chloride ions, combined water, XRD, SEM with EDS, carbonation and chemical resistance to sulfate and chloride.

The analysis of the results indicated that mortars with limestone addition, generally exhibit similar durability properties to that of the OPC mortar.

SOMMAIRE

Études des ciments fillerizées provenant de clinqueres avec haute teneur en C_3A on montré une hydratation acceleré et formation de carboa luminate.

Dans notre travail nous utilison de clínquer avec basse teneur en C_3A et 36 ciments preparés dans le laboratoire avec 5, 10, 15, 25 et 35 pourcentage, a poid, des calcite et calcaire dolomitique pour vérifier leur influence sur la durabilité.

Nous avons essaié pates et mortiers par diffusibilité des ions Cl, eau combiné, DRX, MEB, carbonatation et résistence chimique a les sulfates et clorures.

En analysant les résultats des essais on constate que la durabilité des mortiers fillerizées, généralement, sont similaires a des mortiers de ciment ordinaire.

INTRODUCTION

Portland cement containing finely ground limestone has been studied mainly as an measure for saving energy and resources, for reducing envirommental impact, as well as technical aspects (1). Many papers (2,3,4) pointed out that the addition of $CaCO_3$ to cement with high C_3A content increased the rate of cement hydration and their strength and workability. The ettringite formation accelerated as well as the conversion of ettringite to monosulfate and C_3A reacted with $CaCO_3$ forming calcium carboaluminate.

In comparison, little information with regards to the durability of portland cement with limestone addition is available, and these is no general agreement on the effects of filler addition on cement properties with low C_3A content. Therefore, the main purpose of this present paper is to investigate the effect of limestone content on the durability of the cement with low C_3A clinker.

EXPERIMENTAL

Materials and samples

The chemical composition of ordinary portland cement (OPC) used is shown in Table 1 and the characteristics of calcite and dolomite limestone used as fillers in Table 2. Sand with 91.9% SiO_2, 3.6% feldspar and 1.3% mica was used as an inert filler. Calcite and dolomite limestone were ground to 350 m²/kg 450 m²/kg and 550 m²/kg Spc.Surf. Blaine and quartz to 350 m²/kg. The industrial (OPC) with 6% C_3A content 339 m²/kg Blaine was blended with 5, 10, 15, 25 and 35wt% of filler with different finenesses. This gave the total of 36 mixtures, designated as follows. Po, $C_1$5, $C_1$10, $C_1$15, $C_1$25, $C_1$35, $C_2$5, $C_2$10, $C_2$15, $C_2$25, $C_2$35, $C_3$5, $C_3$10, $C_3$15, $C_3$25, $C_3$35, $D_1$5, $D_1$10, $D_1$15, $D_1$25, $D_1$35, $D_2$5, $D_2$10, $D_2$15, $D_2$25, $D_2$35, $D_3$5, $D_3$10, $D_3$15, $D_3$25, $D_3$35, $Q_1$5, $Q_1$10, $Q_1$15, $Q_1$25 and $Q_1$35. Where Po = OPC without filler, C = calcite, D = dolomite, Q = quartz. The first number indicates specific surface area of filler: 1 = 350 m²/kg, 2 = 450 m²/kg, 3 = 550 m²/kg. The second number indicates the % weight of filler: 5 = 5% etc. .

TABLE 1 - Chemical composition of OPC

Chemical composition (%)									
L.O.I	SiO_2	Al_2O_3	Fe_2O_3	CaO	MgO	SO_3	Na_2O	K_2O	P_2O_5
1.0	18.5	4.5	3.5	59.6	5.3	3.1	0.1	0.5	0.8

TABLE 2 - Composition of calcite and dolomite limestone (%)

Sample	apatite	calcite	dolomite	silicates	magnitite + pyrite
Calcite	2.5	79.6	13.3	2.8	1.2
Dolomite	2.6	42.8	50.1	1.9	2.0

Methods

Pastes were prepared with water to solid ratio of 0.4 sealed into plastic bottles, subjected to continuous rotation at 8 rpm up to 24 hours to prevent segregation, and hydrated at 23°C for designated periods of time. After stopping hydration, the degree of hydration was estimated by the amouth of combined water calcuted by loss on ignition at 1.000 °C and hydrated products were examined with powder XRD. Cℓ ion diffusion was determined by the diffusion cell technique of hardened cements pastes in 28 days water curing, 50 mm diameter x 3 mm thickness. Side I of the cell was filled with deionized water and side II with a 1 M NaCℓ Solution.

Workability of mortar 1:3 (wt) was estimated by water demand for a consistency of 165 ± 5 mm in the flow table test conducted by Brazilian method NBR 7215. The depth of carbonation was determined at the specified

drying period by phenolphthalein indicator method. Specimens 40 x 40 x 160 mm after 7 days water curing were exposed under laboratory conditions at 23°C and 65% RH, outdoor exposed and outdoor covered to provide shelder from raim. The chemical resistances of mortars 40 x 40 x 160 mm after 28 days water curing, and immersed in a 5% $NaSO_4$ and a 1.5% NaCℓ solutions were determined for weight loss after removal of the weak reaction product and flexural strength. The calculated "residual strength" is the ratio between flexural strength of samples immersed in chemical solution and the strength of samples cured under standard conditions with the same age. Samples taken from the broken half were examined with SEM associated with EDS .

RESULTS AND DISCUSSION

Workability

The results (Table 3) indicated that the workability decreases as follows: OPC with limestone addition > OPC without addition > OPC quartz addition. Perhaps the reason for better workability of mortars containing limestone, is that the additional limestone has more suitable texture and fineness, better complementing the particle size distribution of cement and thus improving rheological properties.

TABLE 3 - Workability of mortar

spec.surf area of fillers	OPC	calcite 5,10,15,25,35 wt%	dolomite 5,10,15,25,35 wt%	quartz 5,10,15,25,35 wt%
m^2/kg		W/C for consistency of 165 ± 5 mm		
350	0.49	0.48	0.48	0.50
450		0.48	0.48	
550		0.48	0.48	

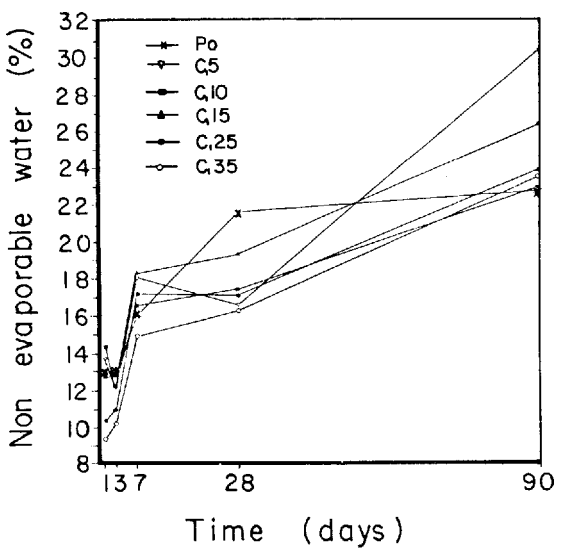

Fig 1 Non evaporable water VS hydration time

Hydration

The rate of hydration was followed by estimating the non-evaporable water. A typical non-evaporable water is shown in Fig. 1. The first seven day stage, rates of hydration of cement with limestone accelerated more rapidly compared to OPC, with the exception of the 35% addition sample.

This confirms that hydration rate is increased in the presence of $CaCO_3$, even for cement with low C_3A content.

XRD analysis

The XRD patterns after 90 days hydration indicated the presence of monocarboaluminate (basal spacing 7.6 Å) with 35% calcite. For lower calcite content, the monocarboaluminate was not detected. Monosulphate was not also detected. This is consistent with that reported by Klemm and Adams (5). They concluded that OPC with a high C_3A content can react readily during hydration with carbonates, forming significant amounts of carboaluminates, whereas for low C_3A the reaction seems to be slower.

Diffusion coeficient of Cℓ ion

The diffusion coeficient of Cℓ ion (Table 4) decreased in the order of calcite (450 m²/kg) addition of 25%, 15%, 35%, 10%, 0% and 5%, the values of D varying between 10^{-9} to 10^{-8} cm²/s. The diffusion coeficient of Cℓ ion for OPC and blended cements varies between 10^{-9} to 10^{-6} cm²/s. Therefore, it can be concluded that the diffusion coefficient of Cℓ ion of cement past with limestone addition is similar to that of OPC .

TABLE 4 - Diffusion coefficient of Cℓ ion

MIXTURE	D (cm²/s)
Po	51.2×10^{-9}
C_25	14.3×10^{-9}
C_210	53.1×10^{-9}
C_215	13.4×10^{-8}
C_225	16.3×10^{-8}
C_235	12.3×10^{-8}

Carbonation

The depth of carbonation (Table 5) decreased in the following exposure conditions: external under cover > controlled laboratory conditions of 23°C and 65% RH > external atmosphere and increased with the time and limestone addition.

At 6 months exposure the results are similar to OPC up to 10% addition.

TABLE 5 - Depth of carbonation of mortar, in mm

MORTAR	LABORATORY 23°C, 65% RH			EXTERNAL ATMOSPHERE			EXTERNAL UNDER COVER		
	DURATION OF CARBONATION IN MONTHS								
	1	3	6	1	3	6	1	3	6
Po	1.0	1.0	2.0	0	0.5	0.5	1.0	1.0	2.0
C_25	0	0	1.0	0	0	0	1.0	1.0	2.0
C_210	1.0	1.0	2.0	0	0	0	0	1.0	2.0
C_215	0	1.0	1.5	0	0	0	0	2.0	3.0
C_225	1.0	2.0	2.5	0	0	1.0	1.0	2.0	3.0
C_335	0	1.0	3.5	0	0	1.0	1.0	2.0	3.5

Chemical resistance

The residual strength ratio of mortars (Fig. 2) immersed in NaCℓ up to 4 months decreased to 0.89 value (15% add) and after that increased, at 6 months, to 1.08 (10% add). For Na_2SO_4 exposure, the residual strength increased up to 1.30 at 2 months (15% add) and decreased at 6 months to 1.03 (35% add). The same trend was observed for dolomite addition. In both solutions no weight loss was observed. The dolomite addition in the sulphate solution showed a slight gain, up to 1%. The performance of chemical resistance of mortars containing limestone may be attributed to filling voids with limestone. Calcite acts as crystallization nuclei, which increase the density of the mortars structure.

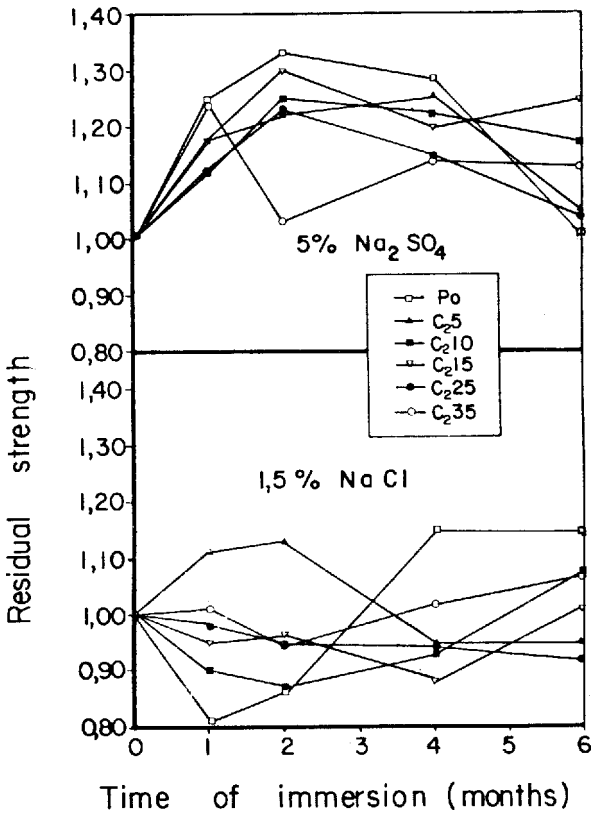

Fig 2 Residual strength VS time of exposure to Na_2SO_4 and NaCℓ sol

SEM examination

Fig. 3 shows morphologival features of some of the mortars near the surface exposed in 1.5% NaCℓ solution and 5.0% Na_2SO_4 solution, after 4 months.

In the mortar containing calcite exposed in Na_2SO_4 solution, a homogeneous intergrowth of ettringite, C-S-H and CH (Fig. 3-a) can be seen.

In the case of mortars containing calcite exposed in NaCℓ solution, plates of calcium chloroaluminate grew together with ettringite and C-S-H (Fig. 3-b).

In general, it was observed that the fractured surface of the mortar containing limestone was more dense and compacted than in the OPC mortar.

In all of the mortars, both immersed in lime water, Na_2SO_4 and NaCℓ solutions, the structure retained its integrity and therefore suggests that the chemicals have limited access to it.

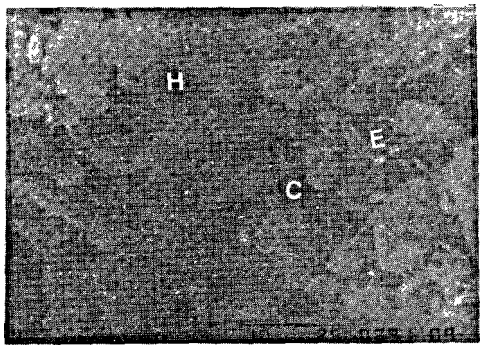

a) OPC + 25% calcite immersed in Na_2SO_4 sol

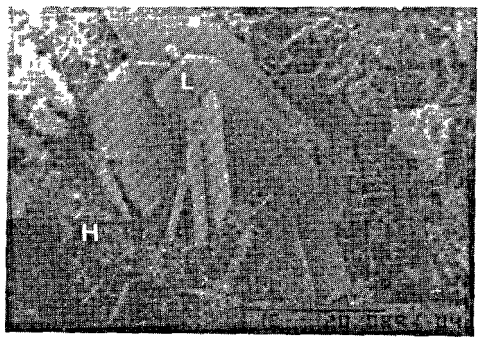

b) OPC + 25% calcite immersed in NaCℓ sol

Fig 3 SEM micrographs of mortars after 4 months immerson in 1.5% NaCℓ and 5.0% Na_2SO_4 sol

(E: ettringite; C: CH; H: C-S-H; L: chloroaluminate)

CONCLUSION

The workability of mortars containing limestone is better than those without it. Therefore, for the same workability, the water to cement ratio can be lowed. The relationships between low W/C ratio and durability is well established.

The diffusion coefficient of Cℓ ion through the cement paste with 5, 10, 15, 25 and 35%wt limestone, is similar to that of OPC.

At 6 months exposure, the OPC and OPC with limestone addition, both showed the same depth of carbonation at up to 10% addition.

No mortar loss weight with or without limestone additions, exposed to 1.5% NaCℓ, 5.0% Na_2SO_4 or lime water solutions was observed after six months exposure.

The good result of mortar containing limestone when exposed to Na_2SO_4 and NaCℓ solutions is due to the fact that its structure is more dense and compacted than that of mortar with OPC as seen by SEM examination.

REFERENCES

1. Baron, J. & Douvre, Ch.: " Technical and economical aspects of the use of limestone filler additions in cement". World Cement, 1987, 18(3), 100-104 .

2. Ramachandran, V.S. & Zhang, C.M.: "Influence of $CaCO_3$ on hydration and microstructural characteristics of C_3S" . Il Cemento, 1986, 3, 129-152 .

3. Soroka, I & Stern, N.: "Calcareous fillers and the compressive strength of portland cement". Cem. Concr. Res. 1976, 6, 367-376 .

4. Bombled, J.P.: "Rhéologie du béton frais, Influence de l'ajout de fillers aux ciments" . 8th Int. Congr. Chem. of Cement, Rio de Janeiro, 1986, IV, 190-196 .

5. Klemm, W.A. & Adams, L.D.: "An investigation of the formation of carboaluminates". ASTM STP 1064, Carbonate additions to cement, Philadelphia, 1990, 60-72 .

INFLUENCE OF GYPSUM CONTENT IN PORTLAND CEMENTS ON SULPHATE RESISTANCE

G Frigione* and F Zenone**

**University of Calabria, Arcavacata (Cosenza), ITALY*
***Cementir-Cementerie del Tirreno, Naples, ITALY*

SUMMARY

The effect of gypsum content on the resistance to sulphates, as a function of the mineralogical clinker composition, has been studied. The results show that the clinker composition and gypsum content strongly affect the behaviour of Portland cement to sulphate attack. A higher sulphate resistance is obtained when the gypsum content is increased as a function of the amount of calcium aluminate in the clinker. Furthermore, polymorphic C_3A forms show pratically identical resistance to sulphate attack, if the cement is suitably dosed with SO_3.

RESUME

Nous nous proposons d'étudier l'influence de la quantite de gypse sur la résistance au sulfate, en tenant compte de la composition minéralogique des clinkers de ciment portland. Les résultats confirment que le comportement du portland à l'attaque du sulfate dépend fortement de la composition minéralogique du clinker, mais que la teneur en gypse a également une grande importance. Pour obtenir une meilleure résistance du portland à l'attaque du sulfate il faut augmenter le contenu en gypse, en function de la teneur en aluminate de calcium. En plus, tous les formes polymorphiques du C_3A montrent la meme résistance à l'attaque du sulfate, si le ciment portland est convenablement dosé en gypse.

INTRODUCTION

An extensive literature about the effect of C_3A on sulphate resistance of cement pastes, mortars and concretes has been published. It is generally recognized that the vulnerability of pastes and mortars to sulphate attack increases with increasing the C_3A content of the cement used (1). According to Blaine et al. (2), on the basis of the multiple regression analysis between the characteristics of the cement composition and the results of the sulphate expansion test, the expansion is a third power function of the C_3A content when this last one is present in the range of 7% to 15%, whereas the linear proportionality occurs with lower C_3A contents.

In cements, C_3A is usually cubic or orthorhombic and sometimes monoclinic (3); however, two phases can coexist. In 60 industrial clinkers, Gourdin et al (4) found 29 cubic, 5 orthorhombic and 26 cubic + orthorhombic C_3A. According to some authors, the crystallographic form of the C_3A can affect the vulnerability of a cement in the presence of sulphate attack. Regourd and Guinier (5) stated that a cement containing 7 wt % cubic C_3A has the same behaviour as a cement containing 16 wt % orthorhombic C_3A in the presence of sea-water attack. Similarly, Mehta (6) showed that the hydrated pastes, made from cements containing cubic C_3A, are attacked by sulphate solutions at a slower rate than pastes made from cements containing C_3A more densely packed. On the other hand, Mather (7) found no correlation between the type of C_3A present in Portland cements and the rate of sulphate attack.

While the influence of gypsum content in Portland cement on the behaviour of the cement itself, with particular reference to the rheologic behaviour, mechanical strengths and volume stability, has been extensively studied (8), there is little indication in the literature concerning the effect of gypsum content on durability and particularly on cement resistance to sulphate attack.

Regourd (9) tested mortars, made from Portland cements (14% C_3A), stored in sea-water and noted that mortars with 12% of gypsum content (ca. 4.8% of SO_3) show a minimum expansion; however, their behaviour is almost similar to that of mortars made from cement with 6% of gypsum content. Frigione and Zenone (10), on the ground of tests made on two Portland cements, one with low and one with medium C_3A content, found that the sulphate resistance improves with the increase in the gypsum amount.

This paper is a contribution to the understanding of the influence of gypsum content on sulphate resistance. The results of a systematic long-term study on Portland cements presenting a wide range of C_3A content have been reported. The effect of the polymorphic form of C_3A in cements has also been considered.

EXPERIMENTAL

Materials

Tests were made on Portland cements prepared by grinding fourteen different industrial clinkers. In the clinkers, the C_3A content varied between 1.6 and 14.0 per cent. The amounts (in wt. %) of the compounds were determined by X-ray diffraction analysis (11) (12). The results are shown in Table 1, where the crystallographic phase of the C_3A are also indicated. The distinction between orthorhombic and cubic phase was determined after silicate dissolution in salicylic acid - methanol (13) (14). In Table 1, the mineralogical compositions, calculated according to Bogue formulae (15), is also reported.

Table 1. Weight percentage of the phases in the clinkers.

Clinker	C_3S		C_2S		C_3A		C_4AF		C_3A pol
	XRD	Bogue	XRD	Bogue	XRD	Bogue	XRD	Bogue	
1	55.4	54.1	25.7	24.1	1.4	1.5	14.1	15.0	C
2	58.2	55.5	19.6	20.8	6.7	7.4	9.8	10.0	C
3	59.1	57.4	21.0	20.2	7.0	7.5	9.1	9.8	C
4	54.8	51.6	24.1	25.0	4.8	4.9	4.6	12.5	C
5	54.0	50.8	23.9	24.5	8.6	8.5	8.2	8.8	C
6	49.3	47.7	28.1	25.5	8.8	8.7	9.1	9.8	O/C
7	50.8	49.3	27.7	26.2	8.8	8.9	8.3	8.8	O
8	49.2	48.8	25.2	23.1	10.0	10.2	9.1	10.2	C
9	46.9	45.9	27.7	27.2	11.0	10.4	9.1	9.5	C
10	44.8	44.5	27.6	26.9	11.6	10.6	9.9	10.4	C
11	47.1	45.4	29.0	29.6	13.2	13.1	6.0	6.8	C
12	44.6	44.8	27.1	26.5	14.0	13.5	6.9	6.9	C
13	56.2	55.4	25.2	25.1	2.7	2.6	8.2	8.5	C
14	55.9	53.2	22.0	22.8	8.1	8.6	8.6	9.0	C

C = cubic O = orthorhombic

The clinkers were ground to the fineness of 400 m^2/kg as determined by the air permeability method (ASTM C 204). Each of the resulting grinds was thoroughly blended with different amounts of gypsum, suitably ground (16). Each of the cements presented a total SO_3 content of 1.5 - 2.0 - 2.5 - 3.0 - 3.5 and 4.0 wt%, respectively.

Testing modes

To evaluate the resistance to sulphate attack, tests on cements, prepared as above described, have been performed:

- by means of visual examination of specimens, measuring 20x20x120 mm, prepared in ISO mortar (17). After storing for the first 21 days in water, they were immersed for 2 years in a Na_2SO_4 solution corresponding to a sulphate ion concentration of ca. 30g/l. The saline solution was renewed every 30 days. Observations were made and photographs taken every six months.

- by means of tests using a method described by Mehta(18): cement paste cube specimens were tested to the compressive strength after prestorage at 20° C for one day and at 40° C for 13 days. Equal prestored specimens were immersed in a 4.0% Na_2SO_4 solution. The solution was maintained at constant pH and sulphate concentration by automatic and continuos titration against N/10 H_2SO_4. After 180 days, the specimens were removed from the solution and the compressive strength was tested. Details of specimens preparation and testing are reported in Mehta (18). Changes in compressive strength of cement paste cubes after 180-day sulphate immersion period compared to those of specimen cubes stored in water, were used as criteria for the evaluation of cement sulphate resistance.

RESULTS AND DISCUSSION

The results of the visual examinations on small specimens after 2 year storage were in perfect agreement with those obtained by using the Metha method.

Hereafter, only these last results will be taken into account, being the values less subjective, obviously.

The percentage strength loss, related to the sulphate resistance, as a function of the C_3A content in the presence of different SO_3 amounts, is given in Figure 1, only for cements containing C_3A in cubic polymorphic form. It appears clear that the resistance to sulphates, for the same C_3A content, increases notably with increasing SO_3 content in the cement. It can be also seen that, within the C_3A limits we experimented, the increase of SO_3 content rises the ideal threshold value of C_3A content corresponding to the passage from sulphate resistant cement to non-resistant cement. Considering, for example, a strength loss equal to 20%, a cement containing 4% C_3A and 1.5% SO_3 and one containing 11% C_3A and 4.0% SO_3 are equally sulphate-resistant.

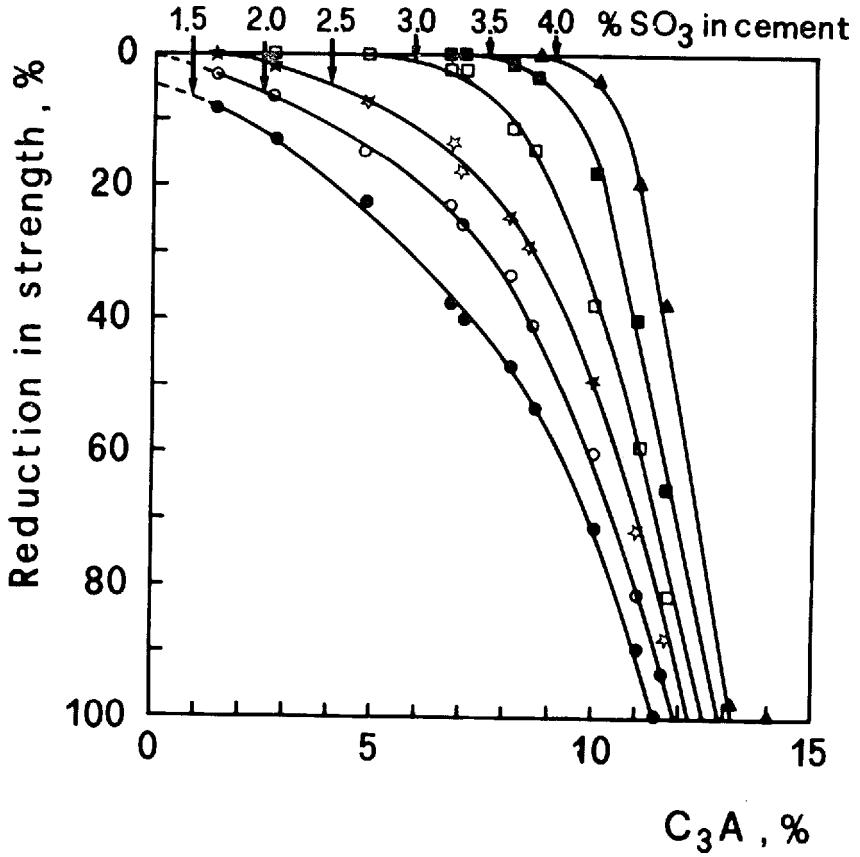

Fig.1. Behaviour of various cements to sulphate attack, as a function of SO_3 content.

It follows that, if the C_3A content is limited, relatively small additions of gypsum give a good sulphate resistance. In particular, cements with a very low C_3A content have always a very good resistance, as also do those with very low SO_3 content.

Figure 2 shows the strength loss of cements made with clinkers similar in C_3A content, but different in their polymorphic form. It can be noted that the cements containing C_3A in cubic form with low SO_3 content behave better than those with

orthorhombic C_3A. For high SO_3 content, the behaviour of both polymorphic forms is practically the same. Thus, one can affirm that the cubic and the orthorhombic C_3A forms behave likewise in the presence of sulphate attack if the cements containing them are suitably dosed with SO_3. Otherwise, the orthorhombic C_3A, with a same SO_3 content, is more vulnerable than the cubic C_3A. This might explain the contradictory results reported in the literature.

CONCLUSIONS

The behaviour of polymorphic, cubic or orthorhombic, forms of C_3A, as regards the sulphate attack, is practically identical if the cement is suitably dosed with SO_3.

However, the influence of C_3A content on cement sulphate resistance is always dependent on SO_3 content in the cement.

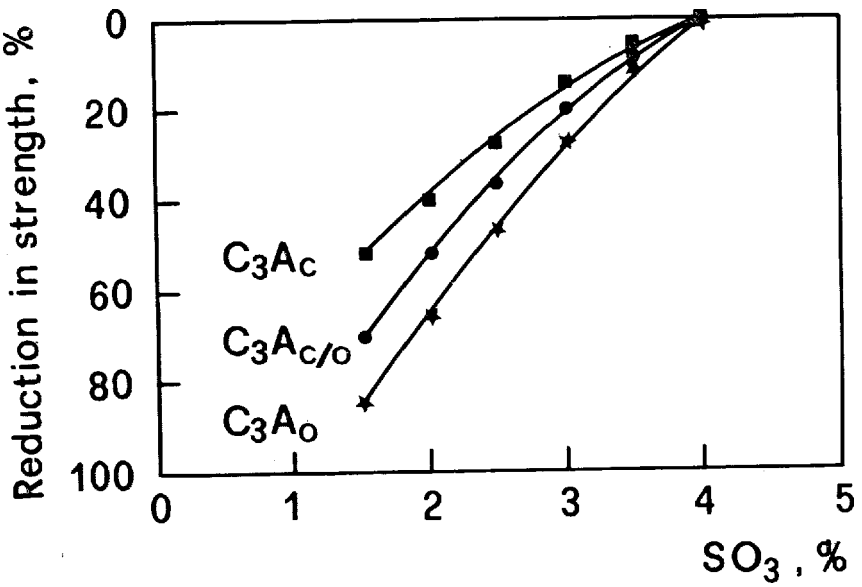

Fig. 2. Behaviour of cements to sulphate attack, as a function of polymorphic forms of C_3A.

C = cubic O = orthorhombic

With increasing C_3A content, a gradual and greater quantity of gypsum is necessary for the cement to resist the aggressive action of sulphates. This may explain why contrasting data are found in the literature regarding cement sulphate resistance for low or medium C_3A contents (19). It can also be noted that the SO_3 values that we have used have always been within a limited range, so as not to create volume instability (20, 21).

A greater sulphate resistance with the increase of SO_3 content in the cements can be attributed to many causes. It can be held that an increase in gypsum content, increasing the amount of non-expansive primary ettringite, leaves a smaller quantity of aluminate which is available to react successively with the sulphates permeating from outside, in order to form expansive ettringite. One may also hypothesize that, with the increase in gypsum content, different hydrated phases or different

microstructures are formed during the cement hydration (22, 23). This causes the cement to behave differently in respect to the aggressive action of sulphates. However, one should not underestimate the fact that, with the increase in SO3 content, a different characteristic of the voids' system is determined (24) as far as size and pore distribution are concerned, with a consequent ability of sulphate ions to diffuse through the pore structure (25, 26, 27) owing to a lower permeability of the cement paste.

The non-vulnerability of the low C_3A content cements toward sulphates, in the light of the results shown by Sersale et al. (24) about the non-effect of SO_3 content on pore size distribution in these cements, can be attributed only to the lack of reagents: anhydrous and hydrate aluminates.

REFERENCES

1. Roy, D.M.: "Mechanisms of Cement Paste Degradation due to Chemical and Physical Factors." **8th Int. Congr. Chem. Cem., Rio de Janeiro,** 1986, **Vol. 1**, 362-380.

2. Blaine, R.L., Arni, H.T. and Evans, D.N.: "Variables associated with expansion in the potential sulfate expansion test". Interrelations between cement and concrete properties. Building Science Series 5, Part 2, Section 4, National Bureau of Standards, 1966.

3. Varma, S.P. and Wall, C.D.: "A Monoclinic Tricalcium Aluminate (C_3A) Phase in a Commercial Portland Cement Clinker". Cem. Concr. Res., 1981, 11(4), 567-574.

4. Gourdin, P., Demoulian, E., Howthorn, F. and Vernet, C.: "Polymorphisme de l'alite et du C_3A. Statistiques". **7th Int. Congr. Chem. Cem., Paris,** 1980, **Vol. II**, I-223-228.

5. Regourd, M., Guinier, A.: "The crystal chemistry of the constituents of Portland cement clinker". **6th Int. Congr. Chem. Cem., Moscow,** 1974. Principal Paper I.2.

6. Mehta, P.K.: "Influence of different crystalline forms of C_3A on sulfate resistance of portland cement". **7th Int. Congr. Chem. Cem., Paris,** 1980, **Vol. IV**, 575-579.

7. Mather, K.: "Factors affecting sulfate resistance of mortars". **7th Int. Congr. Chem. Cem., Paris,** 1980, **Vol. IV**, 580-585.

8. Frigione, G.: **Gypsum in Cement.** Advances in Cement Technology, ed. by S.N.Ghosh. Oxford, Pergamon Press, 1983, p 485-535.

9. Regourd, M.: **Physico-chemical Studies of Cements Pastes, Mortars and Concretes Exposed to Sea Water**. Performance of Concrete in Marine Environment, ACI SP 65, Detroit, 1980, p 63-83.

10. Frigione, G., Zenone, F.: "Influenza del dosaggio di gesso sulla resistenza ai solfati dei cementi". **Convegno AITEC on la Durabilità delle Opere in Calcestruzzo, Padova, Italy,** 1987, **Vol. I**, 93-100.

11. Howard, B.H.: "Preliminary Data on QXRD Analysis of Portland Cement and Clinker Using CeO_2 as the Internal Standard". Cem. Concr. Res., 1984, 14 (5), 729-740.

12. Knudsen, T.: "Quantitative Analisys of the Compound Composition of Cement and Cement by X-Ray Diffraction". Am. Ceram. Soc. Bull. 55, 1976, 1052-1058

13. Mander, J.E., Adams, L.D. and Larkin, E.E.: "A Method for the Determination of Some Minor Compounds in Portland Cement and Clinker by X-Ray Diffraction". Cem. Concr. Res., 1974, 4(4), 533-544.

14. Regourd, M.: **Crystal Chemistry of Portland Cement Phases.** Structure and Performance of Cements, ed. by P. Barnes. London, Applied Science Publishers LTD, 1983, p 109-138.

15. Bogue, R.H.: **La Chimie du Ciment Portland.** Paris, Eyrolles, 1952, 568 p.

16. Frigione, G., Di Leva, R.: "La distribuzione granulometrica dei componenti dei cementi Portland e d'Altoforno". Il Cemento, 1975, 72(1), 13-24.

17. ISO / DIS 679- 1987: "Méthodes d'essai des ciment - Détermination des résistance mécaniques". 1987, 15 p.

18. Mehta, P.K.: "Evaluation of Sulfate Resisting Cements by a New Test Method". ACI Journal, 1975, 72(10), 573-575.

19. Kalousek, G.L., Porter L.C. and Benton E.J.: "Concrete for Long-Time Service in Sulphate Environment". Cem. Concr. Res., 1972, 2(1), 79-89.

20. Soraka, I. and Abayneh, M.: "Effect of Gypsum on Properties and Internal Structure of PC Paste". Cem. Concr. Res., 1986, 16 (4), 495-504.

21. Odler, I. and Abdul-Maula, S.: "Investigations on the Relationship Between Porosity Structure and Strength of Hydrated Portland Cement Pastes. III. Effect of Clinker Composition and Gypsum Addition". Cem. Concr. Res., 1987, 17 (1), 22-30.

22. Feldman, R.F.and Beaudoin, J.J.: "Microstructure and Strength of Hydrated Cement". Cem. Concr. Res., 1976, 6(3), 389-400.

23. Jelenic, I., Panovic, A. and Bezjak, A.: "Hydration and Strength Development in Alite-C_3A-CSH_2-Quartz Pastes Containing Readily Soluble Alkalies". Cem. Concr. Res., 1980, 10 (3), 463-466.

24. Sersale, R., Cioffi, R., Frigione, G., Zenone, F.: "SO_3 Content of Portland and Blended Cements. Porosity and Behaviour of the Resultant Mortars." This Congress.

25. Calleja, J.: "Future Trends in the Research of the Structure, Properties and Behaviour of Blended Cements". **8th Int. Congr. Chem. Cem., Rio de Janeiro,** 1986, **Vol. I**, 233-248.

26. Mehta, P.K.: **Durability of Concrete in Marine Environment - A Review.** Performance of Concrete in Marine Environment, ACI SP 65, Detroit , 1980, p 1-20.

27. Feldman, R.F., Beaudoin, J.J., Philipose, K.E.: "Effect of Cement Blends on Chloride and Sulphate Ion Diffusion in Concrete". Il Cemento, 1991, 88(1), 3-17.

INFLUENCE OF CEMENT CHARACTERISTICS ON THE PROTECTIVE VALUE OF THE CONCRETE COVER

R Torrent and J Gebauer

Holderbank Management & Consulting Limited, Holderbank, SWITZERLAND

ABSTRACT

A quite comprehensive research was carried out to investigate the influence of various factors on the quality of the concrete cover: concrete grade, cement characteristics and curing conditions. Twenty four concrete mixes of mean cube strengths ranging between 25 and 85 MPa were prepared with 9 different cements and subjected to three different curing conditions. Results are presented on the resulting cover qualities, as assessed by their permeability to O_2 and their frost resistance in the presence of de-icing salts.

It has been proved that it is mix characteristics (mainly concrete strength), location and curing conditions which are the main factors affecting the quality of the concrete cover, with cement characteristics playing only a secondary role.

RESUMEN

Se llevó a cabo un completo programa de investigación para estudiar la influencia de distintos factores sobre la calidad del hormigón de recubrimiento: clase de hormigón, características del cemento y condiciones de curado. Se prepararon 24 mezclas de hormigón con resistencias (cúbicas) entre 25 y 85 MPa, utilizando 9 cementos diferentes y aplicando 3 tipos de curado. Se presentan resultados de la calidad de los recubrimientos así obtenidos, evaluada a través de la permeabilidad al O_2 y de la resistencia a la congelación en presencia de sales descongelantes.

Se comprobó que los principales factores que afectan la calidad del recubrimiento son las características de la mezcla (especialmente su resistencia), la ubicación de la superficie y las condiciones de curado, en tanto que las características del cemento juegan solamente un rol secundario.

INTRODUCTION

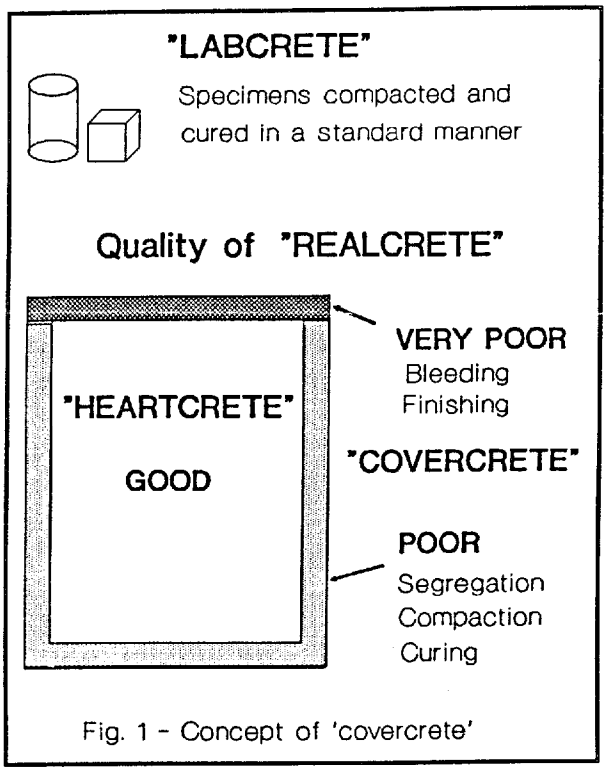

Fig. 1 - Concept of 'covercrete'

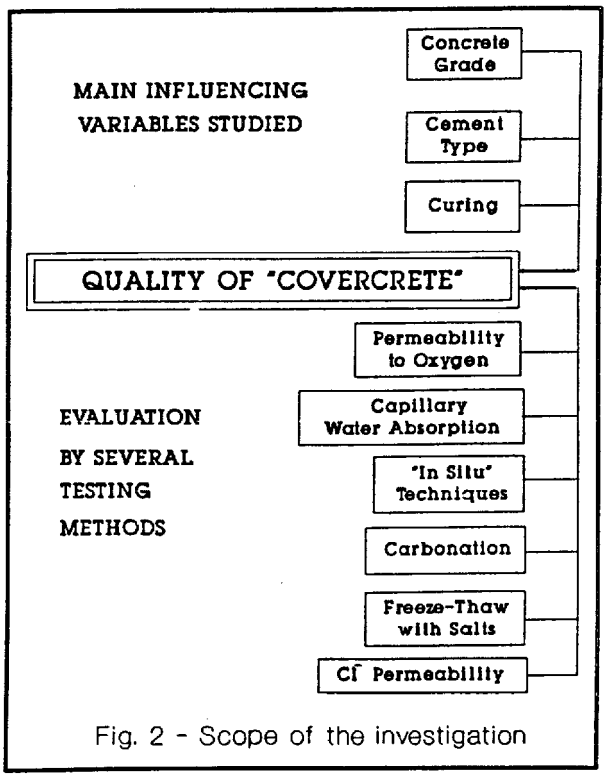

Fig. 2 - Scope of the investigation

While the bearing capacity of a structural member depends on the integral behaviour of the element, its durability against environmental aggressive actions depends basically on the performance of a relatively thin superficial layer of concrete (20-50 mm thick). Indeed, this layer should protect the reinforcing bars against corrosion -be it induced by carbonation or due to the ingress of chlorides- and it is also the most affected by chemical attack, frost, abrasion, etc.

The perception of the vital importance of this layer, in short 'covercrete', for the durability of concrete structures is gaining more and more the attention of researchers and engineers since it is recognized that, due to the proximity of the form walls and re-bars, and to segregation, bleeding, finishing operations, curing, microcracking, etc. the composition and properties of that layer may differ widely from that of the interior ('heartcrete'), see Fig. 1. Moreover, the concrete specimens used for quality control can never represent the quality of the 'covercrete' because they are processed in a completely different manner ("labcrete").

A comprehensive research program was started at "Holderbank" Management & Consulting / Technical Centre in 1989, aimed at studying the effect some technological factors have on the quality of the 'covercrete' as well as to evaluate different testing techniques regarding their suitability to assess that quality, both in the laboratory and on site. Fig. 2 shows the general scope of the research program.

This paper summarizes the more relevant results and conclusions derived from the research and, in particular, those connected with the influence of cement characteristics.

EXPERIMENTAL PROCEDURE

Variables Investigated

As indicated in Fig. 2, the effect of several variables, suspected of influencing the quality of the "covercrete" were investigated, namely: Concrete Grade, as measured by the mean cube compressive strength after 28 days of moist curing, target grades being 25, 35, 45 and 75-85 MPa; Cement Type, a total of nine widely different cement types were employed to prepare concretes of different grades, four portland and five blended (see Table I for their characteristics); Curing, applying moist curing during 0, 7 and 28 days and Location, whereby both the top (trowelled) and bottom (moulded) "covercretes" of slabs were investigated.

	PORTLAND CEMENTS				BLENDED CEMENTS				
	R0	U5	GA	U2	FA	SL	FI	SF1	SF2
COMPOSITION									
C3S	38	48	57	46	80% U2 + 20% Fly Ash	65% U2 + 35% Slag	85% U2 + 15% Lime-stone	92% U2 + 8% Silica Fume	90% GA + 10% Silica Fume
C2S	36	25	18	28					
C3A	11	8	6	9					
C4AF	5	8	11	8					
Alkalis (Na2Oeq)	0.96	0.93	0.52	0.97					
PHYSICAL PROPERTIES									
Density (g/cm3)	3.09	3.14	3.12	3.16	2.98	3.05	3.07	3.05	
Blaine (m2/kg)	247	306	335	290	313	317	301	320	
ISO Compressive Strength (MPa)									
- at 2 days	13.3	20.1	23.0	19.7	17.0	13.1	18.5		
- at 7 days	29.8	31.2	41.6	33.0	28.2	26.8	31.4		
- at 28 days	44.6	41.5	58.0	43.8	41.3	48.2	40.5		
- at 90 days	51.6	53.1	68.0	59.5	61.9	61.2	51.4		
- at 365 days	53.0	62.0	69.8	67.4	71.8	66.1	60.4		

Table I - Composition and Main Characteristics of the Cements

Mix No.	Target Grade (MPa)	Cement Type	Cement Content (kg/m3)	w/c Ratio	AEA (%)	Super-plast. (%)	Aggr. Grad-ing	Slump (cm)	Air (%)	Unit Weight (kg/m3)	Standard Strength (MPa)
1	25	R0	318	0.55	0.12	---	G350	6.5	5.1	2300	28.8
2	35	R0	420	0.44	0.15	---	G450	7.0	5.8	2275	34.0
3	---	R0	448	0.44	---	---	G450	6.5	1.5	2375	39.1
4	25	U5	253	0.66	0.10	---	G250	6.0	4.8	2315	26.9
5	35	U5	333	0.48	0.12	---	G350	6.0	4.8	2327	36.5
6	25	GA	202	0.80	0.15	---	G250	7.5	4.7	2305	26.3
7	35	GA	271	0.60	0.17	---	G250	7.0	5.5	2303	37.3
8	45	GA	430	0.42	0.20	---	G350	10.0	6.0	2289	47.6
9	25	U2	238	0.69	0.15	---	G250	5.0	5.1	2301	25.7
10	35	U2	310	0.53	0.15	---	G350	8.5	5.7	2296	32.8
11	45	U2	484	0.37	0.15	---	G450	6.0	4.2	2350	45.7
12	35	U2	254	0.57	0.30	1.00	G250	3.5	4.2	2356	36.1
13	45	U2	356	0.41	0.30	1.00	G350	5.0	4.2	2377	46.2
14	35	U2	427	0.54	0.07	---	DIN C	4.5	6.0	2220	34.0
18	25	FA	256	0.62	0.20	---	G250	5.5	5.4	2298	25.0
19	35	FA	337	0.47	0.20	---	G350	7.5	5.1	2317	34.5
20	45	FA	443	0.37	0.20	---	G450	7.5	4.1	2347	42.6
21	25	SL	257	0.65	0.20	---	G250	5.0	5.6	2278	26.8
22	35	SL	350	0.47	0.20	---	G350	6.0	5.8	2292	36.0
24	25	FI	275	0.59	0.15	---	G250	4.0	5.0	2309	26.0
25	35	FI	381	0.43	0.18	---	G350	5.5	5.4	2310	34 9
28	45	SF1	291	0.57	---	1.50	G250	10.5	3.9	2338	41.8
29	H	SF1	491	0.26	---	2.50	G450	3.5	2.5	2438	77.1
30	H	SF2	488	0.26	---	2.50	G450	6.5	2.9	2420	87.2

Table II - Composition and Basic Properties of the Mixes

Concrete Mixes

Twenty-four concrete mixes were designed attempting to reach the target grades with a consistency in the plastic range. Table II presents full details of mix composition, properties in the fresh state and standard strength for the 24 mixes. Most concretes were air-entrained (air content= 5±1 %).

Test Methods

The quality of the 'covercrete' was evaluated by means of several test methods (see Fig. 2), applied directly on the concrete surface or on drilled cores 50 mm thick. The results discussed in this paper correspond to the following test methods:

Permeability to Oxygen, acc. to the Cembureau method [1].
Freezing and Thawing with Salts, acc. to Swiss Standards [2].
Impreganted Thin-Sections Optical Microscopy [3].

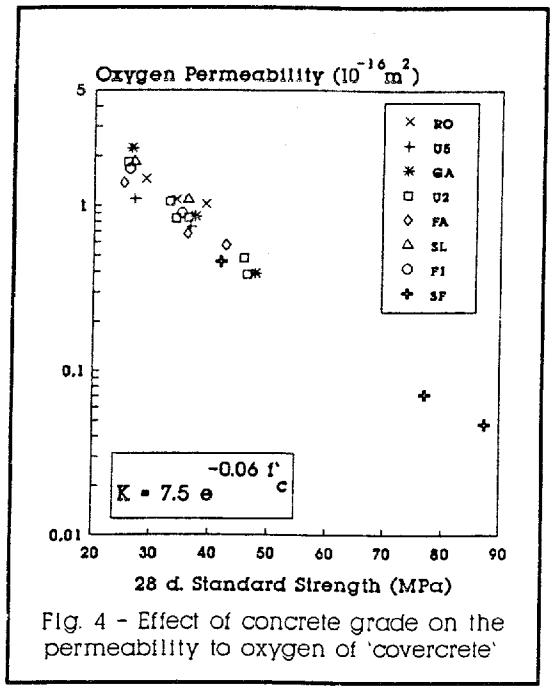

Fig. 4 - Effect of concrete grade on the permeability to oxygen of 'covercrete'

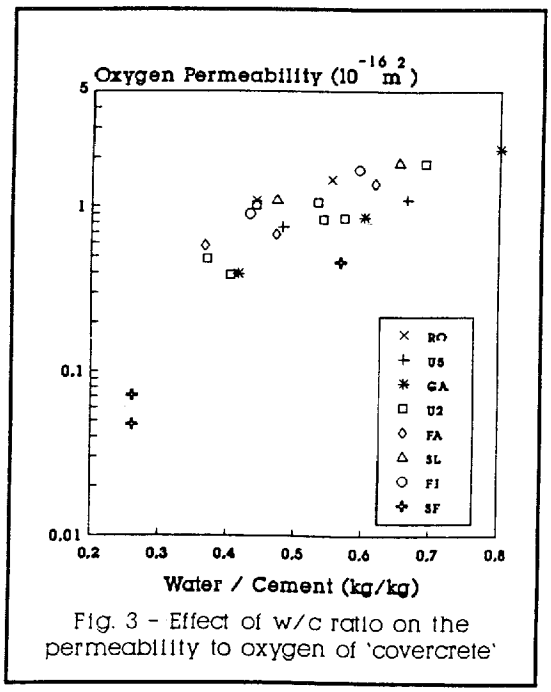

Fig. 3 - Effect of w/c ratio on the permeability to oxygen of 'covercrete'

RESULTS AND DISCUSSION

Effect of Concrete Strength and w/c ratio on O_2 Permeability

Fig. 3 presents the relation between the O_2 permeability K of the 'covercretes' (moist cured for 7 days) and the w/c ratio and Fig. 4 with the 28 days standard strength f'_c (concrete grade) for all the mixes prepared with the different cements.

The following conclusions can be drawn from these results:

Concrete strength is better correlated to O_2 permeability than w/c ratio. As it is easier to control too, codes should ensure durability by specifying minimum strengths rather than maximum w/c ratios, according to severity of exposure.

An increase in concrete strength of 10 MPa reduces the permeability of the 'covercrete' by about 50 percent. In other terms, raising the strength from 25 MPa to 85 MPa reduces the permeability about 40 times.

Concretes of the same strength and well cured exhibit 'covercretes' of similar permeability, irrespective of the cement type used.

However, the use of high-grade cements should be avoided for making concretes of Grade ≤ 25 MPa, since the durability might be jeopardized due to the resulting very low cement contents and high w/c ratios. Justification for this statement can be found in [4].

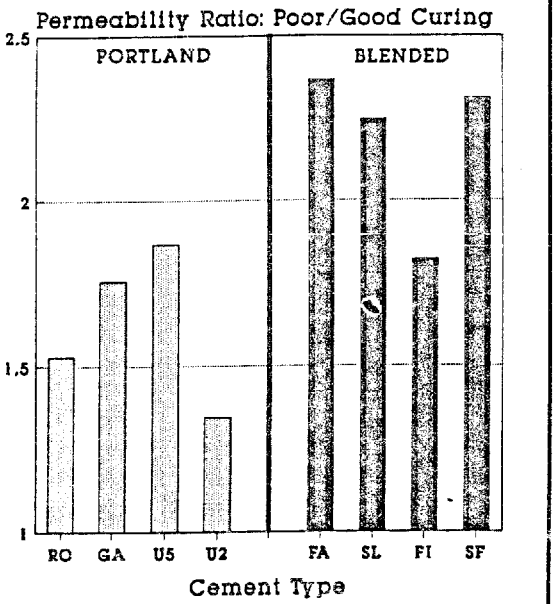

Fig 5 - Increase in permeability of 'covercrete' due to poor curing.

Effect of Curing and 'Covercrete' Location on O_2 Permeability

Fig. 5 shows typical results of the increase in the permeability of the 'covercrete' due to lack of curing.

Fig. 6 shows typical results of the higher permeability of the top, trowelled, 'covercrete' of the slabs, as compared to that of the bottom, moulded, 'covercrete'.

From these results the following conclusions can be drawn:

Poor curing increases significantly the permeability of the 'covercrete'. The effect of bad curing is equivalent to a reduction in concrete Grade of between 5 and 15 MPa.

Blended cements, with the sole exception of limestone filler cements, are more sensitive to bad curing than ordinary portland cements.

Systematically, the top 'covercrete' is 2 to 3 times more permeable than the bottom 'covercrete'. Sole exception are High Performance Concretes, containing silica fume, where no differences were observed.

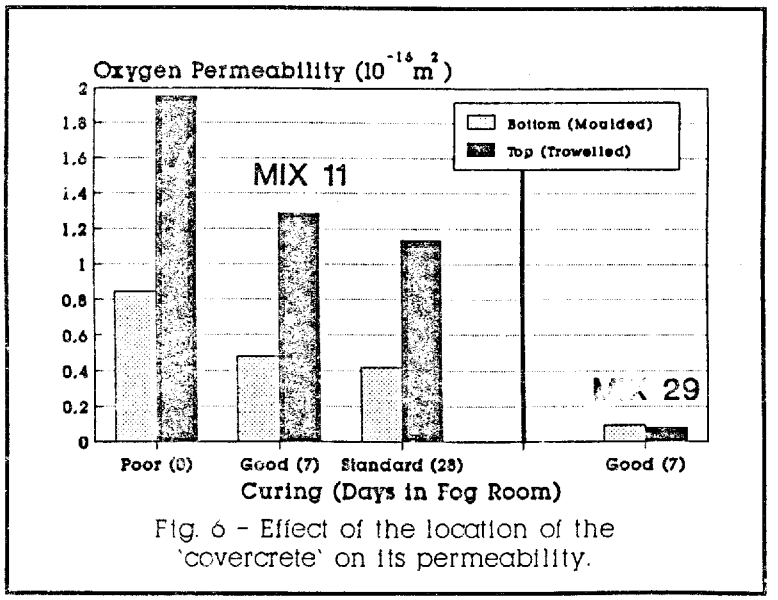

Fig. 6 - Effect of the location of the 'covercrete' on its permeability.

Effect of Air Entrainment and Cement Type on Frost-Salt Resistance

Fig. 7 shows the weight loss of the 'covercretes' (ponded with Nal Cl solution) of several concretes made with different cements, after 30 freeze-thaw cycles.

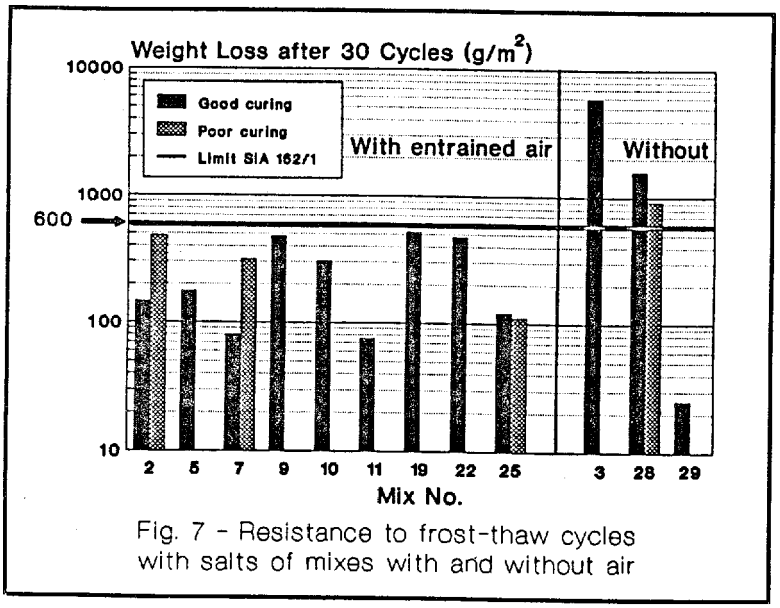

Fig. 7 - Resistance to frost-thaw cycles with salts of mixes with and without air

The following conclusions can be derived:

All air-entrained concretes showed good resistance to freeze-thaw cycles in the presence of de-icing salts, irrespective of the cement type used and of the curing conditions.

Out of the non air-entrained concretes tested, only that belonging to the High-Performance class (very low w/c ratio and with silica fume) showed good resistance to those cycles.

Microscopic Observation of Thin Sections

Microscopic observation of the microstructure of High-Performance Concrete mixes revealed a network of fine microcracks. Hence:

High-Performance (Strength) Concretes presented extensive fine microcracking in their 'covercrete'; nevertheless, their performance regarding permeability and frost-salt resistance was outstanding.

GENERAL CONCLUSIONS AND FURTHER WORK

The main conclusions reached have already been underlined in the paper. In general, it can be said that it is mix characteristics (mainly concrete strength), location and curing conditions the main factors affecting the quality of the 'covercrete', with cement characteristics playing only a secondary role.

As a consequence, we are convinced of the importance of evaluating the quality of the 'covercrete' directly on the structures, because it is virtually impossible to prepare specimens that can simulate the real conditions under which concrete is processed at the jobsite. Thus, in the chain of responsabilities from the materials producers, passing through the ready-mixed concrete producer, to the contractors, the quality of the latter's work is the one that almost invariably goes without control by means of proper testing.

If suitable site methods to measure, for instance, the gas permeability of the 'covercrete' were available, then the resulting quality of the end product (the concrete structure) could be assessed. Going even a step farther we could envisage a future scenario, where both the quality and thickness of the 'covercrete' are specified for given exposure conditions, and the acceptance (in terms of durability) of the structure would be based on such site testing.

It is our opinion that such approach will put more pressure on all parties involved in the concrete construction business, but especially on the contractors, to do a better job, which will result in better, more durable structures, enhancing the image of concrete as a reliable construction material.

HMC has started an investigation in this direction, the first result of which has been the development of a non-destructive test method to measure the coefficient of air-permeability of the 'covercrete' on site [5].

REFERENCES

1. Kollek, J.J., "The determination of the permeability of concrete to oxygen by the Cembureau Method- a recommendation", Mater. & Struct., v.22, 1989, pp. 225-230.

2. Swiss Standards Association, SIA Norm 162/1, # 3 09: Test No. 9, "Freeze-thawing salt behaviour", EMPA Guidelines for testing, Dübendorf, 1989.

3. Jornet, A. and Torrent, R., "Special methods to assess the durability of concrete", 31st 'Holderbank' Technical Meeting, Baden, HMC Report No. MA 90/3767/E, June 1990, 15 p.

4. Torrent, R. and Jornet, A., "The Quality of the *covercrete* of Low-, Medium- and High-Strength Concretes", 2nd. CANMET/ACI Intern. Conf. on Durability of Concr., Montreal, Ed. V.M. Malhotra, Vol.II, pp. 1147-1162, August 4-9, 1991.

5. Torrent, R., "A two-chamber vacuum cell for measuring the coefficient of air-permeability of the concrete cover on site", accepted for publication in Materials & Structures.

OPTIMIZATION OF PORTLAND CEMENT ACCORDING TO FROST RESISTANCE FACTORS

G I Gorchakov and A B Andreyeva

The Moscow Civil Engineering Institute Building Materials Department
Yaroslavsky Shosse, 26 Moscow, RUSSIA

SUMMARY

This paper presents the capabilities of the astringent actuation related to the correction of calcium sulphate content depending on the total content of the tricalcium aluminate and four-calcium alumoferrite as well as on the specific surface of portland cement.

INTRODUCTION

Frost resistance of cement stone and concrete is determined by different factors, the dominant among them being portland composition and porosity of the cement stone (1). The frost resistance factor and the strength of portland cement were determined by tests on standard prisms of size 4 x 4 x 16 cm, made of cement and fine aggregate mixture. The influence of w/c ratio was excluded and a constant ratio of 0.55 was adopted. One needs hardly speak about the importance of this character (w/c) when deciding on the cement for constructions in severely cold climates. Earlier the influence of the aluminate constituent of portland cement on frost resistance was determined (1). In another work an opinion was expressed concerning the deterioration of the technical properties of cement (with higher C_3A contents (2), which limits the use of rapid hardening portland cement in critical constructions.

EXPERIMENTAL

Frost resistance factor was considered as a function of the mineral composition, specific surface and calcium sulphate content of portland cements, made from clinkers of different mineral compositions with C_3A contents ranging from 5 to 14.2% (Table 1).

Table 1

Mineral composition of clinkers

Clinker	Contents of minerals				
	C_3S	C_2S	C_3A	C_4AF	$C_3A + C_4AF$ (A,%)
1	40.7	40.7	6	8.5	14.5
2	58.5	16.4	14.2	4.7	18.9
3	55.7	20.7	5	14.4	19.4
4	41.4	22.7	9	15.5	24.5

Portland cements of three different ranges of specific surface were prepared from each clinker: S = 2300 - 2900, 3500 - 3900 and 4700 - 5100 cm^2/g.

The frost resistance factors of cements of different mineral compositions made from three of the above clinkers and having calcium sulphate contents from 1 to 3.5% (as SO_3) and different specific surface ranges are given in Table 2.

Table 2

Frost resistance factors of portland cement in freeze - thaw cycle

Designation of clinker	Specific surface cement cm^2/g	Frost resistance factor of cements with calcium sulphate content(as SO_3,%)		
		1.0	2.0	3.5
1	2300 -2900	150	130	125
	3500 -3900	125	80	50
	4700 -5100	115	80	75
2	2300 -2900	150	80	50
	3500 -3900	80	120	65
	4700 -5100	50	50	80
4	2300 -2900	50	150	75
	3500 -3900	55	75	150
	4700 -5100	46	75	150

Increasing the specific surface of cement, maintaining the calcium sulphate content constant, decreased the frost resistance. This has been attributed to a change of the actual mineral composition as a result of the selective reduction of the minerals to fragments and unequal distribution of calcium sulphate among the cement fractions. Gypsum is concentrated in the fractions 0 to 7 and 7 to 22 μm whereas C_3A and C_4AF have a tendency to concentrate in the fractions o to 7 and greater than 55 μm (3). Among the clinker minerals C_3A has the highest drying shrinkage and since it is not regulated in large fractions by calcium sulphate, upon hydration, it causes an inner stress, which can lead to deformation of the cement stone structure. That is why the optimization of the frost resistance factor of portland cement must be practically related to mineral composition, specific surface and calcium sulphate contents all of which are interconnected. The results thus obtained form the basis to consider calcium sulphate not only as a regulator of the shrinkage rate and mechanical activity of portland cement, but as a structure generating component too, which can significantly influence the durability of cement stone.

R. Kondo and M. Daimon (3) determined, that in the absence of calcium sulphate, when C_3A contacts with water, a loose layer of hexagonal hydrates C_4AH_{19} and C_2AH_8 is produced on the surface of the particles which had not reacted. In the presence of calcium sulphate, C_3A hydrates form ettringite, and the final products of hydration of C_3A and ferroaluminium phase are $C_3A.CaSO_4.18H_2O$ and solid solution with C_4AH_{19}.

RESULTS AND DISCUSSIONS

The dependence of the optimal dose of gypsum (D) (in terms of SO_3) on the sum of the C_3A and C_4AF (A) contents in the clinker and on the fineness of grinding (S) was studied. The optimal dose with reference to frost resistance and strength factors, worked out experimentally (taking into account the provided standard period of time of cement setting) are given in Table 3.

Table 3

Optimal doses of calcium sulphate

Clinker №	A (C_3A + C_4AF) %	S cm^2/g	Optimal dose of calcium sulphate D,%
1	14.5	2280-2700	1
1	14.5	3520-3690	1 - 2
1	14.5	4690-4865	2
2	18.9	2650-2900	2
2	18.9	3525	2 - 3
2	18.9	4800-5140	3
3	19.4	2600-2800	2
3	19.4	3500-3880	2
3	19.4	4700-4950	3 - 5
4	24.5	2700-2850	3
4	24.5	3500-3700	3
4	24.5	4900-4980	5

CONCLUSIONS

By means of mathematical treatment of the experimental data, the following formula has been obtained. It permits determination of the optimal dose of calcium sulphate as a function of the sum of C_3A+C_4AF contents and the specific surface of portland cement.

$$D = -3.932.10^{-4} (S) - 1.320.10^{-3} (A) + 5.609.10^{-5} (S) (A) + 3.266.10^{-2} \ldots \quad (1)$$

REFERENCES

I. Горчаков Г.И., Капкин М.М., Скрамтаев Б.Г. Повышение морозо - стойкости бетона М., 1965, с. 194

2. Shestoperov V. Influence of C_3A on Some Properties of Cement Stone. International Congress of Cement. M., 1976

3. Kondo R., Daimon M. Phase Composition of Hardened Cement Paste. The Sixth International Congress of the Chemistry of Cement M., 1976

EFFECT OF DIATOMACEOUS EARTH ON BLENDED — CEMENT PROPERTIES

C Urrutia, E Gómez and A Rojas

Departmento de Ingeniería de Materiales (IDIEM), Facultad de Ciencias Físicas Y Matemáticas, Universidad de Chile, Santiago, CHILE

SUMMARY

This research attemptes to evaluate the use of diatomaceous earth as a high-quality pozzolanic additions in the manufacturing of high strength concretes specially in front of agressive environments. Strengths between 5 and 10 MPa are reached when a mortar made of lime and finely ground diatomaceous earth is storaged during 7 days to a temperature of 55 oC and strengths between 10 and 14 MPa when is storaged to a normal temperature during 28 days.

The replacement of 20% cement by diatomaceous earth requires an increase of 20% in mortar-water in order to maintain constant the workability. Several superplasticizers were tested to the end of reducing water requirement. Some of these additives reduced the water amount of mortar to a value similar to that of the control mortar without additive. Using 20% diatomaceous earth along with these additives yielded an increase of 30% in mortar strength at the ages of 28 and 60 days.

The use of diatomites in concrete improves cohesion and bleeding. Water requirement of a concrete increases from 0.53 for control concrete to 0.60 when 20% is replaced by diatomite. Employing water- reducers allowed to lower this value to 0.37 and 0.41, respectively. Compressive strength is increased from 40 MPa exhibited by the control concrete, to values ranging between 68 and 70 MPa when using 10 and 20% diatomite together with additives.

En este trabajo se evalua el uso de kieselguhr como adición mineral al cemento para fabricar hormigones de alta resistencia mecánica y de gran resistencia frente a medios agresivos. Los morteros de cal y kieselguhr, curados durante 7 días a 55 C, alcanzan resistencias de compresión entre 5 y 10 MPa. Los mismos morteros curados a temperatura normal presentan resistencias que fluctuan entre 10 y 14 MPa a los 28 días.

Al reemplazar un 20% del cemento por kieselguhr debe aumentarse en un 35% el agua del mortero para mantener la trabajabilidad constante. Para reducir el requerimiento de agua se probaron una serie de aditivos químicos con poder fluidificante. Con algunos de estos aditivos se logró reducir la cantidad de agua del mortero a un valor similar a la del mortero patrón sin aditivo. El uso de 20% de kieselguhr en conjunto con estos aditivos permitió incrementar la resistencia del mortero a los 28 y 60 días en un 30%.

El uso de kieselguhr en el hormigón mejora la cohesión y la exudación. Para mantener la trabajabilidad constante, se tuvo que incrementar la razón agua/ aglomerante desde 0,53 en el hormigón patrón hasta 0,60 con un reemplazo de 20% de kieselguhr. Mediante el uso de aditivos superfluidificantes se pudo reducir este valor a 0,37 y 0,41 respectivamente. La resistencia a la compresión se incrementó desde 40 Mpa en el hormigón patrón hasta valores entre 68 y 70 MPa a los 56 días, al usar 10 y 20% de kieselguhr con aditivos.

INTRODUCTION

Mineral pozzolanic additions favourably affect some properties of fresh or hardened concrete. Their effect is associated with their great particle-fineness in a mixture such as concrete and, in addition, with their pozzolanic capacity of reaction (1,2).

Fume silica as well as rice-husk ashes and diatomaceous earth have a high contents of amorphous reactive silica and a large reaction -surface. The diatomaceous earth is a natural pozzolan corresponding to an hydrated or opaline form of silica; it is fairly abundant in Chile. In general, mineral deposits contain between 80 and 95% silica and sometimes it is mixed with clay, limestone, sand or salt (3). Diatomaceous earth inconvenience as an addition lies in its high specific surface that reduces concrete workability in an enormous way. This obliges to increase water/cement ratio, thus producing an increment in hardened-concrete porosity and permeability, which adversely affects its mechanical strength and its chemical resistance to aggressive media (4,5). The high water requirement of diatomites has been, perhaps, the factor that contributed more decisively to the loss of interest for using this mineral as a pozzolanic addition for cements. However, these last times chemical additives with a high power to reduce water have been successfully used in cements with silica fume and rice-husk ashes. In these cases, there has been endeavours to make high-strength concrete taking advantage of the extense reactivity of these materials. To this end it has been necessary to maintain or reduce water/agglomerant ratio without diminishing workability in a substantial manner (6,7,8). The likely effect of these same additives on the rheology of cements including a partial replacement by diatomite has not been investigated up to now.

ANALYSYS OF RAW MATERIALS

The diatomites selected for this work were analysed using differential calorimetry, fluorescence and X-ray diffraction. Both minerals are essentially formed by an amorphous phase. Within analysis accuracy, no impurity of the quartz, feldspar or clay type was observed, except in KB-diatomaceous earth which included a fair amount of NaCl. Table 1 shows some of the results and those of portland cement used.

Tabla 1 Properties of raw materials

Component	Composition, in %		
	Diatomac. earth		Cement
	KA	KB	
SiO_2	86.7	85.6	19.2
Al_2O_3	2.2	2.2	6.3
CaO	5.3	2.4	64.6
Fe_2O_3	1.6	0.9	3.1
Na_2O	1.5	4.8	1.3
K_2O	0.6	0.9	0.8
SO_3	1.8	1.0	2.6
P.P.C. (950 °C)	6.7	12.2	0.6
Sp. Surf. (m^2/g)	4.0	2.0	0.38
Sp. Gravity	1.975	2.010	3.100

RESULTS AND DISCUSSION

Diatomaceous earth activity

The puzzolanic activity of the diatomites (KA and KB) was measured in lime mortars cured at 55 ℃ and in lime mortars cured in a moist atmosphere at 23 °C. Using the same amount of lime and diatomite, these experiments show the relatively quick reaction of this last material with lime, and then mortar strength becomes maximum at an age between 21 and 28 days.

This result obliged to modify lime/diatomite ratio to the end of verifying a likely deficit of lime in the mortar. Diatomaceous earth KB yielded an increment in mortar strength while diatomaceous earth KB produced a lowering in compressive strength when lime is increased. In this last instance such a lowering might be due to the strong increase in water requirement for this mortar (Fig.1).

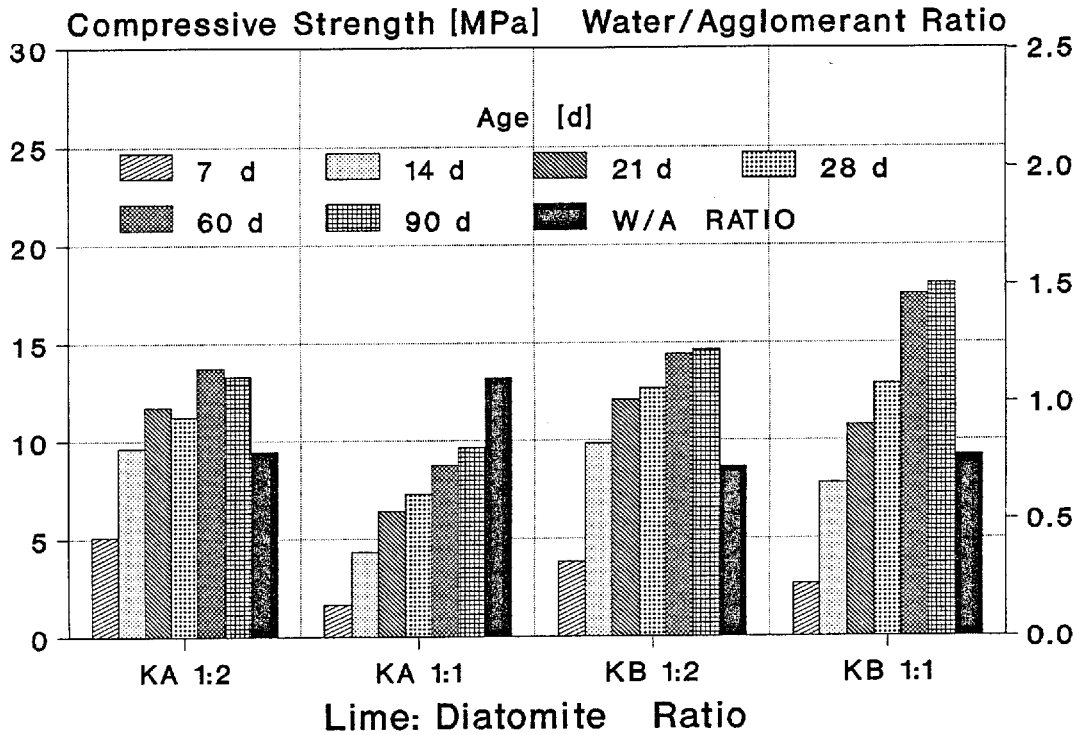

Fig. 1 Pozzolanic activity in a moist atmosphre at 23 °C. Diatomaceous earth/lime ratio 1:1 and 1:2.

Blended Cements with Superplasticizers

Finely ground KA-Diatomite was employed to make blended cement by mixing commercial portland cement with it and homogeneizing the mixture in a ball-mill. Diatomaceous earth contents specially affects the water requirement of the paste and of the mortar of cement. Water of normal consistency is increased by about 17% per each 10% fraction of diatomite that replaces cement. Mixing-water increases along with lower clinker- contents of the cement, delays the initial setting time which shifted from 2:05 hours in portland cement to 3:15 hours in the case of 20% diatomaceous earth addition.

Diatomite addition also affects mortar workability in a strong fashion. Water/agglomerant ratio increased from 0.50 for portland cement to 0.67 when using 20% diatomite, maintaining a constant fluidity of 21 cm. Commercial water- reducers additives allowed a reduction of this ratio, bringing it down to normal levels. Water/cement dosifications determined to maintain a constant fluidity were employed to make mortar prisms, which were tested under compression till fracture; Table 2 shows test results.

Table 2 Effect of the addition of KA- Diatomite and superplasticizer on water demand and compressive- strength

Additive	Addition [%]	Water requirement [%]	Strength (MPa) Curing age, in days			
			3	7	28	90
nil	0	50.0	33.8	35.9	50.9	55.1
	5	52.0	31.7	36.1	50.3	57.9
	10	56.8	27.1	33.0	49.5	57.5
	15	62.0	22.2	30.1	46.3	53.3
	20	67.0	19.7	24.5	41.8	46.8
SF1	0	45.0	35.3	42.5	51.1	57.8
	5	45.6	35.8	43.2	56.7	66.5
	10	46.0	35.8	44.6	60.4	70.3
	15	48.4	34.1	43.8	61.3	70.7
	20	49.6	32.3	42.7	62.5	71.6
SF2	0	44.0	38.8	42.2	50.1	58.2
	5	45.4	36.8	43.4	53.1	63.1
	10	48.0	34.8	40.3	54.3	65.6
	15	48.8	34.5	40.5	58.5	67.8
	20	56.0	28.2	38.6	53.9	59.3
SF3	0	43.8	28.9	35.8	40.5	45.8
	5	45.0	28.4	35.1	47.8	58.5
	10	47.6	26.6	35.9	49.0	60.4
	15	48.4	29.2	38.4	52.2	66.0
	20	54.0	25.9	35.4	52.3	63.7

Increasing additions of diatomaceous earth strongly lower portland cement strength, owing to the high water/agglomerant ratio adopted to make these mortars, and owing to their lower cement-clinker contents. Adding 20% diatomite lowers mortar strength by 41% at 3-day age. This difference is reduced to 31% at 7 days and to 18% at 28 days. When adding 10% diatomaceous earth these differences become much smaller and at the age of 90 days the strength of blended cement is slightly higher than that of portland cement. These results show that diatomite addition contributes to mortar strength within the first weeks of curing.

Superplasticizers allow to lower additionally the W/A ratio to normal levels. With a similar W/A ratio a considerable strength-increase is achieved in all the mortars, when comparing them with the mortar made of portland cement and additive. Some additives such as SF3 contain retarding agents and then, despite the fact that the mortar exhibits a water/cement ratio lower than that of normal mortar, it has a lower strength on short term. This difference even persisted during the whole testing period. Diatomite addition in the presence of these additives permits to increment the mortar strength. The optimum level of diatomaceous earth lies between 15 and 20%

depending on the reducing additive employed. Strength increase varies between 6 and 22% at 28 days, and between 8 and 24% at 90 days.

Hydration heat of cement was measured with the Langavant method following AFNOR Standard NFP15-436. Figure 2 shows some of the results. Portland cement prematurely developed an amount of heat larger than that of the cements including 10 and 20% of diatomite. The larger the kieselguhr addition the greater the difference in the heat thus produced. However, the heat-level defined by portland cement is equaled and even exceeded by the cement with diatomaceous earth. The curve of the heat developed by portland cement in the presence of plasticizer is intersected between 10 and 17 hours with diatomite additions. As overall heat of special cement is equal to, and even larger than the heat of OPC during the first 72 hours. This shows that diatomaceous earth presence favourably alters the reactions of the mineral phases of cement. This phenomenon may be explained through two mechanisms of effect. Thus the intensity of alite reaction may be increased by the adsorption of calcium and hydroxil ions on diatomite surface, profoundizing in this way the dissolution and hidration of this compound. As a second alternative, the fine particles of diatomaceous earth may provide an active surface that is sufficient for the heterogeneous nucleation of portlandite, thus shifting alite-reaction equilibrium.

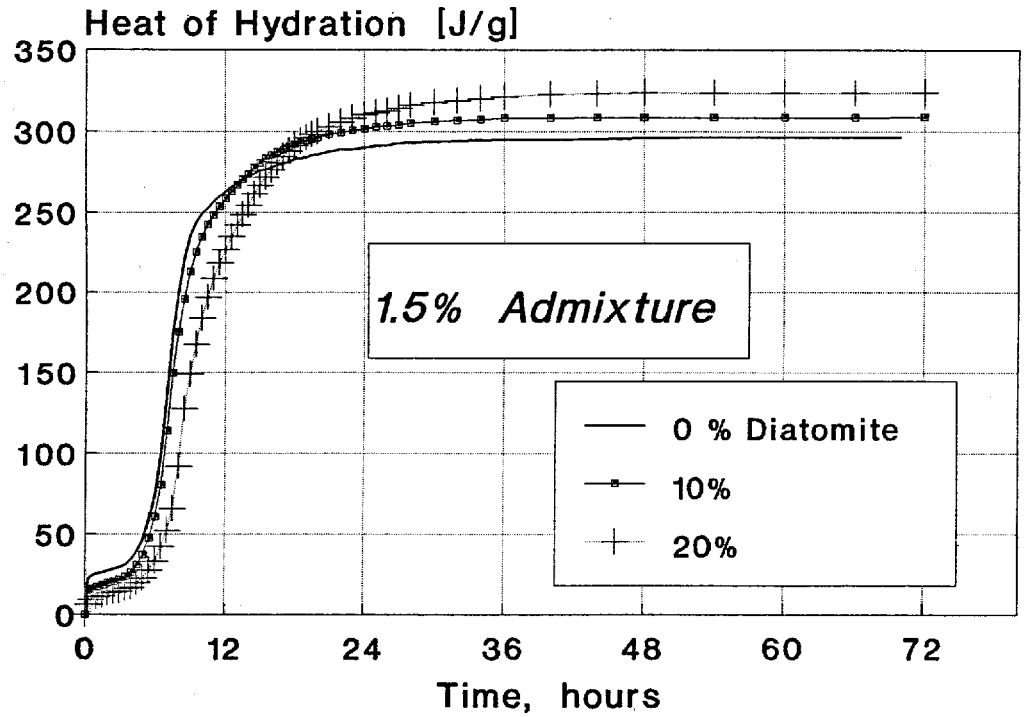

Fig. 2 Effect of the diatomaceous earth on the heats of hydration

At last, cement resistance to sulphate waters was evaluated. Mortar prisms fitted with measuring abutments were dipped in a solution that contained 50 g/l of sodium sulphate. Test specimens were cured before in a moist room for 2 days. It is worth noting that the use of some fluidificating additive, though lowering the water/cement ratio and thus the mortar permeability, was unable to cause a like reduction in mortar expansion. On the contrary, diatomite capacity to reduce expansion is considerable and even it can be observed in mortars devoid of admixture and hence exhibiting a high water/agglomerant ratio. In the extreme instance the

expansion can be eliminated almost completely through the replacement of 15% cement by diatomaceous earth and through the simultaneous inclusion of an additive in order to reduce water/cement ratio.

The effect of this addition was also evaluated on a concrete of 350 kg cement/m3 and a slump of 6 cm. Diatomaceous earth allowed to reduce the bleeding in the concretes made with an excess of bulk aggregate. The compression strength at 90 days is increased from 40 MPa in the pattern concret without admixture to values between 68 and 70 MPa when using 10 and 20% of diatomaceous earth with superplasticizer.

CONCLUSIONS

- In general, diatomaceous earth exhibits a very high water-requirement, which causes an important reduction in mortar strength on short term.
- Water-requirement and reactivity of the diatomites analysed were fairly different. The causes there of might include the presence of minor compounds.
- Superplasticizer permit to reduce water-requirement, of mortar made of cement and diatomite, to levels similar to those of portland cement, and then strength increases of about 20% at 28 days can be obtained in comparison with control mortar strength.
- Diatomite accelerates the hydration reactions of cement, thus increasing the overall heat developed within the first 72 hours.
- Diatomaceous earth reduces the expansion of mortars exposed to sulphated solutions. Adding 15% diatomite and a fluidificating agent allows to avoid expansion completely.

ACKNOWLEDGEMENTS

The authors would wish to express their gratitude to the Fondo Nacional de Desarrollo Científico y Tecnológico (FONDECYT) for financing the present Project N 955/89.

REFERENCES

1. Sersale, R.: "Structure and characterisation of pozzolanas and a fly-ashes". VII International Congress of the Chemistry of Cement, Paris, 1980, V1, IV-1/3.

2. Uchikawa, H.: Theme III Blended and special cements. "Effect of blending components on hydration and structure formation". VIII. Congr. of the Chemistry of Cement, Río de Janeiro, 1986, V1, 249-280.

3. Vila, T.: Recursos minerales no metálicos de Chile. Ed. Universitaria, 1953.

4. Davis, R.E. & Klein, A.: "The effect of the use of diatomite treated with air-entraining agents upon the properties of concrete". Symp. on Use of Pozzolanic Materials in Mortars and Concretes; ACI Sp. Tecn. Publ. No 99, 1949, 93-108.

5. Delvasto, S.: "Pozzolanic activity and characteristics of colombian materials". Proc. 2a Int. Conf. Fly Ash, Silica Fume, Slag and Natural Pozzolans in Cocrete, Madrid, 1986, V1, 77-89.

6. Metha, P.K.: "Properties of blended cements made from rice husk ash". ACI Journal, Proc. 74(9), 1977.

7. ACI- Committee 226: "Silica Fume in Cocrete". ACI Material Journal, 1987.

8. Yogendra, V. & Langan, B. & Haque, M. & Ward, M.: "Silica Fume in very high strength concrete". ACI Materials J., 1987.

THE INFLUENCE OF LIMESTONE ADDITIONS ON RHEOLOGICAL PROPERTIES AND WATER RETENTION VALUE OF PORTLAND CEMENT SLURRIES

Claudio Sbrighi Neto* and Vicente C Campitelli**

**Concrete Technology Group, Instituto de Pesquisas Tecnologicas do Estado de São Paulo, BRAZIL*
***State University of Ponta Grossa, Paraná, BRAZIL*

ABSTRACT

The recent changes on Brazilian specifications for portland cement, in order to permit limestone additions, led to the necessity of knowing its influence in several aspects of the cement behavior when applied in civil construction.

In this paper the rheological properties, basically yeld point and plastic viscosity, are determined in slurries made with cement which has up to 15% of limestone additions, in weight. For the same slurries the water retention value is obtained.

The variations in the yeld point and plastic viscosity showed the "lubricity power" of the smaller particles (below 10 μm). Their amount is increased by the relatively greater grindability of the limestone concerning the clinker.

The limestone additions seem not to change the water retention value.

L' INFLUENCE DES ADDITIONS CALCAIRES SUR LES PROPRIETÉS RHÉOLOGIQUES ET RÉTENTION D' EAU DANS LA PÂTE DE CIMENT PORTLAND

RÉSUMÉ

Les récents changements des normes bresiliennes des ciments portland, dont les additions calcaires sont permises, conduisent au besoin de connaître le comportement des mêmes pendant l' application du ciment aux ouvrage civiles.

Cette étude analyse les propriétés rhéologiques, basiquement la viscosité plastique et le limite d' écoulement determiné sur la pâte de ciment avec un limite supérieur de 15%, en poids de l'addition calcaire. La rétention d'eau est aussi determinée.

Les variations du limite d' ecoulement et de la viscosité plastique démontrent le fort effect des petyts particules (inférieures à 10 μm). La quantité relative des petits particules est augmentée par la rélativement plus grande facilite de la mouture du calcaire utilisé comme source carbonatique. L' addition carbonatique ne change pas la rétention d' eau.

INTRODUCTION

The limestone additions to cement may have several functions (1):
- to complete the granulometric curve of defficient fine grain cement;
- to obstruct capilar pores and make water percolation difficult;
- to influence the rheological parameters of the slurries;
- to take part in the components hydration.

In our present experience, limestone and others additions (slags, fly ash) in percentages below 15%, combined with a finer grinding of the clinker, do not result in significant changes in some properties like pozolanicity, sulfate resistance, heat of hydration and others, at least in the short time.

However, they certainly result in a production cost reduction and should have influence on the long term performance of the paste, specially for characteristics not controled by standards but important for the durability.

In this study we aim to analyse the changes of rheological properties and water retention capacity of cement slurries with limestone additions.

It is a already known the large influence of grain shape, floculation capacity and amount of intersisticial water in the rheological properties and in the total water retention value. The first two are directly dependent of the characteristics of the limestone. On the other hand the compatibility of the limestone with the clinker is fundamental to obtain adequate properties of the mixture.

EXPERIMENTAL ASPECTS

Three types of cement were produced: coarse ($300m^2/kg$), medium ($400m^2/kg$) and fine ($500m^2/kg$). The clinker (Table 1) was ground together with different amounts of limestone (Table 2) and with a balanced quantity of natural gypsum (Table 3), according to ASTM C 563-79 method. The specific surfaces were determined by ASTM C 204-81 and the added limestone quantity varied from 0 to 15%, in weight. The chemical characteristics of the used materials are shown in Tables 1, 2 and 3.

TABLE 1 - Chemical composition of the portland cement clinker

	(%)		(%)
CaO	64.20	insoluble residue	0.82
SiO_2	21.69	ignition loss	0.31
Al_2O_3	6.55		
Fe_2O_3	3.00	C_3S	44.22
MgO	2.35	C_2S	26.56
K_2O	1.02	C_3A	12.29
Na_2O	0.08	C_4AF	9.12
SO_3	0.92	$CaSO_4$	1.56
Free lime	1.85		

TABLE 2 - Chemical composition of the limestone

	(%)		(%)
CaO	51.36	SO_3	0.08
ignition loss	41.42	P_2O_5	0.07
insoluble residue + SiO_2	5.14		
MgO	1.04	CO_2	41.40
Al_2O_3	0.77	$CaCO_3 + MgCO_3$	93.82
Fe_2O_3	0.38	impurities	6.11

TABLE 3 - Chemical composition of the gypsum

	(%)		(%)
SO_3	45.69	MgO	0.26
CaO	32.20	Free water	0.01
combined water	19.46	$CaSO_4 . 2H_2O$	92.98
SiO_2	1.64	$CaSO_4$	4.17
$Fe_2O_3 + Al_2O_3$	0.53	$CaCO_3 + MgCO_3$	0.90
CO_2	0.37	insoluble residue	1.64

In order to determine rheological properties, slurries were prepared according to section 5 of API-RP 10, an American Petroleum Institute Norm. The water/cement ratio used for coarse cement was 0.65 and for the other two cement 0.70, in weight.

For water retention value determination, the slurries were prepared with the previous procedure but "Dispersant/low water loss" commercial additive (base sulphoned nafthalene) was added. This was done in order to permit the use of the apparatus recommended by API norms and 0.44 was the used water/cement ratio.

EQUIPMENTS AND CALCULATION

The rheological properties were determined, according to Appendix H of API - Spec 10, on a direct reading coaxial cylinders viscosimeter, Fann V.G.Model 35 A, at room temperature (25 ± 5°C).

The calculations were based on the Bingham Model (linear relationship between shear stress an shear rate), which has the following fundamental equation:

$$S_s = YP + V_p . S_r$$

where in:
S_s = shear stress, P_a
YP = yeld point, Pa
V_p = plastic viscosity, Pa.s
S_r = shear rate, s^{-1}

The water retention capacity was determined, according to Appendix F of API-Spec 10, on a high pressure filter press apparatus and the calculations were based on the equation:

$$Q_{30} = Qt \cdot 2 \frac{(5.477)}{\sqrt{t}}$$

where in:
Q_{30} = quantity of filtrate in 30 minutes
Qt = quantity of filtrate at time t.

TEST RESULTS AND DISCUSSION

The variations of yeld point and plastic viscosity with the increase of limestone addition are presented in fig. 1 and 2, respectively, and the water retention capacity test results in fig. 3.

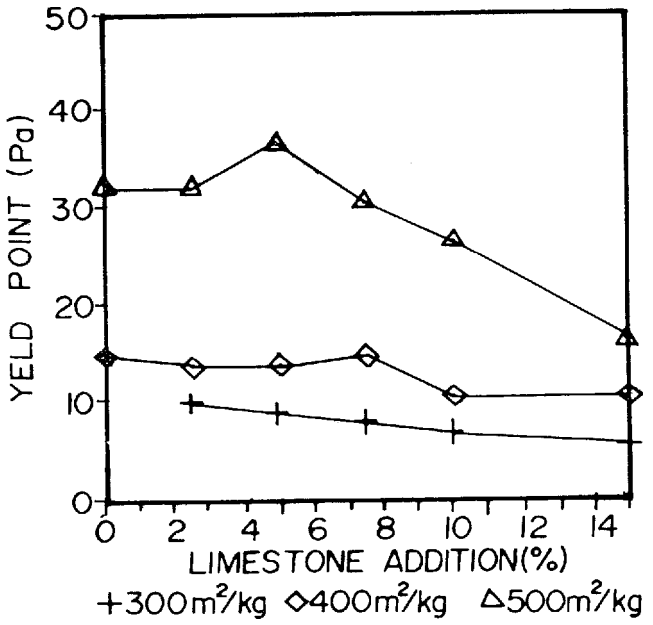

Fig. 1 - Effect of limestone addition on yeld point.

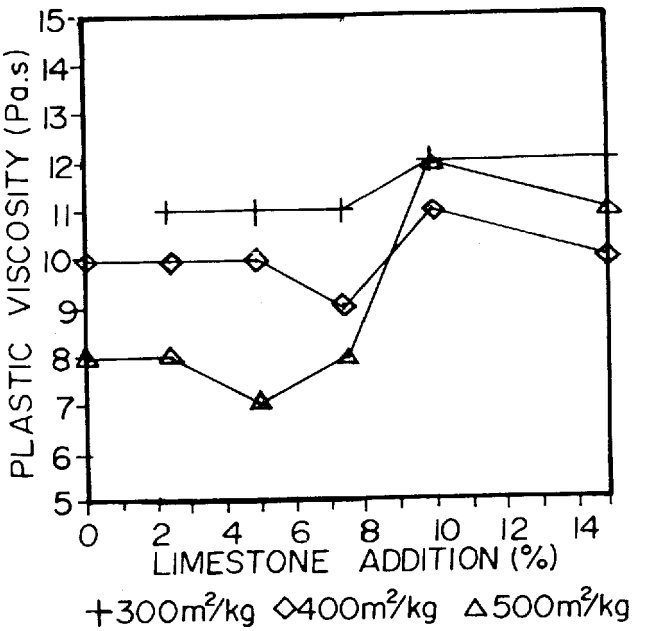

Fig. 2 - Effect of limestone addition on plastic viscosity.

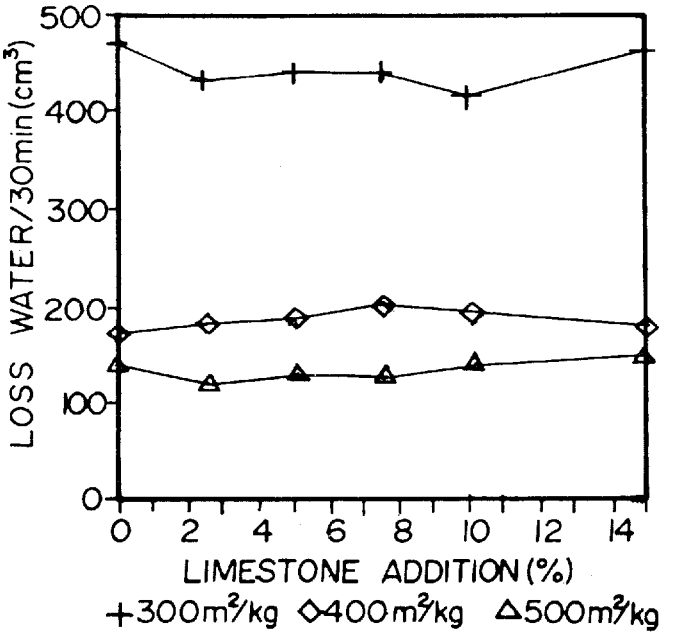

Fig. 3 - Effect of limestone addition on water retention value (loss water).

From the analysis of the first two figures it is possible to detect:

- a tendency of a reduction of the yeld point with the increase of limestone addition. This is more evident for the finest cement (500 m^2/kg);
- a light growing tendency of the plastic viscosity after a certain relation fineness/ limestone content occurs.

The "Lubricity power" of the very fine limestone particles (2) was the most probable reason for this behaviour. It is important to point out two facts: the greater grinding time necessary to prepare the fine cement and the difference of hardness between clinker and limestone. These facts induce that a relatively larger concentration of the limestone in the smaller size particles of the cement occurs. This kind of particles (below 10 µm) has fundamental action on the cohesion and internal friction of the slurry and obviously they have some influence on the rheological properties.

About the water retention value no influence was observed with the increase of limestone content up to 15%.

CONCLUSION

The limestone addition, in level up to 15%, decrease yeld point values specially for finer cement and increase lightly the plastic viscosity after a certain relation fineness-limestone content. In our experimental work these relation are: 300 m^2/kg - 7.5%; 400 m^2/kg - 5.0% and 500 m^2/kg - 2.5%. As it was already mentioned by other authors (3, 4, 5), for the same amount of addition it was a increase of limestone content in the fine blended cement particles (below 10 µm) for the cements fineness growth due to the greater grindability of the limestone.

The limestone used in this research has a relatively high calcium carbonate content perhaps with a purity slightly high than the current limestone used for cement additions. Thus, the clay mineral content and other impurities influence on rheological properties must be verified, specially if they have a floculant behaviour.

REFERENCES

(1) Bombled, J.P. - "Rheology of fresh concrete: Influence of filler addition in the cements" - Proc. of 8th International Congress on the Chemistry of Cement - Vol. IV, p. 190, Rio de Janeiro (1986).

(2) Gegout, P. et alli - "Texture and performance of filler cements" - Proc. of 8th International Congress on the Chemistry of Cement - Vol. IV, p. 197, Rio de Janeiro (1986).

(3) Menetrier-Sorrentino, D. - "Particle size distribution in blended cements" - Proc. of 8th International Congress on the Chemistry of Cement - Vol. IV, p. 60, Rio de Janeiro (1986).

(4) Bombled, J.P., Bellina, G. and Mortureux, B. - "Particle size distribution and specific surface measurements of components of cogrinded blended cements: application to fillers and slags" - Proc. of 8th International Congress on the Chemistry of Cement - Vol. IV, p. 74, Rio de Janeiro (1986).

(5) Tsimas, S., Kasselouris, V., Ftikos, C.H. and Parissakis, G. - "Determination of specific surfaces of co-grinded materials with different grindabilities" - Proc. of 7th International Congress on the Chemistry of Cement - Vol.IV, p.1968, Paris (1980).

THE INFLUENCE OF THE TYPE OF CEMENT ON THE PROPERTIES AND MICROSTRUCTURE OF HIGH-PERFORMANCE CONCRETE

Shondeep L Sarkar and Moussa Baalbaki

Faculty of Applied Sciences, Université de Sherbrooke, Sherbrooke (Québec), CANADA

ABSTRACT

The use of high performance concrete (HPC) is increasing throughout the world for the construction of high-rise buildings, bridges and major structures. The two important contributory factors for the development of HPC are (i) the possibility of using superplasticizers, and (ii) the use of supplementary cementitious materials (SCM) such as slag, fly ash and silica fume.

The authors observed that not all types of portland cement perform equally well in HPC. Although the type of cement does not appear to significantly affect the strength except for its fineness, the differences in the properties of fresh concrete, particularly its rheology can be conspicuous. Supplementary cementitious materials, on the other hand, were found to influence the strength in a notable way.

INFLUENCE DU TYPE DE CIMENT SUR LES PROPRIÉTÉS ET LA MICROSTRUCTURE DES BÉTONS À HAUTE PERFORMANCE

RÉSUMÉ

L'utilisation des bétons à haute performance (BHP) augmente à travers le monde dans la construction des gratte-ciel, ponts et structures majeures. Les deux facteurs importants qui contribuent au développement des BHP sont (i) la possibilité d'utiliser des superplastifiants et (ii) l'utilisation des ajouts cimentaires tels que le laitier, la cendre volante et les fumées de silice.

Les auteurs ont observé que tous les ciments portland ne performent pas de la même façon dans les BHP. Bien que le type de ciment ne semble pas affecter de façon significative la résistance à l'exception de la finesse, la différence au niveau des propriétés du béton frais, particulièrement sa rhéologie, devient significative. Les ajouts cimentaires aussi semblent affecter de façon notable la résistance du béton.

INTRODUCTION

Concrete technologists' constant efforts to improve concrete properties, particularly in achieving significantly higher mechanical strength (compressive, flexural, and tensile), and enhanced durability properties such as higher resistance to freeze-thaw, carbonation, chemical attack, and lower permeability, is converging towards a new family of high-tech concrete with a very low water/cementitious (W/C) ratio, known as high-performance concrete (HPC).

Though in several respects HPC resembles normal strength concrete, ingredients such as cement, water and aggregates being common, HPC can comprise two additional components, namely superplasticizer to reduce the W/C as much as possible (1), and very frequently the incorporation of a SCM like silica fume, fly ash or slag (2). Often a combination of these is used for optimal performance either in the wet or hardened state, and also from an economical point of view. It is needless to emphasize that microstructural studies of HPC are crucially important in order to understand the behaviour of the material ingredients, and to determine the range that can be used without adversly affecting the performance characteristics.

Over the past several years the authors have studied not only the general characteristics of HPC, but also the role of the individual components (3). Experience has shown that every major constituent of HPC plays an important part in its property development. Since HPC effectively is a "composite material," not only does its W/C ratio, but also the properties of the basic ingredients strongly influence its final characteristics.

This paper focusses attention on the importance of the type of cement for making HPC. According to published literature (4) the best cement for making HPC is either Type I or II. As will be shown, this is not always the case. It mainly depends on what one is aiming for, what is the performance level that is being sought, and at what age.

EXPERIMENTAL

Though a vast range of cements were tested, the results presented here are related to five cements to illustrate some of the important aspects of cement characteristics. The particle size distribution pattern of these cements is shown in Figure 1. An arbitrary partition which roughly corresponds to 400 m^2/kg Blaine fineness has been drawn to delineate coarse cements from fine ones. Accordingly, Type I, II, and HTS (a high silica modulus cement) can be classified as coarse with Blaine fineness < 360 kg/m^2, and Type III, and reground Type V cement of Blaine fineness 650 m^2/kg (labelled VR) as fine.

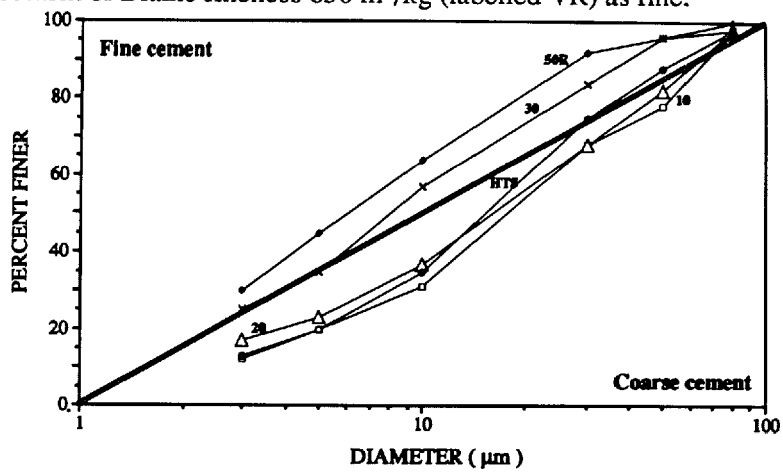

Fig. 1 Particle size distribution pattern of 5 different cements. The diagonal intersect divides them into coarse and fine cements

The Bogue composition of these cements presented in Table 1 shows that in the HTS cement the total silicate phases ($C_3S + C_2S$) exceed 80%. Its other characteristic feature is the extremely low (10.5%) interstitial matrix phases ($C_3A + C_4AF$). In Type VR cement, the C_3A is the lowest (2.3%).

Table 1. Bogue composition of cements used in HPC

Cement Type	C_3S	C_2S	C_3A	C_4AF	Total Silicates	Total Interstitial Phases	Blaine Fineness (m^2/kg)
I	63	13	5.8	11.2	76	17	360
II	46	27	7.8	9.0	73	16.8	360
III	58	17	8.6	5.3	75	13.9	460
VR	61	16	2.3	13.0	77	15.3	650
HTS	62	22	3.6	6.9	84	10.5	320

CONCRETE COMPOSITIONS

Though HPC at several different levels of W/C ratios were tested (5), the range 0.30 to 0.32, readily achieveable in the field, are presented in Tables 2a-c. As can be seen, up to 10% silica fume (as mass replacement of cement) was added to most of the mixes. Not only is its filler action beneficial, its prompt pozzolanicity helps to arrest the generation of macrocrystalline CH in the paste (6). The other types of supplementary cementitious materials used included 40% slag, and 20% fly ash. The advantages of using these industrial by-products have been firmly established (7). The quantity of sodium sulfonate formaldehyde polycondensate superplasticizer shown in Tables 2a-c consists of the total amount used, i.e., added at the time of mixing, and redosed 45 min later. From these tables it is evident that the amount required to make HPC is rather high, this being the only practicable means of drastically reducing the W/C ratio.

RESULTS AND DISCUSSION

The superplasticizer demand in the HTS cement concrete is the lowest (Table 2). Obviously its low interstitial matrix content and coarse grinding imparts less demand on superplasticizer. In contrast, concretes made with the Type V fine reground cement though it contains the lowest amount of C_3A phase, requires much higher superplasticizer. This implies that merely lowering the C_3A content in cement may not necessarily reduce the need for superplasticizer. Parallel to this, one must also consider the fineness of the cement. That coarse cement requires less superplasticizer is further confirmed from the composition of the concretes made with Type I and II cement, which have lower Blaine fineness. The minimum 28 day compressive strength recorded in the present series was 60 MPa. Even without any cement replacement, the strength was as high as 75 MPa with the Type II cement, and 99 MPa with the Type VR cement. The higher strength in the latter is attributable not only to its fine particle size which promotes a greater degree of cement hydration, but also the silicate content of the cement which contributes towards the strength (8). Compared to Type VR cement, the C_3S in Type II cement is lower (Table 1), although it contains the highest amount of C_2S. Nevertheless, belite is slow to hydrate (9), especially when the water content in the system is so low (10). Addition of equal amounts of silica fume (10% by weight of cement) to concretes made with Type I, II and VR cements demonstrate appreciable strength increase. The strength enhancement effect of silica fume and slag is also evident. Despite 50% replacement of cement by these two supplementary cementitious materials, the strength achieved at 28 days is positively higher than the corresponding plain cement concretes. However, when fly ash is added, a strength retrogression at 28 day is observed. It is possible that 20% replacement of cement by fly ash may not be sufficient to induce its pozzolanicity (10). The slump, 100 mm or greater at 45 min (irrespective of the cement type or supplementary cementitious material) can be considered satisfactory.

CH Generation: Decreasing the water content, and adding supplementary cementitious material reduces the amount of well crystallized CH in the paste (known to create inherent weakness in concrete). The 001 CH peak at 18°2θ in the XRD pattern is characterized for its "preferred orientation" (11). A semi-quantitative analysis of this peak is illustrated in Figure 2. Interestingly enough, the concrete with 20% fly ash generates nearly as much CH as the plain cement concretes. CH is distinctly lower in the silica fume concretes despite only 10% cement replacement, confirming its pozzolanicity, whereas in the 50% cement replaced concretes, virtually no oriented CH is produced. One must, however, note that the unusually low quantity of cement is also partially responsible for this phenomenon.

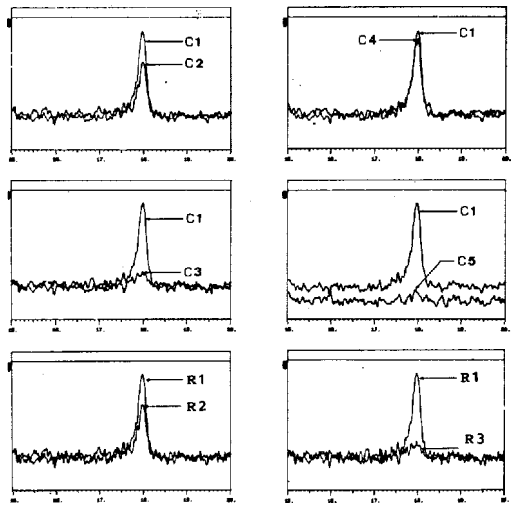

Fig. 2 The 001CH X-ray diffraction peak at 18°2θ in HPCs where C1 and R1 correspond to reference or plain cement concretes in the two series. Composition of C5 HPC is not listed in this paper

Microstructural Characteristics: Compared to normal strength concrete, the paste in HPC is much denser (1), whether it contains only silica fume, fly ash, slag, or a combination. Part of this paste comprises C-S-H gel derived from cement hydration, whereas the rest is either slag or fly ash hydrate. When silica fume is used, its pozzolanic activity produces a low Ca/Si ratio C-S-H (12). Unlike normal concrete, the paste-aggregate bonding in HPC is unusually strong, with little or no oriented CH crystals at the interface (Fig. 3), though fly ash often creates a porous interface due to the presence of unreacted or partly reacted fly ash particles.

The fact that fly ash-HPC produces relatively high quanity of crystalline variety of large CH becomes distinctly visible from SEM examination. Stacked type of CH encapsulating flyash grains is a common occurrence in HPC (Fig. 4). Calcium aluminosulfohydrate minerals, ettringite and monosulfate for example, are rare in HPC.

Owing to the low W/C ratio of HPC, it is not at all unusual to find partly hydrated cement grains in the paste (Fig. 5). The characteristic belite lamellae facilitates detection of this cement phase, compared to alite. The latent hydraulicity of slag and fly ash are well known (13,14). Thus, a number of these grains are invariably present in a partial state of hydration in HPC.

CONCLUSIONS

Today, high performance concrete represents the latest development in concrete technology from the point of view of its high mechanical strength and enhanced durability factors. Thus, research in this exciting new field continues to gain momentum.

The present study shows that the type of cement, i.e., its fineness, composition, amount of interstitial phases, and the total silicate content, together with supplementary cementitious materials (when added) all influence the strength parameter, and the demand for superplasticizer in HPC. Fly ash incorporation fails to augment the performance when tested at 28 days, though slag enhances the strength; silica fume proves to be an excellent material. Drastic reduction in W/C ratio through the use of superplasticizer in addition to the incorporation of supplementary cementitious materials produces a dense paste, and a strong paste-aggregate bonding, that promotes higher strength. Partly hydrated cement and supplementary cementitious material particles are not uncommon in HPC, though oriented CH crystals, and calcium aluminosulfo-hydrate minerals are rare.

REFERENCES

1. Sarkar, S.L. and Aïtcin, P.C., Cem. Conc. Agg., Vol. 9, 1987, pp. 57-64.
2. Mehta, P.K., Proc. IInd. Int. Conf. on FA, SF, Slag, and Natural Pozzolans in Conc., ACI SP-114, 1989, pp. 1-44.
3. Sarkar, S.L. and Aïtcin, P.C., Petrography Applied to Concrete and Concrete Aggregates, B. Erlin and D. Stark, Ed., ASTM STP1061, 1990, pp. 129-144.
4. Howard, N.L. and Leatham, D.M. , Conc. Int., April 1989, pp. 26-30.
5. Aïtcin, P.C., Sarkar, S.L. and Diatta, Y., Mats. Res. Soc. Symp. Proc., Vol. 85, 1987, pp. 261-272.
6. Bache, H.H., Proc. IInd Int. Conf. on Superplasticizers in Conc., 1981, pp. 1-35.
7. Roper, H., Kirby, G. and Baweja, D., Proc. IInd Int. Conf. on FA, SF, Slag and Natural Pozzolans in Conc., ACI SP-91, 1986, pp. 463-482.
8. Taylor, H.F.W., The Chemistry of Cements, Vol. 1, Academic Press, London, 1964.
9. Regourd, M., Annales de l'Institut Technique du Bâtiment et des Travaux Publics, No. 329, 1975, pp. 86-102.

10. Baalbaki, M., Sarkar, S.L., Aïtcin, P.C. and Isabelle, H., Proc. IVth Int. Conf. on FA, SF, Slag and Natural Pozzolans in Conc., to be published, 1992.
11. Lessard, M., Sarkar, S.L., Ksinsik, D. and Aïtcin, P.C., Conc. Int., to be published, 1992.
12. Regourd, M., Mats. Res. Soc. Symp. Proc., Vol. 42, 1985, pp. 3-16.
13. Diamond, S. The Characterization of Fly Ashes, Proc. Symp. N., Mats. Res. Soc. Annual Meet., 1981, pp. 12-23.
14. Sarkar, S.L., Aïtcin, P.C. and Djellouli, H. , Cem. Conc. and Agg., Vol. 12, 1990, pp. 32-37.

Table 2. Summarized composition, physical properties, and 28-day compressive strength of HPC

a) Made with **Type II** cement

	R1	R2	R3
W/C	0.30	0.30	0.32
Cement (%)	100	90	50
Silica fume (%)	--	10	10
Slag (%)	--	--	40
Fly ash (%)	--	--	--
Total Superplasticizer (L/m^3)	9.5	10.0	10.5
Slump (mm) at 45 min	> 180*	190	100
Air content (%)	1.67	1.0	1.5
28d compressive strength (MPa)	75	93	97

* measured at 5 min

b) Made with **Type V reground** cement

	C1	C2	C3	C4
W/C	0.31	0.30	0.31	0.30
Cement (%)	100	90	50	80
Silica fume (%)	--	10	10	--
Slag (%)	--	--	40	--
Fly ash (%)	--	--	--	20
Total Superplasticizer (L/m^3)	15.3	14.0	12.0	13.0
Slump (mm) at 45 min	110	180	220	170
Air content (%)	1.5	1.1	0.8	1.5
28d compressive strength (MPa)	99	116	105	99

c) Made with **Type I, III** and **HTS** cements

	Type I	Type I	Type III	HTS
W/C	0.30	0.30	0.30	0.30
Cement (%)	100	90	90	90
Silica fume (%)	--	10	10	10
Slag (%)	--	--	--	--
Fly ash (%)	--	--	--	--
Total Superplasticizer (L/m^3)	10.5	8.6	10	9.3
Slump (mm) at 45 min	190*	190*	200*	190
Air content (%)	2.7	2.2	1.7	1.5
28d compressive strength (MPa)	60	74	91	74

* measured at 5 min

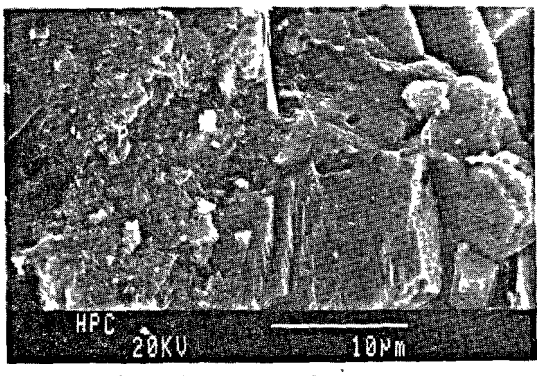

Fig. 3 The strong paste-aggregate bonding in a silica fume HPC devoid of the oriented CH crystals at the interface

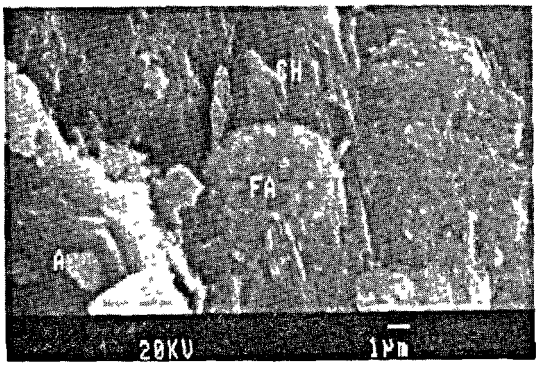

Fig. 4 Stacked type of CH encapsulating a fly ash particle in a HPC

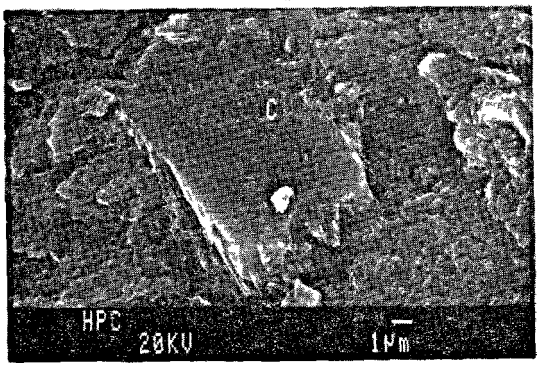

Fig. 5 A partly hydrated cement grain in a HPC

EFFECTS OF THE INITIAL STRUCTURE OF THE CEMENT PASTE IN FRESH CONCRETE ON THE FIRST DEVELOPMENTS OF STRENGTH. INFLUENCE OF SUPERPLASTICIZERS

C Legrand and E Wirquin

Laboratoire Matériaux et Durabilité des Constructions, I.N.S.A. - U.P.S. Toulouse
FRANCE
Association Technique de l'Industrie des Liants Hydrauliques - Paris,
FRANCE

SUMMARY

The strengths of a microconcrete have been measured by means of a very sensitive vane equipment, since the end of the mixing and during the first few hours. At the same time, fine measurements of the heat of hydration have been made.

The results show that during what we use to call the "dorming period", the hydration, as slight as it would be, produces in fact an increase of the strength : the existence of a flocculated structure in the fresh cement paste (responsible of the yield value) explains the immediate reinforcement of the bonds between cement grains as soon as begins the hydration. The filling of pores has a notable effect later.

The same experiments done with the same microconcrete, but added with a superplasticizer, show clearly that, besides the well known hydration delay, hydration beginning does not signify now strength increase. The dispersion of cement grains creates an intergranular minimal distance and decreases the largest pore sizes : the first created hydrates cannot now strengthen an initial structure which does not exist anymore but, on the other hand, the filling of the largest pores will need less hydrates.

RESUME

Les résistances d'un microbéton ont été mesurées à l'aide d'un scissomètre de précision, à partir de la fin du malaxage et pendant les premières heures. Simultanément, des mesures de la chaleur d'hydratation ont été menées.

Les résultats montrent que pendant la période dite "dormante" l'hydratation, aussi faible soit-elle, produit une augmentation de la résistance : la structure floculée de la pâte de ciment (responsable du seuil de cisaillement) explique le renforcement immédiat des contacts interparticulaires par les premiers hydrates formés. Le remplissage des pores n'a un effet notable que plus tard.

Les mêmes expériences effectuées sur le même mortier adjuvanté avec un superplastifiant montrent clairement que le début de l'hydratation n'est plus accompagné d'une augmentation des résistances. La dispersion des grains de ciment a pour effet de supprimer les contacts initiaux et de diminuer la dimension des plus gros pores : les premiers hydrates formés ne peuvent plus consolider une structure qui n'existe plus mais, par contre, le remplissage des plus gros pores nécessite moins d'hydrates que précédemment.

INTRODUCTION

During formation, hydrates first bind the cement particles, then the sand grains and finally the gravel. Concrete acquires strength when the number of bonds is sufficient for the connectivity of the system, i.e. when a percolation threshold appears.

In order to increase concrete strength in the early stages (without changing the water content), chemical reactions are usually speeded up (heating, setting accelerators, fine grinding, etc..). If, however, the initial geometrical arrangement of the cement particles in the fresh concrete can be shown to influence the appearance of a percolation threshold, better early strengths with the same quantity of formed hydrates can be obtained. Cement particles, of course, play the main part in the observed phenomena. Studies of pure cement paste, in spite of a certain academic interest, are not however applicable to concrete. On the other hand, experiments on actual concrete, although indispensable, are difficult to carry out from beginning to end.

This paper concerns the study of the early strengths (0→24 hours) of a microconcrete sample with or without a superplasticizer as a function, not of age as is usually the case, but of the quantity of formed hydrates.

COMPOSITION OF THE TEST MATERIAL

This paper represents a compromise solution following from a previous study of a microconcrete sample composed of :

Cement CPA HP	500 kg/m^3	
Water content	w/c = 0.450	
Siliceous aggregates	0.125 - 0.500 mm	30 %
	0.600 - 1.200 mm	12 %
	1.200 - 2.500 mm	58 %

The admixture, when used, is sulfonate naphthalene (1 % of cement weight) with no change in water content.

MECHANICAL TESTS

Strength measurements must be brief because of the early age of the sample and also to avoid the effects of creep.

The following methodology has been chosen :

- measurement of the shear strength τ_f by vane test for as long as possible after mixing,

- measurement of compressive strength R_c using traditional methods as early as possible.

The same relation as a saturated soil under undrained conditions $R_c = 2\tau_f$ has been used.

QUANTITY OF FORMED HYDRATES

The cement hydration process is so complex that it is impossible to quantify it with a single parameter (1) (2). It is sufficient generally to use a conventional notion of degree of hydration which results from the measurement of a single property such as formation of bound water or heat development.

The first method entails corrections which, at a very early age, are of about the same order as the measured value. The publication of negative quantities of bound water (3) shows the unreliability of this kind of test.

The second method seems more appropriate even using traditional equipment, on condition that the volume of the sample is large enough. The Langavant's calorimeter method recommended by the CERILH has been used (4).

Though the samples used for vane tests and compressive tests are thermically insulated, temperatures in the samples and in the calorimeter evolve differently. At the same age, the degree of maturity (5) is therefore different and it is essential to carry out a correction, based on Arrhenius' law, for calculating the strengths R_c^* at the same degree of maturity (6).

RESULTS

Figure 1 shows the relationships between the corrected strength R_c^* and the heat development during the first hours.

In the case of ordinary microconcrete, the compressive strength increases as soon as there is heat development : close investigation reveals that hydration and hardening occur together as early as the mixing stage.

In the case of microconcrete with added superplasticizer, the strengths remain practically nil, in spite of a certain heat development. So, the retarding effect of superplasticizers is not the only factor responsible for the dormant period. The increase of strengths, when it appears, is slow at the beginning and then accelerates considerably.

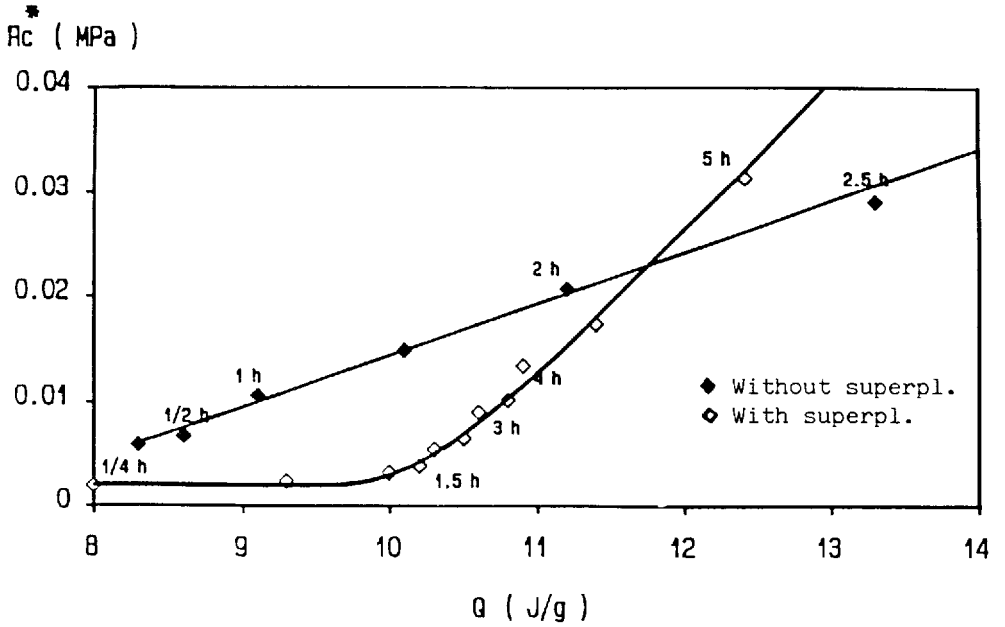

Figure 1

Taking the period (0→24 hours) as a whole, the results presented in figure 2 are obtained (the previous field is represented by rectangle A).

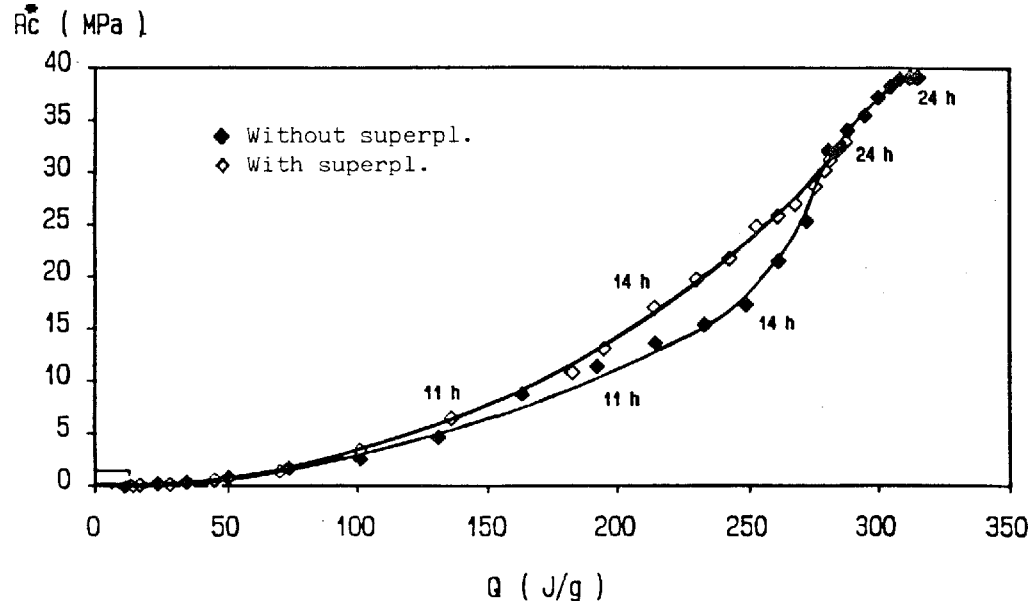

Figure 2

Beyond a certain degree of hydration (figures 1 and 2), the quantity of hydrates needed to produce the same strength is lower in the case of microconcrete with additive, than in that for ordinary concrete.

INTERPRETATION

Fresh cement paste (alone or in concrete), even at reasonably high water contents, presents a yield value and thus has a mechanical strength once mixed. An existing model, based on intergranular bonds by coulombian attraction and Van der Waals' forces, presupposes that the structure of the paste is flocculent (7). The model is particularly useful in explaining rheological viscoplastic behaviour and false thixotropy, the influence of vibration, the evolution of flow characteristics according to the cement concentration, its fineness, etc. (8).

Since there is flocculation, the minimal distances between adjoining grains are practically nil (figure 3a) : it is probable that the first bonds will appear close to these contact areas. Reinforcement by strengthening of the initial intergranular bonds first appears as soon as the first hydrated components are created (9).

Hydrates simultaneously fill the pores but the effect on strength is noticed after a lapse of time. Moreover, hardening kinetics depend on pore size. The largest pores are filled with large amounts of hydrates, as in the case of a flocculent structure. It is possible therefore, in the initial state, to express it as a "weak percolation threshold" due to flocculation, reinforced by the first formed hydrates. A stronger threshold can appear only when enough pores are filled by sufficient hydrates. This is not apparent in figure 1, certainly because of the size of the large pores.

The superplasticizer disperses the particles (figure 3b). At the same water content, there is the same number of cement grains per volume unit, but the dispersion creates an intergranular minimal distance and decreases the size of the largest pores. Of course, the yield value is removed and the first hydrates can no longer strengthen an initial structure which does not exist. On the other hand, pores especially the largest, will need less hydrates. At this stage, the weak percolation threshold no longer exists and more evenly distributed pores need less hydrates to create a strong percolation threshold.

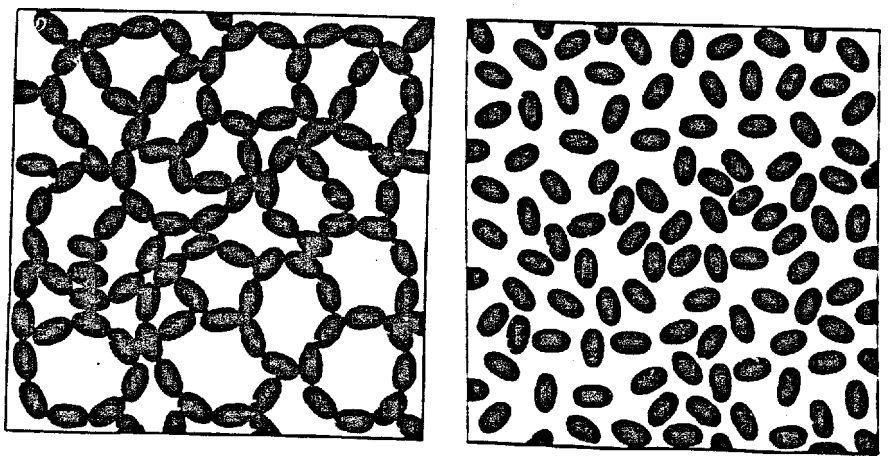

a) floculated b) dispersed

Schematic models of cement paste with the same water content

Figure 3

REFERENCES

1. Baron J. : "Formation de la microstructure ; Hydratation, prise durcissement" Le Béton et l'Eau. Proceedings Seminaire College Int. des Sciences de la Construction, Saint Rémy les Chevreuse, France, 1985, p. 26-45.

2. Torrenti J.M. : "La résistance du béton au très jeune âge". Connaissance Générale du béton, Séminaire, Ecole Nationale des Ponts et Chaussées, Paris, 1989, 24 p.

3. Byfors J. : "Plain concrete at early ages", ed. by Swedish Cement and Concrete Institute, Stockholm, 1980, 464 p.

4. CERILH : "Mesure de la chaleur d'hydratation des ciments par la méthode du calorimètre de Langavant" Internal note, 1976, 16 p.

5. Mamillan M. : "Traitement thermique des bétons", Le Béton Hydraulique, Paris, ed. by Presses de l'Ecole Nationale des Ponts et Chaussées, Paris, 1982, p. 261-269.

6. Gautier E. : "Représentation analytique simple de l'évolution de la résistance du béton en fonction du temps et de la température", CERILH, Internal note, 18 p.

7. Powers T.C. : "The properties of fresh concrete", John Wiley, New York, 1968, p. 432-434.

8. Legrand C. :" Le comportement rhéologique des suspensions de ciment" Le Béton Hyraulique, ed. by Presses de l'Ecole Nationale des Ponts et Chaussées, Paris, 1982, p.115-130.

9. Mutin J.C., Nonat A; and Eddajibi A.H. : "Hydratation et prise". Connaissance générale du béton, ed.by Ecole Nationale des Ponts et Chaussées, Paris, 1989. 39 p.

THE EFFECT OF CURING CONDITIONS ON CHLORIDE DIFFUSIVITY IN SILICA FUME HIGH STRENGTH CONCRETE

Tang Luping and Lars-Olof Nilsson

Division of Building Materials, Chalmers University of Technology, Gothenburg, SWEDEN

SUMMARY

In this study, 150×150×150 mm concrete cubes were cast and cured under six different conditions, that is, sealed in plastic bags, exposed to ambient air, immersed in water, stored in boxes with 100%RH, under Swedish standard condition, and heat cured at 65 °C. A rapid method for determining chloride diffusivity, previously proposed by the authors of this paper, was employed to evaluate the diffusivity at different ages (1, 3, 7, 28, 90, 180 days). The relationship between chloride diffusivity and compressive strength is also discussed in this paper. The experimental results show that water or moisture curing in the early stage of hydration is beneficial to both the developments of strength and resistance to chloride penetration.

摘　要

本文介绍硅灰高强混凝土的养护条件对其氯离子扩散性的影响。在研究中所采用的混凝土试件尺寸为 150x150x150毫米，这些试件在六种不同的条件下养护，即：密封在塑料袋子里；暴露于环境空气中；沉浸在水中；储存在相对湿度为100%的湿气箱内；按瑞典标准条件；以及65摄氏度热养护。该研究采用了本文作者曾提出的氯离子扩散性快速测定法来评定氯离子在不同龄期（1，3，7，28，90，180天）的混凝土中的扩散性。本文还对氯离子扩散性与抗压强度之间的关系进行了讨论。实验结果表明，在水化初期阶段，水养护和湿气养护不仅有利于强度发展，而且还有利于对氯离子渗透的抵抗性的发展。

INTRODUCTION

It is well known that curing conditions greatly affect the properties of concrete. Chloride diffusivity is one of the most important properties regarding the durability of concrete structures. Silica-fume concretes have shown very good resistance to chloride penetration (1-5). Several researchers (1-3) have reported the influence of water-binder ratios on chloride penetration in hardened cement pastes that contain silica-fume. Cabrera and Claisse (4) investigated the electrical resistivity of silica-fume concretes cured in fog room and in water. Recently, Tang and Nilsson (5) reported the relationship between chloride diffusivity and curing time of silica-fume concretes. The present study investigates the effect of curing conditions on chloride diffusivity in silica-fume high-strength concrete.

EXPERIMENTAL

The cement used in this study was Swedish OPC and the silica fume was supplied by Elkem, Norway. The ratio of silica fume to cement (SF/OPC) was 12%, and the water-binder ratio was 0.32. Naphthalene based superplasticizer (Mighty 100 from Japan) was used to obtain sufficient workability. The mix proportion of dry materials is OPC : SF : sand (<8 mm) : gravel (8~12 mm) = 1 : 0.12 : 1.5 : 2.25. The six different curing conditions are listed in Table 1.

Table 1——Curing Conditions

A	air curing, i.e. stored in a laboratory room, RH ≈ 30%~50%, t ≈ 18~22 °C.
B	bag curing, i.e. sealed in a double-layer plastic bag.
W	water curing, i.e. stored in a covered water box under the water level.
M	moisture curing, i.e. stored in a covered water box about 20 mm over the water level.
S	Swedish standard condition, i.e. immersed in water for 5 days before being stored in a climate controlled room at 20 °C and 55%RH.
H	heat curing, i.e. stored in a water box over the water level, heated to 65 °C, kept at 65 °C for 20 hours, slowly cooled to room temperature.

Concrete was mixed in a 250 litre forced mixer and cast into 150×150×150 mm moulds. The top surfaces were covered with plastic film to prevent the water from evaporating. All the concrete cubes, except those to be subjected to heat curing, were cured at room temperature for one day before being demoulded. Later they were cured at different conditions. The cubes cured under the conditions B, W and M were air dried for half a day for samples at an age of 3 and 7 days, and for 2 days for samples at an age of more than 28 days before the strength test. Two hours after casting, the H cubes with their moulds and

film covers were put into a water box about 50 mm over the water level and were subjected to heat curing. After heat curing, the cubes were demoulded and air cured at room temperature for a specified period.

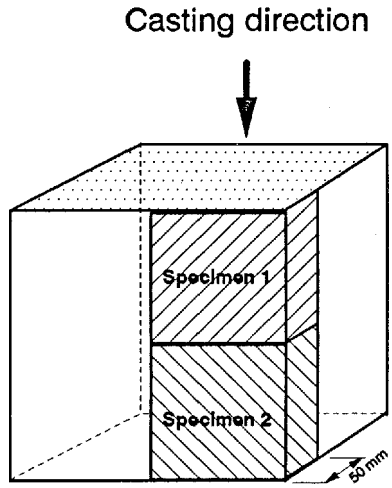

Fig. 1——Positions of the cut specimens.

At the specified age (1, 3, 7, 28, 90, 180 days), the compressive strength of different cubes was tested. For the chloride penetration test, two specimens of thickness 50 mm and cross-section about 70×70 mm were cut out from an intact cube. The positions of the cut specimens are illustrated in Fig. 1.

A newly developed method was employed for rapid determination of the chloride diffusivity, and the experimental procedures of the method have previously been reported (6). If not otherwise stated in this study, the intact surface of the specimen was exposed to chloride solution. The specimens of early age (1 and 3 days) were vacuum saturated with lime water for 8 hours and those of older age (>7 days) for 24 hours. Since the concrete has less porosity than paste and mortar, the concentration of NaCl solution was increased to 6% instead of the 3% used previously (6), so that the penetration depth could be more easily observed. In order to shorten the testing time, the voltage for the specimens older than 7 days was increased to 40 V D.C. The effective diffusion coefficient was calculated by using the following equation:

$$D = \frac{RTL}{zFU} \cdot \frac{x_d - \alpha x_d^{\beta}}{3.6\times10^9 t} \qquad (1)$$

where
- D: effective diffusion coefficient, m^2/s;
- R: gas constant, R = 8.314 J/(K·mol);
- T: solution temperature, K;
- L: thickness of the specimen, mm;
- z: absolute value of ion valency, for chloride, z = 1;
- F: Faraday constant, F = 9.648 $\times10^4$ J/(V·mol);
- U: absolute value of potential, V;
- x_d: chloride penetration depth; mm;
- t: testing time, hr;
- α, ß: constants from a numerical solution of Fick's second law, for T = 298 K (25 °C), L = 50 mm, when U = 30 V, α = 1.061 and ß = 0.589, and when U = 40 V, α = 1.010 and ß = 0.570.

RESULTS AND DISCUSSION

The strength development of the concretes cured under different conditions is shown in Fig. 2. It is seen that there is almost no difference in the compressive strength of concretes cured under conditions B, W and M. As compared with the concretes cured in plastic bag or in water, the concrete cured in air shows slightly higher strength at early ages (i.e. 3 and 7 days), probably due to its lower water content. At an age of 180 days, however, its strength drops a little. This is in agreement with the results of De Larrard and Bostvironois (7). The concrete cured under the Swedish standard condition (S) showed the highest strength. This implies that water or moisture curing in the early stage of hydration is beneficial to the strength development of silica-fume high-strength concrete. The concrete subjected to heat curing reached very high

strength at a very early age (i.e. 1 day), but the further development of its strength became much slower than the others. After 7 days age, the strength of this concrete was even lower than the others.

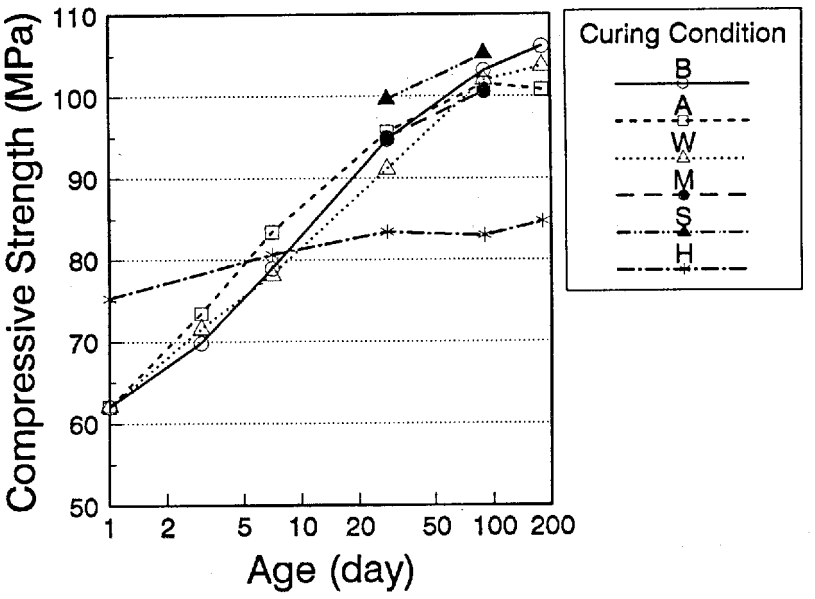

Fig. 2——Strength development of concretes.

The experimental results of chloride diffusivity are listed in Table 2, and the average values of the diffusivity are shown in Fig.3.

Table 2——Chloride Diffusivity ($\times 10^{-12}$ m^2/s) in Concrete Specimens

Age (day)	Specimen No.	Curing Conditions B	A	W	M	S	H
1	1	6.83	"	"	"	"	0.20
1	2	6.50	"	"	"	"	0.34
3	1	3.32	3.32	4.10	n.d.	n.d.	n.d.
3	2	3.76	3.51	3.87	n.d.	n.d.	n.d.
7	1	1.55	1.74	1.64	n.d.	n.d.	n.d.
7	2	1.65	1.72	1.95	n.d.	n.d.	n.d.
28	1	0.48	1.03	0.44	0.37	0.44	2.99
28	2	0.39	1.11	0.48	0.54	0.51	1.59
90	1	0.31	0.48	0.25	0.31	0.27	n.d.
90	2	0.36	0.44	0.36	0.33	0.27	n.d.
180	1	0.24	0.42	0.29	n.d.	n.d.	1.87
180	2	0.20	0.44	0.25	n.d.	n.d.	2.04

n.d.——not determined.

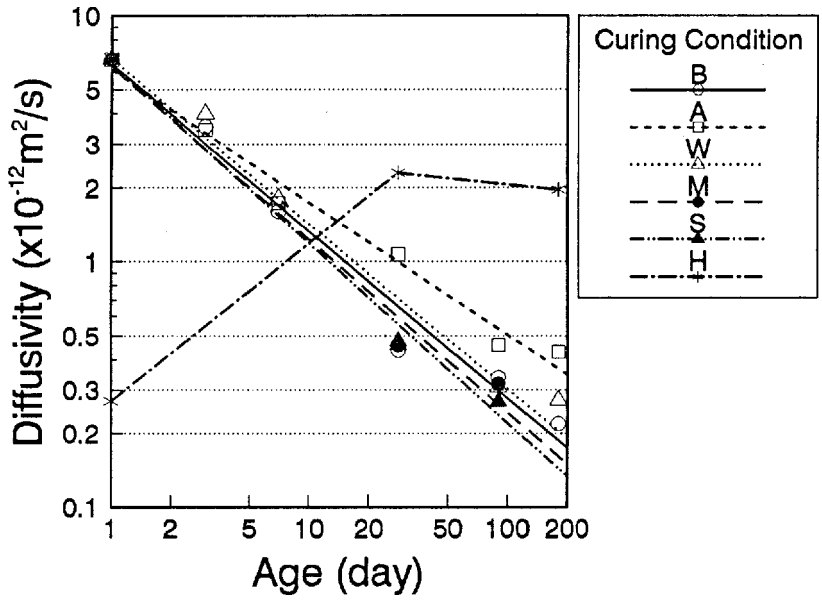

Fig. 3——Chloride diffusivity in concrete specimens.

As expected, chloride diffusivity in all specimens, except those subjected to heat curing, decreased with increased curing time, and the concretes cured under conditions B, W, M and S have shown similar resistance to chloride penetration. After an age of 7 days, however, the diffusivity in air cured concrete became about twice as large as that in the concretes cured under condition B, W, M and S, suggesting that air curing increases micro-cracks. Heat curing results in very low diffusivity at a very early age (i.e. 1 day). However, this low diffusivity could not be maintained. It increased tenfold at an age of 28 days, despite the fact that the strength of the concrete still increased. The large cracks between the paste and the coarse aggregate of H specimens were observed after chloride penetration test. It is apparent that these cracks have given the path for chloride to penetrate into the concrete. A similar phenomenon was generally observed during carbonation (8).

By plotting diffusivity against strength, as shown in Fig. 4, we find that all points, except one (H at the age of 1 day), follow the inverse-power relationship and can be expressed as

$$D = 3.85\left(\frac{1}{R}\right)^{-6.49} \qquad (2)$$

where D is the chloride diffusion coefficient (m^2/s) and R compressive strength (MPa). The square correlative coefficient of this regression equation is 0.92. It can be estimated from this equation, that a decrease in strength by only 10% will double the chloride diffusivity!

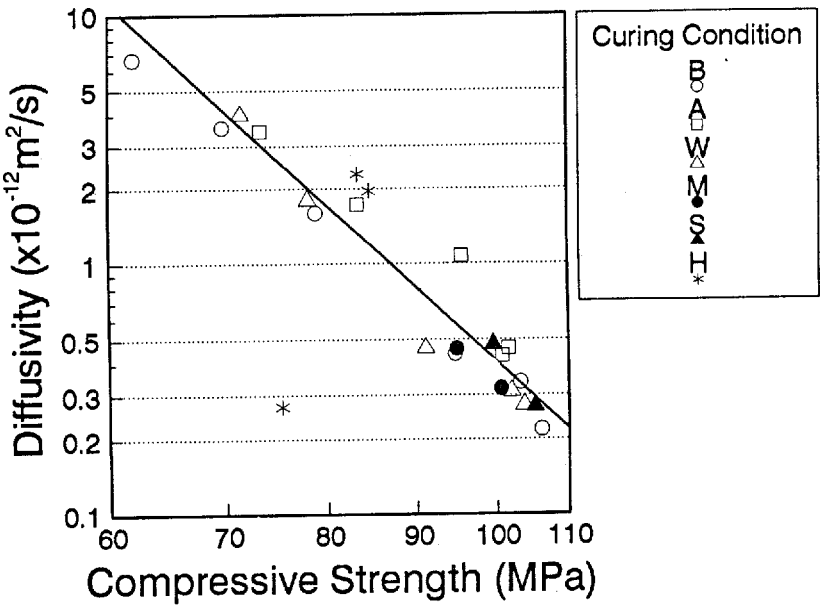

Fig. 4——Relationship between diffusivity and strength.

CONCLUSIONS

From the experimental results the following conclusions can be drawn:

Water or moisture curing in the early stage of hydration is beneficial to both the developments of strength and resistance to chloride penetration.

Curing in a plastic bag has an effect similar to that in water or in moisture. As compared with water or moisture curing, air curing eventually results in lower resistance to chloride penetration, whereas heat curing increases chloride diffusivity by about one magnitude order.

An inverse-power relationship between chloride diffusivity and compressive strength has been suggested. It implies that a small drop in strength might result in a large increase in chloride diffusivity.

REFERENCES

1. Gautefall, O. and Havdahl, J.: "Effect of condensed silica fume on the mechanism of chloride diffusion into hardened cement paste", **3rd International Conference on the Use of Fly Ash, Silica Fume, Slag and Natural Pozzolans in Concrete**, ACI SP-114, Trondheim, ed by V.M. Malhotra, 1989, Vol.II, p 849-860.

2. Marusin, S.L.: "Chloride ion penetration in conventional concrete and concrete containing condensed silica fume", **2nd International Conference on the Use of Fly Ash, Silica Fume, Slag and Natural**

Pozzolans in Concrete, ACI SP-91, ed by V.M. Malhotra, 1986, p 1119-1133.

3. Gautefall, O.: "Effect of condensed silica fume on the diffusion of chlorides through hardened cement paste", **2nd International Conference on the Use of Fly Ash, Silica Fume, Slag and Natural Pozzolans in Concrete**, ACI SP-91, ed by V.M. Malhotra, 1986, p 991-997.

4. Cabrera, J.G. and Claisse, P.A.: "Measurement of chloride penetration into silica fume concrete", **Cement and Concrete Composites**, 1990, **12(3)**, 157-161.

5. Tang, L. and Nilsson, L-O.: "Chloride diffusivity in high strength concrete at different ages", to be published in **Nordic Concrete Research**, Publication No.11, 1992.

6. Tang, L. and Nilsson, L-O.: "Rapid determination of the chloride diffusivity in concrete by applying an electrical field", **ACI Materials Journal**, 1992, **89(1)**, 49-53.

7. De Larrard, F. and Bostvironnois, J.L.: "On the long-term strength losses of silica-fume high-strength concrete", **Magazine of Concrete Research**, 1991, **43(155)**, 109-119.

8. Strunge, H. and Chatterji, S.: "Microscopic observations on the mechanisms of concrete neutralization", **2nd International Seminar on Durability of Concrete——Aspects of admixtures and industrial by-products**, Document D9:1989, Swedish Council for Building Research, ed by L. Berntsson, S. Chandra and L.-O. Nilsson, 1989, p 229-235.

E. 05.03.01 BB

DNR 32205

PERMEABILITY AND DIFFUSION OF GASES IN CONCRETE

U Costa, M Facoetti and F Massazza

Italcementi SpA, Bergamo, ITALY

SUMMARY

Coefficients of air permeability and oxygen diffusion were determined in concretes prepared with portland, pozzolanic and slag cements, and cured up to 180 days.

The total porosity and pore size distributions on the same specimens were calculated by mercury intrusion. Strengths were also determined on all the concretes.

Gas flow coefficients in concretes are highly dependent on the strengths developed by the concretes and not on the type of cement.

It is apparent how all types of cement used permit to obtain impervious concretes through a reduction of the w/c ratio, an adequate cement content and a prolonged curing age.

The diffusion and permeability coefficients of gas maintains an appreciable value also in high-strength concretes when they are dried.

As regards the steel protection the depth of concrete cover is of the utmost importance to avoid that the concrete in the vicinity of reinforcing steel becomes dry.

INTRODUCTION

As is known, corrosion of reinforcing steel is very likely to occur if the alkalinity of the pore solution in concrete is reduced below certain levels by carbonation. The eletrochemical reaction of corrosion is associated with an anodic reaction involving oxidation of iron into ferrous ion as well as a cathodic reaction causing the reduction of the oxygen dissolved in the pore solution.
The condition which makes corrosion start and proceed is the presence of oxygen in the vicinity of the reinforcing steel and the rate at which corrosion occurs will depend on the material's resistance to the oxygen flow.

Gas permeability in concrete is linked to a number of factors which may be categorised as follows:

- Factors inherent to the material: properties of both cement and aggregate, water/cement ratio, cement content, aggressive agents, etc.;
- Environmental factors: aggressive ambient, moisture content, frost action, etc.;
- Technological factors: casting, curing, structural stresses, etc.

The complex interactions occurring among the above factors do not allow simple forecasting models as regards the durability of concrete works to be established. A thorough knowledge of the characteristics of gas and liquid diffusion in concrete may contribute to design and obtain concretes with improved durability features.
This paper is aimed at illustrating the results of a study of air permeability and oxygen diffusion through concretes of different compositions. Coefficients of permeability and diffusion were correlated to concrete strength. Considerations on the importance of an adequate cover depth are also given.

Gas Diffusion and Permeation in Porous Systems

The mechanism of gas flow under a given pressure gradient (permeability) is different from that occurring under a concentration gradient in which no pressure difference is involved (diffusion). Air permeation through concrete follows with good approximation Darcy's law which in is turn derived from the Poiseuille's equation of capillary flow when the gas flow is low and conditions of laminar motion obtain (1) (2). The coefficient of permeability is obtained from experimental measurements of gas flow rates under different pressure gradients.

Gas diffusion in porous solids takes place through mechanisms of transfer which become extremely complex depending on the pore size distribution of the material proper. For example, diffusion is disturbed by the interactions with the pore walls (Knudsen's diffusion) in pores whose dimensions are comparable with the mean free path of gas molecules (approx. 0.1 μm at 1 atm).

Owing to a diffusion process occurring alongside the walls, the gas flow can also be enhanced by the gas fraction adsorbed on the pore walls. The coefficient of gas diffusion will therefore depend not only on the factors connected with volume and pore size distribution but also on the specific interactions occurring between the gas and the pore surfaces. It was however found (3) that, even in complex porous systems such as those present in cement mortars and concretes, diffusion is governed by Fick's first law and this despite some restrictions concerning flows and molecular weights of the gases when they reciprocally diffuse. The simultaneous assessment of permeability and diffusion coefficients in concrete can furnish more precise information about the factors of composition and microstructure which are likely to affect permeability of

concrete.

EXPERIMENTAL

Materials

- Cements
  Four commercial cements, taken at random from the market, were utilised. Their main properties are given in Table 1.

TABLE 1: Cement properties

Composition (%)	C E M E N T S			
	Portland	Fly-ash (*)	Natural Pozzolana	Blast furnace (**)
Loss on Ignition	4.42	6.00	5.52	4.13
MgO	1.47	1.32	2.29	2.98
SO3	2.65	1.25	2.23	2.75
Insoluble Residue	0.83	12.17	4.61	1.33
S--	-	-	-	0.22
Pozzolanicity test	-	pos.	pos.	-
Specific mass g/cm3	3.09	2.88	3.00	3.07
Blaine S.S.cm2/g	3710	3590	6270	3820
Compr. Strength N/mm2				
(***) at 2 days	25	16	10	22
at 28 days	58	39	37	53

*) complying with CEN pozzolanicity test
**) Slag content approx. 35%
***) ISO mortar

- Concretes
  Concretes with different cement contents and w/c ratios were obtained from each of the above cements. Properties of the mixes are given in Table 2. A silico-calcareous river aggregate with a continuous particle size distribution and max diameter of 2 cm was used for making concrete. The aggregate in question did not show any appreciable porosity and therefore did not affect the determination of porosities in the concrete.

TABLE 2: Mix proportions

	WATER (kg/m³)	CEMENT (kg/m³)	AGGREGATE (kg/m³)
MIX 1, w/c = 0.53 slump, cm = 6 flow, % = 28	185	330	1850
MIX 2, w/c = 0.62 slump, cm = 20 flow, % = 80	217	350	1780
MIX 3, w/c = 0.71 slump, cm = 5 flow, % = 25	177	250	1900
MIX 4, w/c = 0.82 slump, cm = 21 flow, % = 80	205	250	1830

Tests Performed

Coefficients of air permeability and oxygen diffusion were determined in the concretes cured up to 180 days. The total porosity and pore size distributions on the same specimens were evaluated by mercury intrusion. Strengths were also determined on all the concretes.

Preparation of Samples

Concretes were poured into cylindrical steel moulds, 80 mm in diameter and 110 mm in length. For 24 hours the moulds were allowed to slowly rotate in order to avoid sedimentation phenomena. Samples were subsequently demoulded and cured in a fog chamber at 20°C.

Upon completion of the prefixed curing age, each cylinder was cut with a diamond saw to obtain two 30-mm thick concrete discs.
Drying of the discs was carried out at 60°C for 10 days up to constant weight. The

absence of drying-induced cracks was ascertained by microscopic examinations.
The choice of testing dried samples was suggested for the purpose of having maximum permeability (4) and of simulating practical conditions occurring in the concrete cover.

Apparatus

Air* permeability measurements were carried out by means of a HASSLER-type cell. Permeability coefficients K were calculated from equation (1) suggested by Grube and Lawrence (5)

$$K = \frac{L\, V_2\, P_2\, \eta}{(P_1^2 - P_2^2)\, A} \qquad 1)$$

where

K	= permeability coefficient,	m^2
η	= fluid viscosity,	$N.s.m^{-2}$
V2	= exit flow rate,	$m.s^{-1}$
P1	= input pressure,	$N.m^{-2}$
P2	= output pressure,	$N.m^{-2}$
A	= sample's cross-section,	m^2
L	= sample's thickness,	m

On the same discs utilised for permeability measurements, determinations of oxygen diffusion were also carried out by means of an apparatus in which O_2 concentrations in the carrier gas (N_2) were assessed by means of a zirconium dioxide probe (6).
Effective coefficients of diffusion (D_{eff}) were determined under steady flow conditions, i.e. with a constant concentration gradient, based on 2)

$$D_{eff} = \frac{n\, O_2\% \, L}{100\, A} \qquad 2)$$

where:

D_{eff}	= effective diffusion coefficient,	$cm^2.s^{-1}$
n	= carrier gas flow rate (N_2),	$cc.s^{-1}$
O_2	= oxygen content in the flow,	%
L	= sample's thickness,	cm
A	= sample's cross-section,	cm^2

From the same discs utilised for diffusion tests three small cylinders, 22 mm in diameter and 30 mm in length, were obtained and subsequently broken up into 3-4 pieces. Fragments were used to prepare mean samples of approx. 25-30 g. Determination of pore size distribution was carried out by means of a Carlo Erba type-2000 porosimeter fitted with an improved cell capable of accommodating not only pulverised material but also fragments of concrete. Total porosity was referred to concrete as well as to the cementitious paste content of concrete. Paste content was calculated by adding cement content to residual water content found in the samples after drying.

---

*) Experiments proved that permeability coefficients do not change if air is used instead of oxygen

Results

Tables 3 summarises the results of the tests on strength, coefficients of permeability and diffusion as well as porosity. Strengths were found to cover a rather wide range of values and to be dependent on the type of cement used as well as the cement content, w/c ratio and curing age. Concrete strength maximum values roughly matched those found on ISO mortar and they were shown to depend more on the strength class than on the type of cement used.

Figures 1 and 2 show that a linear correlation does exist between strength and w/c ratio. It was therefore confirmed that the w/c ratio, at least within the range of concrete mixes investigated and according to the type of aggregate employed, is extremely important among the factors affecting strengths.

Coefficients of permeability and of diffusion were found to decrease rapidly as the w/c ratio decreased, and the cement content and curing age increased. It is to be also noted that concretes having low w/c ratios showed an appreciable permeability and diffusion coefficients also at longer curing ages.

Previous studies (7) have highlighted that the cement matrix-aggregate interface can substantially contribute to carry on gas transfer in concrete and that interface permeability is little reduced as curing proceeds. Porosity tends to diminish at longer curing ages although some values might appear at variance with this rule. Causes for occasional deviations were not analysed but held to be probably due to practical difficulties in obtaining samples with the same homogeneity. For the same w/c ratio, cement content and curing age, total porosity of the matrix is shown to be comparatively lower in portland cement concretes than in those from blended cements. The pore radius distribution curve shown in Figure 3 indicates that little variation is to be expected among concretes made from different cements. In pure pastes (1) (2), porosity is reduced substantially as curing time increases, whereas in concretes only slight reductions or stationary conditions are found.

These results are in agreement with recent data based on which the paste forming in concrete is more porous and most part of extra porosities are larger in diameter than those found in pure pastes (8).

DISCUSSION

Results obtained show that strengths and coefficients of gas flow in the concretes investigated depend on those very factors connected with concrete composition, namely w/c ratio and cement content. As a consequence, a direct functional relation between strengths and coefficients of permeability and diffusion can be expected. In order to verify this assumption, strengths were statistically correlated with K and D_{eff} values by considering at first the values referring to concretes made from the same cement, and subsequently the whole group of values obtained from all concretes.
The best correlation coefficients are in any case obtained from the power correlation function

$$y = Ax^{-B}$$

where:

y = coefficient of permeability or diffusion
x = compressive strength
A, B = constants

TABLE 3: Strength, permeability, porosity of different concretes

		PORTLAND C.					FLY ASH C.				
	Curing	Compressive Strength	Air Permeability	Oxygen Diff.Coeff.	Porosity cm3/100 g		Compressive Strength	Air Permeability	Oxygen Diff.Coeff.	Porosity cm3/100 g	
	days	N/mm2	m2x10	cm2/sx10	concrete	matrix	N/mm2	m2x10	cm2/sx10	concrete	matrix
Mix 1	7	35.8	2.14	9.70	4.4	24.8	24.7	3.52	12.01	4.8	27.6
	90	47.6	1.68	8.23	4.2	24.4	39.8	2.00	6.37	5.2	29.4
	180	46.7	1.03	4.20	4.9	24.4	43.6	0.84	0.69	5.2	28.5
Mix 2	7	30.9	2.97	13.68	5.3	29.2	18.1	6.27	13.93	5.6	30.9
	90	40.0	1.89	10.42	4.6	25.0	34.0	1.75	8.26	5.6	31.4
	180	39.9	1.64	9.79	4.7	25.7	39.2	1.16	1.70	4.8	25.7
Mix 3	7	26.0	13.73	16.60	6.3	46.1	17.6	18.18	16.82	6.8	52.2
	90	34.4	3.53	10.62	4.4	30.9	24.7	9.42	7.14	4.2	31.1
	180	35.0	2.86	3.27	4.7	33.1	26.0	7.63	6.57	4.7	36.4
Mix 4	7	17.6	36.78	22.20	6.1	43.4	10.8	61.92	24.99	7.1	51.6
	90	24.2	10.34	11.02	5.3	36.0	18.1	33.77	15.29	6.1	41.8
	180	25.7	7.18	8.41	5.4	37.0	23.0	19.77	11.70	5.1	36.5

		NATURAL POZZ. C.					BLASTFURNACE C.				
	Curing	Compressive Strength	Air Permeability	Oxygen Diff.Coeff.	Porosity cm3/100 g		Compressive Strength	Air Permeability	Oxygen Diff.Coeff.	Porosity cm3/100 g	
	days	N/mm2	m2x10	cm2/sx10	concrete	matrix	N/mm2	m2x10	cm2/sx10	concrete	matrix
Mix 1	7	18.7	5.70	11.98	5.4	32.1	30.4	2.05	8.65	5.5	31.7
	90	29.9	5.03	6.11	4.7	27.8	48.6	1.05	5.72	4.9	27.2
	180	34.8	1.07	4.99	4.9	28.8	52.2	0.97	5.31	4.5	25.0
Mix 2	7	14.4	15.12	9.86	6.3	36.0	23.6	4.56	10.12	6.1	33.6
	90	27.0	6.94	8.33	6.5	38.2	42.7	1.32	7.82	5.2	28.5
	180	31.0	6.73	6.93	4.2	23.6	46.0	1.30	5.08	5.0	26.8
Mix 3	7	10.6	43.56	23.62	6.3	51.4	19.0	12.94	12.88	5.1	38.6
	90	20.7	5.76	9.51	5.4	44.1	37.0	0.99	6.89	4.5	33.8
	180	22.9	4.27	6.17	4.9	39.3	41.7	0.78	5.54	5.3	40.7
Mix 4	7	6.3	85.86	23.59	6.3	45.6	12.5	43.23	17.27	6.6	48.6
	90	16.0	35.59	13.46	7.7	63.3	24.9	2.57	11.25	6.0	43.3
	180	18.0	16.88	10.53	6.3	50.4	28.7	0.97	7.65	6.1	42.4

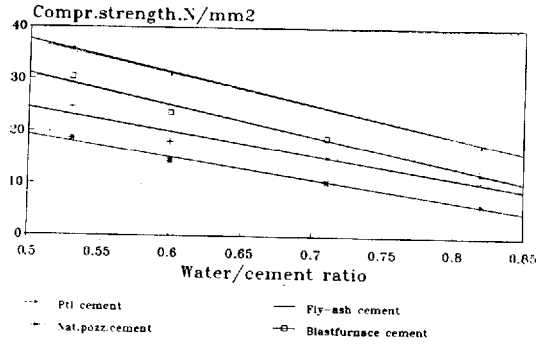

FIG. 1: 7-day compressive strengths in concretes versus w/c ratio

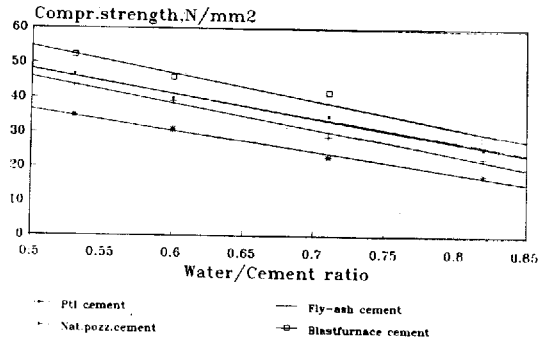

FIG. 2: 180-day compressive strengths in concretes versus w/c ratio

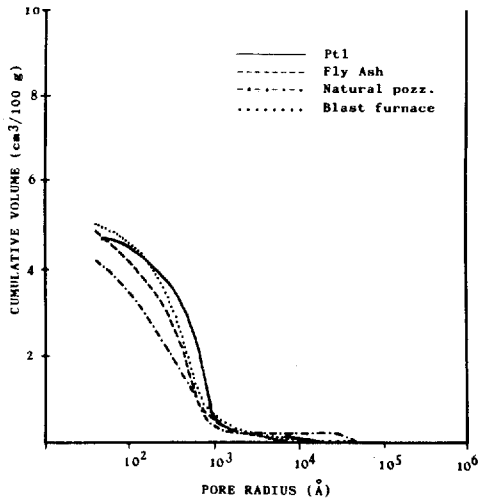

FIG. 3: Pore sizes in concretes:
w/c ratio = 0.60; cement content = 350 kg/m^3
curing age: 180 days

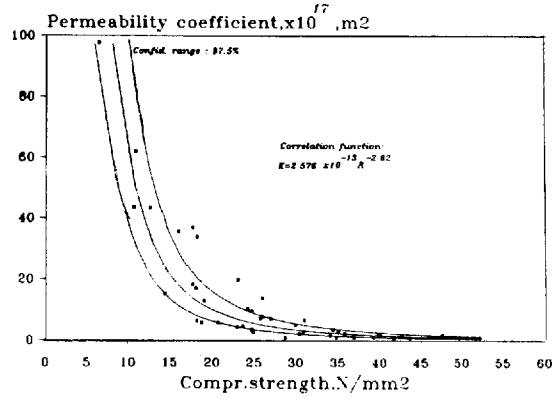

FIG. 4: Air permeability coefficient in concretes versus compressive strength

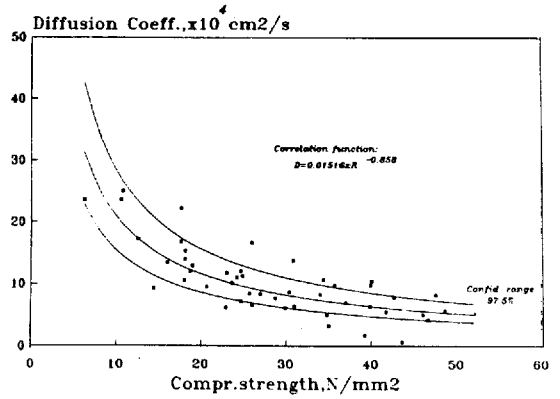

FIG. 5: Oxygen diffusion coefficient in concretes versus compressive strength

The statistical significance of the correlation, expressed by the value of the correlation coefficient R, is entirely equivalent no matther whether the results are grouped for single cements or the data are considered as a whole.

The experimental points and correlation functions which give the best least square fit are illustrated in Figures 4 and 5. It is to be observed that both permeability and diffusion of gases increase rapidly whenever concrete strengths fall below 15 N/mm^2. In order to obtain low permeability concretes, strengths should not be lower than 30 N/mm^2, different types of cements notwithstanding.

CONCLUSIONS

Gas flow coefficients in concretes are highly dependent on the w/c ratio, cement content, curing time and thus also on the strengths developed by the concretes whereas it does not seem that the type of cement used can exert any direct influence on permeability. Influences, if any, are only indirect and depend on the effective strength attained by the concrete upon testing.

It is apparent that all types of cement used permit to obtain low permeability concretes and this is best achieved through a reduction of the w/c ratio, an adequate cement content and a prolonged curing age. The effective diffusion coefficient of oxygen as well as air permeability of concrete show appreciable values also in high-strength concretes when they are dried. This means that high strength alone cannot ensure that reinforcing steel is protected against corrosion. Since the effective diffusion coefficient of oxygen in water is approx. 1/10 of that found in dried concrete, the depth of concrete cover should be such as to allow concrete in the vicinity of the reinforcing steel to be always saturated. This condition depends on relative humidity variations which can vary substantially from site to site. As a consequence, the depth of concrete cover should be determined according to the environmental conditions or, better stated, it should have to be strictly established so as to guarantee steel protection in any case.

REFERENCES

1) **U. COSTA, F. MASSAZZA,** La Durabilità delle Opere in Calcestruzzo (Padova, October, 8-9 1987), 1987, 67-73

2) **U. COSTA, F. MASSAZZA,** EM'88 - 2nd Int. Conf. on Engineering Materials "From Research to applications and Design" (Bologna, June 20-23, 1988), pp. 8

3) **Y. HOUST, F.H. WITTMANN,** Int. Coll. on Materials Science and Restoration (Esslingen, Sept. 2-4, 1986), 629-34

4) **K. KOBAYASHI, K. SHUTTOH,** Cem. Concr. Res. 1991, 21 (2/3), 273-84

5) **C.D. LAWRENCE,** Proc. of the Rilem Seminar on the Durability of Concrete Structures under Normal Outdoor Exposure (Hannover, March 26-29, 1984), 68-79

6) **C. LOCHER, U. LUDWIG,** Betonwerk+Fertigteil-Technik 1987, (3), 177-82

7) **U. COSTA, M. FACOETTI, F. MASSAZZA,** RILEM Int. Symp. on "Admixtures for Concrete: Improvement of Properties" (Barcelona, May 14-17, 1990), 392-401

8) **D. WINSLOW, D. LIU,** Cem. Concr. Res. 1990, 20 (2), 227-35

EVALUATION OF COMPATIBLE-SUPERPLASTICIZER FOR THE PRODUCTION OF HIGH-STRENGTH CONCRETE

M Rollet*, C Levy and R Cavailles****

**Ciment Lafarge, Saint Cloud Cedex, FRANCE*
***Lafarge Coppée Recherche, Viviers sur Rhône, FRANCE*

SUMMARY

When formulating high and very high strength concrete, one of the main difficulties is the choice of the mixture - superplasticizer. The aims are almost always : a maximal water reduction (with an acceptable cost), no rapid concrete stiffening, a good workability and rheology at the jobsite.

After the description of a few admixture - cement incompatibility cases, existent "grout methods" (from CANADA and FRANCE) are explained. They allow us to study the extract grout from the concrete (water, cement, fines, admixtures), which is much easier than concrete batch.

A "modified grout method" was developed and used it in regional H.S.C. (high - strength - concrete) formulations in FRANCE, and in a study of the compatibility of three different kinds of superplasticizers and several cements, which permitted us to determine the most adequate superplasticizer for each cement and the influence of the free lime and the soluble potassium amount.

RESUME

La principale difficulté que l'on rencontre lors de la formulation des bétons à hautes et à très hautes performances réside dans le choix du couple ciment - super-plastifiant. L'objectif est toujours d'obtenir : une réduction maximale de l'eau (à un coût acceptable), une prise retardée du béton, une bonne ouvrabilité et une rhéologie satisfaisante pendant le temps de mise en œuvre.

Après la description de quelques cas d'incompatibilité ciment-adjuvant, on présente les "méthodes des coulis" existantes (canadienne et française). Elles permettent d'étudier le coulis correspondant au béton (eau, ciment, fines et adjuvants), ce qui est plus aisé que d'étudier la gâchée de béton.

Une "méthode des coulis modifiée" a été développée, elle est utilisée en France pour la formulation des bétons régionaux à hautes résistances et pour l'étude de la comptabilité de trois familles de superplastifiants avec plusieurs ciments. Cette démarche a permis de déterminer le superplastifiant le plus efficace pour chaque ciment et l'influence des teneurs en chaux libre et en potassium soluble.

1 - INTRODUCTION

1.1 - Generalities

The use of concrete admixtures and of their utilization on sites have improved the quality and the possibilities of the concrete. But it also caused new problems, like rapid stiffening, flash set, quick workability loss, sticky appearance, segregation, ...
Several cases have been studied in keeping with admixture - cement incompatibility.

1.2 - Lignosulphonate based water-reducer

In 1984, on an important road concrete site in Brittany (FRANCE), pouring and casting difficulties have been recorded. Both the cement and the lignosulphonate based water-reducer admixture were in accordance to French standards, but mixed together in the concrete, stiffening occurred suddenly, after several months of road construction without any problem. As shown in [1], the lignosulphonate molecules, probably because of a selective adsorption effect on the calcium sulphates surface, decrease the solution rate and this reduces noticeably the SO_4^{--} concentration. *A fortiori* , if the anhydrite/gypsum ratio is a little bit higher than needed, the lack of quickly available sulphates (which form ettringite around the cement aluminates) brings about the beginning of the C_3A hydration, and therefore, the paste stiffening. DODSON and HAYDEN [2] have also confirmed the importance of the solution rate of ions SO_4^{--}

As another example, R. RANC studied the influence of the nature of sulphates on the rheology of mortars made with three cements (same Blaine fineness and same SO_3 percentage) mixed with a plasticizer admixture (0.6 % of cement weight) [4,5]. The main results are summed up in the table 1.

Cement sulphates nature	Optimized	Too much anhydrite	Too much hemihydrate
Rheology without superplasticizer	good	good	bad flash set
Rheology with superplasticizer	good	rapid stiffening	better

Table 1
Influence of rheology of mortars depending on cements

It shows that the mortar rheology is directly bound to the quantity of SO_4^{--} ions in the solution. This concentration depends on the cement and the admixture which modifies it. We must choose the adequate quality (nature) and quantity of calcium sulphates in order to avoid a sursaturation (which means a flash set), or a deficiency (which leads to rapid stiffening).

1.3 - High-range water reducers cases

Contrary to lignosulphonate based water-reducers, which at high dosage present harmful secondary effects (severe set retardation, high entrapped-air amount) [3], the superplasticizers (also called high-range water-reducers) can be used a lot more easily. They permit production of high strength concretes (H.S.C. : from 50 to 130 MPa in specific compressive strength) : for instance ; in France today, fluid H.S.C. are available in at least about seventy ready-mix concrete plants.
Anyway, in some cases, stiffening or rapid workability lost were observed, due to wrong superplasticizer/cement combination :

- In 1989, rheology problems occurred on the concrete (average compressive strength on 16 X 32 cm cylinders : 81 MPa) poured for a French bridge-arch. The use of two admixtures (a mixed naphthalene-melamine high - range water reducer and a gluconate retarder) theorically allowed a 20 cm slump concrete maintained for one hour. We tried to quickly elucidate the problem, working on cement pastes and mortars (faster trials than on concrete batches). We suggest to the jobsite another superplasticizer/retarder combination (melamine sulphonate formaldehyde condensate

and a phosphate) and it worked very well. At the end, the contractor decided to try a third couple (melamine and phosphate) and this also worked.

In a ready-mix plant in TOULOUSE, a slump loss problem (i.e. an early stiffening) was experienced with a high strength concrete during summer 89. The initial slump was 20 cm and after five minutes in the truck, the slump dropped to 8 cm. The mix contained a superplasticizer, which is a blend of sulphonated naphthalene and melamine condensates, and a HPR cement with an abnormal amount of anhydrite. This problem was solved by changing the cement (with a normal calcium sulphates addition), or by using different superplasticizers (two differents kinds of melamine based admixtures suited). So, the H.S.C. maintained a good workability for one hour.

2 - THE "GROUT METHODS"

2.1 - The French L.C.P.C. method

The French national highways and bridges laboratory (L.C.P.C.) proposed in 1989 a new method for high strength concrete formulations : the grout method [6]. Starting from a regional optimized concrete formulation, this new approach proposes to extract the grout (cement, water, admixtures), then to improve its strength keeping its fluidity and finally to incorporate this new grout (with less water, the optimal superplasticizer dosage, eventually silica fume) in the granular matrix, in order to obtain a higher strength concrete with nearly the same workability.

The great advantage of this method is to lighten the laboratory trials when formulating a H.S.C., because it is a lot easier to mix grouts and measure their fluidity than batch concretes and measure their slump. This is really interesting when the formulator has the choice between 3 or 4 cements and 5 or 6 superplasticizers (eventually coupled with a retarder admixture ...)
The procedure is to mix the grout in a mortar mixer and to measure the flow time in a Marsh cone (the adjutage is chosen in order to measure fluidity times between 5 and 15 secondes).

2.2 - The canadian Sherbrooke University method

P.C. AITCIN has developped a new apparatus, called the Rheopump, which, in association with a bentonite cone (diameter : 5 mm), permits us to make grouts energetically, and therefore, to appreciate the "rheological reactivity" (which means the water and superplasticizer demand) of a cement mixed with a superplasticizer, as well as the saturation point, i.e. the superplasticizer dosage (% in solids of cement weight) after which any additional amount does not contribute to improve the grout fluidity. Like the previous method, the Rheopump method can be used to determine the influence of different cements and superplasticizers on the grout fluidity during time, the optimal dosage of superplasticizer, and to help the concrete formulations.

2.3 - The modified grout method

2.3.1 - Possibilities of improvement of the existent methods - The two previous methods were the departure points of a "modified grout method". We thought the grout must be energically mixed, so as to replace the "grinding" and dispersing effect of the aggregates in the concrete. We decided to use a simple high turbulence mixer (about 3000 rpm).
The Marsh cone (adjutage : 10 mm) is of common use in FRANCE, so we used it with its nominal adjutage. Smaller diameters lead to too long fluidity times (dispersion risk).

The superplasticizers have an effect on all fine particles, including on the finest sand particles. The quantity of superplasticizer adsorbed on the fine sand particles can influence the saturation point, and therefore the workability of the concrete. This is why we propose adding to the normal grout (cement + water + admixtures) the finest particles of the sand (and possibly of the crushed stone), that is particles finer than 315 µm.

2.3.2 - <u>The modified grout method procedure</u> - For the Ready-Mix Concrete Division, eight regional H.S.C. were studied. For each region, a representative sand (crushed limestone in the south, or natural siliceous around Paris, for instance), the local high strength cement and four superplasticizers of the market were chosen.
The study objectives were to determine the best cement/superplasticizer couple in a given region and to optimize the superplasticizer amount (good workability of the H.S.C. during 1 hour).

Taking an existent H.S.C. formula or calculating a new H.S.C. composition (by french graphic Faury's method), the reference H.S.C. is a good workable 20 cm slump concrete, containing 1.5 % (in % of cement weight which is 425 kg/m^3) of one of the four studied superplasticizer, called RESINE GT.
From the reference H.S.C., we extract : the cement, the sand fine particles (under 315 µm), the useful water (total water minus aggregates absorbed water) and the superplasticizer (the water amount brought by the admixture is substract from the batch water).

The grout is mixed with a high turbulence vertical mixer (at 2800 r.p.m.) during 3 minutes, according to a special introduction order.1.9 liter of the so-prepared grout is poured in the Marsh cone and the flow time for the first liter is measured. For each superplasticizer (one modified melamine resine GT, one pure melamine and two naphthalene-melamine blend based superplasticizers), the flow time evolutions (just after mixing and one hour later) were measured for different increasing admixture dosages (but with a constant water content, the superplasticizer water is substract from the grout batch water).

The curves giving the flow time in terms of superplasticizer percentage of solids shows a saturation point. After this, any over dosage of superplasticizer does not lead to a better grout fluidity (at constant total water content), i.e. to a more workable concrete.
For instance, for the PARIS H.S.C. as shown in figure 1, the saturation points of the four admixtures are different. The modified melamine based superplasticizer (MM) presents the best fluidity (lowest flow time) with the smallest saturation dosage (0.75 % of solids, that is 2.5 % of liquid admixture of cement weight).

Figure 1 : PARIS H S C GROUT FLOW TIME

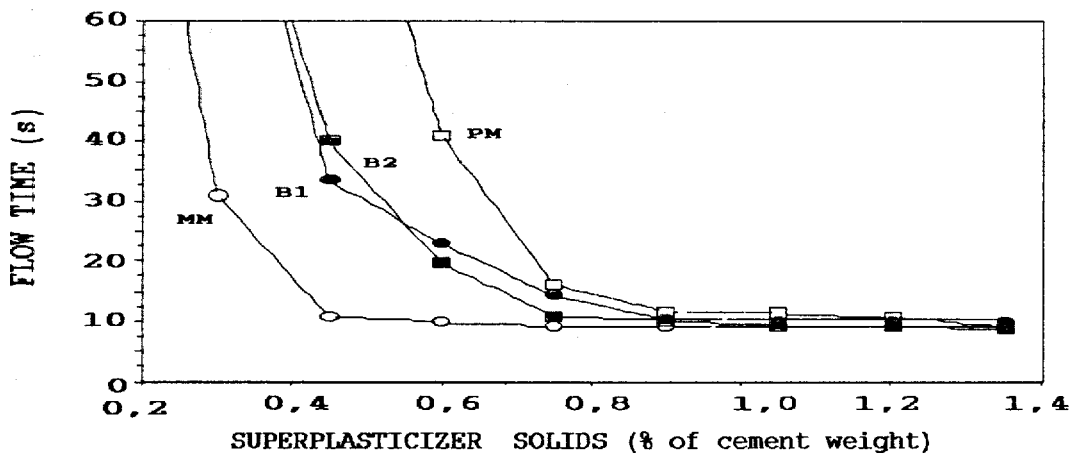

The optimized H.S.C. composition contains, for each of the eight regions, the most efficient superplasticizer at the saturation dosage. The total water content is decreased to obtain a 20 cm slump concrete.
These study results are now applied on the ready-mix concrete plants, corresponding to the studied regions.

In one case (TOULOUSE region), we investigated the influence of the silica fume on the flow time. It was shown that, at low dosage the grout with silica fume is less fluid, but for dosages greater than 0,9 % of modified melamine superplasticizer, it is the opposite.

In another case (LYON region), we found again with the grout method,that a rheological problem discovered on the concrete plant during H.S.C. trial batches, was due to the nature of sand (see table 2).

Sand nature	Concrete workability	Grout flow time at saturation	Saturation dosage (solids)
Rhône river	very good during 1 hour	10 s.	0,6 %
Allier river (with muscovite)	rapid stiffening	14,5 s.	0,75 %

Table 2

3 - STUDY OF THE COMPATIBILITY BETWEEN 3 DIFFERENT KINDS OF SUPERPLASTICIZER AND 18 CEMENTS

3.1 - Aim of the grout trials

For most of the ordinary Portland cements produced in FRANCE by the company, it was very interesting (because of the high-strength concrete development policy) to know their potential to be fluidified, what kind of superplasticizer is t,he most adapted, and tc try to find correlations between these potentials (flow time, saturation point, incompatibility cases, ...) and the main cement characteristics.

3.2 - Investigation method

For each of the 18 ordinary Portland cements and for 3 differents kinds of commercialized superplasticizers (a modified melamine sulphonate formaldehyde condensates (MM), a naphthalene sulphonate formaldehyde condensate (N), a blend of melamine and naphthalene (B1)). The modified grout method was practised, using the same natural siliceous 0 - 0.315 mm sand.
First, the water quantity was determined in order to get a 20 +/- 1 seconds flow time grout with 1.5 % of the melamine based superplasticizer MM (of cement weight ; i.e. 0.45 % of solids of cement weight).
Then, increasing the superplasticizer amount but keeping the same total water content, the flow times were measured in order to find the saturation point for the superplasticizer MM with each cement. The same operations have been done again for the two others admixtures to find their saturation point.

3.3 - Results and discussion

First, as shown in figure 2, the water demand in order to obtain a flow time of about 20 seconds with 1.5 % of melamine superplasticizer MM is very variable from one cement to another.

Figure 2 : WATER/CEMENT RATIOS for a flow time of 20 s.

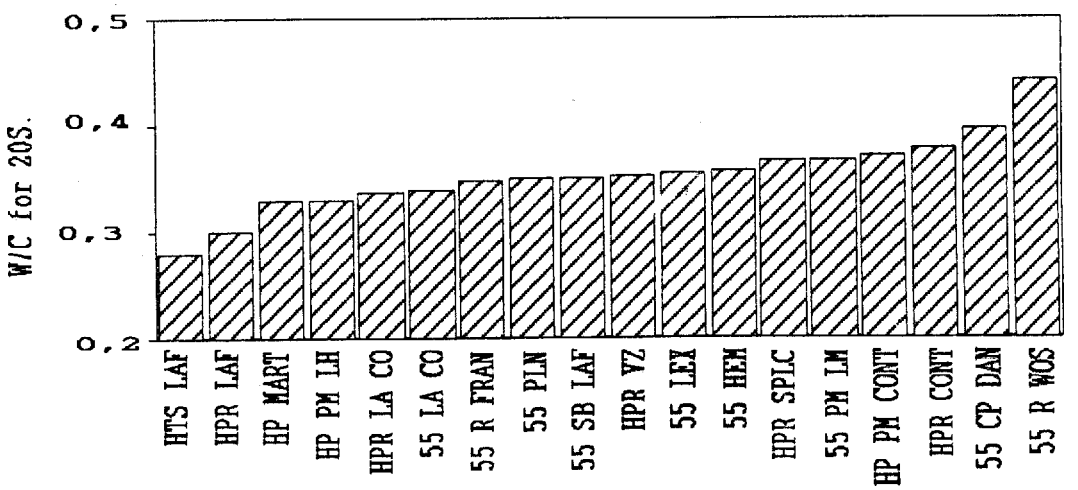

On these 18 cements, correlations between this water demand and the main cement characteristics were determined. It was found that the free lime and the soluble potassium amounts play an important role (see figures 3 and 4). The smaller they are, the easier the cement fluidification is.

Figure 3

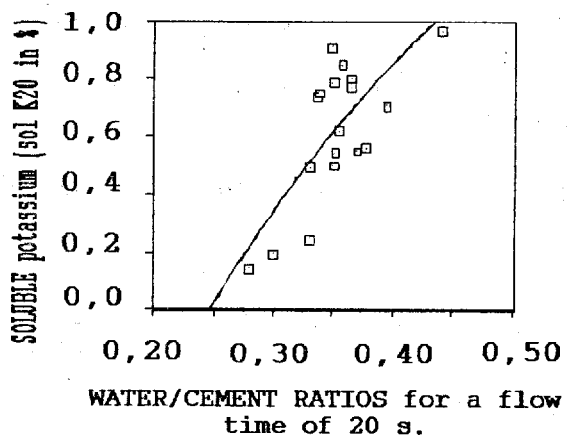

Figure 4

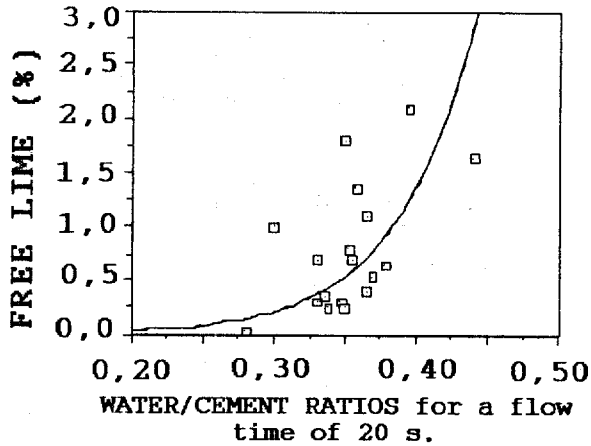

It was interesting to confirm the "flocculating" character of the free lime and not to be able to find a significant correlation with the aluminate phases of the cement (in the modified melamine case),which are said to have a negative influence upon the fluidification.

For each of the 3 superplasticizers and each of the 18 cements, we fixed the saturation points. As known on the jobsites or in the prefab plants, the behavior of the different cements is very variable (saturation dosage, saturation flow time, preference for one or another superplasticizer,...).

For instance, we can see in figure 5 the fundamental behavior differences, on the cement CPA HP MARTRES, between the three kinds of superplasticizers. The modified melamine sulphonate formaldehyde condensate is really the most adapted admixture to this cement. Here, the naphthalene superplasticizer gave bad results. On other cements, it was the best.

Figure 5 : FLOW TIME CPA HP MARTRES

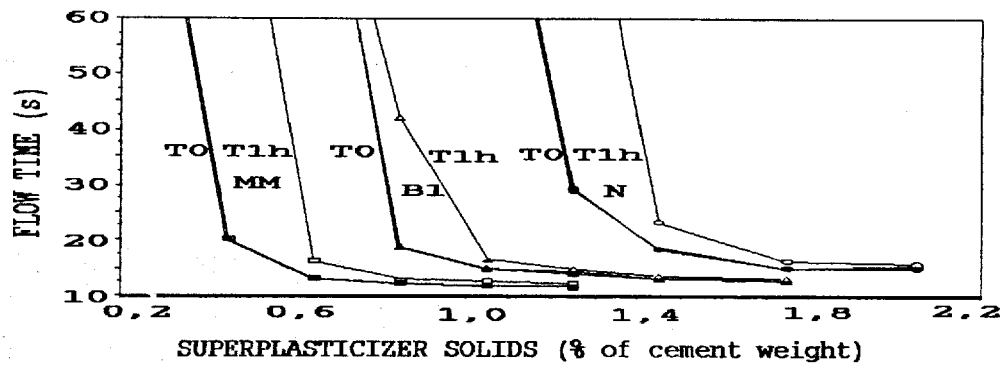

A direct application has been made on concrete batches, with the same water quantity (grout water plus aggregates absorbed water).The figure 6 shows a very good correlation between the grout flow times and the slumps values. The optimal superplasticizer dosage must be about 1 % of solids, this means 3.3 % of liquid melamine superplasticizer (in % of cement weight).

Figure 6 : FLOW TIME VS SLUMP TEST HP MARTRES

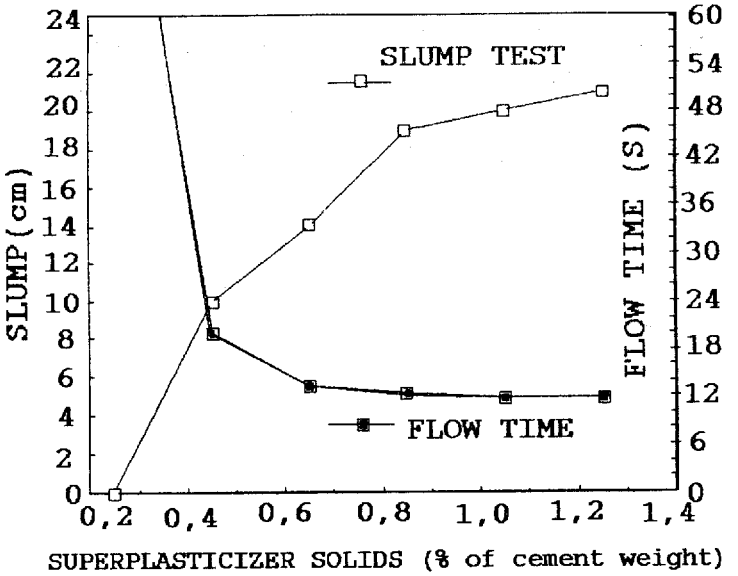

4 - CONCLUSION

The cement/admixture incompatibility is a well-known problem. Numerous cases were studied in our laboratories and elsewhere. In order to avoid this kind of difficulties and to optimize the choice and the dosage of the superplasticizer for the production of high-strength concrete, a method was developed, starting from two existent grout methods. This modified grout method was used for several regional direct applications and for a more theorical study of the compatibility of 3 kinds of superplasticizers and 18 cements,a signification influence of the free lime and the potassium amount contained in the cement was observed.

5 - REFERENCES

[1] PAILLERE A.M. ; ALEGRE R. ; RANC R. ; BUIL M.
Interaction entre les réducteurs - plastifiants et les ciments -Bulletin de liaison du laboratoire des Ponts et Chaussées n° 136 Mars - Avril 1985

[2] DODSON V.H. ; HAYDEN T.D.
Another look at the Portland cement/chemical admixture incompatibility problem - Cement, Concrete and Aggregates, vol. 11 n° 1 - Summer 1989

[3] AITCIN P.C. - Les superplastifiants : des réducteurs d'eau pas comme les autres - Annales I.T.B.T.P. - Mars - Avril 1989

[4] RANC R. - Interactions entre les plastifiants et les ciments. Ciment, bétons, plâtres et chaux n° 782 - Janvier 1990

[5] AITCIN P.C. - BAALBAKI M. - La compatibilité ciment portland/adjuvant - Conférence sur les superplastifiants - Université de Sherbrooke (Canada) Décembre 1990

[6] de LARRARD F. - PUCH C. : La méthode des coulis - Colloque sur les bétons à hautes performances - PARIS - Mars 1989

[7] HANNA E. ; LUKE K. ; PERRATON D. ; AITCIN P.C. - Rheological behavior of Portland Cement in the presence of superplasticizer. Third CANMET international conference - OTTAWA 1989

[8] BAALBAKI M. - La détermination du dosage de saturation - Conférence sur les superplastifiants - Université de Sherbrooke (Canada) Décembre 1990

INFLUENCE OF CEMENT ON THERMAL CRACKING OF CONCRETE AT EARLY AGES

R Springenschmid and R Breitenbücher

Institute for Building Materials, Technical University, Munich, GERMANY

SUMMARY

If the deformations due to temperature changes and/or shrinkage are prevented in concrete members, restraint stresses are caused which can result in cracking. To reduce the risk of cracking the concrete constituents must be selected carefully and the concrete mix must be optimized. For this purpose the influence of cement on thermal cracking of concrete at early ages was studied in laboratory tests with the cracking frame. Investigations have shown that not all cements with a low heat development lead to a low cracking temperature. OPC with low cracking susceptibility normally are ground relatively coarse and contain little alkali and, related to C_3A, much of sulfate.

Werden Verformungen von Betonbauteilen infolge Temperaturbeanspruchung und/oder Schwinden behindert, entstehen Zwangsspannungen, die bei Überschreiten der Zugfestigkeit zu Rissen führen können. Um die Rißgefahr zu vermindern, müssen die Betonausgangsstoffe entsprechend gewählt und die Betonzusammensetzung optimiert werden. Um den Einfluß des Zementes auf die Reißneigung von jungem Beton zu untersuchen, wurden Versuche mit dem Reißrahmen durchgeführt. Die Untersuchungen zeigen, daß nicht alle Zemente mit einer geringen Wärmeentwicklung zu einer niedrigen Rißtemperatur führen. Portlandzemente mit geringer Reißneigung sind meistens grob gemahlen, besitzen einen niedrigen Alkaligehalt und, bezogen auf den C_3A-Gehalt, einen hohen Sulfatgehalt.

1 Introduction

In the absence of external forces, concrete members may crack as early as a few days or weeks after pouring. Such cracks are caused by stresses which are formed when the deformations due to temperature changes or shrinkage are restrained. Especially in thick members, the heat of hydration is thus particularly important. This not only has to be taken into consideration for mass concrete but also for members of more than about 30 cm in thickness, e. g. in concrete walls or tunnel linings [1, 2]. In such cases the temperature maximum is reached about one day after pouring. The concrete then requires about one week to cool down to the ambient temperature. If, during cooling, the restraint (tensile) stresses reach the tensile strength, which is still low, cracks occur.
For solving these problems, up till now low-heat cements have been used. However, by this means only the temperature increase is lowered. To reduce the risk of cracking, more thought must be given to the restraint stresses, which actually cause the cracks.

The development of restraint stresses in concrete at early ages is quite different from that of a linear elastic material without any relaxation. After pouring, the temperature remains constant for some time (Fig. 1, stage I). Following this period the temperature increases due to the onset of hydration and the attendant heat evolution (stage II). In this stage no compressive stresses are produced, since the concrete can still deform plastically. After about 3 to 6 h, compressive stresses are produced due to an increasing modulus of elasticity and further heat evolution (stage III), but these stresses are still reduced by the relatively high relaxation. When the temperature maximum is exceeded, the concrete temperature falls and the residual compressive stresses decrease, because the relaxation is still high and the modulus of elasticity is already higher than during the first heating (stage IV). Due to this the concrete reverts to a stress-free condition at a temperature which is far above the starting temperature and only a few degrees below the temperature maximum. The concrete temperature at this time is called the zero stress temperature, T_Z. On further cooling, relatively high tensile stresses develop (stage V), because the modulus of elasticity has reached a large value. When these tensile stresses exceed the concrete tensile strength, cracking occurs. The temperature at this time is called the "cracking temperature" T_C. Due to the continously increasing modulus of elasticity and relaxation an exact calculation of thermal stresses at early ages greatly depends on realistic assumptions, and calculated values usually show a high disagreement with the experimental data from field and laboratory investigations /3/.

2 The Cracking Frame: A New Test Device

For the investigation of thermal cracking in young concrete it therefore seems more appropriate to make model tests in the laboratory. For this purpose the "cracking frame" was developed at the Institute for Building Materials at the Technical University of Munich /2/.
The cracking frame (Fig. 2) consists of two steel cross-heads, and two massive steel bars with an extremely low coefficient of thermal expansion. Fresh concrete is placed and compacted directly into a formwork which is situated between the two cross-heads. Due to the stiffness of the steel bars longitudinal deformations of the concrete are restrained to a great extent during the whole hardening process. The concrete remains in the frame until a transversal crack occurs. In order

to prevent any loss of water the concrete is covered with a polyethylene foil.

Due to the large cross-section of the specimen (150x150 mm²) and the thermal insulation of the formwork the concrete temperature increases almost adiabatically in the first hours and reaches a maximum after 16 to 22 hours.
The longitudinal stresses in the concrete can be indirectly measured, since the steel bars deform only elastically by a very small amount due to the concrete stresses. These deformations can be measured continuously with strain gauges on the steel bars and the longitudinal restraint stresses developing inside the concrete throughout the test, are determined therefrom.

The temperature and stress development in the test specimen is similiar to that shown in Fig. 1. If the concrete has not cracked after attaining the ambient temperature after 4 days the specimen is further cooled artificially at the rate of 1 ° C per hour. When the tensile stresses exceed the concrete tensile strength a sudden drop in the restraint stresses indicates that a transversal crack has formed. The "cracking temperature" (T_C) characterizes the cracking tendency of the concrete due to thermal stresses in a much better way than the heat of hydration used until now. All the parameters which influence thermal cracking, including the tensile strength, are contained in the cracking temperature. The lower the cracking temperature, the less the cracking tendency of a concrete mix and the less the risk of cracking on site.

3 Tests with Different Cements

In order to quantify the influence of cement on the cracking tendency of concrete, commercially available OPCs and slag cements from different German plants were tested in the crakking frame under identical conditions. The cement content was 340 kg/m^3, and w/c-ratio 0.48. Crushed aggregates with a maximum size of 32 mm were used. The fresh concrete temperature was 20 °C.

Slag cements which are often used as low-heat cements for mass concrete, lead to a relatively small temperature rise during hydration and also to small tensile stresses. However, in some concretes with slag cements a higher cracking temperature was found than in concretes using OPC from the same plant with the same clinker /4/. This is connected with a very slow development of tensile strength in such concretes. Therefore the crack susceptibility of a slag cement is determined mainly by the compositions of the clinker and the slag used.

The cracking temperature for samples with OPC from 17 different plants varied over a very wide range, 6 °C to 22 °C. This could well be expected on account of the difference in heat evolution between the cements (Fig. 3). The temperature in the specimen rose much more, when the cement was ground very fine and/or had a high content of tricalcium aluminate and alkalies. But even this can only partly explain the wide range in the measured cracking temperatures. Also some cements with nearly identical temperature curves led to quite different restraint stresses (Fig. 4).
It can be assumed that this difference in the stresses also points to the presence of additional non-thermally induced contractions or expansions /2, 5/. Swelling in the restrained state causes additional compressive stresses which lead to a decrease in the zero-stress

temperature and hence a reduction in the thermally induced tensile stresses.

To verify the existence of such non-thermally induced deformations, additional tests with the cracking frame were carried out under isothermal conditions, i. e. keeping the temperature of the specimen constant at 20 °C throughout the test. The mix composition of the concrete was the same as for the semi-adiabatic tests mentioned earlier. In one concrete which contained OPC from plant A, tensile stresses under isothermal conditions developed to some extent, probably due to chemical shrinkage (Fig. 5 a). This cement gave a very high cracking temperature of 22 °C in the semi-adiabatic cracking frame test. On the other hand, in concrete with OPC from plant S, compressive stresses were formed under isothermal conditions, such as could arise only from the restraining of an expansion (Fig. 5 b). This concrete cracked at only 6 °C in the semi-adiabatic test, correlating with a low cracking tendency. Such non-thermally induced expansion can be attributed partly to the formation of ettringite during hydration. The sulphate (SO_3) content is decisive for the formation of ettringite, but, to some extent, it is also needed for regulating setting. The extent of this depends, among others, on the content of alkalis and the fineness of the cement /6/.

In view of these considerations a correlate was attempted between the cracking temperature and the other factors as mentioned above of the cement used. Following is the equation so developed /2/:

$$T_C = 22{,}3 - 0{,}143 \cdot \frac{SO_3}{\dfrac{0{,}1149 \cdot C_3A + 1{,}872 \cdot \text{sol A}}{(d' \cdot 0{,}69^{1/n})^2} \cdot C_3A} \qquad (2)$$

where T_C = cracking temperature (°C), SO_3 = sulphate content (%), C_3A = content of tricalcium aluminate (%), sol A = content of soluble alkalis (%) (= sol Na_2O + 0.658 . sol K_2O), d' = position parameter in the RRSB granulometry diagram (µm), and n = slope in the RRSB granulometry diagram (-).
Only the soluble alkalis are taken into account since these alone can bind the sulphate. Figure 6 shows the correlation between the calculated values of cracking temperature and those determined in the cracking frame; the correlation coefficient is 92 %.
Hence it follows that for a low cracking tendency of the concrete the cement should have a low alkali content and, related to the C_3A content, a high sulphate content. Furthermore, it should be ground relatively coarsely.

4 Cements with High Sulphate Content

It therefore appears that the crack susceptibility of a cement can be reduced simply by increasing its sulphate content. However, further investigations showed that this is only true for cements with a low alkali content. In high alkali cements it was not possible to lower the cracking temperature by increasing the sulphate content, because in this case the formation of ettringite is reduced as was also observed in other investigations /6/.
However, in low alkali cements as well, the sulphate content has to be

limited. When the sulphate content is too high, damage to the microstructure can occur due to the formation of excess ettringite.

5 Conclusions

I). Cracking frame tests predict the overall cracking behaviour of a concrete mix and the quantification of the influence of all the parameters of the concrete mix (including temperature).
II). The cracking tendency of a concrete can be characterized by its cracking temperature.
III). Cements with a low susceptibility to thermal cracking are OPCs or blended cements with a low cracking temperature in a semiadiabatic standard test. Usually, cracking temperatures of less than 10 °C are specified.
IV). Due to a slow development in tensile strength and the influence of clinker and slag compositions not all slag cements with a low heat development necessarily give a low cracking temperature.
V). OPCs with a low cracking susceptibility are normally ground relatively coarse and contain little alkali and, related to C_3A, much sulphate.

References

/1/ R. Springenschmid: Die Ermittlung der Spannungen infolge von Schwinden und Hydratationswärme im Beton (Determination of stresses due to shrinkage and heat of hydration in concrete). Beton- und Stahlbetonbau 79, 10, 263-269 (1984).
/2/ R. Breitenbücher: Zwangsspannungen und Rißbildung infolge Hydratationswärme (Restraint Stresses and Cracking due to heat of hydration). PhD thesis, Technical University Munich, 1989.
/3/ R. Springenschmid, R. Breitenbücher, P. Ballardini: Vergleich zwischen Berechnungen und Messungen von Zwangsspannungen im jungen Beton (Comparison of calculated and measured restraint stresses in concrete at early ages). Beton- und Stahlbetonbau 83, 4, 93-97 (1988).
/4/ Springenschmid, R., Breitenbücher, R. and Kussmann, W.: Cracking tendency of concretes with blastfurnace slag cements due to outflow of heat of hydration. Concr. Precasting Plant Technol. 53 (12) (1987) 817-821.
/5/ R. Breitenbücher: Investigation of thermal cracking with the cracking frame. Materials and Structures 23, 172-177 (1990).
/6/ I. Jawed, J. Skalny: Alkalies in Cement: A Review. Part II: Effects of Alkalies on Hydration and Performance of Portland Cement. Cement and Concrete Research 8, 37-52 (1978).

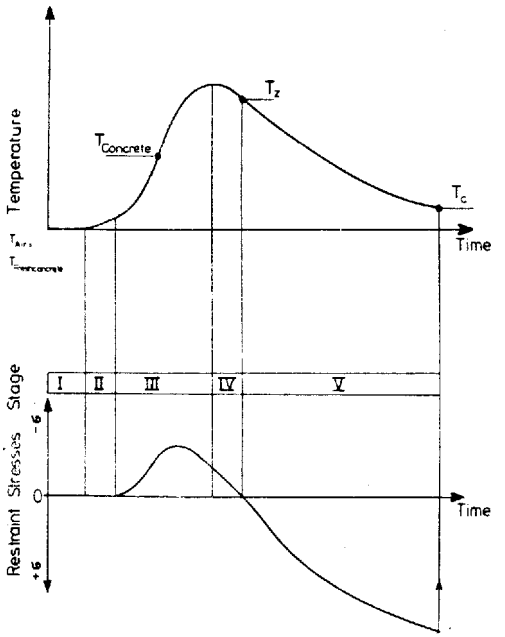

Fig. 1: Temperature and stress development in restrained concrete members during hydratation. $T_{air} = T_{fresh\ concrete}$

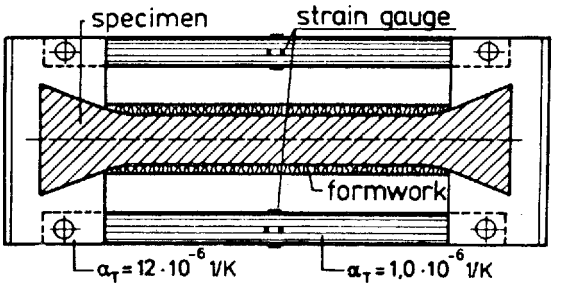

Fig. 2: The cracking-frame

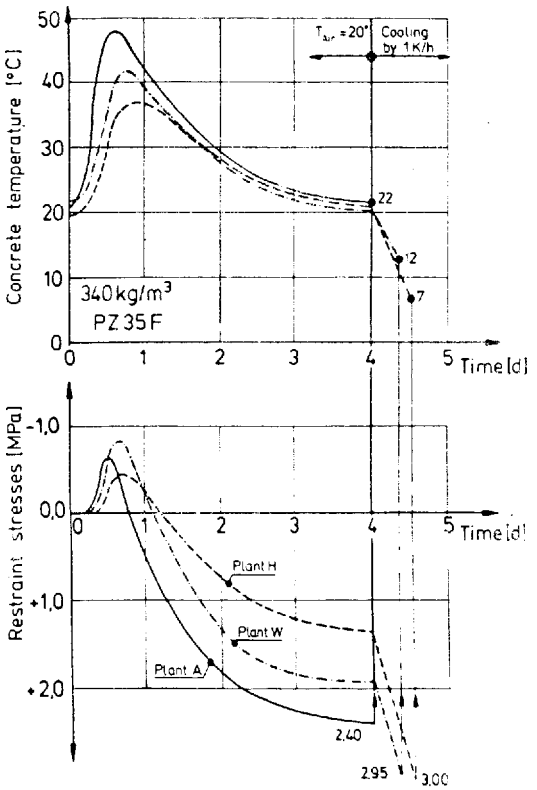

Fig. 3: Temperature and stress curves of concrete with cement (OPC) from different plants.

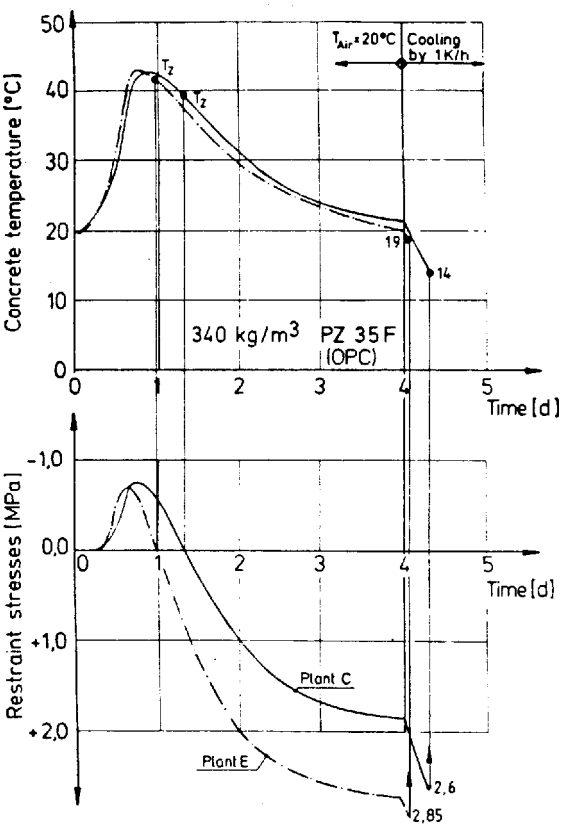

Fig. 4: Differences in the restraint stresses at nearly identical temperatures of concrete with cements from two plants

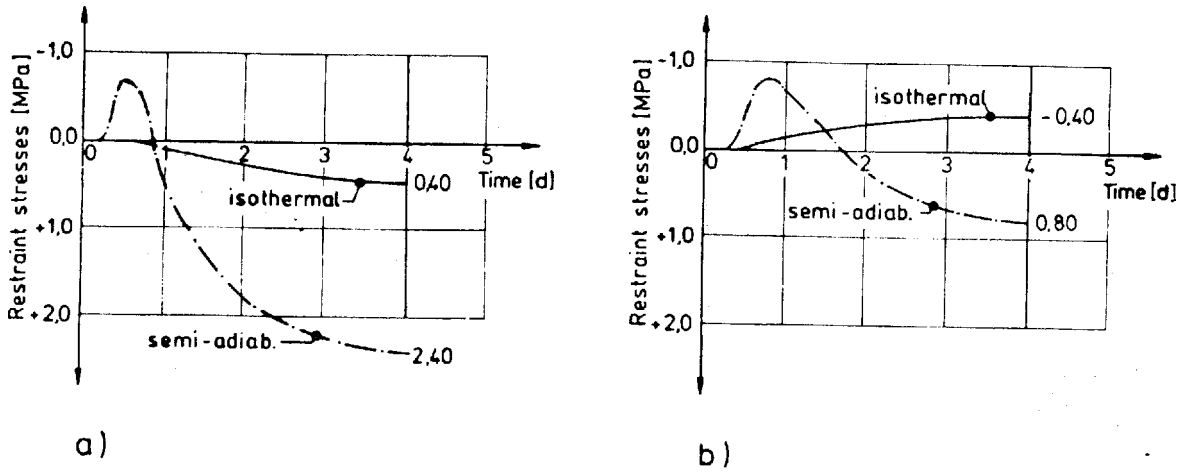

Fig. 5: Restraint stresses measured with the cracking frame under isothermal and semi-adiabatic conditions: a) with OPC from plant A b) with OPC from plant S

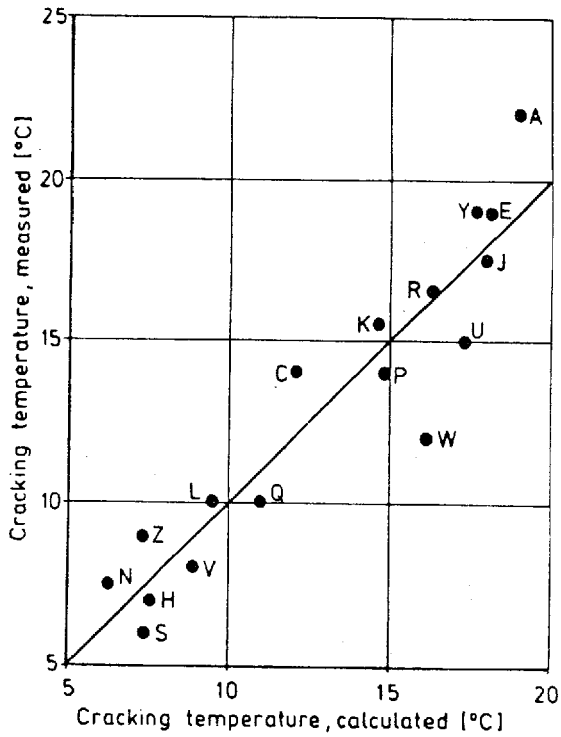

Fig. 6: Comparison of calculated and measured cracking temperatures

RETARDED EXPANSION FOR COOLING SHRINKAGE COMPENSATION IN MASS CONCRETE

Wang Yuqing and Lou Zonghan

Department of Materials Science and Engineering, Zhejiang University, Hangzhou, P.R. CHINA

ABSTRACT

In order that the retarded expansion of concrete caused by periclase hydration in cement paste is used for cooling shrinkage compensation in mass concrete, the hydration rates of clinker periclase in cement paste and rates of retarded expansion at different curing temperature(20℃,50℃,70℃ and 90℃), effect of retarded expansion on strength and pore structure of hardened cement paste were studied. Increase in curing temperature, clinker periclase hydration rate and retarded expansion rate increase. At 50℃, the retarded expansion develops continuously within half one year. Curing temperature changes around 50℃, the final value of expansion of cement made of clinker containing MgO 5.0 wt. % changes slightly, linear expansion is about 0.1%. Retarded expansion caused by clinker periclase has no harmful effect on strength and pore structure of cement if the amount of MgO in clinker is controlled, for example, 5.0 wt. %. A cement exhibiting controlled retarded expansion and high strength can result with the use of 5.0 wt. % MgO in clinker. The retarded expansion develops relatively fast at the temperature inside mass concrete and approximately keeps in step with the cooling shrinkage in mass concrete.

INTRODUCTION

Temperature inside mass concrete, caused by cement hydration heat, can be over 50℃. Concrete shrinks when the temperature decline to environmental temperature outisde, i. e. cooling shrinkage. Cooling shrinkage is the main reason for crack of mass concrete [1]. It is well known that expansive cement have the beneficial effect of compensation of shrinkage. Studies on the volume deform of mass concrete and practical use of low-heat micro-expansion cement in dam pouring have indicated that if concrete itself develops retarded expansion, i. e. expansion develops after cement hardened, and the development of expansion keeps in step with the rate of cooling shrinkage of mass concrete, compensation is more effective [2][3]. On the other hand, it is also well known that the presence of magnesia can cause the retarded expansion of set mortors and concretes, so it is considered that the retarded expansion caused by clinker periclase hydration be used for compensation of mass concrete cooling shrinkage. In order to verify the validity, the hydration rate of clinker periclase and the rate of retarded expansion at different curing temperature, and the effect of retarded expansion on strength and pore structure of hardened cement paste were studied.

EXPERIMENTAL

Materials

The clinkers were synthesized by calcining mixtures of high magnesia limestone and other raw materials in electric resistance furnace at 1385℃ for 45 mins, and then cooled in air. The chemical composition of the clinkers is shown in Table 1. (free CaO<1. 0%)

Table 1. Chemical composition of clinkers (wt. %)

Samples No.	MgO	SiO_2	Al_2O_3	Fe_2O_3	CaO
Cement 1	5. 08	21. 77	5. 06	5. 14	62. 41
Cement 2	0. 79	21. 24	5. 66	5. 63	65. 26

From X-ray diffraction and optical microscopy, there exists free MgO(periclase) in clinker 1, the diameter is about 3—5 μm[4]. Clinker 2 has no free MgO.

Cements were prepared with clinker 96% + gypsum 4% and ground to a Blaine specific surface about 310m^2/Kg. the amount of SO_3 in cement was 1. 8% by weight.

Preparation and Testing

Expansion tests——Sufficient materials of each cement to make twelve 20×20×250mm prisms was weighed out, mixed with 28% by weight of distilled water, and placed in brass moulds. The moulds were stored for 24 hours over water at 20℃ and 100% humidity. After this time the prisms were demoulded, measured and then stored in a water bath at 20℃, 50℃, 70℃ ad 90℃ respectively. Three prisms were tested

in one temperature level. At suitable intervals the prisms were removed from the bath, surface dried, measured and then replaced.

Compressive strength tests——Compressive strength tests were made on 20×20×20mm neat cement paste cubes, cured at 50℃ in water.

X-ray diffraction and DSC analysis——X-ray diffraction and DSC analysis were carried out on the hydration samples of cement 1 cured for different ages at 20℃, 50℃, 70℃ and 90℃ respectively.

Pore analysis——Pore analysis were carried out on the hydration samples of both cement 1 and 2 cured at 50℃ in water by mercury porosimeter.

RESULTS AND DISCUSSIONS

Clinker periclase hydration

X-ray diffraction diagrams are shown in Fig. 1. Clinker periclase hydrates very slowly at 20℃. After one year, periclase hydrates little. However, increasing in the curing temperature, hydration rate increases markedly. Lot of periclase have transformed into brucite only after one month at 50℃, and periclase have hydrated completely within one year. Increasing in curing temperature further to 90℃, periclase hydrates even more quickly.

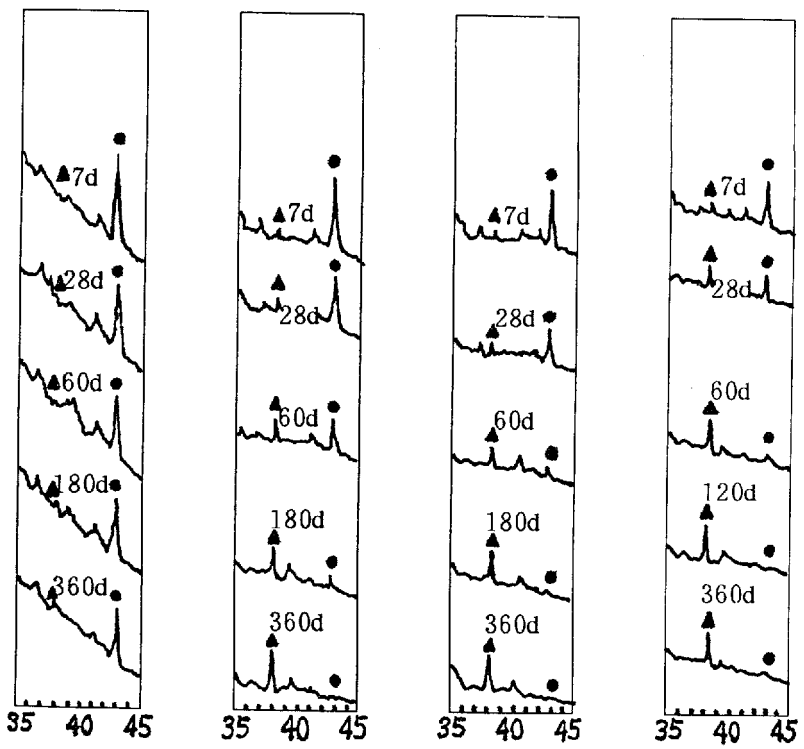

FIG. 1. X-ray diffraction patterns of cement 1

In Fig. 2, the DSC curves for cement 1 cured at different temperature are shown. At 20℃, brucite are formed little after one year, whereas the amount of formed brucite is large at 50℃ just after one month. It substantially confirms the results of X-ray diffraction analysis.

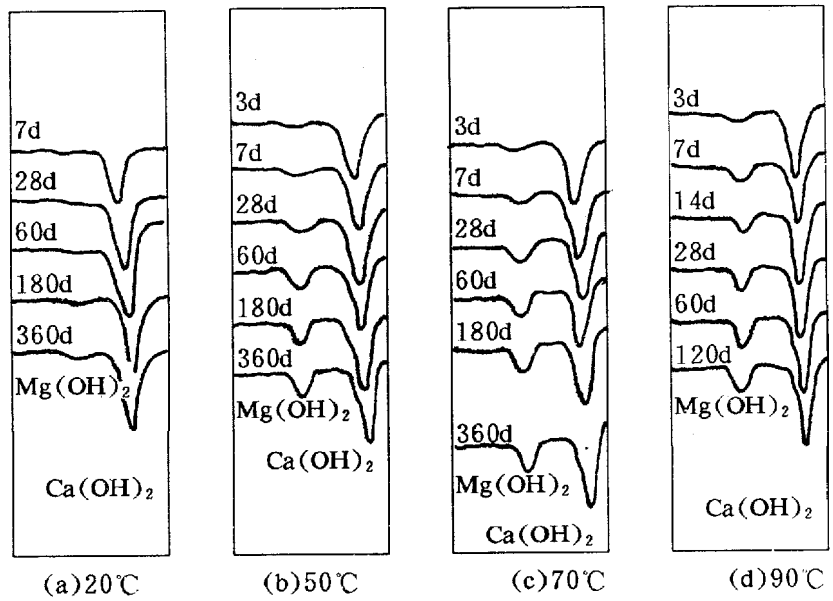

FIG. 2. DSC curves for cement 1

Based on X-ray diffraction and DSC, the rate of periclase hydration can be obtained. The results of X-ray diffraction analysis have indicated that periclase have hydrated completely in cement 1 after one year at 50℃ or 120 days at 90℃. So it is assumed that the area of brucite dehydratd peak of cement 1 cured 50℃ one year or 90℃ 120 days on DSC represents hydration ratio 100 percent. Then from the area of brucite dehydrated peak, the ratio of periclase hydration can be calculated for cement 1 cured at different temperature for different ages.

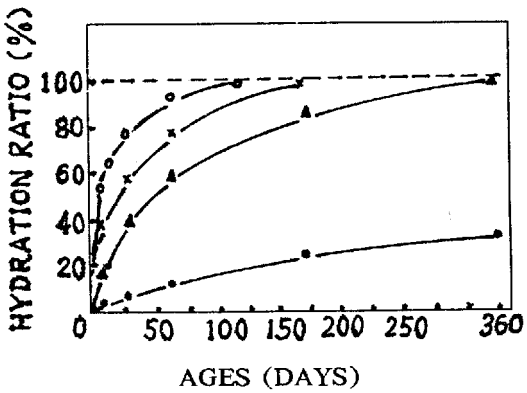

FIG. 3 Clinker periclase hydration rate in cement 1

•——• 20℃ ×——× 70℃

▲——▲ 50℃ ○——○ 90℃

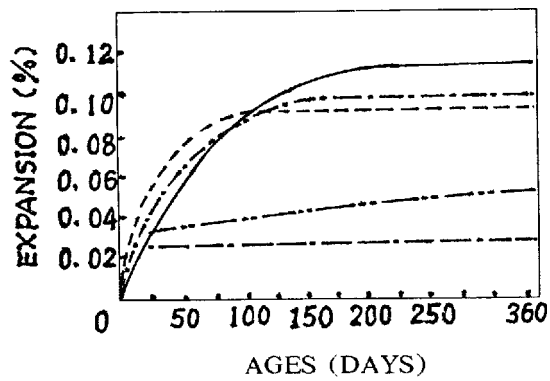

FIG. 4 Expansion of cements cured in different temperature water bath

- - - - cement 1. 20℃, ——— cement 1. 50℃,

—·—·— cement 1. 70℃, – – – cement 1. 90℃

—·—·— cement 2. 50℃

Fig. 3 shows the ratio of periclase hydration as a function of ages for cement 1. At 20℃ the ratio is about 30 percent after one year, whereas, the ratio reaches 40 percent for one month and 80 percent for half one year. It indicates clearly that clinker periclase hydrates relative quickly and most periclase have hydrated within half one year. It implies that the "expansive force" caused by clinker periclase will occur relatively quickly and develop mainly in those ages at 50℃. It is the ages that cooling shrinkage of mass concrete occurs.

Retarded Expansion

Fig. 4 shows the retarded expansion of cement, Cement 2 is no expansion after cement hardened. In the contrast, Cement 1 expands continuously. It indicates that retarded expansion develops when the cement contains periclase.

It can be seen from Fig. 4 that the rate of expansion increases with the curing temperature. At 20℃, the rate of expansion is more slow, after one year little value is obtained. However, at 50℃, expansion develops relatively fast, after approximately half one year, 0.1% linear expansion is obtained, and expansion reaches constant value. Temperature even higher, at 90℃, expansion stops in three months. Compared expansion rate with periclase hydration rate, it indicates that the rate of retarded expansion approximately keeps in step with the rate of periclase hydration.

It can be seen also from Fig. 4 that although the rate of expansion of cement 1 is different cured at 50℃, 70℃ and 90℃, the final value of expansion change slightly, the value is about 0.1%. The reason may be that among the temperature range, only expected effects of increasing the curing temperature are increasing in the rates of hydration and strength development and slight changes in the composition of the tobermorite gel. The results suggest that curing temperature changes around 50℃, the final value of expansion, related to complete periclase hydration, be relatively stable. So, at the temperature inside mass concrete (about 50℃), the retarded expansion is relatively stable, and its effect of compensation for cooling shrinkage in mass concrete is stable.

The retarded expansion develops relatively quickly at relatively early ages, and slowly for longer ages. Correspondingly, inside mass concrete, temperature decreases quickly early and slowly later. So cooling shrinkage develops quickly early and slowly later. From the point of view, the retarded expansion caused by clinker periclase hydration is sufficient for compensation of mass concrete cooling shrinkage. Furthermore, the retarded expansion has benefical effect on volume stablization of mass concrete.

Compressive strength and pore structure

The results of compressive strength tests are given in Table 3. Cement 1 develops strength steadily both at the ages of retarded expansion developing quickly (say 28 days and 60 days) and at the end of expansion. Cement 1 develops strength similarly to Cement 2 at each curing age.

The results of pore analysis are shown in Table 4. There is no marked difference in pore volume between Cement 1 and Cement 2. The results are coincident with the results of compressive strength tests.

Table 3. Compressive strength (in water 50℃, MPa)

Samples No.	Ages(days)						
	3	7	28	60	120	180	360
Cement 1	90.2	110.0	115.5	116.2	114.9	117.6	120.0
Cement 2	96.3	106.3	114.6	117.4	116.1	117.1	120.9

Table 4. Pore size distribution (in water 50℃)

Pore diameter ($nm * 10^{-3}$)	Cement 1				Cement 2			
	7 days	28 days	60 days	one year	7 days	28 days	60 days	one year
75—0.100	0.26	0	0	0	0.18	0	0	0
0.100—0.050	0.18	0.02	0	0.05	0.07	0	0	0
0.050—0.010	5.23	2.99	0.33	1.49	4.60	2.71	0.61	2.93
0.010—0.005	4.15	3.95	5.57	2.12	6.46	6.18	4.90	3.08
0.005—0.0018	5.82	6.90	6.40	7.14	3.87	4.77	7.76	4.62
Total	15.66	13.87	12.30	10.81	15.19	13.67	13.27	10.64

Results of compressive strength and pore analysis indicate that the retarded expansion in cement has no harmful effect on the properties. The possible explanation are that the amount of periclase do not excess the limit, and clinker periclase is fine and well-distributed. The results suggest that the cement exhibiting controlled retarded expansion and high strength can be made through controlling the content of MgO in clinker.

CONCLUSIONS

Increasing curing temperature, clinker periclase hydration rate and retarded expansion rate increase. At 50℃, the retarded expansion develops continuously within half one year. Curing temperature changes around 50℃, the final value of expansion of cement made of clinker containing MgO 5.0 wt. % changes slightly, the linear expansion is about 0.1%. Retarded expansion caused by clinker periclase has no harmful effect on strength and pore structure of cement if the amount of MgO in clinker is controlled, for example, 5.0 wt. %. A cement exhibiting controlled retarded expansion and high strength can be resulted with the use of 5.0 wt. % MgO in clinker. The retarded expansion develops relatively fast at the temperature inside mass concrete and approximately keeps in step with the cooling shrinkage in mass concrete.

REFERENCES

1. F. M. Lea, "The Chemistry of Cement and Concrete", Edward Arnold (Publishers) Ltd, London, 1970.
2. Rikio Iki, "Analysis on the Volume Deform of Mass Concrete", Cement and Concrete, Dec., 1967, pp22-27. (In Japanese).
3. Wu Leifeng, "New Way to Pour Dam", Hydraulic Power Publishing House, April, 1987. (In Chinese).

4. Wang Yuqing and Lou Zonghan, "Studies on Clinker Periclase", Zhejiang Cement, March, 1987, pp18-26. (In Chinese).

5. G. Verbeck and L. E. Copelando, Paper SP32-1, Proc. Menzel symposium on High Presure Stream Curing, 1969, American Concrete Institute, Detroit, pp1-13

DURABILITY OF CONCRETE WITH DIFFERENT CEMENTS AND AGGREGATES UNDER SUSTAINED LOAD

Wojciech G Piasta

Technical University of Kielce, Kielce, POLAND

Abstract:

The influence of cement phase composition and mineral composition of coarse aggregate on concrete durability under complex condition of sustained stress and simultaneous sulphate attack is investigated.

It has experimentally been observed that the effect of the level of sustained compressive and flexural stress and 5% Na_2SO_4 - attack on creep -related deformations or expansion, strength, confirmed also by changes of phase composition of concrete (XRD), are significant.

The studies have been carried out for three portland cements and the cement with slag addition and coarse crushed limestone, granite aggregate and river gravel. The level of compressive and flexural stress has been in the range of 0 to 0.65 and 0 to 0.35, respectively. The effect of compression on concrete behaviour under sulphate attack depends on the level of stress significantly, whereas flexural stress of any value accelerates sulphate attack on concrete.

This experiment indicate more distinct effect of material factors (cement phase composition, kind of aggregate) on the process and rate of deterioration.

Zusammenfassung:

In diesem Aufsatz wurde der Einfluß der Phasenzusammensetzung von Portlandzement und Zuschlägen auf die Beständigkeit von Beton unter der Dauerspannung und dem gleichzeitigen Sulphatangriff vorgestellt.

Es wurde experimentell beobachtet, daß die Einwirkungen der Dauerdruck-und Dauerbiegezugspannungsniveaus und des Angriffs von der 5% Na_2SO_4 - Lösung auf die Kriechdehnung oder das Treiben und die Festigkeit wesentlich sind. Die Einwirkungen wurden auch durch die Veränderungen von Phasenzusammensetzung des Betons bestätigt (XRD).

Die Untersuchungen wurden für 3 Portlandzementen, einen Zement mit Hüttensand und Kalkstein- und Granitzuschlag und Kies durchgeführt. Die Niveaus der Dauerspannungen waren folgend: beim Druck von 0 biszu 0,65; beim Biegezug von 0 biszu 0,35.

Der Einfluß vom Dauerdruck auf das Betonverhalten ist veränderlich und er hängt vom Spannungsniveau ab. Dauerbiegezugspannung auf jedem Niveau beschleunigt den Sulphatangriff auf Beton.

Diese Untersuchung zeigt noch mehr scharf und deutlich den Stoffeinfluß (Phasezusammensetzung vom Zement, Zuschlag) auf den Verlauf des Sulphatangriffs.

INTRODUCTION

Durability of concrete may be defined in general as the capability of this material to maintain its good behaviour in foreseen circumstances during predicted service life [1],[2].
In other words, the durability of concrete is its ability to fulfil the function required in the design of building [3].
However, in the range of civil engineering needs, the research and studies on the durability of concrete as structural material have been insufficiently related hitherto with the conditions of simultaneous action of various factors. It refers to the durability of concrete under sustained load and simultaneous chemical attack. This has not been expressed in the latest research criteria of the sulphate attack on concrete [4] either.

It has been unanimously [5],[6],stated that swelling ettringite is formed under Na_2SO_4 solution attack. In general, two factors seem to be the most important: the permeability of concrete and the content of phase C_3A in cement. The ettringite-related extensive swelling produces concrete that may cause an unknown effect on sustained loaded concrete.
One of significant ways that improves sulphate resistance of portland cements is an addition of blast furnace slag. It reduces the content of C_3A in cement and decreases permeability of cement paste [3]. From the point of view of better resistance to sulphate attack on concrete and performance under sustained load, limestone aggregate should be also taken into account [7].

Applying a long term load on concrete, beside various pores, new elements in the form of any microcracks and cracks occur in section of concrete samples. Under compression first microcracks are observed at the stress below 30 per cent of the ultimate strength in the contact zone. At the stress 40 to 50 per cent of the strength the microcracks appear in the matrix and above 50 per cent of strength the cracks in the contact zones become unstable and bridge between grains. Above the stress level of about 75 per cent the propagation of cracks causes the failure of concrete with time under sustained load (static fatigue) [8]. Under flexure crack propagation is mainly connected with failure crack and some branches in its region. Static fatigue is observed at about 50 to 60 per cent [9].

Development of deformations and different crack propagations that are dependent on the state and level of load should be expected to cause changes of concrete permeability and durability under sustained load [7],[10].

EXPERIMENTAL PROCEDURE

Polish commercial ordinary portland cement 35 (a) with crushed coarse limestone (L) or granite (G) aggregate were applied to produce normal concretes. Tests of durability under flexure were carried out on gravel concretes (RG) with the following commercial portland cements: German OPC 35F (b); Polish OPC 35 (c) and Polish OPC 35 also with the commercial addition of 15 per cent of blast furnace slag (c + 15%bfs)(Table 1).

Table 1: Phase Composition of Cement Clinkers

Cement 35	C_3S	C_2S	C_3A	C_4AF	To tests under
a	70.2	8.5	7.3	8.8	compression
b	67.2	5.0	7.8	11.1	flexure
c ; c+15%bfs	59.2	14.1	13.0	8.8	flexure

The aggregates of two fractions 2 ÷ 8 mm and 8 ÷ 16 mm as coarse fillers and natural quartz sand 0 ÷ 2 mm were applied to make the concrete mixes according to the Table 2.

Table 2: Compositions of Concrete Mixes (kg/m^3)

Concr.	Cement	Sand	Coarse aggregate		Water	w/c	To test under:
			2÷8 mm	8÷16 mm			
G; L	260	600	520	770	200	0.75	compress.
RG	360	650	480	480	270	0.75	flexure

In order to test sulphate expansion, creep-related deformation in compression and compressive strength of concretes G and L, the sample 10×10×30 cm cast and consolided were cured in moist air of 95 per cent RH and t = 18°± 2°C. After 28 days of curing the compressive strength of the concretes was determined and then most of the samples were loaded under sustained uniaxial compression in spring creep-testing machines [7] and immersed with the other in 5% Na_2SO_4 solution and tap water. The stress levels σ/R_{28} were following: 0.20; 0.35; 0.50; 0.65 and they were equal to the values: 4.4; 7.7; 11.0; 14.3 MPa, respectively, for both concretes. Regular measurements of the time-dependent deformations were conducted for 3 years. When the samples were unloaded creep recovery and accumulated expansion were measured for 2 months. Then the residual strength was determined.

In oder to assess performance of the concretes RG with the cements: b, c and c + 15%bfs under sustained flexure and simultaneous sulphate attack, the samples 6.5x6.5x24 cm were cast and consolidated by vibration. After 28 days of curing in tap water the flexural strength was determined. The samples were loaded under sustained 4-point bending (span 20cm) at the stress level: 0.20 and 0.35 and immersed in 5% Na_2SO_4 solution. Every 14 or 30 days the flexural strength was determined. Comparatively, the reference samples (being unloaded) were immersed in 5% Na_2SO_4 and tested in the same way. At the end of investigation the XRD-analysis was carried out.

RESULTS AND DISCUSSION

The dimensional changes of both concretes under the complex conditions of sulphate attack and sustained compressive stress generally appeared to be rather similar for all the cases , respectively (Figs. 1 and 2). Some differences between the time-dependent deformations of these concretes are connected with higher creep-related strains of granite concrete than those of limestone one. This relation was noted after 1 year and 3 years as well. On the other hand, the limestone concrete showed some slight gradual tendency of deformation drop with time, that was only observed for the granite concrete at the stress level 0.20. This stress level is particular for both concretes. The deformation in the third year at this stress level was a restraint expansion, that reached the magnitude of about $250 \cdot 10^{-6}$ and $100 \cdot 10^{-6}$ for granite and limestone concrete, respectively, and was an order of magnitude lower than free expansion ($2000 \cdot 10^{-6}$ and $2400 \cdot 10^{-6}$). The other effect of the interaction of sustained compression and sulphate attack was an untypical accelerated increase in deformation ($250 \cdot 10^{-6}$) of granite concrete at the stress level 0.65 in the second year and thereafter in the third year its decrease ($70 \cdot 10^{-6}$). In comparison with the deformations in water (Table 3) the interaction of sustained compression and sulphate attack results in higher longitudinal

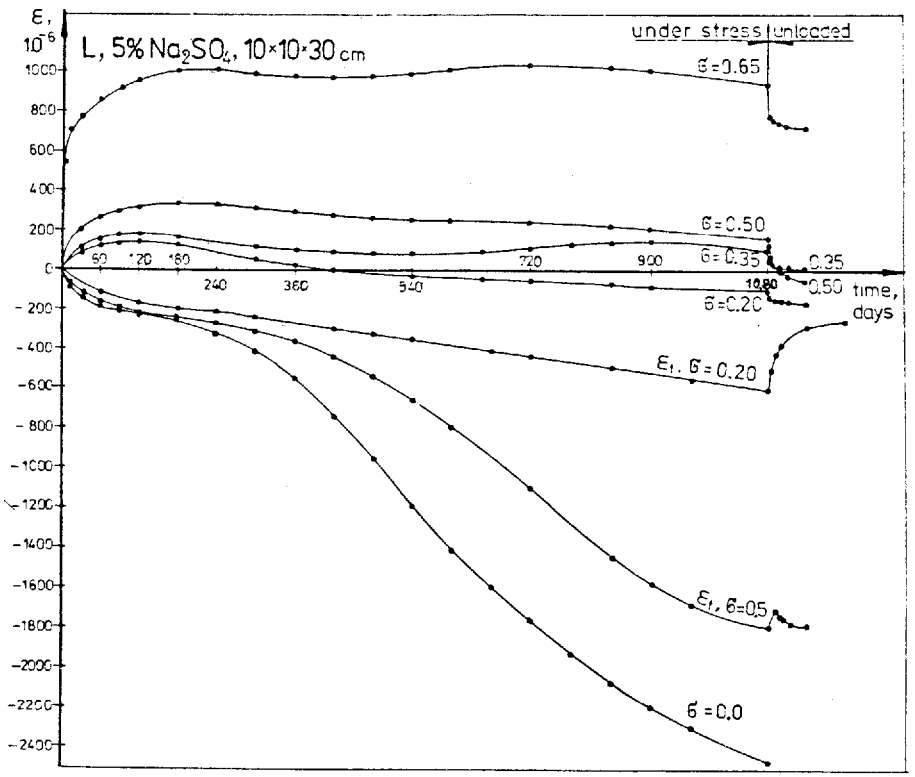

Fig.1. Time-dependent deformations of limestone concrete (L).

ε deformations at the level 0.65 and the phenomenon of restraint expansion at the level 0.20.

It was found that intermediate sustained compressive stress (the level about 0.35) may improve strength (Fig. 3) of concrete under sulphate attack. This is in agreement with the first test [10] of low sulphate resistant concrete. The highest compressive strength for the level 0.35 corresponds to the stable magnitude of the deformation (Figs. 1, 2) of

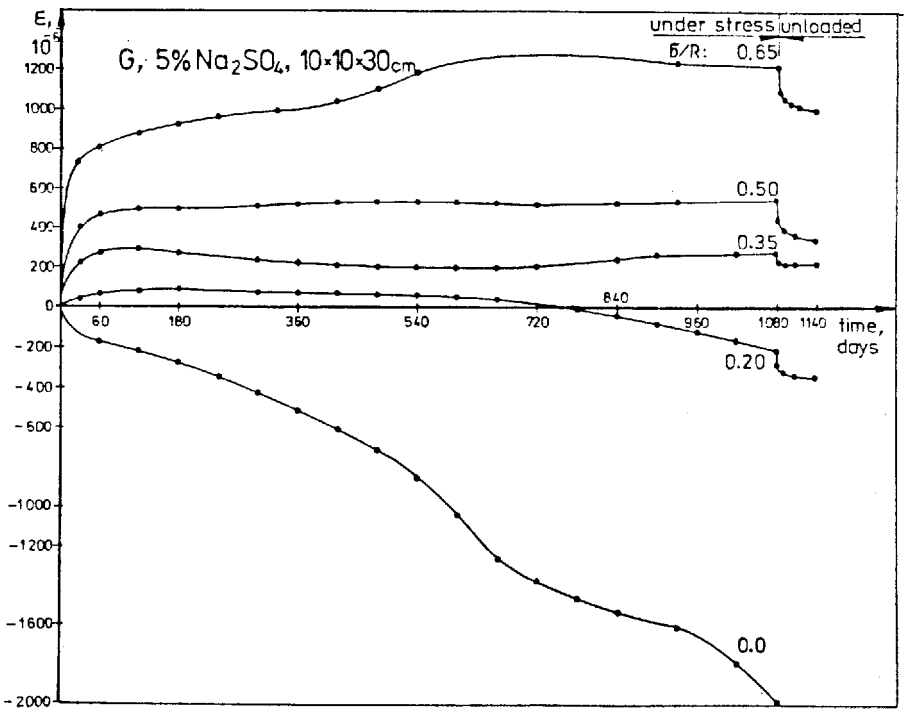

Fig.2. Time-dependent deformations of granite concrete (G).

Table 3: Deformations of concretes after 3 years under sustained compression in tap water ($\times 10^{-6}$)

Concrete	σ/R_{28}	0.0	0.20	0.35	0.50	0.65
L	ε	-270	110	235	320	870
	ε_t	—	-180	—	-510	—
G	ε	-260	40	240	710	1060

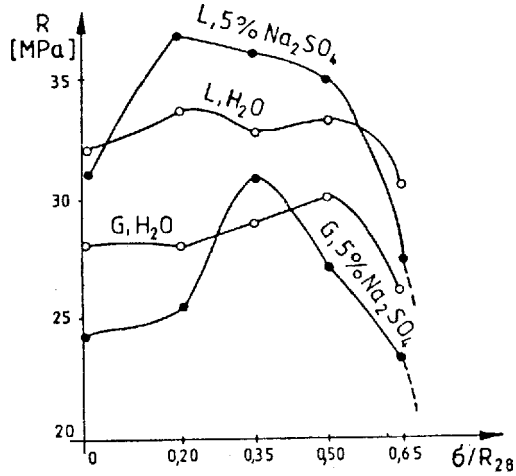

Fig.3. Residual compressive strength after 3 years (R^{G}_{28} = 22.2 MPa; R^{L}_{28} = 22,4 MPa)

both concretes very well. Also the lowest strength of both concretes connected with the stress level 0.65 and sulphate attack is consistent with the increase in their deformations. The improvement of behaviour under the stress of the level about 0.35 and lower strength (Fig. 3) for the highest level are due to initial decrease in the volume of concrete without cracking and to crack occurence, respectively [6]. On the other hand, the influence of the stress level on the strength of concrete is not so significant at the immersion in water. The stress level 0.65 exeedes the limit of linear creep regardless of the environment (Figs. 1, 2; Table 3). The significantly better effect of limestone aggregate than that of granite one on concrete performance was stated under all these complex conditions.

Changes of flexural strength of gravel concretes with various cements (Fig. 4) indicate significant dependence of their durability and service life on load application and stress level. The most accelerated deterioration of the concrete was noted under load of the level 0.35 when the cement c was applied. The level 0.35 appeard to be deleterious for the concretes with both other cements as well. When the concrete with the cement including 15 per cent of blast furnace slag (c + 15%bfs) was loaded the grandual decrease in its flexural strength totally changed the assessment of sulphate resistance of this cement resulting from unloaded concrete. The greatest drop of flexural strength was also found under the stress level 0.35, after 210 days for the concrete with the cement b of rather high sulphate resistance.

The rate of the concrete deterioration observed as strength decrease or as total loss of service ability by the failure (c, 0.35 - 45 days; c, 0.20 - 110 days) was consistent with changes of phase content (Fig. 5).

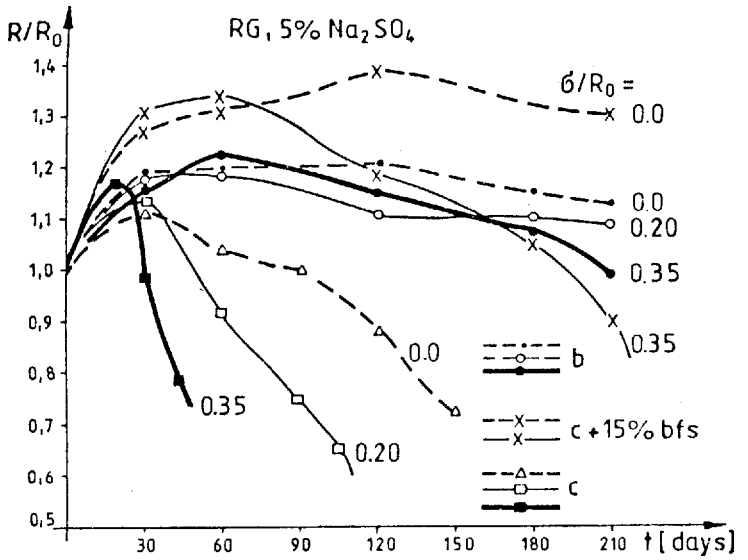

Fig.4. Flexural strength of gravel conretes under sustained bending

R_{28}^{b} = 5,4 MPa

R_{28}^{c} = 4,9 MPa

$R_{28}^{c+15\%bfs}$ = 5,2 MPa

Deleterious formation of ettringite was stated for the concrete with the cement c, alredy after 42 days. Nearly the same amount of ettringite was detected in the concrete with cement c + 15%bfs, however,after 210 days. On the other hand, the amount of the ettringite formed in the concrete with the cement b after 210 days appeared to be much lower than those in both other concretes. Thus, it can be stated that the main phase changes

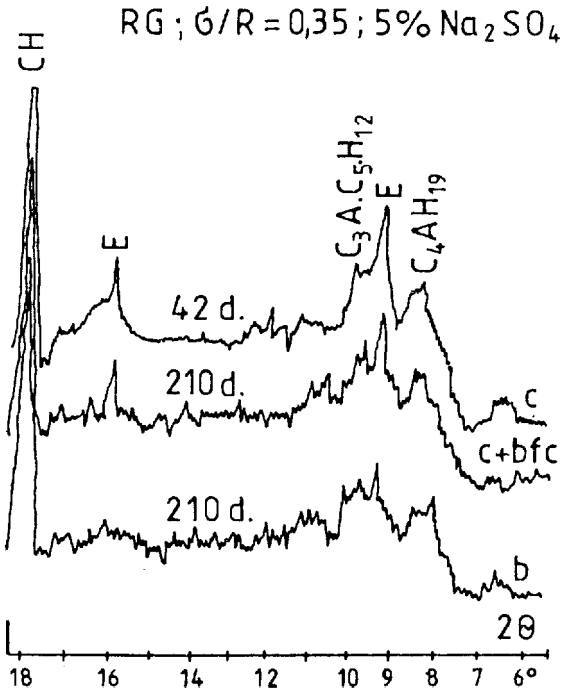

Fig.5. XRD-analysis of gravel concretes.

(formation of ettringite) in concretes under sustained flexure and sulphate attack are the same as those observed in tests of unloaded cement systems [1],[5], however, the loss of service ability is due to the combined interaction of ettringite formation and mechanical effects.

CONCLUSIONS

- The durability of concretes under attack of Na_2SO_4 solution was found the best for the compressive stress level of 0.35 - durability of concrete depends on the interaction of the stress level and severity of sulphate solution.
- Restraint expansion (related to ettringite formation) occured under compressive stress of 4.4MPa. Accelerated creep-related strains and lowest strength were observed at the compressive stress level 0.65, and under sulphate attack, but mainly for granite concrete.
- Better effect of limestone aggregate than that of granite one on concrete durability was found.
- The sustained flexure accelerates the rate of concrete deterioration under sulphate attack. The rate increases with the level of flexural load.
- The main phase change, responsible for the deterioration was ettringite.

REFERENCES

1. Calleja, J.: Durability, **ICCC ,7th, Paris** 1980, Vol. I, VII-2/1-48
2. Valenta, O.: General Analysis of the Methods of Testing the Durability of Concrete, **RILEM Symp. Durability of Concrete, Prague** 1969, Part 1, A3-28
3. Kurdowski, W.: **Mineral Additives for Cement and Concrete Stability**, Monography 106, Tech. Univ.Cracow, 1990,p. 109-120
4. Cohen, M. D.: Mather B.,Sulfate Attack on Concrete- Research Needs,ACI Mater. Jour., 1991, **88**, 62-69
5. Roy, D. M.: Mechanisms of cement paste degradation due to chemical and physical factors, **ICCC, 8th, Rio de Janeiro,** Vol.1, 362-380
6. Mehta, P. K.: **Concrete, Structure, Properties and Materials,** Prentice -Hall, Inc., Englewood Cliffs, New Jersey 1986, 450p.
7. Piasta W. G., Sawicz Z., Piasta J.: Sulfate durability of concretes under constant sustained load, Cem. Concr. Res., 1989, **19**, 216-227
8. Mindess, S.: **Structure and Performance of Cements**, Structure and Performance of Cements, ed. by P. Barnes, Applied Science Publishers, London-N.Y. 1983 p.319-363
9. Klug, P., Wittmann, F.H.: Activation energy and activation volume of creep of hardened cement paste, Mat. Sci Eng., 1974, **15**, 63-66 1989
10. Schneider, U., Piasta, J., Nägele, E., Piasta, W.G.: Stress corrosion of cementitious materials in sulfate solutions, Mater. Struct., 1990, **23**, 110-115

ACKNOWLEDGEMENT

W.G.Piasta would like to thank the Alexander von Humboldt Foundation for the support of his experiments and stydies on durability of concrete.

EFFECT OF PARTICLE PACKING AND MIX DESIGN ON CHLORIDE PERMEABILITY OF CONCRETE

R I A Malek

Materials Research Lab., The Pennsylvania State University, USA

SUMMARY

The 21st Century Concrete Technology will be more concerned with new mix designs that produce highly packed concrete with reduced porosity and low permeability. The experimental work included in the research program reported in this paper was directed towards the assessment of the relationship between chloride permeability and the grain packing of concrete. A computer code for a packing model enabled choosing the mixture proportioning that produces the desired degree of packing. A technique similar to that described in AASHTO T-227 (Rapid Determination of the Chloride Permeability of Concrete) was used to assess the chloride permeabilities of concrete mixtures. It is realized that the aggregate mortar interfaces play a role in concrete resistance to chloride ions penetration. In order to investigate this phenomena, the chloride permeability tests were also made on mortar stripped from fresh concrete samples and cured under the same conditions. Several interesting results were obtained and discussed in detail.

INTRODUCTION

A new method for concrete mix design, based on effective packing of constituents to produce minimum porosity, is introduced in this paper. The effective packing will, in general, lead to a reduction in the permeability of concrete to aggressive agents that move into concrete. Consequently, production of such concrete should result in a net gain in the performance of concrete in various environments.

The mathematical treatment of the new mix design method is based on statistical thermodynamical approach. The method has been used to calculate the packing densities of various concrete mixtures. It has been found that chloride permeabilities as measured by rapid chloride permeability method (AASHTO T-227) show an excellent reciprocal correlation with concrete solid packing densities. In addition, the interfacial porosity play a role in controlling the transport properties in concrete.

CONCRETE MIX DESIGN BASED ON GRAIN PACKING

Review

The effective packing of various size grain mixtures has been recognized as a means of improving the structural integrity of blended materials (both in nature and since old civilizations). In 1922, there appears to have been the first examination of methods of voidage reduction (increased particle packing) based on the simple concept that the interstices in a pack of particles of a given size may be occupied by smaller particles[1]. Furnas[2] was the first to develop the mathematical expressions for voidage reduction (improving particle packing) based on the assumption that small particles fill all the original voids between large particles without increasing the bulk volume of the pack, i.e. each component size fills exactly the voids of the next preceding size. The final volume will be that occupied originally by the largest size particles. In practice, however, it is almost impossible to achieve such system due to the overlap of the size distributions of different grains. Thus, in normal mixing, there is always a net increase in the volume of the packed bed due to the introduction of small particles into the network of large particles. This type of complexions is enhanced by less uniform particle size distributions of various components and presence of irregular-shaped particles due to increased frictions.

The second difficulty in modelling the packing of concrete mixtures is the irregular shapes of its particulate constituents. There has been very little theoretical work done on the packing of grains having irregular shapes due to the complexity of the system. The chemical and nuclear industries, however, developed some programs for calculating the packing densities of non-spherical particles but still with known geometric shapes (cylinders, pellets..... etc.). In concrete systems, the constituents have, in addition to size non-uniformity, a shape non-uniformity, and this makes the mathematical modelling of such system more complex. The problem originates from the fact that non-uniform grains tend to have undefined points of contacts and may have, sometimes, regions of contact.

Many attempts have been made to describe the deviation of particle shape from typically known shape idealizations. There has always been difficulty in applying these attempts to model the packing of particles due to the fact that it is important in the first place to be able to distinguish between the shape of the particle as a whole and the sharpness of its edges. Perhaps, the most acceptable (though not universal) attempt is that by Wadell[3-5]. Due to the limitations in such definitions, its applications to packing problems has been restricted to the prediction of the extent of deviation of particle shape from spherical and rounded edges by comparing calculated and measured packing densities.

The Proposed Model

The proposed method for determining the particle packing in concrete mixtures is based on statistical thermodynamical approach in which the most probable distribution of grains in an assembly of N grain size fractions with a pre-specified total volume fraction of each size category was determined. This approach was adopted to avoid the use of particle shape in the calculations since this has been already encountered in the volume fraction of a particular size category. The maximum number of complexions between particles has been allowed to simulate the actual particle distribution after mechanical mixing of different size fractions. Several descriptors for the particle size that represent the particle size distribution of each size category have been attempted and few were found adequate to be used. The grain size descriptors and volume fractions of the constituents used in the present investigation is presented in Table I. The discussion of values described in this Table is a subject of a separate publication. The calculated packing densities of various concrete mixtures were found to match favorably the measured values (Figure 1).

CONCRETE FORMULATIONS AND CHLORIDE PERMEABILITY TEST

Several concrete formulations covering a range of compositions in the American Concrete Institute (ACI 211) and the American Association of State Highway and Transportation Officials (AASHTO) specifications have been mixed. Some concrete

Table I: Grain Size Descriptors and Volume Fractions of the Concrete Constituents Used.

Material	Grain Size Descriptor (mm)	Volume Fraction
Cement(Type-I)	0.015	0.469
Slag	0.013	0.439
Fly Ash (F)	0.025	0.634
Fly Ash (C)	0.012	0.577
Silica Fume	9.5×10^{-4}	0.099
Sand	1.356	0.658
Angular Crushed Aggregate		
#8	8.055	0.596
#67	14.150	0.613
Rounded Natural Aggregate		
#8	9.422	0.639
#67	11.27	0.690

formulations containing various mineral admixtures were also prepared according to the appropriate ACI recommendations for the use of mineral admixtures. The water to cementitious materials ratio was kept constant (0.47) in all samples, except samples number 8 and 9 which have w/c ratio of 0.42 and 0.53, respectively. The American Society of Testing and Materials (ASTM C-192) guidelines were followed in mixing and curing. Superplasticizers and water reducers were used where needed to attain an equivalent slump without changing the W/C ratio. In addition, mortar samples were stripped from the fresh concrete using #4 sieve. Cylindrical samples of 3 ϕ x 6 inches (76.2 x 152.4 mm) and 3.75 ϕ x 3 inches (95.25 x 76.2 mm) were prepared for compressive strength and chloride permeability tests, respectively. After 24 hours all the samples were demolded and were cured immersed in water at room temperature for 28 days prior to

testing. The cylinders prepared for chloride permeability test were cut on both sides down to 2 inches (27.4 mm) height to expose fresh surfaces before testing. The dry packing densities of these formulation were calculated using the new program. The minimum amount of water required to produce the lowest acceptable workability (25.4 mm slump according to AASHTO specifications for pavements) was found to be that required to fill the intra-particle porosity (1-packing density). A concrete sample was formulated, based on the new program, so as to have the highest possible packing density (lowest porosity) in a combination of cement, sand and #67 crushed aggregate. Attention must be drown to the fact that for each combination of certain cement type, sand and coarse aggregates, there is only **one** formulation that has the highest packing density. Compressive strength development in this sample is higher than that of normal concrete designed according to the traditional methods (Figure 2).

The chloride permeability was measured by monitoring the net charge (coulombs) passing in 6 hours through a disc (95.25 ϕ x 51 mm) mounted in a cell with two compartment, filled with NaCl and NaOH solutions, under the influence of 60Vdc electrical potential (AASHTO T-277). The samples were pre-conditioned by vacuum saturation prior to measurement.

DISCUSSION OF RESULTS

The concrete mixtures characteristics and the chloride permeability data for both concrete and stripped mortar samples (28-days) are presented in Table II. In general, the chloride permeability shows a reciprocal relationship with the solid packing density. Figure 3 demonstrates this relationship. Figure 4 shows a comparison between the concrete mixture that has been designed to have the highest solid packing density and the companion samples designed according to the traditional methods. It is evident that the highly packing sample showed the minimum chloride permeability. Comparing the chloride permeability of this highly packed sample with those of concrete mixtures containing mineral admixtures (Figure 5), it is seen that it has a considerably lower permeability with the exception of silica fume containing samples.

The intra particle interfacial zone plays a role in permeability of concrete. Therefore, increasing the extent of fines will lead to an excess in porosity (interfacial) and that might be reflected as an increase in concrete permeability in general and to chloride ions in particular. It has been found that the chloride permeability of concrete having the same total aggregate volume fraction (sand + coarse aggregate) increase linearly with the fine to coarse aggregate ratio (Figure 6). In addition, the chloride permeabilities of concrete samples are higher than the corresponding values of stripped mortar samples corrected to account for the impermeability of a volume equivalent to the volume of coarse aggregates. The difference is an indicator of the extent of mortar-coarse aggregate interfacial contribution to the total porosity. It has been found to that

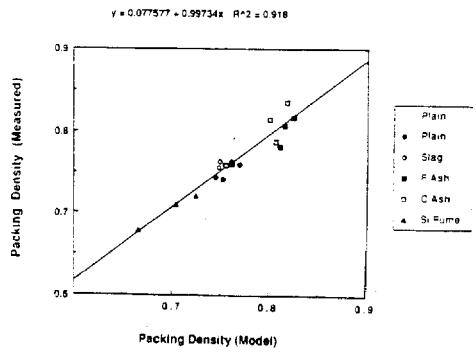

Fig. 1. A comparison between the measured packing densities versus those calculated from the proposed model for plain and mineral admixtures containing concrete.

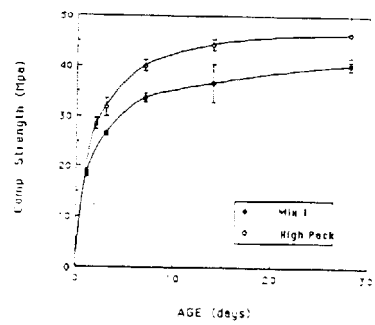

Fig. 2. A comparison of the compressive strength development in the highly packed and normal (#1) concrete samples.

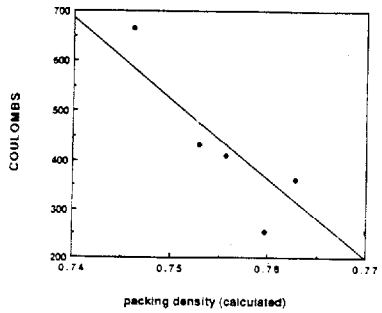

Fig. 3. Variation of chloride permeability in concrete samples versus the solid packing density.

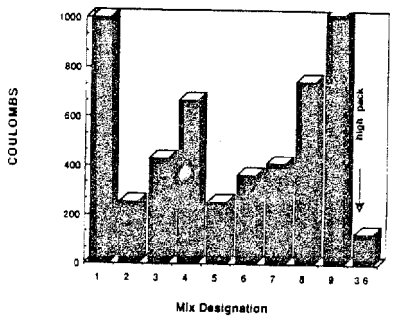

Fig. 4. A diagrammatic representation comparing the chloride permeabilities of different concrete containing #67 crushed aggregate.

the increase in mortar proportion gives rise to a higher interfacial porosities which contributes in increasing the permeability.

CONCLUSIONS

A mathematical model for determining the packing density of concrete mixtures has been developed and successfully tested to aid in concrete mix design optimization. The calculated packing densities were found to correlate with the chloride permeability values as determined by the rapid chloride permeability test (AASHTO 227). Based on the results obtained in the present investigation, several conclusions emerge.

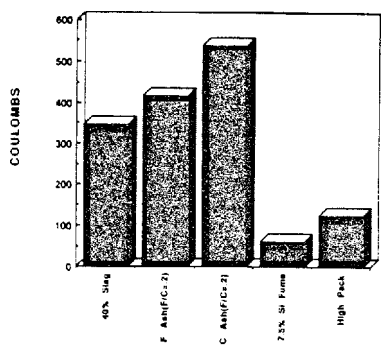

Fig. 5. A diagrammatic representation comparing the chloride permeability of the highly packed concrete with mineral admixtures containing concrete. (All contain #67 crushed aggregate).

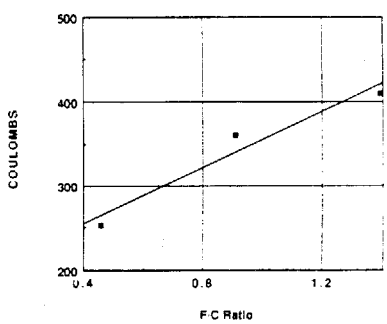

Fig. 6. Effect of the fine to coarse aggregate ratio (at constant total aggregate volume fraction) on the chloride permeability of concrete.

1) The chloride permeability shows a reciprocal relationship with the solid packing density.
2) The concrete samples formulated, based on the new program, so as to have the highest possible packing density (lowest porosity) of their ingredients showed the minimum chloride permeabilities.

3) The highly packed samples have considerably lower permeability than those of concrete mixtures containing mineral admixtures with the exception of silica fume containing samples.
4) The intra particle interfacial zone plays a role in permeability of concrete.
5) Chloride permeability of concrete having the same total aggregate Volume fraction increases linearly with the fine to coarse aggregate ratio.

Table II: Concrete Mixtures Characteristics and their Chloride Permeabilities.

	Sample	Agg. Vol.	F/C Ratio	Packing	Cl (Concrete)	Cl (Mortar)
1	#67 Crushed	0.841	0.562	0.762	1000	4752
2	#67 Crushed	0.823	0.349	0.760	253	4104
3	#67 Crushed	0.817	0.709	0.753	432	3406
4	#67 Crushed	0.818	1.236	0.746	666	3744
5	#67 Crushed	0.866	0.457	0.770	253	2502
6	#67 Crushed	0.866	0.910	0.763	360	1919
7	#67 Crushed	0.866	1.392	0.756	410	1879
8	#67 Crushed+	0.846	0.613	0.763	745	1602
9	#67 Crushed+	0.838	0.512	0.762	1015	10195
10	40% Slag	0.839	0.558	0.756	347	1541
11	60% Slag	0.824	0.558	0.749	40	269
12	65% Slag	0.836	0.558	0.741	69	316
13	80% Slag	0.835	0.558	0.750	33	68
14	F Ash(F/C=.2)	0.832	0.553	0.811	418	2380
15	F Ash(F/C=.5)	0.822	0.543	0.817	228	
16	F Ash(F/C=1)	0.810	0.529	0.824	224	
17	C Ash(F/C=.2)	0.836	0.561	0.806	540	3218
18	C Ash(F/C=.5)	0.838	0.583	0.801	323	
19	C Ash(F/C=1)	0.822	0.580	0.818	612	
20	7.5% Si Fume	0.838	0.556	0.725	60	176
21	10% Si Fume	0.832	0.553	0.704	36	
22	15% Si Fume	0.841	0.546	0.667	0	
23	#8 Crushed	0.841	0.562	0.780	439	2437
24	#67 Rounded	0.842	0.565	0.758	1220	4608
25	#8 Rounded	0.842	0.565	0.745	976	3636
26	#67 Rounded	0.818	0.310	0.726	325	8784
27	#67 Rounded	0.818	0.722	0.715	335	3777
28	#67 Rounded	0.818	1.259	0.752	598	2473
29	#67 Rounded	0.866	0.463	0.734	53	2678
30	#67 Rounded	0.866	0.927	0.722	175	1984
31	#67 Rounded	0.867	1.817	0.719	482	2592
32	#67 Crushed*	0.843	0.576	0.725	281	2588
33	#67 Crushed*	0.843	0.576	0.731	486	2862
34	#67 Crushed*	0.843	0.576	0.751	901	4140
35	#67 Crushed*	0.843	0.535	0.717	781	3442
36	High Pack	0.900	0.435	0.767	124	1490

+ Sample #8 W/C = 0.42, sample #9 W/C = 0.53.
° Samples #10-13, % represent the percent of slag substitution by weight of the cement.
° ° Samples #14-19, F/C = fly ash/cement ratio by volume.
°°° Samples #20-22, % represent the percent of silica fume substitution by weight of the cement.
* Samples #32-35 contain sand of variable gradations.

REFERENCES

1. Schwartz, H.A., Trans. Am. Foundarymen's Soc., pp. 762-781 (1922).
2. Furnas, C.C., Ind. Eng. Chem., 23 [9] (1931).
3. Wadell, H., J. Geol., 40 [5], pp. 443-451 (1932).
4. Wadell, H., J. Geol., 41 [3], pp. 310-331 (1933).
5. Wadell, H., J. Geol., 43 [3], pp. 250-280 (1935).

DETERMINATION OF CONSISTENCY OF CEMENT PASTE - A FRESH LOOK

S G Shashiprakash, T S Nagaraj and B K Raghu Prasad

Department of Civil Engineering, Indian Institute of Science, Bangalore, INDIA

ABSTRACT

Normal consistency is an important property of cement paste, as is considered to be a major parameter in determining the setting time and compressive strength of cement. A number of trials need be made before its value is obtained.

This paper consists of two parts. The first part deals with a 'One point method' of finding normal consistency. Based on the data on cements of different finenesses, a generalized equation is developed for the assessment of normal consistency. This equation leads to a simple and rapid way of assessing normal consistency. It is based on the principle that penetration resistance of cement paste is a measure of shear strength which in turn depends on the physico-chemical interactions between cement and water expressed in terms of generalized water-cement ratios. This method eliminates trials.

The second part consists of the development of an alternative method for the determination of normal consistency. This is developed to minimize the shortcomings like mode of mixing, sample preparation, mode of measurement etc., in the existing Vicat's method. Cone penetrometer, extensively used to determine the liquid limit of soils, has been found to be a viable alternative to Vicat's apparatus. The analysis of the data indicates that, with the analysis of more extensive data, the cone penetrometer itself can be used to determine the setting time of cement besides the normal consistency.

INTRODUCTION

Consistency is the tendency of the cement to get wetted. This is measured by Vicat's apparatus. It is a major parameter for determining the setting time and compressive strength. Though, the method of assessment is the same in Indian (BIS), British (BS) and American (ASTM) codes of practice, normal consistency is defined for different depths of penetration in different codes. IS 4031-1988 (1) and BS 4550-1978 (2) define it as the water content corresponding to a penetration of 5 to 7 mm and 5±1mm from the bottom of the mould, respectively. ASTM C-187 (3) defines it corresponding to a penetration of 10±1 mm from the original surface of the paste. This investigation deals with its assessment as per BS 4550-1978 (2).

PART I ONE POINT METHOD OF DETERMINATION OF CONSISTENCY

In the regular method of finding normal consistency, penetration is measured for different water contents and the water content that gives the standard penetration is taken as normal consistency. The object of this investigation is to determine the normal consistency in a single trial. Popovics (4) had also indicated the possibility of developing a 'One-point method' for the Vicat's test.

Materials

In the first part of the investigation, one brand of cement (brand name 'Veda') was used. The cement was ground to different finenesses with the same chemical composition.

Table 1 Chemical composition of cement (percent by weight)

CaO	SiO_2	Al_2O_3	Fe_2O_3	MgO	SO_3	IR	LOI
60.98	20.00	6.79	3.51	1.41	2.20	2.10	3.36

IR: Insoluble residue LOI: Loss on ignition

The finenesses determined using Blaine's air permeability method are mentioned in figure 1. To verify the validity of this 'One-point method', two other cements were used.

Results and discussions

The normal consistency was determined in accordance with BS 4550-1978. First, tests were conducted using Veda cement with three different finenesses. Penetrations (P) were measured for different water contents (w) for the three cases. A graph of water content versus penetration called flow line, was plotted (Fig.1) and water contents (w_N) corresponding to 5mm penetration from bottom read out. The water contents at different penetrations were generalized by dividing them by the corresponding w_N values. Using this, an equation relating water content, normal consistency (w_N) and penetration of the form,

$$w / w_N = a - bP \qquad (1)$$

where a = 1.008 and b = 0.002, for the data considered, can be developed.

It can be seen from figure 1 that, all the points fall in a narrow band making it possible to represent by an equation.

Two more cements of different brands were tested to assess the validity of this equation for other cements (Table 2). The calculated values are in good agreement with

experimental values. Figure 2 shows the experimental and predicted flow lines cements, when an average value of normal consistency was used in equation 1 to draw the flow lines.

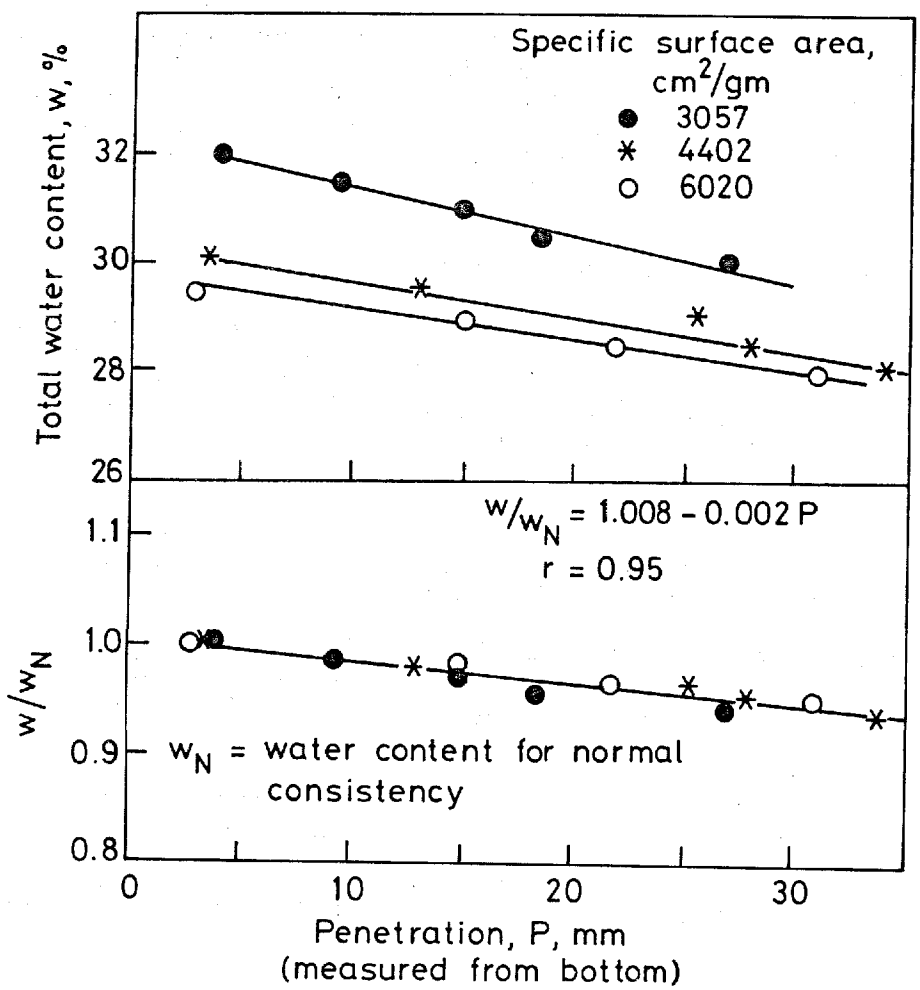

Fig. 1 Relationship between water content and Vicat's penetration for different cements and their normalization

Table 2 Vicat's penetrations for two cements

Sample	Water content (%)	Penetration (mm) measured from bottom	Normal consistency w_N as per eqn. 1)
A	24.0	27.5	25.18
	25.0	13.0	25.46
	25.5	5.5	25.58
B	24.0	23.0	24.95
	24.5	17.0	25.15
	25.0	10.5	25.33

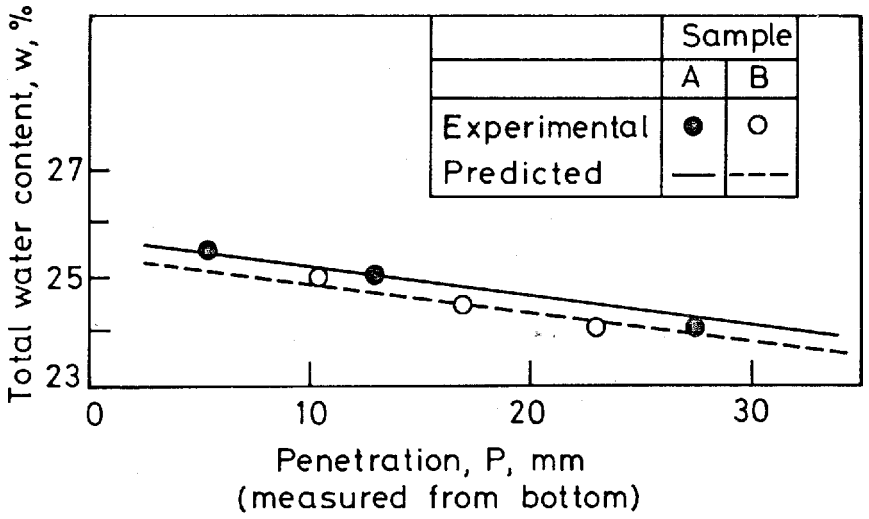

Fig. 2 Experimental and predicted Vicat's penetrations for different water contents using different cements

PART II AN ALTERNATIVE METHOD FOR ASSESSMENT OF CONSISTENCY OF CEMENT PASTE

For the determination of normal consistency, different standards have advocated different methods of mixing, placing and assessment. The Indian and British standards have specified hand mixing, and, American standard mechanical mixing. The paste is filled into the mould as it is, in the case of Indian and British Standards. In the American Standard Method, the paste is made into a ball and tossed 6 times between the hands held 6 inches apart before it is pressed into the mould from the larger end. It is possible that human errors do creep in while doing this experiment. The normal consistency is also defined differently in different codes. Hence, the existing methods merit reexamination.

The alternative method

Cone penetrometer method is an established method for the determination of liquid limit of soils. Liquid limit of soil is analogous to consistency of cement paste. This inference can be made from soil-concrete analogy, by examining the role of the constituents of soil and concrete, and the interaction between clay or cement and water (5). Hence, cone penetrometer can be used in the assessment of normal consistency.

Details of the Vicat's apparatus are given in codes. The standard weight of the plunger is 300 gm and, diameter 10 mm. Only the diameter of the mould varies from one code to other. Indian and British standards specify a diameter of 80 mm. American code specifies a top diameter of 60±3 mm and a bottom diameter of 70±3 mm. The height of the mould in all the cases is 40 mm. The time allowed for penetration is 30 seconds.

Details of the cone penetrometer are available in BS 1377-1975 (6). It has a cone of height 35 mm and apex angle 30°. The total weight of the cone and sliding shaft is 80 gm. The mould is 40 mm in height and 55 mm in diameter. The apparatus is fitted with an automatic release and locking device which restricts the cone penetration to 5 seconds. The dial gauge measures the depth of penetration (from top) to an accuracy of 0.1 mm.

Materials and methods

The first set of tests were conducted on Coromandel cement. The validity of the correlation between the two tests was verified using Dalmia cement. Water content was varied from 23 to 29%.

For Vicat's test, mixing was done manually, as per IS (and BS) code. Penetrations (from bottom) were measured for different water contents. In cone penetration test, mixing was done using a motorized mortar mixer. The paste was placed in two layers; each layer being compacted by giving 25 jolts on a flow table. The penetrations (from top) were measured for different water contents. At least two samples were tested (which were prepared at a time) for each water content. The results are given in figure 3. Similar tests were conducted for Dalmia cement also, for three different water contents.

Results and discussions

The results of tests are shown in figure 3. Penetration values are plotted as obtained, i.e., the Vicat's penetration as measured from bottom and cone penetration from top. The equations are:
For Vicat's test,

$$w_v = 27.3896 - 0.1299\ P_v \qquad (2)$$

and for cone penetration test,

$$w_c = 0.2527\ P_c - 20.0842 \qquad (3)$$

where, P_v and P_c are the Vicat's and cone penetrations and w_v and w_c are the respective water contents.

When the water contents used for the two tests are same, equations (2) and (3) can be combined. i.e., at $w_v = w_c$,

$$P_v = 56.24 - 1.95\ P_c \qquad (4)$$

This equation was used in calculating the values of P_c for various values of P_v. The results are shown in tables 3a and b. It can be seen that the calculated values are in good agreement with the experimental ones.

In Vicat's test, the results are operator dependent. Based on the mode of mixing, the penetration also varies. The variations in the results of cone penetrometer may be due to difference in compaction. But, when the two tests are compared, cone penetrometer test appears to be better. In this case, the cone is allowed to penetrate for only 5 seconds after which it gets locked. In the case of Vicat's apparatus, the penetration is read after 30 seconds. The plunger moves faster for the first ten seconds and then slows down. A major portion of the penetration might have been over in the first ten seconds. Hence measurements of penetrations before this time seems to be quite sufficient.

Another factor that needs to be mentioned regarding operator dependence of Vicat's test is the validity of equation (1). Though, the results obtained in case of consistency tests match well with the calculated values, the equation in its original form could not be used universally. It is not possible to categorically say why it is so. As per the

standards, the cement paste has to be prepared by manual mixing. For different operators, there was a difference in the penetration of the Vicat's needle.

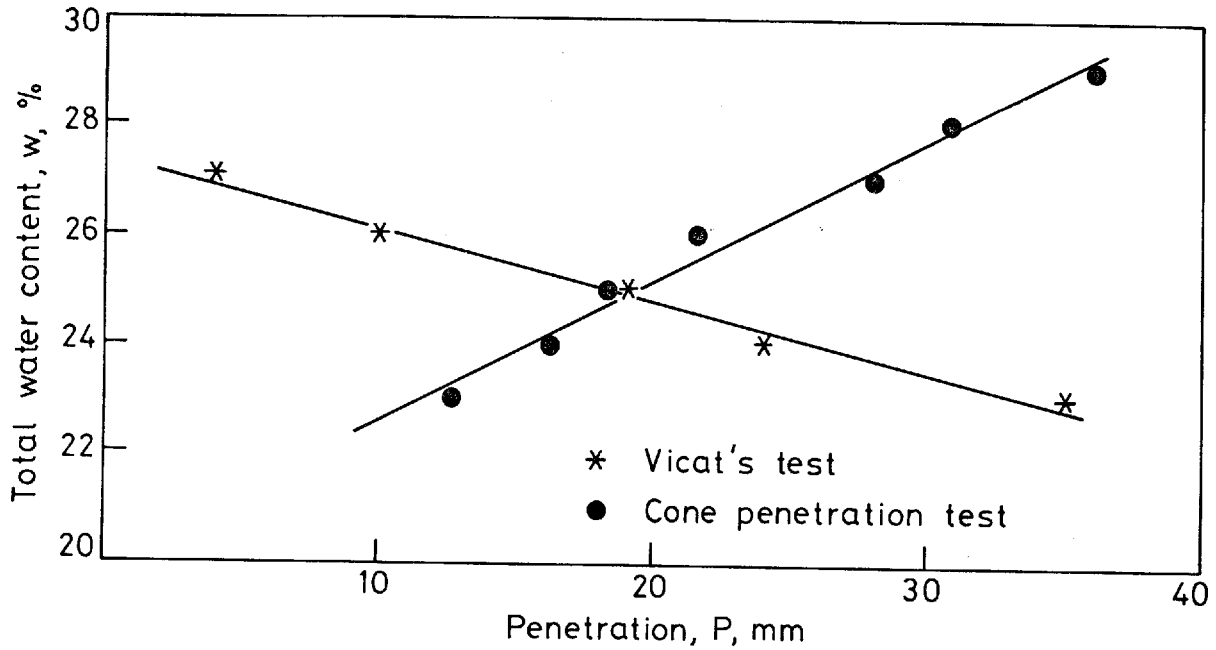

Fig. 3 Relationship between water content and penetration for Vicat's and cone penetration tests

Table 3a Vicat's penetrations

Water content %	Trial No.	Vicat's penetration mm	Calculated cone penetration P_c (cal) mm	Average P_c (cal) mm
25	1	30	13.46	13.20
	2	31	12.94	
27	1	23	17.05	16.79
	2	24	16.53	
29	1	14	21.66	21.15
	2	16	20.64	

CONCLUDING REMARKS

In summary, it can be said that, the equation based on generalization leads to a simple and rapid way of determining normal consistency since the penetration resistance of cement paste is a measure of shear strength which in turn depends on physico-chemical interactions between cement and water expressed in terms of generalized water-cement ratios. This method avoids repetitive trials.

Table 3b Actual and calculated cone penetrations

Water content %	Trial No.	P_c (Actual) 1/10 mm	Average P_c (Actual) mm	Average P_c (Cal) mm	Percentage difference over P_c (Act)
25	1	130			
	2	123	12.43	13.20	-6.19
	3	120			
27	1	168			
	2	158	16.63	16.79	-0.96
	3	173			
29	1	223			
	2	220	21.85	21.15	+3.20
	3	211			
	4	220			

The cone penetrometer appears to be a viable alternative for the Vicat's apparatus. But, additional data is needed before an equivalent parameter for normal consistency is defined. The results are definitely indicative of the possibility of a good correlation between the two tests. These tests are to be extended to cover a wider range of cements and also to define equivalents to the penetration values corresponding to initial and final setting times. The method of compacting should also be changed or can be even avoided.

ACKNOWLEDGEMENTS

This forms a part of the research carried out under a research scheme on `Studies on Superplasticized Concretes' sponsored by Central Board of Irrigation and Power, Govt. of India.

REFERENCES

1. IS:4031-1988: "Indian Standard methods of physical tests for hydraulic cement". Bureau of Indian Standards, New Delhi, India, Part 4, 1988, 2p.

2. BS:4550-1978: "British Standard methods of testing cement". British Standards Institution, London, UK, Part 3, Section 3.5, 1978, 4p.

3. ASTM: C-187-86: "Standard test method for normal consistency of hydraulic cement". Annual Book of ASTM Standards, V04.01, Cement; Lime; Gypsum, ASTM, Philadelphia, 1989, 145-146.

4. POPOVICS, SANDOR: "Predictability of certain properties of soil-water mixtures". Color air photos, Soil properties and tests, 4 reports, Highway Research Record No.63, Washington DC, 1964, 10-21.

5. NAGARAJ, T.S; SUNDARA RAJA IYENGAR, K.T. and SHASHIPRAKASH, S.G.: "Soil-concrete analogy - Principles and potentials". Cement and Concrete Research, 1989, 19(4), 534-546.

6. BS 1377-1975: "British Standard methods of test for soils for civil engineering purposes". British Standards Institution, London, 1975, 143p.

THE DEVELOPMENT OF STANDARDS FOR CEMENTS

P J Jackson* and J M Lawton**

**Sampling & Scientific Services, Rugby, U.K.*
***Cembureau, The European Cement Association, BELGIUM*

SUMMARY

Traditionally, many cement standards have been orientated towards compositional requirements and the successful introduction of a wide range of secondary materials over many years has led to a considerable increase in both their number and complexity.
A parallel development has been to produce standards based on the end use of the cements. It might have been expected that the latter would have their requirements expressed in terms of performance tests, but composition and chemical tests still, in most cases, continue to be adopted to fulfil this role.
This paper reviews the international situation and also indicates how products destined for similar purposes are specified in different ways. The case for common international standards is strong, but requirements for performance will need to be related to rapid chemical and also compositional requirements to enable production to be controlled.

INTRODUCTION

It is customary for standards to define the properties of cements in four different, but complementary ways :

1. Composition
2. Chemical properties
3. Physical properties
4. Performance characteristics

At the beginning of this century, the user had three principal requirements - firstly that when incorporated into grout, mortar or concrete the cement remained workable long enough for it to be put into the desired place, secondly that it developed the required level of strength at the appropriate time and thirdly that once in the hardened state it did not show any marked degree of deterioration after many decades. In those far off days, the first British Standard for Portland cement N°12:1904 (1) contained a compositional requirement which was defined in a limited way through constraints on density and insoluble residue. Chemical requirements included magnesia and sulphuric anhydride - both providing a second order means of ensuring long term stability in the hardened state. A restriction on the amount of coarse material present was also helpful in this connection. The tensile test adopted for strength was performed under conditions which could hardly be considered as sufficiently meaningful for it to be described with any justification as a performance test. The setting time and soundness tests represented performance assessments dealing with placing the material in the plastic state and the long term stability of the structure respectively.
These requirements still appear in standards but in many cases have become inadequate to fully characterize the large numbers of different cements now used for the various applications. Investigation shows that, throughout the world, the number of standards for all types of construction cements has increased from 129 to 282 over the last 30/35 years (2). By far the largest increase has been for those containing secondary materials and the number of countries having standards for cements with these materials increased from 23 to 59 over the same period. In terms of types and classes, the number in this category has increased from 150 to 876.

REQUIREMENTS IN STANDARDS

These fall into two main categories :

1. "Type Requirements" which normally take some considerable time to establish compliance and which are not therefore suited to the direct control of the product and the process. These are referred to in this paper as "Performance Tests"
2. Requirements which are generally considered to be related to the "Type Requirements" but which can be rapidly assessed for compliance and which are therefore suitable for direct process and product control. These are referred to in this paper as "Control Tests"

Performance requirements such as 28 day strengths fall into the former category whilst physical tests such as specific surface area and chemical analyses may be classified in the latter.

In the case of cements which have been used over many decades in the more common applications, there is confidence that the rapid "Control type tests" (2. above) are sufficient. However when materials are introduced which have no such history of successful application but which are attractive economically and/ or environmentally it is not unreasonable for a potential user to seek an assurance that a failure will not occur at either the plastic (concrete) stage or in the hardened state some years later. Such an assurance is normally more meaningful in cases where the secondary material is incorporated in the cement at the plant where the cement is produced. The situation regarding Performance tests and Control tests is illustrated in the following examples :

SULFATE RESISTANCE

As long ago as 1892 Michaelis (3) had ascribed the disintegration of cements in waters containing sulfates to the formation of calcium sulfoaluminates. This work was followed up over the next 30/40 years (4) by many attempts to develop tests to characterize this situation. The most reliable tests involved the retention of specimens in sulfate solutions over many years and quantifying the breakdown of the concrete or mortar by strength, expansion, or weight loss measurements. By 1940 sufficient evidence had been collected to permit a requirement to be put into cement standards limiting the % C_3A (when calculated using the Bogue formula) to a maximum of 5%. This became an effective control test because it was possible to formulate the kiln feedstock to produce Portland cement clinker to meet these requirements.
In many cases this was achieved by converting the C_3A to C_4AF by increasing the addition of iron bearing compounds to the kiln feedstock. However some reservations were raised regarding the conversion of C_4AF to calcium sulfoaluminates and some national standards also include a constraint on the C_4AF level. The present situation (2) is as follows for cements containing 95 to 100% Portland cement clinker and calcium sulfates having a high level of sulfate resistance (to withstand 1500 to 10,000 p.p.m. SO_4 in water (6)).

Number of countries having standards with :

A maximum C_3A level of 5%	9
" " " " " 3/4%	18
" " " " " 4/5 % and $C_3A + C_4AF \leq 22\%$	4
" " " " " 5 % " $2(C_3A) + C_4AF \leq 25\%$	6
" " " " " 3.5/5 % " $2(C_3A) + C_4AF \leq 20/22\%$	10
" " " " " 0% " $C_2F + C_4AF \leq 20\%$	1*
Countries having a performance test as an option	3

4 countries have, in addition, a maximum limit on C_3A level and a max. limit on C_3S
* for "Very high sulfate resistance".

Where Moderate sulfate resistance (to withstand 150 to 1500 p.p.m. SO_4 in water (6)) is required, the number of countries having standards with :

A maximum C_3A of 6%	1
" " " 8%	6
" " " 8% and $C_3S + C_3A \leq 58\%$	2
" " " 8% " $C_3S + C_3A \leq 58\%$ and $SiO_2 \geq 20/21\%$	1
" " " 8% " $SiO_2 \geq 20/21\%$	6*
An Al_2O_3/Fe_2O_3 ratio of 0.7 to 1.0	1

* One country has a maximum limit of 55% on the C_3S instead of the constraint on $C_3S + C_3A$.

These formulations based on Portland cements containing 95% or more of clinker and calcium sulphates have been well tested in practice and through long term performance tests.

The incorporation of secondary materials such as granulated slags (6) (7), pozzolanas (8), and silica fumes (9) into cements has been shown under appropriate circumstances to give enhanced sulfate resisting properties and this is often seen to be an attractive direction in which to proceed. For a given concrete mix, the sulfate resistance achieved in this way would be expected to be dependent upon the characteristics of the Portland cement clinker, that of the secondary component, the relative reactivity of the two (or in the case of some cements three or even four) components, the proportions, and hence e.g. the permeability of the concrete produced. The complexity of this situation may make performance testing an attractive proposition because although the materials themselves may be defined in terms of chemical requirements and the amounts present

can be specified, it is far from easy to predict the manner in which one reacts with the other (10). The problem has however been to develop a performance test which provides meaningful results within a reasonable time. Work in the U.S.A. has proceeded sufficiently far for a performance test to be a mandatory requirement in the ASTM standard for Blended Cements (with moderate sulfate resisting properties) (11).This test (12) involves the preparation of mortar prisms which when they have attained a compressive strength of 20 N/mm² are placed into a solution of sodium sulfate. It is, however, necessary to wait 180 days before the test is completed. In most countries sulfate resistance continues to be defined in terms of compositional requirements and in some cases by specifying certain chemical aspects of the components. The number of countries specifying in different ways is given in the tables below :

High Sulfate Resistance

% C_3A in clinker max.	% * clinker + $CaSO_4$	% slag	% pozzolana	% fly ash	% others	No of countries
2	≤ 30	≥ 70				1
3	≥ 75	<	≤ 25		>	1
3.5	<	no constraints			>	1
4	≥ 85	<	≤ 15	>		1
4 +	<	no constraints			>	1
5 +	≥ 90		< ≤ 10 >			1
5 +	≥ 80	≤ 20	≤ 10			1
5 +	≥ 80	<	≤ 20		>	1
5 +	≥ 65	≤ 35				1
5 +	55-85		< 15 — 40 >			1
5 +	30-65	35-70				1
5 +	<	no constraints			>	1
6 +	72-94		< 6-28 >			1
6 +	65-94	6-35				1
6 + **	<	Pozzolana required to be present			>	1
-	≤ 40	60-75				1
-	≤ 30	≥ 70				3
-	25-60	20-45		20-45		1
-	20-90	10-80				1
-	15-35	65-85				3
-	≤ 15	≥ 85				1

+ % C_4AF + 2 (% C_3A) in clinker ≤ 20/22 : * / ** see under next table

Moderate Sulfate Resistance

% C_3A in clinker max.	% * clinker + $CaSO_4$	% slag	% pozzolana	% fly ash	% others	No of countries
6	≥ 85	≤ 15				1
8	72-94		< 6-38 >			1
8	65-94	6-35				1
8	55-85		< 15-40 >			1
8	30-65	35-70				1
8	<	no constraints			>	2
-	≥ 90			≤ 10		1
-	≥ 85		≤ 15			2 P
-	≥ 80	< ≤ 20	>			1
-	≥ 75	≤ 25				1 P
-	75-80			20-25		1
-	≤ 64	≥ 36				1
-	60-85		15-40			2 P
-	30-75	25-70				3 P
-	≥ 30	<	30-70		>	1
-	<	Pozzolana required to be present			>	1

* In most cases cements **may** contain 3 to 5% minor constituents.

** Cement must meet pozzolanicity requirements.

P Performance test required.

Internationally, a wide range of compositions appears to be permitted for cements claimed to provide a similar level of sulfate resistance - suggesting that there is scope for harmonization and, if practicable, the development of a widely accepted sulfate resistance performance test.

HEAT OF HYDRATION

Since the critical period as far as the heat released from most concrete is less than 5 days then there would appear to be no insurmountable problem in having a common test for both performance and control purposes. Measurements of the heat released under semi-adiabatic conditions are made but the heat of solution method traditionally adopted is time consuming, requires considerable operator skills and has been reported to give misleading results with some cements containing secondary materials. It is not therefore uncommon to supplement it with chemical requirements. The 1991 situation as reported by Cembureau (2) is given below for cements containing 95 to 100% Portland cement clinker and calcium sulfates and related to the number of countries adopting the different approaches :

Low Heat of Hydration

Heat of hydration test required	% C_3A max.	% C_3S max.	% C_2S min.	No of countries	Heat of hydration requirements max. kJ/kg range between
yes	< ——	No constraints	——	> 2	
yes	5	50		1	
yes	5.5			1	
yes	6	40		1 *	
yes	7			1 **	250 &
yes	7	35	40	9	280
yes	7	35		2	at 7 days
yes	8	40	35	1 ***	and 290 &
yes		****		1	320
no	7			1	at 28 days
no	7	35	40	1	
no	7		40	1	
no	8			1	

Moderate Heat of Hydration

yes	6	55		1	
yes	6			1	
yes	8			2	290
yes	8			3 +	at 7 days
yes	8	++		5	and
yes	8	++		4 +	
yes	8	55 ++		1	335
no	6			1	at 28 days
no	6	50	30	1 +++	

* $SiO_2 \geq 21\%$
** $C_4AF + 2C_3A \leq 25\%$
*** Max. specific surface area specified
**** Lime saturation factor to be 0.66 to 0.88
\+ $SiO_2 \geq 20/21\%$
++ $C_3S + C_3A \leq 58\%$
+++ $C_3S + C_3A \leq 53\%$

Where the low heat of hydration cement contains significant amounts of secondary materials the international situation is as follows (2) :

Heat of hydration test required	% clinker + $CaSO_4$	% slag	% pozzolana	% fly ash	% others	No of countries
yes	< ——	No constraints	——	——	—— >	3
yes	60-90 *	< ——	10 to 40 ——	——	—— >	10
yes	60-85		< —— 15-40 ——	—— >		8
yes	10-80 **	20-90				10
yes	20-64	< ——	36-80 ——	——	—— >	2

* Some compositions restrict the clinker C_3A to 5/7 %
** One composition restricts the clinker C_3A to 8 % and the C_3S to 55 %

The heat of hydration maximum requirements in countries using the solution method range between 250/280 kJ/kg at 7 days and 290/320 at 28 days.
For moderate heat of hydration the situation is as follows :

Max. % C_3A in clinker	% clinker + $CaSO_4$	% slag	% pozzolana	% fly ash	% others	No of countries
yes	< ——	no constraints	——	——	>	1
yes	60-90		< —— 10-40	—— >		10
yes	30-75	25-70				6
no	30-75	25-70				1

The heat of hydration maximum requirements range between 293/300 kJ/kg at 7 days and 335 at 28 days

ALKALI AGGREGATE REACTION RESISTANCE

There has been considerable difficulty in producing valid test methods to assess the potential of various cements to inhibit the alkali-aggregate reaction, and as a result only one country, in one of its standards has included a performance type test. The majority of countries adopt requirements which limit the alkali content of the cements (expressed as sodium oxide equivalent $(\%Na_2O)_e$ - which is calculated from $\% Na_2O + 0.658$ $(\%K_2O)$). Other standards rely on compositional requirements. The international situation is as follows (2):

Max % $(Na_2O)_e$ permitted	% clinker + $CaSO_4$	% slag	% pozzolana including fly ash	% others	No of countries
0.6	95-100				17
0.8	95-100				1
1.0	95-100				2
0.6	50-100	0-50			1
0.9	≤ 50	≥ 50			1
0.9	40-65	35-60			1
1.0	40-80	20-60			1
1.0	85	< ——	15 —— >		1
1.0	60-85	< ——	15 —— >	25	1
1.1	36/40-50	50-60/64			2
1.3	30-70	30-70			1
2.0	15-40	60-85			2
2.0	≤ 15	≥ 85			1

It is known (13) that different aggregates can have different demands in respect of alkali requirements and this may have a bearing on the range of values appearing in the various national standards. It must not, however, be assumed that secondary materials are not capable of releasing alkalis themselves when combined with Portland cements (14).

WHITE CEMENTS

White cements would appear at first sight to be one of the easiest materials to specify in terms of their performance. However to do this on an international basis requires that test methods are carefully harmonized and are related to a definitive international "Whiteness" standard. This is not, at present, the case. The other problem is that powder colour and set cement colour are not always directly related.
The present situation in terms of countries having different requirements is as follows:

No requirements in addition to those for ordinary cements	- 11
"Whiteness" requirements " " "	- 7
"Whiteness" and additional chemical requirements * *	- 4
Additional chemical requirements (without "Whiteness")	- 3

* Based on national "Whiteness" standards.
* These place constraints on the iron and on the manganese compounds present.

RAPID HARDENING CEMENTS

The main characteristic that the user is seeking in this type of cement as opposed to the ordinary cements is that it should provide a high strength very soon after placing. Thus a performance requirement at an early age is important.
Despite this, 18 standards exist (2) where the earliest strength requirement is at 3 days.
Where 24 hour and/or 2 days strengths are specified using the CEN EN 196-1 test method - as they are in 24 countries - the 24 hour requirement ranges from 10 to 28 N/mm^2 and that at 2 days 16 to 30 N/mm^2. (In considering these figures it should be borne in mind that some are "Characteristic" requirements and others are of the "Pass/ Fail" type - this is however unlikely to change the situation by more than 2N/mm^2.)

MASONRY CEMENTS

Masonry cements are required to provide their users with a relatively low strength, good "Workability", and good durability in the hardened state. The low strength and to some extent the "Workability" are achieved through the incorporation of a suitable secondary material. The "Workability" is also improved by providing air entraining and water retaining capabilities. Acceptable durability in the hardened state can be assisted by making provision for an adequate air content. The international situation (2) is given below in terms of the number of countries adopting each approach to the question of specification :

No special requirements apart from strength	12
Air content requirements in addition to the above	7
" " and water retention requirements + above	9

No specification constraints on composition	19
≤ 25% secondary material	1
40-50% " " "	1
≤ 50% " " "	3
≤ 60% " " "	4
≤ 80% " " "	2

Masonry cements show a high degree of orientation to performance type testing and specification with air content being adopted as a second order measure of durability.

AIR ENTRAINING CEMENTS

These are confined to standards adopted in the Americas and in Taiwan (2). Apart from the normal requirements adopted in cement standards, an air content test on mortar is required.

SEA WATER RESISTING CEMENTS

France is the only country to have formal standards to cover this type of product and specification is essentially in terms of compositional and chemical requirements as is shown below (2) :

% clinker + $CaSO_4$	% slag	% pozzolana	% fly ash	% C_3A *	% C_3A + 0.27 (%C_3S) max. *	% max. S	% max. SO_3
97-100				8-10	23.5	0.2	2.5
97-100				≤ 8	23.5	0.2	3
≥ 80	≤ 20		≤ 20	11.5		0.5	3
≥ 90		≤ 10		≤ 10		0.2	3
80-90		10-20		≤ 10	26	0.2	3
≥ 90		≤ 10 % Limestone		8-10	23.5	0.2	2.5
≥ 90		≤ 10 % Limestone		≤ 8	23.5	0.2	3
25-40	60-75					2	4
≤ 20	≥ 80					2	5
25-60	20-45		20-45			2	4

* On clinker component

LEACHING RESISTANT CEMENTS

These cements are specified in Italian standards in terms of composition and pozzolanicity (2) :

Degree of leaching resistance	% clinker + $CaSO_4$	% slag	% pozzolana	% C_3S max.	Pozzolanicity test required
moderate	100			40	no
moderate	51-64	36-49			no
high	31-50	50-69			no
very high	≤ 30	≥ 70			no
high	present *		present *		yes
very high	present *		present *		yes

* Percentage range not defined - performance test being developed.

HYDROPHOBIC CEMENTS

There is a formal standard for this product in India where, in addition to the normal cement specification requirements, a hydrophobicity test is included.

DISCUSSION

1. Over the last 30/35 years, the number of standards for the various types of construction cements throughout the world increased from 129 to 282. By far the largest increase has been for those containing secondary materials.

2. Examination of the data presented indicates that different countries often specify cements for similar purposes in different and sometimes apparently conflicting ways. For example, a cement which requires to have high sulfate resisting properties can, with an undefined clinker C_3A level, contain as much as 90% or as little as 15% clinker.
   Almost all the standards for low heat cements include a mandatory heat of hydration requirement but many also constrain the composition, suggesting that compositional requirements are needed to complement the heat of hydration tests.
   With alkali-aggregate reaction resistance, there is one performance test available, but its validity has been questioned (15) (16), and as far as specification by composition is concerned we have one standard permitting up to 2.0% sodium oxide equivalent (Na_2O) for cement containing 40% clinker and another restricting the maximum to 0.9% with 65 % clinker. This supports the suggestion that it is necessary to

take into account the properties of local aggregates, as well as those of the secondary materials. Local guidelines are therefore of primary importance.

3 ASTM in the U.S.A. have, in connection with their C 595 standard for "Blended hydraulic cements", made considerable efforts to produce valid performance tests and associated specification limits. These are still the subject of some criticism, but the experience gained is very important for future developments.

4. In Europe, the CEN Technical Committee (TC/51) dealing with Cement & Building Limes has set up a working group (N°12) which is charged with the identification of any additional test methods for performance which are required to specify cement and are suitable for European standardization.

5. Performance tests, in many cases, require a considerable time before they are capable of showing the acceptability of a product and if they are accelerated excessively they may give misleading results. As such they are often unsuitable for process control purposes and when this situation prevails it is necessary to relate them to the more rapid chemical and physical tests suitable for that purpose.

REFERENCES

(1) British Standards Engineering Standards Committee, (1904), Specification N° 12 "Portland cement"

(2) CEMBUREAU, (1991), "Cement Standards of the World", Cimeurope

(3) W. MICHAELIS, (1892), Tonind. Ztg., 16, 105

(4) R.H. BOGUE, (1955), "The Chemistry of Portland cement" Reinhold, 2nd Edn., 716 - 737

(5) American Concrete Institute, (1985), "Guide to the selection and use of hydraulic cements", ACI Journal, Nov-Dec 1985, 918, clause 6.10.

(6) F.M. LEA, (1956), "The Chemistry of Cement and Concrete", Arnold, 2nd Edn., 424 - 425

(7) Building Research Establishment Digest 250, (1981), "Concrete in sulphate-bearing soils and ground waters"

(8) R. HELMOUTH, (1987) "Fly ash in cement and concrete", Portland Cement Association, 148 - 156

(9) FIP State of Art Report, (1988), "Condensed silica fume in concrete", Thomas Telford, 26

(10) F. HAWTHORN, E. DEMOULIAN, P. GOURDIN, C. VERNET, (1980), "Blastfurnace slags and clinkers - mutual influences" 7th International Congress on the Chemistry of Cement, Editions Septima III 145

(11) American Society for Testing and Materials, (1989), "Standard specification for blended hydraulic cements", C 595

(12) American Society for Testing and Materials, (1989) "Standard test method for length change of hydraulic-cement mortars exposed to a sulfate solution", C1012

(13) CEN TECHNICAL COMMITTEE TC 51, Private communication

(14) D.F. BARLOW and P.J. JACKSON, (1988), "The release of alkalis from pulverised-fuel ashes and ground granulated blastfurnace slags in the presence of Portland cements", Cement and Concrete Research, 18, 235-248

(15) E.C. ROBERT, (1987), "The influence of pulverized fuel-ash on ASR, behavioural differences between mortars containing pyrex glass and beltane opal", Concrete Alkali-Aggregate Reactions, Noyes Publications, 98-103

(16) R.D. HOOTON, "Effect of containers on ASTM C-441-pyrex mortar bar expansions", Concrete Alkali-Aggregate Reactions, Noyes Publications, 351-357

Specific Theme IV B

Cement-aggregate Compatibility and Structure Property Relationship Including Modelling

INFLUENCE OF INTERMILLING SILICA FUME AND RHYOLITE IN ICELANDIC CEMENT ON ALKALI SILICA REACTION

Gudmundur Gudmundsson* and Jón S Möller**

**Icelandic State Cement Works, ICELAND*
***Division of Building Materials, Chalmers University of Technology, Gothenburg, SWEDEN*

SUMMARY

Icelandic cement takes its characteristics from its unusual raw materials. High alkali content in combination with Alkali-Silica reactive aggregates has initiated Alkali-Aggregate reactions in concrete. Research has shown that Alkali-Aggregate reactions can be controlled by intermilling Condensed Silica Fume and Rhyolite with the cement clinker. Eight years continuous measurement of mortarbar expansion of 7.5% CSF cement with active sand shows less than half expansion, compared with the same cement without CSF. Up to 35% replacement with CSF and Rhyolite does not seem to reduce 28 days cement strength significantly.

ZUSAMMENFASSUNG

Die Eigenshaften des Islandischen Zement sind von den ungewönlichen Rohmaterialen abhängig. Der hohe Anteil an Alkalisalzen im Zement hatte zuzammen mit reaktiven Zuschlagmaterialen Alkalischäden im Beton zur Folge. Untersuchungen haben aber gezeigt dass Alkalireaktionen kontrollert und reduziert werden können durch Zugabe von Silikastaub und Liparit bei der Zementvermalung. Kontinuerliche Messungen von Mörtelprismen die jetz acht Jahre dauern beweisen dass eine Zugabe vom 7.5% Silikastaub in einer Mörtelmischung mit reaktivem Sandzuschlag nur die halbe Alkalidehnung aufweist verglichen mit derselben Mischung ohne Silikastaubzugabe. Ein Austausch von 35% Zement gegen eine Mischung von Silikastaub und Liparit scheint die 28 Tage Druckfestigkeit von Zement wenig zu senken.

INTRODUCTION

Concrete, plain or reinforced is the most widely used building material in Iceland. Lack of alternative building materials on one hand and seismic activity and severe climate conditions on the other hand have given concrete this status in modern construction. During the first decades after the second world war there was an explosive expansion in the Icelandic building industry, and therefore a cement production was started in 1958, to replace imported cements.

Iceland has almost exclusively ingenuous geological structure. Through its volcanic activity Iceland is mostly made up of basalt lavas. Substantial deposits of limestone or clay do not exist in the country. Therefore the raw materials used for making cement in Iceland are not traditional, but marine-shell deposits and rhyolite rock.

This paper presents in short terms the composition and properties of the Icelandic cements and the action taken by the Iceland State Cement Works to counteract the risk of damages caused by Alkali-Silica reaction, ASR, in Icelandic concretes.

RAW MATERIALS

The raw materials used for making cement are marine shell sand; 0-2 mm, containing more than 90% $CaCO_3$, as the calcareous part and rhyolite of volcanic origin, type dactic pitchstone with high glass content as the argillaceous part. The rhyolite contains 65-70% SiO_2, 13-14% Al_2O_3 and 5-7% Fe_2O_3.

These extraordinary raw materials have both negative and positive effects on the cement making process. The marine-shell deposits are naturally ground to a fine sand fraction but it is difficult to reach the finest fraction (0.1 mm), whereas rhyolite is rather soft and easy to grind.

The cement is manufactured by the wet process and the burnability of the raw materials is good although the reduced grindability in the finest fraction of the shell sand results in lower lime saturation and less C_3S in the clinker. All precipitator dust from the kiln is disposed.

The clinker produced consists of C_3S=59%, C_2S=23%, C_3A=5% and C_4AF=13%. Alkali content is 1.5% Na_2O eqv., more than double the value, recommended by ASTM for controlling ASR.

ALKALI SILICA REACTION (ASR)

Twenty years ago it was discovered that the concrete aggregates used in the most populated area are sensitive to ASR. In the late sixties and early seventies, tests that were carried out by the ASTM C-289 (Alkali Aggregate Reaction, Quick Chemical Test) and ASTM C-227 (Alkali Aggregate Reaction, Mortar Bar Method) methods, revealed that many Icelandic aggregates are alkali reactive or lie very near the boundary between reactive and non-reactive material as defined by the ASTM standards, (Fig.1) [1,2]. The awareness of this potential danger of Alkali-Aggregate Reaction, AAR, specially in structures subjected to a high degree of moisture, lead to some precautions, such as using selected innocuous aggregates and imported low alkali or pozzolan cements. This was however limited to major structures such as harbours, dams, power stations etc. In general house construction no such actions where taken, partly due to the belief that such constructions where not vulnerable to AAR because of low moisture content, partly because no damage cases had been reported and also because special precautions would have increased building costs [3,4].

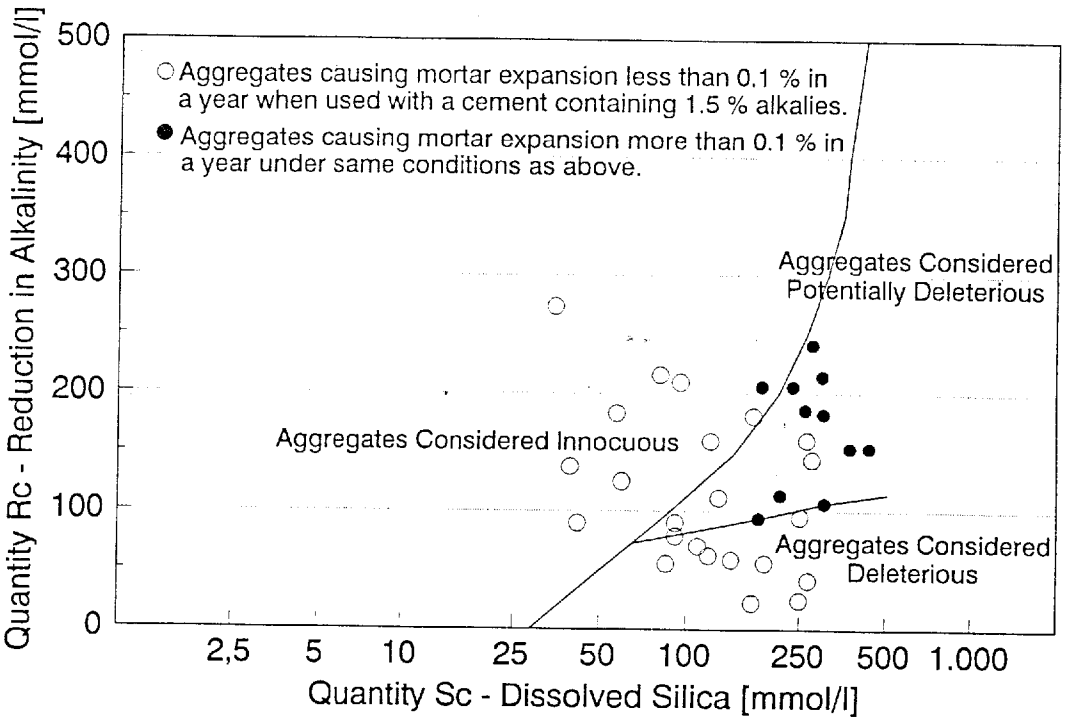

Fig. 1 --- Test results of some Icelandic concrete aggregates according to the Quick Chemical Test and the Mortar Bar Test.

In the late seventies, an intensive field study [5], confirmed that AAR damage was a great problem in housing concrete in the Reykjavík area. Further investigations also showed that the ASR damage was to a great extent due to one aggregate source, Hvaljörd sand. This material, seadredged and unwashed, was used very extensively by the construction industry during the years 1962-1979, and although the potential danger was known, it was ignored [3,4]. Some measures are now taken to wash aggregates from this source, but proofs of effectiveness are limited. Other factors such as high water-cement ratios and unfavourable climate conditions are also believed to have increased the extend of damage.

RESEARCH AND PREVENTIVE MEASURES

It is believed that the ASR can be controlled by the addition of pozzolans, these working as alkali diluents. In Iceland several natural pozzolans are found such as perlite, pumice and rhyolite rock. The rhyolite used as raw material for the clinker process appeared to have rather good pozzolanic properties and for a period of about 5 years all Icelandic cements were interground with 9% rhyolite.

Later on in collaboration with the Building Research Institute, BRI, in Reykjavik, trails were made to use condensed silica fume, CSF, for controlling ASR. Different amounts of silica fumes were used and the alkali silica reaction was measured. The expansion was measured according to ASTM C-227 and ASTM C-289 and the aggregate used in the tests was Hvalfjörd sand. As is seen in Fig.2, with 10% rhyolite the expansion is reduced to less than half compared to the portland cement with no addition. Expansion further reduces with the increase in the amount of rhyolite. Silica fume is seen to be more effective than the rhyolite in controlling expansion. It is also interesting to note that the amount of silica fume needed is also half than that of rhyolite. The expansion further decreases with increase in the amount of silica fume.

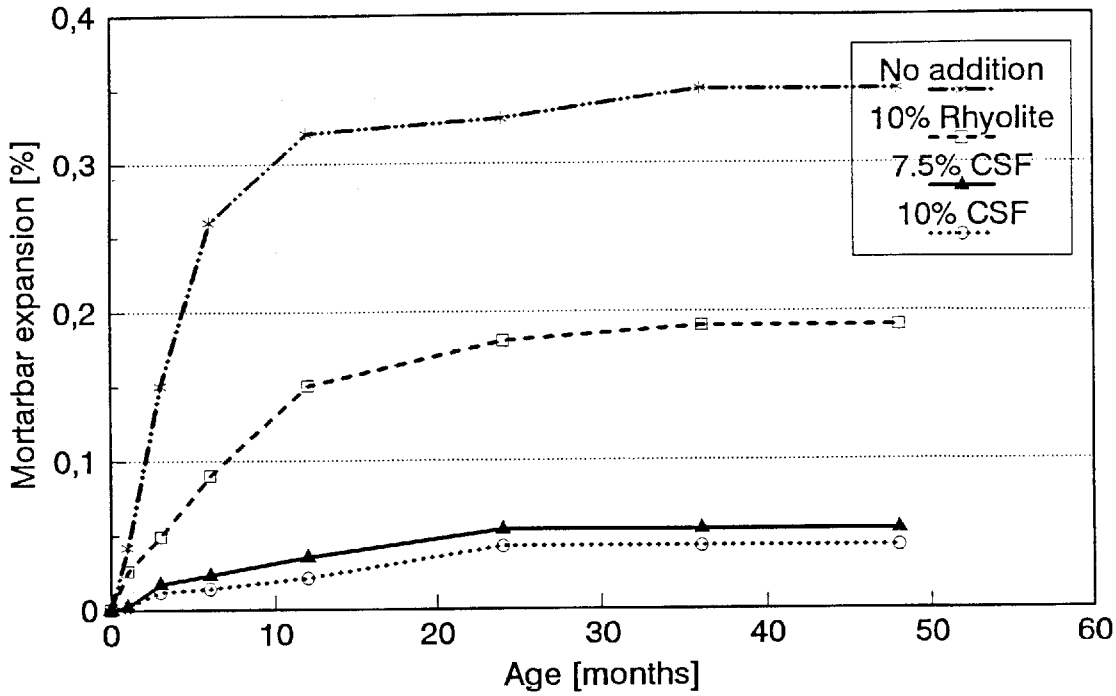

Fig.2 --- Mortarbar expansion of trial interground mixes with Hvalfjörd sand.

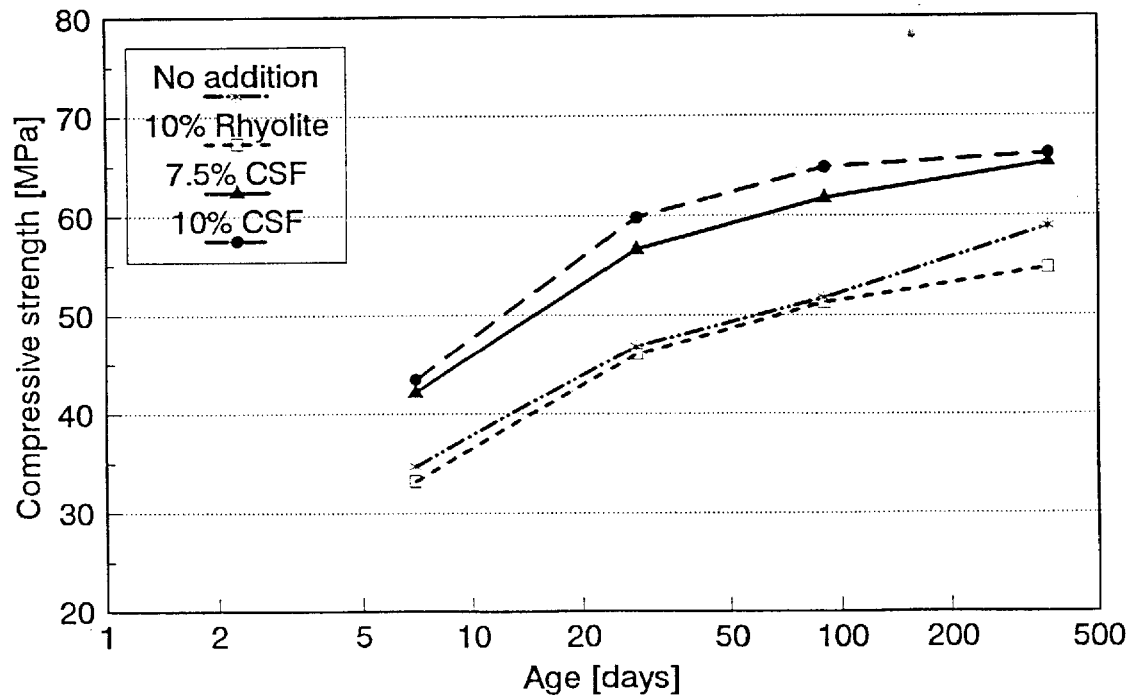

Fig.3 --- Compressive strength of trial interground cements.

In the research the mortarbar expansion was measured up to 4 years. It is seen in the figure, (Fig.2), that the expansion is progressive up to 6-12 months. With 7.5% and 10% CSF the long term ASR is significantly reduced. It was also seen that CSF intergrinding has beneficial influence on many other properties of the concrete such as strength, which was measured up to 365 days, (Fig.3), [6].

There are some contradictory test data on the effectiveness of CSF to control ASR, based upon short time test like 14 days performance in ASTM C-441. The results can be very much misleading and can cause big damages [7]. Results reported on the influence of CSF on the durability properties are also very much controversial. It may be due to the inhomogeneous dispersion of CSF, when blended into the cement in the laboratory or at the concrete mixing plant. In this case CSF will accumulate and will show ball bearing effect. Whereas $Ca(OH)_2$ will precipitate at isolated places, even when CSF present can have the capacity of interacting with all the alkali. This can be the reason for localized damage of concrete [8].

To avoid this problem of dispersion, condensed silica fume is intermilled with the cement in Iceland. Basing upon the test results, 7.5% CSF was decided to be used as a standard measure for controlling ASR. Test series spanning eight years comparing Icelandic Portland Cement with no CSF addition and the same cement with 7.5% intermilled CSF are shown in Fig 4. The figure shows that mortarbar expansion with active sand is less than half for the 7.5% CSF cement, compared with the unblended cement. The expansion is however still active in the blended cement after eight years. This shows that although the ASR process can be slowed down by CSF intermilling, the reactions will still take place if other conditions are ASR favourable.

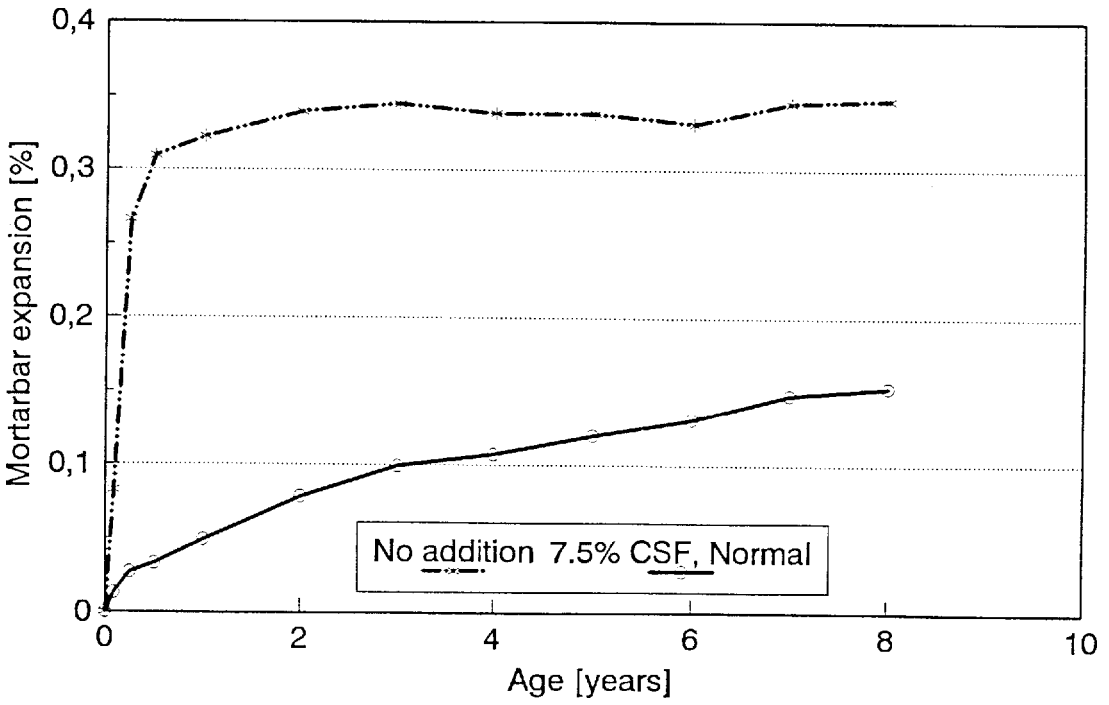

Fig.4 --- Eight years mortarbar expansion with Hvalfjörd sand.

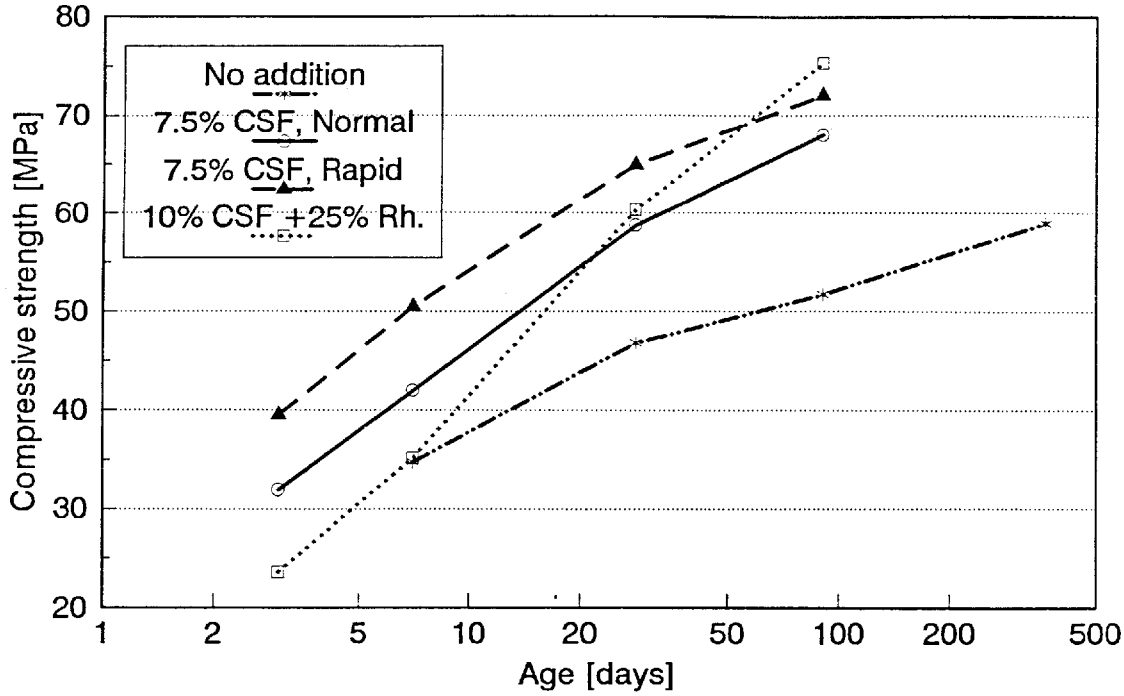

Fig.5 --- Compressive strength; current production, 1991 sample series.

Since the CSF-intermilled cement was put into production, core samples have been taken regularly from concrete walls of dwelling houses in areas where reactive aggregates have been used. No cases of damages due to ASR have been reported and no signs of ASR have been detected in the cores,[4,9].

MODIFICATIONS

Experimental production, where 10% CSF and 25% Rhyolite are interground with the cement clinker has shown encouraging results. This cement has a remarkable good compressive strength development (Fig.5) and seems to have good ability to reduce alkali-aggregate expansion. The cement, which is called "Blöndu" cement, after a hydro power station presently under construction, is being developed to cast thick concrete masses where early heat development can cause problems. Results from long term mortar bar expansion tests with the 10% CSF/25% Rh. cement will be published soon.

Parameter		Cement Type 7.5% CSF Normal	7.5% CSF Rapid	10% CSF + 25% Rh.
SiO_2	%	24.4	24.3	35.6
Al_2O_3	%	4.20	4.12	5.05
Fe_2O_3	%	3.82	3.78	3.40
Free lime	%	1.01	1.08	0.37
Fineness	cm^2/g	3902	6626	6646
Specific gravity	g/cm^3	3.02	2.97	2.73

Table 1. --- Some parameters of cement types in present production.

A rapid hardening variation of the 7.5% CSF cement is also produced. The only difference between the two is the fineness, whereas the composition is almost identical. Some characteristic parameters of the three cement types, currently in production in Iceland are shown in table 1.

CONCLUSIONS

The cements produced in Iceland have very high alkali content. Important concrete aggregates, used in the most populated area, are alkali-silica reactive. This has required some preventive measures to be taken.

The results from intermilling CSF and Rhyolite with the cement clinker have shown very reasonable results during the last decade. Mortarbar expansion with reactive sand is by far slower when the clinker is interground with CSF and Rhyolite.

Up to 35% total replacement does not seem to reduce the compressive strength of the cement considerably, and 7.5% CSF replacement increases compressive strength.

REFERENCES

1. Guðmundsson, G. & Ásgeirsson, H.: "Some investigations on alkali aggregate reaction", **Cement and Concrete Research**, Vol. 5, 1975, p 211-220.

2. Gudmundsson G., "Condensed silica fume in concrete", **University of Trondheim, Report BML 82.610**, Feb 1982, p 135-140.

3. Guðmundsson, G. & Ásgeirsson, H.: "Parameters affecting alkali expansion in Icelandic concretes", **6th International Conference on Alkalis in Concrete, DBF, Copenhagen**, 1983, p 217-221.

4. Olafsson, H.: "AAR problems in Iceland - Present state", **8th International Conference on Alkali-Aggregate Reaction**, Kyoto 1989, p 65-70.

5. Kristjánsson, R.:"Steypuskemmdir-ástandskönnun", **The Icelandic Building Research Institute**, 1979, (In Icelandic)

6. Ásgeirsson, H. & Guðmundsson, G.:"Pozzolanic activity of silica dust", **Cement and Concrete Research**, Vol. 9, 1979, p. 249-252.

7. Chandra, S. Berntsson, L.,"Durability of concrete by mineral admixtures mixing"; **Mineral Admixtures in Concrete** (to be published by ABI Books Pvt Ltd., New Delhi, India.)

8. Bentz, D.P. & Garboczi, E.J.:"Simulation studies of the effects of mineral admixtures on the cement paste- aggregate interfacial zone", **ACI Material Journal**, 1991, 88(5), p 518-529.

9. Kristjánsson, R. & Ólafsson, H.:"Durability of Concrete in Iceland", **Durability of Concrete - G.M.Idorn International Symposium, SP-131, ACI**, 1992,

THE ALKALI-SILICATE REACTION IN SOME BRAZILIAN DAMS

V A Zampieri, Y Kihara* and L Scandiuzzi

Associacao Brasileira de Cimento Portland
**Universidade de São Paulo, São Paulo, BRAZIL*

SUMMARY

Brazilian dams constructed over 15 years ago, without pozzolanic materials, have shown evidences of alkali-silicate reaction. At the time of construction, the aggregates used were considered as non-reactive (gneissic, migmatitic and granulitic rocks of a prevailingly granitic composition).

High temperature conditions (up to 40°C) and humidity oscillations are the main factors affecting the reaction, the intensity of which normally varies in the same structure. Locally, the strain degree of the aggregates is the principal conditioning factor of the reaction, which is more developed on rocks subject to heavier deformation, of a finer grain size. The quartz and feldspars - both strained and with a typical ondulating extinction - appear as the reactive phases in such aggregates.

The reaction products investigated by *SEM* and *EDS* are basically a silico-alkaline gel with a varying *Ca/Si* ratio and a high *K* proportion. Usually, the *Na* content is low in this material. The associated crystallized phases are often more rich in alkalis (mainly *K*) and with varying morphologies, similar to those described in the literature.

SOMMAIRE

Les barrages brésiliens construits depuis 15 ans, sans additions de pouzzolanes, presentent des évidences de réaction alcalins-granulats. Les granulats utilisés (gneiss, migmatites et granulites de composition granitique) ont été considerés comme non réactifs.

Les conditions de haute température (> 40°C), les variations de l'humidité et la disponibilité en alcalins sont les principaux facteurs qui agissent sur l'intensité de la réaction. Le degré de déformation du granulat est le principal facteur conditionnant la réaction. Le quartz et le feldspaths, tous deux à extinction roulante, sont les principaux responsables de la reactivité du granulat.

Dans le béton, les produits de l'alcali-réaction etudiés par la microscopie électronique à balayage avec *EDS*, sont des gels de silicates alcalins avec des rapports *Ca/Si* variés et avec un contenu élevé de *K*. Par contre, le contenu en *Na* est très bas. Les phases cristallines associées sont plus riches en alcalins que les gels et présentent des morphologies variées (rosaces, prismes, feuilles...), similaires à celles décrites dans la littérature.

1 INTRODUCTION

Concrete durability studies focusing alkali-silicate reactions are becoming a growing concern among technologists and researchers involved in civil construction. Evidences of reactions have been systematically and increasingly reported at international symposiums and congresses. In Brazil, the occurrence of alkali-aggregate reactions is scarcely documented. It was only after 1985 that the Brazilian technicians became aware of the occurrence of alkali-silicate reaction in the concrete of the *MOXOTÓ*[1] and the *JOANES II*[2,3] dams, both located in the northeast region of the country (*Figure 1*).

Although the international technical literature on alkali-aggregate reaction is expressive, very little is known about the kinetics and mechanism of the alkali-silicate reaction.

The purpose of this paper is to contribute toward to a better knowledge of the alkali-silicate reaction, reporting the studies developed at Brazilian Portland Cement Association (ABCP) on concretes of some Brazilian dams (Joanes, Pedras and Paulo Afonso).

2 SITE AND CHARACTERISTICS OF THE STUDIED DAMS

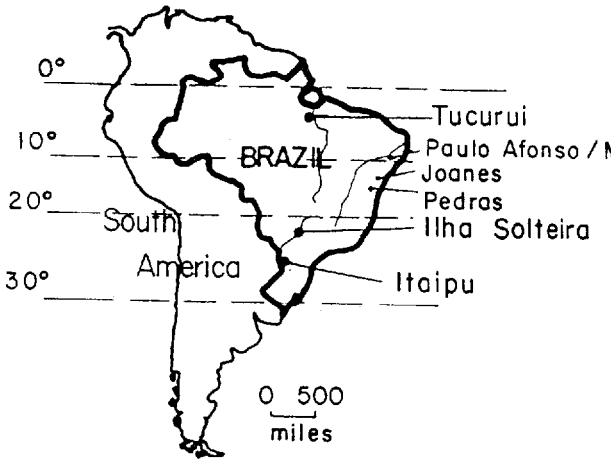

Figure 1 shows the site of the three largest Brazilian dams along with the Moxotó, Joanes, Paulo Afonso and Pedras dams. (For main characteristics see *Table 1*).

TABLE 1 - Main Characteristics of Some Brazilian Dams

Dam	Power Output (MW)	Completion year	Concrete volume (m^3)	Nature of aggregate	Pozzolan used	Site
Itaipu	12,600	1983	12,000,000	Basalt	Fly ash	Paraná river, Paraná State
Tucurui	6,480	1983	5,000,000	Metasediment and basalt	Calcined clay (Flay ash)	Tocantins river, Pará State
Ilha Solteira	3,200	1973	3,675,600	Basalt and gravel	Fly ash and calcined clay	Paraná river, Mato Grosso do Sul State
Pedras*	Flood control and irrigation	1970	308,000	Granulite	-	Contas river, Bahia State
Joanes II*	Water supply	1971	9,360	Gneiss, migmatite and granulite	-	Joanes river, Bahia State
Paulo Afonso I-III*	660	1971	Not available	Granite, gneiss and migmatite	-	São Francisco river, at the boundary of Bahia and Alagoas State
Moxotó	439	1974	514,000	Granite, gneiss and migmatite		

(*) Investigated dams

3 GENERAL CHARACTERISTICS OF STUDIED CONCRETES

The investigated samples - drill-hole cores taken from concretes of the Pedras, Joanes and Paulo Afonso Dams - exhibit textural and structural features consistent with concretes submitted to normal preparation and mixing processes.

They are compact, homogeneous concretes showing a good paste/aggregate adherence. Their cracks are of small importance and localized, without a characteristic standard (random cracking).

The fine aggregates are of natural origing (river sand), of quartzous composition (>90%) and free from reactive phases (opal, chalcedony, etc.). The coarse aggregates (>4,8mm) consist of crushed rocks of a high metamorphic grade (gneisses, migmatites and granulites) and granites, which are resistant, without apparent weathering and of a predominantly ***granitic composition***. More deformed and milonitized types are locally observed.

At an optical microscope the coarse aggregates are shown to be made up of potassium feldspar, calc-sodium feldspar and quartz. Secondarily, there are varying proportions of brown biotite, garnet, amphybole (hornblend) and pyroxene, in addition to opaque and accessory minerals. Usually, the quartz and feldspar crystals occur strained and with a typical ondulating extinction (***Figures 2*** and ***3***). Re-crystallization of quartz are frequently observed.

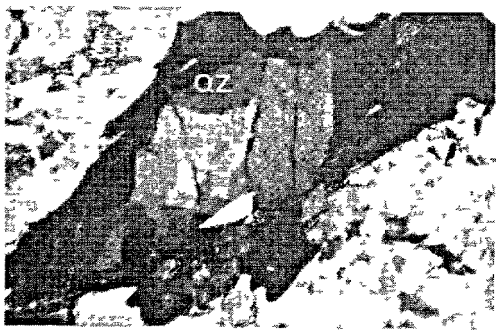

FIGURE 2 – Strained and elongated quartz grain (QZ) following the rock foliation (Pedras Dam) (Ampl. 50x)



FIGURE 3 – Plagioclase (P) and perthitic orthoclase (F) crystals with apparent strain. Qz = quartz (Pedras Dam) (Ampl. 50x).

4 ASPECTS AND PRODUCTS OF THE ALKALI-SILICATE REACTION AT PEDRAS, JOANES AND PAULO AFONSO DAMS

In the studied samples, the alkali-aggregate reaction usually occurs unexpressively, being more intensive in concrete areas subjected to high temperatures and humidity oscillations. Incipient reaction rims and filling of pores with a whitish secondary material are the most usual evidences. Cracking is in general a less common feature. On the few cracking plans and in the area of detaching of coarse aggregates (particularly those of a large size), the occurrence of whitish secondary materials can be noted, similar to those that fill the pores. Gel exsudation is a rare feature.

The visualization of aggregates with developed reaction rims, which occur side by side with others without an apparent reaction, show that the reaction is heavily affected by the textural and compositional characteristics of the coarse aggregates. The rocky types of granitic composition which along the geological time had been subjected to a more intensive strain and shearing or to a high-grade metamorphism appear to be the more reactives.

Tests performed with a Scanning Electronic Microscope (SEM) equipped with an Energy Dispersive Spectrometer (EDS) led to the conclusion that the principal reaction product is a silico-alkaline gel, which can be amorphous or exhibit varying crystallinities and morphologies. From the compositional viewpoint, it consists of silicium and, secondarily, of calcium, potassium and aluminun. Sodium is rather unexpressive.

Normally, the gel which is in contact with the cement paste or fills the pores and cracks tends to show a higher Ca/Si ratio (>1,0) and a lower content of potassium. The nature more basic and smaller contents of alkalis of this external gel apparently account for a more massive aspect and greater stability during sample drying and metallic coating. The internal gel, comparatively richer in alkalis and with a smaller Ca/Si ratio (.4 - .8) shows an intensive cracking process during the drying operation (contraction cracks). This suggests that this phase exhibits a wider expansion capacity. The slim whitish film (reaction rim) which is macroscopically observed surrounding certain areas or the totality of some reactive aggregates, usually at a few millimeters from the edge, would be the outcropping of such reaction products (*Figures 4, 5, 6*).

Moving toward the center of the aggregate, crystalline phases of varying morphologies are observed, which develop into voids or on the weakness planes of the aggregate (cracks, cleavage planes, contact of crystals). Phases of placoid and lamellar foliate habit are frequent. Spear-shaped crystals are seen at a smaller proportion (*Figures 7 - 11*). The compositions of these phases as revealed by the EDS are similar. Only a few changes are observed in the Ca/K ratio and in the Al or Na contents. These latter elements occur normally in low proportions. Hair-thread like filament crystals can be observed, where sodium occurs with a more expressive content.

Although the crystalline phases keep a certain compositional similarity with the external amorphous gel, they are typically richer in alkalis (particularly K). Crystals of ettringite, both isolated or in dense aggregates, as well as carbonate crystals can also occur associated to these materials. The identified reaction products are morphologically similar to those described in the literature[4,5,6].

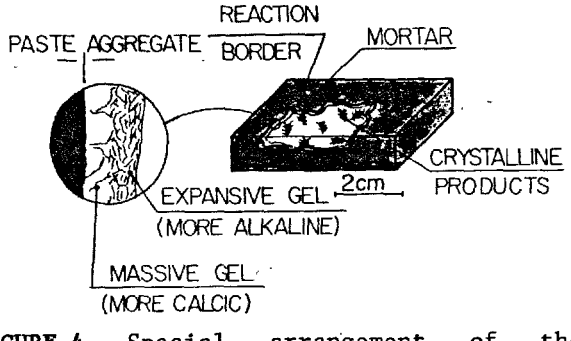

FIGURE 4 - Spacial arrangement of the reaction products.

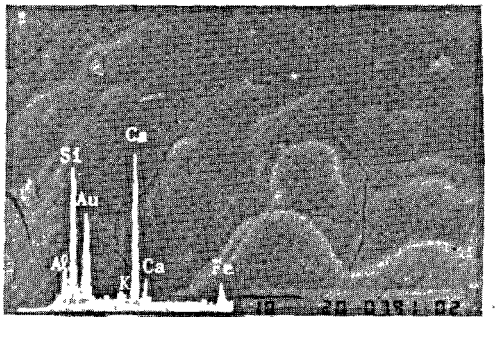

FIGURE 5 - External, more calcic gel (Pedras Dam).

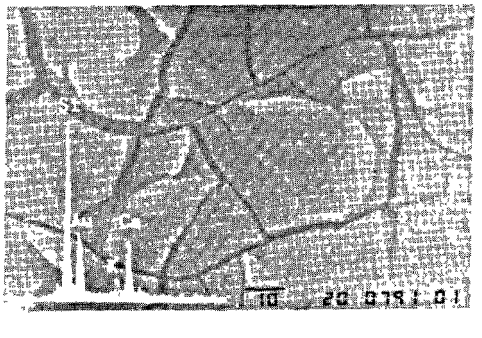

FIGURE 6 - Cracked, more alkaline gel (Pedras Dam).

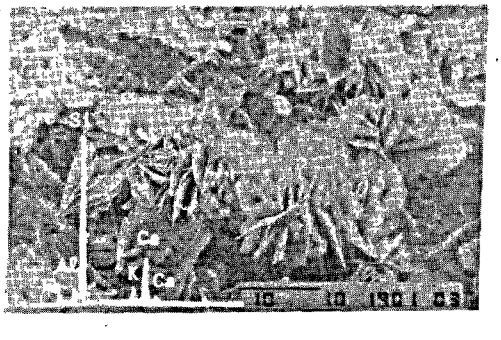

FIGURE 7 - Foliated crystalline phase occuring as rose crystals (Joanes Dam).

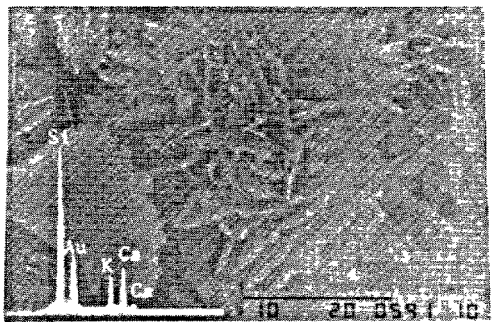

FIGURE 8 - Crystalline spear-shaped phase (Pedras Dam).

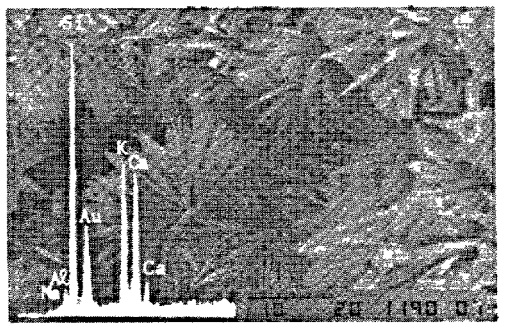

FIGURE 9 - Foliated crystalline phase (Paulo Afonso Dam).

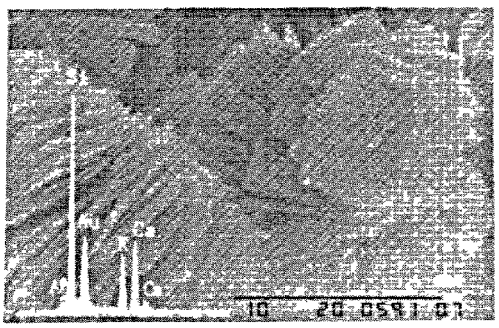

FIGURE 10 - Placoid-quadrangular phase (Pedras Dam).

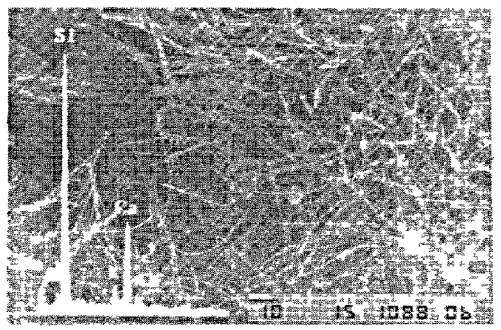

FIGURE 11 - Crystalline more sodic phase (Joanes Dam).

FIGURES 5 - 11 - Morphology and spectra of *EDS* obtained from the crystalline phases observed (Gold peaks result from the coating process).

5 REACTIVITY OF STRESSED QUARTZ AND FELDSPAR

Normally the reactivity of granitic aggregates, which developed expansive reactions of the alkali-silicate type have been attributed to stressed quartz. The role of feldspar in such reactions was investigated by Indian researchers[7,8,9]. *SEM/EDS* studies developed in concretes of Pedras Dam allowed to conclude that also the alkaline feldspar (perthitic orthoclase) and plagioclase must be considered as reactive phases, since these mineral phases develop reaction products similar to those observed in the case of quartz. The products resulting from feldspars are rather rich in aluminum (*Figures 12 - 14*).

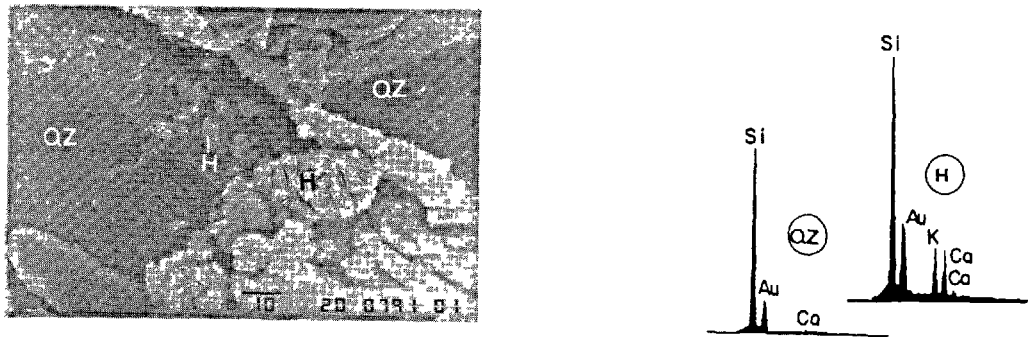

FIGURE 12

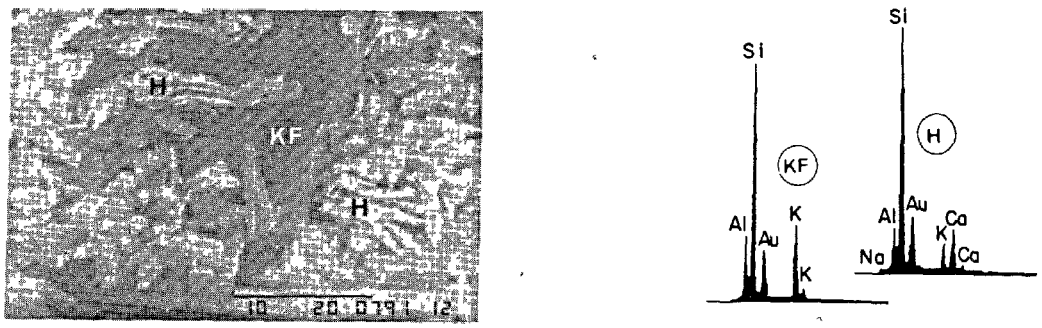

FIGURE 13

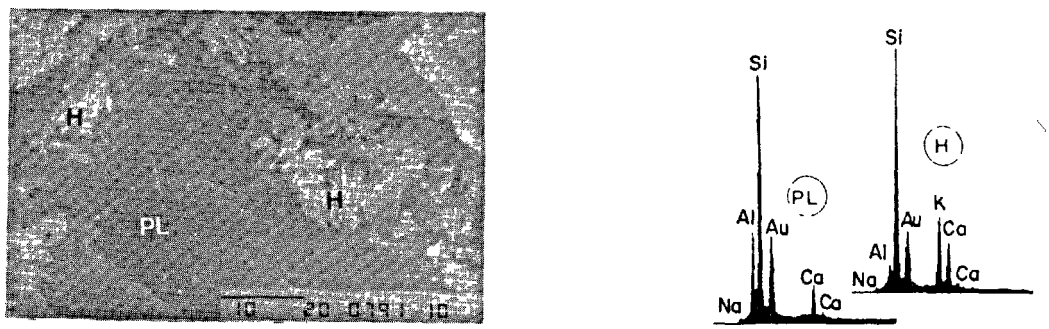

FIGURE 14

FIGURES 12 - 14 - *SEM* - Photomicrographies showing the development of reaction products (H) out from quartz crystals (QZ), alkaline feldspar (KF) and plagioclase (PL). To the righ of each photography the corresponding *EDS* spectra are seen (Pedras Dam).

6 CONCLUSIONS

In addition to Moxotó Dam, which was previously studied[1], the alkali-silicate reaction was also characterized at the Brazilian dams of Joanes, Pedras and Paulo Afonso, all of which located in the northeast region and constructed over 15 years ago using Portland cements (Type I - ASTM) with Na_2O equivalent of .8 - 1.1% and without pozzolans. The coarse aggregates used were obtained from granitic rocks or from rocks of high metamorphic grade (gneisses, migmatites and granulites) of prevailingly quartz-feldspar compositions.

Quartz and feldspars, both stressed, are the reactive phases of these aggregates. The reaction products identified consist basically of a silico-alkaline gel with varying Ca/Si ratio and a high potassium proportion. The crystalline phases that occur associated appear relatively enriched in alkalis and with varying morphologies (placoids, foliate,

lamellar, spear-shaped or filamentous), similar to those described in the literature.

The higher alkali content, particularly potassium, of the crystalline phases observed in the aggregates permits to assume that part of alkalis could derive from feldspars. The crystalline phases rich in sodium are found more frequently at the Joanes Dam, where the cement used presents a Na_2O equivalent close to .8%, with average contents of .7% of Na_2O and .2% of K_2O. However, even at this dam, the crystalline products identified exhibit a larger proportion of K_2O than Na_2O, thus confirming the assumption that the alkaline feldspars are important sources of K_2O.

The paragenetic association of the reaction products suggest that the expansion and cracking process is associated to a more alkaline gel, with a smaller participation of the massive gel (more calcic) and of the associated crystalline phases.

The occurrence of reactive aggregates, the regional climatic conditions characterized by high temperatures (up to 40°C), the high humidity of the concretes (dam concretes) and the presence of available alkalis (partly deriving from feldspar) were the interacting factors which conditioned the development of alkali-silicate reactions in the studied dams.

REFERENCES

1 Cavalcanti, A.J.C.T.: "Alkali-aggregate reaction at Moxotó Dam, Brazil". In: **PROCEEDINGS of the International Conference on Alkali-Aggregate Reaction, 7th**, Ottawa, 1986. Park Ridge: Noyes, 1987. p.168-72.

2 Kihara, Y. and Zampieri, V.A.: "Concrete deterioration by alkali-aggregate reaction: microstructure aspects by scanning electron microscope" (in Portuguese). In: SOCIEDADE BRASILEIRA DE MICROSCOPIA ELETRÔNICA. **SIMPÓSIO Brasileiro de Microscopia Eletrônica e Técnicas Associadas na Pesquisa de Materiais: MICROMAT 88**, São Paulo, 24-6, october 1988. p.5-8.

3 Pimenta, M. de A., Fontoura, J.T.F. and Scandiuzzi, L.: "Investigations and study of alkali-aggregate reaction in concrete of Joanes II Dam" (in Portuguese). In: INSTITUTO BRASILEIRO DO CONCRETO (IBRACON). **REUNIÃO do IBRACON, 31ª**, São Paulo, July 31 - August 4, 1989.

4 Regourd, M. and Hornain, H.: "Microstructure of reaction products". In: **PROCEEDINGS of the International Conference on Alkali-Aggregate Reaction, 7th**, Ottawa, 1986. Park Ridge: Noyes, 1987. p.375-80.

5 Regourd-Moranville, M.: "Products of reaction and petrographic examination". In: **INTERNATIONAL Conference on Alkali-Aggregate Reaction, 8th**, Kyotto, 1989. p.445-56.

6 Davies, G. and Oberholster, R.E.: "Chemincal and swell properties of the alkali-silica reaction product". In: **INTERNATIONAL Congress on the Chemistry of Cement, 8th**, Rio de Janeiro, Sept. 22-7 1986. v.5, p.249-55.

7 Visvesvaraya, H.C., Mullick, G.S., Sinha, S.K. and Wason, R.C.: "Alkali reactivity of granitic rock aggregates". In: **INTERNATIONAL Congress on the Chemistry of Cement, 8th**, Rio de Janeiro, 22-7 Sept. 1986. v.5, p.208-13.

8 Rao, L.H. and Sinha, S.K.: "Textural and microstructural features of alkali reactive granitic rocks". In: **INTERNATIONAL Conference on Alkali-Aggregate Reaction, 8th**, Kyotto, 1989. p.495-9.

9 Mullick, A.K., Wason, R.C., Sinha, S.K. and Rao, L.H.: "Evaluation of quartzite and granite aggregates containing strained quartz". In: **PROCEEDINGS of the International Conference on Alkali-Aggregate Reaction, 7th**, Ottawa, 1986. Park Ridge: Noyes, 1987. p.429-433.

CORRELATION OF CONCRETE STRENGTH WITH CEMENT ACTIVITY AND PHYSICO-MECHANICAL CHARACTERISTICS OF COARSE AGGREGATE

I A Sulkowsky and A G Milrud

The Tashkent State University named after Beruni Tashkent, UZBEKISTAN

SUMMARY

On the basis of the known mathematical approach the concrete dependence strength has been obtained, that one is expressed as the solution function strength and the large aggregate filler. The expression of the given deformation module and Walker formulae has been used for its obtaining.

В статье на основе строгого математического подхода получена зависимость прочности бетона, выраженная в качестве функции прочности раствора и крупного заполнителя. Для её получения использовано выражение приведенного модуля деформации и формула Уокера.

Concrete failure occurs when the flow of a specimen which is equal to the total flow of its components exceeds the tolerance value.

$$\varepsilon_б = (1-\varphi_з)\varepsilon_р + \varphi_з \varepsilon_з \qquad (1)$$

where $\varepsilon_р$ and $\varepsilon_з$ - the mix and aggregates flow respectively,

$\varphi_з$ - the volume content of the coarse aggregate.

The expression (1) was derived to calculate the flow modulus of a concrete as affected by the action of the mix and coarse aggregate.

Knowing the flow modulus concrete strength was calculated employing the worker formula

$$E = \alpha\sqrt{R_б}$$

recommended by the European Concrete Committee.

The efficiency of such an approach has been checked in calculating the load-carrying capacity of brick-work for which the given flow modulus is a more vivid characteristic due to its regular structure, As a result me got a sufficiently precise relation obviating the need for using Onischic's empirical formula.

Passing from flow to moduli in terms of the expression we get the value of the given concrete flow modulus which acquires the following form provided $\alpha_з \approx 0{,}5$:

$$E_{пр} = \frac{2E_р E_з}{E_з + E_р} \qquad (2)$$

Using the Worker formula we can express the given concrete flow modulus and the flow moduli of the components as their strength.

$$R_б = \frac{C R_р}{\left(1 + \frac{1}{K}\sqrt{\frac{R_р}{R_{зк}}}\right)^2} \qquad \ldots \quad (3)$$

where $R_{зк}$ - strength of the discrete aggregates,

$R_{зк} \approx 10\ R_ц$ where $R_ц$ - strength of the aggregates in the cylinder,

K - coefficient of strength growth of the coarse aggregate grains, acting in concrete in the state of tri-axial compression. According to independent experimental data K = 2,5.

C - proportionality factor. This is calculated on condition that concrete strength is equal to mix strength $R_б = R_р = 400$ kgF/cm^2 while using high quality coarse aggregate $R_{зк} = 1200$ kgF/cm^2 and is approximately equal $\approx 1{,}5$.

The relation (3) realistically describes the strength of concrete in terms of aggregates' strength which varies over a wide range.

The strength of the mix, taken into account in formula (3), changes in direct proportion to the cement activity.

Analysis of formula (3) shows that concrete strength can vary in direct proportion to cement activity only for low quality concrete with high quality coarse aggregate, when the value $R_p/R \to 0$.

Thus, if either the mix strength is increased and er ordinary aggregates are used the relation of direct proportionality in formula coases to hold.

The research conducted thus shows that the Bolomey formula

used at present in allowing for the influence of cement activity is not quite precise on concrete strength.

However, above relationship has been refined as below for greater precision on the basis of the experimental data of Z.A.Kiser from the Reinforced Concrete Research Institute

$$R_б = 10\left(\alpha\sqrt{R_ц}\,\frac{Ц}{В} - 10\beta\right) \qquad \ldots (4)$$

where $R_ц$ - cement activity,

$\alpha; \beta$ - experimental coefficients when using high quality materials $\alpha = \beta = 1$.

MICROSTRUCTURE OF INTERFACIAL ZONES BETWEEN HARDENED SULFOALUMINATE CEMENT PASTE AND AGGREGATE

Wang Yanmou*, Li Shaozheng, Lu Yonghua** and Su Muzhen****

**State Administration for Building Materials Industry, P.R. CHINA*
***Cement Research Institute, China Building Materials Academy, Beijing, P.R. CHINA*

SUMMARY

The hydration products, crystal sizes, morphological features and thickness of the interfacial zones between hardened sulphoaluminate cement pastes and limestone aggregates with different gypsum contents have been investigated systematically by means of XRD, SEM / EDAX, TGA etc. The effects of various restraining conditions on the microstructure in interfacial zones have been studied and the bonding strengthes between hardened cement pastes and limestone aggregates have been measured as well. The relationship of microstructure in interfacial zone and mechanical properties of hardened cement paste is discussed.

〔摘要〕

本文采用 XRD、SEM / EDAX、TGA 等测试工具系统地研究了不同石膏掺量的硫铝酸盐水泥系列硬化浆体与石灰石集料界面区的水化产物、晶体尺寸、形貌、界面区厚度以及不同限制条件对上述微结构的影响。同时测定了不同水泥浆体与石灰石集料的粘结强度。讨论了界面区微结构与水泥石力学性能的相关性。

INTRODUCTION

The performances of cement concrete are determined by the properties of its compositions and the bonding characteristics among the compositional materials. Transition zone is the weak, yet crucial part of concrete.

Sulphoaluminate based cement is a new type of cement series, which shows many advantages. With $C_4A_3\overline{S}$ and $\alpha-C_2S$ as the main mineral compositions, sulphoaluminate clinker can be used to produce high early strength, expansive and self-stressing cements by simply controlling the addition of gypsum, applying to various uses. Nevertheless reports concerning the investigation of the microstructure of sulphoaluminate cement and concrete are very few. So it is necessary to study the transition zone of hardened sulphoaluminate cement paste and limestone aggregate.

EXPERIMENTAL

1. Materials

Chemical compositions of clinker and gypsum are shown in Table 1.

Table 1 Chemical compositions of sulphoaluminate cement clinker and gypsum

Sample	Loss	H_2O	SiO_2	Al_2O_3	Fe_2O_3	CaO	SO_3	MgO
Clinker	1.84	—	9.76	29.49	1.58	42.81	10.2	2.49
Gypsum	5.01	17.91	0.53	0.35	0.11	32.05	41.11	2.43

Preparation of cement: cement clinker and gypsum were ground separately, and the ground gypsum was added into clinker in following proportion, 0%, 15%, 25% and 45%, then the mixture was homogenized in a mixer into four cement specimens, marking SA0, SA15, SA25 and SA45 respectively.

2. Sample preparation

2–1 Artificial interface

The aggregate was manufactured into a cylinder of $\Phi 20 \times 20$ cm, which top and bottom surfaces were polished. The top and bottom surfaces were kept as parallel as possible to each other. The cylinder was surrounded by a film which was then fixed with a piece of copper wire to form a mould. After having placed the cement paste ($W/C=0.3$) into the mould and vibrated it, we put the compound specimen into a fog room for curing to the fixed age. The specimen was demoulded by undoing the film and was separated by tapping the interfacial zone of hardened cement paste and aggregate.

2–2 The preparation of three dimensional restrained specimen was described in reference (1).

2–3 Preparation of the specimen for TDA

A thin layer of specimen was scrapped off from the latest hardened cement paste in the interfacial zone for the test of TDA.

2–4 Preparation of the specimen for interfacial bonding strength

The aggregate was made into the specimen of 4×4×2 cm and placed in a form of 4×4×16 cm , in which cement paste was cast and vibrated for forming. The specimen was cured in standard condition to fixed age.

3. Testing Methods

X–ray peak width technique was adopted to measure the average crystal size, refering to data (2).

RESULTS

1. The interfacial zones of limestone aggregate and 4 hardened sulphoaluminate cements are analysed on the ground of the results from XRD multilaminating analysis, and the trend of AFt crystal content in the direction away from the limestone aggregate is shown in Fig.1 (at the age of 28 days). Apparently, AFt crystal is rich on the surface of limestone. The zone rich in AFt crystal is defined as the thickness of interfacial zone which varies with the content of gypsum added, see Table 2.

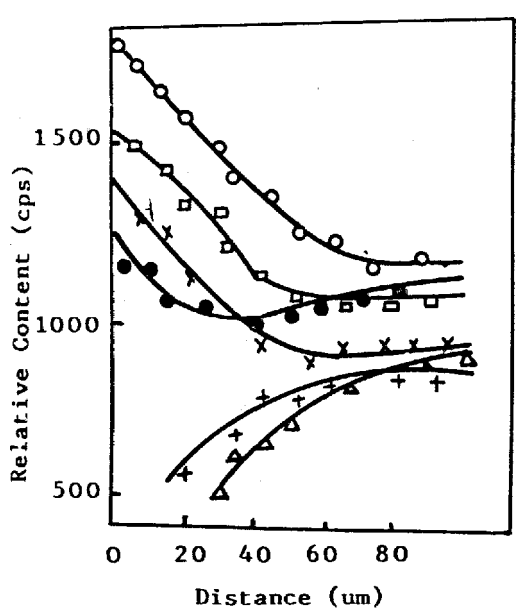

Fig.1 The Variation of AFt crystal distance from limestone

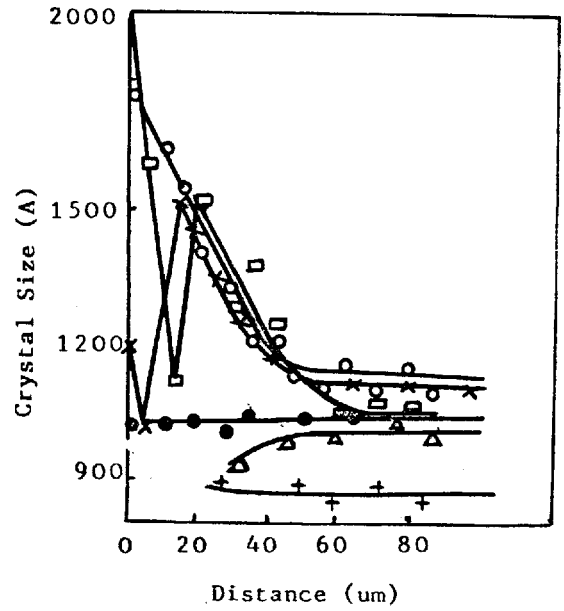

added amount of gypsum x 0; □–5; △ 25; ○ 45; +25 (restrained); ● 45 (restrained)

Fig.2 Mean size of AFt in interface zone with respect to interfacial distance

Table 2 Thickness of interfacial zone

	SA0	SA15	SA25	SA45	Restraining condition	
					SA25	SA45
Thickness (μm)	50	50~60	60~70	70~80	30	30

The results in Table 2 shows that the thickness of interfacial zone increases with the increse of

addition of gypsum, while the thickness of interfacial zone decrease under restraining condition.

2. The variation of AFt crystal size with the distance from limestone aggregate at the age of 28 days, is shown in Fig.2. The average AFt crystal sizes inside interfacial zones are larger than those near the hardened cement pastes (except SA25) and the average AFt crystal sizes inside interfaical zones change considerably with gypsum addition and restraining condition. Under restraining condition the average AFt crystal sizes inside the interfacial zones are similar to those in matrix of hardened cement pastes at the age of 28 days.

3. Morphological and composition analysis of hydration products in interfacial zone

Great difference in morphological features of hydrates in the interfacial zone near the side of aggregate were observed with the variation of gypsum addition and restraining condition. In case of the specimen without gypsum, as shown in Fig.3, EDAX analysis has proved that the hydration products are aluminium gel and ettringite and the characteristic peaks of AFt and AH_3 appears at the temperatures of 134℃ and 260℃ in TGA test (Fig.4), which proved that the area near aggregate is rich in AH_3 gel at first, and then rich in AFt crystal. Its shape is small–fine needle–like crystal.

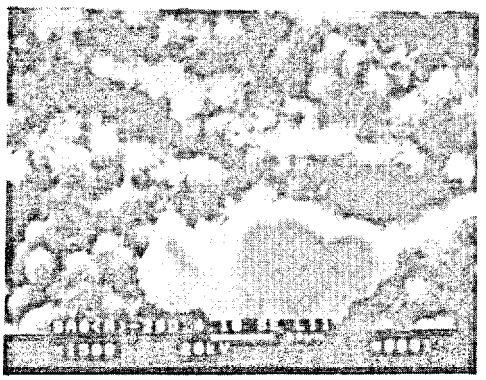

Fig.3 SEM photograph of interfaical zone (0% $C\bar{S}H_2$, 28 days)

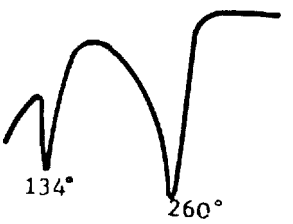

Fig.4 Results of TGA



Fig.5 SEM photograph of interfacial zone (25% $C\bar{S}H_2$, 28 days)



Fig.6 Results of TGA

The hydration products in transition zone become colloidal state when gypsum content reaches

25% (wt%) as shown in Fig.5. The results of TDA are shown in Fig.6, which shows the characteristic peak of ettringite. But no AFt crystal peak appears in the area of 0–30 μm and from the results in Fig.1 and Fig.5 conclude that gel sized and colloidal structure ettringite appears near aggregate at the age of 28 days.

When 15% gypsum was added into the cement, the limestone aggregate surface is rich in tube like AFt crystal (Fig.7), and when gypsum amount was added up to 45%, more AFt crystal appears nearby the limestone aggregate at the age of 28 days. AFt crystal was well grown and like plum blossom, as shown in Fig.8.



Fig.7 SEM photograph of interfacial layer (15% $C\bar{S}H_2$, 28 days)



Fig.8 SEM photograph of interfacial layer (45% $C\bar{S}H_2$, 28 days)

Fig.9 and Fig.10 are the SEM photographes of compound specimens in the interfacial zone covering the area between aggregate and hardened cement paste matrix, which show that a loose and porous interfacial layer exists between aggregate and matrix.

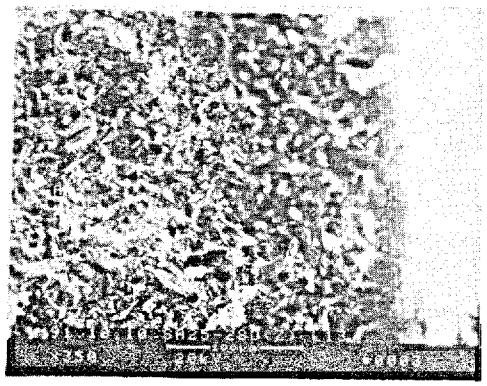

Fig.9 SEM photograph from aggregate (left side) to matrix (25% $C\bar{S}H_2$, 28 days)

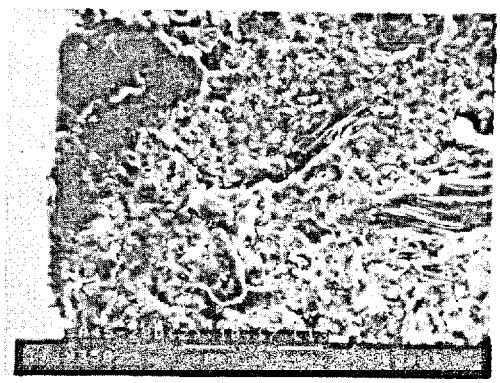

Fig.10 SEM photograph from limestone aggregate (right side) to matrix (45% $C\bar{S}H_2$, 28 days)

4. Interfacial bonding strength

Three point bending test was adopted to measure interfacial bonding strength. Results are shown in Table 3.

Table 3 Interfaical bonding strength

	SA0	SA15	SA25	SA45	Restraining condition	
					SA25	SA45
bonding strength (MPa)	3.29	1.43	0.52	0.39	1.31	0.98

DISCUSSIONS

1. The formation mechanism of interfacial zone

The microstructure in interfacial zone differs remarkably from that inside the hardened cement paste, which is depended on the factors of aggregate property, the dissolubility and hydration rate of cement minerals and migration rate of different ions. According to Maso's (3) theory, when cement paste is cast on the surface of limestone aggregate, a thick water film is formed between aggregate and cement paste, and the cement particles in cement paste begin to diffuse toward water film due to the existence of concentration difference. The main minerals in cement $C_4A_3\bar{S}$, α–C_2S and $CaSO_4 \cdot 2H_2O$ start to dissolute and react with water instantaneously. First $CaSO_4 \cdot 2H_2O$ dissolutes in water and produce Ca^{2+} and SO_4^{2-} while $C_4A_3\bar{S}$ is very easy to hydrate and form AFt and AH_3.

When the concentration of SO_4^{2-} reaches the state of supersaturation, C_2S is also begins to hydrate and produce C–S–H gel and $Ca(OH)_2$.

The migration rate of ions produced in dissolution and hydration follow the following manner: $SO_4^{2-} > Al^{3+} > Ca^{2+}$, and the formation rate of hydration products is in the order of AFt > C–S–H. These ions and hydration products migrate from cement paste and permeate water film to aggregate side in the above order. As to the SA0 cement, the concentration of SO_4^{2-} is very low in solution for no addition of gypsum, therefore Al^{3+} migrates to the side of limestone first according to the migration rate order. This process will continue until the concentration of Al^{3+} become supersaturated and forms a thick layer of AH_3 gel on the surface of aggregate. The following are a layer of ettringite crystal and a little amount of C–S–H; When gypsum content is more than 15%, the state of supersaturation of SO_4^{2-} in solution accelerates the migration of SO_4^{2-}, Al^{3+} and Ca^{2+} to aggregate and secondary reaction of forming AFt takes place. This is the reason that the main hydration products near limestone aggregate is ettringite. Only a small amount of C–S–H and residual $C\bar{S}H_2$ exist in the interfaical zone for the low migration rate of C–S–H. The well grown crystalline hydration products are attributed to the sufficient space in interfacial zone.

2. Microstructural characteristics of interfaical zone

Test results have proved that the compositions of hydrates in interfacial zone vary with the gypsum content added to cement. For the specimen without added gypsum, 2–3 μm or so layer of aluminium gel is formed first on the surface of limestoen aggregate, which is followed by a layer of ettringite crystal and a small amount of C–S–H gel. When gypsum content added to cement is not less than 15%, the interfacial zone consists of a layer of ettringite, $C\bar{S}H_2$ and a bit of C–S–H gel. With the increase of gypsum content, the interfacial zone becomes thicker, wider looser and more porous, as shown in Fig.9, Fig.10.

The water film becomes thinner under restraining condition, so the space for hydrate crystal

growth is limited and the thickness of interfacial zone decreases. The morphological feature of ettringite, characterized by fine and small sized crystal, changes remarkably as the result that the rate of nucleation is faster than that of crystal growth in transition zone in virtue of higher crystal nucleus caused by the thinning of water film.

3. The microstructure in interfacial zone and its effects on macro properties.

The bonding strength between limestone aggregate and hardened cement paste decreases with increase of gypsum added into cement, as shown in Table 3.

In the case of cement without gypsum, 2–3 μm or so aluminium gel layer is formed which is followed by a layer of ettringite crystal in the interfaical zone. The gel which has good bonding performance and dense structure strengthen the bonding strength between aggregate and hardened cement paste both physico chemically and mechanically. With the increase of gypsum content added into the cement, more and more well grown and large–sized ettringite crystall gathers in interfaical zone, and AH_3 gel becomes less and less, So the microstructure of interfacial zone become porous and loose, and bonding strength of interfacial zone decrease with the increase of gypsum content.

Under the state of three dimensional restraining, the thickness of interfacial zone decreases, meanwhile the crystall become small sized and microstructure in interfacial zone grows less porous. Thus the locking action between hydration products and aggregate is strengthened relatively , therefore the bonding strength of interfacial zone is higher than that in free expansion state. Apparently, both proper gel / crystall ratio in interfacial zone and exerting three dimensional restraining on sulphoaluminate cement concrete can improve the bonding strength of interfacial zone effectively.

CONCLUSIONS

1. The interfacial zone of hardened sulphoaluminate cement pastes and limestone aggregate is rich in ettringite. For the specimen without added gypsum, aluminium gel 2–3 μm or so in thick is rich on the surface of limestone firstly, which is followed by a layer of ettringite crystal.

2. With the increase of gypsum content added to cement, the thickness of interfacial zone increases; under the state of restraining, the thickness of interfacial zone decreases and crystal particles become small and fine.

3. The interfacial bonding strength in limestone interfacial zone decrease with the increase of gypsum content. The interfaical bonding strength is improved under restraining condition.

4. Proper gel / crystal ratio in interfacial zone and exerting restraining on expansive sulphoaluminate cement concrete can improve interfacial bonding strength.

REFERENCES

1 Jiangning Liu: "Investigation on the deformation mechancial performances and microstructure of expansive concrete under different restraining condition", Doctorate thesis, 1991.

2 Shengtao Huang "Solid X–ray science" Advanced Education Publishing House, 1978, 308p.

3 J.C. Maso, 7th International Congress on the Chemistry of Cement Vol.I, (1980), VII 1 / 3.

RELATIONSHIPS BETWEEN MECHANICAL PROPERTIES OF MORTARS AND THE HYDRAULIC RADIUS OF THEIR PORES

S P Jiang, Ch Détriche, and J Grandet

Laboratoire de Matériaux et Durabilité des Constructions, I.N.S.A. - U.P.S. Génie Civil, Toulouse Cedex - FRANCE

SUMMARY

Experimental research on the mechanical properties linked to porosity of three hydraulic binder mortars (OPC, Blended cement, Slag cement), has led to a simple law between the strength, the Young's modulus, and the hydraulic radius of the capillary pores. It shows that, for a given cement type, there are biunivocal linear relationships between the strength, the modulus and the reverse of the hydraulic radius of the pores, within a range of capillary porosities comprised between 5 and 20 per cent. So, whatever the age and the water content of the mortar, the hydraulic radius of the pores enable us to characterize the microstructure with an appropriate precision.

RESUME

L'étude de mortiers réalisés avec trois ciments (Ciment portland, Ciment fillérisé au calcaire, Ciment de laitier) permet de dégager une relation simple entre leur microstructure et leurs propriétés mécaniques. Les auteurs montrent que la résistance mécanique et le module d'élascicité sont les fonctions linéaires de l'inverses du rayon hydraulique des pores, dans le domaine de porosité capillaire concernée (entre 5 et 20%). Ces relations biunivoques font apparaître que, pour un ciment donné, quels que soient l'âge et la teneur en eau du mortier, le rayon hydraulique des pores suffit à caractériser la microstructure avec une approximation convenable.

INTRODUCTION

Since Powers' research studies[1] on the relationship between microstructure and mechanical properties of cement-based materials, many models have been put forward, taking into account either the total porosity, the size distribution of the pore[2-6], or their shape[7]. In this research work, we put forward a law linking the hydraulic radius of the pores and their mechanical properties (strength and Young's modulus) of the mortars.

EXPERIMENTAL

The materials used in this study are mortars of three differents cements: an artificial portland cement (CPA), 55HPR grade; a blended cement (lime filler) (CPJ), 45 grade with a 19.6% calcium carbonate content; and a slag cement (CLK). Two types of mortar have been prepared according to the following ratios:

- one part of binder (C), 3 parts of standard sand (French Standard P15-403) and half a part of water (W), giving a ratio W/C = 0.5,
- one part of binder (C), 3 parts of standard sand and 0.4 part of water (W), giving a ratio W/C = 0.4.

Mortars were mixed in 4 x 4 x 16 cm prismatic moulds for the porosity study and for the three-point flexural strength test, as well as in 8 x 16 cm cylindrical moulds for monoaxial compressive test. The removals from the mould of the specimen occurred after 24 hours being kept in a wet chamber (20°C, 100% R.H.), then they underwent wet curing in a 20°C water till the tests were carried out according to a schedule spreading from 3 days to 1 year.

The porosity of the mortars, determined with a mercury porosimeter, is valid for capillary pores the range of which is comprised between 37Å and 75µm. The specific surface of the pores has been determined from the distribution curves of the pore sizes assuming for the calculation that all pores are cylindrical in shape. The hydraulic radius of the pores is calculated from the total porosity and the specific surface of the pores.

The longitudinal deformations were measured by 30mm-long wire probes with a 120 Ω resistance, stuck on the generating lines of the specimen in their mediane span.

The Young's elasticity modulus is obtained experimentally from the slope at the origin of the strain-deformation curve.

RESULTS

a). Relationship between the mechanical strength and the hydraulic radio of the pores

The hydraulic radius of the pores (R_h) is defined as the ratio between the total volume ot the pores (P_t) and the total specific surface of the pores (S_s), giving $R_h = P_t/S_s$. R_h represents the average size of the pores.

Figures 1 et 2 show that individual mechanical strengths do not vary as a linear function of hydraulic radius of the pores. However, for a same hydraulic radius, the strength of the mortars, for a given mortar, is practically independent of the W/C ratio of the mix. On the one hand, for a same hydraulic radius of the pores, the total porosity of mortar for a W/C ratio = 0.5 is higher than that with a W/C ratio = 0.4; on the other hand, considering a same porosity level, the hydrate amount (or hydration degree) is higher with a mortar W/C ratio = 0.5 than with a mortar with a W/C ratio of 0.4[8].

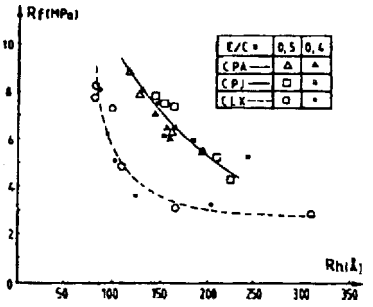

Fig 1 Flexural strength as a function of the hydraulic radius of the pores of the mortars.

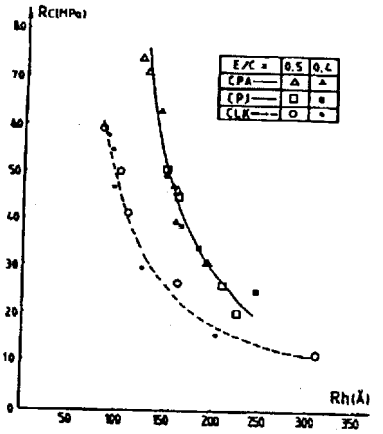

Fig 2 Compressive strength as a function of the hydraulic radius of the pores of the mortars.

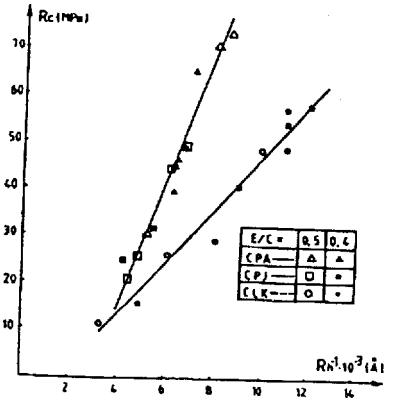

Fig 3 Compressive strength as a function of he inverse value of hydraulic radius of the pores of the mortars.

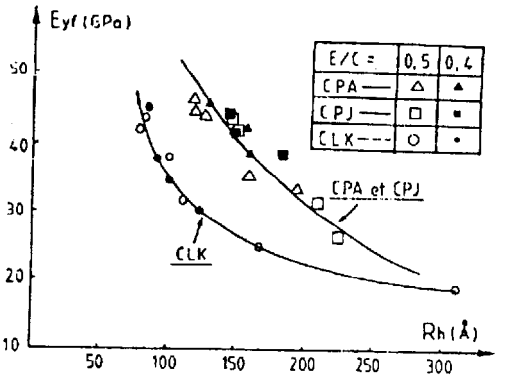

Fig 4 Flexural Young's modulus as a function of the hydraulic radius of the pores of the mortars.

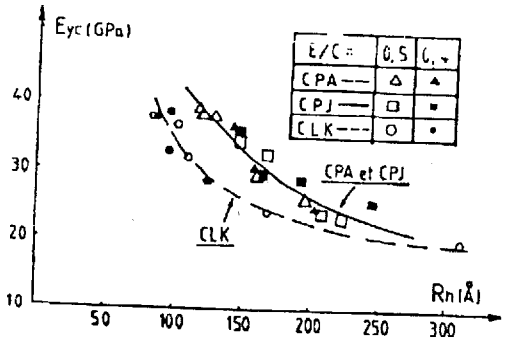

Fig 5 Compressive Young's modulus as a function of the hydraulic radius of the pores of the mortars.

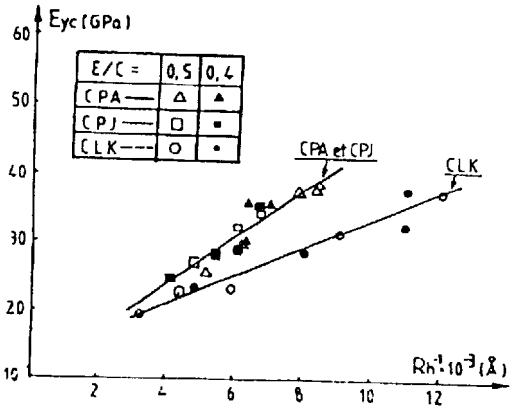

Fig 6 Compressive Young's modulus as a function of the reverse of the hydraulic radius of the pores of the mortars.

The relationship between the compressive strength and the inverse of the hydraulic radius of the pores is given on figure 3. It seems that within the range of porosity under study, it is possible to write:
for slag cement mortar (CLK):

$$R_c = 5,.7 \times 10^3 \ R_h^{-1} - 9.7$$

where R_c is the compressive strength expressed in MPa, R_h is the hydraulic radius expressed in Å. The correlation coefficient Γ is equal to 0.97.
As for portland cement mortar (CPA and CPJ):

$$R_c = 13 \times 10^3 \ R_h^{-1} - 36$$

with a correlation coefficient Γ equal to 0.97.

These relationships show that for a given cement, whatever the age and the water content of the mortar, the mean hydraulic radius of the pores is sufficient to characterize the microstructure with an appropriate precision. So, one has to study and to explain the reason for which the hydraulic radius of the pores varies to understand how are modified the mechanical strengths. This conclusion is worth being confirmed by tests carried out with other W/C values as well as other quite different cements.

b). Relationship between the Young's modulus and the hydraulic radius of the pores

The relationship between the Young's modulus and the mean hydraulic radius of the pores is similar to the relationship between the mechanical strength and the hydraulic radius of the pores, as figures 4, 5, and 6 show it. For a given cement, whatever the age and the water content of the mortar, the Young's modulus varies inversely to the hydraulic radius of the pores.

For the slag mortar, we have :

$$E_{Yc} = 2.07 \ R_h^{-1} + 13.02$$

where E_{Yc} is the compressive Young's modulus (expressed in GPa), whereas R_h is the hydraulic radius of the pores (expressed in Å). The correlation coefficient is equal to 0.95.

For the CPA and CPJ mortars, we have :

$$E_{Yc} = 3.28 \ R_h^{-1} + 10.97$$

The correlation coefficient is equal to 0.85.

CONCLUSION

The results of our research lead to a very simple relationship between properties of a material as complex as mortar, since the compressive strength and the Young's modulus are linear functions of the inverse value of the hydraulic radius of the pores, at least within the range of porosity which has been under research, i.e. between 5 and 20%.

These biunivocal relationships show that, for a given cement, whatever the age and the water content of the mortar, the hydraulic radius of the pores is sufficient to determine the microstructure with a appropriate precision. One has just to analyze and to explain the trend of the hydraulic radius of the pores in order to understand the changes of the mechanical strengths and that of the Young's modulus.

REFERENCES

1. POWERS, T.C: "Structure and Physical properties of portland cement paste", J. of the Amer. Ceramic Soc., 1958, 41, 1-6.

2. FAGERLUND.G.: "Pore structure and properties of materials", in Proc. of RILEM-IUPAC Int. Symp., 1973, 2, D-51.

3. GRANJU J.L. and MASO J.C.: Cem. Concr. Res., 1980, 10, 611-621.

4. ROY, D.M. and GOUDA, G.: "Pore structure and properties of materials", in Proc. of RILEM-IUPAC Int. Symp, 1973, 2, D-53-D73.

5. RÖßLER, M. and ODLER, I.: "Investigations on the relationship between porosity, structure and strength of hydrated portland cement paste. I Effect of porosity",Cem. Concr. Res., 1985, 15, 401-410.

6. GEGOUT,P., HORNAIN,H., THURET,B., MORTUEUX,B, VOLANT,J. and REGOURD,M.: "Texture et performance des ciment fillérisés",in 8th Int. Cong. Chem. Cement, Rio, 1986.

7. KENDALL, K., HOWARD, A.J. and BIRCHALL, J.D.: "The relation between porosity, microstructure and strength, the approach to advanced cement-based materials", in Phil. Trans R. Soc. London, 1983, A310, 139-154.

8. JIANG,S.P. and GRANDET, G.: "Evolution comparée des porosités des mortiers de ciment au laitier et des mortiers de ciment portland", Cem. Concr. Res., 1989, 19(3), 487-496.

CORRELATION BETWEEN FLY ASH EFFECTS ON PERMEABILITY AND SULFATE RESISTANCE OF CONCRETE

Parviz Soroushian and Abdulrahman Alhozaimy

Department of Civil & Environmental Engineering, Michigan State University, USA

ABSTRACT

The effects of fly ash type and content on the permeability and sulfate resistance of concrete were investigated. Correlations were drawn between permeability and sulfate resistance of fly ash concrete in order to check the hypothesis that fly ashes produce physical effects on the capillary pore system, thus influencing permeability and eventually sulfate resistance . The results confirmed that permeability plays a decisive role in the sulfate resistance of concrete.

INTRODUCTION

The most widespread and common cause of concrete deterioration is perhaps due to the action of sulfates on cement paste. Sulfates are often present in groundwater, particularly when high proportions of clay are present in the soil, and in seawater, of which they are a major constituent. In groundwater there may be very high concentrations of sulfates in the vicinity of industrial wastes such as mine tailings, slag heaps, and rubble fills. Sulfates are also present in acid rainfall caused by air pollution, or can be produced by biological sources.[1]

Concretes exposed to sulfates tend to deteriorate gradually with age, thus undergoing cracking, spalling and loss of strength due to the formation of calcium sulphate (gypsum) and calcium sulphoaluminate (ettringite). The reason for this deterioration is that both these compounds occupy a greater volume than the compounds which they replace so that expansion and disruption of concrete take place.

MECHANISMS OF SULFATE ATTACK

Calcium hydroxide and alumina-bearing phases of hydrated Portland cement are more susceptible to the attack by sulfate ions.[2] The hydration of tricalcium aluminate (C_3A)in Portland cement involves reactions with sulfate ions which are supplied by the dissolution of gypsum (calcium sulfate).

$$C_3A + 3CSH_2 + 26H \text{ ---> } C_6AS_3H_{32}$$
tricalcium aluminate + gypsum + water ---> ettringite

At this stage, the formation of ettringite (calcium sulfoaluminate hydrate) is harmless because the concrete is still in a semi-plastic state. If the sulfate is fully consumed before the C_3A has completely hydrated, ettringite is transformed into monosufoaluminate.[1]

Soluble sulfate attack on concrete is generally believed to take place in either or both of the following ways:

1. Sulfate ions except for the case of calcium sulfate attack react with calcium hydroxide to produce gypsum which causes expansion and cracking or softening of concrete.
2. Sulfate ions react with the hydration products of C3A (like hydrated calcium aluminate and monosulfoaluminate) to produce ettringite which can also cause expansion and cracking.

Sulfates ions can come from either calcium, sodium or magnesium sulfate. Magnesium sulfate exerts a more damaging effect than other sulfates because it leads to the decomposition of the hydrated calcium silicates (C-S-H) as well as the $Ca(OH)_2$ and of hydrated C_3A; eventually, hydrated magnesium silicate is formed which has no cementing properties.[3]

In general, the diffusion of sulfate ions into the pores of concrete is controlled by the permeability of concrete. As internal cracking occurs,the effective permeability coefficient of concrete tends to increase, accelerating further sulfate attack.

FLY ASH EFFECTS ON SULFATE ATTACK

The use of fly ash as a Portland cement replacement in concrete improves its chemical resistance, including the resistance to sulfate attack, through pozzolanic reaction. The effectiveness of a fly ash in improving sulfate resistance may depend on the degree of pozzolanic reaction and therefore on the physical and chemical properties of the fly ash; these properties vary with fly ash type and source, and all fly ashes are not equally effective in improving sulfate resistance.[4]

As it has been mentioned earlier, the major factors contributing to the expansion mechanisms under sulfate attack are those reactions involving the calcium hydroxide and hydration products of C_3A. When the fly ash is used as a cement replacement, the C_3A content of cement is diluted; the extent of this dilution, however, may be reduced by using high calcium fly ashes containing measurable amounts of C_3A.[5] The pozzolanic reaction of fly ash reduces the amount of calcium hydroxide in the hardened concrete; this effect is less pronounced with fly ashes which have high calcium oxide contents.[6] Reduced permeability of pozzolanic concretes in the presence of fly ashes also helps in

controlling sulfate attack; the conversion of calcium hydroxide through pozzolanic reaction to low-density calcium silicate hydrate leads to partial blocking of capillary pores and thus reduced permeability of concrete containing fly ash. Mehta (1981)[7] suggests that fly ash influences the sulfate resistance of concrete dominantly by refining capillary pore size distribution rather than modifying the chemical composition.

EXPERIMENTAL PROGRAM

The effects of fly ash type and content on the sulfate resistance of concrete were investigated, and the relationship between sulfate resistance and 28-day permeability were established. The experimental design was based on a replicated 3 x 3 (3 fly ash types x 3 fly ash contents) factorial design (see Table 1). Control tests with no fly ash (two replications) were also performed. The replacement levels of cement with fly ash were 10, 20 and 30% by weight of cement. One replication in this investigation refers to the mean of test results on at least four specimens from two different mixtures.

Table 1. Factorial Design of Experiments.

FLY ASH CONTENT	FLY ASH TYPE		
	F-1st	F-2nd	C
10%	- -	- -	- -
20%	- -	- -	- -
30%	- -	- -	- -

The mortar mixtures considered in this investigation had a sand-binder ratio of 2.75 by weight. Water content was adjusted to give a flow (ASTM C-109) of 100-110%. The materials used in this experimental study were Ottawa sand (ASTM C-109) with a maximum particle size of 0.024 in. (0.6 mm), type I Portland cement, and three fly ash types (two class F and one class C). Table 2 presents the chemical compositions and fineness of the cement and fly ashes used. Distilled water was used for the preparation of all mixtures.

Table 2. Chemical Composition and Fineness of Cement and Fly Ashes (percent).

Property	Cement	Class-F1	Class-F2	Class-C
Silicon dioxide (SiO_2)	20.58	49.30	51.41	32.8
Aluminum oxide (Al_2O_3)	5.35	26.70	28.75	19.7
Ferric oxide (Fe_2O_3)	2.56	8.95	8.43	5.45
Calcium oxide (CaO)	62.44	1.83	1.76	18.60
Magnesium oxide (MgO)	3.46	1.50	1.60	4.82
Sulfur trioxide (SO_3)	3.46	0.52	0.35	5.10
Alkalies as (Na_2O)	0.77	3.80	2.90	8.55
Loss on ignition	2.00	5.50	3.66	0.60
Fineness (% retained on # 325 sieve)	10.70	19.60	34.70	16.00

TEST PROCEDURES

Sulfate resistance tests were conducted on 1 x 1 x 11 in. (25.4 x 25.4 x 285.8 mm) mortar bars. 2 in. (50.8 mm) cubes were used to monitor the development of compressive strength. Mixing was carried out according to ASTM C-305. Two batches were prepared for each mixture composition; six mortar bars in addition to the cubes were made from each mix. A total of 120 bars was prepared. After molding, the specimens were covered with a sheet of plexiglass and sealed. They were then placed in a curing tank containing water at 95 $\pm$ 5 deg.F (35 $\pm$ 3 deg.C) for 24 hours and then removed from molds. The bars and cubes were cured in saturated lime water at a temperature of 74 deg.F (22 deg.C) until a compressive strength of at least 2850 psi (20 MPa) was reached. Thereafter, the initial length was measured.

Mortar bars were subsequently immersed in a water bath containing 5% (0.35 molar) sodium sulfate (Na_2SO_4) solution in distilled water. The sulfate solution in the bath was circulated to eliminate any sedimentation. The proportion of sulfate solution to mortar bars in the water bath was 4 volume of solution to 1 volume of mortar bars.

The mortar bars were tested for length variation after 7, 14, 21, 28, 35, 42, 49, 56, 63, and 70 days. Every 7 days throughout a period of 35 days, the sulfate solution was replaced with a fresh solution having a pH of 7 to 8.

When the bars were immersed in the fresh solution the pH increased to about 11 in less than 24 hours. This can be attributed to the formation of NaOH and the decrease in the amount of SO_4^- as the sulfate attack proceeded.

The sulfate resistance test was accelerated by the addition of sulfuric acid (H_2SO_4) at certain time intervals (Mehta 1975)[8]. The sulfuric acid was added daily in the time intervals from the 22nd day through the 31st day of testing to adjust the pH to about 7 (from 10-11) by titration. The addition of sulfuric acid was stopped when noticeable damage was observed in specimens most susceptible to sulfate attack. Thereafter, The solution was not adjusted while measurement of length change was continued up to the 70th day of the test.

TEST RESULTS AND DISCUSSION

The different mixes considered in this investigation all had comparable levels of workability, i.e. a flow (ASTM C-109) of 100-110%. As shown in Figure 1, the addition of class C fly ash reduces water requirements considerably, whereas the addition of class F fly ashes does not change the flow substantially.

Average expansions at different fly ash contents are shown in Figures 2,3 and 4 for fly ash types F1, F2 and C, respectively. The two class F fly ash types at the 20% and 30% replacement levels, and the class C fly ash of 30% replacement level, are effective in reducing expansions caused by sulfate attack. At 10% replacement level, however, the class F fly ashes did not produce any substantial change in sulfate resistance while the class C fly ash actually increased the expansion under sulfate attack.

Split-plot analysis of variance with repeated measurement was used to analyze the data statically. This analysis of test results confirmed, at 99% level of confidence, that all the variables of this investigation (fly ash type, fly ash content, and the duration of exposure to sulfate solution) as well as their interactions influenced the expansion of concrete materials under sulfate attack.

The separation of means technique was used to identify the ages at which there were significant effects exerted by the fly ash type and content on expansion at 99% level of confidence (see Tables 3 and 4). The class C fly ash at lower replacement levels (10 and 20%) produced larger expansions and faster cracking than the class F fly ashes did. There were also differences in the response of the two class F ashes to sulfate attack. At 30% replacement level, however, the differences between different fly ash types started to diminish.

Table 3. Test Ages (Days) at Which The Effects of Fly Ash Content Were Confirmed at 99% level of Confidence.

Fly Ash Content	Fly Ash Type		
	F1	F2	C
0% Vs. 10%	28	42	28
10% Vs. 20%	28	28	28
20% Vs. 30%	63	35	28

Table 4. Test Ages (Days) at Which The Effects of Fly Ash Type Were Confirmed at 99% level of Confidence.

Fly Ash Type	Fly Ash Content		
	10%	20%	30%
F1 Vs. F2	35	35	63
F1 Vs. C	28	28	a
F2 Vs. C	28	28	63

a: Statistically Comparable at All Ages Considered.

In order to determine the underlying reasons for the fly ash effects on the sulfate resistance of concrete, attempts were made to establish correlations between the sulfate resistance and permeability of concrete. Fly ash reduces concrete permeability by refining the capillary pore system. For the mixes considered in this investigation, rapid chloride permeability test results (AASHTO T277) have been reported by the authors in Ref. 9. The mean values and 95% confidence intervals of the measured 28-day permeability values for concrete specimens, moist-cured for 14 days, are presented in Figure 5. The mean values and 95% confidence interval for expansions following 28 days of exposure to sulfate solution are presented in Figure 6.

The relationship between 28-day permeability and expansion is presented in Figure 7. Correlation coefficient (which shows the validity of the linear relation between the expansion under sulfate attack and permeability) was 0.97 for the three fly ash types and the three replacement levels, indicating a very strong correlation between permeability

and sulfate resistance. This strong correlation suggests that permeability is fundamental to the resistance of fly ash concrete to sulfate attack and largely illustrates the trends in fly ash effects on the sulfate resistance of concrete.

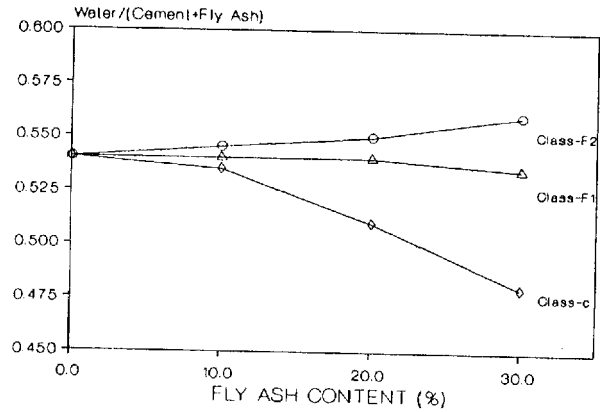

Figure 1. Effects of Different Fly ash Types and Contents on Water Requirement for Constant Workability.

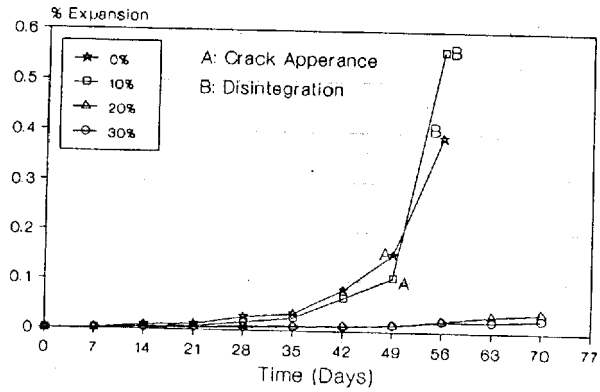

Figure 2. Percent Expansion Vs. Time For Fly Ash F1.

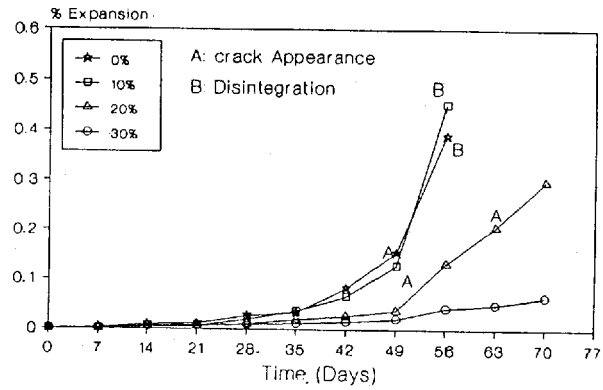

Figure 3. Percent Expansion Vs. Time for Fly Ash F2.

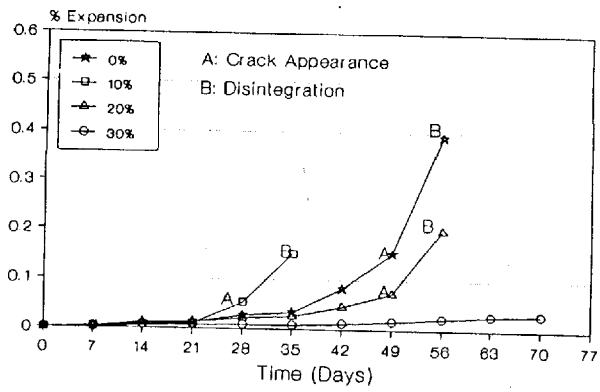

Figure 4. Percent Expansion Vs. Time For Fly Ash C.

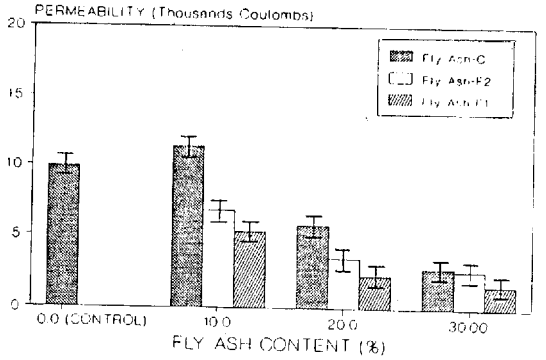

Figure 5. Permeability Vs. Fly Ash Content (Means and 95% Confidence Intervals).

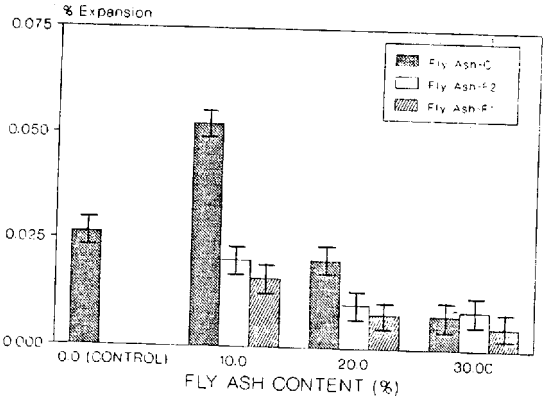

Figure 6. Percent Expansion Vs. Fly Ash Content (Means and 95% Confidence Intervals).

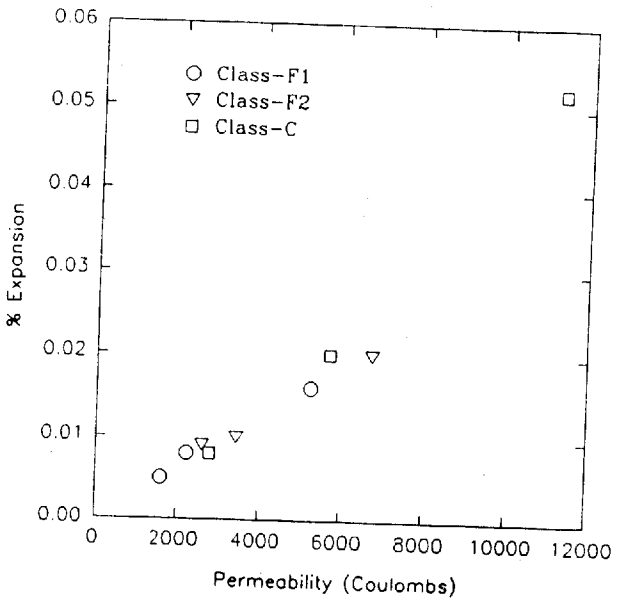

Figure 7. Mean Relationship Between Permeability and Expansion.

SUMMARY AND CONCLUSIONS

The effects of the fly ash type (two class F and one class C) and content (10,20 and 30% by weight of cement) on the sulfate resistance of concrete were investigated through experiments performed under accelerated sulfate attack. Correlations were drawn between the sulfate resistance and permeability of concrete materials. It was concluded that:

1. Fly ash type and replacement level both influence the sulfate resistance of concrete at 99% level of confidence; their interaction was also significant.
2. The two class F fly ashes at 20% and 30% replacement levels, and the class C fly ash at 30% replacement level reduced expansions under accelerated sulfate attack. At 10% replacement level, the two class F fly ashes did not substantially influence sulfate resistance while the class C fly ash increased expansions.
3. At lower replacement levels (10% and 20%), the class C fly ash produced (at 99% level of confidence) larger expansions and faster cracking under sulfate attack than class F fly ashes. There were also differences between the two class F fly ashes. At 30% replacement levels, however, the differences between fly ash types started to diminish.
4. Strong correlations were found between expansion under sulfate attack and permeability for all concrete materials (irrespective of the fly ash type and content). Concrete permeability seems to be fundamental to its sulfate resistance, and fly ash effects on permeability seem to be largely responsible for the corresponding effects on sulfate resistance of concrete.

ACKNOWLEDGMENTS

The authors are thankful to the Research Excellence Fund of the State of Michigan for providing the project with financial support. Contributions of the Composite Materials and Structures Center at Michigan State University are gratefully acknowledged. The fly ashes used in this investigation were provided by the Lansing Board of Water & Light, Detroit Edison and Consumers Power Company, and the cement was contributed by Dundee Cement.

REFERENCES

1. Mindess, S. and Young, J.F.,"**concrete,**" Prentice Hall, Inc.Englewood Cliffs, NJ, 1981. 657p.
2. Mehta, P. K., "**Concrete Structure Properties and Materials,**"Prentice-Hall Inc., Englewood Cliffs, NJ, 1986 441p.
3. Neville, A.M. and Brooks, J.J. "**Concrete Technology,**" Longman Scientific &Technical and John Wiley Sons NY, 1987. 438p.
4. John C. Rosner et al "Sulfate Resistance of Mortar Using Fly Ash as a Partial Replacement for Portland Cement,' The Challenge of Change Sixth International Ash Utilization Symposium Proceedings, March, 1982.
5. Tikalsky P.J. and Carrasquillo R.L., " Sulfate Attack on Concrete Containing Fly Ash," Structural Materials James F.Orofino ed., 1989, p123-137.
6. McCarthy, Gregory, "mineralogy of Western Fly Ash," Cement Concrete Research, Vol. 14, pp 471-478, 1984
7. Mehta, P. K., "Sulfate Resistance of Blended Portland Cement,"Proceedings, 5th International Symposium on Concrete Technology, University of Neuvo Leon, Monterrey, Mar. 1981 pp.35-50.
8. Mehta, P.K., "Evaluation Sulfate-Resisting Cements by a New Method,"ACI Journal, Proceedings V. 72, No. 10, Oct. 1975, pp.573-575.
9. Soroushian, P. and Alhozaimy A., "Fly Ash Effects on Concrete Permeability," ACI Convention, Boston, MA, Mar. 1991.

MODELLING AND VERIFYING PORTLAND CEMENT CONCRETE STRENGTH-TIME RELATIONSHIP UP TO 50 YEARS AGES

C E S Tango

Civil Construction Division, Instituto de Pesquisas Tecnologicas do Estado de São Paulo, São Paulo, BRAZIL

SUMMARY

A long-term compressive strength program has been carried out at I.P.T. - São Paulo - Brazil since 1933 and is expected to be over in 2015. Concrete samples made with 75 ordinary portland cements from 5 Brazilian producers have been tested at ages varying from 2 days up to 50 years.

Two linearizable models are proposed: the simpler one relates compressive strength to time and water/cement ratio, not taking into account the possible effect of the latter in the hydration speed; a second model takes this factor into account, admitting an hypothetical mathematical law relating the hydration speed to the water/cement ratio.

A good adjustment was obtained for both models, but the second one seemed to be more realistic. Variations in the development of strength with the time were observed, mainly between 1 and 10 years, requiring further research on the falling the strength by an eventual restrained expansion of C-S-H gel or other compounds, followed by an autogenous healing.

KEYWORDS: Cement, Concrete, Time Effects, Strength, Mathematical Modeling, Long-Term Testing.

MODÈLES RÉSISTANCE-TEMPS POUR LES BÉTONS DE CIMENTS PORTLAND VERIFIÉS JUSQU' AUX ÂGES DE 50 ANS

RÉSUMÉ

Un programme de longue échéance est developpé à l' I.P.T. - São Paulo - Brésil - depuis 1933 avec les dérniers résultats prévus pour 2015. Échantillons de bétons de 75 différents ciments de 5 producteurs brésiliens ont été essaiés à des âges entre 2 jours jusqu' à 50 ans.

Deux modèles linearisables sont proposés: le plus simple donne la résistance à compression comme fonction du temps et du rapport eau/ciment, sans avoir en compte l'effect possible de ce dernier sur la vitesse de l'hydratation; un deuxième modèle, parcontre, utilise l'hypothèse d'une loi mathematique entre la vitesse de l'hydratation et le rapport eau/ciment.

Les résultats des experiments de longue échéance ont montré que les deux modèles sont sactisfatoires, mais le deuxième est plus realistique. D'ailleurs, des variations sur la croissance de la résistance au cours du temps ont montré la possibilité d'existence des phenomènes expansifs, du gel C-S-H ou des autres components de la pâte hydratée, suivis d'une récuperation autogenique.

INTRODUCTION

A long-term compressive strength test program has been conducted at the Instituto de Pesquisas Tecnológicas - São Paulo - Brazil since 1933 and is expected to be over in 2015. Concretes of 5 mix proportions were made with 75 cement samples from 5 Brazilian producers and tested at ages varying from 2 days up to 50 years. A comparable program, in terms of time extension, is conducted by the University of Wisconsin[1,2,3,4,5]. The objective of this work is to present the derivation of mathematical models for strength-time relationship, and to compare them with the experimental results mentioned above. The theoretical and experimental basis was presented in a previous work[6]; part 2 treats mathematical modeling, and in part 3 the models are adjusted to the test results.

DERIVATION OF MATHEMATICAL MODELS

It seems that the best forms for relating the compressive strength to the structure in a so complex system like the cementitious are the relations with the capilary porosity, the non-evaporable water and the gel specific surface, according to Powers & Brownyard[7] and Powers[8,9] works. The main function may be expressed as:

$f_c = F_1(X)$ (eq. 1) or $f_c = F_2(X^{-1})$ (eq. 2)

where: f_c = compressive strength; F_1 = function relating f_c to X; F_2 = function relating f_c to X^{-1}; X = gel/space ratio (by volume); X^{-1} = space/gel ratio (by volume).

The gel/space ratio is defined as: $X = V_{hc}/(V_{hc} + p_c)$ (eq. 3)
where: V_{hc} = volume of gel; p_c = volume of capilary pores.

If the increasing volume of gel, and the decreasing volumes of anhydrous cement and capilary pores are assumed as having a linear variation with the hydration degree, it follows the eq. 4[6]: $X = K/(1/m_{ec} + x/g_h)$ (eq. 4)

where (considering water specific gravity to be 1): K = volume of gel by weight of hydrated cement; m_{ec} = specific gravity of anhydrous cement; x = water/cement ratio, by weight; g_h = hydration degree, by weight of the actual hydrated material related to the original amount. We also have: $X^{-1} = (1/m_{ec} + x/g_h)/K$ (eq. 5)

where K and m_{ec} are constants depending on the cement and hydration conditions, and we say, according to eqs. 2 and 5: $f_c = F_2'(x/g_h)$ (eq. 6)

Or in other words: the compressive strength is a function of the quocient between the water/cement ratio and the hydration degree. Powers[8] observed that an experimental diagram f_c *versus* x/w_n (where w_n is the non-evaporable water, proportional to the hydration degree) presented a similar configuration to Abrams' Curve, and it would be possible to write the following equations:

$f_c = A/B_1^{x/w_n}$ (eq. 7) or $f_c = A/B^{x/g_h}$ (eq. 8)

where A and B_1 are constants depending on the materials and study conditions, by Powers; w_n = weight of non-evaporable water; B = function of B_1, of specific gravity of water and cement, and of the gel volume produced by weight of hydrated cement[6]. The eq. 8 can be linearized as: $\log f_c = \log A - (\log B) \cdot x/g_h$ (eq. 9)

It can be admitted, in a simplified form[6]: $1/g_h = 1 + (1/g_{ho}').(1/T)$ (eq. 10)

where: g_{ho}' = initial hydration "speed" (it is a virtual speed, once it is the derivative of the hydration degree related to a time function and not to the time); T = time function, expressed as $T = t^n$; n = adjusting exponent, assumed as 1/2 after experimental work[6]. Eq. 10 is grafically represented in Fig.1. From the same point of view g_{ho}' may be assumed as a function of the water/cement ratio x, because it is associated to the hydration speed and the latter may be dependent of the proportion between the interacting agents; consequently we may have: $1/g_{ho}' = 1/g_h'_{max} + (1/g_{ho}'').(1/x)$ (eq. 11)
where: $g_h'_{max} = g_{ho}'$ asymptotic value, for x tending to infinite value, constant depending on the materials and study conditions; g_{ho}'' = derivative of g_{ho}' related to x when x = 0, constant depending on the materials and study conditions.

This function is grafically represented in fig.2. Fig.2 shows that g_{ho}' may be assumed as a constant after a certain value of x. When this possibility prevails, eq. 9 can be expressed, substituting the value given by eq. 10, as:

$\log f_c = \log A - (\log B).x - \{(\log B)/g_{ho}'\}.(x/T)$ (eq.12) or $f_c = A/(B^x.C^{x/T})$ (eq. 13)

where: $\log C = (\log B)/g_{ho}'$

However, if x value is sufficiently low, making valid the use of Fig. 2 diagram, by substituting the values given by eqs. 10 and 11, eq. 9 can be written:

$\log f_c = \log A - (\log B)\,x - \{(\log B)/g_h'_{max}\}(x/T) - \{(\log B)/g_{ho}''\}(1/T)$ (eq. 14)

or: $f_c = A/(B^x . D^{x/T}.E^{1/T})$ (eq. 15)

where: $\log D = (\log B)/g_h'_{max}$ and $\log E = (\log B)/g_{ho}''$

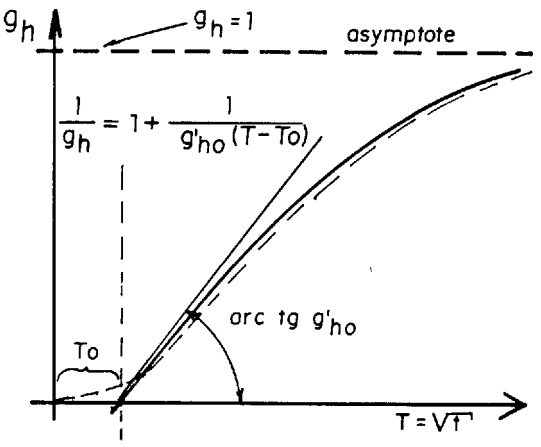

Fig.1 - Simplification of the hydration degree as a function of time diagrams. The dormant period was neglected ($T_0 = 0$) and an homografic function was adopted[6].

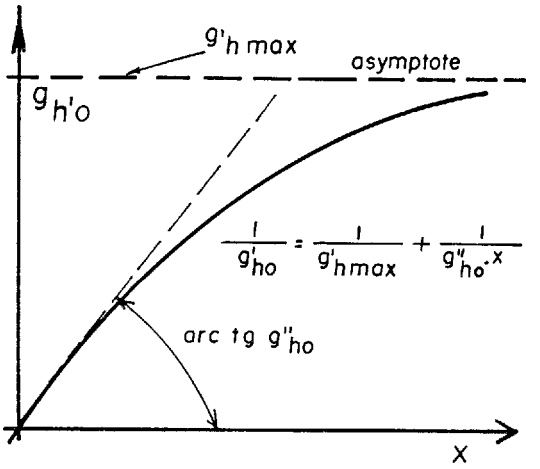

Fig.2 - Adopted diagrams for initial hydration "speed" as a function of the water/cement ratio. It is also an homografic function[6].

Eq. 12 or eq. 13 will be called *first model* and eq. 14 or eq. 15 *second model*. While the second model takes into account an influence of the water/cement ratio on the hydration speed, the first model neglects this factor. For both models, making the time a constant, mathematical expressions with the "Abrams' law" form are obtained: $f_c = A_1/B_1^x$. For the first model, $A_1 = A$ and $B_1 = B.C^{1/T}$; and for the second model, $A_1 = A/E^{1/T}$ and $B_1 = B.D^{1/T}$. Thus, Abrams' expression can be assumed as a particular case for both models, for a constant age $t = T^2$. When the first model is valid, the Abrams' curves for all ages have a common intercept; for the second model, the curves cross theirselves at a common point of virtual water/cement ratio $x = \log E/\log D$. Figs. 3 and 4 show the two cases respectively. Fig. 5 shows the second model, considered as the general case, adopting as 3D coordinates $\log f_c$, 1/T and x. It can be noted that the equation is represented by a surface composed by straight lines parallel to the plane $\log f_c{}^{-1/T}$ or to the plane $\log f_c{}^{-x}$.

EXPERIMENTAL VERIFICATION

The original program planning was made by Ary F. Torres, a notorious researcher engineer at I.P.T. in 1933, for the Cia.Brasileira de Cimento Portland (today extinguished). The first report[10,11] relates the performed program, specimens series, characteristics of concretes, materials, sampling and testing methods and sites for collecting samples. The test programs for the other 4 manufacturers follow the same general rules. The first cement sample was collected and had the concrete tests iniciated in 1933; the last in 1965.

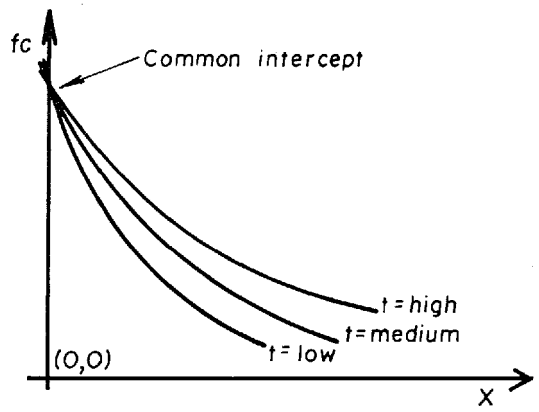

Fig.3 - Abrams' curves for concretes where the water/cement ratio does not influenciate the hydration speed (First Model).

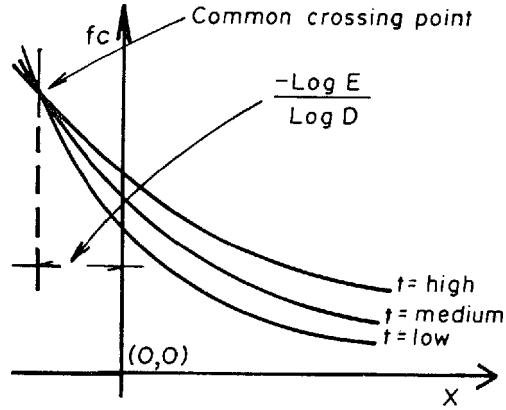

Fig.4 - Abrams' curves for concretes where the water/cement ratio influenciates the hydration speed. (Second Model). First model is a particular case of the second.

In reference (6) are detailed the following informations: The samples and producers were randomly distributed in the period. A number of 75 cement samples are discriminated by test report numbers and each of the 5 manufactures codes. They were collected by the Institute designated personnel in random establishments, including intermediate purchasers and homogenized. The test results of compressive strength, initial setting time, fineness by sieving, amounts of water required for normal consistency of paste and mortar, and chemical analysis for the cement samples, followed A.B.N.T. (Brazilian Technical Standards Association) Methods. All cements were of ordinary portland type without any kind of addition except gypsum; washed sand and gravel from Tietê river (São Paulo State) were used. Gravel had an imposed granulometric curve to obtain total fineness modulus to adequate workability in the different mix proportions. In all the cases, the maximum diameter of aggregate was 38mm and the specific gravity of the aggregate grains was 2,6kg/dm^3. All concretes for the compressive tests were made in room environment conditions with manual mixing in metallic containers. 4 cilindrical 15cm diameter by 30cm height specimens were made by batch. The water/cement ratio for each batch was found by trial an error method to obtain a slump between 8 and 12cm; the specimens were removed from the molding site to a moist chamber around 40 hours after mixing. Respecting adequate proportions between fine and coarse aggregates to obtain the total fineness modulus for each mix proportion, 6 cement:aggregate proportions were made by cement samples: 1:4, 1:5, 1:6, 1:7, 1:8 and 1:9 (1:9 proportion was neglected). In general, only the proportions 1:5, 1:6 and 1:7 had specimens made for all ages, up to 50 years; the rest only up to 1 year age. The test ages were 2, 3, 7 and 28 days; 3, 6 and 12 months; and 2, 3, 5, 10, 25 and 50 years, in general. 3 specimens were made by testing condition. The relative humidity of moist chamber was over 90%. All medium temperatures were monthly calculated. They were all in a range between 18 and 28°C. A computer program using the "BMDP - Statistical Software"[12] was used for multiple linear regressions between the variables compressive strength (f_c), water/cement ratio (x) and time (t). The theoretical models given by eqs. 13 and 15 were the object. Their linearized forms were employed, respectively:

$$\log f_c = \log A - (\log B)\, x - (\log B)\, x - (\log C)\, (x/t^n) \qquad \text{(eq. 16)} \qquad \text{and}$$

$$\log f_c = \log A - (\log B)\, x - (\log D)\, (x/t^n) - (\log E)\, (1/t^n) \qquad \text{(eq. 17)}$$

The input variables in the program were: $\log f_c$ as dependent variables; x, x/t^n, $1/t^n$ as independent variables. Four linear regressions were made by cement sample and by equation above; each one of these four regressions was destined to research the influence of the exponent n in the adjusting degree of the equations, with the arbitrary tentative values of n = 1, 1/2, 1/3 and 1/4. Thus, the total number of regressions was 600. Only a little variation was observed between the values of multiple correlation coefficients and predicting standard deviations for the tentative values of n. The value n = 1/2 was adopted after

verifications of the linearity of the main diagrams $\log f_c$ *versus* $t^{1/2}$, and also for agreement with a related work by Helene[13]. Table 1 presents the parameters for both models admitting $n = 1/2$, including the values of g_{ho}', $g_{h'max}$ and g_{ho}'', calculated as: $g_{ho}' = \log B/\log C$ (eq. 18); $g_{h'max} = \log B/\log D$ (eq. 19); $g_{ho}'' = \log B/\log E$ (eq. 20).

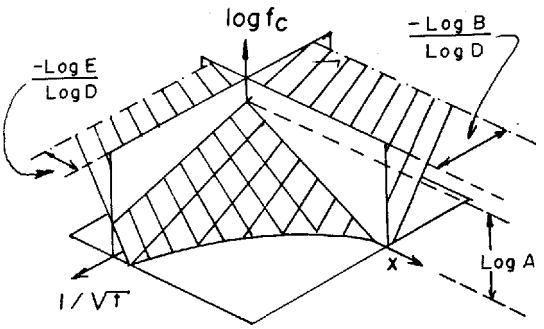

Fig.5 - 3D representation of the function $f_c = f(x,T)$, second model. The coordinates are transformed as indicated. First model is a particular case of the second.

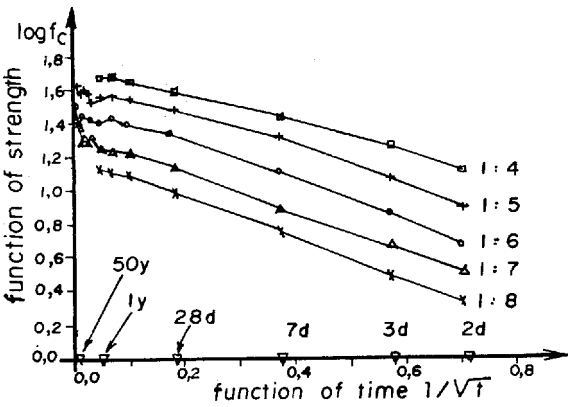

Fig.6 - Developing of strength along the time - a typical case - coordinates are transformed as indicated. Cement sample n.2, Producer n.3, molding in Nov./1935.

DISCUSSION

Satisfactory results are presented by the first model, thus it can be used mainly for concretes with relatively higher water/cement ratios given the reactivity of the cement. In Table 1, the differences between *linear* coefficients are small when comparing the first and the second models. Such correlation coefficients are referred to the *linearized* equations; the linearizations are equivalent to sometimes drastic deformations in the variables' axes, thus the comparison must be made with care. Therefore, in the situation of convergency noted in figs. 3 and 4, it is easy to see that a good adjustment can be obtained for both configurations, because the experimental results are always far away from zero water/cement ratio. Consequently, both models can be accepted as valid alternatives; the second, however, showed better fitting and thus it has been considered more realistic; in the case of using low water/cement ratios the second model is more indicated. A remarkable difference between the two models is the point of crossing the Abrams' curves: when -logE/logD ratio tends to zero, the second model tends to the first model. This ratio is equal to $-g_{h'max}/g_{ho}''$.

The simplifications assumed in the hypothesis, as neglected dormancy period by example, and the assumption of an hydration versus time curve whose configuration is not the classical "S" curve generally accepted, seem reasonable because the dormancy period occurs in a very early time compared to the ages in this study. The models' parameters can be physically interpreted, mainly g_{ho}' for the first model or $g_{h'max}$ and g_{ho}'' for the second. Only the capilary porosity decrease with time is regarded by the models, not other effects like eventual deleterious expansions due to increasing of C-S-H gel or other compounds volumes. These phenomena maybe are responsible for observed distortions in the strength x time diagrams expected form, typically represented in fig. 6. In these curves, falling in the strength was observed generally at ages between 1 and 10 years, with a tendency to back to the original line at around 25 years ages. Some uncontrolled differences in the test conditions between the ages, and human factors are not discarded as possible causes, but the frequency and similarity of these occurences favours further research on the possibility of the expansive phenomena mentioned above. An *autogenous healing* may be responsible for the recuperation of strength, since hydration can be reactivated in case of microcracking when partially unhydrated cement grains are available. The strength falls along the time should not compromise structural stability in normal conditions since the lowest remaining

strengths were always greater than the 28 days' strengths. Other evidence is the utilization of these cements along many decades without structural troubles. Therefore the subject needs to be carefully examinated now, when new design assumptions and new cements with additions with unknown long-term strength curves are used.

Table 1 - Coefficients of equations 12, 13 or 16 (1st model) and 14, 15 or 17 (2nd model), calculated by multiple regression.

sam-		n.of	first model(*)						second model (**)							
ple		cases	r^2	s	log A	log B	log C	$g_{h\infty}'$	r^2	s	log A	log B	log D	log E	$g_{h\infty}'$	$g_{h\infty}''$
1		47	0.9842	0.0429	2.0166	0.86194	1.83909	0.469	0.9874	0.0387	2.11769	1.01656	1.29528	0.35384	0.785	2.873
2		53	0.9805	0.0468	2.03877	0.8322	1.54685	0.538	0.9891	0.0354	2.16934	1.01784	0.80804	0.52628	1.260	1.934
5		51	0.9724	0.053	1.96696	0.80329	1.61823	0.496	0.9755	0.0505	2.04482	0.92489	1.15124	0.30353	0.803	3.047
10	#	49	0.9565	0.0635	1.99864	0.85519	1.48523	0.576	0.9567	0.0641	2.01489	0.88026	1.38984	0.06159	0.633	14.292
11	#	50	0.9783	0.0411	2.01671	0.91763	1.29572	0.708	0.9785	0.0414	2.0353	0.94646	1.18643	0.07141	0.798	13.254
12	#	47	0.9777	0.0372	1.89789	0.76969	1.15324	0.667	0.9778	0.0375	1.91164	0.79072	1.07422	0.05228	0.736	15.125
15		49	0.9725	0.0445	2.07047	0.94956	1.37287	0.692	0.9747	0.0431	2.13617	1.06048	0.97148	0.24177	1.092	4.386
17	#	16	0.9776	0.0267	2.04246	0.77506	1.22577	0.632	0.978	0.0275	1.99816	0.68876	1.55155	0.16722	0.444	4.119
19	#	12	0.9744	0.0218	1.9667	0.67025	0.852	0.787	0.9744	0.0231	1.96528	0.66749	0.86025	-0.00423	0.776	-157.799
20		50	0.9757	0.0609	2.03747	0.97248	1.79528	0.542	0.9786	0.0577	2.12446	1.10156	1.30097	0.33864	0.847	3.253
23	#	49	0.9814	0.0408	2.06575	1.02909	1.3812	0.745	0.9815	0.041	2.04597	0.99897	1.49861	-0.07792	0.667	-12.820
25		50	0.9769	0.041	2.05387	0.99305	1.30223	0.763	0.9794	0.0392	2.11674	1.09637	0.90541	0.24462	1.211	4.482
26	#	50	0.9804	0.0422	2.00472	0.92153	1.55331	0.593	0.9816	0.414	2.05261	0.99895	1.25727	0.18536	0.795	5.389
30		50	0.9742	0.0506	1.84017	0.68494	1.82567	0.375	0.9792	0.046	1.94557	0.86106	1.14956	0.41066	0.749	2.097
32	#	50	0.9803	0.0489	1.98913	0.90036	1.94883	0.462	0.9803	0.0494	1.99508	0.91017	1.91042	0.02359	0.476	38.583
35		50	0.9892	0.0358	1.98722	0.8118	2.13556	0.380	0.9896	0.0355	2.02544	0.87734	1.8797	0.15062	0.467	5.825
40		50	0.9598	0.0609	2.06866	1.00892	1.57943	0.639	0.9656	0.057	2.18551	1.20058	0.82436	0.46637	1.456	2.574
43	#	50	0.9423	0.0737	2.05903	1.00231	1.5783	0.635	0.9431	0.074	2.10307	1.07503	1.3015	1.6967	0.826	0.634
45		50	0.9701	0.051	1.97072	0.77556	1.69832	0.457	0.9775	0.045	2.09142	0.97861	0.91172	0.47337	1.073	2.067
50		50	0.9784	0.0432	2.07981	1.0064	1.49105	0.675	0.9788	0.0432	2.10701	1.05128	1.31644	0.10719	0.799	9.808
54	#	50	0.9785	0.0448	1.97574	0.84061	1.74916	0.481	0.9786	0.0452	1.99052	0.86556	1.65227	0.05816	0.524	14.882
55		50	0.9859	0.0422	2.00636	0.8156	2.22808	0.366	0.987	0.041	2.06388	0.91704	1.83248	0.22722	0.500	4.036
60		50	0.9812	0.0456	2.0178	0.77051	1.89703	0.406	0.9879	0.0369	2.15278	0.988	1.04188	0.53529	0.948	1.846
65		50	0.9664	0.0546	1.8512	0.68965	1.66302	0.415	0.9746	0.048	1.97657	0.8979	0.86532	0.48842	1.038	1.838
70		50	0.9851	0.0392	1.97859	0.8323	1.8351	0.454	0.9907	0.0314	2.10684	1.04532	1.04201	0.48417	1.003	2.159
75		47	0.9672	0.0457	1.95872	0.87397	1.2507	0.699	0.9777	0.0381	2.08658	1.08485	0.46756	0.48054	2.320	2.258

r^2 = squared correlation coefficient (*) see equations 12, 13 or 16 in the text # = 1st model is satisfactory
s = predicting standard deviation of log f_c (**) see equations 14, 15 or 17 in the text
the omitted samples coefficients can be found in reference (6).

CONCLUSION

The concrete compressive strength-time relationship can be modeled with basis on the water/cement ratio and the developing of the hydration with time, for each combination of particular materials and enviromental conditions. Two models are proposed: the first model: $f_C = A/(B^X.C^{X/T})$ and the second model: $f_C = A/(B^X.D^{X/T}.E^{1/T})$. The expected configurations of models were disturbed by the falling of the strengths with a tendency to recuperation at certain levels; this would be probably explained by a destructive expansive phenomenon followed by an autogenous healing and gives margin to further research. The linearization of the models makes easy the extrapolations for the prediction of strength as an application for quality control purposes[14].

This work is only at the beginning, since there are other basic models to be verified, and it is possible to study the influence of cement characteristics on the present models' parameters; and there is a need for research of the possible expansive destructive effect followed by autogenous healing. All these questions will be subject of future works using

the same experimental background, to be completed in 2015. Since at present new cements with several blends are a recognized world tendency, it seems urgent to follow the example of this work using them - now with more technological tools - for the benefit of future generations.

REFERENCES

(1) Withey, M.O. Fifty year compression test of concrete - J. of ACI, n. 6, Proc., V. 58, Dec. 1961.

(2) Washa, G.W.; Saemann, J.C. & Cramer, S.M. Fifty Year Properties of Concrete Made in 1937. ACI Mat. J., Vol. 86, N. 4, Jul., Aug. 1989.

(3) Withey, M.O. Some Long-Time Tests of Concrete. J.of ACI, Proc., V.27, N.6, Feb.1931.

(4) Withey, M.O. & Wendt, K.F. Some Long-Time Tests of Concrete. J. of ACI, Proc., V.29, N.4, Feb. 1943.

(5) Washa, G.W. & Wendt, K.F. Fifty Year Properties of Concrete. J. of ACI, Proc., V.72, N.1, Jan. 1975.

(6) Tango, C.E.S. Um Estudo do Desenvolvimento da Resistência à Compressao do Concreto e do Cimento Portland até 50 Anos de Idade (A Study on the Development of Portland Cement Concrete Strength up to 50 Years Age). Thesis - Doctorate Degree. E.Politecnica U.S.P. S.Paulo. 1990. In Portuguese.

(7) Powers, T.C. & Brownyard, T.L. Studies of the Physical Properties of Hardened Portland Cement Paste. J. of ACI, Vol.18, Oct., Nov., Dec., 1946; Jan., Fev., Mar., Apr. 1947.

(8) Powers, T.C. The Nonevaporable Water Content of Hardened Portland - Cement Paste - It's Significante for Concrete Research and It's Method of Determination. ASTM Bul. n.158, May, 1949.

(9) Powers, T.C. The Physycal Structure of Portland Cement Paste. In: The Chemistry of Cements, Ed. H.F.W. Taylor, Academic Press, London, 1964.

(10) Escola Polytechnica de São Paulo - Laboratório de Ensaios de Materiaes. Ensaio de Concreto de Longa Duração (Long-term Concrete Tests). Ensaio Official n.3931. S.Paulo, 1933. In Portuguese old orthography.

(11) Instituto de Pesquisas Technologicas do Estado de São Paulo. Ensaio de Concreto de Longa Duração (Long-term Concrete Tests). Ensaio Official n. 3931. S. Paulo (1935?). In Portuguese old orthography.

(12) Univ.of California. BMDP Statistical Software Manual. W.J. Dixon, Ch.Ed. UCLA Press, Berkeley, 1985.

(13) Helene, P.R.L. Contribuição ao Estabelecimento de Parametros para Dosagem e Controle dos Concretos de Cimento Portland (Contribution to the establishment of parameters for design and control of Portland Cement Concretes). Thesis - Doctorate Degree. E. Politécnica USP. S.Paulo, 1987. In Portuguese.

(14) Tango, C.E.S. Prévision de la Résistance du Béton jusqu'à 50 ans - une Etude (Predicting Concrete Strengths up to 50 years ages - a Study). RILEM-CEB 2nd. Int. Symp. on Quality Control of Concrete Structures. Ghent, Belgium. 1991. In French.

RELATIONSHIP OF CONCRETE STRENGTH DEVELOPMENT WITH AGE

I A Sulkovsky and A G Milruo

The Tashkent State University named after Beruni Tashkent, UZBEKISTAN

SUMMARY

A suggestion of a more exact dependence of concrete hardening process in time is given. It has been shown that the used proportional coefficient, besides the mineralogical concrete composition, depended on the absolute concrete curing.

В статье предлагается более точная зависимость для описания процесса твердения бетона во времени. Показано, что использованный в ней коэффициент пропорциональности помимо минералогического состава цемента зависит от цементно-водного отношения и абсолютной температуры выдерживания бетона.

Materials containing cement binders are characterised by a slowing down of the hydration process of cement with age. While the formation of hudration products increases the rate of cement strength gain, the fact that the cement grains get coated by the products of their own hydration, retards the subsequent process and decreases the rate of hydration.

The relation, characterising the process of concrete hardening was deduced on the basis of M.I.Strelkov's idea that the rate of increase in concrete strength is inversely proportional to time

$$\frac{dR}{d\tau} = \frac{\beta}{\tau} \qquad \ldots (1)$$

Integration of the expression and substitution of constants reduces it to the formula:

$$R_\tau = R_{28}\left(1 + \beta \ln \frac{\tau}{28}\right) \qquad \ldots (2)$$

where β - is an experimental coefficient of the receding growth of concrete strength and its other characteristics, such as the water-cement ratio of the mix, its temperature and moisture content.

The relation $R_\tau = f(\tau)$ for various values of the β coefficient shows the famili of curves in the usual coordinate system and a bunch straight lines in the semilogarithmic one.

The β coefficient defines in particular the onset of strength formation, which is roughly relatable to the final point of concrete setting.

Indeed, provided $R_\tau = 0$ we get $\tau_0 = 28\, e^{-\frac{1}{\beta}}$

The formula deduced differs from B.G. Skramtaev's logarithmic aquation of the growth in concrete strength, and being a general equation includes the latter as a particular case. The smallest value of the coefficient corresponds to fast hardening cements and the largest values to the slow hardening ones.

Changes in the values of the β coefficient with various characteristics of cement and concrete were calculated through experimental data processing, evaluating the growth in concrete strength during its natural setting within the temperature range 0°- 40°C, as well as the data of growth in concrete strength after hydro-thermal treatment in the temperature range 60°-80°C.

It has been found that the β coefficient is reduced linearly with increase in K quantity defined by the water-cement ratio of the mix.

$$\beta = \alpha(1-K) \quad K = \frac{U}{U+B} = \frac{U/B}{U/B+1} \quad \ldots (3)$$

The logarithm of proportionality factor in the formula (3) is defined as the absolute temperature function

$$\ln \alpha = \frac{A}{T} - B \quad \ldots (4)$$

where A and B - experimental coefficients for portland cement.

$A \approx 1{,}5\ 10^3$; $B \approx 5{,}4$

By substitution in the general equation as below for increase in concrete strength with time as a function of water-cement ratio of the mix, its absolute temperature and time, the strength gain at any age can be calculated

$$R_\tau = R_{28}(1+(1-K)\exp\left(\frac{A}{T}-B\right)\ln\frac{\tau}{28}$$

Processing of a large number of experimental data showed, that the dependence line graph $R_\tau = f(\tau)$ provided T=const in the semilogarithmic system of coordinates that when concrete strength approaches 70% it has a break beyond the limits of which the tangent of angle slope characterizing the hardening rate, decreases abruptly, preserving approximately constant value in the following period.

A MATHEMATICAL MODEL FOR BLENDED CEMENT

G Tognon and S Cangiano

Italcementi SpA, Bergamo, ITALY

SUMMARY

A mathematical model was developed for cement mortars made with blended cements and, for the purpose of comparison, with portland cement. This model is able to provide the maximum admissible content of an addition which can be enveloped by cement particles without vacancies or discontinuities. Numerical results confirm that the aforesaid quantity increases as the maximum grain size of addition increases.

Experimental results, based on compression and flexural tests, show that the geometrical envelope is only a necessary condition for strength preservation or enhancement; for this purpose it is also necessary that a "welding" pozzolanic reaction between cement particles and additions occurs.

INTRODUCTION

In recent years blended cements have been the object of numerous studies (*) chiefly directed to their chemical and physico-mechanical characteristics.

It is a known fact that active additions, whether natural (pozzolanas) or artificial (slag, fly ash, silica fumes) are capable of combining with the lime released during hydrolysis of the clinker's calcium silicates. Since this reaction occurs in a multi-phase system, it depends, other conditions being equal, on the specific surface of the material added and on the availability of lime of hydrolysis. In any case all particles of the addition, whether active or not, must be enveloped by the binder in order to obtain a strong continuum.

The purpose of this work has been to identify the greatest possible quantity of addition that may be completely enveloped by the cement particles. The problem was dealt with by resorting to geometrical models relating to the two systems of particles: the active one (the cement) and the activatable (pozzolanic addition) or inactive one (non pozzolanic addition).

The study has been backed by an experimental investigation whose object has been the testing of the theoretical results.

GEOMETRICAL MODEL

Analysis of the problem

The problem was confronted for a plane particle system (discs of unitary thickness).

After assignment of the number of grain-size classes of the cement (N_c), their weight fractions x(i) (i=1,..N_c) and knowing its specific gravity γ_c, it is possible to calculate the number of cement particles $n_c(i)$ which belong to each grain-size class with reference to the unit of weight:

(1)
$$n_c\ (i) = \frac{x\ (i)}{\pi r^2\ (i)\ \gamma_c}$$

One can imagine the set of cement particles being made up of N_c elementary subsets, each being made up of N_c grain-size classes, such that for each class the following condition is satisfied

(2)
$$n_c\ (i) = N_s\ n_{ce}\ (i)$$

where n_{ce} (i) is the number of particles of the i-th class of the elementary subset. Since in a plane system at least three particles of cement are required to envelop a particle of material added, N_s will be the result of:

(3)
$$N_s = \frac{\{N_c\ (i)\}\ \min}{3}$$

where
$\{n_c\ (i)\}_{min}$ = minimum number of particles present in an i-th cement class.
If N is known, it is possible to calculate by means of (2) the number $N_{ce}(i)$ of particles contained in each of the N classes of the elementary grain-size subset.
Consider a particle (i) of cement belonging to the class of radius r(i), tangential to a particle (j) of radius R(j) of addition. With reference to the symbols shown on fig. 1 one can observe that the following equation subsists:

(4)
$$SEN\ \{\alpha\ (j,i)\} = \frac{r\ (i)}{R(j) + r(i)}$$

(*) see for example [1]

from which the value of angle $\alpha(j,i)$ is obtained, which complies with the condition of tangence:

(5)

$$\alpha\,(j,i) = \text{ARCSEN}\ \frac{1}{1+\dfrac{R(j)}{r(i)}}$$

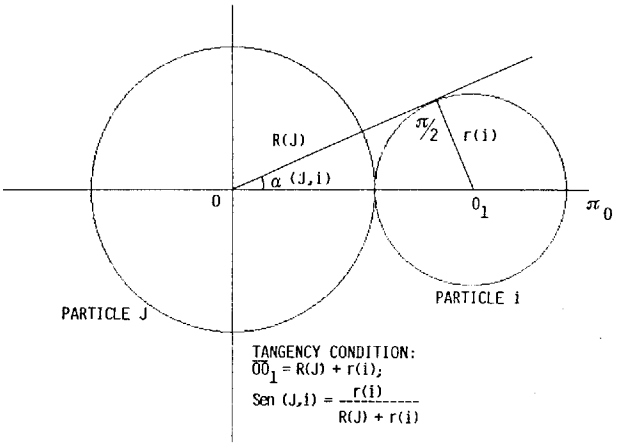

Fig.1 Tangency condition between two circular disk in a bi-dimensional system.

Assuming that only a part of the elementary subset of cement particles made up of (Np) particles divided into (Nsub $\leq N_c$) subsets may phagocytise an added particle (j), the condition of complete envelopment is assured by:

(6)

$$\Sigma_i\ \alpha(j,i) - \pi = 0 \qquad [i = 1,\ldots\ldots,\ N_r]$$

The equation (6) makes it possible, once radii r(i) of the cement particles are known, to determine the radius of the added particle (j) such that it is completely enveloped by the cement particles.

The grain-size curve obtained by the addition will obviously depend on the number and composition of the agglomerate of N_c particles of cement that may envelop an added particle (j). Once the maximum (Rmax) and minimum (Rmin) radius of the particles of the addition have been assigned, and assuming that its grain-size curve is continuous, the maximum (Npmax) and minimum (Npmin) number of cement particles enveloping the particle with Rmax and the particle with Rmin respectively can be calculated.

Admitting that the particles with Rmax and Rmin are enveloped respectively by cement particles that belong to the most numerous grain-size class, an acceptable assumption if one considers the actual relations between the numerousness of the grain-size classes of cement (see table 1), equation (6) becomes:

(6 bis)

$$(Np)\ \text{max, min} = \frac{\pi}{\text{ARCSEN}\left[1+\dfrac{R\text{max, min}}{r}\right]^{-1}}$$

where:

Rmax, min = max and min radii (assigned) of the particles of added material

r = radius of the cement particles that belong to the most numerous cement class.

If one iteratively samples from the grain-size set of cement particles a number Np variable between Npmin and Npmax according to a law of the type:

(7)

$$Np = Npmax - \left[Npmax - Npmin\right]\left[\frac{i}{Ntot}\right]^{k}$$

where
i = number of the iteration, i = 0,....., Ntot
Ntot = total number of cement particles
it is possible to obtain a bundle of grading curves of addition, each of which is defined by a particular value of K.
If Nf is the number of fractions in which the elementary grain-size set of the added particles has been divided, their percentage is given by:
(8)

$$A\ \% = 100\ \pi\ \alpha\ \Sigma j\ R\ (j) \qquad j=1,.....,Nf$$

where α = specific gravity of the addition.

By making recourse to subsequent iterations and using (6) with (7) and (8), it is possible to find the grading curve of addition such as to bring about an assigned per cent of such material.

Numerical processing

The calculation of the maximum percentage of addition, such as to meet the conditions set out in the above paragraph, has been carried out for a plane system of particles. For this purpose a computer program has been developed, whose flow chart is shown on figure 2. Input data are represented by the number of cement classes (N_c), by the average values of radii r(i) of each grain-size class and by the weight fractions x(i). In the input section also the upper and lower limits of the grain-size set of addition has been input.

At step 5 the procedure was such that each grain-size subset sampled, subsequent to the first, had in common with the previous one at least two particles, so as to form a continuous agglomerate of cement particles and filler particles (fig. 3). The calculation R(j) of the particle of addition was carried out by solving equation (6) by means of the Newton-Raphson method [2]. Finally, the condition was introduced of never having a subset overlap the previously generated subsets.

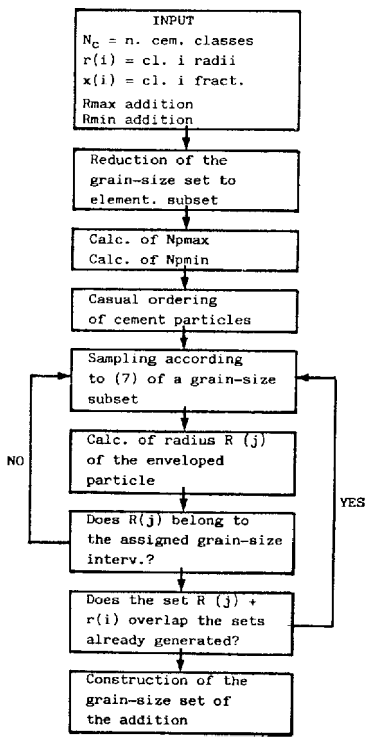

Fig. 2 Program flow chart

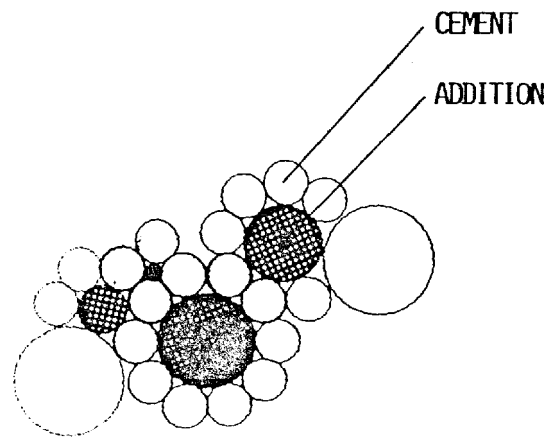

Fig. 3 Agglomerate of cement and addition particles.

Table 1 shows the initial input data relating to the cement considered (high-strength portland type 425), the number of particles for each fraction of the grain-size set referred to the unit of weight, of the elementary subset and the average radii of each grain-size fraction. By collecting in classes the calculated values of the radii of the addition for each subset it is possible to plot the grain-size curve of such material.

Table 1 Grain-size composition expressed in terms of weight-fractions X(I); number of particles contained in 1 gr N (I) and in an elementary sub-set Nel (I) of portland cement type 425.

Weight fraction X (I)	No of particles N (I)	No of particles in subset Nel (I)	Radius (μm)
.3000	100585	5181	1.750
.0460	2332	120	4.500
.1100	2891	150	6.250
.1000	1341	69	8.750
.1000	811	42	11.250
.0800	434	21	13.750
.0600	233	12	16.250
.0490	143	6	18.750
.0280	64	3	21.250
.0320	58	3	23.750
.0950	108	6	30.000

Fig. 4 shows a bundle of grading curves of additions calculated according to different values of k (solid lines); it can be seen that as the content of fractions of large particles increases, larger percentages of additions are admitted. The same figure also shows, for the purposes of comparison, the grain-size curves of the addition used in the experimental part (dashed lines). The parameter k has been made to vary within a field of values such as to approximate the calculated curves to the real ones as much as possible.

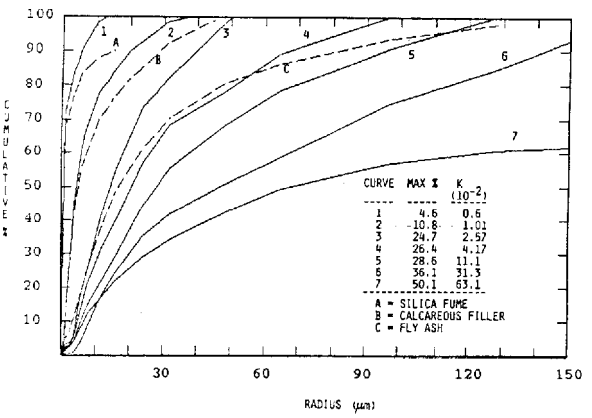

Fig.4 Calculated grading curves (sold lines) and real grading curves (dotted lines) of addition material.

EXPERIMENTAL PART

Materials

Two different types of additions have been used:

- pozzolanic additions:
  - fly ash (from ENEL's thermoelectric power station of Fusine);

- silica fumes
- calcareous additions.

The additions have been admixed with high-strength portland cement type 425 in the following percentages: 0-10%-20%-30%-40%-50%.

The chemical composition of the cement used and of the additions is set out on table II, while fig. 4 shows the grain-size curves (dashed curves).

With the resulting binders plastic mortars have been prepared according to standard EN 196-Part I.

12 beams (40x40x160 mm) have been prepared for each type of mix and placed to age in water for 28 days.

TABLE II
Chemical composition of materials used

Oxide %	Portland Cement	Silica Fume	Fly Ash	Calcareous filler
SiO2	21.67	97.31	43.17	1.45
Al203	4.43	0.13	29.41	0.56
Fe203	1.69	0.02	4.50	0.29
CaO	60.09	0.15	9.38	53.26
MgO	3.18	0.07	1.36	0.84
SO3	2.82	<0.06	0.64	<0.06
Na20	0.22	<0.08	0.26	<0.08
K20	0.75	0.47	0.87	0.1
TiO2	0.20	<0.01	1.34	0.03
Loss on ignition	4.39	1.57	1.85	43.19

Results

At the end of the ageing period the beams were submitted to a three-point bending test; the two stumps were subsequently submitted to compression test.

Figs. 5 and 6 show the values of compressive and flexural strength, as a function of the addition content, referred to the values measured on plastic mortar specimens made with portland cement 425.

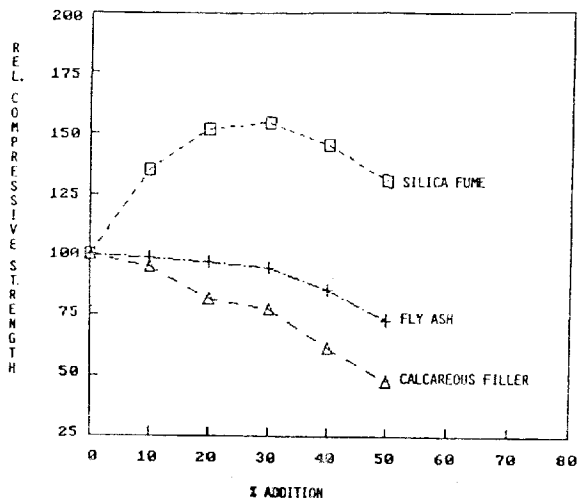

Fig.5 Compressive strength vs. addition percentage.

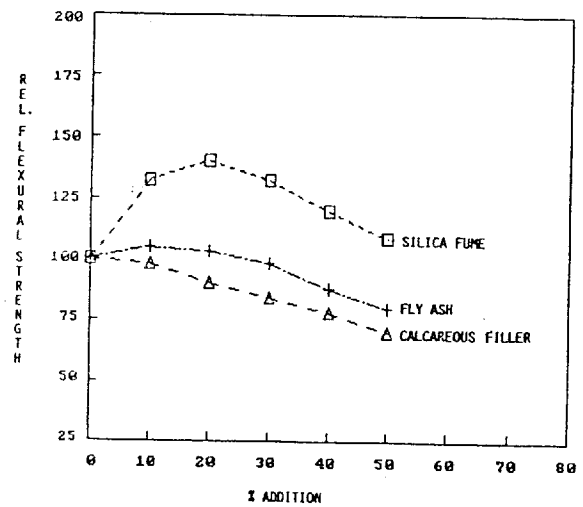

Fig.6 Flexural strength vs. addition percentage

An analysis of these figures reveals:

- the calcareous filler, although it may not be considered inert [3], begins to reduce the strengths, though to a limited extent, already at a content of 10%;
- the strength-reducing effect of fly ash is displaced to a level of 30% of its content in the mix;
- the activity of the silica fume, which starts to become apparent already after two days, with an appreciable increase of the strength, is very much in evidence up to a 20-25% content. Basically this is a high-activity material, whose limit in the addition is not given by the amount of binder required to incorporate it, but by the availability of lime of hydrolysis with which to react and activate.

CONCLUSIVE REMARKS

The two-dimensional model developed defines, within the limits of the assumptions made for the sake of simplicity, the highest content of addition that may be incorporated without discontinuity by the particles of binder.

The geometrical model has shown that the condition of maximum envelopment leads to:

- grading curves of the addition with exponential trend;
- a bi-univocal correspondence between the ϕ_{max} of the particles of this material and their maximum percentage.

The complete incorporation of the addition by the cement particles is not a sufficient condition to ensure the preservation or increase of the mechanical strength of the resulting composite, as compared with the one obtainable with the cement material as is. Also a "welding" reaction (pozzolanic effect) must occur between the components of the mix. This welding, as is known, depends on the nature of the addition and on the kynetics of the pozzolanic reaction. If the welding does not occur, the strengths reduce.

The test results, though they refer to one single cement mixed with three types of addition, derive from one of the infinite combinations of grading curves (that of the binder and that of the addition) which the model may describe by matching the parametric curve with the real one of the addition.

References

[1] Proc. Symp. N "Effects of Flyash Incorporation in Cement and Concrete" (Boston, Nov. 16-18, 1981), S. Diamond Ed.

[2] E. KREYSZIG, Advanced Engineering Mathematics, J. Wiley & Sons, 1979

[3] Carbonate Additions to Cement - ASTM STP 1064, P. Klieger and R.D. Hooton ed., 1990

MATHEMATICAL MODELLING OF THE KINETICS OF BINDER HARDENING AND ITS APPLICATION TO PRODUCTION CONTROL OF CONCRETE

K H Schlüssler

Technische Universität Cottbus
Fakultät Mathematik, Naturwissenschaften und Informatik,
Cottbus, GERMANY

SUMMARY

Hardening of concrete can be seen as a process of evolution, during which its final properties are achieved in depence of the kind of control of the surrounding milieu. Viewing this process different levels (macro, meso, micro) of modelization may be accepted. The paper is based on a phenomenological point of view. Presuming a data set of carefully made measurements an adequate and realistic picture of the evolution of thermo-mechanical properties of concrete can be drawn by mathematical modelization. The heat-transfer problem ist given as an example.

INHALT

Die Erhärtung von Beton läßt sich als ein Evolutionsprozeß darstellen, bei dem seine Endeigenschaften in Abhängigkeit von der Art der Steuerung des ihn umgebenden Milieus abhängen. In der Betrachtung dieses Prozesses kann man unterschiedliche Niveaus (Makro, Meso, Mikro) zugrundelegen. Der Beitrag nimmt einen phänomenologischen Standpunkt ein.

Setzt man das Vorhandensein einer Datenmenge aus sorgfältigen Messungen voraus, so kann durch mathematische Modellierung ein adäquates und realistisches Bild der Evolution der thermo-mechanischen Eigenschaften von Beton gezeichnet werden. Mit dem Wärmetransportproblem wird dafür ein Beispiel gegeben.

INTRODUCTION

Hardening of concrete commonly runs under nonisothermal state conditions. That is the rule for precast concrete, but is still valid for monolithically placed concrete structures. Changes of temperature of the concrete are caused by heattransfer processes from outside (by heating, cooling or meteorological influences) and from inside due to the sources of the hydratationheat of the cement. For known material parameters of the mix (kind of cement, water-cement ratio, porosity of fresh concrete) the appearing course of temperature will be the main influencing factor of the evolution of strength. From this it follows that an optimally designed process only can be achieved, if the interdependance between the characteristic properties of the material and technological parameters (workability of concrete, treating time, scheduled processing temperature, transfer-properties of the form surface) is taken into account. That means the control of a specific technology to accelerate the hardening of concrete (e.g. by heat supply) inevitably must be connected with the mix design. Programs for the mix design and those for processing-control therefore must be seen as a strong unit.

In the following three topics are touched: the background of mathematical modelization of the kinetics of binder hardening, the verification of parameters of the model by measurement data, a heattransfer model for hardening concrete.

1. MATHEMATICAL MODELIZATION OF THE KINETICS OF BINDER HARDENING

When speaking of the modelization of the kinetics of binder hardening it must be clearly said what is the objective of the mathematical description. Naturally there is a big difference whether the whole complexity of the hardening process (dissolution, nucleation, crystallization, growth of CSH gels, polycondensation) should be reflected or some selected properties, being of preferred interest for the technology under consideration. Here we restrict ourselves to a modelization on a macro-level and try to describe essential phenotype properties of the binder. This kind of methodology must not only be seen as a draw back in the sense of missing knowledge in the details or lack of modelization capability. On the contrary experience teachs us, that cements carry a lot of individual features that are related to the circumstances during manufacturing (geological influence to clinker composition, burning temperature, grinding fineness, type of grinding mill etc.). A phenotype modelization thus gives the possibility implicitly to summarize all these effects. It is based on an observation of the kinetics of specific properties of cement stone or concrete by adequate measurement techniques. Available are e.g. differential caloric-, ultrasonic-, strength- respectively (due to chemical shrinkage) volume contraction-measurements. As a result time series for $\dot{Q}(t)$, $v(t)$, $R(t)$ resp. $\Delta V(t)$ are delivered that comprehend the necessary information regarding the evolution characteristics of the processes which are accompanied by stochastic influences. Therefore smoothing splines and/or nonlinear regression calculations are useful preprocessing techniques to rule out this disturbing effects and to get reliable data sets for the derivation of evolution models for concrete properties.

Of special importance is to transform the time series $x(t)$ or $\dot{x}(t)$ (x written instead of one of the above mentioned variables) to the generalized form

$$\dot{x}(t) = f(x(t), T, a_1, a_2, \ldots a_n) , \qquad (1)$$

which connects the rate $\dot{x}$ with the degree x for T (temperature), a_1, a_2, ... a_n being parameters. Using a numerous material of measurement data it was shown that applying a so called Betatype model

$$\dot{x}(t) = \dot{x} \left[\frac{e + x}{e + x_w}\right]^m \left[\frac{1 - x}{1 - x_w}\right]^{s \cdot m} \tag{2}$$

$$x_w = \frac{1 - e \cdot s}{1 + s} \quad \text{or} \quad s = \frac{1 - x_w}{e + x_w} \tag{3}$$

a lot of evolution problems arising in binder hydratation can be modelized. The model contains the degrees of freedom (x_w, $\dot{x}_w$, e, m). The first two determine a switching point of process-evolution of the system (transition from reaction to diffusion control).

The maximal rate $\dot{x}_w$ is strongly dependent on temperature T. That leads to the factorized form of equation (2)

$$\dot{x}(t) = \dot{x}_w(T) \cdot f(x(t)). \tag{4}$$

Viewing the shape function f(x) it must be stated that it reflects only unimodal (with one maximum) evolution rates. Sometimes but seldomly this is a handicap as one can find cases where a one-component model of type (2) is insufficient. But generally the most cements have an evolution behaviour allowing its application.

2. MEASUREMENT DATA

To give a certain background for the chosen way of investigation in the following data are given which are resulting from different measuring principles to hardening pastes of portland cement PZ 4/45 with w/c = 0.50. Figures 1 to 4 show the development of strength, volume contraction due to chemical shrinkage, heat of hydratation and velocity of an ultrasonic signal respectively for different temperatures. From figures 1 to 3 clearly the evolutionary behaviour of structure development can be recognized, which manifests itself in the typical S-shaped curves for the measured state variable. For the velocity of ultrasound of course this is valid too, but here measuring was started after the setting of the paste. Attention again should be directed to figure 5 showing the rate of strength evolution as a function of the already reached values of strength for different temperatures but constant w/c ratio. The data in this constellation are the inputs for the problem of identifying the parameters of equation (2). Repeatedly applying it for different w/c ratios leads to a strength model for hardening concrete, which fully reflects the influence of temperature T, w/c ratio and porosity of fresh concrete for the phenotype cement PZ 4/45. It is without doubt that a lot of experimental work has to be done to supply strength data for the derivation of an evolution model corresponding to equation (2). But it can be seen by comparing figures 1 to 4, that it states with different physical contents, that there are more or less selective influences from hydratation of single clinker components to a specific evolution characteristic. For instance there is no exact congruency between the development of strength and heat of hydratation. Nevertheless differential caloric measurement nowadays presents itself as an undispensable tool to generate a phenotype characterization of a specific cement in its kinetic behaviour.

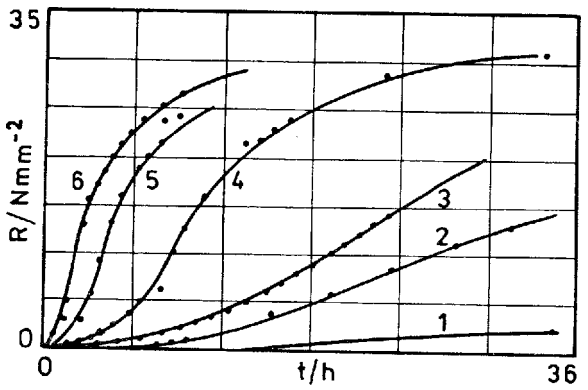

Fig. 1: Strength as function of hardening time for portland cement PZ 4/45 with w/c = 0.50 with T = 1 °C, 13 °C, 20 °C, 35 °C, 50 °C and 80°C.

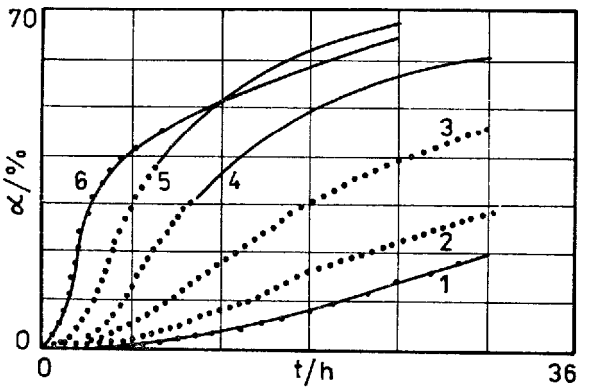

Fig. 2: Degree of hydratation measured by chemical shrinkage as function of hardening time for conditions as in figure 1.

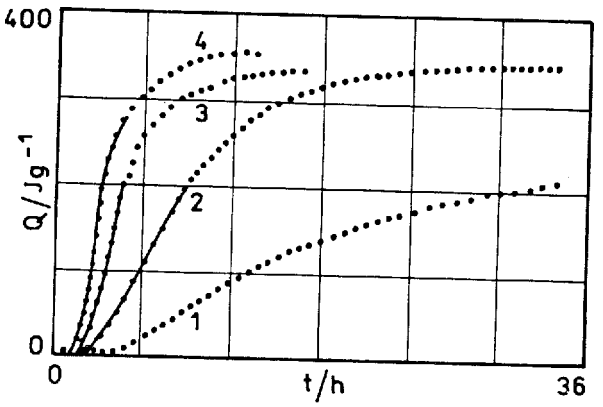

Fig.3: Heat of hydratation an function of hardening time for portland cement PZ 4/45 with w/c = 0.50 and T = 20 °C, 40 °C, 60 °C, 80 °C.

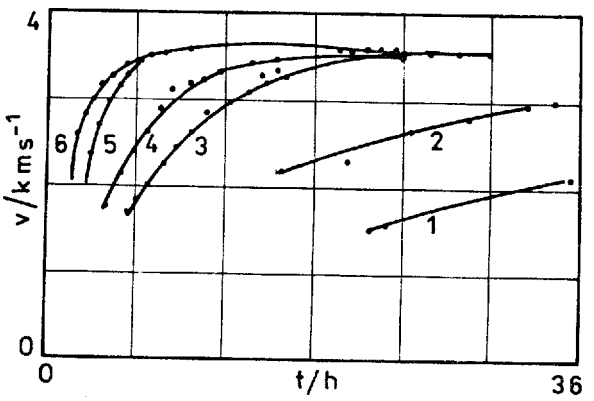

Fig. 4: Velocity of ultrasonic signal as function of hardening time for conditions as in figure 1.

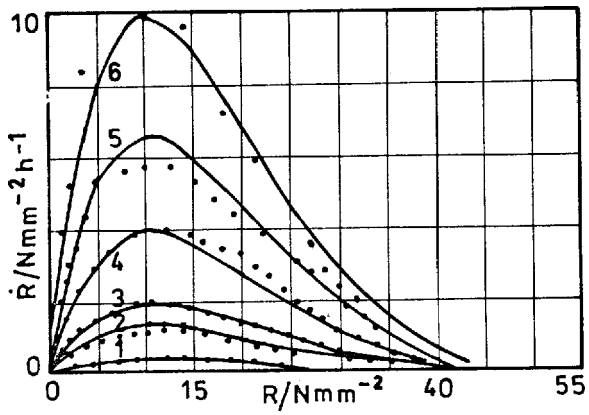

Fig. 5: Rate of strength as function of degree of strength for a cement paste of PZ 4/45 for temperatures as in figure 1.

With regard to ultrasound a correlation to the evolution of strength of concrete was found, if before comparing data an appropriate transformation of the resulting velocity is executed. The idea is to diminish the running time of the signal by the time which is necessary to cross through the volume fraction of the aggregates contained in the mix.

3. A HEAT TRANSFER MODEL FOR HARDENING CONCRETE

The basic assumption for the following is that the kinetics of evolution of strength and heat of hydratation has been modelized separately by equations of type (2) to (4) and that the proof of sufficiently correct representation of the real material properties can be given. Thus the local state of concrete in a continous body (construction) is defined. Note that instationarity is implied in the presented formulation. Now on this background heattransfer problems may be described. If as an example we take plane elements with the direction of heat flux perpendicular to its surface (parallel to x-coordinate) we get the set of nonlinear heattransfer equations:

$$c\,\rho\,T_{,t} = \lambda\,T_{,xx} + Z\,f(Q,T) \qquad (x,t) \in (0,L) \times (0,t_o) \qquad (5)$$

$$Q_{,t} = f(Q,T) \qquad \text{(rate of hydratation heat)} \qquad (6)$$

$$R_{,t} = g(R,T,w/c) \qquad \text{(rate of strength)} \qquad (7)$$

$$\left.\begin{aligned} T(x,0) &= T_o(x) \qquad x \in (0,L) \\ Q(x,0) &= Q_o \\ R(x,0) &= R_o \end{aligned}\right\} \qquad \text{(initial conditions)} \qquad (8)$$

$$\left.\begin{aligned} -\lambda\,T_{,x}(0,t) &= \alpha\,(u(t) - T(0,t)) \\ -\lambda\,T_{,x}(L,t) &= \alpha\,(v(t) - T(L,t)) \end{aligned}\right\} \qquad \text{(boundary conditions)} \qquad (9)$$

The meaning of c, ρ, λ, Z resp. α are: specific heat, mass density, number of heat conductivity, content of cement in the mix resp. heattransfer coefficient at the surface of concrete. The functions u(t), v(t) describe the control temperatures at the boundaries x = 0 and x = L. Partial derivatives are written by comma.

The initial-boundary problem (5) - (9) may easily be transcribed to other types of application. Due to its nonlinearity the solution must be calculated numerically using discrete or semidiscrete methods. In [1,2] details can be found which concern the topic of modelization of hardening kinetics of concrete. The derived model allows state-forecasting with high reliability. An example of calculation is presented in figure 6.

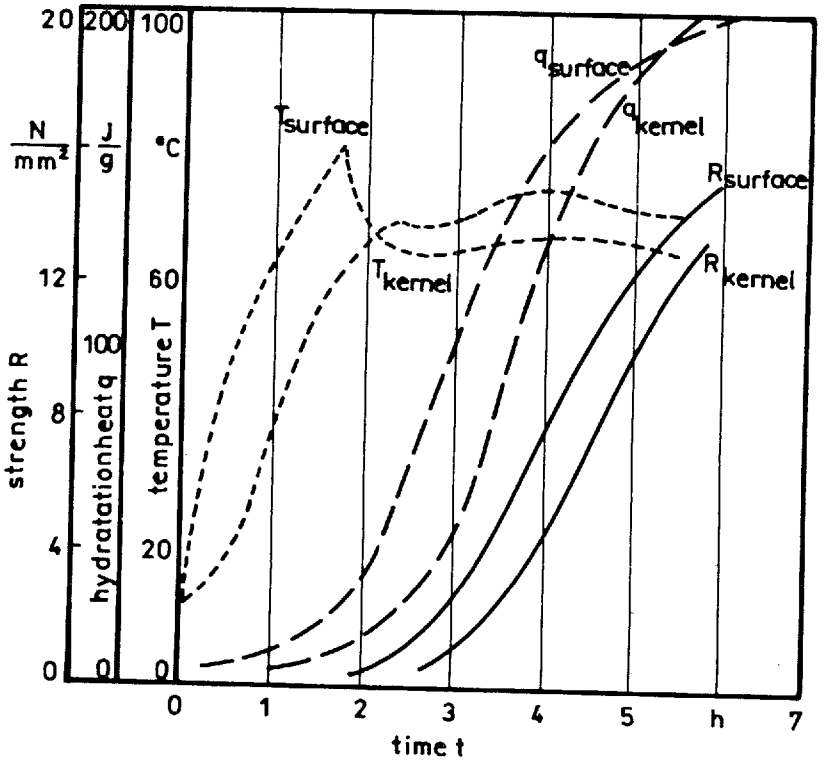

Fig. 6: With help of model equations (5) to (9) calculated evolution of temperature, hydratation heat resp. strength for a concrete plate. Mix: w/c = 0.65, content of cement 350 kg/m³, heattransfer: from 20 °C to 100 °C within 15 min., constant temperature during 1.5 h, then cooling to 20 °C.

REFERENCES

[1] Schlüssler, K.H.: Mathematical modeling of the kinetics of binder hardening, Cement and Concrete Research, Vol. 16, p. 215-226, 1986

[2] Schlüssler, K.H.; Mcedlov-Petrosjan: Der Baustoff Beton - Grundlagen der Strukturbildung und der Technologie, Verlag für Bauwesen Berlin, 1990

Technische Universität Cottbus
Prof.Dr.rer.nat.habil. K.H. Schlüssler
Karl- Marx-Straße 17
D - 7500 Cottbus

MODELS FOR THE DEVELOPMENT OF STRENGTH AND POROSITY WITH TIME IN CEMENTS WITH AND WITHOUT CARBONATE ADDITIONS - A QUALITATIVE DURABILITY EVALUATION

C E S Tango*, M C Florindo* and V C Campitelli**

**Instituto de Pesquisas Tecnológicas do Estado de Sao Paulo-IPT - São Paulo - BRAZIL*
***Escola de Engenharia da Universidade Estadual de Ponta Grossa - Paraná - BRAZIL*

SUMMARY

Eighteen laboratory Portland cements were ground with six calcareous rock/clinker proportions varying from 0% up to 15%, with 300, 400 and 500m^2/kg Blaine's fineness. For each cement, three standard sand mortars were prepared with the same consistency and with different water/cement ratios and cement contents. Compressive strength and porosity tests were made in five ages from 7 days up to 1 year. A mathematical model for porosity-time development is derived and adjusted to the experimental values. A previous model for strength-time development is also adjusted. The trends for strength and porosity may be showed using the models, allowing a comparative evaluation between the cements relative durabilities. References.

"MODÈLES POUR LE DÉVELOPPEMENT DE LA RÉSISTANCE ET DE LA POROSITÉ AU COURS DU TEMPS EN CIMENTS AVEC OU SANS ADDITIONS CALCAIRES"

RÉSUMÉ

Dix-huit ciments de laboratoire ont été broyés avec six proportions calcaire/clinker entre 0% et 15% et finesse "Blaine" 300, 400 et 500m^2/kg. Trois mortiers equi-consistants de sable normal ont été preparés avec chacun des ciments. Des essais à compression et de porosité ont été effectués aux âges de 7 jours jusqu'à 1 an. Un modèle mathematique a été déduit, pour le développement de la porosité au cours du temps, et ajusté aux valeurs expérimentaux. Autre modèle deja déduit a été ajusté aux experiments résistance-temps. On peut montrer les tendences pour la résistance et la porosité avec l'utilisation de ces modèles, et bien aussi faire une evaluation qualitative des durabilités des ciments sans calcaire et avec les divers proportions de l'ajout.

INTRODUCTION

There is a need for a comparative performance avaluation between the new Portland cements with carbonate additions and the old cements, mainly concerning the durability aspects. Accelerated tests give only qualitative answers. However, performance extrapolations also provide a qualitative information, which is more acceptable when the used models are more reliable. This work is based on experimental data obtained at the IPT - Brazil up to 1 year of age, continuing previous works[1,2,3], verifying at this time a mathematical model derived and adjusted for portland cements without additions up to 50 years of age[4, 5, 6, 7, 8] for the strength - time relationship; a new model for porosity - time relationship is also derived with this basis.

EXPERIMENTS

A Portland clinker from a Brazilian manufacturer, natural gypsum and calcareous rock were used[1,2,3]. Three levels for Blaine's fineness were established: 300, 400 and 500 m^2/kg, obtained by grinding the materials together in a laboratory ball mill. Calcareous rock was added replacing clinker in the proportions by weight of 0; 2.5; 5; 7.5; 10 and 15%. Gypsum proportioning was determined by ASTM C-563/79. The 18 experimental cements physical and mechanical characteristics are presented in[1,2,3].

Cylindrical specimens with 5cm diameter and 10cm height were made in the proportions (cements:Brazilian standard sand) 1:2; 1:3 and 1:4, with a flow in the range 160 to 170mm measured in the Brazilian flow table; water/cement ratios were the necessary. Permeable voids volumes were determined following ASTM C-642/82 (adapted for mortars) for each mix proportion (1 specimen by test condition). The compressive strength was obtained by 3 specimens, which were made for each mix proportion and age. The results for 7, 28, 91, 180 and 365 days tests are shown in[1,2,3].

MATHEMATICAL MODELS

Strength as a function of time and water/cement ratio

A mathematical model for the strength as a function of time and water/cement ratio has been previously presented[4,5,6,7,8]: $f_c = A/B^x \cdot D^{x/T} \cdot E^{1/T})$ (eq. 1)

where: f_c = compressive strength; x = water/cement ratio; $T = t^{1/2}$; t = time; A, B, D and E = constants depending on the materials and test conditions.

Equation 1 may be written in the linearized form expressed by equation 2:

$\log f_c = \log A - x \cdot \log B - (x/T) \log D - (1/T) \log E$ (eq. 2)

Linear regressions were made with the results, taking $\log f_c$ as a dependent variable and x/T, x, and 1/T as independent variables, for each one of the 18 researched cements; the values obtained for the constants log A, log B, log D and log E are in Table 1.

Porosity as a function of time and water/cement ratio

The gel capillary pores and anhydrous material evolution volumes in cement paste, during all the hydration, are represented in Figure 1[4,5] (where: V = volume; g_h = hydration degree; x = initial volume of water; m_{ec} = specific gravity of original cement grains; p_c = instantaneous volume of capillary pores; V_{hc} = instantaneous volume of gel; V_c = instantaneous volume of anhydrous cement; $1/m_{ec}$ = initial volume of cement; w_n = virtual volume of non-evaporable water; K = volume of gel after total hydration). In this Figure, it can be observed that the water/cement ratio is numerically equal to the water volume by cement weight ratio for water specific gravity equal to 1. For blended cements with partial or totally inert additions as limestone filler, it can be considered that the inert fraction passes gradually from the anhydrous cement to the gel. It can also be seen:

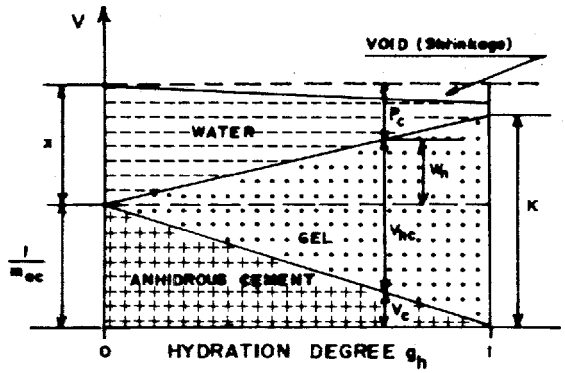

Fig. 1 - Volume evolution as a fraction of the cement weight in the hydration paste.

$$p_c = (x + 1/m_{ec}) - (V_{hc} + V_c) \qquad \text{(eq. 3)}$$

since: $V_{hc} = K \cdot g_h$ and $V_c = (1/m_{ec}) \cdot (1 - g_h)$ equation 3 remains:

$$p_c = x + g_h\,(1/m_{ec} - K) \qquad \text{(eq. 4)}$$

In equation 4, the term in parenthesis is a constant which depends on the particular cement characteristics like specific gravity (m_{ec}) and the resulting volume from hydration of the cement weight unity (K). The hydration degree is given by the following expression[4,5,8].

$$1/g_h = 1 + 1/(g_h'_o \cdot t^{1/2}) \qquad \text{(eq. 5)}$$

where: $g_h'_o$ = initial hydration "speed" (it is not a real speed because of the use of the square root of time instead of the time itself); t = time.

The initial hydration "speed" can be assumed as a function of the water/cement ratio[4,5,8], expressed by the equation:

$$1/g_h'_o = 1/g_h'_{max} + 1/g_h''_o \cdot 1/x \qquad \text{(eq. 6)}$$

where: $g_h'_{max}$ = asymptotic value of $g_h'_o$ for x tending to infinite value, constant depending on the materials and study conditions; $g_h''_o$ = derivative of $g_h'_o$ related to x when x = 0, constant depending on the materials and study conditions.

Substituting equations 6 and 5 in equation 4, we obtain:

$$1/(p_c - x) = 1/(1/m_{ec} - K) + \{1/(1/m_{ec} - K)\}\,(1/g_h'_{max})(1/t^{1/2}) + \{1/(1/m_{ec} - K)\}(1/g_h'_o)\,1/(x \cdot t^{1/2}) \qquad \text{(eq. 7)}$$

It can be observed that equation 7 is linear as it is assumed $1/(p_c - x)$ as dependent variable, $(1/t^{1/2})$ and $\{1/(x \cdot t^{1/2})\}$ as independent variables and the other members as constants now called K_1, K_2 and K_3:

$$1/(p_c - x) = K_1 + K_2(1/t^{1/2}) + K_3\{1/(x \cdot t^{1/2})\} \qquad \text{(eq. 8)}$$

where: $K_1 = 1/(1/m_{ec} - K)$, $K_2 = \{1/(1/m_{ec} - K)\}(1/g_h'_{max})$, $K_3 = \{1/(1/m_{ec} - K)\}(1/g_h''_o)$ (eqs. 9, 10, 11)

The capillary porosity as a function of time and water/cement ratio then remains:

$$p_c = x + 1/\{K_1 + K_2(1/t^{1/2}) + K_3|1/(x \cdot t^{1/2})|\} \qquad \text{(eq. 12)}$$

The experimental results for permeable voids index are the expression of the percentual pore volume by total volume in the researched mortars, i.e.:

$$p_a = (p_c/V_t) \cdot 100 \qquad \text{(eq. 13)}$$

where: p_a = experimentally determined porosity for the mortar; V_t = total volume of the mortar, related to the cement weight unity; p_c = capillary pores volume, related to the cement weight unity.

Calling as: m_{ec} = cement specific gravity; m = aggregate/cement ratio by weight; m_{em} = aggregate specific gravity; x = water/cement ratio, volume/weight; and not taking into account the air volume, we have: $V_t = (1/m_{ec}) + (m/m_{em}) + x$ (eq. 14)

by substituting eq. 14 in eq. 13,

$$p_a = 100 \cdot p_c/(1/m_{ec} + m/m_{em} + x) \quad \text{or:} \quad p_c = (p_a/100) \cdot (1/m_{ec} + m/m_{em} + x) \qquad \text{(eq. 15)}$$

All p_c values were calculated with the eq. 15. The coefficients K_1, K_2 and K_3 were inferred for the eq. 12 by means of its linearization (eq. 6) using a linear regression method and are presented in Table 1.

Table 1 - Finenesses, filler proportions and adjusted coefficients of equations 2 and 12, for the 18 experimental cements.

Cement	Blaine	%	Equation 2					Equation 12			
n.	(m^2/kg)	filler	log A	log B	log E	log D	r^2	K_1	K_2	K_3	r^2
1	300	0.0	2.251	1.125	0.240	0.795	0.995	-5.095	7.969	-5.202	0.588
2	300	2.5	2.307	1.293	0.722	-0.280	0.989	-5.296	2.157	-2.818	0.365
3	300	5.0	2.264	1.226	0.537	0.164	0.994	-5.781	1.820	-3.010	0.304
4	300	7.5	2.246	1.202	0.429	0.428	0.995	-5.263	-1.267	-2.251	0.467
5	300	10.0	2.267	1.273	0.451	0.450	0.993	-5.547	3.533	-3.428	0.482
6	300	15.0	2.219	1.258	0.401	0.521	0.994	-5.793	-15.002	3.327	0.488
7	400	0.0	2.308	1.181	0.335	0.321	0.995	-5.222	10.990	-6.731	0.561
8	400	2.5	2.336	1.257	0.551	-0.019	0.995	-5.035	9.926	-6.937	0.707
9	400	5.0	2.351	1.258	0.561	0.090	0.986	-3.789	-2.927	-3.374	0.680
10	400	7.5	2.261	1.085	0.351	0.566	0.994	-5.470	14.043	-9.034	0.778
11	400	10.0	2.336	1.271	0.457	0.275	0.992	-5.873	11.909	-8.902	0.787
12	400	15.0	2.336	1.317	0.462	0.259	0.998	-5.393	4.009	-4.213	0.680
13	500	0.0	2.347	1.164	0.327	0.289	0.989	-5.030	9.633	-6.319	0.571
14	500	2.5	2.374	1.175	0.448	-0.067	0.998	-5.689	12.276	-6.782	0.572
15	500	5.0	2.352	1.164	0.675	-0.343	0.992	-5.384	11.470	-7.035	0.598
16	500	7.5	2.369	1.188	0.445	0.328	0.993	-6.075	15.988	-8.067	0.591
17	500	10.0	2.347	1.186	0.409	0.284	0.995	-6.063	14.573	-7.772	0.588
18	500	15.0	2.346	1.250	0.396	0.309	0.995	-6.597	18.336	-9.300	0.523

r^2 = squared multiple linear regression coefficient;
number of experiments by cement = 15, except eq. 12, cement 3 with 10 experiments.

Discussion of the models

Compressive strength tests results were less scattered than porosity tests. Thus, the multiple correlation coefficient obtained for adjusting eq. 2 were better than those for eq. 12. In this equation, it must be considered that the experimental values of porosity related to cement weight p_c do not take into account in the calculations the amount for air existing in the mortar. However, this condition is reasonable as the mortar are plastic, with consistency index of 165 ± 5mm. The good correlation coefficients obtained for eq. 2 lead us to assume that the mathematical model is also valid for fillerized cements and not only for ordinary Portland cements, at least up to 1 year age.

With respect to eq. 12, its derivation takes into account that the anhydrous cement with its inert part, after complete hydration, would be transformed into gel, this latter also with its inert part. This assumption is not yet well studied and will be the object of further attention in the adaptation of a valid model for cements containing an addition, at least partially inert as limestone filler. In spite of it's low correlation coefficients, eq.12 expresses the porosity evolution trends with time and with water/cement ratio. This scattering was expected because of the use of a single specimen for determining the porosity, as well as with respect to the limited period of water imersion (48 hours). More accurate methods for determining the porosity must be used in continuing this study. The calculated values for p_c as a function of p_a are certainly affected by the calculations assumptions and determination method limitations and should not be viewed as absolute values, but only as comparative values in this study.

Also the coefficients K_2 obtained should be negative and were in fact positive for an expressive part of the cements. This is another consequence of the scattering and/or the non consideration of the air volume in the sample after saturation or other causes not yet

suspected. The coefficients K_1 are related to the trend for infinite time in spite of the coefficients K_2. Thus, it was considered that the calculated values for eq. 12 adjusted to the experiments are acceptable for a first evaluation of trends.

PERFORMANCE PREDICTIONS

The eqs. 2, 12 and 15 allow us to calculate the water/cement ratio necessary to obtain 32 MPa strength at 28 days and also infinite age properties with this water/cement ratio. It is also possible to interpolate the corresponding value for the aggregate/cement ratio, using the Lyse linear equations inferred for the mortar families for each one of the experimental cements. Table 2 expresses the porosities and strengths at infinite age, which were presented by theoretical mortars with 32 MPa strengths at 28 days of age, made with each one of the cements. Figures 2, 3 and 4 show the strength behaviour with time, related to cement number 1 ($300m^2/kg$, without addition), for the mortars above. It can be observed on Table 2 and Figures 2, 3, 4 and 5 that any additioned cement has nor simultaneously all the parameters indicating better performance; the cements with fineness above or equal to $400m^2/kg$, generally required poorer mixes, but presented higher infinite-time porosities and/or lower strength reserves.

Table 2 - Comparative data for mortars with same consistency and strength (32 MPa) at 28 days of age.

Cement n.	x_{calc} (cm^2/g)	m_{calc} (g/g)	P_{clim} (cm^2/g)	P_{alim} (%)	P_{arel}	f_{clim} (MPa)	f_{cres} (MPa)
1	0.549	3.27	0.353	16.6	1.00	42.9	10.9
2	0.536	3.17	0.347	16.7	1.01	41.0	9.0
3	0.523	3.12	0.350	17.1	1.03	42.0	10.0
4	0.514	2.97	0.324	16.4	0.99	42.4	10.4
5	0.498	2.89	0.318	16.4	0.99	42.9	10.9
6	0.470	2.68	0.297	16.3	0.98	42.4	10.4
7	0.525	3.62	0.403	17.5	1.05	40.2	8.2
8	0.580	3.55	0.381	16.8	1.01	40.5	8.5
9	0.580	3.53	0.316	14.0	0.84	41.8	9.8
10	0.578	3.42	0.395	17.8	1.07	43.0	11.0
11	0.562	3.33	0.392	18.1	1.09	41.8	9.8
12	0.544	3.17	0.359	17.2	1.03	41.6	9.6
13	0.640	3.92	0.441	17.9	1.07	40.0	8.0
14	0.675	4.14	0.499	19.3	1.16	38.1	6.1
15	0.654	3.96	0.468	18.7	1.13	38.9	6.9
16	0.624	3.75	0.459	19.2	1.16	42.5	10.5
17	0.617	3.69	0.452	19.2	1.15	41.3	9.3
18	0.586	3.56	0.434	19.0	1.15	41.1	9.1

x_{calc} = water/cement ratio for 32 MPa strength at 28 days of age;

m_{calc} = aggregate/cement ratio to obtain 160 to 170mm consistency index with x_{calc};

P_{clim} = porosity of the paste, related to the cement weight, calculated at infinite age with water/cement ratio x_{calc};

P_{alim} = porosity of the mortar with water/cement ratio x_{calc}, calculated at infinite age;

P_{arel} = porosity at infinite age, related to cement n. 1, with w/c ratio x_{calc};

f_{clim} = compressive strength at infinite age, to be obtained with the mortar which gives 32 MPa at 28 days of age;

f_{cres} = strength reserve of the mortar with 32 MPa strength at 28 days, i.e., f_{clim} - 32MPa.

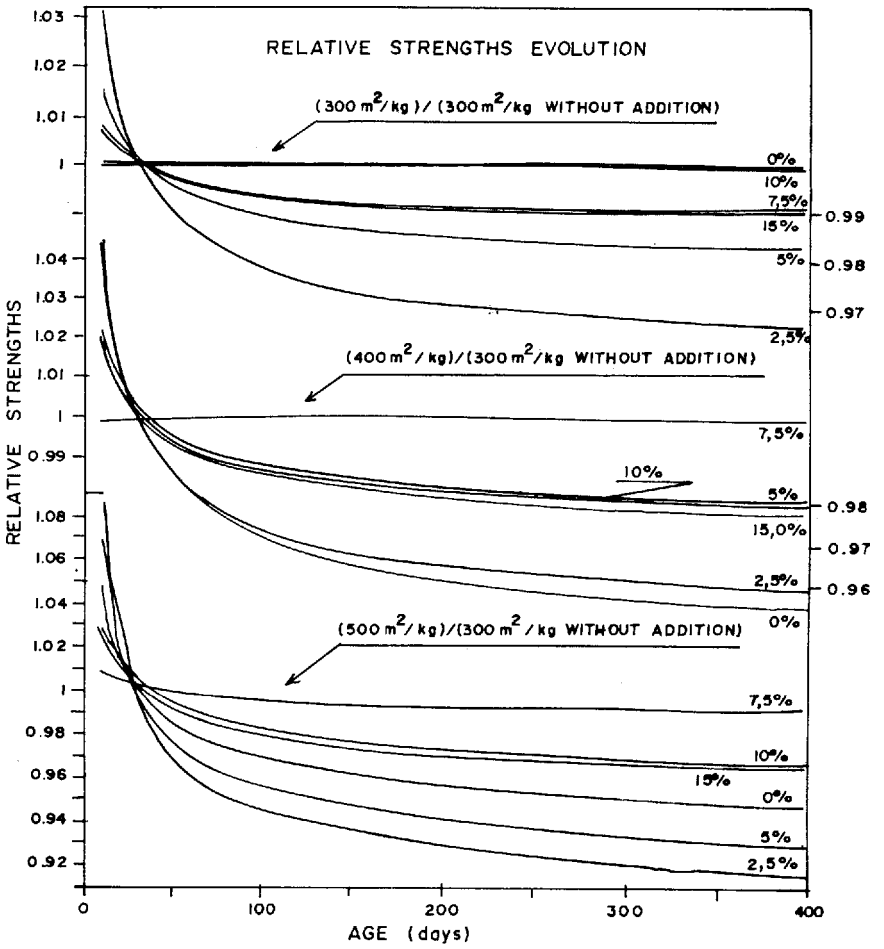

Figs. 2, 3 and 4 - Respectively, relative strength evolutions of cement mortars with 300, 400 and 500m²/kg finenesses, all with 32 MPa strength at 28 days age.

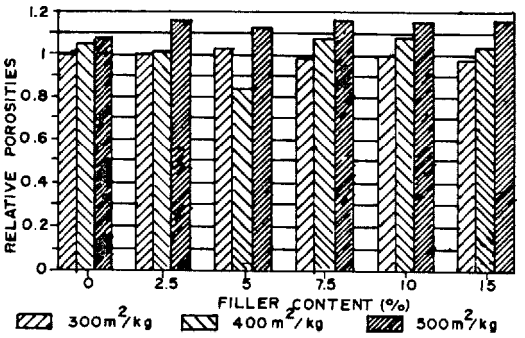

Fig.5 - Calculated porosities at infinite age, of mortars with 32MPa strength at 28 days of age.

However, it cannot be stated that the limestone addition is significantly unfavorable, mainly for 5; 7.5 and 10% filler proportions. In the researched cases it was verified that there is an optimum content of filler for each fineness and probably for each clinker. The low performance of the 2.5% filler cements is remarkable, indicating that variations in the amount of filler can lead to unexpected results.

CONCLUSION

To all the appearances, all the evidences indicate that for the fillerized Portland cements, the mathematical model purposed by eq. 2 is convenient to apply on the development of the strength with the time and water/cement ratio. The model of the eq. 12 requires

further investigation, mainly using more accurate porosity determination methods; also the hypothesis used for the derivation. However, this model was useful for obtaining an approximate idea of the infinite-time porosities.

It was evident that when strength was gained at ages below 28 days, by increasing the fineness and/or additioning limestone, there was a compensation in the later ages, say, lower strengths. Thus, it could be stated that the fillerized cements, in comparison with the cements without addition, would require an increase of the finenesses allied to an increase in the required cement contents for obtaining the same strengths at 28 days, and in the future the porosities of these could be bigger, or the strength reserves could be smaller. Taking into account the relation usually admitted among the porosity and the strength reserve and the durability, it is important to pay attention in verifying the long/term performance of the new cements which are standardized throughout the world.

REFERENCES

1. Campitelli, V.C. Adição de Filler Calcário ao Cimento Portland Comum Simples - Sua Influência em Algumas Propriedades de Pastas e Argamassas, devida a Alterações na Granulometria do Aglomerante. Doctor Thesis. EPUSP - São Paulo, 1989.

2. Campitelli, V.C. & Florindo, M.C. "The Influence of Limestone Additions on Optimum Sulfur Trioxide Content in Portland Cements" - Carbonate Additions to Cement. ASTM - STP 1064 - June, 1988. p.30-40.

3. Campitelli, V.C. Cimentos com Adição Calcária - Aspectos de Desempenho. 2º Congresso Brasileiro de Cimento - ABCP. São Paulo, Nov. 1990, v.1. p.27-44.

4. Tango, C.E.S. Um Estudo do Desenvolvimento da Resistência à Compressão do Concreto de Cimento Portland até 50 Anos de Idade. Doctor Thesis. EPUSP. São Paulo, 1990.

5. Instituto de Pesquisas Tecnológicas. Início de Estudos sobre Resultados de Ensaios de Longa Duração. Report 28.434 - São Paulo, Set. 1990.

6. Tango, C.E.S. Previsão da Resistência do Cocnreto até 50 Anos. Um Estudo. 2º Congresso Brasileiro de Cimento - ABCP - São Paulo, Nov. 1990, v. 2. p.523-542.

7. Tango, C.E.S. Prévision de la Résistance du Béton Jusqu'à 50 Ans - Une Étude. 2nd Int. Symp. on Quality Control of Conc. Structures - RILEM - Ghent - Belgium, 1991.

8. Tango, C.E.S. Modeling and Verifying Portland Cement Strength - Time Relationship up to 50 Years Ages. Submitted Paper, 9th Int. Cong. Chem., Cem. New Delhi, Nov. 1992.

THE DIFFUSION EQUATION OF Cl^- ION THROUGH CEMENT MORTAR

X L Wu, L P Xu, Q B Yang and S Y Huang

Shanghai Institute of Building Materials, Shanghai, P.R. CHINA

SUMMARY

The depth of Cl- diffusion through cement mortar was measured by the color-difference show method with the distinguishable chloride ion concentration about 1200 ppm. It was found that depths measured by this method were correlated to directly measured effective Cl- diffusion coefficients. Therefore this simple and easy method can be used to evaluate the resistance to Cl- diffusion of mortars.

Based on regress of plenty of test results, the diffusion depth may be expressed by the following equation:

$$d = K \cdot C^{0.272} \cdot t^{0.484} \text{ (mm)},$$

where: d - diffusion depth (mm), C - NaCl solution concentration in environment (%), t - exposure time (hour), K = a diffusion coefficient of mortar dependent on the constituent and structure of the mortar (mm/hr).

Test results show that the water-cement ratio, the volume fraction of cement paste in mortar and the curing age may be the main factors influencing the diffusion coefficient of mortar (K). For fly ash cement mortars, besides above mentioned factors the K value is also dependent on the quality of fly ash itself. Some corresponding equations were suggested to calculate the K value in this paper.

文　　摘

本文用色差显示法测定了Cl^-通过水泥砂浆的扩散深度，该方法测得的可见辨的Cl^-浓度约1200 ppm。结果表明用该方法测得的扩散深度与直接测定Cl^-扩散系数是一致的。因此这种简单易行的方法能用来评价砂浆的抗Cl^-侵蚀性能。

根据大量的试验数据回归分析，扩散深度可用下式表达：

$$d = K \cdot C^{0.272} \cdot t^{0.484} \text{ (mm)}$$

其中 d=扩散深度(mm)，C=环境NaCl溶液浓度(%)，t=暴露时间(小时)，K=取决与砂浆组成和结构的砂浆扩散系数(mm/小时)。

试验结果表明，水灰比、砂浆中的水泥浆体含量以及养护龄期可能是影响砂浆扩散系数K的主要因素。对粉煤灰水泥砂浆，除了以上这些因素外，粉煤灰本身的品质对K值也有影响。文中提出了计算K值的几个相关的方程。

INTRODUCTION

As is well known, the chloride-initiated reinforcement corrosion is one of reasons of deterioration of cement exposed to the chloride containing environment. It is important to study the Cl^- ion transfer through concrete and the influence of material constituents and structures on it.

The Cl^- ion transfer from surface to inside of concrete is caused by penetration and diffusion. The Cl^- transfer is dependent mainly on diffusion when the concrete is more or less saturated.

In 1980s, many papers have been published on Cl^- ion diffusion, mainly through cement pastes by direct measurement of the effective diffusion coefficient of Cl^- [1-4]. In this paper, the diffusion depths of Cl^- ion through cement mortars were measured by a colour-difference show method, and diffusion equations of Cl^- ion through cement mortar were also suggested by regression from test results.

EXPERIMENTAL MATERIALS AND METHODS

Materials

The ordinary portland cement of mark 525 according to Chinese Code and fly ash cement made by 70% portland cement and 30 % fly ash were used.

Three kinds of fly ashes were used for making fly ash cement: No.1— ground fly ash, No.2— original fly ash, No.3 — fly ash of high quality, collected by cyclone air separator. Their physical characteristics are shown in table 1.

Table 1 Physical characteristics of fly ashes

No.	Specific Gravity	Bulk density (Kg/m^3)	Residue on 80u sieve (%)	Residue on 45u sieve (%)	Specific surface area (cm^2/g)	Standard consistency (%)	Water requirement ratio (%)	IL. (%)
1	2.11	635	7.1	27.2	5026	47.2	103	5.17
2	2.00	808	22.7	39.0	3123	44.0	107	7.81
3	2.40	593	0	0	5817			3.64

The sand used was standard specially for testing.

Preparation and curing of specimens

The mortar specimens with various mix proportions were made of ordinary cement and fly ash cement. The size of all specimens was 4×4×16 cm. After stored in air for 24 hours, specimens were demoulded and then cured in water of 20 ℃ for 35 days for OPC mortars and 60 days for fly ash cement mortars .

Measurement of depths of Cl^- ion diffusion

After having been cured for given days, specimens were taken out of water. Five surfaces of

specimens were sealed by mineral wax, and one surface was left unsealed. Specimens were immersed again in water for 24 hours, then stored in NaCl solution with different concentrations for given days, and then taken out for testing. The wax was removed and specimens were cut into small pieces with the size of 4×4×2cm. The depth of Cl^- ion diffusion was measured by colour-difference show method, the detail of which had been published in (5).

TEST RESULTS AND DISCUSSIONS

The distinguishable Cl^- ion concentration measured by color-difference method

It has been found that the depth measured by color-difference method was correlated to directly measured effective diffusion coefficient of Cl^- ion [5]. Therefore, this simple and easy method can be used to evaluate the resistence to Cl^- ion diffusion through cement pastes and mortars.

Mortar specimens were prepared with the mix proportion of c : s : w = 1 : 2.5 : 0.5 for determining the distinguishable Cl^- ion concentration (C_a) measured with colour - difference show method. Specimens were immersed in NaCl solution with various concentrations and diffusion depths were measured at different diffusion time by this method.

The distinguishable Cl^- ion concentration (C_x) can be found by means of Fick's second law. The solution of Fick's second law for one dimension equation is:

$$C_x = \frac{C_0}{\sqrt{4\pi Dt}} \exp(-x^2/4Dt) \quad \text{——— (1)} \ [6]$$

where : X —— distance from the diffusion source;
t —— diffusion time;
C_0 —— concentration of diffusion matter for t = 0;
C_x —— concentration of diffusion matter at the point, X distant from the diffusion source as diffusion time being t;
D —— diffusion coefficient.
The boundary condition of the above equation is : if X = 0, then C_x = 0.

The D value can be directly measured by diffusion cell method. That of the mortar with the same mix proportion measured by the present authors is approximately 37.7×10^{-9} cm/s . As C_0, t and D are known, and the distinguishable diffusion depth (d = x) can be measured, the distinguishable concentration C_a can be calculated by equation (1).

Based on test results of 44 series of mortar specimens, the average value of the distinguishable concentration C_a calculated was found to be approximately 1200 ppm.

Correlation of diffusion depth (d) of Cl^- ion through mortar with diffusion time (t) and concentration of NaCl solution (C_a)in surrounding environment

The distinguishable diffusion depths of both ordinary portland cement mortar and fly ash cement mortar (with fly ash No.1) with the mix proportion of c : s : w = 1 : 2.5 : 0.5 were measured with the NaCl solution concentration of 3 , 6 , 9 , 12 , 15 and 18 % and at the diffusion time from 48 hours to 1600 hours.

The relationships between the distinguishable diffusion depth (d), the diffusion time and the concentration of NaCl solution in the surrounding environment were plotted in Fig.1 and Fig.2, and may also be exprssed by the regression equation (2) as follows:

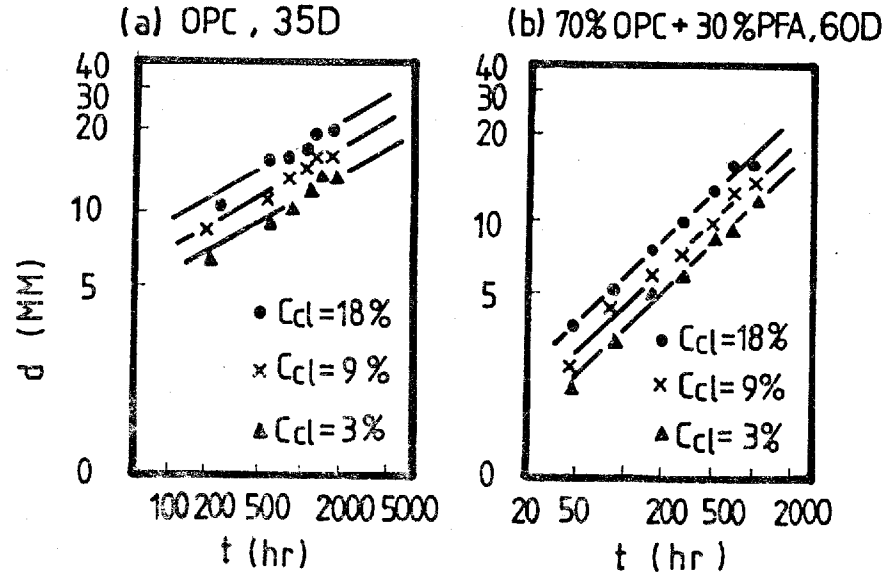

FIG.1 Relationship between (t) and (d) valuves

$$d = K \cdot C_{Cl}^{b_1} \cdot t^{b_2} \qquad (2)$$

where b_1=0.272, b_2=0.484, correlation coefficient r=0.98 and number of samples n=167. K is a coefficient of mortar characterizing its diffusion property dependent on its constituent and structure.

The influence of water-cement ratio (w/c), volume fraction of cement paste in mortar (V_p) on K value

The influence of w/c on K is shown in Fig.3, where the coefficient K is calculated by above

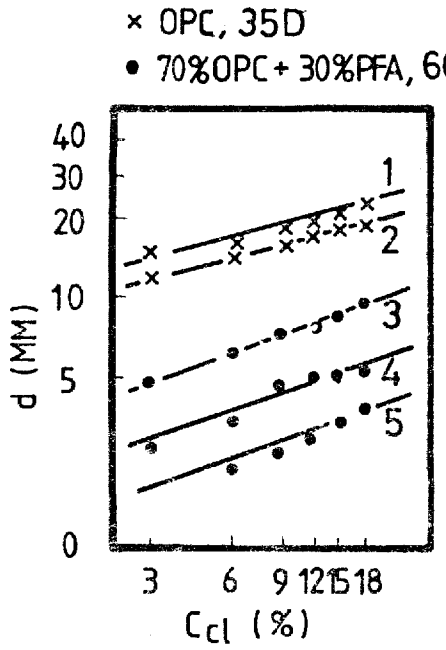

FIG.2 Relationship between C_{cl} and d
1. t=1600 hr 2. t=1060 hr
3. t=317 hr 4. t=89 hr
5. t=48 hr

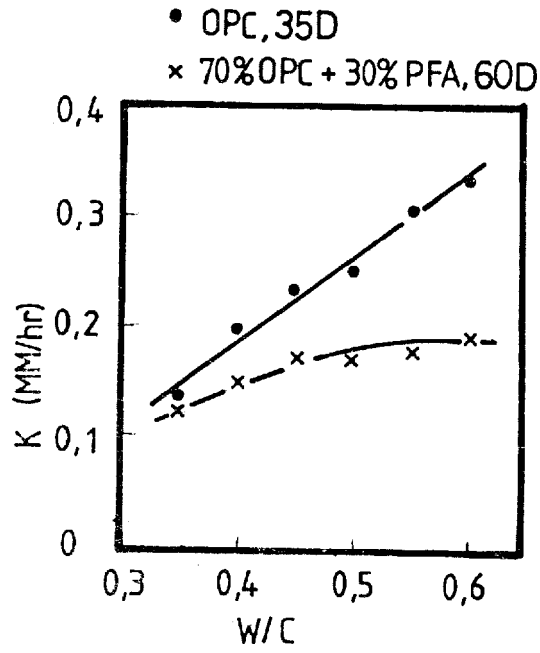

FIG.3 Relationship between W/C and K

mentioned equation (2). It can be seen that the diffusion depth of Cl^- ions or K value increases with the increase in water-cement ratio of the mortar both for OPC mortar and fly ash cement mortar, but the increasing extent of the former is larger than that of the latter.

The effect of volume fraction of cement paste on K value is shown in Fig.4. For ordinary cement mortar, the influence of volum fraction of cement paste in mortar on K values more obvious as w/c is lager. But for fly ash mortar, the influence of V_p on K value seems to be ignorable.

The effect of w/c and V_p on K may also be expressed as follows:

$$K_{OPC}=0.83\ (w/c) + 4.15 \times 10^{-3}\ (V_p) - 0.35 \qquad (3) \quad r=0.78,\ n=24$$

$$K_{OPC/PFA}=0.31(w/c)^{0.88} \qquad (4) \quad r=0.79,\ n=18$$

The effect of the quality of fly ash and curing age on d or K value

In order to investigate the influence of quality of fly ash and curing time on K value, three kinds of fly ash were used for making mortar specimens. According to Chinese Specification JGJ-28-86, they belong to class Ⅱ, Ⅲ and Ⅰ respectively. All specimens cured in water at 20 ℃ for 28, 60, and 100 days were then immersed in 10% NaCl solution for 32 days. The diffusion depth (d) and the K value were shown in fig 5 and table 2 respectively .

Table 2 K values of mortars with different curing time (mm / hr)

Type	28 days	60 days	100 days
OPC	0.20	0.14	0.13
No.1 PFA	0.18	0.10	0.09
No.2 PFA	0.23	0.12	0.11
No.3 PFA	0.15	0.08	0.07

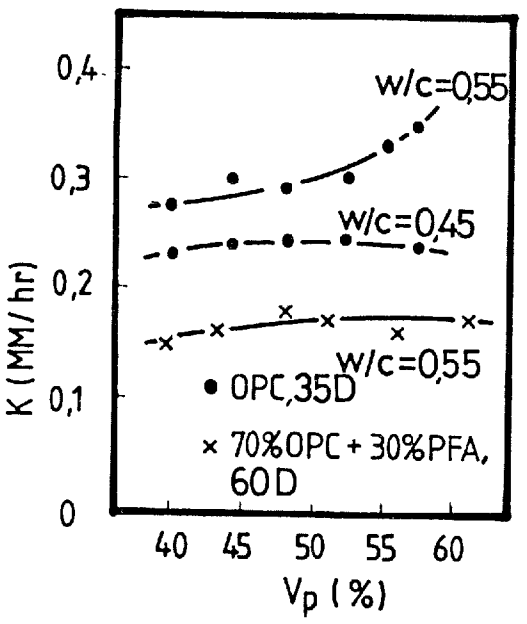

FIG.4 Relationship between V_p and K valuve

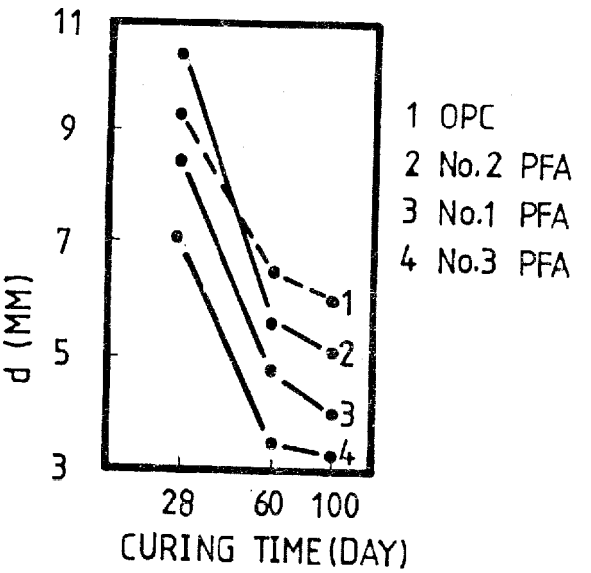

FIG.5 Effect of curing time on d valuves

The X or K value of fly ash cement mortars decreases with the increase in curing time and the X or K value of specimens with fly ash of high quality (No.3) is smaller than that of other fly ash mortars and OPC mortar.

As the K value is apparently affected by the quality of fly ash and the curing time, equation (4) above mentioned for fly ash cement mortars should be revised as follows:

$$K_{opc/pfa}=0.31\ K_f\ K_d\ (w/c)^{0.86} \qquad \text{——————(5)}$$

where: K_f—— a revision coefficient for quality of fly ash, for class Ⅰ, K_f=0.8
class Ⅱ, K_f=1.0
class Ⅲ, K_f=1.3

K_d—— a revision coefficient for curing time, for 28 days, K_d=1.8
60 days, K_d=1.0
100 days, K_d=0.9

4. CONCLUSION

(1). The colour-differential show method can be easily and simply used to evaluate the resistance to Cl^- ion diffusion of cement pastes and mortars.

(2). The diffusion depth of Cl^- ion through mortars is a power function of chloride concentration in surrounding environment and exposure time. It is dependent on the constituent and the structure of the mortar. A regression equation (2) expressing the relationship was shown in this paper.

(3). The main material factors influencing the diffusion depth of Cl^- ion of a mortar are water-cement ratio and cement paste volume, fraction in the mortar. For a fly ash cement mortar, besides those two factors, the quality of fly ash and curing time also influence the diffusion depth. The equations for exepressing the diffusion coefficient K of a mortar have also been given out.

REFERENCES

(1) S.Goto,D.M.Roy: C.C.R,Vol.11,1981,p.751-757.

(2) C.L.Page,N.R.short,W.R.Holden: C.C.R,Vol.16,1986,p.79-86.

(3) A.Kurmar,D.M.Roy: Proc.8th,Int.Cong.Chen.Cem.Vol.V,1986,p.73-79.

(4) Wu XueLi, Xu LiPing, Huang ShiYuan: Journal of Shanghai Institute of Building of Materials,Vol.2,No.3,1989,p.253-259.

(5) Young QuanBing, Wu XueLi: Journal of Shanghai Institute of Building Materials, Vol.3, No.4,1990,p.413-416.

(6) Paul C. Hiemenz: Publication of Peking University, 1977,p.128.

MODELLING OF LIME MORTAR CARBONATION

K Van Balen* and D Van Gemert**

**Center for Conservation of Historic Towns and Buildings, K.U.Leuven (Heverlee), BELGIUM*
***Department of Civil Engineering, K.U. Leuven (Heverlee), BELGIUM*

SUMMARY

The carbonation process in lime mortar is influenced by the diffusion of carbon dioxide into the mortar pare system, by the cinetics of the lime carbonation reaction, by the drying and wetting processes in the mortar. All these phenomena are depending on the presence of water in the mortar. Water is present in liquid form as well as in damp form. Physical models and their mathematical description are given for the factors influencing carbonation. The mathematical description of the carbonation process in lime mortar completes the information to construct a model that allows the simulation of carbonation in conjunction with the drying process.
Simulations at different carbon dioxide concentrations showed a good correlation between experiments and mathematical predictions.

RESUME

Un aperçu général des différents facteurs qui influencent la carbonatation du mortier à la chaux est donné. Il est démontré que le contenu d'eau dans le matériau influence la carbonatation aussi bien à travers un changement de la diffusivité à travers le matériau qu'à travers un changement de la réaction entre le gaz carbonique et la chaux. Un modèle mathématique a été développé qui permet la simulation du processus de la carbonatation en tenant compte de l'évolution du sèchement du matériau dans son environment.
Des simulations avec des concentrations de gaz carbonique différent montrent une bonne corrélation entre les expériments et les prédictions mathématiques.

INTRODUCTION

Although lime mortar has been used for centuries current knowledge is too poor to allow an evaluation of the mechanical behaviour of historic masonry. The slow carbonation of lime mortar makes the mechanical properties of lime mortar and the masonry built with it evolve with time. Recent research <VBAL 1991/2> dealt with this carbonation process and the changes of mechanical and physical properties of lime mortar which are caused by carbonation.

The rate of carbonation is to a great extent influenced by the presence of moisture in the mortar. Therefore, the carbonation process has to be divided into a carbon diffusion process followed by a chemical reaction, in which calcium crystals are formed. The influence of moisture on carbon diffusion parameters in mortar and the influence of moisture on the chemical reaction were studied. A new carbonation model was set up, in which the progress of carbonation takes the drying of the lime mortar into consideration.
The deposit of calcium crystals during carbonation changes the pore structure. Current research shows that this structural change influences the hygric properties of lime mortar.

CARBONATION REACTION

The carbonation reaction proceeds in two stages:

1. Carbon dioxide is dissolved in water;

$$CO_2 + H_2O \rightleftharpoons H_2CO_3 \qquad (1)$$

2. Lime reacts with the hydro carbonate;

$$Ca(OH)_2 + H_2CO_3 \Rightarrow CaCO_3 + 2H_2O \qquad (2)$$

This is confirmed by the slow carbonation of concrete at low relative humidity <Carb 1975>.
Diffusion of carbon dioxide in water is much slower than in the air. The binary diffusion coefficient in the air is 1390 10^{-8} m^2/sec, in water it is 10^4 to 10^5 times less <RICH 1988>. Carbonation is thus retarded when the material is saturated with water.
The optimum water content for carbonation is the water content that corresponds to maximum adsorption on the surface of the pores before capillary condensation.
The water content of the material therefore plays an important role in the diffusion of carbon dioxide in the lime mortar.

FACTORS INFLUENCING CARBONATION

The approach followed distinguishes between mass transport of carbon dioxide, mass transport of water damp and the carbonation reaction.

Factors related to diffusion of carbon dioxide.

a. Time - As for many diffusion problems the progress of carbonation can be expressed in a simple form:

$$x = k*\sqrt{t} \quad or \quad x = e+k*\sqrt{t} \qquad (3)$$

with: x: carbonation depth;
k: a factor;
t: time;
e: a constant.

The k-factor is often determined in an experimental way based on one of the above expressions **(3)**. This k-factor does not correspond to a property of the material, although many researchers are looking for its relation to material properties and using its value to predict carbonation speed <RICH 1988>.

b. Porosity and diffusivity of the material - Both material properties are interconnected as the diffusivity depends on the pore structure of the material. The pore structure of the material also affects the hygroscopic behaviour and as such influences the effect of water content on the diffusion of carbon dioxide in the material.

c. Construction method and cracks - Carbonation speed of site-mixed concrete is faster than that of prefabricated concrete, which in its turn is faster than of prestressed concrete <CURIE in RICH 1988, ref.38>.
In the case of masonry carbon dioxide can also penetrate into the material through the openings between the mortar and the joints and also through the bricks, as was noticed in a British research <HUNT 1980>.
Our research is confined to one-dimensional diffusion in a material assumed to be homogeneous.

d. Geometrical shape - In practice carbonation is often bi- or tri-dimensional. The carbonation front therefore is not always a plane surface.
A greater external surface in relation to the inner mass speeds up carbonation but also the drying in the case of bi- or tridimensional diffusion.

Factors related to the carbonation reaction

This mainly concerns the lime content and the reactivity.
The progress of the carbonation front depends on the amount of lime, which has to react with the carbon dioxide diffusing in the material.
A minimum amount of water in which the carbon dioxide has to be dissolved, is needed for the reaction. The solubility of carbon dioxide and lime decreases with increasing temperature, whereas chemical reactions in general are faster with increasing temperature. Therefore, the optimum carbonation speed is noticed at about 20°C <GRAN 1975, p.181>.
Solubility of lime depends on the particle size. The dissolution of lime is faster than the slow diffusion rate of carbon dioxide.
The solution of carbon dioxide in water depends on the transition coefficient for mass transport between water and air. This coefficient is unknown but under equilibrium conditions, a relation exists between the carbon dioxide concentration in water and the partial pressure in air:

$$[CO_2]_w = K_H * P_k$$
$$[CO_2]_w = K_H * R * T * [CO_2] \qquad (4)$$

$[CO_2]$ carbon dioxide concentration in the air (mole/l) or (mole/m^3);
$[CO_2]_w$ carbon dioxide concentration in water (mole/l) of (mole/m^3);
K_H Henry constant($10^{-1.5}$ mole/l*atm) of($2.92*10^{-4}$ mole/m*N);
P_k partial pressure of carbon dioxide (atm) or (Pa).

The result of carbonation is the formation of calcium carbonate crystals, mostly calcite. Carbonation with high carbon dioxide concentration leads to the formation of aragonite crystals <ROQU 1974, p.912>. This has been noticed on samples carbonated in a 100% CO_2 atmosphere.
The presence of SO_2 can slow down the reaction considerably <SADA 1977/2, p.1502>.

Factors related to drying and wetting

The following climate factors are considered : relative humidity, wind speed, (rain)water and temperature.
The climate affects the carbonation since it influences the water content of the material by wetting and drying.

The drying process is influenced by the wind speed since it influences the mass transfer coefficient, by the temperature and relative humidity of the ambient air. The optimum drying of fresh mortar, after which carbonation can start, is favoured by low relative humidity, strong wind velocity and high temperature.

MATHEMATICAL DESCRIPTION OF CARBONATION

Carbon dioxide diffusion in the air is described by Fick's first law. To describe the diffusion in porous materials the diffusion coefficient is replaced by an effective diffusion coefficient in the material <RICH 1988, p.4>.
Carbon dioxide diffusion is only possible in the open pores. The pore volume is not constant and changes with the water content. Carbonation itself modifies also the pore volume. It has been shown that the total pore volume decreases with carbonation <KROO 1961>. Our own experiments have shown that in lime mortar the relative amount of narrow pores with a diameter between 0.0063 and 0.1μm diminishes with carbonation.
The decrease of porosity and the change of pore size distribution is very small so that we may assume that porosity (ψ) is independent of the degree of carbonation and is only dependent of the water content.
The relation between porosity and water content is deduced from the hygroscopic curve (isotherms). The ratio of the hygroscopic water content (w_H) to the theoretical water content at 100% R.H. may be applied to the total porosity. This method allows taking into account the enclosed air that does not increase the water content but leads to a decrease of the apparent porosity.

$$\psi(w) = \psi_{max} * \left(1 - \frac{w_H}{w_{100\%}}\right) \qquad (5)$$

with: $\psi(w)$: porosity at water content w (m^3/m^3);
ψ_{max} : absolute porosity of the material (m^3/m^3);
w_H : water content at R.H. (kg/m^3);
$w_{100\%}$: water content at R.H. 100% (kg/m^3);

Carbonation reaction.

In a volume dxdydz part of the carbon dioxide is consumed by the reaction. For every mole $Ca(OH)_2$ one mole carbon dioxide is taken up and one mole water is produced. Formula **(6)** expresses the conservation of mass, neglecting the molecular adsorption and the change of the carbon dioxide concentration in the air:

$$\frac{\delta g_{kx}}{\delta x} + \frac{\delta g_{ky}}{\delta y} + \frac{\delta g_{kz}}{\delta z} = -R(w,c) - \psi \frac{\delta c}{\delta t} \qquad (6)$$

or

$$div\left(\frac{D_{kl}}{\mu} * \nabla c\right) + R(w,c) + \psi * \frac{dc}{dt} = 0 \qquad (7)$$

where: g: mass flux of carbon dioxide;
c: carbon dioxide concentration;
μ: diffusion resistance number;
R(w,c): the reaction speed per unity of volume ($mole/s*m^3$);

This **reaction term** R(w,c) expresses that in an elementary volume dxdydz R moles per unit of time and unit of volume of the gas are consumed by the reaction. The consumed carbon dioxide molecules can not participate any more in changing the concentration of the gas in the air of the pore.
The drying is modelled in two stages : drying at the surface and capillary water transport to the surface (first drying phase), the diffusion of water damp to the surface (second drying phase).

We found that the reaction term R can be expressed as :

$$R = k^T * [CO_2] * \alpha(R.V.) * \beta([Ca(OH)_2]) \quad (8)$$

where: $k^T = k^{20} * f(T)$;
$k^{20} = 0.7062\ (s^{-1})$: parameter at 20°C;
$f(T)$: temperature relation;
$[CO_2]$: carbon dioxide concentration in the air of the pore ($mole/m^3$);
$\beta([Ca(OH)_2])$: ratio of pore surface taken in by lime over the total pore surface $[Ca(OH)_2]/[Ca(OH)_2]_0$;
α(R.V.): influence of R.H. on reaction term (see further).

The autocatalytic character of the reaction between calcium hydrate and carbon dioxide <GRAN 1975, p.157> justifies this expression. In <VBAL 1991/2> expressions are given for the different parameters of formula (8).
Water transport at drying can be split up in two phases : the capillary water transport followed by the water vapour diffusion.
During the first drying phase carbonation is assumed to be negligible as the pore structure is not open enough to allow carbon dioxide to diffuse. This drying phase can be calculated independently of the carbonation as nearly no water is produced by carbonation. The period of the first drying phase can be calculated, taking one dimensional drying at one surface <HENS 1981, form. 2.108 b>.
When a full saturated fresh mortar is exposed to carbon dioxide, carbonation in the material will start after the first drying phase[1]. The outer surface of the material can carbonate as the transport of carbon dioxide to it is only hindered by the transfer coefficient, which is more or less independent of the water content in the material. The carbonation at the surface is stopped very quickly and the carbonation will only continue after a time t_{kn} when the first drying phase has passed.

The water damp transport in the second drying phase is expressed as a damp pressure potential, using Fick's law:

$$\overline{g}_{wd} = -\frac{\delta_a}{\mu_{wd}} * \nabla p = -\delta_{wd} * \nabla p \quad (9)$$

μ is a function of p. Due to the shortening of the diffusion path, when the material is filled with water, μ decreases with increasing water content to become about 1 for $w=w_{cr}$ (critical water content at the end of the first drying phase). If the water content still increases the damp diffusion becomes negligible compared with the capillary water transport.
μ as a function of the R.H. (ϕ) can be approximated with the following empirical expression:

$$\mu_{wd} = \frac{1}{a + b * \left(\frac{\phi(\%)}{100}\right)^n} \quad (10)$$

For lime mortar n equals 12 as the hygroscopic curve is very steep, for cement mortar n=2 is a good approximation.

---

[1] This approach neglects diffusion between capillary water content and the critical water content. When this latter is reached capillary water transport to the surface is stopped. Then the water front in the material withdraws due to diffusion of water vapour. Before the critical water content is reached the great pores are free of water and therefore, theoretically, diffusion of carbon dioxide is possible. As the first drying phase, compared with the second one, is very fast the amount of lime that can carbonate in the period that the water content is between w_{cap} and w_{cr} is very small.

From diffusion tests we know that μ=12 for ϕ=75%; μ=1 at w_{cr}. From that the values of a and b of the formula can be determined : a: 0.0833 en b: 0.9167. The value 53.4 in the formula is the water content at 100% R.V in the approximate function in the hygric equilibrium of lime mortar.

$$\mu_{wd} = \frac{1}{0.0833+0.9167*\left(\frac{\phi}{100}\right)^{12}} \qquad (11)$$

This leads for lime mortar to the following curve (Fig. 1).
For the carbonation a diffusion model with a variable diffusion coefficient and variable capacity term is needed.
Both f'(p) and δ depend on the water vapour pressure. The solution procedure of the differential equations will have to take this into account.

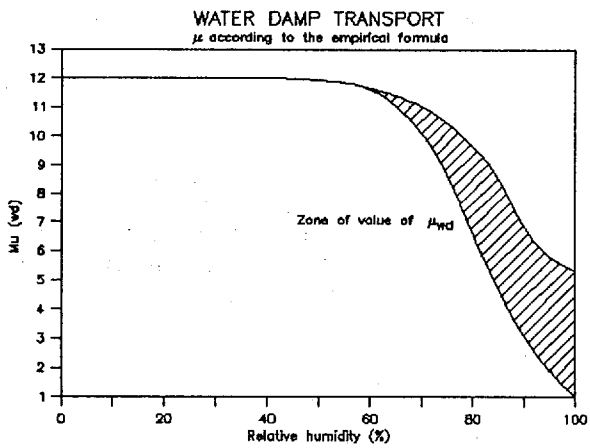

Fig. 1. Evolution of μ_{wd} in lime mortar as a function of R.H.

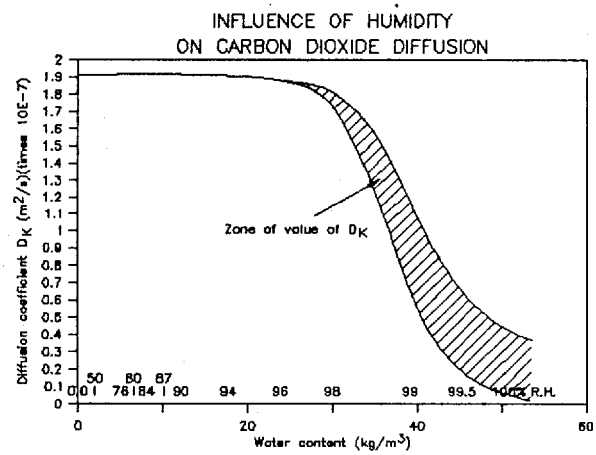

Fig. 2. Evolution of carbon dioxide diffusion coefficient as a function of water content in the material.

The relation between the carbon dioxide diffusion coefficient and R.H. can be approximated by a curve with the inverse form of the hygroscopic curve. It reaches 0 between the capillary and the critical water content, at 100% R.H. At that water content only isolated water islands are present in the material and no diffusion of carbon dioxide is possible. The diffusion coefficient at low R.H. is more or less constant and can be derived from the diffusion resistance number for water vapour (μ) of the material. This diffusion resistance number can be applied to the carbon dioxide diffusion coefficient in the air (D_k).
The diffusion coefficient of lime mortar can be expressed as:

$$D_k = \frac{1}{\left(a+b*\left(\frac{w}{w_{cr}}\right)^{12}\right)} \qquad (12)$$

The lime mortars tested gave μ=12 at 75% R.H., therefore $D_k = 1.9*10^{-7}$ m^2/s. At 100% R.H. D_k is very small, and we consider then D_k 1/100 of $1.9\ 10^{-7}$ m^2/s. It is shown in figure 2.
The influence of relative humidity on the reaction term is calculated in the factor α(R.H.) ($0<\alpha(R.H.)<1$) which expresses which part of the surface is free for the reaction <VBAL 1991/2>.
The result is shown in the following graph for the lime mortar samples tested :

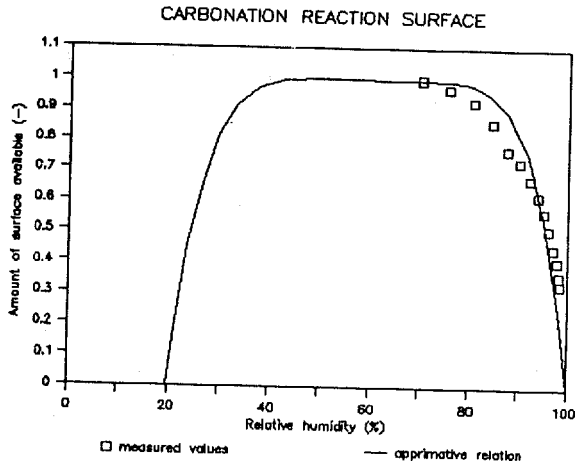

Fig. 3. Ratio of the available pore surface to the total surface, taking into account the influence of molecular adsorbed water and capillary condensation.

Conclusion.

Carbonation can be expressed in the form of a differential equation with a "sink" term. The composition and the structure of the material influence the parameters in the reaction term and the diffusion resistance number.
For the simulation of the carbonation of lime mortar, not taking into account the effect of humidity and assuming that the reaction is much faster than the diffusion, an analytical expression with a new definition of the "sink" term is proposed. This sink term is based on the concentration of lime and of carbon dioxide.

The equations for the description of water vapour transport complete the information needed to construct a model that allows the simulation of carbonation in conjunction with the drying process.

MATHEMATICAL MODEL OF LIME MORTAR CARBONATION

The mathematical formulations expressing carbonation and taking into account the effect of water content in the material are used to construct a computer simulation model. The non-linear coupled differential equations are solved by using a finite difference procedure. Therefore a programm in Turbo Pascal has been made. This allowed us to simulate the one dimensional carbonation process of a lime mortar.
It also allows studying the effect of drying on the progress of the carbonation front in lime mortar. With the appropriate adjustments the same model could be used to simulate the carbonation of concrete.
As an example the carbonation of freshly mixed lime mortar is simulated with the mathematical model in the following figures (Fig. 4 and Fig. 5), which give the evolution of carbon dioxide intake due to carbonation.
The carbon dioxide intake of freshly made lime mortars as studied by Henkel <HENK 1955> has been simulated.
A precise comparison of the simulation with the data given by Henkel is difficult as in the tests of Henkel the carbon dioxide diffusion was not limited to a one dimensional diffusion as it is in the model. Therefore the amount of carbon dioxide fixed in the first phase is very important.

Fig. 4 en Fig. 5 give the calculated carbon dioxide flux at the surface of the lime mortar in an environment with respectively 100% and 20% carbon dioxide concentration. The typical trend of the carbonation intake is found. It is shown that the carbonation of the lime mortar outer surface occurs very fast and that the second diffusion controlled phase of carbonation starts when the lime mortar has dried enough. This leads to a curve with two peaks: a sharp one after a short time and a rounded one after a longer period as found in the experiments of Henkel <HENK 1955>.

CONCLUSION

The mathematical formulations expressing the carbonation and taking into account the effect of water content in the material, were used to produce a simulation model. The non-linear coupled differential equations are solved by using a finite difference procedure.

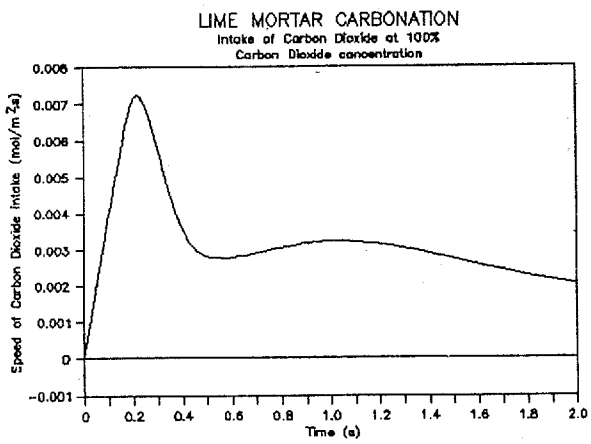

Fig. 4. Carbon dioxide intake of lime mortar carbonating in a 100% CO_2 environment.

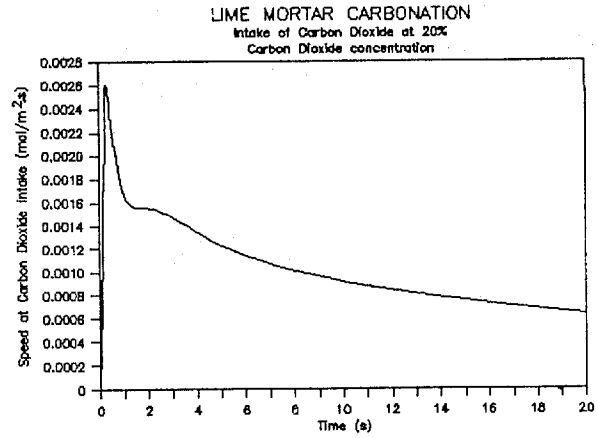

Fig. 5. Carbon dioxide intake of lime mortar carbonating in a 20 % carbon dioxide concentration environment.

The model allows us to study the effect of drying on the progress of carbonation in the studied lime mortar. With the appropriate adjustments the same model can be used to simulate the carbonation of concrete. This model thus contributes to the knowledge and the better understanding of the carbonation process of lime mortars as well as of cement bonded materials.

REFERENCES

<Carb 1975> N., Carbonatatie lichtbeton. Literatuurstudie. (Carbonation of leight-weight concrete. Literature) CUR Rapport, nr. 73, december, 1975, pp. 9-51.

<GRAN 1975> GRANDET J., Contribution à l'étude de la prise et de la carbonatation des mortiers au contact des matériaux poreux. Ph.D. Dissertation, Univ. Paul Sabatier Toulouse, CNRS, 1975, pp. 1-287.

<HENK 1955> HENKEL W., Untersuchungen über die Kohlensaureaufname von Mörteln. *Zement - Kalk - Gips*, nr. 11, 8, 1955, pp. 386-393.

<HENS 1981> HENS Hugo, Bouwfysica 1. Warmte en vocht: Teoretische grondslagen. (Building Physics 1. Heat and humidity: fundamentals.) Leuven, 1981.

<HUNT 1980> HUNT J.H., The loss of alkalinity of brickwork mortars measurements taken on buildings at the B.R.S., Garston, inedit, Building Research Establishment Note, dept. of the Environment, N 149/80, Garston, 1980, 9 p.

<KROO 1961> KROONE B., CROOK D.N., Studies of pore size distribution in mortars. *Magazine of concrete research*, vol.13, n°.39, november, 1961, pp. 127-132.

<RICH 1988> RICHARDSON Mark, Carbonation of reinforced concrete. Its causes and management. Dublin, 1988.

<ROQU 1974> ROQUES H., GIROU A., Kinetics of the formation conditions of carbonate tartars. *Water research*, vol. 8, Great Britain, 1974, pp. 907-920.

<SADA 1977/2> SADA E., KUMAZAWA H., BUTT M.A., Simultaneous absorption with reaction in a slurry containing fine particles (two gases). *Chemical engineering science*, vol. 32, Great Britain, 1977, pp. 1499-1503.

<VBAL 1991/2> VAN BALEN K., Karbonatatie van kalkmortel en haar invloed op historische strukturen. (Lime mortar carbonation and its influence on historic structures.), Ph.D. Dissertation, K.U.Leuven, Leuven, 1991, 281 p.

MODELLING THE RHEOLOGICAL BEHAVIOUR OF FRESH CONCRETE

R I A Malek

Materials Research Laboratory, The Pennsylvania State University, USA

SUMMARY

The 21st Century Concrete Technology holds vast challenges that both the industry and supporting research in the field must be ready to tackle. Looking ahead, a great expansion in the low-cost and time efficient construction can be seen. An investigation of the workability of fresh concrete should constitute an essential part of modern concrete durability studies.

In this paper, an approach to model the rheological behavior of fresh concrete is presented. The model is simple and systematic and relates the mechanical properties of fresh concrete to the fundamental characteristics of the constituents and mixture proportioning. Depending on the forces present, the effect of degree of flocculation of cement particles on the rheological behavior of fresh concrete is considered in developing the model. The model predicts very well several relationships and can be used to calculate the minimum water required to produce flow for a particular aggregate content and others.

INTRODUCTION

Deterioration of concrete (especially in highway systems) is a problem of international concern. Many recent studies of concrete structure failure cases suggest that the rheological properties of the original fresh concrete is an often unrecognized cause of concrete deterioration. Inadequate workability will result in alternating regions of compact and loose concrete which will have an effect on the microstructural development during hardening. This is manifested as an unpredicted decrease in the ability of concrete to restrict the transportation of potentially aggressive species that cause concrete deterioration.

Modeling the rheological behavior of fresh concrete is important to the construction process as it allows the design of mixtures for more consolidated and durable concrete. For decades studies of the rheological properties of cementitious materials were only concerned with that of pastes. In a recent review, Malek[1] summarized the work done to date to model the rheological properties of cement pastes. Bombled and Feneuille[2], Tattersall[3], and Tattersall and Banfill[4] have recently reviewed work on the rheological behavior of concrete. Tattersall[3] in particular, concluded that the flow properties of concrete conform to Bingham model. He and his associates developed an apparatus to determine the rheological properties of concrete based on this model. They pointed out that the workability of fresh concrete is better characterized by two parameters, namely, the yield stress and plastic viscosity rather than the single result provided by other methods.

It is evident that establishing a rheological relationship and choosing the proper technique to determine it depend on the range of shear rate which the concrete will be subjected to. For highway applications, the primary requirement of fresh concrete is that it should be of such workability that it can be readily consolidated in forms and around the reinforcement without excessive bleeding or segregation, and that flatwork can be properly finished without teaming or without surface sprinkling. Of course, many important properties of hardened concrete depend on the success of the consolidation process in meeting these requirements. Since fulfilling these requirements needs low shear values, the domination of yield stress in defining the rheological properties is emphasized.

The main objective of the work summarized here is to find expression to relate the mechanical properties of fresh concrete and particle packing density, which depends on the fundamental characteristics of the constituents and mix proportioning. A summary of the attempt to generate such a model is included. It is recognized that the products of the proposed model must withstand the scrutiny of the concrete technologists and highway engineers and serve their needs.

EXPERIMENTAL

Several concrete mixtures covering a range of compositions in the in the PADOT [Pennsylvania Department of Transportation] guidelines of highway concrete (abstracted from the more generalized AASHTO [American Association of State Highway and Transportation Officials] specifications)were made. These mixes have a range of fine and coarse aggregate proportions and a range of w/c ratios. The cement used was of ASTM type-I. Both crushed limestone aggregate and natural rounded gravel in gradations #8 and # 67 were used. A silicious sand with gradation according to ASTM C-33 was used as fine aggregate. Sieve analyses was made on all batches and necessary adjustments were done to bring all the batches to the same gradation before usage. A computer program for regrading aggregates to match the desired gradation was used for that purpose. In order to avoid batch-to-batch variabilities in physical properties, variations in water content were minimized. This was ensured by bringing the aggregates and sand to the saturated surface dry conditions before mixing. The packing density of each dry mixtures was calculated

using special computer program and justified by experimental determination using the method ASTM C29. Mineral and chemical admixtures were also be used. The general guidelines of ASTM method C-192 were followed for mixing procedure. An Eirich rotating pan mixer was used for this purpose. Rheological and fresh mixture properties were monitored utilizing the slump test and shearing viscometer. The intercept at zero shear rate (on the shear rate-shear stress plot) is proportional to the yield stress. The yield stress value was found to correlate inversely with the results of the slump test. The air content was determined utilizing the pressure method.

THE MODEL

An Approach to a Rheological Model for Concrete

A systematic approach to generate a rheological model for fresh concrete is to find an expression that enables calculation of the mechanical properties of fresh concrete from the fundamental characteristics of the constituents and mix proportioning. It is important that this expression should be as simple as possible and be suitable to the highway environment.

Fresh concrete can be represented by aggregate grains in a continuum of cement particles and water (paste). The aggregate amount and physical properties as well as the microstructure of the continuum will affect the mechanical properties of the concrete mixture. Due to the physical characteristics of cement particles, the particulate structure tends to coalesce and eventually encompass the whole sample in a global network of different size flocs or a gigantic floc. Depending on the forces present this flocculation has a considerable effect on the rheological behavior of fresh concrete. Fluid will be immobilized between the particles that stick together. The floc will have a structure that extends throughout the sample entailing a solid-like rigidity which is reflected in elastic behavior and in the appearance of a yield stress. Finally, the structure can change reversibly under flow causing shear thinning and thixotropy. It is possible to express the mechanical properties of the proposed floc structure by a mathematical expression. For aggregate particles, only the close contact hydrodynamic effects need to be considered, whereas for the continuum the particle-particle interactions constitute an important factor.

Inter-Particle Forces

Two important parameters characterize the rheological properties of concrete: yield stress and plastic viscosity. Yield stress is of primary importance in concrete. It dominates the apparent viscosity at low shear rate (most concrete applications) and is directly responsible for the shape retention-deformation characteristics of concrete. The criteria for the onset of yield stress have not yet been established but in terms of the interparticle interactions, it is the force per unit area necessary to overcome such interparticle interactions, and its magnitude is determined by the overall value of the interparticle interactions. The interparticle interactions are listed in Table I together with the range over which each interaction exists (adapted from References 7-10). It is important to attain a state of balance in the forces between particles by combining attractive and repulsive forces, in order to obtain a stable concrete. If one force dominates the other, the concrete will be unstable giving rise to inferior properties. The net interparticle force is determined by the sum of all forces present. The attractive forces become less significant at high shear rates.

Particle Packing

In the presence of the interparticle forces, and as a result of the size, shape and volume fraction of the particles, a packing array will be adopted which will minimize the overall energy of the concrete floc. The type of packing array determines the number of interactions per unit area, while the packing density and volume fraction control the interparticle distance. If external shear forces are applied, the interparticle distance in the floc is changed and a new equilibrium can be regained after the forces have been removed. The existing interparticle potential provides the restoring forces. This signifies the important role of the water volume fraction which controls the interparticle distance and, subsequently, the interparticle interactions and flow capability of the floc. Therefore the

Table I: Interparticle Interactions

Force	Distance (Å)
Attractive	
van der Waals	3 - 5
Hydrophobic Bonds	1 - 5
Hydrogen Bonds	2 - 3
Liquid Bridges	2 - 5
Shared Counter-ion	2 - 3
Repulsive	
Electrostatic	10 - 100
Steric Hinderance	~ 50

basic requirement to produce a flowable concrete floc is to provide a layer of immobilized water on the surface of particles having a thickness exceeding ~3Å to overcome the interparticle attractive forces (see Table I). This was found to be proportional to the ratio of surface area to volume of the solid fraction. When the minimum water required to produce flowable concrete is subtracted from the actual amount of water used, the resultant "excess water" is directly proportional to the workability (flowability) of the concrete. A representation of such a relationship is given in Figure 1. Negative values on the abscissa (open circles) means water is insufficient to produce the required workability. It is worth noting that the zero point on the abscissa is variable and dependent on the minimum workability limit of concrete. In the present investigation a 1-inch slump was taken as the minimum workability limit (Pennsylvania Department of Transportation and AASHTO specifications).

APPLICATION OF THE MODEL

Effect of Aggregate Proportion and Size on Rheology and Permeability

As mentioned previously, the presence of interparticle forces and as a result of their shape, size and volume fraction, the solid particles tend to acquire a certain packing arrangement in order to minimize the overall energy of the system. As the coarse fraction of the solid particles (aggregate) increases, the packing arrangement will change and the total surface area of the solid particles will generally decrease and, consequently, less water is needed to maintain the distance corresponding to minimum flow requirements. In addition, at a given aggregate volume fraction, increasing the fine to coarse aggregate ratio will increase the total surface area and more water will be needed to maintain a required workability. If the water

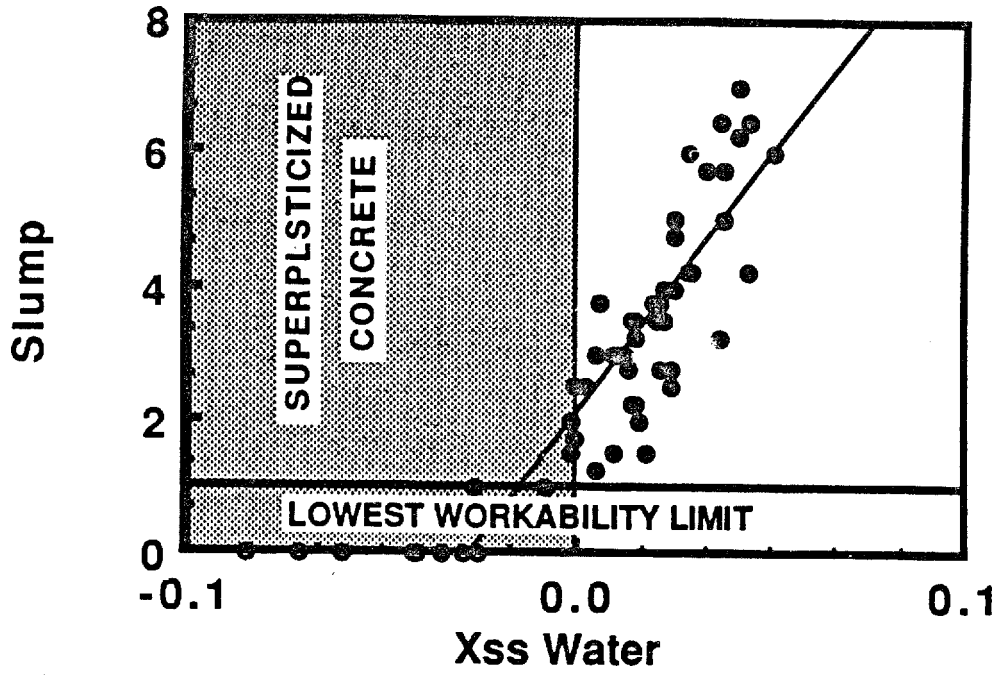

Figure 1. A representation of the relationship between water in excess of that required to produce flowable concrete and the slump value in inches.

content is kept constant (same w/c ratio), a decrease in workability could be observed with increasing F/C (fine/coarse) aggregate ratio. The permeability is thus expected to decrease as the aggregate volume fraction increases (at constant water/solid and F/C ratios) or as the F/C ratio decreases (at the same total aggregate volume fraction and same w/c). Chloride permeability measurements showed such correlations[10,11].

It has been shown[9] that the yield stress increases with the inverse of the particle radius (thus with the ratio of surface area to volume) and with the square of volume concentration. Thus at a fixed aggregate volume fraction, as the aggregate size increases, the yield stress decreases. This is reflected as high slump (higher workability) and high permeability (for chloride[10,11]).

As the axial ratio of the particles increases (i.e. the contact area to volume ratio of the particles increases) the volume concentration of which the particles interact with one another decreases, thus the yield stress decreases, and slump increases. This has been verified experimentally, as more spherical siliceous gravel was found to give concrete with lower yield stress (higher slump) than the corresponding angular limestone of the same gradation.

Effects of Mineral and Chemical Admixtures on Rheological Properties

Mineral admixtures affect the rheological properties of the concrete mixture in two ways. First, the physical characteristics of the mineral particles will affect the overall contact area to volume ratio and thus impose a modified packing order. Second, the chemical nature of the particles will modify the interparticle forces. The overall effect is a change in the water required to produce minimum flowable concrete.

Chemical admixtures (superplasticizers and water-reducers) have one prime function which is to modify the surface charges in the diffused double layers on the surfaces of particles. They tend to diminish the attraction forces between particles and drastically lower the yield stress. The effect of chemical admixtures at higher shear rates is negligible.

Relationship Between Rheology and Interface Properties

The interface properties are expected to be dependent on the rheological properties of concrete in two ways. First, the aggregate volume fraction and the fine to coarse aggregate ratio will affect the interparticle distance (rheology) and eventually the interfacial zone size. Second, the water added in excess of that required for minimum workability will affect both rheological and interfacial properties.

CONCLUSIONS

The workability of fresh concrete plays a significant role in the microstructural development of concrete. The systematic approach to generate a rheological model for fresh concrete is discussed. Emphases were given to the effect of aggregate size and proportion, effect of chemical and mineral admixtures on rheological properties of fresh concrete, and consequences for permeability. In addition the relationship between rheological properties and interface properties has been briefly discussed.

ACKNOWLEDGMENT

Partial financial support of the National Research Council's Strategic Highway Research Program is appreciated.

REFERENCES

1. Malek, R.I.A. "Modelling the Rheological Properties of Cement Pastes, A Review," Ceramic Transactions, Vol. **16**, 31 (1991).
2. Bombled, J.P. and Feneuille, 8th. Intern. Congr. Chem. Cem., Vol. VI, 317 (1986).
3. Tattersall, G.H., 8th. Intern.. Congr. Chem. Cem., Vol. VI, 228 (1986).
4. Tattersall, G.H. and Banfill, P.F.G., The Rheology of Fresh Concrete, Pittman Books, London (1983).
5. Veruray, J.W.E. and Overbeek, J.Th.G., "Theory of the Stability of Lyophobic Colloids," Elsevier, Amsterdam (1948).
6. Gray, H.B., "The Chemical Bond," W.A. Benjamin, Menlo Park (1973).
7. Overbeek, J.Th.G., "Colloid and Surface Chemistry II," MIT Press, Boston (1972).
8. Neville, P.C. and Hunter, R.J., "The Flow Behavior of Sterically Stabilized Latexes," J. Colloid. Interfac. Sci. **49** (2), 204 (1972).
9. Firth, B.A., and Hunter, R.J., "Flow Properties of Coagulated Colloidal Suspensions III," J. Colloid. Interface Sci. **57** (2), 266 (1976).
10. Malek, R.I.A., "Effect of Particle Packing and Mix Design on Chloride Permeability of Concrete, " 9th. Intern.. Congr. Chem. Cem. (1992).
11. Malek, R.I.A., "Chloride Permeability in Highway Concrete," 92nd Meeting of the Amer. Ceram. Soc, Dallas, Tx (1990).

DEPENDENCE OF THE FLOW CHARACTERISTICS OF CONCRETE ON THE DENSITY OF CEMENT STONE

I A Sulkowsky and A G Milrud

The Tashkent State University named after Beruni Tashkent, UZBEKiSTAN

SUMMARY

Ferrey and Wolker formulae use allowed to express the concrete deformation module as well as deformability in the case of the linear density function of the cement stone.

Использование формулы Фере и Уокера позволило выразить модуль деформации бетона и его деформативность в качестве линейной функции плотности цементного камня.

In 1891 y. Fere suggested a basic equation in which the strength of a cement stone is expressed as a function of its density. This equation is known in Soviet practice as the Fere-Simonov formula.

$$R_б = \alpha R_ц \left(\frac{Ц}{\frac{Ц}{\gamma_ц} + В}\right)^2 = \alpha R_ц \left(\frac{\frac{Ц}{В}}{\frac{1}{3{,}1}\frac{Ц}{В} + 1}\right)^2 = \alpha R_ц d^2 \quad (1)$$

where $R_ц$ - cement activity;

α - experimental coefficient allowing for the quality of the materials used.

With increase in cement-water ratio the tangent to the Fere curve is continuously reduced, but provided $\frac{Ц}{В} \to \infty$ the value of the investigated function tends to a constant limit.

The well known formula of Graph, Beliav and Bolomey as well as the formulae of Kiser and Dovjic for light-weight concrete, in which the cement-water ratio of the mix is raised to 2; 3/2, 1; 0,5 power correspon dingly, approximates the initial Fere formula in sections, which is partially proved by a comparison of the values of the concrete strength calculated on their basis.

Use of the Worker formula in conjunction with the Fere equation which has analysed makes it possible to express the concrete flow modulas (E) as a function of cement stone strength (R).

$$E = \beta\sqrt{R} = \beta\sqrt{\alpha R_ц \cdot d^2} = \beta\sqrt{\alpha R_ц d} \quad \ldots (2)$$

$$\beta \approx 1{,}4 \cdot 10^4$$

The flow modulas, evaluated in accordance with the expression (2), changes in direct proportion to the density of cement stone.

The expression in its reduced form E=f(d), explains the cause of the absence of a single valued correspondence between the modulus and its compressive strength.

Indeed, it is clearly seen from the expressions (1-2) that the growth in cement activity affects concrete strength to a considerably greater

extent than its flow modulus.

The maximum concrete flow is also defined in terms of its compressive strength based on the empirical formulae, that do not differentiate between the interaction of the concrete composition and cement activity.

Using the value of the modulus we get by Hooke's law the maximum flow of the concrete compression

$$\varepsilon = \frac{R}{E} = \frac{\alpha \cdot R_4 \cdot d^2}{\beta \sqrt{\alpha \cdot R_4 \cdot d}} = \frac{\sqrt{\alpha R_4}}{\beta} d \quad \ldots (3)$$

The maximum flow, as expressed (3), is also connected with the re-relative strength of the cement stone beeing directly proportional to it.

The equation for defining flow energy as a function of cement stone strength also assumes a sufficiently simple form, as below:

$$W = \frac{R\varepsilon}{2} = \frac{(\alpha R_4)^{3/2}}{2\beta} d^3 \quad \ldots (4)$$

The density of cement stone for various qualities of cement evaluated according to equations 2, 3, 4 lies within the limits of 0,75÷1,5 defining certain bounds, changing its moduli of maximum flow.

The new equation obtained give the simplest relationship between the most important flow characteristics of concrete and its composition which define the density of cement stone.

PHYSICAL DETERMINATION OF CORROSION OF CONCRETE DUE TO EVAPORATION OF PORE LIQUID

I P Vyrodov and V M Lekarev

Polytechnic Institute of Krasnodar, RUSSIA

SUMMARY

This paper suggests a hierarhic model of transportation (convection and diffusion) of aggressive components in capillary porous materials and gives a description of corrosion processes of solution concentration and crystal salts formation due to evaporation of pore liquid. On the basis of the generalized mass transfer equation supplemented with boundary conditions a mathematical model of salt form concrete corrosion under the influence of underground waters and atmosphere has been worked out, with the help of which a multifactor analysis of corrosion resistance and concrete longivity forecast have been done.

КРАТКОЕ СОДЕРЖАНИЕ

В докладе представлена иерархическая модель массопереноса (конвекции и диффузии) агрессивных компонентов в капиллярно-пористых материалах. Описаны коррозионные процессы концентрирования раствора и образования кристаллов солей в результате испарения поровой жидкости. На основе обобщенного уравнения массопереноса, дополненного граничными условиями, разработана математическая модель солевой формы коррозии бетона, с помощью которой проведен многофакторный анализ коррозионной стойкости и спрогнозирована долговечность бетона, подверженного воздействию грунтовых вод и атмосферы.

INTRODUCTION

The urgent problem of increasing corrosion resistance can be effectively solved when all the peculiarities of corrosion processes and their adequatly modelling are taken into account. The phenomenon of corrosion comprises the whole complex of processes with various combinations of factors leading to destruction of material and its performance deterioration. It is difficult to create a universal method of theoretical and phenomenological description of such processes.

However, in many cases some basic factor causing the most intensive destruction of material can be singled out. Salt corrosion is considered as such in the present paper. Because of capillary pressure, through porous space in concrete is filled with solution of salts (underground, sea and other mineralized waters). Due to evaporation of water from the open surface of menisci there takes place concentration of solution and crystallization of salts in pores, the aggressive action upon concrete increasing.

HIERARCHIC MODELLING OF TRANSPORT IN POROUS MEDIA

As a rule physico-chemical processes of corrosion of capillary porous materials are connected with transport (convection and diffusion) of agressive substance to the corrosion front. The complex and irregular structure of concrete [1,2] causes the stochastic character of concentration patterns and flows, the local microscopic values of witch are submitted to the ordinary homogeneous transport equation supplemented with boundary conditions on the inner surface.

Physical conditions for arising of the processes of salt crystallization in the solution are locally assumed by the microscopic parameters, while the corrosion resistance criteria of the material are determined by the measurable macrovalues witch can be obtained by averagening the microvariables in representative elementary volume (REV) of the porous medium. Thus hierarchic (three level) construction of transfer modelling for capillary materials is quite natural. Based on the microstructural transport level in a single capillary (Figure 1a) we pass on by means of averaging to the level REV (Figure 1b) and complete the construction of the hierarchic model by the description of the process in the macrovolume of the total pattern of the porous material (Figure 1c).

TRANSPORT OF AGGRESSIVE COMPONENT IN A SINGLE CAPILLARY

A single cylindrical capillary filled with solution of the aggressive component is considered as a microstructural element of the porous material. The following important peculiarity must be taken into account when constructing the model of mass heat transfer in solutions.Relaxation time neded for the temperature levelling is much more shorter than the time neded for the concentration measurement as the ratio $D_T/D \simeq 10^2 >> 1$ (where D_T- the coefficient of the thermotransport, D - the coefficient of the molecular diffusion in the solution) is taking place.In this case it is assumed to limit oneself to the isothermal approach when describing the mass transfer of the aggressive component in the solution. The equation for the concentration pattern $c(\vec{r},t)$ of each component could be written in general

$$\frac{\partial c}{\partial t} + \mathrm{div}\left(\vec{v}\cdot c - D\cdot \overrightarrow{\mathrm{grad}}\, c\right) + q = 0 \ , \qquad (1)$$

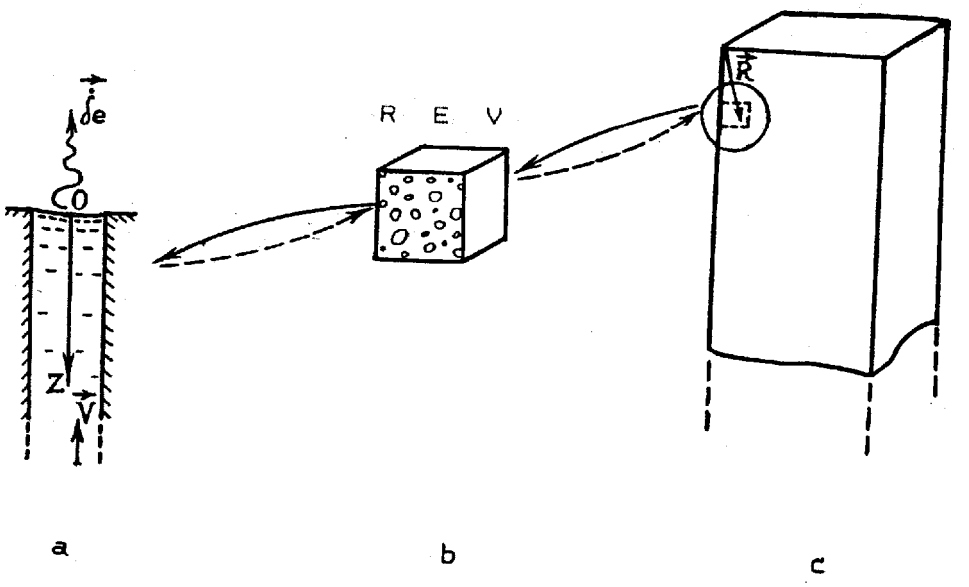

FIG.1 The scheme of the three-level mass transfer modelling in capillary porous materials :
a.- Liquid motion microlevel ($\vec{V}$) in a single capillary opened for evaporation ($\vec{j}_e$) of the solution volatile component from the meniscus surface (Z=0) ;
b.- Representative elementary volume level (R E V) ;
c.- Macrobody level (R macropoint coordinate) ;
differentitation direction
integration synthesizing direction

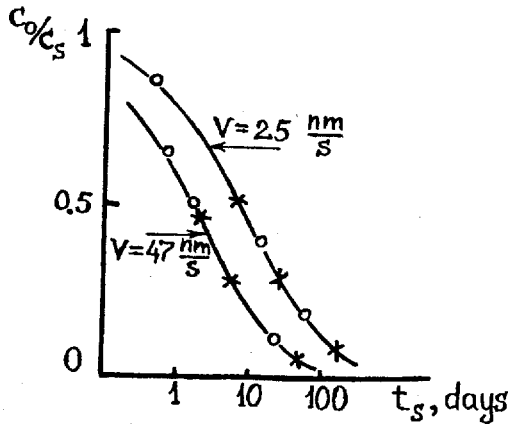

FIG.2 The time dependence t_s of the achieving the limit saturation of the solution (c_s) on the poration surface (Z = 0) upon the relative initial concentration c_o/c_s at the different convective velocity V
x - for $CaCO_3$ solution
o - for $CaSO_4$ solution

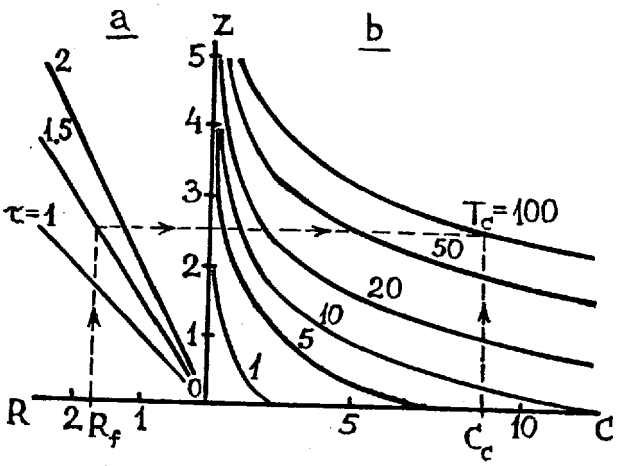

FIG.3 The calculation diagram of the specification time T_c, for which the critical concentration C_c is obtained on the depth R_f of the reinforcement occurance in the concrete (τ-the tortuosity of the pores)

where $\vec{v}$ - the laminar flow velocity of pore liquid, q - the source and discharge strength of aggressive component reflecting a phase change and chemical reactions.

Parallel with a considerable predominance of mass transfer in the axial direction (along the axis z) as compared with the radial direction the isotropy of the solution makes it possible to simplify the equation (1) to one-dimentional form

$$D \cdot \frac{\partial^2 c}{\partial z^2} + v \cdot \frac{\partial c}{\partial z} = \frac{\partial c}{\partial t} + q \quad . \qquad (2)$$

On the open surface of the solution (the meniscus coordinate $z = 0$) the boundary condition is assumed in the form of equality to zero of the total (diffusion and convective) flow of the aggressive component

$$D \cdot \frac{\partial c}{\partial z}\Big|_{z=0} + v \cdot c(0,t) = 0 \quad , \qquad (3)$$

which expresses the non-permeability of the meniscus surface for molecules and iones of the dissolved solts.

Proceeding on the absence of adsorption and chemical inertia of capillary walls ($q = 0$), in case of the uniform flow ($v = \text{const}$) and homogenous initial concentration $c(z,0)=c_o$, the solution in an analytical form can be found

$$C(Z,T) = 0.5(1-Z+T)\cdot\exp(-Z)\cdot\operatorname{erfc}[(Z-T)/2\sqrt{T}] +$$

$$+0.5\cdot\operatorname{erfc}[-(Z+T)/2\sqrt{T}] + \sqrt{T/\pi}\cdot\exp(-(Z+T)^2/4T) \quad , \qquad (4)$$

where nondimentional values $C = c/c_o$, $Z = z \cdot v/D$, $T = t \cdot v^2/D$ and probability integral $\operatorname{erfc}(x) = 1 - 2/\sqrt{\pi}\int_0^x \exp(-x^2)dx$ are used. At each moment of time the aggressive component concentration assumes the maximum value on the surface of evaporation ($Z = 0$):

$$C_m(T) = (1+T/2)\cdot\operatorname{erfc}(-\sqrt{T}/2) + \sqrt{T/\pi}\cdot\exp(-T/4) \quad . \qquad (5)$$

EXPERIMENTAL TEST FOR THE SOLUTION OF MICROSCOPIC EQUATION

According to the equation (5) the monotonic concentration increase leads inevitably at a definite moment of time t_s to achieving of the limit concentration c_s when salt begins to crystallize near the meniscus. Condition $c(0,t_s) = c_s$ for arising of phase transformation in the solution gives an effective possibility to prove clearly acceptability of the equation (4) by means of an experiment.

The experimental test of the model dependence $C(Z,T)$ is carried out on an example of water solutions of the salt ($Ca\,CO_3$, $Ca\,SO_4$ ets.), filling the glass capillary. Water evaporation from the solution to the atmosphere took place on the site of the capillary open face. Atmospheric humidity and temperature were kept under such conditions that the convection velocity remained constant (equal to v_o). Time moment t_s from which the isolation of crystal phase out of the solution close to the meniscus took started was fixed by visual examination for different values of the initial concentration C_o. Experimental results fall on the graph at theoretical curves (Figure 2), calculated on the model formula (5).

MACROSCOPIC TRANSPORT DESCRIPTION IN POROUS MEDIA

Using topological function of tortuosity τ (Fig.3a), let us assume the transition to macrocoordinate $R = f(\tau) \cdot Z$ in the equation (4) for microscopic function $C (Z, T)$. As aresult we obtain the posibility of determining macroparameters basing on the solution of microscopic equation (2). The solution (4) indicates specification time T_S for which the assumed critical value of concentration C_c for the assumed depth of occurance of reinforcement R_c (Fig.3b) is approached (e.g. when the condition of reinforcing-bar steel is violated). The sequence of calculations $R_c \rightarrow Z \rightarrow T_S \leftarrow C_c$ in Fig.3a and 3b is given. If the critical value C_c approaches its limit value C_s for the concentration of solution saturation, formation and grouth of crystals of salt mass m_s in the capillary take place.

The volume averaging of the microscopic value m_s in REV is carried out by means of integral operator

$$\hat{A}_{...} = \frac{1}{\delta} \cdot \int ... \Phi_\delta \cdot d\delta \quad , \qquad (6)$$

where Φ_δ - the density function of the distribution of the volume macrovalue averaging REV δ. It shoud be noted that the thickness of the chosen elementary volume is rather small ($\delta_z \rightarrow 0$), since a considerable increase of the aggressive component concentration takes place close to the meniscus surface (Z=0) according to the formula (4). In this case the volume averaging (6) may be considered as the area averaging of the concrete outer surface where evaporation of pore liquid takes place.

As a result of such averaging the macrovalue of the spesific mass M_s of the crystallized salt distributed irregularly on the surface of concrete is found. The authors [3] noted the position of the maximum value M_s on the concrete piles surface where salt corrosion effect is the greatest.The predicted position of the max M_s on the concrete surface has been prooved by the experience of concrete piles exploitation on salted soils with the high rise of underground waters [3].

CONCLUSIONS AND RECOMMENDATIONS

The suggested physico-mathematical model of the concrete salt corrosion developing under the influence of underground waters and atmosphere makes it possible to calculate time changes of the aggressive component concentration pattern and to estimate the value of the crystal salt formation intensification determining in its turn the velocity of the corrosion front movement into concrete.

Soft ware developed on the basis of the proposed model of aggressive component mass transfer allows with the help of a computer to carry out a multifactor analysis of the corrosion resistance and prediction of concrete piles and foundations longevity under different exploitation conditions. The present model allows to be included as a submodel into broader control programs for the prediction of durability of building on the basis of concrete structures influenced by underground, sea and other aggressive mineralized waters.

REFERENCES

1. Oberholster, R.E.: "Pore structure permeability and diffusivity as related to durability". International Congress on the Chemistry of Cement, 8th, Rio de Janeiro, Brazil, 1986, V1, 324-335.

2. Stroeven, P.: "Structural modeling of plain and fibrereinforced concrete". Composites, 1982, 4, 129-139.

3. Vyrodov, I.P. and Lekarev, V.M.: "Corrosion resistance of concrete columns". Conference on Silicate Industry and Silicate Science, XV, Budapest, Hungary, 1989, 135-136.

KINETICS OF IMPREGNATION OF REINFORCED CONCRETE WITH INHIBITORS AND OTHER SPECIAL SOLUTIONS

I P Vyrodov and V M Lekarev

Polytechnic Institute of Krasnodar, RUSSIA

SUMMARY

This paper presents a description of kinetic processes of impregnation of porous building materials. Dispersion factor for the kinetics of impregnation front along the capillaries with different diameter has been considered. The results of the theoretical calculations have been presented in comparison with experimental data for concrete.

КРАТКОЕ СОДЕРЖАНИЕ

В докладе дано описание кинетических процессов пропитки пористых строительных материалов. Произведен учет дисперсии фронта пропитки по капиллярам различного диаметра. Дано сопоставление результатов теоретических расчетов с экспериментальными данными для бетона.

INTRODUCTION

The knowlege of the kinetics of impregnation of capillary porous building materials is important in such technological processes as concrete treatment with solutions containing inhibitors or impregnation with special solutions decreasing water receptivity. The kinetics of impregnation of the wetting liquid is also used as the method for the determining of the pore structures parameters of concrete. A mathematical model representing the kinetics of impregnation of capillary porous systems may be constructed by the methods of mathematical statistics on the basis of solving the problem of calculating the liquid movement in a single capillary.

RESULTS AND DISCUSSIONS

The meniscus coordinate Z changes with time t at the spontaneous penetration of liquid into the capillary according to the dynamic equation

$$\frac{d}{dt}\left(0.25\pi D^2 \rho \cdot Z \frac{dZ}{dt} \right) = \sigma \pi D \cdot \cos\theta - 8\pi\eta Z \cdot \frac{dZ}{dt}, \qquad (1)$$

where the left part describes the liquid impulse change in the capillary with the diameter D (ρ is the liquid density). In the right part of the equation (1) the first addend expresses the action of surface tension forces (σ is the coefficient of surface tension; for aqueous solutions $\cos\theta \simeq 1$), and the second one expresses the counteraction of friction forces at the laminar flow of viscous liquid (η is the coefficient of the liquid viscosity). The influence of gravity forces is negligible, since the meniscus travel turns out to be considerably less than the liquid balanced rising H in the capillary, i.e. $Z \ll H$

Equation (1) has a solution giving at the initial time moment $t = 0$ a limited velocity value $d Z(0) / dt = Vo$, which is as follows

$$Z(t) = \tau Vo \sqrt{2 \left(t/\tau + \exp(-t/\tau) - 1 \right)} \qquad (2)$$

and

$$dZ/dt \equiv \dot{Z}(t) = V_0 \frac{1 - \exp(-t/\tau)}{\left(\exp(-t/\tau) + t/\tau - 1 \right)^{1/2} \cdot \sqrt{2}}, \qquad (3)$$

where ralaxation time $\tau = \rho D^2 / 32 \cdot \eta$, $V_o^2 = 4 \cdot \sigma / D \cdot \rho$. The quasi-stationary regime of the meniscus transfer is reached at $t \gg \tau$:

$$Z(t) = Vo \sqrt{2 \cdot t \cdot \tau}, \qquad (4)$$

limited by the balanced rising H (i.e. $Z \ll 4\sigma / \rho g D$). Thus the automodel type of the solution (4) is accepted in the broad time interval (e.g. 10^{-8} s $\ll t \ll 10^{7}$ s , for water in the capillary having the diameter D = 1 nm), what is proved by numerous experimental data [1].

The impregnation volume velocity of the cylindrical capillary is expressed in terms of the linear velocity of the meniscus movement as follows

$$v(t) = 0.25 \cdot \pi \cdot D^2 \frac{dZ}{dt}. \qquad (5)$$

The liquid volume absorbed by the capillary for the time t is expressed by

$$w(t) = \int_0^t v(t)\cdot dt = 0.25\,\pi\cdot D^2\cdot Z(t) \qquad (6)$$

One must notice that the minimal diameter of capillaries, where the volume flow of liquid is possible, is limited by the sizes D_m of mesopores. The impregnation kinetics of the monodispersive porous materials is developed in the same way as that in the single capillary which is verified by a number of experimental data.

A characteristic feature of the impregnation of the heterogeneous porous materials is the nonsynchronism of the approaching by the menisci of the given depth Z while moving along capillaries with different diameter, i.e. in this case the dispersion of the impregnation front take place. Such a dispersion can be discribed by a step function

$$L(t-t_c) = \begin{cases} 0\ , & \text{when } t < t \\ 1\ , & \text{when } t \geqslant t_c \end{cases}, \qquad (7)$$

where $t_c = 4\cdot Z_c^2\cdot\eta / \sigma D$ is the time interval for which the menisci penetrate capillaries of the diameter D to the depth Z_c of reinforcement occurance in the concrete.

Then the integral volume velocity of impregnation is expressed by

$$V(t) = N\cdot\int_{D_m}^{\infty} L(t - t_c)\cdot\frac{dZ}{dt}\cdot f_S(D)\cdot dD\ , \qquad (8)$$

where f_S is the differentiational function of the distribution of the capillary area section on the concrete surface, N is the normalization factor depending on the effective porosity of the material and on the initial water saturation of the pore space. The greatest value $V(0)$ is achieved on the surface of the pattern ($Z = 0$) and here it must be limited at maximum allowable leak value (e.c. 0.035 ml/m^2·s). The total liquid volume absorbed by the porous material through the unit area of its surface is given by the function

$$W(t) = \int_0^t V(t)\cdot dt\ . \qquad (9)$$

In accordance with the report data [2] , there has been done the calculations of the kinetic dependence $V(t)$, given by the equation (8) for the tipical function of pore sizes distribution in concrete.The results of the calculation are represented by the Fig.1.The experiment data (Δ- points in Fig.1) and the results of the calculations are adequate.

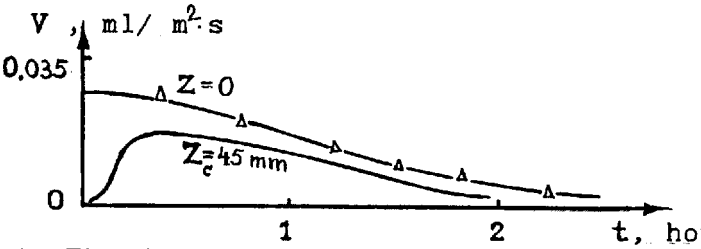

FIG.1 The dependence of the volume velocity V of impregnation upon the time t for the concrete surface ($Z = 0$) and on the depth Z_c of armature steel disposition

REFERENCES

1. Heifec, L.I. and Neimark, A.V.: Multiphase processes in porous media. Moscow, Chemistry, 1982, 319 p.

2. Kondo, R. and Daimon, M.: "Pore Structure and Properties of Concrete". International Congress on the Chemistry of Cement, 6th, Moscow,Soviet Union 1976, V2, 244-257.

Specific Theme IV C

Physico-chemical, Biological and Thermal Degradation Including Environmental Effects

RELATION BETWEEN THE DEGREE OF HYDRATION OF SLAG CEMENT AND THE FROST RESISTANCE OF THE RESPECTIVE MORTAR

H - M Ludwig and J Stark

University of Architecture and Building, Weimar, GERMANY

SUMMARY

In the present investigations the relation between degree of hydration and the properties of mortar have been studied as a function of the grade of slag used and the specific surface of slag, in slag cement. The experiments show that already small changes in these slag properties have serious consequences for the pore size distribution and therefore the frost resistance of the respective mortars.

ZUSAMMENFASSUNG

In den vorliegenden Untersuchungen wurde das Verhältnis zwischen dem Hydratationsgrad und den mörteltechnischen Eigenschaften von Schlackenzementen in Abhängigkeit der Schlackequalität und der spezifischen Oberfläche der Schlacke untersucht.
Die Ergebnisse zeigen, daß bereits geringe Schwankungen dieser Schlackenparameter zu erheblichen Veränderungen in den Porengrößenverteilungen der entsprechenden Mörtel führen, wodurch letztlich auch der Frostwiderstand beeinflußt wird.

0. Abstract

Degree of hydration has a great influence on the properties of mortar and concrete. Correlations of the degree of hydration to total porosity, capillary pore and compressive strength have been described in the literature /1/, /2/.
In the present investigations the relation between the degree of hydration and the properties of mortar have been studied as a function of grade of slag used and the specific surface of slag in slag cement. A portland cement (OPC45) was also included for comparison.

1. Test material

The blended cements used in the trials were produced in a laboratory mill from HOS E and HOS U blastfurnace slags, portland cement (OPC 45) and a mixture of synthetic and natural anhydrites. The specific surface areas of the slags were varied in the range 1000 cm^2/g - 5000 cm^2/g. There were considerable differences in the chemical compositions of the slags. On the basis of the usual parameters for hydraulicity great differences in their hydraulic characteristics would thus be expected. For example, the usual base value (ratio CaO/SiO_2) for HOS U is 1.2, while a value of only 1,05 was found for HOS E.
Using the chemical analysis of the portland cement the following mineral composition can be calculated from the Bogue formula:

C_3S = 50,1 %

C_2S = 18,3 %

C_3A = 6,8 %

C_4AF = 10,6 %

For the determination of degree of hydration, pastes with water/cement ratio 0.5 were prepared from the laboratory cements and stored in closed plastic bottles in the humidity chamber (95-100 % r.h., 25 C) for a pre-determined time. Standard mortar prisms (4 x 4 x 16 cm) were prepared for the determination of the mortar properties.

2. Determination the degree of hydration

Where as there are a number of methods to determine the degree of hydration of PC, it is, generally speaking, problematic for slag cements. Accordingly the slag and the portland cement fractions were evaluated separately for the blended cements.
The determination of the hydrated part of granulated blastfurnace slag was carried out by an extraction method using salicylic acid-acetone-methanol solution /3/. It is based on the fact that unhydrated slag is almost entirely insoluble whereas hydrated slag as well as hydrated and unhydrated portland cement pass into solution with the exception of the clinker phases containing aluminates, the gypsum, and some secondary constituents.
The converted slag is calculated from the measured residue using the

following formula:

$$\alpha_{H,HOS} = (1 - \frac{LR - EW_{COR} \cdot M_{PR} \cdot l_{R,PC}}{EW_{COR} \cdot M_{HOS} \cdot l_{R,HOS}})$$

where

$\alpha_{H,HOS}$ is the quantity of converted slag in %, relative to the total quantity of slag in the cement
LR is the residue from the solution in g determined after the extraction trial
M_{PC} is the mass fraction of portland cement in the unhydrated blended cement in g/g
M_{HOS} is the mass fraction of blastfurnace slag in the unhydrated blended cement in g/g
$l_{R,PC}$ is the specific residue from the solution of the unhydrated portland cement in g/g determined in the preliminary trial
$l_{R,HOS}$ is the specific residue from the solution of the unhydrated blastfurnace slag in g/g determined in the preliminary trial
EW_{COR} is the corrected quantity of sample weighed out in g

The corrected quantity of sample weighed out can be determined from the following formula:

$$EW_{COR} = EW \cdot \frac{100\% - GV}{100\%}$$

where

EW is the quantity of sample weighed out in g
GV is the loss on ignition of the blended cement at 800 °C in %

The results of these investigations are shown in Figure 1. It is discernible that the slag conversion depends on the slag grades and the finenesses of the slag. The HOS U reached a higher degree of hydration than the HOS E slag, especially after a fairly long hydration time.

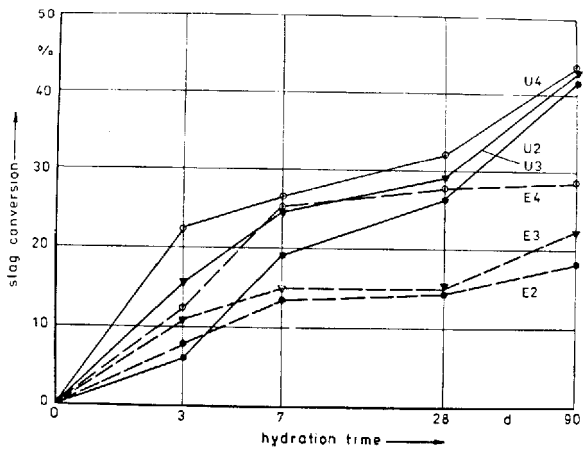

Figure 1:
Dependence of the slag conversion on the hydration time for different slag grades and finenesses

slag cement with

E 2 - blastfurnace slag E, sp. surface area = 2000 cm^2/g
E 3 - blastfurnace slag E, sp. surface area = 3000 cm^2/g
E 4 - blastfurnace slag E, sp. surface area = 4000 cm^2/g
U 2 - blastfurnace slag U, sp. surface area = 2000 cm^2/g
U 3 - blastfurnace slag U, sp. surface area = 3000 cm^2/g
U 4 - blastfurnace slag U, sp. surface area = 4000 cm^2/g

The degree of hydration in the pastes made from pure portland cement was determined from the quantity of chemically combined water. To determine the quantity of chemically combined water at complete hydration a calculation was made of the water bonding values of the clinker phases as obtained from the reaction equations given.

The degree of hydration of the portland cement determined in this way were then transferred to the slag cement taking the percentage content of portland cement into account. Such transfer is possible as an approximation as it was established by x-ray diffraction into the alite decomposition caused by the hydration of the clinker phases in the blended cement proceeds at a similar rate to that in pure portland cement.
The total degree of hydration of the slag cement is found from the individualy degrees of hydration of the slag $\alpha_{H,\ HOS}$ and the portland cement $\alpha_{H,PC}$, and their respective percentages M_{HOS} and M_{PC} in the slag cement.

$$\alpha_{H,G} = \alpha_{H,\ PC} \cdot M_{PC} + \alpha_{H,\ HOS} \cdot M_{HOS}$$

Figure 2 shows a comparison of the progress of hydration of portland cement with that of slag cements which have compositions and specific surface areas close to those of industrially produced cements.
As can be expected, the conversion of the portland cement is significantly higher than that of the slag cements. However, while the difference between the portland cement and the cement containing HOS E remains large over the entire hydration period, that between portland cement and cement containing HOS U becomes progressively smaller after 28 days storage in water.

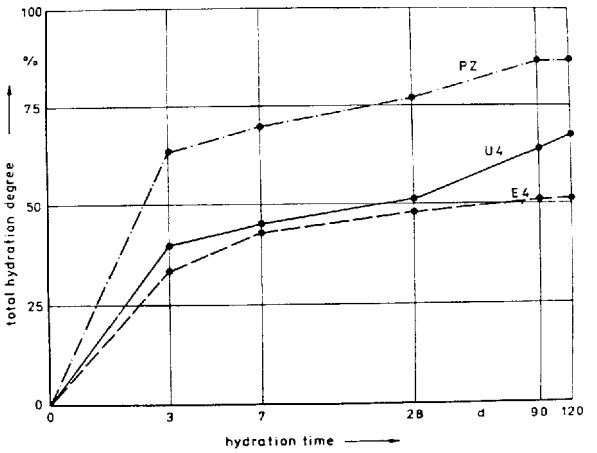

Figure 2:
Dependence of the total degree of hydration on the hydration time for cements with different composition

PZ - OPC 45 portland cement

slag cement
E 4 - blastfurnace slag E, sp. surface area = 4000 cm^2/g
U 4 - blastfurnace slag U, sp. surface area = 4000 cm^2/g

3. Relations between the degree of hydration and slag cement mortar properties

The hydration degrees determined were related to mortar properties such as total porosity, capillary pore, compressive strength and the resistance to freezing and thawing.

3.1.Porosity

The results of the investigations concerning total porosity are shown in Figure 3. The general trend is that increase in the degree of hydration reduced the total porosity. However, there is a difference between the slag cements produced with slag U and slag E, and more particularly between slag cements in general and portland cement.
For this group of blastfurnace slag cements statistical analysis as the results yielded a linear correlaton with a high confidence limit between the degree of hydration and total porosity.

The hydration degree of portland cement as determined shows a higher total porosity as compared to the slag cements and consequently it is not described by the same regression equation.
Still more striking is the fundamental difference in the functional connection between the rate of hydration and structure formation in portland cement in relation to the slag cements when the capillary porosity is considered (Figure 4).

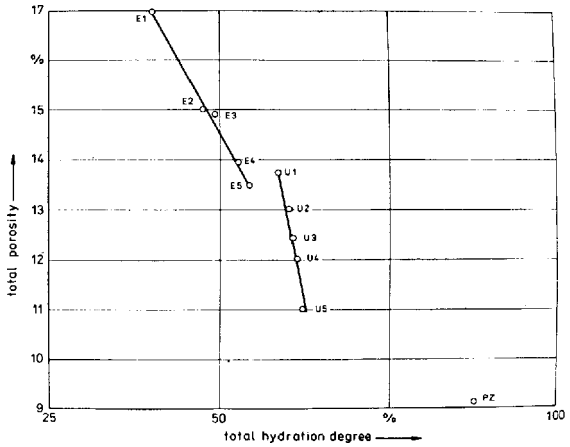

Figure 3:
Dependence of the total porosity on the total hydration degree

PZ - OPC 45 portland cement
slag cements
E/U 1 - sp. surface area = 1000 cm^2/g
E/U 2 - sp. surface area = 2000 cm^2/g
E/U 3 - sp. surface area = 3000 cm^2/g
E/U 4 - sp. surface area = 4000 cm^2/g
E/U 5 - sp. surface area = 5000 cm^2/g

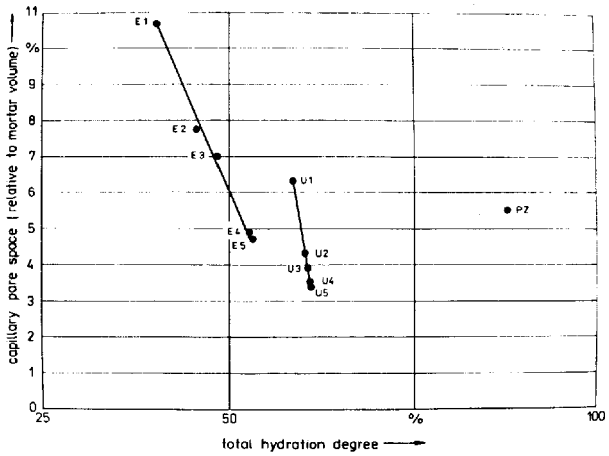

Figure 4:
Dependence of the capillary pore space on the total hydration degree
(capillary pore space was defined after Romberg /3/ - $r = 10^1 - 10^5$ nm)

A distinct decrease of the capillary pore space occurs with the progress in hydration for slag cements. The extent of such decrease is the same regardless of the kind of slag used.
Although there is a small difference between the functional connection of these two magnitudes which is attributable to the grade of slag, it is possible to discuss the slag cements as a group from the statistical angle.
Notwithstanding its greatest degree of hydration (approximately 90 %), portland cement exhibits a relatively high capillary pore space of 5,5 %. Thus it shows a greater capillary porosity than most of the slag cements. However in the case of cements with high quality slag U even mortars with cements with a low specific surface (2000 cm^2/g) show a denser structure in relation to portland cement mortars (A_{oc} = 3500 cm^2/g).

3.2. Compressive strength

The results of these investigations are presented in Figure 5. It is discernible that at the beginning of hydration, in the case of the slag cements, the increase in the degree of hydration was not followed by an equivalent increase in the compressive strength.
Only at longer hydration times does the relation admit of a direct proportionality. The thresold degree of hydration beyond which an increase was accompanied by a proportionate increase in compressive strength was 30 %. Futhermore it becomes evident from Figure 5 that slag cement mortars with slag U achieve a 10 N/mm² higher compressive strength than portland cement mortars in the range of 50 - 70 % hydration degree.

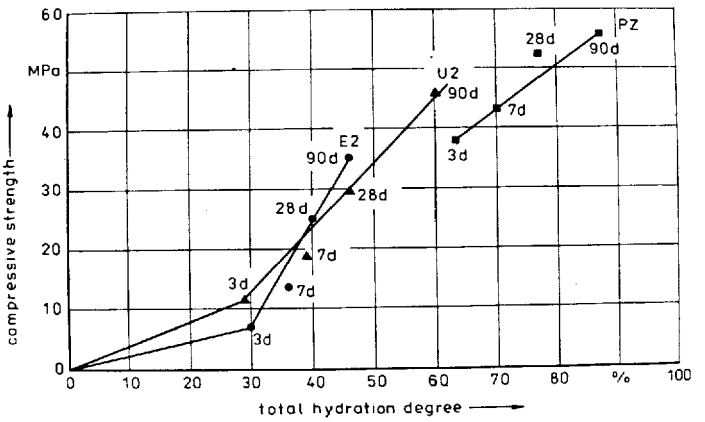

Figure 5:
Dependence of the compressive strength on the total hydration degree

3.3 Resistance to freezing and thawing

Just as relation were established between degree of hydration, on the one hand, and compressive strength, total porosity and pore size distribution or capillary pore space, on the other, a similar relation was obtained between degree of hydration and resistance to freezing and thawing.
The relation between degree of hydration and decrease in ultrasonic pulse velocity across mortar prisms after 150 freeze - thaw cycles is shown in Figure 6.
It can be observed that the two slag cements from HOS U and HOS E exhibit different frost resistance values at similar degrees of hydration. In the range 40 - 50 % hydration degree the cement with HOS U shows about 10 % higher frost resistance than that with HOS E. In the case of the HOS E cement a linear relation between the degree of hydration and decrease in ultrasonic pulse velcity after freezing follows from the statistical evaluation.
For the HOS U cements a break can be observed above 58 % degree of hydration. From here onwards small increase in the hydration degree brings about a higher increase in frost resistance.
Futhermore, it can be seen that a lower hydration degree of the slag cements does not generally lead to a lower freeze - thaw resistance. The mortar prisms of the highly ground slag U (U3 - U5) show a higher frost resistance (decrease in UDV 28 - 41 %) than the portland cement prisms (decrease in UDV 42 %).

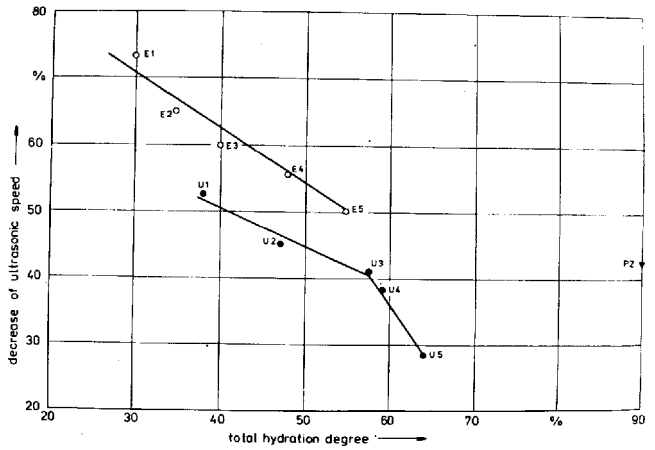

Figure 6:
Dependence of the decrease in ultrasonic pulse velocity after 150 freeze - thaw cycles and the total hydration degree

This is because of the denser structure of slag cement mortars. Figure 7 shows that the portland cement indeed exhibits the lowest total porosity, but the percentage of capillary pores within this porosity is much higher (60.3 %) than in the case of the slag cements (HOS E → 47 %, HOS U → 31.5 %).

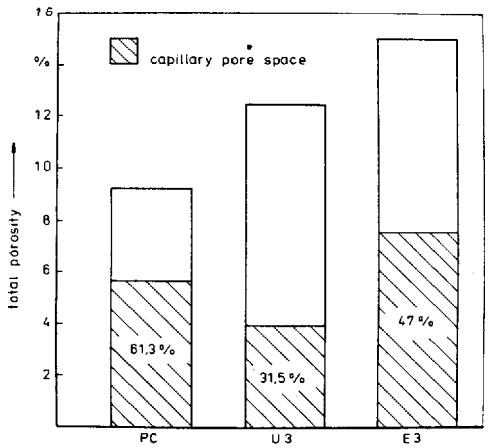

Figure 7:
The total porosity and the capillary pore space of cement with different compositions

4. References

/1/ Keienburg, R.-R.: "Kornverteilung und Normfestigkeit von Portlandzement ", Schriftenreihe der Zementindustrie, Betonverlag, 1976, Heft 4.

/2/ Powers, T. C.: "Physical properties of cement paste". Chemistry on cement. Proc. IV. Symp., Washington 1960, Vol.II, S. 577 - 609.

/3/ Romberg, H.: "Zementsteinproben und Betoneigenschaften". Beton Information, 1978, 18 (5), S. 50 - 55.

CONCRETE DURABILITY ENHANCEMENT BY INTERNAL TIMED RELEASE OF ANTIFREEZE OR ANTICORROSION CHEMICALS FOR INCREASED RESISTANCE TO FREEZE/THAW AND CORROSION

Carolyn M Dry

Architecture Materials Research Lab,
Architecture Research Center, School of Architecture,
University of Illinois, Urbana-Champaign, Illinois, U.S.A.

SUMMARY

Fibers/aggregates and mechanisms to release the chemicals, such as coating dissolution, are the sensors, while the stimulus, such as change in pH or chloride ion amount, and actual release of the chemical work together as actuators. These are thus NOVEL smart materials containing damage sensors and repair actuators acting together are thus designed to be passive, automatically activated, and are distributed throughout the material to provide remedial action anywhere it is needed. The service life of construction materials can be extended without the need for continuous monitoring.

RESUME

Les agrégats/fibres et mécanismes pour libérer les produits chimiques, tels que la dissolution du revêtement sont les détecteurs, alors que les stimulants, tels que la variation dans le degré en pH ou en ion de chlorure, ainsi que le déclenchement réel du produit chimique agissent ensemble comme actionneurs. Ce sont par conséquent des matériaux dignes du NOVEL comprenant des détecteurs de détérioration et des actionneurs de réparation agissant ensemble qui sont de ce fait conçus pour être passifs, actionnés automatiquement, et distribués à travers le matériau pour fournir une action corrective où c'est nécessaire. La longévité des matériaux de contruction peut être prolongée sans surveillance continue.

ABSTRACT

Materials containing various types of hollow porous fibers filled with a chemical which release into the matrix at appropriate times, or over time, are designed to address some issues of cement material performance such as matrix destruction caused by corrosion, and freeze/thaw damage.

The sensing of the corrosion or freezing/thawing of a settable material by a chemical or physical sensor which in the process of sensing, starts the activation of a remedial process, is the subject of this research. It is a distributed system in which sensing and repair occur when and where they are needed.

MATERIALS FOR SENSING OF DAMAGE AND REPAIR ACTION

In these cement materials sensing of damage and attendant actuation of repair occur by the activation of the timed release of a repair chemical into the matrix due to a stimulus which is itself the environmental agent of attack. These are passive smart materials requiring no outside feedback loop nor continuous monitoring. Rather, they are activated by each environmental loading or impetus (see Fig. 1). The sensors and actuators are disturbed throughout the structure. Thus, they are durability enhancing anywhere this is required.

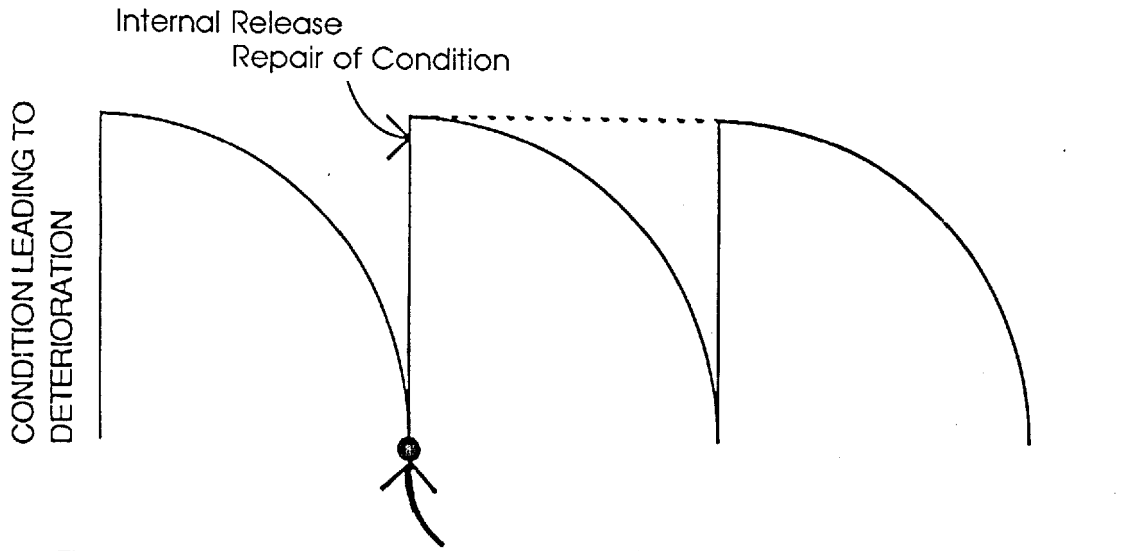

Figure 1. Sensing of Damage and the Repair of Material by Timed Release of Chemicals from Fibers or Aggregate

CORROSION

Corrosion is an electrochemical process that requires an electrical current in a moist and oxygenated condition. The entry of chloride ions or carbonation can cause the pH to be reduced to 11.5 pH, at which point corrosion begins. The addition of calcium nitrite, an anticorrosion chemical, protects the steel. In this design calcium nitrite is put

into hollow porous fibers coated with polyol. Polyol dissolves in an alkalinity of appropriate pH (11.5) or in the presence of chloride ions, thus, releasing the anticorrosion chemical (see Figure 2).

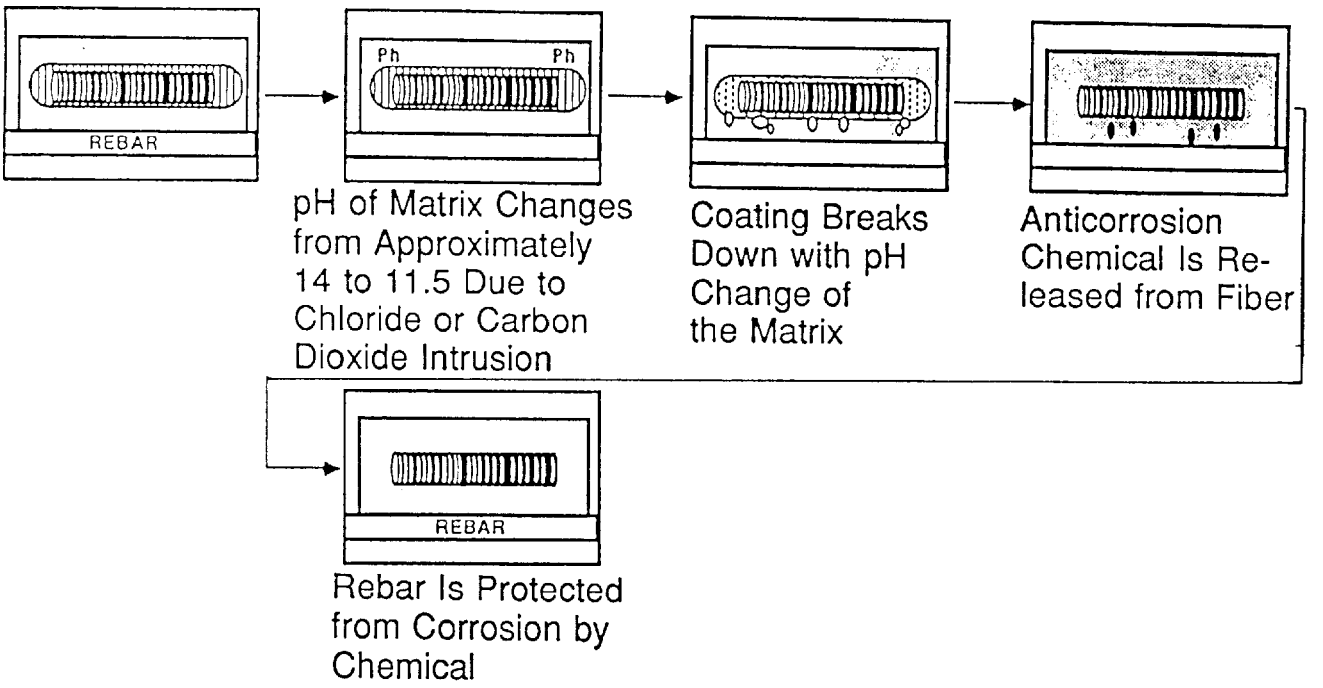

Figure 2. Sequence of Events in Design of Time Release to Protect Against Corrosion

The cause of deterioration, reduction of alkalinity due to chloride or carbonation which causes the corrosion triggers the sensor (coating dissolution) which actuates the remedial action (release of calcium nitrite).

Preliminary results show that the chemicals are released (see Photo 1.) and that the design to prevent corrosion damage will work to retard corrosion (see Figure 3).

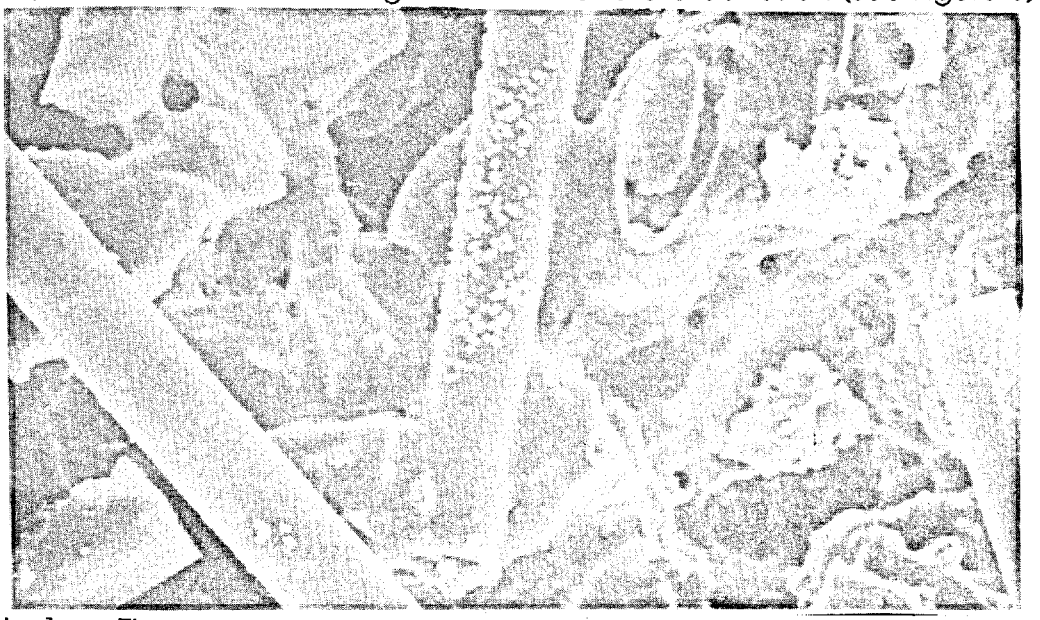

Photo 1. The successful release of chemicals from fibers was documented using a scanning electron microscope.

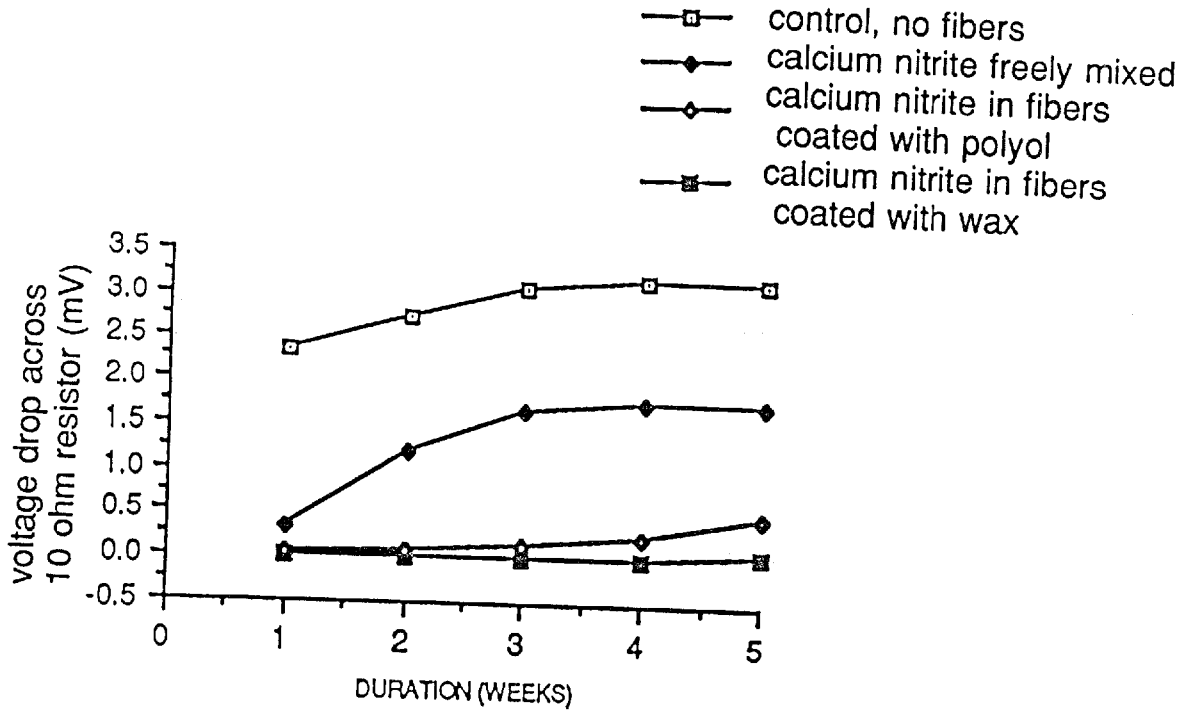

Figure 3. Comparison of Voltage Drop (mV) Across A 10 ohm Resistor of Various Samples Undergoing Corrosion Testing

Each of these tailor-made applications consist of several parts, including: 1.) an agent of internal deterioration, 2.) a stimulus to release the repairing chemical, 3.) a fiber or aggregate, 4.) perhaps a coating or fiber wall which can be removed or changed in response to the stimulus, 5.) a chemical carried inside the fiber or aggregate. Fibers and mechanisms to release the chemicals such as coating dissolution are the sensors, while the stimulus such as a change in pH, and actual release of the chemical work together as actuators. These smart materials containing damage sensors and repair actuators acting together are thus designed to be passive, automatically activated, and are distributed throughout the material to provide remedial action anywhere it is needed.

FREEZE/THAW DAMAGE

Reduction of Freeze/thaw damage or increase of frost resistance is enhanced "if the permeability is high and cooling rate low or permeability low, but space between air void small" (1).

The design to resist frost damage consists of: 1.) adding antifreeze in water solution to hollow porous fibers which is pumped out of the fibers or aggregate, when water expands at freezing (see Figure 4), or 2.) an internal sealant (Xypex) to reduce permeability of air-entrained concrete could be released from hollow porous fibers or aggregate. These are located near the surface. The Xypex could be released as the coating shrinks due to a temperature drop.

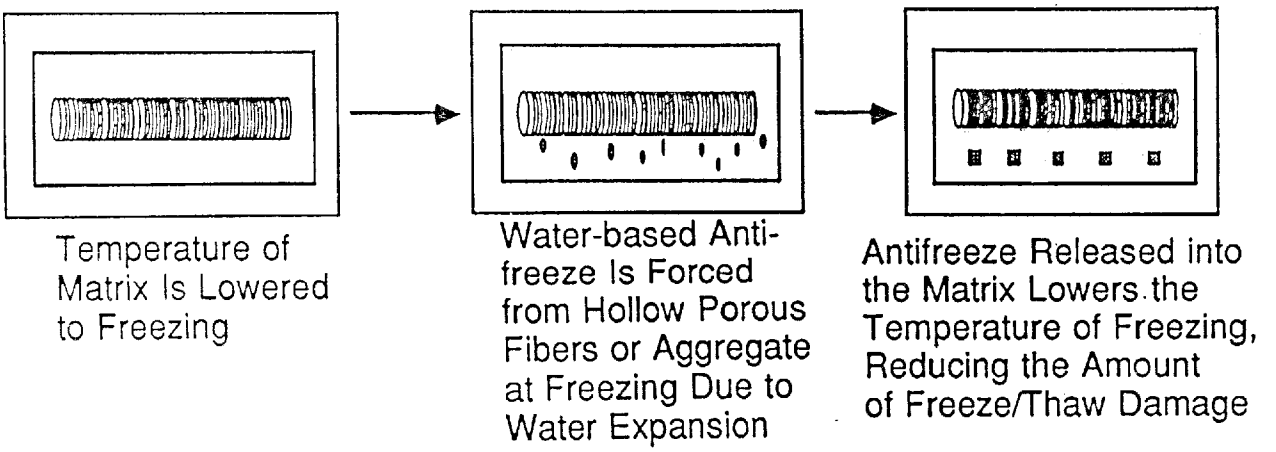

Figure 4. Sequences of Events in Design for Time Release to Protect Against Freeze/thaw Damage

If the above designs are used with porous aggregates, there is an added advantage. It is that the aggregate can substitute for air entraining: "Solid particles having a large porosity in suitable pore size have been added to concrete and act in a manner similar to that of air voids. The optimum particle size should range between 290 and 850 microns, total porosity to particles should be at least 30% by volume, and pore size distribution should be in the range of .0523 microns" (2).

Early results are promising. Limestone aggregate containing antifreeze for timed release performed somewhat better than controls under freeze/thaw conditions as measured by weight loss or weight change (see Figure 5, and Figure 6).

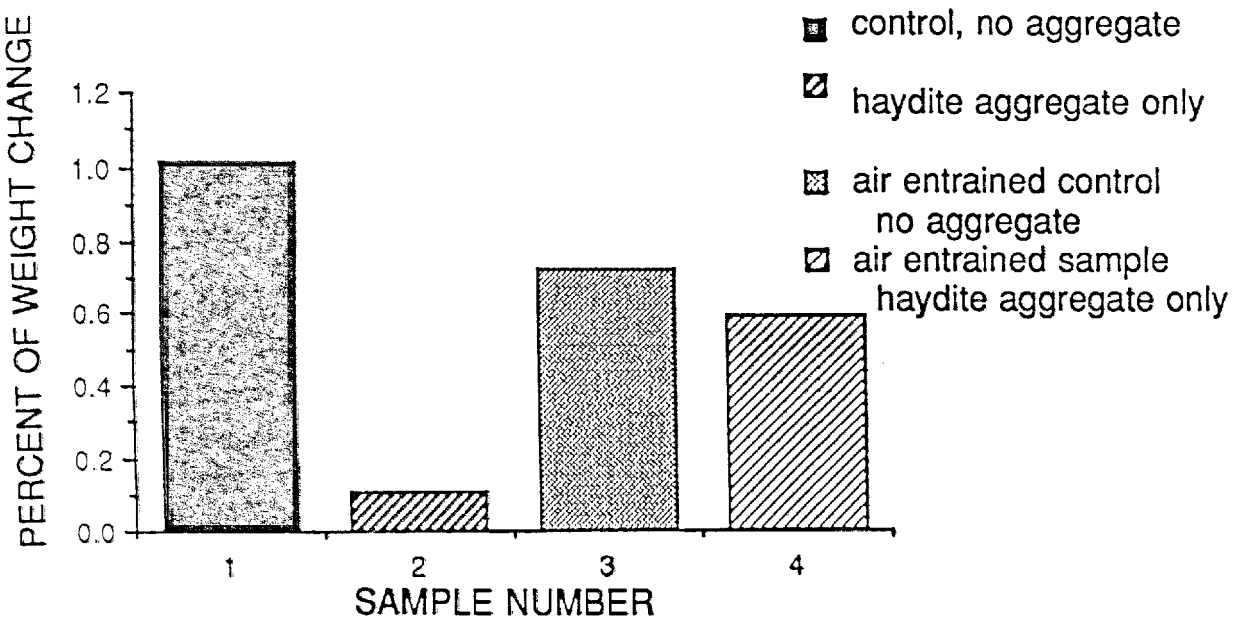

Figure 5. Freeze/Thaw Damage to White Cement with Porous Aggregates Containing Antifreeze Vs. Cement Without As Measured by Weight Change

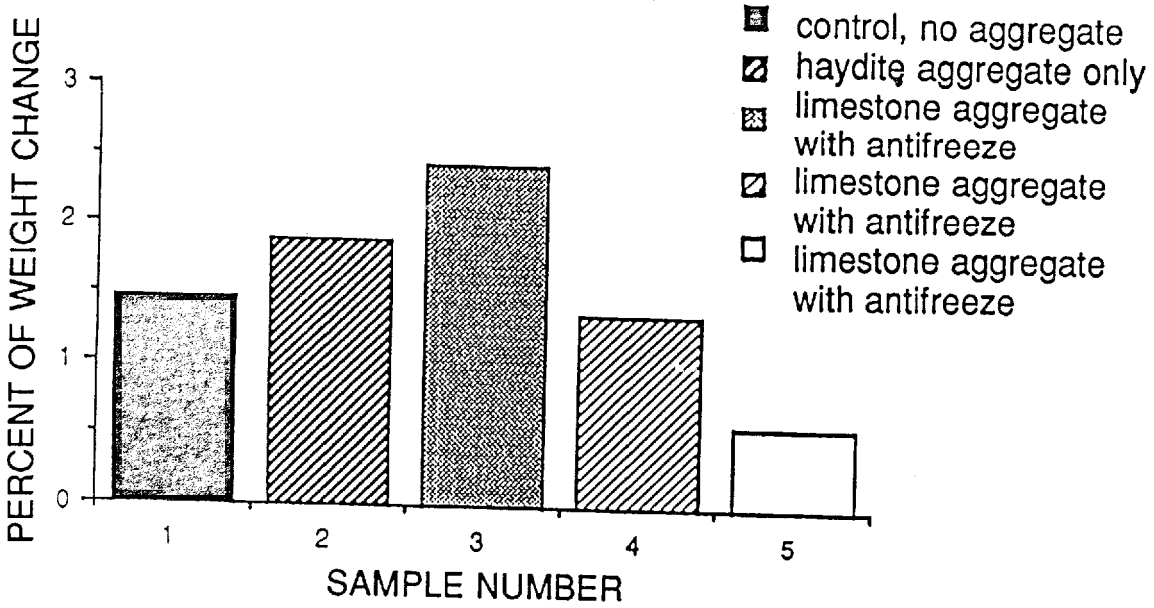

Figure 6. Freeze/Thaw Damage to Portland Cement with Porous Aggregate Containing Antifreeze vs. Cement Without As Measured by Weight Loss

REFERENCES

1. Litvan, E., "Durability of Porous Building Materials", Durability of Building Materials and Components, Proceedings of the First International Conference - Aug. 1978, Editors: P.J. Sereda and G.G. Litian, Philadelphia, Pa., ASTM, 1978, p. 462.

2. American Concrete Institute (ACI) 212: "Chemical Admixture for Concrete", Committee Report No. 86-M27, ACI Materials Journal, May-June 1989, p. 304.

MECHANISMS OF DEICER SCALING OF CONCRETE

Q B Yang, X L Wu and S Y Huang

Shanghai Institute of Building Materials,
Shanghai, P.R.CHINA

SUMMARY

In the present paper, both physical and chemical mechanisms of deicer scaling of concrete were studied. Results showed (1) under the action of freezing-thawing cycles, the scaling of concrete exposed to deicer solutions was much severer than that exposed to water, which was mainly resulted from the increase in the degree of saturation caused by deicer salts; (2) under the action of drying- wetting cycles, the concentrated deicer solution generated a crystallization pressure high enough to expand and damage concrete, which might be another mechanism of deicer scaling of concrete; and (3) $CaCl_2$ solution with low concentration seemed not to cause severe scaling of concrete, but that with very high concentration might cause much severe deterioration of concrete, which might be resulted from the formation of the complex salt $CaCl_2 \cdot Ca(OH)_2 \cdot H_2O$.

摘 要

本文从物理和化学两个方面，研究了去冰盐对混凝土剥蚀破坏的机理。结果表明：(1) 在冻融循环作用下，混凝土的盐冻剥蚀明显高于水冻剥蚀，其主要原因是去冰盐使混凝土的饱水度提高；(2)在干湿循环作用下，高浓度去冰盐可产生足够高的盐结晶压使混凝土破坏，它也可能是去冰盐对混凝土剥蚀破坏的机理；(3) 低浓度$CaCl_2$溶液对混凝土的化学侵蚀很小，但高浓度$CaCl_2$溶液可造成混凝土严重破坏，这可能与复盐$CaCl_2 \cdot Ca(OH)_2 \cdot H_2O$的形成有关。

INTRODUCTION

The deleterious effect of deicing salts on concrete has attracted more and more attention of concrete researchers as the use of deicing salts on highways and bridges rapidly increases in recent years. Under combined actions of deicer solution and freezing-thawing cycles, the surface scaling of concrete is the most common type of damage. Many papers have been published in this field, but scaling mechanisms have not been very clearly understood yet. The various mechanisms (1, 2, 3, 4) on the action of frost seemed to apply mostly to the internal cracking that could result from freezing-thawing cycles. Many research results showed the most dangerous deicer concentration was about 3 % (2, 4), regardless of type of deicer (NaCl, $CaCl_2$, urea or ethyl arcohol). It was thought that the deicer-frost damage might only be physical. However, many researchers (5, 6) have also observed that concentrated deicer solutions caused the severe deterioration of concrete above 0℃, which was resulted from chemical attack.

The purpose of the present paper is to investigate the mechanisms of the effect of deicing salts on concrete both physical and chemical.

EXPERIMENTAL METHODS AND MATERIALS

Mix proportions

Concrete specimens were used in this experimental work. The mix proportion of concrete is W : C : S : G = 0.55 : 1 : 1.77 : 3.28. Air entrainment was not used in order to accelerate the scaling. All specimens were cured in water (20± 2 ℃) for 28 days.

Degree of saturation

Specimens of sizes of 3×3×2.5 cm and 3×3×4 cm after having been cured were dried at 105℃ for 24 hours, cooled to the room temperature, and then soaked in NaCl solutions with various concentrations (0, 4, 10 and 20%) under a vaccum equivalent to 75.8 cm Hg for 4 days and then under the atmosphere pressure for other two days. After that specimens were weighed (M_∞). These prepared specimens were to be used for capillary water-uptake and water loss tests.

Capillary water-uptake test refers to G. Fagerlund' s (1). Prepared specimens of 3×3×4 cm were dried at 105 ℃ for one day, cooled to the room temperature and weighed (M_0). Then the specimen was immersed in water with the depth of immersion of about 4 mm (Fig 1). After immersion for a given time, specimens were weighed again (M_t).

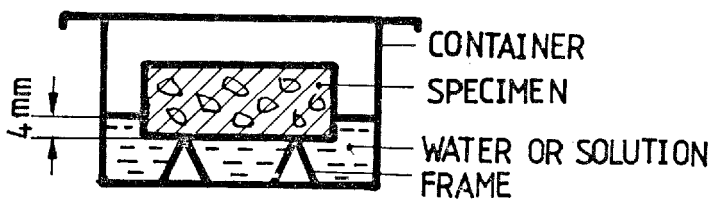

FIG.1 Capillary water-uptake test or freezing-thawing cycles test

In the water loss test, prepared 3×3×2.5 Cm specimens were exposed to the appropriate atmosphere wthin the controlled humidity chambers (75, 83 and 92 %RH were maintained using saturated NaCl, KBr and KNO_3 respectively). Then the specimens were weighed one time two or four days until the equilibrium reached.

The actual degree of saturation (S) was calculated as follows:

$$S = \frac{M_t - M_o}{M_\infty - M_o} \times 100\ \% \quad - - - - - - - - - - - - - - (1)$$

A diagram of degree of saturation (S) versus root of time (T) can be plotted. The degree of saturation (S_e) and the time (T_e) to reach equilibrium may be calculated from the knick-point value (see Fig 2).

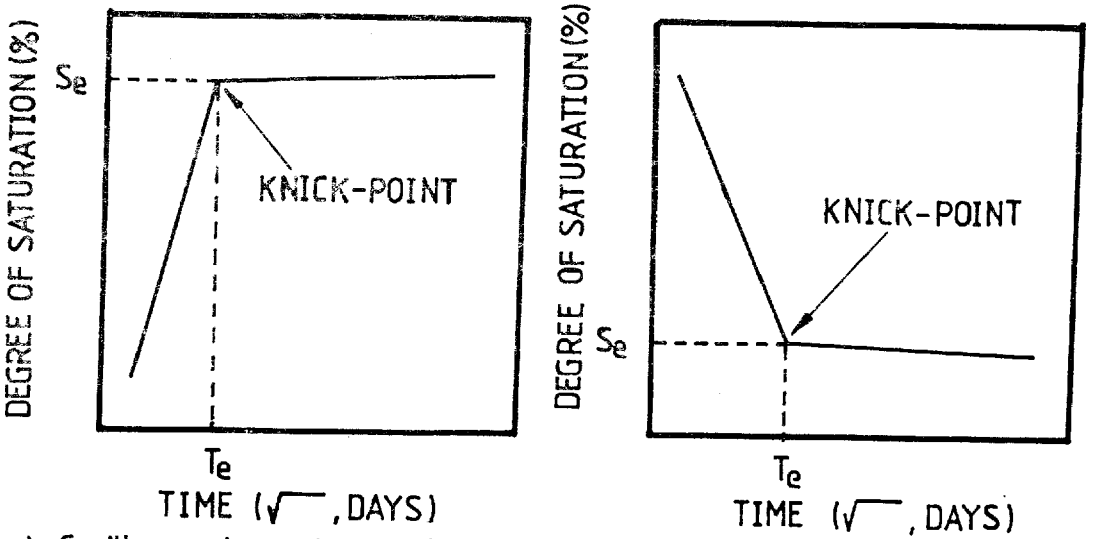

a) Capillary water-uptake test b) Water loss test

FIG. 2 Determination of the degree of saturation and the time to reach equilibrium

Freezing-thawing cycles test

Specimens were immersed in NaCl solutions by one surface with the depth of immersion of about 4 mm (see Fig 1). And then specimens with the container were frozen at -20 ± 2 ℃ for 3 hours with the cooling rate of 0. 5 ~ 0. 7 ℃/min in the freezer and thawed at 20 ± 5 ℃ for 3 hours in air, which constitutes one freezing -thawing cycle.

Drying-wetting cycles test

Specimens cured in water for 28 days were dried at 105 ℃ for one day and soaked in NaCl solutions (0, 4, 12 and 20 %) or immersed by one surface in NaCl solutions (12 and 20 %), which constitutes one cycle. Then the length of specimens was measured after every cycle, and the strength and the mass of scaled particles were measured after 9 cycles.

Chemical attack

Specimens cured in water for 28 days were soaked in various $CaCl_2$ solutions (0, 4, 12 and 20 %) at 10 ± 5 ℃. Then the strength, the length and the mass of scaled particles were measured for a given time, and the pastes (W/C = 0. 26) were analysed by XRD and DTA.

RESULTS AND DISCUSSIONS

Degree of saturation

Table 1 shows the degree of saturation at equilibrium for all specimens under various conditions, which indicates that the degree of saturation increases with the increase in the salt concentration and the relative humidity of the chamber. The degree of saturation at equilibrium of specimens immersed in NaCl solution with higher concentration is much higher than that in water.

Table 1 Degree of saturation and time at equilibrium under various conditions

Type	NaCl	Water loss test						Capillary water-uptake test	
		75 % RH		83 % RH		92 % RH			
	%	Se (%)	t (days)	Se (%)	t (days)	Se (%)	t (days)	Se (%)	t (hrs)
1	0	59	8.4	72	5.8	79	4.8	90	11.6
2	4	66	9.0	77	7.8	87	5.3	94	8.4
3	10	73	11.6	84	10.9	94	7.3	96	5.1
4	20	85	13.7	93	16.4	99	/	99	3.1

Table 1 shows that in the capillary water-uptake test the time to reach equilibrium decreases with the increase in the salt concentration in concrete, and in the water loss test the time increases with the increase in the salt concentration.

In the capillary water-uptake test, a specimen with deicing salt absorbs more water than that without deicing salt because there exists an osmotic pressure due to the concentration difference besides the capillary tension. For the same reason, in the water loss test, the degree of saturation is higher and the time to reach equilibrium is longer for specimens with deicing salt than those without deicing salt.

Freezing-thawing cycles

The mass of scaled particles of specimens was measured after 6 cycles. Fig 3 shows the scaling of specimens exposed to deicer solutions was much severer than that exposed to water; the most dangerous deicer concentration is about 4 % NaCl. These results are in agreement with other authors' (4, 6).

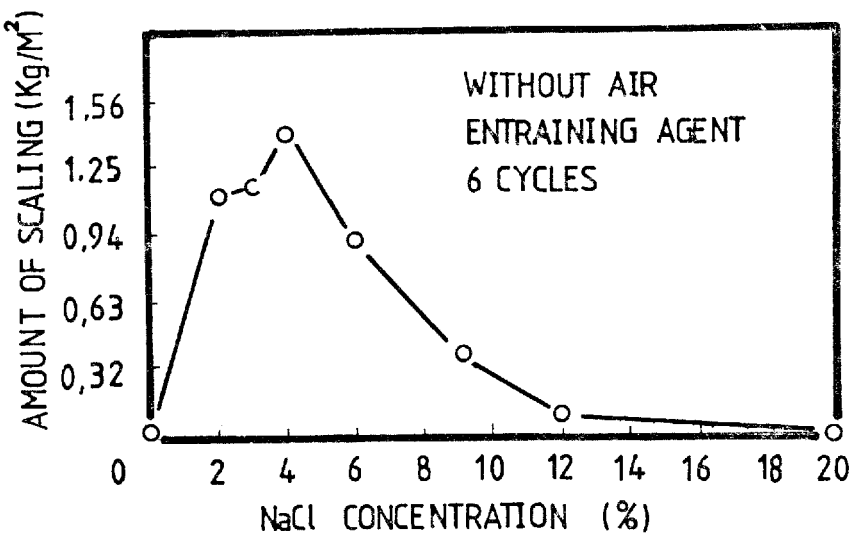

FIG.3 Effect of NaCl concentration on the scaling of concrete

The effect of deicing salts on the frost resistance of concrete is the combined effect of two factors. At first, deicers increase the degree of saturation and thus the amount of ice in concrete with deicer, and moreover, the water in concrete will transfer and accumulate to the surface of concrete exposed to deicer solutions due to the osmotic pressure of deicer, which will cause the surface to be easily damaged and scaled. This is the negative factor on the frost resistance of concrete. But on the other hand, deicers depress the freezing point of water in concrete, which more or less positively influences the frost resistance of concrete. Therefore, the severest scaling of concrete occurs when it is exposed to an intermediate deicer concentration.

Drying-wetting cycles

Test results of specimens under drying-wetting cycles both in water and in NaCl solution are shown in Table 2 and Fig 4. From Fig 4 it can be seen that the effect of drying and wetting in water cycles on the length of specimens is small, and the length after wetting is always larger than the length after drying. But for specimens under drying and wetting in NaCl solution cycles, the length of specimens increase continuously after every cycle, and the length of specimen after drying is always larger than that of the wet specimen before drying, that means the drying process also causes the expansion of specimens with deicing salt.

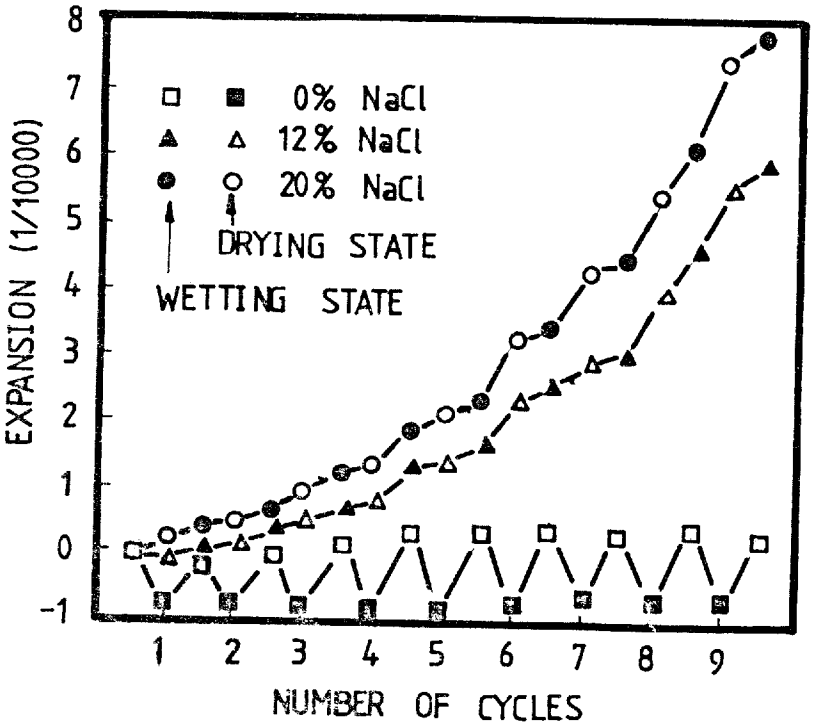

FIG. 4 Effect of NaCl on the expansion of concrete under the drying-wetting cycle condition

From Table 2 it can be seen that the scaling due to drying and wetting in NaCl solution cycles increases with the NaCl concentration, but drying and wetting in water cycles do not cause scaling. Moreover, specimens uptaking NaCl solution by one surface is scaled much more than that soaked in NaCl solution.

Table 2 Effect of NaCl solutions on the compressive strength and the mass of scaled particles of concrete under drying-wetting cycles

NaCl %	Specimens soaked in solutions strength MPa	scaling g/m²	Single surface solution-uptake specimens strength MPa	scaling g/m²
0	40.2	0	/	/
4	41.0	15.6	/	/
12	45.0	71.9	42.0	150.0
20	43.8	135.2	38.7	198.4

Drying-wetting cycles at temperature above 0 ℃ also damage concrete with deicing salt, which could be explained by the crystallization pressure of salt. While drying, the deicing salt crystallizes from oversaturated solution in concrete, which generates very high pressure causing expansion and make concrete deteriorate.

Chemical attack

Very little strength loss (as standard of the strength of specimen cured in water at the same age) and no scaling have been found in the specimens cured for 28 days and then stored in $CaCl_2$ solution with the concentration ≤ 12 %. But for the specimens stored in the concentrated solution of 20 %, the strength reduces a lot and the scaling is much severe, see Table 3.

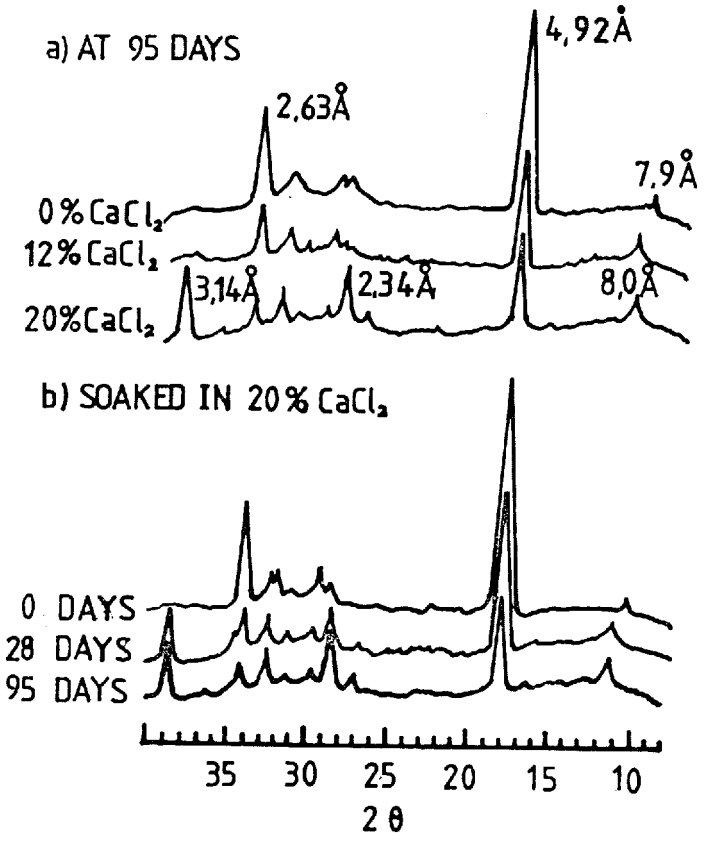

FIG. 5 XRD of specimens soaked in $CaCl_2$ solution at 10±5°C

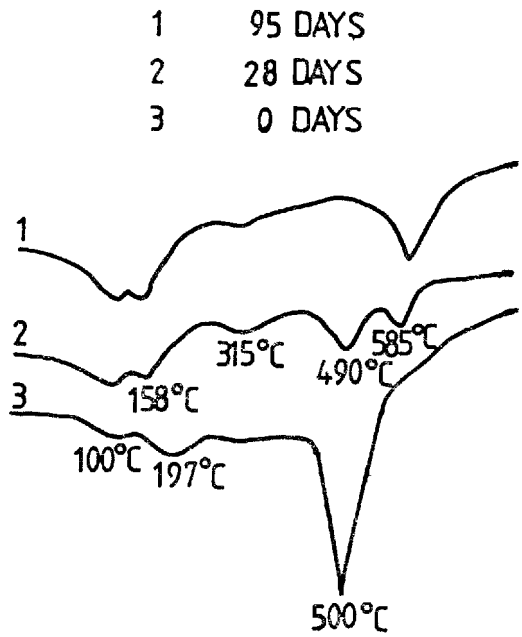

FIG. 6 DTA of specimens soaked in 20%$CaCl_2$ solution at 10±5℃

Table 3 The compressive strength and the amount of scaling of concrete stored in $CaCl_2$ solutions at 10 ± 5 ℃

$CaCl^2$ %	28 days strength MPa	28 days scaling Kg/m²	60 days strength MPa	60 days scaling Kg/m²	95 days strength MPa	95 days scaling Kg/m²
0	52.5	0	57.4	0	58.8	0
4	49.8	0	55.8	0	55.4	0
12	48.9	0	54.0	0	50.6	0
20	30.2	0.63	26.2	1.14	16.2	2.05

From XRD (Fig 5) and DTA (Fig 6) analyses, it can be found that the $Ca(OH)_2$ (4.92 Å and 2.63 Å in XRD; 490～500℃ in DTA) in hardened cement pastes decreases with the increase in the storing time in $CaCl_2$ solution and the concentration of a solution, and the hydrate $C_3A \cdot CaSO_4 \cdot 10H_2O$ (7.9 Å in XRD; 197 ℃ in DTA) in hardened paste reacts with $CaCl_2$ to transform into $C_3A \cdot CaCl_2 \cdot 10H_2O$ (8 Å in XRD; 160 and 314 ℃ in DTA). A new reaction product could be found only in the pattern of cement paste stored in 20 % $CaCl_2$. That is a complex salt $CaCl_2 \cdot Ca(OH)_2 \cdot H_2O$ with its characteristic peaks of 2.34 Å and 3.15 Å in XRD; 580～585 ℃ in DTA. It shows that the deleterious effect of concentrated $CaCl_2$ solution is associated with the formation of the complex salt $CaCl_2 \cdot Ca(OH)_2 \cdot H_2O$

CONCLUSIONS

Under the action of freezing- thawing cycles, the scaling of concrete exposed to deicer solutions is much severer than that exposed to water, which mainly resulted from the increase in the degree of saturation caused by the deicing salt. The most dangerous concentration is about 4 % NaCl.

Under the action of drying-wetting cycles, the concentrated deicer solution generates a crystallization pressure high enough to expand and deteriorate concrete, which may be one of mechanisms of deicer scaling of concrete.

$CaCl_2$ solution with the concentration (< 12%) seems not to cause the scaling of concrete, but that of very high concentration may cause very severe deteriorationof concrete, which may be resulted from the formation of the complex salt $CaCl_2 \cdot Ca(OH)_2 \cdot H_2O$.

REFERENCES

1. Fagerlund, G. : 'The significance of critical degrees of saturation of freezing of porous and brittle materials', Durability of Concrete, SP-47, ACI, 1975, p13-65.

2. Pigeon, M. : 'The frost durability of concrete', **Cement and Concrete —— Science & Technology**, ed by Ghosh, S. N., Kaikaji, New Delhi, India, 1991, Vol I, Part I.

3. Cordon, W. A. : 'Freezing and thawing of concrete — mechanisms and control', Designing for Durable Concrete, SCM-18, ACI, 1988, p373-412.

4. Cantor, T. R. and Kneeter, C. P. : 'Influence of salt on the freeze- thaw deterioration of concrete', Materials Performance, 1977, No 5, p28-31.

5. Mehta, P. K. : **Concrete —— Structure, Properties, and Materials**, ed by Prentice -Hall Inc., Enlewood Cliffs, New Jersy, 1986, p118-129.

6. Chatterji, S. : 'Mechanism of the $CaCl_2$ attack on portland cement concrete', Cement and Concrete Research, 1978. Vol 8, p461-468.

EVALUATION OF VARIOUS CONCRETE DEICERS

P P Hudec*, C MacInnis** and F Achampong**

*Department of Geology,
**Department of Civil & Environmental Engineering,
University of Windsor, Windsor, Ontario, CANADA

SUMMARY

Rock salt (NaCl) remains in use as the principal road deicer in spite of its well-know corrosive properties. It has a eutectic of -23°C, good ice melting rates at low temperatures, and above all, is relatively inexpensive. In the last several years, a search has been conducted for a non-corrosive deicer to replace salt; a leading candidate has been calcium magnesium acetate (CMA), which currently costs about 10 times more than NaCl. In addition to the cost disadvantage, CMA is effective to only about -5°C. Two types of alternatives exist to NaCl: An additive to counteract its corrosiveness without significantly affecting its deicer properties, or a non-corrosive, cost and performance effective replacement. Both alternatives have been investigated in these studies. Phosphate salts have long been suggested as alternate deicers. However, phosphate salts by themselves are not effective, though they do provide corrosion protection. Mixtures of NaCl and various phosphate salts have been shown to be effective non-corrosive deicers. Ca- K- Na-, NH- phosphates all show some promise, especially the mono-valent phosphates. The Ca phosphate is insoluble, but when applied in the acidified state, precipitates in concrete pores and continues to offer protection.

Potassium acetate (KAC) has been shown to have superior de-icing properties, equalling the deicing properties of calcium chloride and far exceeding those of CMA. As with CMA, KAC is non-corrosive and environmentally friendly.

Results of laboratory tests on deicing properties and surface scaling tests for the various deicer combination studies are presented.

Keywords: Deicer, Salts, Durability, Freeze-Thaw, Beneficiation, Adsorption, Cation, Anion, Admixtures, Calcium magnesium acetate, Sodium chloride, Potassium acetate

INTRODUCTION

Deicing salts have become a necessity for paved surfaces in temperate climates, both to prevent accidents, and to reduce legal liability due to accidents. Ice control or prevention of ice formation is required on a large scale on roads and highways, and on a smaller scale on driveways and walkways of public institutions and homes. For the former, sodium chloride, NaCl, remains the dominant deicer, due to its abundance and low cost; for the latter, a variety of deicers are used, but most common are sodium and calcium chloride ($CaCl_2$),or mixtures of the two. The main problem with the chlorides is their corrosive effect on the reinforcing steel of structures, scaling of concrete surfaces, and the accelerated deterioration of aggregates in both cement and bituminous concretes. A new deicer, or a method of modifying the current deicers to alleviate their undesirable effects is needed.

This paper reports the initial results of adding other salts to NaCl to modify its behaviour and still maintain its deicing properties. It also reports on a promising new deicer - potassium acetate - that has deicing properties similar to that of calcium chloride without the undesirable side effects.

THEORIES OF CHLORIDE DEICER FROST DAMAGE

Corrosion of steel by chlorides, both the steel embedded in the concrete (reinforcing bars) and the exposed steel (girders, railings, cars, etc.) is well known. Corrosion of rebars is a chemical process, aided by the physical deterioration of the concrete by the freezing and thawing cycles. The physical deterioration theories that will be discussed briefly. The understanding of the physical deterioration process and the role of the deicing salt (NaCl) in it is essential before an alternate deicer can be found. The main variables in the frost damage of porous materials are the nature of the pore surface, pore and capillary size, pore and capillary size distribution, and the total internal surface area per unit volume.

Nature of pore surface

All surfaces, including mineral surfaces, posses a surface charge; the amount of charge is a function of the nature of the surface. In minerals that make up the rock used as natural aggregate, the surfaces can be mineral faces (rarely), cleavage faces, or fracture faces. The latter are the most active, since fracture surface breaks randomly across chemical bonds of the mineral; cleavage faces represent a direction of minimum bonding between elements of the crystal and are less active. Furthermore, if the crystal is 'imperfect', i.e., has an incomplete lattice, or a lattice in which under-or over-size elements substitute, or has a lattice that has been tectonically strained, the surfaces of that mineral will possess a greater charge.

The charge on the surfaces is generally negative. The negative surfaces attract polar water molecules and the cations of deicing salts. For instance, the Na+ of NaCl is adsorbed to the surface. Polar water molecules, in turn, are attracted to the cation, increasing the amount of tightly held water above that which the surface would normally hold. The action is similar to that of sorption of cations onto clay particles - the "double layer" theory. The concentration of cations is greatest near the surface, and diminishes gradually away from the surface. Adsorbed water, having lost some of its free energy as heat of adsorption, has lower vapour pressure than 'normal' or bulk water.

Pore Size

The size of the pore determines the proportion of the adsorbed vs. 'normal' water held in the pore. The water adsorbed at close to 100 percent relative humidity at 20°C completely fills capillaries of up to 5 μm radius, as shown by the Kelvin equation. If the material contains a greater proportion of small size pores in the 'critical' range, more will be filled with adsorbed water and the ratio of adsorbed to absorbed water in the porous material increases. The adsorbed water in the pores has lower vapour pressure; the vapour pressure of the water is proportional to the pore radius - thus, the water in very small pores has a lower vapour pressure than water in larger pores. If the porous material is fully saturated by immersion, the larger pores contain mostly bulk, normal vapour pressure water, and a vapour pressure potential exists between large and small pores. Because of this difference, higher vapour pressure water is compelled to move towards lower vapour pressure water by osmosis. The pressure in the small pores increases proportionately to the vapour pressure difference; if the osmotic pressure exceeds the tensile strength of the pore walls, a crack develops. The cracks, in turn, become the new generation of small pores, advancing the deterioration process.

The effect of deicers

If the pores hold adsorbed deicer cations, the upper limit of the pore or capillary size that is filled with adsorbed water may increase several times. The amount of increase is a function of the concentration of the cations in the pore, the ionic size to charge ratio, and the clustering geometry of the water-ion system. Generally, the smaller the ionic radius and the ionic size to charge ratio, the greater is the water clustering ability of the cation. The net effect of deicer cations is to increase the number of pores and capillaries occupied by adsorbed water, and to increase the proportion of adsorbed water in the pore system. Thus a greater number of pores become osmotically active, and the deterioration is accelerated. The freezing and thawing of the pore system serves to concentrate the cations in the pores. The concentrated cations increase the osmotic pressure difference, and the severity of the deterioration.

The relationship between adsorbed water content and the degree of freeze-thaw deterioration is shown in Figure 1. The results shown are for a wide range of aggregates used in concrete in Ontario, Canada. They include all the usual rock types: limestone, dolomite, granite, diorite gabbro, gneiss, volcanics and argillite, more or less in their order of frequency of occurrence. The freeze-thaw deterioration was determined by saturating the aggregates in a 3% NaCl solution, and freezing them in air in 100% humidity conditions for 5 cycles - 16h freezing at -16°C, 8h thawing at room temperature (22°C). Adsorption was determined by exposing the oven-dried aggregate to 98% relative humidity (RH) conditions at 22°C for 72h and determining the weight gain.

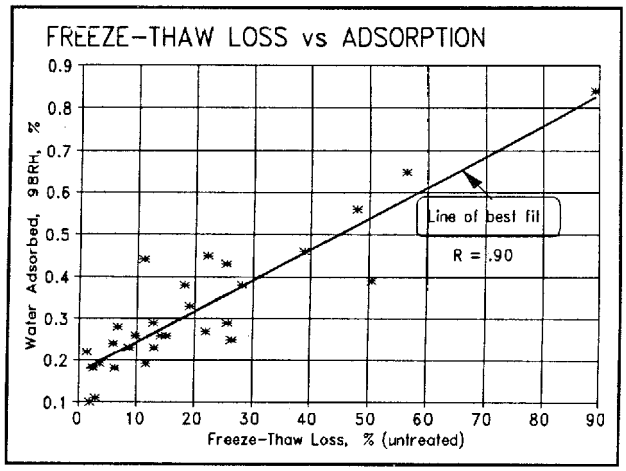

Figure 1 Relationship of adsorbed water on the freeze-thaw loss of aggregates.

Figure 1 shows a good correlation between freeze-thaw damage and water adsorption (R=.95). The effect of adsorbed water on the freeze-thaw durability is clearly demonstrated.

REDUCING THE DEICER SALT DAMAGE - RESULTS OF EXPERIMENTS

Assuming the above scenario of deicer salt damage is correct, then to reduce the physical deterioration due to the fine pore system requires that the osmotic differential among the pores be reduced. The osmotic difference will be reduced if the proportion of adsorbed, low vapour pressure water is reduced.
Two potential remedies are suggested: 1. Satisfy the cations of the current deicer salts (NaCl) by substituting a strong anion that will preferentially bind to the cation at the expense of the water molecule, thus reducing the amount of adsorbed water; or 2. Develop a deicer that does not cluster water molecules and does not increase the adsorbed water content. The first suggestion can be accomplished by admixing a large ionic size, strongly electronegative anion salt to NaCl or CaCl deicer. The second remedy requires testing a variety of salts for their effectiveness in melting ice without causing scaling damage to the porous materials.

Preventive treatments with existing deicer (nacl)

Numerous chemical compounds were tested for their effectiveness as NaCl additives. The compounds were chosen mainly on the basis of their active anion, with the theory that the anion would bond with the adsorbed Na cation and interfere with water adsorption. Some of the major anion groups tested were nitrates, borates, other chlorides, and phosphates. The latter was found to be most effective, especially the mono cation phosphates: mono sodium, potassium, and calcium phosphates. Ammonium phosphates were also effective.

Salt Treatment - Figures 2 and 3 show the effect of mixing 5% of NaCl with 5% of the mono sodium and mono calcium phosphates respectively. The salts were dissolved in water, aggregates saturated, and the freeze-thaw test was carried out as described above. The results are compared to the 'untreated' solution, i.e., one containing only 5% NaCl. The figures show that the Na phosphate -salt mixture significantly reduced the freeze-thaw breakdown; Ca phosphate was somewhat less effective. The difference in effectiveness may be due to the almost infinite solubility of Na phosphate, whereas Ca phosphate is insoluble under normal pH conditions, and can only be dissolved in an

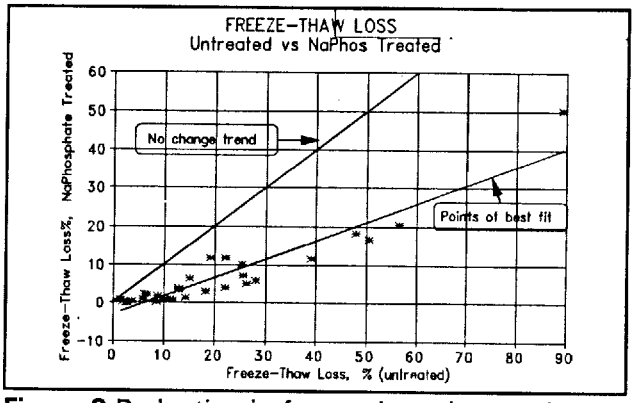

Figure 2 Reduction in freeze-thaw damage by 1:1 admixture of Na phosphate to NaCl.

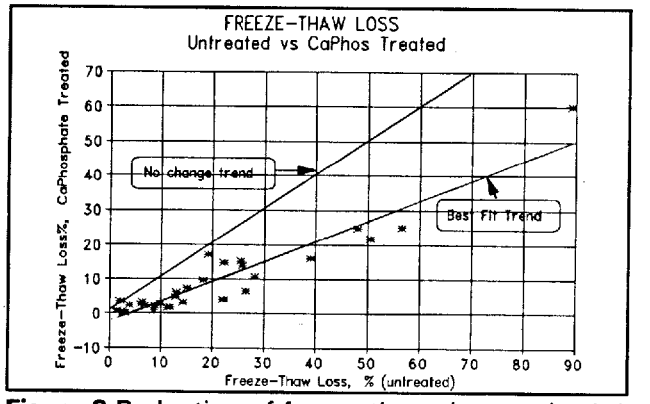

Figure 3 Reduction of freeze-thaw damage by 1:1 admixture of acidified mono calcium phosphate to 5% NaCl.

environment of pH of less than 3. Upon contact with reducing conditions (such as carbonate aggregate), the phosphate precipitates as a film in the pores. This may confer a longer-lasting protection, as will be seen later.

Treating Aggregates - In some experiments, the aggregates were immersed in the Ca phosphate solution briefly, dried, and then saturated in a 5% NaCl test solution. The treatment was also effective in reducing the freeze-thaw damage, as shown in Fig. 4. Phosphate treatment is capable of 'beneficiating' or improving the performance of a marginal quality aggregate. The period of exposure to the phosphate solution has an effect on the results, as shown in Fig. 5. The results of ammonium phosphate are displayed here; similar results were obtained with calcium phosphate. The figure shows that, although more prolonged exposure to the 20% phosphate solution provides increasing protection, most of the protection is conferred within the first minute of immersion of the sample. The short exposure time would make the phosphate treatment fit easily into an aggregate plant process.

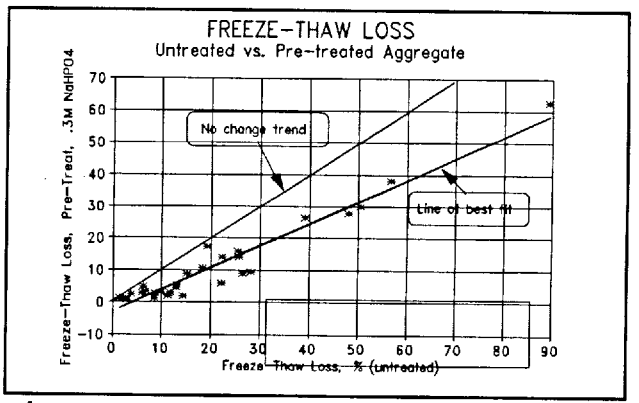

Figure 4 Aggregate pre-treated in mono calcium phosphate prior to freeze-thaw test in 5% NaCl.

If treatment of aggregates to reduce the freeze-thaw damage in the presence of deicers is viable, the long-term effectiveness of the treatment needs to be determined. The main process to reduce effectiveness will be leaching of the treatment salt. A leaching experiment was set up during which treated aggregate, after drying, was washed in running water for specified time periods, dried, washed again, and after three cycles of washing, tested for freeze-thaw resistance. The experiment was designed to simulate three periods of rain with intervening drying periods.The results are shown in Figure 6. The figure shows that a nominal loss in the effectiveness of the treatment was detected. The figure also gives results for some of the other treatment chemicals tested in addition to phosphate.

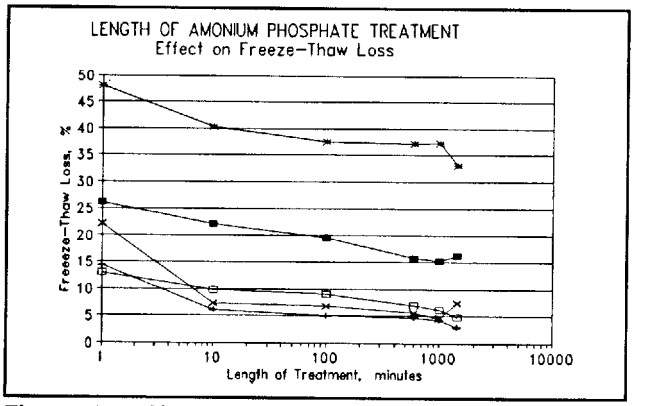

Figure 5 Effect of length of treatment in mono calcium phosphate solution on freeze-thaw resistance.

All of the above treatments were applied on 'fresh' aggregate. Can a salt contaminated material be improved by treatment? Figure 7 shows the results of experiments designed to answer this question.

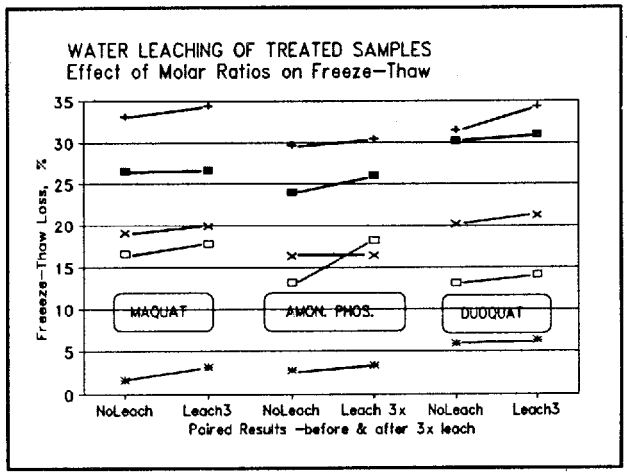

Figure 6 Leaching of aggregates after treatment - effect on freeze-thaw resistance.

Aggregate was first immersed in a 5% NaCl solution for 24h, dried, and immersed in a solution of ammonium phosphate of different concentrations for 5 minutes. After treatment, the aggregate was dried, and re-immersed in the 5% NaCl solution for 24h and subjected to freeze-thaw testing.

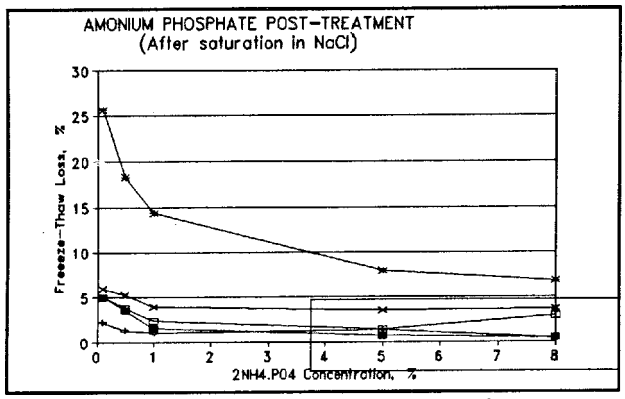

Figure 7 Treatment of salt-contaminated aggregate - effect on freeze-thaw resistance.

The results show that phosphate is effective in reducing freeze-thaw damage of salt-contaminated aggregate. This finding has wider implications: i.e., salt-contaminated concretes could be 'beneficiated' by treatment with soluble phosphate solutions, and made more resistant to spalling and scaling due to freezing and thawing. Experiments along these lines are continuing.

Summary

The results presented above suggest that adding treatment chemicals to deicing salt, or treating the aggregate with the chemicals has a beneficial action in controlling the deterioration of the material due to freezing and thawing in a NaCl environment. Phosphates, either Na or Ca monophosphate, are the treatment chemicals shown to be the most effective.

Phosphates are well known as corrosion inhibitors. Rather simple experiments have shown that even a small amount of phosphate in a NaCl solution is effective in reducing or reducing rust formation. Calcium monophosphate is insoluble in water, but slightly soluble in NaCl solution. Sufficient phosphate anion may be dissolved in deicer water to reduce the rebar corrosion.

ALTERNATE DEICERS

Chloride-based deicers as a group are corrosive to concrete, embedded steel, cars and are damaging to the environment. In the last several years, a search has been conducted for a non-corrosive deicer to replace salt; a leading contender has been calcium magnesium acetate (CMA) (1,2,3,4). During the winter of 1986-87, CMA was used as a deicer on selected roads in Ontario (Canada), and in three U.S.A. states (California, Massachusetts, and Wisconsin) (5). Although CMA was found to be an effective deicer, it is somewhat slower acting than NaCl, and at temperatures below -4°C it takes a long time to start noticeable melting; below -9°C no melting takes place without traffic. In addition to being less effective, CMA currently costs approximately 20 times more than NaCl.

Research in our laboratories has shown that a deicer of the same acetate family - a potassium acetate (KAC) - while possessing the same favourable properties of CMA is similar in its effectiveness to calcium chloride which is known as one of the most effective deicers at low temperatures.

Melting Rates of Potassium Acetate (KAC)

As part of a study to compare the various deicers, established and potential, a melting rate study was carried out. The study consisted of applying a measured quantity of the deicer, usually 20g, to a standard quantity of ice, usually 200g, at a given constant temperature of freezing. The temperatures chosen were -5, -10, -15, and -20 degrees

centigrade. The amount of ice melted was measured at 15, 30, 45, and 60 minute intervals.

The results are presented in the next four figures (Figures 8 through 11). Four deicers are compared: NaCl, $CaCl_2$, CMA, and KAC. Figures 8 and 9 show the melting rates of the four deicers at -10°C and at -20°C respectively as function of time. It is seen that KAC is equivalent in its melting rate to $CaCl_2$, and about twice as effective as NaCl. CMA, on the other hand, is very ineffective at -10°C - it takes almost 30 minutes to initiate any melting. It does not melt any ice at -20°C.

Figures 10 and 11 show the effect of temperature on the rate of melting. KAC and $CaCl_2$ behave similarly, and melt almost 3 times as much ice as NaCl at any given temperature. CMA melts only small quantities of ice over the equivalent period, and virtually none below -10°C.

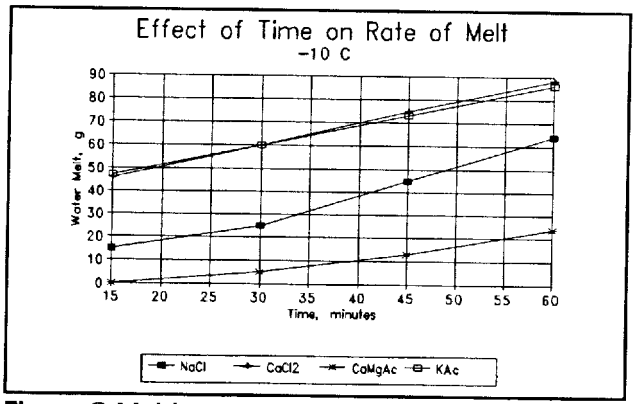

Figure 8 Melting rate of ice under various deicers at -10°C as function of time.

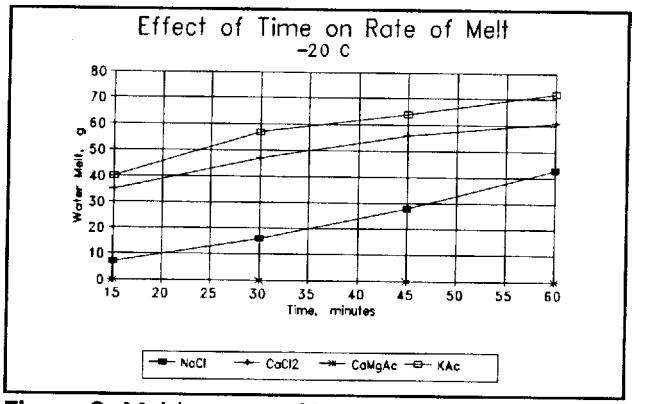

Figure 9 Melting rate of ice under various deicers at -20°C as function of time.

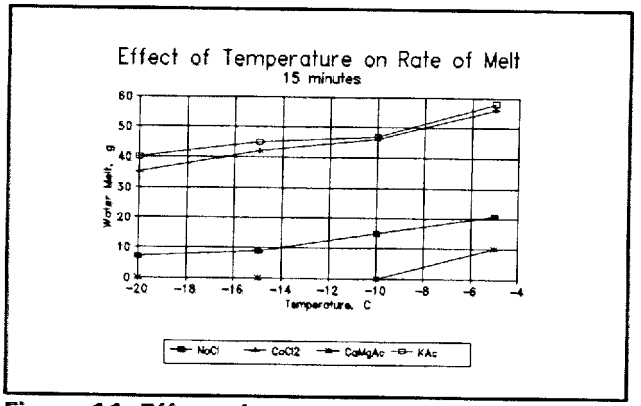

Figure 11 Effect of temperature on the melting of ice after 15 minutes exposure to deicers.

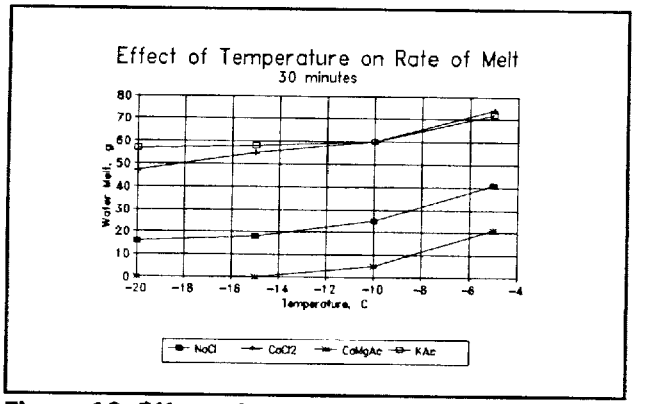

Figure 10 Effect of temperature on the melting of ice after 30 minutes exposure to deicers.

Scaling tests

The scaling of mortars exposed to some of the above deicers were determined. The scaling was determined as follows: At age of 28 days, triplicate samples of two inch cube mortars were placed on a carpet saturated in the 3% test solutions in an air-tight container. The closed container was frozen at -16°C for 16h, and thawed for 8h at room temperature (22°C) for 5 cycles. The samples were then visually rated for deterioration of the face in contact with the saturated solution. A rating system of 0 to 5, where 5 is the full face deterioration, was used to rate the scaling potential of the solution. The results (Figure 5) show that the acetates caused no scaling, while the chlorides, as expected, showed severe scaling. Thus, KAC, while exhibiting strong deicing capabilities, shows none of the deleterious effects associated with the chloride deicers. Although metal corrosion tests have not been carried out with KAC, it should not behave differently from CMA - i.e., it should be non-corrosive. The scaling test used was non-standard; however, the comparative results should be valid.

Relationship of scaling, de-icing effectiveness, and water adsorption

A deicer must be hygroscopic and hydrophillic at temperatures in the freezing range to be effective. Tests were carried out to determine the amount of water adsorbed at -3°C and at room temperature (22°C). Mortar cubes saturated for 24h in the various deicer solutions were dried, and exposed to 95% humidity at 22°C in a humidity chamber. After 72h, the gain in mass due to water sorption was measured.

The results at -3°C, combined with scaling rating, are shown in Figure 13. The figure shows that the chloride-saturated mortars show the greatest water adsorption, and also the greatest scaling. None of the acetates show scaling, and they also show reduced water adsorption compared with the chlorides. As a suggestion, a limit is proposed to the maximum water adsorption above which scaling is likely to take place. There are no theoretical basis for this at present. When the deicing property of KAC is better understood, an explanation may be evident.

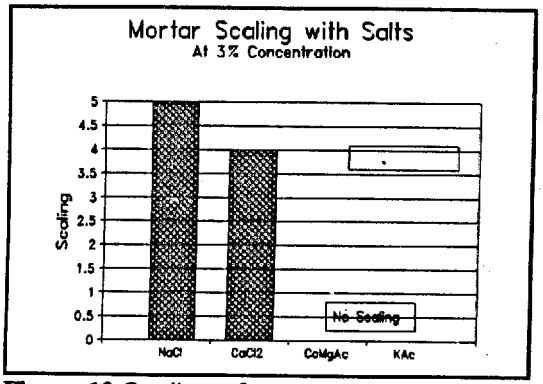

Figure 12 Scaling of mortar cubes exposed to various deicers.

SUMMARY AND CONCLUSIONS

There are four ways of controlling the damage caused by deicers:

1. Do not use deicers. Control ice by sanding. However, sanding tends to plug drains.
2. Use additives to common chloride deicers to minimize their deleterious effects. Phosphates, especially Na and Ca monophosphates, have been shown to be effective in reducing scaling (and corrosion) due to use of NaCl as a deicer.
3. Use non-chloride deicers. Calcium magnesium acetate has been shown to be effective at near freezing temperatures, but ineffective at lower temperatures. The deicer proposed in this paper, potassium acetate, is as effective as the best chloride deicer, but in common with other acetates, is benign to concrete and the environment.

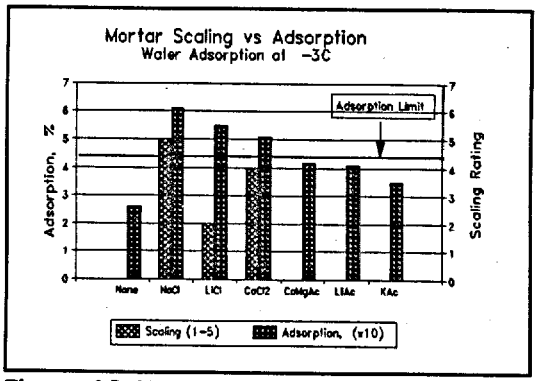

Figure 13 Water adsorption and scaling of mortar cubes exposed to various deicers.

ACKNOWLEDGEMENT

The work reported in the paper has been supported by an operating research grant to the two senior authors from the Natural Science and Engineering Research Council (NSERC) of Canada.

REFERENCES

1. Dunn, S.A., and Schenk, R.U.: "Alternative Highway Deicing Chemicals", Transportation Research Board Special Report 185, TRB, NRC, Washington, D.C., 1979.

2. Erns, D.D., Demish, G., and Wieman, T.:: "Calcium Magnesium Acetate in Washington State":, Transportation Research Record 1019, TRB, NRC, Washington, D.C., 1985.

3. Hsu, M.T.: "Production and Testing of Calcium Magnesium Acetate in Maine", Transportation Research REcord 962, TRB, NRC, Washington, D.C., 1984, p 77-82.

4. Horner, R.R., "Environmental Monitoring and Evaluation of Calcium Magnesium Acetate", NCHRP Report 305, TRB, NRC, Washington D.C., April 1988.

5. Collar, B.H., "Field Evaluation of Calcium Magnesium Acetate During the Winter of 1986-1987", Public Roads 52(1), June, 1988, p. 13-18.

INFLUENCE OF THE TYPE OF CEMENT ON THE CORROSION BEHAVIOUR OF STEEL IN CONCRETE

P Schießl and M Raupach

Institute for Building Research, RWTH Aachen, GERMANY

SUMMARY

The test results discussed in this paper are based on an extensive research project on the influence of concrete composition and environmental conditions on the corrosion behaviour of steel in concrete induced by chlorides. As testing method the measurement of the currents between locally separated anodes and cathodes within special concrete specimens called corrosion cells has been used.

The results reported in this paper show, that the use of blastfurnace slag, pulverized fuel ash and silica fume as blending agents in concrete leads to a significant increase of the electrical resistivity and a decrease of the corrosion rate of the reinforcement in the case of chloride induced corrosion.

ZUSAMMENFASSUNG

Die Versuchsergebnisse, die in dieser Veröffentlichung diskutiert werden, basieren auf einem umfangreichen Forschungsprojekt zum Einfluß der Betonzusammensetzung und Umgebungsbedingungen auf das Korrosionsverhalten von Stahl im Beton bei Chlorideinwirkung. Als Prüfverfahren wurden Elementstrommessungen zwischen örtlich getrennten Anoden und Kathoden in speziellen Betonprüfkörpern, sogenannten Korrosionszellen, durchgeführt.

Die Versuchsergebnisse zeigen, daß die Verwendung von Hüttensand, Steinkohlenflugasche und Silikastaub als Zusatz- bzw. Zumahlstoffe im Beton zu einer deutlichen Erhöhung des elektrolytischen Widerstandes und einer Verringerung der Korrosionsgeschwindigkeit bei chloridinduzierter Korrosion der Bewehrung führt.

INTRODUCTION

During the last years corrosion of the reinforcement in concrete structures caused by chlorides, carbonation of the concrete or low quality of the concrete cover lead to several serious damages.

To be able to assess the corrosion risk of existing reinforced concrete structures and to plan durable repair measures it is necessary to know the factors influencing the corrosion process. To study the parameters influencing chloride induced corrosion of steel in concrete an extensive research program has been carried out using so called concrete corrosion cells (see e. g. (1, 2)). In this paper the results regarding the influence of the type of cement are presented and discussed.

THE CONCRETE CORROSION CELL

The features of the concrete corrosion cell are shown in Fig. 1. At first, a layer of chloride containing concrete is placed in an air- and watertight vessel. After the hardening of the concrete a chloride-free second layer of concrete is placed upon the first. Steel electrodes are installed in these two concretes. The electrodes are electrically connected, enabling the macrocell current flowing between them to be measured.

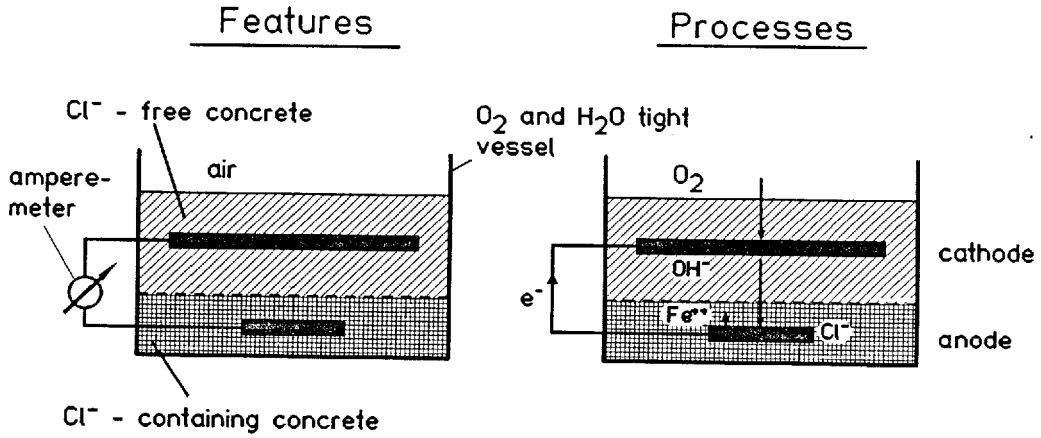

Fig. 1: Schematic representation of the set-up and the operation of the concrete corrosion cell

The electrode installed lower down works as the anode, provided that the chloride content is above a critical limit value. The second electrode is installed near the upper surface of the chloride-free concrete and, being protected by the alkalinity of the concrete, it only can work as cathode.

The rate of corrosion is directly related to the electric charge carried between anode and cathode: 100 µA correspond to 911 mg of iron removal at the anode per year. The relation between macrocell current and steel removal at the anode has been investigated in (3). It was found out, that there is as very good agreement between the

calculated (integration of macrocell currents) and the directly measured weight loss. That means that micro cell action at the anode is negligible for this test set up.

EXPERIMENTAL RESULTS

The macorcell currents have been measured automatically with an instrumentation that allows to store the currents of 192 corrosion cells on a personal computer continuosuly.

The investigations have been carried out with 400 cm² large cathodes and 20 cm² large anodes placed in a distance of 7.5 cm from one other. The influence of the geometrical design of the corrosion cell has been investigated in (3). The concrete mix design of the corrosion cells used for the investigations on the influence of blastfurnace slag and fly ash are given in Table 1. The aggregate grade curve was A16/B16 according to DIN 1045 except for specimens No. 7 (A32, see Table 1).

Table 1: Parameters of the corrosion cells used to investigate the influence of the blastfurnace slag content and fly ash

Type of cement	Slag content	Fly ash content
-	M.-%	M.-%
OPC 35 F	0	-
PBC 35 F	20	-
BFC 35 L	42	-
SR BFC 35 L	74	-
FAC 35 L	-	26

→ → → → →

No.	cement content	w/c - ratio	curing	concrete cover
-	kg/m³	-	d	mm
1	300	0,60	0	25
2	300	0,60	2	25
3	300	0,60	7	25
4	300	0,60	0	10
5	300	0,60	2	10
6	300	0,60	2	40
7	300	0,50	2	25
8	360	0,50	2	25
9	450	0,40	2	25
10	450	0,40	7	40

The test series on the influence of the C_3A content of the cement and the silica fume content of the concrete have been carried out using the concrete composition described in the following chapters and a concrete cover of 25 mm. After a curing period of two days the specimens have been stored at 20 ± 1 °C and 80 ± 5 % r. h.. The influence of the chloride content on the macrocell currents was inverstigated in (1). The following tests have been carried out with an addition of 2 % chlorides (Cl^-) relative to the cement content if there is no special remark.

INFLUENCE OF THE BLASTFURNACE SLAG AND FLY ASH CONTENT OF THE CONCRETE

Fig. 2 shows the mean values of the macrocell currents of 10 corrosion cells made with different blastfurnace slag and fly ash contents (alltogether 5 x 10 specimens, see Table 1). The reduction of the corrosion rates in the course of time is mainly caused by the storage conditions (drying out, no penetration of chlorides into the

corrosion cells after concreting). More detailed information about the time dependent behaviour of the macrocell currents is given in (4) and (5). Increasing the blastfurnace slag content and using fly ash lead to a significant reduction of the macrocell currents compared to the corrosion cells without additives.

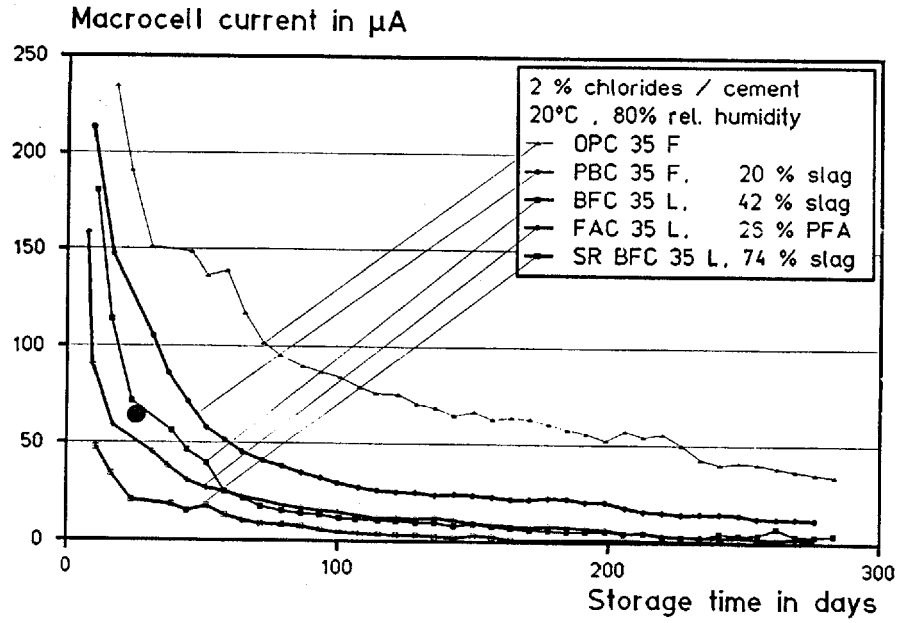

Fig. 2: Mean values of the measured macrocell currents of 10 concrete corrosion cells (see Table 1)

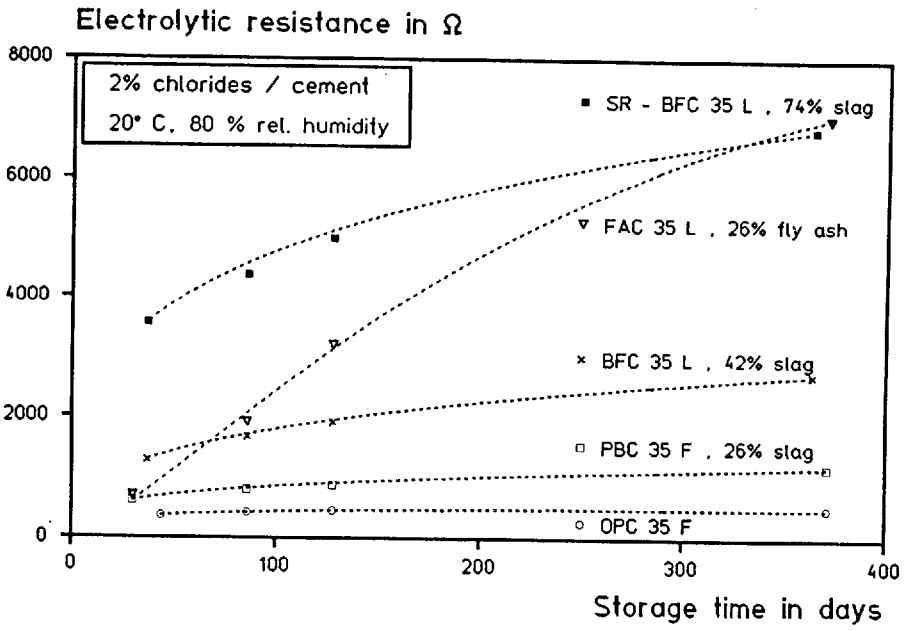

Fig. 3: Mean values of the measured electrolytical resistances of the concrete of 10 concrete corrosion cells (see Table 1)

As additional test the electrolytic resistance of the concrete between anodes and cathodes of the corrosion cells have also been measured. To eliminate polarisation effects at the electrodes an alternating voltage (50 or 1000 Hz) was applied to the steel electrodes. The results of the AC resistance measurements show that the elctrolytic resistance of the concrete increased in the course of time and with increasing blastfurnace slag of fly ash contents considerably (see Fig. 3) The electrolytic restistance of the concrete containing 26 % fly ash/cement increased very slowly and was as high as the resistanc of the concrete containing 74 % blastfurnace slag/cement after one year. This behaviour can be explained by the pozzolanic reaction of the fly ash and consequently the change of the pore structure.

These investigations show that the use of blastfurnace slag and fly ash leads to an increase of the electrolytical resistance of the concrete and a reduction of the corrosion rate of the reinforcement induced by chlorides. The main reason for this effect is the change of the pore structure of the concrete which causes a restriction of the mobility of the ions chlorides moving to the pits during the corrosion process (6).

INFLUENCE OF SILICA FUME

To investigate the influence of silica fume on the corrosion rate of steel in concrete, three corrosion cells containing 0, 10 and 20 % silica fume/cement have been produced. Superplaticiser was added to the concrete, so that the consistency of the three concretes was nearly the same (flow spread ~ 36 cm).

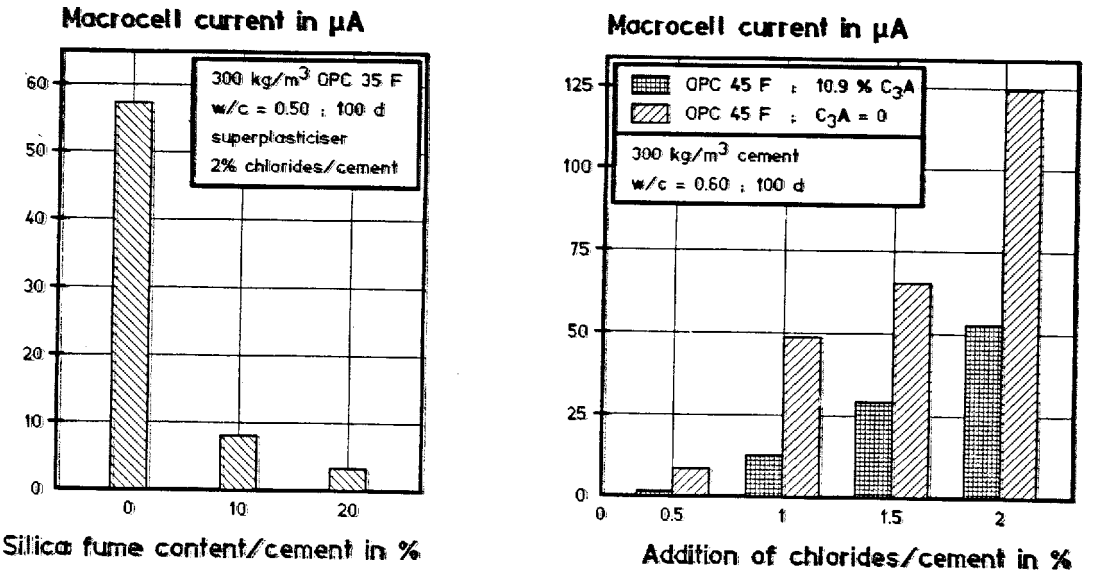

Fig. 4: Influence of the silica fume content of the concrete and the C_3A content of the cement on the corrosion rates of the concrete corrosion cells

Fig. 4 shows, that the macrocell currents decrease significantly, when the silica fume content of the concrete increases. Although 2 % chlorides/cement have been added, the corrosion currents came down to practically zero when adding at least 20 % silica fume. The increase of the silica fume content also caused a considerable increase of the electrolytic resistance of the concrete from 795 Ω without silica fume to 16750 Ω (20 % silica fume/cement) after one year.

INFLUENCE OF THE C_3A-CONTENT OF THE CEMENT

To investigate the influence of the C_3A-content of the cement on the corrosion rate corrosion cells made with different C_3A contents and chloride additions have been produced. Fig. 4 shows that the corrosion rates of the specimens containing cement without C_3A were much higher compared to a cement containing 10,9 % C_3A.

As known from previous work, the chloride binding capacity of the C_3A-free cement and the resistance against chloride diffusion are very low (see e. g. (6)). Both effects stimulate the anodic dissolution of iron at the anode.

CONCLUDING REMARKS AND FURTHER OUTLOOK

The tests reported here show, that the use of blastfurnace slag, pulverized fuel ash and silica fume as blending agents in concrete leads to a significant increase of the electrical resistivity and a decrease of the corrosion rate of the reinforcement in the case of chloride induced corrosion. The main reason for this favourable effect is the change of the pore structure of the concrete causing a restriction of the mobility of ions in the pore solution and the mobility of chlorides moving to the pits during the corrosion process. Cement without C_3A caused the highest corrosion rates correlating with its low chloride binding capacity and it low resistance against chloride diffusion which stimulates the anodic dissolution of iron. This type of cement should only be used in the case of sulphate attack, when there is no additional chloride attack.

REFERENCES

1. Schießl P. ; Raupach, M.: Influence of Concrete Composition and Microclimate on the Critical Chloride Content in Concrete. London : Elsevier, 1990 - In: Corrosion of Reinforcement in Concrete, International Symposium, Wishaw, Warwickshire, UK - 21-24 May 1990, S. 49-58

2. Schießl, P. ; Raupach, M.: Macrocell Steel Corrosion in Concrete Caused by Chlorides. - In. Second CANMET/ACI International Conference on Durability of Concrete, August 4-9, 1991 in Montreal, S. 565-583

3. Schießl, P. ; Schwarzkopf, M.: Chloridinduzierte Korrosion von Stahl in Beton. In: Betonwerk und Fertigteiltechnik 52 (1986), Nr. 10, S. 626-635

4. Schießl, P. ; Raupach, M.: Influence of Blending Agents on the Rate of Corrosion of Steel in Concrete. Stockholm : Swedish Council for Building Research, 1989 - In: Durability of Concrete, June 1989, S. 205-214

5. Schießl, P. ; Raupach, M.: Einfluß der Betonzusammensetzung und der Umgebungsbedingungen auf die chloridinduzierte Korrosion von Stahl in Beton: Ergebnisse von Untersuchungen mit Betonkorrosionszellen. In: Betoninformation 30 (1990), Nr. 4, S. 43-54

6. Schießl, P.: Corrosion of Steel in Concrete. RILEM Report 60 CSC. New York : Chapman and Hall, 1988

CORROSION SUSCEPTIBILITY OF GALVANIZED AND MILD STEEL REINFORCEMENT IN BLENDED CEMENT CONCRETES

Kalyan Dass*, S S Rehsi*, Tilak Raj*, P C Gupta* and K B Jain**

**Central Building Research Institute, Roorkee, INDIA*
***Hindustan Zinc Ltd., Udaipur, INDIA*

SUMMARY

Investigations were carried out to determine the corrosion susceptibility of galvanised and mild steel reinforcement in blended cements namely, portland pozzolana (PPC), portland slag cement (PSC) and supersulphated cement (SSC). Parallel tests were carried out with ordinary portland cement (OPC). The extent of corrosion was assessed on the basis of data obtained by time potential measurements, weight loss measurements and bond strength test on concrete test specimens reinforced with galvanised and mild steel bars, before and after subjecting them to weathering by alternate wetting and drying cycles. Time-potential and weight loss measurements were also made on galvanised and mild steel bars immersed in cement-water suspensions.

The data obtained and reported in the paper show that under normal environmental conditions and in the absence of chloride, galvanised steel will resist corrosion better than mild steel. In the presence of chloride,e the galvanised steel bars embedded in OPC, PPC, PSC and SSC concretes show significantly higher loss in weight on weathering than mild steel bars, indicating thereby that galvanised steel shall corrode more in chloride bearing environment.

Intoduction

Amongst the various techniques of protecting steel from corrosion distress in concrete when subjected to adverse conditions, much attention has been given to providing protection by galvanizing the steel reinforcement. Literature survey, however, reveals variable results regarding the extent of protection provided by the galvanized reinforcement (GI) vis-a-vis mild steel (MS) (1-7).

An invesetigation was carried out to evaluate the corrosion susceptibility of GI and MS in concrete made with ordinary portland cement and different types of blended cements. The rsults obtained are reported and discussed here.

Materials Used

Ordinary Portland Cement (OPC), Portland Pozzolana Cement (PPC), and Portland Slag Cement (PSC), Sand, Coarse aggregate and water used were conforming to relevant Indian standards. Super Sulphated Ceemnt (SSC) haaving 3, 7 & 28 days compressive strength 75, 128 and 427 kg/cm^2, respectively was used. The thickness of the zinc coating was about 100 μm & was chromated using standard hot dip process.

Experimental Procedure

(a) Studies in Solutions

Time-potential and weight loss measurements of MS and GI bars immersed in cement water suspension/extract, with and without NaCl and in tap water were carried out.

(b) Studies in Concrete :

Time-potential, bond strength and weightl loss of MS and GI reinforcement in concrete prepared with different cements were determined, under following conditions :

- After taking time-potential measurements in tap water for first 60 days the specimens were placed in 3% NaCl solution and measurements continued upto 300 days.
- Bond strength and weight loss measurements of GI & MS rods in concrete specimens were carried out after subjecting the test specimens to alternate wetting and drying cycle; one cycle consisted of wetting in 3% NaCl solution and drying at 50^oC.

Results and Discussion

Potential of GI in Cement Water Suspension

The data on potential of GI bars in cement-water suspensions and tap water are shown in Fig. 1. The pH of different cement water suspensions over a period of time is shown in Fig. 2. It can be seen, the potential of GI decrased as the pH increased at 5 days. Thereafter potential shifted to more negative values after about 60 days and became closer to each other in the corrosive range. The pH at this point becomes 11.5 or less. In SSC water suspension, the potentials are in the corrosive range from the beginning and remains more or less constant throughout. On the other GI in tap water having a pH of about 8 show continuous increase in potential indicating better protection. This

observation is also supported by the data on weight loss measurements in tap water (Table 1). This difference can be attributed to the fact that cement water suspension unlike tap water are corrosive in nature due to high alkalinity and presence of certain other constituents dissolved from cements.

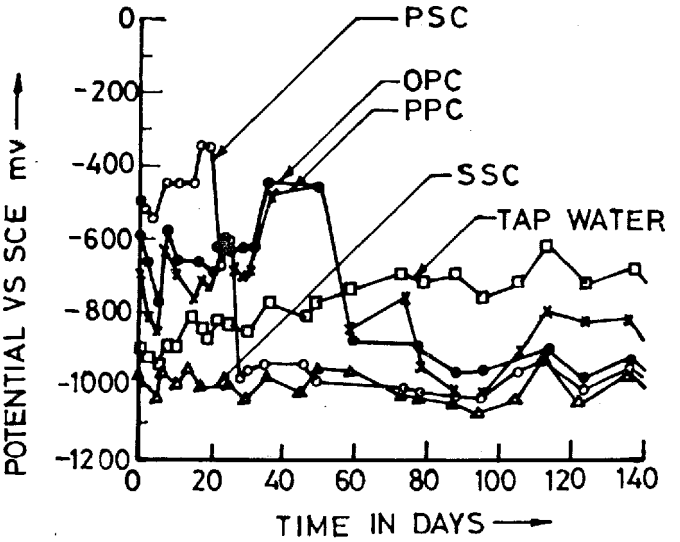

FIG. 1 TIME-POTENTIAL CURVES OF G.I IN DIFFERENT CEMENT - WATER SUSPENSIONS AND TAP WATER

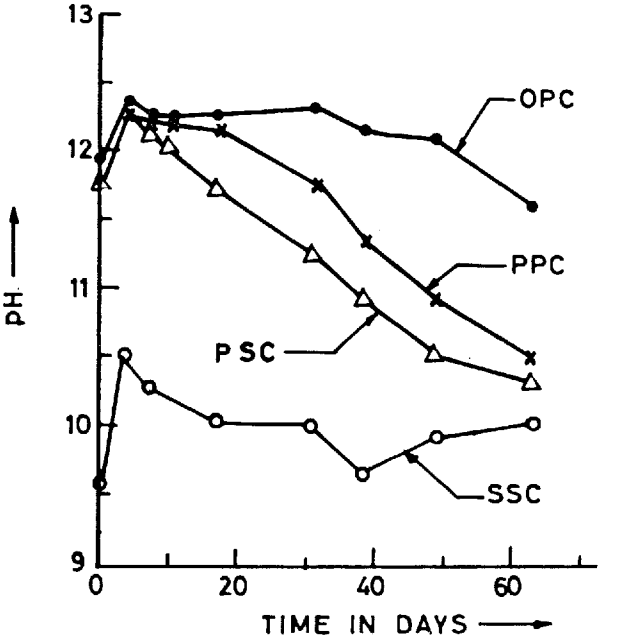

FIG. 2 TIME- pH CURVES OF DIFFERENT CEMENT - WATER SUSPENSIONS

Weight Loss in Cement Water Suspension

Data on weight loss measurements of GI immersed in suspension of OPC, PPC, PSC and SSC in water are shown in Table 1 alongwith weight loss in tap water.

Considering slight variation in weight loss from cement to cement as insignificant the data show that under normal conditions in the absence of chloride, the corrosion of GI in OPC, PPC, PSC oncrete is likely to be more or less similar. In SSC concrete due to its lower alkalinity, the corrosion of GI is expected to be lower so long as the zinc coating remain intact on the reinforement. The effect of chloride in OPC - water suspension/extract on weight loss is also shown by the data given in Table 1. While there is hardly any weight loss of MS in chloride free cement-water suspension having pH about 12.4, the loss in weight of GI increases with passage of time upto 265 days. With addition of NaCl in cement-water extract, the weight loss of MS and GI increases. The loss in weight of GI is much higher than MS. The data clearly show poor resistance of GI in presence of chloride vis-a-vis MS. The pattern of weight loss changes when MS and GI are immersed in cement water extract (pH = 10.4) having NaCl additions. In this case, the weight loss of MS is much greater in than GI. This is due to the fact that while lower pH is beneficial to GI it is highly detrimental to MS which remains passive only at pH more than 12.4.

Table 1 : Loss in weight of GI and MS bars in different media.

Medium	Bar	Per cent loss in weight after immersion for 60 days	115 days	150 days	196 days	240 days	265 days
1. SSC-water Suspension	GI.	0.113	0.158	0.182	0.195	0.264	0.310
2. PSC-water Suspension	GI.	0.074	0.227	0.298	0.313	0.376	0.390
3. PPC-water Suspension	GI.	0.087	0.137	0.191	0.253	0.322	0.335
4. OPC-water Suspension	GI.	0.063	0.0196	0.308	0.404	0.463	0.510
	MS.	0.00	0.02	0.07	0.247	-	-
5. OPC-water extract (pH=12.4) +1% NaCl	GI.	0.62	1.34	1.63	1.90	2.13	2.26
	MS.	0.26	0.565	0.84	1.37	1.73	1.88
6. OPC-water extract (pH=10.4) + 1% NaCl	GI.	0.177	0.206	0.235	0.26	0.284	0.350
	MS.	0.596	0.850	0.99	1.16	1.36	1.50
7. Tap water	GI.	0.068	0.04		0.05	0.056	0.067
	MS.	-	0.207		0.338	0.338	0.349

Measurements in Concrete

Time Potential Measurements

Superimposed time potential curves of MS and GI in OPC, PPC, PSC & SSC concretes in tap water and 3% NaCl solution are shown in Fig. 3. It can be seen that:

(i) Potentials of MS bars embedded in OPC, PPC and PSC concretes move towards more positive directions in tap water indicating passivity. SSC exhibits corrosive behaviour from the beginning. In 3% NaCl the potentials in OPC, PPC, PSC concretes shift to more negative values showing corrosion tendency. In SSC concretes the potential of MS although does not deviate more than that in tap water, remain in corrosion range and final potentials are more negative than rest of the concretes.

(ii) Potentials of GI in tap water as compared to MS shifts to more negative values in all the concretes including SSC. The shift is of the order of about 400 milivolts. This shift may be due to basic difference in the electrochemical potential of the two metals; that is Iron and Zinc Potentials of GI in OPC, PPC and PSC show wide fluctuation and swing between passive and corrossive range. As com-pared to this, the potentials in SSC concrete though in corrosive range varies within very narrow range right from the beginning.

In 3% NaCl solution the potentials in all cases are in corrosive range. The values for different concretes do not vary widely from each other, except SSC where potential moves towards more positive side with passage of time, showing better protection against corrosion of GI in presence of chloride.

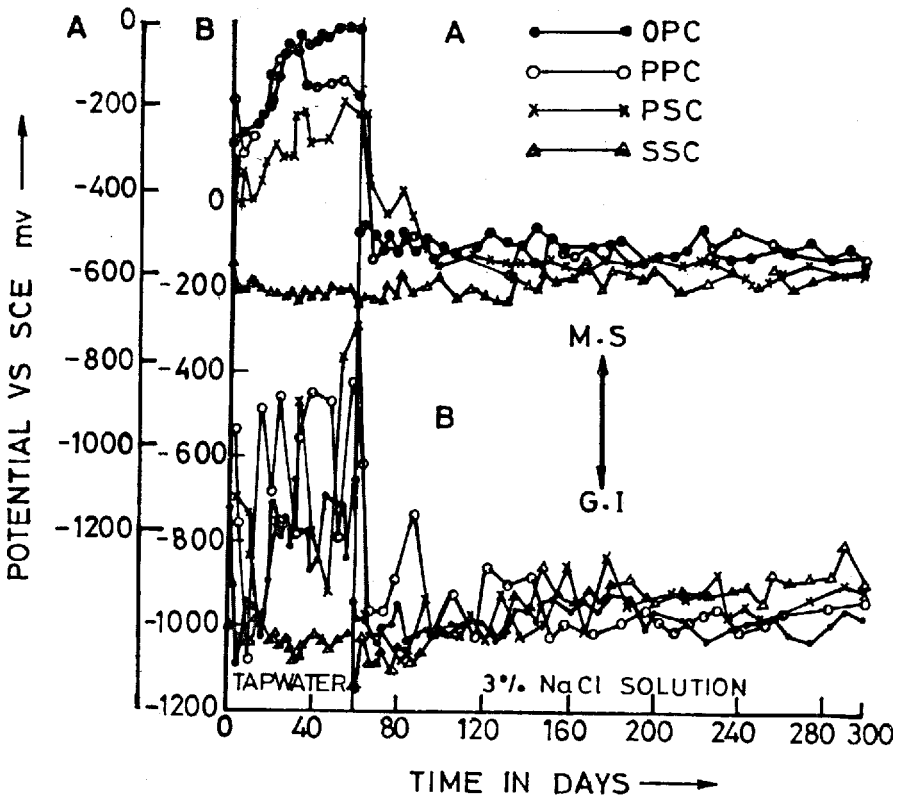

FIG. 3 SUPERIMPOSED TIME-POTENTIAL CURVES OF G.I. M.S. IN DIFFERENT CEMENT CONCRETES IN TAP WATER AND 3% NaCl SOLUTION

Bond Strength

The bond strength of MS/GI bars embedded in OPC, PPC, PSC and SSC concretes obtained at 28 days of water curing and after 8, 16 and 26 cycles of accelerated weathering are shown in Table 2. It can be seen that as compared to MS, the GI bars developed lower bond strength in OPC, PPC and PSC concrete at 28 days. In SSC, GI develop higher bond strength. This can be attributed to the difference in alkalinity levels in these concretes (Table 2). As the development of bond is age dependent the time required to develop full bond between steel and concrete may thus be greater for GI than MS. The difference in bond strength observed at 28 days is therefore likely to be levelled off over a period of time. The observation is supported by the bond strength data obtained on ageing under accelerated weathering cycles. Ingress of chloride during accelerated cycles in 3% NaCl and drying also accelerated the kinetics of hydration in all concretes leading to improved bond.

At 26 weathering cycles except for SSC there is a decrease in bond strength of MS. This may be due to loosening of bond due to rust formation and increase in volume. The increase in bond strength in GI may be attributed to the fact that increase in volume due to zinc

corrosion is less than due to steel corrosion.

Table 2 : Bond Strength of MS/GI Bars in Concrete

Concrete	pH of the Concrete Extracts 28 Days Water Cured	Rein-force-ment	Bond Strength (Kg/cm^2)			
			28 Days	After Accelerated Weathering Cycles		
OPC	12.35	MS	30.0	60.7	91.9	81.2
		GI	10.0	59.7	96.3	92.2
PPC	12.40	MS	22.8	39.1	73.0	61.87
		GI	11.3	34.9	72.8	80.3
PSC	12.30	MS	38.3	40.9	71.8	66.3
		GI	14.1	40.8	73.8	74.8
SSC	11.20	MS	45.9	86.7	83.5	93.0
		GI	52.3	74.7	91.9	-

Weight Loss Measurements

The data on loss in weight of MS and GI bars embedded in OPC, PPC, PSC and SSC concretes subjected to alternate cycles of wetting in 3% NaCl and drying are shown in Table 3.

Table 3 : Loss in Weight of MS/GI Bars Embedded in Concretes

Concrete	Concrete Cover Thickness (mm)	% Weight Loss No. of Weathering Cycles					
		8 Cycles		16 Cycles		26 Cycles	
		MS	GI	MS	GI	MS	GI
OPC	12	0.61	3.07	2.02	4.25	2.30	4.31
	25	0.56	2.50	0.96	3.96	2.10	3.96
PPC	12	0.36	2.89	1.73	4.03	3.70	5.00
	25	0.42	2.68	1.60	3.35	1.72	3.96
PSC	12	0.41	2.16	1.48	3.21	3.73	4.57
	25	0.37	2.00	1.22	2.39	1.73	3.75
SSC	12	1.10	2.58	2.70	3.90	6.04	7.18
	25	1.38	2.78	3.40	4.88	6.13	6.50

It can be seen that loss in weight in GI rods is significantly higher than MS rods embedded in all types of concrete. It is further seen that under the condition of test increasing cover thickness from 12 mm to 25 mm does not provide greater protection against corrosion. The data confirm the findings of the earlier workers (3, 6) that GI corrode more in chloride containing environments.

The data obtained in potential-time measurements, bond strength and accelerated weight loss measurements show that the protective behaviour of OPC, PPC, and PSC in respect of GI is more or less similar. Initial

pH of these concretes is also almost equal. The behaviour of SSC concrete is different mainly due to its low initial alkalinity and greater sulphate content.

As seen earlier the GI is likely to perform better in SSC concrete. However, the use of SSC concrete is restricted to situation where ambient temperature does not exceed 40°C and where sulphate attack is problem.

Conclusions

From the present study it can be concluded that

(1) GI is prone to corrosion in high alkaline environment (pH = 12.4 or more) obtainable in OPC, PPC, PSC where MS does not corrode.

(2) In the presence of chlorides and high alkaline environment the corrosion of GI is greater than MS.

(3) In low alkaline environments (pH = 11 or less) obtainable in SSC and in presence of chloride the corrosion of GI is lower than MS.

Acknowledgement

The study referred in this paper was sponsored by M/s Hindustan Zinc Ltd. Uda ipur and is published by permission of Director, CBRI.

References

1. Frazier, K.S., "Value of Galvanized Reinforcing in Concrete Structures", Materials Protection; May, 1965.

2. Cornet, Israel and Gresler, Brois, "Corrosion of Steel & Galvanized Steel in Concrete", Materials Protection, April, 1966.

3. Haruo Shimada, Seiya Nishi, "Sea Water Corrosion Attack on Concrete Blocks Embedding ZInc Galvanized Steel Rebars", Corrosion of Reinforcement in Concrete Construction, Ed. Alan, P. Cranc, Ellis Horwood Ltd., Publ. 1983, pp. 407-418.

4. Jiro-Satake, Masashi Kamakura, Kiyoshi Shirakawa, Naoto, Mikami and Narayanswamy, "Long Term Corrosion Resistance of Epoxy Coated Reinforcing Bars", Corrosion of Reinforcement in Concrete Construction, Alan, P. Crance, Eills Horwood Ltd., Publ. 1983, pp. 357-377.

5. Tripler, Arch. B, et. al. "Method for Reducing Corrosion of Reinforcing Steel", National Cooperative High Way Research Programme Report 23, High Way Research Board, 1966.

6. Everett, L.H. and Treadway K.W.J., "The use of Galvanized Steel Reinforcement in Buildings", BRS Current Paper CP 3/70, Jan., 1970, pp. 2.

7. Bird, C.E., "The Bond of Galvanized Steel Reinforcement in Concrete", Nature, VI, 194, No. 4380, pp. 798.

CORROSION CHARACTERISTICS OF STEEL IN BLAST FURNACE SLAG-PORTLAND CEMENT BLENDS

H T Cao, D E Macphee, L Bucea and V Sirivivatnanon

CSIRO Div of Building, Construction & Engg,
AUSTRALIA

Abstract

The present paper reports on the corrosion characteristics of steel embedded in slag blended cement pastes of different slag contents of up to 80 percent in the normal situations and under the influence of chloride. Information obtained from potentiodynamic anodic polarization are summarised. The results indicate that anodic dissolution characteristics of steel were significantly modified by the presence of slag, particularly at high percentages. In cement pastes containing high percentages of slag, the electrochemical data suggest that the corrosion layer formed on steel surface may not be the conventional iron (III) layer at early age of hydration. This is attributed to the reducing characteristics of slag. Despite the difference in the protective nature, electrochemical data indicate that there were no significant difference in the corrosion behaviour of steel under the influence of chloride between slag blended cement and portland cement. Observations of steel embedded in slag blended cement pastes using scanning electron microscopy and measurements of galvanic corrosion current are also given.

Introduction

Steel reinforcement embedded in concrete is protected against corrosion by the formation of the passive layer on its surface. There are three factors that directly affecting the formation of this passive layer, namely the alkalinity of the surrounding pore solution, the presence of oxidizers or a high oxidizers/reducers ratio and a low corrosive surface-acting anions/inhibitors ratio. All of these factors are time-dependent due to the effects of the hydration process of the particular binder used or due to the interaction of the hardened cement paste with the environment.

It has been known that the passive layer formed on the steel surface is a product of a corrosion process itself. In other words, there are anodic reactions and cathodic reactions involved. However in the case of passivation the corrosion products are adherent to the steel substrate forming a dense non-porous 3-D layer. The formation of this layer retards the subsequent rate of iron dissolution. Glasser and Sagoe-Crentsil [1] indicated that the passive layer of steel in concrete consists of two distinct layers. The inner layer is mainly Fe_3O_4/γ-Fe_2O_3 while the outer layer is mainly α-FeOOH and spinel phases. Nodules of $Ca(OH)_2$ and (evidence indicating) other cement hydrated products are present in varying amounts in both layers.

The formation of the passive layer, its growth and its stability are depended on the relevant cathodic and anodic reactions occurring on the steel surface. These in turn depends on the chemistry of pore solution.

Blended cements made with ground granulated blast furnace slag have been used for many years. The effect of slag on the engineering properties of the blended cement concrete has been reported in the literature [2]. With regard to durability aspects, the incorporation of slag has been associated with increase in resistance to chloride penetration and sulphate attack [3]. The use of slag blended cements in general tends to provide equal to or better protection to steel reinforcement in comparison to portland cements. However since blast-furnace slag is produced in a reducing atmosphere, it contains a certain amount of reducing species. During the hydration of slag blended cements these reducing species are released [4] which can affect the formation and the maintenance of the passive layer [5].

The work presented in this paper is aimed at investigation the characteristics of the passivation of steel embedded in cement pastes made with slag blended cements after different ages of hydration. In this investigation, potentiodynamic anodic polarization experiments using steel-embedded-in-cement-paste samples were performed with supporting evidence obtained from microscopy work and galvanic corrosion current measurements.

Materials and Experimental procedures

One portland cement (type A - AS 1315 - 1982) and one ground granulated blast furnace slag (BFS) were used in this work. The chemical compositions of the materials are given in Table 1.

The configuration of samples of steel-embedded-in-cement paste used as working electrodes for potentiodynamic anodic polarization work [6] is shown in Figure 1. The paste was made with a water-to-binder ratio of 0.8. The procedures used for anodic polarization were similar to those described in ASTM G 5 - 87. The samples were kept in saturated condition to minimize the effect of variation in moisture content. The scan rate was $0.17 mV.sec^{-1}$. Anodic polarization experiments were performed in lime saturated solution at 23°C starting at -1200 mV vs SCE to +800 mV vs SCE. Graphs of the anodic polarization curves are plotted with potential E in mV vs SCE and current in $\mu A/cm^2$. Three sets of samples were used. The first set of samples was continuously cured in lime-saturated water. This set of sample was used to investigate the effects of slag content and age of hydration on anodic behaviour of steel. The second set of samples was prepared with and cured in lime saturated water containing 0.04 M NaCl to simulate the effect of Cl^- contamination in the mixing water. The third set of samples was cured for 7 days in lime saturated water prior to immersion in water containing 0.5 M NaCl to simulate the effect of chloride penetration by sea water. It is noted that the water-to-binder ratio of 0.8 used in this work was adopted to facilitate the chloride penetration. Procedures and sample configuration used for the galvanic corrosion current measurement were established in a previous investigation [8].

Table 1

Chemical compositions of portland cement and BFS

Oxides	PC	BFS
SiO_2	21.3	33.4
Al_2O_3	4.95	13.4
TiO_2	0.2	0.7
Fe_2O_3	2.5	1.5
CaO	64.4	40.7
MgO	1.55	6.5
SO_3	2.6	1.0
K_2O	0.95	0.38
L.O.I.	1.2	0.2
Fineness ind.	-	384

Figure 1

Configuration of sample as working electrode for anodic polarization experiment

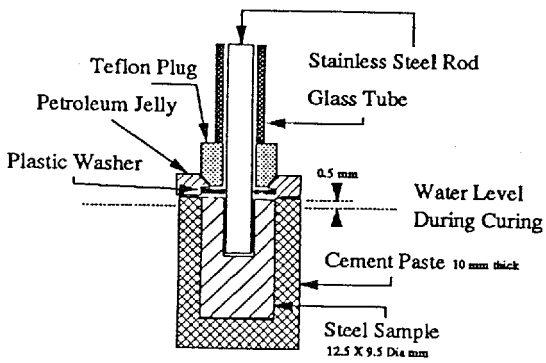

Results and discussion

Figure 2 shows the anodic polarization curves of steel embedded in BFS blended cement paste with different BFS loadings after one day of curing. In the case of OPC, the anodic dissolution characteristics of steel showed the different regions of iron oxide formation and a passive range as expected. The rest potential of the steel was about -300 mV vs SCE and was in the passive range. This implies that the passive layer formation of steel embedded in this particular portland cement was reasonably fast.

The overall shape of the polarization curves of steel embedded in BFS blended cement paste shown in figure 2 was very similar to that of portland cement paste after one day of hydration when the slag content was equal to or less than 60%. This denotes that the tendency for the steel to be passivated in slag blended cement paste was similar to that of portland cement. However it was noted that the rest potential of the steel in BFS blend was generally lower than that of in portland cement. At this age, the rest potential of steel was in the range of -400 to about -650 mV vs SCE. In some cases, the rest potential of the steel was outside the passive range. This indicates that although the trend of steel to be passivated appears to be unchanged with the presence of slag, its formation in slag blends may not be as readily as in the case of portland cement. It is noted that the passive layer is a result of an corrosion process in which the corrosion product is a dense iron (III) layer.

Figure 2

Potentiodynamic anodic polarization curves of steel embedded in OPC-BFS blends - 1 day

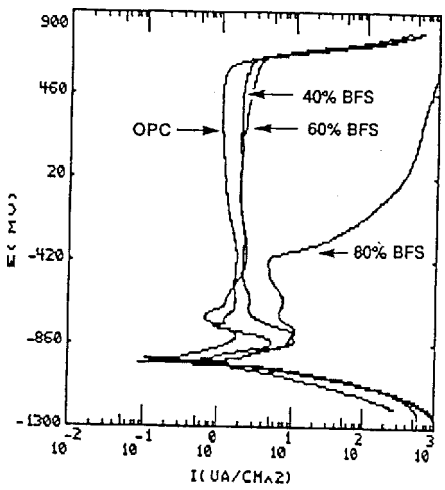

In order for this layer to form a certain ratio of oxidizers-to-reducers must be maintained. In slag blend, it appears that at early age, the ratio of the oxidizers-to-reducers in the solution is not favourable to the formation of a iron (III) layer. In the case of 80% BFS blend, apart from the above mentioned effect, the anodic polarization curve of steel was modified significantly as shown in figure 2. This figure shown that, the passive region of the steel was limited and there was suggestion of pitting corrosion. This indicates that the evolution of reducing species at very high level of slag content can be as early as after one day of hydration. It has been suggested that the release of reducing species such as S^{2-}

and HS^- and their dissociation can lead to H^+ production and therefore locally reduced pH [5]. In BFS blended cement, previous work [4] denoted that the E_h of the pore solution of a blend containing 75 to 85% of BFS becomes negative after 1 to 3 months of hydration. In this work, the electrochemical data indicates that apart from this, there would be a release of reducing species from slag at a much earlier age. At high slag content, this is not compensated by the hydration of the portland cement component. It was noticeable the passive currents (in the case of 40 and 60% BFS) in slag blended cement paste were considerably higher than that shown in portland cement. This denotes that even if the passive layer of steel in slag blended cement is formed by external polarization, it would not be as dense as that in portland cement.

As the hydration proceeded from 1 to 7 days, there were little variation in the anodic behaviour of steel in portland cement and in BFS blends containing 40% slag. However the characteristics of the polarization curves for steel embedded in 60% and 80% BFS blends after 7 days of hydration were very different from those after 1 day of hydration as shown in Figure 3.

Figure 3

Potentiodynamic anodic polarization curves of steel embedded in OPC-BFS blends - 7 days

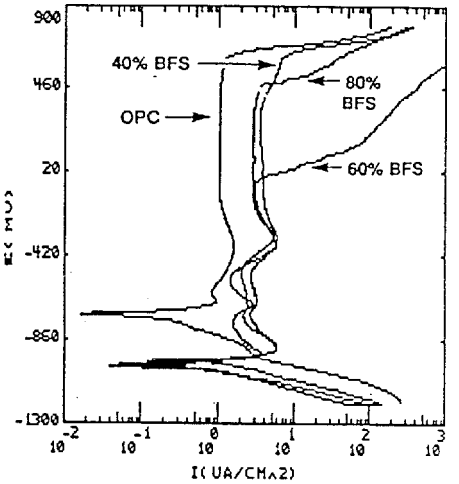

Figure 4

Potentiodynamic anodic polarization curves of steel embedded in OPC-BFS blends - 28 days

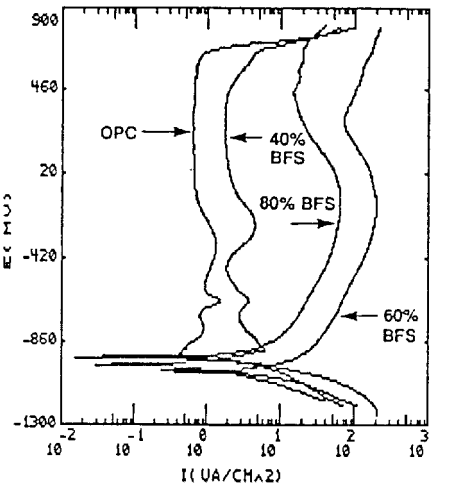

From this figure it can be seen that, the anodic behaviour of steel in 60% BFS had been modified as shown by the shorten passive range, whereas in the 80% BFS, a "full" range of the passive region was observed. This denotes that in the case of 80% BFS blend after the initial release of the reducing species, the hydration of portland cement would to be the dominant factor in determining electrochemical behaviour of steel. In 60% BFS blend, the situation was reversed. This also denotes the variability in the electrochemical behaviour of steel in BFS blended cement caused by slag hydration. This effect was not apparent in the case of OPC. After 28 days of hydration (Figure 4), there was only minor variation to the anodic behaviour of steel embedded in 40% BFS blended cement paste. At this age, the anodic polarization curves of steel embedded in either 60% or 80% BFS showed significant difference in characteristics to that of portland cement. In both cases, the anodic curves did not exhibit the "normal" maxima associated with the iron hydroxides, iron (II) and iron (III) oxides as the anodic polarization progressed. There appears to be only one maximum on the curve. This suggests that at this age of hydration, the corrosion layer would not be that of iron (III) layer as in portland cement. The corrosion layer in high slag content blended cement appears to be that of either iron (II) or combination of iron (II) oxide and hydroxide. At this stage, the electrochemical data suggests that steel is in a reducing environment created by the BFS blended cement matrix if the slag content is greater than 60%. Similar anodic behaviours of steel in BFS blends were observed after 56 days of hydration as shown in Figure 5.

In general, the results obtained from these anodic polarization experiments indicate that the presence of slag can modified significantly the anodic behaviour of steel embedded in cement paste. The effect of slag was found to be dependent on the age of hydration and on the percentage of slag used. The anodic polarization work suggest that particularly at high loading of slag, the "conventional" protection mechanism from the formation of iron (III) oxides is not prevalent.

In slag blended cement it appears that the corrosion layer at the steel surface would be that of iron (II) compounds as a result of the reducing characteristics of the slag blended cement. An iron (II) layer would be more porous than an iron (III) layer in terms of resistance to further iron dissolution as noted in the literature [7]. In order to the iron (III) oxide layer to form in slag blended cement, additional polarization or oxygen availability is required. The polarization experiments in this work were performed in saturated condition, the solubility of oxygen is limited. In practice, it is suspected that with BFS blended concretes being drying out, it is possible that an iron (III) oxide layer may still be formed. It should be noted that although information regarding the possible states of the steel-paste interface can be obtained from anodic polarization curves, correlation between current values obtained from these experiments to corrosion rates of steel is not appropriate.

Figure 5
Potentiodynamic anodic polarization curves of steel embedded in OPC-BFS blends - 56 days

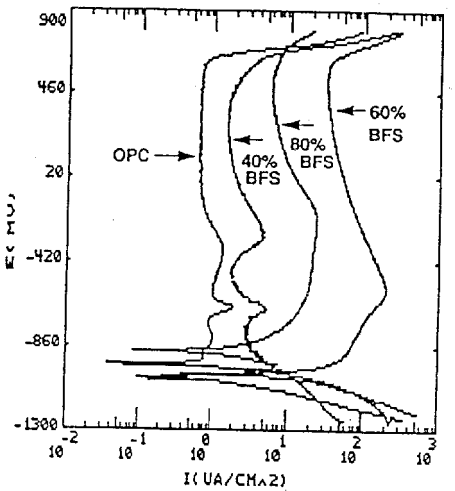

Figure 6
Fe-image of Steel/OPC-BFS interface

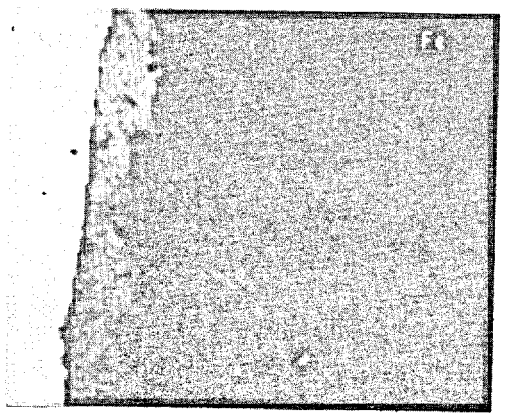

Figure 7
Fe-image of Steel/OPC interface

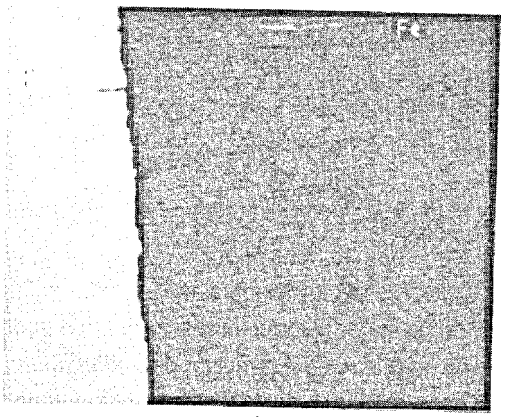

Examination using scanning microscopy [5] has indicated that there is a marked difference in the characteristics of the steel-paste interface in blended cement containing high BFS content and OPC as shown in Figure 6 and 7 respectively. In the case of BFS-OPC, the interface is characterized with an Fe-rich board diffuse band, whereas this band is absent in the case of OPC. Apart from the difference in the interface characteristics, previous work has also shown that during the first few days of hydration, the galvanic corrosion current [8] between steel embedded in BFS blended cement paste and graphite counter electrode was found to be higher initially than that in OPC as shown in Figure 8.

Figure 8
Galvanic corrosion current between steel embedded in cement paste and graphite electrode

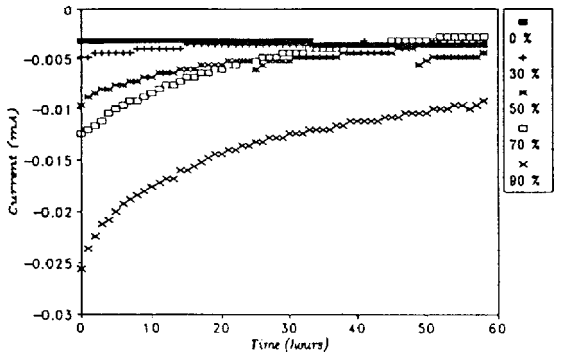

The results obtained from the examination of the steel-paste interface and galvanic corrosion current measurement support the observations gained from potentiodynamic anodic polarization study. The board Fe-rich band at the interface and the high early galvanic corrosion current suggest higher dissolution rate of Fe ion and a different type of corrosion layer at the steel-paste interface in BFS blends in comparison with that in OPC, particularly with high BFS loading and at early age. The ease of the early dissolution rate of Fe is consistent with the suggestion made previously regarding the formation of the iron (II) layer in BFS blends.

Some anodic polarization curves of steel embedded in cement pastes made with and cured in water containing 0.04M NaCl for 7 days are shown in Figure 9.

Figure 9
Potentiodynamic anodic polarization curves of steel embedded in OPC-BFS blends - made with water containing 0.04M NaCl - 7 days

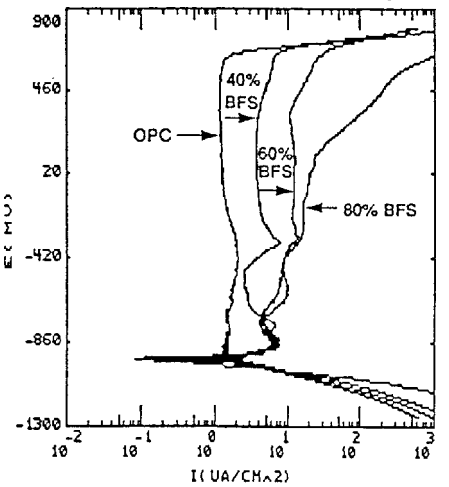

Figure 10
Potentiodynamic anodic polarization curves of steel embedded in OPC-BFS blends - 7 days initial moist curing - 6 months in 0.5 M NaCl solution

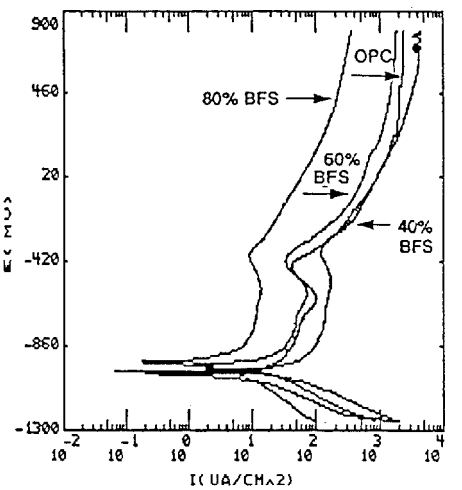

At this level of chloride ion contamination in the mixing water, it can be seen from figure 9 that as the percentage of BFS increases, the passive current increases and the passive range becomes more limited. The shape of the anodic polarization curve also suggests that pitting corrosion would be more prevalent in the paste containing high BFS loading. These results indicate that in the case of chloride contamination in the mixing water, the protective characteristics of BFS blended cement paste may not be as good as that of OPC in the early age of hydration.

Figure 10 shows the potentiodynamic anodic polarization curves of steel embedded in BFS blends immersed in 0.5 M NaCl solution after an initial moist curing period of 7 days. This figure shows that in the case of penetrating chloride, there is little difference in behaviour of OPC paste and paste containing BFS up to 60 percent after 6 months of immersion in salt solution. In all cases, no passive range was observed. Both pitting and general corrosion are expected. However, in the case of steel in 80% BFS, the curve tends to suggest that the tendency of steel dissolution would be much less than either in OPC or in BFS blends with 60% slag and lower. The resistance to polarization appears to be higher in the case of 80% BFS blend after 6 months of immersion. Possible explanations for this

behaviour would be either the better resistance to chloride penetration of BFS blended cement paste, particularly at high BFS content [9] or the limited oxygen availability in reducing environment. It has been noted in the literature [10] that in the regions of higher oxygen potential, chloride ions are released from the soluble complexes of iron (II) chloride to further attack the steel. The reducing characteristics of paste containing high BFS loading would lessen the availability of oxygen. Hence it appears that although the reducing characteristics of slag blended cement would not be conducive to the formation of the iron (III) oxide layer, in the case of chloride ingress, it effects can be beneficial as long as the concrete remains uncracked. It should be emphasised that only preliminary results are presented in this paper. Further work is needed to further examine the implication of the reducing characteristics of high slag blends and its variation at different water-to-binder ratio. It should also be noted that there is no reasonable reason at this stage to infer that the corrosion rate of steel in BFS blend would be any higher than that in equivalent OPC. This is due to the reasoning that the reducing characteristics of slag pore solution would limit the availability of oxygen which in turn can increase the degree of concentration polarization of the cathodic reaction or can lessen the effect of chloride attack resulting from the beakdown of complexes of iron (II) chloride.

Conclusions

The results presented in this paper indicate that the corrosion characteristics of steel embedded in slag blended cement paste are quite different than that in OPC paste. This is attributed to the reducing characteristics of the slag which tends to promote the formation of the iron (II) layer rather than iron (III) layer at the steel-paste interface, particularly at high loading of BFS. The mechanism of protection against steel corrosion provided by BFS blended cement would be different from that provided by OPC.

References

1 Glasser, F.P. and Sagoe-Crentsil, K.K., "Steel in Concrete: Part II Electron Microscopy Analysis", Mag. Concr. Res., 41, (149), 213-20, (1989).

2 Malhotra, V.M., "Properties of fresh and hardened concrete incorporating ground granulated blast furnace slag", Chap. 5 in Supplementary Cementing Materials for Concrete, SP 86-8E, Ed. V.M. Malhotra, CANMET, 291-336, (1987).

3 Douglas, E., "Blast furnace slag cement mortar and concrete: durability aspects", Chap. 6, ibid, 337-372, (1987).

4 Angus, M.J. and Glasser, F.P., "The chemical environment in cement matrices", Proc. Mat. Res. Soc., 50, 547-556, (1986).

5 Macphee, D.E. and Cao, H.T., "Theoretical description of the impact of blast furnace slag on steel passivation", (in preparation, 1991)

6 Cao, H.T., Bucea, L. and Sirivivatnanon, V., "Corrosion rate of steel embedded in cement paste", (submitted to Cement and Concrete Research, 1991).

7 Lorenz, W.J. and Heusler, K.E., "Anodic dissolution of iron group metals", Chap. 1 in Corrosion Mechanism, Ed. F. Mansfield, Marcel Dekker Inc., New York, (1987).

8 Macphee, D.E. and Harrison, R.S., "Galvanic current measurements to assess the corrosion characteristics of steel in BFS-OPC matrices", (in preparation, 1991).

9 Cook, D.J., Hinczak, I, Jedy, M. and Cao, H.T., "The behaviour of slag cement concretes in marine environment - chloride ion penetration" Proc. 3rd Int. Conf. on Fly Ash, Silica fume, Slag and Natural pozzolans in Concrete, Trondheim, Norway, June, 1989, 1467-1483, (1989).

10 Foley, R.T., "The role of chloride ion in iron corrosion", Corrosion - NACE, 26, 58-70, (1970).

SULPHATE ATTACK ON CONCRETE: PREDICTION OF THE AFt STABILITY FROM PHASE EQUILIBRIA

D Damidot and F P Glasser

Dept. of Chemistry, University of Aberdeen, Aberdeen, Scotland, U.K.

SUMMARY

The calculation of the phase diagram for the CaO-Al_2O_3-$CaSO_4$-H_2O system at 25°C, enables the equilibrium between ettringite and pore fluid to be predicted. Good agreement is obtained between calculated and observed results. Modifications to the ettringite stability domain when soluble ions such as sodium are introduced, can be calculated readily despite the chemical complexity of five components. However, results can be depicted in form of an easily understood two dimensional diagram. The results are used to predict the aqueous phase compositions able to attack cement by precipitating ettringite.

RESUME

La construction de diagramme de phase pour le système CaO-Al_2O_3-$CaSO_4$-H_2O à 25°C, permet de prédire le domaine d'équilibre entre l'ettringite et la solution contenue dans les pores de la pâte de ciment. Les modifications du domaine de stabilité de l'ettringite quand d'autres constituents comme Na_2O sont introduits, peuvent aussi être calculées malgrè la complexité du system contenant cinq composés. De plus, les résultats peuvent être présentés sous la forme de diagrammes en deux dimensions plus facilement assimilables. Les résultats sont utilisés afin de définir les compositions de solutions permettant la formation d'ettringite et ainsi pouvant attaquer le ciment par lixiviation.

INTRODUCTION

When cement concretes are exposed to sulphate-containing water, formation of ettringite, which belongs to the AF_t family, results in destructive expansion. This process is well-known from empirical observations and can be simulated in the laboratory. Nevertheless the conditions which lead to ettringite formation are not known precisely. The position of ettringite equilibrium surface in the $CaO-Al_2O_3-CaSO_4-H_2O$ system appears to be relatively well established through the studies of Jones (1) and D'Ans and Eick (2). Some additional data are available on the role of soluble species, notably sodium, which alters ettringite solubility relations in the $CaO-Al_2O_3-CaSO_4-H_2O$ system.

Despite these important studies, it is still not possible to treat certain important aspects of sulphate attack. Firstly, the complex phase diagram is often presented in graphical form and, in order to compress three or even four dimensions onto paper, the ability to undertake quantitative graphical calculations is lost. Secondly, ettringite formation occurs in response to a changing equilibrium, but the pathway taken to reach the new equilibrium is not always apparent from simplified graphical presentations of phase equilibria, nor is it easy to treat diffusional changes as occur, for example, when pore water commingles or interdiffuses with sulphate-bearing waters.

The purpose of this paper is to lay the foundations of a new and more flexible approach. The necessary equilibria are solved by computer, and the agreement between thermodynamic calculation and experiment compared. The computer-based solutions suggest a simpler graphical approach to sulphate attack.

EXPERIMENTAL

The background portion consists in making computer programs that calculate the equilibrium curves, their intersections (boundary curves and invariant points) and draw these curves in a 2 or 3-dimensional space. All these programs were written in Fortran and run on an IBM-PC compatible computer.

RESULTS AND DISCUSSION

Construction of the $CaO-Al_2O_3-CaSO_4-H_2O$ phase diagram

Details concerning the calculation and the drawing of the tri-dimensional phase diagram have been reported previously (3) and only the basic equations are reported in this paper. To simplify the calculations, speciation was not taken into account and four master species were used: Ca^{2+}, $Al(OH)_4^-$, SO_4^{2-} and OH^-; solubility products were defined using these master species. The values of the solubility products were obtained from experimental data at 25°C obtained at Aberdeen (4):

- Ettringite (Et.):

$$K_{sp1} = (Ca^{2+})^6.(Al(OH)_4^-)^2.(SO_4^{2-})^3.(OH^-)^4 = 2.80E\text{-}45$$

- Monosulfoaluminate (Mono.):

$$K_{sp2} = (Ca^{2+})^4.(Al(OH)_4^-)^2.(SO_4^{2-}).(OH^-)^4 = 3.71E\text{-}30$$

- Hydrogarnet (C_3AH_6):

$$K_{sp3} = (Ca^{2+})^3.(Al(OH)_4^-)^2.(OH^-)^4 = 2.91E\text{-}23$$

- Calcium hydroxide ($Ca(OH)_2$):

$$K_{sp4} = (Ca^{2+}).(OH^-)^2 = 8.90E\text{-}6$$

- Gibbsite (AH_3) (crystalline form):

$$K_{sp5} = (Al(OH)_4^-) / (OH^-) = 3.99E\text{-}2$$

- Gypsum ($CaSO_4.2H_2O$):

$$K_{sp6} = (Ca^{2+}).(SO_4^{2-}) = 3.72E\text{-}5$$

For isotherms other than 25°C, the method of calculation is identical, but numerical values of the solubility

products change. The Davies equation is used to calculate the activity coefficients. By solving the systems formed by one, two or three of these equations together with charge balance, it is possible to define respectively, the equilibrium surfaces, the boundary curves and the invariant points. The phase diagram was drawn from the boundary curves and the invariant points (Fig 1). This representation is easier to visualize than the complete diagram drawn from the surface of equilibrium of the hydrates (some parts of which are hidden). From this diagram, the ettringite surface of equilibrium is defined by four boundary curves: AH_3-Et., C_3AH_6-Et., CH-Et. and gypsum-Et. These curves intersect in four invariant points, defined previously by Jones (1): H2 (C_3AH_6-Et.-AH_3), E2 (AH_3-Et.-gypsum), F (CH-Et.-gypsum) and G (C_3AH_6-Et.-CH). The sequence of the invariant points, relative to the sulphate concentration, enables characteristic ranges of sulphate concentrations to be divided into seven segments, each of which indicates a change in hydrates in equilibrium with solution:

$0 < [SO_4^{2-}] < 0.015$ mM/l	: AH_3, C_3AH_6 and CH
$0.015 \leq [SO_4^{2-}] \leq 0.030$ mM/l	: AH_3, C_3AH_6, ettringite and CH
$0.030 < [SO_4^{2-}] < 11.4$ mM/l	: AH_3, ettringite and CH
$[SO_4^{2-}] = 11.4$ mM/l	: AH_3, ettringite, CH and gypsum
$11.4 < [SO_4^{2-}] \leq 15$ mM/l	: AH_3, ettringite and gypsum
$15 < [SO_4^{2-}] \leq 15.12$ mM/l	: AH_3 and gypsum
$15.12 < [SO_4^{2-}] \leq 15.2$ mM/l	: gypsum

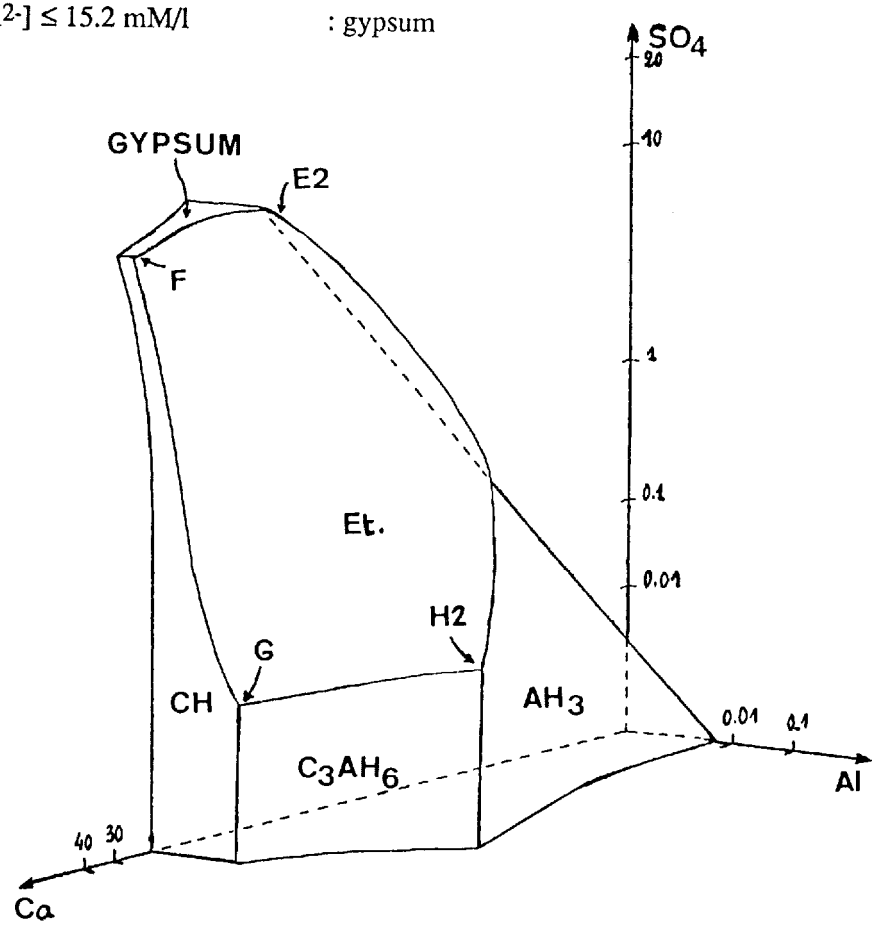

FIG. 1. $CaO-Al_2O_3-CaSO_4-H_2O$ system at 25°C. Total calcium, aluminium, sulphate concentrations in solution are used as axis (mM/l).

These results agree with the experimental data at higher concentrations as reported by Jones (1) and D'Ans and Eick (2). For example the compositions of solutions at the invariant points is generally in good accord (table 1) except for those at concentrations lower than 1mM/l. Also, crystalline gibbsite was considered during the calculation instead of a mixture of gibbsite and bayerite (more or less crystalline) reported by Jones. This helps

explain differences of aluminate concentration. However the same segmentation can be applied to divide the range of sulphate concentration into regimes although with different boundary concentrations.

In the above calculations, monosulphoaluminate never appears to be a stable phase at 25°C; monosulphoaluminate is always metastable with respect to C_3AH_6 or to ettringite. This is in agreement with the Jones and D'Ans and Eick works (1,2) and experiments carried out at Aberdeen to determine the solubility of monosulphoaluminate (4).

Ettringite is stable in segments 2 to 5 which represent the main part of the sulphate concentration range: 0.015 to 15.0 mM/l. However two domains exist (segment 1 and segments 6-7) in which ettringite is always metastable. If foreign ions soluble in the aqueous phase, such as sodium, are added to the system, the sulphate concentrations that delimit the previously defined segments change but the seven segments still exist (3). The ionic strength of the aqueous phase and the solution activity coefficients are changed, but solubility products remain constant.

Invariant Point	[Ca] mM/l	[Al] mM/l	[SO_4] mM/l
G (C)	21.25	0.01	0.015
G (E)	21.46	0.025	0.107
H2 (C)	5.04	0.386	0.03
H2 (E)	3.1	0.158	0.263
F (C)	31.3	0.0003	11.4
F (E)	32.8	0.027	12.2
E2 (C)	15.17	0.001	15
E2 (E)	15.13	0.09	14.82

Table 1. Composition of the aqueous phase at invariant points: (C) calculated and (E) experimental from D'Ans and Eick (2).

Prediction of the formation of ettringite for solutions of known compositions

Using the computer programmes, the stability of the ettringite in contact with a solution of known composition can be predicted from the sulphate concentration of the solution. If sulphate concentrations lie in one of the metastable domains (segment 1 and segments 6-7), it can be concluded that ettringite will not precipitate and if it already exists, it will dissolve. On the other hand, if sulphate concentrations lie in segments 2 to 5, it is more difficult to conclude: the composition of the solution has to be drawn on the phase diagram and compared with the ettringite equilibrium surface. As the phase diagram has three dimensions, it is not easy to visualise the aqueous phase composition relative to the ettringite equilibrium surface. To overcome this problem, the ettringite equilibrium surface and the composition of the solution can be projected on the calcium-aluminate, calcium-sulphate, aluminate-sulphate planes, to obtain three two-dimensional representations. If the composition of the solution is contained in all the projected surfaces, ettringite can precipitate or remain as a stable phase if it exists already. The idea of using two dimensional representations, enables us to define a simpler method to predict the ettringite stability. In the simplest case, where the sulphate concentration is known, the phase diagram can be restricted to the two dimensions of the calcium-aluminate plane, so that calculations of the phase diagram can be restricted to the unique sulphate concentration that represents a section of the tri dimensional phase diagram perpendicularly to the sulphate axis. This method is more rapid and easier to solve as the system has only two equations: the solubility product of the hydrate and the electrical balance.

To illustrate this method, the phase diagram has been calculated for three solutions similar in composition except increasing for sodium concentration (table 2).

Solution Number	[Ca] mM/l	[Al] mM/l	[SO_4] mM/l	[Na] mM/l
1	3.85	0.035	0.1	0
2	3.85	0.035	0.1	50
3	3.85	0.035	0.1	100

Table 2 Composition of the solutions studied

The first solution appears to be undersaturated with respect to ettringite (Fig. 2). Therefore ettringite will not precipitate or, if present, it will dissolve. In this case, AH_3, ettringite and CH are the stable phases. However in the two solutions containing sodium, C_3AH_6 is also a stable phase. Solution number 2 is slightly supersaturated with respect to ettringite (Fig. 3) while the third example is slightly supersaturated with respect to C_3AH_6 (Fig. 4). It can be predicted that ettringite will precipitate only in solution 2. No precipitation occurs with the first solution and C_3AH_6 precipitates with the third one. Thus the conclusions concerning the cement attack by ettringite formation in these three solutions are very different, even through the aqueous phase compositions are similar except for alkali contents. This simple example demonstrates that all the ions contained in the solution have to be taken into account to predict whether ettringite will form or not.

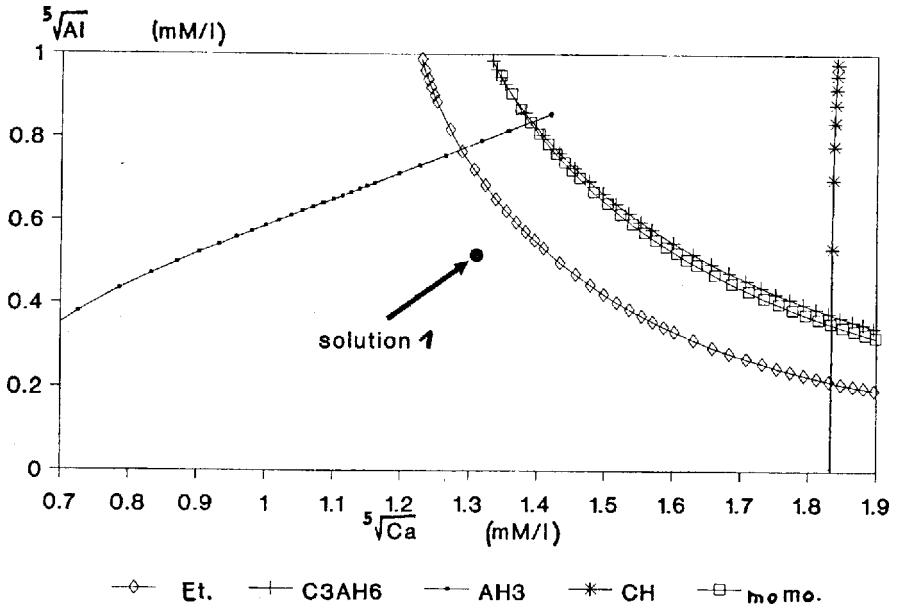

FIG. 2. Equilibrium curves of AH_3, C_3AH_6, ettringite (Et.), monosulphoaluminate (Mono.) and CH in the calcium-aluminate plane, at a sulphate concentration equal to 0.1mM/l and no sodium.

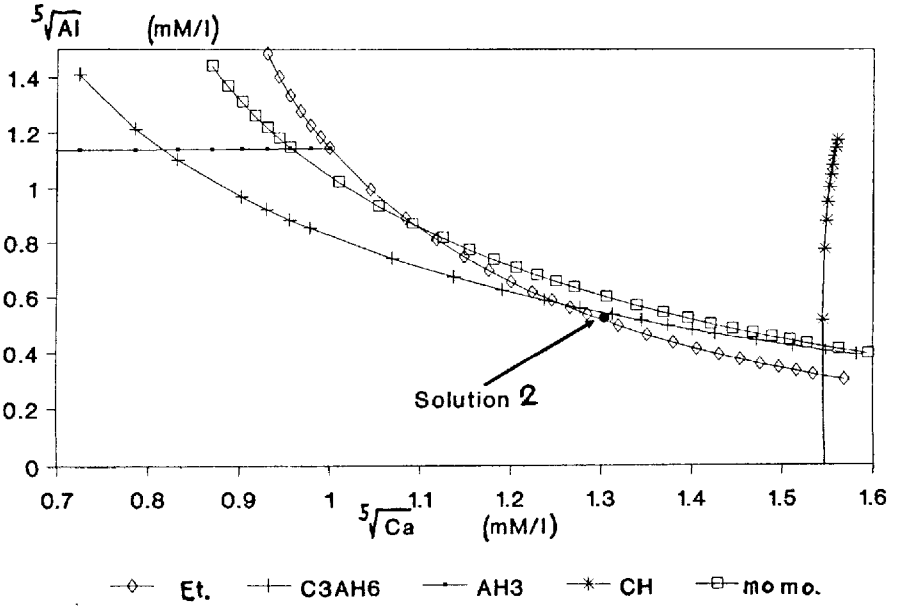

FIG. 3. Equilibrium curves of AH_3, C_3AH_6, ettringite (Et.), monosulphoaluminate (Mono.) and CH in the calcium-aluminate plane, at sulphate concentration equal to 0.1mM/l and 25mM/l Na_2O.

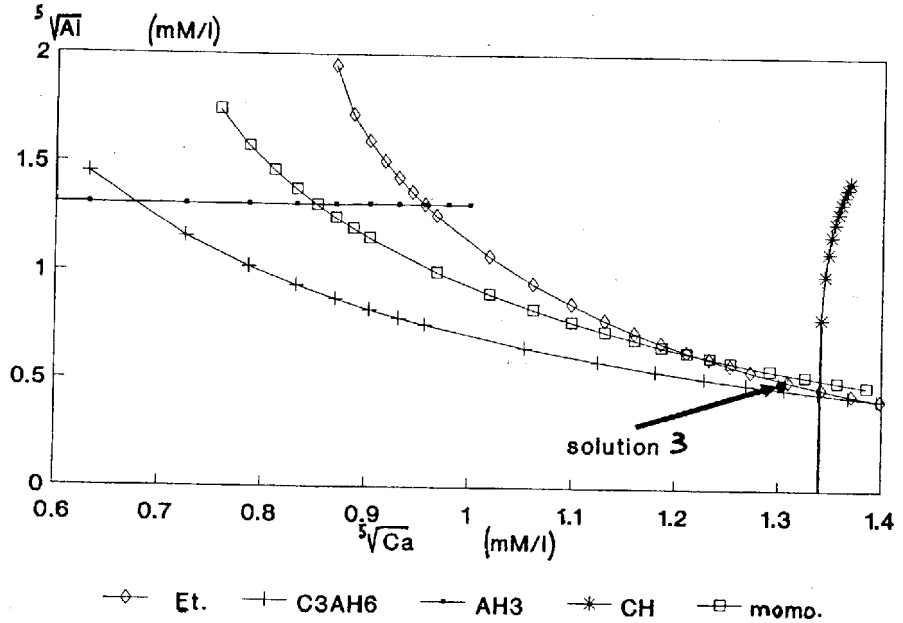

FIG. 4. Equilibrium curves of AH_3, C_3AH_6, ettringite (Et.), monosulphoaluminate (Mono.) and CH in the calcium-aluminate plane, at sulphate concentration equal to 0.1mM/l and 50mM/l Na_2O.

CONCLUSION

From calculations of phase equilibria in the system $CaO\text{-}Al_2O_3\text{-}CaSO_4\text{-}H_2O$, the ettringite surface of equilibrium can be defined. The ettringite surface of equilibrium is very sensitive to soluble ion concentration even at low levels. Computer simulations are fast, accurate and far more flexible than graphical solutions: examples are given in which the role of soluble alkali is calculated. This method will be developed further to predict cement attack due to the action of groundwater containing sulphates and to classify the more aggressive ones.

ACKNOWLEDGEMENTS

This work has been supported by the Commission of the European Communities, contract number FI2W-CT90-0035.

REFERENCES

1. Jones, F.E. "The quaternary system $CaO\text{-}Al_2O_3\text{-}CaSO_4\text{-}H_2O$ at 25°C: Equilibria with crystalline Al_2O_3. $3H_2O$, alumina gel and solid solutions", J. Phys. Chem.,1944,48,311-356
2. D'Ans, J. and Eick, H. "Das System $CaO\text{-}Al_2O_3\text{-}CaSO_4\text{-}H_2O$ bei 20°C", Zem. Kalk Gips,1953,6,302-311
3. Damidot, D. and Glasser, F.P. "Thermodynamic Investigation of the $CaO\text{-}Al_2O_3\text{-}CaSO_4\text{-}H_2O$ System at 25°C and the Influence of Na_2O", Cement and Concrete Research,to be published in 1992
4. Atkins, M., Macphee, D., Kindness, A. and Glasser, F.P. "Solubility properties of ternary and quaternary compounds in the $CaO\text{-}Al_2O_3\text{-}SO_3\text{-}H_2O$ system", Cement and Concrete Research,1991,21,991-998

EFFECT OF SEA WATER ON CALCIUM MONOSULFATE HYDRATE CONTAINING AMINO ACID

Naomitsu Tsuyuki , Satoshi Suzuki* and Junichi Kasai**

Department of Chemistry, College of Science and Technology, Nihon University, JAPAN
**Kawasaki Works, Kokan Mining Co., Ltd., JAPAN*
***Department of Industrial Chemistry, College of Industrial Technology, Nihon University, JAPAN*

SUMMARY

One of the factors contributing to lower durability of concrete structures is the effect of carbonation. Another factor is salt attack, i.e., corrosion of reinforcing bars by the infiltration of Cl^- resulting from erosion by sea water or use of sea sand. In this study, C_3A which reacts with Cl^- most actively was synthesized and allowed to react with $CaSO_4 \cdot 2H_2O$ to prepare monosulfate. The purpose of the study was to clarify the effect of Cl^- on cement minerals and to investigate a method for improving durability. Monosulfate was crushed after 7 days curing and dispersed in a Cl^--containing solution. The authors examined the behavior of the dispersed monosulfate, attempted to add an amino acid at the stage of preparing a hardening body to control its reaction and investigated the effect of the amino acid on hydration.

コンクリート構造物の耐久性低下の要因として、炭酸化の影響がある。また、海水の侵食や海砂の使用によって Cl^- が侵入することによる鉄筋の腐食がある。本研究では、Cl^- と最も反応活性な C_3A を合成し、$CaSO_4 \cdot 2H_2O$ と反応させることによってモノサルフェートを作成した。本研究の目的は、セメント鉱物に及ぼす Cl^- の影響や、これが耐久性に及ぼす影響について明らかにすることである。モノサルフェートを材令7日後に粉砕し、Cl^- を含む溶液 ($NaCl + MgCl_2$) 中に分散させた。そして分散させたモノサルフェートの挙動は液相中に溶解している種々のイオン濃度を測定することにより行った。また、その反応を支配するために硬化体作成時にアミノ酸を添加することを試み、水和に及ぼすアミノ酸の影響を検討した。

1. Introduction

One of the factors contributing to lower durability of concrete structures is the effect of carbonation. Another factor is salt attack, i.e., corrosion of reinforcing bars by the infiltration of Cl^- resulting from erosion by sea water or use of sea sand. This study was investigated in order to clarify the effect of Cl^- on cement minerals, and was attempted as a method of improving durability. The diffusion of Cl^- in hardened cement paste was reported by S. Goto and his coworkers[1].

After monosulfate was synthesized as a hardening body, it was crushed and dispersed in quasi sea water. The authors attempted to add amino acid at the stage of preparing a hardening body, and investigated the effect of amino acid on hydration.

2. Experiment

2.1 Synthesis of monosulfate

C_3A was synthesized, 20 wt.% of $CaSO_4 \cdot 2H_2O$ was hydrated and hydrated at W/S = 0.65. The hardening body obtained after 7 days curing was crushed to less than 200 mesh, the hydration was stopped by methanol and acetone. From the XRD data of this sample, it was found that unreacted C_3A still existed after 7 days of curing although monosulfate had been predominantly synthesized. Similarly, another hardening body was prepared using water solution of glycine as amino acid having the lowest molecular weight ($H_2N\text{-}CH_2\text{-}COOH$, molecular weight = 75.07). The concentration of amino acid was 5 wt.% or 10 wt.% based on C_3A.

2.2 Quasi sea water

Quasi sea water was prepared by dissolution of NaCl and $MgCl_2$ and adjusting them to the same concentrations as in sea water. It was a solution containing 27.4 g NaCl/l and 5.06 g $MgCl_2$/l.

2.3 Experiments

At first, the rate of heat liberation was determined to clarify the effect of amino acid on C_3A, and the electric conductivity of C_3A dispersed in solution of amino acid was also measured.

Next, 2 g of crushed monosulfate was dispersed in 100 ml of quasi sea water at 25°C, stirred for a definite time, and filtered the solution to obtain solid and liquid. In the solid phase, the product of hydration was identified by XRD, and its surface structure was observed by SEM. In addition, the adsorption behavior of amino acid was determined by FT-IR. The pH of the liquid phase was measured, and the concentrations of cations (Ca^{2+}, Al^{3+}, Na^+, Mg^{2+}) were determined by ICP and those of anions (Cl^-, SO_4^{2-}) by chromatography.

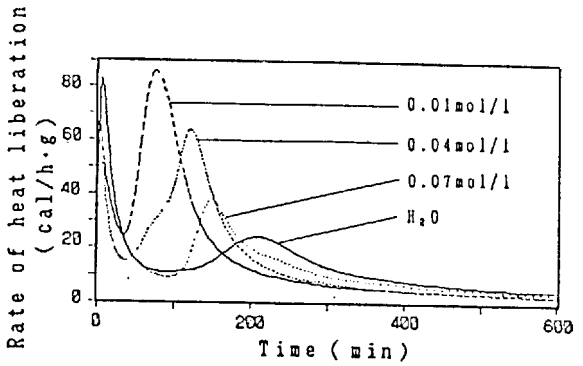

Fig. 1. Conduction calorimetric curves of C_3A and $CaSO_4 \cdot 2H_2O$ (20 wt.%) hydrated with amino acid (W/solid = 5).

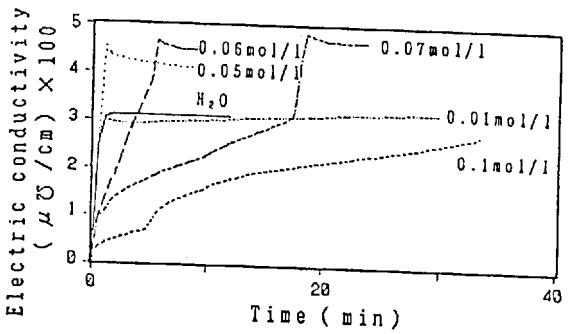

Fig. 2. Electric conductivities of amino acid dispersed C_3A (W/solid = 100).

3. Results

3.1 Rate of heat liberation of C_3A-amino acid system

The rate of heat liberation was determined to clarify the effect of amino acid on hydration of C_3A. When C_3A was mixed with 20 wt.% of $CaSO_4 \cdot 2H_2O$ and hydrated using of amino acid solution. The heat liberation characteristics shown in Fig. 1 were obtained.

3.2 Electric conductivity of C_3A-amino acid system

To clarify the elution behavior of ions when 1 g of C_3A was dispersed in each of 100 ml of solutions containing 0.01～0.10 mol/l of amino acid, and the electric conductivity was measured at 30-second intervals. The results are given in Fig. 2.

3.3 Conversion of monosulfate

When synthesized monosulfate ($C_3A \cdot CaSO_4 \cdot 12H_2O$) was dispersed in quasi sea water, the solid phase varied with hydration time. This process was clarified based on the XRD data. The XRD of monosulfate added with or without 5 wt.% amino acid are given in Fig. 3. In addition to AFm phase of $C_3A \cdot CaCl_2 \cdot 10H_2O$ (d=7.81), and $C_3A \cdot 0.5CaSO_4 \cdot 0.5CaCl_2 \cdot 10H_2O$ (d=8.32) was produced. The changes with time in XRD intensity of monosulfate added with or without 5 wt.% amino acid were plotted using the respective values of d. The results are given in Fig. 4. The SEM photograph of hydrate after 1 day curing is given in Fig. 5.

3.4 Elution of cations from monosulfate

When crushed monosulfate was dispersed in quasi sea water, the concentrations of eluting Ca^{2+} and $Al(OH)_4^-$, and pH were measured. The changes with standing time of these concentrations were determined in terms of CaO and Al_2O_3. The concentration of Na^+ in the liquid phase was calculated as Na_2O. The concentrations of cations in monosulfate added with or without 5 wt.% amino acid are shown in Fig. 6.

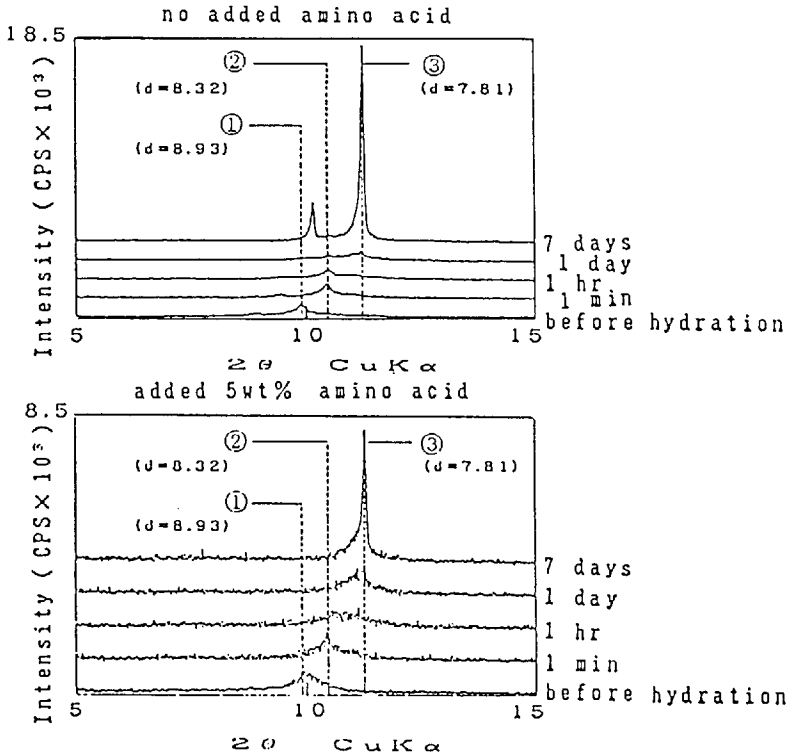

Fig. 3. XRD patterns of monosulfate in pseudo sea water.

①: $C_3A \cdot CaSO_4 \cdot 12H_2O$
②: $C_3A \cdot 0.5CaSO_4 \cdot 0.5CaCl_2 \cdot 10H_2O$
③: $C_3A \cdot CaCl_2 \cdot 10H_2O$

3.5 Concentrations of anions existing in quasi sea water

The Cl^- existing in quasi sea water reacted with monosulfate, permeated and reacted with the solid phase and was fixed there. The change with standing time of the concentration of Cl^- in quasi sea water was measured. The results are given in Fig. 7. Similarly, the change with standing time of the concentration of SO_4^{2-} eluting from monosulfate is shown in Fig. 8.

3.6 Adsorption of amino acid by C_3A

In the hydration process of C_3A, amino acid was adsorbed between the layers of hydrate. The adsorption behavior was measured by FT-IR. The difference spectrum between hydrate of C_3A added with or without amino acid (the quotient of their spectra) was determined. Also the difference of the spectrum between hydrate of C_3A and amino acid with or without the presence of $CaSO_4 \cdot 2H_2O$ was determined. The results are given in Fig. 9.

4. Discussion

(1) When C_3A is hydrated with amino acid, the rate of heat liberation increases quickly irrespective of the concentration of amino acid. As seen from Fig. 1, when C_3A is mixed with $CaSO_4 \cdot 2H_2O$, the secondary peak resulting from the formation of monosulfate appears quickly, indicating accelerated hydration. Such increase in the rate of heat liberation is a rare case because this rate usually decreases with the addition of organic admixtures[2]. The reason for this probably is that amino acid is having two functional groups of both -COOH and $-NH_2$.

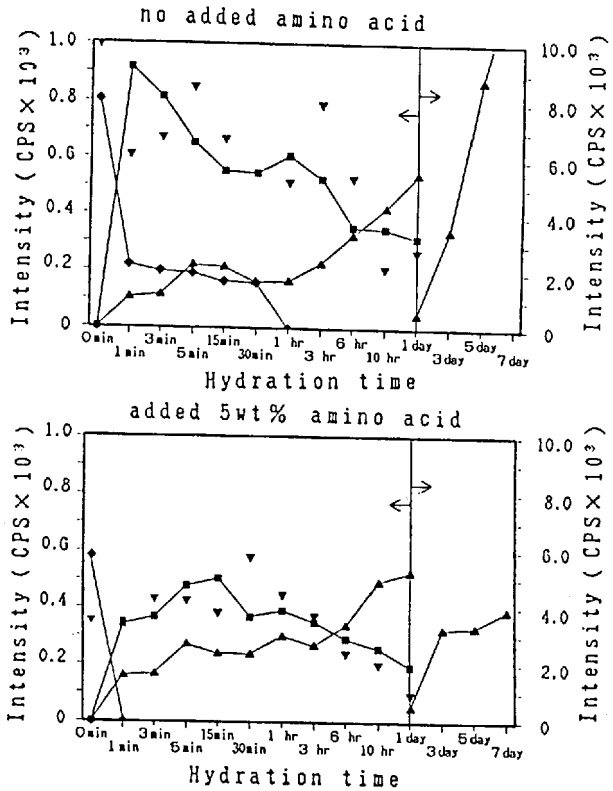

Fig. 4. Change of XRD intensities vs. hydrantion time.

◆: $C_3A \cdot CaSO_4 \cdot 12H_2O$

■: $C_3A \cdot 0.5CaSO_4 \cdot 0.5CaCl_2 \cdot 10H_2O$

▲: $C_3A \cdot CaCl_2 \cdot 10H_2O$

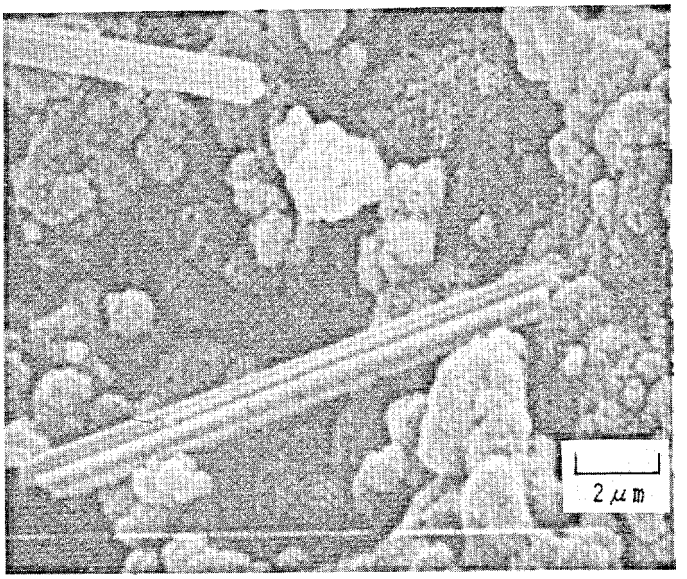

Fig. 5. SEM photograph of hydrate of C_3A-$CaSO_4 \cdot 2H_2O$-amino acid after 1 day curing.

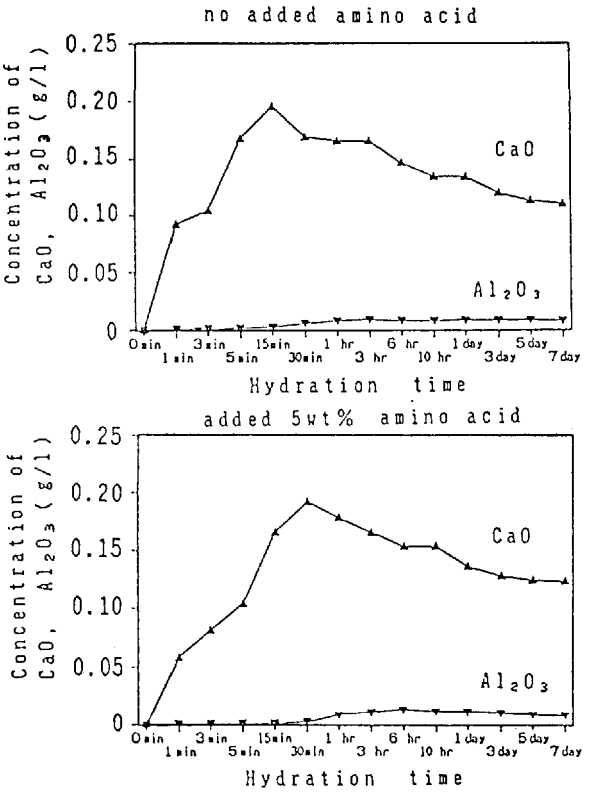

Fig. 6. Concentration of CaO, Al_2O_3 eluted from monosulfate in pseudo sea water vs. hydration time at 25°C.

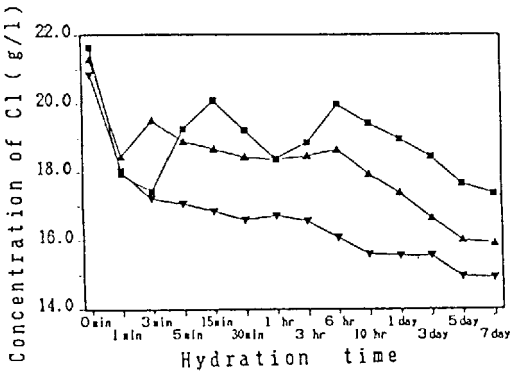

Fig. 7. Concentration of Cl^- in pseudo sea water by dispersion of monosulfate vs. hydration time at 25°C.
■ : no added amino acid
▲ : added 5 wt.% amino acid
▼ : added 10 wt.% amino acid

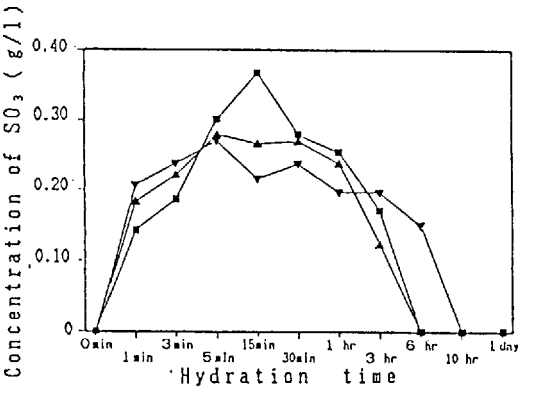

Fig. 8. Concentration of SO_4^{2-} eluted from monosulfate in pseudo sea water vs. hydration time at 25°C.
■ : no added amino acid
▲ : added 5 wt.% amino acid
▼ : added 10 wt.% amino acid

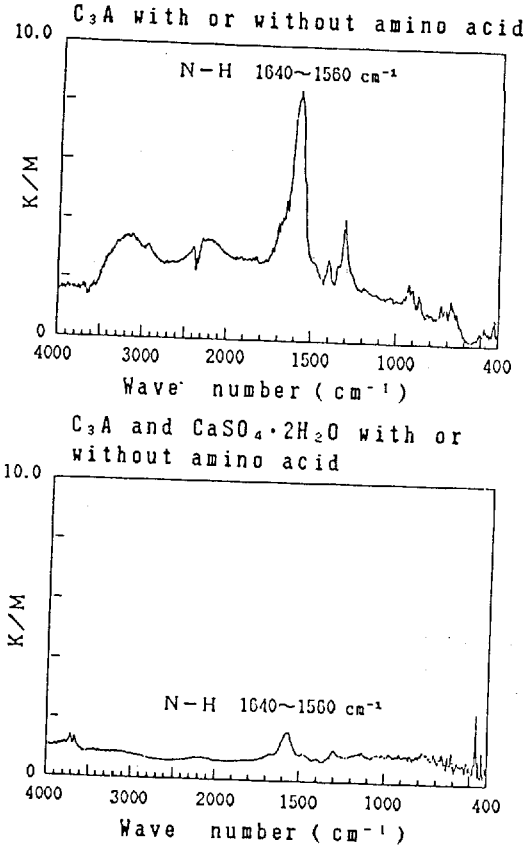

Fig. 9. FT-IR (spectrum of degree) of hydrates of C_3A with or without 5 wt.% amino acid.

(2) As seen from Fig. 2, the electric conductivity increases quickly when C_3A is dispersed in water, showing that Ca^{2+} and $Al(OH)_4^-$ elute vigorously from C_3A. The rate of increase in conductivity in the solution of amino acid lowers depending on the concentration of amino acid. This is because Ca^{2+} react with amino acid, gradually slowing down the movement of electric charges. However, when this reaction ends, these ion species elute more vigorously from C_3A, causing the conductivity to increase quickly.

(3) As seen from Fig. 3, monosulfate ($C_3A \cdot CaSO_4 \cdot 12H_2O$) is attacked by Cl^- in quasi sea water and converts to AFm phase of $C_3A \cdot CaCl_2 \cdot 10H_2O$ type. However, this process is not completed at a stretch, but through the formation of two-component solid solution ($C_3A \cdot 0.5CaSO_4 \cdot 0.5CaCl_2 \cdot 10H_2O$). This solid solution is produced immediately after dispersion in quasi sea water, but disappears with the lapse of time. The XRD data show that the solid solution is amorphous and then converts to $C_3A \cdot CaCl_2 \cdot 10H_2O$. Thus, the two-component solid solution becomes amorphous and is then restructured for conversion to $C_3A \cdot CaCl_2 \cdot 10H_2O$. When added with amino acid, monosulfate exhibits the same tendency. As seen from Fig. 4, monosulfate finally converts to AFm phase of $C_3A \cdot CaCl_2 \cdot 10H_2O$ type, but this conversion is suppressed by the presence of amino acid. The reason is that amino acid suppresses the reaction of monosulfate with Cl^-.

(4) As described in 2.1, the presence of unhydrated C_3A in synthesized monosulfate is observed by XRD. Accordingly, it is considered that the surface layer of grain is monosulfate, but the inner layer contains unhydrated C_3A. Elution of Ca^{2+} and $Al(OH)_4^-$ from such monosulfate of layered structure is at a much lower rate than is in the case of hydrating C_3A. Particularly $Al(OH)_4^-$ does not elute. Moreover, the rate of elution is low irrespective of the addition of amino acid. Therefore, it seems

that the elution behavior shown in Fig. 6 is not attributable to unhydrated C_3A, but is explained by elution of Ca^{2+} from monosulfate existing in the surface layer.

(5) As seen from Fig. 7, the change with standing time of the concentration of Cl^- in quasi sea water gradually diminishes irrespective of the addition of amino acid, but this diminution is greater with higher concentration of amino acid. This is because the higher concentration of amino acid allows more Cl^- in quasi sea water to be incorporated in the solid phase, resulting in lowering the concentration of Cl^-. Consequently, Cl^- reacts with monosulfate to convert it to two-component solid solution and hence to AFm phase of $C_3A \cdot CaCl_2 \cdot 10H_2O$ type. On the other hand, the concentration of SO_4^{2-} in quasi sea water in every case increases with the lapse of time and then decreases as shown in Fig. 8. As SO_4^{2-} does not exist at the start, its elution is from monosulfate. This decrease in concentration of SO_4^{2-} corresponds to that of Ca^{2+} shown in Fig 6. As a result, $CaSO_4 \cdot 2H_2O$ precipitates. This has been identified as a columnar crystal on the SEM photograph.

(6) In the hydration process of C_3A, by elution of Ca^{2+} and $Al(OH)_4^-$ to elute from the surface of grain and C_4AH_{13} is formed from solution reaction. Amino acid is adsorbed between the layers of this hydrate to form an interlayer compound[3]. Fig. 6 shows that the difference spectrum is largely affected by the presence of $CaSO_4 \cdot 2H_2O$. It has been found that the presence of $CaSO_4 \cdot 2H_2O$ in monosulfate suppresses the adsorption of amino acid, so the formation of monosulfate precedes the reaction of C_3A with amino acid.

5. Conclusions

The effect of Cl^- on monosulfate added with amino acid was studied.
(1) Monosulfate is attacked by Cl^- in quasi sea water and is converted to AFm phase of $C_3A \cdot CaCl_2 \cdot 10H_2O$ type through the formation of $C_3A \cdot 0.5CaSO_4 \cdot 0.5CaCl_2 \cdot 10H_2O$.
(2) In the case of monosulfate added with amino acid, the conversion of (1) is suppressed. This is because amino acid suppresses the reaction of monosulfate with Cl^-.
(3) Cl^- in quasi sea water is consumed by reaction with monosulfate. In the case of monosulfate added with amino acid, the higher concentration of amino acid allows more Cl^- to be incorporated in it.
(4) In quasi sea water, Ca^{2+} and SO_4^{2-} are caused by the attack of Cl^- to elute from monosulfate, but $Al(OH)_4^-$ virtually does not elute from it. As a result, $CaSO_4 \cdot 2H_2O$ precipitates.
(5) In the hydration process of C_3A, amino acid is adsorbed between the layers of hydrate to form an interlayer compound. However, this adsorption is suppressed when $CaSO_4 \cdot 2H_2O$ coexists.

Reference

1) S. Goto, M. Tsunetani, H. Yanagida and R. Kondo, Yogyo-Kyokai-Shi, 87, 126-33 (1979).
2) N. Tsuyuki, R. Oka, T. Miyakawa and J. Kasai, J. of the Ceramic Society of Japan, 98, 332-38 (1990).
3) J.F. Young, Cement and Concrete Research, 2, 415-33 (1972).

Acknowledgement
This study has been supported by the Fifth Bounty of the Cement Association of Japan. The authors heartily express their gratitude to the association.

THE BEHAVIOUR OF A LOW ENERGY CEMENT AND TWO BLENDED CEMENTS IN Na_2So_4 AND SEA WATER MEDIA

M T Blanco, S Garcia, S Giménez, A Palomo, F Puertas and T Vázquez

Instituto de Ciencias de la Construcción, "Eduardo Torroja" (C.S.I.C.), Madrid, SPAIN

ABSTRACT

Starting from an industrial cement obtained by milling a new low energy cement and gypsum, two cements containing 20% wt of fly ashes and 10% wt of limestone respectively, have been prepared. After their characterization, the behaviour of the three cements in Na_2SO_4 dissolution and sea water has been studied. The results have been compared with those obtained when the cements were immersed in distilled water. The method used for testing was the Kock-Steinneger one.

As a consequence of the study it can be said that the three cements keep a good behaviour in all the aggressive media although the strengths are lower (independently of the age of the specimens) in Na_2SO_4 and sea water than in distilled water.

Also, the composition of the hydrated pastes conserved in the aggressive liquids for different periods of time has been studied. The techniques used in this investigation were XRD and SEM. The evolution of the content of $Ca(OH)_2$, gypsum and $Mg(OH)_2$ of the pastes as well as the variations observes in the morphology of C-S-H gel along the time and in function of the aggressive medium, seem to keep a good correlation with the strengths evolution.

Finally it has been concluded that those cements prepared with the new low energy cement have such a composition that makes them to be resistant to the sulphate attack.

RESUMEN

Se han preparado dos cementos, a partir de un cemento industrial de bajo costo energético y 20% de cenizas volantes y 10% filler calizo. Se han caracterizado los 3 cementos y se ha estudiado su comportamiento en disolución de Na_2SO_4 al 4,4% y agua de mar. Los resultados se comparan con los obtenidos cuando los cementos se conservaron en agua destilada. El método usado para el ensayo fue el de Koch-Steinnerger.

De los resultados se deduce que los tres cementos se comportan satisfactoriamente en los dos medios agresivos, si bien las resistencias mecánicas de las probetas son menores (independientemente de la edad de las muestras), cuando se conservan en disolución de Na_2SO_4 o agua de mar, que cuando se conservan en agua destilada.

Así mismo, se ha estudiado la composición de las pastas de cemento conservadas durante diferentes periodos de tiempo en los medios descritos. Las técnicas utilizadas han sido XRD y SEM. Se observa una buena correlación entre la evolución de las resistencias y del contenido en $Ca(OH)_2$, yeso, $Mg(OH)_2$ de las pastas así como las variaciones observadas en la morfología del gel C-S-H.

Finalmente se concluye que los cementos preparados con el clinker de bajo costo energético son resistentes al ataque por sulfatos.

INTRODUCTION

An amount of about 1.000 tons of clinker, white Portland type, have been obtained through a new manufacturing process. Previous works on this subject have been described in several publications (1), (2), (3).

Summarily speaking, the product was obtained starting from gypsum, fluorspar, limestone, kaolin, and sand, by properly dosifying a raw mixture, the chemical analysis of which is shown on Table I. That Table also shows the mineralogic composition of the clinker industrially obtained. The material was obtained through a wet process, and the maximum clinkering temperature neared 1.350ºC.

It has been observed that the qualitative composition of this new clinker does not significantly differ from that of conventional clinker, but in the presence of fluorellestadite and sulfo-and fluoaluminates.

The technical balance-sheet of the industrial process tested with the new procedure gave, generally speaking, positive results. The mechanical characteristics and the physic-chemical behaviour of the cement manufactured by the joint grinding of the clinker with 3% of gypsum were advantageous as compared with the cement made by the usual method (3).

The economic balance-sheet of the process indicated, also in general terms, that a minimum saving of 8% was reached through the new process.

Giménez et al. have studied the behaviour shown by cement along time and face to aggressive solutions (4).

The new manufacturing process was initially applied to the making of white cement. This trial was considered as a pilot test, as a previous step to the application of the new process in a grey cement manufacturing line.

This justifies the durability studies conducted with the new cement, to which fly ashes (20%) and limestone (10%) were respectively added; the results from the study are presented here.

EXPERIMENTAL PROCEDURE

In the present study three different cements were used: CB (cement obtained by applying the production method for the low-energy clinker); CBC (80% of CB plus an addition of 20% fly ash); and CBCa (90% of CB plus 10% calcareous filler).

The durability of cements towards aggressive solutions was evaluated by the Kock-Steinegger method. The solutions used were: deionized water, Na_2SO_4 4.4% solution and artificial salt water ASTM D 1141-76.

The corresponding specimens were gradually extracted from the aggressive solutions, at pre-determined ages and tested at flexural and compression. The evolution of the mineralogic composition with time was studied by X-Ray diffraction, IR spectroscopy and SEM, as used and described in (4).

TABLE I

Raw Mix Chemical and Clinker Mineralogic Analysis

RAW MIX (% wt)	SiO_2 14.7	Al_2O_3 1.5	Fe_2O_3 0.2	CaO 45.4	MgO 0.4	SO_3 2.3	CaF_2 0.8	I.L. 34.5
CLINKER (% wt)	C_3S 69.5	C_2S 6.8	FL* 14.0	CaO 3.0	C_3A 3.0	C_4A_3S 2.0	CAF** 0.5	H*** 0.7

* Fluorellestadite
** $C_{11}A_7.CaF_2$
*** $CaSO_4.1/2H_2O$

RESULTS AND DISCUSSION

New white cement (CB)

Table II shows the flexural and compressive strengths disclosed by CB cement mortars submerged in the three media described above until 545 days.

TABLE II

Flexural and Compressive Strengths of CB Mortars in Agressive Media

AGES days	WATER		4.4% Na_2SO_4 SOL.		SEA WATER	
	FLEX. MPA	COMPR. MPA	FLEX. MPA	COMPR. MPA	FLEX. MPA	COMPR. MPA
1	5.60	37.24	6.25	39.99	5.73	45.99
7	5.58	32.36	6.06	33.25	5.19	26.99
28	6.17	49.35	6.61	38.61	5.44	39.50
56	6.47	52.92	5.49	41.25	4.56	44.11
90	6.34	63.81	5.42	52.67	5.04	48.23
180	6.57	58.23	5.27	40.96	4.61	53.13
270	6.31	63.31	5.33	30.37	4.57	48.33
365	5.95	54.31	4.43	31.28	4.61	53.41
545	6.32	61.27	4.65	32.70	4.53	55.25

In order to estimate the evolution in time crystalline compounds in the cement paste of the new procedure (CB), when mortars of the aforementioned cement are submerged in different solutions, the intensity of the reflections described in (4) was measured and the value was divided into the fluorellesteadite reflection value ($2\Theta = 25.64$). It must be pointed out that both I_{Ett}/I_{FL} and $I_{calcite}/I_{FL}$ quotients remain constant both in time and in all media.

In Figure 1 the values of the following quotients: ICH/I_{FL}, I_{gypsum}/I_{FL} and $I_{Mg(OH)2}/I_{FL}$ are shown versus time in the different media.

The use of a fluorellesteadite reflection as internal standard is justified by the fact that this compound is a constituent of the clinker and because of its high insolubility, because it does not suffer any modification with time.

From Figure 1 it is important to emphasize:

a) The content in $Ca(OH)_2$ is at 7 days similar in CB cement pastes in contact with the three media, although those from Na_2SO_4 solution and sea water are slightly lower. During the treatment time, the content in $Ca(OH)_2$ decreases in the pastes exposed to aggressive media compared to those preserved in water.

b) In the case of mortars obtained using the new cement and preserved in a Na_2SO_4 solution it should be observed that simultaneously to the decrease in the quantity of $Ca(OH)_2$ there is also an important increase of the content of gypsum which is the major crystalline phase already at the 180 day stage.

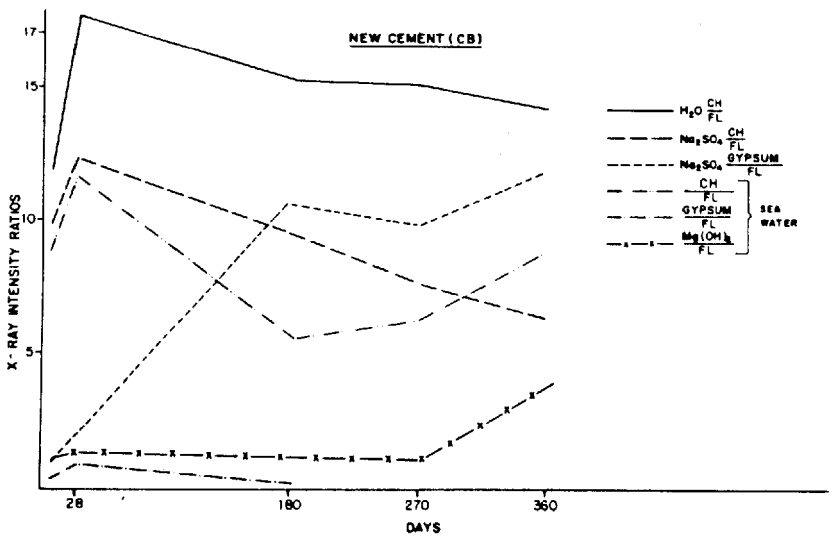

FIGURE 1

The following conclusions could be drawn from the results described above:

a) Mortars obtained from CB cement and preserved in water reach between 28 and 56 days similar endurance to the one obtained at 545 days.

b) CB cement mortars submerged in Na_2SO_4 solution show up to the 28 day stage greater endurance than those mortars kept under H_2O, due to gypsum formation (at the expense of $Ca(OH)_2$) that makes the system become more dense.

The massive gypsum formation with detriment to $Ca(OH)_2$, because of its expansive nature, brings along an endurance decrease in a long-term basis.

In addition it seems probable that the C-S-H gel evolution process, in reference to its morphology and qualities, could become altered because of the existence of SO_4^{2-} and Na^+ ions and that the endurance decrease could not only be due to the gypsum expansive formation process (4).

c) The endurance decrease of CB mortars preserved in sea water in relation to those preserved in water could be partly due to $Mg(OH)_2$ formation at the expense of $Ca(OH)_2$ which would be dissolved (the $Mg(OH)_2$ molar volume is ≈ 2/3 lower than the $Ca(OH)_2$ one).

It seems that in some way the C-S-H gel microstructure is being modified by the aggressive (4).

New white cement with 20% fly ashes (CBC)

Table III shows the flexural and compressive strengths displayed at different ages by the mortar specimens made with CBC cement and submerged in the three media mentioned before.

TABLE III

Flexural and Compressive Strengths of CBC Mortars in Agressive Media

AGES days	WATER		4.4% Na_2SO_4 SOL.		SEA WATER	
	FLEX. MPA	COMPR. MPA	FLEX. MPA	COMPR. MPA	FLEX. MPA	COMPR. MPA
1	5.01	38.17	4.95	27.04	5.15	28.3
7	4.81	33.87	5.31	28.27	4.66	22.24
28	5.72	32.80	5.54	35.54	4.90	28.44
56	6.97	54.79	5.32	47.16	6.05	34.73
90	7.02	48.47	7.07	50.67	5.54	37.19
180	7.49	62.06	5.80	49.71	6.34	48.28
270	8.29	66.83	6.02	52.26	5.29	35.36
365	7.69	71.88	5.63	43.97	6.05	44.59
545	8.33	70.58	4.92	49.14	5.68	-

The mineralogic constituents of the CBC cement pastes are/naturally the same as those of the CB standard cement, whichever the conservation media used. However, a clear variation in the proportions and evolution of the phases is found.

Figure 2 shows the values of the ratios:

$$\frac{I_{Ca(OH)_2}}{I_{Fe11}} \qquad \frac{I_{CaSO_4 \cdot 2H_2O}}{I_{Fe11}} \qquad \frac{I_{Mg(OH)_2}}{I_{Fe11}}$$

versus time in the different media.

It may be observed in that Figure that the amount of $Ca(OH)_2$ decreases in water-cured specimens with respect to the contents in the samples without any addition (Fig. 1), due to the pozzolanic reaction of ashes with $Ca(OH)_2$.

The increase in the CB cement strengths with respect to those shown by CB cement is due to the mentioned pozzuolanic reaction with the production of CSH gel, a product which densifies the system.

The evolution with time of the $Ca(OH)_2$ contents in the specimens kept in Na_2SO_4 solution is similar to that of the specimens kept in water.

There is a gradual increase of the gypsum contents in the specimens submerged in Na_2SO_4 solution, but to a lesser degree than those corresponding to the CB cement. This is due to the lesser amount of $Ca(OH)_2$ available and to the higher density of the system which hinders access to sulfate ions.

In these specimens there are two concurring reactions: the pozzuolanic reaction of the fly ashes and the formation of gypsum by reaction of sulfates with $Ca(OH)_2$.

In spite of the fact that the pozzuolanic reaction takes place in these mortars, their long-term strengths did not augment as could be expected, as it happens in specimens kept in water. This is due to the expansive process of the formation of gypsum. Additionally, studies conducted through SEM have disclosed that the presence of sulfate ions does alter to a certain degree the morphology and properties of the CSH gel, by delaying and even partially inhibiting the densifying process experienced by the CSH with time.

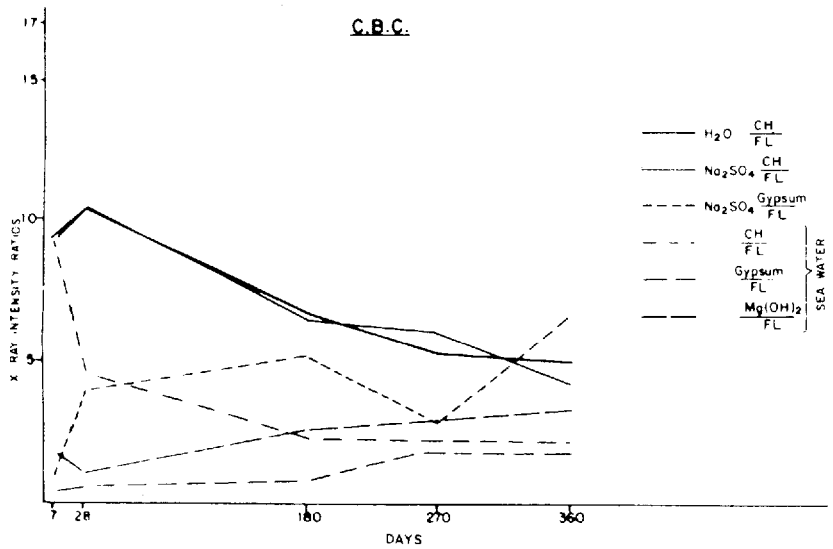

FIGURE 2

Finally, a gradual and more intense decrease of the $Ca(OH)_2$ contents is observed in the samples kept in sea water, as well as an increasing augmentation in the gypsum and brucite contents along time.

The strength behaviour of CBC cement mortars kept in sea water is quite similar to that shown by the same mortars conserved in Na_2SO_4 solution.

The microstructural explanation of this behaviour could be found in the following reactions:

$$Ca(OH)_2 + MgSO_4 \longrightarrow CaSO_4.2H_2O + Mg(OH)_2$$

$$MgSO_4 + \text{C-S-H gel} + H_2O \longrightarrow CaSO_4.2H_2O + Mg(OH)_2 + SiO_2$$

The former reaction implies an expansive process and the latter a destruction of the CSH gel.

New white cement with 10% limestone (CBCa)

Table IV shows flexural and compressive strengths of mortar specimens made with CBCa cement and submerged in the different media described and at different ages.

The nature and evolution of the mineralogic constituents is very similar to those already described for CB cement without any admixture.

The $Ca(OH)_2$ contents decreases significantly and progressively in the mortars kept in sea-water and Na_2SO_4 solution. These mortars do already contain gypsum at one day's age, the proportion of which increases with time.

Specimens kept in sea water show a small gypsum contents (but in this case at up to 28 days' age) and increasing $Mg(OH)_2$ contents.Therefore, the degradation mechanisms of the material seem to be the same in CBCa cement mortars as with CB cement, what would justify the similar mechanical behaviour, at least in the case where the aggressive medium used is sea water

TABLE IV

Flexural and Compressive Strengths of CBCa mortars in Agressive Media/

AGES days	WATER		4.4% Na_2SO_4 SOL.		SEA WATER	
	FLEX. MPA	COMPR. MPA	FLEX. MPA	COMPR. MPA	FLEX. MPA	COMPR. MPA
1	4.93	34.82	5.98	41.67	4.86	32.53
7	4.88	34.63	5.95	31.81	4.26	18.48
28	5.97	37.48	4.56	36.41	4.69	26.11
56	6.22	47.68	3.74	37.53	4.34	36.60
90	5.74	46.55	4.69	36.79	4.22	40.38
180	5.57	47.14	4.23	30.76	4.22	45.03
270	6.35	49.95	4.09	30.29	3.90	29.48
365	5.95	54.53	3.47	31.52	4.28	45.96
545	6.29	57.06	3.40	31.09	4.34	-

This behaviour seems to be somewhat different when the aggressive medium is Na_2SO_4 solution, since strength decreases appear of about 20% with respect to the strengths shown by CB cement mortar specimens. This diminution cannot be due to a chemical interaction of the limestone added to the system. However, such admixture modifies the microstructure of the paste, since its grains can behave like small inert aggregates, so that $Ca(OH)_2$ crystals would grow around them, which would facilitate the access of the sulfate ions and the expansive reaction of the formation of gypsum.

As a general conclusion, it may be stated that the new cement produced, as well as its derivatives, display a satisfactory behaviour face to the aggressive media studied.

ACKNOWLEDGEMENT

The authors wish to thank to the Dirección General de Investigación Científica y Técnica for the sponsorship of the project PB87-0293.

REFERENCES

1.- M.T. Blanco-Varela, T. Vázquez and A. Palomo. Spanish Patent nº 542691 (1985)

2.- M.T. Blanco-Varela, T. Vázquez and A. Palomo. Cem. Concr. Res. Vol. 16 pp. 97-104 (1986)

3.- S. Giménez, M.T. Blanco-Varela, A. Palomo and F. Puertas. Zement Kalk Gips 1 pp. 12-15 (1991)

4.- S. Giménez, S. García, M.T. Blanco, A. Palomo: The behaviour of a low cement energy cement in Na_2SO_4 and sea water media. Cement and Concrete Research (in press).

MECHANISM OF DETERIORATION OF GYPSUM-CEMENT BINDER MATERIALS

C Ostrowski

Cracow University of Technology, Kraków, POLAND

SUMMARY

The aim of carried out investigations was to determine the mechanism of deterioration of gypsum-cement binder materials. In order to confirm the hypothesis on the complex mechanism of deterioration of these binder materials, which was based on the expansive reactions of the formation of ettringite and thaumasite and its solid solutions with ettringite, some complex investigations of changes of the phase composition of the binder materials were carried out. The results of these investigations showed that the ettringite content increased mostly till 28 days of hydration and till 1 year the increase was slight. Whereas the expansion of the binder material in contact with water occurred chiefly between the 3rd and 12th months. As a result of the investigations carried out, it was proved that in the later period the crystallization of thaumasite and its solid solutions with ettringite occurred. The formation of thaumasite was also shown not only from the ettringite phase but also form the silicate phases.

RÉSUMÉ

On présente dans cet article une étude experimentale du mechanisme de deterioration de la metière composée du ciment et du plâtre. La deterioration est due à des reactions de formation de l'ettringite et de la thaumasite et leur solution solide. On observe une nette augmentation de teneur de l'ettringite jusqu'à 28-eme jour de la hydratation, après cette période l'augmentation est faible. Une expansion de la matière en contact avec l'eau se produit surtout 3-eme et 12-ème mois. Les resultats montrent que la cristalisation de la thaumasite de sa solution solide avec l'ettringite se présente dans une étape finale. On observe que la thaumasite ne se forme pas seulement de la phase de l'ettringite mais aussi des phases de silicates.

1. Introduction.

Chemical and mineral composition of Portland cement has been known for over 100 years and the composition of hemihydrated gypsum for even longer. Naverthelees, an energy-sparing technology of producing durable gypsum-cement materials for a variety of purposes associated with construction engineering has not yet been developed. Differences in opinions on the mechanism of the deterioration of the above materials lie in disagreements over opinions as to the changes which take place mainly in the aluminate phases. The hydration processes of C_3A, which take place in the gypsum-cement material are characterized by the crystallization of ettringite and thaumasite associated with expansion. In extreme cases this can prevent the formation of a stable solid structure.

2. Experimental procedures.

2.1. Formation of expansive phases in swelling gypsum-cement materials.

The aim of the work was to study the conditions under which expansive reactions occur and to find efficient methods of controlling and limiting the extent of those reactions. In order to verify a hypothesis concerning the mechanism of deterioration of gypsum-cement materials assumping of the expansive formation of ettringite and thaumasite and their solid solutions, a comprehensive study of the changes in the phase composition and physical properties (mechanical strength, linear changes) of gypsum-cement materials has been carried out.

2.1.1. Materials.

Chemical composition of the Portland clinker "Wiek" (%wt):

loss on ignition	SiO_2	Al_2O_3	Fe_2O_3	CaO	MgO	SO_3	Na_2O	K_2O	CaO free
0,4	22,3	4,0	3,4	67,7	0,6	0,3	0,12	0,38	2,18

Mineral composition determined microscopically technique (%wt):

C_3S	β-C_2S	C_3A	C_4AF
72,5	8,8	7,7	10,6

Portland clinker "Wiek" is an alite clinker with a low belite content. The alite crystallites vary in size from 1 to 90 μm and the belite ones from 20 to 60 μm. The spaces between calcium silicate crystals are filled by ferro-aluminates. Free calcium oxide particles are distributed irregularly and their sizes are up to 15 - 40 μm.

Chemical composition of builders gypsum (%wt):

loss on ignition	SiO_2	Al_2O_3	Fe_2O_3	CaO	MgO	SO_3
8,10	4,10	1,26	0,56	36,8	0,07	48,30

Identified by X-ray analysis: β-$CaSO_4 \cdot 0{,}5H_2O$, $CaSO_4 \cdot 2H_2O$, $CaSO_4$ II, $CaCO_3$ with some quartz, kaolinite and muskovite.

Chemical composition of fly ash (%wt):

loss on ignition	SiO_2	Al_2O_3	Fe_2O_3	CaO	MgO	SO_3	Na_2O	K_2O	TiO_2
0,8	47,8	23,5	8,5	3,8	4,4	0,3	0,8	2,4	0,7

68% of the particles were less than 60 μm in diametr. The pozzolanic activity, determined according to ASTM-C-379-56T was 16,2%

2.1.2. Preparation of batches of gypsum-cement binder materials and experimental results.

Gypsum-cement pseudo-mixtures were prepared from pulverized clinker with the addition of 20%wt of fly ash from the "Rybnik" thermal-electric power

plant with a specific surface (Blaine) area of 450m^2/kg. 5%wt of gypsum was also added. The composition of the mixtures is given in Table 1. Three series of bar-shaped samples of with dimensions 4x4x16 cm, were prepared from homogenized gypsum-cement mixtures. One series of samples was kept for one year in air, the second underwater, and the third one under "mixed" conditions (7 days in water, 7 days in air), respectively. The water, in which the samples were kept was changed every week because of the high concentration of $Ca(OH)_2$ and $CaSO_4$ which promoted the auto-corrosion of the samples. Changes in the compressive strength of the samples with time are illustrated in Fig. 1. Linear changes of the gypsum-cement pastes were measured using theGraf-Kaufmann apparatus. The results are shown in Fig. 2.

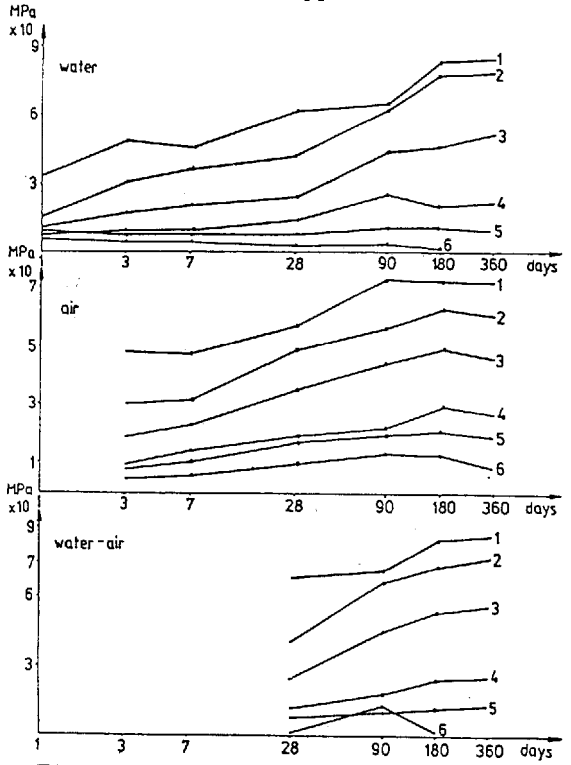

Fig. 1.
Changes of the Compressive Strength of the Samples of Hardened Gypsum-Cement.

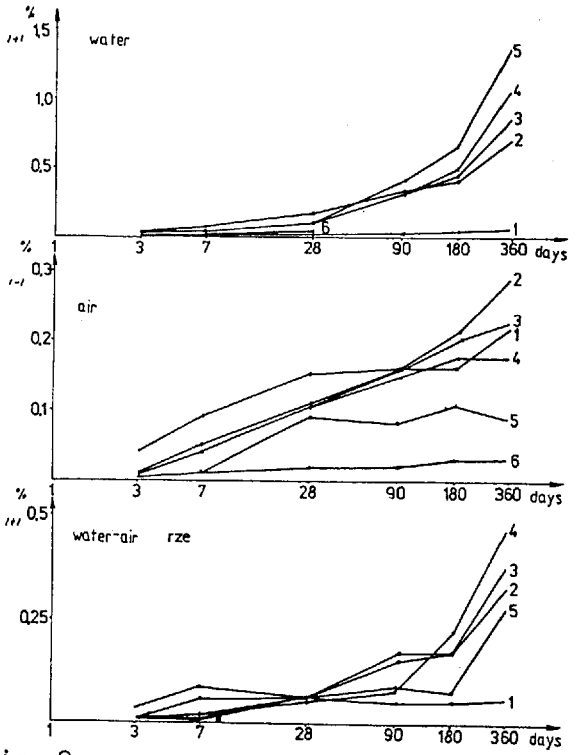

Fig. 2.
Linear Changes of the Samples of Hardened Gypsum-Cement Pastes.

1. 100% cement 2. 80% cement + 20% hemihydrate 3. 60% cement + 40% hemihydrate
4. 40% cement + 60% hemihydrate 5. 20% cement + 80% hemihydrate 6. 100% hemihydrate

Table 1. The composition of mixture gypsum hemihydrate - cement.

No	Cement %wt	Gypsum hemihydrate %wt	Addition of retarder %wt	Ratios water / cement+hemihydrate	Standard consistency cm
1.	100	0	1,5	23,5	18
2.	80	20	1,5	34,5	18
3.	60	40	1,5	34,9	18
4.	40	60	1,5	41,8	18
5.	20	80	1,5	44,6	18
6.	0	100	1,5	50,0	18

The ettringite content in hardened pastes was determined using the method of Uchikawa and Uchida [4]. The results are given in Table 2

Table 2. The content of ettringite in the hardened gypsum-cement mortars.

Cementitious content in mixture %wt	$C_3A * 3\ CaSO_4 * 32\ H_2O$ %wt			
	1	28	180	360 days
100	3,84	3,20	2,74	2,92
80	3,84	8,05	6,57	8,10
60	2,81	6,66	7,90	7,50
40	1,82	3,19	5,66	6,11
20	1,71	3,20	2,47	3,60

The results of the X-ray analysis of samples of the hardened gypsum-cement binders are illustrated in Fig. 3. The X-ray diffraction patterns for samples of the anhydrous mixed binders contain lines characteristic of alite, belite, braunmillerite, hemihydrate and gypsum and also of admixtures of kaolinite, muscovite, anhydrite, calcite. Marked changes in the phase composition were observed even after 1 day of hydration. Hemihydrated gypsum is converted into gypsum during the first few hours of contact with the aqueous phase. The intensity of alite peaks decreased with time (d_{hkl} = 0,176 nm) and distinct peaks of CH (d_{hkl} = 0,49 nm) and ettringite (d_{hkil} = 0,972 nm) appeared. The CH content in the samples reached a maximum after 28 days of hydration. In the hardened pastes containing 20%wt of cement, CH disappears after 180 days as a result of reactions with the mineral constituents of the fly ash, rich in a pseudo crystalline silica and active aluminium oxide. In cement - rich mixtures the saturation of the liquid phase by Ca^{+} and SO_4^{2-} ions creates favourable conditions for the crystallization of ettringite. The

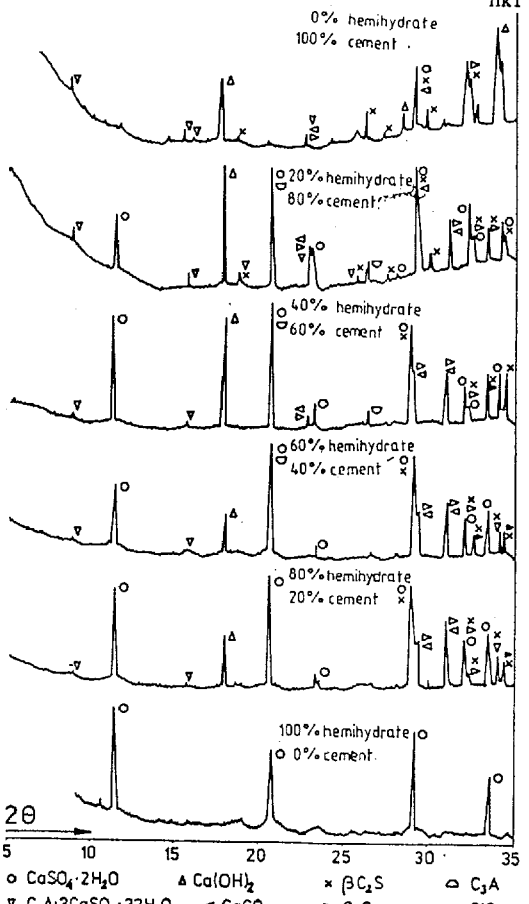

Fig. 3. X-ray Diffraction Patterns for Samples of Hardened Gypsum-Cement Pastes after 1 Days of the Hydration.

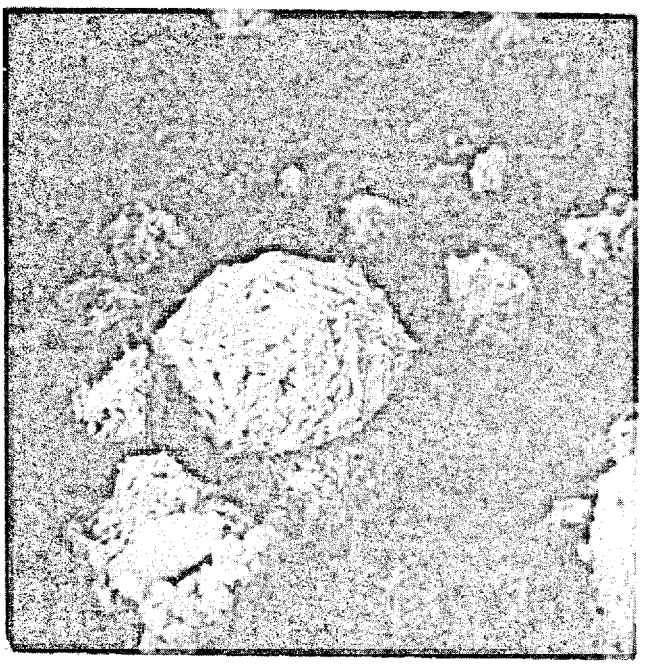

Fig. 4. The SEM Photographs of Thaumasite. Magnification 2000 X

concentration of ettringite reached a maximum after 28 days of hydration. A lower rate of crystallization of ettringite, observed in hardened binders rich in gypsum, is caused by change in the ionic composition of the liquid phase, i. e. a decrease in the Ca^{2+} ion concentration. The maximum ettringite concentration is reached after 180 days of hydration. After 180 days the concentration of ettringite in the samples decreases as a result of secondary reactions with atmospheric carbon dioxide. Braunmillerite has been identified in samples of cement and gypsum-cement pastes after 1, 28, 180 days of hardering. This phase is not observed in samples prepared on the basis of cements from other cement plants in Poland. Because of this fact cement used for obtaining gypsum-cement binders should be tested for the activity of the ferrite phase. There is no possibility of following the changes in the intensity of the C_3A peaks in the X-ray diffraction pattern because they coincide with those for gypsum. Thaumasite and calcite are present in paste samples containing 20%wt of cement after 180 days of hydration under combined conditions, which is illustrated in Fig. 4. A large number of agglomerations of thaumasite and calcite crystals can be seen in paste samples after 1 year of conditioning under combined conditions. The formation of thaumasite is accompanied by the presence of micro fractures in the gypsum-cement materials.

2.2. Prevention of the crystallization of expansive phases.

2.2.1. Determination of the conditions for the formation of thaumasite.

Thaumasite has not yet been synthesized at room temperature. According by to Leifeld [5], thaumasite is stable only below 12^0C but according to Bensted [6] up to 110^0C. After partial dehydration ettringite and thaumasite can be regenerated [7]. The formation of thaumasite in concretes and in contact layers between concrete and gypsum plaster indicates, however, that this compound could crystallizate at room temperature given sufficient time. It was assumed that thaumasite could be formed from ettringite as a result of isomorphic heterovalency substitution of Al (r= 0,051 nm) by Si (r= 0,042 nm). Thaumasite could also be formed from silicate phases in the presence of gypsum, calcite and CO_2(g). To start with mono mineral substances like calcium aluminates were used and then also multi phase systems (Portland clinker, blast furnace slag). Syntheses were carried out using the following pseudomixtures:

$C_3A + 3\ C\bar{S}H_{0,5} + 10\%\ CH + 20\%\ SiO_2 + aq + CO_2(g) \xrightarrow{20^\circ C}$ ettringite

$\xrightarrow{20^\circ C}$ solid solution ettringite and thaumasite $\xrightarrow{20^\circ C}$ thaumasite,

$C_3S + C\bar{S}H_{0,5} + C\bar{C} + aq \xrightarrow{4^\circ C}$ thaumasite,

$\beta\text{-}C_2S + C\bar{S}H_{0,5} + C\bar{C} + aq \xrightarrow{20^\circ C}$ thaumasite,

$C\bar{S}H_{0,5}$ + Portland clinker with a high alite content and with a low content of

$C_3A + C_4AF + aq + CO_2$ (g) $\xrightarrow{20^\circ C}$ thaumasite,

$C\bar{S}H_{0,5}$ + blast-furnace ash $\xrightarrow{-20^\circ C\ \%\ 20^\circ C}$ thaumasite.

For example, a sample of the last mixture, containing 70% slag + 30% gypsum, was mixed with water and then pressed into a slab 15x15x0,5 cm. The sample was kept on an outside window ledge from September to March. During that period the temperature varied between 22^0C and -20^0C. By the end of March the sample had turned into a white sludge, which after drying at 40°C changed into a fine white powder. The X-ray diffraction patterns of the thaumasite separated from the sample is illustrated in Fig. 5. Mass spectrometric analysis of the gaseous products given off during the thermal decomposition of the sample is illustrated in Fig. 6. Hydration of the mixture $C_3A + 3\ C\bar{S}H_{0,5}$ + 10% CH + 20%

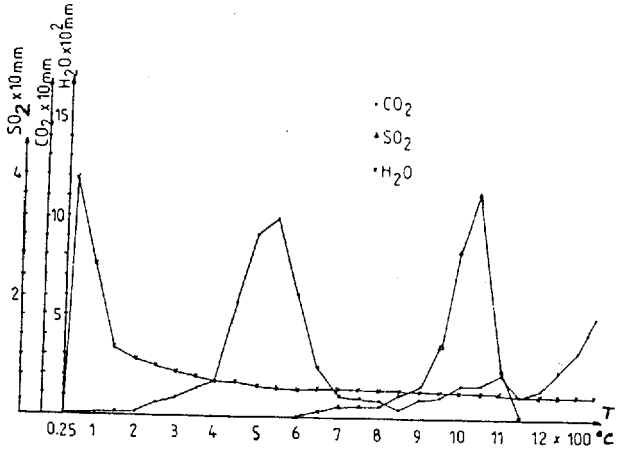

Fig. 6.
Mass Spectrum of Separated Thumasite Sample.

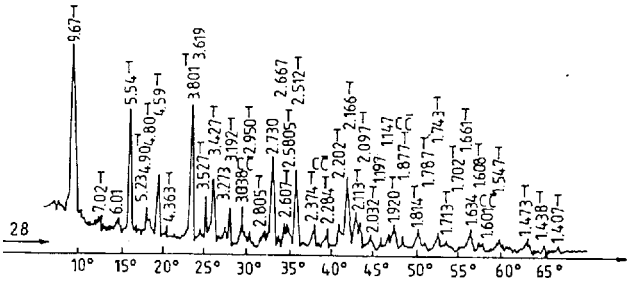

Fig. 5.
X-ray Diffraction Patern for Thaumasite.

S leads to rapid crystallization of ettringite. Between the 7th and 28th day of hardening it is possible to distinguish strong lines of ettringite, gypsum and weak ones for CSH. The introduction of CO_2 causes the formation of $C_3A * C\bar{C} * H_{11}$. The quantitative determination of silica in etringite by the chemical method indicates that gradual replacement of Al by Si occurs. The solid solution formed after 180 days corresponds to $Ca_6[Al_{0,37}Si_{0,63}(OH)_6 \cdot 12H_2O]_2[SO_4,CO_3]_2$. It can be supposed that the Si contained in thaumasite comes from CSH. The latter phase disappears in the corroded layer. In the presence of gypsum and calcite the hydration products of C_3S and β-C_2S contain free silica (the surface layer of the bar samples). This confirms strong carbonization of CSH, associated with its decomposition. The formation of thaumasite precedes the decomposition of CSH into SH_2 and $C\bar{C}$.

Blocks formed from hemihydrated gypsum and clinker stored under combined conditions of hydration initially contracted and then exhibited gradual swelling of 0,38% after 180 days, and then fell apart. The corrosion front moved from the surface to the interior of the samples. Over 180 days cracks formed and the corrosion layer acquired an appreciable thickness. By using different techniques (X-ray powder analysis, IR spectroscopy, thermal analysis, microscopic examination) it was shown that thaumasite was present, formed from ettringite. The crystallochemical resemblance between thaumasite and ettringite made the identification of the latter by X-ray and thermal analysis methods very difficult. The technique of Van Aardt [8] was very useful here. This method makes it possible to decompose ettringite and gypsum in the mixture by treating the material with a 5% solution of Na_2CO_3. Transformation of ettringite into thaumasite through the action of SiO_2 and gaseous CO_2 and with the participation of the liquid phase is one of the reasons for the deterioration of the gypsum-cement materials in the later stages of hardering. At low temperatures, thaumasite crystalizes also from CSH in the presence of gypsum and calcite, the latter reaction being probably preceded by the decomposition of CSH into $C\bar{C}$ and SH_2, under the influence of CO_2 from the atmosphere. This mechanism is confirmed by information about the synthesis of thaumasite from CaO, SiO_2, $CaSO_4 \cdot 2H_2O$ and $CaCO_3$ at about 4^0C [9]. The first change, i. e. the transformation of ettringite into thaumasite is associated with the deterioration of cohesion of gypsum-cement materials, and

the second one, the formation of thaumasite from CSH takes place without volume changes but it is accompanied by considerable loosening of the structure and loss of cohesion. An essential role in the breaking of Si-O bonds and the passing of Si to ion exchange sites is played by alkali metal ions. Some lattice points in the anion sub lattice of thaumasite may be occupied not by SO_4^{2-}, but $B(OH)_4^{1-}$ [11]. The structure of the mineral juravskite $Ca_6Mn_2(SO_4)_2(CO_3)_2(OH)_{12}*24H_2O$ is analogous to that of thaumasite [12]. Thus the deterioration of their strength in water, as a result of crumbling or considerable weakening of the structure is a great disadvantage of gypsum-cement materials. If a sufficient amount of the gel phase is formed in the early stages of hydration, it seals the gypsum-cement material, which helps to decrease to a minimum the extent of its carbonation. The introduction of adducts of sucrose and urea prevents the changing of the coordination of Si from tetrahedral to octahedral, hindering the crystallization of thaumasite from the liquid phase (combining silica and alkali). Controlling the process of the degradation of gypsum-cement materials made it possible to produce in Poland 3mln m^2 of the self-levelling, monolithic floors in residential blocks.

3. Conclusions.

The mechanism of the deterioration of gypsum-cement materials is associated with the crystallization of expansive ettringite - thaumasite solid solutions out of the ettringite phase and thaumasite from hydrated calcium silicates. The crystallization of ettringite can be prevented by blocking the passing of Si from tetrahedral to octahedral coordination in $[Si(OH)_6]^{2-}$

4. References.

[1] Alksnis,F.F.: **Twardnienie i destrukcja gipsocementowych materiałów kompozycyjnych**. 1st ed. Leningrad, Stroijzdat, 1988.

[2] Bensted,J. "Some problems of ettringite and of thaumasite in the gypsum plaster - cement contact area". **Proceeding of the International RILEM Symposium on Calcium Sulphates and Derived Materials, Saint Rémy - Lès Chevreuse, France**, May 1977.

[3] Kollmann,H. & Strübel,G. & Trost,E. "Mineralsynthetische Untersuchungen zu Treibursachen Durch Ca-Al-Sulfat-Hydrat und Ca-Si-Carbonatsulfat--Hydrat". Tonind. Ztg. 3, 1977, 63.

[4] Uchikawa,H. & Uchida,S. "The analysis of ettringite in hardened cement paste". Cem. Concr. Res., 4, 1974, 821.

[5] Leifeld,G. & Munchberg,W. & Stegmaier,W. "Ettringite und Thaumasite als Treibursache in Kalk-Gips Putzen durch Ettringit und Thaumasit". Zement-Kalk-Gips, 4, 1970, 174.

[6] Bensted,J. "Thaumasite - a detrioration product of hardened cement structures". Il Cemento, 1, 1988, 3, ibid 3, 1977, 81.

[7] Pauri,M. & Collepardi,M "Thermo-hygrometrical stability of thaumasite and ettringite". Il Cemento, 3, 1989, 177.

[8] Van Aardt, S. Visser, Cem. Concr. Res. 5, 1975, 225.

[9] Bensted,J. & Varma,J. Studies of thaumasite, part I, Silicates Ind., 2, 1973, 29.

[10] Ostrowski,C. **Mechanism of deterioration of gypsum-cement binder materials**. Opole University of Technology 1986, 138 p.

[11] Dun,P.J. "Charlesite, a new mineral of the ettryngite group from Franklin, New Jersey". Am. Mineralogist, 68, 1983, 1033.

[12] Granger,M.M. & Protas,J. "Determination et etude de la structure cristalline de la jouravskite, Acta Crystallographica", B25, 1969, 1943.

[13] Ostrowski,C. et al., Polish Patent No 146 757, 1990.

CEMENT TYPE INFLUENCE ON PROPERTIES AND DURABILITY OF MORTARS PREPARED WITH WATER AND SEA WATER IN SEA AGRESSION CONDITIONS

Bogomil D Daraktchiev

University of Architecture, Civil Engineering and Geodesy, Sofia, BULGARIA

The Paper treats the results of long-term research of properties and durability of mortars prepared with water and sea water and different types of cement. Types of cement differ in mineral content /C_3A content is 3.98, 8.47 and 11.26%/ quantity and type of mineral additives. The influence of cement type and sea water is established on: change of strength properties of mortars seasoning in sea water for 10 years; durability of samples in changing zone conditions; additional swelling of samples provoked by sea water activity; changes in volume and size of pores in the cement stone; changes in the cement stone new formations.

Im Vortrag werden die Ergebnisse von langzeitigen Untersuchungen der Eigenschaften und der Bestandigkeit von Morteln dargestellt, die mit und Meereswasser, sowie aus verschiedenen Zementarten gefertigt wurden. Die Zementarten unterscheiden sich nach ihrer Mineralzusammen - setzung (C_3A = 3.98, 8.47 und 11.26%), nach Menge und Art der orga - nischen und Mineralzuschlage. Es wird der Einfluss der Zementart und des Meereswassers auf die folgenden Eigenschaften untersucht :

- die Anderung der Festigkeitseigenschaften bei einer bis zu 10 - jahrigen Aussetzung dem Meereswassers; die Bestandigkeit der Proben in der veranderlichen Zone; das zusatzliche Quellen der Proben, verursacht vom Meereswasser; die Veranderung von Volumen und Masse der Poren im Zementstein; die Veranderungen der Neubildungen im Zementstein.

INTRODUCTION

The aim of this report is to reveal the results of research on the properties of mortars, prepared with cements of different mineral composition, with different additions and waters /ordinary and sea water/, placed in sea medium. This research has been carried out for many years and some data on the long-lasting properties of mortars and concrete prepared with sea water have been published.

COMPOSITION OF THE SEA WATER

The concentration of salts in the waters of the Black Sea is 14.5 - 18.0 g/dm^3, which is about 2 - 2.5 times lower than the one in the oceans. The percentage of the different salts is similar to that in the ocean waters: NaCL 78%, $MgSO_4$ 4.6%, $CaSO_4$ 3.5%, K_2SO_4 2.5%, $CaCO_3$ 0.35%, $MgCl_2$ 10.7%. For the Black Sea pH=8.05.

MATERIALS AND COMPOSITION OF THE MORTARS

The researches have been carried out with five types of cements /Table 2/, which were obtained from three types of clinkers I, II and III with mineral composition as given in Table 1 and with contents of C_3A 11.26%, 8.47% and 3.98% respectively.

TABLE 1 MINERAL COMPOSITION OF THE CLINKERS

Clinker	C_3S	C_2S	C_3A	C_4AF
I	40.08	34.15	11.26	10.43
II	59.56	11.96	8.47	10.43
III	54.91	26.26	3.98	15.21

Clinker I was used only in the preparation of cement No.1 together with 15% combined mineral addition of limestone and blast furnace slag /BFS/, 7.5% each. Clinker II was used for the preparation of three types of cements: No.2 - without mineral additions, No.4 - with the above mentioned combined mineral addition and No.5 - with 30% BFS. Clinker III was used only in preparation of cement No.3 without mineral additions. 3.5% natural plaster was added to all the cements.

Seven types of cement-sand mortars were prepared on the basis of these five cements /Table 2/. In six of them /No.1,2,3,4,5 and 7/ the mass ratio cement: 1:2.2 and the water-cement ratio is W/C=0.5. In No.6 the ratio is 1:1.05 and W/C=0.34. 0.01% to cement weight neutralized colophony resin was added in mortar No.7. The neutralized colophony resin /NCR/ has the effect of increasing the air contents of the mortar. The used sand had modulus of fitness f=2.9.While preparing samples from all the mortars, both ordinary and natural sea water from the Black Sea /salt contents - 16.1 g/dm^3/ were used.

TABLE 2 CHARACTERISTIC OF THE USED CEMENTS AND CEMENT-SAND MORTARS

Mortar No.	Cement				Composition of Mortar	
	No.	Clinker	C_3A%	Addition	Cement:Sand	W/C
1	1	I	11.26	15% comb.	1:2.2	0.50
2	2	II	8.47	-	1:2.2	0.50
3	3	III	3.98	-	1:2.2	0.50
4	4	II	8.47	15% comb.	1:2.2	0.50
5	5	II	8.47	30% BFS	1:2.2	0.50
6	2	II	8.47	-	1:1.05	0.34
7	1	I	11.26	15% comb. 0.01%NCR	1:2.2	0.50

TABLE 3 COMPRESSIVE AND BENDING STRENGTH OF WATER-SATURATED SAMPLES, PREPARED WITH WATER AND SEA WATER

Mortar No.	Compressive Strength, MPa/%			
	28 days	1 year	2 years	10 years
1w	30.9/100	45.2/146	41.3/134	40.6/131
1sw	25.0/100	36.0/144	37.9/152	38.0/152
2w	31.0/100	38.6/125	44.5/144	47.2/152
2sw	32.2/100	46.8/145	44.1/137	40.5/126
3w	39.0/100	58.0/149	59.2/152	60.5/155
3sw	40.2/100	57.5/143	59.5/149	64.4/160
4w	27.8/100	36.5/131	43.0/155	37.5/136
4sw	27.2/100	41.0/151	43.5/160	38.0/140
5w	26.0/100	43.0/165	43.5/167	38.2/146
5sw	30.1/100	44.3/147	43.7/145	40.6/135
6w	50.7/100	70.2/138	76.0/150	79.5/157
6sw	55.6/100	74.2/133	79.5/143	82.5/149
7w	24.2/100	39.0/161	40.0/165	38.0/157
7sw	20.2/100	-	-	35.4/175

Mortar No.	Bending Strength, MPa/%			
	28 days	1 year	2 years	10 years
1w	6.4/100	7.3/114	7.6/119	6.6/103
1sw	5.3/100	6.7/126	6.9/130	6.4/121
2w	6.2/100	8.1/131	8.4/135	8.4/135
2sw	6.4/100	9.3/145	9.4/147	8.6/132
3w	6.6/100	9.0/136	9.3/141	9.5/144
3sw	6.7/100	8.8/131	9.2/137	9.5/142
4w	6.1/100	8.6/141	8.8/144	7.0/115
4sw	6.3/100	8.5/135	8.4/133	8.0/127
5w	5.3/100	8.6/162	8.7/164	7.2/136
5sw	5.4/100	9.6/178	8.9/165	8.4/156
6w	8.1/100	10.0/123	10.9/135	10.8/133
6sw	8.5/100	10.3/121	10.6/125	10.8/127
7w	4.2/100	7.3/174	8.5/202	7.1/169
7sw	3.8/100	-	-	7.8/205

Note: w - means that the mortar had been prepared with ordinary water;
sw - means that the mortar had been prepared with sea water.

TESTING METHODS AND RESULTS

1. Long-lasting test under the conditions of uninterrupted seasoning under sea water.

The mortar prisms 4x4x16 cm were made using water and sea water, which were placed in a moist medium (φ >90%, t=293±3 ^{0}K) up to the 28th day and were in sea water afterwards. The results from the tests on compressive and bending strength at the age of 28 days, 1, 2, and 10 years of the different mortars are given in Table 3.

The results show that the samples prepared with sea water /with the exception of No.1 and No.7, which were made from cement having C_3A=11.26%/ had better strengths. A long-lasting retaining and increase of strength was shown by the samples prepared with the two types of water on condition that the contents of C_3A is low /No.3/ or that they contain a considerable quantity of BFS /No.5/, NCR /No.7/ or have a low water-cement proportion /No.6/, regardless of the high contents of C_3A.

2. Behaviour of the mortars under conditions modelling the changeable zone.

After the 28th day samples from the seven mortars /Table 2/, prepared with water

and sea water, with dimensions 4x4x16 cm were subjected to a hundred freeze-thaw test condition cycles /from 258 up to 293°K/ and to a hundred wet-dry test condition cycles /from 293 up to 333°K/ in sea water. The procedures were changed alternatively each ten cycles. Table 4 shows /for the sake of brevity/ only the decrease of the compressive and bending strength of the so treated samples in per cent in comparison to the respective control /not treated/ samples that were lying uninterrupted in sea water.

TABLE 4 DECREASE OF STRENGTH DUE TO CHANGEABLE INFLUENCE

Mortar No.	1w	1sw	2w	2sw	3w	3sw	4w	4sw	5w	5sw	6w
Decrease of the compr. strength,%	21.3	24.3	13.9	16.2	13.2	15.3	16.1	16.8	14.1	15.8	7.9
Decrease of the bending strength,%	16.1	14.2	9.2	17.9	7.8	16.8	19.8	22.4	17.9	20.2	0.4

continuation ---------

6sw	7w	7sw
8.6	16.5	16.3
0.3	11.6	14.6

The analysis shows that, generally speaking, all the samples, prepared with sea water have a slightly lower durability /greater decrease of the ultimate strengths/ in comparison to the ones prepared with ordinary water. Analogous results were obtained as a result of the test on 200 freeze-thaw cycles. No matter the test results dispersion, the greatest decrease of ultimate strength demonstrate the mortars prepared with cements with high percentage of C_3A /11.26 and 8.47%/ and containing mineral additions /mortars No.1,4, and 5/. An increase in the durability of these mortars, using sea water during preparation, can be achieved by decreasing the water-cement ratio and by adding air entraining agents such as the neutralized colophony resin.

3. Swelling of the samples placed under water from the sea

The aim of the research is to determine, following the method proposed here, the degree of the formation of swelling newly formed compunds /mainly ettringite/ in the seven mortars /Table 2/, prepared only with ordinary water, in the course of long-time staying under sea water. The samples from each mortar with fixed dubbs for the measurement of the deformations and dimensions 4x4x16 cm. After the initial measurement of the deformations on the 28th day, half of the samples from each mortar /3 pieces/ were placed under ordinary water, and the other half - under sea water. These stayed there 365 days. The additional swelling wkich had been caused by the sea water and which brings about internal stress in the material, was calculated as the difference between the swelling of the samples that had been staying in ordinary and sea water /Table 4/.

TABLE 4 ADDITIONAL SWELLING ON THE 365th DAY OF THE SAMPLES STAYING UNDER SEA WATER IN COMPARISON TO THOSE STAYING UNDER ORDINARY WATER

Mortar No.	Swelling, mm/m		Additional swelling caused by the sea water, mm/m
	in water	in sea water	
1w	0.475	0.625	0.150
2w	0.419	0.513	0.094
3w	0.369	0.431	0.062
4w	0.344	0.437	0.093
5w	0.356	0.412	0.056
6w	0.510	0.561	0.051
7w	0.454	0.610	0.156

The results that were achieved with this method show that the additional swelling can be lowered by decreasing C_3A contents in the cement, by the application of mineral additions or by lowering the water-cement proportion.

4. Pore structure

We shall consider here only the influence of the cement type and that of the alter-

nating changeable treatment /100 freeze-thaw and 100 wet-dry cycles/ as described in .2. on the volume and the dimension of the pores of mortar No.1 /C_3A = 11.26%/ and No.3 /C_3A = 3.98%/, prepared with ordinary water. Pore sizes were measured using "Carlo Erba" porositimeter made in Italy, with range from 5 to 10 000 nm.

Figure No.1 shows the integral curves of the porousness of a sample from mortar No 1 after having stayed under sea water for two years /curve No.1/ and after the alternating changeable treatment /curve No.2/. Curve No.3 is the integral curve of a sample from mortar No.3 after the alternating changeable treatment. The volume of the pores within the range of the apparatus respectively for curves No.1,2 and 3 is V = 0.059cm/g V = 0.077cm/g and V = 0.031cm/g

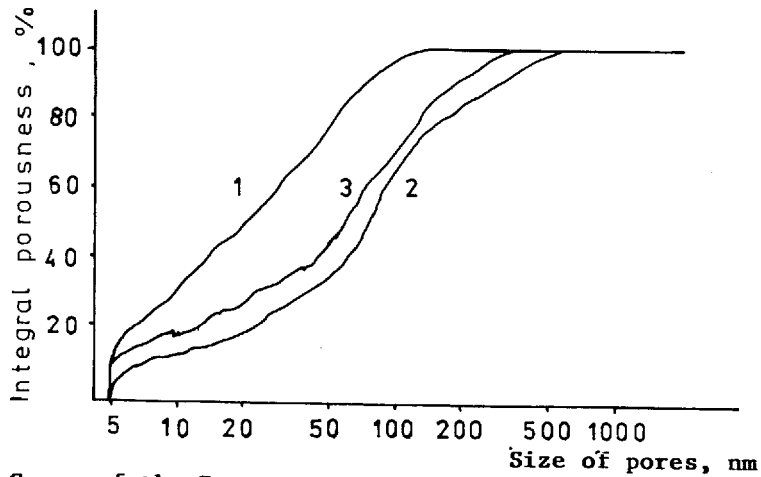

Figure No.1 Integral Curve of the Porousness of Samples, Prepared from Mortars No.1 and No.3
Curve No.1 - a sample from mortar No.1 after having stayed under sea water for two years
Curve No.2 - a sample from mortar No.1 after the alternating changeable treatment
Curve No.3 - a sample from mortar No.3 after the alternating changeable treatment

The test results show that the volume of the pores in the sample prepared from mortar No.1 increase with 30%, while the porous structure grows larger. This can be explained with widening action of the ice crystals in the pores and the increased pressure of the water in the pores. The increased volume of the pores has a negative effect on the ultimate strength and a porousness over 100nm accelerates the process of corrosion. The volume of the pores in the sample, prepared with mortar No.3 /C_3A = 3.98%/ is considerably lower and that makes the cement stone more resistant to corrosion.

5. Phase composition of the cement stone

Here we are going to reveal the influence of the water the cement has been made with /ordinary or sea water/ upon the phase composition of the cement stone that was obtained on the basis of clinkers I and II, 4% natural plaster and 35% water. The phase composition was analysed using x-ray diffractometer mark TuKM-62. The test was performed using CuK radiation and Ni filter. Figure No2 shows the diffraction patterns of the cement stone on the 7th day after having stayed in moist air /φ >90%/ and t = 293°K. Every diffraction pattern on the figure is marked with I or II according to the type of the clinker and with a subscript according to the type of the water /w stands for ordinary water and sw for sea water/.

It can be seen from the diffraction patterns that the lines of the $Ca(OH)_2$ /d = 4.91 A, 3.11 A etc./ have greater intensity in all the samples prepared with sea water, which demonstrates an accelerated hydration of the cement. In the case of clinker I the

product of the hydration of C_3A not withstanding the type of the used water is C_4AH_{13} /d = 7.7 A°, 3.9 A° etc./, while the product from the hydration of clinker II with the sea water is $C_3A.CaCl_2.10H_2O$ /d =7.9 A°, 3.83 A° etc./

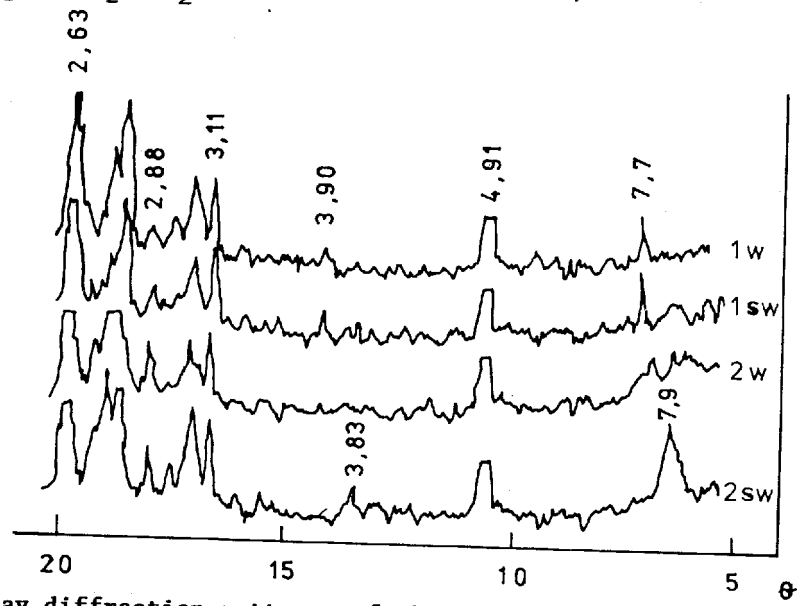

Figure No.2 x-ray diffraction patterns of the cement mortar

CONCLUSIONS

The use of sea water in the preparation of cement modifies partially the phase composition of the cement mortar and its properties. It accelerates the hardening process giving greater ultimate strengths on the 28th day on the condition that the quantity of C_3A in the cement does not surpass a value of about 10%. While the behaviour of these mortars in the conditions of a sea medium is analogous, in the changeable zone they show a lowered durability. It is established that an additional swelling takes place, developing internal stresses which are deleterious to the durability properties.The influence of the C_3A upon the change of the volume of the pores and the porous structure of the mortars subjected to the changeable influence of the sea water has been observed.

REFERENCE

1. Taylor M.A., Kuwairi A. Effects of the ocean salts on the compressive strength of the concrete. Cement and Concrete Research, 1978, vol.8, No.4
2. V.S.Ramachandran and al. Influence of sea water solution on mortar containing calcium carbonate. Materials and Structures, Nov. 1990, vol.23, No.138
3. Popovics S. Concrete-making materials. Washington,1979
4. Gjorv O.E. Long-time durability of concrete in sea water. A.C.I.J. January 1971

INVESTIGATION INTO DELAYED ETTRINGITE FORMATION IN CONCRETE

J Stark, K Bollmann and K Seyfarth

Department of Building Materials, University of Architecture and Building at Weimar, Weimar, GERMANY

SUMMARY

This paper presents some results of an extensive research programme at the University of Architecture and Building Weimar, dealing with the durability of concrete in connection with ettringite formation.

Investigations have shown that in addition to the temperature of heat treatment the temperature during the utilization of hardened concrete is of great influence on the durability of concrete.

Especially in concrete with a dense structure (low w/c-ratio) even an SO_3-content of 3,3 % in cement in connection with drying-temperatures of 60 °C and longer moisture-periods may result in structural damages.

ZUSAMMENFASSUNG

In diesem Beitrag werden einige Ergebnisse eines umfangreichen Forschungsprogrammes der Hochschule für Architektur und Bauwesen Weimar vorgestellt, das sich mit der Dauerhaftigkeit von Beton im Hinblick auf eine späte Ettringitbildung beschäftigt.

Die Untersuchungen haben ergeben, daß neben der Wärmebehandlungstemperatur auch die Temperatur während der Nutzung des erhärteten Betons einen großen Einfluß auf die Dauerhaftigkeit des Betons hat.

Besonders bei Beton mit dichtem Gefüge (niedriger W/Z-Wert) kann es bereits bei einem SO_3-Gehalt von 3,3 % im Zement in Verbindung mit Trocknungstemperaturen von 60 °C und längeren Feuchteperioden zu Gefügeschäden kommen.

INTRODUCTION

In the past few years there have been some special problems in durability of concrete made with Portland cement. In use, heat-treated precast concrete but also that hardened under normal temperatures have exhibited structural damage connected with crack formation and loss of strength. The damage has occured in concrete, which frequently or for a longer time was exposed to high moisture and changing temperatures. With reference to some other publications, for instance by LUDWIG, NECK, SYLLA, ODLER, the possibility of delayed ettringite formation as the cause of damage cannot be excluded.

A research programme at the University of Architecture and Building Weimar deals with the durability of concrete in connection with ettringite formation.

EXPERIMENTAL PROGRAMME

The experiments were performed on specimens of different shape: prisms (40x40x160 mm), cubes (100x100x100 mm), beams (100x100x400 mm) and panels (50x150x600 mm) of concrete with a maximum aggregate size of 8 mm. The aggregate consists of pure quartz, which is said to be inert.

The investigations include as the following:

A) different water-cement-ratios and cement-contents as given in Table 1.

Table 1.: Composition of mixture

water-cement-ratio	aggregate-cement-ratio	cement kg/m^3	water kg/m^3	aggregate kg/m^3
0.35	2.68	577	202	1546
0.50	4.24	400	200	1696
0.65	5.96	300	195	1788

B) a variation of the type of cement:
cements with SO_3-contents of 2,3 %, 2,8 %; 3,3 %; 3,9 %; 4,5 % and Na_2O-equivalent of 1,04 % were used

C) normal hardening at 20 °C (prisms, beams, panels, cubes) and heat treatment at different temperatures at 60 °C, 75 °C, 90 °C (beams, cubes)

D) standard curing and curing without evaporating protection up to the 28th day

E) different ways of storage (variation of moisture and temperature conditions) from the age of 28 days, to simulate environmental conditions during utilization - these are listed in Table 2.

Table 2.: changing storage conditions from the age of 28 days
case 1)...5): prisms (up to the age of 3 years)
case 6) : baems and cubes
case 7) : panels and cubes

case	drying period time d	humidity %	temp. °C	moisture period time d	humidity %	temp. °C
1)	28	63	20	28	water	20
2)	28	63	20	130	water	20
3)	21	< 1	60	130	water	20
4)	14	< 1	105	130	water	20
5)	1	< 1	60	1	water	20
6)	90 + 7	80 < 1	10 60	90 + 8 times freezing and thawing	water	20
7)	permanent open-air-storage					

For the assessment of structural changes, periodic velocity of ultrasonic pulse, mass, change in length, and strength were determined. In addition scanning electron microscopy and micro-analysis investigations were applied.

RESULTS

Results on prisms

Considerable damages have already occurred in small specimens (prisms) (figure 1).

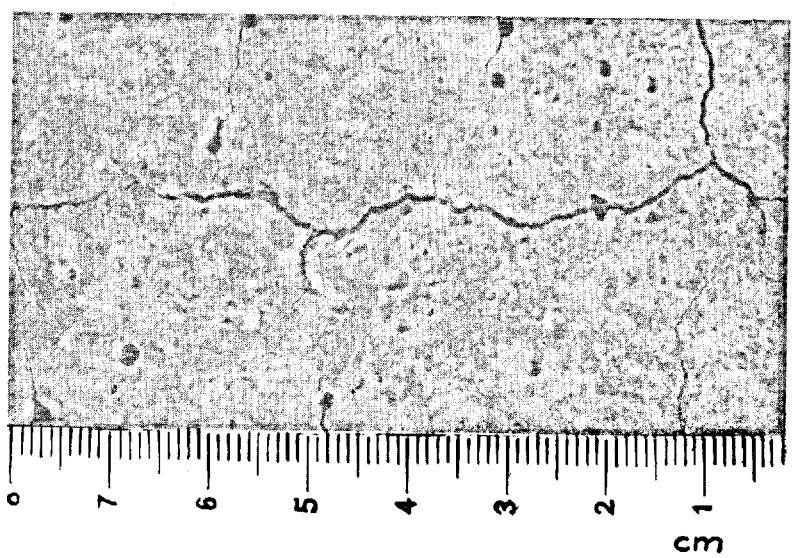

Figure 1: Crack-formation on concrete after two long drying and miosture periods
(case 3: drying temp. = 60 °C; w/c = 0,35; SO_3-cont. = 3,3 %)

The structural change depends on the various factors of influence mentioned above.

A) Water-cement-ratio and curing

Especially concrete with a dense structure (w/c = 0,35; standard curing) shows many defects in form of cracks (width up to 0,5 mm), connected with an expansion of up to 10,5 mm/m, a decrease in the modulus of elasticity (determined from the periodic velocity of ultrasonic pulse), and a loss of strength.

B) SO_3 -content of the cement

The extent of damage (cracks) depends on the SO_3-content. Concrete of a w/c-ratio of 0,35 shows most defects at a SO_3-content of 3,9 %.

C) Changing storage conditions

Damages (crack formation) only occur in concrete (prisms) repeatedly affected by temperatures of 60 °C or 105 °C during long periods of changing storage conditions (case 3 and 4). The maxima in expansion, in decrease in the modulus of elasticity and in loss of strength are to be found at temperatures of 60 °C (case 3). Short periods of changing storage conditions (case 5) do not result in crack formation.

In all these cases the damaged concrete was hardened under normal temperatures. Hence it follows that concrete which is not heat-treated may show damages due to higher temperatures during utilization. The determination of temperature in the concrete-panels permanently stored in the open air shows that the high temperatures of up to 60 °C are realistic under intensive sun-radiation.

Some of the results received on prisms after two long drying and moisture periods at drying temperatures of 60 °C and 105 °C (case 3 and 4) are represented in figures 2, 3 and 4.

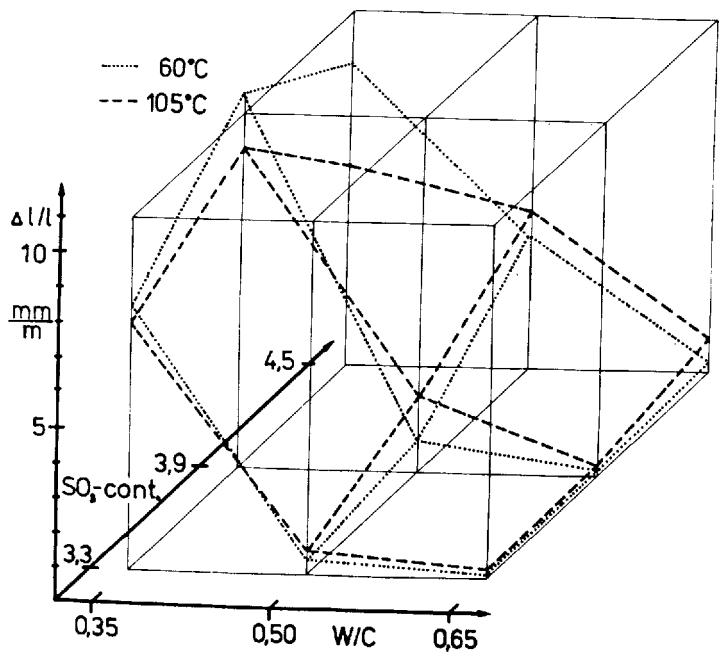

Figure 2: Expansion of prisms (from the age of 28 days); $\Delta l/l$ versus w/c-ratio and SO_3 -content

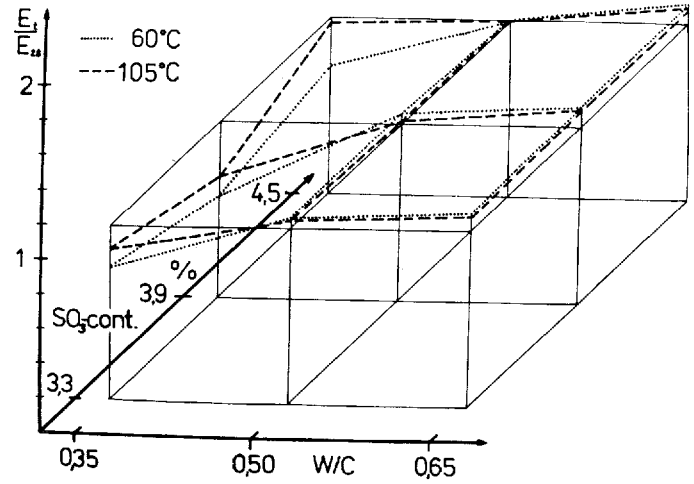

Figure 3: Variation in the modulus of elasticity; E_t/E_{28} versus w/c-ratio and SO_3-content

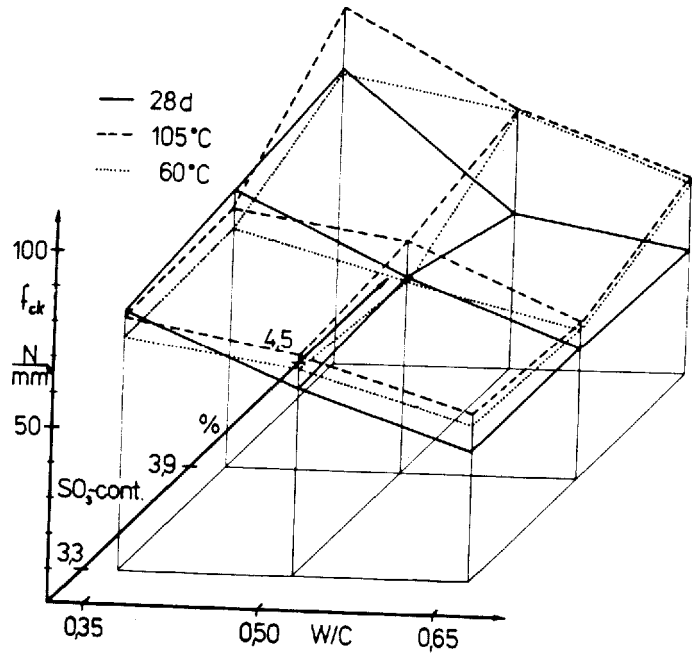

Figure 4: Compressive strengths at the age of 28 days and after two long drying and moisture periods at drying temperatures of 60°C and 105°C; f_{ck} versus w/c-ratio and SO_3-content

The structural damages become apparent in crack formation, high expansion above 0,5 mm/m (figure 2), decrease in the modulus of elasticity determined from decrease of periodic velocity of ultrasonic pulse (figure 3) and loss of strength. The flexural tensile strength, $f_{ct,fl}$, declines proportionally to the modulus of elasticity. However compared to it the compressive strength, f_{ck}, remains relatively high (figure 4).

The findings are corroborated by the SEM, which show secondary formation of phases (figure 5). The micro-analysis proves the phases to be ettringite modifications.

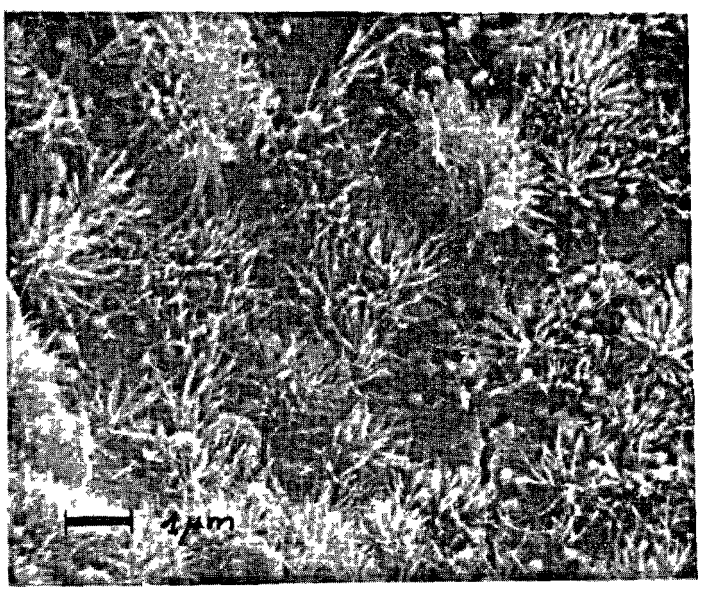

Figure 5: SEM-picture of a crack-surface in concrete after two long drying and moisture periods
(case 3: drying-temp.= 60 °C; w/c = 0,35; SO_3-cont.= 3,9 %);
formation of needle-shaped ettringite-modifications

Results on beams, panels and cubes

First cracks in concrete beams and cubes have occured as a result of heat treatment at temperatures of 75 °C and 90 °C. The greatest extent of damage was noticed on concrete heat-treated at 75 °C. The investigations are not finished yet. The results find out on beams up to the age of 2 years show in tendency the same effects like on prisms. But on big specimens the effects appear later and to a less degree. The first cracks became more extensive during further storage connected with loss of strength and with decreasing periodic velocity of ultrasonic pulse.

Results of micro-analysis and SEM show a secondary formation of needle-, bunch- and ball-shaped ettringite modifications in cracks and pores.

The measurements at the concrete panels permanently stored in the open air for to years show up to now normal effects in shrinkage, expansion and strength development.

CONCLUSIONS

In addition to the temperature of heat treatment the temperature during the utilization of hardened concrete is of great influence on the durability of concrete.

Especially in concrete with a dense structure (low w/c-ratio)a SO_3-content of 3,3 % in cement in connection with drying-temperatures of 60 ^{o}C and longer moisture-periods may result in structural damages.

Damages become apparent at first on small specimens.

REFERENCES

1. Bollmann, K. and Stark,J.: "Ein Beitrag zur Dehnung von Beton unter Einwirkung von Feuchte und erhöhten Temperaturen", 11. Internationale Baustoff- und Silikattagung, Weimar, Bundesrepublik Deutschland, 1991, Vortrag, Tagungsunterlagen, Band 1, 103-114.

2. Seyfarth, K., Stark, J.: "Zur Dauerhaftigkeit wärmebehandelter Betone", 11. Internationale Baustoff- und Silikattagung, Weimar, Bundesrepublik Deutschland, 1991, Vortrag, Tagungsunterlagen, Band 1, 179-190.

3. Ludwig, U.: "Probleme der Ettringitrückbildung bei wärmebehandelten Mörteln und Betonen", 11. Internationale Baustoff- und Silikattagung, Weimar, Bundesrepublik Deutschland, 1991, Vortrag, Tagungsunterlagen Band 1, 164-179.

4. Neck, U.: "Auswirkungen der Wärmebehandlung auf Festigkeit und Dauerhaftigkeit von Beton", Beton, 1988, 38/12, 488-493.

5. Sylla, H.-M.: "Reaktionen im Zementstein durch Wärmebehandlung", Beton, 1988, 38/11, 449-454.

6. Heinz, D., Ludwig, U., Rüdiger, I.: "Nachträgliche Ettringitbildung an wärmebehandelten Mörteln und Betonen", Beton- und Fertigteiltechnik, 1989, 55/11, 56-61.

7. Odler, I., Abdul-Maula, S.: "Possibilities of quantitative determination of the Aft-(ettringite) and Afm-(monosulphate) phases in hydrated cement pastes", Cement and concrete resaerch, 1984, 14, 133-141.

THE RESISTANCE OF PFA CONCRETE TO ACID GROUNDWATERS

J D Matthews

Building Research Establishment, Garston, Watford, UK

SUMMARY

A wide-ranging research programme to assess the durability of pfa concrete in a variety of exposure conditions was established at BRE several years ago and includes studies of the resistance of pfa concrete to different aggressive solutions and waters such as sulphate solutions, acid groundwaters and seawater. Variable parameters in the programme included three different sources of Portland cement, four different sources of pfa, total binder contents ranging from 180 to 500 kg/m³ and pfa contents of 20-40%.

This paper reports data on strength and weight loss of concretes with and without pfa immersed for up to five years in slow-flowing natural moorland groundwater of pH in the range 3.5 to 4.5.

The results indicate that the quality of the concrete, measured by 28-day compressive strength or water/binder-ratio, is a more important factor in determining performance in acid conditions than is the composition of the cement, with pfa content having little overall influence. There is some evidence, however, that concretes made with cements having high C_3S contents, which liberate greater amounts of calcium hydroxide on hydration than cements with low C_3S, are attacked slightly more rapidly whether or not they contain pfa.

INTRODUCTION

The damaging effect of acids on all types of Portland cement concrete is well known. The degree of attack depends upon the nature and concentration of the particular acid and usually takes the form of a leaching of calcium hydroxide from the concrete surface, ultimately dissolving the cement matrix and leaving an 'exposed aggregate' finish. If the concrete contains a limestone aggregate this too will be dissolved.

In a review of concrete behaviour in acidic soils and groundwaters, Eglinton (1) noted that although the national standards of a number of European countries recommended the use of pozzolanic or blastfurnace cements in acid conditions the literature generally indicated that the quality of the concrete was more important than the type of cement used in determining resistance of concrete to acids. Harrison (2) also discussed this point and noted that the evidence in the literature was conflicting on whether such cements could improve chemical resistance. He concluded that, for the particular requirement of acid resistance, data in the literature did not seem to justify any specific recommendation for the type of cementitious binder, although it was acknowledged that the consensus seemed to point to a slower rate of attack on properly cured concretes with reduced lime contents such as occurs when pozzolanic cements are used. However, Harrison notes that a number of the papers drawing attention to the reduced vulnerability of such cements are based upon theoretical considerations, and some of the limited amount of documented test data suggest little improvement in performance due to the use of pozzolanic or blastfurnace cements. An exception to this may be slag cements with very high slag contents, such as supersulphated cement, which have been considered (3) to offer improved chemical resistance in acid conditions down to pH 3.5 provided that the concrete was dense and with low w/c ratio.

Recently, the Building Research Establishment (BRE) has revised its recommendations for producing durable concrete in sulphate-containing soils and groundwaters which now include recommendations relating to acid conditions (4). No specific recommendations for cement type for acid resistance are made and the Digest simply makes reference to the reduced calcium hydroxide content and reduced porosity in well cured slag and pulverised-fuel ash (pfa) concretes as being generally regarded as beneficial in reducing the rate of attack.

Some years ago, BRE commenced an extensive programme of tests to investigate various aspects of the durability of concrete containing pfa. This programme included work on sulphate resistance and resistance to marine conditions and, in the absence of any recent UK test data on the acid resistance of concrete containing pfa of the quality currently available in the UK, it was decided to include tests for acid resistance in the programme. Consequently, a site where specimens could be exposed in naturally occurring moorland water of low pH was sought and established. This paper reports the results of exposure tests of up to five years duration carried out on this site on concretes of a wide range of qualities containing different sources of cement and pfa.

EXPERIMENTAL

Materials

A series of concrete mixes was cast using three different sources of Portland cement and four different pfas. Since the programme also included testing for sulphate and seawater resistance, the cements were chosen to encompass a range of tricalcium aluminate (C_3A) contents and included one sulphate-resisting Portland cement (SRPC, reference no 831) and two ordinary Portland cements (OPCs) with calculated C_3A contents of 7% (reference no 852) and 14% (reference no 814) respectively. All four pfas complied with the chemical requirements of the British Standard (5) for pfa for use as a cementitious component in concrete. Two of the ashes (nos 1,2) complied with the maximum value of 12.5% for the residue on a 45 μm sieve specified in this Standard, whilst a third ash (no 3) fell just outside this limit (14.6% residue). The fourth ash (46.1% residue, no 4) was very much coarser and was chosen deliberately to provide an example of an ash which did not produce a water

reduction in concrete. The loss-on-ignition value of this ash (6.1%, compared with a maximum BS limit of 7%) was also higher than those of the other three ashes and would have contributed to the lack of water-reducing properties. Aggregates used throughout were Thames Valley flint gravel (coarse and fine). Compound compositions of the cements calculated by the Bogue formula are given below:

Compound	SRPC 831	OPC 852	OPC 814
C_3S	65.04	60.09	51.57
C_2S	8.96	14.05	17.86
C_3A	0.78	6.99	14.07
C_4AF	16.32	9.21	7.72

Concrete mixes

In all, 55 concrete mixes were made with comparisons between Portland cement control mixes and pfa mixes being made on the basis of equal workability and equal binder content at levels of 300 kg/m³ and 400 kg/m³. Some additional control mixes at reduced cement contents (270 kg/m³ and 360 kg/m³ respectively) were made in order to provide a closer comparison in terms of 28-day strength with the corresponding pfa mixes. For SRPC, cement contents at the extremes of the normal practical range were also investigated. Pfa contents were mainly 20% and 40% by mass of total binder, but a small number of mixes with 30% pfa were made.

The workability of the concrete mixes was deliberately chosen to be relatively high in order to reflect the type of mix that may be used, for example, in piling. The criterion set for workability was that the compacting factor should be 0.95 ± 0.02 and this was successfully achieved. Slump values were also recorded and, with five exceptions, these all fell in the range 95 ± 20 mm. Two mixes were made at a lower workability (CF 0.91, slump 45 mm). The matrix of mixes cast is shown in Table 1.

Since specimens were cast for a variety of tests, each mix was cast in two or three batches of between 60 and 85 litres. All tests on 100 mm cubes, including the testing in acid groundwaters reported here, were carried out on three replicate specimens. Specimen numbers were randomised throughout, the only constraint being that at least one specimen was selected from each batch of a mix to make up the three replicates.

Curing and exposure

All specimens were kept for the first 24 hours after casting under damp hessian and polythene before demoulding. Specimens for testing in acid groundwaters were then cured in water at 20°C until they reached a minimum age of 28 days. In practice, three or four mixes were transported to the BRE acid water exposure site in a single journey so that, at the time of initial exposure, specimen ages actually ranged between 28 and 56 days.

Specimens were exposed at a site owned by the South West Yorkshire Water Authority at Butterley reservoir near Marsden in South Yorkshire. The natural moorland water in this area is highly acidic. The exposure facility consists of two steel tanks, through which compensation water from the reservoir is allowed to flow slowly over the specimens. Specimens were placed in open plastic crates each fitted with wooden dividers to keep the specimens apart and to ensure that the water had access to all faces of the specimens. Measurements of pH of the water in the tanks were made at regular intervals during the period of test, the pH being found to vary mainly within the range 3.5-4.5. The water had low temporary hardness (8-10 ppm $CaCO_3$) and contained only small quantities of aggressive carbon dioxide (2-6 ppm) and the aggressive nature of the water is believed to be derived essentially from its content of humic acid.

Table 1 Matrix of mixes cast

Ash Content (%)	Total Cementitious Content (kg/m³)	SRPC 831 (0.8% C_3A)					OPC 852 (7.0% C_3A)					OPC 814 (14.1% C_3A)				
		–	1+	2	3	4	–	1	2	3	4	–	1	2	3	4
Nil	180	✓					–					–				
	200	✓					–					–				
	270	✓*					–					✓				
	300	✓*					–					✓				
	360	✓					✓					✓				
	400	✓					✓					✓				
	450	✓					–					–				
	500	✓					–					–				
20	300		✓	✓	✓	✓		✓	✓	–	✓		✓	✓	✓	✓
	400		✓	–	✓	–		✓	–	✓	–		✓	–	✓	–
30	300		–	–	–	–		–	–	–	–		✓	–	–	–
	350		–	–	–	–		–	–	–	–		✓	–	–	–
	400		–	–	–	–		–	–	–	–		✓	–	–	–
40	300		✓	✓	✓	✓		✓	✓	–	✓		✓	✓	✓	✓r
	350		–	–	–	–		–	–	–	–		✓	–	–	–
	400		✓	–	✓	–		✓	–	✓	–		✓	–	✓	–

+ pfa reference no; * = 2 mixes of different workability; r = repeated mix

Testing of specimens

Specimens were recovered for test after periods of exposure of two and five years. Further specimens remain for test at ten years. Upon recovery, specimens were observed to be coated with a deposited layer of dark brown silt. Before test, the silt was removed by gentle scrubbing in water. The appearance of the specimens was that of an 'exposed-aggregate' concrete, indicating that the cement matrix had been dissolved from the surface. The specimens were weighed in a saturated surface-dry condition before testing for compressive strength. In order to determine the weight loss of specimens for a given mix, the mean weight of the three replicate specimens at each age of test was subtracted from a 'baseline' weight for each mix. Since further specimens from each mix were weighed and tested for compressive strength after storage in water at 20°C at 1, 2 and 5 years, and it was observed that no systematic increase in weight occurred over this period, it was decided to take the average weight of these water-stored specimens at 1, 2 and 5 years (ie nine specimens) as the 'baseline' weight for each mix.

RESULTS

Five-year weight loss, expressed as a percentage of the 'baseline' weight, is plotted against 28-day water-stored compressive strength in Figure 1. When all the data for the 55 mixes are considered, a correlation coefficient of -0.601 is obtained, a value which is greater than 99.9% significant. A closer examination of Figure 1 reveals no dependence of percentage weight loss upon the pfa content. However, the data do give some indication of separate relationships for the different Portland cements and the 'best-fit' lines for each cement are therefore also shown. The data for the SRPC mixes and the OPC 852 mixes both have very high correlation coefficients of approximately -0.83, whilst the data for the OPC 814 mixes give a somewhat lower level of correlation ($r = -0.513$, between 95% and 99% significant for the 21 data points).

A good correlation was also obtained between the compressive strength at five years of the acid water-stored specimens, expressed as a percentage of the corresponding 20°C water-stored strength (referred to as 'percentage strength

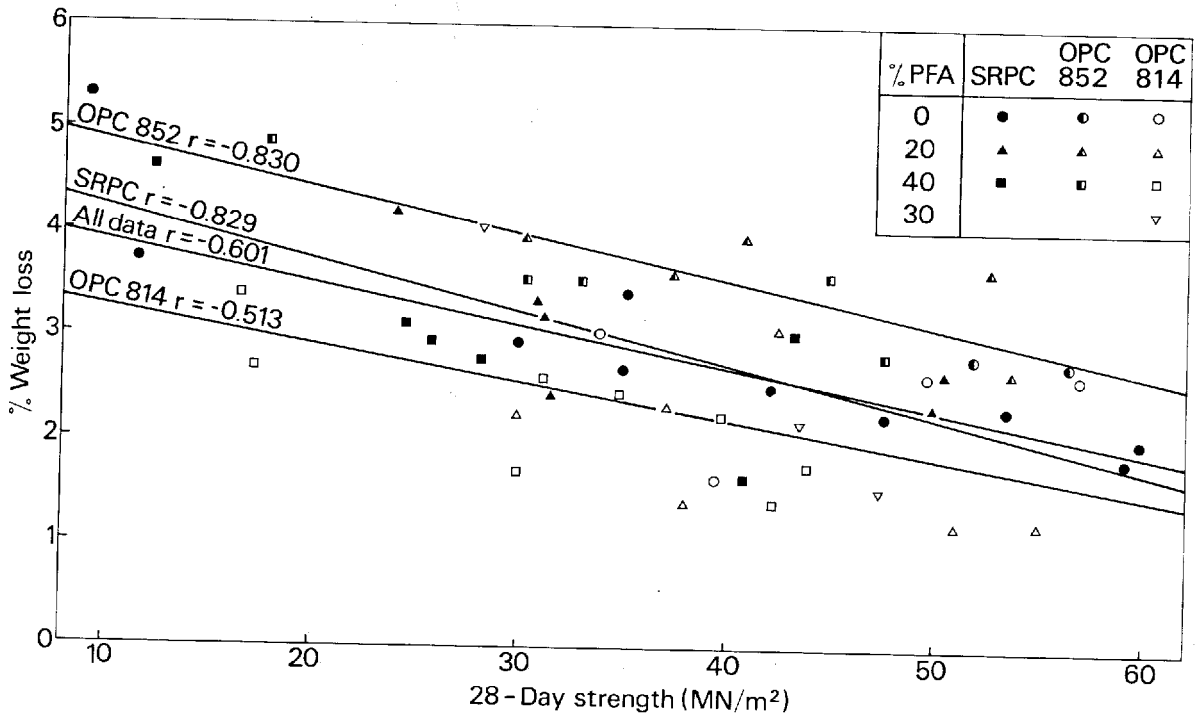

Figure 1: Percentage weight loss at 5 years v. 28-day compressive strength

retained'), and 28-day water-stored compressive strength (r = 0.567). Once again there was no dependence upon pfa content but there were indications of separate relationships for the three different cements and this is reflected in the separate correlation coefficients (r = 0.717, 0.686 and 0.665 for SRPC, OPC 852 and OPC 814 data respectively).

A good relationship was also found between percentage weight loss and the estimated free water/binder ratio (binder = cement plus pfa) for each mix (Figure 2, r = 0.547), the correlation coefficient being greater than 99.9% significant for the 55 data points. Individual correlation coefficients for the different cements are shown in Figure 2. A poorer correlation (r = -0.380) was found between percentage strength retained and free water/binder ratio.

DISCUSSION

The degree of deterioration of specimens after five years' exposure in acid groundwater, whether expressed as percentage weight loss or percentage strength retained, clearly depends upon the quality of the concrete which can be expressed in terms of its 28-day compressive strength or free water/binder ratio. There is no indication of any dependence upon pfa content.

Nevertheless, despite this statistical dependence upon concrete quality, the range of performance levels of the concretes is relatively small and there is only a limited difference in performance between the highest quality and lowest quality concretes. The percentage strength retained at five years varies between 49% and 82%, but the values for 45 of the 55 mixes fall in the range 53-68%; the mean value is 62%. Although two-year data are not reported here, it was generally observed that loss of both weight and strength occurred progressively between two and five years. At two years, the range of percentage strength retained values was 63-89% but, again, 43 of the 55 values fell in the range 67-83% with a mean value of 77%.

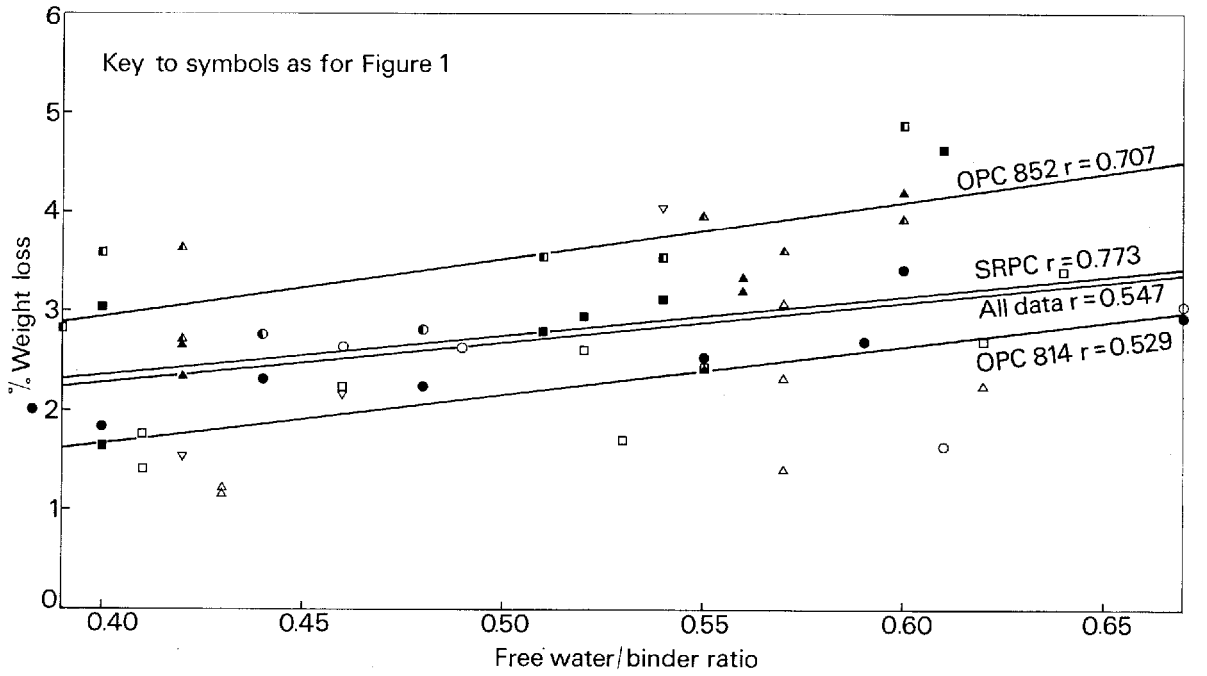

Figure 2: Percentage weight loss at 5 years v. free water/binder ratio

Comparable results were obtained by Halstead (6) in a similar experiment to the present one. Percentage strength retained at various ages in Halstead's work and the current work were as follows:-

Age (years)	0.5	1.0	1.5	2.0	3.5	4.0	5.0
% strength retained: Halstead	86	78	62	-	51	45	-
Present work	-	-	-	77	-	-	62

Halstead's work included a range of cement types,namely ordinary Portland, rapid-hardening, Portland blastfurnace, high alumina, sulphate-resisting, low heat and supersulphated, and he commented that strength loss of concrete using any of the cements tested was fairly uniform. Strength loss was, however, less with concrete of high strength and greater with concrete of lower strength although the differences were not large. Entirely comparable results (albeit on a smaller range of cement types) have been obtained in the current work. The rather lower values of percentage strength retained obtained in Halstead's work compared with the current work can probably be traced to the fact that almost half of Halstead's mixes had a w/c ratio as high as 0.8, indicating the likelihood of a faster rate of attack by acid water.

The apparent lack of dependence of acid resistance upon pfa content is of interest. As noted in the Introduction to this paper, the evidence in the literature is contradictory on whether cements containing pozzolanic materials such as pfa or latent hydraulic binders such as granulated blastfurnace slag are effective in improving acid resistance. The work of Halstead (6) referred to above found little difference in the performance of cements with and without slag. More recently, Fattuhi and Hughes (7) found that coatings to concrete were considerably more effective in improving acid resistance than were 'admixtures' which included pfa. Harrison (2) observed that the literature was conflicting but gave examples of test data where the use of slag or pfa offered little improvement (including the work of

Halstead and Fattuhi and Hughes). Other work which was cited as demonstrating an improved performance appeared to be confined to the use of cements with high slag contents. Although concluding that consensus appeared to point to a slower rate of attack on concretes with reduced lime content, the comment was made that many papers arrived at this view through theoretical, rather than practical, considerations.

The current work appears to support the view that the quality of the concrete is of greater significance to acid resistance than is the nature of the cement and, in particular, within the range tested (0-40%) there appeared to be no dependence upon pfa content.

It is, however, of interest to compare the performances of mixes containing the three different sources of Portland cement used in this study. As noted above and shown in the Figures, separate relationships between percentage weight loss or percentage strength retained and the indicators of concrete quality are suggested for the different cements. The compound compositions of the cements calculated by the Bogue formula indicate that the cement which has performed best (OPC 814) has the lowest C_3S and highest C_2S contents.

Although it must be stressed that the differences in performance in acid water between all three cements and their blends with pfa are small, nevertheless these data suggest that cements with higher C_3S contents, and consequentially lower C_2S contents, may not perform as well as cements with low C_3S contents. This appears to be recognised for example in the French Standard (8) for concrete in aggressive environments since, although OPC is permitted in the slightly and fairly aggressive degrees of exposure, it is recommended that the OPC should have low contents of C_3S and C_3A, (the latter for sulphate resistance purposes). Since C_3S liberates more calcium hydroxide on hydration than does C_2S, this would be compatible with the point noted by Harrison (2) that the consensus in the literature appears to point to a slower rate of attack on concretes with reduced lime contents. However, in the present mixes, the $Ca(OH)_2$ liberated by C_3S or C_2S will be at least partially combined by pfa with the formation of further quantities of calcium silicate (and aluminate) hydrates. If the pfa content appears to have little effect on acid resistance but the cements forming higher amounts of $Ca(OH)_2$ perform less well, this suggests that the acid resistance is reduced not only if the quantity of available $Ca(OH)_2$ is high but also if the quantity of calcium silicate hydrates is high. This is perhaps not unexpected since acid waters are, in time, able to leach lime from cement hydrates as well as uncombined $Ca(OH)_2$ from hardened concrete.

CONCLUSIONS

(i) The exposure of concrete specimens for five years in acidic groundwater has resulted in a gradual dissolution of the cement matrix from the concrete surface.

(ii) Rate of deterioration of concrete has been measured by percentage weight loss and by percentage strength retained.

(iii) There are correlations between these indicators of concrete deterioration and the quality of the concrete, whether measured by 28-day compressive strength or free water/binder ratio.

(iv) Despite the relationship between deterioration and concrete quality, the range of degrees of deterioration was relatively small for a wide range of concrete mixes.

(v) There appeared to be no relationship between acid resistance and pfa content.

(vi) Although quality of the concrete was the over-riding factor, there was some suggestion that cements with higher C_3S contents which liberate greater quantities of calcium hydroxide on hydration may be more susceptible to acid attack.

(vii) Conclusion (vi) appears to hold true even when the calcium hydroxide is combined by pfa to form further calcium silicate hydrates suggesting that it is the total quantity of lime-containing phases, rather than simply the uncombined $Ca(OH)_2$ content, which determines the overall acid resistance of the concrete.

ACKNOWLEDGEMENTS

The author would like to thank South West Yorkshire Water Authority for permission to establish the testing facility at Butterley reservoir and in particular the reservoir keeper, Mr John Shaw, for all his practical assistance at the site. Thanks are also due to all of those BRE colleagues who have assisted with preparation, transportation and testing of specimens.

REFERENCES

1. Eglinton, M.S., 'Review of concrete behaviour in acidic soils and ground waters', CIRIA Technical Note No. 69, 1975 (available to members of CIRIA only).

2. Harrison, W.H., 'Durability of concrete in acidic soils and waters', Concrete, 1987, 21, (2), 18-24.

3. Building Research Establishment, 'Concrete in sulphate-bearing soils and groundwaters', BRE Digest 174, 1975 (now withdrawn).

4. Building Research Establishment, 'Sulphate and acid resistance of concrete in the ground, BRE Digest 363, 1991.

5. BS 3892 : Part 1 : 1982. 'Pulverized-fuel ash for use as a cementitious component in structural concrete', British Standards Institution, London England, 1982.

6. Halstead, P.E., 'An investigation of the erosive effect on concrete of soft water of low pH value', Magazine of Concrete Research, 1954, 6, (17), 93-98.

7. Fattuhi, N.I. and Hughes, B.P., 'Effect of acid attack on concrete with different admixtures or protective coatings', Cement and Concrete Research, 1983, 13, 655-665.

8. French Standard P 18-001, 1985. 'Concretes: classification of aggressive environments', Association Francaise de Normalisation (AFNOR), Paris, France 1985.

STUDIES ON THE CARBONATION OF HYDRATED CEMENT AND ITS EFFECT ON MICROSTRUCTURE AND STRENGTH

H Matsusato, K Ogawa, M Funato and T Sato

Central Research Laboratory, Nihon Cement Co., Ltd.,
Tokyo, JAPAN

SUMMARY

Portland cement mortar specimens which were precured for 28 days at 20 °C 95% R.H. were carbonated at an accelerated pace up to 1 year. The strength of the specimens was measured through these curing ages. The progress of carbonation was monitored by the phenolphthalein method and by quantitative analysis of CaCO3 and silica gel (1). Pore size distribution and microstructure of the specimens were investigated. The influence of alkali and w/c of mortar upon the rate of carbonation were examined.

It was found that the progress of carbonation of Ca(OH)2 and C-S-H in the mortar specimens occurred concurrently, and alkali influenced rate of carbonation to a lesser extent than w/c. The strength of the specimens increased with the progress of carbonation, and no decline in strength occurred even if all the Ca(OH)2 and C-S-H in the specimens had reacted with CO2 to yield CaCO3 and silica gel. Pore volume higher than 6 nm was decreased by carbonation, this reduction in porosity led to increase in strength. A change in pore size distribution was also observed with carbonation, that is, the pores between approximately 80 nm and 300 nm were decreased. This change in pore size distribution was apparently related to the difference in morphology between C-S-H and carbonated products such as silica gel or calcium carbonate.

概要

20℃－95%R.H.で 1ヵ月間前養生したポルトランドセメントのモルタル試験体を 1年間迄促進炭酸化した。この養生期間を通じて試験体の強さを測定した。フェノールフタレイン法及び炭酸カルシウムとシリカゲルの定量(1) によって炭酸化の進行を追跡した。細孔径分布及び微細構造を調べた。また，炭酸化速度に対するアルカリ及びモルタルの w/cの影響を調べた。

モルタル試験体中での$Ca(OH)_2$とC-S-Hの炭酸化反応は同時に進行すること，炭酸化速度に対するアルカリの影響は w/c と比較して小さいことが分った。炭酸化の進行に伴って強さが増大し，試験体中の全ての$Ca(OH)_2$とC-S-H がCO_2と反応して$CaCO_3$とシリカゲルを生成しても強さの低下は生じなかった。炭酸化により，6nm 以上の全細孔容積が減少した。この空隙率の減少は強さの増大と対応している。炭酸化によって細孔径分布が変化した。即ち，約80nmと300nm の間の空隙が減少した。この細孔径分布の変化はC-S-H と炭酸化生成物(シリカゲルや$CaCO_3$) の間の形態の差と関連している。

INTRODUCTION

A number of studies have appeared in the literature on the neutralization of concrete in the context of steel reinforcement corrosion (2). Most of these studies on carbonation of the hydrated cement have been concerned with the reaction of Ca(OH)2 with CO2 to form CaCO3. But it is also known that not only calcium hydroxide but also all the other hydrated compounds react with CO2 when atmospheric carbon dioxide diffuses into concrete (3,4). However, little has been reported on the influence of carbonation reaction of C-S-H on the microstructure or the strength of hardened cement. This is largely because both C-S-H and silica gel which is produced by carbonation of C-S-H are poor in crystallinity and therefore there was no effective method to analyze them quantitatively.

This investigation was taken up to reveal the influence of carbonation of C-S-H on the microstructure and strength of hydrated cement, by applying a quantitative analytical method of silica gel as proposed by the authors (1). The influence of water to cement ratio (w/c) and alkali content on the progress of carbonation were also examined.

EXPERIMENTAL

Specimens

Mortar specimens of 4x4x16 cm were prepared at w/c = 0.5 (cement:sand = 1:2) and w/c = 0.7 (cement:sand = 1:2.8) using ordinary Portland cement and Toyoura standard sand which is described in JIS R 5201. The chemical composition of the cement is shown in Table 1. In order to examine the influence of alkali on the progress of cement, two samples of the cement, one in which the alkali content (as equivalent Na2O) was adjusted to 1.16% by adding NaOH reagent and the other the original cement as such which contained 0.56% of alkali were used. Mortar specimens from these were carbonated at an accelerated rate, or cured in ordinary atmosphere, as shown schematically in Fig.1.

Table 1 Chemical composition of the cement sample

(mass %)

Loss on ignition	Insol.*	SiO_2	Al_2O_3	Fe_2O_3	CaO	MgO	SO_3	Na_2O	K_2O	TiO_2	P_2O_5	MnO	Total	(R_2O**)
1.0	0.3	22.0	5.5	3.1	63.2	1.6	1.9	0.26	0.45	0.37	0.19	0.14	100.01	(0.56)

*Insoluble residue **; equivalent Na_2O

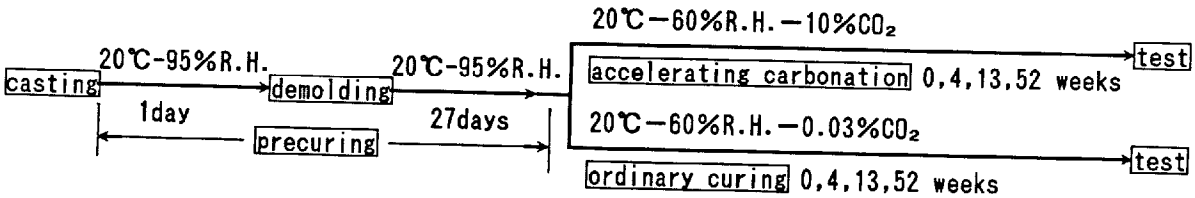

Fig.1 Curing conditions of the specimens

Testing method

(i) Strength

The flexural and compressive strengths of the mortar specimens were measured up to the age of 1 year.

(ii) Rate of neutralization

The depth of neutralization was measured by spraying an ethanolic solution of phenolphthalein on the surface of broken specimens of 10x10x40 cm.

(iii) Phase composition

A sample of 4x4x3 cm was cut off from the center of the mortar specimen of 4x4x16 cm, as shown in Fig.2, then crushed to below 5 mm and immersed in acetone to stop hydration. The following investigations were performed with the sample after D-drying. Loss on ignition of the sample was measured after ignition for 1 hour at 950°C. The CaCO3 content was calculated from the carbon content which was analyzed with a carbon analyzer. The silica gel content was analyzed by the procedure schematically represented in Fig.3 (1). The sand content was evaluated based on the assumption that it was equal to the insoluble part of the specimen as shown in Fig.3. The CaCO3 and silica gel contents were referred to the weight of anhydrous cement. Infrared spectroscopy was used to ascertain the decomposition of C-S-H and the formation of silica gel.

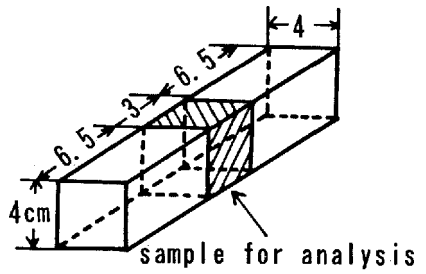

Fig.2 Sampling position of the sample for analysis

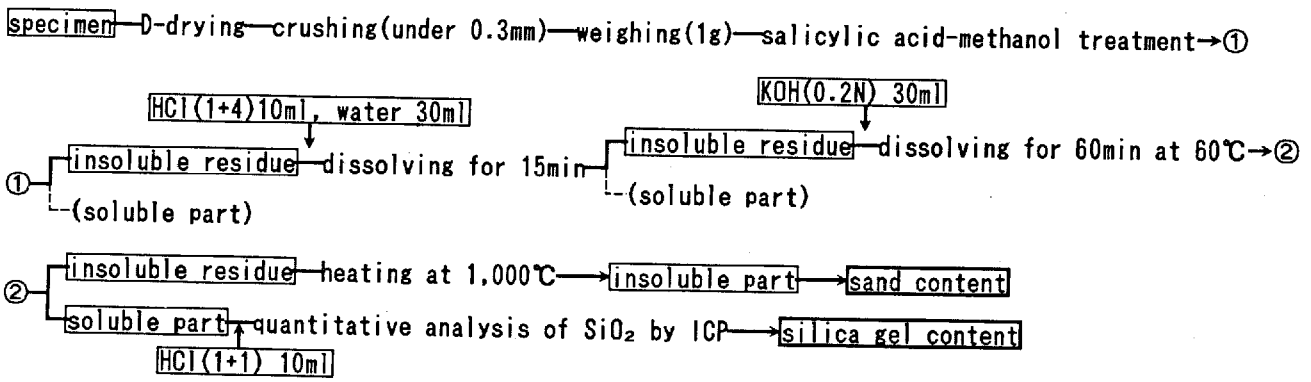

Fig.3 Procedure for analysis of silica gel (1)

(iv) Microstructure in the mortar specimen

The inside of the cut-off sample from the mortar specimen which was cured for 1 year in ordinary atmosphere and the outside of the mortar specimen which was subjected to accelerated carbonation for 1 year were used as the non-carbonated sample and the carbonated sample respectively. The pore volume and the pore size distribution of these samples were observed to be in the range 6 nm to 100,000 nm by mercury intrusion porosimetry. SEM observation was also performed to reveal the difference in microstructure between the non-carbonated and the carbonated samples.

RESULTS AND DISCUSSIONS

Flexural as well as compressive strengths of the mortar specimens which underwent accelerated carbonation were higher than those of the specimens cured in ordinary atmosphere, as shown in Figs.4 and 5.

The depth of neutralization of 10x10x40 cm specimen is shown in Fig.6. The values of coefficient k as obtained from the following equation going the rate of neutralization of these specimens are shown in Table 3.

$$A = k \times \sqrt{t} + b \qquad (1)$$

where A: depth of neutralization(mm)
k: coefficient of the rate of neutralization
t: curing time (week) b: coefficient

From these results, it can be seen that w/c has a greater influence than alkali content of the cement on the rate of neutralization.

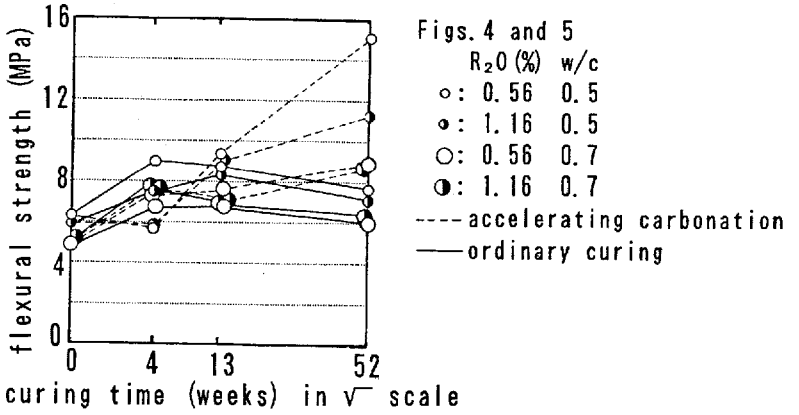

Fig.4 Flexural strength of the mortars

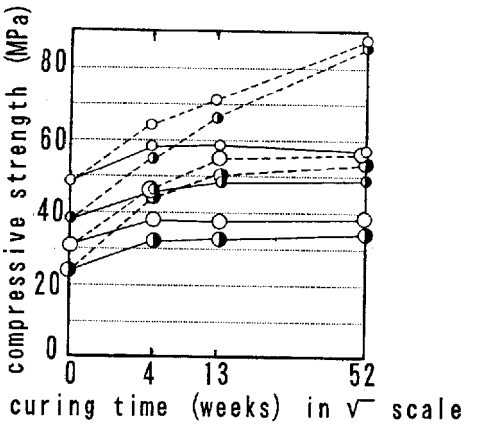

Fig.5 Compressive strength of the mortars

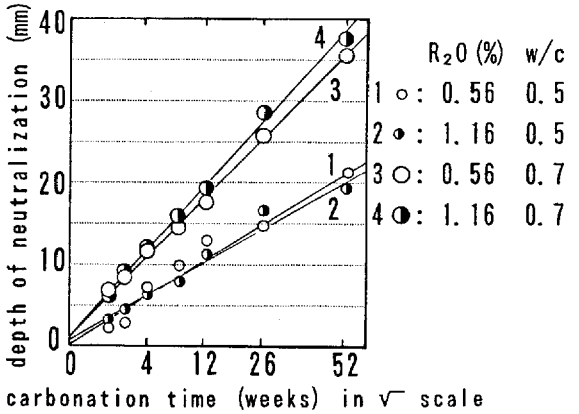

Fig.6 Depth of neutralization of the specimens subjected to accelerated carbonation

Table 2 The value of coefficient in equation of rate of neutralization

	w/c = 0.5		w/c = 0.7	
	R_2O=0.56%	R_2O=1.16%	R_2O=0.56%	R_2O=1.16%
k	3.0	2.8	4.8	5.2
r*	0.974	0.986	0.997	0.998

*; coefficient of correlation

Changes in CaCO3 and silica gel contents with curing time are shown in Figs.7 and 8. As can be expected, CaCO3 and silica gel contents increased with curing time in all cases. Amongst them, the specimens which contained 1.16% of alkali showed higher CaCO3 and silica gel contents than those low in alkali (0.56%), in the case of w/c = 0.5. It was observed in these specimens that just after precuring for 28 days the Ca(OH)2 and non-evaporable water contents for the specimen high in alkali were lower than for the specimen low in alkali, and the porosity of the specimen high in alkali was higher than that of the specimen low in alkali see Table 3 and Fig.9(a) . From these results, the influence of alkali content on the carbonation reaction comes out to be as follows : a coarser microstructure is formed in the hardened mortar high in alkali, as alkali slows down the progress of hydration, and this coarser microstructure enable CO2 to easily diffuse into the specimen. Little accelerating effect on carbonation by alkali was found when w/c = 0.7. In this case, the porosity of the specimens just after precuring for 28 days was higher irrespective of the alkali content, as shown in Fig.9(b), so the influence of alkali on carbonation seems to have been little.

Table 3 Ca(OH)2 and non-evaporable water contents of the mortar after precuring

(g/100g-cement)

	w/c = 0.5		w/c = 0.7	
	R_2O=0.56%	R_2O=1.16%	R_2O=0.56%	R_2O=1.16%
$Ca(OH)_2$	20.1	15.3	20.0	18.1
water*	23.8	20.6	24.0	21.6

*;non-evaporable water

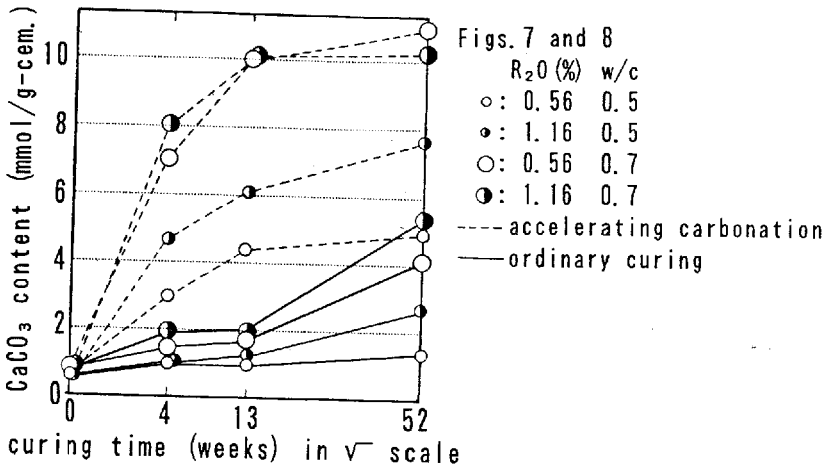

Fig.7 Changes of CaCO3 in the specimens with curing time

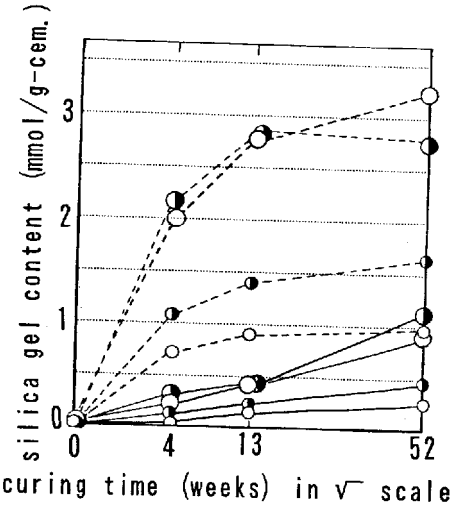

Fig.8 Changes of silica gel in the specimens with curing time

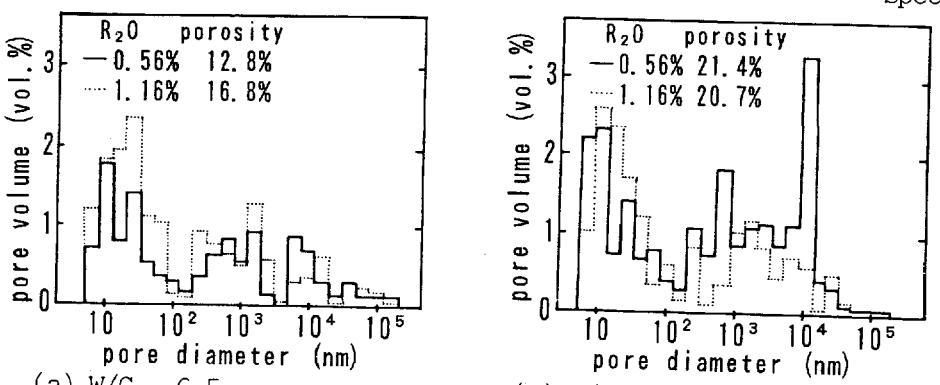

(a) W/C = 0.5 (b) W/C = 0.7

Fig.9 Pore size distributions of the mortars after precuring

From the results of changes in strength and carbonation in Figs.4 to 8, it can be seen that strength increased with progress of carbonation. As the CaO and SiO2 contents of the cement used were 11.2 mmol/g and 3.67 mmol/g respectively, almost the entire CaO and SiO2 had existed as CaCO3 and silica gel in the specimens whose w/c = 0.7 and which underwent accelerated carbonation for 52 weeks. This means that the whole Ca(OH)2 and C-S-H in the specimens had already reacted with CO2 to form CaCO3 and silica gel. The IR spectra of these specimens showed one absorption band at a wave number of around 1,040 cm-1 which was attributed to silica gel and another one around 870 cm-1 attributed to CaCO3. However, the absorption band may be seen around 950cm-1 due to C-S-H was not observed, as in Fig.10. The results thus showed that if all the Ca(OH)2 and C-S-H in the specimens had reacted with CO2 to yield CaCO3 and silica gel, no decline in strength occurred. The interrelationship between CaCO3 and silica gel contents resulting from the carbonation reaction are shown in Fig.11. It was revealed that the carbonation of C-S-H and Ca(OH)2 in mortar specimen start and proceed simultaneously, because a small amount of silica gel was detected with a small amount of CaCO3 even at the start of carbonation, and the CaCO3 content increased in proportion to the silica gel content.

The content of CaCO3 due to carbonation of C-S-H was estimated assuming the molar ratio of Ca/Si of C-S-H in the specimen to be 1.7, as shown in Fig.11, in which line 1 shows the relationship [CaCO3]= 1.7 x [silica gel] (in mmol). The CaCO3 content originating from Ca(OH)2 as shown in Fig.11 was calculated by the difference of Ca(OH)2 content between the non-carbonated part at the inside of the mortar cured in ordinary

atmosphere and the carbonated part at the outside of the mortar subjected to accelerated carbonation. The content of CaCO3 resulting from carbonation of other hydrates, such as AFm, in Fig.11 were estimated by subtracting the sum of the CaCO3 contents originating from both Ca(OH)2 and C-S-H from the total CaCO3 content.

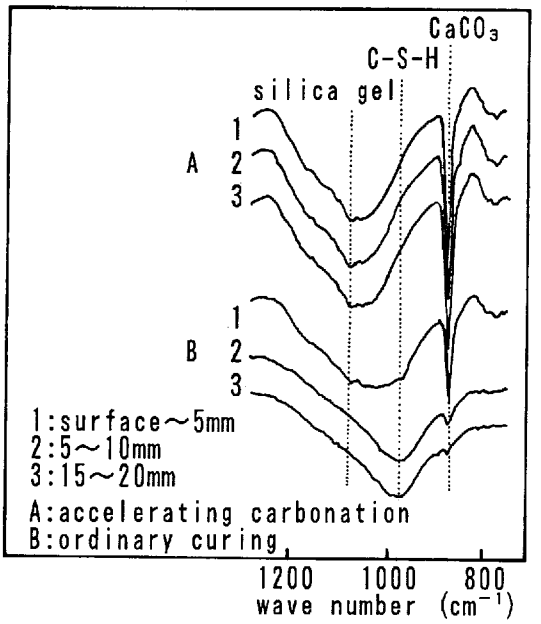

Fig.10 IR spectra of non-carbonated and carbonated part

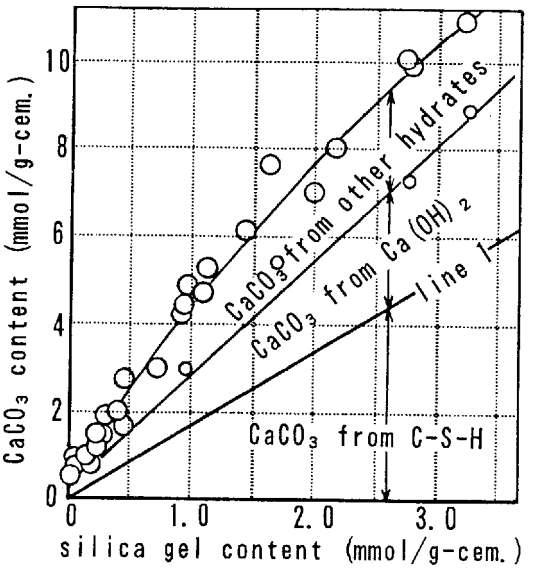

Fig.11 Relationship between CaCO3 and silica gel content

Fig.12 shows the pore size distributions of the carbonated and the non-carbonated parts of the specimens. The pore volume greater than 6 nm and in the range of around 80 to 300 nm were reduced by carbonation. This reduction in porosity caused an increase in the strength.

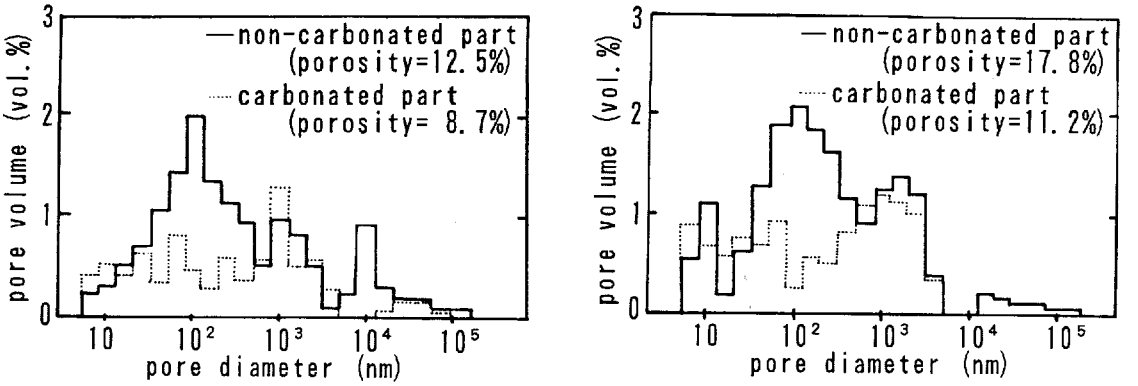

(a) W/C=0.5, R2O=0.56% (b) W/C=0.7, R2O=0.56%

Fig.12 Pore size distributions of non-carbonated and carbonated part of the mortars cured for 1 year

Fig.13 shows the SEM images of the fracture surface of mortar specimen. A large, layer structure of Ca(OH)2 crystal with a smooth surface and a sharp edge can be seen in the non-carbonated part of the specimen, as shown in Fig.13(a). Fig.13(b) shows the fracture surface of the carbonated specimen which are considered as the cluster of CaCO3 yielded by carbonation of Ca(OH)2. The surface of this carbonate is rough, and consists of a few ten nm's of grains. Fig.13(c) is a SEM image of non-carbonated, typical C-S-H of 20 to 50 nm in thickness and around 300 to 1,000 nm in length. Fig.13(d) is a SEM image of the carbonated part which shows the cluster of spherical

grains around 30 to 50 nm in size. These grains are taken to be calcium carbonate and silica gel yielded by carbonation of C-S-H, since the original shape of C-S-H can still be seen. Thus, these carbonated products are formed in situ from the non-carbonated hydrates without substantial change in the configuration of the hydrates.

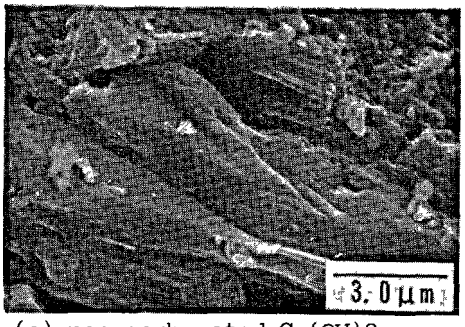

(a) non-carbonated Ca(OH)2

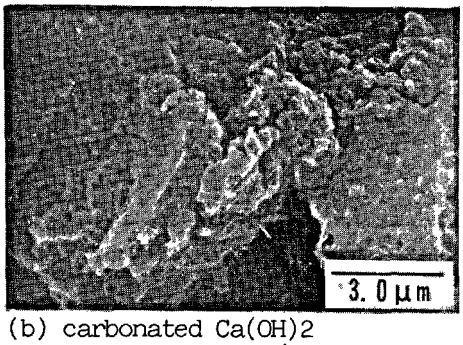

(b) carbonated Ca(OH)2

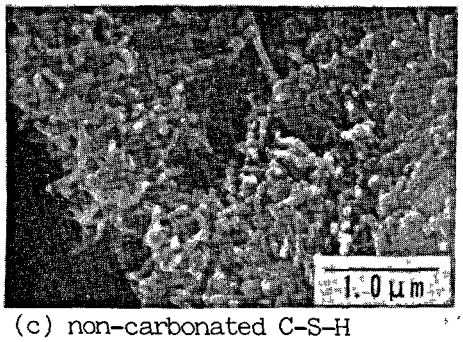

(c) non-carbonated C-S-H

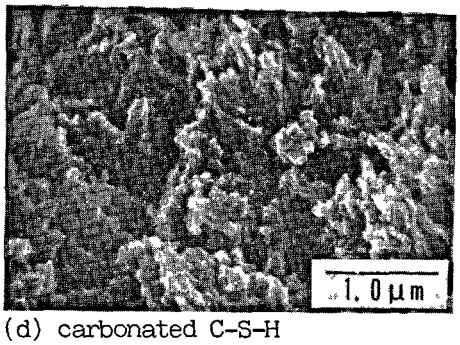

(d) carbonated C-S-H

Fig.13 SEM images of non-carbonated and carbonated part of the specimens

From these SEM observations, it is revealed that the configurations of non-carbonated hydrates are retained through carbonation of the hydrates to form the finer carbonated products.

4. Conclusions

i) The carbonation of Ca(OH)2 and C-S-H in hydrated cement progress concurrently.
ii) The influence of alkali on the acceleration of the carbonation of Ca(OH)2 and C-S-H is less than that of w/c. This effect of alkali is considered as mainly due to the retardation of cement hydration and the formation of coarser microstructure.
iii) Mortar strength is increased as the carbonation progress. No decline of strength occurs even if all the Ca(OH)2 and C-S-H in the specimens have reacted with CO2 to yield CaCO3 and silica gel.
iv) The volume of pores greater than 6 nm and between approximately 80 and 300 nm are decreased by carbonation. The configurations of non-carbonated hydrates are retained through carbonation of the hydrates to form the finer carbonated products.

REFERENCES

1) M.Funato, M.Hashimoto and S.Kuramochi: "Studies on quantitative analysis of silica gel formed by carbonation of cement hydrates", CAJ Proc. Cem. Concr. 1991, No.44, 252-257
2) L.J.Parrot: "A review of carbonation of reinforced concrete", Cement and Concrete Association, Building Research Establishment, C&CA/BRE special publication, 1987
3) J.Calleja: "Durability", 7th ICCC, 1980, Vol.I, VII 2/1-2/48
4) D.M.Roy: "Mechanism of cement paste degragation due to chemical and physical factors", 8th ICCC, 1986, Vol.I 362-380

CARBONATION OF PORTLANDITE SINGLE CRYSTALS AND PORTLANDITE IN CEMENT PASTE

J R Johnstone and F P Glasser

Department of Chemistry, University of Aberdeen, Aberdeen, Scotland, U.K.

SUMMARY

It is generally regarded that the durability of reinforced concrete can be drastically reduced by carbonation. Some complex investigations involve modelling the physicochemical processes associated with cement and concrete carbonation. This study hopes to augment these with a simpler, more direct approach. Calcium hydroxide crystals and cement paste specimens were prepared and subsequently carbonated under accelerated conditions and two different humidity conditions, for 21 days. Electron microscopy of the calcium hydroxide crystals identified 'rims' of calcium carbonate around the crystal. The calcium carbonate present was a mixture of calcite and vaterite. From X-ray analysis, no preferred orientation was detected for either polymorph, and initial indications suggest that the surface nucleation of the carbonate material is random. The carbonation of the calcium hydroxide content of the cement specimens could not be observed by electron microscopy, but the apparent destruction of ettringite, due to the lowering of the pH in the carbonated regions, was noted. This study suggests that calcium hydroxide is not directly converted to calcium carbonate, but that a dissolution-reprecipitation process accounts for a large part of the transformation.

RESUME

Il est généralement admis que la durabilité du béton armé peut être profondément altérée par la carbonatation. La carbonatation est souvent étudiée par des voies compliquées qui mettent en oeuvre la modélisation des processus physico-chimiques intervenant dans les ciments et les bétons. La présente étude est au contraire basée sur une approche plus simple et plus directe du problème. Des cristaux d'hydroxide de calcium ainsi que des échantillons de ciments ont été préparés puis carbonatés sous des conditions accélérées; 21 jours sous deux humidités différentes. L'étude par microscopie électronique des cristaux d'hydroxide de calcium révèle la formation d'une couche de carbonate de calcium formée autour des cristaux. Le carbonate de calcium est composé d'un mélange de calcite et de vatérite. Aucune orientation préférentielle n'a été détectée pour la calcite aussi bien que pour la vatérite par diffraction de rayons X. Les premières informations suggèrent plutot que la nucléation est alléatoire. La carbonatation de l'hydroxide de calcium contenu dans le ciment n'a pu être observée directement par microscopie électronique. Cependant il apparait que l'ettringite est détruite dans la zone carbonatée. Cette étude suggère que l'hydroxide de calcium n'est pas directement transformé en carbonate de calcium. Un mécanisme de dissolution-précipitation semble intervenir au cours de cette transformation.

INTRODUCTION

One of the most deleterious processes affecting the durability of reinforced concrete is generally regarded to be carbonation. The two major phases present in the hydrated cement component, namely C-S-H (calcium silicate hydrate) and CH (calcium hydroxide) react readily with CO_2 (carbon dioxide).

$$C\text{-}S\text{-}H(s) + CO_2(g) \rightarrow CaCO_3(s) + H_2O(l) + \text{"amorphous silica"}(s) \quad (1)$$

$$Ca(OH)_2(s) + CO_2(g) \rightarrow CaCO_3(s) + H_2O(g,l) \quad (2)$$

Investigations into the effect of carbonation on cement and concrete systems have been carried out [1-5] with general agreement on the observed reactions and conclusions. Recent work [6-9] has involved the derivation of complex systems which mathematically model the physicochemical processes involved in cement and concrete carbonation. The combination of defined reaction conditions with assumed unsteady state dynamics, results in the development of expressions which describe and predict the carbonation process. To fully understand the carbonation mechanism of cement paste, such models, which provide useful and accurate data, need to be augmented by a simpler, more direct study of the process. Of all the cement phases which undergo carbonation, CH is seen as one of the most susceptible to CO_2 attack. There is some debate [2,10], as to whether CH or C-S-H is preferentially carbonated but, for simplicity, only the carbonation of CH itself and CH in cement paste (Equation.2) is considered here.

Before looking at carbonation itself, it is prudent to firstly consider the morphology of the CH in the cement paste, as this will have a direct bearing on subsequent reactions with CO_2. It is thought [11], that the morphology of CH in cement paste changes during ageing. With ongoing hydration, fresh CH is continually being formed, and along with the dissolution of small CH crystals, areas of supersaturated CH solution are thermodynamically possible. This may establish concentration gradients within the fine pore system which, in turn, can lead to the diffusion of CH to the larger pores and voids, where large CH crystals tend to grow at the expense of the smaller ones. CH may also be finely distributed through the C-S-H gel and capillary pores.

With this wide range in size of CH in cement paste, the reactivity with respect to carbonation will also be very different; the smaller and less crystalline regions of CH being more reactive than the larger, more regular CH crystals. The carbonation process only adds another level of complexity to the reactions within cement paste, so in trying to develop an insight into the carbonation reaction it is hoped that an actual mechanism may be postulated.

EXPERIMENTAL

CH single crystals were grown by an adapted slow diffusion process in solution [12,13]. In a CO_2-free atmosphere, 30% solutions of sodium hydroxide and calcium chloride were prepared, and 250ml of each were placed in separate plastic bottles. The bottles were placed in the bottom of a large desiccator, which was slowly filled with degassed, double-distilled water, to a level approximately 50mm above the open tops of the plastic bottles. The desiccator was stored in a cool, thermally stable environment for 5 weeks, after which CH crystals (ca. 2-3mm in size) formed. These were removed, dried, and subsequently stored under nitrogen until required.

Cement paste specimens (10x10x50mm) were prepared using Ordinary Portland Cement (OPC) to BS 12 with a water/cement ratio of 0.4. The cement bars were demolded after 24 hours and cured for 7 days at 100% relative humidity in a CO_2-free environment before carbonation.

The carbonation of the CH crystals and the cement specimens was carried out under accelerated conditions in a 100% CO_2 atmosphere. Two carbonating chambers were constructed (Figure 1), one at 100% relative humidity and the other at a calculated relative humidity of less than 1%. It was originally intended to have a continuous flow of CO_2 through each chamber, but the suggestion by Reardon et. al. [14] of purging the system every 3-4 days for 1 hour to enable an equilibrium between the CO_2 and the specimens to be established was adopted.

Specimens were immediately carbonated for 21 days.The cement specimens in the dry carbonating chamber were not dried to an equilibrium level, but were initially moist at the start of carbonation. It was thought that this would simulate more accurately the conditions in which cement undergoes carbonation in dry climates. Non-carbonated CH crystals and cement bars were stored under similar humidity regimes, in a CO_2-free atmosphere for a similar length of time.

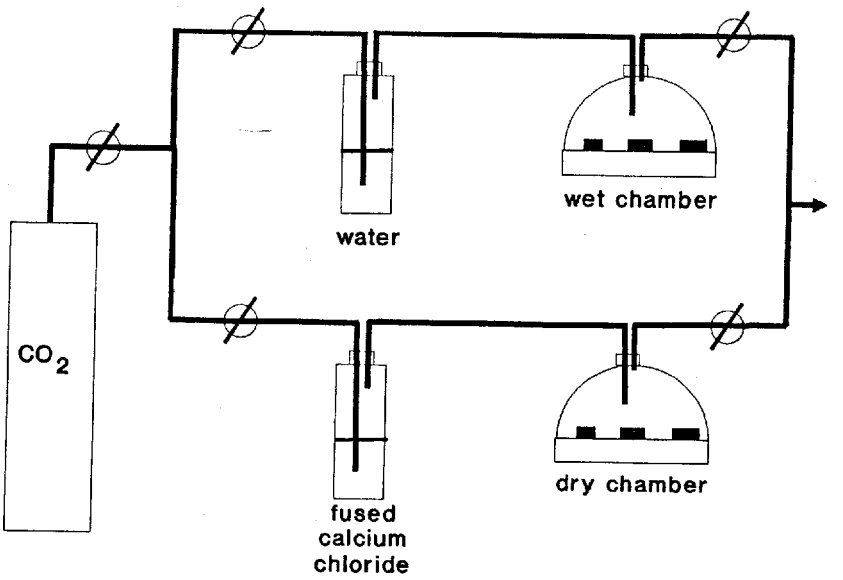

Figure 1: Schematic Representation of the Carbonating Chambers.

RESULTS AND DISCUSSION

Electron microscopy of the moist and dry carbonated CH crystals showed a marked change in appearance and, upon examination of cross sections, the formation of "rims" around the crystal (Figure 2). These "rims", subsequently determined as $CaCO_3$ (calcium carbonate), had not formed on the outer surface of the crystal, but had ingressed into the crystal forming a "skin" of carbonate material around an interior of, as yet, uncarbonated CH. The appearance of these carbonate "rims" were similar in both the moist and dry carbonated CH crystals. Wet conditions produce condensation on the crystal surfaces aiding reaction, but under dry conditions surfaces of CH crystals do not act as sites for capillary condensation of water. However, if direct reaction occurs between CH and CO_2 and $CaCO_3$ is formed, pores may develop and these do appear to offer sites for capillary condensation, particularly as water is evolved. Compared to the surface and near-surface of non-carbonated CH crystals (Figure 3), the morphology of the carbonated region appears very different to the general appearance of the interior CH. Severe cracking of the carbonated region occurs perpendicular to the crystal face (Figure 2), suggesting that the formation of the $CaCO_3$ may have occurred in a strained environment.

Calculations of the difference in molar volumes of the solid phases shows that the carbonation process, assuming calcite to be the solid product, is accompanied by an increase of approximately 11%. X-ray analysis of the CH crystals revealed that the $CaCO_3$ formed was a mixture of two polymorphs; calcite and vaterite. It is generally regarded [4] that calcite, being the most stable polymorph, is the "ultimate" product of carbonation, and that the vaterite formed was an intermediate product. From X-ray films, estimated line intensities seem to indicate that when examined *in situ* on the CH crystal, there is no preferred orientation of either the calcite or vaterite product. Work is continuing to determine whether there is any directionality of the carbonation of CH crystals, but the preliminary indications are that surface nucleation and subsequent growth of the $CaCO_3$ is random (Figure 4).

Differential Thermal Analysis of the moist carbonated CH crystals determined that the amount of $CaCO_3$, by weight, and hence an indication of the degree of carbonation, was approximately 6% in 21 days.

This is significantly less than observed in the carbonation of cement paste, but can be accounted for in terms of the difference in the morphology, size and perfection of CH crystals, relative to those present in cement paste. CH crystals are generally less reactive than CH present in cement, as their smooth surfaces, with well defined edges and few surface defects, tend to act as a good barrier against the attack and subsequent diffusion of CO_2. The accompanying volume increase associated with the carbonation process suggests that $CaCO_3$ product will increase the density of the layers on and just below the surface, thus restricting diffusion of CO_2 and slowing further carbonation.

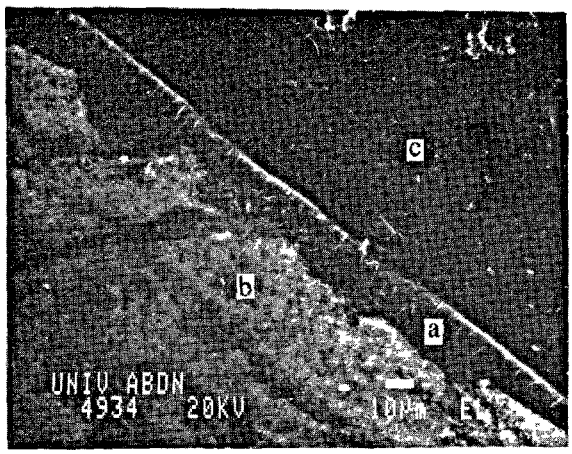

Figure 2: Carbonated CH Crystal showing region of carbonated material (a), uncarbonated CH (b) and inert mounting resin (c).

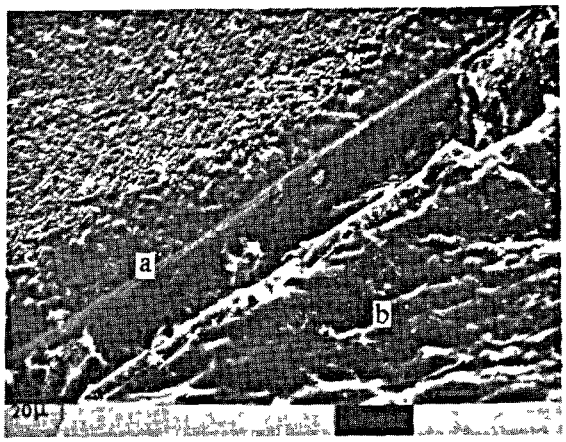

Figure 3: Noncarbonated CH Crystal (a), with etched surface and mounting resin (b).

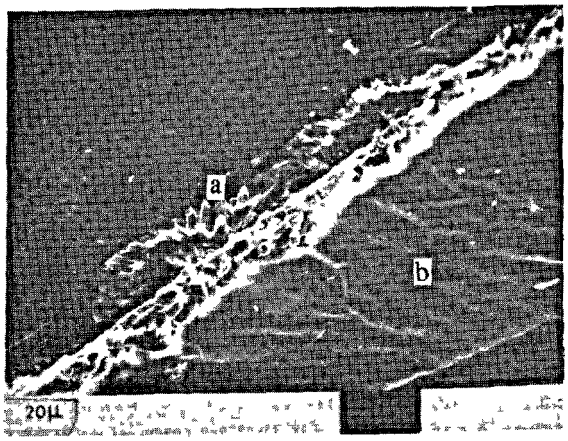

Figure 4: Carbonated CH Crystal showing $CaCO_3$ Growth in Random Orientations (a), on the crystal surface and mounting resin (b).

The carbonation of hardened cement paste is more complex, since several other hydrated phases present also react with CO_2. The carbonation of the CH component in cement, though, is considered to be of great importance, as it appears to react preferentially with CO_2, and has been described in great detail [1-8]. The mechanism proposed by Powers [15] is now generally thought to involve the dissolution of CO_2 and CH in the pore fluid, followed by reprecipitation of $CaCO_3$, mainly as the thermodynamically favourable polymorph

calcite, although vaterite and aragonite may also be observed in practice. Diffusion of calcium, through the establishment of high concentration gradients in solution, is thought to assist the carbonation of CH. With the carbonation process consuming CH, the diffusion of yet more calcium to the carbonation front is accelerated. This is thought to partially account for the high rate of carbonation after the induction period and during the early life of the cement. The subsequent slowing of the carbonation rate is thought to be the consequence of lowering concentration gradients, resulting in slower transport of calcium to the reaction front, as well as the increase in volume of solids, reducing the connected porosity of the cement. X-ray analysis shows the presence of calcite, CH and unreacted cement phases (mainly C_2S), in both the moist and dry carbonated specimens. The calcite detected is semi-crystalline nature, giving broadened diffractions.

A rough approximation of the depth of carbonation was obtained by spraying a 1% phenolphthalein solution onto freshly broken surfaces and measuring the depth of carbonation. This was observed to be on average, 1.55mm for the dry carbonated specimens and 1.85mm for the moist carbonated specimens.

Electron microscopy of coated, fracture surfaces of the cement specimens are unable to show the carbonation of CH and the subsequent formation of calcite. What the micrographs do show is that in the noncarbonated regions of the cement (Figure 5), the typical morphology of the early forming ettringite (AFt), phase is observed. In the carbonated region of the cement, (Figure 6), the AFt phase is no longer present and would appear to have been destroyed by the carbonation process [4].

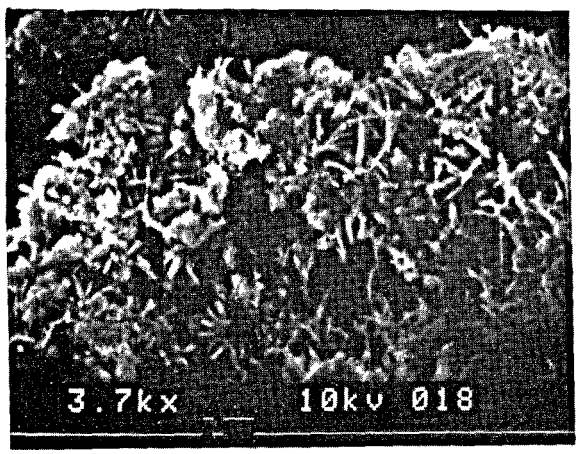

Figure 5: Noncarbonated OPC showing the typical morphology of AFt.

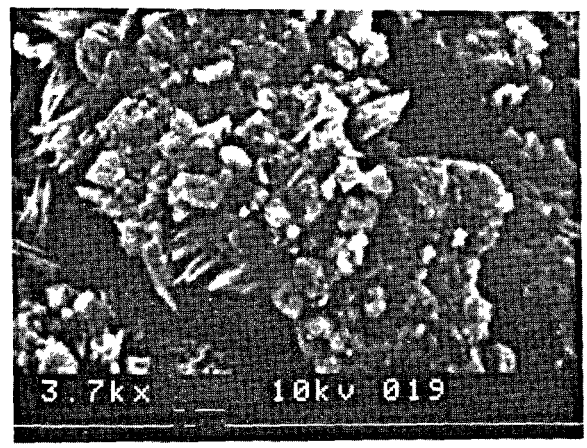

Figure 6: Carbonated OPC with no apparent AFt.

Such observations help to determine that direct transformation of CH to $CaCO_3$ in cement paste is highly unlikely. Indirect evidence, such as the lack of a topotactic transformation and the difficulty of accommodating a volume increase of up to 11% associated with the conversion, supports the belief that CH is not wholly converted to $CaCO_3$ by direct reaction. The presence of large CH crystals in cement paste will, however, lead to large local stress accumulations during carbonation. On that account, it may be desirable to control crystallite formation, by either using a low w/c ratio, or additive materials such as superplasticizers, which inhibit crystal growth [16].

CONCLUSIONS

(i) The carbonation of CH crystals produced "rims" of $CaCO_3$ which ingress into the crystal. The cracking of these "rims" is thought to be due to the strain resulting from the volume increase upon carbonation.

(ii) Direct reaction between CH and CO_2 appears to be restricted to initial stages during dry carbonation. Once pores and cracks are established, offering sites for capillary condensation, the carbonation process of CH crystals is similar to that of cement paste.

(iii) The $CaCO_3$ formed is a mixture of calcite and vaterite, with calcite seen as the "ultimate" carbonation product and vaterite as an early intermediate form. There is no preferred orientation of the $CaCO_3$ and surface nucleation seems to occur randomly.

(iv) The relative humidity during carbonation of both CH crystals and cement paste in the dry carbonating chamber was raised significantly due to the initial moisture released by the cement specimens. This makes it difficult to correlate carbonation with relative humidity, because local disequilibrium occurs within pores and cracks.

(v) The carbonation of CH in cement paste is thought to progress through a dissolution-reprecipitation process, which results in the formation of semi-crystalline $CaCO_3$, mainly calcite. The transport of the CH to the reaction front is thought to account for the initial high carbonation rate, which is subsequently reduced by the slowing of the CH and CO_2 counter-diffusion.

(vi) There is no evidence to suggest that CH in cement paste is directly transformed to $CaCO_3$.

(vii) The large volume increase accompanying carbonation of CH suggests that the presence of large crystals of CH could lead to unacceptable local stresses.

REFERENCES

1. Hamada M.: "Neutralization (Carbonation) of Concrete and Corrosion of Reinforcement Steel". **Proc. 5th Intl. Symp. Cement Chem (Tokyo)**, 1969, 343-69.

2. Calleja J.: Carbonation Section of Principle Report on Durability. **Proc. 7th Intl. Symp. Cement Chem (Paris)**, 1980, **VII**- 2/1.

3. Parrott L.J.: "Carbonation, Corrosion and Standardisation". **Protection of Concrete, Intl. Conf.**, (Dundee), 1990, 1009-24.

4. Richardson M.G.: **Carbonation of Reinforced Concrete.**, Citis Ltd., (Dublin), 1988.

5. Smolczyk H.G.: "Physical and Chemical Phenomena of Carbonation". **RILEM Symp. Carbonation of Concrete**, 1976, Paper 1.1.

6. Fukushima T.: "Theoretical Investigation on the Influence of Various Factors on Carbonation of Concrete". **4th Intl. Conf. Durability of Building Mater. and Components (Singapore)**, 1987, 662-70.

7. Papadakis V.G. et.al.: "Fundamental Concrete Carbonation Model and Application to Durability of Reinforced Concrete". **Proc. 5th Intl. Conf. Durability of Building Mater. and Components (Brighton U.K.)**, 1990, 27-38.

8. Ying-yu L.; Qui-dong W.: "The Mechanism of Carbonation and its Dependence on Pore Structure". **Concrete Durability - Katherine and Bryant Mather Intl. Conf. SP-100, Amer. Concrete Inst.**, 1987, **2**, 1915-43.

9. Cowie J.; Glasser F.P.: "The Reaction Between Cement and Natural Waters Containing Dissolved Carbon Dioxide". Adv. in Cement Res. (in press)

10. Slegers P.; Rouxhet P.: "Carbonation of the Hydration Products of Tricalcium Silicate (C_3S)". Cement and Concrete Research, 1976, **6**, 381-88.

11. Bache H.H. et. al.: "Morphology of Calcium Hydroxide in Cement Paste". **Symp. on Structure of Portland Cement Paste and Concrete. Highway Research Board (Washington)**, 1966, 154-74.

12. Ashton F.W.; Wilson R.: "The Preparation and Optical Properties of Calcium Hydroxide Crystals". Amer. Jou. Sci., 1927, **13**, 209-18.

13. Johnston J.: "The Utilization of Diffusion Processes in the Preparation of Pure Substances". Jou. Amer. Chem. Soc., 1914, **36**, 16-19.

14. Reardon E.J.; Dewaele P.: "Chemical Model for the Carbonation of a Grout/Water Slurry". Jou. Amer. Ceram. Soc., 1990, **73**[6], 1681-90.

15. Powers T.C.: "A Hypothesis on Carbonation Shrinkage". Jou. Portland Cement Association., 1962, **4**, 40-9.

16. Yilmaz V.T.; Glasser F.P.: "Crystallization of Calcium Hydroxide in the Presence of Sulphonated Melamine Formaldehyde Superplastcizer". Jou. Mater. Sci. (Letters), 1991, **10**, 712-15.

EFFECTS OF SOME ADDITIVES ON DYNAMICS OF CARBONATION OF CONCRETE

B Skenderovic

Faculty of Civil Engineering, Subotica, YUGOSLAVIA

SUMMARY

The effect of adding dispersion of synthetic polymers and of the replacement the part of cement with fine ground slag (30%) or with silica-fume (10%) on dynamics of carbonation of concrete in variable natural conditions was tested. Test prisms, made of cement mortar, were cured in water for 28 days, afterwards, they were exposed to the action of the atmosphere of various degrees of air-pollution. The depth of the carbonation layer, as well as the change of the strength and the water absorbing capacity were measured after the period of two years.The pH,and the % of bound CO_2 in mortar layers of various depths were also measured.

The results of investiqations have shown that by replacement of 30 % of cement with fine ground slag (5300 cm^2/g), the carbonation of concrete practically does not speed up. By replacement of 10% of cement with silica-fume, the carbonation substantially speeds up, though, the porosity of concrete is remarkably decreased.

INTRODUCTION

It is known that carbonation in concrete is faster if the porosity and water absorbing capacity are bigger, and the contents of lime ($Ca(OH)_2$) is lower. By adding fly-ash and other puzzolanas to cement the porosity is increased, and the pH and the contents of free $Ca(OH)_2$ is decreased in hardened concrete, by that, the carbonation of concrete, considerably speeds up /2,3,7,8/. Additives (silica-fume, dispersions of polymers) which remarkably decrease porosity and water absorbing capacity of concrete, reducing the quantity of free $Ca(OH)_2$ in it, are used more and more, as they help to increase the resistance of concrete against corrosive action of various liquids /2,3,7/. The similar effect has the replacement of the part of cement by fine ground slag /2,7,8/, its hydraulic activity is significantly increased by fine grinding. By adding the combination of fine ground slag and dispersion of synthetic acrylates /7/, mortars and concretes of very good mechanical and physical characteristics were obtained, which were at the same time very resistant to the corrosive effect of aggressive liquids. A logical question apears how vill this kind of additives influence the speed of concrete carbonation. By reduction of porosity they should slow down the process of concrete carbonation, and by the decrease of the quantity of $Ca(OH)_2$ it should be speeded up. There is no answer to this in published literature, only Angelmayer /1/ has established that by adding dispersion of acrylates the process of concrete carbonation is slowed down. Therefore, we decided to test the influence on the dynamics of carbonation if the part of cement is replaced by fine ground slag or by silica-fume, with or without addition of water dispersion of synthetic acrylates.

EXPERIMENTAL

Test prisms (4.4.16 cm) made of cement mortar (1:3), using standard three-fractional sand, were used. The composition of cement binder was various due to different additives:

Sample mumber	The quantity of additives in %			
	Cement	Slag	Silica-fume	Dispersion of polymers
1	100	-	-	-
2	70	30	-	-
3	70	30	-	15
4	90	-	10	-

All test prisms were cured in water for 28 days at room temperature, afterwards, they were exposed to various atmospheric conditions outdoor for 2 years under different degree of air pollution, after that period compressive and bending strengths, water absorbing capacity and the thickness of carbonated layer were measured. The depth of carbonated layer was measured after the treatment of the fresh crashing of prism with 1% solution of phenolphthalein indicator. The water absorbing capacity is the percentage of water which is absorbed by test prisms kept in water for 24 hours.

In order to define better how deep progressed the carbonation process in test mortars the % of CO_2 and the pH in three layers of test prisms were established by chemical analyses. The layers were separated by cutting - the first layer was the surface layer of 5 mm, the second one was

the next of same thickness, the third layer was in fact the remaining, central part of the prism. The quantity of chemically bound water was determined by DTA analysis.

RESULTS AND DISCUSSION

The usual method of studying carbonation of concrete or cement mortar is to measure the depth of carbonated layer, that is, the layer where the pH is reduced below 9, it is possible to detect by phenolphthalein indicator which changes colour around pH 9. Results are shown in Table 1. Conrol specimens and specimens with 30% fine ground slag (5300 cm^2/g), show practically the same thickness of carbonated layer. It means that by replacement up to 30% of cement with fine ground slag the carbonation speed of cement mortar (concrete), is not siqnificantly changed. According to the data of published literature /2,3,7,8/ it may be expected that the presence of slag causes certain speeding up of carbonation process, however, it should be taken into consideration that very fine ground slag (5.300 cm^2/g) is used in these experiments and its hydraulic activity is increased by fine grinding.

Table 1 Results of measurements of carbonated layer depth

Kind and quantity of additives in %	Depth of carbonated layer in mm, specimens from				
	Vilage	Town	Chemical factory	Special Chamber	Average values
Without add.	1,64	2,54	2,75	2,50	2,36
30% slag	2,05	2,55	2,39	2,52	2,38
30% slag+15% disp.polymers	1,50	1,82	1,24	2,00	1,64
10% silicafume	2,25	3,70	2,26	4,03	3,06

In the case when besides 30% of fine ground slag also 15% of water dispersion of synthetic acrylates is added the thickness of carbonated layer formed for the period of two years substantially decreases. It means that in such way a kind of cement mortar (concrete) is obtained in which the carbonation is significantly slowed down. This result is consistent with the results of Angelmayer /1/ and is the consequence of decreased porosity of cement mortar (concrete). Because, by the change of the part of cement with silica-fume, the porosity of cement mortar (concrete) is also remarkably decreased, it was expected that the obtained carbonated layer in specimens with 10% of silica-fume will be thinner than in control specimens, but the obtained carbonated layer was even thicker.

Faster carbonation is, probably, the consequence of less free $Ca(OH)_2$ and lower pH (Table 2), this being a result of the reaction of active SiO_2 from silica-fume with $Ca(OH)_2$ in mortar.

The process of carbonation takes place in a layer of mortar(concrete) which is gradually shifting from the surface towards depth. There is different degree of carbonation in different depths, because the relation between $Ca(OH)_2$ and $CaCO_3$ is different, and the pH is also different.

By measuring the thickness of carbonated layer by means of phenolphthalein indicator, only the depth of concrete with pH<9 is established, which is considered as carbonated. Howerer, this method does not show the

degree of carbonation of next layer where the process of carbonation is in progress, but the quantity of $Ca(OH)_2$ is still sufficient to keep pH above 9. In the layer where the carbonation process is in progress the relations of the quantities of $Ca(OH)_2$ and $CaCO_3$ are different, as well as the pH values. It is enough for the practice to establish only the thickness of the carbonated layer (with pH < 9), but in research work it is interesting to find out what occurs ahead of this layer. We are also interested to establish how much is the fall of pH (conc. of $Ca(OH)_2$) and the quantity growht of $CaCO_3$ (bound CO_2) in various depths of test mortar (concrete), that is, to find out how deep is the start of the carbonation (front of carbonation). Our procedure was similar to the one of Parrott et al. /5/, the measurements of pH and % CO_2 were carried out in three layers of test mortars. The results are given in Table 2. Besides the measured values (first column) also the differences of pH and % CO_2 in the second and third layers were calculated in regard to the values in the third layer (there no carbonation has yet occured).

Table 2 Results of chemical analyses of mortar layers

Kind and quantity of additives in %	Layer mumber	pH		% of bound CO_2	
		Measured	Diff.in %	Measured	Diff. in %
Without additives	1	12,51	-2,34	4,31	+600
	2	12,80	-0,08	0,91	+31,4
	3	12,81	0	0,59	0
30% slag	1	11,85	-7,06	4,07	+846
	2	12,75	0	0,53	+23,3
	3	12,75	0	0,43	0
30% slag +15% disp.pol.	1	11,57	-0,60	2,30	+207
	2	11,58	-0,51	1,44	+105
	3	11,64	0	0,75	0
10% silica-fume	1	11,18	-3,45	2,48	+353
	2	11,51	-0,60	0,95	+58,3
	3	11,58	0	0,60	0

In all kinds of mortars the pH is the lowest and the quantity of bound CO_2 is the biggest in the first, the most carbonated layer. At the same time, the biggest are the differences between the first and second layers, but they are considerably smaller between the second and third, if any, as the second layer is poorly carbonated. The difference in pH and % of CO_2 between the first and second to the third layer (it is not carbonated) is essential for noticing the front and establishing the region of initial carbonation. The results are measured in % and shown in separate columns in Table 2, the graphic representation is in Fig. 1.

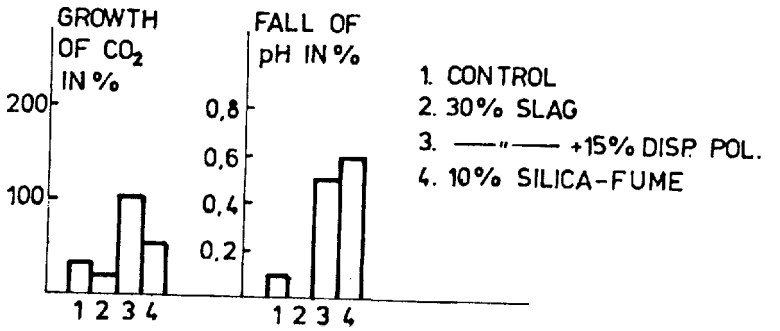

Fig 1 Decrease of pH and increase of CO_2 i secound layer in relation to the third layer of mortar

According to the measured values of pH and % of CO_2 in first layers (Table 2), and the fall of pH and the growth of % of CO_2 in regard to the third layer (Table 2, Fig. 1) it is concluded that the carbonation is speeded up by addition of slag and silica-fume, while on the other hand, when dispersions of synthetic acrylates are added the carbonation of mortar (concrete) is remarkably slowed down. Howerer, the differences of pH and % of CO_2 between the second and third layers (Table 2, Fig. 1) obviously show that in the second layer (depth: 5-10 mm) there is no fall of pH and growth of % of CO_2 in control specimens without additives, as well as in specimens with addition of slag (30%). In the second layer of specimens with addition of 15% dispersion of polymers or 10% of silica-fume, the fall of pH and the increase of contents of CO_2 is noticed in relation to the third non- carbonated layer. It means that the front of carbonation made even deeper progress than 5 mm in these specimens, and it has already reached the second layer (depth: 5-10 mm). From the results in Table 2, and Fig. 1 it can be concluded that by replacement of the part of cement by slag the carbonation of concrete is slightly speeded up, but the presence of silica-fume considerably increases the thickness of carbonated layer (pH<9), but also the layer in which the carbonation is in progress.

By addition of dispersion of synthetic acrylates the thickness of carbonated layer is remarkably decreased, but the layer in which the carbonation is in progress is wider. It is hard to explain so far why the thickness of the layer where the process of carbonation takes place increases by addition of silica-fume and dispersions of polymers, as these mortars (concretes) are less porous and it would be expected that CO_2 and SO_2 from atmposphere penetrate with more diffcalty into them.

Tabel 3 Changes of strengths of test mortars of 2 years

Kind nad quantity of additives in %	Bending strength in MPa			Compressive strength in MPa		
	Starting 28 days	After 2 years	Diff. in %	Starting 28 days	After 2 years	Diff. in %
Without additives	6,78	6,09	-10,2	42,0	46,7	+11,2
30% slag	7,35	6,26	-14,8	42,7	54,3	+27,2
30% slag+15% disp.pol.	7,32	7,27	- 0,7	32,4	53,4	+64,8
10% silica-fume	6,95	4,56	-34,4	38,6	46,8	+21,2

The changes of strength of test mortars for the period of two years are shown in Table 3, the changes of water absorbing in Table 4. As it is seen in Table 3 the compressive strength has significantly increased in all test mortars for 2 years, this being the consequence of prolonged hydration of cement. Especially big is the increase of compressive strength in mortars to which besides 30% of slag, also 15% of dispersion of acrylates is added. This proves that the presence of acrylates hinders teh hydration of cement and fine ground slag in the beginning (low strength after 28 days), but this loss is made up in their presence by intensified additional hydration. Because of continued process of cement hydration the bending strength, should also be increased and decreased the water absorbing capacity in test mortars. Meanwhile, as it is seen in Tables 3 and 4 for the period of 2 years, significant decrease of bending strength occured, and the water absorbing capacity increased in most of test mortars. The growth of water absorbing capacity and the reduction of bending strength is the biggest in mortars in which 10% of cement is replaced by silica -fume, on the other hand it is relatively small in control specimens and

in specimens with slag addition. Test mortar with 15% of added acrylates dispersion did not show the decrease of bending srength and the water absorbing capacity was even considerably decreased. The growth of water absorbing capacity and the decrease of bending strength of mortars (concretes) which are exposed to precipitations and frequent changes of temperature and relative humidity are probably the consequence of forming microcracks in the surface layer. This layer being exposed to great mumber of cycles of alternate wetting and drying, and during winter to the influence of frost, too. It is known that mortars (concretes) in presence of silica-fume are brittle and shrink more at drying. Therefore, in such mortars, probably, greater number of microcracks are formed causing considerable fall of bending streangth and growth of water absorbing capacity. This is, perhaps, besides low contents of $Ca(OH)_2$, the reason of faster carbonation of mortar (concrete) to which silica-fume is added. By addition of dispersions of synthetic polymers the brittleness and the shrinkage is reduced at alternate wetting and drying of mortar. Thus, it seems, that less microcracks are formed in surface layer and as consequence less water is absorbed and slower is the carbonation of cement mortar (concrete).

CONCLUSION

According to the results of these experiments it is concluded:

1. By replacement of the part of cement (to 30%) with fine ground slag the speed of carbonation of cement mortar (concrete) is not essentially changed.
2. By replacement of the part of cement (10%) with silica-fume the process of carbonation is speeded up, though, the porosity of cement mortar (concrete) is decreased.
3. By addition of water dispersions of synthetic acrylates the carbonation of cement mortar (concrete) is considerably slowed down.

REFERENCES

1. Angelmayer K. : "Betonschutz und Betonsanierung",Kunstharz Nachrichten 1991, br. 17, firma Hoechst.

2. Hamada M.: "Neutralization of Concrete and Corrosion of Reinforcing Steel", Proc. of the 5th Int. Symp. on the Chem. of Cement, Tokyo,1968 343.

3. Ilknur B. : "Über die Carbonatisierung von Mörteln und Betonen nach Literaturergebnissen und eigenen Untersuchungen", disert.,Aachen,1980.

4. Jungerman B.: "The chemical Process of hte Carbonation of Concrete", Betonwerk+Fertigteil-Techn., 1982, 6, 358.

5. Parrot L.Y., Killoh C.C.: "Carbonation in 36-year old. in-situ Concrete", Cem. and Concr. Res., 1989, 19, 649.

6. Reardon E.J., James B.R., Abouchar J.: "High Pressure Carbonation of Cementitious Grout, Cem.Concr. Res., 1989, 3, 385.

7. Skenderović B.:"Uticaj raznih dodataka na dinamiku karbonatizacije maltera(betona)", Zbornik radova Građevinskog fakutleta Subotica, 1991,7, 142.

8. Skenderović B.: "Influence of Slag and Fly-ash on Dynamics of Carbonation of Concrete", FIP Sympos. 92, Budapest, 1992.

EFFECTS OF AIR-POLLUTION ON CHEMISM AND DYNAMICS OF CONCRETE CARBONATION

B Skenderovic*, and G Lomic**

**Faculty of Civil Engineering, Subotica,*
***Faculty of Technology, Novi Sad,*
YUGOSLAVIA

SUMMARY

The effect of SO_2 concentration on dynamics and chemism of carbonation process in concrete, under conditions of steady as well as changeable temperature and relative humidity, was tested. test prisms (4.4.16 cm), made of cement mortar (1:3), which were exposed to the action of the atmosphere of various degrees of air-pollution (village, town, industrial region), and of intensified concentrations of CO_2 and SO_2 in laboratory conditions at room temperature, were used.

It was established that in outdoor climatic conditions frequent and significant temperature and relative humidity changes, as well as bigger concentration of SO_2 (intensified air-pollution), cause considerable increase of speed of cement mortar (concrete) carbonation. In laboratory conditions, without changes of temperature and relative humidity the influence of air-pollution is less expressed. Some evidences are noticed that perhaps SO_2 causes also sulphate corrosion in carbonated layer of concrete.

INTRODUCTION

By intensification of air-pollution the concentration of SO_2 and nitrogen oxides is very intense, whereas, the concentration of CO_2 does not change significantly. Engelfried /1/ has established, on the basis of tests in laboratory conditions, that the quantities of SO_2 found in the most polluted industrial regions in Germany, do not speed up the process of neutralization (carbonation) of concrete. We have not found any data in published literature about the effect of air-pollution on dynamics of concrete carbonation in natural conditions where frequent and large variations of temperature and relative humidity take place. Some latest researches, published in literature /3,4/, as well as our preliminary investigations /5/, have shown that the process of carbonation may be remarkably speeded up at frequent and remarkable changes of temperature and humidity. Therefore, a conclusion can be drawn that in changeable natural conditions the influence of air-pollution could be different than in relatively uniform laboratory conditions.

EXPERIMENTAL

Test prisms (4.4.16 cm), made of cement mortar (1:3), using standard three-fractional sand as aggregate, were applied. In some of test mortars the part of cement was replaced by (10%) silica-fume or (30%) fine ground (5.300 cm^2/kg) slag. At making one kind of test mortar 15% of dispersion of acrylates was added. Test prisms were cured in water for 28 days, they were afterwards exposed to changeable climatic conditions on three places of various degrees of air-pollution (village, town, industrial region), and to laboratory conditions in special chamber with high concentration of CO_2 (9 g CO_2/m^3) and SO_2 (10 mg SO_2/m^3). There was no artificial air circulation in the chamber, the temperature and relative humidity were slightly varying. The concentration of CO_2 in outdoor atmosphere did not differ much at all three test locations (about 300 mg CO_2/cm^3) but there were considerable differences in SO_2 concentration. There was no, or only a trace of SO_2, from time to time, in the village. On two other locations the concentrations of SO_2 were very changeable - they showed variations from 0 to 0,03 mg/m^3 in the town, meanwhile, in industrial regions they were high and varied in the limits between 0,010-0,220 mg SO_2/m^3, the average annual value being 0,066 mg/m^3.

After the period of 2 years the water absorbing capacity, strength and the thickness of carbonated layer were measured in test prisms. Besides, the pH and the % of bound CO_2 as well as the chemically bound water in layers of different depths in mortar were measured. The layers were separated by cutting, the first one was the surface layer up to 5 mm thick, the next one was of the same thickness (5-10 mm), and the remaining - central part of test prisms was used as the third layer.

Water absorbing capacity was measured by the mass increase of test prisms which were kept in water for 24 hours, at room temperature. The quantity of chemically bound water in test mortars was determined by DTA analyses.

RESULTS AND IDSCUSSION

In Table 1 there are given the results of measurements of the thickness of carbonated layer of test prisms after the period of two years. It is easy to observe that the thickness of carbonated layer is bigger when there is higher degree of air-pollution, that is, greater concentration of SO_2 in the atmosphere. We expected greater depths of carbonated layers

in specimens kept in special chamber with high concentrations of CO_2 (9 g/m^3) and SO_2 (10 mg/m^3). Relatively slow carbonation of test mortars

Table 1 Results of measurements of depth of carbonated layer

Location	Depth of carbonated layer in mm, specimens with:				
	Without additives	30% slag	30% slag +15% disp. pol.	10% silica-fume	Average values
Village	1,64	2,05	1,50	2,25	1,86
Town	2,54	2,55	1,82	3,70	2,65
Industrial region	2,75	2,39	1,24	2,26	2,73
Special chamber	2,50	2,52	2,00	4,03	2,76

in a chamber with high concentration of CO_2 and SO_2 is, probably, the consequence of steady temperature and little variations of relative humidity in the laboratory and chamber, as well as the static conditions of the air in the chamber. Specimens kept outdoors in an industrial region were exposed to the influence of the atmosphere with considerably lower concentrations of CO_2 and SO_2. The migration of moist was all the time taking place in specimens because of frequent alternate wetting and drying of mortar due to frequent and significant variations of temperature and relative humidity, and also because of periodical precipitations. According to some results of recent investigations /3,4/ the migration of moist in concrete remarkably speeds up the carbonation process. This is, probably, the reason of difference between our results and these of Engelfried /1/ which were carried out in laboratory conditions. Consequently, the influence of the concentration of SO_2 in the atmosphere (degree of air-pollution) as it seems depends in great deal also on other factors,especially, on the degree and frequency of temperature and relative humidity changes, more exactly, on moist migration in the surface layer of concrete.

Table 2 Results of chemical analyses of different layers of test mortars

Location	Layer mumber	pH	% of bound CO_2	% of chem.bound water	
				Measured values	Difference in %
Village	1	11,43	4,54	3,49	+ 3,04
	2	12,23	1,44	3,44	+ 1,47
	3	12,56	0,42	3,39	0
Town	1	11,45	4,73	3,43	+ 7,08
	2	12,34	1,65	3,32	+ 3,83
	3	12,57	0,60	3,20	0
Industrial region	1	11,32	3,95	3,57	+11,60
	2	11,44	1,67	3,50	+ 9,37
	3	12,49	0,44	3,20	0
Special chamber	1	11,82	3,55	3,19	+12,72
	2	12,52	1,47	2,90	+ 2,47
	3	12,62	0,50	2,83	0

The results of measurements of pH, % of bound CO_2 and chemically bound water are given in Table 2. The results of pH measurements in dif-

ferent layers of test mortars affirm that the neutralization penetrated the deepest in test mortars exposed to outdoor changeable atmospheric conditions, with intensified concentration of SO_2 (industrial region). Less quantities of CO_2 in the first layers in specimens kept in the atmosphere with higher concentration of SO_2 (industrial region, chamber) are, probably, the consequence of partial conversion of $CaCO_3$ into $CaSO_4 \cdot 2\,H_2O$ under the action of SO_2. On the possibility of forming gypsum in surface carbonated layer, especially in more polluted atmosphere, points out the increase of chemically bound water in the first two layers in regard to the third, non-carbonated layer. We have calculated in % this increase of the quantity of chemically bound water, and the results are shown in a separate column in Table 2, and as a graphic representation in Fig. 1.

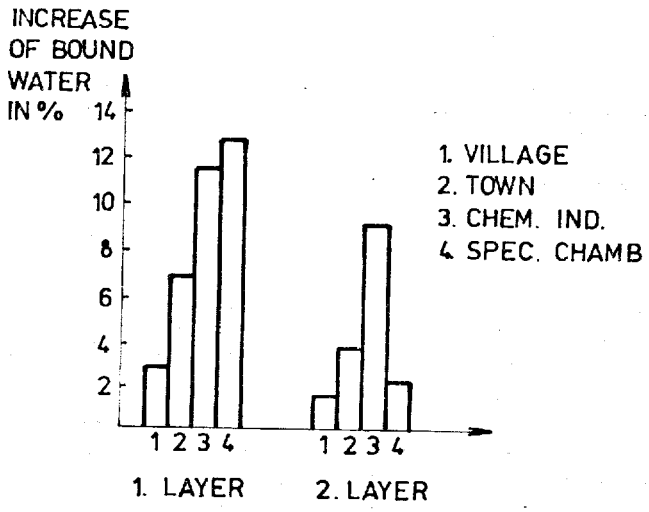

Fig 1 Relative increase of the quantity of chemically bound water in the first and second layers of test mortars

The growth of the quantity of chemically bound water in the first layer of mrotar is as much bigger as bigger is the concentration of SO_2 in the air (higher pollution). More considerable increase of the quantity of

Table 3 Results of measurements of strengths and water absorbing capacity of test prisms

Location	Compressive strength in MPa		Bending strength in MPa			Water absorbing capacity in %		
	28 days	2 years	28 days	2 years	Diff. in %	28 days	2 years	Diff. in %
Willage	36,2	49,7	6,58	5,88	-11,40	3,56	3,76	+ 5,62
Town	36,2	47,9	6,58	6,57	- 0,15	3,56	3,79	+ 6,46
Ind. region	36,2	49,0	6,58	6,17	- 6,23	3,56	4,39	+23,31
Special chamber	36,2	43,7	6,58	4,18	-37,23	3,56	6,12	+71,91

chemically bound water in the second layer is only in specimens exposed to moist migration and higher concentration of SO_2 (industrial region). Less quantities of chemically bound water in all there layers of mortar

in specimens kept in a chamber is, probably, the consequence of incomplete additional hydration of cement because of the lack of moist.

The results of hte measurements of strengths and water absorbing capacity of test prisms after 28 days and 2 years are shown in Table 3. As it was expected the compressive strength is considerably increased for two years, this being the consequence of prolonged hydration of cement and additives. This growth of strength is much less in specimens kept in the chamber under laboratory conditions because of the lack of moist for the hydration process. As a result of hydration of cement and additives, also the bending strengths should be increased, but the porosity and water absorbing capacity of test prisms should be decreased. However,as the data in Table 3 indicate, certain fall of bending strength, and some growth of water absorbing capacity is established in all test prisms. It is, probably, the consequence of forming micro-cracks in surface layer of mortar. The cause of forming these micro - cracks in specimens kept outdoors in changeable climatic conditions could be the action of frost,as well as the great mumber of cycles of alternate wetting and drying of surface layer, at the same time, mortar is exposed to alternate swelling and shrinkage which may also cause forming of micro-cracks. According to the literature carbonation is followed by some shrinkage of concrete(mortar), but it is not very likely that it has bigger action on forming micro-cracks. The fact that the biggest fall of bending strength and the growth of water absorbing capacity are established in specimens kept in chamber at realtively high concentration of SO_2, and small changes of relative humidity, points at the possibility that one of the most important factors of forming micro-cracks is swelling, which is caused by sulphat corrosion under the action of SO_2.

In favour of this assumption speak also the results of bigger quantity of chemically bound water in the first layer of specimens kept in polluted outdoor conditions (industrial region).

These are, naturally, only assumptions which should be checked by detailed and complete researches. Our intention is to continue the investigations on the specimens after four years of treatment.

CONCLUSION

According to the obtained results it is concluded:

1. In changeable climatic conditions, with frequent and considerable temperature and relative humidity variations, and at periodical precipitations,the concentration of SO_2 in the air essentially effects the speed of neutralization (carbonation) of cement mortar (concrete).
2. The influence of the concentration of CO_2 and SO_2 is remarkably less in laboratory conditions where the temperature and the relative humidity are uniform.
3. There are some evidences that sulphate corrosion takes place in surface carbonated layer under the action of SO_2.

REFERENCES

1. Engelfried R.:"Einfluss der Feuchte und dess Schwefeldioxidgehaltes der Luft auf die Carbonatisation des Betons", Betonwerk+Fertigteil--Technik, 1985, 11, 722.

2. Jungerman B.: "The Chemical Process of the Carbonation of Concrete", Betonwerk+Fertigteil-Technik, 1982, 6, 358.

3. Kobayashi K., Uno Y.: "Influence of Alkali on Carbonation of Concrete Part I. Preliminary Tests with Mortar Specimens", Cem.and Concr. Res., 1988, 18, 636.

4. Parrot L.Y., Killoh D.C.: "Carbonation in 36-year old in - situ Concrete", Cem. and Concr. Res., 1989, 19, 649.

5. Skenderović B.: "Uticaj stepena aerozagađenja na dinamiku karbonatizacije betona", Zbornik radova savetov. "Zaštita životne sredine u procesnoj ind.", Dubrovnik, 1991, 180.

EFFECT OF THE CARBONATION PROCESS ON THE CONCRETE DETERIORATION BY $CaCl_2$ AGGRESSION

M Collepardi and S Monosi

Department of Materials Science,
Ancona University, ITALY

SUMMARY

A concentrated aqueous solution of $CaCl_2$(30%) causes a strong deterioration in mortars manufactured with Portland cement. X-ray diffraction analyses indicate the formation of large amounts of hydrated calcium oxychloride accompanied by the consumption of hydrolysis lime. The cement paste carbonation makes the mortars durable against the $CaCl_2$ attack. In this case, X-ray diffraction analyses show the conversion of $Ca(OH)_2$ into $CaCO_3$.

INTRODUCTION

The de-icing salts based on calcium chloride are responsible for the severe deterioration of the concrete structures. The deteriorating process causes cracks and swelling of concrete and a rapid decrease in compressive strength (1-4).

This severe attack is accompanied by the formation of small amounts of chloroaluminate hydrate ($C_3AxCaCl_2x10H_2O$). In a previous paper (5) it was assumed that the oxychloride product is formed by the reaction

$$3Ca(OH)_2 + CaCl_2 + 12H_2O \longrightarrow 3CaOxCaCl_2x15H_2O$$

between lime produced by Portland cement hydration and calcium chloride which diffuses through the concrete.

In order to confirm that hypothesis, mortar specimens partly or completely carbonated have been exposed to the $CaCl_2$ attack.

MATERIALS AND PROCEDURES

Prismatic mortar specimens (40x40x160) were produced by using high strength Portland cement and two water/cement ratios (0.65 and 0.35).

After 1 day, the specimens of each water/cement ratio, were demoulded and divided into 3 groups: the specimens of the first group were kept under water, the ones of the second group were cured in the air, whereas the specimens of the third group were exposed to the CO_2-rich room (30% by volume) and at R.H. of 60%.

After 60 days, the carbonation depth by the phenolphtalein test was measured on all specimens. Then each group was divided into two subgroups: the specimens from the first subgroup were kept under water at 20°C, while those of the second subgroup were immersed under a 30% $CaCl_2$ aqueous solution. This solution was maintained for 15 days at 20°C and then at 5°C because the deterioration due to $CaCl_2$ attack is mainly exhibited at low temperatures of about 5°C.

On all the specimens, compressive strength tests and X-ray diffraction analyses were carried out.

RESULTS AND DISCUSSION

Carbonation

The specimens exposed to the CO_2-rich room were completely carbonated after 15 days, while the carbonation depth was about 1.5 mm after 60 days for those exposed to air.

In the mortar specimens with a water/cement ratio of 0.35, cured in the CO_2-rich

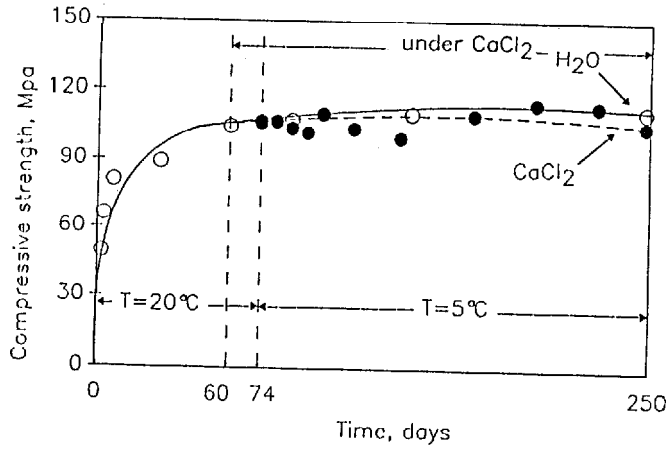

Fig.1 Compressive strength versus time of the specimens (w/c=0.35) exposed to the CO_2-rich room before the immersion under water or under $CaCl_2$ aqueous solution.

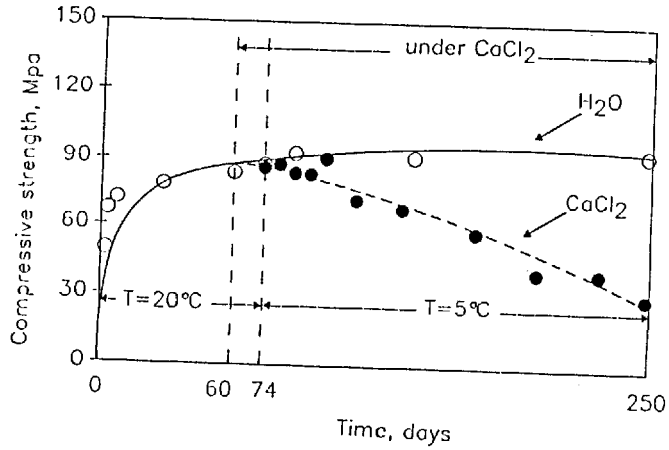

Fig.2 Compressive strength versus time of the specimens (w/c=0.35) kept under water before the immersion under water or under a 30% $CaCl_2$ aqueous solution.

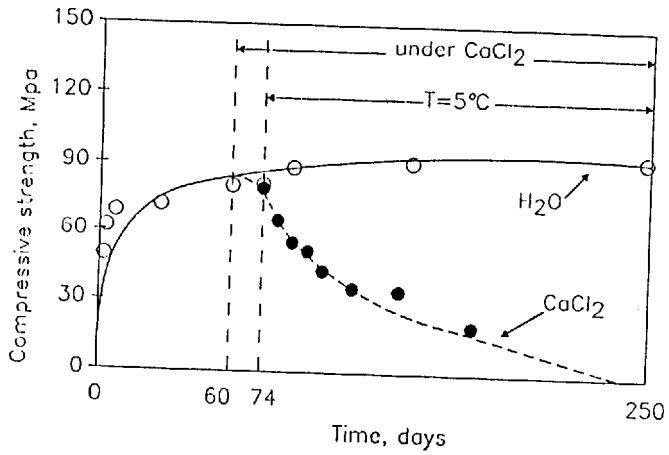

Fig.3 Compressive strength versus time of the specimens (w/c=0.35) kept in the air before the immersion under water or under 30% $CaCl_2$ aqueous solution.

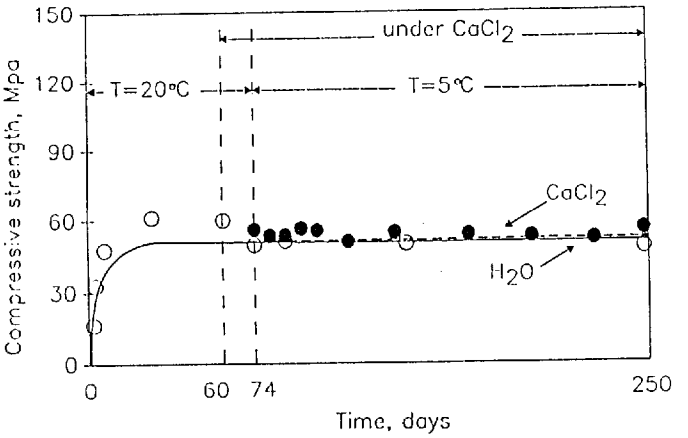

Fig.4 Compressive strength versus time of the specimens (w/c=0.65) exposed to the CO_2-rich room before the immersion under water or under 30% $CaCl_2$ aqueous solution.

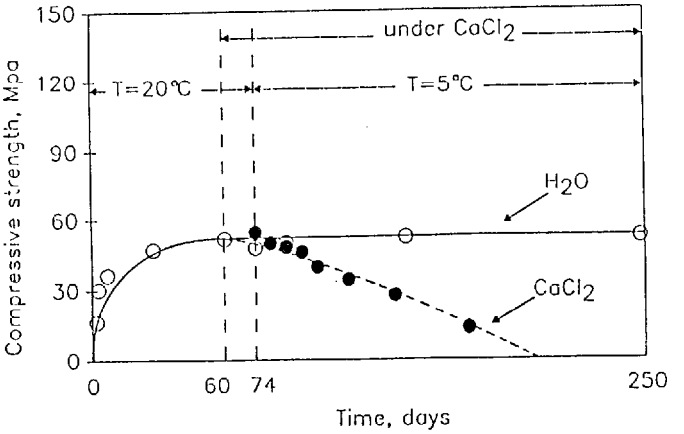

Fig.5 Compressive strength of the specimens (w/c=0.65) kept under water before the immersion under water or under 30% $CaCl_2$ aqueous solution.

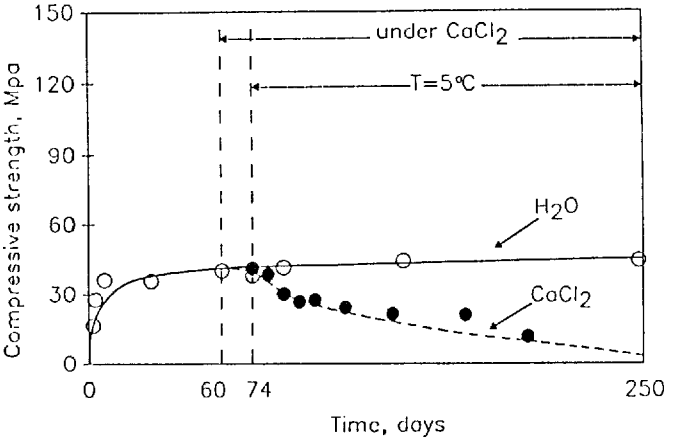

Fig.6 Compressive strength of the specimens (w/c=0.65) kept in the air before the immersion under water or under 30% $CaCl_2$ aqueous solution.

room, the carbonation depth was about 6 mm, while those exposed to air had a carbonation depth of 1 mm.

Compressive strength

The evolution of the compressive strength of the mortar specimens was determined by the type of preliminary cure.

Figures 1-3 show the compressive strength versus time of the specimens with a water/cement of 0.35.

The comparison of the curve indicates that the compressive strength was increased by exposure in the CO_2-rich room. After the immersion in the $CaCl_2$ aqueous solution, the specimens cured in the CO_2-rich room keep the same strength as that of the corresponding specimens cured under water. Substantially, the exposure to the $CaCl_2$ attack did not cause any mechanical decrease. A progressive decrease in strength after immersion in the aggressive solution was recorded in the specimens preliminarly cured under water or in the air. In particular, after one month of immersion in the $CaCl_2$ solution, the specimens cured in the air, which are in the same condition as for the concrete structures before exposure to the de-icing salts, show a strength decrease of about 30% with respect to the value found before immersion.

Similar results can be noted on Figs. 4-6 concerning strength evolutions of the specimens with w/c of 0.65. Even in this case, the immersion in the aggressive $CaCl_2$ solution caused a rapid decrease in strength of the specimens cured under water or in the air. The specimens preliminarly cured in the CO_2-rich room, even after 6 months of immersion in the $CaCl_2$ aqueous solution, conserved the same compressive strength as the corresponding specimens cured under water.

Moreover the strength decrease in the specimens with w/c of 0.65, caused by exposure to the aggressive solution, is less rapid than that registered in the specimens with w/c of 0.35. This result appears apparently paradoxal since a faster deterioration in the cement mortar made with a lower water/cement ratio and therefore of better quality is expected.

X-Ray diffraction analyses

The deterioration of the mortar specimens preliminarly stored under water or in the air (independently to their w/c ratio) exhibiting a significant compressive strength decrease, were explained by X-ray diffraction analysis.

This analysis showed a progressive formation of the calcium oxychloride and the simultaneous decrease in lime content. Figure 7, for instance, shows the XRD pattern of the cement mortar (w/c = 0.35) preliminarly cured under water, after 6 months of immersion in the $CaCl_2$ solution. The typical XRD peaks of calcium oxychloride were observed, whereas the $Ca(OH)_2$ peaks were absent, due to the combination of lime with

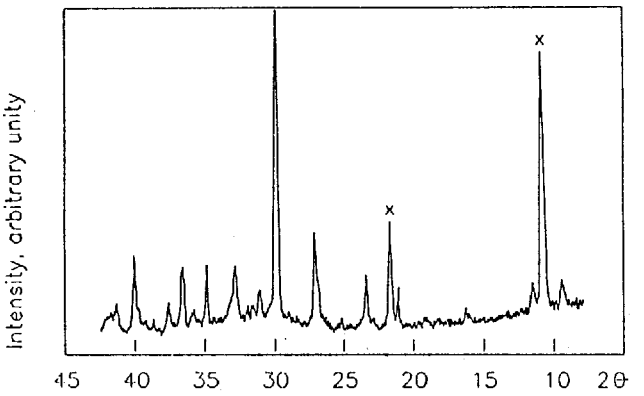

Fig.7 X-ray pattern of cement mortar (w/c=0.35) after 6 months of immersion in $CaCl_2$ aqueous solution and preliminary curing under water ($X=3CaO.CaCl_2.15H_2O$).

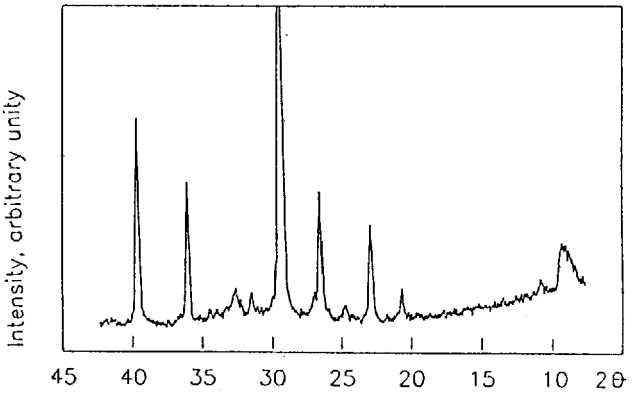

Fig.8 X-ray pattern of cement mortar (w/c=0.35) taken from outer surface of the specimens after 6 months of immersion under $CaCl_2$ solution and preliminary exposure to the CO_2-rich room.

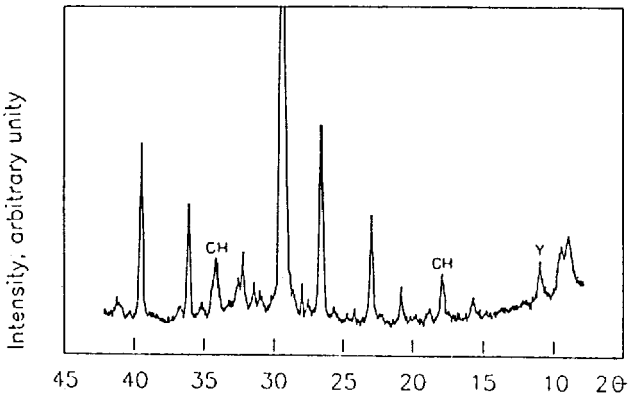

Fig.9 X-ray pattern of cement mortar (w/c=0.35) taken from inner part of the specimens after 6 months of immersion under $CaCl_2$ solution and preliminary exposure to the CO_2-rich room ($CH=Ca(OH)_2$; $Y=C_3A.CaCl_2.10H_2O$).

$CaCl_2$.

X-ray diffraction analyses carried out on the carbonated mortar specimens preliminarly cured in the CO_2-rich room have shown the absence of hydrolysis lime (Fig. 8). Only in the inner part of the specimens with w/c of 0.35, are the lime reflexes still noticeable (Fig. 9). Obviously in these specimens the carbonation has started but has not completed.

In fact, by means of the colorimetric test, a complete carbonation can be shown in the outer part only up to a thickness of about 6 mm, after 60 days; neverthless, the typical XRD peaks of calcium oxychloride in the carbonated outer portion and in the inner one where the lime is still present, are not observed.

CONCLUSIONS

The results of the present work mean that the aggression of the $CaCl_2$ against cement mortars is due to the calcium oxychloride ($3CaOxCaCl_2x15H_2O$) that is formed by the reaction between $CaCl_2$ diffused through the material and lime produced by Portland cement hydration.

When the hydrolysis lime is transformed into $CaCO_3$ because of the carbonation, the $CaCl_2$ penetration is not able to cause the oxychloride formation growth and therefore material damage does not occur.

These results indicate that the calcium oxychloride hydrate, is responsible for the concrete structures damage when exposed to the de-icing salts based on $CaCl_2$.

REFERENCES

1. Chatterji, S. and Jensen, A.D.: "Studies of the mechanism calcium chloride attack on Portland cement", Nordisk Beton, 1975, 19, 5-6.

2. Chatterji, S.: "Mechanism of the $CaCl_2$ attack on Portland cement concrete", Cement and Concrete Research, 1978, 8, 461-468.

3. Berntsson, L. and Chandra, S.: "Damage of concrete sleepers by calcium chloride", Cement and Concrete Research, 1982, 12, 87-92.

4. Conjeau, M.: "Mecanisme d'attaque des ciments Portland par $CaCl_2$", **Seminario Internazionale sugli alluminati di calcio, Torino, Italy,** 1982.

5. Monosi, S. and Collepardi, M.: "Chemical attack of calcium chloride on the Portland cement paste", Il Cemento, 1989, 2, 97-104.

AGGRESSIVITY OF PHENOL HOMOLOGUES SOLUTIONS AND CAUSED CORROSION OF CEMENT COMPOSITES

V Živica

Inst. of Construction & Architecture, Slovak Academy of Sciences, Bratislava, CSFR

SUMMARY

This paper represents the results of long-term study of the action of phloroglucinol, cresol, phenol, pyrocatechol, hydrochinone, pyrogallol and resorcinol on the cement composite. The obtained results show that these phenols represent components with very different aggressivity and cause acidic corrosion. The relatively most aggressive medium is the resorcinol solution, which causes a very dangerous kind of corrosion. Its causes and the properties of phenols as parameters of their aggressivity are given.

La contribution mentionne les résultats de la recherche à long terme da l'action des solutions des homologues du phénol au composé du ciment. Les résultats obtenus montrent que ces solutions présentet les milieux avec l'agressivité diverse et ils causent la corrosion acide. Le milieu relativement le plus agressif est la solution du résorcinol qui produit la sorte da la corrosion très dangereuse. Ses causes et les propriétés des phénols comme les paramètres de leur agressivité sont présentées.

INTRODUCTION

Phenol and its homologues can occur in waste waters from various industrial branches and can present as aggressive substances a danger for concrete structures /1,2/. Information is rare and practically limited to the basic homologue - phenol. Simirarly information about the chemism of caused corrosion is limited. From the point of view of phenol homologues aggressivity their acidity is an important property.It is known that acid substances can cause acidic corrosion of cement composites, resulting in decomposition of their hydration products. In water soluble products of this destruction can be leached out. The result of this process is a gradual decomposition of the binding agent in the composite and subsequently degraded physical properties, including the strength of the attacked material.

The aim of this study was to determine the aggressivity of phenol homologues and its factors.

EXPERIMENTAL

Preparation of the test specimens

The cement used was an ordinary Portland cement of class 400 according to standard ČSN 722112 /Table 1/. An natural silica sand according to standard ČSN 721208 was used.

2-cm cubes and 2x2x12 cm prisms, made from mortar (cement:sand 1:3, w/c=0,6) were used for the study. After the curing of the test specimens 24h at 95% relative humidity and 27 days in tap water, the test specimens were put in saturated solutions of phloroglucinol, hydrochinone, paracresol and phenol and in 10% solutions of pyrocatechol, pyrogallol and resorcinol. A part of the test specimens were stored for control in tap water. Temperature of the curing was 20 ± 2°C.

Testing

The following properties of the test specimens were studied: visual state, physical properties (bulk density, compressive strength, dynamic modulus of elasticity, length changes) chemical and phase composition, using chemical and thermal analysis (Q-derivatograph for DTA, GT and DGT curves determination) and X-ray analysis (diffractometer Philips), pore

Table 1 Composition and Properties of Used Cement

Chemical Composition - %							
Loss on ignition	Insoluble residue	SiO_2	Al_2O_3	Fe_2O_3	CaO	MgO	SO_3
2.00	1.50	20.28	5.74	3.13	60.63	2.57	2.57

Bogue Potential Compounds-%					Physical Properties			
C_3A	C_4AF	C_3S	C_2S	$CaSO_4$	spec. weight $kg.m^{-3}$	spec. surface $m^2.kg^{-1}$	Setting time min. Initial	Final
9.76	9.82	40.83	27.47	4.18	3143	355.9	190	310

structure, using total porosity determination (calculation from bulk density and specific weight values) and mercury porosimetry (porosimeter mod.70 H, Carlo Erba, Milano).

RESULTS AND DISCUSION

Fig.1 shows that the action of phenol homologues solutions on compressive strength and dynamic modulus of elasticity was quite different. The phloroglucinol solution caused only retardation of the development and the hydrochinone solution a moderate decrease of compressive strength. The solutions of further phenol homologues caused a pronounced degradation of the mentioned properties of mortar. In the case of the action of the resorcinol solution was this pronounced degradation connected with the expansion and cracking of the test specimens /Fig.2/. The interior of these test specimens contained a pasty like matter proving the decomposition of mortar by the resorcinol solution.

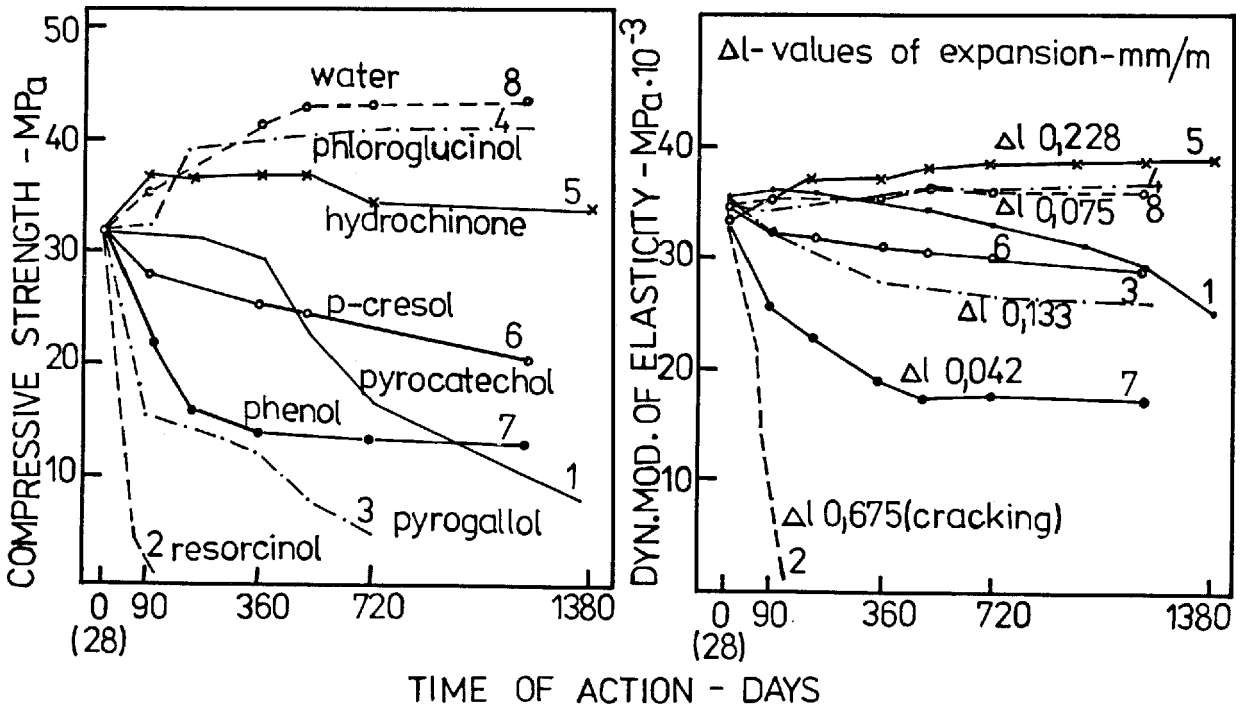

Fig.1 COMPRESSIVE STRENGTH AND DYNAMIC MODULUS OF ELASTICITY OF MORTAR EXPOSED TO THE ACTION OF PHENOL HOMOLOGUES SOLUTIONS

According to the obtained results, given in Table 2, the phenol homologues solutions caused the decrease in CaO and $Ca(OH)_2$ content and the adverse effect on pore structure (total porosity and pore median increase) of attacked mortar. No common reaction products of phenol homologues and of mortar components have been found in attacked mortar. Our further study of the phase composition of reaction products, resulting from phenols action upon on C_3A, C_4AF and C_3S hydration products, proved the destructive action of phenol homologues too. Again no common reaction products have been found /3/.

The phenol homologues solutions, with exception of phenol, para-cresol and resorcinol solutions, at the contact with mortar test specimens turned black and were precipitated black or dark powder products. This phenomenon was caused by oxidation of phenol homologues with OH groups in ortho and para positions /4/. The effect of this process (decrease of phenol homologues concentration in attacking solution and partially filling of pores in mortar by solid oxidation products) evidently was one of the causes of decreased aggressivity of these phenol homologues - compared to the aggressivity of solution of stable resorcinol (OH groups in meta position).

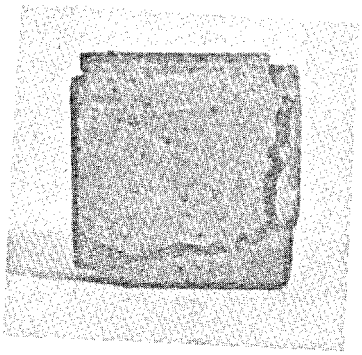

Fig.2 Destructed test specimen by resorcinol solution, exposition time 90 days

The found effects of the phenol homologues solutions - the decrease in $Ca(OH)_2$ and CaO content, the degradation of the pore structure and the characteristic continous decrease of compressive strength and of the modulus of elasticity of mortar attacked by the studied phenol homologues solutions represent an

Table 2 Composition and Pore Structure of Mortar Exposed to the Action of Phenol Homologues Solutions

Solution	Time of exposition days	CaO content %	CaO bound in $Ca(OH)_2$ and $CaCO_3$ %	Total porosity %	Pore median nm
Phenol	720	5.85	1.37	33.91	100.0
Para-cresol	720	10.32	4.13	29.74	36.0
Resorcinol	90	4.67	1.20	46.07	124.4
Pyrogallol	720	4.63	1.57	39.12	390.0
Phloroglucinol	1260	11.37	4.58	28.28	-
Water	1260	14.54	5.39	26.01	54.0

acidic corrosion. In the case of the attack by the resorcinol solution this acidic corrosion was accompanied by increased expansion an mainly by cracking and at last by disintegration of the attacked test specimens, unusual at this type of corrosion. These effects are known as symptoms of expansive corrosion. However, this type of corrosion is still accompanied by further symptoms - as an existence of voluminous reaction product in the attacked material and its typical transient strengthening and final disintegration as a result of the rising of this product. All mentioned symptoms accompany e.g. such expansive corrosion as is the well known sulphate corrosion. However, the two last mentioned important symptoms in the case of resorcinol corrosion have not been observed at the study.

According to the obtained results the cracking of the mortar attacked by the resorcinol solution was not caused by the process of expansive corrosion. It is possible to suppose that this cracking is a result of the interaction of acidic corrosion and of the effect of surface activity, as a result of acidity and surface active properties of resorcinol. The result of this interaction is probably the synergistic strengthening of the destructive effect of the resorcinol solution on cement composite. The surface activity of resorcinol is proved by decreased surface tension of its 10% solution with a value of 0.045 N/m comparing with water with a value of 0.070 N/m. The opinion about the supposed role of surface activity at the described corrosion is supported by its known effects - the decrease of surface tension of solutions and the facilitation of their penetration into the pore structure of solids, the improvement of their wetting, adsorption on solids, the dispersive effects on solids, the possibility to cause tensions in pore structure of cement composites reaching values until to 5 MPa /5/.

On the basis of the obtained results for aggressivity of phenol homologues their following properties seem as the deciding ones: solubility in water, acidity, number and position of OH groups in homologue molecule and surface activity. The given factors and the degradation effectnivness of the studied phenol homologues are in Table 3 summarized.

Table 3 Comparison of Properties of Phenol Homologues and of Caused Corrosion of Mortar

Phenol homologues	pKa Value	Solubility in water %	Concentration of solutions used at the study - %	Corrosion degree of mortar	Determined corrosion type
Phloroglucinol	7.97	1.12	saturated solution /SU/	6.03 / 720	acidic corrosion
Hydrochinone	9.69	6.7	saturated solution /SU/	18.49 / 760	acidic corrosion
Para-cresol	10.26	1.8	saturated solution	47.55 / 720	acidic corrosion
Phenol	10.00	9.3	saturated solution	69.07 / 720	acidic corrosion
Pyrocatechol	9.45	31.2	10 /SU/	62.51 / 760	acidic corrosion
Pyrogallol	9.28	31.5	10 /SU/	88.36 / 720	acidic corrosion
Resorcinol	9.44	63.7	10	97.02 / 90	acidic corrosion cracking

SU - solution in contact with mortar unstable
Corrosion degree: values over the line - decrease of compressive strength of attacked mortar expressed in % of strength of control test specimens, values under line - exposition time in days

The increase of degradation effectnivness of studied phenol homologues solutions and of homologues aggressivity respectively represents this order: phloroglucinol, hydrochinone, para-cresol, pyrocatechol, phenol, pyrogallol and resorcinol. Especially aggressive homologue is re-

sorcinol. These results displaces the opinion about indentity of phenol homologues aggressivity.

CONCLUSION

Phenol homologues solutions can cause acidic corrosion of cement composites. Their aggressivity seems to be in comparison with aggressive inorganic media a very complex property, which besides the homologues acidity is influenced by further mentioned factors. Danger of acidic corrosion of cement composites in phenol homologues media represents increased demands on anti-corrosive protective measures of concrete structures in such media.

The mentioned complexity of aggressivity and of corrosion processes may be expected even at the action of further aggressive organic media on cement composites. There is a possibility of destructive action of acidic corrosion and its combination with destructive co-effect of organic substances surface activity and of destructive co-effect of their contingent voluminous reaction products with cement composites components. A further possible factor of complication of attack of cement composites by organic media seems to be possible unstability of organic substances at contact with them and caused chemical changes of attacking solutions. The role of surface activity in processes of cement composites destruction requires further research.

REFERENCES

1. Smith, M.N.: "The Effect of Phenol upon Concrete", Concrete Research 1985, 37(133), 234-237.

2. Smith, M.A.: "Identification and Assesment of Ground Conditions Aggressive to Concrete", Concrete in Ground, London, 20.-21.may 1984 The Concrete Soc., 1985.

3. Živica, V.: "Action of Phenols Solutions on the Hydration Products of Portland Cement", /in Slovak/, Stavebnícky časopis, 1992, 40/3/.

4. Červinka, O., Dědek, V. and Ferles, M.: "Organic Chemistry" /in Czech/, SNTL/ALFA, Praha, 1980, 792 p.

5. Kuročka, P.N. and Černov, A.V.: "About the Role of Capillarity Phenomena in the Procces of Porous Solid Destruction", /in Russian/, Izvestija VUZ, Stroitel'stvo i Architektura, 1985, No.7, 59-62.

CORROSION OF HARDENED CEMENT PASTES BY FORMIC ACID SOLUTIONS

A Bajza

Slovak Technical University, Bratislava, CZECHOSLOVAKIA

SUMMARY

The action of formic acid (HCOOH) solutions leads to the deterioration of the structure, degradation of the physico-mechanical properties and the change of the chemical and phase composition of the hardened portland cement (HPC) pastes.

The formic acid causes the formation of the layer structure, substantial decrease of the compressive strength, weight and bulk density of hardened portland cement paste and to the increase of total porosity, micropores volume and median of the micropores radius determined by MIP.

Besides the common tests, the course of the corrosion was studied by XRD, DTA, MIP and SEM.

ZUSAMMENFASSUNG

Die Wirkung der Ameisensäurelösungen hat zur Folge Strukturstörungen, Verschlechterung der physikalisch-mechanischen Eigenschaften und eine Veränderung der chemischen und Phasenzusammensetzung der erhärteten Zementpasten.

Die Ameisensäure verursacht einerseits die Bildung der Schichtenstruktur, deutliche Verringerung der Druckfestigkeit, des Gewichts und der Rohdichte der erhärtenen Zementpasten, andererseits führt sie zum Anstieg der gesamten Porosität, des mittels der Queksilberhochdruckporosimetrie festgelegten Porenvolumens und des Medianmikroporenradius.

Ausser herkömmlichen Versuchen wurde der Korrosionsverlauf anhand der RDA, DTA, Hg-Porosimetrie und REM studiert.

INTRODUCTION

The corrosion of the cement composite materials by formic acid (HCOOH) occurs in concrete constructions the chemical, paint, textile, furrier, food-stuff industry, in medicine, agriculture, etc. Formic acid is acting there either as a chemical or a product of the bio-degradation. After Moskvin (1) this corrosion can be classified as Type II. Due to the decomposition of the hydrated and unhydrated cement compounds it leads to the severe degradation of the technical properties of composites. The end products of it are soluble calcium salts as well as hydrated oxides $SiO_2.aq$, $Al_2O_3.aq$ and $Fe_2O_3.aq$ (1,2,3).

While $SiO_2.aq$ is insoluble (except HF) in acid solutions, the solubility of $Al_2O_3.aq$ and $Fe_2O_3.aq$ depend on the pH value of the acting solution. The hydrated oxide $Al_2O_3.aq$ is in the solid state at pH values above 3,5 and $Fe_2O_3.aq$ at pH values above 1,5. At the lower pH values they dissolve (4).

Medgesi (5) studied the concrete corrosion by organic acids including HCOOH. He found that the rate of corrosion had increased with increasing solubility of the calcium salts formed and it was not essentially influenced by the type of cement. Medgesi (6) also published results on the DTA investigation of the cement matrix of concrete corroded by HCOOH and other chemicals. According to the data published by Bajza (7) composites based on portland cements do not withstand to the action of HCOOH. To achieve their longer service life it is necessary to use efficient protecting coatings.

EXPERIMENTAL

A commercial portland cement having a calculated compound composition (Bogue) of 64,77 % C_3S, 5,55 % C_2S, 9,08 % C_3A, 8,94 % C_4AF and 3,26 % $CaSO_4$ has been used.

Cylinders 30x30 mm from cement pastes of the water to cement ratios 0,1 (pressed at 100 MPa), 0,3 and 0,4 (vibrated) were prepared. After 28 days of water curing (pastes having w/c=0,1) or 1 day moist curing followed by 27 days in water (pastes having w/c=0,3 and 0,4) a part of samples was further cured in water at room temperature and a part was placed in a 0,5, 3 and 5 % HCOOH solutions for 1, 7, 28, 91, 365 and 1460 days. During the first 6 months of storage the aggressive solutions were replaced every 28 days, during successive storage after every 84 days. The samples were tested at the age of 1, 28, 29, 35, 56, 119, 393 and 1486 days, irrespective of the treatment method.

At the particular treatment period the appearance of the tested samples were assessed, their changes in weight, thickness of corroded layer, porosity (calculated from the loss of the weight after drying and the sample volume), compressive strength, pore size distribution, chemical and phase composition and morphology were determined.

Experimental technique such as chemical gravimetry, XRD, DTA, MIP and SEM were used.

RESULTS AND DISCUSSIONS

The corrosion of the hardened cement pastes by HCOOH solutions causes formation of the layered structure. The properties of the corrosion products layer differ from not yet corroded "core" of the samples. As the corrosion proceeds the corrosion layer becomes thicker. At any stage of samples storage in aggressive solutions, it is possible to separate the corroded layer easily from them.

Table 1. Properties of Hardened Portland Cement Pastes

Designation	w/c	Solution	Age (Samples Storage in Solution)	Change in Weight $\frac{m_\tau - m_{28}}{m_{28}} \cdot 100$	Bulk Density of Saturated Samples	Compressive Strength	Total Porosity
			days	%	$kg.m^{-3}$	MPa	%
PI_3	0,4	Water	1		2030	21,3	42,8
			28		2058	62,5	38,4
			393		2068	79,7	35,8
			1488		2072	86,0	34,4
PI_2	0,3		1		2173	37,1	33,7
			28		2203	91,9	30,2
			393		2215	116,1	27,6
			1488		2228	129,4	27,1
PI_1	0,1		1		2548	139,7	18,3
			28		2551	225,4	16,6
			393		2566	271,5	15,1
			1488		2575	296,8	14,4
M_1I_3		0,5 % HCOOH	29(1)	- 0,7	2050	58,2	39,2
			56(28)	- 1,3	2030	50,0	41,4
			393(365)	- 10,1	1887	39,1	47,6
			1488(1460)	- 15,3	1730	16,1	52,7
M_2I_3	0,4	3,0 % HCOOH	29(1)	- 4,1	2034	48,5	41,2
			56(28)	- 10,1	1928	40,9	46,4
			393(365)	- 51,6	1264	0,6	79,5
			1488(1460)	- 52,2	1227	-	81,9
M_3I_3		5,0 % HCOOH	29(1)	- 4,9	1963	43,5	43,2
			56(28)	- 15,4	1816	26,6	52,4
			393(365)	- 52,9	1214	0,5	80,2
			1488(1460)	- 53,8	1201	-	82,2
M_2I_2	0,3	3,0 % HCOOH	29(1)	- 3,2	2163	74,7	34,1
			56(28	- 7,4	2101	58,1	39,7
			393(365)	- 48,3	1288	1,3	78,3
			1488(1460)	- 50,2	1248	-	79,5
M_2I_1	0,1		29(1)	- 2,5	2490	175,5	20,3
			56(28)	- 5,9	2418	147,7	22,3
			393(365)	- 39,6	1575	13,5	62,9
			1488(1460)	- 47,3	1331	-	74,3

The data of Table 1 show, that the properties of the samples cured in water were improved with the time of curing, those stored in formic acid solutions were severely corroded. The corrosion led to their substantial decrease of the weight, bulk density, compressive strength and increase of the total porosity.

The effect of corrosion by HCOOH solutions can be observed from the compressive strength data, (Tab. 1). In the most cases were found to be negligible after 1 year of storage and most unmeasurable after 4 years, respectively. The corrosion effectiveness increased mainly with the increasing solutions concentration and partly also with the increasing water to cement ratio of the cement paste. The smaller influence of the water to cement ratio on the rate of corrosion can be explained by the fact that it depends on the permeability of the corrosion products layer (its thickness and pha-

Table 2. Bulk Density and Results of Mercury Intrusion Porosimetry

Designation	Age (Sample Storage in Solution	Bulk Density of Dry Samples	Pore Volume 3,75-7500 nm x 10^{-3}	Median of Micro pores Radius	Pore Size Distribution			
					3,75-10 nm	$10-10^2$ nm	10^2-10^3 nm	$10^3-7{,}5\times10^3$ nm
	days	$kg.m^{-3}$	$m^{-3}.kg$	nm	%	%	%	%
PI_3	28	1674	0,169	37	12,7	81,2	3,1	3,0
	393	1710	0,100	31	4,8	90,4	2,6	2,2
PI_1	28	2385	0,033	26	3,0	96,2	0,5	0,3
M_2I_3	119(91)	942	0,320	283	20,3	51,0	28,0	0,7
	393(365)	470	0,677	477	4,7	21,8	46,2	27,3
M_3I_3	119(91)	582	0,462	581	7,6	18,6	34,5	39,3
	393(365)	412	0,689	636	4,0	19,5	35,6	40,9
M_1I_1	393(365)	2089	0,041	38	3,6	84,7	6,9	4,8
M_2I_2	393(365)	946	0,382	248	4,6	29,5	59,9	6,0
M_3I_1	393(365)	571	0,533	385	3,8	25,1	61,4	9,7

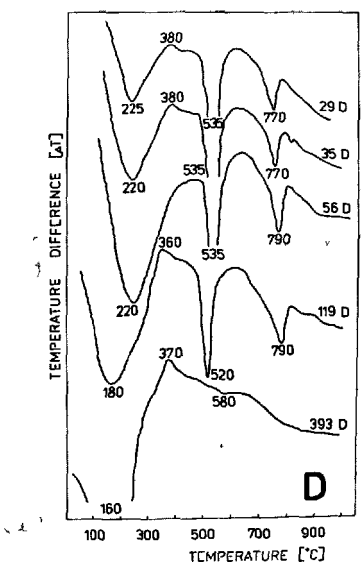

Fig. 1. DTA curves of HPC pastes stored in formic acid solutions.

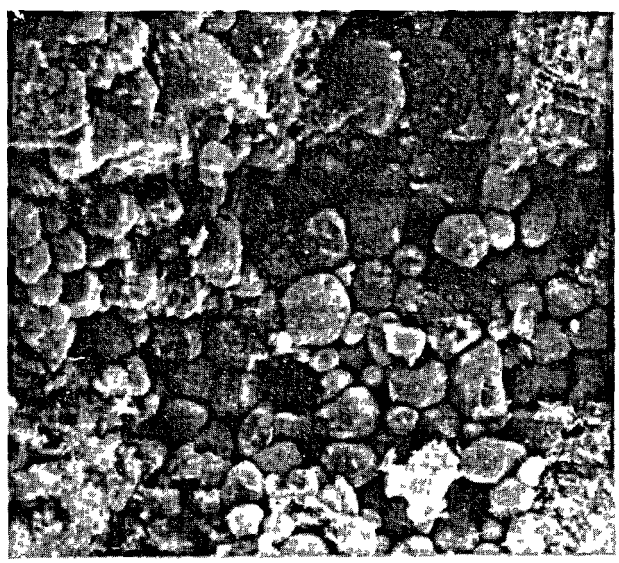

Fig. 2. SEM micrograph of HPC paste (w/c=0,4) stored 365 days in 3 % HCOOH solution. Magnification: x1000.

se composition) and does not depend on the permeability of uncorroded hardened cement paste (1).

The results of MIP (Table 2) correspond with the properties discussed above. The higher water to cement ratio, solutions concentration and their longer acting time led to higher degradation of the hardened cement pastes structure. With the progress in corrosion increased their micropores volume and the amount of micropores with larger radii (the median of micropores radius is increasing).

X-ray diffraction analysis of the samples stored in aggressive solutions made possible to identify at earlier stages the same phases as in those which were cured in water. X-ray diffraction analysis is showing the continuous decrease of the amount of unhydrated and hydrated components of cement. After 1 year of storage the characteristic diffraction lines of the hydration products and clinker minerals were already absent. That documents the amorphous character of the corrosion products or the fact that they were due to their higher solubility dissolved into the solution.

DTA curves (Fig. 1) of the corroded samples in their earlier stages of storage are similar to the control ones cured in water. In later stages the characteristic peaks of the portlandite (at about 520 ^{o}C) and those of calcite (above 750 ^{o}C) are absent. Large endothermic peaks in the range of 160-225 ^{o}C can be seen, which correspond as well to the decomposition of the non-corroded hydration products as to the main corrosion products SiO_2.aq, Al_2O_3.aq and Fe_2O_3.aq. No charakteristic peaks of calcium formate decomposition were found.

On the DTA curve published by Medgesi (6) it is to see endothermic effects at about 100 ^{o}C and 570 ^{o}C. They characterize the presence of the amorphous gel phase and the transformation of the aggregate quartz content, respectively.

SEM studies of the corroded layer show that the structure do not have a distinct morphology, it is very porous and fragile (Fig. 2).

Chemical gravimetry data (Table 3) show big differences between the composition of the water cured control samples and those stored in the aggressive solutions. While the amount of CaO in all control samples is high, in corroded layers of the samples stored in aggressive solutions is very low. The amount of CaO is decreasing with the solutions concentration and their acting time. On the contrary the amount of SiO_2 is increasing. The content of Al_2O_3 and Fe_2O_3 in corroded layers is always higher than in water cured samples. The amount of these oxides is influenced by the pH values of the aggressive solutions. It is necessary to note, that the chemical composition of the same age water cured samples and that of not yet corroded cores of samples stored in aggressive solutions is similar.

For corrosion studies of hardened portland cement pastes it was found that the thickness of the corroded layer of the sample is one of the most convenient characteristic. For the conditions used (portland cement, w/c=0,4, samples height and diameter 30 mm, solutions concentration 0,5-5 %, time of exposure 1-1460 days) the following equation can be written

$$t_\tau = 0{,}174\ C^{0{,}579}\ \tau^{0{,}583} \qquad (1)$$

where t_τ is the thickness of the corroded layer (mm),
C - the solutions concentration (%),
τ - the exposure time (days).
This equation corresponds rather well with the theoretical one $t_\tau = A\sqrt{\tau}$ published by Polak (8).

CONCLUSION

The obtained experimental data show that formic acid solutions severely corrode hardened portland cement pastes.

The course of corrosion is influenced mainly by the water to cement ratio of the cement paste, the concentration and acting time of formic acid solution

Table 3. Chemical Composition of Non-corroded and Corroded Hardened Portland Cement Pastes

Designation	Age (Samples Storage in Sol.)	SiO_2 + Ins. Res.	Fe_2O_3	Al_2O_3	CaO	MgO	Loss on Ignit.
	days	%	%	%	%	%	%
PI_3	28	19,25	2,40	4,72	52,78	1,43	18,00
	119	18,44	2,62	7,26	51,64	0,64	14,60
M_1I_3	393(365)	18,58^c	2,56^c	6,04^c	48,40^c	2,08^c	17,44^c
		53,73	8,57	14,14	5,70	2,65	13,51
M_2I_3	56(28	54,41	6,96	11,36	7,75	0,43	15,68
	119(91)	17,32^c	2,82^c	7,68^c	51,40^c	1,80^c	12,37^c
		67,90	4,31	9,13	3,64	0,29	13,95
	393(365)	86,34	1,25	2,71	1,04	0,30	8,31
M_3I_3	119(91)	16,96^c	2,69^c	7,43^c	50,32^c	1,52^c	18,25^c
		72,37	2,32	5,84	3,43	0,26	14,31
	393(365)	88,14	0,43	1,00	0,40	0,00	8,29
PI_1	393	18,80	2,92	6,09	58,58	1,34	7,56
M_2I_1	393(365)	18,86^c	2,83^c	7,24^c	59,38^c	1,48^c	8,28^c
		68,68	7,19	7,24	2,04	0,27	13,12

c - core

It is a typical acidic corrosion characterized by the formation of the layer structure.

The composition and properties of the corrosion products layer are very different from those ones of yet not corroded samples core or of the control water cured samples.

The microstructure of the corroded layer is very porous and without the presence of morphologically typical hydration products.

For the thickness of the corrosion products layer as the convenient characteristic of corrosion studied the general exponential equation can be written

$$t_\tau = k\, C^a \tau^b \qquad (2)$$

REFERENCES

1. Moskvin, V.M., Ivanov, F.M., Alexejev, S.N. and Gusejev, E.A.: Corrosion of concrete and reinforced concrete, methods of their protection (in Russian). Moscow, Strojizdat, 1980, 536 p.

2. Biczók,I.: Concrete corrosion, protection of concrete (in German). Budapest, Verlag der Ungarischen Akademie der Wissenschaften, 1960, 396 p.

3. Regourd,M.: "Physical and chemical corrosion of concrete". Durability of reinforced concrete (in French). Zurich, Switzerland, SIA, 1985, 15-22.

4. Moskvin, V.M., Rubeckaja, T.V. and Ljubarskaja, G.V.: "Corrosion of concrete in acid medium and methods of its investigation" (in Russian). Beton i železobeton, 1971, (10), 10-12.

5. Medgyesi, I.: "Comparaison de l'effet corrosif de certaines acidic organiques". Rilem Symposium Durability of Concrete. Prague, Czechoslovakia 1969, Preliminary Report, Part II, C 431 -C 445.

6. Medgyesi, I., Bozsidár, M. and Marton, M.: "Derivatographic results in the research of concrete corrosion". Proc. 4th Intl. Conf. Thermal Anal., Budapest, Hungary 1974, V3, 533-542.

7. Bajza, A.: Corrosion of hardened cement pastes by NH_4NO_3 and acetic and formic acids. Pore Structure and Permeability of Cementitious Materials, ed by L. R. Roberts & J.P.Skalny. Pittsburgh, MRS Proc. 137, 1989, p. 325-334.

8. Polak, A.F., Cabibullin, R.G., Jakovlev, V.V. and Latypov, V.M.: "Generalized mathematical model of concrete corrosion in aggressive solutions" (in Russian). Beton i železobeton, 1980, (9), 44-46.

ELECTROCHEMICAL DEGRADATION OF CEMENTITIOUS MATERIALS

A Gerdes and F H Wittmann

Institute of Building Materials, Swiss Federal Institute of Technology, Zurich, SWITZERLAND

SUMMARY

Concrete elements may be exposed to long lasting electric fields. The reinforcement may act in some cases like an electrode. If the concrete elements are water saturated migration of ions will take place under the influence of an imposed electric field. This transport mechanism will locally reduce the equilibrium ion concentration and hence induce dissolution of solid phases. A model will be described to predict quantitatively this degradation process. The predictions of the model are compared and verified by experimental results. Measures to prevent this corrosion process are discussed.

Betonbauteile können längerfristig elektrischen Feldern ausgesetzt werden. In einigen Fällen fungiert dabei die Bewehrung als Elektrode. Bei mit Wasser gesättigten Bauteilen kann unter dem Einfluss elektrischer Feldern eine Ionenmigration stattfinden. Dieser Transportmechanismus kann örtlich die Konzentration der im Gleichgewicht stehenden Ionen beeinflussen und zum Abbau der Hydratationsprodukte führen. Ein Modell wird entwickelt, um diesen Schadensmechanismus quantitativ zu beschreiben. Die Annahmen dieses Modells werden mit Analyseergebnissen verglichen und verifiziert. Weiterhin werden Möglichkeiten diskutiert, um diesen Korrosionsprozess zu verhindern.

1. INTRODUCTION

Tap water reservoirs are often built as a reinforced concrete structure. For hygienic reasons the inner surfaces of the concrete structure are usually coated [1]. In Europe organic coatings are more and more replaced by cement based mortar coatings. For this application white cements are often used. In many cases the service life of the cement based coating has been shown to be well above ten years. In some cases, however, the coating locally becomes soft within penny-shaped areas. The material from these areas can easily be washed out. Sometimes the soft areas can be detected by their brownish colour.

Detailed analyses have shown that chemical attack by tap water and microbiological corrosion can be excluded as origin for this type of damage [2]-[4]. Recently several authors have found that cement based materials can be severly attacked under the influence of an electric field.

SAITO and NAKANE [5] placed concrete specimens between two carbon electrodes. One electrode works as a cathode (-), the other one as an anode (+). Under the influence of a potential difference, forced directional ion migration through the porous structure of hydrated cement paste takes place. The authors indicate that the appearance and composition of the mortar changes distinctly after a short time. The surface facing the cathode showed clearly a coarser texture by visual inspection and it was found that the porosity and permeability increased. The chemical analysis of the mortar indicated that the $Ca(OH)_2$ content continually decreased, subsequently the decomposition of CSH takes place. This has been measured by following the Ca/Si ratio.

MENZEL and AKTAS [6] investigated the effect of an electric current on concrete. They described that the mortar near the anode gets a spongy appearance, showing particles of brownish colour, while the cathode area remains dense and shows white stains. The results of DTA- and XRD-analysis confirmed that the lime was completely dissolved. In this case other hydration products, like CSH gel, were dissolved due to the action of hypochloric and hydrochloric acid, produced by electrolysis.

Based on these results we propose in this paper a hypothesis for the deterioration of concrete under an electric field. The prediction of this model will be discussed and verified by comparison with experimental results.

2. THE MODEL : CHEMICAL REACTIONS UNDER THE INFLUENCE OF AN ELECTRIC FIELD

The deterioration of concrete under the influence of an electrical field is assumed to be due to a series of migration processes and subsequent reaction mechanisms. The proposed model is schematically shown in Fig. 1.

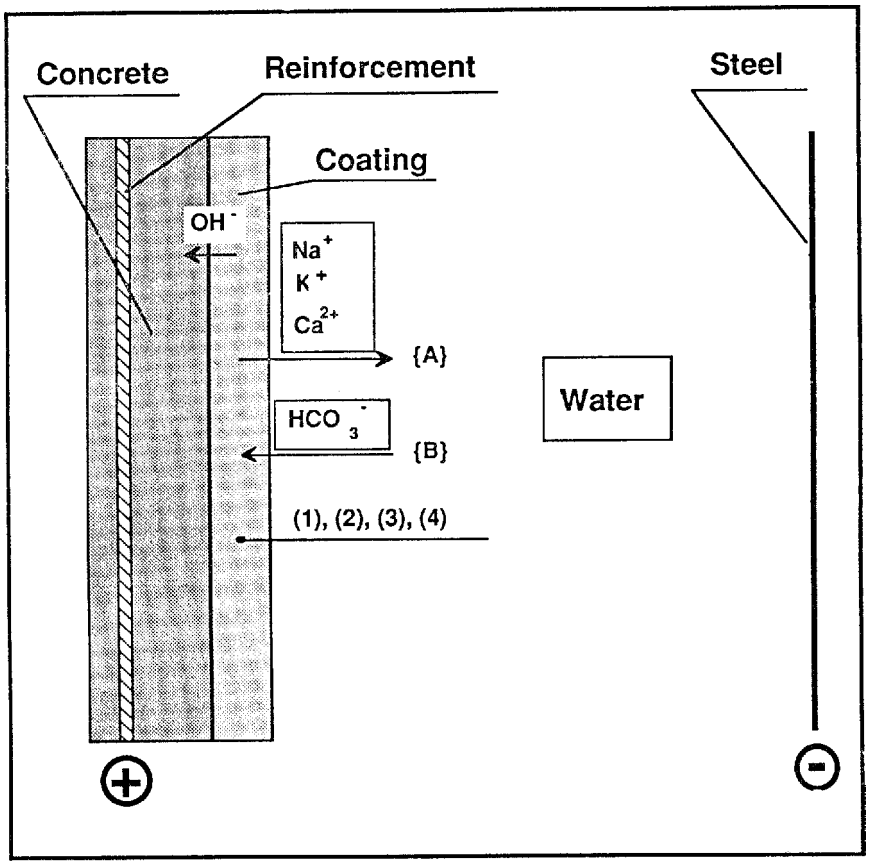

Fig. 1 Model of the deterioration of concrete under the influence of an electric field

Under the influence of an electric field anions like Ca^{2+}, Na^{+} or K^{+} ions dissolved in the pore water of concrete and the cement based coating will migrate towards the negative electrode. This process is characterized by {A} in Fig. 1. On the other hand, cations like HCO_3^- ions dissolved in the tap water migrate towards the positive electrode and enter the coating. This process is characterized by {B} in Fig. 1. Sometimes the HCO_3^-- concentration in tap water is very high, for instance up to 40 French degrees of hardness which corresponds to 400 mmol/l ions of alkaline earth metals. In the solution in the pore system the concentration of HCO_3^- ions increase.

As a consequence of equilibrium of CO_3^{2-}/HCO_3^- and the solubility products of carbonates, only insoluble $CaCO_3$ precipitates :

$$Ca^{2+} + 2\,HCO_3^- \;<===>\; CaCO_3 + CO_2 + H_2O \qquad (1)$$

The reaction product CO_2 can dissolve $Ca(OH)_2$ and hydrates of the calcium aluminate phases. At the same time Ca^{2+} and OH^- ions can be dissolved from the CSH gel. The amount of dissolved Ca^{2+} ions depends on the CO_3^{2-}/HCO_3^- equilibrium.
The reactions involving $Ca(OH)_2$ may be represented by the following equations :

$$CO_2 + 2\,OH^- \;\text{<===>}\; CO_3^{2-} + H_2O \qquad (2)$$

$$Ca^{2+} + CO_3^{2-} \;\text{<===>}\; CaCO_3 \qquad (3)$$

Cement hydrates like calcium aluminate hydrate, monosulphate or ettringite decompose into $CaCO_3$, Al_2O_3 and in the case of monosulphate or ettringite in addition to $CaSO_4$.
The decomposition of CSH is characterized by the decrease of the Ca/Si ratio. This can be described by equation (4):

$$x\,CaO{\cdot}SiO_2(aq) + z\,H_2O \;\text{--->}\; y\,Ca^{2+} + 2y\,OH^- + (x\text{-}y)\,CaO{\cdot}SiO_2(aq) \qquad (4)$$

The dissolution of the CSH gel is further accelerated by the destruction of the protective layer [7], [8] . Finally, decomposition of the cement hydrates lead to the formation of silica, alumina and iron oxide [9].

3. ON THE ORIGIN OF ELECTRIC FIELDS

Among the possible origins for an electric field in concrete structures like water reservoirs range corrosion cells or stray field currents, induced for instance by transformers, electrified railway systems or trams. In general a corrosion cell is built up if two different materials, characterized by different corrosion potentials, are connected with one another and when they are in in contact with an electrolyte.
In the case of water reservoirs a corrosion cell consisting of corroding steel in contact with reinforcing steel in concrete can be formed. This is schematically shown in Fig. 2.

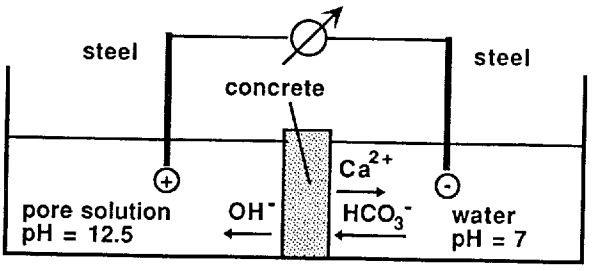

Fig. 2 Model of a corrosion cell

For the reinforcing steel in concrete stored under water, a corrosion potential of - 500 mV can be measured, using a $Cu/CuSO_4$ cell as reference electrode. By connecting the reinforcing steel in concrete to the corroding steel a corrosion potential ranging from 350 up to 600 mV can be expected [10]. Under these conditions the migration of Ca^{2+} ions and HCO_3^- ions occur as outlined in section 2.

4. EXPERIMENTAL VERIFICATION: ANALYSIS OF THE CEMENTITIOUS COATING

4.1 Visual inspection

Recently some reservoirs with the characteristic damage described above have been examined. The diameter of the damaged areas is typically 2 to 5 cm. Sometimes a regular pattern following the reinforcement of the concrete structure can be observed. The coating in the damaged areas is soft and can be easily removed.

4.2 Chemical analysis

Extensive chemical analyses have been carried out on the undamaged and the damaged mortar coating. Some typical results shall be presented here. Results of a chemical analysis of undamaged material (sample 1) and damaged material (sample 2) are shown in Table 1. Values are given in weight-%.

Sample No.	HCl-insolub. residue	HCl-solub. SiO_2	Cement content	Fe^{3+}	SO_4^{2-}
1	43.09	6.54	31.90	0.17	0.72
2	58.81	0.42	2.07	0.16	0.03

Table 1: Chemical analysis of (1) the undamaged and (2) damaged coating material

The cement content was determined by measuring the HCl-soluble SiO_2. The SO_4^{2-} content was determind by gravimetric analysis. The Fe-content was analyzed by means of photometry.
These data show, that the cement and sulphate content of the damaged mortar was significantly reduced, while the amount of Fe is found to be almost constant.
Moisture content (loss of weight at 300 °C), content of $Ca(OH)_2$ (loss of weight at 400-500 °C) and the amount of $CaCO_3$ (loss of weight at 550-850 °C) were determined by thermogravimetry. The results of TG analysis are shown in Table 2. All values are given in weight-%.

Sample No.	moisture content	$Ca(OH)_2$ content	$CaCO_3$ content
1	9.5	9.1	8.8
2	16.9	n.n	29.9

Table 2: TG analysis of (1) the undamaged and (2) damaged coating material

4.3 Scanning electron microscopy

The morphology as seen by SEM is shown in Fig. 3 and Fig. 4 for the undamaged and damaged coating material.

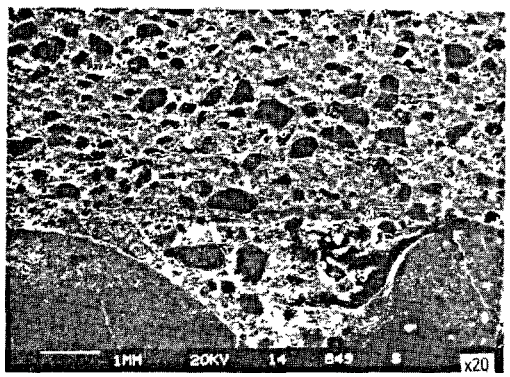

Fig. 3 Undamaged cement based coating material

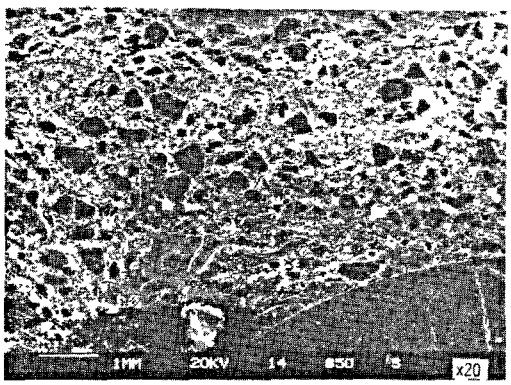

Fig. 4 Damaged part of the same coating material as shown in Fig. 3

In Fig. 3 the original surface of the coating can be seen. The binding matrix near the surface of the damaged material has been destroyed and can be seen that the mortar desintegrates.

5. DISCUSSION

The deterioration of a cementitious coating material can be described by the following model. Under the influence of an electric field built-up by a corrosion cell for instance migration of ions occurs out of and into the coating. The decrease of Ca^{2+} ions and the increase of HCO_3^- ions in the pore system of the coating respectively lead to a chemical attack of the cementitious material. As a result of this attack, which in essence is similar to carbonation, $Ca(OH)_2$ is dissolved, cement hydrates are decomposed and transformed into $CaCO_3$.
The proposed mechanisms of deterioration can be verified by results of visual inspection, chemical analysis and SEM observation. Further experiments to verify the model quantitatively will be carried out.
This type of corrosion can be avoided by electrical disconnection of the active electrodes [11].

6. CONCLUSIONS

A model to describe electrochemical degradation of cementitious materials is proposed. Based on the model and using the results of the analysis of damaged coating material the following conclusions are obtained:

- A complete decompositon of cementitious materials, stored under water, is possible if a corrosion cell can develop and/or a equally oriented electric field is applied.

- The model presented here explains the mechanisms and the velocity of deterioration observed in water reservoirs.

- This type of deterioration can be avoided by careful design of the metallic components in a reservoir or by averting metallic reinforcement.

7. REFERENCES

1. H. Kollmann: "Instandsetzung von Trinkwasserbehältern aus Stahlbeton", Bautenschutz und Bausanierung, 1989, 12, 12-18

2. S. Karlsson, A.C. Albertsson, "The biodegradation of a biopolymeric additive in building materials", Materials and Structures, 1990, 23, 352-357

3. K. Kirstein, W. Stiller, E. Bock, "Mikrobiologische Einflüsse auf Betonkonstruktionen", Beton- und Stahlbetonbau, 1986, 202-205

4. A. Schiffers, Chr. v. Oppel, H. Kaltwasser, "Untersuchungen der Zerstörung von Asbestzementplatten und Beton im Naturzugkühlturm des Kraftwerkes Ensdorf", Energie, 1976, 28, 252-254

5. H. Saito, S. Nakane, "Preliminary experimental study on the deterioration of cementitious materials by acceleration method", (will be published in Nuclear Engineering and Design, (1992)

6. K. Menzel, M. Aktas, "The effects of galvanic current on concrete", Otto Graf Journal, 1991, vol.2, 217-232

7. E. Koelliker, "On the hydrolytic decomposition of cement paste and the behaviour of calcerous aggregates during corrosion of concrete by water", Betonwerk + Fertigteiltechnik, 1986, 234-239

8. H. Grube, W. Rechenberg, "Betonabtrag durch chemisch angreifende saure Wässer", Beton, 1987, 446-451, 495-498

9. H.F.W. Taylor, **Cement Chemisty**, Academic Press, London, 1990, 383-387

10. H. Hildebrand, C.L. Kruse, W. Schwenk, "Einflussgrössen der Fremdkathoden aus Bewehrungsstahl in Beton auf die Erdbodenkorrosion von Stahl", Werkstoffe und Korrosion, 1987, 38, 696-703

11. R. Müller, "Korrosionsprobleme in Abwasseranlagen- Grundlagen, Beispiele, Massnahmen" Verband schweizerischer Abwasserfachleute (Hrg.), Verbandsbericht Nr. 381, Zürich, 1988

AN IMPACT OF THERMAL-TREATED ARGILLACEOUS OCHRE ON PROPERTIES OF DECORATIVE CEMENT

N A Sirajiddinov, Kh L Usmanov and D K Adylov

Institute of Chemistry, Uzbek Academy of Sciences
Tashkent, UZBEKISTAN

SUMMARY

The work contains results of an examination of the feasibility of using thermally-treated argillaceous ochre on such properties of decorative cement as strength, frost- , weather- and sulphate resistance. It has been established that under thermal treatment, aluminates, silicates and ferrites, being in the composition of argillaceous ochre, were subjected to structural changes, and thus, they positively influenced the properties of decorative cement.

АННОТАЦИЯ

В работе приведены результаты исследования о возможности использования термообработанной глинистой охры на такие свойства декоративного цемента, как прочность, морозо-, атмосферо- и сульфатостойкость. Установлено, что вследствие термообработки алюминаты, силикаты и ферриты, находящиеся в составе глинистой охры, претерпевают структурные изменения и тем самым положительно влияют на свойства декоративного цемента.

In the production of red cement an expencive pigment is generally used as a clouring admixture and the red cements thus obtained are characterized by a low fading resistance. That is why search of a new abundantly available colouring admixtures for improving the properties of coloured cemenets seems necessary.

For this purpose, we examined natural argillaceous yellow ochre and a white clinker of the integrated building materials factory in Angren. The chemical composition of these raw materials is presented in Table I.

TABLE I

CHEMICAL COMPOSITION OF THE RAW MATERIALS

Materials	SiO_2	Al_2O_3	Fe_2O_3	CaO	SO_3	P_2O_5	MgO	Na_2O	R_2O	
White clinker from Angren	23.35	6.42	1.05	67.44	0.30	-	0.42	-	1.67	99.65
kn=0.90 r=6.26 n=3.0										
Yellow argillaceous ochre	51.68	20.39	15.85	0.82	0.11	-	0.65	0.1	1.39	90.89

In the X-ray diffractograms of non-fired ochre mainly the lines corresponding to the following compounds can be observed: quartz (-SiO_2) - 0.334; 0.244; 0.180; 0.165; 0.153; 0.137 nm; grinalite - $Fe_3/OH/_4 \cdot Si\ {}^{\cdot}O_2$ - 0.712; 0.355 nm; limonite - $FeHO_2$ or (FeOOH)- 0.421; 0.244; 0.226; 0.180; 0.165; 0.136 nm; diklite - $Al\ /OH/_4 \cdot Si_2\ O_5$ - 0.233; 0.165 nm.

When heating up to 700-900°C the colouring matter - yellow argillaceous ochre , including a compound goethite - $FeHO_2$ (FeOOH), transforms to hematite Fe_2O_3 (red).

$$- FeOOH \xrightarrow{600 - 800^{\circ}C} - Fe_2O_3$$

That is why it was interesting to examine the impact of thermal treatment of the yellow argillaceous ochre over 200-1000°C on its properties. At 800°C minerals of the yellow argillaceous ochre are successively dehydrated and rendered partially amorphous as a result of the deformation and breakdown of the crystal lattice of the mineral.

In the X-ray diffractograms of the thermally treated argillaceous ochre the lines 0.442; 0.334; 0.186; 0.181 and 0.158 nm are indicated, corresponding to -quartz and the ones 0.270; 0.250; 0.185 nm - Fe_2O_3 (hematite).

Mixtures in which a part of the red ferro oxide pigment was substituted with the thermally treated ochre were forpassed for an examination of the impact of the latter on the physical and mechanical properties of the decorative cement.

According to the results of the trials, the decorative cement specimens, containing ochre can stand higher bending, tension and compression as compared to the ochreless ones (TABLE II). The positive influence of ochre on the activity of the decorative cement can be explained by the fact, that thermal treatment of the ochre results in the dehydration of ferro-containing compounds of montmorillonites, dikkites and other argillaceous minerals, which leads to structural changes and, in turn, increase in its activity.

An examination of the impact of the thermally treated ochre on weather and frost-resistance has been conducted on specimens of dimensions 4 x 4 x 16 cm and composition 1 : 3 (binder : aggregate ratio). The weather resistance was determined by bending and compression tests of the specimens after one year`s exposure to natural weather conditions and comparing their strength with that of control specimens kept under normal conditions in a humid medium as bar standard (2). The coefficient of weather-resistance of the specimens, containing up to 11.5% of thermally treated ochre were found to be 0.94 - 1.45.

TABLE II

RESULTS OF PHYSICAL AND MECHANICAL TESTS OF THE CEMENTS

No	Material used			Rated thickness (%)	Setting time (h/min.)		Ultimate strength MPa, in a day					
							Bending			Compression		
	White cement	Argillaceous ochre	Red ferro-oxide		initial	final	3	7	28	3	7	28
1.	91.5	-	8.5	29.0	1:08	2:42	36.9	42.7	58.2	183	290	323
2.	85.0	11.5	3.5	31.5	1:00	1:27	30.7	48.2	58.8	322	400	560
3.	85	10.5	4.5	32.5	1:05	2:05	40.9	50.5	59.8	330	426	580
4.	85	8.5	6.5	33.8	1:30	2:50	36.2	40.2	56.5	288	399	490
5.	82.5	9.5	8.0	30.1	1:10	1:55	36.1	40.5	47.4	294	357	420

Frost resistance trials were conducted in a freezing chamber at $20^{\circ}C \pm 2^{\circ}C$. Defrosting was conducted in water at room temperature not lower than $+10^{\circ}C$. The trials comprised 300 phase-thaw cycles. After each 25 cycles the specimens were weighed and visually examined. The results indicated that after 300 cycles the specimens showed no defects in outer appearance. The tests on physical and mechanical properties also indncated a not much fall in strength for some specimens; the coefficient of the weather resistance ranged from 0.93 to 1.13%.

Prism specimens (2 x 2 x 10 cm) were made from a white portland cement, a red portland cement with an admixture of a red ferro-oxide and from another red one with an admixture of the thermally treated ochre, using a binder to aggregate ratio of 1 : 3. After a 28-day hardening in water the specimens were transferred to glasses filled with sand and 1-3% salt solutions ($MgSO_4$, Na_2SO_4 and $MgCl_2$). Visual examination of the specimens after 3 months indicated that in those of white and red cement, containing the red ferro-oxide a slight film of salts on the surface could be observed.

At the end of one year the film increased mostly in the specimens from the white cement. By three years , the specimens showed big cracks, evident salt filming and failures, mostly in the solutions of Na_2SO_4, which was the most agressive. However, the specimens containing the thermally treated ochre showed no such intensive salt filming and outer defects under the same conditions. Only in the 3% solution of Na_2SO_4 a slight film of salts on the surface of the specimens could be observed, but without cracks. This phenomenon can be explained as follows. In the process of hardening of the decorative cement, the aluminates and the silicates, activated in the thermal treatment of the argillaceous ochre, interact with the $Ca(OH)_2$, released during the hydration of the cement materials and form hydroaluminates and hydrosilicates of calcium. And this prevents formation of hydrosulphoaluminates and hydrosulphoferrites of calcium.

Thus, the use of thermally treated ochre as colouring admixture to white cement improves such basic properties as the physical and mechanical ones as well as frost-, weather- and salt-resistance.

REFERENCES

1. Kontorovich S.I., Segalova E.E., Rebinder P.A.: "Reports, Acad.Sci. USSR, 1959, 129 (4), 847. (Russian).

2. Butt Yu.M., Timashev V.V.: "A Practical Work on Chemical Technology of Binding Materials". "Vysshaya Shkola" Publishing House, 1973, 127-260. (Russian).

DURABILITY OF CONCRETE ON HIGH-ALUMINATE PORTLAND CEMENT AT ACTION OF THE SIGN-VARIABLE TEMPERATURES

Vas I Kolomiets, B I Popov and Val I Kolomiets

Far-Eastern research, designing and technological institute on construction of Russia state construction commission,
Complex research and industrial concern "Cesson" Nakhodka,
RUSSIA

ANNOTATION

The paper presents the results of an investigation on alternate freezing and thawing resistance for high-aluminate alite portland cement concretes of Spassk plant (C3A > 10%), and also for sulfate resistant belite cement of Templuiski plant (C3A ~ 4%). The addition of the modifiers ZC, LCT, C-3 has been shown to be effective for influence on the liquid phase of the cements. So, the 0,5% addition of ZC to the liquid phase allows to decrease the concentration of CaO in the filtrate of cement suspension to 28%.

According to the crushing strength tests, the addition of complex reactive antiaggregate modifiers on the base of ZC + LCT (C-3) increase the freeze resistance in 2.5 times in relation to the standard high-aluminate portland cement concrete.

Аннотация

В данной работе представлены результаты исследований стойкости бетона на высокоалюминатном алитовом портландцементе (ВАЦ С3А > 10%) и сульфатостойком белитовом цементе (СБЦ) Темлюйского завода (С3А ~ 4%) при воздействии циклических знакопеременных температур. Показано, что при введении модификатора ЗЩ-0,5% к жидкой фазе в фильтрате цементной суспензии осталось 28% CaO.

Соблюдая принцип равнонадежности на основании предельно допустимых напряжений (рд) показано различие в механизмах разрушения бетонов на ВАЦ и СБЦ. Достигнутая высокая морозостойкость (F-300 и выше) с комплексным модификатором ЗЩ + ЛСТ(С-3) позволяет рекомендовать расширение области использования ВАЦ.

INTRODUCTION

For use in cold regions, the resistance to low temperature (freeze resistance) is one of the basic characteristics of cement. Due to high structural and technical properties, the high-aluminate portland cements (HAPS) are the object of a great practical interest, but their use is restricted by phase changes during the time of hardening, low water stability C3A, and high concentration shrinkage. These factors decrease in a considerable degree the durability of cement stone.

The negative effect of C3A can be compensated by transference of high-solutive compounds to hard-solutive ones. It is known, that the formation of the high-basic calcium hydrosilicates is followed by formation of low-basic calcium hydrosilicates after binding of free calcium oxide and lowering of pH to 10.5 - 9.4 (1). The solvated Ca++ ions take the most part in the formation of low-basic silicates.

The properties of liquid phase are known to have considerable effect on the cement hydration process (2,3). The presence of the excessive OH- ions in the mixing water intenses the hydration processes for low-basic calcium silicates (4,5). Due to high condensation of silicate-oxygen radicals (SiO4 - octahedrons), the durability of low-basic hydrosilicates of tobermorite group is very high in relation to the durability of high-basic calcium hydrosilicates (6). In these conditions the dissolution kinetics of binder is determined, first of all, by concentration of H+ and OH- ions in the solution. On the water-binder boundary, the concentration is increased by dissociative adsorption of H2O on active centers (6,7). At the normal temperature the major products of hydration are CSH and Ca(OH)2, in proportion 1.5 - 2.0 (8).

On the other hand, the destruction of solid medium is accompanied by inter crystalline microcracking in the areas of portlandite and calcium hydrosilicates. Silica and alumina hydrogels are resist the increasing of the microcracking due to relaxation of microstresses. Besides, the acicular crystals of calcium hydrosilicate and ettringite enforce the gels. The maximum crashing resistance of cement stone (about 65 MPa) is conditioned by presence of calcium hydrosilicates. If the concentration of Ca(OH)2 is higher then 23 - 25 mass % (it is possible, when the concentration of C3S is 65 - 70%), durability does not increase, and sometimes becomes even lower (9). These factors initiated the working out of crystallizers as initial reagents for synthesis of two major bearer of durability - ettringite (for early durability) and calcium hydrosilicate (for continuous hardening).

Therefore, the investigations of freeze stability of alite HAPS have a considerable theoretical and practical interest. In the present study we have attempted to increase the stability by some complex modifiers and to understand their role in the processes of hardening and freeze-thaw destruction.

EXPERIMENTAL DATA

The objects of our study were HAPC concretes (A > 10%) of Spassk plant, and belite sulfate- resisting cements (SRC) of Teploozersky plant (A=4%). Each test series included the samples with the reactive modifiers ZC, LST, and C-3, together with the standard control samples without modifiers (table 1). The complex use of the modifiers has

co-reactive effect and improves binder plasticity. Volume ration of coarse and fine aggregates (r) was constant and equal to 0,36.

Freezing of cubic samples (100 mm) was performed in Nema thermobarocamera till 223 K with keeping at this temperature for 2,5 h and posterior thawing for 2.5 h in sea water.

Table 1

Composition code	Concrete composition, kg/m3					Strength, R compr., MPa in the specific points R(N)			Number of cycles of specific point R(N)	
	Z	B	ZC	LST	C-3	Ro	R*	RD	N*	Nd
OP	450	220	-	-	-	42.7/1.00	49.3/1.55	43.2/1.01	3	9/468
2P	450	220	0.05	-	-	37.1/1.00	44.9/1.21	29.6/0.80	5	99/3770
3P	-"-	-"-	-"-	0.20	-	37.5/1.00	45.4/1.21	26.5/0.71	6	90/3336
5P	-"-	-"-	0.2	0.4	-	37.5/1.00	41.5/1.11	32.4/0.86	6	105/4005
6P	409	200	-	-	0.60	41.7/1.00	45.9/1.10	31.2/0.75	5	102/3892
8P	-"-	180	-	-	1.0	40.0/1.00	49.1/1.23	40.3/1.01	24	108/5088
OS	416	203	-	-	-	40.4/1.00	40.9/1.01	33.4/0.83	9	42/1661
2S	-"-	-"-	0.05	-	-	40.0/1.00	44.0/1.10	40.5/1.01	3	12/553
3S	-"-	-"-	-"-	0.20	-	38.9/1.00	42.1/1.08	37.2/0.96	22	46/1890
5S	409	200	0.2	0.40	-	40.8/1.00	43.6/1.07	32.5/0.78	10	36/489
6S	-"-	-"-	-	-	0.60	40.7/1.00	46.2/1.44	39.7/0.98	24	46/2040
7S	409	190	-	-	0.60	43.6/1.00	49.5/1.14	38.9/0.89	13	74/3417

Note: 1. R*, Rd, N*, and Nd - crushing strength and cycle number at the points of maximum and destruction correspondently (10). In the nominator of "cycle number" column, the coefficient of structure formation finishing in the corresponding points is given. In the nominator of "Nd" column - the integral Jm . 2. Code "P" for HAPC M-500, "C" for SRC.

RESULTS AND DISCUSSION

Following the principle of equal reliability based on the maximum admissible stress (Rd), the present study assumes to show a mechanism of HAPC concrete destruction under freezing and thawing. The results obtained (11) give the opportunity to consider calcium sulfate not only as a regulator of mechanical reactivity and hardening, but also as a structure forming component, which effects to a considerable extent on longevity of cement stone.

The experimental data obtained show in case of injection of ZC=0.5% in relation to liquid phase in the cement suspension filtrate 1:5, 28% of CaO was remained (see Table 2).

Table 2.

Concentration of CaO (g/l) in the cement suspension filtrate (1:5) in case of ZC, % to liquid phase								
0	0.02	0.05	0.1	0.3	0.5	0.8	1.2	1.5
1.77	1.72	1.46	1.44	1.22	0.49	0.57	0.38	0.29
100	97	82	81	69	23	32	22	16

Analysis of ZC role in hardening mechanism, and also experimental data analysis let suggest, that the origin of fine disperse phases promotes the dense structure formation of cement stone.

A mechanism of the elastic-plastic failure near the crack tip is affected by history of loading and sizes of plasticity zones (12) which are related to changes of the plastic zone size and respective residual stresses for variable cycles of loading and unloading.

Therefore, the process of material failure are necessary to be considered in the historical consequence that allows us to use a confidential interpretation of analysis results (10). Kinetics of concrete strength for freezing-thawing is given by

$$LnR' = x*(a+bx) + c*\sin(r), \qquad (1)$$

where $R' = R/R0$ -relative strength of concrete in freeze-thaw process, "a", "b", "c" are coefficients expressing the intensity of running of construction and destruction processes; w is the circular frequency of harmonic function, rad.

According to the present understanding, the mechanical strength of the solid bodies, especially in the initial moment of sinking, is to great extent determined by dislocations (13).

Forming the high-energetic wing of the concrete strength function at initial time shows the presence of other, apart from further cement hydration, processes, for example, relaxation and "collapsing dislocation holes" (see Figure). Sign-variable temperature effects, transforming into the sign-variable concrete deformations, give rise the continuous micro- and macro- displacements of the structure. Approaching the grain or block boundary, dislocations are interrupted. For moving new dislocations in the next grain or block, additional forces caused the strength increase of the structure concerned are needed: there is constructional process - 1 period (10). Therefore, absolute value of maximum strength (R*) characterizes the resistability and completeness of the structurization. (see Figure).

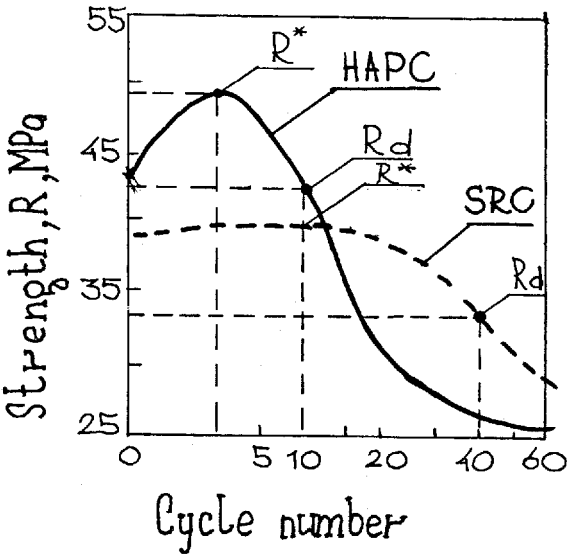

Figure. Kinetics of concrete strength in case of cyclic effect of sign-variable temperatures. (Tg = 223 K)
1- concrete composition (OP) on high-aluminate portland cement of Spassky plant (M500)
2- concrete composition (OS) on SRC of Teploozersky plant.

On the other hand, it is known that tobermorites are able to take up water and increase in volume with retention of crystal integrity (14). It follows that the increase of tobermorite structure in solid phase of cement stone must lead to sufficient variations of the material strength indices. In addition, main crack-formations for such structures must be value of the maximum concrete strength for freezing-thawing.

Thus, an extent of the structurization completeness of capillary-porous bodies (cement systems) for freezing-thawing is determined by

$$Z = R(Nd)/Rc \qquad (2)$$

where R(Nd) is value of the kinetics function of concrete strength in freeze-thaw process at the point of destruction, MPa.

Analyzing the obtained results based on the criterion "rm" is should be noted that concrete on the basic of HAPC cement without admixtures has proved must less cold-resistant than SRC. For this, an extent of the structurization completeness for the "OP" composition is equal to 1.01 while the "OS" composition has a value equal to 0.83 (see Table 1).

When injecting ZC admixture into liquid cement phase, the

greater cold-resistance will always have larger value of this integral (Jm). Comparing values Jm for 2P and 2S compositions, it should be noted that in the former case this value is 6.8 times more (see Table 1).

Cold-resistance is to greatest extent increased when complex admixture ZC+LST (SAS) is introdused into liquid phase of hardening cement. This admixture is especially efficient in case of HAPC.

In the course of initial structurization, a portland cement with alkali-containing admixture ZC+LST in liquid phase is characterized by reduced concentration of calcium ions as compared with the reference one (see Table 2). Antiaggregating effect of lignosulfates and alkaline compounds favours forming the fine-dispersed structure of cement stone. Trend of microstructure formation in early period increases significantly its resistibility against cyclic effects of sign- variable temperatures.

A cold-resistance is to greatest extent increased when complex admixture ZC+LST (SAS) is introduced into liquid phase of hardening cement. This admixture is especially efficient in case of HAPC.

In the course of initial structurization, a portland cement with alkali-containing admixture Z C+LST in liquid phase is characterized by reduced concentration of calcium ions as compared with the reference one (see Table 2). Antiaggregating effect of lignosulfates and alkaline compounds favours forming the fine-dispersed structure of cement stone. Trend of microstructure formation in early period increases significantly its resistibility against freeze - thaw destructive processes.

CONCLUSION

The performed study shows, that HAPC and SRC concretes have not only different freeze resistance, but different mechanisms of destruction. So, HAPC concrete without modifier has structurization coefficient 1.01, while SRC concrete - 0.83 (Jm 438 and 1661 correspondently)

Addition of the complex modifier ZC + LCT (C-3) at the early stadium of structurization to HAPC liquid phase decreases in a very considerable degree the concentration of calcium ions, promoting the generation of low-based calcium hydrosilicates. Besides, the anti - coagulator property of lignosulfates improve the conditions of fine structure formation in cement stone.

Addition of more reactive modifier compounds decrease the gypsum concentration in HAPC liquid phase, and allows to obtain the low-gypsum portland cement with high content of the aluminate phase directly in the construction industry. This method has high technological effectiveness and is characterized by accelerated formation of fine-dispersed structure of cement stone. Besides, alkali cations of sodium remaining in liquid phase considerably activates the aggregate surface. In the final analysis, these factors promote the increasing of strength, density and longevity of the HAPC concretes.

References

1. Teylor, H.F.W.: Chemistry of cement, Moscow, Stroyisdat, 1969, 499 p.

2. Kaushansky, V.E. :"Effect of the mixing water structure and composition on the cement hydration process". All-Union Scientific -technical Conference on chemistry and technology of cement, 8th, Section I and II, Moscow, Russia 1991, 230p.
3. Kaushansky, V.E.: Journal of applied chemistry (JAC), 1982, 9.
4. Kaushansky, V.E. & Tikhomirov, I.M.: JAC, 1979, 5.
5. Dobronravova, L.A., Butt, Yu.M., Kolbasov, V.M. and Tyusheva, Z.V.: Proceedings of D.I.Mendeleev Moscow Chemistry-Technological Institute, 1974, 82.
6. Ilykhin, V.V., Kuznetsov, V.A., Lobatchev, A.N. and Bashkutov, V.S.: Caltsium hydrosilicates. Moscow, Nauka, 1979, 186p.
7. Kapranov, V.V.: Hardening of binder and binder based materials. Cheluabinsk, South-Ural Books Firm, 1976, 189p.
8. Taulor, H.F.W. and Roy D.M.: Intern Congress Cement, 7th, Paris, 1980.
9. Kuznetsova, T.V.: "Achivements and problems in science and technics of cement obtaining". CEMENT, 1986, 7, 1-3.
10. Kolomiets, V.I.: "Modelling of moment extreme failures for estimating concrete low-resistance". International Conference on concrete and ferro-concrete, 23rd, Moscow, 1991, 84-88.
11. Horchakov, G.I., Orentlikher, L.P. and Andreeva, A.B.: "Portland cement optimization according freezing ability index". All-Union Scientific -Technical Workshop, 8th.
12. Brock, D.: Fatique Crack Propagation. Elementary Engineering Fracture Mechanics. 3rd ed. Hengham, Martinus NijHoff, Mass., 1982, 250-287p.
13. Ekorobi, T.: Physics and mechanics of failure and strength of solid bodies. Moscow, 1971, 84-88p.
14. Shpunova, S.K.: Physico-chemical principles of the cement stone structure formation. Lvov, Vistcha shkola, 1981, 156p.

EQUIPMENT TO MEASURE THERMAL EXPANSION OF CEMENTITIOUS MATERIALS

R I A Malek

Materials Research Laboratory, The Pennsylvania State University, USA

SUMMARY

Thermal expansion is an important characteristic of cementitious systems in a variety of applications. Oil well cementing, industrial and radioactive waste disposal, and rock repository shaft sealing are a few examples of such applications. In these systems, the exposure to heat is likely to occur and it is extremely important to establish a thermal expansion compatibility with the host material. The thermal expansion should be of such value as to ensure effective sealing without causing creep to the host material. Accurate monitoring of thermal expansion constitutes an essential part for these technologies. Because of the nature of the cementitious systems, normal dilatometers could not give accurate thermal expansion values. In the present paper, new equipment for thermal expansion determination of cementitious materials is presented. In this system, the thermal expansion is accurately monitored while the sample is subjected to controlled conditions of humidity and if desired, pressure. The results and their implications on the performance of selected examples will be discussed.

INTRODUCTION

Cementitious systems are widely used in supporting and sealing several underground structures. Oil wells, industrial and radioactive waste disposal sites, and rock repository access shafts are a few examples of these structures. The underground high temperature and pressure may interfere with the performance of cementitious materials under such conditions.

Cementitious materials response to heating is different from other materials. Heating in air, the cementitious materials expand or sometimes shrink. The behavior may be different if heating takes place in a closed environment or under pressure. This is almost entirely controlled by the physical and chemical (phase) changes. There is no published data on the thermal expansion of cementitious systems under a

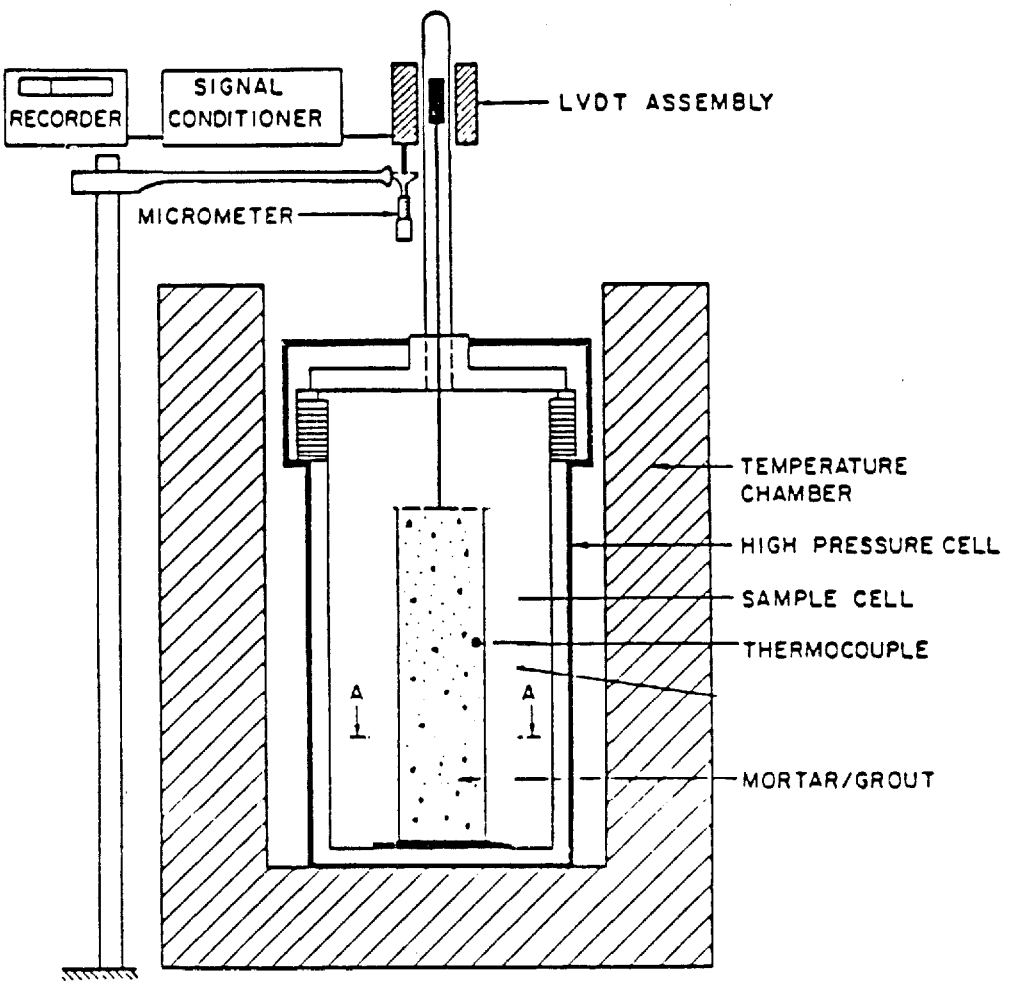

Figure 1. Equipment for thermal expansion of cementitious systems.

closed environment. This is due to the lack of dilatometers adequate for the cementitious systems. In addition to heating in an open systems most dilatometers use small-size samples not representative of the highly heterogeneous cementitious systems.

In the present paper, a new equipment for the determination of thermal expansion of cementitious materials is presented. In this system, the thermal expansion is accurately monitored while the sample is subjected to a controlled environment.

THE EQUIPMENT

The new equipment for determining the thermal expansion in cementitious systems under a controlled environment is represented diagrammatically in Figure 1.The equipment consists of a high pressure cell containing the sample and adjusted to the desired conditions of humidity and pressure. A 1 square inch x 7.25 inch (645.16 square mm x 184.15 mm) rectangular or cylindrical sample is placed vertically on the center bottom of the cell. An outer furnace assembly permits controlled temperature change. The length of change is determined by using a linear variable displacement transducer (LVDT) and its accessory signal conditioner/amplifier. This LVDT has an accuracy of $\pm$ 2 x 10^{-4} inches ($\pm$5.08 x 10^{-3}).

APPLICATION

An example on the use of this equipment was presented in this paper. It is used to measure the thermal expansion of two cementitious formulations and a rock. The cementitious formulations are proposed for the access shaft sealing of a high level waste repository site in tuff rock. The formulations are given in Table I.The samples were cured for 28 days at 38°C and 100 % relative humidity.

The cementitious samples and the tuff rock were run separately by placing each sample in the cell. The test cell was then sealed in a saturated water vapor environment at atmospheric pressure. Temperature

Table;e I: Composition of Cementitious Mixtures (weight percent).

INGRADIENTS	FORMULATION I	FORMULATION II
Type K cement	33.8	-------
Class H cement	--------	18.6
Deionized water	15.9	15.5
Silica fume	7.3	4.2
Low-calcium fly ash	8.2	-------
Minusil	-------	11.1
Slag	-------	23.2
ASTM C 109 sand	33.8	13.4
Fine sand	-------	13.4
Dispersant	0.5	0.5
Defoamer	0.005	0.02
	----------	----------
Total	99.51	99.9

rise was programmed from room temperature (27°C) to 100°C at a rate of 2.5°C per hour to maintain thermal equilibrium during the entire run. A change in length was detected by the LVDT assembly and recorded. Δl/l was determined and plotted versus temperature in Figure 2.

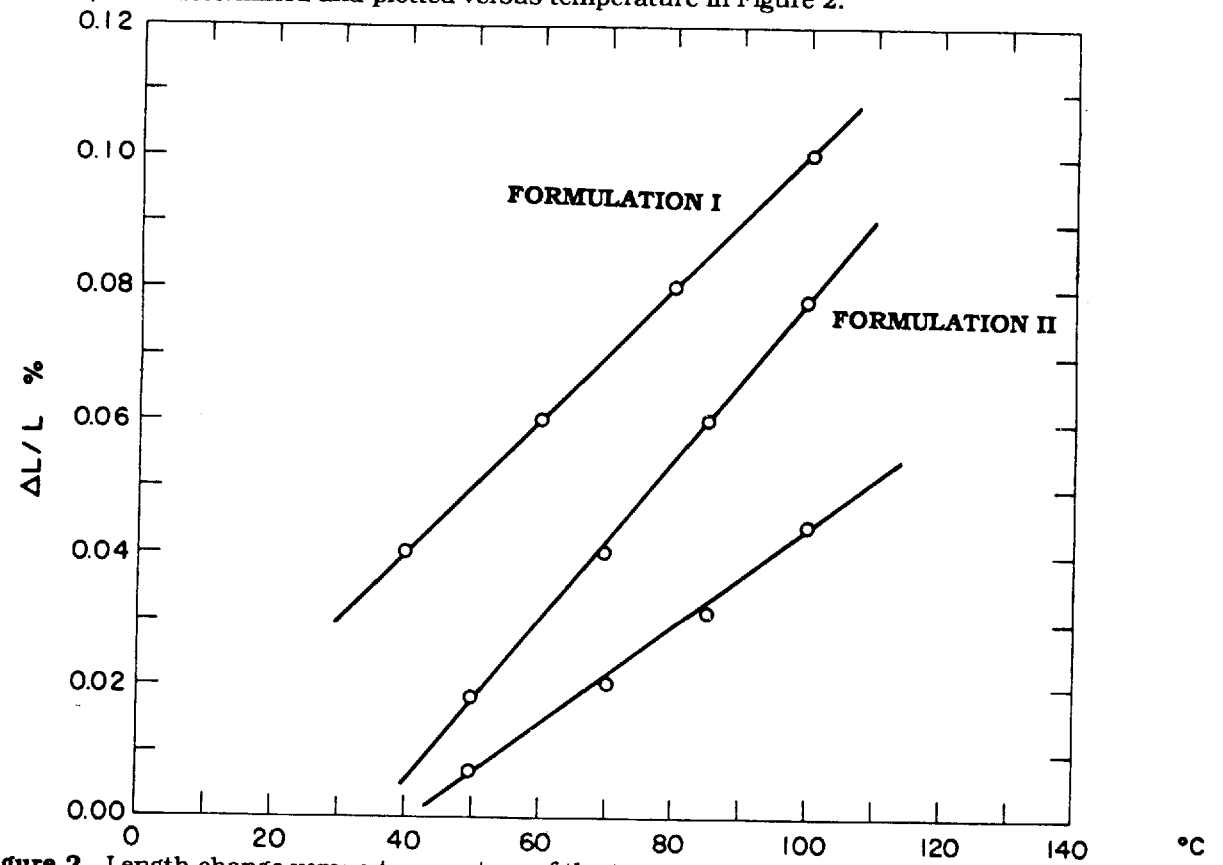

Figure 2. Length change versus temperature of the two cementitious formulations and the tuff rock.

RESULTS AND DISCUSSION

Under the test conditions described above, the two formulations show more thermal expansion than the tuff rock. This ensures that, at elevated temperatures, the two formulations will keep an effective sealing of the access shaft. The performance of formulation I, however, is much better since its expansion is not excessive with respect to the tuff rock. This will ensure an effective sealing without causing creep of the host rock. While the present paper does not address the particular issue of differences in performance, it is believed that an explanation of this could easily be reached.

CONCLUSIONS

New equipment for thermal expansion determination of cementitious materials is designed. In this system the thermal expansion is accurately monitored while the sample is subjected to controlled conditions (humidity, temperature, and if desired, pressure). The results and their implications on the performance of selected examples is important in order to predict the in situ performance of cementitious materials under different field conditions.

PORE STRUCTURE AND TRANSPORT PARAMETERS OF CONCRETES CONTAINING BLENDED CEMENTS

P Distler, J Kropp and H K Hilsdorf

Institute for Building Materials, University of Karlsruhe, Karlsruhe, GERMANY

SUMMARY:

Reactive or inert additions in blended cements have very different effects on the pore structure of mortars and concrete made thereof. This pore structure is mainly connected with the transport parameters and therefore with the durability of cementious materials.
In this investigation the influence of different additions on structural and transport parameters is explained in relation to the duration of curing. Also the alternation of the pore structure due to carbonation is taken in account.
For this hcp prisms and concrete cubes of 6 different blended cements have been manufactured and, after curing periods of 3, 7 and 28 days, kept under different CO_2-concentrations.
The depth of carbonation and the pore structure were investigated on the cement hcp prisms; different transport parameters like the permeability index for air and the initial surface absorption were determined on carbonated and not-carbonated concrete cubes.

ZUSAMMENFASSUNG:

Reaktive oder inerte Zumahlstoffe in Kompositzementen wirken sich sehr unterschiedlich auf die Porenstruktur daraus hergestellter Mörtel und Betone aus. Diese Porenstruktur ist eng mit den Transporteigenschaften und damit der Dauerhaftigkeit zementgebundener Werkstoffe verknüpft.
In dieser Untersuchung wird der Einfluß verschiedener Zumahlstoffe auf Struktur und Transportparameter in Abhängigkeit von der Nachbehandlungsdauer erläutert. Auch die Veränderung der Porenstruktur durch Karbonatisierung wird mit berücksichtigt.
Dazu wurden aus 6 verschiedenen Zementen Zementstein- und Betonproben hergestellt, die nach Nachbehandlungsdauern von 3, 7 und 28 Tagen in unterschiedlichen CO_2-Konzentrationen gelagert wurden.
An den Zementsteinprismen wurden Karbonatisierungsfortschritt und Porenstruktur untersucht; die Betonproben dienten zur Bestimmung von Oberflächenpermeabilität gegenüber Luft und Wasseraufnahme nach ISA-Test.

1 Introduction

The durability of cementitious materials is closely related to the ingress of deleterious substances from external sources penetrating the pore system of the hydrated cement paste matrix. Transport parameters which may serve as an indication for the resistance of a given material against physical and/or chemical attack are strongly controlled by the pore structure of the matrix. The pore structure is mainly influenced by the w/c-ratio and degree of hydration, however, also the type of cement as well as the type and amount of reactive or inert additions are essential parameters. Additionally, carbonation may alter the pore structure thus also affecting the transport characteristics.

In an experimental investigation the development of pore structure with duration of curing was monitored for blended cements containing ground granulated slag, fly ash, natural puzzolana, combinations thereof and ground limestone. The rate of carbonation was observed for exposure to accelerating conditions in 2% CO_2 by volume as well as for normal laboratory air. The pore structure of the carbonated surface zone then has been compared to the non-carbonated matrix. Measurements of the air permeability index and initial surface absorption were performed in order to evaluate the perviousness of the surface near regions.

2 Test program

2.1 Materials

In Table 1 the different types of cements used are summarized. These cements are standard cements according with the German Standard DIN 1164, in column 2 the table gives also information on their future classification according to the draft European standard prENV 197 /1/. Hydrated cement paste prisms and concrete cubes have been manufactured with a w/c-ratio of w/c=0.5 for all test series. For the concretes a cement content of 300 kg/m^3 was chosen and 1170 kg/m^3 of aggregates were used.

Table 1: Composition of the different cements used

Cement No.	Type	clinker content(%)	ggbfs(%)	filler(%)	nat. pozzolan(%)	fly ash(%)
1	CEI	95		5		
2	CEII	60	20			20
3	CEIIC	80				20
4	CEIIF	80		20		
5	CEIII	40	60			
6	CEIV	60			40	

2.2 Sample preparation, curing and exposure conditions

The fresh mixes have been cast in steel moulds and compacted on a vibrating table. For curing the specimens were kept under wet burlap up to an age of 3, 7 and 28 days respectively.
After the curing period samples were stored in either normal laboratory air or were kept in an atmosphere of 2% CO_2 by volume to accelerate carbonation. For several test series a set of samples was also stored in carbon dioxide free air to prevent carbonation of the surface zones. For all storing conditions the relative humidity of the air was controlled to 65% r.h. at 20°C.

2.3 Test methods

After various time periods samples were split and the depth of carbonation was measured by means of the phenolphthalein test. If a sufficient depth of carbonation has been reached, i.e. approximately 5 mm, the carbonated layer was cut off and its pore structure was investigated by mercury intrusion porosimetry. Transport characteristics of the different test series were investigated on the concrete cubes. The surface permeability index was measured by means of a suction device and the capillary absorption of water was measured by placing the bottom side of the cubes into water for a depth of approximately 2 mm. Weight gain was then recorded at various time intervals.

3 Test results

In Fig. 1 the depth of carbonation of hydrated cement paste prisms stored for six months in normal laboratory air is presented. In Fig. 2 the change in pore volume which is accessible to mercury penetration is given. In this diagramm the total pore volume intruded at the maximum presure of 200 N/mm^2 for carbonated hcp samples is related to the corresponding value of the non-carbonated paste. These ratios are given for curing periods of 3,7 and 28 days. Fig.3 shows a comparison between the pore size distribution of the different hcp series for a carbonated and a non-carbonated matrix for 4 different cements. These distribution curves have been measured on oven dried material and the contact angel was taken as 116°C. In Figure 4 the air permeability index of concrete surface zones is presented. In this diagramm the permeability index determined on concrete cubes with carbonated surface zones has been related to the permeability index which was observed on compagnion specimes stored in CO_2-free air, therefore, no carbonation could take place. No seperate pre-conditioning of the test specimes was necessary because all cubes had been stored in air of 65% r.h. for approx. 1 year. Therefore the moisture content and its distribution especially in the surface near regions was identical for all test series. Details of the test method and evaluation of the results are presentated elsewhere /2/.

Also for the water absorbtion tests, no spezial pre-condition of the samples was necessary, due to the same reasons. In Fig. 5 the take up of water of concrete cubes with and without carbonated surfaces zones is presented and for the initial absorption the take up of water after 30 minutes of contact with water was chosen. This short term absorption was of interest because the depth of carbonation for the carbonated test specimes was approx. 6mm only.

4 Discussion

Carbonation of cementitious materials is a diffusion controlled process and the incress of CO_2 into interior sections of the material is the rate controlling factor. Fig.1 illustrates that increasing hydration due to prolongued curing forms a denser structure thus reducing the rate of carbonation. Depending on the typ of cement, however, different periods of curing are necessary to attain a sufficient tightness of the paste.

Carbonation in turn also affects the porosity and pore structure of the paste, and for cements with a high clinker content the pore volume accessible to mercury penetration is reduced (c.f. Fig. 2). This fraction of the total pore volume essentially contains the capillary porosity. Fig.3 shows for 4 different cements that also the distribution of the pore sizes in this range is affectet and for some systems coarser pores develop on carbonation, even though the total volume intruded may reduce. These coarse pores may increase the perviousness of the paste.

Figures 4 and 5 show the effect of carbonation and the changes in the pore structure on two different transport characteristics of the surface near regions, i. e. the air permeability index and the initial absorption of water. In most cases the deposition of calcium carbonates in the pore spaces caused a reduction of air permeability (Fig.4) as well as in the absorption of water (Fig.5).

It had been shown earlier /3/ that the changes in the pore structure occuring upon carbonation depend on the extent to which the individual hydration products are decomposed. For cements with a high clinker content a reduction in pore volume as well as in the size of pores had been observed due to the deposition of calcium carbonates, whereas cements with low clinker content exhibited a coarsening of the pore structure.
This was attributed to the excessive formation of porous silicia gel resulting from the decomposition of CSH. These changes in the pore structure were associated with changes in permeability for water in liquid and vapour phase.

5 References

/1/ prENV 197, Cement, Composition, Specification and Conformity Criteria, CEN, 1989

/2/ Schönlin, K.; Hilsdorf H. K.: Evaluation of the effectiveness of curing of concrete structures; Concrete Durability, Katherine and Bryant Mather Internationale Conference, ACI SP 100, Detroit 1987

/3/ Bier, Th.; Kropp, J.; Hilsdorf, H. K.: The formation of silica gel during carbonation of cementious systems containing slag cements; ACI SP 114-69, Detroit 1989

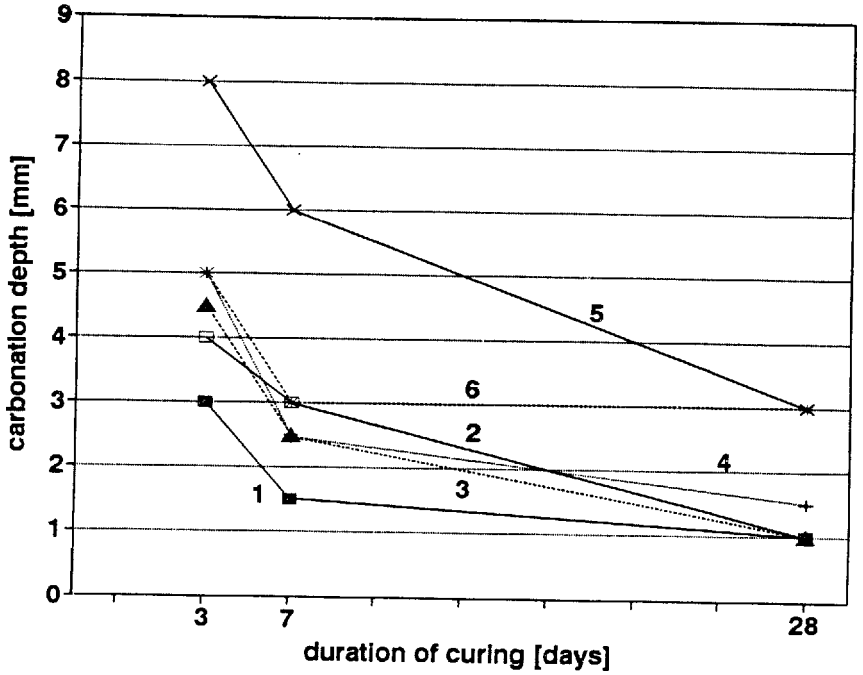

Figure 1: Depth of carbonation in hcp prisms, w/c=0.5, cured for 3, 7 and 28 days and subsequently exposed to laboratory air of 65% r.h. at 20°C. Figures describe the type of cement acc. to table 1.

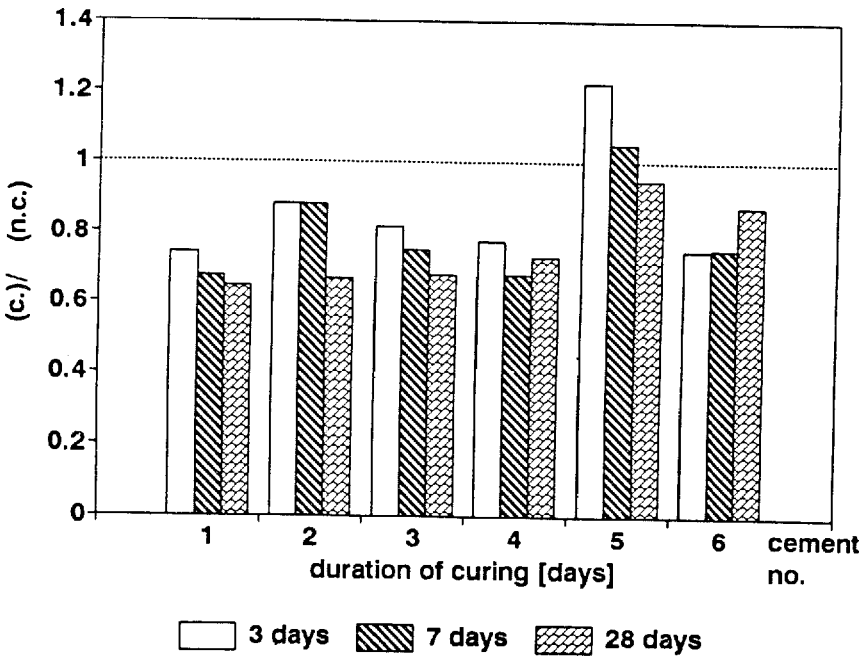

Figure 2: Mercury intruded pore volume in carbonated hcp in relation to intruded pore volume in non carbonated paste. Type of cement acc. to table 1.

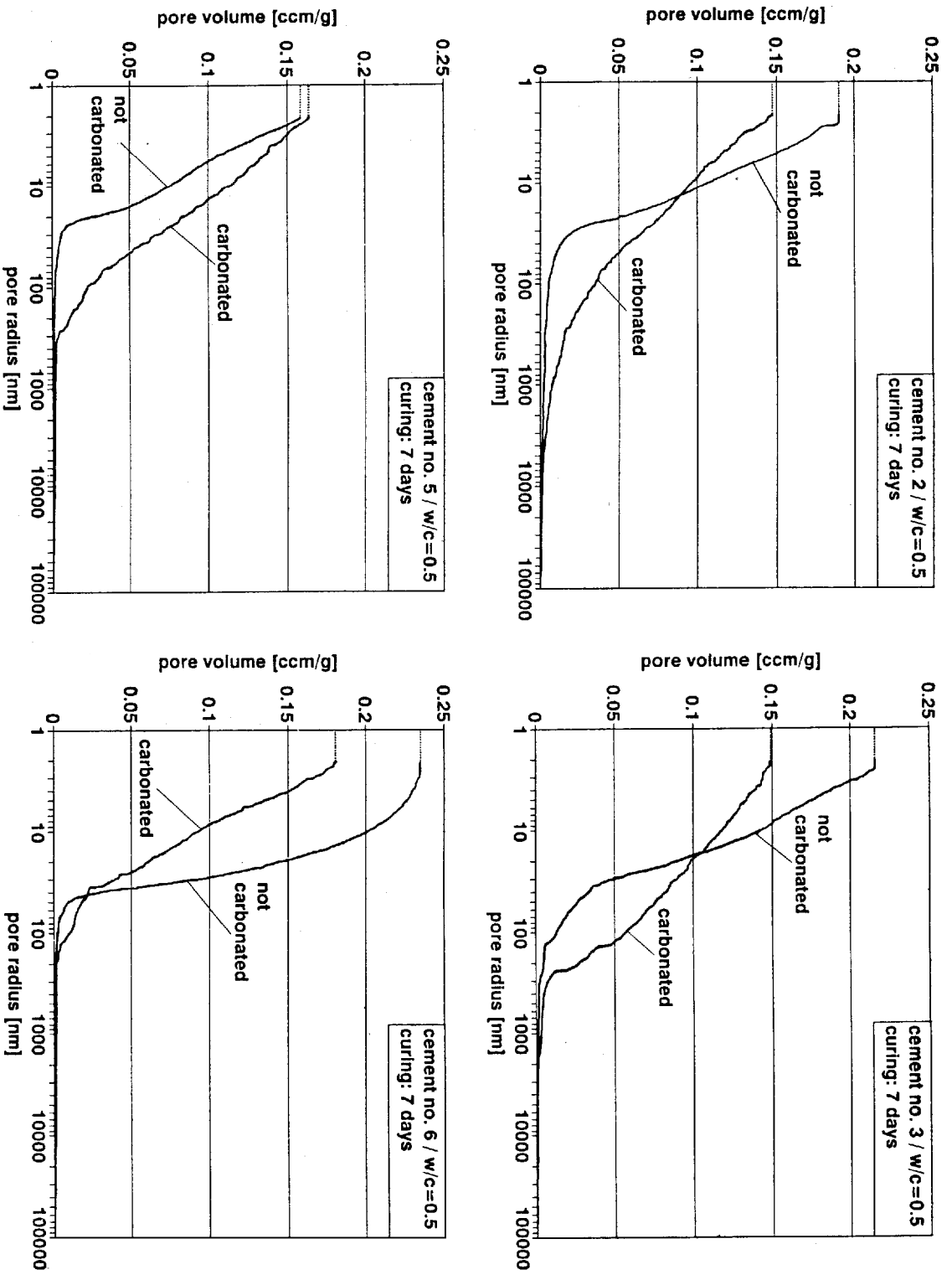

Figure 3: Cumulative poresize distribution in hcp for carbonated materials. The type of the cements represented in the diagrams is given in table 1.

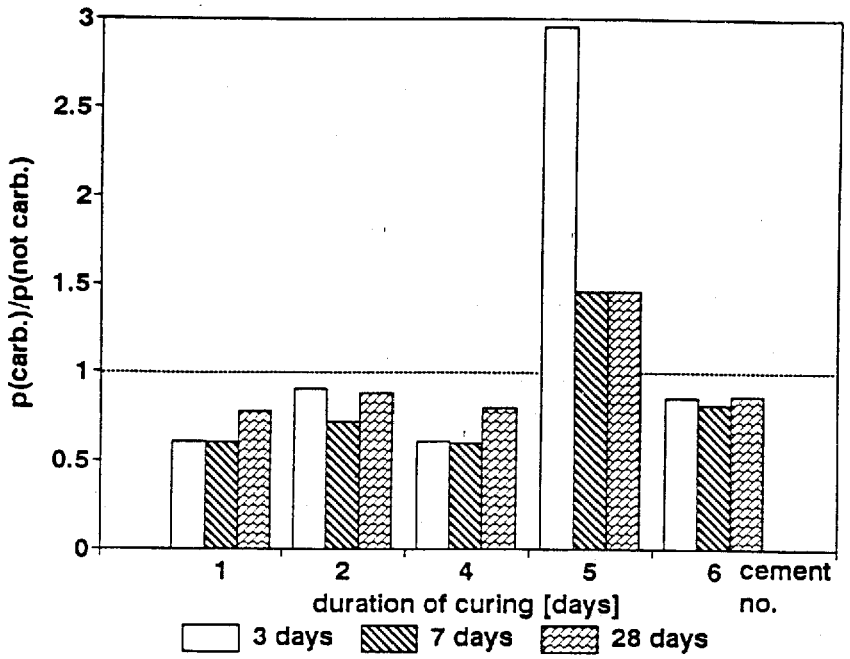

Figure 4: Surface permeability index of concretes with carbonated surface zones in relation to the respective surface permeability index of not carbonated concrete surfaces. The type of cement refers to table 1.

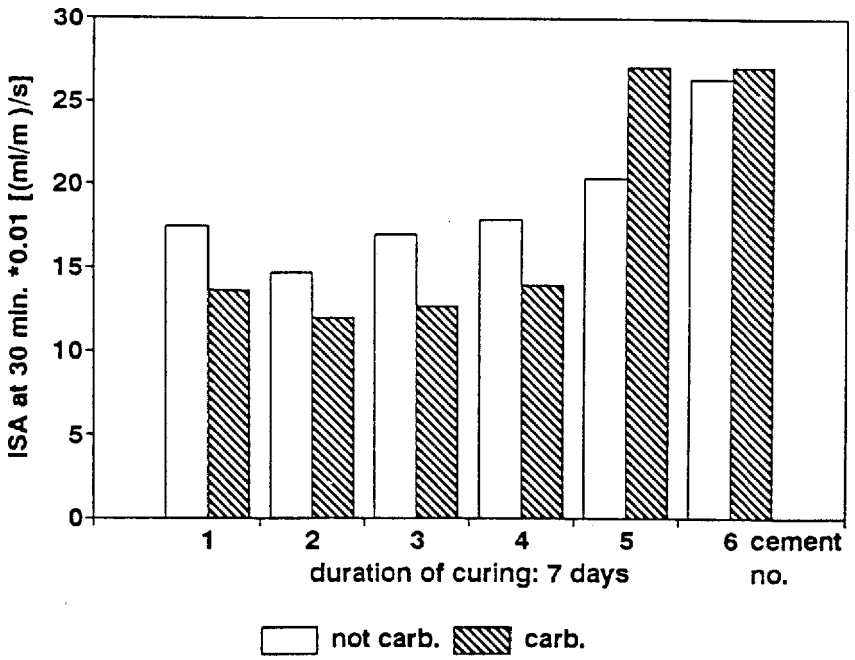

Figure 5: Initial surface absorption (ISA) of water for concrete cubes with and without carbonated surface zones. The type of cement refers to table 1.

DURABILITY EVALUATION OF PLAIN AND BLENDED CEMENTS IN AGGRESSIVE MEDIA

O S Baghabra Al-Amoudi, Rasheeduzzafar, Mohammed Maslehuddin and Sahel N Abduljauwad

Department of Civil Engineering, King Fahd University of Petroleum & Minerals, Dhahran, SAUDI ARABIA

SUMMARY

This study was carried out to evaluate the durability performance of plain and blended cements in natural sea water (Cl^- 3.7%, and SO_4^{--} 0.5%) and simulated sabkha groundwater (Cl^- 15.7% and SO_4^{--} 2.1%). Specimens made with two types of ordinary portland cement and three blending materials were used and the performance of these cements was evaluated by conducting compression tests and monitoring reinforcement corrosion at periodic intervals. Blended cements exhibited a higher physical deterioration leading to a substantial reduction in strength compared to plain cements after about two years of exposure to the sabkha groundwater. The reduction in compressive strength was observed to be higher in plain cement specimens placed in sea water compared to blended cement concretes. The reinforcement corrosion activity was, however, lower in blended cements compared to the plain cements in both the environments.

الملخص

أجريت هذه الدراسة لتقييم أداء أنواع الإسمنت الإعتيادية والمضافه في مياه البحر الطبيعية (كل ٧ر٣٪ و ك أ٤ $^-$ ٥٥ر٠٪) وفي محلول مماثل للمياه السبخيه (كل $^-$ ٧ر١٥٪ وكب أ٤$^-$ ٥٠ر٠٪) . وتم عمل عينات من نوعين من الإسمنت الإعتيادى وثلاثة أنواع من المواد الإضافيه ، وتقييم أداء هذه الانواع من الاسمنت بعمل إختبارات قوة الضغط ومراقبة صدأ حديد التسليح وذلك على فترات متعاقبة . وتدل نتائج هذه الدراسة أن تدهور أنواع الإسمنت المضافة قد أدى الى نقصان كبير فى القوة مقارنةً مع أنواع الإسمنت الاعتيادية وذلك بعد سنتين من التعرض للمياه السبخية . وكان النقص في قوة الضغط لانواع الإسمنت الإعتيادية أعلى منه فى اسمنت المواد المضافه عند التعرض لمياه البحر . وقد كان نشاط صدأ حديد التسليح في أنواع إسمنت المواد المضافه أقل منه في أنواع الإسمنت الإعتيادية وذلك في كلا البيئتين .

INTRODUCTION

Deterioration of concrete due to reinforcement corrosion and softening/expansion of the cement paste matrix due to the reaction between certain compounds in the hardened concrete and the sulfate salts in the service-environment is a phenomenon commonly observed in the marine structures and foundations placed in soils and groundwaters charged with high concentrations of chloride and sulfate salts. While cement has been extensively used in these structures, and has performed very well, the changes in the cement manufacturing processes over the last few years of this century, have brought about changes in its physico-chemical characteristics. Failures in certain structures, built of late, and exposed to marine and other aggressive media, have been reported. Also, mineral admixtures like natural pozzolan, and industrial by-products like fly ash, silica fume and blast furnace slag are commonly used in concrete these days. While there is considerable data on the sulfate resistance performance of these cements [1,2] and also some data are available on the performance of these cements in chloride environments [3,4], data are fairly sparse at this time on the durability performance of these cements in environments characterized by high concentrations of chloride and sulfate ions. In the absence of such data, a more rigorous approach towards the selection of appropriate composite binder is required before its use can be recommended in such aggressive environments. This type of evaluation is of particular importance for the Arabian Gulf area where the concentration of chloride and sulfate salts in the sea and groundwater along the coastal areas is extremely high [5].

MATERIALS AND TECHNIQUES

ASTM C 150 Type I (C_3A: 8.5%) and Type V (C_3A: 3.5%) cements were used in preparing plain cement specimens. ASTM C 618 class F fly ash was used as 20% replacement by weight of Type I cement to prepare portland cement fly ash blended cement specimens. Silica fume was used as 10% replacement by weight of Type I cement in the silica fume-cement mortar specimens. In addition, one blast-furnace slag cement, containing 60 percent granulated blast-furnace slag, was also used. A sand to cement ratio of 2.75 was used for mortar specimens, while a cement content of 350 kg/m^3 was used in the reinforced concrete specimens used for evaluation of reinforcement corrosion.

Mortar cube specimens, 25 mm in size, were used to determine the compressive strength. Concrete cylinders, 75 mm in diameter and 150 mm in height, with a centrally embedded 12 mm reinforcing bar were used for corrosion monitoring. After casting, the specimens were covered with wet burlap for 24 hours prior to demolding. After demolding, the specimens were cured in potable water for a further period of 13 days. After this period, the specimens were placed in natural sea water (Cl^- 3.7% and SO_4^{--} 0.5%).

The second group of specimens were placed in a simulated sabkha groundwater (Cl^- 15.7% and SO_4^{--} 2.1%). Mortar specimens, 25 mm cubes, were tested in compression after 3, 6, 12, 18 and 24 months using a special 200 kN automatic compression testing machine suited for testing small cubes.

Reinforcement corrosion was monitored by measuring half-cell potentials and measuring corrosion current density at regular intervals. The half-cell potentials were measured using a high impedance voltmeter and recording the potentials with respect to a saturated calomel electrode (SCE). Linear polarization resistance technique was used to measure the corrosion current density.

RESULTS

Strength Reduction

The reduction in compressive strength of the plain and blended cement mortar specimens immersed in sea water for a period of up to two years is shown in Fig. 1. These data indicate a nearly linear relationship between the time of immersion and the reduction in compressive strength in both plain and blended

cements. Highest strength reduction, after two years of exposure, was observed in Type I cement (C_3A: 8.5%). Strength reduction of about 50% was observed in mortar specimens made with this cement compared to 28% observed in Type V cement. The strength reduction in blended cements was in the range of 13 to 28%. The lowest reduction of 13% was indicated by blast furnace slag cement mortar specimens. The strength reduction in silica fume blended cement mortar specimens was approximately 25%. The reduction in the compressive strength in specimens immersed in sabkha groundwater is shown in Fig. 2. The reduction in strength after two years of exposure was about 85, 81 and 46% respectively in blast furnace slag, silica fume and fly ash blended cement mortar specimens. The strength reduction in Type I and Type V cement mortar specimens was 55 and 30% respectively.

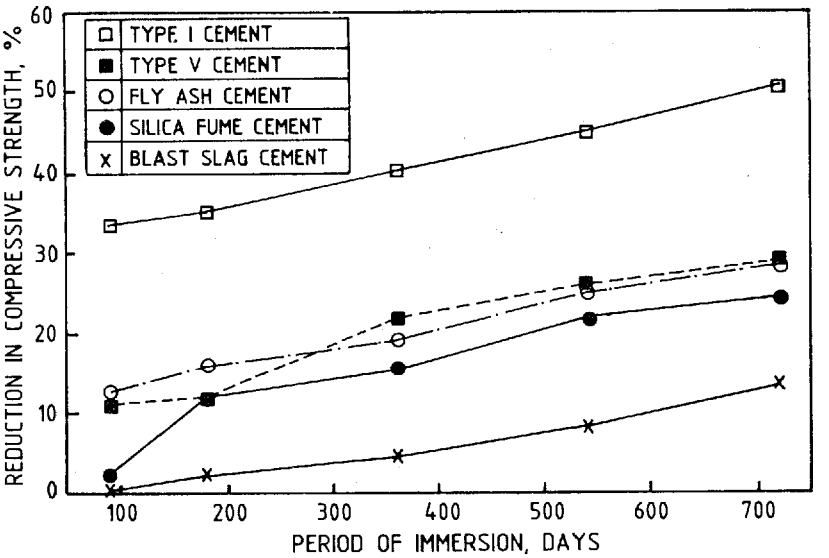

Fig. 1: Strength reduction in specimens immersed in sea water

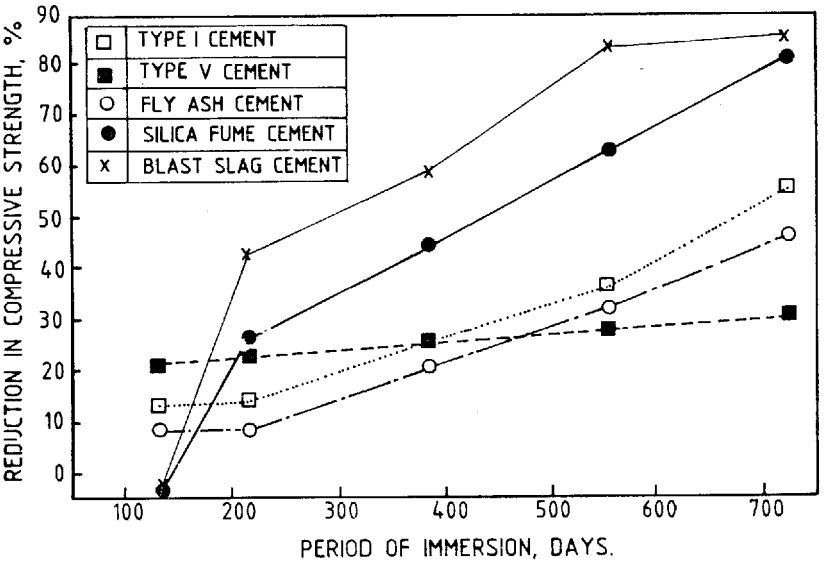

Fig. 2: Strength reduction in specimens immersed in simulated sabkha groundwater

Reinforcement Corrosion

Fig. 3 is a time-half-cell potential record for specimens immersed in the sea water. The half-cell potentials provide a qualitative indication of the reinforcement corrosion. Potential values more negative than -270 mV vs saturated calomel electrode (SCE) indicate initiation of reinforcement corrosion. The potential-time curves in Fig. 3 indicate initiation of corrosion after 114, 75 and 130 and 560 days in Type I, Type V and fly ash and silica fume cement concrete specimens immersed in the sea water respectively. The time to initiation of corrosion in the above specimens was 162, 106, 210 and 552 days respectively, (Fig. 4) when placed in the sabkha groundwater. The corrosion potentials of steel in blast furnace slag cement concrete specimens was more than -270 mV from the time of immersion of these specimens in both the solutions. This indicates that the ASTM C 876 criterion of -270 mV SCE is not useful for detecting the onset of corrosion in blast furnace slag cements [7].

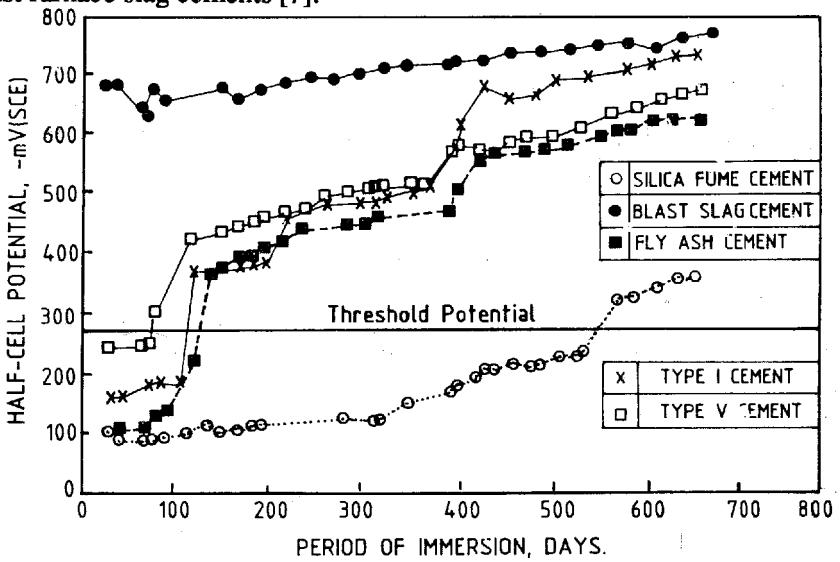

Figure 3: Half-cell potential-time record for specimens immersed in sea water

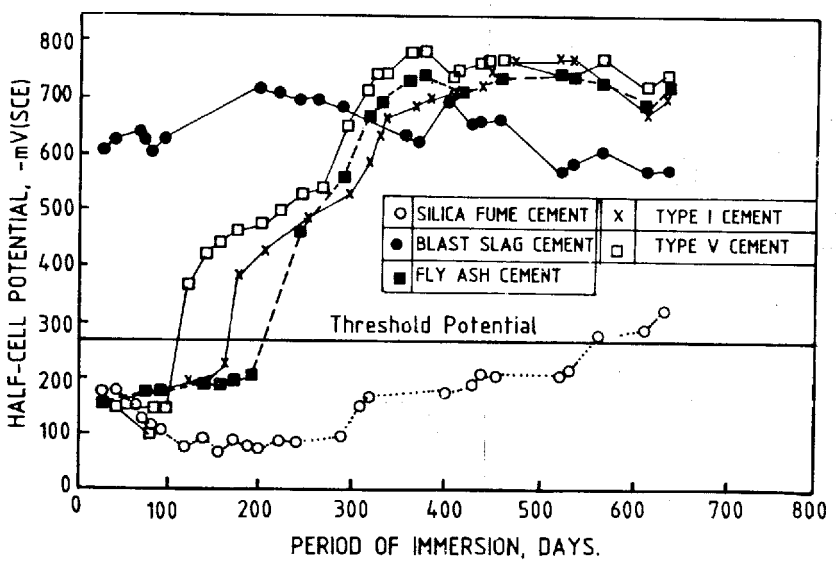

Fig. 4: Half-cell potential-time record for specimens immersed in simulated sabkha groundwater

The data on corrosion current density for bars embedded in plain and blended cement concrete specimens and immersed in the sea water are shown in Fig. 5. The corrosion current density on steel in plain cements was in the range of 3.07 to 3.20 $\mu A/cm^2$ while the corrosion current density on bars in blended cements was in the range of 0.13 to 1.17 $\mu A/cm^2$. The corrosion current density on steel in Type I and Type V cement concrete specimens immersed in the sabkha groundwater was 4.17 and 6.18 $\mu A/cm^2$ respectively (Fig. 6). The corrosion current density on steel in blended cements was in the range of 0.21 to 1.73 $\mu A/cm^2$. Minimum corrosion activity was indicated in silica fume cement concrete specimens immersed in both solutions.

DISCUSSION

The compressive strength data indicate a higher strength reduction in blended cements, particularly blast furnace slag and silica fume blended cement specimens compared to plain cement specimens immersed in the simulated sabkha groundwater. The strength reduction, on the other hand, was observed to be higher in plain cement mortar specimens which were immersed in sea water compared to blended cement mortar specimens. The higher deterioration, as reflected by a higher strength reduction in the compressive strength, in the blast furnace slag and silica fume blended cement mortar specimens placed in the sabkha groundwater compared to plain cements may be attributed to the softening of the cement matrix due to reaction of the secondary calcium silicate hydrate (C-S-H) with the high concentrations of sulfate salts, particularly magnesium sulfate, associated with the groundwaters. This sort of deterioration is manifested by softening and deterioration of the surface skin leaving the aggregates exposed to environment (scaling). This effectively means a reduction in the load carrying capacity of the specimen. Schroder and Smolzyck [6] related the surface deterioration to the glass content of the slag. A minimum glass content of the slag (> 61%) was found to be necessary for improving the sulfate resistance of the blend. The reduction in strength in silica fume cement mortar specimens is attributed to the presence of Mg^{++} cations associated with sulfate salts. Mg^{++} cation is known to be destructive to the secondary calcium silicate hydrate (C-S-H) gel by partially converting it to a cohesionless, porous, reticulated magnesium silicate hydrate (M-S-H) gel. The enhanced deterioration of silica fume blended cement paste in the magnesium sulfate environment has also been observed by Cohen and Bentur [8] and Bonen and Cohen [9].

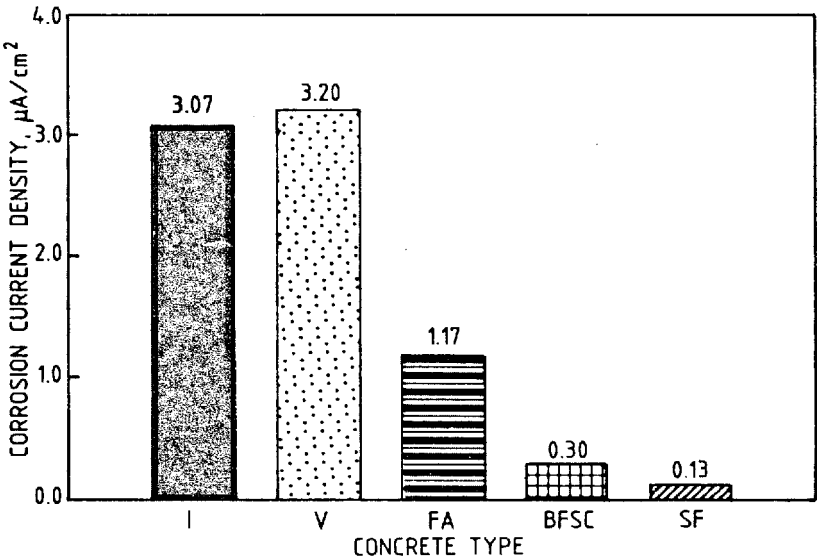

Fig. 5: Corrosion current density on steel in specimens placed in sea water

The reinforcement corrosion data indicate superior performance by blended cements in resisting reinforcement corrosion compared to plain cements in both sea water and sabkha groundwater. The corrosion current density on steel in fly ash, blast furnace slag and silica fume cement concrete specimens was four to thirty times lower than in plain cement concretes. This is indicative of their usefulness in enhancing the useful-service life of structures placed in marine and sabkha environments. Further, the superior corrosion resistance performance of silica fume and blast furnace slag cement concretes indicates that the higher reduction in strength observed in specimens immersed in the sabkha groundwater does not accelerate the reinforcement corrosion process. However, additional precautionary measures, like application of a water-resistant epoxy-based coating is necessary when silica fume and blast furnace slag cement structures are to serve in environments charged with high concentrations of chloride and sulfate salts.

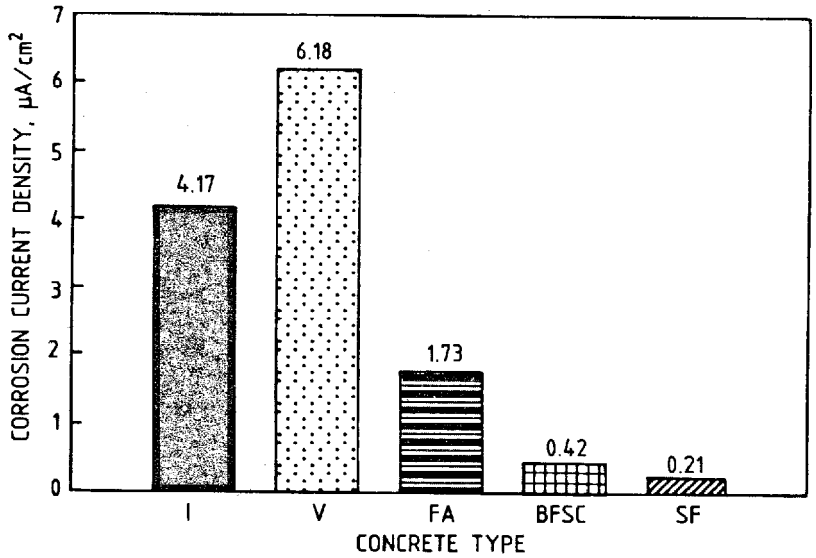

FIG. 6: Corrosion current density on steel in specimens placed in simulated sabkha groundwater

CONCLUSIONS

Higher reduction in compressive strength was observed in blended cement specimens placed in the simulated sabkha ground water compared to plain cement mortar specimens. The performance of blended cements was superior to plain cement mortar specimens when placed in sea water. The higher strength reduction observed in silica fume and blast furnace slag cements placed in sabkha groundwater compared to plain cements is attributed to the reaction of the magnesium cation associated with the sulfate salts with the calcium silicate hydrate gel.

Reinforcement corrosion in silica fume and blast furnace slag cement concretes was lower than in plain and fly ash cement concrete specimens. This trend was observed in specimens placed in both sea water and sabkha groundwater. This indicates that use of silica fume and blast furnace slag will be helpful in mitigating reinforcement corrosion in aggressive environments such as sabkha. However, protective measures like coating the exterior surface with a water-resistant epoxy-based coating will be necessary to protect concrete from deterioration due to magnesium-based sulfate salts.

ACKNOWLEDGEMENT

Authors gratefully acknowledge King Fahd University of Petroleum and Minerals, Dhahran Saudi Arabia for support of this research.

REFERENCES

1. Lawrence, C.D. Sulfate Attack on Concrete. *Magazine of Concrete Research*, 42, No. 153, Dec. 1990, pp. 249-264.

2. Wong, G., and Poole, T., *Sulfate Resistance of Mortars made with Portland Cement and Blends of Portland Cement and Pozzolan or Slag*, Technical Report SL-88-34, Department of the Army, Vicksburg, 1988, 143 pp.

3. Rasheeduzzafar, Dakhil, F.H., and Mukarram, K., Influence of Cement Composition and Content on the Corrosion Behavior of Reinforcing Steel in Concrete. ACI SP-100, 1987, American Concrete Institute, Detroit, pp. 1477-1502.

4. Page, C.L., Short, N.R., and Holden, W.R., The Influence of Different Cements on Chloride-Induced Corrosion of Reinforcing Steel. *Cement and Concrete Research*, Vol. 16, No. 1, 1986, pp. 79-86.

5. Johnson, H., Kamal, M.R., Pierson, G.O., and Ramsay, J.B. Sabkhas of Eastern Saudi Arabia. *Quarternary Period in Saudi Arabia*, Al-Sayyari S.S. and Zotl, J.G., (Eds.) Springer-Verlag, Austria, 1978, pp. 84-93.

6. Schroder, F., and Smolczyk H.G., Blast Furnace Slags and Slag Cements. Behavior in Aggressive Solutions. *Proc. 5th Int. Symp. on the Chemistry of Cement*, Vol. IV, Tokyo, 1968, pp. 181-199.

7. Maslehuddin, M., Al-Mana, A.I., Saricimen, H., and Shamim, M., Corrosion of Reinforcing Steel in Concrete Containing Slag or Pozzolans, *Cement Concrete and Aggregates*, Vol. 12, No. 1, 1990, pp. 24-31.

8. Cohen, M.D., and Bentur, A., Durability of Portland Cement-Silica Fume Pastes in Magnesium Sulfate and Sodium Sulfate Solutions. *ACI Materials Journal*, May-June, 1988, pp. 148-157.

9. Bonen, D., and Cohen, M.D., Magnesium Sulfate Attack on Portland Cement Paste, I. Micro Structural Analysis, *Cement and Concrete Research*, Vol. 22, No. 1, 1992, pp. 169-180.

PERFORMANCE AND DURABILITY OF CEMENT CONCRETE USING PORTLAND POZZOLANA CEMENT

S C Maiti and N K Jain

National Council for Cement and Building Materials,New Delhi, INDIA

SUMMARY

Results of investigation on engineering properties of concrete made with commercially available cements are presented. The investigation includes strain capacity, creep, corrosion potential and long term performance of concrete specimens and prestressed concrete beams. The average strain capacity of concrete made with portland pozzolana cement (PPC) was found to be about 25 percent higher than that with ordinary portland cement (OPC) at 180 days. Concrete made with PPC exhibited slightly higher specific creep (14 - 18%) than that with OPC at 90 days. Anodic polarisation studies upto 9 months on concrete specimens with high tensile wire indicate that PPC is comparable to OPC in their performance in normal environments. But concrete specimens kept in 3.5 percent NaCl solution indicate corrosion of reinforcements, as expected, for both PPC as well as OPC. The half-cell potential measurement and flexural test on prestressed concrete beams indicate satisfactory performance of concrete, when they were exposed to normal environmental conditions for 10 years.

1 Ø INTRODUCTION

For thermal shrinkage cracking related to either internal temperature effect in mass concrete or external temperature effects on other structures in extreme climates, the significance of strain capacity of concrete is of great importance (1). Houghton (2) provided a simple method to determine this by rapid loading of the test specimens, and measuring the ultimate elastic strain. The tensile strain capacity can be used to calculate the rapid temperature drop that a fully restrained concrete can undergo.

The creep of concrete is inversely proportional to the rapidity of hardening of the cement used. More hardened the cement paste, the more rigid it is and the lower is its creep potential at a given applied stress. Since concrete with PPC has lower strength at early ages than that with OPC, and the rate of hardening of such concrete is lower at early ages, for a given age of loading (3 or 7 days), creep of concrete made with PPC is higher than that with OPC (3).

Regarding measurement of corrosion potential of steel in concrete, the galvanostatic (i.e. measurement of potential as a function of time at constant current density) anodic polarisation technique at low current densities was found to be a reliable accelerated test for the prediction of the corrosion activity on steel embedded in concrete specimens (4). But for monitoring corrosion potential of steel reinforcements in structural elements, the method of free corrosion potential measurement using copper-copper sulphate half cell (5) is preferred. This test is suitable for identifying corrosion activity in steel reinforcements in concrete members, regardless of their size and at any time during the service life.

2.Ø SCOPE OF THE PRESENT INVESTIGATION

Experiments were conducted to measure tensile strain capacity of PPC - as well as OPC concrete. There is a general apprehension that use of PPC might increase the creep of concrete. To investigate the validity of this, tests were carried out using OPC and PPC (made with 15% burnt clay pozzolana) from the same source and having comparable physical characteristics (Table 1). The ages of loading were 3 - and 7 days. The concrete mix proportions and the stress-strength ratio were kept same for the two concretes. The creep as well as creep recovery were measured under the same conditions of temperature and relative humidity.

The incidence of corrosion of reinforcemet in the environment of PPC was another aspect to be investigated. In the present investigation, high tensile wires (5 mm dia.) were inserted in concrete cylinder specimens made with M3Ø and M4Ø grades of concrete. The corrosion potential was measured in normal as well as in aggressive chloride solution, using the anodic polarisation technique.

TABLE 1

CHARACTERISTICS OF CEMENTS

PARTICULARS	ORDINARY PORTLAND CEMENT	PORTLAND POZZOLANA CEMENT
1 Physical properties:		
i) Initial setting time, minutes	175	185
ii) Final setting time, minutes	295	260
iii) Specific gravity	3.08	3.10
iv) Fineness (Blaine), Cm^2/g	3039	3672
v) Compressive strength, N/sq.mm		
a. at 3 days	28.2	22.4
b. at 7 days	38.7	33.7
c. at 28 days	46.2	40.7
2 Chemical composition (percent):		
i) Loss on ignition	3.95	4.04
ii) Silica (SiO_2)	24.07	33.16
iii) Iron oxide (Fe_2O_3)	3.99	4.24
iv) Alumina (Al_2O_3)	4.00	5.08
v) Calcium oxide (CaO)	59.76	49.28
vi) Magnesium oxide (MgO)	1.59	1.30
vii) Sulphate (SO_3)	2.04	2.09
viii) Insoluble residue	5.34	16.12

Prestressed concrete beams (15 cm x 15 cm x 150 cm) with concrete grade M40, were water-cured for 28 days and then kept outside the laboratory for 10 years in normal environmental conditions. These beams were tested for free corrosion potential using a copper-copper sulphate half cell, and for flexural strength. The reinforcements of these beams were examined for corrosion . The concrete samples from these beams were tested for pH and X-ray diffraction.

3.0 DISCUSSION OF THE TEST RESULTS

The average strain capacity of PPC concrete was found to be about 25% higher than that of OPC concrete at the age of 180 days. This means, PPC concrtete can withstand rapid temperature drop, better than that by OPC concrete.

The instantaneous creep recovery was found to be lower than the elastic strain at the age of loading, as expected (6). The specific creep of PPC concrete was 14-18% higher than that of OPC concrete at 90 days (Fig. 1). For M30 Grade of PPC concrete

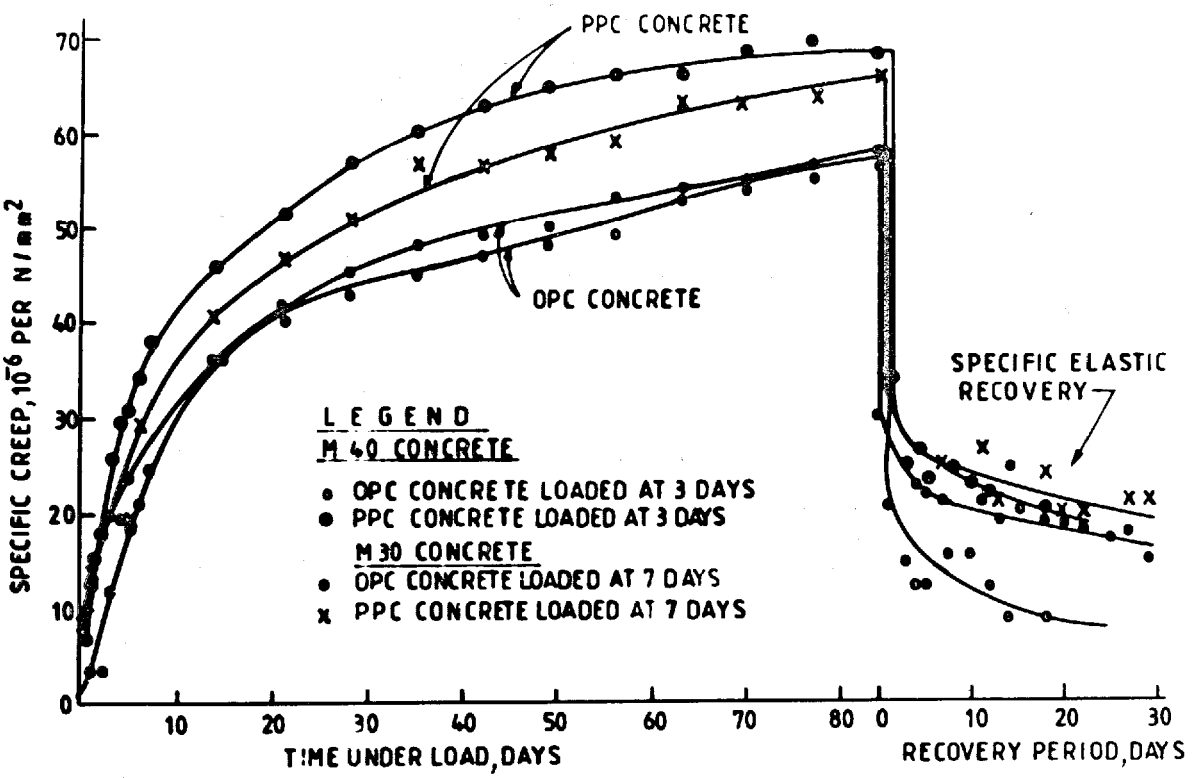

FIG 1 SPECIFIC CREEP OF CONCRETE MADE WITH DIFFERENT CEMENTS

loaded at 7 days, this was expected so, as the compressive strength was lower, at the time of application of the load, the rate of hardening of concrete being almost same in the two cases. For M40 grade of concrete loaded at 3 days, the strength of PPC concrete at the time of application of the load was not lower, but the higher creep was probably due to the lower rate of hardening observed thereafter.

The test results on anodic polarisation studies upto 9 months for high tensile wires in concrete, indicate the performance of PPC comparable to that of OPC, so far as non-incidence of corrosion of reinforcements in normal environment is concerned. When concrete specimens were kept in 3.5% NaCl solution, corrosion of reinforcement did occur in the specimens made with OPC as well as PPC, as expected (Fig.2).

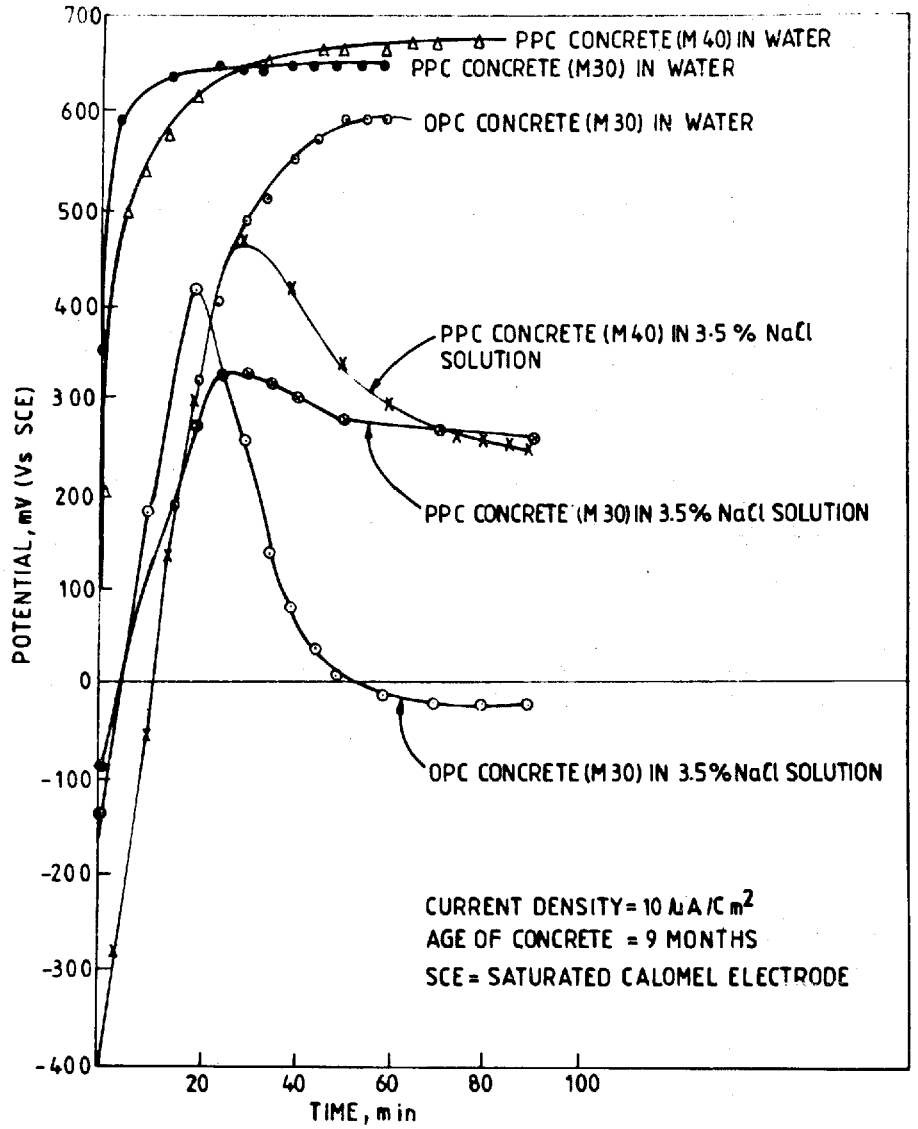

FIG 2 TIME Vs POTENTIAL FOR DIFFERENT CONCRETES

The free corrosion potential of high tensile wires in prestressed concrete beams made with PPC as well as with OPC exposed to normal environmental conditons for 10 years, showed that there was no corrosion of wires, as the potentials were more positive than -0.35 V with reference to copper-copper sulphate half cell (Fig.3). The beams were tested for flexural strength and the prestressing wires were exposed, after breaking the beams. The test results indicate satisfactory performance of the beams for the flexural strength, and the wires were found to be not corroded.

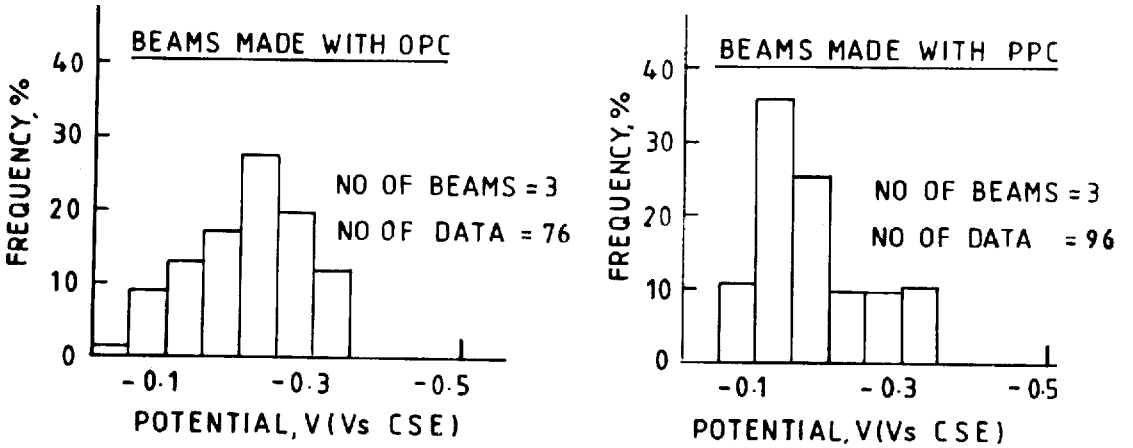

FIG 3 FREE CORROSION POTENTIAL OF STEEL IN PRESTRESSED CONCRETE BEAMS AFTER TEN YEARS EXPOSURE

Both the concrete samples (with PPC as well as with OPC) have pH of the order of 11.90. The XRD studies (Fig.4.) indicate presence of comparable amount of $Ca(OH)_2$ in concretes made with PPC and OPC. Thus the reduction of alkalinity of 10 years old concrete made with PPC towards a possible corrosion hazard, was not observed.

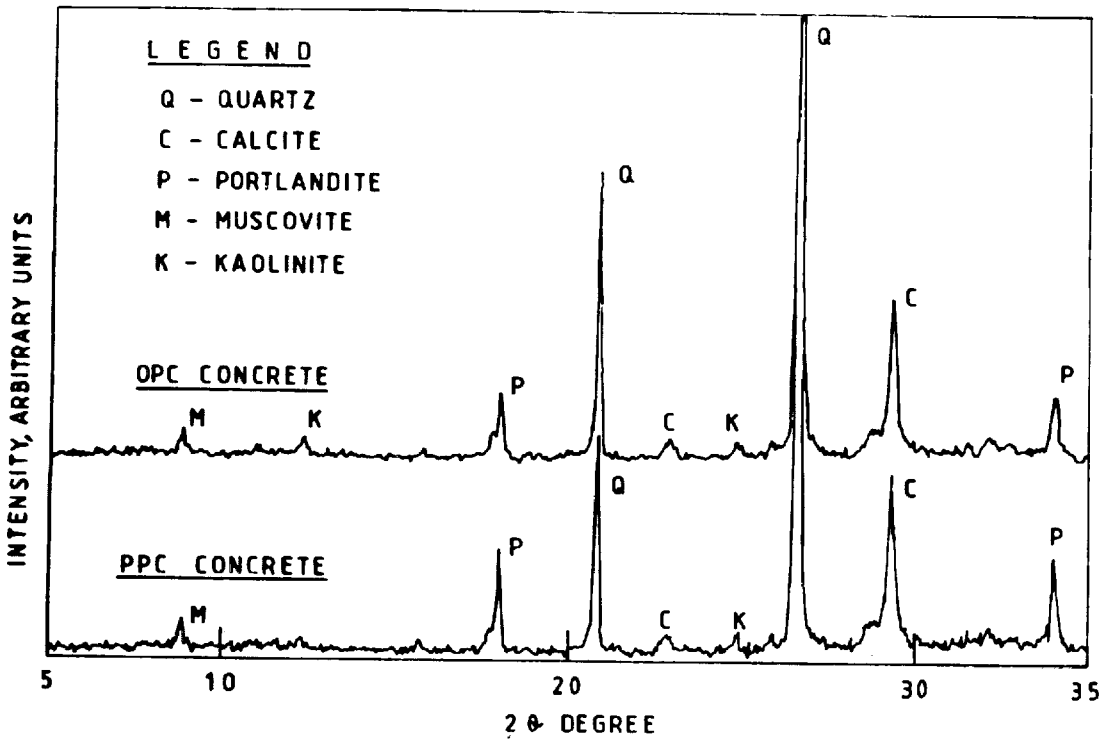

FIG 4 X-RAY DIFFRACTION OF CONCRETE SAMPLES OBTAINED FROM PRESTRESSED CONCRETE BEAMS EXPOSED TO NORMAL ENVIRONMENT FOR TEN YEARS

4.0 CONCLUSIONS

The strain capacity of PPC concrete was found to be higher than that of OPC concrete, which means PPC concrete can withstand rapid temperature drop, better than that by OPC concrete. The observed higher specific creep of PPC concrete was due to lower strength of concrete at the time of loading, and due to lower rate of hardening thereafter, in the present case. The accelerated test for predicting corrosion potential of steel in concrete cylinder specimens, indicated performance of PPC concrete comparable to that of OPC concrete. No incidence of corrosion was observed in prestressing wires of prestressed concrete beams made with PPC and exposed to normal environment for ten years.

ACKNOWLEDGEMENT

The authors have freely drawn upon completed R&D work of the National Council for Cement and Building Materials. This paper is published with the permission of the Director General of the Council.

REFERENCES

1. MEHTA,P.K.:**Concrete: Structure, Properties and Materials.** Prentice-Hall International, 1986,450 p.

2. HOUGHTON, D.L.: "Determining tensile strain capacity of mass concrete". Proceedings,**Journal of American Concrete Institute**, 1976, 73 (12), 691 - 700.

3. NEVILLE, A.M.: **Creep of concrete: Plain, Reinforced and Prestressed.** North - Holland Publishing Company, Amsterdam, 1970, 622 p.

4. GOUDA,V.K, SHATER,M.A and MIKHAIL,R.: " Hardened Portland blast - furnace slag cement pastes II. The corrosion behaviour of steel reinforcement." **Cement and Concrete Research**, 1975, 5 (1), 1 - 13.

5. ASTM C876 - 87 :" Standard test method for half cell potentials of reinforcing steel in concrete." American Society for Testing and Materials, Philadelphia, 1990, 429-433.

6. NEVILLE, A.M. AND BROOKS, J.J.: **Concrete Technology.** Longman Scientific & Technical, 1987, 438 p.

SOME CHARACTERISTICS OF A FIFTY YEAR CONCRETE

M A Cincotto and V M John

Instituto de Pesquisas Tecnológicas do Estado de São Paulo S.A. IPT - BRAZIL

SUMMARY

XRD, SEM/EDX, mercury intrusion porosimetry, TG and chemical analysis have been employed to determine the characteristics of specimens of fifty year age concrete prepared with the same materials in three different mix proportions. It was concluded that the w/c ratio did not influence the combined water but influences carbonation that increases with w/c ratio. The curves of cumulative volume of intruded mercury is flattened compared with that obtained for pastes. The transition zone has different composition with mix proportion, being rich in portlandite for higher cement content concrete and rich C-S-H for the lower one.

RÉSUMÉ

Trois éprouvettes, agées de 50 ans, préparées avec les mêmes matériaux, dans trois proportions ciment-aggrégats, ont été caractérisées par analyse chimique, analyse aux rayons X, microscopie à balayage, thermogravimétrie et porosimétrie au mercure.

Ces résultats ont permis de conclure que: la proportion eau/ciment n'influence pas la teneur d'eau d'hydratation mais le taux de carbonatation; la courbe cumulative du volume de pores est aplatie par rapport aux courbes obtenues pour les pâtes de ciment; la composition de l'auréole de transition qui entoure l'aggrégat se différentie selon la teneur en ciment du béton, étant prédominante en portlandite pour le mélange plus riche en ciment et prédominante en C-S-H pour le moins riche.

INTRODUCTION

Portland cements of different producers had their compressive strength determination extended until the age of fifty years besides their chemical and physico-mechanical characterization. In another paper of this Congress are presented the data obtained during this period and suggested a mathematical model for the evolution of the strength resistance related to water/cement ratio and curing age (1).

To complement these data the study of the microstructure of the concretes is going on which first results related to one type of cement is now being presented on this paper. The sample studied is the number 10 of the cited paper.

MATERIALS

Specimens prepared with pebble and Brazilian standard sand in proportions: 1:5:0.486, 1:6:0.6 and 1:7:0.715 (cement-agregate:water, by weight), and slump of 10 ± 2cm were maintained in moist curing chamber.

Table 1 - Compressive strength evolution (cylinders 15 x 30cm)

Specimen	Compressive strength (MPa)					
	3d	7d	28d	1y	25y	50y
1:5.00:0.486	14.0	25.6	33.7	34.0	42.8	50.3
1:6.00:0.600	9.31	18.0	26.0	23.9	33.9	37.2
1:7.00:0.715	6.37	11.9	18.2	18.3	33.6	33.9

The original cement had a chemical composition in weight percentage: 20.3 SiO_2, 5.17 $A\ell_2O_3$, 3.11 Fe_2O_3, 63.6 CaO, 5.47 MgO, 1.17 SO_3, 0.03 Na_2O, 0.13 K_2O, 1.24 LOI, 0.07 insoluble residue and 0.80 free lime. The alkalis were determined in the concrete and calculated on the base of cement content of concrete. The percentual Bogue composition was 59.3 C_3S, 13,3 C_2S, 8.44 C_3A, 9.45 C_4AF and 2.52 gypsum.

EXPERIMENTAL

A slice of 3cm thick was taken for the essays 2cm away from the base of the crushed cylinder. Some bits were cut off and prepared for polished section observation in the SEM. From other bits, the cement stone was separated by hand of the coarse aggregate. A fraction of little grains was separated for mercury porosimetry in Carlo Erba Porosimeter and another one ground to 0,075mm fineness and dryed for chemical, thermal and X-ray diffraction analysis. Its content of cement was determined as the soluble fraction in hydrochloric acid.

RESULTS AND DISCUSSION

The XRD patterns were qualitatively the same for the three samples, showing the lines characteristics to C-S-H, calcite, portlandite and hydrogarnet, the lines of a sulfoaluminate or magnesium hydroxide were not identified (Fig. 1).

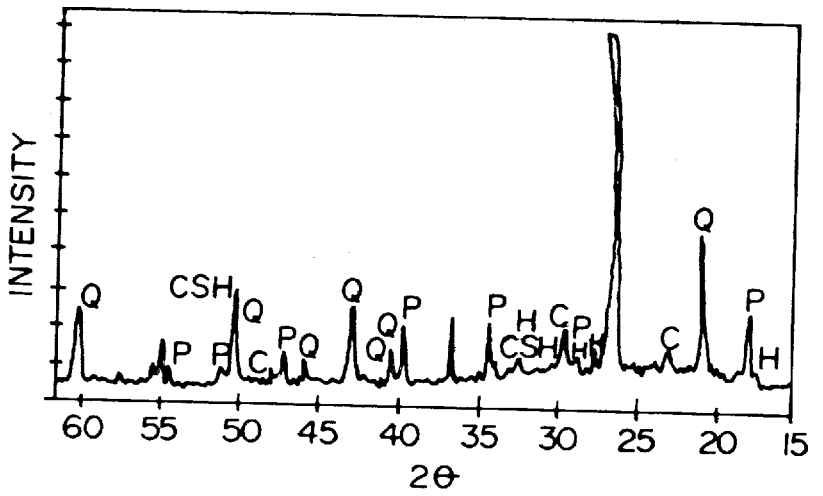

Q - Quartz

P - Portlandite

H - Hydrogarnet

C - Calcite

Fig. 1 - XRD patterns of the cement stone.

The TG-DTG curves obtained in air atmosphere (10°C/min) have the profile shown in Fig. 2, with a loss weigth at 60°C of adsorbed water and the others corresponding to the dissociation of C-S-H, $Mg(OH)_2$, $Ca(OH)_2$ and $CaCO_3$ (Fig.2). The corresponding weight losses, refered to the same content of cement (35,5%) are indicated in Table 1. It is clear that the carbonation increases with the diminished content of cement in the concrete. Admiting that the calcite originates from portlandite, its corresponding carbon dioxide content expressed as water hydration and added to the other results gives the total water hydration. (Table 2).

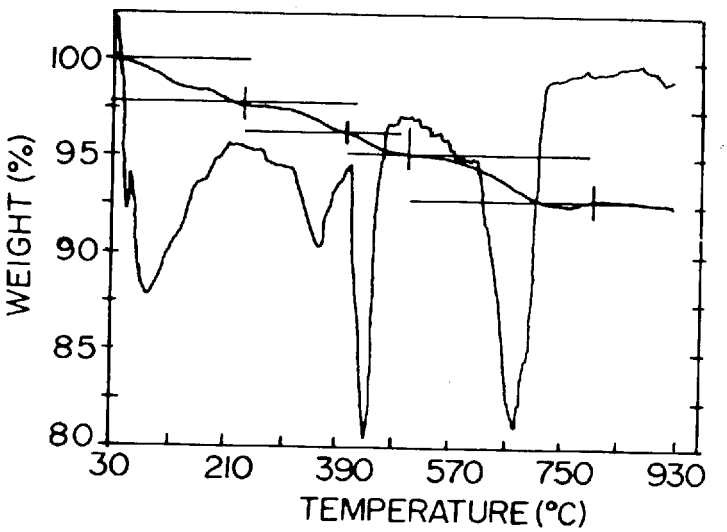

Fig. 2 - DTG curves for concrete 1:7 in air atmosphere free of CO_2.

Table 2 - TG Weight loss (%)

Compound	Concrete		
	1:5	1:6	1:7
C-S-H	2.624	2.959	2.538
$Mg(OH)_2$	1.711	2.040	1.738
$Ca(OH)_2$	1.787	1.521	1.253
$CaCO_3$	1.267	2.073	2.804
TOTAL	7.389	8.593	8.333

As the LOI of the anhydrous cement is known the corresponding content of anhydrous cement for each sample was calculated and therefore, estimated the combined water. The results obtained were 20% for 1 :5.00, 22% for 1:6.00 and 20% for 1:7.00 concretes.

The curves of cumulative volume of intruded mercury plotted against pore diameter (Fig.3) are very similar for concretes 1:6.00 and 1:7.00 and also their total volumes, that is, 0,10cm³/g and 0,095cm³/g, in the range of 15-0,76µm. Although having different w/c ratio the second one has higher degree of carbonation. For concrete 1:5,00 the total volume is 0,08cm³/g. It was observed that the curves are flatter than published ones for pastes with lower degree of hydration, although the w/c ratio of 0,486 has shown a maximum in the range of 0,02-0,1µm range, as observed by Odler at 180 days (2). This flattening results in a different profile of the cumulative penetration volume curve shown in Fig.3.

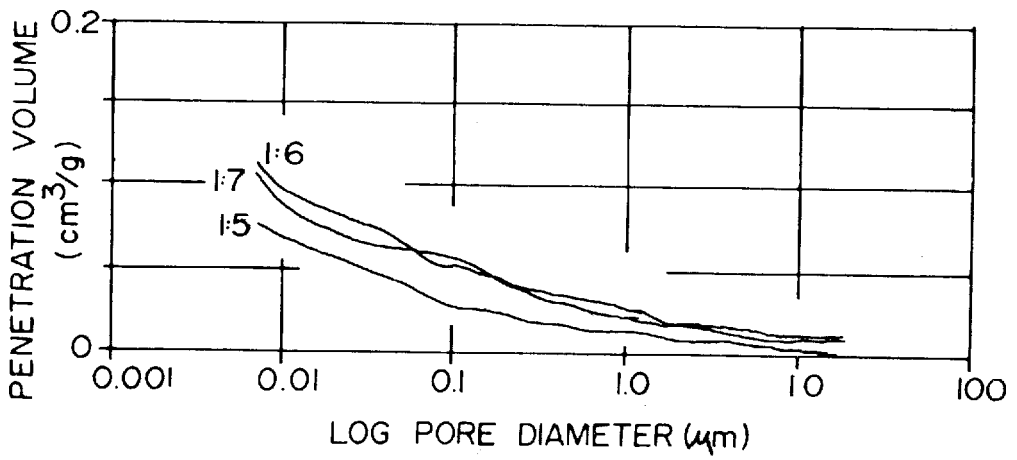

Fig. 3 - Curves of cumulative volume of intruded mercury for concretes (mix proportion: 1:5, 1:6, 1:7).

The backscattered electron images of polished sections showed a transition zone between the aggregate and the paste, more evident in 1:7.00 concretes as large as 4,8m (Fig.4). The crack surrounds the aggregate but runs out of the observed transition zone.

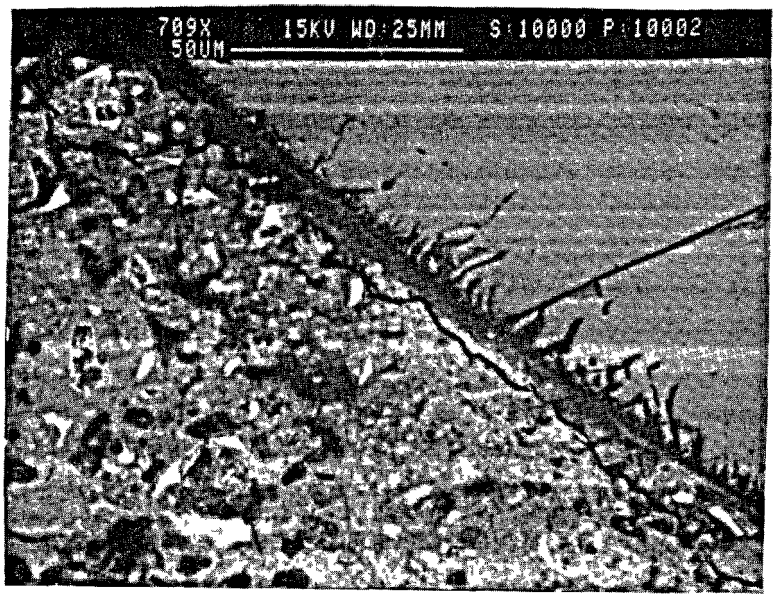

Fig. 4 - BEI of the transition zone with crack.

For the 1:7 concrete between closer aggregates the paste is very porous as shown in Fig.5. In Fig. 6 it is shown a paste region far from the aggregates, for the cement concrete richest with a feature similar to the anhydrous cement.

A spot analysis by EDX for the three samples were made, of the inner region of the aggregate, of its border, the transition zone and of a point far from the aggregate, and then calculated the atom ratios: Si/Ca, Si/Ca+Mg, Al+Fe/Ca.

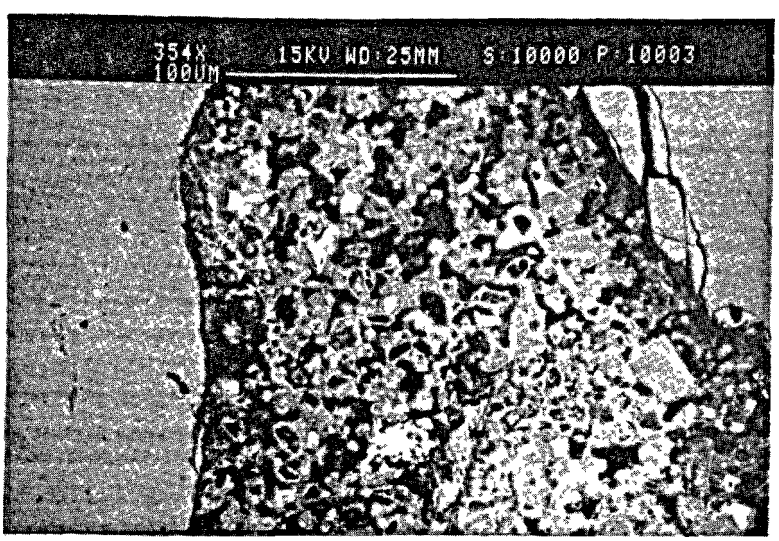

Fig. 5 - BEI porous zone characteristic of concrete 1:7.

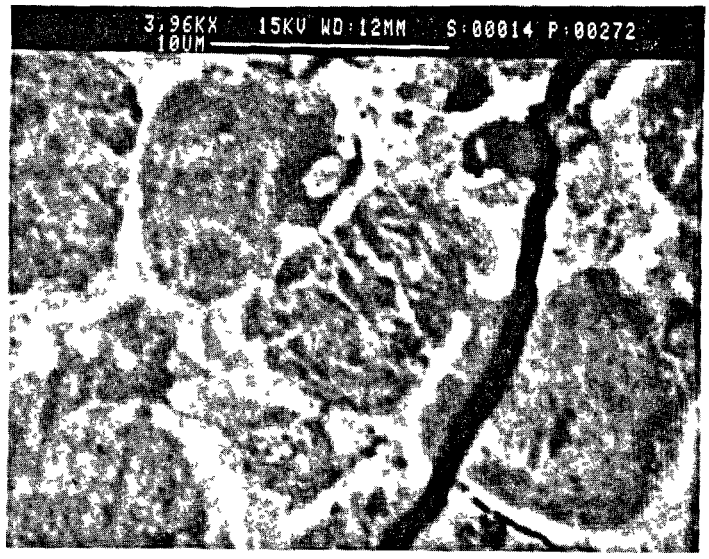

Fig. 6 - BEI image of hydration paste similar to original cement grains, rich in magnesium.

Based on the results of Taylor (4) it can be concluded that: a) the transition zone is rich in portlandite in 1:5 concrete, with portlandite and C-S-H in 1:6 concrete and high in C-S-H in 1:7 concrete; b) magnesium is found predominantly in granular regions rich in C-S-H and with a considerable content of Al and Fe; c) the interstitial zone is very high in Al and Fe, but low in Si and Ca and was not considered as hydrogarnet phase. The aggregate border have a considerable percentage of calcium.

CONCLUSIONS

The results permit to conclude that the w/c ratio did not influence the resulting combined water. The porosity curves are different and the total volume is lower than that observed for pastes of lower degree of hydration. The concretes with w/c ratios of 0.600 and 0.718 have similar total porosities and compressive strength. The higher percentage of carbonation may explain this fact. In the concrete 1:5 the transition zone is rich in portlandite and for the 1:7 rich in C-S-H. The considerable percentage of calcium found in the border of the aggregate, points to a reaction between quartz and calcium of the transition zone.

ACKNOWLEDGEMENTS

The authors thanks Dr. Jivaldo do Rosário Matos (Instituto de Química-Laboratory of Thermal Analysis) and the Departamento de Metalurgia-SEM Laboratory, both of the University of São Paulo and our colleague Valdecir Angelo Quarcione for Chemical analysis.

REFERENCES

(1) TANGO, C.E.S.: "Modeling and verifyiing portland cement concrete relationship up to 50 years age". (Paper published in this Congress).

(2) ODLER, I., ROSSLER, M.: "Investigation on the relationship between porosity, structure and strength of hydrated portland cements, 2: effect of pore structure and and of degree of hydaration". Cem. Conc. Res. 1985. 15 (4), 401-410.

(3) MEHTA, P.K. , MANMOHAN, D. :"Pore size distribution and permeability of hardened cement pastes". International Congress on the Chemistry of Cement, 7th, Paris, 1980. v.3, VII-1-5.

(4) TAYLOR, H.F.W., NEWBURY, D.E.: "An electron microprobe study of a mature cement paste". Cem. Conc. Res., 1984, 14(4), 565-73.

Specific Theme IV D

Special Concrete and Cement Composites

CONSTITUTION OF MORTARS AND PULL-OUT OF STEEL FIBRES

B Marchese and G Marchese

Dipartmento di Ingegneria dei Materiali e della Produzione, Facolta' di Ingegneria, Universita' di Napoli, Piazzale Tecchio, Napoli, ITALIA

SUMMARY

The pull-out resistance of steel fibres embedded in cementitious matrix gives useful indications on the mechanical behaviour which is significantly affected by the constitution of paste or mortar. A special dichotomy characterizes the interfacial region: the smooth and almost simple steel surface on one side, and the matching surface of the very complex cementitious matrix on the other side. Microstructures of the matching surfaces of the interfacial zone were revealed by SEM. Pull-out tests on single fibres, performed by a Controlled Displacement Machine, are shown to be related to several parameters. Among them, the shape of the fibre, either straight- or hooked- ended, the age and the composition of the matrix.
In OPC pastes and mortars, the interfacial layer was shown to be very rich in $Ca(OH)_2$ and sufficiently smooth to replicate the steel surface. However, the POZ pastes and mortars, though having a much less $Ca(OH)_2$ content, manage to form a thin, not so continous film. In contacting areas, a higher strength of this film might be supposed.
A larger post-peak area for POZ pastes and mortars was noted and related to the different composition of the bonding interfacial layer. The two types of mechanisms operating in the fibre pull-out, in terms of either debonding or frictional energy, were discussed.

RÉSUMÉ

La rèsistence à l'extraction des fibres d'acier plongèes dans des matrices en ciment peut donner des indications valuables sur le comportement mechanique qui est considerablement influencè par la constitution de pâtes au mortiers de ciment.
Une dichotomie particuliere caracterise la règion à l'interface: d'une cotè, la surface lise et presque simple de l'acier, de l'autre, la surface compagne de la matrice complexe de ciment. Les microstructures des surfaces compagnes de la bande à l'interface on ètè ètudièes par SEM. Des essais de dèsefilement de chaque fibre, accomplis à l'aide d'une machine a deformation controllèe, on montrè d'être governès par plusieurs parametres, en particulier: la forme des fibres, l'âge et la composition de la matrice. Dans les pâtes ou mortiers en ciment Portland, la coche à l'interface se montre riche en CH et suffisament lisse pour repèter la surface de l'acier. Au contraire, les pâtes ou mortiers en ciment pouzzolanic, bien que le contenu de CH soit moins èlevè, moutrent la formation d'un film mince et moins continu. Dans la bande de contacte l'on doit supposer une rèsistence plus èlevèe de cet film.

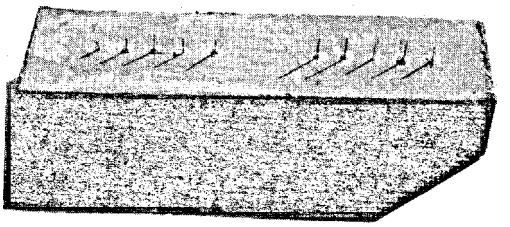

FIG.1. Typical 28 days cured POZ mortar specimen embedding 10 steel fibres.

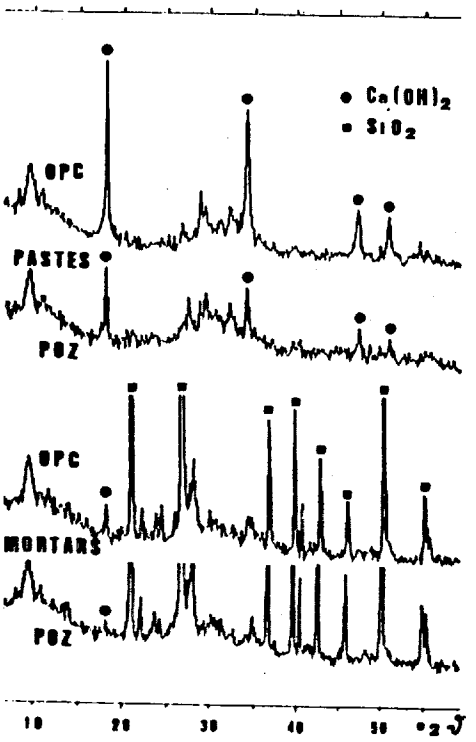

FIG.4. XRD diagrams of both OPC and POZ pastes and OPC and POZ mortars.

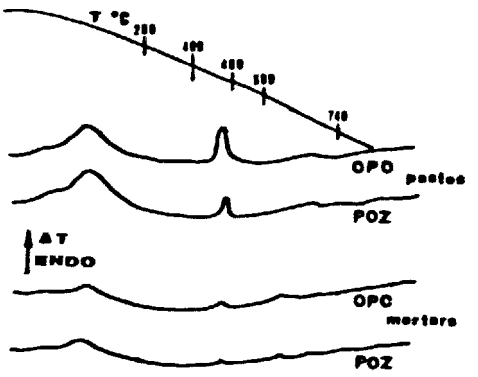

FIG.5. DTA curves of the same specimens in FIG.4, with temperature profile superimposed.

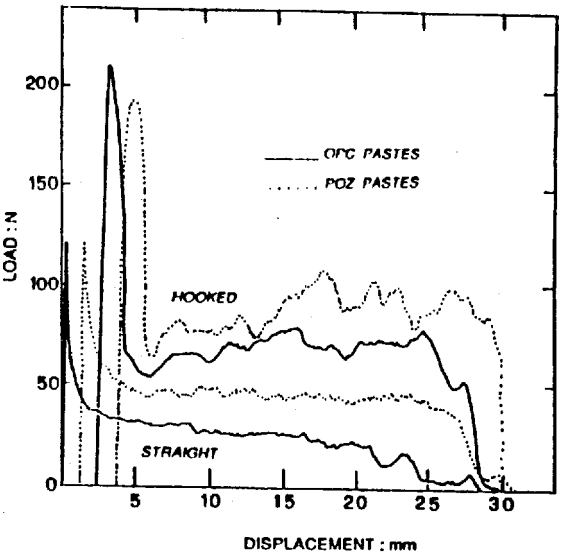

FIG.2. Load-displacement pull-out curves of 2 straight and 2 hooked fibres embedded 3cm in OPC and POZ pastes.

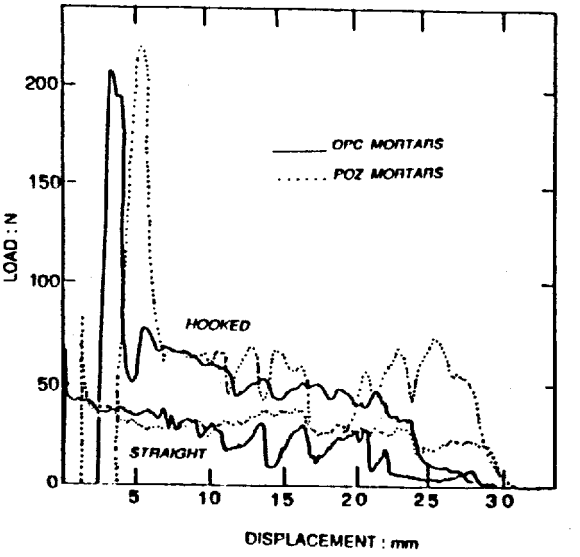

FIG.3. Load-displacement pull-out curves of 2 straight and 2 hooked fibres embedded 3cm in OPC and POZ mortars.

INTRODUCTION

The enhanced properties of cementitious pastes, mortars and concretes for the inclusion of steel fibres come from the peculiar properties of the single components and of the originating interfacial regions (1,2,3,4). To transfer mechanical load at the interface steel-matrix, the ductile steel and the brittle cementitious matrix need to show highest compatibility, fundamental property of each composite (5,6,7,8).

Besides composition, steel fibres operate with parameters like shape, size, length/diameter ratio, surface condition, etc., which remain almost constant with age in the interfacial zones. On the contrary, the cementitious matrix represents a very complex system whose compositional characteristics derive from both type of cement and aggregate, and their modifications with age. SEM observations revealed that the cementitious matrix segregates a more or less thick layer having composition and microstructure quite different from the one of the bulk mass (10,11,12).

The pull-out test represents the more direct method to investigate the mechanical behaviour of the interfacial region originating at the contact of the embedded ductile fibre with brittle cementitious matrix (13,14,15). The pull-out curve evidences two basic processes in the interfacial zone: initial debonding and eventual frictional slip of the fibre (16,17,18,19).

Aim of this paper is to correlate the mechanical behaviour of single steel fibres, embedded in pastes and mortars, with compositional and morphological aspects of the interfacial regions.

EXPERIMENTAL

Pastes and mortars of both OPC and POZ cement were used. In the latter, with the 30% substituting pozzolana was used. Prisms of 4x4x16 cm size with water:cement:sand = 0.5:1:3 in mass were prepared. Steel fibres of BEKAERT, type DRAMIX ZC50/.50, were used. In each prism, ten fibres , five with and five without the terminal hook, were embedded for a 3cm length, at 1cm of distance from each other, according the method of Mansur (4), Fig.1.

After 28 days of curing, each fibre was pulled out at a rate of 2.54 mm/min by an Instron 4301 tensile machine. X-Ray Diffraction (XRD) was carried out in a Philips PW1820 diffractometer. A Stanton Redcroft simultaneous thermal analyzer was used for Differential Thermal Analysis (DTA) and Thermogravimetry (TG). The heating rate was 10 ^{o}K/min in flowing N_2 atmosphere. A Stereoscan Cambridge 240 was used for SEM observation .

RESULTS AND DISCUSSION

In Fig.2 typical pull-out curves of single fibres from OPC and POZ plain pastes are reported. The solid lines represent the pull out of straight fibres and the dotted lines the pull out of hooked fibres, respectively. The four profiles show an initial sharp increase of load up to a maximum value which represents the debonding of the whole steel surface from the cementitious matrix surface. Adhesional and frictional bonds are broken for shear and tensile stress, helped by local section diminution due to Poisson effect (5).

More load is necessary to pull-out the hooked fibres because of the mechanical anchoring of the hooked end. As a matter of fact, the cementitious matrix is not able to follow the high strains due to its brittleness. This should affect a larger volume beyond the interfacial region into the bulk mass. After debonding, the fibre begins to slide: the load rapidly decreases. The decrease eventually slows

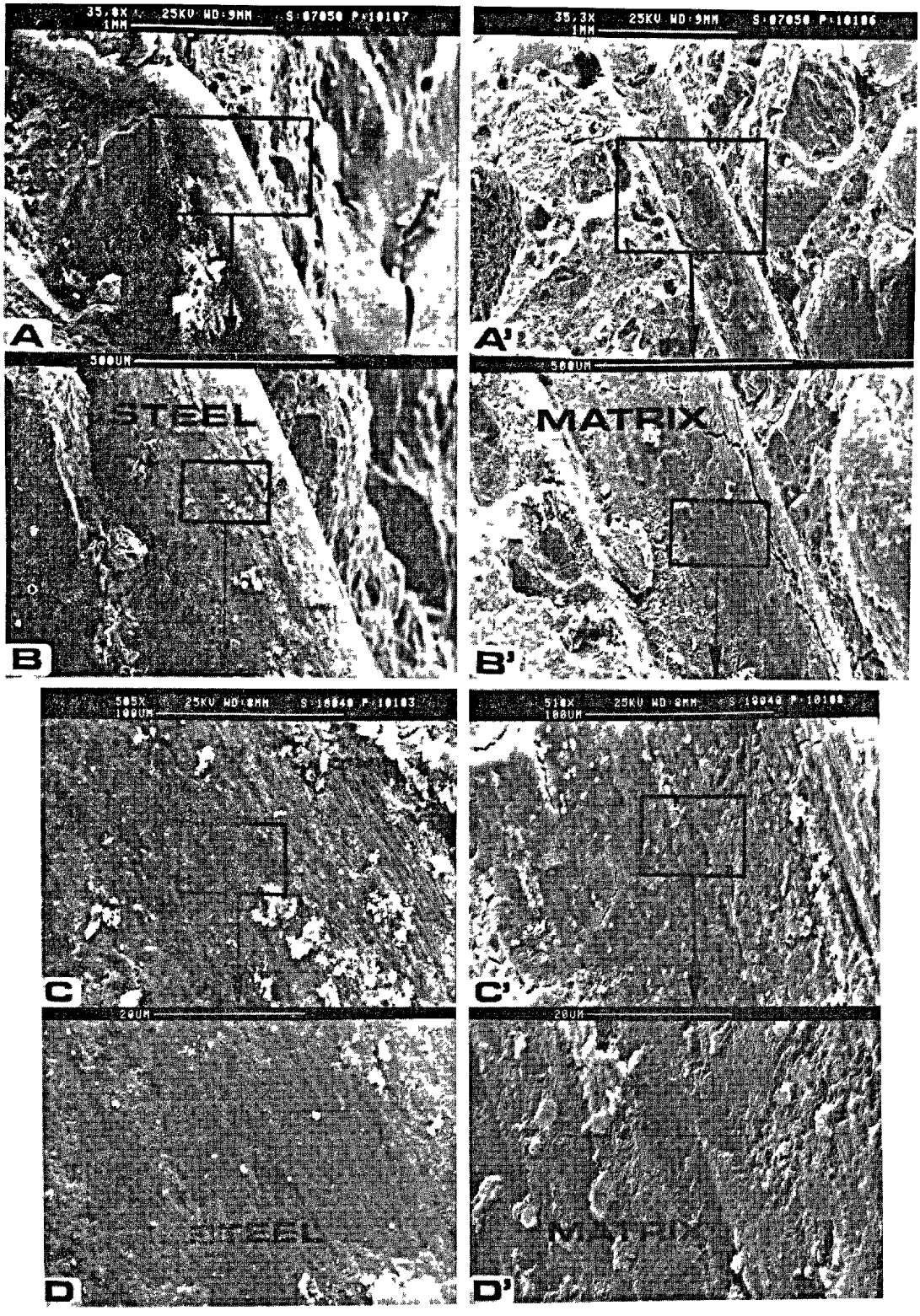

FIG.6. SEM micrographs of matching surfaces of the steel fibres, A, and OPC mortar, A'. The marked areas are enlarged in B, C, D and in B', C' and D', respectively.

down showing a characteristic sliding friction. The two straight fibres show the most regular profile gradually diminishing for the minor contact surface. The two hooked fibres show a delayed decrease of load. The enclosed area between the maximum at about 200N and the lower value at about 75N, could indicate the energy for the straightening of the hooked end. The irregularities of the profiles have to be attributed to the detachment of fragments of the matrix and to their eventual shifting.

In Fig.3 the pull-out curves from OPC and POZ mortars show very similar profiles. The load decreases very sharply after the maximum for the two straight fibres. In mortars, the presence of grains of different size and high elastic strength causes strong irregularities in frictional behaviour (13,14). As for the pastes, the correspondent areas for the hooked fibres are larger than those for the straight fibres. However, the energy values for the pastes and the mortars are not too much different at these curing times. The use of POZ cement seems to induce a slightly larger post-peak areas.

At the interfacial region, the steel surface remains practically unaltered with age, unless of dangerous corrosion phenomena coming from outside. However, the complex composition of the cementitious layer can be modified with casting and age. Several phases are the principal constituents of pastes and mortars.

In Fig.4 the most intense peaks of the XRD diagrams indicate that the abundant crystalline phases are the CH for pastes and SiO_2 quartz for mortars.

These phases were detected together with other ones for the same samples by DTA, Fig.5. The plain OPC pastes show the large endotherm peak due to water loss up to 280 ^{o}C of several hydrated phases: C-S-H gel, hydrated Ca mono- and tri-sulphoaluminate. The endothermic peak between 400 and 560 ^{o}C is attributed to dehydroxilation of the CH. Finally, the endothermic peak between 650 and 800 ^{o}C is indicative of the $CaCO_3$ decarbonation. In mortars, the predominant sand content in respect to the paste content is revealed by the small endotherm at 576 ^{o}C for the structural transition from alfa into beta quartz.

Simultaneous TG curves were used to derive quantitative data of phases. In respect to the residue at 740 ^{o}C, the CH content was 24.3% and 14% in OPC and POZ pastes, reduced to 3.5% and 2.1% in OPC and POZ mortars, respectively.

Morphologies at steel/matrix interface were detected by SEM (20,21). Fig.6 shows a typical fracture surface of OPC mortar with a steel fibre partially embedded, A, and the matching surface of matrix, A'. The "twin" micrographs demonstrate that the fracture path propates very easily along the boundary of the two different materials. The magnifications of area marked in A reveal the smooth steel surface with a few adherent relicts of paste, B,C and D. On the other hand, magnifications of the area marked in A' show that the matrix can reproduce the finer details of the steel surface , B', C' and D', because of the existence of a Ca-rich layer. It is actually well known that the CH content in this layer can reach the 20% and even the 40% of the content of the bulk mass (10).

In Fig.7 some significant morphologies of the fracture surface of POZ mortar at interfacial region are reported. The steel surface seems to be covered by numerous fragments of paste, C and D. The adherent layer of matrix appears to be not so homogeneous as to replicate the steel surface, C' and D', due to the less amount of CH able to segregate into the surface film. However this non continous film can give a high adhesion strength. This hypothesis could justify the similar values of peak detected in the load-displacement diagrams.

CONCLUSION

Pull-out of single fibres of a ductile material like steel from a brittle material like cementitious matrix represents the most direct method for studying the mechanical strength in the interfacial zone.

The maximum value of load, indicative of debonding strength, appears to be very similar for the OPC and POZ pastes and also for mortars, at 28 days age. The embedded hooked end causes a doubling of the load.

The post-peak profile characterizes the progressive friction sliding through the paste or the mortar. The POZ cement seems to enhance the correspondent values. Higher energies, measured by the areas, are detected for sliding the hooked end of fibre.

The OPC pastes and mortars have a larger CH content able to give a continous adherent film that also replicates finer details of the steel surface. The POZ pastes and mortars form a Ca-poor layer. One may suppose that the superficial film, even if rather discontinous, could show a high strength.

ACKNOWLEDGEMENTS

This research was financially supported by Consiglio Nazionale delle Ricerche, Progetto Finalizzato Edilizia, SP3.

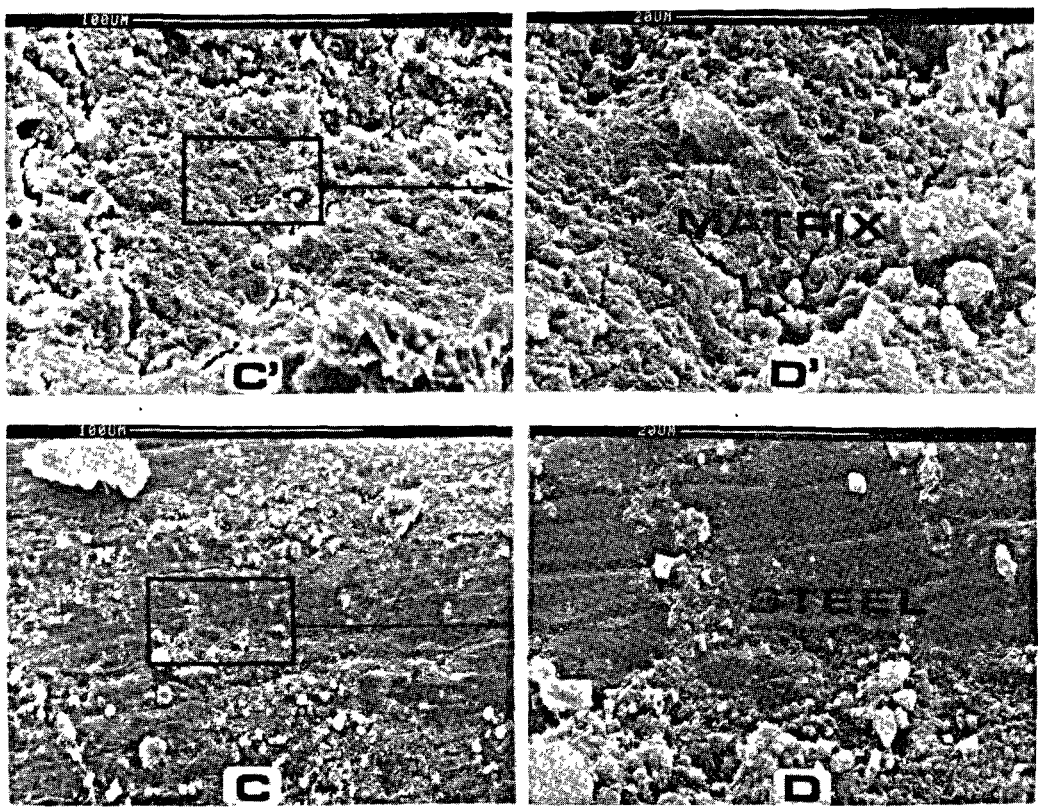

FIG.7. SEM micrographs of matching surfaces of the steel fibres, C, and POZ mortar, C'.
The marked areas are enlarged in D and in D', respectively.

REFERENCES

1. Shah S.P.: "Fiber Reinforced Concrete" Concrete International, 1990, **12**(3), 81-82.
2. Grande D.H., Mandell J.F. & Hong K.C.C.: "Fibre-Matrix Bond Strength Studies of Glass, Ceramic, and Metal Matrix Composites"Journal of Materials Science, 1988 **23**(1), 311-328.
3. Naaman A.E., Argon A.S.& Moavenzadeh F.: "A Fracture Model for Fiber Reinforced Cementitious Materials" Cement and Concrete Research, 1973 **3**(4), 397-412.
4. Mansur M.A., Nagataki S., Lee S. H.& Oosumimoto Y.: "Torsional Response of Reinforced Fibrous Concrete Beams" ACI Structural Journal, 1989, **86**(1), 36-44.
5. Kerans R.J., Hay R.S.& Pagano N.J.: "The Role of the Fiber-Matrix Interface in Ceramic Composites" Ceramic Bulletin, 1989, **68**(2) 429-442.
6. Evans A.G.: "Perspective on the Development of High-Toughness Ceramics" Journal of American Ceramic Society, 1990, **73**(2), 187-206.
7. Hsueh C.: "Fibre Pullout against Push-down for Fibre-reinforced Composites with Frictional Interfaces" Journal of Materials Science, 1990, **25**(2A), 811-817.
8. Hsueh C.: "Interfacial Friction Analysis for Fibre-reinforced Composites during Fibre Push-Down (Indentation)" Journal of Materials Science, 1990, 25(2A), 818-828.
9. Favre J.-P.& Jacques D.: "Stress Transfer by Shear in Carbon Fibre Model Composites" Journal of Materials Science, 1990, **25**(2B), 1373-1380.
10. Pinchin D.J.& Tabor D.: "Interfacial Phenomena in Steel Fibre Reinforced Cement I: Structure& Strength of Interfacial Region" Cement& Concrete Research, 1978, **8**(1), 15-24.
11. Page C.L.: "Microstructural Features of Interfaces in Fibre Cement Composites" Composites, 1982, **13**(2), 140-144.
12. Bentur A., Diamond S.& Mindess S.: "Cracking Processes in Steeel Fiber Reinforced Cement Paste" Cement and Concrete Research, 1985, **15**(3), 331-342.
13. Bartos P.: "Analysis of Pull-Out Tests on Fibers Embedded in Brittle Matrices" Journal of Materials Science, 1980 **6**(12), 3122-3128.
14. Gray R.J.: "Analysis of the Effect of Embedded Fiber Length on Fiber Debonding and Pull-Out from an Elastic Matrix, Part 1, Review of Theories" Journal of Materials Science, 1984, **19**(3), 861-870.
15. Currie B.& Gardiner T.: "Bond Between Polypropylene Fibres and Cement Matrix" Intern. Journal of Cement Composites & Lightweight Concrete, 1989, **11**(1), 3-10.
16. Banthia N.& Pigeon M.: "Load Relaxation in Steel Fibres Embedded in Cement Matrices" Intern. Journal of Cement Composites & Lightweight Concrete, 1989, **11**(4), 229-234.
17. Banthia N., Trottier J.-F.& Pigeon M. "Fiber pull out mechanisms: effect of fiber geometry, loading rates and sub-zero temperatures" FIBRE REINFORCED CEMENTS& CONCRETES: RECENT DEVELOPMENTS, Ed. R.N. Swamy& B.Barr INTERNATIONAL CONFERENCE 18-20 SEPTEMBER 1989, CARDIFF UK p. 136-145.
18. Thouless M.D., Sbaizero O., Sigl L.S.& Evans A.G.: "Effect of Interface Mechanical Properties on Pullout in a SiC-Fiber-Reinforced Lithium Aluminum Silicate Glass-Ceramic" Journal American Ceramic Society, 1989, **72**(4), 525-532.
19. Ezeldin A.S.& Balaguru P.N.: "Bond Behaviour of Normal& High-Strength Fiber Reinforced Concrete" ACI Materials Journal, 1989, **86**(5), 515-524.
20. Bentur A., Mindess S.& Diamond S.: "Pull-out Processes in Steel Fibre Reinforced Cement" Intern. Journal of Cement Composites & Lightweight Concrete, 1985, **7**(1), 29-37.
21. Tashiro C.& Tatibana S.: "Bond Strength Between C_3S Paste and Iron, Copper or Zinc Wire and Microstructure of Interface" Cement and Concrete Research, 1983, **13**(3), 377-382.

INTERFACE AND INTERNAL COMPATIBILITY IN A COPPER FIBRE CEMENT COMPACT COMPOSITE

P Kittl, G Diaz and V Martinez

Dept. de Ciencia e Ingeniería de Materiales, IDIEM, Facultad de Ciencias Físicas y Matemáticas, Universidad de Chile, Santiago, CHILE

ABSTRACT

This paper presents the mechanical behaviour of a compacted composite formed by short ductile copper fibres ramdomly distributed in portland cement paste. The samples, a half with fibres and the other without them, were subjected to compression fatigue. So, 1 Hertz and the value of stress corresponding to the 1% of the probability of fracture by gradual load were used. Diagrams of cumulative probability of fracture against cycles are obtained for both types of samples. Scanning electron microscopy shows that the mechanisms of fracture are different in each case. Samples of compacted neat-cement paste finish their life with a catastrophic fracture whereas samples of composite behaves like a pseudoductile material devoid of catastrophic failure.

RESUMEN

En este trabajo se presenta el comportamiento mecánico de un compuesto compactado formado por fibras cortas de cobre dúctil que se distribuyen aleatoriamente en una matriz de cemento portland. Las muestras, una mitad con fibras y la otra sin ellas, se sometieron a fatiga a la compresión. Se usó 1 Hertz de frecuencia y el valor de esfuerzo correspondiente al 1% de probabilidad de fractura por carga gradual. Se obtuvieron diagramas de probabilidad acumulativa de fractura versus el número de ciclos para ambos tipos de muestra. Por medio de microscopía electrónica de barrido se observa que los mecanismos de fractura son diferentes en cada caso. Las muestras de pasta pura de cemento compactadas fallan por fractura catastrófica mientras que las muestras de compuesto se comportan como un material pseudodúctil con ausencia de falla catastrófica.

INTRODUCTION

In general, fibrocement using metallic fibres includes steel fibres because the expansion coefficients of both materials are similar. This property is important when the fibre percentage is large, but when this content is very small this property becomes unimportant. The last of our research works were based on the main idea that, owing to the circumstance that copper-fibre expansion coefficient differs from that of cement, around such fibres there are produced microcracks able to stop fatigue fissures growing within the matrix when the material is subjected to fatigue. But now, in the present work, although the difference of expansion coefficient between the copper-fibre and the cement produces microcracks, the mechanical fatigue is not going to produce them, but it is going to interact with them in some way. Another property of copper fibres is that their ductility allows them to undergo a certain amount of deformation without breaking at fatigue cracks. Copper fibre ductility makes them cheaper than steel fibres and thus a composite devoid of catastrophic failure can be made for manufacturing prefabricated elements. Such elements may be piping, corrugated plates, tiles and the like. In addition, some investigation work was made in connection with corrosion resistance of copper fibres embedded in the cement matrix.

The first fundamental research work about this fibrocement was related to decohesion [1] of the copper-fibre cement interface followed by the complete fracture statistics theory of a short ductile-fibre unidirectional composite [2]. That mentioned first work supplied the elements required for producing a compacted copper-fibre reinforced cement composite [3] and the optimum fibre-cement and the optimum fibre-length were ascertained in this later work. The cumulative probability of fracture was determined using fracture statistics, and our theory regarding fatigue was verified thereafter [4]. An electron-microscopy study about the cement matrix surrounding the fibre was studied by Kittl and Díaz [5]. Thermal fatigue of asbestos-cement composite was studied and compared with that of copper-fibre cement composite [6]. The compatibility between the copper-fibres and the cement matrix can be improved by a controlled corrosion [7,8]. The improvement of the mechanical properties in tiles made of compacted fibrocement composite was recently studied by Kittl, Díaz, Alvarez and Aldunate [9].

EXPERIMENTAL PROCEDURE

Short ductile copper-fibres of diameter 0.00016 m and length 0.018 m were ramdomly distributed in portland cement devoid of additives. 310 cylindrical samples with diameter 0.02 m and length 0.03 m were made. A half of the total number of samples was made without fibres and the other half with them. For the composite, the proportion of fibres used was 4% by weight of the cement matrix whereas the water/cement ratio was 0.04. The compacting was reached by appying 35 MPa pressure into a steel mould. Once made, the test specimens were kept into a moist room for 24 hours at temperature of 295° K, and after immersed in water until saturation. Afterwards, the samples were placed again in the moist room for six days. Later, 48 samples of compacted neat cement paste and 50 samples of copper-fibre cement compact composite were subjected to static compression which allowed to obtain a diagram of cumulative probability of fracture by gradual application of the load. So, the fatigue load was the load corresponding to the 1% cumulative probability of fracture by applying slow load. Finally, 107 samples of composite and 105 samples of neat cement paste were tested to compression fatigue. The experimental configuration consisted of a fatigue machine constituted of an arm connected to a rotating cam putted in motion by a motor. The load was applied introducing a fixed weight of 37 Kg into a recipient hung of the arm. So then, using a frequency of 1 hertz, the samples were subjected to fatigue until fracture, pointing the number of cycles for the event. The limit number of cycles for a particular specimen was approximately 50,000. A greater number of cycles is not considered because of the long time required to end the test. Some of the

samples were observed by scanning electron microscopy so as to elucidate the mechanisms of fracture.

RESULTS AND DISCUSSION

The data of number of cycles for fracture were ascendantly ranked. Then the cumulative probability of fracture was determined by using the formula $F(N)=(i-1/2)/n$, where n is the total number of similar samples tested and i is the number of samples that failed at number of cycles at most equal to N. This cumulative probability can be plotted against logN, number of cycles for fracture to occur, which allows to obtain a cumulative probability of fatigue fracture diagram. Figure 1 corresponds to this diagram of cumulative probability of fatigue cycles for fracture for the samples of neat cement paste. Likewise, figure 2 shows the said diagram for the samples of copper-fibre cement compact composite.

There is an increase of the performance of 10% in the samples of cement with fibres. This would not justify its use, but the difference is ,that in the case of the neat cement paste the sample is broken by catastrophic fracture whereas in cement with fibres the samples continue resisting. In the case of fatigue by thermal shock, fissures are produced in the interface, which makes to decrease the adherence between the fibre and the matrix. This implies a diminution of the fatigue resistance. In the case of mechanical fatigue there no exist this production of fissures and the cement-fibre interface does not suffer damage. The samples broken by fatigue continue with their shape as is shown in figure 3, whereas in the fatigued samples without fibres there is no much propagation of cracks because this is catastrophic, as is shown in figure 4. In the figure 5, it is observed that the surface of the interface has broken up in such a way that some parts remain sticked to the fibre, whereas in figure 6 is shown as the mentioned fibre holds the broken parts together. So finally, the use of fibrocement composites would

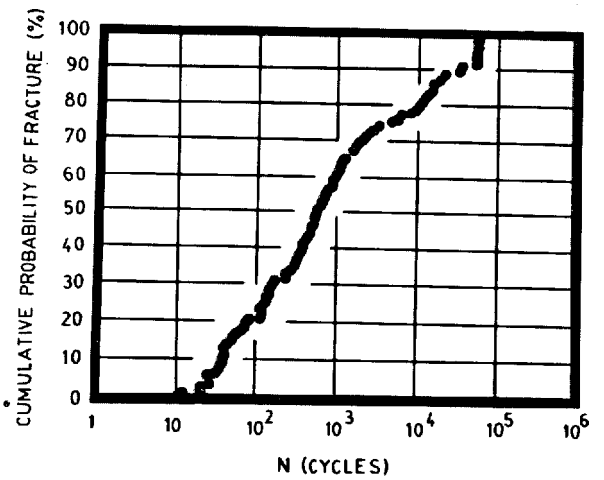

Fig. 1 Cumulative probability of fatigue cycles for fracture to occur. Samples of compacted neat cement paste.

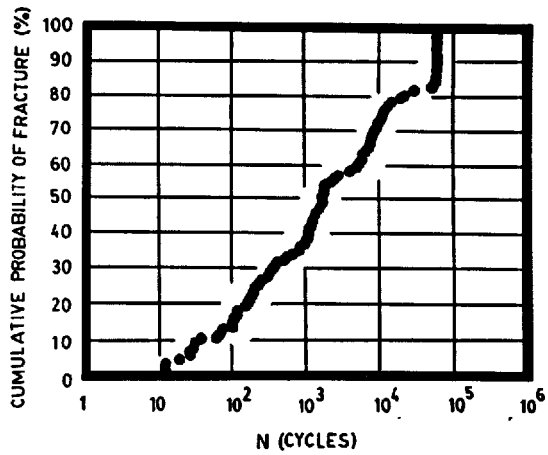

Fig. 2 Cumulative probability of fatigue cycles for fracture to occur. Samples of copper-fibre cement compact composite.

be justified; in the practical case there probably is a superposition of both mechanical and thermal fatigue. It must be understood that an improvement of the fatigue properties implies an improvement of the durability to fatigue.

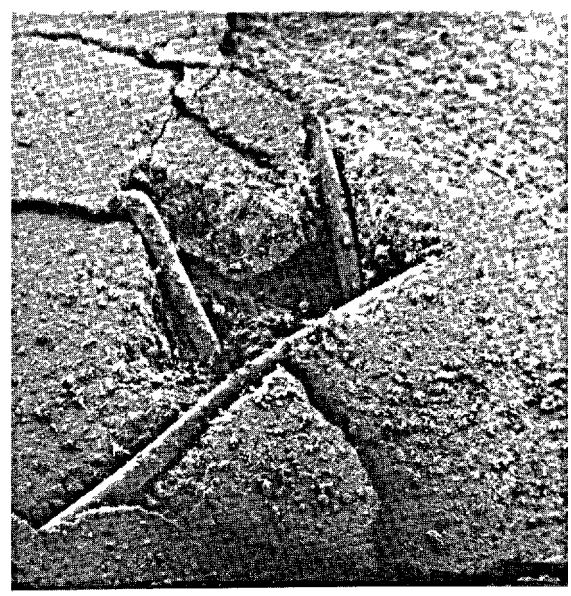

Fig. 3 Sample of copper-fibre cement compact composite fractured by fatigue. The broken parts are maintained assembled. (20X).

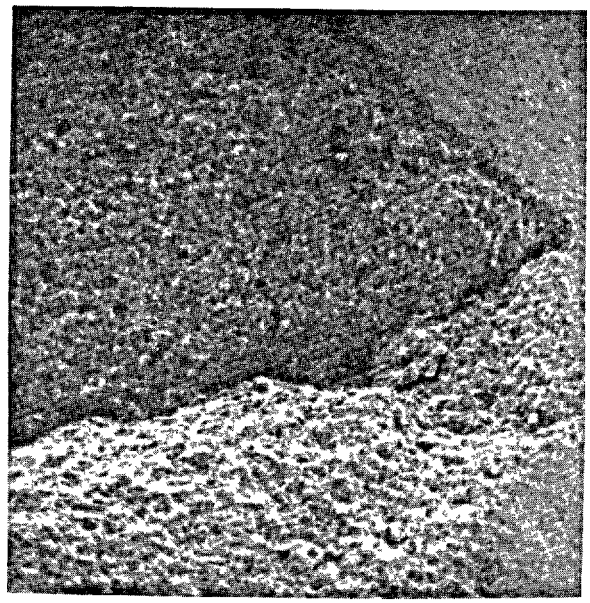

Fig. 4 Sample of compacted neat cement paste fractured by fatigue. (30X).

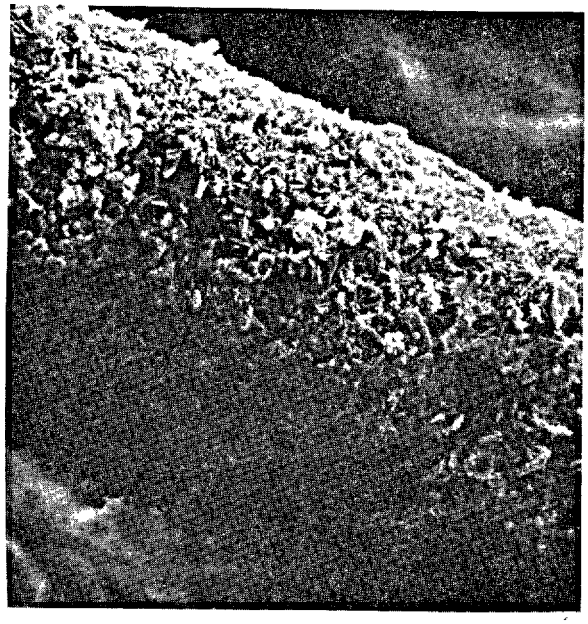

Fig. 5 Surface of a copper-fibre covered with the hidrated cement as is shown after the fracture by mechanical fatigue. (360X).

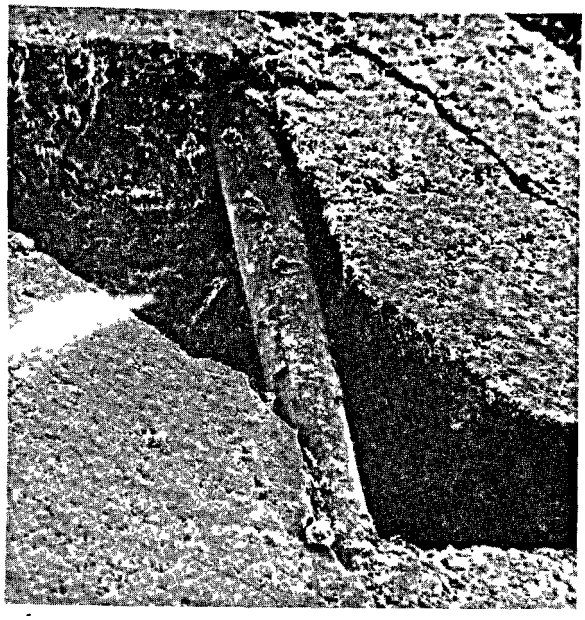

Fig. 6 A copper-fibre operated as a retainer of parts in the sample fractured by mechanical fatigue. (72X).

ACKNOWLEDGEMENTS

The authors wish to thank to the Fondo Nacional de Desarrollo Científico y Tecnológico (FONDECYT) for their grants N° 516/88 and 1195/91.

REFERENCES

1. Kittl, P. and Galleguillos, E.: Statistical analysis of decohesion in a Cu Wire/Cement interface, Res Mech. Lett., 1981, 1, 445-449.
2. Kittl, P. and Díaz, G.: Fracture statistics of pull-out of a brittle composite and a short-fibre composite, Res Mech., 1985, 13, 43-54.
3. Kittl, P., Galleguillos, E. and Díaz, G.: Properties of compacted copper fibre reinforced cement composite, Int. Cem. Comp. Light-Weight Concr., 1985, 7, 193-197.
4. Díaz, G., Kittl, P. and Galleguillos, E.: Statistical mechanics of fracture and fatigue of compacted copper fibre-cement composite, Int. Cem. Comp. Light-Weight Concr., 1986, 8, 101-107.
5. Kittl, P. and Díaz, G.: Compatibility of copper fibre with compacted cement and low thermal-shock fatigue thereof, 8 th. Int. Congress on the Chemistry of Cement, 1986, III, 438-443.
6. Kittl, P. and Díaz, G.: Fracture statistics and low thermal-shock fatigue of asbestos-cement composite, Cem. Concr. Res., 1987, 17, 31-36.
7. Kittl, P., Díaz, G., Perret, R. and Alvarez, N.: Research work on copper-fibre cement carried out at the IDIEM, Copper 87, Ed. by A. Varschavsky and P. Kittl, Santiago, Chile, 1987, 1, 279-290.
8. Kittl, P., Perret, R., Alvarez, N. and Díaz, G.: On durability and mechanical properties improvement of a compacted copper-fibre cement composite subjected to general corrosion, Cem. Concr. Res., 1988, 18, 539-544.
9. Kittl, P., Díaz, G., Alvarez, N. and Aldunate, R.: Comparative testing of small samples of compacted neat-cement paste and of a compacted copper-fibre cement composite, Eng. Frac. Mech., 1990, 36, 233-237.

HIGH-STRENGTH AND DURABLE COMPOSITES WITH NON-METALIC REINFORCEMENT

V V Glukhovskiy, N Z Mikhailishina and V P Serbin

Kiev Polytechnical Institute, Kiev, UKRAINE

SUMMARY

The results of an investigation in the main properties of composites based on mineral binders and glass reinforcement distinguished from the known glass fiber materials by a high durability.

АННОТАЦИЯ

Изложены результаты исследования основных свойств композитов на основе минеральных вяжущих и стеклянной арматуры, отличающихся от известных стекловолокнистых материалов высокой долговечностью.

INTRODUCTION

As is generally known, the abnormally high level of strength of glass fibers originally inherent in the idea of creation of glass fiber reinforced cement is the function of the state of its surface. This underlies the dependence of durability of glass fiber-based cement on the chemical activity of the system components (1). It was found that a friable film of new formations is formed on the surface of fibers as a result of active chemical interactions taking place between the fibers and the matrix (1-5). It is noted in this case that optical properties of central areas of fibers do not change in long-term interaction with binder (6) and the value of Young's modulus of fibers also remains invariable (4). This gives the grounds to believe that the decrease of the level of strength of glass fibers in the environment of the hardening binder takes place as a result of a sharp increase in the number of defects on its surface and it is to a lesser degree related to the decrease of diameter of fibers as a result of their surface interaction with new formations of binder .In the context of the foregoing, it might be believed that along with the wellknown methods of obtaining durable composites based on inorganic fibers and mineral binders(1, 7, 8), elements can be proposed for the reinforcement of cements which do not change their strength as a result of intensive chemical impacts taking place in the zone of their contact with matrix.

Results of tests of concretes reinforced with glass rods of alkali-resistant glass 4.2 mm in diameter are presented in (9). The bending strength levels of 4.0-8.8 MPa achieved by the authors do not allow to speak about a high efficiency of the proposed reinforcement technique.A similar proposal was indirectly mentioned also in (10) where it was proposed to use prestressed macrothreads of glass ceramic 0.25-25.4 mm in diameter as reinforcing components.

EXPERIMENTAL

Results are presented below obtained in investigating specimens reinforced with glass rods of different chemical composition 4 and 2 mm in diameter arranged along the whole length of the specimen. Portland cement, alumina cement and gypsum have been used as binders. Tensile strength in bending was determined in specimen tests according to three-point scheme.

Results of bending strength (R_{tb}) variation presented in Fig. 1 point to the fact that an increase in the number of reinforcing ratio to 20-30 % is accompanied with the growth of the composite strength. A further increase of reinforcement factor is unsuitable since it does not lead to the growth of strength. Bending strength of specimens at the same reinforcement ratio grows as the time of hardening increases.And with the growth of hardening time, the specimens which were hardened in water feature higher strength characteristics than those hardening in hydraulic seal. In the first case, the composition features after five years of hardening a bending strength of 62 MPa and in the second case 50 MPa. This is apparently the result of the dependence of strength characteristics on the intensity of binder hydratation processes which are more intensive at the hardening of portland cement in water.

Results presented in Fig. 2 confirm this conclusion and show that the steaming at 95° C enables the level of strength to be obtained peculiar to compositions hardening under natural conditions during 5 years. A following hardening of the same specimens during additional 2 years enables bending strength of 60-65 MPa to be achieved.

Use for binder of alumina cement (Fig. 3) which is characterized by the aggressivity with respect to the reinforcing glass elements lower than that of portland cement shows that in this case the composites feature both a lower level of initial

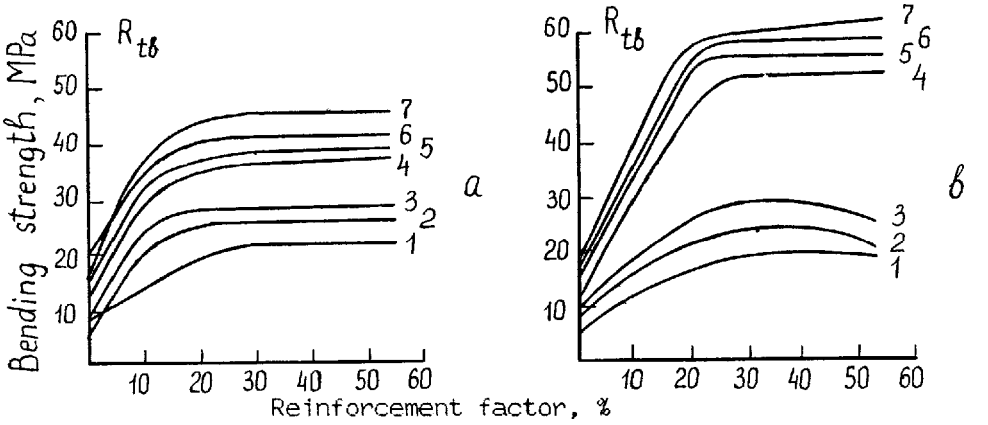

FIG.1 R_{tb} OF SAMPLES BASED ON PORTLAND CEMENT WITH REINFORCEMENT 4 MM IN DIAMETER IN HARDENING IN HYDRAULIC SEAL (a), IN WATER (b) : 1 -3 days; 2 -7 days; 3 -28 days; 4 -180 days; 5 -1 year; 6 -2 years; 7 -5 years

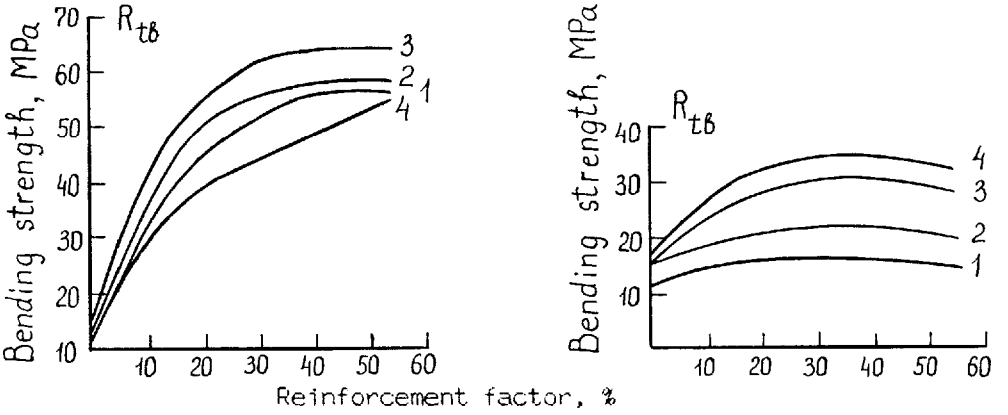

FIG.2 R_{tb} OF SAMPLES BASED ON PORTLAND CEMENT HARDENING AFTER THERMAL-MOISTURE TREATMENT : 1 -1 day; 2 -180 days; 3 -2 years; 4 -autoclave treatment

FIG.3 R_{tb} OF SAMPLES BASED ON ALUMINA CEMENT :1 -3 days; 2 -7 days; 3 -1 year; 4 -2 years

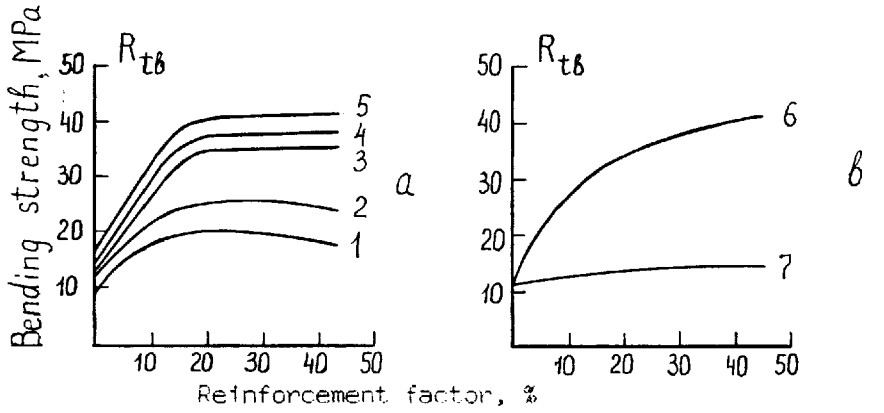

FIG.4 R_{tb} OF SAMPLES BASED ON PORTLAND CEMENT WITH REINFORCEMENT 2 MM IN DIAMETER IN HARDENING UNDER NATURAL CONDITIONS (a), AFTER HEAT-MOISTURE TREATMENT (b): 1 -3 days; 2 -7 days; 3 -28 days; 4 -1 year; 5 -2 years; 6 -steamed; 7 -autoclaved

strength (20 MPa) and a lower intensity of its growth in time (37-39 MPa). Using as the binder gypsum whose environment is practically inert with respect to glass, we can obtain composites with the level of bending strength not over 10.5 MPa. This confirm the earlier conclusions about the substantial dependence between the strength characteristics of the compositions being studied and the intensity of the processes of chemical interaction in contact zone of new formations of binder with the surface of reinforcing elements. In this case, as distinct from compositions reinforced with glass fibers, the strength of the composite increases as the intensity of the interaction in contact zone grows.

When investigating strength characteristics of composites reinforced with thinner rods (diameter 2 mm), glass was used with the thermal coefficient of linear expansion differing from the similar characteristic of the matrix material more than twofold. The results of investigation of the strength of compositions based on portland cement and rods 2 mm in diameter presented in Fig. 4 confirm regularities obtained earlier but the absolute value of the bending strength of specimens with the same amount of reinforcement is higher in the initial hardening periods (3, 7, 28 days) when thinner rods have been used. The subsequent growth of strength with the increasing binder hardening time comes about in this case less intensively as compared with specimens reinforced with rods 4 mm in diameter. Thermal wet treatment at 95 C makes it possible in this case also to achieve the level of the strength of samples which were hardened during 2 years under natural conditions. The autoclaving of samples (175°C)results in a sharp decrease of the strength of the composite down to 14 MPa. It should be pointed out in this case that a similar treatment of samples with the reinforcement 4 mm in diameter made from glass which is characterized by the thermal coefficient of linear expansion close to this characteristic of the material matrix also results in some decrease of the strength of specimens (Fig.2, curve 4), but this decrease is less substantial and makes it possible to obtain composites with bending strength of 40 - 52 MPa depending on the value of reinforcement factor. The results of investigations of the strength characteristics of a composite with the optimal quantity of reinforcement with basalt rods are presented in Table 1. In this case, a high chemical stability of the applied glass prevents the obtaining of composites with the strength similar to that for the specimens reinforced with glass of compositions described earlier. However, it is possible to obtain strength levels within 26 to 37 MPa also in this case.

Table 1

Relationship between tensile strength in bending portland cement specimens with basalt rods of different diameter and hardening conditions

Rod diameter, mm	Bending strength, MPa, in specimens hardening under			
	Natural conditions during		Steaming	Autoclaving
	28 days	1 year		
2	33.5	35.9	31.2	24.8
3	26.7	37.0	30.4	22.8
4	29.8	36.7	26.6	22.4

Results of the investigations of the value of bond of the used rods with the matrix material which were carried out using the value of the rods drawing out force, show that the maximum value of bond of 3.25 MPa is characteristic of glass and portland cement after their steaming. When composite is hardened under natural conditions in water and in hydraulic seal, the parameter being studied makes up 3.10 and 2.61 MPa, respectively, when portland cement is used. The strength of bond between matrix based on portland cement and a basalt rod makes up 1.7, 1.26 and 1.79 MPa, respectively at hardening in water after steaming and autoclaving.

As a result of comprehensive physical and chemical investigations of the zone of contact of the reinforcing components and the matrix material which have been carried out by means of X-ray diffraction, derivatographic, infrared spectroscopy and electron microscopic analysis, it was found that with the use of portland cement the process of interaction between the new formation of binder and the suface of the reinforcing components is accompanied by the decrease of concentration of calcium hydroxide in contact zone.Investigations of the surface of reinforcing elements withdrawn from the hardened matrix carried out by means of elektron microscope have shown that in case of the use of portland cement, the surface is covered with a layer of new formations featuring a sufficient strength but in case of the use of alumina cement and gypsum, the surface of the reinforcing elements is rather smooth and differs slightly from the surface of the original rods. Similar investigations of model systems consisting of portland cement and finely pulverized glass have confirmed results obtained earlier and pointing to intensive binding of free calcium hydroxide as a result of interaction taking place in composites being studied.

CONCLUSIONS

In conclusion it should be emphasized that the presented results point to the possibility to obtain durable and highstrength composites based on inorganic binders and mineral fibres in which the properties of the initial components are combined rather efficiently and a high chemical activity of the ingredients of the system which provides their joint work does not result in weakening of the system and ensures its high durability and efficiency as distinct from composites reinforced with thin glass fibres. An increase in the degree of chemical interaction in the zone of contact between the rods and the matrix is the source of the growth of composite strength.

REFERENCES

1. Pashchenko, A.A.,Serbin,V.P.,Glukhovskiy,V.V. et al.:REINFORCEMENT OF INORGANIC BINDING AGENTS WITH MINERAL FIBRES. Moscow, Stroyizdat, 1988, 200 p, (in Russian)

2. Pashchenko, A.A. & Serbin,V.P.:REINFORCEMENT OF CEMENT STONE WITH MINERAL FIBRE. Kiev, Vishcha skola, 1979,222 p, (in Russian)

3. Budnikov, P.P., Pashchenko, A.A. & Serbin, V.P.:"Investigations of structure of cement stone reinforced with mineral fibre".Izv. AN SSSR. Inorganic materials, 1966, V2(4), p 741-744, (in Russian)

4. Majumdar, A., West, J. & Larner, L.:"Properties of glass fibres in cement environment". J. Mater. Sci., 1977, 5, p 927-936

5. Stucke, M. & Majumdar, A.:"Microstructure of glass fibre-reinforced cement composites". J. Mater. Sci., 1976, 11, p 1019-1030

6. Budnikov, P.P., Slobodyanik, I.Ya., Pashchenko, A.A. & Serbin, V.P.:"Cement stone reinforced with glass fibre". Stroitelniye materialy, 1966, 4, p 17, (in Russian)

7. Biryukovich, K.L., Biryukovich, Yu.L. & Biryukovich, D.L.:GLASS-FIBRE REINFORCED CEMENT IN CONSTRUCTION. Kiev, Budivelnik, 1986, 95 p, (in Russia)

8. Serbin, V.P., Glukhovskiy, V.V. et al.:GLASS CONCRETE BASED ON INORGANIC BINDERS. Kiev, UkrNIINTI, 1988, 35 p,(in Russian)

9. Gunosekaran, M.:"Alkali-resistant glass "cane" reinforcement for structural lightweight concrete". Indian Concrete Journal, 1974, 10, p 314-315

10. USA Patent No 4341835, 27 July 1982. "Composite materials reinforced with macrofibers".

COMPOSITES: CEMENT AND GLASS FIBRE

V P Serbin, V V Glukhovskiy and R V Serbina

Kiev Polytechnical Institute, Kiev, UKRAINE

SUMMARY

The questions of durability of glass fibre-based cement composites are considered as well as the problems of selection of efficient technological conditions in developing compositions with preset properties and the experience of their application for manufacturing nonpressure pipes.

RESUME

On a examine des questions qui concernent de la durabilite des composites en cement renforce a la fibre de verre, des problemes de choix du regime technologique effectif lors de l'elaboration des compositions aux proprietes donnees et aussi l'exprience leur utilisation a la fabrication des tuyaux travaillant sans pression.

INTRODUCTION

Modern civil engineering places heavy demands on materials and products, in addition to their economical efficiency, both on the properties of the material and on a high degree of readiness, finish and configuration of products. Interesting architectural design can obtained due to a high tensile and bending strength which provides the required stiffness of elements with a large area and small thickness. The use of glass fibre-based cement makes it possible to decrease the cost of construction due to the smaller mass of products when compared with those made of reinforced concrete, to reduce the thickness of the walls on retention of the required heat transfer coefficient, to decrease the expenditures for prevention measures due to the increased fire-resistance of the products, to reduce the products in transportation due to the increased impact resistance of the material, to vary the finish of panal surface. Thus, the economic expediency of the use of glass fibre-based cement products is determined by their technical advantages and by the possibility to save costs in construction (1,2,4).

The experience of application of glass-concrete structures and products in the world practice has revealed the versatility of the properties and fields of application of glass fibre-based cement: as a finishing coat for various kinds of concrete and ferroconcrete products; fibre-reinforced plaster for tunnel, shaft and mining engineering; roofing panels, facing slabs, lightweight facade with sound insulation or without it; multilayer wall panels and dividing walls; box units for land-based and underwater construction; warmed and non-warmed space shells; materials for construction of oil storage tanks, silos, tubings for tunnel and mine construction; ventilation skips, pipings, ducts, air conduits, water conduit channels, hydraulic seal of reservoirs of various purpose; thin-walled shells for protection of thermal insulation of pipelines, not turned-over concrete forms, fire-resisting layer or plates, ets (1,5,6).

EXPERIMENTAL

An important characteristic of composites based on cement matrix and glass fibre reinforcement is their durability since glass fibre is subject to corrosion in alkaline medium of hardening cement. A method of forecasting the properties of glass fiber-based cement compositions has been developed at Kiev Polytechnical Institute (3,4) which makes possible to model the "ageing" process practically to any age from data of short-time experiments, to estimate the stability of the glass fibre reinforcement and to study the properties of the "aged" composites.

RESULTS AND DISCUSSIONS

Series 1

Thus, studies have been made into durability of two compositions of fibrous concrete with content of glass fibre reinforcement of 1.5 and 2 % . Portland cement brand 400, sand with gradation factor 1.6 and alkali-resistant fibre with 40 mm long fibres have been used as source materials. Cement-to-sand ratio was 1:1, water-to-cement ratio was 0.45. The mixture of components was prepared in a spiral-whirling mixer and then it was put to a form and compacted with overweight on vibrating table. After preliminary hardening, the samples have been subjected to comprehensive test: accelerated ageing according to the developed technique, air resistance, freeze resistance and environmental resistance under conditions of Kiev. Physical and mechanical properties of composites have been determined in definite time intervals. The results of testing for tensile bending strength are presented in Fig.1. Based on the results of the studies into the forecasting of durability of glass fibre concrete of the compositions under consideration, the following strength stabilization coefficients depending on environment conditions have been obtained: in atmospheric conditions of Kiev 0.76; in premises with damp air 0.60; in premises with dry air 1.00 at a temperture of 50 C and 0.73 at a temperature of 90 C .

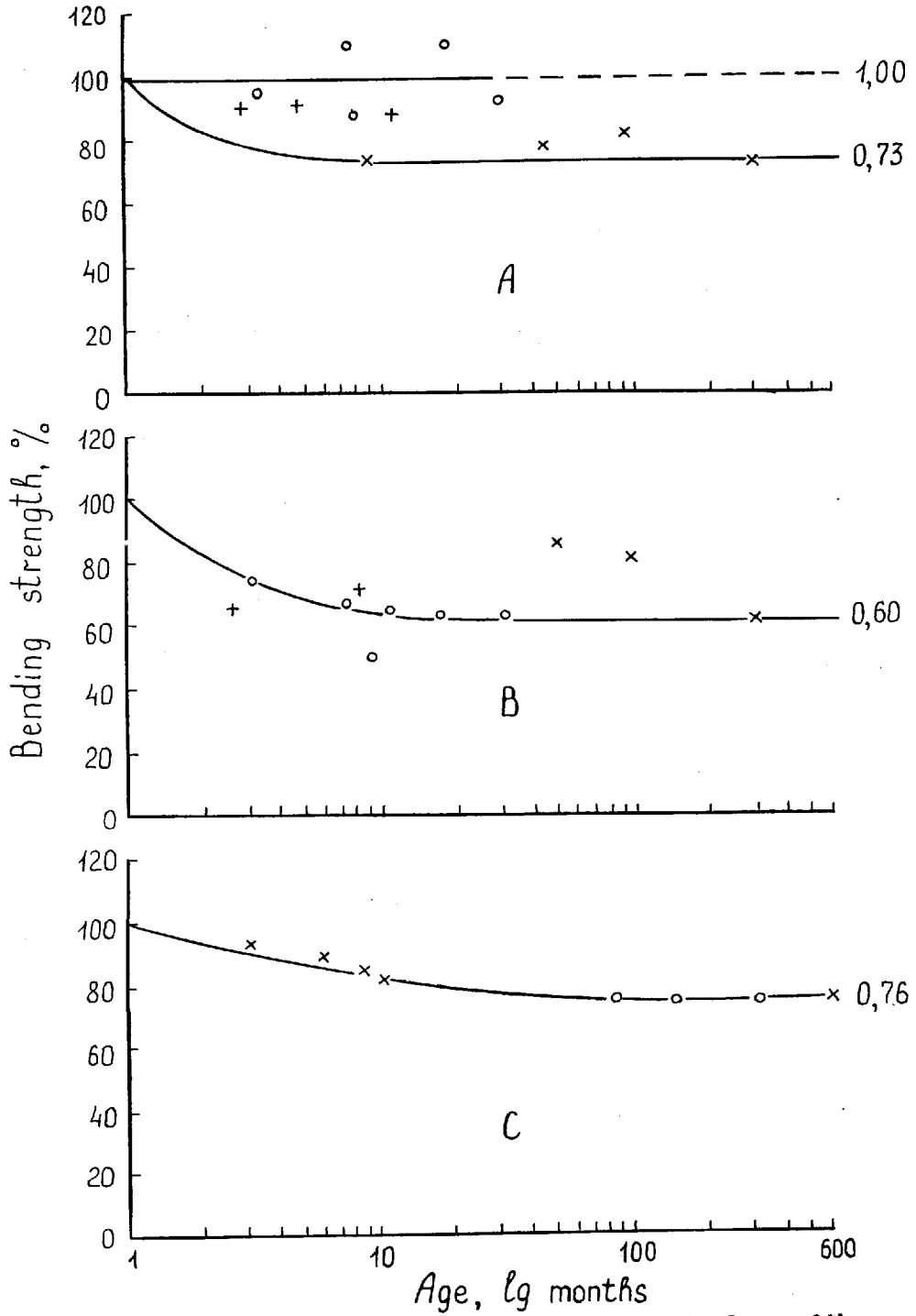

FIG.1 Forecasting of tensile bending strength of glass fibre-concrete (compositions 1,5 & 2%, initial strength of 28 days composite is taken for 100%):

A - dry premises (20°C - +, 50°C - o, 90°C - x)

B - wet premises (20°C - +, 50°C - o, 90°C - x)

C - atmospheric conditions (air resistance & freeze resistance - o, atmospheric resistance - x)

Series II

A higt strength and resistance to cracks of glass fibre based cement compositions determine their promising future in manufacturing pipes of various application. Tests on industrial equipment of a plant were conducted to check the technological possibility to manufacture nonpressure glass-concrete pipes by the centrifuge method.

The formation of 5 m long nonpressure glass-concrete pipes with inside diameter 400 and 500 mm and wall thickness 50 and 60 mm, respectively, was carried out in a roller centrifuge. Mortar 1:1 was used of portland cement brand 400 and quartz sand with gradation factor 1,6 . Water-to-cement ratio was 0.45 . Cuts of glass-fiber reinforcement with polyorganic coating protecting it from the action of the hardening portland cement environment in amounts of 2 % (the length of fibres was 50 mm) and the mortar have been distributed in layers in chute feedder. Centrifuging and heat and moisture treatment have been carried out in accordance with the plant conditions for reinforced-concrete pipes. Tests conducted with the manufactured glass fibre-based concrete tubes have shown that they meet the requirements of standart "Reinforced-concrete nonpressure pipes". A batch of glass fiber based concrete pipes is in operation in the industrial waste-water disposal system of the plant boiler house. Technical and economic efficiency of nonpressure glass fibre-based concrete pipes consists in the increase of the quality of products, in saving metal and crushed stone, in the decrease of materials consumption, in the increase of waterproofness, in the reduction of production and operating costs.

The qualitative aspect of solution of the problem of creation of glass fibre-based cement compositions is shown in Fig.2 : the ways of creation of composites with the preset properties are determined and concrete examples of the use of this material are presented (4). The developed bases of glass fibreer-based cement composites show that a selection of the composite contert is determined by the area of their application, be it structures and products of short-time or long-term application. The choce of the kind and amount of glass fibre reinforcement depends on the design features of products, on technnological and operational loads as well as on the chosen manufacturing technology.

It is advisable to manufacture glass fibre-based cement structures and products of short-time application (where the use of high strength characteristics is accounted for by the time of preservation of high strength of glass fibre reinforcement) on the basis of widely produced materials: portland cement and fiber of alkali or alkali-free composition. For products of long-term application, compositions should be used in which the preset strength of the glass fiber reinforcement is stable in time. Such compositions can be obtained on a basis of low-alkali binding materials (alumina cement and its modifications, gypsum binding agents, belite portland cement, sulfocontaining binders), through the introduction into the traditional binder of additions decreasing the alkalinity of the hardening medium and of glass fibre armature of glass of alkali-resistance composition or of fibres of usual compositions with protective coating.

An increase in the density of glass-fibre-cement composition, a decrease of its porosity and water absorption, carbonization hamper the processes of corrosion of glass fibre reinforcement. An additional treatment of composites with coatings which impedes the penetration of moisture contributes to the same. The properties of cement matrix be controlled through the introduction of additives of various purpose. Strength characteristics of glass fibre-based cement compositions are determined largely by the condition of the fibre, by the kind, quantity and orientation of reinforcement in the composite, by the material or product manu-facturing technology (3,7).

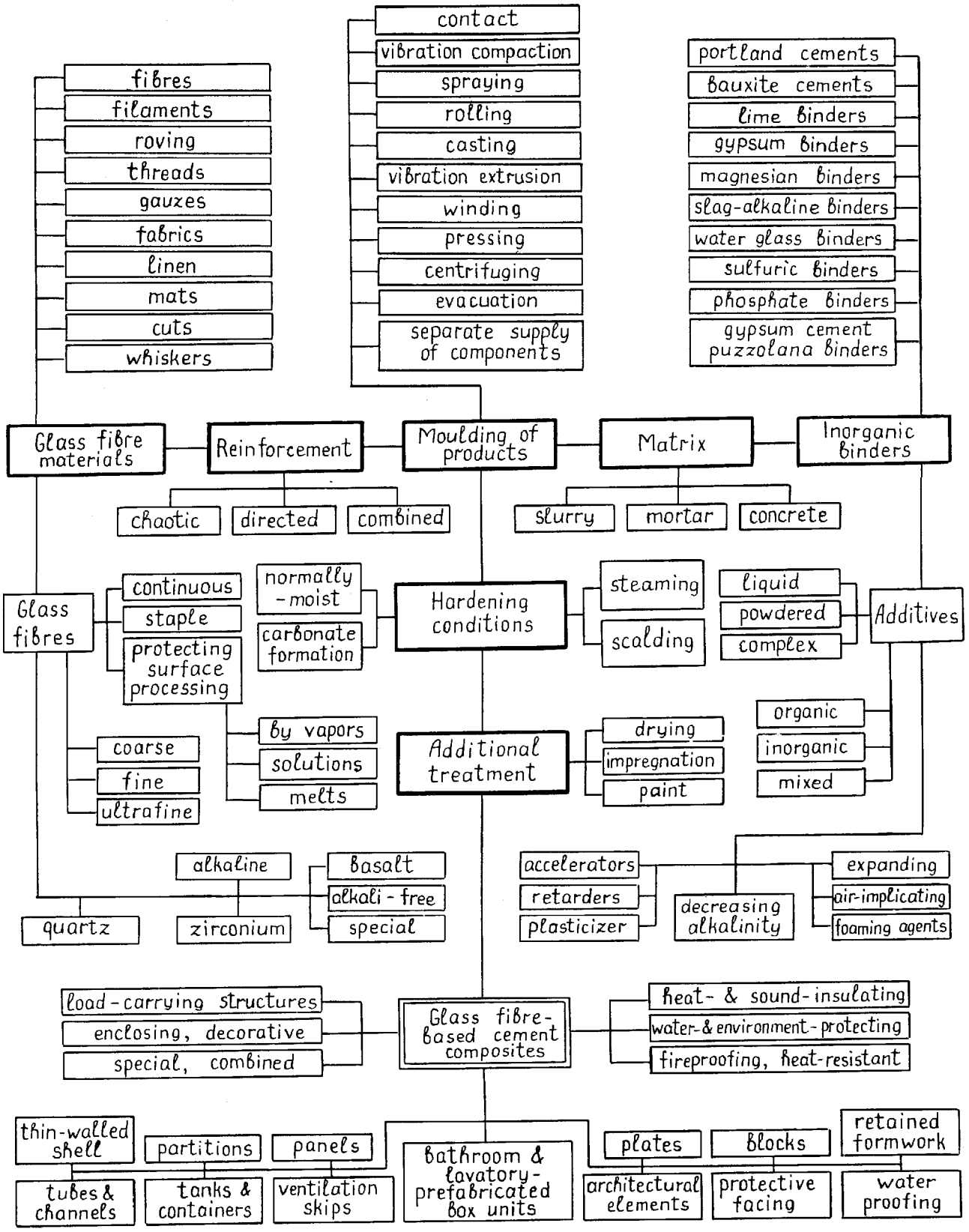

FIG.2 Diagram of creation of glass fibre-based cement composites

CONCLUSIONS AND RECOMMENDATIONS

Wide possibilities to vary glass fibre-based cement for-mulations make it possible to obtain compositions with a high strength, impact resistance, resistance to cracks, atmospheric durability and frost resistance, fire-resistance, waterproofing and a wide variety of other special properties. Due to many positive properties and in particular as a material enabling metal to be saved, glass fibre-based cement has received wide recognition. The rise in output and in application of glass fibre-based cement composites in civil engineering substantially depends on their longevity and efficiency.

REFERRENCES

1. "Concrete'90 - conference report", N 2, Concr. Constr., 1990, 34, Nov., p 8-12.

2. Biryukovich, K.L., Biryukovich, Yu.L. & Biryukovich, D.L.: GLASS-FIBRE REINFORCED CEMENT IN CONSTRUCTION. Kiev, Budivelnik, 1986, 95 p.

3. Pashchenko, A.A., Serbin, V.P., Glukhovskiy, V.V. et al.: REINFORCEMENT OF INORGANIC BINDING AGENTS WITH MINERAL FIBRES. Moscow, Stroyizdat, 1988, 200 p.

4. Serbin, V.P. ELABORATION & APPLICATION OF GLASS FIBRES-BASED CEMENT COMPOSITES. Kiev, Znanie, 1982, 34 p.

5. Meyer, A.: "Konstruktions- und Bemessungregin fur Glasfaser-beton", Betonwerk + Fertigteil fur Techn., 1990, 56, N 12, p 49-53.

6. Newby, M.R.: "Glass reinforced cement as permanent formwork incorporation architectural form & detail", N 2, Concr. Constr., 1990, 34, Sept., p 6-11.

7. Bentur, A.: "Fibre reinforced cementitions materials", Mater. Sci. Concr. J., Westerville (Ohio), 1989, p 223-284.

FRC REINFORCED WITH SHORT POLYPROPYLENE FIBERS FRACTURE PROCESS

J R L Dyczek and M A Petri

Technical University of Mining & Metallurgy, Faculty of Ceramics and Materials Science, Kraków, POLAND

SUMMARY

Investigations of the mechanical properties were performed using uniaxial tension test. Tensile strength, modulus of rupture, work of fracture of FRC reinforced with short polypropylene fibres, were determinated. From the obtained values for the work of fracture the average values of the fibre-matrix bond strength were calculated as a function of curing time and curing conditions. It has been found that in the case of samples cured under normal conditions only the pulling out of fibres from the matrix was observed whereas in autoclaved samples (160°C) the fibres were torn off.

RÉSUMÉ

Investigations des propriétés mécaniques ont été effectués par tension uniaxiale. Pour les éprouvettes de FRC on déterminaté la résistance à la traction, module de rupture, la travail de rupture. Pour des valeurs obtenus de la travail de rupture on a calculé des valeurs moyennes de la résistances à la limite fibre-matrix en fonction du temps et des conditions. On a mis en évidence normales pendant de rupture les fibres on été étirés. En cas des éprouvettes autoclavés (160°) on a observés le casse des fibres.

INTRODUCTION

The cracking process of composites reinforced with short fibres and having brittle matrix, as it is the case with FRC,begins with the destruction of the matrix begins. Depending on the mechanical properties and the geometry of the fibres, their distribution in the matrix and the strength of the fibre-matrix interfacial boundary, the development of the matrix crack, may be stopped at a certain depth or it may proceed further.When analyzing the cracking process of FRC from the stress-strain curve we can distinguish three characteristic.
- the value of the first crack at which the stress initiates the cracking process of the matrix (FC)
- modulus of rupture (MOR), i.e. the maximal unit value of the stress which may be sustained by the fibres after the matrix fracture,
- work of fracture (WOF), illustrating the total amount of energy needed to separate the material into two parts.

All the above quantities are a function of the amount of the reinforcing fibre (V_f) its length (l), diameter (d_f),strength (δ_f), adhesion of the fibre to the matrix (τ) and the dispersion of the fibres in the matrix. All the above factors, except τ , can be easily measured, only the determination of the real strength of the fibre-matrix boundary is a problematic. In case of FRC this problem becomes still more complicated since this boundary has a composite non-homogeneous micro structure [1,2].It may be assumed that it is just the boundary which will be the weakest part in the material taken as a whole. There exist several methods which permit to determine the value of τ, however it is not always possible to apply them. When short fibres are used as the reinforcing element, with the so-called "rough rendered" surface, produced only in the form of cut fibres, the methods of direct measurements cannot be used.
When analyzing the measurable properties of FRC reinforced with short polypropylene fibres, space distributed (3D) in the matrix, i.e. FC, MOR and WOF,taking into consideration both the variation from and the compatibility of the obtained results with the prevailing theories, it has been established that in the case under consideration it is possible to estimate the value of τ from the relation WOF Vs Vf. The method was discussed in detail by the authors at the RILEM Congress [3]. The work expenditure in the process of the composite separation can be divided into three components: work connected with the formation of new surfaces, work used for pulling out the fibres from the matrix (or their tearing off and pulling out of the ends) and the work connected with the secondary distribution of stresses. The total expenditure of energy can be described by the formulae:

- in case the fibres are torn off

$$WOF_I = \left(\frac{\tau \cdot l^2}{12 \cdot d_f} + \frac{\tau^2 \cdot l^2}{12 \cdot E_f \cdot d_f}\right) \cdot V_f + \left(1 - \frac{V_f}{2}\right) \cdot \gamma_m \qquad (1)$$

- in case they are pulled out from the matrix

$$WOF_{II} = \left(\frac{l_c^2 \cdot \sigma_f}{12 \cdot d_f} + \frac{\sigma_f^3 \cdot d_f}{12 \cdot E_f \cdot d_f} + \frac{V_f}{2} \cdot \gamma_m\right) V_f + \left(1 - \frac{V_f}{2}\right) \cdot \gamma_m \qquad (2)$$

The above equations represent a straight line equation:
$WOF = A \cdot V_f + B$ (3), where the variables are WOF and V_f. The value of τ may be calculated from the directional coefficient A.

EXPERIMENTAL

Polypropylene fibres produced by Denaklon were used to make FRC. Its properties are listed in Table 1.

TABLE 1 Properties of used fibres, Denaklon, Krenit Standard

	Units	Producers data	Data for computation
Length	mm	6	$l = 6$
Thickness	μm	35-46	$a = 37.5$
Width	μm	100-250	$b = 175$
Density	g/cm^3	0.9	$\rho = 0.9$
Tensile strength	MPa	450-500	$\sigma_f = 475$
E - modulus	GPa	13-18	$E_f = 15.5$
Ultimate strain	%	6-8	$\varepsilon_f = 7$
Diameter	μm	-	$d_f^* = 61.7$

d_f^* - was calculated as: $d_f^* = 4 \cdot \frac{A_f}{P_f}$

where: A_f - cross-sectional area of fibre
P_f- perimeter of fibre

The cement matrix was modified with an addition of silica fume, and in case when the samples were to be autoclaved sand quartz ground to the specific surface 280 m^2/kg was added. Mix proportions and curing conditions of the samples are shown in Table 2.

TABLE 2 Mix proportions of matrix

	Cement	Silica fume	Quartz sand	w/c	w/ss	Cure
A	100	-	-	0.33		3,7,14,28d/water
B	90	10	-	0.33		3,7,14,28d/water
C	47.5	5	47.5	0.54	0.26	28d/water
D	47.5	5	47.5	0.54	0.26	autoclav.8h/160°C
E	47.5	5	47.5	0.54	0.26	autoclav.8n/180°C

The samples were made by the casting method, out gassed by vacum treatment and vibrated. Their mechanical properties were examined under uniaxial tension, at the strain rate 15.64 x 10^{-3} cm/min. The measured values of FC, MOR as the mean values derived from 6 measurements are listed in Tables 3 and in the figures 1-3.

TABLE 3 Measured values of the first crack of matrix, FC [MPa], and of modulus of rupture, MOR [MPa]

		Fracturing of matrix			Modulus of rupture		
	Curing	Volume part of fibers			Volume part of fibers		
	time	0.01	0.02	0.03	0.01	0.02	0.03
A	3 days	1.82	2.04	2.41	1.97	2.58	2.92
	7 days	2.12	2.74	3.39	1.83	2.51	3.17
	14 days	2.12	2.57	2.83	1.33	1.98	2.56
	28 days	1.89	2.12	2.72	1.23	2.03	2.46
B	3 days	1.94	2.20	2.53	1.43	1.98	2.71
	7 days	2.10	2.29	2.72	2.11	2.81	3.52
	14 days	2.25	2.62	2.89	2.07	2.64	3.17
	28 days	1.99	2.31	2.68	1.86	2.58	3.07
C	28 days	2.72	2.96	3.72	1.29	2.31	3.05
D	aut.160°C	2.88	3.18	4.36	1.22	2.09	2.36
E	aut.160°C	2.15	3.38	4.75	-	-	-

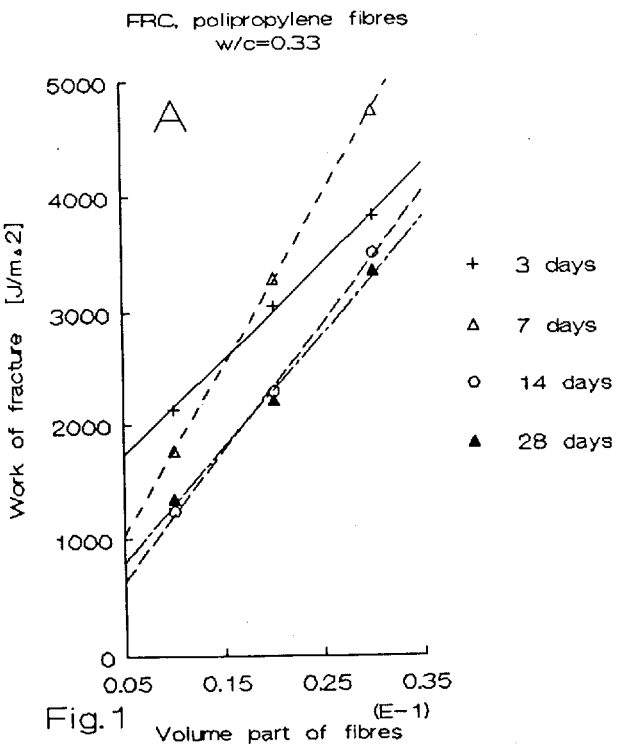

Fig.1

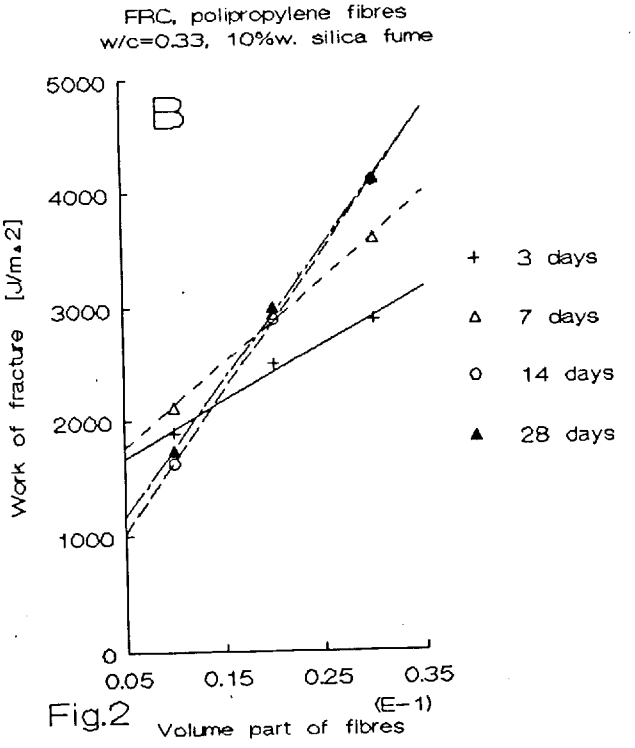

Fig.2

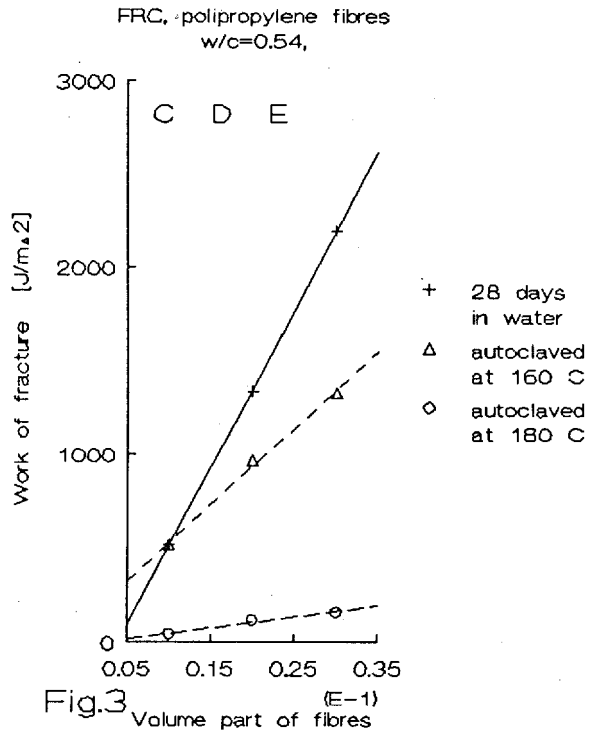

Fig.3

The values of the strength of the fibre-matrix interfacial boundary τ, are listed in Table 4 and potted on a fig.4.

Table 4 Calculated values of the fibre-matrix bond strength (τ)

	Cure	A_I or A_{II}	τ [MPa]
A	3 days	84950	1.73
	7 days	148850	3.01
	14 days	113250	2.30
	28 days	100400	2.04
B	3 days	49850	1.02
	7 days	74180	1.51
	14 days	123150	2.50
	28 days	118400	2.40
C	28 days	83950	1.71
D	aut.160°C	40900	4.62*

A_I, A_{II} - direction coefficients of the $WOF=A \cdot V_f+B$ equation
* - τ was calculated from A_{II}

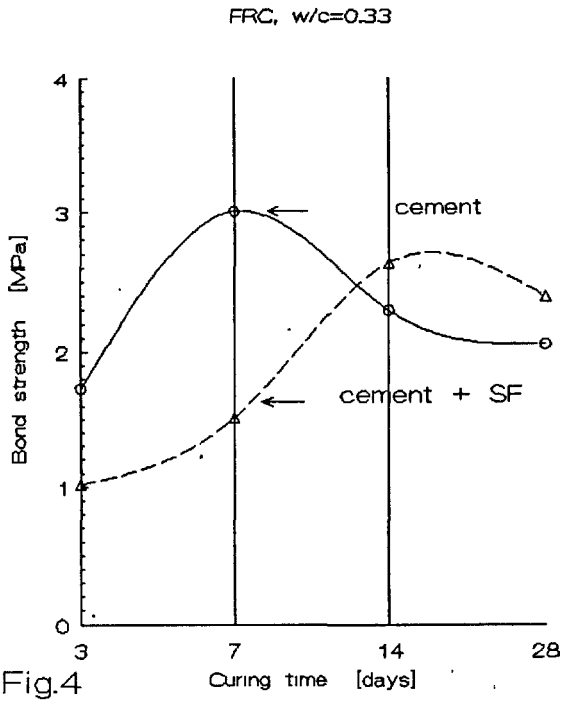

Fig.4

The SEM photos of the fibres for two cases: when the fibre is being pulled out from the matrix (curing in natural conditions) and torn off (autoclaved at 160°C) are shown in Figs 5 and 6.

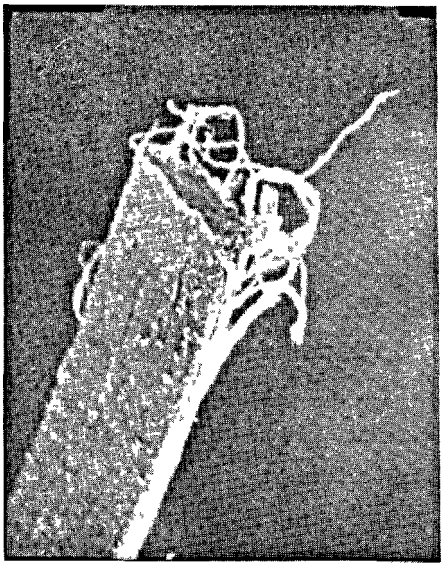

Fig.5.
Indyvidual fibre pull outed from matrix (FRC nat. cured)

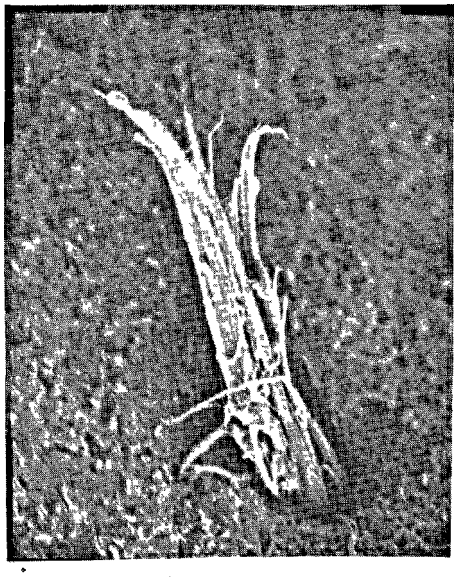

Fig.6.
Fibbre torn off in fracturing process of FRC autocl. at 160°C

DISCUSSION

From the experimental data presented in Table 3 and in the diagrams 1-3 for the samples of the A and B series,(curing under normal conditions) it follows that the values FC, MOR and WOF are combined function of the curing time of the samples. In case of samples from the C (control) series and autoclaved samples (D, E), prepared according to the same recipe, it has been observed that the process of hydrothermal treatment increased the strength of the matrix with simultaneous reduction of the ability of the material to carry load under after-cracking conditions.The autoclaved material at 180°C showed brittle fracture which is evidence that polypropylene fibres have been destroyed at this temperature. SEM observations of the surface of the broken samples has revealed that in case of materials of the A,B,C series the fibres were pulled out from the matrix and not torned off (Fig.6). In both cases the damages of the fibres surfaces could be seen clearly. When calculating the values of τ, listed in Table 4, for FRC of the A, B, C series equation 1 was used, whereas in case of the D series - equation 2 was used. For materials autoclaved at 180°C, considering the absence of the pseudo plasticity effect the above calculations could not be made. The values of the strength of fibre-matrix interfacial boundary, listed in Table 4 and shown in Fig.4, for FRC cured in normal conditions are a function of the curing time of the samples.Changes in τ correlate with the changes in the mechanical properties of the materials, listed in Table 4. This phenomenon may be explained as being due to the rebuilding of the microstructure of the interfacial boundary, occurring under the influence of the curing time of cement and the additive (in this case silica fume).

CONCLUSIONS

On the basis of the τ values calculated from the relation WOF vs V_f, it is possible to conclude that:
- the strength of the interfacial boundary: polypropylene fibre-cement matrix changes with the curing time of the material, but it cannot be represented by a linear function
- silica fume addition to cement causes changes in the strength of τ,
- in case of samples cured under normal conditions only the pulling out of fibres from the matrix was observed in the fracturing process of FRC, whereas in autoclaved samples the fibres were torn off.

REFERENCES

1. Bentur A., Interfaces in Fibre Reinforced Cements, **Mat. Res. Soc. Symp.** Proc. **Vol. 114** (1988)
2. M. Kawamura, S.Igarashi, Significance of Microstructure of the Glass Fiber-Cement Paste Interfacial Zone in Long Term Durability of GFRC Composites, **Durability of Concrete** Second International Conference, **Vol.II**, Montreal (1991)
3. J.R.L. Dyczek, M.A. Petri, Polypropylene FRC Fibre-Matrix Bond Strength, will be publish in **Fourth RILEM International Symposium** on Fibre Reinforced Cement and Concrete Proc., Sheffield (1992)

STRENGTHENING AND TOUGHENING MECHANISMS IN CARBON FIBER REINFORCED CEMENTS

N Banthia*, J Sheng and M Pigeon****

*Department of Civil Engineering, The University of British Columbia, Vancouver, B.C., CANADA

**Department of Civil Engineering, Laval University, Sainte-Foy, P.Q., CANADA

SUMMARY

Strength and toughness of cements reinforced with discontinuous pitch-based carbon fibres was measured by conducting static and impact tests. Improvements both in strength and toughness were noted. Some processing difficulties and reinforcing mechanisms in these composites are discussed through microscopic fracture observations. Various possible applications of these composites in structural and non-structural applications are enumerated.

INTRODUCTION

For researchers investigating cement-based materials, the most important challenges are the poor tensile strength and low fracture toughness exhibited by these materials. These undesirable attributes lead to an easy nucleation and propagation of cracks limiting the range of their use. One effective method of improving the mechanical behaviour of cementitious materials is by "fibre reinforcement". The improvements in the properties of cementitious materials by fibre inclusion is, among other things, in direct proportion to the volume fraction of the fibres included.

There are inherent difficulties in mixing large steel fibres (20-60 mm in length and 0.1-1.0 mm in diameter) at high volume fractions. At the limiting volume fraction (≈ 1.5%), steel fibres are known to provide only a marginal improvement in strength. The improvements in toughness or energy absorption, however, are exceptional (1). It is believed that a substantial improvement in the tensile strength may be obtained only through an effective control of fracture at the micro-level by using very fine fibres at a large volume fraction. These fine fibres with their diameters almost as small as the particles of cement are often collectively called "micro-fibres". While carbon is the most used micro-fibre so far (2), other micro-fibres of steel and polypropylene have also been researched (3).

Carbon fibres used as cement reinforcement may be divided into two types: high modulus polyacrylonitrile (PAN-based) fibres, and the low-modulus pitch-based fibres derived from petroleum pitches. Properties of these two types of fibres are given in Table 1. Considerable improvements in cement properties were reported with PAN-based fibres in their continuous form (4). However, the prohibitive cost of the PAN-based fibre did not allow its large scale commercialization and lately the attention has shifted almost entirely to the inexpensive pitch-based carbon fibre.

This paper describes some fracture characteristics of cements reinforced with pitch-based carbon fibres in the discontinuous form. Carbon Fibre Reinforced Cements and Concretes are often abbreviated as "CFRC".

Table 1 Carbon Fibres for Reinforcing Cements

Fibre Type	Diameter (μm)	Specific Gravity	Tensile Strength (MPa)	Young's Modulus (GPa)	Approximate Cost Ratios
PAN-based	7-8	1.6-1.7	3000-4000	250-400	7
Pitch-based	14-18	1.7-1.8	600-2000	30-200	1

EXPERIMENTAL

Carbon fibres used for the purpose of this investigation had the following properties—Type: Pitch-based; Diameter: 18 μm; Length: 6 mm; Tensile Strength: 590 MPa; Elastic Modulus: 30 GPa; Elongation at Break: 1.4%.

Given the high specific surface area of carbon fibres, mixing by conventional means was found to be difficult. Ordinarily, carbon fibres tend to ball and disperse non-uniformly. Condensed silica fume, previously proven effective (5), was used as the fibre dispersing agent. A conventional mortar mixer was used for mixing. The water/cement ratio was maintained throughout at 0.30. Fibre volume fractions of up to 5% were investigated. With simultaneous external vibration, the following specimens were cast:

1. Beams 19 mm x 19mm x 150 mm for flexural testing; and,
2. Tensile briquettes 25 mm x 25 mm critical section for instrumented impact tests under uni-axial tension.

The mixes in the fresh state with high fibre volume fractions had only a moderate flowability, but the moldability and finishability were good. CFRC mixes ordinarily required longer than usual compaction times. The specimens were demoulded 24 hr after casting and cured at least for 28 days at 23 ± 2°C and 95 % r.h. before testing. Figure 1 shows a well hydrated CFRC section.

The properties and characteristics of CFRC, like any other composite, depend upon the circumstances and conditions that exist at the time of their processing, i.e. at the time of their mixing, casting and curing. One major processing concern is the low modulus of the fibre itself, which may cause fibres to deform during the mixing operation. Figure 2 shows such a possibility. The other processing concern is the induced stresses in the fibres, the interfaces and the surrounding matrix as a result of composite dimensional changes in the curing stage. However,

once hardened, the elastic moduli of pitch-based carbon fibres and the hydrated cement paste are not all that different and some dimensional changes may be tolerated.

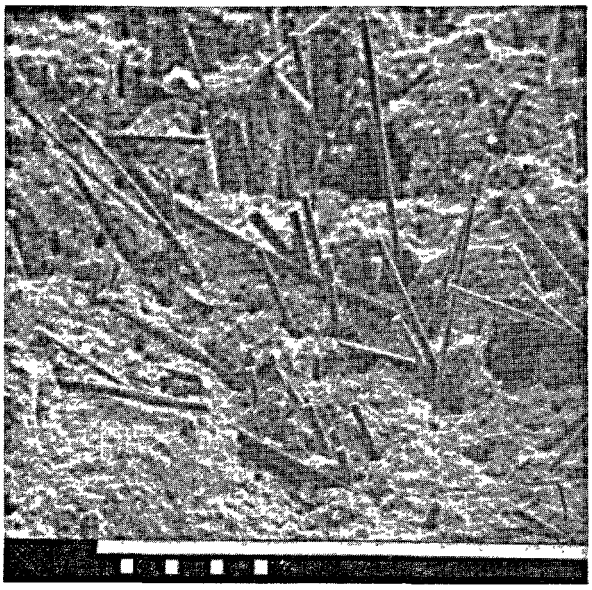

Figure 1. A Well-Hydrated CFRC Section

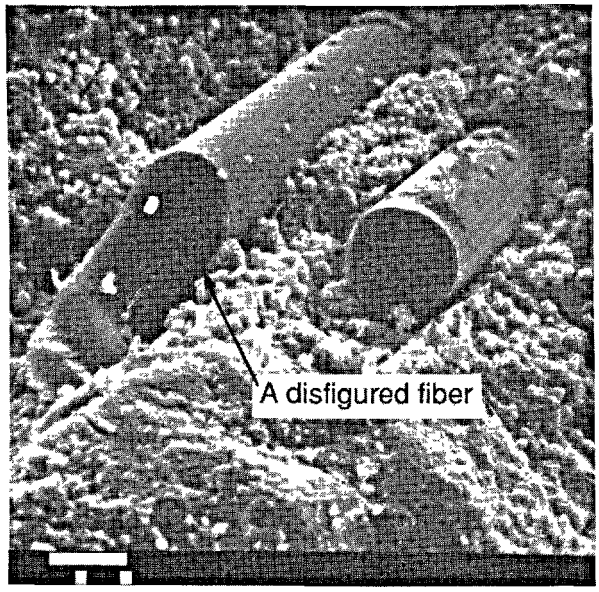

Figure 2. Some Fibre Disfiguring during Mixing

RESULTS

Flexure

In the flexural test setup, the 19 mm x 19 mm x 150 mm beams were supported on an unsupported span of 130 mm and the load was applied at the mid-point through a knife-edge (Figure 3). The beam displacement at the center was measured by means of a deflectometer and the applied load versus beam center-point displacement plots were obtained. Figure 4 shows some typical plots. Notice that considerable strengthening as well as toughening occurred due to carbon fibre reinforcing.

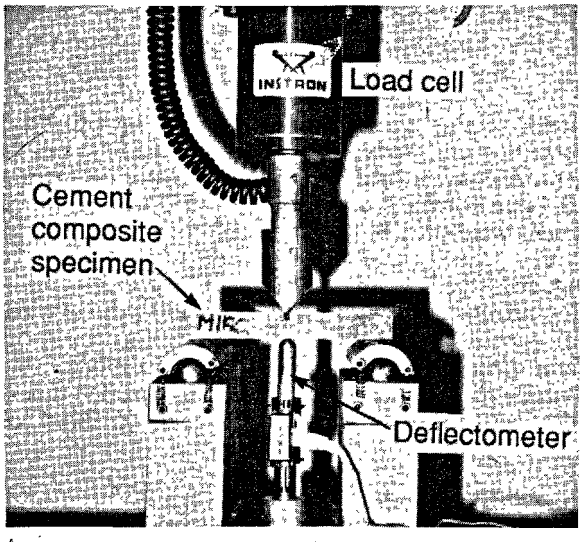

Figure 3. Flexural Test Setup

As opposed to unreinforced cements, where the failure occurred in the elastic range itself, the load-displacement plots for the composites had a general shape consisting of:

–A linear elastic region up to the BOP (Bend Over Point);

–A distinct strain hardening region following the BOP up to the occurrence of the ultimate load; and,

–A stable strain softening region after the ultimate load with substantial energy absorption. When integrated, these curves provided the values of fracture energies consumed by the specimens.

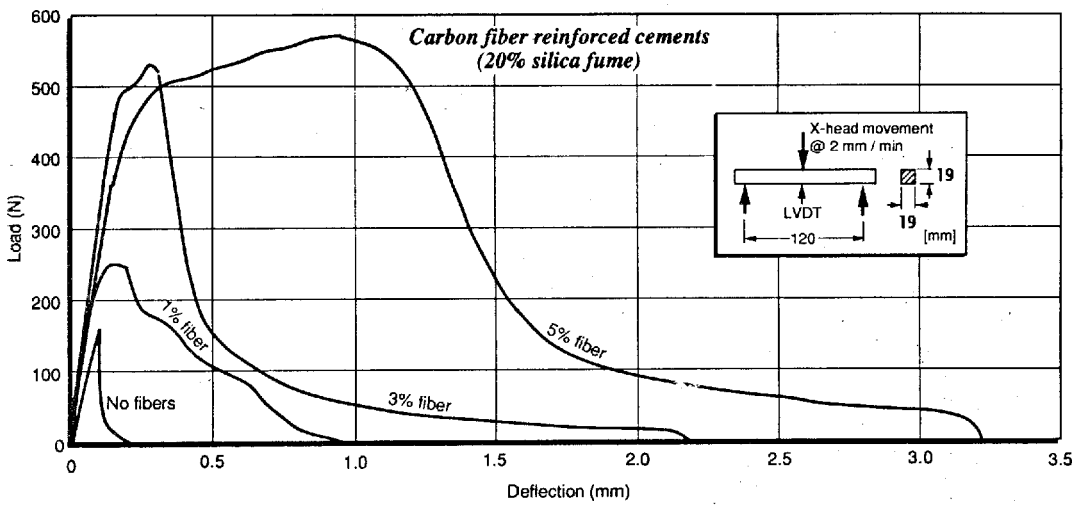

Figure 4. Some Typical Load-Deflection Plots in Flexure

As can be noticed in Figure 4, carbon fibres were capable of providing significant strengthening in the elastic range itself. A 3-fold increase in the first crack strength at 5% fibre content was noted. Along with the improvements in the first crack or the elastic strength, equally remarkable improvements occurred in the ultimate load carrying capacity and the fracture energy values. These quantities are plotted in Figures 5(a) and 5(b), respectively, as a function of fibre volume fraction. Note a 6-fold increase in the ultimate strength at high fibre volume fractions and a one to two orders of magnitude increase in the fracture energy consumption.

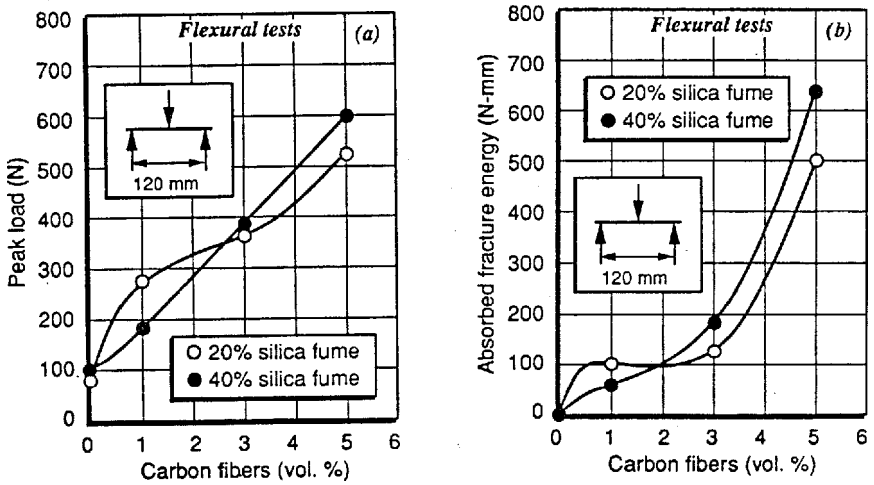

Figure 5. (a) Ultimate Load Carrying Capacity and (b) Absorbed Fracture Energy for CFRC

Impact Resistance

Improvements in the impact resistance due to carbon fibre reinforcing have been reported in some previous investigations (5,6) where multiple drop-weight tests were conducted.

In the present investigation, instrumented impact tests were performed on CFRC in uni-axial tension mode. Figure 6 shows the modified Charpy impact test setup. The equipment, its construction and functioning are described in details elsewhere (7). Briefly, the specimen support system had two parts, one movable (Part A in Figure 6 called 'the trolley') and the other fixed (Part B in Figure 6), with the specimen bridging in-between. The

trolley was struck by the swinging pendulum with an instrumented striker at its elevated deck which placed the specimen under a uni-axial tensile impact load. After fracture, the frictionless trolley traveled towards the shock absorbers and on its way intercepted a pair of photocell assemblies that recorded its post-fracture velocity. By subtracting the post-fracture kinetic energy of the trolley from the energy lost by the hammer, the fracture energy consumed by the specimen was obtained. Similarly, by placing an accelerometer on the trolley, the inertial part of the measured hammer load could be obtained which could then be used to obtain the true specimen stressing load (1, 8).

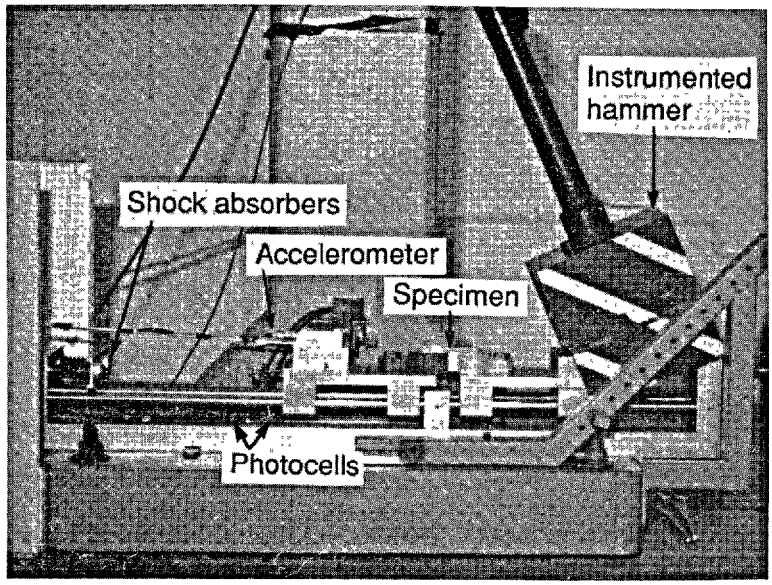

Figure 6. Instrumented Impact Setup with Trolley Mounted Specimen Support System

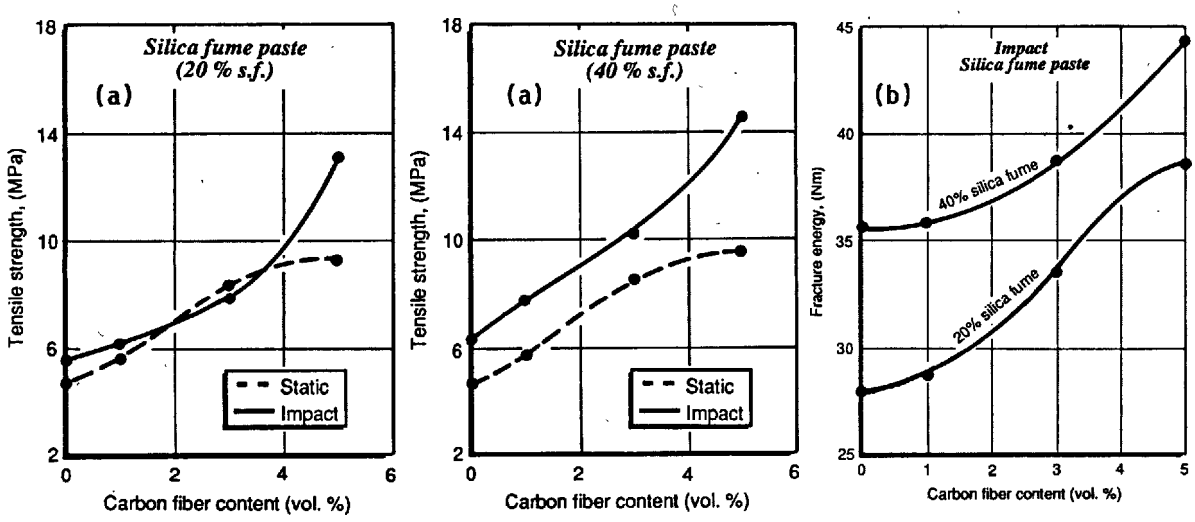

Figure 7. (a) Tensile Strength and (b) Fracture Energy Consumption of CFRC under Impact

Figures 7a and 7b show the observed tensile strength and the computed fracture energies, respectively, under impact. The remarkable improvements in the impact resistance could also be noted from the hammer-specimen contact load vs. time pulses recorded in these impact tests. CFRC specimens always had longer hammer-specimen contact times and the areas under these curves were proportional to the fibre volume fraction.

DISCUSSION

The toughening and strengthening mechanisms furnished by carbon fibres in cementitious matrices are not so well understood. Based on simple calculations for fibres aligned in the direction of loading, the critical embedded length for pitch-based carbon fibres is shown to be about 1-2 mm (9). It follows, therefore, that when CFRC is loaded in tension directly or indirectly, most of the fibres should fracture. Similar argument was extended by Akihama, Suenaga and Nakagawa (Ref. 10). As seen in Figure 8, fibre fractures were seen to occur frequently in CFRC loaded in flexure. However, given the fact that at fracture, the strain supported by pitch-based carbon fibres is not very high (≈1%), for high composite toughness some fibre pull-out must occur. Indeed, some fibre pull-out was also found to exist. Finally, in some fibres, even a combination of the two modes—fibre fracture occurring within the embedded length followed by fibre pull-out—was observed. It appears possible that this type of behaviour may be due, in part, to the existence of residual processing stresses in the fibres.

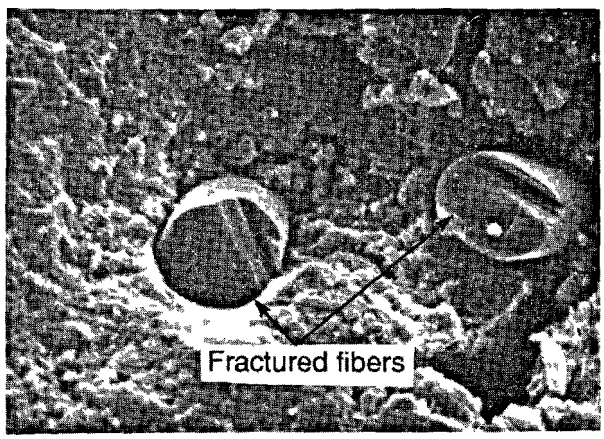

Figure 8. Fractured Surface of CFRC Showing Fibre Fractures

It is clear from the results that both strengthening and toughening occur as a result of carbon fibre reinforcing. Some possible explanations for the observed strengthening and toughening in continuous fibre reinforced systems have been previously provided (11, 12). The proposed concept of *multiple crack formation* has also been proposed for CFRC with discontinuous fibres (3). Although the data reported here is preliminary in nature, the observed improvements in the mechanical properties are impressive and future research is warranted. In particular, the influence of fibre characteristics and interface properties on composite performance should be thoroughly investigated for optimization.

The combination of two or more fibre types in the same mix (hybrid fibre systems) should be studied with the aim of obtaining a desired combination of strength, toughness and cost. Some trials combining carbon and steel micro-fibres have produced promising results (9, 13).

APPLICATIONS OF CARBON-CEMENT COMPOSITES

Given the improvements in the mechanical properties of weak and brittle cement matrices by carbon fibre reinforcing and the interesting physical properties of these composites, there are numerous possible uses.

One of the major uses of these composites is in thin precast products such as roofing sheets, panels, tiles, curtain walls, ferrocements, wave absorbers, permanent forms, free-access floor panels, and I- and L- shaped beams. The first large scale application of CFRC was in the form of panels with tile cladding in the Al Shaheed Monument in Iraq. CFRC curtain walls have been used in Japan for some time now.

In cast-in-place applications, CFRC has potential for use in mortars for external walls especially for structures in seismic regions, for small machinery foundations, etc.. Latex modification of CFRC has been shown to improve water absorption and durability (14), and the use of these composites for thin repairs appears promising (15). The good electrical conductivity of these composites (16) may be put to use in the secondary anode system in the cathodic protection of reinforced concrete bridge decks, in conductive floor panel systems and also in the concrete for lightning arresters.

Numerous non-structural applications of CFRC have also been suggested. The potentially beneficial applications include uses in the electrical and electronics industries. On the highly unconventional side, the use of CFRC in the motorcycle engine as the cylinder head has also been attempted (17).

CONCLUDING REMARKS

The improvements in the strength and toughness of cement-based materials by reinforcing them with low modulus pitch-based carbon fibres are encouraging. There are numerous possible applications of these composites

in structural as well as non-structural areas. However, extensive research efforts are needed prior to a wholehearted use of these composites.

REFERENCES

1. Banthia, N., Mindess, S. and Bentur, A. Impact Behaviour of Concrete Beams, Materials and Structures (RILEM), 20(119), 1987, pp. 293-302.

2. Banthia, N. Pitch-Based Carbon Fibre Reinforced Cements: Structure, Performance, Applications and Research Needs, The Canadian Journal of Civil Engineering, Feb. 1992 (to appear).

3. Banthia, N. and Sheng, J., Proc. Second Canadian Symposium on Cement and Concrete (Ed. S. Mindess), Vancouver, 1991.

4. Ali, M.A., Majumdar, A.J. and Rayment, D.L. Carbon Fibre Reinforcement of Cement, Cement and Concrete Research, 2, 1972, pp. 201-212.

5. Ohama, Y., Amano, M. and Endo, M. Properties of Carbon Fibre Reinforced Cement with Silica Fume, Concrete International, March 1985, pp. 58-62.

6. Soroushian, P., Bayasi, Z. and Nagi, M. in Fibre Reinforced Cements and Concretes: Recent Developments (Eds. R.N. Swamy and B. Barr) Elsevier Applied Science Publishers, 1989, pp. 167-178.

7. Banthia, N. and Ohama, Y. in Fibre Reinforced Cements and Concretes: Recent Developments (Eds. R.N. Swamy and B. Barr) Elsevier Applied Science Publishers, 1989, pp. 251-260.

8. Banthia, N., Mindess, S., Bentur, A. and Pigeon, M. Impact Testing of Concrete Using a Drop Weight Impact Machine, Experimental Mechanics (USA), 29(2), 1989, pp. 63-69.

9. Banthia, N. and Sheng, J. Micro-Reinforced Cementitious Materials, Materials Research Society Symposium Proceedings, Boston, Volume 211 (Eds. S. Mindess and J. Skalny), 1991.

10. Akihama, S., Suenaga, T. and Nakagawa, H. Carbon Fibre Reinforced Concrete, Concrete International, 10(1), January, 1988 pp. 40-47.

11. Aveston, J., Cooper, G.A. and Kelly, A. in The Properties of Fibre Composites, Proc. Conf. National Physical Laboratories, IPC, Science and Technology Press, UK, 1971 pp. 15-24.

12. Mobasher, B., Stang, H. and Shah, S.P. Microcracking in Fibre Reinforced Concrete, Cement and Concrete Research, 20, 1990, pp. 665-676.

13. Banthia, N., Reinforcement of Cements with Micro-Fibres of Carbon and Steel, Proc. of First Canadian University-Industry Workshop on Fibre Reinforced Concrete (Ed. N. Banthia), Quebec, 1991.

14. Soroushian, P., Aouadi, F. and Nagi, M. Latex Modified Carbon Fibre Reinforced Mortar, ACI Materials Journal, 88(1), 1991, pp. 11-18.

15. Banthia, N. and Dubeau S. Micro-Reinforced Cementitious Composites for Thin Repairs, Proc. ACI Int. Conf. on Evaluation and Rehabilitation of Concrete Structures, 1991, Hong Kong.

16. Banthia, N. Djeridane, S. and Pigeon, M., Electrical Resistivity of Micro-Fibre Reinforced Cements, Cement and Concrete Research, 1991 (accepted).

17. Kanno, M., Ohama, Y., Kawai, H. and Demura, K. Proc. of 32nd Japan Congress on Materials Research, The Society of Materials Science, Kyoto, Japan, 1989, pp. 209-212.

STRUCTURE/PERFORMANCE CHARACTERISTICS OF ARAMID FIBRES REINFORCED MDF CEMENT

R I A Malek* and M N Salama

**Materials Research Laboratory*
The Pennsylvania State University, USA

SUMMARY

The 21st Century Concrete Technology is expected to show considerable shifts toward new materials such as macro-defect-free and fiber reinforced materials. The major objective will be to produce concrete of improved mechanical properties.

The use of high performance fibres in many diverse engineering applications is well known. However, the introduction of such fibres in macro defect free (MDF) cement matrices has imposed several processing difficulties. The production of high performance composites based on MDF matrices reinforced with aramid fibres to acquire high a degree of ductility offers an additional new material for a variety of applications. Structural and mechanical characteristics and efforts to improve the interface bond strength are presented. The structure/performance relationship of such composites are discussed.

INTRODUCTION

New developments in the making of cementitious materials with improved mechanical properties have resulted from different combinations of modifying composition and processing. Together, these developments have resulted in about ten fold enhancement in their properties, which approach those of modern composites[1]. One of the most recent developments is the approach of preparing the so-called macro-defect free (MDF) cement. Originally discovered at Imperial Chemical Industries and Oxford University[2] and later pursued at this laboratory, these composites are prepared with a major amount of inorganic cement, a lesser amount of organic polymer and water, and minor amounts of other components. These composites have shown to have great potential for increased toughness. Such materials are already being used in novel applications, which include construction purposes (pre-fabricated houses, wall panels, .. etc.) in different parts of the world. A great advantage of these meterials is their high tensile strength and their capability to transmit loads to high performance fibres for added toughness.

The purpose of this paper is to report on the processing, structural and mechanical characteristics of high performance composites based on MDF matrices reinforced with aramid fibres to acquire high degree of ductility for a variety of applications. Efforts to improve the interface bond strength through mechanical and chemical anchorage are presented. The structure/performance relationship of such composites are discussed.

EXPERIMENTAL

The aramid fibres are obtained as chops consisting of a number of filaments held together with glue. Excess glue exists as an outgrowth on the fiber surface enhancing its mechanical anchorage when embedded in the cementitious matrix. The chop diameter is 25 mm x 0.5 mm. Some mechanical properties of the fibres are given in Table I.

Table I: Specific Gravity, Tensile Strength, and Young's Modulus of the Aramid Fibres Compared to That of Steel.

Fiber	Specific Gravity (g/cm^3)	Tensile Strength (Kgf/mm^2)	Young's Modulus (Kgf/mm^2)
Aramid	1.5	120	6,600
Steel	7.8	30	21,000

Composites of aramid fibres with MDF cement mixtures of Type I Portland Cement (Keystone Cement, PA), water, and polyacrylamide (Polysciences, U.S.A.) are prepared. Two fabrication techniques are used. The first is the mixing of the MDF cement ingredients together with the aramid fibres in a normal cement mixer at high speed. This procedure requires a high water to cement ratio of 0.25-.35 and the use of a

superplasticizer. After mixing, the fresh composite is molded, pressed to about 2000 psi and cured at room temperature.In the second fabrication technique, the MDF components (polyacrylamide/ cement = 0.15, and w/c ratio = 0.10) are separately mixed in a high shear mixer (Brabender). The resulting dough is extruded in the form of sheets of 3 mm thickness. The composite is fabricated by aligning the aramid fibres (3% by weight) in one direction and laminating between several sheets of MDF cement with more fibres on the tension side. The laminated composite is then pressed at about 2000 psi and cured at room temperature. A reference sample is prepared using the same lamination technique but with no fibres.

Small diameter fibres are known to arrest microcracks generated in the cement matrix as a result of loading. It is thought that using the small fibres in addition to the large fibres will add favorable mechanical properties to the resulting composite. The small fibres are 10-20 microns in cross sectional area and 1 mm in length aramid fibres (DuPont). The short fibres are mixed with the MDF in proportion equal to 4-7% replacement of the cement. The samples containing the two types of fibres are fabricated by the lamination technique.

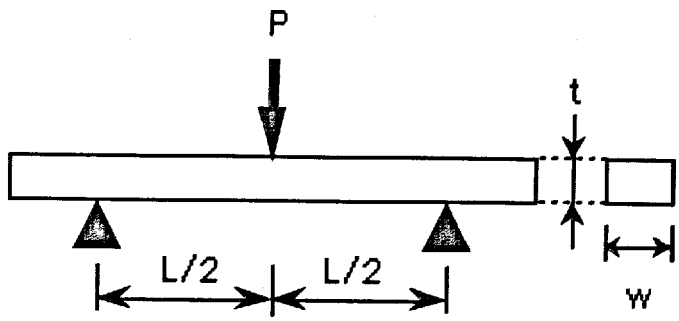

Figure 1. Schematic and Conditions of the 3-Point Bending Test

Note: Max. flexural stress is calculated by the following formula: $3PL/2wt^2$.
Elastic modulus can be calculated by the following formula: $PL^3/4wt^3Ymax$:
Ymax is the displacement at the center.
Half span depth ratio (L/2t): 1.5-1.3; L=76.2mm, t=25.4-28.6mm.
Stroke control loading; Cross-head speed: 0.051mm/min.

Attempts to enhance the matix-fibre interface bond strength through chemical anchorage is made by using silane coupling agents. Epoxy silane, $(CH_3)_3$ Si CH_2 CH_2 CH_2 OCH_2 CH-O-CH_2 (Dow Corning Z6040) is used. The coupling agent is applied to the fibre surface from acidified aqueous solutions and allowed to dry at 110°C.

After 28 days, the mechanical properties of the samples are tested by the three point bending test. Figure 1 schematically shows the conditions of the test and the equations applied[3]. Although the ultimate strength of the composite is reached in 7 days, the current samples are tested in 28 days in order to compare the results with parallel samples which are exposed to wet-dry cycles to test their moisture resistance. The latter samples are not included in the present publication.

RESULTS AND DISCUSSION

The stress-strain curves of the composites are presented in Figures 2-4. Figure two shows a comparison between the results of the unreinforced MDF matrix, fabricated by lamination, and the fibre reinforced one, fabricated by mixing. Although the matrix maximum strength has dropped to one third its value due to the mixing procedure, the fibre reinforced sample shows almost the same composite maximum strength. The horizontal area at the point of matrix failure represents a transition stage during which the load is transmitted from the matrix to the fibres. During this stage, a rearrangement in the microstructure of the fibre-matrix interfacial to new equilibrium conditions takes place to handle the increasing load. The gradual failure of the composite is a clear indication of the excellent interfacial bond strength in these composites.

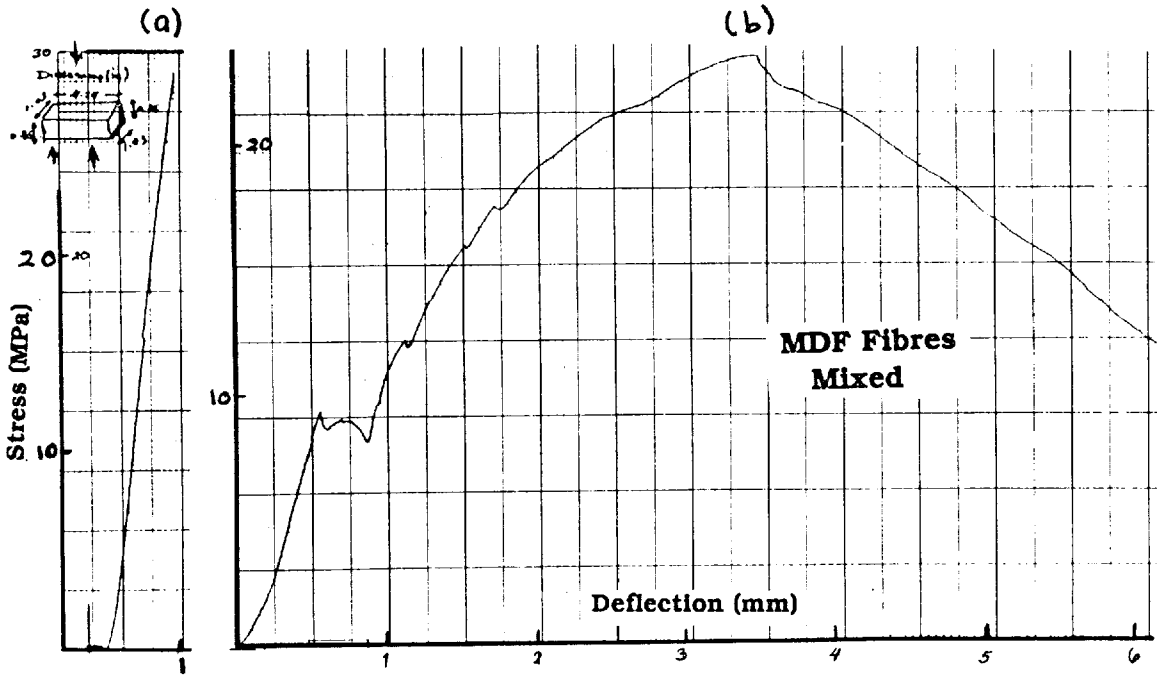

Figure 2. Stress-strain curves of the MDF cement matrices, a) laminated, unreinforced; b) mixed, reinforced

Figure 3 represents the stress-strain relationship of the large fibre reinforced MDF matrix fabricated by lamination with unidirectional fibre orientation. Here, the benefits of fibre inclusion combined with the fabrication technique is clearly reflected as a net increase in the maximum strength of both the matrix and the composite. The close proximity of the maxima indicates a an excellent interfacial bond strength.

Figure 4 presents the stress-strain relationships of the MDF matrices containing large and small aramid fibres. In the sample whose interface has not chemically modified (curve a) the two maxima have the same maximum strength reflecting the role of the small fibres in arresting microcracks and delaying the failure of the matrix. The initial sudden failure of the composite might indicate, unexpectedly, a little decrease in fibre-matrix anchorage. This is rectified when epoxy silane is used to enhance the interfacial

bond strength (curve b). The improved interface properties is clearly reflected in the presence of only one maximum of an integral structures.

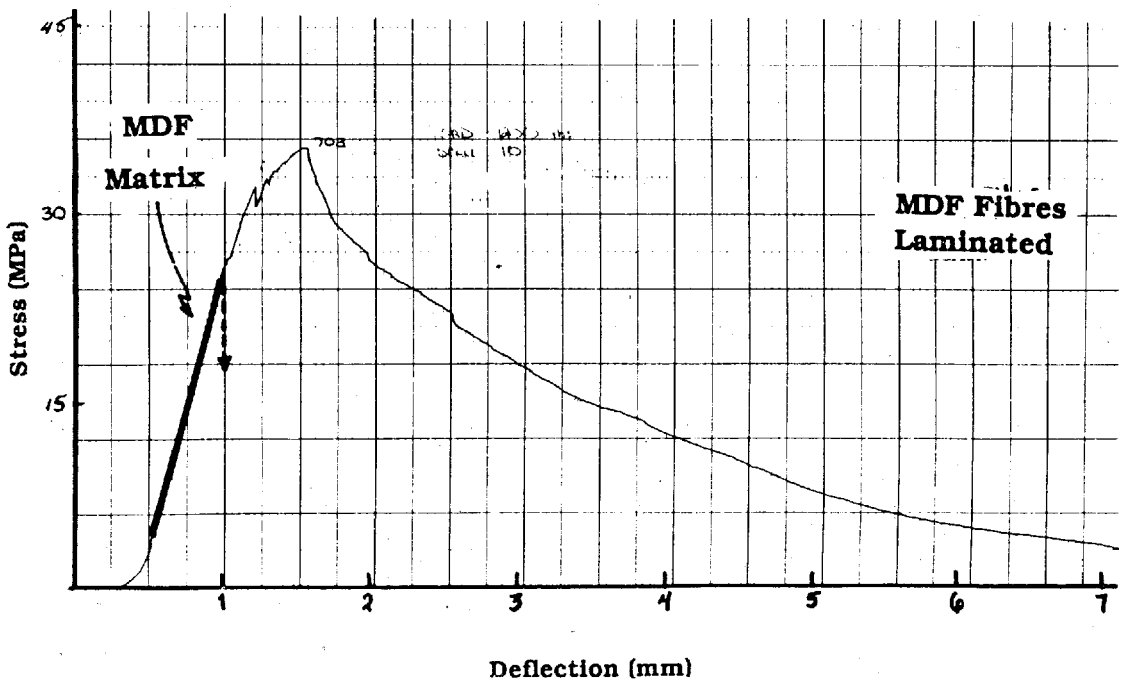

Figure 3. Stress-strain curves of the laminated MDF matrices containing large aramid fibres.

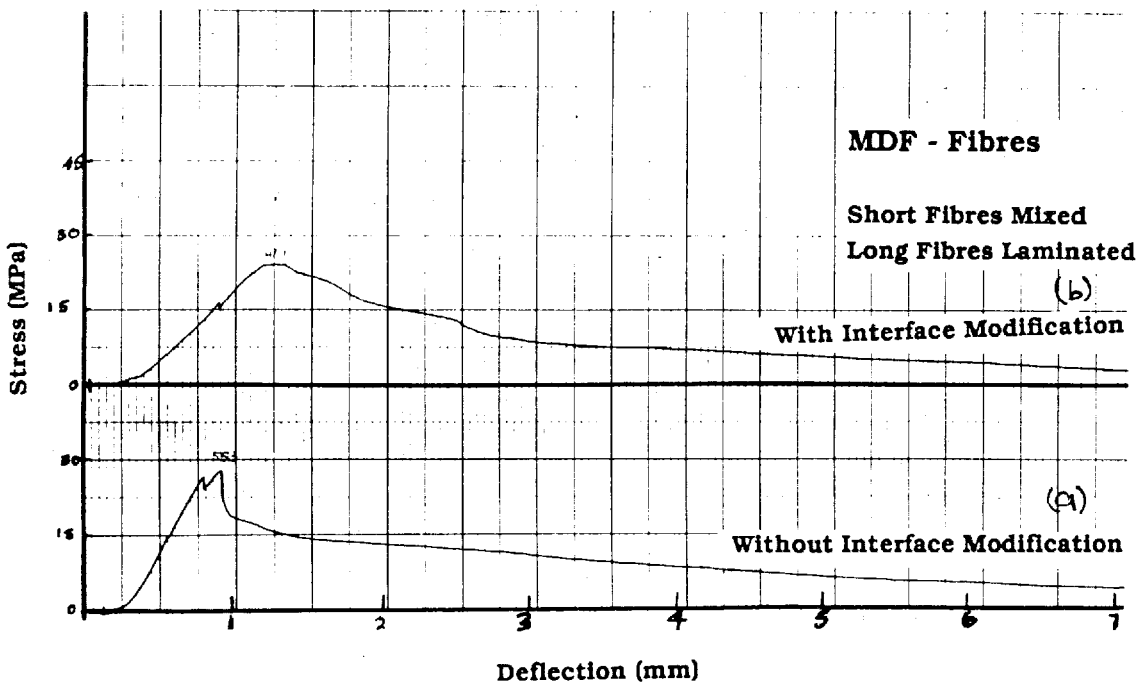

Figure 4. Stress-strain curves of the laminated MDF matrices containing different length fibres, a) chemically unmodified interface; b) epoxy silane treated interface.

CONCLUSIONS

Structural and mechanical characteristics of aramid fibre reinforced MDF cement and efforts to improve the interfacial bond strength are presented. The inclusion of the aramid fibres has resulted in several fold improvement in the elastic mechanical properties of the composite and makes approach those of metals.

ACKNOWLEDGEMENT

This research has been supported by the National Science Foundation.

REFERENCES

1. Roy, D.M., Science, **238**, 651-8 (1987).
2. Birchall, J. D., A. J. Howard, and K. Kendall. Nature **289**, 388-9 (1981).
3. Timoshenko, S.P., and J.N. Goodier, Theory of Elasticity, 3rd Ed., McGraw & Hill (1982).

PHYSICAL, CHEMICAL AND MECHANICAL CHARACTERIZATION OF GEOPOLYMERS

A Palomo, A Macías, M T Blanco and F Puertas

Instituto de Ciencias de la Construcción "Eduardo Torroja" (C.S.I.C.) - Madrid, SPAIN

ABSTRACT

Silicate cements based on metakaolin are being investigated as they seem to have a promising future. The mechanical characteristics of geopolymer mortars are a proof of such affirmation. Compressive strengths of about 49 MPA after curing the mortars during 1 hour at 80ºC, and 84.3 MPA after 24 hours at 80ºC, show the potential of these materials.

Two different pathways for synthetic a geopolymer with a starting molar composition of Na_2O/SiO_2 = 0.40, SiO_2/Al_2O_3 = 3.21, H_2O/Na_2O = 10, Na_2O/Al_2O_3 = 1.28, have been compared. The final products obtained have been characterized. Measurements of the mechanical strength and mercury porosimetry, as well as analyses through X-ray Diffraction, IR Spectroscopy and DTA-TG analyses, have been carried out. The results show the influence of the mixture of raw materials at early ages (about 1 hour), when a geopolymer is synthesized.

RESUMEN

Se han estudiado cementos de silicatos basados en metacaolín, a los que se les promete un importante futuro. Las características mecánicas de los morteros de geopolímero son una prueba de tal afirmación. Las resistencias a compresión de estos morteros, con valor de 49 MPA en aquellos curados durante una hora a 80ºC y de 84, 3 MPA después de 24 horas a 80ºC, muestran el potencial de estos materiales.

Se han comparado dos caminos diferentes de síntesis de geopolímero, con relaciones molares iniciales de Na_2O/SiO_2=0.40, SiO_2/Al_2O_3=3.21, H_2O/Na_2O=10, Na_2O/Al_2O_3 = 1.28. Los productos obtenidos han sido caracterizados, Se han realizado ensayos de resistencia mecánica y prosimetría de mercurio, así como análisis a través de difracción de Rayos X, espectroscopía IR y ATD-TG. Los resultados obtenidos muestran la influencia que tiene la mezcla de las materias primas a las primeras edades (dentro de la primera hora) en el proceso de síntesis de geopolímero.

INTRODUCTION

Cements other than portland cement are under study in order to increase the range of the cementing systems available.

Silicate cements based on metakaolin were described for the first time by Davidovits (1,2). These products, named geopolymers, have the general formula:

$$M_n\ [-(Si-O_2)_z-Al-O]_n\ .wH_2O$$

where z is 1, 2 or 3, and n is the degree of polymerization. Similar patterns have been proposed for the formation of zeolites and zeolite precursors (3), in which Al and Si, initially available for solution, react with each other to form polyhydroxyaluminosilicate complexes. No doubt, a certain resemblance seems to exist with regard to the formation of zeolites and geopolymers; both processes require reactive precursor materials and, besides the concentrations of the reagents (especially of OH^-) are often critical, as are the time and the temperature conditions of curing. However, differences between both products are also clear; zeolites are crystalline products and their synthesis is often aimed at producing loose, free flowing powders (4), while geopolymers appear to be amorphous on X-ray diffraction and form massive-dimensionally stable compacts.

In this study, the investigation has concentrated on one of the parameters which in a previous work (5) was demonstrated to influence some of the characteristics of the geopolymers; this is the order of addition of the raw materials to the reaction mixture. Two different pathways for obtaining the geopolymers have been considered, and the products so obtained studied.

EXPERIMENTAL

Materials

The materials used in the synthesis processes have been: sodium hydroxide (Merck), sodium silicate (Probus) and metakaolin obtained from kaolin supplied by CAOBAR S.A. (Guadalajara - Spain). The kaolin was activated by treatment at 750ºC for 24 hours.

Analytical data for these materials are given in Table I.

TABLE I

CHEMICAL COMPOSITION OF THE STARTING MATERIALS

COMPONENT (wt %)	SODIUM SILICATE	METAKAOLIN
SiO_2	30.32	55.50
Al_2O_3	-	42.38
Na_2O	11.05	0.02
H_2O	58.47	*
CAO	-	0.92
Fe_2O_3	-	0.70
SO_3	-	-
MgO	-	0.39

* Weight loss of kaolin precursor is 12.98% to 750ºC in air

Methodology of the preparation of geopolymer mortars

Two methods were studied:

A) 1.- 47.3 g of NaOH (pellets) + 80 ml H_2O (stirring during 2 minutes).

2.- 180 g of metakaolin + alkaline solution (15 minutes in a mixer).

3.- Addition of 142.6 g of sodium silicate to the mixer (15 minutes of mixing).

4.- Addition of 1350 g of sand to the mixer (10 minutes of mixing). A geopolymer paste:sand ratio of 1:3 was fixed.

5.- Moulding.

6.- Curing at 80ºC (specimens cured for 1 hour, 4 hour and 24 hours were prepared).

B) 1.- 47.3 g of NaOH (pellets) + 80 ml H_2O (stirring during 2 minutes)

2.- Mixing of alkaline solution with 142.6 g of sodium silicate (stirring during 5 minutes).

3.- 180 g of metakaolin + alkaline liquid (25 minutes in a mixer).

4.- Addition of 1350 g of sand to the mixer (10 minutes mixing).

5.- Moulding.

6.- Curing at 80ºC (specimens cured for 1, 4 and 24 hours were prepared).

Evaluation of physical and mechanical characteristics

The pore size distribution (Hg porosimetry) of the pure geopolymer has been determined. The obtainment of a pure geopolymer involves the elimination of the 4th step in the synthesis methodology.
A mechanical study of the geopolymer mortars has also been carried out:
* Compressive strength on cylinders of 3 cm diameter
* Flexural strength on a prism of 1x1x6 cm.

Chemical Characterization

X-ray Diffraction, IR Spectroscopy and DTA analyses have been used in order to make structural comparison between the geopolymers obtained through the two pathways tested.

RESULTS AND DISCUSSION

Tables II and III, as well as figures 1,2,3,4 and 5, show the results obtained with the geopolymers after subjecting them to the physical and mechanical tests and to the chemical characterization.

TABLE II

MECHANICAL STRENGTHS OF MORTAR GEOPOLYMER

	TIME OF CURING AT 80ºC (HOURS)	METHOD A	METHOD B
COMPRESSIVE STRENGTHS (MPA)	1 4 24	50.38 73.87 87.93	38.93 57.79 67.03
FLEXURAL STRENGTHS (MPA)	1 4 24	10.18 10.84 12.18	8.60 10.69 12.94

TABLE III

Hg – POROSIMETRY OF PURE GEOPOLYMERS

GEOPOLIMER OBTAINED THROUGH	TOTAL INTRUSION VOLUME (ml/gr)	TOTAL PORE AREA (m^2/gr)	MEDIAN PORE DIAMETER (VOLUME) (μm)	MEDIAN PORE DIAMETER (AREA) (μm)	AVERAGE PORE DIAMETER (4V/A) (μm)	BULK DENSITY (gr/ml)	APPARENT DENSITY (gr/ml)	STEM VOLUME USED (%)
Method A 1 h cured	0.2216	32.791	0.0289	0.0230	0.0270	1.5766	2.4230	30
Method A 4 h cured	0.2657	36.126	0.0306	0.0256	0.0294	1.3008	1.9877	121
Method A 24h cured	0.2676	26.962	0.0476	0.0373	0.0397	1.2898	1.9697	35
Method B 1h cured	0.2573	38.945	0.0273	0.0247	0.0264	1.3830	2.1468	44
Method B 4 h cured	0.2182	31.272	0.0285	0.0258	0.0279	1.3113	1.8369	35
Method B 24h cured	0.1928	22.839	0.0401	0.0323	0.0338	1.3556	1.8354	26

Physical and Mechanical Data

From the mechanical point of view, the strength values in Table II show the potential of geopolymers as a material to be used with structural purposes.

Samples obtained by method A develop (after 1 hour of curing) higher compressive strengths (about 22% higher) than the specimens prepared by method B (see Table II). However, the evolution of the strengths at longer ages is quite similar for both methods. From the results, it can be concluded that the reaction of formation of a geopolymer is initially faster by method A than by method B. This reaction rate is similar for both methods at longer ages.

Whit regard to the porosity of the geopolymers, it can be deduced from Table III that for those specimens tested at early curing ages, there is a correlation between the total porosity of the products, or their average pore diameters, and their mechanical strengths. In fact, the geopolymers having the highest compressive strengths (method A, 1 h curing), are also those with the lowest total porosity and the lowest average pore diameter. However, at longer curing times, there is not a satisfactory agreement between the porosity data and the mortar strengths. This may be due to the fact that porosity measurements were conducted on pure geopolymer prisms and the presence of some crystalline products was detected in some of those prisms. That - probably accidental - crystallization could be the reason for the porosity data increasing with time (see Table III). Anyway, this is a point which requires to be clarified in future investigations.

Chemical Characterization

It can be seen through X-ray diffraction that the only solid raw starting material (metakaolin) and the final reaction product (geopolymer) are both amorphous solids with a low content of crystalline SiO_2 (quartz). However, IR spectroscopy provides a useful method for following changes occurring during reaction. So, in figure 1(a), the metakaolín IR spectrum is shown: the bands at 1080 and 460 cm^{-1} are Si-O vibrations, while the Al-O vibrational band has shifted to 800 cm^{-1}. This band is characteristic of tetrahedrally coordinated Al.

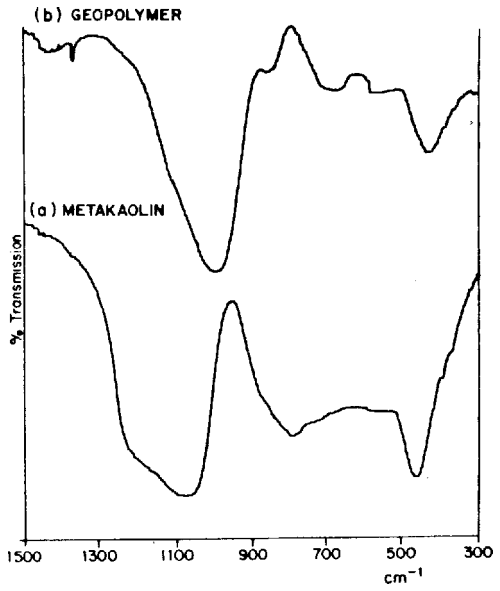

Fig. 1

IR spectra metakaolin (a) and pure geopolymer (method A, 4 hours) (b)

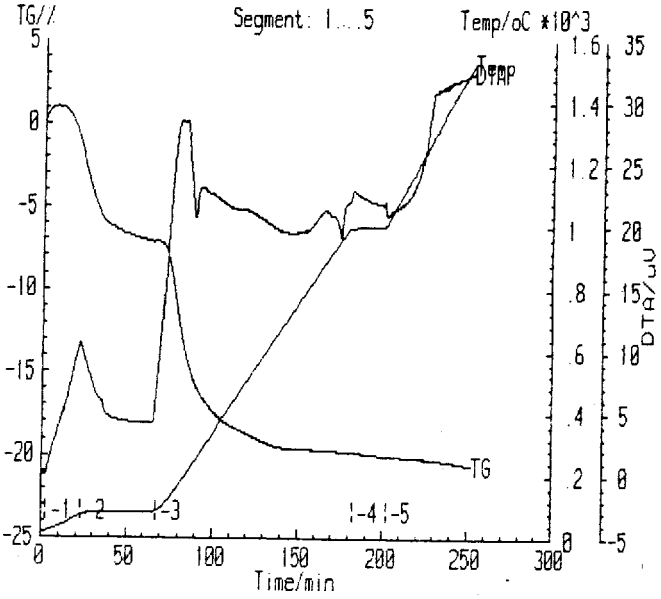

Fig. 2

DTA and TG curves of the geopolimer obtained through method A and 4 hours of curing regime

The geopolymer IR spectrum is quite different (see figure 1 (b)): The Si-O vibrational bands have moved to lower frequencies (1000 and 440 cm^{-1}), and in this spectrum the bands due to Al-O vibrations are located at 850 and 700 cm^{-1}. More details about the IR study of the formation reaction of the geopolymers were given in (5). The important aspect which should now be emphasized is that all the geopolymers obtained in the present work have an IR spectrum identical to that shown in figure 1(b).

Differential Thermal Analyses (DTA) were carried out in samples obtained through each method. Figure 2 is an example of the DTA and TG curves of these materials (there are no differences between the DTA and the TG results of the total samples tested). In the DTA curve of figure 2, some peaks are observed. The first two at 80ºC and 160ºC are endothermic and respectively due to a loss of water in the sample (adsorbed water in the first peak and constitutional water in the second). This loss of water can be quantified in about 15% wt of the sample. There are no more weight variations with increasing temperature.

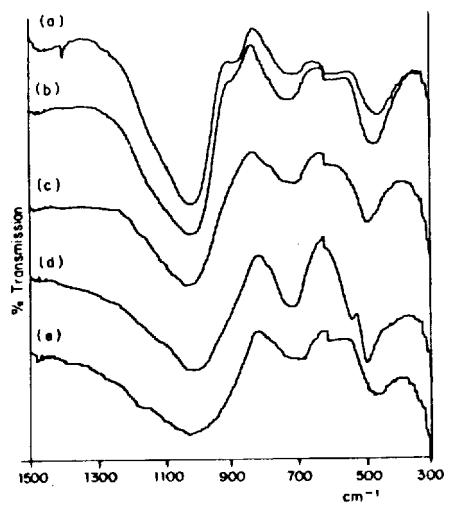

Fig. 3

IR spectra of geopolymer (method A, 4 h) heated at 200ºC (b), at 750ºC (c), at 1050ºC (d), 1400ºC (e) and geopolymer (method A, 4 h)

Other signals are observed in the DTA curve : one broad and small endothermic peak at about 900ºC and an almost vertical variation of the base line at 1300ºC. The peak at 900ºC has been assigned to a chemical transformation (nepheline formation) and the signal at 1300ºC to the melting of the sample.

The IR spectra of geopolymers quenched at 200º, 750º, 1050º and 1400ºC (figure 3 (b), (c), (d) and (e) respectively) and the X-ray diffraction patterns of the same samples (figures 4 and 5) confirm such a hypothesis. A detailed observation of these IR spectra can show the evolution of the geopolymer with temperature. The band at 870 cm^{-1} begins to change at 200ºC and has completely disappeared at 750ºC. At 1050ºC and 1400ºC this band does not appear in the spectra. Simultaneously, the band at 450 cm^{-1} starts moving towards lower frequencies, changing its profile at 200ºC, and it does constantly so as temperature increases. At 1050º, that band is small and sharp and located at 475 cm^{-1}. In the IR spectrum of the geopolymer quenched at this temperature, the development of a new band at 515-520 cm^{-1} can be observed. The band at 1000 cm^{-1}, corresponding to Si-O vibrations moves towards lower frequencies as the

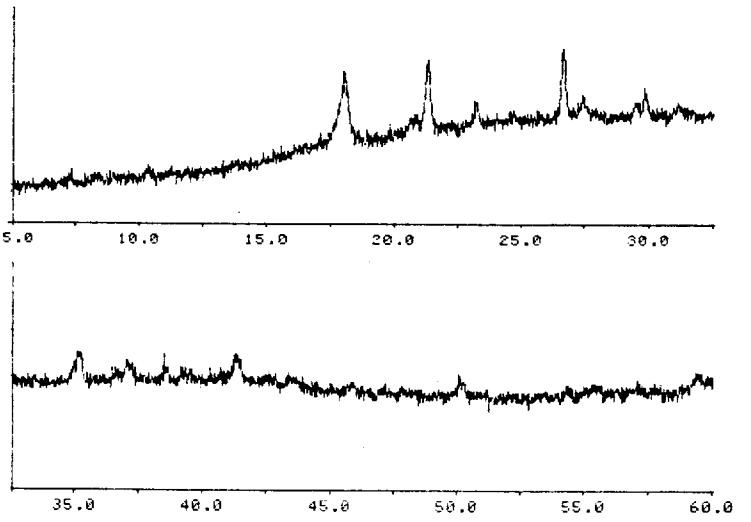

Fig. 4

X-Ray diffraction pattern of geopolymer A 4 h after 30' a 750ºC

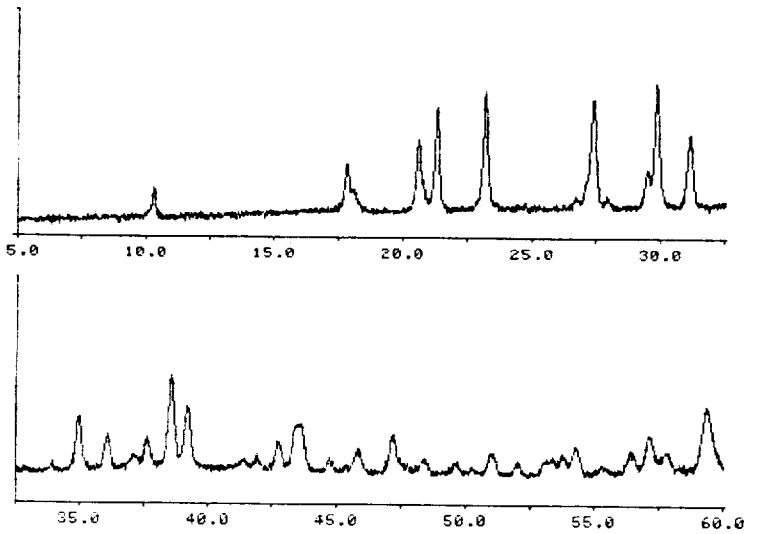

Fig. 5

X-Ray diffraction pattern of geopolymer A 4 h after 30' a 1050ºC

treatment temperature of the material increases. These alterations of the spectra (displacement of the bands at 450 and 1000 cm^{-1}), together with the development of another at 515 cm^{-1}, may be useful to confirm the presence of nepheline.

Generally speaking, it can be said that the geopolymers, independently of the synthesis pathways followed in the above mentioned experiments and also of the curing conditions, undergo a transformation with temperature which involves a microstructural rearrangement upon losing constitutional water, in the first place, and upon producing crystalline nepheline ($NaAlSiO_4$) in the second place. While nepheline has completely crystallized at 1050ºC (see figure 5), the first nepheline traces were found at 750ºC (see figure 4). At the highest temperature, 1300ºC a molten phase is produced.

CONCLUSIONS

The following conclusions can be drawn from this study:

1.- Compressive mechanical strengths at early curing times (1 hour) are higher in geopolymers obtained by method A than in those obtained by method B. There is not such a marked difference between the evolution of compressive strengths of the materials obtained by each of these methods at longer curing times.

2.- From the microstructural point of view, the x-ray diffraction patterns, as well as the IR spectra of the samples, seem to show that both methods, A and B, for obtaining geopolymers, do not lead to different materials.

3.- The evolution of geopolymers with temperature can be considered to have three stages:

a) losing of constitutional water at about 150ºC.

b) Transformation in nepheline at about 900ºC.

c) Melting at about 1300ºC.

ACKNOWLEDGEMENT

The authors wish to thank the "Comunidad de Madrid" for the financial support given to project C115/91.

REFERENCES

1.- Davidovits, J. "Mineral Polymer and Methods of Making them". U.S. Patent 4349386 (Sep. 1982).

2.- Davidovits, J. "Early High Strength Mineral Polymers". U.S. patent 45009985 (April 1985).

3.- Madani, A; Aznar, A.; Sanz, J and Serratosa, J.M. J. Phys. Chem. 94, 760-765 (1990).

4.- Drszaz, B.; Hocevar, S. and Pejovnik, S. "Zeolites: Synthesis, Structure, Technology and Applications". Elsevier (Amsterdam) (1985).

5.- Palomo, A and Glasser, F.P. Br. Ceram. Trans and Jour. (Submitted for publication)(1991).

STRENGTH PROPERTIES OF EPOXY-MODIFIED MORTARS WITHOUT HARDENER

Y Ohama*, K Demura* and T Endo**

**College of Engineering, Nihon University, Koriyama, Fakushima-ken, JAPAN*
***Onoda Autoclaved Lightweight Concrete Co., Ltd., Owariasahi, Aichi-ken, JAPAN*

SUMMARY

In the production of conventional epoxy-modified mortars, the use of any hardener is indispensable for the cure of epoxy resin. The authors have drawn attention to the fact that the epoxy resin can harden in the presence of alkalis, and successfully developed epoxy-modified mortars without any hardener. As a result, the disadvantages of the two-component mixing of the epoxy resin and hardener have been overcome. The epoxy-modified mortars without any hardener are prepared with various polymer-cement ratios, and tested for strength and adhesion. For comparison, the epoxy-modified mortars with a hardener are also prepared, and tested in the same manner. From the test results, polymer-cement ratios of 5 to 10% are recommended for the purpose of improving the strength and adhesion of cement mortars by modifying with the epoxy resin excluding the hardener.

要　約

従来のエポキシ樹脂混入ポリマーセメントモルタルの製造においては，硬化剤の使用がエポキシ樹脂の硬化のために不可欠である。著者らは，エポキシ樹脂がアルカリの存在下で硬化する事実に着目し，硬化剤を用いないエポキシ樹脂混入ポリマーセメントモルタルの開発に成功している。その結果，エポキシ樹脂と硬化剤の二成分混合の欠点が克服された。本研究では，硬化剤無添加エポキシ樹脂混入ポリマーセメントモルタルを各種ポリマーセメント比で調製し，強さ及び接着強さを試験している。又，比較のために，硬化剤添加エポキシ樹脂ポリマーセメントモルタルも調製し，同様に試験している。その試験結果からは，ポリマーセメント比5から10%が，硬化剤無添加エポキシ樹脂ポリマーセメントモルタルの強さ及び接着強さの改善のために推奨される。

INTRODUCTION

Epoxy resin has superior properties such as high adhesion and chemical resistance, and has widely been used as adhesives and corrosion-resistant paints in the construction industry in the world. Incorporation of the epoxy resin into cement mortar can be expected to impart its superior properties to the mortar. In the preparation of conventional epoxy-modified mortars, the use of any hardener is indispensable for the cure of the epoxy resin(1). The authors have drawn attention to the fact that the epoxy resin can harden in the presence of alkalis(2,3), and successfully developed epoxy-modified mortars without any hardener. As a result, the disadvantages of the two-component mixing of the epoxy resin and hardener have been overcome. The epoxy-modified mortars without any hardener are prepared with various polymer-cement ratios, and tested for strength and adhesion. For comparison, the epoxy-modified mortars with a hardener are prepared, and tested in the same manner.

MATERIALS

Cement and Aggregate

Ordinary portland cement and Toyoura standard sand specified in JIS (Japanese Industrial Standard) were used for all the mortar mixes.

Epoxy Resin and Hardener

A diglycidyl ether of bisphenol A was used as an epoxy resin, and a modified aliphatic amine as a hardener. The properties of the epoxy resin are indicated in Table 1. The constitutional formula of the epoxy resin is expressed below.

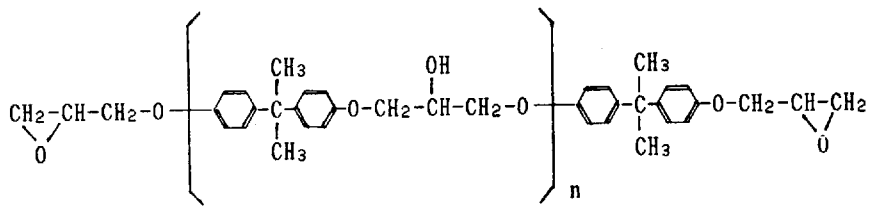

n=0.1-0.2

Table 1 Properties of Epoxy Resin.

Epoxide Equivalent	Molecular Weight	Hue (Gardner)	Specific Gravity (20°C)	Viscosity (cP, 20°C)	Flash Point (°C)
184～194	380	≦0.6	1.17	45000	>150

TESTING PROCEDURES

Preparation of Specimens

According to JIS A 1171 (Method of Making Test Sample of Polymer-Modified Mortar in the Laboratory), mortars were mixed with the mix proportions given in Table 2, and their flow was adjusted to be constant at 170±5. Beam specimens 40x40x160mm were molded, and then subjected to a 2-day-20°C-80%R.H.-moist plus 5-day-20°C-water plus 21-day-20°C-50%R.H.-dry cure.

Mortar substrates and specimens for adhesion test were prepared as follows ; According to JIS R 5201 (Physical Testing Methods for Cement), ordinary cement mortar was mixed with a ratio of cement to standard sand 1:2 and a water-cement ratio of 65.0%. Mortar substrates 70x70x20mm were molded, and then subjected to a 1-day-20°C-80%R.H.-moist plus 6-day-20°C-water plus 7-day-20°C-80%R.H.-moist cure. Then the bonding surfaces of the mortar substrates were treated with abrasive papers. The cured mortar substrates were bonded in a size of 40x40x10mm as shown in Fig.1 by the mortars mixed with the mix proportions given in Table 2, and then given a 2-day-20°C-80%R.H.-moist plus 5-day-20°C-water plus 21-day-20°C-50%R.H.-dry cure.

Table 2 Mix Proportions of Epoxy-Modified Mortars.

Cement: Sand (By Weight)	Polymer-Cement Ratio(%)	Hardener Content* (wt%)	Water-Cement Ratio (%)	Flow
1 : 3	0	0	75.5	170
	1	0	75.5	168
	3		75.5	173
	5		75.5	170
	10		75.5	172
	20		75.5	171
	40		75.5	172
	60		75.5	171
	80		75.5	173
	1	65	68.0	168
	5		68.0	169
	10		70.0	166
	40		80.5	170
	80		80.5	170

Note, * : Hardener Content (wt%)=(Hardener/Epoxy Resin)x100

Strength Test

Beam specimens were tested for flexural and compressive strengths in accordance with JIS A 1172 (Method of Test for Strength of Polymer-Modified Mortar).

Adhesion Test

As shown in Fig.1, bonded specimens were tested for adhesion in tension in accordance with JIS A 6915 (Wall Coatings for Thick Textured Finishes) by using the Instron universal testing machine.

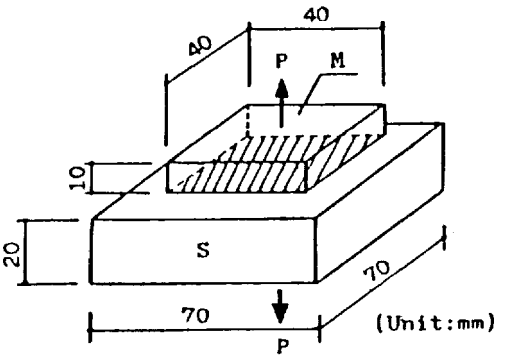

P : Load
S : Mortar substrate
M : Bonded mortar
▨ : Bonding joint

Fig. 1 Specimen for Adhesion Test.

TEST RESULTS AND DISCUSSION

Figs.2 and 3 represent the flexural and compressive strengths of epoxy-modified mortars without and with a hardener. The flexural and compressive strengths of the epoxy-modified mortars without the hardener increase with raising polymer-cement ratio, and reach the maximums at a polymer-cement ratio of 10%. By contrast, the flexural and compressive strengths of the epoxy-modified mortars with the hardener decrease with an increase in the polymer-cement ratio, and attain the minimums at a polymer-cement ratio of 1%. The maximum flexural and compressive strengths of the epoxy-modified mortars without the hardener are about 1.7 and 1.3 times respectively, the strengths of unmodified mortar. They are considerably higher than the strengths of the epoxy-modified mortars with the hardener at the same polymer-cement ratio. Furthermore, the maximum flexural strength of the epoxy-modified mortars without the hardener is much the same as that with the hardener at a polymer-cement ratio of 80%. Likewise, the maximum compressive strength of the epoxy-modified mortars without the hardener is about the same as that with the hardener at a polymer-cement ratio of 40%. In the preparation of conventional epoxy-

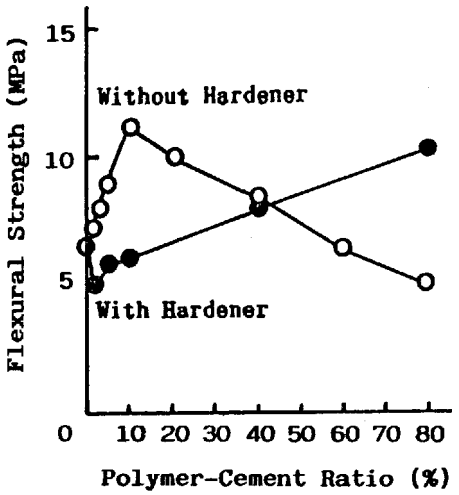

Fig.2 Polymer-Cement Ratio vs. Flexural Strength of Epoxy-Modified Mortars without and with Hardener.

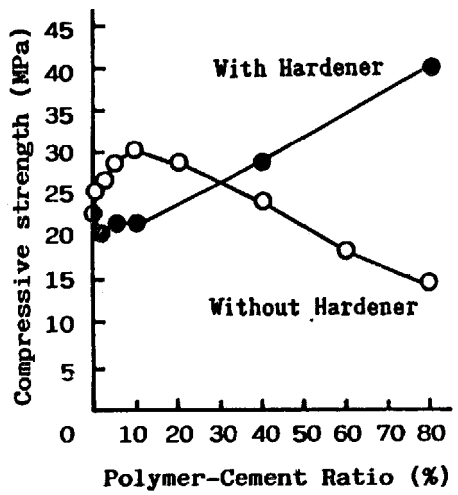

Fig.3 Polymer-Cement Ratio vs. Compressive Strength of Epoxy-Modified Mortars without and with Hardener.

modified mortars, the use of any hardener is generally indispensable for the cure of epoxy resin. However, in this study, the flexural and compressive strengths of the epoxy-modified mortars without the hardener at polymer-cement ratios of 40% or less are higher than those of the unmodified mortar. Therefore, it is considered that the epoxy resin can harden in the presence of the alkalis in the mortars. The hardening reaction between the epoxy resin and alkalis [e.g., $Ca(OH)_2$] is expressed as follows :

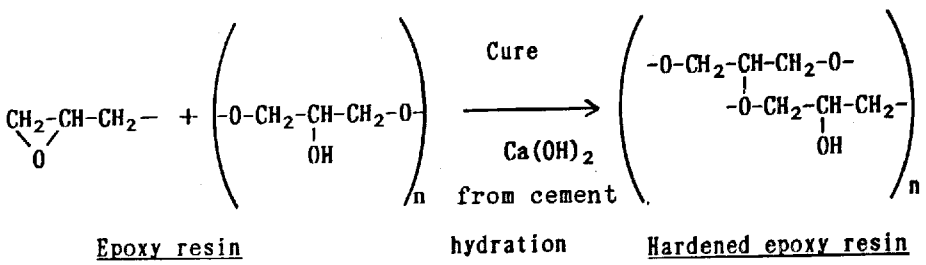

Photo 1 shows a hardened epoxy resin in the epoxy-modified mortars without the hardener at a polymer-cement ratio of 10%. Reductions in the flexural and compressive strengths of the epoxy-modified mortars without the hardener at polymer-cement ratios of 20% or more may be explained to be due to the presence of a considerable amount of the epoxy resin which can not harden in the epoxy-modified mortars without the hardener.

Fig.4 exhibits the adhesion in tension of epoxy-modified mortars without a hardener to ordinary cement mortar. The adhesion in tension of the epoxy-modified mortars without the hardener to ordinary cement mortar increases with raising polymer-cement ratio, and reaches the maximum at a polymer-cement ratio of 5%. The maximum adhesion in tension is about 1.5 times the adhesion of unmodified mortar. A marked decrease in the adhesion in tension of the epoxy-modified mortars without the hardener to ordinary cement mortar at polymer-cement ratios of 20% or more may be attributed to the same reason as stated on the strength reductions. The failure modes of the epoxy-modified mortars without the hardener to ordinary cement mortar were the mixed failures which are the combination of the cohesive failures in the epoxy-modified mortars and the adhesive failures.

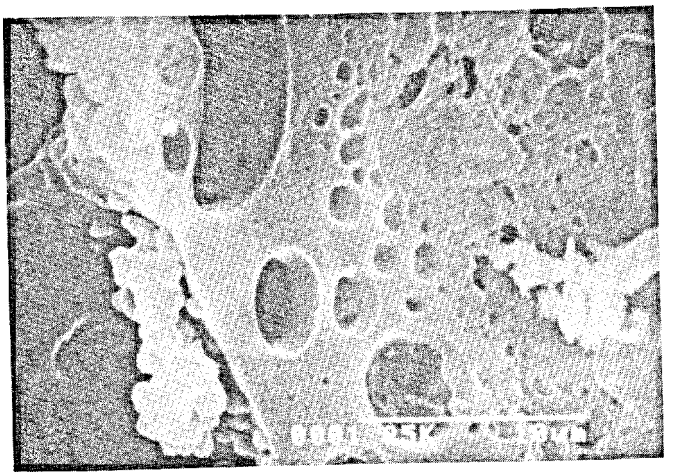

Photo 1 Electron Micrograph of Epoxy-Modified Mortar without Hardener at Polymer-Cement Ratio of 10% (x4000).

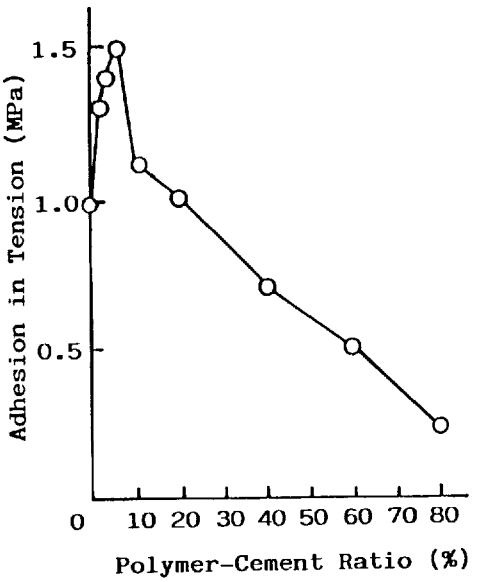

Fig.4 Polymer-Cement Ratio vs. Adhesion in Tension of Epoxy-Modified Mortars without Hardener.

CONCLUSIONS

From the test results, the following conclusions can be summarized :

(1) The flexural and compressive strengths of epoxy-modified mortars without a hardener reach the maximums at a polymer-cement ratio of 10%. The maximum flexural and compressive strengths are about 1.7 and 1.3 times respectively, the strengths of unmodified mortar. They are considerably higher than the strengths of the epoxy-modified mortars with the hardener at the same polymer-cement ratio.

(2) The adhesion of epoxy-modified mortars without a hardener to ordinary cement mortar attains the maximum at a polymer-cement ratio of 5%. The maximum adhesion is about 1.5 times the adhesion of unmodified mortar.

(3) From the strength and adhesion test results, it is concluded that polymer-cement ratios of 5 to 10% could be recommended to improve the strength and adhesion of cement mortar by modification with epoxy resin without any hardener.

REFERENCES

1. Ohama, Y., Demura, K. and Ogi, T.:"Mix Proportioning and Properties of Epoxy-Modified Mortars", **Brittle Matrix Composites 2**, Elsevier Applied Science, London, 1989, p 516-525.
2. Butt, Yu.M., Topil'skii, G.V., Mikul'skii, V.G., Kozlov, V.V., and Gorban', A.K.: "Issledovanie Vzaimodeistviya Epoksidnogo Polimera s Portlandtsementami (in Russian)", Izvestiya Vuzov Stroitel'stovo i Arkhitektura, 14(1), 1971, 75-80.
3. Kakiuchi, H.: **New Epoxy Resins (in Japanese)**, Shokodo, Tokyo, May 1985, p140-141.

SEVERAL ASPECTS CONCERNING MODIFICATION OF CEMENT COMPOSITIONS BY POLYMER AGENTS

L J Lavrega

Byelorussian Polytechnical Academy, Minsk,
Republic of BELARUS

SUMMARY

Structure formation in some polymer-cement compositions was studied with regard to porosity variations, as well as X-ray, thermografic and electron-microscopic analyses. Physico-mechanical properties of compositions, their water- and corrosion resistance were studied in parallel.

Efficiency of modofication of cement compositions by polymer agents may be achieved subject to the following conditions: technologies for preparation of mixtures and for decreasing quantity of polymer admixtures shall be separated. This may be proved by examples illustrating cynetics of hardening of modified cements, their microstructural and physico-mechanical properties.

РЕЗЮМЕ

Формирование структуры некоторых полимерцементных композиций изучалось по изменению пористости, а также при помощи рентгеноструктурного, термографического и электронномикроскопического анализа. Параллельно изучались физико-механические свойства композиций, их водо- и коррозионная стойкость.

Эффективность модификации цементных композиций полимерными добавками достигается при соблюдении двух условий: раздельной технологии приготовления смесей и уменьшения количества полимерной добавки до разумного минимума. Это подтверждается приведенными данными кинетики твердения модифицированных цементов, их микроструктурными характеристиками и физико-механическими свойствами.

INTRODUCTION

Modifying cement compositions by various polymer admixtures in view of applying a number of valuable properties to materials and structures has become the most commonly used practice in construction. For example, when arranging floors and pavements, addition of polymer emulsions into cement compositions may increase their wear resistance and impact strength, in comparison with concrete floors by factor of 1.5 to 20, raise up water- and corrosion resistance, eliminate dust formation, etc.
The similar effect may be achieved using polymer-cement compositions in water-proof mortars, roofing, cladding and white-washing (1). Modifiers such as co-polymers of butadiene/styrene, butadiene/metacryl acid, butadiene/vinulpyridine and other monomers, polyvinylacetate and polyethylene dispersions, epoxy-, carbamido-formaldehyde-, phenol- and other water-soluble polymers have found a widespread application in construction works.

Successful application of this or that modifier depends on many factors, and neglection of at least one of these factors may reduce the expected effect to zero. Among the above factors we may highlight the following ones: quantity of modifier, technology of modification (type of addition, sequence, activation processes), availability of various stabilizing and surface-active accompanying agents, technological process (pressing, centrifuging, casting, vibrating, guniting), technological modes of hardening and expedient maintenance conditions. For instance, polyvinylacetatecement plasters and coatings are effective for indoor dry structures. If similar stuccos are used for outdoor structures, within the period of 0.5 - 1 year break-downs and cracks start to appear.

EXPERIMENTAL

Studying interaction of the two different materials - mineral binder and polymer modifier in complex multicomponent system - is a very actual problem. This may be quite understood since determination of the nature of running processes in these systems and parameters of the hardened compositions allows an optimum of components and technologies to be revealed. Thus we may ensure determination of maximum and moreover, the required properties of polymer-cement compositions in the required maintenance conditions.

We studied structure formation and properties of polymer-cement compositions containing butadienestyrene latexes in combination with surface-active substances of non-ionogenic type and salts-electrolytes. Acid carbonates were used as the latter salts. Medium-aluminate cements from Byelorussian plants served as mineral components. One of the most important factors of the hardened compositions is the character of their porosity and porous structurewhich were studied in complex with X-rayographic, thermographic and electron-microscope analyses. The investigations were conducted by Dr. Yambor's method (Slovakian Academy of Sciences) /3/.

Quantity of the added polymer agents was varied from 0 to Max. The investigations were carried out using high-pressure mercury porosimeter (type 70H, Carlo Erba, Milan).

Quantity of water in samples was varied so that mobility of the cement-polymer-water system should correspond to normal thickness, (K_{Hr} = const).

RESULTS AND DISCUSSIONS

Analysis of the results showed that as quantity of polymer agent increased, general porosity of the system rose up and consequently its strength decreased (Fig. 1).

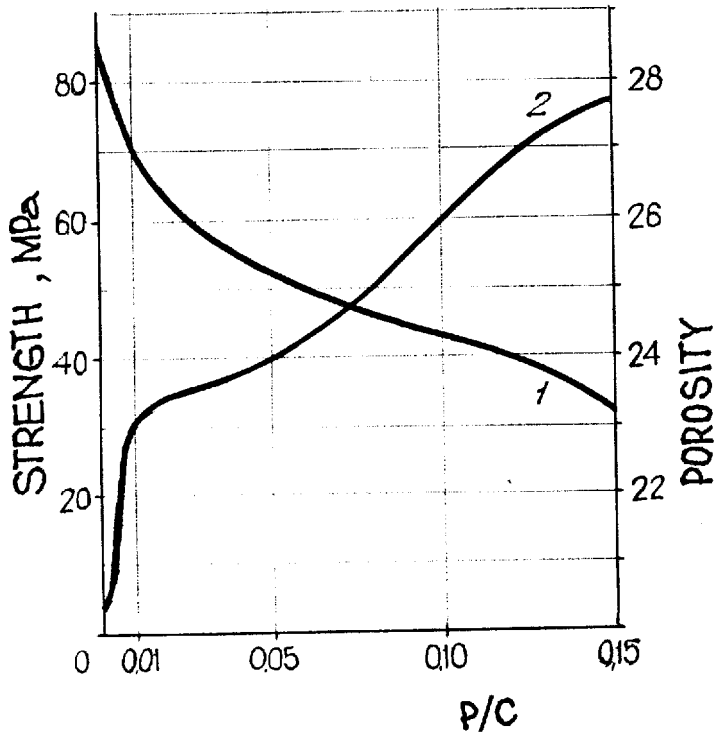

Fig. 1. Change in strength (1) and porosity (2) of polymer-cement systems as a function of polymer-cement ratio.

Volumetric mass of samples decreased from 2.364 to 1.921 g/cm^3. Study of the porous structure revealed availability of the following main dimensions of pores:

a) micropores of 3.7 to 7500 nm radius;
b) macropores of 7.5 to 600 μm radius;
c) macropores of > 0.6 mm radius.

Pores of a) and b) groups were determined directly using the mercury porosimeter, and macropores were calculated.

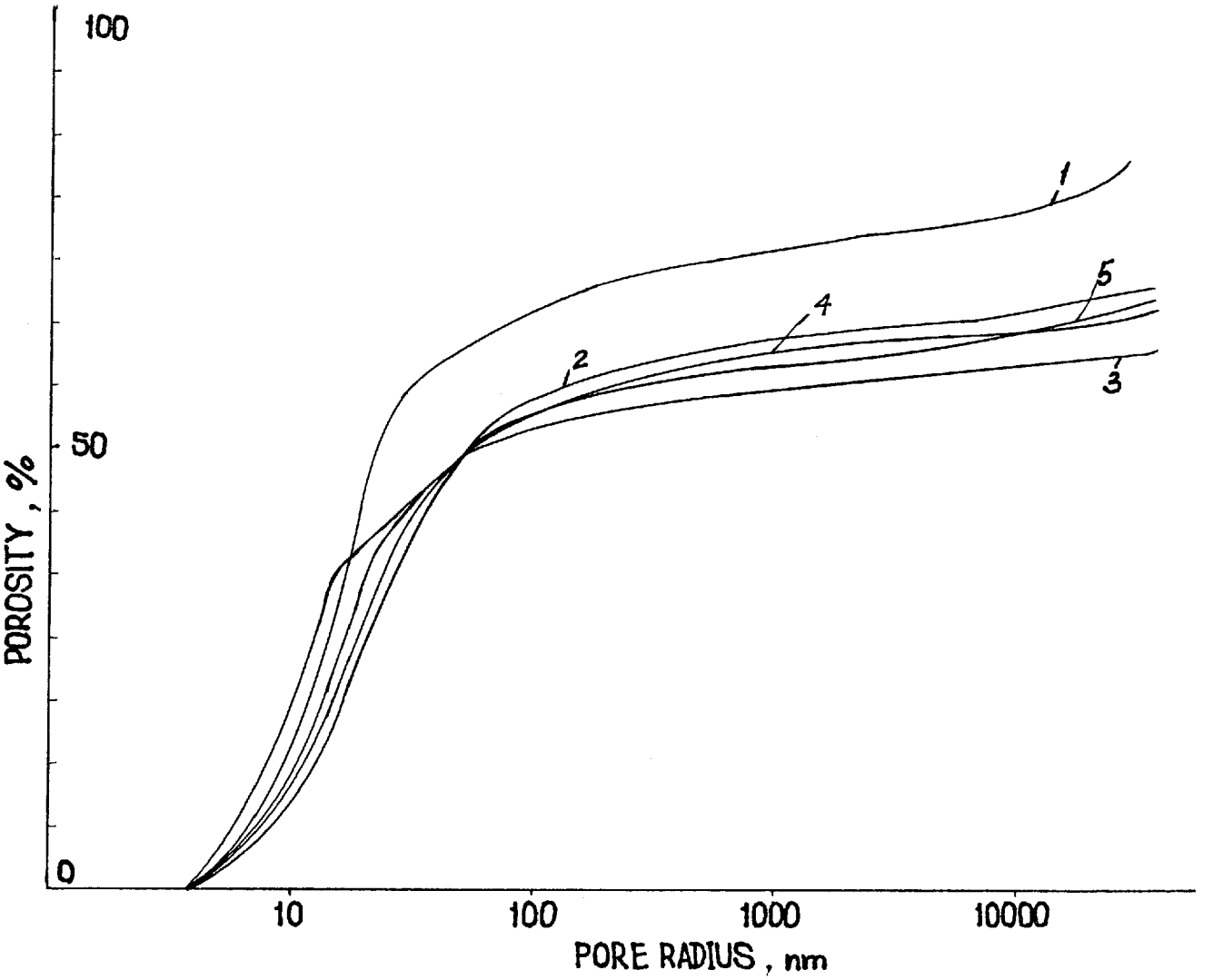

Fig. 2. Curve of micropores' arrangement in polymer-cement systems: 1 - without admixture; 2 - polymer-cement (P/C) = 0.01; 3 - P/C = 0.05; 4 - P/C = 0.10; 5 - P/C = 0.15.

According to (2), pores of $\leqslant$ 1 μm radius belong to hydrational category, and depend on type and total volume of hydrational newformations in the system. The remaining pores of $>$ 1 μm form a group of technological pores which reflect technological factors of structure formation. Volume of micropores of $\leqslant$ 7500 nm radius varies from 9.4 to 14.7%, and it is characteristic that samples without agents have minimum quantity of these pores inasmuch as samples containing small quantity of agent (P/C = 0.01) have maximum quantity. In systems where quantity of agent varies from P/C = 0.05 to P/C = 0.15, the volume of these pores remains practically stable. However, there is one more interesting pattern: as median of micropores' radius in "cement-water" systems decreases while strength increases (formation of structu-

re intensifies), the same median in "cement-polymer-water" systems decreases while content of P/C increases and strength decreases. Thus, in this case the character of pores is subject to a strong adjustment by polymer component.

Volume of micropores of 7.5 to 600 μm radius and, particularly, those of 650 μm radius tends to increase (from 11.1 to 15.1%) as content of P/C increases. However, similar to other cases, with minimum P/C content, the volume of these pores is considerably lower than in all other samples, including those without modifiers.

Value of porosity and porous structure are in a well-known connection with the character and volume of hydrational new formations. Complex thermal analysis (Table 1) of test samples allows estimation (provided there is a slight error in factor related to the burn-out of polymer component) that losses at burning within temperature intervals of 100-450°C correspond to the relative volume of hydration products being formed.

Table 1

Properties	Value with P/C composition 1, 0.0	2, 0.01	3, 0.05	4, 0.10	5 0.15
Moisture up to 100°C, %	1.1	1.1	0.8	1.0	1.2
Losses at calcination (100-450°C), %	6.1	5.7	5.9	7.3	9.1
Losses at calcination (450-600°C), %	0.5	0.4	1.8	1.9	3.2
Losses at calcination (600-1000°C), %	6.0	6.8	7.8	8.4	8.7
Total losses at calcination up to 1000°C, %	13.7	14.0	16.4	18.6	22.2

X-ray-diffractional phase analysis showed an increase in quantity of clincker minerals, $Ca(OH)_2$ and crystallizationally imperfect hydration products type CSH1 - CSH2 in all the samples. Presence of a weak line of 0.514 nm indicates availability in some samples of an aluminate phase of C_3AH6. Comparing maximums of intensity of C_3S line with interplane distance d=0.2195 nm and maximums of intensity of Ca(OH) line with interplane distance d=0.1928 nm allows estimation of relative content of C_3S and $Ca(OH)_2$, and consequently of obtained hydration rate of the test P/C compositions.

The above data show that the least hydration value is observed in

composition N°3 where content of C_3S is about 25%. As for other samples, hydration value there is approximately invaried and the content of C_3S is 20%. Calculating these results in terms of volumetric mass shows that as porosity and P/C-ratio of compositions increases, the volume of the binding phase decreases.

Thus, increasing quantity of the polymer modifier may give rise to porosity (mainly due to macroporosity), decrease volume of the binder and reduce strength. However, the character of microporosity allows a conclusion that the polymer modifier may enhance properties of compositions provided an optimum quantity of the agent has been added.

Table 2

Results of the Diffractional/Phase Analysis

Composition N°	CpS lines of C_3S 0.2195 nm	CpS lines of $Ca(OH)_2$ 0.1928 nm
1	156	119
2	159	113
3	197	117
4	149	102
5	150	119

The given phenomena are closely connected not only with quantity of the polymer binder, but also technology for preparing P/C binder. Both our investigations and research work carried out by other authors (V.M.Hruiov, R.S.Iskhakov, S.A.Inozemtseva) /1/ showed that application of a two-stage technology for mixture preparation allows elimination of the main disadvantage of compositions with water-dispersed polymer, i.e. retardation of cement hydration processes and reduction of composition's strength. According to the technology proposed, the surface-active substance is to be mixed with the binder, and then a non-stabilized polymer emulsions added. Extra peptization of cement will take place, solution rate will increase, and thus, according to B.V.Ratinov /4/, crystallization processes will start earlier.

Accelerated hardening may be explained by the fact that research work revealed that surface-active substance may change the ratio between C_3A solution rates and crystallization hydrates to the benefit of the former.

Retardation rate of cement's hydration process with the polymer modifier (at P/C = 0.05) aged 1 day is 28%. Application of a separate technology allows reduction to 8%. This is proved by X-rayographic and differential-thermal analysis. Suitable minimization of the polymer modifier in combination with the separate technology allow compositions with stable corrosion resistance to be obtained (Table 3).

Table 3

Corrosion Resistance of Polymer/Cement Concretes

Properties		Value		
		test composition	P/C=0.03	
			separate technology	standard technology
1. Bending strength, MPa:				
- after steaming		3.7	5.0	4.0
- 28 days		4.74	6.06	5.46
- after curing in:				
aggressive media / water	7 days	3.4 / 3.8	4.98 / 5.55	3.88 / 4.2
	28 days	3.5 / 4.37	4.91 / 5.85	3.17 / 4.88
	60 days	3.5 / 4.75	5.5 / 6.97	3.68 / 4.44
	90 days	4.2 / 3.95	5.8 / 5.59	3.24 / 5.20
2. Absorption, %				
aggressive media / water	2 days	6.4 / 6.6	4.1 / 4.5	6.3 / 5.4
	7 days	6.8 / 7.6	3.8 / 4.3	5.8 / 5.9
	28 days	6.3 / 6.2	4.8 / 4.2	6.1 / 6.8
	60 days	8.6 / 10.3	4.7 / 4.9	7.5 / 7.3
	90 days	7.5 / 9.3	4.6 / 6.9	6.4 / 7.9

Corrosion-resistance durability of P/C compositions modified by butadiene-styrol latex was determined using beam-samples (4x4x16 cm) of 1:3 ratio according to change in mass, compression and bending strength while curing in water and aggressive media, concentration of SO_4", Cl" and NH_4' being 322, 1024 and 1470 mg/l accordingly.

Compositions were prepared using standard and separate technologies

and different P/C contents. Several properties are given in Table 3.

CONCLUSIONS

The investigations have opened to a certain extent the essence of a positive effect of the polymer modifier on concretes. As for disadvantages, such as retardation of hydration processes, lower strength and corrosion resistance with time, etc., they may be successfully avoided by decreasing quantity of the polymer agents to a suitable minimum, and applying an effective technology.

ACKNOWLEDGEMENTS

The author appreciates the help of Y.Jambor from the Slovak Academy of Sciences in carrying out experimental work and analysis of results. The paper is published with the permission of Rector of the Byelorussian Polytechnical Academy.

REFERENCES

1. Tcherkinski Yu.S., Lavrega L.Y.: "Polimery i tsementy v stroitelstve". Tiumen' , 1990, p.252.

2. Tcherkinski Yu.S.: "Polimertsementny beton". M.,Strojizdat, 1984, p.203.

3. Jambor Y.: "Porosita pórosá structúra a pevnost' cementovúch kompozitov." Stavebnicky casopis, 33, c.9, Veda, Bratislava, 1985, s.743-763.

EFFECTS OF ADDITION OF DIFFERENT QUANTITIES OF POLYMER DISPERSIONS ON HYDRATION OF PORTLAND CEMENT AND CHARACTERISTICS OF MORTAR

B Skenderović

Faculty of Civil Engineering, Subotica, YUGOSLAVIA

SUMMARY

The effects of different quantities (0,10,20,30%) of water dispersions of synthetic acrylates on the dynamics of hydration of Portland cement and the characteristics of mortar have been investigated.

At the beginning (2-3 days) synthetic acrylates slow down the process of hydration of Portland cement, but later, the hydration is faster in the presence of acrylates and after 90 days mortar has better bending and compressive strength than control mortar without acrylates. By adding dispersions of acrylates the adhesion of mortar to concrete is considerably increased, the porosity, water absorption and vapour-permeability are decreased. In presence of acrylates the shrinkage at drying of mortar is remarkably decreased, and the consequence of it is the smaller danger of micro-cracks in hardened mrotar (concrete).

INTRODUCTION

It is known that by adding water dispersions of synthetic polymers the bending strength and adhesion may be increased, and the porosity and water absorbing capacity of concrete and mortar decreased. However, some of our researches have shown that the presence of synthetic polymers slows down the process of hydration of Portland cement in the first 28 days. Therefore, we considered, that for better understanding of the effect of dispersion of synthetic polymers on the process of hydration of Portland cement, the dynamics of hydration and properties of mortar should be followed for a longer period.

EXPERIMENTAL

Prisms (4x4x16 cm) made of cement mortar (1:3) with addition of different quantities (0,10,20,30 %) of water dispersion of synthetic polymers (acrylate) were used for tests. Test prisms had been cured in water for 28 days, afterwards, they have been kept for 90 days in the air (about 20°C) in a laboratory or outdoor in variable atmosphere for 2 years. The changes of speed of supersonic vibrations pasing through, volume changes, strength (7,28,90 days), adhesion strength to concrete (28 days) were measured, and after 90 days, the porosity, water absorbing capacity, vapour-permeability of test mortars were also measured.

Shrinkage of test prisms has been measured by Graff-Kaufmann method, and the porosity by Hg-porosimeter (Erba 2000). Water absorbing capacity was determined by measurement of mass increase of test prisms in water during 24 hours.

EXPERIMENTAL RESULTS AND DISCUSSION

The results of our previous research have shown that mortars containing acrylate dispersions had lower pH and % of $Ca(OH)_2$ (Table 1),and smaller compressive strength (Table 2), than control mortars without acrylates after 28 days curing in water. From the results presented in Tables 1 and 2, can be concluded that the process of cement hydration in the presence

Table 1 Mechanical properties of test prisms

Disper.of acrylate %	Bending strength (MPa), after:		Compress strength (MPa) after:	
	7	28 days	7	28 days
0	6,68	8,49	38,1	44,5
10	7,95	9,19	40,0	42,1
20	9,33	10,48	34,7	37,5
30	11,87	11,02	32,4	33,7

Tabel 2 Chemical properties of mrotars

Disper.of acrylate %	% of $Ca(OH)_2$ 28 days	pH, after	
		7	28 days
0	4,70	12,36	12,61
10	-	12,35	12,60
20	1,07	12,35	12,60
30	-	12,30	12,56

of acrylates was a bit slower than in control mortar without acrylates. Cement hydration does not stop after 28 days and it is very interesting to find out what will be the action of different quantities of acrylates in mortar on dynamics of cement hydration at room temperature in laboratory conditions (till 90 days), and outdoor in the atmosphere with many changes of temperature nad humidity during the year and day.Cement hydration process had been controlled by the measurement of speed, the ultrasonic waves passed through test prisms (1,3,7,28,90 days), and by the measurement of bending and compressive strengths (7,28,90 days) of test prisms. The results of these measurements are presented in Fig. 1 and Table 3. Ultrasonic waves are moving faster in mortar with more solid phase produced as a result of cement hydration (CSH-gel). Therefore, bigger speed of ultrasonic waves through test mortars means better and faster hydration of cement. It is obvious from Fig. 1 that there was much slower hydration of cement in mortars with 20 ar 30% of added acrylate dispersion during three days, but in the period between 3 and 7 days cement hydration was faster in the presence of acrylates and as a result after 7 days we obtained almost the same quantity of solid material in all test mortars, or we can say, that we reached almost the same cement hydration level in all test mortars. This hydration level did not considerably change in the period between 7 and 28 days. It is interesting that small (10%) quantities of acrylate dispersion speeded up cement hydration in the beginning. After curing in water (from 28 to 90 days) test prisms were kept in dry air at room temperature, and as it is seen in Fig. 1 the process of cement hydration continued slowly. As a result of that hydration the strength of test mortar had also considerable increased especially in mortars to which 10 and 20% of water dispersion of acrylates was added (Table 3).From Table 3 it can be seen that by addition of at least 20% acrylate dispersion we can considerably improve the bending strength of cement mrotar (concrete), what is well known. From the results presented in Fig. 1 and Table 3 it can be concluded by addition of acrylate dispersions the hydration of portland cement is retarded for 2 or 3 days, but it is speeded up later. After 7 (28) days there is practically the same cement hydration level in mortars with 10 and 20% added acrylate dispersion as in mortars without acrylates. If 30% of acrylate dispersion is added cement hydration is retarded and mortar with lower compressive strength is got after 7 and 28 days. The presence of acrylates in mortars is beneficial concering cement

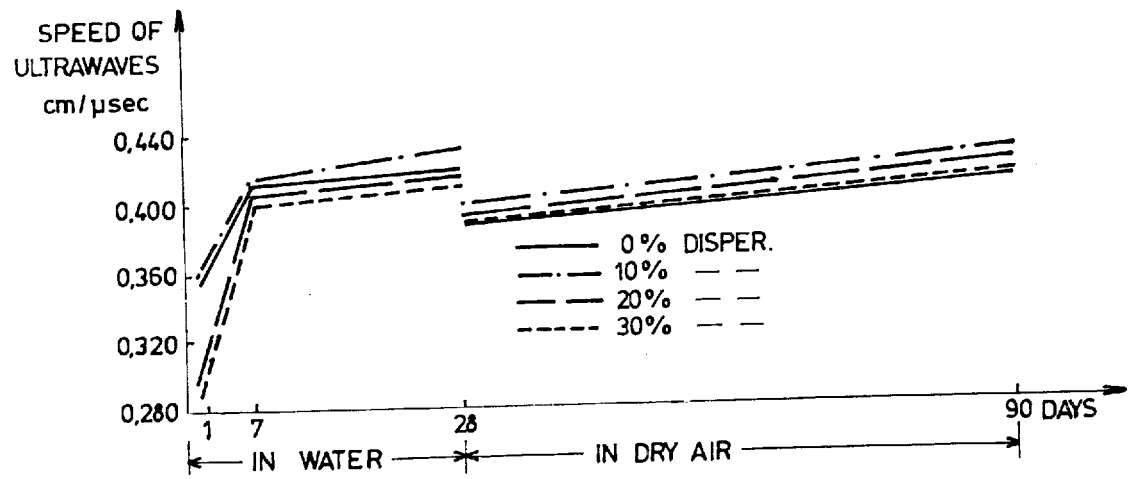

Fig 1 Speeds of ultrasonic waves through wet and dry test prisms

Table 3 Mechanical properties of test prisms

Disper. of acrylate %	Bending strength (MPa), after:			Compress.strength (MPa), after:		
	7	28	90 days	7	28	90 days
0	5,17	8,00	9,59	35,5	39,2	46,9
10	5,31	9,45	9,69	35,2	41,1	60,5
20	5,89	9,59	12,71	32,2	38,8	60,9
30	5,71	12,54	13,14	27,7	33,8	58,4

hydration after 28 days of curing in water, and as a result after 90 days compressive (and bending) strengths were bigger in mortars with addition of acrylate dispersions. From results presented in Fig. 1 and Table 3 it is clear that best mechanical properties has mortar to which 20% of water dispersion of acrylate has been added, meanwhile, the producer recommends 30%.

The presence of acrylates has big influence on some physical properties of cement mortar (concrete), as it can be seen from the results presented in Table 4. Porosity, water absorption and vapour diffusion of

Table 4 Physical properties of test mortars

Disper.of acrylate %	Porosity in % after 90 days	Water abs.in %, after:		Adhesive force N/mm^2 after 28 days	Vapour diff. after 28 days
		28	90 days		
0	18,06	7,75	5,19	0,080	12,9
10	11,98	3,84	3,48	0,480	-
20	10,75	2,37	1,79	1,080	28,3
30	12,76	0,91	0,83	-	-

mortar is considerably lessened, and adhesion towards concrete is very

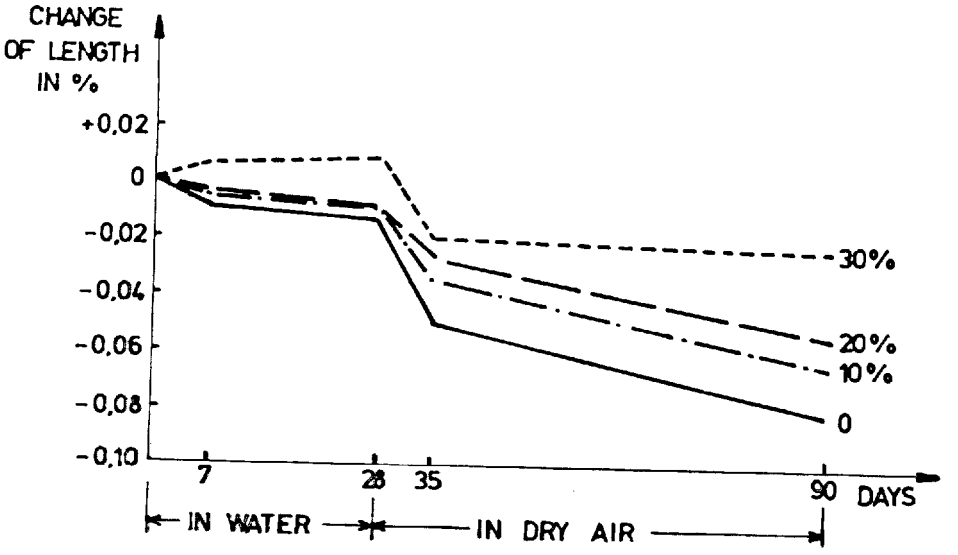

Fig 2 Shrinkage of test prisms

much increased by addition of acrylate dispersions. The drying of wet mortar causes shrinkage, and as a consequence of repeated shrinkage micro-cracks can be formed on the surface. The presence of micro-cracks has bad consequences on mechanical and physical properties of mortar (concrete), they have especially bad influence on bending strength. Water absorption is increased, and the durability of mortar (concrete) is considerably decreased if micro-cracks are present. As it can be seen from Fig. 2 shrinkage of mortar is considerably decreased if acrylates are present. From Table 3 it can be concluded that, in the presence of aerylates, bending strength of mortar is increased. because of smaller shrinkage and better bending strength of mortar containing acrylates, the danger of formation micro-cracks is decreased. The results presented in Table 5 prove these assumptions. In Table 5 there are the results of measurements of bending and compressive strengts and water absorption of test mortars after curing

Tabel 5 Results of strength and water absorption measuremeuts

Disper.of acrylate %	Mortar without acrylate after:			Mortar wih 15% acryl. after:		
	28 days	2 years	Differ. in %	28 days	2 years	Differ. in %
Compr.strength in MPa	42,7	54,3	+27,2	32,4	53,4	+64,8
Bending streng.in MPa	7,35	6,26	-14,8	7,32	7,32	-0,68
Water absorp. in %	2,72	3,52	+24,4	3,23	2,35	-27,2

(28 days) and after keeping 2 years outdoor under conditions of changeable temperatures and humidity. The results of bending strength and water absorption measurements are somehow unexpected as it would be logical that as the result of prolonged hydration also the bending strength increases, and the porosity as well as water absorption decrease. The reason of the fall of bending strength and of the growth of water absorption of test mortars is, probably, the consequence of forming micro-cracks in surface layer of mortar. Other causes of forming micro-cracks could be: the action of frost, great number of alternate cycles of wetting and drying in surface layer of mortar and corrosive action of SO_2 from polluted atmosphere. An important finding for us is the following: in specimens with 15% addition of acrylate dispersions the fall of bending strength did not ocur, the water absorption was even decreased. This is,probably, the consequence of positive influence of acrylates on bening strength and on the decrease of mortar shrinkage at drying, accordingly, it decreases the possibility of forming micro-cracks in the surface layer of mortar.

CONCLUSION

According to the obtained results of investigations, it may be concluded:

1. The hydration of Portland cement is considerebly slowed down during the first days in the presence of dispersion of synthetic acrylates. However, this is made up by later faster hydration of cement,so that after 90 days there is higher degree of hydration in the presence of added dispersion of acrylates (10 and 20%).
2. By adding optimum quantity of water dispersion of synthetic acrylate

the adhesion of mortar to concrete, and the bending strength are considerably increased, and the final compressive strength is also increased to a certain degree. The porosity and water absorption of cement mortar (concrete) is remarkably decreased if acrylates are present, but also the vapour-permeability is decreased.

3. By addition of dispersion of acrylates the shrinkage of cement mortar is significantly decreased, the consequence of it is the forming of less micro-cracks in surface layer.

REFERENCES

1. Angelmayer K.: "Betonschutz und Betonsanierung", Kunstharz Nachrichten, 1991, 17, firma Hoechst.

2. Skenderović B., Tot A., Stipić L.: "Ispitivanje uticaja dodataka raznih vrsta i količina vođenih disperzija sintetičkih polimera na mehaničke i fizičke osobine betona", Zbornik radova Građevinskog fakulteta Subotica, 1988, 4, 172.

3. Skenderović B., Stipić L., : "Uticaj dodavanja finomlevene zgure i disperzija sitnetičkog polimera na osobine cementnog maltera", 3.Jug. posvet. o sanac. zgradb. in okolja, Maribor, 1989, 244.

THE APPLICATIONS OF POLYMER CONCRETE BASED ON METHYLMETHACRYLATE FOR THE MACHINE TOOL INDUSTRY

Peter J Koblischek

INTERACRYL GmbH, Frankfurt, GERMANY

SUMMARY

This Polymer Concrete (PC) as specified in the Patents /1/ is based on more than 20 years of experience. It is a modified PC made from calcite, quartz and a reactive methylmethacrylate resin with the viscosity of water and corresponds to **DIN 51 290: Polymer Concretes (PC) in Mechanical Engineering.** The application is very easy, because this system consists only of two components which are mixed and put into a mould or metal construction. After compacting with vibrators, the hardening process is finished in one hour and the machine part is ready. This technology permits the low energy-production of machine bases with a high degree of finish and an enormous freedom of design, comparable to that of grey cast iron. The total energy consumption for producing a machine base of this PC is only one-fifth of the energy required for the same cast iron base. Also the possibility of the recycling of this PC is given. So the degree of damping in comparison with grey cast iron is 10 times and with steel 20 times higher. Comparative tests have been made conducted on similarly constructed high speed cutting machines, with regard to various Polymer Concretes based on MMA-PC = MOTEMA®-AC, polymethacrylate resin (PMMA), epoxi resin (EP) and unsaturated polyester resin (UP).

ZUSAMMENFASSUNG

Dieser Polymerbeton (PC), der in den Patenten /1/ spezifiziert ist, resultiert aus mehr als 20 Jahren Erfahrung. Er ist ein modifizierter PC, hergestellt aus Calcit, Quarz und einem Reaktionsharz auf Basis von Methylmeth- acrylat mit der Viskosität von Wasser. Er entspricht DIN 51 290: Prüfung von Reaktionsharzbeton (PC) im Maschinenbau. Die Anwendung ist sehr einfach, da dieses System nur aus zwei Komponenten besteht, die miteinander vermischt und danach in eine Form oder Metallkonstruktion gegeben werden. Nach Verdichten mit Vibratoren ist die Aushärtung in einer Stunde beendet und das Maschinenteil ist fertig. Diese Technologie erlaubt die Herstellung von Maschinenteilen mit niedrigem Energiebedarf, geringer Nachbearbeitung und hoher großer Gestaltungsfreiheit, vergleichbar der von Grauguß. Der gesamte Energiebedarf für ein Maschinenteil aus diesem PC ist nur ein Fünftel von der Energie, die zur Herstellung eines vergleichbaren Gestells aus Gußeisen erforderlich ist. Auch das Recycling von diesem PC ist gegeben. Die Dämpfung im Vergleich zu Grauguß ist 10-fach, zu Stahl sogar 20-fach höher. Vergleichende Tests wurden an baugleichen Hochgeschwindigkeitsfräsmaschinen durchgeführt, die aus unterschiedlichen Polymerbetonen auf Basis von MMA-Harz = MOTEMA®-AC, Polymethylmethacrylatharz = (PMMA), Epoxidharz = EP und ungesättigten Polyesterharz = UP hergestellt waren.

INTRODUCTION

Machine tool bases are the stressed parts of a machine tool on which the aggregates required for machining, such as motors, gears, supports for tools and workpieces and feeder units, are mounted. They are meant to receive the forces accuring during machining of the pieces, which in this case are mainly vibrations, and to absorb them as far as possible. Machine bases have preferably been made of cast iron, cast steel, welded steel constructions and to a lesser degree of cement concrete. Cement concrete as a material for machine bases has the following advantages: low material costs, high absorption properties, thermal expansion like steel, and high sound absorption. However, there are the following disadvantages: long setting period, virtually no absorption of tensile forces, significant cost increases because of indispensable steel reinforcement or expensive prestressing technique, altering of dimensions by absorption of water or insufficient chemical resistance. On the other hand, MOTEMA®-AC has the same advantages as cement concrete, but without its disadvantages. This kind of concrete differs from an hydraulically hardened concrete (cement concrete) insofar as a matrix of fine fillers and a reactive resin based on methyl-methacrylate is used as bonding agent for the usual mineral aggregates instead of cement glue. The setting reaction must be induced and takes place by polymerization of the bonding agent and is concluded within one hour. /2/

Table 1:

Characteristic Data of M O T E M A®-A C

	Unit	Value
Specific gravity	g/cm^3	2,3
E-modulus:	kN/mm^2	
from tension test		23,9
from bending test edgeways		31,0
from bending test flat		39,5
from sympathetic vibration of a longitudinally activated 32 mm ø bar		46,0
Compressive strength	N/mm^2	120,0
Bending tensile strength	N/mm^2	29,0
Tensile strength	N/mm^2	11,5
Constant reverse bending strength	N/mm^2	3,2
Poisson's ratio	μ	0,35
Damping (log. decrement Λ)		0,048
Material damping Λ GG25 : Λ AC		1:10
Shore hardness	Sh	80,0
Abrasion	$cm^3/50\ cm^2$	4,3
Waterabsorption	%	0,2
Coefficient of expansion	mm/m/°C	0,015
Thermal dimensional stability DIN 53 461	°C	106,0
Thermal conductivity	W/m · k	2
Transient resistance	Ω · cm	10^{15}-10^{16}
Surface resistance	Ω	10^{13}-10^{14}
Static adhesion to metallic surface	N/mm^2	7-12

With MOTEMA®-AC three times as much geometrical moment of inertia is necessary in comparison with grey cast (GC). In practice, at least three times the wall thickness is used in comparison with GC. This way, the increase in the geometrical moment of inertia is automatically achieved. Assuming that the same rigidity criterion (EI) is required, the following demand is made on the basis of the characteristic data:

Table 2.

Rigidity Criterion: $E_{GC} \cdot I_{GC} = E_{AC} \cdot I_{AC}$
E_{GC} = Elastic modulus for Grey Cast Iron (GC)
E_{AC} = Elastic modulus for MOTEMA®-AC
I_{GC} = Geometrical moment of inertia of Grey Cast Iron (GC) component
I_{AC} = Geometrical moment of inertia of MOTEMA®-AC component

The same weights are thereby arrived for constructions made of GC and MOTEMA®-AC, on the basis of the different specific weights. An approx. 10-fold damping is achieved in comparison with grey cast iron. Due to the sealed form of construction, higher rigidities are generally achieved against deflection and torsion. This will be demonstrated by similarly constructed frames for high-speed grinding machines made of MOTEMA®-AC, Grey Cast Iron and other Polymer Concretes as said before.

TEST RESULTS

Comparison with Grey Cast Iron

These high-speed grinding machines are subjected to extreme dynamic loads. One particular advantage shown by the machine frame made of MOTEMA®-AC is the fact that no critical resonance points lie within the main excitation areas involved in the machining operation. /3/ The results of measurements are shown below:

Table 3.

Characteristic frequencies (Resonance figures) in Hz						
MOTEMA®	32,9	-	-	-	247,4	321,6
GCI	40,6	52,9	127,2	164,4	248,1	318,9

Comparison of Polymer Concretes (PC)

At the Institute of Cutting Technology and Machine Tools (ITW) of the TH-Darmstadt high-speed cutting has been tested since 1978. High-speed machining makes extremely also high demands on the dynamic performance of machine tools, and so the first frame of a machine for high-speed milling made of MOTEMA®-AC was already processed in 1980. Because of the fundamental studies conducted with this, two more machine-frames made of MOTEMA®-AC were produced, exactly in time for the "ICPIC 84", and could be exhibited. All of these frames are fully equipped and are working highly satisfactory. Very good surface qualities at high dimensional accuracy were achieved with aluminum alloy at the cutting speed range between $2000 \leq V_f \geq 6000$ m/min. at a higher rate of cutting. The main time-saving amounted to 50 %. The second machine-frame made of MOTEMA®-AC was set up and compared to other equally constructed frames of Epoxi- (EP), Polymethyl-methacrylate- (PMMA) and Polyester- (UP) concrete (shrink resistant) in the course of the "United Research Project High Speed Millings". /4/
The sizes of these machines are the same: 1500 x 1500 x 2150 mm.

Dynamic behavior

The dynamic elasticity of the machine frames was examined using modal analysis in a frequency range between 0 Hz and 500 Hz. The Table 4 shows that the fourth frequency of the MOTEMA®-AC machine frame is over 500 Hz.

Table 4.

Characteristic Frequencies in the range from 0 Hz to 500 Hz				
Frame	1.	2.	3.	4.
E P	202,5	249,1	383,5	474,5
U P	208,8	252,7	404,8	460,8
MOTEMA®-AC	217,2	265,8	412,9	-

Damping

In contrast, a marked dependence on resin was established in the damping values. The degree of damping varied here in comparison with Grey Cast Iron (GC). These results have been conducted on the similarly high-speed cutting machines. /5/

Table 5.

Degree of Damping	
Grey Cast Iron (GC)	1
Epoxi Concrete (EP)	4
Unsaturated Polyester Conc. (UP)	6
Polymethacrylate Concrete (PMMA)	6
M O T E M A® - AC	10

Static behaviour

The static behaviour of the machine frames was examined with centric load (simulation of drilling), defined forces of up to 10 kN being introduced via a hydraulic cylinder. The qualitative dislocation of check points 1 and 3 is outlined as a function of the load. As can be clearly seen, the machine frame made of MOTEMA®-AC is noticeably stiffer when subjected to bending strain than the same structure made of Epoxi-concrete. This behaviour can probably be attributed to the fact that the EP-frame was not tempered after manufacture, so that the degree of cross-linkage could not be optimized. The following Figure 1 on the next page shows the Static Behaviour and Load Deflection response of equally machine frames made of MOTEMA®-AC and EP-PC at identical Check Points. /6/

Long term behaviour

Not only the mechanical characteristics are important - also the thermal material characteristics and the long-term behaviour of the PCs are of significance. As was shown by Groche on the basis of comparative long-period creep tests, the long-term behaviour of PC, based on methacrylic resins is most favorable, i.e. the smallest deformations occur in methacrylic concrete, while the deformations that can be expected in standard epoxi resin concrete and polyester resin concrete are several times higher. /7/

Figure 1: Static Behaviour

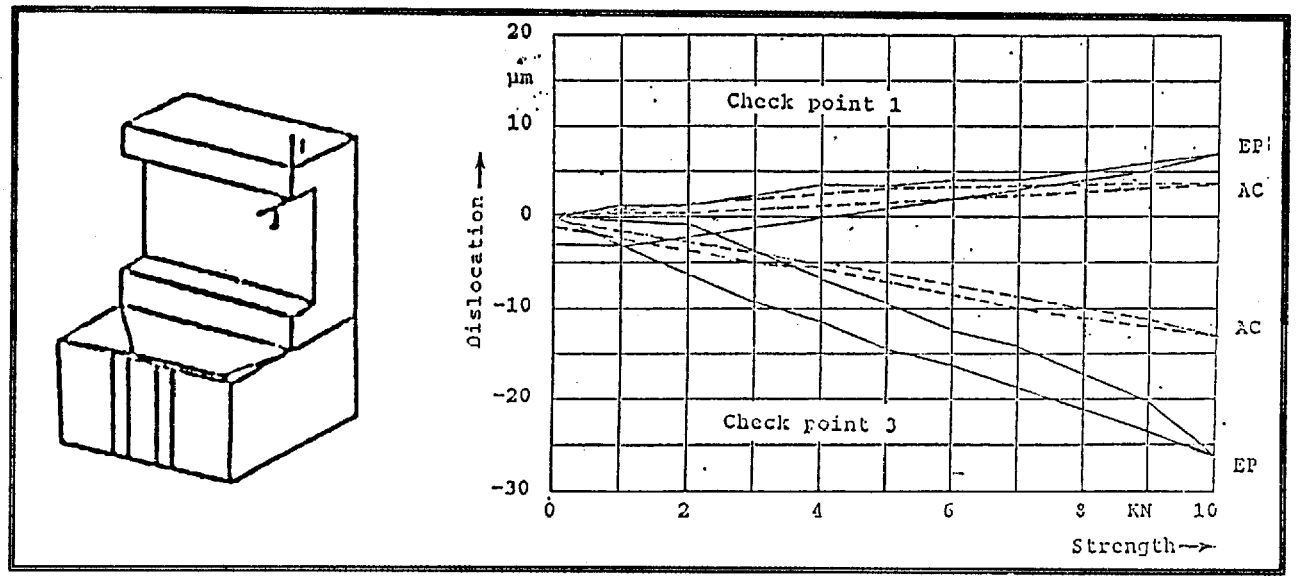

Yet, there are also epoxi resins, i.e. Araldit 167, which have the same long-term behavior as MOTEMA®-resin used for tests at the Institute of Technology and Machine Tools of the TH- Darmstadt; by EP at least up to the temperature range of approx. 50°C and by MOTEMA®-AC over 80°C. The results (1981) were expected since it is well known, that at room temperature cured EP-PC is loosing mechanical strength beginning at 40°C until 50°C. /8/ /9/

A new low-viscosity epoxi-system for machine bases with a binder content of 7 % and aggregates of 93 % has nearly the same mechanical strength as MOTEMA®-AC. Subjected to temperatures of up to 60°C the following graph shows the reduction in compressive and tensile strength and the E-modulus. /10/

Figure 2: Strengths of EP-PC dependent on temperature

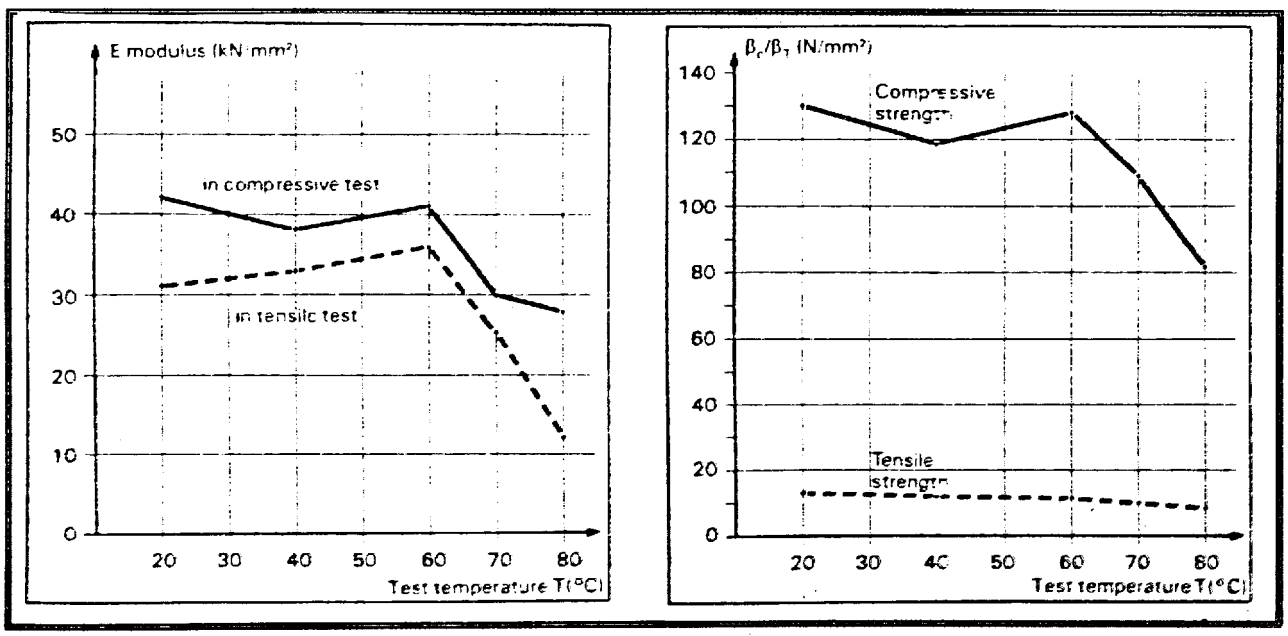

Test specimen: 40x40x160 mm
Prisms cured for 6 days at 20°C and 1 day at60°C.

DISCUSSION

In the author's opinion the Polymer Concretes are the best materials for machine tool bases, not only in combination with grey cast iron and welded steel constructions but also as a replacement material. Today economical and ecological pressure and high technical standard call for an optimum on static, dynamic and thermal performance of the machine bases and for a possibility of recycling. This all is given by the MOTEMA●-AC-technology of the author. /11/

Therefore it is not justifiable to cure machine bases at increased temperatures with the weight of several tons, without achieving the thermal dimensional stability of MOTEMA●-AC, because of the increase of costs and the necessary energy. The total energy consumption for producing a MOTEMA●-AC machine base is only one-fifth of the energy required for the same cast iron base. The following Table 6 gives a general view for the energy consumption for some materials.

Table 6: Energy Consumtion

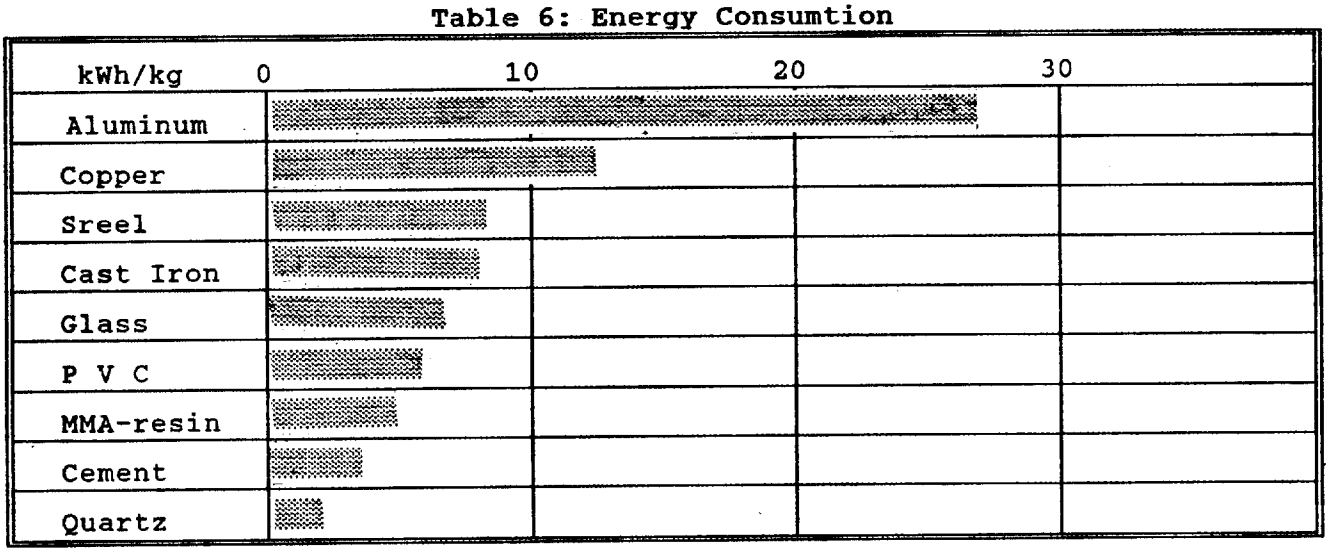

PROGNOSIS

PC will never become a material such as, for example, normal concrete. The advantages are its high chemical constancy, its dimensional stability due to its impermeability to moisture and pollutants and its ability, also when unreinforced, to absorb tension. The comparatively quick curing and therefore prompt availability of the product save time and money. Procuring, seasoning and machining of cast iron bases takes many weeks to months. MOTEMA●-AC bases are ready for assembling within days. The manufacturing costs are up to 30% less than cast iron bases. The machine tool builder can produce bases in his own workshop on a Just-In-Time basis with all the technical advantages for the future, e.g. the growing importance of noise reduction.

CONCLUSION

In an industry where time equals money, reduced inventories and Just-In-Time manufacturing at even less cost is a strong incentive to the use of MOTEMA●-AC. Through the test results as mentioned before and practical application those requirements have been met for years:

* production right in time
* fast availability
* high damping
* high rigidity
* dynamic stability
* long-time stability
* long-temperature stability
* corrosion-resistant
* low need of energy
* reduction of noise
* possibility of recycling

The MOTEMA®-AC Technology provides all these advantages together with the very easy processing.

REFERENCES

1. Patents: DBP: 30 30 914. US: 4,670,208; 4,826,127. EP: 0046272; Japanese: 1,622,731; Spain: 504,724.

2. Koblischek, P.J.: "Toolmachine Frames, made of Acrylic Concrete", **Third International Congress on Polymers in Concrete, ICPIC '81,** College of Engineering, Nihon University, Koriyama, Japan, May 13-15. 1981, 1116 p.

3. Schulz, H.: "Machine Tool Frames made of Polymer Concrete". Werkstatt und Betrieb, 1981, 114(10), 747-752.

4. Koblischek, P.J.: "MOTEMA-acrylic concrete for machine tool frames", The International Journal of Cement Composites and Light-weight Concrete, 1985, 7(1), 55-57.

5. Koblischek, P.J.: "Non-Metallic Casting Materials", **IMTS 86, Chicago, The Third Biannual International Machine Toll Technical Conference,** U.S.A. Sept. 3-10, 1986, V4B, 4-61 p.

6. Dey, H.-J. & Schulz, H.: "Experience in the use of high-speed milling/cutting machines made of reaction resin concrete", **Colloquium Polymerbeton THD'87,** THD-Darmstadt, Febr. 18th, 1987.

7. Groche, F. : "Materialeigenschaften und Anwendungsmöglichkeiten von Polymerbeton", VDI-Berichte 384, VDI-Verlag, Düsseldorf, 1980.

8. Koblischek, P. J. : "MOTEMA-AC the non-metallic casting material-6 years after this introduction", **5th ICPIC '87,** Brighton-Polytechnic, GB, Sept. 21-24, 1987, 139 p.

9. Koblischek, P. J. : "Polymer concrete bases for high-speed cutting machines", **Eastern Manufacturing Technology Conference,** Springfield, MA. U.S.A. Nov. 10-12, 1987, 5, 209 p.

10. Phillips, T.J. : "A specific Polymer Concrete for Machine Structures", **5th ICPIC '87,** Brighton-Polytechnic, GB, Sept. 21-24, 1987, 127 p.

11. Koblischek, P. J. : "MOTEMA-AC, the material with the highest damping and rigidity-ideal for bases for laser machines", **ECLAT'90 3rd European Conference on Laser Treatment of Materials,** Erlangen, Sept. 17-19, 1990, 949 p.

INFLUENCE OF SOME WATER SOLUBLE POLYMERS ON THE MECHANICAL PROPERTIES OF CEMENT POLYMER COMPOSITES

Kamala Gopinathan and D V Ramana Rao

National Council for Cement and Building Materials, New Delhi, INDIA

SUMMARY

The studies carried out on the influence of four water soluble/compatible polymers on compressive, flexural and tensile strengths, porosity and resistance to corrosion of cement polymer composites are presented. An accelerated curing process was adopted for the preparation of the specimens. The results indicate that the presence of the polymers enhance the properties substantially and confirm the correlation between increase in flexural and tensile strengths and the decrease in porosity. A relationship between porosity reduction and water solubility of the polymers was also observed.

INTRODUCTION

The ordinary portland cement, though high in compressive strength, has low tensile and flexural strengths. These can, however, be improved as shown by the preparation of macrodefect free (MDF) cements by Birchall et.al (1). However, the MDF cements differ significantly from conventional cements and as such should be mainly viewed in the context of advanced engineering materials (2). Another approach to the improvement of properties of cement products is the addition of organic polymers. These compounds, either by acting as a continuous reinforcing network or by interaction with the hydrated cement to form stable compounds (3) enhance the strength and durability properties of the composites. This work, undertaken in view of these considerations, studies the effects of certain water soluble polymers on the properties of OPC products. The approach was to use varying amounts of different water soluble/compatible polymers and simultaneously to adopt an accelerated curing process. The polymer content was kept relatively low so as to assess their effectiveness even in small amounts. The properties studied include compressive, flexural and tensile strengths, porosity and corrosion. The preparation of specimens of the polymer cement composites and the modified curing process are described in this paper. The various properties of the composites have been measured and are related to the nature and quantity of the polymer used.

EXPERIMENTAL.

Materials: The materials used are given in Table 1

Table 1 Materials used in the preparation of polymer cement composites

MATERIALS USED				
Polymer	Cement			
1. Polyacrylamide (4) (PAA)*	Ordinary Portland Cement			
2. Poly (N-methylol acrylamide) (5) (NMPAA)*	Composition	(Percentage)		
3. Polyvinyl alcohol (PVA)*	CaO	63.57	Na_2O	0.32
4. Microcrystalline cellulose polymer (MCCP)*	SiO_2	21.21	K_2O	0.641
	Fe_2O_3	4.94	Insolubles	0.33
	MgO	1.10	Loss on	1.68
	Al_2O_3	5.59	ignition	

* Only these abbreviations are given in figures 1 to 4.

Sample Preparation

For compressive strength studies, normal curing processes were observed while for the other parameters an accelerated curing process was adopted. Four series of mortar samples with one blank and three polymer cement ratios (0.1,0.3 and 0.5 w/w) were prepared.Compressive strengths were tested at 28, 60, 90 and 120 days. The w/c ratio in each case was 0.4.

For studies on flexural and tensile strengths, a different method of sample preparation was adopted. The required amounts of cement, polymer and water were mixed in an orbital blender for 3 minutes. The mixture was transferred to moulds and subjected to vibration for 2 minutes. The mix was smoothed over and kept at 90% R.H at r.t for 24 hours. The specimens were demoulded after 24 hours at 90% R.H and subjected to wet curing at 50°C at 90% R.H for another 24 hours. They were then dry cured at 80°C for 24 hours. After this rapid curing, the specimens could be kept at r.t indefinitely without any deterioration in their strengths. The water/cement ratio used was 0.2.

For porosity measurements, the broken specimens from the flexural strength studies were used, while for corrosion studies cubes (7.07 cm^3) were cast as in compressive strength measurements, but the accelerated curing method was adopted.

METHOD OF INVESTIGATION

Compressive strength measurements were carried out on Schenk Trebel Equipment Type RB 600-2, 1979 Capacity 600 KN. Averaging was done on three identical cubes.

Flexural strength measurements were done on equipment (0.5 tonne capacity) supplied by AIMIL India. The specimen dimensions were 16x4x4 cm. The flexural strength was determined by centre point loading using the expression $f=3\ Pl/2bd^2$ where P is the load of fracture, l is the distance between the supports, b is the beam width and d is the beam depth.

Tensile strengths were measured on equipment supplied by AIMIL India. The specimens were according to specifications by Bureau of Indian Standards. Porosity,p, of the samples was calculated from $p = 1 - dB/dT$ where dB is the bulk density (i.e the mass of specimen divided by its volume of material including pores) and dT the true density (mass of specimen divided by its volume excluding pores). The values were obtained by using a density bottle to find dT on the ground specimen of particle size $<150\ \mu m$ and an immersion method to measure dB.

Resistance to corrosion was measured by determining the weight loss suffered by the cubes after immersion in 5% Hydro chloric acid for 10 days.

RESULTS AND DISCUSSIONS

Consistency measurements indicated that the addition of the polymer increased the plasticity of the mix. It was observed that, for the w/c ratio used, OPC gives a mix of dry consistency whereas the polymer modified mix has a liquid consistency which can be poured into the mould. In the case of PVA, however, there was only a marginal increase in plasticity.

A study of the compressive strengths of composite mortars show no increase over the blank even up to the age of 120 days. The inferior strength characteristics even at this stage may be due to wet curing (6). However, further studies have to be carried out before any definite conclusions can be drawn. The values of flexural strength, tensile strength and porosity for the various polymer cement composites studied indicate a marked improvement over the unmodified cement pastes.

The variation of flexural strength with polymer content is given in Fig.1. There is a clear indication that as the polymer content increases, the flexural strength increases. This is true for all the polymers although the strength enhancing effect

is less pronounced in the case of Polyvinyl alcohol. It is noticed that in the case of Polyacrylamide and its N-methylol derivative the strength has increased four fold with a polymer content of 5%. The trend is not linear but there is no levelling off upto the maximum concentration studied (5%) with any of the four polymers.

The same trend is noticed in the case of tensile strengths also (Fig.2). Though the effect appears less than in the case of flexural strengths, the strength improvement is substantial with an almost twofold increase at a polymer content of 5%.

There are two factors to be considered in the strength increasing mechanism, a low water cement ratio and a low total porosity. At very low w/c ratio, the mix becomes unworkable but the presence of these polymers give high workability and thus contribute to strength enhancing. It may be noted that polyvinyl alcohol which does not impart much workability is less efficient in improving strengths. The special curing method also accelerates strength development (7). Thus curing at room temperature takes several days for developing flexural strengths. But humid curing followed by dry curing, both at high temperatures, develops high flexural strength in 48 - 72 hours.

The results of the porosity studies confirm the correlation between the strength increase and a lowering of the total porosity. Fig.3 shows the variation of porosity with polymer content. It is observed that porosity decreases with increasing polymer content and as noticed in the case of flexural strengths, there is no levelling off upto the maximum studied (5%) polymer content.

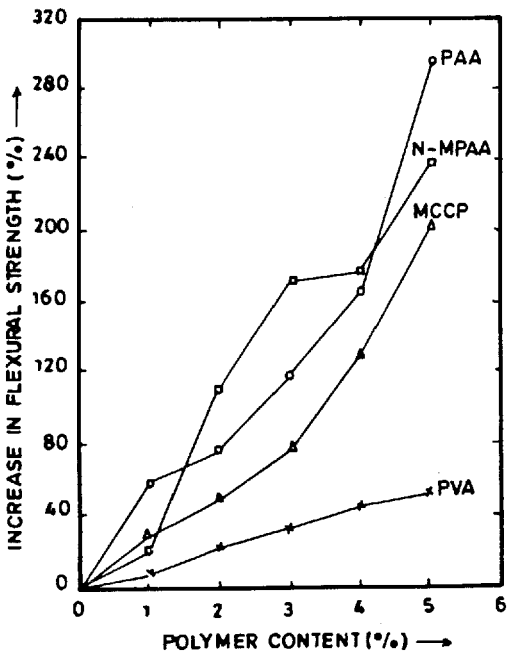

Fig.1. Variation of flexural strength with polymer content

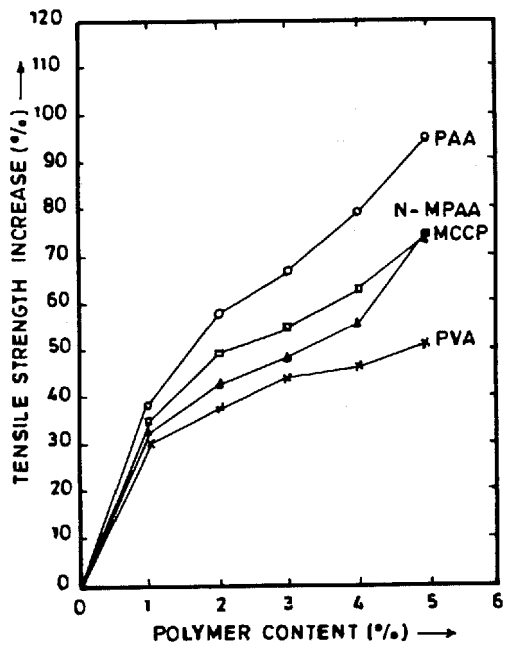

Fig. 2. Variation of tensile strength with polymer content

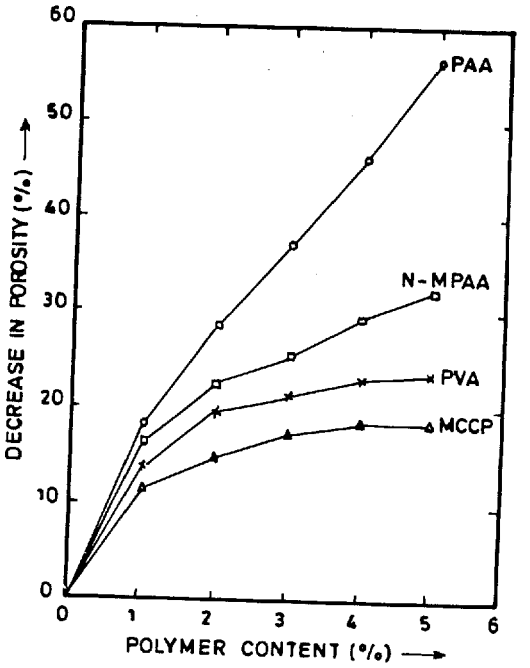

Fig.3. Porosity reduction by polymers in polymer cements

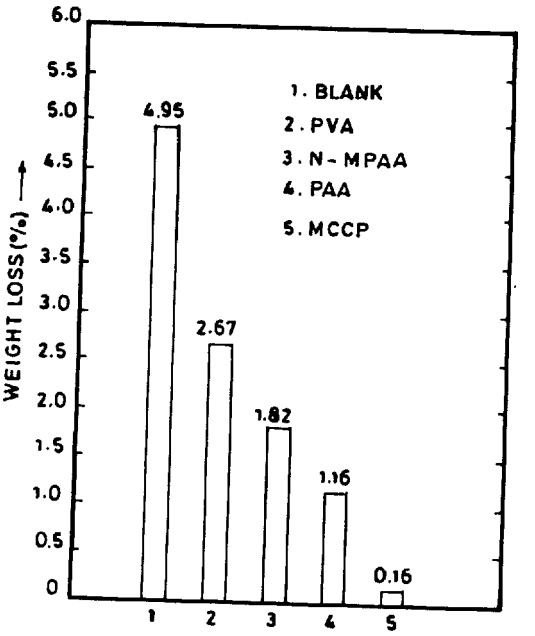

Fig.4. Corrosion resistance of polymer-cements

Figs.1, 2 and 3 clearly indicate that as porosity decreases, flexural and tensile strengths increase. The results show that the incorporation of even small amounts of these polymers produce a substantial reduction in the porosity with consequent increase in strength.

The porosity studies reveal an interesting relation between solubility and porosity reduction i.e the higher the solubility, the greater is the porosity reduction. Thus polyacrylamide, which is the most soluble of the four, produces a porosity reduction of 56.8% at a concentration of 5% whereas microcrystalline cellulose polymer, which is the least soluble produced a porosity reduction of only 18% at the same concentration. The effect may be due to the fact that the molecules of the highly soluble polymer are able to penetrate better into the interstitial spaces and fill the voids and consequently reduce the porosity. This aspect, however, requires further detailed study.

The resistance to corrosion of the polymer cement composites, measured by the weight loss of the cubes after 10 days immersion in 5% HCl is shown in Fig.4 As can be seen, the weight loss is much less in the composite as compared to the blank, showing that all the polymers are able to impart some corrosion resistance to the cement. This confirms earlier studies (8) on corrosion resistance of polymer composites. The effect is most pronounced in the case of microcrystalline cellulose polymer and least in polyvinyl alcohol.

CONCLUSIONS

The studies indicate that polymer modified cements prepared by the accelerated curing process possess substantially higher flexural and tensile strengths compared to the ordinary cements. This increase has been related to the decrease in porosity

and enhanced workability imparted to the cement by these polymers. The decreased porosity may be due to their high water solubility. The polymer modified cements are also more resistant to corrosion.

ACKNOWLEDGEMENTS

The authors are grateful to the Director General, NCB for permission to present this paper. The help given by the Staff of Building Technology Lab, Civil Engg. Dept, IIT Madras in the use of their equipment is gratefully acknowledged.

REFERENCES

1.Birchall,J.D. : "Cement in the context of new materials for an energy expensive future" Phil. Trans. R.Soc. Lond 1983, A 310, 31 - 42.

2.Tan,S.R., Howard,A.J. & Birchall, J.D. : "Advanced materials from hydraulic cements". Phil. Trans.R.Soc. Lond. 1987, A 322, 479 - 491.

3.Ben-Dor,L., Heitner-Wirguin,C & Diab, H. : "The effect of ionic polymers on the hydration of C_3S" Cem.Concr. Res. 1985, 15, 681 - 686.

4.Sorensen,W.R. and Campbell,T.W. Ed. Preparative methods of polymer chemistry,Interscience, New York, 1962.

5.Thomas,W.M. "Acrylamide Polymers: Encyclopedia of Polymer Sciences and Technology" 1964, Vol.I.

6.Montanaro,L., Festa D.,Bachiorrini,A. & Penati,A. : Influence of added polymer emulsions on the short-term physical and mechanical characteristics of plastic mortar" Cem.Concr. Res. 1990, 20, 62 - 68.

7.Brackenbury,W.R.E., Grzeskowiak,R., Reid,N.L. & Lynn, M.E.: "Flexural strengths of polymer modified cement pastes prepared by a novel curing process". Cem.Concr.Res. 1988, 18, 971 - 979.

8.Diab,H., Ben-Dor,L., Heitner-Wirguin,C. & Bonen, D. : "The porosity and compressive strength of polymer-cement" Cem.Concr.Res. 1985, 15, 1061 - 1067.

INCREASING WATER-RESISTANCE OF PHOSPHOGYPSUM BY POLYMER ADMIXTURES

M V Chumak and O S Popova

Byelorussian Polytechnical Academy, Minsk
Republic of BELARUS

SUMMARY

Phosphogypsum, as well as other gypsum binders is characterized by low water-, freeze- and corrosion resistance which, however, may be improved by using polymer admixtures. Compositions of phosphogypsum binders with composite polymer emulsions and silicones showing high strength and water-resistance properties have been developed.

The experiments conducted revealed a close relationship between the structure and properties of phosphogypsum and made it possible to find some effective ways of the phosphogypsum properties regulation.

РЕЗЮМЕ

Фосфогипс, как все гипсовые вяжущие, обладает низкой водостойкостью и взаимосвязанными с ней низкими морозо- и атмосферостойкостью, что поддается изменению с помощью полимерных добавок. Разработаны композиции на основе фосфогипсового вяжущего с добавлением комплексных полимерных эмульсий, характеризующиеся высокими прочностью и водостойкостью.

Проведенные исследования показали тесную взаимосвязь между структурой и свойствами фосфогипса и позволили определить некоторые эффективные пути урегулирования свойств фосфогипса.

INTRODUCTION

Phosphogypsum - well-known raw material - is one of the mass production wastes. Utilization of phosphogypsum may both extend raw-material base of construction and solve a great number of urgent ecological problems. Our country alone produces about 20 to 22 mln tons of phosphogypsum. Presense of $CaSO_4 \cdot 2H_2O$ (up to 98%) in phosphogypsum makes it a promising gypsum-containing material. It is distinguished by high strength and manufacturability, fireproofness, biological resistance, low energy-intensive production and other qualities. However, like all gypsum materials, it has low water resistance and interrelated low frost- and atmospheric resistance.
The cause of it lies in porosity of the traditional gypsum binder and the character of the porous structure which is formed during evaporation of the excess moisture.

There are some familiar methods for improving durability of phosphogypsum-based building materials:

- removal of the excess moisture from phosphogypsum binder by pressing (1);
- integration of phosphogypsum binders with material admixtures which may regulate water-demand of mixtures as well as their hydraulic properties;
- addition of complex hydrophobizing polymer agents which render a great deal of new properties to the phosphogypsum stone (2).

The last-mentioned method is the most promising because of its simplicity and ease of production.

EXPERIMENTAL

Our experiments involved the study of structure formation of the phosphogypsum stone containing complex polimer agents and formation of microstructure with properties of a hardened binder.

It is known that phosphogypsum is a multi-tonnage waste of fertilizer production. It is obtained by treating apatites with sulphur acid from the following formula:

$$Ca_5(SO_4)_3F + 5H_2SO_4 + 10H_2O = 2H_3PO_4 + 5CaSO_4 \cdot 2H_2O + HF \qquad (1)$$

Pressureless heat treatment or pressure treatment being used, phosphogypsum can be processed into β-and α-semihydrates, respectively.

The experiments were conducted on phosphogypsum binders taken from "Voskresenski PO Minudobrenia" works. Acryl emulsions with finishing agents and fine-dispersed active mineral agents were used to hydrophobize the phosphogypsum binder. The action of complex polymer-mineral agents on properties of the phosphogypsum binder was determined by studying phase composition of the source and modified binders and the character of their porous structure.

Phase composition was determined by complex thermal analyses and

radiography difractional phase analyses. Derivatograph OD 102 ("MOM", Budapest), difractograph ("Philips") with radiogoniometer PY 1050, proportional impulse computer and monitoring transistor device were used in the experiments. The approximate quantity of starting phases was calculated by the results of the gravimetric thermal analysis.

Porosimetric analysis of the source and modified binders samples was conducted using high-pressure mercury porosimeter type P2000 ("Carlo Erba", Milan). The porosimeter was equipped with a computer and monitoring device for detecting micropores of 200 μm radius.

RESULTS AND DISCUSSIONS

Phase analysis of the source and modified binders revealed a prevailing presence of 2 phases in the harden stone - dihydrate $CaSO_4 \cdot 2H_2O$ and gypsum $CaSO_4$ $0.5H_2O$. The presence of the latter may be controlled by a samples' moulding technology (pressing, casting) and chemical activation. High content of semi-hydrates in pressed samples (11.5 - 24.8%) may be reduced by several fold owing to special techniques. Difractograms of the phosphogypsum stone with various content of modified agents are given in Fig. 1.

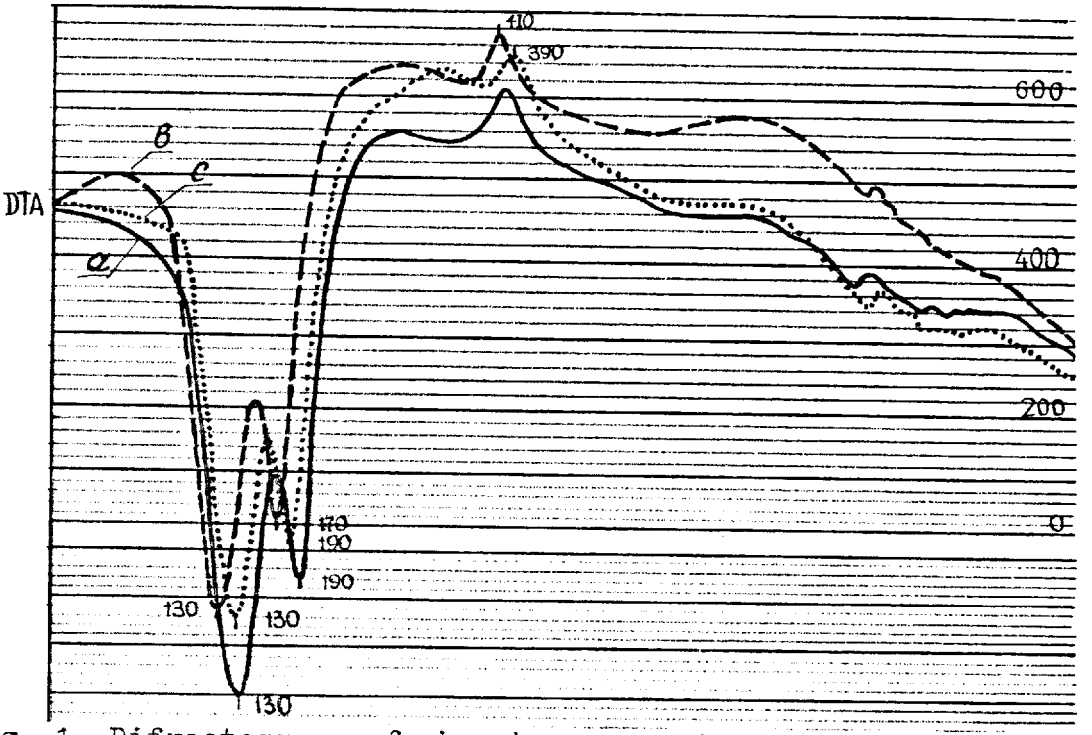

Fig. 1. Difractograms of phosphogypsum stone:
a) without agents b) with 0.25% modifying agent
c) with 0.5% modifying agent

The study of the porous structure shows that as the quantity of modifying agents increases, the curve of pores distribution is shifted manifesting itself in shortening the median of micropores radius (see Table 1).

Table 1

Porous Structure of Modified Phosphogypsum

Property	Value		
	test sample	0.25% Modifying agent	0.5% Modifying agent
Basic physico-mechanical properties			
1. Bulk density (wet), $g \cdot cm^{-3}$	2.134	2.16	2.169
2. Bulk density (dry), $g \cdot cm^{-3}$	2.126	2.152	2.160
3. Moisture content, %	0.4	0.37	0.41
4. Density determined by picknometric method, $g \cdot cm^{-3}$	2.463	2.460	2.465
5. Total porosity, %	12.8	12.6	12.4
Results of the porosimetric analysis			
6. Bulk density, $g \cdot cm^{-3}$	2.155	2.228	2.206
7. Volume of micropores of radius $\leq$ 7500 nm in $mm^3 \cdot g^{-1}$, %	54.387 11.83	45.527 10.22	49.739 10.96
8. Volume of pores of radius 7.5 - 200 μm $mm^3 \cdot g^{-1}$	2.075	1.767	2.246
%	0.45	0.40	050
9. Total volume of pores $mm^3 \cdot g^{-1}$	56.462	47.294	51.985
%	12.28	10.62	11.46
10. Radius median of micropores, nm	37.318	32.128	50.712
11. Radius median of pores, nm	38.192	33.314	53.205
12. Specific surface of pores, $m^2 \cdot g^{-1}$	3.269	3.320	2.294
13. Content of pores of 200 μm radius, %	1.68	1.00.	0.84

As for the internal surface of pores it decreases. The character of pores structure of the phosphogypsum stone (even with a small content of agents) exerts a considerable influence on the main physicomechanical properties. Thus water-absorption of samples aged 14 days decreases as quantity of modifying agents increases (from 5.3% for the test sample to 2.3% for a tolerable quantity). Softening factor raises up from 0.68 to 1.04 (at optimum quantity of modified agents). Change in strength is the most noticeable at the early stages of hardening (Fig.2).

A considerable increase of heat resistance in the phosphogypsum stone is also of great interest. For instance, heat resistance factor raises up from 0.69 to 1.16 after 25 cycles of alternate exposure at +300°C for 2 hours followed by cooling in the open air.

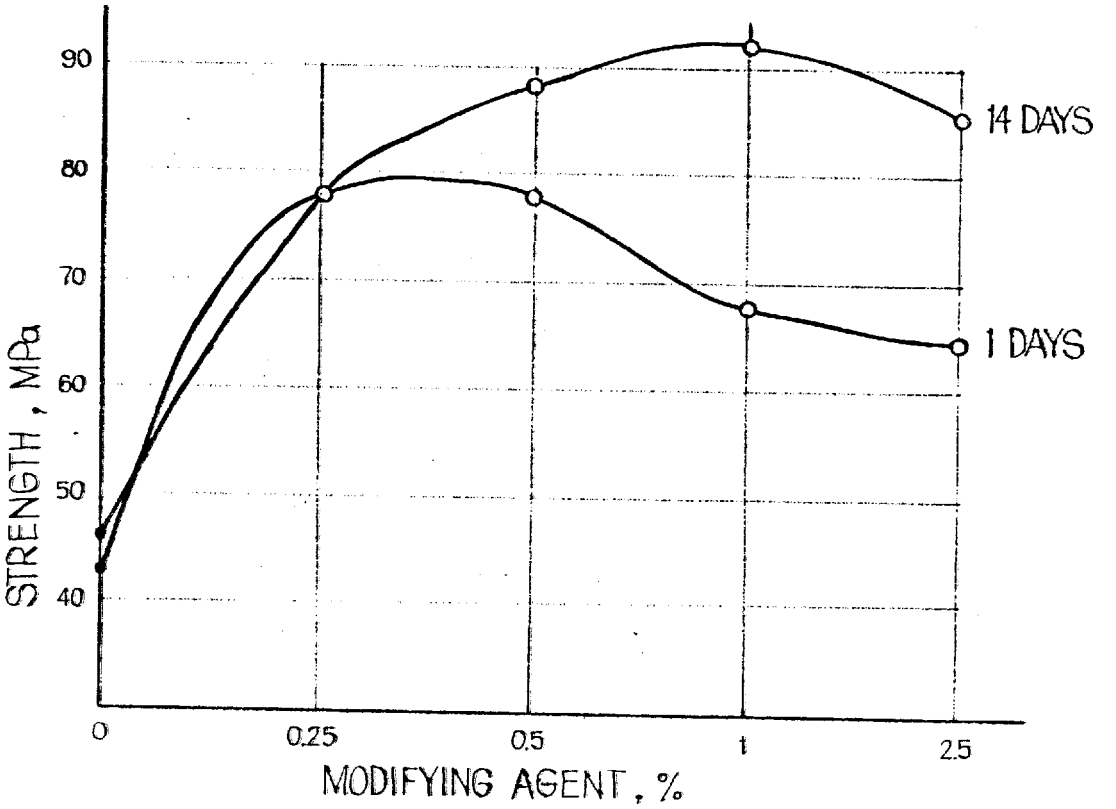

Fig. 2. Strength of modified phosphogypsum stone.

CONCLUSIONS

Experiments showed that modification of phosphogypsum binders using composite polymer admixtures facilitates the formation of a thinner porous structure. Median of micropores radius in modified phosphogypsum, as well as the inner surface of pores, are smaller than that of standard phosphogypsum. Therefore, products, made of phosphogypsum binders shall have lower water-absorbing capacity and higher water-resistance property. Regulating quantity of the polymer agent allows production required stress-strain behaviour.

ACKNOWLEDGEMENTS

The authors appreciate the help of J.Jambor from the Institute of Construction and Architecture, Slovak Academy of Sciences in carrying out experimental work and analyses of results. The paper is published with the permission ofRector of the BPA.

REFERENCES

1. Liashkevitch I.M.: "Effectivnye stroitelnye materialy na osnove gipsa i fosfogipsa", Minsk, Vysshaya Shkola, 1989, pp.58-69.

2. Altykis M.G. et al.: "Primemenie polimerfosfogipsobetona dlia trotuarnyh plit", V sb. "Teoria i praktika primenenia polimertsentov v proizvodstve stroitelnyh materialov i stroitelstve, Tbilisi, 1984, pp.58-60.

3. Meschcheryakov Yu.G.: "Gipsovye poputnye promyshlennue produkty i ih primenenie v proizvodstve stroitelnyh materialov", L.,Strojizdat, 1982, pp.80-90.

IMPROVING DUCTILITY OF CONCRETE BY INCORPORATING NATURAL RUBBER LATEX

B Kameswara Rao*, K T Sundara Raja Iyengar and T S Nagaraj****

**National Council for Cement and Building Materials, New Delhi, INDIA*
***Indian Institute of Science, Bangalore, INDIA*

SUMMARY

Polymeric admixtures modify the properties of the processed concrete. This investigation deals with the development of a method of incorporating natural rubber latex into concrete ingredients with only marginal effects on the compressive strength of base plain concrete. This retention of the strength has been possible by reducing the water/cement ratio with the aid of a superplasticizer. The quantity of natural rubber latex is expressed as the dry rubber content by percentage of volume of concrete. Natural rubber latex has also been used in the concrete along with steel fibers. The combination latex and fibers yielded improved deformation characteristics in the concrete.

INTRODUCTION

Portland cement concrete lends itself to a variety of innovative designs as a result of its many desirable properties. Concrete possesses high compressive strength and stiffness with properties durable under normal environmental conditions. Two characteristics, however, limited its use. Concrete inherently is brittle and weak in tension. Several methods have been developed to impart ductile behaviour. Broadly, these methods can be grouped as mechanical and chemical. Loading concrete under confined condition and reinforcing concrete by discrete fibers are the mechanical means of imparting ductile behaviour. Incorporation of polymeric materials form the chemical method of developing the ability of the material to exhibit ductile response. In the present investigation, the chemical and the combination of mechanical and chemical methods have been exploited.

The results of earlier study (1) conducted prior to this investigation indicate that strength reductions upon incorporation of natural rubber latex is so large that even the improved ductility of the material can not be used gainfully for structural applications. This study is mainly to develop a method of processing natural rubber latex concrete such that the processed concrete acquires ductile characteristics without losing strength of plain concrete.

After arriving at the suitable processing technology with natural rubber latex, it was planned to use this material with the combination of steel fibers. The combination of these two materials imparted higher degrees of strain capacity in the hardened concrete. The combination of polymeric and fibrous materials was also tried by Mangat and Swamy (2,3). They also obtained good results in their studies.

NATURAL RUBBER LATEX

Natural rubber latex is collected from Hevia trees. It is an alkaline material with a pH of 11. In the fresh state, latex particles repel each other due to negative charge. On exposure to atmosphere, lactic acid bacteria will attack the latex, there by reducing the pH value to 4. This results in the reduction of repulsion with a tendency for coagulation. In order to retain the latex in a stable state as well as to prevent premature coagulation, an alkaline environment is essential. To realise this environment, ammonia is generally used. Since ammonia is highly volatile, the moment the latex is added to concrete, it evaporates causing instantaneous coagulation of the rubber. In order to avoid this situation, the earlier investigators suggested the use of alkaline salts such as sodium carbonate and sodium silicofluoride. The main disadvantages noticed with these salts are considerable reductions in workability and strength of concrete.

DEVELOPMENT OF NATURAL RUBBER LATEX MODIFIED CONCRETE

Latex modified concrete fall under the purview of Polymer Cement Concretes (PCC). Most of the earlier investigators, who worked on PCCs, used synthetic rubber latexes to improve the ductility of the concrete. As for as the authors are aware, only one investigation has been reported (1) in the literature on natural rubber latex. In all these investigations, the ductility could be improved with significant reduction in the strength of the concrete. But in the present investigation, it was aimed to improve the strain capacity of the concrete by using natural rubber latex without much reduction in the compressive strength. Naphthalene type of superplasticizer was used to reduce the water/cement ratio and thereby to enhance the compressive strength of the latex modified concrete.

Some trial experiments were conducted to find out the required dosages of superplasticizer for different of workability in all the mixes. These experiments were conducted on cement mortar and the workability was measured with the help of a flow table 2. In these experiments, it was found that the usage of the alkaline salts such as, sodium carbonate and sodium silicofluoride was not required to avoid the premature coagulation of the natural rubber latex, since the superplasticizer was found to serve this purpose also.

While doing these experiments, the water/cement ratio of the plain mortar was kept at 0.5. In the latex mortar mixes, the quantities of latex and superplasticizer were adjusted such, that the total volume of water, latex and superplasticizer in each mix is same as that of water content in the plain mortar mix. The quantities of latex are expressed as latex/cement ratio (L/C ratio) by weight and the quantities of superplasticizer are expressed as percentage by weight of the cement. The quantities of the latex and the corresponding dosages of the superplasticizer are as shown below:

Latex/Cement Ratio by Weight	Superplasticizer (% by Weight of cement)
0.05	0.5
0.10	1.8
0.15	2.7

For the quantities of latex for L/C ratios beyond 0.15, it was found that the latex gets coagulated irrespective of the quantity of superplasticizer. So, the maximum quantity of latex that could be used as an admixture was 15% by weight of cement. It was further explored to reduce water content in mixes with latex/cement ratios less than 0.15 for the same level of 2.7% of superplasticizer. This information was quite useful, subsequently, in proportioning of latex concrete mixes with reduced water requirements.

In all the earlier studies, the quantity of latex has been expressed as L/C ratio. This has the following two inconsistencies:

i) Ductile behaviour is mainly due to rubber in the latex. The quantity of rubber varies for different latexes from different sources. So, even for the same ratio of L/C, the quantity of rubber available for imparting ductility would be different.

ii) There can be variation in the quantity of cement for a concrete of specified strength. So, the quantity of latex varies even when L/C ratio is the same.

To tide over these inconsistencies, the possibility of expressing quantity of latex in terms of Dry Rubber Content (DRC) as a percentage by weight of the concrete was examined. But, this led to another difficulty. The concrete which can develop the same level of strength can have different unit weights depending upon the specific gravities of cement, fine and coarse aggregates and their corresponding quantities for a unit volume of concrete. Hence, the quantity of dry rubber content or natural rubber latex varies with respect to the unit weight of the concrete. Finally, it has been found that expressing the quantity of latex by dry rubber content (DRC) by the percentage of volume of the concrete (volume fraction of rubber v_R) would overcome all the inconsistencies for relative comparison of the properties.

Cylindrical concrete specimens of size 10 cm dia x 20 cm height were prepared for testing them for stress-strain relation. The water/cement ratio of the plain concrete was 0.5, aggregate/cement ratio was 5.84 and the ratio between fine and coarse aggregates was 1:2.26. Graded aggregate of 20 mm maximum size and sand conforming to Zone II was used. Ordinary portland cement conforming to IS:269-1976 was used in this investigation. The physical and chemical properties of the cement are as given below:

TABLE 1 PROPERTIES OF CEMENT

Physical	Chemical
a) Fineness = 3150 cm^2/g (Blaine's)	a) LOI = 1.27 %
	b) MgO = 1.21 %
b) Setting Time Initial = 110 min Final = 4h 20 min	c) IR = 1.10 %
	d) SO_3 = 2.15 %
c) Soundness Le-Chatelier exp = 1 mm	e) LSF = 0.82 %
d) Compressive strength 3 days = 245 kg/cm^2 7 days = 380 kg/cm^2 28 days = 540 kg/cm^2	

Natural rubber latex concrete mixes with dry rubber content of 1 to 3%, in steps of 0.5% increase were formulated. The reduction in total fluid content, with reference to water/cement ratio of 0.5 for plain concrete, indicated in table 2 have been effected only to water with quantity of latex and superplasticizer remaining constant. Latex concrete mix proportions with reduced water/ cement ratios are listed in the table 2.

The specimens were cast in the usual manner. The latex concrete specimens were cured under wet burlap for seven days and were transferred to a pond, where they were cured for 21 days at ambient temperature. The specimens were tested for stress-strain relation in direct compression. Compression tests were carried out in a 500 KN capacity displacement rate controlled testing machine. The rate of the movement of platen was fixed at 0.0525 mm/min. Figure 1 shows the compressive stress-strain curves for plain and natural rubber latex concretes with varying percentages of dry rubber content.

It can be seen that for dry rubber contents up to 2%, the maximum compressive strength is almost same compared to that of plain concrete, but with a pronounced increase in the strain capacity. This reflects a marked increase in the ductile behaviour of latex concretes. Beyond a dry rubber content of 2%, although the ductile behaviour is pronounced, latex concretes result in strength reductions to the extent of 15% to 30% over the strength of plain concrete. The decrease in the strength of natural rubber latex content beyond DRC of 2% is due to the presence of more rubber as soft inclusion with simultaneous reductions in attractive forces among cement gel particles. The reduction in water/ cement ratio that could be effected in this study could compensate only for the otherwise strength reductions due to weak inclusion of rubber particles in latex concretes only up to DRC of 2%.

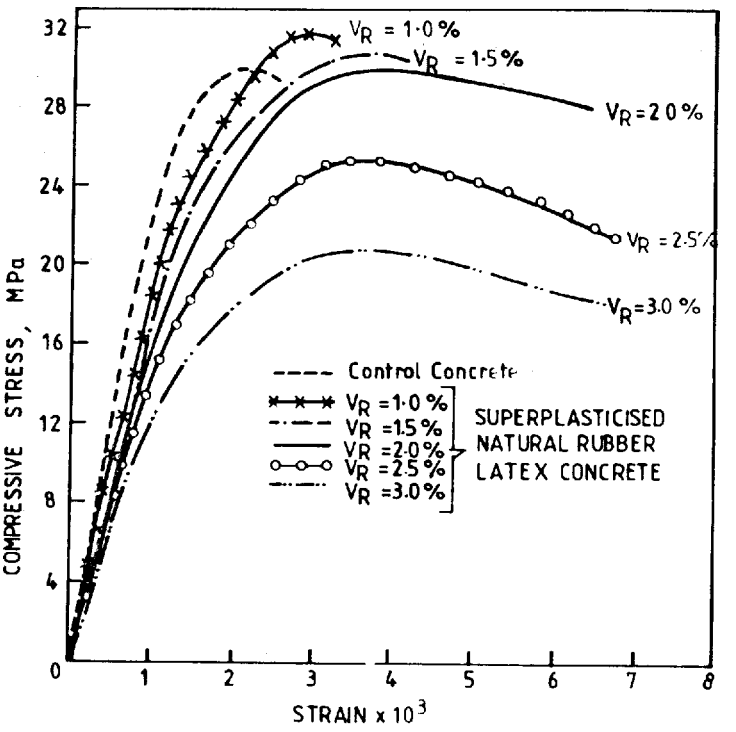

FIG 1 STRESS-STRAIN RELATION FOR LATEX MODIFIED CONCRETES

TABLE 2 LATEX CONCRETE MIX PROPORTIONS

Cement:Sand:Coarse Aggregate = 1:1.79:4.05

Dry Rubber Content	Reduction in Total Fluid Content(%)*	Water/ Cement Ratio	Latex/ Cement Ratio	Super-plasti-cizer (%)	Bulk Density (kg/m^3)	Cylinder Compressive strength (kg/cm^2)
Plain Concrete	0.00	0.50	0.000	0.0	2414.00	295
1.0	10.70	0.37	0.042	2.7	2444.34	315
1.5	8.70	0.36	0.064	2.7	2437.82	305
2.0	6.35	0.35	0.086	2.7	2437.60	285
2.5	4.15	0.34	0.108	2.7	2425.12	243
3.0	2.00	0.33	0.130	2.7	2419.00	195

* Total fluid content refers to total volume of water, latex and superplasticizer

INCORPORATION OF STEEL FIBERS IN THE LATEX MODIFIED CONCRETE

The marked improvements in the ductility of the latex modified concretes, prompted to probe further by incorporating steel fibers in the latex modified concretes. It was assumed that the failure of the interface between the steel fibers and latex concrete

would be more ductile, because of the presence of rubber. In order to verify this assumption, steel fibers of 1.5% of the volume of concrete were incorporated in the latex concrete of 2% DRC. Specimens also were prepared by incorporating the same percentage of fibers in the plain concrete to make a comparative study. In both the concretes, the mix proportions were same as explained earlier. The stress strain relations of these concretes are shown in Figure 2. Remarkable improvement in the strain capacity can be seen in the case of combined latex and fiber reinforced concrete.

Hence, it is evident that natural rubber latex plays an important role in improving the ductility of the concrete.

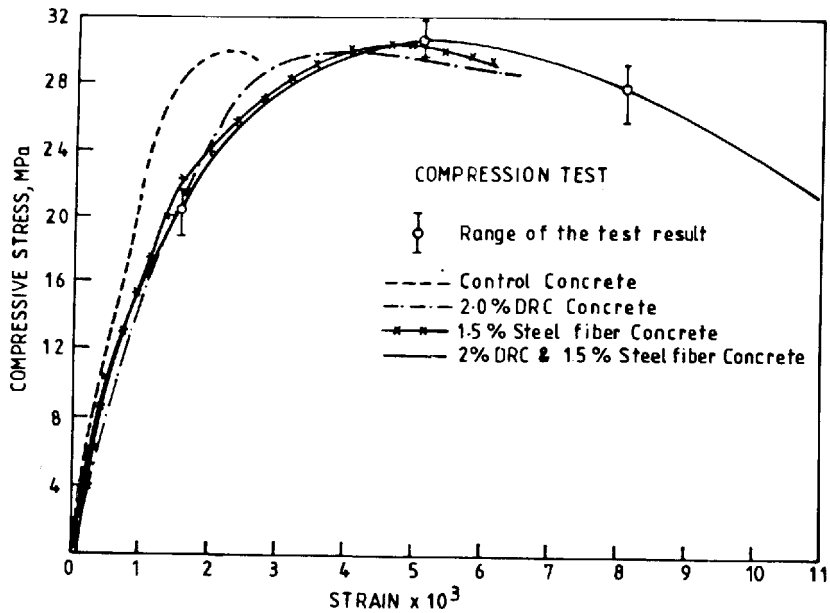

FIG 2 STRESS-STRAIN RELATION OF CONCRETE WITH STEEL FIBERS & NATURAL RUBBER LATEX

CONCLUDING REMARKS

On the basis of the experimental findings, the following concluding remarks are made:

i) With natural rubber latex as an admixture, the ductility of the concrete gets enhanced.

ii) The use of superplasticizer helps to reduce the water content and also to delay the coagulation of the rubber.

iii) The quantity of the natural rubber latex can be expressed as the dry rubber content being the percentage of volume of the concrete.

iv) A dosage of 2% dry rubber content is found to be the optimal dosage.

v) The combination of natural rubber latex and steel fibers yielded more ductile behaviour to the concrete.

REFERENCES

1. Ravindra Rajah, R.: "Effect of Natural Rubber Latex on the Properties of Portland Cement Paste, Mortar and Concrete". **Third International Congress on Polymers in Concrete**, 1981, **V1**, p 380-394.

2. Mangat, P.S. and Swamy, R.N.: "Properties of Polymer Modified Plain and Fiber Reinforced Concrete". **Proceedings of the First International Congress on Polymers in Concrete**, London, May 1975, Construction Press, 1976, p 296-299.

3. Mangat, P.S. and Swamy, R.N.: "Some properties of Fiber-Polymer Concrete Systems". RILEM, Materials and Structures, Nov-Dec 1977, 10(60).

EXPERIMENTAL INVESTIGATION OF FRACTURE PROPERTIES OF ORDINARY CONCRETE AND POLYMER CEMENT CONCRETE

Wang Xinyou, Chen Gaixin and Wu Keru

Department of Materials Science and Engineering, Tongji University
Shanghai, P.R. CHINA

SUMMARY

This paper reports on an experimental study of the fracture properties of ordinary concrete and polymer cement concrete. The polymer used was styrene butadience latex, and it was randomly mixed in concrete at different volume fractions The complete load-crack opening displacement curve, fracture toughness and fracture energy of the concretes have been obtained by means of wedge splitting test. The test results indicated that water cement ratio and volume fractions of polymer greatly affects the fracture properties of the concretes, and polymer cement concrete is much tougher than ordinary concrete due to the addition of polymer.

摘　要

本文使用楔入劈裂法实测了普通混凝土和掺丁苯胶乳聚合物水泥混凝土的荷载—裂纹张开位移全曲线、断裂韧性、断裂能和抗压强度等力学性能。试验结果表明，水灰比及聚合物掺量对混凝土的断裂性能有较大影响，由于掺加聚合物，混凝土的韧性将得到较大改善。

INTRODUCTION

Concrete-polymer composites are the complicated engineering materials which are made by properly arranging inorganic materials and the organic materials. The development of the concrete-polymer composites was a very important progress in the concrete materials. In last decade, more and more researchers have paid great attension to the concrete-polymer composites with increasing use of these materials (1). However, most of the previous investigations is mainly to study the physical and chemical properties of the concrete-polymer composites, very few researcher has studied the macro mechanical properties, especialy the fracture properties of them. In this paper, the complete load-crack opening displacement curve, fracture toughness and fracture energy have been determined by means of the wedge splitting test (2) for studyting the fracture characteristics of ordinary concrete and polymer cement concrete with a styrene-butadiene latex.

MATERIALS

Ordinary concrete was prepared using the following materials: No. 525 Portland cement, river gravel with a specific gravity of 2.65 which has the maximum aggregate size 15mm, river sand with a specific gravity of 2.61, and high range water reducing agent only for preparing high-strength concrete. Polymer cement concrete (PCC) was prepared using all the materials similar to those for the ordinary concrete and a styrene-butadiene (SBR) latex as a polymer for PCC. Table 1 gives the properties of the latex used in this study.

Table 1 Properties of latex

Total solid content (%)	PH (20° C)	Viscosity (CP)	Surface tension dyn/cm (20° C)	Specific gravity (20° C)	Average particle diameter (μm)	Glass transition temperature (° C)
51	6.5-9.5	<1000	50	1.01	0.18	-7-+10

In this study, water-cement ratio W/C of ordinary concrete and PCC and the polymer content of PCC were considered as the variables of investigation, their mix proportions are listed in Table 2.

Table 2 Mix proportions of ordenary concrete and PCC

Mix series		Mix proportions (by weight) Cement:Sand:Gravel:Water	Polymey content (vol.%)	Polymer cement ratio(%)
OA	OA1	1:1.93:3.14:0.70	0	0
	OA2	1:1.93:3.14:0.60	0	0
	OA3	1:1.93:3.14:0.50	0	0
	OA4	1:1.93:3.14:0.45	0	0
	OA5	1:1.93:3.14:0.40	0	0
PA	PA1	1:2.21:3.47:0.48	6	5
	PA2	1:2.27:3.56:0.45	11	10
	PA3	1:2.36:3.70:0.43	16	15
	PA4	1:1.25:3.21:0.29	20	15
PB	PB1	1:1.20:3.07:0.31	13	10
	PB2	1:1.28:2.98:0.34	13	10
	PB3	1:1.77:3.15:0.38	12	10
	PB4	1:2.27:3.56:0.45	11	10

EXPERIMENTAL

Wedge Splitting Test

Preliminary test results and theoretical analysis had shown that the wedge splitting(WS) test is a good method to determine the fracture properties of concrete. Therefore, WS test was selected for this studyl. Test apparatus is shown in Fig.1. The test results obtained by WS test are the complete load-crack opening desplacement(P -COD) curves, and the fracture toughness K_{IC} and fracture energy G_F was calculated on the basis of the equations through these complete P-COD curves. These calculation equations have been inferred by the authors (3) according to the loading and geometry conditions of WS test.

Preperation of Specimens

The sizes and geometry of specimens with a saw-cut notch required by WS test arw shown in Fig.2. Compressive strength of concrete was also obtained for every mix propertion using the cube specimens 100mm 100mm 100mm.

All specimen were cast according to the standard methods. The specimens of ordinary concrete were cured at room temperature for 24 hours, demolded, and then moved to the standard curing room to the test time. PCC specimens were cured at room temperature for 24 to 48 hours, demolded, and then moved and cured at the standard curing room for 7 days. Prior to testing, the PCC specimens were removed to the room conditions and cured to the testing time. The test age is 28 days, and the initial depth of the notch is 50mm for all the specimens.

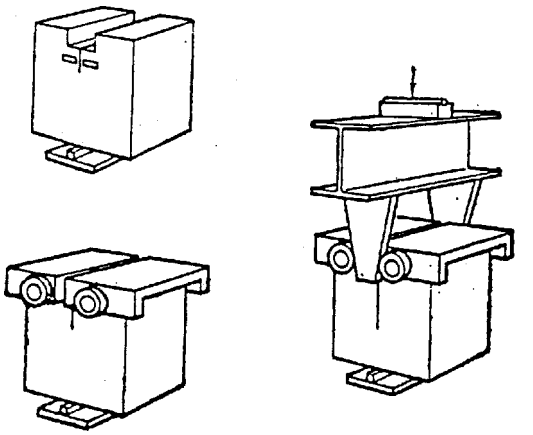

Fig. 1 Setup of wedge splitting test apparatus

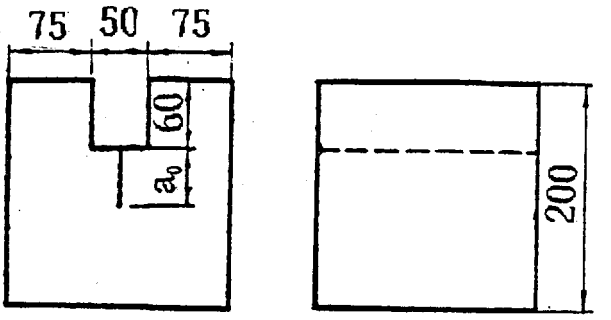

Dimenion: mm

Fig 2 Geometry of specimen

RESULTS AND DISCUSSION

The complete P-COD curves can be stably detected by means of WS test. Fig. 3 and 4 show the typical P-COD curves for concrete OA and PA. The fracture properties of concrete, such as fracture toughness K_{IC}, fracture energy G_F, the maximum load P_{max}, the crack opening displacement at the peak load COD_0, and so on, can be gained from the measured P-COD curves. The compressive strength f_c are determined by means of standard compressive test. All the experimental results are given in Table 3.

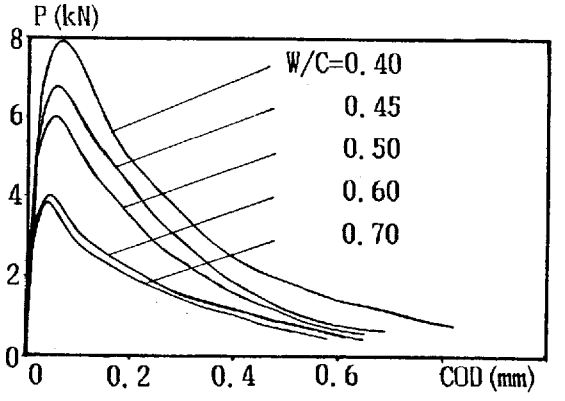

Fig. 3 Effect of water -cement ratio on the P-COD curves forconcrete OA

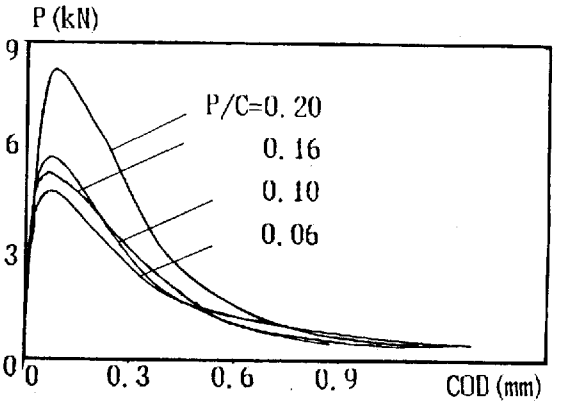

Fig. 4 Effect ofthe ploymer content on the P-COD curves for concrete PA

Table 3 Fracture mechanical properties of ordinary concrete and PCC

Concrete		Compressive strength	Wedge splitting test: Peak load	COD at peak load	Fracture energy	Fracture toughness
		f_c (MPa)	P_{max} (N)	COD_0 (mm)	G_F (N/m)	K_{IC} (kN/m$^{3/2}$)
OA	OA1	19	3825	0.036	99	553
	OA2	31	4000	0.042	116	579
	OA3	43	6000	0.052	159	866
	OA4	46	6750	0.054	163	977
	OA5	47	7875	0.060	218	1138
PA	PA1	35	4730	0.065	189	708
	PA2	36	5700	0.068	191	857
	PA3	32	5050	0.078	203	773
	PA4	49	8200	0.084	254	1207
PB	PB1	54	8870	0.086	294	1348
	PB2	47	7560	0.063	274	1122
	PB3	46	6720	0.081	232	1012
	PB4	36	5700	0.068	191	857

Influence of Water-Cement Ratio

The influence of water-cement ratio on the fracture properties and compressive strength of ordinary concrete and PCC is shown in Fig. 5 and 6. It is clear that W/C greatly affects the concrete properties, and these properties have almost same changing tend and range with the increase of W/C for ordinary or PCC. On the other hand, W/C plays more important role on the properties of ordinary concrete than those of PCC, as shown in Table 3. This difference may be caused by different microstructure of ordinary concrete and PCC. Because PCC contains the polymer, it is certain that its mechanical properties are not only depend on W/C, but also related to the volume fractions of polymer.

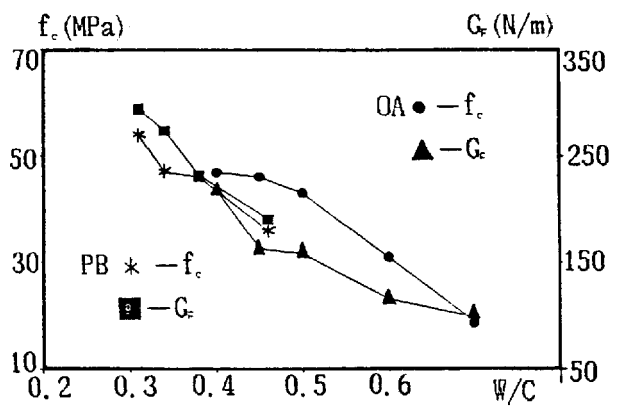

Fig. 5 Variation of fracture energy and compressive strength of ordinary concrete and PCC with water-cement ratio

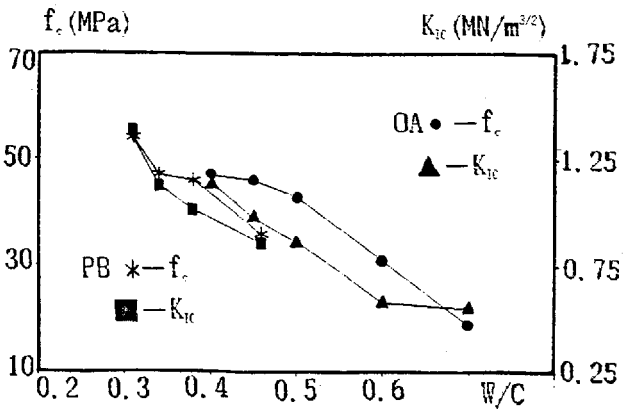

Fig. 6 Variation of fracture toughness and compressive strength of ordinary concrete and PCC with water-cement ratio

Influence of the Volume fractions of polymer

Fig. 4 indicates that the volume content of polymer heavily affects the complete P-COD curves. With the increase of the polymer content, the compressive strength and fracture toughness will decrease, and reach the minimum, but the fracture energy will increase all the time as shown in Fig. 7 and 8.

When the polymer is added to ordinary concrete and a net work structure of polymer phase is formed, the bond capability between aggregate and matrix, and bond capability between get particles of cement are then improved. Thesefore, the tensile strength and toughness of PCC are then improved. According to the failure mechanism of concrete, the compressive strength of the concrete is indirectly increased. On the other hand, because of the lower glass transition temperature of the latex, the latex gives the state of soft and high elasticity, and its elasticity modulus is smaller than that of hardended cement paste. When PCC is loaded in compression, the polymer phase is not strong and stiff to the load, that is, that the polymer provides a 'sub void' phase, and thus weakens the compressive strength of PCC. This means that the compressive strength and fracture energy of PCC are depend on the combined effect of the above two aspects. It is clear that no matter which effection isdominant in PCC with different polymer contents, fracture energy of PCC always increases with increasing polymer content. However, when the polymer content is smaller, the compressive strength decreases and reach to its minimum value with the increase of the polymer contents. When the ploymer content surpass 0.15, the microstructure of PCC will be evener and denser with increasing polymer content, and compressive strength then increases.

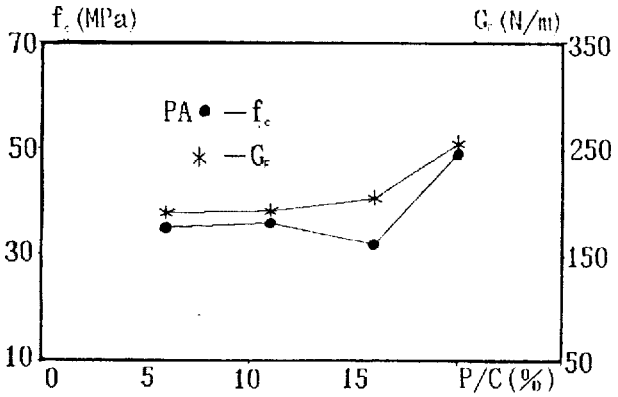

Fig. 7 Variation of fracture energy and compressive strength of PCC with the polymer content

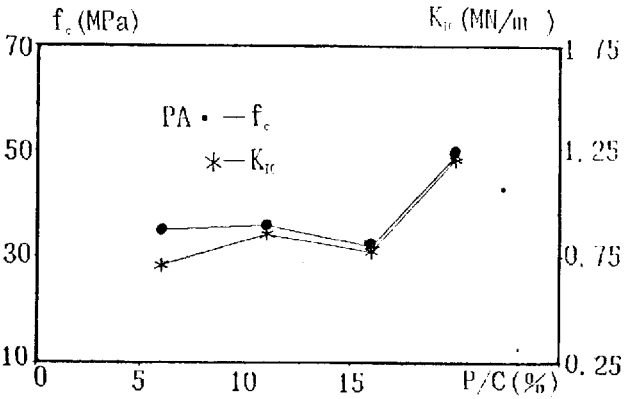

Fig. 8 Variation of fracture toughness and compressive strength of PCC with the polymer content

Comparison of Fracture Properties of Ordinary and PCC

In general, the complete P-COD curves for ordinary concrete are more steeper than those of PCC. If the maximum load of them are the same, the displacement at the maximum load, maximum displacement and fracture energy of ordinary concrete are

smaller than those of PCC as shown in Fig.3 and 4. It is also observed that the decending branch of the complete P-COD curve for PCC has a longer tail, and there are no brustic and brittle failure of the PCC specimens in test. When the compressive strength of ordinary concrete is the same or close to that of PCC, the fracture energy of PCC is much bigger than that of the ordinary concrete. From these test results and phenomena, it can be concluded that after the polymer is added to the ordinary concrete, the toughness of the composite will be improved to a great extent.

The mechanism of improving toughness of PCC may be explained as follows: (1) The polymer exist mainly in cement paste in the state of three-dimensional continuous net work structure which is similar to the 'micro fibers', and then improves ability resistant to cracking due to the good ductility and high tensile strength of the polymer. Kuhlman (4) has ever taken a photo showing clearly the toughness- improving mechanism of these 'micro fibers' of the polymer structure. (2) Due to the existance of various surface active subtances in the polymer, the ability of surfaces of aggregate particles and imersing the surface pores of the aggregate particles in fresh concrete is strengthed. At the same time, a lot of the dispersed particles of the polymer are absorbed to surface, and sometimes enter the surface flaws of the aggregate particles themselves. Therefore, polymer films form and stick to the surfaces of the aggregate particles. This leads the results of improving the bond capacity between PCC and the aggregate, and effectively prevents the formation and propagation of the cracks.

CONCLUSIONS

1. The water-cement ratio has the same influence on the mechanical properties of ordinary concrete and on those of PCC. Meanwhile, the mechnical properties of ordinary concrete are more heavily depend on water-cement ratio than those of PCC.

2. Fracture energy of PCC with SB latex used in this study increases with increasing polymer content, but the compressive strength and the peak load will reach the minimum values, and then increase.

3. PCC has high toughness. This is primarily due to affection of the 'micro fibers' mechnism of the polymer structure and the higher bond ability between aggregate and cement paste improved by the polymer active subtances.

REFERENCE

1. Polymers in Concrete, Proceedings of 6th International Congress on Polymer in Concrete, September 24-27, 1990, Shanghai, China, ed by Huang Yinyuan, Wu Keru and Chen Zhiyuan, International Academy Press, Beijing, 1990.
2. Tschegg, E.K. and insbaner, H.N., Test methods for the determination of fracture mechnics properties, Patent Specification, No. A-233/86, Australian Patent Office, 1986 (in German)
3. Wang Xinyou and Wu Keru, Study on the wedge splitting test method for determining fracture parameters of concrete, Journal of Shanghai Institute of Building Materials, Vol. 3, No. 4, December 1990, pp357-367 (in Chinese)
4. Kuhlman, L.A., Latex-Modified Concrete, ACI, SP69-8, pp. 123-144.

THE COMPOSITION, PROPERTIES AND APPLICATION OF COMPOUND EXPANSIVE AGENT

Wang Yanshen, Jiang Yunan, Zhang Gueiqing and Ma Kueihong

China Building Materials Academy, Guanzhuang, Beijing, P R CHINA

ABSTRACT

This paper introduces the composition, properties and application of a compound expansive agent (CEA) and comparison between the CEA and calcium sulphoaluminate expansive agent.

〔摘　要〕

本文介绍了复合膨胀剂的组成、性能和应用实例并与硫铝酸钙型膨胀剂作了对比。

To lower concrete shrinkage and lessen concrete cracking, we developed a CEA and have used it for decades in underground constructions, water resources engineerings, bridges and prestressed concrete constructions with satisfactory application results.

COMPOSITION AND PROPERTIES CEA

The CEA is made by mixing expansive clinker, natural alunite and gypsum in proper proportion, then grinding the mixture into fine powder with a specific area of 230～270 m^2 / kg. When 8—12% CEA is used to replace ordinary portland cement in concrete, one can get suitable amount of expansion and strength compensation, and cracking of concrete is remarkably reduced, impermeability improved, architectural perfomance bettered.

Expansive clinker consists of limestone, clay and iron oxide powder, and formed by calcination under 1350—1400℃. The mineral composition of expansive clinker includes 45—50% C_3S and 35—40% crystal CaO particles of size 15–35 μm. 40–60% CaO crystal particles are enclosed by C_3S, C_3A and C_4AF.

Natural alunite is the raw material for alum, its main composition being $K_2SO_4 \cdot Al_2(SO_4)_3 \cdot 4Al(OH)_3$ with α—SiO_2 and kaolinite.

CEA Compositions Table 1

Loss	SiO_2	Al_2O_3	Fe_2O_3	CaO	MgO	SO_3	K_2O	Na_2O	f–CaO	Σ
1.02	18.76	4.10	1.76	66.96	0.53	6.20	0.53	0.41	35.86	100.17

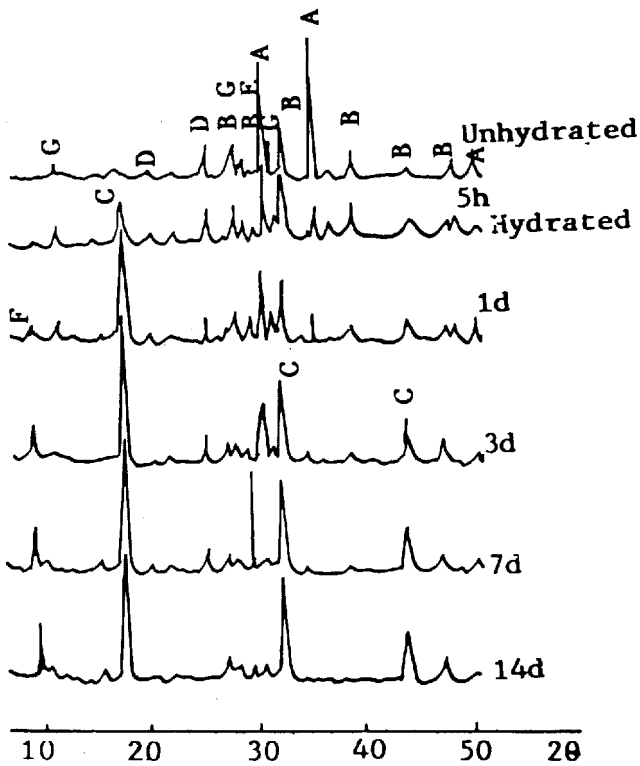

Fig.1 XRD diagrams of CEA hydrated for different ages

A–CaO; B–C_3S; C–$Ca(OH)_2$;
D–α–SiO_2; E–$(Na,K)Al_2(SO_4)_3 \cdot (OH)_6$;
F–$C_3A \cdot 3CaSO_4 \cdot 32H_2O$; G–$CaSO_4 \cdot 2H_2O$

When CEA starts to hydrate $Ca(OH)_2$ appears after 5 hours. The $Ca(OH)_2$ grows steaily with the increase of hydration age while the CaO peaks decrease gradually, until CaO is completely exhausted at 7 days. Ettringite appears at the age of 1 day and increases with the hydration time. Alunite decreases and fades away slowly. At the age of 14 day, its peak is just visible, see Fig.1.

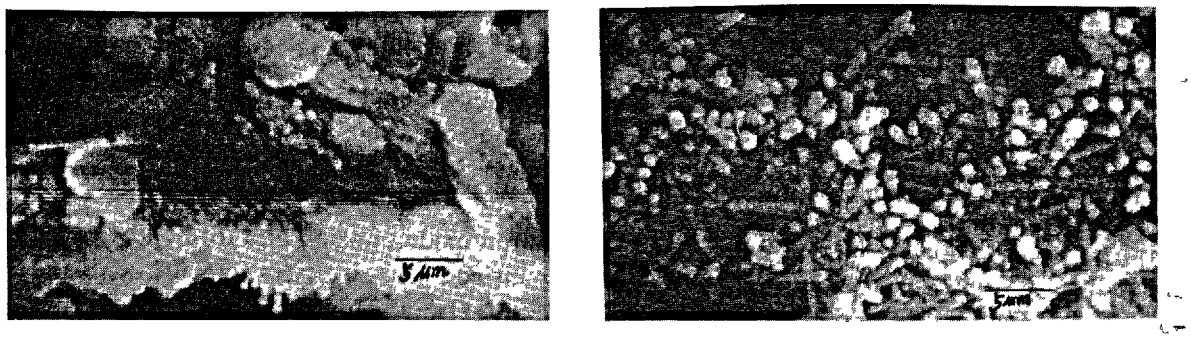

(a) 3d (b) 7d

Fig.2 SEM photographs of CEA hydrated for 3d, 7d

SEM observations have proved a thin layer of collodial hydrated products on the particle surface at 5 hours. At the age of 1 day, the colloidal range increases and at 3 days the collidal products turn into hexagonal crystal and flowery $Ca(OH)_2$, and a little bit ettringite (Fig.2a). Ettringite crystal size become larger which interlock wiht the colloid at the age of 7 day (Fig.2b).

525 grade ordinary portland cement incorporated with 10% CEA has a inintial setting of 2：00 ~2：30 and final setting of 3: 30~4: 50.

Mortars containing 10% CEA with cement sand ratio of 1:2 and water cement ratio of 0.4 were demoulded after curing in moisture for 16~18 hours. Then their initial lengths were measured and placed in 20±3℃ water till testing age. The size of specimen was 25×25×280mm and the specimen for strength test was 40×40×160mm.Results are given in Table 2.

Properties of Mortar Containing 10% CEA with Cement Sand Ratio of 1:2 Table 2

Items	3d	7d	28d	3m	6m	1y	3y	6y
Compressive strength (MPa)	27.4	40.2	59.0	70.3	74.3	75.9	81.7	83.1
Flexural strength (MPa)	6.5	7.5	9.9	10.0	10.1	10.0	10.1	10.1
Restrained expansion (%)	0.021	0.032	0.043	0.048	0.049	0.048		
Self-stress (MPa)	0.58	0.38	1.18	1.31	1.37	1.29	1.32	
OPC compressive strength (MPa)	32.1	45.8	64.0					
OPC flexural strength (MPa)	6.8	8.2	10.2					

To observe the shrinkage characteristics of CEA in dry air circumstance, we prepared 1:2 mortars in which 10%, 20%, 30% and 40% CEA were added for strength and expansion tests. The specimens were cured in 75% rh air to 1, 3, 5, 7 and 28 days for testing. The specimen incorporating 10% calcium sulphoaluminate expansive agent (CSA) was also made for comparison. The test results are shown in Fig.3.

Compressive Strength (MPa)

		3d	7d	28d
1–CEA	10%	30	31.5	43.4
2–CEA	20%	23.0	25.0	31.5
3–CEA	30%	13.3	17.5	20.4
4–CEA	40%	7.6	8.3	18.7
5–CSA	10%	25.0	32.2	37.0

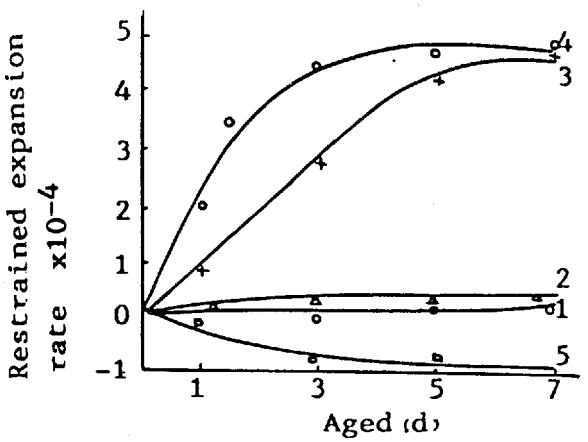

Fig.3 The restrained expansion value cured in air of 75 rh.

The results in Fig.3 have proven that the specimens incorporating CEA have a expansion effect in the environment of 75% rh air, and expansion increases with the increase of CEA content. Strength results show the reverse trend. But the specimen containing 10% CSA demonstrates shrinkage in the same condition.

For concrete expansion test, we prepared 10 × 10 × 30 cm specimens. The mixing preportion of concrete mixture is (cement+CEA) : sand: gravel:water= 1: 1.87: 2.93:0.52. The dosage of CEA was 10%. Test results are given in Fig.4.

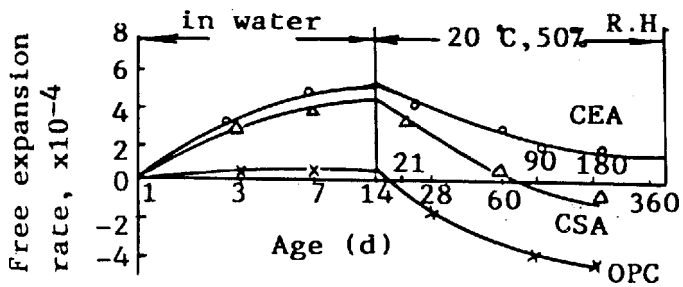

Fig.4 Free expansion of CEA concrete

The expansion value of CEA concrete cured in water for 14 days is 4.5×10^{-4}, later the specimens kept in air of 20℃ and 50% rh for 1 year, show expansion of 1.1×10^{-4}, a expansion drop 3.4×10^{-4}. Considering the fact that the expansion drop of calcium sulphaluminate expansive agent in half a year is 5.3×10^{-4} under same condition and shows shrinkage rather than expansion, and OPC concrete shrinkage reaches 5.8×10^{-4} in half a year, CEA has the lowest shrinkage and most favorable for preventing cracking.

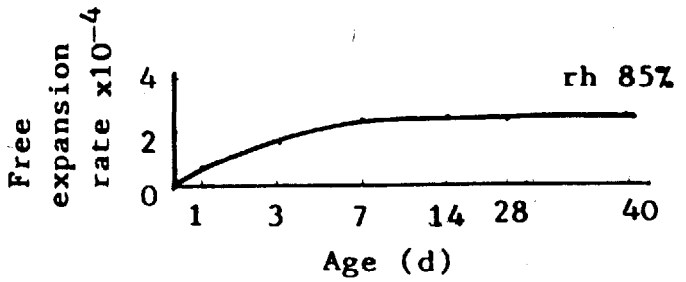

Fig.5 Expansion value of CEA concrete (rh 85%)

The expansion value of CEA concrete cured in damp atmosphere with a rh over 85% can reach 2.5×10^{-4}. With the percentage of reinforcement of 0.25~ 1.75%, CEA concrete can produce a self-stress of 0.3~1.0MPa.

The strength of CEA concrete Table 3

Dosage		Mix proportion	Slump	Strength (MPa)						
PC	EA	(C+A):S:G:W	cm	3d	7d	28d	3m	6m	1y	3y
88	12	1:1.84:2.83:0.55	11		20.74	35.1	45.9	48.2	49.8	52.4
90	10	1:1.64:3.65:0.525	15	21.2	37.2	46.0				
*100	0	1:1.69:3.65:0.53	14.6	18.41	36.6	43.2				

* OPC

The strength values in Tab.3 are obtained in a frec state. Test results have demenstrated that the strength of concrete in restrained condition will inereases 10~20%.

The impermeability grade of CEA concrete prepared with the mix proportion in Tab.3 can reach S34. In case of casting-in-place, CEA concrete impermeability varys between S_{10}~ S_{30}. It also has the freez-resistance grade of D250. The weight and strength loss are respectively 0.2% and 2.53% after 250 freeze-thaw cycles. The freeze-resistance grade of calcium sulphoaluminate expansive agent concrete is D100~D150.

Embeding Φ16 × 50mm smooth bar in CEA concrete, and curing concrete to 28 days, 2 months, 3 months and 6 months, no corrossion occurred on the surface of the smooth bar.

CEA caused no alkali-aggregate reaction and slump loss. If 0.15~ 0.25% lignosulfonate or 0.2% superplasticizer, or 0.1% naphthalene based water reducer are added in CEA concrete, concrete strength can increase 30% at 3 day, 10% at 28 day while its expansive property is not affected.

ANALYSES AND DISCUSSIONS

1. In the early age of hydration, CaO and H_2O react and form into $Ca(OH)_2$, and expansion appears. Activated by $Ca(OH)_2$ and $CaSO_4$, alunite in solution formed ettringite which fills the space in cement and concrete. As this prcess progresses, the structure become denser, the porosity decreases and pore distribution is improved [1] . At the late stage of hydration, alunite still exists and formation process of ettingite takes place over a long period of time. So the expansion of CEA belongs to the type of slow steady expansion, which is desired to keep cement and concrete expanding steadily to effeciently compensate concrete shrinkage, and prevent cracking. The ingenious combination of different expansive ingredient becomes the unique feature of CEA expansive agent.

When expansion process is in a dominant state and exceeds the capacity the strength can bear, strength will decrease with the increase of expansion, therefore the optimum effects can be achieved only if strength and expansion develop coordinately.

2. Why the expansion drop of CEA concrete is lower than that of calcium sulphaluminate expansive agent conerete?

According to reference [2] the number of crystalized water molecules in ettringite varies between 30~33, and changes with drying condition. When vapor pressure reaches p = 0.52 m.m. mercury, it drops to nearly 18, and when p = 0.49, to 16,P's further reduction will lead water molecules to drop to about 10. Ettringite will become transient product when it dehydrates in the drying process. The structure and composition will depend on the position and bond strength of water in AFt crystal.This phenomen can suggests the trend of ready dehydration of the hydrates produced by calcium suphoaluminate expansive agent in dry condition. The expansion is mainly contributed by $Ca(OH)_2$ which is insensitive to the drying process. Furthermore expansion from ettringite is very slow in CEA conerete, so it is expected to reduce the shinkage recession and prevent cracking.

3. Reference [3] has confirmed that $C_4A_3\underline{S}$ and CA react separately with $CaSO_4 \cdot 2H_2O$ and H_2O to form ettringite. Complete hydration of $C_4A_3\underline{S}$ and CA to form ettringite needs 58.15~63.17% water, and only 34.79% water would be needed for CEA to hydrate completely. Reference to Fig.3, mixing water in CEA concrete can meet the requirement of full hydration. This unique point suggests that strict water curing is not imperative for CEA concrete to achieve suitable expansion, thus is convenient for prepares.

ENGINEERING APPLICATION CASES

1. Beijing Xidan Underground Railway Station, including a underground bazaar, and two sections of the station. The structure is 260 meters long. 21 meters deep, 27 meters of span. Total CEA shrinkage compensating concrete consumption was 30000 m^3, mixing proportion was cement 400 kg / m^3, CEA 10% (weight of cement).

2. Beijing Urban and Rural Trade Exchange Center, 4 storeys underground with total square area of 39600 m^2, circumference 490 meters height of 15 meters, thickness 50 cm. CEA concrete was need for this project, CEA dosage 8.5~11%, compressive strength at 28 day reached 34~36 MPa. No cracking and leakage have been found after 4 years service.

3. Beijing Asian Games Gymnasium, 2400 m^2 floor was cast in place and no shrinkage joints

were preset. Concrete strength at 28 day reached 34.3~43.1 MPa. Expansion in moist environment was 2×10^{-4}. No cracking or leakage were observed.

4. Fujian Longmentan Dam partition. Dam length 104 meters, height 40 meters, bottom substrate thickness 60 cm, top layer 35 cm, cast in place, no transverse shrinkage joint, constructed from CEA conerete.

5. No.2 Qian Tang Jiang Bridge, includes 1700 meter highway and 2800 meter railway. To assure the close connection between the bridge beck and piers, 1:2.5 CEA mortar was used as grout.

CONCLUSIONS

1. CEA is made by grinding a mixture of expansive clinker, natural alunite and gypsum. The expansion from the formation of $Ca(OH)_2$ occurs at the early age of hydration, and expansion caused by ettringite happens at late age and continues at a low rate.

2. The developments of strength and expansion of CEA mortar and concrete carry out coordinately and steadily. CEA mortar and concrete possess good impermeability and freeze resistance. Compared to calcium sulphoaluminate expansive agent, they show lower shrinkage and better freeze resistance, and do not require strict water curing.

3. CAE concrete has obtained good applications results in the field of waterproof marine structure, bridge and building industry. Furthermore, low cost and rich raw material resources of CEA render it promising building material.

REFERENCES

1. Wang Yansheng , Zhang Gueiging et al: "The Compound Expansive Agent for Concrete". Journal of Chinese Ceramic Soceity, 1987, 15[5] 472–477.

2. К.Г. Красильников, Л.В. Никитина, et al: "Physical and Chemical Process of Cement Expansion". Proc. of 6th Intern Cem. Chem. Vol 3. Cement and its Properties, China Building Publication, Beijing, 1980, 258–262.

3. Xue Jungan, Wu Zhongwei: "Expansive and Self–Stressing Cement". China Building Publication, Beijing, 1979, 272–334.

PROPERTIES OF UEA SHRINKAGE-COMPENSATING CONCRETE AND ITS APPLICATION IN ENGINEERING FOR ASIAN GAMES

You Baokun, Wu Wanchun, Yu Faming, Han Lilin and Chen Fuyin

China Building Materials Academy, Guanzhuang, Beijing, P R CHINA

ABSTRACT

In this paper the properties of UEA shrinkage–compensating concrete is introduced and the principle of crack resistance and impermeability for the UEA concrete is explained, the practice of engineerings for Asian Games in Beijing using UEA concrete, technical and economic benefits, and the future use of UEA concrete in physical construction are described.

[摘　要]

阐述了掺U型膨胀剂（UEA）的补偿收缩混凝土的性能及其抗裂防渗原理。文中介绍了该混凝土在亚运工程中应用情况和技术经济效果。补偿收缩混凝土在体育建筑中的应用有广阔的前景。

UEA can be added to portland cement or portland cement with additions blast furnace slag, fly ash or other pozzolana. The setting time for these cements with UEA is normal. They do not bleed basically, but their slump loses slightly faster.

Table 1 gives the physical properties of cements with and without UEA. Table 2 shows the properties of concretes with different amount of UEA. It is seen from Table 1 and 2 that the strength for the concrete with the substitution rate for cement of 10～12% UEA (internal mixture) is not affected on the whole — the early strength is increased and the long time strength continues to grow. The strength for restrained expansive concrete increase by 10–20% compared with unrestrained expansive concrete. Hence, UEA concrete is a reliable structural material.

Physical Properties for UEA Cements Table 1

No.	UEA Added	Setting Time		Restrained Expansion Rate ($\times 10^{-4}$)				Compressive Strength (MPa)			Bending Strength (MPa)		
		initial	final	in water		in the air		3days	7days	28days	3days	7days	28days
				3days	7days	14days	28days						
1	0	2:17	3:25	−0.2	0.14	−1.6	−2.8	19.8	34.5	58.4	3.6	5.9	7.8
2	10	1:50	3:15	2.5	3.0	1.5	0.05	26.7	39.3	58.2	4.5	6.4	8.1
3	12	1:20	2:50	2.8	3.5	2.0	0.08	25.7	36.4	56.3	4.1	6.2	7.6

Properties for UEA Concrete Table 2

No.	UEA Added (%)	WC (%)	Slump (cm)	Restrained Expansion Rate (10^{-4})				Compressive Strength			Impermeability Grade
				3days	7days	14days	28days	3days	7days	28days	(S)
0	0	0.52	5.6	0.67	0.67	0.50	0.10	28.0	31.6	40.8	S10
1	10	0.52	5.4	1.75	2.00	2.10	2.50	31.5	33.2	42.5	S30
2	12	0.50	5.1	2.12	2.50	2.80	3.01	28.2	30.6	40.6	S30
3	15	0.50	5.2	2.58	3.62	3.82	4.10	19.5	28.7	35.7	S20

The restrained expansion rate is increased with the amount of UEA added. For the internal mixture of 10–14% UEA the rate is 200–400$\mu\varepsilon$, converted to 0.2–0.7 MPa pre-compressive stress. The expansion ends within 14 days, and the expansive stability is in a good state.

The UEA concrete has roughly the same modulus of elasticity and poisson's ratio as ordinary concrete. Its bond strength with steel bars is 20–30% greater than that for ordinary concrete. It does not rust steel bars and resists sea water well. The impermeability grade of UEA concrete is greater than S30, the frost resistance grade greater than D150.

UEA has good miscibility with other admixtures and can be used in pumped concrete, fluidizing concrete and antifreezing concrete.

1. INTRODUCTION

The statistics shows that drying shrinkage and temperature deformation can cause racking of structure. Cement chemists tried to make an expansive cement able to compensate the cement shrinkage [1] . In 1936, H. Lossier made the material for the first time and later the Soviet Union, Japan and the United States developed the material and applied it to engineerings. China began its study of the expansive–self–stressing cement in 1956 and put it into use in the mid–seventies. This paper introduces type–U expansive agent (UEA), a concrete agent having selected the essence of expansive cements in the world, passed the technical appraisement of ministerial level in 1988 produced in ten factories of China, and rated as a new product of national class.

Many countries have mass–used shrinkage compensating concrete in large scale constructions. A skating rink was built in Sapporo Hokkaido in Japan, using shrinkage–compensating concrete with 11% expansive agent for the Winter Olympic Games in 1972 [3] . The rink, 60 m long, 30 m wide and 12 cm thick, was constructed of jointless concrete with freezing pipes embedded in it. Type K shrinkage–compensating cement concrete was used for the ice hockey rink in the Metropolitan Sports center of Bloomington, Minn. the United States. The 1653.6 m^2, 15.2 cm thick slab with the refrigeration piping under playing surface was placed continuously by pump [4] . The monolithic self–stressing concrete was used to reconstruct V.I. Lenin Stadium and "Dinamo" Stadium in the Soviet Union for the XX11 Olympic Games [5]

Since 1986, China has applied the shrinkage–compensating concrete with UEA to the construction of physical facilities, for example, the bleachers of the stadium of track and field, the overhead passages of sports centre, the natatorium, the amusement palace, the museum of physical culture, the boxing gymnasium, the bleachers of hockey field and the sportsmen inspection and registration office were built in the north suburb of Beijing for Asian Games 1991, resulting in good structural self–waterproofing. The world's engineering practice indicates that the application of shrinkage–compensating concrete to the physical construction and other civil engineerings has broad prospects.

BASIC PROPERTIES FOR UEA CONCRETE

UEA consists of sulfoaluminate, aluminium sulfate, alumina, calcium sulfate. It is white powder with specific gravity 2.90. When the cement with addition of UEA hydrates, the expansive ettringite ($C_3A \cdot 3CaSO_4 \cdot 32H_2O$) forms and the concrete expands. The concrete is restrained by reinforcing bars and the neighbouring concrete and tensile stresses are created in steel bars by the concrete. 0.2～0.7 MPa pre–compressing stress builds up in the concrete and counteracts the tensile stress resulting from drying shrinkage of the concrete. In addition, the UEA concrete delays onset of shrinkage, and the tensile strength increases sufficiently so as to withstand the shrinkage stresses before shrinkage of concrete takes place. The combination of the effects of a small chemical pre–stress and the delayed shrinkage caused by UEA concrete prevents or decreases the shrinkage cracks. That is the principle for crack–resistance of UEA shrinkage–compensating concrete.

Moreover, the crystalline ettringite formed during hardening of UEA concrete fills, spearates capillary pores and reduces the pore size and total porosity. Therefore, the impermeability of UEA concrete is 1–2 times more than that of ordinary concrete.

UEA APPLIED TO ENGINEERINGS FOR ASIAN GAMES

Bleachers of Stadium

The total construction area for the track and field stadium of China Olympic Sports Centre is 30653 m^2 with bleachers on the east section and the west section. Each section is divided into five units with joints between. There are decorated rooms under the second to fourth floors for physical use. The bleachers have a total area of 21400 m^2 with average thickness 8 cm.

The bleachers must be waterproofed. The original design suggested using waterproofing rolls or importing waterproofing paint from U.S.A. the exports of China discussed the issue and decided to use UEA concrete as structural self–waterproofing material. This is the first application in China.

The proportioning of UEA concrete for the bleachers is shown in Table 3, and their properties in Table 4.

Proportioning for UEA Concrete Used in Bleachers of Track and Field Stadium Table 3

No.	Cement Grade	Materials Used (kg / m^3)						Proportion
		Cement	UEA*	Sand	Stone	Water	Reducer	
1	325#	349	48	716	1167	177	2.38	1:1.8:2.94:0.45
2	425#	304	42	735	1200	170	2.08	1:2.12:3.47:0.49
3	525#	265	36	754	1230	172	1.81	1:3.50:4.09:0.57

* UEA substitution for cement 12%

Properties for UEA Concrete used in Stadium Bleachers Table 4

No.	Design Grade (MPa)	Restrained Expansion Rate (%)			Compressive Strength (MPa)			Strength Achieved Design Strength (%)	Impermeability Grade
		3days	7days	28days	3days	7days	28days		
1	25.0	0.015	0.038	0.042	20.1	28.5	35.2	140	S20
2	25.0	0.019	0.036	0.039	19.2	25.3	37.1	148	S22
3	25.0	0.020	0.037	0.045	23.4	30.2	39.9	160	S20

UEA concrete was mixed in a drum mixer for 2 min. with various materials added together, and the concrete slump 6–8 cm. The accelerating and antifreezing admixtures were used for winter operation. The concrete was cured by specially trained persons for more than 14 days, and the exposed concrete surface kept wet all the time. For construction at temperature below freezing (0℃) the concrete should be covered by multi–layer rock wool felt for insulating.

The UEA concrete for the bleachers was poured in June 1988, and the construction completed in December. A large number of concrete tests were made on the spot. The average strength grade was greater than 35 MPa, impermeability grade greater than S20, restrained expansion rate 300–400 $\mu\varepsilon$, and self–stress 0.2–0.7 MPa. All the design reqirements were reached. No crevice and seepage for the bleachers has been found through three rainy seasons and winters.

The bleacher area for the hockey field is 3000 m^2 with thickness 20–25 cm. China Building Materials Academy offered the structural self–waterproofing technology of UEA concrete. The design grade of strength for the concrete was 250#, and that of impermeability S8. 525# ordinary portland cement was used with 11–22% UEA, 2% antifreezing agent. The proportion of the concrete was 1:2.33:3.80:0.53. Test results on the site showed the average strength > 30 MPa, restrained expansion rate 0.02–0.031%, self–stress 0.2–0.4 MPa. Three years service of the bleachers is satisfactory.

Overhead Passages for Sports Centre

The overhead passages for sports centre in the north suburb of Beijing, connecting fields and gymnasium, are main throughfare for motor vehicles and viewers. The total avea for the passages is 47000 m^2 with thickness 20–30 cm. The external waterproofing rolls were designed originally for the passage paving, but later the whole using UEA concrete as self–waterproofing material was decided. The concrete proportioning in Table 3 was used for the most paving concrete, 300# pumped concrete was partially used. 13% UEA was added to replace cement. The concrete proportion was 1:1.93:3.16:0.49, the amount of cement used 325 kg / m^3, slump 16 cm. Only one or two seepages were found during past three years.

Natatorium

The ordinary waterproofing concrete was used for swimming pools of the natatorium in the North Suburb of Beijing. In order to improve its impermeability, UEA concrete was applied to 20 cm thick bottom. 425# 322 kg / m^3 cement was used with 13% UEA, proportion of the concrete 1:2.25:3.74:0.48 and slump 6–8 cm. The tests on the spot showed the average compressive strength 29.5 MPa, impermeability S12, exceeding design grade (200). The waterproof area for swimming pools is around 600 m^2, and the test showed no seepage.

Amusement Palace

The structure of Amusement Palace for Asian Games is complicated. Total of 1500 m^3 UEA concrete and motar was used for 1200 m^2 dampproof course, 1000 m^2 waterproof roof and 400 m^2 area of pools in water–amusement park. Pumped concrete was used with cement 352 kg / m^3, UEA 13%, proportion 1:1.66:2.71:0.47, slump 16 cm, average strength for test cubes > 31 MPa, impermeability > S8, and design reqirements attained.

Underground Construction

The structural self–waterproof concrete mixed with composite expansive agent was used for a 2500 m^2 basement of the physical museum and a 2400 m^2 basement of the gymnasium for martial arts. If the waterproof rolls required by the original design had been used, the operation would have been very complicated. The two basements had the same concrete proportion 1:2.18:3.17:0.48 with cement 300 kg / m^3, expansive agent 12%, slump 6–8 cm. The average strength of tests on the site 25.9 MPa, impermeability > B8, expansion rate 0.015–0.003%, and self–stress 0.1–0.3 MPa. No crevice and seppage has been found since the completion of two basements in 1988.

Secondary Pouring

There are several post–poured joints in the bottom and side walls of Chaoyang Gymnasium for Asian Games. The dimension for one such joint is 96 × 1 × 2.5 m, reqiring 300 m^3 concrete. UEA concrete was used as the joint filler. The concrete proportion was 1:1.63:3.24 with cement 350 kg/m^3, UEA 10% and 0.6% UNF (reducer). Results of tests on the site showed compressive strength 40.3–50.6 MPa, expansion rate 0.055%, impermeability > S11, max. S20. The secondary pouring was finished in 1987 with good quality.

Rigid Waterproofed Roof

We cooperated with Beijing Institute of Architectural Design and No.3 Municipal Construction Company appling minute expansive concrete to the rigid waterproofed roof for the sportsmen inspection and registration office. The roof concrete was mixed with 30 mm size fine aggregates, 13% UEA, restrained by φ6–300 steel bars, divided into squares with seams sealed with caulk and finally covered by 20 mm thick 1:2.5 motar with 10% UEA. No leakage has been found in the roof in rainy seasons.

According to incomplete figures, 1230 t. UEA has been used in various engineerings for Asian Games, converted into 30000 m^3 concrete. It is seldom that in such large area and multi engineerings to use shrinkage compensating concrete in physical construction.

TECHNO–ECONOMIC EVALUATION

UEA is a kind of concrete agent for crack–resistance and impermeability. A great deal of engineering practices shows that UEA concrete is a close combination of load–bearing structure material and waterproofing material, having structural self–waterproofing function. It breaks the traditional waterproofing mode and leads to new progress in building waterproofing and construction technique.

The use of UEA concrete has notable economic and social effects. Constructions and Buildings, for example, of sports centre for Asian Games in the north suburb of Beijing have a waterproofing area of 81,500 m^2. The cost for organic waterproffing rolls would be 2.85 million yuan (RMB), and that for UEA concrete only 0.37 million yuan, thus 2.48 million yuan of material cost can be saved. The expenses of more than 3 million yuan were cut down for considering the factor of shortening the working time.

CONCLUDING REMARKS

Studies and engineering practices in the Soviet Union, U.S.A., Japan, India and China indicate that use of the shrinkage–compensating concrete in physical construction is wide, and is an effective measure in solving shrinkage cracks of buildings and structures. Especially application in structural self–waterproofing has marked techno–economic resuts. It is believed that application of the new material to physical construction and other civil engineerings has a bright future.

REFERENCES

1 Xue Jungan and Wu Zhongwei et al.: "Expansive and Self-stress Cements, and their Application" (in Chinese), China Building Industry Press, 1985 pp.1–12.

2 You Baokun, Wu Wanchun et al.: "Construction Technique" (in Chinese) 1987, No.5, pp13–15.

3 Masatane Kokubu: "Klein Symposium on Expansive Cement Concrete", ACI Publication SP–38, Detroit, 1973, p.361.

4 R.E. Price: "New Materials in Concrete Construction", Proceedings of the Conference, University of Illinois, Illinois at Chicago Circle, Chicago, 1971, p.20–III.

5 Y.A. Dykhovichnyi and V.A. Maksimenko: "Concrete and Reinforced Concrete (USSR)", 1980, No.4, p.9.

EFFECTIVENESS OF EXPANSIVE ADDITIVES IN AVOIDING EARLY AGE THERMAL CRACKING

L Ebensperger* and R Springenschmid**

**"Holderbank" Management & Consulting Ltd., Holderbank, SWITZERLAND*
***Institute for Building Materials, Technical University of Munich, Munich, GERMANY*

SUMMARY

The influence of expansive additives on the early age behaviour of concrete was investigated. The free and restrained deformations, the development of thermal stresses in a cracking frame, the compressive strength and the elasticity of concrete specimens were thereby measured. Tests were carried out with 4 expansive additives based on free lime CaO or calciumsulphoaluminate CSA, which were mixed at dosages between 0 and 15% of cement weight to different ordinary Portland cements (OPC) of strength class 35F. The effect of w/c-ratio, temperature and curing was also studied.

The expansion increased substantially at higher dosages resulting in an additional strong decrease in compressive strength. Considering the chemical composition of the binders used the interrelation between both properties could be explained. In comparison with the dosage of the expansive additive, the influence of w/c-ratio and temperature is negligible, but not so the effect of a good curing during the first days. The addition of dosages of nearly 10% led to a permissible remaining expansion. Similar dosage also led to compressive stresses sufficient to compensate the early ages restrained tensile stresses. The risk of thermal cracking could be avoided in this way.

Die Zugabe von Quellzusätzen auf die Eigenschaften des jungen Betons wurde untersucht, um deren Wirksamkeit zur Kompensation von Zwangszugspannungen infolge Hydratationswärme abzuklären. Dazu wurden die Verformungen an spannungsunbehinderten und behinderten Betonproben, der Druckspannungsaufbau, die Reissneigung in einem Reissrahmen, die Druckfestigkeit und die E-Modulentwicklung ermittelt. 4 Quellzusätze, welche auf einer Freikalk (CaO) oder Calciumsulfoaluminate (CSA) Basis beruhen, wurden verschiedenen Portlandzementen beigemischt. Der Einfluss des w/z-Faktors, der Temperatur und der Nachbehandlung wurde in die Untersuchungen miteinbezogen.

Höhere Quellzusatzdosierungen führten erwartungsgemäss zu grösseren Verformungen, was aber in einigen Fällen unverzüglich zu einer Druckfestigkeitsabnahme führte. Der Zusammenhang zwischen den beiden Eigenschaften kann erklärt werden, wenn der Chemismus des Bindemittels miteinbezogen wird. Gegenüber der Quellzusatzdosierung ist der Einfluss des w/z-Faktors und der Temperatur von untergeordneter Bedeutung. Die Notwendigkeit einer ausreichenden Feuchtbehandlung während der ersten Tage ist dagegen bestätigt worden. Quellzusatzsdosierungen von ca. 10% erzeugten bei guter Nachbehandlung ein noch zulässiges Restquellvermögen und führten zu einer wesentlichen Verringerung der Reissneigung des jungen Betons. Die während der Reaktion des Quellzusatzes entstehenden Druckspannungen konnten die infolge der abfliessende Hydratationswärme hervorgerufenen Zugspannungen teilweise oder vollständig kompensieren.

INTRODUCTION

The risk of cracking in concrete structures increases when tensile stresses are produced by restrained changes in volume . At early ages these changes are mostly due to cooling after the maximum temperature resulting from the heat of hydration has been reached, and later to the action of drying shrinkage. When the resulting tensile stresses exceed the tensile strength, concrete cracks. Figure 1 shows schematic the stresses occurring normally at concrete together with the zones of high cracking risk /1/.

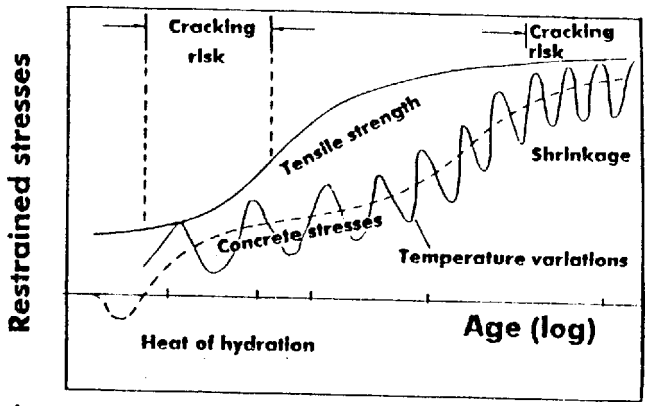

Figure 1: Normal stresses at concrete and zones with high cracking risk./1/

Different solutions are available to minimize the cracking risk of concrete. By means of constructive solutions, the main idea is to reduce the degree of restraint of the structure. In this way the developed tensile stresses are proportionally reduced. By shortening the concrete segments or with the use of special thin layers on the contact zones this aim is reached. By means of technological solutions it is intended to favourably influence the deformations and properties of concrete. In this instance solutions such as cooling of the fresh concrete, use of cements with low sensitivity against cracking, reduction of cement content, use of aggregates with low temperature coefficient, etc. are applied.

Experience gained in many countries such as U.S.A. /2,3/, Japan /4,5/, Russia /6/ and Italy /7/ has shown that the use of expansive additives based on the formation of calcium hydroxide (from free CaO) or ettringite (from calciumsulphoaluminate CSA) is advantageous to avoid drying shrinkage cracking. In this case compressive stresses are developed which compensate, to some extent, the tensile stresses. However, the conditions for avoiding early age thermal cracking are different, because in this case the expansive action of the additives should start when the concrete has already achieved sufficient stiffness, so that early compressive stresses can be developed. On the other hand, the expansive action should be limited to avoid late destruction of concrete due to excessive expansion (Figure 2).

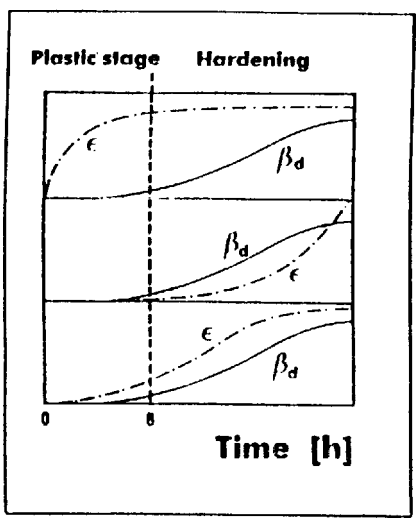

Figure 2: Premature, delayed and adjusted expansive reaction ϵ in comparison with development of compressive strength β_d/1/

MATERIALS AND METHODS

Tests were carried out using four expansive additives, two of each type. Q1 and Q2 correspond to additives based on CSA and Q3 and Q4 are based on free CaO. Their chemical analysis and composition with the values for physical properties are given in Table 1 together with the four Portland cements X, Y, Z and W. Expansive additives Q3 and Q4 show, apart from CaO, also a high $CaSO_4$ content and silicate phases. The density and Blaine of the cements are almost the same, but there are differences in their chemical composition. Instead the sulphate content is the same, the free lime, periclase and silicate phases varied. There are also critical differences in the alkali and C_3A content.

CHEMICAL	CEMENTS				EXPANSIVE ADDITIVES			
ANALYSIS	X	Y	Z	W	Q1	Q2	Q3	Q4
CaO	61.96	64.40	63.70	64.70	53.38	51.83	72.77	68.33
SiO_2	19.96	19.90	19.20	19.30	2.74	0.48	6.45	7.69
Al_2O_3	6.17	5.31	5.34	5.21	11.29	12.71	0.98	2.18
Fe_2O_3	3.91	3.09	4.24	3.36	0.81	0.45	1.08	1.01
SO_3	2.80	2.77	2.82	2.81	28.43	31.33	17.59	17.20
free CaO	0.55	1.48	1.40	1.16	20.30	19.10	33.70	31.00
MgO	1.77	2.77	2.01	1.92	2.22	2.09	1.04	1.30
A_{eq}	1.54	0.49	1.19	0.86				
PHYSICAL PROPERTIES								
Density [g/cm3]	3.17	3.27	3.17	3.13	2.88	2.92	3.10	3.06
Blaine [cm2/g]	3100	3220	3340	3130	3850	3930	4800	4200

CHEMICAL	CEMENTS				EXPANSIVE ADDITIVES			
COMPOSITION	X	Y	Z	W	Q1	Q2	Q3	Q4
C_3S	43.30	62.90	63.40	68.90	-	-	24.50	29.20
C_2S	24.60	9.60	7.20	3.40	-	-	-	-
C_3A	9.70	8.90	7.00	8.10	-	-	0.80	4.10
C_4AF	11.90	9.40	12.90	10.20	2.50	-	3.30	3.10
$CaSO_4$	4.80	4.70	4.80	4.80	41.70	51.90	29.90	29.20
CSA	-	-	-	-	16.20	6.10	-	-
$C_{12}A_7$	-	-	-	-	5.30	18.80	-	-
2 C_2S C_8	-	-	-	-	11.00	-	-	-
$Ca(OH)_2$	-	-	-	-	11.90	5.30	3.20	10.70
CaO	0.60	1.50	1.40	1.20	11.30	15.10	31.30	22.90
MgO	1.80	2.80	2.00	1.90	2.20	2.10	1.00	1.30

Table 1: Chemical analysis and composition of the cements and expansive additives.

Limestone was used as an aggregate on the fractions 0/4, 4/8 and 8/16 mm, with a grading curve AB16 according to DIN 1045 /8/. The standard mix was prepared with a binder (cement + additive) content of c=340 kg/m^3 and w/c=0.55. It was mixed for 3 mins. at 20°C and cured over 3 days at 20°C under a plastic sheet. From here on the w/c-ratio (0.45, 0.50, 0.60 and 0.70), the mix and curing temperature (10°C and 30°C) and the curing humidity conditions (without plastic sheet or under a wet burlap during the whole measurement) were varied.

The first question to be answered was to define the permissible dosage of expansive additive according to the German Standard DIN 1164 /9/. The total sulphate content in Germany is limited to 3.5%, which means, for the the CSA additives, a maximal dosage of less than 2.7%, and for CaO-additives less than 4.7%. Besides this, at preliminary tests at the Institute for Rock Products Technology in Aachen /10/, it was found that some of the cements showed a very high sensitivity against the additive. Considering these two points, the dosage of expansive additive (replacement) was varied between 0% and 15% of cement weight.

The effectiveness of expansive additives was determined by measuring the free and restrained deformations on 15x15x50 cm^3 concrete specimens, as well as the development of compressive stresses and the remaining expansive potential under water curing. Moreover, the long-term properties such as compressive strength and elasticity of concrete were studied.

For the determination of the free deformation and the development of compressive stresses under restrained conditions, a special technique was implemented. A steel reinforcement bar was placed inside a plastic tube between two steel plates 15 mm thick. The steel bars were fixed externally in the middle of the steel plates with nuts. The variation of the amount of steel reinforcement allowed different restraints between 0.39 and 2.9%. With strain gauges placed on the steel the restrained deformations were measured. The free deformations were measured with two inductive transducers, one at each side (Figure 3).

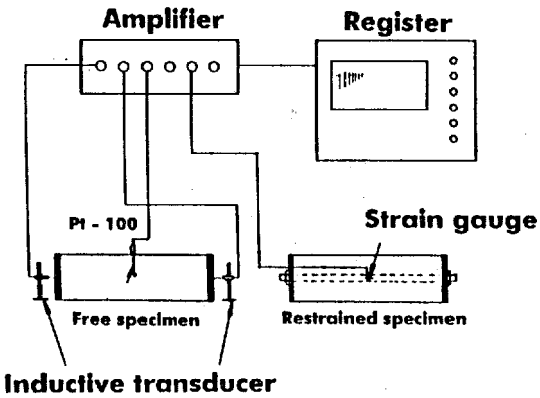

Figure 3: Equipment to measure free and restrained deformations. /1/

The measurement of deformations started 4 hours after mixing and were continuously recorded up to 10 days. Afterwards the free specimens were stored underwater to determine the remaining expansive potential. The effectiveness of expansive additives in compensating restrained tensile stresses was studied with a cracking frame /11/, which exerts a much higher degree of restraint (Figure 4).

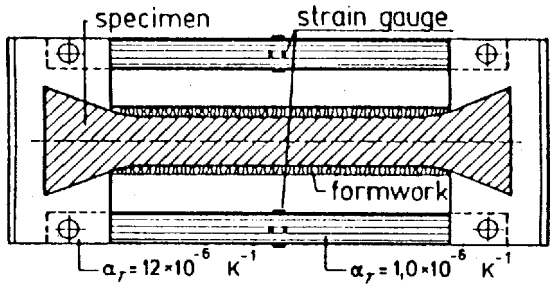

Figure 4: Cracking frame/11/

RESULTS AND DISCUSSIONS

The **compressive strength** behaviour of concretes containing expansive additives should be related to the developed expansion. Deformations that exceed the elastic strain of the chemical bonds are accompanied by a decrease in strength. Through the application of a known definition for an optimum sulphate content /12/, this behaviour was explained.

$$\text{opt } SO_3 = 0{,}789 + 0{,}1149 \cdot C_3A + 1{,}872 \cdot A_{eq}$$

where: $A_{eq} = Na_2O + 0{,}658 \cdot K_2O$ C_3A = Tricalciumaluminate in [mass %]

Defining the sulphate ratio as Sg = total SO_3 / optimum SO_3 (Table 2) it was found that: for cements with sulphate ratios lower than 1.0 the addition of expansive additive does not lead to a decrease in compressive strength, as long as the total sulphate content of the binder (cement + additive) is lower than the optimum sulphate content. On the other hand, for cements with nearly the optimum sulphate content, any addition of expansive additive leads to decreases in compressive strength (Figure 5).

CEMENT	X	Y	Z	W
total SO_3 [%]	2.80	2.77	2.82	2.81
optimum SO_3 [%]	4.78	2.73	3.82	3.33
sulphate ratio Sg	0.59	1.02	0.74	0.84

Table 2: Sulphate ratio of the used Portland cements

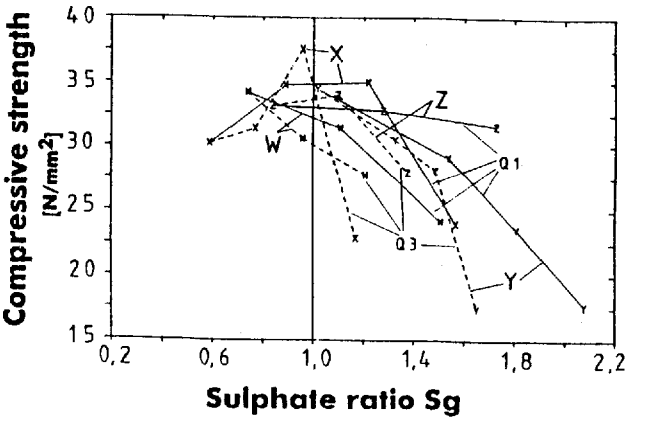

Figure 5: Relation between compressive strength and sulphate ratio for the different concrete mixes

Expansive deformations up to 3.5 $^{o}/_{oo}$ were measured on **free** specimens. As expected, higher dosages of expansive additive led to higher deformations. At higher dosages the deformations were also more significant and an exponential growth was observed. As long as the dosage of expansive additive is lower than 10%, only a negligible effect of the type of additive was observed (Figure 6). However, differences were observed in relation to the Portland cement used; higher deformations and a sensitive behaviour were observed for the cements which nearly show an optimum sulphate content.

The strength and expansion behaviour of expansive concretes indicates that cements with a lower sulphate ratio (e.g. cement X) should be preferred for the application with expansive additives. Hence, the maximum permissible dosage of the expansive additive should be based on the **sulphate ratio** rather than on the existing sulphate content of the binder. That means, the definition of the permissible dosage according to the standard is not appropiate.

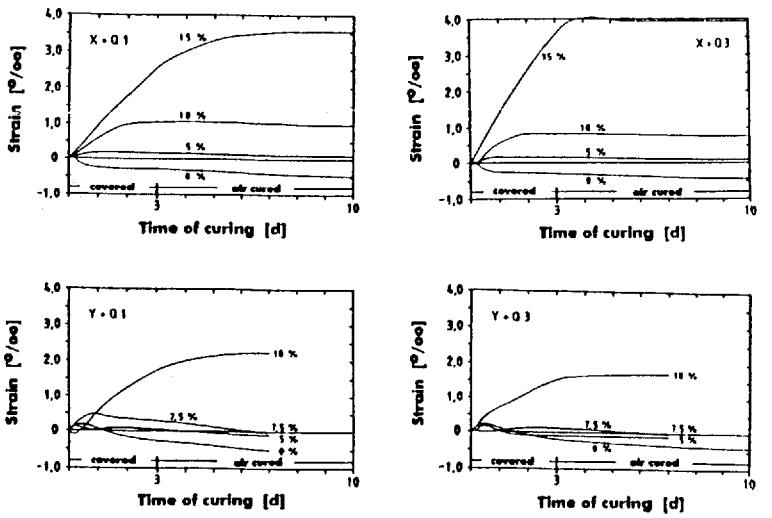

Figure 6 : Free deformation at concretes with different cements and dosages of expansive additive.

The **w/c-ratio** and **temperature** have a minor influence compared to that of the dosage of expansive additive (Figure 7). At constant cement content variations of the w/c-ratio in the practical range between 0.50 and 0.70 did not produce substantial differences in the expansive action. At lower w/c-ratios the chemical reactions took place only partlially due to the insufficient water supply for hydration. The main influence of temperature was to accelerate or to delay the chemical reactions.

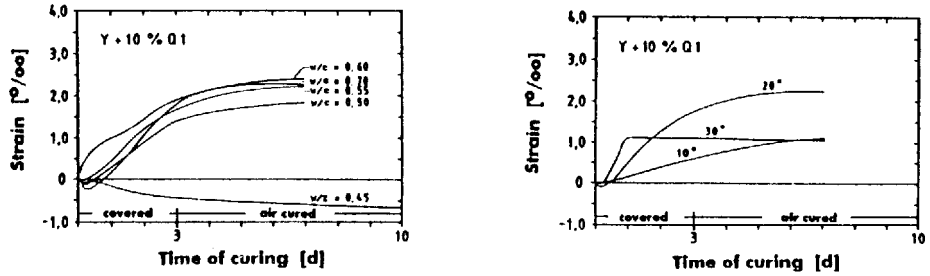

Figure 7 : Free deformation at concretes with 10 % additive and different w/c-ratios and mix temperature.

The need for a **good curing** to secure an optimum reaction of the expansive compounds was proved. Curing under adequate humidity conditions during hardening increased the expansive deformation by 50% in comparison with the normal curing (under plastic sheet).

For the investigated expansive concretes with normal or good curing and a dosage of expansive additive lower than 10%, the **remaining expansive potential** after 90 or 180 days under water curing was with 0.7 ‰, approx. the double of normal concrete. For higher dosages and for bad curing conditions that value is exceeded.

The determination of the **modulus of elasticity** in normal and expansive concretes with 10% expansive additive showed that the modulus of elasticity has a similar behaviour as compressive strength. That means, the addition of expansive additives influences both concrete properties in the same manner. Perhaps expansive concretes show, under compressive action, a slower development of the modulus of elasticity together with a higher capacity of deformation.

The higher the percentage of steel, the higher the **compressive stresses** developed in the concrete. The maximum values reached after 3 days amounted 1.5 N/mm^2 and were maintained, or just slighty diminished till the end of the experiment after 10 days. For steel ratios higher than 3.0% just a small increase in compressive stresses has to be expected (Figure 8).

Through the addition of expansive additives at dosages of nearly 10% the **cracking risk** at early age in concrete was substantially reduced. The compressive stresses developed during the heating period reached up to 2.0 N/mm^2 and despite a considerable relaxation, they were enough to compensate partially or totally the restrained tensile stresses (Figure 9). Here the cracking stress almost did not change, but the cracking temperature was dropped down from near 15°C to temperatures under 0°C. Consequently the risk of thermal cracking was strongly reduced.

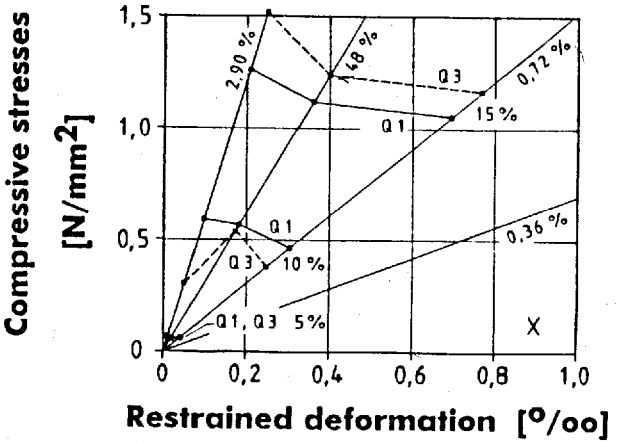

Figure 8: Relation between compressive stresses and restrained deformation for concrete with different dosages of additive.

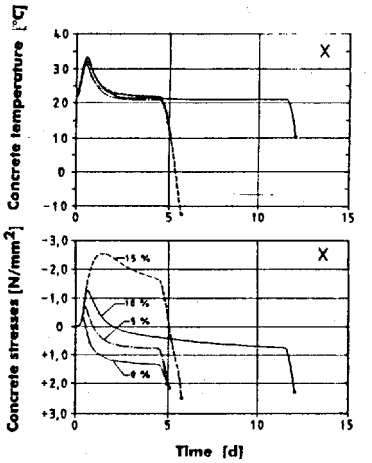

Figure 9: Temperature and stress development at the cracking frame for concretes with different dosages of additive.

CONCLUSIONS

In brief it can be asserted that it is possible to make concretes with expansive additives, so that at early ages a compressive stress will be developed and maintained. Under these conditions an effective compensation of tensile restrained stresses at early ages is achieved. Hereby it can also be certain that through the use of cements with lower sulphate content and expansive additives up to certain dosages which depends on the sulphate ratio of the binder, the compressive strength will not be diminished and only a reduced remaining expansive deformation will occur.

REFERENCES

1. *Ebensperger, L.* : Wirksamkeit von Quellzusätzen im Beton zur Kompensation von Zwangsspannungen infolge Hydratationswärme, Dissertation TU München (1990).
2. *ACI SP-38*: Alexander Klein Symposium on Expansive Cement Concrete, ACI, (1972)
3. *ACI SP-64*: Cedric Willson Symposium on Expansive Cement Concrete, ACI, (1980)
4. *Kokubo, M.*: Use of Expansive Components for Concrete in Japan, ACI SP-38 (1972), S.353-378
5. *Nagataki, S.*: Expansive Cement Concretes in Japan, ACI SP 64 (1980, S.43-79.
6. *Budnikov, P.P. Kravchenko, I.*: Principal Paper-Expansive Cements, Proc. of 5th Int. Symp. on Chemistry of Cement, Vol.4, Tokyo (1968) S.319-330.
7. *Dilacon Anic*: Expansivo per cemento, ANIC Spa., Italy (1982)
8. *DIN 1045*: Beton und Stahlbeton, Bemessung und Ausführung Dezember (1978).
9. *DIN 1164*: Portland-, Eisenportland- Hochofen- und Traβzement, November (1978).
10. *Ludwig, U.*: Sachstandsbericht zu: "Eigenschaften und Wirkungen von Quellmittelr mit Normzementen", DFG-Forschungsprojekt, RWTH-Aachen (1989).
11. *Springenschmid, R.*: Die Ermittlung der Spannungen infolge von Schwinden und Hydratationswärme in Beton, Beton- und Stahlbetonbau 10 (1984), S. 263 - 269.
12. *Jawed I.; Skalny J.*: Alkalies in Cement. A Review. II. Effect of Alkalies in Hydration and Performance of Portland Cement, CCR Vol. 8 (1978), S. 37 - 52

FaL-G: THE LUCID CONCRETE MEDIA

P Veerabhadra Rao*, N Kalidas and N Bhanumathidas****

**Department of Engineering, Gandhi Institute of Technology & Management, Visakhapatnam, INDIA*
***Bhanu International, Visakhapatnam, INDIA*

PREAMBLE

Concrete is a diluted version of neat cement, of course, simultaneously to maintain the dimensional stability of cast element by minimising shrinkage effect of cement. In the process, the Ordinary Portland Cement (OPC) is diluted from its characteristic strength of 600-800 kg/cm^2 to 150 kg/cm^2 (M15) and 200 kg/ cm^2 (M20) by appropriate changes in mix design of concrete viz. 1:2:4 and 1:1½:3 respectively. Of course, M10 and M15 are more popularly used concrete grades with strength characteristics sufficient to meet the requirements of majority of structural elements.

When such high rate of dilution is involved, why the high strength cement like OPC is needed? Why not some low strength substitutes, at lower costs?

This is where a ground blend of flyash (Fa), Lime (L) and calcined gypsum (G), called FaL-G cement, christened keeping in view its ingredients, with its neat strength of about 50% to that of OPC could be successfully used to develop concrete grades such as M10, M15 and M20, with due change in mix designs.

A live structure is successfully constructed incorporating a slab of 2000 sft (186 sq mtr) and beams of 250 rft (76.2 mtr) which also include two tie beams of 15 ft and 18 ft length, all executed with pure reinforced FaL-G cement concrete (RFCC). Also a demonstrative road of 15 ft x 50 ft is laid with FaL-G concrete to demonstrate the product in practical reality.

DEUTSCHE UEBERSETZUNG - PRAEAMBEL

Beton ist durch zuschlagstoffe gemagerter zement. Diese magerung verbessert die masshaltigkeit der gegossenen elemente durch minimierung der zementtypischen ausdehnungsverluste. In den gebraeuchlichen betonquali-taeten ist die mechanische festigkeit des normalen Portland zements von 600-800 kg/cm^2 auf 100 (M10), 150 (M15) oder 200 (M20) kg/cm^2 durch entsprechende variationen der zuschlagstoffe verringert. Die betonquali-taeten M10 und M15 sind mengenmaessig dominierend, ihre festigkeitscharakteristik ist ausreichend fuer die mehrzahl der betonanwendungen.

Wird bei solch starker verringerung der urspruenglichen festigkeiten ein hochfestes bindemittel wie Portland zement benoetigt? Reicht nicht ein kostenguenstiges bindemittel mit niedrigeren festigkeiten aus?

FaL-G zement, eine mischung von flugasche, kalk and kalzineirtem gips von kontrolleirter zusammensetzung und bindemittelfestigkeiten von ca. 50 prozent verglichen mit Portland zement wurde erfolgreich eingesetzt zur erzeugung von betonqualitaeten gemaess M10, M15 oder M20.

Den erfolgreichen einsatz von FaL-G beton demonstrieren ein gebaeudemit einer platte von 186 m^2, traeger von 76,2 m und 2 zugtraeger von 4,6 und 5,5 m laenge, ausgefuehrt ausschliesslich mit stahlarmiertem FaL-G zement-beton sowie eine strassenmusterflaeche von 15 x 4,6 m.



Column structure with slab (2000 sft) and beams (250 rft) cast out of FaL-G concrete. The wall construction with FaL-G concrete blocks and FaL-G cement mortar in progress.

(Location: Office of M/s Bhanu International, Visakhapatnam)

MIX DESIGN

In view of low neat strength, FaL-G cement has to be added in higher dosage in comparison to OPC. During the study of different mix designs, it is observed that $1\frac{1}{2}$ times of FaL-G cement by weight to that of OPC, keeping the proportions of aggregates same, renders the same grade strength.

Mix design (by weight)

OPC	Grade	FaL-G	WCF	Compressive strength (N/mm^2)		
				7 days	14 days	28 days
1:2:4	M15	$1\frac{1}{2}$:2:4	0.57	11.57	13.99	16.53
1:$1\frac{1}{2}$:3	M20	$1\frac{1}{2}$:$1\frac{1}{2}$:3	0.57	14.52	17.91	21.05

The above mixes have been prepared manually. However, keeping in view the chemistry of FaL-G with reference to the sensitive factor of minimising water towards better cohesive bond, but without sacrificing the plasticity, the traditional lime mortar mixing mechanism has been conceived and adopted. The results are impressive with 0.25 to 0.30 of water consistency factor (WCF), otherwise noted as water/ cement ratio, and strength improvement by about 30-50%. The cube (15 cm), beam (100 x 100 x 500 mm) and cylinder specimens with $1\frac{1}{2}$:2:4 mix, which rendered M15 grade by manual mixing, tested for respective technical strengths, have yielded the following results when the mix is prepared in a Pan Mixer with WCF of 0.25 attaining the same plasticity :

Strengths at 28 day (N/mm^2)	Recorded strength of FaL-G	Grade strength of OPC
Compressive strength	27.50	15.00
Beam MOR	3.92	2.71
Cylinder compression	19.93	12.00

ANALYSIS OF STRENGTHS

MOR for concrete varies as $0.7 \sqrt{f_{ck}}$ (Ref: IS:456; Clause 5.2.2). Thereby grade value of MOR of M15 OPC concrete is $0.7 \sqrt{15} = 2.71$ N/mm^2. Relatively in FaL-G, the same value is required to be $0.7 \sqrt{27.5} = 3.67$ N/mm^2 whereas the recorded value is 3.92 N/mm^2.

Shape factor

For OPC concrete, ratio of cylinder compressive strength to cube compressive strength is normally recorded as not less than 0.8. With FaL-G, this ratio was 0.72 which is closely agreeing with the standard requirements.

The above strength factors have been recorded based on 3 specimens for each test which is not sufficient for drawing conclusions. Studies on standard deviations and coefficient of variation of cube compressive strengths are in progress which may unfold striking values to enlarge the scope of FaL-G concrete applications.

Preparation of concrete in a Pan Mixer not only reduces the WCF but also renders a viscously cohesive cement paste with high gelatinous plasticity and impressive workability. It is observed that such concrete gives an improved cementitious coat on reinforcement for longer life in addition to improving characteristic strengths remarkably.

The strengths recorded in this paper are based on the physical blending of raw material inputs of FaL-G cement devoid of intergrinding. Nevertheless, the plant level manufacturing of FaL-G cement after thorough intergrinding of inputs is expected to improve the strengths. A study is in progress to correlate the factors among grindability, fineness, water consistency and strengths which are interrelated.

COST ECONOMICS

Comparing to concrete mixer, Pan Mixer is not expensive in the light of the following data :

	Concrete Mixer	Pan Mixer
Cost (Rs)	55,000	45,000
Power	5 HP	7.5 HP
Output/hour	100 cft	100 cft
Strength	Normal grade strength	Minimum 30% high for same input of cement

Cost of concrete

			For M15	
			OPC	FaL-G
Cement	0.8 t	@ Rs 1800/ton	1440	-
FaL-G	1.2 t	@ Rs 800/ton	-	960
Sand	48 cft	@ Rs 2.25/cft	108	108
Chips	96 cft	@ Rs 7.00/cft	672	672
			2220	1740
Output			100 cft	120 cft
Cost/cft (Rs)			22.20	14.50
Savings			----------35%----------	

CONCLUSIONS

Taking into view the chemistry of various flyashes and corresponding monitoring of raw material composition in order to achieve uniform FaL-G specifications based on any flyash, drafting of specifications for FaL-G cement is in the process of deliberations. Also, the exhaustive studies on consistency factors are in progress and further data is awaited.

Though the chemistry of FaL-G and rheological behaviours permitted the postulations to believe that the corrosion effect on reinforcement would be lesser than that of OPC, systematic studies are in progress to corroborate the same with practical data.

A substitute to OPC does not imply that it should meet all the criteria. When the mankind witnesses the legendary structures of centuries old built with lime mortar of 30-60 kg/cm^2 strength, a substitute like FaL-G cement with much improved chemistry and capability of concrete development in M10 to M20 should be viewed with receptivity and pragmatism. Wherever necessary, FaL-G cement may be drafted with its own product and applicational standards/codes instead of keep comparing it to OPC and get worried with certain deviations of specification.

OPC is undoubtedly the virtuous cement for its amenability to play with strengths, casting prestressed concrete elements and high strength applicational areas. The object of FaL-G cement concrete is to rationalise the use of OPC wherever the applicational requirements are met, as a substitute rather than a total replacement. In the present day's context of global concern to conserve natural resources and minerals on one hand and utilisation of industrial wastes on the other, FaL-G cement meets both the objectives in a single go and thereby deserves effective promotional efforts by all concerned right thinking intelligentia.

ACKNOWLEDGEMENTS

The authors gratefully acknowledge Mr Gunther Erlenstaedt, expert in utilisation of calcareous and siliceous industrial wastes and M/s Salzgitter Anlagenbau, Germany for the technical guidance and support in these studies.

STRENGTHENING EFFECT OF DEHYDRATED PHASES OF CALCIUM SILICATE HYDRATE ON CEMENT CONCRETE

Feng Naiqian and Ji Xihuang

Department of Civil Engineering, Tsinghua University, Beijing, P R. CHINA

SUMMARY

The main composition of ALC is calcium silicate hydrate. The dehydrated phases(DP), which are the waste of ALC calcined at different temperatures, are used to study the strengthening effect on cement concrete.

The DP is of high activity, while the DP calcined at 800°C is the most active. When 10% of cement is replaced by the DP at 800°C, the strength of the concrete(W/C=0.3) at 3, 7, 28-day is 9%, 27%, and 15% higher than that of the control concrete without DP.

The strengthening effect of the mixtures of the DP and natural zeolite finely ground together at different ratios is also studied. The strength of the concrete(W/C=0.3) at 7, 28-day containing the DP and zeolite natural zeolite at the ratio of 20:80, which replaces 5% of cement, increases by 17% and 21% respectively.

The strengthening regularity and strengthening mechanism of the dehydrated phases of calcium silicate hydrate on cement concrete are studied in the article.

目前国际上广泛使用的加气混凝土其主要成分为水化硅酸钙，加气混凝的生产中常有很多废料。本实验把经不同温度脱水的加气混凝土废料作为水化硅酸钙脱水相，研究其对水泥混凝土的增强作用.

试验发现，脱水相具有较高的化学活性，而其中以经800℃脱水相的活性最大，当以之置换10%水泥时，混凝土(W/C=0.30)的3天，7天，28 天强度分别比不掺脱水相的空白混凝土高9%，27%，和15%。

本文研究了以不同比例混合磨细后的脱水相和沸石对水泥混凝土的增强效果.当脱水相和沸石以20:80的比例混磨后，以之置换5%的水泥，混凝土(W/C=0.30)的7，28 天强度分别比空白混凝土增加了 7% 和 21% 。

本文研究了水化硅酸钙脱水相的增强规律和增强机理。

INTRODUCTION

There is a great deal of waste of ALC in the production of ALC in China, eg. the waste of ALC remained in Peking ALC Factory is up to 50 thousand tons every year. The waste not only causes the pollution of environment but also takes a lot of land unless some measures are taken to make full use of it. The waste of ALC used in this study as the dehydrated phases is added to concrete to replace some of the cement to strengthen the concrete. The DP, when finely ground with zeolite, can be used to make super-high strength concrete.

EXPERIMENTAL RESULTS AND DISCUSSIONS

The DP in this test are the waste of ALC calcined at 700°C, 800°C, 900°C for 2 hours. The ALC is produced by using sand, cement and lime autoclaved at 180°C, 10 atm for 8 hours. The XRD pattern of the ALC is shown in Fig.1. The main compositions are tobermorite, CSH(B), and a little of xonolite(1). All the DP and zeolite used in the study pass the sieve of 4900 hole/cm².

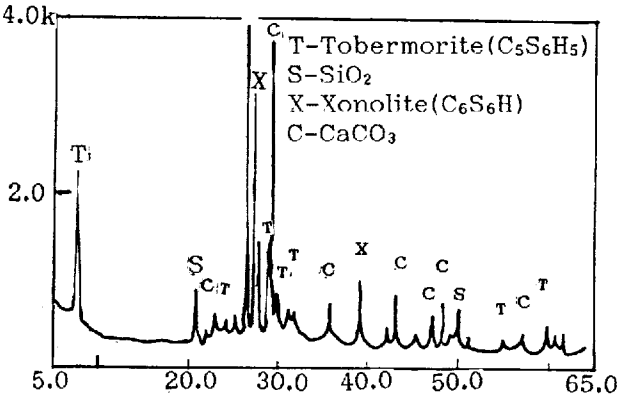

FIG.1 XRD of ALC

1 Strengthening Effectiveness of the DP at different temperatures in cement concrete

Materials used in the test: Portland cement(strength grade #525), river sand, crushed gravel with the Dmax=30mm, Water reducer(UNF), and DP (at 700°C, 800°C, 900°C for 2 hours, used to replace 10% of the cement in concrete)

The Composition of concrete and the test results are given in Table 1 and Table 2 respectively.

TABLE 1 Composition of the concrete

No	Calcination Temp.of DP	W/C	S	Material(kg/m³ concrete)						Slump (cm)
				DP	Cement	Water	Sand	Gravel	UNF	
0	----	0.3	0.35	--	500	150	630	1170	5	3.5
1	Uncalcined	0.3	0.35	50	450	150	630	1170	5	3.5
2	700°C	0.3	0.35	50	450	150	630	1170	5	2.8
3	800°C	0.3	0.35	50	450	150	630	1170	5	3.0
4	900°C	0.3	0.35	50	450	150	630	1170	5	3.0

TABLE 2 Compressive strength of the concrete

No	Compressive strength(MPa)			Calcination Temp. of DP
	3-day	7-day	28-day	
0	44.28 (100%)	55.39 (100%)	74.97 (100%)	-----
1	48.13 (108.7%)	60.60 (109.4%)	81.04 (108.1%)	Uncalcined
2	49.02 (110.7%)	70.01 (126.4%)	84.27 (112.4%)	700°C
3	48.31 (109.1%)	70.40 (127.1%)	85.99 (114.7%)	800°C
4	47.11 (106.4%)	63.48 (114.6%)	84.04 (112.1%)	900°C

Test results in Table 2 show that the 3-, 7-, 28-day strength of the concrete containing DP calcined at different calcination temperatures, which replaces 10% of cement, is higher than that of the control concrete without DP; The strength of the concrete with DP at 800°C is the highest. The Table also shows that the waste of ALC uncalcined can also a bit increase the strength of concrete.

2 Strengthening Effectiveness of the Mixture of the DP and Natural Zeolite in Cement concrete

It is found by orthogonal test that there is an optimal ratio of DP at different calcination temperatures to the natural zeolite to strengthen concrete. The following tests are the repetition tests of the orthogonal test. The materials used in the test are the same as those in Table 1. The composition of control concrete without the mixture(No.0 in Table 4) is the same as that of the concrete No.0 in Table 1. As for the concrete with the mixture(Table 4),The W/C ratio(W/C=0.30), sand ratio(S=0.35) and the amounts of water, sand and gravel in the following concrete (Table 4) remain the same as those of the control concrete except the different amount of the cement replaced by the mixture and the different ratios of DP to natural zeolite.

TABLE 4 The proportion of cement replaced by the mixture of DP and natural zeolite at the different ratios and the test results

No	Calcination	Mixture	Material(kg/m³ concrete)				Compressive strength(MPa)
	Temp.of DP	DP:Zeolite	DP	Zeolite	Cement	7-day	28-day
0	---	---	---	---	500	60.19(100%)	76.63(100%)
1	---	0:100	0	25	475	66.03(109.7%)	80.70(105.3%)
2	Uncalcined	20:80	5	20	475	67.89(112.8%)	87.40(114.1%)
3	700°C	20:80	5	20	475	70.12(116.5%)	84.30(110.1%)
4	800°C	20:80	5	20	475	70.66(117.4%)	92.65(120.9%)
5	900°C	20:80	5	20	475	64.46(107.1%)	85.69(111.8%)
6	---	0:100	0	50	450	68.91(114.5%)	82.92(108.2%)
7	Uncalcined	35:65	17.5	32.5	450	68.86(114.4%)	83.52(109.0%)
8	700°C	35:65	17.5	32.5	450	71.20(118.3%)	84.35(110.1%)
9	800°C	35:65	17.5	32.5	450	65.66(109.1%)	87.44(114.1%)
10	900°C	35:65	17.5	32.5	450	65.19(106.3%)	87.12(113.6%)

The test results show that the natural zeolite can increase the strength of concrete, while the mixture of DP at different calcination temperatures and zeolite can greatly increase the strength of the concrete. eg. when 10% of the cement is replaced by the mixture of DP at 700°C and zeolite (DP : Zeolite = 35:65), the 7-day and 28-day strength of the concrete is increased by 9.1% and 14.1% respectively. It is noticeable that when the mixture of DP (at 800°C)and zeolite (DP:Natural zeolite=20:80) replaces 5% of the cement, the strength of the concrete is 93 MPa, increased by 21% as compared with the control concrete(No.0). It can be used to make super-high strength concrete.

STRENGTHENING MECHANISM OF DP IN CEMENT CONCRETE

1 Structure changing process of the calcium silicate hydrate in dehydration

The DTA curve of the waste of ALC and XRD patterns of the dehydrated phases at 700°C, 800°C, 900°C are given in Fig 2, Fig 3, Fig.4, Fig.5 respectively.

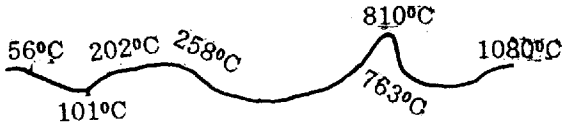

FIG.2 DTA of ALC

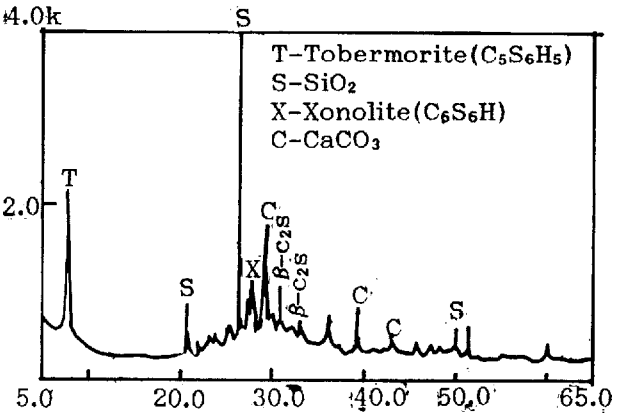

FIG.3 XRD of DP at 700°C

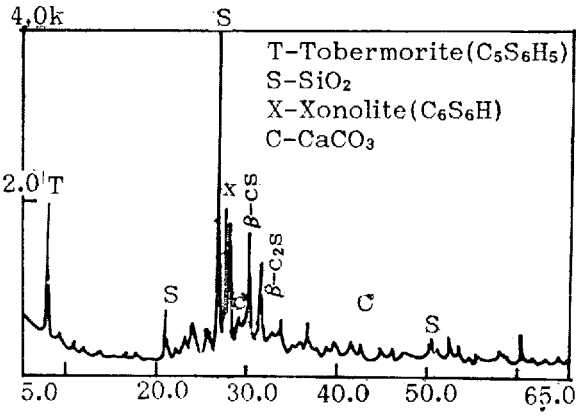

FIG.4 XRD of DP at 800°C

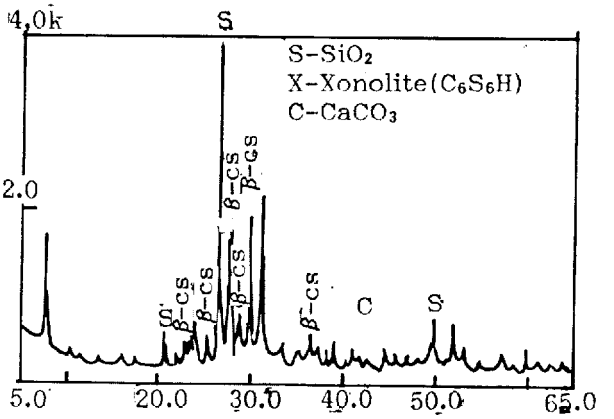

FIG.5 XRD of DP at 900°C

The Fig.2 shows that (1) There is an endothermic peak in the temperature range of 56°C-202°C, the free water and inter-layer water in the calcium silicate hydrate are quickly dehydrated in this temperature range, but the structure of the calcium silicate hydrate is not affected; (2) There is a widen endothermic peak in the temperature range of 258°C-763°C, the OH^- ions , which have different bond force in the calcium silicate hydrate, are released gradually, the structure of calcium silicate hydrate is destroyed seriously, and at about 763°C the structure is completely destroyed; (3) At about 810°C there is an exothermic peak which corresponds to the formation of β -CS. It can be seen from Fig.3 and Fig.4 that there isβ -C_2S in the dehydrated phases at 700°C, 800°C, it can also be seen from Fig.5 that the tobermorite is turned intoβ-CS. when the temperature is over 820°C. There is no new crystal phase formed in the

dehydrated phase of calcium silicate hydrate when the temperature does not exceed 810°C, and the dehydrated phase ,with a high specific surface,is in the amorphous and substeady state and is of high reactive activity(2) (3).

2 Activity of DP

It is due to the high reactivity of DP that there is strengthening effectiveness in cement concrete. It is found that there is high content of soluble SiO_2 and Al_2O_3 in DP (see Table 5).

TABLE 5 Content of soluble SiO_2 and Al_2O_3 and strength of DP mixed with CaO

Calcination Temperature	700°C	800°C	900°C
Soluble SiO_2 (%)	23.42	23.31	22.33
Soluble Al_2O_3 (%)	5.89	6.24	5.62
Strength of DP with CaO(MPa)	7.3	7.05	3.44

The 28-day strength of DP mixed with water (water/solid=0.45) is only 1.58 MPa, but when it mixed with CaO at DP:CaO:Water=2:1:1.5, the strength is increased quite a lot.(see Table 5). The DP can react with $Ca(OH)_2$ produced in the hydration process of cement,and turns into CSH gel(the SEM of hydration product of DP and CaO are shown in Fig.6), therefore the concrete is strengthened. The table also shows that the reactive activity is reduced when the temperature exceeds 820°C because of the formation of new crystal phase.

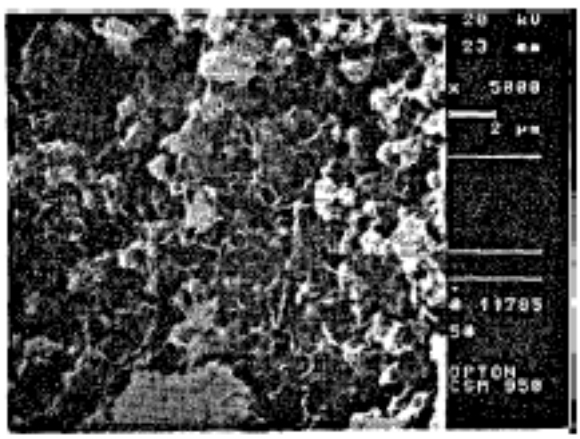

FIG. 6 SEM of hydration products of DP at 800°C reacted with CaO(autoclaved at 100°C for 16 hours)

It is found by the comparing tests between the pure hcp and the hcp with DP at 800°C that the intensity of $Ca(OH)_2$ peaks in hcp with DP replacing 10% of cement at 2θ =18.1 and 2θ=34.1 is weaker than that of the pure hcp (Table 6).

TABLE 6 XRD Intensity of $Ca(OH)_2$ in hcp with and without DP at 800°C

Position of peak	2θ=18.1°		2θ=34.1°	
Age	3-day	28-day	3-day	28-day
Intensity of $Ca(OH)_2$ in pure hcp	3.1	3.2	2.8	2.7
Intensity of $Ca(OH)_2$ in hcp with DP	2.6	2.7	2.3	2.3

STRENGTHENING MECHANISM OF THE MIXTURE OF DP AND NATURAL ZEOLITE

It is known from the discussion above that the DP can react with $Ca(OH)_2$. The natural zeolite, which is of porous and micro-crystal structure, can also react with $Ca(OH)_2$ to produce CSH gel(4), on the other hand, the mixture can also offer the outer space for the hydration products, hence improves the distribution of the hydration products.

1 The Mixture Can Improve The Pore Structure Of The Hardened Cement Paste

Table 7 is the pore content and accumulated pore content of the pure hcp and the hcp with the mixture(DP:Zeolite=20:80) which replaces 10% of cement at 7, 28-day. The water/solid=0.30.

Table 7 Pore content(in $10^{-2}cm^3/g$) and accumulated pore content of the pure hcp and the hcp with mixture

Pore diameter	7-day				28-day			
	Pore Content		Accum. pore content		Pore Content		Accum. pore content	
(A)	Pure*	Mixture*	Pure*	Mixture*	Pure*	Mixture*	Pure*	Mixture*
7500	0.285	0.186	0.285	0.186	0.045	0.139	0.045	0.140
1816	0	0.093	0.285	0.279	0.134	0.046	0.179	0.186
938	0.475	0.047	0.76	0.325	0.223	0.139	0.402	0.326
625	0.95	0.743	1.710	1.068	0.268	0.326	0.670	0.652
375	4.133	4.179	5.843	5.247	2.500	2.746	3.170	3.397
214	2.233	2.276	8.075	7.523	1.563	1.861	4.732	5.258
125	1.853	1.904	9.928	9.427	1.205	1.582	5.937	6.841
75	1.4251	1.254	11.353	10.681	1.652	1.163	7.589	8.004
54	0.523	0.836	11.875	11.516	0.833	0.698	8.482	8.702
42	0.143	1.300	12.018	12.817	0.714	0.326	9.163	9.028
38	0.143	0.325	12.16	13.142	0.223	0.233	9.420	9.260

* Pure=pure hcp, Mixture=hcp with the mixture of DP and zeolite

The Table 7 shows that harmful large pore(diameter>938A) in hcp is greatly reduced by the mixture, and the micro-pore(diameter<625A) in the hcp with mixture is a bit higher. The mixture can not only improve the hydration products but also the porosity structure.

2 The Mixture Can Improve The Interface Structure

The results of the micro-strength on surface of the interface zone are shown in Table 8. The computed CaO/SiO_2 analysed by EDX(Energy Dispersion of X-ray) is also shown in Table 8.

TABLE 8 Micro-strength and CaO/SiO_2 on the surface of the interface zone

Micro-strength on surface of hcp(10^7Pa)								CaO/SiO_2 (wt%)			
Distance to interface(um)	25	50	100	150	200	250	300	20	40	60	80
Hcp	46	36	73	95	117	112	117	2.3	1.2	3.6	1.9
Hcp+Mixture	73	97	109	116	120	125	123	1.7	1.9	2.3	0.1

Table 8 shows that the micro-strength of surface in interface zone of the hcp with mixture is larger than that of pure hcp, and the CaO/SiO_2 in the interface zone is lower,it is caused by the activated SiO_2 and Al_2O_3 which absorbs a great deal of the flake-like $Ca(OH)_2$ in the interface zone, the $Ca(OH)_2$ is harmful to the bond strength between the hcp and aggregate, so the interface structure is improved by the mixture.

Conclusions

1. The DP i.e. the waste of ALC calcined at 800°C is the most active,when 10% of cement is replaced by it the strength of concrete(W/C=0.3) at 28-day is 15% higher than that of the control concrete

2. The DP can produce CSH gel in the presence of $Ca(OH)_2$, furthermore, it has the effect of micro-crystal and can accelerate the hydration process of the cement, hence increase the early strength of the concrete.

3. The mixture of DP at 800°C and zeolite can be used to make super-strength concrete, when W/C=0.3, 5% of cement is replaced by it, the strength of the concrete at 28-day is 93 MPa,21% higher as compared with the control concrete.

4. The mixture of DP and zeolite can improve the porosity and the interface zone structure, hence the strength of the concrete is increased.

References

1. Pu Xincheng: **Science of Concrete**, China Press of Architecture and Civil Engineering, March 1984, p215-246.

2. Yuan Runzhang: "Structure Changing Process of Calcium Silicate Hydrate in Dehydration", Journal of Wuhan Technology University,No.3 1988, p8-13.

3. Gao Qiongying et al: "Study on the Rehydration of the Dehydrated Phases of CSH", Journal of Wuhan Technology University, No.1 1990, p25-33

4. Feng Naiqian: "The Strength Effect of the F-Mineral Admixture on Cement Concrete", Journal of Wuhan Technology University, No.4 1988 p43-47

PREPARATION OF NOVEL POROUS MATERIALS FROM FLY ASH, GYPSUM AND PORTLANDITE BY MEANS OF STEAM CURING - UTILIZATION OF LIMESTONE SLIME AND MEASUREMENT OF PHYSICAL PROPERTIES OF FIRED BODIES

K Ikeda and C Tashiro

Department of Advanced Materials Science and Engineering, Yamaguchi University, Ube, JAPAN

SUMMARY

Novel porous materials called FGL have been prepared from fly ash, gypsum and portlandite. III-anhydrite was used as gypsum source and portlandite was sythesized from limestone slime. Precursors made from slurry mixtures of the three raw materials were steam-cured and water resistant porous materials were obtained. Physical properties, such as bulk density, shrinkage and flexural and compressive strengths were measured after firing the FGL up to 1,000°C. Blending more gypsum component yielded superior results, being resistant up to 600°C firing without cracking.

SUMARIO

Nuevos materiales porosos llamados FGL han sido preparados a partir de ceniza liviana de carbón, yeso y portlandita. III-anhidrita fué usada como fuente de yeso y la portlandita fué sintetizada a partir de caliza limosa.
Los precursores hechos a partir de mezclas suspensión de los tres materiales crudos fueron expuestos al vapor y se obtuvieron materiales porosos resistentes al agua.
Propiedades físicas, tales como densidad aparente, resistencia a la contracción, a la flexión y compresión, fueron medidas después de calcinar el FGL hasta 1000°C. Mezclando más el componente yeso, se dieron resultados superiores siendo resistente hasta 600°C de calcinación, sin rompimiento.

INTRODUCTION

General characteristics of a novel class of porous materials designated as FGL have already been studied at ambient temperature (1, 2, 3). FGL bricks are prepared easily from slurry mixtures of fly ash, gypsum and portlandite through steam curing. To facilitate the rapid consolidation of the slurries hemihydrate or III-anhydrite is used as gypsum source. The precursors obtained are demoulded in a short period of time, air-dried generally at ambient temperature for several days and then steam-cured at 80°C and 90%RH. Thus, water resistant light weight porous bricks are prepared. It has been suggested that FGL would have practical applications for heat insulation and acoustic purposes as building materials to realize energy saving as well as sound insulation in buildings and houses.

In limestone mines producing high grade limes and concrete aggregates the excavated limestones are washed with water to purify the limestones. After that a huge amount of limestone slime containing mainly silica is discarded as a waste.

In this paper utilization of the such limestone slime is discussed in preparation of FGL. The physical properties of the FGL so prepared, especially after firing at elevated temperature are discussed.

EXPERIMENTAL

The chemical composition of the limestone slime collected from a mine is shown in Table 1. In order to prepare the portlandite (slaked lime) the slime was decarbonated by firing at 1,000°C for 3.5 h. Then, the slaked lime was synthesized by the steam hydration technique at 70°C for 1 h.

Desulphurization gypsum was supplied from a power plant. It contains a small amount of calcite and has 99% purity. The gypsum was ground in a ball-mill for 3 h to get finer powders with water grinding media. After drying it was screened on 100-mesh sieve. It was then kept in a 200°C oven to decompose into III-anhydrite and weighed immediately on being taking out of the oven every time.

Fly ash was supplied from a power plant. Coarse particles were eliminated from it using a cyclone separator, and under 30 μm powders were collected. The chemical composition of the fly ash is shown in Table 1. Fly ash is essentially glassy with traces of quartz and mullite detected by XRD.

The physical characteristics of the three raw materials are represented in Table 2. The mixing proportions were decided on the basis of previous work. The gypsum/portlandite molar ratios, G/P, of which are presented in Table 3 (1). Precursors were prepared by slip-casting with W/S 0.8. The consolidated slurries were demoulded after 40-50 min and left to dry at ambient temperature for 3 days. They were then steam-cured at 80°C and 90% RH for 18h.

The steam-cured bodies, 2 x 2 x 8 cm, were fired at elevated temperature from 100°C to 1,000°C in steps of 100°C. The 100 and 200°C firings were performed in an oven for 1 h, introducing the specimens directly, but the higher firings were carried out in a

Table 1. Chemical compositions of fly ash and limestone slime.

	SiO_2	TiO_2	Al_2O_3	Fe_2O_3	MnO	CaO	MgO	Na_2O	K_2O	SO_3	CO_2	Ig.l	Total
Fly ash	63.15	1.26	23.27	4.22	0.06	1.92	1.38	0.72	0.85	0.13		2.76	99.72
Slime	2.0		0.57	0.4	0.01	53.9	0.34	0.1	0.06		42.3*		99.68

* Calculated value.

Table 2. Physical characteris of the raw materials.

	Fineness, cm^2/g, Blaine	Apparent density, g/cm^3
Fly ash	4,280	2.24
Gypsum	6,360	2.28*
Portlandite	13,920	2.13

* Apparent density of original gypsum.

Table 3. Mixing proportions of the raw materials.

	G/P molar ratio	Fly ash	Gypsum(III-anhydrite)		Portlandite
A	0.9	55.7	30.0	(23.7)	14.3
B	0.7	51.6	30.0	(23.7)	18.4
C	0.3	51.3	20.0	(15.8)	28.7

programming muffle furnace at heating rate of 20°C/min. The specimens were kept for 1 h after holding. All the specimens were taken oup rapidly after firing.

Bulk density, shrinkage, 3-point flexural and compressive strengths were measured for each specimen after firing. Photographs of the specimens after firing were also taken.

RESULTS AND DISCUSSION

The bulk density and shrinkage of nonfired specimens are summarized in Table 4. Green bodies showing around 1.5 g/cm^3 bulk density were getting lighter according to the degree of air-drying and 0.87-0.90 g/cm^3 bulk densities were reached at the end of steam curing. It has already been reported that bulk density depends on w/s and 0.99 g/cm^3 has been reported as the minimum value so far (2, 3, 4). Though no marked contraction is generally observed, a slight contraction was detected in specimens C. A very small expansion was noticed in specimens A after steam curing, probably due to the formation of ettringite.

Variation in bulk density after firing is summarized in Fig.1. Generally two weight loss regions are noted. The first one below 200°C may be due to the dehydration of ettringite and C-S-H. After the dehydration the bulk densities become nearly constant. Around 800°C the specimens again lose weight. This second one may be due to the decarbonation of calcite formed by the carbonation of the portlandite during air-drying. After decarbonation the bulk densities rise again due to sintering. It is interesting that the

Table 4. Bulk density and shrinkage of nonfired specimens, w/s 0.8.

	Bulk density, g/cm^2			Shrinkage, %		
	Green	Air-dry	Steam	Green	Air-dry	Steam
A	1.48	1.09	0.90	nil	nil	nil*
B	1.47	0.99	0.89	nil	nil	nil
C	1.46	0.91	0.87	nil	0.05	0.06

* see the text.

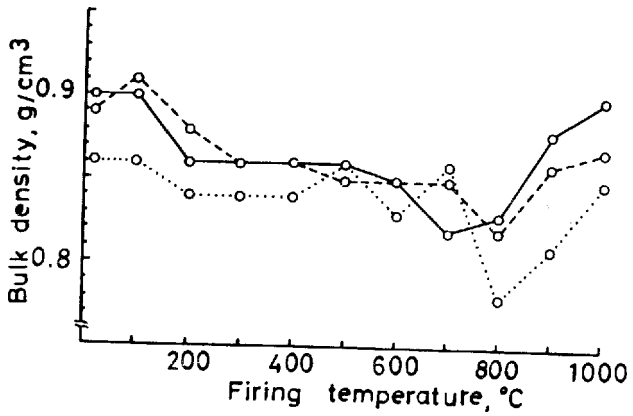

Fig. 1. Variation of bulk density.

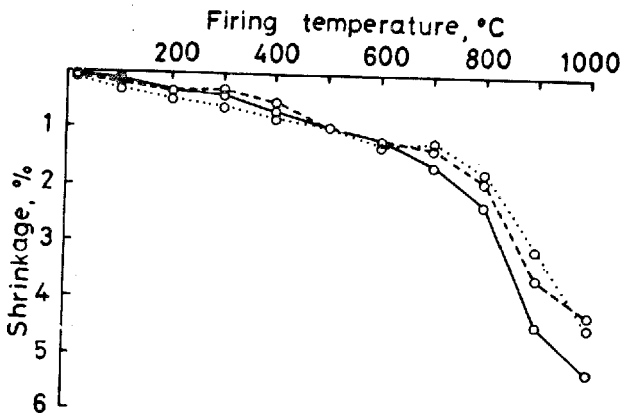

Fig. 2. Variation of shrinkage.

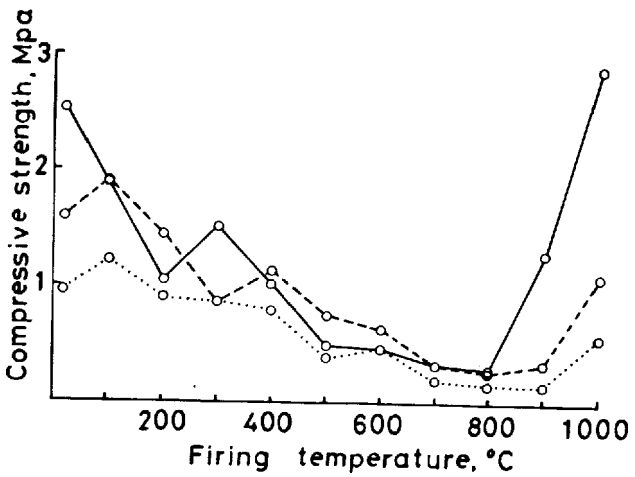

Fig. 3. Variation of compressive strength.

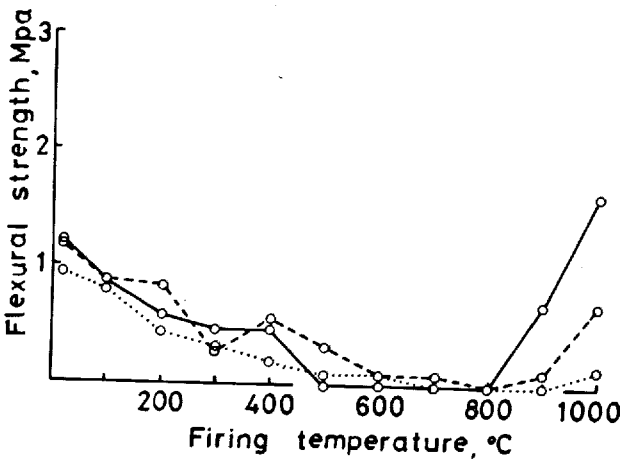

Fig.4. Variation of flexural strength.

——— G/P 0.9 ------- G/P 0.7 ····· G/P 0.3

density values as of 1,000°C are as equal to those of nonfired bodies, but their light weight charactor is retained.

Variation of linear shrinkage is represented in Fig. 2. Fired bodies show gradual contraction until 800°C and marked contraction, 3-5 % beyond that due to sintering. Specimens A containing more ettringite shrink most at higher temperature regions.

Results of compressive strength test are summarized in Fig. 3. Generally, the strength decreases gradually with increasing firing temperature until 800°C. Then, it begins to rise with the temperature, probably due to sintering. In case of specimen A the final strength becomes exceeding that of room temperature after firing at 1,000°C. The fired bodies lose strength considerably in medium temperature firing. The same trend is seen in the results of flexural strength test summarized in Fig. 4. It is noted that flexural

strength becomes quite weak after firing around 500-800°C.

The overall appearance of fired specimens A is shown in Fig.5. It is evident that 700°C firing resulted in bad cracking but the specimen could still stand. Though strength test gives minimum values at 800°C, the specimens fired at this temperature exhibit only slight cracking. It is interesting to note that specimens fired at 800, 900 and 1,000°C show "bending phenomena" with a little cracking on the outer surface. It is strange that the specimens are stable and straight inside the furnace but they suddenly begin to bend after taking out. This is probably due to the formation of γ-C_2S after transformation with cooling. We observed the presence of β-C_2S, but no evidence of γ-C_2S in this instance. Specimens, B and C, also give nearly similar results, i.e., badly cracked after 700°C firing as well. However, specimens C are not so fire resistant in the region 500-800°C, exhibiting cracking to a greater or smaller degree.

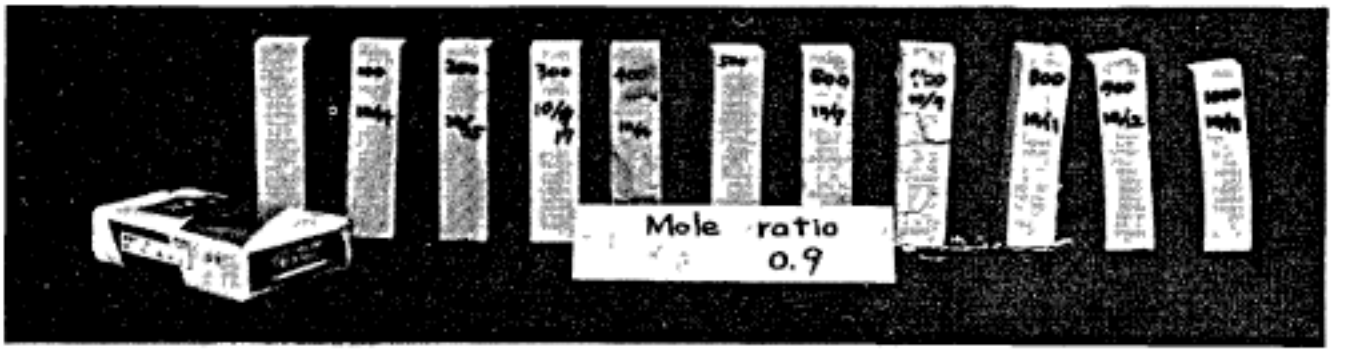

Fig. 5. Overall view of the specimens after firing. Nonfired body to fired bodies from left to right every 100°C.

CONCLUSION

Specimens of porous materials having three different chemical compositions have been prepared, using sythetic portlandite from limestone slime. Some physical properties have been measured after firing up to 1,000°C. The following conclusions have been drawn.

(1) Limestone slime is applicable as portlandite source despite being impure.
(2) Generally bulk densities decrease with higher firing temperatures and minimum values were reached after 800°C firing. Then, the bulk densities increase again toward 1,000°C firing.
(3) Measurements of linear shrinkage show gradual contraction up to 800°C firing. The conttaction then begins to enhance toward 1,000°C firing.
(4) Compressive strength decreases gradually up to 800°C firing. Then, it begins to increase toward 1,000°C firing due to sintering. The same trend is observed on flexural strength, too.
(5) Photographs of overall views of specimens revealed that specimens fired at 700°C are badly cracked. Specimens fired at 800, 900 and 1,000°C are deformed with a little cracking after cooling. Specimens C containing much more portlandite component are not so fire resistant as specimens B and C.
(6) The strength of specimens decreases with firing temperature, but no marked cracking was observed below 600°C firing for specimens A and B. Therefore, FGL materials prepared with higher G/P molar ratio can be used as heat insulating materials up to 600°C, although flexural strength becomes weak.
(7) The strength is regained after firing around 1,000°C. Thereby, bending phenomenon was encountered with cooling of the fired bodies.

ACKNOWLEDGEMENT

Thanks are due to Mr. H. Inn, then the student of Yamaguchi University for his

assistance in this work. Chuden Chemical Enfineering and Nittetsu Mining Companies are also acknowledged for providing the fly ash and the limestone slime, respectively.

REFERENCES

1. Ikeda, K. and Tomisaka, K.: "Fundamental Studies on the Preparetion and Strength of Steam-Cured Porous Materials Made From the Mixtures of Fly Ash, Gypsum and Lime", Journal of the Ceramic Society of Japan, 1989, 97(4), 478-483. -in Japanese but English version available.
2. Ikeda, K. and Tomisaka, T.: "Utilization of Solid Wastes Derived from Power Stations" , Fine Ceramics, 1989, 10(3), 117-125. -in Japanese.
3. Ikeda, K. and Tomisaka, T.: "The Thermal Conductivity of Steam-Cured New Porous Materials Prepared from Fly Ash, Gypsum and Portlandite, Proceedings of the 2nd BISCC, Beijing, 1989, 3, 365-372.
4. Ikeda, K. and Tomisaka, T.: "Physical Properties of FGL, Novel Porous Materials Prepared from Fly Ash, Gypsum and Lime with Special Emphasis to the Thermal Conductivity", Fortschrittsberichte der DKG (FOB) 1992, 7(1) 84-91.

IMPROVED FORMULATIONS WITH HIGH EARLY STRENGTH AND REGULATED SET

M M Ali, S K Handoo, N K Jain and S C Ahluwalia

National Council for Cement and Building Materials,
New Delhi, INDIA

SUMMARY

Rapid hardening high early strength composite formulations are used for specific applications such as rapid repair of cracks in dams, damaged runways, strata control in mines, preparation of grout mixes etc. The formulations generally used either tend to cause corrosion, being chloride based, or are useful only under specified curing conditions. In the present paper, inorganic formulations have been developed based on CSH-sulfoaluminate hydrate system. These composites set in a few minutes and attain compressive strength up to 200 kg/cm2 at two hours. The high early strength was achieved through controlled formation and crystallization of ettringite along with accelerated hydration of silicates. The gelatinous hydrates fill the pores at early ages leading to a dense compact hardened mass. The strength gain in the first two hours could be related mainly to the concentrations of reactive sulfate and aluminate components in the composite. The parameters favouring activation of the components have also been identified and discussed.

INTRODUCTION

Portland cement has long been a standing basic components in preparation of composite mixes for various special applications. Inorganic systems, consisting of finer portland cement activated with agents such as alkali metal carbonates, hydroxides, chlorides etc, are used for rapid setting and high early strength requirements. The pozzolanic additions with alkali activation, such as silica gel and sodium carbonate, with cement develops properties of rapid setting and high early strength (1-3). Similarly sodium silicate - sea water portland cement grouts at w/c ratio of 2 to 3 have been used for a number of years for void filling in the foundation of offshore concrete gravity platforms. Various other inorganic systems having rapid hardening compositions have been developed based on portland cement, calcium sulfate, aluminates, slags and alkali metal carbonates (4-8). The organic systems generally consist of polymerisable resins and have been used for rapairs of damaged concrete structures. These are mostly epoxies and polyurethanes (9). While in general the formulations developed are adequate for certain purposes, they do not provide both rapid setting and high early strengths under ordinary curing conditions (10). A large number of patent literature on these cements is available, some of the important papers are referred here (11-15).

The present paper develops composite formulations through acceleration reactions in CSH-sulfoaluminate system. Studies at NCB relate to composite formulations with set regulation and high early strength generation to meet requirements of some of the applications such as repair of damaged runways, anchoring bolts in mines, repair of dams and shotcreting.

EXPERIMENTAL

The experiments were planned in two parts (i) development of admixture formulation and (ii) development of composite mix consisting of admixture and OPC.

The admixture consisted of adequate mix proportions of synthesized calcium monoaluminate (CA) cement, reactive calcium sulfate, alkali carbonate and retarder based on hydroxy carboxylic acid. Monocalcium aluminate cement was prepared in the laboratory from high grade limestone (CaO > 50%) and bauxite (Al_2O_3 > 80%), using 1:1 molar mix proportion corresponding to CaO and Al_2O_3. A homogeneous mix of the limestone and bauxite powder was fired in an electric furnace at 1400oC for two hours. The sintered mass was ground to a fineness of 200 cm2/gm Blaine and refired at 1400oC for two hours. The powdered sample indicated by XRD a predominance of CA. The fineness of the finally prepared CA was maintained at about 3000 cm2/gm Blaine. Reactive calcium sulfate was prepared by calcining high purity mineral gypsum at 700oC for one hour. The X-ray diffraction indicated formation of stable anhydrite. The calcined sample was ground to a fineness around 3000 cm2/gm Blaines. Mixes of calcium aluminate and calcium sulfate corresponding to Al_2O_3/SO_3 molar ratios of 1 to 4 were prepared with 5% by weight of sodium carbonate. The mixes were interground to a fineness of 3000 cm2/gm Blaine.

The composite mixes consist of OPC, admixture and filler such as sand for mortars, and sand and aggregate (<10 mm size) for concrete. The composite mixes were prepared by replacing 10 to 30 percent of OPC by weight of admixture and using 1:1 cement sand mix for mortar and 1:1:2 for concrete. The composite mixes were evaluated for hydrated phases and performance characteristics. Mortar mixes hydrated for 2 hrs, 5 hrs, 24 hrs

and 28 days were prepared using a w/c ratio of 0.4. The hydration was arrested by acetone treatment. The hydrated admixture samples both with and without sodium carbonate, were also prepared to study the effect of acceleration on hydration. The hydrated samples were evaluated for mineral phases using x-ray diffraction and fracture surface morphologies using scanning electron spectroscopy. The XRD was carried out on Rigaku model D/Max-C using voltage/ current 30 KV/20 mA and scanning speed of 3 deg/min.

The mixes with and without retarder formulations prepared were evaluated for setting time using Vicat apparatus and compressive strength on mortar (1:1) mix. Water cement ratio for compressive strength determination was fixed at 0.4. To regulate setting time retarder citric acid was used, 0.1 percent by weight of admixture. The retarder was mixed by dissolving in water.

RESULTS AND DISCUSSIONS

Physico-Mechanical Properties

The composite mix formulations were found to set in 2 to 15 minutes with the rate of setting fastest with admixtures having higher Al_2O_3/SO_3 ratio. The setting time could be increased to 30 minutes by using about 0.1 percent citric acid by weight of the admixture.

The compressive strengths of composite mortar samples are shown in Table 1. In a typical mix proportion prepared by replacing 20 percent of OPC by admixture, compressive strengths were found to increase with an increase in total Al_2O_3/SO_3 ratio derived from all the components of the mix. The composite formulations having Al_2O_3/SO_3 ratios greater than 2.0 achieve high early strength. The flexural strength of composite mixes having Al_2O_3/SO_3 more than 2.0 were found to be in the range of 30-40 kg/cm2 at two hours.

TABLE 1

Compressive Strength of Composite Mix having Different Al_2O_3/SO_3 Ratios (Mix replacing 20%) of OPC by admixture)

Composite Al_2O_3/SO_3 Ratio	Compressive Strength (kg/cm2) 2 h	5 h	24 h
1.13	6	10	135
1.82	10	16	160
2.34	34	57	200
2.72	68	108	215
3.15	90	140	220

Fineness of OPC is 2750 cm^2/gm Blaine

X-ray diffraction studies of a typical composite mix hydrated have shown formation of poorly crystalline ettringite (Fig. 1) at different ages. The intensity of peak is not markedly increased with the time of reaction. Substantial amount of unhydrated cement phases were seen even at 24 hours.

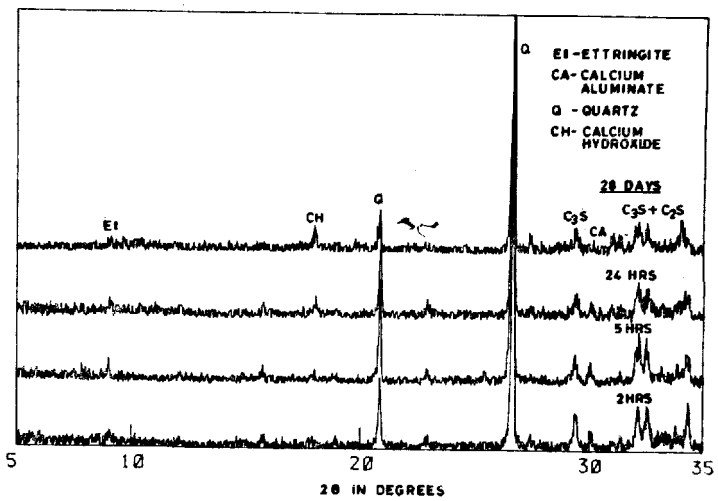

Fig 1 : XRD of Hydrated composite samples

The lack of crystallization is owing to the presence of Ca(OH)2 released from hydration of OPC (6). Hydration of an admixture sample without and with sodium carbonate (ADM I & ADM II) have shown that in presence of alkali carbonate, ettringite is predominant at, 120 minutes while an admixture without alkali carbonate forms monosulfate, as shown by XRD (Fig. 2). It is evident that alkali carbonate increases availability of reactive sulfate ions for the formation of ettringite and formation of monosulfate hydrate does not take place in appreciable quantity.

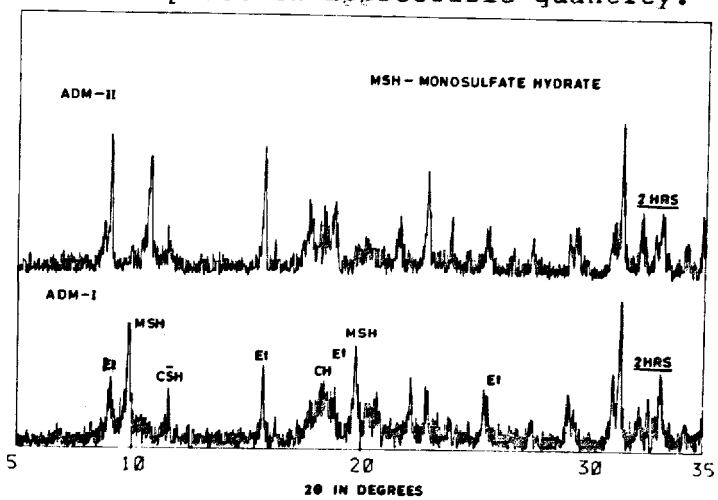

Fig 2 : XRD of Hydrated admixture samples

Scanning electron microscopic studies of hydrated samples have shown formation of gelatinous hydrates (Fig. 3) which increases with the increase in Al2O3/SO3 ratio as well as the amount of admixture (Table 1). At lower Al2O3/SO3 ratio, i.e 1.13, highly porous structures are seen at 2 hrs. When Al2O3/ SO3 is raised to 2.34, a relatively much higher amount of hydration could be seen. Abundant gelatinous hydrate phases are seen around the particles. With increasing ratio i.e at Al2O3/SO3 of 2.72, a dense structure is developed. An increase in reaction time develops strong structures (Fig.3). The gelatinous hydrates fill the void spaces and lead to

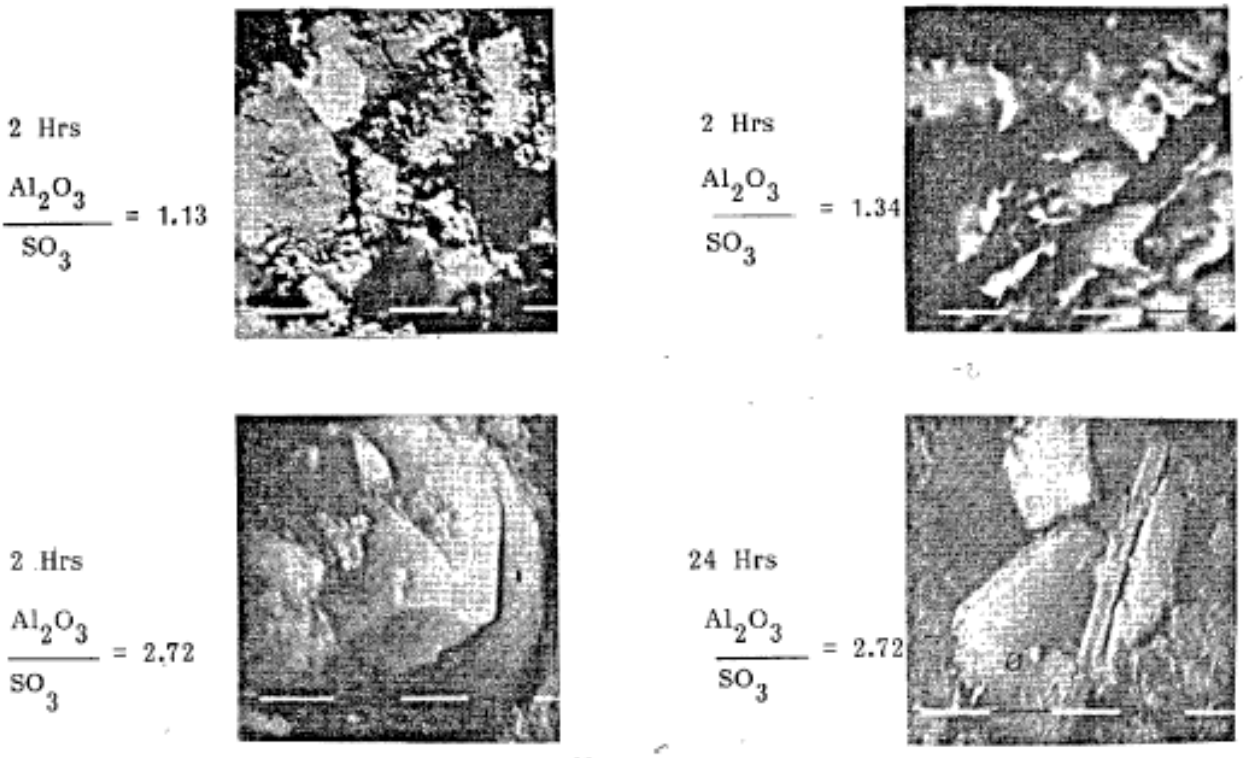

Fig 3 : SEM of Hydrated Samples at Different Ages

increases in compressive strength : the quantity of admixture determines the strength of the structure. The densification is further evident from porosity measurement by mercury porositimetry of the hardened mortar which indicates that at two hours the average porosity was found to be about 15 percent which is reduced to 8 percent at 12 hours.

The fineness of cement has been found significant in determining the early strength. At higher fineness of OPC i.e 4200 cm2/g Blaine, the 2 hr compressive strength of a typical composite mix is about 68 kg/cm2 compared to 30 kg/cm2 at fineness of 2750 cm2/gm. This is due to generation of a denser compact mass using finer cement.

The mix formulations developed were found suitable for various applications. The field trials were carried out for shotcreting at a tunnel site where rebound losses were substantially reduced. The mix formulations capable of yielding as high as 200 kg/cm2 compressive strength were also developed which were found suitable for emergency repairs, such as damaged runways.

CONCLUSIONS

1 The composite mix formulation developed is based on bulk precipitation of ettringite at early ages leading to rapid setting and high early strength.

2 The performance characteristics of formulations could be varied depending upon the fineness and strength of OPC mix proportions and accordingly the formulations could be tailor-made to suit the requirement in field.

3 Successful field trials for shotcreting were carried out wherein substantial saving in rebound losses were attained during shotcreting.

ACKNOWLEDGEMENT

This paper is based on the results of a R&D project at Newer Materials and Process Division of the National Council for Cement and Building Materials. The paper is published with the permission of Director General of the Council.

REFERENCES

1 Ali, M M, Handoo, S K and Ahluwalia, S C. Improved formulations with high early strength and regulated set. Third NCB International Seminar on Cement and Building Materials, New Delhi, 21-25 January 1991, VII-21-27.

2 Majumdar, A J. New Rapid Hardening Cement Developed, Building Research Establishment, BRE News of Construction Research, April 1989.

3 Mudbahatkl, G A, Parmeswaran, P S, Heble, A S, Pai, B V B and Chatterjee A K. Non-Alitic Cement from Calcium Sulphoaluminate Clinker, Brazil Sym. Vol.4, 1986, 370-364.

4 Nakagawa, K, Daimon, W Y. Hydration Mechanism & Quick Hardening Mechanism of Amorphous Calcium Aluminate with Anhydrous Gypsum, Gypsum and Lime, Jan, 1989, 12-17.

5 Collepardi, M, Turriziani, R and Marcialis, A. The Paste Hydration of 4 CaO.3Al2O3SO3 in presence of calcium sulphate, Tricalcium Silicate and Dicalcium Silicate, Cem & Conc. Res. 2(2), 1972, 213-223.

6 Mehta, P K. Effect of Lime on Hydration of Pastes Containing Gypsum and Calcium Aluminates on Calcium Sulfoaluminate, J Amer, Ceram Soc, Vol 56 (6), 1973, 315-319.

7 Lukas, W, Rock R and Hagleitner, K. 'Energy Dispersive Analysis of Ettringites in Cement Paste Samples', Translation ZKG No. 7/77(328-330).

8 Mchedlov, O P - Petrossyan, Gribko, W F, Omel, A F Chevko, Kholodny, A G. 'Influence of Ettringite Formation Kinetics on Special Cement Properties', Third NCB International Seminar on Cement & Building Materials, New Delhi, 21-25 Jan. 1991, Vol 4, VIII-78-83.

9 Nagele, E and Schneider, U. Properties of organo-mineral cements, Advances in Cement Res. 3(10), 1991, 75-79.

10 U S Patent Number 640, 715, 3 February 1987.

11 German Patent DE 3, 527, 978, 05 February 1987.

12 South African Patent ZA 8809, 199, 30 August 1989.

13 Japanese Patent, 01, 226, 756, 11 September 1989.

14 German Patent DD 271, 897, 20 September 1989.

15 Japanese Patent 0238, 350, 07 February 1990.

DURABILITY OF HIGH STRENGTH CALCIUM SULPHATE FREE CEMENT

I P Yanev*, M Z Radenkova-Yaneva**

*Scientific Institute for Building Materials,
**University of Architecture, Civil Engineering and Geodesy,
Sofia, BULGARIA

Cement on the base of ordinary portland cement clinker and calcium sulphate free ratarder of setting time is made. The latter is a waste lignosulphonate blended with taking-away-water additives in connection with its favourable use in cement grinding. From this cement mortar samples are made according to the standard methods. One batch of the specimens is put immediately after demoulding in high corrosive artificial medium (100 g salts in 1 dm^3 water). Two others are put in the same solution after having been kept 14, respectively 28 days in fresh water. At different ages (1, 3,6 and 9 months) the bending and compressive strengths are obtained. The results received are compared to the strength properties of the samples having been hardened in fresh water and natural sea water (from the Black sea). Coefficients of durability for each batch of the samples investigated are calculated. A high durability is established for mortars subjected to the corrosive medium in early age of hardening. This is of a great importance for building constructions, which are brought in exploatation immediately after demoulding.

Un ciment a la base d'un clinker de Portland et d'un retardateure de prise sans plâtre est obtenu. Le dernier représente un lignosulfonate de rebit mélangé avec un additif anhydre en vue son utilisation favorable lors de mouture du ciment. Des échantillions des mortiers sont moulés du ciment obtenu par des procédés stsndards. Après le décoffrage une partie des échantillons est mise immédiatement dans un milieu artificiel à forte corrosion (100 g de sels dans 1 dm^3). Deux autres séries sont mises dans la même solution après un durcissement durant 14 jours, respectivement - 28 jours, dans l'eau. Les resistances de flexion et de compression sont déterminées ades âges différents (1, 3, 6 at 9 mois).

Les résultats obtenus sont comparés aux données des recherches sur les propriétés de résistance des échantilloms âgés dans une eau potable et dans une eau de mer naturelle (de la Mer noire). Les coefficients de résistance de chaque série d'échantillons étudiés sont déterminés. On a établi une haute résistance ala corrosion des mortiers de ciment soumis aux effets des milieux agressifs lors des périodes initiaux du durcissement. Ceci est d'une importance singuliere pour la construction des ouvrages hydrotechniques maritimes mis en exploitation à l'instant même.

INTRODUCTION

The cement-stone and concrete corrosion is one of the most important aspects in assessment of the possibility of the constructions to be used in specific conditions. Under the influence of the liquid aggressive media (river, sea, underground and other kinds of water) the cement hydration products are attacked. Conditions for their decomposition or their interaction with aggressive liquids and formation of the compounds with a greater volume are created. In connection with this it is of a great importance to estimate the durability of the cement stone. The latter is especially important when a new kind of binder is put into practice.

Recently a new binder on the base of ordinary portland cement clinker has been made (1,2). This binder has high initial and final strengths (2), the cement stone has high density (3) and the mortars and concretes obtained can be used for constructions that can quickly brought into use (4). In this work the results of determination of durability of calcium sulphate free cements are shown. The results will allow to characterize entirelly the properties of the new tipe of binder and to estimate the possibility of its use in building of hydrotechnical constructions, working in different corrosive media.

MATERIALS AND EXPERIMENTAL PROCEDURE

In the investigation, calcium sulphate free cement obtained from the ordinary portland cement clinker without additive of calcium sulphate (regulator of setting time) is used (1,2). Durability of cement is determined by assessment of the strength of the mortars immersed in the oorrosive media. This method accounts for two kinds of corrosion - dissolution of the hardened cement's components and formation of compounds with great volume. Change of the strength with time characterizes quantitatively the corrosion processes so that one can follow those properties which are of a greater importance and have a real particular significance. As aggressive media natural sea water and water containing 80,16 g NaCl, 6,812 g $MgSO_4$, 9,62 g $MgCl_2$ and 3,42 g $CaSO_4$ in 1 dm^3 (artificial sea water) are used. The proportions of the salts corresponded to Black sea water but their concentration is about 6,7 times higher than that of sea water (5). In this way the processes of interaction between the cement stone and the salts of water are intensified and in a shorter time results can be obtained that can serve for estimation of the durability of cement.

Samples prisms 20x20x80 mm are made from mortars with cement to sand ratio one to three by weight. Sand with definite granulometry - fraction between 0,15 and 0,50 mm - is used. Water to cement ratio is equal to 0,58 and corresponds to a spreading of the mixture equal to 155 mm. The composition of the mortars is chosen so that the conditions of carrying out the experiments to be similar to the conditions of using of the binders in practice. In this way the work of Kalousek on cement pastes (6) can be used only partially in the interpretation of our results.

One batch of the specimens is put immediately after demoulding in the corrosive solution. Two other batches are put in the same kinds of solutions after having been kept 14 respectively 28 days in fresh water. At different ages (1, 3, 6 and 9 months) the bending and compressive strengths are determined. Coefficients of durability which are equal to the ratio between the strengths (compressive or bending) of the specimens kept in corrosive solutions and the corresponding strengths of the controle samples hardened in fresh water is calculated. The conditions of carrying out the experiments are according to (5).

The quantity of the aggressive media is 200 cm^3 for each sample. The solutions are stirred with air and the samples are carefully examined every day. By means of thermal analysis some of the products of interaction between the compounds of the cement stone and aggressive solutions are determined.

RESULTS AND DISCUSSION

The results of the strength properties obtained during experiments are shown in Table 1. Coefficients of durability are shown in Table 2.

Table 1.

Strength Properties of the Mortars

Condition of samples examination		Bending strength, MPa				Comptessive strength, MPa			
		at the age, days							
		30	90	180	270	30	90	180	270
Immediately after demoulding	fresh water	6,4	7,1	8,4	6,6	30,4	32,5	32,8	33,7
	sea water	6,9	6,5	8,7	7,3	29,8	28,5	27,8	21,3
	artificial sea water	7,5	7,3	7,0	6,0	29,5	24,8	21,8	19,2
After 14 days keeping in fresh water	fresh water	6,6	7,2	8,5	8,8	30,6	32,9	33,5	33,8
	sea water	8,7	7,9	7,3	7,1	29,1	28,0	28,3	24,6
	artifisial sea water	8,1	5,9	4,8	3,0	25,4	21,7	16,9	13,8
After 28 days keeping in fresh water	fresh water	6,8	7,4	8,7	8,8	31,8	33,0	33,8	34,0
	sea water	8,3	7,2	6,7	7,0	28,1	25,6	21,0	15,4
	artificial sea water	9,0	6,0	4,3	3,0	27,9	25,2	19,0	13,0

Table 2.

Coefficients of Durability

	Immediately after demoulding		After 14 days keeping in fresh water		After 28 days keeping in fresh water	
	sea water	artificial sea water	sea water	artificial sea water	sea water	artifisial sea water
K_6, bending	1,05	0,83	0,86	0,65	0,77	0,49
K_6, compressive	0,84	0,66	0,84	0,59	0,62	0,56

In the interpretation of the results the following special features of the investigated cement can be shown. The high degree of hydration of the calcium sulphate free cement in the first days of hydration (1 to 3 days) provides a very dense structure of the cement stone which is formed from calcium hydrosilicates with high CaO/SiO_2 ratio. These

hydrocilicates are the main bearer of the strength properties of this kind of cement, as in the cement stone calcium hydrosulphoaluminate is not formed.The high density of the cement stone received during the hardening of the cement investigated on its turn is a precondition for the increased sensibility of the structure under inner attacks. This means that when compounds with high volume are formed in dense structure the latter is demolished quickly.At the same time due to its lower permeability for aggressive solutions the heterogenous chemical reactions take place in the superficial layer of the samples.

If we assume that in the first days the hydration is quite advanced, the following processes of hardening in aggressive media are connected with some additional processes such as: leaching of $Ca(OH)_2$ in aggressive solution because of the increased solubility of $Ca(OH)_2$ in the presence of NaCl (7); interaction of $Ca(OH)_2$ with Mg^{2+} of the aggressive solution and formation of amorphous $Mg(OH)_2$; decomposition of hydrosilicates with release of $Ca(OH)_2$ and C - S -H phase with lower CaO to SiO_2 ratio; diffusion of SO_4^{2-} and Cl^- in the inner part of the samples, their interaction with calcium hydrosilicates and formation of compounds with higher volume (7,8).

On the basis of the above mentioned processes the results obtained are discussed. The strength properties of the samples cured in fresh water increase up to the end of the experiments (9 months). However the increase of the compressive strengths in comparison with those at the age of 28 days, is about 10 percent. The already described complex interactions are connected with the decreasing of the strengths of the samples immersed in aggressive solution. However the moment of immersing of the samples in the solutions is of a great importance. If it take place immediately after demoulding, the coefficients of durability have higher values (table 2). If the immersing in aggressive solution is after 14, respectively 28 days hardening in fresh water, the strengths of the samples are lower. These results can be connected with the additional processes of densifying and recrystalisation of the structure during hardening in fresh water. At the same time the increased concentration of the salts in the aggressive solution has undoubtedly a great influence - the decrease of the strengths is considerable (table 1, table 2).

The interaction in the system investigated has a heterogenous character. It is an exchange of substances inside the samples accompanied by chemical reactions. In this case the total rate of the process is determined by the rate of diffusion as well as by the rate of the chemical reaction and can be expressed in the following way (9) :

$$\frac{dq}{d\tau} = \sqrt{D'.K'.C}$$

where: $\frac{dq}{d\tau}$ - is the quantity of the substance, reacting on the surface.

D' - is the effective coefficient of diffusion.

K' - is the effective rate constant.

C - is the concentration.

At the same time the depth of penetration (X) of the aggressive substances in the volume of the materials depends on the rate of diffusion (V_1) and the rate of the chemical interaction (V_2):

$$X = \sqrt{V_1.V_2}$$

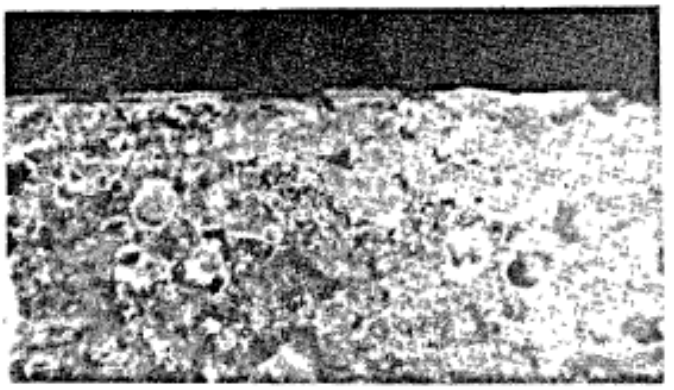

Fig.1. Stereo-micrograph of the specimen kept in natural sea water, x 90.

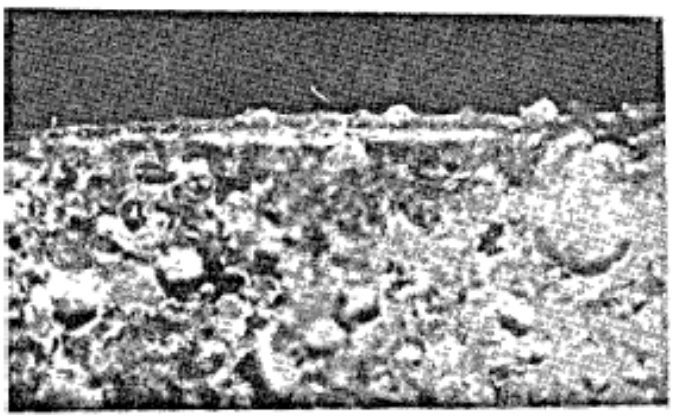

Fig. 2. Stereo-micrograph of the spesimen kept in artificial sea water, x 90.

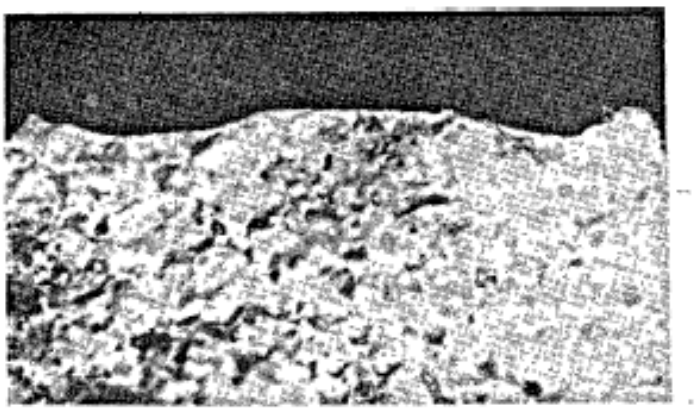

Fig.3.Stereo-micrograph of the specimen kept in fresh water, x 90.

The driving force of the process of diffusion is the gradient in the concentration and the bigger its valus is, the higher the rate of diffusion will be. The rate of the chemical interaction also depends on the concentration of the reagents, respectively on the concentration of the aggressive agent. In this sense the samples subjected to the action of artificial sea water show greater degree of corrosion as well as a greater depth of penetration in the volume of the material. This is clearly seen on fig. 1 and fig 2. It must be said, that in samples kept in fresh water no destruction in the macrostructure of the superficial layer is noticed (fig. 3). At the same time morphological changes in the C-S-H phases occur and the strength of the samples decreases (10).

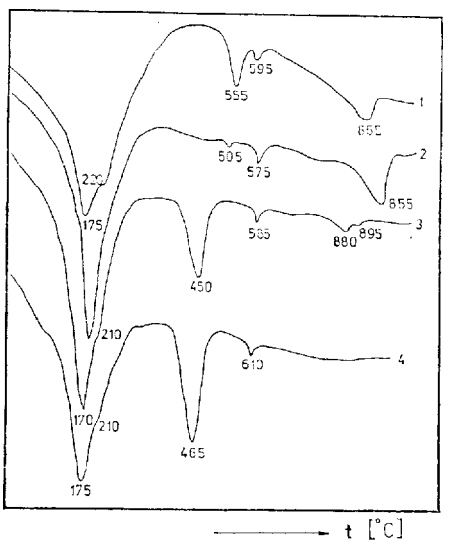

Fig.4. Shapes of DTA curves for the samples investigated 1/ kept in fresh water; and put in natural sea water 2/immediately after demoulding, 3/ after keeping 14 days and 4/ after keeping 28 days in fresh water. The age of testing 270 days.

The results of the thermal investigation of samples from the superficial layer of the specimens are shown on fig 4. Under the action of sea water (natural and artificial) $Mg(OH)_2$ is obtained (11). It accumulates mainly in the superficial layer, because Mg^{2+} do not diffuse in the volume of the specimens (6). The great endothermal effect in the temperature 170-180°C is connected with the decomposition of the gypsum (160 -180°C), the calcium hydrosulphoaluminates (120-150°C) and hydrosilicates with high CaO to SiO_2 ratio (100-200°C).

On the base of the determined coefficients of durability at the age of 6 months it can be said that the investigated calcium sulphate free cement is resistant to corrosion ($K_6 > 0,8$ (5)) in the cases when the action of the aggressive medium take place not later than 14 days from the demoulding. In this sence the high sterngth calcium sulphate free cement can be used for building of hydrotechnical constructions which can be immediately brought into use and work in marine conditions.

REFERENCES

1. Bulgarian Patent No 35653,21 November 1984. "Binder for mortars and concretes".
2. Yanev, I.:"Highstrength calcium sulphate free cement", Technitsceska misal, 23, No 6, 1986, pp. 65-70.
3. Yanev, I., Radenkova-Yaneva,M.:" Structure of cement stone with high density". Proceedings of the International Conference on Mechanics and Technology of Composite Materials, Varna, Bulgaria, 2-4 October, 1985.
4. Yanev,I., Radenkova-Yaneva,M.:Compositions for restoration". Proceedings of the Conference on Material Science and Restoration, 2nd, Esslingen, Germany, 2-4 September 1986.
5. Butt,U.M.- Practical works on Technology of Binders, Moscow,1953.
6. Kalousek,G.L.: Mechanism of Seawater Attack on Cement Pastes". A.C.I.Journal, February, 1970.
7. Moskvin,V.M.: Corrosion of the Concrete, Moskow,1980.
8. Magnesium-sulphate and Acid Corrosion of Cements, Editor I.Kanzepolski, Tashkent, Uzbekistan, 1975.
9. Ratinov,V., Ivanov,B.: Chemistry of Civil Engineering, Moskov, 1968.
10. Isogai,J., Kondo,R.:"Hardened Cement Paste Affected by Sea Water", Proceedings of the Sixth International Congress on the Chemistry of cement, Volume II, Moscow, 1976.

VOLUME STABILITY OF HIGH MAGNESIA CEMENTS

K M Sharma*, R Bhargava*, S C Ahluwalia* and K C Narang**

**National Council for Cement and Building Materials, New Delhi, INDIA*
***Dalmia Cement (Bharat) Ltd., New Delhi, INDIA*

SUMMARY

National standards world over specify limits on the presence of MgO in cement to overcome the problem related with the anticipated delayed hydration of MgO in the set mortar/ concrete under normal conditions of mixing, placing and curing of cement structures. This has resulted in selective use of limestone particularly with respect to MgO, thereby reducing the life of the quarries and the cost of raising it. Solutions have been reported both in terms of improving the heating and cooling schedules as well as using reactive and non reactive additives during grinding of clinker. However, contribution of the individual parameters to reduce expansion due to MgO and the mechanism of the process are not clearly established. Investigations at National Council for Cement and Building Materials (NCB) were directed towards quantifying the effect of reactive and mineral additives on the various aspects of the problem of expansion. Effect of chemical composition of clinkers and the cooling conditions on the autoclave expansion of the resultant cements has been discussed. Studies with regard to the effect of cement and additive fineness and periclase size on autoclave expansion and the hydration characteristics of the cements have also been reported. A correlation of these properties with the autoclave expansion has been attempted.

INTRODUCTION

It is well established that magnesia in portland cement clinker in the form of periclase is an undesired component leading to uneven volume changes in hardened cement, particularly when present in high quantities. Because of this, most national standard specifications on cement have a tolerance limit on MgO and this limit in IS:269-1989 is 6% (Max). The presence of periclase in clinker not only introduces an element of uneven volume change in hardening cement but also limits the raw material choice for cement industry (1). The volume change on long term expansive behaviour of cements has been mainly attributed to the areaction of expansive MgO i.e periclase, with water to form $Mg(OH)_2$ (brucite) and the rate of this reaction is very slow. However, the expansion in cements is not proportional to the amount of periclase present (2). In addition to periclase, factors such as free lime, sulphate, alkalies, C_3A, burning and cooling conditions are also responsible for expansive behaviour of cement. However, contribution of the individual parameters to reduce expansion due to MgO and mechanism of the process are not clearly established. Investigations at National Council for Cement and Building Materials (NCB) were directed towards quantifying the effect of reactive and mineral additives on the various aspects of the problem of expansion. The present paper deals with the physico chemical and mineralogical characteristics of clinkers of varying chemical composition prepared in laboratory under different cooling conditions. Studies with regard to the effect of cement and additive fineness and periclase size on autoclave expansion and the hydration characteristics of the cements have also been reported.

EXPERIMENTAL

The raw materials used in the present investigations are limestone (LS-OC and LS-OD) and clays (F-CLY, HF-CLY and CLY). The elemental composition carried out by using gravimetric cum volumetric methods are given in Table 1. Experiments were conducted as per the details given below to see the effect of clinker properties on autoclave expansion :

A/ Effect of Clinker Composition

Raw mixes were designed to prepare clinkers as per the details provided in table 2 at a fineness level of 10 % residue on 90 micron sieve. Additional quantities of raw mix Ia were also prepared at a fineness level of 3, and 5 % residue on 90 micron sieve. Mineral composition, morphology and microstructure of the clinkers were determined by XRD and optical microscopy and are presented in Fig.1 and Plate 1 for clinkers Ia and IIb. The cements obtained from above clinkers were subjected to the determination of autoclave expansion (Table 3).

B/ Effect of Cooling Conditions

Keeping in view the limit of MgO in cement the raw mixes RM-Ib and RM-IIb were fired at 1400°C for 25 minutes in a laboratory furnace and cooled under different conditions : i/ Water quenching ; ii/ Clinkers removed from furnace at 1400°C and cooled in air to ambient temperature (rapid cooling) ; iii/ Clinkers cooled in the furnace at the rate of 8-10° C/min upto 1100°C and then cooled in air to ambient temperature (slow cooling).

X-ray diffractograms of clinker IIb prepared under different cooling conditions are presented in Fig.2. Clinkers were ground with 4 percent

gypsum to a fineness level of 300 ± 5 m2/kg and the resulting cements were subjected to autoclave expansion (Table 4).

C/ Effect of Additives on Autoclave Expansion

Effect of addition of flyash, granulated blast furnace slag and inert additives such as limestone in various ratios in cement prepared from slowly cooled clinker IIb on autoclave expansion was studied. The results are presented in Fig.3.

D/ Effect of Fineness

i/ Effect of Cement Fineness

The clinker sample IIb was ground alongwith 4 percent gypsum to fineness levels of 300, 350, 400 and 450 m^2/kg. The results are plotted in Fig.4.

ii/ Effect of Fineness of Additives

The additives flyash, slag and limestone of finenesses 250, 350 and 450 m^2/kg were added to cement of 300 m^2/kg fineness in ratio of 15, 35 and 5 percent respectively. The results are given in Fig.4.

E/ Hydration Studies

Cements prepared from clinker IIb and with 15 percent flyash, 35 percent slag and 5 percent limestone were subjected to hydration studies. The hydration was arrested at particular age with acetone and dried under vaccum. The samples were analysed by X-ray diffraction and SEM techniques for identification of hydration products (Fig.5 and Plate 2).

RESULTS AND DISCUSSIONS

The results of chemical analysis in Table 1 indicate that limestone LS-OC is of high grade containing only 0.83 percent MgO whereas LS-OD is of low grade and contains as high as 13.14 percent of MgO. Two clay samples contain 2.55 and 9.29 percent Fe_2O_3 and the lateratic clay contains high percentage of Fe_2O_3 (73.85). The results indicate that single limestone can not be used for obtaining the raw mixes of desired chemical composition.

TABLE 1
ELEMENTAL ANALYSIS OF RAW MATERIALS

S. No.	Sample Number	Constituents determined (Percent)								
		LOI	SiO_2	Fe_2O_3	Al_2O_3	CaO	MgO	Na_2O	K_2O	TiO_2
1	Limestone (LS-OC)	39.54	6.51	0.70	0.85	51.17	0.83	0.08	0.03	-
2	Limestone (LS-OD)	44.09	2.10	0.60	0.15	39.81	13.14	0.05	0.02	-
3	Clay (F-CLY)	9.91	58.22	2.55	26.16	1.09	-	0.36	0.19	1.56
4	Clay (HF-CLY)	6.28	12.47	73.85	5.15	0.47	0.42	0.42	0.20	0.40
5	Clay (CLY)	6.77	63.07	9.29	13.87	3.74	1.07	0.45	1.30	-

Effect of Fineness of Raw Mix

Raw mix RM-Ia with 3 and 5 percent residue on 90 micron sieve yielded good clinkers whereas on the basis of 10% residue on 90 micron sieve led to the formation of clinkers with relatively poor mineral composition. Free lime content of all the clinkers was found to be lower than 1.5 percent. The optical microscopic investigations have revealed that the size of periclase increases from 10 to 25 u with decrease in fineness of raw mix. Similarly the autoclave expansion of the resultant cement increases from 0.25 to 0.78 percent with decrease in fineness.

Effect of Chemical Composition

Clinker composition obtained by Bogue's calculations was found to be close to the potential phase composition (Table 2).

TABLE 2
DESIGN PARAMETERS OF CEMENT RAW MIX AND OF RESULTANT CLINKER

S. No.	Sample No.	LOI	SiO_2	Fe_2O_3	Al_2O_3	CaO	MgO	Clinker Phase Composition C_3S	C_2S	C_3A	C_4AF
		Percent									
1	RM-Ia	36.08	12.19	2.93	2.25	42.90	3.05	56.22	18.45	5.29	14.36
2	RM-Ib	36.45	11.84	2.93	2.18	41.97	4.05	55.36	17.00	5.19	14.45
3	RM-Ic	36.77	11.52	2.92	2.14	41.19	4.91	55.66	16.55	4.88	14.48
4	RM-IIa	36.42	12.51	1.72	2.28	43.14	3.06	56.93	19.52	8.43	9.10
5	RM-IIb	36.88	12.02	1.50	2.60	42.45	4.02	56.24	18.35	10.25	8.06
6	RM-IIc	37.71	11.74	1.56	2.42	41.67	4.90	56.75	16.98	9.44	8.37

The periclase content in clinkers having MgO content of 4.5 percent was observed to be 1% and particle size varied between 2 to 6 u. In clinkers with 6 percent MgO content the periclase content was found to be 2 percent with particle size varied between 4 to 10 u. The periclase content of clinker with 7 percent MgO jumped suddenly to 4 percent with a size of 10-20 u. The results of optical microscopy (Plate 1) and XRD studies (Fig.1) show the formation of normal phases in all the clinkers. The results also showed even distribution of MgO in various clinker phases. X-ray diffractograms and optical micrographs of some representative samples are given in Fig.1 and Plate 1 respectively.

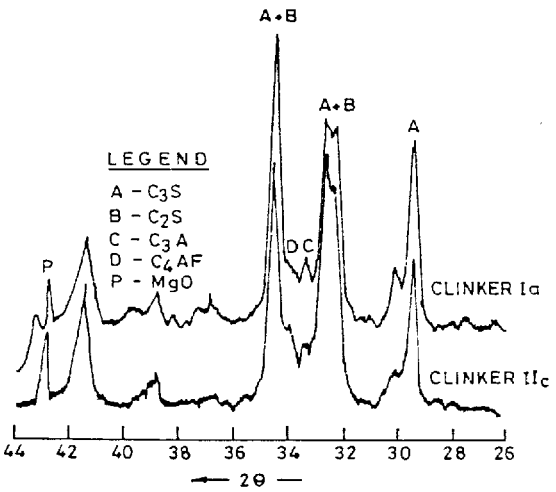

FIG 1 : XRD OF LABORATORY CLINKERS

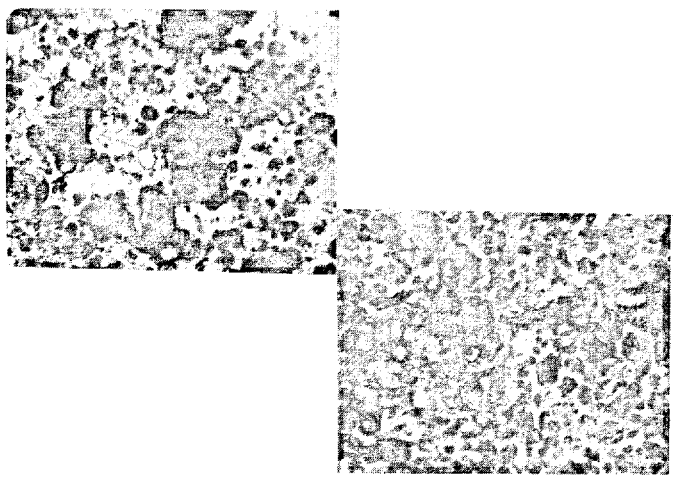

PLATE 1 : OPTICAL MICROGRAPHS OF CLINKER SAMPLES

Results in Table 3 indicate that the autoclave expansion of cements increases with increase in periclase content and size. The cements with same overall MgO content but different periclase content both in size and shape showed drastically different autoclave expansion. The autoclave expansion also increases with increase in C3A content at a constant MgO level.

TABLE 3
EFFECT OF CHEMICAL COMPOSITION OF CLINKER ON AUTOCLAVE EXPANSION OF CEMENT

Sl. No.	Sample Number	MgO content	C_3A content	Autoclave expansion
1	C-Ia	4.54	5.29	0.45
2	C-Ib	6.04	5.19	0.78
3	C-Ic	7.35	4.88	2.65
4	C-IIa	4.57	8.43	0.59
5	C-IIb	6.04	10.25	2.20
6	C-IIc	7.40	9.44	3.01

Effect of Cooling Conditions

The optical microscopic results indicate that the quantity and crystal size of periclase increases with decrease in rate of cooling. The effect of cooling rate is more apparent for clinkers with higher MgO content. X-ray diffractograms (Fig.2) of clinker IIb suggest the lowest periclase contents in water quenched clinkers. This is supported by the lowest autoclave expansion in the resultant cement (Table 4).

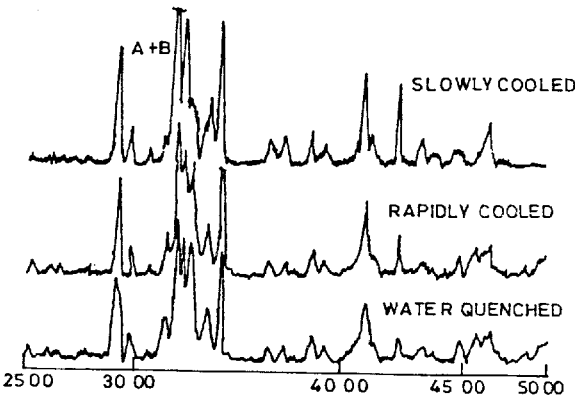

FIG 2 XRD OF CLINKER PREPARED UNDER DIFFERENT COOLING CONDITION

TABLE 4
EFFECT OF COOLING CONDITIONS ON AUTOCLAVE EXPANSION OF CEMENTS

Sl. No.	Sample number	Cooling condition	Autoclave expansion
1	C-Ib	Slow	5.00
2		Rapid	0.78
3		Water	0.30
4	C-IIb	Slow	6.20
5		Rapid	2.20
6		Water	0.80

Effect of Additives

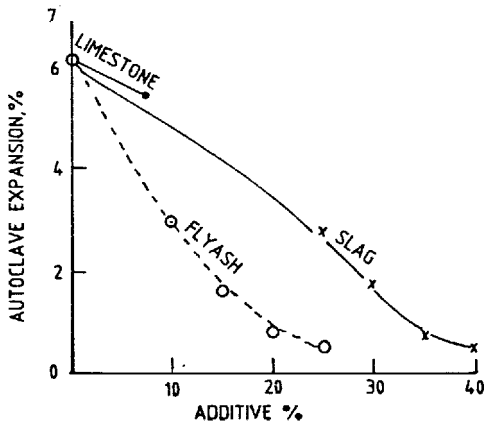

FIG.3 EFFECT OF ADDITIVES ON AUTOCLAVE EXPANSION OF CEMENT

Flyash, blast furnace slag and other pozzolanas have been widely used for making high MgO cement volume stable (3-5). Studies on cement IIb having autoclave expansion of 6.2 percent indicate that the replacement of cement by 10, 15, 20 and 25 percent flyash resulted in lowering of autoclave expansion to 3.4, 1.67, 0.79 and 0.48 percent, whereas replacement of cement by 25, 30, 35 and 40 percent slag resulted in lowering of autoclave expansion to 2.81, 1.73, 0.65 and 0.50 percent level. Addition of reactive silica brings down the CaO/SiO_2 ratio in the resultant cement and on hydration,

$Ca(OH)_2$ formed reacts with the reactive silica to form C-S-H which generates additional strength to offset some of the expansive forces generated by hydration of periclase whereas in case of slag $Ca(OH)_2$ liberated from the hydration of cement activates the slag component which in turn gives additional C-S-H. Study conducted with inert material such as limestone revealed that there is only marginal reduction in autoclave expansion upto an addition of 7 percent. The results are plotted in Fig.3.

Effect of Fineness

Effect of fineness of cement on autoclave expansion plotted in Fig.4 reveals that with increase in fineness the autoclave expansion decreases. The reduction is more pronounced in the fineness range of 350 to 400 m^2/kg.

The results plotted in Fig.4 indicate the reduction in autoclave expansion with increase in fineness of additive at a given percentage.

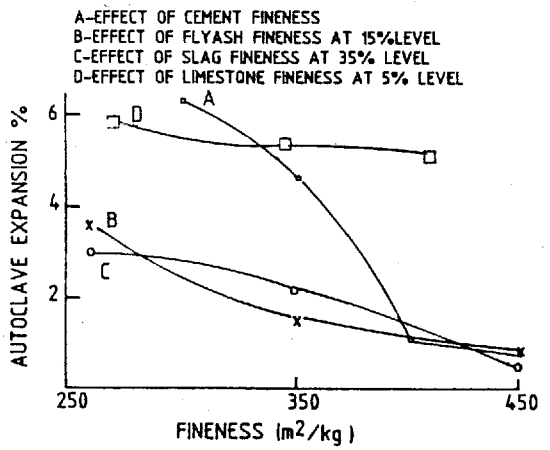

FIG 4. EFFECT OF CEMENT AND ADDITIVE FINENESS ON AUTOCLAVE EXPANSION

Hydration Studies

The hydration studies carried out upto 28 days revealed that the formation of $Ca(OH)_2$ is maximum in the control OPC and increases with

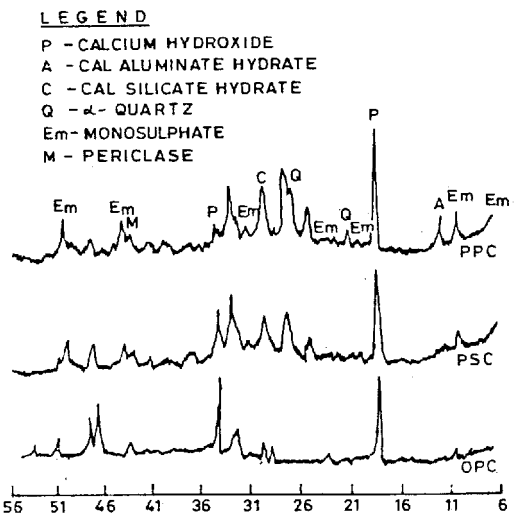

FIG 5 : XRD OF HYDRATED SAMPLES AT 7 DAYS

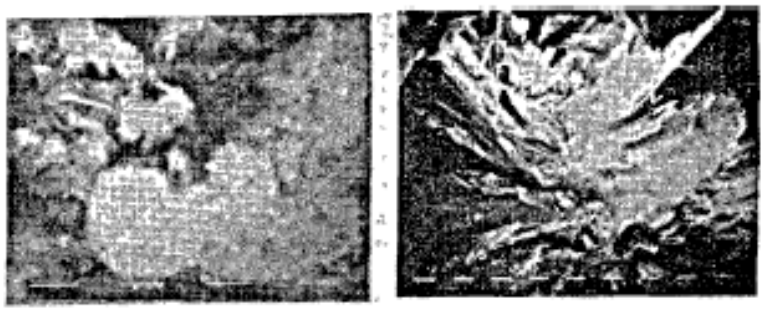

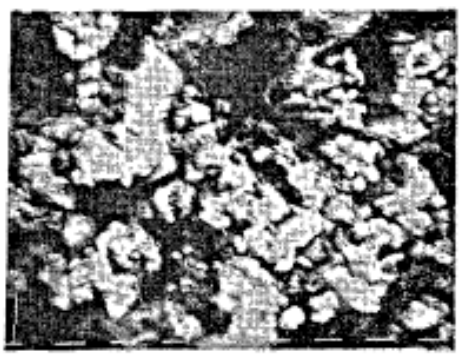

PLATE 2 : SEM's OF HYDRATED SAMPLES AT 7 DAYS —10μ

the age of hydration. The reaction appears to follow; the release of $Ca(OH)_2$ through OPC hydration, followed by activation of slag which in turn releases more lime and produces C-S-H. In case of pozzolana, the librated lime from cement hydration combines with pozzolana to give C-S-H. The hydration products identified at different ages are $Ca(OH)_2$, ettringite and solid solution of the tri and monosulphate, C_4AH_3 and C-S-H which are similar to hydration products of OPC, slag and pozzolana cements. The C-S-H obtained in the case of pozzolana and slag cements are of lower CaO content as expected. The selected X-ray diffractogram and SEMs of hydrated samples at 7 days are given in Fig.5 and Plate 2 respectively.

CONCLUSIONS

Clinkers prepared with varying MgO and C3A content and under different cooling conditions were subjected to grinding and the resultant cements were tested for autoclave expansion. The results are summarised here :

i. At fixed level of MgO, the autoclave expansion increases with increase in C3A content.

ii. Out of three coooling conditions studied, the lowest autoclave expansion was observed in water quenched sample.

iii. Keeping other factors constant, the autoclave expansion decreases with increased percentage of additives such as limestone, flyash and slag.

iv. Similarly keeping other factors constant, autoclave expansion decreases with increase in fineness of cement. The autoclave expansion also decreases with increase in fineness of additives at a given percentage.

ACKNOWLEDGEMENT

The authors have freely drawn upon completed R&D work/status reports of NCB. This paper is being published with the permission of the Director General, NCB, New Delhi, India.

REFERENCES

1. CRI :" Unsoundness of Clinkers with MgO Content well Below Permissible IS limit ". Pub. No. RB-22-82, March 1982. Cement Research Institute of India, New Delhi.

2. Ramchadran V.S.:" Unsoundness of Cements containing MgO and CaO". ill cemento, Sept. 1980, 77(3), 159-68.

3. Gille F.:" Investigations on expansion tendencies of Portland Cement due to MgO". Zement-Kalk-Gips, 1952, 142, p 5.

4. Rosa J. : " Portland Cement with High MgO content". Zement- Kalk-Gips, 1965, 54(9), 460-70.

5. Dolezsai K.: " High Magnesia Portland Cement". Proc. seventh conference on silicate industry, 1963.

STUDY OF HIGH-STRENGTH BLENDED FERRO-ALUMINATE CEMENT MORTAR AND CONCRETE

Wang Yanmou*, Zhang Liang, Su Muzhen** and Deng Junan****

**State Administration for Building Materials Industry, P R CHINA*
***China Building Materials Academy, Beijing, P R. CHINA*

SUMMARY

In this paper, the authors have compounded a new blended cement by using ferro–aluminate clinker mixed with fly ash, silica fume and gypsum. The mortars and crushed stone concrete prepared from this cement shows very high compressive and flexural strength in the presence of super–plasticizer and using conventional technology. Hydration products of the blended cement, effects of active additions, pore structure and interfacial zone of hardened blended cement concrete have also been discussed.

〔摘　要〕

本文采用铁铝酸盐水泥熟料与硅灰，粉煤灰和少量二水石膏配制成铁铝酸盐混合水泥．使用这种水泥，采用高效减水剂在一般工艺可以制备具有高抗压和抗折强度的砂浆及碎石砼．并对混合水泥的水化产物、混合材的作用效果、混合水泥砼的孔结构和集料—浆体的界面区进行了分析．

INTRODUCTION

Cement concrete is the most-widely used man-made construction material. With the improvement on the quality of engineering materials and the development of civil engineering such as highrise buildings, large-span structures and ocean engineering, the demand for high and super-high strength concrete is increasing.

Since concrete is a cement-based composite material, enhancing the strength of hardened cement paste is the premise of improving the strength of concrete. The well-known effective technological means of improving cement paste strength is to add some active additions such as silica fume, fly ash and slag into cement and reduce water / cement ratio greatly by means of the dispersion of superplasticizer. Feerro-aluminate Cement, which was developed by China Building Materials Academy in 1984, is a new type of high-effective, energy-saving and widely-used cement series with outstanding performances such as high-early strength and high-strength, impermeability, only claims, no details. The practical technological method for further improving some properties and reducing production costs of ferro-aluminate cement can be achieved by studying the effects of additions and admixtures.

RAW MATERIALS AND TEST METHODS

Ferro-aluminate clinker (FA) and commerical ferro-aluminate cement (FAC) are now commorcially produced and supplied. Better to avoid nams. The mineral compositions of FA are shown in Table 1. Some properties of FA and FAC are shown in Table 2. Chemical compositions of FAC, silica fume (S) and fly ash (F) are shown in Table 3.

Table 1. Mineral compositions of FA

Minerals	$C_4A_3\bar{S}$	C_2S	C_4AF
Content (%)	61	15	24

Table 2. Properties of FA and FAC

	Compressive Strength (MPa)		Flexural Strength (MPa)		Setting Time (hour:minute)	
	1d	3d	1d	3d	initial	final
FA	4.71	74.7	1.18	11.4	0:30	1:03
FAC	63.4	67.2	7.78	8.34	0:41	1:20

Table 3. Chemical compositions of raw materials

Composition (%)	Loss	SiO_2	Fe_2O_3	Al_2O_3	CaO	MgO	SO_3	MnO	K_2O	Na_2O
F	3.73	55.85	8.60	24.35	3.01	1.23	0.73	0.18	1.23	0.45
S	1.34	93.79	1.34	0.23	0.60	0.75	0.31	0.18	0.98	0.36
FAC	6.22	5.69	6.64	26.42	40.44	1.53	11.48		0.14	0.05

The coarse aggreagte used was crushed lime–stone with the particle size of 5～10 cm. The fine aggregate was the standard sand (according to GB178–77). The superplasticizer is FDN (manufactured in China). Mixtures of mortar and crushed stone concrete were cast into 4×4×16 cm moulds and vibrated on the vibrating table (frequency 2800～3000 times per minute) 4～6h, after casting the specimens were demolded and then cured in the water of 20℃ till the designated age for testing of compressive and flexural strength. Fluidity of mortar are determined by the fluidity meter of mortar and pore structure of concrete are measured by MIP.

RESULTS

Fluidity—The fluidity of mortar can be shown by the diameter on a fluidity meter of cement mortar (a bouncing table). Table 4 shows the results of the fluidity of the blended cement mortars with only fly ash or with both silica fume and fly ash. Apparently, the fluidity of mortar can be greatly improved if part of fly ash is replaced with silica fume. That indicates that fine particles have been uniformly dispersed into cement paste. Therefore, cement mortars and concretes with good workability can be obained at low W / C ratio through the comprehensive effects of good particle size distribution and dispersion of superplasticizer.

Table 4. Mix proportion and fluidity of the blended cement mortars

Mix	Additions (by weight)	Admixture	Blended cement / sand	Water / blended cement	Diameter of spreading (cm)
FAF	30% F	2% FDN	1:1	0.20	108
FAFS	20%F+10%S	2% FDN	1:1	0.20	197

Mechanical Properties of Hardened Mortar— The blended ferro–aluminate cements (BFAC) are compounded by mixing different amounts of fly ash and 10% silica fume. The mechanical properties of the mortars made of them at low W / C ratio are shown in Table 5. From the results we can see that super–high compressive, especially super–high flexural strength mortars can be made with the blended cements. Meanwhile, the increasing of the dosage of fly ash in blended cements does not cause the obvious reduction of the compressive and flexural strength of mortars.

Table 5. Mix proportion and mechanical properties of super–high strength mortars

Mix	Additions (by weight)	BFAC / Sand	Water / BFAC	Admixture	Compressive strength (MPa)		Flexural strength (MPa)	
					3d	28d	3d	28d
M1	10% S	1:1	0.15	2% FDN	99.0	124.4	17.41	26.25
M2	10F%+10%S	1:1	0.15	2% FDN	97.8	125.6	17.88	26.25
M3	20%F+10%S	1:1	0.15	2% FDN	102.8	130.7	21.10	26.91
M4	30%F+10%S	1:1	0.15	2% FDN	103.2	124.8	22.80	23.82

Mechanical Properties of Crushed Stone Concrete — The blended cement with 20% fly ash and 10% silica fume was selected to make super–high strength crushed stone concrete. The controll

crushed stone concrete was also made with FAC under the same workability as the former. The results are shown in Table 6. We can see that the crushed stone concrete made of BFAC can reach not only high compressive strength but also very–high flexural strength.

Table 6. Mix proportion and mechanical properties of crushed stone concretes

Mix	Cement	Cement Concrete (kg/m^3)	Proportion (cement:sand: aggregate)	W/C	Admix–ture	Compressive strength (MPa)			Flexural strength (MPa)		
						1d	7d	60d	1d	7d	60d
C0	FAC	650	1:0.79:1.85	0.45	2% FDN		72.2			8.04	
C1	FAFS	650	1:0.79:1.85	0.20	2% FDN		138.8			19.45	
C2	FAFS	650	1:0.79:1.85	0.20	2% FDN	97.0	143.7	147.2	8.51	18.98	20.02

DISCUSSION

Hydration products — The hydration products of blended high–strength cement are investigated by XRD and DTA as shown in Figure 1. Results show that they are mainly composed of AFt, C–S–H gel, AH_3 and FH_3 gel, and there are also a large amount of unhydrated cement remains which may act as microaggregate in hardened cement paste. The morphology of the hydration products was investigated by SEM as shown in Figure 2. Some garrulous ones which are bound together are observed but good–crystallized AFt can not. Therefore, we regard that in the BFAC hardened paste with very–high strength, AFt exists as crystal–structure but gel–size and interweaves close together with other gel products. The hydrated cement composed of crystallite and gel is very advantageous to the improvement of compressive and flexural strength of concretes and mortars.

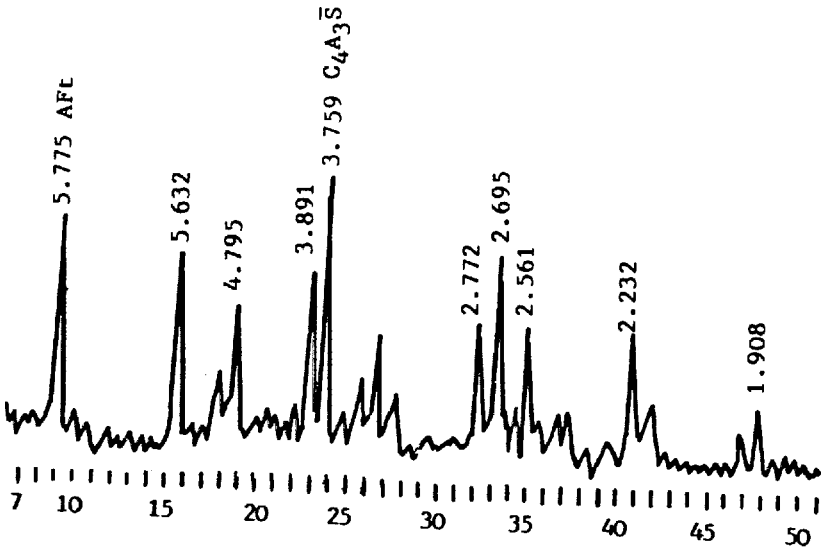

(a)

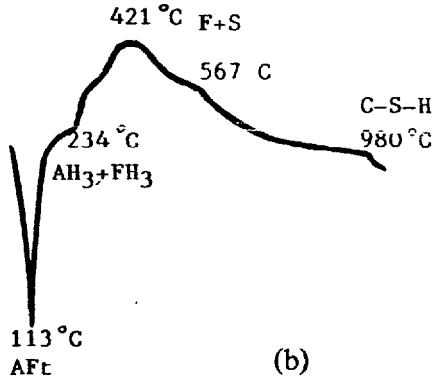

Fig.1 Results of XRD (a) and DTA (b) on the hydration products (W / C = 0.15, 28 days' age)

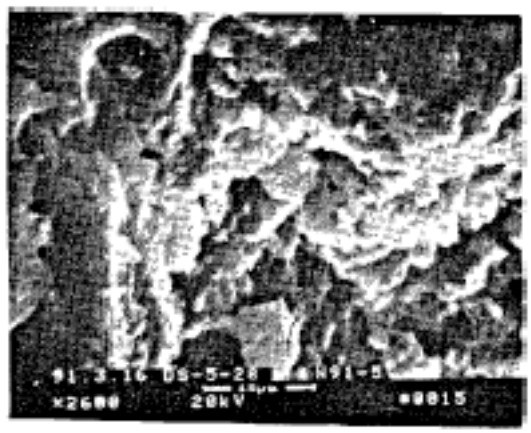

Fig.2 Morphology of the hydration products in hardened high–strength BFAC paste (W / C = 0.15, 28 days' age)

Effect of active additions — In BFAC, silica fume has the physical filling and densification effects and hydrates to form C–S–H gel at early age. It is worthy of note that in the BFAC system the activity of fly ash can be brought into full play. From Figure 3 we can see clear reaction rims around some fly ash particles and thin filiform hydration products ettringite inside hollow glass particles [Figure 3(b)]. The reasons of activating fly ash may be as follows: (1) hydrated BFAC system is alkaline; (2) activation of porous, quickly–dissolved high–active clinker minerals of $C_4A_3\bar{S}$ etc. and gypsum; (3) through dissolution–precipitation reaction, clinker minerals and gypsum hydrate to form hydration products to deposite onto the surfaces of fly ash particles and active $Al_2O_3$and $SiO_2$of their surfaces which are activated simultaneously take part in hydration. With the deepening of hydration, the water absorbed in gel pore and calcium ion diffuse through the hydration products layers around some particles inside them to make hydration go on, thus cementing fly ash very tightly with cement paste. For that reason, the mortars can still maintain high–strength even if part of clinker in the blended cements is replaced with fly ash.

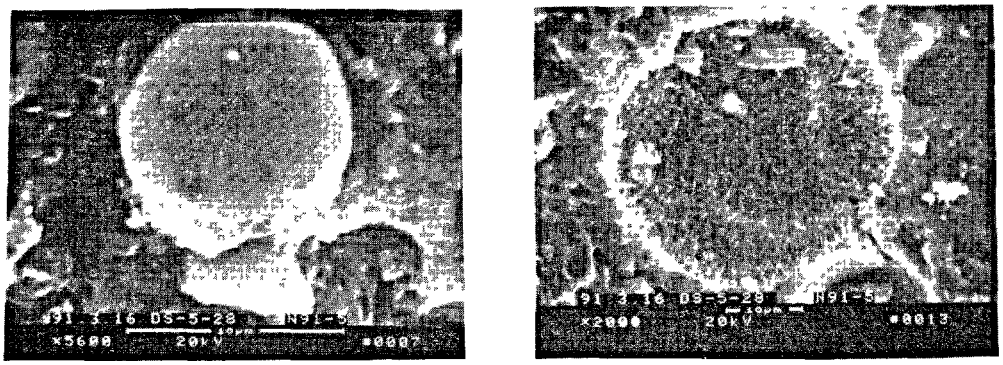

(a) (b)

Fig.3 Fly ash particles with clear reaction rims in hardened BFAC paste

Pore structure — The pore structures of the crushed stone concretes of C0 and C1 in Table 6 were investigated by MIP. The results of pore size distribution and total porosity are shown in Table 7, compared with the controll FAC concrete C0 with lower strength, the content of air void of the BFAC concrete C1 with higher strength is reduced significantly and its pore sizes are much finer for the diameters of 65% of the total pore are less than 100Å. That is attributed to the effect of filling and compact of additions and water–reducing of superplasticizer.

Table 7. Pore size distribution of crushed stone concretes

Pore size (Å) / Pore volume(%)	> 10000	10000 ~1000	1000 ~500	500~250	250~100	100~ 50	50~18	Total porosity (%)
C0	12.08	36.92	9.00	5.96	6.38	4.65	25.01	19.12
C1	15.82	7.48	4.79	4.00	4.66	3.06	60.19	7.51

Interface—The microstructures of the aggregate—cement paste interficial zone in the concretes with different strengthes are very different. In the low strength concrete C0, we can observe interficial zones for example as seen in Figure 4, But in the high strength concrete C1, the difference between interfacial zone and cement paste in itself can be hardly recognized as shown in Figure 5. The improvement of interficial zone microstructure is one of the most principal reasons of that FBAC mortars and concretes possess high strength.

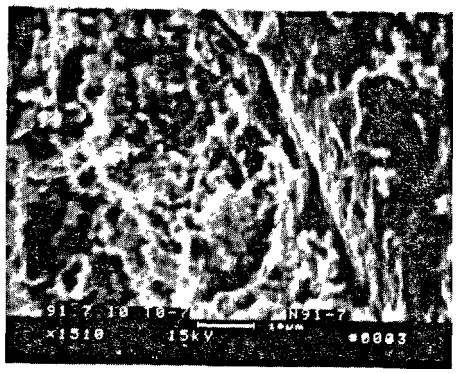

Fig.4 Porous interfical zone in the low strength crushed stone concrete C0

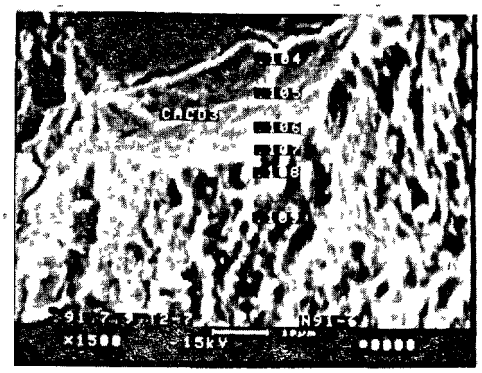

Fig.5 Dense interficial zone in the high strength crushed stone concrete C1

CONCLUSIONS

In the ferro–aluminate cement system, active additions such as silica fume and fly ash can be well activated. Using BFAC, very–high early and later strength (including flexural and compresive strength) mortars and concretes can be obtained at low W / C ratio with superplasticizer. That affords us a practical technological method to do further research on high–toughness and high–strength concretes. The reasons that BFAC mortars and concretes can reach very–high strength own to the comprehansive effects of super–plasticizer dispersion, high–activity of ferro–aluminate clinker minerals, gel and crystallite in hydration products, good particle size distribution and improvement of pore structure and interfacial zone.

1. P.K.Mehta "High Iron Oxide Hydraulic Cement" July 19, 1977 4036657

2. Wang Yanmou, Su Muzhen and Deng Junan "Study of Ferro–Aluminate Cement" 《Cement》 No.8, 1982

3. Guo Yong, Wang Yanmou, Su Muzhen, etc. "Research on Characteristics of Hydration of Ferric Phase in Ferro Aluminate Cement" 《Journal of Chinese Ceramics Society》 Vol.17, No.4, 1989

THE HYDRATE CHARACTER AND DURABILITY OF GANGUE CEMENT

Xu Bin

Sichuan Building Materials University, Mianyang
P R. CHINA

SUMMARY

In studies on concrete with gangue as an additive to cement,good results have been obtained and the durability of this type of concerte is now under consideration.This thesis discusses and compares the hydrate characteristics of gangue cement and portland cement.Also the durability of gangue cement concrete's carbonate resistance,frost resistance and sulphate attack resistance.By the method of cross experimental design and multiple linear regression,it analyses the effect of many factors acting on every durability index, and from the tests and analysis of the results, defines the best mix and technological design for gangue cement concrete to meet the durability requirements. Because of "the second hydration",it seems that some durability test methods can't be used in gangue cement concrete in the same way as on portland cement concrete, so a new method was introduced to solve this problem.

摘　要

这篇论文在详细分析和比较煤矸石水泥与普通硅酸盐水泥水化特征的基础上，运用正交分析的方法，研究和讨论了煤矸石水泥制品的耐久性问题。试验表明，由于煤矸石的"二次水化"作用，目前应用的一些测定普通水泥制品耐久性的方法不适于煤矸石制品的耐久性测定。因此作者提出了一种较为简便且能同时适用于普通水泥制品和煤矸石水泥制品的耐久性测定的方法。

INTRODUCTION

Broiled gangue is a kind of hydraulic binding material.The effective silicon and effective aluminium in it produce latent hydration activity which may be stimulated by the calcium hydroxide.It's likely that the hydration of gangue is on as follows:

$$2SiO_2+6Ca(OH)_2+aq \longrightarrow 3CaO \cdot 2SiO_2 \cdot nH_2O+3Ca(OH)_2$$
$$Al_2O_3+3Ca(OH)_2+28H_2O \longrightarrow 3CaO \cdot Al_2O_3 \cdot 3CaSO_4 \cdot 31H_2O$$
$$Al_2O_3+3Ca(OH)_2+CaSO_4+9H_2O \longrightarrow 3CaO \cdot Al_2O_3 \cdot CaSO_4 \cdot 12H_2O$$

This has been proved by X-ray phase analysis. That is to say, the hydration of gangue is dependent on the calcium hydroxide which was produced in the process of cement clinker hydration. In other words, the hydration of gangue has the character of hydrate hysteresis -- which was called "the second hydration". Because of "the second hydration",gangue as addition to cement may bring about the following effects:

①.About the strength. In the hydration process of gangue cement, the latent hydration activity of gangue must be stimulated by calcium hydroxide which is produced by the hydration of cement clinker. On the other hand, in ordinary temperatures, the rate of hydration of cement clinker is not fast and it would take a long time to complete hydration. This means that the cement clinker can't provide sufficient calcium hydroxide to stimulate the latent hydration activity of gangue in a short time. For this reasion,compared with portland cement,the extent of the hydration of gangue cement is lower in the early time but will be enhanced later. Also the strength of gangue cement concrete is lower in the early stage but stronger in the later stage.

②.About the hydrates. The rate of hydration and the lime-silica rate of hydrates of silicate minerals in cement clinker depend on the consistency of the calcium hydroxide in the liquid phase around the reactive face(the surface between cement clinker granulas and water) . If the consistency of calcium hydroxide is lower, then the rate of hydration will be faster and the lime -silica rates of the hydrates will be smaller, and vice versa. The absorption or adsorption o calcium hydroxide of gangue in the hydratation process of cement clinker may bring about the consistency of calcium hydroxide in the liquid phase around the reactive face lower. This will not only accelerated the hydration of cement clinker, but will also cause the high-alkali calcium silicate hydrates to translate into low-alkali ones. The latter has a higher strength and cause the product to be more compact.

③.About the alkalinity of concrete. "The second hydration" consumed part of the calcium hydroxid produced by the hydration of cement clinker. Compared with portland cement concrete, gangue cement concrete has a lower alkalinity. This is not a favorable property of concrete as regards to carbonate resistance and steel protection but it will not have much influence on the resistance to sulphate attack.

④.About the structure of concrete. As the gangue's hysteretic hydration takes place, the hydrates fill in the structure which has been formed by the hydration and hardening of the cement clinker. This not only increases the later density and strength, but also increases the ability of resist the deleterious materials intruding into the concrete in some degree.

PROPERTIES OF THE GANGUE

Gangue is a kind of mineral which exists between coal seams, actually, it is a mixture of minerals which contains carbon. The composition and properties varied with the geological age of the coal seam, the composition of the coal seam and the method of mine coal exploitation. Previously, the gangue used in the study was collected by experience or aspect. In this way, we have obtained some knowledge of the mineral. However, there is some disparity between the study and the applications. For the propose this study can be more directly and easily put into application, the gangue used in this study was collected at Chongqing Zhongliangshan coal mine from different gangue heaps which contained with gangue from different coal seam at different times.The chemical composition of gangue is presented in Table 1.

Table 1. Chemical composition of gangue

SiO_2	Al_2O_3	Fe_2O_3	CaO	MgO	SO_3	TiO	Igloss
31.84	20.11	9.17	4.14	0.87	1.41	2.00	25.12

X-ray analysis shows that the gangue is mainly composed of kaolinite, quartz, calcite and hematite etc. The gangue was broiled at 800 ℃ for 2. 5 hours and quenched in air immediately. Then the gangue was ground to about 3500 cm^2 /g. The result of the ISO method test shows that the broiled gangue was up to the standard of pozzolanicity.

CARBONATION RESISTANCE

Cross experiment design method was used in this study and eight series of concrete mixes (shown in Table 2) were tested at the age of 28 days. For the carbonate depth test, 100 mm cubes were used. For the carbonate coefficient test,2 mm cubes were used.The carbonate resistance test was carried out in carbonation chambers. The process of carbonation was accelerated by CO_2 enriched (20%) air maintained at 50% relative humidity and the temperature at 20℃.The results of the carbonate coefficient test and the extreme deviation analysis are shown in Table 2; and the variance analysis are shown in Table 3.

Table 2. The cross experiment design scheme and the results of extreme deviation of the carbonate coefficient test.

factor / row No. / test No.	A (gangue content%)	B (W/C)	C (curing method)	D (gypsum) (SO_3 %)	E (lime) (f-CaO%)	carbonate coefficient
	1	2	3	4	5	
T-1	1(0)	1(0.4)	2(standard)	2(2%)	1(0)	1.32
T-2	3(30%)	2(0.6)	2(standard)	1(0)	1(0)	1.76
T-3	2(10%)	2(0.6)	2(standard)	2(2%)	2(5%)	1.06
T-4	4(20%)	1(0.4)	2(standard)	1(0)	2(5%)	0.95
T-5	1(0)	2(0.6)	1(steam)	1(0)	2(5%)	0.97
T-6	3(30%)	1(0.4)	1(steam)	2(2%)	2(5%)	0.56
T-7	2(20%)	1(0.4)	1(steam)	1(0)	1(0)	1.09
T-8	4(10%)	2(0.6)	1(steam)	2(2%)	1(0)	1.17
K1	2.29	3.92	3.79	4.77	5.34	Σ=8.88
K2	2.15	4.96	5.09	4.11	3.54	
K3	2.32					
K4	2.12					
R	0.20	1.05	1.30	0.67	1.80	

Table 3. The result of variance analysis.

source of variance	deviation square	freedom degree	mean-square deviation	F value	critical value	noticeable extent
A	S =0.0154	3=fe	0.005=Se		F 0.05(1,3)	
B	S =0.1365	1	0.1365	27.30	=10.10	**
C	S =0.2096	1	0.2096	41.92	F 0.01(1,3)	***
D	S =0.0536	1	0.0536	10.72	=34.10	**
E	S =0.4073	1	0.4073	81.46		***
Total	S =0.8224	7				

Note: *** -- very noticeable; ** -- noticeable; * -- there is some influence.

The results of the extreme and variance analysis shows that the influence order of the five factors acting on the carbonation coefficiente are: lime content→curing method→water-cement ratio→gypsum content→gangue content.Among them,the lime content and the curing method are very noticeable factors; water-cement ratio and gypsum content are also noticeable factors;the gangue content has little effecte on the carbonate coefficient of the concrete.

The experiment design of the carbonate depth test was the same as the carbonate coefficient test, and the results show that the influence order of the factors acting on the carbonation depth are: curing method→gangue content→W/C→lime content→gypsum content; the gangue content has a noticeable influence on the carbonate depth,while the other factors have little influence.

From the results of the carbonation resistance tests we know that:①.Within the limit of 30 %, it will not cause noticeable influence on the carbonate resistance property of concrete when gangue as additive to cement. ②. The most noticeable factor that influences the carbonate resistance property of gangue cement concrete is the curing method; Steam curing is not beneficial for the carbonate resistance property. ③. Although lime may have the function of intensify the hydration of gangue, it is not beneficial for the carbonate resistance property of gangue cement concrete.

FROST RESISTANCE

Six series concrete (see Table 4) and 100 mm cubes were tested at the age of 28 days. The freezing was carried on in an ordinary deep-freezer held at the constant temperature of -20℃ for 4 hours; and the thawing was done in a box filled with water at a constant temperature of 20 ℃ for 4 hours. After 50 freezing and thawing circles, the strength and weight of the specimens were measured and compared with the corresponding ones that withou t freezing. The latter were measured at the time of the relative age. The void structures were determined by mercury penetration method and the results are shown in Table 5.The results of frost resistance are also shown in Table 5. By the method of multicomponent regress analysis, a regress equation was established between the main influential factors and the relative index for the frost resistance property as in equation(1),and the results of variances analysis are shown in Table 6.

Table 4. Concrete mixes used.

test number	cement clinker (Kg/M³)	gangue (Kg/M³)	W/C	coarse aggre-gate (Kg/M³)	fine aggre-gate (Kg/M³)
D-1	224.4	0	0.6	951.5	408.4
D-2	202.0	22.4	0.6	951.5	408.4
D-3	179.5	44.9	0.6	1427.5	612.7
D-4	157.1	67.3	0.5	1427.5	612.7
D-5	188.5	80.8	0.4	956.0	371.6
D-6	235.6	101.0	0.3	962.7	302.9

$$Y = 10.39 - 0.04X_1 + 0.13X_2 + 169.0X_3 - 0.42X_4 \quad (1)$$

$$R = 0.81$$

Where: Y -- strength loss; X_1-- W/C; X_2-- gangue content; X_3-- total voids volume; X_4 -- capillary content; R-- liner relative coefficient.

The study of frost resistance shows that: ①. The influential order of these factors is: gangue content→capillary content→total volume of voids→ water-cement ratio. ②. Water-cement ratio , gangue content and total volume of voids are inversely proportional to frost resistance and the capillary content is directly proportional to it. ③. The inter pore structure is a decisive factor for frost resistance and on which the strength has only a little influence. ④. The addition of gangue is not favorable to frost resistance.Nevertheless,having appropriate W/C, the frost resistance property of gangue cement concrete may be better.

Table 5. Results of frost test

test number	total volume (ml/g)	total area (M^2/g)	average diameter (μ m)	capillary content (%)	weight loss(g)	strength loss(MPa)
D-1	0.1303	12.4991	0.0208	71.9937	-11 -4 -4	1.28 4.10 2.67
D-2	0.1339	13.3423	0.0201	74.1249	-3 -15 -11	1.57 3.45 3.78
D-3	0.1213	12.2263	0.0198	66.9087	-2 0 4	5.52 6.17 5.82
D-4	0.1411	16.7901	0.0168	78.2988	-1 -2 3	7.65 4.73 4.04
D-5	0.1123	15.3871	0.0146	69.2295	-8 1 -2	3.80 4.41 4.65
D-6	0.0958	13.0691	0.0147	58.3264	-9 -2 -4	5.75 5.67 6.30

Table 6. The results of variance analysis.

source of variance	deviation square	freedom degree	mean-square deviation	F value	critical value	noticeable extent
X1	0.0017	1	0.0017	0.0014	F0.01(1,13)	
X2	17.6768	1	17.6768	14.5960	= 9.10	***
X3	4.8582	1	4.8582	4.0115	F0.05(1,13)	*
X4	8.9676	1	8.9676	7.4046	=4.70	**
Error	15.7440	13	1.2111			
Total	46.4018	17				

Note:*** -- very noticeable; ** — noticeable; * - there is some influence.

At the age of 28 days,the frost resistance of gangue cement concrete is rather poor,as "the second hydration " is carried on with the age,the frost resistance may be enhanced.

SULPHATE ATTACK RESISTANCE

Six mixes of concrete were used in this study.The gangue content and W/C were the same as the frost test,the specimens were made from cement mortar and the cement-sand ratio was 1:3. The specimens which were formed as 2 mm cubes were immersed with 4. 4% magnesium sulphate solution at the age of 28 days. Strength of the specimens were determined at the time when they had been inpregnated with the magnesium sulphate solution for 3, 7, 14, 28, 60, 120 days. Fig 1 shows the strength variation of the specimens in the process of the magnesium sulphate attack.

On the other hand,in the depth of 1.5 mm,the density of magnesium sulphate were determined by photoelectron spectrograph when the specimens have been inpregnated in the solution for 120

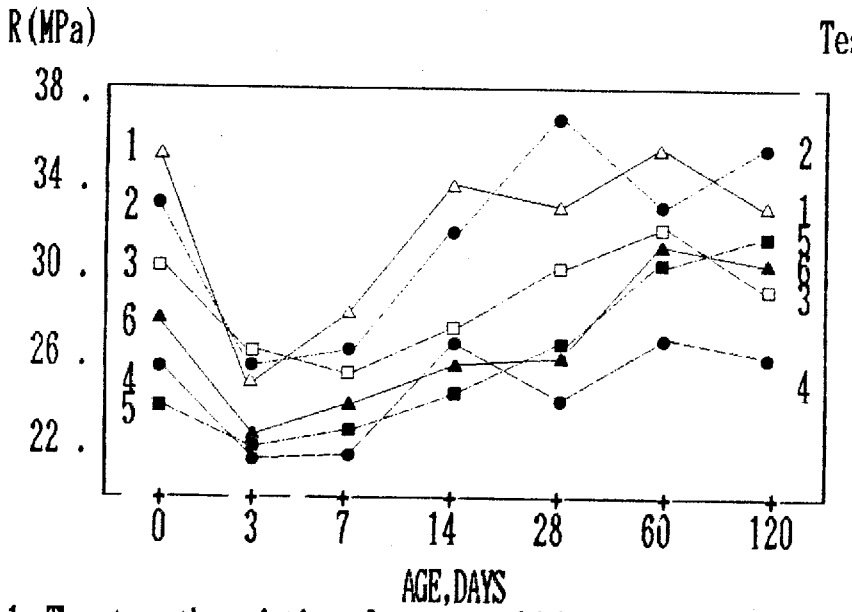

Test No.	Gangue (%)	W/C
1	0	0.6
2	10	0.6
3	20	0.6
4	30	0.5
5	30	0.4
6	30	0.3

Fig 1. The strength variation of concrete which were inpregnated in a 4.4% magnesium sulphate solution.

days. Then a regressive analysis was done between the strength variation and the density of the magnesium sulphate.The results show that there isn't much relationship between them.

A regress equation (see equation (2)) was established between the main factors and the relative index for the sulphate attack resistance property of gangue cement concrete.

$$Y = 74.04 - 0.03X_1 - 0.41X_2 - 68.53X_3 - 14.47X_4 \qquad (2)$$
$$R = 0.772$$

where: Y -- variation of strength; X_1-- water-cement ratio; X_2-- gangue content; X_3-- voids ratio; X_4-- percentage of C_3A; R -- regression coefficient.

The results of the sulphate attack resistance shows that:①. The sulphate attack resistance property of the concrete was improved noticeable after cement clinker was partly replaced by gangue, and in the limit of 30%, the more gangue content, the better the sulphate attack resistance. ②.The amount of C_3A in cement had a noticeable influence on the sulphate attack resistance property of the concrete;The results of X-ray quantitative analysis shows that in the process of gangue content addition, the C_3A content reduced. Variance analysis shows that the more the C_3A content in cement, the more the sulphate attack on the concrete.③.There isn't much relationship between the magnesium sulphate attack resistance property of gangue cement concrete and the amount of magnesium sulphate which intruded into the concrete. The sulphate attack resistance is mainly decided by other properties of the concrete such as density, C_3A content etc. ④. The influence order for the main factors on magnesium sulphate resistance are: gangue content→C_3A content→voids ratio→water cement ratio.

DISCUSSION

For the reasion of "the second hydration", the structure formation and strength growth of this kind of concrete is slow early on but the strength growth increase is larger than that of portland cement concrete later. So it is not suitable to use gangue cement concrete the same way as portland cement concrete. In my opinion we should use this kind of concrete at a later age such as 90 days when the structure has been fully formed, which will benefit both the strength and durability property of the concrete.

In the tests,it was found that gangue cement concrete has a specific property of incomplete carbonation. That is to say, in the process of carbon dioxide intrusion into gangue cement concrete,it seems that the carbon dioxide didn't neutralize all the alkali on the way,but passed quickly and then neutralized the remaining alkali later. So the method of measuring the depth of carbonation by using phenolphthalein -sprint reagent to indicate the carbonate depth is not suitable for gangue cement concrete, because there isn't a distinct dividing line between the carbonated area and the area without carbonation. To solve this problem, as it appears to me, a chemical analyse method should to be used to determine the content of calcium hydroxide existing in the concrete.Then from the relationship between the calcium hydroxide content of the concrete and carbonation,we can determine the degree of carbonation.The method is based on the follofwing principle. Although many hydrates can be carbinated by carboinc acid, numerous tests have proved that the principal products of carbonation of concrete is calcium carbonate. So by the method of measuring the amount of calcium carbonate in the definite volume of the concrete, we can determine the extent of carbonation taking placed in the concrete. By this method, the amount of calcium carbonate in concrete can be determined by an analytical chemistry method and the samples can be made very small and placed directly in the air. So the results we get may be more actual.This method can be used for both gangue cement and portland cement concrete.

CONCLUSION

1.Compared with portland cement concrete, the carbonation rate of gangue cement concrete is faster at the age of 28 days, but the carbonate coefficient is not low when the mix is properly prepered. Steam curing is not beneficial for the carbonate resistance property of gangue cement concrete.

2.The greatest single factor that acts on the frost resistance property of concrete is the presence of air voids in the paste. The more voids in the concrete, the poorer the frost resistance property. The addition of gangue increased the unmber of voids in the concrete, so we should take methods to produce W/C as well as the gangue content from increasing.

3.Gangue has not much influence on the sulphate attack resistance property of concrete.With the proper mix and techological design,gangue cement concrete can be better than portland cement concrete in this aspect of it's properties.

4.Gangue has the specific property of incomplete carbonation, so the method of using phinolphthalein-sprint reagent to indicate the carbonate depth can not be used for this kind of concrete and it should be replaced by other methods.

REFERENCES

1. Pan Yixiang: " The Hydrates and Microstructure of Gangue Cement", The Journal of Chongqing architacture and engineering institute,1986,4,43-49.

2. F. M. Lee, translated by Tang Mingshu: "Cemenet and Concrete Chemistry",Chinese Engineering Industry Press,1980,p 345-473.

3. Wang Zuxian: "The Application of Cross Experiment Design in Concrete", Chinese Engineering Industry Press,1985,86-175.

4. Rachil J. Detweiler: "Assessing the Durability of Concrete in Freezing and Thawing", ACI Materials Journal,1989,4,41-49.

5. W. H. Gutt etc: "Blastfurnance Slay as Coarse Aggregate for Concrete Stored in Sulphate Solutions for 22 Years",Magzine of Concrete Research,1989,3,p 23-31.

6. R.K.Dhir: "Near Surface Characteristics of Concrete: Prediction of Carbonation Resistance", Magzine of concrete Research,41,No.148,21-28.

7. Dhir R.K.etc:"Near Surface Characteristics and Durability of Concrete- An Intial Apprasal", Magzine of Concrete Research,1986,3,34-41.

DURABILITY OF CEMENT MATERIALS MODIFIED WITH MELTED SULPHUR

D A Ugincius, K I Mokritsky and L I Degteriova

Building Institute, Kharkov, UKRAINE

SUMMARY

Concrete-sulphur materials offer potential advantages of high durability (as wall as strength) as compared with conventional concrete. Howerer have shown that melted sulphur may be react with calcium hydroxide of cement stone during impregnation process. Thermodinamical calculations, analitical chemistry studies were conducted to obtain highly full information on the reaction between melted sulphur and calcium hydroxide. Have shown that plaster is the main product of this chemical interaction and that is no serious danger of the secondary calcium hydrosulphoaluminate formation in the porous space of the cement stone.

РЕЗЮМЕ

Бетоны, пропитанные серой, обладают высокой коррозионной стойкостью (как и прочностью) по сравнению с аналогичными бетонами. В то же время показано, что расплав серы может вступать в реакцию с гидроксидом кальция цементного камня в процессе пропитки. Термодинамические расчеты, химический анализ позволили получить более полную информацию об этих реакциях и идентифицировать продукты реакции между расплавленной серой и гидроксидом кальция. Показано, что основным продуктом этого химического взаимодействия является гипс, и отсутствует серьезная опасность образования вторичного гидросульфоалюмината кальция в поровом пространстве цементного камня.

Sulphur-Impregnated Concretes (1,2) have a very high durability in acid, sulphate, salt and alkaline liquid media (3-6), but this technology is comparatively new and some problems connected with it are not studied or studied not enogh. One of this questions is chemical interaction of sulphur with soaked material as in the process of the impregnation as during its following exploitation.

It is known that melted sulphur can form with oxides of alkaline and alkaline-earth metals several sulphides, sulphates and polysulphides. In connection with this it was made an attempt by means of DTA method to identificate the products of interaction of cement stone and sulphur (7), existing of such interaction was established. And it was set proposition that calcium hydroxide takes place in this reaction. There exists suggestion (8) that calcium hydroxide interacting with sulphur (in the presence of water) forms at first polysulphides and thiosulphates which than come into sulphates, more frequently into ettringite. It can call in its turn destruction of concrete by well known manner (we did not study formation of primary ettringite during the exploitation of concrete so as this process precedes contact of concrete with sulphur and is known well).

With the purpose of analysis of correctness of such proposition we carried out of thermodynamical calculations of reactions of interaction of sulphur with main products of cement hydration: $Ca(OH)_2$; $3CaO \cdot AL_2O_3 \cdot 6H_2O$; $2CaO \cdot Al_2O_3 \cdot 8H_2O$; $CaO \cdot Al_2O_3 \cdot 10H_2O$; $4CaO \cdot Al_2O_3 \cdot 13H_2O$; $4CaO \cdot Al_2O_3 \cdot 19H_2O$; $2CaO \cdot SiO_2 \cdot 3H_2O$; $4CaO \cdot 3SiO_2 \cdot 1,5H_2O$; $6C_aO \cdot 6SiO_2 \cdot H_2O$; $5CaO \cdot 6SiO_2 \cdot 3H_2O$; $5CaO \cdot 6SiO_2 \cdot 5,5H_2O$; $5CaO \cdot \underline{6}SiO_2 \cdot 10,5H_2O$; $CaO \cdot 2SiO_2 \cdot 2H_2O$; $CaO \cdot Al_2O_3 \cdot 2SiO_2 \cdot 2H_2O$; $2CaO \cdot 2Al_2O_3 \cdot 8SiO_2 \cdot 7H_2O$. Possibility of existing of reactions and their preference with comparison with other reactions was defined as to magnitude and sigh of isobaric - isothermal potential $G_T°/nS$ (where n - the number of moles, taking place in the reaction). The main of examined reactions and their thermodynamical analysis are done in table 1.

Data in the table 1 say about the principle possibility of formation as plaster and ettringite. Unfortunately we had no thermodynamical data of calcium thiosulphate that is who we could not consider reactions with the formation of this combination. In connection with it we calculated the limits of stability of $S_2O_3^{2-}$ with other sulphur-containing ions and plotted the results on the diagram Eh-pH in the System sulphur-water whish is done in literature (9).

Table 1

Reactions of sulphur with several cement minerals. Dependence G°_{T} on temperature.

Reactions	G°_{T}/mole S by T,K, ccal/mole			
	298	333	373	433
$CaO \cdot Al_2O_3 \cdot 10H_2O + 1{,}5O_2 = CaSO_4 \cdot 2H_2O + 5H_2O + Al_2O_3 \cdot 3H_2O$	-162,5	-251,9	-618,3	-1619,8
$6(CaO \cdot Al_2O_3 \cdot 10H_2O) + 3S + 4{,}5O_2 = 5(Al_2O_3 \cdot 3H_2O) + 3CaO \cdot Al_2O_3 \cdot 3CaSO_4 \cdot 31H_2O + 14H_2O$	-164,1	-251,3	-514,5	-
$5CaO \cdot 6SiO_2 \cdot 10{,}5H_2O + 5S + 7{,}5O_2 = 5(CaSO_4 \cdot 2H_2O) + 6SiO_2 + 0{,}5H_2O$	-167,0	-200,2	-311,8	-599,9
$Ca(OH)_2 + S + 1{,}5O_2 + H_2O = CaSO_4 \cdot 2H_2O$	-158,0	-134,9	-221,2	-360,9
$Ca(OH)_2 + S = CaS + H_2O + 0{,}5O_2$	+43,0	+38,1	+21,2	-21,5

Table 2

Reactions and equations determined limits of fields of stability of $S_2O_3^{2-}$ ion and other sulphur-containing ions

Number of reaction	Reactions	Equations
1	$S_2O_3^{2-} + 5H_2O = 2SO_4^{2-} + 10H^+ + 8e^-$	$Eh = 0{,}296 - 0{,}073ph - 0{,}00711g \frac{S_2O_3^{2-}}{SO_4^{2-}}$
2	$2H_2S + 3H_2O = S_2O_3^{2-} + 10H^+ + 8e^-$	$Eh = 0{,}303 - 0{,}073ph - 0{,}00711g \frac{S_2O_3^{2-}}{H_2S}$
3	$2S^{2-} + 3H_2O = S_2O_3^{2-} + 6H^+ + 8e^-$	$Eh = 0.006 - 0{,}044ph + 0{,}00711g \frac{S_2O_3^{2-}}{S^{2-}}$
4	$2HS^- + 3H_2O = S_2O_3^{2-} + 8H^+ + 8e^-$	$Eh = 0{,}201 - 0{,}059ph + 0{,}00711g \frac{S_2O_3^{2-}}{HS^-}$
5	$2S + 2H_2O = S_2O_3^{2-} + 6H^+ + 4e^-$	$Eh = 0{,}456 - 0{,}088ph + 0{,}01411g S_2O_3^{2-}$
6	$S_2O_3^{2-} + 5H_2O = 2HSO_4^- + 8H^+ + 8e^-$	$Eh = 0{,}275 - 0{,}059ph + 0{,}00711g \frac{HSO_4^-}{S_2O_3^{2-}}$

Reactions 1 - 6 from table 2 and corresponding them equations Eh = f(ph) determine the limits of stability between thiosulphate ion $S_2O_3^{2-}$ and other sulphur-containing ions. However this limits take place beyond the fields of stability of the main sulphur-containing ions and sulphur (dotted lines on figure 1).

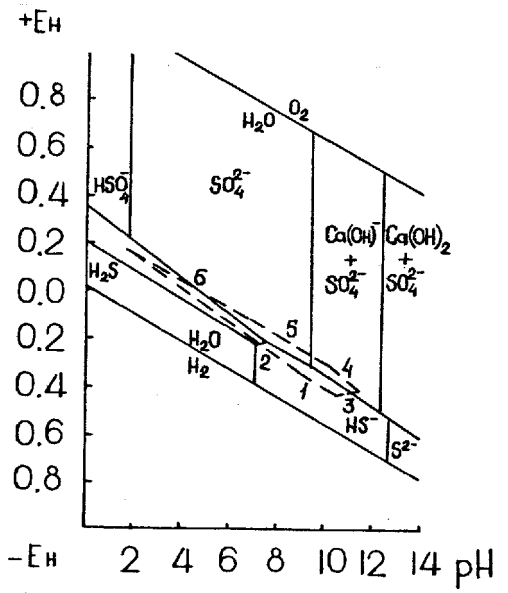

Fig.1 Fields of equilibrum of combinations in the system "sulphur - water"

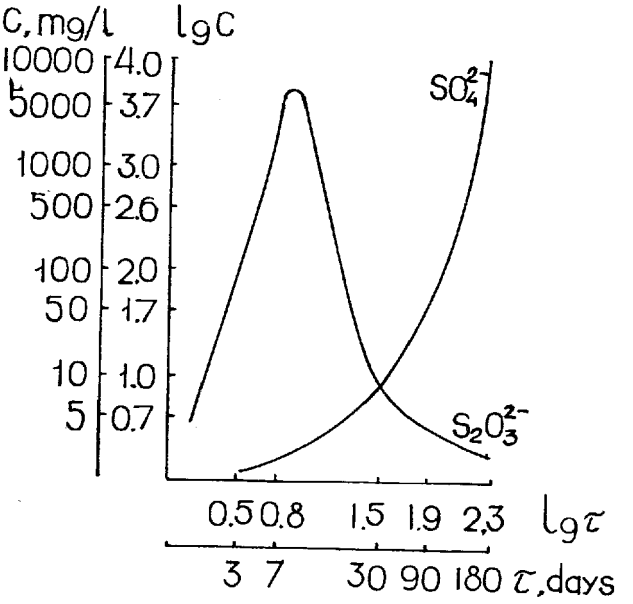

Fig.2 Changing of concentration of interaction products in the system "sulphur - C_3S".

That witnesses about metastability of thiosulphate-ion $S_2O_3^{2-}$. However such counted metastability of Thiosulphate ion does not contradicted to formation of the latest as intermediate product in the process of oxidation of the sulphur to the sulphat-ion SO_4^{2-}. In connection with this we studied kinetics of interactions of sulphur and hydrated C_3S with purpose of the identification of this interaction products. C_3S was chosen as one of the main clincer mineral having strong hydration capacity.

Hydrated C_3S samples soaked with melted sulphur after that crushed and placed into retorts with aqua distillate ate water/solid ratio w/s =20. During this experiment continuing for half an year sumple were uninterruptedly mixed and concentration of thiosulphate ions in the filtrate was periodically analysed.

On the fig.2 kinetics of concentration of $S_2O_3^{2-}$ ions changing was shown. It is necessary to note that are formed immediately at the moment

of contact of sample with water and the maximum concentration takes place in seven days. At the same time the appearance of sulphate-ions is registered and its concentration is increased very sharply at the time when thiosulphate-ions concentration quickly falls.

So, the metastability of thiosulphate ions is proved during this experiment. It is evidently that oxidation of sulphur in water alkaline solutions goes on at two stages:

$$2S + 3H_2O = S_2O_3^{2-} + 6H^+ + 4e^- ;$$

$$S_2O_3^{2-} + 5H_2O = 2SO_4^{2-} + 10H^+ + 8e^- ;$$

at sulphate-ion is the final product of reaction.

So, thermodinamical calculations confirmed the probability of interaction of sulphur and cement in concrete and shown that plaster or ettringite may be products of this interaction. An analitical method confirms that thiosulphate-ion is metastable in this system.

It was necessary to know the practical meaning of this chemical process. For this purpose the phase composition of soaked with sulphur samples was studied by differential thermal analysis, X-ray diffractometry and scanning electron microscopy methods (5,6). The analysis of experimental data allows to confirm that in all camples soaked with melted sulphur and also in exposed in acid, sulphate, salt and alcaline liquid media pla media plaster was found only. High density of concrete soaked with sulphur provides the formation of plaster only on the surface layers of material on the depth no more 1-2 mm. Be cause of this the formation of ettringite are not realised too.

Thus in real nature conditions the probability of destruction of concrete soaked with sulphur in the result of formation of ettringite and plaster is quite insignificant. The high durability of such concretes in acid, sulphate, salt and alkaline liquid media (6) certainly confirms it, because it is well known that this media are strongly agressive as to concrete.

REFERENCES

1. Platou, J.:"Sulphur-impregnated concrete", Sulphur Inst.Journal, 1975, 11(1), 2-4.

2. Malhotra, V.M.; "Sulphur-infiltrated concrete", Concrete constr., 1975, 20(3), 91-93.

3. Berry, E.E.; Soles, J.A. and Malhotra, V.M.: "Leaching of Sulphur and Calcium from Sulphur-Infiltrated Concrete by Alkaline and Neutral Aqueous Media," Cem. and Concr. Res., 1977, 7, 185-190.

4. Feldman, R.F. and Beaudoin, J.J.:"Some factors affecting durability of sulphur-impregnated porous bodies", Ibid., 1978, 8, 273-282.

5. Ugincius, D.A., Babushkin, V.I., Mokritsky, K.I. and Degteriova, L.I.: "The interaction of sulphur and cement stone components in concretes impregnated with sulphur", Cem.and Chem.Techn., 1987, 30(8), 68-71, Ivanovo (in Russian).

6. Mokritsky, K.I.:"Corrosion Resisting of Concrete Pipes Impregnated with Melted Sulphur", Dissertation, 1985, Rostov/Don (in Russian).

7. Jashi, N.A.:"Chemical interaction of hydrated cement and melted sulphur", In: Questions of mechanics and technology of the Railway precast Reinforced Concrete, 1981, 81-86, Dniepropetrovsk (in Russian).

8. Orlovski, J.I. and Mansi, V.N.: "Properties of concretes soaked with melted sulphur", Constr. and Arch., 1980, 1, 78-81, Novosibirsk, (in Russian).

9. Garrels, R.M. and Kreist, Ch.L. : Solutions, minerals, equilibra. Moscow, Mir, 1968, 128 p. (in Russian).

DEVELOPMENT OF DURABILITY - IMPROVING ADMIXTURES FOR CONCRETE

Y Ohama*, K Demura*, K Tachibana, T Endo*** and Y Sato******

*College of Engineering, Nihon University, Koriyama, Fukushima-ken, JAPAN
**Hodogaya Chemical Co., Ltd., Minato-ku, Tokyo, JAPAN
***Onoda Autoclaved Lightweight Concrete Co., Ltd., Owariasahi, Aichi-Ken, JAPAN
****Showa Shell Sekiyu K.K., Atsugi, Kanagawa-ken, JAPAN

SUMMARY

The present paper deals with a basic study on the development of chemical admixtures for improving the durability of concrete. An alkyl alkoxy silane as a chemical admixture and polymer dispersions as cement modifiers were added to concrete at various contents of the alkyl alkoxy silane and a constant polymer-cement ratio of 5 %. Concrete specimens were prepared, and tested for compressive strength, chloride ion penetration, carbonation and drying shrinkage. It is concluded from the test results that the addition of the alkyl alkoxy silane and polymer dispersions to the concrete considerably improves their resistance to chloride ion penetration and carbonation, and drying shrinkage without strength reduction. The newly developed chemical admixtures may be effectively used as durability-improving admixtures for the concrete.

要　約

本論文では，コンクリートの耐久性改善用化学混和剤の開発における基礎的研究について述べる。化学混和剤としてのアルキルアルコキシシランは添加率を変え，各種ポリマーディスパージョンはポリマーセメント比５％一定でコンクリートに添加して，供試体を作製し，圧縮強度，塩化物イオン浸透，中性化及び乾燥収縮試験を行った。試験結果から，コンクリートへのアルキルアルコキシシラン及びポリマーディスパージョンの添加は，コンクリートの強度の低下なしに，塩化物イオンの浸透及び中性化に対する抵抗性と乾燥収縮を相当に改善することが分かる。従って，この新しく開発された化学混和剤は，コンクリートのための耐久性改善用混和剤として，効果的に用いられ得る。

INTRODUCTION

In recent years, the rapid deterioration of various reinforced concrete structures has been reported, and become a serious social problem in the world. The cause of the rapid deterioration is the wet corrosion of reinforcing bars because of the penetration of carbon dioxide, oxygen, water and chloride ions into concrete. Currently, polymer-modified concretes and mortars using various polymer dispersions have widely been used in construction works because they have excellent flexural strength, adhesion, waterproofness, carbonation resistance and chloride ion penetration resistance (1). On the other hand, the authors have reported that the addition of alkyl alkoxy silane to mortar and concrete considerably improves their properties such as waterproofness and resistance to chloride ion penetration (2).

The objective of this study is to develop the durability-improving admixtures for concrete which are used to prevent the deterioration of reinforced concrete structures. Concretes are prepared with various contents of alkyl alkoxy silane as a chemical admixture and polymer dispersions as cement modifiers, and tested for compressive strength, chloride ion penetration, carbonation and drying shrinkage. The combined effects of the alkyl alkoxy silane and polymer dispersions on the properties of the concretes are discussed.

MATERIALS

Cement and Aggregate

Ordinary portland cement as specified in JIS (Japanese Industrial Standard), river sand (size, 2.5mm or finer) and river gravel (size, 5-20mm) were used for all the mix proportions.

Admixtures

Alkyl alkoxy silane (AAS) was used as a chemical admixture. Polymer dispersions used as cement modifiers were a styrene- butadiene rubber (SBR) latex, and an ethylene-vinyl acetate (EVA) emulsion and a polyacrylic ester (PAE) emulsion. Their basic functions are listed in Table 1. Table 2 gives the properties of the polymer dispersions. Before mixing, a silicone-emulsion-type antifoamer was added to the polymer dispersions in a ratio of 0.7 % of the silicone solids in the antifoamer to the total solids in the polymer dispersions. A polyoxyethlene nonyl phenol ether-type nonionic surfactant with an HLB

Table 1 Basic Functions of Admixtures.

Type of Admixture		Basic Function
Chemical Admixture	Alkyl Alkoxy Silane (AAS)	Inhibition of the penetration of H_2O and Cl^- due to the water-repellent capillaries formed inside concrete and mortar
Cement Modifier	Polymer Dispersions (SBR Latex, EVA and PAE Emulsions)	Prevention of the penetration of H_2O, Cl^-, CO_2 and O_2 due to the polymer film barriers formed inside concrete and mortar

Table 2 Properties of Polymer Dispersions.

Type of Polymer Dispersion	Specific Gravity (20°C)	pH (20°C)	Viscosity (20°C, cP)	Total Solids (%)
SBR	1.021	9.7	64.0	45.0
EVA	1.060	4.9	2370.0	44.9
PAE	1.026	8.9	121.0	44.9

(hydrophile-lipophile balance) value of 5.7 was employed as a stabilizer for the polymer dispersions.

TESTING PROCEDURES

Preparation of Specimens

According to JIS A 6204 (Chemical Admixtures for Concrete), concretes were mixed using the mix proportions given in Table 3. Concrete specimens having the desired shapes

Table 3 Mix Proportions of Polymer-Modified Concretes with AAS.

Type of Concrete	Water-Cement Ratio (%)	Sand-Aggregate Ratio (%)	Polymer-Cement Ratio * (%)	AAS Content (wt% of Cement)	Nonionic Surfactant Content (wt% of Cement)	Unit Water Content (kg/m³)	Mix Proportion by Weight (kg/m³)			Air Content (%)	Slump (cm)
							Cement	Fine Aggregate	Coarse Aggregate		
Unmodified	65.0	42.0	0	0	0	182	280	780	1075	2.0	7.0
SBR-Modified	63.5	42.0	5	0	0	177	280	780	1075	5.9	7.6
	65.5			0.5	0.5	182				2.3	7.0
	65.5			1.0	0.3	182				2.5	7.0
EVA-Modified	54.0	42.0	5	0	0	151	280	780	1075	5.2	8.0
	65.0			0.5	0.5	182				4.0	7.1
	65.0			1.0	0.5	182				3.5	7.0
PAE-Modified	55.9	42.0	5	0	0	157	280	780	1075	8.3	7.5
	60.8			0.5	1.0	170				4.3	9.0
	59.9			1.0	1.0	168				3.8	8.0

Note. *;Calculated on the basis of total solids in polymer dispersions.

and sizes were molded, and then subjected to a 2-day-20°C-80%R.H.-moist plus 1-day-70°C-water plus 7-day-20°C-50%R.H.-dry cure (except for the concrete specimens for drying shrinkage test).

Strength Test

The cured cylindrical specimens 10x20 cm were tested for compressive strength according to JIS A 1108 (Method of Test for Compressive Strength of Concrete).

Chloride Ion Penetration Test

The cured cube specimens 10x10x10 cm, whose two sides, casting and bottom surfaces were coated with an epoxy resin paint, were immersed in 2.5% sodium chloride solution at 20°C for 28 days for chloride ion penetration. After immersion, the cube specimens were split, and the split crosssections were sprayed with 0.1% sodium fluorescein solution and 0.1N silver nitrate solution as prescribed in UNI 7928 (Concrete - Determination of the Ion Chloride Penetration). The depth of the rim of each crosssection changed to white color was measured with slide calipers as a chloride ion penetration depth as illustrated in Figure 1.

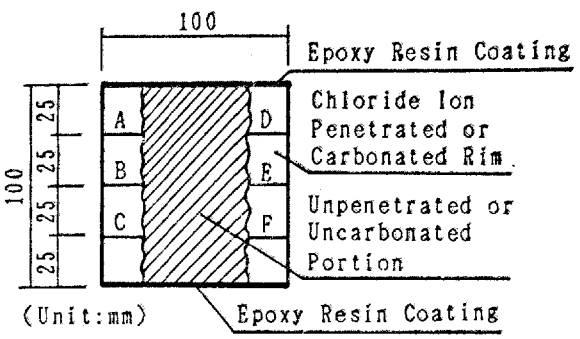

A, B, C, D, E and F:
Measured for Chloride Ion Penetration or Carbonation Depth, and Averaged.

Fig. 1 Crosssection of Specimen after Chloride Ion Penetration or Carbonation Test.

Accelerated Carbonation Test

The cured cube specimens 10x10x10 cm were placed in a nonpressurizing carbonation test chamber for 28 days, in which temperature, humidity and CO_2 gas concentration were controlled to be 30°C, 60%R.H. and 5% respectively. After accelerated carbonation, the cube specimens were split, and the split crosssections were sprayed with 1 % phenolphthalein alcoholic solution. The depth of the rim of each crosssection without color change was measured with slide calipers as a carbonation depth as shown in Figure 1.

Drying Shrinkage Test

Immediately after the beam specimens 10x10x40 cm were given a 2-day-20°C- 80%R.H.-moist plus 5-day-20°C-water cure, the original length of the beam specimens was measured. Then the specimens were cured at 20°C and 50%R.H. for 28 days, and their drying shrinkage was measured by the comparator method specified in JIS A 1129 (Method of the Test for Length Change of Mortar and Concrete).

TEST RESULTS AND DISCUSSION

Figure 2 represents the 28-day compressive strength of polymer-modified concretes with AAS. In general, the compressive strength of SBR- and PAE-modified concretes with AAS are almost the same as that of SBR- and PAE-modified concretes without AAS regardless of AAS content. The compressive strength of both polymer-modified concretes is about 90 % of that of unmodified concrete. On the other hand, the compressive strength of EVA-modified concretes with AAS decreases with increasing AAS content, and is lower than that of unmodified concrete at an AAS content of 1.0 %. It seems that the addition of AAS to SBR- and PAE-modified concretes does not affect their compressive strength.

Figures 3 and 4 exhibit the weight change and chloride ion penetration depth of polymer-modified concretes with AAS. Irrespective of polymer type, the weight change of the polymer-modified concretes with AAS is markedly reduced with increasing AAS content. In particular, the weight change of the polymer-modified concretes with an AAS content of 1.0 % is about one-third of that of unmodified concrete. Like their weight change, the chloride ion penetration depth of the polymer-modified concretes with AAS tends to increase with raising AAS content regardless of polymer type. The chloride ion penetration depth of PAE-modified concrete with an AAS content of 1.0 % is a half of that of the unmodified concrete. The reason for the excellent resistance to the chloride ion penetration of the polymer-modified concretes with AAS can be explained to be due to the combined effects of the good water repellency of AAS and the polymer film formation by polymer dispersions.

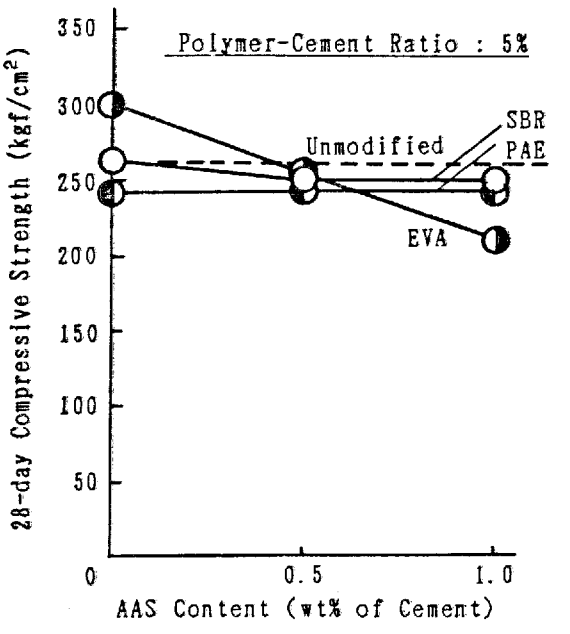

Fig. 2 28-day Compressive Strength of Polymer-Modified Concretes with AAS.

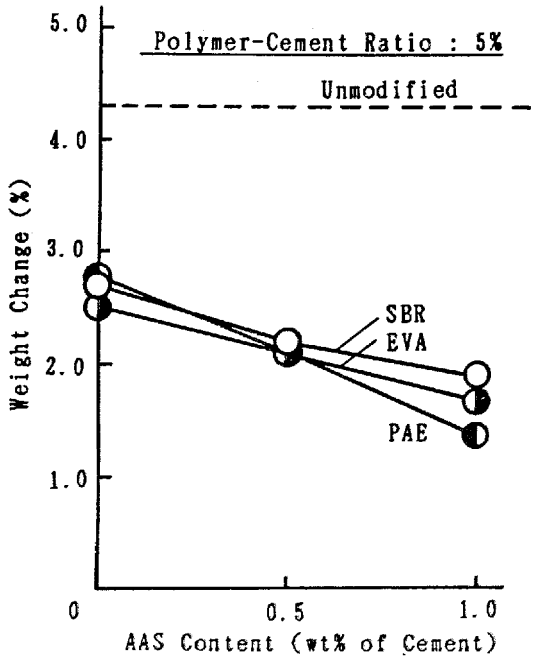

Fig. 3 Weight Change of Polymer-Modified Concretes with AAS, Immersed in 2.5% NaCl Solution for 28 Days.

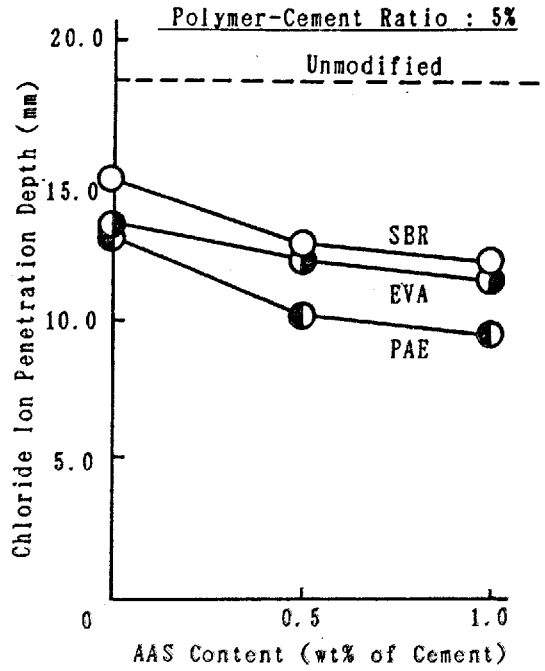

Fig. 4 Chloride Ion Penetration Depth of Polymer-Modified Concretes with AAS, Immersed in 2.5% NaCl Solution for 28 Days.

Figure 5 illustrates the carbonation depth of polymer-modified concretes with AAS. Regardless of polymer type and AAS content, the carbonation depth of the polymer-modified concretes with AAS is considerably reduced, and becomes about two-third or less of that of unmodified concrete. The effect of the AAS content on the carbonation of the polymer-modified concretes is hardly recognized; therefore, the superior carbonation resistance of the polymer-modified concretes with AAS may be considered to be greatly dependent on the addition of polymer dispersions.

Figure 6 gives the 28-day drying shrinkage of polymer-modified concretes with AAS. Irrespective of polymer type, the drying shrinkage of the polymer-modified concretes without AAS is lower than that of unmodified concrete. Furthermore, the drying shrinkage of the polymer-modified concretes is decreased by combining AAS addition, and turns out to be about two-third or less of that of the unmodified concrete.

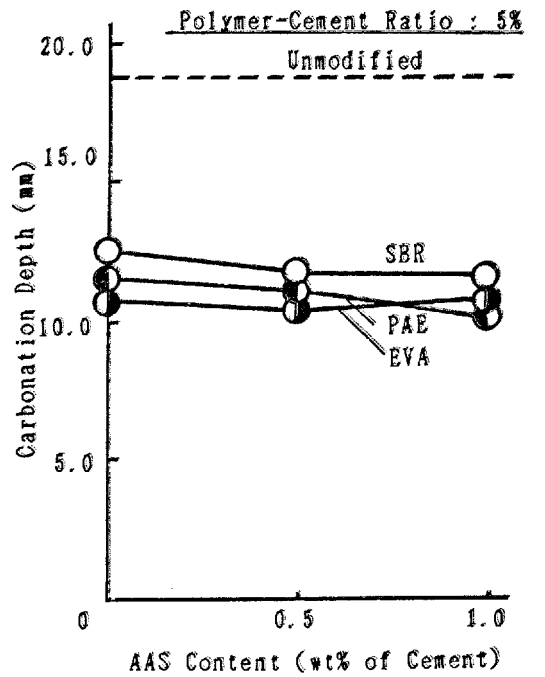

Fig. 5 Carbonation Depth of Polymer-Modified Concretes with AAS, Exposed to Air with CO_2 Gas Concentration of 5% at 30°C and 60% R.H. for 28 Days.

CONCLUSIONS

From the test results, the following conclusions can be obtained.

(1) In general, the compressive strength of SBR- and PAE-modified concretes with AAS is almost the same as that of unmodified concrete, but the compressive strength of EVA-modified concrete with AAS tends to decrease with raising AAS content.

(2) Irrespective of polymer type, the weight change and chloride ion penetration of polymer-modified concretes with AAS decrease markedly with raising AAS content.

(3) The carbonation depth of polymer-modified concretes with AAS is considerably reduced regardless of polymer type and AAS content.

(4) In comparison with unmodified concrete, the drying shrinkage of polymer-modified concretes with AAS decreases regardless of polymer type and AAS content.

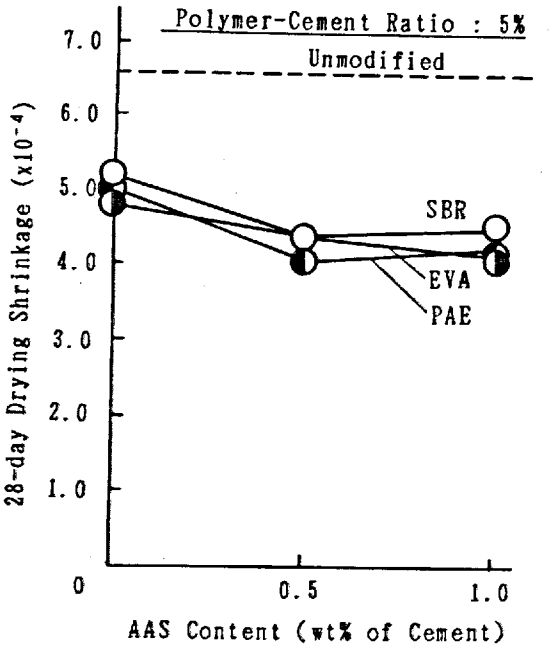

Fig. 6 28-day Drying Shrinkage of Polymer-Modified Concretes with AAS.

(5) Accordingly, the simultaneous use of polymer dispersions and AAS considerably improves the resistance to chloride ion penetration and carbonation, and drying shrinkage of concretes although the compressive strength of the concretes using the polymer dispersions and AAS is the almost same as that of unmodified concrete. In consideration of a good balance between the cost and performance, a polymer-cement ratio of 5 % and an AAS content of 0.5 % are recommended when the polymer disperions and AAS are used as durability-improving admixtures for concrete.

REFERENCES

1. Ohama, Y., "Principle of Latex Modification and Some Typical Properties of Latex-Modified Mortars and Concretes", **ACI Materials Journal**, 1987, 84(6), 511-518.

2. Ohama, Y., Demura, K., Satoh, Y., Tachibana, K. and Miyazaki, Y., "Development of Admixtures for Highly-Durable Concrete", **Proceedings of the Third International Conference on Superplasticizers and Other Chemical Admixtures in Concrete, SP-119, American Concrete Institute, Detroit**, 1989, 321-342.

STRUCTURE FORMATION OF CEMENTLESS CONCRETE MADE WITH SLAG SAND AND HIGH-CALCIUM ASH FROM THERMAL POWER PLANTS

S I Pavlenko and A B Oreshkin

Siberian Metallurgical Institute, Novokuznetsk, RUSSIA

SUMMARY

This paper presents results of a laboratory investigation into the processes of structure formation (at 24 hr, 28 days, 3 and 6 months) of cementless fine-grained concrete containing high-calcium fly ash, slag sand from thermal power plants and silica fume developed by the Siberian Metallurgical Institute for use in load-bearing and enclosing structures. Physico-mechanical, deformation and specific properties (frost resistance, heat conductivity, protection of reinforcement from corrosion) of the above concrete have also been investigated.

РЕЗЮМЕ

В докладе представлены результаты лабораторных исследований процессов структурообразования во времени (сутки, 28 суток, 3 и 6 месяцев) разработанного нашим институтом бесцементного мелкозернистого бетона для несущих и ограждающих конструкций на основе высококальциевой летучей золы, шлакового песка ТЭС и кремнеземистой пыли. Также исследованы физико-механические, деформативные и специальные свойства (морозостойкость, теплопроводность, защита арматуры от коррозии) указанного бетона.

INTRODUCTION

In the papers presented at the international conference in Shef - field in September 1991 (1) and at the 4th international conference in Istanbul in May 1992 (2) we spoke about the development of fine-grained cementless concrete on the basis of high-calcium fly ash, slag sand from thermal power plants and silica fume. Neither natural aggregates such as gravel, rubble, sand nor artificial porous materials (claydite, agloporite, foam polystyrene and others) are used in the concrete. High - calcium fly ash is used as a binder. The proportioning of concrete mixtures is given in Table 1.

Table 1 - Mixture Proportions

No	Application	Quantities, kg/m^3					Mixture Slump, cm	Average Density, kg/m^3	Compressive Strength, MPa
		Fly Ash	Silica Fume	Slag Sand	Water	Air-entraining Admixture			
1.	For load-bearing Structures	650	70	720	480	-	8 to 10	1920	15 to 20
2.	For enclosing structures	500	50	500	330	5.4	8 to 10	1385	4.5 to 5.5

The purpose of the study is to investigate the process of structure formation, phase minerological composition of concrete (at 24hr, 28 days, 3 and 6 months) and its physico-mechanical,deformation and specific properties such as frost resistance, heat conductivity, reinforcement corrosion.

MATERIALS

Fly Ash

Fly ash from the Novosibirskaya Thermal Power Plant is a fine-dispersed powder of a light brown colour with the average specific surface of 4000cm^2/g. The positive characteristics of this fly ash are its high contents of bound calcium oxide (30%) and silicon oxide (37.6%), small amounts of potassium and sodium oxides (0.66%), of sulfur (2.53%) and of unburnt particles (2.48%). The fly ash has good binding properties.On the other hand, the ash contains a high amount of magnesium oxide (6.44%) and free calcium oxide (5.5%) affecting the irregularity of concrete volume change.

Slag Sand

The slag sand had a particle size distribution of 0 to 5mm and fineness modulus of 2.7 mm; its colour varied from dark brown to black and the alumina-silicate glass was mostly in the radioamorphous state.It contained neither unburnt particles nor sulfuric compounds.

Silica Fume

Silica fume is a super-dispersed powder of a grey colour with the average specific surface of 20000 cm^2/g.

Air-Entraining Admixture

The air-entraining admixture used was a synthetic detergent called "Progress", the secondary sodium alkyl sulphate. It is usually supplied as a liquid having a density of 1.084 tn/m^3.

Structure of the materials is shown in Fig.1 (a,b,c) and their physical properties and chemical analysis are given in Tables 2 and 3.

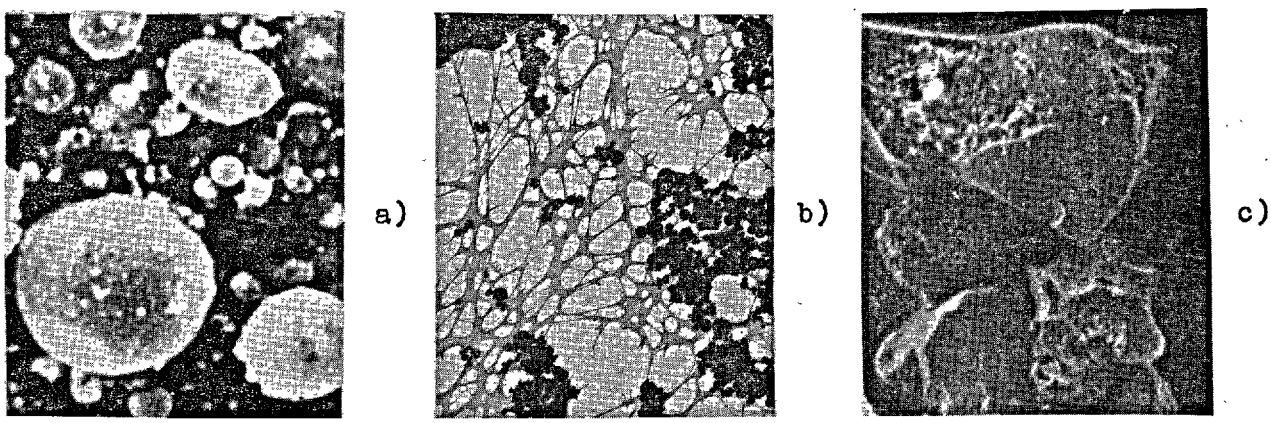

FIG.1 (a,b,c) Structure of the materials: a) fly ash, b) silica fume, c) slag sand. Electron micrograph.

Table 2 - Physical Properties

Characteristics of materials	Materials		
	Fly Ash	Slag Sand	Silica Fume
Bulk density, kg/m^3	1200	1400	230
True density, kg/m^3	2550	2350	2200
Specific surface, cm^2/g	3990	-	20000
Fineness modulus, mm	-	2.7	-
Colour	light brown	dark green	light grey

Table 3 - Chemical Composition

Oxides, %	Materials		
	Fly Ash	Slag Sand	Silica Fume
SiO_2	37.13	62.20	90.11
CaO total	35.53	1.70	0.71
CaO free	5.51	-	-
Al_2O_3	7.52	23.37	1.93
Fe_2O_3+FeO	8.87	6.44	1.82
MgO	6.44	2.16	0.97
K_2O+Na_2O	0.66	2.59	2.03
TiO_2	0.47	0.06	0.02
MnO_2	0.15	0.22	0.20
P_2O_5	0.04	0.03	0.19
SO_3	2.53	-	0.89
Loss on ignition	2.48	-	2.25

EXPERIMENTAL

The presence in the ash of high-temperature forms of CaO, MgO and slowly hydrating glass phase deteriorates the properties of ash as a binder. The surface of the particles of free CaO is often covered by the fused coaling which hampers its contact with water. The hydration process of such CaO is slow. Calcium hydroxide is formed in the artificial stone when the stabilizing crystallization structure has already been formed. During this process the considerable internal stresses appear causing the irregular volume change of the hardening system which is the most important criterion of durability, deformation and even destruction of the artificial stone. We observed this effect while proportioning concrete mixtures. Concrete specimens didn't shrink but increased in volume, had hair cracks and broke being immersed in water at the age of 28 days and more. The above deformations are shown in Fig.2 (a,b).

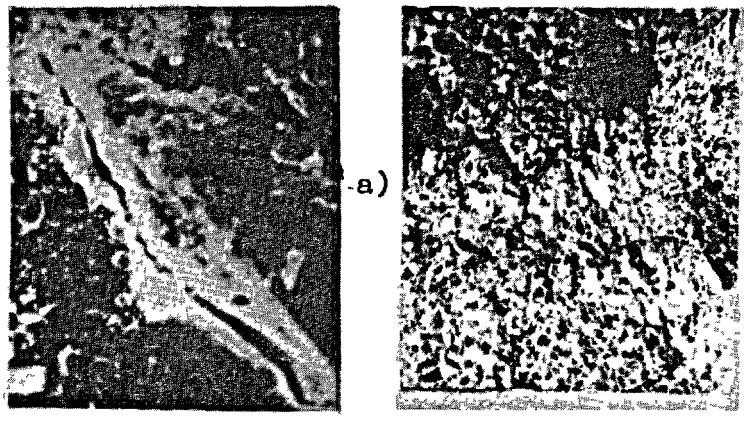

FIG.2 (a,b) The Deformation of concrete.
a) The Microdeformation
b) The Macrodeformation

To eliminate the negative effect of the slowly hydrating free CaO, we used hot water for mixing concrete and introduced silica fume suspension affecting the hydration process (Fig.3).

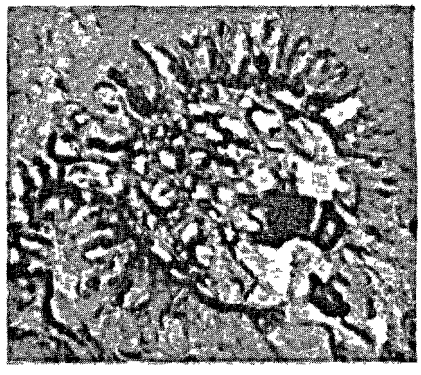

FIG.3 Reaction of hydration of free CaO with silica x 14600. Electron micrograph.

Besides, concrete specimens were cured in the laboratory steam curing chamber in order to accelerate free $CaO+SiO_2+H_2O$ reaction. the best results were obtained with:

temperature of water + 60° C
curing specimens at room temperature for 4 to 6 hours
curing specimens in the laboratory steam-curing chamber at the temperature of 95 to 100°C using 3+12+3 hour cycle.

Structure formation processes, phase-mineralogical composition of concrete at 24 hours, 28 days, 3 and 6 months, its physico-mechanical and deformation properties have been investigated on the above specimens. The latter are left to be used for a long term investigation (1year, 2 years and more).

Main physico-mechanical and deformation properties of two types of concretes are shown in Table 4.

Table 4 - Main Physico-Mechanical and Deformation Properties of Cementless Concrete over 6 Months Period

Characteristics of concrete	Test Duration, days			
	1	28	90	180
1. For Load-Bearing Structures				
Compressive Strength, MPa	15	20	22	23
Relative Shrinkage, mm/m	0.28	0.61	0.65	0.66
Total Value of Creep Deformations when $= 0.5\ R_{prism}$, mm/m	-	0.36	0.38	0.39
Initial Modulus of Elasticity, $E \cdot 10^{-3}$	95	121	125	130
pH	12.6	12.4	12.1	12.0
2. For Enclosing Structures				
Compressive Strength, MPa	4.5	5.5	5.8	5.7
Relative Shrinkage, mm/m	0.52	0.68	0.74	0.76
Total Value of Creep Deformation, mm/m	-	0.38	0.39	0.41
Frost Resistance, cycle	-	51	53	56
Heat Conductivity, W/m°C	0.44	0.36	0.32	0.26

As can be seen from the Table 4, the main properties of concrete improve with time, except for the slight decrease in compressive strength of concrete for enclosing structure at the age of 180 days as compared with 90 days. Since shrinkage and creep have not yet been stabilized, the results will be more exact at the age of 1,2 years.

The process of structure formation over the given period (up to 6 months) was studied using four methods: radiostructural and differential-thermal analyses, electronic microscope and chemical analysis. Fig.4(a,b, c,d) illustrates this process.

a) at 24 hours

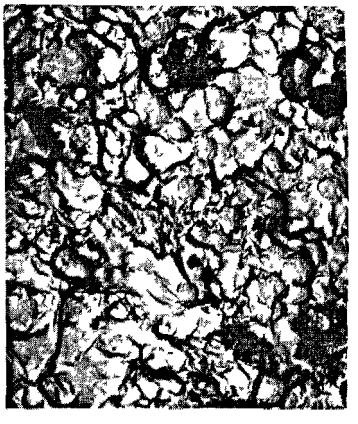

b) at 30 days



c) at 90 days



d) at 180 days

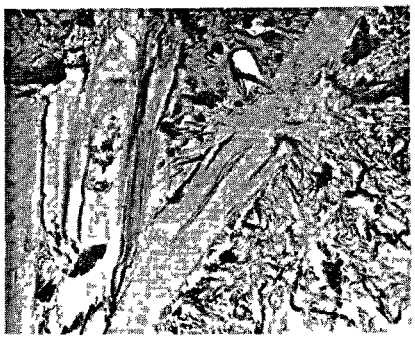

FIG.4 Structure of cementless fine-grained slag ash concrete: a) aggregated ash particles x 14600; b) crystals of C_2SH_2 x 14600; c) new formations x 11400; d) large crystals of calcium hydrosilicate x 12400

Relative change in the quantity of free CaO in concrete was determined by chemical analysis. If the quantity of free CaO in fresh concrete mixture is taken as 100% (free CaO will constitute 1.71% by the total concrete mixture) its quantity is equal to 0.53%, 0.41%, 0.29% and 0.26% at 24 hours, 28, 90 and 180 days, respectively.X-ray photographs of materials and concrete also indicate that the formation of hydrosilicates of calcium occur not only due to the hydration of minerals but also due to binding free calcium oxide by silicon oxides and their interaction with water. X-ray photographs will be illustrated in slides.

Differential-thermal analysis and dynamic weighing of specimens during heating were used to determine the degree of ash hydration by the quantity of hydrate water in it, the amount of new formations being defined by the loss in weight in the limits of corresponding effects. (The thermographs are given in slides.)

CONCLUSION

Cementless concrete incorporating high-calcium ash, slag sand from thermal power plants and 10 to 15% silica fume prepared with hot water and after its curing at the temperature of 95% to 100° C may be used for the construction of single, two-storey block of flats in normal conditions.

REFERENCES

1. Pavlenko S.I. Lightweight cementless concrete on the base of high-calcium fly ash and slag sand from TPP. Blended cements in Construction. Edited by R.N.Swamy, Elsevier Applied Science, London and New York. September, 1991, pp.95-106.

2. Pavlenko S.I. Fine-grained cementless concrete made with high-calcium fly ash and slag sand from thermal power plants.Fourth CANMET/ACI International Conference on Fly Ash, Silica Fume, Slag Sand and Natural Pozzolans in Concrete, May 3-8, 1992, Istanbul, Hilton Hotel, Istanbul, Turkey.

ACTIVATED MIXED BINDERS AND CONCRETES BASED UPON THEM

L A Kuznetsova, V M Dymsky, G A Korableva and T N Kobystcha

Far-Eastern Research Institute for Construction,
Vladivostok, RUSSIA

SUMMARY

This paper presents results of laboratory investigations concerning the obtained effective mechanoactivated mixed binders based upon portland cement with use of mineral agents as well as to study properties of concretes based upon those binders.

The results of investigations showed that it was possible to use activated mixed binder in concretes and mortars for production of both built-up and cast-in-place constructions as well as other building articles.

АННОТАЦИЯ

В данной работе представлены результаты лабораторных исследований в направлении получения эффективных механоактивированных вяжущих на основе портландцемента с использованием минеральных добавок и изучения свойств бетонов на основе этих вяжущих.

Результаты исследований показали возможность использования активированного смешанного вяжущего в бетонах и растворах для изготовления сборных и монолитных конструкций, а также мелкоштучных блоков и других строительных изделий.

INTRODUCTION

Far-Eastern Research Institute for Construction (Vladivostok) carried out investigations to obtain effective mechanoactivated mixed binders upon high-aluminate cement where low-calcium acid fly ash or natural sand were utilized as mineral agents, as well as to study properties of concretes based upon those binders.

EXPERIMENTAL

To obtain mixed binders we used portland cement of such brands as PC 400-D20 and PC 500-D5 produced by cement plants of the Far-Eastern Association, named "Spasskcement". The cement contained from 5% to 18% of its weight as an active mineral agent, i.e. a volcanic tuff which activity to absorb calcium hydroxide from its saturated solution was 80...110 mgCaO/g of the agent. Mineralogical analysis of a clinker utilized in the cement production was as follows : C_3S-59...62%, C_2S - 12...14%, C_3A - 9-11%, C_4AF - 11...12%. The cement contained 1.2...1.8% of its weight as alkali (in terms of Na_2O). Specific surface of the cement was 290... 320 m^2/kg.

A fly ash (of dry separation) utilized for the mixed binder production was formed during pulverized-coal burning of lignites from the far-eastern coalfields. Its chemical analysis (% of its weight) is as follows : silicon oxide is 58...61%, aluminium oxide is 24...27%, ferrum oxide is 3.6...5.4%, calcium oxide is 3.2...4.8%, magnesium oxide is 1.2...2.2%, pottassium oxide is 1.2...2.6%, sodium oxide is 0.3...0.5%, sulphuric anhydride is 0.1...0.2%. A content of soluble silica is 0.8...0.9%. Losses on ignition are 0.3...0.4% at 550°C and 0.5...0.9% at 950°C. Specific surface of ash (by Blane) is 290...330 m^2/kg. True density is 2.07...2.18 g/cm^3.

According to data of thermography and X-ray phase analysis, fly ash contains considerable amount of vitreous phase and quartz, solid-phase mullite crystallization in amorphous clay substance and alumino-silicate vitreous phase, some hematite.

Mineralogical analysis of the fly ash was made by dr.E.Galibina in Research Institute on Construction (Tallinn). According to solubility in different media the analysis was presented as follows : vitreous phase- up to 16.5%, orthoclase - 7.4%, mullite - up to 25%, hematite - up to 3.5%, quartz - up to 22%, SiO_2 in silicaglass insoluble in 3% HCl - up to 11.7%. It is obvious that given analysis is rough, Calculated amount of mullite was overestimated, evidently, because a portion of aluminium oxide was a part of the vitreous phase. Refraction value of the vitreous phase was generally 1.5-1.6, indicating silica and aluminosilicate composition.

The next mineral agent is quartz sand from Volsky deposite. It contained from 98 to 99% of its weight as silica, from 0.5 to 0.9% as pulverized or clay matter. Its grain dimensions were generally 0.5... 0.9 mm.

When producing the mixed binders, a dry super plasticizer S-3 or a dry waste of biochemical production of nutrient yeast, named "caramel", were utilized as chemical agents-modifiers.

Mineral agents were injected as 20...50% of the binder weight, super plasticizer S-3 as 1% and "caramel" as 0.18...0.2% of cement weight. To control data when the binders set or the other properties,

we added calcium sulphate having double or semiwater content, an amount of which was determined experimentally.

We obtained mixed binders through joint comminution of agents in a ball mill or powder dispenser of toroid-spiral type. In case of utilization of natural sand as mineral agent, the binder was obtained in two stages. The first stage included sand comminution to such fine grains that were characterized by a specific surface value 500...650 m^2/kg (by Blane). In this case, super plasticizer S-3 or "caramel" were added at the first stage, since they intensify the comminution. When the fly ash was utilized, the binders were produced during one-stage comminution of components to a dispersivity that corresponded to a specific surface value 500...660 m^2/kg.

An activity of binders was determined by standard methodology, on samples of 1:3 cement-and-sand mortar. Beams-samples that were 4x4x16 cm overall hardened both under water conditions at 20±2°C of water temperature and under damp atmospheric conditions at 20±2°C of atmospheric temperature and 100% of humidity.

Strength properties of mechanoactivated mixed binders were evaluated and shown in Table 1.

Table 1

A binder, name and amount of a mineral agent	Specific surface m^2/kg	Cement and sand mortar, 1:3		Strength Limit, MPa			
				Damp-air hardening		Underwater hardening	
		v/c	cone spread, mm	28 days	180 days	28 days	180 days
				Bend* Comp*	Bend Comp	Bend Comp	Bend Comp
Initial plane cement	302	0.40	115	- -	- -	7.1 52.1	9.2 66.2
The same, mechanoactivated	505	0.43	112	- -	- -	8.2 53.7	- -
Cement + 30 % of sand	498	0.42	111	- -	- -	5.2 38.3	- -
Cement + 30 % of sand + S-3	518	0.33	108	- -	- -	7.1 56.0	- -
Cement + 30 % of sand + "caramel"	515	0.40	110	- -	- -	5.8 40.9	- -
Cement + 20 % of ash +S-3	520	0.36	108	10.3 64.3	11.0 81.8	9.0 58.0	9.7 70.9
Cement + 30 % of ash + S-3	545	0.34	106	10.0 62.2	10.7 73.5	9.0 57.8	9.6 70.6

Initial "old" cement	305	0.40	107	- -	- -	6.3 44.2	- -
The same + 30% of ash + S-3	516	0.34	107	- -	- -	6.6 58.0	- -
The same +30 % of ash + "caramel"	501	0.43	106	- -	- -	5.9 46.4	- -
Cement + 40 % of ash + S-3	513	0.36	106	9.3 60.3	9.7 71.8	7.8 55.7	9.0 69.7
Cement + 50 % of ash + S-3	528	0.37	106	8.2 54.3	9.1 70.3	7.9 54.4	8.6 69.6
Cement + 30 % of ash + "caramel"	518	0.43	107	8.1 49.7	8.5 58.3	8.7 50.6	8.9 56.4

*Bend-Bending, Comp-Compression

We ought to say that due to choosing of an optimal amount for the control agent, named calcium sulphate, all the binders had practically the same period of setting, i.e. the beginning in 1.5...2 hours, the end in 3...4 hours. A mortar plasticity being the most important technological value was equalized through variability of water-cement proportion and was also practically the same in all mixes.

Testing of mechanochemical activated mixed binders revealed that quartz sand even in fine grains was an inert agent while the fly ash acted as an active mineral agent in any case.

Mechanochemical activation with utilization of super plasticizer S-3 permitted to obtain rather effective mixed binder even an old cement was used.

Strength of samples from all mechanoactivated mixed binders with the fly ash and super plasticizer S-3 were increasing by six months of hardening under water/damp air conditions, but not decreasing at all. At the same time, the strength of samples with different content of the fly ash (especially during 6-month hardening in water) were equalizing.

Most probably, it was caused by appearance of additional amount of calcium hydroaluminates and hydrosilicates due to reaction of interaction between the vitreous phase of the ash particles and products of hydrated clinker minerals when contacts of these products with the more dispersed ash particles were increasing in number.

When passing a standard test for mechanoactivated mixed binders on samples of cement-and-sand mortars, "caramel" agent was not considerably effective. But when these binders were tested in concretes, they were effective due to air-entraining property.

On base of cement-ash binder activated by joint comminution of components in the ball mill there were produced the concretes of different types and for different purposes.

As a result, we indicated a possibility of obtaining a gas-ash concrete that was hardening non-steam-and-pressure-cured, classified as B2...B7.5(2.5...10 MPa strength), dense as 650...950 kg/m^3 and resistant to no less than 25 cycles of freezing-defrosting by turns. Due to dense aggregates we obtained a concrete classified up to B40 (M500 brand), wheresaving in cement was 30% and in mixed binder it was within 80...100 kg/m^3 as compared to standard cement consumption recommended by Standards and Manuals in the field of Construction.

As an agent for the mixed binder dry super plasticizer S-3 permitted to make a strength rate of a heavy concrete 1.4 times as high while cement saving was 30% and 1.2 times as high while cement saving was 50%.

Using a porous aggregate and the cement-ash binder containing 50% of ash and "caramel" agent we obtained structural insulating concretes classified as B2.5...B3.5 (M35...M50 brands) where the binder was consumed under standard requirements.

The cement-ash binder activated in powder dispenser of VNIIG construction permitted to obtain concretes on dense aggregates of the higher strength rate while hardening both under normal-humidity conditions and after thermal treatment as in comparison with non-activated and activated portland cement. The concrete had a strength rate B45 (M600 brand) while portland cement saving was 30%, and its strength rate was B35 (M450 brand) while the cement saving was 50%.

CONCLUSIONS AND RECOMMENDATIONS

The proposed method of obtaining activated mixed binder allow recommended for using in concretes and mortars for production of both build-up and cast-in-place constructions,as well as small-scale blocks and another products for construction.

ACKNOWLEDGEMENTS

This paper is based on the results of planned works of the Far-Eastern Research Institute for Construction, Russian Ministry of Construction.

The authors appreciate the help of their colleagues in carrying out experimental permission of the Institute scientifical and technical council.

USE OF CIRCULATING SAND ACTIVATORS IN SEPARATE MIXING TECHNOLOGY OF CONCRETE

B V Gusev, A G Milrud, A E Lutin, I A Sulkowsky and B B Akhmedov

The Tashkent State University named after Beruni Tashkent, UZBEKISTAN

SUMMARY

The description of a new construction activator as well as the positive results of its appliance while introducing the separate concrete preparation technology use are given.

В статье дается списание активатора новой конструкции и сообщаются положительные результаты его использования при внедрении раздельной технологии приготовления бетона.

A number of experimental tests as well as comparative tests carried out by the Reinforced Concrete Research Institute on tubulent mixers used in separate mixing technology of concrete showed this technique to be not very. efficient.

The results of the research revealed the possibility of successful introduction of the separate mixing technology of concrete by recourse to mix pretreatment in circulating sand activators of a principally new design.

The circulation sand activator is a vertical double bearing shaft with flat discs, mounted in the cylindrical body of the activator.

To create the necessary head and bring about mass circulation, a working impeller is installed at the lower section of the shaft.

The action of the high revolution discs and the impeller discharges the mix under pressure into narrow annular slots between the rotating discs and the fixed body, which represent the areas of active dispersion of sand grains and cement.

According to the results of granulometric analysis during the activation of the sand-water system in the circulation sand activator a significant quantity of extremely fine particles with specific surface of 6000 cm^2/g is formed at the expence of sand grain surface abrasion.

A correlation between the quantity of the extremely fine fraction (Π) formed and the activation time has been deduced as follows:

$$\Pi = \Pi_0 + \frac{\alpha t}{1 + \beta t}$$

where α and β are proportionality factors.

Provided $t \to 0$ the factor defines the slope of the tangent at the initial position of the graph.

Provided $t \to \infty$ the observed function tends to the limit $\frac{\alpha}{\beta}$ which defines the maximum possible content of the fine dispersion particles.

Analysis of the calculated values of the proportionality factor shows that the maximum number of particles of the fine dispersion fraction, which can be formed during the sand activation in the circulation sand activator, is approximately equal to the space between the grains.

The specific power consumption $\frac{kWh}{m}$ calculated allowing for the number of fine dispersion particles formed in the circulation sand activator whithin the 2-minute activation period adopted in the separate mixing technology of concrete , is approximately 2,5 times lower than for ball mills.

Thus it has been found that to get a product of such fine dispersion, it is more efficient to use the principle of sand grain surface abrasion , realized in a circulation sand activator than crushing grains in a ball mill.

Results of the tests conducted revealed the possibility of introducing the intensive separate mixing technology of concrete employing the circulation grain activator for mixing concrete of various grades up to M300 including moderately high-flow concrete mix of OK=3...6 cm with coarse and medium sized plasticized sand grains. This would enable a 15 to 25 % saving in cement.

The expedience of using sand activated in the circulation sand activator for producing items througt the plateholding technology has been determinated. A 20% saving of cement has been shown.

Ways possible by this have been found for of utilising the fine dispersion fraction that is obtained as a microaggregate in the process.

The efficiency of activation of the cement-water system in the circulation sand activator has been estimated.

Circulation sand activator of the porposed design has been successfully used in the intensive separate mixing technology of concrete at the enterprises of the Ministry of Civil Engineering in the Uzbekistan.

ADVANCES IN USE OF SEA WATER FOR PREPARING OF CONCRETE MIXTURES FOR REINFORCED CONCRETE BY MEANS OF A SPECIAL WATER TREATMENT

Bogomil D Darakchiev and Lyubomira V Pantofchieva

University of Architecture, Civil Engineering and Geodesy, Sofia BULGARIA

SUMMARY

The paper presents the results of testing of the strength properties of concrete samples prepared with different making waters, received from sea water being treated in an ion exchange way. The strength characteristics attained have been juxtaposed with those of control samples prepared with plain potable water.

In cosequence of the investigations it has been established that by the ion exchange method, depending on the anionic form, concretes of higher compressive strength (than the control samples) have been realized, the concentration of Cl^- and SO_4^{2-} being strongly diminished.

РЕЗЮМЕ

В докладе представлены результаты испытаний прочностных свойств бетонов, изготовленных с помощью морской воды, обработанной ионообменным способом, с целью снижения концентрации хлоридов и сульфатов из-за необходимости коррозионной безобасности арматуры бетона.

Установленно, что с помощью анионированной морской воды, в зависимости от анионной формы смолы, получены бетоны разной прочности, в большинстве случаев бо́льшей прочности на сжатие (по сравнению с контрольными образцами с питьевой водой), отвечающие строжайшим требованиям нормативных документов по отношению концентраций хлоридов (сульфатов).

INTRODUCTION

The content of chloride ions in reinforced concretes has been limited according to the national standards and C E B - F I P Model Code, 1990. Because of the danger of reinforcement corrosion the percentage of Cl^- in reinforced concretes must be below 0,1 % by weidht of the cement mass, [1, 2, 3, 4].

In case of higer concentrations of Cl^- different inhibitors have been applied with varying success, [5, 6, 7].

In this paper the possibilities for use of sea water as making water for preparing of reinforced concrete mixtures have been concidered; at that, the corrosion effect of the significant concentrations of the chlorides and sulphates on the reinforcement had to be avoided. To this end, the sea water was processed in a special way that decreased the concentrations of Cl^- and SO_4^{2-} up to the minimum desired.

TREATMENT OF THE SEA WATER

The method proposed is based on the filtration ion exchange. The sea water has been subjected to a treatment by means of suitable selected anion exchanger in appropriate salt form of its active functional groups. A strong basic or a weakly basic anion exchange resin in an anion exchange column has been converted into the necessary ionic form by means of regenerating agent — solution of the corresponding salt or acid. After the regeneration the anion exchanger has been rinsed with water and then it is ready to work.

The sea water to be treated flows through the anion exchange resin bed, during the interaction loses its Cl^- (and SO_4^{2-} and other anions), exchanging them for the anions loading the active groups. The outlet fluid contains a significantly decreased concentration of Cl^- and SO_4^{2-}, and an increased concentration of the exchangeable anion. Due to the

equivalent ion exchange a new making sea water has been received, non-containing corrosion aggressive concentrations of Cl^- (SO_4^{2-}) .

The mechanism of the thus described process represents stoichiometrical ion exchange. It can be realized in ion exchange columns of any size, giving possibilities to produce treated making sea water as much as necessary. The concentrations of the regeneration solutions are about 4 - 6 %.

REAGENTS USED FOR REGENERATION AND KINDS OF TREATED MAKING WATERS

A great number of regenerating reagents were used: solutions of sodium hydrocarbonate, sodium phosphate, sodium tartarate, sodium tetraborate, sodium acetate, sodium ethylenediamine tetraacetate (EDTA), orthophosphoric acid, acetic acid. The effluent from the ion exchange column treated sea waters can be used singly or in combinations in different ratios. The aim is to attain improved kinetics of induration and improved strength properties of the concrete. Experiments have been conducted with the following combinations of separately treated sea waters as making waters: HCO_3^- / PO_4^{3-} = 1 : 1 ; HCO_3^- / CH_3COO^- = 1 : 1 ; CH_3COO^- / / PO_4^{3-} = 1 : 1 ; EDTA / PO_4^{3-} = 1 : 4 .

CHARACTERISTICS OF THE RAW SEA WATER USED

In the experiments presented raw water from Black Sea was used to produce making water for preparing reinforced concrete non-containing corrosion aggressive concentrations of Cl^- and SO_4^{2-} . The concentration of the solids in the Black Sea water varies between 14,5 and 18,0 g / dm^3, that is about 2,0-2,5 times lower than the ocean total dissolved solids concentration. The other characteristics of the raw sea water:

	meq / dm^3	mg / dm^3
total alkalinity A_{mo}	3,25	
total hardness	64,40	
Ca^{2+}	15,20	304,0
Mg^{2+}	49,20	984,0

		meq / dm^3	mg / dm^3
Cl^-		277,50	9 850
SO_4^{2-}		26,25	1 260
pH	8,05		

MATERIALS AND COMPOSITION OF THE CONCRETE

The investigations have been accomplished using cement from production batch containing 20% mineral addition (8% limestone and 12% blast furnace slag) and the following mineral content:

	%
C_3S	50,5
C_2S	31,3
C_3A	10,2
C_4AF	10,2

All the tests have been conducted with concrete of the same composition (kg / m^3): cement - 350, middle-grained sand - 650, gravel - 1 150, and water - 1 150 . As making waters potable water, natural sea water and treated sea waters with diminished content of Cl^- and SO_4^{2-} have been used. Seven of the latter were singly and four of them were in combinations used. The samples prepared with potable water were control samples (comparative ones).

The concrete samples (cubes) stayed in standard conditions according to Bulgarian State Standard 505 / 84. The tests for their compressive strength have been conducted on the 3rd, 7th , 28th and the 180th day.

RESULTS OF THE INVESTIGATIONS

Investigations data about the influence of the kind of making water (potable, sea and treated sea waters) upon the compressive strength are presented in the Table 1. All the experiments preparing the concrete with treated sea water, have ensured such a decreasing of the Cl^- (SO_4^{2-}) -concentration, that completely satisfied the most stringent requirements

Table 1

COMPRESSIVE STRENGTH OF CONCRETES PREPARED BY MEANS OF POTABLE-, SEA- AND TREATED SEA WATER WITH DIMINISHED CONCENTRATION OF Cl^- AND SO_4^{2-}

N°	KIND OF MAKING WATER	CONCENTRATION IN THE MAKING WATER (mg/dm^3)		COMPRESSIVE STRENGTH (MPa)			
		Cl^-	SO_4^{2-}	3rd	7th	28th	180th DAY
1.	POTABLE WATER	20	30	9,6 (100)	16,0 (100)	29,7 (100)	39,2 (100)*
2.	SEA WATER	9 850	1 260	14,1 (147)	19,6 (123)	30,1 (101)	40,8 (104)*
3.	TREATED SEA WATER WITH ANIONITE IN:						
3.1.	PO_4^{3-} FORM	1 930	430	13,8 (144)	22,1 (138)	35,3 (119)	42,5 (109)
3.2.	PO_4^{3-} FORM	360	180	10,5 (109)	18,9 (118)	35,5 (120)	40,6 (104)
3.3.	E D T A FORM	720	200	0,7 (7)	- -	10,6 (36)	- -
3.4.	HCO_3^- FORM	1 520	635	- -	15,6 (98)	28,3 (95)	36,0 (92)
3.5.	TARTARATE FORM	1 070	20	slow induration			
3.6.	ACETATE FORM	710	150	12,0 (125)	18,6 (116)	33,4 (112)	42,0 (107)
3.7.	$B_4O_7^{2-}$ FORM	360	30	2,8 (29)	7,0 (44)	12,0 (40)	18,0 (46)
3.8.	EDTA/PO_4^{3-} = 1:4	1 290	190	12,0 (125)	20,3 (127)	32,8 (110)	40,9 (104)
3.9.	HCO_3^-/PO_4^{3-} = 1:1	1 160	405	11,2 (117)	18,3 (114)	30,1 (101)	33,6 (86)
3.10.	HCO_3^-/CH_3COO^- = 1:1	710	150	11,6 (121)	17,0 (106)	29,3 (99)	37,9 (97)
3.11.	PO_4^{3-}/CH_3COO^- = 1:1	710	180	11,5 (120)	23,2 (145)	29,2 (98)	34,3 (88)

* In brackets - % ratio of the compressive strength of the sample to that one of the control sample, prepared with potable water.

of the normative documents concerning the content of chlorides in reinforced concretes (0,1 % by weight of the cement).

The results for the compressive strength of the samples prepared with potable water, sea water, and treated sea waters are juxtaposed in Table 1. The analyses shows that the concrete samples with acetate (№ 3.6) and phosphate (№ 3.1 and 3.2) making waters have the best strength characteristics. Their compressive strength at the 28th day exceeds that of the control samples with plain potable water with 12% and 19-20% respectively. At the same time these making waters speed the enduration in the early age (3rd day) from 9 to 44%. This positive trend goes on also six monthes later. The increase of the compressive strength in the early age of the samples with phosphate making water, having very low Cl^- concentration (№ 3.2), is weaker in comparison with that of the samples possessing higher Cl^- concentration (№ 3.1). Very good results have been received for the compressive strength of the samples prepared by means of mixed making water EDTA / PO_4^{3-} = 1 : 4, (№ 3.8). Samples prepared with tartarate, tetraborate and EDTA - making waters have shown too low compressive strength.

CONCLUSIONS

The results up to now received for the concrete prepared by means of treated sea waters (acetate, phosphate and combined EDTA/PO_4^{3-} = 1 : 4 making waters) pretend to be very good. They afford the opportunity to satisfy the strongest demands of the standards preparing reinforced concretes without danger of reinforcement corrosion.

REFERENCES

1. Corrosion of Metals in Concrete, ACI Journal, 1985, Vol.82, №1.

2. Travaux, 1985, № 598, p.84.

3. Browne R. - Durability of Reinforced Concrete Structures, "New Zealand Concrete Construction", 1989, № 9.

4. Vinayaka M.R. - Durability of Concrete: Resistance to Chloride,

Sulphate and Acid Attak., "Ind.Concrete J.", 1986, Vol. 60, N° 11.

5. James M.Gaidis et al. - The Inhibition of Chloride-induced Corrosion in Reinforced Concrete by Calcium Nitrite, "Cement, Concrete and Aggregates", 1987, Vol. 9, N° 1.

6. Alekseev S.N. et al. - Inhibitori korozii stali v železobetonnih konstruktsijah, Moskva, 1985.

7. Andrade C. et al. - "Cement,Concrete and Aggregates", 1986, Vol. 8, N° 2.

NEW TECHNIQUE TO EXAMINE HOMOGENEITY OF PARTICLE DISPERSION IN SLAG / CEMENT BLEND AND ITS EFFECT ON CONCRETE DURABILITY

R I A Malek

Materials Research Laboratory, The Pennsylvania State University, USA

SUMMARY

The 21st Century Concrete Technology's major objective will be to produce economic durable concrete of low permeability and low or no environmental impact. The use of mineral admixtures is expected to be wider. The specification and quality assurance/ control will be modified to use testing techniques for examination of concrete to ensure their integrity and good performance. Rehabilitation and remaining service life may be assessed on existing concrete structures by periodic examination utilizing these testing techniques. A new testing technique for this purpose is presented. The technique examines the effectiveness of particle dispersion in slag or pozzolanas/cement blends in the paste portion of concrete and its relation to concrete performance. Several specimens from existing concrete structures in the U.S., England, Iceland, Germany, and Sweden were examined and the results accurately predict the performance of these concrete.

INTRODUCTION

The deterioration of concrete originates in its microstructure. Appreciable differences in reactivities of slag and cement particles have an adverse effect on the properties of concrete made of their blends with inadequate particle dispersion. A technique to examine the effectiveness of particle dispersion in slag or pozzolanas/cement blends in the paste portion of concrete and its relation to performance is discovered. In this technique freeze-dried polished slices of the concrete samples are subjected to the incident electron beam in a SEM. Use was made of the properties of the backscattered electron beam (BSE) to differentiate between slag particles and other particles in the matrix. An interactive computer-controlled electron beam, described in detail in this paper, is used to examine the polished concrete slices.

EXPERIMENTAL

Several concrete samples have been received from different constructions in the U.S., England, Iceland (2 samples), Germany, and Sweden. The concretes contain different proportions of blast furnace slag. Freeze-dried polished slices of the concrete samples are subjected to the incident electron beam in a SEM. The inverted mode of the backscattered electron imaging is used, in which, the darkness of a particular area or particle is inversely proportional to the average atomic weight of the constituent elements.

The homogeneity of particle dispersion in the slag or pozzolanas/cement blended paste of concrete is examined using a computer interactive scanning electron microscope provided with an image analysis utility. In this technique, the electron beam is allowed to sweep in successive lines. When the beam strikes particles with BSE intensities above a previously set threshold level, it stops and remains on the particle surface for four seconds. During that time, eight diameters are drawn across the particle's center and the characteristic x-ray signals, excited from the particle central region, are analyzed by the EDX unit. Memory stored coordinates will prevent analysis of the same particle twice. For the purpose of the present analysis, a minimum separation of two microns between two particles is required to analyze them as separate entities. The elemental count percentage, particle cross sectional area, average particle diameter and shape are determined by the computer software. The results of this analysis can be obtained either for individual particles or as an average certain group of particles with specific chemical composition.

RESULTS AND DISCUSSION

SEM-EDX Examination

An SEM/EDX examination of the aggregates in the six samples revealed the presence of various type aggregates in the samples. The coarse aggregates were Limestone and silicious gravel in the U.S. and English samples, respectively. Silicious sand was the fine aggregate present in both samples. The existence of potassium and aluminum together with silicon might indicate a feldspathic composition for some of the fine aggregate particles; alkali feldspar is detected in the x-ray diffraction. The analysis showed limestone as the major constituent of both the coarse and fine aggregates in the two concretes from Iceland The Swedish concrete, on the other hand, contains dalomitic limestone as a major constituent of coarse and fine aggregates. Of interest is the presence of large slag fragments as part of the coarse and fine aggregates (which is mainly composed of sandstone) in the German sample. The chemical composition of the slag particles in the U.S. and English samples is given in Table I. It is evident that the chemical composition is within the normal compositions of slag.

The quantitative EDX analysis of the samples from Iceland show the average oxide composition of both types of slag particles as presented in Table I. The low CaO content in these samples may suggest that these particles are actually natural pozzolanas and not a slag. This is confirmed by the existence of very large grains of similar chemical composition as the slag particles, exhibiting air bubbles in a large glassy matrix which may possibly indicate that some type of glassy volcanic rocks have been used as aggregates in these samples.

The German sample appears to exhibit a somewhat unique composition. It seems made mainly of slag as is evident from the dominance of bright particles in the backscattered image. The average chemical (oxide) composition of the matrix is presented in Table I. Additionally, some of the slag particles are too large to be considered as part of the cementitious matrix. The latter might have been added as a portion of the coarse aggregates (composition given in Table I).

The slag particles in the Swedish sample seem to exhibit apparent differences in their sizes, being larger in the outer portions and smaller in the inner. That this is an indication of a poor hydration at the outer portions is partially verified by the noticed spalling and poor aggregate-matrix bond near the outer portions of the sample. An average chemical composition of the slag particles in both locations is presented in Table I. The low SiO_2 content in these samples may suggest that it is not slag.

Table I. Quantitative EDX Analysis Showing the Average Chemical Composition of the Slag/Pozzolanas Particles in the Different Samples .

	Al_2O_3	CaO	MgO	K_2O	Na_2O	SiO_2	SO_3
U.S.A.	8.22	44.91	5.96	0.31		37.53	3.07
England	9.60	44.7	6.20	9.00		38.90	0.60
Iceland I	12.51	5.27	11.86	0.71	0.22	54.79	
Iceland II	14.67	14.145	6.31	0.05	2.22	33.03	3.82
Germany	15.81	41.47	5.63	0.43	0.12	36.36	
Sweden	23.78	38.5	18.97			10.21	0.65

Determination of the Effectiveness of Particle Dispersion

Tables II, III,and IV show the results of the analyses made on the concrete sepecimens. Three analyses on the U.S. specimen were made at three locations: top (2-3 mm from the top), middle (25 mm from the top), and bottom (100 mm from the top). The analyses on the english specimen were made at three locations: top, middle (70mm from the top) and a blue area (120mm from the top).

It appears from the data on the U.S. specimen that the average area of the cement particles do not change with depth whereas for slag it is higher in the top layer and lower in the middle and bottom layers. This may be a reflection of a variable hydration degree of slag particles that could be ascribed to variable wet and dry conditions at different depths of concrete. Of concern is the high standard deviation of both slag and cement particles in the top layer compared to the lower (approximately equal standard deviation in the middle and bottom layers). That this is an indication of an inhomogeneous dispersion of slag particles in the top layer is partially verified by the fact that the top layer may have been subjected to preferential segregation due to excess water for trowling.

The data obtained for the blue area in the english slag indicates the existence of a higher concentration of particles of similar composition to the slag particles. That this is an indication of a highly concentrated slag particles in the blue areas as a result of poor dispersion is under an ongoing investigation.

It appears that the two samples from Iceland contain about 40% of the cementitious mixture as pozzolanas. The sample Iceland II concrete seems to contain finer pozzolanas than sample Iceland I. The dispersion of pozzolanic particles in sample Iceland II seem a little better than in sample Iceland I.

TABLE II. SEM-DEX Chemical Classification Analysis of the U.S. Concrete. Summary of Statistical Data

a. General Analysis of All Classes

	TOP	MIDDLE	BOTTOM
Features	823	1085	685
Frames	15	17	13
Total Area Analyzed (Sq. Cm)	2.02×10^{-3}	2.14×10^{-3}	1.57×10^{-3}
% Feature Area per Frame	7.56	11.4	7.18
Sigma	3.84	10.6	4.16

b. Specific Analysis of the Chemical Macroclasses

	TOP		MIDDLE		BOTTOM	
	Slag	Cement	Slag	Cement	Slag	Cement
POP	72	256	96	457	39	297
POP%	8.8	31.1	8.9	42.1	5.7	43.4
Features/sq.cm ($\times 10^4$)	3.6	12.7	4.49	21.4	2.48	18.9
Average particle area	26.3	13.9	15.0	12.1	16.6	17.1
Average area per unit frame area ($\times 10^{-3}$)	12.6	24.0	7.6	25.9	4.9	27.8
Sigma	12.4	4.3	5.1	17.3	4.6	18.6

The concrete sample from Germany seems made mainly of slag. The slag particles seem fairly large in size (low Blaine slag). In addition, the sample seems to contain large pieces of slag that have been added as part of the coarse aggregate.

The concrete sample from Sweden seems to contain about 40% slag of normal fineness. The large average slag per unit frame area might be a reflection of poor hydration. The dispersion of slag particles, on the other hand, seems fairly good.

TABLE III. SEM-DEX Chemical Classification Analysis of the English Slag. Summary of Statistical Data.

a. General Analysis of All Classes

	TOP	MIDDLE	BLUE AREA
Features	818	1032	636
Frames	15	10	13
Total Area Analyzed (Sq. Cm)	1.82×10^{-3}	1.36×10^{-3}	1.46×10^{-3}
% Feature Area per Frame	8.8	13.8	9.36
Sigma	5.38	5.97	3.84

b. Specific Analysis of the Chemical Macroclasses

	TOP		MIDDLE		BLUE AREA	
	Slag	Cement	Slag	Cement	Slag	Cement
POP	45	350	78	484	34	315
POP%	5.5	42.8	7.6	46.9	5.4	49.5
Area%	5..0	47.7	5.4	49.9	4.8	48.6
Features/sq.cm ($\times 10^4$)	2.5	5.7	19.2	35.6	21.6	2.3
Average area per frame (sq. μm)	17.8	21.8	13.0	19.3	19.5	21.1
Sigma	25.4	28.0	19.9	53.6	39.5	48.5
Average area per frame area ($\times 10^{-3}$)	4.4	42.0	7.4	67.2	4.5	45.5
Sigma	5.2	44.6	5.5	22.6	4.5	37.5

Table IV. SEM-DEX chemical classification analysis of the Samples from Iceland, Germany, and Sweden. Summary of statistical data.

a. General Analysis of All Classes

	ICELAND I	ICELAND II
Features	1332	720
Frames	8	5
Total Area Analyzed (sq. cm)	1.25×10^{-3}	7.57×10^{-4}
% Feature Area per Frame	9.85	4.93
Sigma	2.14	2.2

Table IV. Ctd.

b. Specific Analysis of the Chemical Macroclasses.

	ICELAND I		ICELAND II	
	Cement	Slag	Cement	Slag
POP	642	372	340	137
POP %	48.2	27.9	47.2	19.0
Features/sq. cm ($x10^4$)	51.6	30.0	45.0	18.0
Average particle area (sq.μm)	9.8	8.9	4.9	5.1
Average area per unit frame area ($x10^{-3}$)	53.4	26.7	20.9	8.8
Sigma	17.5	6.7	11.6	5.8

a. General Analysis of All Classes

	GERMANY	SWEDEN
Features	1512	995
Frames	8	8
Total Area Analyzed (sq. cm)	1.8×10^{-3}	1.21×10^{-4}
% Feature Area per Frame	17.3	9.9
Sigma	4.4	4.2

b. Specific Analysis of the Chemical Macroclasses.

	GERMANY		SWEDEN	
	Cement	Slag	Cement	Slag
POP	53	1015	291	119
POP %	3.5	67.1	29.3	12.0
Features/sq. cm ($x10^4$)	2.9	55.0	24.0	9.8
Average particle area (sq.μm)	21.9	23.6	7.9	11.1
Average area per unit frame area ($x10^{-3}$)	6.8	137.2	20.2	16.0
Sigma	4.5	43.6	7.5	7.8

CONCLUSIONS

A new technique to examine the homogeneity of particle dispersion in slag or pozzolanas/cement blends in the paste portion of concrete is discovered. The technique is useful in predicting the deterioration of concrete resulting from inadequate particle dispersion. The technique represents a powerful tool in quality assurance/control and inspection of concrete structures.

ACKNOWLEDGMENT

Partial financial support of the American Concrete Institute is appreciated

AUTHORS INDEX
(VOLUME V)

A

Abduljauwad, S N — 438
Alhozaimy, A — 196
Achampong, F — 289
Adylov, D K — 416
Ahluwalia, S C — 602, 614
Aitcin, P-C — 21
Akhmedov, B B — 658
Ali, M M — 602
Andreyeva, A B — 74

B

Baalbaki, M — 21, 89
Baghabra Al-Amoudi, O S — 438
Bajza, A — 402
Banthia, N — 492
Battagin, A F — 46
Bhanumathidas, N — 585
Bhargava, R — 614
Blanco, M T — 329, 505
Bollmann, K — 348
Breitenbucher, R — 122
Bucea, L — 309

C

Campitelli, V C — 84, 226
Cangiano, S — 213
Cao, H T — 309
Carolyn M Dry — 276
Cavailles, R — 115
Chen Fuyin — 571
Chen Gaixin — 557
Chumak, M V — 544
Cincotto, M A — 452
Collepardi, M — 389
Costa, U — 107

D

Damidot, D — 316
Daraktchiev, B D — 342, 661
Degteriova, L I — 635
Demura, K — 512, 641
Deng Junan — 621
Detriche, Ph. — 191
Diaz, G — 468
Distler, P — 431
Djanikian, J G — 53
Dyczek, J R L — 485
Dymsky, V M — 653

E

Ebensperger, L — 578
Endo, T — 512, 641
Ezirim, H — 39

F

Facoetti, M — 107
Fedner, L A — 9
Feng Naiqian — 589
Florindo, M C — 226
Frigione, G — 60
Fuhr, C — 26, 32
Funato, M — 363

G

Garcia, S — 329
Gebauer, J — 67
Gerdes, A — 409
Gimenez, S — 329
Glasser, F P — 316, 370
Glukhovskiy, V V — 474, 479
Gomes Jr, D — 53
Gomez, E — 78
Gorchakov, G I — 74
Grandet, J — 191
Gudmundsson, G — 167
Gupta, P C — 302
Gusev, B V — 658

H

Han Lilin — 571
Handoo, S K — 602
Hilsdorf, H K — 431
Honda, M — 14
Huang, S-Y — 233,283
Hudec, P P — 289

I

Ikabata, T — 14
Ikeda, K — 596

J

Jackson, P J — 157
Jain, K B — 302
Jain, N K — 445, 602
Ji Xihuang — 589
Jiang Yunan — 564
Jiang, S P — 191
John, V M — 452
Johnstone, J R — 370

K

Kalidas, N —585

Kalyan Dass — 302
Kamala Gopinathan — 538
Kasai, J — 322
Kelham, S — 3
Kihara, Y — 174
Kittl, P — 468
Knöfel, D — 26, 32
Koblischek P J — 531
Kobystcha, T N — 653
Kolomiets Val. I — 420
Kolomiets Vas. I — 420
Korableva, G A — 653
Kropp, J — 431
Kuznetsova, L A — 653

L

Lavrega, L Y — 517
Lawton, J M — 157
Legrand, C — 95
Lekarev, V M — 256, 262
Levy, C — 115
Lou Zongham — 129
Li Shaozheng — 184
Lomic, G — 383
Lu Yonghua — 184
Ludwig, H-M — 269
Lutin, A E — 658

M

Ma Kueihong — 564
MacInnis, C — 289
Macias, A — 505
Macphee, D E — 309
Maiti, S C — 445
Malek, R I A — 143, 247, 427, 499, 668
Marchese, B — 461
Marchese, G — 461
Martinez, V — 468
Martins, J M — 53
Maslehuddin, M — 438
Massazza, F — 107
Matsusato, H - 303
Matthews, J D — 355
McCarter, W J — 39
Mikhailishina, N Z — 474
Milrud, A G — 181, 210, 253, 658
Moir, G K — 3
Mokritsky, K I — 635
Möller, J S — 167
Monosi, S — 389
Müllar, A — 26

N

Nagaraj, T S — 150, 550
Narang, K C — 614
Neto, C S — 84
Nilsson, L-O — 100

O

Ogawa, K — 512, 641
Ohama, Y — 512, 641
Oreshkin, A B — 647
Ostrowski, C — 335

P

Palomo, A — 329, 505
Pantofchieva, L V — 661
Pavlenko, S I — 647
Petri, M A — 485
Piasta, W G — 136
Pigeon, M — 492
Popov, B I — 420
Popova, O S — 544
Prasad, B K R — 150
Puertas, F — 329, 505

R

Radenkova-Yaneva, M — 608
Rao, B K — 550
Rao, D V R — 538
Rao, P V — 585
Rasheeduzzafar — 438
Raupach, M — 296
Rehsi, S S — 302
Rojas, A — 78
Rollet, M — 115

S

Salama, M N — 499
Sarkar, S L — 89
Sato, T — 363
Sato, Y — 641
Scandiuzzi, L — 46, 174
Schießl, P — 296
Schlußler, K H — 220
Serbin, V P — 474, 479
Serbina, R V — 479
Seyfarth, K — 348
Sharma, K M — 614
Shashiprakash, S G — 150
Sheng, J — 492
Shestoperov, V S — 9
Sirajiddinov, N A — 416
Sirivivatnanon, V — 309
Skenderovic, B — 372, 383, 525
Soroushian, P — 196
Springenschmid, R — 122, 578
Stark, J — 269, 348
Su Muzhen — 184, 621
Sulkowsky, I A — 181, 210, 253, 658
Sundara Raja Iyendar, K T — 550
Suzuki, S — 322

T

Tachibana, K — 641
Tagnit-Hamou, A — 21
Tang Luping — 100
Tango, C E S — 203, 226
Tashiro, C — 596

Tezuka, Y — 53
Tilak Raj — 302
Tognon, G — 213
Torrent, R — 67
Tsuyuki, N — 322

U

Ugincius, D A — 635
Urrutia, C S — 78
Usmanov, Kh. L — 416

V

Van Balen, K — 239
Van Gemert, D — 239
Vasiliev, J E — 9
Vazquez, T — 329
Vyrodov, I P — 256, 262

W

Wang Xinyou — 557
Wang Yanmou — 184, 621
Wang Yanshen — 564
Wang Yuqing — 129
Wirquin, E — 95
Wittmann, F H — 409
Wu Keru — 557
Wu Wanchun — 571
Wu X-L — 233, 282

X

Xu Bin — 628
Xu, L P — 233

Y

Yanev, I — 608
Yang Q B — 233, 282
Yokota, N — 14
You Baokun — 571
Yu Faming — 571

Z

Zampieri, V A — 174
Zenone, F — 60
Zhang Gueiqing — 564
Zhang Liang — 621
Zivica, V — 396

9th International Congress on the Chemistry of Cement New Delhi, India, 1992

VOLUME VI

REPORTS ON SPECIAL PANEL DISCUSSIONS
AND POSTER PAPERS

NATIONAL COUNCIL FOR CEMENT AND BUILDING MATERIALS
NEW DELHI

9th International Congress on the Chemistry of Cement New Delhi, India, 1992

REPORTS ON SPECIAL PANEL DISCUSSIONS AND POSTER PAPERS

Volume VI

Organised by

NATIONAL COUNCIL FOR CEMENT AND BUILDING MATERIALS
NEW DELHI

Co-sponsored by :

Department of Scientific & Industrial Research
Ministry of Science & Technology
Govt. of India

Cement Manufacturers' Association, India

The India Cements Ltd

J K Cement Works

Madras Cements Ltd

Narmada Cement Co Ltd

Orissa Cement Ltd

This volume is a part of six-volume series of the Congress Papers.
Title of each volume is given below :

I—Congress Reports
II—Communication Papers–Theme I
III—Communication Papers–Theme II
IV—Communication Papers–Theme III
V—Communication Papers–Theme IV
VI—Reports on Special Panel Discussions and Poster Papers

Published by :
National Council for Cement and Building Materials (NCB)
M-10 South Extension Part II New Delhi 110 049 INDIA

No Part of this publication be reproduced without the written permission of the Publishers.

The views expressed in the technical papers printed in this publication are those of authors and not necessarily of the Publishers.

Printed in India by Tara Art Press, New Delhi

PREFACE

Commencing with a one-day meeting in London on 14 January 1918 arranged by the Faraday Society, to discuss "The setting of cements and plasters", which is taken as the first Symposium to deal solely with the chemistry of cement, the subsequent International Symposia and Congresses on the Chemistry of Cement have been held in Stockholm (1938), London (1952), Washington DC (1960), Tokyo (1968), Moscow (1974), Paris (1980) and Rio de Jenairo (1986). At the conclusion of the Rio Congress, it was decided that the next Congress will be held in India. Accordingly, the 9th International Congress on the Chemistry of Cement is being held in New Delhi, India, from 23 to 28 November 1992.

The preparatory and organisational work for this 9th Congress was commenced immediately after the 8th Congress. To start with, all the participants in the previous two Congresses and a large number of individuals and organisations interested in the subject of the Congress were contacted through an extensively worked out and widely distributed Questionnaire. The response was most encouraging. The responses were carefully analysed and the directions which would meet the views of the largest number of participants towards advancing the cement sciences were determined. Based on these findings the first Bulletin was issued in August 1988, providing the necessary preliminary information on the Congress and outlining its scope and essential organisational aspects.

The objectives of the Congress were set to advance the knowledge of chemistry of cements with emphasis on application of this knowledge in both the manufacturing aspects and utilization of cements in practice. Within this broad scope, the thrust was on tracking the scientific progress made in the field since the last Congress, assessing the status of exploitation of the results by the industry and the society, and mapping of the new frontiers of knowledge.

The overall organisation of the Congress was governed by a National Organising Committee which was responsible for all organisational aspects including financial arrangements. Taking into account the suggestions received from various quarters, the International Scientific Committee consisting of 67 experts from 39 countries all over the world was formed which was responsible to finalise : (a) the themes and sub-themes of the Congress, (b) procedures for inviting, receiving and reviewing of papers, (c) selection of authors for general and special reports, and (d) the system for conduct of the proceedings of the sessions and other related scientific and technical matters.

The International Scientific Committee held two meetings in New Delhi in November 1989 and in January 1991. In addition, informal meetings were held with representative groups in Seoul, Tokyo, Paris, Washington DC and Montreal. The International Scientific Committee finalised the Generic and Specific Themes of the Congress. It was decided that for each Generic Theme, there shall be one Principal Review Paper, which shall cover the progress achieved in the area of the Generic Theme between the two Congresses. For each Specific Theme, there shall be one Congress Paper highlighting trends of research and realisation of the results in the industry in the areas related to the Specific Theme. Under each Specific Theme, in addition to the invited Congress Papers, there shall also be Communication Papers. Both the principal review papers as well as the Congress papers were to be presented by the invited experts identified after deliberations of the International Scientific Committee.

Preliminary Abstracts of communication papers were solicited through the Second Bulletin in May 1991. 537 Abstracts were received which were scrutinised by a panel of Indian experts and 513 were short-listed. Authors were requested to send full manuscripts of the paper for detailed review and acceptance for publication and presentation. As many as 412 communication papers from 40 countries were received which were reviewed by a panel of international experts. As a result, 346 communication papers belonging to the four themes of the Congress were finally

accepted for presentation and publication. These were in addition to 21 State-of-the-Art Congress Reports received from invited authors; reports on two Specific themes could not be had because the authors selected expressed their inability at a late stage, making replacement difficult.

In addition to the papers on deliberative thematic sessions, a poster session is being organised on "Advances in Physico-Chemical Evaluation, Characterisation and Quality Control Techniques and Systems" for Clinkers, Particulate Cements, Hydrated Systems and Concrete Systems. The State-of-the-Art Report would be presented by an invited expert and 24 contributions made in the form of posters will be presented during the Congress. In addition, Special Panel Discussions are being organised to survey the newer frontiers of knowledge in the areas of computerisation in cement science and concrete systems; resource economy in cement and concrete making; and cement in hazardous waste management.

The proceedings in six Volumes contain all the above contributions received for the Congress. This **Volume VI** contains the invited **Reports on Special Panel Discussions and the Poster Papers.**

A novel feature of the 9th Congress will be that, in addition to the normal sessions as in the earlier Congresses, there will be three sessions to bring out the technological and techno-ecnomic impact of the scientific advances on the industry. These are intended to provide a better appreciation of the implications of the scientific advances specially on the process control machinery and related industries as well as on operational aspects related especially to energy conservation and environmental improvement. Texts of these Special Lectures will be published in Volume VII of the Proceedings to be brought out after the Congress, along with the texts of Addresses at the Inaugural and Concluding Sessions and List of nearly 550 delegates from 42 countries who are expected to attend the Congress.

I am grateful to the members of the International Scientific Committee for their whole-hearted co-operation, to those who reviewed the Abstracts, and to the International Panel of Reviewers of Manuscripts for providing very useful technical and editorial comments on the communication papers. The co-operation of the authors in accepting and implementing the reviewers' suggestions and revising their manuscripts accordingly is greatly appreciated. Thanks are also due to those authors whose communication papers could not be accepted essentially because the contributions did not fit in with the themes of the Congress and not because of any technical deficiency. We recommend that the authors have those papers published elsewhere.

The unstinted efforts put in by my colleagues in the National Council for Cement and Building Materials in all aspects of organising this Congress, is thankfully acknowledged.

A K Mullick
Chairman
International Scientific Committee
9th International Congress
on the Chemistry of Cement

New Delhi
14 September 1992

CONTENTS

Volume VI

SPECIAL PANEL DISCUSSION I : Computerisation in Cement Science and Concrete Systems

1. Computer-Based Models of the Microstructure and Properties of Cement-Based Materials 3
   E J Garboczi and D P Bentz

2. Computer Modelling of Microstructure of Cement-Based Materials 16
   R T Coverdale and H M Jennings

3. Numerical Simulation of Hydration and Structural Development of Cement-Based Materials 22
   K van Breugel

4. Time-Dependent Temperature Distribution in an Heterogeneous Material 28
   H Sadouki and F Wittmann

SPECIAL PANEL DISCUSSION II : Resource Economy in Cement and Concrete Making

5. Resource Economy in the Production of Cement 39
   R Bastier, J Cantacuzene and J P Schaer

6. Integral Lamination : An Energy-Saving Factor 46
   Ph Martin

7. The Use of Pozzolanic Materials as an Additive to Clinker : Experience of a Moroccan Cement Plant 66
   Y Ennadifi

8. Resource Economy in Concrete Making 73
   F Howthorn and P Jaugey

SPECIAL PANEL DISCUSSION III : Cement in Hazardous Waste Management

9. The Use of Waste Fuels in the Cement Industry 77
   Ferenc D Tamás

10. Cementitious Materials in Nuclear Waste Management 88
    Della M Roy

11. Application of Cements to the Treatment and Conditioning of Toxic Wastes 114
    F P Glasser

12. Hazardous Waste (Organic, Heavy Metal) : Cement Disposal 119
    Michael W Grutzeck

13. Storage Systems for Hazardous Waste : Evolution and State-of-the-Art 126
K van Breugel

14. Cement in Waste Management : Use of Non-conventional Materials in the Cement Industry 132
J Beretka

POSTER PAPERS

15 Contribution of ^{29}Si High-Resolution NMR to the Study of Concrete Alkali-Aggregates Reaction 141
L Fernandez, H Zanni-Théveneau, R Couty, P Barret and D Bertrandie

16. Progress in the ^{27}AL MAS NMR Spectroscopy : Monitoring the Hydration of Calcium Aluminate Cements 148
D Müller, A Rettel, W Gessner, J P Bayoux and A Capmas

17. Development of Instrumentation and Techniques to Study Cement Suspensions at High Temperatures and Pressures (Up to CA. 200°C) 155
G V M Teodoru, H Hartmann and P Jackmuth

18. On Line Bulk Analysis of Raw Material in Cement Plant by Neutron Irradiation and Capture Gamma Ray 162
J P Baron, J Alexandre, L Debray and X Dupont-Wavrin

19. X-Ray Diffractometry in Prediction of Cement Strength 168
G Goswami and J D Panda

20. Influence of Various Cement Types on Concrete Durability in Marine Environment 175
Shigemi Sakoda, Nobufumi Takeda and Shigeyuki Sogo

21. An Approach to the Prediction of Portland Clinker Grindability and Strength by Microscopy 182
Yushiro Kihara, Sergio L Centurione and Flavio Andre da Cunha Munhoz

22. Evaluation of Cement Clinker for Estimation of Compressive Strength by Optical Microscopy 189
L H Rao, P K Akhouri and S K Sinha

23. Mössbauer Spectroscopy Used for Determining Composition of Calcium Aluminoferrites in Portland Clinker 194
V K Klassen, I I Miroshnichenko, S F Mindolin and V I Belyaeva

24. Carboxylic Acid Anions : The Reaction Mechanisms and Products with the Aluminate Phase of Cement 198
Herbert Poellmann

25. Additions Method in Analysis of Cement Materials by Ion-Selective Electrode Potentiometry 205
I K Gromozova

26. Methods of Performing Adiabatic and Isothermal Calorimetry 210
R I A Malek

27. Dielectric Study of the Hydration Process in Portland Cement 216
A Anagnostopoulou-Konsta and D Daoukaki-Diamanti

28. Portland Composite Cements with Regulated Alkali-Buffer Behaviour 223
Roland Herr, Wolfgang Wieker and Cornelia Hübert

29. The Hydration of Pozzolanic Cement on the Base of Fired Clay Bricks 233
Jonjaua Ranogajec and Ljiljana Fišang

30. Study of Pozzolanic Activity in Opaline Rocks Using Particle Size Variations 240
M Frias, M I Sanchez De Rojas, M P Luxan and N Garcia

31. Water Sorption and Weight Change on Heating of a Portland Cement Depending on Pretreatment 247
E T Stepkowska, J M Bijen, J L Perez-Rodriguez and A Justo

32. Alkali Aggregate Reaction : Proposals for a Kinetic Test on Aggregates 254
D Sorrentino, J Y Clément and S Sabio

33. Self-Desiccation in Concrete 261
Kristina Norling-Mjörnell

34. Mechanical Behaviour of Advanced Cementitious Materials 268
W Jiang and D M Roy

35. Development of Remote Sensing Technique for Prediction of Limestone Quality 275
M Imran, D K Panda and G V K Prasad

36. The Hydration Chemistry of some Blended Cements 281
Hans S Pietersen and Jan M Bijen

EXPLANATORY NOTES

The following symbols, which have been universally recognised by cement chemists for formulating more complex compounds, are used interchangeably with the respective oxide formulae throughout this volume :

A	:	Al_2O_3	K	:	K_2O
C	:	CaO	M	:	MgO
$\bar{C}$	:	CO_2	N	:	Na_2O
CH	:	$Ca(OH)_2$	P	:	P_2O_5
F	:	Fe_2O_3	S	:	SiO_2
H	:	H_2O	$\bar{S}$	:	SO_3

Commonly used abbreviations of more general nature are as follows :

DTA	—	differential thermal analysis
EPMA	—	electron probe micro analysis
IR	—	infrared
NMR	—	nuclear magnetic resonance
RH	—	relative humidity
w/c	—	water-cement ratio
XRD	—	X-ray diffraction
SEM	—	scanning electron microscope
EDAX	—	energy dispersive analysis of X-rays

Special Panel Discussion I

Computerisation in Cement Science and Concrete Systems

COMPUTER-BASED MODELS OF THE MICROSTRUCTURE AND PROPERTIES OF CEMENT-BASED MATERIALS

E J Garboczi and D P Bentz

National Institute of Standards and Technology
USA

Abstract

As computers, with larger memories and faster computational speeds, have become more available to scientists and engineers, new uses have been found that are systematically transforming many areas of science and engineering. The field of cement-based materials is no exception. The use of computer-based models has, in the past 5-6 years, made possible for the first time semi-quantitative theoretical understanding of some aspects of microstructure and properties of cement-based materials. This paper focuses on this specific area. We summarize the nature of, and results from, available computer-based models, classify them using the concept of a fundamental model, and discuss each model's intended users and computer requirements.

I. INTRODUCTION

There is no denying that the availability of computers is quickly transforming the fields of industry, government, science, and engineering. Old, recurring problems become more easily solvable, repetitive tasks are done much more quickly and automatically, and problems can now be tackled that never could before. This has also been happening in the world of concrete, in manufacturing and in research. This panel, entitled "Advancing frontiers of computerization in cement science and concrete systems," was designed to survey some of the ways that computers are affecting the world of cement. Since we cannot cover everything in a few short papers and a 90 minute discussion period, we have chosen to focus on the area of models of microstructure and properties of cement-based materials, for two reasons: 1) its high scientific and technological importance, and 2) because progress in this area is only possible at all with the use of computers, so it serves as a sensitive barometer of the influence of computers. Three other areas to which computer-based models of microstructure and properties have strong ties are expert systems, data bases, and computer networks. These important relationships have been reviewed recently [1].

This paper is divided into two parts. We first survey available computer models of microstructure and properties of cement-based materials, classify them, and try to indicate how various computer development trends affect their use. Specific results from most of these models will be covered in the papers of the other panel members, who are primarily the developers of these models. Secondly, we present a survey of results from digital-image-based models, which have been our contribution to this field.

II. MODEL SURVEY AND CLASSIFICATION

One definition of the term 'computer-based model of microstructure and properties' is: "A theoretical construct, which is made using valid scientific principles expressed in mathematical language, that can be used to make quantitative predictions about a material's structure and/or properties" [2]. A model is a mathematical representation of a physical system, usually with some simplifying assumptions. A traditional mathematical model uses deterministic equations to represent the physical system. A computer-based model

represents the physical system of interest numerically, by storing the relevant numbers in memory. To qualify as a model of microstructure, a computer-based model must make some attempt to numerically represent the amount and spatial distribution of the different phases of the material being studied. To further qualify as a model of properties, the computer-based model must have the power to predict, directly from the numerical representation of microstructure, properties that can be checked directly against experimental measurements. Recent reviews have appeared that discuss these concepts at greater length [2,3].

A classification of computer-based models can be made based on the idea of a "fundamental model" of a material. A fundamental model is defined [2] as a model that deals directly with the microstructural elements that determine the properties of interest. For example, a fundamental model for the microstructure and properties of vapor-deposited crystalline diamond films must deal with microstructure at the atomic level, which is the level where the properties are determined. On the other hand, in order for a model of cement paste to be considered fundamental, it need not be at the atomic level, but rather must deal with individual cement particles and their hydration products, and how the microstructure is built up from these constituents. Furthermore, a model for the mechanical properties of concrete could be considered fundamental if individual aggregates and interfacial zones were dealt with, while at the same time considering the cement paste to be a continuum with known properties. Also, upon further thought since the review of Ref. 2 was written, we now extend the definition of a fundamental model to include the requirement that properties must be able to be exactly calculated from the numerical representation of the microstructure, such that if the model microstructure were an exact replication of the real microstructure, the predicted property would give the exact experimentally measured value, allowing of course for experimental error and the limits of numerical precision. We can now classify a variety of models, according to the concept of a fundamental model defined above. It is important to keep in mind that calling a model fundamental as opposed to non-fundamental is not a value judgement, but simply a classification. All the following models are computer-based models of microstructure and properties, but not all are fundamental.

We begin with a model developed by L.J. Parrott [4] that links hydration reactions, reaction product formation, and engineering properties. This model is not a fundamental model, since there is no direct representation of microstructure at the cement particle level, and properties are not exactly calculated from a numerical representation of microstructure. Microstructure is dealt with at the level of average phase volumes, which are functions of time and variables like moisture history, cement fineness, etc. [4]. Properties are predicted, mainly as a function of porosity, using empirical relations that summarize experimental knowledge, not by direct calculation. The greatest utility of this model is that it forms a convenient summary of known experimental results, and relates these carefully and systematically to important variables like degree of hydration and total porosity. There are clear similarities with expert systems as defined in Ref. 1, so that this model can in some sense be considered to be an expert system. It is operated on a personal or microcomputer (PC), and does not have large memory or computational speed requirements. Emerging computer technology will probably affect the use of this model mainly through making PC's cheaper, more available, and more portable, so that the information obtainable by this model is also more available. It is capable of systematic refinement as more experimental information becomes available.

A model similar in some ways to Parrott's model, which, however, takes microstructure into account at a somewhat deeper level, is that recently developed by van Breugel [5,6]. In this model, the growth of a single cement particle is treated in detail, while interaction with other hydrating particles is treated statistically. The particle size distribution of the original cement particles is used as input. The model has reaction kinetics built into it, with parameters that are fit to experiment. This model was designed, like Parrott's model, to be of use to practicing engineers, and so both models are designed to run on present generation PC's. This choice of computer capability to some extent determines the scope of the model, for example in the choice to represent hydrating cement particle interactions statistically, rather than as many

individual particles [6]. Van Breugel's model is not a fundamental model, because it does not take into account directly the formation of microstructure and the spatial arrangement of reaction products, and calculations are not made exactly from a numerical representation of microstructure. Calculations of properties other than those referenced [5] will have to depend on empirical relations fitted to experimental results, as in Parrott's model. Good agreement with experimental results, using fitted parameters, has been obtained for degree of hydration vs. time for various water:cement ratio pastes. Further details are available in van Breugel's paper in this proceedings [6]. New advances in PC availability and power will enable more sophisticated treatments of microstructure to eventually be built in, and new properties to be computed. Finally, it should be noted that this model is in a fairly early stage of development.

The next model, which is classified as a fundamental model, is by Wittman and co-workers [7,8]. This is a model of concrete in which cement paste is treated as a continuum with known properties but individual aggregate shapes and sizes are treated directly. A picture was generated of a two dimensional slice through a concrete sample, which was then gridded with a finite element grid. Exact (within numerical precision) calculations were then made of thermal conductivity, diffusion coefficients, and elastic moduli. This model qualifies as a fundamental model of concrete, although it still has simplifying assumptions such as perfect bonding between aggregate and cement paste matrix, and it is two dimensional. This was the first fundamental computer-based model of microstructure and properties to appear in the literature. Further advances in computer speed and memory will be of help to this model, since a three dimensional version would require many more finite elements to be used, implying much longer computational times for the gridding process and for the solution process, and potentially large memory requirements for the many finite elements needed. This model is not designed to be used by the practicing engineer, but is rather a research tool, designed to explore directly the relationships between properties and concrete composite structure at the aggregate level. Extensions of this modelling approach are to be found in the paper by Wittmann in these proceedings [9].

The first fundamental model for cement paste microstructure to be developed was that due to Jennings and Johnson [3,10]. This model attempts to simulate directly the development of the microstructure of hydrated C_3S paste by starting with a numerical representation of the initial cement particle/water mixture, and then operating cyclically on this stored information with an algorithm for consuming cement and generating hydration products. Cement particles are modelled by spheres whose diameters are taken from measured cement particle size distributions. This model directly represents cement paste microstructure, but direct, exact (within numerical error) calculations of various cement paste properties have not yet been carried out. These calculations would entail using either finite element or finite difference techniques to discretize the model, and enable the appropriate equations to be solved. The memory requirements for this model are not great, as individual particles are stored as spheres, meaning that only four numbers--the three Cartesian coordinates of the center and the radius--must be stored for each particle. The computational requirements for generating the microstructure are not great either, and the model has been adapted to run on a PC, although run times are significantly more than a few minutes, but, in order to carry out finite difference calculations of properties, large memory and high speed computers would be necessary.

III. DESCRIPTION OF DIGITAL-IMAGE-BASED COMPUTER MODEL

In this section, we review what has been accomplished with our digital-image-based microstructure and properties model. This model is a fundamental model, since it provides a cement particle level numerical description of microstructure, and allows for exact calculations of various physical properties. A review of our earlier work has recently appeared [2].

To set the model discussion in the proper context, it is first necessary to discuss briefly the impact of computers on the image analysis of cement-based materials. Storage of images requires large amounts of memory (e.g., 512 x 512 pixels x 256 gray levels = 0.25 MByte). Over the last 5 or 10 years, major

advances in image analysis have been made possible due to the availability of much larger memory capacities and faster processors on computer systems.

Image analysis is concerned primarily with quantifying images. In dealing with the data produced it is critical to consider the limits to accuracy imposed by the randomness inherent in the structure and the limitations on the area that can be analyzed. Any measure is only an estimate of the value for the whole sample. Such estimates will always contain random variance and the size of this can be approximated by statistical means (e.g. standard error). Great care must be taken to avoid systematic errors or bias, by correctly selecting sections and areas to be analyzed, particularly if the cement paste or concrete is anisotropic. For example, to measure microstructural gradients around aggregate particles within acceptable levels of error it has been found necessary to average measurements over some 50 images [11].

The power of scanning electron microscopy (SEM) to image directly, and the power of computers to then quantify, microstructure is undisputed. The digital-image-based microstructure model we describe next was based explicitly on digital image techniques in order to exploit this quantitative imaging power [12]. Visualization capability is an important consideration for computer simulation models in general, and microstructure development models in particular. By implementing the digital-image-based model on a graphics workstation, the researcher is able to watch a model microstructure evolve. In addition to allowing for rapid debugging of model algorithms and code, visualization also provides the researcher with added insight into the underlying processes of the model and the dynamic effects of changing model parameters.

The digital-image-based model has been described in detail elsewhere [13,14]. For the model, two-dimensional area or three-dimensional volume is represented by a set of pixels each identified as a particular phase of concrete. Standard cement chemistry notation is used (C $\equiv$ CaO, S $\equiv$ SiO_2, and H $\equiv$ H_2O). Relevant phases are cement (which is assumed to be pure C_3S), calcium hydroxide (CH), calcium silicate hydrate (CSH), porosity, aggregate, and mineral admixtures. Thus, a cement particle is represented as a collection of contiguous pixels assigned a phase of C_3S. In this manner, real cement particle shapes may be utilized as well as circles and spheres in generating simulated cement microstructures. Figure 1 shows an image of real cement particles (obtained using SEM and image analysis) placed randomly around a simple square aggregate and the same system after 77% simulated hydration. In the latter image, the cement particles are bright white, CH is light grey, CSH is dark grey, and pore space is black.

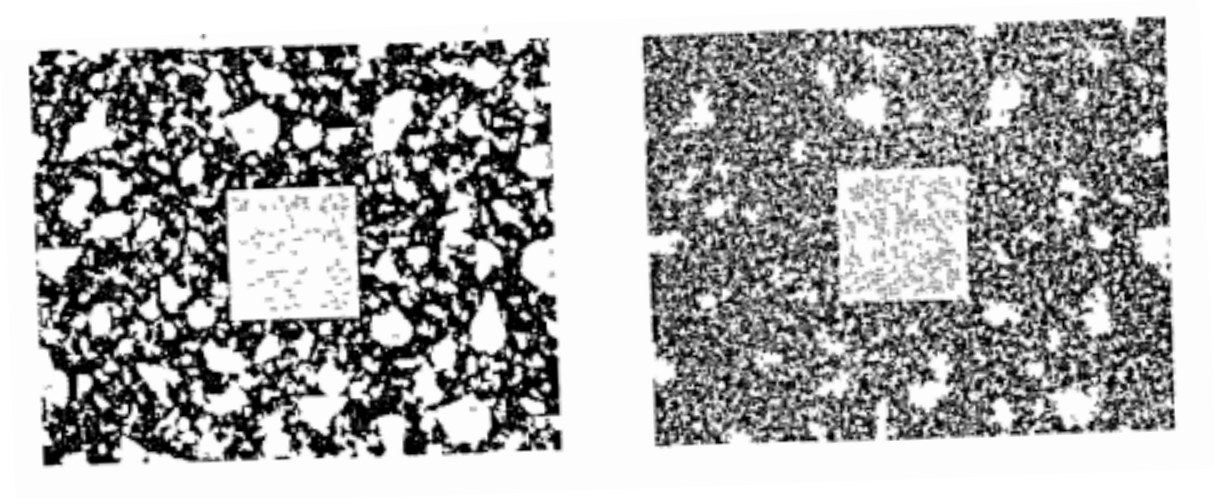

Fig. 1. Cement particles placed around aggregate (w/c=0.47) a) before and b) after 77% hydration.

Hydration is simulated by operating on all the pixels present in the cement paste volume or area. The two reactions considered in this study are the hydration of C_3S to form CH and CSH and the pozzolanic reaction between CH and silica (found in silica fume or fly ash) to form secondary or pozzolanic CSH. The assumed reaction stoichiometry is [15]:

$$C_3S + 5.3H \rightarrow C_{1.7}SH_{4.0} + 1.3CH$$
$$S + 1.7CH + 2.3H \rightarrow C_{1.7}SH_{4.0}$$

In terms of volumes, each unit of reacted C_3S produces 1.7 units of CSH and 0.61 units of CH. For the pozzolanic reaction, each unit volume of silica is capable of reacting with 2.08 units of CH to produce 4.6 units of pozzolanic CSH.

Hydration is executed in discrete cycles consisting steps which we term dissolution, diffusion, and reaction. During dissolution, all C_3S pixels in contact with water-filled porosity are given a chance to dissolve and produce diffusing CH and CSH species. The dissolution probability is based on the area of C_3S surface in contact with water. During diffusion, the CSH and CH diffusing species execute random walks within the available pore volume (area) until reaction occurs. CSH forms on the surfaces of the original cement particles or on previously deposited solid CSH. CH forms crystals by a nucleation and growth mechanism within the available pore space. Additionally, when silica is present, the CH diffusing species react at silica surfaces to form pozzolanic CSH. When all diffusing species generated from one dissolution step have reacted, a cycle is complete and a new dissolution step is begun. By monitoring how much of the cement is left after any given number of hydration cycles, the degree of hydration, α, of the system can be determined.

Especially for 3-D studies, the digital-image-based model is dependent on having large memory, high speed computers available. A typical complete study, which uses a 100^3 pixel unit cell, requires about 50 MBytes of memory and 60 hours of central processor time on the NIST Cray-YMP supercomputer. A 3-D version of this model, called HYDRA3D, is available to researchers along with documentation [16] through the Cementitious Materials Modeling Laboratory at the National Institute of Standards and Technology. In work with this model to date, the two main thrusts have been to simulate interfacial zone microstructure and to compute cement paste transport properties. Results from these studies will be reviewed next.

IV. SIMULATION OF INTERFACIAL ZONE MICROSTRUCTURE

As a composite material, a concrete's performance must be expected to depend on the properties of the interfaces between its two major components: aggregate and cement paste. The dependence of mechanical properties on interfacial microstructure has been reviewed by Bentur [17] but durability will also be influenced strongly by interfacial zone microstructure and its effect on transport properties. Indeed, increases in electrical conductivity due to interfacial zones have been observed by Ping et al. [18], while Costa et al. [19] have observed similar effects on permeability, both using simplified specimen geometries.

Over the years, the general microstructural features of interfacial zones in ordinary portland cement concrete have been explored by a number of researchers [20,21]. The general consensus reached is that the interfacial zone consists of a region, up to 50 μm wide around each aggregate, containing less cement and more porosity and larger pores than the bulk cement paste, and often containing large crystals of calcium hydroxide. Due to these features, the interfacial zone is often considered to be the weak link in a concrete composite with respect to mechanical performance and durability.

To simulate an interfacial zone in concrete using the digital-image-based model, a single non-reactive, zero porosity aggregate is first placed in the hydration volume (area) and then the cement particles are

placed at random locations such that no particles overlap. Absorptive aggregates and cement clinker aggregates have also been simulated [22].

Causes of interfacial zone microstructure

The application of the microstructural model to simulating interfacial zones has been described by Garboczi and Bentz [23]. The results obtained from a simulation similar to the system in Fig. 1 but with circular cement particles, indicated that the interfacial zone region should contain less cement and CSH, and more porosity and CH than the bulk paste, in accord with what has been observed in real concretes. Although particle packing effects obviously contributed to these characteristic features of the interfacial zones, a secondary one-sided growth mechanism also plays a role. Here, in the interfacial zone, available pore space is being filled with hydration products growing from one direction only, unlike the bulk paste where products are growing inward from all directions. Using simulation, it was possible to separate these two effects. By first placing the cement particles in the system and then overlaying the aggregate, it was possible to remove any effects of the initial particle packing (i.e. the wall effect) and study only the one-sided growth effect. This system could then be contrasted against one in which the aggregate is placed first followed by the cement particles, where both the wall and one-sided growth mechanisms would be present.

Results are shown in Fig. 2 in terms of the porosity present as a function of distance from the aggregate surface for the initial and fully hydrated systems for both system configurations mentioned above. The one-sided growth mechanism is seen to be a secondary but significant contributor to the increased porosity in the interfacial zone. The cement particles used in this simulation were monosize and 21 pixels in diameter, so that the thickness of the interfacial zone is seen to be nearly the same as the diameter of the cement particles. Further results given in Ref. 21 indicate that interfacial zone thickness scales as the median (weight basis) cement particle size, and is independent of water:cement ratio, so that cement fineness is one variable which will strongly influence interfacial zone characteristics.

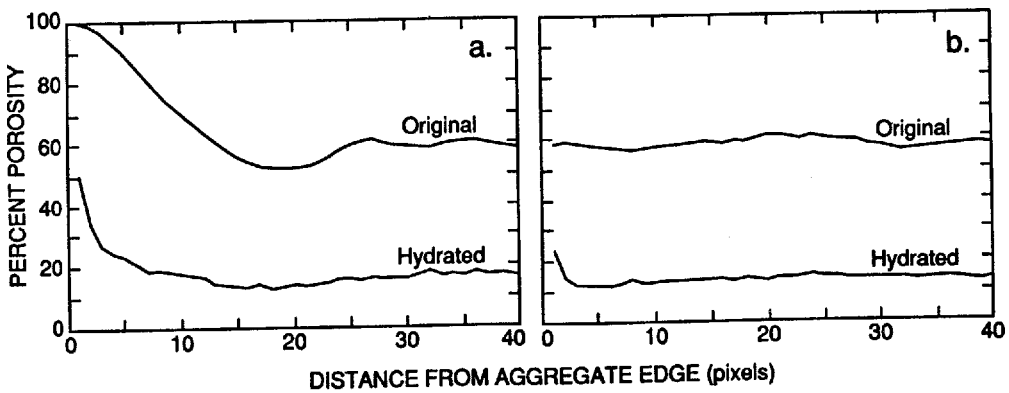

Fig. 2. Porosity vs. distance from aggregate surface before and after hydration for a) wall and one-sided growth mechanisms and b) one-sided growth mechanism only.

Use of mineral admixtures

The densification of interfacial zone microstructure due to the addition of silica fume has been well

documented by Scrivener et al. [24]. When properly prepared, concrete containing silica fume exhibits interfacial zones which are nearly as dense as the bulk paste. This is due both to the small size of silica fume which allows it to pack more efficiently near the aggregate surface, and its high pozzolanic activity which converts CH into more CSH. Utilizing simulation, both the size and reactivity of mineral admixtures such as silica fume and fly ash can be varied [14]. Since in the 3-D version of the model, a pixel is typically 1 μm on a side, well dispersed silica fume can be represented by small particles one pixel in size. Conversely, fly ash or agglomerated silica fume can be represented by larger particles, being the same size as the cement particles present in the system. Pozzolanic activity is varied by specifying how many volume units of CH each volume unit of mineral admixture may consume via the pozzolanic reaction. According to the reaction given earlier, pure silica would be able to consume 2.08 units of CH. Fly ash must be assigned a lower reactivity as it is typically only about 50% silica. Thus, 1.04 might be a reasonable maximum activity to be expected while 0.47 appears to be a more likely value to be achieved in practice based on data provided by Hooton [25].

Results have been summarized in terms of the total phase fraction of cement + CSH + mineral admixture present, assuming these to be the major load bearing phases in the cement paste matrix. Figure 3 shows the distribution of these phase fractions near an aggregate for a variety of concretes at a constant w/s ratio of 0.45 after 77% simulated hydration. In Fig. 3, size refers to the size of the mineral admixture particles while reactivity is equivalent to the pozzolanic activity discussed above. Small silica fume (System F) added at a 20% replacement for cement on a weight basis results in a nearly uniform distribution of these load bearing phases throughout the concrete microstructure. Fly ash is not nearly as effective, although the results do suggest that utilizing very fine fly ash should be beneficial if its ultimate pozzolanic activity of 1.04 is achieved (System E) due to the exposure of all available silica surfaces. Berry et al [26] have obtained experimental results in support of this hypothesis. Thus, small pozzolanic mineral admixtures are seen to somewhat offset the wall effect while not affecting the one-sided growth effect, and they do offer the additional benefit of converting CH into a larger volume of pozzolanic CSH.

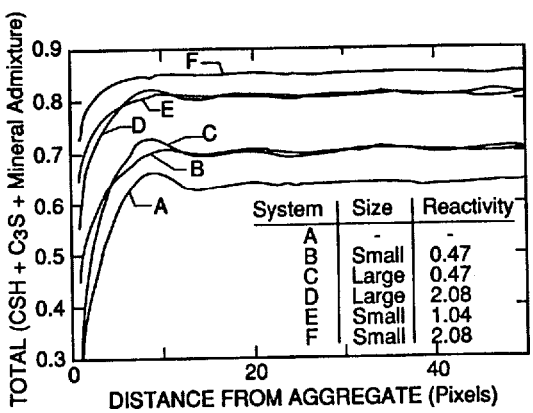

Fig. 3. Total load bearing phases vs. distance from aggregate for concretes containing 20% of various mineral admixtures.

Comparison between model and real microstructures

The digital-image-based cement paste microstructural model has been more rigorously verified by

quantitatively comparing the interfacial zone microstructures of model and real specimens for systems containing 0, 10, and 20% silica fume [27]. Real specimens consisting of cement paste and coarse aggregate were prepared and then quantified with respect to phase fraction distributions using scanning electron microscopy and image analysis. Results are shown in Fig. 4 for the total cement+CSH+silica fume and porosity phase fractions. In Fig. 4, the model results have been scaled along the x-axis so that the average cement particle size is equivalent in the model and real systems. In general, agreement between the two systems is quite good. The cement+CSH+silica fume and porosity phase fractions are nearly homogeneous throughout the 20% silica fume concrete.

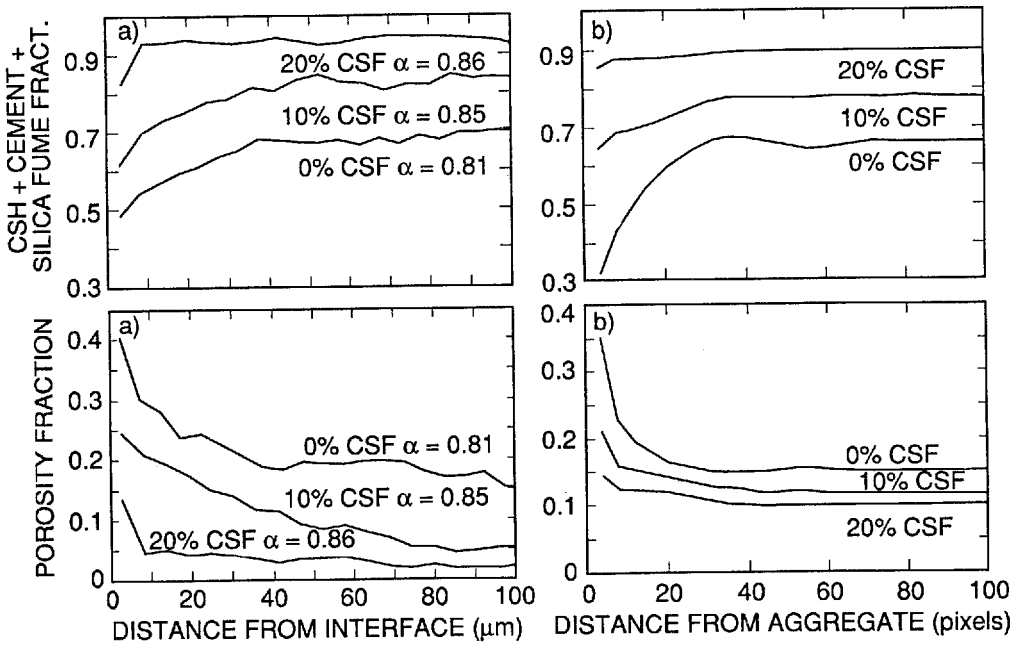

Figure 4: Showing cement + CSH + silica fume and porosity phase fractions vs. distance from the aggregate for a) experiment, and b) simulation.

V. ELECTRICAL CONDUCTIVITY OF CEMENT PASTE

The dc electrical conductivity of cement paste, σ, is an important transport parameter, and can be used as a probe of microstructural development [28]. Also, of particular practical significance, ionic diffusivities can be obtained from the Nernst-Einstein relation [29] by using the relative conductivity σ/σ_o, where σ_o is the pore fluid conductivity. Scientifically sound quantitative relationships between microstructure and σ/σ_o have never been made. This is because of both the lack of an adequate theory, and the lack of a program of careful, systematic measurements. We now present a preliminary comparison between simultaneous experimental measurements of σ and σ_o using impedance spectroscopy, and computer simulation predictions of σ/σ_o.

In general, for a material containing pores that are filled with a conductor, the bulk conductivity σ can be written [30] as $\sigma = \beta\ \phi\ \sigma_o$, where ϕ is the porosity, σ_o is the conductivity of the material filling the pores, and β is a dimensionless factor summarizing parameters like pore connectivity and tortuosity. The factor ϕ corrects for the cross-sectional area available for flow. The time-dependent d.c. electrical conductivity of cement paste may be described as $\sigma(t) = \Gamma(t)\ \sigma_o(t)$, where the relative conductivity $\Gamma(t)$ is defined by $\Gamma(t) = \sigma(t)/\sigma_o(t) = \beta(t)\ \phi(t)$. The dependence on time t is explicitly shown. By this choice of

variables, we have separated the bulk conductivity into a microstructure-dependent part, Γ, and a pore fluid part, σ_o. By simultaneously measuring σ and σ_o, we can monitor microstructure via Γ, and hydration chemistry via σ_o.

Cement pastes were prepared from ASTM Type I white Portland cement and deionized water, with a water:cement ratio of 0.5. Experimental details regarding materials and methods are given elsewhere [31]. White cement was used in these experiments due to its high calcium silicate content, making it the best approximation to C_3S without the difficulty of synthesizing pure C_3S, the cement component on which the computer model of hydration is based. The bulk paste conductivities, σ, were obtained by impedance spectroscopy [32], which allowed bulk and electrode resistances to be separated. Impedance data was collected with a low frequency gain-phase/impedance analyzer interfaced to a microcomputer. The value of real impedance at the minimum in the imaginary impedance between the electrode and bulk arcs gave the d.c. bulk resistance [28].

The pore fluid within the paste was extracted using a steel die according to previously defined procedures [33]. Pore fluid conductivity (σ_o) data was obtained within hours of extraction using an in-line conductivity probe. Degree of hydration α and thereby capillary porosity, were obtained by loss on ignition measurements [34]. Capillary porosity, ϕ, was calculated from α assuming that cement paste consists of unhydrated cement, hydration product, and capillary porosity. This being true, the relation between these two parameters is given by $\phi = (1 + 1.3\alpha)/(1 + 3.2w/c)$ [35].

The algorithm for computation of electrical conductivity has been described in detail elsewhere [29]. Once a three-dimensional microstructure has been built up in the computer, Laplace's equation is solved for the structure using a finite-difference technique and a conjugate gradient method [29]. The pore fluid conductivity is normalized to unity, so that a conductance of 1 is assigned to adjacent pairs of pixels representing capillary pore space. This means that the computed bulk conductivity will be given in units of σ_o, so that $\sigma = \Gamma$. Since the CSH gel phase contains very fine continuous micropores, it is assigned a finite but much smaller conductance of 0.0025. This number has been calibrated by experimental chloride diffusivities measured for 28-day or older samples [2]. In the time range studied, the conductivity was dominated by the capillary pore space, so that the exact value of the conductivity assigned to the CSH phase would have only minor effects on the results. All measured capillary porosities were greater than 28%, well above the percolation threshold of 18%, where the capillary pore space becomes discontinuous [35].

Figure 5 shows simulation and experimental results for the relative conductivity Γ, plotted as a function of capillary porosity. This data represents hydration times from about one hour up to approximately 200 hours, with a maximum degree of hydration of about 0.65. Over the entire range of capillary porosities studied, the simulation results and the experimental results agree reasonably well. For the highest porosities, there appears to be some systematic disagreement between simulation and experiment, with the experimental data lying above and following a different functional form than the simulation data. The dashed line in Fig. 5, which goes through the high porosity experimental points fairly well, is of the functional form $\phi^{1.5}$, as explained below.

In the case of simple suspensions of insulating particles in a conducting fluid, Γ is experimentally known to generally follow a power law [36]: $\Gamma = \phi^m$, where $m \approx 1.5$ for spherical particles. A paste of water:cement ratio 0.5 has an initial capillary porosity of $\phi = 0.62$, so that the initial value of Γ might be expected to be $\Gamma \approx 0.48$. In this limit, the simulation data appear to obey a power law with a slightly higher power, which is probably an artifact of the finite resolution with which the initially spherical cement particles are represented. The power law form, as well as the simulation, assume only uniform, bulk conduction processes in the conducting fluid. The experimental data seem to agree well with this assumption. It is interesting to note that the experimental conductivities appear to break away from the $\phi^{1.5}$ power law at a porosity of about 50%. This capillary porosity is realized at a degree of hydration of 0.23, which is very close to the degree of hydration at the final set point. When the cement paste has set,

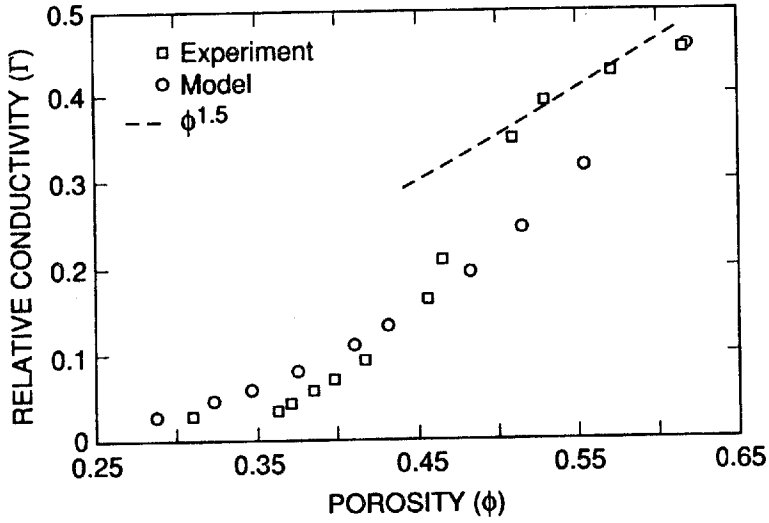

Figure 5: Showing the simulation and experimental results for relative conductivity $\Gamma = \sigma/\sigma_o$, plotted vs. capillary porosity, for an 0.5 water:cement ratio white cement paste.

implying the existence of a continuous solid phase, the description of the paste as a suspension will certainly not be correct.

Experimentally measured electrical conductivities are the mathematical product of σ/σ_o, a microstructural parameter, and σ_o, a chemically determined parameter. If two samples had the exact same microstructure and so the exact same value of σ/σ_o, but were saturated with two different pore fluids having different values of σ_o, then their measured conductivities would of course also be different. This elementary observation finds relevance in recent uses of the "Rapid Chloride Permeability Test" (RCPT) [37] on silica fume modified concretes.

There is compelling recent evidence [28] that the pore fluid conductivity in silica fume modified cement pastes is much lower than that in the same water:solid plain cement pastes. The reason seems to be the up-take of alkali ions by the pozzolanic CSH formed by the reaction of the silica fume with CH [28]. Therefore, even if silica fume did nothing to modify the microstructure, the measured conductivity and thus the total current passed in the RCPT would be lower. For example, if a silica fume concrete gave an RCPT number of 500, and a plain Portland cement concrete gave the same number, the actual resistance to chloride penetration of the plain cement concrete could be significantly

greater than that of the silica fume concrete. The RCPT, if valid results are desired, must be used with care when any material changes are made that could change the composition of the pore fluid from that of plain portland cement concrete. Christensen et al. [28] also shows the strong effect that the electrodes have on the apparent d.c. resistance of a cement paste, and the necessity for using a.c. techniques in order to measure the true d.c. resistivity, which is the quantity that is the proper predictor of chloride diffusivity, via the Nernst-Einstein relation [29].

VI. CONCLUSIONS

It is clear that the use of computers, both at the personal computer (PC) level and at the supercomputer level, is having a great impact on the ability to quantitatively model the microstructure and properties of cement-based materials, using both non-fundamental and fundamental models. Some of the models are reasonably compatible with present day PC technology, but would be helped by wider availability of this technology, while others push the limits of current supercomputer technology, so that their capabilities will improve directly as the memory capacity and speed of supercomputers continue to improve. The models described in this paper have already added to our knowledge and understanding of cement-based materials, and have a tremendous potential to do even more. The results from these models need to be understood and absorbed by those doing experimental research, and more experiments need to be planned, from the very start, with the object of collecting the data that is needed by the models. In the increasingly high-tech world of high-performance materials, ultimately progress is only going to be made by close collaboration between computer-based models of microstructure and properties, and experimental investigations.

VII. ACKNOWLEDGEMENTS

The authors would like to thank the National Science Foundation Science and Technology Center for Advanced Cement-Based Materials (ACBM) for partial support of this work, and G. J. Frohnsdorff and J.R. Clifton for encouragement and valuable discussions. We would also like to thank our ACBM colleagues at Northwestern University, B.J. Christensen, T.O. Mason, and H.M. Jennings, with whom some of the work in this paper was done. Finally, we would like to thank K.L. Scrivener of Imperial College, London, for supplying text and suggestions on the effect of computers on image analysis of cement-based materials.

VIII. REFERENCES

* Building Materials Division, 226/B348, Building and Fire Research Laboratory, Technology Administration, U.S. Department of Commerce.

1) Frohnsdorff, G.J., Clifton, J.R., Jennings, H.M., Brown, P.W., Struble, L.J., and Pommersheim, J.M.: "Implications of Computer-Based Simulation Models, Expert Systems, Data Bases, and Networks for Advancing Cement Research". Ceramics Bulletin, 1988, 67(8), p. 1368-71.
2) Garboczi, E.J. and Bentz, D.P.: "Fundamental Computer-Based Models of Cement-Based Materials". Materials Science of Concrete II, edited by J. Skalny and S. Mindess. Westerville, Ohio, USA, American Ceramic Society, 1991.
3) Jennings, H.M., "Towards Computer-Based Microstructure Models for Cement-Based Systems".
4) Parrott, L.J., "Modeling of Hydration Reactions and Concrete Properties". Materials Science of Concrete I, edited by J. Skalny. Westerville, Ohio, USA, American Ceramic Society, 1989.
5) van Breugel, K.: Simulation of hydration and formation of structure in hardening cement-based materials. Ph.D. thesis, Department of Civil Engineering, Delft University of Technology, 1991.
6) van Breugel, K.: "Numerical Simulation of Hydration and Structural Development of Cement-Based Materials". Proc. of the 9th Int. Congress on the Chemistry of Cement. New Delhi, India, 1992.
7) Wittmann, F.H., Roelfstra, P.E., and Sadouki, H.: "Simulation and Analysis of Composite Structures". Mater. Sci. Eng., 1984, 68, p. 239-248.
8) Roelfstra, P.E., Sadouki, H., and Wittmann, F.H.: "Le beton numerique". Mater. Struct., 1985, 18, p. 327-35.
9) Sadouki, H. and Wittmann, F.: "Time-Dependent Temperature Distribution in an Heterogeneous Material". Proc. of the 9th International Congress on the Chemistry of Cement. New Delhi, India, 1992.
10) Jennings, H.M. and Johnson, S.K.: "Simulation of Microstructure Development During the Hydration

of a Cement Compound". J. Am. Ceram. Soc., 1986, 69, p. 790-95.
11) Scrivener, K.L., personal communication.
12) Bentz, D.P. and Garboczi, E.J.: "Digitized direct simulation model of the microstructural development of cement paste". Physical Phenomena in Granular Materials, edited by G. Cody, T. Geballe, and P. Sheng. Pittsburgh, Pennsylvania, USA, Mater. Res. Soc., 1990, p. 523-530.
13) Bentz, D.P. and Garboczi, E.J.: "A digitized simulation model for microstructural development". Advances in Cementitious Materials, edited by S. Mindess. Westerville, Ohio, USA, American Ceramic Society, 1989, p. 211-226.
14) Bentz, D.P. and Garboczi, E.J.: "Simulation studies of the effects of mineral admixtures on the cement paste-aggregate interfacial zone". ACI Mat. J., 1991, 88, 518-529.
15) Young, J.F. and Hansen, W.: "Volume relationships for CSH formation based on hydration stoichiometries". Microstructural Development During Hydration of Cement, edited by L.J. Struble and P.W. Brown. Pittsburgh, Pennsylvania, USA, Mater. Res. Soc., 1987, p. 313-322.
16) Bentz, D.P. and Garboczi, E.J.: "Guide to Using HYDRA3D: A Three-Dimensional Digital-Image-Based Cement Microstructural Model". Gaithersburg, Maryland, USA, National Institute of Standards and Technology Internal Report (NISTIR 4746), 1991.
17) Bentur, A.: "Microstructure, interfacial effects, and micromechanics of cementitious composites". Advances in Cementitious Materials, edited by S. Mindess. Westerville, Ohio, USA, American Ceramic Society, 1989, p. 523-550.
18) Ping, X., Beaudoin, J.J., and Brousseau, R.: "Flat aggregate-Portland cement paste interfaces, I. Electrical conductivity models". Cem. and Conc. Res., 1991, 21, 515-522.
19) Costa, U., Facoetti, M., and Massazza, F.: "Permeability of the cement-aggregate interface: Influence of the type of cement, water:cement ratio, and superplasticizer". Admixtures for Concrete: Improvement of Properties, edited by E. Vazquez. London, Chapman and Hall, 1990, p. 392-401.
20) Uchikawa,R.: "Similarities and discrepancies of hardened cement paste, mortar, and concrete from the standpoint of composition and structure". J. Res. Onoda Cem. Co., 1988, 40, 1-24.
21) Scrivener, K.L. and Gartner, E.M.: "Microstructural gradients in cement paste around aggregate particles". Bonding in Cementitious Composites, edited by S. Mindess and S.P. Shah. Pittsburgh, Pennsylvania, USA, Materials Research Society, 1988, p. 77-85.
22) Bentz, D.P., Garboczi, E.J., and Stutzman, P.E.: "Computer Modelling of the Interfacial Zone in Concrete". Proc. of Conference on Interfacial Zone. Dijon, France, RILEM, 1992.
23) Garboczi, E.J. and Bentz, D.P.: "Digital simulation of the aggregate-cement paste interfacial zone in concrete". J. Mat. Res., 1991, 6(1), 196-201.
24) Scrivener, K.L., Bentur, A., and Pratt, P.L.: "Quantitative characterization of the transition zone in high strength concretes". Adv. in Cem. Res., 1988, 1, 230-237.
25) Hooton, R.D.: "Permeability and pore structure of cement pastes containing fly ash, slag, and silica fume". Blended Cements, edited by G. Frohnsdorff. Philadelphia, Pennsylvania, USA, American Society of Testing Materials, 1986, p. 128-143.
26) Berry, E.E., Hemmings, R.T., Langley, W.S., and Carette, G.G.: "Beneficiated fly ash: Hydration, microstructure, and strength development in portland cement systems". Fly Ash, Silica Fume, and Natural Pozzolans in Concrete, edited by V.M. Malhotra. Detroit, Michigan, USA, American Concrete Institute, 1989, p. 241-273.
27) Bentz, D.P., Stutzman, P.E., and Garboczi, E.J.: "Experimental and simulation studies of the interfacial zone in concrete". Cem. and Conc. Res, 1992, in press.
28) Christensen, B.J., Mason, T.O., and Jennings, H.M.: "Influence of Silica Fume on the Early Hydration of Portland Cements using Impedance Spectroscopy". J. Am. Ceram. Soc, 1992, in press.
29) Garboczi, E.J. and Bentz, D.P.: "Computer Simulation of the Diffusivity of Cement Paste", J. Mater. Sci., 1992, in press.
30) Garboczi, E.J.: "Permeability, Diffusivity, and Microstructural Parameters: A Critical Review". Cem. and Conc. Res., 1990, 20, 591.
31) Christensen, B.J., Mason, T.O., Jennings, H.M., Bentz, D.P., and Garboczi, E.J.: "Experimental and Computer Simulation Results for the Electrical Conductivity of Portland Cement Paste". Proc. of

Symposium on Advanced Cementitious Systems, edited by F. Glasser. Pittsburgh, Pennsylvania, USA, Materials Research Society, 1992, in press.
32) Bonanos, N., Steele, B.C.H., Butler, E.P., Johnson, W.B., Worrell, W.L., McDonald, D.D., and McKubre, M.D.H.: "Applications of Impedance Spectroscopy". Impedance Spectroscopy: Emphasizing Solid Materials and Systems, edited by J.R. McDonald. New York, Wiley and Sons, 1987, p. 191-238.
33) Barneyback, R.S., Jr. and Diamond, S.: "Expression and Analysis of Pore Fluids from Hardened Cement Pastes and Mortars". Cem. Concr. Res., 1981, 11(2), 279-285.
34) Mindess, S. and Young, J.F.: Concrete. Englewood Cliffs, New Jersey, USA, Prentice-Hall, 1981, p. 103.
35) Bentz, D.P. and Garboczi, E.J.: "Percolation of Phases in a Three-Dimensional Cement Paste Microstructural Model". Cem. and Conc. Res., 1991, 21, 325-344.
36) De La Rue, R.E. and Tobias, C.W.: "On the Conductivity of Dispersions". J. of the Electrochem. Soc., 1959, 106, 827-833.
37) Whiting, D.: "Rapid Determination of the Chloride Permeability of Concrete". Washington, D.C., USA, Federal Highway Administration, 1981, Report No. FHWA/RD-81/119.

COMPUTER MODELLING OF MICROSTRUCTURE OF CEMENT-BASED MATERIALS

R T Coverdale* and H M Jennings**

**Department of Materials Science and Engineering*
***Department of Civil Engineering*
Northwestern University, Evanston
USA

ABSTRACT

A general approach and associated guidelines for microstructural modelling are described. Verification of microstructural models is discussed in terms of a single model that makes predictions at many different levels. Since large amounts of information must be processed in order to satisfy the discussed guidelines, microstructural models are computer models. Microstructural modelling of cement paste is discussed in terms of two existing computer models. A new technique which simulates impedance measurements of cement paste, and which may serve as a basis to modelling other bulk properties, is described.

I. Introduction

A model may be described as "an alternative, usually simpler, representation of a real object, concept, or process[1]", or "a theoretical construct, which is made using valid scientific principles expressed in mathematical language, that can be used to make quantitative predictions about a material's structure or properties.[2]" A model is validated by comparing its output with measured observations. Once a model accurately represents a system or process, it can be used to make predictions that have not yet been observed and a good model can make predictions outside of the range of data that was used to formulate the model. This typically requires a mechanistic understanding of the processes. In the general area of cements and concrete, models have been developed that produce a singular output, e.g., rate of reaction, strength, etc.

A computer model allows the storage and ready access of large amounts of information, and can manipulate this information at high speed. Well developed algorithms perform calculations on this information and thus produce output of the computer model. The ability to make decisions based on specified criteria is an integral part of a computer model. The beauty of a well developed computer model is the ability to make predictions addressing several different aspects of the material. For example, a computer model should be able to predict strength, permeability, and rate of reaction as well as other characteristics. Simply using a computer to solve a complicated set of analytical equations does not constitute a computer model. This paper describes a general approach to computer modelling and discusses some guidelines that must be satisfied. Specifically microstructural models are discussed; following the principles of Materials Science, they form the basis of connecting processing to properties.

II) Modelling Microstructure

The following is a description of a fully developed ideal model of microstructure. A general flow chart is shown in Figure 1 (after Jennings and Johnson[3]). The first requirement of a microstructural computer model is that it describe and represent physical space. The model space should be large enough so that the microstructure contained within it is an average representation of the entire system being modelled. Another requirement relating to the scale of the model is that the model must deal with features of the microstructure that determine the bulk properties. These two requirements are basically the same as those for a "fundamental model"[2]. As shown in Fig. 1, computer models manipulate information and make predictions at several levels. One level of information deals with the reactions of the individual phases and the products produced. Another is how the products converge in physical space. At still another level, the physical arrangement of phases produces various bulk properties. Since most properties are determined by the microstructure, a computer model of the microstructure should be able to compute almost any property that is desired.

III) Verification of Computer Models

The simulated microstructure must accurately represent the real microstructure in every aspect. In order to determine if a model meets this requirement the description of the microstructure must be such that quantitative characteristics can be computed and, in turn, properties can be predicted. Verification can be achieved qualitatively and quantitatively. At one level, displaying the microstructure graphically allows visual comparison with micrographs, while image analysis provides quantitative comparison of amounts, arrangements, and distributions of phases.

While this type of comparison is important, perhaps the most practical way to verify the model is to compare measurements of bulk properties to the properties calculated from the model. For example, based on the elastic properties of each phase or component of the microstructure, and their arrangement within the microstructure, calculation of the elastic modulus of the bulk material is possible, and the result could then be compared to the measured value. This type of analysis serves to verify the model.

A generalized flow chart for computing properties is shown in Fig. 2. The process starts with two independent events: 1) a representative microstructure in "model space" is determined, and 2) a property, based on fundamental scientific principles, is assigned to each phase in the microstructure. The model space is segmented (pixels) and transformed into property space by assigning each pixel a property. Neighboring segments are then related to each other, thus modelling segment interaction for the property of interest. All the segment relations in property space are combined to produce an average bulk property representing the entire microstructure. A similar approach has been used by Bentz et. al.[4]

The process of calculating bulk properties from simulated microstructures may be as extensive as modelling the microstructure itself. This is necessary, however, if the model is to provide useful information in the development of higher performance materials, particularly when a property depends on microstructure and not simply on average composition.

IV) Modelling the Microstructure of Cement Paste

Since the microstructure of cement paste is random in some respects, it is very difficult to extract macrostructural properties using analytical equations and relationships alone. Thus, cement paste is a material that can be usefully studied through microstructural modelling. In other words, microstructural modelling will provide theoretical calculations of properties, based on fundamental scientific principles, that were previously unavailable because of the random nature of cement paste.

A significant portion of the literature describes mathematical models which address macrostructural properties of cement paste, e.g., porosity, moisture content, percent hydration etc. These models are typically based on empirical relationships and consider only average quantities. A significant effort of this type has been pursued by Parrott[5]. This category of modelling has been previously reviewed [6,7], and has been classified as non-fundamental[2]. To this point, fundamental computer models of the microstructure of cement paste have shown great promise in becoming a useful way to gain insight into the relationship between microstructure and properties[8,9,10,11,12]. Furthermore detailed information about the distribution of phases as well as their average quantity is proving to influence physical properties. The influence of strength on the size of pores, and clusters of pores, as well as volume fraction is perhaps, an obvious example.

Currently , to the authors' knowledge, only two fundamental models of cement microstructure exist that successfully address some of the criteria set forth in Section II. The first model of this kind was developed by Jennings and Johnson[3], and the second by Bentz and Garboczi[13]. Both of these models have a structure shown in the flow chart in Fig. 1, and have been reviewed by Garboczi in this proceedings. The main difference between the two approaches is in the way each accounts for physical space. The Jennings-Johnson approach is to model particles of the microstructure as spheres, keeping track of their location and size with an array of records, each particle having its own record. The Bentz-Garboczi model divides space up into very small cubes of equal size and registers the phase occupying each individual cube. While the Bentz-Garboczi model is more computer intensive than the Jennings-Johnson model, the format of the former allows the microstructure to be more easily characterized, i.e., it is already segmented.

V) A New Approach

Work is currently underway to reliably analyze the microstructure of cement paste using impedance spectroscopy[14,15]. An alternating voltage is applied to a specimen, over a range of frequencies, and the resulting current and phase angle are measured. From this, the complex impedance ($Z(w) = Z' + Z''i$, where Z' and Z'' are the real and imaginary parts of impedance, respectively) is determined for the bulk material. By plotting the results in the form of a Nyquist plot[16], useful information about the microstructure can be obtained without damaging the sample.

Using a digitized microstructure that is finely divided into pixels (Bentz-Garboczi model), the impedance spectrum of cement paste is simulated. This process follows closely the flowchart in Figure 2. Phases of the simulated microstructure are assigned simple RC circuits (convert to property space), the R and C values being based on the physical properties of the individual phases. The pixels are then connected together by electrical bonds that represent series combinations of the RC elements (establish relationships between adjacent segments, see Fig. 3). A voltage is applied to the electrical network and the resulting impedance is calculated (determination of average bulk property).

Preliminary results from this technique, applied in two dimensions, have shown that it is possible to qualitatively duplicate experimental impedance curves[17]. Figure 4 shows two simulated Nyquist plots, each containing the same amounts of phases, but with different arrangements. The plots are parameterized by applied frequency, with frequency increasing from right to left. The equivalent DC resistance is the point where the imaginary impedance is a minimum. The portion of the impedance curve to the right of the minimum is the electrode arc, and is due to polarization effects between the sample and electrode surfaces. The portion of the curve to the left of the minimum is the bulk arc, and it is this part of the curve that provides information about the microstructure of cement paste. This figure shows the sensitivity of the technique to amounts and distribution of phases. It is important to note that complex impedance is a physical property that depends on the distribution of phases as well as the average quantities present.

Further research is currently underway to pursue this technique in three dimensions, the goal being exact quantitative duplication of experimental results. This will provide significant insight into the relation between microstructure and the impedance curve. Modelling is significant because the microstructure in the model is explicitly known, and therefore details of the impedance curve can be traced to specific aspects of the microstructure. Another goal of this research is to use this same format to predict other bulk properties of cement paste. For example, Young's modulus can be simulated by summing the elastic properties of individual segments.

VI) Present Limitations and Challenges

Perhaps the biggest challenge of this type of modelling is to find means of scaling so that the microstructure includes the fine structure such as that of C-S-H, as well as coarse structure such as that of aggregate. This challenge must be addressed because many average properties depend on the properties of segments in both scale ranges.

Another major challenge is to track the microstructure as it deforms. Rheology, creep, shrinkage, and fracture are related to movement at the microstructural level.

VII) Summary

Two generic flow charts are presented that may help define the functions of a microstructural model. One describes a model in which the microstructure is numerically represented and serves as the basis for computing properties. The other describes recent efforts to compute quantitative electrical properties, and may serve as the basis for computing other properties. This entire approach is justified because bulk properties of cement depend not only on the fundamental properties of the microstructural phases, but also on the amounts and distributions of each phase. Future directions and challenges are considered.

VIII) Acknowledgment

The authors wish to acknowledge the National Science Foundation's Center for Science and Technology for Advanced Cement Based Materials, grant # DMR-08432, for financial support of this work.

IX) References

1) H.M. Jennings, *Microstructural Development During Hydration of Cement*, Mat. Res. Soc. Symp. Proc., Vol. 85, pp. 291-300 (1987)
2) E.J. Garboczi and D.P.Bentz, in *Materials Science of Concrete II*, Edited by J. Skalny and S. Mindess, The American Ceramic Society, pp. 249-277, 1991
3) H.M. Jennings and S.K. Johnson, J. Am. Ceram. Soc., Vol. 69, No. 11, pp. 790-795 (1986)
4) D.P. Bentz, D. Gingold, E.J. Garboczi, C.J. Lobb, and H.M. Jennings, Proc. ACerS/NIST Conference on Advances in Cementitious Materials, Gaithersburg, MD (1990)
5) L.J. Parrott, *Research on the Manufacture and Use of Cements*, Edited by G. Frohnsdorf, Engineering Foundation, pp.43-73, 1986
6) J. Pommersheim and J.R. Clifton, *Cements Research Progress*, Chap. 13, 1979
7) G. Frohnsdorf and J.R. Clifton, *Cements Research Progress*, Chap. 13, 1980
8) W. Ku, O.J. Gregory, and H.M. Jennings, J. Am. Ceram. Soc., Vol. 73, No. 2, pp.286-296 (1990)
9) E.J. Garboczi and D.P. Bentz, J. Mat. Sci., Vol. 27, pp. 2083-2092 (1992)
10) E.J. Garboczi and D.P. Bentz, Proc. ACerS/NIST Conference on Advances in Cementitious Materials, Gaithersburg, MD (1990)
11) E.J. Garboczi and D.P.Bentz, J. Mat. Res., Vol. 6, No.1, (1991)
12) D.P Bentz and E.J. Garboczi, Cem. and Conc. Res., Vol. 21, pp. 325-344 (1991)
13) D.P. Bentz and E.J. Garboczi, Proc. ACerS/Nist Conference on Advances in Cementitious Materials, Gaitherburg, MD (1990)
14) C.A. Scuderi, T.O. Mason, and H.M. Jennings, J. Mat. Sci., Vol. 26, pp. 349-353 (1991)
15) B.J. Christensen, T.O. Mason, and H.M. Jennings, J. Am. Ceram. Soc., Vol. 75, No. 4, pp. 939-945 (1992)
16) *Impedance Spectroscopy: Emphasizing Solid Materials and Systems*, Edited by J.R. MacDonald, Wiley, New York, 1987.
17) R.T. Coverdale, E.J. Garboczi, H.M. Jennings, B.J. Christensen, and T.O. Mason, submitted to J. Am. Ceram. Soc.

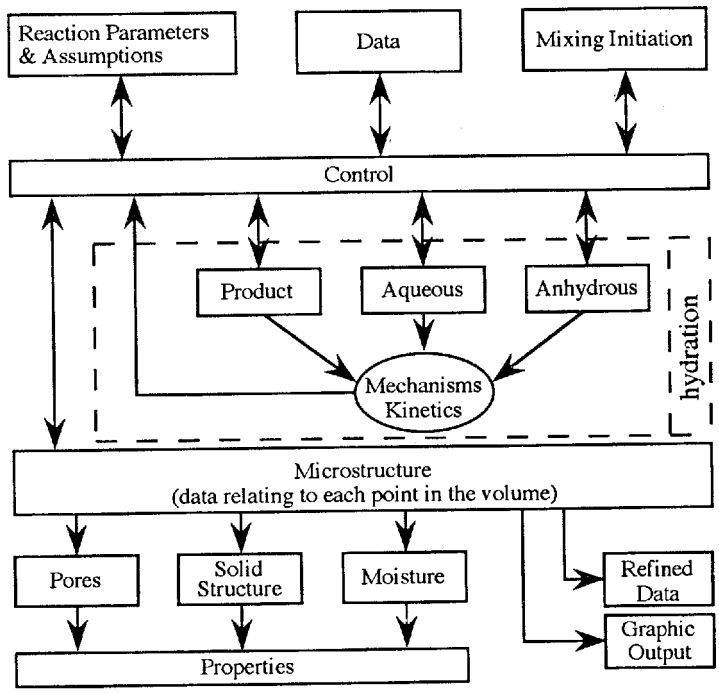

Fig. 1 - Functional flow chart for simulating the hydration process. Each box represents a number of subroutines each of which performs a particular function. Arrows indicate the direction in which information can flow. (after ref. 3)

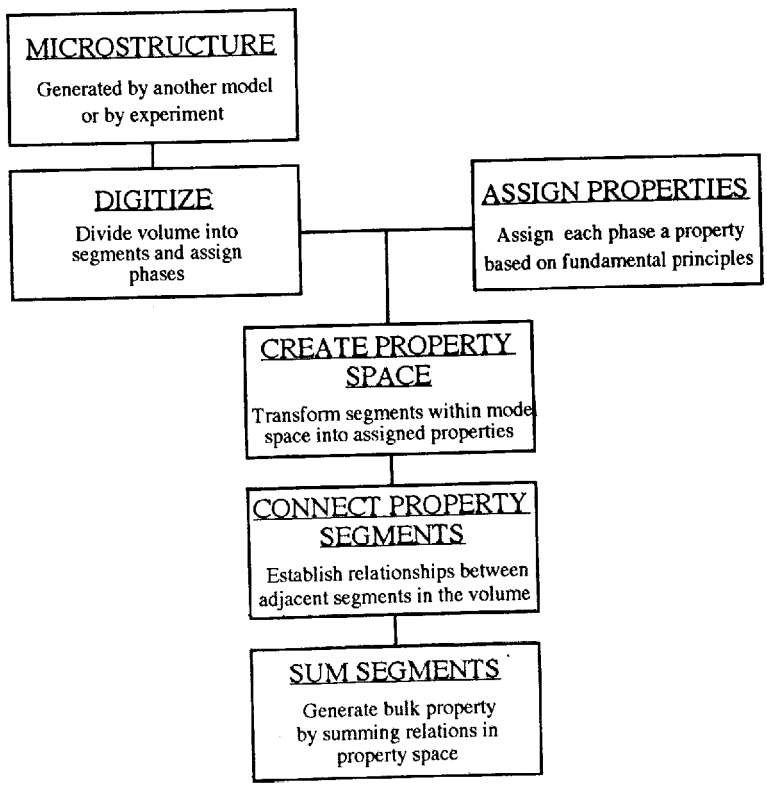

Fig. 2. Functional flow chart for extracting bulk properties from microstructural model.

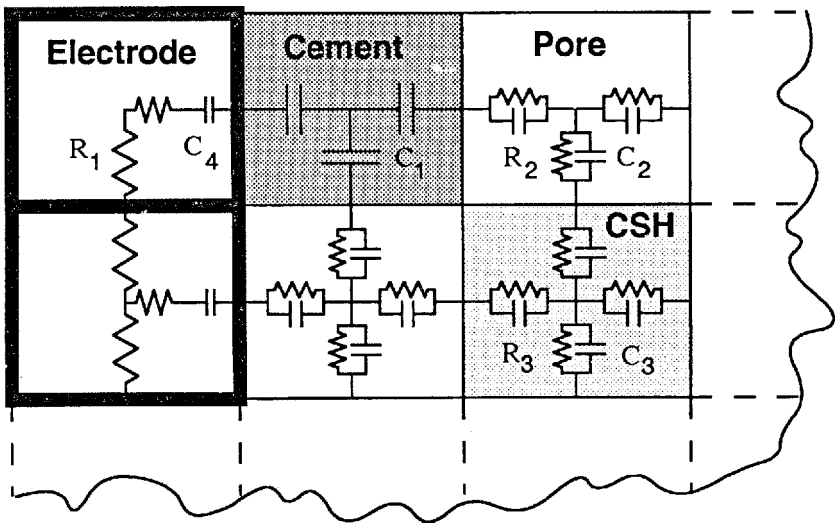

Fig. 3 - Sample of 2D simulated microstructure where different RC circuits represent the AC electrical properties of the different phases of the microstructure.

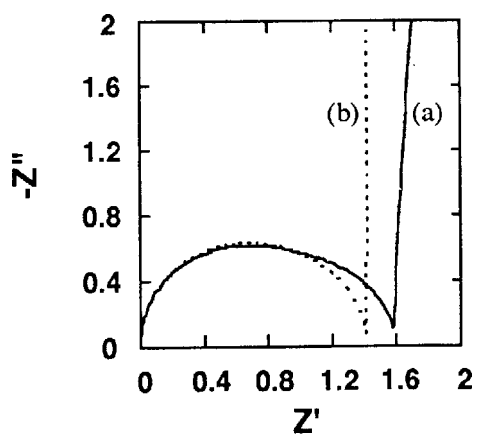

Fig. 4 - Nyquist plot for two simulated microstructures with the same volume fractions of phases, but different distributions; a) random microstructure, b) highly clustered microstructure.

NUMERICAL SIMULATION OF HYDRATION AND STRUCTURAL DEVELOPMENT OF CEMENT-BASED MATERIALS

K van Breugel

Delft University of Technology, Delft
THE NETHERLANDS

SUMMARY

A computer-based numerical model is presented which simulates hydration and micro-structural development in Portland cement-based materials. The model, called HYMOSTRUC, the acronym for HYdration, MOrphology and STRUCtural formation, enables to predict hydration curves as a function of the particle size distribution and chemical composition of the cement, the water/cement ratio and the actual reaction temperature. The influence of microstructural development, i.e. the formation of interparticle contacts, on the rate of hydration is modelled explicitly. Parameters used for quantification of particle interactions are discussed in view of their correlation with strength development. Calculations of the porosity in the matrix-aggregate interfacial zone are briefly mentioned.

ZUSAMMENFASSUNG

Ein "Computer-Based", numerischer Model wird presentiert, der den Hydratationsvorgang und die Entwicklung der Mikrostruktur in Portland-Zement gebundenen Materialen simuliert. Dieser Model, HYMOSTRUC genannt (Akroniem für HYdratation, MOrphology und STRUCtural development), ermöglicht es Hydratationskurve zu berechnen als Funktion der Kornverteilung und chemische Zusammensetzung des Zementes, der Wasser/Zement Wert und der Temperatur während der Reaktion. Der Einfluss der Entwicklung der Mikrostruktur, dass heisst der Entwicklung von Kontakten zwischen Zementkörner, auf der Hydratationsgeschwindigkeit is explizit modelliert worden. Parameter, die benutzt werden für der Bestimmung von Kontakten zwischen Zementkörner werden diskutiert im Beziehung auf ihre Korrelation mit der Festigkeitsentwicklung. Die Bestimmung der Porosität in der Matrix-Zuschlag Zone wird kurz erwähnt.

1. INTRODUCTION

Quality control on the building site is one of the major challenges in engineering practice in our days. In this framework computer programs have been developed for analyzing the risk of early-age thermal cracking in concrete structures. The input for most of these macro-level programs consists of, among other things, either an adiabatic or an isothermal hydration curve of the mix in view. There is in increasing demand for predictive models with which these curves can be generated numerically. Just for this purpose a numerical model has been developed with which the engineer's wishes were fulfilled as good as possible and is, on the other hand, also as consistent as possible with present views on processes and mechanisms involved in hydration and structural formation. It will be obvious that, bearing in mind the complexity of the subject, rigorous systematization was required of the predominant characteristics of the cement itself, of the hydration products and of the mechanisms and processes involved in hydration and structural development. For a more comprehensive survey of numerical models for simulation of hydration and structural formation reference is made to [1,2].

2. SIMULATION MODEL FOR HYDRATION AND MICROSTRUCTURAL DEVELOPMENT

2.1. Background Considerations And Model Assumptions

In the model the development of microstructure in cement-based materials is considered to be a process of making contacts between expanding cement particles. Expansion occurs because the volume of the reaction products exceeds the volume of the dissolving cement grains by a factor ν, i.e. about 2.2. Numerical simulation of the formation of interparticle contacts is based on the assumption that:

1. Reaction products are formed in the close vicinity of dissolving cement grains [6];
2. The density of the reaction product (gel) is constant throughout the hydration process and independent of the place where it is formed;
3. Both dissolution and expansion of the cement particles occur concentrically.

With progress of the hydration process small particles, located in the vicinity of the surface of bigger particles, will gradually become embedded in the outer shell of the bigger particles. For quantification of this "interaction process", the *stereological aspect* of microstructural development is of paramount importance and compels to consider the particle size distribution and the spatial distribution of the cement particles in the paste.

2.2. Particle Size Distribution And Stereological Aspects

For the particle size distribution of the cement the well-known Rosin-Ramler distribution

$$G(x) = 1 - \exp(-nx^{n}) \qquad [g] \qquad (1)$$

has been adopted, with x [μm] the particle diameter and b and n constants which are determined so that $G(x\rightarrow\infty) = 1$ g. The cement particles are, actually, randomly distributed in the paste. Since each particle has, therefore, a unique position in the system, the process of formation of interparticle contacts, as well as the effect of this process on the hydration kinetics of each particle, will be different for each individual particle. If we would decide to follow the hydration process of each particle explicitly, the computation times required for a simulation of a representative polysize sample would soon exceed what can be considered realistic if these calculations are to be run on present generation personal computers (which was considered a prerequisite). To overcome this computation time problem a so-called "pseudo-probabilistic" approach has been chosen. In this approach the cement particles are at first assumed to be equally spaced in the paste. An arbitrary particle x is considered to be located in the center of a "cell", and is called the "central particle". For this homogeneous distribution of the cement particles it is relatively easy to determine the *amount of cement* present in a fictitious *shell* around an arbitrary central particle x. For the purpose a *shell density factor* $\zeta_{sh;x,d}$ has been defined, viz.:

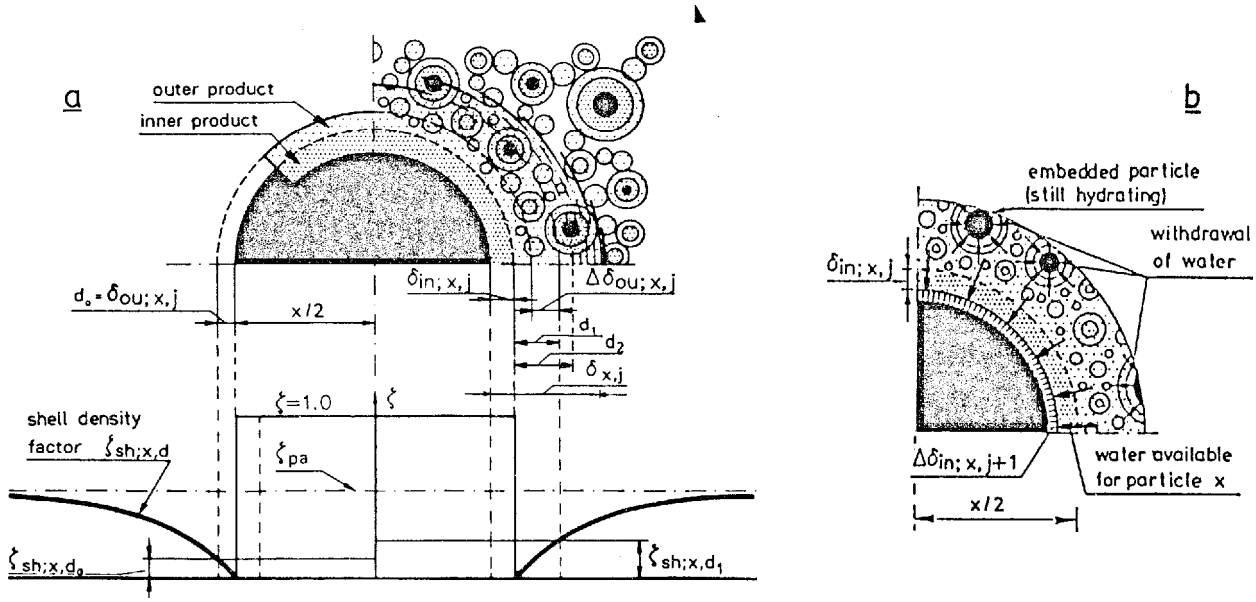

Fig. 1. Schematical representation of expansion mechanism and water withdrawal.
a. Upper part - Left: No embedding of particles
Upper part - Right: Enhanced expansion caused by embedding of neighbour particles
Bottom part: Shell density curves $\zeta_{sh;x,d}$
b. Water withdrawal mechanism: schematical

$$\zeta_{sh;x,d} = \frac{\text{amount of cement } [\mu m^3] \text{ in a spherical shell with thickness d}}{\text{total volume } [\mu m^3] \text{ of the shell}} \qquad (2)$$

An example of the course of a shell density factor is shown in the bottom part of Fig. 1a. Going from the periphery of the particle x in outward direction the shell density gradually increases from zero at the surface of the anhydrous cement particle to the bulk density $\zeta_{pa} = [1+\omega_0 * \rho_{ce}]^{-1}$, in which ω_0 is the w/c ratio and ρ_{ce} the specific mass of the cement.

In order the allow, in a way, for the actual randomness of the particle distribution it is assumed in further numerical evaluations that the cement present in a fictitious shell around a central particle x consists of particles with diameters < x μm. A consequence of the chosen procedure is that the *number* of particles involved in the interaction process must be counted carefully on penalty of counting them more than once.

Particles, which are not embedded in the outer shell of bigger particles, are identified as *free* particles. It is assumed that embedded particles, which are not fully hydrated at the moment when they become engulfed by an expanding particle, hydrate at the same rate as free particles of the same size.

2.3. Particle Expansion Mechanism. Basic Structure Of The Algorithm

An arbitrary stage in the hydration process of a central particle x is shown schematically in the upper part of Fig. 1a. At a certain time, say t_j, the degree of hydration of particle x is $\alpha_{x;j}$. For the corresponding *penetration depth* $\delta_{in;x,j}$ of the reaction front it holds:

$$\delta_{in;x,j} = (x/2) * [1 - \{ 1-\alpha_{x,j} \}^{1/3}] \qquad (3)$$

The volume of outer product of particle x corresponding with the degree of hydration $\alpha_{x;j}$ follows from:

$$V_{ou;x,j} = (\nu - 1) * \alpha_{x,j} * V_x \qquad (4)$$

with v_x the volume of particle x in its anhydrous state. If no cement would be found in the spherical outer shell which is filled up with outer product of the expanding particle, the outer radius $R_{ou;x,j}$ of particle x would be:

$$R_{ou;x,j} = [\frac{v_{ou;x,j}}{4\pi/3} + (x/2)^3]^{1/3} \quad (5)$$

For the thickness $\delta_{ou;x,j}$ of the outer shell it would follow:

$$\delta_{ou;x,j} = R_{ou;x,j} - x/2 \quad (6)$$

In reality a certain amount of cement will be present in the outer shell. The volume of the cement in a shell with thickness $\delta_{ou;x,j}$, called the *directly embedded cement volume* $v_{em;x,j}$, is determined by multiplying the shell volume $v_{ou;x,j}$ with the corresponding shell density factor $\zeta_{ou;x,d_0}$ (with $d_0 = \delta_{ou;x,j}$):

$$v_{em;x,j} = \zeta_{sh;x,d_0} * v_{ou;x,j} \quad (7)$$

The volume of the embedded, partly hydrated, cement accounts for an additional expansion $\Delta\delta_{ou;x,j}$ of the outer shell of particle x. This additional expansion, on its turn, results in an increase of the amount of embedded cement. The amount of cement found in the shell with a thickness $\Delta\delta_{ou;x,j}$ is called the *indirectly embedded cement volume*. The total volume of directly and indirectly embedded cement can be calculated analogously to the procedure for the determination of the directly embedded cement (formulae (2) and (7)), albeit that the shell density factor is a little higher now because of the increase of the thickness of the outer shell (Fig. 1a, bottom part: $\zeta_{sh;x,d_1} > \zeta_{sh;x,d_0}$). The increase of the amount of embedded cement, on its turn, causes another additional increase of the outer shell, etc. This expansion mechanism can be written in the form of a geometrical series. Numerical evaluation results in workable expressions for the thickness of the outer shell of particle x and for the total thickness of the layer of reaction products at time t_j, viz. $\delta_{x,j}$, as well as for the amount of cement embedded in the outer shell of particle x. Adding the amounts of cement embedded in the outer shells of all free particles in the system yields the amount of cement involved in the interaction process at time t_j.

2.4. Rate Of Penetration Of The Reaction Front

The rate of penetration of the reaction front in an individual cement particle x at time t_j is computed with a *rate formula* which, in a reduced form, looks as follows:

$$\frac{\Delta\delta_{in;x,j+1}}{\Delta t_{j+1}} = K_0(.)*\Omega_1(.)*\Omega_2(.)*\Omega_3(.)*F_1(.) * [\, F_2(.) * (\frac{\delta_{tr}}{\delta_{x,j}})^{\beta_1}\,]^{\lambda} \quad (8)$$

with $\Delta\delta_{in;x,j+1}$ the increase of the penetration depth in time step Δt_{j+1}, $K_0(C_3S)$ the basic rate factor [μm/hr], $\delta_{tr}(C_2S)$ the transition thickness [μm], being the total thickness of the product layer $\delta_{x,j}$ at which the reaction for the particle in view changes from a *boundary reaction* ($\lambda = 0$) into a *diffusion controlled reaction* ($\lambda = 1$). β_1 is an empirical constant.

The factor $\Omega_1 = \Omega_1(x,\alpha_j)$ accounts for the effect of *water withdrawal* by the embedded and still hydrating particles on the rate of penetration of the reaction front in particle x. The water withdrawal mechanism is schematically shown in Fig. 1b, whereas Fig. 2 shows examples of the values of the reduction, or partition, factors for three different particle sizes. The factors $\Omega_2 = \Omega_2(\alpha_j)$ and $\Omega_3 = \Omega_3(\alpha_j)$ are reduction factors, allowing for the *distribution* and the *amount* of capillary water in the pore system of the hydrating paste, respectively. The function $F_1(.) = F_1(\alpha_j,T_j,C_3S)$ accounts for the effect of the reaction temperature on the rate of momentary operating processes and mechanisms and was found to be a function of the degree of hydration α_j, the curing temperature T_j and the cement composition. A second temperature function $F_2(.)$ accounts for the effect of the curing temperature on the morphology and density, i.e. the ν-value, of the reaction products (see [2]).

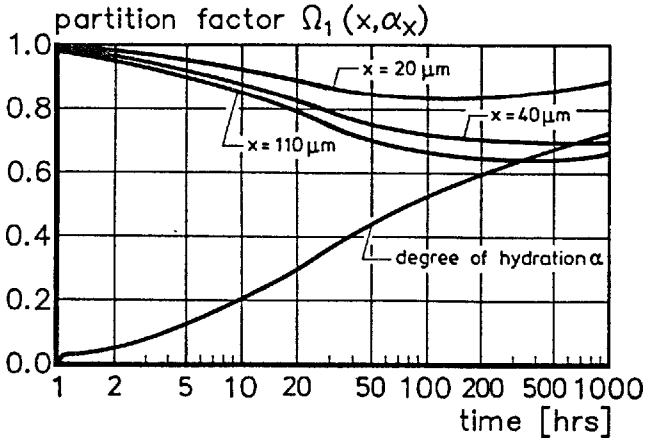

Fig. 2. Water withdrawal mechanism. Reduction factor $\Omega_1(x,\alpha_{x,j})$ [2].

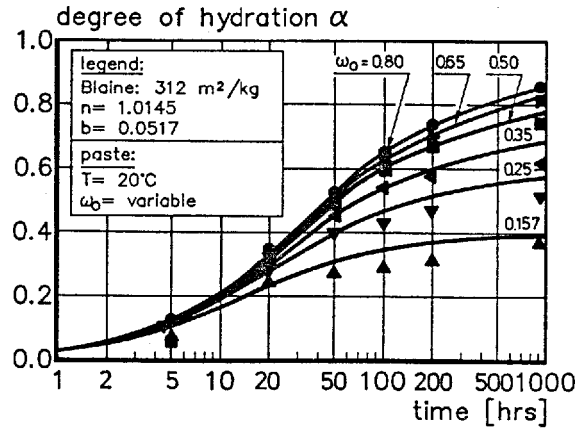

Fig. 3. Effect of water/cement ratio on rate of hydration. Test data: [7].

2.5. Model Parameters

The model parameters $K_0(C_3S)$, $\delta_{tr}(C_2S)$ and β_1 have been determined in an extensive evaluation program. In this program over 60 hydration tests were involved, comprising 27 different types of cement with C_3S contents ranging from 15% to 70%. The w/c ratios varied from 0.16 to 0.8, particle size distributions with n-values (R-R function) ranging from 0.73 to 3.15 and curing temperatures from 4°C up to over 50°C. The model parameters were determined so as to achieve a satisfactory fit of the experimental data. It was found that the K_0-values could be written as a function of the C_3S content according to:

$$K_0(C_3S) = 0.02 + 6.6\ 10^{-6} * [C_3S\%]^2 \qquad [\mu m/hr] \qquad (9)$$

with a standard deviation $\sigma(K_0) = 0.008$ μm/hr. The transition thickness δ_{tr} appeared to be weakly correlated with the C_2S content. For a slow cement values ranged from 2 to 4 μm, whereas for rapid hardening cements values from 3 to 6 μm would hold. These values seem to be consistent with those that could be deduced from the experimental work of Bezjak et al. [3] and Alujevic et al. [4]. For the factor β_1 a value of 2 appeared to be applicable in the majority of cases.

3. RESULTS

Fig. 3 shows a comparison of the calculated and measured effect of the w/c ratio on the rate of hydration of isothermally hydrating pastes (experimental data of Taplin [7]).
For mortars with w/c ratios 0.4 and 0.5, Fig. 4 shows the correlation between the amount of embedded cement, per μm^3 paste, and the compressive mortar strength. As the correlation seems to be independent of the w/c ratio, the embedded cement volume is supposed to be a more universal strength parameter than, for example, the degree of hydration, since in the latter case the w/c ratio is known to affect the correlation between strength and degree of hydration quite significantly.

Since HYMOSTRUC accounts for the stereological aspect of microstructural formation explicitly, evaluation of the effect of the *packing of particles* on the porosity of the paste in the matrix-aggregate interfacial zone is possible. For a cement of moderate fineness Fig. 5 shows the thickness and porosity in this zone. Experimental data of Scrivener are inserted as a reference.

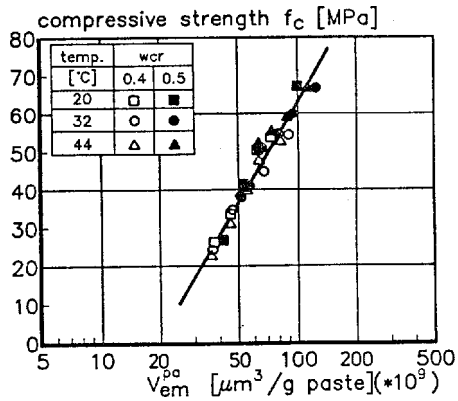

Fig. 4. Mortar strength as function of calculated embedded cement volume per cm^3/paste [2].

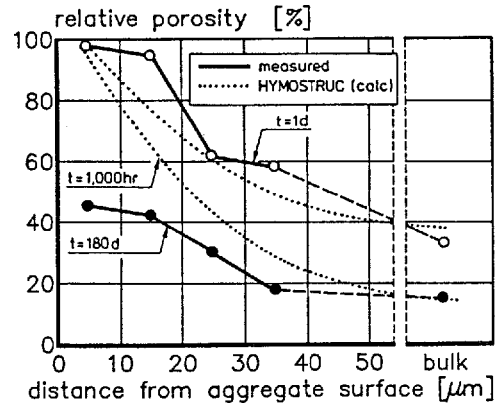

Fig. 5. Porosity in the matrix-aggregate interfacial zone. Experimental data: Scrivener [5].

4. DISCUSSION AND CLOSURE

Computer-based simulation programs are powerful tools to make huge files of data concerning chemical, physical and stereological aspects of hydration and structural development operational and accessible for engineering practice. The model briefly presented in this paper, called HYMOSTRUC, is an example of such a model. It appeared to be possible to predict adiabatic and isothermal hydration curves for a wide variety of cement pastes, mortars and concretes quite satisfactory. The model bridges, to a certain extent, the gap between the micro- and meso-level on the one hand, and the macro- or engineering level on the other hand, as it can be applied as a research tool for investigating the effects of the chemical composition and the particle size distribution of the cement, the w/c ratio and the initial mix temperature on temperature fields and development of material properties in actual concrete structures. Examples of both theoretical and practice-oriented evaluations performed with HYMOSTRUC are found in [2].
The step-wise calculation procedure according to which the model operates makes it possible to consider a large number of non-linear phenomena and mechanisms from which we would have to refrain if we would stick to a purely analytical "closed solution" approach. Although promising results have been obtained already, it is emphasized that the model is still in its early stage of development. Further research is planned as regards the difference between paste hydration and hydration in actual concretes, modelling of hydration of non-Portland cements, the effect of extra fines and pore water chemistry.

5. REFERENCES

1. Garboczi, E.J.: "Computer-Based Models of the Microstructure and Properties of Cement-Based Materials". 9th Int. Conf. Chem. Cements, New Delhi, 1992.
2. Breugel, K. van: **Simulation of Hydration and Formation of Structure in Hardening Cement-Based Materials.** PhD., Delft University of Technology, 1991, 295 p.
3. Bezjak, A., et al.: "Kinetic analysis of extraction of calcium silicates with methanolic solution of salicylic acid". Cement and Concrete Research, Vol. 10, No. 4, 1980, p 553-563.
4. Alujevic, V., et al.: "Kinetic study of the hydrothermal reaction of CaO-quartz system". Cement and Concrete Research, Vol. 16, No. 5, 1986, p 695-699.
5. Scrivener, K. et al.: "Quantitative characterization of the transition zone in high strength concretes". Advances in Cement Research, Vol. I, No. 4, 1988, p 230-237.
6. Taylor, H.F.W., et al.: "An electron microprobe study of a mature cement paste". Cement and Concrete Research, 14, 1984, p 565-573.
7. Taplin, J.H.: "A Method for following the hydration reaction in Portland Cement Paste". Austr. Journ. Appl. Sci., 10, 1959, p 329-345.

TIME-DEPENDENT TEMPERATURE DISTRIBUTION IN AN HETEROGENEOUS MATERIAL

H Sadouki and F Wittmann

Institute for Building Materials
ETH-Hönggerberg, SWITZERLAND

SUMMARY

A random composite structure is generated. The large aggregates are chosen to follow the Fuller distribution function. Small aggregates are considered to be smeared out in the mortar matrix. This composite structure is represented by finite volumes. Temperature distributions in the composite structure are calculated. First the case of hardening concrete is considered. In concrete with large aggregates and when rapid hardening cement is used the obtained local temperature distribution is influenced by the characteristics of the composite structure. The local temperature field caused by heating or cooling of the surface is also depending on the characteristics of the composite structure.

RESUME

Pour étudier l'influence de l'hétérogénéité du béton sur les champs de température qui y sont induits par la libération de la chaleur d'hydratation du ciment ou par une éventuelle variation de la température ambiante, on a représenté le matériau par une structure composite à deux phrases. Dans cette structure composite, les diamètres des plus gros granulats sont répartis selon une distribution de Fuller. Les granulats de moindre taille sont supposés uniformément répartis dans une matrice de mortier. Cette structure est par la suite finement subdivisée en volumes finis. Au moyen de la méthode des volumes finis, on a calculé les distributions spatio-temporelles de la température au sein de la structure composite. On a considéré en premier lieu le cas du béton composé de gros granulats pour lequel un ciment à durcissement rapide a été utilisé, les distributions de température obtenues sont influencées par le caractère hétérogène du matériau. Le champ de température induit par un réchauffement ou un refroidissement de la surface dépend également des caractéristiques physiques et géométriques de la structure co nposite.

INTRODUCTION

In massive structures the temperature gradients originated by the liberation of heat of hydration of the cement may cause a risk of crack formation at early age. There are computer programs available to predict the temperature distribution in an arbitrary shaped concrete structure taking the concrete composition and the type of cement into consideration (see for instance [1]).

In all these attempts concrete is considered to be a homogeneous material and the liberation of heat is assumed to be smeared out over the total volume. In reality, however, heat is only generated in the cement matrix surrounding the inert aggegates. Concrete and especially old dry concrete is also heterogeneous with respect to heat conduction. The coefficient of thermal conductivity of the aggregates and the dry mortar matrix can differ by a factor of four. In this contribution the influence of the heterogeneous structure of concrete on the global and local temperature distribution shall be studied. Two different cases will be analyzed in detail here: the temperature distribution in a hydrating young concrete and the temperature distribution induced by heating up the surface of a concrete element.

SIMULATION OF THE COMPOSITE STRUCTURE OF CONCRETE

In concrete technology aggregates are usually chosen to follow a predetermined size distribution. Often the Fuller distribution is taken:

$$f(d) = \sqrt{\frac{d}{d_{max}}} \qquad (1)$$

In [2] it is shown how two- and three-dimensional composite structures can be simulated. It is also possible to represent the characteristic shape of the aggregates in a realistic way. For the sake of simplicity circular inclusions have been considered in this study exclusively.

Fig.1 shows one example of a simulated concrete structure. In this case the aggregates with a diameter between 4 mm and 32 mm are randomly placed in a square with a side length of 100 mm.

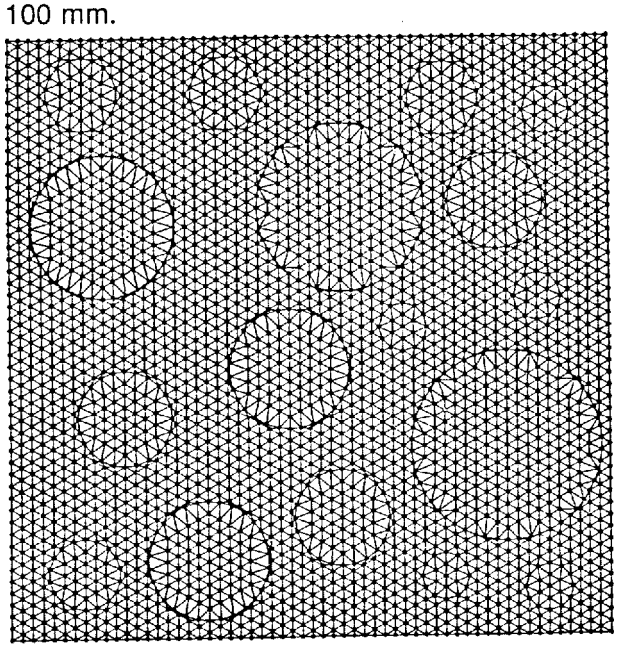

Fig. 1: Finite volume representation of a computergenerated random composite structure.

All finer particles are considered to be smeared out and in a homogeneous mortar matrix. The simulated composite structure is finally represented by a mesh of finite volumes. In the case shown in Fig.1 the composite structure is subdivided into 5858 finite volumes.

The temperature distribution in space and time in the mortar matrix is calculated with the finite volumes method using the well-known thermal diffusion differential equation:

$$c_v^m \frac{\delta T}{\delta t} = \frac{\delta}{\delta x}\left[\lambda^m \frac{\delta T}{\delta x}\right] + \frac{\delta}{\delta y}\left[\lambda^m \frac{\delta T}{\delta y}\right] + \dot{Q}^m(t) \qquad (2)$$

In this equation c_v^m stands for the heat capacity of the mortar, λ^m represents the coefficient of thermal conductivity of the mortar, and finally Q^m is the specific heat of hydratation of the cement used.
For the temperature distribution in the inclusions an analogous diffusion differential equation is used:

$$c_v^i \frac{\delta T}{\delta t} = \frac{\delta}{\delta x}\left[\lambda^i \frac{\delta T}{\delta x}\right] + \frac{\delta}{\delta y}\left[\lambda^i \frac{\delta T}{\delta y}\right] \qquad (3)$$

the upper index i symbolizes the corresponding values for the inclusions.

At the surfaces of the specimen under consideration different boundary conditions can be chosen, either a prescribed temperature (Dirichlet) or a prescribed flux boundary condition (Newman).

RESULTS

Temperature Distribution in Hardening Concrete Elements

In the first example a normal concrete is considered. Three faces of the square shown on Fig.2a are assumed to be thermally isolated while the upper surface is in contact with air having a temperature of 20°C. For the calculation λ^m has been chosen to be 2,4 and λ^i 4W/m°K. In this case a usual transfer coefficient for a concrete air interface has been adopted: α = 11,5 W/m²°K. A characteristic rate of liberation of heat for normal Portland cement has been used [3]. The temperature evolution has been plotted for four different points in the structure. It is obvious that a global thermal gradient between the inner parts and the surface is generated.
In Fig. 2b the spatial temperature distribution along two lines has been plotted for the same type of concrete and in the same structure. Points on the right line indicated by small circles are all situated in the mortar matrix while points on the left line in Fig. 2b, indicated by triangles, are partly in inclusions and partly in the mortar matrix. It can be seen from Fig. 2b that there is no significant difference between the temperature gradient along the two lines. In this case the material can be considered to be homogeneous with respect to the temperature field. No significant local gradients are built up.

It can be anticipated that the influence of the composite structure becomes more important when the diameter of the aggregates increases and when the heat of hydratation is liberated more

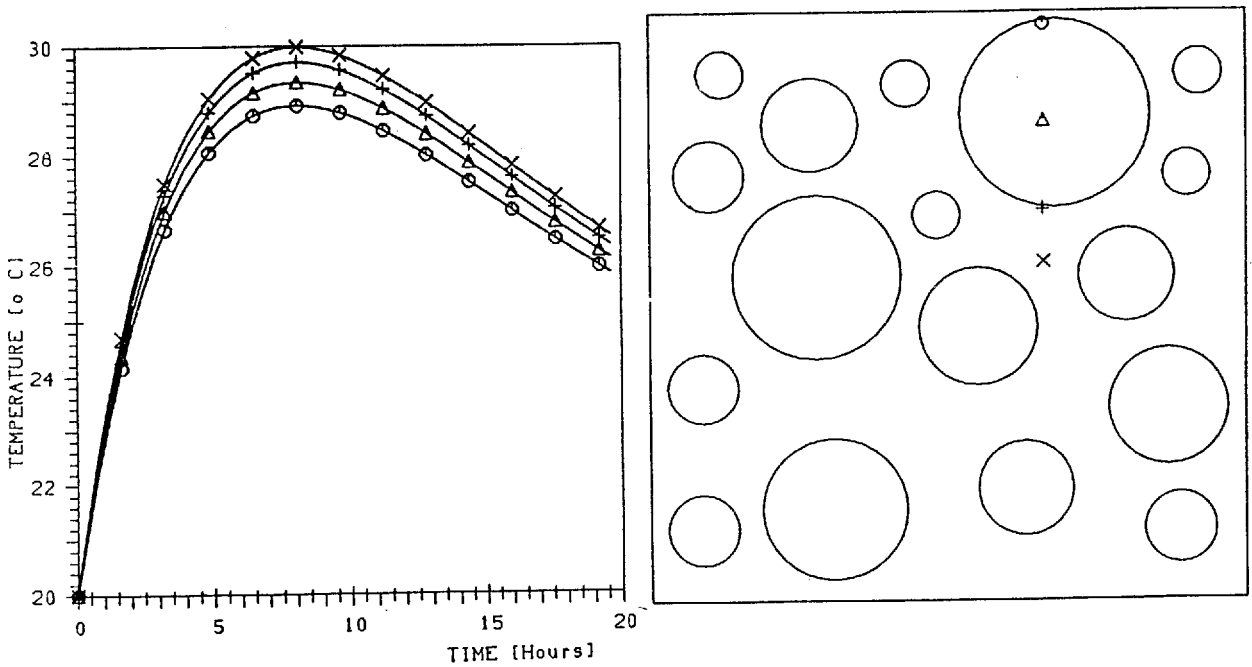

Fig. 2a: Temperature evolution at four different points in the composite concrete-like structure as function of the duration of hydration.

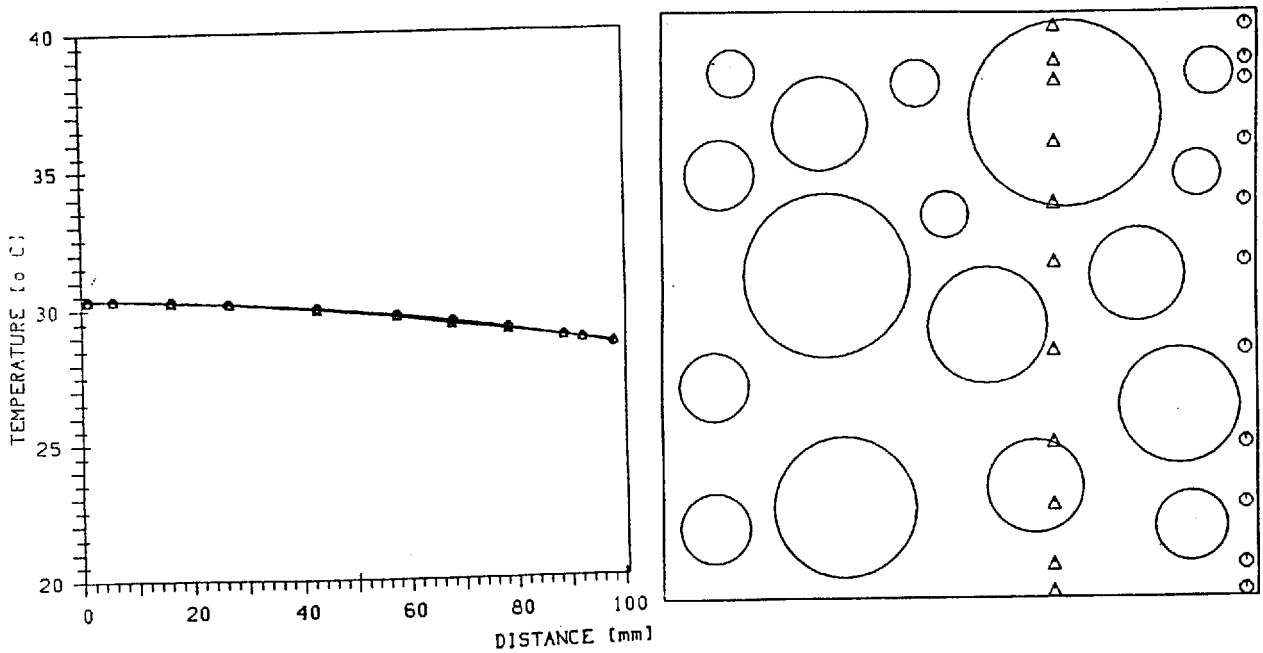

Fig. 2b: Temperature distribtution in a hardening normal concrete cube of an age of 6 hours as determined as function of the distance from the surface along two lines: (a) the entire length of the line in the matrix (circles) and (b) the line crosses two aggregates (triangles).

quickly. Therefore we have studied in the second example the temperature evolution in a cube made of dam concrete. The maximum aggregate size in this case is 150 mm and the cube length is 500 mm. All other parameters are identical with the values in the first example.

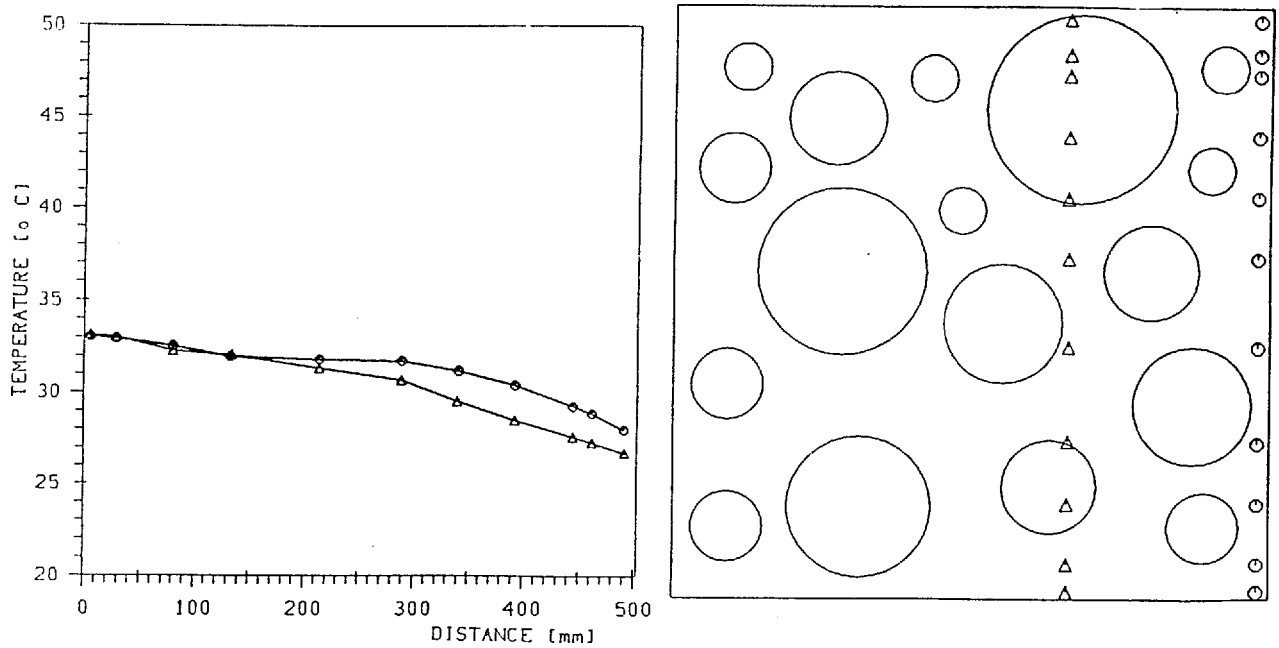

Fig. 3: Temperature distribution in a hardening dam concrete (maximum aggregate size = 150 mm) at an age of 4 hours as determined as function of the distance from the surface along two different lines (see Fig. 2).

The temperature profiles along the two selected lines are shown in Fig.3. It can be seen that the high thermal conductivity of the large aggregate leads to a relatively quick cooling of this zone. In this example the temperature distribution is severely perturbed by the composite structure and the thermal flux necessarely becomes twodimensional. As a result local temperature gradients are developed.

In order to study the influence of rate of hydratation on local temperature gradients the situation in a hardening polymer concrete has been considered as third example. In this case the dimensions of normal concrete have been used again. For the polymer matrix λ^m has been measured to be 0,63 W/m°K. The temperature evolution at four different points in the structure is shown in Fig.4a. Along the same lines as in the previous examples the temperature profiles have been plotted. in Fig.4b. As a example temperature profiles at a reaction-time of 1,28 hours are shown. The difference in temperature at the same distance from the surface can reach values up to 15°C. This perturbation of the temperature field can certainly not be neglected when thermal stresses are to be calculated.

The examples shown so far are characteristic for surface near zones of a hardening concrete element. In order to study the temperature distribution in a composite structure in the centre of a massive element we have considered a cube of dam concrete under adabatic conditions. A typical result is shown in Fig.5. The cement mortar matrix heats up quickly while the temperature evolution in the centre of the aggregates is remarkably delayed depending on the aggregate size.

Temperature Distribution behind a Heated Surface

We consider now a concrete element equilibrated at 20°C. Then the upper surface is heated within 12 minutes to 40°C while the three other surfaces are considered to be thermally isolated. In this example it is assumed that the concrete has dried before this heat treatment (old concrete) and therefore λ^m is chosen to be 1 W/m°K. The temperature profiles along the two lines as calculated 15 minutes after heating started are shown in Fig.6 The profile in the mortar matrix corresponds to a profile which can be expected for a homogeneous material. The profile which is

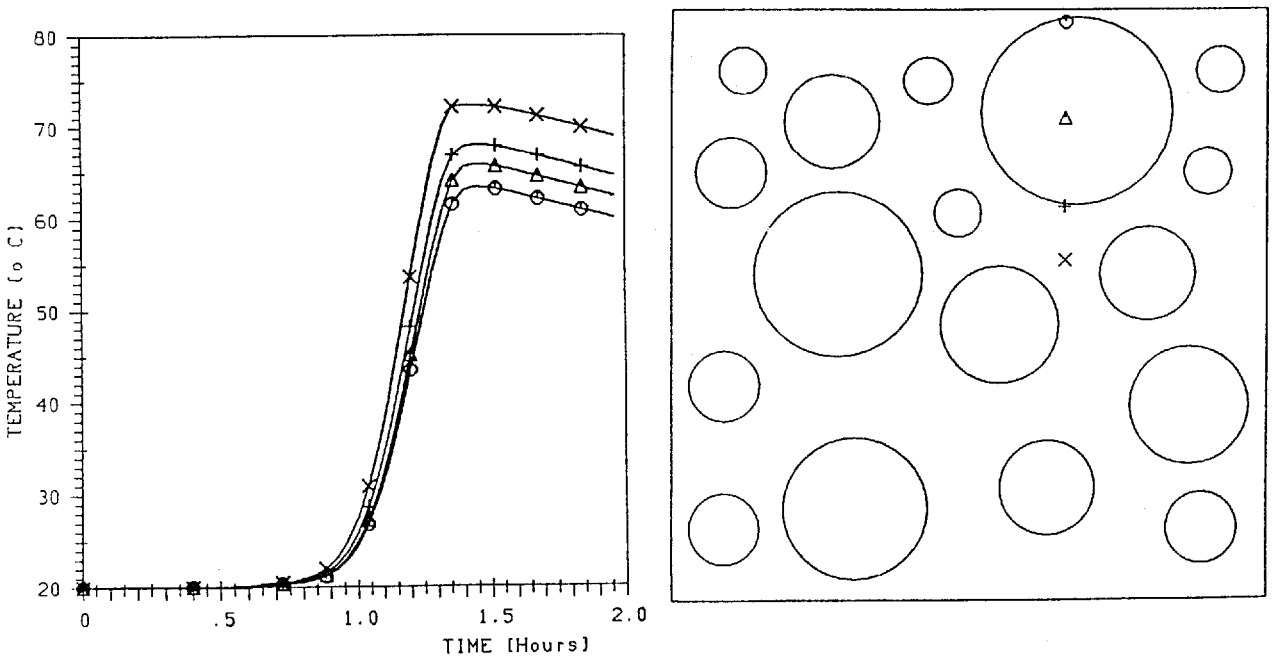

Fig. 4a: Temperature evolution at four different points in the composite structure of hardening polymer concrete.

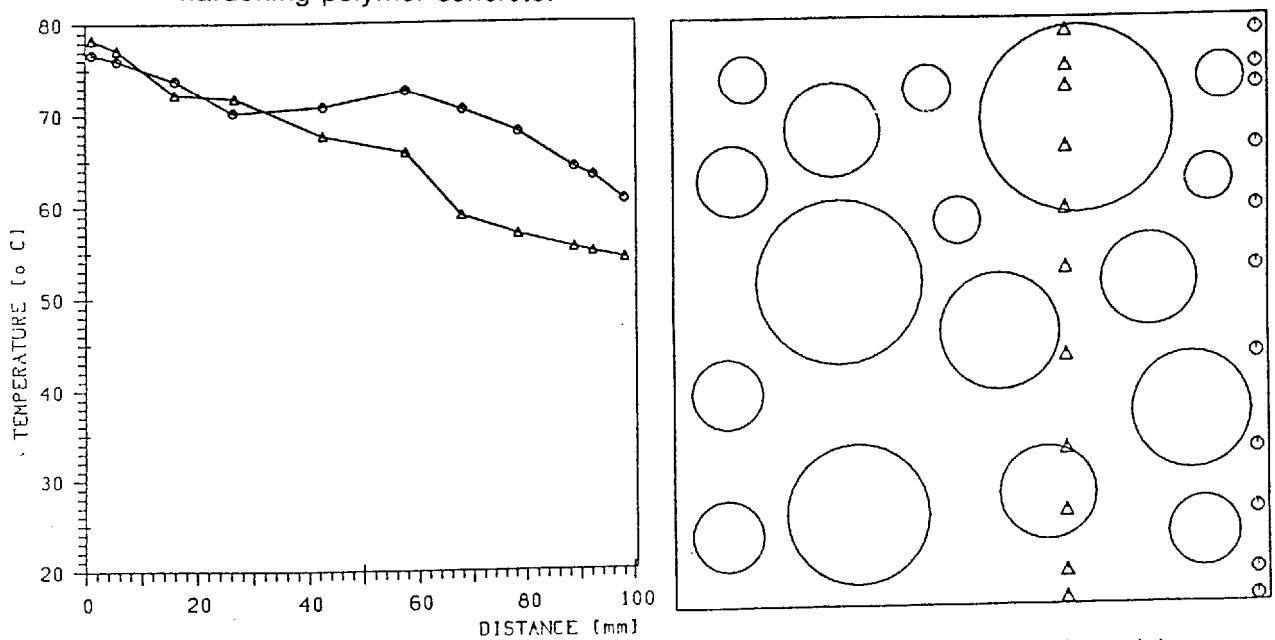

Fig. 4b: Temperature distribution in hardening polymer concrete 1.28 hours after mixing as determined as function of the distance from the surface along two different lines (see Fig. 2).

crossing the aggregates, however, is severely perturbed. A temperature difference of up to 5°C can be observed. This temperature difference will induce a local stress distribtution.

In the last example the same temperature history is imposed to a concrete cube with aggregates having a higher thermal conductivity : $\lambda^i = 6$ W/m°K. Results are shown in Fig.7. It is obvious that in this case the temperature field locally is even more perturbed. Thermal local stresses will therefore depend both on the dimensions of the heterogeneous structure and the difference between λ^m and λ^i.

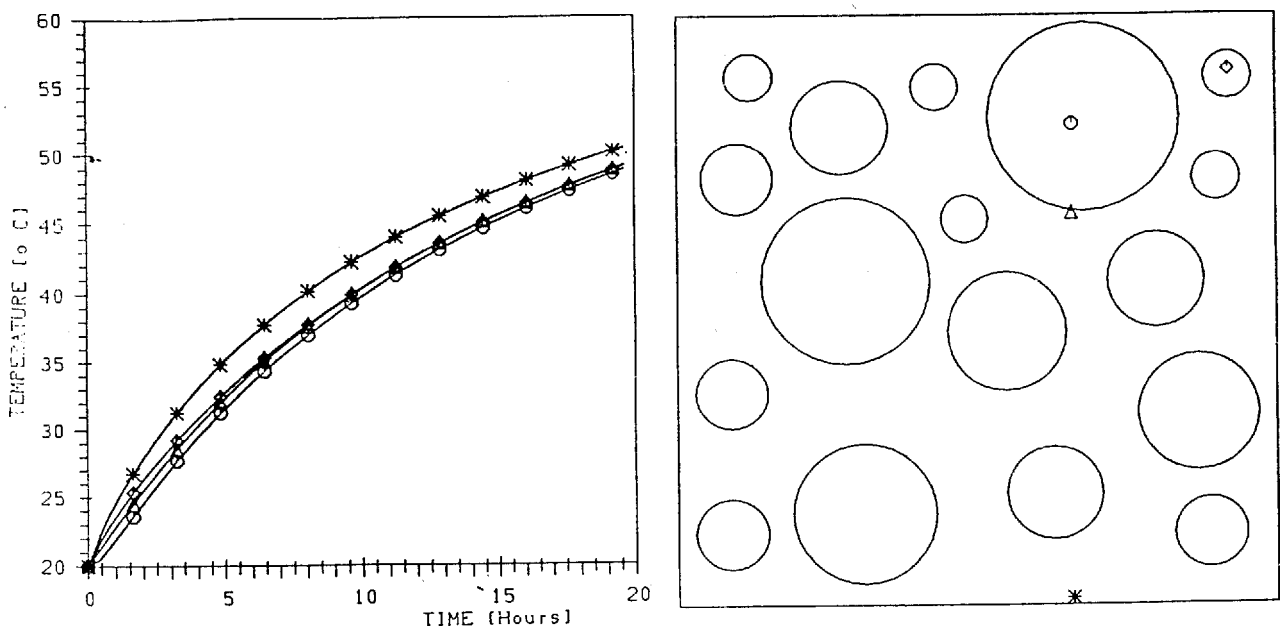

Fig. 5: Temperature evolution in hardening dam concrete under adiabatic conditions as determined at four different points in the composite structure.

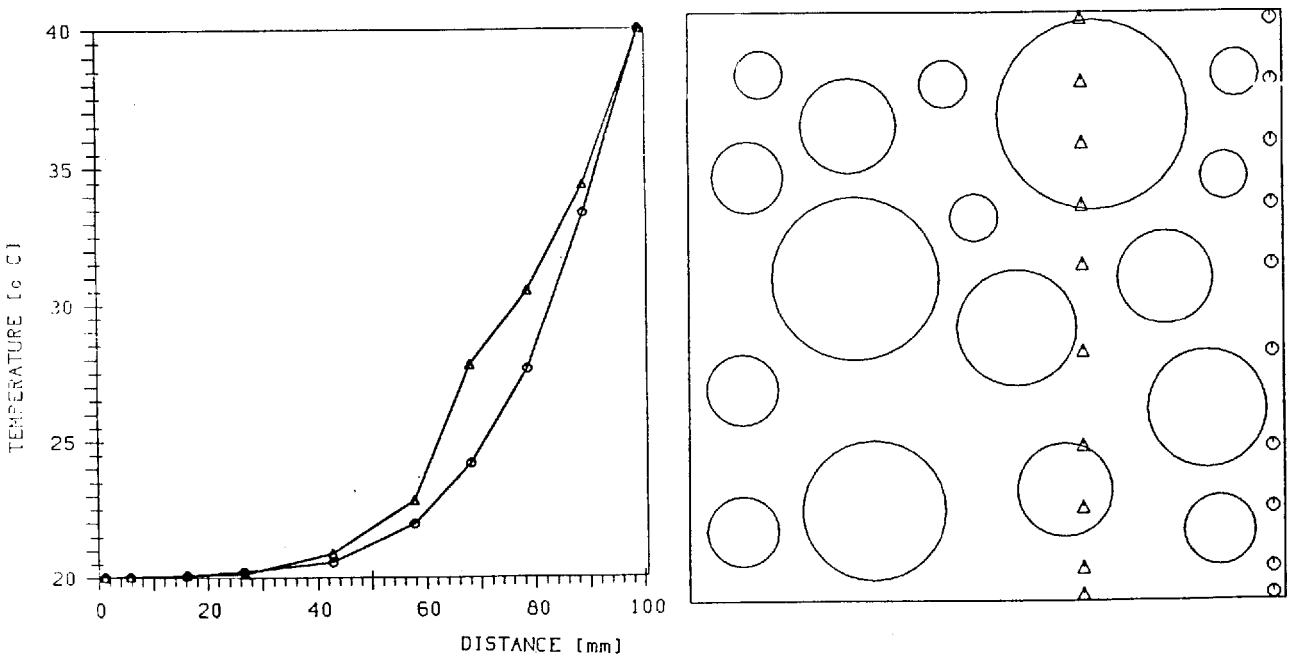

Fig. 6: Temperature distribution in a dried normal concrete having 20°C after being heated from the upper surface. The temperature is shown as function of the distance from the surface along two different lines after a heating time of 15 minutes. λ^m of the matrix is chosen to be 1 W/mK and λ^i of the aggregates 4 W/m°K.

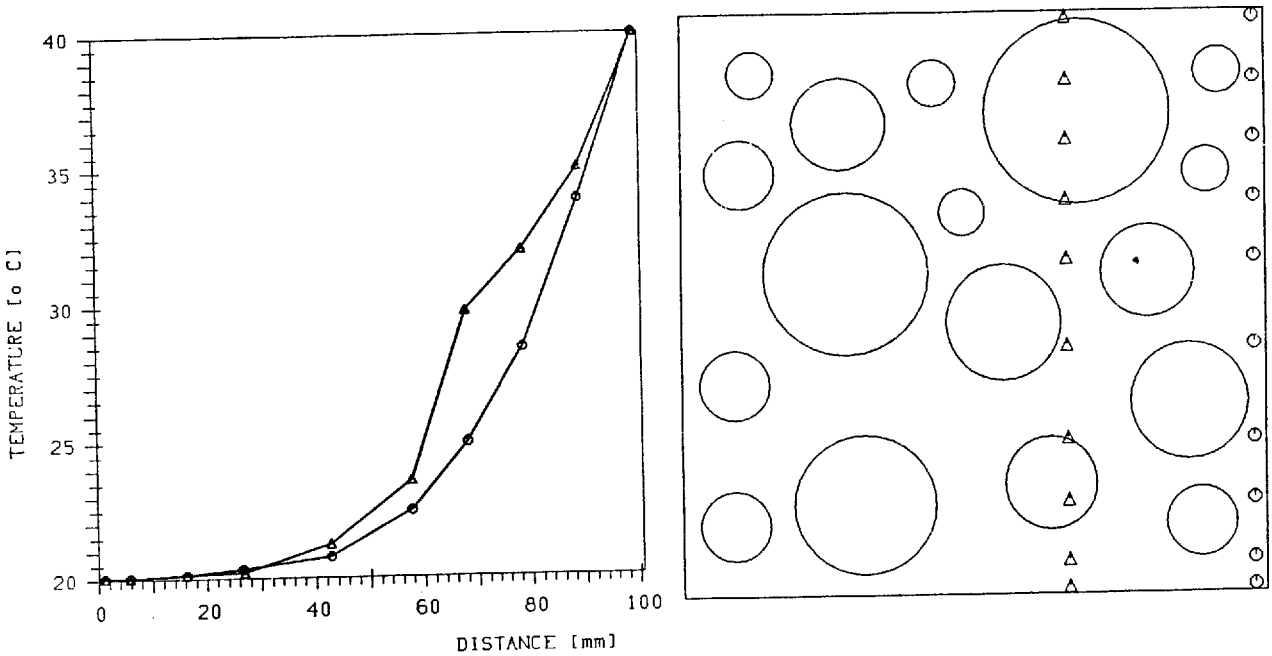

Fig. 7: Similar results as shown in Fig. 6 but calculated with the assumption of λ^i by 6 W/m°K.

CONCLUSIONS

Time-dependent temperature distributions in concrete elements are usually calculated assuming a homogeneous material. For normal Portland cement and concrete with aggregates not exceeding 32 mm this assumption is justified for the calculation of the temperature distribution and global thermal stresses in hardening concrete. In dam concrete having much larger inclusions and for rapid hardening cements the temperature distribution is influenced by the characteritics of the composite structure. Strong local temperature gradients can occur. In this case local thermal stresses will be superimposed to the global thermal stress field. The temperature distribution following heating or cooling of the surface strongly depends on the characteristics of the composite structure. If thermal stresses in concrete are to be calculated the perturbation of the global temperature field by the composite structure has to be taken into account.

LITERATURE

1. P.E. Roelfstra and M.Sadouki, Heat/1, Finite Element Modules for Materials Science and Structural Engineering, Swiss Federal Institute of Technology Lausanne (1984).

2. H. Sadouki, Simulation et analyse numérique du comportement mécanique de structures composites, Thèse No.676, Swiss Federal Institute of Technology Lausanne (1987).

3. K. Wesche, Baustoffe für tragende Bauteile, Vol.2, Beton Verlag, Wiesbaden (1981).

Special Panel Discussion II

Resource Economy in Cement and Concrete Making

RESOURCE ECONOMY IN THE PRODUCTION OF CEMENT

R Bastier, J Cantacuzene and J P Schaer

Ciments Francais Group
FRANCE

The experience of performance diagnosis and performance improvement among a large number of cement plants allows to define a methodology and to select priorities in technical and financial means allocation.

Performance diagnosis is designed to make sure that assets are properly kept and operation results really represent sustainable activity. It also considers differences of output or specific consumptions related to the intrinsic capabilities of more or less modern equipment and more or less stringent quality requirements.

Global performance comparison is developped to determine realistic standards regarding the major cost factors, so as to evaluate the potential savings resulting from capital addditions or technical support.

Three year plans are built in order to define the sequence of actions which are implemented and the set of parameters which tell that performances are improved as expected.

ECONOMIE DE RESSOURCES DANS LA PRODUCTION DU CIMENT

L'expérience du diagnostic des performances et de leur amélioration dans un nombre important de cimenteries permet de définir une méthodologie et de sélectionner les priorités dans l'affectation des moyens techniques et financiers.

Le diagnostic de performances est conçu pour s'assurer que les actifs sont correctement préservés et que les résultats opérationnels sont réellement significatifs d'une activité durable. Il étudie aussi les différences de production et de consommations spécifiques liées aux capacités intrinsèques d'équipements plus ou moins modernes et aux exigences plus ou moins contraignantes de qualité.

La comparaison des performances globales est élaborée pour définir des normes réalistes relatives aux principaux facteurs de coût, et d'évaluer les économies potentielles résultant d'investissements ou d'assistance technique.

Le plan à 3 ans est construit pour établir la séquence d'actions à mettre en oeuvre et définir la série de paramètres qui permettent de confirmer que les performances progressent comme prévu.

RESOURCE ECONOMY IN THE PRODUCTION OF CEMENT

J.P. SCHAER - Director of Cement Performance

Ciments Français Group.

Ciments Français has built a strong and wide experience in analyzing the cost factors in the production of cement, and in implementing the adequate methods to achieve the potential improvements. In some cases, pulling down old production lines or selecting a new location to build brand new works may prove cost-effective. But more often, improving already existing facilities appears to be a much wiser process.

We will exhibit the basic principles and the major results of the "Performance Program" at Ciments Français through the following steps :

- a performance diagnosis determines the effectiveness of the organization, the condition of the equipment, the reliability of the informations regarding technical and economical parameters ;
- a comparison between all the cement plants allows to define performance standards for a given plant and the potential improvements in specific areas ;
- a three-year plan, agreed with the operation managers, summarizes the actions to be implemented and the parameters which will make sure that the expected results are achieved.

Such a program appears to be much more reliable than the traditional approach based on capital addition studies, whereby the accumulated earnings derived from equipment supplier quotations very often reach irrealistic levels.

1. The performance diagnosis

The experience shows that it is relatively easy to exhibit good operating performance (high output, low cost of production and maintenance), at least for a short period of time, by keeping the assets in a poor way. Cement industry is intensive in capital, technology and professionalism, and earnings may result from spending the assets. Such a way of managing the business has often effects on quality control, environment or safety.

1.1. Conservation of the assets

Several fields should be paid careful attention :

- Raw materials owned reserves and long-term availability of purchased raw materials is the most critical factor ; attention is often focused on legal status and tonnage of the reserves, and not enough on the long-term consistency of the quality supplied to the cement plant ; this relies on an ongoing prospecting program, the day-to-day analysis of the quarried material and the yearly update of the reserves, based on the analytical results ; when the level of information is sufficient, a computer aided prospecting and quarrying plan should be implemented. Obviously, the lifetime of the reserves determines the rest of the operations.

- Equipment condition is a very sensitive matter, since reducing the maintenance expenses is the easiest way to improve operating profits for one or two years. And, because the cement industry is capital intensive, the cost of maintaining the equipment in good operating conditions is often underestimated. In case some pieces of equipment are supposed to be shutdown after a given number of years or in case the facilities have suffered from short maintenance in the past, specific adjustments on performance diagnosis may be necessary. But, in the other cases, a survey should be performed over 2-3 years in order to analyze the number of outages, their origin, their duration and the actions to correct the failures. This survey is essential, in addition to the direct inspection, and to the in-depth inspection reports, to determine whether the equipment is running under stable conditions.

- Manpower knowledgeability and responsibility is the third area where assets - intangible assets in this case - are vital regarding the future. The survey should focus on the organization, where filling or not some key positions often reveals the effectiveness of the organization (especially positions like equipment, quality, environment and safety inspection). The major rule is to clearly separate operating positions (production of raw materials, raw meal, clinker, cement, finished products) from support positions (maintenance, quality control, process, environment, personnel, marketing and sales, information processing). A clear diagnosis must be performed to check that all positions are properly filled and that replacement plans exist. This can be achieved through the analysis of the information system reliability, of the market perception, and of the compliance with internal procedures and external regulations.

Making sure that the operations are running in stable and safe conditions is a prerequisite to performance evaluation.

1.2. Performance evaluation

The major problem which we face is to get measurements which allow a comparison between cement plants which are not operated under the same conditions, in terms of economical parameters (relative cost of electric power and fuel, relative cost of manpower and capital additions, ...), or in terms of technicality (manpower background, industrial environment and support, ...). Each cement plant is different, but still, the experience shows that comparisons can be made and help selecting the operations to be improved in priority.

- Quality assurance should be considered first. Quality assurance means, in the same time, high quality standards all along the process, high consistency, and strong motivation of the operators towards quality objectives. The experience shows that optimizing the long-term quarry and supply plans with the primary target of getting a consistent raw mix also helps reducing the transportation and prehomogenization costs. Milling and homogenizing the raw mix with the primary target of getting a raw meal which is consistent both in chemical composition and size distribution also helps the efficient use of a given preheater and increases the burnability of the meal. Operating the kiln and the cooler with the primary target of getting a clinker both highly reactive and easy to grind, also helps minimizing the refractory consumption and optimizing the secondary air temperature. Running the finish mill with the primary target of achieving the cement specifications with as coarse fineness as possible also helps reducing the energy costs in the mill and in the separator. All this clearly indicates the list of quality parameters to be analyzed before talking about output and specific consumptions.

- Performance evaluation of each major piece of equipment is a useful intermediate step before evaluating the global performance of a given plant. Experimental results show how different types of kiln, mills (raw meal, solid fuel, cement), and separators perform in terms of output and specific consumptions when they are optimized. By comparing the operating conditions of a given piece of equipment, potential performance improvements can be measured.

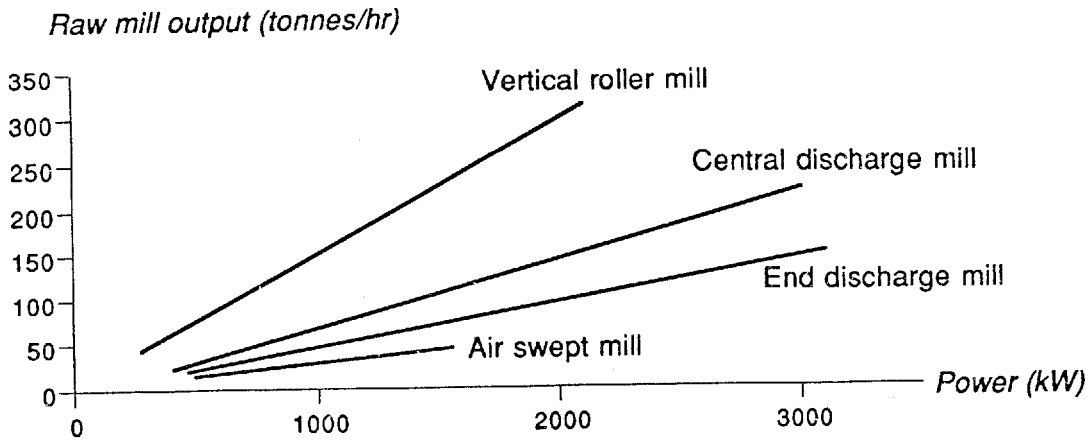

Chart n°1 : Raw mill output versus power consumption

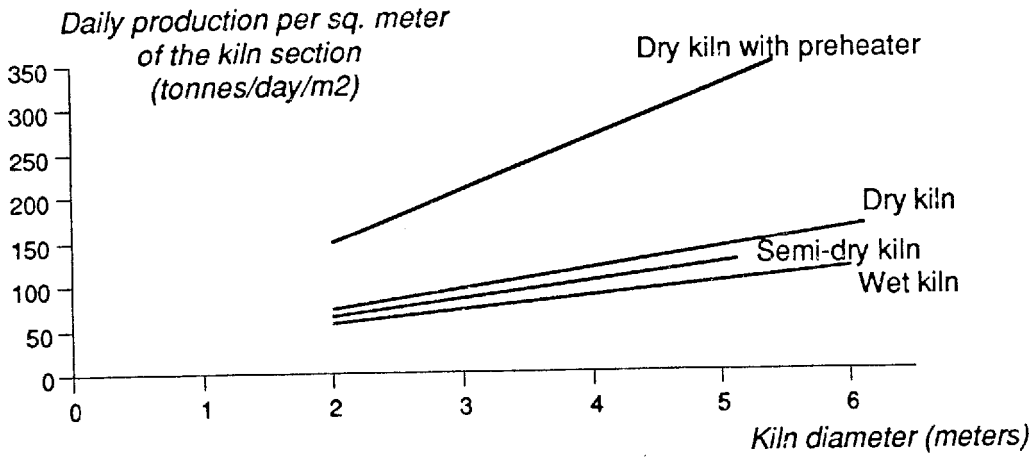

Chart n°2 : Kiln output versus kiln diameter

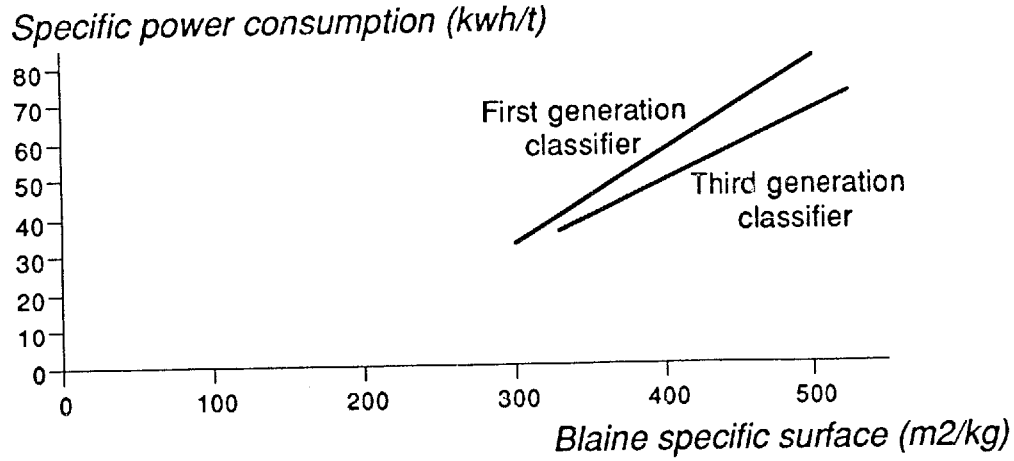

Chart n°3 : Power consumption versus cement fineness

2. The global performance comparison

Because of the differences in size and design of cement plants, but also because of the differences in the available raw materials and in the way the various steps of the production process have been optimized, a global comparison looks more difficult.

The analysis is based upon the observation that scale effects in the cement industry are often correlated with process improvements. The performance of a plant which produces 1 Mt/year with a single kiln is higher than the performance of a plant which operates three kilns to get the same tonnage.

Therefore, a plant which can produce 1 Mt of clinker per year with three kilns, the capacity of which is 0,2 Mt, 0,3 Mt and 0,5 Mt, should be considered as the addition of three plants which would have a "reference-capacity" of 0,38 Mt each.

The calculation may be refined if the production is only 0,75 Mt because the smaller kilns are used at 50 % of their capacity ; the "reference production" would then be 0,315 Mt. If productions are Pi for Ci capacities, the "reference production" is :

$$P = \frac{P_1C_1 + ...P_iC_i ..... + P_nC_n}{C_1 + ...C_i ....+ C_n}$$

In comparison, the "reference production" of a plant which produces 0,75 Mt when its capacity is 1 Mt with only onekiln, remains 0,75 Mt.

An additional refinement is necessary to calculate the "reference production" of cement, depending on the capacities of the cement mills involved, and the additions to clinker (pouzzolane, fly ash, limestone).

This will not be developed here ; it results in a production which may be very different from the total output of a given plant, but much more relevant to the potential performance.

In order to illustrate the conclusions, we shall focus on two major cost factors : energy and maintenance.

2.1. Performance in energy consumption

The basic observation shows that saving thermal energy generally requires increased electrical energy (by drawing more gases through the preheater, or the cooler, or by drawing tertiary air to the precalciner, ...). Of course the trade-off depends on the relative cost of fuel and power, in various countries or even in various provinces for a given country. But, in order to compare the total energy consumed to produce the reference tonnage in each plant, we selected the ratio 1 : 7 (the cost of 1 kWh of electrical energy is considered equivalent to the cost of 7 kWh of thermal energy). The result, as shown by chart n° 4, is interesting.

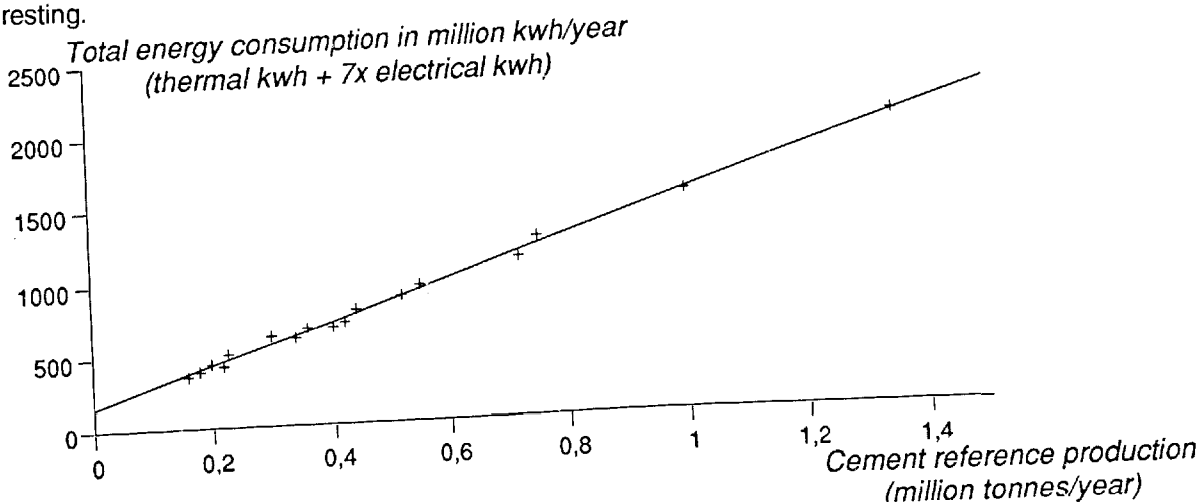

Chart n°4 : Total energy consumption versus cement production

Of course, for confidentiality reasons, the names of the plants are not given, but the chart is based on measured results.

It clearly appears that a great number of plants are very close to a base straight line which starts at a positive level when the production is zero (which means that the consumption of total energy results from the addition of a fixed term and a variable term, which is proportional to the tonnage produced) and reaches about 1500 kWh/t of cement for 1 Mt/year (for example 725 th/t of clinker or 800 thermal kWh/t of cement, plus 100 electrical kWh/t of cement or 700 equivalent thermal kWh/t of cement).

Of course, brand new plants may achieve better results in terms of total energy consumption, but this is not the scope of the study, which focuses on plants which have been in existence for many years, and were optimized step by step to achieve at least stable performances.

The chart also shows the plants which are over the base line, and the importance of the gap which is measured. Considering the cost per thermal kWh in a given plant, immeadiately tells the potential savings which are achievable through fuel and power optimization. This is a very strong help when a decision is to be made about where to allocate the efforts first, both in capital addition and technical support.

2.2. Performance in maintenance

The cost of maintenance should be considered here as the yearly average, over five years or so, of the total operating expenses and small capital additions which allow the plant to run in a stable way. Depending on the legislation or the financial situation, some expenses can be considered capital additions or not : they should be incorporated as well. Depending on the industrial environment, maintenance costs may cover in-house personnel or outside services ; spare-parts can be produced in the plant shop or bought ; all such costs should be added as well as refractories, grinding media, or lubricants. This is the only way which allows a fair comparison between plants which, by nature or because of the context, implement different maintenance policies : full preventive programs and early replacement against repair on failure, sub-contracting against in-house maintenance, ...

On chart n° 5 each plant is represented by its total maintenance cost and its reference production. The total maintenance cost is expressed as a percentage of the cost of a new 1 Mt/year plant, again for confidentiality reasons.

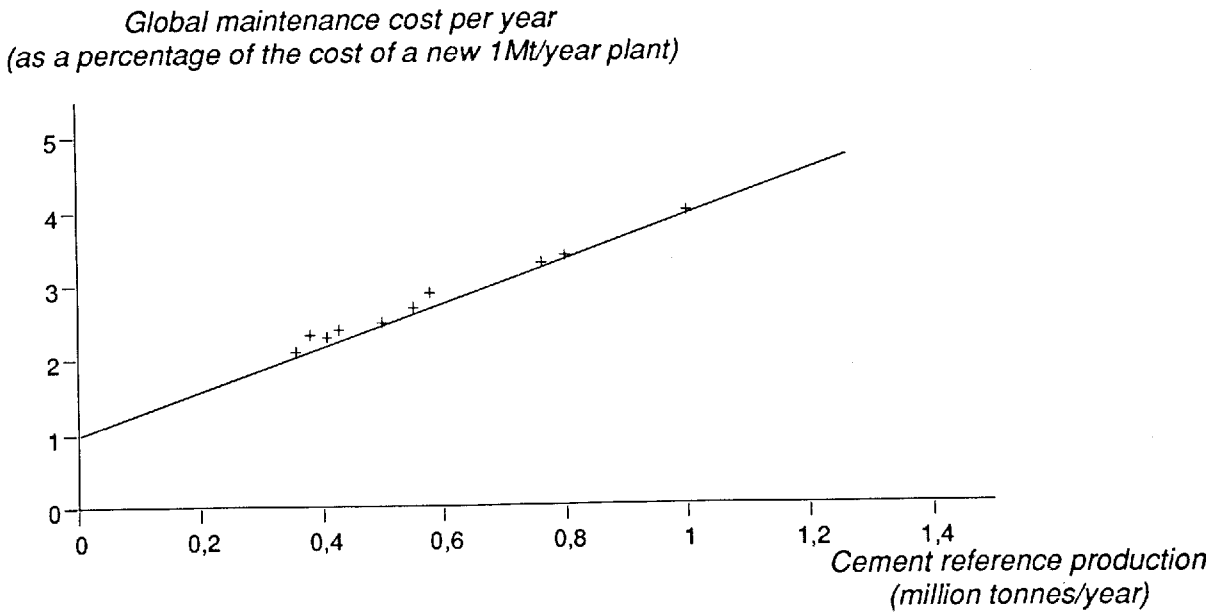

Chart n°5 : Global maintenance cost versus reference production

As for the energy consumption, this chart shows that many plants are close to a base line which starts at a positive level (the cost for maintening a mothballed plant) and reaches about 4 % of the cost of a new 1 Mt plant, when the actual production is 1 Mt/year. Similarly, some plants show expenses higher than expected, which indicates either that the equipment design is not optimum, or that the effort to keep the plant running is exceptionnally high, for whatever reason.

Of course, one should be very cautious when drawing conclusions from such observations, but, at least, it helps selecting the most promising targets where to put financial and technical efforts.

3. The three-year plan

Based on the performance diagnosis and the evaluation of potential earnings, it is possible to determine a sequence of actions in various areas in order to achieve performance improvements. In order to be effective, such a plan should follow a certain number of simple rules.

3.1. A long-term scheme

A clear view of what the plant should look like in the next decade is useful like town planning, to determine the location of future buildings or equipment, the traffic in, out, and through the plant. Too often, additions are designed upon short-term considerations and badly hinder the future development of the plant.

Doing so is not often easy because of the market uncertainty, and it may be necessary to design an alternative scheme in case a more or less important part of the plant is expected to be shutdown. But even in that case, the possibility to view one or two scenarios is important to avoid spending money on areas with little future.

3.2. A yearly reappraisal

The evolution in the market or the techniques require some flexibility when designing a three-year plan. Switching from one fuel to another, from one computer aided process control to another, may prove very cost-effective, and the plan cannot be considered as a strict directive. But the procedure for revising the plan should be clear enough too, in order to avoid irresponsible attitudes.

3.3. A strong personnel involvement

The construction of the plan should be top-down and bottom-up in the mean time, in order to develop the proper motivation among the whole personnel.

Performance improvement often means personnel evolution, in terms of numbers, skills, adaptation, etc ... This cannot be effectively achieved without involving the personnel from the starting point.

3.4. A set of parameters to measure performance improvement

Too often, objectives are not reached because of a lot of good reasons. When the effort is made, from the beginning, to set up the performance parameters which are expected to show whether actions were successful or not, it becomes much easier to track the real problems which always happen. It also helps deciding whether a specific action should be implemented in others locations, where conditions are more or less the same.

Conclusion

Above considerations regarding performance in the production of cement may look trite, and obviously, to a certain extent, they are.

Our major purpose was to show how the analysis of industrial operations can help selecting priorities in resource economy. And the main conclusion is that cement plant managers should not focus on improving the performance of any specific piece of equipment without looking at the connections between the various steps of the process. In order to achieve a global performance improvement, they should make sure that quality assurance and process control all along the production line guarantees quality consistency in the raw materials, raw meal, clinker as well as in finished cement.

INTEGRAL LAMINATION : AN ENERGY-SAVING FACTOR

Ph Martin

Process Department, Engineering Division, Technodes SA
Group Ciments Francais
FRANCE

SUMMARY

Tests were conducted in an integral lamination pilot mill by varying the following parameters :

- **fineness**
- **SO_3**
- **hemihydrate**

The resulting cements were compared to a paste, and to mortars and concretes, using a control sample made industrially in a ball mill.

In Iso mortars, the resistance of laminated cements is greater at 1 and 2 days ; at 7 and 28 days, it equals that of the control sample with the same Blaine.

With constantly workable concrete, the resistance of laminated cements is greater at 1 and 2 days; at 7 and 28 days, it is less than that of the control sample.

Specific electrical energy saving per grinding tool is 45%.

It should be noted however that the re-circulating load of an integral laminating mill is twice that of a ball mill thus; the capacities of the separator and its filter must be accounted for.

RESUME

Des essais ont été menés sur un atelier pilote de laminage intégral en faisant varier les paramètres suivants :

- **finesse**
- **SO_3**
- **hemihydrate**

Les ciments obtenus ont été comparés sur pâte pure, mortiers et bétons à un témoin fabriqué industriellement en broyeur à boulets.

Les résistances des ciments laminés sont sur mortiers Iso supérieures à 1et 2 jours et égales à 7 et 28 jours à celles du témoin pour une même surface Blaine.

Les résistances des ciments laminés sont sur béton à maniabilité constante supérieures à 1 et 2 jours et inférieures à 7 et 28 jours à celles du témoin.

L'économie d'énergie électrique spécifique est de 45 % pour l'outil broyant.

Il faut toutefois préciser que la charge circulante d'un atelier de laminage intégral est double de celle d'un atelier de broyeur à boulets, ce qui oblige à bien dimensionner le séparateur et son filtre notamment.

1. GOAL OF THE STUDY

The goal of this study was to determine the influence of fine milling, of total SO_3 content and of hemihydrate content on the characteristics of mortars and concretes made with cements from an integral lamination plant.

Moreover, we compared the performance of these cements in mortars and concretes to those of industrial cement made in a ball mill equipped with a cyclone separator.

2. PROPOSED CHARACTERISTICS OF CEMENTS TO BE STUDIED

To accomplish this, we have sought to make OPC, HP and HPR cements; that is, resistance at 2 days greater than 30 Mpa and resistance at 28 days greater than 60 Mpa on Iso mortar having the following characteristics:

Cement	Blaine value	SO_3 total	Hemihydrate
Industrial ball mill	4 100	3.45	1%
Pilot lamination F	3 700	3.30	0
Pilot lamination G	4 300	3.30	0
Pilot lamination H	4 300	3.30	1%
Pilot lamination I	4 300	3.70	1%
Pilot lamination J	4 300	3.70	1,5%

Variation in the fineness of laminated products is obtained only by variation in the rotor speed of the separator. Variation in the hemihydrate content of laminated products was obtained by heating the air admitted into the separator by a gas furnace.

A comparison of F and G cements allows the influence of blaine to be estimated, SO_3 and hemihydrate content are hold constant.

A comparison of G and H cements allows the influence of cement temperature to be estimated, SO_3 and Blaine are hold constant.

A comparison of H and I cements allows the influence of total SO_3 content to be estimated, Blaine and Hemihydrate are hold constant.

A comparison of I and J cements allows the influence of a Higher hemihydrate content to be estimated, Blaine and SO_3 are hold constant.

A comparison of these laminated cements in relation to the ball mill industrial sample allows the characteristics of laminated cement to be chosen based on the cement quality required.

3. CHARACTERISTICS OF THE CLINKER EMPLOYED

M.Khül	M.S.	M.A/F	K_2O	SO_3		C_3A	Ferrite		C_2S	C_3S	
							cubic				
96.3		2.30	1.45	0.13%	0.25%		6.4%	12%		29%	52%

Calculated according to Bogue

C_3A cubic	Ferrite	C_2S	C_3S
8.2%	11.2%	18%	56%

4. CHARACTERISTICS OF OBTAINED CEMENTS

The cement obtained in the pilot plant has a narrower grading curve owing to a third generation seperator. This influences on that part of the curve greater than 8 μm. APPENDIX 1.

5. CHARACTERISTICS OF PASTES AND MORTARS APPENDIX 2

5.1. PASTE CONTENT IN WATER

As with all cases of grading profile narrowing, the water content of the paste is increased due to the lower rheology of the powder.

Hemihydrate and SO_3 contents do not affect paste water content and initial set.

5.2. MORTAR WORKABILITY

As with the case of paste, mortar workability is also slightly eroded...

5.3. ISO MORTAR RESISTANCE

APPENDICES 3 and 4.

5.3.1. Influence of fineness

A 500 Blaine value increase in fineness (13.5%) increases resistance at 1 day by 12.7%, at 2 days by 10.6%, at 7 days by 3.5% and at 28 days by 1% for an 8.3% increase in electrical consumption.

5.3.2. Influence of hemihydrate content

An increase in hemihydrate content (0.2 to 0.9%) has a harmful effect on resistance at 1 day (- 7.6%), but has almost no effect on resistance at 2, 7 and 28 days.

5.3.3. Influence of total SO_3 content

By estimating the mortar resistance of H cement at Blaine value 4 550, a one-point increase (3.25 to 4.27%) in SO_3 content reduces resistance at 1 day (- 5%) but does not affect resistance at 2, 7 and 28 days.

5.3.4. Correlations

$R_{1\ day}$ = 4.62 + 0.006295 x Blaine value - 1.199 x SO_3 - 202.735 Hemihydrate
R^2 = 0.812

$R_{2\ days}$ = 11.163 + 0.006107 x Blaine value
R^2 = 0.9076 The introduction of SO_3 and hemihydrate does not improve the correlation coefficient

$R_{7\ days}$ = 37.966 + 0.00399 x Blaine value + 0.826 x SO_3 - 52.26 hemihydrate
R^2 = 0.99

or $R_{7\ days}$ = 40.40 + 0.00401 x Blaine value
R^2 = 0.94

There is no correlation possible on $R_{28\ days}$.

For this laminated clinker, the significant correlations show the harmful influence of hemihydrate content, notably at 1 day; this contradicts normal ball mill observations.

5.4. COMPARISON WITH INDUSTRIAL CEMENT

Laminated cement ground 300 Blaine value less than ball-milled industrial cement has the same resistance at 1 and 2 days and less resistance, on the order of 3%, at 7 and 28 days.

It is necessary to grind laminated cement 300 Blaine value more than ball-milled industrial cement to obtain the same performance at 7 and 28 days.

6. CHARACTERISTICS OF CONCRETES

APPENDIX 5.

6.1. RHEOLOGY APPENDIX 6.

As has already been seen with regard to pastes and mortars, the workability of laminated cements is eroded in relation to that of ball-milled industrial cement.

Regardless of the fineness of laminated cements (between 3,700 and 4,500 cm^2/g inclusive), their hemihydrate content (0 to 1.6%) or their SO_3 content(3.3 to 4.3%), their application in water is 5% greater (10 liters of water per m^3 of concretes) to that of cement ground in ball mills, whatever the slump (4, 8 or 17 cm).

6.2. RESISTANCE ACCORDING TO SLUMP APPENDICES 7, 8, 9, 10, 11, 12, 13

Despite a greater water application on concrete for laminated cements than for the control sample, resistance of the concrete is always greater at 1 and 2 days (an exception is laminated cement at 3,700 Blaine value, which has less resistance than the control sample at 2 days).

The effect of supplementary water application of laminated cements is not really felt until 7 and 28 days, when their resistance is less than that of the control sample.

The increase of resistance on concrete at 1 day varies from 6 to 17%, with an 8 cm slump in relation to the control sample.

The resistance at 2 days varies from - 7.7% to 15%, with an 8 cm slump in relation to the control sample.

The resistance at 7 days varies from - 10.5% to 0%, with an 8 cm slump in relation to the control sample.

The resistance at 28 days varies from - 7.5% to - 5.5%, with an 8 cm slump in relation to the control sample.

6.3. COMMENTARY

The conclusions reached concerning concrete differ slightly form those which had been reached concerning mortar. Resistance in mortars identical to the control sample at 7 and 28 days were obtained with a grind 300 Blaine points higher than the control sample. The equivalent resistance in concrete at 7 and 28 days is never obtained. The resistance of laminated cements at 1 and 2 days is always greater than cement ground in ball mills with the same Blaine value.

7. GRINDING ENERGIES

In the case of the cement studied, the grinding energy spent on the roller press alone is 26 kWh/T as compared with 48 kWh/T for the industrial ball mill. The electrical energy saved is therefore 45%.

APPENDICES 14 and 15

It should be noted, however, that the re-circulating load of an integral lamination shop is 2.5 times greater than the recirculating load of a plant equipped with a ball mill.

In comparison with a classical ball mill plant which produces the same throughput, an integral lamination plant will require the enlargment of the elevator, separator and separator filter.

8. CONCLUSIONS

With regard to the clinker employed, the study has shown that, for laminated cements :

- The hemihydrate has a harmful effect on mortar resistance.
- They are less susceptible to SO_3 fluctuations than cements ground in a ball mill.
- Their short-term resistance is greater, and their long-term resistance weaker, than those of ground cements.
- They consume 45% less electrical enery in the grinding tool alone.

ANNEXE 1

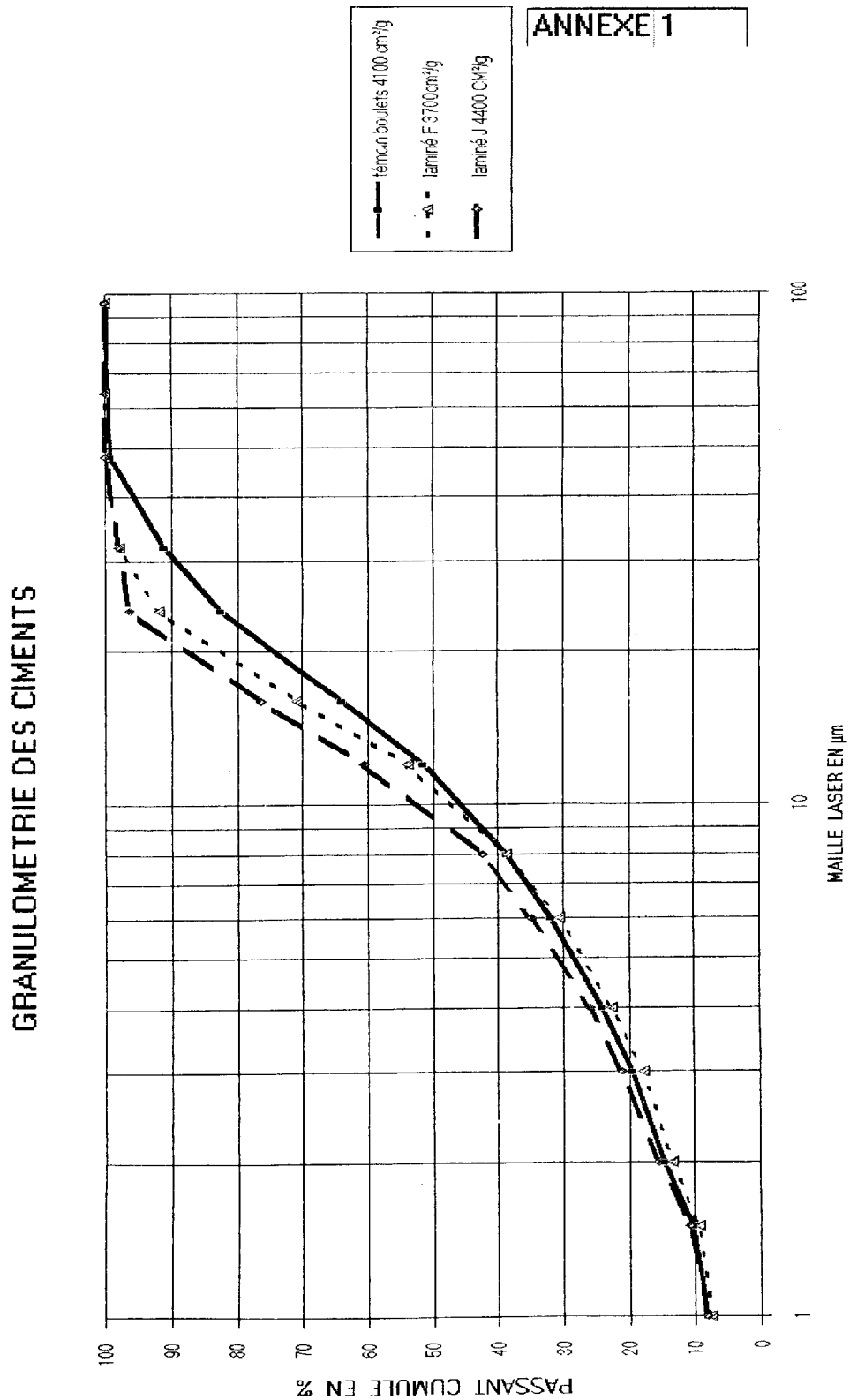
GRANULOMETRIE DES CIMENTS
témoin boulets 4100 cm²/g
laminé F 3700cm²/g
laminé J 4400 CM²/g
PASSANT CUMULE EN %
100
90
80
70
60
50
40
30
20
10
0
1
10
100
MAILLE LASER EN µm

ANNEXE 2

REFERENCE DES CIMENTS	CARACTERISTIQUES DES CIMENTS					CARACTERISTIQUES DES PATES ET MORTIERS					
	BLAINE	LASER		SO3	hémi-hydrate	EAU Pat pure	début de prise	mania. E/C=0.5	RESISTANCES A LA COMPRESSION		
		32µm	24µm	total					1	2	7	28
témoin CPA HP BR. à BOULETS 1992	4080	8.8	17.3	3.45	1.00%	30.8	2h45	11"	24.1	35	58.2	71.6
pilote CPA HP LAMINAGE F	3765	2	8.1	3.15	0%	32.8	2h15	11"	24.5	34.1	55.6	69.9
pilote CPA HP LAMINAGE G	4270	2.1	3.6	3.3	0.20%	33.8	2h00	20"	27.6	37.7	57.5	70.7
pilote CPA HP LAMINAGE H	4325	3.7	4.4	3.25	0.90%	34	2h20	19"	25.5	36.9	57.6	67.7
pilote CPA HP LAMINAGE I	4550	3.1	3.5	4.27	1.20%	34.2	2h35	15"	25.4	38.5	59.1	70.8
pilote CPA HP LAMINAGE J	4465	2	3.7	3.8	1.60%	32.6	2h10	14"	25.4	39.1	57.9	71.9

ANNEXE 3

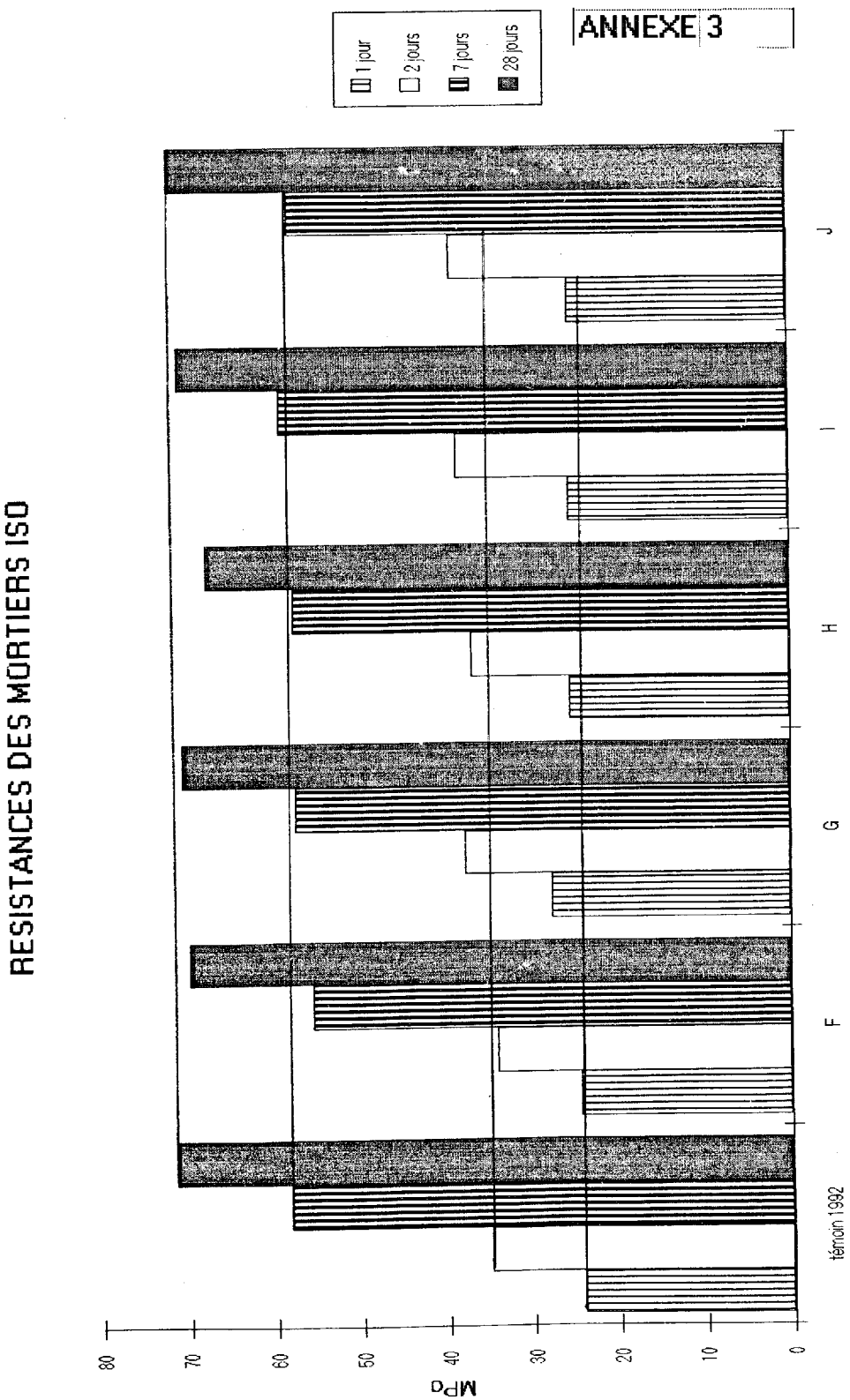
RESISTANCES DES MORTIERS ISO
1 jour
2 jours
7 jours
28 jours
J
I
H
G
F
témoin 1992
MPa
80
70
60
50
40
30
20
10
0

ANNEXE 4

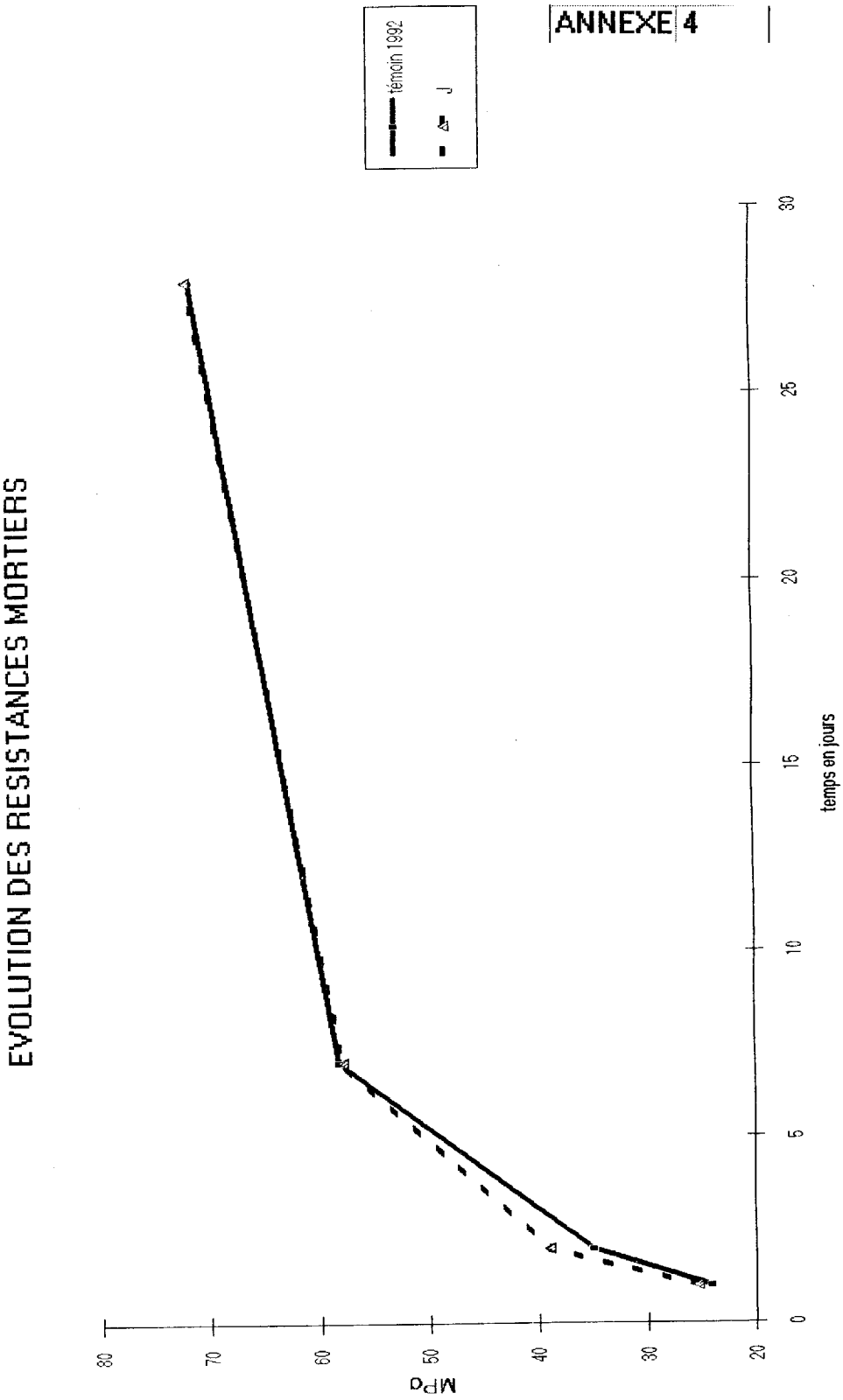
EVOLUTION DES RESISTANCES MORTIERS
témoin 1992
J
MPa
80
70
60
50
40
30
20
0
5
10
15
20
25
30
temps en jours

ANNEXE 5

REFERENCE DES CIMENTS	CARACTERISTIQUES DES CIMENTS					CARACTERISTIQUES DES BETONS							
	BLAINE	LASER		SO3 total	hémi-hydrate	EAU EN L/M3	E/C	SLUMP EN CM	RESISTANCES A LA COMPRESSION :				RESSU. en ml
		32µ	24µ						1	2	7	28	
TémoinCPA HP BR à BOULETS 1992	4080	8.8	17.3	3.46	1.00%	165	0.47	4	19.3	30.2	45.9	56.6	15
						175	0.5	8	17.3	26.5	43	53.9	23
						185	0.53	15	13.7	22.1	37.9	49.3	39
PiloteCPA HP LAMINAGE F	3765	2	8.1	3.15	0%	175	0.5	4	21.2	28.9	42.1	50.7	24
						185	0.53	8	18.7	24.3	38.6	49.8	38
						195	0.56	17	16	20.5	33.9	46.2	55
PiloteCPA HP LAMINAGE G	4270	2.1	3.6	3.3	0.20%	175	0.5	5	19.8	28.5	43.3	54.3	17
						185	0.53	9	17.7	26.2	40.3	49.4	25
						195	0.56	17	15.5	23.1	36.1	46.9	44
PiloteCPA HP LAMINAGE H	4325	3.7	4.4	3.25	0.90%	175	0.5	4	22.5	29.1	42.8	53	13
						185	0.53	8	19.9	26.7	38.7	49.5	22
						195	0.56	17	17	22.4	35.8	44.7	33
PiloteCPA HP LAMINAGE I	4550	3.1	3.5	4.27	1.20%	175	0.5	5	19.3	30.4	41.5	52	15
						185	0.53	8	18.1	28.4	40.7	50	24
						195	0.56	17	14.9	24.1	36	44.3	38
PiloteCPA HP LAMINAGE J	4455	2	3.7	3.8	1.60%	175	0.5	6	21.1	31.8	42.2	53.7	15
						185	0.53	10	20.1	28.9	41.4	49.3	25
						195	0.56	17	17.8	26.5	36.4	44.8	36

ANNEXE 6

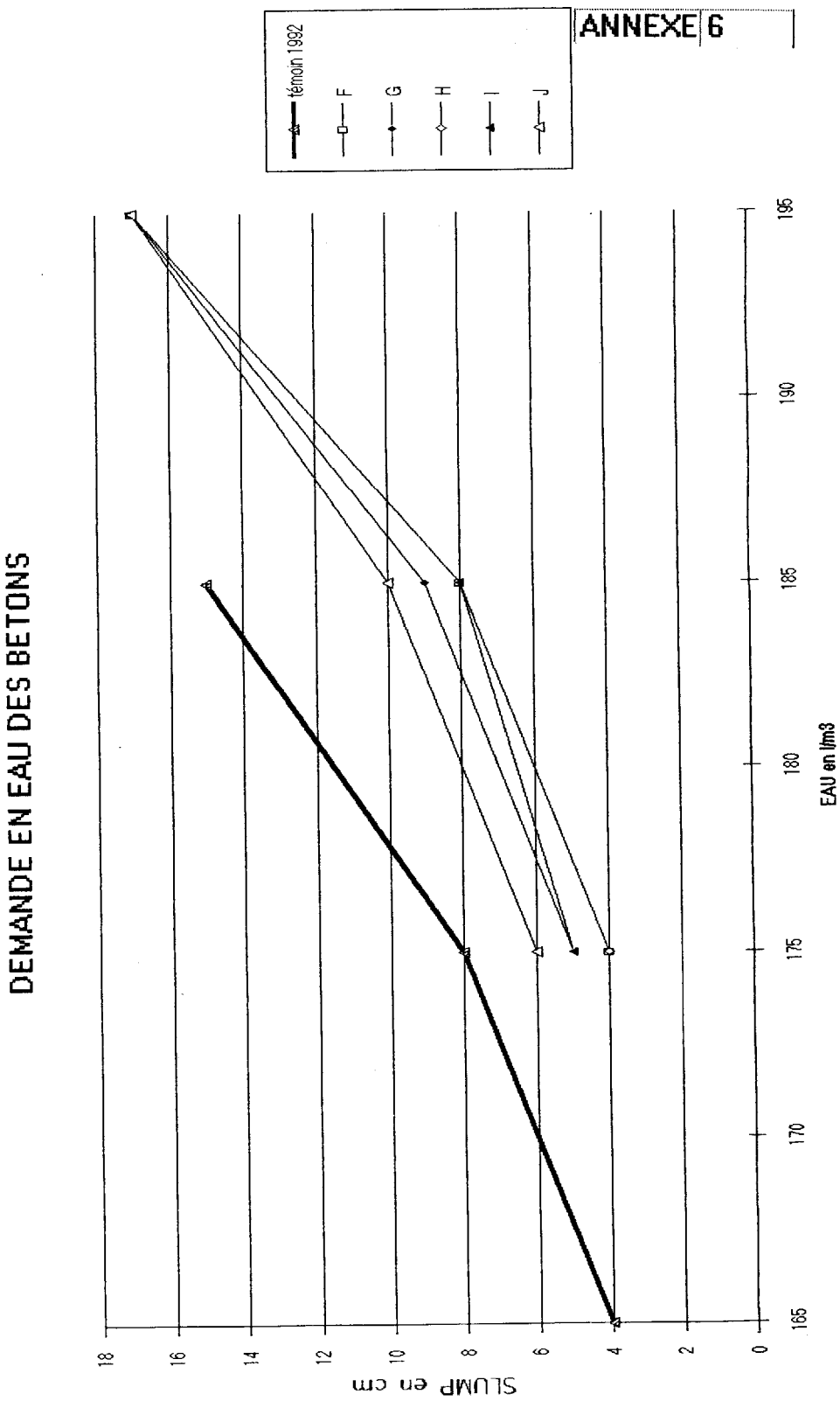
DEMANDE EN EAU DES BETONS
témoin 1992
F
G
H
I
J
SLUMP en cm
0
2
4
6
8
10
12
14
16
18
EAU en l/m3
165
170
175
180
185
190
195

ANNEXE 7

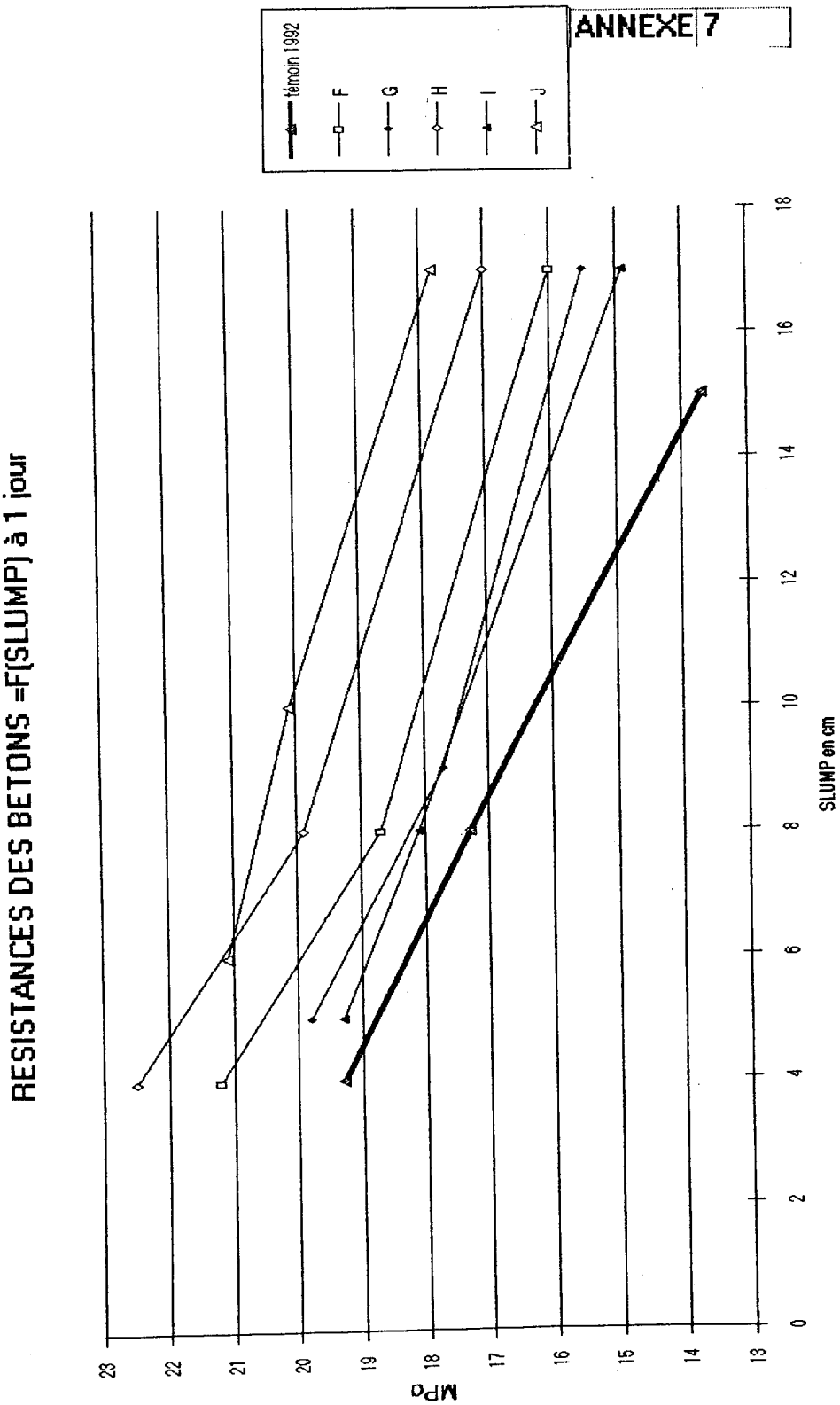
RESISTANCES DES BETONS =F(SLUMP) à 1 jour
témoin 1992
F
G
H
I
J
MPa
23
22
21
20
19
18
17
16
15
14
13
SLUMP en cm
0
2
4
6
8
10
12
14
16
18

ANNEXE 8

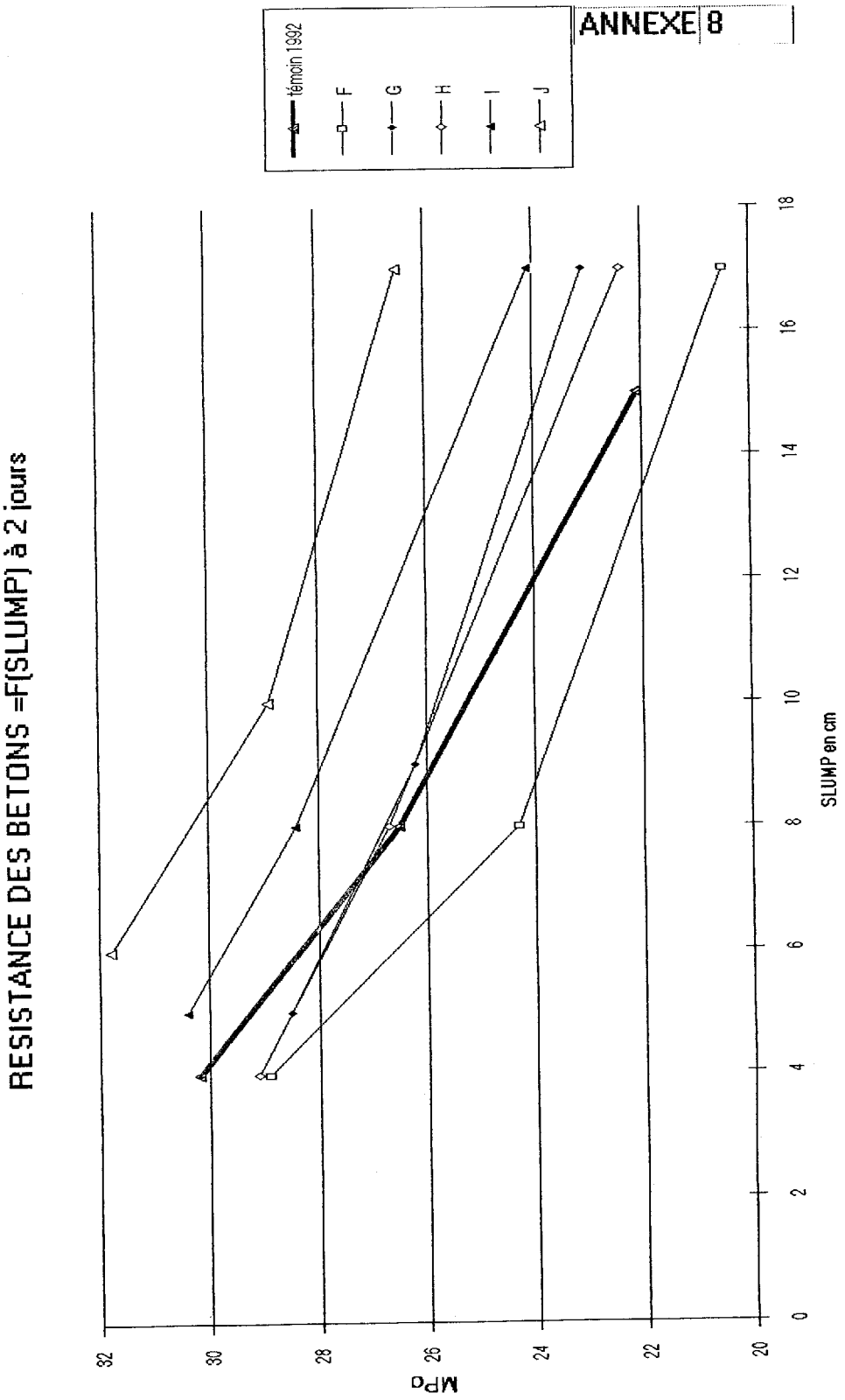
RESISTANCE DES BETONS =F(SLUMP) à 2 jours
témoin 1992
F
G
H
I
J
MPa
32
30
28
26
24
22
20
0
2
4
6
8
10
12
14
16
18
SLUMP en cm

ANNEXE 9

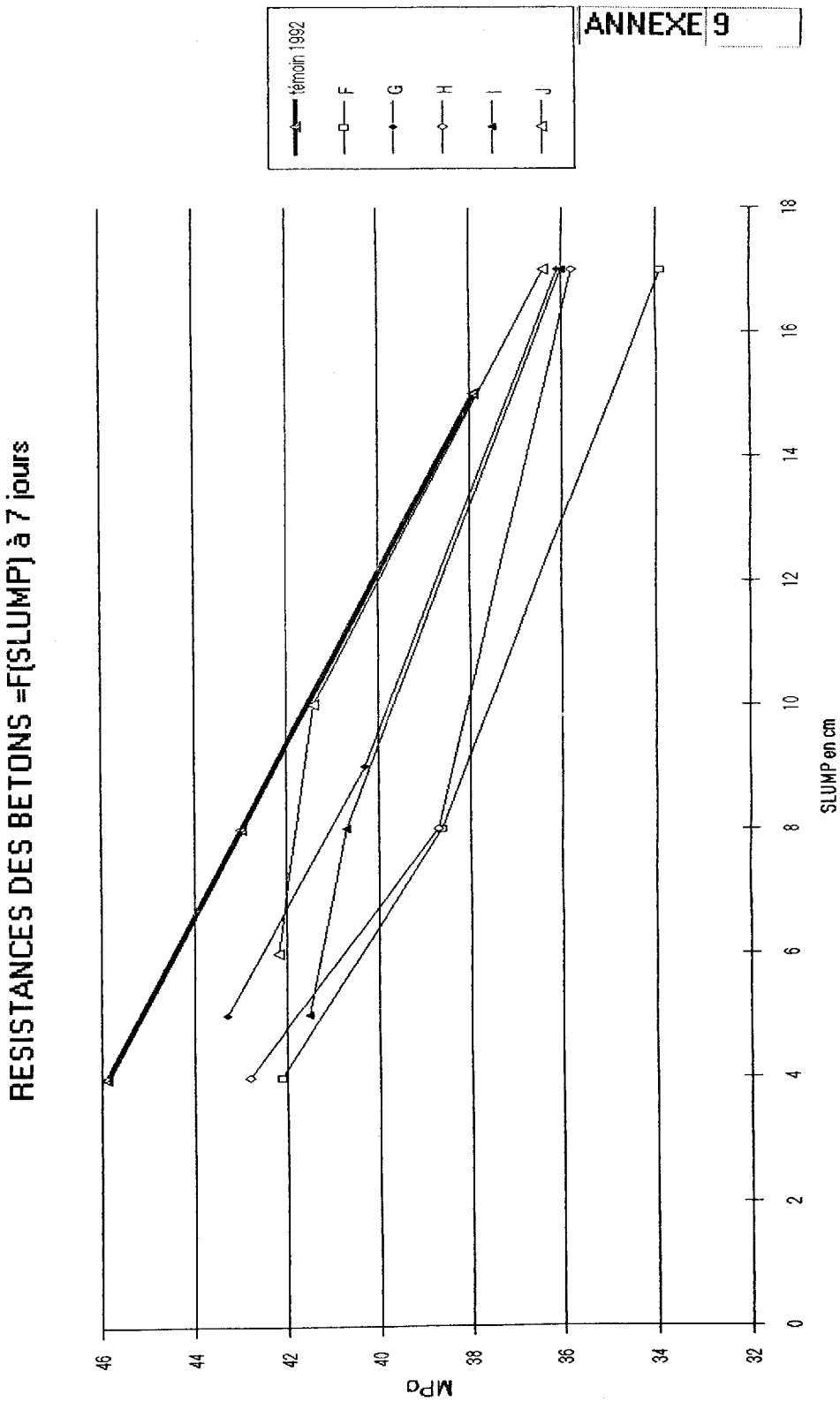
RESISTANCES DES BETONS =F(SLUMP) à 7 jours
témoin 1992
F
G
H
I
J
MPa
46
44
42
40
38
36
34
32
SLUMP en cm
0
2
4
6
8
10
12
14
16
18

ANNEXE 10

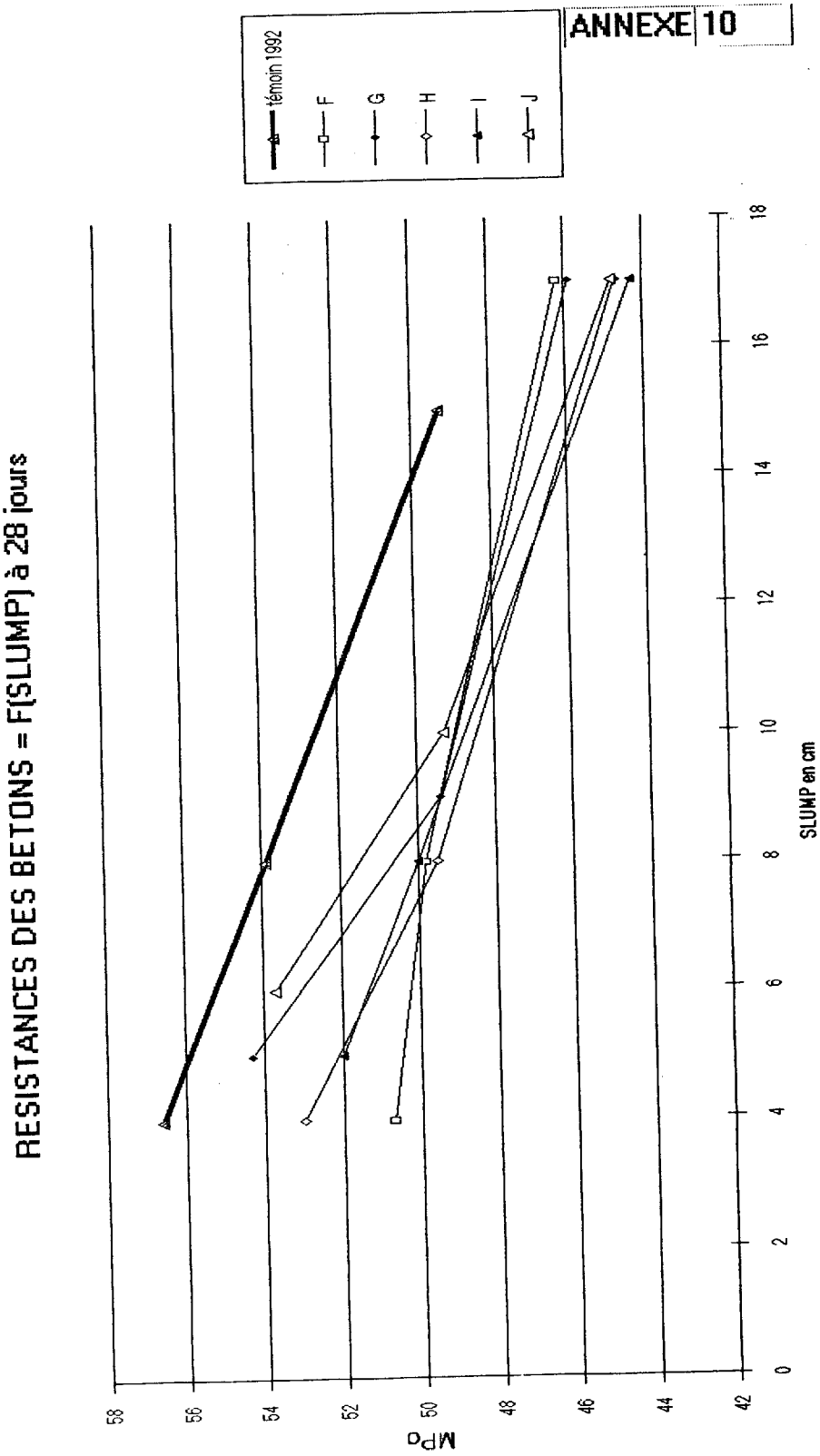
RESISTANCES DES BETONS = F(SLUMP) à 28 jours
témoin 1992
F
G
H
I
J
MPa
58
56
54
52
50
48
46
44
42
0
2
4
6
8
10
12
14
16
18
SLUMP en cm

ANNEXE 11

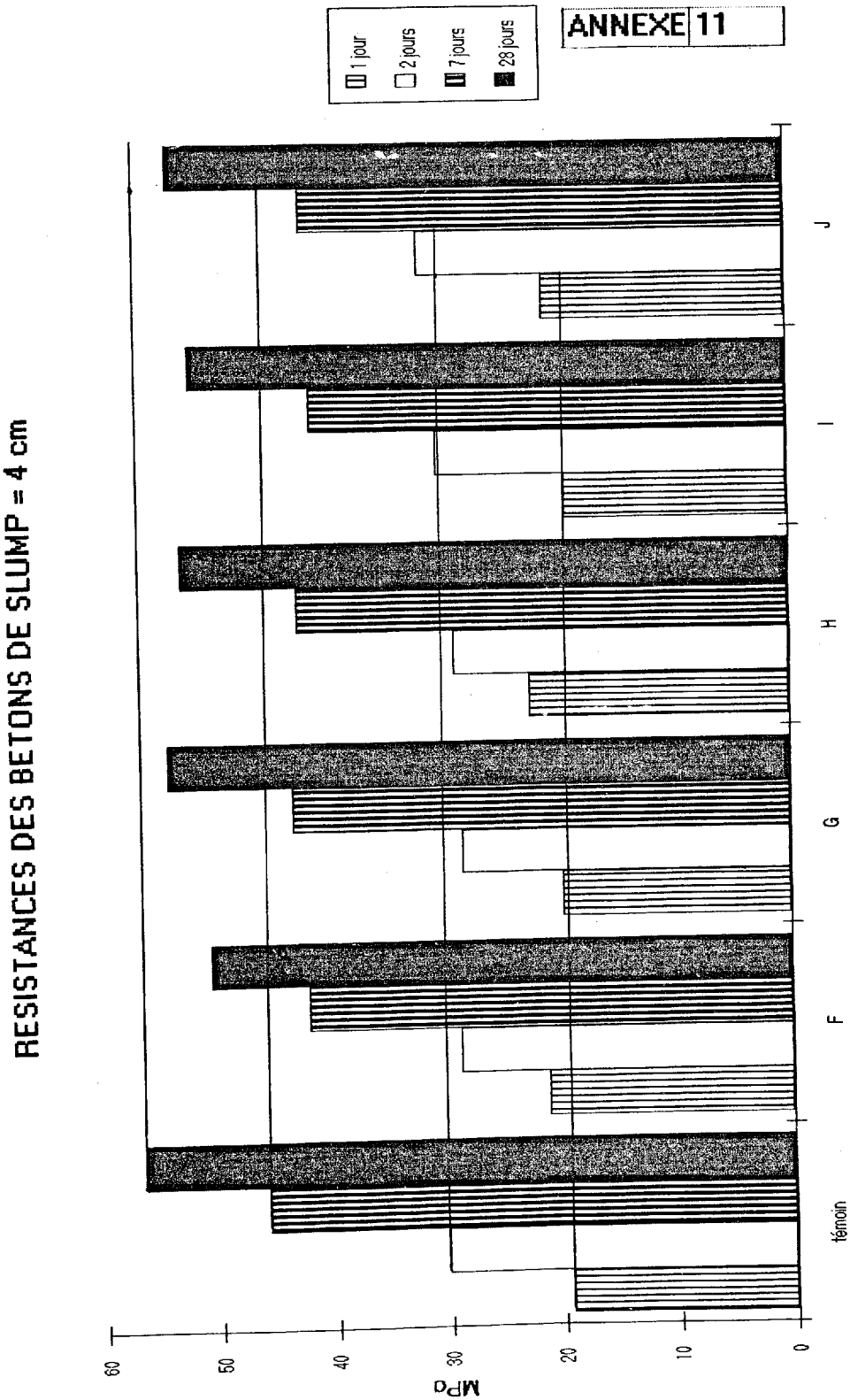
RESISTANCES DES BETONS DE SLUMP = 4 cm
1 jour
2 jours
7 jours
28 jours
MPa
0
10
20
30
40
50
60
témoin
F
G
H
I
J

ANNEXE 12

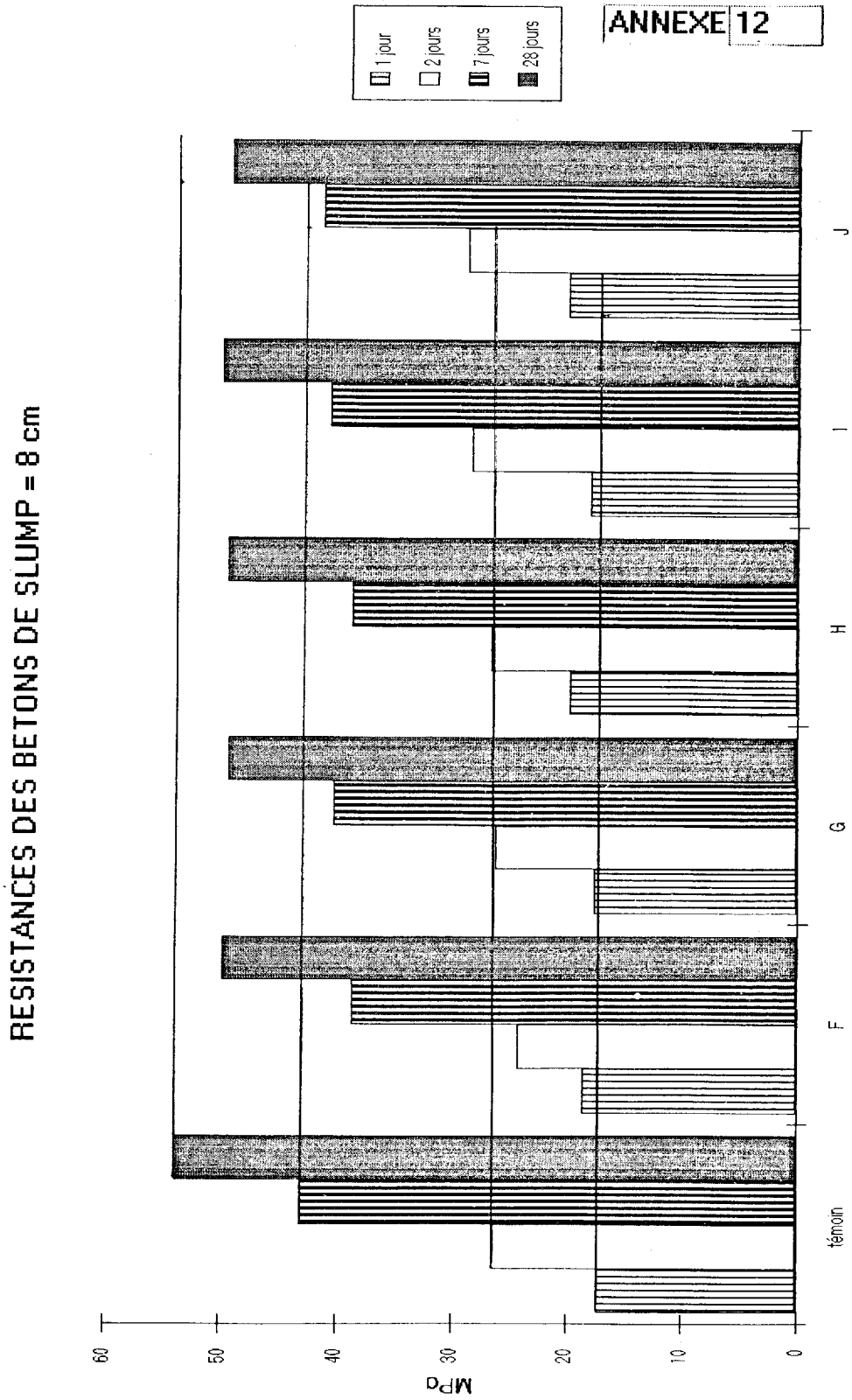
RESISTANCES DES BETONS DE SLUMP = 8 cm
1 jour
2 jours
7 jours
28 jours
MPa
0
10
20
30
40
50
60
témoin
F
G
H
I
J

ANNEXE 13

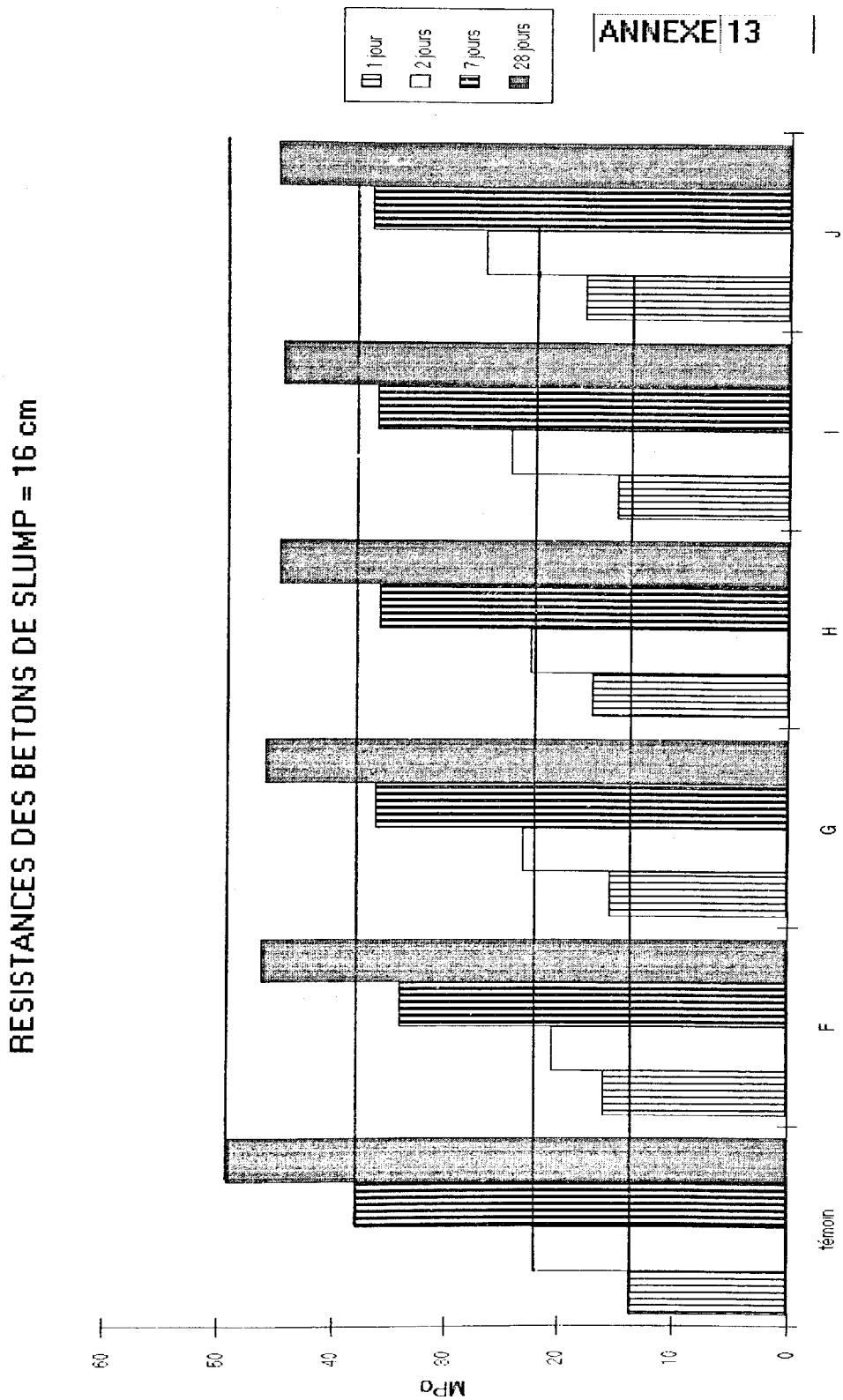
RESISTANCES DES BETONS DE SLUMP = 16 cm
1 jour
2 jours
7 jours
28 jours
MPa
0
10
20
30
40
50
60
témoin
F
G
H
I
J

ANNEXE 14

REFERENCE DES CIMENTS	CARACTERISTIQUES DES CIMENTS					PROCESS			
	BLAINE	LASER		SO3 total	hémi-hydrate	Temp. ciment	Débit T/H kWh/T	Refus/ Alim.
		32µm	24µm					
témoin CPA HP BR. à BOULETS 1992	4080	8.8	17.3	3.45	1.00%	85°C	47 T/h 48 kWh/T	5
pilote CPA HP LAMINAGE F	3765	2	8.1	3.15	0%	49 °C	0.827 T/h 24 kWh/T	11.7
pilote CPA HP LAMINAGE G	4270	2.1	8.6	3.3	0.20%	40 °C	0.787 T/h 26 kWh/T	13.2
pilote CPA HP LAMINAGE H	4325	3.7	4.4	3.25	0.90%	85 °C	0.837 T/h 25 kWh/T	12.9
pilote CPA HP LAMINAGE I	4550	3.1	8.5	4.27	1.20%	85 °C	0.825 T/h 27 kWh/T	13.2
pilote CPA HP LAMINAGE J	4455	2	8.7	3.8	1.60%	95 °C	0.849 T/h 26 kWh/T	12.7

ANNEXE 15

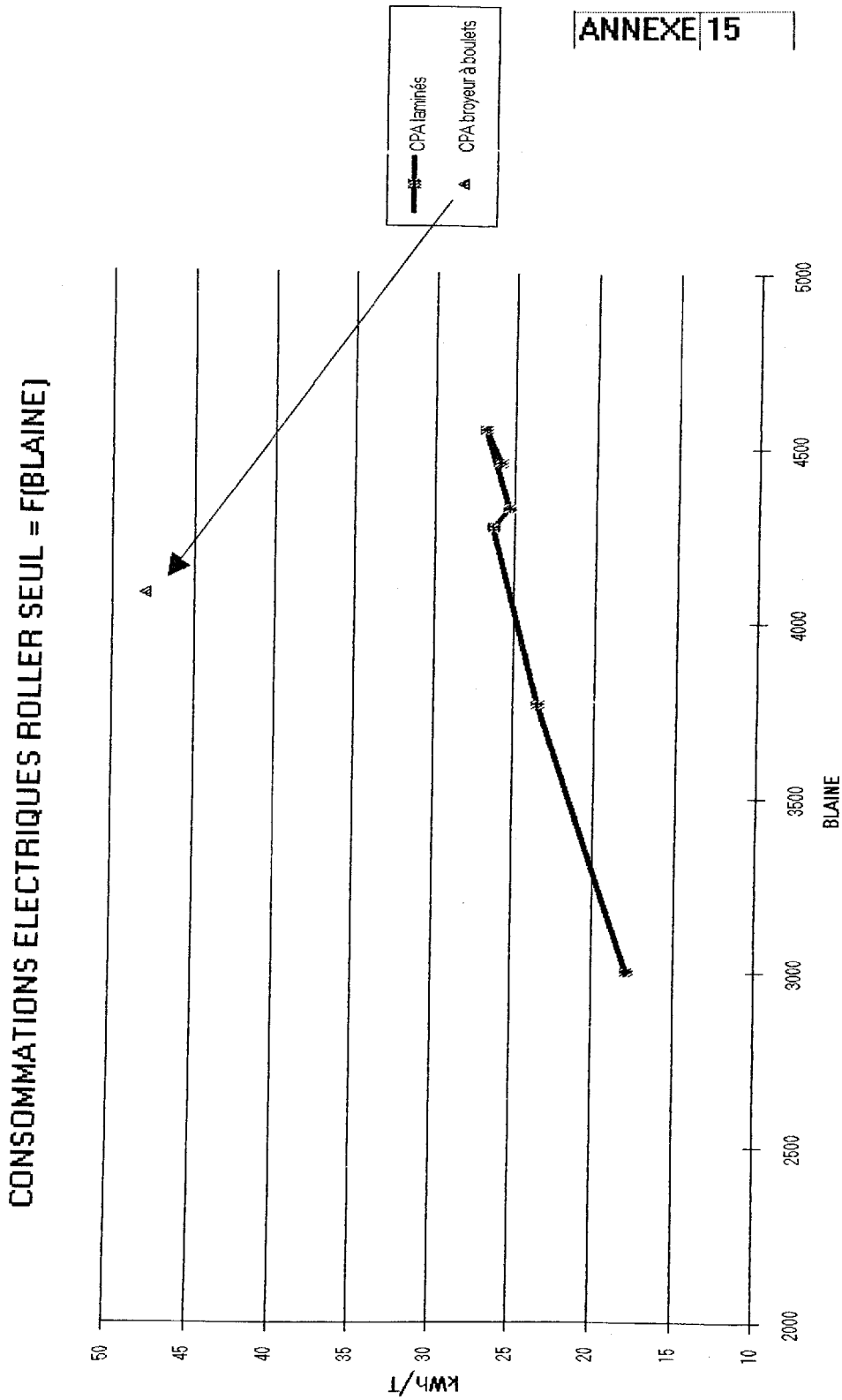
CONSOMMATIONS ELECTRIQUES ROLLER SEUL = F(BLAINE)
CPA laminés
CPA broyeur à boulets
kWh/T
50
45
40
35
30
25
20
15
10
2000
2500
3000
3500
4000
4500
5000
BLAINE

THE USE OF POZZOLANIC MATERIALS AS AN ADDITIVE TO CLINKER : EXPERIENCE OF A MOROCCAN CEMENT PLANT

Y Ennadifi

Societe Cimenterie De L'oriental-CIOR
MOROCCO

Summary

It is estimated today that approximately 1.2 million tons of additives are used in Morocco to produce 6 million tons of compound cements. More than half of compound cements is made with pozzolana ; the rest, with fillers.

Reserves of more-or-less active pozzolane are estimated at several million tons.

The ever-growing use of materials with pozzolanic properties is the result of selective research involving these materials and of industrial production tests on compound cements.
However, it is estimated that the means established to profit by these materials are not yet sufficient, given the wide variety of both volcanic and sedimentary pozzolanas.

In this study, we describe the experience, over a period of ten years, of a Moroccan factory (the Oujda Cement Plan) concerning the use of volcanic ashes with pozzolanic properties in the production of compound cements.

1) INTRODUCTION

Pozzolanic cements are standardized in Morocco since 1971. Compound cements were standardized in 1986. The enforcement of the standard and the production of compound cements have allowed the Moroccan Cement Industry to save (in comparison with the old standard) 220,000 tonnes of clinker and the equivalent of 20,000 tonnes oil equivalent annually ; which means about 15 % reduction in energy consumption.
These savings have been accompanied by a noticeable improvement in the characteristics of cements.

The use of pozzolana as an additive began at the CIMENTERIE DE L'ORIENTAL in 1983. The desired goal was, on the one hand, to save clinker after the increase in the price of energy, and, on the other hand, to produce cements with active additives designed for some projects where special resistance is requested, in particular to aggressive water.
In fact, Morocco lacks black furnace slags and does not produce enough fly-ashes.

2) GENERAL REMINDERS

a) Pozzolana :

Pozzolana is a rock including constituents which, in the presence of water and at normal temperature, are capable of combining chemically with lime to form insoluble minerals in the water and which are endowed with binding properties. Numerous rocks, such as certain volcanic glass, zeolite tuffs and diatomites, have pozzolanic properties.

Minerals formed by reaction with lime are mainly hydrated calcium silicates and aluminates.

b) Pozzolanic activity :

Pozzolanic activity depends on the proportion of minerals which are formed through the alkaline reaction of lime on acid silicates and which lead to mechanical resistance after the hardening process

c) Moroccan standard :

The Moroccan Standard MN 10 01 F 004 currently in force defines different categories of cement, a category being characterized by its composition and the different classes corresponding to it.
Each class is characterized by the compressive strength resistance obtained by a specific date.
There are two categories of cements depending on the proportion of clinker contained (excluding gypsum): pure Portland cements contain at least 97 % clinker, (CPA, or artificial Portand cements), and compound cements (CPJ) contain at least 65 % clinker, which means less than 35 % secondary constituents. The standard enlarges the list of secondary constituents to include artificial pozzolanas and fillers.

Resistance classes are defined by a bracket which indicates minimal and maximal compressive strength resistance after 28 days.

To meet the particular needs of certain users, the standard provides sub-groups 45 R and 55 R (R = Rapid) for groups 45 and 55, specifying resistance at 8 days.

3) CHARACTERIZATION OF PROSPECTED NATURAL POZZOLANAS

Prospected rocks are located at the foot of the Gurugu volcanic range which dominates the city of Nador, a major port on the Mediterranean coast. It is a volcanic formation which features a great diversity in the different series of volcanic eruptions. One finds the entire range of volcanic magmas, from rhyolites to basanites, including trachytes, andesites and latites.

Table 1 in the Appendix gives the detailed chemical composition and the soluble phase of the four pozzolanas examined.

a) Tuff :

This concerns non-sedimented aerial tuffs found on the large areas of the median parts of the Gurugu volcanic range. The rocks beneath the surface are homogeneous. They are soft, with small grains less than 2 mm in diameter, principally constituted of clay, quartz, small amounts of orthose and with a vitreous phase. Silicates and silica are the main components of the vitreous phase.

b) Trachyte :

This trachyte is found just below the tuff level. It has a porous rock shape and is homogeneous ; it is pale blue and dry.

It is principally composed of sanidine and tridymite, with a vitreous phase made of silica and silicates.

c) Cinerite :

This is a rock which is composed of both fine and consolidated elements. It is found some ten kilometers from the Gurugu volcano, close to the sea.
It seems that part of the volcanic projections was the object of a reshaping and alteration process in the sea which gave rise to this rock with lamellibranchiate fossils, currently used at the OUJDA factory as pozzolanic material. The rock is covered by a layer of fine clay-and-limestone cinerite elements. X-ray diffractometry shows that these cinerites are composed of fine quartz and glass.

d) Latite :

This rock consists of blocks, 200 mm in diameter, with a large variety of crystalization.
It is composed principally of quartz, orthose and glass.
The vitreous phase is essentially composed of silicates and silica.

4) TEST RESULTS AND DISCUSSION

4.1. Different tests have been carried out to measure pozzolanicity ; the results are given in the table below :

	Soluble Silica %	Milligrams of lime fixed by one gram of pozzolana	AFNOR Test (Solubility Graph)	ASTM Test with sand and lime 8 days compressive strength resistance (MPa)
TUFF	4.40	420	Negative	0.5
TRACHYTE	4.90	260	Limited	1.1
CINERITE	6.80	280	Positive	10.6
LATITE	20.50	500	Positive	7.0

Mineralogical analysis by x-ray diffraction gave the following results :

	TUFF	TRACHYTE	CINERITE	LATITE
Active Constituent (glass or amorphous)	H	M	H	M
Inactive Constituents				
QUARTZ	H	-	H	H
TRIDYMITE	-	H	-	-
ORTHOSE	M	-	M	H
SANIDINE	-	VH	-	-
CLAY	VH	-	M	-
HEMATITE	-	H	-	-
CALCITE	-	M	H	M

VH = very high
H = high
M = medium

The above analyses show that each pozzolana is composed of an active and an inactive part.
The x-ray diffraction tests have shown the presence of glass (active consistuent) in the four pozzolanas examined.

This presence of glass is confirmed by all the pozzolanic power measuring tests. However, owing to humidity, grindability and behavior in cement mills, impact on the resistance of compound cements is different.

The four pozzolanas are arranged below in decreasing order according to the degree of pozzolanicity and long-term resistance.

Classification in Decreasing Order	Soluble Silica %	Fixed lime Quantity	AFNOR Pozzolanicity Test	ASTM Pozzolanicity Test	Compressive Strength Resistance at 28 days
1	Latite	Latite	Cinerite	Cinerite	Cinerite
2	Cinerite	Cinerite	Latite	Latite	Latite
3	Trachyte	Trachyte	Trachyte	Trachyte	Trachyte
4	Tuff	Tuff	Tuff	Tuff	Tuff

Although the pozzolanic nature is connected to the fixed lime quantity, the test results given above show that this pozzolanicity does not present a strong correlation with the increase of compound cement resistance.

For this reason, the choice of pozzolana retained for the production of compound cements was based on the results of resistance tests.
From our point of view, it shows that the performance of compound cements depends on other parameters which, at the present stage of our research, we have not yet been able to identify.

4.2. Behavior of compound cements in relation to seawater :

We have studied the test-tube behavior of compound cements made with the four pozzolanas in comparison with pure cements.

The compound cements were prepared in the laboratory and ground to a Blaine value fineness of 3500 cm2/g.

Test tubes with five types of cement were immersed in seawater for three months ; seawater was renewed every three days.

Visual checks made from the eighth week showed a noticeable dissolution of the surface crust in the pure cement test tubes in comparison with those of the pozzolana-additive cements.

The addition of pozzolana therefore confers on concrete a protective layer by making the active phase of pozzolana react with hydrolysis lime during cement hydration.

4.3. Long-term resistance tests :

The results of the resistance tests given in Table 2 demonstrate that the pozzolanic power of the four types of additive begins to reveal itself between 28 days and 3 months.

The resistance attained by the four types of compound cements at the end of three months is superior to that of pure cements.

In conclusion, the study and the choice of a pozzolana for the production of compound cements has allowed, on the one hand, substantial savings of energy and, on the other hand, an improvement in the characteristics of concretes made with compound cements, particularly with regard to durability, resistance to aggressive water and hydration heat.

Table 1 : Chemical Composition of Pozzolanas

NATURAL POZZOLANAS				
	TUFF	TRACHYTE	CINERITE	LATITE
Humidity Loss of ignition	17 19.28	0.11 0.35	17 17.40	5 4.33
Insolubles	56,94	89,33	54,70	61,60
Si02 Al203 Fe203 CaO MgO K2O Na2O	4,40 0,10 0,10 0,10 0,15 0,70 0,36	4,90 0,33 0,46 0,20 0,10 2,10 1,10	6,80 0,55 0,60 0,58 0,40 0,90 N.D.	20,50 1,65 0,90 0,79 0,70 2,60 0,20
TOTAL	99,10	99,08	98,93	98,27
Si02 Al203 Fe203 CaO MgO Ti02 MnO SO3 K2O Na2O P205	54,26 14,38 3,31 1,24 3,33 0,96 0,00 0,00 1,47 1,36 0,11	67,50 15,07 5,03 1,53 0,43 0,18 0,00 0,00 6,67 3,76 0,02	61,52 11,59 2,34 2,18 1,81 0,19 0,00 0,00 2,89 N.D. 0,04	64,63 16,01 0,92 0,25 0,23 0,88 0,00 0,00 9,28 0,46 0,20
TOTAL	99,58	100,59	99,52	99,06

1st part : Chemical analysis of the elements of the soluble part
2nd part : Total chemical analysis

Table 2 : Comparison of mechanical resistance in MPa observed in mortar test tube

Evidence of the pozzolanic effect of various pozzolanas

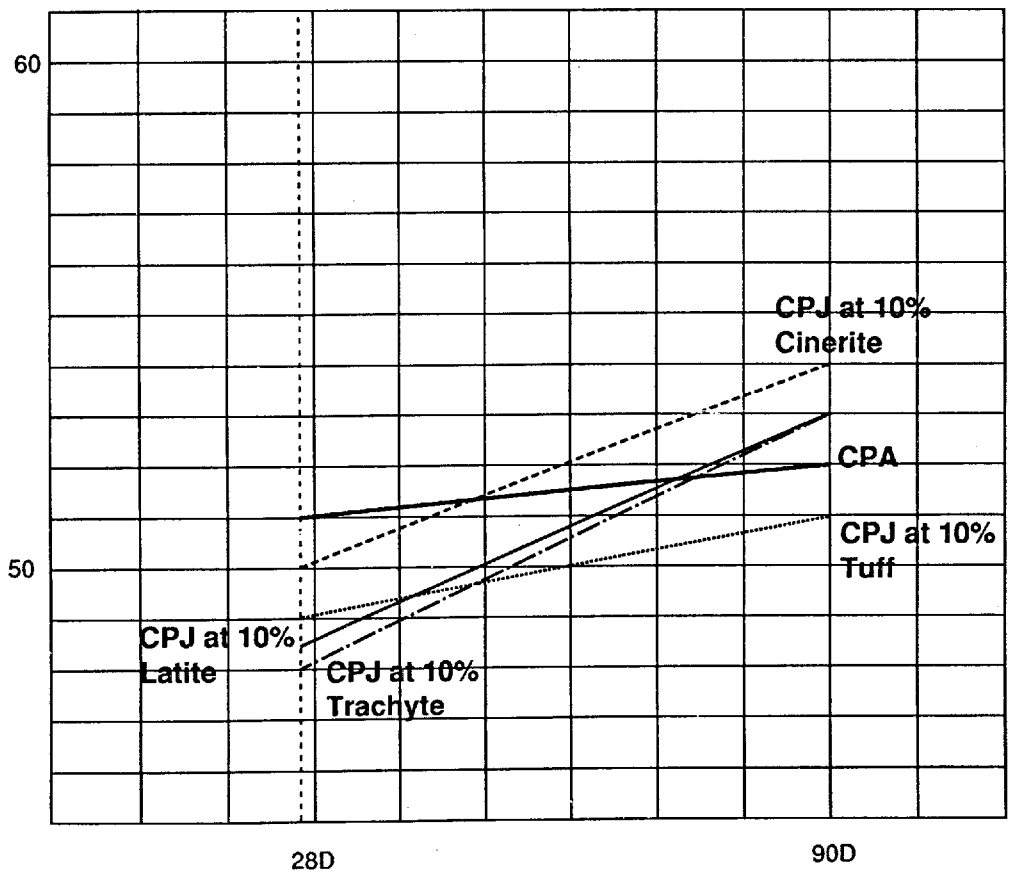

MAP

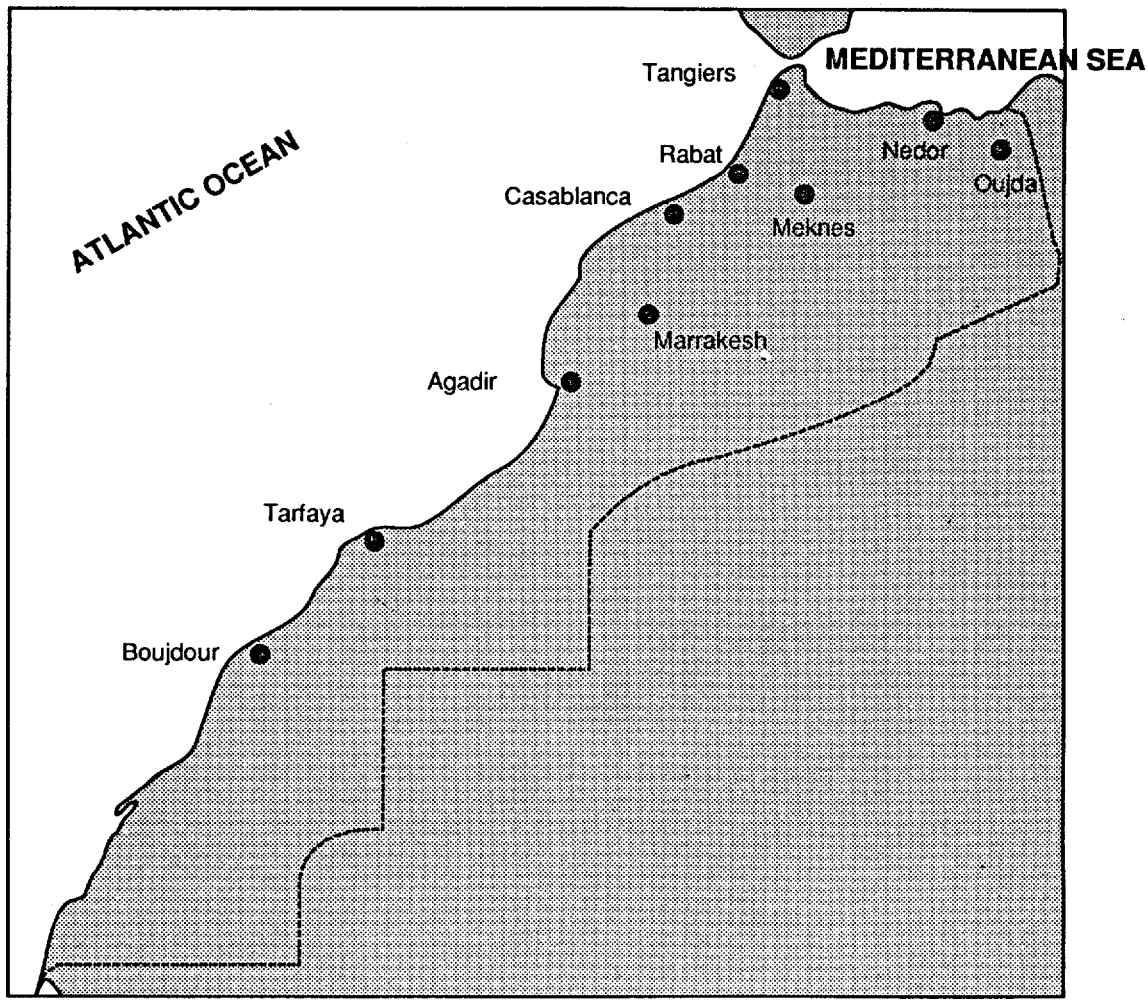
MEDITERRANEAN SEA
Tangiers
ATLANTIC OCEAN
Rabat
Nedor
Oujda
Casablanca
Meknes
Marrakesh
Agadir
Tarfaya
Boujdour

RESOURCE ECONOMY IN CONCRETE MAKING

F Hawthorn and P Jaugey

Ciments Francais Group
FRANCE

Resource economy in ready mix concrete industry results in optimizing the raw materials, the mix designs and the process of producing and delivering. As a whole, it can be expressed as an improved control of the energetic, environmental and social costs of the delivered concrete.

After the Second World War, mineral additives, fly ashes, pozzolan and limestone filler, generally available as by-products of other industries, were used as raw materials of cement and concrete manufacturing. They are of common use either as components of blended and/or special cements or as direct additives in concrete mixes at lower extent. More recently the development of admixture technology enabled a tremendous improvement of the mechanical properties of the concrete, resulting in drastic reductions of volume and costs in concrete structures. These new technologies open a promising field for the use of low grade aggregates and recycled crushed concrete. There are also important sources of saving in the process of mixing and delivering concrete itself. As an example, the improvements of weighting units and the use of security margin for achieving a designed strengh. The environmental regulations for recyling the aggregates and washing waters which are more and more edicted and enforced to the concrete industry will also bring a contribution to the natural resource economy.

Special Panel Discussion III

Cement in Hazardous Waste Management

THE USE OF WASTE FUELS IN THE CEMENT INDUSTRY

Ferenc D Tamás

Department of Silicate Chemistry and Technology
University of Veszprém
HUNGARY

ABSTRACT

Wastes containing burnable organic materials are very common. Their disposal can cause considerable difficulties, as many of them are hazardous. Incineration is a safe method, provided that the temperature is high, the atmosphere is oxidising and the residence time of waste-laden gases is long. The burning of wastes as supplementary fuels in cement kilns is a technically and environmentally viable method, as here all three provisions are definitely more than adequate. Even the most stable hazardous organics can be safely destructed in cement kilns, without the slightest environmental hazard. Waste co-firing however may cause considerable difficulties during cement manufacture, as some elements in the supplementary fuel (mainly halogens and sulfur) create volatile compounds which in turn promote ther formation of rings and other adherent layers in the kiln and/or heat exchangers, unless precautionary measures (gas-, meal- and/or dust-bypasses) are built.

ZUSAMMENFASSUNG

Abfälle, die brennbare organische Materialien enthalten, sind sehr häufig. Ihre Entsorgung kann beträchtliche Schwierigkeiten verursachen, da viele als gefährlicher Sondermüll gelten. Die Verbrennung ist eine sichere Lösung, falls die Temperatur hoch, die Atmosphäre oxydierend und die Aufenthaltsdauer der abfallbeladenen Gase lang genug sind. Eine technisch und umweltbedingt günstige Methode ist die Verbrennung in Zementöfen, da hier alle drei Voraussetzungen sicher gegeben sind. Selbst die stabilsten gefährlichen organischen Stoffe können ohne die geringste Gefahr für die Umgebung in Zementöfen sicher entsorgt werden. Die Zusatzbefeuerung mittels Abfälle kann allerdings in der Zementherstellung zu großen Problemen führen, da einige Elemente im Zusatzbrennstoff (vor allem Halogene und Schwefel) solche flüchtigen Verbindungen bilden, welche wiederum Ringe und andere anhaftende Schichten im Ofen und/oder in den Wärmeaustauschern ausbilden, falls keine Vorsorgemaßnahmen (Gas-, Mehl- und/oder Staubbypäße) getroffen werden.

INTRODUCTION

Hazardous organic wastes can be safely and completely destructed to nonhazardous products by a controlled exposure to a high temperature, among oxidizing conditions. If temperature, excess oxygen and the time of exposure are adequate, then the carbon and hydrogen content of the waste is transformed to carbon dioxide and water, respectively, i.e. materials which are always present in the atmosphere; while nitrogen, sulfur and halogen contents are transformed into elementary nitrogen (or, to a small part to nitrogen oxides), sulfur dioxide and hydrochloric acid, respectively. Nitrogen is a natural ingredient of Earth's atmosphere, while NO_x, HCl and SO_2 and definitely less hazardous than the parent organics; and, if necessary, can be subsequently removed.

Cement-making kilns, where temperatures are over 1400°C, (flame temperatures exceeding even 2000°C), the atmosphere is always strongly oxidizing (cement contains ferric components, the presence of ferrous iron would deteriorate the quality of cement), and, due to the extremely large volume of the rotary kilns, the exposure time of the waste within the destruction zone is very long, seem to be an ideal alternative for the thermal destruction of hazardous wastes. Besides that, there are some other features which make this type of thermal destruction attractive: the environment is basic, i.e. acid products of destruction (SO_2, HCl) are almost fully absorbed in the clinker or in the dust; and as all modern cement-making kilns are equipped with efficient precipitators, in most cases there is no need to invest for further exhaust gas purification equipment (scrubbers, fabric filters, etc.). The calorific value of the waste is utilized for cement burning, thus enables savings in primary fuel consumption.

Several sorts of wastes can be succesfully destructed in cement making rotary kilns,: solids, liquids, gases, or even sludges, etc. Experiences with incinerating used car tires, waste rubber, municipal or household waste, sewage sludge, landfill gas have been reported; but the most important waste fuel, used extensively in several cement factories is the group of waste solvents, from the pharmaceutical, paint, metallurgical etc. industries. Some solvents can be easily desctructed, but other ones, e.g. chlorinated hydrocarbons are persistent, and need high temperatures for incineration. The most important member of this group is PCB (polychlorinated biphenyl), which is extremely stable, and, still worse, its products of incomplete destruction (PID), such as polychlorinated dibenzo furanes (PCDF) or polychlorinated dibenzo dioxins (PCDD) are highly toxic. Experience proved that cement kilns, with properties mentioned above are almost ideal for incinerating PCB, as here the amount of PID-s is very low, usually in the ppb range and often below detection limits.

From the environmental point, the destruction of hazardous organic wastes can be considered fully safe; but from the point of cement technology, their use as substitute fuels can bring considerable difficulties, esp. in case of chlorinated wastes (which are very common among the solvents), as volatile chlorides are formed from the alkali contents of the raw material, which, in turn, get into various internal circuits within the kiln, cause rings and other adherent layers and deteriorate, or even comp-

letely block the operation of the cement-making line. Thus, unless special precautions (bypassing gas or solid flows, or cutting circuits by other measures) are made, the cement industry is reluctant in using waste solvents.

THE HISTORY

Although the idea of controlled destruction of combustible hazardous wastes in cement kiln is quite old, the first publication (in the author's knowledge) dealing with this problem was published 15 years ago[1]. (Some internal reports, by the Canadian environmental authorities, date back to somewhat earlier years. The reports describe some trial runs made at St. Lawrence Cement, Missisauga, Ontario, in 1976). In the paper, referred to above, authors describe that cement-making rotary kilns, esp. the wet-process ones, where gas flow is slow and consequently combustion gases are kept for a long time in the hot zone, are suitable for the safe destruction of chlorinated hydrocarbons, including even PCB. Later tests were made at Stora Vika Test center in Sweden[2], in a coal-fired wet-process kiln. Highly chlorinated organic waste, PCB, and even Freon were successfully destructed. A detailed description of waste co-firing tests carried out in Norway was published in 1983[3]. In this experimental series, made in NORCEM's Slemmestad factory, a long, wet-process, coal-fired kiln was used for the co-firing of tar, solvents, emulsions, PCB oil. As neither PCB, nor products of incomplete combustion (PIC) were found in the emitted gases, and the economy was also on the safe side, the author concluded that "The wet kiln using waste is competitive to a modern dry kiln using conventional fuels.... Incineration in a cement kiln should make an important contribution towards the safe disposal of hazardous waste in the future".

Since these early experiments several tests were made all around the world, with conventional and non-conventional kilns. The use of "chemically derived fuels" (CDF) or "waste derived fuels" (WDF) is a standard practice in many cement-making rotary kilns.

THE ENVIRONMENTAL SIDE

Destruction of hazardous organics in a cement kiln can be considered as being absolutely safe from the environmental point of view, a proper operation of the kiln, and some precautionary measures presupposed. Such measures include the safe storage and handling of the waste, and an automatic system which immediately stops the addition of the waste if the temperature drops below a certain level (e.g. failure of the main fuel burner, collapse of refractory lining, etc.). Destruction and removal efficiencies (DRE) of principal organic hazardous constituents (POHC) are usually better than 99.99, sometimes even 99.9995% or more (environmental experts usually express these data in 'non' units (number of nines), i.e. 4 and 5.5 resp. for the two above data). Besides the very high DRE values, in most cases no significant changes were found in the conventional emissions either; moreover some emissions are reduced when waste co-firing is used, for instance particulates, or sulfur oxides, in case of coal-fired kilns. The same is true for the emission of toxic heavy metals, often contained in coal. Their emission is obviously the lower, the higher was the share of the waste.

In case of WDF's containing chlorinated hydrocarbons, however, a novel

type of emission, usually absent among "normal" conditions must be taken into consideration: hydrochloric acid, from the chlorine content of these substances. (This is definitely less hazardous than PIC's; after all, hydrochloric acid is present in our stomachs too). Actual measurements however show that this is not a significant danger, as the majority of chlorine is bound in the cement clinker or in the dust collector, and only a slight part is emitted. A good forecast of WDF-induced emissions was presented in 1984[4].

Several reviews have been published[5, 6, 7, 8] on co-firing hazardous wastes in cement kilns. In the forthcoming paragraphs some more detailed data will be given.

Solid Wastes

Solid urban wastes can be well used as alternative fuels in rotary cement kilns. Brocco et al.[9] studied in 1983 the trace organic pollutants of the emission and claimed that no changes occurred if WDF's of solid urban wastes were co-fired with coal in a cement kiln. No PCDD or PCDF traces were found over the detection level, nor did the total concentration of polycyclic aromatic hydrocarbons increase in the emissions. The operational experiences of co-firing solid industrial wastes was checked by Haley[10] in the Blue Circle plant in Westbury, UK. Such waste fuels are well utilised, esp. when the waste is processed before burning to eliminate non-burnable inorganics, etc. A special refuse processing plant, of approx. 80000 tons/yr capacity was established in England, to serve the Westbury plant[11]. In his review on the 1988 IEEE Cement Industry Technical Conmference, Michard[12] reports on the use of WDF for co-firing a dry-process, 4-stage cyclone preheater kiln in Italy with municipal solid waste, after the removal of paper, plastics, metals amd glass.

Not only municipal solid wastes, but other burnable solids can be used for co-firing in cement kilns, and thus save primary fuel and at the same time help the safe disposal of wastes. The most frequently used solid of this type is waste tires of cars, lorries, buses, etc. A complete, computerised system exists for their handling: tires are placed onto a roll track and transported to a weigh feeder which detects the weight of each individual tire, while a computer calculates the time interval for further transportation to the kiln through a double tipping valve to the kiln feed end. The rubber burns completely in the high-temperature zone, while metals melt and end up oxidic in the clinker phases. Approx. 25% savings in primary fuel have been reported[13]. Besides fuel savings, the quality of clinker is improved too, decarbonisation degree of limestone gets higher, and the productivity of the kiln may increase by 3-5%[14]. An alternative system for the utilisation of waste tires as fuels is described by Saito et al.[15]. Here nonsliced tires are introduced to a gasifier, including a fluidised bed and a moving bed thermal combustion chamber, and the generated fuel gas is used as an additinal gas for cement burning. The gasifier needs no auxiliary fuel except for ignition.

Acid resin, a viscous, honey-like waste from the acid refining of lube oils is hazardous as it contains free sulfuric acid (has a pH value of zero). Formerly this was disposed of by landfilling, but this is not permitted any more. This waste has a high calorific value by its resin and

hydrocarbon content but is very difficult to handle. After neutralisation it becomes particulate, coal-like and can be used as a supplementary fuel in cement kilns. Neutralisation can be done by powdered limestone, or, still better, by the highly basic dedusting or baghouse powder of the cement kiln. Thus the waste from one industry can be neutralised by another waste from a different industry and finally disposed of properly in the first industry again[16]. Spent bleaching earth, hard rubber residues etc. can be incinerated in cement kilns too[1]

Liquid wastes.

Burnable liquid wastes have been incinerated and thus safely disposed of in cement kiln. Such wastes may come from several industrial branches: mainly from the pharmaceutical industry, but almost all chemical plants, where solvents or various sorts of oil products are used, produce such wastes. The production and use of paints, lacquers, plastics, cleaning agents, lubricating oils, then degreasing operations in machinery, dry-cleaning etc. are good examples to show the immense field where burnable liquid wastes are produced; their commercially viable, and at the same time, absolutely safe disposal is thus of extreme economic and environmental importance.

Burnable liquid wastes can be subdivided into two groups: some of them can be easily destructed, at rel. low temperatures, and without the formation of toxic substances. Simple hydrocarbon oils, non-halogenated solvents, etc. belong to this group. Other wastes, as halogenated hydrocarbons (particularly those containing polynuclear aromatics), or solvents which contain heavy metals (e.g. coming from the paint making industry) can be destructed with extreme care only, as their PIC's are very toxic, and cause substantial environmental danger when emitted. Thus a high DRE is not sufficient; a low quantity of emitted hazardous substances, be it PIC or heavy metal or anything else is of equal importance. Wastes belonging to the first group can be safely incinerated in industrial boilers too; but the absolutely safe disposal of second-group wastes need extreme precaution. Thermal destruction in a cement kiln is near-ideal for such wastes. Several authors quote this technique as being the BDAT (Best Demonstrated Available Technology) of disposal, esp. in case of PCB.

Co-firing of non-PCB liquid wastes. -Low-Cl waste liquids, containing mainly trichloro-ethane, toluene, methylene chloride and methyl ethyl ketone, fired in a dry-process kiln[18] also showed a total destruction of the POHC's (principal organic hazardous components), and no increase of particulate or gaseous emissions, as contrasted to the baseline, coal-only state. This is important, as all previous experiments, mentioned earlier were carried out in long, wet-process kilns, where conditions are more favourable for destruction (long retention time due to the length and large volume of the kiln).

Good reports on extended (over 5 months) operational experiences of burning wastes in the San Juan Cement Co. factory in Puerto Rico were published by Peters et al. in 1984.[19,20]. Co-fired wastes contained chlorinated monocarbon compounds, as CH_2Cl_2, $CHCl_3$, CCl_4, or non-chlorinated waste solvents, composed mainly of methyl ethyl ketone. In the first of

these publications[19] the authors report insufficient DRE values of an average 95%, with hardly 91% in the worst case. The cause of the low DRE was the absence of waste atomisation; but even in that case PCDD or PCDF formation was not detectable, approx. 82% of input Cl appeared in the clinker, the rest in the baghouse dust and only 0.3% was emitted. The introduction of waste atomisation improved DRE drastically, being over 4.5 non in all cases[20].

A report of 1984[21], describing the use of liquid wastes (of non-specified composition) claims that 40% of the primary fuel (petroleum coke) was saved in a 3-month test period, and no significant increase in the emissions from the kiln stack was observed and nor is there any adverse effect on the plant products. Similar results were obtained by Branscome et al.[22], although in this study a somewhat increased emission of HCl and of Pb was observed. The majority of these pollutants, however are retained in the process solids, mainly in clinker.

The best report, summarizing practical experiences of waste destruction, both in wet, dry and preheater kilns, in the U,S., Canada and Sweden was published in 1988[23]. A satisfactory (>4 non) DRE was measured in all cases; a slight increase of particulates was measured when chlorinated wastes were burned, but only in case of kilns with an electrostatic precipitator. Those kilns equipped with fabric filters showed no change in emissions.

In former works, cited earlier, emission of HCl was mentioned several times. Recent results[24] however show that Cl^--ions emitted might be in the form of NH_4Cl. However no sufficient data exist to prove the validity of this finding, as HCl and NH_3 can be emitted even simultaneously.

Co-firing of PCB liquid wastes. -As mentioned earlier the safe disposal of polychlorinated biphenyls (PCB) is one of the most challenging and important problem of hazardous waste management, due to the extreme stability of the substance, and to the extremely toxic nature of products of when incinerated incompletely. This is why one of the first reports on using cement kilns for this purpose has dealt with the safe disposal of PCB[1]. At this time only long wet-process kilns seemed to be adequate for this purpose; although the destruction was practically complete (no high molecular weight chlorinated hydrocarbons found and light ones, as CCl_4 or CH_2Cl_2 in ppb quantities only), an increase of precipitator dust and emission of particulate matter was observed[25]. The EPA standards are met in normal operation by a generous margin, and DRE values of > 5 non easily obtained in a kiln co-firing coal and PCB-containing oil, as experiences from New Zealand show[26, 27].

Not only wet-process kilns can be used for the destruction of PCB: Krogbeumker[28] reports on successful, large scale (> 500.000 tons per year) incineration of PCB-containing waste oils in a Dopol-type dry-process kiln. Destruction was practically complete in this case too: PCB emissions under the detection limit (0.1 ppm), and PID's (mainly PCDD and PCDF) in the ng/cu.m range, i.e. well below the natural background. A Norwegian report[29] indicates a still higher DRE value, of > 6 non. The emission of particles,

and even of organic micro pollutants is influenced by operation conditions to a much higher extent than the fuel incinerated. In case of improper operation, these emissions can be rather high even in the absence of supplementary fuel.

A Czechoslovak test run[30] shows the complete destruction of PCB too; concentrations in clinker and in kiln dust were as low as 0.09 and 0.11 ppb. Unfortunately no data on PIC's (e.g. PCDF or PCDD) are given. Other recent studies[31,32] however indicated that even PIC's are below the detection limit in flue gases, if a proper atomisation of the auxiliary fuel is granted.

THE CEMENT TECHNOLOGICAL SIDE

General

In former paragraphs more than adequate reference was given that the high temperature, the excess oxygen and the long retention time of gases assures the total destruction of burnable organics, including even the most stable ones; and, in case of chlorine-containing wastes, the majority of Cl is not emitted, but absorbed in the basic milieu, mainly in the cement, and, to a lesser extent, in the kiln dust. Unfortunately, only scarce references mention the experience that co-firing of waste, particularly of used tires and of halogenated hydrocarbons can cause very serious difficulties during the manufacture of cement, and a definite upper limit must be kept to avoid them.

Earlier investigations[33] gave this level as 0.7% Cl/kg clinker; this however might not be true in some cases. The most frequently encountered difficulties are the formation of adherent rings and/or layers in the kiln or in the heat exchangers.

The difficulties already begin with the proper handling of the waste. Their chemical composition must be exactly known, esp. their halogen content. Such determination is not an easy task, as waste may come from various sources, form mixtures or emulsions, thus sampling is a very important problem. Moreover, for safety reasons, all containers, pipelines, etc. must be kept under inert gas to avoid self-ignition, and in a confined area to avoid spillouts. Detailed procedures were established for evaluating and accepting the wastes and for use of the wastes as supplemental kiln fuel[34]. Safety valves must automatically stop the flow of supplementary fuel if the temperature drops under a certain level. A fully controlled and automatic system exists, among other factories, in Norway's NOR-CEM works in Brevik[35].

Wastes may introduce materials into the process, which are either completely absent or present in low concentrations only, among normal ("no-waste") conditions. These, in turn, can change process parameters to a considerable extent. Particularly important are the inputs of chlorine, and, to a lesser extent, sulphur, as they may cause cycles and disturb kiln operation due to the formation of buildups and adherent coatings on the refractory lining of the kiln and/or preheater[13]. Chloride-containing wastes are used very often as alternative fuels; but in their presence (over a certain limit) alkalis, thallium and some other substances yield volatile

chlorides which get vaporised in the hot zone of the kiln, and condense again at cooler zones. In this way, cycles are formed, which, unless interrrupted, cause very serious troubles, as in a saturated cycle the concentration of a substance may be higher by orders of magnitude than that of the original input. Two sorts of cycles exist: besides the internal cycle, just discussed, also external cycles may occur when precipitator dust is recycled to the kiln with the feed.

The most common method of interruption is the use of a bypass (gas- or hot meal-bypass), located at the transition between kiln and preheater. A gas bypass removes a portion of the kiln exit gases which contain vaporised cycle-forming compounds, as alkali- and heavy metal-chlorides, or various sulphates. A hot meal bypass removes some of the preheated feed material which is enriched with condensed cycle compounds. The dust bypass takes out filter dust and thus interrupts external cycles[36].

Combustible wastes can be used obviously in a combined form, making them an integral part of the preheating - calcining - cooling industrial process. A German patent describes this sort of waste utilisation[37].

A practical experience

A cement factory in Hungary uses the dry-process technology, with a four-stage cyclone preheater. The kiln is heated by heavy fuel oil. No bypass exists. In a set of experiments four different states were thoroughly investigated for emissions: 1./ clinker burning with fuel oil only; 2./ burning with fuel oil + waste tires; 3./ burning with fuel oil + waste halogenated solvents. 4./ burning with fuel oil + waste tires + + waste halogenated solvents. In the two latter cases the halogen load was adjusted in four levels (1, 2, 3 and 4 kg Cl per tonnes of clinker).

Results show that emission of particulates was in all cases well below the permitted value in all cases. Emission of carbon monoxide is slightly decreased by co-firing waste solvents, and increased by tire co-firing (but even in this case below the permitted level. Nitrogen oxides are decreased by solvents. SO_2 is below detection limits in all cases. Among toxic heavy metals the emission of Hg, Cd and Tl was lower by one order of magnitude of the permitted value, and remained unchanged by waste co-firing. Joint emission of As, Se, Ni, Co and Te was approx. 20% of the permitted, slightly increasing by tire co-firing, but unchanged by solvent firing. Joint emission of Pb, Cr, Cu, V, Sn Mn and Sb was approx. 25-30% of the permitted, increased to the double, and remained unchanged by co-firing tires and solvents, resp. The emission of HCl was, in State 1./, approx. 5-20% of the permitted value, increasing to a slight extent, but proportionally with halogen load in State 4./, but remaining unchanged in State 3./. HF was not emitted in any state, being one order of magnitude less than the permitted level. Emission of PCDD and PCDF, as well as mutagene effect of flue gas condensate and emitted particulates was measured too. Dioxines are slightly increased by tire, and slightly decreased by solvent co-firing, being somewhat below the permitted value in all states. Mutageneity is approx 5 - 10% of aerosol mutageneity in city air.

It is thus evident from these results that co-firing of these wastes

is an absolutely safe method of their disposal, from the environmental aspect. The cost of additional safety equipment, as described earlier, is covered by the savings of the primary fuel.

Waste co-firing, on the other hand, caused very serious technological difficulties. Thick adherent layers were formed in several parts of the kiln and the heat exchangers, even at the most cautious supervision. The layers consisted of clinker minerals, cemented together by spurrite and other sulfur- and/or chlorine- containing compounds, and, at highest halogen loads even free KCl (sylvine) was observed. These rings havesometimes almost completely stopped the flow of solid materials. This is why the management has discontinued waste co-firing until a bypass built.

REFERENCES

1. Black,.W. & Usher, D.: "Safe DisposaL of PCB". **Proc. Natl. Conf. Treatment & Disposal of Industrial Residues**, 1977, 4-6

2. Ahling, B.: "Destruction of chlorinated hydrocarbons in a cement kiln" Envir. Science & Technol. 1979 13(11) 1377-79

3.Trovaag, K.: "Hazardous waste incineration in a cement kiln" World Cement Technol. 1983 14(2) 59-62

4. Sprung, S.: "Emission forecast for the use of waste-derived fuels" Zement - Kalk - Gips 1984 37(10), 519-22

5. Lauber, J.D.: "Burning chemical wastes as synthetic fuels in cement kilns" **Proc. Annual Meeting of APCA (Air Pollution Control Association)** 1981 74(3) Paper No. 81-51.1

6. Weitzmann, L.: "Cement kilns as hazardous waste incinerators". Environ. Progress. 1983 2(1) 10-14

7. Mourninghan, R.E., Peters, J.A. & Branscome, M.R.: "Effects of burning hazardous wastes in cement kilns on conventional pollutant emissions" **Proc. Annual Meting of APCA** 1985 78(5) Paper No. 85-68.1

8. Chadbourne, J.F. & Freeman, H.M.: "Hazardous waste as fuel in cement kilns" **Hazardous Waste: Detection, Control, Treat. Proc. World Conf.** 1987 Part B. 1315-24.

9 .Brocco, D , Cecinato, A., Liberti, A.& Rotatori, M.:" Solid urban wastes as alternative fuel in a cement kiln; trace organic pollutants in the emissions". Riv. Combust. 1983 37(9-10) 243-49

10. Haley, C.A.C.: **4th Agric.** "Solid waste as a cement kiln fuel" **Indust. Municip. Waste Management in To-day's Environment. Conf.** p. 143-4

11. Haley, C.A.C. & Chatterton, M.H.: "Solid wastes as a fuel in the cement industry in the UK" Energy Prog. 1985 5(2) 84-88

12. Michard, D.: "Using kilns for incineration" Rock Products 1988(7) 80-82

13. Neumann, E., Duerr, M. & Kreft, W.: "The substitution of fossil fuels in cement kilns" World Cement 1990 21(3) 80-88

14. Shubin, V.I., Burlov, Yu.A., Kalabukhov, V.A. & Khnykin, Yu.F.: "Modernisation of rotary kilns for combustion of used automobile tires" Tsement. 1989 (1) 17-18

15. Saito, I., Sakae, K., Ogiri, T. & Ueda, Y.: "Effective use of waste tires by gasification in cement plant" World Cement 1987 18(7) 264-69

16. Hungarian Patent, No. 195,941, 6 April 1984. "A Composition for the Utilisation for Oil Refinery By-Products, esp. their Use in the Silicate Industries"

17. Riganti, V.: "Use of the rotary cement furnace for disposing of industrial waste" Not. Ecol., 1985 3(2) 9-13

18. Higgins, G.M. & Helmstetter, A.J.: "Evaluations of hazardous waste incineratiom in a dry process cement kiln "U.S. Envir. Protection Agency Res. Dev. Report 1983 243-52

19. Peters, J.A., Hughes, T.W., McKendree,, J.R., Cox, L.A. & Hughes, B.M.: "Evaluation of hazardous waste incineration in cement kilns at San Juan Cement Co." Gov. Report Announce Index (U.S.) 1984 84(23) 135

20. Peters, J.A., Hughes, T.W. & Mourningham, R.E.: "Evaluation of hazardous waste incineration in a cement kiln at San Juan Cement Co." U.S. Envir. Protection Agency Res. Dev. Report 1984, 210

21. Robb, A.F.: "Energy from waste in a cement kiln" Proc. 31th Ont. Ind. Waste Conf. 1984 195-229

22. Branscome, M.R., Westbrook, W., Mourningham, R.E., Bolstad, J. & Chehaske, J.: **Summary of testing at cement kilns co-firing hazardous wastes.** In: Incinerating hazardous wastes, ed. by H.M. Freeman, Lancaster, Pennsylvania, Technomic Publ. Co. 1988, p 185-90

23. Mourningham, R.E. & Branscome, M.R.: "Hazardous waste combustion in industrial cement and lime kilns" Gov.Report Announce. Index (U.S.) 1988 88(6) 1 - 76

24. Trenholm, A.R. & Hlustick, E.R.: "Emissions from a cement kiln burning hazardous waste" **Proc. A & WMA Annual Meeting** 1990, 83(2) Paper No. 90/29.5 p. 1 - 19

25. McDonald, L.D., Skinner, D.J., Hopton, F.J. & Thomas, G.H.: "Burning waste chlorinated hydrocarbons in a cement kiln" Gov. Report Announce. Index (U.S.) 1878 78(16) 258

26. Holden, R., Tyson, M.O. & Hodgkinson, E.J.: "The destruction of polychlorinated biphenyl waste oils in a cement kiln" Chem. New Zealand 1983 47(2) 31-4

27. Holden, R., Tyson, M.O. & Hodgkinson, E.J.:"A demonstration of the safe destructionof PCB waste oil in a coal fired cement kiln" **CHEMECA-83, Chem. Eng. Today, Barton, Australia** 1983 763-70

28. Krogbeumker, G.: "Safety arrangements for the supplementary combustion of waste oils containing polychlorinated biphenyls (PCB) in rotary cement kilns" Zement - Kalk- Gips 1988 41(4) 188-92

29. Benestad, C.: "Incineration of hazardous waste in cement kiln" Waste Management Res. 1989 7(4) 351-61

30. Lishak, P. & Zemanova, E.: "Elimination of wastes containing polychlorinated biphenyls" Chem. Prum. 1990 40(2) 86-91

31. Krogbeumker, G.: "Thermal utilisation of PCB-containing used oils in cement manufacture" Umwelt 1990 20(3) L36-L40

32. Krogbeumker, G.: "Thermal utilisation of polychlorinated biphenyl containing waste oils in cement manufacture" Brennstoff-Wärme-Kraft 1990 42(3) 36-40

33. Black, M.W. & Swanson, J.R.: "Destruction of PCB's in cement kilns" Pollut. Eng. 1983 15(6) 50-53

34. Peters, P., Higgins, G.M. & Chadbourne, J.: "Hazardous waste as a supplemental fuel for cement kilns" **Proc. 12th Natl. Waste Process. Conf.** 1986 65-69

35. Langfeldt, F.: "Recycling of liquid industrial wastes in cement making rotary kilns" **Symposium, organised by Norcem-Invenco, Budapest, 1992**

36. Kreft, W.: "Environmental protection concepts in the cement industry" Zement-Kalk-Gips 1988 41(4) 193-201

37. German patent No. 3,411,144. 10. Oct. 1985. "Treatment of Combustible Wastes in the Preparation of Cement Clinker"

CEMENTITIOUS MATERIALS IN NUCLEAR WASTE MANAGEMENT

Della M Roy

Materials Research Laboratory
The Pennsylvania State University
USA

I. INTRODUCTION

Cementitious materials have been investigated extensively to establish their role, and enable a prediction of their performance, when used for radioactive waste isolation. A number of applications have been addressed, ranging from those in high-level waste management, where their prime roles would be physical such as in sealing an underground waste repository, mechanical to serve as a protective cask for transport, or under certain conditions, both chemical and physical in the solidification of high-level waste. Cements also have been explored for their use in forming primary casks for containment of spent fuel assemblies. For the disposal of low-level (and in some countries, immediate-level) waste, a cementitious matrix may be used to encapsulate the waste, thereby generating an integral waste form (Burns, 1971;Roy, 1978). In addition, concretes will be required to perform special structural roles, used to construct trenches, vaults, and other disposal units. Also, there are numerous applications where grouts are used for sealing purposes (Roy and Burns, 1982). This summary paper addresses briefly each of these areas.

The durability of cementitious materials in radioactive waste disposal depends upon many factors which are understood in part through in the studies of concrete durability. The resistance of hardened cement paste and concrete to chemical and physical degradation when exposed to an aggressive environment, or when interaction takes place between potentially reactive internal components and the external environment, is not related strictly to the mechanical strength of the material; i.e., strong materials do not always resist attack and disintegrative forces in any environment in which they are placed. Nevertheless, it is true that higher strength cement pastes are generally less permeable, and thereby will provide better resistance to chemical attack and physical degradation than low strength materials. It is also a well-known fact that water content (and w/c ratio) of a cement paste is probably the most important single factor in determining the subsequent porosity and permeability of the hardened paste, and that decreasing water content serves to decrease porosity and usually increases strength.

The porosity and pore structure of cement pastes exert major control on the ingress of potentially deleterious substances, or the release rate of potentially harmful species such as radionuclides. The pore structure and microstructure constitute major rate-controlling factors for potentially harmful transport processes, whether the species being transported is water (to give rise to alkali-silica expansion), sulfate ions (causing sulfate attack), chloride ions (to depassivate the protective layer on reinforcing steel), acids, oxygen or carbon dioxide, to weaken the concrete structure, or leaching, transport, and release of radioactive spaces (Roy, 1986).

The resistance of hardened cement paste and concrete to chemical attack and physical degradation thus is the result of compositional and microstructural factors combined with environmental exposure conditions. Factors controlling the initial microstructure development and its effect on the operation of forces of degradation will be discussed along with some of the research applicable more specifically to nuclear waste management. In cases with waste disposal, there are high demands for performance and durability of the cementitious material, ranging from hundreds to thousands of years. Many of the findings of such studies are applicable as well to hazardous waste management, or mixed waste management/disposal. In addition, although there is considerable overlap in the applicability of the knowledge gained in the two major areas, the high-level and the low-level applications will, in general, be discussed separately.

II. APPLICATIONS IN WASTE SOLIDIFICATION

Introduction

As an alternative to other waste forms designed for the immobilization of the lesser active wastes, solidification with cement offers three major advantages: 1) The technology involved in the fabrication of the waste form is simple and available as are the starting encapsulating materials; 2) a series of studies throughout the world has verified the viability of properties of tailored cementitious formulations; and 3) perhaps most importantly, there is a potential advantage of the near-thermodynamic stability offered by a hydrated (hydroxylated) encapsulent host material designed for immobilization of waste in a geological repository.

An objective of any waste form design is to achieve a product that is as near to thermodynamic equilibrium as possible with its environmental/geological surroundings in order to minimize the potential for alteration. With the exception of the simple four-coordinated oxides of Si, Ti, U and Th, all potential host phases are hydrated at the normally cited conditions of temperature and pressure of underground geologic repositories. Because of this basic observation of the phase stability of materials, it is likely that all but a hydrated host phase will have the potential to alter to a more thermodynamically stable form under geologic repository conditions and thus alter the source term utilized to model the stable repository (R. Roy and D. Roy, 1981). For these reasons, the hydrated products of silicate-, aluminate- or phosphate-based cements offer the potential to be more nearly in thermodynamic equilibrium with the geological environment than other host phases. (R. Roy, 1982).

The use of cementitious materials to deal with the disposal and immobilization of radioactive wastes is widespread within the European Waste Management community and have been used for about three decades in the U.S. for the fixation of low-and intermediate-level radioactive wastes at power reactor plants (Kibbey and Godbee,1974). The necessary research to certify the disposal of lower level reactor waste, e.g., resins, etc has been carried out in a number of cases (Christensen, 1980) and successfully utilized radiation levels in excess of those that would be encountered in the typical waste. Cements thus are currently used, and therefore expected to find increasing use of solidification of low-level radioactive wastes (Hespe, 1971, Roy, 1978, Passant, 1988). In addition, they have been used (Weeren, 1977; Moore et al, 1977) and are currently being considered for solidifying intermediate level wastes (Passant, 1988). Although there are some concerns with limits of thermal stability, modified cement processing may be also considered as an option for generating waste forms permitting higher thermal loading (Roy, 1978; Roy and Gouda, 1974, 1978; Roy et al., 1979b; Roy, 1987a; Dole et al, 1983).

Two major types of hydraulic cement are used for these purposes portland and high alumina cements (Stone, 1979). In addition, blended or chemically modified cements

have been proposed to have considerable advantage (McDaniel et al, 1989). These types of cement can be used as matrices for incorporating primary waste containment forms, which may serve to replace the usual "aggregate" of concrete. When mixed with water or waste solution, the cements hydrate, harden, and form a dense "cement paste", which integrates the waste form to produce a monolith which may compare in strength and hardness to many types of natural rock.

The most valuable engineering properties of normal cement pastes, cement composites and concrete are their workability, durability (against atmospheric weathering, chemical attack), water tightness, and dimensional stability (to shrinkage and/or expansion after setting). Beyond this, the relevant properties of concrete that should be examined when considering its usefulness as a material for incorporating radioactive waste are its ease of forming a monolithic mass, permeability, resistance to leaching, relative thermodynamic stability, thermal stability and conductivity, and radiation stability. Strength development is frequently correlated with other properties; it appears generally to be adequate and may be enhanced by special processing (Roy, 1987b). Many of the basic properties of cement paste and concrete-e.g., density, durability, strength, and shrinkage-depend strongly on the porosity of the cement paste matrix, which in turn depends on the amount of water used in processing, which will be discussed later. Volume stability is probably not critical, but in the event that it leads to the formation of microcracks, a decrease in strength and an increase in leachability may occur (Roy, 1978, 1986, 1987).

Intermediate to High Level Solidification

Among the alternatives which have been considered are three that use cement and concrete: (1) Conversion to concrete (with separated residual salt); (2) Shale fracturing; (3) Shale Cement; (4) warm pressed dense forms; and (5) FUETAP (Roy, 1978; Roy and Gouda, 1974, 1978; Roy et al, 1979, 1982; Moore et al, 1977; Dole et al, 1983).

Disposal of intermediate-level waste has been carried out for a number of years at Oak Ridge National Laboratory by shale fracturing using a modified grout (Weeren et al, 1979). In this technique, a grouting consisting of liquid sludge, or dried sludge waste forms mixed with a blend of cement and other additives is pumped down a well (Weeren et al, 1979) and injected into a shale formation (DeLaguna et al, 1968). The grouts were blended from portland cement, fly ash (class F), drilling clay, pottery clay, and a retarder. The shale is first fractured by pressure from a small volume of water, and the grout is then injected into the initial fracture. As the crack propagates, it is filled with grout. Injection continues until the batch of waste-grout is depleted. The grout sets a few hours after injection, permanently fixing the radioactive waste in a rock-like sheet of cement composite within the shale formation. Subsequent injections ideally form sheets parallel to and a few feet above the first. The leach rates (rates of release of cesium, strontium, plutonium, and curium) were determined and were stated to be equivalent to that of a borosilicate glass. Effective diffusion coefficients (Deff) of the various species were calculated. One superior grout showed Cs Deff $\cong 10^{-12}$ to 10^{-14} cm^2 sec^{-1}. Strontium typically was 5×10^{-12}; while curium and plutonium were 10^{-16} to 10^{-17}. The leach rates were calculated as follows:

$$\sum \frac{a_n}{A_o} \cdot \frac{v}{s} = 2\left(\frac{D_e t_n}{\pi}\right)^{\frac{1}{2}}$$

where a_n/A_o is the fraction of the radionuclide leached in time t_n (sec), v is the specimen volume, cm^3; s is surface and exposed to leaching, cm^2 (Godbee, 1980; Moore, 1981). The low leaching rate was attributed to the presence of critical blending

components. Stinton et al (1984) have shown in examining 20-year old grouts in core drilling found, e.g., that cesium was associated with the illitic clay in the grout. Further, no migration of Cs occurred outside the grout after 20 years.

Related research on high-level waste forms established that, in addition to glass waste forms which are scheduled to begin production at Savannah River in 1990 (Hindman, 1988), there is much merit in the relative inertness of ceramic/crystalline mineral model waste forms (R. Roy, 1978, 1980, 1982; McCarthy and Roy, 1981; Rusin et al, 1979, Vance et al, 1986). At the same time, the consideration of natural mineral models and thermodynamic considerations establish the virtue of low temperature hydroxylated forms. Roy and co-workers (Roy et al, 1981; Barnes and Roy, 1983; Barnes et al, 1982; and Scheetz et al, 1985) researched the development of high performance cementitious waste forms and investigated their properties as well as characterized the behavior of individual components. While initial research was keyed into Hanford waste compositions, later work used Savannah River waste compositions. Ross et al (1983) in comparative studies of various types of transuranic waste form based on the Rocky Flats plant had in fact shown that both densified and cast cementitious waste forms in many respects compared favourably to alternatives (borosilicate glasses, etc). In work at Mound Laboratories, Lewis (1983) showed that it was feasible to produce a pelleted high density cement waste form based on the Roy and Gouda (1974, 1978) concept.

Solutions containing up to intermediate-level waste (ILW) have been solidified in concrete drums in Germany (Koster, 1985). The waste form was found to have a low Cs release rate in brines with composition characteristic of the salt mines in which they would be stored. In addition, a containerless disposal method has been explored, in which such a waste form be pumped directly into a non-accessible underground salt cavern (Kramer and Kroebel, 1982). Additional concepts were developed to stabilize spent high-temperature gas-cooled reactor fuel with a cementitious grout at elevated temperatures (Wilbourn, 1985). Furthermore, a cementation process for TRU waste for deep burial has also been explored, which appears favourable (Schneider and Ledebrink, 1984). Plans have also been developed in the United Kingdom for solidifying ILW in cement (BNFL, 1988) of which a slag-cement is a likely candidate (Forrester, 1986). In France, a concrete immobilization process has been designed for sludges from liquid radwastes with activities up to 1.1×10^{10} Bq.m^{-3} activity to which has been added salt concentrates of up to 800 g.L^{-1} concentration (Mangin et al, 1988).

In other high-level waste studies, a new radiophase for ceramic nuclear waste forms was found, having the $NaZr_2P_3O_{12}$ structure (Komarneni and R. Roy, 1982; R. Roy et al, 1983; Alamo and R. Roy, 1986). This phase is relatively insoluble, immobilizes the relatively mobile Cs^+ species, and serves as an extraordinarily good host for actinides, as well as providing an additional smaller cation site for fixation of smaller ions. The properties of a waste form prepared by mixing this phase in tailored cement compositions were investigated (Roy et al, 1984; Wei et al, 1985). In fact, some of the most insoluble cementitious waste forms produced to date were generated in such encapsulated materials prepared by warm pressing high-silica matrix cements (containing slag and silica fume).

Phases such as pollucite, a cesium aluminosilicate ($CsAlSi_2O_6$) had been identified as an insoluble component for fixation of Cs in a polycrystalline mineral/ceramic waste form; powellite ($SrMoO_4$) for transuranics and rare earths, and sodalite (I-sodalite $Na_8[AlSiO_4]_6I_2$) for iodine (McCarthy and Roy, 1981; Roy, 1982). These phases were investigated individually, or in combination, when solidified/encapsulated in cements (Roy et al, 1981; Barnes et al, 1982; Barnes and Roy, 1983; Scheetz et al, 1985).

Low Level Waste Solidification

Many of the properties of cementitious materials which make them appropriate for consideration for use as a matrix for encapsulating wastes have been discussed briefly

in the previous section. The performance demands for low level wastes, however, are not as high as with the intermedite to high-level waste disposal, because of the lower activities involved. The reverse of the transport of ions or chemical species into a cement paste is the movement of water through the paste and removal of species, leaching, which depends on the pore structure and water permeability of the paste. As water permeation involves the transport of a liquid through a porous medium under a pressure gradient, leaching involves the transport of species under a concentration gradient, e.g., in the case with very pure water in contact with cement paste.

Most of the studies related to low-level nuclear waste isolation are concerned with the release of trace species or radionuclides present in small concentrations, in attempt to control the release of toxic or harmful species, but a number of concerned with the release of major elements as well (Kumar et al, 1986, 1987; Atkinson et al, 1984; Atkinson, 1983; Roy, 1979; Roy et al, 1979; Roy et al, 1982, 1984, 1985; Barnes and Roy, 1983; Scheetz et al, 1985; Wei et al, 1985; Dole, 1985; Zamorani, 1986; Malek et al, 1986). Various disposal concepts examined in recent years have investigated alternatives to shallow-land burial for low-level radioactive waste, in which leaching and transport are still primary properties of concern. This shallow-land burial alternative proposes a standard trench with a reinforced concrete floor, backfilling the trench voids with concrete and possibly using a concrete cap covered with clay and topsoil. The use of concrete backfilled trenches in a geologically stable, semi-arid area can provide an additional degree of safety, but their use in a geologically unfavourable area could possibly create problems. Three reasons for using concrete backfill are: better intruder barriers, creation of a concrete monolith, and lower susceptibility to subsidence (Salsman, 1985).

Low-level waste (salt solution) at Savannah River after reprocessing will be mixed with (granulated) blast furnace slag, fly ash, and cement to form a grout. The grout will then be pumped to a reinforced concrete vault for solidification and disposal as a monolith called saltstone (Langton et al, 1983; Malek et al, 1986; Wilhite et al, 1988). Properties have been investigated in the laboratory which include leaching of radioactive species and cementitious components, and numerous physical and mechanical properties to be used for performance prediction (Barnes et al, 1985, 1986; Malek et al, 1986; Malek and Roy, 1987; Kaushal et al, 1986, 1987).

There are numerous bases for selecting cement-based waste forms, among them the ability to reduce the release rates of radionuclides such as ^{90}Sr, ^{137}Cs, and various anionic species. Kumar and Roy (1986a,b) and Kumar et al (1987a,b) have extensively investigated the diffusion of Cs^+ in various types of cements, as has Atkinson (1984).

Hoyle and Grutzeck (1988) have found that secium release rates can be diminished through reactions taking place at higher temperatures, from 38° to 90° C, of cementitious compositions, suitable to the formation of Cs-containing zeolitic phases (a wairakite analog); while Kaushal et al (1989) have reported that both cesium and strontium leachability were reduced in slag and fly-ash containing mixtures in which a zeolitic phase with the nosean structure was formed. It should be noted that such zeolitic materials can only persist for prolonged periods in modified compositions for which the zeolitic component is a stable phase. Hoyle and Grutzeck (1986) reported strontium retention in cementitious compositions with added silica and/or alumina.

Roy et al (1981), Ross et al (1983) and various others have shown also the general effectiveness of cementitious materials in reducing the release of trans-uranic elements and rare earths.

Tallent et al (1988), Malek and Roy (1987) and others have addressed considerations in the immobilization of soluble anions such as NO_3 and technetium in oxidized

form. They have found that granulated blast furnace slag is effective in reducing the leachability of technetium while keeping the nitrate ion leachability reasonably low (Tallent et al, 1988; McDaniel et al, 1989). Langton (1987) has reported that also chromium releases from saltstone can be significantly reduced by substituting hydraulic blast furnace slag for portland cement in the formulation designs. The use of iron filings in a cementitious waste form have also been effective in reducing the release of soluble technetium (Bostick et al, 1989).

Serne et al (1989) presented leach rate data for several radionuclides (^{60}Co, ^{90}Sr, ^{99}Tc, ^{129}I, ^{137}Cs, and ^{241}Am) in studies on experimental grouts for disposal of Hanford double-shell tank waste, to be used in the prediction of long-term performance. A typical formula mixed 1 L of liquid waste with 1080 g dry blend grout mix (47.5 wt% slag, 47.5% class F Fly ash, and 5% Type I/II portland cement). As was found in other studies also, the iodine, technetium, nitrite, nitrate and sodium leached more rapidly than other species.

Many radioative wastes also contain toxic elements of concern and may be classed as mixed wastes. Komarneni et al (1987, 1988) addressed the mechanisms of heavy metal fixation in a number of crystalline calcium silicate cementitious materials. In reactions with the crystalline phases tobermorite, xonotlite, and wollastonite they found that Pb^{2+}, Cd^{2+}, Mn^{2+}, Zn^{2+} and Cu^{2+} appear to replace surface Ca^{2+} ions, but that Co^{2+} and Ni^{2+} irreversibly replace Ca^{2+} causing amorphization. Zamorani et al (1989) reported that Cr, Ni and Cd were immobilized by replacing Ca^{2+} in the presence of chlorides.

Additional evidence for the mechanisms of ion fixation, and especially waste ion fixation, may be found from examining the pore solution in the solidified cementitious material. Malek and Roy (1983) found that saturated $Ca(OH)_2$ solutions in contact with blast furnace slag-cement pastes and opal would lose their Ca ions first before the alkali ions. Glasser and Marr (1984, 1985) found that when all are present at 15% replacement level, silica fume is more effective in removing alkali and hydroxyl ions from solution than are blast furnace slag, fly ash or a natural pozzolan; while at 65% replacement level of high-alkali (1.02%) cement, Silsbee et al (1986) found that blast furnace slag by 28 days had reduced the pore solution alkali content by ~3 times (dropping from ~0.78 N to ~0.25 N), after passing through a slight maximum at ~12 days.

Atkinson and others have attempted thermodynamic modeling of the solution composition in contact with cement, beginning with the simple CaO-SiO_2-H_2O system (Atkinson et al, 1987). In prior studies they reported that slag blends were more effective in maintaining a relatively high pH, as compared to pure portland cement and other portland cement blends (Atkinson, 1985). This is considered important for long time durability, which is presumed to be dependent on several factors, among them the development of a fine pore solution.

For more detailed treatments of the subject, the reader is also referred to recent conference proceedings which contain substantial inputs on the behavior of cementitious materials in waste management (Waste Management 87; Waste Management 88; Spectrum 88; Scientific Basis for Nuclear Waste Management XII; Scientific Basis for Nuclear Waste Management XIII, MRS, 1989, In Press).

III. NUCLEAR WASTE REPOSITORY SEALING MATERIALS

Introduction

In addition to the considerations above related to nuclear waste isolation which are concerned with the release of trace species or radionuclides present in small

concentrations, a number are concerned with the release of major elements as well. The leaching of major elements is of especial concern for the sealing of geologic repositories for radioactive waste, where the cementitious sealing materials should maintain low permeability for prolonged periods (Roy, 1980, 1987a, 1989b; Roy and Burns, 1982; Roy et al, 1985; Grutzeck and Roy, 1985; Wakeley et al, 1981; White et al, 1979; Scheetz and Roy, 1985).

Materials for sealing radioactive waste repositories constitute an important component of the total waste isolation system, because the emplaced seals will provide a major contribution to adequate waste isolation. Penetrations through geologic repository formation strata, which compromise the natural barriers to ingress and egress of groundwaters, provide the most likely pathways for radionuclide release from the stored waste. Properly constituted penetration seals will contribute greatly to the restoration of a repository site to a state approaching its pristine condition, to prevent release of harmful amounts of radionuclides. The seals are required as structural components of shafts and drifts to provide mechanical support, to provide general fill, and in certain critical areas, to provide impermeable barriers restricting fluid flow (Roy, 1981, 1987a).

The use of cementitious materials (cements, grouts, mortars, concrete, and other composites) provides an extensive record (Roy, Grutzeck, and Licastro, 1979) from applications for underground sealing in the oil and gas and mining industries, as well as in other underground storage (Rennick et al, 1972; Herndon and Smith, 1976; Office of Nuclear Waste Isolation, 1979). The particular range of properties of these materials and their versatility suggest that they are likely to be used extensively in geologic repositories. Applications in nuclear waste repository sealing are subject to the overriding constraint that the other desired properties must be combined with the requirement of long-term performance. Numerous materials studies in recent years, therefore, have placed a strong emphasis on studies relating to longevity.

The major requirements for repository seal materials include: (1) mechanical adequacy; (2) good bonding to the host rock; (3) very low permeability to fluids, particularly in the interfacial zone between seal material and host rock; (4) stability and chemical durability; (5) compatibility with the surrounding rock and groundwater environment; (6) resistance to destructive expansion and contraction; and (7) resistance to radionuclide transport. These properties are important over the long time period of repository isolation.

Cementitious materials, either alone or in combination with other compatible plug component materials, are likely to satisfy the requirements, and therefore research is addressing specific problems related to their applications as repository seal materials. First materials selection and evaluation studies have been performed to determine the properties and characteristics related to hardening, placing, and other early stage properties; followed by characterization of starting materials and products.

Materials selected for further study on the basis of their performance in short-term tests have been investigated intensively to provide information on their longevity. This type of information is obtained from a variety of sources, including tests on experimental mixtures and formulations. The studies include detailed characterization of experimental seal materials or, where possible, specimens from plugs that have served in the field for extended time periods; evaluation of the thermodynamic stability of the material; determination of reaction rates and kinetic factors; determination of selection criteria based on knowledge of natural mineral associations; studies of ancient concrete prototype materials; and investigations of other special factors relevant to determining probable stability of seal material and host-rock-environment combinations (Roy, 1981, 1987; Scheetz and Roy, 1989a,b,c; Licastro et al, 1989).

Among early stage properties the relationship between viscosity and volume concentration of cement has been investigated for a large number of mixtures; this is one type of rheological information used in designing potential seal material mixtures (Roy and Asaga, 1981; Buck et al, 1985). The optimum amounts of chemical admixtures and other components that produce lower viscosities or more workable mixtures were determined from a given volume concentration of cementitious solids.

Another important factor affecting both early stage properties and structure development is the rate of heat evolution of a hydrating mixture. Calorimetric studies are made to quantify the heat effects and indicate the time at which the peak rate of heat evolution is achieved, its magnitude, and the effect of material parameters on the total heat-effect pattern (Rousan, 1982; Gotsis et al, 1984, 1986; Kaushal et al, 1987, 1989).

Kumar (1982) and others have investigated the effects of particle size and size distribution upon properties of the material. Cement was classified into three different surface-area fractions by the removal of finer fractions of cement particles. Particle-size distribution, chemical analysis, and setting time measurements provided initial characterization. Effects of fine particle size pozzolan (silica fume) additions on the early heat of hydration and dimensional change of pastes were investigted; SEM, TG and x-ray methods were used to study microstructural features and chemical reaction in the neat pastes and mortars. Recent studies have also shown how important particle size distribution and rheology are for concrete microstructural development (Scheetz et al, 1990).

Longevity of Seal Materials

Parallel with selection and evaluation studies, factors which more specifically determine the potential longevity of seal materials have been examined.

Thermodynamic Stability

The materials most likely to perform for long periods of time are those which are thermodynamically stable both intrinsically and under the environmental effects of the geologic repository. The studies of thermodynamic factors to date have included literature studies, calculations, and generation of needed new thermodynamic data. These studies have as their objective to determine the appropriate thermodynamic equilibria and to determine the lowest free energy (i.e., most stable) state for the intrinsic seal material compositional systems or subsystems and also the potential response of the seal materials under the expected environmental conditions (Sarkar et al, 1982). Preliminary calculations using some measured concentrations of solutions existing in contact with portland cement-waste systems (Roy et al, 1981) have shown that some liquid compositions appear to lie within the stability field for the zeolite, leonhardite (Roy and Burns, 1982). Atkinson et al (1987) have discussed the CaO-SiO_2-H_2O system itself.

Continuing studies are examining the effects of groundwater compositions on cementitious phase stabilities, and the compatibilities of intermixed seal component phases, i.e., cement minerals, with clays or zeolites. The early results show that some reaction of high-calcium content cements with clays or zeolites takes place at elevated temperatures, but that the reaction products have favourable sorption properties for radionuclide ions such as cesium (Komarneni et al, 1982). Freeborn and Roy (1983a,b) have investigated in a preliminary way the stability in a tuff environment and in a salt environment, based on thermodynamic considerations.

At the other extreme, studies have been made of ancient concretes, mortars, and plasters which have performed for a very long time and may provide an analog of modern

concrete seal materials. A first stage report detailed the compositions, properties, and microstructures of a few of these remarkably durable materials, derived from widely different sources (Langton and Roy, 1980), while other studies examined intermediate age concretes and old Roman, Greek and Cypriot materials dating back to as early as the 6th century B.C. (Roy and Langton, 1989c; Langton and Roy, 1981, 1983). Specimens were obtained from some structures used for water confinement, which remain in excellent condition.

Permeability, Porosity, and Pore Size Distribution: Potential for Ionic Diffusion

Key definitive seal material properties affecting long-term durability include permeability of the seal system to fluids, which related to both their potential for restricting water flow and, hence, radionuclide release in common with cementitious waste form properties. Typical materials with relatively high strengths have been found to have permeabilities lower than 10^{-8} Darcy (um^2) after 14 to 28 days curing, at all the temperatures studied, which exceed the goals set for the seal material performance. It has been shown that there is a general increase in porosity and permeability with increasing w/c ratio, when other factors are kept constant (Goto and Roy, 1981). However, the pore size distribution is probably the more important measure for predicting material transport and is not a direct function of the porosity (Kumar, 1985; Kumar and Roy, 1986a, b; Feldman, 1986, 1989). In some studies of cementitious materials relationship between water permeability and mean pore radius was found. Finally, a series of linear relationships was also found between the rapid chloride "permeability" (coulombs charge transported under an electric field) and mean pore radius for type I cement paste and for each of three lefvels of fly ash substitution. Within each material, the chloride transport rate increased nearly with mean pore size. The relationships between "rapid chloride permeability" and water permeability follow similar trends (Li and Roy, 1986).

Porosity, mean pore radius and pore size distributionin cementitious materials are very important microstructural characteristics; they are related to a series of properties of materials, such as flexural strength, fracture toughness, durability, and resistance to ionic diffusion. Kumar and Roy (1986) and Li and Roy (1986) have found that the pore structure of some materials is essentially affected by the cement fineness, w/s ratio, chemical composition, and pozzolanic reaction. Chloride ion diffusion under an applied electric field appears to be affected not only by the pore structure of the materials, but also by the diffusion mechanism.

The relationship between porosity, pore structure and ionic diffusion which was developed as follows:

$$\alpha = [C_a r^{Cb}]^3/\varepsilon$$

Where C_a and C_b are constants; ε is porosity, r is median pore radius, α = ratio of theoretical to effective diffusion. Values for C_a and C_b were generated for the neat portland cement pastes and $C_a = 10.3 \pm 2.6$ and $C_b = -0.41 \pm 0.13$ for Cl^- diffusion and $C_a = 4.6 \pm 2.5$ and $C_b = -0.62 \pm 0.08$ for Cs^+ diffusion were obtained over the temperature range of 27° to 60° C (Kumar, 1985; Kumar and Roy, 1986).

In a further refinement of porosity models, a preliminary model has been developed (Shi et al, 1989) for describing the distribution of pore sizes in cement paste. Experiments performed at normal and elevated temperatures have been carried out to determine phase stabilities of cementitious materials, the species present in the liquid phase, and to use the latter for calculating the dissolution rates of cementitious sealing materials, dependent on reasonable ranges of porosity, permeability, and interfacial sealing characteristics (Scheetz and Roy, 1989a,b; Scheetz et al,1989a,b; Scheetz and Anderson,1985). Recent studies (Haworth et al, 1989)

have also used thermodynamic models of cements (Berner, 1987), geochemical codes such as PHREEQE (Parkhurst et al, 1985) and coupled chemistry-transport models such as CHEQMATE (Haworth et al, 1988) model and leaching of cement, Onofrei et al (1989) in recent experimental studies investigated the grouting of fractures in granite, and found that both rock and grout compositions were important, and that under certain conditions self-healing of fractures was possible.

Dimensional Change/Expansivity

It is considered generally an advantage for sealing if slight expansion occurs on consolidation of the grout or concrete, as this builds a protection against later shrinkage and opening of fractures. Numerous studies have addressed the methods of determining expansion/sealing effectiveness (Gotsis et al, 1986; Licastro et al, 1985; Roy et al, 1984) as well as the development of cementitious materials to possess a slight expansive or non-shrinking characteristic (Christensen et al, 1983; Buck, 1985; Buck et al, 1985; Gulick et al, 1982; Fermnandez and Freshley, 1985; Gulick and Wakeley, 1989; Licastro et al, 1989; Grutzeck and Roy, 1985; Ogawa and Roy, 1981; Roy et al, 1985; Roy et al, 1982a, b, 1983a,b,c; Wakeley et al, 1981a,b; Wakeley and Roy, 1983; Wakeley, 1986).

The need for adequate concrete performance at temperatures up to 100° C and pressures up to 30 MPa, under varying moisture conditions from dry to saturated or under more extreme conditions has also been stressed (Kelsall et al, 1985; Fernandez and Freshley, 1985).

Interfacial Properties, Bonding, Stability

The interfacial integrity with host rock is the most difficult component of the seal system to guarantee, as suggested above, and presents special challenges to characterizatin (Roy, 1989c). Detailed interfacial, microstructural, and chemical characterization studies have been made via scanning electron microscopy (SEM), optical petrography, and other qualitative methods (Grutzeck and Roy, 1980), coupled with measurement of tensile strength of the bond between grout and rock materials (Das, 1985) which is one indicator of chemical and physical compatibility between these materials; and finally, permeability, which is the final measure of seal effectiveness (Wakeley and Roy, 1982).

Bench scale tests of simulated borehole seals have also been carried out to more realistically approach field conditions for evaluating seal effectiveness (Lingle et al, 1983; Scheetz et al, 1986a,b). Scheetz and Anderson (1985) have also calculated by means of a preliminary dissolution model the "time to failure" of grouted fracture (faults, barrier seals) in tuff rock, using experimentally determined dissolution characteristics, and different assumptions of hydraulic head, etc, finding that these times are in excess of the 10^4 to 10^6 years usually considered adequate for isolation of a repository. The dissolution rate is dependent on both physical characteristics and chemical characteristics of the seal system.

SUMMARY

Cementitious waste forms for low-and intermediate-level waste solidification/ disposal, in common with cementitious repository sealing materials place high demands on the long-term performance of the materials. The adequate performance and its counterpart, degradation of hardened cemetitious materials has been investigated in numerous studies, and has been shown to involve various chemical and physical factors, both those inherent in the cement paste composition and microstructure and those resulting from interaction with the environmental exposure conditions. To predict the performance of cement paste, cementitious waste, forms, or sealing grouts and

concretes, in different environments, it is necessary to consider the development of the cementitious material structure beginning with the fresh state, during mixing, placing and consolidation, and through the curing period, before being able to determine the probable effects of long-term exposure. A number of authors have emphasized that it is necessary when making durable concrete to develop a dense and well-homogenized microstructure, and establish that the concrete is well cured (Roy et al, 1989c). The effects of undesirable cracking developed as result of thermal stresses, resulting from uncontrolled excess heat evolved during hydration should be minimized, as they are critical in influencing long-term durability. The mechamisms of molecular and ionic transport are important in the operation of disruptive forces of degradation, whether drying shrinkage, freezing and thawing, carbonation, or intrusion of undesirable chloride, sulfate, or other salts or chemicals;alkali-aggregte reaction; or leaching or release of undesirable encapsulated toxic or radioactive waste species to the environment. The pore structure of the matrix material is citical in transport processes (Roy, 1986).

These mechanisms then act cooperatively;there is an interaction with chemical features either inherent in the cementitious matrix composition itself, or with the aggregate; or with ions or gases diffusing in or out of the cementitious material. In addition to characterizing the solids, the investigation of the chemistry of pore solutions is useful for monitoring chemical changes taking place, which combine the effects of the initial nature of the cementitious material with its response to changes from the environment. The thermodynamic stability of phases is important in controlling degradation processes as, e.g., the free energy change to produce carbonated or other reaction products.

Favorable free energy changes facilitate reaction during curing, and others are favorable to "pozzolanic" reactions of portland cement with siliceous (and alumino-silicate) pozzolans, producing a more chemically stable form of C-S-H, which is part of the reason for the apparently enhanced durability of pastes containing such admixtures. The free energy change is also important in assessing stability of sealing materials in a particular host environment.

Considerable advances have been made in understanding mechanisms of degradation of release of harmful species to the environment; however, much remains to be determined, particularly concerning the cooperative phenomena, i.e., the interaction of the numerous early-stage developmental controlling factors, the consequent physical and chemical characteristics of the hardened cement paste and its microstructure, and the potentially disruptive physical and chemical forces of degradation. The current studies in progress and the unanswered questions (MRS, 1989) provide additional evidence of the sustained and substantial effort needed in this important area.

ACKNOWLEDGEMENT

The author acknowledges partial support of NSF Grant DMR-8812824. Much of the earlier research quoted was supported by the U.S. Department of Energy and through the Office of Nuclear Waste Isolation, Los Alamos National Laboratory, and Sandia National Laboratory. Recent studies made under the Strategic Highway Research Program, National Research Council (USA) and Martin-Marietta Energy Systems, Inc. and its predecessors have also been quoted. The author thanks especially numerous colleagues who have contributed to the various studies.

REFERENCES

James Alamo and Rustum Roy. Crystal Chemistry of the $NaZr_2(PO_4)_3$, NZP, or CTP, Structure Family, J. Mat. Sci., 22, 444-450 (1986).

A. Atkinson, A.K. Nickerson, and T.M. Valentine. Radioactive Waste Management and the Nuclear Fuel Cycle, 4, 357-378 (1984).

A. Atkinson. Radioactive Waste Management and the Nuclear Fuel Cycle, 3, 371-386 (1983).

A. Atkinson, U.S. Atomic Energy Authority Report, AERE-R11777 (1985).

A. Atkinson, J.A. Hearns and C.F. Knights. Aqueous Chemistry and Thermodynamic Modelling of $CaO-SiO_2-H_2O$ Gels, AERE R12548, UKAEA Harwell, July 1987.

M.W. Barnes, B.E. Scheetz, L.D. Wakeley, S.D. Atkinson, and D.M. Roy. Stability of I and Sr Radiophases in Cement Matrices, pp. 147-154, Scientific Basis for Nuclear Waste Management, Vol. 6, Ed. S.V. Topp, North-Holland, NY; Materials Research Society Symposium Proceedings (1982).

M.W. Barnes and D.M. Roy. The Buffering Mechanisms in Leaching of Composites of Cement with Radioactive Waste, Scientific Basis for Nuclear Waste Management, Vol. VI, Ed. Douglas C. Brookins; North-Holland, NY, pp. 159-166; Symposium Proceedings, Materials Research Society (1983).

M.W. Barnes, D.M. Roy, and L.D. Wakeley. Leaching of Composites of Cement with the Radioactive Waste Forms Strontium Powellite and Iodine Sodalite at 90°C, Advances in Ceramics, Am. Cer. Soc., 406-412 (1984).

R.H. Burns. Solidification of Low and Intermediate-Level Wastes, Atomic Energy Review, 9, 547-599 (1971).

BNFL (British Nuclear Fuels PLC), Technology and Engineering, 20 pp. BNFL Engineering, Risley, UK (1988).

M.W. Barnes and D.M. Roy. Activity Diagrams for Calcium/Hydrogen, and Potassium/Hydrogen, and H_4SiO_4 and Their Relation to Reactions in Systems Containing Radioactive Waste Forms, Cement, and Rock in the Presence of Water, Scientific Basis for Nuclear Waste Management, Ed. G. McVay, North Holland, 697-710 (1984).

M.W. Barnes, D.M. Roy and C.A. Langton. Leaching of Saltstone, Mat. Res. Soc. Symp. Proc., Vol. 44, Scientific Basis for Nuclear Waste Management, VIII, Eds. C. M. Jantzel, J. A. Stone and R. C. Ewing, 865-874 (1985).

M. W. Barnes, D.M. Roy and C.A. Langton. Leaching of Saltstones Containing Fly Ash, in Fly Ash and Coal Conversion Byproducts: Characterization, Utilization and Disposal II, Mat. Res. Soc. Symp. Proc. Vol. 65, Eds. G. J. McCarthy, F. P. Glasser, and D. M. Roy (1986).

L.D. Bates and S.D. Van Hoesen. Development of the Central Waste Facility, Waste Management 85, Amer. Nucl. Soc., 147-153 (1985).

U. Berner. Modelling the Incongruent Dissolution of Hydrated Cement Minerals, Radiochimica Acta, Proc. Int. Conf. Migration 87 (1987).

W.D. Bostick, J.L. Shoemaker, P.E. Osborne, and B.E. Evans-Brown, Treatment and Disposal Options for a Heavy Metals Waste Containing Soluble Technetium-99, K/QT-230-R, Martin Marietta Energy Systems, Inc. (22 pp.) (1989).

A.D. Buck. Development of Two Candidate Mixtures (Salt, Nonsalt) for Repository Sealing Applications, Miscallaneous Paper SL-85-8, U.S. Army Engineer Waterways Experiment Station, Vicksburg, Mississippi (1985).

A.D. Buck, J.A. Boa, Jr. and D.M. Walley. Development of a Sanded Expansive Salt Grout for Repository Sealing Application, Miscellaneous Paper SL-85-11, U.S. Army Engineer Waterways Experiment Station, Vicksburg, Mississippi (1985).

R.H. Burns. Solidification of Low and Intermediate Level Wastes, Atomic Energy Review 9, 547-599 (1971).

C.L. Christensen, C.W. Gulick and S.J. Lambert. Sealing Concepts for the Waste Isolation Pilot Plant (WIPP) Site, SAND81-2195 Revised, Sandia Laboratories, Albuquerque, NJ (February 1983).

H. Christensen. Solidification of Nuclear Waste in Concrete, Alternate Nuclear Waste Forms and Interactions in Geologic Media, ORNL Conf-8005107, Gatlinburg, TN, p. 217 (1980).

J.E. Carlson. Containment of Radioactive Wastes Using Improved Cementitious Binders, Waste Management 87, 533-537 (1987).

A. Das, M.S. Thesis, The Pennsylvania State University (1985).

L.R. Dole. Overview of the Applications of Cement-Based Immobilization Technologies Developed at U.S. DOE Facilities," Waste Management 85, Vol. II, Am. Nucl. Soc., Chicago, IL, 455-464 (1985).

L.R. Dole, G.C. Rogus, M.T. Morgan, D.P. Stinton, J.H. Keasler, S.M. Robinson, and J.G. Moore. Cement-Based Radioactive Waste Hosts Formed Under Elevated Temperatures and Pressures (FUETAP Concretes) for Savannah River Plant High-Level Defense Waste, ORNL/TM-8579, Oak Ridge National Laboratory (1983).

W. DeLaguna, T. Tamura, H.O. Weeren, E.G. Struxness, W.C. McClain, and R.C. Sexton. Engineering Development of Hydraulic Fracturing as a Method for Permanent Disposal of Radioactive Wastes, ORNL-4259, Oak Ridge National Laboratory (1968).

J.S. Devgun and D.H. Charlesworth. Impact of Past Experiences on Engineering a Shallow Land Burial Facility, Waste Management 87, 205-211 (1987).

R.F. Feldman, Theme 4.1, Proc. 8th Intl. Congr. Chem. Cement, Brazil, V.I. (1986).

R.F. Feldman, Proc. 5th Intl. Symp. Monterey, 261-288 (1981).

R.F. Feldman. The Porosity and Pore Structure of Hydrated Portland Cement Paste, Mat. Res. Soc. Symp. Proc., Vo. 137, 59-74 (1989).

J.A. Fernandez. Repository Sealing Plan for the Nevada Nuclear Waste Storage Investigations Project Fiscal Years 1984 through 1990, SAND84-0910, Sandia National Laboratories, Albuquerque, New Mexico (1985).

J.A. Fernandez and M.D. Freshley. Repository Sealing Concepts for the Nevada Nuclear Waste Storage Investigations Project, SAND83-1778, Sandia National Laboratories, Albuquerque, New Mexico (1985).

J.A. Forrester. Personal communication, Aug. 29 (1986).

W.P. Freeborn and D.M. Roy. Low Temperature Phase Equilibria in the System Concrete-Tuff: Thermodynamic Calculations, Experimental Studies, and Natural Assemblages (124 pp.), Report to Los Alamos National Laboratory (April 1983a).

W.P. Freeborn and D.M. Roy. The Stability Field of Ettringite in Cements for Salt Repository Sealing (27 pp.), Report to Office of Nuclear Waste Isolation (Oct. 1983b).

H.W. Godbee et al. Application of Mass Transport Theory to the Leaching of Radionuclids, from Waste Solids, Nucl. Chem. Waste Manage., 1, 29 (1980).

S. Goto and D.M. Roy, The Effect of W/C Ratio and Curing Temperature on the Permeability of Hardened Cement Paste, Cem. Concr. Res. 11 (4), 575-580 (1981).

C. Gotsis, D.M. Roy, P.H. Licastro and S. Kaushal. Thermal and Thermomechanical Analysis of a Cylindrical Cementitious Plug Hydrating in a Borehole, Properties of concrete at Early Ages, 49-78, Ed. J.F. Young, American Concrete Institute, SP-95, Detroit (1986).

C. Gotsis and D.M. Roy. Parametric Analysis of the Heat Evolution During Hydration of a Cementitious Plug in a Borehole, Cem. Concr. Res. 14 (6), 847-854 (1984).

F.P. Glasser and J. Marr. British Ceramic Proc. 35, 419 (1984).

F.P. Glasser and J. Marr. Il Cemento, 85-94 (1985).

M.W. Grutzeck and D.M. Roy. Morphology and Microstructure of Cement Paste/Rock Interfacial Regions, in Proc. 7th Intl. Congr. on the Chemistry of Cement, Communications, Vol. VIII, pp. VII-127—VII-133, Septima, Paris (1980).

M.W. Grutzeck and D.M. Roy. Experimental Characterization and Stability of Salt- and Nonsalt-Containing Grouts and Mortars, BMI-ONWI-568, ONWI, Battelle Memorial Inst., Columbus, OH (1985).

M.W. Grutzeck, B.E. Scheetz, E.L. White and D.M. Roy. Modified Cement-Based Borehole Plugging Materials: Properties and Potential Longevity, Borehole and Shaft Plugging Proceedings OECD/USDOE, Columbus, OH (7-9 May 1980), 353-368, OECD, Paris, France (1980).

C.W. Gulick, Jr., J.A. Boa, Jr. and A.D. Buck. Borehole Plugging Materials Development Program, SAND81-0065, Sandia National Laboratories, Report 3, Albuquerque, New Mexico (1982).

C.W. Gulick and L.D. Wakeley, Reference Properties of Cement-Based Plugging and Sealing Materials for the WIPP, Tech. Rept. SL-89-17, Sandia National Labs., Doc. #63-5609 (1989).

R.H. Guymon, L.D. Vaneslow and G.D. Campbell. The Grout Treatment Facility, Spectrum 88, 95-98 (1988).

A. Haworth, S.M. Sharland, P.W. Tasker and C.J. Tweed. A Guide to the Coupled Chemical Equilibria and Migration Code CHEQMATE, NSS Report NSS-R113 (1988).

A. Haworth, S.M. Sharland and C.J. Tweed. Modelling of the Degradation of Cement in a Nuclear Waste Repository, Mat. Res. Soc. Symp. Proc., Vol. 27, 447-454 (1989).

J. Herndon and D. Smith. Plugging Wells for Abandonment, ERDA Report Y/OWI/Sub-76/99068, Office of Waste Isolation, Union Carbide Corp., Nuclear Division, NTIS (1976).

E.D. Hespe. International Atomic Energy Agency, Leach Testing of Immobilized Radioactive Waste Solid, A Proposal for a Standard Method, Atomic Energy Rev., 9 (1), 19-207 (1971).

Hindman, T.B., Defense Radioactive Waste Management: Status and Challenges, Spectrum 88, Am. Nucl. Soc., 12-14 (1988).

R.D. Hooton. Permeability and Pore Structure of Cement Pastes Containing Fly Ash, Slag, and Silica Fume, Proc. ASTM C-1 Symp. on Blended Cements, Denver, 128-143 (1985).

R.D. Hooton and L.D. Wakeley. Influence of Test Conditions on Water Permeability of Concrete in a Triaxial Cell, Mat. Res. Soc. Symp. Proc., Vol. 137, 157-164 (1989).

S. Hoyle and M.W. Grutzeck. Effect of Phase Composition on the Strontium Leachability of Cement-based Waste Forms, Advances in Ceramics 2 (1986); Nucl. Waste Management 2, 275-84.

J.K. Johnstone, R. Peters and P.F. Gnirk. Unit Evaluations of Yucca Mountain, Nevada Test Site: Summary Report and Recommendations, SAND83-0372, Sandia National Laboratories, Albuquerque, NM (1984).

S. Kaushal, D.M. Roy, and P.H. Licastro. Modelling of Temperatures in Large Cementitious Works, Fly Ash, and Coal Conversion: Byproducts: Characterization, Utilization and Disposal III, Mat. Res. Soc. Symp. Proc., Vol. 86, 265-276, eds. G.J. McCarthy, F.P. Glasser, D.M. Roy, and S. Diamond (1987).

S. Kaushal, D.M. Roy, P.H. Licastro, and C.A. Langton. Thermal Properties of Fly Ash Substituted Cement Waste Forms for Disposal of Savannah River Plant Salt, in Fly Ash and Coal Conversion Byproducts: Characterization, Utilization, and Disposal II, Mat. Res. Soc. Symp. Proc. Vol. 65, eds. G.J. McCarthy, F.P. Glasser, and D.M. Roy, 311-320 (1986).

S. Kaushal, D.M. Roy, P.H. Licastro and S. Komarneni. Heat of Hydration and Characterization of Reaction Products of Adiabatically Cured Fly Ash and Slag Mixtures, Fly Ash and Coal Conversion By-Products: Characterization, Utilization and Disposal, Mat. Res. Soc. Proc. Vol. 136, 87-97 (1989), Eds. R.T. Hemming, E.E. Berry, G.J. McCarthy and F.P. Glasser, Mat. Res. Soc., Pittsburgh, PA (1989).

P.C. Kelsall, D. Meyer, J.B. Case and W.E. Coons. Schematic Designs for Penetration Seals for a Repository in the Paradox Basin, BMI/ONWI-563, Prepared by IT Corporation for Office of Nuclear Waste Isolation, Battelle Memorial Institute, Columbus, OH (1985).

A.H. Kibbey and H.W. Godbee. A Critical Review of Solid Radioactive Practices at Nuclear Power Plants, ORNL-4924, Oak Ridge National Lab, March (1974).

S. Komarneni, E. Breval, D.M. Roy and R. Roy. Reaction of Some Calcium Silicates with Metal Cations, Cem. Concr. Res. 18, 204-220 (1988).

S. Komarneni and D.M. Roy. Mechanisms of Immobilization of Nuclear Waste Elements by Cement Minerals, Cement, and Mortar, Cem. Concr. Res., 11, 789-794 (1981).

S. Komarneni and D.M. Roy. Hydrothermal Interactions of Cement or Mortar with Zeolites or Montmorillonites, in Scientific Basis for Nuclear Waste Management, VI, Mat. Res. Soc. Symp. Proc., Vol. 15, Ed. Douglas G. Brookins, North-Holland, New York, pp. 55-62 (1983a).

S. Komarneni and D.M. Roy. Tobermorites: A New Family of Cation Exchangers, Science 221, 647-648 (1983b).

S. Komarneni and D.M. Roy. New Tobermorite Cation Exchangers. J. Mat. Sci., 20, 2930-2936 (1985).

S. Komarneni, D.M. Roy, and A. Kumar. Cation Exchange Properties of Hydrated Cements, pp. 441-447 in Advances in Ceramics 8, Nuclear Waste Management, Ed., G.A. Wicks and W.A. Ross, Amer. Cer. Soc., Columbus, OH (1984).

S. Komarneni, D.M. Roy, and R. Roy. Al-Substituted Tobermorite: Shows Cation Exchange, Cem. Concr. Res., 12, 773-780 (1982).

S. Komarneni and R. Roy. Use of γ-Zirconium Phosphate for Cs Removal from Radioactive Waste, Nature, 299, 707-708 (1982).

S. Komarneni, R. Roy and D.M. Roy, J. Mat. Sci. Lett. 6, 91-92 (1987).

S. Komarneni, R. Roy, D.M. Roy, C.A. Fyfe, and G.J. Kennedy. Al-Substituted Tobermorite—The Coordination of Aluminum as Revealed by Solid State^{27} Al Magic Angle Spinning (MAS) NMR, Cem. Concr. Res., 15, 723-728 (1985).

S. Komarneni, R. Roy and D.M. Roy. Pseudomorphism in Xonotlite and Tobermorite with Co^{2+} and Ni^{2+} Exchange for Ca^{2+} at 25°C, Cem. Concr. Res. 16, 47-58 (1986).

R. Köster. Cementation of Radioactive Wastes in the Federal Republic of Germany, Waste Management, 85, Ed., R.G. Post and M.E. Wacks, Amer. Nucl. Soc., 487-491 (1985).

Kramer, R. and R. Kroebel, In Situ Solidification of Low and Medium Level Wastes, Mat. Res. Soc. Symp. Proc., Vol. 11, Ed. W. Lutze, 849-858 (1982).

A. Kumar, M.S. Thesis, The Pennsylvania State University, University Park, PA (1982).

A. Kumar, Ph.D. Thesis, The Pennsylvania State University, University Park, PA (1985).

A. Kumar, S. Komarneni, and D.M. Roy. Diffusion of Cs^+ and Cl^- Through Sealing Materials, Cem. Conr. Res., 1, 153-160 (1987a).

A. Kumar and D.M. Roy. Retardation of Cs^+ and Cl Using Blended Cement Admixtures. J. Am. Ceram. Soc., 69 (4), 356-360 (1986a).

A. Kumar and D.M. Roy. Pore Structure and Ionic Diffusion in Admixture Blended Portland Cement Systems, Proc. 8th Intl. Congr. Chem. Cement, Brazil, V. V, 73-79 (1986b).

A. Kumar and D.M. Roy. Pore Structure Studies of High Early Strength Portland Cement Containing Silica Fume, Trans. Indian Cer. Soc., 47, (1), 11-15 (1988).

A. Kumar, D.M. Roy, and D.D. Higgins. Diffusion Through Concrete, Concrete, 31-32, Jan. (1987b).

A. Kumar, S. Komarneni, and D.M. Roy. Diffusion of Cs^+ and Cl Through Sealing Materials, Waste Management 86, Am. Nucl. Soc. (1986).

C.A. Langton. Slag-Based Saltstone Formulations, Scientific Basis for Nuclear Waste Management XI, 61-72, Eds. M.J. Apted and R.E. Westerman (1987).

C.A. Langton, M.D. Dukes, and R.V. Simmons. Sci. Basis for Nucl. Waste Management VIII, ed G.V. McVay, MRS Proc., Elsevier, NY, 575-582 (1983).

C.A. Langton and D.M. Roy. Longevity of Borehole and Shaft Sealing Materials. 2. Characterization of Cement-Based Ancient Building Materials, Report ONWI-202, The Pennsylvania State University, University Park, PA (1980a).

C.A. Langton and D.M. Roy. Longevity of Borehole and Shaft Sealing Materials: II. Characterization of Cement-Based Ancient Building Materials. Topical Report to Office of Nuclear Waste Isolation, Battelle, (ONWI-202), Oct. (1981).

E.L. Lewis. Pelletized Waste Form Demonstration Program, Vol. II, Description and Performance, MLM-3045, Mound Laboratory, Feb. (1983).

S. Li and D.M. Roy. Investigation of Relations Between Porosity, Pore Structure, and Cl Diffusion of Fly Ash and Blended Cement Pastes, Cem. Concr. Res. 16, 749-759 (1986).

P.H. Licastro, R.I.A. Malek and D.M. Roy. Expansive Stresses of a Grout Plug on the Walls of a Borehole, Waste Management '85, Proc., Symp on Waste Management at Tucson, AZ, March 24-28, Am. Nucl. Soc., Vol. 3, 475-478 (1985).

P.H. Licastro, D.M. Roy and J.A. Fernandez. Mechanical Compatibility between Selected Cementitious Material and Topopah Spring Member Tuff, SAND86-0558, Sandia National Laboratories (in press, 1989).

R. Lingle, D.D. Bush and B.G. DiBona (TerraTek Engineering, Salt Lake, UT) and P.H. Licastro, D.M. Roy and B.E. Scheetz. Full Scale Borehole Sealing Test in Basalt Under Simulated Downhole Conditions, Report to Office of Nuclear Waste Isolation (Sept. 1983).

D. Mangin, M. Guerin, C. Lattand, A. Malfondet. Immobilization into Concrete of Liquid Radwaste, Nuclear, and Hazardous Waste Management: Spectrum 88, Am. Nucl. Soc., LaGrange Park, IL, 264-267.

R.I.A. Malek and D.M. Roy. Effect of Slag Cement and Aggregate Type on Alkali-Aggregate Reaction and its Mechanisms, 6th Intl. Conf. on Alkalis in Concretes, Research and Practice, Copenhagen (1983), 223-230; Danish Concrete Assn., Copenhagen, Eds. G.M. Idorn, Steen Rostam.

R.I.A. Malek, P.H. Licastro, D.M. Roy, and C.A. Langton. Slag Cement-Low Level Radioactive Waste Forms at Savannah River Plant, Ceram. Bull., 65, 1578-1583 (1986).

R.I.A. Malek and D.M. Roy. Dissolution Kinetics of Tuff Rock and Mechanism of Chemical Bond Formation at the Interface with Cement Grout, Mat. Res. Soc. Symp. Proc., Vol. 44, 943-950, Eds. C.M. Jantzen, J.A. Stone and R.C. Ewing (1985).

R.I.A. Malek and D.M. Roy. Stability of Low-Level Cement-Based Waste Systems, Waste Management 87, Tucson, V. 3, 363-368; Amer. Nucl. Soc., (1987).

R.I.A. Malek, D.M. Roy and Y. Fang. Pore Structure, Permeability, and Chloride Diffusion in Fly Ash adn Slag Containing Pastes and Mortars, Fly Ash and Coal Conversion By-Products: Characterization, Utilization and Disposal, Mat. Res. Soc. Proc., Vol. 136, 255-262, Eds. R.T. Hemming, E.E. Berry, G.J. McCarthy and F.P. Glasser, Mat. Res. Soc., Pittsburgh, PA (1989).

Materials Research Society (1989), Scientific Basis for Nuclear Waste Management XIII, Mat. Res. Soc. Symp. Proc., Vol. 176, Eds. V.M. Oversby and P.W. Brown, Materials Research Society, Pittsburgh, PA (to be published, 1990).

G.J. McCarthy and R. Roy. A Review of Ceramic Nuclear Waste Forms Through 1978, Alternative Nuclear Waste Forms and Interactions in Geologic Media, pp. 37-43, Ed., L.A. Boatner and G.C. Battle, Jr., DOE CONF-8005107 (1981).

C.E. McCulloch, M.J. Angus, F.P. Glasser, and A.A. Rahman. Sci. Bas. for Rad. Waste Man., 413-418 (1984).

E.W. McDaniel. Cement Technology for Borehole Plugging: An Interim Report on Permeability Measurements for Cementitious Solids, ORNL/TM-7092, Oak Ridge National Laboratory, Oak Ridge, TN (January 1980).

E.W. McDaniel. Quality Assurance Consideration for Cement-Based Grout Technology Programs at Oak Ridge National Laboratory, Waste Management 87, 103-106 (1987).

Earl W. McDaniel, Othar K. Tallent, Terry L. Sams, Dianne B. Delzer and William D. Bostick. Basis for Selecting Cement-based Waste Forms for Immobilizing Radioactive Waste, Scientific Basis for Nuclear Waste Managmenet XII, Mat. Res. Soc. Symp. Proc., Vol. 127, Pittsburgh, PA (1989).

J.G. Moore et al. Cement Technology for Borehole Plugging: Interim Report on the Effects of Fly Ash and Salt on the Physical Properties of Cementitious Solids, ORNL/TM-7106, Oak Ridge National Laboratory, Oak Ridge, TN (1980).

J.G. Moore et al. Cement Technology for Plugging Boreholes in Radioactive Waste Repository Sites, Progress Report for the Period October 1, 1977 to September 30, 1978, ORNL-5524, Oak Ridge National Laboratory, Oak Ridge, TN (August 1978).

J.G. Moore, H.W. Godbee, and A.H. Kibbey. Leach Behavior of Hydrofracture Grout Incorporating Radioactive Wastes," Nuclear Technol., 32, 39-52, Jan. (1977).

J.G. Moore. A Survey of Concrete Waste Forms, Alternate Nuclear Waste Forms and Interactions in Geologic Media, ORNL CONF-8005107, Gatlinburg, TN, 194-216 (1981).

K. Ogawa and D.M. Roy. C_4A_3S Hydration, Ettringite Formation, and Its Expansion Mechanism: I. Expansion, Ettringite Stability, Cem. Concr. Res. 11, 741-750 (1981).

M. Onofrei, M.N. Gray, L.D. Keil and R. Pusak. Studies of Cement Grouting Techniques for Sealing a Nuclear Fuel Waste Disposal Vault, Mat. Res. Soc. Symp. Proc., Vol. 137, 349-359 (1989).

V.M. Oversby. Reaction of the Topopah Spring Tuff with J-13 Water at 120°C, Lawrence Livermore National Laboratory Report UCRL-53574 (July 1984).

D.L. Parkhurst, D.C. Thorstenson and L.N. Plummer. U.S. Geological Survey, Water-Resource Investigations, 80-96 (1985).

F.H. Passant. Low Level Waste Management Developments in UK Nuclear Power Stations, Proc. Int. Top. Mtg. on Nuclear and Hazardous Waste Management, Spectrum 88, Am. Nucl. Soc., LaGrange Park, IL (1988).

I.B. Plecas, J.D. Drlijaca, A.M. Kostadinovic, A. D'Peree, L. Gradisar. Co-60 Leaching from Various Formulations of Concrete in Shallow Land Disposal System, Waste Management 87, 503-506 (1987).

G.E. Rennick, J. Pasini, R.F. Armstrong and J.R. Abrams. Plugging Abandoned Gas and Oil Wells, Min. Congr. J. 58, 37-42 (1972).

W.A. Ross, J.H. Westik, Jr., F.P. Roberts, and C.O. Harvey. Comparative Leach Testing of Alternate Waste Forms, Cer. Bull., 62, 1026-1029; 1035 (1983).

A.A. Rousan. A Methodology for Thermal Characterization of Cementitious Materials, Ph.D. Thesis, The Pennsylvania State University, University Park, PA (1982).

A.A. Rousan and D.M. Roy. A Thermal Comparator Method for Measuring Thermal Conductivity of Cementitious Materials, I&EC Product Research and Development 22, 349-351 (1983).

D.M. Roy. Cement Based Nuclear Waste Solidification Forms, Proc. Conf. on High-Level Radioactive Solid Waste Forms, U.S. Nuclear Regulatory Commission (Dec. 18-21, 1978), Denver, CO, pp. 479-516, NUREG/CP-0005, Ed., L. Casey, April (1979).

D.M. Roy. Borehole and Shaft Plugging Proceedings, OECD/USDOE, Columbus, OH (7-9 May 1980), 369-384, OECD, Paris, France (1980).

D.M. Roy. Geochemical Factors in Borehole-Shaft Plug Longevity, The Technology of High-Level Nuclear Waste Disposal, Vol. 1, 338-353, Ed. P.L. Hofmann, DOE/TIC-4621, Technical Information Center, U.S. Dept. of Energy (1981).

D.M. Roy. Mechanisms of Cement Paste Degradation Due to Chemical and Physical Factors, Proc. 8th Intl. Congr. Chem. Cement, Brazil, V. I, 362-380 (1986).

D.M. Roy. Recent Progress in Repository Sealing Materials Studies, The Technology of High-Level Nuclear Waste Disposal, Ed., P.L. Hofmann, Battelle Memorial Institute, Project Management Div., Columbus, OH, 71-92 (1987a).

D.M. Roy. New Strong Cement Materials: Chemically Bonded Ceramics, Science, 651-658, Feb. 6 (1987b).

D.M. Roy. Hydration, Microstructure, and Chloride Diffusion of Slag-Cement Pastes and Mortars, Proc. Third Intl. Conf. on the Use of Fly Ash, Silica Fume, Slag, and Natural Pozzolans in Concrete, Trondheim, Norway, Vol. 2, 1265-1281, Ed. V.M. Malhotra, Am. Concr. Inst., Detroit, MI (1989a).

D.M. Roy. Relationships Between Permeability, Porosity, Diffusion, and Microstructure of Cement Paste, Mortar, and Concrete at Different Temperatures, Mat. Res. Soc. Symp. Proc. 137, Eds. L.R. Roberts and J.P. Skalny, 179-190 (1989b).

D.M. Roy and K. Asaga. Rheological Properties of Fresh Cement Mixes for Repository Sealing Applicatiosn: Effects of Superplasticizers, Mixing Procedures and Time, A Topical Report for Office of Nuclear Waste Isolation, Report ONWI-199, The Pennsylvania State University, University Park, PA (1981).

D.M. Roy (with P.W. Brown, P.D. Cady, M.W. Grutzeck, Y. Li, G. Lui, P.H. Licastro, W. Ma, R.I.A. Malek, J.M. Pommersheim, B.E. Scheetz, D. Shi, M. Silsbee, G.M. Idorn, V. Johansen, B. Osbaeck and N. Thaulow). Concrete Microstructure, First Quarterly Report Year 2, to Strategic Highway Research Program, National Research Council, Washington, DC (Apr. 14, 1989c).

D.M. Roy and F.L. Burns. Recent Advances in Repository Seal Materals, Scientific Basis for Nuclear Waste Management, Vol. 11, Ed. W.L. Lutze, North-Holland, NY, pp. 631-640 (1982); Symposium Proceedings, Materials Research Society.

D.M. Roy and G.R. Gouda. Hot Pressed Cement in Radioactive Waste Management, Final Report to Nuclear Waste Technology Program, Subcontract BSA-481, Battelle Pacific Northwest Laboratories, Aug. (1974).

D.M. Roy and G.R. Gouda. High Level Radioactive Waste Incorporation into (Special) Cements, Nucl. Tech., 40, 214-219 (1978).

D.M. Roy, M.W. Grutzeck and P.H. Licastro. Evaluation of Cement Borehole Plug Longevity, A Topical Report for ONWI, DOE Report ONWI-30, The Pennsylvania State University, NTIS (1979a).

D.M. Roy, M.W. Grutzeck, K. Mather and A.D. Buck. PSU/WES Interlaboratory Study of an Experimental Cementitious Repository Seal Material, ONWI-324, prepared by Materials Research Laboratory, The Pennsylvania State University, and Structures Laboratory, U.S. Army Engineer Waterways Experiment Station for Office of Nuclear Waste Isolation, Battelle Memorial Institute, Columbus, OH (1982a).

D.M. Roy, M.W. Grutzeck and L.D. Wakeley. Selection and Durability of Seal Materials for a Bedded Salt Repository: Preliminary Studies, ONWI-479, Office of Nuclear Waste Isolation, Battelle Memorial Institute, Columbus, OH (1983a).

D.M. Roy, M.W. Grutzeck and L.D. Wakeley. Selection and Durability of Seal Materials for a Bedded Salt Repository: Preliminary Studies, Tech. Report, ONWI-447, prepared by Materials Research Laboratory, The Pennsylvania State University, for Office of Nuclear Waste Isolation, Battelle Memorial Institute, Columbus, OH (1983b).

D.M. Roy, B.E. Scheetz, L.D. Wakeley, E.L. White and M.W. Grutzeck. Selection and Durability of Seal Materials for a Tuff Repository: Preliminary Studies, A Report for Office of Nuclear Waste Isolation, (draft) 63 pp. (1983c).

D.M. Roy, M.W. Grutzeck and L.D. Wakeley. Salt Repository Seal Materials of the BCT Family: A Synopsis of Cementitious Material Development, ONWI-479, Topical Report by Materials Research Laboratory, The Pennsylvania State University, for Office of Nuclear Waste Isolation, Battelle Memorial Institute, Columbus, OH (Dec. 1983d).

D.M. Roy, M.W. Grutzeck and L.D. Wakeley. Salt Repository Seal Materials: A Synopsis of Early Cementitious Materials Development, BMI/ONWI-536, Office of Nuclear Waste Isolation, Battelle Memorial Institute, Columbus, OH (1985).

D.M. Roy and A.M. Johnson. Investigations of Stabilities of Calcium Silicate Hydrates at Elevated Temperatures and Pressures, Proc. Conf. on Calcium Silicate Buildin Products, SCI Special Publication (Soc. of Chem. Industry, London), 114-1212 (1965).

D.M. Roy, S. Kaushal, P.H. Licastro and C.A. Langton. Thermal Properties of Fly Ash Substituted Cement Waste Forms for Disposal of Savannah River Plant Salt, Fly Ash and Coal Conversion Byproducts: Characterization, Utilization and Disposal II, Mat. Res. Soc. Symp. Proc., Vol. 65, Eds. G.J. McCarthy, F.P. Glasser and D.M. Roy, 311-320 (1986).

D.M. Roy, A. Kumar, and J.P. Rhodes. Diffusion of Chloride and Cesium Ions in Portland Cement Pastes and Mortars Containing Blast Furnace Slag and Fly Ash, Fly Ash, Silica Fume, Slag and Natural Pozzolans in Concrete, Vol. 2, SP-91, Ed., V.M. Malhotra, 1423-1444, American Concrete Institute, Detroit (1986).

D.M. Roy and C.A. Langton. Characterization of Cement-Based Ancient Building Materials in Support of Repository Seal Studies, A Topical Report for Office of Nuclear Waste Isolation, The Pennsylvania State University, BMI/ONWI-523, May (1983).

D.M. Roy and C.A. Langton. Studies of Ancient Concrete as Analogs of Cementitious Sealing Materials for a Repository in Tuff, LA-11527-MS, Los Alamos National Lab., Los Alamos, NM, 101 pp., March (1989).

D.M. Roy, M. Perez, B.E. Scheetz and P.H. Licastro. Changes in Length and Volume of Cementitious Grouts, in Innovative Cement Grouting, ACI Special Publication SP-83, Am. Concr. Inst., Detroit, MI, pp. 43-60 (1984).

D.M. Roy, B.E. Scheetz, and M.W. Barnes. Preparation of Cement Composite Nuclear Waste Forms and Their Physical and Chemical Properties, PSU-021, The Pennsylvania State University, Report to Rockwell International, Contract DE-AC09-79ET41900 with the U.S. Department of Energy, Sept. (1981).

D.M. Roy, B.E. Scheetz, M.W. Grutzeck, L. Wakeley, and S.D. Atkinson. Low Temperature Ceramic Waste Form: Characterization of Monazite Cement Composites, Scientific Basis for Nuclear Waste Management, Vol. 2, pp. 343-349, Ed., C.J.M. Northrup, Plenum, NY (1980).

D.M. Roy, B.E. Scheetz, M.W. Grutzeck, A.K. Sarkar, and S.D. Atkinson. A Low Temperature Ceramic Radioactive Waste Form, 136-142, Proc. Intl. Symp. Ceramics in Nuclear Waste Management, Cincinnati, OH (April 30-May 2, 1979), Eds., T.D. Chikalla and J.E. Mendel, Nucl. Div., Am. Ceram. Soc. and USDOE Conf., 7990420 (1979b).

D.M. Roy, B.E. Scheetz, M.W. Grutzeck, A.K. Sarkar and S.D. Atkinson, Proc., Intl. Symp. Ceramics in Nuclear Waste Management, Cincinnati, OH, pp. 136-142, Eds. T.D. Chikalla and J.E. Mendel, Nucl. Div., Am. Ceram. Soc. and U.S.D.O.E., Conf.-790420 (1979).

D.M. Roy, B.E. Scheetz, C.A. Langton and M.W. Grutzeck. Selection and Durability of Seal Materials for a Basalt Repository: Preliminary Studies, MRL-C/PSU-022, Materials Research Laboratory, The Pennsylvania State University, University Park, PA, 117 pp. (Sept. 1982b).

D.M. Roy, B.E. Scheetz, L.D. Wakeley, and M.R. Barnes. Leach Characterization of Cement Encapsulated Wastes, Conference on Leachability of Radioactive Solids, Gatlinburg, TN, Dec. 9-11, 1980, Nucl. and Chem. Waste Mgt., 3, 35-42 (1982).

D.M. Roy, Wei Fajun, and M.W. Grutzeck. NZP-Cement Composite Waste Forms, Advances in Ceramics, Nuclear Waste Management, 8, 401-405, Am. Ceram. Soc., Columbus, OH (1984).

D.M. Roy and W.B. White. Borehole Plugging by Hydrothermal Transport, A Feasibility Report for Oak Ridge National Laboratory, Materials Research Laboratory, The Pennsylvania State Uniersity, University Park, PA, ORNL/SUB-4091-1 (May 30, 1975).

R. Roy. Stabilities of Alternate Waste Forms. Proc. Conf. High-Level Radioactive Solid Waste Forms, pp. 757-773, Denver, USNRCEG/CP-0005 (1978).

R. Roy. Nuclear Waste--The Penn State Connection, Earth and Min. Sci. Bull., 50, 13 (1980).

R. Roy and D.M. Roy. New Low Temperature Hydroxylated Radioactive Waste Forms, International Seminar on Chemistry and Process Engineering for High Level Waste Solidification, Julich, Germany, June (1981).

R. Roy. Radioactive Waste Disposal, Vol. 1, The Waste Package, pp. 232, Pergamon Press, NY (1982).

R. Roy, E.R. Vance, and J. Alamo. [NZP], A New Radiophase for Ceramic Nuclear Waste Forms, Mat. Res. Bull., 17, 585-589 (1982).

R. Roy, L.J. Yang, J. Alamo, and E.R. Vance. A Single Phase ([NZP]) Ceramic Radioactive Waste Form, Scientific Basis for Nuclear Waste Management, Vol. 6, pp. 15-21, Ed., Douglas G. Brookins, Elsevier Science Publishing Co., Inc., New York (1983).

G. Rudolph and R. Köster. Immobilization of Sr and Cs in Intermediate Level Wastes by Solidification in Cements, Sci. Basis for Nuclear Waste Management, V. 1, Ed., G.J. McCarthy, Plenum Press, NY, 467-470 (1979).

J.M. Rusin, J.W. Wald and R.D. Lokken, Alternative Waste Forms—A Comparative Study, Scientific Basis for Nuclear Waste Management, Vo.. 2, 255-264, Ed. C.J.M. Northrup, Jr., Plenum, NY (1979).

J.M. Salsman. Considerations for Creating a Free-Standing Monolith, Waste Management 85, Am. Nucl. Soc., Chicago, IL, 133-136 (1985).

A.K. Sarkar, M.W. Barnes and D.M. Roy. Longevity of Borehole and Shaft Sealing Materials. I. Thermodynamic Properties of Cements and Related Phases, A Topical Report for Office of Nuclear Waste Isolation, Report ONWI-201, The Pennsylvania State University, University Park, PA (1982).

B.E. Scheetz, see Roy et al., 1989c; Appendix C (1989).

B.E. Scheetz and G. Anderson. Preliminary Dissolution Model Calculations, A Report to Los Alamos National Laboratory, prepared by Materials Research Laboratory, The Pennsylvania State University, University Park, PA (1985).

B.E. Scheetz, M.W. Grutzeck, L.D. Wakeley and D.M. Roy. Characterization of Samples of a Cement-Borehole Plug in Bedded Evaporites, DOE Report ONWI-70, The Pennsylvania State University, NTIS (1979).

B.E. Scheetz, P.H. Licastro and D.M. Roy. A Full-Seal Borehole Sealing Test in Anhydrite Under Simulated Downhole Conditions, Vol. 2, BMI/ONWI-581(2), prepared by Materials Research Laboratory, The Pennsylvania State University, for the Office of Nuclear Waste Isolation, Battelle Memorial Institute, Columbus, OH (May 1986a).

B.E. Scheetz, P.H. Licastro and D.M. Roy. A Full-Scale Borehole Sealing Test in Salt Under Simulated Downhole Conditions; Vol. 2, BMI/ONWI-573(2), Office of Nuclear Waste Isolation, Battelle Memorial Institute, Columbus, OH (May 1986b).

B.E. Scheetz, R.I.A. Malek, P.J. Andersen, V. Johansen and D.M. Roy. Packing and Rheological Models and Their Predicting Capacity for Concrete Properties, TRB, Washington, DC (Jan. 1990).

B.E. Scheetz and D.M. Roy. Performance Evaluation and Characterization of a Cementitious Seal Material for application in the Topopah Spring Tuff at the Nevada Test Site, Proc. Mat. Res. Soc. Symp., Vol. 44, Scientific Basis for Nuclear Waste Management VIII, Eds., C.M. Jantzen, J.A. Stone, and R.C. Ewing, 935-942 (1985a).

B.E. Scheetz and D.M. Roy, Cer. Bull. 64 (32), 452 (1985b).

B.E. Scheetz and D.M. Roy. Preliminary Survey of the Stability of Silica-Rich Cementitious Mortars 82-22 and 84-12 with Tuff, LA-11222-MS, Los Alamos National Lab., Los Alamos, NM, 51 pp. (March 1989a).

B.E. Scheetz and D.M. Roy. Reactivity of a Tuff-Bearing Concrete; CL-40 CON-14, LA-11532-MS, Los Alamos National Lab., Los Alamos, NM, 84 pp. (April 1989b).

B.E. Scheetz and D.M. Roy. Reactivity of a Tuff-Bearing Concrete: CL-40 CON-14, LA-11532-MA, April (1989c).

B.E. Scheetz, D.M. Roy and C. Duffy. Elevated Temperature (Hydrothermal) Stability of Cementitious Sealants for a Deep Geological Repository in Tuff, Waste Management 9, 253-259 (1989a).

B.E. Scheetz, D.M. Roy and C. Duffy. Physical and Mechanical Properties of Thermally Altered Cementitious Sealing Materials for a Nuclear Waste Repository in Tuff, Third Intl. Conf. on the Use of Fly Ash, Silica Fume, Slag, and Natural Pozzolans in Concrete, Trondheim, Norway, Vol. 2, 1597-1614, Ed. V.M. Malhotra, Am. Concr. Inst., Detroit, MI (1989b).

B.E. Scheetz, D.M. Roy, C. Tanner, M.W. Barnes, M.W. Grutzeck, and S.D. Atkinson. Properties of Cement Solidified Radioactive Waste Form with High Levels of Loading, Am. Ceram. Soc. Bull., 64, 687-690 (1985).

V.W. Schneider and F.W. Ledebrink. Cementation of TRU Waste by a New Process, Advances in Ceramics, Vol. 8: Nuclear Waste Management, Eds., G.G. Wicks and W.A. Ross, Amer. Cer. Soc., Columbus, OH, 394-400 (1984).

R.J. Serne, W.J. Martin, R.D. Lokken, V.L. LeGore, C.W. Lindenmeier and P.F.C. Martin. Leach and EP Toxicity Tests on Grouted Waste Form Tank 106-AN, PNL-6960, Pacific Northwest Laboratory, Richland, WA (1989).

D. Shi, P.W. Brown and S.K. Kurtz. A Model for the Distribution of Pore Sizes in Cement Paste, Mat. Res. Soc. Symp. Proc., Vol. 137, 23-34 (1989).

M. Silsbee, R.I.A. Malek and D.M. Roy. Composition of Pore Fluids Extruded from Slag-Cement Pastes, Proc. 8th Intl. Conr. Chem. Cement, Brazil, V.IV, 263-269 (1986).

D.P. Stinton, E.W. McDaniel, and H.O. Weeren. Partitioning of Cesium in Phases Produced by Grouted Waste Injection, Scientific Basis for Nuclear Waste Management VII, Ed., G.V. McVay, North Holland, NY (1984).

J.A. Stone. Studies of Concrete as a Matrix for Solidification of Savannah River Plant Radioactive Waste, DP-1448, Savannah River Lab., Aiken, SC (1977).

J. Stone, et al. Preliminary Evaluation of Alternative Forms for Immobilization of Savannah River Plant High-Level Waste, DP-1545, E.I. DuPont de Nemours, Aiken, SC (1979).

J.C. Stormont. Development and Implementation: Test Series A of the Small Scale Seal Performance Tests, SAND85-2602, Sandia National Laboratories, Albuquerque, NM (1986a).

O.K. Tallent, E.W. McDaniel, G.D. Del Cul, K.E. Dodson and D.R. Trotter. Immobilization of Technetium and Nitrate in Cement-Based Materials, Mat. Res. Soc. Symp. Proc., Vol. 112, 23-30, Eds. M.J. Apted and R. Westermann, Materials Research Society, Pittsburgh, PA (1988).

G.H. Tattersall and P.F.G. Banfill. The Rheology of Fresh Concrete, Pitman Books Ltd., London, 356 pp. (1983).

E.R. Vance, S. Urquart, D. Anderson, and I.M. George. Immobilization of Uranium-Rich High-Level Nuclear Waste, Advances in Ceramics, Vol. 20, Nuclear Waste Management II, 249-258 (1986).

L.D. Wakeley, B.E. Scheetz, M.W. Grutzeck and D.M. Roy. Characterization of Samples of a Cement-Borehole Plug in Bedded Evaporites from Southeastern New Mexico, Cem. Concr. Res. 11 (1), 131-142 (1981a).

L.D. Wakeley, B.E. Scheetz, M.W. Grutzeck and D.M. Roy. Cem. Concr. Res. 11 (1), 131-142 (1981b).

L.D. Wakeley, D.M. Roy and M.W. Grutzeck. Experimental Studies of Seal Materials for Potential Use in a Los Medanos-Type Bedded Salt Repository, ONWI-325, prepared by Materials Research Laboratory, The Pennsylvania State University, for Office of Nuclear Waste Isolation, Battelle Memorial Institute, Columbus, OH (1981a).

L.D. Wakeley and D.M. Roy. Cementitious Materials for Sealing Access Shafts Through Evaporite and Clastic Rocks to a Radioactive-Waste Repository, Mat. Res. Soc. Symp. Proc., Vol. 44, Scientific Basis for Nuclear Waste Management VIII, Eds. C.M. Jantzen, J.A. Stone and R.C. Ewing, 951-960 (1985).

L.D. Wakeley. Dependence of Expansion of a Salt-Saturated Concrete on Temperature and Mixing and Handling Procedures, Technical Report SL-87-(in prep), U.S. Army Engineer Waterways Experiment Station, Vicksburg, Mississippi (1986).

L.D. Wakeley and A.D. Buck. Effects of Different Fly Ashes and Silica Fume on Selected Properties of an Expansive Grout, pp. 1261-1278, in Fly Ash, Silica Fume, Slag and Natural Pozzolans in Concrete, ACI SP-91, Ed. V.M. Malhotra, Vol. 2, CANMET/ACI (1986).

L.D. Wakeley and J.P. Burkes. Distribution of Chloride in a Salt-Saturated Grout in Contact with Halite Rock, Cem. Concr. Res. 16, 267-274 (1986).

L.D. Wakeley and T.S. Poole. Post-Test Analysis of a Laboratory-Cast Monolith of Salt-Saturated Concrete, Miscellaneous Paper No. SL-86-13, U.S. Army Engineer Waterways Experiment Station, Vicksburg, Mississippi (1986).

L.D. Wakeley and D.M. Roy. Experimental Concretes for Sealing Radioactive-Waste Repositories in Evaporite Strata, Cem. Concr. Res. 13, 97-106 (1983).

L.D. Wakeley and D.M. Roy. A Method for Testing the Permeability Between Grout and Rock, Cem. Concr. Res. 12, 533-534 (1982).

Wei Fajun, M.W. Grutzeck, and D.M. Roy. Leaching of Warm-Pressed CsZP-Cement Composite Waste Forms, Mat. Res. Soc. Symp. Proc., Vol. 44, Scientific Basis for Nuclear Waste Management, VIII, Eds., C.M. Jantzen, J.A. Stone, and R.C. Ewing, 899-902 (1985).

E.L. White, B.E. Scheetz, D.M. Roy, K.G. Zimmerman and M.W. Grutzeck. Scientific Basis for Nuclear Waste Management, Vol. I, pp. 47-478, Mat. Res. Soc. Proc., Ed. G.J. McCarthy, Plenum, NY (1979).

R.G. Wilbourn. Development of a Grout-Based Stabilization Method for Spent High-Temperature Gas-Cooled Reactor Fuel, Waste Management 85, 503-510 (1985).

E.L. Wilhite, C.A. Langton, H.F. Sturm, R.L. Hooken, and E.S. Occhipirti. Saltstone Processing Start-Up at the Savannah River Plant, Spectrum 88, Am. Nucl. Soc., LaGrange Park, IL, 99-101 (1988).

H.O. Weeren. Waste Disposal by Shale Fracturing at ORNL, Nucl. Eng. Design, 44, 291-300 (1977).

H.O. Weeren, J.G. Moon, and E.W. McDaniel. Waste Disposal by Shale Fracturing at ORNL, Sci. Basis for Nucl. Waste Management, Vol. 1, 257-264, Plenum Press, NY (1979).

E. Zamorani, G. Serrini, and H. Blanchard. Cem. Concr. Res., 16 (3) (1986).

E. Zamorani, I.A. Sheikh, M. Della Rossa and G. Serrini, Physical Properties and Leachability of MLW Stream Containing Cr, Ni and Cd Immobilized in a Cement Matrix, Scientific Basis for Nuclear Waste Management XII, Mat. Res. Soc. Symp. Proc., Vol. 127, Eds. W. Lutze and R. Ewing, 489-494 (1989).

APPLICATION OF CEMENTS TO THE TREATMENT AND CONDITIONING OF TOXIC WASTES

F P Glasser

Department of Chemistry
University of Aberdeen, Scotland, UK

Abstract

Some of the issues, problems and perspectives in the use of cement for the treatment and conditioning of toxic and hazardous wastes are presented as an introduction to a panel discussion.

VERWENDUNG VON ZEMENTEN FÜR DIE BEHANDLUNG UND KONDITIONIERUNG VON TOXISCHEN UND ANDEREN GAFÄHRLICHEN ABFÄLLEN

ZUSAMMENFASSUNG

Einige Diskussionspunkte, Probleme und Perspektiven der Anwendung von Zementen in der Behandlung und Konditionierung von toxischen und anderen gefährlichen Abfällen werden als Einleitung zu einer Paneldiskussion erörtert.

1. Introduction

These notes are meant as a basic introduction to the subject; space precludes an exhaustive review. At first sight, cements appear to offer a barrier action against the escape of toxic wastes into the environment. Indeed, they are used in engineered barriers. But in this application they may be in competition with other, less sophisticated barrier systems, e.g., plastic membranes. However physical barriers are subject to potential disruption; brittle materials, including both aged plastic and concrete, are inherently liable to cracking. This disadvantage may be overcome by the use of soft, low strength barriers, e.g. those made of cement-bentonite slurries. But cement and blended cements can also be used as matrix-formers; these applications are technically the most challenging and form the basis of this contribution.

Setting Reactions

The set of cement is a colloidal reaction and direct incorporation of waste may interfere. It is well known that a wide range of materials interfere with cement set while a more restrictive range of materials exist which accelerate set. Set retarders include substances which complex Ca, e.g. EDTA, citrate, or which form insoluble precipitates which coat cement grains and block hydration, e.g. borate and phosphate. On the other hand,substances which remain soluble in the cement environment may sometimes accelerate set, e.g. sodium salts, calcium chloride, etc. Most conditioning operations therefore require to establish a "window" of waste species concentrations within which the conditioning process will give an acceptable performance. The substitution of cement, in whole or in part, by fly ash, slag and/or natural pozzolans often increases the sensitivity of the set to interference. In the writer's experience, strong set accelerators or retarders always affect the microstructure, with inevitable consequences to the porosity-permeability characteristics of the matrix.

Given the complexity of most real waste streams, there is a need for empirical testing, to ensure compliance with specifications and to demonstrate that proposed waste form/cement combinations are compatible. But there are also concerns about the longer term behaviour, which can only be addressed by basic research on immobilisation mechanisms.

Immobilisation Mechanisms

The behaviour of hazardous wastes in cement has a rather poorly-documented science base. An extensive review of a wide range of industrial processes for fixation is given by Conner (1), and progress in the specialised field of cement solidification has been described in a recent American Chemical Society Symposium (2).

Much of the advantage of cement-based solidification arises from physical matrix-forming effects; liquids, sludges and dusts are converted into solid forms. These have low mobility,low surface area:volume ratios and on that account are less susceptible to leaching. However cements comprise an intrinsically microporous matrix and are thus potentially more susceptible to leaching than might be assumed from geometric surface area. Fortunately cements also have a chemical immobilisation potential which contributes to fixation.

The source of the chemical immobilisation potential arises from:-

- sorption on high surface area cement phases, e.g. C-S-H
- structural incorporation into one or more of the cement hydration phases
- precipitation, by reaction with one or more of the cement constituents
- physical retardation by the solid matrix, which facilitates slow reactions.

It is not always possible to make clearcut distinctions between mechanisms, but wherever possible it is desirable to distinguish the fixation mechanism(s) to develop an adequate methodology with which to extrapolate performance-related data to predict long-term releases.

The cement environment is characteristically wet and is also rich in soluble ions. On account of the range of soluble cations (Na, K, Ca) and anions (OH, SO_4; possibly also Cl and CO_3) considerable competition exists for sorption sites. Therefore, any ion/neutral species which are to be effectively sorbed, given that they may be present at low concentrations, must have very favourable distribution coefficients.

The crystalline cement hydrate phases have structures which permit some crystallochemical substitution. Since the level of toxics which need to be incorporated is frequently low, solid solution could be an important mechanism for fixation. Thus ettringite, the AF_t phase, has a range of structural sites favourable for incorporation of both anions and cations; for example sulfate may be partly replaced by borate, chromate and arsenate (3).

Precipitation is however the single most effective chemical mechanism of fixation. Elementary chemical considerations suggest that a wide range of metal ions will precipitate at the high pH characteristic of cement systems (4). The so-called amphoteric elements (i.e. those elements which have a minimum solubility at near-neutral pH's but which become soluble at both low and high pH's) deserve special mention. For example, Al is normally very soluble at the high pH's characteristic of cements but nevertheless remains virtually insoluble; it is preciptated as hydrogarnet, $3CaO{\cdot}Al_2O_3{\cdot}6H_2O$, and ettringite. Both these solubility-limiting phases are congruently soluble and their solubility product data are known (5,6).

Data are available for some specific waste constituent - cement interactions. For example, Bishop (7) gives data for cadmium, chromium and lead, and found that solubility-limiting ternary metal silicate hydrates formed. Similarly, studies of uranium point to calcium uranium hydrate, or silicate hydrates, as the source of immobilisation potential (8). Undoubtedly, more species-specific mechanistic studies are needed: the Panel may wish to discuss the present state of the data and what research needs require to be met.

Another factor relevant to waste conditioning is the redox potential (E_h) This has been measured for cement systems and found to be oxidising, in the range +100 to +200mV relative to a standard hydrogen electrode. But chemically-reduced materials, such as metallurgical slags, drastically lower the redox potential perhaps to -400mV (9). The presence in wastes of metal and of decomposing organics can be expected to favour a low E_h, and many natural disposal sites, for example those sited in clay, may also have a low E_h. The level of E_h may affect release rates: for example, chromium is much less soluble at high pH in its Cr(III) (reduced) speciation than as Cr(VI) (oxidised).

Leach Testing

Performance-based tests are an essential requirement of most legislative codes. Since cements influence the pH of the leachant medium, and since pH is an important factor in controlling leach rates, there is a need to determine whether accelerated leach tests are relevant, and if so what correlation is achieved between laboratory performance and site monitoring. In this context the Panel may also wish to discuss the applicability of existing standards to the testing of cemented products.

Future Performance

The factors which contribute to controlling toxic releases from cemented wastes depend on internal chemical potentials and on the physical integrity of the matrix. The rate of property decay, and its impact on release

rates is uncertain. The reaction of organic material with cement is a particularly important area in which we lack knowledge: the position is only marginally better for inorganics. Considerable progress has been made in predicting the performance of cements intended for the immobilisation of low-level radioactive wastes, and it is suggested that technology transfer would be useful: predictive exercises, using coupled geochemical codes together with information on cement properties developed for radioactive wastes, could be adapted for hazardous wastes. It is also possible to use treatments developed for static and dynamic aspects of other leachates, e.g. combustion waste (10,11). A weakness of these codes is that we lack basic input data on waste-cement interactions, as well as of cement-near field interactions. But computer based codes do provide a useful framework with which to make predictions and, given the chemical complexity of the waste-cement system, may be essential. In any event, simple extensions of actual test data lacks credibility when extrapolated over long time scales; conceptual models capable of quantification are needed. The extent to which cements will provide controlled release rates in the long term, the quantification and prediction of these rates, might also be discussed.

Summary

Many issues are suggested for the panel discussion. These are technical as well as economic. Ultimately, the economic cost-benefit ratio will be an important factor in choice of disposal scenario, so use of cement-based technology will have to be justified on the basis of performance as well as cost. To date, there seems to be only limited awareness of the scientific basis for validating the performance of cement systems,of the need to establish acceptable leach protocols, for predicting long-term performance and comparing alternative strategies.

References

1. Conner, Jesse R: **Chemical Fixation and Solidification of Hazardous Wastes.** Van Nostrand Reinhold 1990, 692pp. ISBN 0-442-20511-2.
2. Spence, R.D.: **Chemistry and Microstructure of Solidifed Waste Forms** Lewis Publishers (in press) ISBN 087371-748-1.
3. McCarthy, G.J., Hasser, D.J. and Bender, J.A. "**Synthesis, Crystal Chemistry and Stability of Ettringite: a Material with Potential Applications in Hazardous Waste Immobilisation**". Materials Re. Soc. Proceedings Vol. 245 (Ed. F.P. Glasser) in press.
4. Garrels, R.M. and Christ, C.L. "**Solutions, Minerals and Equilibria**". Freeman, Cooper & Co. 1965 450pp. ISBN 0-87735-333-6.
5. Atkins, M., Bennet, D., Dawes, A., Glasser, F.P., Kindness, A. and Read, D. Proceedings of European Materials Res. Soc. (in press) Elsevier (Amsterdam).
6. Atkins, M., Macphee, D., Kindness, A. and Glasser, F.P. **Solubility Properties of Ternary and quaternary Compounds in the CaO-A_2O_3-SiO_2-H_2O System** (in press) Cement and Concr. Res.
7. Bishop, P.L. "**Leaching of Inorganic Hazardous Constituents from Stabilized/Solidified Hazardous Wastes**" Hazardous Wastes and Hazardous Mater. (1988) 5[2] 129-143.
8. Atkins, M., Beckley, N., Carson., S., Cowie, J., Glasser, F.P., Kindness, A., Macphee, D., Pointer, C., Rahman, A., Jappy, T., Evans, P.A., McHugh, G., Matingley, N.J. and Wilding, C. (1991) Report EUR 13542 EN, Commission of the European Communities, Brussels.
9. Cote, P. 1986 **Contaminant Leaching from Cement Based Waste Forms Under Acidic Conditions** (1986) PhD Thesis, McMaster Univ. Hamilton, Ontario, Canada.

10. Land and Water Quality News Electric Power Research Institute, Palo Alto CA) 6 (1) March 1991, p3.
11. Groot, G.J., Wijkstra, J., Hoede, D., and van der Sloot, H. "**Leaching Characteristics of Selected Elements from Coal Ash as a Function of the Acidity of the Contact Solution and the Liquid/Solid Ratio**". (1989) A.S.T.M. Standard Tech. Pub. 1033, 170-183; 125-149.

HAZARDOUS WASTE (ORGANIC, HEAVY METAL) : CEMENT DISPOSAL

Michael W Grutzeck

The Pennsylvania State University
USA

Introduction

Two choices involving cement technology are available for dealing with the disposal of hazardous waste (organic, heavy metal). The waste (if it is flammable) can either be incinerated in a cement kiln or solidified/stabilized in a cementitous material (grout, concrete).

Kiln-based incineration studies have shown that the use of selected organic wastes such as Freon 113, 1,1,1-trichloroethane, and methylethylketone as a partial replacement for fuel, is not only cost effective, but environmentally sound. Destructive and removal efficiencies (DER) for this process often exceed EPA's mandate of 99.99% [1-6]. More recently it has been demonstrated in Norway that even PCB's could be successfully incinerated. Using a dry cement Kiln, they have shown a DER of ≥ 99.9999% for PCB. They also demonstrated that the emission of cyclic particulates, polynuclear aromatic hydrocarbons, and other cyclic organic hydrocarbons were more a factor of kiln operating conditions than the material being incinerated[7].

Since the last ICCC in Rio de Janeiro, there has been a greater acceptance of the solidification/stabilization of organic hazardous waste using cementious materials, although the trend has been away from using ordinary (ASTM Type I) portland cement (OPC). The majority of papers report a greater use of blended cements containing pozzolona, fly ash, ground granulated blast furnace slag, and clays. Several recent papers have dealt with the optimization and microstructure of OPC-based hazardous waste forms[8-12], and others with the design and advantages of pozzolanic portland cements[13-18]. The patent literature includes blast furnace slag activated with ≤ 10% anhydrite[19], and one with a clay-portland cement blend[20]. In general, the addition of organics to the cementitious host tended to either radically change the microstructure/phase development or have no effect. The latter behavior is in part attributed to the fact that some wastes are not miscible with water, e.g. chloronaphthalene. When the organic waste was soluble to some degree i.e. trichloroethylene (C_2HCl_3) or 3-chlorophenol (and contained chlorine) ettringite tend to be stabilized, inhibiting its conversion to monosulfate and slowing the overall cement hydration reaction. The general consensus seems to be that the solidification/stabilization of organics with cementitious materials are more problematic than heavy metals. Some of the more detailed analyses of work in each of these two areas will be given below.

Heavy Metals

The use of portland cement and blended portland cement to solidify/stabilize heavy metals is well documented[21-27]. The successful immobilization of heavy metals such as Cr, Pb, Ba, Hg, Cd, and Zn in cement is generally attributed to adsorption and precipitation of hydroxide phases. Pb and Zn tend to retard setting of the cement, but solid state ^{29}Si NMR tends to suggest that $Pb(NO_3)_2$ enhances the degree of silicate polymerization, whereas $Zn(NO_3)_2$ tends to retard polymerization. Although cementitious waste forms are stable under high pH, their use to solidify/stabilize pickling liquor or their exposure to acid tended to degrade both the cement and its ability to retain heavy metals in its structure. One reported use of portland cement to solidify/stabilize waste containing As_2O_3 described adverse effects on the mechanical properties of the cement waste form[28]. Compressive strength was observed to decrease from 11 to 6 MPa with a 7.5% addition of arsenic oxide. However, leach rates were extremely low, arsenic in the leachate was ~10^4 times lower than the equilibrium solubility of As_2O_3 in water. A dynamic leaching test was carried out on four samples containing synthetic sludge (As, Cd, Cn, and Pb) formulated from lime and fly ash, opc and fly ash, opc and bentonite, and opc and soluble silicates. The tests were run for 665 days. Arsenic leached the most easily of the four metals[29]. A permeability study on cement based waste forms containing Zn, Cd, and Hg showed that the waste forms containing Zn had the highest permeability, followed in succession by Cd and Hg[30]. Pore structure seemed to correlate with permeability.

Organics

Solidification/stabilization of organic species using portland cement and portland cement blends is a different matter entirely. Organics such as phenols tend to degrade the performance of cement-based materials, whereas other organics such as methyl alcohol have little or no effect. Whereas, in the case of heavy metals, it is less of an issue, the nature of the waste stream, in terms of the organic phases present in the material, becomes extremely important. For example, the phenols (parachlorophenol, pentachlorophenol and 2, 4, 5 - trichlorophenol) tend to degrade the mechanical properties of the waste form and lead to poor leaching performance[31-34]. Microstructures at early ages are different than undoped control samples and surprisingly porosity tends to decrease rather than increase as lower strengths would seem to imply. Samples containing pentachlorophenol decreased in strength from 13 to 7 MPa (composed to control) and leach testing showed a 12% release of organic in 120 days. A review of the performance of five different binders (OPC, OPC and fly ash, OPC + activated carbon, OPC and bentonite and OPC and soluble silicates) combined with 20 organic priority pollutants at 3 different levels of concentration (10, 100 and 1000 mg/g solidified waste)[35]. It is implied that waste form and organic waste must be evaluated on a case by case basis! Finally, it has also been reported that PCBs were immobilized by a cement matrix[36].

A large amount of work on leach testing, mechanisms of incorporation and phase formation has been carried out at Louisiana State University, Baton Rouge[37-42]. The authors used ethylene glycol and p-bromophenol as their representative organic materials and solidified/stabilized them with portland cement. They used a wide variety of techniques (x-ray and election diffraction, EDX, SEM/TEM) to characterize the waste form and identify host phases for the wastes. As mentioned earlier, p-bromophenol did not alter the cement matrix to any great extent; however, the ethylene glycol did. There was a decidedly smaller amount of

crystalline material present in the latter sample, which was more amorphous. Interestingly the authors found what they believe is evidence of a new phase in their p-biomophenol samples. The phase contains approximately 34% waste, and is crystalline as evidenced by yet unidentified x-ray diffraction peaks. The authors also found a heterogenous distribution of the p-biomophenol in the calcium silicate hydrate phase (C-S-H). They further report a general decrease in Tobermonite-like material associated with organic additions. Chloride ions were associated with Al in Al x-ray maps, but not with Ca. Finally, both Ca $(OH)_2$ as well as $Mg(OH)_2$ were found to have surface coatings of organics, evidence of weak attraction.

A new predictive technique is under development at Brookhaven National Lab (USA). It is claimed that using this model one will be able to predict the reliability and quality of a cement-based hazardous waste form prior to its use[43, 44]. Finally, in this same vein, researchers are developing more realistic leaching tests[45]. Column leach testing of cement-based waste forms containing phenol and trichloroethylene was carried out on 3 and 28 day cured waste forms. The leachability index values for phenol were 7.7 and 8.2, respectively. The scale varies from 5 (very mobile) to 15 (immobile). The test may be a useful way to rank performance, however, it could not be used for trichloroethylene, because it was suspected that this organic was prone to vaporization/decomposition during the test.

Summary

Two very good books giving an overview of hazardous waste science and technology have recently been published. They are entitled Stabilization and Solidification of Hazardous Wastes[46] and Hazardous Waste Treatment Technologies[47], respectively. The first book is an excellent compilation of material dealing with all aspects of stabilization/solidification science and technology. The second book addresses types of hazardous waste and potential ways of dealing with its disposal (biological, wet air oxidation, chemical fixation and solidification, chemical oxidation). Both books are excellent reviews, touching on many of the items discussed above. These are worthy additions to the libraries of those new to the field of hazardous waste disposal.

References.....

References

1. R. E. Mournighan, J. A. Peters, and M. R. Branscome, "Effects of Burning Hazardous Wastes in Cement Kilns on Conventional Pollutant Emissions," Proceedings-APCA Annual Meeting, 78th, (vol. 5), 85-68.1, 20 (1985).

2. J. N. Bolstad, J. Chehaske, M. Branscome, C. W. Westbrook, R. G. Mournighan, Proceedings-APCA Annual Meeting, 78th, (vol. 5), 85-68.2, 15 (1985).

3. P. Peters, G. M. Higgins and J. Chadbourne, "Hazardous Waste as Supplemental Fuel for Cement Kilns," Proceedings National Waste Processing Conference, 12th, 65-9 (1986).

4. W. Kemner and R. Mournighan, "When is DRE not DRE?," Proceedings - APCA Annual Meeting, 79th, (vol. 3), 86-49.1, 18 (1986).

5. R. E. Mournighan and M. Branscome, "Hazardous waste Combustion in Industrial Processes: Cement and Lime Kilns," EPA Report 600/2-87/095, 76 (1987).

6. J. F. Chadbourne and H. M. Freeman, "Hazardous Waste as Fuel in Cement Kilns," Hazardous Waste: Detection, Control, Treatment, Proceedings World Conference (1987), Elsevier, Amsterdam, Ed. R. Abbou, Pt.B 1315-1324 (1988).

7. C. Benestad, "Incineration of Hazardous Waste in Cement Kilns," Waste Management Research 7 (4), 351-361 (1989).

8. T. El-Korchi, K. Melchinger, B. Kolvites and D. Gress, "The Effect of Heavy Metals and Organic Solvents on the Microstructure of Cement Stabilized Hazardous Waste," in Proceedings International Conference Ceramic Microstructures, 8th, 132-143, Eds. J. Bayles, G. R. Gouda, and A. Nisperos, International Ceramic Microstructure Association, Duncanville, TX (1986).

9. H. S. Shin and P. Sujiwalthana, "Factors affecting Solidification of Hazardous Materials," Hazard Waste: Detection, Control, Treatment, Proceedings World Conference (1987), Pt.B 1549-60, Ed. R. Abbou, Elsevier Amsterdam (1988).

10. H. S. Shin, R. N. Her, and J. K. Koo, "Design Optimization for Solidification of Hazardous Wastes", Hazard Waste Hazard Materials 5, (3), 239-250 (1988).

11. D. M. Montgomery, C. J. Sollars, R. Perry, S. E. Tarling, P. Barnes, and E. Henderson, "Treatment of Organic - Contaminated Industrial Wastes Using Cement-Based Stabilization/Solidification - I. Microstructural Analysis of Cement-Organic Reactions," Waste Mange. Res. 9, (2), 103-111 (1991).

12. Ibid, "Treatment of Organic - Contaminated Industrial Wastes Using Cement-Based Stabilization/Solidification - II. Microstructural Analysis of the Organophilic Clay as a Pre-Solidification absorbent", Waste Manage. Res. 9 (2), 113-125 (1991).

13. D. Barnes, D. J. Cook, P. A. Fitzgerald, R. McFarland, "Characteristics of Leachate from Chemically Fixed Toxic Metal Bearing Wastes," in Proceedings - Aust. Water Wastewater Association, Int. Conv. 572-580, Aust. Water Wastewater Association, Melbourne (1985).

14. P. E. Rushbrook, G. Baldwin, and C. B. Dent, "A Quality Assurance Procedure for Use at Treatment Plants to Predict the Long-Term Suitability of Cement-Based Solidified Hazardous-Wastes Deposited in Landfill Sites," ASTM Spec. Tech. Publ. 1033, 93-113 (1989).

15. W. E. Razzell, "Chemical Fixation, Solidification of Hazardous Waste," Waste Manag. Res. 8 (2), 105-11 (1990).

16. T. D. Schultz, "Spray Dryer Spent Sorbent Hazardous Waste Fixating and Cementitious Properties," Report HWRIC-RR-033, Order No. PB90-160748, 114 (1989).

17. K. G. Partymiller, D. R. Jackson, and W. E. Grube, Jr. "An Overview of the Soliditech, Inc. Site Demonstration," Proceedings- A & WMA Annual Meeting, 83rd, 1 90/14.2, 12 (1990).

18. W. E. Grube, Jr., "Physical and Morphological Measures of Waste Solidification Effectiveness, Proceedings - A & WMA Annual Meeting, 83rd 1, 90/14.3, 14 (1990).

19. C. W. J. Hooykaas, "Method for Rendering Toxic Waste Harmless," EUR. Pat. Appl., EP 361614 A1, April 4, 1990, 5 (pending).

20. C. W. J. Hooykaas, "Process for Immobilizing Environmentally NOXIOUS Metals and Organic Substances," EUR. Pat. Appl., EP 398410 A1, November 22, 1990, 6 (pending).

21. W. Shively, P. Bishop, D. Gress, and T. Brown, "Leaching Tests of Heavy Metals Stabilized with Portland Cement," J. Water Pollut. Control Fed. 58 (3), 234-41 (1986).

22. T. M. Gilliam, L. R. Dole, and E. W. McDaniel, "Waste Immobilization in Cement-based Grouts," ASTM Spec. Tech. Pub., 933, 295-307 (1986).

23. P. L. Bishop, "Prediction of Heavy Metal Leaching from Stabilized/Solidified Hazardous Wastes," Toxic Hazardous Wastes, Proceedings Mid-Atl. Ind. Waste Conference, 18th, 236-52, Ed. G. d. Boardman, Technomic, Lancaster, PA (1986).

24. P. L. Bishop, "Leaching of Inorganic Hazardous Constituents from Stabilized/Solidified Hazardous Wastes", Hazardous Waste Hazardous Materials 5 (2), 129-43 (1988).

25. D. J. Oretego, S. Jackson, G. S. Yu, H. McWhinney, D. L. Cocke, "Solidification of Hazardous Substances - a TGA and FTIR Study of Portland Cement Containing Metal Nitrates," J. Environ. Sci. Health, Part A A26 (6), 589-602 (1989).

26. F. Bigelli, "Neutralizing Process for Toxic Waste Material," Eur. Pat. Appl., EP 375044 A2, June 27, 1990, 12 (1990).

27. J. Ortego, Y. Barroeta, F. K. Cartledge and H. Akhter, " Leaching Effects on Silicate Polymerization. An FTIR and Silicon-29 NMR Study of Lead and Zinc in Portland Cement," Environ. Sci. Technol. 25 (6), 1171-4 (1991).

28. I. A. Sheikh, E. Zamorani, and G. Serrini, "Characterization of Cement Containing Arsenic Trioxide (As_2O_3), Comm. Eur. Communities, [REP] EUR, EUR 11926, 16 (1988).

29. P. L. Cote, T. W. Constable, and A. Moreira, "An Evaluation of Cement-based Waste Forms Using the Results of Approximately Two Years of Dynamic Leaching," Nucl. Chem. Waste Manage 7 (2), 129-39 (1987).

30. C. S. Poon, A. J. Clark, R. Perry, A. P. Barker, and P. Barnes, "Permeability Study on the Cement based Solidification Process for the Disposal of Hazardous Wastes," Cement Concrete Research 16 (2), 161-72 (1986).

31. H. C. Eaton, M. B. Walsh, M. E. Tittlebaum, F. K. Cartledge, and D. Chalasani, "Organic Interference of Solidified/Stabilized Hazardous Wastes," Environ. Monit. Assess. 9 (2), 133-42, (1988).

32. D. G. Skipper, H. C. Eaton, F. K. Cartledge, and M. E. Tittlebaum, "The Microscopic Fracture Morphology of Hardened Type I Portland Cement Paste Containing Parachlorophenol," Hazardous Waste Hazardous Materials 4 (4), 389-402 (1987).

33. M. Riaz and E. Zamorani, "Testing of Ordinary Portland Cement for the Immobilization of Pentachlorophenol," Comm. Eur. Communities, [Rep.] EUR, EUR 12044, 13 (1989).

34. Ibid, "A Study of the Degradation of Cement Matrixes Containing 2, 4, 5-Trichlorophenol," Comm. Eur. Communities, [Rep] EUR, EUR 11619, 18 pp. (1988).

35. R. J. Caldwell, P. L. Cote, and C. C. Chao, "Investigation of Solidification for the Immobilization of Trace Organic Contaminants," Hazard Waste Hazard Mater. 7 (3), 273-82 (1990).

36. M. Riaz and E. Zamorani, "Dynamic and Static Water Leachability of Polychlorinated Biphenyls Immobilized in Cement," Comm. Eur. Communities, [REP] EUR, EUR 12122, 19 (1990).

37. M. B. Walsh, H. C. Eaton, M. E. Tittlebaum, F. K. Cartledge, D. Chalasani, "The Effect of Two Organic Compounds on a Portland Cement - Based Stabilization Matrix," Hazardous Waste Hazardous Materials 3 (1), 111-23 (1986).

38. M. E. Tittlebaum, H. C. Eaton, F. K. Cartledge, M. B. Walsh, and A. Roy, "Procedures for Characterizing Effects of Organics on Solidification/Stabilization of Hazardous Wastes," ASTM Spec. Tech. Pub. 933, 308-18 (1986).

39. A. C. Chou, H. C. Eaton, F. K. Cartledge, and M. E. Tittlebaum, "A TEM Study of the Interactions Between Certain Organic Hazardous Wastes," Congr. Int. Quim. Cimento, [An], 8th, 6 589-93, Secr. Geral. 8° CIQC: Rid de Janeiro, Brazil (1986).

40. A. C. Chou, H. C. Eaton, F. K. Cartledge, and M. E. Tittlebaum, "A Transmission Electron Microscopic Study of Solidified/Stabilized Organcis," Hazardous Waste Hazardous Materials 5 (2), 145-53 (1988).

41. A. Roy, H. C. Eaton, D. Skipper, F. K. Cartledge and M. E. Tittlebaum, "Phase Formation in Cement/Organic Mixtures," Proceedings Int. Conf. Cem. Microsc. 8th, 47-51, Eds. J. Bayles, G. R. Gouda, and A. Nisperos, Int. Cem. Microsc. Assoc., Duncanville, TX (1986).

42. D. Skipper, H. C. Eaton, F. K. Cartledge, and M. E. Tittlebaum, "Scanning Electron Microscopy/Energy Dispersive x-ray Analysis of Type I Portland Cement Pastes Containing p-Chlorophenol," Proceeding Int. Conf. Cem. Microsc. 8th, 93-107, Eds. J. Bayles, G. R. Gouda, and A. Nisperos, Int. Cem. Microsc. Assoc. Duncanville, TX (1986).

43. B. G. Rushbrook, and C. G. Deut, "A Method for the Reliable Prediction of the Quality of Cement - Based Solidified Hazardous Wastes at the Time of Preparation," Management Hazardous, Toxic Wastes Process Ind., [Int. Congr.], 328-41, Ed. S. T. Kolaczkowski and B. D. Crittenden, Elsevier, Appl. Sci., London (1987).

44. C. G. Deut, P. E. Rushbrook and G. Baldwin, "A Method for Predicting Quality in Solidified Hazardous Wastes," U. S. Environ. Prot. Agency Res. Dev. [Rep] EPA, EPA/600/9-87/018F, Proc. Int. Conf. New Front. Hazard Waste Mange 2nd, 1987, 331-40 (1987).

45. B. Kolvites and P. Bishop, "Column Leach Testing of Phenol Trichlopethylene Stabilized/Solidified with Portland Cement," ASTM Spec. Tech. Pub. 1033, 238-50 (1989).

46. E. F. Barth, P. de Percin, M. M. Arozarena, J. L. Zieleniewski, M. Dosani, H. R. Maxey, S. A. Hokanson, C. A. Pryately, T. Whipple, R. Kravitz, M. J. Cullinane, Jr., L. W. Jones, and P. G. Malone, Stabilization and Solidification of Hazardous Wastes, 390, Noyes Data, Park Ridge, NJ (1990).

47. A. P. Jackman and R. L. Powell, Hazardous Waste Treatment Technologies, 276, Noyles Publications Park Ridge, NJ (1991).

STORAGE SYSTEMS FOR HAZARDOUS WASTE : EVOLUTION AND STATE-OF-THE-ART

K van Breugel

Department of Civil Engineering
Delft University of Technology, Delft
THE NETHERLANDS

SUMMARY

The complexity of today waste problems has evidenced, that this problem is a multi-disciplinary one. It is recognised more and more, that the solution of the problem is not in the hands of one discipline, but in the hands of the many, finally in the hand, of the whole society. In this contribution the evolution in waste management is presented in so far storage systems for intractable wastes are concerned. Since the most remarkable developments in recent years are undoubtedly in the field of non-nuclear waste management, emphasis will be on storage systems for this type of waste. At first different possibilities to minimize and control the emission of contaminating elements are briefly mentioned. The terms "multi-barrier system" and "system technology" are explained then and elucidated with examples. Controllability, repairability and renewability are mentioned as prerequisites for modern storage facilities for intractable wastes. The state-of-the-art as regards handling and storage of nuclear-waste is briefly mentioned. A survey of literature, including references to several comprehensive recent state-of-the-art reports, is given.

ZUSAMMENFASSUNG

Die Komplexität der heutige Abfallproblematik macht klar, dass wir mit einem multi-disziplinairen Problem zu tun haben. Mehr und mehr wird gesehen, dass die Lösung des Abfallproblems nicht in die Hände liegt von nur einer Disziplin, sondern in die Hände von der ganzen Gesellschaft. In diesem Bericht wird die Evolution in der Abfallentsorgung beschrieben in so weit es Bauwerke für Abfall-Lagerung betrifft. Weil die meist interresante Entwicklungen auf dem Gebiet der nicht-nucleaire Abfall-Lagerung gefunden werden, wird dieser Bericht sich darauf konzentrieren. Angefangen wird mit ein Uebersicht verschiedener Möglichkeiten um der Emission von Umweltgefährdenden Stoffen einzuschrenken. Das Multi-Barriere Konzept und der Begriff Systemtechnik werden besprochen und mit Beispiele verdeutlicht. Kontrollierbarkeit, Repareirbarkeit und Erneuerbarkeit sind die Stichworte für moderne Lagerungssysteme. Ein "state-of-the-art" im Bezug auf Abfälle im Kerntechnik wird kurz besprochen.

INTRODUCTION

Handling, treatment and storage of hazardous wastes has become a major issue in recent decades. Among the different types of waste one can distinguish between [14]:

1. Wastes containing significant quantities of intractable inorganic elements, such as heavy metals like cadmium, mercury, arsenic, selenium, lead, zinc and copper.
2. Radioactive wastes
3. Wastes containing significant quantities of toxic, hazardous or polluting organic compounds, which cannot be re-processed or recycled utilizing current technology.

For a discussion on whether, and when, a material has to be considered a waste material reference is made to lit. [10]. In the framework of this paper it suffices to define waste as a substance, which may cause a hazard to the people and the environment if no precautions are taken in the form of controlled storage or if no special treatment of this substance would have been undertaken.
Measures aiming at minimizing the environmental risk associated with handling of hazardous waste are: 1) solidification and stabilization (s/s-) techniques, 2) encapsulation and 3) containment for interim or long-term storage. With these measures one should aim at reducing the release of toxic or intractable hazardous elements to an environmentally acceptable levels. A reasonable criterion could be that the rate at which hazardous materials are released should not exceed the capacity of the biosphere to reabsorb them without excessive disturbance of the existing (local) eco-system [14].

WASTE TREATMENT STRATEGY: MATERIAL TECHNOLOGY and SYSTEM TECHNOLOGY

Once release criteria are fixed, decisions have to be made concerning the strategy to be followed to meet these criteria. Solidification and stabilization of toxic and hazardous wastes with, for example, cementitious materials is one of the possibilities [12,16, 18]. A major point of concern refers to the long-term behaviour of the resulting products [4,7,8]. Laboratory tests generally refer to the short term behaviour, while in most cases a well-defined cocktail of only a limited number of intractable substances are considered. Most often, however, the chemical composition of the wastes is difficult the determine and, moreover, unpredictable [5]. Leaching mechanisms or bacterial action may act as a vehicle for re-entering of toxic or hazardous materials into the biosphere in amounts which may endanger the environment. These mechanisms and processes make it hard to guarantee that s/s techniques will adequately immobilize intractable elements for a required period of may be some hundreds of years. Particularly in those cases, where the consequences of uncontrolled releases of toxic wastes are unpredictable on the basis of presently available knowledge, caution should be exercised with large-scale application of s/s-techniques. In this respect it is worthwhile to recall in mind that mechanisms and processes involved in degradation of cement-based materials are not fully understood yet [13,19]. As long as this situation exists, it will be hard to prove that leaching will not occur and long-term stability is assured.

Forgoing considerations has led to the conviction that the waste problem cannot be solved by *material technology* only. *Complementary* to the material technology one should adopt the so called *system technology* [1,4]. In system technology the focus of attention is on aspects like *inspectability* and *controllability*. In so far as bulk storage of waste is part of this system technology and storage structures are involved in it, *repair* and *renew* of these structures should remain possible during their entire lifetime.

STORAGE SYSTEMS FOR NON-NUCLEAR WASTE

Dumping

A dump, or deposit, is generally considered a place where the waste is stored for an unlimited period of time. Most of these dumps are carried out as landfills which generally have four essential components, viz. [5]: 1) An appropriate (or inappropriate) natural geologic setting; 2) One of more liners below the wastes; 3) A final, permanent cover and 4) A leachate collection system. The liner systems may comprise natural sealings made of clay or of some synthetic membrane, for example made of high density polyethylene (HDPE).

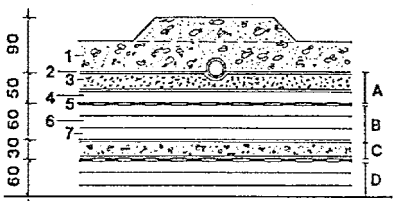

1 gravel
2 geotextile
3 gravel 0/32
4 bentoniet
5 plastic liner
6 illite
7 caolite
A Protective layer
B First mineral sealing
C Control layer
D Second mineral sealing

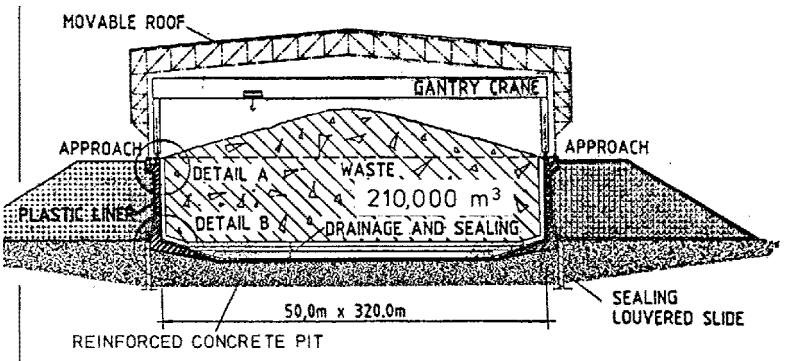

Storage system for intractable chemical waste [9]

Fig. 1. Multi-layered combination sealing (left) [1]; Improved landfill design (right)

The performance of landfills have been thoroughly evaluated by Montague for the US-situation [5]. In his evaluation aspects like differential settlements of the subsoil, chemical resistance of the (synthetic) liner material and volume changes of the waste body on the integrity of the storage system were taken into account. With reference to the second law of thermodynamics Montague concluded, that, left to itself, a system becomes as disordered as possible and that, when applied to liner systems, these (synthetic) liners will sooner or later start leaking. A similar conclusion would hold for the durability and hence reliability of the landfill's cover. Montague's conclusions are substantiated by a large number of laboratory and field studies and are endorsed by the Environmental Protection Agency to a large extent [25]. All this has led to the conclusion, that traditionally designed landfills cannot be considered as the adequate solution for our waste problems. Apart from doubtful reliability and, in essence, shifting our problems to future generations, it is remarked that dumping almost definitely excludes re-use of increasingly scarce materials.

Improved Landfills

The reliability of a landfill can be improved by using multiple-liner systems [26, 27] and, as regards the leakage control system, the construction of control tunnels located at the bottom of the waste body [6]. An example of an improved landfill has recently been taken into operation in the Rotterdam area in The Netherlands [9]. This dump consists of a rectangular box-shaped reinforced concrete tank, 300 m long, 50 m wide and 11 m high. Wall and bottom thickness varied form 1.2 to 0.8 m. The tank walls are provided with a 2 mm thick HDPE liner at the inside, whereas the bottom liner consists of a crack-bridging rubber bitumen membrane and a 100 mm thick cast-asphalt layer, which forms a sealing layer. A leachate collection system is installed and a control and security system has been provided under the tank to monitor possible ground water pollution. The landfill is built for storage of non-treatable waste such as metal and leather tanning sludge and gas scrubber sludge. A separate section of the tank (one fifth) has been created for storage of waste containing more than 2% by weight of lead, chromium, copper and nickel. This waste has a certain potential for re-use in the near future.
Although this structure has been judged to be the most advanced landfill system built so far, several open questions remain [1]. The expected lifetime of the structure of 150 year immediately rises the question: "And than?". In case of leakage of the HDPE liner and/or the concrete, repair will be quite difficult. Finally, the drawback of taking scarce raw materials out of the materials cycle, typical for dumping, remains.

Multi-Barrier Concept

General - Similarly to the safety strategy in the nuclear industry, also for storage of non-nuclear waste the multi-barrier concept is adopted [2,22]. The concept has been encountered, in a way, in the foregoing sections already when discussing the multiple-liners systems for landfills. In a more explicit form this multi-barrier system is present in those systems which are designed to meet the most stringent requirements regarding con-

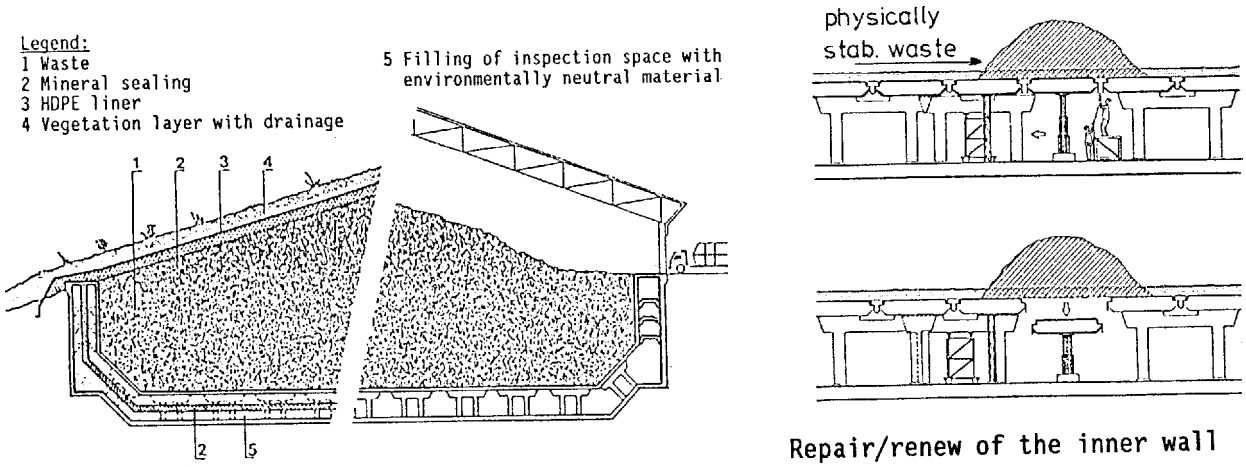

Fig. 2. Double walled storage system for interim storage of non-treatable waste [1].

trollability, repairability and renewability. The major reason for requiring repairability and renewability of the system is anticipation on unpredictable reactions of the waste with the containment material. Multi-barrier systems with the option of repairability and renewability are considered now as the only acceptable solution for storage of high toxic and otherwise undefinable hazardous waste with a risk of unpredictable consequences in case of uncontrolled release to the biosphere.

Double Wall Systems For Interim Storage - The multi-barrier concept as just outlined has got shape in the double wall storage system for interim storage of wastes which cannot be recycled economically yet or wait for new treatment techniques [1,4]. An example is shown shown in Fig. 2. Emphasis is clearly on system technology. The inner container is built of panels which can be replaced by new one in case unforeseen chemical attack of the wall material compels to do so. The repair procedure is schematically shown in Fig. 2b.

CONCRETE AND CONCRETE STRUCTURES AND THE STORAGE OF NUCLEAR WASTE

Concrete And Radiation

Although there are still problems which wait for final solutions, the problems with storage of nuclear waste are easier than that of non-nuclear waste in the sense that the hazard source, i.e. radiation, is quite well-defined now. Among the different types of radiation, viz. alpha-, beta-, gamma- and neutron radiation, the gamma- and neutron radiation is of major importance [11].
Absorbtion of *gamma-radiation* takes place via interaction with electrons. Since the number of electrons per gram material is about constant, the absorption of gamma-radiation strongly depends on the specific mass of the shielding material. The shielding capacity of steel is about three times that of concrete and that of lead about five times as much. To enhance the shielding capacity, high density concretes using heavy aggregates like limonite, magnetite, barytes, steel and iron shot and lead can be applied, resulting in specific masses between 3 and 6 g/cm^3. In normal weight concretes the intensity of the gamma-radiation is reduced by a factor 10 with 300 mm concrete. The reduction of radiation intensity is associated with the production of heat.
Shielding against *neutron-radiation* is based on, firstly, slowing down of the fast neutrons, for which the shielding material should contain some heavy elements, and, secondly, slowing down of intermediate neutrons and capturing the slow neutrons, for which purpose a certain quantity of hydrogen, i.e. water, should be available. Since both heavy elements and water are normally present in concrete, this material is most suitable for shielding purposes. To assure the presence of sufficient water in the concrete throughout the desired lifetime of the structure special aggregates with high amounts of crystal water may be used, for example serpentin with about 13 percent water by mass. Secondary gamma-radiation associated with the adsorption of neutrons produces heat.
More recent field investigations have confirmed the suitableness of concrete for shielding

against nuclear radiation. Strength reductions appeared to be less than expected from more classic literature data [21].

Treatment And Handling Of Nuclear Waste: The Role Of Concrete And Concrete Structures

Classification of Nuclear Waste - Radioactive wastes are generally classified into low, intermediate and high level radioactive wastes [3,23,24]. High level radioactive waste can be heat producing or non-heat producing. According the level of reactivity different levels of shielding must be applied. Also the stage of aggregation of the waste, i.e. gaseous, liquid or solid, determines how the waste is treated.

Low Level Radioactive Waste - Liquid and/or solid nuclear waste with a low level of radioactivity can be stored in steel drums or, more and more, cast in concrete blocks. When cast in concrete the radiation at the surface of the blocks is generally so low, that handling is possible without additional protective measures. The drum/blocks are stored in specially designed concrete storage structures.

Intermediate Level Radioactive Waste - Treatment and storage of intermediate radioactive waste is similar to that of low radioactive waste to large extent. The higher radiation level, however, requires additional shielding, generally realized in the form of a second barrier of concrete.

High Level Radioactive Waste - Non Heat Producing - Materials which have been submitted to radiation can be put, together with a concrete slurry, in drums of stainless steel. These drums are stored in specially designed concrete protective structures, which should assure that radiation outside the structure shall not exceed certain limits.

High Level Radioactive Waste - Heat Producing - Both the fact that the level of radiation may be very high and that heat is produced over a long period of time requires special provisions. The waste can be pre-treated, i.e. immobilized, in a glasseous substance. The primary container for this type of waste is generally made of stainless steel, for example (double-wall) steel drums. Special provisions are taken so as to limit radiation [15]. The steel drums are place in a concrete protective structure where they are continuously cooled in either a wet (water) or dry (air) cooling process. Increasing concern about safety has led to designs for concrete protective storage structures which meet about the same stringent criteria as a nuclear reactor. Hence, this thickness of above-ground storage structures is determined largely by the required thickness for aircraft impact, i.e. 2.0 to 2.5 m (Phantom II).
The concrete should be free from form macrocracks. For this purpose the concrete is normally prestressed with steel prestressing cables, ensuring a residual compressive stress in the concrete. Microcracking is reduced by limiting the temperature differences over the cross section of the concrete. Microcracking due to different expansion of matrix and aggregate should be reduced by limitation of the absolute temperature in the concrete in all stages of the structures lifetime, including construction and hardening period and operation. To prevent rapid corrosion of the steel drums the temperatures should preferably be kept below 60°C. When corrosion of steel is no issue, temperatures should be kept below 100°C to prevent physico-chemical degradation of the cement matrix and microcracking [21].

CONCLUDING REMARKS

Our to-day world is borrowed from those who come after us! It is the responsibility of all disciplines involved in waste management to inform each other about their possible contribution to preliminary or final solutions of the waste problem, aiming at a world which will remain clean enough to live in. A predominant trend in the engineering approach of the problem is that of "system technology" [1,4,17]. It is based on the philosophy that in those cases, where either the long-term behaviour of a waste or the consequences of uncontrolled release of a particular waste are unpredictable, storage should be realized in systems which can are controllable and can be repaired and renewed when necessary without any hazard for the environment. It can hardly be doubted that the evolution in waste storage systems will develop according to this system technology concept as to one of the most advanced and environmentally amicable concepts available yet.

REFERENCES

1 Rudat, D.: "Design principles and examples of structures for treatment and containment of hazardous waste". Proc. Int. Symp. FIP, Budapest, 1992 (to be published May 1992).
2 Brandl, H.: "Altlasten und Deponien". Symp. Entsorgung für Morgen, Wien, 1989, p 33-78.
3 Vrijen, J.: Environment-compatible solutions for storage of nuclear waste. Concrete for protection of the environment against nuclear radiation. ed. Dutch Concrete Society, Gouda (NL), 1988, p 21-30 (in Dutch).
4 Bomhard, H.: "Prevention and containment of large-scale technology-related accidents". Shell and spatial structures as protective and safety measures. IASS-bulletin, Vol. 32, No. 107, 1991, p 138-148.
5 Montague, P.: The limitations of landfilling. Beyond Dumping, ed. by B. Piasecki, London, 1984, p 3-18.
6 "Kontrolltunnel für Mülldeponie". Beton- und Stahlbetonbau, 87, No. 1, 1992, p 17.
7 Hahn, J.: "Anforderungen an Chemikalienlager aus der Sicht des Boden- und Grundwasserschutzes". Proc. Symp. Umweltsicherheit beim Umgang mit wassergefährdenden Stoffen, Aachen, 1988, p 257-267.
8 Kyles, J.H., Malinowski, K.C., Leithner, J.S., Stanczyk, T.F.: "The effect of volatile organic compounds on the ability of solidification/stabilization technologies to attenuate mobile pollutants". Proc. Hazardous waste and hazardous materials, Washington, 1987, p 152-157.
9 Sijberden, H.L.: "Design and construction of the C2-landfill Maasvlakte Rotterdam".
10 Dietrich, G.N.: Information burdens and difficulties in conceptualizing the crisis: A reappraisal. Beyond Dumping, ed. by B. Piasecki, London, 1984, p 19-26.
11 Hilsdorf, H.K., Kropp, J., Koch, H-J.: Der Einfluss radioaktiver Strahlung auf die mechanischen Eigenschaften von Beton. Deutscher Ausschuss für Stahlbeton, 1976, 41 p.
12 Sugi, T., Kataoka, K., Yamada, S., Ando, Y.: "Solidification of sludges with cement-slag-$CaSO_4$". Proc. 8th. ICCC, Rio de Janeiro, 1986, 649-652.
13 Chou, A.C., Eaton H.C., Cartledge, F.W., Tittlebaum, M.E.: "A TEM study of the interaction between certain organic hazardous wastes and Type I Portland Cement". Proc. 8th. ICCC, Rio de Janeiro, 1986, 589-593
14 Taylor, S.J., Holmes, R.E.: "Isolation of toxic and hazardous waste in the environment". Proc. Int. Conf. Concrete for Hazard Protection, Edinburgh, 1987, p 291-297.
15 Geevers, F.: Design of storage structures for radioactive waste. Concrete for protection of the environment against nuclear radiation. ed. Dutch Concrete Society, Gouda (NL), 1988, p 31-36 (in Dutch).
16 Bijen, J.M.J.M.: "Concrete and hazardous materials". Proc. Seminar Concrete and Environment, STUTECH-report No. 9, 1991, p 37-50 (in Dutch).
17 Close, S.R., Jorgensen, Ib.F.: "Prestressed Concrete Tanks for Hazardous Liquids". Concrete International, Vol. 13, No. 10, 19.., p 47-51.
18 Emery, J.J.: "Stabilizing industrial sludge for fill applications". Proc. 8th. ICCC, Rio de Janeiro, 1986, p 644-648.
19 Litvan, G.G.: "Mechanism of cement paste degradation due to chemical and physical processes". Proc. 8th. ICCC, Rio de Janeiro, 1986, p 359-361.
20 Bhatty, J.F. Reid, K.J.: "Compressive strength of municipal sludge ash mortars". ACI-Journal, Vol. 86, No. 4, 1989, p 394-400.
21 Buck, A.D.: "Characterization of radioactive concrete by petrographic and physical testing". ACI-Materials Journal, Vol. 85, No. 1, 1988, p 55-58
22 Brenk, H.D.: "Möglichkeiten de Uebertragbarkeit von Sicherheitssystemen aus anderen Bereichen". Proc. Symp. Umweltsicherheit bei Umgang mit wassergefährdenden Stoffen, Aachen, 1988, p 269-300.
23 Amalray, R.V.: Storage tanks for liquid radioactive wastes: Their design and use. Int. Atomic Energy Agency, Vienna, Technical report series No. 135, 1972, 55 p.
24 IAEA: Handing and storage of high-level radioactive liquid wastes requiring cooling. Technical report series No. 191 (of IAEA), 1979, 115 p.
25 Allegri, T.H.: Handling and Management of Hazardous Materials and Waste. London, 1986, p 458.
26 Ruetten, M.G., Lattz, W.W.: "Construction of multiple-lined hazardous waste Landfills". Proc. Hazardous waste and hazardous materials, Washington, 1987, p 169-173.
27 Mason, G.S., Pyle, R.T.: "An improved protective cover design for hazardous waste Landfills". Proc. Hazardous waste and hazardous materials, Wash. 1987, p 174-177.

CEMENT IN WASTE MANAGEMENT : USE OF NON-CONVENTIONAL MATERIALS IN THE CEMENT INDUSTRY

J Beretka

CSIRO Division of Building, Construction and Engineering
Victoria, AUSTRALIA

ABSTRACT

This paper reviews the current state of utilisation of non-conventional materials, particularly industrial wastes and by-products, in the cement industry. Some of these materials, particularly fly ash and blast furnace slag, have been used for cement replacement for over 50 years. However, there are others, viz. silica fume, rice husk ash, by-product gypsum, non-ferrous slags, tailings, etc., which, although in smaller quantities, have found gradually increasing application in the cement and concrete industries in the past 10–20 years. The use of the above materials is not limited to cements and concretes made from ordinary Portland cement, but extends to special cements termed aluminous, expansive, shrinkage resistant, fast setting and hardening, very high strength, and low energy cements.

ZUSAMMENFASSUNG

Die Arbeit gibt einen Überblick über die gegenwärtige Nutzung von nichtkonventionellen Stoffen in der Zementindustrie, insbesondere von Industrieabfällen und -nebenprodukten. Einige dieser Materialien, zum Beispiel Flugasche und Hochofenschlacke, sind seit über 50 Jahren in Gebrauch. Es gibt aber andere Stoffe, wie Silica-Rauch, Reisschalenasche, Gips als Nebenprodukt, Nichteisenschlacken, Abraum, usw., die in den vergangenen 10 bis 20 Jahren zwar in kleineren, doch aber in zunehmenden Mengen in der Zement- und Betonindustrie zur Anwendung gekommen sind. Die Verwendung obengenannter Stoffe is nicht auf Zemente und Betonqualitäten aus gewöhnlichen Portlandzement beschränkt, sondern erstreckt sich auf solche Spezialzemente wie aluminat-, schwell-, schwindresistent-, schnell abbindend oder erhärtend-, Hochfestigkeits- und Niederenergie-Zemente.

INTRODUCTION

Industry worldwide generates large quantities of industrial wastes and by-products, many of which are siliceous, cementitious and pozzolanic, and as such have found widespread application in the cement and concrete industries. The principal waste materials from the point of view of the cement industry are fly ash and pelletised blast furnace slag; and to a lesser extent, silica fume and rice husk ash. The common characteristic of the above materials is that they are poorly crystalline, or non-crystalline, and in fact they are amorphous and 'glassy', and are reactive in the finely divided form. Cements incorporating the above mentioned materials are termed 'composite cements' (1). In these cements the particular inorganic mineral additive takes an important part in the hydration reaction and contributes substantially to the product of hydration.

The use of fly ash and blast furnace slag for cement replacemant has been practiced in western Europe and Japan, since the early 1940s. The use of these materials, and some new ones like silica fume and rice husk ash, attracted worldwide attention in the 1960s. Since 1983, four international conferences have been held on this topic (2–5). Furthermore, the last five International Congresses on the Chemistry of Cement (6) saw a progressively increasing number of publications on fly ash, blast furnace slag and silica fume, and also lesser known materials derived from various industrial processes. The incorporation of sulphate (usually in the form of natural gypsum or anhydrite) in Portland cement (OPC) as a set retarder has been broadened by the application of by-product gypsums, particularly phosphogypsum and sulphogypsum.

OPC is a widely used binder for the stabilisation of wastes which are considered to be toxic, and contain heavy metals or radioactive elements. The popularity of OPC is due to the fact that it is produced in virtually every country, it is relatively cheap, and its physical and chemical properties are well established. OPC can bind metals in insoluble form, and can be formulated to reduce the leachability of toxic metal ions by forming metal oxide/silica compounds of low solubility, which can encapsulate the metal ions in a silicate or metal silicate gel matrix. However, the discussion of the encapsulation of toxic wastes, heavy metals or radioactive elements is outside the scope of this paper.

This review discusses the utilisation of several commonly used materials (fly ash, blast furnace slag, silica fume) and some lesser-known waste materials (rice husk ash, non-ferrous slags, tailings, etc.) in the cement and concrete industries. Large-scale utilisation of these wastes results in reduced exploitation of natural resources, protection of the environment, energy saving, cost reduction and, by reduced production of carbon dioxide emission, it contributes to the reduction of the greenhouse effect. Because many trace elements, including radioactive trace elements, usually concentrate in the waste materials during industrial processes, the potential radioactivity of them will also be discussed briefly.

Fly Ash

The principal waste from the burning of coal in coal-fired power stations is fly ash, which is collected from the flue gases by cyclones, bag filters or electrostatic precipitators. The fineness of the ash depends on the degree of grinding of the coal, and its composition on the type and quantity of mineral matter present in the coal. During combustion, the mineral matter (clay, shale, feldspar, quartz, etc.) fuses at high temperature, then solidifies on cooling to fine, spherical, and largely non-crystalline, glassy particles.

In general, fly ash derived from anthracite or bituminous (black) coal is pozzolanic and is suitable for cement replacement, whereas that derived from sub-bituminous (brown) coal or lignite contains high percentages of soluble salts (sulphates or chlorides of calcium or magnesium) and is less suitable or unsuitable as pozzolan. From the point of view of the cement industry, fly ash may be sub-divided according to the origin of the coal it is derived from (7–9), viz.

(a) cementitious and pozzolanic, high calcium (>10% CaO) fly ash, usually derived from lignite or sub-bituminous coal (ASTM Class F), and
(b) normal pozzolanic, low calcium (<10% CaO) fly ash produced by burning anthracite or bituminous coal (ASTM Class C).

Numerous other classifications have been suggested according to carbon content, SiO_2 reactivity, SiO_2 solubility, pozzolanic activity, etc.

It is difficult to obtain correct figures for the worldwide generation and utilisation of fly ash. It has been stated (9) that >170 million tonnes are produced annually. A recent compilation of data has been published by RILEM (9) and is shown in condensed form in Table 1. This table does not include data from several industrial countries, the (former) USSR, and several eastern European, South American, and third-world countries.

Table 1. Annual production and utilisation† rates of siliceous by-products (t)*

Country	Fly ash x 10^6 t (1986/87)		Blast furnace slag x 10^6 t (1984)‡		Condensed silica fume x 10^3 t (1984)	
	Production	Utilisation	Production	Utilisation	Production	Utilisation
Australia	5.2	0.56	4.7	0.12	60	20
Canada	3.2	1.1	2.9	0.2	23	11
China	41.0	9.5	22.0	16.0	nil	nil
Denmark	1.2	0.9	nil	nil	nil	nil
France	2.2	1.3	10.4	1.9	60	nil
Germany§	2.9	2.2	15.0	2.8	25	nil
Hungary	4.1	1.1	n.a.	n.a.	n.a.	n.a.
India	39.0	1.2	7.8	2.8	nil	nil
Japan	3.3	0.96	24.0	8.2	25	nil
Netherlands	0.74	0.72	1.1	1	nil	nil
Norway	n.a.	n.a.	0.1	nil	140	40
South Africa	13.0	0.58	1.5	0.6	43	nil
Spain	7.4	1.5	n.a.	n.a.	n.a.	n.a.
Sweden	0.14	0.08	0.1	0.03	10	1
UK	10.4	5.9	1.5	0.25	nil	nil
USA	38.3	8.0	13.0	1.0	100	2

* Table combined from Refs 7 and 9.

† The utilisation data represents only the amount of material used as pozzolanic and/or cementitious constituents of hydraulic cements and structural concretes.

‡ Figures include all iron blast furnace slag, including air-cooled slag. Utilisation data only for granulated or pelletised slag.

§ Former West Germany only.

It is generally accepted that the cementitious and pozzolanic properties of fly ash depend mainly on its particle characteristics (size and shape) and its mineralogical composition, and not on chemical composition. Fly ashes consist mainly of mineral matter (50–90%) in the form of glass. Mineralogically those derived from bituminous coal consist of mullite, quartz, magnetite, hematite and free CaO. Again, it is generally agreed that those with >35–50% SiO_2, or > 55% combined $SiO_2 + Al_2O_3$, and <7–10% CaO have better pozzolanic activity than ashes outside these limits (8–10).

The particle size of ashes varies from 0.5–200 μm; most particles are >1 μm, and the median range is 5–20 μm. National standards usually specify maximum residue in per cent on a 45 μm sieve, and the recommended figure varies between 12 and 50%. Specific surface varies between 250 and 1000 m^2/kg and, in general, the higher the surface area, the higher the reactivity of the ash. Other parameters determined are the density, water requirement, pozzolanicity (the amount of free lime remaining in a fly ash–lime mix after reaction for a predetermined period, usually 28 d), soundness, colour, moisture content and radioactivity.

In addition to particle size and shape, and mineralogy, the carbon content (originating from the unsatisfactory combustion of the coal) is another important parameter affecting technological properties of concrete incorporating fly ash such as workability and ultimate strength. It is measured by the loss on ignition of the ash. This figure also includes the content of carbonates and some clay minerals; but mainly (about 90%) represents unburnt carbon. It is generally accepted that the figure should be <6% for good quality ash.

Fly ash is usually added to cement at the replacement level of 20–30%, but additions of 50–80% are possible for special applications (9,10). Fly ash additions to concrete has several technological advantages: it reduces water demand, improves workability, may suppress alkali-aggregate reaction, reduces water segregation (bleeding), and reduces air content and consequently the permeability. It also reduces the heat of hydration in large pours, and thus concrete will be less susceptible to thermal cracking. However, the addition of fly ash increases the setting time, and it may reduces early (1, 7 d) strength, but the later or ultimate strength (28 d to 1 yr) at the level of 25–30% addition will be the same as OPC, concrete or even higher, due to the pozzolanic reaction between the fly ash particles and lime. The above parameters and technological properties of cements and concretes have been extensively discussed and reviewed recently (1, 7–11).

Other possible uses of fly ash include (a) its incorporation in the raw mix for the production of OPC clinker (low quality fly ash); (b) raw material and fuel in the kiln (high carbon ash); and (c) replacement for clinker for the production of OPC–fly ash cement (low-carbon, high quality ash) (12).

Blast Furnace Slag

Blast furnace slag is the by-product of the manufacture of molten iron. It results from the fusion of limestone and other fluxes with the ash from the coke and the siliceous and aluminous components of the ferrous burden. By varying the rate and manner of cooling of the molten slag, several forms of slag are produced. If allowed to solidify in air, a dense crystalline material termed 'air-cooled slag' is produced. Alternatively, the slag may be rapidly cooled/foamed with air and small amounts of water to give an expanded material termed 'foamed', or 'pelletised' or 'expanded slag'; or the slag is rapidly quenched with water to form 'granulated slag'. Air-cooled slag is mainly polycrystalline, whereas pelletised or foamed slags are partly crystalline and partly glass. Granulated blast furnace slag is almost entirely glass and is the type of slag used for cement replacement, after grinding.

The largest producers of molten iron, and consequently of blast furnace slag, are Japan, China, Germany, France and USA, as shown in Table 1 (7). The figures include all three types of slags mentioned above, of which mainly the granulated slag and, to a lesser extent, the pelletised slag is used for cement replacement. Its usage varies from country to country, from a low 2–3% to about 35% in Japan, India and Italy.

Chemically, pelletised slag is silica glass, containing calcium, magnesium and aluminium. The principal crystalline phase that may be present in small quantities is melilite, which is the term applied to any solid solution in the series extending from akermanite ($2CaO.MgO.2SiO_2$) to gehlenite ($2CaO.Al_2O_3.SiO_2$) (1,8,11). The quenched material consists of small granules or pellets about 1–3 mm in size, which are dried and ground to <45 μm (about 400–500 m^2/kg, Blaine) in size, giving angular particles with fineness similar to OPC clinker.

In general, pelletised blast furnace slag can be incorporated in cement and concrete by three different methods (13): (a) by intergrinding it with OPC clinker (and gypsum) to produce Portland blast furnace cement, which is the most widely practised method; (b) by grinding the slag separately followed by dry mixing the resulting powder with OPC at the cement plant; or (c) by grinding the slag separately then adding it at the mixer as partial replacement for OPC. This last method is usually applied to large structures or concrete pours. It could be expected that the intergrinding process should lead to a more uniform distribution of the slag and clinker particles than the other two methods, and thus it should give greater contribution to the strength of concrete. It is generally accepted that the differences between the above three methods of slag addition has little effect on the compressive strength of the resulting cement and concrete. However, it has been noted that intergrinding can provide slightly higher early strength, whilst the other two methods can provide higher strength at later ages. One can conclude that the mode of application of blast furnace slag gives wide flexibility to the user, irrespective of the methods of incorporation in the mixes. Activation of blast furnace slag with alkali (1,8) improves the early strength of blended slag-cement mortars and concretes.

The replacement levels vary, from a low 20–35% to a high 70–90%, particularly for concretes with high resistance to sulphate attack. It has been used at 60–65% replacement levels to reduce alkali-aggregate expansion. The hydration and microstructure of slag cement pastes and mortars has been extensively studied over the years (see, for example, Refs 1 and 8). One important finding is that the hydration products of cements incorporating blast furnace slag are similar to those of OPC. Apart from the obvious economic advantages, blast furnace slag also improves the resistance of pastes to chloride diffusion (14).

Silica Fume

Condensed silica fume, termed 'silica fume', is generated during the production of silicon metal or ferrosilicon alloy, and it is collected by bag filters or cyclones at the plants (1,7,8,11). A comprehensive review of all aspect of silica fume research and application may be found in Ref. 15. The material consists of very fine (<0.1 μm) spherical particles of amorphous silicon dioxide, usually >90% purity, with several percentages of Fe_2O_3, Al_2O_3, C, and alkali metal impurities. It is the most reactive pozzolanic material available, with very high surface area of the order of 15 000 to 20 000 m^2/kg (by BET). The material is rather difficult to handle, unless it is pelletised or used in the form of a slurry. The quantities generated and used at some of the major industrial countries is shown in Table 1 (7).

Silica fume is increasingly being used in concretes either as a partial replacement for, or as an additive to cement. It has a dual role: first as a filler because of its fine particle size, and secondly as a pozzolanic material

because of its high surface area and reactivity with lime. If properly applied, it improves mechanical strength and durability, and reduces alkali-aggregate reaction. The usual level of addition is limited to about 5–10%, unless water-reducing admixtures are used. In the latter case, the levels can be increased to 20–30%. Silica fume, due to its extreme fineness and high reactivity, can fill voids in cement paste and concrete, it accelerates the hydration of cement and, by special processing, very high strength (>270 MPa) concretes can be produced. It has been observed that silica fume greatly enhances the mechanical strength of concretes mainly due to the water-reducing effect of superplasticisers, and not to the pozzolanic reaction between the silica fume and free lime (16). Silica fume can be incorporated in concretes containing OPC alone or in concretes containing fly ash, blast furnace slag, or other siliceous additives.

Rice Husk Ash

The term 'rice husk ash' is applied to the siliceous residue produced by the controlled combustion, at 400–600°C, of rice husk in many rice-growing countries (1,8,11). The rice husk ash consists of irregularly shaped, fine (<45 μm) amorphous silica particles, which are highly reactive and pozzolanic, similar to silica fume. It usually contains >90–92% SiO_2 and low levels of impurities, viz. Fe_2O_3, Al_2O_3, CaO, MgO, Na_2O, P_2O_5, 1–2% K_2O, and 1–5% carbon. The main impurity that can have a major effect on its reactivity is carbon, which greatly reduces the reactivity of the ash particularly above the level of 10%. At >20% carbon content, the material becomes unreactive. Rice husk ash also has a very high specific surface area (of the order of 60 000 m^2/kg) (by BET). Rice husk ash has already found practical use in some localities either by blending it with OPC to produce concrete with high resistance to acid attack, or by reacting it with lime at ambient or preferably elevated temperatures to produce calcium silicate building materials (17).

Non-ferrous Slags and Tailings

A number of other waste materials, such as slags from the production of steel and non-ferrous metals, and tailings from industrial processes, have also been examined for use as mineral additives in composite cements (18). These include basic oxygen steel slags, and slags derived from the manufacture of chrome, copper, zinc, nickel, tin, lead, oil shale and other metals. Some of the above slags contain high percentages of CaO (e.g. steel slag), and are low in SiO_2. Some of these materials, e.g. zinc slag, have a strongly retarding effect on OPC (19). Most of these materials are only of potential interest at present. A comprehensive listing and discussion of these materials may be found in Ref. 20. One material which is of particular interest in manufacturing of special cements is red mud. It is derived from the production of alumina from bauxite by the Bayer process. In the process, bauxite is digested in caustic soda at elevated temperatures, producing an insoluble residue termed 'red mud', and sodium aluminate solution. Red mud is washed to recover caustic soda, then pumped in the form of a slurry into a residue disposal area. Its composition is variable from plant to plant, and country to country. Chemically it contains 10–35% SiO_2, 6–50% Fe_2O_3, 6–25% Al_2O_3, and small quantities of CaO, TiO_2 and SO_3. Mineralogically it consists of hematite (or goethite), quartz, and boehmite (AlO.OH) or sodalite ($3Na_2O.3Al_2O_3.5SiO_2.nH_2O$). The relatively high content of alumina in the red mud makes it attractive for use in special cements (21).

By-product Gypsum

Large quantities of by-product gypsum, also known as chemical gypsum, is generated annually throughout the world. These by-product gypsums are usually named after the relevant manufacturing process, e.g. phosphogypsum, sulphogypsum, saltgypsum and titanogypsum (22). The two principal by-product gypsums are phosphogypsum derived from the manufacture of phosphoric acid for fertilisers, and sulphogypsum derived from the flue gas desulphurisation process. Both materials can be used as retarders in the cement industry to replace natural gypsum (or anhydrite), particularly in countries where natural gypsum is in short supply (e.g. Japan). World production of phosphogypsum is quoted to be of the order of 120–150 million tonnes annually (23). In OPC production, about 3.5–4% by weight of gypsum is added to the clinker at the milling stage. It is known that the presence of phosphate in phosphogypsum can retard the setting of cement at early ages, but it does not affect the strength at later ages. This has been verified by Mehta and Brady (24) and several other researchers. Experiments were also carried out on the refining of phosphogypsum by various methods, but relatively little fresh information has surfaced since the excellent paper by Murakami (22). Sulphogypsum, which contains mainly chlorides, water soluble magnesium salts and calcium sulphite as impurities, is finding increasing application in the plaster industry (25), and a more limited application as a retarder for OPC (26).

SPECIAL CEMENTS

Special cements may be classified as aluminous, expansive, shrinkage resistant, fast setting and rapid hardening, very high strength or low energy cements (27). They are binders used for specific applications, and are manufactured outside the limits for OPC composition, and of OPC processes.

A special group of these cements are modified Portland cements (1), to which gypsum or anhydrite, and separately synthetised calcium sulfoaluminate, $C_4A_3\overline{S}$, is added. $C_4A_3\overline{S}$ in the presence of gypsum hydrates to ettringite, $C_6A\overline{S}_3.H_{32}$, providing expansion within the OPC matrix.

Apart from the 'classical' calcium aluminate cements (Ciment Fondue) which incorporates bauxite, the common characteristics of special cementsis the use of high percentages of alumina derived not only from bauxite, but also from fly ash, blast furnace slag or clay (28). This group of binders, which usually set rapidly, are also termed 'low-energy cements' (29). They rely on the manufacture of a clinker containing $C_4A_3\overline{S}$, which hydrates in the presence of gypsum to ettringite. Such cements can be made from limestone, natural gypsum, aluminous materials, clay, etc., and also from phosphogypsum, fly ash, ferrous and non-ferrous slags, and other waste materials. The main phase composition of these cements is $C_4A_3\overline{S}$, C_2S, C_4AF, CaO, and other minerals; and the main hydrated products are ettringite, C_2S, and C–S–H. Increasing research effort is being invested in such cements with the view of utilisation of fly ash, by-product gypsums and other waste materials; and also for the purpose of saving energy.

RADIOACTIVITY

Most natural materials contain various elements in trace quantities, including uranium (238–U), thorium (232–Th), their radioactive daughters (e.g. 226–Ra) and potassium (40–K). During industrial processes, e.g. burning of coal, production of molten iron, and the manufacture of phosphoric acid for fertilisers, etc., the trace elements usually accumulate in the waste materials, i.e. in the fly ash, slag, phosphogypsum, respectively. Consequently, their radioactivity can raise to unacceptably high levels of >370 Bq/kg (30). Furthermore, many of these trace elements concentrate in the fine fractions of the particular waste materials. With fly ash and phosphogypsum, it was found that the radioactivity levels of these materials could be reduced by sieving the fine –45 μm fraction, and discarding the fines (31) Ground blast furnace slag had relatively low radioactivity, but the levels were about the same in all the sized fractions. Red mud had exeptionally high radioactivity, which could not be reduced by sieving and discarding the fines (31). It is imperative that the trace element content and the gamma ray activity of waste materials is determined prior to their application in building materials, in order to ensure that they do not emit radioactivity levels which may have a harmful effect on the general public (32).

REFERENCES

1. Taylor, H.F.W.: **Cement chemistry**, Academic Press, London, 1991, 475 p.
2. Malhotra, V.M. (Ed.): **Proc. First International Conference on Fly Ash, Silica Fume, Slag and Other Mineral By-products in Concrete**, Montebello, Canada, 1983, ACI Publications SP–79, Detroit, USA.
3. Malhotra, V.M. (Ed.): **Proc. Second International Conference on Fly Ash, Silica Fume, Slag and Natural Pozzolans in Concrete**, Madrid, Spain, 1986, ACI Publications SP–91, Detroit, USA.
4. Malhotra, V.M. (Ed.): **Proc. Third CANMET/ACI International Conference on Fly Ash, Silica Fume, Slag and Natural Pozzolans in Concrete**, Trondheim, Norway, 1989, ACI Publication SP–114, Detroit, USA.
5. **Proc. Fourth CANMET/ACI International Conference on Fly Ash, Silica Fume, Slag and Natural Pozzolans in Concrete**, Istanbul, Turkey, 3–8 March 1992.
6. **Proc. International Congress on the Chemistry of Cement**: 4th, Washington, 1960; 5th, Tokyo, 1968; 6th, Moscow, 1974; 7th, Paris, 1980; and 8th, Rio de Janeiro, 1986.
7. RILEM Technical Committee 73–SBC: "Siliceous by-products for use in concrete, Materials and Structures", 1988, **21**, 69–80.
8. Mehta, P.K.: "Pozzolanic and cementitious by-products in concrete – another look", Ref. 4, 1989, V1, Paper SP 114–1, 1–44.

9. Wesche, K. (Ed.): "Fly ash in concrete: properties and performance", Report of RILEM Technical Committee 67–FAB, Use of Fly Ash in Building, E & F.N. Spon, Chapman and Hall, London, 1991, p. 255.
10. McCarthy, G.J., Glasser, F.P., Roy, D.M. & Hemmings, R.T. (Eds): "Fly ash conversion by-products: characterisation, utilisation and disposal IV", Materials Research Society, Pittsburgh, 1988.
11. Hiroshi Uchikawa: "Effect of blending components on hydration and structure formation", Ref. 6, 1986, Theme III, Blended and Special Cements, 249–280.
12. Bijen, J. & Waltje, H.: "Alternative raw materials and building materials for Portland cement: Pt IV – Slag-fly ash cement", Ministry of Housing, Physical Planning and Environment, Leidschendam, Netherlands, 1985.
13. Longo, A. & Torrent, R.J.: "Methods of addition of blast furnace slag: their effect on the compressive strength of mortars and concretes", Ref. 2, 1986, Paper SP 91–68, 1381–1400.
14. Roy, D.M.: "Hydration, microstructure and chloride diffusion of slag-cement pastes and mortars", Ref. 3, 1989, Paper SP 114–61, 1265–1281.
15. Federation Internationale de la Precontrainte: "Condensed silica fume in concrete", Thomas Telford, London, 1988.
16. Olivier, J.P., Carles-Gibergues, A. & Hanna, B.: "Pozzolanic activity and voids filling effect of a CFS introduced in the pastes of high strength concretes" (in French), Cement and Concrete Res., 1988, **18(3)**, 438–448.
17. Hara, N., Yamada, H., Inoue, K., Inoue, N. & Noma, H.: "Hydrothermal reactivity of rice hush ash and its use for calcium silicate products", Ref. 3, 1989, Paper SP 114–23, 499–516.
18. Regourd, M.: "Characteristics and activation of blending components", Ref. 6, 1986, Theme 3.1, 199–232.
19. Arliguie, G. & Grandet, J.: "Influence de la composition d'un ciment Portland sur son hydration en presence de zinc", Cement and Concrete Res., 1990, **20**, 517–524.
20. Gutt,W. and Nixon, P.J.: "Use of waste materials in the construction industry", Materiaux et Constructions, 1979, **12**, 255–305.
21. Ikeda, K.: "A new type of pozzolanic cement utilising red mud and fly ash", Ref. 6, 1986, Seminar 4, Posters, 389.
22. Murakami, K.: "By-product gypsum from various chemical industries as a retarder for the setting of cement", Ref. 6, 1986, Session IV–5, 457–503.
23. Carmichael, J.B.: "Worldwide production and utilisation of phosphogypsum". Proc. 2nd Int. Symp. Phosphogypsum, 1988, Florida Institute of Phosphate Research, Bartow, Florida, **1**, 8–35.
24. Mehta, P.K. & Brady, J.R.: "Utilisation of phosphogypsum in portland cement industry", Cement and Concrete Res., 1977, **7**, 537–544.
25 Ellison, W. & Luckevich, L.M.: "FGD waste: long-term liability or short-term asset?", Power, 1984, **128(6)**, 79–83.
26. Knauf, A.N.: "The problems of flue gas gypsum", Zement-Kalk-Gips, 1983, **36(5)**, 271–274.
27. Kurdowski, W., George, C.M. &and Sorrentino, F.P.: "Calcium aluminate and other non-silicate cements", Ref. 6, 1986, Sub-theme 3.3, Special Cements, 292–318.
28. Sudoh, G., Ohta, T. & Harada, H.: "High strength cement in the $CaO–Al_2O_3–SiO_2–SO_3$ system and its application", Ref. 6, 1980, 152–157.
29. Mehta, K.: "Investigations on energy-saving cements", World Cement Technology, 1980, **21**, 166–177.
30. OEDC: "Exposure to radiation from the natural radioactivity in building materials", Report by a Group of Experts of the OECD Nuclear Energy Agency, 1979, Paris, France.
31. Beretka, J. & Mathew, P.J.: "Natural radioactivity of Australian building materials, industrial wastes and by-products", Health Physics, 1985, **48**, 87–92.
32. International Commission on Radiological Protection: "Lung cancer risk from indoor exposures to radon daughters", ICRP Publications 50, Ann. ICRP, 1987, **17(1)**, 1–60, Pergamon Press, Oxford.

Poster Papers

CONTRIBUTION OF ^{29}Si HIGH-RESOLUTION NMR TO THE STUDY OF CONCRETE ALKALI-AGGREGATES REACTION

L Fernandez*, H Zanni-Théveneau*, R Couty, P Barret*** and D Bertrandie*****

**Laboratoire de Physique et de Mécanique des Milieux Hétérogénes and Université Pierre et Marie Curie, Paris, FRANCE*
***Laboratoire de Géologie de 1'ENS, Paris, FRANCE*
****Laboratoire de Recherche sur la Réactivité des Solides Faculté des Sciences Mirande, Dijon, FRANCE*

SUMMARY

We report here a ^{29}Si NMR investigation related to the alkali-aggregates reaction of concrete. In order to understand how a swelling gel can develop in concrete, we worked on a model system consisting in silica gel in interaction with a NaOH (or KOH) aqueous solution. The high resolution NMR techniques allowed us to identify two types of solids which can precipitate from the solutions under the action of calcium compounds. Their structures depend on those of their molecular precursors in solution, themselves depending on the silica and sodium (or potassium) concentrations in solution.

RESUME

Nous présentons ici une étude de RMN de ^{29}Si en relation avec la réaction alcali-granulats des bétons. Afin de comprendre comment un gel peut se développer dans le béton, nous avons étudié un système modèle constitué par du gel de silice en interaction avec une solution aqueuse de soude (ou de potasse). Les techniques de la RMN haute résolution nous ont permis d'identifier deux types de solides pouvant précipiter à partir de ces solutions sous l'action de composés de calcium. Les structures de ces précipités dépendent de celles de leurs précurseurs moléculaires en solution, elles-mêmes déterminées par les concentrations de silice et d'alcalin en solution.

INTRODUCTION

The alkali-aggregates reaction (1), first reported in 1935, consists in the growth in concrete, of a swelling siliceous gel, which can induce a degradation of the buildings. It is due to the attack of some siliceous aggregates of concrete, said to be reactive, by the very alkaline intersticial water contained in cement pores. Besides the tremendous work devoted to this problem (2), the nature and the formation mechanisms of the swelling gel are not yet understood.

In this study our purpose was to use the ^{29}Si high resolution NMR techniques to investigate which kind of gels may develop in such a very alkaline reactive medium. It is well known (3) that the great property of ^{29}Si NMR is to get the connectivity of SiO_4 tetrahedra which are the basic elements of silicates and silica structures*.

A first ^{29}Si NMR investigation of some concrete aggregates (see Fig.1.), starting from non reactive quartz and going to some aggregates, like opals, known to be very reactive, conviced us to take again the modelizing approach of L. Dent Glasser et al (4). Indeed, the NMR spectra and especially those obtained by CP-MAS techniques clearly show the structural differences between the well crystallized structure of quartz (characterized by a narrow Q^4 line at -107,4 ppm) and those of aggregates (characterized by a broadening of the Q^4 line and the onset of Q^3 and even Q^2 entities) which present some similarities with the silica gel spectrum.

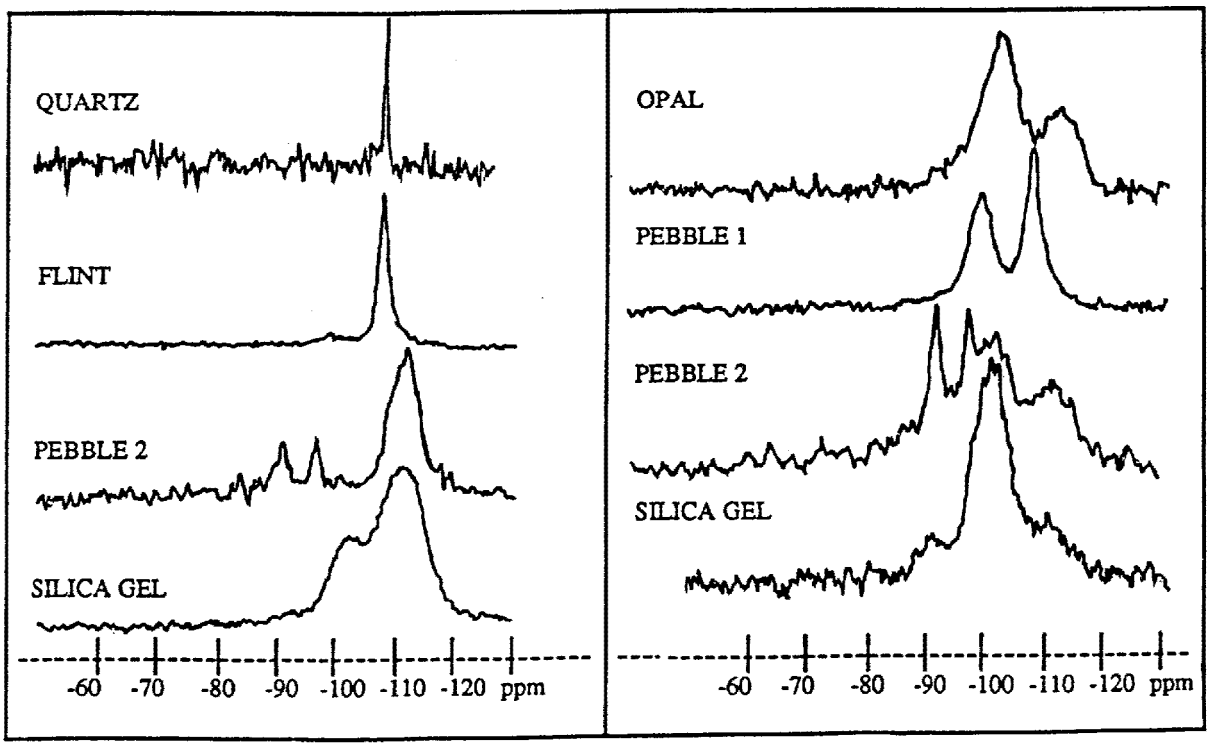

Fig. 1. ^{29}Si NMR spectra of some siliceous minerals used as aggregates in concrete, compared with those of quartz and commercial silica gel.
(left side: MAS spectra; right side: CP-MAS and proton decoupling spectra).

*Q^n notation: index n stays for number of bridging oxygens pro Q (SiO_4-) unit

So, we decided to study the reaction of silica gel, playing the role of reactive aggregate, with a NaOH (or KOH) solution, the concentration of which (0.7N) being equivalent to that of cement water. This reaction leads to the formation of silica alkaline solutions undergoing transformation from the ionic to the colloïdal state along with the increase of silica concentration to the saturation point, called pessimum (4). At this point, some residual silica gel no longer passes in solution and has been considered as the gel which can swell in time (4).

Z. Wen (5) extended this approach, showing that, indepently of the phenomenon of residual gel, other potentially pathogen gels could precipitate from the solution. Indeed, whatever is the concentration of silica in the solution, which means that the solution may be either ionic or colloïdal, solids may precipitate under the action of electrolytes, especially calcium electrolytes and particularly calcium salts and hydroxyde, $Ca(OH)_2$, the portlandite, always present in a cement medium. This reveals the role of calcium in the formation of these gels, an idea also developped by Chatterji et al. (6) and more recently by Dron (7).

EXPERIMENTAL

Samples

Silica gel (MERCK, grain size: 60 to 160 µm, specific or massic area: 750 gm^{-2}) was previously dried during 2 hours at 250°C. Silica solutions were prepared by adding different masses of silica gel in a definite volume of a 0.7 N aqueous NaOH (or KOH) solution.

Solutions were characterized by two SiO_2/Na_2O (SiO_2/K_2O) molar ratios: the initial molar ratio corresponding to the total amount of solid SiO_2 added to the solution and denoted by R_{mt} and the actual molar ratio in solution, determined by flame atomic absorption spectrometry and denoted by R_{ms}. The R_{ms} curves plotted versus R_{mt} were observed to pass through a maximum reached for a given mass of added silica gel. In these conditions, so called "pessimum" conditions, the silica concentration reached a maximum at the end of a time long enough to consider that equilibrium was realized. The values of R_{mt} and R_{ms} were 4.75 and 4.56 respectively. Before the maximum, the values of R_{ms} did not differ from those of R_{mt}; after the maximum,

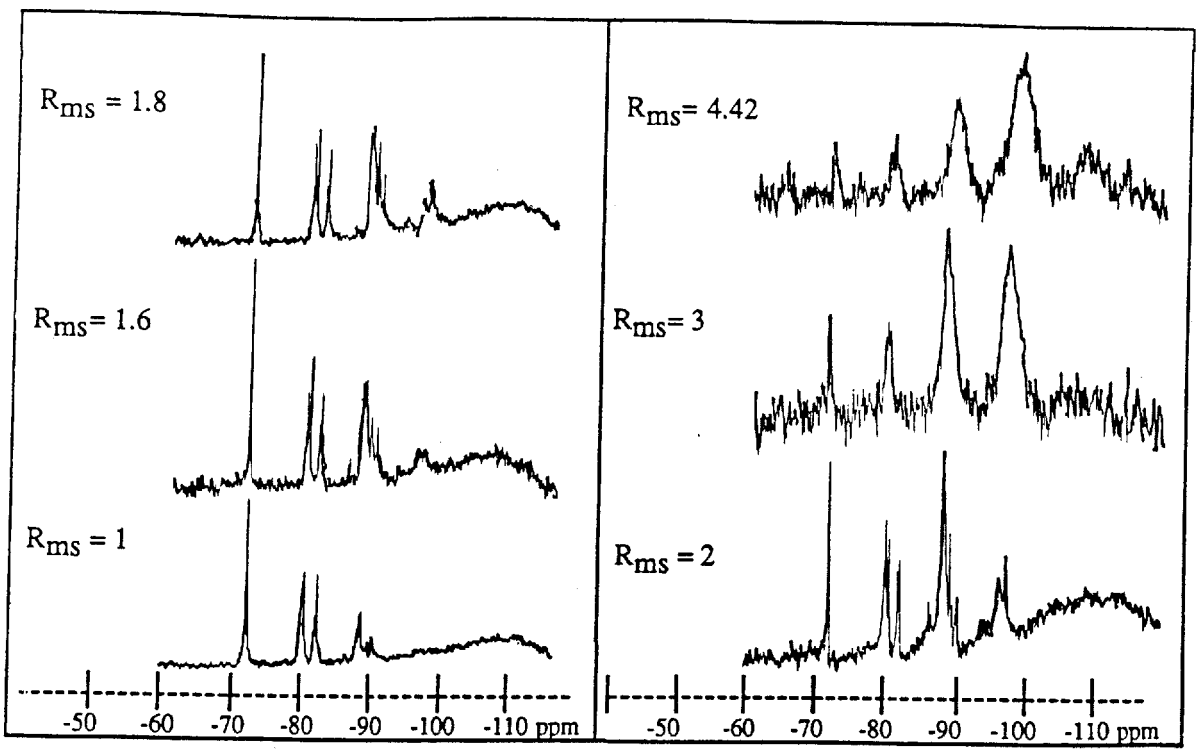

Fig.2. ^{29}Si NMR spectra of the alkaline solutions for different R_{ms} ratios

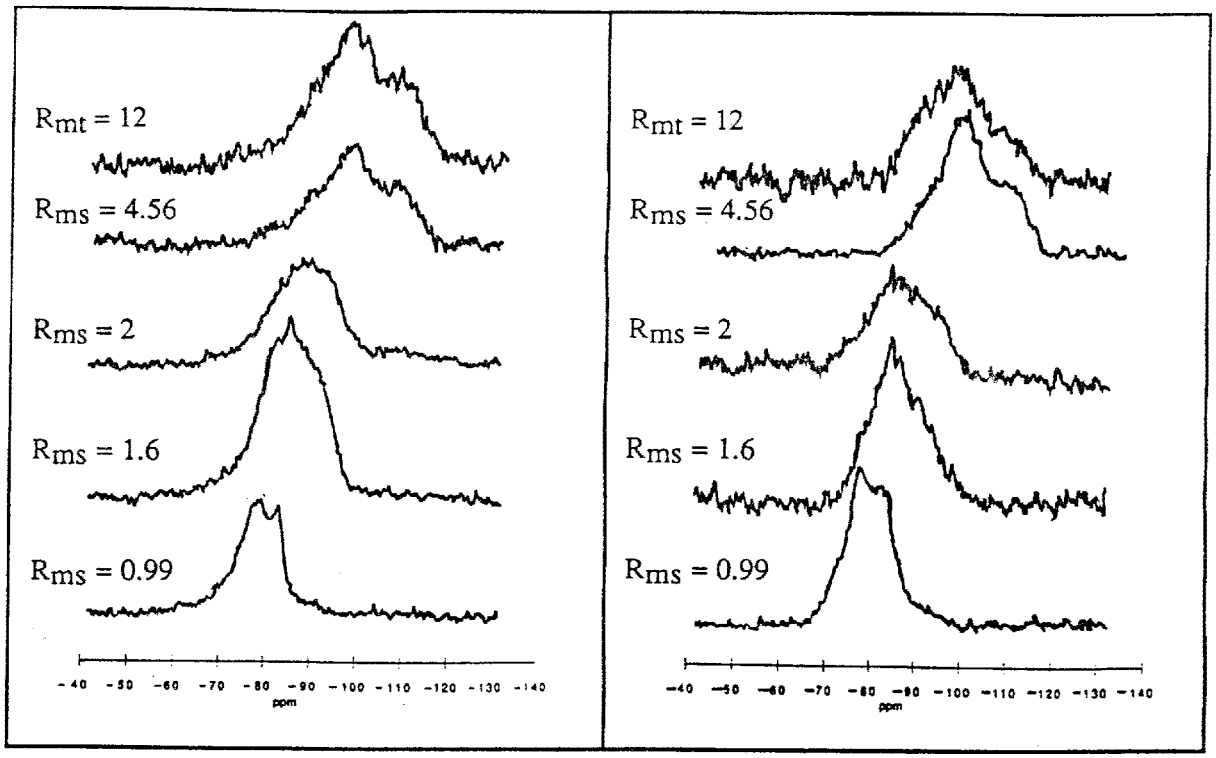

Fig.3. ^{29}Si NMR spectra of the precipitates obtained from the alkaline solutions for different SiO_2/Na_2O ratios.
(left side: MAS spectra; right side: CP-MAS, proton decoupling spectra).

second one some informations about silanols location in the structure, since CP experiments selectively reveal silicon nuclei in interaction with protons.

The two types of experiments show the evolution of the precipitates structure when increasing the R_{ms} ratio. Solids obtained from ionic solutions (R_{ms} = 0.99, 1.6 and 2) are composed of Q^1 and Q^2 entities only, lying in the range -73 to -89 ppm, like the calcium silicate hydrates, the CSH, resulting from cement hydration (9). Precipitates issued from colloidal solutions (R_{ms} = 4.56) are built with Q^2, Q^3 and Q^4 entities, the two last ones centered at - 99 and - 108 ppm.

We have verified that after the pessimum, solutions were always colloidal and that one could obtain precipitates from them. For instance, we have reported on Fig.3. the spectra corresponding to R_{mt} = 12; they are similar to those of precipitates obtained before the pessimum.

On Fig.4. are presented the spectra of residual silica gel, obtained by filtration of the saturated solutions near the pessimum and after (R_{mt} ratios equal to 4.75, 12; and 20). MAS spectra reveal an evolution in the Q^3/Q^4 intensities ratio between the original gel and the residual ones: near the pessimum (R_{mt} = 4.75) the two entities seem to have the same intensities; then Q^3 intensity decreases (R_{mt} = 12) and is rather the same than in the original silica gel for R_{mt} = 20. CP-MAS spectra also show some differences in the silanols sites between the original silica gel and the residual gels: in particular one observes a shift of the Q^3 peak maximum. One must notice that the residual silica gel structures differ from that of precipitates.

R_{mt} increased from 4.75 to 25 and R_{ms}, measured in solution, decreased from 4.56 to about 2.3 and remained constant even though R_{mt} increased. That came from the simultaneous decreases of SiO_2 and NaOH (KOH) concentrations due to the absorption of NaOH (KOH) by the residual silica gel (4).

In all these cases, solutions were stirred during 5 days at less and equilibrium detected by pH stabilization.

Solid precipitates were obtained, whatever was the silica concentration in solution, by adding solid $CaCl_2$ to the solutions (5). Then they were dried by aceton-ether.

NMR Experiments

^{29}Si NMR experiments in solutions were performed on a BRUKER AM 250 NMR spectrometer in a field of 5.87 Tesla, at a frequency of 49.69 MHz.

^{29}Si NMR experiments on solids were performed on a BRUKER CXP 300 NMR spectrometer, in a field of 7.03 Tesla , at a frequency of 59.62 MHZ, using the high resolution solid state NMR techniques: Magic Angle Spinning, Proton Decoupling and ^{1}H - ^{29}Si Cross-Polarization .

$(Si(CH_3)_3)8Si_8O_{20}$, the Q_8M_8,was used as a secondary standart, the major peak being at 11.6 ppm relatively to TMS, the tetramethylsilane $Si(CH_3)_4$.

After identifying the different Q^n entities present in the spectra, which necessitated the spectra decomposition in the case of the solid precipitates, the mean degree of connectivity of the SiO_4 tetrahedra, n, defined by

$$n = \Sigma\ n\,Q^n / \Sigma\,Q^n$$

where n = 0, 1 ....4, was calculated

RESULTS

On Fig.2. are presented, for instance, the ^{29}Si spectra of sodic solutions corresponding to different R_{ms} ratios. They clearly show the passage from ionic to colloidal state with the increase of R_{ms} ratio. For low R_{ms} ratios (1 to 2), the polymerization degree in the solution is weak. The spectra present intensive monomeric Q^0 peaks, located at -72 ppm, dimeric Q^1 and cyclic Q^2 peaks located in the range -80 to -82 ppm, linear Q^2 entities at -88 ppm and also a weak Q^3 signal at -90 ppm. The broad signal in the range -105 to -120 ppm is due to Q^4 entities of the borosilicate tube containing the solutions but for higher R_{ms} ratios (3, 4.42) we worked with silica-free tubes.

The onset of the colloidal state is revealed by two features: the broadening of the whole spectrum and the growth of Q^3 and Q^4 entities with the decrease of poorly polymerized entities, Q^0,Q^1,Q^2 and even the disappearence of monomeric Q^0 near the pessimum. Our results are in agreement with previous results (3, 8) but we have extented the study to higher SiO_2/Na_2O molar ratios, till the saturation of the solution.

The same results are obtained in the case of potassic solutions.

The ^{29}Si NMR spectra of solids precipitated from the different solutions are presented in Fig.3. For each sample we have achieved MAS experiment and CP-MAS, ^{1}H decoupling experiments. From the first kind of spectra, we can obtain the contribution of each particular Q^n entity in the structure of gels and from the

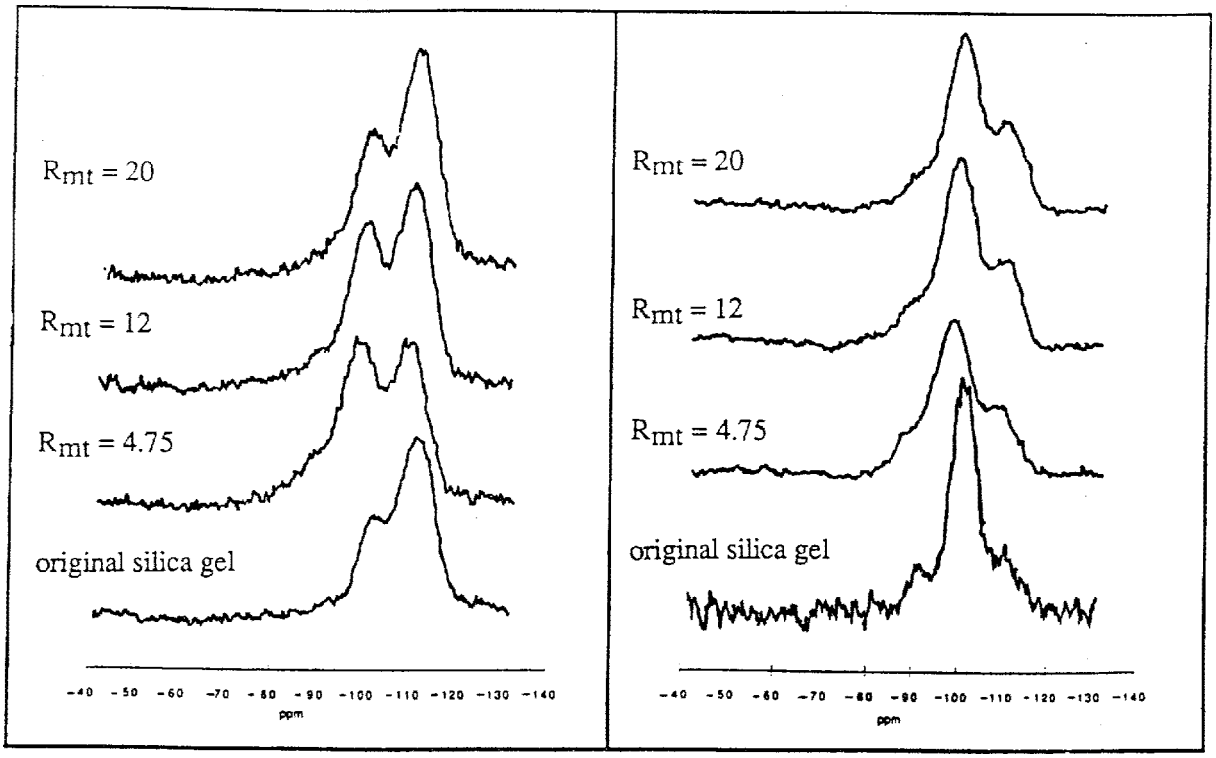

Fig.4. ^{29}Si NMR spectra of the initial silica gel and of the residual silica gel for different R_{mt} ratios after the "pessimum"
(left side: MAS spectra; right side: CP-MAS, proton decoupling spectra).

Finally, on Fig. 5., we have plotted the R_{ms} ratio of the sodic and potassic solutions versus the mean degree of connectivity of the SiO_4 tetrahedra in the molecular precursors in solutions and also in the precipitates obtained from these solutions.

First, one can observe that there is no difference between sodic and potassic solutions and between sodic and potassic precipitates.

Then, the mean degree of connectivity of the precipitates has the same behaviour with the R_{ms} ratio than the mean degree of connectivity of the molecular precursors. Even this ratio is not enough, alone, for characterizing the structure of the precipitate, it appears to be a relevant parameter to obtain a precipitate with a particular structure.

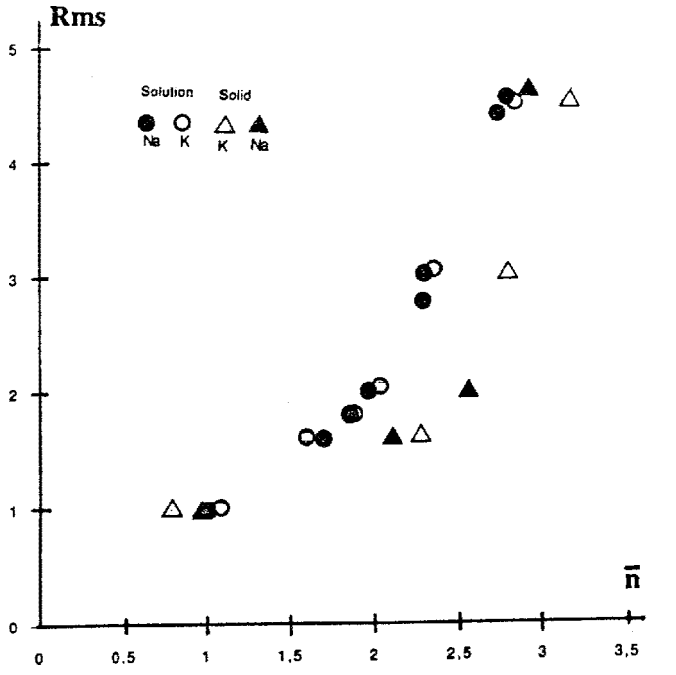

Fig. 5. Relation between the R_{ms} of the silica alkaline solutions and the mean degree of connectivity, n, of the molecular precursors and of the precipitates.

CONCLUSION

This NMR investigation of the system silica gel-alkaline solution, modelizing the alkali-reaction phenomenom, has confirmed the previous results (5) showing that whatever is the solution concentration, the action of calcium compounds leads to gels precipitation. As far as ionic solutions are concerned, precipitates have a Q^1, Q^2 structure, identical to that of cement silicate hydrates, the CSH (9). In the case of colloïdal solutions, a sol-gel transformation takes place on each side of the pessimum, which leads to compounds analogous to silica gel (i.e. consisting of Q^2, Q^3, Q^4 units) the structures of which are different from the structure of the residual silica gel. The mean degrees of connectivity, reflecting the degrees of polymerization, were measured for the molecular precursors in solution and for the precipitates: they are clearly connected together along with the R_{ms} ratios in solution, SiO_2/Na_2O (or SiO_2/K_2O). But it is obvious that the gels structure depends not only on the R_{ms} ratio but also on the SiO_2/CaO_2 ratio as shown by Grutzeck et al. (10) in their study of calcium silicate hydrates. Quantitative analysis of the spectra is in progress along with ^{23}Na NMR experiments and chemical analysis.

We hope that these results, obtained in the case of a model system, should help to identify the swelling gel observed in actual situations.

ACKNOWLEDGEMENTS

This work has been achieved in collaboration and with the financial support of ATILH (Association Technique de l'Industrie des Liants Hydrauliques, France).

REFERENCES

1 Diamond, S.: "ASR- another look at mechanisms". **8th Int. Conf. AAR, Kyoto, Japan,1989** edited by Okada, K., Nishibayashi, S. and Kawamura, M., Elsevier Applied Science, 83-94.

2. Nine international conferences have been devoted to alkali-aggregate-reaction since 1974; the last one was held in London, july 1992.

3 Engelhardt,G. and Michel, D.: "**High Resolution ^{29}Si NMR of silicates and zeolites**". Wiley, 1989, 485 p.

4 Dent Glasser, L. and Kataoka, N.: "The chemistry of 'alkali-aggregate' reaction". Cem. Concr. Res., 1981, **11**, 1-9.

5 Wen, Z.: "Formation et caractérisation de sols alcalins de silice. Conditions de leur transformation en gel au contact de sels et d'hydroxydes, notamment de ceux qui sont présents dans le béton. Etude particulière du rôle de la portlandite". Thesis, Université de Bourgogne, Dijon, France, 1989, 71 p.

6 Chatterji, S., Jensen, A.D., Thaulow, N. and Christensen, P.: "Studies of alkali-silica reaction. Part 3. Mechanisms by which NaCl and $Ca(OH)_2$ affect the reaction". Cem. Concr. Res. 1986, **16**, 246-254.

7 Dron, R.: "Thermodynamique de la réaction alcali-silice". Bulletin de liaison des Laboratoires des Ponts et Chaussées, mars-avril 1990, Paris.

8 Wijnen, P. W. J. G., Beelen, T. P. M., de Haan, J. W., Rummens, C. P. J., van de Ven, L. J. M. and van Santen, R. A.: "Silica gel dissolution in aqueous alkali metal hydroxydes studied by ^{29}Si-NMR". J. Non-Cryst. Sol., 1989, **109**, 85-94.

9 Rassem, R., Zanni-Théveneau, H., Schneid, I.and Regourd, M.: "^{29}Si high-resolution NMR study of tricalcium silicate hydration". J. Chim. Phys., 1989, **86**, 1253-1264.

10 Grutzeck, M. W., Benesi, A. and Fanning, B.: "Silicon-29 Magic Angle Spinning Nuclear Magnetic Resonance study of calcium silicate hydrates". J. Am. Ceram. Soc., 1989, **72**, 665-668.

PROGRESS IN THE ^{27}AL MAS NMR SPECTROSCOPY : MONITORING THE HYDRATION OF CALCIUM ALUMINATE CEMENTS

D Müller*, A Rettel*, W Gessner*, J P Bayoux**.and A Capmas***

*Centre of Inorganic Polymers, Berlin, GERMANY
**Lafarge Coppee Recherche, Viviers, FRANCE
***Lafarge Fondu International, Neuilly sur Seine, FRANCE

^{27}Al magic-angle spinning nuclear magnetic resonance spectroscopy (MAS NMR) in combination with proton decoupling was applied to the study of hydration of calcium aluminate cements. It is shown that herewith not only the hydration process can be followed quantitatively in terms of the degree of hydration but also separately the formation of hydrogarnet. Beyond this, under favourable circumstances, also the formation of the other hydration phases, and especially of aluminium hydroxide, can be studied individually. The method described was applied to study the hydration of monocalcium aluminate.

^{27}Al MAS NMR Spektroskopie in Verbindung mit Protonenentkopplung wurde angewendet zur Untersuchung der Hydratation von Calciumaluminatzementen. Es wird gezeigt, daß mit dieser Technik der Verlauf des Hydratationsprozesses nicht nur wie bisher quantitativ mittels der Bestimmung des Hydratationsgrades verfolgt werden kann, sondern auch separat die Bildung der Hydratphase C_3AH_6. Darüber hinaus läßt sich in günstigen Fällen auch die Bildung der anderen Hydratphasen und insbesondere die des Aluminiumhydroxids individuell verfolgen. Die beschriebene Technik wurde zur Untersuchung der Hydratation von Monocalciumaluminat eingesetzt.

INTRODUCTION

Previous studies [1,2] have shown the applicability of the high-field ^{27}Al magic-angle spinning nuclear magnetic resonance spectroscopy (MAS NMR) to the investigation of the hydration of monocalcium aluminate. By monitoring the conversion of tetrahedral into octahedral Al the hydration process can be followed quantitatively in terms of the degree of hydration (Al^{six}/Al_{total}). However, under the experimental conditions described (spinning rates of about 6 kHz), it was not possible to separate the signals of the different individual hydration products (C_3AH_6, AH_3, C_2AH_8, CAH_{10} ; [3]) involved. In this contribution we report the combined application of high-power proton decoupling and high-field ^{27}Al MAS NMR. It is shown that herewith the formation of C_3AH_6 can be followed separately. Beyond this, under favourable circumstances, a complete deconvolution of the spectrum of the hydration products is possible.

EXPERIMENTAL

The ^{27}Al MAS NMR spectra were recorded on a spectrometer MSL 400 (Fa. BRUKER) at 104.3 MHz under high-power proton decoupling conditions. Spinning frequencies of about 5 kHz were applied. For a correct quantitative analysis short excitation pulses of 0.6 us with repetition times of 10 s had to be used. For the deconvolution of the spectra the simulation programs LINESIM [4] (only for gaussian/lorentzian lines) and POWDER [5] (including quadrupole interaction) were used. The hydration process of the samples (w/c = 0.5) was stopped with acetone and ether in the usual manner, the measurements were performed at room temperature.

SEPARATION OF THE C_3AH_6 SIGNAL

In Fig. 1 the influence of additional proton decoupling on the MAS spectra of various synthetic mixtures of the hydration phases is shown. It can be seen that the application of high-power proton decoupling leads to a significant line narrowing of the ^{27}Al MAS NMR signal of the C_3AH_6 phase whereas the signals of the other hydration products cannot be narrowed sufficiently and coincide as before at about 8 ppm.

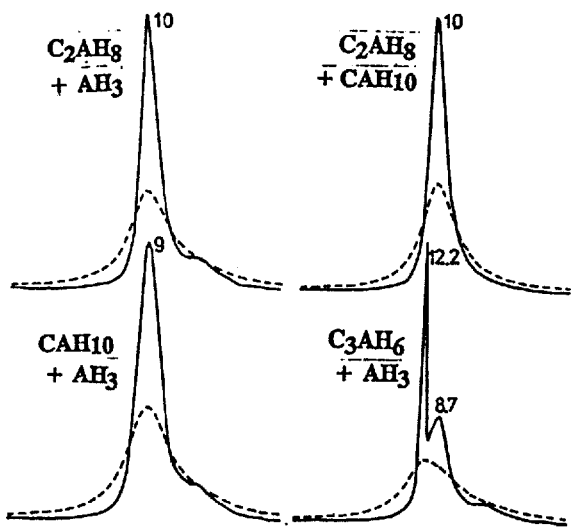

Fig. 1 Line narrowing by ^1H decoupling

The favourable behaviour of the C_3AH_6 signal is due to the low electric field gradient (quadrupole coupling constant of about 0.7 MHz) at its Al site causing a characteristic sharp peak at 12 ppm after proton decoupling. Similar narrowing effects and an effective proton decoupling can also be achieved by only MAS measurements with modern high-speed MAS probes providing spinning rates of about 15 kHz. With recent double-oriented rotation (DOR) experiments, however, no resolved spectra could be obtained without additional proton decoupling.

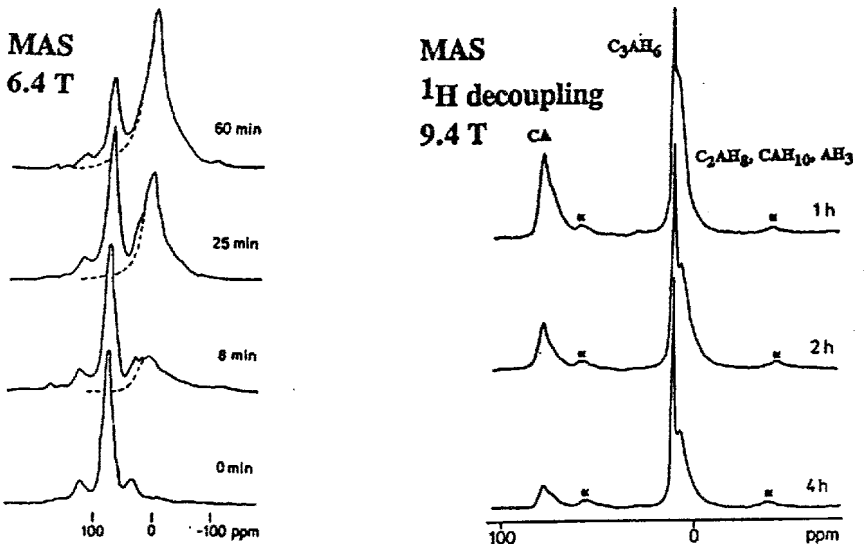

Fig. 2 Historical [1] (a) and recent (b) NMR spectra of hydrated CA

Fig. 2 illustrates the achieved apparative progress of the application of the ^{27}Al MAS NMR spectroscopy to the investigation of the hydration of monocalcium aluminate since the first studies in 1984 [1], (hydration at 70 °C, samples in b) precured for 3 days at 7 °C).

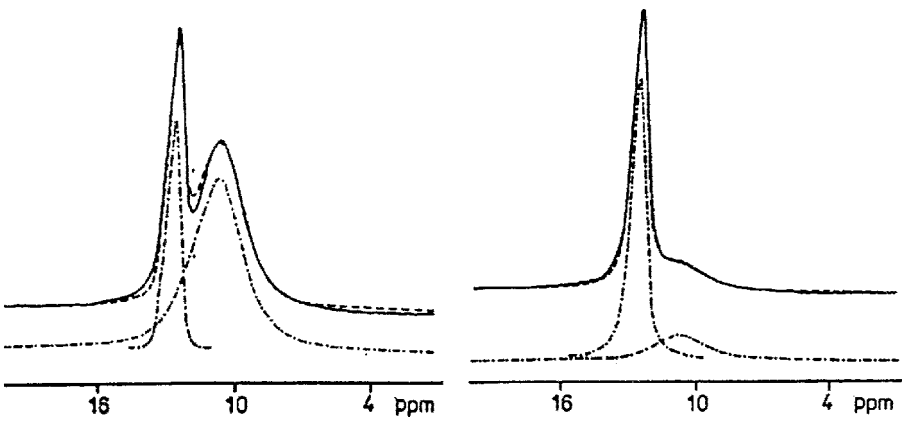

Fig. 3 Peak deconvolution

In Fig. 3 examples of a quantitative analysis of two C_3AH_6/C_2AH_8 mixtures with molar ratios of 1 : 3 and 3 : 1, respectively, are shown.

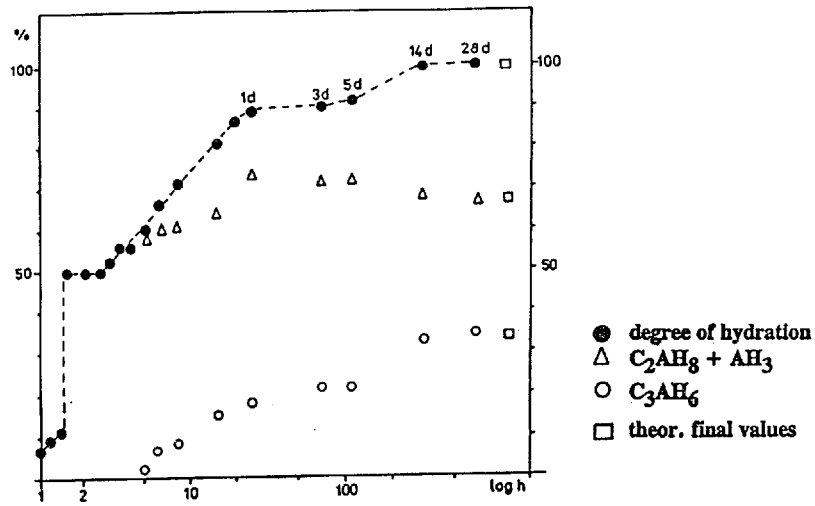

Fig. 4 Hydration of CA at 50 °C

The method described was applied to study the hydration of monocalcium aluminate. Fig. 4 shows the progress of the formation of C_3AH_6 under hydration at 50 °C. Simultaneously, as difference to the total hydration reaction, the amount of C_2AH_8 + AH_3 is plotted. As expected from powder diffraction data the formation of C_3AH_6 starts significantly not before 5 hours. It should be noted that after 28 h hydration time the final composition of the hydration product corresponds to the theoretical molar ratio of 1 : 2 for C_3AH_6 and AH_3 which is expected after a complete reaction according to eq. (1)

$$\begin{array}{lll} 6CA + 33\,H \longrightarrow & 3\,C_2AH_8 & + 3\,AH_3 \\ & \downarrow & \downarrow \\ & (2\,C_3AH_6 + AH_3 + 9\,H) & + 3\,AH_3\ . \end{array} \qquad (1)$$

In contrast, samples precured 3 days at 7 °C under the formation of CAH_{10} and after a subsequent hydration for several days at 70 °C did not show such a theoretical ratio of 1 : 2, but ratios of 1 : 3 reflecting an incomplete conversion. This behaviour can only be explained by remaining amorphous intermediates since no powder diffraction reflections of the corresponding crystalline phases (C_2AH_8 or CAH_{10}) were detected. The same behaviour was observed during conversion of the pure CAH_{10} phase.

Separation of the AH_3 signal

Because of a missing line splitting a direct separation of the AH_3/C_2AH_8 and AH_3/CAH_{10} signals is not possible as in the case of C_3AH_6 . However, the crystalline AH_3 provides a characteristic and structured lineshape with an additional hump at -2.5 ppm and a high-field wing extending to chemical shift ranges outside of the other signals. This lineshape is understood in terms of two crystallographically different Al sites with different electric field gradients of the octahedra. Fig. 5 shows the experimental and

fitted ^{27}Al MAS NMR spectrum of a crystalline AH_3 standard. According to the simulation the two Al sites correspond to the following fitting parameters:

	Al(1)	Al(2)
quadrupole coupling constant	2.2 MHz	4.3 MHz
asymmetry parameter of the efg	0.8	0.2
relative intensity	50 %	50 %
chemical shift	11.5 ppm	11 ppm

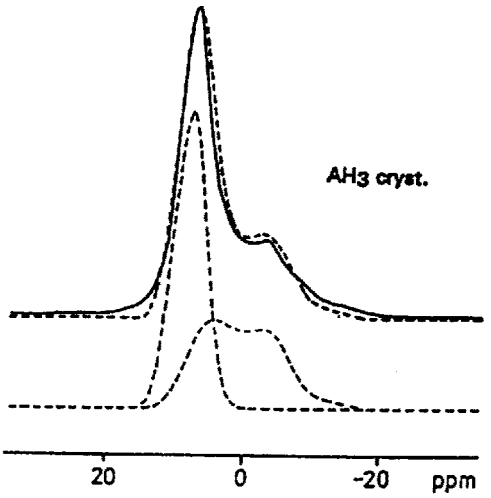

Fig. 5 Simulation of the AH_3 spectrum

The feature of the AH_3 spectrum can be used for a separation by extrapolating the non-superimposed high-field tail on the basis of the known lineshape. The procedure was tested with two synthetic mixtures of AH_3 with C_2AH_8 and CAH_{10}, respectively, with ratios of 1 : 1 . In both cases the extra-polation gave correct results (see Fig. 6). Correspondingly, the theoretical composition was obtained analyzing a three-component mixture of C_3AH_6 with C_2AH_8 and AH_3 of equal amounts. In this case the C_3AH_6 contribution was separated in the usual manner and from the remaining signal AH_3 was separated by extrapolation.

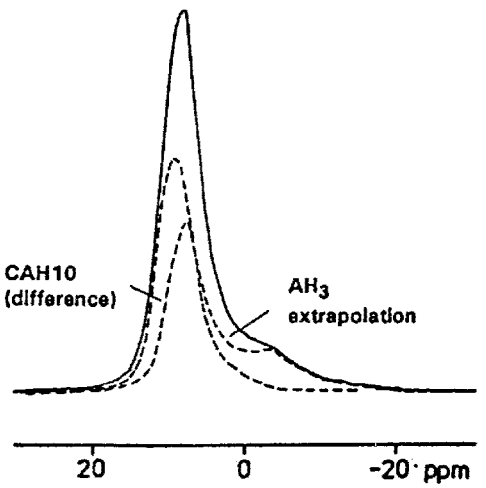

Fig. 6 Deconvolution of a synthetic mixture (CAH_{10}/AH_3)

In real hydration products, however, the resulting spectrum cannot be treated as a mere superposition of the lineshapes of the individual phases. This holds as well for the crystalline C_3AH_6 (a slight broadening) as for AH_3 (smoothening of the spectrum).

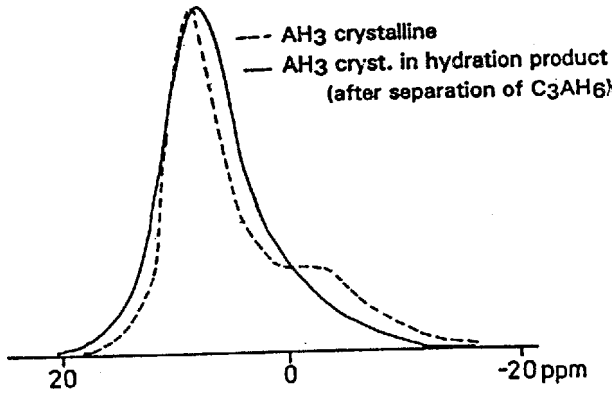

Fig. 7 Comparison of AH_3 lineshapes

Fig. 7 compares the spectra of the pure crystalline AH_3 phase with that of crystalline AH_3 in a completely reacted hydration product after the separation of the C_3AH_6 signal. Though diffraction method evidenced polycrystalline hydroxide without C_2AH_8 interferences, the NMR lineshape of this phase in the real hydration product aside C_3AH_6 is similar to that of freshly precipitated amorphous hydroxide. Since this lineshape still provides a prolongated but smoothened high-field part, the attempts of a separation procedure must base on the actual lineshape and not the ideal one.

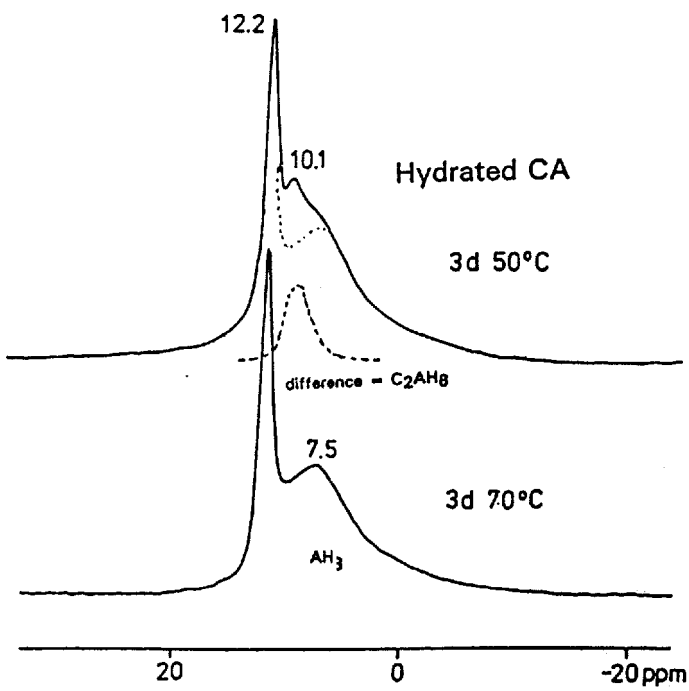

Fig. 8 Hydration of CA

Fig. 8 shows the spectra of CA samples hydrated 3d at 50 and 70 °C, respectively. The sample hydrated at 50 °C definitely still contains C_2AH_8 as reflected by the peak at 10 ppm and the difference between both spectra (dashed line). Deconvolution of the spectrum yields approximately 30 % C_3AH_6, 5 % C_2AH_8 and 65 % AH_3.

CONCLUSIONS

Recent ^{27}Al MAS NMR spectroscopy can be applied to hydration studies of calcium aluminate cements not only monitoring the progress of the hydration reaction but also the formation of the individual hydrate phases, especially C_3AH_6. The investigations are still in progress.

REFERENCES

[1] MÜLLER, D., RETTEL, A. & GESSNER, W. : "An Application of Solid-State Magic-Angle Spinning ^{27}Al NMR to the Study of Cement Hydration", *J. Magn. Reson., 1984, 57, 152 - 156.*

[2] RETTEL, A., GESSNER, W., MÜLLER, D. & SCHELER, G.: "On the Hydration of $CaAlO_4$ at Various Temperatures", *Br. Ceram. Trans. J., 1985, 84, 25 - 28.*

[3] Notation used: C=CaO, A=Al_2O_3, H=H_2O

[4] Barron, P.,: Bruker Software Package

[5] Müller, D. & Heidemann, D. : Bruker Software Package

DEVELOPMENT OF INSTRUMENTATION AND TECHNIQUES TO STUDY CEMENT SUSPENSIONS AT HIGH TEMPERATURES AND PRESSURES (UP TO CA. 200°C)

G V M Teodoru, H Hartmann and P Jackmuth

College of Applied Sciences, Cologne
GERMANY

SUMMARY

This paper presents new developments made in order to do microscopic investigations on cement suspensions treated at high temperature and the corresponding high pressure. An original "pressure-chamber" was projected basing on an existing microscopical heating accessory Leitz 350. Mainly the pressure-chamber resulted as a space between two quartz glasses, separated through a 0.2 mm polytetrafluorethylene gasket.The heating up to 200°C of the cement suspension was done electrically, by 2.2 A and 17 V for 30 minutes. The paper contains details referring to the construction of this original imaginated pressure-chamber and to the necessary insulation. A Leitz microscope type Orthoplan was used in order to follow the crystallization in the heated cement suspension and in solution of C_4AF as completion of the formerly reported results /2, 3/. On the Fotokina Exhibition in Cologne, autumn 1990 from 3 to 10 October, it was possible for the first time to follow the process of crystallization in cement suspensions at high temperatures (ca. 200° C) with the help of the described instrumental developments, a video camera and a monitor (fig. 3).

ZUSAMMENFASSUNG

Der Beitrag stellt neue Entwicklungen vor, die Beobachtungen an Zementsuspensionen, behandelt bei hohen Temperaturen und entsprechendem Druck, ermöglichen sollen. Eine originale "Druck-Kammer" wurde entworfen, ausgehend von der vorhandenen mikroskopischen Zusatzeinrichtung Leitz 350. Im Prinzip besteht die Druck-Kammer als freier Raum zwischen zwei Quarzglasscheiben, getrennt durch eine 0,2 mm starke Teflondichtung. Die Erwärmung bis auf 200° C der in diesem Raum befindlichen Zementsuspension geschieht durch elektrischen Strom bei 2,2 A und 17 V während 30 Minuten. Mitgeteilt wurden Einzelheiten über die Konstruktion dieser neu entworfenen Kammer und über ihre Isolierung. Als Ergänzung zu den bereits früher mitgeteilten Ergebnissen /2, 3/ wurden Beobachtungen der Kristallisierung in Suspensionen von Zement bzw. C_4AF mit dem Mikroskop Type Orthoplan durchgeführt. Auf der Fotokina-Ausstellung in Köln im Herbst 1990, zwischen dem 3. und 10. Oktober, war es zum ersten Mal möglich, den Prozess der Kristallisierung in den Zementsuspensionen bei hohen Temperaturen (ca. 200° C) mit Hilfe der vorgestellten Einrichtung, einer Videokamera und eines Monitors, zu verfolgen (Fig. 3).

1 INTRODUCTION

The author carried out since 1967 systematic research works on concretes subjected to a hydrothermal treatment. The quantification of influences of hydrothermal treatment in relation to tests made is most important for its practical use, since it is possible that structural components are hardened **with or without hydrothermal treatment on the same building site** (e.g. Hotel Maritim in Cologne few years ago). Additionally, accelerated curing and testing of concrete specimens come into being because of the need to know faster, if possible only after 10 to 24 hours, the quality of the concrete placed in structure and not after 28 days /1/. The cement is the "active" element in the concrete and therefore the studies are to be concentrated on it.

2 DEVELOPMENT OF INSTRUMENTATION

For the simulation of cement hydration at temperature of ca. 200° C and corresponding high pressure, carrying on former research, a special pressure-chamber was constructed. The fig. 1 shows the components of this chamber and in fig. 2 is given a cross section through the whole system. The specimen (3) - e.g. cement powder and distilled water - find themselves between two circular quartz glass pieces (2) and (4) which are brought to

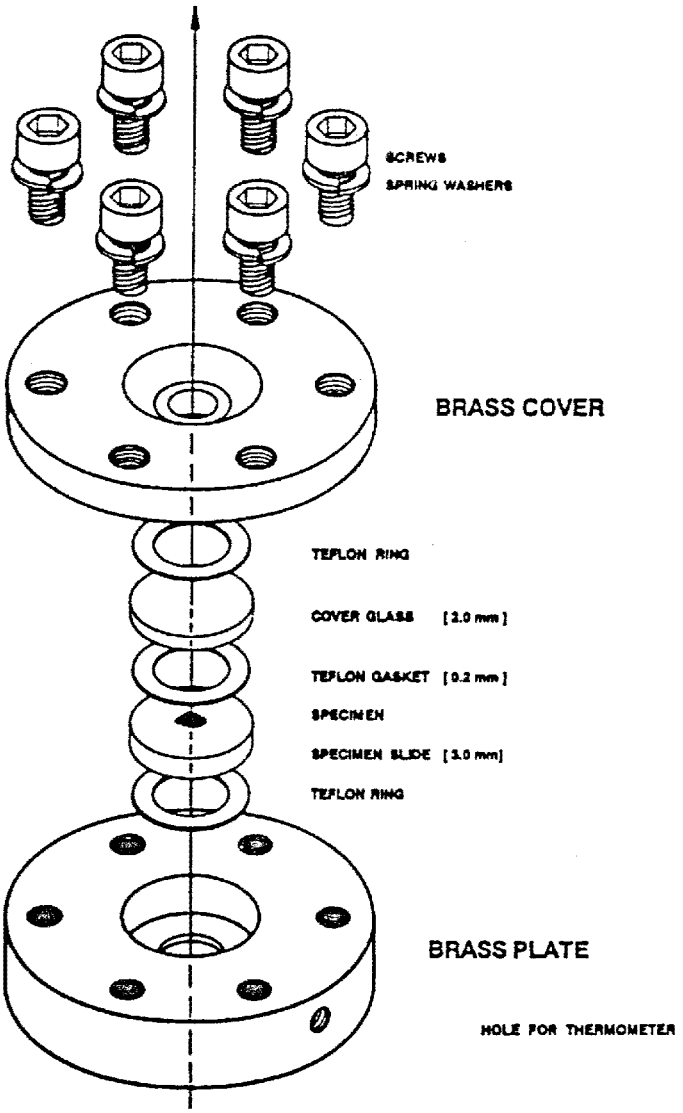

Figure 1 Pressure-chamber ; Components

a certain distance with a circular teflon gasket o.2 mm thin, having also the function to isolate the suspension from the out side. Cover glass (2) and specimen slide (4) are pressed together as uniformly as possible with the help of two brass covers held together by 6 screws. The screws, provided with spring washers, are drived home succeeding one another, by very small steps with a torquewrench,as far as to arrive a torque of ca. 1.5 Nm. Between the brass cover plates and the cover glass and specimen slide respectively, there are again teflon gaskets, so that the glass pieces cannot be damaged. The lower brass plate is found to be on a ring-formed heating plate. A hole is provided into the brass plate to place a thermometer. To hold the temperature constant over a long time period, this system is placed in an insulated block of gas concrete which has a hole for the light source and for the microscope objective respectively.

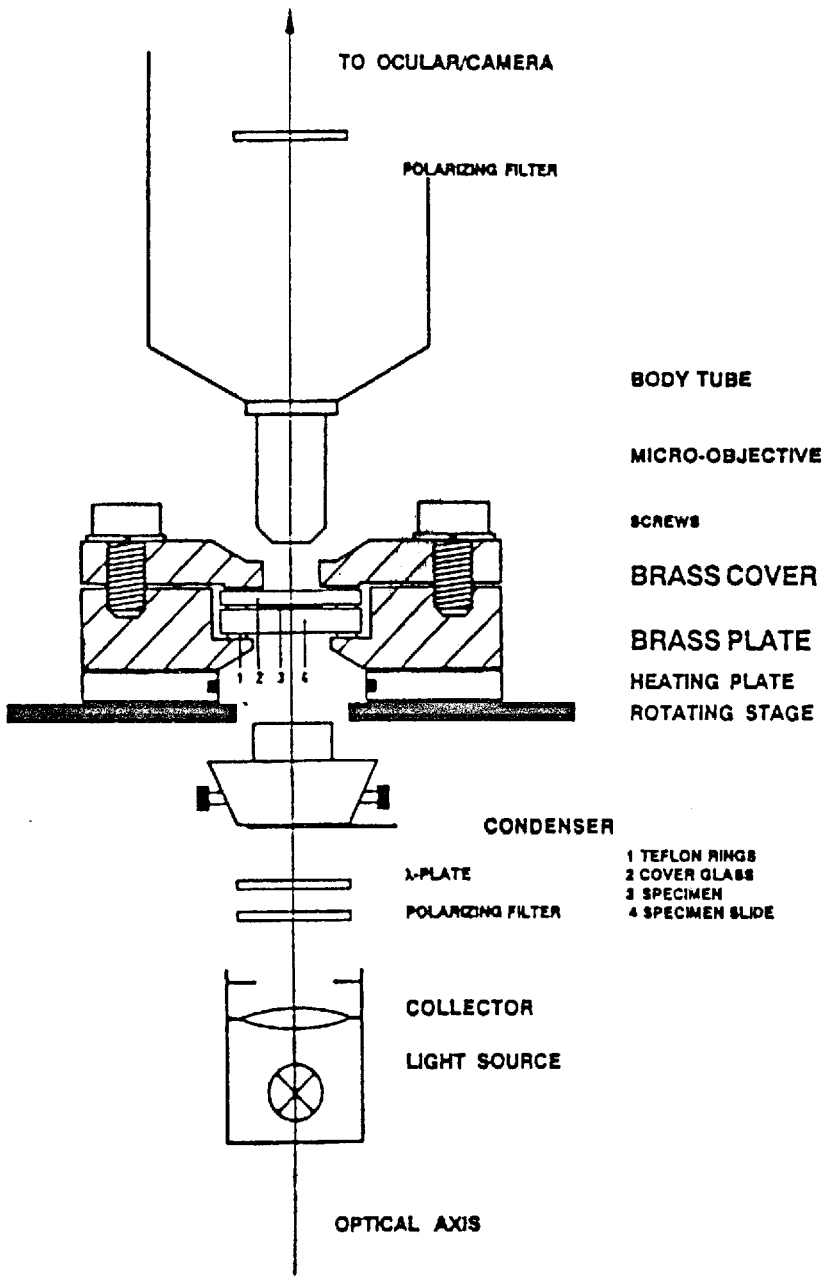

Figure 2 Pressure-chamber ; Cross section

The closed pressure-chamber is placed on the heating plate, closed with the insulation cover and the whole placed on the rotation table of the microscope. The specimen will be brought to the desired temperature by heating it up uniformly. To avoid damages to the microscope objective, this will be removed from the insulation cover during the examination pauses's and another cover placed instead. A special heat-resistant objective should be used, corrected because of the 2 mm thickness of the cover glass. For lighting one needs a condenser with a focal distance as high as possible because the distance between the glass slide and the rotating table is of a few centimeters. In order to observe the evolution of the crystallization in the cement suspension, a video camera was adapted on the microscope ocular and connected to a monitor (fig. 3). On the Fotokina International Exhibition in Cologne (October 3-10 1990) it were shown for the first time different phases of the crystallization process in cement suspensions, in their evolution, at high temperatures (ca. 200° C).

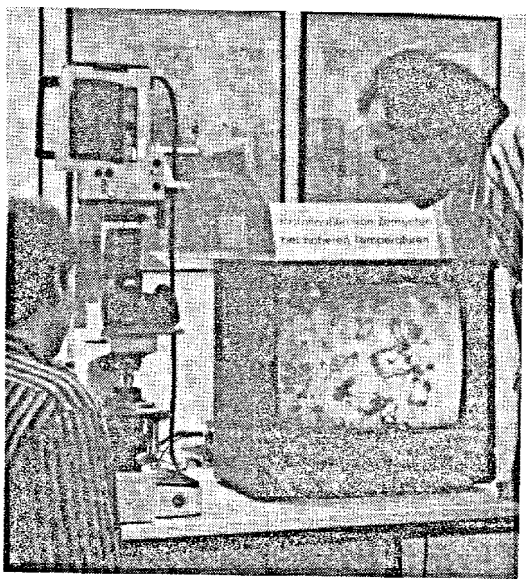

Figure 3 Television of cement suspension in evolution.

The heating table has the following performances:

- maximum current intensity (I) : 3.2 A~
- maximum current voltage (U) : 25 V~
- maximum temperature (T) : 350°C

The rise of temperature depending upon I, U and time is given in Table 1.

Table 1

I (A), U (V)	2A, 14V		2.2A, 17V						2.8A, 20V							
Minutes	5	10	13.5	15	18	20	22.5	25	27	28.5	29	32	33	35	37.5	38.5
Temperatures °C	70	98	125	137	160	167	180	194	200	210	220	230	238	248	255	260

I (A), U (V)	3A, 21.7V											
Minutes	41.5	43	44.5	46.5	48.5	49	50.5	51	52.5	53	55.5	56
Temperatures °C	270	280	287	293	307	310	318	320	329	330	338	340

3 RESEARCH ON C_4AF SUSPENSIONS

In previous research /2, 3/ the author studied the reaction of the cement and cement compounds - C_3S, C_2S and C_3A - with water at the same above temperature, mainly from the point of view structure. Now will be presented the results obtained with the pressure - chamber described above, by C_4AF suspension treated at 200° C. As element of comparison served the reaction with water at 20° C and 95° C respectively.

3.1 Preparation

For the preparation following steps are necessary. At first all the components of the pressure-chamber are to be cleaned, especially the teflon rings. In the lower brass plate will be put one teflon ring and over this, the glass slide. Another teflon ring follows. One water drop will be put on the glass slide, exactly in its midst, and after having shared the powder into the liquid, in this case C_4AF, the cover glass, followed by another teflon ring and the upper brass plate isolate the system. The two brass plates are pressed together with the screws.

3.2 Observations

The pressure-chamber is ready and the rise of temperature can begin. Some 10-15 minutes after filling it and rise of temperature, only few crystals can be seen, which are also very small. They are irregularly distributed and can be seen in polarised light, bright on a dark background. With time, the number and size of the crystals increase and their distribution is regular after ca. 2 hours. It seems that in fig. 4 besides smaller

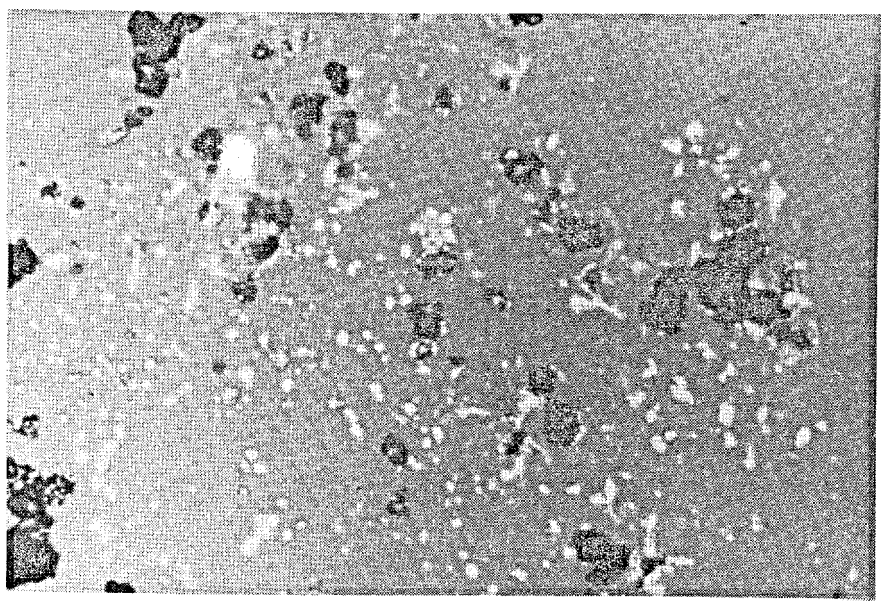

Figure 4 C_4AF suspension at 195° C (x 180)

crystals of C_3AH_6 also hematite was formed. Regularly formed, plate-shaped crystals, having essentially almost all the same size are equally distributed. Nearly these crystals, needle-shaped crystals are also formed (fig. 5a). These are comparatively fewer and irregularly distributed. They are formed on such places, where still nonhydrated particles can be found. Partly, at such places "tufted" agglomerations of needle-shaped crystals are found, which lie close together (fig. 5b).

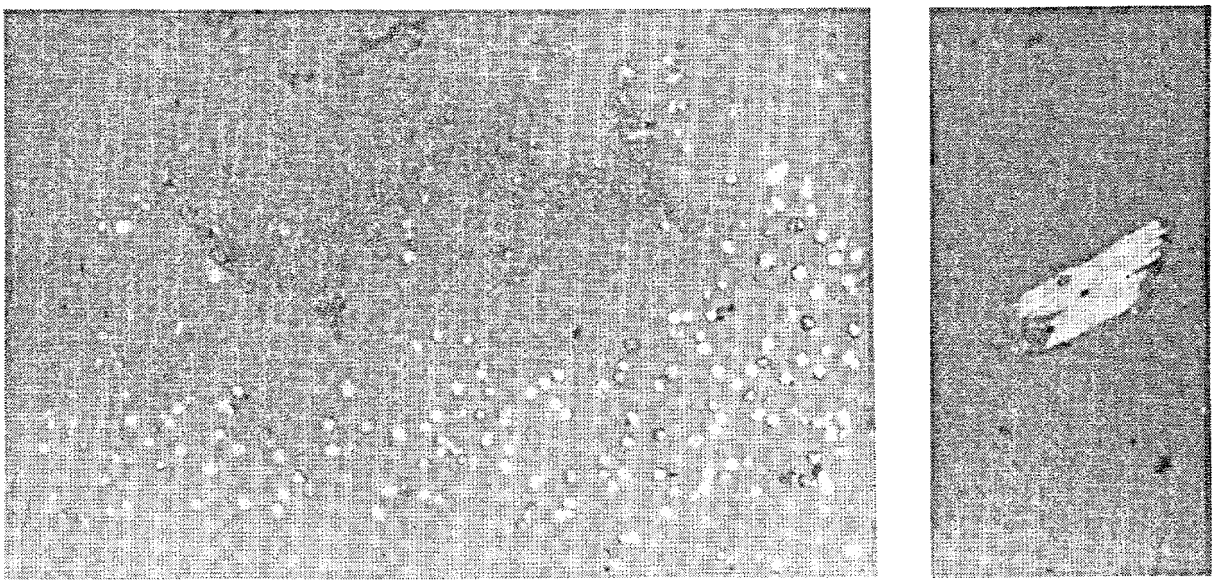

5a 5b

Figure 5 Small crystals of C_3AH_6 /a/ and needle-shaped crystals /b/ (x 170)

After ca. 30 minutes at 120° C, fine needle-shaped crystals could be seen. At the end of the treatment (running time 3 hours 50 minutes, final temperature 195° C) many brown crystals, either separately or together are to be found.They cannot be distinguished from those formed at 20° C and 95° C respectively. In addition to these, many needle-type crystals could be seen, which are finely branched themselves, and are not to be found by other temperatures. The big needles (comparable to those formed by 95° C) are not clearly defined, fact attributed to the hexagonal plate-shaped crystals formed on them and therefore their aspect is rather irregular. Regularly formed crystals of C_3AH_6 are very small but in great number, in a variety of forms such as: cubes, octahedra, do-

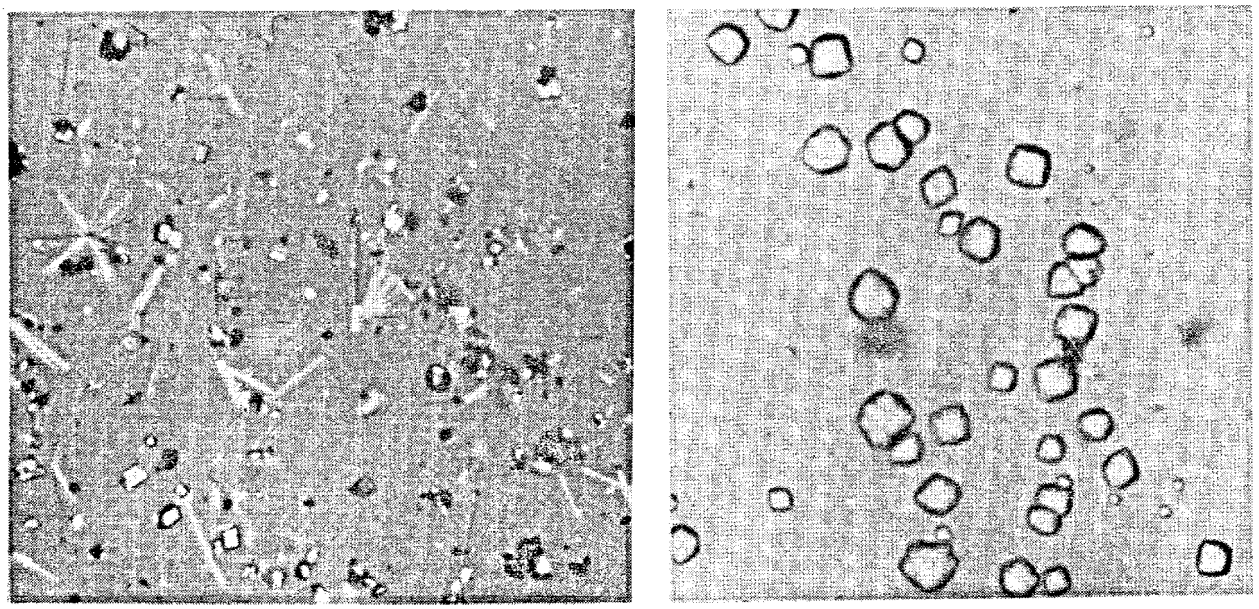

Figure 6 Aspects of C_4AF suspension at 95° C after 6 days (x 180).

decahedra, rhombic and combinations of these formes. Hereby less irregularly formed big crystals are created, as well as spatial ones. As by the suspensions at 95° C, agglomerations of very small crystals could be seen, but clearly smaller than by 95° C. Big hexagonal plate-shaped crystals are not at all present here. Adversely shows the suspension of C_4AF by treatment at 95° C very many large, well formed needle-shaped crystals, either alone or in agglomeration (fig. 6). At the same time the crystals of C_3AH_6 are also observed, but larger than by 195° C formed ones.

4 CONCLUSIONS

A pressure-chamber was presented with all constructional details. It enables to heat electrically specimens up to 350° C and to do microscopical observations under these conditions also in connection with a video camera and monitor. The results obtained on suspensions of C_4AF at 195° C are presented, comparatively with treatment at 95° C. The C_4AF reacts rapidly with water to form C_3AH_6 (but smaller crystals than by 20° C or 95° C respectively). Calcium hydroxide is not, or less than normally formed. Probably a formed CFH decomposes to $Ca(OH)_2$ and hematite.

5 REFERENCES

1. Teodoru, G.V.M.:**Zerstörungsfreie Betonprüfungen. Insbesondere Anwendung von Ultraschall. Kritische Betrachtungen**, Beton-Verlag Düsseldorf, Germany, 1989 162 pp.

2. Teodoru, G.V.M.:"Structures et résistances mécaniques sous des traitements hydrothermiques", 7th International Congress on the Chemistry of Cement, Paris, France, 1980 Vol. IV p. 318-323.

3 Teodoru, G.V.M.: "Influence des conditions de durcissement sur la durabilité de la pâte de ciment et du béton", 8th International Congress on the Chemistry of Cement, Rio de Janeiro, Brasil 1986, Vol. V p.80-84.

ON LINE BULK ANALYSIS OF RAW MATERIAL IN CEMENT PLANT BY NEUTRON IRRADIATION AND CAPTURE GAMMA RAY

J P Baron*, J Alexandre*, L Debray and X Dupont-Wavrin****

**Laboratorie Central des Ponts et chaussées (LCPC)-Nantes, FRANCE*
***Ciments Lafarge-Saint Cloud, FRANCE*

ABSTRACT

In collaboration with the "Ciments Lafarge" company, the LCPC has developed a technique involving a neutron irradiation method for on-line bulk analysis of raw material quality, on the input line to a cement plant, by determination of the following elements : Calcium, Silicon, Aluminium and Iron. A system has been built and experimented in a cement plant in actual service conditions. This system consists of a sampler placed on the on-stream line supplying the plant at a rate of 1000 tons/hour. An analyzing hopper, incorporating the neutron irradiation system consisting of a 14 MeV neutron generator tube and the gamma ray detection system comprised of a sodium iodine scintillator associated with a photomultiplier is coupled to this sampler. This system is continuously fed with the raw material to be controlled. The gamma radiation spectra supplied by the detector are analyzed on two distinct measurement channels. One of these channels processes the nuclear radiations generated by the neutron capture phenomena, whereas the other channel processes the nuclear radiations resulting from the neutron activation phenomena. Both the system and operating method have been experimented in actual service conditions. The information data collected in the said operating conditions, practically in real time, allows readings to be obtained every two minutes for Silicon, Calcium, Aluminium and Iron, as a result of a suitable processing method applied to the gamma capture and activation spectra. A comparison has been made between these measurements and the results of an analysis of the same piles conducted simultaneously through a sampling tower delivering, at an hourly rate, a sample analyzed in accordance with the fluorescent X-ray process. The comparison of the results obtained from both analyzing methods highlights the advantages featured by the neutron irradiation process.

RESUME

En collaboration avec Ciments Lafarge, le LCPC a développé une méthodologie utilisant une technique d'irradiation neutronique pour contrôler on-line la qualité de la matière crue à l'entrée d'une cimenterie, en dosant les éléments : Silicium, Calcium, Aluminium et Fer. Un dispositif a été construit et expérimenté dans une cimenterie en conditions réelles. Il comporte un échantillonneur placé sur la veine de matière alimentant l'usine à 1 000 tonnes/heure. A cet échantillonneur, se trouve associée une trémie d'analyse comportant le système d'irradiation aux neutrons constitué par un tube générateur de neutrons de 14 MeV et le système de détection gamma constitué par un scintillateur à iodure de sodium associé à un photomultiplicateur. Cet ensemble est alimenté en continu par la matière crue à contrôler. Les spectres de rayonnements gamma fournis par le détecteur sont analysés sur deux voies de mesures distinctes. L'une permet une exploitation des réactions nucléaires dues aux phénomènes de capture neutronique. L'autre permet une exploitation des réactions nucléaires dues aux phénomènes d'activation neutronique. Ce dispositif et cette méthodologie ont été expérimentés en usine dans des conditions réelles d'utilisation. Les informations obtenues dans ces conditions, quasiment en temps réel, permettent d'avoir une mesure toutes les deux minutes des quatre éléments Silicium, Calcium, Aluminium et Fer, par une exploitation judicieuse des spectres de gamma de capture et d'activation. Une comparaison de ces mesures a été effectuée avec une analyse de ces mêmes tas faite en parallèle au moyen d'une tour d'échantillonnage délivrant toutes les heures un échantillon analysé par fluorescence X. La comparaison des résultats obtenus par ces deux méthodes d'analyse met en évidence les avantages du contrôle par irradiation neutronique. Le LCPC et Ciments Lafarge ont breveté le procédé et l'installation d'analyse par cette technique et envisagent maintenant la construction d'un analyseur industriel basé sur cette technique innovante.

1. INTRODUCTION

The neutron activation and capture analyzing technique has been used for twenty years or so in specialized laboratories for the determination operations of chemical elements, generally under the form of traces in small samples. However, the particular features of neutrons have rapidly caused an evolution of the situation toward other types of determination processes offering wider applications. Indeed, this elementary particle the neutron is, may propagate over distances of several centimeters in a material subjected to neutron bombing. This particular feature of the neutron makes it the privileged particle for "sounding" the material and proves to be the means of performing a bulk analysis of the materials subjected to its irradiation without any preparation.

On the ground of these principles, the "Laboratoire Central des Ponts et Chaussées (LCPC) has developed a method aimed at determination, both on site and during drilling operations, of the major chemical elements (Si, Ca, Fe, Al) involved in the materials used in civil engineering applications. Subsequently, in collaboration with Ciments Lafarge, the LCPC has conducted further work in order to develop a method using the neutron irradiation technique for on-line bulk analysis of the raw materials supplied to a cement plant, by determination of the elements : Silicon, Calcium, Iron and Aluminium.

2. INTEREST OF RAW MATERIAL IN-FEED CONTROL IN A CEMENT PLANT

In a cement plant, keeping the quality of the cement under control is closely linked to the chemical composition of the raw material. Accurate determination of lime (CaO), Silicon (SiO2), alumina (Al203), and iron oxide (Fe2O3) contained in the raw material, enables cement clinker to be produced.

The disparity between the geological layers of the quarry causes fairly high variations in the composition of the raw material and of the four basic elements.

Currently, repeatability of component determination is obtained through pre-homogeneisation plants. Monitoring of pile average composition is performed through a sampling tower installed upstream of the prehomogeneisation plant. The tower supplies a sample, theoretically representative of the raw material before its introduction into the milling plant, and subsequently into the kiln. After preparation in the laboratory, this sample is analyzed according to the fluorescent X-ray process. Chemical corrections are then introduced at the milling stage, hereby ensuring correct dosing of the raw material. Currently, information is available only at an hourly rate, in the best conditions. The processed sample is tiny, weighing a few grammes ... and representativity problems may occur.

To gain full control over the raw material without any specific preparation process, the LCPC and Ciment Lafarge have conducted joint researches aimed at studying the possibility of using this fabulous projectile that neutron is for direct on-line analysis of the chemical composition of raw materials. Indeed, owing to essential characteristics associated with the neutron irradiation analyzing techniques, it is possible to design a neutron irradiation analyzing technique giving results on a quantity of materials 50 000 times as big as with the fluorescent X-ray technique associated with a sampling tower. In such conditions, the representativity problems are practically eliminated. Besides, this new technique can be implemented in order to give results on a quasi real time basis, thus enabling its direct insertion to be envisaged into the cement plant process, in the future.

3. PRINCIPLES DEVELOPED TO IMPLEMENT THE SYSTEM

Preliminary tests conducted in laboratory on raw material specimens and samples have enabled the definition and development of an instrumental neutron irradiation technique on the one hand, and a method on the other hand, in order to obtain signals capable of being used for the purpose of analyzing and determination of the chemical elements involved in cement fabrication. On the said basis, an experimental system has been designed to demonstrate, in a cement plant, the feasibility of the continuous control process applied to raw materials in accordance with the neutron irradiation technique, during the constitution of the prehomogeneisation piles. This system has been designed and installed in the Ciments Lafarge plant situated at Saint Pierre La Cour (France), where the experiments have been conducted.

3.1 Mechanical system

Account taken of the structure of the sampling tower in the Saint Pierre La Cour cement plant, it was decided to install an analyzing hopper in order to monitor the raw material taken by a disk type sampler scale 1/60 on the conveyor belt conveying the material into the plant. Figure 1 shows a simplified schematic diagram of the system. The analyzing hopper consists of a small inverted steel cone, 2 m high approximately, with an average diameter of 0.60 m. The selection of such a diameter is based on the necessity of irradiating the complete flux of material within a sphere of influence of the neutrons, having a radius of 0.3 m or so. The selected height eliminates the so-called "border" phenomena generated by the predictable variations of the level of material in the hopper.

A polyethylene tubing is placed in the centre of the hopper. This tubing is designed to introduce the analyzing sensor into material core.

This analyzing hopper is fed continuously. A vibration discharge system ensures continuous, fairly homogeneous flow of material within the volume of the sphere of influence.

3.2 Analyzing sensor and associated instruments

The analyzing sensor is comprised of two essential elements :

- A 14 MeV neutron generator tube enabling irradiation of the material to be analyzed. This tube is now manufactured in France by SODERN.
- A gamma ray detector consisting of a sodium iodur crystal associated with a photomultiplier. The crystal is placed at a distance of 30 cm or so from the neutron emission point. A shielding consisting of 30% bore laden polyethylene is placed between the crystal and the neutron generator tube in order to protect the crystal from the neutron flux.

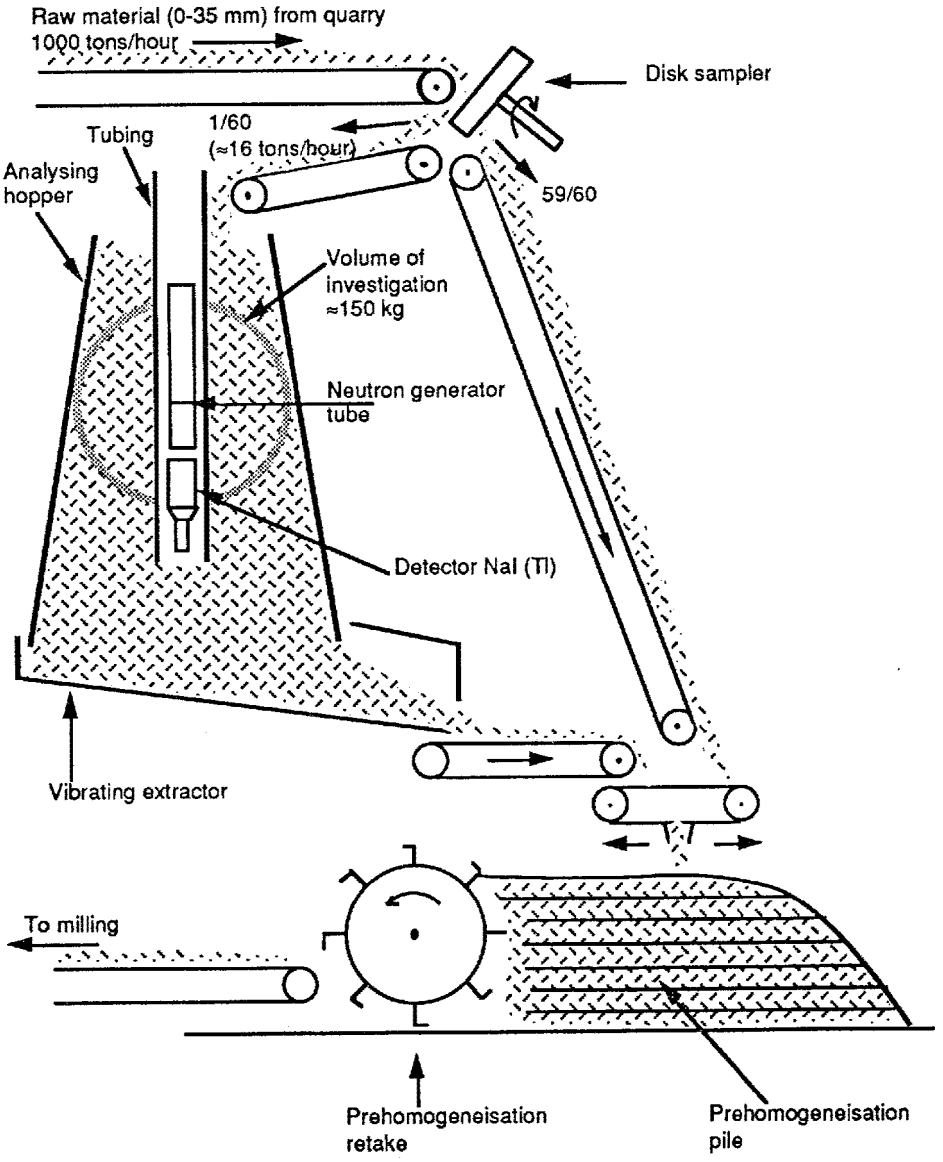

Fig. 1. Synoptic scheme of raw material analysing process by neutron irradiation

To obtain the gamma ray spectra, a high performance multi-channel analyzer is associated with the analyzing sensor. A micro-computer of the PC-AT type ensures the piloting functions of the multi-channel analyzer, processes the obtained spectra, stores the collected information and displays the results on an almost real time basis.

3.3 Operating principle of the system in the pulsed mode

Two possibilities are available to irradiate bulk material for analysis purposes : using an isotropic source, or a neutron generator tube. In the method jointly developed by the LCPC and Ciments Lafarge, the solution involving

the neutron generator tube has been retained. This choice has been made on the basis of the criteria enabling the development of an analyzing method well suited to industrial applications, while featuring high analytical performances. Indeed, the utilization of an isotropic source has the drawback of requiring the enforcement of stringent rules concerning protection and safety, especially in industrial environments. Besides, the flux of neutrons supplied by an isotropic source decreases in the long run, and emission is performed continuously. A neutron generator tube involves less stringent safety rules when operated in industrial environment, as neutron emission is controlled by electrical and electronic systems. Besides, the advantage of this particular feature is not essentialy related to the safety aspect, as neutron emission can also be envisaged in the pulsed mode. In such conditions, the analyzing methods are more widely diversified than with an isotropic source, as differentiation is possible between the various types of nuclear reactions. Figure 2 shows how the irradiation and gamma ray detection phases are organized in terms of the time.

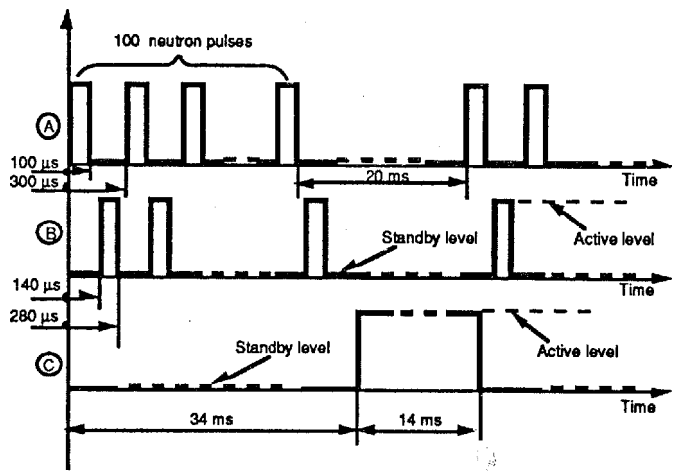

Fig. 2. Time structures of experimental conditions for neutron irradiation and gamma ray detection

Ⓐ : Time structure of neutrons irradiation pulses series

Ⓑ : Measuring channel 1 for spectrum acquisition, representative of neutron captures and neutron activation reactions

Ⓒ : Measuring channel 2 for spectrum acquisition, exclusively representative of neutron activation reactions

This pulse irradiation method and the gamma detection technique between each such pulse enables two gamma ray spectra to be obtained simultaneously. The spectrum obtained on channel 1 is representative of the activation and capture phenomena which occured in the material so irradiated. The spectrum obtained on channel 2 is representative of the activation phenomena exclusively, as sufficient time (4 milli-seconds) has been allowed to elapse after the trailing edge of the last pulse out of the 100 neutron pulses, to render this channel operative. The difference between the spectra obtained on channels 1 and 2 thus enables obtaining the spectrum representative of the capture phenomena, exclusively.

Thus, with the use of a neutron generator tube, it can be seen that a method, both original and innovative, can be developed, which does feature enhanced characteristics as compared to an isotropic source. Thus, access to the differentiation of the capture and activation phenomena is possible for interpreting the spectra.

3.4 Spectrum exploitation method

Figure 3 shows the spectra obtained after differentiation of the capture and activation phenomena. Owing to the fact that a sodium iodur detector has been used, it appeared difficult to extract the photo-electric peaks of the Compton background to set-up a process enabling determination of the chemical elements to be dosed. Our interest has been preferentially aimed at extended spectral regions enabling :

- Characterization of the concentration of an element to be dosed (Ca, Si, Al, Fe)
- Taking into account the parameters having effects on the measurement

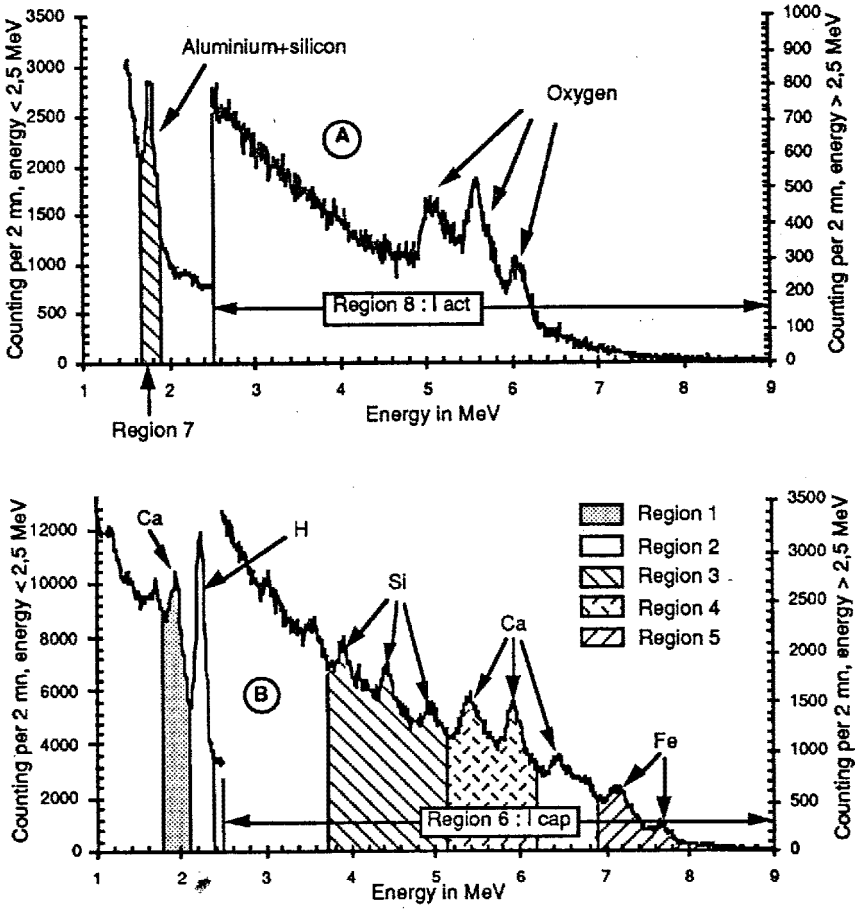

Fig. 3. Typical spectrums obtained in the analysing hopper with raw material

(A) : Spectrum exclusively representative of neutron activation reactions

(B) : Spectrum exclusively representative of neutron captures reactions

Studies have enabled regions of specific interest to be highlighted in the gamma ray radiation spectra, resulting from the capture and activation phenomena respectively. These regions of interest each encompass at least one characteristic photo-electric peak of one of the investigated elements. The studies of the said regions of the spectrum resulting from the capture phenomenon have demonstrated that the following system of equations could be established

$$C_{Ca} = (P_1 N_{Ca1} + P_2 N_{Ca2} + P_3 N_{Si} + P_4 N_{Fe})/I_{cap} + P_5$$

$$C_{Si} = (P'_1 N_{Si} + P'_2 N_{Ca1} + P'_3 N_{Ca2} + P'_4 N_{Fe})/I_{cap} + P'_5$$

$$C_{Fe} = (P''_1 N_{Fe})/I_{cap} + P''_2$$

$$C_{Al} = (P'''_1 N_{Al} + P'''_2 C_{Si}) \times I_{act}/I_{cap} + P'''_3$$

- N_{Ca}, N_{Si}, N_{Fe}, N_{Al} are the intregrals of the regions of interest retained in the spectra in association with the elements Ca, Si, Fe ands Al
- C_{Ca}, C_{Si}, C_{Fe}, C_{Al} are the concentrations of the elements Ca, Si, Fe, Al present in the material subjected to the neutron irradiation process in the pulsed mode
- I_{cap} is the integral ranging between 2.5 and 10 MeV, in the spectrum resulting from capture phenomena
- I_{act} is the integral ranging between 2.5 and 10 MeV, in the spectrum resulting from activation phenomena.

4. CALIBRATION METHOD - ACCURACY AND REPRODUC-TIBILITY MEASUREMENT

The calibration of the suggested method consists in determining the P_i coefficients of the above system of equations. This determination can be made by multiple linear regression on spectra obtained with various materials the chemical composition of which is known. Then, the proportional contents of any other unknown material can be assessed under the same conditions. The accuracies have been studied by comparisons made between the reference analysis by X fluorescence on samples, and those determined by the neutron irradiation technique. The typical

standard deviations between the differences so observed between both methods can give an idea of the accuracies in question. For analyzing times in the range of ten minutes, we have obtained for the standard deviation σ :

- For CaO $\sigma = 0.40$
- For SiO2 $\sigma = 0.40$
- For Fe203 $\sigma = 0.15$
- For Al203 $\sigma = 0.20$

On the basis of the said calibration, we have conducted an experiment bearing on repeated measurements still on the same raw material (material composition not variating in terms of the time). The purpose of these tests was to assess the accuracy and repeatability of the measurements. Knowledge of this characteristic is of high interest, as it is an expression of the intrinsic stability of the analyzing method linked to the instrumentation and count statistics.

Over an extended period of time (9 hours approximately) we have performed successive measurements of 2 mn each, on a moving average value of 5 measurements at a time. These measurements have been used to determine the four elements Ca, Si, Fe, Al. The standard deviations σ obtained on these determinations are as follows :

- For Cao $\sigma = 0.34$
- For SiO2 $\sigma = 0.37$
- For Fe2O3 $\sigma = 0.06$
- For Al203 $\sigma = 0.11$

The same experiment has been resumed two months later, and has given the same results. Under such conditions, it can be admitted that the performances of the raw material analyzing method by the neutron irradiation process are acceptable for process control purposes in a cement plant.

5. CONTROL OF PREHOMOGENEISA-TION PILES - RESULTS

Using the system and method described in the foregoing, we have followed the constitution of three prehomogeneisation piles of 12 000 tons each. The information data collected on a quasi real time basis have enabled a determination of the four elements Silicon, Calcium, Iron and Aluminium to be obtained every two minutes.

In parallel with the said tests, the sampling tower associated with the fluorescent X-ray system did supply a determination of the same elements at an hourly rate. A comparative representation of both types of measurements is given in Figure 4 for pile N° 2 (determination of Fe203 and Al203) and pile N° 3 (determination of CaO and Si02). These results have been selected as they are fairly representative of the data obtained on all piles controlled within the scope of this survey. It is noted that the results as a whole are in fairly good agreement with those obtained from the sampling tower and fluorescent X-ray system. Globally, they appear to be satisfactory for contemplating the development of an industrial analyzer based on the stated principles.

6. DISCUSSION - CONCLUSION

The tests conducted on the site at the Saint Pierre La Cour cement plant of Ciments Lafarge on the analysis of unprepared raw materials by the neutron irradiation method did constitute an important step for applying laboratory know-how to industrial process control applications. The analysis of prehomogeneisation pile follow-up in real time gave positive results.

X-RAY DIFFRACTOMETRY IN PREDICTION OF CEMENT STRENGTH

G Goswami and J D Panda

Dalmia Institute of Scientific and Industrial Research
Orissa, INDIA

SUMMARY

The paper describes a rapid method for predicting both 3-days and 28-days compressive strength (CCS) of cement mortar cubes based on X-Ray Diffractometry (XRD) of cement clinkers. The process is based on an index X derived from the ratio of XRD pulse counts (Cu-K_α) at 2 θ 30.2 (d=2.959) and 31.1 (d=2.874) corresponding to alite (hkl-202) and belite (hkl-120). The equations derived for a particular plant :

1. 3 days CCS = X x 240 kg/cm^2, when $X_n \leq 1$
   and 240 + 26 (X_n -1) kg/cm^2, when $X_n > 1$,
   where X_n maximum = 5.5

2. 28 days CCS = $C + \frac{C \times I_n}{100}$
   where C = 3 days CCS estimated by XRD
   I_n = 90-10 X_n, where X_n max = 5.5

Calculated CCS values, in average, vary from the test values by +5.9 to -5.4% in case of 3-days and by +3.8 to -3.5% in case of 28- days CCS.

INTRODUCTION

A number of attempts have been made to predict cement strength from the examination of the corresponding clinker and thus to control the clinkering process. The reported methods are generally based on microstructures and optical properties of clinker phases, phase composition and chemistry like alkali contents, phase compositions and fineness of cement and microhardness of clinker phases and hydrated and autovlaved cement. In continuation of our endeavour to develop a method for quick prediction of cement strength by X-Ray Diffractometry (1-3), a comprehensive method for prediction of 3- and 28- days compressive strength (CCS) of cement mortar is presented here.

EXPERIMENTAL

Daily average clinker samples were collected from a cement kiln and then crushed to -0.2mm size in a laboratory ball-mill. A representative sample of about 100 gm was taken from the crushed material for XRD analysis and the rest was further ground with prefixed amount of gypsum for making Ordinary Portland Cement (OPC). Physical properties of the cement samples including specific surface (Blaine) and CCS at different ages were determined according to the Indian Standard, I.S. 4031-1988.

XRD patterns of the clinker samples were taken, using Cu-K_α radiation with Ni-filter at 40 KV, 20mA. Ten seconds pulse counts were taken at 2 θ 30.2 (d=2.959 Å) and 31.1 (d=2.874 Å)corresponding to alite (hkl=202) and belite (hkl=120) respectively, and counts for back-ground were deducted from each of them. After back-ground correction, an index X_n was derived by dividing counts at 30.2 (2θ)by that at 31.1 (2θ). An example of calculation of X_n index is shown in Table-1, corresponding to Fig.1.

Table - 1

Example of calculation of X_n index from XRD pulse counts (Cu-K_α)

Scan	Pulse counts		X_α- Index
	Position A	Position B	
	2 θ = 30.2 (Cu-K_α)	2 θ = 31.1 (Cu-K_α)	Counts at A divided by Counts at B
1.	230	110	2.1 ; 2.15
2.	212	97	2.2 ;

In Fig.2, X_n is plotted against I_n, the latter being the increase of CCS from 3 days to 28 days curing, expressed as the percentage of the 3 days CCS. From this figure, it is conceivable that the index X_n has a distinct relationship with the increase of strength from 3 days to 28 days curing. Their correlation co-efficient is found to be 0.78. The same value for about 90% samples is found to be 0.88 which is significantly high. From this relationship, attempts were made to derive an equation to calculate the possible increase in strength based on the XRD index X_n. The best possible relationship is found to be :

$$I_n = 90-10\ X_n, \text{ where } X_n \text{ maximum is } 5.5 \quad (\ I\ )$$

In Fig.3, actual I_n , derived from the tested 3 days and 28 days cement strength is plotted against I_n calculated from X_n (Equation I). It is found that the calculated and actual I_n bear a high degree of positive linear correlation.

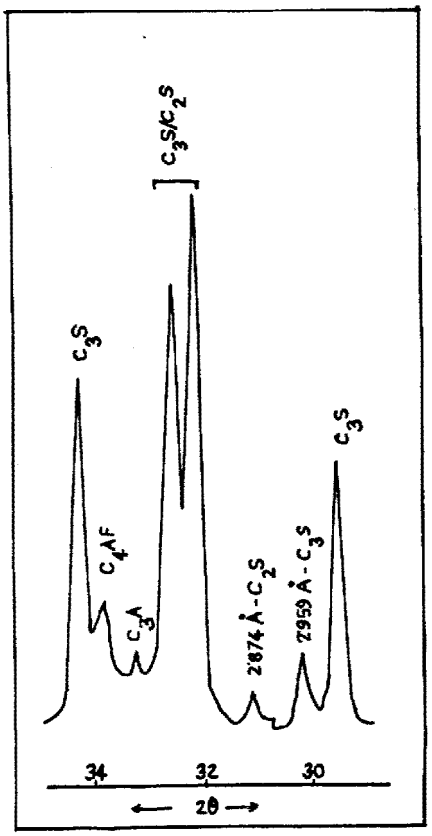

Fig.1 XRD pattern (Cu-K_α) of cement clinker, showing the diffraction peaks (d= 2.959 and 2.874 Å) taken for X_n index.(common cement notations are used).

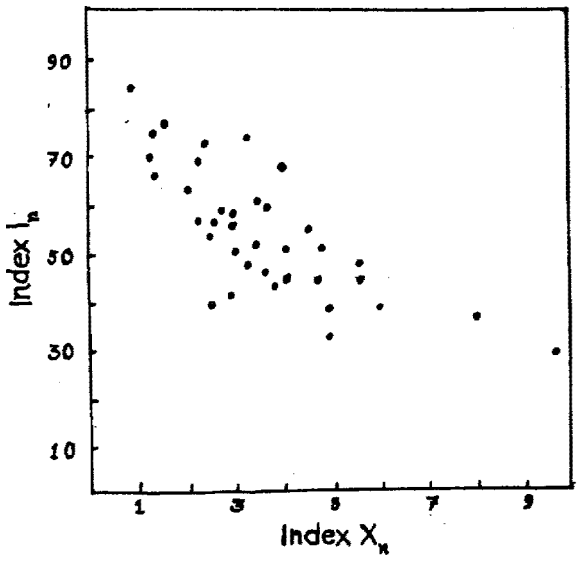

Fig.2 Relation between the Index X_n and I_n.

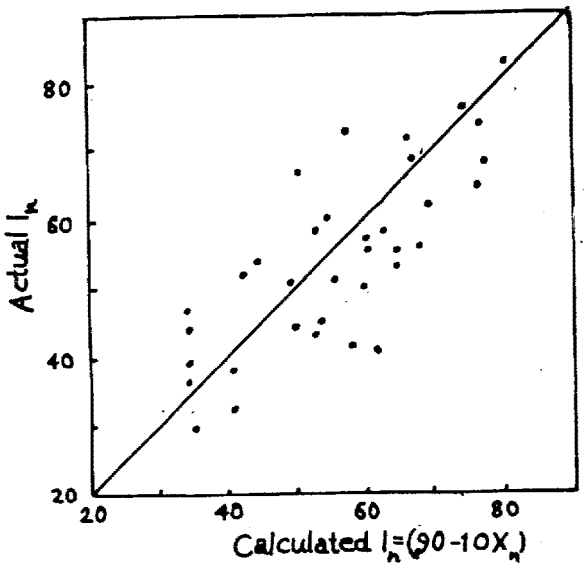

Fig.3 Relation between the actual and calculated I_n.

RESULTS

3-Days CCS

The possible relationship between the index X_n and 3 days strength (CCS) of the cement mortars was attempted in different ways. The best relationships derived between them are as follows :

When $X_n < 1$, 3 days CCS = $X_n^2 \times 240$ kg/cm^2 (II)

When $X_n > 1$, 3 days CCS = $240 + 26 (X_n - 1)$ kg/cm^2 ,

where X_n maximum = 5.5 (III)

The relationship between the tested and calculated CCS values is shown Fig.4. Their correlation co-efficient is found to be 0.88. The average tested and clculated CCS values of 42 samples are 296.4 and 294.7 kg/cm^2 respectively. In average calculated CCS values vary from tested values by + 5.9 to -5.4% only. Root mean square error is 6.33. Inspite of having wide variation in tested CCS values (195 to 360 kg/cm), predicted strength values for 33 of the samples are within 100 kg/cm^2 of the former.

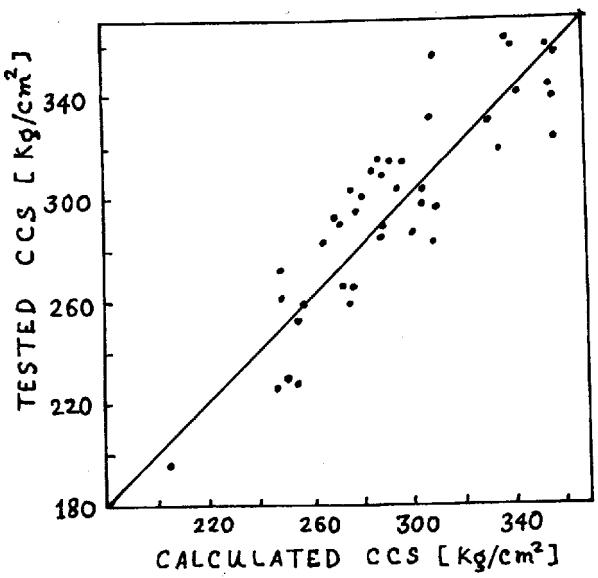

Fig.4 Relation between the tested and calculated 3 days CCS (kg/cm^2).

28-Days CCS

As I_n is the increase of CCS from 3 days to 28 days curing, expressed as the percentage of the former, it is conceivable that

$$\text{28 days CCS becomes} = \text{3 days CCS} + \frac{\text{3 days CCS} \times I_n}{100} \quad \text{(IV)}$$

An illustration of calculation of CCS from X_n is given below :

$X_n = 2.0$

So $I_n = 90-10\ X_n = 90-20 = 70$ (I)

$$\text{3 Days CCS} = 240 + 26\ (X_n - 1)\ \text{kg/cm}^2 \quad \text{(III)}$$

$$= 240 + 26\ (2-1)\ \text{kg/cm}^2$$

$$= 266\ \text{kg/cm}^2$$

$$\text{Hence 28 days CCS} = \text{3 days CCS} + \frac{\text{3 Days CCS} \times I}{100}\ \text{kg/cm}^2 \quad \text{(IV)}$$

$$= 266 + \frac{266 \times 70}{100} = 452\ \text{kg/cm}^2$$

(Tested value = 457 kg/cm^2)

Applying the equation IV, 28 days CCS of 35 samples were calculated from their calculated 3 days CCS. It is found that averages of calculated and tested 28 days CCS of 35 samples are 464 and 462 kg/cm^2 respectively. Variation of the calculated CCS from the tested values is in average within + 3.8 and - 3.5%.

The predicted CCS values for 50% of the test samples are within 10 kg/cm^2 or about ± 2% of the test values. Tested and calculated 3- and 28- days CCS values of cement mortars at different X_n levels ranging from 0.8 to 5.5 (at an interval of 0.5) are shown in Table-2. It is found that while both 3- and 28- days CCS, in general, increase with the increase of X_n, the range of variation in 28- days CCS is much less than that in 3 days.

Table - 2

Tested and calculated 3- and 28-Days CCS of cement mortar samples at different X_n levels (Plant I)

X_n	I_n	CCS (kg/cm^2)			
		3 Days		28 Days	
		Tested	Calcu-	Tested	Calcu-
0.8	82	195	192	357	349
1.5	75	255	253	450	443
2.0	70	282	266	457	452
2.5	65	294	279	451	460
3.0	60	308	292	461	467
3.5	55	302	305	483	473
4.0	50	302	318	454	477
4.5	45	329	331	508	480
4.9	41	343	341	474	481
5.5	35	338	357	498	482

Prediction for a second plant

Applicability of the method was further examined by testing clinker and corresponding cement samples from another plant. Examination of 18 samples shows that X_n ranges from 1 to 2.8. The equations for 3 days CCS were derived as :

When $X_n < 1$, 3 days CCS = $X_n \times 276$ kg/cm^2

When $X_n > 1$, 3 days CCS = $276 + (X_n - 0.5)\ 90$,

where X_n maximum = 2.0

The average testedf and calculated CCS values of 18 samples are 372.8 and 374.8 kg/cm^2 respectively. Variation of calculated CCS from the tested values in average is within ± 3.6 %.

For this plant, I_n is found to be 65-10 X_n, where X_n max. = 2.0 28 days CCS values were calculated using the equation IV. It is found that averages calculated and tested CCS values are 552.8 and 559.4 kg/cm^2 respectively. Variation of the calulated CCS from the tested values in average is within + 4.0 and -3.6 %.

DISCUSSION

The d - spacings 2.959 and 2.874 Å, taken for calculation of X_n, are the characteristics of alite and belite phases respectively. Thus X_n shows the relative amount of alite present in the clinker, although it is not the ratio of the actual amounts of alite and belite present. As the early and late strengths of cement is generally guided by alite and belite contents respectively, it is conveivable that the higher X_n causes higher 3 days CCS and lower degree of strength increase at a later stage (28 days). The reverse is the case with lower X_n. This is reflected in an almost inversely proportional relationship between X_n and I_n (Fig.2) and in the fact that the variation in 28 days CCS values is much less than that in 3 days.

The equation derived is applicable for ordinary portland cement of a significantly wide range of fineness and SO_3 contents, e.g. in the first plant fineness varied from 2780 to 3125 Cm^2/gm and SO_3 contents from 1.5 to 2.1%, with tested 3 days CCS ranging from 195 to 360 kg/cm^2 . However, as each kiln and kilns in each plant are known to have their individual characters, which controls the clinker quality, it is accepted that any regressive equation, based on microscopic examination of clinker is limited to one kiln only (4) and none of the equations without any modification are universally applicable (5-10). Thus cements having much differences in physical and chemical parameters and in pyro-processing may need a little modification in the present equiation derived for 3 days CCS and also in determination of I as found in cases of the two plants examined here. As the 28 days CCS is derived from the calculated 3 days CCS and I_n , the equation for the same does not need any modification.

CONCLUSION

The method developed can predict 3- and 28- days strength of cement mortar with negligible variations from the conventionally tested values. The method is very rapid and actual testing time is around 15 minutes only. The data are collected from the display of the XRD unit and thus the method avoids any element of personal judgement involved in microscopic method. As the test results are achievable within a very short time, the method coupled with the XRD test for clinker burning condition (11) can be used for any corrective measures that may be necessary in the kiln for the control of the clinker quality.

ACKNOWLEDGEMENT

The authors are very grateful to Mr.A.H.Dalmia, President, Messrs Orissa Cement Limited, Rajgangpur for his keen interest in the study and thanks the colleagues for their help in testing the Cement samples.

REFERENCES

1. Goswami, G., "Quick Prediction of Cement Strength by X-Ray Diffractometry" TIZ Int. Powder Magazine 1989, 113 (10) 819-820.

2. Goswami, G. & Panda, J.D., "X-Ray Diffractometry in defining the increase of cement strength from 3 days to 28 days curing" Indian Cem. Review 1990, 5 (3) 25-27.

3. Goswami, G. & Panda, J.D. "Quick Prediction, of 28 days cement strength by X-Ray Diffractometry" TIZ Int. Powder & Bulk Mag. 1991, 115 (5) 208-210.

4. Ono, Y., "Microscopic observation of clinker for the estimation of burning condition, grindability and hydraulic activity" 3rd Int. Conf. on Cem. Micr. Houston, 1981, 198-210.

5. Relis, M., Ledbetter, W.B. & Harris, P. "Prediction of mortarcube strength from cement characteristics" Cem. Conc. Res. 1988, 674-686.

6. Fundal, E. "Optical measurements of cement clinker" World Cem. 1982, 13 (8) 318-24.

7. Aldridge L.P. "Accuracy and precission of an X-Ray Diffraction method for analyzing portland cement" Cem. Conc. Res. 1982, 12 437-46.

8. Campbell, D and Weiss, S. "Some effect of kiln atmosphere and flame shape on clinker characteristics" 9th Int. Conf. on Cem. Micr., Reno, 1987, 147-64.

9. Arbelaez, C. "Problem in Cement strength decrease and its solution using microscopy" 10th Int. Conf. on Cem. Micr., Antonio 1988, 178-201.

10. Aizawa, T., Nakase, K. and Deguchi, Y. "Advanced control system for cement plants" Journ. Res. Onoda Cem. 1991, 43 (124) 44-55.

11. Goswami, G., Mohapatra, B.N. & Panda, J.D. "Characterization of Burning condition of cement clinker by X-Ray Diffractometry", Cem. Conc. Res. 1991, 21 (6) 1176-79.

INFLUENCE OF VARIOUS CEMENT TYPES ON CONCRETE DURABILITY IN MARINE ENVIRONMENT

Shigemi Sakoda*, Nobufumi Takeda and Shigeyuki Sogo****

**Tokai University, JAPAN*
***Obayashi Corporation, JAPAN*

[SUMMARY]

To evaluate the durability of a reinforced concrete structure in a marineenvironment, it is important to know the state of progress of reinforcing bar corrosion in the concrete. Exposure tests in a marine environment of concretes using various types of cement were performed to grasp the permeation velocities of chloride ions into concrete and the condition of progress of reinforcing bar corrosion.

In this paper, the diffusion coefficient of chloride ions in concrete is determined based on diffusion theory, and the results of prediction and analysesof long-term permeation quantities are described. The influences of environmental conditions and cement varieties on the progress of reinforcing bar corrosion in concrete are touched upon.

As a result of exposure tests, it was recognized that permeation ofchloride irons and progress of corrosion of reinforcing bars are slow. As fordurability of structures, it was revealed that conditions are severest in the order of parts in the splash zone, underwater, and in air offshore.

These results are considered to be effective for establishing a design method for offshore concrete structures considering design service life and environmental conditions.

1. Introduction

Concrete structures in marine environments are adversely subject to the gradual penetration and accumulation of chloride ions, in such a way that the rate of penetration can affect a structure's durability, while the amount of accumulation is critical in the growth of rebar corrosion. The penetration rate can vary according to such factors as environment, cement type, and construction conditions, however the extent to which these factors contribute to rebar corrosion has not been fully discussed. This paper reveals the results of the study on long-range estimation analysis of chloride ion penetration and the influence of chloride ions on the growth of rebar corrosion in concrete made using various types of cement, based on exposure tests in marine environments.

2. Test and Analysis Methods

2.1 Test Specimens

Two types of specimens were prepared: columns (cylinders) with 15 cm diameter and 15 cm length, and prisms simulating beams 90 cm long with embedded rebars. Fig.1 shows the shape and dimensions of the beam specimens. Deformed steel bars with 19 mm diameter were embedded in the beam specimens with a covering depth of 2 cm, with some of them being prepared with construction joints in the center or cracks of 0.05 - 0.1mm wide. Some of the side of the beam specimens were coated with epoxy resin, to allow unidirectional penetration of chloride ions.

Table 1 shows the mix proportions of concrete used for specimens. Four types of cement were used : normal portland cement (NP), blast furnace slag cement type-B (BB), sulfate resisting portland cement (SR), and normal portland cement of which 15% was replaced with silica-fume (SF). Table 2 shows the chemical composition of the cements. Physical properties of the other materials are shown in Table 3.

2.2 Environmental Conditions of Exposure

The specimens were exposed to three environments : in the splash zone of a mole affected by the tide (A), in seawater at a depth of about 11m below the surface of the sea (B), and in the marine atmosphere over the pier (C) of Shimizu Port, opening to the Pacific Ocean. Table 4 shows the environmental conditions of the exposure test site.

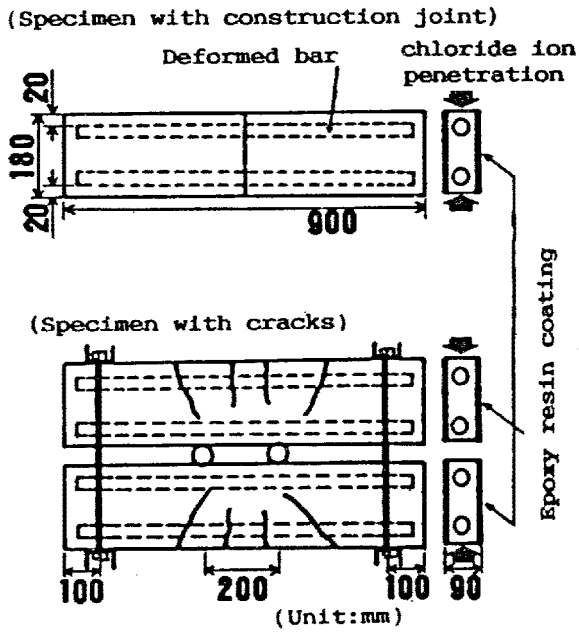

Fig. 1 Shape and Demensions of the Beam Specimens

Table 1 Mixture Proportion of Concrete

Type of cement	Gmax (mm)	W/C* (%)	s/a (%)	Unit weight (kg/m³) W	C	S F	WRA	HRWR
N P	15	50.0	48.0	168	332	–	0.83	–
B B				162	324		0.81	
S R				166	332		0.83	
S F				166	282	50	–	6.48

C* = C+SF, SF=silica-fume
WRA :Air-entaining water-reducing admixture
HRWR:High-range water-reducing admixture

Table 2 Chemical Composition of cements

Type of cement	Chemical Composition (%) igloss	insol	SiO_2	Al_2O_3	Fe_2O_3	CaO	MgO	SO_3
N P	0.6	0.3	21.7	5.3	3.0	64.7	1.3	2.2
B B	0.9	0.5	25.2	7.3	2.2	57.5	2.8	1.7
S R	0.8	0.1	22.1	4.1	4.5	64.3	1.0	1.9

Table 3 Physical Properties of Materials

Materials	Physical Properties
Slica-fume	·Specific gravity 2.25 ·average diameter 0.36 m ·SiO_2 92.6%
Fine aggregate	·Pit sand ·Fineness modulus 2.67 ·Specific gravity 2.58 ·Absorption 1.64%
Coarse aggregate	·crushed stone ·maximum size of aggregate 15mm ·Specific gravity 2.66 ·absorption 1.09%
Air entaining water-reducing admixture	Lignin sulfonic acid
High-range water-reducing admixture	Lignin sulfonic acid

Table 4 Environment Condition of Exposure

position		Environment Condition
A	Splash zone	Between H.W.L.(+1.7m) and L.W.L.(0.0m)
B	Underwater	Average tempartuer 18.4 ℃, pH 8.29 Chloride ion concentration 18.4 ‰ Insoluble oxygen 7.98ppm
C	marine atmosphere	Zone of 5m higher than L.W.L. Affected by spindrift and sea dreeze

Table 5 Measurement Items and Method

Items	Method
Concrete quality	Compressive strength, Modulus of ststic elasticity
Chloride ion content	Quantitative determination of total saites by potentiometric titration using chloride ion selective electrodes
Rebar corrosion	Sketch the corroded parts and assess by percentage of corrosion area
Self potentials of rebar	In compliance with ASTM C 876, using saturated copper sulfate solution as reference electrodes

2.3 Measurement Items

Measurements were taken at ages of 1, 3 and 6 years (5 years for SF). Table 5 shows the measurement items and methods. Concrete powders taken from the column specimens at intervals of 2 cm in depth were used for chloride ion content analysis. Corrosion of rebars were examined by overhauling the beam specimens.

2.4 Method of Analysis for Chloride Ion Penetration

Diffusion of chloride ions is generally expressed by Fick's Law, Equation (1) below [1]. In this study, a specimen's surface chloride ion content (Co) and diffusion coefficients (Dc) in Equation (1) were calculated by least squares from the content of chloride ions measured at 3 and 6 years of exposure.

$$C = Co \left\{ 1 - \mathrm{erf} \left(\frac{x}{2\sqrt{Dc \cdot t}} \right) \right\} \quad \cdots\cdots \quad (1)$$

x : Depth below surface (cm)
t : Elapsed time (Sec)
C : Chloride ion content at a depth of x cm (%)
Co: Chloride ion content at surface (x=0) (%)
Dc: Diffusion coefficient of chloride ions (cm^2/sec)
erf: Error function $\mathrm{erf}(x) = 2/\sqrt{\pi} \int e^{-t}\, dt$

3. Results of Tests and Analysis

3.1 Change in Concrete Quality

Change in the compressive strength of the specimens over time is shown in Fig. 2. Submerged NP, BB,and SR specimens showed greater compressive strengths than the control speciments under standerd curing from the age of 1 year to 3 years, but at the age of 6 years the strengths of NP, BB and SR decreased by 10% , 9% and 5% , respectively, from those at 3 years. The specimens exposed to the marine atmosphere showed similar compressive strengths to the controls from the age of 1 year to 3 years, but they showed a reduction in strength at 6 years: NP by 8%, BB by 6% and SR by 6%. The compressive strength of the SF specimens reductions from the ages of 3 to 6 years were 7% in the sea and 3% in the air.

It is considered that in the marine environments ettringite is formed by the reaction between tricalcium aluminate (C_3A) in the cement gel and sulfate in the seawater. This results in a tightening of the composition of the concrete by filling in voids, as well as an increase in the compressive strength up to an age of 3 years, whereas thereafter the ettringite swells to cause a decrease in the compressive strength. This tendency is particularly noticeable in NP, which contains a large amount of tricalcium aluminate.

3.2 Penetration of Chloride Ions

The amount of chloride ion penetration in NP specimens after 6 years of exposure is shown in Fig. 3. The penetration amount is the greatest in the splash zone specimens, followed by those in the sea and in the air in descending order. Chloride ion contents at the surface of the specimens in the sea were 2.5 times greater, and those in the splash zone were 3 times greater than those in the air.

Fig. 4 shows the amount of chloride ion penetration in various types of concrete specimens exposed in the sea and in the air. In the seawater the chloride ion contents in BB were greater than in NP from the surface of the specimens down to the depth of 3cm, whereas they were smaller than in NP further inside. Those in SR were as great as in NP, while those in SF were smaller than in NP. In the marine atmosphere the penetration amounts of chloride ions were almost the same regardless of the types of cement.

In Fig. 5 changes in the penetration contents over the years are shown. Up to 3 years of exposure the chloride ion contents at the surface of NP, BB and SR both in the sea and in the air increased, but they tended to remain constant thereafter. Up to 5 years of exposure those in SF continued to increase. Thus,the penetration rates varied depending on the types of cement used.

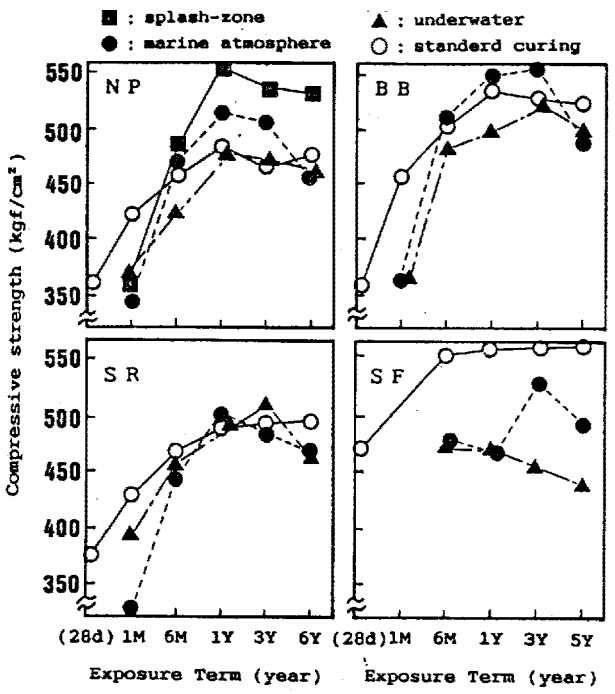

Fig. 2 Change in the Compressive Strength over Time

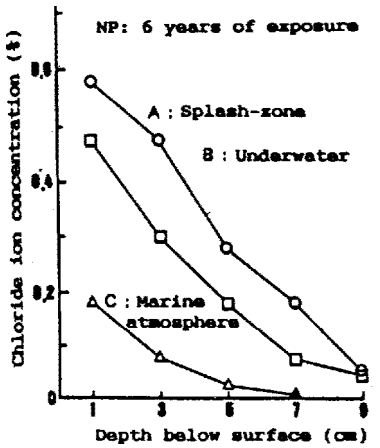

Fig. 3 Amount of Chloride Ion Penetration after 6 years of Exposeur (in NP)

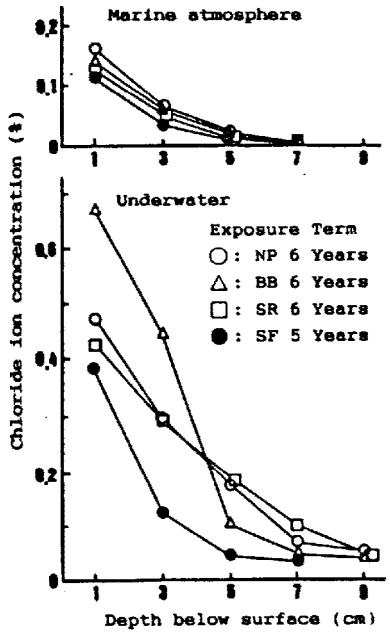

Fig. 4 Amount of Chloride Ion Penetration in Various Types of Concrete

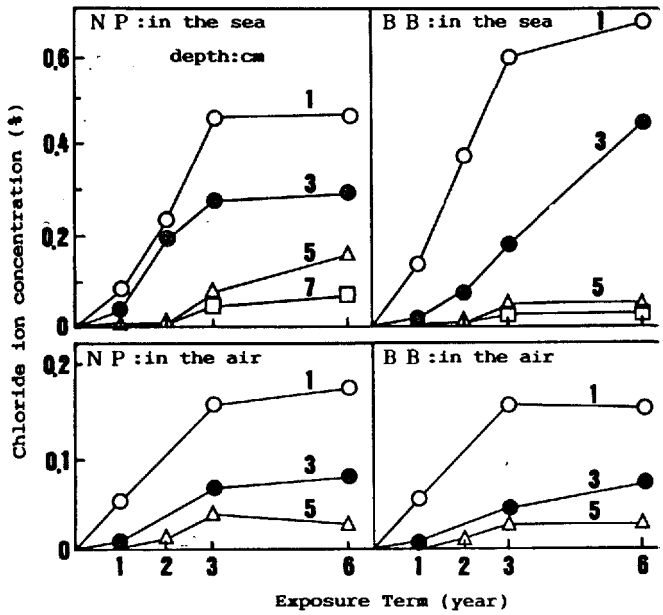

Fig. 5 Changes in the Penetration Conteuts over the Years

Table 6 Surface Chloride Ion Concentration and Diffusion Coefficient

Condition of mix and environment		Surface chloride ion concentration Co(%)			Diffusion Coefficient Dc($\times10^{-8}$cm^2/sec)		
		3 Y	6 Y	ave.	3 Y	6 Y	ave.
N P	A	0.74	0.70	0.72	4.9	4.5	4.7
	B	0.61	0.57	0.59	3.9	3.1	3.5
	C	0.20	0.24	0.22	3.2	1.2	2.2
B B	B	0.76	0.87	0.82	2.2	2.1	2.2
	C	0.20	0.21	0.21	2.7	1.5	2.1
S R	B	0.55	0.50	0.53	4.7	4.0	4.4
	C	0.17	0.16	0.17	4.7	1.6	3.2
S F*	B	0.32	0.39	0.36	1.9	1.8	1.9
	C	0.11	0.19	0.15	4.0	1.2	2.6

* Calculation value for measurement at age of 5 years

3.3 Result of chloide Ion Penetotation Anarysis

The amount of chloride ion penetoration at 3 and 6 years (5 years for SF) of exposure were substituted into Fick's equation. The obtained values of chloride ion concentration at the surface (Co) and Diffusion coefficients (Dc) are shown in Tabel 6.

In the marine atmosphere the chloride ion concentration at the surface (Co) values were in the range of 0.15- 0.21%, regerdless of the types of cement, whereas in the seawater the contents varied with the types of cement: BB, NP, SR, and SF in descending order. The Co values under the sea were 3-4 times greater than those of the specimens in the air of the same mix design.

The diffusion coefficients (Dc) in the air showd on great differences among the cement types: all of them fell in the range of 2.6~3.2 $\times10^{-8}$ cm^2/sec. The diffusion coefficient of air exposed specimens may fluctuate greatly in the environmental conditions where wave and wind influence is strong.

No great differences were observed among the submerged speciments, due to the stable environmental conditions there, but the diffusion coefficients varied with regard to the types of cement : SR, NP, BB, and SF in descending order. Therefore, it was confirmed that the presence of blast furnace slag and silica-fume in cement have the effect of inhibiting chloride ion penetration concrete.

The surface concentration of chloride ions and diffusion coefficients for NP specimens in the splash zone were as great as 0.72% and 4.7 $\times10^{-8}$ cm^2/sec : in the splash zone the rate of chloride ion penetoration was higher than in the other two environments.

3.4 Long-Range Estimates of Chloride Ion Penetration

Fig. 6 shows the results of chloride ion penetration estimations for 10 and 50 year spans, calculated using the values shown in Table 6. In the air, no wide variations are estimated in the concrete's chloride ion penetration distribution in 50 years. Under the sea, it is estimated that it will take longer for the same amount of chloride ion to penetrate deep into BB and SF than into NP concrete, due to the smaller diffusion coefficients of BB and SF than that of NP concrete.

Table 7 shows the projected chloride ion contents in concrete at a depth of 10 cm in 10 and 50 years. The chloride ion amount in 10 years at a depth of 10 cm are estimated to be 0.83, 1.58,and 0.92 for BB, SR, and SF in the air, compared with NP as 1, while in the sea the amounts are estimated at 0.59, 1.21, and 0.17 for BB, SR and SF. The effect of inhibiting chloride ion penetration by blast furnace slag and silica-fume is expected to continue even after 10 years of exposure to marine environment.

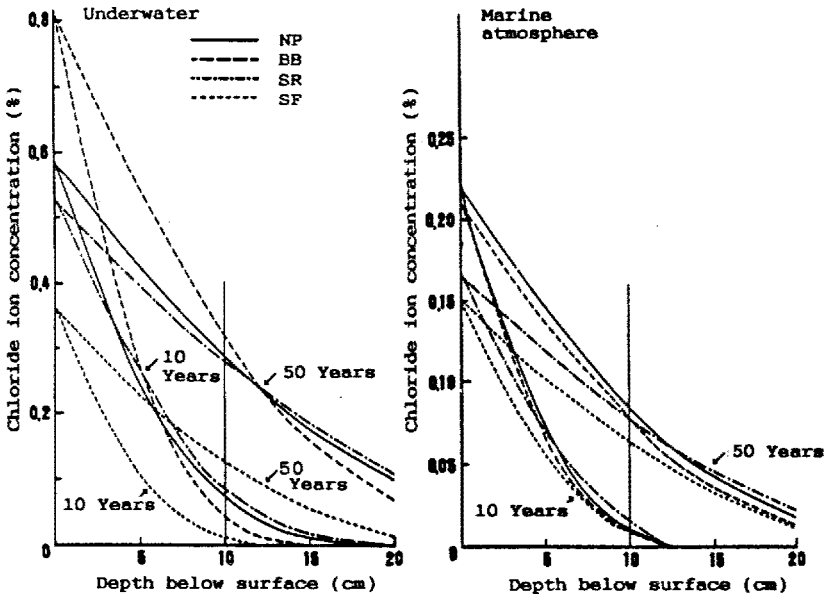

Fig. 6 Chloride Ion Penetration Estimation for 10 and 50 Year Spans

Table 7 Chloride Ion Content in 10 and 50 Years after

Condition of mix and environment		Chloride ion content at a depth of 10cm(%)	
		10 years	50 years
NP	A	0.137	0.400
	B	0.076	0.293
	C	0.012	0.086
BB	B	0.045	0.320
	C	0.010	0.080
SR	B	0.092	0.287
	C	0.019	0.081
SF	B	0.013	0.133
	C	0.011	0.064

BB and SR both in the sea and in the air are estimated to have the same amount of chloride ions as NP at a depth of 10 cm from the surface after 50 yeras. In SF, however, the level is estimated to be 25 ~50% lower than in NP.

If NP is used, the chloride ion level in the air exposed concrete is estimatated to be 1/6 of the level of the submerged concrete, and the level in the splashed zone exposed is estimated to be 1.8 times as high as the submerged concrete after 10 years. Compared with the submerged concrete, the figures for the air exposed concrete and splash zone concrete are estimated to be 1/3 and 1.4 times as high after 50 years.

3.5 Growth of Steel Corrosion in Concrete

Fig. 7 shows the percentages of corrosion area on the rebars in the beam specimens and also chloride ion amounts in the covering concrete. Corrosion was observed after 1 year of exposure in the splash zone, and it developed rapidly as the years exposure increased. On the other hand, in the submerged NP specimen, corrosion area increased when the chloride content was over about 7 kg/m^3 (0.3% concentration) , but scarcely any growth of corrosion was observed between 3 and 6 years of exposure. This delay in corrosion growth may be due to the low oxygen supply in the sea.

Although the amounts of chloride ions in the covering concrete of BB and SF were as high as more than 7kg/m^3 after 5 or 6 years of exposure, no corrosion was observed on the rebars. This suggests that the threshold values of chloride ions necessary to initiate corrosion of rebars are higher in BB and SF than in NP. In the air exposed specimens the chloride ion levels in the covering concrete were in the range 1.0~2.0 kg/m^3, and no corrosion was observed in concrete of any cement type.

Thus the splash zone was found to be the most corrosion environment, followed by the seawater (about 10m deep) and the marine atmosphere environments in descending order.

3.6 Influence of Cracks and Construction Joints on Rebar Corrosion

Fig. 8 shows the changes in chloride ion levels at the suface of cracks and construction joints and the changes in rebar corrosion area percentage. In all three environments corrosion was initiated earlier in the speciments with cracks. Since the chloride ion levels at the surface of the cracks are no greater than those of the specimens with no cracks, it is considered that the accelerated initiation of corrosion is due to the direct access of oxygen and chloride ions to the rebars through the cracks.

Submerged specimens with cracks displayed larger area of corrosion than those with no cracks, but the speed of corrosion development was slow. The decreased rate of corrosion development may be due to the low supply of oxygen in the sea. In the air exposed specimens corrosion development was also slow : the reason may be because the passive film of

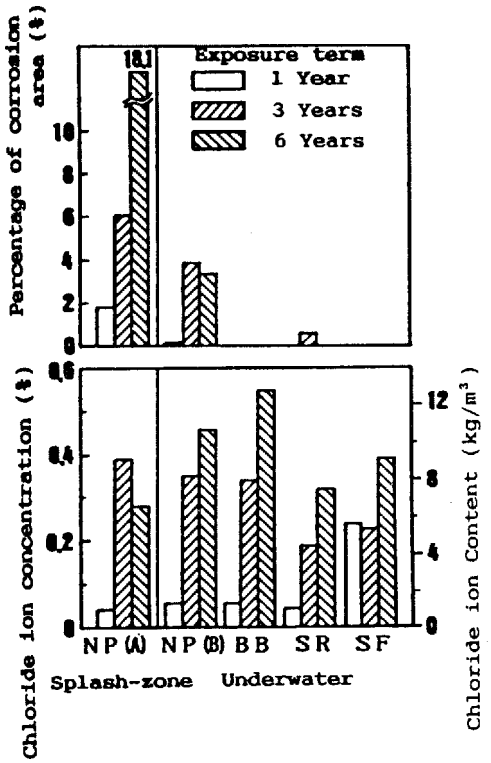

Fig. 7 Percentages of Corrosion Area on Rebars and Chloride Ion Amount in the Covering Concrete

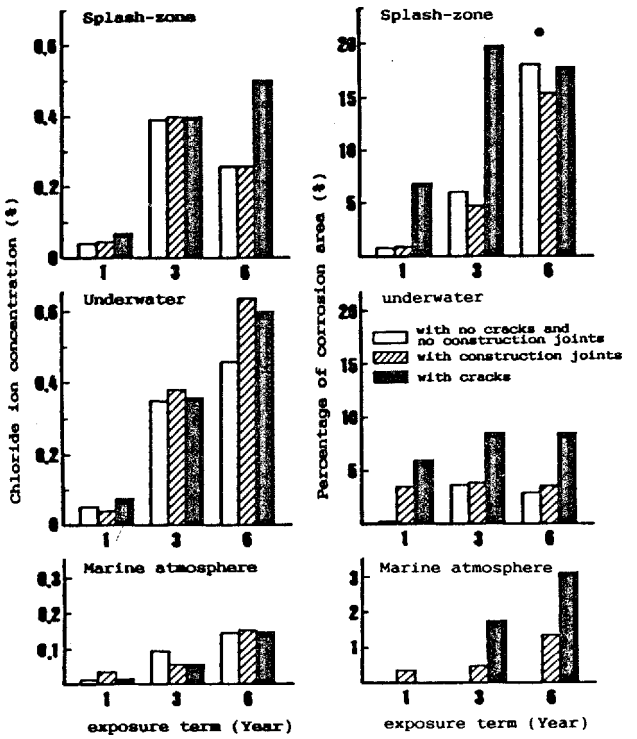

Fig. 8 Changes in Chloride Ion Levels at the Surface and in Rebar Corrosion Area Percentage of Cracks and Construction Joints

therebars were not destroyed completery, due to the insufficient penetration of chloride ions. The rapid corrosion development in the splash zone exposed speciments may due to sufficient supply of oxygen and chloride ions.

Cracks in concrete in marine in environments accelerate corrosion. Corrosion is initiated at construction joints if there are any. These joints are weak point from the standpoint of corrosion prevention. Special care should be taken in the construction of such joints.

4. Conclusion

The following conclusions are obtained from the study:

(1) In marine environments ettringite is formed as a result of a reaction between tricalcium aluminate (C_3A) in cement gel and sulfates in sea water, and it gradually fill voids in the concrete,densifying the composition and increasing the compressive strength up to an age of 3 years. However, thereafter the ettringite swells futher, to cause a decrease in strength.

(2) From the chloride ion penetration levels obtained from the marine environment exposure tests, their diffusion coefficients through concrete specimens were caluculated; it was revealed that the coefficient are small in the specimens containing blast furnace slag and silica-fume, thus demonstrating that both are capable of inhibiting chloride ion penetration.

(3) In the splash zone environment rebar corrosion develops more rapidly than in other environments, due to sufficient oxygen supply, high chloride penetration, and the presence of the appropriate amount of water. In the seawater and in the marine atmosphere corrosion develops relatively slowly if either oxygen or chloride ions is insufficient.

Reference

[1] R. D. Browne: Mechanism of Corrosion of Steel in Concrete in Relation to Design, Inspection and Repair of Offshore and Coastal Stractures, ACI SP-65, 1980 ,etc.

AN APPROACH TO THE PREDICTION OF PORTLAND CLINKER GRINDABILITY AND STRENGTH BY MICROSCOPY

Yushiro Kihara*, Sergio L Centurione and Flavio Andre da Cunha Munhoz****

**Universidade De Sao Paulo*
***Associacao Brasileira De Cimento Portland*
Sao Paulo, BRAZIL

S U M M A R Y

Grindability and cement strength development are influenced by raw mix characteristics and clinker portland manufacturing process. The clinker microstructure analysis brings important technological data for monitoring cement manufacturing stages and for prediction of the potential grindability and strength.

A laboratorial expeditious method for clinker grindability and 28 days cement strength prediction was developed based on microscopic parameters obtained by reflecting light microscopy and on clinker fineness data.

Correlation calculations show that grindability is lowered when the ***mineralogical coefficient*** (KM = alite/belite x 1/Ø alite) decreases. Clinker fine fraction (<4,8mm) also influences adversaly the grindability. The potential strength development of clinker could be estimated using the ***mineralogical coefficient*** and clinker fineness data.

1 INTRODUÇÃO

The evaluation of clinker grindability and prevision of its 28 days strength are themes of technological interest in the portland cement industry. Important contributions were given by SCHEUBEL & BALZER[1], ONO[2], KNÖFEL[3], HARGAVE et al.[4], BRUGGEMAN & BRENTRUP[5], among others, which demonstrated that besides clinker compositional factors, textural characteristics and the presence of minor components have significant effect of the clinker comminution process and cement strength development.

The final portland cement strength depends on its binding capacity (cement quality), porosity and pore structure of the system[6]. The possibility of expressing mathematically the cement strength is based on parameters such as phase content, chemical composition and fineness.

The purpose of this paper is to present an expeditious method for clinker grindability and 28 days cement strength prediction in a quick and simplified way, thus completing the microscopical control of portland clinker manufacturing conditions.

2 ACTING FACTORS ON CLINKER GRINDABILITY AND CEMENT STRENGTH DEVELOPMENT

The behaviour of clinker fragmentation is determined by its specific energy of rupture, microfissure sizes and characteristics of the mineralogical phase[7]. The porosity, granulometry and clinker texture also affect the clinker grindability.

Alite (C_3S) is the most fragile mineralogical component of clinker, followed by C_3A, C_4AF and belite (C_2S)[7]. SCHEUBEL & BALZER[1] verified that alite and belite contents and crystal sizes have an important bearing on grindability. Belite cluster is one of the most important parameters on clinker comminution[8].

The interstitial phase (C_3A and C_4AF), free lime and periclase also act on clinker grindability, but less pronouncedly than silicatess (alite and belite). Their influences are masked by other more significative parameters.

Clinker porosity favours fineness increase of the grounded product, but for specific areas above 200m^2/kg this influence is less pronounced[9,1]. On the other hand, the grindability of clinker is reduced when the proportion of dust is increased, rising the power consumption[10].

The cement strength development depends fundamentally on the compositional and mineralogical characteristics of portland clinker. Each of the portland clinker phases contributes to the strength development, and the extent of its effects change in time and intensity among these phases. The silicates, mainly C_3S, have a well-marked effect on all age strengths in [6].

A good statistical correlation between 28 days strength and clinker phase composition is shown by the KNÖFEL factor ($3C_3S + 2C_2S + C_3A - C_4AF$). Small (30-35 μm) and well shaped alite crystal favours the grindability and the 28 days strength in [6].

The cement fineness has a decisive influence over the reaction kinetics. Increasing fineness rises the reaction surface and consequently improves the cement hydratation rate and the strength development.

Several investigators have proposed methods for strength prediction based on combination of chemical (e.g. Bogue's composition, soluble alkali, sulphates), mineralogical and physical (e.g. fineness, water/cement ratio) parameters. Taking into account the complexity of hydration process and many factors which interact in the cement components reactivity, there is no consensus about the most adequate parameters to foresee the 28 days strength. Most of the proposed methods do not have much application in routine characterization, due to the analitical diversity and complexity.

3 EXPERIMENTAL

Twenty nine Portland clinker samples obtained from 13 Brazilian plants were studied. They were produced from raw materials with distinct geological and chemical characteristics. For cement strength studies 12 experimental samples were prepared from 2 manufacturing units (plants A and B).

3.1 Optical Microscopy

The studies of clinker microstructure and mineralogical composition were carried out through reflected light microscopy.

The results of clinker microstructure studies referring to silica grinding conditions and alite size together with clinker mineralogical compositions obtained by point counting of clinker phases are summarized in *Table 1*.

3.2 Expeditious Analysis of Grindability

An expeditious analysis of grindability was developed for 150g clinker samples, comminuted for 5 minutes in a Herzog disk mill, with useful capacity of $350cm^3$, without a central grinder body. Previously, the sample was quartered, dried and crushed (< 4,8mm). Afterwards, the fineness was determined through 37 μm sieve residue, by mechanical sieving.

Table 1 shows the fineness obtained through the proposed method together with *mineralogical coefficient* values (KM) calculated through alite/belite ratio, alite size and fine fraction contents (<4,8mm) obtained through clinker granulometrical analysis. Two out twenty nine samples were eliminated in the statistical correlation analysis because their values fell away from the average and presented different characteristics: high KM (A-5) and low interstitial phase content (M-29).

3.3 Compressive Strength analysis

The 3, 7 and 28 days compressive strengths (*Table 2*) were determined in 12 laboratorial cements, obtained from portland clinker samples from plants A and B.

The experimental cement samples with 4% of natural gypsum were prepared from 5kg of material, previously crushed (<0,2cm) and comminuted in ball mill until a defined Blaine fineness ($364 \pm 10 m^2/kg$) was attained. The grinding times needed for obtaining the desirable fineness were used in calculation of Blaine/time expression (*Table 2*).

4 RESULTS AND DISCUSSION

Statistical studies of correlation between the fineness (% >37μm), obtained by expeditious analysis of grindability, and mineralogical coefficient KM (alite/belite x 100/Ø alite) showed a correlation coefficient of r = 0,90, while the mineralogical coefficient between the fineness (% >37μm) data and clinker fine percentage (<4,8mm) was r = 0,63, in a whole of 27 samples (*Figures 1A* and *1B*).

These results obtained showed to be valid for clinker grindability in a 99% probability level, thus allowing the following considerations:

a) the clinker grindability is improved when KM increases. However, this correlation is not linear for KM values higher than 40 (sample A-5);

b) the unsatisfactory quartz grindability leads to belite clusters formation, which promotes a decrease in alite/belite proportion, low KM (<12) and fineness values (*Figure 1A*), favouring dust formation;

c) clinkers with KM values higher than 20 are considered of better grindability while those with KM values smaller than 12 are of difficult grindability, with a higher power conssumption; and,

d) clinkers with low content of interstitial phase (<10%) may present an easier grindability than expected (sample M-29).

Calculation of multiple linear correlation among clinker fineness data (represented by >37μm residue), mineralogical coefficient KM and clinker fines percentage, in a whole of 27 samples from 12 plants, showed a correlation coefficient r = 0,91 explicit in the following equation:

Fineness = 34,1283 - 0,3052 KM + 0,0126 fines

The standardized partial regression coefficients are -0,860 and 0,069 for mineralogical coefficient KM and clinker fines percentage, respectively, showing the significative influence of the mineralogical coefficient on grindability.

With the purpose of investigating the influence of mineralogical and physical parameters: fineness, (obtained by expeditious analysis of grindability), KM, *KNÖFEL* factor and Blaine/t values were undertaken. These studies were developed in 12 experimental clinker samples prepared with clinkers from two plants (A and B). *Table* 3 contains these results.

TABLE 3 - Results of simple linear correlation (r) between cement strength and the following parameters: fineness (>37μm), mineralogical coefficient (KM), *KNÖFEL factor* and Blaine/t.

Compressive strength (days)	Coefficient of linear correlation (r)*			
	Fineness (fraction >37μm)	KM	KNÖFEL	Blaine/t
3	0,80	0,78	0,58	0,70
7	0,85	0,89	0,66	0,86
28	0,90	0,88	0,75	0,92

* for a probability of 99% and a whole of 12 samples, the correlation is valid when r >0,71.

The analyses of these values permits the following considerations:

a) the best correlation indexes were obtained through 28 days strength;

b) the clinker grindability, represented by fineness (% >37μm) has an important role in cement strength development: the better the grindability, the higher the strength (*Figure 1C*);

c) the mineralogical coefficient (KM) also has an influence on strength development: the higher the alite/belite ratio and the smaller the alite size, the higher the strength, represented by high KM values (*Figure 1D*);

d) the correlation coefficient obtained for the *KNÖFEL factor* (r = 0,75) was the smallest among the choosen parameters; and,

e) the Blaine/t ratio, where t is the time necessary to attain the desired fineness, showed a good correlation with 28 dayss strength, thus showing the importance of clinker grindability for clinker fineness.

Statistical studies of multiple linear correlations among 28 days strength and the choosen parameters (fineness, KM and *KNÖFEL factor*) showed the best correlation between the mineralogical coefficient (KM) and the fineness (% >37μm) resulting in the following equation:

28 days strength = 46,5073 - 0,3058 x fineness + 0,0556 KM,

when the correlation coefficient is r = 0,93 and the standardized partial regression coefficient are -0,0564 and 0,394 for fineness and mineralogical coefficient (KM), respectively.

Statistical studies permit to conclude that microstructural and compositional characteristics have a strong influence on clinker grindability, permiting a valuation of its brittleness, notwithstanding the greatly different range of clinker samples (27), produced from distinct raw materials and under different manufacturing conditions. In addition, although in a more restricted universe of samples (12), it was observed that the utilization of mineralogical parameters and fineness data permit a valuation of potential clinker strength development.

5 FINAL CONSIDERATIONS

The studies undertaken showed that, among the chemical, mineralogical and granulometrical parameters, the compositional and textural characteristics of calcium silicates are those which have the largest influence over clinker grindability, the larger alite frequency and the minor alite crystal size favouring the clinker grindability. On the other hand, the minor frequency of belite, mainly in clusters, decreases the clinker grindability. These parameters can be related through a mineralogical coefficient (KM), represented by the product between alite/belite ratio and the inverse of alite size (KM = alite/belite x 100/Ø of alite). KM increases with clinker grindability, but it is poorly affected by fine fraction (clinker fraction < 4,8mm). Clinkers with KM values higher than 20 are considered of good grindability and lower than 12 of difficult grindability (hard clinker). Likewise, KM values also has an influence on strength development: the higher the KM values, the higher the strength.

The clinker grindability has an important bearing on cement fineness: the better the grindability, the smaller the power consumption (to obtain the desired fineness) and the higher the cement strength. The statistical correlations between clinker fineness, obtained through an expeditious method of clinker grindability, and mineralogical coefficients (KM) make it possible to estimate the potential development of clinker strength and the grindability. Occasional changes of clinker grindability and cement strength can be antecipated through this proposed method, allowing for a quick performance of the operator on clinker manufacturing processes.

REFERENCES

1. Scheubel, B. & Balzer, H.J.: "Microscopic examinations of cement clinker using the linear traverse technique for determination of clinker grindability". Zement-Kalk-Gips, 34(11):624-627, nov.1983.

2. Ono, Y.: "Microscopical estimation of burning condition and quality of clinker". In: **INTERNATIONAL Congress on the Chemistry of Cement, 7th**, v.2, I-206-11, Paris, 1980.

3. Knöfel, D.: "Relationship between chemism, phase content and strength in portland cements". Zement-Kalk-Gips, 32(9):448-54, set.1979.

4. Hargave, R.V., Venkateswaran, D., Deshmukh, V.V. & Chatterjee, A.K.: "Quantification of OPC clinker microstructure - An approach for prediction of cement strength". In: **INTERNATIONAL Congress on the Chemistry of Cement, 8th**, v.2, 167-172, Rio de Janeiro, 1986.

5. Bruggeman, H. & Brentrup, L.: "Correlation between mineralogical clinker parameters and cement strength". **PROCEEDINGS of the Eleventh International Conference on Cement Microscopy**, 226-245, 1989.

6. Odler, I.: "Strength of Cement (final report)". Materials and Structure, 24:143-157, mar.1991.

7. Hornain, H. & Regourd, M.: "Fissuration et broyabilité du clinker". In: **INTERNATIONAL Congress on the Chemistry of Cement, 7th**, v.2, I-276-81, Paris, 1980.

8. Dorn, J.D.: "The influence of coarse quartz in kiln feed on the quality of clinker and cement". **PROCEEDINGS of the Seventh International Conference on Cement Microscopy**, 10-23, 1985.

9. Decker, M.: "The grindability of cement clinker". Zement-Kalk-Gips, Wiesbaden, v.25, n.9, sept.1972, p.445-48.

10. Buchanan, C.E.Jr. & Bayles, H.J.: "Effects of clinker size on grindability". **PROCEEDINGS of the Seventh International Conference on Cement Microscopy**, 196-212, 1985.

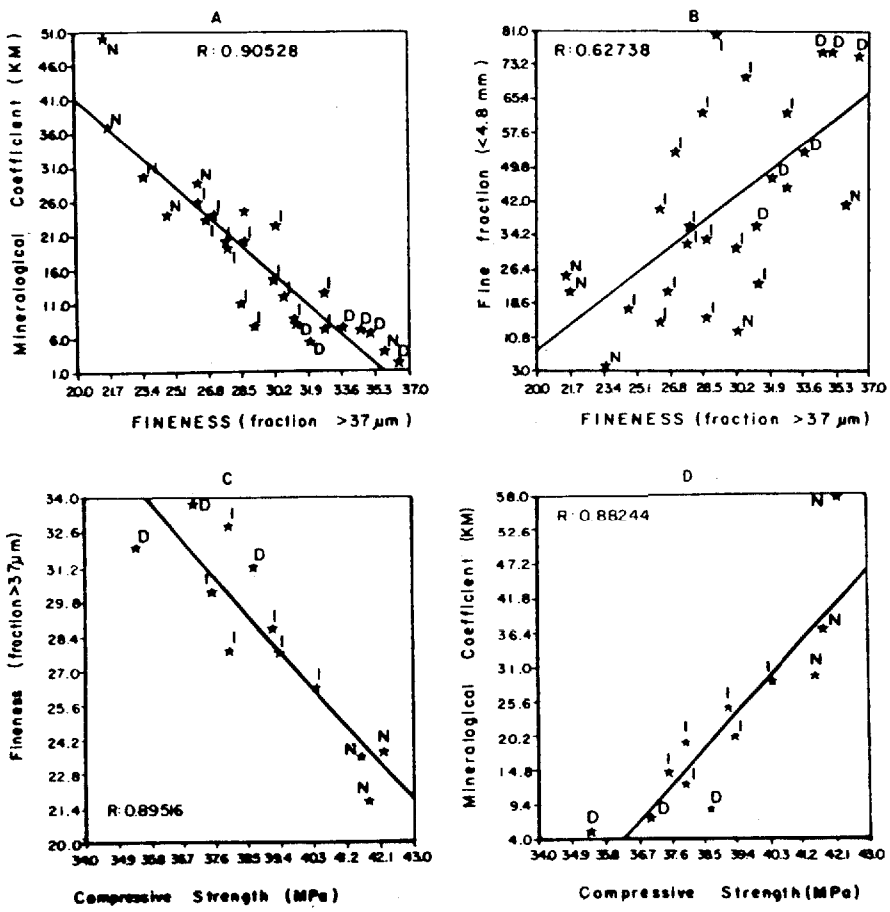

FIGURE 1 – Graphics of linear regression analyses comprising fineness, mineralogical coefficient, compressive strength and fine fractions, associated with silica grinding conditions (N = normal, I = unsatisfactory and D = deficienty).

TABLE 1 - Microscopic analyses, mineralogical coefficient, fine fraction and fineness of clinkers samples.

Sample (plant-Nº)	Silica grinding conditions	Alite Size (μm)	Mineralogical Composition						Mineralogical coefficient (KM)	Fine Fraction (<4,8mm)	Fineness (fraction >37μm)
			alite	belite	C_3A	C_4AF	Free CaO	Periclase			
A-1	I	30	68,2	9,3	3,8	12,1	1,8	4,8	24,4	33	28,7
A-2	N	35-40	69,8	6,3	4,2	14,2	0,3	5,2	29,5	4	23,5
A-3	I	30	67,5	11,3	3,6	12,1	1,3	4,2	19,9	32	27,7
A-4	N	30-35	72,9	6,1	2,8	14,1	0,1	4,0	36,8	21	21,7
A-5	N	35	74,3	3,7	3,3	12,8	0,9	5,0	57,4	18	23,7
A-6	I	30-35	72,2	7,8	3,5	12,3	0,2	4,0	28,5	14	26,3
B-7	I	40-45	67,0	11,0	4,3	13,1	1,1	3,5	14,3	31	30,2
B-8	I	50	64,6	10,4	5,3	15,4	1,3	3,0	12,4	45	32,8
B-9	D	50	59,8	16,7	6,9	12,2	1,1	3,3	7,2	53	33,7
B-10	D	55-60	64,1	13,0	5,0	14,4	0,8	2,7	8,6	36	31,2
B-11	D	45-50	54,2	22,2	3,0	14,2	3,0	3,4	5,1	47	32,0
B-12	I	50	70,3	7,4	4,6	13,6	1,0	3,1	19,0	36	27,8
B-13	D	55	60,6	17,1	16,6		1,7	4,0	6,4	76	35,1
B-14	D	40-45	57,9	20,1	15,9		1,8	4,3	6,8	76	34,6
C-15	I	30	67,8	9,8	6,6	11,3	3,3	1,2	23,1	21	26,7
C-16	I	35-40	70,2	7,3	5,1	14,9	1,6	0,9	25,7	40	26,3
C-17	I	35-40	70,8	7,9	4,6	14,0	2,1	0,6	23,9	53	27,1
D-18	I	50-55	63,7	17,6	2,7	14,6	0,4	1,0	6,9	62	32,8
D-19	D	40-45	37,9	43,5	16,1		1,0	1,5	2,0	75	36,5
D-20	I	45	65,1	12,3	19,0		2,8	0,8	11,8	70	30,7
E-21	N	40-45	76,5	3,6	17,6		0,5	1,8	50,0	25	21,5
F-22	I	25-30	65,0	21,6	5,8	6,3	1,3	-	10,9	62	28,5
G-23	N	70-80	57,8	21,5	3,3	15,8	0,4	1,2	3,6	41	35,8
H-24	I	25-30	67,1	12,2	4,7	8,7	2,1	5,2	20,0	15	28,7
I-25	N	50	74,7	6,7	15,8		0,9	1,9	22,3	12	30,3
J-26	I	35	72,1	8,6	4,9	9,0	2,1	3,2	23,9	17	24,7
K-27	I	30-35	56,8	23,7	10,4	6,7	1,0	1,4	7,4	80	29,2
L-28	I	40-45	59,3	17,8	8,7	11,2	0,2	2,8	7,8	23	31,3
M-29	D	34	61,4	28,4	8,6	1,3	0,3	-	6,4	13	23,1

N - normal D - deficient I - unsatisfactory

TABLE 2 - Compressive Strength and Fineness Results of Laboratorial Cements

Sample (plant-Nº)	Blaine ($m^2.kg^{-1}$)	Blaine/Time ($m^2.kg^{-1}m^{-1}$)	Compressive Strength (MPa)		
			3 days	7 days	28 days
A-1	367	6,12	27,6	33,6	39,2
A-2	374	6,68	30,3	35,5	41,6
A-3	366	6,10	28,8	33,9	39,4
A-4	369	6,96	33,4	35,8	41,8
A-5	360	6,42	32,7	36,6	42,2
A-6	358	6,50	29,4	33,9	40,4
B-7	362	5,25	27,4	33,2	37,5
B-8	358	5,77	27,4	32,8	38,0
B-9	355	4,61	27,4	32,5	37,0
B-10	372	5,47	30,2	33,0	38,7
B-11	372	4,13	26,2	30,5	35,4
B-12	370	5,98	27,2	32,2	38,0

EVALUATION OF CEMENT CLINKER FOR ESTIMATION OF COMPRESSIVE STRENGTH BY OPTICAL MICROSCOPY

L H Rao, P K Akhouri and S K Sinha

National Council for Cement and Building Materials
New Delhi, INDIA

SUMMARY

The paper highlights the application of microstructural and granulometric studies of portland cement clinker to estimate its 28-day compressive strength. The various microstructural parameters and physical and chemical characteristics of large number of industrially produced Indian cement clinkers from different processes, such as wet, semi-dry, dry and vertical shaft kiln were studied in detail. Polished clinker samples were analysed and the regression analyses were carried out on the data obtained. The result off statistical analysis showed that definite quantity of silicate phases in a particular grain size range of a clinker exhibited characteristic compressive strength pattern. Further multi statistical analysis of the four optical parameters viz (i) phase quantity of alite, (ii) phase quantity of belite, (iii) average grain size of alite and (iv) average grain size of belite, selected as significant parameter has led to the development of a mathematical model for rapid measurement of 28-day compressive strength of cement.

INTRODUCTION

Optical microscopic study of cement clinker is an important technique in identifying the parameters responsible for contributing appreciably to compressive strength. Even when more sophisticated and advanced laboratory tools are available in cement research, microstructural study still remains a useful and a frequently employed supplementary technique in systematic study of portland cement for estimation of 28-day compressive strength.

The study of microstructural and morphological characters of clinkers are used to substantiate burnability result. Microstructural parameters such as the shape, size of alite and belite, as well as the nature of grain boundaries play a major role in the hydraulic property of clinkers and their 28-day compressive strength.

Based on the careful perusal of several earlier attempts (1,2) for the estimation of compressive strength of cement, the National Council for Cement and Building Materials (NCB) has developed a quick and comprehensive technique (3) taking into account four optical parameters. viz (i) phase quantity of alite, (ii) phase quantity of belite, (iii) average grain size of alite and (iv) average grain size of belite,This technique has served as a viable physical method for quality control of OPC. The present study mainly deals with granulometry for establishing grain size ranges vis-a-vis compressive strength.

METHODOLOGY

The clinker samples collected from various processes were embedded in epoxy resin and subjected to vacuum impregnation. After final grinding, polishing was done on the satin cloth using 9,6 and 3 micron diamond lapping compound and studies were conducted in reflected light.

QUANTIFICATION OF ALITE, BELITE AND THEIR GRANULOMETRY

Grain size was measured by a polarising microscope, with a micrometer attached to the ocular. The calibrated values of the micrometer are easily converted to actual grain size, using polarising constant. The phase quantities were determined by point counting developed by Chayes (4). The averaging of grain size was done after observing the distribution of grains in different size ranges (5). The grain size measurements were carried out on a large number of grains so as to represent the different size ranges. The distribution of alite and belite in different range intervals is represented by histograms.

Correlation of Alite Grain Size with 28-Day Compressive Strength

The general behaviour of the alite grain size with respect to cement strength is such that increases in grain size lead to decreases in 28-day compressive strength whereas detailed granulometric study revealed that the 28-day compressive strength varies with different grain size ranges. Alite contents of 30-40% with grain size range 20-25μm increase cement compressive strength. Beyond 25μm, no change in strength is observed, whereas cement with 40-45% alite content exhibited a gradual decrease in cement strength with increasing grain size; alite contents between 45-50% showed a sharp decrease in strength even for small variations of grain size. Alite contents of 50-55% in the 12-15μm size range showed increases in strength, while for 15-22μm, the strength gradually decreased (Fig 1).

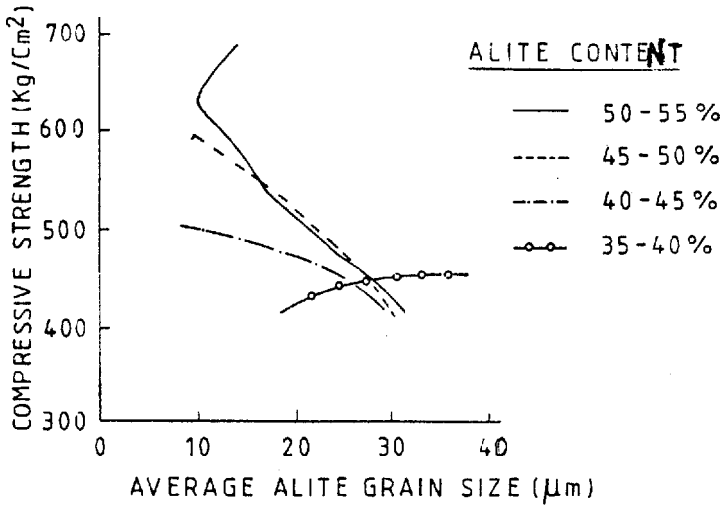

FIG 1 BEHAVIOUR OF ALITE GRAIN-SIZE WITH RESPECT TO 28 DAY COMPRESSIVE STRENGTH

Correlation of Belite Grain Size with 28-Day Compressive Strength

The general behaviour of belite grain size is such that increases in grain size shows increases in strength. The belite content of 10-25% showed a sharp decline of strength in the 15-18μm size range, whereas a content of 25-30% showed increase in strength with the increase in the grain size, to about 605 kg/cm. Beyond this limit the grain size of belite had no influence on the strength characteristics. It was observed that for 30-35% of belite content, a small increase in the grain size led to appreciable increase in strength (Fig 2).

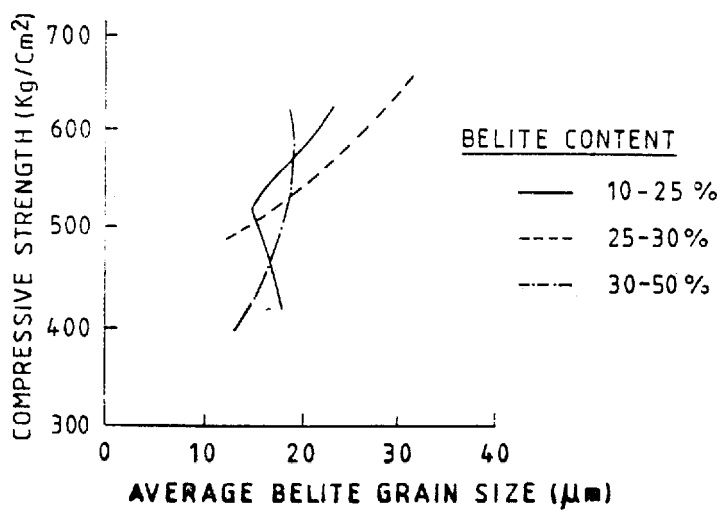

FIG 2 BEHAVIOUR OF BELITE GRAIN-SIZE WITH RESPECT TO 28 DAY COMPRESSIVE STRENGTH

Histograms were plotted from the data obtained on alite (Fig 3) and belite (Fig 4) grain size ranges to establish grain size distribution patterns.

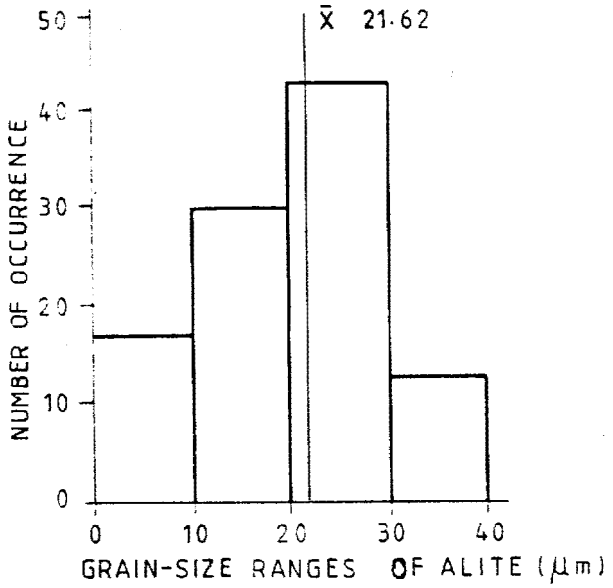

FIG 3 GRAIN-SIZE DISTRIBUTION OF ALITE IN CLINKER

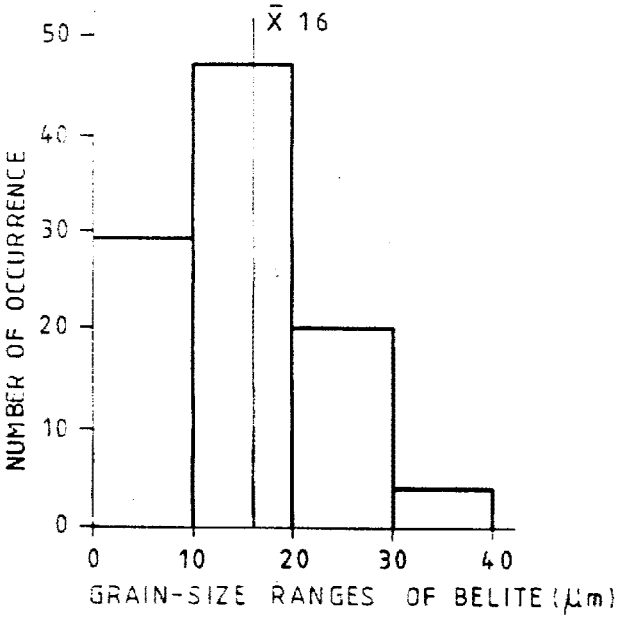

FIG 4 GRAIN SIZE DISTRIBUTION OF BELITE IN CLINKER

The mean and standard deviations were calculated for both alite and belite grain sizes. In the case of alite it has been found that out of a total of 112 grains, the range intervals 20-30 μm with a population of 43 showed most predominant number ofoccurrence, followed by 30 in the range of 10-20 μm. The calculated mean gives a value of 21.62 which falls in the class interval of 20-30 μm and corresponds with the maximum frequency. Similarly in the case of belite out of the total of every 100 grains measured, the class interval showing most predominant frequency of occurrence 45, is 10-20 μm followed by 29 in the size interval of 1 to 10 μm. The calculation of mean gives a value of 16 which falls in the size interval of 10-20 μm and is in correspondence with the maximum frequency.

The data obtained after analysing a large number of samples from various processes were subjected to multivariate statistical analysis by computer (6). Depending on the regression coefficient and regression equation as well as the weightage obtained for the various microstructural parameters, a mathematical model has been developed for estimation of 28-day compressive strength of cement clinker.(3)

$$Y \ (kg/cm^2) = 81.6+7.5X_1 + 1.11X_2 - 3.63X_3 + 5.73X_4$$

where X_1 = phase quantity of alite (%)
X_2 = phase quantity of belite (%)
X_3 = average grain size of alite (μm)
X_4 = average grain size of belite (μm)

The compressive strength results were plotted and a good correlation between expected and measured compressive strength was obtained (Fig 5).

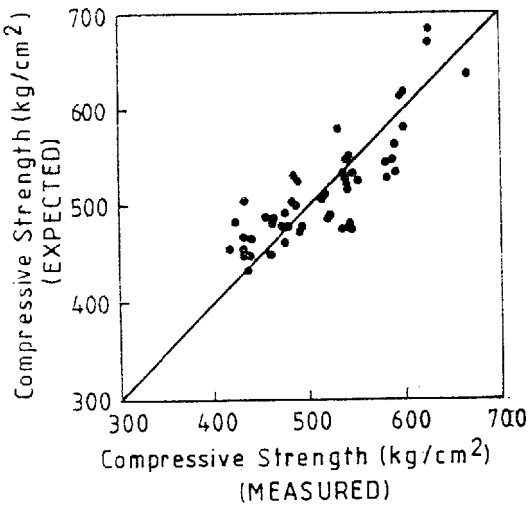

FIG 5 CORRELATION BETWEEN 28 DAY COMPRESSIVE STRENGTH Vs EXPECTED STRENGTH BY NCB TECHNIQUE

CONCLUSION

The mathematical model developed by NCB for the estimation of 28-day compressive strength is being implemented and good correlation has been obtained between the measured and expected compressive strength on a large number of OPC clinker samples derived from various processes.

ACKNOWLEDGEMENT

The authors have freely drawn upon completed R&D reports of NCB. This paper is being published with the permission of the Director-General NCB, New Delhi.

REFERENCES :

1. Ono Y. Microscopical observation of clinker for the estimation of burning condition grindability and hydraulic activity. Proc. 3rd Int. Conf. on Cement Microscopy. Houston, U.S.A., 198, 1981.

2. Hargave R.V., Venkateswaran. J. Deshmukh V.V and Chatterjee A. K., Quantification of OPC clinker microstructure - An approach for prediction of Cement Strength. Proc. 8th Int. Conf. on Chemistry of Cement, Rio-de-Janerio, Brazil, 167, 1986.

3. Sinha, S.K., Rao L.H., and Akhouri P.K. Rapid estimation of 28-day compressive strength of clinker by optical microscopy. Proc. 13th Int. Conf. on Cement Microscopy, Florida, 1991.

4. Chayes F. Petrographic model analysis, an elementary statistical appraisal. John Willey and Sons, New York,1956.

5. Cariau, B. et al. Industrial application of quantitative Study of Portland Cement clinker through reflected light microscopy Proc. 10th Int. Conf. on Cement Microscopy San Antonio, Texas, 1988.

6. Davis J.C Statistics and data analysis in geology. John Willey and Sons Inc. New York, 1973.

MÖSSBAUER SPECTROSCOPY USED FOR DETERMINING COMPOSITION OF CALCIUM ALUMINOFERRITES IN PORTLAND CLINKER

V K Klassen, I I Miroshnichenko, S F Mindolin and V I Belyaeva

Technological Institute of Building Materials
Belgorod, RUSSIA

SUMMARY

The technique is proposed for determining composition of calcium aluminoferrites in industrial clinkers, based on dependence of Néel temperature upon Fe paramagnetic ions concentration.

РЕФЕРАТ

Предложена методика определения состава алюмоферритов кальция в промышленных клинкерах, в основе которой лежит зависимость температуры Нееля от концентрации парамагнитных ионов железа.

Solid solutions of calcium aluminoferrites $Ca_2(Al_{1-x}Fe_x)O_5 (x > 0.3)$ are one of the minerals in cement clinker, and what is more it is known that ferrite phase in Portland cement is located in the area of C_6AF_2-C_6A_2F compositions. Determining aluminoferrite phase is a vital problem in manufacture of portland clinker when solving tasks connected with calculation of clinker mineralogical composition and selection of optimal raw material mixture, as well as obtaining "aluminoferrites composition - strength properties" correlations.

In order to viden the scope for Mössbauer spectroscopy technique when determining composition of aluminoferrites in clinkers the authors carried out theoretical and experimental studies of effect of Fe^{3+} paramagnetic ions for Al^{3+} diamagnetic ions substitution upon dicalcium ferrite properties. The Heisenberg Hamiltonian of the following form was used to describe magnetic properties of dilute antiferromagnet $Ca_2Fe_2(1-x)Al_{2x}O_5$:

$$H = -\frac{1}{2}\cdot\sum_i\cdot\sum_j P_{ij}\cdot C_i\cdot C_j\cdot I_{ij}\cdot(\vec{S}_i\cdot\vec{S}_j), \qquad (1)$$

where I_{ij} - parameter of exchange interaction between S_i and S_j spin moments of Fe^{3+} paramagnetic ions located in the lattice sites of the given ferrite;
C_i and C_j - quantities taking values 1, if i and j sites are occupied by Fe^{3+} ions, and Pij - if linkage between sites is in the form of Fe-O-Fe. The authors were a success to establish the following dependence for Néel temperature:

$$T_N(x) = \frac{P\,[C_1(I_{11} + |I_{12}|) + C_2(I_{13} + |I_{14}|)]}{I_{11} + |I_{12}| + I_{13} + |I_{14}|}\,T_N(1), \qquad (2)$$

$T_N(1)$ - Néel temperature of pure dicalcium ferrite;
$T_N(x)$ - Néel temperature of diamagnetically dilute ferrite;
C_1 - Fe^{3+} ions concentration in octahedric crystallographic sublattice;
C_2 - Fe^{3+} ions concentration in tetrahedric crystallographic sublattice;
P - probability of leakage in the sites for Fe^{3+} ions in the dicalcium ferrite lattice.

In order to determine the constants appearing in this expression the experimental data on Néel temperature obtained for calcium aluminoferrite solid solutions with the help of Mössbauer spectroscopy have been used. This resulted in the following dependence:

$$T_N(x) = P(0.53\,C_1 + 0.47\,C_2)T_N(1)$$

Experimental value $T_N(1) = 737$ K.

Dependence of probability of leakage in the sites for Fe^{3+} ions in the dicalcium ferrite lattice upon Fe^{3+} ions concentration should be examined in more detail. The given dependence is shown in Fig.1.

Originally, when we have pure dicalcium ferrite all the Fe^{3+} ions are connected by Fe-O-Fe linkages and thus represent linked system, i.e. infinite cluster. As Fe^{3+} ions are replaced with Al^{3+} ions, Fe-O-Al and Al-O-Al linkages occur together with Fe-O-Fe linkages which leads to decrease in linking the given ferrite lattice. The figure shows that probability of leakage is equal to 1 for aluminoferrites of C_2F - C_4AF compo-

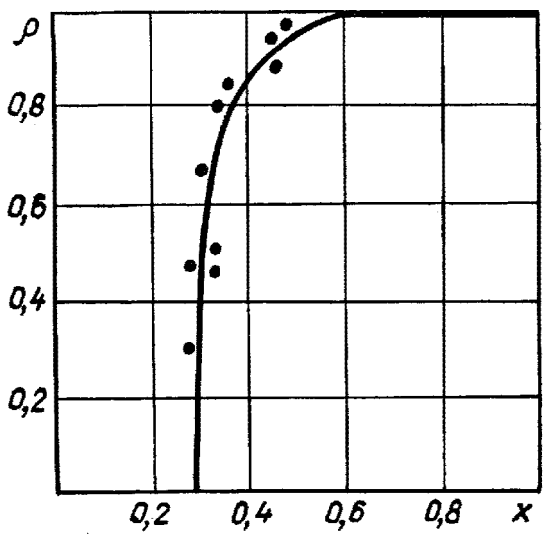

Fig.1. Dependence of probability of leakage P upon Fe^{3+} ions concentration x. The results of numerical modelling are shown by points.

sition, i.e. all the Fe^{3+} ions belong to infinite cluster. For cx = 0.3-0.5 aluminoferrites (for C_4AF - C_6A_2F compositions) P begins to decrease rapidly reaching zero value with x_c = 0.32, the quantity which is usually called critical concentration or leakage threshold. Above x_c there is Fe^{3+} ions infinite cluster in the lattice, and consequently it is possible to arrange antiferromagnet order in the lattice. Below the given concentration the lattice is aggregation of isolated finite clusters, i.e. the substance is paramagnet. Consequently concentration magnetic change takes place in the point x_c = = 0.32.

It should be noted that quantity of critical concentration is close to quantity of Fe ions concentration with which replacement of Fe with Al is still possible. The replacement is possible if it is infinite cluster of Fe^{3+} linked ions in the lattice of the given ferrite. Thus, probability of leakage in the Fe-O-Fe linkages in the lattice of ferrite at issue determines structural phase change as well - the other aluminate phases C_3A and $C_{12}A_7$ emerge below the critical concentration.

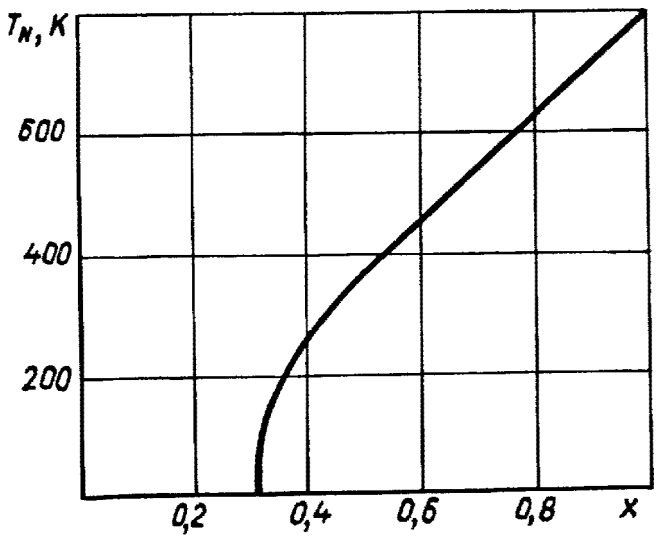

Fig.2. Dependence of Néel temperature T_N on Fe^{3+} ions concentration.

Fig.2 shows dependence of Néel temperature on Fe^{3+} paramagnetic ion concentration.

In the interval of x = = 0.5-1.0 concentrations the given dependence is of linear nature and Néel temperature decrease in this interval is defined by decrease of Fe^{3+} ions concentration, probability of leakage is practically equal to 1. In the interval of 0.32-0.5 concentrations the effect of probability of leakage upon Néel temperature of the given ferrite prevails. In this range of concentrations the given factor sharply increases Néel temperature responsivity to diamagnetic additives in the dicalcium

ferrite lattice, that is why it is offered to use dependence of Néel temperature for determining diamagnetic additives concentration in the C_2F lattice including Al^{3+} ions.

It is known that besides Fe ions there may be ions of K, Na, Li alkaline elements in the dicalcium ferrite lattice of industrial clinkers. In order to determine the effect of these ions upon Néel temperature Mössbauer spectres of aluminoferrites have been obtained where concentration of alkaline elements varied in a wide interval of 1 - 80%. The experimental data show that with concentration of ions of alkaline elements being high enough the spectre is represented by superposition of two sextets, referring to Fe ions disposed in dicalcium ferrite lattice and paramagnetic doublet. Presence of the given doublet in the spectre is connected with the fact that in synthesised specimen besides dicalcium ferrite there is a different phase which may be classified as alkaline ferrite. The following values of the limiting concentrations have been determined by the paramagnetic doublet intensity: Li - 3.12, Na - - 2.095, K - 1.48 (mole %) hence presence of alkaline elements in the lattice of the ferrite at issue will lead to slight decrease in its Néel temperature. So the most substantial parameter affecting the decrease of Néel Temperature is Al^{3+} ions concentration.

In order to check the possibility of use of the technique proposed and determine aluminoferrites composition in industrial clinkers of the Stary Oskol cement works the Mössbauer spectres in the temperature interval of 80 - 300 K have been obtained. Close concentration values (x=0.4) have been obtained for all the specimens according to Néel temperature which conformed with $C_2A_{0.6}F_{0.4}$ or $C_5A_{1.5}F$ aluminoferrite composition.

It should be noted that the technique proposed offers a number of merits as compared to known before. First, the technique proposed covers all the range of compositions of calcium aluminoferrite solid solutions. Secondly, sensitivity of this new technique is higher, especially with small values of Al^{3+} ions concentration. Moreover, the given technique enables to determine directly Fe^{3+} ions concentration in aluminoferrites which is extremely important in case when there are admixtures in their composition. In the similar cases the other types of analyses, for instance, will indicate considerably greater error due to the change in C_2F crystal lattice parameters both by Al^{3+} ions and alkaline element ions.

CARBOXYLIC ACID ANIONS : THE REACTION MECHANISMS AND PRODUCTS WITH THE ALUMINATE PHASE OF CEMENT

Herbert Poellmann

Mineralogical Institute of University
Erlangen-Nuremberg, GERMANY

ABSTRACT

Organic admixtures are increasingly used as additives for cements to establish definite setting and hardening conditions or improve workability. Only few data are available on the chemistry of the new hydration products which are formed under these special conditions. Under the influence of organic additives not only cristalline precipitates are formed but also gel-structures and chelate complexes. The formation conditions as a function of the concentration will be discussed.

Different aliphatic, aromatic and substituted carboxylic acids and their salts were used as additives. Acceleration and reatrdation as a function of concentration can occur.

Only formate can enter the ettringite-structure. No other ettringite-like compounds with carboxylic acid anions could be synthesized. Instead at high concentrations of these anions different calcium salts are precipitating.

Carboxylic acid anions are normally fixed in the interlayer of lamellar salts with the typical composition as follows :

$$Ca_4\{Al_2(OH)_{12}\}^{2+} \quad \{(\ R\ )_m \cdot nH_2O\}^{2-}$$

$R = H\text{-}(CH_2)_n\text{-}COO^-$

$R = (C_6H_5)\text{-}(CH_2)_n\text{-}COO^-$

$R = {}^-OOC\text{-}(CH_2)_n\text{-}COO^-$

R = hydroxy carboxylic acid

Partially these new hydrates form complex solid solution series with tetracalcium aluminate hydrate.

The course of hydration was studied using heat flow calorimetric methods. The different cristalline and semi-cristalline hydrates were characterized.

INTRODUCTION

The practical use of additives is usually based on empirical data. To improve the knowledge on the hydration behaviour of the aluminate phase of cements under the influence of additives it is necessary to do some basic research. To optimize the interactions of additives with the cement it is useful to understand how they work. The chemical controlled hydration behaviour in the case of organic additives is strongly dependant on the concentration of the used agent. Often besides cristalline hydrates, semicristalline hydrates and amorphous phases are formed. Normally only the resulting effect of the additive on special products is documented, especially for practical purposes. Confirmatory tests are necessary at all time in these multicomponent systems. In technical applied additives often minor components are the dominant reacting agent. Slight changes in concentration can have drastic effects or even can turn round the behaviour.
This is well known for some substances which can act as retarding or accelerating agent depending solely on the used concentration.

In this study a combination of the resulting effect of the additive due to its concentration and the cristallochemical behaviour of the reactions was investigated. Therfore a lot of different carboxylic acids and their salts were applied and their reaction behaviour directly measured by heat flow calorimetry. The new crystallizing hydrates were characterized by pure synthesis and their properties were dermined. Transformations of basic research studies to knowledge on commercial cements were undertaken in the case of high alumina cements.

EXPERIMENTAL

In the present investigation two main ways of synthesizing hydration products were undertaken.

1. Synthesis of pure new compounds to establish properties and chemical compositions. This was normally done by controlling reaction parameters and additionally long term studies to obtain equilibrium conditions. Reagent grade chemicals, CaO, freshly synthesized CA and H_2O with organic additives were used. Investigations at different temperatures and reaction times up to 1 year were used. The reaction mixtures were shaken in polyethylene bottles and were treated carefully using a glove-box at definite conditions.

2. Reaction behaviour and the course of hydration was studied by heat flow calorimetry and combined X-ray diffraction and infra-red techniques. Usually different concentrations of various additives were added as solutions to commercial high alumina cement and the heat flow maxima was determined. As a function of concentration a shift to acceleration or retardation could be measured. Broadening effects at increasing concnetrations were sometimes observed. The resulting hydration products were carefully investigated for their cristalline and amorphous hydrates. In this stage of research it was doubtless necessary to have knowledge on the properties of phases synthesized in step 1. Especially the X-ray powder data which were determined for the various phases containing organic molecules could be successfully used in the interpretation of the hydrates. Optical, Interference and scanning electron microscopy were used to documente hydration stages and new products formed in the course of hydration.

RESULTS

To study the influence of simple organic carboxylic acids and their different Ca-salts the following chemicals were used :

1. Monocarboxylic acids	Formic acid, Acetic acid, Propionic acid
2. Dicarboxylic acids	Oxalic acid, Malonic acid, Succincic acid
3. Phenylcarboxylic acids	Benzoic acid, Phenylacetic acid, Phenyl-propionic acid, Phenyl-butyric acid
4. Hydroxicarboxylic acid	Tartaric acid, Mendelic acid, Malic caid, Salicylic acid

Scanning electron micrographs of hydration products show typical hexagonal shaped lamellar calcium aluminum hydroxi salts containing carboxylic acid anions in the interlayer. The X-ray data of these new hydrates could be ob tained. In Fig.1 and Fig.2 typical hydrates formed in the course of hydration are formed. In both cases these hydrates contain organic ions in their crystal lattice.

FIG. 1 : Lamellar hydrates on surface of aluminate-phase

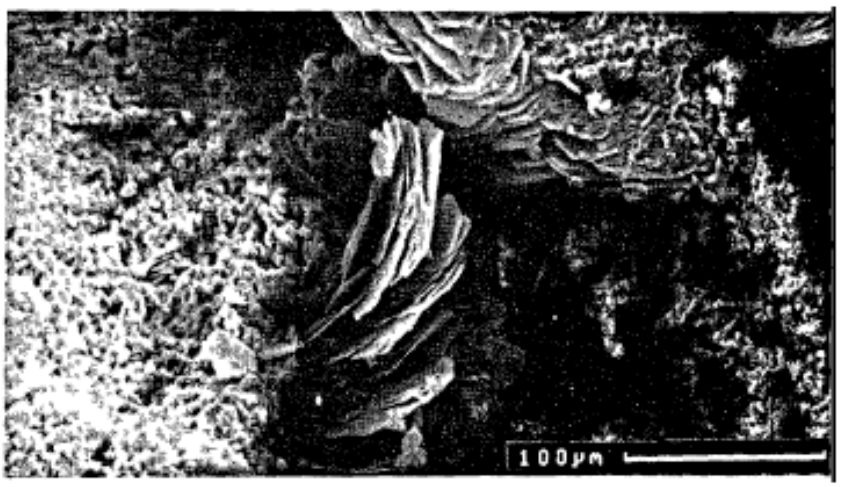

FIG. 2 : Pure crystals of lamellar phase containing organic ions

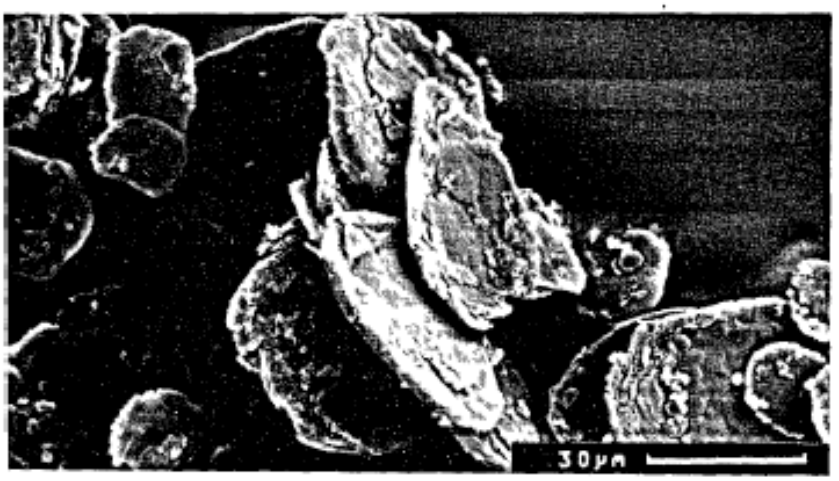

The course of hydration of high alumina cement under the influence of different concentraions of additives is documented in Fig. 3 - 17. The usage of additives was restricted to Ca-salts of different carboxylic acids to investigate especially the behaviour of the organic parts of these salts Chemically the hydration products can be described as derivatives of the lamellar structure of tetracalcium aluminate hydrate. The interlayer anion OH^- is partially or completely replaced by carboxylic acid anions. The chemical formula can be given by :

$$Ca_4\{Al_2(OH)_{12}\}^{2+} \quad \{(R)_m \cdot nH_2O\}^{2-}$$

$R = H\text{-}(CH_2)_n\text{-}COO^-$

$R = (C_6H_5) - (CH_2)_n\text{-}COO^-$

$R = {}^-OOC - (CH_2)_n\text{-}COO^-$

R = substituted carboxylic acid anion

The maxima of heat evolution of high alumina cement under the addition of different concentrations of Ca-salts of organic acids are given.

FIG.3: Addition of $Ca(HCOO)_2$

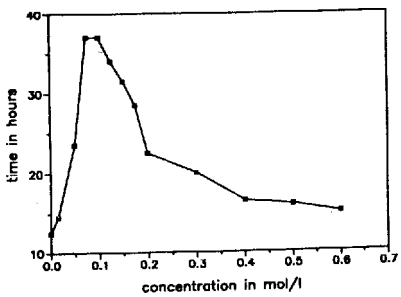

FIG: 4: Addition of $Ca(CH_3COO)_2 \cdot H_2O$

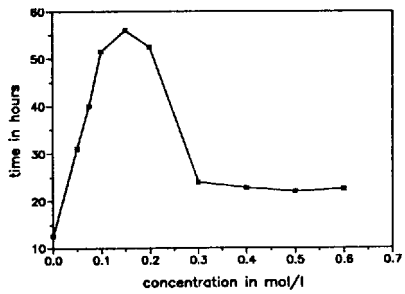

FIG.5: Addition of $Ca(CH_3CH_2COO)_2 \cdot H_2O$

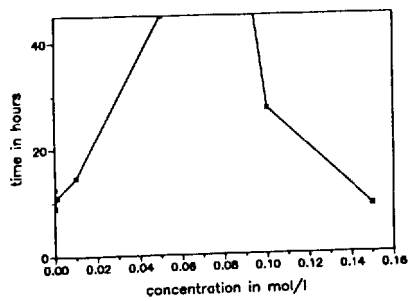

FIG. 6: Addition of $CaC_2C_4 \cdot H_2O$

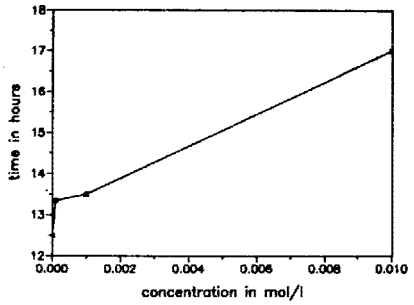

FIG. 7: Addition of $CaCH_2(COO)_2 \cdot aq$

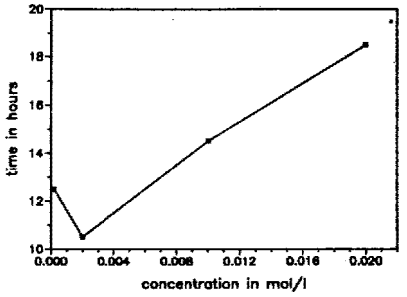

FIG. 8: Addition cf $Ca(CH_2)_2C_2O_4 \cdot nH_2O$

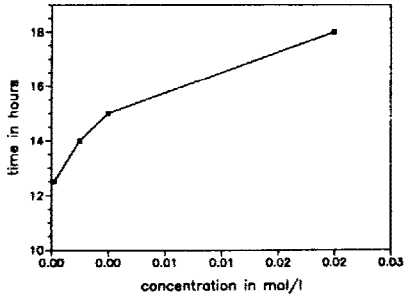

FIG. 9: Addition of $Ca(CH_2)_3(COO)_2 \cdot aq$

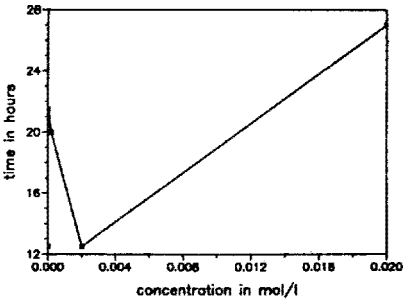

FIG. 10: Addition of $Ca(C_6H_5COO)_2 \cdot aq$

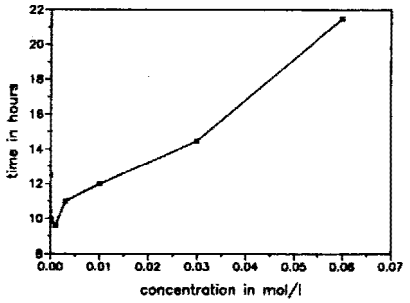

FIG. 11: Addition of $Ca(C_6H_5CH_2COO)_2 \cdot aq$

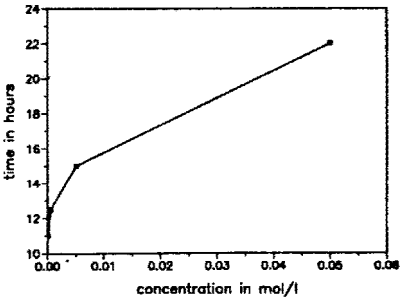

FIG. 12: Addition of $Ca(C_6H_5(CH_2)_2COO)_2 \cdot aq$

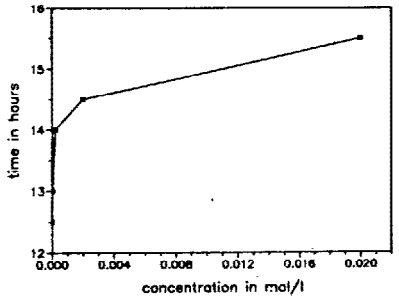

FIG. 13: Addition of $Ca(C_6H_5(CH_2)_3COO)_2 \cdot aq$

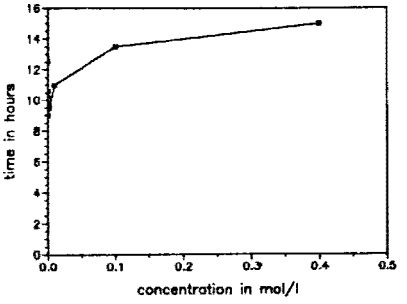

FIG. 14. Addition of $Ca(C_4H_4O_6)\cdot 4H_2O$

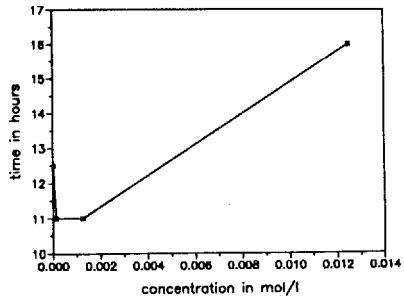

FIG. 15: Addition of $CaC_5H_5O_4\cdot 2H_2O$

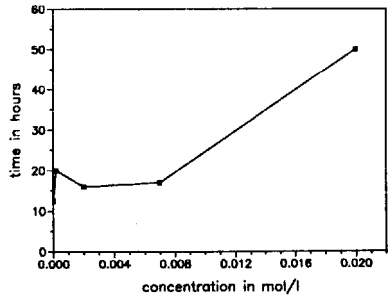

FIG. 16: Addition of $Ca(C_6H_5CHOHCOO)_2$

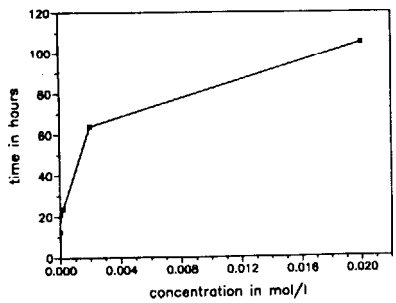

FIG. 17: Addition of $Ca(C_6H_5OHCOO)_2$

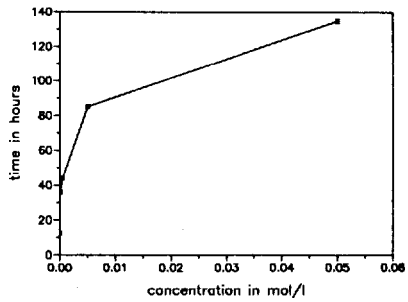

DISCUSSION AND SUMMARY

The results on the addition of calcium carboxylic acids to high alumina cements clearly indicate that depending on the concentration acceleration or retardation can occur. Anions and cations can influence the hydration behavicur. Besides cristalline hydration products semi-cristalline phases, chelates and gel-structures can be observed.

The cristalline hydrates can be written by derivatives of tetra-calcium aluminate hydrate. With increasing length of carbon chains of the carboxylic acids the lattice parameter of the layer structure increases in c_o direction. This effect can easily be measured by X-ray methods and used for identification of the new phases. Carboxylic acid anions can not enter the structure of ettringite (only formate-ettringite cristallizes). Hydroxy carboxylic acids do have increased influence on the hydration behaviour in comparison to unsubstituted acids.

With increasing chain length of carbon-atoms in these acids an increased effect at similar concentrations can be measured. Sometimes additives have contrary effects at different concentrations. This si due to other types of hydrates formed under these conditions. Additional molecular water can enter the interlayers of the hydrates and increase the viscosity of the slurries, despite no ettringite is crystallizing.

LITERATURE

1. Carrel, Greskowlak, Midgley, H.G. & Parsonage, J.R.(1987) : "Acceleration and retardation of set high alumina cement by additives", Cem. Concr.Res. 17(3), 422 - 432

2. Poellmann,H.:"Study of the hydration mechanisms and formation of new hydrates applying organic additives to the aluminate phase of cement"
Proc.Int.Con.Cem.Mict., (1989), 287-305

3. Poellmann,H.:"Mineralogical and Crystallographic Investigations on the hydration behaviour of the aluminate phase of cements"
Two Volumes, Habilitationsschrift, Erlangen, (1990)

4. Ramachandran,V.S.:"Concrete Admixtures Handbook" - Noyes Publications (1984)

5. Wilding,C.R., Walter,A. & Double,D.D.:"A classification of inorganic and organic admixtures by conduction calorimetry"
Cem.Concr.Res. 14, (1984), 185-194

6. Young,J.F.:"Effect of organic admixtures on the interconversion of calcium aluminate hydrates"
Cem.Concr.Res. 1, (1971), 113-122

ADDITIONS METHOD IN ANALYSIS OF CEMENT MATERIALS BY ION-SELECTIVE ELECTRODE POTENTIOMETRY

I K Gromozova

Design and Research Institute of Cement Industry, "GIPROCEMENT"
St Petersburg, RUSSIA

SUMMARY

The many-year operation experience of the institute of Giprocement with ion-selective electrodes provides support for advantages of measurements conduction by the standard additions method. Examples of this method application to the ion-selective analysis of cement materials are given in the paper. A simple method of ion concentrations calculation is proposed.

РЕЗЮМЕ

Многолетний опыт работы института Гипроцемент с ионселективными электродами подтверждает преимущества проведения измерений по способу стандартных добавок. В докладе приводятся примеры применения способа к ионселективному анализу цементных материалов. Предлагается простой способ расчёта концентрации ионов.

INTRODUCTION

The Institute of Giprocement has gained many-year operation experience in the field of the electrochemical analysis, mainly, by ion-selective electrode potentiometry methods (1,2,3). The ion-selective method of fluorine determination developed by Giprocement for raw materials and finished product is included into the new edition of the State standard for chemical methods of analysis of cement materials along with the photocolorimetric method. Both standardized methods of fluorine content control in raw mixes, clinkers, fluorspars envisage concentration measurements using a calibration curve (4).

With the use in the cement production sphere of new non-traditional fluorine-containing mineralizers of technogenous origin (e.g. silicofluoric acid, fluorine-chlorine-bearing waste with up to 30% chlorine content, fluoric concentrate containing up to 40% fluorine and more) there was observed a decline in accuracy of the ion-selective and photocolorimetric analysis of fluorine at its concentration measuring by calibration curve. Even choice of proper dilutions of controlled sample solutions and account of their salt composition as it has been done previously for fluorspars (1) did not improve the accuracy of the results. Further investigations on application of the standard additions method for carrying out quantitative potentiometric measurements of fluorine and other ion concentrations made it possible to choose optimum conditions of their ion-selective analysis.

EXPERIMENTAL DATA AND THEIR DISCUSSION

The measurements were taken on И120М ionometer. They involved the use of home electrodes developed by the University of St.-Petersburg as well as of the fluoride electrode produced in the town of Verkhnyaya Pyshma (has been in operation for more than 15 years). Procedure of analysis recommended for control of fluorine content (from 1 to 40% and more) will be as follows: 0.1 g of sample is fused with a mix of potassium-sodium carbonate and borax (2:1). The melt is dissolved in the hydrochloric acid. Then an aliquot of 5 ml is taken to a graduated beaker, 20 ml of concentrated urotropine solution is added and the first measurement of electromotive force of this solution (E_1) is conducted. It is followed by introduction of additive of 1 ml of standard sodium fluoride solution with concentration equal to 10^{-2} m fluorine/l. Then the electromotive force of the solution with additive (E_2) is measured. Fluorine content is calculated from a simple formula:

$$\%F = \frac{9.135}{a-0.96},$$

where $a = 10^{\Delta E/S}$. $E = E_1 - E_2$, and S - electrode function slope (Nernst factor) is determined by two sodium fluoride solutions with fluorine concentration of 10^{-3} m/l and 10^{-4} m/l. The parameter "a" is found from a precompiled Table 1 given below. The simplified expression given above for calculation of fluorine concentration is obtained through transformation of known equation for determination of ion concentrations by the additions method (5-8).

Procedures of potentiometric analysis of fluorine by the additions method have been developed both for raw mixes and clinkers where fluorine content was from hundredths of per cent up to 1% and for cinder slurries containing 1-2% fluorine and up to 30% iron oxide. The additions method has considerably reduced labour content of analysis and cut

time for its conduction by 1.5-2 times since there is no need in electrode calibration by standard samples. Evaluation of electrode function slope is conducted at regular intervals by two standard solutions. At permanent operation the Nernst-factor varied only a fair, by 1-2 units which practically had no influence on $10^{\Delta E/S}$ value (refer to Table 1).

Table 1

ΔE	$a = 10^{\Delta E/S}$		
	S = 56	S = 59	S = 60
1	1.04	1.04	1.04
2	1.08	1.08	1.08
3	1.13	1.12	1.12
4	1.18	1.17	1.17
5	1.23	1.22	1.21

At the same time accuracy of ionometric measurements by the additions method is increased appreciably due to decrease of action of chemical composition of units analyzed. Examples of determination of fluorine--ion, nitrate-ion, carbonate-ion by means of direct potentiometry using the additions method as well as with the use of calibration curves are illustrated in Tables 2,3,4,5.

Table 2. Results of Potentiometric Analysis of Fluorine in Standard Samples of Raw Mixes

F introduced, %	F(C) determined by ion-selective analysis			
	Calibration curve		Additions methods	
	C,%	ΔC against introduced, %	C,%	ΔC against introduced, %
0.19	0.15	-0.04	0.17	-0.02
0.10	0.08	-0.02	0.12	+0.02
0.05	0.07	+0.02	0.04	-0.01
0.90	0.94	+0.04	0.92	+0.02
		$\bar{\Delta}C = \pm 0.03$		$\bar{\Delta}C = \pm 0.02$

Table 3. Results of Potentiometric Analysis of Nitrate-Ion Concentrations in Standard Samples of Cement Raw Mix

NO_3^- introduced in %	Nitrate (C) determined by ion-selective analysis			
	Calibration curve		Additions method	
	Calibration by KNO_3 solutions		C,%	ΔC against introduced, %
	C,%	ΔC against introduced, %		
0.61	0.94	+0.33	0.55	-0.06
3.07	3.56	+0.49	3.07	0.00

Table 4. Analysis of Water Extract of Electrostatic Precipitator Dust of the Korkinsky Cement Plant for Content of Free CO_3^{2-}-ion

Sample	Chemical analysis	Ion-selective analysis by additions method
Dust 1 of electrostatic precipitator stage 1	1.52	1.37

Table 5. Results of Fluorine Analysis in Samples of Complex Chemical Composition (C,%)

Srl. No.	Material analyzed	Photocolorimetric method (KФK)	Ion-selective method (Additions method)	
		C,%	C,%	ΔC against KФK, %
1	Calcium flubride	1.95	2.02	+0.07
2	Calcium fluoride	18.12	18,54	+0,42
3	Electrothermophosphoric slag	7.50	7.68	+0,18
4	Fluorine-chlorine-bearing mineralizer	23.17	22.84	-0,33
5	Fluoric concentrate	38.00	37.60	-0.40
6	Silicofluoric acid	65.71	66.6	+0.90

CONCLUSIONS

Data presented confirm once again advantages of the ionometric analysis by the standard additions method. The additions method is particularly effective for samples of composite chemical analysis for which it is difficult to choose calibration standard samples of similar matrix. The simple method proposed for calculation of ion concentrations does not require computer application.

REFERENCES

1. Gromozova, I.K., Bogdanova, I.V., Kots, Ye.A. & Avdeyeva, Yu.V.: "Ion-selective method of fluorine determination in cement materials without separation of interfering elements". 8-th All--Union Scientific-Technical Conference on Cement Chemistry and Technology, Moscow, 1991, 250-252.

2. Gromozova, I.K., Svatovskaya M.B. & Avdeyeva, Yu.V.: "Features of fluorine ion determination in the presence of higher silicium concentrations". 8-th All-Union Scientific-Technical Conference on Cement Chemistry and Technology, Moscow, 1991, 79-81.

3. Moskvin, L.N., Grigorieva, M.F., Kots, Ye.A. & Gromozova, I.K.: "Determination of ferrous iron in slags and cements by voltammetry method". Tsement, 1988, (8), 19-20.

4. GOST 5382-91: "Cements and materials of cement production. Methods of chemical analysis". The State Building Committee of the USSR, Moscow, 1991, 94p.

5. Ion-selective electrodes (under the editorship of R.Darst) (translation from English). Moscow, "Mir", 1972, 430p.

6. Kamman, K.: Ion-selective electrodes operation. Moscow, "Mir", 1980, 283p.

7. Nikolsky, B.P., Materova, Ye.A.: Ion-selective electrodes. Leningrad, "Khimiya", 1980, 289p.

8. Lakshminarayanaiah, N.: Membrane electrodes. New York, Academic Press, 1976, 368p.

METHODS OF PERFORMING ADIABATIC AND ISOTHERMAL CALORIMETRY

R I A Malek

The Pennsylvania State University
Materials Research Laboratory
USA

SUMMARY

The 21st Century Concrete Technology is expected to be more concerned with the heat of hydration data. Such data is important to the quality assurance/control of concrete, microstructure development, control of the rate of heat evolution, and inputs to various maturity models for monitoring strength development and predicting the possibility of high thermal gradient.

Experimental methods for performing adiabatic and isothermal hydration calorimetry are discussed, and their use and applications detailed for cementitious materials. Examples are given in their applications for portland cement pastes and concrete. Differences between the isothermal and adiabatic characteristics suggest that it is desirable for determination of the behavior of larger mass concrete to use data from adiabatic calorimetry or multiple temperature isothermal data sets. A far more reaching goal of the author of the present paper is to be able to extend these techniques to non destructive test methods for in-situ determination of the heats of hydration.

INTRODUCTION

In recent years, heat of hydration data has become an important factor for both the cement chemist and the cement practitioner. Such data is important in a number of areas including:

- Quality Assurance of both ingredients and mixes.
- The study of microstructure development under both adiabatic and isothermal conditions.
- Determining the effect of mineral admixtures, i.e. fly ash, slag, etc., as well as retarders in controlling rate of heat evolution.
- Inputs to various maturity models for determining strength development.
- Predicting the possibility of high thermal gradient within massive pours.
- Aid in determining thermal stability of cementitious materials used in subsurface waste isolation, i.e. borehole plugging, shaft sealing, etc.
- Establishing thermal limits for waste processing, i.e. selection of waste form.

Heat of hydration results from the complex exothermic reactions taking place as the cement changes from a fluid mixture of dry cement and water to a solid. The rate of heat evolution is most commonly determined using a number of techniques, i.e. isothermal (conduction) calorimetry, adiabatic calorimetry, solution calorimetry and semi-adiabatic.

1. Isothermal calorimetry

a. Solution Calorimetry, Heat of Hydration, Heat of Solution

A method for determining the heat evaluation during cement or cement components hydration is the heat of solution method described in ASTM C186-68. The British standards adopt a similar method (BS 1370) but differ in minor details. The method depends on the measurement of the heat of solution of the original cement and of the set cement. Applying Hess' law of heat summation equality to the difference between the heats of solution of fresh and set cement, the heat of hydration can be calculated. The heats of solutions are determined to the ignited weight basis by determining the heat loss on ignition. The heat of solution of set cement is determined on a ground sample cured up to a certain age at 73.4°F.

The calorimeter used is an open thermal flask with a cork stopper through which passes a Beckmann thermometer and a stirrer. The interior wall are covered with wax and the entire assembly is placed inside an insulated box. The heat capacity of the system is predetermined with zinc oxide whose heat of solution is known. The heat of solution is determined in a solvent consisting of hydrofluoric and nitric acids. The method required much precaution since considerable error can result from changing the properties of the sample (carbonation, particle size and size distribution, solubility of components and rate of heat evolution).

b. Conduction Calorimeters

In this case, the heat conducted away to a controlled temperature bath or to metal. The rate of heat evolution is determined from the temperature gradient between sample and bath . An example of this type of calorimeter is the Seebeck envelope whose composition and operation is discussed in detail elsewhere[1].

2. Semiadiabatic Calorimetry (Vacuum Flask Method)

The heat evolved during hydration of cement or cement components can be measured up to a few days by using a vacuum flask and correcting for the heat losses. The method cannot be used over a long period of time or when the heat evolved is not considerably high.

3. Adiabatic Calorimeters

The adiabatic methods for determining the heat evolution depends on placing a sample in an adiabatic calorimeter. This is achieved by surrounding the sample container with an outer bath, the temperature of which is raised automatically with a rate that is exactly the same rate as that of the sample. The temperature rise can be calculated as calories per gram knowing the specific heats of the cement or concrete sample and that of the calorimeter. The length of experiment depends on the efficiency of adjusting the temperature of the outer bath.

Temperature-Matched Curing System

A calorimeter is developed to study (a) the adiabatic temperature rise in cement and by concrete systems; and (b) to be used for curing concrete specimens at elevated temperature cycles. Two types of these calorimeters have been developed, the first[2] of them uses a temperature cycle that has been previously recorded on a separate concrete sample. In a modified version of the apparatus[3] a concrete control cube is cast in an insulated plastic mold provided with two thermocouples, sheathed in an oil-filled copper tube, cast in its center. The water temperature in the baths are then controlled to follow that of the control cube. The system is composed of three curing tanks interconnected through a network of perfectly insulated copper cubes. One of the three tanks is the heating tank in which water is heated and circulated by heat pumps. The system is also provided with a chiller unit which, if required, allows the water to be precooled to a starting temperature below ambient. The temperature measurement, power control and data storage are performed by a microcomputer and associated peripheries. Three pre-calibrated thermocouples are placed in each of the two curing tanks for monitoring temperature. To prevent the water temperature from lagging behind or overshooting the concrete temperature, a control program was used to calculate the power input into the system.

If proportional control alone was used, the power input is adjusted to be approximately equal to the temperature difference. The equation used to control the power would be:

$$Q = P(T_C - T_W) \qquad (1)$$

where

- P = proportionality constant
- T_C = concrete temperature (°C)
- T_W = water temperature (°C)
- Q = power input to heaters.

The proportional control damps out any temperature oscillations (on-off controllers) but causes an offset between the two temperatures. To eliminate this offset an integral or reset term is added to the equation:

$$Q = P(T_C - T_W) + c_1 \int (T_C - T_W)dt \qquad (2)$$

where c_1 is an integration constant. Using this equation the offset is reduced to zero. To prevent overshooting, a third derivative is added:

$$Q = P(T_C - T_W) + c_1 \int (T_C - T_W)dt + c_2 \frac{d}{dt}(T_C - T_W) \qquad (3)$$

where c_2 is a derivative constant.

The temperature distribution throughout the water in the curing tanks is controlled by regulating the flow rates of heated water into tanks by system values so that the maximum difference does not exceed 0.5°C and the "between tank" variation to 1.0°C.

The considerably large volume of the curing tanks makes it difficult to control the temperature of the bath to match the reference sample temperature especially in the acceleration period or when using high early strength cement (Type III).

The PENN STATE Calorimeter

A system has been developed at The Pennsylvania State University's Materials Research Laboratory[4] that separates the adiabatic calorimeter from the adiabatic curing tanks. The adiabatic calorimeter is unique and versatile in that it is much smaller in size and the temperature control is quicker. A recorded temperature profile allows the duplication of the entire heat cycle precisely with the curing tanks.

The adiabatic system essentially consists of a microcomputer, a water/oil bath and an auxiliary bath for larger samples. The computer is used to acquire and store the data as well as send out appropriate control signals to the bath. It is connected to a plotter, a printer and a disk drive. An ADALAB card manufactured by Interactive Microware, Inc., State College, Pennsylvania, is used to interface the computer to an 8-channel input multiplexor and a signal amplifier. This card also contains 12 bit analog to digital and digital to analog converters.

Individually calibrated chromel-alumel thermocouples are used for the temperature measurements. They were selected for their high voltage signal output and their resistance to oxidizing atmospheres. The thermocouple for monitoring the sample temperature was placed in the center of the sample.

The thermocouple output is approximately 0.04 mV/°C. Cold junction compensators were used to compensate for room temperature variations. The signal is amplified by the amplifier (ADA-AMP) and then converted by the A/D converter. The program converts this to a temperature through the calibration constants for the thermocouple. A control signal is also sent about every 30 seconds to the bath through the D/A converter to heat the bath to a temperature equal to the sample temperature at that time. The computer program which inputs the data, converts the signals to the appropriate temperatures, sends control signals to the bath and stores data on disk.

The temperature difference between various portions of the sample was checked by placing thermocouples at various points inside the sample. It is found to be less than 0.2°C at all times and to be of a random nature. The total temperature rise in a cementitious sample was found repeatable within 1°C over the entire course of an experimental run.

Simplified Adiabatic Calorimeter

There is an argument[5] that regardless of the several measures taken to ensure that the temperature of the bath matches the concrete temperature, the true equilibrium condition between concrete and surroundings is not existing and the system is to a variable extent far from true adiabatic conditions. Therefore, it is more convenient to use simpler calorimeters that are far less expensive and less operationally complicated and correct for the drift from equilibrium conditions. The equation used is as follows:

$$(\Delta T_C^*) = \left(1 + \frac{c_c}{c_{col}}\right)[(\Delta T) + a] \qquad (4)$$

where

ΔT_C^* is the true adiabatic temperature rise
ΔT is the measured temperature rise
c_s is the heat capacity of the calorimeter
c_{cal} is the heat capacity of the concrete
a is called error of adiabatism and it estimates the drift of temperature over long periods (24 hours) in the absence of heat evoluation.

4. Measurement of the Specific Heat of Concrete

Two methods are used to determine the specific heat of concrete; namely, the method of mixtures and the electrical method.

(a) Method of Mixtures. This is a classical method of calorimetry and is described in detail in literature[6-8].The procedure consists of heating a given amount of crushed concrete up to a fixed temperature and in dipping it quickly in the water (at ambient temperature) contained in a calorimeter. The change in water and concrete temperatures allows the specific heats to be obtained.

(b) The Electric Method. In this method[9] a resistor of known value (R) and invariable with temperature, is immersed in the mass of fresh concrete. At the end of the calorimetric test, and after coating the sample to ambient temperature, a current of known intensity (I) is passed through the resistor for a time (t). Therefore, by the Joul effect the sample receives a quantity of heat defined by

$$Q = \frac{RI^2t}{4184} \qquad (5)$$

and the heat capacity is calculated as follows

$$C = \frac{Q}{\Delta T} = \frac{RI^2t}{4184\,\Delta T} \qquad (6)$$

where ΔT is the temperature rise of the calorimeter and by differentiation,

$$\frac{d\Delta T}{dt} = \frac{RI^2}{4184\,C} \qquad (7)$$

Since the right-hand side of this equation is constant, plotting ΔT versus time is a straight line. The heat capacity of the calorimeter can be determined and that of the concrete can be estimated from the plot of ΔT versus time. The specific heat of concrete could, thus, be calculated.

REFERENCES

1. Adams, L.D. "The Measurement of Very Early Hydration Reaction of Portland Cement Clinker by Thermoelectric Conduction Calorimeter," Cem. Concr. Res. 6 (2), 793 (1976).
2. Bell, F.H. "An Apparatus for Curing to a Predetermined Time-Temperature Function," Magazine of Concrete Research, Vol. 24, No. 78, pp. 43-45 (March 1972).
3. Wainwright, P.J., and J.J.A. Tolloczho, "A Temperature-Matched Curing System Controlled by Microcomputer," Magazine of Concrete Research, Vol. 35, No. 124, pp. 164-169 (September 1983).
4. Kaushal, S. "Thermal Properties and Modelling of Aluminosilicate Materials for Low-Temperature Bath Applications," Ph.D. Thesis, The Pennsylvania State University (1988).
5. Costa, U. "A Simplified Model for Adiabatic Calorimetry," Il Cemento 2, 75 (1979).
6. "Method of Test for Mean Specific Heat of Hydraulic Cements, Cement Pastes and Other Materials (Method of Mixture)," Handbook for Concrete and Cement, U.S. Army Waterway Experimental Station, Vicksburg, CRD-242-54.
7. "Method of Test for Specific Heat of Aggregates, Concrete and Other Materials (Method of Mixtures)," Handbook for Concrete and Cement, U.S. Army Waterways Experimental Station, Vicksburg, CRD-C124-73.
8. Whitting, U. , A. Litvin and S.E. Goodwin, "Specific Heat of Selected Concrete," J. ACI 75 (7), pp.299-305 (1978).
9. Costa, U. "A Simplified Model for Adiabatic Calorimeters," Il Cemento 2, 75 (1979).

DIELECTRIC STUDY OF THE HYDRATION PROCESS IN PORTLAND CEMENT

A Anagnostopoulou-Konsta and D Daoukaki-Diamanti

National Technical University of Athens
GREECE

ABSTRACT

The variation of the dielectric behaviour of portland cement during the solidification process was studied with the thermally stimulated depolarization currents (TSDC) technique, in the temperature range 77 to 300 K. Three large TSDC peaks are recorded between 150 and 210 K in newly formed samples, shifting to higher temperatures as the setting proceeds. Analysis of the behaviour of these peaks has shown that: a) a sudden discontinuity in the position of all recorded peaks is displayed after 5 -9 hours of hydration time, in accordance with other authors, b) no free or loosely bound water has been detected, even in newly formed samples, contrary to results reported in literature, and c) freezing of the sample causes total hindering of the setting process.

RESUME

La variation du comportement dielectrique du ciment Portland pendant le processus de solidification a ete etudie au moyen de la methode des thermocourrants de depolarization entre 77 et 300 K. Dans les echantillons fraichement prepares trois pics ont ete enregistre entre 150 et 300 K, se deplacant vers les temperatures plus elevees avec le temps d'hydratation. L'analyse de la forme et du comportement de ces pics a montre que: a) une variation plutot brusque de la position de ces pics est apparente apres 5 a 9 heures de duree d'hydratation, en accord avec des resultats reportes par les autres auteurs, b) on n'a pas detecte dans les echantillons de l'eau libre ou faiblement liee, contrairement aux resultats obtenus par des methodes differentes, et c) la prise du ciment s'arrette completement au dessous de la temperature de congelation.

1. INTRODUCTION

The electrical properties of cement paste are strongly related to the state of water in the system and may thus vary extensively during the cement setting. Therefore, the evolution of the electrical behaviour of cement with hydration time may successfully be used as a method for monitoring the curing of this material, as reported by a number of authors [1-5 and references cited]. The d.c. conductivity and the dielectric properties of portland cement have been measured in the frequency range from about 1 Hz up to 13 MHz as a function of time since mixing for up to 100 days, or more [1-4]. Results have been analyzed and interpreted in various ways, e.g. in terms of a dipole relaxation process reflecting the change of physical properties during setting [4], via plausible equivalent circuits with discussion of possible physical interpretation [5], as a function of the amount of unbound water remaining in the sample [1], or even in terms of polarization and diffusion at fractal pore surfaces [3].

Dielectric spectroscopy has been also applied to MDF cement [6,7], a possible application of which is considered for large-ares low-cost substrates in electronic packaging. Dielectric constant and loss factor from 10^0 Hz to 1 MHz and d.c. resistivity of these cements, processed in various ways, have been measured as a function of their composition, processing conditions and humidity. The higher dielectric constant and loss values at lower frequencies ($< 10^5$ Hz) have been attributed to unbound water and plasticisers present in the sample. Results of efforts to inhibit the effects of high humidities on the electrical properties are also reported.

In this work, we report, for the first time to our best knowledge, on the investigation of the dielectric behaviour of portland cement during the solidification process by means of the Thermally Stimulated Depolarization Currents (TSDC) method in the temperature range 80-300 K. The obtained results are analyzed and discussed as compared to findings reported by other authors on similar materials [1-7] and with reference to results obtained with the same method on a variety of samples [10-12].

2. EXPERIMENTAL

The principal of the TSDC technique is the following. The sample is polarized by applying an electric field at some suitable polarization temperature T_P for a time t_p large compared with the relaxation time at T_P. With the electric field still applied, the sample is cooled down to a temperature T_0 sufficiently low to prevent depolarization by thermal energy. The field is then switched off and the sample is heated at a linear heating rate b, while the resulting depolarization current, as the dipoles relax, is detected by an electrometer. Thus for each polarization mechanism an inherent current peak can be detected. In the case of a single relaxation process obeying the Arrhenius equation,

$$\tau(T) = \tau_0 \exp[W/kT] \tag{1}$$

the depolarization current density J(T) is given by the equation

$$J(T) = \frac{P_0}{\tau_0} \exp[-W/kT] \exp\left[-\frac{1}{b\tau_0}\int_{T_0}^{T} \exp[-W/kT']\,dT'\right], \tag{2}$$

where τ is the relaxation time, W the activation energy of the relaxation, τ_0 the pre-exponential factor, T the absolute temperature, k the Boltzmann constant and P_0 the initial polarization. By analysis of the shape of this curve the activation energy, W, the pre-exponential factor, τ_0, and the contribution of the peak to the static permittivity, $\Delta\varepsilon$ may be evaluated [8].

Characteristic features of the TSDC method are: its high resolving power, its sensitivity (dipole concentrations as low as 0.1 ppm can be measured) and the special experimental techniques it offers, by means of which it is possible to resolve relaxation processes, arising from different sets of dipoles with slightly different relaxation times, into their simpler components [8-10].

A standard equipment described in [10] was used for TSDC measurements in the temperature range 77-300 K. If not otherwise cited the experimental conditions used were the following: E_P = 3 kV cm^{-1}, t_P = 5 min, cooling rate 10 K min^{-1} and heating rate between 3 and 4 K min^{-1}.

Our samples were prepared by compressing a mixture of PCSO5 cement powder and water into cylindrical pellets. After preparation, the samples were immediately inserted between the measuring capacitor plates and TSDC measurements were recorded approximately every hour during the solidification process. The water/cement ratio in the samples varied between 10 and 40%.

Several kinds of contacts were used: silver paste, direct contact of the sample with the brass electrodes of the measuring capacitor, thin insulating foils (teflon, mica) or conducting (Au, Al, Cu) foils between the sample and the brass electrodes, in symmetrical and asymmetric arrangements.

3. RESULTS

In Fig. 1 we show TSDC plots recorded at different hydration times with the same sample. Three large peaks, numbered I, II and III in the order of increasing temperature, appear at about 150 K, 185 K and 210 K respectively in newly formed samples. As the cement setting progresses, the position and shape of the peaks remain unaltered up to a certain hydration time ranging between 5 and 9 hours. At the end of this time interval all peaks shift to higher temperatures reaching eventually the values of 120 K, 230 K and 250 K respectively (Fig. 2). It was, however, remarked that the recorded TSDC spectra remained completely unaltered with time, if the samples were not kept at room temperature (or higher) during several minutes between successive measurements.

The dependence of the peaks on the polarizing voltage V_P is shown in Fig. 3, where the maximum current I_M of peaks I and II is plotted as a function of V_P. I_M for peak I increases linearly with V_P while its position remains constant, providing a first evidence of the dipolar origin of this peak, contrary to peaks II and III, which display a quite different behaviour.

Fig. 4 shows TSDC plots obtained with the use of thin insulating foils between the sample and the capacitor electrodes. It is seen that peaks II and III are eliminated whereas peak I, although remarkably reduced, remains unaltered as far as its position and shape are concerned. This fact provides a further support for the dipolar origin of this peak.

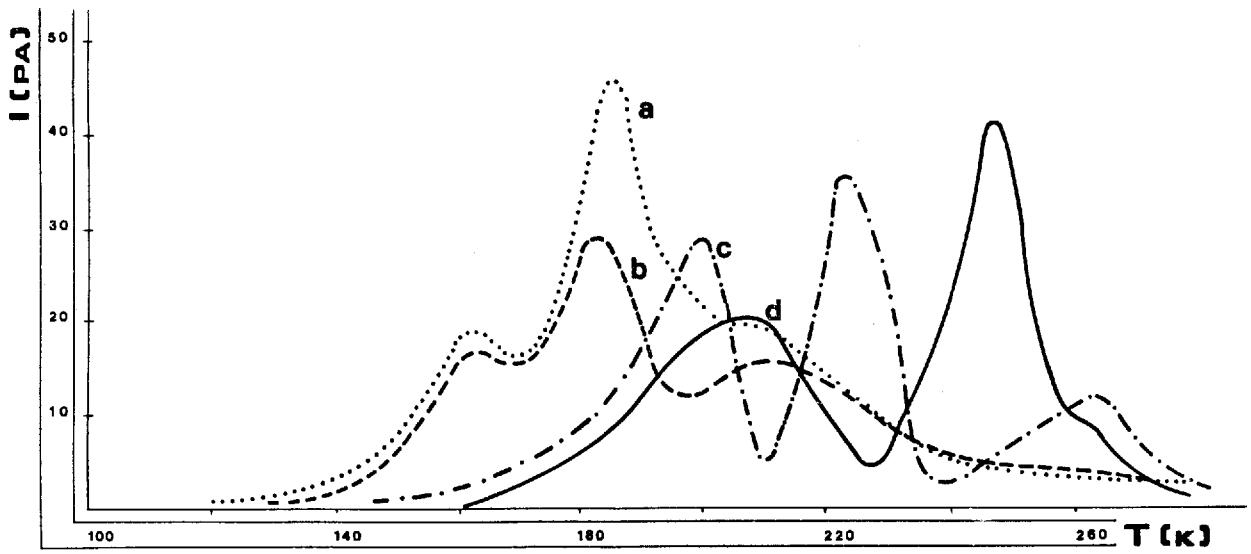

Fig. 1. TSDC plots of a portland cement sample for four different hydration times: (a) 1.5 h, (b) 3 h, (c) 850 h, and (d) 3,300 h.

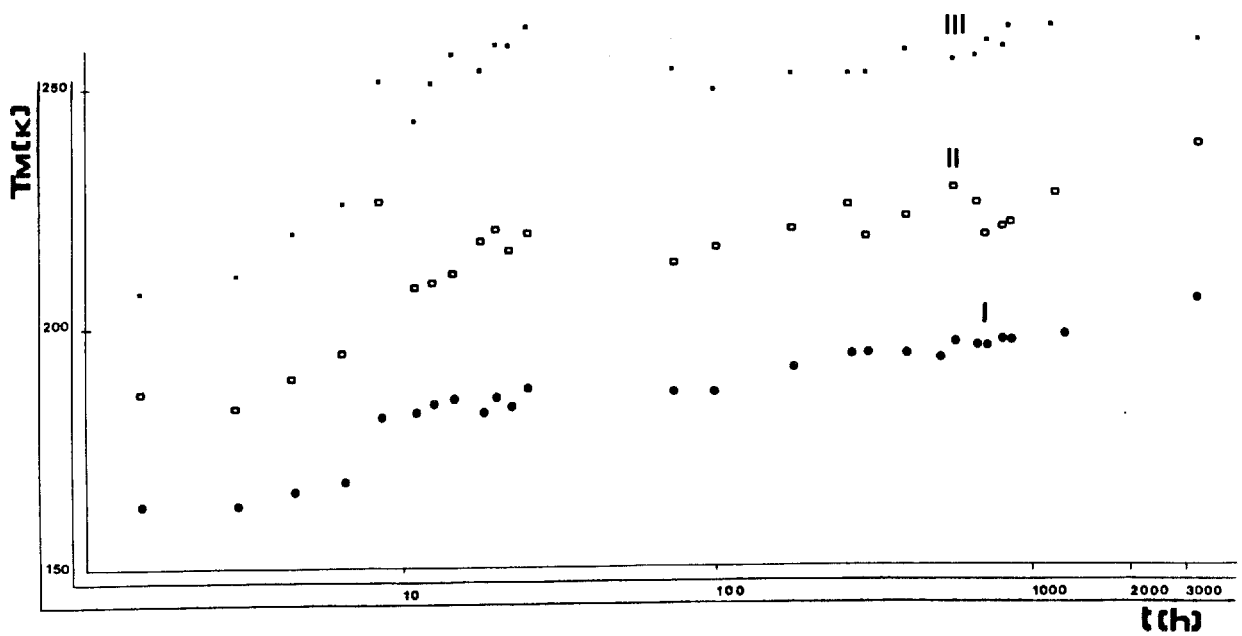

Fig. 2. Peak temperature T_m vs hydration time t for peak I (•), peak II (□) and peak III (▪).

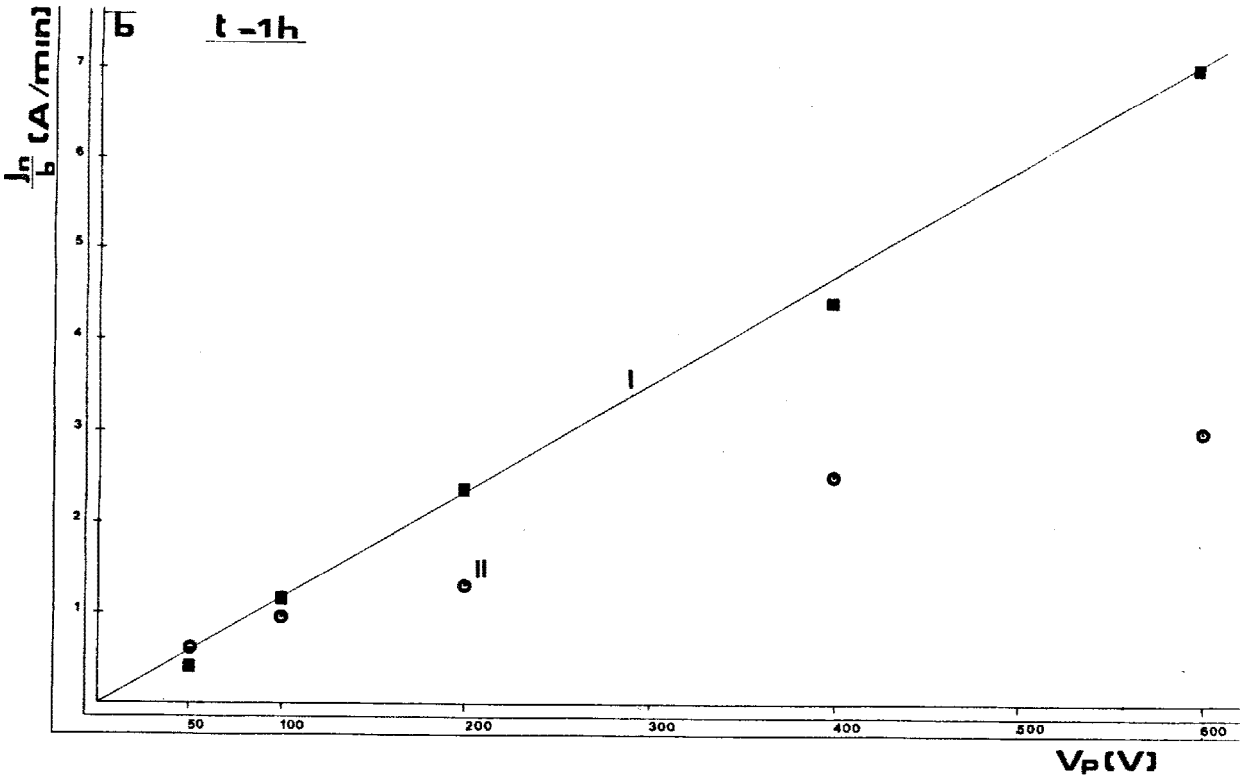

Fig. 3. Current maximum I_m divided by heating rate b vs polarizing voltage V_p for peaks I and II. T_p and t_p were kept constant.

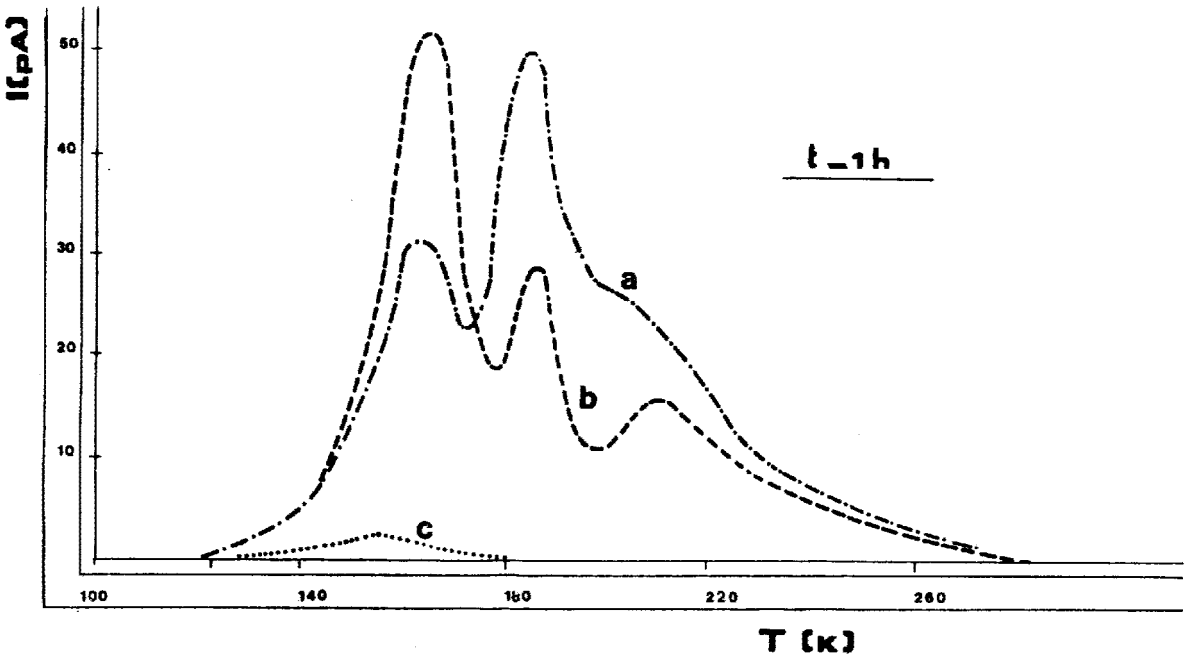

Fig. 4. TSDC plots of a Portland cement sample provided with brass electrodes (a), Cu contacts (b) and insulating electrodes (c).

Use of asymmetrical electrode arrangements shows that, except for peak I, recorded spectra are strongly influenced by the polarity of the forming field (Fig. 5).

Systematic analysis of peak I with the use of the partial heating technique [4] has shown that two relaxation mechanisms are likely to contribute, with activation energies in the range 0.35 - 0.42 eV and 0.52 - 0.58 eV respectively. The pre-exponential factor τ_0 was found equal to 2.1 (+ 0.5) x 10^{-14} s for both mechanisms and the contribution of the whole peak to the static permittivity was between 65 and 76 depending on electrode material (increasing with increasing electric contact conductivity).

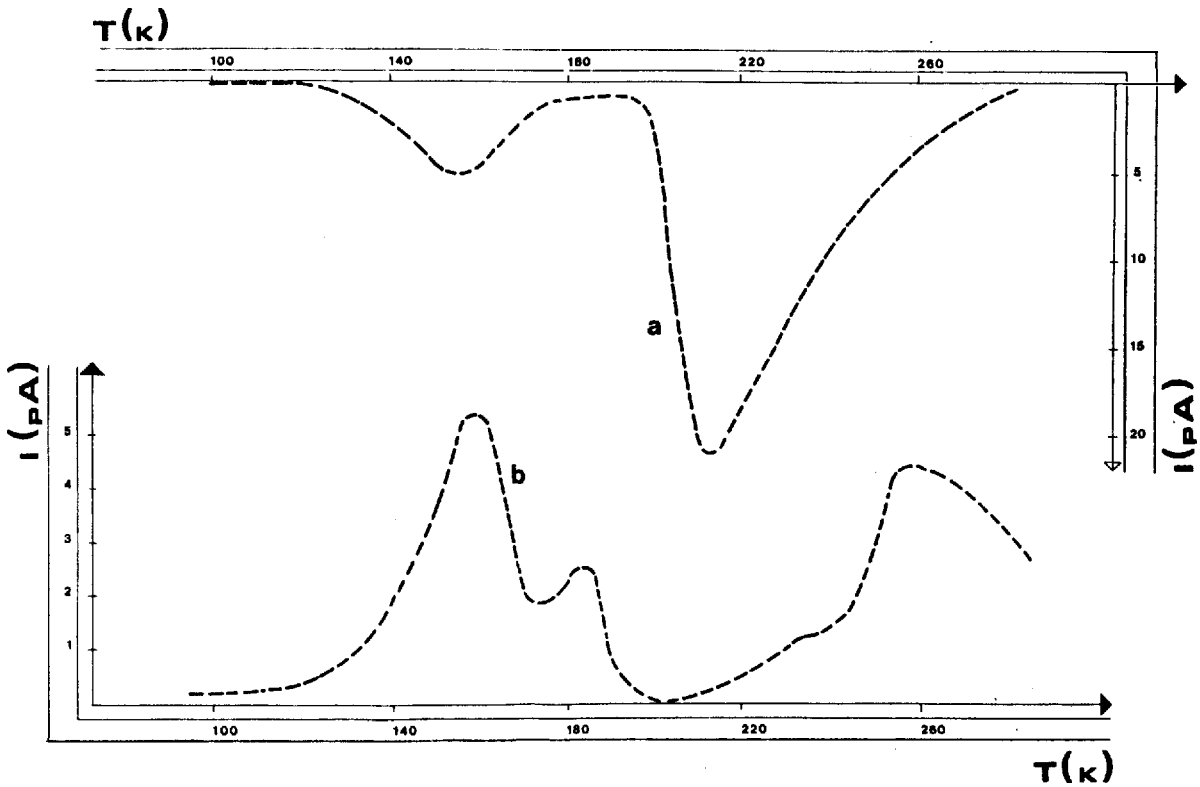

Fig. 5. TSDC plots of a cement sample in the brass-sample-Hostaphan configuration (a) and the same sample after inversion of the polarity of the polarizing field (b).

4. DISCUSSION

The dependence of peaks II and III on the polarizing field value (Fig. 3) and on the electrode material and arrangement (Fig. 5) suggests that part of peak II at least and peak III as a whole are related to dc-conductivity 11] and can reasonably be ascribed to injected electron carriers trapped in the bulk of the sample (II) and at the interfaces between sample and electrodes (III) as revealed also by measurements performed with other asymmetric electrode arrangements (not shown).

The origin of the dipoles responsible for peak I is not clear, nevertheless it is certain that they cannot be ascribed to free or loosely bound water molecules of the type observed in hydrated organic substances [10-12] contrary to other authors [13,14] who support that free and physically adsorbed water exist even in saturated cement paste. It is not excluded, however, that this peak, as well as part of peak II, is related to interlayer and/or intrapore water. These water molecules would become more strongly bonded (evolving to water bonded in the gel phase) as hydration proceeds, as witnessed by the displacement of the peaks towards the higher temperatures as the setting proceeds. Tightly (in the sense of irrotationally) bound water is not expected to be detected by this technique, according to our previous experience [11,12].

According to results obtained also by other authors with different dielectric techniques [4,7] and NMR [13,14], the sudden discontinuity observed in the position and shape of all three peaks in the interval between 5 and 9 hours of hydration time (Figs 1 and 2) corresponds to the "dormant" period of the setting process, during which the cement paste is still plastic.

Finally, the fact that TSDC spectra do not evolve with time when the samples are constantly kept at low temperatures (mostly sub zero temperatures) during successive measurements, shows that freezing of the samples causes complete hindering of the setting process.

REFERENCES

1. P.R. Camp and S. Bilotta, J. Appl. Phys. **66** (1989) 6007-13.
2. M.G. Abd El Wahed, J. Mat. Sci. Lett. **9** (1990) 35-38 .
3. G.A. Niklasson, A. Berg, K. Bratervik, B. Hedberg and L.O. Nilsson, Solid State Comm. **79**, (1991) 93-96 .
4. H.C. Kim and S.S. Yoon, J. Phys. D: Appl. Phys. **21** (1988) 1215-20.
5. C.A. Scuder, T.O. Mason and H.M. Jennings, J. Mat. Sci. **26** (1991) 349-53.
6. P.Sliva. L.E. Cross, T.R. Gururaja and B.E. Scheetz, Mat. Lett., **4** (1986) 409-413 and 475-80.
7. G.V. Chandrashekhar, E.I. Cooper and M.W. Shafer, J. Mat Sci. **24** (1989) 3356-60.
8. J. van Turnhout, in "Electrets", ed. G.M. Sessler, Springer Verlag (1980), 81-215
9. J. Vanderschueren and J. Gasiot, in "Topics in Applied Physics" vol. 37, "Thermally Stimulated Relaxation in Solids", ed. P. Braunlich, Springer Verlag (1979) 135-223.
10. P. Pissis, D. Diamanti, G. Boudouris, J. Phys. D **16** (1983) 1311-15.
11. A. Anagnostopoulou-Konsta and P. Pissis, J. Phys. D: Appl. Phys. **20** (1987) 1168-74.
12. A Anagnostopoulou-Konsta, L. Apekis, C. Christodoulides, D. Daoukaki P. Pissis and E.G. Sideris, in "Biologically Inspired Physics", ed. L. Peliti, Plenum Press, N.Y. (1991) 229-240.
13. L.J. Schreier, J.C. Mactarish, L. Milcovic, M.M. Pintar, R. Blinc, G. Lahajnar, D. Lasic and L. Reeves, J. Am. Ceram. Soc. **68** (1985) 10-16.
14. R. Blinc, J. Dolinsek, G. Lahajnar, A. Sepe, I. Zupancic, S. Zumer, F. Milia and M.M. Pintar, Z. Naturforsch. **43a** (1988) 1026-38.

PORTLAND COMPOSITE CEMENTS WITH REGULATED ALKALI-BUFFER BEHAVIOUR

Roland Herr, Wolfgang Wieker and Cornelia Hübert

Centre of Inorganic Polymers, Berlin
GERMANY

Summary

Pyrogenous pozzolanas formed in a high temperature process and hydratic pozzolanas formed in a chemical precipitation or leaching process show significant differences in their chemical reaction rate in alkaline environments, e.g. in pure alkali hydroxide solutions and in cement paste pore fluids. Based on this finding Portland composite cements (PCC) were developed having a well regulated and precalculable alkali buffer behaviour. The regulated alkali buffering is achieved by a qualified selection of the t y p e s and q u a n t i t i e s of pozzolanas introduced in the cement making process. Mixtures of pyrogenous and hydratic pozzolanas in PCC exhibit in the hydration process a less competitive but a more marked superposition effect with respect to alkali buffer behaviour of the cementitious system.
The pyrogenous pozzolanas used were aluminosilicatic lignite coal fly ash, silica fume, copper slag and a synthetically made cristobalite.
The hydratic pozzolanas applied were silica-rich residues of hydrometalurgical mineral acid extraction processes of alumina and rare earthes from calcinated clays and from wollastonitic phosphorous slag and a silica gel precipitated in a technical siccative making process.
Investigations by pore solution chemistry and mortar bar expansion tests have proved the aptitude of the new cement type reliably to prevent expansion and map pattern cracking of concrete associated with AAR.

Zusammenfassung

Pyrogene Puzzolane (die aus einem Hochtemperaturprozeß stammen) und hydratische Puzzolane (die aus einem chemischen Fällungs- oder Laugungsprozeß kommen) zeigen bemerkenswerte Unterschiede in ihrer Reaktionsgeschwindigkeit in alkalischen Medien. Auf der Grundlage dieses Befundes wurden Portland-Komposit-Zemente (PKZ) entwickelt, die Mischungen aus pyrogenen und hydratischen Puzzolanen enthalten und sich bei der Hydratation durch eine vorausberechenbare Alkalitätsentwicklung auszeichnen.
Für die Herstellung der PKZ wurden als pyrogene Puzzolane alumosilicatische Braunkohlenflugaschen, Silica Fume, Kupferschlacke und ein synthetischer Cristobalit verwendet. Als hydratische Puzzolane wurden die kieselsäurereichen Rückstände aus den hydrometallurgischen Aufbereitungsverfahren zur Gewinnung von Tonerde und seltenen Erden aus kalzinierten Tonen und aus wollastonitischer Phosphorofenschlacke verwendet.
In Untersuchungen mittels Porenflüssigkeitsanalyse und Mörtel-Prismen-Dehnungstests wurde nachgewiesen, daß diese neue Zementsorte eine betonschädigende Alkali-Zuschlagstoff-Reaktion zuverlässig verhindert.

INTRODUCTION

The use of natural or artificial pozzolanas as admixtures to high alkali Portland cements is a well established method for preventing expansion and map pattern cracking of concrete associated with alkali-aggregate reaction (AAR).
The effect of pozzolana addition to Portland cements is based on the chemical properties of pozzolanas and pozzolana-like materials to react with the highly alkaline cement paste pore fluid much quicker than the coarser sand and gravel-size aggregates. The pozzolanic reaction is an essential part of the hydration reaction of a blended cement and results in the formation of non-swellable alkali bearing CSH phases with a relatively low C/S ratio. The alkali uptake by the solid phases is reflected in the lowering of the cement paste pore fluid alkalinity level.
Briefly stated, the kinetics of the pozzolanic reaction plays a dominating role in counteracting AAR.
This paper deals with our findings on the chemical reactivity of artifical pozzolanas in alkaline environments both in pure alkali hydroxide solutions and as admixture components in pozzolanic Portland composite cements (PCC) containing different types and quantities of pozzolanas.

MATERIALS AND EXPERIMENTAL

In our experiments 3 types of materials were used:

A) Basic materials: Pure potassium hydroxide solution, 0.50 Moles KOH/1; high alkali Portland cement PZ 45 (PC 1), Na_2Oeq. 1.25 %; low alkali Portland cement PZ 45 NA (PC 2), Na_2Oeq. 0.43 %, the both cements according to German standard DIN 1164.

B) Pyrogenous pozzolanas: Synthetic Cristobalite (SyC) sintered at 1400°C; Copper slag (CoS) metallurgical waste product; aluminosilicatic lignite coal fly ash (BFA).

C) Hydratic pozzolanas: Silica gel (SG) precipitated in a technical siccative making process; SiO_2-rich residues of a hydrometallurgical mineral acid extraction process of Al_2O_3 from calcinated clays (RCE); SiO_2-rich residues of a hydrometallurgical mineral acid extraction process of rare earthes from a wollastonitic phosphorous slag (RPSE).

The chemical and physical data of the investigated materials are shown in Table 1 and 2.

Conductometric measurements. The reactivity of pozzolanas was characterized on the basis of the rate of hydroxide consumption from a given 0.50 Molar potassium hydroxide solution at 20 °C and 60 °C monitored by electrical conductometry. The reaction curves (Figure 1) were mathematically interpreted by means of the AVRAMI-EROFEEV equation / 1 /.

Cement paste preparation, squeezing technique and pore fluid analysis. Blended cements were prepared by mixing up to 20 mass-% of different types of pozzolanas with PC 1 cement. Changes in the total sulphate content of the cements, caused by the substitution method of cement preparation, were corrected by small additions of anhydrite. The total SO_3-content in each pozzolana-containing Portland cement was 3.35 %. The cement pastes were mixed with distilled water in plastic bottles using a water-solid ratio of 0.50. After mixing, the bottles were tightly closed and subsequent stored in containers in a damp atmosphere at 20 °C for a 400-days hydration period. At the various ages, the cement paste pore fluids were squeezed applying a maximum squeezing stress of 320 MPa in each case. The paste pore fluids were filtered through a 0.20 µm PTFE-syringe filter and diluted for analysis. The ion concentrations of Na^+ and K^+ were determined by flame photometry, Ca^{++} by complexometric titration, OH^- by acidimetric titration and SO_4^{--} by ion chromatography, respectively.

Table 1: Chemical data of cements and pozzolanas, mass-% *)

oxides	PC 1	PC 2	SyC	CoS	BFA	SF	SG	RCE1	RPSE
SiO_2	19.7	20.7	98.5	47.2	47.5	95.5	84.6	71.8	88.9
Al_2O_3	5.17	4.90	0.0	17.4	31.4	0.80	0.0	12.9	0.14
Fe_2O_3	3.10	1.90	0.0	4.1	6.6	0.81	0.0	2.07	0.04
CaO	62.90	64.40	0.0	19.3	4.0	0.0	0.0	0.06	0.47
MgO	2.34	1.40	0.0	7.6	1.5	0.70	0.0	0.06	0.04
SO_3	3.36	3.40	0.0	0.0	0.2	0.0	0.0	0.0	0.02
K_2O	1.43	0.50	0.0	2.1	2.1	1.54	0.0	1.01	0.02
Na_2O	0.31	0.10	0.0	0.92	0.2	0.33	0.0	0.03	0.05
Na_2O-eq.	1.25	0.43	0.0	2.30	1.8	1.34	0.0	0.70	0.05
L.O.I.	0.85	1.80	1.0	0.80	2**)	1.07	15.4	8.51	4.46
Insol.	0.40	0.30	n.d.	n.d.	n.d.	n.d.	n.d.	n.d.	n.d.

*) 110 °C dried samples; **) carbon

Table 2: Physical data of cements and pozzolanas

type	PC 1	PC 2	SyC	CoS	BFA	SF	SG	RCE1	RPSE
BET-surface m^2/g	1.5	1.4	1.43	1.0	3.0	27.0	632	163	94
50 % sieve passing µm	22	20	22	19.5	23	0.22	5	7	6
chemically bond water mass-%	<0.5	<0.5	<0.5	<0.5	<0.5	0.5	5.55	3.61	4.0

Cement mortar strength and mortar bar expansion measurements. Cement mortar strength and mortar bar expansion were measured by means of 4 x 4 x 16 cm prism test acc. to German standard DIN 1164, parts 2, 5, 6 and 7. For AAR expansion measurements, 20 mass-% of the quartz sand within the fractions 0.16-0.50, 0.50-1.0 and 1.0-2.0 mm was replaced with crushed and sieved Pyrex glass or 8 mass-% Beltane Opal as alkali sensitive aggregate components. The expansion prisms were kept in closed containers above water at a temperature of 40 °C.

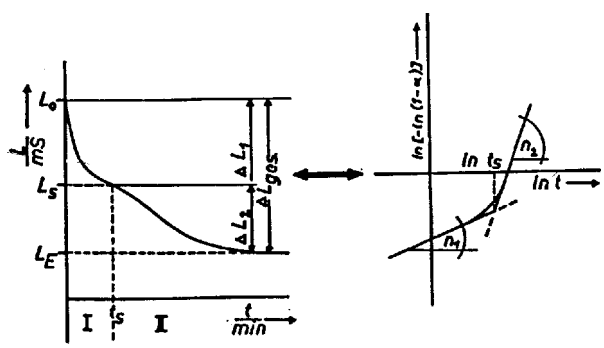

Fig. 1

Principle of the mathematical interpretation of the conductivity-time curves of pozzolana-potassium hydroxide suspensions according to AVRAMI-EROVEEV equation.

RESULTS AND DISCUSSION

Conductometric measurements. The results of the hydroxide consumption test on the pyrogenous pozzolana SF (silica fume) and pozzolana RCE1 in 0.50 Molar KOH/l are exemplified in Figure 2. As can be seen the pozzolana SF reacts in the alkaline environment and gives a linear function in a double logarithmic diagram. From this finding we conclude that the dissolution of silica fume can be described as a 1-stage mechanism mainly including the

$$\geq Si - O - Si \leq + OH^- \dashrightarrow \geq SiO^- + \geq SiOH \qquad \text{(eq. 1)}$$

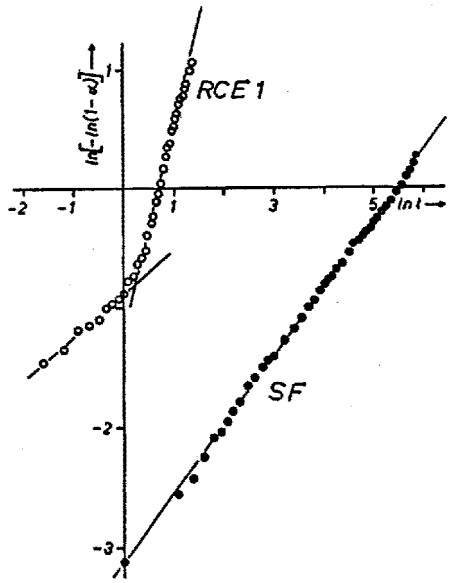

Figure 2: Results of the interpretation of the conductometric hydroxide ion consumption test. Pozzolanas: RCE1 and SF; KOH 0.50 M; temperature 60 °C; molar ratio Si : OH = 1 : 1.

breaking of the siloxan bridges.

In contrast to this finding the hydratic pozzolana RCE1 is shown to react so as to give two linear functions with a clearly point of intersection. This means that the dissolution of the SiO_2-residues from calcinated clays can be described as being in a certain analogy to pure silica gel, e.g. as a 2-stage mechanism, the both stages overlapping each other. At stage 1, the dominant reaction is the neutralisation reaction of the acid silanol groups.

$$\equiv SiOH + OH^- \dashrightarrow \equiv SiO^- + H_2O \quad \text{(eq. 2)}$$

At stage 2 the dominating reaction is similar to equation 1 and leads to breaking of the siloxan linkages.

Additionally, the reaction rate constants k_2 (reaction stage 2) of the Si-O-Si bond degradation of the pozzolanas SG, RPSE, RCE, SF, BFA and Aerosil in 0.50 Molar KOH solution at 20 °C and 60 °C (molar proportions Si : OH = 1 : 1) were calculated. The results are listed in Table 3. The results demonstrate clearly that hydratic pozzolanas having a large specific surface occupied by surface standing OH-groups are essentially more reactive than pyrogenous ones.

type of pozzolana	k_2 (min^{-1})	
	20 °C	60 °C
- hydratic		
SG	0.2250	4.953
RPSE	0.0136	0.589
RCE	0.0100	0.507
- pyrogenous		
Aerosil	0.0084	0.126
SF	$< 10^{-4}$	0.004
BFA	$\ll 10^{-4}$	n.d.

Table 3:
Reaction rate constants k_2 (reaction stage 2) of the Si-O-Si bond degradation of pozzolanas in 0.50 M KOH-solution at 20 °C and 60 °C (molar proportions Si : OH = 1 : 1.

Cement paste pore fluid compositions of mono-pozzolanic cements. The evolution of cement paste pore fluid compositions of mono-pozzolanic cements containing on the one hand a typical pyrogenous pozzolana (SF) and on the other hand a typical hydratic pozzolana (RCE1) is exemplified in the Figures 3 and 4.

Fig. 3 shows the pore fluid composition of cements containing 10 % and 20 % of the typical pyrogenous pozzolana silica fume (SF). Alkalinity increases up to 7 days and then decreases with increasing hydration time and amounts of SF. In a similar way the other pyrogenous pozzolanas investiga-

ted here (BFA, CoS, SyC) behave. The sequence of the reactivity is as follows:

SF >> BFA >> CoS = SyC

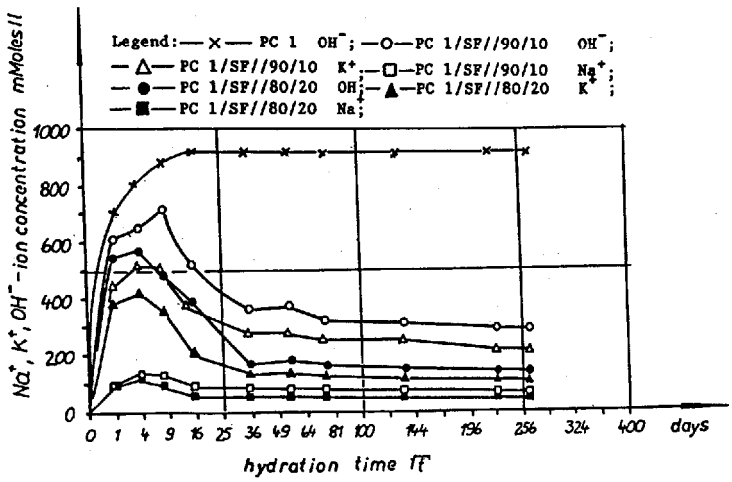

Fig. 3

Cement paste pore fluid composition of high alkali Portland cement PC 1, of PC 1/SF//90/10 and of PC 1/SF//80/20 mono-pozzolanic cement pastes versus the hydration time (temperature 20 °C; W/S 0.50).

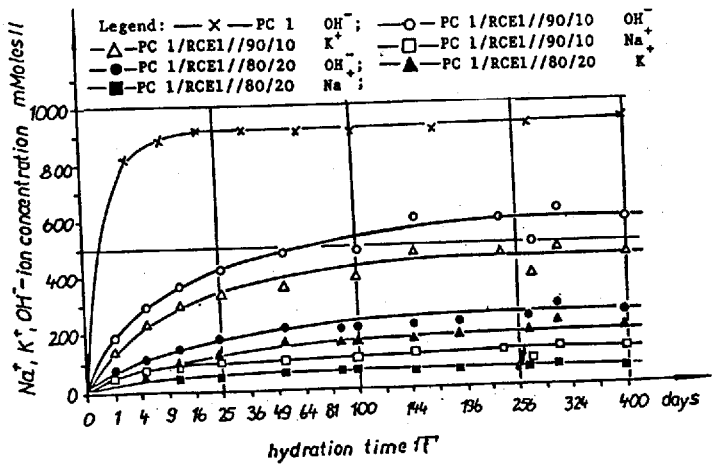

Fig. 4

Cement paste pore fluid composition of high alkali Portland cement PC 1, of PC 1/RCE1//90/10 and of PC 1/RCE1//80/20 versus the hydration time (temperature 20 °C; W/S 0.50).

Fig. 4 shows the pore fluid composition of the cements containing 10 % and 20 % of a typical hydratic pozzolana, e.g. a silica-rich residue of clay extraction (RCE1). This pozzolana brings about a decrease in both alkalinity and alkali concentration in the early stage of hydration and does not show the maxima given in Fig. 3. In a similar way behave the other hydratic pozzolanas. RCE1 shows a little bit lower chemical reactivity than that of SG and RPSE. The sequence of the reactivity of the investigated hydratic pozzolanas is

SG > RPSE > RCE1

The technical advantage in the use of cements containing hydratic pozzolanas, is that this type of cement exhibits a larger alkali buffer rate than alkali sensitive aggregates. By using this type of alkali buffering cement AAR can be prevented reliably / 2 /. Doubtless, a technological disadvantage in the use of this type of pozzolanic cement is its bad early strength development which is more drastic deminished than that of a low alkali Portland cement.

In this perspective, we started investigations for optimizing the proper-

ties of pozzolana containing cements by using properly selected mixtures of pyrogenous and hydratic pozzolana components.

Fig. 5 shows that the moderate alkali buffer effect of a lignite resp. a brown coal fly ash (20 mass-%) in a blended cement can be improved remarkably by replacing BFA with 5 - 10 % RCE1. The Portland composite cement PC 1/BFA/RCE1//80/10/10 shows an alkalinity development which approximates to that of an original low alkali Portland cement, e.g. PC 2, Na_2Oeq. 0.43 % (Table 6).

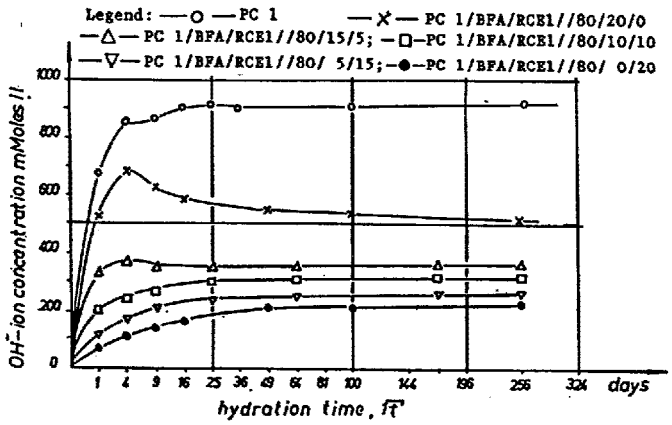

Fig. 5

Cement paste pore fluid composition of high alkali Portland cement PC 1 and of Portland composite cements composed of PC 1 and different BFA/RCE1 pozzolana mixtures versus the hydration time (temperature 20 °C; W/S 0.50).

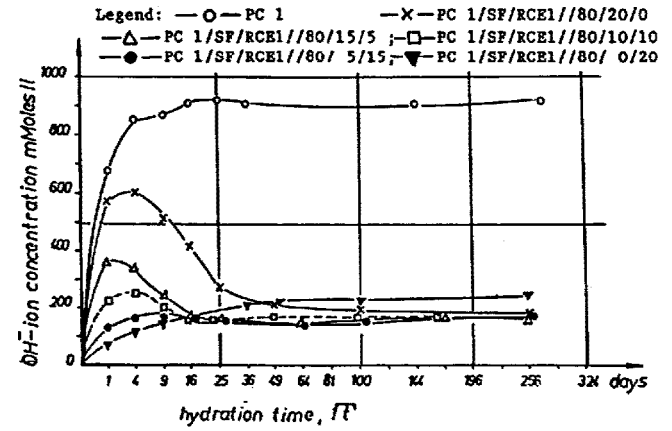

Fig. 6

Cement paste pore fluid composition of high alkali Portland cement PC 1 and of Portland composite cements composed of PC 1 and different SF/RCE1 pozzolana mixtures versus the hydration time (temperature 20 °C; W/S 0.50).

Fig. 6 shows a similar effect in the Portland composite cement PC 1/SF/RCE1. By decreasing SF/RCE1 ratio the maximum alkalinity of the cement paste decreases and within a few weeks it can be reduced to a level comparable to that of an original low alkali Portland cement.

Based on the trend of the alkalinity curves it was assumed that each of the two pozzolanas in the pozzolana mixtures behave more or less individually and therefore a precalculation of the alkalinity level as a function of the t y p e and q u a n t i t y of the pozzolanas used should be possible.

In order to prove the superposition effect of pozzolanas in Portland composite cements we determined the so-called specific efficiency coefficient (SEC) of the pozzolanas SF, RCE1 and BFA in PC 1/SF 90/10 and 80/20, PC 1/RCE1 90/10 and 80/20 and in PC 1/BFA 90/10 and 80/20 mixtures. For this reason the OH^- ion concentration of the cement paste pore fluid was measured after 250 days of hydration at normal temperature. The slope of the linear function ranging between 0 and 10 % pozzolana content in the blended cement is considered as the specific efficiency coefficient SEC. The

various calculated SEC-values are listet in Table 4.

Table 4: Specific efficiency coefficients SEC of different types of pozzolanas, valid for W/S ratio 0.50, hydration temperature 20 °C and hydration time 250 days.

type of pozzolana	SEC (mMoles OH^-/1 · %)
SF	- 42.5
RCE1	- 34.0
BFA	- 22.0

On the basis of the SEC-values and the mass proportions of the pozzolanas, the hydroxide ion concentrations expected to be found in the pore solutions of the hardened Portland composite cements after hydration of 250 days were calculated. Table 5 shows the results of the measurements and calculations.

Table 5: Measured and calculated OH^- ion concentration values in the pore fluid of Portland composite cements after 250 days hydration at 20 °C (W/S ratio 0.50; squeezing stress 320 MPa)

cement composition	OH^- ion concentration mMoles/1 measured	calculated
PC 1 pure	920	950 1) 891 2)
PC 1/SF/RCE1 80/ 5/15	165	197
PC 1/SF/RCE1 80/10/10	170	155
PC 1/SF/RCE1 80/15/ 5	156	113
PC 1/BFA/RCE1 80/ 5/15	260	300
PC 1/BFA/RCE1 80/10/10	320	360
PC 1/BFA/RCE1 80/15/ 5	370	420

1) calculated by equation $Y = 724\ X + 45$ / 3 /
2) calculated by equation $Y = 699\ X + 17$ / 4 /.

The measured and the calculated OH ion concentration values are well approximated to each other. From these findings we conclude that pozzolana mixtures composed of pozzolanas with different chemical activity exhibit a less competitive but a more marked superposition effect with respect to alkali buffer behaviour in the cementitious system. This result was surprising indeed as we had expected to find a stronger dominance of the more active pozzolana component.

Characteristic data of optimized Portland composite cements are shown in Table 6. These data show that Portland composite cements have a well regulated alkali buffer behaviour, a good strength development, a high final compressive strength and an excellent reduction of AAR caused mortar bar expansion.

GENERAL CONSIDERATIONS ON RESULTS AND CONCLUSIONS

In pure Portland cement pastes (Fig. 7a) the curves of the cement paste pore fluid alkalinity is determined essentially by the cement alkali content. The curve A is typical for a high alkali cement, e.g. PC 1 in our investigation (Na_2Oeq. 1.25 %) and curve B is typical for a low alkali cement, e.g. PC 2 in our investigation (Na_2Oeq. 0.43 %).

In cement pastes containing one pyrogenous pozzolana only (Fig. 7b) the

Table 6: Results of alkalinity development, expansion behaviour and compressive strength increase of Portland-, Portland pozzolana- and Portland composite cement mortars (hydration temperature 20 °C; W/S ratio 0.50)

hydration time, days	1	3	7	28	90	180	360
Portland cement PC 1, Na_2Oeq. 1.25 %							
alkalinity mMoles/l	680	840	860	918	920	921	918
expansion [1] mm/m	n.d.	0.25	0.65	2.40	5.75	6.80	7.20
compressive [2] strength, MPa	18.5	32.0	38.1	47.0	48.5	51.3	n.d.
Portland cement PC 2, Na_2Oeq. 0.43 %							
alkalinity mMoles OH/l	150	280	300	325	330	326	317
expansion [1] mm/m	n.d.	0.10	0.10	0.12	0.13	0.15	0.14
compressive [2] strength, MPa	12.1	26.5	36.0	44.4	53.2	53.5	n.d.
Portland pozzolana cement PC 1/BFA//80/20							
alkalinity mMoles OH/l	520	690	650	554	542	518	500
expansion [1] mm/m	n.d.	0.12	0.17	0.34	0.52	0.68	0.77
compressive [2] strength, MPa	14.5	26.5	34.5	43.6	48.9	56.3	58.4
Portland composite cement PC 1/SF/RCE//80/15/5							
alkalinity mMoles OH/l	345	340	260	180	178	178	183
expansion [3][4] mm/m	0.14	0.23	0.22	0.20	0.20	0.20	0.20
compressive [2][3] strength, MPa	16.1	30.2	44.3	64.0	73.1	75.2	75.7
Portland composite cement PC 1/BFA/RCE//80/12/8							
alkalinity mMoles OH/l	210	242	261	305	310	315	314
expansion [1][3] mm/m	n.d.	0.10	0.10	0.14	0.16	0.16	0.15
compressive [2][3] strength, MPa	14.3	29.1	36.5	48.5	56.0	62.3	63.4

legend:
1) Mortar 1 : 3 : 0.50; replacement of 20 mass-% aggregate quartz sand within the fractions 0.16-0.50, 0.50-1.0 and 1.0-2.0 mm by crushed Pyrex glass; 40 °C storage in moist air.
2) Mortar 1 : 3 : 0.50; 100 % aggregate quartz sand.
3) Addition of 2 mass-% superplastisizer related to cement mass.
4) Mortar like 1) containing 8 mass-% crushed Beltane Opal.

alkalinity level of the cement paste pore fluid can be regulated within the field A-C by means of the type of pozzolana selected and the quantity used.

In cement pastes containing one hydratic pozzolana only (Fig. 7c) the alkalinity of the cement paste pore fluid can be regulated within the field A-D by means of the type of hydratic pozzolana chosen and the quantity used.

Finally, in cement pastes containing at least one pyrogenous and one hydratic pozzolana component (Fig. 7d) the alkalinity of the cement paste pore fluid can be regulated within the field A-E by means of a proper selection of the types and quantities of pozzolanas. The curve E characterizes an extremely alkali buffered cement type.

The field A-E in Fig. 7d occupies a much larger area than the other fields A-C (Fig. 7b) and A-D (Fig. 7c) and therefore it characterizes the extended possibilities in the manufacture of alkali buffered cements / 5 /.

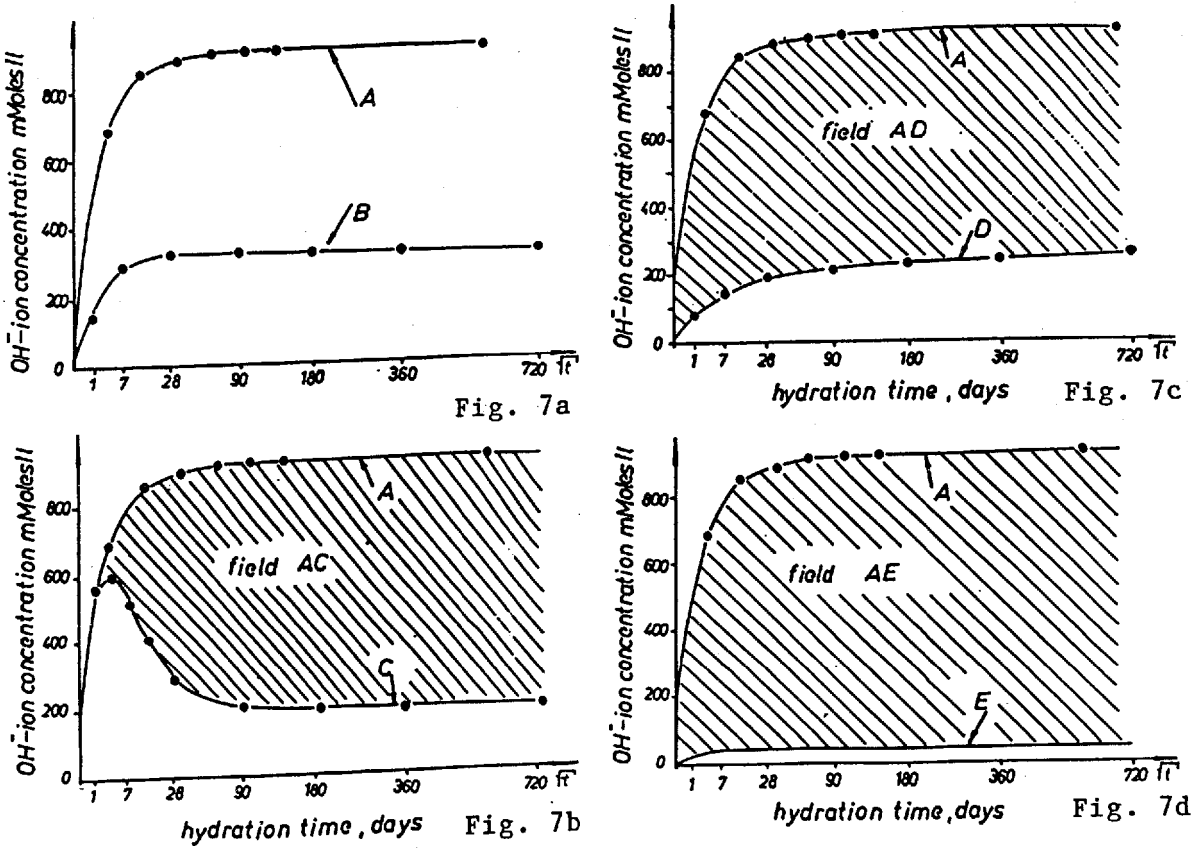

Fig. 7: General considerations on the possibilities of the regulation of cement paste pore fluid alkalinity level in pure Portland cement cement pastes (Fig. 7a), in mono-pozzolanic Portland cement pastes containing pyrogenous pozzolanas (Fig. 7b), in mono-pozzolanic Portland cement pastes containing hydratic pozzolanas (Fig. 7c) and in Portland composite cement pastes containing mixtures of pyrogenous and hydratic pozzolanas (Fig. 7d).

From this finding we can conclude that Portland composite cements made of Portland cement clinker rich in alkalis, gypsum or anhydrite and properly selected pozzolana mixtures based on industrial by-products represent a new cement type which would be most suitable in terms of a reliable pre-

vention of map pattern cracking and expansion of concrete associated with alkali-aggregate reaction.

REFERENCES

1. C. Hübert: Investigations of the alkaline degradation of silica gels. Thesis 1988, Academy of Sciences of GDR, Berlin (in German).

2. R. Herr, W. Wieker and G. Priem: Early strength Portland pozzolana cement with increased chemical corrosion resistance. GDR patent specification DD 155 059, 05.12.1980.

3. R. Herr, W. Wieker et al.: Development of procedures for binding and buffering of reactionable alkalis in concrete. Unpublished contract research report for VEB Zementkombinat Dessau, Sept. 1983 (in German).

4. S. Diamond: ASR - Another look at mechanisms. Proc. 8th Intnl. Conf. on Alkali-Aggregate Reaction, Kyoto, Japan. 1989, p. 83 - 94.

5. R. Herr, W. Wieker and R. Ilgner: Alkali regulated high strength Portland composite cement and procedure for making high strength and durable concrete. GDR patent specification DD 287 473 A5, 17.3.1989.

THE HYDRATION OF POZZOLANIC CEMENT ON THE BASE OF FIRED CLAY BRICKS

Jonjaua Ranogajec* and Ljiljana Fišang**

**Faculty of Technology, Novi Sad, YUGOSLAVIA*
***Beocin Cement Factory, Beocin, YUGOSLAVIA*

Summary

The hardening characteristics of a number of mixtures on the base of thermally activated brick clay materials, burnt at 960°C in laboratory and industrial conditions and mixed with 30% mass. of portlandite (water/solid = 0,60) are investigated. Feldspars, carbonates and peat component presented in the green samples, which were also involved in the thermal activation, suport the pozzolanic activity of the initial material.

The use of fresh burnt bricks, as the base pozzolanic material gives the weakest mixtures in the contact with portlandite. Part of the free CaO, from the burnt material, conversing to $CaCO_3$ during the 14 day maturing period (old bricks), dramatically increases the rate of hydration process.

Amorphous character of the heated samples have a remarcable influence on the hidration process and the formation of specific crystal types from the groups of C - S - H and C - A - H, as well as ettringite crystal form.

Resumé

Les recherches ont portées sur une série de mélanges constitués de mineraux d'argile activées thermiquement par cuisson à 960°C et de portlandite (30% mass). La présence du feldspath, du calcaire et des minéraux argilex, dans les matières pnemières canduit à des phases désorganisées après de la calcination des pouzzolanes, ayant la possibilité de activer le processus hydraulique, donnant des phases hydratées; C - S - H and C - A - H.

Les résistances, les plus faibles ont ete observées dans les mélanges avec des briques fraiches. Les brigues anciens, après une conversation de CaO $\rightarrow CaCO_3$ des 14 jours, ont montrées un bon compartement de durissement.

1. Introduction

The thermal activation of the burnt clay material presents one of the ways to obtain ceramic system with remarcable pozzolanic character. Ghorab /1/ has analysed different types of clay materials; bentonite, kaolin and their mixtures with talc and feldspars in the field of pozzolanic characteristics, after a specific thermal activation. Changes in the internal surface area of these materials have been studied as the function of temperature and in the presence of portlandite. The mixtures of thermally activated kaolinite and bentonite give higher stregth values than those obtained from each individual minerals. In these systems the ratio thermally activated clay/calcium hydroxide has had a remarcable influence on the strength of samples /2/. The presence of iron oxides has a close influence on the pozzolanic effect of the clay materials, increasing with the ratio kaolin+ $+Fe_2O_3$/quartz.

Same of the papers have analysed the reactions among feldspars and water/2,3/. At 39^oC the alkali feldspars produce tetra-calcium aluminate hydrates, alkalics and/or calcium aluminate hydrates. In the case of Ca-feldspars, more tetra-calcium aluminate hydrates were produced /3/, which in turn formed ettringite in the presence of sulphates. Matousek and Sauman /4/ have reported the expansion characteristics of expanding cements based on Portland cement, metokaolinite and gypsum. In the case of the mixture which contains 20% mass. of metakaolinite, complete consumption of gypsum had occured between the 7th and the 10th day. The expansion continued up to the 14th day. After that period ettringite had stopped. Chatteriji /5/ was first who reported that in the system C_3A-$Ca(OH)_2$-gypsum-water, expansion continues even when ettringite was disappearing and monosulfate was forming.

Lou Zonghan /6/ has studied 24 slag glasses from the system CaO-Al_2O_3-SiO_2. His investigations were laid on the dissociation reaction of aluminium and the formation of ettringite under alkaline conditions. C-S-H gel together with ettringite were the phases which were rapidaly formed by the surface reaction between the slag glass and alkaline solution. The expansion of ettringite does not always depend on CaO concentration /7/ but depends on pH value in pore solution within the paste. Than the authors related the expansion of the systems with pH value no CaO concentration in the case that alkali is present in the paste.

In the system CaO-Al_2O_3-CO_2-H_2O, it is possible to obtain phases like $C_4A\bar{C}H_{11}$, C_2AH_8 and CAH_{10}. To escape the formation of cubic form C_3AH_6, one of the phases which can destroy the structure of the cement paste, $CaCO_3$ can be used as positive influence on the hydration of tricalcium-aluminate (C_3A phase) /8/.

One of aims of the infastigations of this paper was to clarify the influence of $CaCO_3$ in the binder paste. The crystal form $C_3A \cdot CaCO_3 \cdot Hn$ like $C_4A\bar{C}H_{11}$ is the main product of hydration in the system CaO-Al_2O_3-CO_2-H_2O. The results of our invastigations permit the explanation of the positive effect of ground $CaCO_3$ admixture in practical concrete technology. Chatteriji in his paper /5/ concluded that the addition of finely ground $CaCO_3$ to ordinary Portland cement decreased the sulphate expansion of cement by decreasing monosulphate formation. His results were conected with ours, having in mind the fact that we used fired brick clays instead of metakaolinate.

1. Experimental

For the experiments we have used:

1. Laboratory fired bricks (t=960°C) of particular mineral compositions fresh systems I and II with the particles which have been ground below 100 μm and than mixed with portlandite in the ratio 70/30 mass.%. The ratio of water/solid was 0.60. The systems have presented the field of our investigations with the aim to put in the evidence the pozzolanic proprieties of the fiered clays (bricks). The obtained mixtures presented the base for the designed prisms 60x x10x10 mm dimensions, which have been stored 2, 3, 7 and 28 days in the water of 25°C. The phase composition of the hydrated samples has been investigated by SEM and X-ray diffraction.

2. Bricks from the ordinary production, ground below 100 μm with the specific state: "fresh" and "old". Time of maturing of "old" bricks was 14 days. The ground bricks have been used for designing prisms of the same dimensions, as in the point 1 of experimental procedure, using water/solid ratio of 0.60. The hardering characteristics and phase composition of "fresh" and "old" samples after 2,3,7 and 28 days have been determined.

3. Discusions

The X-ray analysis of the pastes after 2, 3, 7 and 28 days of curing time put in evidence the pozzolanic proprieties of the fired bricks. The difference between chemical and mineral compositions of the laboratory systems (point 1 of the experimental part); more Al_2O_3 and Na_2O oxides in the case of fired system I, was the main reason for obtaining specific hydrates of the group C-A-H. Namely, the presence of C_3AH_6 crystals can be evident in the case of paste on the base of brick I. This phase presents the intermediar field for ettringite formation (Fig. 1), whose crystals with its particular shape can destroy just formed microstructure of the hidrated sample.

Hydrogarnet, C_3AH_6, in the analysed samples (specific in the case of paste on the base of brick I) is the dominant C-A-H phase before the final set (Fig. 1) of the sample. This is the consequence of the chemical instability of the first period of the hydration process; CAH_{10} and C_2AH_8. Which forms tend to "covert" over time to C_3AH_6 (hydrogarnet) and AH_3. This convertion is accompained by up to 50% densification, increases in porosity and dramatic loss of strength. The standard C-S-H phases are presented in both mixtures (Fig. 2), but their presence cannot influence too much on the expansion of the hydrogarnet form.

Table I The chemical composition* of the burnt clay bricks I and II

Oxides	Brick I	Brick II
	% mass.	
L.O.I	0,89	0,95
SiO_2	59,82	60,12
Al_2O_3	19,19	16,41
Fe_2O_3	3,88	7,90
CaO	5,92	5,27
MgO	6,06	5,84
K_2O	2,29	2,11
Na_2O	1,48	1.06
Σ	99,53	99,61

* The initial materials before burning process, could be specified as raw materials with the presence of clay materials (illit, chlorite , carbonates (dolomite and calcite), quartz, feldspars mica and peat component (X-ray diffraction, DTG and DSC analysis).

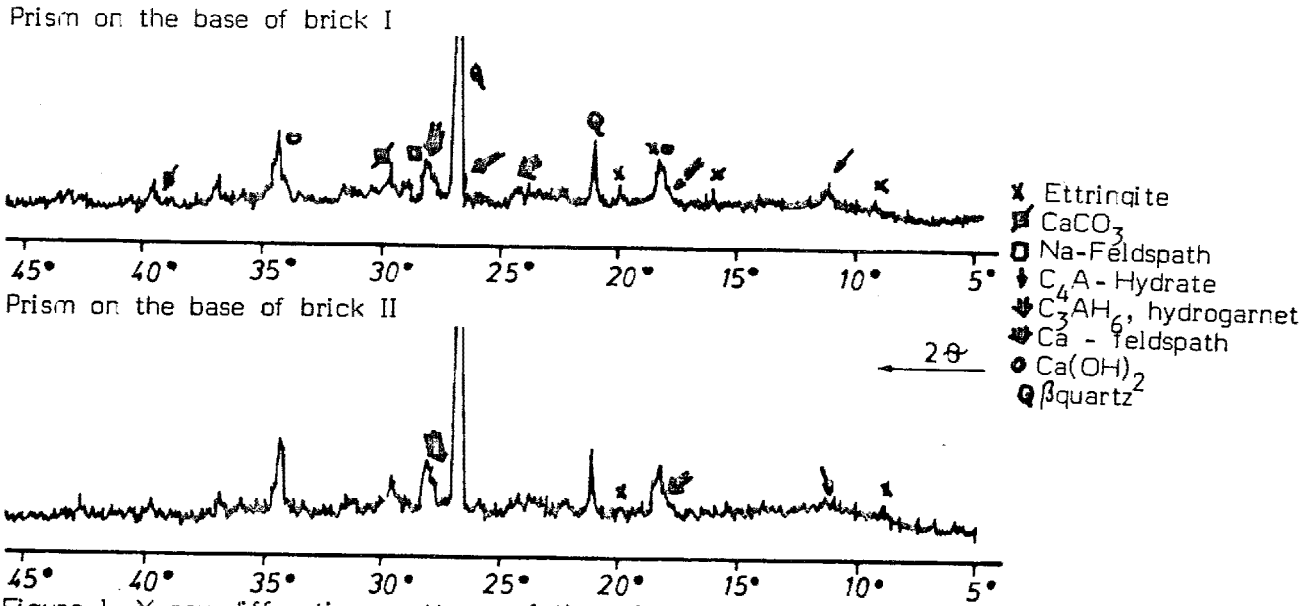

Figure 1. X-ray diffraction patterns of the prisms on the base of laboratory burnt brick clays I,II and portlandite, curing time 28 days.

Prism of the brick I

Prism of the brick II

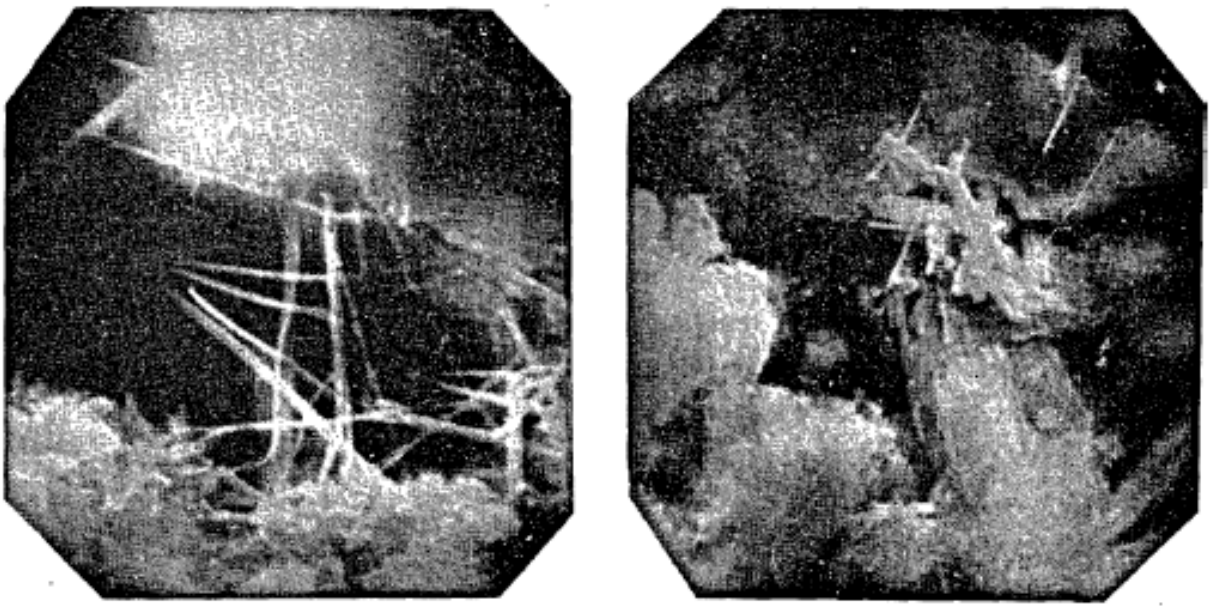

SEM x 10 000

SEM x 10 000

Figure 2. SEM-analysis of the broken surface of the prisms made from laboratory burnt brick I i II and portlandite, curing time 28 days.

The second part of the experiments includes ground "fresh" and "old" bricks of the same chemical and mineral compositions (Table II). Time of maturing for the "old" sample was 14 days before grinding. The idea was to obtain $CaCO_3$ (after the converstion of free CaO, in the presence of water and CO_2 component), and than use this type of material for further hydration process. The pozzolanic reaction of the systems; fired bricks + $Ca(OH)_2$ has been followed in the period of 28 days and the hardening characteristics have been determined after 2, 3, 7, and 28 days of storage in water of 25°C (Fig. 3).

Table II Chemical composition of the fresh and old bricks

Oxide	Old brick	Fresh brick
	% mas.	
L.O.I.	0,74	0,68
SiO_2	60,89	61,10
Al_2O_3	15,41	15,81
Fe_2O_3	6,26	6,16
CaO	8,83	8,31
MgO	3,44	3,44
SO_3	0,24	0,34
Na_2O	1,38	1,50
K_2	2,35	2,37
Σ	99,54	99,71

The increase of mechanical characteristics was notable in the case of pastes made from the "old" system (Fig. 3). The X-ray diffraction of this paste, after 28 days of curing (Fig. 4), indicates a notable presence of $CaCO_3$ which is not in the case of paste on the base of "fresh" brick. SEM analysis (Fig. 5) give more information about the presence of the crystals of ettringite, which crystals are "enveloped" from the $CaCO_3$ phase. This role, $CaCO_3$ does not have in the case of paste on the base of "fresh" system (Fig. 5), where crystals of ettringite show a significant growth, forming large fibrous bundes.

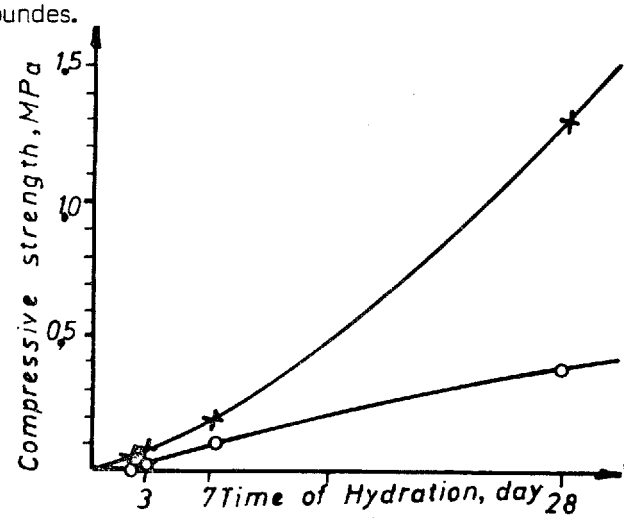

Fig. 3. Compressive strength development of the prisms
x-x-x- prism on the base of old brick
-o-o-o- prism on the base of fresh brick

Prism on the base of fresh brick

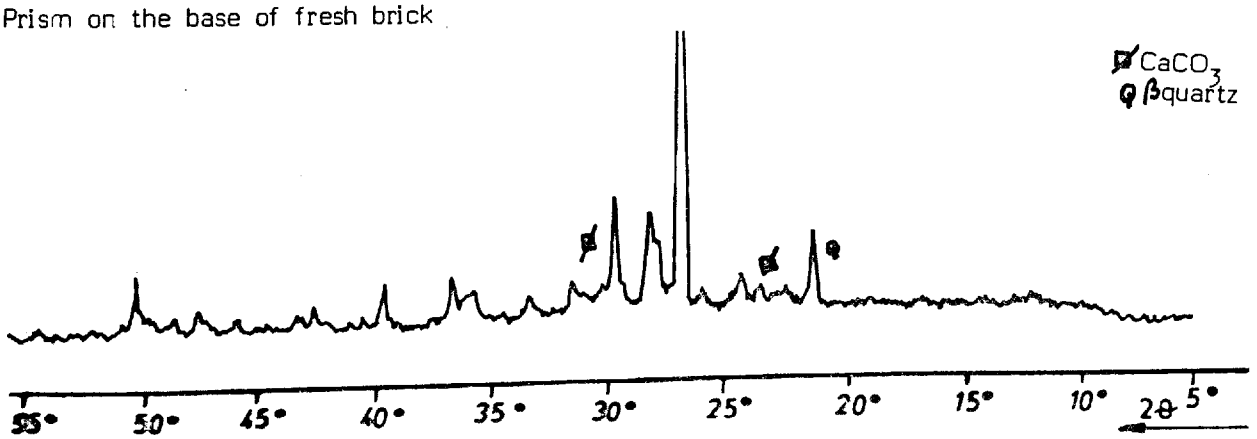

Prism on the base of old brick

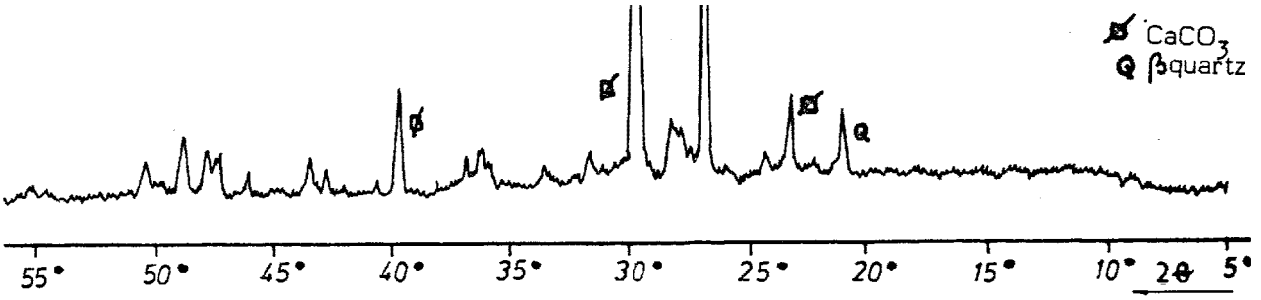

Figure 4. x-ray diffraction patterns of the pastes on the base of old and fresh brick, curing time 28 days

Prism on the base of old brick

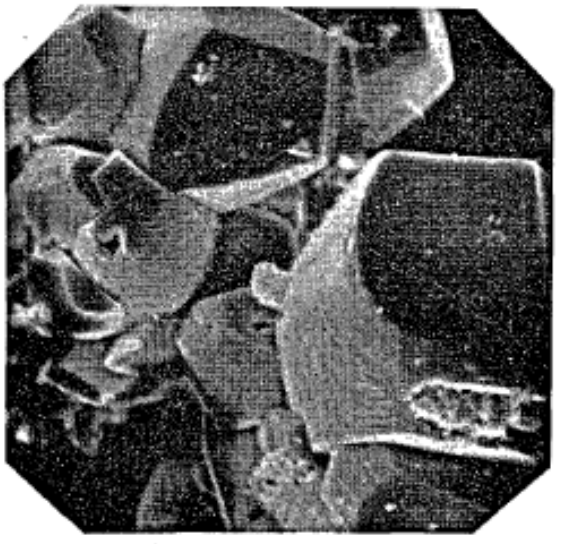

SEM x 1000

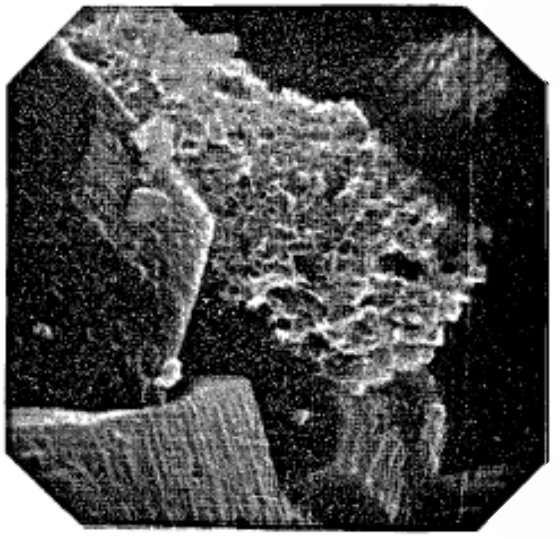

SEM x 4000

Prism of the base of fresh brick

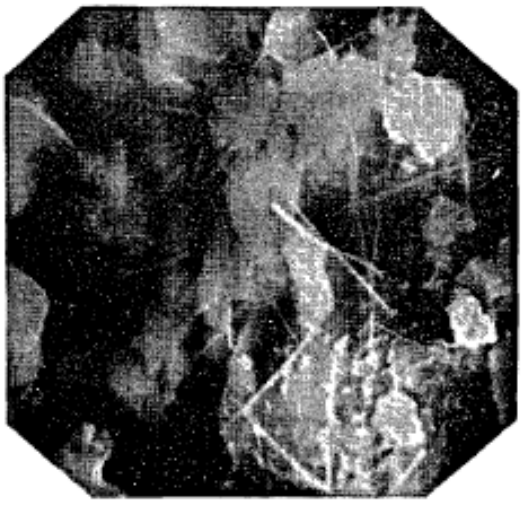

x 10 000



x 6 000

Figure 5. SEM analysis of the broken surfaces of the prism on the base of fresh/old bricks and portlandite

Taking into consideration the experiences which concern the influence of $CaCO_3$ on the hydration of tricalcium-aluminate - C_3A, we can admit the intermediar formation of $C_3A \cdot CaCO_3 \cdot H_n$ which posses a high binding capacity and a great influence on the structure of paste (causes a more compact structure). The presence of this phase can be supposed in the hydrated system, which will,in the future form crystals of $CaCO_3$ phase. In this way, the formation of C_3AH_6 and ettringite crystal phases has been stopped in their growing. At the same time, the net of small needles of ettringite covering the specific part of the system (which includes the glass on the base of Al_2O_3 oxide) makes it unreachable for the further water attack (Fig. 5). The structure of pores was changed (the new crystal form with its volume has a great influence on it) and the samples have remarcable mechanical characteristics.

4. Conclusions

Brick clays, thermally activated at 960°C in the presence of portlandite (70/30 mas. ratio, water/solid = 0,60) have showen satisfied pozzolanic proprietios. The oxides Al_2O_3 and Na_2O from the amorphous systems, obtained after thermal activation, presented good milieu for the developing process of C_3AH_6 and C_4A--hydrates and the intermediar phases for ettringite form. The concequences were, low mechanical characteristics of the hydrated pastes. This effect was overcome thanks to the $CaCO_3$ phase which enveloped the net of the crystals of ettringite stoping their futher growth and the attack of the water on the glass phase of the same system.

5. References

1. Ghorab, H.Y., Abdelalim A.M.K., and Ahmed O.M, Hardening characteristics of same clay minerals, Zement-Kalk-Gips, 11, 578-581, (1991)
2. Murat M., Ambroise J., and Pera J., Les differents procédés d'activation des mineraux argileux permettant d'élaborer des liants pouzzolaniques a resistances optimales. The different activation processes of clay minerals to obtain pozzolanic binders with optimal strengths, Proceeding of 8th International Congress on the Chemistry of Cement, Volume IV, 535-591 (1986)
3. Van Aardt J.H.P., and Visser S., Sulphate expansion of cement products made with aggregates containing Ca-rich feldspars, Proceeding of 7th International Congress on the Chemistry of Cement, Volume IV, 400-403,(1980)
4. Matousek M. and Sauman Z., Contribution to the hydration of expansive cement on the basis of metakaolinite, Cement and Conc. Res. 4,113-122,(1974)
5. Chatterji S., Mechanism of sulfate expansion; A reappraisal of literature, Proceding of the 7th International Congress on the Chemistry of Cement, Volume IV 586-591,(1980)
6. Longhan L., Ligun Y and Qizhong S., Dissociation of aluminium from slag glasses and formation of ettringite, Proceeding of 8th International, Congress on the chemistry of Cement, 30-36 (1986).
7. Shan-Ba Y., Snag-Xing J., Yin-Jiang L. and Ke-Yong Hu., Effect of alkali on the expansive properties of sulfoaluminate cement pastes, Proceeding of the 8th International Congress on the Chemistry of Cement, 301--306,(1986).
8. Bachiorrini B., Quilhat B., Murat M., Negro A., Sonstelle M., and Fourmier A.A., Hydration of monocalcium aluminate with calcite, Proceeding of the 8th International Congress on the Chemistry of Cement, 376-385 (1986).

STUDY OF POZZOLANIC ACTIVITY IN OPALINE ROCKS USING PARTICLE SIZE VARIATIONS

M Frias, M I Sanchez De Rojas, M P Luxan and N Garcia

Institute E Torroja (CSIC), Madrid
SPAIN

Sedimentary opaline rocks from the Western Iberian Peninsula present a pozzolanic character which makes them suitable for use as active additions for cements.

Earlier papers have used different method to study pozzolanic activity in opaline rocks. This study employs and assesses the usefulness of a new method to evaluate pozzolanic activity in opaline rocks that is based on variations in particle size.

The technique consists of granulometric analysis using laser diffraction and specifically studies the density distribution curves obtained with laser diffraction.

Pozzolanic behaviour is examined here by observing granulometric variations of the opaline rocks over time in two different media: a reactive liquid, which gives rise to a pozzolanic reaction with these materials, and a nonreactive aqueous medium.

Las rocas opalinas de origen sedimentario, procedentes del Oeste de la Península Ibérica, presentan un carácter puzolánico, por lo que son idóneas para su incorporación como adiciones activas en cementos.

La actividad puzolánica de las rocas opalinas ha sido estudiada, mediante diferentes métodos, en anteriores trabajos de investigación. En este estudio se presenta la aplicabilidad a las rocas opalinas de un nuevo método de evaluación de la actividad puzolánica de materiales, basado en las variaciones de los tamaños de partícula.

La técnica utilizada es la difracción de rayos laser para análisis granulométrico y, concretamente, las curvas de densidad de distribución obtenidas mediante dicha técnica.

El comportamiento puzolánico de las rocas opalinas se estudia mediante la observación de las variaciones granulométricas con el tiempo en distintos medios: un líquido reactivo, con estos materiales, que de lugar a la reacción puzolánica y un medio acuoso no reactivo).

1.- INTRODUCTION

Numerous investigations have been carried out on the phenomenon of the pozzolanic activity of materials. An evaluation of this activity is extremely difficult and therefore a multitude of tests have been set up with this intention, always seeking results that are a reflection of the material in practice (1).

In this work a method is presented based on g anulometric variations that take place when a pozzolanic materials is placed in contact with a solution of calcium hydroxide, and represents a new view within the study of pozzolanic activity.

The technique used is laser beam diffraction, normally used for the granulometric analyses of particles and the method represents the applicability of this technique in the following of chemical reactions.

The study was carried out with opaline rocks of sedimentary origin whose pozzolanic characteristics have been the object of different research works in the last few years (2).

2.- EXPERIMENTAL

2.1.- Materials

During the development of this work, six opaline rock samples of sedimentary origin were selected, coming from different locations in Spain and designated: SA1, SA2, SA3, ZA1, ZA2 and AV.

The characterization of the materials was made taking into account chemical, mineralogical, physical and pozzolanic activity characteristics.

* **The chemical analysis** of these materials, indicates that they are mainly formed of silicon, aluminum and small amounts of iron, calcium and alkaline oxides.

* **The principal mineralogical** component of this type of material is silica that contains all the transitions between amorpha (opaline A) and the more or less crystallized (opaline CT). Also present are quartz kaoline, mica and alunite may appear sporadically.

* **Among the physical characteristics** to be considered in opaline rocks is fineness, the factor that has the greatest influence in the earliest ages on the reaction speed of a material and, therefore, on its pozzolanic activity.
The degree of fineness of these materials is reflected in the specific surface values, which for the different opaline rocks are found in the interval of 4.500 to 5.000 cm2/g.

* **Pozzolanic activity** in these materials has been studied through their behaviour with calcium hydroxide.
Figure 1 shows the amounts of lime fixed by the different materials. These amounts are obtained by a valuation of the calcium ions proceeding from a mixture of saturated lime solution and opaline rocks, at different ages, and contrasted with the saturated lime solution used as a control (2), which has no solid material.

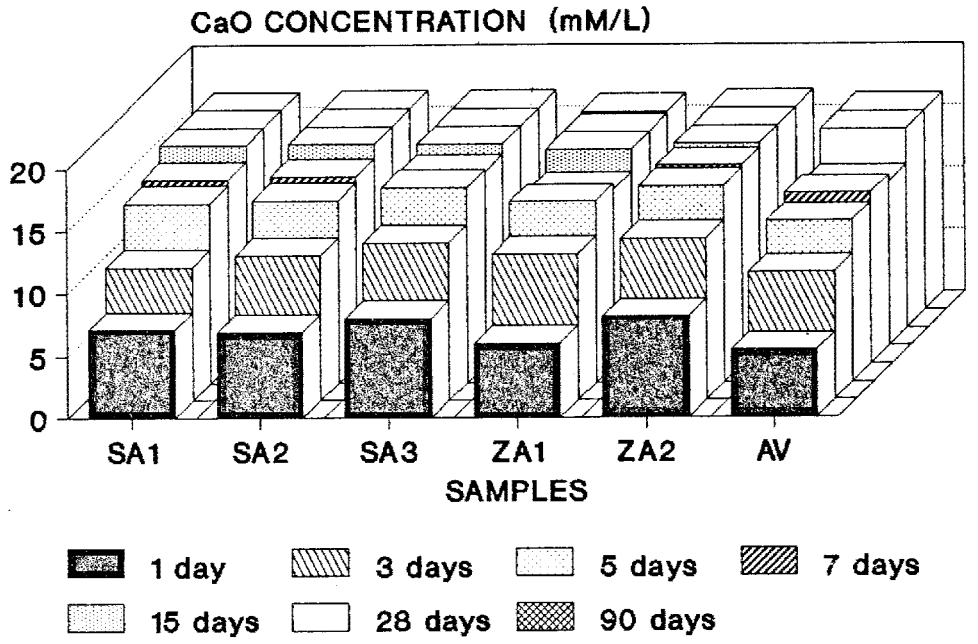

Fig. 1.- Pozzolanic activity test. Fixed CaO over time

The results shown strongly indicate the existence of a significant difference between the samples studied, principally in the early ages, so that it is possible to make a classification between them, according to their greater or lesser reactivity with the lime:

$$AV < ZA1 \approx SA1 \approx SA2 < SA3 = ZA2$$

2.2.- Test method

The equipment used is a Helos 12K granulometric analyser based on laser beam diffraction spectrometry.

The tests were carried out with two systems:

(a) Opaline rock / distilled water
(b) Opaline rock / saturated lime solution

In this way intended to check the effect of calcium hydroxide in granulometric variations, in contrast to the effect of distilled water.

The method used consisted of adding an amount of dry sample, between 0.5 and 1.0 g, to the feed and dispersion cell in liquid phase, in which had previously been introduced some 450 cm3 of distilled water for system (a) and saturated lime solution, previously prepared and evaluated, as used in the pozzolanic activity evaluation method, for system (b).

In both cases the resulting solution was shaken using two stirrers included in the apparatus, and thereafter ultrasonic equipment was connected for a predetermined time to eliminate possible aglomerations.

Test execution times are established for all the samples analysed: 0, 5, 15, 25, 40, 55, 70, 85 and 115 minutes, applying ultrasonic 10 seconds before each measurement and with agitation and solution temperature constant. At the end of this period the corresponding granulometric analyses are determined.

Granulometric figures thus obtained are shown graphically in the form of density distribution curves, since the variations taking place in the particle sizes in clearly observed.

3.- RESULTS AND DISCUSSION

In the first place the results of investigations carried out with the opaline rock - distilled water system will be given, as a contrast with the results with the opaline rock -saturated lime solution system.

(a) Opaline rock - distilled water systems

Having obtained the corresponding density distribution curves for opaline rocks in distilled water, it can be seen that no granulometric evolutions exists over time in any of the samples analysed, which indicates a lack of reaction by these materials in the water.

For this reason only the curves of three of the opaline rocks have been given, Figure 2: a)SA1, b)ZA1 and c)AV.

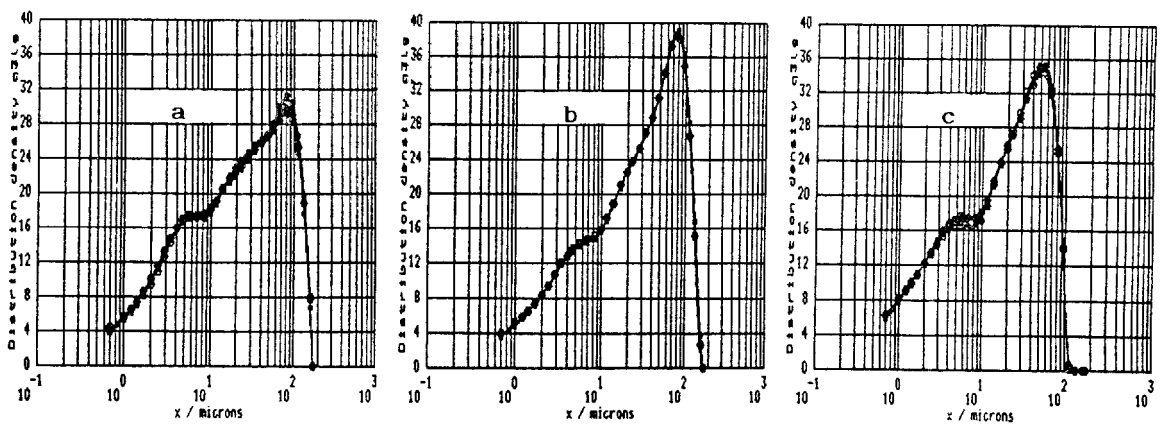

Fig. 2.- Granulometric density curves evolution over time with water. a)SA1 b)ZA1 c)AV

(b) Opaline rock - saturated lime solution system

The behaviour of this type of materials in the presence of saturated lime solution is totally different from that observed in the opaline -

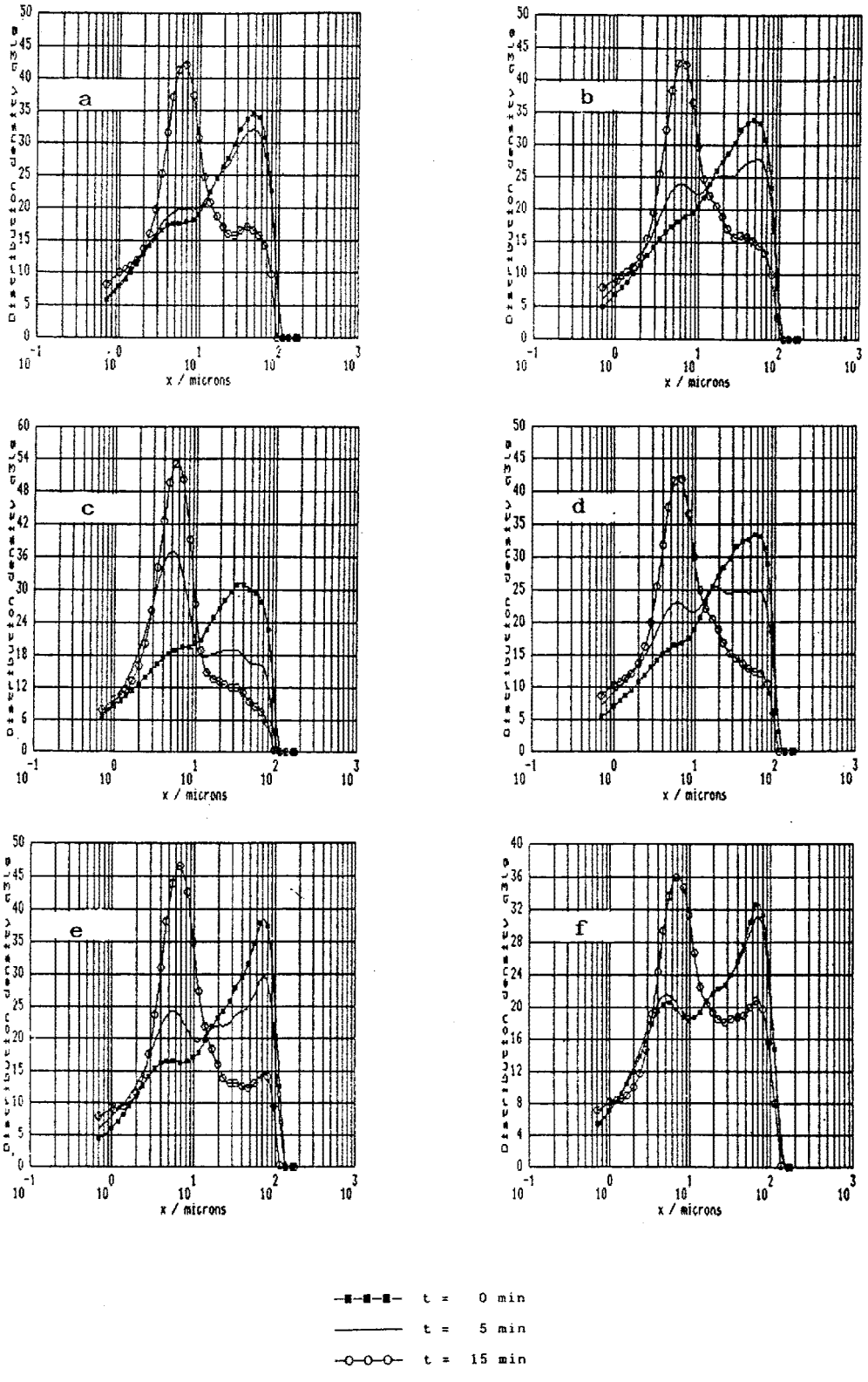

Fig. 3.- Granulometric density curves over time with saturated lime solution up to 15 minutes.
a) SA1 b)SA2 c)SA3 d)ZA1 e)ZA2 f)AV

water system, due mainly to interaction phenomena between the lime and the acid constituents in the rocks.

The graphic representation of the granulometric results is given using the corresponding accumulated granulometric curves during two different stages of the test:

* During the initial period up to a time of 15 minutes (Figure 3: a)SA1, b)SA2, c)SA3, d)ZA1, e)ZA2 and f)AV).

* And during the period from the beginning to the end of the test (final test time = 115 minutes) when all the granulometric curves are found together.

Since the evolution is analogous in relation to the effect observed over time, only two figures are given as an example (Figure 4: a)ZA2 and b)AV).

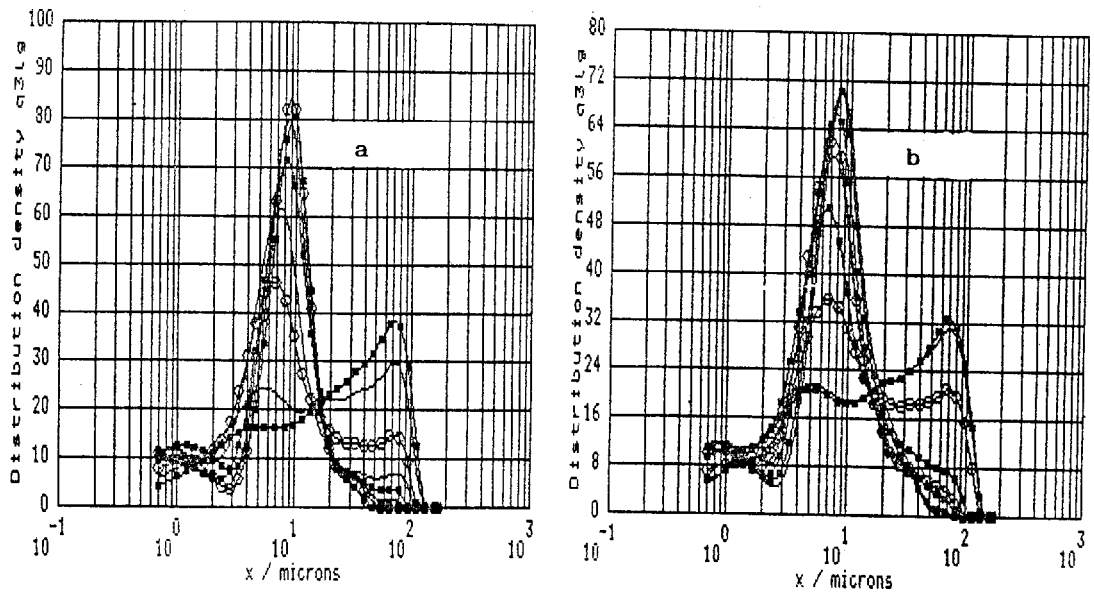

Fig. 4.- Granulometric density curves over time with saturated lime solution up to 115 minutes.
a)ZA1 b)AV

In general it may be seen from a detailed study of granulometric curves given that the opaline rocks studied show similar granulometric behaviour with lime.

When comparing the density distribution curves of the materials (t=0 min) with those obtained after the first 15 minutes of the test, it may be observed that a maximum of some 6 µm appears that increases progressively in intensity with time, and that it moves slowly towards higher particle sizes.

Figure 5 shows the intensities of this maximum at 15 minutes and 115 minutes respectively.

From the granulometric point of view, the opaline samples show different reaction speeds. Those designated SA1, SA2, ZA1 and AV do not undergo such noticeable granulometric differences as samples SA3 and ZA2. These data concur with the reaction tests with lime carried out chemically, shown in Figure 1.

A relationship has been observed between the increase in intensity of the granulometric maximum formed at the first 15 minutes and activity with lime of these materials, evaluated chemically, so that the greater the speed of pozzolanic reaction the greater the intensity of this maximum.

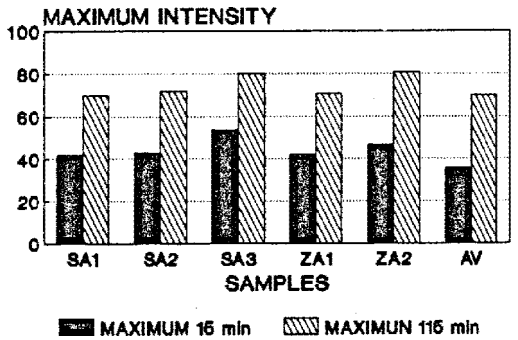

Fig. 5.- Pozzolanic activity test. Laser method

4.- FINAL CONSIDERATIONS

* By means of the analysis carried out with the material-water system, it has been shown that opaline rocks has no granulometric variations in this medium. Therefore granulometric changes taking place in the material-saturated lime solution system are due to chemical reactions taking place with this liquid as reagent.
* The laser technique appears available to follow chemical reactions through observation of granulometric variations over time.
* The distribution density curves obtained for the different materials show, with the saturated lime solution, the formation of a granulometric maximum that increases with time and whose intensity differs from one sample to another, so that with greater pozzolanic activity in materials during the first ages, the greater the intensity shown by the said maximum.
* Studies on granulometric variations carried out using laser technique give similar results regarding pozzolanic activity to those carried out chemically.

Laser beam diffraction technique allows a differentiation to be made between pozzolanic behaviour in materials, and the establishment of orders of degree of activity in the same.

5.- REFERENCES

1. SERSALE, R. (1980): Structure et caractérisation des pouzzolanes et des cendres volantes. 7th Int. Congr. Chem. Cem., IV-1/3-21, Paris.
2. LUXAN,M.P.and Col (1987): Structure and reactivity of various natural siliceous materials,vol.1, Ed. Maso-Chapman and Hall, pp 191-194.

WATER SORPTION AND WEIGHT CHANGE ON HEATING OF A PORTLAND CEMENT DEPENDING ON PRETREATMENT

E T Stepkowska*, J M Bijen, J L Perez-Rodriguez*** and A Justo*****

*Institute of Hydroengineering, POLAND
**Technical University, Delft, THE NETHERLANDS
***Istituto de Ciencia de Materials, CSIC, SPAIN

SUMMARY

Water sorption/retention of a Portland cement powder was measured at the relative water vapour pressures p/p_o = 0.5; 0.95 and 1.0, followed by static heating at 110°C, 220 °C, 400 °C and 800 °C. Water sorption at p/p_o = 0.5 indicates the specific surface of powder grains in dry state. Water sorbed at the high p/p_o and evaporating at 110°C or 220°C indicates the specific surface and accumulated water both in hydrated state. Oven dry weight increased pronouncedly after sorption test.Portlandite forms on storage in water vapour and heating at 220°C and on heating in air at 400°C it transforms into carbonates, which decompose at 800°C; this was proved by XRD and TG. Results depend on storing conditions and ageing of the cement. Thus this procedure may give valuable informations on cement quality and its variation with time.

ZUSAMMENFASSUNG

Die Wassersorption (-retention) von einem Portlandzementpulver wurde bestimmt bei den relativen Wasserdampfdrücken p/p_o = 0.5; 0.95 und 1.0. Nachher die Gewichtsänderung bei den Temperaturen 110°C, 220°C, 400°C und 800°C wurde gemessen. Wassersorption bei p/p_o =0.5 ist der spezifischen Oberfläche des trockenen Zementpulvers proportional. Das Wasser, das bei einem hohen p/p_o sorbiert wird und bei 110°C oder 220°C entdämpft, ist der spezifischen Oberfläche im hydratiertem Zustand proportional und das in diesem Zustand akkumuliertes Wasser angiebt. Der Portlandit entsteht während der Aufbewahrung im Wasserdampf und der Erhitzung bei 220°C und er in die Karbonate übergeht, falls er in der Luft bei 400°C erhitzt wird (das wurde durch XRD und TG gezeigt). Diese Karbonate bei 800°C zerstört werden. Die Ergebnisse sind von den Aufbewahrungsbedingungen und von dem Zementalter abhängig. Solche Untersuchung kann also wertvolle Informationen liefern über die Zementqualität und ihre Veränderung mit der Zeit.

1 INTRODUCTION

During the study of cement-bentonite-water mixtures, used in Civil Engineering for construction of impermeable screens, water sorption and weight loss on heating were measured both of parent materials and of their mixtures. A strange behaviour of a Portland cement was observed, thus it will be presented here, as this may be useful in evaluation of cement quality (see also [1]). Two slag cements gave qualitatively similar results, which is discussed elsewhere [2].

Water sorption was measured by the method derived for clays. This problem is comparatively well understood, which is not the case in cements, where the hydration mechanism is still not clear [3], see [4].

The components of the total sorbed water content may be considered as: (1) physically bound, adsorbed water, escaping below 110°C, (2) hydrating water escaping below 400°C (3) chemically bound water.

At $p/p_o > 0.8$ a three molecular water layer of the thickness of 8-9Å is adsorbed by the surface of cement grains [5]. It remains in the system on desorption at $p/p_o = 0.8$. At full saturation of water vapour ($p/p_o = 1.0$) a six molecular layer is adsorbed [6]. The physically bound water may amount to 0.15 g H_2O per g anhydrous cement [7], [8], see [4].

An increased density by about 10% of the adsorbed water is usually assumed, due to strong adhesion forces [7] and to "surface tension" (capillary forces) at saturated water vapour pressure. This factor resulted in dense arrangement of bentonite powder grains, when stored initially at $p/p_o = 1.0$ [9]. In cements it may possibly hinder a full hydration.

Cement hydration may be due to: (1) liberation of Ca^{2+} ions from the grain edges, followed by transformation into $Ca(OH)_2$ [10] and (2) after dissolution of anhydrous grains the hydration occurs and precipitation of hydration products on the grain surface [4].

At full hydration about 0.2 to 0.26 g H_2O per g cement is chemically bound [4] and thus the total quantity of accumulated water may amount to 40%.

The chemically bound water content depends on time and on cement constituents. Powers [7] gives the following values for half year curing (in g H_2O per g cement): 0.187 for alite C_3S, 0.158 for belite C_2S, 0.665 for C_3A, 0.213 for C_4AF. In one year alite is almost completely hydrated and belite - to about 70% [11], i.e. 0.688 g/g and after 7 years it decreases to 0.18 g/g [12].

To study cement quality, the water sorption was measured at three relative water vapour pressures, followed by stepwise static heating. Results are interpreted in reference to broad experience in water sorption and thermogravimetry of clay minerals. Some samples were subject to XRD study.

2 MATERIAL

Portland cement CBR P–50 was investigated, supplied by prof. J.M.Bijen (Delft). It contains (XRD): calcium silicates, alite Ca_2SiO_5 (C_3S) and belite Ca_2SiO_4 (C_2S), calcium aluminium silicate $CaAl_2SiO_6$ (CA_2S) and possibly tobermorite $Ca_5Si_6O_{16}(OH)_2 \cdot 8H_2O$.

3 METHODS AND RESULTS

3.1. Water sorption (WS) of air dry (a) and oven dry (o) and water "retention" (WR) of air dry specimens were studied by successive storage for two weeks at 30°C and at normal pressure in aluminium containers 2×3 cm in desiccators at $p/p_o = 0.5$; 0.95 and 1.0 in WS and in inverse order in WR (series I, tripple sample, $G_o = 5.0$ g). In series II (single sample, ceramic crucible, $G_o = 2.6$ g), only $p/p_o = 0.5$ and 0.95 was applied. Thereafter all the samples, including the untreated ones (SH, single sample) were subjected to static heating at 110°C (1d), 220°C (8h), 400°C (4h) and 800°C (1h). After heating at 220°C the WS and WR samples, series I, were transferred to ceramic crucibles and left overnight in the cool oven (which operations caused an appreciable increase in weight) and the heating was proceeded.

Sorbed water content and change in weight on heating

$$\Delta G = [G(t) - G_o]/G_o$$

were related to the initial wight of the air dry cement ($W_0 = 0.3\%$ in series I and 0.5% in series II). The oven dry weight increased both after WS and WR test (Table 1 and Fig. 1).

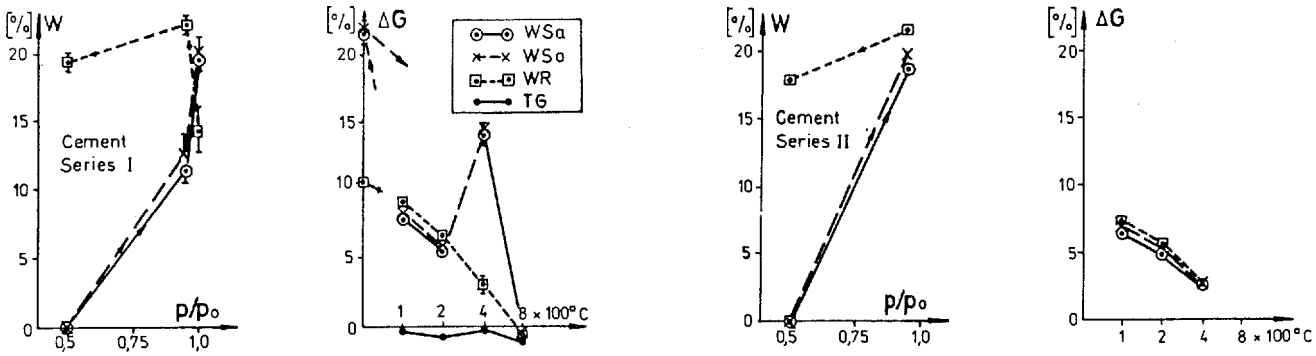

Figure 1: Water sorption and weight loss on heating of Portland cement

Table 1. Water sorption and thermal change in weight ΔG of Portland cement, related to air dry weight (in percent)

Series	W_o	Test	Water content at p/p_o =			ΔG from air dry to:				
			0.5	0.95	1.0	110°C	220°C		400°C	800°C
	%					1d	8h		4h	1h
		WSa	0.11	11.4	19.6	7.9	5.5	21.6	14.1	-0.4
			± .02	1.0	.7	.3	.2	.6	.4	.1
I	0.30	WSo	0.05	12.6	20.2	8.2	5.7	21.8	14.5	-0.4
			± .02	1.4	1.0	.4	.4	.5	.4	.1
		WR	19.5	22.2	14.3	9.1	6.6	10.5	4.1	-0.5
			± .5	.6	1.7	.3	.1	.1	.6	.1
		SH				-0.33	-0.83		-0.05	-1.1
		WSa	0.06	18.7	–	6.3	4.8		2.6	–
II	0.52	WSo	-0.22	19.8		6.8	5.4		2.8	
		WR	17.88	21.6		7.3	5.7		2.6	

Surprisingly a high increase in weight, with respect to weight at 220 °C, was observed in samples WSa and WSo after the contact with air and heating at 400°C (about 9%), but it was not the case in WR samples. Also the SH sample indicated a small weight increase (1%) on heating between 220°C and 400°C.

To check the reason by XRD, another series II of WS/WR test was prepared. In this case a smaller increase in oven dry weight was found and the weight at 400°C was in all samples smaller than that at 220°C. Selected samples, series II after WR test were studied by XRD.

3.2 XRD was performed by Siemens Kristalloflex D 501, equipped with a graphite monochromator CuKα and a computer SICOMP PC 16-20 with files of basal spacings of various standard minerals. Most of the peaks are present independent on sample pretreatment, but their relative intensity vary. Only the tobermorite peak at 3.49 Å, observed in the air dry cement, disappeared after WR test and heating at 220°C (Fig. 2).

Some peak intensities are presented in Table 2, related to the alite peak intensity at 2.77 Å:,

$$I_r = I(peak)/I(2.77\text{Å})$$

4 DISCUSSION

After storage in water vapour at $p/p_o = 0.5$ the water content, close to that in dry state, gives information on the specific surface of unhydrated cement grains. If the coefficient derived for clays is applied here, the approximate value of this specific surface may be calculated as:

series I: S = 0.0041 cm^3 H_2O/g cement x 585 m^2/gH_2O = 2.4 m^2/g

series II: S = 0.0058 = 3.4 m^2/g

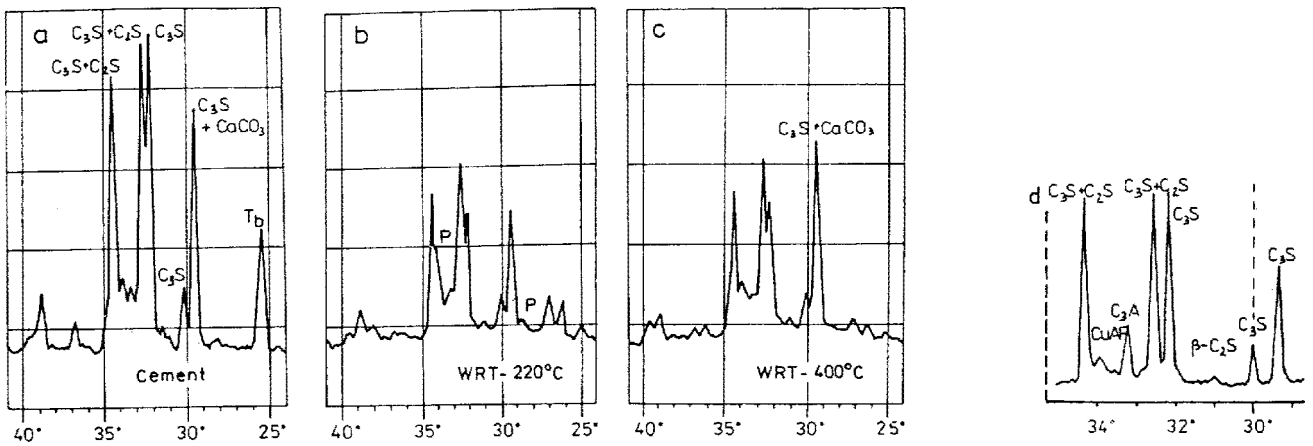

Figure 2: XRD of Portland cement after various treatments (a-c) and of alite (d), from P. Barnes, *Structure and Performance of cements*, Appl. Sci. Publ., Lomdon 1983. M. Regourd, p. 109-138.

Table 2. Relative intensities of XRD peaks of Portland cement after certain pretreatment

Compound	Peak Å	Relative intensity I_r		
		Cement	WR 220°C	WR 400 °C
Tobermorite	3.49	0.38	–	0.08
Portlandite	4.92	–	0.30	–
	3.10	–	0.19	–
	2.64	–	0.66	?
C_3S + $CaCO_3$	3.025-3.03	0.75	1.00	1.42
C_3S	2.96	0.19	0.36	0.36
β-C_2S	2.87	0.04	0.19	0.19
C_3S	2.77-2.78	1	1	1
its intensity		80%	33%	31%
C_3S + C_2S	2.74	0.96	1.37	1.28
C_3Ac	2.684	0.21	?	0.33
C_4AF	2.638	0.25	?	0.44

Table 3. "Accumulated" water content %

Series	Test	p/p_o = 0.95	1.0	Series	Test	p/p_o = 0.95
I	WSa	(5.9)	14.1	II	WSa	13.9
	WSo	(6.9)	14.4		WSo	14.4
	WR	15.5	(7.7)		WR	16.0

This coefficient assumes a certain molecular thickness of water layer [13], which for cement may be thicker, thus the coefficient would be smaller.

Storage for four weeks successively at $p/p_o = 0.95$ and 1.0 (in WS test or vice versa in WR test) gives information on the amount of water, which may be accumulated by cement grains from the cement-water paste or from the cement-aggregate-water paste.

If it is assumed that at $p/p_o = 1.0$ (0.95 in WR) the adsorbed water forms a six-molecular layer (thickness about 1.8 nm) on the surface of hydrated cement grains [7] and it evaporates at 110°C, the specific surface in hydrated state would be:

WSa: S = (0.196 - 0.079) cm^3/g : 1.8 nm = 65 m^2/g
WSo: S = (0.202 - 0.082) cm^3/g : 1.8 nm = 67 m^2/g
WR : S = (0.222 - 0.091) cm^3/g : 1.8 nm = 73 m^2/g

the accumulated water being 11.7%, 12% and 13% respectively. The difference is due to different pretreatment and storage conditions. Also the age of the cement sample may be of importance.

A part of this water, sorbed on the hydrated surface, may be more strongly bound and may possibly escape between 110°C and 220°C (2.4–2.5%). If this is included into specific surface calculations, the result would be:

WSa: S = (0.196 - 0.055) cm^3/g : 1.8 nm = 78.3 m^2/g
WSo: S = (0.202 - 0.057) cm^3/g : 1.8 nm = 80.6 m^2/g
WR : S = (0.222 - 0.066) cm^3/g : 1.8 nm = 86.7 m^2/g

with accumulated water content 14.1%, 14.5% and 15.6% respectively.

A similar S value would be obtained assuming, that the lowering of p/p_o from 0.95 to 0.5 in WR test would result in desorption of a monomolecular layer, of the thickness about 0.3 nm:

WR : S = (0.222 - 0.195) cm^3 H_2O/g cement: 0.3 nm = 90 m^2/g

If the results obtained in various series are compared, the WS in series II (W = 0.5%) at $p/p_o = 0.95$ is almost double that in series I ($W_o = 0.3\%$) and close to that measured at $p/p_o = 1.0$. If the accumulated water is compared (difference between WS/WR values and ΔG at 220°C), the following is obtained as presented in Table 3.

Values in parantheses are underestimated by 1-2% as the weights at 220°C were measured after a longer sorption time than the sorption value used in calculation.

It is possible that the higher values indicated in Table 3 correspond to a six molecular layer of sorbed water, whereas the lower ones – to three molecular water layer on the surface of hydrated cement grains.

Also the difference in the values measured at $p/p_o = 1.0$ in WS and WR test, may be due to difference in sorption time (two weeks in WR test and almost double that in WS test, as it was preceeded by two weeks at $p/p_o = 0.95$). Some geometrical hindrances may also be of importance due either to,

(1) "surface tension" exerted on cement grains by water molecules at the saturated water vapour pressure [7], [9] or

(2) cementation of cement grains at the sorbed water content (some chemical bonding).

For geometrical hindrances speak low values of resorption after heating at 220°C of WR samples (see below). Only slight differences were observed in behaviour of oven dry (WSo) and air dry (WSa) samples.

After the WS/WR test the oven dry weight at 110°C was by 8-9% higher than that before the test. Only one third of it escaped at 220°C, i.e. 2.4–2.5% as it was mentioned above, thus about 5.6–6.6% of the increased weight remained on heating at 220°C. This retention could be due to following reasons:

(1) some sorbed water remaining on internal surfaces of cement grains,

(2) hydration of C-S-H gel and other eventual gels; this water should escape below 400°C,

(3) formation of portlandite, which was detected by XRD in the WR sample, series II, heated at 220°C (Table 2 and Fig. 2, also in unheated one, unpublished data for another series).

Sanman [14] has shown that under hydrothermal conditions the main product of hydration of pure C_3S^x are α-C_2 S-hydrate and a considerable amount of $Ca(OH)_2$, which is also the case in the study presented here (Table 2 shows increase in relative intensity of C_2S + C_3S peak and of portlandite peaks after WR

test). $Ca(OH)_2$ was observed by SEM on the edges of one year old C-S-H gel [14] and also on the second day of curing of soil-cement-water mixtures [15].

Water escaping both at 110°C and 220°C after the sorption test leaves free pores in hydrated cement grains, which pores as well as the external grain surface, being water "thirsty" accumulate it quickly during the contact with atmospheric air.

The total accumulation amounts to a value somewhat higher (by about 2 %) than the final weight after WS test (21.6 %) and to about half its value after WR test (10.5 %). More informative is the value of accumulation calculated by subtraction of the weight at 220°C, i.e. $\Delta G - \Delta G$ (220°C) = 16% in WS and 3.9%. in WR. These values may give interesting information, but conditions of resorption measurements should be better established.

Resorbed water and hydrating (gel) water escaped on heating at 400°C and the decrease in weight thus measured was: 7.4% in WSa, 7.3% in WSo and 6.5% in WR.

The final weight at 400°C was in WS samples higher than that at 220°C by 8.8% in WSa, 8.7% in WSo but it was lower by 2.6% in WR. The formation of calcite at 400°C (and possibly at lower temperatures) was proved by increase in relative intensity of calcite peak (Table 2). Conditions of its formation were apparently less favourable in WR samples than in WS ones, possibly due to smaller pores (see above) or smaller pore necks, less available for CO_2 molecules, which are bigger than water molecules and do not indicate any dipole moment.

It should be mentioned that the untreated cement indicated also an increase in weight on heating at 400°C by 0.8% as compared to the weight at 220°C.

All the carbonates formed during the test decomposed at 800°C, as the sample weight was by about 0.4% lower than the initial one. This weight loss from 400°C to 800°C represents (1) content of carbonates, which were formed during the whole procedure, (2) eventual chemically bound water from compounds which decompose within this temperature range.

The untreated cement (sample SH) after heating at 800°C indicated the weight by 1.1% smaller than the initial one, which should be accounted for in eventual evaluation of carbonates formed during the WS/WR test.

After due consideration the amount of portlandite and of carbonates formed during the whole treatment may be inferred from these thermogravimetric data. It should be mentioned that the temperature of formation and/or decomposition of these compounds is unusually low.

These data are important parameters pertaining to properties of cement and concrete: for a mud mixed with some additives to improve its geotechnical properties, correlations were found between strength and weight loss on static heating between 110°C and 400°C (escape of hydrating water, probably from calcium aluminate silicate hydrate, which was found by XRD) and weight loss on dynamic heating between 20°C and 1000°C (decomposition of calcite). The correlation coefficient exceeded 0.8. Thus both these substances influence the strength of the system [16].

Values presented above are quantitatively not constant, but measurement results depend on sample storage time, i.e. ageing (compare series I and II; also unpublished data of next series). Thus the problem of ageing may be studied by this procedure.

Observations made here may have even a wider application, e.g. in storage of solar energy [17].

5 CONCLUSIONS

Some information pertaining to cement quality may be inferred from water sorption/retention measurements, followed by determination of weight change on heating.

(1) water sorbed at low relative humidity conditions indicates the specific surface in dry state,

(2) water sorbed at a high relative humidity (p/p_o = 0.95 to 1.0) and evaporating at 110°C or at 220°C indicates both the quantity of water accumulated in hydrated state and the specific surface in this state; internally sorbed water may evaporate at temperatures exceeding 220°C,

(3) hydrating (gel) water, evaporating between 110°C and 400°C; it may be masked by carbonatization of calcium hydroxide formed previously in cement,

(4) chemically bound water and carbonates, which develop during the testing procedure and decompose between 400°C and 800°C, thus at unusually low temperatures, which may have practical application.

6 REFERENCES

1. E.T. Stępkowska, J.L. Perez-Rodriguez, A. Justo, P.J. Sanchez-Soto, M.A. Aviles and J.M.J.M. Bijen, *13th Nordic Symposium on Thermal Analysis and Calorimetry*, Stockholm, 1992.
2. E.T. Stępkowska, J.M.J.M. Bijen, J.L. Perez-Rodriguez, A. Justo, P.J. Sanchez-Soto, M.A. Aviles, sent to Ed. Sh. Yariv for J.Therm. Analys.
3. A.R. Ramahandran et al., *Symp. on Microstructural Development During Hydration of Cement*, Boston, Mat. Res. Soc., 1986, Proc. Vol. 85, p. 33-38.
4. K. van Breugel, *Simulation of Hydration and Formation of Structure in Hardening Cement-Based Materials*, 1991, Techn. Univ. Delft.
5. T.C. Powers, C& CAss. London 1968, p. 319-344.
6. J. Hagymassy et al., J. of Colloidal and Interface Science, 1969, Vol. 29, Nr 3, p. 152-155.
7. T.C. Powers et al., J. of American Concrete Institute, 1946/1947, Part 1-9.
8. F. Keil, *Zement*, Springer Verlag, 1971.
9. E.T. Stępkowska and S.A. Jefferis, Thermochimica Acta, 1987, Vol. 114, p. 179-186.
10. E.E. Lachowski and S. Diamond, *Cement and Concrete Research*, 1983, Vol. 13, p. 177-185.
11. Z. Larionova, L. Nikitina and V. Garashin, *Phase composition, microstructure and strength of cement stone and concrete*, Stroyizdat, 1977, Moscow, (in Russ.).
12. L.E. Copeland et al., Proc. 6th Internat. IAEG Congress, 1990, Balkema, p. 3147-3154.
13. E.T. Stępkowska, *Sorption test for estimation of particle interactions in Soil Mechanics* (in Polish), I Nat. Conf. "Clay Minerals", Bolesławiec, 1979.
14. Z. Sanman, *Silikaty*, 1964, Vol. 8, p. 185-195.
15. R. Angelova & D. Evstatiev, Proc. 6th Internat. IAEG Congress, 1990, Balkema, p. 3147.
16. E.T. Stępkowska, C. Maqueda, J.L. Perez-Rodriguez, A. Justo, E. Gomez, Proc. 7th EUROCLAY Conf. DRESDEN 1991, p. 1001-1005.
17. J.M. Criado, M. Macias, A. Macias-Machin, 1991, Report of Istituto de Ciencia de Materiales, 41072 Sevilla, Spain.

ALKALI AGGREGATE REACTION : PROPOSALS FOR A KINETIC TEST ON AGGREGATES

D Sorrentino, J Y Clément and S Sabio

Lafarge Coppée Recherche, Viviers
FRANCE

SUMMARY

The ASTM C-289 standard test method for potential reactivity of aggregates known as the Chemical Method, has been reappraised. Several important points have been the object of a detailed research programme. Noticeable improvements have been brought about, which allow us to propose a renewed chemical test, called the kinetic test. It has been accepted as a tentative French AFNOR standard P 18-589.

A new qualification diagram has been defined ; the experimental values (silicates and sodium concentrations) are expressed, in the form of their molar ratio (SiO_2/ Na_2O), as a function of the time. As previously, the new diagram includes three areas, each of them representing a different type of reactivity. The separation lines have been established, based on the field performance record of the materials and / or on the results of the conventional expansion tests at 38° C : mortar bars tests for the fine aggregates, concrete prisms tests for the coarse ones.

RESUME

La norme ASTM C-289, destinée à qualifier la réactivité potentielle des granulats, communément appelée Méthode Chimique, a été reconsidérée sous plusieurs aspects. Les résultats, issus d'un programme de recherches portant sur plusieurs points critiques, nous permettent de proposer des améliorations sensibles à la méthode chimique. Ceci fait l'objet, en France, d'une norme expérimentale AFNOR P 18-589.

Un nouvel abaque de qualification des granulats a été défini ; les valeurs expérimentales (concentration en ions silicates et sodium), sont exprimées sous forme du rapport molaire SiO_2 / Na_2O, en fonction du temps. Le nouveau diagramme, comme le précédent, est divisé en trois zones, chacune d'entre elles correspondant à un type de réactivité différente. Les limites entre ces zones ont été établies à partir du comportement des granulats dans les ouvrages et /ou des essais conventionnels d'expansion à 38° C : essais sur barres de mortiers pour les sables et sur prismes de béton pour les gravillons.

1- INTRODUCTION

In the alkali aggregate reaction field, two main types of approach have been developed to determine the potential reactivity of the aggregates : expansion tests on mortar bars or concrete prisms and direct determinations on aggregates, like the petrographic examination (ASTM C 295 standard) or the ASTM C 289 Chemical Method.

This chemical method has had a worldwide success, because it is quick, easy to do and does not require a large quantity of material. However, from the time it first appeared as a standard (1952), many authors have reported that it suffers from several defects : lack of reliability and too narrow a range of application, are the main ones. The detailed bibliography cannot be reported here, see for example : evaluation of test methods for alkali aggregate reactivity [1] ; the text of the standard itself says : "while not completely reliable in all cases...".

We have tried to overcome or at least improve this situation, establishing a five point research programme. Explaining the reasons why such parameters have been investigated and the synthesis of the results obtained, are the main objectives of this paper. Each point will be the purpose of a separate section but, a brief summary of the ASTM C 289 standard will be given first.

2-THE ASTM C 289 STANDARD TEST METHOD for POTENTIAL REACTIVITY of AGGREGATES

First issued in 1952, the current edition was approved in March 1987. Its scope is reported :" this test method covers chemical determination of the potential reactivity of an aggregate with alkalies in a portland cement concrete as indicated by the amount of reaction during 24 h at 80° C between 1N sodium hydroxide solution and aggregate that has been crushed and sieved to pass a 300 µm sieve and be retained on a 150 µm sieve ".

The amount of reaction is evaluated by the measurement of the silica dissolved into solution (Sc) and the reduction in alkalinity (Rc), being the difference between the alkalinity of the original NaOH solution and, theoretically, the remaining OH^-, following completion of the test, (determined by HCl titration, using the phenolphtalein end point). Aggregates are considered innocuous, potentially deleterious or deleterious, depending on the location of the representative point of the Sc, Rc values in the diagram (Fig.1).

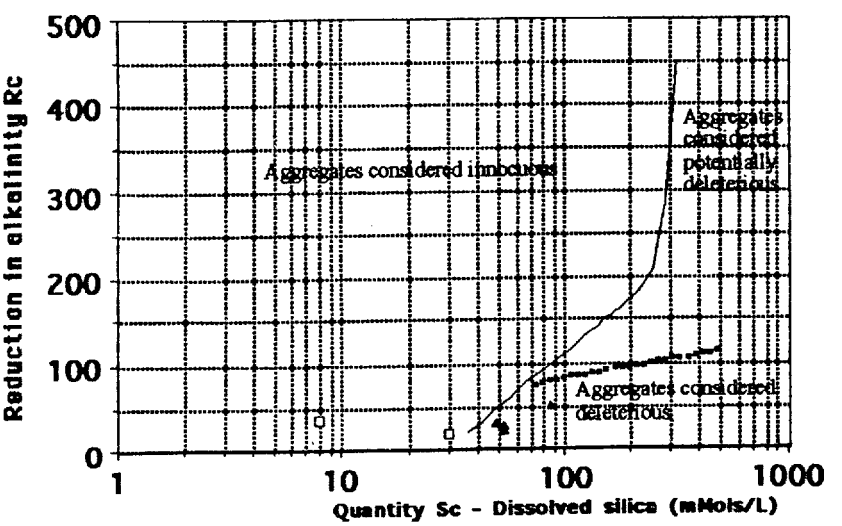

FIG. 1-Illustration of division between innocuous and deleterious aggregates on basis of reduction in alkalinity test

3 - GRAIN SIZE OF THE MATERIALS

The material passing the 150 µm sieve is discarded and, to ensure that all material finer than 150 µm has been removed, the sample is washed. Several experimental facts disagree with this decision to remove the fine particles; a well known case will be quoted : the deleterious reactivity of the Potsdam sandstone from the Beauharnois dam (Canada) is not revealed, using the conditions prescribed in the standard [2]. From petrographic examinations, it appeared to us that the failure of the method to show correctly the reactivity of this sandstone was related to the elimination of the fine and soft particles, which are also the reactive ones.

This aggregate consists of large, compact and spherical crystals of quartz embedded in a porous thin layer of minute particles of silica and argilaceous matter. One can easily imagine indeed, that when the coarse aggregate particles are crushed, the fracture will preferentially occur within this porous and soft interstitial phase. Those dusty loose particles now being at the surface of the reduced size grains, will be easily detached from each other, will form the fine size fraction and will therefore be preferentially eliminated during the sieving and washing processes.

Experimental verifications have been made by preparing two batches of samples : one, according to the standard and a second where the finest particles are thorougly retained (the grain size of the particles therefore ranges from 0 to 300 µm) : Sc in this case is much higher [3]. Also the reactivity of these aggregates was not shown by the mortar bar test ASTM C 227, presumably for the same reason.

In fact this is not an exception ; it can occur with many other types of aggregates presenting heterogeneities and including "strong " and "weak" materials; this very broad definition can relate to a large variety of situations : hard and soft minerals, compact and porous or layered materials, well crystallized and microcrystalline or amorphous materials. In all these cases, the weak materials which will be drastically disturbed by the crushing process, will be easily discarded in the subsequent step of sieving.

We have not really made investigations to check if the 300 µm limit was a good choice or not ; we have only tried a few experiments, limiting the particles size at 100 µm. In such a case almost all the minerals become highly reactive, liberate large quantities of silica into solution, findings which are in agreement with P.G. Bellew previous results [1]. Therefore we abandoned this limit and maintained the 300 µm one.

For these reasons, the test we now practice is made on particles ranging from 0 to 300 µm. This choice means, that special attention has to be paid to the sample preparation. As the production of overground particles has to be avoided, we recommend following section 7.2 of the ASTM Chemical method, i.e : reduce the material retained on the 300 µm sieve by repeated passes through a disk type pulverizer, with sieving after each pass. From a practical point of view, several types of grinder, manual or mechanical, are suitable but as soon as a few percent of fine particles are generated, they must be removed from the grinding circuit, sieved on a 100 µm sieve, weighed each time for control ; once the grinding has been completed, they should be mixed and homogenized with the larger particles. The percentage of particles smaller than 100 µm should range 35 to 45.

4 - AN ADDITIONAL IMPORTANT PARAMETER : THE TIME

When making mortar bar or concrete prisms tests, the length changes are measured as a function of the time; on the contrary to the chemical method where the duration of the alkaline attack is constant and lasts for 24 hours. Time is not a parameter and this is surpriszing ! It is interesting to draw in the same figure (Fig.2) the expansion of equivalent concrete prisms, made of two deleterious aggregates : the siliceous limestone Spratt's aggregate (Ontario, Canada), which is now considered as a reference aggregate of the alkali silica reaction, and the Sudbury's aggregate, also from Ontario, which represents the slow/late alkali-silica/silicate reaction, abbreviated as SLEASS [4].

The same shapes of curves have been obtained by Rogers and appear in figure 4 of the previous reference.

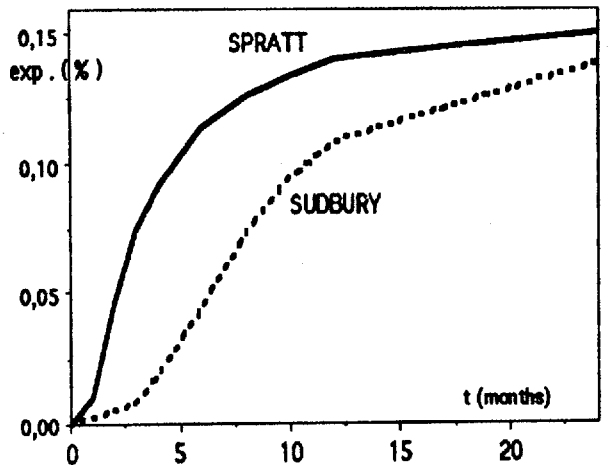

Fig. 2 -Expansion against time for concrete prisms made of two reactive aggregates . Spratt is an alkali silica reactive aggregate, Sudbury is an alkali silicate reactive aggregate.

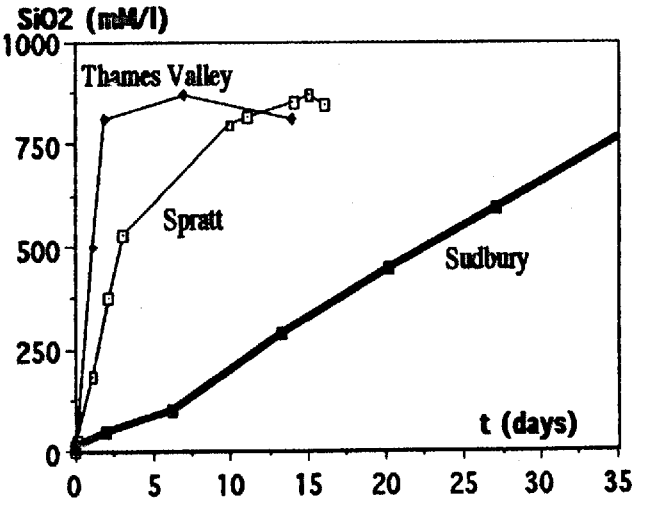

Fig. 3 - Dissolution rate of silica from three aggregates, determined with stirred suspensions.

The expansion kinetics for the Sudbury's aggregate is slow during 3 months but the ultimate expansion is probably as high if not higher. From this, we have made the assumption, that the dissolution kinetics of the silica from these two types of aggregates could follow the same laws : fast dissolution rate for the siliceous limestone, slow initial rate but ultimate, large quantity of reaction for the polyphasic Sudbury's aggregate. In order to check the validity of this assumption, the following experiments have been made : ground aggregates (0-300 μm) have been placed at 80°C, in a thermoregulated vessel, made of teflon and stirred with a 1N or 2N NaOH solution. This type of experiment is now being used as an industrial quality control test, to determine the reactivity of hydraulic binders (Portland clinkers, Aluminous cements).

The quantity of silica released as a function of the time, of sodium and OH^- consumed by the silica network, have been determined at selected times, using the I.C.P to analyse silica and a flame photometer to determine the sodium. The results obtained with three aggregates : Spratt, Sudbury and the Thames Valley sand from the U.K are very interesting, when presented in the same figure (Fig. 3).

It clearly shows that the reaction kinetics of silica dissolution from Sudbury's aggregate is slow during the first few days, but the dissolution rate, which is almost linear, remained constant for the 35 days of the experiment. This fits with P.G.Bellew assumption, that the % of reactive minerals may be as high as 70%, in such type of material [5].

The conclusion to be drawn from this is that the deleterious character of the Sudbury's aggregate can be revealed by the chemical test, but that the 24 hours allowed is not long enough : 30 mmols/L silica were found.

Based on this type of findings, we have decided to include time as a parameter. Instead of using 24 hours only, we now make tests at three ages, at least : 24, 48 and 72 hours. The reason why we call it a KINETIC test is to emphasize on the importance of time and we consider this as an important progress factor. This will help to evaluate correctly the aggregates developing a slow alkali silicate reaction, which was not the case with the regular ASTM C 289 method. Preliminary investigations were made up to 144 hours but it was then shown that there was no need to go this far. However, if the answer is not quite clear after 72 hours, an additional experiment at 96 hours should be made. This idea is not new indeed; authors like Oberholster [6] and Mullick [7] already called attention upon it.

5- THE REDUCTION IN ALKALINITY Rc

The validity of determining an alkalinity reduction, Rc, by an acidic titration with HCl, using phenolphtalein, has been questioned many times in the literature ; due to this, Rc has been abandoned by many authors, who simply determine Sc. A 50 or 100 mMols limit for Sc has been proposed [1], but for reasons explained in section 7, this is unfair for some families of aggregates, especially those containing large quantities of flint.

We will not detail all the complaints on this subject ; some basic explanations were discussed by L. Dent Glasser and Kataoka [8]. From this it appears that the choice of the parameter OH^-, is neither correct from a theoritical point of view, because it is involved within two reactions, nor from a practical point of view since the HCl titration, using the phenolphtalein does not indeed measure OH^-, but the concentration of some anions, including part of the carbonates, silicates and others, if they are partially or totally soluble (e.g : chlorides, sulfates). The titration to the phenolphtalein end point not being independent of dissolved silica, means that Rc is a function of Sc ; this shows that the choice of this second parameter Rc is incorrect.

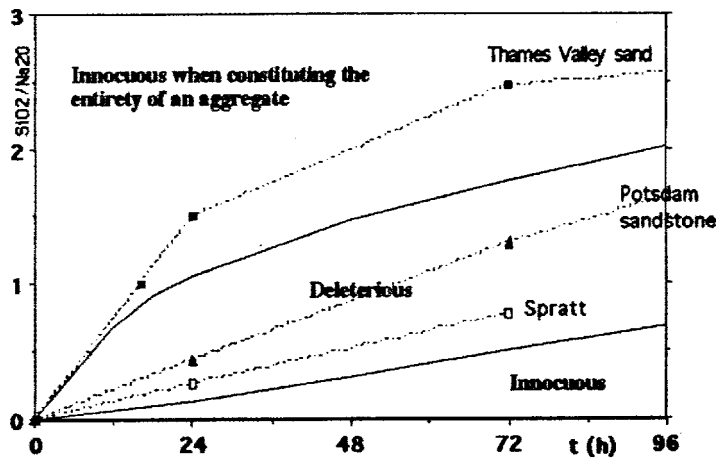

Fig.4 - Interpretation diagram of the kinetic test.
The limits have been established, based on performance of aggregates in concrete structures and or on conventional concrete prisms tests (coarse aggregates) and mortar bars prisms (sands).

Following the advice provided in this publication and in several later papers, we now measure the Na^+ concentration remaining in the liquid phase after the alkaline attack. The results are expressed as the molar Na_2O/SiO_2 ratio (see the y axis of fig.4)

Flame photometry is a suitable method and, as it is often calibrated for K_2O, it additionnally provides the K_2O concentration, due to the release of alkalies by minerals. We have already observed, although the approach is still rough and on a qualitative basis, that the aggregates which liberate K_2O during this NaOH attack are the same which give releasable alkalies, determined in a $Ca(OH)_2$ solution maintained at the boiling point for 7 hours. We consider that it is worthwile to develop this point further.

6- SILICEOUS LIMESTONES

This type of aggregate is common in Canada ; especially on the East coast, the Spratt's aggregate, belongs to this group : the rock consists of calcite and small amounts of dolomite with an insoluble residue of 10%, which itself consists of quartz with small amounts of illite and pyrite.

Practising the ASTM C 289 on the whole aggregate, does not show its deleterious nature : we found 25 mMols silica, which agrees with previous results. The problem originates from several reasons :

- a low silica content compared to the very high $CaCO_3$ level,
- a very high Rc if using the experimental HCl titration, because Rc includes part of the carbonates ; this shift of the representative point into the upper part of the diagram (Fig.1) can move it out of the deleterious region.

To overcome these problems, a solution has been tried, which consists in realizing the NaOH attack on the siliceous insoluble residue and not on the entire aggregate. The quantity of silica dissolved is usually extremely high, the insoluble residue being essentially made of reactive silica ; however the interpretation of the results remains delicate because the true reactivity of the materials is far from being that of the insoluble residue, even

if corrected to the % of the insoluble residue.

Using the modified conditions, explained above in sections 3, 4 and 5, we have applied the kinetic test to the Spratt's aggregate first and repeated it with French limestones (Tournaisis). The results expressed in the new diagram, figure 4, show that their deleterious behaviour is easily evidenced.

A special mention shall be made for aggregates which contain a few percent of calcite and simultaneously slowly reacting forms of silica or silicates. A problem may arise in this case, which leads to an underestimation of the soluble silica. At the beginning of the alkaline attack, the silica concentration is low : a few millimols; at the same time, minute amounts of lime can be released from the calcium carbonate, but this is enough to be over saturated with respect to CSH, which may then precipitate. This precipitation of CSH will withdraw calcium and silicates ions from the liquid phase, therefore the measured soluble silica will be underestimated. This type of reactivity has seldom been met, until now, with French aggregates, but seems more common in Canada.

The lesson to draw from this is that, to avoid any misinterpretation of the test, a complete chemical analysis of the aggregate, and an XRD pattern are essential and detailed petrographical determinations are strongly recommanded.

7- AGGREGATES AND COMBINATIONS OF AGGREGATES BEARING A PESSIMUM EFFECT

The pessimum effect has been known since the earliest AAR research, but has received a great deal of attention by researchers from the UK (Hobbs, Sims, Jones, Nixon ...), because it is a typical case they have to deal with.

The pessimum can be simply defined as the reactive silica content or reactive aggregate content corresponding with the maximum expansion. It occurs in the distressed structures in the UK with some aggregates containing flints and cherts, when these types of sands or gravels (Trent Valley, Bristol Channel, isle of Wight), were used in combination with a non reactive limestone or coarse granite aggregate; otherwise their field performance record is good.

The ASTM C227 mortar bar test produces misleading results, as recently documented by Sims [9] : " the mortar bar test is insensitive to those circumstances encountered in the UK which depend upon the occurrence of a critical combination of constituents and conditions ". The accelerated tests are in trouble too, for the same basic reason, that they are not able to give a flexible answer. The Canadian concrete prism test and the broadly equivalent French standard P 18 587, may be right or wrong, but their answer is in any case incomplete. What is indeed evaluated is a particular combination of the coarse aggregate with a non reactive sand but nothing else ; it neither gives the reactivity of the coarse aggregate, nor the reactivity of any other combination! Therefore extension of the results to any other composition may be dangerous. One has to be very careful with this type of aggregates and one has to think in terms of reactivity of the combination of the aggregates. Concerning the expansion tests, the only valid approach will be the evaluation of the job mix concretes (presently under investigation in France).

The ASTM C 289 chemical test is also insensitive to the pessimum effect and because these rock types contain highly reactive forms of silica from a chemical point of view, (large amounts of silica are released into solution during the first hours of the alkaline attack; see curve figure 3), they would be classified as deleterious or potentially deleterious, which is unjustified most of the time.

We have taken these observations into consideration and, working with a large series of aggregates showing such a type of reactivity (there are plenty in France), we are now able to give a better image of the reality.

The upper part of the new diagram represents the reactivity of the aggregate alone ; it means that, if used alone or in combination with aggregates of an equivalent reactivity, there will not be an expansive reaction, but it is important to note that it is not an innocuous aggregate, as in the lower part of the diagram. If combinations of this type of aggregate are to be made with aggregates of a different reactivity, it will be a necessity to make tests on this particular combination. The kinetic test can do this. We have prepared and tested a series of

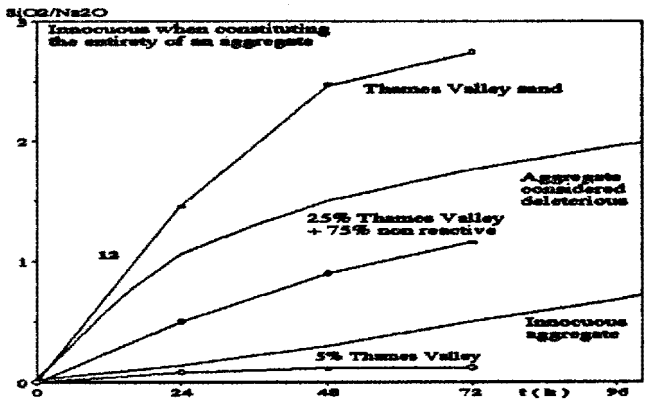

Fig. 5 -Modification of the position of the curve, as a function of the Thames Valley sand %.

mixes, with varying % of Thames Valley sand and another non reactive material ; the representative curves are located in the three parts of the diagram, depending on the respective proportions of the materials : figure 5. This apparently complicated situation represents the reality.

The capability of the kinetic test to easily detect the aggregates showing a pessimum content and to provide the range of proportion of the mixes giving the pessimum expansion is of a great importance.

8- CONCLUSIONS

A quick chemical test is very attractive to characterize the potential reactivity of the aggregates ; the world-wide known ASTM C 289 Chemical method has revealed cases of failure. Based on the published complaints and our knowledge in the cement hydration field, the main problems have been investigated ; an improved version of this test is now proposed, which is termed kinetic test to emphasize the importance of the time.

The following points have been considered : granulometric size, alkalinity reduction, time. The modifications included in the kinetic test allow its application to a much larger number of aggregates : the slowly reacting aggregates and the siliceous limestones can be correctly evaluated.

A great advantage of this test is its capability to detect the aggregates showing a pessimum effect. Its detailed answer fits better with reality. Up till now, this test has been applied to about 150 aggregates, with a large degree of success.

REFERENCES

[1] P.G. Bellew. Evaluation of test methods for alkali aggregate reaction . Proc. 6th ICAAR, pp 303,314, Copenhagen, 1983.

[2] J. Bérard, R. Roux. La viabilité des bétons du Québec : le rôle des granulats. Can.J Civ. Eng. vol. 13, pp 12-24,1986.

[3] D. Sorrentino, S. Sabio, D.Junique. Attaque alcaline des granulats : mise au point d'un test cinétique. Annales ITBTP, n° 499 dec. 91, Série Essais et Mesures 235, pp 91-103.

[4] C.A. Rogers. Concrete prism expansion testing to evaluate slow/late expanding alkali-silicate /silica reactive aggregates. Proc. of a workshop held on march 19 1990 at the ACI convention, Toronto. Published as Materials Report 92, march 1990, by the Ministry of Transportation, Ontario.

[5] C.A. Rogers. General information on standard alkali reactive aggregates from Ontario Canada. Ministry of transportation report, 1988.

[6] R.E. Oberholster.Alkali reactivity of siliceous rock aggregates. pp 419-423, 6th ICAAR, Copenhagen,1983.

[7] A.K. Mullick. Evaluation of ASR potential of concrete aggregates containing strained quartz. NCB Quest. Vol, 1, n° 1,pp 35-46,aug.87.

[8] L.Dent,Glasser, N. Kataoka. Some observations on the rapid chemical test for potentially reactive aggregate.Cement Concrete Research pp 191-196, 1981.

[9] I.Sims. The importance of petrography in the ASR assessment of aggregates and existing concretes. 7th ICAAR, pp359-367, Ottawa, 1986.

SELF-DESICCATION IN CONCRETE

Kristina Norling-Mjörnell

Division of Building Materials
Chalmers University of Technology
SWEDEN

Summary

Long drying-times are one problem associated with concrete slabs in buildings. If the concrete does not dry out sufficiently before the surface is covered by tight vinyl flooring, the relative humidity beneath the flooring will be too high. The concrete must dry out to an average moisture content corresponding to a recommended level of relative humidity (RH) before tight flooring is laid. Since the drying of concrete is very slow the drying-times become unreasonably long.

However, the RH in concrete also reduces due to the consumption of water during the hydration process. In concrete with a low water to cement ratio, a major part of the water is bound to the cement and the amount of excess moisture is fairly low. Even under sealed conditions, there is a decrease in the RH because of internal drying also known as self-desiccation. This self-desiccation seems to be influenced by different factors, such as the water to cement ratio, cement-type and curing temperature. The mineral additive condensed silica fume also contributes to self-desiccation. The influences of these factors have been estimated in this work. To summarize the results very briefly: a low water to cement ratio, an ordinary Swedish portland cement as well as a high curing temperature and the addition of CSF all have a reducing effect on the relative humidity in concrete. Based on this knowledge, we have designed a quick-drying concrete. This concrete may be used for slabs in buildings that would otherwise require unreasonably long drying times.

Sammanfattning (in Swedish)

Långa torktider är ett problem som förknippas med betongplattor i byggnader. Om betongen inte får torka ut tillräckligt innan ytan täcks med en tät PVC-matta kommer relativa fuktigheten under mattan att bli allt för hög. Betongen måste torka ut till en medelfukthalt motsvarande den relativa fuktighet som rekommenderas innan mattläggningen kan påbörjas. Eftersom uttorkning i betong går långsamt resulterar det i väldigt långa torktider.

Men, relativa fuktigheten i betong minskar också på grund av att vatten förbrukas under hydratationen. I en betong med lågt vattencementtal binds en stor del av vattnet till cementet och mängden överskottsvatten är obetydlig. Även i de fall där ingen uttorkning sker utåt minskar relativa fuktigheten till följd av inre uttorkning, också kallad självuttorkning. Självuttorkning i betong verkar påverkas av flera faktorer. Bland dessa kan nämnas vattencementtal, cementtyp, härdningstemperatur. Även tillsats av silika bidrar till en viss självuttorkning. I den här studien har man tittat på hur dessa faktorer påverkar självuttorkningen. För att sammanfatta några av resultaten väldigt kortfattat: Ett lågt vattencementtal, ett vanligt svenskt standardcement såväl som en hög härdningstemperatur har en minskande effekt på RF. Så har även tillsats av silika. Med utgångspunkt från detta försöker vi nu tillverka en snabbuttorkande betong. Betongen kan användas i betongplattor som annars skulle kräva orimligt långa torktider.

Introduction

Built-in moisture is one of the major problems associated with concrete slabs in buildings. Much damage to flooring is caused by moisture. One common reason is that the level of humidity in the concrete had been too high when the surface was covered by tight flooring. We come across this problem in many different constructions. One is concrete ground slabs placed on a tight polythene sheet. Another is concrete slabs placed on permanent shuttering. It becomes more and more common today to use a formwork which is not removed after the casting of the concrete. The formwork is either made of profiled corrugated steel sheets or of a thin slab of high strength concrete. Common to these constructions is a rather thick cast-in-place concrete slab placed on a tight underlying material. The drying is very slow and therefore drying times are unreasonably long. Since the building industry of today strives towards shorter construction times, it is important to reduce the drying-time as well as to prevent damage to buildings caused by moisture.

Drying of concrete

Concrete initially contains a large amount of mixing water. During the curing period, some of the water gradually becomes chemically bound to the cement, i.e. hydration takes place. Yet there is still much water left in the pore system when the hydration diminishes. A substantial amount of moisture referred to as excess moisture has to dry out before materials sensitive to moisture are combined with the concrete. Since the drying procedure is very slow, excess moisture is present in the concrete for a very long time.

The drying starts when the moisture can evaporate from the surface and proceeds as a combination of moisture flow inside the material and evaporation at the surface. The transportation of moisture continues until the equilibrium moisture content is reached. If a tight layer is applied while the concrete is drying, it prevents moisture evaporating from the surface. However the moisture flow still continues up to the surface until a new equilibrium is reached. With a very tight surface, the moisture load on the surface layer corresponds to the average of the remaining moisture content when the flooring was laid.

This is why the concrete must dry out to a certain moisture content corresponding to a recommended level of relative humidity (RH) before a tight flooring is laid. The average RH should not exceed 85 - 90% for a vinyl flooring. One solution might be thin slabs. However, these do not match the design standards and requirements concerning acoustic properties. Another possibility is to use high-strength concrete with liquid damp proofing. This concrete contains less mixing water as well as less excess moisture.
It would be more appropriate to call this concrete low water content concrete rather than high-strength concrete, as we make use of the low water content and not the high strength of the concrete.

Self-desiccation in concrete

Low water content concrete has a low water to cement ratio and a higher cement content than normal concrete. Thus, a mayor part of the mixing water becomes chemically bound to the cement during hydration. What is left is a small amount to be physically combined and sometimes a minor amount of moisture to dry out. Even in sealed conditions, there is a decrease in RH because of internal drying, also known as self-desiccation.

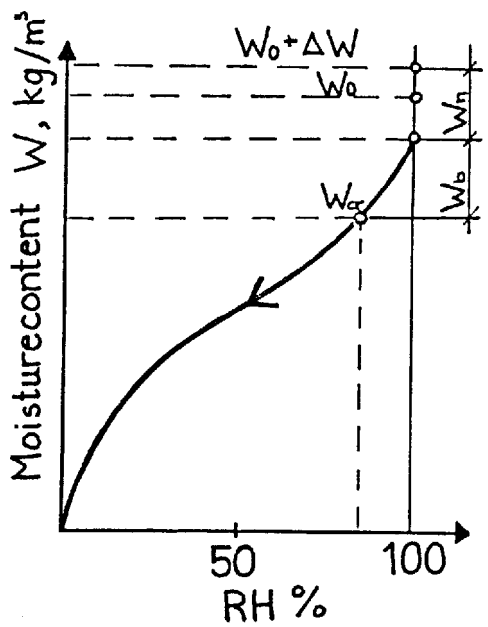

W_0 = mixing water

ΔW = additional water during curing (rain)

W_n = Chemically bound water

W_{cr} = Moisture content corresponding to the critical RH

W_b = Excess moisture

Figure 1. The moisture content in concrete. For sealed conditions $\Delta W = 0$.

If any additional water is added during curing, the RH may increase and the effect of self-desiccation is lost. On the other hand this concrete is much more dense and probably more impermeable to water than ordinary concrete. Before this property is further examined, it is important to protect the surface from any additional water, for example rain water, during curing. The surface is usually covered by a tarpaulin. Many liquid damp proofing products are used but it is not very likely that they will keep the rain water out completely.

Mineral admixtures such as condensed silica fume, CSF, seem to have a positive effect on the internal drying of concrete. Due to CSF's very high surface area, it is likely to refine the pore structure, and consequently the RH decreases.

Hydration in self-desiccating concrete

During hydration, water reacts with the cement. The chemically bound water is fixed to different cement components as hydrate water and hydroxide. The degree of hydration is a measure of the amount of bound water. The rate of hydration is affected by the W_0/C-ratio as well as by the RH in the pore structure. At an RH lower than 80% the rate of hydration is very low. Consequently, the hydration becomes slow and stops at an early stage. Due to self-desiccation, concrete with a low W_0/C-ratio dries out to a low RH and the hydration diminishes early. Work is in progress to study the relationship between the amount of chemically bound water, the rate of hydration and the RH.

Measuring the relative humidity (RH) in concrete

RH was measured directly with a capacitive RH-sensor made by Vaisala, Finland. For the small-scale experiments in the laboratory, the RH-gauge is placed into a sealed test tube containing the sample. When measuring the RH in concrete slabs in a building, the RH-gauge is put into a drilled hole with the desired depth. The RH can be read when equilibrium conditions have been reached in the enclosed air. The reading is preferably done after about eight hours.

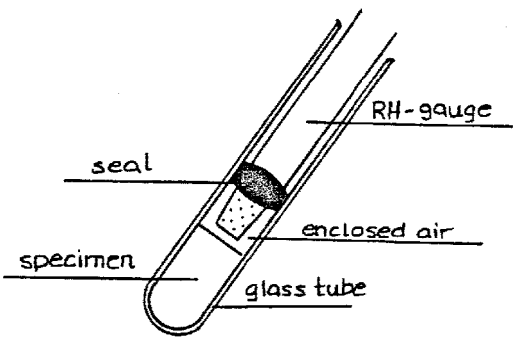

Figure 2. Method of measuring RH in the laboratory.

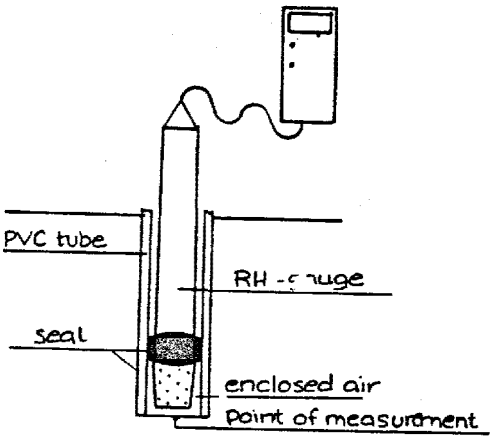

Figure 3. Field measurements of RH.

Experimental arrangements and measurements

Laboratory tests

The results show that the RH in a young concrete is influenced by different factors such as the water to cement ratio, cement type and curing conditions. Mineral admixtures like condensed silica fume also play an important role for internal drying. Experiments have been carried out in order to estimate what effect these factors have on internal drying and how they influence the self-desiccation capacity of the concrete. Small-scale experiments were made with cement paste and cement mortar. Specimens were placed in jars or test tubes and cured under sealed conditions at a constant temperature. The relative humidity was measured regularly according to the method described earlier. The following variable factors were included in the studies: water to cement ratio, cement type, amount of CSF and curing temperture.

Cement paste:

Factors	Levels
W_0/C	0.36, 0.40, 0.44, 0.50
Cement types	Slite, Skövde, Degerhamn (For cement types: see next page)
Curing temperatures	5°C, 20°C
Amount of CSF	0 or 10% of the cement weight

Cement mortar:

Factors	Levels
W_0/C	0.35, 0.40
Cement types	Slite, Degerhamn
Curing temperature	20°C
Amount of CSF	0 or 10% of the cement weight

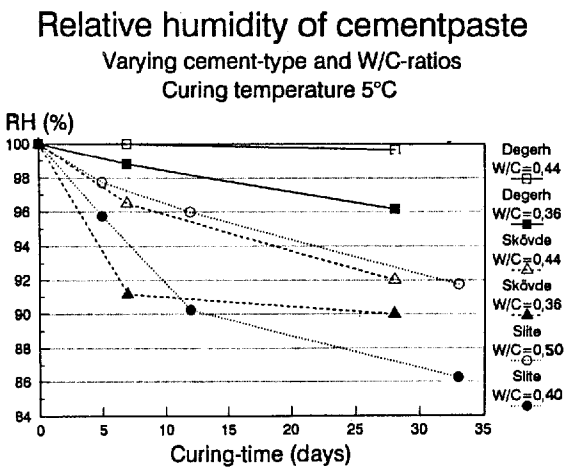

Figure 4. The effect of cement type on RH in cement paste.

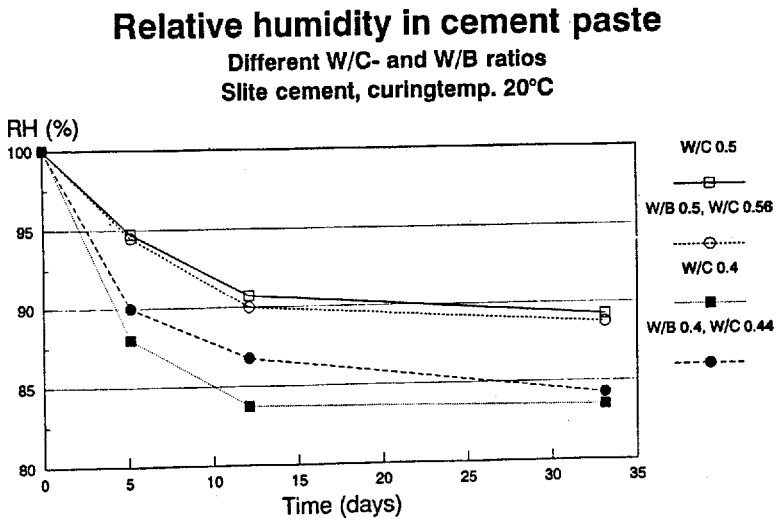

Figure 5. The effect of W_0/C- and W_0/B-ratios on RH in cement paste.

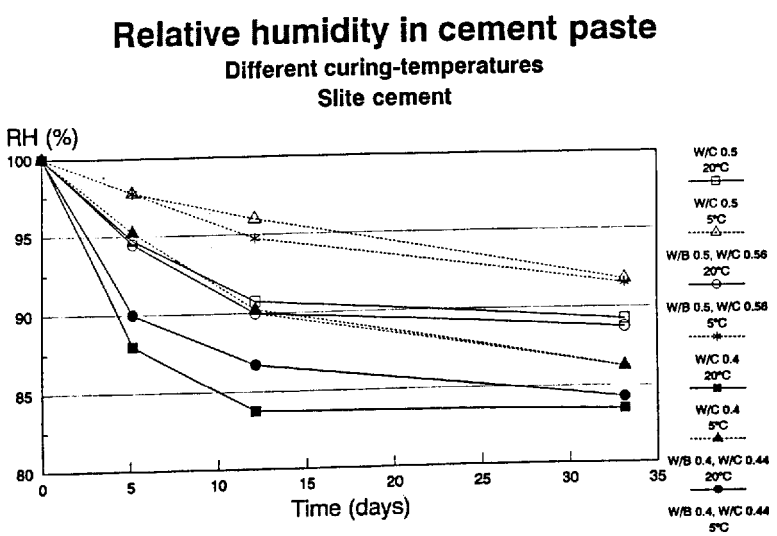

Figure 6. The effect of curing temperature on RH in cement paste.

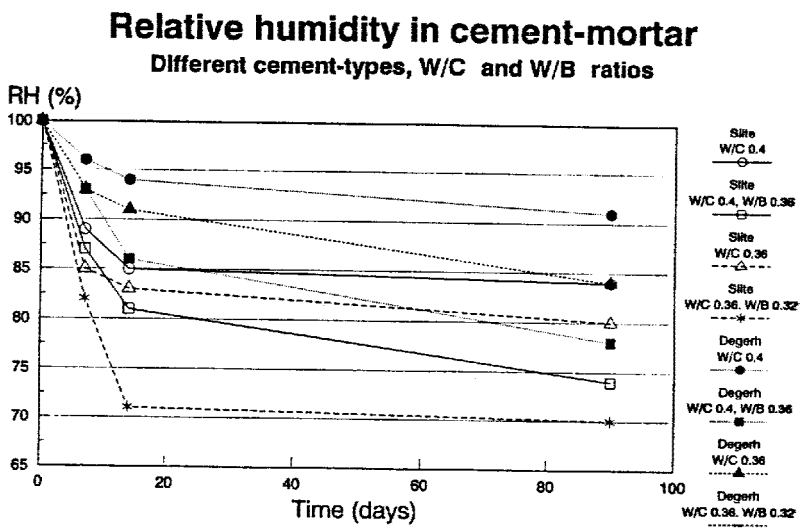

Figure 7. The effect of W_0/C- and W_0/B-ratios on RH in mortar.

Results

Not unexpectedly, the two dominating factors observed were water to cement ratio and the type of cement used. Less important but still significant were the effects of the curing temperature and the addition of CSF.
There is a considerable difference in the self-desiccating capacity at early age for different cement types. The difference in RH between cement paste made of Degerhamn cement which is a low-alkali, low-heat sulphant resistant cement, and one made of Swedish ordinary portland cement, OPC, from Skövde or Slite is about 5% if the same water to cement ratios are compared. The OPCs from Skövde and Slite have the higher self-desiccating capacity which decreases the RH. Increasing the water to cement ratio from 0.40 to 0.50 for one cement type gives an increase in RH of approximately 5% RH. The effect of curing in 5°C instead of 20°C is a few percent higher RH. In mixes where CSF is added, it amounts to 10% of the cement weight. It is included when calculating the water to binder ratio: $W_0/B = W_0/(C+CSF)$. CSF is a puzzolanic material and reacts with water forming hydration products similar to those of the cement. CSF has a minor effect on the initial stage of self-desiccation whereas the long-term effect seems to be greater.

Overall, the studies of the RH in cement pastes and mortars show similar results and follow general trends.

Field studies

The next natural step was to study these phenomena in reality. We had the opportunity to follow the drying of concrete with various compositions in different constructions at two building sites. The first was a concrete ground slab. The concrete was made according to the guiding outlines for mixing a low water content concrete or a "self-desiccating concrete". The water to cement ratio was 0.45, the water to binder ratio was 0.43 and the addition of CSF 6% by the cement weight. Because of the high cement content, a superplasticiser was needed to increase the workability of the concrete. The slab was covered by a tarpaulin during the first week and after that exposed to the outside climate (winter-spring in the middle of Sweden). The curing temperature varied between 0 and 10°C. The RH in the concrete was a little more than 90% after one month.

In the other test area, two types of concrete mixes were examined, one with a water to cement ratio of 0.51 and the other with 0.45. No CSF was added in either of the mixes. As the slabs were placed at different times and exposed to very different curing conditions, it is very difficult to draw any conclusions. We can, however, identify one difference between the two W_0/C-ratios. The concrete with the lower W_0/C-ratio dried out to the recommended RH before the flooring was laid. This was not the case with the concrete with the higer W_0/C-ratio.

It is important to keep in mind, when looking at the results from the field studies, that the measurements are very approximate, since it is very difficult to measure the RH in this environment and since the slabs were exposed to totally different curing and drying conditions.

Conclusions

Concrete slabs in buildings may require a quick-drying concrete to prevent damage caused by high humidity. If the flooring is tight, the humidity beneath the flooring will finally come up to a relative humidity corresponding to the average moisture content in the concrete when the flooring was laid. The RH in the concrete must decrese below a critical level before the surface is covered by tight vinyl flooring.

Concrete with a W_0/C-ratio of about 0.40 dries even under sealed conditions due to self-desiccation. Also some types of cement have a great influence on the RH in young concrete. Both of the Swedish ordinary portland cements, Skövde and Slite, decrease the RH more than the low-heat sulphant resistant Degerhamn cement. To add condensed silica fume apparently accelerates the self-desiccation in concrete. CSF plays both the role of a filler, due to its fine particle size, and the role of a puzzolanic material, due to its large surface area and its ability to combine with lime. Thus it refines the pore structure and reduces the RH. The curing temperature also influences the RH. A higher curing temperature accelerates the self-desiccation and reduces, not unexpectedly, the RH.

The knowledge of how these factors influence self-desiccation enabled the design of a quick-drying concrete. Furthermore, it is important to study how this concrete works in real constructions in buildings. The concrete might be exposed to various drying conditions, such as additional water and low curing temperatures.

References:

Hygroscopic Moisture in Concrete - Drying, Measurements and Related Material Properties, Nilsson, L.O, Report TVBM-1003, Lund Institute of Technology, Sweden 1980.

MECHANICAL BEHAVIOUR OF ADVANCED CEMENTITIOUS MATERIALS

W Jiang and D M Roy

Materials Research Laboratory
The Pennsylvania State University
USA

Summary

The topic of this paper is focusing on the latest advances in cementitious materials mechanical properties and laboratory technology. There are numerous pathways for achieving what is desired with respect to high-strength cementitious materials, i.e. the different routes to generating strong materials, including chemical modification, high-shear mixing with polymer addition, and the making of fibre and particulate composites. The Strengthening mechanisms were studied. The measurement of fracture toughness of cement paste and concrete were conducted by the experimental technique based on the *J*-integral in an indirect way using small-sized specimens by the single-edge-notch-beam method in the three-point bending test.

INTRODUCTION

Normal cementitious materials have a low tensile strength (approximately one-tenth its compressive strength) and exhibits limited ductility, especially in tension. The distinguishing mechanical property of cementitious is brittleness - that is, catastrophic failure following an almost entirely elastic deformation. Cementitious materials can thus be classified as a brittle material containing many inherent flaws in the form of air voids and microcracks. But recent advances in this area have led to the development of novel materials that include composites some of these new strong and high-quality materials are being developed for more sophisticated applications. A schematic stress-strain diagram of three types of concrete is shown in Figure 1. Cementitious materials of the new generation have strengths that are greater by an order of magnitude than those of conventional cements. Though these specialty materials are too expensive to use in voluminous quantities for everyday building, their special strong mechanical properties make them ideal for a number of other applications.

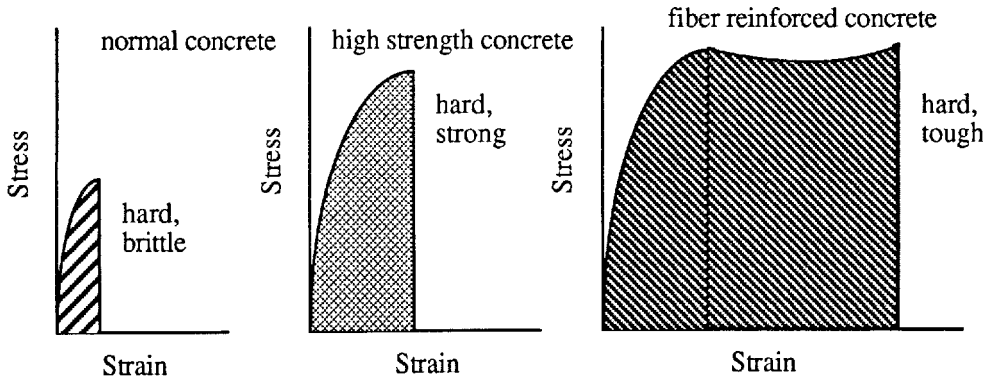

Figure 1 Schematic stress-strain diagram for three type concretes

J-integral

Earlier investigations in the fracture of quasi-brittle materials assume the validity of linear-elastic fracture for the laboratory specimens employed and their toughness parameters such as K_{1c} and G_{1c} are determined. However, such parameters as obtained from normal laboratory sized specimens are found to be dependent on the specimen size. As a result, very large specimens (over 1 meter) are required to obtain the true K_{1c} value. Such specimens sizes are clearly impractical in the laboratory[1,2]. The objective of the present investigations is to develop the experimental technique based on the *J*-integral in an indirect way using small-sized specimens.

The *J*-integral introduced by Rice can be interpreted as the area of tension-softening curve [1], which is defined as the functional curve between the traction across a crack plane and the separation distances of the crack faces in a uniaxial tension specimen quasi-statically loaded to complete failure. The path independent nature of this integral allows the integration path to be taken close or sufficiently far from the crack tip[3,5]. It is equivalent to the critical energy release rate G_c under small scale yielding condition. G_c is related to through the equation

$$J_c = G_c = (K_{1c})^2 / E \qquad \text{(for plane stress conditions)}$$

From this relation, the linear-elastic fracture parameter K_{1c} can be obtained. *J*-integral can be obtained experimentally from a compliance test by loading two precracked specimens with slightly different crack lengths. If the load P and the load point displacement Δ are measured simultaneously in the test, *J* can be obtained in terms of d from the area $A(\Delta)$ between the two *P*-Δ curves up to a load point displacement value of Δ.

$$J(\Delta) = (1/B)[A(\Delta)/(a_2-a_1)]$$

Where *B* is the width of the specimen and (a_2-a_1) is the difference in crack length.

Strengthening and Toughening Mechanisms

The history of the attempts to strengthen concrete is almost its history of engineering. Numerous mechanisms for strengthening concrete have been advanced. New concrete have been developed with and without such knowledge. Table 1 gives the description of some of the mechanisms involved and the processes employed.

TABLE 1
Major concrete strengthening mechanisms

Mechanisms	Associated effect
Admixture-modified	
a) Chemical	effective dispersant promotes denser packing, reducing water requirement
b) Mineral	DSP(densified systems containing homogeneously arranged, ultra-fine particles of silica fume or fly ash)
c) Polymer (water soluble)	MDF(macro-defect-free); allows high shear processing
Mechanical compaction	utilizes intense mechanical compaction which overcomes the inter-locking surface forces and pack the concrete as densely as permitted
Fiber reinforcing	the cracks are stopped or deflected by the presence of the fibres at the interface and the work of fracture is often dramatically increased
Polymeric reinforcing	polymer fills tiny pores and flaw, increases density, improves the cement-aggregate bonding, reduces stress concentrations
Autoclave curing	fine and close in the texture, well and high percentage crystalline hydrate

EXPERIMENTAL

Specimens Preparation

Cement used in this research was the Lafarge product "Secar 71" high alumina cement. Fine aggregates were ASTM standard sands. Coarse aggregate is sieved before use so that the maximum sized aggregate can pass through a No. 8 screen. The mix proportions: for concrete, cement: sand: aggregate :water were 1.0: 2.75: 2.75: 0.35; for mortar, 1.0: 2.75: 0 : 0.3. Specimen size dimensions for the three-point bending test: for mortar and concrete, 350x80x40, for cement paste 60x10x10mm. The two different a/w (crack depth/beam depth) ratios were 0.4 and 0.5. The notch was cut in a tension side of the beam using a 0.2mm thick diamond saw. Table 2 illustrates the preparation of specimens tested in this work. Further details can be found in the relevant reference.The specimens were tested at an age of 28 days.

Hot pressing cement paste: Specimens were pressed in specially designed cell at 350-50 MPa for 0.5-1hr temperature variable.[6]

MDF cement paste: The term MDF refers to macro-defect-free cement paste. The use of several percent of a water-soluble polymer at a low water/cement ratio combined with processing by high shear mixing and extruding changes the pore structure of the paste. Their relatively high strength in bending, as high as 150MPa or higher, was proposed to be due primarily to the absence of large flaws.[8] Now even higher strengths are achieved. Typical MDF composition was shown in Table 3.

TABLE 3
Typical MDF composition

Ingredients	OPC	Polyacrylamide	Glycerin	Water
Wt. %	78.0	8.0	0.5	13.5

Test Method

The measurement of fracture toughness of cement paste, mortar, and concrete have been conducted by the single-edge-notch-beam method, in the three-point bending test. The load and load point displacement were measured simultaneously. Signal output was recorded by computer data acquisition system and sent immediately to an IBM PC where the data were stored. The data are analyzed numerically. For each set of raw data, values are obtained by interpolation.

Young's moduls of elasticity was obtained from the flexure of a beam using the equation

$$E = (kl^3/4bd^3)*10^{-3}$$

Where E is Young's moduls of elasticity (GPa), k the slope of the load-deflection plot (Nmm^{-1}), b the beam width (mm), d the beam depth (mm) and l the beam span (mm).

TABLE 2
Preparation of specimens

Materials	Preparation	Reference
1. hcp (hydrated cement paste)	water/cement = 0.3	
2. hot pressing paste	50,000 psi, 80 °C	[6]
3. MDF paste		[7]
4. mortar	ASTM C109	
5. polymer impregnated mortar		[8]
6. plain concrete	ASTM C116	
7. DSP concrete	5% silica fume	[11]
8. PIC (autoclaved)		[8]
9. carbon FRC	8% Vol, 6mm (Stackpole)	[9]
10.steel FRC	2% Vol	[12]
11.polypropelene FRC	2%, 0.5"	[10]

PIC = polymer impregnated concrete; FRC = fiber reinforced concrete.

RESULTS AND DISCUSSION

The Factors Affecting Strength

Total porosity: Only by using intense mechanical compaction was it possible to overcome the inter-locking surface forces and pack the cement as densely as permitted by the particle geometry-typically corresponding to a low water/cement ratio- resulting in very high strengths. The strength of the cement paste is strongly dependent on both the total porosity and the maximum pore size of the materials. Dense packing is the essential feature of cementitious materials necessary to reduce both the total porosity and maximum pore size (critical flaws). The packing of particle systems is strongly dependent on the mechanical placing of particles, i.e. the kinematics of the arrangement of particles. Normally, denser packing can be obtained by shear deformation, repeated shear deformation, or balanced vibration. In Figure 2 the curve shows the relationship between compressive strength and porosity of hardened cement paste in small-scale laboratory experiments under special hot-pressing conditions.[6] Much higher strengths have also been achieved; in particular, the highest also combined the effects of dense particle packing.

Maximum pore size: The Griffith criterion s, which is normally defined as $(ER/\pi C)^{1/2}$, where R is the fracture energy and C is the crack (pore) length, can be modified to incorporate porosity (p), to yield

$$\sigma = [E_0R_0(1-p)^3\exp(-kp)/\pi C]^{1/2}$$

where k is a constant and E_0 and R_0 are E and R for a nonporous reference state. The data on the MDF cement in Figure 3 agree with this theory fairly well.[14]

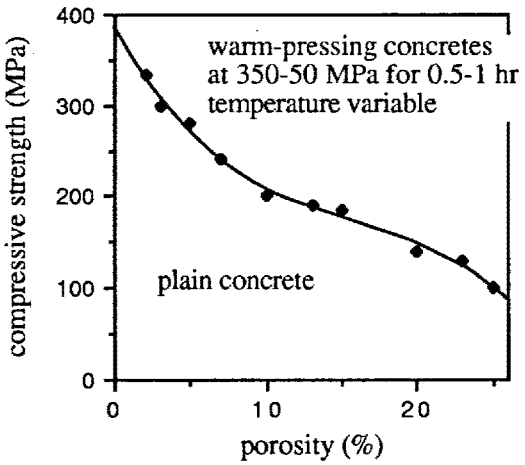

Fig. 2 The relationship between compressive strength and porosity

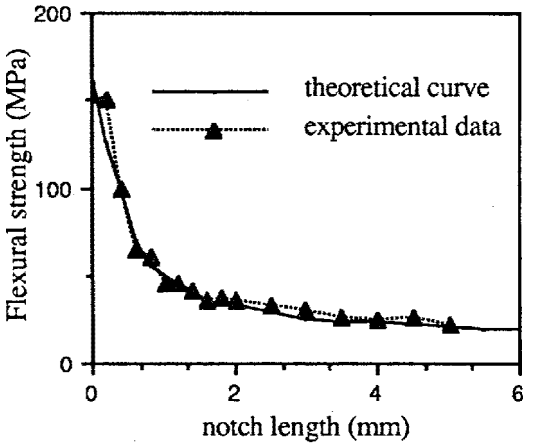

Fig. 3 Notched beam test of the flexural strength of MDF cement paste

Toughening Mechanisms

Fibre Reinforcing: Broadly, the reason why weak, brittle cementitious materials are made stronger and tougher by very small additions of fibre is that cracks are stopped or deflected by the presence of the fibres at the interface and the work of fracture is often dramatically increased; in practice, this is generally equivalent to a substantial improvement in tensile strength, although the stiffness may not be greatly improved. When a low volume fraction of fibers is used, the role of fibers is apparent after the cracks have formed in the materials. In such cases -assuming there is no fiber fracture- the fiber debonding and pullout processes have a significant influence on the total energy consumption and overall toughness of the composite[2]. Figure 4 shows toughness, bending strength of cementitious materials as compared with plastics, aluminum, wood, glass and steel. Figure 5 shows the effect of the fiber content on values of *J*-integral.

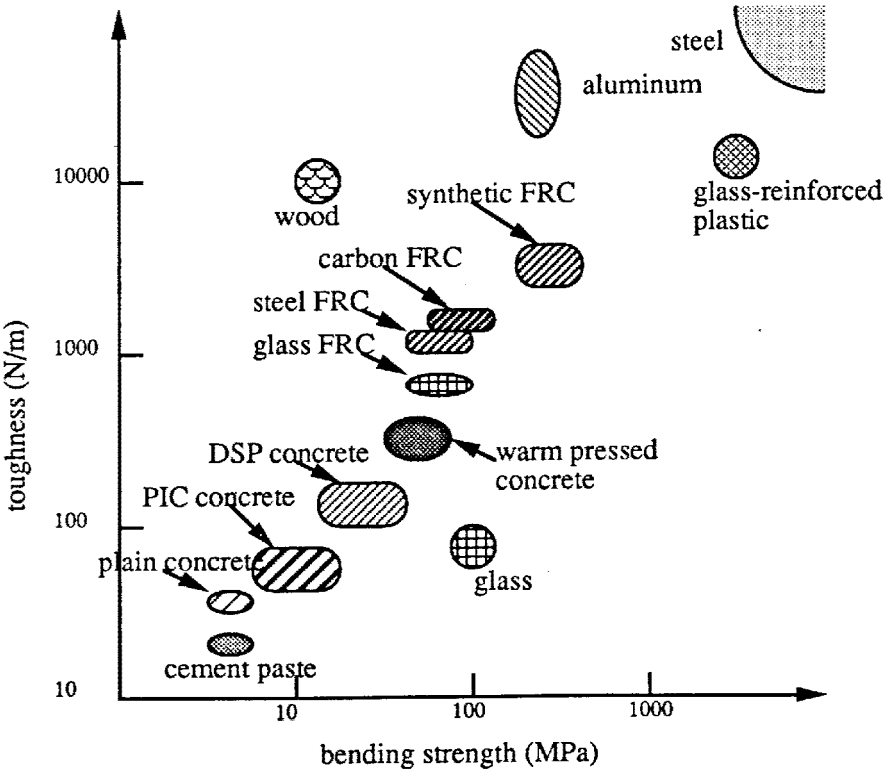

Fig. 4 Toughness, bending of strength of cementitious materials as compared with plastics, aluminum,wood, glass and steel

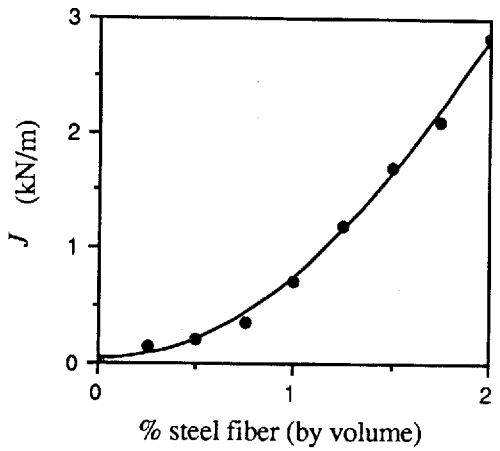

Fig. 5 J-intergral against load point displacement

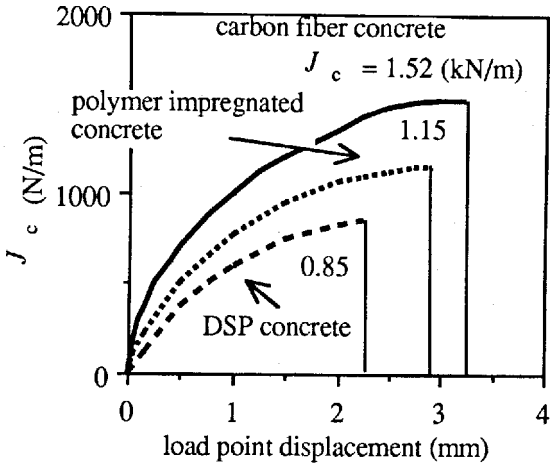

Fig. 6 Effect of fiber content on values of J-integral

Densified with small particles: The term DSP refers to Densified Systems containing homogeneously arranged, ultra-fine Particles. In the actual context, the densely packed are normally cements and the ultra-fine particles are silica fumes or, less commonly, fly ashes. The latter are chemically less reactive than cement, especially the fly ash, and achieve dense packing while eliminating the problem of the too rapid hardening encountered with very fine cements; in addition, the silica fume ensures the formation of a coherent structural skeleton between the cement particles, resulting in a fine, dense microstructure. [11] Experimental results of toughness under effect of different toughening mechanisms are shown in Figure 6. Table 4 lists J-integral, Young's modulus of elasticity (E) obtained from the test, and critical stress intensity Factor, K_{1c} which was calculated from the equation of $J_c = (K_{1c})^2/E$ for different concrete, mortar and paste. Figure 7 shows the range of fracture energy obtained for various concretes, mortar and paste based on J-integral of the multiple-specimen method.

The difference between the J-integral technique we used here and the RILEM GF test [4] is that in their test, pre-cracked specimens with only one crack size are needed and only the apparent critical energy release rate can be determined,whereas in our test, two kinds of crack size are used and more information is provided. Furthermore that the value of G_c we obtained is expected to subject to a much smaller size dependence than the RILEM test value. The size dependence is mainly due to damages outside the cracking plane which tends to increase with the specimen size. In our case, G_c is obtained from the different in energy of two specimens with slightly different crack size. The irrecoverable losses will tend to compensate each other for the two specimens and hence the size dependence can be greatly reduced.

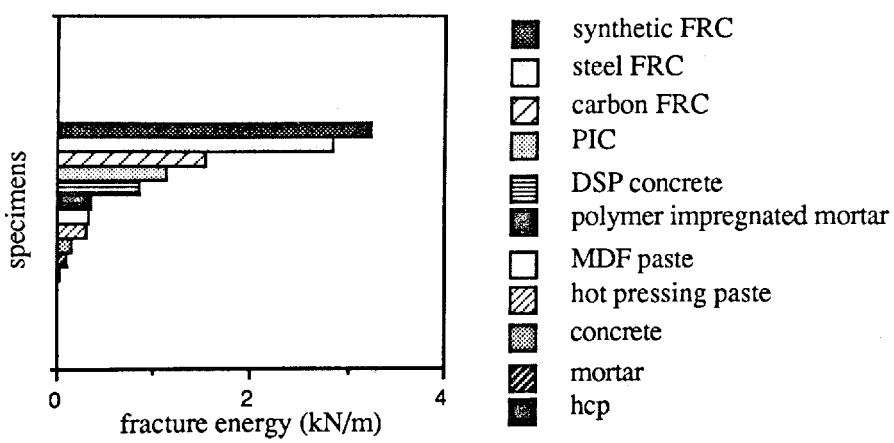

Fig. 7 Fracture energy of various specimens

TABLE 4
J-integral, Young's modulus of elasticity and critical stress intensity Factor

Materials	*J*-integral (kN/m)	E (GPa)	K_{1c} (MPa·m$^{1/2}$)
1. hcp (hydrated cement paste)	0.016	11	0.419
2. hot pressing paste	0.31	24	2.78
3. MDF paste	0.32	25	2.82
4. mortar	0.11	20	1.48
5. polymer impregnated mortar	0.35	26	3.01
6. plain concrete	0.16	22	1.87
7. DSP concrete	0.85	28	4.88
8. PIC (autoclaved)	1.12	30	5.79
9. carbon FRC	1.52	34	6.97
10.steel FRC	2.83	35	9.95
11.polypropelene FRC	3.23	41	11.51

CONCLUSIONS

Major advances have been made in mechanical properties of cementitious materials critical to modern technology. The challenge remains to better understand the mechanisms involved in generating strength and toughness, the effects of compositional and microstructural modifications, and the range of feasible processing parameters which control the properties of such composites. *J*-integral, an indirect experimental technique is developed to obtain the critical stress intensity Factor, K_{1c}. Three-point bending test was employed. The test involved only laboratory-sized specimens and can be easily performed without the need of mortification of testing machines. Our results are found to be in good qualitative agreement with those obtained by the other tests.

REFERENCES

1. Leung, C.K.Y. and Li, V.C., Determination of fracture toughness parameter of quasi-brittle materials with laboratory-size specimens. J. Mater. Sci., 1989, **24**, 854-62.
2. Ouyang, C. and Shah, S.P., Geometry-dependent R-curve for quasi-brittle materials. J. Am. Ceram. Soc., 1991, **74** [11], 2831-36.
3. Westerlind, B.S., Carlsson, L.A. and Andersson, Y.M., Fracture toughness of liner board evaluated by the *J*-integral, J. Mater. Sci., 1991, **26**, 2630-36.
4. Karihaloo, B., Fracture Mechanics Test Methods for Concrete, ed. S.P Shah and A. Carpinteri, Chapman and Hall, London, 1991, pp. 1-69.
5. Gdoutos, E.E., Fracture Mechanics Criteria and Applications, Kluwer Academic Publishers, The Netherlands, 1990, pp. 171-76.
6. Roy, D.M. and Grouda, G.R., High strength cement paste, hot pressing, Cem. Concr. Res. 1973, **3**, pp. 807-20.
7. Park, C.K., Silsbee, M.R. and Roy, D.M., Toughening of MDF-OPC Composites, Mat. Res. Soc. Symp. Proc. Vol. 211, 1991, pp. 237-246.
8. Feldman, D., Polymeric Building Materials, Elsevier Science Publishers, England, 1989, pp.209-251.
9. Li, V.C., Fracture Resistance Parameters for Cementitious Materials and Their Experimental Deterinations, In Application of Fracture Mecanics to Cementitious Composites, ed. S.P. Shsh, HATO-ARW, 1984, pp.431-449.
10. Li, V.C., Backer, S., Wang, Y., Ward, R. and Green, E, Toughened Behavior and Mechanisms of Synthtic Fiber Reinforced Normal Strength and High Strength Concrete, In Fiber Reinforced Cements and Concrete: Recent Developments, ed. E.N. Swamy and B. Barr, Elsevier Science Publishers, England, 1989, pp.420-433.
11. Bache, H.H., CBL report No. 40 from Aalborg Portland, Denmark, 1981.
12. Mindess, S., Lawence, F.V. and Kesler, C.E., The J-integral as a fracture criterion for Fiber Reinforced Concrete, Cem. Concr. Res. 1977, **7**, pp. 731-42.
13. Roy, D.M., New Strong Cement Materials: Chemically Bonded Ceramics, Science, 1987, **235**, pp. 651-58.

DEVELOPMENT OF REMOTE SENSING TECHNIQUE FOR PREDICTION OF LIMESTONE QUALITY

M Imran, D K Panda and G V K Prasad

National Council for Cement and Building Materials
New Delhi, INDIA

SUMMARY

The solar refelectance spectra, which is a measure of the amount of light reflected by a material, is a consequence of the chemical composition and structure of the material modified by environmental factors and the physical conditions of the material. This is expressed in satellite data by photographic tone or colour and has been extensively employed for lithological discrimination.

The present paper highlights an integrated approach using visual interpretation, ground reflectance and digital image processing techniques as employed for grade prediction of limestone with specific case studies.

INTRODUCTION

The use of term "remote sensing" usually refers to the gathering and processing of information about the earth's environment and resources, through the use of remotely recorded data obtained with the help of air borne or space borne spectral imaging instruments.

The National Council for Cement and Building Materials (NCB) has carried out pioneering work by using this technique for assessment of cement grade limestone through development of remote sensing keys and discovering new deposits estimating about 3600 million tonnes. The present paper highlights the details of remote sensing techniques employed for grade prediction through visual interpretation of Satellite data, measurement of ground reflectance and digital image processing technique with specific case studies.

BASIC CONCEPT

Spectral reflectance is a measure of the amount of light reflected by a material and expressed in images by photographic tone or colour. This has been widely employed for lithologic discrimination based on the assumption that the spectral behaviour of rock types/surface materials depends on the composition of the rock type/surface materials. The physical appearance of the rock type/object is governed by its mineral constituents/chemical composition and thus will influence the spectral behaviour.

GRADE PREDICTION THROUGH VISUAL INTERPRETATION

As the tonal variation in the satellite data is the function of spectral behaviour of rock types, an attempt was made to correlate the same with the grade of limestone. The False Colour Composites of bands 2,3 and 4 (Blue-Green-Red) of Landsat TM and IRS-LISS II data enlarged to 1:50,000 scale were selected for two areas in Andhra Pradesh and one in Rajasthan. Initially the limestone and associated rocks were delineated using the remote sensing keys developed earlier (3). During ground truth studies, the systematic samples were collected for darker and lighter tone areas separately and were analysed for CaO and SiO2 content. It was observed that the lighter toned areas almost invariably, were indicative of higher silica content (more than 15%) as compared to darker tone areas (tables 1 & 2).

TABLE- 1
REMOTE SENSING KEYS OF VARIOUS LIMESTONE LITHO UNITS ON IRS-1A,LISS-II FCC IMAGERY. BANDS COMBINATION 2 , 3 , 4 (B-G-R)

LIMESTONE LITHO-UNITS	TONE/ COLOUR	TEXTURE	TOPOGRAPHY	DRAINAGE
Dolomitic	Light yellow	Mottled	Conical Hills	Coarse dendritic
High grade	Dark blue	Fine	Undulating	Coarse , partly internal
Low grade shaly	Light blue, alternate bands	Fine	Undulating	Dendritic,coarse
Lime kanker	Dull white	Mottled	Undulating	Coarse , partly internal.

TABLE-2

SILICA CONTENT IN LIMESTONE

Sample No.	Colour of Limestone on the F C C Light Blue SiO2%	 Dark Blue SiO2%
1.	16.38	10.12
2.	15.17	08.32
3.	14.11	09.61
4.	15.92	10.11
5.	16.32	11.02
6.	15.17	11.12
7.	17.68	09.68
8.	15.11	08.38
9.	17.18	06.11
10.	15.31	07.66

SPECTRAL REFLECTANCE STUDIES FOR GRADE PREDICTION

It has been observed that various physical as well as chemical characteristics of minerals, rocks and soils influence their spectral emission. Some of these include mineralogy, particle size, packing, moisture and organic content. Additional variables that may influence remotely sensed data are target temperature and temperature gradient, radiations from surrounding terrain reflected by the target, micrometeorology, surface roughness of the target, reflected and direct atmospheric radiations.

In order to establish a relationship between field reflectance and grade of limestone, reflectance data was collected using Ground Truth Radiometer (GTR) designed by ISRO's Space Application Centre. The equipment enables collection of reflectance data in the range of 485 to 837 nm compatable to 4 bands of TM/IRS and three bands of SPOT.

The data was normalised by eliminating the effects due to varying intensity and inclination of the incident radiation, cloud cover, surface orientation of the object and height of the instrument etc using GTR calibration plate. The percentage relative reflectance is obtained by using the following equation

$$\text{Relative Reflectance \%} = \frac{RQ}{RB} \times \frac{GB}{GQ} \times 100$$

Where RQ = Reflectance of the object
RB = Reflectance recorded with barium sulphate plate
GB = Gain Setting for plate
GQ = Gain Setting of object

The observations were recorded using all the 11 bands in the available range at about 50 different stations corresponding to various types of limestone. Representative samples of limestone were collected from the respective locations and were chemically analysed for major oxide constituents. The spectral reflectance curves were plotted with respect to CaO and SiO2 content of limestone (fig 1).

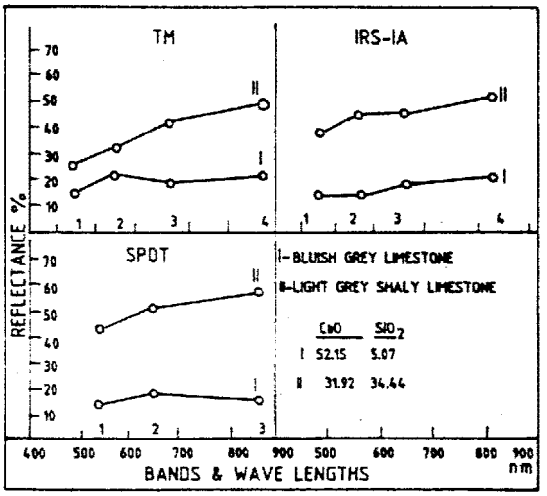

FIG. 1 : Field Reflectance of Limestone

The following observations were made :

a) High calcium limestone exhibits lower reflectance as compared to high silica limestone.

b) The intensity of reflected beam is lesser in case of rough rock surface as compared to smooth/even surface.

c) The reflectance increases with the increase in wavelength.

d) The solar angle, which is governed by the time of observation also has a direct bearing on reflectance data.

GRADE PREDICTION THROUGH DIGITAL IMAGE POCESSING OF SATELLITE DATA

Satellite images consist of tiny, equal areas of picture elements, arranged in regular rows and columns. The position of any picture element or pixel is determined on X-Y Co - ordinate system. Each pixel has a numerical value called the digital number and reflects the intensity of electromagnetic energy, measured for the ground resolution cell represented by that pixel. The digital numbers vary from 0 to 255.

Digital Image Processing is a collection of techniques for improving the image quality for interpretation and classification. For the present study, the ISROVISION - an indigenously developed digital image processing system supported by SACIMAGE software package was used.

The system accepts the image data in the form of Computer Compatible Tape (CCTs) or floppy products from different satellites, viz. Landsat series, IRS and SPOT etc.

To further corroborate the earlier observation for grade prediction through visual interpretation and field reflectance value, the digital image processing was carried out for an area covered by upper Vindhyan rocks in SE Rajasthan.

The rock types identified in the area include limestone of varying grade, shale,sandstone,quartzite and trap rock. Soil cover, vegetation and water bodies have also been observed through supervised classification technique. The grey values of all the rock types, vegetation and water bodies were plotted against the wavelength (Fig 2). It was observed that with the increased wavelengths, the grey values of the objects were increasing. However, each object had its characteristic wavelength range. It was evident that the grey value of quartzite is highest and for water it is the lowest. The grey value of limestone was in the range of 28-29 (band-2), 32-34 (band-3) and 42-43 (band-4). The increase in grey value of limestone in a particular band was indicative of higher silica content. High magnesium (dolomitic) limestone showed lower reflectance value as compared to high calcium limestone.

The digitally processed images (fig 3) were found to be useful in classification of rock types based on the grey values. The limestone of various grades could be broadly classified based on the change in grey values and provided definite clues for grade prediction.

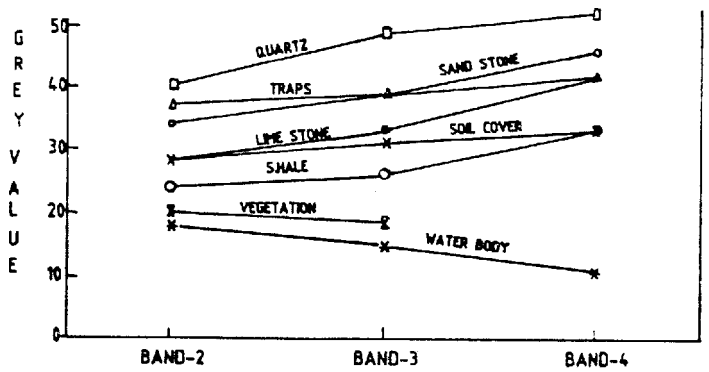

FIG.2 : Grey Values of Litho-Units Obtained Through Digital Image Processing



FIG.3 : Digitally Processed Image Showing Limestone (1) and associated rocks.

CONCLUSION

1. Apart from identification of rock types, the remote sensing technique was found to be helpful in predicting the grade of limestone through visual interpretation, ground reflectance data and digital image processing.

2. While collecting the field reflectance data, the physical properties of rocks including colour and roughness of the surface should be recorded. When a rough rock is placed on the sample stage, part of it would be slightly out of focus and the intensity of the reflected beam from these areas would be lesser. A proper calibration would therefore be required to know the influence of roughness of the rock surface.

3. As the human eye has its own limitation, the subtle tonal variation may quite often, be un-noticed in FCC during visual interpretation. The digital image processing may, therefore, be considered more reliable in predicting the grade.

4. The remote sensing technique has been found extremely useful in selecting the areas of interest during reconnaissance prospecting. It can considerably reduce the time and cost of exploration of virgin deposits. However, the prediction should be considered as indicative and for ultimate quality assessment, limited ground truth studies are essential.

ACKNOWLEDGEMENT

This paper is based on the R&D project work carried out by the Geological, Mining Development and Raw Mixes (GMR) Programme under the Cement Research Institute (CRI) of National Council for Cement and Building Mateials. The authors are thankful to Shri S Chatterjee, Head - CRI and Shri U R Raju, Programme Leader - GMR for guidance in preparing this paper. This paper is being published with the permission of the Director General of the Council.

REFERENCE

1. Gladwell, D.R., Lett, R.E., and Lawrence,P.: "Application of reflectance spectrometry to mineral exploration using portable radiometer". **Econ. Geol.** 1983, Vol 78, p 699-710.

2. Hunt, G R ,and Salisbury, J W :"Visible and near infrared spectra of minerals and rocks", I. Silicate materials: **Modern Geolgy**,1970, Vol I, p 283-300.

3. Imran, M.,Prasad, G V K , Panda,D K :" Remote sensing applications in evaluation of limestone deposits. **Second NCB International Seminar on Cement and Building Materials, New Delhi**, 30 Jan. to 3 Feb.1989, Seminar Papers, Vol. I p-1-14.

4. Lyberis, N., Parrot,J F., Chorowicz, J , and Rudant, J. P.: "Geological features of the Spitsbergan region obtained from multispectral SPOT data and field radiometer measurements". **Int. Jour. of remote sensing**, 1990, Vol.11, No. 2, p 253-265.

5. Whitney, G., Abrams, M J., Goetz, A F H.: " Mineral discrimination using a portable ratio-determining radiometer". **Econ. Geol.**1983, Vol.78, p 685-698.

THE HYDRATION CHEMISTRY OF SOME BLENDED CEMENTS

Hans S Pietersen* and Jan M Bijen*

Materials Science Section, Faculty of Civil Engineering
Delft Technical University, Delft
THE NETHERLANDS

ABSTRACT

The hydration of portland cement alone, as well as cement composites containing several physically and chemically different class-F fly ashes (20% m/m), metakaolinite (20% m/m), silica fume (20% m/m) and granulated blast furnace slag (70% m/m), was evaluated using a microprobe, a transmission microscope and ^{29}Si MAS-NMR.

Both the microprobe as well as the TEM study indicated that the fly ash reacts with the cement by slowly forming micron sized reaction rims around the glassy fly ash spheres. The microprobe study further indicated that the composition of the CSH of the portland cement and those of the fly ash varied in minor details, mainly indicating an increased alumina content. Silica contents of the CSH were approximately similar. All analytical methods applied indicate that the finest and most glassy fly ash initially reacts the fastest; upon time however, all fly ash blends indicate pozzolanic reactions. In most cases, evidence was found for the existence of strätlingite, or CSH/strätlingite mixtures.

The alumina contents of the CSH in the metakaolinite blends is higher compared to the fly ash blends. The silica fume blend displays the highest SiO_2/CaO ratios; alumina contents are of course very low. The slag cements also clearly indicate a reaction between the cement and the slag; after 6 months usually 5-20 μm wide reaction rims developed around slag grains.

Quantitative ^{29}Si MAS NMR was used to monitor the changes in amorphous components, like CSH (inner- and outer product, resp. Q^2 and Q^1), silica fume and metakaolinite; the highest Q^2/Q^1 ratio was found in the silica fume cements.

(* also Intron BV, Institute for Materials and Environmental Research, Houten, The Netherlands)

1. INTRODUCTION

Increasing environmental pressures are currently resulting in the widespread use of secondary materials in composite cements. The best known examples of such secondary materials are fly ashes, granulated blast furnace slag and silica fume. An understanding of the mechanism with which these materials react with ordinary portland cement (or other cementitious binders or activators) will stimulate their use and may result in "tailored" composite materials with specific, and in many cases, improved characteristics, compared to ordinary portland cements. It also decreases the environmental pressures related to portland cement manufacture (CO_2 emission and land excavation).

In this article, several relatively new methods of analysis will be discussed with reference to the hydration mechanism of composite cements. The results will be referenced against recent thermodynamic evidence regarding the composition of fully hydrated cements. The analytical methods applied included a microprobe, a transmission microscope and ^{29}Si MAS-Nuclear Magnetic Resonance.

Microprobe study

Only a limited number of electron optical studies reporting quantitative data have been published [1;2;3;4 and ref. therein]. The interpretation of previous results has suffered by the complexity and extremely small scale variations of the phenomena studied. In general, the CSH in composite cements containing PFA is believed to display somewhat higher Si/Ca atom ratios (0.6-0.7) as well as slightly higher Al/Ca ratios (up to 0.3 instead of ≈ 0.1). The interpretation provided by Harrison and co-workers [1] indicates that older (> 3 days) PFA cement pastes show a progressive increase with time in mean Si/Ca and mean Al/Ca ratios, which they attributes to the pozzolanic reaction. The pozzolanic reaction leads to additional CSH in the space previously occupied by PFA, pore solution or CH. In slag cements a Mg containing reaction product, differing from CSH, is formed; hydrotalcite (HT) [4]. Recent solubility experiments carried out with synthetic compounds known or suspected to be present in PFA- and slag-cements indicate that thermodynamic "equilibrium assemblages" will consists of either 1) CH + CSH (1.7) + C_3AH_6 + AFt + HT + aq. or 2) CSH (variable ratio) + Si-hydrogarnet (C_3AH_6 <===> C_3ASH_4) + AFt + aq [5]. In situation where a lot of Al and Si is available, like high replacement class-F PFA or metakaolinite blended cement strätlingite (C_2ASH_8; an AFm phase) may be formed. Silica fume blended cements are well known to produce CSH displaying a distinctly higher Si/Ca ratio.

Transmission Electron Microscopy

Transmission electron microscopic (TEM) studies have also been limited to a few studies. In principle, chemical analysis with TEM provides more realistic and detailed chemical information on reaction products formed. Rodger and Groves [6] studied a C_3S-PFA paste by TEM and found that the fly ash particle was often surrounded by a reacted zone consisting largely of radially fibrillar material, described as CSH, with denser regions of Si-hydrogarnet (experimentally $C_{12}A_3FS_4H_{16}$), and dense outer regions CSH and CH. Studies of a 885 day old granulated blast furnace slag cement [7] with analytical electron microscopy revealed that both a cement hydration product (CHP), other than CSH, as well as an "inner slag hydrate" (ISH), resembling a hydrotalcite-like phase, were formed. Other studies also indicated the presence of low- or non-calcium bearing magnesium-aluminium hydroxide, similar to the naturally occurring mineral hydrotalcite, but of variable composition [8;9].

29Si-MAS-NMR

Since the first solid state ^{29}Si NMR experiments by Lippmaa and coworkers [10], much research has been devoted to silica polymerization reactions, in particular to cement hydration; reviews may be found in the references 11, 12 and 13. In this study, ^{29}Si NMR has been employed as a tool to characterize the hydration reaction of several composite cements, up to 6 to 9.5 months.

2. EXPERIMENTAL

Materials used were three class-F fly ashes, differing mainly in physical properties (EFA, LM and LB), a granulated blast furnace slag (CEMIJ), silica fume (SF) and metakaolinite (MK). As a reference material (inert) quartz flour was used (KW). The cement used was an ordinary portland cement A (PCA). Apart from the slag-cement all materials contained 20% m/m of fly ash, silica fume, metakaolinite or quartz flour. The slag-cement contained 70% m/m slag. The water/solids ratio was 0.40; Details about chemical and physical properties of all materials used are summarized in table 1. All composite cement specimen were cast in small plastic containers, sealed and cured for a specific time. Further hydration of the samples was prevented at the required time either by freeze drying or methanol exchange followed by heating at 105°C.

The microprobe study was performed using polished thin section of the cements cured for 180 days. The analysis and micrographs were made using a JEOL JXA-8600 Superprobe, equipped with a Tracor EDS analysing system and five wavelength dispersive spectrometers.The accelerating voltage was 15 KV and the beam current 100 pA with a live time of 30 or 40 seconds. The TEM study was performed using a Phillips EM-400 microscope on ion-milled samples. The NMR spectra were obtained on a Bruker AM 500 spectrometer equipped with a Bruker solid-state accessory. Details of the analytical details have been presented in Pietersen et al. [13].

3. RESULTS AND DISCUSSION

Unreacted cement

Limited data were obtained for unreacted clinker minerals like alite and belite; the ferrite and aluminate phases are generally too small in size to provide an accurate chemical analysis with a microprobe. The analytical results are summarized in table 1. The analysis in this table were obtained using X-ray fluorescence on glass pearls.

Hydration products in portland cement paste

In order to prevent analysis of anhydrous clinker phases in the data on hydration products, all analysis above 85 % were excluded in the following graphs, unless stated otherwise. A survey of the data is made by plotting the Al2O3/CaO against the SiO2/CaO ratios; the division by CaO is made in order to minimize the effect of analysis of the hydrates with very low totals. This presentation has been applied previously by Harrison and co-workers [1;2].

Figure [1] provides an example of such a graph for ordinary portland cement. hydrated for 180 days. Most of the analysis plot either near to a composition representing CSH (SiO_2/CaO = 0.5-0.65; Al_2O_3/CaO = 0.05), or on lines connecting the CSH compositional area with CH (origin) or AFm (SiO_2/CaO = 0.05; Al_2O_3/CaO = 0.6). The sample points on both lines may represent mixtures between the two phases on both ends of the lines.

Hydration products in PFA - portland cement paste

The data handling procedure in the fly ash composite cements was similar to the previously described method. From figure [2], representing the PCA blended with the very glassy fly ash EFA, it may be seen that a significant amount of Al-containing CSH is formed, with a Al_2O_3/CaO ratio of 0.15. In the figure, the potential equilibrium phase assemblages are indicate with on open square. Evidence for a Si-hydrogarnet phase, such as C_3ASH_4 seems likely. Some data points suggest a high Si-strätlingite-like composition; on the other hand, these analysis may also reflect the analysis of the PFA/CH transition zone.

A much clearer evidence of Si-hydrogarnets, strätlingite and a Al-CSH is found in the cement blended with fly ash LB in figure [3]; this fly ash displays a high alumina content, and is also rather glassy. The Al_2O_3/CaO ratio of the CSH is in this sample significantly higher compared to the previous sample, and is designated Al-CSH. All data points in the Al-CSH filed originated from reacted zones around fly ash particles, such as shown in photograph 1.

A detail of such a zone may be seen in the TEM photograph 2, in which the fibrillar nature of the reaction zone can be seen clearly; the material in this zone appeared to be amorphous and the chemical analysis also indicate a relatively high CaO/SiO_2 ratio (1.9). Both the presence of alumina containing CSH and silicious hydrogarnets, as well as the observed formation of micrometer thick "reaction zones" around fly ash particles are a clear evidence of the pozzolanic reaction taking place.
The data in figure [4] relate to the cement blended with fly ash LM, which is the least glassy one. It is remarkably that in this cement alumina containing hydration products seem to be restricted to silicious hydrogarnets and possibly a high calcium strälingite-like phase; an high Al-CSH can not be detected clearly. It is assumed that the presence of abundant Al-CSH is a clear evidence of extensive pozzolanic reaction. On the other hand, not all fly ashes display a similar kind of reaction.

The ^{29}Si solid state MAS-NMR analysis also points at an extensive pozzolanic reaction in fly ash blended cements, but of different intensity. As can be seen in figure 5, the hydration of ordinary portland cement results in the formation of two distinguishable CSH hydration products. In the course of hydration the intensity of Q^0 at -71 ppm, representing C_3S and C_2S, decreases. The intensity of the chemical shifts of the hydration products Q^1 and Q^2 (chemical shifts of resp. -79 and -84 ppm) increases.

Compared to portland cement, the spectra of the fly ash blends (figure 6 and 7), indicate an increase in the amount of silica middle groups (Q^2-type, or "inner product CSH") at -84 ppm, relative to the amount of silica end groups (Q^1-type, or "outer-product CSH) at -79 ppm. This indicates an increased tendency to form more polymerized, and

longer, CSH chains. In the fly ash blended cements the size distribution as well as the glass content of the fly ashes used apparently influence the hydration reaction; the finest and most glassy fly ash (EFA; German wet bottom boiler) displays somewhat higher Q^2/Q^1 ratios and an increased initial hydration, compared to the coarser fly ash (LM; Dutch low-NOx furnace). Fly ash fineness is generally accepted to be one of the key factors regarding fly ash reactivity [e.g. 14;15;16].

Hydration products in metakaolinite - portland cement paste

In figure 8 microprobe analysis of a portland cement blended with 20 % m/m metakaolinite are shown. Comparison with the chemically related fly ash cement blends shows that here all CSH contain significant amount of alumina, clearly reflecting the enhanced reactivity of metakaolinite over fly ash. Evidence for C_2ASH_8-like phase assemblages is also more pronounced. Remarkable is the evidence for reaction products having a SiO_2/CaO ratio of 0.35-0.45 and Al_2O_3/CaO of 0.1-0.2; these may represent analysis of intimately mixed CH and C_2ASH_8 or Si-hydrogarnet. Evidence exists that not all of the metakaolinite did react, by the data points towards a metakaolinite composition.

^{29}Si NMR studies of the metakaolinite cements (figure 9) indicated that, it is not possible to deconvolute the Q^1 and Q^2 chemical shifts at all ages, due to changes in the shift maxima Q^1 and/or Q^2. This may also be attributed to the formation of amorphous or non-crystalline alumina containing reaction products, such as strätlingite (C_2ASH_8) or silicious hydrogarnets. Clear evidence exists for the presence of unreacted metakaolinite, even after 180 days.

Hydration products in silica fume - portland cement paste

In figure 10 the microprobe results of the silica fume blended cement are shown. Contrary to the fly ash and metakaolinite blended cements, this cement indicates CSH compositions with significantly lower Al_2O_3/CaO ratios (0.04 - 0.07). Evidence for strätlingite or silicious hydrogarnet formation is lacking. This is not to be expected because of the relative scarcity of alumina in these cement systems. There is however evidence for only partially reacted silica fume, as indicated by the low Al but high Si data points.

^{29}Si NMR studies of the silica fume blended cements (figure 11) indicate that this cement develops a markedly increased amount of Q^1 and Q^2 species, with a notably increased amount of Q^2 compared to Q^1. As in the metakaolinite blends, the silica fume does not react completely at 180 days.

Hydration products in granulated blast furnace slag cements

Figure 12 show Al_2O_3/CaO versus SiO_2/CaO microprobe results of the granulated blast furnace slag cement hydrated for 180 days. The CSH composition in this cement varies from the previous cements because it contains some magnesium, as well as somewhat more alumina compared to ordinary portland cements. In figure 12 the unhydrated slag grains are indicated by square brackets; these form a relatively isolated group in the diagram. Sample points around this area indicate the formation of a slag hydration products, slag rims or slag relicts (signed 1) as well as intimately mixed slag reaction products and CSH (signed 2). The slag hydration product indicate an approximate SiO2/CaO ratio of 0.6 - 0.8 and a variable Al2O3/CaO and MgO/CaO ratio (figure 13). From figure 13 it can be seen that the slag hydration products all fall on a remarkably straight line which may be described as [Al2O3/CaO = 0.1 + MgO/CaO]. This corresponds closely to the atom ratios found by Harrison et al. [1]. This line is directed towards hydration products with a hydrotalcite-like ($M_xA_yH_z$) composition. The data in figure 12 also indicate the presence of a silicon and magnesium containing hydrogarnet phase (signed 3), although it may not be excluded that they represent analysis of intimately mixed CH and unhydrated slag grains.

The chemical shift of the glassy blast furnace slag at -73 ppm appeared too broad and overlapped the Q^0, Q^1 and Q^2 chemical shifts of the (un)hydrated cement; a successful deconvolution of the slag cement could therefor not be obtained.

CONCLUSIONS

The CSH composition of blended cements is influenced by the addition of PFA, metakaolinite, silica fume or slag, which is mainly reflected by different Al_2O_3/CaO ratios. The combined use of three physically different analytical techniques all point at a pozzolanic reaction, or in the case of the slag, hydraulic behaviour. The pozzolanic reaction of the fly ash results in the formation of hydration products resembling the ones predicted on thermodynamic grounds. The extend of the pozzolanic reaction of fly ash in pastes cured for 180 days is however variable; one of the variables seems to be the glass composition, as well as the total glass content. The pozzolanic reaction of metakaolinite, which is chemically related to fly ash, indicates a similar trend; the formation of very alumina rich CSH, as well as silicious hydrogarnets of variable composition and strätlingite. In granulated blast furnace slag

cements a hydrotalcite-like phase is developed. In the silica fume blended cement the reaction mechanism is relatively simple; only a very silicious CSH, with a Ca/Si ratio up to 2. Both metakaolinite and silica fume do not appear to react completely, as indicated by the microprobe analysis and the ^{29}Si NMR results. ^{29}Si NMR results indicate that in both the silica fume as well as in the activated kaolinite blend, the reaction of the anhydrous calcium-silicates is initially (first 7 days) accelerated with respect to the reference portland cement. In the fly ash blends this effect is less pronounced.

ACKNOWLEDGEMENTS

This study formed part of a contract between Delft University of Technology and NOVEM, the Dutch Society for Energy and Environment BV, contract nr.11238.p117.

REFERENCES

1. Harrisson, A.M., Winter, N.B. and Taylor, H.F.W. 8th International Congress on the Chemistry of Cement, Theme 3, Volume IV, 170-175, 1986, Rio de Janeiro, Brazil.
2. Harrisson, A.M., Taylor, H.F.W. and Winter, N.B. Cem. Concr. Res., 15, 775-780, 1985.
3. Uchikawa, H. 8th International Congress on the Chemistry of Cement,Volume I, 249-280, 1986, Rio de Janeiro, Brazil.
4. Taylor, H.F.W. Cement Chemistry, 290-305, 1990, Academic Press, London.
5. Atkins, M, Bennett, D.G., Dawes, A.C., Glasser, F.P., Kindness, A. and Read, D. A Thermodynamic Model for Blended Cements, DoE Report No: DoE/HMIP/RR/92/005, December 1991.
6. Rodger, S.A. and Groves, G.W., Adv. Cem. Res. (1988), 1, 84.
7. Feng, Q.L. and Glasser, F.P. Mat. Res. Soc. Symp. Proc., Vol. 178, 1990, 57.
8. Richardson, I.G., Wilding, C.R. and Dickson, M.J., Adv. Cem. Res. (1989), 2, 147.
9. Richardson, I.G., Rodger, S.A. and GRoves, G.W., Mat. Res. Soc. Symp. Proc., Vol. 176, 1990, 63.
10. E. Lippmaa, M. Mägi, A. Samoson, G. Engelhardt and A.R. Grimmer, "Structural studies of silicates by solid state high-resolution ^{29}Si NMR"; J. Amer. Chem. Soc., Vol. 102, 4889-4893 (1980).
11. H. Justnes, J.O. Bjorgum, J. Krane, I. Meland and T. Skjetne, The utilization of Nuclear Magnetic Resonance (NMR) in Cement and Concrete Research, SINTEF Report STF65 A89071 (Trondheim, Norway, 1989).
12. Grimmer, A.R. and Colombet, P. (Eds.), Application of NMR Spectroscopy to Cement Science, Gordon and Breach Science Publishers, (in press, 1992).
13. Pietersen, H.S., Kentgens, A.P.M., Nachtegaal, G.H., Veeman, W.S. and Bijen, J.M. "The Reaction Mechanism of Blended Cements: A ^{29}Si NMR Study", in 4th CANMET-ACI Conf. on Fly Ash, Silica Fume, Slag and Natural Pozzolans in Concrete, Istanbul, May 3-8, 1992.
14. Pietersen, H.S. "Reactivity of fly ash and slag in cement", PhD thesis, Delft Technical University, Faculty of Civil Engineering, Materials Science Section, 1992.
15. Helmuth, R. "Fly ash in cement and concrete", Portland cement association, 1987.
16. Wesche, K. "Fly ash in concrete - properties and performance", Rilem Report 7, Chapman and Hall, 1991.

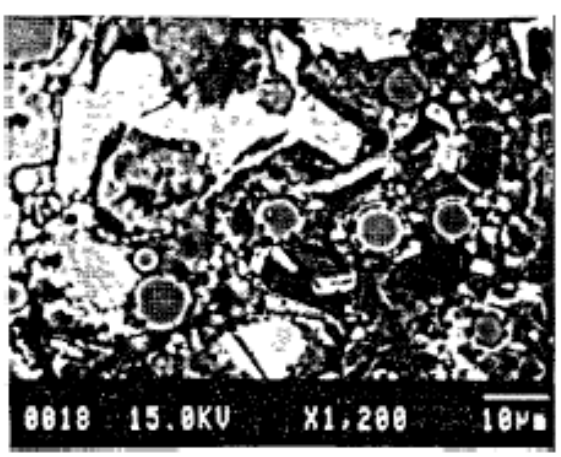

Micrograph 1.
Backscattered image of a fly ash blended cement paste. The rims around the fly ash grains represent a reaction zone, due to the pozzolanic reaction.



Micrograph 2.
Transmission microscopy image of a fly ash grain (10 μm) which developed a reaction zone.

Table 1. Analysis of portland cement (PCA), fly ashes (EFA, LB, LM), granulated blast furnace slag, metakaolinite (MK) and silicafume (SF). n.d. = not determined.

COMPONENT	PCA	EFA	LB	LM	SLAG	MK	SF
SiO_2	21.26	50.46	55.57	53.93	30.80	55.60	95.09
Al_2O_3	4.91	25.74	30.14	34.16	17.14	41.18	0.58
Fe_2O_3	2.87	6.53	6.05	4.87	0.30	0.68	1.06
TiO_2	n.a.	1.19	1.74	1.66	0.85	0.05	0.02
MgO	1.63	2.24	0.89	0.56	10.70	0.35	0.60
CaO	64.42	4.32	1.00	2.06	36.44	0.03	0.11
Na_2O	0.21	2.04	0.31	0.36	0.30	0.12	0.27
K_2O	0.69	4.43	2.56	0.92	0.51	2.44	0.73
H_2O	0.35	0.18	0.12	0.17	0.06	0.34	0.59
LOI[a]	0.55	3.95	4.66	4.74	0.00	0.83	1.60
AA[b]	n.d.	1.29	0.30	0.22	n.d.	n.d.	n.d.
Alk. (Eq. Na_2O)	0.69	n.d.	n.d.	n.d.	n.d.	n.d.	n.d.
Insoluble	1.10	n.d.	n.d.	n.d.	n.d.	n.d.	n.d.
MULLITE	-	2.1	16.2	22.8	-	-	-
QUARTZ	-	1.8	5.6	5.1	-	-	-
FE-SPIN.	-	0.7	0.7	0.5	-	-	-
GLASS[c]	-	95.4	77.5	71.6	>99	-	-
D_{50}	n.d.	5.9	46.6	25.9	n.d.	n.d.	n.d.
span[d]	n.d.	7.1	3.3	3.3	n.d.	n.d.	n.d.
Specific Surf. (M^2/gr)	n.d.	1.5	1.0	1.2	n.d.	14.8	19.3

[a] LOI = Loss On Ignition (total carbon)

[b] AA = Available Alkali (ASTM C618)

[c] Glass = 100 -(Σ % mullite + % quartz + % Fe-spinel)

[d] D_{50} = 50 % of all particles is smaller than this size (μm); span = $(D_{90}-D_{50})/D_{50}$

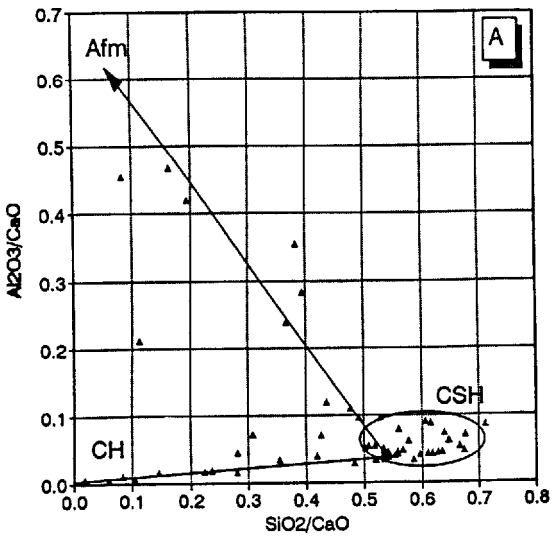

Figure 1.
Microprobe analysis of ordinary portland cement (180 days; w/s = 0.4).

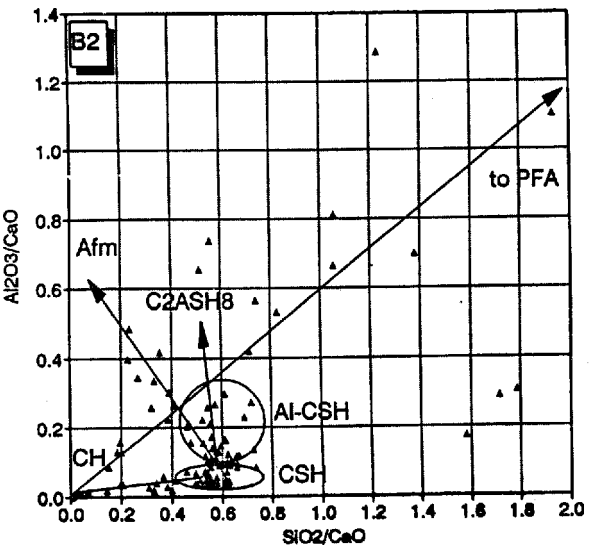

Figure 2.
Microprobe analysis of ordinary portland cement blended with 20 % m/m fly ash EFA (180 days; w/s = 0.4).

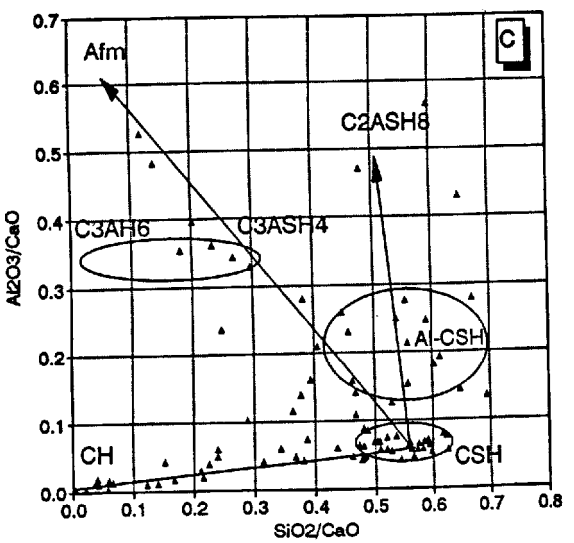

Figure 3.
Microprobe analysis of ordinary portland cement blended with 20 % m/m fly ash LB (180 days; w/s = 0.4).

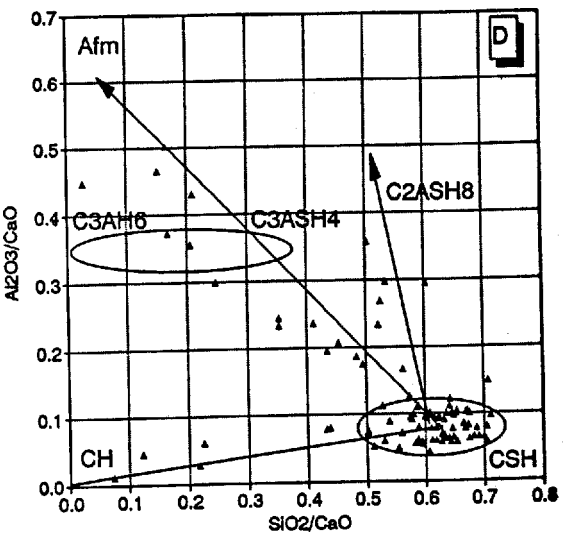

Figure 4.
Microprobe analysis of ordinary portland cement blended with 20 % m/m fly ash LM (180 days; w/s = 0.4).

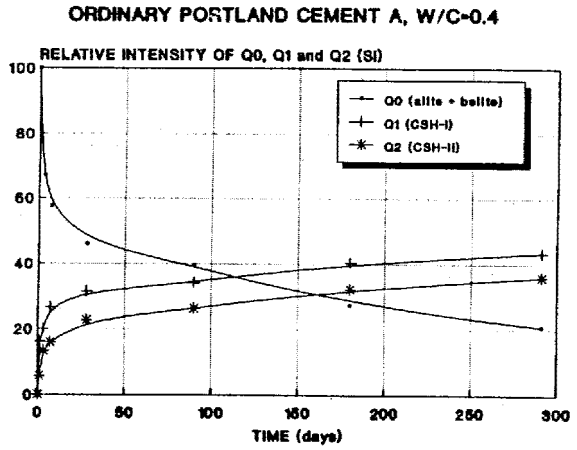

Figure 5.
Progressive hydration of ordinary Portland cement. Unhydrated portland cement displays a chemical shift at approximately -71 ppm, representing both C_3S and C_2S.

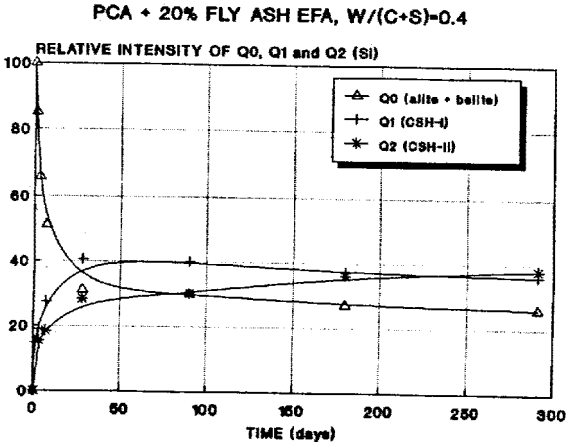

Figure 6.
Hydration of ordinary portland cement blended with 20% m/m class-F fly ash EFA. Fly ash displays a chemical shift at -100 ppm, comparable with synthetic aluminium-silicate glasses [14].

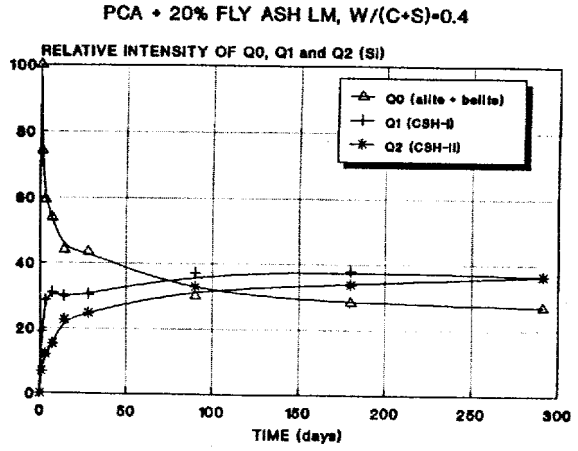

Figure 7.
Progressive hydration of ordinary portland cement blended with 20% m/m class-F fly ash LM.

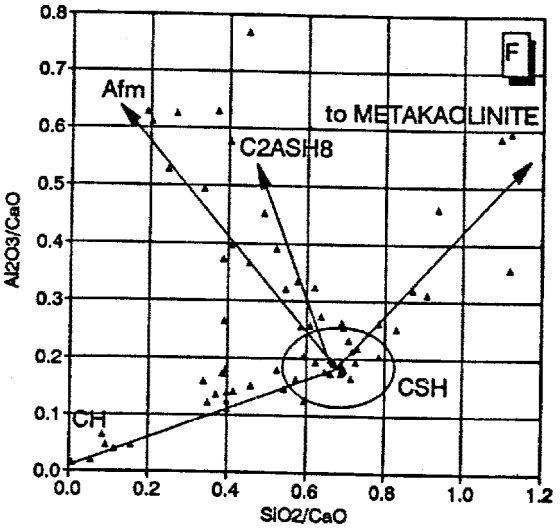

Figure 8.
Microprobe analysis of ordinary portland cement blended with 20 % m/m metakaolinite (180 days; w/s = 0.4).

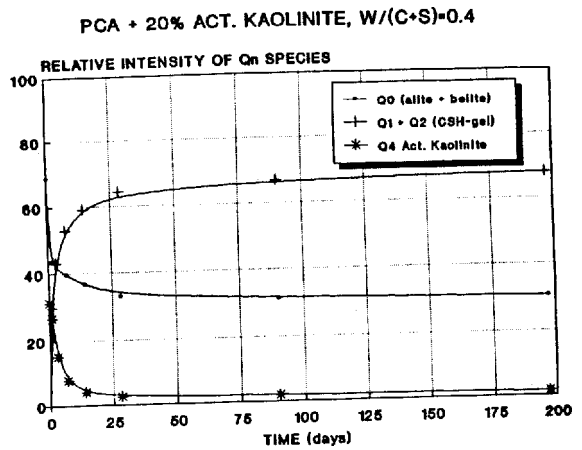

Figure 9.
Hydration of ordinary portland cement blended with 20% m/m metakaolinite. The metakaolinite has a chemical shift at -100 ppm.

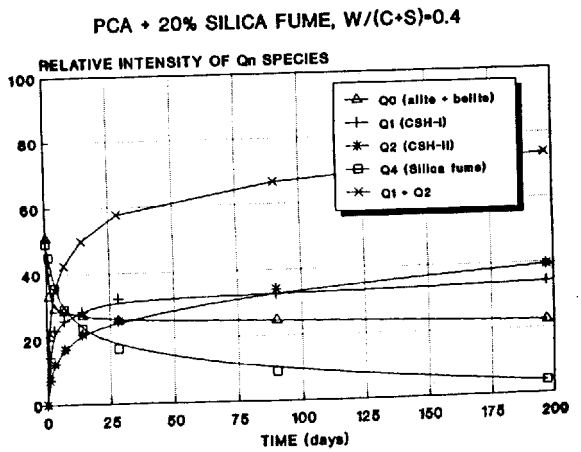

Figure 11.
Hydration of ordinary portland cement blended with 20% m/m silica fume. The chemical shift of silica fume is -110 ppm.

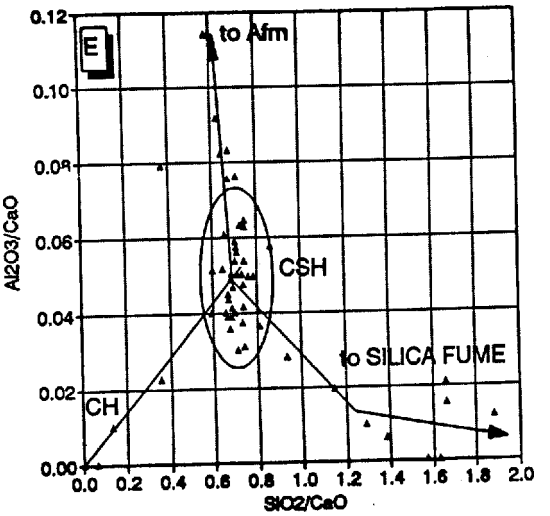

Figure 10.
Microprobe analysis of ordinary portland cement blended with 20 % m/m silica fume (180 days; w/s=0.4).

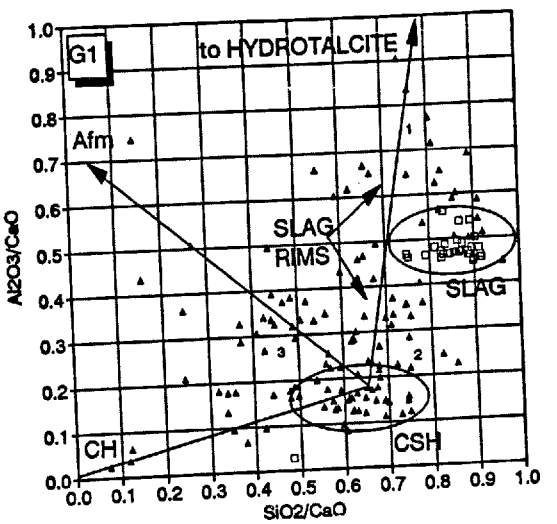

Figure 12.
Microprobe analysis of blast furnace slag cement containing 30 % m/m ordinary portland cement (180 days; w/s=0.4); SiO_2/CaO versus Al_2O_3/CaO.

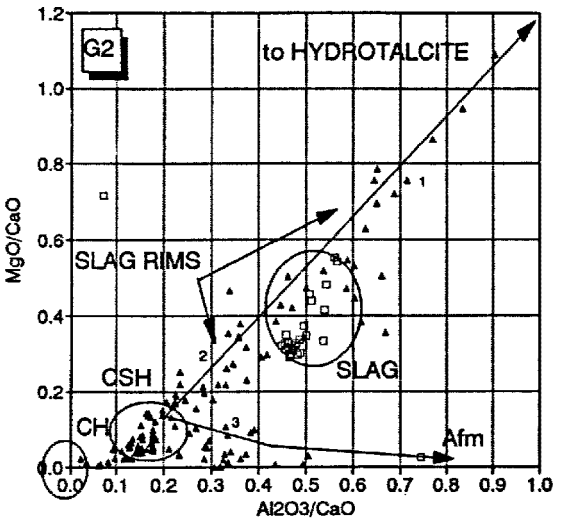

Figure 13.
Microprobe analysis of blast furnace slag cement containing 30 % m/m ordinary portland cement (180 days; w/s = 0.4). Al_2O_3/CaO versus MgO/CaO.

AUTHORS INDEX
(VOLUME VI)

A

Akhouri, P K – 189
Alexandre, J – 162
Anagnostopoulou-Konsta, A – 216

B

Baron, J P – 162
Barret, P – 141
Bastier, R – 39
Bayoux, J P – 148
Belyaeva, V I – 194
Bentz, D P – 3
Beretka, J – 132
Bertrandie, D – 141
Bijen, J M – 247, 281

C

Cantacuzene, J – 39
Capmas, A – 148
Centurione, S L – 182
Clément, J Y – 254
Couty, R – 141
Coverdale, R T – 16

D

Daoukaki-Diamanti, D – 216
Debray, L – 162
Dupont-Wavrin, X – 162

E

Ennadifi, y – 66

F

Fernandez, L – 141
Fišang, L – 233
Frias, M – 240

G

Garboczi, E J – 3
Garcia, N – 240
Gessner, W – 148
Glasser, F P – 114
Goswami, G – 168
Gromozova, I K – 205
Grutzeck, M W – 119

H

Hartmann, H – 155
Hawthorn, F – 73
Herr, R – 223
Hübert, C – 223

I

Imran, M – 275

J

Jackmuth, P – 155
Jaugey, P – 73
Jennings, H M – 16
Jiang, W – 268
Justo, A – 247

K

Kihara, Y – 182
Klassen, V K – 194

L

Luxan, M P – 240

M

Malek, R I A – 210
Martin, Ph – 46
Mindolin, S F – 194
Miroshnichenko, I I – 194
Müller, D – 148
Munhoz, F A da C – 182

N

Norling-Mjörnell, K – 261

P

Panda, D K – 275
Panda, J D – 168
Perez-Rodriguez, J L – 247
Pietersen, H S – 281
Poellmann, H – 198
Prasad, G V K – 275

R

Ranogajec, J – 233
Rao, L H – 189
Rettel, A – 148
Roy, D M – 88, 268

S

Sabio, S – 254
Sadouki, H – 28
Sakoda, S – 175
Sanchez De Rojas, M I – 240
Schaer J P – 39
Sinha, S K – 189
Sogo, S – 175
Sorrentino, D – 254
Stepkowska, E T – 247

T

Takeda, N – 175
Tamás, F D – 77
Teodoru, G V M – 155

V

van Breugel, K – 22, 126

W

Wieker, W – 223
Wittmann, F – 28

Z

Zanni-Théveneau, H – 141

9th International Congress on the Chemistry of Cement New Delhi, India, 1992

VOLUME VII

ADDRESSES AT PLENARY SESSIONS AND SPECIAL LECTURES

NATIONAL COUNCIL FOR CEMENT AND BUILDING MATERIALS
NEW DELHI

9th International Congress on the Chemistry of Cement New Delhi, India, 1992

Volume VII

ADDRESSES AT PLENARY SESSIONS AND SPECIAL LECTURES

Organised by

NATIONAL COUNCIL FOR CEMENT AND BUILDING MATERIALS
NEW DELHI

Co-sponsored by :

Department of Scientific & Industrial Research
Ministry of Science & Technology
Govt of India

Cement Manufacturers' Association, India

The India Cements Ltd

J K Cement Works

Madras Cements Ltd

Narmada Cement Co Ltd

Orissa Cement Ltd

This volume is the last of the seven-volume series of the Congress Proceedings Title of each volume is given below :

I	–	Congress Reports
II	–	Communication Papers - Theme I
III	–	Communication Papers - Theme II
IV	–	Communication Papers - Theme III
V	–	Communication Papers - Theme IV
VI	–	Reports on Special Panel Discussions and Poster Papers
VII	–	Addresses at Plenary Sessions and Special Lectures

Published by :
National Council for Cement and Building Materials (NCB)
M-10, South Extension Part II, New Delhi 110 049 (INDIA)

No part of this publication be reproduced without the written permission of the Publishers.

The views expressed in the technical papers printed in this publication are those of authors and not necessarily of the Publishers.

Printed in India by THE OFFSETTERS, New Delhi.

PREFACE

The 9th International Congress on the Chemistry of Cement, which is held once in six years in different parts of the world, was held in New Delhi from 23 to 28 November 1992. Organised by NCB, the Congress was co-sponsored by the Department of Scientific & Industrial Research, Govt of India, Cement Manufacturers' Association, and Messrs India Cements Ltd, J K Cement Works, Madras Cements Ltd, Narmada Cement Co Ltd and Orissa Cements Ltd.

The objectives of the Congress were set to advance the knowledge of chemistry of cements with emphasis on application of this knowledge in both the manufacturing aspects and utilization of cements in practice. Within this broad scope, the thrust was on tracking the scientific progress made in the field since the last Congress, assessing the status of exploitation of the results by the industry and the society, and mapping of the new frontiers of knowledge. A Technical Exhibition was organised as a part of the Congress; two cultural events were staged on two evenings during the Congress.

The Congress was inaugurated by Smt Krishna Sahi, Hon'ble Minister of State for Industrial Development, Govt of India. At the Concluding Session of the Congress, the Valedictory Address was delivered by Shri P R Kumaramangalam, Hon'ble Minister of State for Science & Technology, Govt of India.

More than 500 scientists and researchers, including 250 from 27 overseas countries participated in this Congress. Twentyone Principal Reports and 348 Communication Papers belonging to the four themes of the Congress were presented. In addition to the papers on deliberative thematic sessions, a Poster Session on "Advances in Physico-chemical evaluation, characterisation and quality control techniques and systems" for clinkers, particulate cements, hydrated systems and concrete systems were organised. The state-of-the-art reports, invited lectures and 24 contributions made in the form of posters were presented during the Congress. In addition, Special Panel Discussions were organised to survey the newer frontiers of knowledge in the areas of computerisation in cement science and concrete systems; resource economy in cement and concrete making; and cement in hazardous wastes management. The first six volumes of proceedings contain all the above contributions received for the Congress.

This Volume VII contains the texts of the Addresses delivered at the Inaugural and Concluding Sessions and the Special Lectures presented during the Congress, besides the list of delegates who attended this prestigious Congress. The complete set of seven volumes of the Proceedings will be a report of the event and also serve as a reference source on the latest developments in the frontiers of cement chemistry and related research for the benefit of cement industry and cement users world-wide.

The International Scientific Committee which met during the Congress, decided that the next (10th) Congress be held in Sweden. We wish the organisers good luck and the Congress every success.

I am grateful to the members of the International Scientific Committe of the Congress for their whole-hearted cooperation, to those who reviewed the Abstracts and to the International Panel of Reviewers of Manuscripts for providing very useful technical and editorial comments

on the communication papers. The cooperation of the authors in accepting and implementing the reviewers' suggestions and revising their manuscripts accordingly is greatly appreciated. Thanks are also due to those authors whose communication papers could not be accepted essentially because the contributions did not fit in with the themes of the Congress and **not** because of any technical deficiency.

The unstinted efforts put in by my colleagues in the National Council for Cement and Building Materials in all aspects of organising this Congress, is thankfully acknowledged.

A K Mullick
Chairman
International Scientific Committee
9th International Congress
on the Chemistry of Cement

New Delhi
25 January 1994

CONTENTS

Volume VII

PREFACE iii

INAUGURAL SESSION

1. Welcome Address 3
Shri N Srinivasan, Chairman NCB and Chairman, Organising Committee, 9th ICCC

2. The Congress Perspective 5
Dr A K Mullick, Director General NCB and Chairman, International Scientific Committee, 9th ICCC

3. Presidential Address 8
Shri Suresh Kumar, Secretary to the Govt of India, Dept of Industrial Development

4. Inaugural Address 10
Smt Krishna Sahi, Hon'ble Minister of State, Industrial Development

5. Vote of Thanks 12
Dr C Rajkumar, Organising Secretary, 9th ICCC

CONCLUDING SESSION

6. The Congress Overview 15
Shri N Biswas, Secretary to the Govt of India and Director General, Technical Development

7. Valedictory Address 17
Shri P R Kumaramangalam, Hon'ble Minister of State, Science and Technology

8. Summing up and Closing 19
Dr A K Mullick, Director General, NCB and Chairman, International Scientific Committee, 9th ICCC

SPECIAL LECTURES

I. Present Problem in Cement Manufacturing 23
Prof Dr Eng Hiroshi Uchikawa, Executive Director, Research and Development, Onoda Cement Co Ltd, Japan

II. Advances in Portland Cements and Utilisation of Industrial Wastes -- Towards Sustainable Development 58
Dr A K Mullick, Director General NCB

ADDENDA

1 Energy-Saving Belite-Pozzolanic Cement 83
A Garbacik and S Peukert, Research Institure for Mineral Building Materials, Cracow, Poland

2 Production Performances and Utilisation of a Special Superplasticized Cement 88
V Alunno Rossetti, Sapienza University, Engineering Faculty, and F Curcio & L Gussino, Unicem Spa, Guidonia Research Centre, Rome, Italy

CONGRESS ALBUM

LIST OF DELEGATES 95

EXPLANATORY NOTES

The following symbols, which have been universally recognised by cement chemists for formulating more complex compounds, are used interchangeably with the respective oxide formulae throughout this volume:

A	:	Al_2O_3	K	:	K_2O
C	:	CaO	M	:	MgO
$\overline{C}$	:	CO_2	N	:	Na_2O
CH	:	$Ca(OH)_2$	P	:	P_2O_5
F	:	Fe_2O_3	S	:	SiO_2
H	:	H_2O	$\overline{S}$	:	SO_3

Commonly used abbreviations of more general nature are as follows:

DTA	-	differential thermal analysis
EPMA	-	electron probe micro analysis
IR	-	infrared
NMR	-	nuclear magnetic resonance
RH	-	relative humidity
w/c	-	water-cement ratio
XRD	-	X-ray diffraction
SEM	-	scanning electron microscope
EDAX	-	energy dispersive analysis of X-rays

INAUGURAL SESSION

WELCOME ADDRESS

by

Shri N Srinivasan
Chairman NCB and Chairman Organising Committee of the Congress

Hon'ble Smt Krishna Sahi, Shri Suresh Kumar, Dr Mullick, Dr Rajkumar, Distinguished Delegates, Ladies and Gentlemen:

On behalf of the National Council for Cement and Building Materials (NCB), Cement Manufacturers' Association (CMA) and on my own behalf, I have the privilege and pleasure of welcoming you all to the 9th International Congress on the Chemistry of Cement. This Congress has brought together on a common platform over 500 delegates representing scientists, engineers and technologists concerned with the manufacture and utilisation of cement. With nearly 250 overseas participants from 42 countries – this important global event will go a long way in facilitating exchange of knowledge and experience on the latest developments in the cement world.

We welcome Hon'ble Minister, Smt Krishna Sahi whose services to the nation in various capacities are well-known. She is not only keenly interested in the industrial development but also a firm believer in the key role that science and technology can play in the industrial development. Her presence here is the evidence of her abiding interest in the development of this important core sector industry of cement and her firm conviction to the major role that cement industry has to play in the development of the country.

I am glad to welcome Shri Suresh Kumar, Secretary to the Government of India, Department of Industrial Development, who has distinguished himself by his dynamism and in-depth knowledge of cement industry in guiding the affairs of the cement industry in India.

My special words of welcome to our distinguished guests from overseas; we look forward to benefiting from the variety and richness of their knowledge and experience. We are indebted to the Ministry of Industry, Department of Science and Technology, Cement Manufacturers Association, and cement industry at large for their catalytic role in supporting this Congress.

Food, clothing and shelter have been the three basic needs of humanity right from the beginning. Developed nations have met these needs adequately but not the teeming millions of developing countries; majority are still without adequate shelter. For over 150 years now cement has been the main construction material. Today, more than ever, there is greater need – through innovation of science and technology - towards reducing unit inputs of fuel and power in the manufacture of cement. The bulk nature of cement also calls for renewed efforts to further minimise the freight element. This could go a long way in providing shelter to a large number of inhabitants of the developing countries.

India has a rich tradition and cultural heritage expressed not only through its art and crafts, and literature, but also through its ancient monuments and historical buildings built from a variety of indigenous durable binding materials. From the days of traditional building materials, the country, through acquisition of new knowledge and expertise, has come a long way to manufacture and utilise modern material – cement – and has won recognition amongst the cement producing countries of the world both quantitatively as well as qualitatively. It is indeed a measure of the stature of Indian cement industry, and that of the host organisation, National Council for Cement and Building Materials (NCB) that the 9th International Congress on the Chemistry of Cement is being held under its aegis in India. The only other Asian country to host this Congress earlier was Japan in 1968.

The pragmatic Government policies have been giving a fillip to the cement industry which, as a result, was able to modernise and also expand rapidly. Many wet process plants were modernised and converted to dry

process units and several new state-of-the-art energy efficient million tonne plants were set up. With new generation modern plants having been set up, the industry can take pride that the latest technology in use in India today is comparable to that anywhere else in the world. India is the fifth largest producer of cement in the world, with production at 54 million tonnes in 1991 besides being a leading industrialised country with a large Science and Technology base.

As materials economy and fuel economy have been the driving force in bringing technological changes in the cement manufacturing process, technological advancements in these areas are to be stepped up manifold in view of changed situation. Newer technologies for cement manufacture need intensive exploration. The basic technology of clinker manufacture has not changed for many years and I do hope there will be a breakthrough in the near future. Apart from OPC and blended cements, a number of special cements, formulations and composites with high early strength and rapid setting properties for specific application areas are becoming popular all over the world. Newer approaches in manufacture of cement clinker, such as fluidisation process, which many countries have tried and are continuing to try, and radiation synthesis of cement clinker being tried in the former Soviet Union, for which India also has a Joint Cooperation Programme seems to be promising area; the successes achieved in this direction are quite encouraging.

The industry has been conscious of its obligations towards environment and has been working on utilisation of industrial wastes and inert fillers like ground limestone or silica dust in the manufacture of cement. How far these will be techno-economically feasible, beside being environment-friendly has to be examined in-depth. There is no doubt that our improved research and development capabilities has today enhanced our understanding of the chemistry, the structure and properties, quality, performance and durability of cements. Yet we are far away from our goal of developing economically viable indigenous methods of their processing as appropriate to socio-economic conditions.

There is a wide range of research, investigation and scientific information available on the subjects of the Congress and we need to sift through it to get answer to what is really important and critical to our needs. There cannot be any other forum more appropriate than the present Congress which is aimed at reviewing the state-of-the-art of cement sciences and tracking the scientific development and progress in the field since the last Congress.

The issues like raw materials and energy conservation, development of newer materials, enhancement of performance of concrete, etc, highlighted in the themes of the Congress are well selected and are of vital importance to the cement industries all over. The excellent efforts put in by NCB and various national and international fora of the Congress under the leadership of its Director General Dr Mullick and his colleagues in organising this unique Congress very well illustrates the significant role NCB is playing – to promote science and technology in the cement industry. I am confident that 400 technical reports and papers – that will be presented will stimulate active participation from the delegates and we are looking forward to a very fruitful outcome from the deliberations of the Congress towards latest developments at the frontier of chemistry of cement and its research for the benefit of cement industry and cement users world wide.

Before I conclude, I would like to mention that as a part of this event, a technical exhibition on cement and allied industries has been organised where both national and international organisations are participating. The National Awards for Energy Efficiency in the Indian cement industry for the year 1990-91 and 1991-92 will also be given away at the Concluding Session of the Congress on 28 November 1992.

With your permission, Madam, I would now request Dr Mullick, Director General, NCB and Chairman of the International Scientific Committee of this Congress, to present the Congress Perspective.

THE CONGRESS PERSPECTIVE

by

Dr A K Mullick
Director General
National Council for Cement and Building Materials

Hon'ble Minister Smt Krishna Sahi, Shri Suresh Kumar, Shri Srinivasan, Dr Rajkumar, Distinguished Delegates, Ladies and Gentlemen:

I have great pleasure in welcoming you all to this International Congress on the Chemistry of Cement, the deliberations of which are commencing now. The first symposium to deal solely with the chemistry of cement was held on 14 January 1918 in London; the subsequent meetings were held in Stockholm (1938), London (1952), Washington DC (1960), Tokyo (1968), Moscow (1974), Paris (1980) and Rio de Janeiro (1986). Now we are at the threshold of the 9th meet in the series. Recalling these events is like tracking the history of development of cement sciences in the last eight decades.

The deliberations of these meetings have always been of paramount importance for the growth of the cement industry. The Congresses in the past have served to chronicle the developments in the science and technology of manufacture and use of cement. The deliberations have identified the more important problems faced by the industry and their possible solutions through the inputs of science. These have also served as a sounding board for exploring possibilities of newer and better cements and paving the path for future advances. The relevance of the Congress is therefore, in the symbiosis of evolving solutions to today's problems and exploring the opportunities for the future.

When we outline the agenda of the deliberations for the next six days, it is purposive to do so in the perspective of the current situation. With global production of over 1200 million tonnes annually, cement continues to be the leading building material the world over. However, the generally weakening economic activities in most countries are also reflected in the cement and construction industries. The strategy for survival and possible economic recovery primarily includes steps for lowering manufacturing costs and improving production efficiency, in addition to cost-reduction through appropriate management measures. The key to success will, therefore, be in improving the manufacturing operations in what is being produced today and in the products that will be required for tomorrow's needs.

Environmental protection and measures for environmental improvement continue to be important items for consideration in cement manufacture and use. However, environmental issues need not necessarily mean higher costs. Environment and economics may be made to converge as mutually reinforcing areas and in fact can even create new profit areas. In such a sustainable development for the cement industry, conservation of energy and raw materials form the main driving force for cost reduction.

The main constituents of cement are calcium, silica, oxygen, alumina and iron. These, incidentally are also the major elements in the earth's crust. So is also the case of various industrial wastes like slags, flyash, sludges, etc, which are used in cement manufacture. To this list, one can now include polymers, which, although man-made, are produced in substantial quantities, surpassing metals in terms of volume sold. From the point of view of raw materials, cement thus has a wide base.

The initial spurt of cement research was on the composition of cement and its hydration. Soon the scope was enlarged and the fundamental questions of cement chemistry were being addressed to the problems of manufacture of cement and its use in constructions. The emphasis also gradually shifted from laboratory clinkers to those produced on commercial scale in cement plants. From the beginning, the study of composition of cements have mainly progressed in terms of ternary system lime - alumina - silica and later, the quaternary system lime - alumina - iron - silica; either by investigation of the four major phases present

in the cement clinker or investigation of the role of minor components by phase equilibria methods. The minor components are known to enter into solid solution with major components and influence the atomic arrangement and crystal structure of the major cement compounds, which can improve the hydraulic properties. Enhancement of activity of the main cement phases were thereafter explored in the presence of MgO, alkalis and sulphates as well as halides. As a result of such investigations, the equilibrium phase assemblage of the clinker minerals were seen to be different from the idealised chemical entities. The cement clinker that comes out of a manufacturing plant can be understood and explained only in terms of such wider compositions.

How the deliberations in these Congresses have reflected the progressive advancement in the knowledge of cement, can be illustrated by one simple example. As was mentioned earlier, the first international meeting in 1918 arranged by the Faraday Society, was to discuss the "setting of cements". As is to be expected, almost all the ten papers were devoted to understanding the mechanisms of setting of cements and how it is influenced by the cement composition. A period followed when we lived with the controversy of "gel" versus "crystalline" theories of setting. It was nearly four decades ago that the issue seemed to have been resolved by the knowledge that the substance of set cement is crystalline, but of colloidal dimensions. However, the pursuit of knowledge continued. Today, one can say with a fair degree of confidence that the mechanisms of setting, hardening and gaining of strength of cement upon hydration are well understood. Due to the awareness created by such deliberations, one can now have a cement in mortar or concrete which can set very quickly, say within two to three minutes after mixing with water, and used for emergency repairs in a construction. This is achieved by tailoring the chemical composition of the cement system or by use of accelerators. On the other hand, one can also have cement, the setting of which can be delayed in concrete for hours or probably even for days, by incorporating set retarders, to enable placement of large volumes of concrete without joints, as in roller-compacted concrete for dams.

In the modern dry process cement plants equipped with preheater-precalcinator systems, the scope of reduction in energy consumption through improved plant and machinery at present stem mostly from better comminution systems in grinding of coal, raw materials, raw mix and the cement clinker. New grinding systems would aim at increasing the activity of raw materials by mechano-chemical effects and thereby lower the sintering temperature. Till then, reduction in thermal energy is perhaps possible mainly through improved plant operations and input of materials science into optimum cement formulations. The technology of cement manufacture is quite complex in terms of the reactions involved, but improvements in the manufacturing processes have taken place in tandem with progress of knowledge of what happens at each stage in manufacture, particularly the interaction of raw materials with the fuel in the atmosphere inside the cement kiln.

Let us consider the opportunity for reducing energy costs in manufacture and aiding environmental protection as offered through the use of waste-derived fuels, both as supplementary fuels and as raw materials. The impetus for using various types of wastes like used rubber tyres, battery casings, reclaimed oil, wood chips, rice hulls and even municipal trash was derived from the fact that cement kilns, used as incinerators, are one of the most environmentally sound means of managing industrial wastes. Since these wastes also have fuel value, they are used as part substitute of the main fuel. During the processes of burning of cement raw materials, components of the fuels can get absorbed in the clinker, eg, ash in case of coal firing, or as condensations in main cement minerals, eg, through intakes of alkalis, sulphur, chlorine and heavy metals in volatiles. Cement plants in India who have switched over to lignite as part substitute of coal as fuel, had to take into account differences in the ash content as well as in the composition of the ash between the two, affecting the silica absorption in the clinker. The crystal structure of clinker can also be different in case of coal or lignite as compared to natural gas or oil. Effect of incorporation of waste-derived fuels on the chemistry and mineralogy of cement clinkers has thus to be looked into.

Another example where the dictates of energy conservation, environmental control and conservation of prime raw materials can be made to coincide, is in the development of low-lime cements. The heat required for cement manufacture in dry process plants is essentially to dissociate the calcium carbonate and to heat the feed to the clinkering temperature. Thus, energy conservation can be brought about by reducing the

proportion of limestone in the raw mix and lowering the clinkering temperature. Emission of carbon-di-oxide, which increases greenhouse effect, is unavoidable in cement manufacture. However, nearly two-third of CO_2 emitted is due to decarbonation of limestone; use of less limestone in the raw mix is desirable from this point of view also. Lastly, use of low-lime raw mixes will enable use of marginal grade limestones, thereby conserving limestone reserves of richer quality. Use of industrial wastes like slag, flyash and sludges go to serve the same purpose.

Apart from blended cements, which are well known, cement systems of low-lime content, activated belite cements, higher iron oxide cements and other formulations have received wide attention in all countries. Mineralisers and fluxes have been used to lower the clinkering temperature. Activators like alkali halides or organic chelating agents can be used to lower the temperature of decarbonation of limestone. However, it must be realised that the net energy saving in these cases is not directly proportional to the lowering of temperature of clinkerisation or decarbonation, but somewhat less.

The economic resurgence that is expected in most of the countries in the near future would hopefully involve considerable investments towards building of infrastructures like housing, roads, bridges etc. Apart from cement of the types as commonly marketed today, newer formulations that were hinted above would also be required for such usages. One paramount requirement will be adequate durability and performance of such cements. Many cement formulations in low-lime mixes and incorporating sulpho-aluminates, ferrite or halide-bearing phases could not find wide market adaptation so far, because of lack of adequate data on the long-term durability of concrete made with them. The emphasis on performance of cement and concern for the durability of concrete constructions have coincided with voluminous research throughout the world for more than 50 years now, including deliberations of these Congresses in the past. In spite of tremendous advances in the understanding of durability in various aggressive environments, it remains the foremost problem for the structural concrete used today. The deliberations in this Congress would hopefully lead to a holistic view of the concrete structure and its interaction with the load and service environments, in which, the type of cement is an important consideration just like other aspects of structural design, detailing of reinforcement and the workmanship.

Alongside development of infrastructure, many countries in the world would have to pay attention and spend considerable resources at rebuilding of the distressed concrete structures. Suitable repair materials based on cement would require special properties like very quick setting, high early strength, compatible modulus of elasticity and adequate durability under the service environment. This will be one of the thrust areas for many new cement systems which have been reported, in conjunction with established repair materials of polymeric origin.

Study of cement sciences is the study of chemical reactions and analysis of structures of the reactants, the products formed at high temperature in the kiln and its reaction with water in cement pastes, mortars and concrete. With the advances in electronic technologies and computer methods, newer techniques and instruments are put into use in the analysis of the composition, the structure and the texture of the materials. The entire Poster Session in this Congress has been devoted to this subject.

Lastly, industrial progress is not mere possession of, or access to scientific and technological knowledge. It depends even more on our ability to adapt and put such science and technology to intelligent and productive use. The commonality of scientific and technological issues among the various countries impels that there is a lot to be gained by pooling our expertise and experiences. The International Congresses on the Chemistry of Cement have always been conceived in this perspective and have succeeded in a large measure in achieving the objectives, as I hope will our deliberations in the next few days.

Thank you.

PRESIDENTIAL ADDRESS

by

Shri Suresh Kumar
Secretary (Industrial Development)
Govt of India

Hon'ble Minister, Shri Srinivasan, Dr Mullick, Distinguished Delegates, Ladies and Gentlemen:

It gives me immense pleasure to be in your midst at the Inaugural Session of the 9th International Congress on the Chemistry of Cement which is being held in India for the first time. This is a prestigious global event in the field of cement technology taking place in different parts of the world once in six years and I understand that each Congress has been successful in advancing the science of cement. As the future of cement rests in the realm of the related science and technology, I would like to take this opportunity to commend the progress of these Congresses which have acted as catalysts in the development and growth of cement industry worldwide.

Cement industry of India is nearly eight decades old. With the current progressive policies set in motion by the Government, the industry has entered a new phase of growth in the eighties. Not only has the growth taken place in terms of installed capacity and actual output, but even the structure of the industry has undergone a significant change in terms of plant size and technical processes. The industry has been investing in technological upgradation and modernisation. However, in order that the industry remains competitive, it would have to reach a level where it modernises itself not only in the national context but from an international perspective.

Indian cement industry is set to make its presence felt on the international scene, quantitatively as well qualitatively. There has been a rise in cement production by about 150 per cent in the last decade and if this rate of growth is sustained throughout the next decade, Indian cement industry will overtake the cement industries of some of the more developed countries. These advantages are to be consolidated through further improving our operational efficiencies so that the industry is on a dynamic growth path during the nineties and beyond.

In order to retain such a position, cement industry has to continuously strive to exploit the large potentials for technological advancement in terms of process improvements, product diversification, and cost reduction, and strike a harmonious balance in effective utilisation of resources, ecological protection and optimal levels of energy conservation. Conservation of energy and material resources should receive priority attention in such an exercise.

This holds good not only for Indian cement industry but also for the cement industry in other countries. However, important scientific, R&D and technological issues relating to production and utilisation are to be taken into consideration vis-a-vis each country's techno-economic and social realities. As factors of production have their own peculiar characteristics in various countries, there is a greater need for pragmatism appropriate to those conditions. As all countries are not equally endowed with the requisite quality of raw materials, fuels and other energy resources, it becomes imperative to make the most of what is available through efficient methods keeping in view the present needs as well as conservation for future.

The changing cement scenario world-wide and technology associated with the manufacture and utilisation of cement points unmistakably to development of newer cements in the foreseeable future. With advances taking place in material sciences, coupled with technological and engineering improvements in the design of plants and machineries equipped with computerised facilities, our industries have to move fast towards this goal through better cementitious materials and cementitious systems.

In the manufacturing process as well as the utilisation of cement and its products, industries have to pay greater attention to environmental considerations. There is a need to adopt a positive approach by giving the

lead in environmental protection through greater emphasis on self-regulation rather than just meeting the various regulatory provisions.

India has an age-old tradition of environmental conservation in tune with which conscious efforts are being made for maintaining environmental security along with developmental advances. The action points in this regard include a judicious mix of promotional and regulatory steps with focus on environment related policies and operations in industries, with specific reference to pollution control and waste management besides environmental impact assessment plans for mining and quarrying activities for industries like cement.

Lastly, the cement industry in various countries have to prepare themselves for sustaining cement quality and improving their performance. The quality considerations should not stop with quality checks at the manufacturing end, but must reach down to the product that ultimately goes into use as part of a total quality system.

In this Congress, which is aimed at the advancement of knowledge of chemistry of cement and application of this knowledge in both manufacturing aspects and utilisation of cements in practice, such like issues will be most relevant for discussion on which collective thinking and cross-fertilisation of ideas is necessary for finding rational solutions. I sincerely hope that this Congress, where a galaxy of experts from all over the world have gathered, would provide a valuable opportunity to arrive at solutions which seem potentially fruitful in our pursuit of knowledge on the chemistry of cement towards better cementitious materials and cementitious systems.

With these words may I now request Hon'ble Minister to kindly inaugurate this Congress.

INAUGURAL ADDRESS

by

Smt Krishna Sahi
Minister of State, Industrial Development
Govt of India

It is pleasure to be here with you to inaugurate the 9th International Congress on the Chemistry of Cement. The holding of this prestigious event in India is indeed a milestone for the Indian cement industry. Such meetings provide valuable opportunities to share thoughts, exchange views and discuss experiences among leading scientists, technologists, researchers, industry representatives and others from all over the globe.

Cement is the pre-eminent building material throughout the world. Over the years a lot of research has gone into the chemical and physical processes involved to develop suitable varieties of cement possessing the desired adhesive properties, strength and durability. Our late Prime Minister, beloved Indiraji, while laying the foundation for the National Council's main laboratory block, had stressed, "Research is an indispensable part of planning for industrial progress. Purposeful research demands close co-ordination between the research scientists and the users of research". I am sure the participants are looking forward to interacting meaningfully on the latest advances in the technological aspects of production, economic utilisation, and their impact on industry and users, so as to arrive at an in-depth understanding of the various interconnected issues.

This International Congress is taking place in India at a time when our Government is implementing wide ranging economic reforms. We are seeking to unshackle our unparalleled human resources to make India a major partner of the developed and developing nations, working together for a better world. The new financial, trade and industrial policies are market-oriented and investor-friendly in order to enable entrepreneurs to take decisions based on their commercial judgement. We are seeking to rapidly upgrade our technology and quality to world standards and make our industry internationally competitive in price, quality, productivity and efficiency. There are no longer any controls on the manufacture, distribution and pricing of cement. Import of foreign technology, plant and equipment and the employment of foreign technicians is by and large automatic. I would urge the distinguished delegates assembled here to fully understand the changes that India is going through and go away with the conviction that not only is our Government fully committed to these reforms but also that India is a land of opportunity.

Cement is an essential infrastructure industry whose technological and economic aspects underpin modern development. No limits can be set to the possible improvements in the manufacture of cement or diversification of its application. Research and development is a crucial component of industrial and economic growth aimed at improving social and economic conditions and ensuring sustainable development. If cement has to keep pace with the fast tempo of advances in materials science, much additional scientific investigation and research is needed not only on the physical and chemical properties of inputs and associated ingredients, but also in process improvement, end-use diversification, etc.

It is also essential that the needs of industry and the results of research are speedily and efficiently integrated into the industry and research institutions through interactive linkage systems. I am happy to note that the National Council for Cement and Building Materials is fulfilling this role as an industrial support organisation at the national level, devoted to research, technology development and transfer, education and industrial services in the field of cement and building materials. With a view to upgrade technology and keep abreast of international developments, the Indian corporate sector has also been building up its research capabilities. Many cement plants have in-house R&D laboratories which interact with the NCB.

The Indian cement industry has much to be satisfied about. It possesses the latest manufacturing technologies and has highly skilled manpower. It is almost self-reliant in terms of raw materials. It is well

equipped to absorb and assimilate the latest global technological advances. Indian cement technologists and engineers have made important contributions to the understanding of the chemistry and technology of cement both in India and overseas. The honour bestowed on the industry and the National Council in holding this Congress here is, therefore, well deserved.

The international cement industry has many challenges to face. Production must increase at an accelerated rate in the coming years to cater to the fast growing needs of the developing economies. It will also be necessary to continuously develop and improve processes, technologies and standards to reach even higher levels of efficiency in output, energy use, natural resource conservation and environmental preservation. Simultaneously, the search for alternative raw materials, energy sources and cement-like products must continue. The economic advantages of increased efficiency in operations and product performance are obvious. They would help make cement production and development more economically viable, environmentally safe, socially beneficial and sustainable.

Before I end, I would submit a thought for this august gathering to ponder over. Our ultimate aim is to improve the quality of life. Though we have achieved levels of scientific and technological development unimaginable a few decades ago, thousands of millions live in conditions of terrible poverty all over our planet. As an international gathering of experts, opinion-leaders and enlightened world citizens, could we resolve to direct our endeavours to optimise the R&D capabilities of developing countries through bilateral, regional and international collaboration and cooperation. This will help the vast majority of developing countries to become active participants in the global S&T system. I would appeal to the representatives of developed countries with their formidable R&D achievements and diverse experience of technologies to take the lead in unifying and promoting research for mutual benefit thus helping the developing countries in their quest for better standards of living.

I wish you fruitful work on cement – the truly universal binding material. Science and technology will serve humanity the day it discovers how to cement the hearts of people of all shades and creeds for the peace and prosperity of Planet Earth. I have no doubt that the contributions from this Congress will truly culminate in a synthesis of various ideas and proposals reflecting the latest trends in research and technology on cement. With these words, I have great pleasure in inaugurating the 9th International Congress on the Chemistry of Cement.

VOTE OF THANKS

by

Dr C Rajkumar
Jt Director, NCB and Organising Secretary, 9th ICCC

Hon'ble Smt Krishna Sahi, Shri Suresh Kumar, Shri Srinivasan, Dr Mullick, Distinguished Delegates, Ladies and Gentlemen:

With the Inaugural Session of this 9th International Congress coming to its close, it is my pleasant privilege to propose the Vote of Thanks.

With the inspiring Inaugural Address by the Hon'ble Minister we have just now listened to, this prestigious international meet is all set for a good start. Madam, we are aware of your busy schedule, despite which you have favoured us with your presence. Your Address is a source of great inspiration to all the participants to have a meaningful deliberation in the coming six days. We are indeed grateful to you for kindly inaugurating this Congress.

We are thankful to Shri Suresh Kumar, Secretary to the Govt of India, Ministry of Industry, for having graced this occasion with his presence and for delivering the Presidential Address. Sir, we are thankful to you for giving your valuable views on the issues relating to the cement industry today. This Congress will take note of these during its deliberations.

We are indeed thankful to Shri Srinivasan, Chairman NCB and Chairman of the Organising Committee of this Congress. Your continuous guidance, Sir, in every aspect of this Congress right from the first day, has given us both encouragement and support in organising this event. The guidance and directions given by Dr A K Mullick as Chairman of the International Scientific Committee of this Congress, in all scientific and technical matters, have been of immense benefit to the Congress, for which we thank you Sir.

Our special thanks are due to the various organizations who have co-sponsored this Congress. Our thanks are due in no less measure to the distinguished invited speakers who have taken pains to prepare excellent Congress Reports and to personally participate and present them. I also take the opportunity to thank all the authors who have made contributions to the Congress and those who are present here. I shall be failing in my duty if I do not thank the Members of the International Scientific Committee, the Organising Committee, and the Reviewers, whose views and guidance have greatly enhanced the quality of this Congress. Our heartiest thanks are due as much to the participants in the Technical Exhibition.

We are thankful to the Press and the Electronic media for covering this event. To achieve smooth operation and a comfortable environment, many agencies have joined hands with us and we are thankful to them for their services.

Lastly I wish to place on record my grateful thanks to my colleagues from NCB who have worked hard for months towards the success of this Congress.

CONCLUDING SESSION

THE CONGRESS OVERVIEW

by

Shri N Biswas
Secretary TD & DGTD
Govt of India

Hon'ble Minister for Science and Technology Shri Kumaramangalam, Shri Srinivasan, Dr Mullick, Shri Singh, Distinguished Delegates, Ladies and Gentlemen:

I am happy to be present amongst this distinguished audience during the concluding session of the 9th Congress on the Chemistry of Cement. This Congress has been held at a very appropriate time when the cement industry all over the world is gearing up to meet the challenges posed by the present economic situation and is drawing up strategies for improved efficiency and cost reduction through appropriate measures.

A thorough assessment of the progressive advancements in the knowledge of cement chemistry, plant and machinery design and effective utilisation of energy and material resources would indeed be a very positive step towards this direction. The deliberations in this Congress during the last six days have been able to achieve this objective effectively. This Congress has indeed been useful and purposive in dealing with the enormous challenges which have been posed of late by the dwindling natural raw material resources, scarcity of power and fuel, impact of the industrial activity on the possible degradation of the environment and increasing need of improved performance of cement in constructions.

With this background, the presentation of the state-of-the-art reports by eminent international experts on the various generic and specific themes which were identified, and nearly 380 communication papers provided the much desired impetus.

The reports and papers presented in this Congress brought out the results of intensive investigations, which will influence both the cement formation characteristics and the effect of minor components on the properties of cement as a whole. The relationship between the characteristics of the cement raw-mix and the clinker formed, and the role which the melt phase plays in improving the performance of cement have been debated at length. The developments in pyroprocessing are indicative of still nascent stationary kiln systems and improved performance through the developments in grinding technology. For the first time, this Congress has laid due emphasis on the use of non-traditional raw materials and low grade fuels and combustible wastes. Research work in this area has established the feasibility of using non-traditional raw materials such as lime bearing carbonate sludges from paper, sugar, fertilizer and chemical industries such as soda ash and acetylene plants and wastes from iron, aluminium, phosphorous and other metallurgical industries.

Recycling of hazardous and non-hazardous waste fuels in cement manufacture has been the most promising development during the period under review. Considerable progress has been reported in design engineering and construction of waste derived fuel facilities in many parts of the world. The developments in the cement clinker technology and the use of non-traditional raw materials and waste fuels have also opened up unique opportunities for energy conservation and environmental improvement which must be harnessed to the maximum possible extent in the service of mankind.

With the pressure on cement industry mounting to consume less raw materials, reduce specific fuel consumption and curb harmful emissions, the role of minor components has come under very close scrutiny and work has been reported in the direction of quantifying the gain ensuing from their use. Considerable research work has also been reported in the fixing up of heavy metals in cement clinker to render them harmless. The effects of the measures to reduce energy consumption and pollution control on the quality of clinker have also been discussed at length.

Although various papers in this Congress have emphasised the development of low-energy, low lime cement to substitute ordinary portland cement, no threat seems to be emerging to the dominance of ordinary portland cement as the major binding material for construction. Blended cements, which have occupied a pivotal place as more energy economical and cost effective cements, shall continue to occupy prominent place in future also.

The Congress evinced keen interest in the hydration studies of cements which is evident from a very large number of papers presented on the subject. Newer techniques like nuclear magnetic resonance, transmission electron microscopy etc have no doubt led to a much better knowledge on the complex problems of hydration of clinker components, portland cement and blended cements, which shall lead to diversifying the application of these cements.

Due attention has been paid to the most common causes of deterioration to concrete, emphasising the role of mineral additions on pore structure refinement and durability of cement mortar and concrete. Extended application of multi-component blended cement for manufacture of advanced fibre reinforced bonded composite densified systems, macro defect free cement, etc, shall remain important areas of development for years to come.

Corrosion of reinforcement, frost action, carbonation, alkali aggregate reactions and sulphate attack are the major causes which adversely influence the durability of concrete structures. Use of super-plasticizers and mineral admixtures have helped to considerably enhance the durability of concrete in service. The laboratory tests currently used to evaluate concrete need to be made field oriented to yield more meaningful results. To solve these problems, future efforts shall have to be concentrated towards a holistic understanding of the durability issues.

While concluding, I would like to specially highlight a unique feature of this Congress in the form of special panel discussions and special lecture sessions at the end of each day's deliberations, which brought out the technological and techno-economic impact on the industry of the various scientific advances deliberated in the Congress under the various theme sessions. These special sessions together with an excellent technical exhibition organised during the Congress could clearly establish the much needed interface amongst the scientists, manufacturing industry and the users to enable the effective utilisation of the scientific advances. Thus, in my opinion, the 9th Congress could indeed achieve its objective of pooling expertise and experiences from different parts of the world with a view to adapt and put such scientific and technological knowledge to productive use.

Thank you.

VALEDICTORY ADDRESS

by

Shri P R Kumaramangalam
Minister of State, Science and Technology
Govt of India

Shri Biswas, Shri Singh, Shri Srinivasan, Dr Mullick, Dr Rajkumar, and Distinguished Delegates, Ladies and Gentlemen:

It gives me immense pleasure to be in the midst of this august gathering for the valedictory address on the successful conclusion of this six-day International Congress. I am indeed grateful to the organizers for giving me this opportunity. In fact, holding of this prestigious Congress in Delhi is also a matter of great honour for this historic city. This Congress, as you all know, is held once in six years and it is only the first time that it is being hosted by India and only the second time for Asia.

Today the scientific community readily acknowledges the stark reality of technological inter-dependence. No country and no scientific institution can work in isolation. In fact, the breakneck speed with which technological frontiers are being explored and penetrated together with the high rate of technological attrition has only highlighted the need for technological inter-dependence.

Such international meets serve as effective media of technology transfer, apart from bringing together the experts and scientific organisations connected with the field. With science and technology making breath-taking strides, no human endeavour can flourish without actively being involved in the various developments taking place around joint consultations of this type with active involvement of all concerned is particularly useful as ultimately much of the problems have to be dealt through active interaction and exchange of views between those who are seized of all problems.

I understand that the Congress has been attended by over 500 delegates, including 250 from overseas countries representing leading experts from R&D organizations, technical institutions, cement manufacturing sector and user agencies. The discussions in various technical sessions have been frank and free, marked by high technical levels and enriched by exchange of knowledge and experience on the latest developments in cement industry overseas. Innovations in technologies and processes for the production and utilisation of cement were discussed with emphasis placed on materials and energy conservation environment and development of newer cementitious materials.

With an installed capacity of 66 million tonnes and targeted capacity of 55 million tonnes for this year, India today ranks fifth amongst the top cement producing countries in the world. The Indian cement industry is getting modernized at a rapid pace. It does have a unique scientific and technical base at the NCB and CSIR which is comparable to the best anywhere else in the world. However, we still have a long way to go in exploiting fully the new technologies and processes. I am sure that this is well within the means and capacity of our cement industry to master and exploit these new technologies and emerge in the frontline in this arena. Emphasis will have to be simultaneously laid on indigenisation, adoption and upgradation of technologies. Today, efficiency, absorption and adaptation of technologies and processes has assumed strategic importance to attain technological competitiveness and this serves as a very important stepping stone for the technological self-reliance.

Cement has been and continues to be the prime building material in construction activities all over the world. The multifarious demands are leading to more and more exacting diversified requirements. They are creating unprecedented pressure on raw materials, the energy resources, the environment, the plant equipment and machinery, manpower and technological adaptiveness. The deliberations of this Congress have revealed that cement manufacturing technologies have undergone phenomenal developments all over the world during the past few years.

The present scenario of energy crisis and the spectre of growing pollution hazards, unique efforts are on to develop relevant technologies. In the last two decades attempts have been made to investigate low energy cement and cementitious materials from natural resources as well as industrial by-products. The development and production of new cements have become imperative due to energy intensive raw materials and depletion of natural fossil fuels. A closer look at the economics of production of portland cement shows that energy inputs account for 58% of the total cost of production (28% on power + 30% for fuel). Mineralizers, additives, grinding aids and slurry thinner are some of the cost effective propositions for cement industries.

Commendable R&D has also been done by the Central Building Research Institute, Roorkee especially in substitute materials and construction techniques in order to conserve more valuable and scarce material, that cement is. Lime research has been given a new impetus in order to exploit deposits of such limestones not hitherto used or to improve lime quality as produced from different types of kilns and finally ending up with the required effective designs of lime kilns and lime hydrator, the latter for introducing lime into market in the hydrated form.

A number of variations of cement, like non-shrinking cement, and the popular portland pozzolana cement, masonry cement, high magnesia cement and oilwell cement have been developed and in some cases even pilot plants set up to demonstrate the technical feasibility of their production. Such properties of cement or of a cement based product as strength at normal and high temperatures, porosity and permeability, water resistance and volume stability and weathering resistance under different exposure conditions dictate their field application. A clear and deeper understanding of basic nature and characteristics of these materials leads to a rational and economic utilization. With the growing popularity and sophistication in the manufacture of cement, the cost continues to rise. It is a big drain on the national economy of many a developing nations to import portland cement. With the development of steel industry by-product slag – the air-cooled variety as concrete aggregate and granulated variety as a major admixture in portland cement are the most popular developments. Hydraulicity of slag glasses due to variations in raw materials would continue to form the research topic for many cement chemists but economics and saving in energy, if any, in the production of slag cements should be given higher priority. The same could be said about portland flyash pozzolana cement. If there is any real economy to the consumer or the nation in the manufacture and use of these cements, it should be given prime considerations. In this context, it would be worthwhile to examine the feasibility and suitability of super sulphated cement with 70-75% slag content, as this cement would be more economical both in cost and consumption of energy.

In today's context it is very clear that energy efficiency and conservation of scarce material will form the mainstay for technological innovations in the cement industry. I am very happy to learn that the deliberations during the last few days in this Congress have brought out the tremendous scope which material science offers towards energy conservation in cement manufacture. The deliberations have also brought out the importance of using industrial wastes in cement and concrete construction. The research done in this regard by NCB, CBRI and other laboratories in the CSIR family is indeed commendable. The utilisation of this industrial waste has made important contribution towards energy conservation apart from environmental improvement.

I heartily congratulate the winners of the National Awards for Energy Efficiency for this year and for the previous year. At the same time, I would like to commend the efforts of others who participated in the scheme of awards. In the process of their participation, they would certainly have streamlined their production and monitoring practices and derived energy benefits in terms of energy savings which is a reward in itself.

I think that the Congress has served its purpose very well by focusing attention on these important aspects of chemistry of cement with emphasis on energy conservation and environmental concern. The Congress has made a significant contribution by opening up of vistas of knowledge through mutual discussions and exchange of viewpoints, and I would like to congratulate the members for the successful conclusion of this conference.

SUMMING UP AND CLOSING

by

Dr A K Mullick
Director General
National Council for Cement and Building Materials

With the inspiring valedictory address of Shri Kumaramangalam, Hon'ble Minister of State for Science and Technology, we come to the end of this evening's function as well as the six days' deliberations of the 9th International Congress on the Chemistry of Cement. A total of 372 papers and congress reports were deliberated upon in 46 sessions. We are happy to say that the total number of delegates was 533 and they came from 45 countries. The countries were Australia, Austria, Bahrain, Belgium, Bhutan, Brazil, Canada, Colombia, Costa Rica, Denmark, Finland, France, Germany, Greece, Hungary, India, Indonesia, Iran, Italy, Japan, Kenya, Korea, Lithuania, Malaysia, Mongolia, Morocco, Nepal, Netherlands, Norway, Peoples' Republic of China, Pakistan, Philippines, Poland, Romania, Russia, Saudi Arabia, South Africa, Spain, Sweden, Switzerland, Thailand, UAE, UK, USA and Ukraine.

Shri Biswas, in his Congress overview has touched upon the main points of the deliberations. At the inaugural session, the main issues were identified as cost reduction, energy conservation, environmental improvement and improvement in performance characteristics of cement. Deliberations were adequately addressed to all these issues in a symbiotic manner. We noticed the emerging trends of industrial practices as related to energy and, material conservation and environmental improvement, making an imprint on the on-going research and the way chemistry of cements has a bearing on each of these were very ably brought out. For the first time, computerisation and modelling of the microstructure and mechanics of material received a focus which is fast emerging as an important area of research. With this Congress, we had started a novel scheme of having Special Invited Lectures to bring out the technological and techno-economic impact of the scientific advances, on the industry – intended to provide a better appreciation of the implications of the scientific advances specially on the process control machinery and related industries as well as operational aspects related especially to energy conservation and environmental improvement.

The Hon'ble Minister has just given away the National Awards for Energy Efficiency in the Indian Cement Industry. I am happy to say that these awards, which are being given for the last six years, have fulfilled the objective to motivate a competitive improvement in performance and improved energy consciousness in the Indian cement industry, by giving national recognition to the efforts for realisation of low energy consumption. Energy conservation is a multi-faceted activity and requires inputs from many sources. If NCB awards have served a catalytic purpose of bringing in the needed improvement, even in a small measure, we would consider our efforts have been amply rewarded.

The deliberations of the Congress in very many details were planned by the International Scientific Committee with 65 members from 37 countries and organizations. In the two meetings of the Committee held during these last six days, significant decisions have been taken about the future of the Congress. A suggestion has been made that the gap between the successive congresses could be brought down from six years to perhaps four or five years; the choice has been left to the organizers of the next Congress. An idea has also been mooted to have some sort of a system of time capsule of cements and concretes which can be unveiled for scientific investigations after suitable intervals of time, to enable a direct comparison of both the materials development as well as the developments in the analytical techniques. We have to work out the fuller details about this.

Another significant decision taken by the International Scientific Committee was about the venue for the next Congress, i e the 10th International Congress on the Chemistry of Cement. I am happy to announce that it has been decided that the next (10th) ICCC will be held in Sweden.

This is the occasion when we would like to express our sincere thanks to the various people who helped

in making the Congress a success. We are thankful to the Hon'ble Minister of State for Science and Technology for delivering the valedictory address and giving away the energy awards. We are thankful to the Hon'ble Minister of State for Industrial Development, Smt Krishna Sahi who inaugurated the Congress on the first day. We are also thankful to the Hon'ble Minister of State for Science and Technology, Government of Haryana, Prof Ram Prakash who inaugurated the Technical Exhibition. We thank the Secretary, Industrial Development, Shri Suresh Kumar who presided over the inaugural session, Secretary Technical Development, Shri N Biswas for giving the Congress overview and the Secretary Water Resources, Dr C D Thatte for chairing a Special Session.

We thank Shri N Srinivasan, Chairman, NCB and the NCB's Board of Governors and members of the Board's Committees for their continuous support, guidance and directions for the last six years, ever since the bid to host this Congress in India, was made in 1986. Our thanks are due to the Members of the International Scientific Committee and the Organising Committee for their guidance in the technical matters connected with the Congress deliberations. We thank the various co-sponsors of the Congress – the Indian cement industry through the Cement Manufacturers' Association, the Department of Scientific and Industrial Research, Govt of India and the individual cement companies who co-sponsored this Congress. We are thankful to the Ministry of Power for joining NCB in sponsoring the National Energy Awards. Our thanks are due to those who chaired the Technical Sessions and authors of the papers and reports.

Our thanks are due to all the delegates who participated in this Congress. Our thanks are due to the media in no less a measure. I would like to express my thanks to Dr C Rajkumar, the Organising Secretary of this Congress and all my colleagues in NCB who worked for this Congress tirelessly all these years.

Much of our organisational experience in conducting events of this magnitude came from the International seminars that we have been regularly holding. Enquiries have been received as to when the Fourth NCB International Seminar, which was deferred in view of this Congress, would be held. It has been internally discussed and we would like to hold it in the winter of 1994; the exact dates will be announced later. We hope to see many of you again during that seminar.

It was only six days ago when we were recalling the earlier Congresses as a part of historical records of the progress in the realm of cement chemistry. With this 9th Congress coming to an end, in a few moments from now, the 9th Congress and the beautiful logo would also be consigned to the history. What will remain is the memory of the last six days with you all. I can only say that it was wonderful to have all of you with us and we sincerely hope you found the deliberations rewarding and your stay in India fruitful and enjoyable. We thank you once again for being with us and for your help and participation in making the Congress a success.

Namaste.

SPECIAL LECTURES SESSION

PRESENT PROBLEM IN CEMENT MANUFACTURING

Prof Dr Eng Hiroshi Uchikawa

Executive Director
Research and Development, Onoda Cement Co Ltd, Japan

1. INTRODUCTION

The cement industry has steadily progressed for purposing the improvement of the constitution of resource- and energy- intensive industry, the establishment of environmentally benign industrial structure and the steady supply of low cost, high-performance multi-functional products by the modernization of the industry including through reduction of manufacturing and distribution costs and the positive, advanced environmental preservation.

The manufacturing cost is mainly reduced by labor, energy and resource savings. The trends of the labor productivity and energy consumption in Japan are shown in **Fig. 1**.

The measures for remarkably improving the labor productivity include the enlargement of plant capacity, the introduction of an automatic sampling and analysis system, the distribution and steady emolument of computer-based operation control and the abolition of inefficient, obsolete facilities.

Energy conservation was achieved mainly by the conversion of operation process and the modifications of a process.

The burning process has rapidly changed for twenty years through the dry process, dry process with filter, long kiln in the wet process, shaft kiln, Lepol kiln, long kiln in the dry process, lime-calcination process and SP process to the SP with precalciner process which has predominated in the burning process since Rio de Janeiro Congress in 1986 as illustrated in **Fig. 2**. The cement industry has tided over two oil crisis by switching the fuel from oil to coal as illustrated in **Fig. 3** and the industrial waste has recently been used as the fuel alternative to coal.

The grinding efficiency of the grinding process has been improved by enlarging the diameter of ball mill, changing the feeding position of raw materials, reducing the diameter of ball, using the classifying liner, introducing the roller mill and using the closed circuit by employing high-efficiency classifiers. The conspicuous improvements made since Rio de Janeiro Congress include the introduction of preliminary grinding of the raw materials or product with a roll press or roller mill, the challenge to the grinding process without ball mill using only a roll press, and activation of the materials to be ground by a mechanochemical effect in the attrition grinding using shear stress.

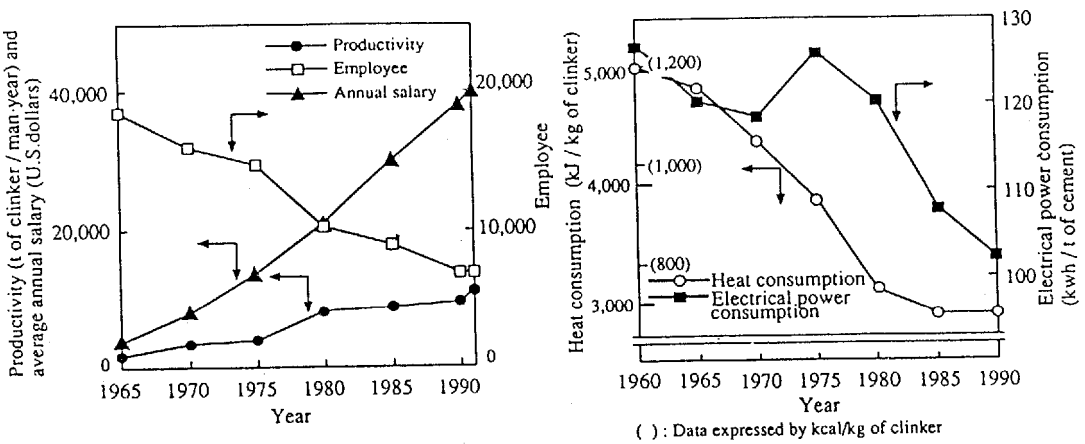

Fig.1 Productivity, number of employee, average annual salary of employee, and specific heat and electrical power consumption of Japanese cement industry

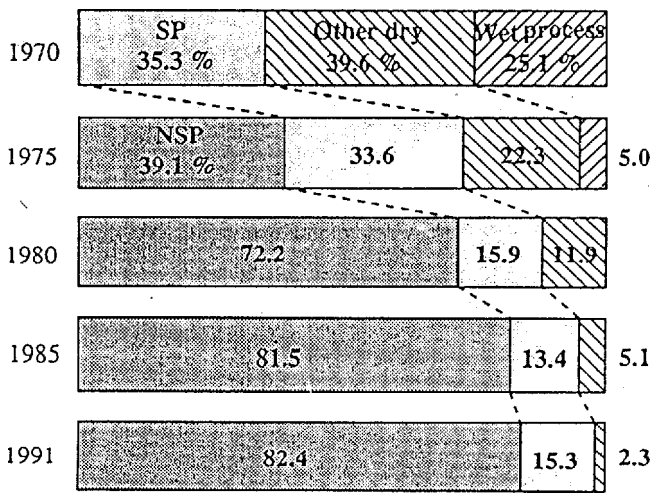

NSP : Suspension preheater with precalciner type
SP : Suspension preheater type

Fig.2

Type of kiln in Japan

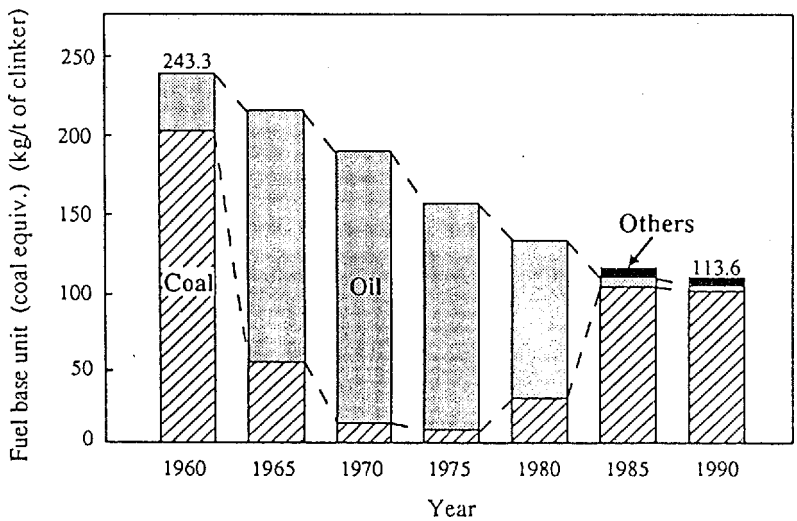

Fig.3

Change of fuel base unit (coal equivalent)

For saving resources, the use of industrial waste contributes to the reduction of the consumptions of natural raw materials and fuel. Recently, however, the situation of the cement industry is developing for social requirements of the disposal of industrial waste as well as reducing the manufacturing cost of cement.

The cement industry is also tacking the environmental problems in the global scale to keep the environment of our rich life. Technical development and investment in equipment have been aggressively made for reducing the emissions of harmful materials including air pollutants such as NOx, SOx and dust, green house gases such as CO_2 and water pollutants and meeting the requirements of the strict regulations established by the governments of countries.

Reviewing cement itself for the energy conservation and the measures to counter the environmental pollution has been carried on since Rio de Janeiro Congress and a great effort has been spent to develop new types of cement for meeting the diversified demands and needs of the industry as well. The development and progress in the application of superplasticizer and advanced technology for composite materials can improve the performance of cement as concrete. Environmental load-

reducing cement including blended cement, belite cement, modified belite cement and alinite cement are being developed.

Meanwhile, the trend of the investment in the equipment of the cement industry in Japan is illustrated in **Fig. 4**. The figure reveals that the overseas investment is increasing in and after 1989 since the modernization investment made a pause in that year.

The reduction of manufacturing cost of cement by the developments in the cement manufacturing process and the modifications of it conducted since Rio de Janeiro Congress in 1986, the effect of them on the quality of cement, problems in the operation by using industrial waste alternative to raw materials and fuel, the development of the environmental load-reducing types of cement and the measures in using the new type cement for assuring the quality of concrete will be described hereafter from the practical aspect rather than the scientific aspect.

2. REDUCTION OF MANUFACTURING COST BY THE DEVELOPMENTS OF NEW PROCESSES AND MODIFICATION OF PROCESS

Energy conservation as well as labor and natural resources saving causes not only the manufacturing cost reduction but also the reduction of quantity of pollutants discharged from cement manufacturing plants. Conventional energy conservation in the cement industry has been attained mainly by enlarging the plant scale accompanied with the increased demand, converting the conventional process to a new one with the progress of technology, stabilizing the operation by computer control and abolishing obsolete plants. As of 1991, the production of cement in NSP and SP kilns in Japan account for 82.4 and 15.3 %, respectively, of the total production of it. Sprung of Germany and Delort of France[1] indicates, however, in their Principal Paper that energy will not be substantially reduced by only improving and optimizing the process in a state-of-the-art plant. Nevertheless, most of the cement manufactures are still concentrating their efforts on energy conservation with minor improvements of the process expecting that the cumulative effect will be large though the effect of each measure is small. The new processes of cement manufacturing reported after Rio de Janeiro Congress in 1986 and the measures for energy conservation carried out "maintaining the quality of cement unchanged" for the last ten years in Onoda Cement will be described hereafter.

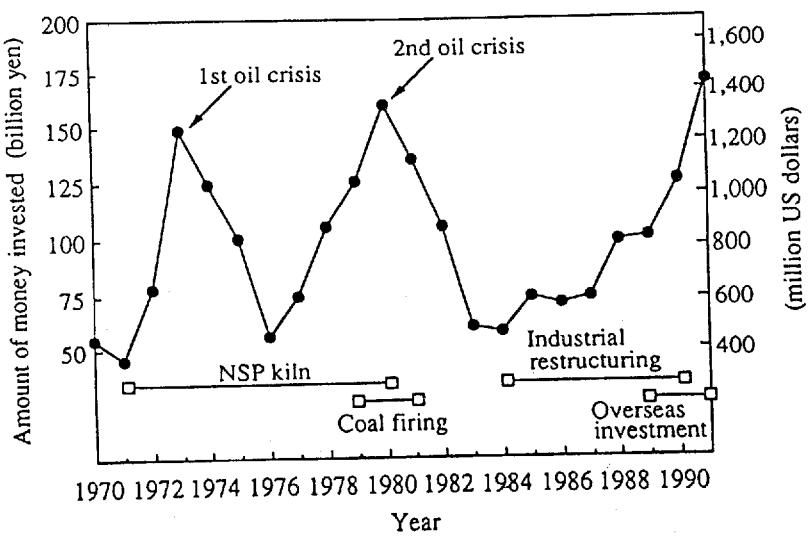

Fig.4

Machinery and equipment investment

2.1 New manufacturing Process

2.1.1 Fluidized bed reactor

The fluidized bed reactor has recently been gained attention because it is characterized by suitability for a small scale plant in inland areas, less emissions of NOx, low consumption refractory due to static low-temperature reactor and low maintenance cost due to easy maintenance. Although forty years have passed since the fluidized bed reactor was developed in the U.S. as Pysel process in 1940, it has never been scaled up larger than the experimental scale. Fuller Co. in the U.S. has recently released a fluidized bed reactor for white portland cement as illustrated in **Fig. 5**. A mixture of the raw materials with 5 to 9% (70 to 90% of the total fuel) of coal or coke and 5% or less of white portland cement as the binder is pelletized and thus prepared pellets 1.2 to 4.7mm in diameter are fed into the fluidized bed reactor. It is estimated from the data obtained by test reactors 12.7 and 45.7cm in diameter that the diameter of a 300t/d-commercial reactor will be 4.9m and the specific consumption of heat will be a 6,052kJ/kg of clinker (1,441kcal/kg of clinker)[2].

Two group of Kawasaki Heavy Industry, Sumitomo Cement and Technical Institute of Coal [4], and Ishikawajima-Harima Heavy Industry and Chichibu Cement[3] have constructed separately pilot plants as illustrated in **Fig. 6** and **Fig. 7** and long term test operation is being carried out in each pilot plant. The former is characterized by the combination of a spouted bed reactor and a high-temperature fluidized bed reactor with multi-stage cyclone preheater and fluidized bed and moving bed coolers and self-pelletizing (2 to 3mm in diameter) of raw materials heated in the spouted bed. A 20 t/d-pilot plant is being operated at present. It is said that the quality of cement manufactured in the pilot plant is almost the same as the product manufactured in a rotary kiln as shown in **Table 1**[3].

The latter comprises a spouted, fluidized bed reactor, a suspension preheater equipped with a precalciner, a fluidized bed cooler and packed cooler as shown in **Fig. 7**. A part of the product clinker is crushed and circulated to the fluidized bed reactor as the seed clinker to nodulate the raw materials in the reactor. A 50t/d- pilot plant is being operated at present. The operational data of a 330t/d- commercial plant estimated for the data obtained from the pilot plant are compared with those of a rotary kiln. The result is shown in **Table 2**[4]. The emissions of NOx and the investment and maintenance costs are lower than those of a large SP kiln with precalciner. There are, however, still many problems awaiting solution including techniques for thoroughly sintering the clinker and reducing the variation of quality. Since the process has high heat transfer efficiency at low temperature, it may be applicable to manufacturing such cement as belite cement burnt at low temperature.

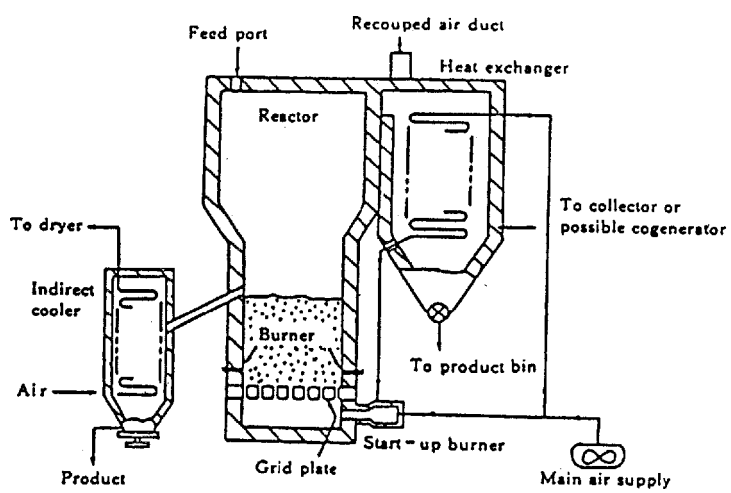

Fig.5

Fluidized bed reactor designed by Fuller

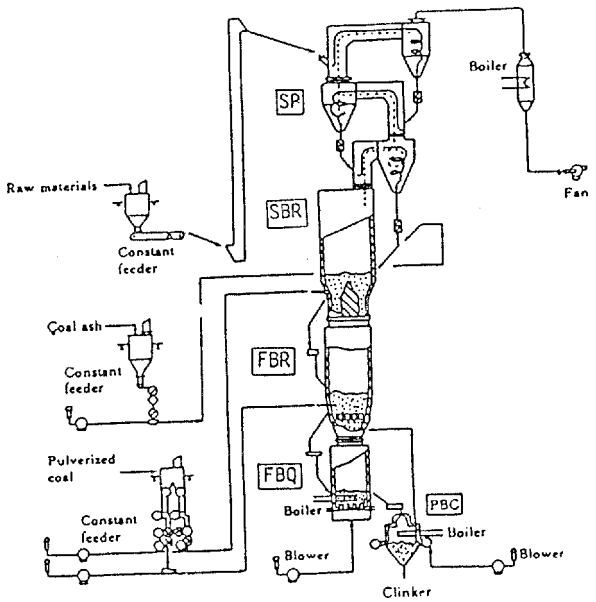

SP : Suspension preheater, SBR : Spouted bed reactor,
FBR : Fluidized bed reactor, PBC : Packed bed cooler,
FBQ : Fluidized bed quenching cooler

Fig.6

Fluidized bed reactor designed by KHI-Sumitomo

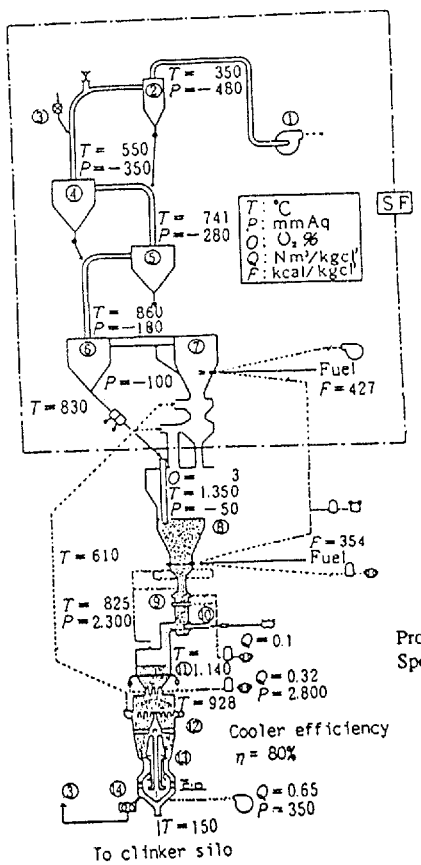

① Exhaust fan
② Fire stage cyclone
③ Raw meal containing clinker
④ Second stage cyclone
⑤ Third stage cyclone
⑥ Fourth stage cyclone
⑦ Precalciner
⑧ Spouted bed - type fluidized reactor
⑨ Classifier
⑩ Clinker slitter
⑪ Fluidized bed cooler
⑫ Packed bed cooler
⑬ Clinker discharger
⑭ Roller Crusher

Production rate : 330 t / day
Specific heat consumption : 3276 kJ / kg of clinker
(780 kcal / kg of clinker)
(coal combustion)

Fig.7 Fluidized bed reactor designed by IHI-Chichibu

Table 1 Quality of clinker manufactured by fluidized bed reactor

		Blaine specific surface area (cm^2/g)	45μm R (%)	Compressive strength (N/mm^2) 1day	3day	7day	28day
OPC	FBR	3,200	16.5	—	14.0	22.1	37.0
				—	(143)	(226)	(378)
	RK	3,250	12.5	—	13.9	22.6	35.7
				—	(142)	(231)	(364)
HPC	FBR	4,550	10.0	12.6	21.5	29.5	42.7
				(129)	(219)	(301)	(436)
	RK	4,540	10.4	13.0	22.2	29.7	39.8
				(133)	(227)	(303)	(406)

Note; OPC: Ordinary portland cement, HPC: High-early strength portland cement, FBR: Manufactured by fluidized bed reactor, RK: Manufactured by conventional rotary kiln, ( ): Data expressed by kgf/cm^2

Table 2 Estimated operational data of fluidized bed reactor and rotary kiln

	Fluidized bed reactor	Rotary kiln
Specific heat consumption (kJ/kg of clinker)	3,264 (780)	4,393 (1,050) (4-stage SP)
Specific electric power consumption (kwh/t of clinker)	35-45	30-40 (4-stage SP)
Exhaust temperature of clinker (°C)	150	150
NOx *1 (ppm)	< 50	< 400
Ratio of energy cost (%)	61	100
Ratio of construction cost (%)	75	100
Maintenance and repair cost	Low	High

Note; *1: In the case of using crude oil
Capacity of fluidized bed reactor : 0.1 million t/year (330t/d)
( ) : Data expressed by kcal/kg of clinker

2.1.2 Vortex reactor

Improving the heat exchanging of powders suspended in a vortex gaseous stream with the gas has already been carried out in the vortex chamber in the preheaters of NSP kilns as shown in **Fig. 8**. Ryzhik et al [5] of Russia reported in Communication Paper on the burning of cement in the vortex reactor equipped with a cyclone preheater. The raw materials partially decarbonated by preheating is supplied into the vortex reactor in which the raw materials is heated and decarbonated in the vicinity of the wall surface by the fuel and combustion air blown in the tangential direction of the reactor and the sintering reaction is terminated in the central part of the reactor. It is considered, however, that thus manufactured product is not sufficiently sintered as cement in this process because the average retention time of the raw materials in the reactor is as short as one second or less and the temperature of clinker is not high enough owing to the endothermic reaction of the decarbonation. It is, therefore, expected to develop the technology and improve the equipment for increasing the combustion rate of fuel and extending the retention time of the raw materials in the reactor. The vortex reactor is applicable as a simple facility to manufacturing a low-burning temperature, low-production special cement and cement containing corrosive, pollutive components. The facility should be, therefore, developed by determining the use and narrowing down the purpose.

2.1.3. New pregrinding system

The grinding process has been relatively markedly advanced in the cement manufacturing process as stated by Johansen of Denmark and Kouzetsova [6] of Russia in Principal Paper.

A multiple grinding system having an impeller breaker or hammer mill for the raw materials and a rod mill for clinker installed ahead of the ball mill has been put in practice from long ago. Since these pregrinding facilities have been abolished owing to the improvement by enlarging the ball mill and balls used in the first compartment in the ball mill, most of them have disappeared in the latter half of the 1970's. The introduction of the pregrinding system has been investigated again for saving energy and minimizing the investment in equipment in the latter half of the 1980's from the different viewpoint as follows:

(1) Prevention of energy applied by the collision of media from being lost as heat or sound,
(2) Lessening the effects of the variations of crushability and grindability derived from the different characters of clinker by separately crushing and grinding in each optimum facility, and
(3) Application of the mechanochemical effect by attrition using shearing stress.

Grinding is an operation producing new surfaces by cutting the atomic bonds with mechanical energy. The mechanical energy other than that consumed for producing the new surfaces generates heat and sound which change the crystal structure and composition and develop lattice defects. Such a phenomenon changing the characters of a material with the mechanical energy is called the mechanochemical effect. The effect activates a material up to the metastable state, improves the reactivity, decreases the sintering temperature and increases the rate of hydration reaction.

The pregrinding in the roll press is based on a patent on the application of a roll press to the finish grinding process of cement applied by Professor Schoenert of Clausthal Institute of Technology in Germany in 1987[7]. Since the grinding system as illustrated in **Fig. 9** has been completed, it is being introduced to the cement-grinding process. In this system, clinker is collapsed in a roll press into flakes which are disintegrated and coarser particles outputting the roll press are ground in the successive ball mill. A part or the all of coarser particles classified in a classifier is generally returned to the roll press. Since the load of the low-efficient ball mill is remarkably alleviated in this system, the specific consumption of electric power is also reduced.

The pregrinding system using a roller mill also is spreading by the same concept.

The operational results obtained from a grinding system comprising a roll press with rolls 120cm in diameter and 45 cm long installed ahead of a 150kW-two compartment-ball mill 305cm in diameter and 975cm long and a grinding system comprising roller mill with three roller of 123cm in diameter each and a table 180cm in diameter installed ahead of a 5,500kW-two compartment-ball mill 510cm in diameter and 1,400cm long are shown in **Table 3**.

The electric power consumption is reduced by 9.7% and 15.7% and the grinding capacity is increased by 31.0% and 35.5% by installing the roll press and roller mills ahead of the ball mill in those systems.

2.1.4 Grinding without ball mill

The actual result of a grinding system comprising only a roll press acting as the main grinder, a disintegrator and a classifier as illustrated in **Fig. 10** has recently been reported [8]. It is considered, however, that some problems including the particle size distribution and quality of the cement will be solved in the near future. The break-through concept of the grinding system without ball mill will be applied soon to the raw materials and slag which are easier grindable.

2.1.5 Impact-shear (attrition) grinding mill

The improvement of the sintering reactivity has been tried by activating the raw materials particles with the mechanochemical effect. A planet mill, a typical impact-attrition mill, has such a structure as illustrated in **Fig. 11**[9], thereby enhancing the reactivity of the raw materials by the attrition derived from the shear destruction. Sulimenko [10] of Russia describes in Communication Paper

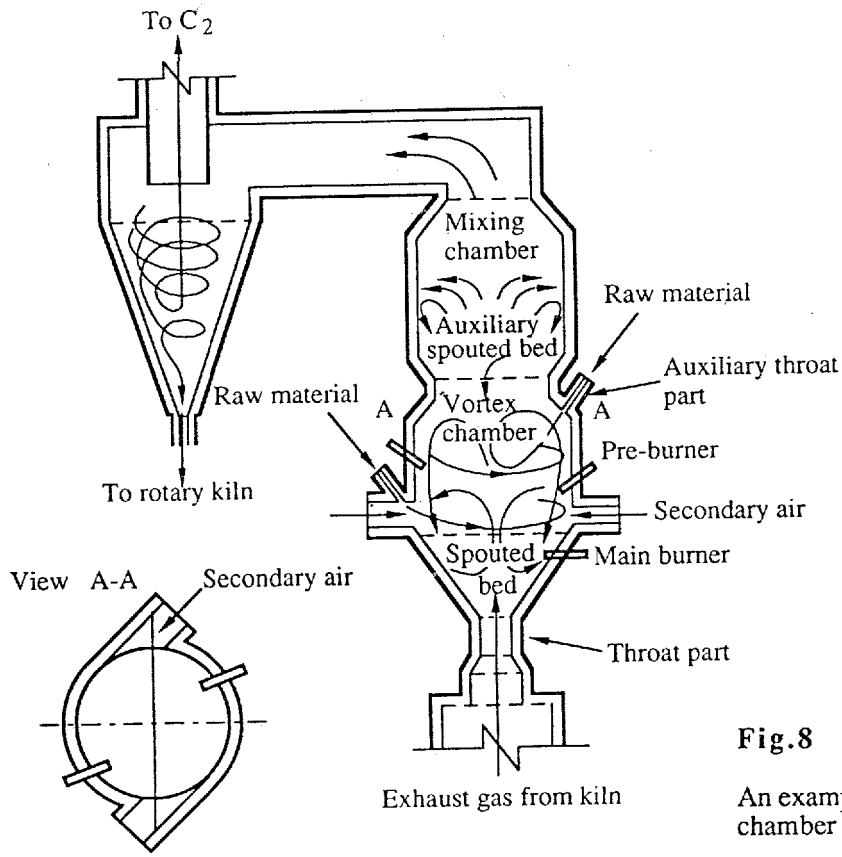

Fig.8

An example of vortex chamber in NSP kiln

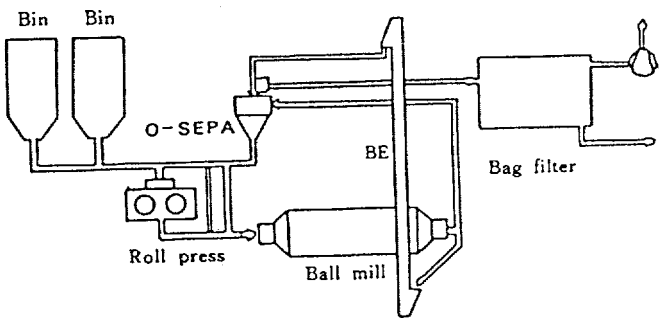

Fig.9

Roller press pre-grinding system

Table 3 Operational data of roll press and roller mill pre-grinding system for cement grinding

		POLYCOM system	CKP + ball mill system
Blaine specific surface area		3,200 cm^2/g	3,250 cm^2/g
Production rate	With pre-grinding	76.0 t/h	210.0 t/h
	Without pre-grinding	58.0 t/h	155.0 t/h
	Increasing rate	31.0 %	35.5 %
Specific electric power consumption	With pre-grinding	28.8 kwh/h	28.0 kwh/h
	Without pre-grinding	31.9 kwh/h	33.2 kwh/h
	Decreasing rate	9.7 %	15.7 %

Note; POLYCOM : Polysius pre-grinding roll press + ball mill system
CKP : Chichibu- KHI pre-grinding mill

that the crystal size of raw material ground in the planet mill is as small as 1/2 to 1/4 that ground in the ball mill and the lattice strain of it is increased, whereupon the sintering of clinker is terminated at 1300°C for ten minutes.

For generalizing this method, it is necessary to successfully construct a larger-sized mill, reduce the power consumption in the practical operation and demonstrate the superior economics and quality of product to the other sintering reaction -accelerating methods and the burning and grinding processes in the terms of energy consumption, because there are other methods including using a flux and a mineralizer for reducing the burning temperature of clinker and accelerating the sintering reaction and the electric power consumption of the planet and vibrating mills are higher than those of the ball and roller mills.

2.1.6 Introduction of computer-integrated manufacturing

The development and introduction of an automation system are being made using a computer, the artificial intelligence and the fuzzy theory for purposing the unmanned, stable operation of the process for manufacturing cement. Not only the computer control systems of the raw materials preparation and the grinding and burning process have recently been used but also the computer-integrated manufacturing (CIM)[11] involving the effective operation, plant maintenance and management controls are introduced for efficiently producing the products meeting the requirements of quality and cost and supplying it to the customers according to the production and delivery programs. CIM contributes to the modernization of the cement industry.

2.2 Energy Conservation by Minor Improvements of Process

2.2.1 Measure for energy saving

The consumption of the heat and electric power in Onoda Cement Co., Ltd. are illustrated in **Fig. 12** and **13**, respectively. The specific consumption of heat decreases from 3,260 KJ/kg of cement in 1981 to 3,010 KJ/kg of cement in 1990 and the ratio of the consumption of the industrial waste fuel to the total consumption of heat increases from 3.1 to 8.3 %, while the consumption of the electric power per ton of cement decreases from 110.5 to 100 kwh in that period of time. The measures taken for the energy saving for each process are listed in **Table 4**.

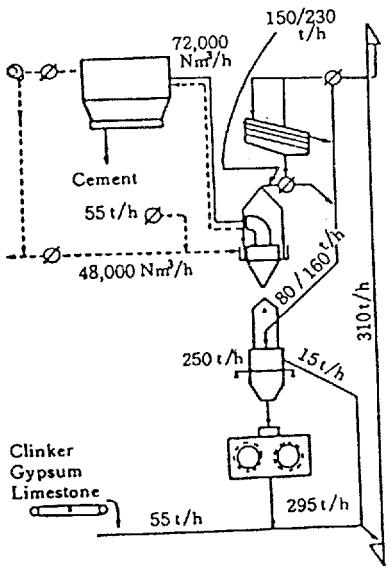

Fig.10 The latest roller press grinding system without ball mill

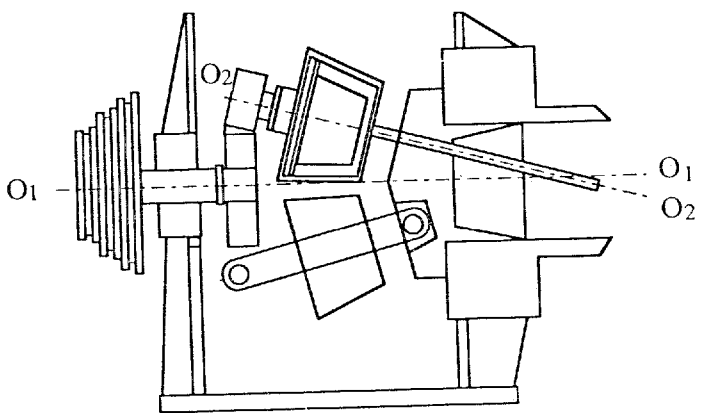

Fig.11 Planetary mill for researching mechanochemical process [9]

The consumption of heat has been reduced by the cumulative result obtained from minor improvement of the equipment and operation including the reduction of the carry-over latent and radiant heats of clinker and exhaust gas, the use of reactive raw materials, the stabilization of the operation and the use of industrial waste. In addition, the cost has been reduced by using inexpensive oil coke, though it is less combustible, as the fuel.

The consumption of electric power has been reduced in the raw material, burning and finish processes.

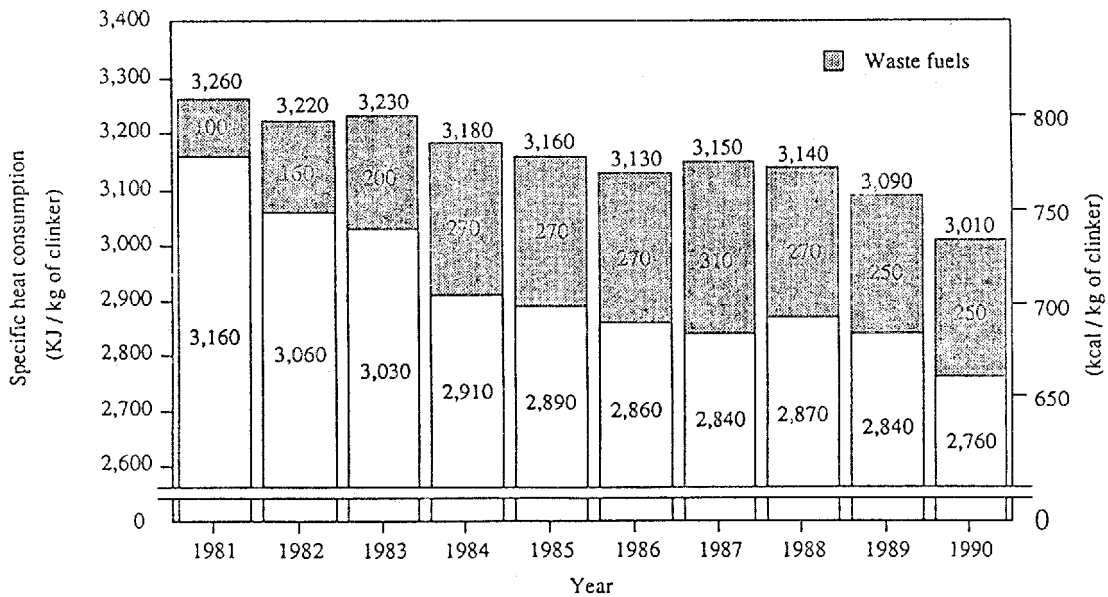

Fig.12 Change of specific heat consumption and amounts of industrial waste used for cement burning in Onoda in recent ten years

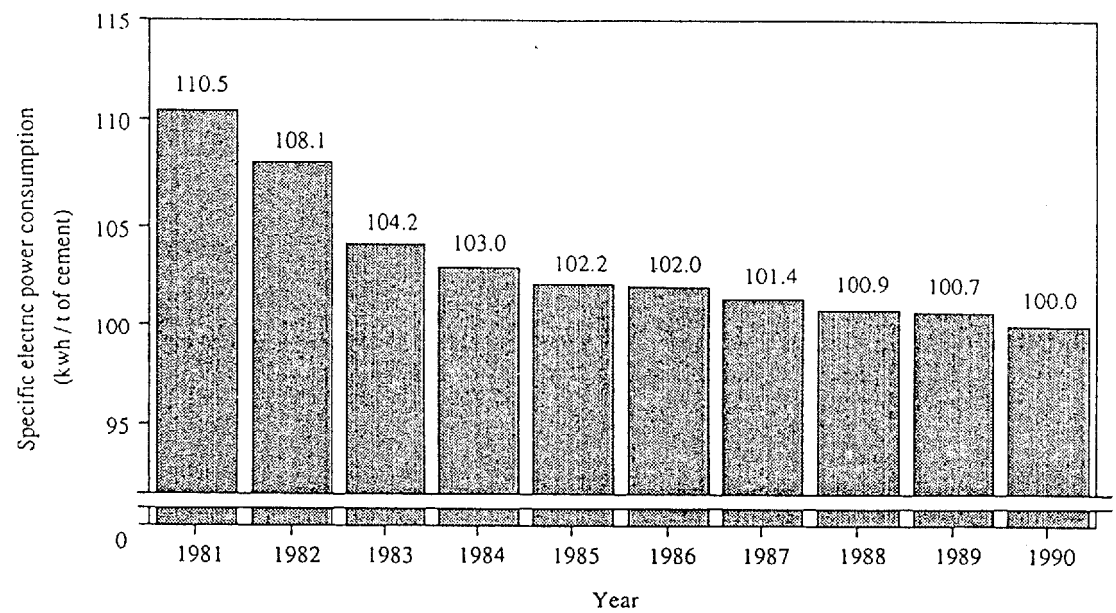

Fig.13 Change of specific electric power consumption of cement manufacturing in Onoda in recent ten years

Table 4 Measures for reducing specific heat and power consumption

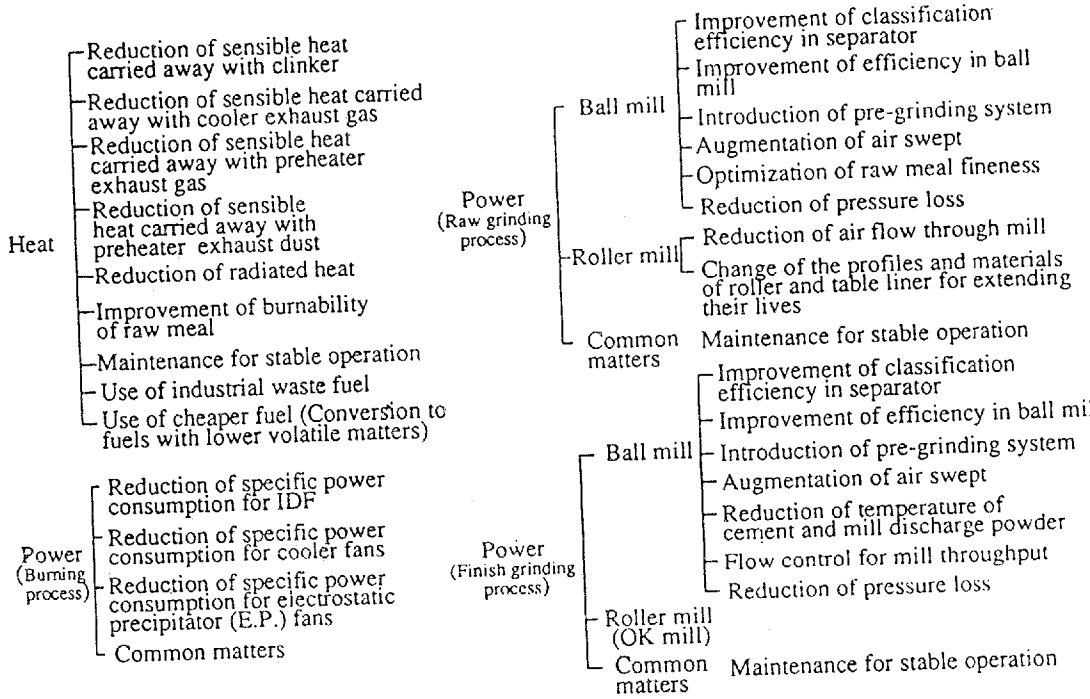

In the ball mill system in the raw material-grinding process, energy has been saved by introducing an high performance classifier, enhancing the classification efficiency by improving the selector blade in the classifier, improving the grinding efficiency by introducing new liners with higher ball-classifying and lifting functions including Magotteaux-Slegten, angular spiral and duo-lift liners, by improving the air-sweeping function and by changing the material for bag filter cloth, improving the shape of opening blade ring and reducing the flow rate of air passing through the mill by optimizing the external circulation. In the roller mill system, the grinding efficiency has been improved and the service life of mill has been lengthened by improving the shapes of the roller and table and changing the material of them. In addition to the mechanical improvement of equipment, the energy consumption has been reduced by changing the control level including the decrease of the fineness of kiln feed.

The consumption of electric power in the burning process has been mainly reduced in the induced fan (IDF), cooler fan and electrostatic precipitator (EP) by reducing the exhaust gas from the preheater, lowering the draft at the inlet of preheater, reducing the electric power consumed for IDF by employing the Scherbius system, optimizing the flow rate of air passing through the cooler, the capacity of the fan and flow rate of gas passing through EP, and reducing the electric power of fan.

In the finish process, the specific consumption of electric power has been reduced keeping the quality of cement unchanged by installing a control system of the passing through rate of powder in the mill, cooling the cyclone of the separator with water and lowering the cement temperature by water spray in second compartment in the mill.

2.2.2 Example of measures of energy saving

Some example of the measures for reducing the consumptions of heat and electric power are described hereafter.

2.2.2.1 Reduction of heat consumption

(1) Optimum brick arrangement

Various measures have been implemented to reduce the radiant heat from the shell of the rotary kiln

after commercial plant test. Then, bricks were arranged as illustrated in **Fig. 14** using insulating bricks 20 m from the end of kiln. As a result, the heat conductivity was decreased to 0.5 kcal/mh°C at 350 °C.

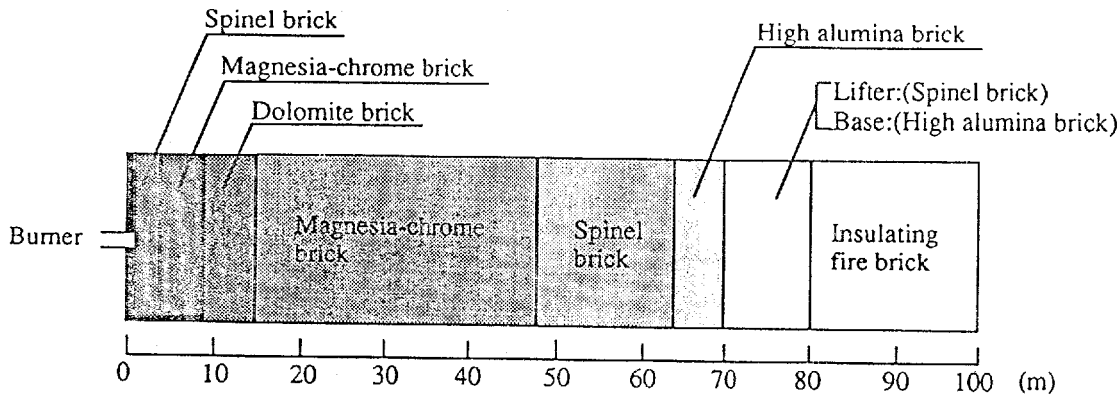

Insulating fire brick data

		SiO_2	Al_2O_3
Chemical composition	(%)	57	40
Refractoriness	(SK)	34	
Apparent porsity	(%)	40	
Bulk density	(-)	1.6	
Cold crushing strength	(kgf/cm^2)	150	
Thermal conductivity at 350 °C	(kcal / mh °C)	0.5	

Fig.14 An example of refractory and heat-insulating brick arrangement

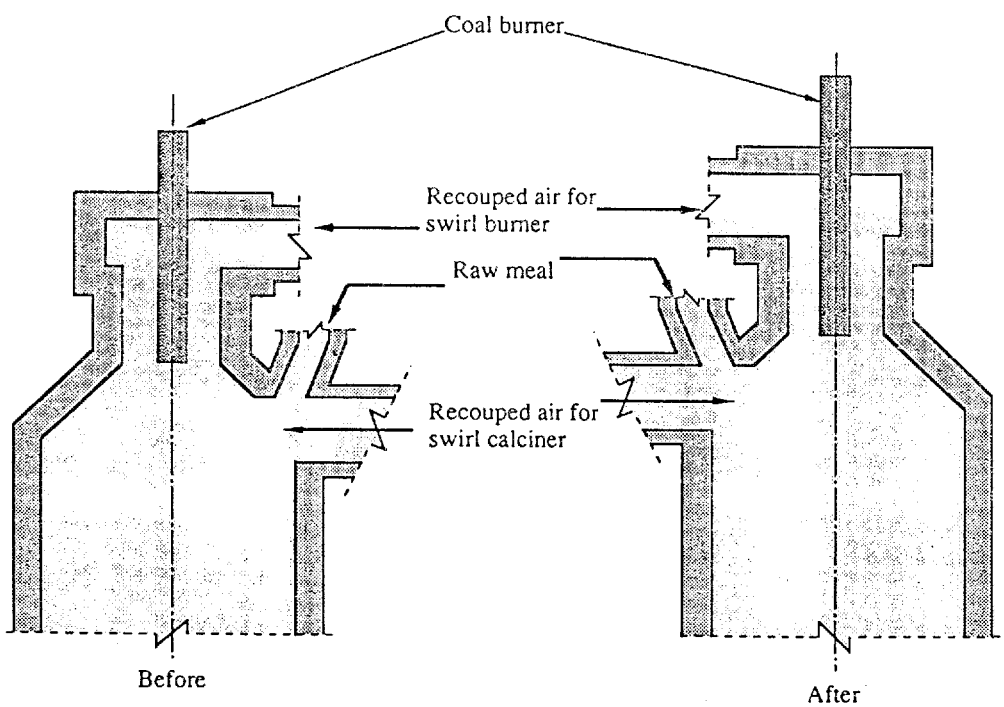

Fig.15 Improvement of precalciner

(2) Improvement of precalciner

The fuel has been rapidly converting from heavy oil to coal in around 1980 in Japan as shown in **Fig. 3**. In order to prevent the inside temperature dropping of the precalciner caused by the decrease of the combustion rate accompanied with the fuel conversion, the retention time of the feed was lengthened as shown in **Fig. 15** by injecting coal from the tangential line of the swirl burner of the precalciner for the suspension preheater and enlarging the sectional area of the air duct to the burner so as to increase the air volume by 15 to 20 % and the volume of the bottom combustion room as well. Thus the heat consumption was reduced by 34 to 42 KJ/Kg of cement (8 to 10 Kcal/kg of cement) by the improvement.

(3) Improvement of rotary kiln burning

The combustion rate of coal in a burner of the rotary kiln depends upon the uniform mixing of the finely ground coal with the primary air and the high-temperature secondary air coming from the cooler. Since most of the burners have such a structure that air-borne finely ground coal is injected between the straight flowing fresh air stream and the swirling internal air stream as illustrated in **Fig. 16**, the burner was improved so that the greater part of the high-temperature secondary air flowed directly into the center of flame by installing a fin dividing the air flow at the outlet of the fresh air. The mixing of the fuel with the air can be improved by further installing a spiral fin at the outlet of finely ground coal stream.

(4) Installation of double path to cooler

A double path was installed at the cooler to separately blow the air of 200 to 300°C discharged from the electrostatic precipitator for the exhaust gas of the cooler into the second and third compartments in the cooler for cooling the clinker as shown in **Fig. 17**. Since the temperature of secondary air was raised, the consumption of heat per kg of cement was reduced by 42 KJ or 10 Kcal.

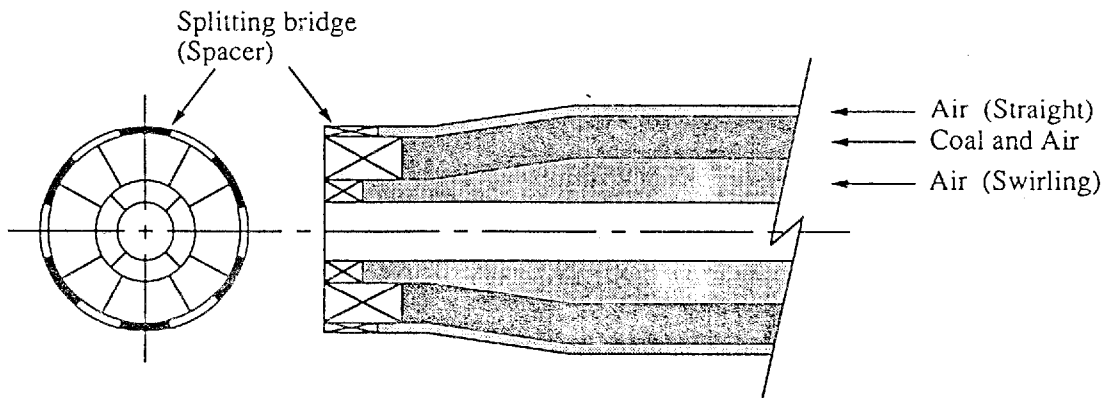

Fig.16 Mod ..ion of burner

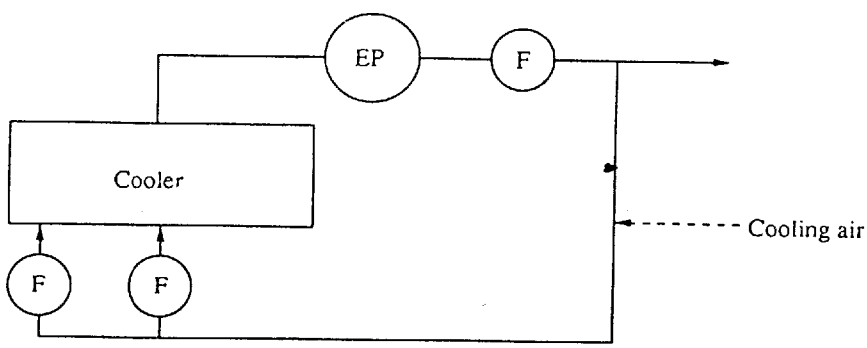

EP : Electric precipitater
F : Fan

Fig.17

Double path cooling system in cooler

(5) Cooler width control
The inclined cooler was reconstructed to be horizontal and the thickness of clinker bed was increased by decreasing the effective width at the inlet of clinker in the cooler to increase the heat recovered as the secondary air by preventing the channeling of the cooling air caused by the segregation of clinker as shown in **Fig. 18**. As a result, the consumption of heat per kg of cement was reduced by 82 KJ or 20 Kcal.

(6) Homogenizing and HM-reducing of kiln feed
The consumption of heat per kg of cement is increased by 29 KJ and the production rate of clinker is decreased by 1.4 to 1.7 t/hr with every 0.01 increase of HM. The consumption of heat per kg of cement is increased by 46KJ and the production rate of clinker is decreased by 2.6 t/hr with every 0.01 increase of standard deviation of HM(σ_{HM}). The strength of JIS mortar at the age of 7 and 28 days are decreased by 0.64 N/mm^2 (6.5 kg/cm^2) and 0.39 N/mm^2 (4.0 kg/cm^2), respectively, with every 0.01 decrease of HM. The composition of clinker is controlled in Onoda Cement Co., according to the standards shown in **Table 5** established from the actual results of operation.

2.2.2.2 Reduction of power consumption

(1) Reduction of pressure loss in suspension preheater
The suspension preheater was modified to reduce the pressure loss in it as shown in **Table 6**. A total of 300 mm Aq of the pressure loss or 1.5 kwh per ton of cement was reduced by repeatedly modifying the cyclone at each stage and the duct. Deposit is easily formed in the inlet duct of kiln, constrictions of duct and the chute of bottom cyclone shown in **Fig. 19**. In order to prevent the deposition, therefore, the inner walls of them were coated with anti-adhesion SiC castable refractory and the level of chorine content of the feed and coal was controlled to reduce to 150ppm as well as a total of 100 air blasters were installed there to remove the deposit by operating every 5 to 20 minutes.

(2) Decreasing fineness of kiln feed
Since the large SP kiln equipped with a precalciner with large heat load per sectional area and large production rate of clinker was developed, the heat transfer to the feed was remarkably improved. Even though the fineness of feed is considerably decreased, therefore, the sintering reaction of clinker can be proceeded easier than the conventional kiln. As a result, even the sintering temperature became possible to be decreased as shown in **Fig. 20**. The results obtained by repeating the laboratory and commercial plant tests taking the reactivity of feed into consideration indicate that the fineness of feed can be decreased from 12 % to 30 % as the residue over the 88 μm-water sieve or from 4 % to 10 % as the residue over the 200 μm-air jet sieve without deteriorating the quality of cement as shown in **Table 7**. When the ball mill is operated at the same capacity of kiln, the weight of balls can be reduced as much thereby decreasing the circulation ratio of ground material. The capacity of the transportation system was, therefore, optimized to reduce the electric power. Implementing those measures in the commercial plant, the grinding rate was able to be increased by 3 to 5 % reducing the consumption of power per ton of cement by 5 kwh.

(3) Optimization of particle size distribution of cement
The content of coarser particles 30 μm or over in cement was reduced by using an grinding aid, developing a high-performance classifier and applying the roller mill to the grinding of clinker as shown in **Fig. 21**. Since the content of the particles 5 μm or under is decreased and that of the particles 5 to 30 μm are increased so that a sharp particle size distribution is obtained and the n-value in the Rosin-Rammler's formula is increased.

Meanwhile, the volume of water required for keeping a constant fluidity increases with increasing the sharpness of the particle size distribution as shown in **Fig. 22**. Although high-strength can be developed from cement with sharp particle size distribution by the standard test made at the constant water cement ratio, the quantity of water required for obtaining the constant slump and flow of practical concrete needing appropriate workability and fluidity so much increases that setting of concrete is retarded and the strength is decreased.

In the practical operation, therefore, the power consumed in the grinding and classification required for producing the cement particles with the constant specific surface area is not minimized

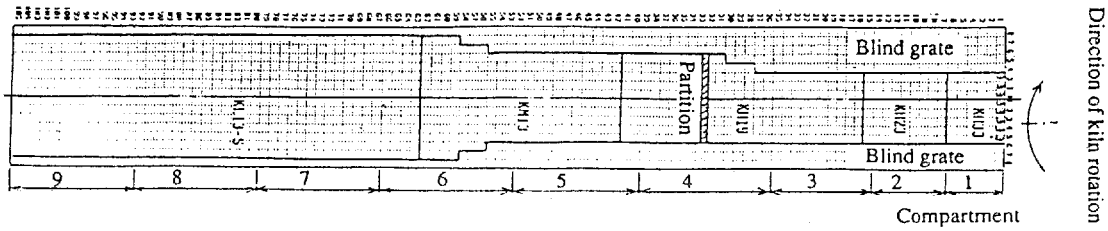

Fig.18 Cooler width control of horizontally set cooler

Table 5 Target level for homogenization of raw meal

	Mean or equipment for homogenization	Standard deviation of HM	Remark
Raw meal · Storage silo feed	On-line real time proportioning by computer control system with continuous on-line fluorescent x-ray analyzer	≤ 0.060	Standard deviation within a day
· Kiln feed	Air blending silo	≤ 0.025	Standard deviation within a month (by daily data)
Clinker		≤ 0.020	Standard deviation within a month (by daily data)

Table 6 Measures for reduction of pressure loss in preheater

Modification of cyclone and connecting duct	Reductions of pressure loss
(1) Cyclone 1 (bottom)	
a) Cyclone inner tube is removed	30-50 mmAq
b) Cyclone inlet duct is expanded	20-40 mmAq
c) Connecting duct 1 is expanded	50 mmAq
(2) Cyclone 2	
a) Cyclone inner tube is cut, and the diameter increased	20 mmAq
b) Straightening vanes are fitted in the cyclone inner tube	20-30 mmAq
c) Cyclone inlet duct is expanded	20-30 mmAq
d) Resistance plate is fitted in the cyclone	30-50 mmAq
e) Connecting duct 2 is expanded	20-50 mmAq
(3) Cyclone 3	
a) Cyclone inner tube is expanded, and straightening vanes fitted	30-40 mmAq
b) Resistance plate is fitted in the cyclone	50 mmAq
c) Connecting duct is expanded	20 mmAq
(4) Cyclone 4	
a) Straightening vanes are fitted in the cyclone inlet duct	10 mmAq
b) Straightening vanes are fitted in the cyclone inner tube	15 mmAq
c) Spiral cone is fitted under the cyclone inner tube	40-50 mmAq
Total	300 mmAq

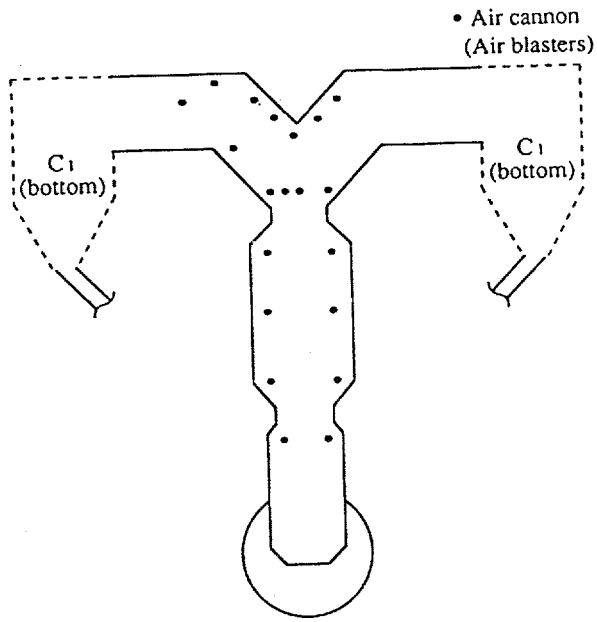

Number of air blaster	20	(this side)
	100	(total)
Cycle times	5 - 20	min.

Fig.19

Disposition of air blaster around the kiln inlet duct

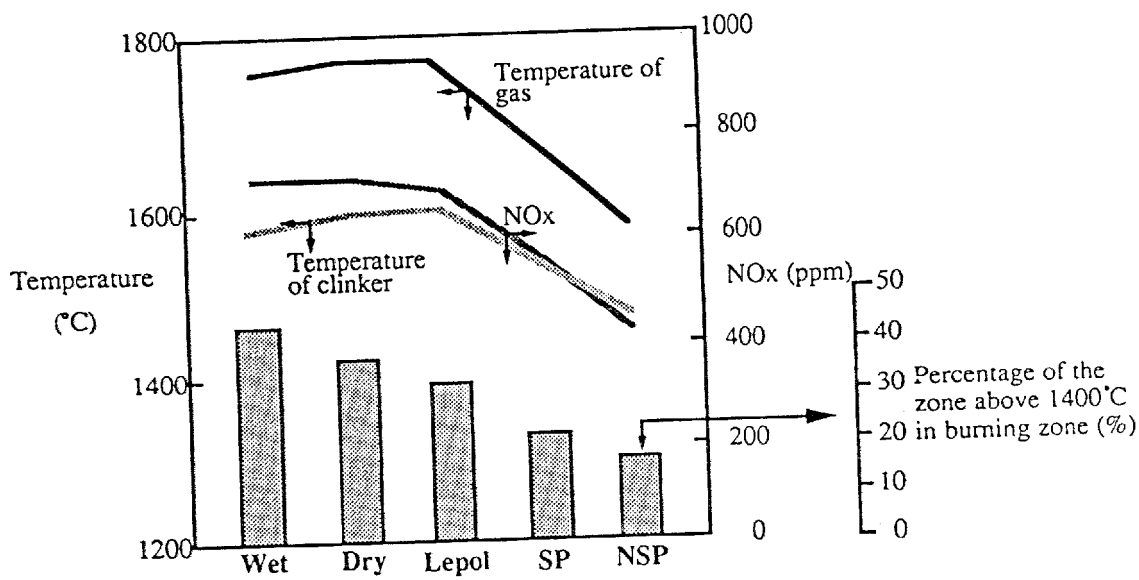

Fig.20 Temperature of clinker and gas, and amounts of NOx produced in burning zone in various types of kiln

but the cement with an appropriate particle size distribution of approximately 1.2 of n is produced though the power consumption is increased to some extent. The fineness and the particle size distribution of the cement meeting the requirements of the characters of clinker and the type of cement can be easily controlled by combining the control by changing the number of revolution and air flow of classifier and the control of circulation ratio in the grinding and classification systems.

Since the dehydration degree of gypsum is decreased and the state of it is changed by decreasing the temperature of mill in the grinding and classification systems using the high-performance classifier and roller mill, the workability and fluidity of concrete are affected by decreasing the temperature. Recently, therefore, an operation at a higher grinding temperature above the conventional concept has been carried out.

Table 7 Amount of free lime in clinker and 28 day strength of mortar with the change of raw meal fineness

Year	200μm R *1 (%)	Free lime (%)	28day compressive strength *2 (N/mm²)
1980	4.9	0.7	39.3 (385)
1981	6.0	0.7	40.6 (398)
1982	9.6	0.5	40.8 (400)
1983	11.4	0.6	41.3 (405)
1984	14.1	0.5	41.5 (407)
1985	14.5	0.6	40.9 (401)
1986	17.8	0.3	41.3 (405)
1987	13.8	0.6	42.0 (412)
1988	13.3	0.5	42.0 (412)
1989	13.3	0.5	42.2 (414)
1990	12.6	0.5	42.5 (417)
1991	10.8	0.7	43.8 (429)

Note; *1 : 200μm residue of raw meal measured by air jet sieve, *2 : Test data of JIS mortar, ( ) : Data expressed by kgf/cm²

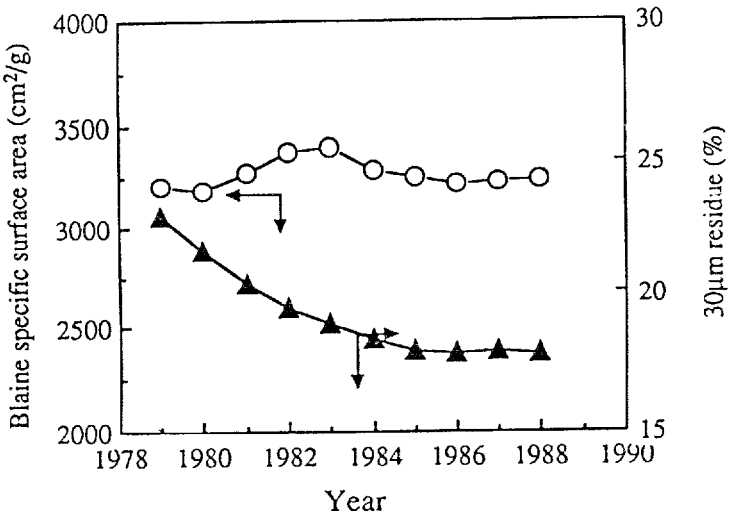

Fig.21

Blaine specific surface area and 30μm residue of cement

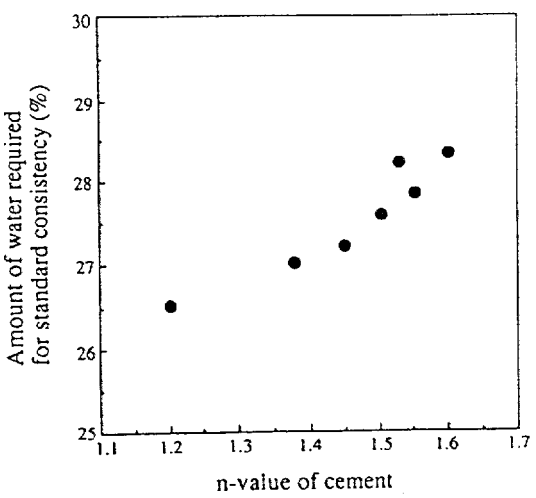

Fig.22

Relationship between n value

2.2.3 Shaft kiln

The shaft kiln spread in the 1960's because of low capital investment, low heat loss and high thermal efficiency. It has, however, shortcomings including insufficient sintering reaction of clinker, high content of residual free-lime and low quality of cement product because an appropriate heating and cooling temperature pattern can be hardly obtained in the sintering of clinker and an stable, high burning temperature can be hardly maintained. Since the shaft kiln has additional shortcomings of too much emissions of CO and dust to carry out a mass production of cement. It has also inferiority in the amounts of productions, labor productivity, heat and power consumptions, stability of operation, environmental pollution and quality of product to the latest facilities including the NSP kiln, its has disappeared in developed countries. There is, however, the potential local demand for the low-cost shaft kiln to manufacture lower grade cement for structures and general purposes in China, India and Australia.

The latest examples of the improvements in the shaft kiln include homogenizing the raw materials components, modernization of acceptance facilities of raw materials and coal, weighing, mixing, grinding and storing facilities, stabilization of the burning zone, increasing of burning temperature, reduction of the emission of dust and modernization of the finish-grinding process.

The stabilization of burning zone and the increasing of burning temperature by preventing the incomplete combustion will be attained by making a lot of air blowing duct with blowing holes at the circumference slightly below the burning zone of the shaft kiln as illustrated in **Fig. 23** to blow part of the air coming from the bottom of the kiln into poor-ventilation parts. The system is provided with valves operated by detecting the poor-ventilation parts from the temperature distribution in the burning zone.

The electrostatic precipitator and bag filter are unsuitable for collecting dust discharged from the shaft kiln considering the temperature, moisture content and composition of gas. A facility developed alternative to those facilities concurrently collects the dust and preheats the pellets composed of ground raw materials and coal with the exhaust gas passing through the bed of pellets to be supplied to the kiln as illustrated in **Fig. 24**. The heat and power consumptions are reduced by 10 % each and the content of dust in the exhaust gas is reduced to 1 / 10 or under. The content of free lime in clinker is reduced as low as 2.0 % or less as shown in **Table 8**.

Qin [12] of China presents in Communication Paper that clinker was produced by rapid burning with quantity of heat as low as 625 kcal / kg of clinker (2625 kJ / kg of clinker) which was surprisingly low value. Since the epoch-making improvement of shaft kiln is indispensable for rapidly burning clinker at high temperature, it is expected to release the technology for the progress of the cement industry.

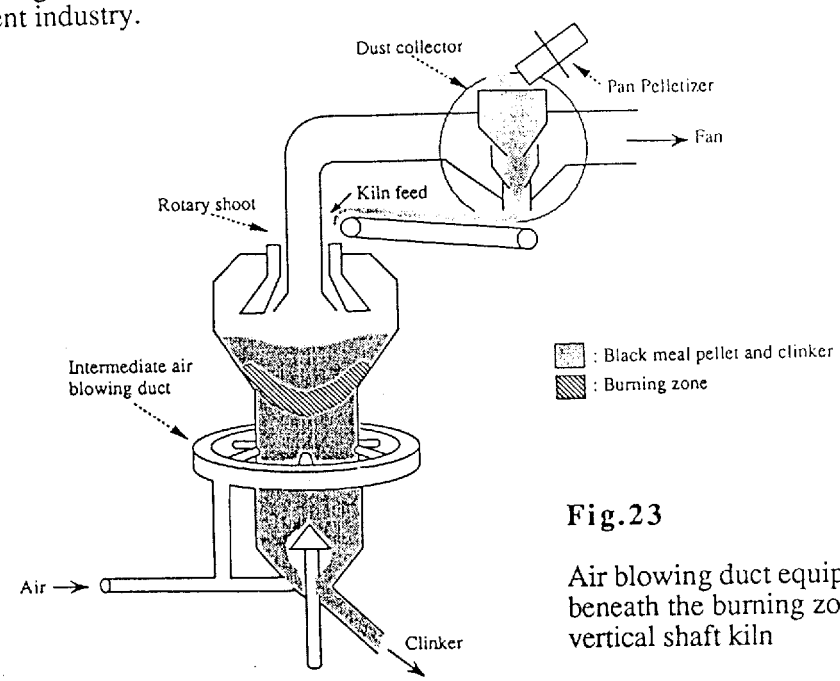

Fig.23

Air blowing duct equipped beneath the burning zone of vertical shaft kiln

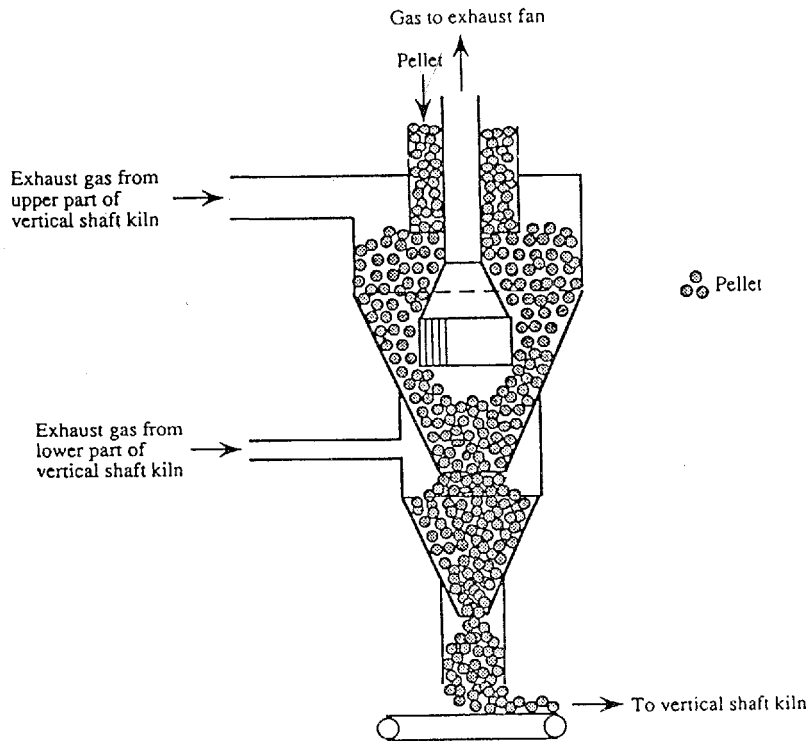

Fig.24 Dust collector for vertical shaft kiln (pellet filter)

Table 8 An example of operation data of vertical shaft kiln

	Improved kiln	Conventional kiln
Specific heat consumption (kJ/kg of clinker)	3,570 (850)	3,990-4,200 (950-1,000)
Specific electric power consumption (kwh/t of cement)	110	115-120
Amount of dust in exhaust gas (mg/Nm^3)	100	700-3,400

( ) : Data expressed by kcal/kg of clinker

Since the retention time of clinker in the cooling zone of the shaft kiln is as long as several hours and the clinker is cooled slowly, most of belite transforms into β and γ-form and the hydration reactivity is decreased. Therefore, the composition of raw meal fed to shaft kiln is designed to increase the quantity of alite and to decrease the quantity of belite, that is, about 0.95 of lime standard, 1.8 to 2.0 of SM and 1.2 to 1.6 of IM adding approximately 0.5 % each of fluorite and anhydrous gypsum as F and S. Raina et al. [13] of India stated that the clinker manufactured in the shaft kiln is low liter weight and porous and has high early strength and energy required for grinding is approximately 20 % lower than that of the clinker manufactured in the rotary kiln. The production of the porous clinker may be caused by the combustion of finely ground coal contained as much as 10 to 15 % in the raw meal pellets and the insufficient densification by the sintering due to the temperature at the burning zone as low as approximately 1300 °C. The high early strength may be attributed to the alite-rich composition. Although the lower electric power consumption may be caused by the decrease of tough-to-grind belite, a grinding method suitable for the pore structure of clinker should be selected for further reducing the grinding energy [14] because the crushability and grindability of clinker depends upon the pore structure as described in 2.1.3.

Ahluwalia et al.[15] of India states in Communication Paper that SM extremely affects the burnability and free-lime content in clinker and is related to the morphology of clinker minerals. It may safely be said that the result of Ahluwalia's study proves that SM is a determinant of the properties of clinker including quantity of melt, surface tension and viscosity and the reaction of alite formation.

3. APPLICATION OF INDUSTRIAL WASTE TO MANUFACTURING OF CEMENT

The quantities of industrial waste and municipal disposal have rapidly increased in recent years with the advances of the industries and the rise in the standard of living. It is necessary to prevent the environmental pollution including the air and water pollutions caused by the industrial activities and daily life. An urgent, important problem in the civilized society is to efficiently treat the industrial waste in conformity with strict regulations in Japan in the same way as in advanced countries.

Administrative agencies including local governments in Japan asked the cement industry for the use of the industrial waste as raw materials or fuels alternative to the natural resources to solve the above-mentioned problem. The cement industry started the development of the application technologies approximately ten years ago from the economical point of view by the manufacturing cost reduction of cement as well as from the social responsibility. Recently, the quantity of the industrial waste practically used for cement manufacturing has increased every year. The types and quantities of the main industrial waste are listed in **Table 9**.

The principles to be observed for using the industrial waste as part of the raw material or fuel for cement manufacturing are as follows:

(1) The industrial waste is more economical than conventional raw materials or fuels.
(2) The industrial waste does not detrimentally affect the quality of cement.
(3) The use of industrial waste does not cause environmental pollution.
(4) The industrial waste is stably supplied.

In order to keep those principles, therefore, it is necessary to closely and carefully make the technical and economical studies considering the existing technical power, the investment required for new equipment for treating the industrial waste and the environmental and emission regulations of harmful materials established by proper local governments. Communication Paper of Balwerk[16] in Germany is a superior reference judging from this point of view.

3.1 Establishment of Acceptance Inspection Standards and Application to Administrative Agency for Use

The acceptance inspection is made by analyzing the following items of the industrial waste at the

research laboratory in the proper company or an authorized inspection office including a certified environmental measurement office and by checking the data submitted by the supplier of industrial waste:

(1) Harmful elements including Hg, R-Hg, Cd, Pb, Cr^{+6}, As, CN^- and R-P and harmful substances including PCB,
(2) Smelly materials including H_2S, mercaptan and NH_3,
(3) Elements or substances detrimentally affecting the quality of cement including listed in **Table 12**,
(4) Elements alternative to the main elements including Si, Al, Fe and Ca and component alternative to heat value, and
(5) Moisture causing troubles in the operation by sticking raw materials or product in conveyors and chutes and consuming energy for drying, halogen elements including chlorine clogging the cyclone, chute and duct attached to the suspension preheater by producing low-melting point compounds at 800 to 1000 °C due to concentration during circulation in the gas, and extraneous matter including metal piece which may break the facilities for cement manufacturing.

Then, the data including the composition of exhaust gas, the contents of heavy metals and water-soluble harmful components contained in the raw material, clinker and dust and bad smell are collected by practically applying the industrial waste to the commercial plant.

Table 9 Kind and amount of industrial waste in Japan (1990)

Category	Kind of industrial waste	Amount of industrial waste (t)
Oil or solvent	Reclaimed oil, waste oil	141,347
Acid or alkali soil	Waste clay	37,892
	Others	3,000
	Subtotal	40,892
Rubber or plastics	Used tire	101,038
	Others	100
	Subtotal	101,138
Wood	Wood waste	6,670
Slag	Blast furnace slag	12,790,713
	Copper slag	1,232,726
	Molding sand	168,501
	Debris	1,600,476
	Others	230,884
	Subtotal	16,023,300
Ash	Coal ash	2,020,975
Sludge	Organic sludge	19,942
	Inorganic sludge	289,306
	Subtotal	309,248
Gypsum as by-product	Chemical gypsum	875,561
	Desulfurization gypsum	1,424,148
	Subtotal	2,299,709
Soot or dust	Dust	477,970
Others	Remainder of animal and plant origin	196
	Waste from construction	6,164
	Others	118,991
	Subtotal	125,351
Total		21,546,600

It is indispensable to establish the acceptance inspection standards of industrial waste by comprehensively investigating whether or not the acceptance, transportation, weighing and feeding of the industrial waste can be smoothly carried out and what facilities is additionally required if it is unable to be smoothly handled. An example of the acceptance inspection standards is shown in **Table 10**. Since industrial waste contains more or less harmful matter, the standards have to provide for the delivery method using a closed container including container bag and covered wagon to prevent the industrial waste from spreading in environment. The environmental and emission criteria of harmful matter for the prevention of environmental pollution in Japan are shown in **Table 11**.

The environmental data collected by using the industrial waste in the commercial plant have to be submitted to the competent local administrative office for obtaining the approval of the use of industrial waste.

3.2 Development of Application Technology and Investment in Equipment

Although the industrial waste meeting the requirements of the acceptance inspection standards is used in the processes shown in **Fig. 25**, some investment in equipment is required to smoothly continue the operation in each process. As indicated by Chatterjee et al [17] of India in Communication Paper, the greatest care has to be taken in the type, composition and properties in one type of it, particularly between different types of it.

The industrial wastes containing moisture and free from it are fed into the clay preparation system before the clay dryer and the process before the raw material grinding mill, respectively. For precisely controlling the composition of industrial waste, storage facilities and weighers by the types of industrial waste have to be newly installed. For properly preparing different types of industrial waste with diversified compositions and properties, on-line, real-time continuous analytical and control technologies and new analyzers and controllers based on them are required.

The industrial waste as fuel is fed into a kiln through the burner or from the end of kiln, into the precalciner for the suspension preheater directly or through the burner and into the process after gasification. The industrial waste commonly used as raw material and fuel is mixed with the natural raw material. Fine, high combustion rate wastes are fed from the kiln head at the same time as the feed of finely ground coal. Meanwhile, coarse, relatively fire-retardant particles including EP dust containing unburnt carbon produced in a thermal electric power plant are stored in a stockyard of oil coke and ground together with coal and feed with finely ground coal. Although waste tires are usually fed into the kiln from the end of it, they are sometimes gasified in a separate gasifier and the gas produced is blown into the precalciner. Oil waste is injected into the precalciner for the suspension preheater for the mixed combustion with finely ground coal. Smaller combustible solid waste than 1 in^3 including plastics waste and scrap wood is fed into the suspension preheater from the bottom through the drum mixer and the pressure constant feeder for suspension firing.

Development of combustion technologies and installation of equipment suitable for treating each type of industrial waste are required for implementing those plants. For instance, a conveyor, air-tight constant feeder and gasifier of waste tire have to be developed for using it, and the performances of the constant feeder, combustion rate controller and extraneous matter remover and the abrasion resistant of equipment have to be improved for using the industrial waste alternative to fuel. And technical development for preventing the reaction of NH_3 with SO_3 is required for using the EP dust discharged from the thermal electric power plant where the NOx in exhaust gas is reduced with ammonia. Since the whole plant has to be closed so that the industrial waste does not escape from it, investment in the reconstruction of the plant is required. The technical development and the investment in equipment have to be precisely investigated from balancing with the profits obtained by the reduction in the raw material and fuel cost and the benefits obtained from the reciprocal trade of industrial waste producers.

3.3 Expansion of Application Scope

Many types of industrial waste contain the components usable as the mineralizer and flux for cement as well as the main components. Active research and development are also required for

Table 10 An example of acceptance inspection standard of industrial waste

Name of industrial waste	Acceptance inspection standard of industrial waste	
	Quality and property	Type of packing and method of transportation to the plant
Waste tire	Car tire (any tire is accepted) Cut tire or tire without cutting	Bulk
Waste oil	Liquid or mud , Low volatile matter, Chlorine content < 1000ppm, Heat generation > 12.5 MJ/kg, Water < 20%	Tank lorry or Drum (Tank lorry is preferable)
Petroleum oil, Heavy oil, Naphtha, Unburnt dust	Water < 25% Heat generation > 12.5MJ/kg	Bulk vehicle with pressurized air unloader or container bag (Bulk vehicle is preferable)
Sludge	Water < 25% R_2O < 1% Chlorine < 100ppm	Bulk dump truck (Moisture control is essential to dusty waste)
Waste sand from cast iron process	SiO_2 > 75%, R_2O < 1% Water < 10% Without any foreign matter	
Waste wood, Waste plastics	Chlorine < 1000ppm Water < 10% Size < 250x250x250mm	Bulk dump truck or container bag
Coal ash, Evacuated waste from furnace	Chlorine < 100ppm R_2O < 1%	Bulk vehicle with pressurized air unloader
Aluminum sludge or aluminum ash	Al_2O_3 or Al > 60% Chlorine < 100ppm Water < 70%	Bulk vehicle with pressurized air unloader Bulk dump truck (Moisture control is essential to dusty waste)
Materials containing iron	Fe_2O_3 or Fe > 30% Chlorine < 100ppm Only small amount of metal such as Cr, etc. Powder, cotton-type or grindable material	Bulk dump truck or container bag

Other conditions : No bad odor, Content of harmful component (Hg, R-Hg, Cd, Pb, Cr^{6+}, As, CN, R-P or PCB) should be under the legal limit, No foreign matter such as metal, etc.

Table 11 Environmental and emission criteria for harmful components in Japan

Environmental criteria

Air

	SO_2	CO	Suspended dust	Oxidant	NO_2
Average *1	< 0.04ppm	< 10ppm	< 0.10mg/m^3	< 0.06ppm	< 0.06ppm
Maximum	< 0.1ppm *2	< 20ppm *3	< 0.20mg/m^3 *2		

*1: Average amount in a day, *2: Average amount for a hour, *3: Average amount for eight hours

Water

Cd	CN	O-P	Pb	Cr^{6+}	As	Hg	R-Hg	PCB
< 0.01ppm	nd	nd	< 0.1ppm	< 0.05ppm	< 0.05ppm	< 0.5ppb	nd	nd

nd: Not determined

Emission criteria for cement industry

Exhaust gas

- SOx SOx is regulated by K value
  $q = K He^2 \times 10^{-3}$
  q : Amount of SOx in exhaust gas (Nm^3/h)
  He : Equivalent height of chimney (m)
  K : Specified locally by government ranging from 1.75 to 17.5
- Soot < 0.1 g/Nm^3
  < 0.05 g/Nm^3 (Specified area)
- NOx < 250ppm (In case that the amount of exhaust gas exceeds 100,000Nm^3/hr)
  < 350ppm (In case that the amount of exhaust gas doesn't exceed 100,000Nm^3/hr)

Dust: Regulated according to the criteria regarding the structure, operation, use and control of the equipment

using such industrial waste. Pan [18] of China presents in Communication Paper that molybdenum residue produced in the treatment process of iron ores improves the early strength of cement because the formation of C_3S is accelerated by the decrease of the viscosity of liquid phase. Rajczyk et al.[19] of Poland present in Communication Paper that the Ba-containing waste produced in the manufacture of BaS so much lowers the sintering temperature of belite cement that the energy consumption is reduced. It is expected that those technologies will be demonstrated in commercial plant.

One of the useful methods for using variously reactive industrial waste containing diversified components as raw material is to improve the reactivity by pretreatment. Chatterjee et al. [20] of India present in Communication Paper that an application example of the sol-gel method for the sintering of advanced ceramics to the clinker burning using industrial waste, which may be used as the pretreatment mentioned above. However, attention must be paid to the cost performance .

3.4 Effect on quality of cement

The type of industrial waste and the elements contained in it are diversified. The contents of minor and trace components in commercially available types of cement in Japan are shown in **Table 12**. The minor components is defined as the components other than the four major components and the trace component is defined as the components contained as low as 0.1 % or 1000 ppm or less.

The effects of those components introduced in the cement-manufacturing process as the alternative raw materials and fuel on the operation and quality are listed in **Table 12**. Although some effects on the quality vary according to the papers, those which the author considered to be reasonable are listed.

Table 12 is put to practical use as the basic data for developing the acceptance inspection standards of industrial waste described in 3.1.

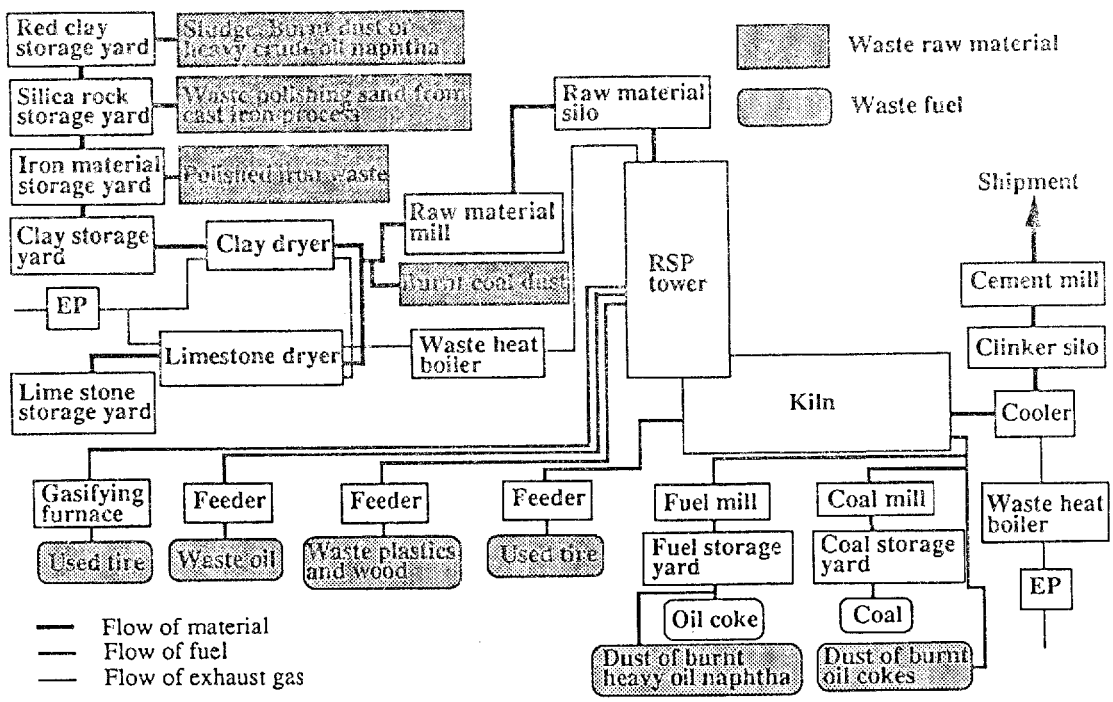

Fig.25 An example of the flowchart of industrial waste utilizing processes

Table 12 Influence of minor components on burnability of raw meal, manufacturing process and quality of cement

Element	Content	Volatile or non-volatile	Origin	Influence on human body	Regulation*1 W*2 (ppm)	Regulation*1 T*3 (ppm)	Influence on manufacturing process: Burnability	Influence on manufacturing process: Others	Influence on hydraulic reactivity	Influence on quality of cement: Setting	Strength: Early	Strength: Late	Others	Special remarks
Minor MgO	0.8-2.5%	non-v *4	limestone	harmless	—	—	• 1.0-1.5% ↑[1] • Max.=2.0% • >2.0% ↓[2,3]	• Gr. *5	in ad. amnt.*6[4] C_3S ↑		up[5]	down(>2%)	• problem in soundness[6]	Pericalse causes expansion
SO_3	0.2-0.9%	volatile	fuel, limestone	harmless, SO_x, harmful	—	—	the less, the better (<0.5%)	• Gr. • coating in Pr *7 and Kn*8 ↑[7,8]	C_2S ↑ C_3S ↓ C_3A ↓[9]	accel.*9	up	down(>0.5%)	• caution for A.A.R. *10	Alkali sulfate is easily formed
P_2O_5	0.11-0.34%	non-v	limestone	harmless	—	—	• 0.1-0.3% ↑ • Max.<0.5% • >0.5% ↓[10]	• coating in Pr ↓[8]	C_3S ↓	remarkably ret.*11 if soluble	up down	up down(>0.5%)[10]	(<0.5%)[10] (take care of p-gypsum *12)[11]	
Na_2O K_2O (R_2O)	0.1-0.5% 0.4-1.2% 0.4-1.0%	volatile volatile	clay clay	harmless harmless	— —	— —	• 0.2-0.4% ↑ • Max.<1.0% • >1.0% ↓[12]	• coating in Pr ↑[13]	in ad. amnt. C_3S ↑ C_2S ↑	accel. accel.	up up	down[14,15] down[14,15]	• A.A.R.[16] >0.6% of R_2O	Alkali sulfate is easily formed
TiO_2	0.2-0.6%	non-v	clay	harmless			• <1.0% ↑ • lower melt forming temperature[17]		in ad. amnt. C_3S ↑[4]	ret.[13]	up	undefinite[17,18] (<1.0%) many contradictory results on strength		
Trace Cl	30-80 ppm	volatile	coal	harmful HCl:harmful Cl_2:harmful			↑	• coating in P ↑ (>100ppm) • metal-corrosion ↑ • brick damage ↑	C_3A ↑	accel.	up	undefinite	• metal-corrosion (<300 g/m³ - concrete)	
Zn	280-590ppm	volatile	limestone	—			↑ • max.=1.5%[19]	• coating in P and Kn ↑[13]	C_3S ↓[4]	ret.[20]	down	down(>0.5%) (optimum: 700ppm[20])		Zn stablizes R-C_3S easily but hydraulic reactivity is low[4]
Cr	24-100ppm	non-v	brick, clay	Cr^{6+}: harmful			↓? no effect[18]	• coating in Kn ↑[13]	C_3S ↑[13]	accel.	up down	(<0.5%)[21] down(>0.5%)[10]		Cr^{6+} content become high in high temperature burning, cement color change to green[10]
Mn	170-350ppm	non-v					↑? flux effect[22]		C_3S ↑ C_2S ↑ C_3A ↑ C_4AF ↑		up down	down(<1/2 subst. *13)[23] down(>1/2 subst. *13)[23]		Cement color changes to green or blue[10], Strength at later age increases by 1% addition[24]
SrO BaO	900ppm	non-v	limestone						C_2S ↑[25] C_3A ↑		down down down down	down[13] down[26]		Lattice defect is decreased in Sr[13] bearing C_3S, Lattice distortion is decreased in Ba[26] bearing C_3S High in amount of substitution[13]
F	310-440ppm	l-vol *14					↑, Max.=2% • $C_3A \rightarrow C_{11}A_7$[27]	• coating in P and Kn ↑ (>0.3%)	C_3S ↑		up	up(<0.5%)[13]		Cost merit is ambiguous by using F as flux
Cd	1-28ppm	volatile		harmful	1.5	2.0								
As	17-25ppm	l-vol		harmful	3	10								
V	24-33ppm	l-vol		harmful										
Pb	81-174ppb	volatile	coal	harmful	1	100	no remarkable effect in the amount existed in cement			no effect				
Cu	70-180ppm	non-v		harmful										
Hg	119-148ppb	non-v		harmful	5ppb	500ppb								
Sb	24-36ppm	non-v		harmful										
NH_3				harmful						delay[11] (0.1%)	down[28]			
CN				harmful	1.5	3.0								

note; *1: Regulation for water pollution, *2: Water soluble amount, *3: Total amount, *4: Non-volatile, *5: Easy to be ground, *6: In adequate amount, *7: Preheater, *8: Kiln, *9: Accelerated, *10: Alkali-aggregate reaction, *11: Retarded, *12: Phosophogypsum, *13: Substitution for Fe_2O_3 in C_4AF, *14: A little volatile

References in this table are separately listed at the end of the paper expressed by the number with prefix T.

3.5 Example of Industrial Waste used for Cement Manufacturing

Since the quantity of industrial waste used for cement manufacturing in all the manufacturing plants in Japan is unavailable, the actual result in the main three plants of Onoda Cement Co. in FY1990 is listed in **Table 13** for reference. Twenty-six types of industrial waste delivered from 252 firms were annually consumed as 131,000 tons as fuel and 424,000 tons as raw material. Accordingly, 110,000 tons of coal and 382,000 tons of raw material were saved in year, namely, the fuel and raw material costs were reduced by 6.9 and 7.0 %, respectively. The investment in equipment reached, however, to 9.2 billion yen or 73.6 million US$ and the interest and depreciation expenses account for 130 % of the reduced cost assuming that the invested money will recovered in ten years, which will increase in the future.

3.6 Future Problem

In order to meet the requirements in the four principles for using industrial waste alternative to fuel and raw material and expedite the use of it, cement manufactures and industrial waste producers have to implement the following items by self-help:

(1) The measures to reduce the contents of harmful elements detrimentally affecting the environment, quality of cement and process for cement manufacturing to their tolerance limits or under,
(2) Development of application technologies of industrial waste
 ·Development of new types of cement using harmful elements as useful elements,
 ·Development of efficient dehydration and handling techniques for industrial waste with high content of water,
 ·Development of technique for homogenizing industrial waste with diversified contents and properties,
 ·Acceleration of labor saving and unmanned operation in the process using industrial waste
(3) Apportionment of cost caused by using industrial waste between the cement manufacturer and industrial waste producer.

Table 13 Utilized industrial waste in three major plants of Onoda (1990)

Plant	Kiln			Amount of industrial waste used (1,000t/y, dry base)			Amount of raw meal and fuel saved (1,000t/y)						Reduced cement manufacturing cost (%)	
	No.	Type	Capacity (t/d)	Fuel	Raw meal	Total	Coal	Clay	Silica sand	Lime stone	Iron material	Total	Fuel	Raw meal
Ofunato	1	RSP	3,000	0.5	82.0	82.5	0.4	45	16	12	1	74.4	1.9	2.6
	2	RSP	3,000											
	5	RSP	4,900											
	Total		10,900											
Fujiwara	4	RSP	2,500	70.3	149.1	219.4	69	82	29	21	2	203	17.1	13.2
	5	RSP	5,200											
	Total		7,700											
Tsukumi	3	RSP	3,800	42.3	193.3	235.6	41	106	38	27	3	215	5.0	8.2
	4	RSP	5,200											
	5	RSP	5,200											
	Total		14,200											
Sum. Total			32,800	113.1	424.4	537.5	110.4	233	83	60	6	492.4	6.9	7.0

It is estimated, however, that the use of industrial waste will be increased in the future for meeting the social demand as illustrated in **Fig. 26**, and that even the industrial waste which cannot be used at present due to the variable quality will be compelled to be used in the near future, whereupon the technical development cost and the investment in equipment will be increased to provide for using such industrial waste. A Principal Paper by Sprung of Germany and Delort of France [1] revealed that the heat required for a process is not necessarily reduced by using industrial waste alternative to the fuel. It is estimated that the cost including the interest and depreciation expenses for the investment in equipment will be higher than that without using the industrial waste in the near future. The following incentives to expediting the use of industrial waste meeting the social demand effectively using the resources and protecting the clean environment should be administratively employed in the future:

(4) Administrative guidance in the indication of chemical composition of industrial waste.
(5) Tax credits for technical development and investment to equipment to provide for using industrial waste.
(6) Financing the firms with low-interest funds.
(7) Financial assistance including subsidy.

The final treatment of municipal refuse and waste building materials as well as industrial waste is becoming an important social problem. Since the disposal of such massive refuse and waste gives increasing rise to financial and land-use difficulties, those incentives will become profitable.

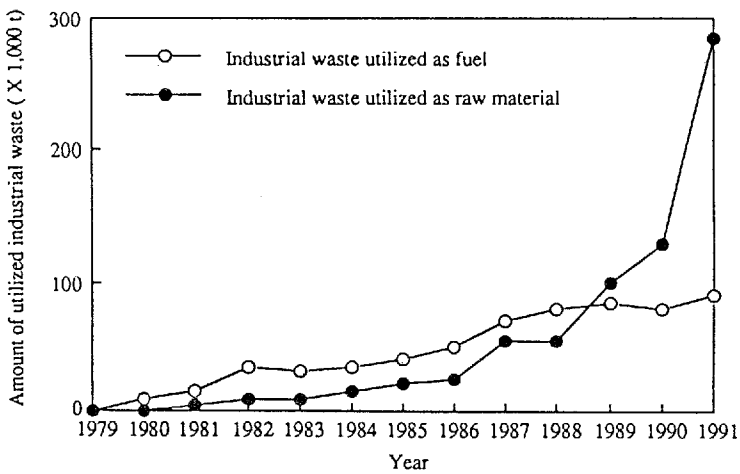

Fig.26

Amount of industrial waste used in Onoda's Fujiwara plant

4. DEVELOPMENT OF ENVIRONMENTAL LOAD-REDUCING CEMENT

The process for manufacturing cement has an intrinsical problem that a large quantity of CO_2 and too much NO_x for environment are emitted because a large quality of limestone is used as a raw material and the burning temperature is high. Accordingly, the reduction of the emissions of CO_2 requires the decrease of fuel and limestone consumption and the reduction of the emission of NOx requires the lowering of the burning temperature. For the reduction of fuel consumption requires the decrease of the unit consumption of limestone and the lowering of the burning temperature. Judging from this point of view, the changing of clinker composition and the improvement of blended cement have been implemented and the environmental load-reducing cement is being developed for saving resources and energy as well as for protecting environment.

4.1 Belite Cement

The changing of the clinker composition to the belite-rich type is required for the reduction of the unit consumption of limestone and the lowering of the burning temperature and meets the requirements of the development of low-hydration heat cement for mass concrete used for the

construction of giant structures on the increase in recent years.

The belite cement composed of 2 % of C_3A, 8 % of C_4AF and the rest of belite requires the limestone 90 kg/t of clinker less than ordinary portland cement, thereby decreasing the quantity of heat required for decarbonating the limestone by 149.5 kJ/kg of clinker (35.6 kcal/kg of clinker). Considering the increment of the heat of formation of clinker minerals as much as 139.9 kJ/kg of clinker (33.3 kcal/kg of clinker), the theoretical quantity of heat required for manufacturing belite cement clinker is 1512 kJ/kg of clinker (360 kcal/kg of clinker) which is approximately 16 % lower than that for ordinary portland cement clinker.

Assuming that the thermal efficiency of a large SP with precalciner kiln is 60 %, the quantity of heat required for burning belite cement clinker is 483 kJ/kg of clinker (115 kcal/kg of clinker) less than that for ordinary portland cement and the quantities of carbon dioxide derived from the raw meal and fuel are decreased by 40 and 60 kg/t of clinker (16 kg of coal/t of clinker), respectively, 100 kg/t of clinker in total, which accounts for 10 % of the total production of CO_2. Meanwhile, electric power consumption in grinding is a few kwh/t of clinker increased by using much amount of poor grindable silicious rock as the raw materials in the raw meal preparation process and several kwh/t of clinker increased by increasing the content of belite in clinker in finish grinding process. The quality of the belite cement varies according to the content of belite as shown in **Table 14**. The heat of hydration become low and the setting is delayed and the early strength is lowered with increasing the content of belite at the water cement ratio of 0.65 according to JIS.

The enhancement of the hydration reactivity of belite is investigated in an laboratory scale to improve the early strength of it. It is necessary to quench belite clinker at a rate of 800 °C/ min. or higher [21] or stabilize α– and α'- modifications of belite containing P, Na, K, V and S [22] having a high hydration reactivity at room temperature. The application of such super air quenching to the commercial equipment is, however, difficult and the water cooling by dropping clinker into water which is realized in the manufacturing white portland cement requires high cost for the heat recovery in the cooler and the drying of clinker. Even though the target crystalline modification of belite is stabilized at room temperature, the hydration reactivity is hardly improved by producing the solid solution containing those special components. Konznetsova et al.[23] of Russia describe in Communication Paper that the hydration reactivity is improved by the increasing of the dissolved amount of minor element to belite and lattice strain because the temperature of the raw meal partially replaced by carbon containing industrial waste is locally raised to approximately 2100 °C by the combustion of carbon in it. If the solubility limits of the components by the local temperature-raising at the high temperature, the keeping of it as the solid solution without deposition by the cooling and the relationship between the type and quantity of component species and the hydration reactivity will be demonstrated, this process will be accepted. Singh et al.[24] of India determined the thermodynamic constants and reaction rate constant from Jander's formula based on the study on the effect of the starting material species on the hydration reactivity of belite. And they state in Communication Paper that $Ca(NO_3)_2$ has a superior effect and that the hydration rate of β-C_2S produced is related to the lattice defect in the β-C_2S. This study will be feasible at a location where a large quantity of $Ca(NO_3)_2$ is available at a lower cost than limestone as the source of Ca. Although it is known that a little addition of Ba improves the hydration reactivity of belite, the study of Teoreanu et al.[25] of Rumania supports it, Yang et al.[26] of China described that β-C_2S obtained by heating hillebrandite, a hydrothermal reaction product, at 850 to 950 °C has so large specific surface area that the strengths at one and three day are equal to those for ordinary portland cement. There are still many problems to be solved till commercialization including the selection of the raw material appropriate for the hydrothermal synthesis, the installation of large-sized autoclave and a comparative study of the energy required for the hydrothermal synthesis with that for the conventional process.

Since the performance of the organic admixtures including superplasticizer and fluidizing agent has recently been improved, the workability of concrete at low water cement ratio is remarkably improved by combining the adjustment of the particle size distribution of cement with the addition of such an organic admixture. Since this procedure is effective for compensating insufficient properties of cement for preparing concrete, it is a practically valuable technique. The low early strength, the largest drawback of belite cement, is markedly improved by this technique as shown

in **Table 15**. The bonding strength between the belite cement paste and the aggregate is high and the final strength is high and stable, because the water cement ratio are so low that the precipitation of $Ca(OH)_2$ around aggregate by the hydration is repress and the transition zone is hardly formed in the vicinity of the aggregate. In Japan, recently, belite cement has been used for the mass concrete by making the best use of it and the use will be further extended in the future.

Table 14 Characters and properties of belite cement

Sample	Mineralogical composition (%)				Density (g/cm^3)	Fineness (Blaine specific surface area) (cm^2/g)
	C_3S	C_2S	C_3A	C_4AF		
A	43	45	2	10	3.16	3,300
B	30	58	2	10	3.17	3,310
C	21	67	2	10	3.17	3,280
D	10	80	2	8	3.18	3,320
E	0	90	2	8	3.19	3,310

Sample	Setting time			Heat of hydration (J/g)			JIS mortar strength (N/mm^2)			
	Water (%)	Initial set (h-m)	Final set (h-m)	7 days	28 days	91 days	3 days	7 days	28 days	91 days
A	27.7	2-10	4-00	245.6 (58.7)*1	314.6 (75.2)	357.7 (85.5)	10.8 (110)*2	15.9 (162)	38.7 (395)	55.7 (568)
B	27.7	2-55	5-25	206.7 (49.4)	269.0 (64.3)	327.2 (78.2)	9.7 (99)	13.1 (134)	35.3 (360)	62.8 (641)
C	27.7	3-15	6-10	186.6 (44.6)	250.2 (59.8)	320.5 (76.6)	6.7 (68)	9.5 (97)	31.4 (320)	61.9 (632)
D	27.5	4-05	7-55	101.7 (24.3)	222.2 (53.1)	294.6 (70.4)	0.8 (8)	1.1 (11)	12.3 (126)	52.1 (532)
E	27.5	5-10	9-30	77.4 (18.5)	173.6 (41.5)	270.3 (64.6)	0.5 (5)	0.8 (8)	19.6 (200)	53.2 (543)

*1 ( ) : Data explained by cal/g, *2 ( ) : Data explained by kgf/cm^2

Properties of concrete

Sample	Mix proportion (kg/m^3)				Slump (cm)	Air (%)	Strength (N/mm^2)			Adiabatic temperature rise of concrete at 28 days (°C)
	Water	Cement	Sand	Gravel			7 days	28 days	91 days	
A	158	300	797	1059	11.1	3.6	13.2 (135)	34.8 (355)	48.9 (499)	38.0
B					11.9	3.8	11.3 (115)	33.7 (344)	56.1 (572)	31.5
C					11.7	3.6	8.3 (85)	31.9 (326)	60.7 (619)	29.5
D					11.3	3.8	2.1 (21)	15.3 (156)	50.8 (519)	28.3
E					11.2	3.5	1.3 (13)	26.5 (207)	46.7 (477)	27.2

( ) : Data explained by kgf/cm^2

Table 15 Properties of belite cement concrete with low water/cement ratio

Mixing proportion

	Water (kg/m^3)	Cement (kg/m^3)			Sand (kg/m^3)	Coarse aggregate (kg/m^3)	W/C	Super plasticizer (%)
		Cement	Coarse particle*1	Fine particle*2				
1 Ordinary portland cement	200	400			790	869	0.50	
2 Belite cement C	140	400			871	951	0.35	0.7
3 Belite cement C	174	870			540	856	0.20	1.62
		609	174	87				

*1: Coarse particle of ordinary portland cement clinker ranging from 50 to 200μm
*2: Fine particle of calcite powder of which particle size is less than 3μm

Properties of concrete

	Air (%)	Slump (cm)	Slump flow (cm)	Compressive strength (N/mm^2)			
				3days	7days	28days	91days
1 Ordinary portland cement	4.7	18.5	—	15.0 (147)	23.5 (230)	35.6 (349)	40.5 (397)
2 Belite cement C	4.0	18	—	19.9 (195)	35.9 (352)	59.2 (584)	88.8 (868)
3 Belite cement C	2.8	22.0	45x46	58.1 (570)	72.9 (714)	110.9 (1087)	138.9 (1361)

( ): Data expressed by kgf/cm^2

4.2 Modified Belite Cement

In addition to the improvement of the hydration reactivity of belite for increasing the early strength of belite cement as mentioned in 4.1, the method for adding an early strength-developing mineral together with belite is being explored. The materials to be added include $C_4A_3\overline{S}$, $C_{11}A_7{\cdot}CaF_2$ and C_4AF which have rate of high hydration reaction and produce ettringite in the presence of calcium sulfate.

The modified belite cement containing those minerals together with belite can be burnt at a temperature 200 to 300 °C lower than ordinary portland cement. Since $CaSO_4$ and CaF_2 much contained in the raw meal of modified belite cement are converted into low melting point compounds in the burning process and these compounds are deposited on the cyclone, precalciner and duct of the suspension preheater and sometimes clog up them, this type of cement is not manufactured in the SP and SP with precalciner kilns but in an old type facility which is used for another reason that the market demand is low. The heat consumption is, therefore, not necessarily reduced though the burning temperature is low.

The facilities suitable for the raw material preparation and clinker-grinding processes should be developed and improved to reduce the quantity of heat consumed for manufacturing such a type of cement and the merits of manufacturing modified belite cement should be discussed comprehensively viewing from standpoints of the power consumption, product quality and environmental load.

4.2.1 Belite-sulfoaluminate cement

The belite-sulfoaluminate cement is mainly composed of belite and calcium sulfoaluminate. Since it is burnt at a temperature rage from 1200 to 1300 °C where belite and $C_4A_3\overline{S}$ ($3CaO{\cdot}3Al_2O_3{\cdot}CaSO_4$) can coexist, the belite burnt at this temperature is the ß-form (type II).

Boikova et al [27] of Russia presents in Communication Paper that the minerals produced other than belite vary according to the Al_2O_3/Fe_2O_3 ratio in the system $CaO\text{-}SiO_2\text{-}Al_2O_3\text{-}MgO\text{-}SO_3$, increasing $C_4A_3\overline{S}$ with the increase of IM, increasing the ferrite solid solution, C_6AF_2, with the decrease of IM and coexisting of $C_4A_3\overline{S}$ and the iron solid solution in the intermediate

composition. The result almost agrees with that for the $CaO-SiO_2-Al_2O_3-Fe_2O_3-MgO-CaSO_4-K_2SO_4$ system obtained by Kapralik et al [28].

Su et al [29] of China states in Communication Paper that clinker containing 55 to 75 % of $C_4A_3\overline{S}$ and 15 to 25 % of α -C_2S is produced from limestone, bauxite and anhydrous gypsum by burning at 1300 °C in a dry rotary kiln, rotary kiln equipped with shaft preheater and rotary kiln equipped with RSP and it is small porous particles with the bulk density of 650 to 850 g/l and that calcium sulfoaluminate in that clinker is a solid solution produced by substituting Mg for Ca, Si for Al and Ti for Fe and K_2O mainly supplied from bauxite produces a columnar alkali-containing phase which causes the flash setting and expansion exceeding a certain limit. Although the temperature of the gas entering into suspension preheater may be lower than that in the burning of ordinary portland cement, it is a success that the clogging trouble caused by the coating of raw material on the walls of SP and RSP sections was solved. It is expected that the data concerning the operational measures, heat and electric power consumption will be disclosed.

The belite-sulfoaluminate cement has not been developed and commercialized to save energy and improve the early strength of cement but to meet the requirements of the market in the terms of physical properties of cement in Japan[30]. The clinker is composed of 60 to 70 % of $C_4A_3\overline{S}$ and 30 to 40 % of belite. Since the blended cement manufactured by blending slag and gypsum to the clinker shows no breeding, compensates the shrinkage, hardly produces efflorescence and is of a low-alkaline, high-early-strength type, it is used for glass fiber reinforced concrete and precast concrete.

4.2.2 Belite-fluoroaluminate Cement

Jet cement or regulated set cement manufactured by adding 8 to 12 % of gypsum anhydride, a little gypsum hemihydrate, Na_2SO_4 and $CaCO_3$ so as to adjust the SO_3/Al_2O_3 ratio to 1.0 to 1.2 to the clinker composed of 55 to 60 % of alite, 5 to 10 % of belite, 20 to 25 % of $C_{11}A_7{\cdot}CaF_2$ and 4 to 8 % of C_4AF is on sale in Japan, China, Germany and U.S.A. [31].

Belite-fluoroaluminate cement is the cement in which alite is substituted for belite in the jet cement. Although the burning temperature of the clinker is approximately 150 °C lower than 1350 °C of the jet cement, the strengths at middle ages including 3- and 7- days ages are hardly increased.

Yang et al.[32] describes in Communication Paper that it is necessary to decrease the content of $CaSO_4$ in the raw materials to 1.0% or less for repressing the production of $C_4A_3\overline{S}$ and improve the hydration reactivity. The burning temperature of clinker is decreased to 950 to 1150°C by controlling the composition to contain 30 to 60% of C_6AF_2, 10 to 40 % of $C_{11}A_7{\cdot}CaF_2$ and 5 to 30% of $C_2\overline{S}$ and to increase the content of iron and using $CaSO_4$ as a flux.

The sintering reaction of clinker proceeds producing low melting point compounds at low temperature in high-alumina composition with more iron and CaF_2 and $CaSO_4$. However, when the melting phase in the clinker exceeds a certain limit, the raw material is deposited on the refractory lining of the rotary kiln and large lumps are formed. Therefore, it becomes impossible to continue the stable operation even if there is a slight variation of the burning temperature. The heat consumption is not reduced as expected from the lowering of the burning temperature and it exceeds sometimes that for ordinary portland cement. It is, therefore, desired to consider the measures for the actual operation taking those points into consideration.

4.3 Alinite Cement

Alinite cement was developed in Soviet Union in 1977[33]. The cement is produced by substituting alinite ($Ca_{9.9}Mg_{0.8}\square_{0.3}(SiO_4)_{3.4}(AlO_4)_{0.5}O_{1.9}Cl$, where $\square$=vacancy) for alite, $C_{11}A_7{\cdot}CaCl_2$ for C_3A, and adding several percent of gypsum dihydrate to clinker which contains 60 to 80% of alinite, 10 to 30 of belite, 5 to 10 % of $C_{11}A_7{\cdot}CaCl_2$ and 2 to 10 % of ferrite. The clinker contains 1.0 to 2.9 % of chlorine. The temperature range producing each mineral component is shown in **Fig. 27**. The figure reveals that the burning temperature is as low as 1000 to 1200 °C by flux effect of $CaCl_2$. Calcium chloride silicates considered to be produced in addition to alinite include $C_2S{\cdot}CaCl_2$. The hydration reactivity is high and the later strength is fairly lower though early strength is higher than that of ordinary portland cement. Although the early strength is increased

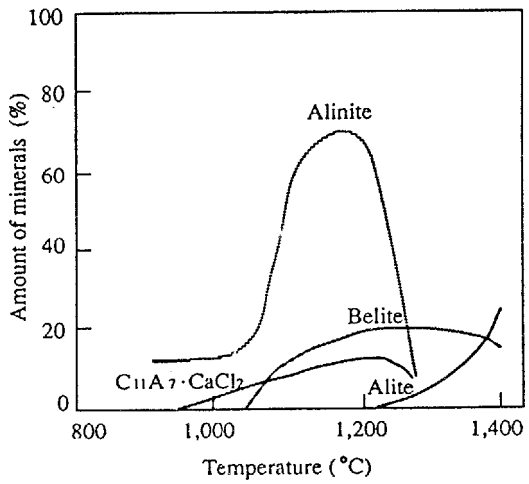

Fig.27

Temperature-phase relationship in the formation of alinite clinker

by increasing the contents of $C_{11}A_7 \cdot CaCl_2$ and gypsum, the stability is lowered. Part of Cl is fixed as a hydrate in the hydration process and the fixed chlorine is released again by the conversion and decomposition of hydrate. Since reinforcements and prestressing wires are remarkably corroded by the released chlorine, the alinite cement is used for the unreinforced concrete and foundation-improving material requiring for neither high-strength nor durability. Although more than ten years have passed since the alinite cement was developed, it is produced only in a 15t/d-miniplant located at Research-industrial Association Institute in the Republic Kazaf. Since the burning temperature of alinite cement is low and chlorine-containing industrial waste can be used as the raw material of the cement, attention has recently been paid to this cement. There are, however, still many problems awaiting solution in commercial production including the quality, corrosion of manufacturing equipment by chlorine, troubles caused by coating, recovery of chlorine from the exhaust gas, prevention of it from emitting to environment and accumulation of harmful elements contained in the industrial waste in clinker though the content of chlorine is limited as low as 2.5 % or less taking the quality of alinite cement into consideration. Attention is paid to the research by Ryzhik et al [5] of Russia on the application of the vortex reactor to the manufacturing of the alinite cement as a development of a facility for the cement.

4.4 Blended cement

Blended cement is a typical environmental load-reducing cement viewing from the standpoint of the manufacturing of cement. The characters, properties and performance of the blended cement have been elucidated by the research and development for a long time [34] and the manufacturing technologies and supply system have been established. Although the use of it is limited to mainly civil engineering works, the demand will continuously increase in the future.

Taking the opportunity of the 2nd oil crisis, the specification of portland cement were so revised in world nations that 5 to 10 % or less of particles including slag, fly ash and lime stone and so on are allowed t be contained in the portland cement besides clinker and gypsum. Although the deterioration of the physical properties including strength by addition of blending components are prevented by increasing HM of clinker. As mentioned in 2.2.2.1(5), the increase of HM generally increase the heat consumption and decrease the production and varies the electric power consumption by grinding blending components. Utilization of blending components to portland cement should, therefore, be done so as to minimized the loads on the environment and manufacturing cost referring above-mentioned facts.

5. CONCLUSIONS

In order to continue the further prosperity of the cement industry toward the next century in the unstable international-political and global-economical situations, it is indispensable to establish a production system pursuing the ultimate manufacturing cost, construct an international production

and distribution system, establish an international cooperative research system and buckle down to the protection of environment for assuring the healthy and comfortable life.

The resource- and energy-intensive cement industry is required to thoroughly save labor, resources and energy not only for the cost reduction but also the protection of environment, particularly to reduce the unit consumptions of fuel and limestone for reducing the emission of CO_2, to decrease the burning temperature for reducing the emission of NOx and play a role as the venous industry for cleaning the environment by using industrial waste and municipal refuse.

For implementing those measures in the actual manufacturing process of cement, it is important to develop a new process, improve the efficiencies of the current equipment and process, develop the technology, invest in equipment and establish the social system for using industrial waste alternative to raw material and fuel, establish reliable environmental- and quality-control systems and develop the environmental load-reducing cement.

This lecture introduced to the scientific and technological progresses of the above-mentioned items made since Rio de Janeiro Congress, pointed out the problems and described the author's view from the practical aspect. Since all of those problems are difficult to be solved, it is necessary for solving them and completing the technologies to put many hours in them, employ capable men, raise a lot of funds for research and development and invest in equipment for commercializing the results of research and development. Finally I would like to express my sincere expectation that breaking through conventional framework this New Delhi Congress will be the initial step to the advanced international research and technical cooperation toward the 21st century.

REFERENCES

1) S.Sprung and M.Delort; "Effect of Energy Conservation and Environmental Control Measures on Clinker Properties", 9ICCC, Principal Paper, Theme I, New Delhi (1992)
2) S.M.Cohen and W.E.Lindquist; "New Fluid Bed Process for Production of White Cement", Zement-Kalk-Gips, Vol.41, p.209-213 (1988)
3) M.Yagi, I.Hashimoto, T.Sekiwa and K.Mukai; "Pyro System of Fluidized Bed Reactor", in Japanese, The Cement Manufacturing Technology Symposium, No.46, p.7-12 (1989)
4) K.Sutoh and Z.Kawai; "Development of Fluidized Bed Reactor for Cement", in Japanese, Fuel and Combustion Engineering, Vol.54 No.6, p.1-9 (1987)
5) A.B.Ryzhik, M.V.Kougiya and A.V.Alexandrov; "Thermal Treatment of Cement Raw Materials Through Intensive Heat Exchange", 9ICCC, Communication Paper, Theme I, New Delhi (1992)
6) V.Johansen and T.V.Kouznetsova; "Clinker Formation and New Processes", 9ICCC, Principal Paper, Theme I, New Delhi (1992)
7) K.Schoenert; German Patent No.270853. 1 (1981)
8) G.R.Gouda; "Technical Aspects of Communication in the Cement Industry", World Cement Technology, Vol.12, p.112-122 (1981)
9) G.Jinbo; "Powder Technology in Soviet Union", in Japanese, Journal of the Society of Powder Technology, Vol.24(3), p.188-191 (1987)
10) L.M.Sulimenko; "Mechanoactivation of Portland Cement Raw Mixes", 9ICCC, Communication Paper, Theme I, New Delhi (1992)
11) H.Uchikawa; "The Future for Cement/Concrete in Japan - The Way to the Prosperity of Japanese Cement Industry through Self-Renewal -", Onoda Pacific Conference, Vol.2, p.Uchikawa 1-77, Sydney (1990) / Journal of Research of the Onoda Cement Company, Vol.42, No.122, p.1-62 (1990)
12) Z.G.Qin; "The Study and Application on High-Quality Cement Clinker Calcining with Low Heat Consumption in Shaft Kiln", 9ICCC, Communication Paper, Theme I, New Delhi (1992)
13) K.Raina and R.Bhargava; "Effect of Thermal Treatment on the Reactivity of Clinker Minerals Produced from Vertical Shaft Kiln", 9ICCC, Communication Paper, Theme I, New Delhi (1992)

14) H.Uchikawa; "Advances in Physico-Chemical Characterization and Quality Control Techniques for Cement and Concrete", 9ICCC, Principal Paper, Poster session, New Delhi (1992)
15) S.C.Ahluwalia and K.Raina; "Morphology and Microstructure Features of Clinker from Vertical Shaft Kiln", 9ICCC, Communication Paper, Theme I, New Delhi (1992)
16) R.Bolwerk; "The Reduction of Dioxin in Connection with the Use of Waste-Derived Fuels in the Cement Industry", 9ICCC, Communication Paper, Theme I, New Delhi (1992)
17) V.K.Gore, S.A.Khadilkar, P.G.Lele, C.H.Page and A.K.Chatterjee; "Conservation of Raw Material through Use of Industrial Wastes in Cement Manufacture", 9ICCC, Communication Paper, Theme I, New Delhi (1992)
18) Pan Yi Zhou; "Studies of Producing Portland Cement with Tailings of Molybdenum-Iron Ore", 9ICCC, Communication Paper, Theme I, New Delhi (1992)
19) K.Rajczyk and W.Nocun-Wczelik; "Studies of Belite Cement from Ba containing By-Product", 9ICCC, Communication Paper, Theme I, New Delhi (1992)
20) V.Varadarajan, C.H.Thombare, S.A.Borkar, C.H.Page and A.K.Chatterjee; "Experiences in Use of Industrial By-Product Sludge for Cement Manufacture by Sol-Gel Technology", 9ICCC, Communication Paper, Theme I, New Delhi (1992)
21) I.Mielke, A. Muiller and J.Stark; "Active Belite Cement", 9ICCC, Communication Paper, Theme I, New Delhi (1992)
22) F.M.Lea; "The Chemistry of Cement and Concrete", p.155, Edward Arnold (1970)
23) T.V.Kouznetsova, A.P.Osokin, V.G.Akimov and V.N.Panyuskin; "The Structure and Properties of Low-CaO contained Clinker", 9ICCC, Communication Paper, Theme I, New Delhi (1992)
24) N.B.Singh, S.P.Singh and A.K.Shukla; "Formation and Solid State Properties of ß-Dicalcium Silicate", 9ICCC, Communication Paper, Theme I, New Delhi (1992)
25) I.Teoreanu and E.Andronescu; "Orthosilicate Composition in CaO-SrO-BaO-SiO_2 System and Their Water Reactivity", 9ICCC, Communication Paper, Theme I, New Delhi (1992)
26) N. Yang, B. Zhong and Z. Wang; "An Active ß-Dicalcium Silicate Preparation and Hydration", 8ICCC, Communication Paper, Theme 2, Vol.III, p.28-33, Rio de Janeiro (1986)
27) A.I.Boikova, O.I.Fomicheva and L.V.Grishchenko; "Effect of SO_3 and MgO on Phase Relations and Crystal Chemical State of Phases in Belite-Aluminoferrite Clinker", 9ICCC, Communication Paper, Theme I, New Delhi (1992)
28) I.Kapralik and F.Hanic; "Phase Improvements in the System CaO-Al_2O_3-SiO_2-Fe_2O_3-MgO-$CaSO_4$-K_2SO_4 in Air up to 1300 °C referred to Sulphoaluminate Cement Clinker", Trans. J. Br. Ceram. Soc., 85, p.131-136 (1986)
29) M.Su, J.Deng, Z.Wu and X.Liu; "Research on the Chemical Composition and Microstructures ofSulpho-Aluminate Cement Clinker", 9ICCC, Communication Paper,Theme I (1992)
30) I.Uchida, T.Sohma and M.Tanaka; "Hydration and Alkalinity of the System Calcium silicate-Hauyne-Slag", CAJ Review of the 38th General Meeting, p.39-41 (1983)
31) H.Uchikawa and K.Kohno; "Ultra-rapid hardening cement (Jet Cement)", New Concrete Materials, Surrey University Press, England, p.70-136 (1983)
32) Y. Yang, W. Haung, G. Qian and Y. Qi; "The Influence of SO_3 in $C_2A_xF_{1-x}$ - $C_{11}A_7 \cdot CaF_2$ - C_2S System on Formation of $C_{11}A_7 \cdot CaF_2$", 9ICCC, Communication Paper, Theme I, New Delhi (1992)
33) B.I.Nudelman et al; U.S.S.R. Patent SU-2397380 (1977)
34) H.Uchikawa; "Effect of Blending Components on Hydration and Structure Formation", 8ICCC, Principal Paper, Theme 3, Vol.I, p.249-280, Rio de Janeiro (1986)

References of Table 12

T-1) H.Muller-Hesse, H.E.Schwiete; "Uber die Einlagerung von MgO in einige Zementklinker-mineralien", Zement-Kalk-Gips Vol.9, p.386-389 (1956)
T-2) M.Kristmain; "Portland cement clinker. Mineralogical and Chemical Investigation", Cem. Concr. Res., Vol.7, p.649-658 (1977)
T-3) E.Spohn, E.Woermann and D.Knofel; "A Refinement of the Lime Standard Formula",

5ICCC, Vol.I, p.172-179, Tokyo (1968), "Eine verfeinerte Kalkstandardformel", Zement-Kalk-Gips, Vol.22, p.55-60 (1969)
T-4) Y.Ono, T.Uno and Y.Soda; "The Mortar Strength of Each Polymorphic Form of Ca_3SiO_5", CAJ Review of the 20th General Meeting, p.53-57 (1966)
T-5) Y.Soda, K.Mizukami and M.Shirasaka; "On the Decline in the Development of the Strength of Portland Cement by the Increase of Magnesia", CAJ Review of the 32nd General Meeting, p.48-51 (1978)
T-6) K.Miyazawa and K.Tomita; "Der Einfluss von MgO auf die Eigenschaften des Portlandzementes", Zement-Kalk-Gips, Vol.19, p.82-85 (1967)
T-7) M.Amafuji and A.Tsumagari; "Formation of Double Salt in Cement Burning ", 5ICCC, Vol.I, p.136-156, Tokyo (1968)
T-8) H.M.Sylla; "Untersuchungen zur Buldung von Ansatzringen in Zementdrehofen", Zement-Kalk- Gips, Vol.27, p.499-508 (1974)
T-9) W.Gutt and M.A.Smith; "Studies of the Role of Calcium and Sulphate in the Manufacture of Portland Cement Clinker", Trans. Brit. Ceram. Soc. Vol.67, p.487-509 (1968)
T-10) K.Akatsu, K.Maeda and I.Ikeda; "The Effect of CrO_2 and P_2O_5 on the Strength and Color of Portland Cement Clinker", CAJ Review of the 24th General Meeting, p.20-23 (1979)
T-11) W.Lieber; "The Influence of Lead and Zinc Compounds on the Hydration of Portland Cement", 5ICCC, Vol.II, p.444-454, Tokyo (1968)
T-12) G.K.Moir and F.P.Glasser; "Mineralizers, Modifiers and Activators in the Clinkering Process", 9ICCC, Principal Paper, Theme I, New Delhi (1992)
T-13) R.Bucchi; "Influence of the nature and preparation of raw materials on the reactivity of raw mix", 7ICCC, Vol.I, p.I-1/3-1/41, Paris (1980)
T-14) B.Osbaeck; "Der Einfluss von Alkalien auf die Festigkeigenschaften von Portlandzement", Zement-Kalk-Gips, Vol.32, p.72-77 (1979)
T-15) J.Gebauer and M.Kristmann; "The influence of the composition of industrial clinker on cement and concrete properties", World. Cem. Technol., Vol.10, p.46-51 (1979)
T-16) K.Nakano and S.Nagano; "Some Properties of Cement Affecting Mortar-Linig by Centrifugal Force", CAJ Review of the 38nd General Meeting, p.88-91 (1984)
T-17) D.Knofel; "Beeinflussung einiger Eignschaften des Portlandzementklinkers und des Portlandzements durch TiO_2 ", Zement-Kalk-Gips, Vol.30, p.191-196 (1977)
T-18) D.Knofel; "Der Einbau von TiO_2 in die Phasen des Portlandzementklinkers", Zement-Kalk-Gips, Vol.32, p.35-40 (1979)
T-19) G.Xu, W.Huang, Z.Lu and G.Qian; "The Effect of ZnO on Burning of Portland Cement Clinker in Rapid Heating-Up Burning", 9ICCC, Communication Paper, Theme I, New Delhi (1992)
T-20) K.Akatsu, K.Ikawa and K.Maeda; "Some Effects of Zinc Oxide in the Raw Mix on the Portland Cement and Clinker", CAJ Review of the 22nd General Meeting, p.40-43 (1968)
T-21) T.Sakurai, T.Sato and A.Yoshinaga; "The Effect of Minor Components on the Early Hydraulic Activity of the Major Phases of Portland Cement Clinker", 5ICCC, Vol.I, p.300-321, Tokyo (1968)
T-22) V.Valkov, M.M.Sitchiov, L.Gigova and Yu.V.Nikiforov; "Common Influence of BaO and Mn_2O_3 on the Obtaining and the Properties of the Portland Cement", 7ICCC, Vol.II, p.I-95-98, Paris (1965)
T-23) K.Akatsu and I.Monna; "Effect of Mn on the Portland Cement Clinker and Cement", CAJ Review of the 20th General Meeting, Vol.20, p.41-45 (1966)
T-24) R.Parkash, S.C.Ahluwalia, N.K.Kathal and V.K.Mathur; "Role of Manganese on the Kinetics of Formation and Hydration of C_3S Phase", 9ICCC, Communication Paper, Theme I, New Delhi (1992)
T-25) K.Suzuki, S.Shibata and S.Ito; "The Hydration and the Strengths of High Temperature Phase of $2CaO{\cdot}SiO_2$ ", CAJ Review of the 32nd General Meeting, p.37-38 (1978)
T-26) Y.M.Butt, V.V.Timashev and V.E.Kaushanski; "Properties of Tricalcium Silicate and its Solid Solutions", Proc. 9th Conf. Silicate Ind. (Siliconf 1967) Budapest, 59 (1968)
T-27) J.A.Hedvall; "Einfuhrung in die Festkorperchemie", Vieweg u. Shon, Braunschweig. (1952)
T-28) C.Tashiro, K.Okuni and K.Mino; "Effect of Heavy Metal Oxides on the Hydration of C_3S and Microstructure of its Hardened Mortars", in Japanese, Semento-Gijutsu-Nenpo, Vol. 32, p.82-85 (1978)

ADVANCES IN PORTLAND CEMENTS AND UTILISATION OF INDUSTRIAL WASTES – TOWARDS SUSTAINABLE DEVELOPMENT

Dr A K Mullick

Director General
National Council for Cement and Building Materials

INTRODUCTION

We had the privilege of listening to the special lecture on "Present-day Problems in Cement Manufacture" yesterday; there is another presentation planned for tomorrow, covering performance aspects. Keeping these two presentations in view, I had to search for an area to focuss. After some considerations, I have chosen "**Advances in Portland Cements and Utilisation of Industrial Wastes - Towards Sustainable Development**" as the subject. We are talking of sustainable development which is aimed at meeting the material needs of present generations without compromising the ability of future generations to meet their needs (1). In this particular case, we have to dovetail the developments towards the search for low-waste and non-waste technology for cement to mitigate the increasing shortage of major resoures, ie, raw materials, energy and the environment.

From the deliberations of the last few days, it is clear that this Congress has identified the following as the main issues facing the cement and construction industries :

* cost reduction through energy and materials conservation;
* improvements in efficiency of operations;
* environmental protection; and
* improved performance in constructions.

Taken together, these form the key issues to sustainable development.

Although the issues are listed separately, in so far as development of cement systems and building materials are concerned, there is considerable overlap between them. In other words, more than one objective can indeed be achieved through one solution.

Invited Congress Reports as well as Communication Papers presented in Theme II on this topic have been taken into account in making this presentation, besides relevant information in the published literature and from the industry sources. Instead of elaborating on the scientific information at any great length, I will endeavour to examine the developments from the view point of adaptation by the cement manufacturing industry and the construction industry.

ENERGY AND MATERIAL RESOURCES

Cement manufacture is energy-intensive and therefore, reduction in thermal and electrical energy have always received considerable attention as will be reflected by the trend of energy consumption in different countries. What is shown in **Figs 1 and 2** is the trend in the Indian cement industry, which are the weighted average values for the whole industry and is influenced by the relative shares of wet and dry process plants at different points of time (2). It may be seen that the average values of specific thermal energy (in kCal/kg of clinker) and specific electrical energy (in kWh/tonne of cement) have progressively decreased as aided by various technological developments. The specific thermal energy has come down gradually with the switching over to dry process of cement manufacture, introduction of pre-heater and precalcinator systems, and adoption of modern million tonne plants. Further reductions have been possible with the adoption of six stage preheater systems, low pressure drop cyclones and kilns of smaller L/D ratio (**Fig 1**).

In case of specific electrical energy, it increased somewhat with the switchover to dry process plants, but again started declining as more and more efficient grinding systems were introduced in the industrial stream (**Fig 2**).

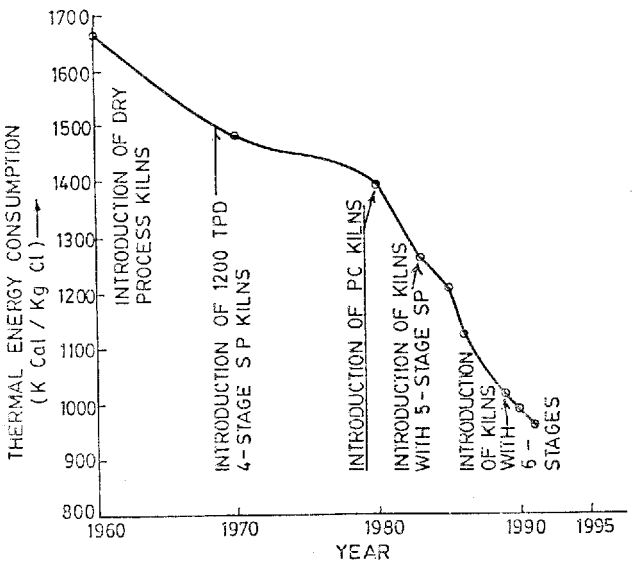

Fig 1

Trend of thermal energy consumption in cement manufacture in India (NCB data)

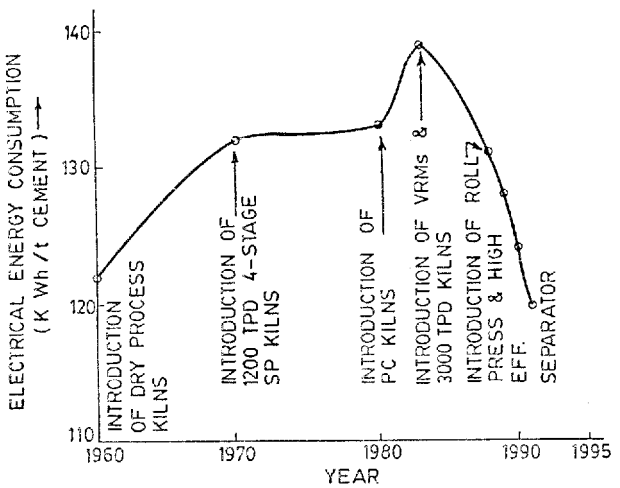

Fig 2

Trend of electrical energy consumption in cement manufacture in India (NCB data)

It is now believed that while further reduction in specific power consumption would still be possible with better grinding systems, reduction in specific thermal energy consumption can be effected only through improved plant operations and input of material science in the formulation of cement systems. The experience of a number of cement plants in India has shown that by adopting efficient operational practices and good housekeeping, unit energy consumption rate has steadily declined during the last few years (2,3). These include :

* Minimising false air infiltration in the Preheater-ESP-Raw Mill circuits;
* Process optimisation for improved combustion and increased cooler efficiency;
* Replacing higher rating motors by optimum rating and reducing idle running of equipment;
* Proper control of feed and product sizes to grinding mills;
* Rationalisation of compressed air utilisation;
* Introduction of slip power recovery systems for speed control on fan motors;
* Installation of high efficiency fans;
* Replacement of pneumatic conveying by mechanical transport like bucket elevators, belt conveyors etc;
* Providing variable speed drives and frequency controllers for fan drives.

Any large capital investments were not involved in bringing about the improvement.

Coming to the raw material scene, the total cement grade limestone deposits in India are estimated at 95,000 million tonnes. (**Fig 3**). The figure in itself is impressive, but once we realise that only 18 percent of it is in the "measured" category, and on the other hand, 27 percent of the total reserves are in the "marginal" grade, and lastly, major limestone deposits are concentrated only in a few States in the country, certain disquieting thoughts come in. For example, as a perspective for the 8th Five Year Plan period, it has been suggested that unit plant capacity should go up to 1.5 million tonnes, ie, 4500 tpd single line streams. But then it is found that limestone deposits which can sustain cement plants of this size are occurring only in such States, most of which are even now surplus in cement production over the demand (4).

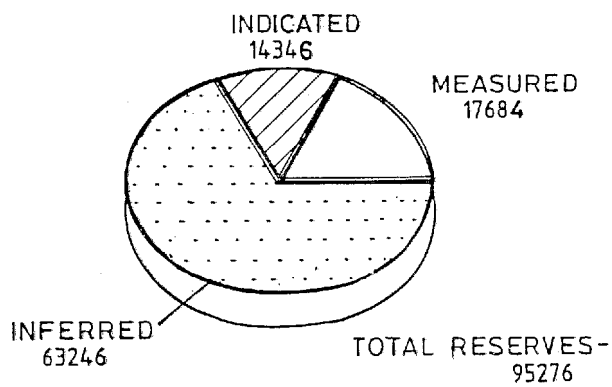

Fig 3

Estimates of cement grade limestone reserves in India (in million tonnes)

On the other hand, substantial quantities of wastes are generated in the country which has the same elemental compositions as the principal raw materials used in the manufacture of cement or other building materials. It is estimated (5) that the volume of various industrial, agricultural and urban wastes produced annually in India are :

Industrial, including Mining Wastes	250 m tonnes
Agricultural Wastes	500 m tonnes
Rural and Urban Wastes	1900 m tonnes

Exploitation of these wastes in the cement and building materials industries will achieve the purpose of raw material conservation as well as environmental improvement through wastes utilization.

Another problem unique to countries like India is, use of coal as fuel for cement manufacture, its high ash content and also the variable quality. This results in increasing coal consumption for cement manufacture, but then there is a limit of how much coal ash can be absorbed in the cement clinker. On the other hand, if the amount of coal fed as fuel is reduced because of ash content and requisite thermal energy is not provided, the temperature attained inside the kiln would be lower than required.

AVENUES FOR THERMAL ENERGY CONSERVATION IN CEMENT

As it has been mentioned above, the three approaches for energy conservation would be through improved plant and machinery, improved formulations for cement composition and improved plant operations. In so far as specific thermal energy consumption in cement manufacture is concerned, it is now believed that in modern dry process cement plants equipped with preheater-precalcinator systems, for saving in thermal energy, one has to fall back upon material science approach (6).

In the dry process of cement manufacture, the heat required is essentially for the dissociation of calcium carbonate in the raw mix and to heat the feed to the clinkering temperature of around 1450°C. In the wet process, further heat is required for drying out the moisture. We will not consider wet process technology in any great detail in this presentation. The strategy for lowering the thermal energy, would be through means of three possible steps :

(a) whether the dissociation of calcium carbonate as well as formation of clinker can be accomplished at relatively lower temperature, by use of activators as well as mineralisers and fluxes;

(b) whether the lime content in the raw mix can be reduced.

These two taken together, can be classified as approach to portland cements of lower clinkerisation temperature and for low-lime mixes.

(c) incorporation of latent hydraulic, pozzolanic or inert fillers in blended cements and composites, where the proportion of cement clinker is considerably reduced.

ADVANCES IN PORTLAND CEMENTS

A number of developments following the approach to lower clinkerisation temperature and low-lime mixes have been investigated in many countries in the world. Apart from conservation of energy and raw material resources, some of these systems also aim at improving the product performance. The approaches are tabulated in **Table 1** (7) and described below.

Mineralisers and Fluxes

If mineralisers and/or fluxes are used with normal cement raw-mix of LSF about 0.95, the clinkerisation temperature can be brought down from 1450° to around 1300°C. Mineralisers prompt formation of C_3S phase and fluxes lower the temperature at which the formation of liquid phase commences and also decrease the viscosity of the clinker melt (6). The line dividing these two functions are quite often thin.

Table 1

Cements of Lower Clinkering Temperatures

Sl No	Type	Clinkering Temp. °C	Main Clinkering Phases	Raw Materials
1	With Mineralisers	1300-1400		CaF_2 Fluorosilicates as Mineralisers
2	Active Belite	1250-1350	α' -C_2S C_3S C_3A C_4AF	Low Grade Limestone Clay, Shale etc
3	Belite Sulpho-Aluminate	1150-1250	β -C_2S $C_4A_3\bar{S}$ CA, $C_{11}A_7$	Low Grade Limestone Low Grade Bauxite Gypsum
4	Belite Sulpho-ferrite	1200-1250	β -C_2S C_4AF $C_4A_3\bar{S}$ $C\bar{S}$	Limestone, Gyupsum, Laterite, Iron Ore
5	Alinit	1100-1150	Alinite $2C_4S.CaCl_4$ $C_{11}A_7.CaCl_2$ $C_4AF.CaCl_2$	Limestone, Clay, Calcium Chloride
6	Low Temperature Cement	900-1150	$C_3S.CaF_2$ $C_{11}A_7.CaF_2$	Limestone, Clay, Bauxite, CaF_2

Fluorides and silico-fluorides are among the more common mineralisers which have been investigated along with gypsum as well as heavy metals like zinc, copper, cobalt etc (8,9). Improvements result from modifications in the mineralogy, morphology and microstructure of the main cement minerals. Entering into solid solution with main clinker minerals, these dopants can improve the strength characteristics, besides improving the burnability of the raw mix.

Although the clinkerisation temperature could be lowered by upto 150°C, the resultant energy saving is proportionately much less, because lower burning zone temperature also lowers the temperature of the waste heat that is recovered in the process. Although the heat losses of the kiln are reduced with less fuel energy input, there is always energy to be recovered from the clinker cooler and the net energy saving could only be of the order of 5 per cent (10).

In many situations it has been seen that this saving of energy does not compensate the cost of the mineraliser which has led to the use of the combination of mineralisers like fluorine and gypsum (11). The performance of mineralisers cannot be generalised, but would vary from case to case and control of mineralising effect

would sometime become difficult; problems of material flow may occur due to the volatiles and inhomogenity of dispersion of the mineralisers. If temperature reached inside the kiln is not controlled, melting may take place at the transition zone or even earlier and local damage to refractory take place. The kiln control, therefore, becomes more difficult and may lead to clinker ring formation if proper care is not taken.

Use of mineralisers should be viewed more as a necessity when the raw materials encountered are marginal and adequate burnability of the raw mix can be achieved only with the use of suitable mineralisers in some cases. It may also help in the coating formation of the refractories. In India, mineralisers have been used to encounter problems of marginal grade raw materials and coal of relatively lower calorific value (12). In addition, many commercial clinkers are found to have been inadvertantly mineralised by impurities in the industrial raw materials.

Low-lime Mixes

The effect of reducing the $CaCO_3$ content in the raw-mix on the theoretical energy required for clinkerisation is expressed in **Fig 4** (13). As a typical estimate, it has been stated that if the lime saturation factor of the raw mix decreases from 0.97 to 0.80, the reaction enthalpy of formation of cement clinker decreases from about 440 kCal/kg to about 390 kCal/kg, ie, a decrease of about 50 kCal/kg (6). Such lowering of lime factor means lower proportion of C_3S and higher proportion of C_2S phase in the clinker, and therefore the clinker formation can take place at a temperature lower than the usual (1450°C). Such a cement with high C_2S content will be relataively slower in gaining strength. Very rapid cooling of the clinker can stabilise the high temperature modifications of C_2S phase and the reactivity increased due to introduction of crystal defects. Such rapid cooling would mean higher heat losses in the clinker cooler and as a consequence the net saving in fuel energy becomes much smaller than from reaction enthalpy calculations. Higher percentage of C_2S phase, which is more harder to grind, may also increase the energy consumption in grinding and the net energy cost may not show appreciable difference. In addition, the cement may have to be ground finer, which also would increase the consumption of electrical energy (6).

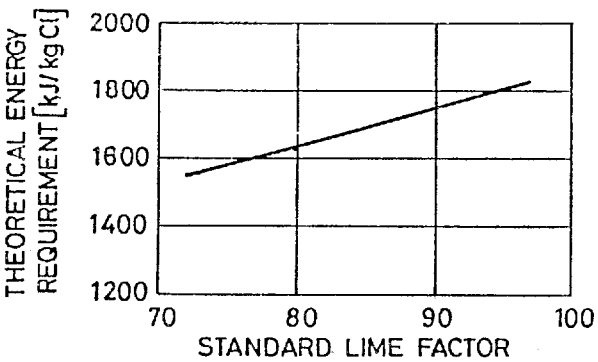

Fig 4

Influence of standard lime factor on theoritical energy requirement for cement manufacture (13)

As we will discuss later on, such cements having higher proportion of C_2S and therefore slower early strength, do not permit addition of significant quantity of slag or pozzolans in the manufacture of blended cements. The net effect of these developments would be that virtually there would be no energy saving.

The belite phase can also be activated in the presence of alkalis and other additives introduced in the raw mix (6). Such belite cements do often result when marginal grade limestones and low calorific value fuels are used, even when such

activation is not specifically planned. A cement plant is unlikely to have special arrangements for very rapid cooling for the clinker and grinding to higher fineness is, therefore, resorted.

Another approach, which would permit LSF in the raw-mixes even as low as 0.75, is in the formations containing sulpho-aluminate, ferrite and sulpho-ferrite phases (14,15). The strategy is to counter the slower strength development of C_2S phase with formation of ettringite by aluminate phases and sulphate ions. Referring to Table 1, one would notice one common feature being, near or total absence of C_3S phase. $C_4A_3\bar{S}$ - calcium slupho-aluminate is an important phase in these cements. As is well known, this phase is present in expansive cement, where initial expansion and strengths at early ages are due to formation of ettringite. Another phase which has received considerable attention is the compound $12CaO.7Al_2O_3$ ($C_{12}A_7$) which has the ultimate formula $C_{11}A_7.CaO_2$ in which the two oxygens atoms can be replaced with two fluorine or chromium atoms or two hydroxyl groups (16). Formation of derivatives of the type $C_{11}A_7.CX_n$ are alternative methods of stabilising the structure of $C_{12}A_7$, in which X is either F, Cl, S, SO_2 (16,17).

The compound $C_{11}A_7.CaX_2$ can be used independently or with gypsum and admixtures for giving quick setting formulations. Similarly, the ternary mixtures of OPC, HAC and gypsum allows early strength by formation of ettringite and expansion characteristics.

The cement based on $C_4A_3\bar{S}$ containing C_2S and free lime are prepared by burning a raw material containing SO_3/Al_2O_3 in a ratio of 1.3/1.9. The strengths of the order of 27 MPa at three hours and 59 MPa at 28 days was reported by Sudoh et al and as quoted in Ref 17. The same Ref 17 lists a high early strength formualtion based on $C_4A_3\bar{S}$, C_2S and $C\bar{S}$ which is obtained by burning a raw material ratio of SO_3/Al_2O_3 0.4/1.7 moles and C/A is equal to 0.5/1.2 moles to a temperature of 1200 to 1300°C. This is a high early strength cement having a strength of 15 to 24 MPa at four hours (17).

Alumina-belite cements typically contain 60 to 65 percent of β-C_2S and the clinker is formed at a temperature between 1250 and 1300°C. The cements are required to be ground to a fineness about 400 m^2/kg so as to result in compressive strength comparable to normal OPC. The early strength of such formulation is due more particularly to the formation of ettringite and calcium aluminate hydrates and usual calcium silicate hydrates (CSH) formed contribute only at a substantially later stage (6).

In the present Congress, considerable details of synthesis as well as structural details of $C_4A_3\bar{S}$ phase have been described. It has been reported that $C_4A_3\bar{S}$ could be synthesised from limestone, phospho-gypsum, and bauxite as raw materials at 1170°C (18). When blended with separately synthesised C_2S and CS, strength of the order of 18-31 MPa at 1 day and 37-42 MPa at 28 days were obtained. $C_4A_3\bar{S}$ phase can also contain upto 9 percent Fe_2O_3 in solid solution (19). A number of other additives like BaO, SrO, $CaCl_2$, TiO_2 ... were also found to enter into solid solution with $C_4A_3\bar{S}$ and modify the ettringite phase in the hydration process (20). Assimilation of MgO in C_3S phase suggested possible use of dolomitic limestone in manufacture of sulfoaluminate cement (21).

Cements containing sulphated calcium ferrites in C-F-$C\bar{S}$ system are reported to be commercially produced in Russia. The clinkering temperature is 1200 to 1300°C. These have expansive properties and develop compressive strength of the order of 80 MPa at 28 days (22). Mass production of quick setting and rapid hardening special

cements in the $C_{11}A_7.CaF_2$ - β C_2S system have been reported from China, which gave concrete strength of 25 MPa at 3 hours and 46-58 MPa at 28 days (23).

Mehta had described an iron oxide cement which consists on an average 35 percent of C_2S, 30 percent C_4AF, 20 percent $C_4A_3\bar{S}$, and 15 percent $CaSO_4$ can be burnt at 1200°C. At a fineness of 350 m^2/kg, the strengths are reported to be comparable to those of normal OPC (14).

Blends of OPC and High Alumina Cement and gypsum are often used for formulations of expansive cement systems. In India such a system has been widely used for grouting of heavy machinery foundations (**Fig 5**). The typical hydration products are CSH, ettringite and Calcium Hydroxide. The ettringite phase is quite stable even after long years in service (**Fig 6**) (24). Separate formation of $C_4A_3\bar{S}$ phase and then blending with OPC in 10-15 percent by weight has been reported. However, during the process of clinkering, $C_4A_3\bar{S}$ based cement, care must be taken to prevent the decomposition of $CaSO_4$ to obtain a suitable clinker and avoid SO_3 volatalisation (17).

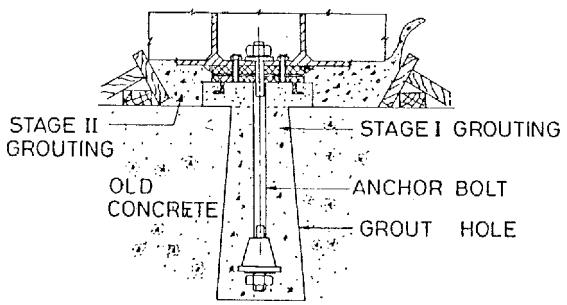

Fig 5

Typical arrangement for grouting machinery foundation with non-shrink grout (24)

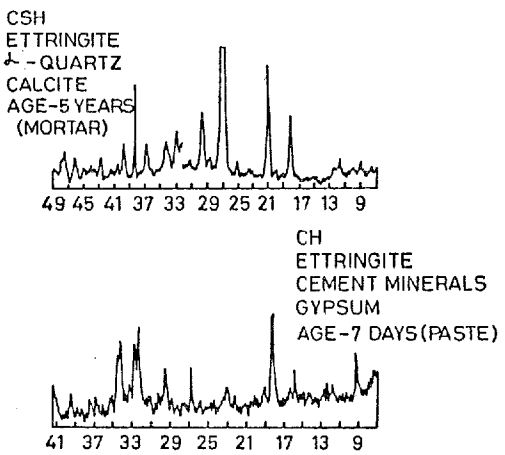

Fig 6

XRD patterns of CRI-NS Grout formulations (24)

Another formulation reported from India is of a fast setting high early strength on the basis of ettringite formation and accelerated CSH formation. In a typical shotcrete mix for tunnel lining, early setting time - up to two to five minutes, and compressive strength of 10 to 20 MPa in two hours was obtained. Rebound in placement was reduced. The hydration phases included ettringite, CSH, Calcium hydroxide, gypsum and ammonium sulphate hydrate (25).

Industrial Adaptation

While considerable laboratory research on various aspects of such modified portland cements has been reported, it must be admitted that it has not caught up on the industrial stream. As was pointed out, the net energy saving by lowering the clinkering temperature by 150 to 200°C is perhaps not more than 5 percent, which would not justify creation of separate cooling arrangements and additional cost of dispensation of the additives, their procurement, storage and handling. It is quite

unlikely that a large cement plant of capacity 3000 tonnes per day or more would be exclusively manufacturing such cements at least in the near future and therefore commercial application must be relegated to smaller capacity plants. Practical problems of pyroprocessing and kiln control that can accompany such formulations when the temperature of clinkerisation is not precisely controlled, as well as the interaction with the refractory system has not been reported.

While the hydration phase of these systems have been adequately reported, the resultant durability in constructions, specially for the inclusions in contact with the matrix, ie, aggregates or the reinforcements, have not been reported much in detail. It may be recalled that although commercial production of alinite cement, where the clinker formation takes place in a salt melt, was reported, its use in reinforced concrete has not been encouraged, due to the risk of reinforcement corrosion (6). On the other hand, desired performance characteristics like rapid setting or high early strength or expansion for compensation of shrinkage can always be obtained in the system of OPC/HAC/Gypsum and some accelerators (17,24).

Cement based on calcium aluminates are capable of rapid strength development and superior chemical resistance specially in sulphatic environment. Use of high alumina cement which imbibes all these properties are however not favoured for structural concrete because of progressive reduction in the strength of the concrete that takes place over the years due to conversion of hexoganal calcium aluminate hydrates to cubic hydrates, specially with increase of temperature and humidity. Significant research has been reported from BRE in England wherein blends of high alumina cement and granulated blast furnace slag have been found to give very satisfactory performance in terms of compressive strength in prolonged moist curing and of temperature up to 40°C (**Fig 7**) (26).

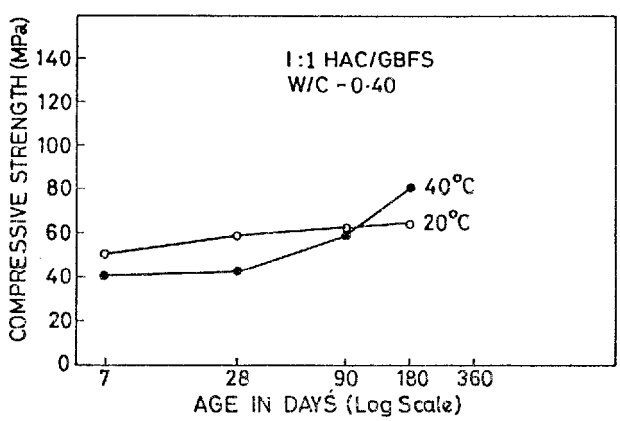

Fig 7

Compressive strength development of high alumina cement and granulated blast furnace slag mixes at 20°C and 40°C (26)

USE OF INDUSTRIAL WASTES AS RAW MATERIALS

Because of the similarity of main elemental composition between them, the various types of industrial wastes can be substitutes for naturally occurring raw materials in the manufacture of cement, as well as other binders and building materials (5). A list of various industrial wastes which can be used for cement and building materials industries, and their availability in India, are shown in **Table 2**. Considerable research and development work have been carried out in many countries on the techniques of utilisatiaon of such industrial wastes and the technologies are well established.

For the conservation of basic raw material in the manufacture of cement, use of flyash, lime sludges and red mud can be mentioned. Because of its substantial lime content, use of various sludges are more common. A summary of typical chemical composition of various sludges available in India, indicating $CaCO_3$ content as well as other impurities, which restrict their utilisation in cement manufacture, is shown in **Table 3** (5).

Table 2

Availability of Industrial Wastes for Building Materials in India

Sl No	Wastes	Source	Availability MT/annum
1	Flyash	Thermal Power Station	36.0
2	Blast Furnace Slag	Iron & Steel Industry	7.8
3	Lime Sludge	Paper, Sugar, Fertilizer Acetylene, Chromium Industry	6.0
4	Phospho-gypsum Fluo-gypsum	Production of Phosphoric acid, Hydrofluric acid	5.5
5	Red Mud	Aluminium Industry	2.0
6	Ferro alloy & other metal-lurgical slags	Ferrochrome, Ferro-manganese & Ferrosilicon alloys and smelting of zinc & copper, non-ferrous metal industry	10.0
7	Silica dust	Production of Silicon, Ferro silicon, Manganese silicon	very small
8	Kiln Dust	Cement Industry	5.0
9	Rice Husk	Rice shellers	40.0

Table 3

Chemical and Mineralogical Composition of Indian Lime Sludges from different industries

Constituents	Paper	Fertilizer	Acetylene	Sugar	Chromium	Soda Ash
LOI	35-40	34-38	25-30	40-50	20-35	32-35
CaO	45-50	45-50	60-70	42-50	35-40	44-48
Al_2O_3	2-5	0.3-0.5	1-3	2.0-2.5	3-5	1.5-3.0
Fe_2O_3	1-1.5	0.3-0.5	0.10-0.25	2.0-2.5	--	1-2
SiO_2	4-6	3-5	4-6	1.5-4.5	4-6	4-7
SO_4	--	8-10	0.2-0.3	1-2	--	--
P_2O_5	--	1.5-2.0	Traces	--	--	--
F^-	--	1-2	--	--	--	--
Cl^-	--	--	0.2	--	--	6-10
MgO	1.5-2.0	--	0.2-0.5	4-10	3-6	1-2
$Na_2O + K_2O$	0.5-1.5	--	0.02-0.20	1-2	1.0-1.8	--
Cr_2O_3	--	--	--	--	18-20	--
Major Phase	Calcite	Calcite	Calcium hydroxide	Calcite	Calcite	Calcite
Minor Phase	Quartz Silicate	Quartz Silicate	Quartz Silicate	Quartz Silicate	Chromite Ferrite	Quartz Silicate
Contami-nations	Alkalies	Phosphates Fluorides Ammonia	Alkalies Chloride	Organic matter	Chromium oxide Alkalies	Chloride

Press mud is obtained in India as waste from sugar industry, containing 45-50 percent moisture and 9-12 percent organic matter. After disposal, the sludge dries out in the field, and on a dry basis, has 18-20 percent organic matter and a lime content of 38-40 percent. Since the organic matter is light material, it has to be separated before grinding with the other raw materials, so as to enable its use as a part substitute to limestone.

Carbide sludge contains a high percentage of lime (56 percent) and chloride (0.46 percent). Because of the presence of chloride ions, it cannot be used in total substitution to limestone in cement manufacture in which the total chloride content is required to be restricted to 0.05 percent as per Indian Standard Specifications (5). Depending upon the chloride content in the carbide sludge, the content of sludge in the raw mix shall have to be limited. Rheological properties of raw mixes containing carbide sludge are also important. Taking into consideration the flowability and pumpability of cement raw meal slurry in a wet process plant about 30 percent sludge can be utilised. A 600 tpd commercial cement plant is in operation in India, using carbide sludge to partially substitute limestone.

Calcium carbonate sludge (phosphochalk) contains about 10 percent SO_3. A maximum of 10 percent phosphochalk can be substituted for limestone in the raw mix. Use of phosphochalk beyond 10 percent may not be favoured because of the presence of high SO_3, P_2O_5 and $\bar{F}$ contents (Table 3).

Red mud, a waste from the aluminium industry, contains high alumina and iron. Therefore use of red mud has to be restricted to keep the potential clinker liquid and the moduli values under control. Because of high percentage of R_2O_3 group of elements such as iron and aluminium (60-65 percent) a maximum of 8-10 percent red mud can be incorporated in the raw mix, where no clay is used. Use of red mud lowers the temperature of liquid formation by about 100-150°C.

Phospho gypsum is used as set controller for cement manufacture in partial replacement of mineral gypsum. Presence of impurities like P_2O_5 and F adversely affects performance of phospho gypsum unless these impurities are reduced by beneficiation (5). Use of flyash containing high SO_3 content has been suggested for set control, in place of gypsum (27).

A general problem of use of waste lime sludges is that the moisture content in the filtered cake is 35 to 50 percent. In case of slurry the solid content is 5 to 10 percent. Both handling and transportation of wet sludges and pre-drying before use are required. For handling and transportation of phosphogypsum, systems are required both at the fertiliser and the cement plants. At the fertiliser plant, the phosphogypsum slurry from the pond can be pumped by conventional slurry pumps to the washing system. Washed slurry is fed to either filter press or centrifuge or to sun-drying. The dried phosphogypsum is required to be transported to the cement plant in bulk.

Use of flyash as a raw material for cement manufacture is not common in India because of lack of plastic properties (for wet process) and volatalisation of sulphates and alkalis in dry process plants, which may lead to ring formation. Variability in the composition of flyash will render control of raw meal composition difficult. In any case, high ash coal used as fuel in India does not enable any silicious addition in the raw mix in large dosages. However, instances of use of flyash, blast furnace slag and phosphogypsum for manufacture of special cements containing $C_4A_3\bar{S}$ phase has been suggested. It has been pointed out that impurities

present in such industry-derived material can reduce the temperature of synthesis of $C_4A_3\bar{S}$ from 1350 to 1170°C (18).

INDUSTRIAL WASTES AS ADDITIVES IN BLENDED CEMENTS

A number of latently hydraulic, pozzolanic or inert fillers can be used as additions to blended cements or as mineral admixtures in concrete, with granulated blast furnace slag and flyash (also called pulverised fuel ash) leading the way. A classification of such additives is given in **Table 4** (28). The basis of reactivity of such mineral additions and the chemistry of hydration with cements are too well known to be repeated (27). We may summarise that hydration reactions of slags can be activated in presence of lime, typically derived from the hydration of cement.

Table 4

Classification of Additives

Classification	Industrial Waste
Cementitious	Rapidly-cooled blast furnace slag
Cementitious and Pozzolanic	High-calcium fly ash (>10% CaO)
Highly Pozzolanic	a) Condensed silica fume b) Rice husk ash produced by controlled incineration
Normal Pozzolanic	Low-calcium flyash (<10% CaO)
Others	Air-cooled blast furnace slag

In case of pozzolans like flyash, cementitious products are formed in combination with lime and in presence of moisture, as in hydration when blended with ordinary portland cement. The hydraulicity of blast furnace slags and pozzolanicity of fly ash etc depends upon its chemical composition, mineralogy and fineness and particle size distribution, and therefore experiences in different countries may not match in a quantitative sense. For example, Indian slags, although containing 90 to 95 percent glassy phase, are characterised by relatively lower lime content and higher alumina content. The glass content in Indian flyashes are only 30 to 35 percent and the lime content is low. The pozzolanicity, therefore, is considerably lower, compared to other flyashes with much higher glass content or with high lime content (5).

From basic considerations it would appear that a blend of 70 to 80 percent ground granulated blast furnace slag with adequate hydraulicity can be activated with lime liberated by the hydration of say 20 to 30 percent cement. However, from practical considerations of relative grindability of slags and clinker as well as the need of fulfilling the requirements of strength specifications at early ages (3, 7 and 28 days) at par with ordinary portland cement, the slag content in commercial cements in India are much lower. To a large extent, the same situation exists in case of portland pozzolana cements where pozzolana like flyash or calcined clay are interground with cement clinker. The fineness of the blended cement to which it has to be ground as well as the pozzolana percentage are arrived at by trials with the cement clinker.

A typical trial is as shown in **Table 5.** Although cement specifications in India permit addition up to 25 percent pozzolans in blended cement, the usual proportion seldom exceeds 15 percent, lest the initial strength of the blend would be lower and may create marketing problems (29).

Table 5
Results of Typical Trials to Optimise Flyash Content in PPC

Trial No	Sample	Flyash %	Fineness M^2/kg	Compressive Strength, MPa		
				3d	7d	28d
1	OPC-Control	-	299	21.6	28.5	55.0
2	PPC-1	10	318	21.1	25.8	52.8
3	PPC-2	15	306	20.3	23.9	49.7
4	PPC-3	20	310	19.1	22.3	47.6
5	PPC-4	25	305	17.8	20.2	44.7
6	PPC-3	20	310	19.1	22.3	47.6
7	PPC-3A	20	345	21.6	27.5	50.0
8	PPC-3B	20	392	23.1	30.7	51.0

The relative merits of whether it is more advisable to use the mineral admixtures in manufacture of blended cements in the cement plants rather than mixed with cement and other components of concrete in the mixer at the construction site has often been debated. The preferred practice in any country depends upon the historical development of the industry. While the chemical reactions in the final concrete mix may be the same, there are intrinsic differences in the amount of additions that can be made. For blended cements whose performance requirements including early age strength are to be at par with ordinary portland cement, would quite often not permit larger additions as would be permissible in a concrete mix, where the strength of the mix can be specified as per the site requirements and even at a much later age, eg 90 days or even one year in case of concrete dams. On the other hand, manufacture of blended cements at the plant is claimed to ensure better quality control and thorough blending of the cement and the additive.

Many advantages claimed of blended cements can be realised only with prolonged moist curing. Longer duration of moist curing and delayed form removal in structural concrete are necessitated due to slower rate of gain of strength upto, say, 28 days, for which the concrete mixes are customarily designed. Other parameters remaining the same, the compressive strength of concrete is generally related to strength of cements as in standard mortar tests. Because of lower early age strength, mineral additions may increase the volume of cement produced but not necessarily the volume of concrete made with it. Advantages of blended cements should thus be searched in the realm of improved durability.

It must be recalled that blended cements like portland slag cement and portland pozzolana cement were intended to render specific engineering properties to the blend like low heat of hydration, increased sulphate resistance etc. Adequate reactivity of the slag and flyash to be blended is, therefore, essential. Present-

day trend in UK is to further process the flyash by classification techniques, which result in uniformity in grain-size distribution (30). There is considerable data reported on the durability of concrete when either slag or flyash are incorporated (31,32,33,34). Most significant improvements are reported in the case of increase to corrosion resistance (**Figs 8,9,10**) as well as alleviating alkali silica reaction (**Figs 11,12**).. Similar results of improved durability has also been reported in case of high-volume low-calcium flyash concrete (35). Improved sulphate resistance can result in portland slag cements, if the slag percentage is very high; otherwise it would essentially depend upon the C_3A content in the parent cement (36).

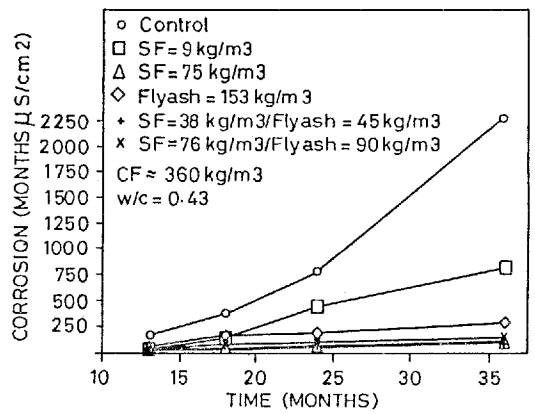

Fig 8

Influence of silica fume and flyash additions on total corrosion of reinforcement in concrete exposed to 3% NaCl solution (31)

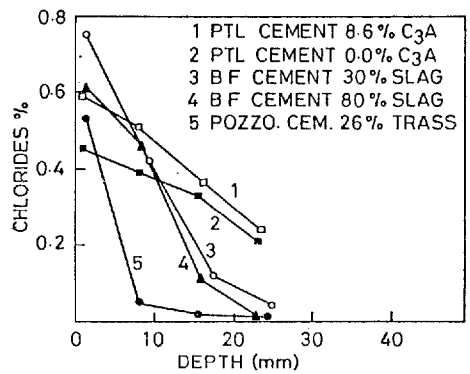

Fig 9

Effect of the cement type on the amount of chloride ion penetration after six months exposure to sea water (32)

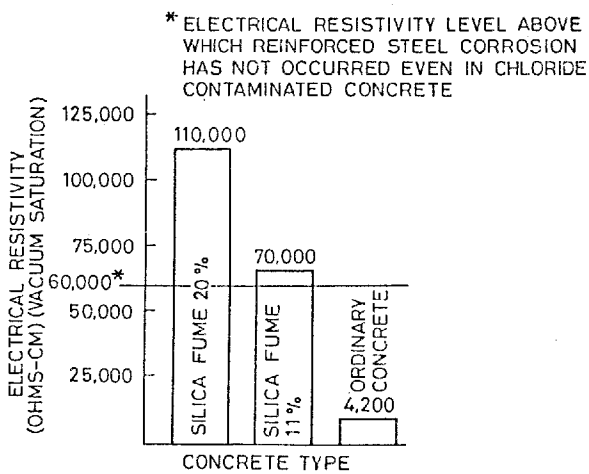

Fig 10

Effect of incorporation of silica fume on the electrical resistivity of concrete (33)

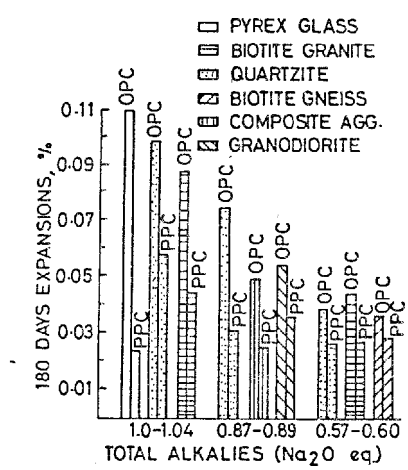

Fig 11

Comparative performance of Ordinary Portland Cement (OPC) and Portland Pozzolana Cement (PPC) on mortar bar expansion tests for ASR with reactive aggregates (34)

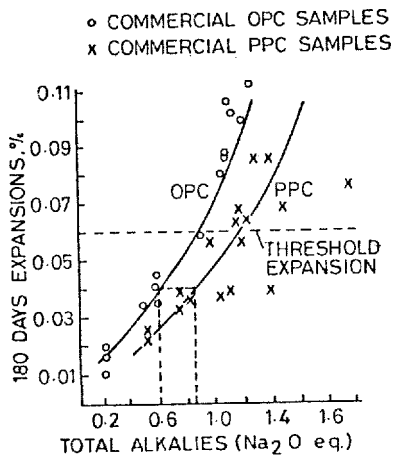

Fig 12

Influence of cement type on mortar bar expansion at 60°C (34)

Because significant slag reactions or pozzolanic reactions cannot be expected by 28 days, such blended cements, especially portland pozzolana cement in India, are generally ground to about 500 cm^2/g (Blaines) finer and still result in about 10 percent lower compressive strength till 28 days (**Table 6**)(29). From these considerations, it will appear that in commercially produced portland slag cements containing typically 45 to 50 percent slag there would still be some scope for pozzolanic reactions with flyash. Attention has therefore shifted towards ternary blend of ordinary portland cement, slag and flyash along with gypsum (37). For a blend of 50 percent ordinary portland cement, 40 percent slag and 10 percent flyash, perhaps the later age (90 days) strengths could be comparable with the parent 50-50 portland slag cement. Where the slag percentage is high, no pozzolanic reactions on addition of flyash can be expected (37).

Table 6

Comparison of Strengths of PPC & OPC - Plant Data

Cement Plant	Fineness cm^2/g		Ratio of Strength PPC/OPC	
	OPC	PPC	7 days	28 days
1	3755	3800	0.65	0.74
	4090	4355	0.61	0.74
2	2755	3325	0.92	0.85
3	2965	3000	0.96	0.94
4	3086	3473	0.98	0.95
5	2855	3863	0.88	0.97
	2519	3863	0.88	0.97
	3074	3872	-	0.87
6	3474	3608	0.72	0.63
7	2871	3413	0.91	0.87
8	2941	3504	0.87	0.90
9	3546	3782	0.89	0.90
10	3453	3826	1.24	1.02
11	3726	3826	1.00	1.06
12	3050	3453	0.52	0.70
13	3293	3696	0.82	0.78
14	3826	3896	0.78	0.74
15	4659	4684	0.90	1.03
16	3765	3750	0.80	0.79
17	3300	3655	0.98	1.02
18	2822	3252	1.10	1.10
19	3395	3375	0.78	0.83
20	3020	3128	0.91	1.07
21	3113	3273	0.87	0.91

In general, in order to manufacture a blended cement with good performance it is recommended to choose a clinker of high quality, with C_3S and C_3A and alkali content higher than that of a clinker for plain portland cement (27). This is one of the disadvantages of lowlime mixes like belite cement which may not offer energy and material economy by allowing blending with such mineral admixtures (13). However, instances have been reported where the compressive strength up to 28 days in a low-heat cement containing 51 to 65 percent C_2S increased with addition of blast furnace slag upto 60 percent (**Fig 13**) (38). The heat of hydration however remained lower than that of the low heat cement. In this instance the blast furnace slag seem to assist develop the microstructure of low heat cement. Increase in compressive strength of the low heat cement blended with flyash (20 to 30 percent) was observed at one year age (38).

One significant trend in the manufacture of portland slag cement is the separate grinding of clinker and gypsum on the one hand and slag on the other, with overall power consumption of the order of 43 to 44 kwH/tonne against 55-60 kWh/tonne in case of combined grinding (39).

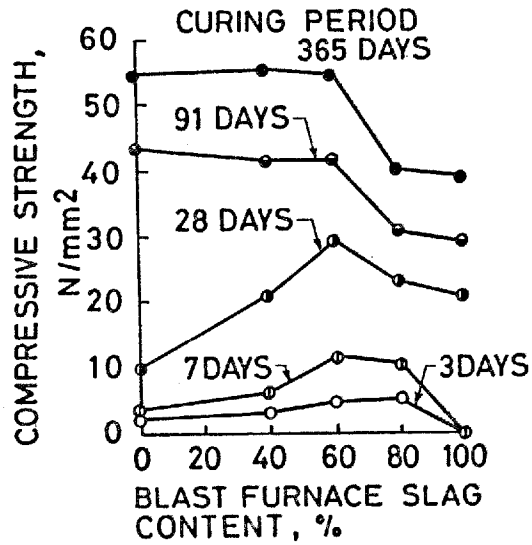

Fig 13

Compressive strength development of blends of low heat cement and blast furnace slag (38)

Inert Fillers

With the introduction of a common European Standard Specification in line with countries like France, which permit addition of inert calcarious fillers, eg, ground limestone or silicious fillers, eg, silica dust, considerable research has been reported on the effect of addition of such inert fillers. Addition of ground limestone upto 5 percent is claimed to result in a beneficial reaction with the C_3A in ordinary portland cement, leading to formation of calcium carbo-aluminate, thereby participating in set control, with possibly no adverse effect on the strength. However, the effect will essentially depend upon the chemical composition and characteristics of the parent cement (40).

Alkali Activation

Alkaline activation of slag is known for long time when slag-lime binders were marketed and used in the thirties. Apprehension of long term durability and development in ordinary portland cement led to general decline in its application (15). Renewed interest has now been focussed on activation of slags in the presence of alkalis. Such activators being sodium hydroxide, gypsum, calcium hydroxide, water glass, alkalis, sodium carbonate etc (41,42,43). Very high compressive strengths upto 80 to 90 MPa or even higher, have been reported (**Fig 14**) (42). In general, a combination of activators have been preferred (43). Development of activated slags and its blend with flyash were attempted in NCB to result in non-portland cements - blended cements having strength properties at par with ordinary portland cement, and were recommended for use as masonry cement (44). Flyash-slag blend activated with sodium silicate has been reported to have a strength of about 50 MPa and with increase in strength with time (45).

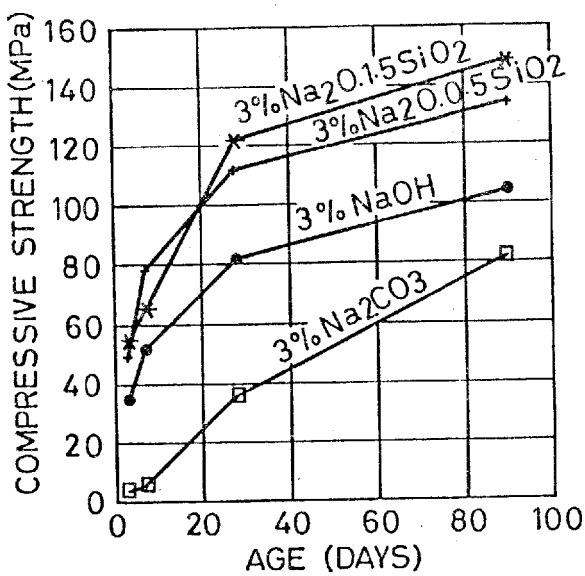

Fig 14

Effect of different additives on strength development of alkali-phosphorus slag cements (42)

Attention has been given to the utilisation of air-cooled slags which are not hydraulic and the disposal of which is becoming a problem in many countries. Alkali activation (NaOH, $Na_2 CO_3$) along with thermal processing at 1300 to 1350°C for further granulation and then water quenching has been reported to result in satisfactory hydraulicity of such activated slags (46).

BUILDING MATERIALS FROM INDUSTRIAL WASTES

From the discussions above, it will be clear that industrial wastes can certainly conserve the basic raw material for manufacture of cement and result in binders for masonry purposes even without ordinary portland cement. The full potential of such mineral additions cannot be achieved in blended cements because of strength requirements of specifications and market demands for cements with high early strength. On the other hand, such blends have demonstrated improved durability in the concrete and separate addition at the concrete mixer in larger volumes would be more useful for large volume use of such wastes provided they are available and marketed in such usable forms.

Relative proportion of the wastes generated in a country, vis-a-vis the cement production would dictate whether large volume use of such waste materials can be found through the cement concrete route. For example, in India which currently produce 55 million tonnes of cement, and perhaps 35 million tonnes of flyash, obviously all the flyash cannot be used by cement and concrete. On the other hand, considerable potential exists for manufacture of alternate binders/building components using flyash. A typical status projection is depicted in **Fig 15** from which it will appear that for large volume structural use of flyash blocks as replacemenmt of fired (burnt) clay bricks for walling in housing construction has the largest potential (47). The basic route for utilisation of flyash in such application would be what can be called as "hydro thermal" processing. The soluability of the silica in the flyash can be increased both with temperature and in combination with lime (**Fig 16**) (48). On this logic, the flow chart for generation of hydro thermal processing of flyash has been suggested which is reproduced in **Fig 17** (48). It is interesting to note that satisfactory building blocks can be manufactured at

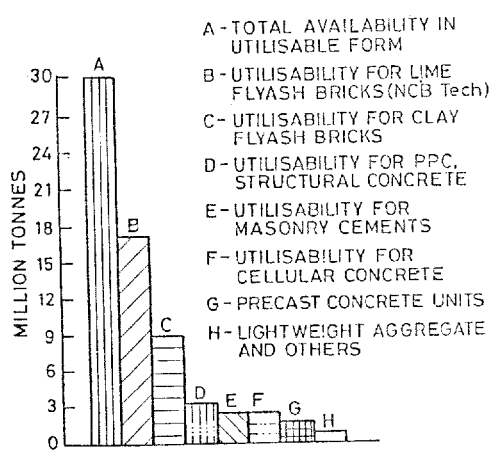

Fig 15

Potentials of use of flyash for various applications in India (47)

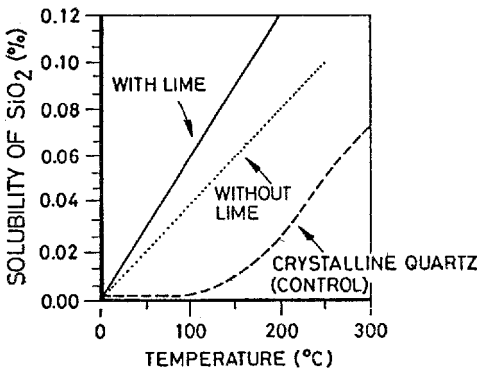

Fig 16
Solubility of SiO_2 in Class F flyash (48)

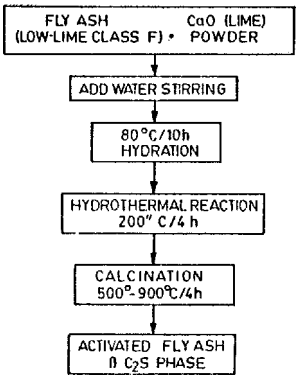

Fig 17
Flow chart of the general procedure for the hydrothermal processing of flyash to make cement (48)

the stage following initial steam curing. A technology on this approach is depicted in **Fig 18** (49). The strength of such lime-flyash bricks are comparable to what is obtained in commercial clay bricks, and higher strengths are indeed possible by suitable changes in the formulations. Further hydro thermal treatment involving autoclaving has also been suggested as a technology by some other laboratories and naturally the strength of the blocks is higher (50). Following further calcination the hydro thermal cement made from activated flyash containing β C_2S phase resulted in satisfactory strength properties (**Fig 19**) (48). Continuing research in these lines will be required for development of binders as well as building units from industrial wastes and at the same time solving the problem of their disposal.

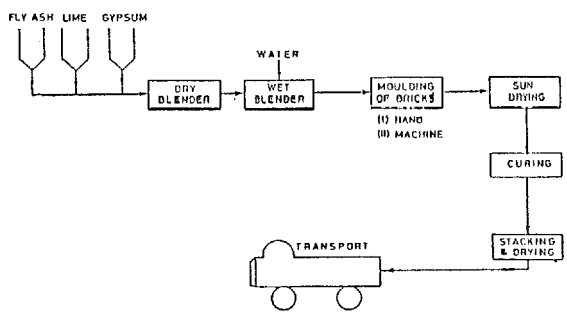

Fig 18
Schematic diagram for manufacture of lime-flyash bricks as per NCB technology (49)

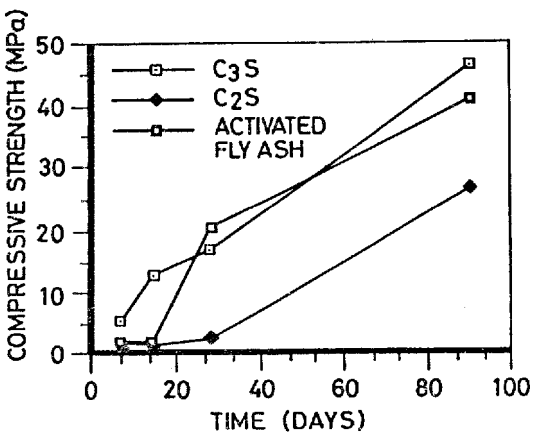

Fig 19
Compressive strength of mortars prepared from flyash cement compared with those from C_3S and C_2S (48)

CONCLUSION

1. Advances in portland cements has been reported which has the potential of lowering the clinker temperature, but concommittant energy saving is perhaps not very large. These cements do render special properties to concrete like high early setting, high early strength or increased durability against

sulphates etc. It will be proper to approach these developments in terms of such impoprtant properties rather than from the angle of energy conservation alone.

2. These developments would, however, be very useful when one has to use a marginal grade raw material and marginal fuel as in India. Any energy saving would be an added benefit.

3. Not much commercial manufacture of such cements are reported or anticipated in large scale in the near future. It has not been possible to assess the operational problems in the manufacturing of these systems as a continuous process in large size cement kilns, the problems of temperature control, interaction with the refractories etc.

4. Data on long-term durability of concrete in service, made with such modified cements should be collected to allow unhindered application of such cements, wherever manufactured commercially.

5. The manufacture and use of blended cements are well established. However, it has not been possible to realise the full potential in terms of volume addition because of competitive strength requirements to be at par with ordinary portland cement. Such additions result in increased durability, specially resistance to corrosion of reinforcement and alkali silica reaction, which should be highlighted. Larger volumes of the additions are possible in concrete mixes rather than in cement plants. The kind of utilisation, ie, in the cement plant or in the concrete mixers, depends on the historical development of the industry in any country.

6. Non-portland binders on the basis of activation of slags and flyashes do hold promise for applications in low-cost housing. However, it is more practical to make building blocks rather than binders, which will help in the construction and site management and at the same time enable larger volume utilisation.

ACKNOWLEDGEMENT

A number of unpublished reports and data available at the National Council for Cement and Building Materials (NCB) have been freely consulted in the preparation of this paper.

The author is grateful to Dr V M Malhotra of CANMET Canada and Prof (Dr) F W Locher of ZKG Germany for their reviewing the manuscript and making very useful suggestions for its improvement.

REFERENCES

1. Bergen Ministerial Declaration on Sustainable Development in the ECE Region, Bergen, Norway, 14-16 May 1990, UNEP Industry and Environment, Vol.13, No.2, Apr-Jun 1990, p.54-56.

2. Mullick A.K., Saxena J.P., Kumar K, and Pahuja A, "Energy Use Analysis of Indian Cement Industry - An Overview", VDZ Congress, Dusseldorf, Oct 1993, Technical Subject 5.

3. Energy Conservation in Cement Industry : A Resume of National Awards for Energy Efficiency in Indian Cement Industry (1988-89 and 1989-90), NCB publication, Jul 1992, 20 pp.

4. Mullick A.K., Chatterjee S, and Imran M : Availability and Utilization of Limestone for Indian Cement Industry, NCB Quest, Vol 4 No 2, Nov 1990, p.1-14.

5. Mullick A.K and Ahluwalia S.C : Utilization of Wastes in Indian Cement Industry, International Symposium "Cement Industry Solutions to Waste Management", Calgary, Canada, Oct 1992.

6. Locher F.W : Low Energy Clinker Formation, 8th International Congress on the Chemistry of Cement, Rio de Janeiro, Brazil, Sep 1986, Vol.I, p.57-67.

7. Stark J., and Muller A : International Development trends in Low Energy Cements, Zement Kalk Gips, No.4, Apr 1988, p.162-165.

8. Odler I and Abdul Maula S : Einflu ß Von Mineralisatoren auf das Brenner des Portland Zement Klinkers, ZKG, 33 (1980) No 3, p.132-136 & 278-282.

9. Toropov N.A, Luginina I.G, and Luginin A.N : Ober den Chemischen Einflu ß Von Zusatzen auf die der Klinker-bildung vorange henden prozesse - Zur Be Schleunigung der klinker bildung durch zustaz von Mineralisatoren, Silikatteche 22 (1971) No.7, p.220-222.

10. Christensen N.H and Johansen V : Role of Liquid phase and mineralizers, J. Skalny (Editor), Cement Production and Use, Engineering Foundation, US Army Research Office, 1979, p.55-69.

11. Moir G.K and Glasser F.P : Mineralizers, Modifiers and Activators in the Clinkering Process, 9th International Congress on the Chemistry of Cement, New Delhi, Nov 1992, Vol.I, p.125-152.

12. Chatterjee A.K and Page C.H : Industrial Applications of Mineralizers for Improved Clinker Burning - Illustrative Case studies, All India Seminar on Cement and Allied Building Materials, CRI, New Delhi, Jan 1984, Vol.III, p.192-209.

13. Sprung S and Delort M : Effect of Energy Conservation and Environmental Control Measures on Clinker Properties, 9th International Congress on the Chemistry of Cement, New Delhi, Nov 1992, Vol.I, p.155-176.

14. Mehta P.K : Investigations on Energy Saving Cements, World Cement Technology, 11 (1980), No.4, p.166-177.

15. Narang K.C : Portland and Blended Cement, 9th International Congress on the Chemistry of Cement, New Delhi, Nov 1992, Vol.I, p.213-257.

16. Kouznetsova T.V : Special Cements, Calcium Aluminate and other no-silicate cements, 8th International Congress on the Chemistry of Cement, Rio de Janeiro, Brazil, Sep 1986, Vol.I, p.283-291.

17. Kurdowski W, George C.M and Sorrentino F.P : Special Cements - Principal Paper, Ibid, p.292-318.

18. Beretka J, Santoro L, Sherman N and Valenti G.L : Synthesis and Properties of Low Energy Cements Based on C_4A_3S, 9th International Congress on the Chemistry of Cement, New Delhi, Nov 1992, Vol.III, p.195-200.

19. Krivobovodov Y.U. R & Samchenko, S.V : Sulphate-bearing Solid Solution of Calcium Aluminates and Ferrites, Ibid p.209-215.

20. Ivashchenko, S.I : Cements Based on Modified Portland and Sulfoaluminate-Belite Clinkers, Ibid p.222-226.

21. Ali, M.M, Sharma, P.S and Bhargava, R : Potentials of Using Dolomitic Limestone in Making Sulfoaluminate-Silica Cements, Ibid, p 227-232.

22. Osokin, A.P, Krivoborodov, Yu R and Dyukova, N.F : Sulfoferrite Cements, Ibid, p.256-261.

23. Liu Kezhong, Deng Zhongyan, Yuan Mingdong and Tang Jinshu : Study on Cement in the $C_{11}A_7.CaF_2$-C_2S System, Ibid, p.268-276.

24. Development of Cement Based Non-shrink Grout, Technology Digest, National Council for Cement and Building Materials, New Delhi, May 1982, 7 pp.

25. Ali, M.M, Hando, S.K and Ahluwalia, S.C : Improved Formulations with High Early Strength and Regulated Set, Third NCB International Seminar on Cement and Building Materials, New Delhi, Jan 1991, Vol.4, p.VII-21.

26. Majumdar, A.J, Singh, B and Edmonds, R.N : Hydration of Mixture of Cement Fondu and Granulated Blast Furnace Slag, Cement and Concrete Research, Vol.20, No.2, 1990, p.197-208.

27. Sersale, R : Advances in Portland and Blended Cements, 9th International Congress on the Chemistry of Cement, New Delhi, Nov 1992, Vol.I, p.261-302.

28. Mehta, P.K : Pozzolanic and Cementitious By-products in Concrete - Another Look, ACI, SP-144-I, I (1989).

29. Mullick, A.K, Babu,K.H and Rao, P.B : Evaluation of Pozzolanic Activity and its Impact on Specification of Blended Cements, 8th International Congress on the Chemistry of Cement, Rio de Janeiro, Brazil, Sep 1986, Vol.VI, p.308-311.

30. Edwards, P and Foster, A : Making the most of a National Resource, Concrete, Vol.26, No.3, May/Jun 1992, p.15-16.

31. Berke, N.S, Scali, M.J, Regan, J.C and Shen, D.F : Long-term Corrosion Resistance of Steel in Silica Fume and/or Flyash Containing Concretes, Durability of Concrete, Second International Conference CANMET/ACI, Montreal, 1991, SP-126, Vol.1, p.393-422.

32. Massazza, F and Oberti, G : Durability of Pozzolanic Cements and Italian Experience in Mass Concrete, Ibid, Vol.2, p.1259-1283.

33. Wolsiefer, J.T. Sr : Silica Fume Concrete - a Solution to Steel Reinforcement Corrosion in Concrete, Ibid, Vol.1, p.527-558.

34. Mullick, A.K and Wason, R.C : Performance of Commercial Blended Cements and their Role in Alleviating ASR, Proc. International Seminar on Durability of Concrete, Aspects of Admixtures and Industrial By-products, Gothenburg, Sweden, Jun 1989, p.138-148.

35. Malhotra, V.M, Carette, G.G, Bilodeau, A and Sivasundaram, V : Some Aspects of Durability of High Volume ASTM Class F (Low-Calcium) Fly Ash Concrete, Durability of Concrete, Second International Conference CANMET/ACI, Montreal, 1991, SP-126, Vol.1, p.65-82.

36. Osborne, G.J : The Sulphate Resistance of Portland and Blast Furnace Slag Cement Concretes, Ibid, Vol.2, p.1047-1070.

37. Sharma, K.M, Sharma, R.N, Yadav, D and Narang, K.C : Effect of Pozzolanic Additions on Hydration and Performance of Portland Slag Cement, 9th International Congress on the Chemistry of Cement, New Delhi, Nov 1992, Vol.III, p.187-192.

38. Yoshida, K and Igarashi, H : Strength Development and Heat of Hydration of Low Heat Cement, Ibid, p.16-22.

39. Verma, N.P : Energy Efficient Method of Portland Slag Cement Grinding, Third NCB International Seminar on Cement and Building Materials, New Delhi, Jan 1991, Vol.3, p.V-29.

40. Ingram, K.D and Daugherty, K.E : Limestone Additions to Portland Cement Update, Chemistry and Effects, 9th International Congress on the Chemistry of Cement, New Delhi, Nov 1992, Vol.III p.180-186.

41. Tango, C.E.S and Vaidergorin, E.Y.L : Some Studies on the Activation of Blast Furnace Slag in Cements without Clinker, Ibid, p.101-107.

42. Dai, L and Cheng, J : An Investigation on Blast Furnace Slag-Fly Ash-Alkali System, Bulletin of Chinese Silicate Society (In Chinese), 1988, 16(1), p.25-32.

43. Chen Zhi Yuan and Liao Xin : The Selection of Stimulation Agents for Alkali-Slag Cement, 9th International Congress on the Chemistry of Cement, New Delhi, Nov 1992, Vol.III, p.305-311.

44. Narang, K.C : Investigations on Microstructural Behaviour and Performance of Non-Portland Binders, 10th International Congress on Cement Microscopy, Texas, USA, 1988, p.71-81.

45. Changgao Lu : The Research of the Reactive Products and Mineral Phase for FKG Cementitious Material, 9th International Congress on the Chemistry of Cement, New Delhi, Nov 1992, Vol.III, p.319-324.

46. Sharma, K.M, Bhargava, R, Yadav, D and Ahluwalia, S.C : Metallurgical Slags as Blending Materials for Cement Manufacture, Ibid, p.121-127.

47. Mullick, A.K : Approaches to Utilization of Flyash in the Building Materials Industries, Shanghai International Conference on the Utilization of Flyash and other Coal Combustion By-products, 1991.

48. Jiang, W and Roy, D.M : Hydro-thermal Processing of New Flyash Cement, Ceramic Bulletin, Vol.71, No.4, 1992, p.642-647.

49. Rajkumar, C and Ray, S.C : Utilization of Flyash in Manufacture of Building Bricks, Shanghai International Conference on the Utilization of Flyash and other coal Combustion By-products, 1991.

50. Rai, M, Chandra, D, Gupta, R.L., and Jain, S.K : Production of Calcium-silicate Bricks from Flyash, National Workshop on Utilization of Flyash, May 1988, Roorkee, India, Proc. p A.59-62.

ADDENDA

ENERGY-SAVING BELITE-POZZOLANIC CEMENT

A Garbacik and S Peukert

Research Institute for Mineral Building Materials
Cracow, POLAND

SUMMARY

In this paper a very effective belite-pozzolanic cement technology is described. Belite-pozzolanic cement is produced by intergrinding of active belite clinker with appropriate additions of gypsum, and fly ash from coal combustion. The essential technological requirement here, is to use active low-temperature belite clinker containing a large quantity of free lime. Using special raw materials, it is possible to reduce the clinkering temperature down to 1250 - 1300° C. Soft burnt free CaO is utilized in pozzolanic reaction and has no negative effect on the soundness of cement. It is possible to enhance considerable the hydraulic activity of belite clinker and pozzolanic reaction by increasing the fineness of cement. Owing to the very good grindability soft sintered belite clinker that effect can be obtained at low energy consumption coefficient in cement grinding process. In this paper an industrial trials of belite clinker and belite-pozzolanic cement manufacturing are described. The properties of clinker, field of application of cement and economic efficiency belite-pozzolanic cement production are given.

RÉSUMÉ

Dans l'article on présente une technologie effective de production du ciment bélito-pouzzolanique. Le ciment bélito-pouzzolanique est fabriqué au moyen de pulvérisation du clinker bélite actif mélangé à des additifs spéciaux de gypse et de cendres volantes provenant de la combustion du charbon. L'usage du clinker bélite actif de basse température, contenant une grande quantité de chaux libre en est une condition technologique primordiale. Grâce à l'addition des produits spéciaux, il est possible d'abaisser la température de clinkérisation à 1250 - 1300 C. La chaux libre peu cuite est utilisée dans la réaction pouzzolanique. Sa présence n'a pas d'influence négative sur le constance de volume de ciment. Le bas dergé du frittage du clinker et sa bonne pulvérisabilité améliorent considérablement l'activité hydraulique du clinker et de la réaction pouzzolanique au moyen d'un haut degré de pulvérisation du ciment tout en gardant un bas niveau de consommation de l'énergie au cours de la pulvérisation.

INTRODUCTION

One of the methods to reduce the heat consumption in the burning process of OPC clinker is by the modification of its compound composition, essentially an increase of its belite content. A reduction of heat of decarbonation and clinkering temperature of low-lime raw mixes results in lower energy consumption of the belite clinker sintering process.

The fundamental problem in belite cement technology is the low hydraulic activity of belite at early stage of hydration. Therefore, to obtain an energy-saving belite-rich clinker with strength development comparable to OPC clinker, the problem of poor hydraulic activity of belite must be solved. For C_2S, the high-temperature forms and modifications containing defects in its structure are known to be more reactive. Thus the possibilities to improve the hydraulic activity of belite by the modification of the dicalcium silicate structure are explored. The stabilizing process of the active forms of belite can be effective under appropriate sintering conditions including crystallochemical and crystallophysical methods of modification of the belite lattice structure (1-6). However from the technological point of view, physical activation is more useful and utilized for production of rapid-cooled (1-4) and low-temperature active belite clinkers (5-6).

In this paper the results of industrial tests on low-temperature active belite clinker are reported. This clinker was used for production of belite and belite-pozzolanic cements. The latter, produced with fly ash addition, is described.

BASIC FEATURES OF BELITE-POZZOLANIC CEMENT TECHNOLOGY

Belite-pozzolanic cement is produced by grinding of active belite clinker with appropriate addition of gypsum, and fly ash from coal combustion. The essential technological requirement here is to use low-temperature active belite clinker containing a large quantity of free lime. Soft sintered uncombined CaO is favourably utilized in pozzolanic reaction and has no negative effect on the soundness of cement. The highest hydraulic activity is obtained from belite clinker burnt from special raw materials, with high silica modulus and high burnability (7). Low burning temperature and high silica modulus of clinker are favourable for synthesis of extremely fine-crystalline active forms of silicates. It is feasible to enhance the hydraulic activity of belite clinker and pozzolanic reaction in belite-pozzolanic cement by increasing the fineness of cement. The energy consumption in grinding such a cement is low, owing to the very good grindability of soft-burnt belite clinker.

PLANT PRODUCTION OF BELITE-POZZOLANIC CEMENT OF STRENGTH CLASS 40

Production and properties of clinkier

Belite clinkier was produced from highly reactive chalky raw materials in a long wet-process rotary kiln with planetary coolers. The temperature in the burning zone, and hence the degree of sintering were regulated by the amount of the coal fed into the kiln. Free lime content and litre weight of the clinker served as the means of evaluating the burnability of the clinker. The parameters of the belite clinker were as follows:

- lime saturation factor	0.77	-	0.80
- silica modulus	3.0	-	3.5
- belite content	45	-	50 % by mass
- alite content	30	-	35 % by mass
- free lime content	2.0	-	3.0 % by mass
- litre weight	1.05	-	1.10 kg/l
- burning temperature	1250	-	1300 °C

The examination of phase content showed that the silicate phase of the clinker is composed of very fine crystalline irregular grains of β-C_2S and alite. The crystal sizes of alite and belite range from 5 to 10 μm. The clinker is soft and very porous. These factors contribute to the excellent grindability of the clinker and its mixes with fly ash. The grindability coefficient of belite clinkers as a function of fineness is shown in Figure 1.

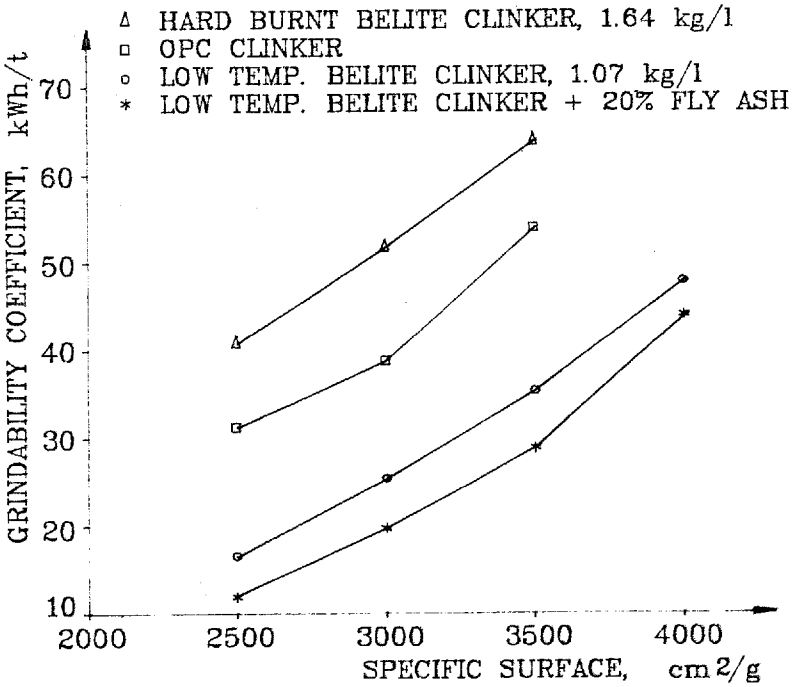

Fig.1. Grindability coefficient of belite clinkers as a function of fineness (according to Mittag method)

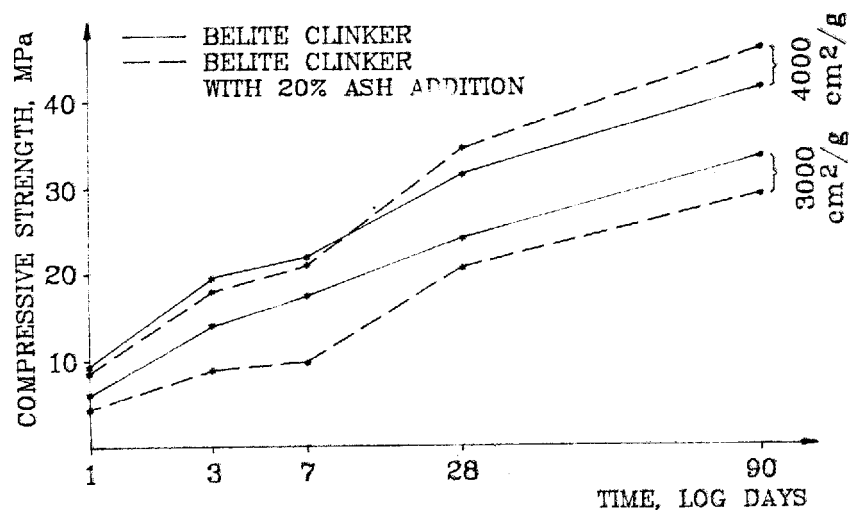

Fig.2. Evaluation of compressive strength of low-temperature belite clinker (belite content 48%, free lime content 2.6%, litre weight 1.07 kg)

The possibilities of activation of the belite and belite-pozzolanic cements by increasing the cement fineness have been studied. Figure 2 shows the results of compressive strength measurements of low-temperature belite at different finenesses. It can be stated that cement fineness particularly strongly influences belite-pozzolanic cement strength.

Production and properties of cement

Belite-pozzolanic cement was produced in open-circuit two-compartment mills. The belite clinker obtained as stated above was ground with additions of 15 to 20% fly ash and 5 to 6% gypsum, to a specific surface area of 3500 to 4000 cm^2/g (Blaine). The compressive strengths of cement mortar (ISO) prepared from different lots of belite-pozzolanic cement are presented in Table 1.

As can be seen, the belite-pozzolanic cement produced meets the strength requirements for OPC strength class 40. The data of heat of hydration shown in Table 2 confirm the high hydraulic activity of the belite-pozzolanic cement.

Comprehensive laboratory and field tests showed that other technological properties of belite-pozzolanic cement are comparable to those of OPC containing fly ash addition. In accordance with field tests the belite-pozzolanic cement can be used as a substitute for portland-pozzolanic cements, especially advantageously for autoclaved cellular concretes.

Table 1. Strength of belite-pozzolanic cement

No of cement lot	Specific surface cm^2/g	Compressive strength in MPa after days				
		3	7	28	90	180
1	3770	18	27	42	51	55
2	3850	21	27	45	53	58
3	3960	20	25	48	55	60
4	3880	20	27	43	54	58
5	3850	21	26	42	51	56

Table 2. Heat of hydration of belite-pozzolanic cement

Cement	Heat of hydration in J/g after hours				
	6	12	24	48	72
Belite-pozzolanic cement (No 5 in Table 1)	27.2	100.4	175.8	213.5	230.3
OPC with 20% addition of slag	15.9	54.4	182.1	234.5	259.6

Economic efficiency of cement production

Comprehensive industrial trials have confirmed the merits of low-temperature belite clinker manufacturing, claimed in numerous publications /5,6/. It was proved that in comparison to OPC clinker burning process it is possible:

- to reduce considerably the heat consumption in clinker burning process - by approx. 15% in the wet method;
- to utilize as fuel a poor quality coal with calorific value below 2.10^4 kJ/kg;
- to reduce by 50% the volatilization rates of alkalies and sulfur;
- to reduce SO_3 and NO_x emission;
- to improve the clinker grindability by 35 - 40%

CONCLUSION

Advantages in the production process and properties of low-temperature belite clinkers can be very effectively exploited through the energy-saving belite-pozzolanic cement technology.

REFERENCES

1. Müller, A., Stark, J. and Rümpler, K.: "Zum Stand der Entwicklung eines aktiven Belit-Zementes", Zement-Kalk-Gips, 1985, 38, 303.

2. Stark, J., Müller, A. and Rümpler, K.: "Produzione di cemento alla belite attiva ai fini della riduzione del consumo di energia", Cemento, 1987, 3, 239.

3. Gies, A. and Knöfel, D.: "Influence of alkalies on the composition of belite-rich cement clinkers and the technological properties of the resulting cements", Cem.Concr.Res., 1986, 16, 411.

4. Gies, A. and Knöfel, D.: "Influence of sulfur on the composition of belite-rich cement clinkers and the technological properties of the resulting cements", Cem.Concr.Res., 1987, 17, 317.

5. Ludwig, U. and Pohlmann, R.: Investigations on the production of low lime portland cements", Ciments-Béton-Plâtres-Chaux, 1988, 773, 257.

6. Bei, R. and Ludwig, U.: "Hydraulische Reaktivität belitreicher Portlandzemente", Zement-Kalk-Gips, 1990, 43, 506.

7. Kurdowski, W. and Garbacik, A.: "Energy-saving cements", Beijing Int. Symp. on Cement and Concrete, China, 1985.

PRODUCTION PERFORMANCES AND UTILISATION OF A SPECIAL SUPERPLASTICIZED CEMENT

V Alunno Rossetti* and F Curcio** & L Gussino**

*Sapienza University, Engineering Faculty, Rome, ITALY
**Unicem Spa, Guidonia Research Centre, Rome, ITALY

SUMMARY

Since the introduction of superplasticizers in concrete technology, two particular problems have been noticed: the first one is the possibility of absorption of the product in the aggregate porosity, the second one is the effect of the addition time on the fluidifying action. In order to overcome these problems a special cement, to which the admixture is added in the cement factory, has been produced at one Italian plant. In this paper the characteristics and the performances of this cement are described.

1. INTRODUCTION

The use of superplasticizing admixtures has greatly changed the concrete practice in many countries, due to the great benefits attainable with their use, in terms of performances, reliability and econonomy.

One problem arising with the use of superplasticizing admixtures is the variability of the effects, as a function of the time of addition to the mix. A second interesting aspect is that the effect of the superplasticizers is believed to be essentially due to adsorption phenomena on the cement particles surface, while the admixture absorbed by the porosity of aggregate particles or adsorbed on it should be ineffective: it could be supposed that a previous adsorption, limited to the cement surface, should minimize the aggregate influence.

In order to reduce the above mentioned variability and to increase the performance of the admixture, the possibility of a direct addition to the cement, instead of the usual addition in the concrete mix, has been studied and a research has been conducted since about 3 years ago. The results obtained in the laboratory were satisfactory and after some experience with a pilot plant, an industrial production at one italian cement plant is now regularly carried on.

In this paper some information is given on the production, performances and applications of this special Super Plasticized Cement (SPC).

2. ADVANTAGES TO FORESEE FROM A SPC

As above outlined, two advantages could be foreseen in using a superplasticized cement.

2.1 Reduced effect of the addition time

The effect of a superplasticizer on the rheological properties of the cementitious mixes, normally depends on the time of addition, in the presence of water.

This effect has been observed both in laboratory tests and in industrial practice, on cement pastes and on concrete. For concrete mixes in industrial practice, Kasami and coworkers (1) for example, found a remarkable increase of slump and slump increment; Collepardi and coworkers (2), examined the effect of an immediate or delayed addition of a sulphonated naphtalene formaldehyde polymer to cement pastes, and found a remarkable effect on their fluidity as measured by means of the minislump test.

To underline the unpredictability of the results, it is worth mentioning that in at least one case the opposite effect (reduced workability for delayed addition) has been claimed (3).

In the industrial practice the addition time can be the very first moment of the contact of the cement with water (as when the admixture is contained in the latter), or it can be quite longer, since the admixture producers, to obtain the best performances of the product, sometimes ask the user to delay the addition to the mix, after that all or the greater part of the required mixing water has been added and the concrete has been thoroughly mixed. In some cases, the admixture is added in the truck mixer at the job site, a long time after the water addition.

The dependence of the effect of the superplasticizer on the time of addition, in some cases can be certainly objectionable: it means indeed that, expecially when a strict control of the timing of concreting operations is not possible, the effect of the superplasticizer is not always and not completely predictable; in turn this can lead to variations of the w/c ratio in attempting to mantain the slump at the prefixed value.

2.2 Effect of the adsorption

The second reason for trying to develop a SPC is the fact, commonly accepted, that the fluidifying effect of the superplasticizers is associated to adsorption phenomena on the surface of the cement particles. It could be supposed that if, due to the production process, the polymer is already adsorbed on the cement surface when the cement comes into contact with water, and if moreover for the same reason the polymer is not or is less adsorbed/absorbed by the aggregates, the fluidifying effect should increase.

It could be objected to this last point, that this is a very simplified way of looking at the phenomenon: many parameters indeed have been taken into account to explain the action of the superplasticizers; among those the most significant could be the amount of adsorption on the individual phases, anhydrous and hydrated. According to Ramachandran (4) for example, the admixture is greatly adsorbed by C3A and C3A-gypsum mixture, leaving only small amounts for the dispersion of the silicate phases. By late addition the admixture is less adsorbed, and more of it is left in solution for dipersing the silicate phases.

Another way of reasoning is that the addition of the admixture to the cement could be seen as a slightly delayed addition in concrete, since its presence as a dispersion of solid particles does not imply immediate appearance in solution and the possibility of immediate action; on the contrary a certain amount of time is required for the solubilization of the product.

3. PRODUCTION OF A SUPERPLASTICIZED CEMENT

On the basis of the preceding considerations a study has been carried out since 1988, in cooperation with an admixture producer, with the task of producing a cement containing the admixture since its production in the cement factory.

The first attempts were based on the addition of a normal sulfonated naphtalene superplasticizer solution to the cement, during the final grinding. The results so obtained, even if encouraging, were not satisfactory, both for the fluidifying effect and for the duration of the effect. Only the availability of a purposely made admixture (again of the sulfonated naphtalene type), gave the possibility of reaching good performances of the product. Also the way of mixing the admixture with the cement has a marked effect on those performances and required the set up of a special stage in the production.

In this way a pilot plant and then a full scale plant for the production of the cement have been set up and today a regular industrial production is carried out.

4. PROPERTIES OF THE SUPERPLASTICIZED CEMENT

4.1 Standard tests

The base cement for the SPC produced so far, is a portland cement (PD) , of the italian type "525" (a rapid hardenig cement, having a crushing strength higher than 52.5 MPa at 28 days). This type was selected since the SPC was meant to have high performances, in view of an initial test utilization in precast and prestressed concrete elements; other types of cement can of course be used.

In table 1 SPC typical characteristics and performances are given, in comparison with those measured on the "parent" portland cement (both according to italian standards). It can be observed that the performances of the two cements are practically the same; if tested on the basis of a constant water/cement ratio this holds for the compressive strength too. On the contrary, when tested on the basis of the same flowability the SPC, requiring about 25 % less water, gives compressive strengths quite higher than the PC.

Cement	PD 525	SPC	
SSB, cm^2/g	4030	3980	
Retained at 40 μm, %	4.4	5.2	
L.O.I. %	0.75	1.6	
Insoluble, %	0.41	0.41	
SO_3	3.30	3.35	
C_3S (clinker)	56.2		
C_2S	19.7		
C_3A	7.7		
C_4AF	9.4		
Paste water dem., %	25.6	20.2	
Initial set, mins	95	300	
Final set, mins	125	395	
		Same w/c	Same consistency
Mortar w/c	0.5	0.5	0.37
Mortar flow, %	118	>200	117
R_{c1}, MPa	26.4	24.2	38.9
R_{c3}, MPa	44.1	44.3	67.0
R_{c7}, MPa	53.3	52.0	81.0
R_{c28}, MPa	64.0	62.9	95.5
R_{f28}, MPa	8.8	7.1	12.4

Tab. 1 - Characteristics of the cements.

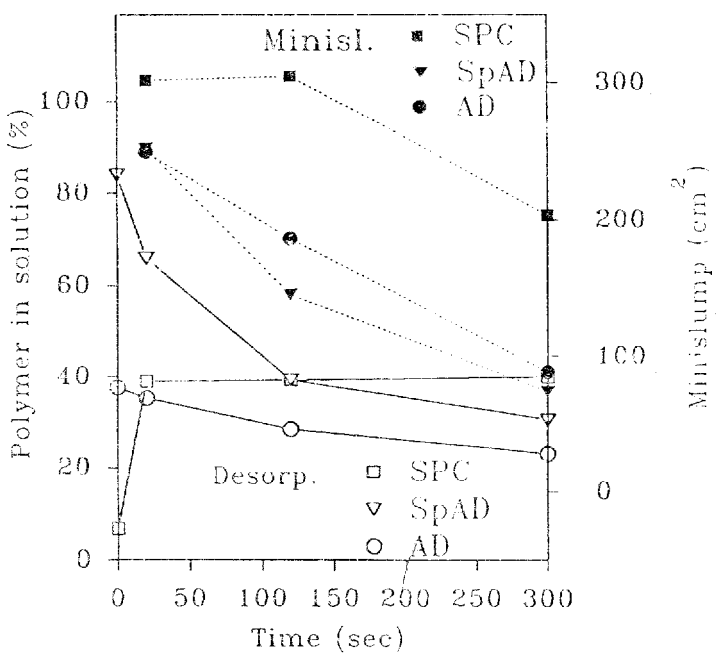

Fig. 1 - Adsorbtion and minislump tests.

4.2 Minislump and absorption tests

In order to obtain some indications on the adsorption phenomena, tests of polymer adsorption and of minislump were performed. For all the tests, the same cement sample was used, and three ways of addition:

- addition of the special admixture (SpAD) to the dry cement in the pilot plant (SPC sample),

- addition of the same admixture (SpAD), but added together with the mixing water (SpAD sample),

- addition with the mixing water of a superplasticizing admixture (AD) having very high performance, commonly used for concrete (AD sample).

As abovesaid, all the admixtures were based on sulfonated naphtalene polimers, and the same quantity was added (1.8 % by weigth of cement).

The minislump (6) tests were performed by energic mixing of the cement with 35% by weight of water (or water + admixture), for periods of time of 20, 120 and 300" and measuring the pat area immediately after the end of the mixing.

In the same samples, part of the mix was used for separating the solution by filtration and measuring the concentration of the polymer, by means of UV absorption spectrometry.

The concentration of the polymer in the solution has been plotted in fig.1 as a percentage of the polymer initially present in the paste; the proportion of polymer adsorbed on the cement can be evaluated by difference. The test for the concentration of the admixture in solution was also performed at "zero time"; this means that water (in the case of SPC) or admixture in water, was passed through the cement, directly over a filtering device.

In fig. 1 results of the adsorption and minislump tests are presented.

The adsorption results indicate that both SpAD and AD are adsorbed until a not very different percentage of the admixture initially present has been dissolved in the contact solution; the SPC cement releases a high proportion of the polymer to the solution, so that at 300" the concentration is the highest, but similar to those already found in the former cases.

The minislump results indicate that the SpAD admixture added to the cement with the mixing water (immediate addition) is equivalent to the AD admixture at 20" and slightly less effective in the same conditions at later times; the SPC, containing the SpAD admixture shows higher fluidity at 20" and is more fluid also at later times.

It can be observed that in a quite short period of stirring, the fluidifying admixture reaches its full effect in all cases; in this period the mean concentration of polymer in solution is quite low for the SPC, having the highest fluidity, because it goes from 7 to 40% of the quantity initially present; on the contrary the concentration of polymer in solution in this period is the highest for SpAD and AD. The fact that the full effect of the polymer is reached for a high concentration of polymer in solution (SpAD and Ad) in one case, and for a low concentration in the other case, could be explained in two ways:

- the polymer in the SPC can really be effective because of the adsorption on the cement particles during the production process,

- the high efficacy in the case of SPC is due to the retarded availability in solution; this is due to the time required for the solid polymer to be dissolved.

To obtain some more information, minislump tests have been made with the SpAD in delayed addition. The highest minislump value (about 300 cm2) has been obtained with the following procedure: addition of water, 60 seconds of mixing, admixture addition (2") and final mixing (58"). This result seems to confirm the great influence of the delayed addition for the system studied; anyway on the basis of the obtained results the hypotesis of the influence of a previous adsorption cannot be rejected.

5. PROPERTIES OF THE CONCRETE

The properties of the concrete obtainable with the SPC are the same that can be obtained with a normal cement PD 525, since they depend essentially on the w/c ratio. For this reason only a few particular aspects are dealt with in this paper. Those aspects are not normally specified by the client or the designer, but in some cases can be significant. It can also be observed that the use of a particular type of admixture and the addition time are seldom specified if ever; this leads to a large variation of the examined properties if the possibility of using different admixtures to obtain the same specified performances of concrete is also taken into account.

5.1 Slump loss

As abovesaid the workability of fresh concrete in the presence of superplasticizers is related to the time of addition and some effect is also observed on the slump loss in time(6). The SPC cement is characterized by a slump loss of 50% of the initial value in 45 min at 20 Centigrade; normal superplasticized concretes show a wider variation as a function of the addition time: taking into account also the type of admixture, the half slump loss time can vary from 10 to 40 minutes about.

5.2 Strenght variability

Data of compressive strength as a function of the cement content, obtained at 18 hours and 28 days on concrete specimens in the same laboratory conditions, are presented in fig. 2 and 3. The PD 525 cement and the SPC are obtained with a clinker produced in the same kiln. The aggregate used is the same reference material, purchased in large dry batches of 7 different grain sizes and having a constant water absorption. For all concretes the slump is 220 $\pm$ 15 mm, obtained in the case of PD 525 using a superplasticizer.

The results in fig. 2 are obtained as a control in concrete of the industrial production of 6 months of the SPC and reflect clinker and cement properties variations. Results in fig. 3 have been obtained during the same period as a control in concrete of the PD 525 cement production, and reflect the variation in the cement properties already mentioned as well as not strictly controlled addition times for different types of superplasticizing admixtures. In the writers opinion these data represent the variability of results that can be espected in producing concretes of the same target strenghts, when only strength and slump values are specified.

In both the figures, the regression line (continuous) and the 95% confidence interval (dashes) for the regression line have been traced. It can be observed that the interval is about twice for the PD 525 concretes.

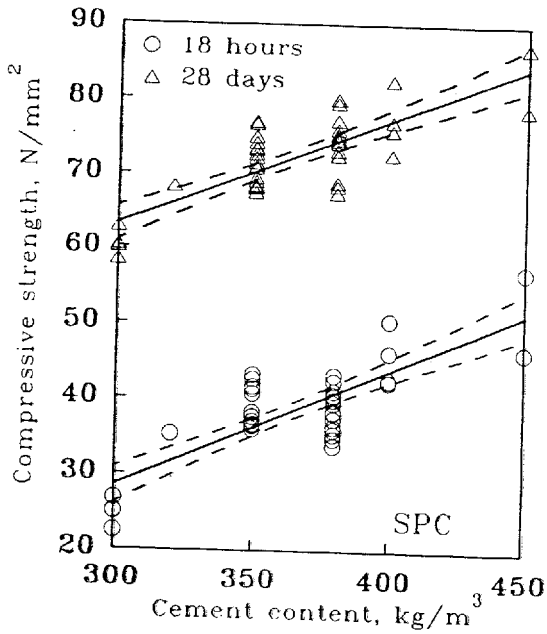

Fig. 2 - SPC strength in concrete.

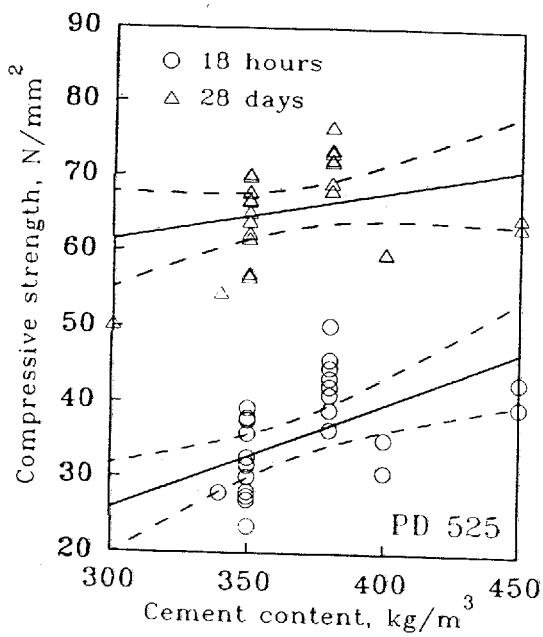

Fig. 3 - PD strength in concrete.

Even if the SPC is already used in precast concrete elements production, homogeneus statistical data are not yet available.

6. CONCLUSION

Industrial production and laboratory testing confirm the advantages of the use of a special cement, containing a superplasticizer added in the cement factory, essentially in reducing the variability of strenght, and in improving the reliability of the concrete.

REFERENCES

1) Kasami H., Ikeda T., Yamane S., in Proceedings of an International Symposium on Superplasticizers in Concrete, Ottawa, Canada (1978)

2) Collepardi M., Corradi M., Baldini G., Pauri M., in VII Int. Congr. on the Chem. of Cement, VI, 20, Paris (1980)

3) Hewlett P.C., in Proceedings of an International Symposium on Superplasticizers in Concrete, Ottawa, Canada (1978)

4) Ramachandran V.S., "Concrete Science", Ed. Heyden / London (1981)

5) Perenchio W.F., Whiting D.A., Kantro D.L., in Proceedings of an International Symposium on Superplasticizers in Concrete, Ottawa, Canada (1978)

6) Alunno Rossetti V., Unpublished data.

CONGRESS ALBUM

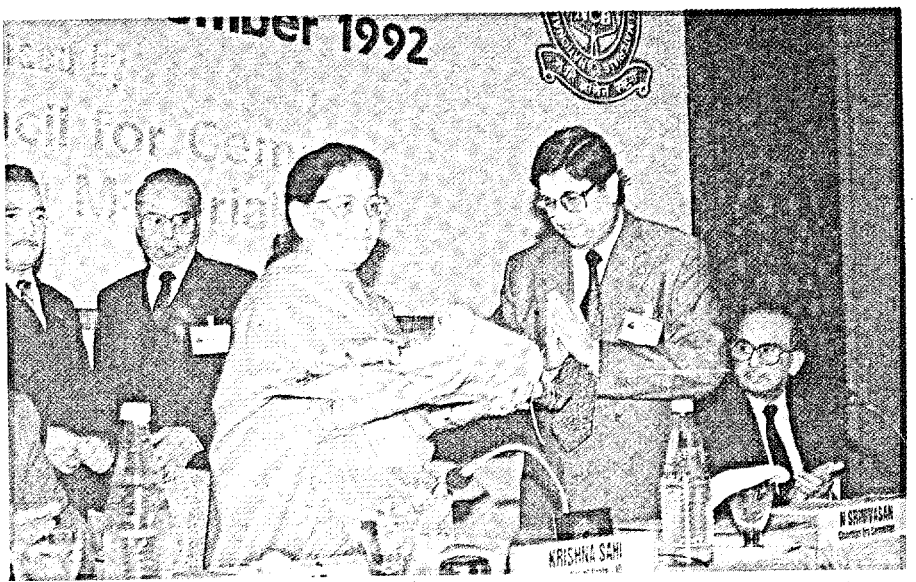

Mrs Krishna Sahi, Hon'ble Minister of State, Industrial Development, receives a welcome bouquet from Mr N Srinivasan, Chairman, Organising Committee 9th ICCC and NCB

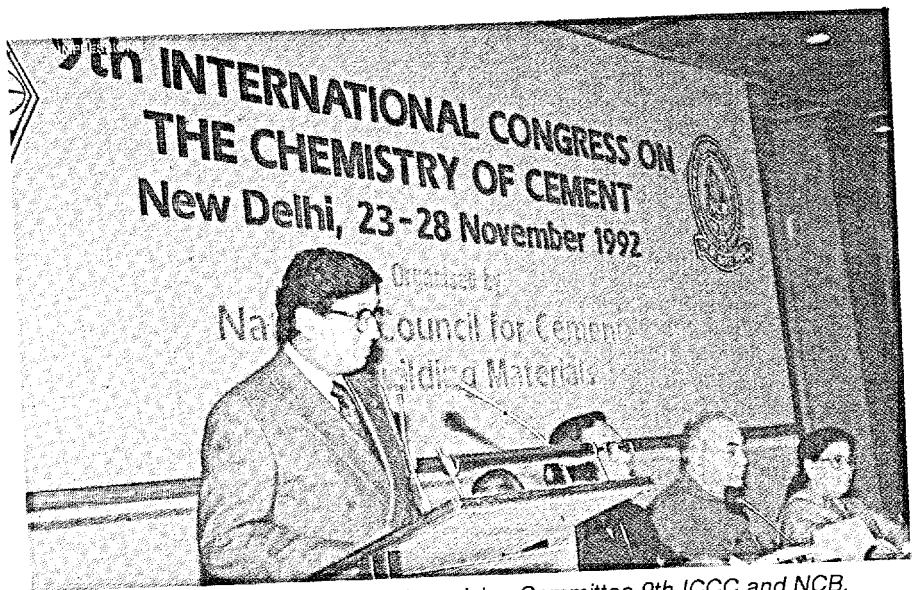

Mr N Srinivasan, Chairman, Organising Committee 9th ICCC and NCB, delivering the Welcome Address

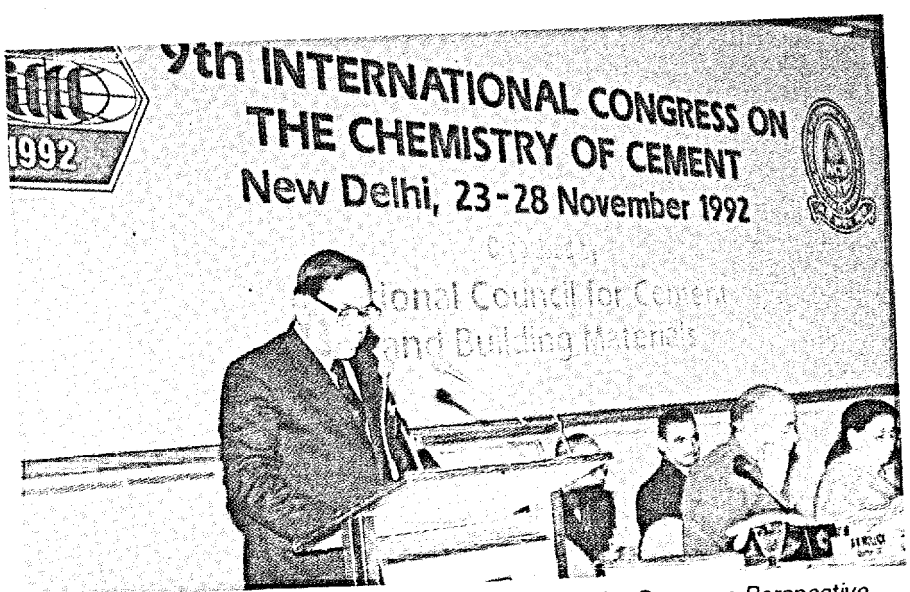

Dr A K Mullick, Director General NCB, presenting the Congress Perspective



Mrs Krishna Sahi, Hon'ble Minister of State, Industrial Development, at the informal get-together

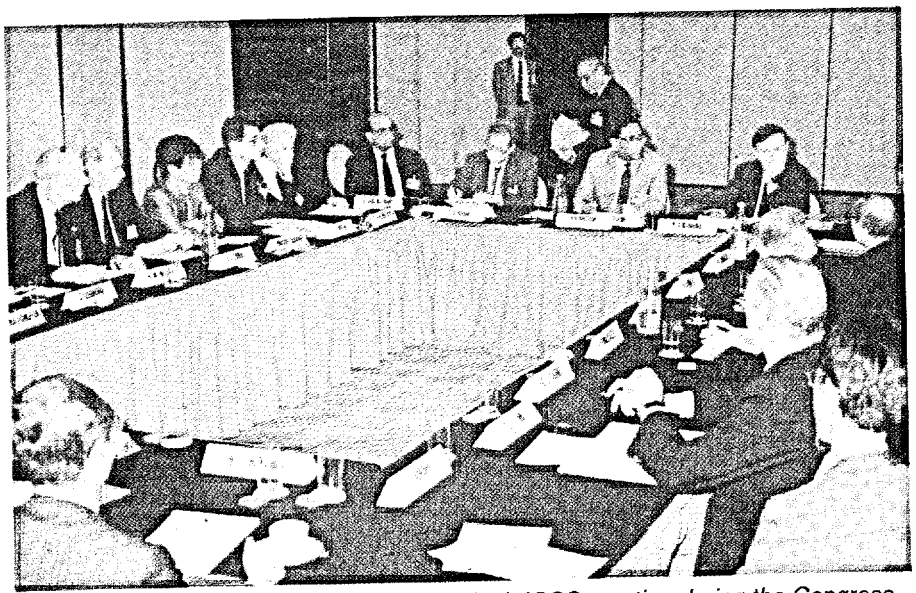

The International Scientific Committees of 9th ICCC meeting during the Congress

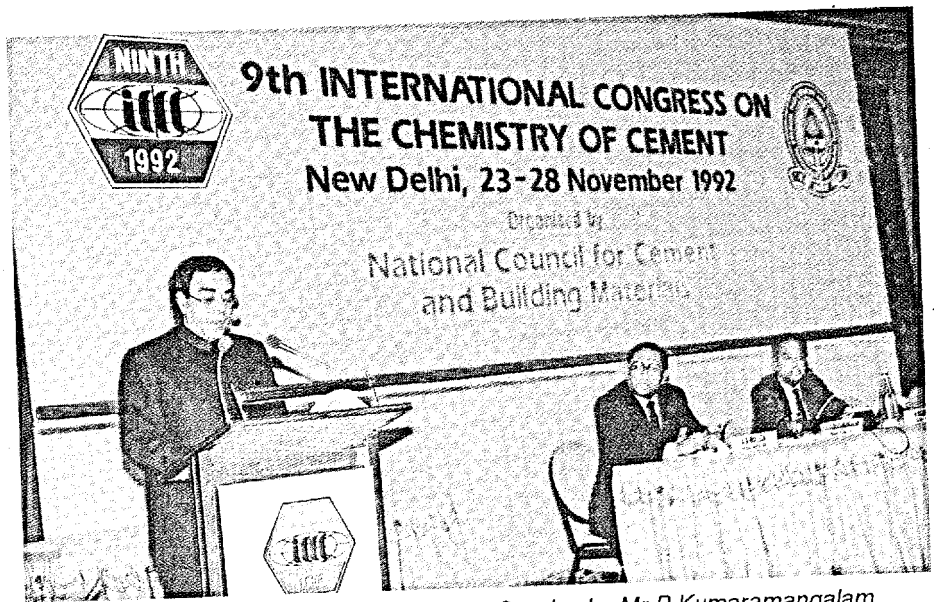

Valedictory Address at the Concluding Session by Mr P Kumaramangalam, Hon'ble Minister of State, Science and Technology

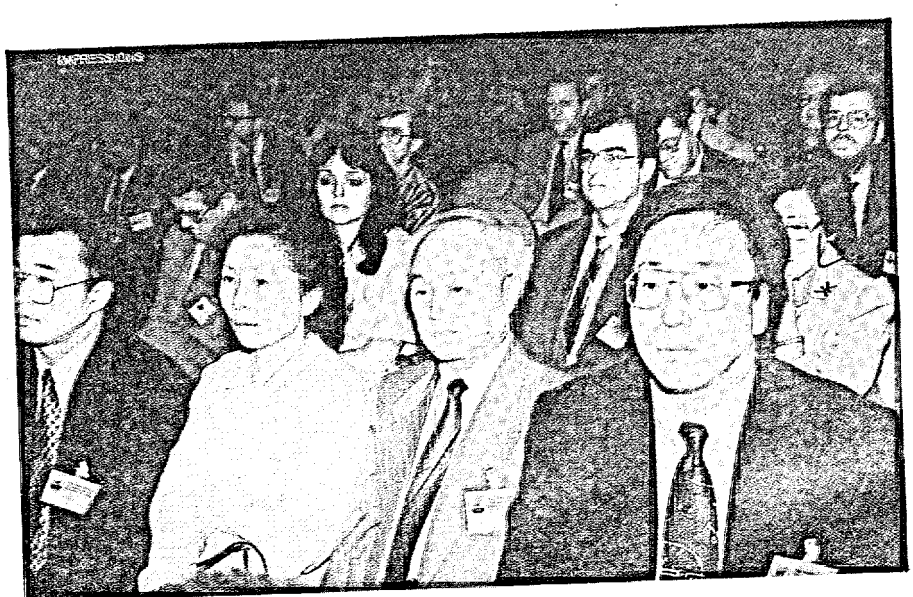

A section of the delegates



A moment of serious consultation between Prof F P Glasser, University of Aberdeen, UK and Prof Hiroshi Uchikawa, Onoda Cement Co Limited, Japan



Lady delegates from China at Tea break

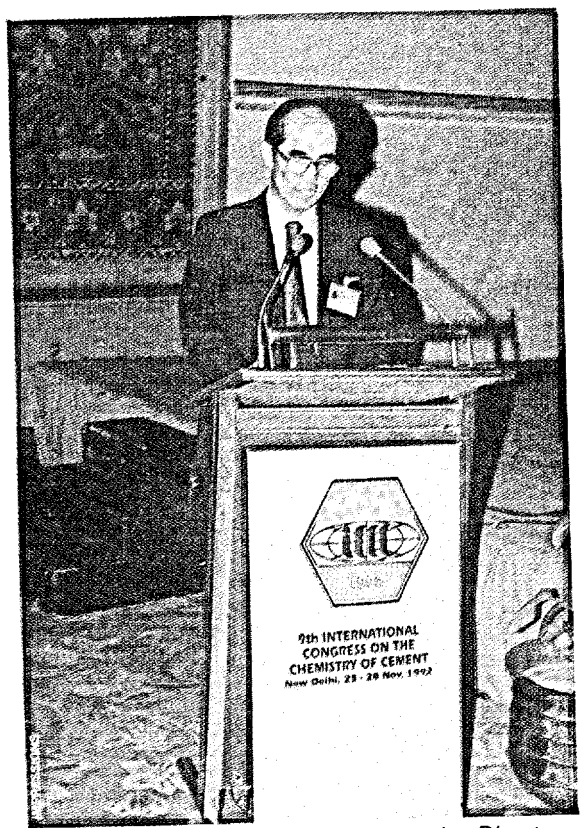

Prof Dr Eng Hiroshi Uchikawa, Executive Director, Research and Develoment, Onoda Cement Co Limited, Japan, delivering his Special Lecture

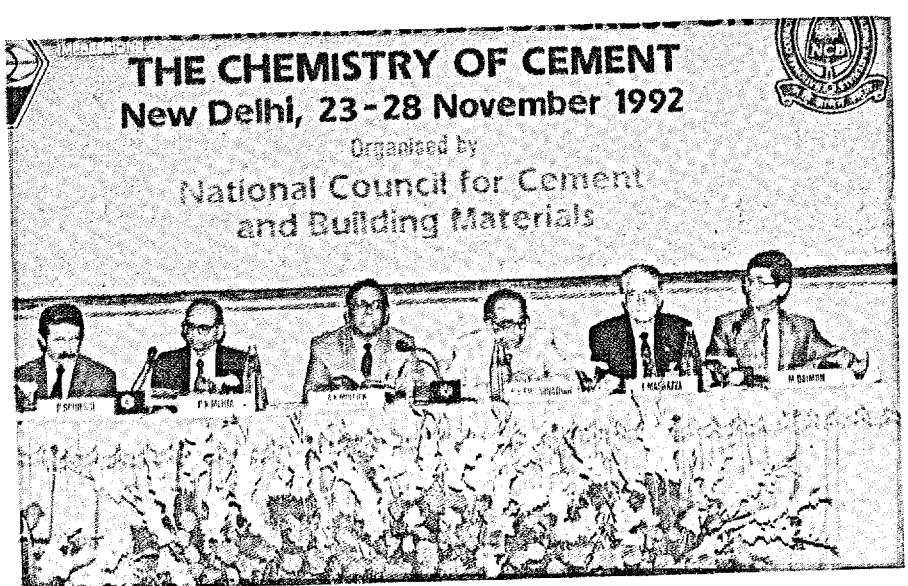

Making introductory remarks at Session II is the Chairperson Dr K V Swaminathan (Third from right)

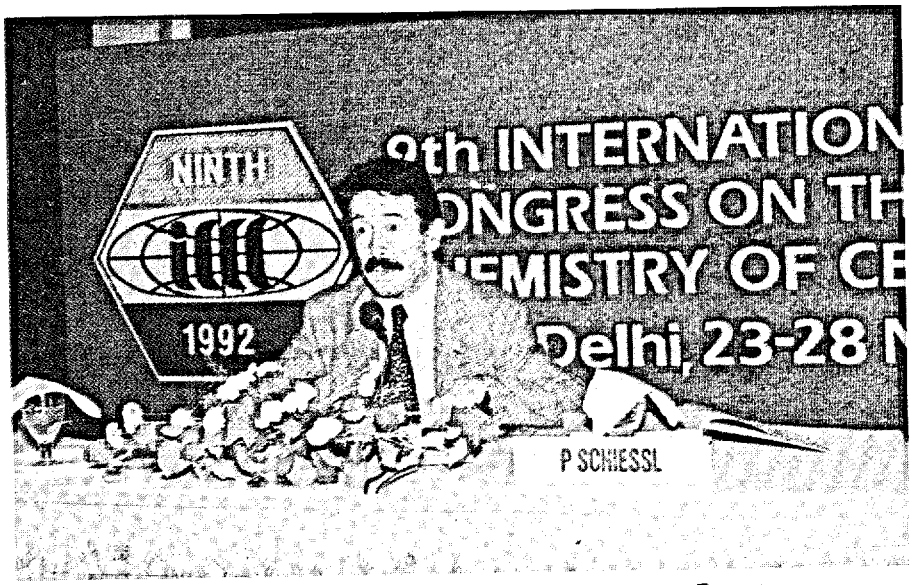

Dr P Schiessel (Germany) presents his Congress Report



Dr A J Majumdar (UK) presents his Congress Report, Chairperson of the Session, Dr M Daimon (Japan) is third from left at the table



Presiding over Special Session I is Dr V M Malhotra (centre) *of CANMET, Canada. He is flanked by Dr A K Mullick* (left) *Director General, NCB and Dr H Uchikawa*



Dr F H Wittmann (Switzerland), invited speaker at Special Session III, and the Chairperson Dr P K Mehta



Prof Della M Roy (USA) presenting her paper

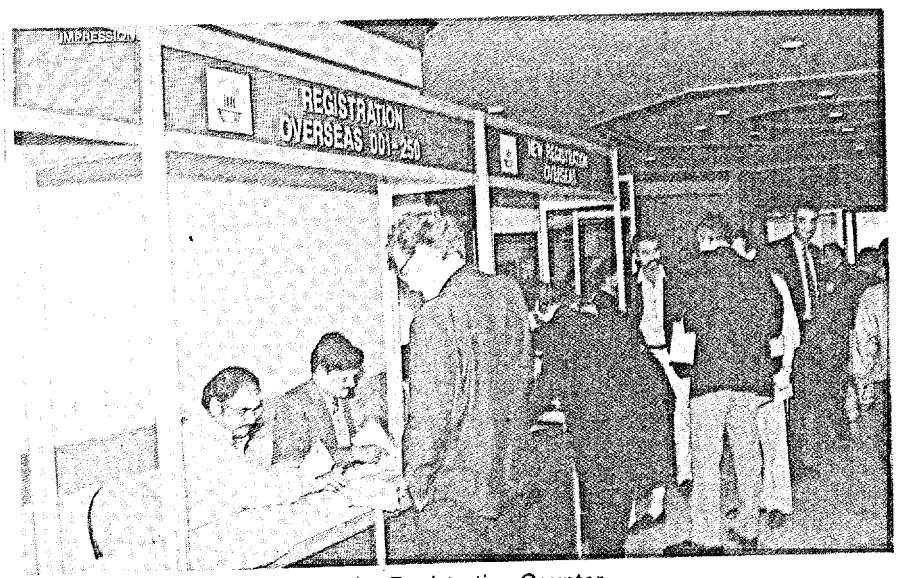

At the Registration Counter

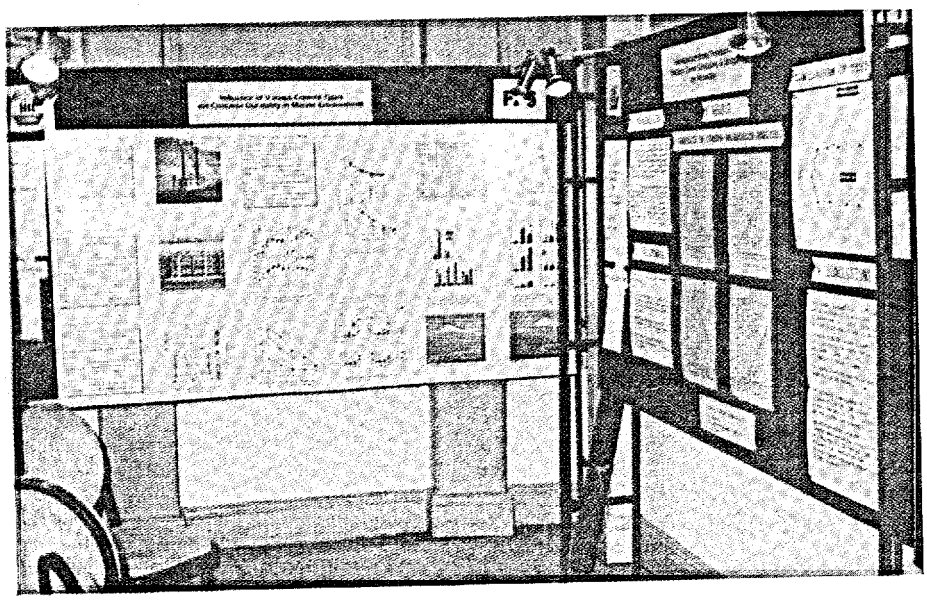

A section of the Poster Papers enclosure

9TH INTERNATIONAL CONGRESS ON THE CHEMISTRY OF CEMENT

SPECIAL LECTURE

ADVANCES IN PORTLAND CEMENTS AND UTILISATION OF INDUSTRIAL WASTES – TOWARDS SUSTAINABLE DEVELOPMENT

Dr A K Mullick
Director General
National Council for Cement
and Building Materials

DRAFT - FOR LECTURE

TO BE CHECKED BEFORE PUBLICATION

ADVANCES IN PORTLAND CEMENTS AND UTILISATION OF INDUSTRIAL WASTES — TOWARDS SUSTAINABLE DEVELOPMENT

Dr A K Mullick
Director General
National Council for Cement and Building Materials

INTRODUCTION

We had the privilege of listening to the special lecture on "Present-day Problems in Cement Manufacture" yesterday; there is another presentation planned for tomorrow, covering performance aspects. Keeping these two presentations in view, I had to search for an area to focuss. After some considerations, I have chosen "**Advances in Portland Cements and Utilisation of Industrial Wastes - Towards Sustainable Development**" as the subject. We are talking of sustainable development which is aimed at "meeting the material needs of present generations without compromising the ability of future generations to meet their needs". In this particular case, we have to dovetail the developments towards the search for low and non-waste technology (for cement) to mitigate the increasing shortage of major resoures, ie, raw materials, energy and the environment.

From the deliberations of the last few days, it is clear that this Congress has identified the following as the main issues facing the cement and construction industries :

* cost reduction through energy and materials conservation;
* improvements in efficiency of operations;
* environmental protection; and
* improved performance in constructions.

Taken together, these form the key issues to sustainable development.

Although the issues are listed separately, in so far as development of cement systems and building materials are concerned, there is considerable overlap between them. In other words, more than one objective can indeed be achieved through one solution.

Invited Congress Reports as well as Communication Papers presented in Theme II on this topic have been taken into account in making this presentation, besides relevant information in the published literature and from the industry sources. Instead of elaborating on the scientific information at any great length, I will endeavour to examine the developments from the view point of adaptation by the cement manufacturing industry and the construction industry.

ENERGY AND MATERIAL RESOURCES

Cement manufacture is energy-intensive and therefore, reduction in thermal and electrical energy have always received considerable attention as will be reflected by the trend of energy consumption in different countries. What is shown in Figs 1 and 2 is the trend in the Indian cement industry, which indicates that the average values of specific thermal energy (in kcal/kg of clinker) and specific electrical energy (in kWh/tonne of cement) have progressively decreased as aided by various technological developments. The specific thermal energy has come down gradually with the switching over to dry process of cement manufacture, introduction of pre-heater and precalcinator systems, and adoption of large million tonne plants. Further reductions have been possible with the adoption of six stage preheater systems, low pressure drop cyclones and kilns of smaller L/D ratio (Fig 1).

In case of specific electrical energy, it increased somewhat with the switchover to dry process plants, but again started declining as more and more efficient grinding systems were introduced in the industrial stream (Fig 2).

It is now believed that while reduction in specific power consumption would still be possible with better grinding systems, reduction in specific thermal energy consumption can be effected only through improved plant operations and input of material science in the formulation of cement systems. The experience of a number of cement plants in India has shown that by adopting efficient operational practices and good housekeeping, unit energy consumption rate has steadily declined during the last few years. These include :

* Minimising false air infiltration in the Preheater-ESP-Raw Mill circuits;
* Process optimisation for improved combustion and increased cooler efficiency;
* Replacing higher rating motors by optimum rating and reducing idle running of equipment;
* Proper control of feed and product sizes to grinding mills;
* Rationalisation of compressed air utilisation;
* Introduction of Slip power recovery systems for speed control on fan motors;
* Installation of High efficiency fans;
* Replacement of pneumatic conveying by mechanical transport like bucket elevators, belt conveyors etc;
* Providing Variable speed drives and frequency controllers for fan drives.

No capital investments were involved in bringing about the improvement.

Coming to the raw material scene, the total cement grade limestone deposits in India are estimated at 95,000 million tonnes. (Fig 3). The figure in itself is impressive, but once we realise that only 18 percent of it is in the "measured" category, and on the other hand, 27 percent of the total reserves are in the "marginal" grade, and lastly, major limestone deposits are concentrated only in a few States in the country, certain disquieting thoughts come in. For example, as a perspective for the 8th Five Year Plan period, it has been suggested that unit plant capacity should go up to 1.5 million tonnes. But then it is found that limestone deposits which can sustain cement plants of this size are occurring only in such States, most of which are even now surplus in cement production over the demand.

On the other hand, substantial quantities of wastes are generated in the country which has the same elemental compositions as the principal raw materials used in the manufacture of cement or other building materials. It is estimated that the volume of various industrial, agricultural and urban wastes produced annually in India are :

Industrial, including Mining Wastes	250 m tonnes
Agricultural Wastes	350 m tonnes
Rural and Urban Wastes	1800 m tonnes

Exploitation of these wastes in the cement and building materials industries achieve the purpose of raw material conservation as well as environmental improvement through wastes utilization.

Another problem unique to countries like India is, use of coal as fuel for cement manufacture, its high ash content and also the variable quality. This will result in increasing coal consumption for cement manufacture, but then there is a limit of how much coal ash can be absorbed in the clinker. On the other hand, if the requisite thermal energy is not provided, the temperature attained inside the kiln would indeed be lower than required.

AVENUES FOR THERMAL ENERGY CONSERVATION IN CEMENT

As it has been mentioned above, the three approaches for energy conservation would be through improved plant and machinery, improved formulations for cement composition and improved plant operations. In so far as specific thermal energy consumption in cement manufacture is concerned, it is now believed that in modern dry process cement plants equipped with preheater-precalcinator systems, for saving in thermal energy, one has to fall back upon material science approach.

In the dry process of cement manufacture, the heat required is essentially for the dissociation of calcium carbonate in the raw mix and to heat the feed to the clinkering temperature of around 1450°C. In the wet process, further heat is required for drying out the moisture. However, we will not consider wet process technology in any great detail. The strategy for lowering the thermal energy, would be through means of three possible steps :

(a) whether the dissociation of calcium carbonate as well as formation of clinker can be accomplished at relatively lower temperature, by use of activators as well as mineralisers and fluxes;

(b) whether the lime content in the raw mix can be reduced.

These two taken together, can be classified as approach to portland cements of lower clinkerisation temperature and for low-lime mixes.

(c) incorporation of latent hydraulic, pozzolanic or inert fillers in blended cements and composites, where the proportion of cement clinker is considerably reduced.

ADVANCES IN PORTLAND CEMENTS

A number of developments following the approach to Lower Clinkerisation Temperature and Low-lime Mixes have been investigated in many countries in the world. Apart from conservation of energy and raw material resources, some of these systems also aim at improving the product performance. The approaches are tabulated in Table 1 and described below.

Mineralisers and Fluxes

If mineralisers and/or fluxes are used with normal cement raw-mix of LSF about 0.95, the clinkerisation temperature can be brought down from 1450° to around 1300°C. Mineralisers prompt formation of C_3S phase and fluxes lower the temperature at which the formation of liquid phase commences and also decrease the viscosity of the clinker melt. The line dividing these two functions are quite often thin. Fluorides and silico-fluorides are among the more common mineralisers which have been investigated along with gypsum as well as heavy metals like zinc, copper, cobalt etc. Improvements result from modifications in the mineralogy, morphology and micro-structure of the main cement minerals. Entering into solid solution with main clinker minerals, these dopants can improve the strength characteristics, besides improving the burnability of the raw mix.

Although the clinkerisation temperature could be lowered by upto 150°C, the resultant energy saving is proportionately much less, because lower burning zone temperature also lower the temperature of the waste heat that is recovered in the process. Although the heat losses of the kiln are reduced with less fuel energy input, there is always energy to be recovered from the

clinker cooler and the net energy saving could be of the order of 5%.

In many situations it has been seen that this saving of energy does not compensate the cost of the mineraliser which has led to the use of the combination of mineralisers like fluoride and gypsum. The performance of mineralisers cannot be generalised, but would vary from case to case and control of mineralising effect would sometime become difficult; problems of material flow may result due to the volatiles and inhomogenity of dispersion of the mineralisers. If temperature reached inside the kiln is not controlled, melting may take place at the transition zone or even earlier and local damage to refractory takes place. The kiln control therefore becomes more difficult and may lead to clinker ring formation if proper care is not taken. Use of mineralisers should be viewed more as a necessity when the raw materials encountered are marginal and adequate burnability of the raw mix can be achieved only with the use of suitable mineralisers in some cases. It may also help in the coating formation of the refractories. In India, mineralisers have been used to encounter problems of marginal grade raw materials and coal of relatively lower calorific value.

Low-lime Mixes

The effect of reducing the $CaCO_3$ content in the raw-mix on the theoretical energy required for clinkerisation is expressed in Fig 4. As a typical estimate, it has been stated that if the lime saturation factor of the rawmix decreases from 0.97 to 0.80, the reaction enthalpy of formation of cement clinker decreases from about 440 kcal/kg to about 390 kcal/kg, ie, a decrease of about 50 kcal/kg. Such lowering of lime factor means lower proportion of C_3S and higher proportion of C_2S phase in the clinker, and therefore the clinker formation can take place at a temperature lower than the usual (1450°C). Such a cement with high C_2S content will be relataively slower in gaining strength. Very rapid cooling of the clinker can stabilise the high temperature modifications of C_2S phase and the reactivity increased due to introduction of crystal defects. Such rapid cooling would mean higher heat losses in the clinker cooler and as a consequence the net saving in fuel energy becomes

much smaller than from reaction enthalpy calculations. Higher percentage of C_2S phase, which is more harder to grind, may also increase the energy consumption in grinding and the net energy cost may not show appreciable difference. In addition, the cement may have to be ground finer, which also would increase the consumption of electrical energy.

As we will discuss later on, such cements having higher proportion of C_2S and therefore slower early strength, do not permit addition of significant quantity of slag or pozzolans in the manufacture of blended cements. The net effect of these developments would be that virtually there would be no energy saving. The belite phase can also be activated in the presence of alkalis and other additives introduced in the raw mix. Such belite cements do often result when marginal grade limestones and low calorific value fuels are used even when such formulations are not specifically planned. A cement plant is unlikely to have special arrangements for very rapid cooling for the clinker and grinding to higher fineness is therefore resorted.

Another approach, which would permit LSF in the raw-mixes even upto 0.75, is in the formation of what has been called Active Belite Cement containing sulpho-aluminate and sulpho-pherite phases. Referring to Table 1, one would notice one common feature being, near or total absence of C_3S phase. $C_4A_3\bar{S}$ - calcium slupho-aluminate is an important phase in these cements. As is well known, this phase is present in expansive cement, where initial expansion and strengths at early ages are due to formation of ettringite. Another phase which has received considerable attention is the compound $12CaO.7Al_2O_3$ ($C_{12}A_7$) which has the formula $C_{11}A_7.CaO_2$ in which the two oxygens atoms can be replaced with two chlorine or chromium atoms or hydroxyl group.

The compound $C_{11}A_7.CaX_2$ can be used independently or with gypsum and admixtures for giving quick setting formulations. Similarly, the ternary mixtures of OPC, HAC and gypsum allows early strength by formation of ettringite and expansion characteristics.

The cement based on $C_4A_3\bar{S}$ containing C_2S and free lime are prepared by burning a raw material containing SO_3/Al_2O_3 in a rtio of 1.3/1.9. The

strengths of the order of 27 MPa at three hours and 59 MPa at 28 days was reported by Sudoh et al. A high early strength formualtion based on $C_4A_3\bar{S}$, C_2S and $C\bar{S}$ is obtained by burning a raw material ratio of SO_3/Al_2O_3 0.4/1.7 and C/A is equal to 0.5/1.2 to a temperature of 1200 to 1300°C. This is a high early strength cement having a strength of 15 to 24 MPa at four hours.

Alumina-belite cements typically contain 60 to 65% of β - C_2S and the clinker is formed at a temperature between 1250 and 1300°C. The cements are required to be ground to a fineness about 400 m^2/kg so as to result in compressive strength comparable to normal OPC. The early strength of such formulation is due more particularly to the formation of ettringite and calcium aluminate hydrates and usual calcium silicate hydrates (CSH) formed contribute only at a substantially later stage.

In the present Congress, considerable details of synthesis as well as structural details of $C_4A_3\bar{S}$ phase have been described. It has been stated that $C_4A_3\bar{S}$ could be synthesised from phospho-gypsum, flyash, slag and bauxite as raw materials at 1170°C. When blended with separately synthesised C_2S and CS, strength of the order of 18-31 MPa at 1 day and 37-42 MPa at 28 days were obtained. $C_4A_3\bar{S}$ phase can also contain upto 9% Fe_2O_3 in solid solution. A number of other additives like BaO, SrO, $CaCl_2$, TiO_2 ... were also found to enter into solid solution with $C_4A_3\bar{S}$ and modify the ettringite phase in the hydration process. Assimilation of MgO suggested possible use of dolomitic limestone.

Cements containing sulphated calcium ferrites in C-F-$C\bar{S}$ system are reported to be commercially produced in Russia. The clinkering temperature is 1200 to 1300°C. These have expansive properties and develop compressive strength of the order of 80 MPa at 28 days. Mass production of quick setting and rapid hardening special cements in the $C_{11}A_7.CaF_2$ - β C_2S system have been reported from China, which gave concrete strength of 25 MPa at 3 hours and 46-58 MPa at 28 days.

Mehta had described an iron oxide cement which consists on an average 35% of C_2S, 30% C_4AF, 20% $C_4A_3\bar{S}$, and 15% $CaSO_4$ can be burnt

at 1200°C. At a fineness of 350 m^2/kg, the strengths are reported to be comparable to those of normal OPC.

Blends of OPC and High Alumina Cement and gypsum are often used for formulations of expansive cement systems. In India such a system has been widely used for grouting of heavy machinery foundations (Fig 5). The typical hydration products are CSH, ettringite and Calcium Hydroxide. The ettringite phase is quite stable even after long years in service (Fig 6). Separate formation of $C_4A_3\bar{S}$ phase and then blending with OPC in 10-15% by wt has been reported. However, during the process of clinkering, $C_4A_3\bar{S}$ based cement, care must be taken to prevent the decomposition of $CaSO_4$ to obtain a suitable clinker and avoid SO_3 volatalisation.

Another formulation reported from India is of a fast setting high early strength on the basis of ettringite formation and accelerated CSH formation. In a typical shotcrete mix for tunnel lining, early setting time - up to two to five minutes, and compressive strength of 10 to 20 MPa in two hours was obtained. Rebound in placement was reduced. The hydration phases included ettringite, CSH, Calcium Hydroxide, gypsum and ammonium sulphate hydrate.

Industrial Adaptation

While considerable laboratory research on various aspects of such modified portland cements has been reported, it must be admitted that it has not caught up on the industrial stream. As was pointed out, the net energy saving by lowering the clinker temperature by 150 to 200°C is perhaps not more than 5%, which would not justify creation of separate cooling arrangements and additional cost of dispensation of the additives like their procurement, storage and handling. It is quite unlikely that a large cement plant of capacity 3000 tonnes per day or more would be exclusively manufacturing such cements at least in the near future and therefore commercial application must be relegated to smaller capacity plants. Practical problems of pyroprocessing and kiln control that can accompany such formulations when the temperature of clinkerisation is not precisely controlled, as well as the interaction with the refractory system has not been reported.

While the hydration phase of these systems have been adequately reported, the resultant durability in constructions, specially for the inclusions in contact with the matrix, ie, aggregates or the reinforcements, have not been reported much in detail. It may be recalled that although commercial production of alinite cement, where the clinker formation takes place in a salt melt, was reported, its use in reinforced concrete has not been encouraged, due to the risk of reinforcement corrosion. On the other hand, desired performance characteristics like rapid setting or high early strength or expansion for compensation of shrinkage can always be obtained in the system of OPC/HAC/Gypsum and some accelerators.

Cement based on calcium aluminates are capable of rapid strength development and superior chemical resistance specially in sulphatic environment. Use of high alumina cement which imbibes all these properties are however not favoured for structural concrete because of progressive reduction in the strength of the concrete that takes place over the years due to conversion of hexoganal calcium aluminate hydrates to cubic hydrates, specially with increase of temperature and humidity. Significant research has been reported from BRE in England wherein blends of high alumina cement and granulated blast furnace slag have been found to give very satisfactory performance in terms of compressive strength in prolonged moist curing and of temperature up to 40°C (Fig 7).

USE OF INDUSTRIAL WASTES AS RAW MATERIALS

Because of the similarity of main elemental composition between them, the various types of industrial wastes can be substitutes for naturally occurring raw materials in the manufacture of cement, as well as other binders and building materials. A list of various industrial wastes which can be used for cement and building materials industries, and their availability in India, are shown in Table 2. Considerable research and development work have been carried out in many countries on the techniques of utilisatiaon of such industrial wastes and the technologies are well established.

For the conservation of basic raw material in the manufacture of cement, use of flyash, lime sludges and red mud can be mentioned. Because of its substantial lime content, use of various sludges are more common. A summary of typical chemical composition of various sludges, indicating $CaCO_3$ content as well as other impurities, which restrict their utilisation in cement manufacture, is shown in Table 3.

Press mud is obtained as waste from sugar industry, containing 45-50 percent moisture and 9-12 percent organic matter. After disposal, the sludge dries out in the field, and on a dry basis, has 18-20 percent organic matter and a lime content of 38-40 percent. Since the organic matter is light material, it has to be separated before grinding with the other raw materials, so as to enable its use as a part substitute to limestone.

Carbide sludge contains a high percentage of lime (56 percent) and chloride (0.46 percent). Because of the presence of chloride ions, it cannot be used in total substitution to limestone in cement manufacture in which the total chloride content is required to be restricted to 0.5 percent as per Indian Standard Specifications. Depending upon the chloride content in the carbide sludge, the content of sludge in the raw mix shall have to be limited. Rheological properties of raw mixes containing carbide sludge are also important. Taking into consideration the flowability and pumpability of cement raw meal slurry in a wet process plant about 30 percent sludge can be utilised. A 600 tpd commercial cement plant is in operation in India, using carbide sludge to partially substitute limestone.

Calcium carbonate sludge (phosphochalk) contains about 10 percent SO_3. A maximum of 10 percent phosphochalk can be substituted for limestone in the raw mix. Use of phosphochalk beyond 10 percent may not be favoured because of the presence of high SO_3, P_2O_5 and $\bar{F}$ contents (Table 3).

Red mud, a waste from the aluminium industry, contains high alumina and iron. Therefore use of red mud has to be restricted to keep the potential clinker liquid and the moduli values under control. Because of high percentage of R_2O_3 group of elements such as iron and aluminium (60-65 percent) a

maximum of 8-10 percent red mud can be incorporated in the raw mix, where no clay is used. Use of red mud lowers the temperature of liquid formation by about 100-150°C.

Phospho gypsum is used as set controller for cement manufacture in partial replacement of mineral gypsum. Presence of impurities like P_2O_5 and F adversely affects performance of phospho gypsum unless these impurities are reduced by beneficiation. Use of flyash containing high SO_3 content has been suggested for set control, in place of gypsum.

A general problem of waste lime sludges is that the moisture content in the filtered cake is 35 to 50%. In case of slurry the solid content is 5 to 10%. Both handling and transportation of wet sludges and pre-drying before use are required. For handling and transportation of phosphogypsum, systems are required both at the fertiliser and the cement plants. At the fertiliser plant, the phosphogypsum slurry from the pond can be pumped by conventional slurry pumps to the washing system. Washed slurry is fed to either filter press or centrifuge or to sun-drying. The dried phosphogypsum is required to be transported to the cement plant in bulk.

Use of flyash as a raw material for cement manufacture is not common in India because of lack of plastic properties (for wet process) and volatalisation of alkalis in dry process plants. However, instances of use of flyash, blast furnace slag and phosphogypsum for manufacture of special cements containing $C_4A_3\bar{S}$ phase has been suggested. It has been pointed out that impurities present in such industry-derived material can reduce the temperature of synthesis of $C_4A_3\bar{S}$ from 1350 to 1170°C.

INDUSTRIAL WASTES AS ADDITIVES IN BLENDED CEMENTS

A number of latently hydraulic, pozzolanic or inert fillers can be used as additions to blended cements or as mineral admixtures in concrete, with granulated blast furnace slag and flyash (also called pulvarised fuel ash) leading the way. A classification of such additives is given in Table 4. The basis of reactivity of such mineral additions and the chemistry of hydration

with cements are too well known to be repeated. We may summarise that hydration reactions of slags can be activated in presence of lime, typically derived from the hydration of cement. In case of pozzolans like flyash, cementitious products are formed in combination with lime and in presence of moisture, as in hydration when blended with ordinary portland cement. The hydraulicity of blast furnace slags and pozzolanicity of fly ash etc depends upon its chemical composition, mineralogy and fineness and particle size distribution, and therefore experiences in different countries may not match in a quantitative sense. For example, Indian slags, although containing 90 to 95% glassy phase, are characterised by relatively lower lime content and higher alumina content. The glass content in Indian flyashes are only 30 to 35% and the lime content is low. The pozzolanicity, therefore, is considerably lower, compared to other flyashes with much higher glass content or with high lime content.

From basic considerations it would appear that a blend of 70 to 80 percent ground granulated blast furnace slag with adequate hydraulicity can be activated with lime liberated by the hydration of say 20 to 30% cement. However, from practical considerations of relative grindability of slags and clinker as well as the need of fulfilling the requirements of strength specifications at early ages (3, 7 and 28 days) at par with ordinary portland cement, the slag content in commercial cements in India are much lower. To a large extent the same situation exists in case of portland pozzolana cements where pozzolana like flyash is interground with cement clinker. The fineness of the blended cement to which it has to be ground as well as the pozzolana percentage are arrived at by trials of the nature shown in Table 5. Although cement specifications in India permit addition up to 25% pozzolans in blended cement, the usual proportion seldom exceeds 15%, lest the initial strength of the blend would be lower and may create marketing problems.

The relative merits of whether it is more advisable to use the mineral admixtures in manufacture of blended cements in the plants rather than mixed with cement and other components of concrete in the mixer at the site has often been debated. While the chemical reactions in the final concrete mix may be the same, there are intrinsic differences in the amount of additions

that can be made. For blended cements whose performance requirements including early age strength are to be at par with ordinary portland cement, would quite often not permit larger additions as would be permissible in a concrete mix, where the strength of the mix can be specified as per the site requirements and even at a much later age, eg 90 days or even one year in case of a concrete dam.

Many advantages of blended cements can be realised only with prolonged moist curing. Longer duration of moist curing and delayed form removal in structural concrete are necessitated due to slower rate of gain of strength upto, say, 28 days, for which the concrete mixes are customarily designed. Other parameters remaining the same, the compressive strength of concrete is generally related to strength of cements as in standard mortar tests. Because of lower early age strength, mineral additions may increase the volume of cement produced but not necessarily the volume of concrete made with it. Advantages of blended cements should thus be searched in the realm of improved durability.

It must be recalled that blended cements like portland slag cement and porrtland pozzolana cement were intended to render specific engineering properties to the blend like low heat of hydration, increased sulphate resistance etc. Adequate reactivity of the slag and flyash to be blended is therefore essential. Present-day trend in UK is to further process the flyash by grinding, so as to obtain uniformity in grain-size distribution. There is considerable data reported on the durability of concrete when either slag or flyash are incorporated. Most significant improvements are reported in the case of increase to corrosion resistance as well as alleviating alkali silica reaction (Figs 8 to 12). Similar results of improved durability has also been reported in case of high-volume low-calcium flyash concrete. Improved sulphate resistance can result in portland slag cements, if the slag percentage is very high; otherwise it would essentially depend upon the C_3A content in the parent cement.

Because significant slag reactions or pozzolanic reactions cannot be expected by 28 days, such blended cements are generally required to be ground to about 500 cm^2/g (Blaines) greater and still result in about 10% lower

compressive strength till 28 days (Table 6). From these considerations, it will appear that in commercial slag cement containing typically 45 to 50% slag there would still be some scope for pozzolanic reactions with flyash. Attention has therefore shifted towards ternary blend of ordinary portland cement, slag and flyash along with gypsum. For a blend of 50% ordinary portland cement, 40% slag and 10% flyash, perhaps the strengths could be comparable with the parent 50-50 portland slag cement. Where the slag percentage is high, no pozzolanic reactions on addition of flyash can be expected.

In general, in order to manufacture a blended cement with good performance it is recommended to choose a clinker of high quality, with C_3S and C_3A and alkali content higher than that of a clinker for plain portland cement. This is one of the disadvantages of low-lime mixes like belite cement which may not offer energy and material economy by allowing blending with such mineral admixtures. However, instances have been reported where the compressive strength up to 28 days in a low-heat cement containing 51 to 65% C_2S increased with addition of blast furnace slag upto 60% (Fig 13). The heat of hydration however remained lower than that of the low heat cement. In this instance the blast furnace slag seem to assist develop the microstructure of low heat cement. Increase in compressive strength of the low heat cement blended with flyash (20 to 30%) was observed at one year age.

One significant trend in the manufacture of portland slag cement is the separate grinding of clinker and gypsum on the one hand and slag on the other, with overall power consumption of the order of 43 to 44 kwH/tonne against 55-60 kWh/tonne in case of combined grinding.

Inert Fillers

With the introduction of a common European Standard Specification in line with countries like France, which permit addition of inert calcarious fillers, eg, ground limestone or silicious fillers, eg, silica dust, considerable research has been reported on the effect of addition of such inert fillers. Addition of ground limestone upto 5% is claimed to result in a beneficial reaction with the C_3A in ordinary portland cement, leading to formation of calcium

carbo-aluminate, thereby participating in set control, with possibly no adverse effect on the strength. However, the effect will essentially depend upon the chemical composition and characteristics of the parent cement.

Alkali Activation

Alkaline activation of slag is known for long time when slag-lime binders were marketed and used in the thirties. Apprehension of long term durability and development in ordinary portland cement led to general decline in its application. Renewed interest has now been focussed on activation of slags in the presence of alkalis. Such activators being sodium hydroxide, gypsum, calcium hydroxide, water glass, sodium carbonate etc. Very high compressive strengths upto 80 to 90 MPa or even higher, have been reported (Fig 14). In general, a combination of activators have been preferred. Development of activated slags and its blend with flyash were attempted in NCB to result in non-portland cements - blended cements having strength properties at par with ordinary portland cement, and were recommended for use as masonry cement. Flyash-slag blend activated with sodium silicate has been reported to have a strength of about 50 mpa and with increase in strength with time.

Attention has been given to the utilisation of air-cooled slags which are not hydraulic and the disposal of which is becoming a problem in many countries. Alkali activation (NaOH, $Na_2 CO_3$) along with thermal processing at 1300 to 1350°C for further granulation and then water quenching has been reported to result in satisfactory hydraulicity of such activated slags.

BUILDING MATERIALS FROM INDUSTRIAL WASTES

From the discussions above, it will be clear that industrial wastes can certainly conserve the basic raw material for manufacture of cement and result in binders for masonry purposes even without ordinary portland cement. The full potential of such mineral additions cannot be achieved in blended cements because of strength requirements of specifications and market demands for cements with high early strength. On the other hand, such blends have demonstrated improved durability in the concrete and separate addition at the concrete mixer in larger volumes would be more useful for large volume

use of such wastes provided they are available in such usable forms.

Relative proportion of the wastes generated in a country, vis-a-vis the cement productin would dictate whether large volume use of such waste materials can be found through the cement concrete route. For example, in India which currently produce 55 million tonnes of cement, and perhaps 35 million tonnes of flyash, obviously all the flyash cannot be used by cement and concrete. On the other hand, considerable potential exists for manufacture of alternate binders/building components using flyash. A typical status projection is depicted in Fig 15 from which it will appear that for large volume structural use of flyash blocks as replacemenmt of fired (burnt) clay bricks for walling in housing construction has the largest potential. The basic route for utilisation of flyash in such application would be what can be called as "hydro thermal" processing. The soluability of the silica in the flyash can be increased both with temperature and in combination with lime (Fig 16). On this logic, the flow chart for generation of hydro thermal processing of flyash has been suggested which is reproduced in Fig 17. It is interesting to note that satisfactory building blocks can be manufactured at the stage following initial steam curing. A technology on this approach is depicted in Fig 18. The strength of such lime-flyash bricks are comparable to what is obtained in commercial clay bricks, and higher strengths are indeed possible by suitable changes in the formulations. Further hydro thermal treatment involving autoclaving has also been suggested as a technology by some other laboratories and naturally the strength of the blocks is higher. Following further calcination the hydro thermal cement made from activated flyash containing β C_2S phase resulted in satisfactory strength properties (Fig 19). Developments in these lines will be required for development of binders as well as building units from industrial wastes and at the same time solving the problem of their disposal.

CONCLUSION

1. Advances in portland cements has been reported which has the potential of lowering the clinker temperature, but concommittant energy saving is perhaps not very large. These cements do render special properties to concrete like high early setting, high early

strength or increased durability against sulphates etc. It will be proper to approach these developments in terms of such impoprtant properties rather than from the angle of energy conservation alone.

2. These developments would, however, be very useful when one has to use a marginal grade raw material and marginal fuel as in India. Any energy saving would be an added benefit.

3. Not much commercial manufacture of such cements are reported. Therefore, operational problems in the manufacturing of these systems as a continuous process in large size cement kilns, the problems of temperature control, interaction with the refractories etc have to be assessed.

4. Data on long-term durability of concrete in service, made with such modified cements should be collected.

5. The manufacture and use of blended cements are well established. However, the full potential in terms of volume addition has not been possible to be realised because of competitive strength requirements to be at par with ordinary portland cement. Such additions result in increased durability, specially resistance to corrosion of reinforcement and alkali silica reaction, which should be highlighted. Larger volumes of the additions are possible in concrete mixes rather than in cement plants.

6. Non-portland binders on the basis of activation of slags and flyashes do hold promise for applications in low-cost housing. However, it is more practical to make building blocks rather than binders, which will help in the construction and site management and at the same time enable larger volume utilisation.

REFERENCES

(To be added)